Can. J. Chem. Downloaded from www.nrcresearchpress.com by 210.87.254.5 on 09/05/12
For personal use only.

Canadian Journal of Chemistry

Published by THE NATIONAL RESEARCH COUNCIL OF CANADA

VOLUME 48 JANUARY 1, 1970 NUMBER 1

Perchlorate catalysis of the methanolysis of triphenylmethyl chloride in benzene solution and its relation to special salt effects in solvolysis reactions

K. T. LEFFEK

Department of Chemistry, Dalhousie University, Halifax, Nova Scotia

Received August 25, 1969

The kinetic form of the suppression of the perchlorate catalysis of the methanolysis of triphenylmethyl chloride in benzene solvent by tetra-*n*-butylammonium chloride has been investigated. This is consistent with a catalysis brought about by a simple perchlorate ion, suppressed by a competition between such ions and alkylammonium chloride ion-pairs for the alkyl halide ion-pair.

The results are discussed in relation to the qualitatively similar special salt effects observed in acetolysis reactions by Winstein and co-workers, with particular reference to the necessity of the concept of intimate and solvent-separated ion-pairs in the interpretation of these effects.

Canadian Journal of Chemistry, 48, 1 (1970)

Introduction

The study of the nucleophilic substitution reactions of triphenylmethyl chloride in benzene solvent by Swain and co-workers and by the Hughes–Ingold school led to controversy over the mechanism of the reaction (1–8). After the correction of experimental errors on the part of both groups, the mechanisms presented by them were essentially the same, even though the statements differed in detail (3, 8).

The alkyl chloride ionizes to a very slight extent to yield an ion-pair which is subsequently attacked by the reagent. In the alcoholysis reactions, the attack on the ion-pair by the alcohol molecule is the slowest step in the reaction, whereas in the radiochloride exchange, the initial ionization is rate determining. When the alcohol concentration is greater than 0.01 *M* the reagent also acts as a co-solvent giving an indeterminant order in alcohol greater than unity. In the presence of a tertiary base, such as pyridine, significant changes in the kinetics are observed, which have been studied by Leffek and Waterfield (9).

Part of the investigation made by Hughes *et al.* on the methanolysis of triphenylmethyl chloride concerned the catalysis of the reaction by saline perchlorate and the suppression of this catalysis by the common-ion chloride salt (6). The catalyzed reaction was found to have a kinetic order of one half with respect to the tetra-*n*-butylammonium perchlorate catalyst, which was interpreted to mean that the catalysis was brought about by single perchlorate ions. On the basis of this result the authors re-interpreted the perchlorate catalysis observed by Winstein and co-workers (10–14) on the solvolyses of several alkyl sulfonates in acetic acid solvent, as being due to simple perchlorate ions at low concentration and ion-pairs at higher concentration. Winstein prefers to explain this catalysis as an interaction involving the perchlorate ion-pair alone and has carried out a kinetic analysis to prove this (15). This paper included a criticism of Ingold's interpretation of the behavior of triphenylmethyl chloride in benzene, particularly with respect to the application of the steady state approximation to the mechanistic schemes proposed by Ingold *et al.* It is stated that a common-ion retardation of the methanolysis rate as observed by Hughes *et al.* (6) is not to be expected on the basis of the steady state approximation. However, the common-ion retardation was confirmed by Leffek and Waterfield (9) and the experimental behavior was fitted to an equation derived by use of the steady state approximation, from a mechanism which is essentially the same as that of Hughes and

TABLE 1

Suppression of the perchlorate catalysis of the methanolysis of triphenylmethyl chloride by saline chloride in benzene solvent*

$[(n\text{-}C_4H_9)_4NClO_4] = 5 \times 10^{-5}\ M$		$[(n\text{-}C_4H_9)_4NClO_4] = 1 \times 10^{-4}\ M$		$[(n\text{-}C_4H_9)_4NClO_4] = 2 \times 10^{-4}\ M$	
$10^6[(n\text{-}C_4H_9)_4NCl]$	$10^5k_1(s^{-1})$	$10^6[(n\text{-}C_4H_9)_4NCl]$	$10^5k_1(s^{-1})$	$10^6[(n\text{-}C_4H_9)_4NCl]$	$10^5k_1(s^{-1})$
0	11.0	0	14.4	0	19.1
0.2	10.7	1.0	12.0	2.0	15.4
0.5	8.4	2.0	8.2	3.0	12.6
1.0	8.4	4.0	7.6	4.0	12.3
1.2	7.9	7.0	6.4	5.0	9.8
1.5	7.6	—	—	8.0	7.8
2.0	7.8	—	—	—	—
$[(n\text{-}C_4H_9)_4NClO_4] = 5 \times 10^{-4}\ M$		$[(n\text{-}C_4H_9)_4NClO_4] = 1.0 \times 10^{-3}\ M$		$[(n\text{-}C_4H_9)_4NClO_4] = 2 \times 10^{-3}\ M$	
$10^6[(n\text{-}C_4H_9)_4NCl]$	$10^5k_1(s^{-1})$	$10^6[(n\text{-}C_4H_9)NCl]$	$10^5k_1(s^{-1})$	$10^6[(n\text{-}C_4H_9)_4NCl$	$10^5k_1(s^{-1})$
0	24.1	0	28.6	0	33.6
1.0	24.7	3.0	27.4	5.0	26.9
2.0	17.5	6.0	19.4	10.0	20.6
4.0	19.1	8.0	19.6	15.0	19.8
7.0	13.6	10.0	15.6	20.0	13.7
10.0	9.6	13.0	12.2	30.0	11.4
16.0	7.6	15.0	10.0	40.0	10.4
20.0	7.4	20.0	9.4	—	—
—	—	25.0	8.6	—	—

*$[(C_6H_5)_3CCl] = 0.05\ M$; $[CH_3OH] = 0.1\ M$.

Ingold except that the quadrupoles postulated by these authors were omitted for simplicity as these do not affect the derivation of the rate equation.

Winstein *et al.* have stated (15) that the work of Ingold *et al.* needs clarification and Bethell and Gold in a review (16) have called for a detailed consideration of Winstein's results from the viewpoint of the Ingold model. The present paper seeks to provide such clarification in the area of the perchlorate catalysis of the methanolysis, and examines again the compatibility or otherwise of the catalysis with the corresponding phenomenon observed by Winstein for solvolysis of sulfonates in acetic acid.

Results and Discussion

The results of Hughes *et al.* (6) have been extended in a detailed kinetic study of the suppression of the perchlorate catalysis by common-ion salt. These workers fitted this effect to the equation

$$[1] \qquad k_1^{pc} - k_1^{00} = \frac{k_1^{p0} - k_1^{00}}{1 + \rho c}$$

where the superscripts refer to the rate constants in the presence of a concentration of perchlorate (p) and chloride (c), and ρ is a competition factor between the chloride and other competitors for the carbonium ion-pair.

Six series of runs were carried out using constant concentrations of alkyl chloride and methanol, and within each series, the perchlorate concentration was held constant while the catalysis was suppressed by gradually increasing the concentration of added alkylammonium chloride (17). The results are collated in Table 1 and three of the series are plotted, in the form $(k_1^{pc} - k_1^{00})^{-1}$ vs. c, in Fig. 1. (The value of k_1^{00} is $5.6 \times 10^{-5}\ s^{-1}$.) Each plot shows a linear dependence, as observed by Hughes *et al.* (6), after an initial curvature which they did not report. The slope of each straight line provides a value for ρ, the competition factor, and these ρ values are shown in Table 2. The ρ values vary with the tetra-*n*-butylammonium perchlorate concentration and a plot of $\log_{10}\rho$ against $\log_{10}[(n\text{-}C_4H_9)_4NClO_4]$, shown in Fig. 2, has a slope of $-\frac{1}{2}$.

If eq. [1] is rewritten, substituting $A/p^{\frac{1}{2}}$ for ρ,

Can. J. Chem. Downloaded from www.nrcresearchpress.com by 210.87.254.5 on 09/05/12
For personal use only.

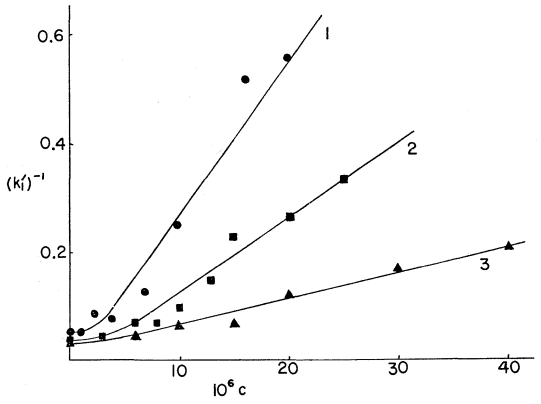

FIG. 1. The reciprocal of the catalyzed initial specific rate ($k_1' \equiv 10^5(k_1^{pc} - k_1^{00})$) plotted against the concentration of tetra-*n*-butylammonium chloride. Initial concentrations: triphenylmethyl chloride, 0.05 *M*; methanol, 0.1 *M*; tetra-*n*-butylammonium perchlorate; line 1, 0.5×10^{-3} *M*, line 2, 1×10^{-3} *M*, and line 3, 2×10^{-3} *M*.

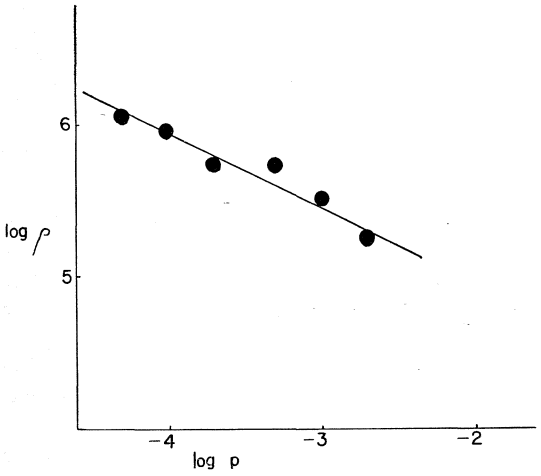

FIG. 2. The logarithm of the competition factor ρ plotted against the logarithm of the tetra-*n*-butylammonium perchlorate concentration. Initial concentrations: triphenylmethyl chloride, 0.05 *M*; methanol 0.1 *M*.

where *A* is a constant and *p* the concentration of tetra-*n*-butylammonium perchlorate, then

$$[2] \qquad (k_1^{pc} - k_1^{00}) = \frac{(k_1^{p0} - k_1^{00})}{1 + \frac{Ac}{p^{\frac{1}{2}}}}$$

Hughes *et al.* (6) showed that the catalyzed rate constant $(k_1^{p0} - k_1^{00})$ is proportional to $p^{\frac{1}{2}}$, indicating that the catalysis was brought about by a simple perchlorate ion. Equation [2] substantiates this in that it proves that the competition for the triphenylmethyl chloride ion-pair is between the tetra-*n*-butylammonium chloride ion-pair and the simple perchlorate ion.

TABLE 2

Variation of competition factor ρ with tetra-*n*-butylammonium perchlorate concentration*

$10^4[(n\text{-}C_4H_9)_4NCl]$	$10^{-4}\rho$
0.5	112
1.0	91
2.0	54
5.0	54
10.0	32
20.0	18

*$[(C_6H_5)_3CCl] = 0.05$ *M*; $[CH_3OH] = 0.1$ *M*.

In eq. [2], $(k_1^{p0} - k_1^{00})$ may be replaced by a factor $Bp^{\frac{1}{2}}$ as noted above, where *B* is another constant. Thus

$$[3] \qquad (k_1^{pc} - k_1^{00}) = \frac{Bp^{\frac{1}{2}}}{1 + Ac/p^{\frac{1}{2}}}$$

$$\therefore (k_1^{pc} - k_1^{00}) = \frac{Bp}{p^{\frac{1}{2}} + Ac}$$

Thus if

$$Ac > p^{\frac{1}{2}}, \quad (k_1^{pc} - k_1^{00}) \propto \frac{p}{c}$$

and if

$$Ac < p^{\frac{1}{2}}, \quad (k_1^{pc} - k_1^{00}) \propto p^{\frac{1}{2}}$$

Therefore, at extremely low concentrations of tetra-*n*-butylammonium chloride, the catalyzed rate will not be suppressed by this added chloride, but as soon as the factor *Ac* becomes significantly greater than $p^{\frac{1}{2}}$, the inverse proportionality between the catalyzed rate constant and *c* will be observed. From the graphs in Fig. 1, it is clear that the non-linear portion extends over a greater range of alkylammonium chloride concentration as the perchlorate concentration is increased. It can also be seen that if the dependence of $(k_1^{pc} - k_1^{00})$ on the perchlorate concentration is determined at extremely low alkylammonium chloride concentration, say 2×10^{-6} *M*, it will be identical to that found by Hughes *et al.* (6), since the plots are essentially horizontal at this point. However, at 10×10^{-6} *M* chloride, $\log_{10}(k_1^{pc} - k_1^{00})$ plotted against $\log_{10}[(n\text{-}C_4H_9)_4NClO_4]$ gives a straight line with

Can. J. Chem. Downloaded from www.nrcresearchpress.com by 210.87.254.5 on 09/05/12
For personal use only.

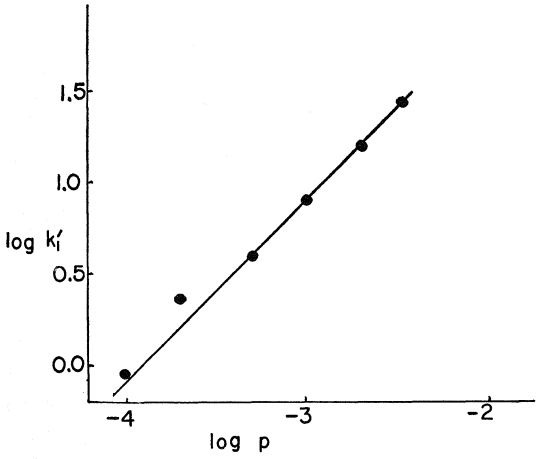

FIG. 3. The logarithm of the catalyzed initial specific rate ($k_1' \equiv 10^5(k_1^{pc} - k_1^{oo})$) plotted against the logarithm of the tetra-*n*-butylammonium perchlorate concentration. The line shown has a slope of unity. Initial concentrations: triphenylmethyl chloride, 0.05 *M*; methanol, 0.1 *M*; tetra-*n*-butylammonium perchlorate, 1×10^{-5} *M*.

a slope of unity, as predicted by the above analysis. This graph is shown in Fig. 3.

Thus, there can be little doubt that the catalysis and its suppression by common-ion salt behave as if the simple perchlorate ion is responsible for the rate increase at the concentrations studied. Since the mass-law equation [1] which these results fit so satisfactorily is of the standard form, well-known in physical–organic chemistry for many years, it would seem unnecessary to introduce the ideas of Winstein concerning intimate and solvent-separated ion-pairs. Nevertheless, these different types of ion-pairs are considered essential by Winstein *et al.* (15) in explaining the perchlorate catalysis in other systems, and this school has had considerable success in rationalizing a large amount of data concerning rates of solvolysis in terms of ion-pairs generally (18).

Notwithstanding this general success of ion-pairs, the kinetic distinction between intimate ion-pairs and solvent separate ion-pairs is not as firmly established as it appears to be. Winstein *et al.* (15) have offered a kinetic analysis of their special salt effect of lithium perchlorate in the acetolysis of 1-*p*-anisyl-2-propyl *p*-toluenesulfonate to prove that the effect is due to $LiClO_4$ ion-pairs and not to simple ClO_4^- ions. They plot (in Fig. 2 of reference (15)) a factor *Z*, a compound of two rate constants, against $LiClO_4$ concentration and also against the square root of this concentration. A steady state derivation of the rate law from Winstein's scheme, involving intimate and solvent-separated ion-pairs, requires that the former should be a straight line and the latter a curve. The authors state that this is so, whereas in fact both plots are curves, but the plot of *Z* vs. $[LiClO_4]$ is fairly close to a straight line. If these quantities are replotted in the form of $\log_{10}Z$ vs. $\log_{10}[LiClO_4]$, the relation between them could be found exactly, if such a plot is linear. Figure 4 (line 2) shows that no simple relation of the form $Z \propto [LiClO_4]^x$ exists between these two quantities. Thus the claim that the special salt effect is a result of scavenging by perchlorate ion-pairs of the solvent-separated R^+X^- ion-pairs (19) has not been quantitatively proved.

The same results from which *Z* was calculated (Table IV of reference (15)) may be used in an analysis in Ingold's terms. Line 1 of Fig. 4 shows

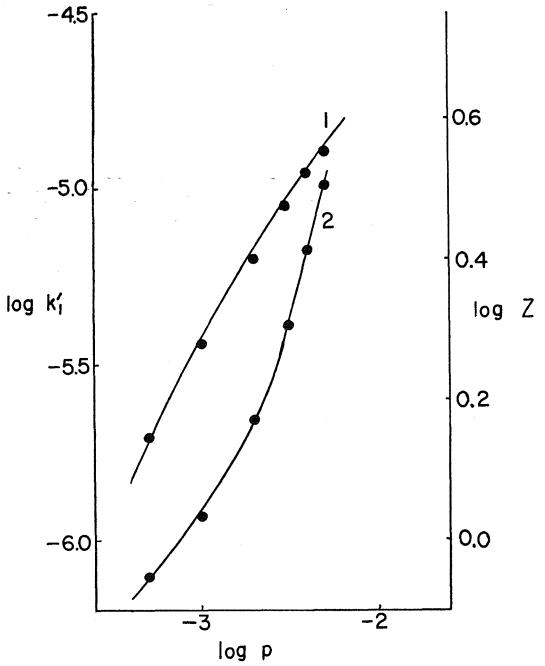

FIG. 4. Line 1. The logarithm of the catalyzed specific rate ($k_1' \equiv (k_1^p - k_1^o)$) plotted against the logarithm of the tetra-*n*-butylammonium perchlorate concentration. Line 2. The logarithm of Winstein's *Z* factor plotted against the logarithm of the tetra-*n*-butylammonium perchlorate concentration. The rate constants refer to the acetolysis of 1-*p*-anisyl-2-propyl *p*-toluenesulfonate.

Can. J. Chem. Downloaded from www.nrcresearchpress.com by 210.87.254.5 on 09/05/12
For personal use only.

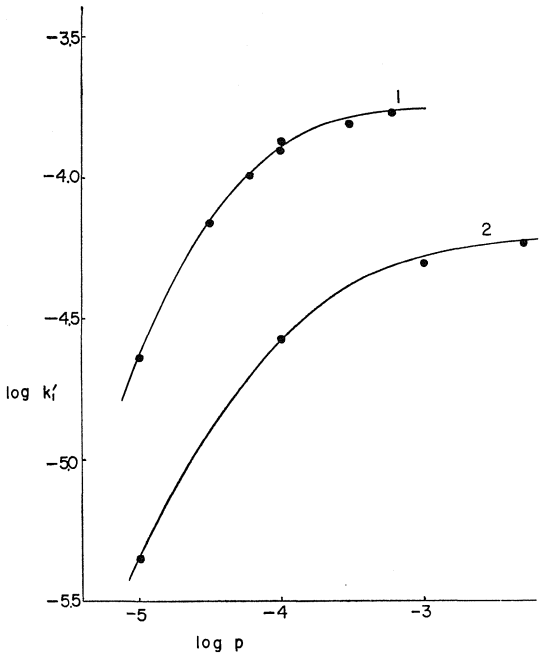

FIG. 5. The logarithm of the catalyzed specific rate ($k_1' \equiv (k_1^p - k_1^0)$) plotted against the logarithm of the tetra-*n*-butylammonium perchlorate concentration for; line 1, the acetolysis of cholesteryl *p*-toluenesulfonate; line 2, the acetolysis 2-(2,4-dimethoxyphenyl)ethyl bromobenzenesulfonate.

a plot of the logarithm of the catalyzed rate ($k_1^p - k_1^0$) vs. $\log_{10} p$, where p is the $LiClO_4$ concentration. This, too, is seen to be a curve, but closer to a straight line than Winstein's Z factor. Over the same range, line 1 has an average slope of about 0.8.

Winstein and co-workers have observed several examples of special salt effects and it is of interest now to analyze them on Ingold's model to see if any substantiate his claim (footnote at end of ref. (8)) that they are close to a square root dependence of the catalyzed rate on $LiClO_4$ concentration. None of these other examples was studied in as great detail as 1-*p*-anisyl-2-propyl *p*-toluenesulfonate but they all include a sufficient number of measurements to make plots of $\log_{10} (k_1^p - k_1^0)$ vs. $\log_{10} [LiClO_4]$. Seven plots have been made with the aid of which three types of catalysis can be distinguished. The graphs for cholesteryl *p*-toluenesulfonate and 2-(2,4-dimethoxyphenyl)ethyl bromobenzenesulfonate (14) are shown in Fig. 5. These are curves indicating no relationship of the type $(k_1^p - k_1^0) \propto [LiClO_4]^x$. In contrast to these, the plots in Fig. 6 are straight lines for substrates *trans*-2-*p*-anisylcyclopentyl *p*-bromobenzenesulfonate, *trans*-2-*p*-anisylcyclohexyl *p*-bromobenzenesulfonate, and *erythro*-3-*p*-anisyl-2-butyl *p*-bromobenzenesulfonate (13). The slopes of the log–log plots are 0.74, 0.82, and 0.56 respectively. Two more curved plots are found in Fig. 7 for *o*- and *p*-anisylethyl *p*-toluenesulfonate. Thus only one compound shows the square root dependence expected by Ingold.

The three types of perchlorate catalysis, there fore, are the normal catalysis observed by Winstein for which the catalyzed rate is proportional to $[LiClO_4]$, the special catalysis for which $(k_1^p - k_1^0) \propto [LiClO_4]^x$ where x may be any value between ½ and unity, and an "extra-special" catalysis where x is not constant. Neither the theory of Winstein involving solvent-separated ion-pairs, nor that of Ingold involving catalysis by simple perchlorate ions can accommodate all of these results quantitatively. The

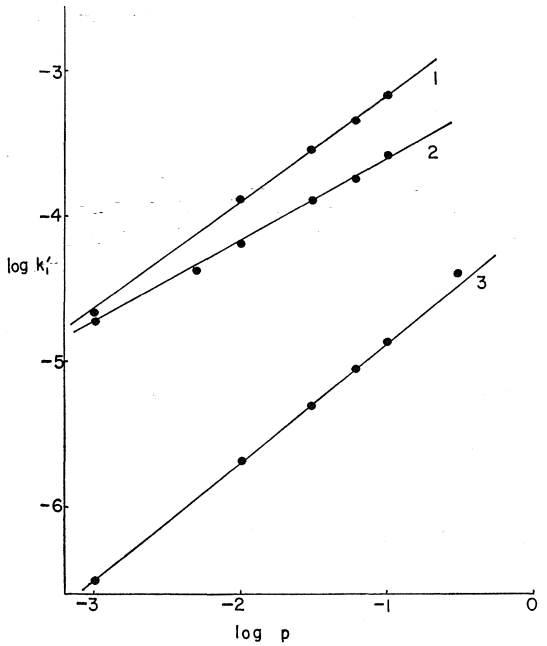

FIG. 6. The logarithm of the catalyzed specific rate ($k_1' \equiv (k_1^p - k_1^0)$) plotted against the logarithm of the tetra-*n*-butylammonium perchlorate concentration for; line 1, the acetolysis of *trans*-2-*p*-anisylcyclopentyl *p*-bromobenzenesulfonate; line 2, the acetolysis of *erythro*-3-*p*-anisyl-2-butyl *p*-bromobenzenesulfonate; line 3, the acetolysis of *trans*-2-*p*-anisylcyclohexyl *p*-bromobenzenesulfonate.

Can. J. Chem. Downloaded from www.nrcresearchpress.com by 210.87.254.5 on 09/05/12
For personal use only.

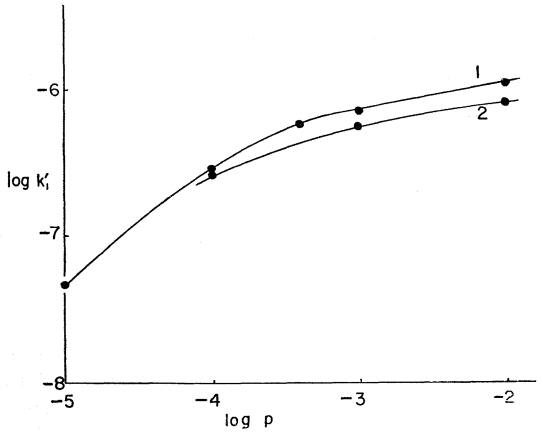

FIG. 7. The logarithm of the catalyzed specific rate ($k_1' \equiv (k_1^p - k_1^o)$) plotted against the logarithm of the tetra-*n*-butylammonium perchlorate concentration for: line 1, the acetolysis of *p*-anisylethyl *p*-toluenesulfonate; line 2, the acetolysis of *o*-anisylethyl *p*-toluenesulfonate.

Ingold theory has the advantage that it makes use of simpler concepts of single ions and ion-pairs, and the success of this approach with the reactions of triphenylmethyl chloride in benzene is striking, suggesting that this may represent a limiting case. Obviously, the effects observed in acetolysis are more complicated, but may be interpreted in terms of simultaneous catalysis by single ions and ion-pairs, to give relationships involving the perchlorate concentration between a square root and a linear dependence. The non-linear dependences show an initial catalysis similar to the linear plots but this falls off as the perchlorate concentration is increased, with the graph passing through an inflexion point when the concentration is such that the normal catalysis begins to take over. This behavior is not readily rationalized in specific terms but may be taken to indicate that the special salt effects are quite distinct from the normal ones.

Thus, although neither of the theories which have been offered is clearly more satisfactory than the other, it can be concluded that the kinetic significance of the solvent-separated ion-pair in solvolysis reactions has not been quantitatively proved, and that special salt effects are by no means completely explained either in these terms or by simple ion catalysis.

Experimental

The preparation and purification of materials have been described (9).

The kinetic method was the simple titration of the product hydrogen chloride against standard triethylamine solution in acetone solvent, as used before (6, 9). All the first order rate constants quoted are extrapolated initial values, obtained from a plot of the instantaneous rate constants, calculated from the integrated first order equation, against the percent reaction completed. All the runs were carried out at 25°.

1. C. G. SWAIN. J. Amer. Chem. Soc. **70**, 1119 (1948).
2. C. G. SWAIN and M. M. KREEVOY. J. Amer. Chem. Soc. **77**, 1122 (1955).
3. C. G. SWAIN and E. E. PEGUES. J. Amer. Chem. Soc. **80**, 812 (1958).
4. E. D. HUGHES, C. K. INGOLD, S. F. MOK, S. PATAI, and Y. POCKER. J. Chem. Soc. 1220 (1957).
5. E. D. HUGHES, C. K. INGOLD, S. PATAI, and Y. POCKER. J. Chem. Soc. 1230 (1957).
6. E. D. HUGHES, C. K. INGOLD, S. F. MOK, and Y. POCKER. J. Chem. Soc. 1238 (1957).
7. E. D. HUGHES, C. K. INGOLD, S. PATAI, and Y. POCKER. J. Chem. Soc. 1256 (1957).
8. E. D. HUGHES, C. K. INGOLD, S. F. MOK, S. PATAI, and Y. POCKER. J. Chem. Soc. 1265 (1957).
9. K. T. LEFFEK and R. G. WATERFIELD. Can. J. Chem. **45**, 1497 (1967).
10. A. H. FAINBERG and S. WINSTEIN. J. Amer. Chem. Soc. **78**, 2763 (1956).
11. A. H. FAINBERG and S. WINSTEIN. J. Amer. Chem. Soc. **78**, 2769 (1956).
12. A. H. FAINBERG and S. WINSTEIN. J. Amer. Chem. Soc. **78**, 2780 (1956).
13. A. H. FAINBERG, S. WINSTEIN, and G. C. ROBINSON. J. Amer. Chem. Soc. **78**, 2777 (1956).
14. S. WINSTEIN and E. CLIPPINGER. J. Amer. Chem. Soc. **78**, 2784 (1956).
15. S. WINSTEIN, P. E. KLINEDINST, JR., and G. C. ROBINSON. J. Amer. Chem. Soc. **83**, 885 (1961).
16. D. BETHELL and V. GOLD. Quart. Rev. **12**, 173 (1958).
17. K. T. LEFFEK. Ph.D Thesis. University of London, London, England. 1959.
18. S. WINSTEIN, B. APPEL, R. BAKER, A. DIAZ. Chem. Soc. (London), Spec. Publ. **19**, 109 (1965).
19. S. WINSTEIN, P. E. KLINEDINST, JR., and E. CLIPPINGER. J. Amer. Chem. Soc. **83**, 4986 (1961).

Can. J. Chem. Downloaded from www.nrcresearchpress.com by 210.87.254.5 on 09/05/12
For personal use only.

Infrared spectra of acetonitrile sorbed on porous glass

M. J. D. Low and P. L. Bartner
Department of Chemistry, New York University, New York, New York 10453

Received July 18, 1969

Infrared spectra were recorded of acetonitrile sorbed on highly degassed porous glass as well as on silica and B-, Al-, and Zr-impregnated porous glass and silica. Most of the acetonitrile was weakly and reversibly adsorbed, becoming hydrogen-bonded to surface hydroxyls. A small amount of the adsorbate formed weakly bound surface complexes with Al- and Zr-, but not with B-impurities.

Canadian Journal of Chemistry, **48**, 7 (1970)

Can. J. Chem. Downloaded from www.nrcresearchpress.com by 210.87.254.40 on 09/05/12
For personal use only.

Introduction

Roev, Filimonov, and Terenin (1) recorded infrared spectra of acetonitrile adsorbed on silica, porous glass, and on a silica–alumina catalyst and concluded that hydrogen bonds were formed between the acetonitrile molecules and the surface hydroxyls of the three solids. The weakly held acetonitrile could be desorbed easily. However, the spectrum of the silica–alumina catalyst, recorded after the hydrogen-bonded acetonitrile had been removed, showed bands indicating the presence of an additional, more tightly bound surface species. The symmetrical C≡N stretching absorption of these was shifted in a manner analogous to the C≡N shifts found with acetonitrile – metal chloride complexes, leading Roev *et al.* to assume that specific adsorption centers possessing an electron-acceptor nature existed on the silica–alumina catalyst. Similar effects were not reported for acetonitrile on silica or on porous glass.

The absence of the more tightly bound acetonitrile species on pure silica is not surprising. However, porous glass contains oxide impurities which markedly affect the reactivity of its surface. For example, Little, Klauser, and Amberg found isomerization, cracking, and polymerization reactions occurring on porous glass to be very dependent on the concentrations of alumina and zirconia impurities (2), and Cant and Little found evidence pointing to the binding of ammonia to electron-deficient surface boron atoms (3). More recently, the oxide impurities were found to affect the adsorption of NH_3 (4), HCN (5), pyridine (6), aniline (7), and trimethylamine (8). The apparent lack of reactivity of porous glass to acetonitrile was consequently not in keeping with a general trend. We have, therefore, recorded infrared spectra of acetonitrile adsorbed on porous glasses and silicas with the dual purpose of establishing whether acetonitrile–surface species could form, and extending our studies of the sorption of nitrogenous materials on siliceous surfaces.

Experimental

The glass adsorbents were 10 × 25 × 1 mm pieces of Code 7930 porous glass purchased from Corning Glass Works. Cab-O-Sil (G. Cabot Co., Boston, Mass.) and Aerosil (Degussa, Inc., Kearny, N.J.) were impregnated with B, Al, or Zr, using aqueous H_3BO_3, $Al(NO_3)_3$, or $Zr(SO_4)_2$ solutions, by the incipient wetness method. Porous glass samples were impregnated by similar procedures. Most experimental procedures have been described elsewhere (4–11). The porous glass samples were degassed at 600 °C, heated in 30 Torr O_2 for 1 h at 600 °C, and then degassed at 750 °C for 40 h. Spectral-grade acetonitrile was degassed by alternate freezing and thawing in vacuum. Spectra were recorded with Perkin–Elmer Models 521 and 621 spectrophotometers.

Results and Discussion

Spectra were recorded of acetonitrile adsorbed on highly degassed porous glass and pure silica, as well as on B-, Al-, or Zr-impregnated porous glass and silica samples. The data indicate that some surface complexes were formed in addition to the hydrogen-bonded, weakly adsorbed acetonitrile. Consequently, it is convenient to consider the two types of adsorption separately.

Weak Adsorption

The general characteristics of the weak adsorption were like those described earlier (1). However, some aspects of the weak adsorption will be considered, because the earlier study was very brief.

The prominent features of highly degassed porous glass (spectrum *A*, Fig. 1) were the 3748-cm^{-1} absorption of free silanols and the 3703-cm^{-1} absorption of free B—OH groups (9–11). When such a sample was exposed to successively increasing pressures of acetonitrile vapor at

Can. J. Chem. Downloaded from www.nrcresearchpress.com by 210.87.254.40 on 09/05/12
For personal use only.

TABLE 1

Infrared spectra of weakly adsorbed acetonitrile

Frequency (cm^{-1})						
Adsorbed acetonitrile						
Porous glass						
Low coverage	High coverage	Cab-O-Sil	Porous glass, silica, SiO_2–Al_2O_3 Roev, *et al.* (1)	Acetonitrile* Liquid	Acetonitrile* Vapor	Assignment†
3748	3748	3748	3750			ν(O—H), free surface Si—OH (9–11)
3703	3703					ν(O—H), free surface B—OH (9–11)
3460	3430	3430	3450			ν(O—H), perturbed hydroxyls
	3170	~3170		3165	3179	$\nu_2 + \nu_4$
~3000	3004	~3000		3002	3010	ν_5, degenerate C—H stretch
~2947	2945	2950	2950	2944	2954	ν_1, symmetric C—H stretch
	2630			2628	2620	$\nu_2 + \nu_8$
	2410			2411	2417	$\nu_3 + \nu_7$
2292	2296	2303	2300	2293	2306	$\nu_3 + \nu_4$
2265	2258	2268	2266	2254	2267	ν_2, symmetric C≡N stretch

*See ref. 12.

†See Venkateswarlu (12); ν_3, symmetric CH_3 deformation; ν_4, symmetric C—C stretch; ν_7, degenerate CH_3 rock; ν_8, degenerate C—C≡N bend.

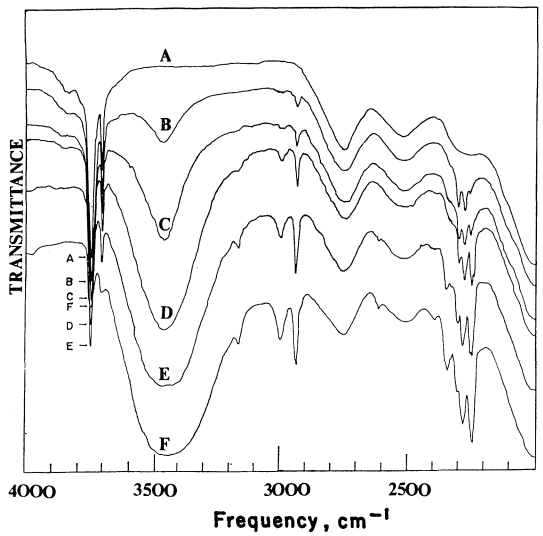

FIG. 1. Sorption of acetonitrile on porous glass. *A*, background spectrum of porous glass after degassing for 40 h at 750 °C. The degassed glass was exposed to acetonitrile vapor at 25 °C at the following pressures in Torr: *B*, 1.5; *C*, 4.5; *D*, 15; *E*, 38; *F*, 80. The ordinates are displaced to avoid overlapping.

25 °C, e.g., Fig. 1: (*a*) Both the free Si—OH and B—OH groups declined in intensity but did not change in frequency. (*b*) A band appeared near 3460 cm^{-1}; broadened, and shifted its center to near 3430 cm^{-1}; additional bands were observed in the 3200–2200 cm^{-1} range. These are listed in Table 1. (*c*) The four bands of adsorbed acetonitrile (column 1, Table 1) increased in intensity and shifted slightly in frequency when the acetonitrile pressure was increased (column 2, Table 1). Some bands were quite weak and were observed only when the amount of adsorbed acetonitrile had become appreciable (column 2, Table 1; spectra *E* and *F*, Fig. 1). Also, (*d*) there were changes in intensities and frequencies of absorptions below 2400 cm^{-1}; some apparent shifts were caused by the overlapping of bands and will be considered later.

The broad 3460-cm^{-1} band and other bands below 3200 cm^{-1} given in columns 1 and 2 of Table 1 were entirely eliminated by pumping at 25 °C for approximately 2 h, with the exception of the 3004- and 2945-cm^{-1} bands; quite weak bands remained near those positions (and also below 2400 cm^{-1}) after the other bands had been eliminated. Similar effects were observed when acetonitrile was adsorbed on Cab-O-Sil silica. The band positions are given in column 3 of Table 1. All such bands could be completely eliminated by pumping at 25 °C for 30 min.

The weak, reversible adsorption on porous glass at low coverage and on Cab-O-Sil is mainly ascribed to hydrogen bonding of acetonitrile molecules to surface hydroxyls, as pointed out by Roev, Filimonov, and Terenin (1), the 3460-cm^{-1} band being caused by that interaction. Only the ν_2 C≡N vibration (columns 1 and 3, Table 1) was slightly perturbed, other modes of adsorbed acetonitrile being largely unaffected, as would be expected for structures such as

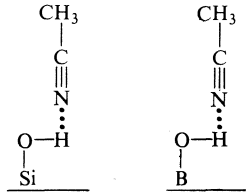

It is interesting to note that the band frequencies for acetonitrile adsorbed on porous glass became more like those of liquid acetonitrile (12) when the surface coverage was increased, as suggested by the shift of the $\nu_3 + \nu_4$ and ν_2 modes. Possibly some capillary condensation occurred within the highly porous glass samples at the highest acetonitrile pressures. Such an effect would not be expected with non-porous Cab-O-Sil.

Surface Complexes

After the weakly bound acetonitrile had been removed from porous glass, two weak bands were observed near 3000 and 2950 cm^{-1}, as well as a group of three bands near 2300 cm^{-1}, e.g., Fig. 2. All five bands decreased in intensity on degassing and, although some remnants of the bands were detectable after pumping at 200 °C for 1 h, all bands were eliminated at 300 °C. The three bands near 2300 cm^{-1} (Table 2) shifted in frequency by several wavenumbers and changed in relative intensity, although the precise frequency–intensity relations could not be established because the bands were weak. The five bands were not observed with Cab-O-Sil.

In general, the results with porous glass pointed to the existence of surface groupings which gave rise to distinct absorptions near 2300 cm^{-1} and which were somewhat more difficult to desorb (and consequently somewhat more tightly bound

Can. J. Chem. Downloaded from www.nrcresearchpress.com by 210.87.254.40 on 09/05/12
For personal use only.

TABLE 2
Infrared spectra of surface complexes of acetonitrile

Frequency, cm^{-1}					
	Al-impregnated		Zr-impregnated		
Porous glass	Porous glass	Cab-O-Sil	Porous glass	Cab-O-Sil	Assignment
~2345	2348	2348			C≡N stretch of Al-complex
~2318	2318	2318	2319	2317	Combination band
~2292			2293	2292	C≡N stretch of Zr-complex

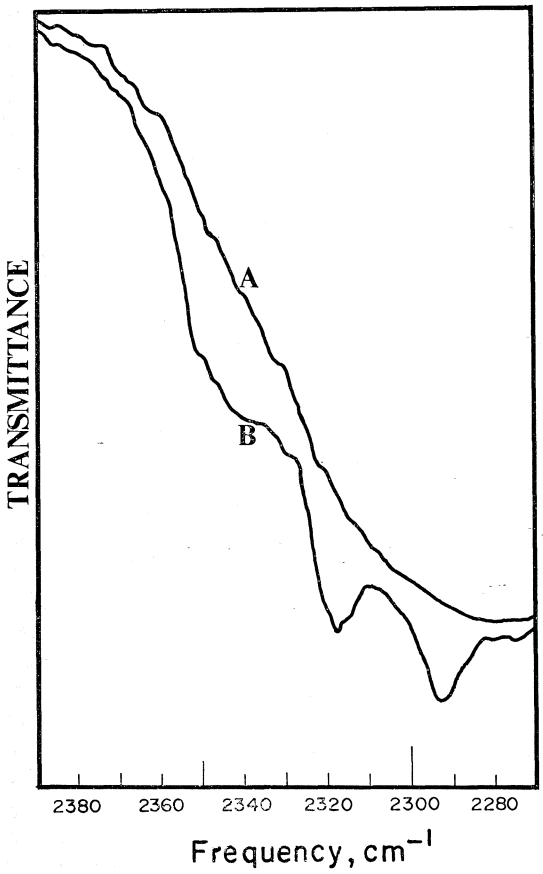

FIG. 2. Acetonitrile on porous glass: *A*, background spectrum of degassed porous glass; *B*, after exposure to 80 Torr acetonitrile at 25 °C, followed by degassing for 100 min at 25 °C. Both spectra were recorded at 10× ordinate scale expansion.

to the surface) than the hydrogen-bonded acetonitrile. The observation of a more tightly bound species on silica–alumina (1) and the existence of acetonitrile complexes (1, 13–15, and references therein) would suggest the occurrence of surface species such as

where M is an atom of one of the minor constituents or impurities on the glass surface. The formation of the surface complex, as in the case of acetonitrile complexes, would perturb the C≡N stretching mode and would shift the C≡N band to higher wavenumbers (14, 15). However, the porous glass spectra (Fig. 2, and Fig. 3, spectrum *A*) exhibited three absorptions, suggesting that more than one surface species was formed. A series of experiments involving the adsorption of acetonitrile on B-, Al-, or Zr-impregnated porous glass and Cab-O-Sil was consequently carried out in order to obtain information about the nature of the surface complexes.

The results obtained with impregnated adsorbents can be summarized as follows (band positions are given in Table 2). (*a*) The Al-impregnation of porous glass led to the enhancement of two of the three bands in the 2300-cm^{-1} region (Fig. 3, spectrum *B*); a third band observed near 2292 cm^{-1} with porous glass (e.g. Fig. 3, spectrum *A*) was eliminated. (*b*) Another pair of bands at 2319 and 2293 cm^{-1} was enhanced with Zr-impregnated porous glass (Fig. 3, spectrum *C*), while the weaker band near 2345 cm^{-1} of porous glass (Fig. 3, spectrum *A*) was eliminated. (*c*) Bands were not accentuated with B-impregnated porous glass. (*d*) Bands analogous to those found with the impregnated porous glasses were found with Al- or Zr-impregnated Cab-O-Sil. Spectrum *D* of Fig. 3 is an example, showing the weak but sharp 2317- and 2292-cm^{-1} bands observed with

Can. J. Chem. Downloaded from www.nrcresearchpress.com by 210.87.254.40 on 09/05/12
For personal use only.

Can. J. Chem. Downloaded from www.nrcresearchpress.com by 210.87.254.40 on 09/05/12
For personal use only.

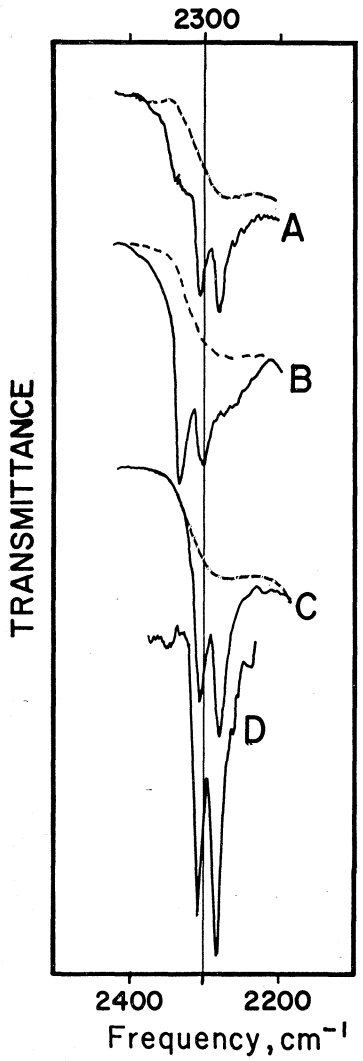

FIG. 3. Acetonitrile on impregnated adsorbents: *A*, porous glass; *B*, Al-impregnated porous glass (3 wt. % Al_2O_3), after exposure to 80 Torr acetonitrile at 25 °C, followed by degassing at 25 °C for 3 h; *C*, Zr-impregnated porous glass (2 wt. % ZrO_2), after exposure to 80 Torr acetonitrile at 25 °C, followed by degassing at 25 °C for 3 h; *D*, Zr-impregnated Cab-O-Sil (2 wt. % ZrO_2), after exposure to 80 Torr acetonitrile at 25 °C, followed by degassing at 25 °C for 2.5 h. The dashed lines are backgrounds. The ordinates were displaced to avoid overlapping. Trace *D* was recorded at 5× ordinate expansion.

Zr-impregnated Cab-O-Sil. No bands attributable to a species more tightly bound than hydrogen-bonded acetonitrile were observed with B-impregnated Cab-O-Sil. (*e*) The bands of surface complexes formed on Al- or Zr-impregnated Cab-O-Sil could be removed or greatly decreased by pumping for about 1 h at room temperature. (*f*) No bands of surface complexes were observed with porous glass which had been leached (2) to remove Al- and Zr-oxide impurities.

The various results suggest that the three absorptions observed with porous glass (Fig. 2) were caused by two pairs of bands, overlapping occurring near 2318 cm^{-1}. For porous glass, the 2345, 2318 cm^{-1} pair is attributed to a small number of surface Al–acetonitrile complexes, and the 2318, 2292 cm^{-1} pair to a larger number of corresponding surface Zr–acetonitrile complexes. The band near 2318 cm^{-1} found in all cases (Table 2) is assigned to a combination analogous to the $\nu_3 + \nu_4$ mode of acetonitrile which would not be significantly affected by the formation of the surface complex. The two bands near 3000 and 2950 cm^{-1} are attributed to the C—H modes of the surface complexes. The 2348- and 2292-cm^{-1} bands are assigned to the perturbed C≡N stretching modes of the respective surface Al- and Zr-complexes.

The shifts of the C≡N bands of the surface complexes (94 cm^{-1} for the surface Al-complex and 38 cm^{-1} for the surface Zr-complex, with respect to the C≡N band of liquid acetonitrile) are quite close to the shifts of 90 cm^{-1} for the $2CH_3CN{\cdot}AlCl_3$ complex and 36 cm^{-1} for the $2CH_3CN{\cdot}ZrCl_4$ complex (15). A shift of 96 cm^{-1} was reported (15) for $CH_3CN{\cdot}BCl_3$, so that the C≡N group of a hypothetical surface B-complex might be expected to absorb near 2350 cm^{-1}. Such a band was not observed with B-impregnated silicas, indicating that no detectable amount of a surface B-complex was formed (similarly, a surface B–NCH complex was not found in an earlier study (5) on the interaction of HCN with porous glass). The lack of coordination of the nitrile to the surface boron cannot be adequately explained in view of the existence of bulk acetonitrile – boron halide complexes. Perhaps the acceptor strength of the boron impurity was decreased with respect to that of BCl_3 because the boron atoms were in close proximity to surface oxygen atoms. Such an effect was found with the series (in decreasing acceptor strength) $BCl_3 > RO{\cdot}BCl_2 > (RO)_2BCl > (RO)_3B$, where only the first formed adducts with nitriles (13).

Support by a grant from the National Center for Air Pollution Control is gratefully acknowledged.

1. L. M. Roev, V. N. Filimonov, and A. N. Terenin. Opt. Spektrosk. **4**, 328 (1958).
2. L. H. Little, H. E. Klauser, and C. H. Amberg. Can. J. Chem. **39**, 42 (1961).
3. N. W. Cant and L. H. Little. Can. J. Chem. **42**, 802 (1964).
4. M. J. D. Low, N. Ramasubramanian, and V. V. Subba Rao. J. Phys. Chem. **71**, 1726 (1967).
5. M. J. D. Low, N. Ramasubramanian, P. Ramamurthy, and A. V. Deo. J. Phys. Chem. **72**, 2371 (1968).
6. M. J. D. Low and V. V. Subba Rao. Can. J. Chem. **46**, 3255 (1968).
7. M. J. D. Low and V. V. Subba Rao. Can. J. Chem. **47**, 1281 (1969).
8. M. J. D. Low and V. V. Subba Rao. Unpublished results.
9. M. J. D. Low and N. Ramasubramanian. Chem. Commun. 20, 1965.
10. M. J. D. Low and N. Ramasubramanian. J. Phys. Chem. **70**, 2740 (1966).
11. M. J. D. Low and N. Ramasubramanian. 152nd Meeting of the American Chemical Society, New York, Sept. 1966; preprints, Division of Petroleum Chemistry, p. 133.
12. P. Venkateswarlu. J. Chem. Phys. **19**, 293 (1957).
13. W. Gerrard, M. F. Lappert, and J. W. Wallis. J. Chem. Soc. 2178 (1960).
14. W. Gerrard, M. F. Lappert, H. Pyszora, and J. W. Wallis. J. Chem. Soc. 2182 (1960).
15. E. Oikawa and S. Kambara. Polym. Lett. **2**, 649 (1964).

Can. J. Chem. Downloaded from www.nrcresearchpress.com by 210.87.254.40 on 09/05/12
For personal use only.

Sorption of dimethyl ether on silica gel

E. ROBINSON[1]
Department of Chemistry, College of Technology, Belfast, Northern Ireland
AND
R. A. ROSS
Department of Chemistry, Lakehead University, Port Arthur, Ontario
Received September 3, 1969

The adsorption of dimethyl ether has been studied at its boiling point on a range of silica gels by measurement of adsorption/desorption isotherms and isothermal calorimetric heats of adsorption. Data were determined on gels heat treated at 240, 500, 700, and 900 °C and also on gels impregnated with 0.274% w/w aluminum. On 240 °C gels, heats of adsorption varied from around 20 through 12 to 7 kcal/mole at $\theta = 0.01$, 0.50, and 0.90, respectively. Hysteresis loops are analyzed and the initial adsorption trends explained by hydrogen bond formation between the ether oxygen and surface hydroxy groups. The enhanced amounts of ether adsorbed after aluminum impregnation are explained by the creation of either Brønsted acid sites on gels treated at 240 °C or Lewis acid sites on gels treated at the highest temperatures.

Canadian Journal of Chemistry, **48**, 13 (1970)

Can. J. Chem. Downloaded from www.nrcresearchpress.com by 210.87.254.42 on 09/05/12
For personal use only.

Introduction

Recently, studies of the adsorption of ring ethers on silica gel surfaces have been reported (1, 2). For these systems, heats of adsorption were determined from calorimetric and adsorption isotherm measurements made in the region of the boiling points of the gases. These data, when supplemented by measurements of gel properties such as surface areas and hydroxyl group concentrations, were used to interpret the nature of the adsorbate/adsorbent interactions. This work has now been extended to include data on the adsorption of dimethyl ether.

While comprehensive studies of the adsorption of diethyl ether on silica gel have been made (3), little or no heat measurements are available for dimethyl ether. McDonald (4) used dimethyl ether in an infrared study of surface hydroxyl groups of amorphous silica and found that "moderately strong" hydrogen bonds were formed between the ether oxygen atom and the surface hydroxyls. The rapid desorption of ether, which left a surface spectrum identical to that prior to adsorption, indicated that chemisorption probably did not occur.

Experimental

Materials

Davison 923 chromatographic-grade silica gel with a particle size range of 75–150 μ was used. This had a surface area of 660 m^2/g (Brunauer, Emmett, and Teller (B.E.T.); N_2; −196°) and a lump density of 1.20 g/cm^3 after activation at 240 °C for 15 h. Aluminum impregnation (5) was carried out by immersion of the gel in a solution of aluminum nitrate. This treatment gave an aluminum content of 0.274% w/w and reduced the surface area to 590 m^2/g. Methyl ether (Matheson) had an average purity of 99.8% w/w; methyl alcohol was the principal impurity. The ether was further purified by vacuum distillation in the adsorption apparatus, with the first and last fractions discarded.

Apparatus and Procedure

Adsorption isotherms were determined in an all-glass, quartz-spring vacuum balance (6) and heats of adsorption by calorimetry (1).

Results

Complete adsorption/desorption isotherms were determined at the boiling point (7), 248.2 °K, on gel pretreated (8) at 240, 500, 700, and 900 °C (Fig. 1). The isotherms obtained exhibit hysteresis loops which in each case extend over the same limits of pressure, but diminish in area as the activation temperature is increased.

Hysteresis loops changing in this manner may be analyzed graphically (9). The variation in loop height is assessed by plotting the vertical separation of the boundary curves (ΔW) against log p and the loop width is evaluated by plotting the horizontal separation of the boundary curves, expressed in terms of log p, as a function of the amount of gas adsorbed (W). The plots are shown in Fig. 2. The width of the loop, at its maximum, declines almost linearly with the temperature of activation between 240 and 700 °C, while the

[1]Present Address: Lambeg Research Institute, Lisburn, County Antrim, N. Ireland.

Can. J. Chem. Downloaded from www.nrcresearchpress.com by 210.87.254.42 on 09/05/12
For personal use only.

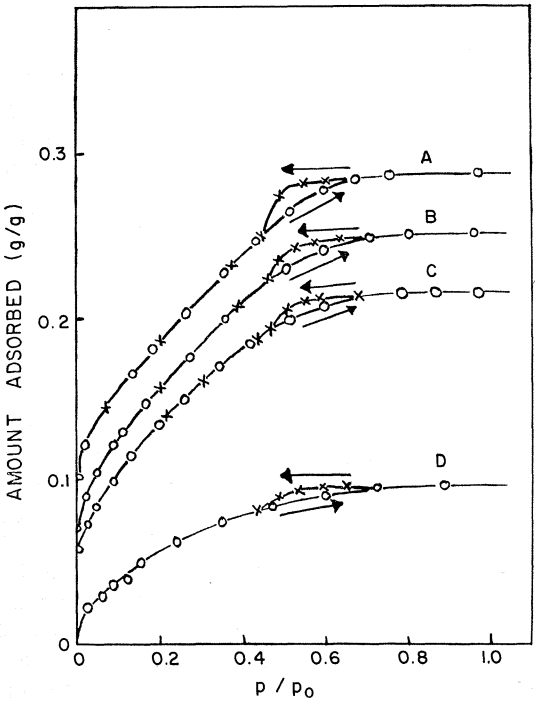

FIG. 1. Adsorption/desorption isotherms for dimethyl ether at 248.2 °K on *A*, 240; *B*, 500; *C*, 700; and *D*, 900 °C gels.

loop height shows a greater drop between 240 and 500 °C than between 500 and 700 °C. The width is a measure of the difference between the chemical potential of the adsorbate, when the same amount is present in the adsorbent, in the two extreme states represented by the boundary curves of the loop (9).

The amounts of gas adsorbed at monolayer completion obtained from B.E.T. plots (6) and the amounts adsorbed at $p = p_0$ are given in Table 1.

The isotherm obtained with the 240 °C aluminum-impregnated material was similar to that of the 240 °C gel. Only a very slight increase in the monolayer adsorbed amount was observed, 0.154 g/g, along with a diminution in area of the hysteresis loop, vertical separation = 0.010 g/g, at $p/p_0 = 0.53$ (cf. 240 °C gel, 0.013 g/g). However, thermal treatment at 900 °C of the aluminum-impregnated material had a marked effect on the adsorption isotherm when compared with that obtained on normal 900 °C gel. The amount of gas adsorbed below $p/p_0 = 0.05$ was more than doubled (0.060 g/g, cf. 0.027 g/g) while the amount

TABLE 1

Methyl ether adsorption data at 248.2 °K

Activation temperature (°C)	Monolayer adsorbed amount (g/g)	Monolayer value of p/p_0	Amount adsorbed at $p = p_0$ (g/g)
240	0.153	0.095	0.288
500	0.130	0.115	0.250
700	0.109	0.120	0.213
900	—	—	0.095

adsorbed at $p = p_0$ increased by 0.077 g/g. The hysteresis loop extended over the same limits as the other dimethyl ether isotherms but it had a greater area than that for the 900 °C normal gel.

Isothermal heats of adsorption were determined calorimetrically for dimethyl ether at 248.2 °K on both 240 and 500 °C gels. Figure 3 shows the variation in the heat of adsorption with surface coverage. Unlike the ring ethers previously studied (1, 2), the heat of adsorption of dimethyl ether barely exceeds 20 kcal/mole below $\theta = 0.01$. At $\theta = 0.5$, the heats are 12.4 and 11.2 kcal/mole for 240 and 500 °C gels, respectively.

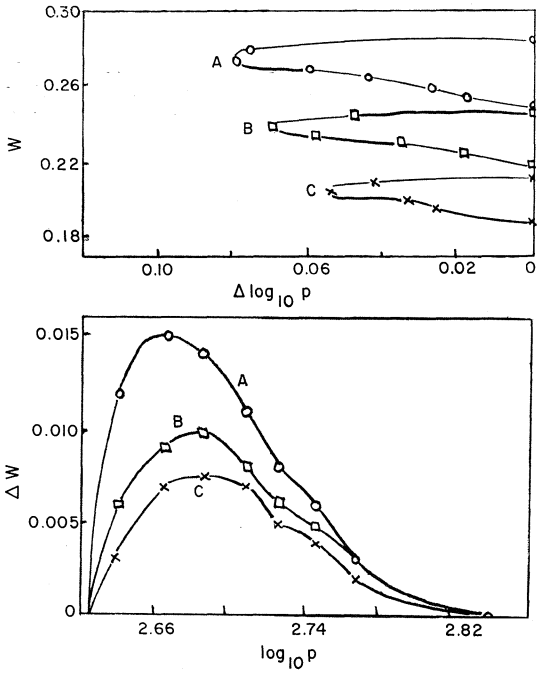

FIG. 2. Hysteresis loop analysis of dimethyl ether isotherms on *A*, 240; *B*, 500; and *C*, 700 °C gels.

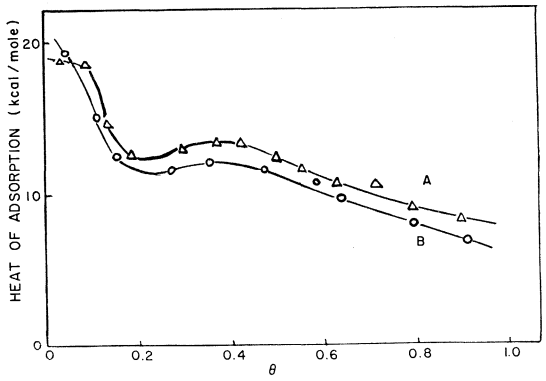

FIG. 3. Variation of heat of adsorption with surface coverage on *A*, 240; and *B*, 500 °C gels.

Discussion

The heats of adsorption of dimethyl ether in the region $\theta = 0.01$ to 0.10 lie between 20 and 16 kcal/mole. Such moderately high values are usually explained by surface heterogeneity where the most labile silanol groups interact first with the adsorbed molecules. In the case of ethylamine adsorption (8), probably surface complexes of an ionic nature are formed at these coverages when heats of adsorption are > 30 kcal/mole. The values for dimethyl ether are comparable with those obtained for dimethyl sulfide (10), and a similar model of adsorption is probably applicable, with strong hydrogen bonds formed between adsorbate and adsorbent at this low coverage.

The angle of the C—O—C bond in dimethyl ether (11) is 111 ± 4° which indicates (12) that the oxygen atom uses sp^3 hybrid orbitals, two half-filled sp^3 orbitals overlapping with those of carbon atoms, and two occupied by electron pairs. These electron pairs are available for hydrogen bond formation with silanol groups.

The heat of adsorption at $\theta = 0.5$ on 240° gel is 12.4 kcal/mole, comparable with 14.2 kcal/mole for diethyl ether (13) and about 12 kcal/mole for dimethyl sulfide (10). The comparisons are particularly useful when considered along with the values of the heats of liquefaction of the three gases (5.1 (14), 6.5 (13), and 6.4 (15) kcal/mole for dimethyl ether, diethyl ether, and dimethyl sulfide, respectively). The heat of adsorption of diethyl ether (3, 16) has been attributed to double hydrogen bond formation between the oxygen atom of the ether and pairs of suitably arranged hydroxyl groups.

The monolayer coverage with dimethyl ether at 248.2 °K was equivalent to 5 μmole/m^2 on 240° gel with the surface hydroxyl group concentration (5) 7.9 μmole/m^2. This would suggest mainly dual-site adsorption with some single-site adsorption occurring also. The latter mode of attachment may become more predominant as the surface coverage increases, in agreement with the decline in the heat of adsorption beyond $\theta = 0.5$.

After impregnation of gels with aluminum, the monolayer and total amounts of dimethyl ether adsorbed increased, particularly with the 900 °C sample. The impregnated material showed acidity to *p*-dimethylamino azobenzene, pK = +3.3 (17), which was not shown by the pure gel. Such acidity can be explained by the creation of surface Brønsted acid sites through the incorporation of aluminum into the surface. Several workers (18, 19) have suggested that treatment of silica gel with aluminum nitrate results in the absorption or condensation of a basic form of aluminum on a surface hydroxy group, and that the aluminum complex formed can interact subsequently with an adjacent hydroxy group causing it to dissociate a proton and thus yield a Brønsted site (20). Molecules of dimethyl ether initially adsorbed on these sites could accept the labile proton and form a charged surface species around and above which subsequent adsorbing molecules would cluster, thereby increasing the amount of dimethyl ether adsorbed.

Dehydration of the Brønsted centers is considered (20) to lead to the formation of Lewis acid sites where the aluminum atom is bonded to three oxygen atoms, leaving an electron-pair vacancy in its valence shell. Hence the increased adsorption of dimethyl ether on 900° impregnated gel may be explained by the interaction of the ether oxygen atom with these Lewis sites.

The adsorption branch of the hysteresis loop obtained with 240 °C gel, Fig. 1, rises gradually between $p/p_0 = 0.045$ and 0.70 (range 0.25). The desorption curve closes steeply between $p/p_0 =$ 0.52 and 0.45 (range 0.07). This shape of loop corresponds to that designated by de Boer (22) as Type *E*. It indicates the presence of cylindrical pores, radius r_n, which contain large cavities with variable radius, r_w, while $r_w > 2r_n$. Thermal treatment reduces the height of the loops, Fig. 2, which may be related to the disappearance of some pore constrictions (8, 21). The greatest diminution generally occurs above 500 °C, in harmony with

Can. J. Chem. Downloaded from www.nrcresearchpress.com by 210.87.254.42 on 09/05/12
For personal use only.

the rapid loss of surface area and pore volume (8) above this temperature.

We thank the British Petroleum Company for the award of a research scholarship (E.R.).

1. E. ROBINSON and R. A. ROSS. J. Chem. Soc. A. In press.
2. E. ROBINSON and R. A. ROSS. J. Chem. Soc. A. In press.
3. A. V. KISELEV and V. I. LYGIN. Russ. Chem. Rev. **31**, 175 (1962).
4. R. S. MCDONALD. J. Phys. Chem. **62**, 1168 (1958).
5. E. ROBINSON and R. A. ROSS. J. Chem. Soc. A, 2137 (1968).
6. T. W. BOYLE, W. J. GAW, and R. A. ROSS. J. Chem. Soc. 240 (1965).
7. Matheson gas data book. Matheson Company Inc., New Jersey. 1966. p. 195.
8. R. A. ROSS and A. H. TAYLOR. Proc. Brit. Ceram. Soc. **5**, 167 (1965).
9. D. H. EVERETT. The solid–gas interface. Vol. 2. *Edited by* E. A. Flood. Edward Arnold, London. 1967. p. 1055.
10. W. J. JONES and R. A. ROSS. J. Chem. Soc. A, 1787 (1968).
11. Interatomic distances. The Chemical Society, London. 1958.
12. W. HERZ. The shape of carbon compounds. W. A. Benjamin, Inc., New York. 1963. pp. 27, 96.
13. V. YA. DAVYDOV, A. V. KISELEV, and B. V. KUZNETSOV. Russ. J. Phys. Chem. **39**, 1096 (1965).
14. J. E. HAGGENMACHER. J. Amer. Chem. Soc. **68**, 1633 (1946).
15. R. C. REID and F. K. SHERWOOD. The properties of gases and liquids. McGraw-Hill Book Company, Inc., New York. 1966. p. 157.
16. L. H. LITTLE. Infrared spectra of adsorbed species. Academic Press, Inc., London. 1966. p. 263.
17. See e.g., A. I. VOGEL. Textbook of quantitative inorganic analysis. Longmans, Green, and Co., Ltd., London. 1966. p. 55.
18. K. G. MIESSEROV. Dokl. Akad Nauk S.S.S.R. **87**, 809 (1952).
19. R. C. HANSFORD. Ind. Eng. Chem. **39**, 849 (1947).
20. J. E. MAPES and R. P. EISCHENS. J. Phys. Chem. **58**, 1059 (1954).
21. W. J. JONES and R. A. ROSS. J. Chem. Soc. A, 1021 (1967).
22. J. H. DE BOER. Proc. Symp. Colston Res. Soc. **10**, 68 (1958).

Can. J. Chem. Downloaded from www.nrcresearchpress.com by 210.87.254.42 on 09/05/12
For personal use only.

Can. J. Chem. Downloaded from www.nrcresearchpress.com by 210.87.254.105 on 09/05/12
For personal use only.

Radiolysis in the adsorbed state. III. Methyl iodide adsorbed on silica gel[1]

N. H. SAGERT,[2] J. A. REID,[3] AND R. W. ROBINSON
Physical Chemistry Branch, Chalk River Nuclear Laboratories, Atomic Energy of Canada Limited, Chalk River, Ontario

Received July 31, 1969

The ^{60}Co γ-radiolysis of methyl iodide adsorbed on silica gel has been studied by examining the hydrocarbon products, which are mainly methane and ethane. These products are formed in large yields, indicating that a large fraction of the energy absorbed in the silica gel is able to cause decomposition of the methyl iodide. The "energy transfer" is thought to occur by electron or excitation transfer to the methyl iodide, leading to the production of methyl radicals.

Evidence has been obtained that the silica gel takes part in the system as a chemical reactant as well as being an energy transfer medium, and that changing the nature of the surface changes the course of the reaction. This is most clearly shown in two ways. The ratio of methane to ethane decreases as the surface hydroxyl concentration decreases, and it is concluded that excited methyl radicals form methane by abstraction of hydrogen from surface hydroxyls. Experiments using methyl iodide-d_3 adsorbed on protiated silica gel confirm the participation of hydrogen from the silica gel, as the methane is over 85% CD_3H, while the ethane is over 95% C_2D_6.

The effect of additives such as N_2O and SF_6, which are known to be electron scavengers, was also studied. It was shown that methyl iodide is a much better electron scavenger than N_2O and is as good an electron scavenger as SF_6 in this system.

Canadian Journal of Chemistry, **48**, 17 (1970)

Introduction

Allen and co-workers (1–3) have shown that a form of energy transfer is observed when certain materials are irradiated while adsorbed on high surface area solids. Larger yields of products are obtained than would be expected if only the energy absorbed in the adsorbate were causing the decomposition, and the conclusion they reached is that energy originally absorbed in the solid is causing decomposition of the adsorbate.

We previously studied radiolysis of N_2O on silica gel to examine the role of electrons in the radiolysis of substances adsorbed on silica gel (4), and found that up to 4.1 molecules of nitrogen were produced for each 100 eV absorbed in the silica gel plus the N_2O ($G(N_2) = 4.1$). At least 3.0 of these molecules (3.0 G units) came from electrons, as determined by competition with SF_6 and CCl_4. However, this system is somewhat ambiguous as the stoichiometry, that is, the number of nitrogen molecules produced per electron scavenged, is uncertain because of possible secondary reactions.

In the study reported here we have examined the radiolysis of methyl iodide adsorbed on silica gel, since reaction [1]

[1] $$CH_3I + e^- \rightarrow CH_3\cdot + I^-$$

is quite well known (5). Wong and Willard (6), using electron spin resonance (e.s.r.) techniques, have determined $G(CH_3) = 1.4 \pm 0.2$ for the radiolysis of CH_3Br on silica gel at −196 °C. In other adsorbate – silica gel systems investigated by Wong and Willard (6), the yield of electrons was higher, and we hoped that a study of the products of the system would help resolve this discrepancy. Work by Fujimoto *et al.* (7) on the photolysis of methyl iodide adsorbed on porous vycor has shown that methane and ethane are the chief hydrocarbon products of that system.

Isotopic labelling techniques were used to determine the origin of the products, since previous work with the cyclohexane-d_{12} – silica gel system has shown that the silica gel can act as a chemical reactant as well as an energy transfer medium (8). Competitive electron scavenging with other electron scavengers (N_2O and SF_6) was also used in an attempt to see if electrons actually were precursors of the observed yields.

Experimental

The silica gel was the same as that used previously, and for which the surface area, total water content, surface hydroxyl concentration, and adsorption isotherms of N_2O and SF_6 have been measured (4, 8). Methyl iodide (Fisher certified reagent) and methyl iodide-d_3 (Merck, Sharp, and Dohme) were used as received. The CD_3I

---

[1]A.E.C.L. No. 3484.

[2]Present Address: Materials Science Branch, Whiteshell Nuclear Research Establishment, Pinawa, Manitoba.

[3]A.E.C.L. Summer Student 1968. Present address: Department of Chemistry, University of Waterloo, Waterloo, Ontario.

Can. J. Chem. Downloaded from www.nrcresearchpress.com by 210.87.254.105 on 09/05/12
For personal use only.

contained 1.9% CD_2HI, as determined by mass spectrometry. The N_2O (Canadian Liquid Air Co.) and SF_6 (Matheson) were used as received.

The silica gel was dried at 120 °C in air, and samples of 0.5 to 2.0 g were weighed into cylindrical vessels fitted with break seals. The samples were evacuated, raised to the desired temperature, and kept overnight at that temperature while being evacuated to 10^{-6} Torr. The methyl iodide was measured out as a liquid, degassed, passed through a 6 in. column of P_2O_5, and transferred to the silica gel. The transfers were done on a grease-free, mercury-free vacuum line. The samples were then warmed to 60 °C to facilitate uniform mixing and were cooled. They were irradiated at 0 °C in a ^{60}Co γ-source at a mean dose rate of 6.1×10^{17} eV/g min in silica gel, as determined by Fricke dosimetry using $G(Fe^{3+}) = 15.6$.

The products were pumped off the gel, which was warmed to 50 °C to promote desorption. Methyl iodide was separated from the more volatile products using a short column of Porapak Q (Waters Associates), and the products were analyzed on a 5 ft column of Porapak Q at 50 °C. For analyses of hydrogen and nitrogen, products volatile at −196 °C were measured volumetrically and analyzed mass spectrometrically. Isotopic analyses of products were done on a Consolidated 21–130 mass spectrometer at 68 V. Cracking patterns for C_2D_6 and all the substituted methanes were determined using samples obtained from Merck, Sharp, and Dohme. All mass spectra were corrected for ^{13}C content. Substituted methyl iodides were determined on the same mass spectrometer at 9.9 V uncorrected ionizing voltage.

Results

The major hydrocarbon products from the radiolysis of methyl iodide adsorbed on silica gel are methane and ethane. They are produced with yields of several tenths of a G unit, based on energy absorbed in the entire system. Other minor products are hydrogen, ethylene, propane, and *n*-butane, all produced with yields less than 0.02 G units. It should be emphasized that all G values reported in this work are based on energy absorbed in the entire system of silica gel plus adsorbate.

Figure 1 gives the dose dependence of the yields of methane and ethane from 1×10^{19} to 4×10^{19} eV/g, for a gel degassed at about 300 °C and containing 15.5% of a monolayer of methyl iodide. For convenience, the methyl radical yield is defined as $G(CH_4) + 2(C_2H_6)$ and is shown in Fig. 1. With gels degassed at 700 °C, yields of methane and ethane were strictly linear over this range of absorbed dose. Extremely small yields of methane and ethane were produced when methyl iodide was distilled at −196 °C onto either unirradiated silica gel or silica gel irradiated to a dose of 4×10^{19} eV/g at −196 °C and the system allowed

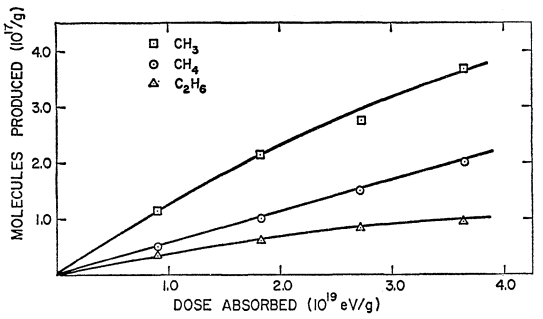

FIG. 1. Dose dependence of products formed from the methyl iodide – silica gel system. $\theta_{CH_3I} = 0.15_5$. Evacuation temperature = 298 °C.

to warm to room temperature, although in the latter case the blue color of the irradiated gel was bleached. The irradiations were done at −196 °C in an attempt to trap any long-lived species capable of causing decomposition. Thus, the phenomena we are observing are the results of radiation effects which occur during the irradiation. When the gel was irradiated without methyl iodide a small yield of hydrogen was observed (10^{-2} G units), which could account for some of the small hydrogen yield from the methyl iodide – silica gel system.

In Figs. 2 and 3, yields of the major products are shown as a function of the surface coverage of methyl iodide at a constant dose of 1.8×10^{19} eV/g. Results with a gel degassed at about 300 °C are shown in Fig. 2, and with one degassed at about 700 °C in Fig. 3. Coverages of methyl iodide were calculated using 24.2 $Å^2$ for the area

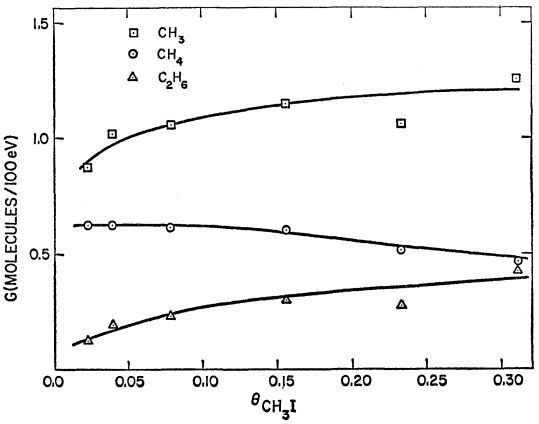

FIG. 2. Dependence of product yields on the fraction of a monolayer (θ) of methyl iodide on the gel. Dose = $1.8_2 \times 10^{19}$ eV/g. Evacuation temperature = 298 °C.

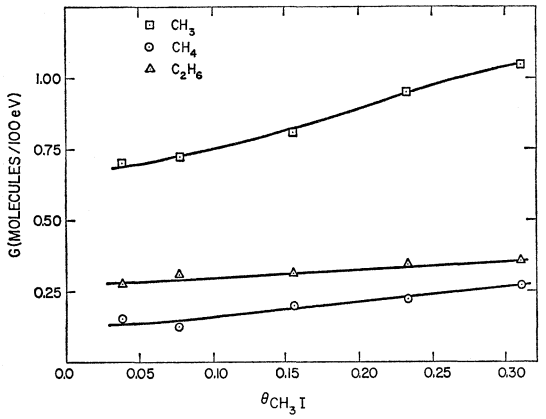

FIG. 3. Dependence of product yields on the fraction of a monolayer (θ) of methyl iodide on the gel. Dose = $1.8_1 \times 10^{19}$ eV/g. Evacuation temperature = 695 °C.

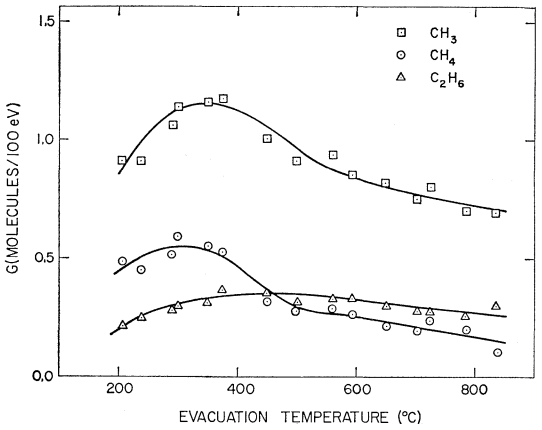

FIG. 4. Dependence of product yields on the degassing temperature of the gel. Dose = $1.8_2 \times 10^{19}$ eV/g. $\theta_{CH_3I} = 0.15_6$. $G(CH_3)$ is defined as $G(CH_4) + 2\,G(C_2H_6)$.

of a methyl iodide molecule. This value was calculated from the liquid density of methyl iodide (9).

Yields of methane and ethane remained large at the smallest coverages to which we could conveniently work. Although, of course, no products were obtained at zero coverage, our yields did not extrapolate smoothly to zero, indicating that "energy transfer" occurs over a considerable distance. This is in agreement with the results obtained by Wong and Willard at −196 °C using e.s.r. techniques (6).

Gels degassed at 300 °C and at 700 °C give very different results. The methyl yield is much higher on the low temperature gel. The ratio of methane to ethane is much larger than unity over gels degassed at 300 °C, particularly at lower coverages, whereas it is considerably less than unity on gels degassed at 700 °C. This is shown more clearly in Fig. 4, which shows yields obtained at 15.6% of a monolayer of methyl iodide at a dose of 1.8×10^{19} eV/g for a number of gels degassed at various temperatures. The methyl radical yield is defined as the methane yield plus twice the ethane yield. Here it is shown that methane is produced in larger yield over gels degassed below 450 °C, whereas ethane is in larger yield over gels degassed above this temperature. Ethane yields are relatively independent of degassing temperature above a degassing temperature of 300 °C, whereas the methane yields tend to correlate with the surface water content of these gels given previously in Fig. 4 of ref. 8, and with nitrogen yields from the radiolysis of N_2O over this gel (4).

In an attempt to discover the source of the methane and ethane, deuterated methyl iodide was irradiated on protiated silica gel and the methane and ethane yields were studied as a function of dose, coverage, and evacuation temperature. In all cases the ethane yield was virtually all C_2D_6, although over gels degassed at the highest temperatures up to 5% C_2D_5H was obtained. The methane, on the other hand, was largely CD_3H with a small amount of CD_4. Yields of CD_3H and CD_4 are shown as a function of degassing temperature in Fig. 5 for a constant coverage of 15.6% of a monolayer of CD_3I and a dose of 1.9×10^{19} eV/g. At the highest degassing

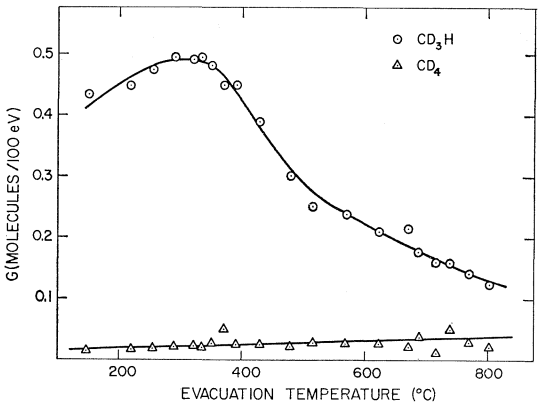

FIG. 5. Methane yields from the radiolysis of CD_3I on silica gel as a function of degassing temperature of the gel. Dose = $1.9_0 \times 10^{19}$ eV/g. $\theta_{CD_3I} = 0.15_6$.

Can. J. Chem. Downloaded from www.nrcresearchpress.com by 210.87.254.105 on 09/05/12
For personal use only.

Can. J. Chem. Downloaded from www.nrcresearchpress.com by 210.87.254.105 on 09/05/12
For personal use only.

temperatures, up to 0.05 G units of CD_2H_2 were obtained. More CD_2H_2 was also produced at doses greater than 2×10^{19} eV/g. With gels degassed at 700 °C, the proportion of CD_4 remains constant above a coverage of 15% of a monolayer, whereas with gels degassed at 300 °C, the proportion of CD_4 increases with coverage.

The recovered deuterated methyl iodide was examined using low voltage mass spectrometry to see if there was any exchange of H into the methyl iodide, as had been noted previously for the radiolysis of c-C_6D_{12} on light silica gel (8). No evidence was found for the formation of CD_2HI to within our limits of detection, which would correspond to 0.2 G units.

Nitrous oxide (10) and sulfur hexafluoride (11) are known to react with electrons by

[2] $$N_2O + e^- \rightarrow N_2 + O^-$$

[3] $$SF_6 + e^- \rightarrow SF_6^-$$

In an attempt to assess the role of electrons in the radiolysis of this system, we added both N_2O and SF_6. Nitrous oxide had little effect on the methane yields on gels degassed at 200 or 700 °C as shown in Fig. 6 for 7.8% of a monolayer of methyl iodide at a dose of 2.0×10^{19} eV/g. The surface area of the nitrous oxide molecule was taken as 16.8 Å^2 (9). Ethane yields increased, however, although the results were extremely irreproducible. Nitrogen was produced with a yield of about 1 G unit, similar to yields obtained from the radiolysis of N_2O on silica gel in the presence of other electron scavengers, compared with up to 4 G units for the radiolysis of N_2O alone on silica gel. Adding up to 5% of a monolayer of SF_6 decreased the methane yields somewhat and increased ethane yields, but the results were extremely irreproducible. Both N_2O and SF_6 coverages were corrected for unadsorbed gas, using isotherms measured previously (4).

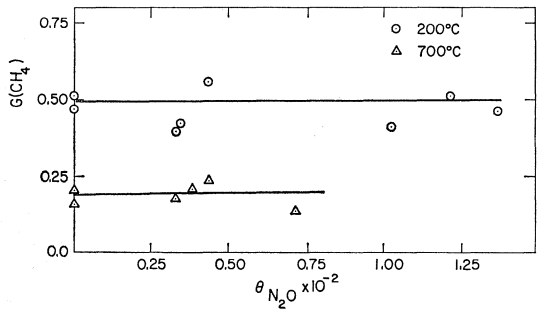

FIG. 6. Methane yields in the presence of added N_2O for gels degassed at 200 and 700 °C. Dose = $1.9_8 \times 10^{19}$ eV/g. $\theta_{CH_3I} = 0.078$.

Discussion

The discussion of the results will be based on the premise that we are dealing with the radiolysis of methyl iodide which is physically adsorbed on the surface of the silica gel. This is a reasonable postulate, since Hertl and Hair (12) have measured an isosteric heat of adsorption of 6.0 ± 1.0 kcal/mole for methyl iodide adsorbed on an aerosil. This is of the same order as that measured for cyclohexane and benzene which are known to be physically adsorbed (13). In agreement with this low heat of adsorption, we were able to recover our unreacted methyl iodide quantitatively by pumping at 50 °C, even for the smallest coverages used.

The yields of methane and ethane are much larger than would be expected if the silica gel were acting as an inert support for the methyl iodide. A surface coverage of methyl iodide of 15.6% of a monolayer corresponds to a mole fraction of methyl iodide of 2.2×10^{-2} and an electron fraction of 3.9×10^{-2}. Since $2G(C_2$ products$) + G(CH_4)$ from the radiolysis of liquid methyl iodide is 3.1 (14), then $G(CH_3)$ from the direct radiolysis of the methyl iodide would be 0.12 G units at this coverage, compared with the observed yield of 1.1_5 G units from a gel evacuated at 300 °C, and 0.83 for one degassed at 700 °C. At lower coverages the relative increases in yields are even larger, even though the actual yields are decreased slightly at the lower coverages. It is also apparent that energy absorbed in the silica gel is able to cause decomposition of the methyl iodide with only about 1/3 of the efficiency of energy absorbed directly by the methyl iodide. As our yields do not extrapolate smoothly to zero at zero coverage, this "energy transfer" acts over large distances in the gel. This agrees with the results obtained by Wong and Willard (6), who found yields independent of coverage at much lower coverages than we could use.

A mechanism for methyl radical formation involving electrons and positive holes formed initially in the gel as well as, possibly, direct excitation would explain our results

[4a] Solid $\rightsquigarrow \oplus + \ominus$

[4b] $\rightsquigarrow$ Solid*

Can. J. Chem. Downloaded from www.nrcresearchpress.com by 210.87.254.105 on 09/05/12
For personal use only.

[5a] $\oplus + \ominus \rightarrow$ Solid**

[5b] $\rightarrow$ Deactivation

[6] $\ominus + CH_3 \rightarrow CH_3I^-$

[7] $CH_3I^- \rightleftarrows [CH_3\cdot + I^-]_{caged} \rightarrow CH_3\cdot + I^-$

[8] CH_3I^- or $[CH_3\cdot + I^-]_{caged} + \oplus \rightarrow CH_3I$ or $[CH_3\cdot + I\cdot]_{caged}$

[9a] $[CH_3\cdot + I\cdot]_{caged} \rightarrow CH_3\cdot + I\cdot$

[9b] $\rightarrow CH_3I$

[10] Solid* + $CH_3I \rightarrow CH_3\cdot + I\cdot$ + solid

where Solid* and Solid** are unspecified excited states of the solid which may or may not be distinguishable from each other. The participation of CH_3I^+ may be ruled out since the ionization potential of CH_3I is about 9.5 eV (15), whereas it is now considered that the band gap of silica is at most 8.1 eV (16).

The total methyl radical yield is about 1.2 *G* units, whereas the electron yield from silica gel has been reported to be from 2.1 to 4.7 *G* units (4, 6). Evidence from experiments using N_2O and SF_6 as competitive scavengers, to be discussed below, indicates that CH_3I is an efficient electron scavenger in this system. Hence the methyl iodide scavenges up to 4.7 *G* units of electrons but only gives 1.2 *G* units of methyl radicals. It is postulated that the CH_3I^- formed in reaction [6] has a relatively long lifetime compared with anion – positive hole combination (reaction [8]). This long lifetime could be caused by a back reaction favored by caging effects in the narrow pores of the gel (reaction [7]). Such a reaction has been used by Willard and his co-workers (17, 18) to explain first order decay of methyl radicals in organic glasses.

Anion – positive hole recombination (reaction [8]) will give methyl radicals, some of which will be highly excited since up to 8 eV is available, but may also give back a methyl iodide molecule, particularly when combination occurs in narrow pores of the gel where caging effects may be appreciable (17, 19). It is also possible that caging keeps the methyl radicals formed in reaction [7] close to the iodide ion. When this iodide ion is neutralized to give an iodine atom, methyl iodide could be reformed. The extent of the participation of reactions [4b] and [5a], followed by reaction [10], has not been determined in this work, as we shall see when we consider the effects of electron scavengers on the system.

Some methyl radicals produced in reaction [9] may contain excess energy. Since they are initially formed in a tetrahedral configuration, they may contain as much as 10 kcal/mole of vibrational energy (5, 20), although more recent estimates suggest that they contain from 4 to 5 kcal/mole in the ν_2 mode (21, 22). Thus they may abstract from methyl iodide (20) or from the surface hydroxyl groups by reaction [11], written for deuterated methyl iodide

[11a] $CD_3\cdot + CD_3I \rightarrow CD_4 + \cdot CD_2I$

[11b] $CD_3\cdot + \equiv SiOH \rightarrow CD_3H + \equiv SiO\cdot$

Both reactions [11a] and [11b] are expected to have activation energies of at least 9 kcal/mole (23, 24), but may occur, particularly if the methyl radicals have excess energy. The correlation of the methane yield with the known (8) surface hydroxyl content of the gel indicates that reaction [11b] is more important in our system. This view is strongly supported by the observation that the major portion of the methane yield from the radiolysis of CD_3I on protiated silica gel is CD_3H. Apparently at -196 °C, methyl radicals from the radiolysis of CH_3Br on silica gel are not capable of abstracting from surface hydroxyl groups, since Wong and Willard see 1.4 *G* units of trapped methyl radicals from that system (6).

The ethane produced is considered to come mainly from combination of methyl radicals (reaction [12])

[12] $CH_3\cdot + CH_3\cdot \xrightarrow{\text{solid}} C_2H_6$

The absence of propane and *n*-butane in the major products is taken as evidence that methylene radicals play no important part in this system. This is supported by the observation that the methane yield from the deuterated methyl iodide is CD_3H, whereas the ethane yield is C_2D_6. Any methylene addition to methane would be expected to give mainly C_2D_5H.

On gels degassed at low temperatures, the surface hydroxyl concentration is high and a large portion of the methyls abstract from the surface hydroxyls, giving methane. On gels degassed at higher temperatures, the surface hydroxyl concentration is lower so that a larger fraction of the radicals combine with each other to give ethane.

The variations in the relative yields of methane to ethane with coverage also require explanation. On a gel degassed at 300 °C, the results in Fig. 2

Can. J. Chem. Downloaded from www.nrcresearchpress.com by 210.87.254.105 on 09/05/12
For personal use only.

show that at high coverage ($\theta_{CH_3I} = 0.3$) the ratio of ethane to methane increases. Now the results using CD_3I show that the methane is formed largely by reaction [11*b*] even at high coverage. Hence an increase in the surface coverage must favor reaction [12] over [11*b*]. This could arise if vibrationally excited radicals produced in reaction [7] are moderated by interaction with methyl iodide molecules. Methyl radicals are thought to form long-lived collision complexes with methyl iodide which would facilitate exchange of vibrational energy (23). Thermal radicals would then combine to give ethane. It is also possible that excited methyl radicals could give ethane by reaction [13] at high coverages (25).

[13] $$CH_3\cdot + CH_3I \rightarrow C_2H_6 + I\cdot$$

A third possibility is that the methyl iodide is adsorbed in such a way as to cover some of the surface OH groups and prevent their participation in reaction [11*b*]. On gels degassed at 700 °C, ethane is always the major product and the ratio of methane to ethane varies little with coverage.

No hydrogen was exchanged into the CD_3I when irradiated with gels degassed at any temperature. Thus, a carbonium ion induced exchange of the type envisaged for *c*-C_6D_{12} (8) does not operate here. On gels degassed at the higher temperatures, small yields of C_2D_5H and CD_2H_2 were noted, and these yields are probably the result of a carbonium ion induced exchange. These products were particularly noticeable at the highest doses, in agreement with the results of Kohn (26) on radiation-induced exchange between methane and silica gel.

Both N_2O and SF_6 are known to be good electron scavengers (10, 11) and hence were used in competition with the methyl iodide. The methane yields were not affected by N_2O for gels degassed at 200 or 700 °C. Thus, either electrons are not participating in the energy transfer or, more likely, N_2O is not competing effectively with the methyl iodide for the free electrons or negative holes. The nitrogen yields obtained resemble those for the γ-radiolysis of N_2O on silica gel in the presence of SF_6 and CCl_4. Thus methyl iodide, behaving like SF_6 and CCl_4, apparently suppresses the nitrogen yield, giving a smaller nitrogen yield than from the N_2O – silica gel system. The postulate that N_2O is an inefficient competitor with methyl iodide for the electrons is therefore reasonable.

With SF_6, some decrease in methane yields was noted, indicating that SF_6 may be capturing electrons, but not to the extent expected. However, the scatter was very large and no real conclusions can be drawn. The relative efficiencies of some electron scavengers in the vapor phase have been calculated by Holtslander and Freeman (27), who gave a value of 10 as the ratio between SF_6 and N_2O. Because the influence of N_2O and SF_6 on the methyl iodide system was not substantial, methyl iodide appears to be an extremely efficient electron scavenger, at least comparable to SF_6.

The irreproducible yields of ethane in the presence of N_2O or SF_6 probably result from chain reactions induced by $O^\cdot$, O^-, or F^- (28, 29). In aqueous media, SF_6^- is known to produce 6 F^- ions and a SO_4^{2-} ion (30). Similar reactions may well occur in the presence of surface hydroxyl groups. Hence any quantitative treatment of the effect of N_2O and SF_6 on this system is of little value at present.

We would like to thank Dr. A. O. Allen and Prof. J. E. Willard for useful discussions, and Drs. D. A. Armstrong, A. W. Boyd, and D. R. Smith for comments on this manuscript.

1. J. M. Caffrey, Jr. and A. O. Allen. J. Phys. Chem. **62**, 33 (1958).
2. J. W. Sutherland and A. O. Allen. J. Amer. Chem. Soc. **83**, 1040 (1961).
3. J. G. Rabe, B. Rabe, and A. O. Allen. J. Phys. Chem. **70**, 1098 (1966).
4. N. H. Sagert and R. W. Robinson. Can. J. Chem. **46**, 2075 (1968).
5. M. Shirom and J. E. Willard. J. Phys. Chem. **72**, 1702 (1968).
6. P. K. Wong and J. E. Willard. J. Phys. Chem. **72**, 2623 (1968).
7. M. Fujimoto, H. D. Gesser, B. Garbutt, and A. Cohen. Science, **154**, 381 (1966).
8. N. H. Sagert and P. J. Dyne. Can. J. Chem. **45**, 615 (1967).
9. D. M. Young and H. D. Crowell. Physical adsorption of gases. Butterworths Scientific Publications, London. 1962. p. 226.
10. F. S. Dainton and D. B. Peterson. Proc. Roy. Soc. London, Ser. A, **267**, 443 (1962).
11. R. S. Davidow, R. A. Lee, and D. A. Armstrong. J. Chem. Phys. **45**, 3364 (1966).
12. W. Hertl and M. L. Hair. J. Phys. Chem. **72**, 4676 (1968).
13. J. M. Thorp and J. B. Woolf. Trans. Faraday Soc. **64**, 2190 (1968).
14. R. C. Petry and R. H. Schuler. J. Amer. Chem. Soc. **75**, 3796 (1953).
15. V. I. Vedeneyev, L. V. Gurvich, V. N. Kondrat'yev, V. A. Medvedev, and Ye L. Frankevich. Bond energies, ionization potentials, and electron affinities. Edward Arnold Publishers, London. 1965.

16. R. W. DOUGLAS. *In* Interaction of radiation with solids. *Edited by* A. Bishay. Plenum Press, New York. 1967. pp. 563–591.
17. R. F. C. CLARIDGE and J. E. WILLARD. J. Amer. Chem. Soc. **87**, 4992 (1965).
18. W. G. FRENCH and J. E. WILLARD. J. Phys. Chem. **72**, 4604 (1968).
19. R. F. POTTIE, W. H. HAMILL, and R. R. WILLIAMS, JR. J. Amer. Chem. Soc. **80**, 4224 (1958).
20. C. D. BASS and G. C. PIMENTEL. J. Amer. Chem. Soc. **83**, 3754 (1961).
21. L. ANDREWS and G. C. PIMENTEL. J. Chem. Phys. **47**, 3637 (1967).
22. D. E. MILLIGAN and M. E. JACOX. J. Chem. Phys. **47**, 5146 (1967).
23. J. R. MAJER and J. P. SIMONS. Advan. Photochem. **2**, 137 (1964).
24. P. GRAY and A. A. HEROD. Trans. Faraday Soc. **64**, 2723 (1968).
25. R. E. REBBERT and P. AUSLOOS. J. Chem. Phys. **48**, 306 (1968).
26. H. W. KOHN. J. Phys. Chem. **66**, 1017 (1962).
27. W. J. HOLTSLANDER and G. R. FREEMAN. J. Phys. Chem. **71**, 2562 (1967).
28. W. J. HOLTSLANDER and G. R. FREEMAN. Can. J. Chem. **45**, 1661 (1967).
29. R. R. HENTZ and S. J. RZAD. J. Phys. Chem. **72**, 1027 (1968).
30. K.-D. ASMUS and J. H. FENDLER. J. Phys. Chem. **72**, 4285 (1968).

Can. J. Chem. Downloaded from www.nrcresearchpress.com by 210.87.254.105 on 09/05/12
For personal use only.

Can. J. Chem. Downloaded from www.nrcresearchpress.com by 210.87.254.6 on 09/05/12
For personal use only.

$Hg(^3P_1)$ photosensitized decomposition of 2,5-dihydrofuran

B. Francis and A. G. Sherwood
Department of Chemistry, Simon Fraser University, Burnaby 2, British Columbia

Received[1] October 2, 1968

The mercury photosensitized decomposition of 2,5-dihydrofuran was studied in the vapor phase at 25 ± 2 °C. Major products are carbon monoxide, propene, and hydrogen, while biallyl, allene, methylacetylene, furan, 2,3-dihydrofuran, tetrahydrofuran, and small amounts of three unidentified products are also produced. The quantum yields of all products are decreased by increasing substrate pressure, indicating collisional deactivation of an excited state precursor which, at low pressures, decomposes according to the scheme

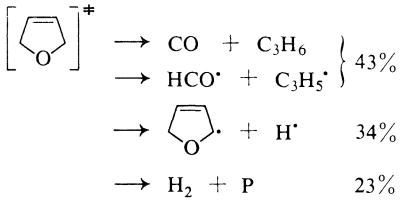

The product P is not furan and its possible identity is discussed. The free radical component of the reaction was further studied by carrying out the reaction in the presence of nitric oxide. The results are consistent with the above processes.

Canadian Journal of Chemistry, **48**, 25 (1970)

Introduction

The mercury photosensitized reactions of cyclic compounds are of interest because of the possibility of ring cleavage in the primary process to yield a triplet biradical. In the case of cycloparafins larger than cyclopropane, the most important primary process is the cleavage of a C—H bond to give a hydrogen atom and a cycloalkyl radical whose chemical behavior is not significantly different from that of straight chain analogues (1). The reaction of cycloolefins produces compounds originating from free radical reactions, as well as ring contracted compounds, which suggest that a part of the primary process produces a biradical with free electrons separated by several carbon atoms (2, 3). Isomerization of these biradicals results in the observed products, vinyl cyclopropane from cyclopentene (2), and vinyl cyclobutane from cyclohexene (3).

The presence of a hetero atom in the ring would also be expected to change the nature of the primary process from that observed in the case of the cycloparafins. The reactions of the epoxides of ethylene (4, 5) and of butene-2 (6) produce excited molecules which, at low pressure, can decompose with cleavage of the ring. Little work has been done on heterocyclic compounds with larger rings. Srinivasan has studied the mercury photosensitized reaction of furan (7, 8). The main reaction products, cyclopropene and carbon monoxide, were suggested to arise from the decomposition of a biradical intermediate

[1] 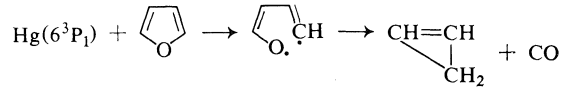

The formation of 3-methylcyclopropene from 2-methyl furan suggests that the double bond in the cyclopropene product was formed between carbon atoms 3 and 4 of the substrate molecule. It also appears that the substrate molecule underwent Diels–Alder additions to monoolefins, suggesting another biradical intermediate which may be represented as

We have undertaken a study of the mercury photosensitized decomposition of 2,5-dihydrofuran (2,5-DHF). The C—O bond, in a position

[1]Revision received October 6, 1969.

allyl to the double bond, represents a likely site for bond cleavage, i.e.

[2] $Hg(6^3P_1)$ + $\longrightarrow$ 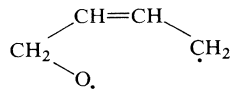

The resulting biradical should be compared to that suggested by Cvetanović and Doyle (9) as the intermediate formed by the addition of ground state oxygen atoms to butadiene

[3] $O(^3P) + CH_2{=}CH{-}CH{=}CH_2 \rightarrow \dot{O}{-}CH_2{-}\dot{C}H{-}CH{=}CH_2$

This biradical differs from that produced in reaction [2] only in the positions of the double bond and the free electrons. These structures may be regarded, in valence bond terminology, as representing contributions to a resonance hybrid structure which may be written $\dot{O}{-}CH_2{-}\overset{\text{- - - - - - - - - - -}}{CH{-}CH{-}CH_2}$.

The products of the O-atom – butadiene reaction were butadiene monoxide, formed by pairing of the unpaired electrons of the biradical represented in reaction [3]; 3-butenal, formed by a hydrogen shift in this biradical; and carbon monoxide, formed by its decomposition. Because the major emphasis of these authors was on the higher molecular weight products, some of their work was repeated. Propylene and CO, in roughly equimolar amounts, were found to be the major products.

In relation to the present work, the most interesting observation of Cvetanović and Doyle was that no 2,5-DHF was produced. The intermediate formed in reaction [3] does not cyclize to any extent to give a 5-membered ring. It is tempting to interpret this observation as indicating that the structure $\dot{O}{-}CH_2{-}CH{=}CH{-}\dot{C}H_2$ does not contribute significantly to the structure of the biradical intermediate. On the other hand, the exclusive formation of the 3-membered ring may be the result of an interaction between the unpaired electrons which controls the direction of the reaction from the moment of addition of the oxygen atom.

It was considered likely that a study of the 2,5-dihydrofuran photosensitization would contribute to the understanding of this question.

Experimental

The substrate (Aldrich Chemical Co. Inc.) was purified by gas chromatography on a 6 ft Carbowax 600-on-celite column. The main impurities were furan and tetrahydrofuran which, as well as being difficult to remove, were formed in a slow but perceptible dark reaction. Reactions were carried out in a cyclindrical quartz cell, 5 cm diameter × 10 cm long, irradiated through a Vycor 7910 filter with a low pressure mercury arc. Mercury vapor was present in the cell at equilibrium vapor pressure at ambient temperature (25 ± 2 °C). After reaction, the cell contents were separated into three fractions by trap-to-trap distillation. Each fraction was analyzed by gas–liquid chromatography (g.l.c.). The fraction which condensed at −112 °C was analyzed on a Carbowax 600-on-celite column, the fraction which condensed at −196 °C was analyzed on a Porapak P column, and the non-condensables on a molecular sieve column. Hydrogen was measured by two methods. The yields of CO, analyzed by g.l.c., were subtracted from the total yields of non-condensables. This gave values which were consistent with those obtained directly by g.l.c. using argon as a carrier gas.

Actinometry was done by extrapolation of nitrogen yields from the mercury photosensitized decomposition of *n*-butane – nitrous oxide mixtures, assuming that the quantum yield of N_2, extrapolated to zero butane pressure, was equal to unity (10). The absorbed light intensity measured in this way was 0.81 ± 0.02 μeinsteins min^{-1}.

The quenching cross section of 2,5-DHF was also measured by the N_2O method (10) using the values $\sigma_{n\text{-butane}}{}^2 = 3.6$ Å^2, $\sigma_{DHF}{}^2 = 28.4 \pm 1.4$ Å^2.

Results and Discussion

The main products of the reaction are hydrogen, carbon monoxide, and propylene. Smaller quantities of allene, biallyl, furan, 2,3-dihydrofuran (2,3-DHF), and tetrahydrofuran were also formed. Identification of these components was verified by mass spectrometry, infrared (i.r.) and nuclear magnetic resonance (n.m.r.) spectroscopy. An authentic sample of 2,3-DHF was prepared by the method of Paul, Fluchaire, and Collardeau (11). The n.m.r. spectrum of this sample agreed with that reported by Korver *et al.* (12). The i.r. spectrum of this sample agreed with that of the product identified as 2,3-DHF.

Small amounts of three less volatile products were also obtained. These will be referred to as A, B, and C. Their identification was attempted but their quantum yields were so low as to yield only poor i.r. and mass spectra. Tentative identification will be discussed later. The yields of these products are indicated in Table 1 in terms of g.l.c. peak areas since calibrations were impossible.

The quantum yields of products as a function of reaction time are given in Table 1. Taking into account the large experimental uncertainty in the

Can. J. Chem. Downloaded from www.nrcresearchpress.com by 210.87.254.6 on 09/05/12
For personal use only.

TABLE 1

Mercury photosensitized decomposition of 2,5-dihydrofuran*

Time (min)	Quantum yield								
	H_2	CO	Propene	Allene	Methyl acetylene	Biallyl	Furan	2,3-DHF	THF
1	0.29	0.27	0.28	0.013	0.010	0.067	0.067	0.048	0.057
2	0.17	0.32	0.29	0.012	0.014	0.046	0.046	0.014	0.020
3	0.18	0.37	0.30	0.021	0.014	0.045	0.045	0.023	0.026
4	0.20	0.31	0.29	0.018	0.016	0.047	0.047	0.029	0.025
5	0.19	0.33	0.26	0.017	0.015	0.046	0.046	0.026	0.024
7	0.18	0.36	0.26	0.019	0.017	0.046	0.046	0.016	0.018
10	0.17	0.36	0.27	0.020	0.014	0.041	0.041	0.025	0.025
13	0.16	0.35	0.28	0.022	0.015	0.046	0.046	0.021	0.020
16	0.15	0.33	0.24	0.018	0.014	0.033	0.033	0.020	0.018
20	0.17	0.32	0.27	0.019	0.015	0.033	0.033	0.018	0.019
25	0.17	0.34	0.26	0.021	0.015	0.035	0.035	0.019	0.019
30	0.19	0.31	0.26	0.023	0.018	0.031	0.031	0.020	0.020
40	0.15	0.32	0.26	0.022	0.017	0.036	0.036	0.021	0.022
50	0.13	0.29	0.24	0.020	0.017	0.033	0.033	0.019	0.020

*Substrate pressure = 10 Torr.

analysis of very short runs, the quantum yields of all products except A, B, and C are essentially independent of time, indicating that none of these products are the result of secondary reactions. A small amount of nonvolatile material was observed in very long runs but this does not appear to be an important product.

The variation of quantum yields of products

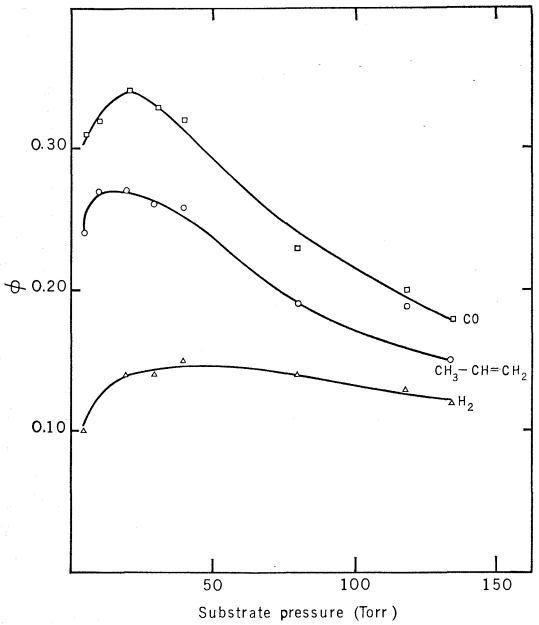

FIG. 1. Quantum yield of products as a function of pressure, reaction time = 20 min.

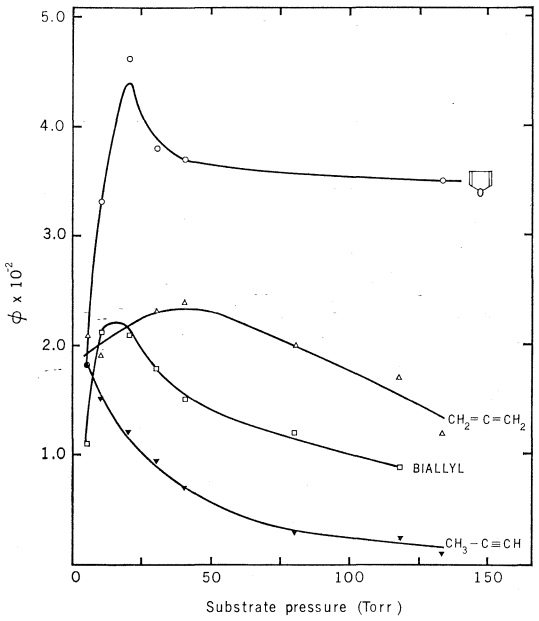

FIG. 2. Quantum yield of products as a function of pressure, reaction time = 20 min.

with substrate pressure is indicated in Figs. 1 and 2. 2,3-DHF analysis was impossible at higher pressures due to inadequate resolution of the g.l.c. peaks. All products show behavior characteristic of the decomposition of an excited molecule subject to collisional deactivation. In order to test this idea runs were done in which CF_4 was present. The results, shown in Figs. 3

Can. J. Chem. Downloaded from www.nrcresearchpress.com by 210.87.254.6 on 09/05/12
For personal use only.

and 4, have been corrected for the small amount of quenching of triplet mercury by the CF_4. It can be seen that the quantum yields of all products (except allene) are decreased by the presence of the added inert gas.

The following mechanism is suggested

[4] $Hg(6^1S_0) + h\nu \longrightarrow Hg(6^3P_1)$

[5] $Hg(6^3P_1) +$ $\longrightarrow Hg(6^1S_0) +$

[6] 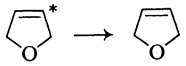

[7] $\longrightarrow$ $+ H_2$

[8] $\longrightarrow CH_3{-}CH{=}CH_2 + CO$

[9] $\longrightarrow$ $+ H^{\bullet}$

The free radical formed in reaction [9] may also be written as

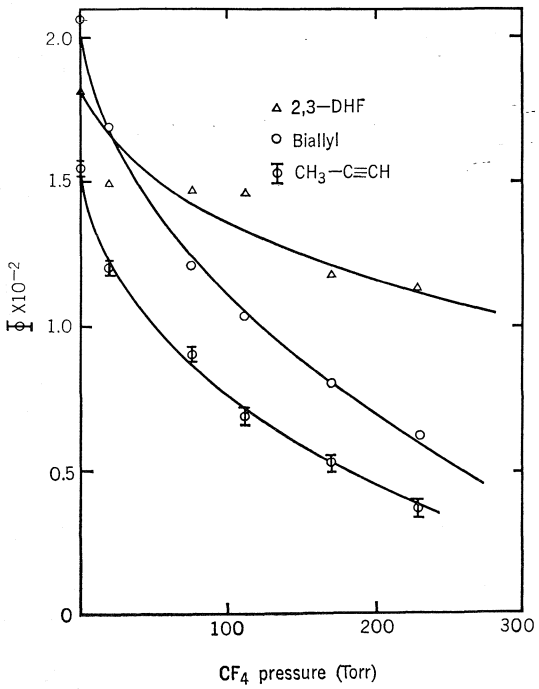

FIG. 3. Quantum yield of products as a function of pressure of added CF_4, reaction time = 20 min.

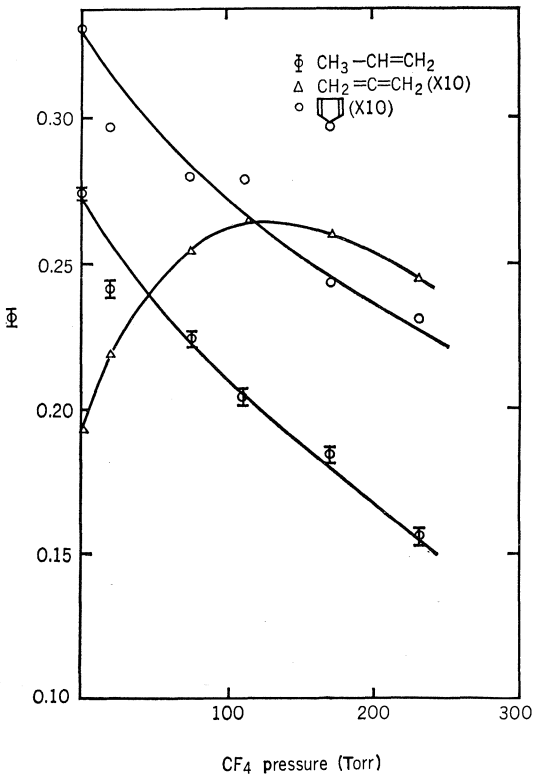

FIG. 4. Quantum yield of products as a function of pressure of added CF_4, reaction time = 20 min.

To represent the delocalization of the free electron, we may represent the structure as

Disproportionation of this radical would be expected to give either 2,3-DHF or 2,5-DHF or both. The H atom probably adds to a substrate molecule to give a tetrahydrofuranyl radical

[10] $H +$ 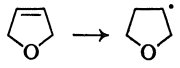

The cyclic products of the reaction are accounted for in terms of disproportionation reactions of these radicals

[11] 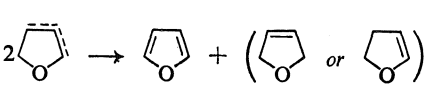

[12] 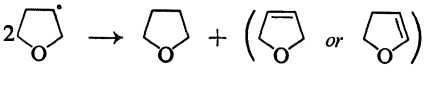

Can. J. Chem. Downloaded from www.nrcresearchpress.com by 210.87.254.6 on 09/05/12
For personal use only.

[13] 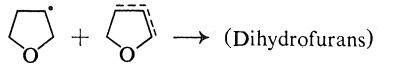 (Dihydrofurans)

[14] 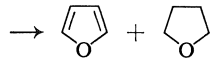

NO Inhibition

This mechanism was tested by introducing NO into the system. The results, again corrected for competitive quenching, are shown in Table 2. Acrylonitrile and H_2O, although identified, were not determined quantitatively because of bad overlap of their g.l.c. peaks with that of the substrate. The CO yield is slightly increased while the propylene yield is decreased by a factor of some 33% in the case of the shorter runs. The further decrease observed in the longer runs suggests consumption in secondary reactions. To the extent of this 33%, then, propylene must have a free radical precursor. It may be formed by the decomposition of excited 2,5-DHF molecules by way of the ring opened biradical suggested in the Introduction.

[15] 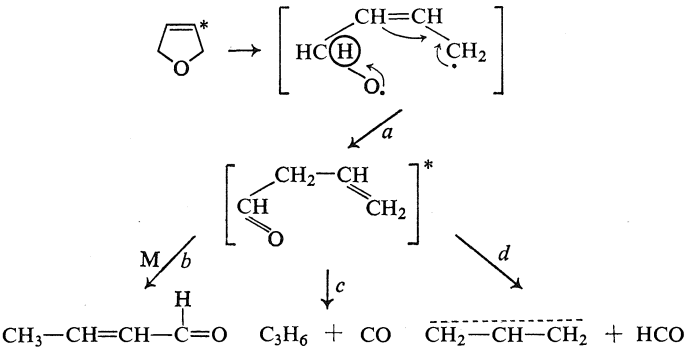

If the biradical intermediate is too short-lived to react with NO, the above scheme is consistent with the experimental observations.

The 3-butenal formed in reaction [15*a*] would be excited to the extent of approximately 112 kcal/mole and could react in three ways. Reaction [15*c*] would yield directly carbon monoxide and propylene whose formation would not be inhibited by NO. Reaction [15*d*] would produce formyl and allyl radicals. Allyl may yield additional propylene by disproportionation with formyl radicals

[16] $\dot{C}H_2—CH—\dot{C}H_2 + HCO \rightarrow CH_3—CH=CH_2 + CO$

Such disproportionations of formyl with other radicals have been reported (13). Formation of propylene by this route would be inhibited by NO. The presence of allyl radicals in this system is indicated (14) by the formation of acrylonitrile by the reaction

[17] $\dot{C}H_2—CH—\dot{C}H_2 + NO \rightarrow CH_2=CH—CH_2—NO \rightarrow CH_2=CH—CN + H_2O$

The decrease in yield of crotonaldehyde caused by the presence of NO indicates a free radical origin of some of this product, probably the combination of allyl and formyl radicals.

Combination and disproportionation of allyl radicals are probably the source of the allene and biallyl formed when NO is absent

[18] $2\dot{C}H_2—CH—\dot{C}H_2 \rightarrow CH_2=CH—CH_2—CH=CH_2$

[19] $\rightarrow CH_3—CH=CH_2 + CH_2=C=CH_2$

The ratio of allene to biallyl suggests a disproportionation-to-combination ratio of approximately 0.5. This value constitutes an upper limit because of the possibility of allyl disproportionating with other radicals present to yield allene.

The maximum in the curve for allene in Fig. 4 may be the result of a changing disproportionation-to-combination ratio as "hot" allyl radicals are collisionally deactivated.

The small yield of methylacetylene is not

Can. J. Chem. Downloaded from www.nrcresearchpress.com by 210.87.254.6 on 09/05/12
For personal use only.

Can. J. Chem. Downloaded from www.nrcresearchpress.com by 210.87.254.6 on 09/05/12
For personal use only.

TABLE 2

Effect of NO on mercury sensitized decomposition of 2,5-dihydrofuran*

[NO] (%)	Reaction time (min)	Quantum yield†											Gas chromatograph peak areas		
		H_2	CO	$CH_3—CH=CH_2$	N_2O	$CH_3—C\equiv CH$	$CH_2=C=CH_2$	Biallyl	2,3-DHF	Furan	THF	Crotonaldehyde	A	B	C
0	10	0.17	0.32	0.27	0	0.014	0.02	0.041	0.025	0.041	0.025	0.048	838	980	511
3.7	5	0.17	0.42	0.19	0.17	0.010	0	0	0	0.27	0	‡	0	0	241
10.2	5	0.17	0.42	0.20	0.18	0.014	0	0	0	0.25	0	0.025	0	0	253
11.4	30	0.165	0.38	0.18	0.12	0.012	0	0	0	0.24	0	0.024	0	0	1178
15.5	30	0.17	0.42	0.17	0.12	0.011	0	0	0	0.25	0	0.023	0	0	1201

*Substrate pressure = 10 Torr.
†Corrected for competitive quenching by NO.
‡Not determined.

Can. J. Chem. Downloaded from www.nrcresearchpress.com by 210.87.254.6 on 09/05/12
For personal use only.

effected by NO and so may be the product of a molecular decomposition.

With reference to reaction [15*a*], McDowell and Sifniades (15) have studied the photolysis of crotonaldehyde and have suggested the decomposition of an excited state to give *either* propylene and CO *or* allyl and formyl. Allen and Pitts, in a more recent paper (16), have suggested the intermediacy of propenyl radicals in the crotonaldehyde photolysis. The participation of 1-propenyl radicals in the present reaction would have been indicated by the formation, in the NO-inhibited runs, of HCN and formaldehyde (17).

[20] $CH_3—CH=CH + NO \rightarrow CH(—O—N)—CH=CH \rightarrow CH_3—C(=O)H + HCN$

The absence of these products supports reactions [15*a*] to [15*d*] as the sources of propylene.

The formyl radicals in the presence of NO give HNO and CO (18, 19).

[21] $HCO + NO \rightarrow HCO(—NO) \rightarrow HNO + CO$

This is consistent with the small effect of NO on the CO yield and with the formation of N_2O and H_2O by the process

[22] $2HNO \rightarrow H_2O + N_2O$

Table 1 indicates that the yield of furan undergoes almost an 8-fold increase when NO is added. This additional furan is probably formed by reaction of dihydrofuranyl radicals with NO.

[23] 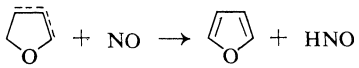

Such disproportionations of free radicals with NO occur to some extent in the case of ethyl radicals (20) to give ethylene and HNO, in the case of vinyl radicals (21) to give acetylene and HNO, and in the case of isopropoxy (22), to give acetone and HNO. No addition product of the reaction of dihydrofuranyl radicals with NO could be found. Assuming that the yield of furan in the presence of NO represents the quantum yield of the processes [7] and [9], the small yield of cyclic products in the uninhibited reaction indicates that disproportionation reactions [11] and [14] favor the re-formation of substrate.

Compounds A and B are not produced when NO is present, a fact which suggests that they have free radical precursors. The mass spectrum of A indicates a molecular weight of 110. The i.r. spectrum indicates absorption at 1640, 990, and 935 cm^{-1}, suggesting an allyl group, while the peak at 1090 cm^{-1} suggests a dihydrofuranyl ring. These observations suggest that A is the combination product of an allyl and a 2,5-DHF radical, i.e.

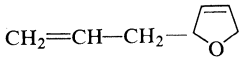

Although the relative nonvolatility of compound B suggests a molecule considerably larger than the substrate, the mass spectrum taken with an electron energy of 10 eV contains only an ion mass of 69. The i.r. spectrum of this compound has a peak characteristic of the 2,3-DHF ring at 1090 cm^{-1}. These observations suggest in a very tentative way that compound B may be the combination product of two dihydrofuranyl radicals, i.e.

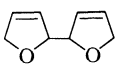

Product C, whose formation was not inhibited by the presence of NO, was produced in such small amounts that no useful spectra could be obtained.

Summation of the carbon content of products of the reaction in the presence of NO is, within experimental error, equal to the value in the absence of NO. This suggests that a radical chain mechanism which consumes substrate is not important.

Reaction [7] is written as if the products were H_2 and furan. The quantum yield of H_2 at 100 Torr pressure is 0.14 while that of furan is only 0.036. Since no other isomer with mass 68 was found, we must conclude that the product of reaction [7] is reactive. Srinivasan (6, 7) has identified an excited state of furan which reacts with olefins to give Diels–Alder addition products. If the same species is formed in reaction [7], its addition to the substrate would be expected. We are at present investigating that possibility.

Conclusion

It appears, in summary, that a quenching collision between triplet mercury and 2,3-DHF yields an excited molecule which may decompose

in the following ways. (*1*) Cleavage of a C—H bond to give a dihydrofuranyl radical and an H atom (34%). (*2*) Ring cleavage to give a biradical which may decompose to give propylene and CO *or* to give formyl and a free radical precursor of propylene (43%). (*3*) Molecular decomposition to give hydrogen and the unknown reactive species (23%).

The difference between the products of this reaction and those of oxygen atom – butadiene reaction indicates that the same biradical intermediate is not involved. Electron delocalization in the intermediate species, $\dot{O}—CH_2—\dot{C}H—CH=CH_2$ and $\cdot O—CH_2—CH=CH—CH_2\cdot$, may not be complete enough to make the two identical. An alternative explanation is that in either or both reactions, the formation and isomerization of the initially formed intermediate represents a single concerted process without involving an identifiable biradical intermediate.

The authors gratefully acknowledge financial support received from the National Research Council of Canada and from the President's Research Fund of Simon Fraser University.

1. J. G. CALVERT and J. N. PITTS, JR. Photochemistry. John Wiley and Sons, Inc., New York. 1966. p. 102.
2. W. A. GIBBONS, W. F. ALLEN, and H. E. GUNNING. Can. J. Chem. **40**, 568 (1962).
3. G. R. DEMARE, O. P. STRAUSZ, and H. E. GUNNING. Can. J. Chem. **43**, 1329 (1965).
4. M. K. PHIBBS, B. DE B. DARWENT, and E. W. R. STEACIE. J. Chem. Phys. **16**, 39 (1948).
5. R. J. CVETANOVIĆ. Can. J. Chem. **33**, 1684 (1955).
6. R. J. CVETANOVIĆ and L. C. DOYLE. Can. J. Chem. **35**, 605 (1957).
7. R. SRINIVASAN. J. Amer. Chem. Soc. **89**, 1758 (1967).
8. R. SRINIVASAN. J. Amer. Chem. Soc. **89**, 4812 (1967).
9. R. J. CVETANOVIĆ and L. C. DOYLE. Can. J. Chem. **38**, 2187 (1960).
10. R. J. CVETANOVIĆ, W. E. FALCONER, and K. R. JENNINGS. J. Chem. Phys. **35**, 1225 (1961).
11. R. PAUL, H. FLUCHAIRE, and G. COLLARDEAU. Bull. Soc. Chem. France, 668 (1950).
12. P. K. KORVER, P. J. VANDER HAAK, H. STEINBERG, and TH. J. DEBOER. Recueil, **84**, 129 (1965).
13. J. G. CALVERT. J. Phys. Chem. **61**, 1206 (1957).
14. O. P. STRAUSZ, P. J. KOZAK, G. N. C. WOODALL, A. G. SHERWOOD, and H. E. GUNNING. Can. J. Chem. **46**, 1317 (1968).
15. C. A. MCDOWELL and S. SIFNIADES. J. Amer. Chem. Soc. **84**, 4606 (1963).
16. E. R. ALLEN and J. N. PITTS, JR. J. Amer. Chem. Soc. **91**, 3135 (1969).
17. A. G. SHERWOOD and H. E. GUNNING. J. Amer. Chem. **85**, 3506 (1963).
18. I. M. NAPIER and R. G. W. NORRISH. Proc. Roy. Soc. London, Ser. A, **229**, 337 (1967).
19. O. P. STRAUSZ and H. E. GUNNING. Trans. Faraday Soc. **60**, 347 (1964)
20. W. A. BRYCE and J. CHRYSOCHOOS. Trans. Faraday Soc. **59**, 1842 (1963).
21. A. G. SHERWOOD and H. E. GUNNING. Unpublished results.
22. G. A. HUGHES and L. PHILLIPS. J. Chem. Soc. Ap. 894 (1967).

Can. J. Chem. Downloaded from www.nrcresearchpress.com by 210.87.254.6 on 09/05/12
For personal use only.

Can. J. Chem. Downloaded from www.nrcresearchpress.com by 210.87.254.40 on 09/05/12
For personal use only.

Theory of molecular size distribution in multichain polymers[1]

S. G. WHITEWAY, I. B. SMITH, AND C. R. MASSON
Atlantic Regional Laboratory, National Research Council of Canada, Halifax, Nova Scotia

Received[2] May 13, 1968

Expressions are derived for the most probable distribution of molecular sizes in multi-chain polymers formed by the self-condensation of the monomer A—R—X_{f-1}, where A and X are functional groups and X may be either A or B. It is assumed that all functional groups of the same kind are chemically equivalent and that intramolecular condensation may be neglected. For the case A—R—B_{f-1} the results are identical with those of Flory, although it is shown that this is fortuitous and due to a cancellation of two errors in Flory's method. For the case R—A_f the results differ significantly from expressions derived by Flory and sources of error in previous work are discussed. In theory, the mole and weight fractions of individual x-mers vary continuously with the extent of reaction α over the entire range up to $\alpha_{max} = 2/f$. The ratio of the weight average to the number average degree of polymerization is finite for all values of α below α_{max}. The critical point for the formation of infinitely large (wall-to-wall) molecules occurs, not at $\alpha = 1/(f-1)$ as predicted by Flory, but at $\alpha = 2/f$. The prediction of actual gel points is discussed in terms of the largest molecule which can have a physically meaningful existence at any fixed value of α.

Canadian Journal of Chemistry, **48**, 33 (1970)

Introduction

Expressions have been derived by Flory (1, 2) for the most probable distribution of molecular sizes in multi-chain polymers formed by the self-condensation of monomers of the types A—R—B_{f-1} and R—A_f, where A and B are functional groups. In the former case it is considered that A can condense with B, but self-condensation of like functional groups is forbidden. In the latter case it is assumed for simplicity that self-condensation of A groups on the same molecule is forbidden.

Both types of polymer may be regarded as derived from the monomer A—R—X_{f-1}, where X may be either A or B. The simplest case of such a polyfunctional condensation is represented in Fig. 1, which illustrates the structure of the polymers formed for $f = 3$. Numerous isomeric structures are obviously possible and the complexity increases with increasing chain length and increasing functionality, f.

Although, as pointed out by Flory (2), examples of polymers of the former type are scarce, the correct evaluation of molecular size distributions in this case is important because such polymers form a natural link between relatively simple unbranched polymers on the one hand and the more complex polymers formed in ordinary polyfunctional condensations, on the other.

In our laboratory we have been interested in the average size and distribution of polymeric species in silicate and phosphate melts. The former may be regarded as derived from the tetrafunctional monomer SiO_4^{4-} and the latter from the trifunctional monomer PO_4^{3-}. Our work has led to a re-examination of the expressions derived by Flory for the molecular size distribution in such systems.

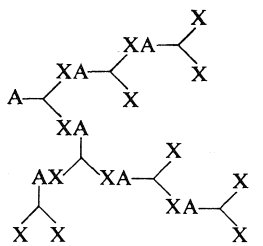

FIG. 1. Polymer formed by self-condensation of the monomer A—R—X_{f-1}, for $f = 3$.

Molecular Distributions

Consider the self-condensation of the monomer A—R—X_{f-1} to yield polymers of the type illustrated in Fig. 1. We assume that all functional groups of the same kind are chemically equivalent (principle of equal reactivity) and that intramolecular condensation does not occur.

As illustrated in Fig. 1, the polymers may be regarded as derived from A, X, and XA groups; these groups may, therefore, be considered as the "building units" of the system. The problem of calculating the molecular distribution is that of deciding how these groups are distributed among all molecules in the system at equilibrium.

[1]NRCC No. 11 013.
[2]Revision received September 24, 1969.

Can. J. Chem. Downloaded from www.nrcresearchpress.com by 210.87.254.40 on 09/05/12
For personal use only.

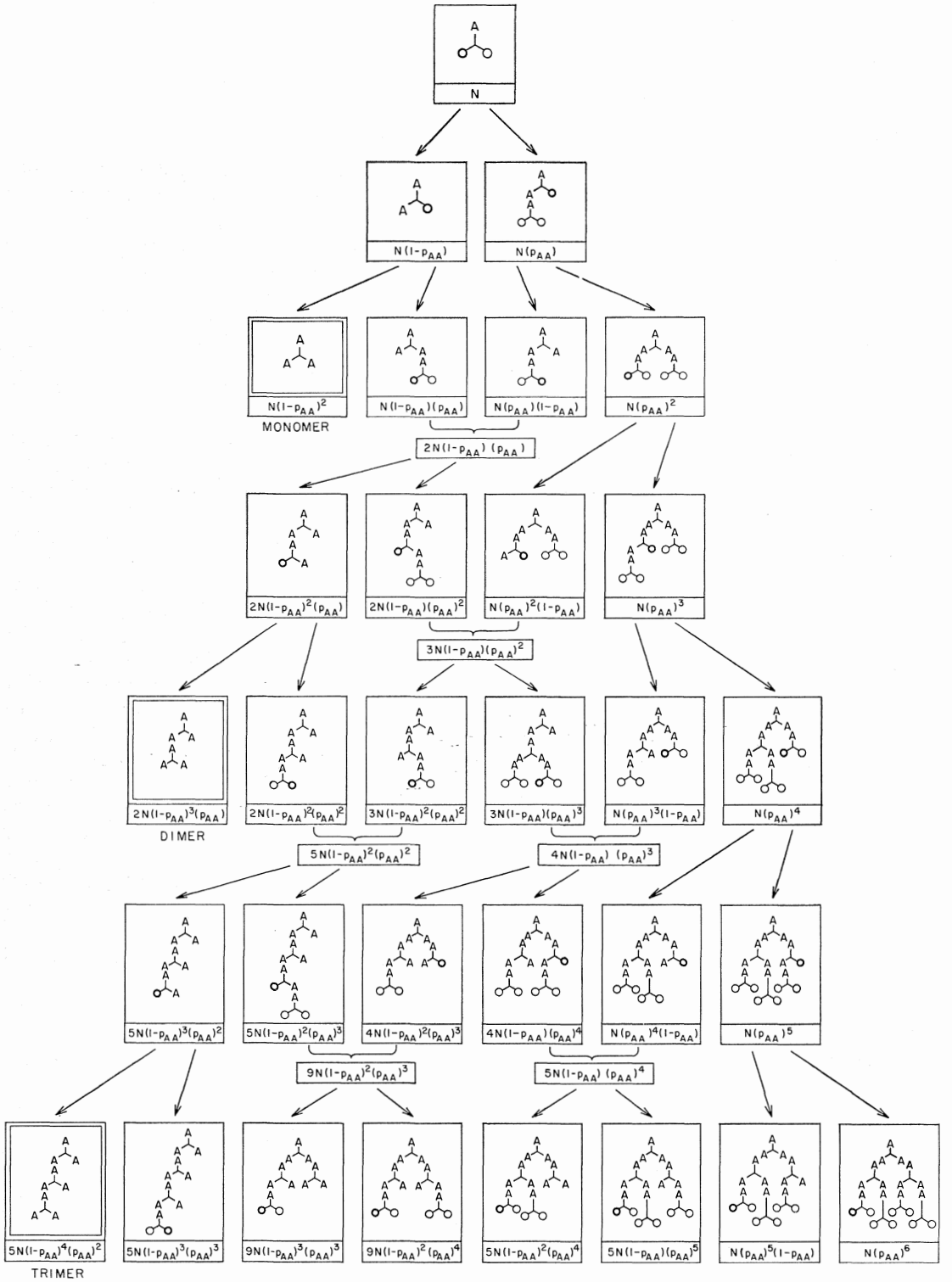

FIG. 2. Derivation of molecular size distribution for polymers derived from the monomer R—A_3. N is the total number of molecules in the system. Each circle denotes either an A group or an AA pair. Bold circles indicate groups for which a decision is about to be made as to whether it is A or AA, as indicated by the arrows. The number in each box indicates the number of molecules of that structure.

Can. J. Chem. Downloaded from www.nrcresearchpress.com by 210.87.254.40 on 09/05/12
For personal use only.

This problem has two aspects (see also Appendix IV). First, if N is the number of molecules in the system, the location of N groups, A or X, is automatically determined: each is *committed* to start one molecule, and may not be considered for any other location. Second, we have no such definite information regarding the location of the remaining groups, and may assume only that they are distributed randomly among all molecules.

It must be emphasized that our recognition of the presence of committed and uncommitted groups in the system in no way violates the principle that all functional groups of the same kind are chemically equivalent. In particular it must be stressed that we do not in any way specify which A or X groups belong to particular locations. To do so would, indeed, violate the above principle. That there are N A or X groups committed to certain locations is a property of the system and involves no act of choice or artificial specialization on our part. This point is fundamentally important towards a correct evaluation of the molecular size distribution.

In the following discussion it is assumed for convenience that each molecule is started by an A group. This is not a necessary condition, however, and identical results are obtained if the molecules are considered started by X groups or a mixture of A and X groups. It may be noted that XA groups cannot be used as starting points for the molecules. Such a procedure would immediately exclude the monomers from consideration.

In any x-mer there are $fx - 2x + 1$ X groups and $x - 1$ XA groups. The total, $x(f - 1)$, when summed over all molecules yields $N_0(f - 1)$ as the number of uncommitted groups which have randomly assigned positions, where N_0 is the number of structural units[3] in the system. We define a probability p_{XA} to be

[1] p_{XA} = number of XA groups/$N_0(f - 1)$

This is the probability that any group selected at random from the uncommitted groups will be an XA group.

The System R—A_f

If α, the extent of reaction, is the fraction of A groups initially present which have reacted, the number of AA groups is $\alpha f N_0/2$. Therefore, from eq. [1]

[2] $$p_{AA} = \alpha f/2(f - 1)$$

Figure 2 illustrates the use of p_{AA} for determining the size distribution for the system RA_3. Each box represents molecules of a certain structure. Groups which are known to be either A or AA are so indicated; groups for which a decision has not been reached are drawn as circles. In addition, the expression under each box gives the number of molecules of that structure. Thus the single box in the first row indicates that there are N molecules for which the only information yet available is that each consists of one terminal A group that is attached to two groups, either of which may be A or AA.

The second row shows the two possible structures of the molecules obtained by deciding how many of the N groups indicated by the bold circle in row 1 are AA (and at the same time, how many are A). The only possible decision is that based on the odds for randomly selecting an AA group from the uncommitted groups. Therefore, $N(p_{AA})$ molecules have an AA group at the location in question, while $N(1 - p_{AA})$ molecules are terminated at that site by an A group.

In row 3, similar decisions are made concerning the bold circles of row 2. One result is that the number of molecules of monomer is $N(1 - p_{AA})^2$ and the mole fraction of monomer, N_1, is $(1 - p_{AA})^2$. The manner in which the mole fractions of larger molecules are obtained is obvious from Fig. 2. Molecules for which the power of p_{AA} is the same may be combined in number. This simplifies the scheme considerably but makes it impossible to obtain directly the distribution of isomers within a particular x-mer fraction.

After the scheme has been carried to the stage of tetramer the mole fractions are

$$N_1 = (1 - p_{AA})^2$$
$$N_2 = 2(1 - p_{AA})^3(p_{AA})$$
$$N_3 = 5(1 - p_{AA})^4(p_{AA})^2$$
$$N_4 = 14(1 - p_{AA})^5(p_{AA})^3$$

where $p_{AA} = 3\alpha/4$.

The scheme which leads to these specific results may be regarded as a diagrammatic solution of the Bernoulli binomial probability function (3), and has been introduced for illustrative purposes. The probability function itself will now be used to

[3]In general, the same terminology as used by Flory is employed. In the case under consideration, a structural unit is identical with a repeating unit in the polymeric structure.

Can. J. Chem. Downloaded from www.nrcresearchpress.com by 210.87.254.40 on 09/05/12
For personal use only.

derive the general expression for the mole fraction of x-mer.

If p is the probability of a favorable outcome at each trial, then the probability P that in n trials an event will be favorable exactly $n - r$ times and unfavorable r times, is

$$[3] \qquad P = \frac{n!}{r!(n-r)!}\, p^{n-r}(1-p)^r$$

We define a favorable outcome to be, for our case, that of selecting an AA group in a choice between AA and A groups, so that $p = p_{AA}$. The number of trials equals the number of sites in an x-mer where such a choice is made, and is $fx - x$, while the number of favorable events necessary to obtain an x-mer is $x - 1$. The factorial part of eq. [3] gives the number of sequences of $x - 1$ favorable and $fx - 2x + 1$ unfavorable choices, regardless of order. However, when considering polymerization, the order in which favorable and unfavorable choices occur is important. For example, a dimer ($f = 3$) is selected by choosing three A groups (apart from the starting A) and one AA group. Equation [3] predicts four possible sequences of the four choices, and they are: AA,A,A,A; A,AA,A,A; A,A,AA,A; A,A,A,AA. Only the first two sequences are specific for dimer; the last two are unsuccessful as they imply prior selection of monomer. In general, the probability function must be divided by x to allow for unsuccessful sequences, and the modified probability gives directly the mole fraction of x-mer

$$[4] \qquad N_x = \frac{(fx-x)!}{(fx-2x+1)!x!}\,(p_{AA})^{x-1} \times (1-p_{AA})^{fx-2x+1}$$

where $p_{AA} = \alpha f/2(f-1)$. In the following discussion we denote by ω_x the factorial term in eq. [4]

$$[5] \qquad \omega_x = \frac{(fx-x)!}{(fx-2x+1)!x!}$$

It is identical with the combinatorial term derived in a different way by Flory (1) (ref. 2, p. 365).

Mole fraction distributions as given by eq. [4] are illustrated in Fig. 3 for trifunctional condensations for various values of α. Figure 4 shows the mole fractions of various species up to the tetramer as functions of α.

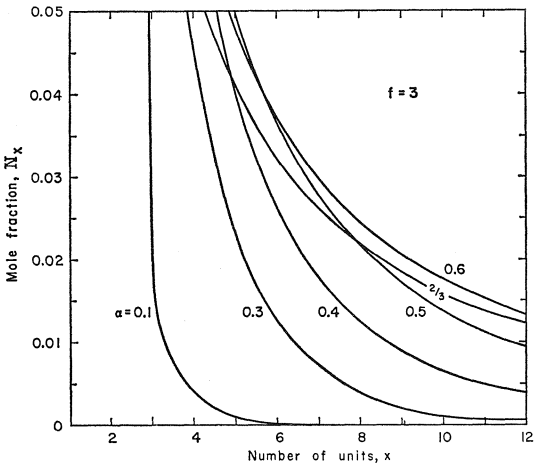

FIG. 3. Distribution of mole fractions for a polymer formed by the self-condensation of a trifunctional monomer, for various extents of reaction α.

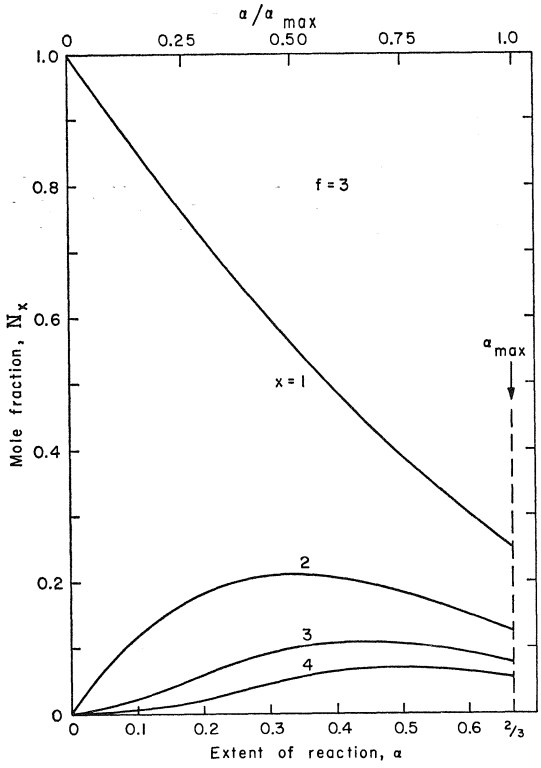

FIG. 4. Mole fractions of various species plotted against the extent of reaction, α, for a trifunctional condensation.

Can. J. Chem. Downloaded from www.nrcresearchpress.com by 210.87.254.40 on 09/05/12
For personal use only.

The System A—R—B_{f-1}

If α_B is the fraction of B groups which have reacted, then the number of BA groups is $(f-1)N_0\alpha_B$. Therefore, from eq. [1]

$$[6] \qquad p_{BA} = \alpha_B$$

Figure 5 illustrates the use of p_{BA} for determining the size distribution for the system A—R—B_2. Figures 2 and 5 are constructed somewhat differently in that, in the latter, separate boxes are retained for isomers of molecules having the same powers of p_{BA}. After the scheme has been carried to the stage of tetramer the results for the mole fractions are

$$N_1 = (1-\alpha_B)^2$$

$$N_2 = 2(1-\alpha_B)^3\alpha_B$$

$$N_3 = 5(1-\alpha_B)^4\alpha_B{}^2 \text{ (2 isomers, in ratio 4:1)}$$

$$N_4 = 14(1-\alpha_B)^5\alpha_B{}^3 \text{ (3 isomers, in ratio 8:4:2)}$$

The general expression may be derived in a manner analogous to the R—A_f case, and is

$$[7] \qquad N_x = \omega_x(p_{BA})^{x-1}(1-p_{BA})^{fx-2x+1}$$

where $p_{BA} = \alpha_B$.

Comparison with Flory's Expression

In Fig. 6 are plotted (line 2) the results of eq. [4] for the system RA_f with $f = 3$ and $x = 1$, as well as (line 1) the results of Flory's corresponding expression (ref. 1 and ref. 2, p. 372, eq. [35]), which is

$$[8] \qquad N_x = \frac{3(2x)!}{(x+2)!x!}\,\frac{(1-\alpha)^{x+2}(\alpha)^{x-1}}{\left(1-\frac{3\alpha}{2}\right)}$$

The discrepancy between these two results is large. In the method used by Flory, an A group is chosen at random in the system and the probability of its being part of an x-mer of a particular configuration calculated. The overall probability that this A group is attached to an x-mer of any configuration is next calculated by multiplying by the number of configurations, ω_x. Finally this is equated to a probability, calculated independently as a function of N_x, that an A group chosen at random belongs to an x-mer. There are two errors in this method (see also Appendix II).

The first error arises because the expression used for ω_x requires the singling out of one particular A on each configuration. This implies that the original A was chosen at random from a set of N A's comprised of only one A from each molecule, rather than from all A's ($3N_0(1-\alpha)$) in the system. Thus Flory's expression

$$\omega_x\alpha^{x-1}(1-\alpha)^{fx-2x+1}$$

should have been equated by him to N_x, because the probability of selecting an x-mer by choosing one of this set of pre-identified A's is equal to the mole fraction of the x-mer.

The second error arises from using α rather than p_{AA}, thus treating AA groups as if they were only A groups. The situation that arises from this error can be regarded in several ways. From one point of view, Flory calculates the probability of forming molecules of the type indicated in Fig. 1 with XA groups replaced by A groups. Regarded in another way, Flory's method implicitly assigns a probability of unity to the chance of finding the second A of an AA group, as α refers only to the chance of finding "singly-reacted" A groups. Thus the basic premise that the probability of reaction is constant and is an *a priori* probability equal to α is violated. In any case it should be clear that the correct procedure is to calculate the probability of finding, at random, the building units of the system, in this case A and AA groups. This correct procedure should include, in Flory's method as in ours, the taking into account of the A groups that were arbitrarily assigned starting positions in the molecules. As noted in the discussion of error 1, Flory's method implies selecting every molecule by one A group before examining the remainder of the molecule.

On the other hand, the 2 methods give identical results for the A—R—B_{f-1} case. This is a result of the stoichiometry of this system. As there is only one A group per molecule, error 1 cannot be made. Similarly, error 2 is not made, as eq. [6] shows that α_B fortuitously equals p_{BA}. The same is true for the R—A_f system when $f = 2$, and for this case also, the Flory expression for mole fractions becomes identical to that derived here.

Significance of Mole Fractions when $\alpha \to \alpha_{max}$

The requirement of no intramolecular condensation places a limit, α_{max}, on the fraction of A groups that have reacted. For R—A_f structural units, $\alpha_{max} = 2/f$. When $f > 2$, eq. [8] indicates that mole fractions approach infinity at

Can. J. Chem. Downloaded from www.nrcresearchpress.com by 210.87.254.40 on 09/05/12
For personal use only.

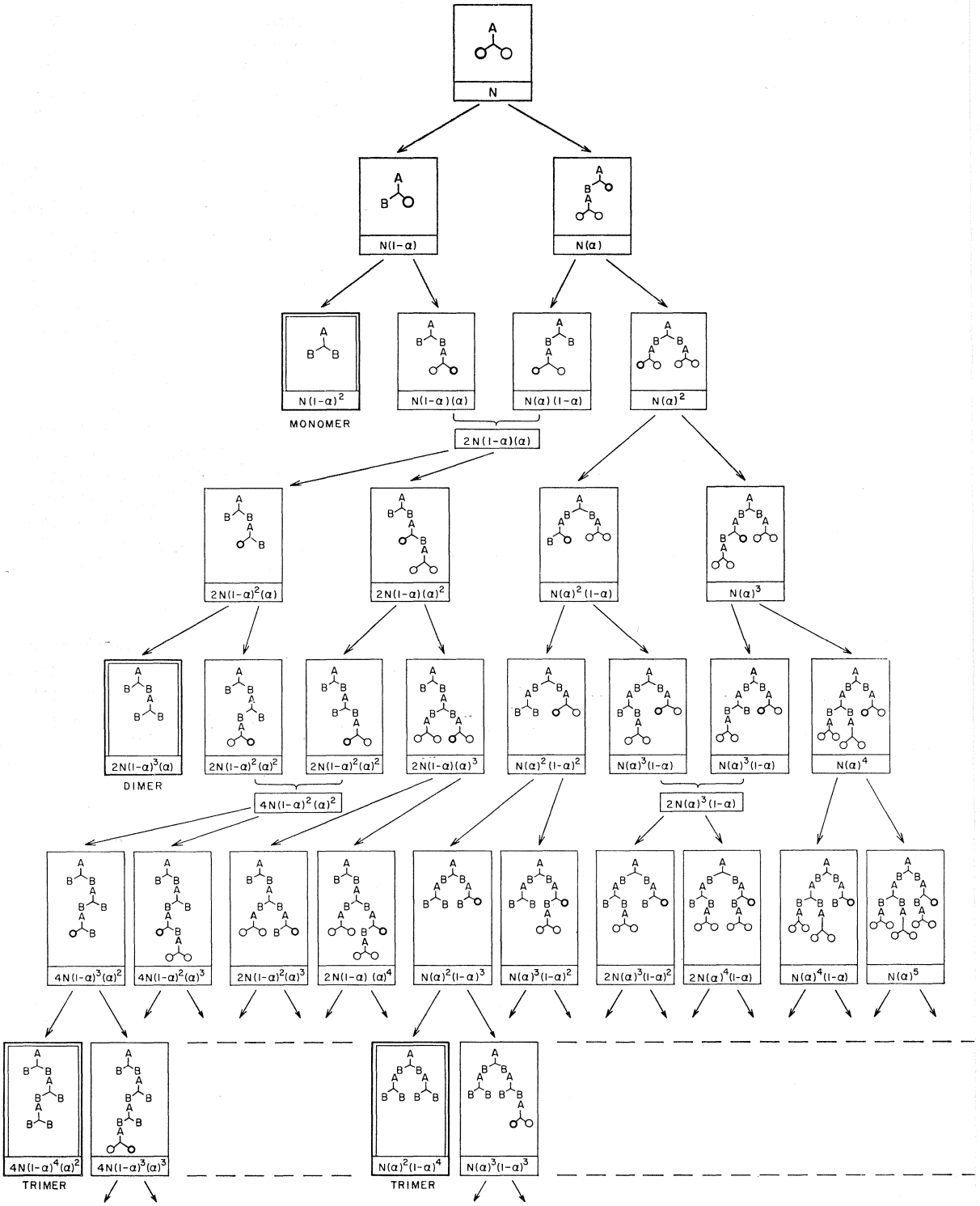

FIG. 5. Derivation of molecular size distribution for polymers derived from the monomer A—R—B_2. *N* is the total number of molecules in the system. Each circle denotes either a B group or a BA pair. Bold circles indicate groups for which a decision is about to be made (as indicated by the arrows) as to whether it is B or BA. The number in each box indicates the number of molecules of that structure.

Can. J. Chem. Downloaded from www.nrcresearchpress.com by 210.87.254.40 on 09/05/12
For personal use only.

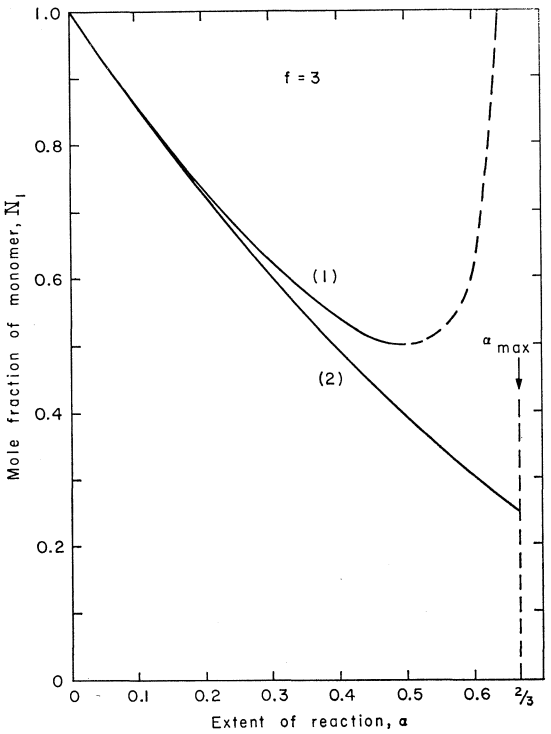

FIG. 6. Mole fraction of monomer plotted against extent of reaction α for the self-condensation of a trifunctional monomer. (1) Work of Flory, (2) this work.

α_{max}, an anomalous result explained by Flory as part of the gelation phenomenon. The present expressions predict no such anomaly: in theory, finite mole fractions occur in the range $0 < \alpha < \alpha_{max}$.

For example (Fig. 6) when $f = 3$, $N_1 \rightarrow 0.25$ as $\alpha \rightarrow 2/3$. It is interesting to examine the significance of this particular result. At the limit, when $\alpha = 2/3$, the expression $N = N_0(1 - 3\alpha/2)$ indicates that the existence of only one molecule requires an infinite number of structural units: the system is composed of one molecule of infinite size. As α is only 2/3, p_{AA} is 1/2 and this molecule must be branched, although not completely so. Obviously at this limit the mole fraction of monomer cannot be 0.25, but one may ask what the mole fraction would be if this one infinitely large molecule were depolymerized the least amount possible. This least amount corresponds to breaking any single bond in the molecule; consequent on which bond is broken, monomer, dimer, trimer, etc. is formed. Therefore, we may ask instead, "of all bonds in an infinitely large molecule, how many yield a monomer when broken?"

It is clear that for a linear molecule no monomer will, in the limit, be formed. A linear x-mer has $(x - 1)$ bonds, of which only the two terminal ones yield monomer when broken. The mole fraction of monomer, therefore, is $2/(x - 1)$, which approaches 0 as x approaches infinity.

For the other extreme we may consider the very large, radially symmetrical, fully branched x-mer shown in Fig. 7. Bonds are depicted as lying in shells characterized by numbers 0, 1, 2,..., m. The outermost shell contains $3(2^m)$ bonds, any of which yield monomer when broken. The total number of bonds, B, in such a molecule is given by

$$B = 3\sum_0^m 2^m \simeq 6(2^m)$$

The approximation becomes increasingly valid as m increases, and is already good to 1% when m is 5. For a reasonable amount of material, say 1 mole of monomer, m is about 77, and the error in the approximation is vanishingly small. Therefore, the probability of finding a bond which, when broken, yields monomer is

$$N_1 = 3(2^m)/6(2^m) = 0.5$$

The values of 0 and 0.5 represent the limits of N_1 as $\alpha \rightarrow 2/3$ for all possible molecules of the type R—A_3 that are infinitely large. The intermediate value of 0.25 predicted by eq. [4] is

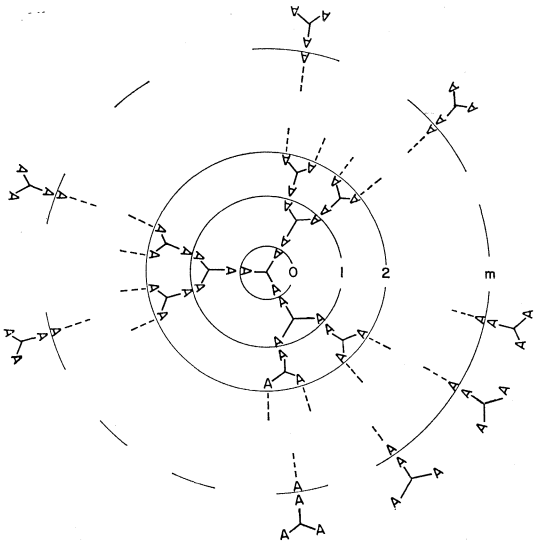

FIG. 7. Radially symmetric, fully branched x-mer, $f = 3$. The number of bonds lying in any shell is $3(2^{\text{shell number}})$.

Can. J. Chem. Downloaded from www.nrcresearchpress.com by 210.87.254.40 on 09/05/12
For personal use only.

acceptable considering that the infinitely large molecule envisaged is not completely branched. Further, on this basis, Flory's expression does not yield an acceptable value. It is interesting to note that when $f = 2$, only linear molecules are possible, and both eqs. [4] and [8] predict $N_1 \rightarrow 0$ as $\alpha \rightarrow \alpha_{max}$, as expected. In addition, both methods yield the above result, $N_1 \rightarrow 0.25$, as $\alpha \rightarrow \alpha_{max}$ for the A—R—B_2 system.

Incompletely branched molecules may be simulated for the R—A_3 case, at $\alpha = \alpha_{max}$, by beginning with an

configuration (cf. Fig. 2) and flipping a coin ($p_{AA} = 1/2$) to determine whether A or AA groups should occupy particular positions in the structure. One large "molecule" constructed in this way contained 497 bonds, of which 118 would have yielded monomer if broken. The mole fraction of monomer could then be calculated to be 118/497 = 0.24, in good agreement with the value 0.25 predicted for an infinitely large molecule. A similar game was played to construct molecules of the type RA_4. At α_{max}, $p_{AA} = 1/3$, and a die was rolled with two faces marked "AA" and 4 faces marked "A". Large "molecules" constructed in this way had ratios of terminal bonds to total bonds in good agreement with the predicted limiting value of 0.296.

Gelation Phenomena

Flory (2) has noted that the extent of reaction at which the probability of chain branching equals $1/(f - 1)$ is a critical point for a polymerizing system and has identified it with the experimental gel point. The behavior of various mathematical expressions at this point, discussed by Flory, is demonstrated in Fig. 2 for $f = 3$. When $p_{AA} = 0.5$, the number of circles at any stage equals the number of circles in the preceding stage. Consequently at the critical point the scheme requires an unlimited supply of groups.

We have shown for the system R—A_f that p_{AA} and α are related by the expression

$$[2] \qquad p_{AA} = \alpha f/2(f - 1)$$

From the definition of a critical point given above we have

$$[9] \qquad (p_{AA})_c = 1/(f - 1)$$

From eqs. [2] and [9]

$$[10] \qquad \alpha_c = 2/f$$

However, we also have

$$[11] \qquad \alpha_{max} = 2/f$$

The conclusion is that when p_{AA} is correctly expressed in terms of α, the critical point occurs at α_{max}, and therefore not within the physically realizable range of α. It is no longer possible to identify with the critical point experimental gel points which occur at some value of α less than α_{max}.

It is important to determine whether there is any other feature of the mathematical expressions which might predict the existence of gel points. Some insight into this problem may be gained by examining the expression for N_x. This expression may be used, along with the appropriate equation for N, to find N_x, the number of molecules of a particular x-mer. At a sufficiently large value of x it is possible for N_x to be considerably less than unity, even when N_0 is of the order of Avogadro's number. One interpretation of this result is that the probability of finding a molecule of this size is so small that for practical purposes such molecules may be considered to have no meaningful existence. On the other hand, molecules with values of N_x considerably larger than unity may be considered always present in the system. It is of interest to calculate, as a function of α, the largest molecule which, according to this arbitrary criterion, can have a meaningful existence. We need to determine x_{max} (i.e. the value of x when $N_x \simeq 1$) and this calculation reduces to solving the equation $N N_x = 1$ for x.

The results of such calculations for $f = 2$, 3, and 4, taking N_0 to be 4×10^{24}, are shown in Fig. 8, where x_{max} is plotted against α/α_{max}. Stirling's approximation was used to evaluate the factorials occurring in N_x when $f > 2$. The figure shows that relatively large molecules exist at values of α appreciably below α_{max}. This is particularly true for $f > 2$; for such cases x_{max} increases rapidly in the range $0.7 < \alpha/\alpha_{max} < 0.85$. If gelation is due to the presence of such large molecules there is some reason to anticipate gel points in the above range. The prediction of actual gel points would require additional information and is not within the scope of this paper. The role of intramolecular condensation, considered in

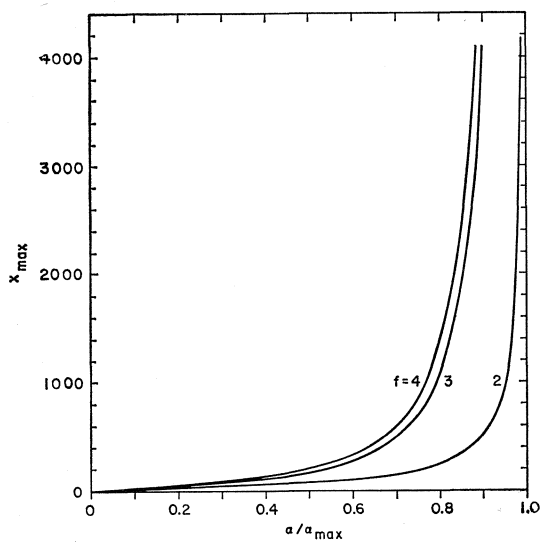

FIG. 8. Chain length, x_{max}, of largest physically meaningful molecule plotted against α/α_{max} for various values of f.

this discussion not to occur, is not well established. It may be pointed out that one effect of intramolecular condensation is, for a given α, to yield smaller molecules.

The above conclusions are in line with many experimental observations. For example, Solomon, Loft, and Swift (4) showed that for numerous alkyd resins, calculations of the gel point based on the theory of Flory did not agree with the experimental values. For the systems studied, gelation always occurred at much lower extents of reaction than predicted by expressions based on Flory's assumptions. Failure of the principle of equal reactivity of functional groups with increase in molecular size was suggested as a possible cause; although such effects may be important, it is now clear that expressions based on Flory's critical value of α cannot be expected to apply. Bobalek *et al.* (5) have pointed out that in most industrial practice, theoretical prediction of the gel point in alkyd resins is ignored and empirical procedures are used instead. They have also presented data which show that side reactions such as intramolecular condensation, not allowed for in the theory, can account for only a small part of the observed deviations.

The results obtained in this study will allow more exact expressions to be derived for the ionic distributions in silicate melts. The revised distributions will not differ markedly from those already reported (6, 7), as the Flory expressions were not used in the derivations. Application of the above concepts to silicate and phosphate melts will be discussed in a subsequent communication.

The authors are grateful to A. G. McInnes for many helpful comments and discussions.

1. P. J. FLORY. J. Amer. Chem. Soc. **74**, 2718 (1952).
2. P. J. FLORY. Principles of polymer chemistry. Cornell University Press, Ithaca, New York. 1953.
3. J. R. GRAY. Probability. Oliver and Boyd Ltd., Edinburgh. 1967.
4. D. H. SOLOMON, B. C. LOFT, and J. D. SWIFT. J. Appl. Polym. Sci. **11**, 1593 (1967).
5. E. G. BOBALEK, E. R. MOORE, S. S. LEVY, and C. C. LEE. J. Appl. Polym. Sci. **8**, 625 (1964).
6. C. R. MASSON. Proc. Roy. Soc. London, Ser. A, **287**, 201 (1965).
7. C. R. MASSON. J. Amer. Ceram. Soc. **51**, 134 (1968).

Appendix

I. Evaluation of Other Relationships

We first evaluate summations required for calculating the weight fraction of x-mer, w_x, and the weight average degree of polymerization, $\bar{x}_w$, in ordinary polyfunctional condensations. These summations are of the type

$$[12] \quad S_m = \sum_{x=1}^{\infty} (fx - x)!x^m\delta^x/(fx - 2x + 1)!x!$$

where

$$[13] \quad \delta = p_{AA}(1 - p_{AA})^{f-2}$$

or, in general

$$[14] \quad S_m = \frac{p_{AA}}{1 - p_{AA}} \sum x^m N_x$$

Proceeding in a manner analogous to that described by Flory (ref. 2, pp. 366 and 367) we have

$$[15] \quad S_0 = p_{AA}/(1 - p_{AA})$$

$$[16] \quad S_1 = p_{AA}/(1 - p_{AA})[1 - p_{AA}(f - 1)]$$

$$[17] \quad S_2 = \frac{p_{AA}[1 - p_{AA}^2(f - 1)]}{(1 - p_{AA})[1 - p_{AA}(f - 1)]^3}$$

With the aid of these results, the following are obtained. The weight fraction distribution, w_x, is given by

$$[18] \quad w_x = xN_x/\sum xN_x$$
$$= xN_x[1 - p_{AA}(f - 1)]$$
$$= [(1 - p_{AA})/p_{AA}][1 - p_{AA}(f - 1)]x\omega_x\delta^x$$

Can. J. Chem. Downloaded from www.nrcresearchpress.com by 210.87.254.40 on 09/05/12
For personal use only.

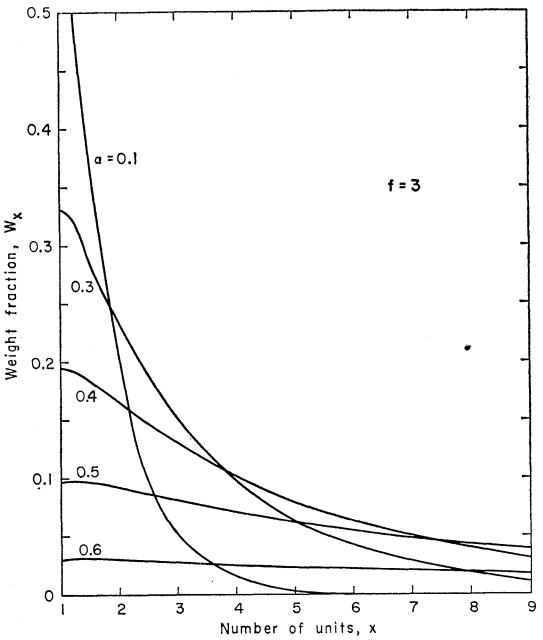

FIG. 9. Distribution of weight fractions for a polymer formed by the self-condensation of a trifunctional monomer, for various extents of reaction, α.

Figure 9 illustrates the weight fraction distributions, for various values of α, for $f = 3$. The weight fractions of various species are plotted in Fig. 10 as functions of the extent of reaction α.

The weight average degree of polymerization is given by

$$[19] \qquad \bar{x}_w = \frac{\sum x^2 N_x}{\sum x N_x} = \frac{S_2}{S_1}$$

Substituting for S_1 and S_2 from eqs. [16] and [17] gives

$$[20] \qquad \bar{x}_w = \frac{1 - p_{AA}{}^2(f-1)}{[1 - p_{AA}(f-1)]^2}$$

and, on substituting for p_{AA} from eq. [2], we have

$$[21] \qquad \bar{x}_w = \left(1 - \frac{(\alpha f)^2}{4(f-1)}\right) \Big/ \left(1 - \frac{\alpha f}{2}\right)^2$$

The number average chain length $\bar{x}_n$ may be written directly without recourse to the distribution, as $\bar{x}_n$ = number of structural units/number of molecules

$$[22] \qquad \bar{x}_n = 1 \Big/ \left(1 - \frac{\alpha f}{2}\right)$$

However, $\bar{x}_n$ may be defined also in terms of the distribution, i.e. $\bar{x}_n = \sum x N_x$. Evaluation of this summation by the use of eq. [14] also gives $\bar{x}_n = 1/[1 - (\alpha f/2)]$. That our distribution gives the required result is a necessary, but not sufficient, test of the distribution, and implies only that the summation is convergent in the range $0 < \alpha < \alpha_{max}$. It should be noted that Flory's distribution satisfies this test also.

Finally, by combining eqs. [21] and [22] we have

$$[23] \qquad \frac{\bar{x}_w}{\bar{x}_n} = \left(1 - \frac{(\alpha f)^2}{4(f-1)}\right) \Big/ \left(1 - \frac{\alpha f}{2}\right)$$

The ratio $\bar{x}_w/\bar{x}_n$ is plotted against the extent of reaction α in Fig. 11 for $f = 2$, 3, and 4. The ratio is finite for all values of α below $\alpha_{max} = 2/f$. For functionalities greater than 2, $\bar{x}_w/\bar{x}_n$ asymptotically approaches infinity as $\alpha \to 2/f$. These results are in marked contrast to the results obtained by Flory (ref. 2, p. 373), who concluded that both $\bar{x}_w$ and $\bar{x}_w/\bar{x}_n$ tend to infinity as $\alpha \to 1/(f-1)$.

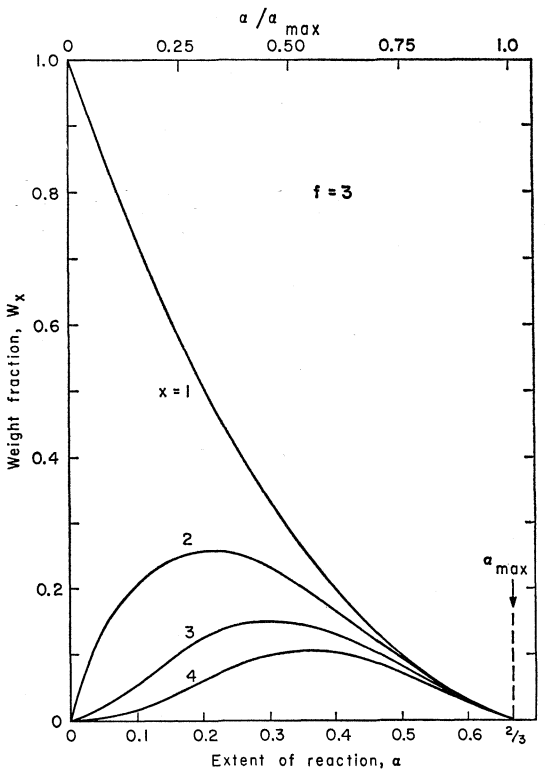

FIG. 10. Weight fractions of various species plotted against the extent of reaction, α, for a trifunctional condensation.

Can. J. Chem. Downloaded from www.nrcresearchpress.com by 210.87.254.40 on 09/05/12
For personal use only.

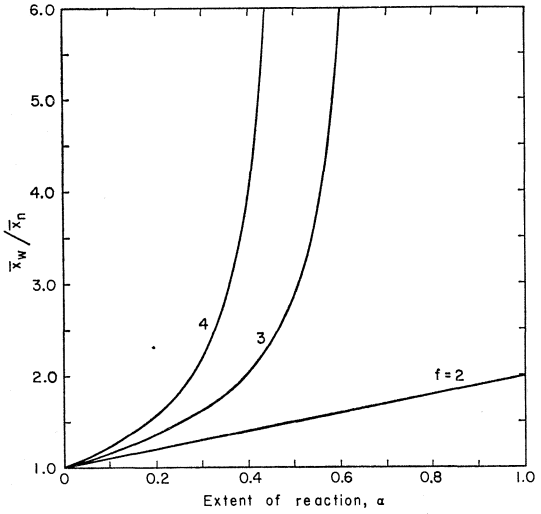

FIG. 11. Ratio of weight average to number average degree of polymerization plotted against extent of reaction α for various values of the functionality, *f*.

II. Modification of Flory's Treatment

It can be shown by the following argument that Flory's treatment cannot be correct. Flory says, in effect, "Let us postulate that intramolecular condensation does not occur." He then derives theoretical expressions for the mole fractions of various species. Anomalous results are obtained at $\alpha = 1/(f-1)$. He identifies this with the gel point and claims it is associated with the onset of intramolecular condensation, *previously postulated not to occur.*

There is a fundamental error in logic here. This cannot be resolved by arguing that the anomaly at $\alpha = 1/(f-1)$ is due to the "neglect" of intramolecular condensation. Such an argument would only be valid if theory and experiment were compared. The theory, by itself, can obviously yield no information about intramolecular condensation if, in setting up the theory, this is postulated not to occur. Nor can it be resolved by claiming that the assumption of no intramolecular condensation "applies only to the sol fraction." The initial postulates cannot be altered to rationalize anomalous results. It is clear that the expressions derived by Flory cannot be correct because they are at variance with his initial assumptions.

Molecular distributions in the R—A_f case may be correctly evaluated by Flory's procedure if it is modified. Flory's method (ref. 2, p. 371) for this case is based on a certain similarity to the A—R—B_{f-1} case. For example, whereas the structures

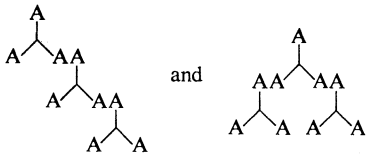

are not different, "marking" an A group creates the 2 different configurations

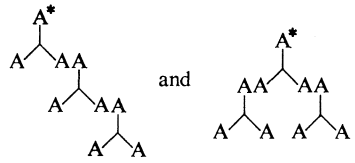

which correspond to two configurations in the A—R—B_{f-1} system

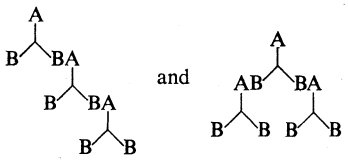

The "marking" of one of the A groups is an artifice which allows using for ω_x a value originally derived by Flory for the A—R—B_{f-1} case. However it must be recognized that implicit in this method is the assumption that every molecule carries one such "marked" A. The following derivation follows Flory's method, but takes account of this and other points.

Select at random any A from among the $fN_0(1-\alpha)$ unreacted A's. The probability that this is one of the $N_0(1-\alpha f/2)$ "marked" A's is $(1-\alpha f/2)/f(1-\alpha)$. Now consider the further probability that this marked A is part of an *x*-mer. When the marked A occupies one particular position in the *x*-mer this probability is

$$\omega_x p_{AA}{}^{x-1}(1-p_{AA})^{fx-2x+1}$$

(The necessity of using p_{AA} rather than α already has been discussed.) However, as the marked A can occupy any one of $fx - 2x + 2$ positions, the overall probability that any unreacted A

Can. J. Chem. Downloaded from www.nrcresearchpress.com by 210.87.254.40 on 09/05/12
For personal use only.

Can. J. Chem. Downloaded from www.nrcresearchpress.com by 210.87.254.40 on 09/05/12
For personal use only.

selected at random is part of an x-mer of any configuration whatever is

$$[24] \quad P_x = \frac{(fx - 2x + 2)(1 - \alpha f/2)\omega_x}{f(1 - \alpha)} \times {p_{AA}}^{x-1}(1 - p_{AA})^{fx-2x+1}$$

The remainder of the argument is identical with that of Flory. P_x is also equal to the number of A's on x-mers divided by the total number of A's in the system

$$[25] \quad P_x = \frac{(fx - 2x + 2)N_x}{N_0 f(1 - \alpha)}$$

where N_x is the number of x-mers. From eqs. [24] and [25]

$$[26] \quad N_x = N_0(1 - \alpha f/2)\omega_x {p_{AA}}^{x-1} \times (1 - p_{AA})^{fx-2x+1}$$

Dividing by the total number of molecules, we obtain for the mole fraction of x-mer

$$[27] \quad \mathcal{N}_x = \omega_x {p_{AA}}^{x-1}(1 - p_{AA})^{fx-2x+1}$$

which is identical with eq. [4].

III. Effect of Solvent and of Product of Condensation

In the derivation of eq. [4] for the mole fraction of x-mer, it was tacitly assumed that the polymerization occurs in bulk. It is of interest to examine the more general situation when polymerization is allowed to occur in solution.

In this case, the total number of molecules is

$$[28] \quad N = N_0(1 - \alpha f/2) + N_s$$

where N_s is the number of molecules of solvent. The mole fraction of x-mer thus becomes

$$[29] \quad \mathcal{N}_x = N_x/[N_0(1 - \alpha f/2) + N_s]$$

Substituting for N_x from eq. [26]

$$[30] \quad \mathcal{N}_x = \frac{(1 - \alpha f/2)\omega_x {p_{AA}}^{x-1}(1 - p_{AA})^{fx-2x+1}}{(1 - \alpha f/2) + (N_s/N_0)}$$

From eq. [26]

$$N_s/N_0 = N_s(1 - \alpha f/2)\omega_x {p_{AA}}^{x-1} \times (1 - p_{AA})^{fx-2x+1}/N_x$$
$$= \mathcal{N}_s(1 - \alpha f/2)\omega_x {p_{AA}}^{x-1} \times (1 - p_{AA})^{fx-2x+1}/\mathcal{N}_x$$

as $N_s/N_x = \mathcal{N}_s/\mathcal{N}_x$.

Substituting for N_s/N_0 in eq. [30] and simplifying, one gets

$$[31] \quad \mathcal{N}_x = \omega_x {p_{AA}}^{x-1}(1 - p_{AA})^{fx-2x+1}(1 - \mathcal{N}_s)$$

where, as before

$$[2] \quad p_{AA} = \alpha f/2(f - 1)$$

and

$$[5] \quad \omega_x = (fx - x)!/(fx - 2x + 1)!x!$$

Equation [31] is the desired expression for the mole fraction of x-mer in the presence of an inert solvent. Comparison with eq. [4] shows that, for the same extent of reaction α, the mole fractions of individual species in the presence of solvent are each decreased by the fraction $\mathcal{N}_s$ of the corresponding bulk values.

Equation [31] also applies if the polymerization is performed in bulk and the product of condensation (e.g. H_2O) is allowed to accumulate in the system. In this case $\mathcal{N}_s$ is the mole fraction of the product at equilibrium. Equation [31] will be used later for the derivation of activities in binary silicate melts.

The number average chain length in the presence of solvent (or product of condensation) may be obtained by substituting for $\mathcal{N}_x$ from eq. [31] in the expression

$$[32] \quad \bar{x}_n = \sum x\mathcal{N}_x/\sum \mathcal{N}_x$$

The result is

$$[22] \quad \bar{x}_n = 1/(1 - \alpha f/2)$$

which is the same as for the bulk polymerization if α is unchanged. The expression for the weight average degree of polymerization is similarly unchanged if polymerization proceeds to the same extent as in bulk.

IV. Some General Comments on Statistical Distribution of Groups

In deriving molecular distributions in the system A—R—X_{f-1} it is necessary, as discussed above, to distinguish clearly between two categories of functional groups in the system at equilibrium. If α_x is the fraction of X groups that have reacted, the system contains $N = N_0[1 - (f - 1)\alpha_x]$ molecules. We then have: (*a*) $N_0[1 - (f - 1)\alpha_x]$ A groups which have become

committed to specific locations in the system. In the general case this is the number of A or X groups which have to be assigned starting positions in the N molecules; in the A—R—B_{f-1} case this also happens to be the total number of A groups in the N molecules; (*b*) X and XA groups that are uncommitted to specific locations. These are the groups we must assume to be distributed statistically among the N molecules. There are $(f-1)N_0(1-\alpha_x)$ X groups and $(f-1)N_0\alpha_x$ XA groups.

The total number of groups in the system is thus

$$N_t = N + (f-1)N_0$$

It is interesting to note that, of this total, the committed groups vary in number with the extent of reaction, α_x, whereas the number of uncommitted groups is constant for all values of α_x. Although the number of groups in the uncommitted category is independent of α_x, the composition of this category (i.e. the relative numbers of XA and X) does depend, of course, on α_x.

Can. J. Chem. Downloaded from www.nrcresearchpress.com by 210.87.254.40 on 09/05/12
For personal use only.

Methods of numerical differentiation in the analysis of thermodynamic data for the mercury–solution interface

W. R. Fawcett and J. E. Kent
Department of Chemistry, University of Guelph, Guelph, Ontario
Received July 29, 1969

Methods of numerical differentiation for the calculation of surface charge densities and relative surface excesses from electrocapillary data are considered. Estimates of the random error in calculated derivatives are made by testing eight different differentiation methods with artificial data containing known levels of random error. The relative merits of these techniques and the number and spacing of data points needed to perform numerical differentiation precisely are discussed.

Canadian Journal of Chemistry, **48**, 47 (1970)

Can. J. Chem. Downloaded from www.nrcresearchpress.com by 210.87.254.40 on 09/05/12
For personal use only.

Introduction

Several papers describing the use of digital computers in the analysis of thermodynamic data for the mercury–solution interface have appeared in the literature recently (1–3). As might be expected, these calculations make use of both numerical integration and numerical differentiation techniques. Methods of numerically integrating real data are well known (ref. 4, chap. VI). The precision of the calculated integrals is usually greater than that of the original data since random errors in the latter tend to cancel one another on addition. Numerical differentiation is a more difficult operation (ref. 4, chap. V and ref. 5). The important step in this calculation is the fitting of an analytical expression $y = f(x)$ to a finite array x_i,y_i where both the independent and dependent variables have associated random error. The best curve fitting technique for a given data set depends on the values of the true derivatives in the given range, the spacing of the data points, and the errors in the data. The differentiation calculation is unavoidably "noisy" since random errors are magnified in the associated division calculation.

Various methods of numerical differentiation have been described for the analysis of electrocapillary data. Barradas, Kimmerle, and Valeriote (1) calculated surface charge densities from experimental surface tension – potential data by fitting the results to a seventh order ordinary polynomial over the whole potential range (at least 25 data points). Mohilner and Mohilner (2) proposed a variety of segmental techniques for performing the same calculation. According to one of these, a segment of the electrocapillary curve containing 4 data points was fitted with a cubic equation, and the derivative was calculated at one central point. This operation was repeated adding one point at one end of the segment and dropping one at the other until all the data points had been considered. These authors noted that smoothing is often necessary and suggested several methods based on the moving segment technique, for instance, fitting 4 points to a quadratic equation using the least-squares method. Lawrence, Parsons, and Payne (3) calculated relative surface excesses from surface tension – activity data by fitting the data points over the whole range to a cubic equation. They pointed out that this particular calculation is especially difficult since the number of data points obtained by most workers is usually less than 10. The order of the "best" polynomial was determined by comparing the results of an nth order fit with that of an $(n + 1)$th order fit. Another method used to determine optimum smoothing has been to compare the results of numerical differentiation with those of graphical differentiation (6). Both of the above criteria are necessarily subjective since the true value of the derivative is unknown. Both Mohilner and Mohilner, and Lawrence *et al.* have stressed the necessity of determining thermodynamic data at more concentrations than has been customary, in order to improve the precision with which surface excesses may be calculated.

In the present paper, objective criteria for determining the optimum differentiation technique for given data characteristics are established by testing a variety of empirical and statistical curve fitting methods with artificial electrocapillary data containing known amounts of random error. In addition, these calculations are

Can. J. Chem. Downloaded from www.nrcresearchpress.com by 210.87.254.40 on 09/05/12
For personal use only.

used to show how many experimental points should be determined in a given concentration range in order to obtain the maximum precision in calculated relative surface excesses.

Generation of Artificial Electrocapillary Data

In the present case, the artificial data were precise values of surface tension, relative surface excess, and electrode potential determined as functions of both electrode charge density and bulk activity of the adsorbing species. In order that these data would accurately reflect reality they were based on two examples of anionic adsorption — one of weak adsorption, the other of strong adsorption — studied by Payne (7, 8). In both cases Payne found that the amount of specifically adsorbed anion, q_{sa}, was given by the Frumkin isotherm

$$[1] \qquad \ln\left(\frac{q_{sa}}{q_m - q_{sa}}\right) + \frac{g q_{sa}}{q_m} = \ln \beta a_{\pm}$$

where q_m is the limiting amount of specifically adsorbed anion in $\mu C\ cm^{-2}$, g, a lateral interaction parameter, $a_{\pm}$, the mean activity of the salt whose anion is adsorbed, and β, the adsorption coefficient. It was observed for the above cases that $\ln \beta$ is a linear function of the electrode charge density, q. The contribution to the anionic surface excess from the diffuse double layer, $q_-{}^d$, was calculated from the Gouy–Chapman theory.

$$[2] \qquad q_-{}^d = -\left(\frac{q + q_{sa}}{2} - A\right) - \left[\left(\frac{q + q_{sa}}{2}\right)^2 + A^2\right]^{\frac{1}{2}}$$

A is equal to $(RT\varepsilon c/2\pi)^{\frac{1}{2}}$ where ε is the solvent's dielectric constant and c, the bulk concentration of the salt. For the present case where only 1–1 electrolytes are considered, c is assumed to be equal to $a_{\pm}$. Thus the total surface excess of anions, q_-, is $q_{sa} + q_-{}^d$.

The relationships between surface tension, electrode potential, and the anionic surface excess are given by interfacial thermodynamics (9). When the electrode charge density is chosen as independent variable, and if the solution contains a simple 1–1 electrolyte, Gibbs adsorption isotherm may be written

$$[3] \qquad d\xi_+ = E_+\, dq - \frac{2RT}{F} q_-\, d \ln a_{\pm}$$

where E_+ is the electrode potential with respect to a reference electrode reversible to the cation and $\xi_+ = \gamma + qE_+$, γ being the surface tension. On integrating the above expression at constant charge, the function ξ_+ may be calculated.

$$[4] \qquad \xi_+ = (\xi_+)_0 - \frac{2RT}{F}\int_{(a_{\pm})_0}^{a_{\pm}} q_-\, d \ln a_{\pm}$$

The subscript "0" refers to the value of the particular quantity at the lowest or reference activity. In order to calculate the surface tension from ξ_+, E_+ must first be determined. From eq. [3]

$$[5] \qquad \left(\frac{\partial E_+}{\partial \ln a_{\pm}}\right)_q = \frac{-2RT}{F}\left(\frac{\partial q_-}{\partial q}\right)_{a_{\pm}}$$

and from eqs. [1] and [2]

$$[6] \qquad \left(\frac{\partial q_{sa}}{\partial q}\right)_{a_{\pm}} = \frac{1}{\beta}\left[\frac{q_m q_{sa}(q_m - q_{sa})}{q_m{}^2 + g q_{sa}(q_m - q_{sa})}\right]\frac{\partial \beta}{\partial q}$$

and

$$[7] \qquad \left(\frac{\partial q_-{}^d}{\partial q}\right)_{a_{\pm}} = -\left[\frac{1}{2} + \frac{1}{2}\left(\frac{\partial q_{sa}}{\partial q}\right)_{a_{\pm}}\right] \times \left\{1 + \left(\frac{q + q_{sa}}{2}\right)\Big/\left[\left(\frac{q + q_{sa}}{2}\right)^2 + A^2\right]^{\frac{1}{2}}\right\}$$

Having determined $(\partial q_-/\partial q)_{a_{\pm}}$, E_+ was calculated at constant charge by integrating eq. [5]

$$[8] \qquad E_+ = (E_+)_0 - \frac{2RT}{F}\int_{(a_{\pm})_0}^{a_{\pm}} \left(\frac{\partial q_-}{\partial q}\right) d \ln a_{\pm}$$

In order to evaluate E_+ and ξ_+ according to eqs. [4] and [8], the values of these variables must be known at the lowest concentration. $(E_+)_0$ was calculated from eq. [9] (7, 8)

$$[9] \qquad (E_+)_0 = C_0 + \frac{q}{K_q{}^i} - \frac{q_{sa}}{K_{q_{sa}}{}^i} + \phi_2 - \frac{RT}{F}\ln (a_{\pm})_0$$

ϕ_2 is the potential at the outer Helmholtz plane as calculated by the Gouy–Chapman theory

$$[10] \qquad \phi_2 = \frac{2RT}{F}\sinh^{-1}\left(\frac{q + q_{sa}}{2A}\right)$$

C_0, $K_q{}^i$, and $K_{q_{sa}}{}^i$ are constants related to the capacity of the inner layer. Having calculated $(E_+)_0$ as a function of q, $(\xi_+)_0$ was found by

Can. J. Chem. Downloaded from www.nrcresearchpress.com by 210.87.254.40 on 09/05/12
For personal use only.

TABLE 1
Representative values of artificial electrocapillary data

Activity a (moles l^{-1})	Electrode charge density q ($\mu C\ cm^{-2}$)	Electrode potential E_+ (V)	Anionic surface excess q_- ($\mu C\ cm^{-2}$)	Surface tension γ ($\mu J\ cm^{-2}$)
Weak adsorption				
0.01	15.0	1.0521	−14.6535	36.1333
	0	0.1229	− 0.5525	42.5000
	−15.0	−0.7002	− 0.5624	36.6833
0.1	15.0	0.9301	−17.8307	36.0668
	0	0.0478	− 2.4915	42.3357
	−15.0	−0.7011	1.6189	36.7890
1.0	15.0	0.8278	−20.2551	35.3262
	0	−0.0641	− 5.3289	41.8738
	−15.0	−0.7086	3.7633	36.9858
Strong adsorption				
0.01	15.0	1.3128	−20.4616	29.7592
	0	0.1445	− 2.3750	38.6500
	−15.0	−0.7599	0.6579	32.2705
0.1	15.0	1.1582	−24.2602	29.4202
	0	0.0253	− 5.1776	38.2052
	−15.0	−0.7612	1.8632	32.3891
1.0	15.0	1.0126	−26.4300	28.5862
	0	−0.1148	− 7.6571	37.4385
	−15.0	0.7709	4.1321	32.5912

integrating eq. [3] at constant activity

$$[11] \qquad (\xi_+)_0 = \gamma_0 + \int_0^q (E_+)_0 \, dq$$

where γ_0 is the surface tension at the point of zero charge for the lowest concentration.

Calculation of the artificial data was carried out on a digital computer. Initially q_{sa} was evaluated for values of charge density in the range −15 to 15 $\mu C\ cm^{-2}$ at 1 $\mu C\ cm^{-2}$ intervals (31 values), and for values of activity in the range 0.01 to 2.51 M for increments of 0.02 in $\log a$ (121 values). The parameters q_m, g, β, C_0, K_q^i, $K_{q_{sa}}^i$, and γ_0 were taken from Payne's papers (7, 8). Newton's method was used to calculate q_{sa} for given values of q and $a_\pm$ in eq. [1]. The integrals in eqs. [4], [8], and [11] were evaluated by Simpson's method. Finally, the surface tension was calculated from ξ_+, q, and E_+ according to the relation $\gamma = \xi_+ - qE_+$. The precision of the resulting surface tension data was ± 0.0001 $\mu J\ cm^{-2}$; this is at least 100 times greater than that achieved experimentally to date. Values of surface tension at the electrocapillary maximum agreed well with those tabulated by Payne. Calculated values of γ, q_-, and E_+ for representative values of activity and charge density are given in Table 1.

In order to test the effectiveness of the various differentiation techniques, the precise values of surface tension were modified using a standard technique (10) so that they contained a normally distributed random error with a known standard deviation. Six levels of random error corresponding to standard deviations of 0.001, 0.002, 0.005, 0.01, 0.02, and 0.05 $\mu J\ cm^{-2}$ were used.

Methods of Differentiation

Two types of differentiation methods were considered: (*1*) those in which a curve was fitted to the data over the whole range of the independent variable x, and (*2*) those in which a curve was fitted to a segment which contained a fixed number of data points and which was moved over the range of x, one point being gained and one lost per move.

In the first method (AOV), an ordinary polynomial in x was fitted to the data by least-squares, the optimum order of the polynomial being determined by a statistical test (11). In order to test the significance of the $(m + 1)$th term in an mth order polynomial, the following ratio was calculated

$$[12] \qquad F = \frac{(S_{m-1}^2 - S_m^2)(n - m)}{S_m^2}$$

Can. J. Chem. Downloaded from www.nrcresearchpress.com by 210.87.254.40 on 09/05/12
For personal use only.

where

$$S_k^2 = \sum_{i=1}^{n} (y_i - a_0 - a_1 x_i - a_2 x_i^2 - \ldots\ldots - a_k x_i^k)^2$$

S_k^2 is the estimated variance when a kth order polynomial is fitted to n data points. If the experimental F was greater than that tabulated for 1, $n - m$ degrees of freedom at a 5% significance level (12), the $(m + 1)$th coefficient was regarded as significant. Consequently, the calculation procedure involved fitting first a quadratic and then a cubic equation to the data. If the 3rd order term was found to be significant by the F-test, a 4th order polynomial was fitted to the data. This procedure was repeated until the F-test indicated that the $(m + 1)$th term was not significant. An assumption inherent in the use of the above test is that the estimated variance is equal to the true variance. Of course, the accuracy of this estimation and therefore the usefulness of the procedure increases with the total number of data points.

An additional condition imposed in determining the order of the fitted polynomial was that the estimated variance for the chosen fit be less than 1.25 times the variance for the error level in the independent variable, S_y^2. This precaution was necessary when higher order polynomials were involved. For example, when the best fit is obtained with an 8th order polynomial, the 5th order term may not be significant whereas the 6th, 7th, and 8th order terms are. The estimated variance for a 5th order polynomial, S_5^2 would be considerably greater than S_y^2, whereas S_8^2 would approximately equal S_y^2.

The above calculation was time consuming since the coefficients of the polynomial had to be recalculated each time that the order was increased. When the independent variable is equally spaced, curve fitting can be carried out much more effectively with orthogonal polynomials; for example, Chebyshev polynomials (ref. 4, chap. V and ref. 13, chap. 11). In this case, when the polynomial order is increased, the coefficients of the lower order terms remain the same. Normally, real electrocapillary data are equally spaced with respect to electrode potential but not with respect to the logarithm of activity. The artificial data calculated here were unequally spaced with respect to both the above variables.

As pointed out by Lanczos (4), polynomial approximation to a data set over its whole range is not always a good curve fitting technique. For instance, as may be the case with electrocapillary data, the random error associated with the dependent variable may change over the range of the independent variable. However, polynomial approximation over a sufficiently small range is always safe. For this reason the moving segment technique would seem preferable.

Several types of moving segment methods with varying amounts of smoothing were tested. The amount of smoothing increases with the degrees of freedom, f, associated with the curve fitting technique. If ns is the number of data points in the segment and m, the order of the polynomial, then $f = ns - m - 1$. In total, five empirical moving segment methods with $f = 0, 1, 2, 3$, and 4 were tested.

The first method (CBFT4) involved fitting a cubic equation to a moving segment of 4 points. The fitted curve was used to calculate the derivative at the second point of the segment, so that for n data points, $n - 3$ derivatives were calculated, none being determined at the 1st, $(n - 1)$th, and nth points. This technique involved no smoothing. In the second (CBFT5) and third (QDFT5) methods, cubic and quadratic equations, respectively, were fitted to a 5-point segment. The derivative was calculated from the fitted curve at the central point in the given segment, so that derivatives were not obtained for the two points at each end of the data range. The last two empirical methods involved fitting cubic and quadratic equations in a 7-point segment (CBFT7 and QDFT7). Again the derivative was only calculated at the central point of the segment. This rule was broken for the first and last segments where derivatives were calculated from the fitted curves for the third and $(n - 2)$th points so that a total of $n - 4$ derivatives were obtained. These procedures involved the most smoothing, having 3 and 4 degrees of freedom, respectively.

The last two moving-segment methods tested (AOV5 and AOV7) made use of the F-test. The size of the segments was 5 points and 7 points, respectively; the movement of the segment, the calculation procedure, and the total number of derivatives calculated were the same as described above for the empirical methods. The order of the polynomial was in the range 2 to $ns - 1$ and was determined by the F-test. It was not anticipated that these methods would be very successful

TABLE 2
Differentiation methods and their characteristics

Differentiation method	Range of curve fitting	Order of polynomial	Degrees of freedom
AOV	Whole range of data	(Determined by F-test)	$n - m - 1$ ($m < n$)
AOV5	5 points	(Determined by F-test)	$5 - m - 1$ ($m < 5$)
AOV7	7 points	(Determined by F-test)	$7 - m - 1$ ($m < 7$)
CBFT4	4 points	Cubic	0
CBFT5	5 points	Cubic	1
CBFT7	7 points	Cubic	3
QDFT5	5 points	Quadratic	2
QDFT7	7 points	Quadratic	4

since the small number of data points would not permit a good estimate of the variance.

A summary of the various methods together with their important characteristics is given in Table 2. The least-squares calculation involved, namely solution of the normal equations, was carried out on a digital computer in double precision (16 significant figures). The augmented matrix for these equations was reduced by the Gauss–Jordan elimination method with normalization (ref. 14, chap. 8).

Results and Discussion

The artificial data for the cases of weak and strong anionic adsorption with various known levels of random error were subjected to the eight differentiation techniques described above. The surface tension, $\gamma(E,a)$, was differentiated with respect to potential, at constant activity, and the function $\xi(q,a)$, with respect to the logarithm of activity at constant electrode charge density. In general, for the function $f(x,y)$ tabulated for k values of x and n values of y, $n(k - o)$ values of $\partial f/\partial x$ or $k(n - o)$ values of $\partial f/\partial y$ were calculated, where o is the number of points at the ends of the data array which are omitted in the differentiation technique. For the described techniques o was equal to 4 (2 points at each end), except in the case of CBFT4 where it was 3. The level of random error in the calculated derivative was estimated by summing the squares of the differences between the known true derivatives and those calculated. The observed error is reported as its root-mean-square value, σ. For example, when values of surface charge density were calculated using AOV, σ_q was calculated as follows

$$\sigma_q = \left\{ \frac{\sum_{j=1}^{n} \sum_{i=3}^{k-2} \left[\left(\frac{\partial \gamma}{\partial E} \right)_{i,j} - q_{i,j} \right]^2}{k(n-4)} \right\}^{\frac{1}{2}}$$

The higher levels of random error introduced in the artificial data were chosen to cover the range of errors reported for real data (3, 6, 8). Typically, surface tension, electrode potential, and the logarithm of activity have been measured with precisions of 0.02 μJ cm^{-2}, 0.0002 V, and 0.001, respectively. Most workers have made observations for increments of 50 mV in E_+ and 0.3 in log $a_\pm$. The maximum change in ξ_+ for both increments is the order of 1 μJ cm^{-2}, so that the minimum relative error in ξ_+ is about 0.03 as compared with relative errors of 0.006 in E_+ and 0.005 in log $a_\pm$. Thus, errors in the independent variables may be considered negligible as far as differentiation is concerned.

The results of the test of the differentiation methods for the case of surface charge determination are given in Table 3. The level of error in q, σ_q, was not significantly different for the cases of weak and strong anionic adsorption, so that average values are reported. As expected, σ_q depended on the error level in the surface tension, σ_γ. The best methods for the range of σ_γ considered were AOV and AOV7. The orders of the polynomials chosen by the F-test in AOV were in the range 3 to 12 and depended on the type of data, the activity, and σ_γ. In AOV7, the chosen polynomials were usually either 2nd or 3rd order. The

Can. J. Chem. Downloaded from www.nrcresearchpress.com by 210.87.254.40 on 09/05/12
For personal use only.

TABLE 3

Level of error in calculated surface charge density, σ_q ($\mu C\ cm^{-2}$)

	Level of error in surface tension data, σ_γ ($\mu J\ cm^{-2}$)*					
Method	0.001	0.002	0.005	0.01	0.02	0.05
CBFT4	0.02	0.04	0.11	0.20	0.43	1.23
CBFT5	0.02	0.03	0.08	0.16	0.35	0.94
CBFT7	0.02	0.02	0.04	0.09	0.16	0.45
QDFT5	0.03	0.03	0.04	0.07	0.11	0.29
QDFT7	0.06	0.06	0.06	0.07	0.09	0.18
AOV	0.02	0.03	0.05	0.08	0.10	0.19
AOV7	0.02	0.03	0.05	0.09	0.11	0.20

*Size of array: $k = 31$, $n = 6$.

results for AOV5 are not reported, since, in this case, the order chosen was always 3.

According to the results obtained, the method used by Barradas *et al.* (1) for this calculation, namely fitting a 7th order polynomial over the whole data range, cannot be used for all types of data. At the same error level reported by these authors, 0.01 $\mu J\ cm^{-2}$, the order of the best polynomial for weak adsorption was either 5 or 6, whereas for strong adsorption it varied between 4 for the lowest activity to 8 for the highest. The second method reported in the literature (2), CBFT4, was found not to be as precise as the other methods for the higher error levels.

As pointed out earlier, in testing methods of determining surface excesses, the effects of both total number of data points and error level in the dependent variable ξ were considered. Usually, electrocapillary curves have been measured at 3 activities per activity decade. For the present artificial data this corresponded to activities of 0.01, 0.02, 0.05, and so on, up to 2.00 *M* for a total of 8 activities. The testing was also carried out for 5 activities per decade (0.01, 0.016, 0.025, 0.040, and 0.063 *M* in the lowest decade with a total of 13 activities) and 10 activities per decade (0.01, 0.013, 0.016, 0.02, 0.025, 0.032, 0.040, 0.05, 0.063, and 0.079 *M* in the lowest decade with a total of 25 activities).

The results of the test are summarized in Table 4. Separate values of σ_Γ for weak and strong adsorption and results for AOV5 are not reported for the reasons stated previously. A striking aspect of the results was the marked dependence of σ_Γ on the spacing of the data points for the segmental methods. This effect was undoubtedly due to the small variation in the dependent variable in the given range of the independent variable. From Table 1, the maximum total change in ξ_+ over the activity range varied from the order of 10 $\mu J\ cm^{-2}$ at high positive surface charge densities to the order of 1 $\mu J\ cm^{-2}$ at high negative surface charge densities. This is to be compared with a total change in γ of the order of 10 $\mu J\ cm^{-2}$ in either direction from the electrocapillary maximum at constant activity. When the total change in y, Δy, is small and σ_y is large, methods with no smoothing (CBFT4) are very noisy whereas those with large amounts of smoothing (QDFT7) are not. Furthermore, as Δx becomes smaller, the total Δy associated with the interval in the segmental method becomes smaller and the noise level increases.

Another interesting result of the test was that the precision of the calculated surface excesses by the best method for a given σ_ξ at 3 activities per decade was not increased significantly by increasing the number of observations in the given activity range. This is also attributable to the small change in the dependent variable over the range. AOV was the best method at spacings of 5 and 10 activities per decade but not at the widest spacing because of the small number of observations. In the latter case the method with the lowest σ_Γ varied with σ_ξ. The order of the polynomial fit in AOV varied between 2 and 6 and depended on σ_ξ, q, data spacing, and data type. At the widest spacing and for $\sigma_\xi = 0.01$ $\mu J\ cm^{-2}$, the order was usually 2 or 3. This result compares favorably with that of Lawrence *et al.* (3) who used non-statistical criteria in choosing a third order polynomial fit for the same conditions.

In general, it is concluded that the best differentiation technique for this type of data with a constant error level is AOV. An important con-

Can. J. Chem. Downloaded from www.nrcresearchpress.com by 210.87.254.40 on 09/05/12
For personal use only.

TABLE 4

Level of error in calculated anionic surface excess, σ_Γ (μC cm^{-2})

Method	Level of error in ξ, σ_ξ (μJ cm^{-2})					
	0.001	0.002	0.005	0.01	0.02	0.05
*3 activities per decade**						
CBFT4	0.03	0.06	0.15	0.31	0.61	1.53
CBFT5	0.03	0.04	0.12	0.22	0.48	1.07
CBFT7	0.03	0.03	0.06	0.12	0.24	0.59
QDFT5	0.07	0.07	0.07	0.10	0.19	0.43
QDFT7	0.11	0.11	0.11	0.11	0.17	0.35
AOV	0.03	0.04	0.08	0.12	0.20	0.43
AOV7	0.03	0.04	0.09	0.13	0.19	0.40
5 activities per decade†						
CBFT4	0.04	0.09	0.25	0.45	0.96	2.61
CBFT5	0.04	0.08	0.19	0.37	0.78	2.11
CBFT7	0.02	0.04	0.11	0.21	0.41	1.08
QDFT5	0.03	0.04	0.08	0.14	0.27	0.70
QDFT7	0.05	0.05	0.07	0.11	0.19	0.46
AOV	0.02	0.03	0.06	0.11	0.17	0.36
AOV7	0.03	0.05	0.08	0.14	0.27	0.66
10 activities per decade‡						
CBFT4	0.09	0.18	0.48	0.93	2.05	4.93
CBFT5	0.07	0.15	0.39	0.76	1.65	3.97
CBFT7	0.04	0.08	0.21	0.41	0.88	2.08
QDFT5	0.03	0.05	0.13	0.27	0.57	1.35
QDFT7	0.02	0.04	0.09	0.20	0.37	0.89
AOV	0.02	0.03	0.06	0.10	0.18	0.33
AOV7	0.03	0.06	0.12	0.28	0.53	1.27

*Size of array: $k = 31$, $n = 8$.
†Size of array: $k = 31$, $n = 13$.
‡Size of array: $k = 31$, $n = 25$.

sideration in choosing this technique is that the degrees of freedom associated with the fitted curve be high. It is pertinent to point out that since a curve is fitted to the data over the entire range, the derivative at any point in the range will depend on all the observations, not just those in its vicinity. Thus, the experimenter who wishes to apply this technique must have a good knowledge of the random errors in the data. When the random error varies over the range, the method can be used if the individual observations are weighted. The segmental techniques are preferred in cases where knowledge of random errors in the data is less exact. In almost all cases, a segmental technique with an error level as good as that of AOV is available for a given range of σ_y.

In the determination of surface excesses more observations should be made, preferably over a wider range of activities. Obviously, there is no gain in precision in making measurements at 10 activities per decade, but a spacing of 5 activities per decade should provide sufficient data in the activity range normally studied.

The authors wish to thank Dr. T. D. Newton and J. Longmuir of the University of Guelph for helpful discussions and assistance with the computer programming, and the Institute of Computer Science for the use of their facilities. The financial support of the National Research Council of Canada is gratefully acknowledged.

1. R. G. Barradas, F. M. Kimmerle, and E. M. L. Valeriote. J. Polarogr. Soc. **13**, 30 (1967).
2. D. M. Mohilner and P. R. Mohilner. J. Electrochem. Soc. **115**, 261 (1968).
3. J. Lawrence, R. Parsons, and R. Payne. J. Electroanal. Chem. **16**, 193 (1968).
4. C. Lanczos. Applied analysis. Pitman, London. 1957.
5. D. M. Koenig. Chem. Eng. **73** (19), 186 (1966).
6. J. O'M. Bockris, K. Muller, H. Wroblowa, and Z. Kovac. J. Electroanal. Chem. **10**, 416 (1965).
7. R. Payne. J. Electrochem. Soc. **113**, 999 (1966).
8. R. Payne. J. Chem. Phys. **42**, 3371 (1965).
9. R. Parsons. Can. J. Chem. **37**, 308 (1959).
10. IBM System/360 Scientific Subroutine Package (360A-CM-03X) Version III. 4th ed. p. 77.
11. D. H. Menzel. Fundamental formulas of physics. Vol. 1. Dover, New York. 1960. pp. 121–123.
12. M. Abramowitz and I. A. Stegun. Handbook of mathematical functions. Applied Mathematics Series 55. National Bureau of Standards, Washington, D.C. 1964. p. 987.
13. S. S. Kuo. Numerical methods and computers. Addison–Wesley Publ. Co., Inc., Reading, Mass. 1965.

Can. J. Chem. Downloaded from www.nrcresearchpress.com by 210.87.254.40 on 09/05/12
For personal use only.

Spectroscopy of chromium compounds in molten salts

H. C. BROOKES[1] AND S. N. FLENGAS

Department of Metallurgy and Materials Science, University of Toronto, Toronto 181, Ontario

Received February 24, 1969

Modifications to the Hitachi Perkin–Elmer 139 ultraviolet–visible spectrophotometer are described which enable absorption spectra of molten salts to be measured to 865 °C. The instrument can be readily reconverted for ambient temperature measurements. The solubilities and the limiting heats of solution of Ag_2CrO_4 and $PbCrO_4$ in equimolar $NaNO_3$–KNO_3 have been measured spectrophotometrically from 250 to 350 °C. The absorption spectrum of dilute solutions of Cr(III) in CsCl has been measured, the octahedral $CrCl_6^{3-}$ being present in solution at 700 °C.

Canadian Journal of Chemistry, **48**, 55 (1970)

Can. J. Chem. Downloaded from www.nrcresearchpress.com by 210.87.254.5 on 09/05/12
For personal use only.

Introduction

Visible and ultraviolet absorption spectroscopy in molten salts provides valuable information about the concentrations of species present in solution, about the interactions between species, and enables investigations of physicochemical properties of fused salts to be made.

Several modifications of existing spectrophotometers for measurements at high temperatures have been described (1–3). The desirability of being able to continue using the instruments for room temperature measurements has been emphasized (4) and the value of having both sample and reference solution at the same temperature has been indicated (5). This paper describes spectrophotometric measurements using a modification of the Hitachi Perkin–Elmer 139 ultraviolet–visible spectrophotometer. This appears to be the first single-beam grating instrument for which modifications for high temperature spectroscopy have been described. The instrument has an accuracy of at least 0.5 mμ over its entire wavelength range and, unlike a prism instrument, a constant bandwidth can be used over this range. The modified instrument has both sample and reference cells at the same temperature and it can be operated at ambient temperatures immediately after completing high temperature measurements.

The solubilities of $PbCrO_4$ and Ag_2CrO_4 in equimolar $NaNO_3$–KNO_3 have been determined over the temperature range 250–350 °C by measuring the absorptivity of saturated solutions at 371 mμ, and the heats of solution have been calculated. Work in this laboratory necessitated determination of the coordination of Cr^{3+} in molten CsCl solutions and spectra of dilute solutions of $CrCl_3$ in CsCl have been obtained from 650 to 750 °C for this purpose.

Experimental

Spectrophotometer and Furnace

The regular light sources compartment of the Hitachi Perkin–Elmer 139 is easily removed from the monochromator to which it is attached by one clamp, and can be replaced by a furnace containing both sample and reference cells which are simultaneously heated. For regular low-temperature operation the instrument is assembled according to the sequence

light source – monochromator – samples – detector

For operation up to 865 °C, the sequence (5)

light source – hot samples – monochromator – detector

is used, the original empty sample compartment is left in place ready for normal operation when required. Since, in the regular sequence, the light beam is focussed on the entrance slit of the monochromator, the high temperature sequence resulted in a decreased light intensity at the detector. However, the photomultiplier detector provided with the instrument enabled measurements described in this report to be obtained with slit widths never greater than 0.3 mm.

The furnace assembly, geometrically similar to the designs of Sundheim and Greenberg (3) and others (6–8), consisted of a rectangular machined lava-stone block 5 cm × 5 cm × 13 cm in the center of which 1.4 cm square cross-section reference and sample compartments were cut, 11 cm deep and 0.6 cm apart. Six 3.2 mm holes surrounding the sample compartments contained No. 20 chromel wire heating elements connected in series of 12 Ω total resistance. Two Pt – Pt 13% Rh measuring thermocouples and one chromel–alumel controlling thermocouple were inserted in horizontal wells, the couples being placed adjacent to the optical cells. For reproducible and precise positioning of the 1 cm square optical cells, 0.5 cm diameter threaded boronitride positioning rods fitted through horizontal side holes were used. The furnace block was centrally placed inside a water-cooled cylindrical steel shell 20 cm × 15.7 cm o.d.,

[1]Present address: Department of Chemistry, University of Natal, Durham, Natal, South Africa.

Can. J. Chem. Downloaded from www.nrcresearchpress.com by 210.87.254.5 on 09/05/12
For personal use only.

closed on both ends. The block was held in place with hard-setting fibrefrax insulation. Rectangular light beam channels cut through the fibrefrax were only slightly larger than the light beams so as to minimize heat losses.

Lava stone is well suited for the purpose used here as it is easily machined but hardens once heated above 800 °C, and it has suitable thermal properties which enable an even temperature distribution (±2 °C) to be maintained. The furnace assembly and light-source compartment were mounted on separate carriages which rode on an optical bench enabling precise alignment of the monochromator, sample cells, and light source. The monochromator and detector were also mounted on a platform fastened to the optical bench. A water-cooled plate covered the area surrounding the monochromator entrance slit and this light entrance was covered with an optical grade 1.6 mm quartz window. These precautions prevented furnace radiation from heating the monochromator above room temperature.

The furnace could be rapidly heated to the desired temperature and then automatic control switched in which resulted in a temperature control of ±2 °C at 800 °C. The light source and monochromator fitted flush against the furnace assembly light ports, which were copper tubes 2.5 cm long, projecting 6 mm from the furnace shell.

Optical Cells

These were of fused silica with 49 mm × 10 mm windows as supplied by Fisher Porter Manufacturing Co., New York. Path lengths of 1 mm were obtained using Beckmann 9 mm precision quartz inserts, lengths being checked by micrometer measurements on cells and inserts. The cells were extended at their open ends by 7 cm lengths of 8 mm quartz tubing, and were sealed under vacuum once filled with salts.

Materials

All starting materials were Fischer certified reagents. Twice recrystallized sodium and potassium nitrates were dried at 250 °C in vacuo for 1 week. Then equimolar mixtures were prepared, intimately mixed, and the mixtures further dried as before. Silver chromate was precipitated from aqueous solutions of recrystallized $AgNO_3$ and K_2CrO_4, washed, and dried. Lead chromate was similarly prepared using lead nitrate. Anhydrous chromium trichloride was prepared from the hydrate $CrCl_3 \cdot 6H_2O$ (9); CsCl and $CrCl_3$ were dried in vacuo at 500 °C for 1 week.

Procedure

Optical cells were filled in a drybox under dry argon and sealed under vacuum. Calibration spectra of K_2CrO_4 in 1:1 $Na/K(NO_3)_2$ were measured over the concentration range 5×10^{-4} to 3.4×10^{-3} molal and from 250 to 350 °C. Beer's law was verified over this concentration range at 253, 293, and 347 °C at 371 mμ (10). These solutions were used as calibration standards, and the molal absorptivity of the chromate ion, ε, at 371 mμ was found to vary linearly with temperature from 247 to 358 °C according to the equation

$$\varepsilon_{molal} = -7.645T + 11\,124$$

Different initial concentrations, from 0.02 to 0.3 molal, for silver chromate or lead chromate in the nitrate mixture, were used for each set of measurements. Mixtures were prepared by weight and intimately mixed on a ball mill in certain cases. In other cases, pellets of solute were weighed directly into the cells containing the solvent. For the $CrCl_3$ in CsCl, four mixtures from 0.007 to 0.118 molal were prepared.

The solutions were equilibrated in vacuum sealed cells at a constant temperature for 2 to 4 days before readings were commenced, care being taken to ensure the quartz inserts were accurately aligned in the cells. The sample and reference cells were compared with each other when filled with pure solvent and all absorbances were corrected for any small differences found. Sample and reference cells were interchanged periodically and no significant variation in absorbance was detected. The absorbance of K_2CrO_4 in KNO_3 at 362 °C was measured and the results agreed with those of Smith and Boston (10) within the limits of experimental error, indicating that the equipment was functioning satisfactorily.

Attempts to prepare Ag_2CrO_4 in situ from $AgNO_3$ and K_2CrO_4 in $Na/K(NO_3)_2$ were unsatisfactory in that the undissolved precipitate did not settle to the bottom of the cell, but adhered to the walls. With the procedure described above, a small amount of chromate precipitate still remained in the light path and the resulting light loss was corrected for as follows. Neither nitrate solvent nor dissolved chromate absorb at 550 or 590 mμ. Absorbances were measured relative to the pure blank at these wavelengths and subtracted from total apparent absorbance at 371 mμ. The correction was never more than 0.02 absorbance units. At the completion of a series of measurements the cells were inverted and the molten salt cooled in the quartz tube attached to the cell in order to prevent cracking of the cell windows (11). Since the saturated solutions of Ag_2CrO_4 are sufficiently strongly absorbing to give absorbances near the upper limit of the instrument, viz. 2 absorbance units, a differential spectrophotometric procedure was adopted to increase the precision of these results. A $Na/K(NO_3)_2$ blank of 1.0 cm path length was used, the absorbance of which was measured against the 1 mm path length solvent cell. The absorbance of the 1.0 cm reference was measured periodically against several 1 mm blanks and no variation was found within the limits of experimental error. At high absorbances the slit width was varied at fixed wavelengths and no significant variation in absorption was detected, indicating that measurements were being made within the stray light limits of the instrument. Measurements were made when the equilibrium temperature had been approached from above and below.

That the salts were thoroughly dry was indicated by the fact that, with $CrCl_3$ and CsCl at 760 °C for several days, no etching of the quartz cells was detected.

Results and Discussion

The absorption spectrum of $CrCl_3$ in CsCl at 656 and 757 °C is shown in Fig. 1. It is seen to consist of a very strong absorption edge below 500 mμ with two broad, weaker bands centered at 580 and 830 mμ with molal absorptivities of

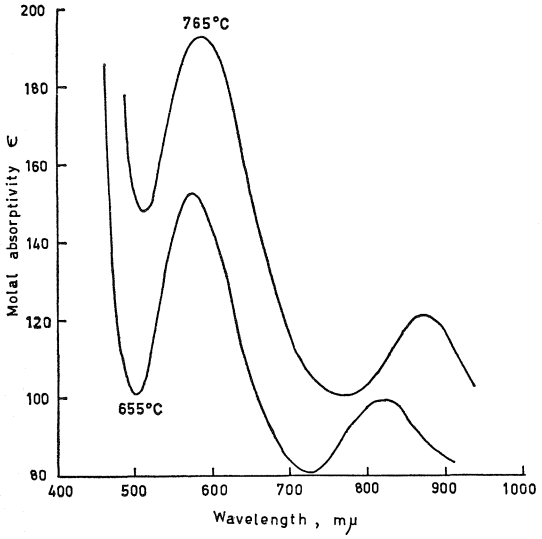

FIG. 1. Absorption spectra of Cr(III) in CsCl.

about 200. A slight bathochromic shift, from 575 to 585 mμ, was found over the temperature range 655 to 765 °C. The bands have shifted some 30 mμ to longer wavelengths in the CsCl solvent compared to the LiCl–KCl eutectic (12, 13), but the essential similarity with the spectrum in the latter solvent suggests the presence of the octahedrally coordinated $CrCl_6^{3-}$ in CsCl, the 580 mμ band corresponding to the $^4A_2 \rightarrow {}^4T_2$ (^4F) transition and the 830 mμ band to the $^4A_2 \rightarrow {}^4T_1$ (^4F) transition, as indicated by others (12, 13). The bathochromic shift of these bands in CsCl relative to LiCl–KCl might be associated with the decrease in polarizing power of the large Cs^+ cation relative to K^+, Li^+. The Cs^+ ions surrounding the $CrCl_6^{3-}$ will not attract the electron cloud away from the chromium as much as the K^+, Li^+ cations. The resulting electron repulsions in the 3d shell will be smaller and the shielding of the chloride nuclei will increase. This polarization of the chromium and its coordination shell will affect the electron states and thus the coordination geometry and absorption spectrum.

Measurements of the absorptivity of dilute solutions of Ag_2CrO_4 and $PbCrO_4$ in the nitrate solvent, using known concentrations well below the saturation limit, showed that the absorptivities, ε, of Ag_2CrO_4, $PbCrO_4$, and K_2CrO_4 at 371 mμ were identical at the same temperatures within experimental error.

The solubility of Ag_2CrO_4 in 1:1 $Na/K(NO_3)_2$ increased from 3.10×10^{-3} molal at 250 °C to 3.51×10^{-3} molal at 350 °C, and the solubility of $PbCrO_4$ in this solvent increased from 1.79×10^{-3} molal at 250 °C to 2.55×10^{-3} molal at 350 °C.

The solubility of $PbCrO_4$ in equimolar $Na/K(NO_3)_2$ has been measured by a colorimetric method from 250 to 300 °C (Duke and Iverson (14)). Their equilibration times were much smaller than those of this work, viz. several hours as opposed to several days, and their solubility of 7×10^{-4} molal at 300 °C was smaller than our value of 2×10^{-3} molal at 300 °C. However, their precision was ±15%, while that of the present spectrophotometric work is ±3%.

For the reaction

$$(M_xCrO_4)_{solid} \rightleftharpoons (xM^+ + CrO_4^{2-}) \text{ in solution}$$

$$[1] \qquad d \ln X_{M_xCrO_4} = \frac{\bar{\Delta}\bar{H}_{M_xCrO_4}}{R} d\left(\frac{1}{T}\right)$$

where $\bar{\Delta}\bar{H}$ is the limiting heat of solution of pure

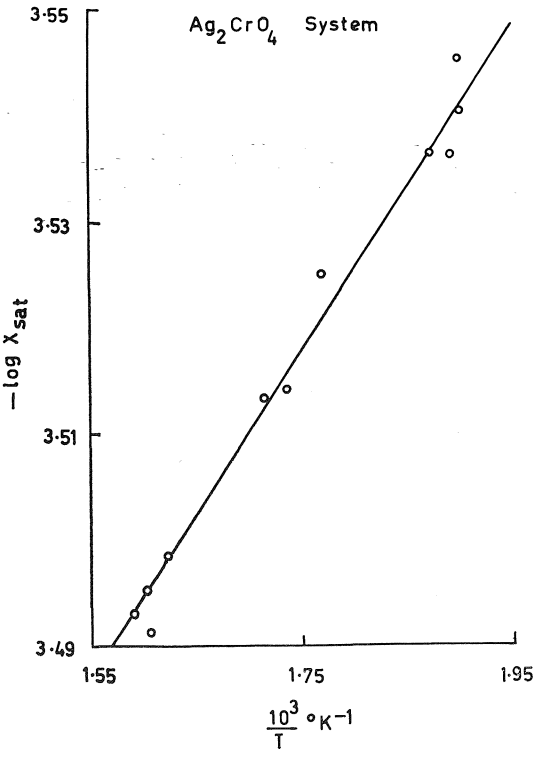

FIG. 2. Plot of $-\log X_{sat}$ against $1/T$ for Ag_2CrO_4 in an equimolar $NaNO_3$–KNO_3 mixture.

Can. J. Chem. Downloaded from www.nrcresearchpress.com by 210.87.254.5 on 09/05/12
For personal use only.

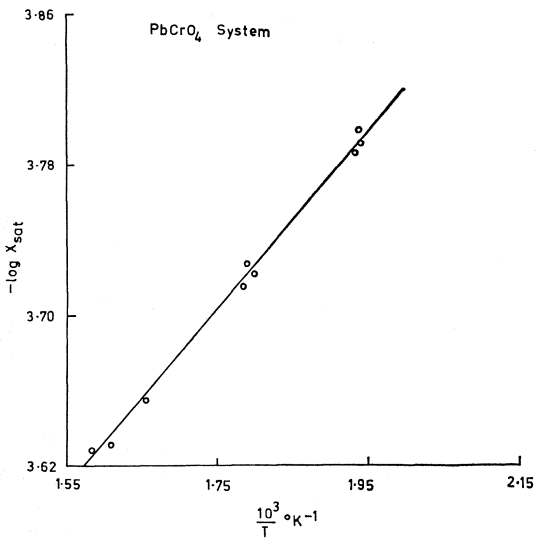

FIG. 3. Plot of $-\log X_{sat}$ against $1/T$ for $PbCrO_4$ in an equimolar $NaNO_3$–KNO_3 mixture.

solid M_xCrO_4 in the melt and M is, respectively, Ag for $x = 2$ and Pb for $x = 1$. Figures 2 and 3 are plots of eq. [1] for Ag_2CrO_4 and $PbCrO_4$, respectively. They are linear over the temperature range covered and give limiting heats of solution of 0.72 kcal/mole and 2.09 kcal/mole for Ag_2CrO_4 and $PbCrO_4$, respectively. The respective solubility products at 350 °C are $K_s = 1.716 \times 10^{-7}$ mole/1000g^3 for Ag_2CrO_4 and $K_s = 6.5 \times 10^{-6}$ mole/1000g^2 for $PbCrO_4$.

The authors wish to acknowledge the award of a National Research Council of Canada Postdoctoral Fellowship to H.C.B.

1. J. R. MORREY and A. W. MADSEN. Rev. Sci. Instrum. **32**, 799 (1961).
2. R. A. BAILEY and G. J. JANZ. The chemistry of non-aqueous solvents. Vol. I. *Edited by* J. J. Lagowski. Academic Press, Inc., New York. 1966. Chap. 7.
3. B. R. SUNDHEIM and J. GREENBERG. Rev. Sci. Instrum. **27**, 703 (1956).
4. D. N. HENTY and D. H. KERRIDGE. J. Sci. Instrum. **42**, 756 (1965).
5. D. M. GRUEN. J. Phys. Chem. **66**, 57 (1962).
6. D. M. GRUEN and R. L. MCBETH. J. Inorg. Nucl. Chem. **9**, 290 (1959).
7. D. M. GRUEN and R. L. MCBETH. J. Phys. Chem. **66**, 57 (1962).
8. R. A. BAILEY and J. A. MCINTYRE. Rev. Sci. Instrum. **36**, 968 (1965).
9. Inorganic syntheses. Vol. II. *Edited by* W. C. Fernelius. McGraw-Hill Book Co., Inc., New York. 1946. p. 193.
10. G. P. SMITH and C. R. BOSTON. Ann. N.Y. Acad. Sci. **79**, 930 (1960).
11. C. R. BOSTON and G. P. SMITH. J. Phys. Chem. **62**, 409 (1958).
12. G. HARRINGTON and B. R. SUNDHEIM. Ann. N.Y. Acad. Sci. **79**, 950 (1960).
13. D. M. GRUEN and R. L. MCBETH. Pure Appl. Chem. **6**, 23 (1963).
14. F. R. DUKE and M. L. IVERSON. J. Phys. Chem. **62**, 417 (1958).

Can. J. Chem. Downloaded from www.nrcresearchpress.com by 210.87.254.5 on 09/05/12
For personal use only.

Can. J. Chem. Downloaded from www.nrcresearchpress.com by 210.87.254.6 on 09/05/12
For personal use only.

Versatile heteronuclear-decoupler for use with a Varian HA-100 spectrometer[1]

R. BURTON AND L. D. HALL[2]
Department of Chemistry, University of British Columbia, Vancouver 8, British Columbia
Received June 30, 1969

Specific details are given for double-tuning the Varian V-4333 probe for use in the following heteronuclear magnetic double resonance experiments: observe ^{1}H at 100 MHz; irradiate ^{2}H, ^{19}F, or ^{31}P; observe ^{19}F at 94 MHz; irradiate ^{1}H, ^{2}H, or ^{31}P. An inexpensive source of audiofrequency-noise is described which, in conjunction with the double-tuned probe and several commercially available components, constitutes the basis of a versatile heteronuclear-decoupler. Examples are given which illustrate the effectiveness of this decoupler. Double-tuning of the Varian V-4333 probe by introducing a second transmitter coil is also described.

Canadian Journal of Chemistry, **48**, 59 (1970)

Introduction

Proton–proton nuclear magnetic double resonance (n.m.d.r.) experiments are now used (1) routinely in the course of many structural studies. With a few notable exceptions, routine applications (2, 3) of heteronuclear n.m.d.r. experiments have been less widespread even though some suitable equipment is commercially available.[3] Prompted initially by an interest in the n.m.r. spectra of organo–fluorine and organo–phosphorus derivatives, we have developed a versatile heteronuclear-decoupler for use with a Varian HA-100 spectrometer. The key features of this decoupler are as follows. (*a*) It does not interfere with the routine operation of the instrument, and can itself be used "routinely". (*b*) Rapid changeover between the nuclei to be irradiated can be effected merely by changing a "double-tuned" probe adaptor. (*c*) It can be used (in principle) to irradiate any chosen nuclear species. (*d*) The modification of the Varian V-4333 probe[4] can be performed by "semi-skilled" personnel and is readily "reversible".

Although our initial aim was the development of heteronuclear-decoupling using a single, "coherent", radiofrequency (hereafter referred to as continuous-wave (c.w.) decoupling), we were intrigued by the possible uses of the "incoherent" heteronuclear-decoupling technique (more commonly known as the "noise-decoupling" technique) developed by Ernst (4). Ernst demonstrated that a radiofrequency field used for a heteronuclear-decoupling experiment could be made to cover a wide spectral region if the radiofrequency unit used as the source of the decoupling frequency was modulated with a suitably broadband source of audiofrequency ("white-noise"). The audiofrequency noise-source used by Ernst was a pseudo-random sequence generator,[5] which is a reasonably expensive item if purchased commercially.[6] We shall describe here an alternative inexpensive method for effecting noise-modulation, which appears to be sufficiently versatile for many experiments.

Experimental

A block-diagram of our decoupler as used for c.w. experiments is given in Fig. 1*A*. The "decoupling" frequency is derived from a Hewlett–Packard synthesizer-driver (model 5110 B) and a Hewlett–Packard frequency synthesizer (model 5105 B), which has a maximum output frequency of 500 MHz. The output of the synthesizer (4 mW maximum) is amplified to a maximum of 5 W with a Hewlett–Packard power amplifier (model 230 A).

Double Tuning of the Varian V-4333 Probe

The versatility of this decoupler is dependent on the double-tuning of the Varian V-4333 probe by means of

---

[1]This paper also constitutes Part IV of a series entitled "Studies of carbohydrates by nuclear magnetic double resonance".

[2]To whom all correspondence should be addressed.

[3]Nuclear Magnetic Resonance Specialities Inc., New Kensington, Pennsylvania, market a modulized unit. Varian Associates, Palo Alto, California have recently marketed a "proton-decoupler", which can be used to irradiate proton resonances while observing the resonance of other nuclear species.

[4]Prior to starting our work, we had a most helpful correspondence with Professor D. H. Whiffen who was then at the National Physical Laboratory, U.K. He informed us of his groups' work with the Varian V-4332 probe. The space available in the V-4333 probe is not sufficient for that particular modification to be made conveniently.

[5]This now forms the basis of a 100 MHz "proton-decoupler" marketed by Varian Associates.

[6]For example, Hewlett–Packard model 3722A.

a selection of double-tuned probe-adaptors.[7] Figure 2*A* shows the Varian V-4333 probe after modification. The transmitter cable has been disconnected from "x" and replaced with the B.N.C. jack (UG-657/U) shown. The transmitter coil connection was removed from its tuning network and connected directly to the jack.

Each of the double-tuned modules is conveniently housed in a cut-down, Hammond chassis, as indicated typically in Fig. 2*B*. The B.N.C. (UG-88/U) plug (C) provides the sole support for the module. If desired, one side of the box may be lined with a perspex sheet, to which the individual components may be glued once the tuning is completed.

The circuit diagrams for the modules constructed so far are given in Fig. 3. The values of the components used for these modules are as follows:

^1H - $\{^{19}F\}$ *and* ^{19}F - $\{^1H\}$

C_4 and C_5: each 3–15 pF variable ceramic.
C_6 and C_7: each 60 pF parallel with 9–35 pF variable ceramic.
L_2 and L_3: each $2\frac{1}{4}$ turns of 16 gauge wire, 3/16 in. diameter.
L_4 and L_5: each slug-tuned, 13 turns of 26 gauge wire on 3/16 in. diameter form.

^1H - $\{^2H\}$ *or* ^{19}F - $\{^2H\}$

C_1 and C_2: each 3–15 pF variable ceramic.
C_3 : 9–35 pF variable ceramic.
C_8 : approximately 220 pF.
L_1 : 8 turns of 26 gauge wire, 5/32 in. diameter.

^1H - $\{31P\}$ *or* ^{19}F - $\{31P\}$

C_1 and C_2: 3–15 pF variable ceramic.
C_3 and C_4: 9–35 pF variable ceramic.

Because of the fairly high frequencies involved, wiring capacitance contributes significantly to the circuit performance. Consequently, each module must be individually tuned after it has been assembled; both transmitters must be connected to the module during the tuning process. In building and tuning these modules, we found that a standing-wave-ratio (s.w.r.) meter was indispensible; two s.w.r. meters, one on each transmitter cable, proved to be even better.[8]

The tuning procedures for each of the two classes of modules is detailed below; the ^{1}H - $\{^{19}$F$\}$ module is the more difficult to tune.

^1H - $\{^2H\}$, ^{19}F - $\{^2H\}$, ^1H - $\{^{31}P\}$ *or* ^{19}F - $\{^{31}P\}$

The s.w.r. meter is connected between the module and the output of the decoupler (ω_2). Capacitors C_1 and C_2 are tuned for a maximum received signal from the ω_1 source as indicated by the detector-level meter of the V-4311 r.f. unit. Capacitors C_3 and C_8 are tuned to a minimum s.w.r. on the ω_2 line (as indicated by the s.w.r. meter). One repeat of the above cycle usually suffices for optimal tuning.

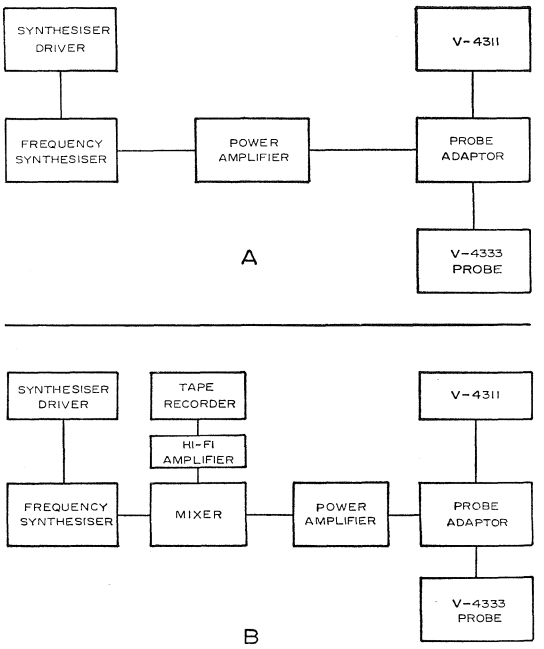

FIG. 1. Block diagram of the components used for heteronuclear-double-resonance experiments: (*A*) continuous-wave decoupling, (*B*) "noise-modulated" decoupling.

^1H - $\{^{19}F\}$ *and* ^{19}F - $\{^1H\}$

Initially, this module should be tuned with low power on the ω_2 line to avoid damage to the V-4311 r.f. unit (ω_1).

(*1*) Connect s.w.r. meter between the ω_1 source (V-4311 r.f. unit) and the probe and adjust C_6 for minimum leakage of ω_2 power back into the V-4311 unit. (*2*) Adjust C_7, C_4, and L_4 for maximum reading on detector level meter on the V-4311 unit. (*3*) Connect s.w.r. meter in the ω_2 line and adjust C_5 and L_5 for a low s.w.r. (*4*) Since the individual circuit components interact strongly, it is necessary to repeat each of the above steps. Perfect adjustment would have the s.w.r. on both lines unity, and no power from either transmitter leaking into the other one. In practice a s.w.r. of 1.5 and less than 0.5 W leakage performs adequately.[9]

We have also investigated the possibility of using a second transmitter coil for the decoupling frequency. Figure 4 shows the modification of a 40.5 MHz Varian V-4333 probe. The new transmitter coil was made as similar as possible to a Varian 100 MHz transmitter coil and was attached to the outside of the insert by "Scotch-tape". This coil was matched to the 100 MHz source by

[7]This is the method used by Nuclear Magnetic Resonance Specialities Inc.

[8]It is a pleasure to thank Mr. Eric Fisher of this Department for this suggestion.

[9]In the case of the ^{1}H - $\{^{19}$F$\}$ and ^{19}F - $\{^1$H$\}$ module, we were perturbed that any failure of the adaptor might result in the full power-output of the decoupler damaging the attenuator of the V-4311 r.f. unit. To preclude this possibility, separate trap-circuits were connected between the attenuator and the transmitter output jack (J 307) of the V-4311 unit.

Can. J. Chem. Downloaded from www.nrcresearchpress.com by 210.87.254.6 on 09/05/12
For personal use only.

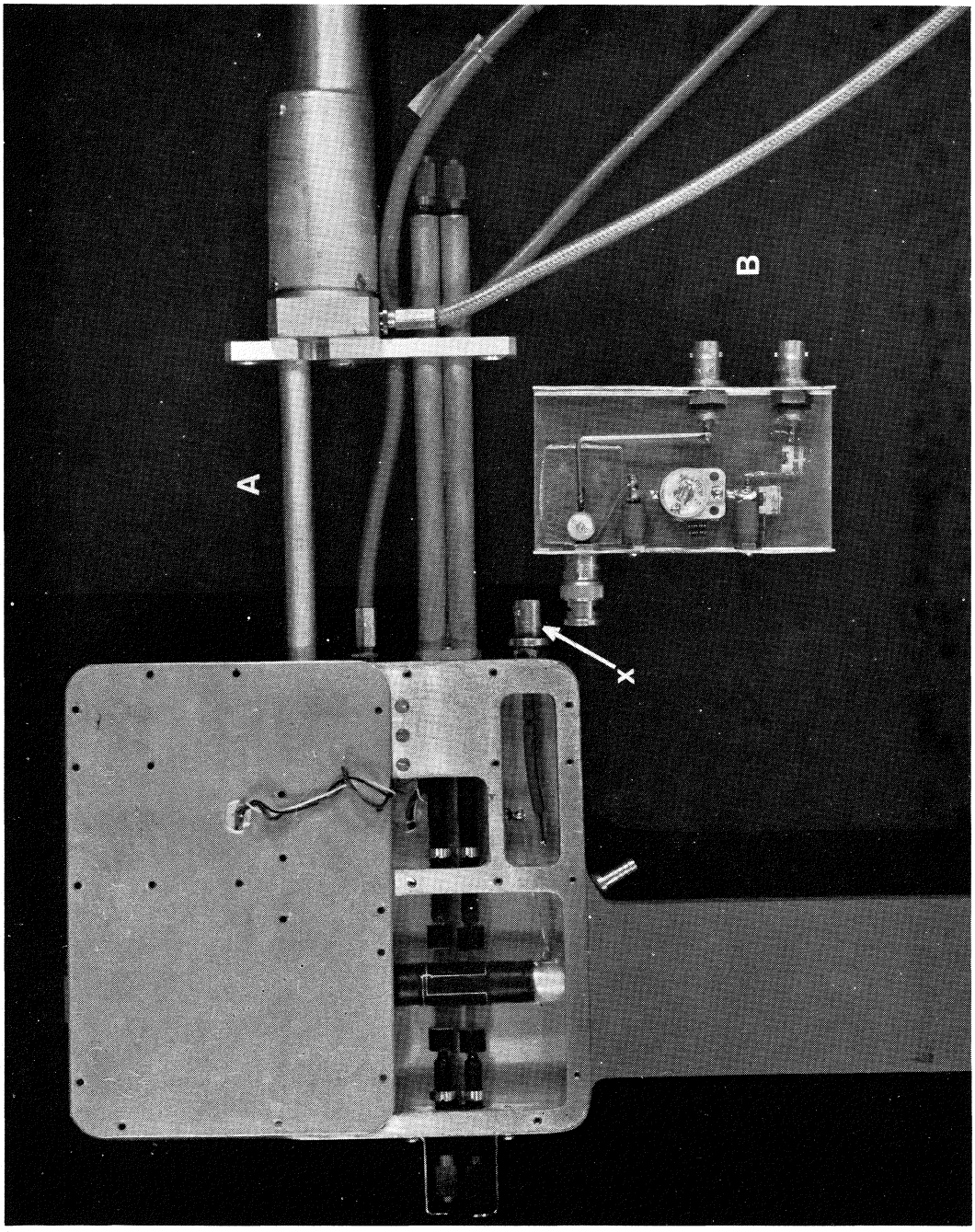

FIG. 2. (*A*) A Varian V-4333 (100 MHz) probe modified for heteronuclear-decoupling experiments. (*B*) The double-tuned probe adaptor (module) used for ^{1}H - $\{^{31}P\}$ experiments.

Can. J. Chem. Downloaded from www.nrcresearchpress.com by 210.87.254.6 on 09/05/12
For personal use only.

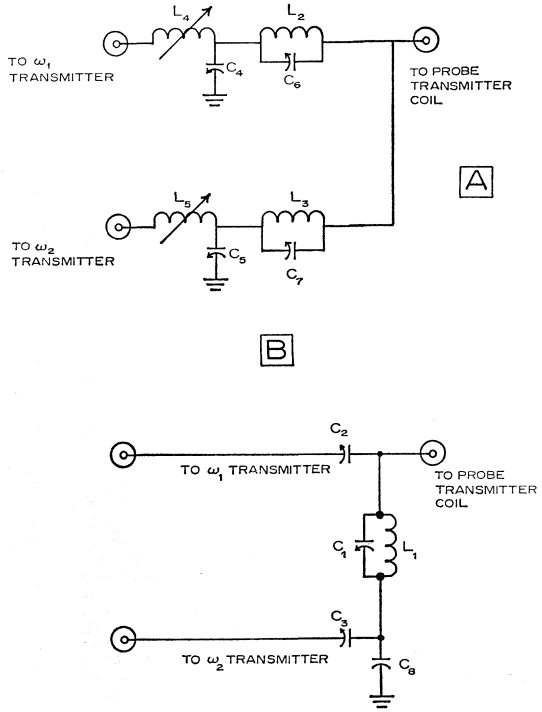

FIG. 3. (*A*) Circuit diagram of module used for ^1H - $\{^{19}F\}$ and ^{19}F - $\{^1H\}$ experiments. (*B*) Circuit diagram of modules used for ^1H - $\{^2H\}$ ^{19}F - $\{^2H\}$, ^1H - $\{^{31}P\}$, and ^{19}F - $\{^{31}P\}$ experiments.

the circuit shown in Fig. 5; the circuit was tuned for a minimum s.w.r. at 100 MHz.

This second transmitter coil did not appear to degrade the resolution of the spectrometer; neither did it affect the probe balance to any appreciable degree. One minor disadvantage of this method is that it is less easily "reversed" and we consider this method to be the less versatile.

The same basic modification suffices for ^{31}P - $\{^{19}F\}$ studies. For these experiments the second coil should be matched to 94 MHz as described above for 100 MHz.

Noise-Modulated Experiments

A block diagram of the components used for these experiments is given in Fig. 1*B*. This sequence is similar to that used by LeRoy F. Johnson (5), for ^{13}C - $\{^1H\}$ experiments, and developed independently of us. A wide-band of audio-noise, provided by either a Bucta (model 160) or a Mooge (model 903S) white-noise generator, was filtered to the required bandwidth by a cascaded pair of Krohn–Hite filters (model 3100R). A wide selection of bandwidths was separately recorded with a Sony (model 250) tape-deck. In each case the above filters were used to define the high-frequency limit, while the low-frequency limit was that of the recording circuitry of the tape-deck. Closed loops of this tape were then used, with the tape-deck and a Heathkit high fidelity audio amplifier (model AA-161), as a noise-source. The output of the audio-amplifier, suitably attenuated by a series resistor, was connected to the input "X" of a Hewlett–Packard mixer (model 10514A). Connection of the frequency-synthesizer to input "L" resulted in a noise (amplitude) modulated radio-frequency source; the basic synthesizer frequency is not transmitted, only the "sum" and "difference" of the noise- and radio-frequencies. Care must be taken that the mixer is not overloaded.

We were concerned that a possible disadvantage of using the conventional high fidelity audio components as the basis for a noise-modulated decoupler might be their low-frequency cut-off (ca. 50 Hz). Prompted by this concern, we constructed a pseudo-random sequence generator similar to that used by Ernst in his original study.[10] Later in this paper, the performance of this unit is compared with that of the taped-noise approach.

Results and Discussions

Since the many possible applications of the equipment described in Experimental are best discussed in relation to particular chemical problems, we shall only give here a minimum of illustrative examples. We shall not illustrate deuterium decoupling, which is very readily effected and has already been widely used, most notably by Anet and his co-workers (6). It should be noted that all the spectra shown in the figures were obtained on a "first-run" basis and no attempt was made to select the best spectra which were actually obtainable; on this basis these can be taken as genuinely "typical" results, and are in some respects below the calibre which we normally anticipate for specific research problems.

The spectra shown in Fig. 6 illustrate simple applications of continuous-wave heteronuclear spin-decoupling, using a deuterochloroform solution of the diphenyl phosphate ester of 1,1,1-trifluoroethanol.[11] The "normal" 100 MHz p.m.r. spectrum is shown in Fig. 6*A*. Continuous-wave irradiation at the fluorine resonance frequency (94.087,140.0 MHz), shown in Fig. 6*B*, leaves only the coupling (8.4 Hz) with the phosphorus. Similarly, irradiation at the phosphorus resonance frequency (40.480,340.0 MHz), Fig. 6*C*, leaves only the ^{19}F coupling (8.2 Hz). It is worthwhile commenting that the interval between the experiments shown in Figs. 6*B* and 6*C* was ca. 10 min, which is a typical changeover time and includes the readjustment of field

[10]We are indebted to Mr. Berry of the Electrical Engineering Department, University of British Columbia, who helped us greatly with this phase of the study.

[11]We thank Mr. Bruce Donaldson for this sample.

Can. J. Chem. Downloaded from www.nrcresearchpress.com by 210.87.254.6 on 09/05/12
For personal use only.

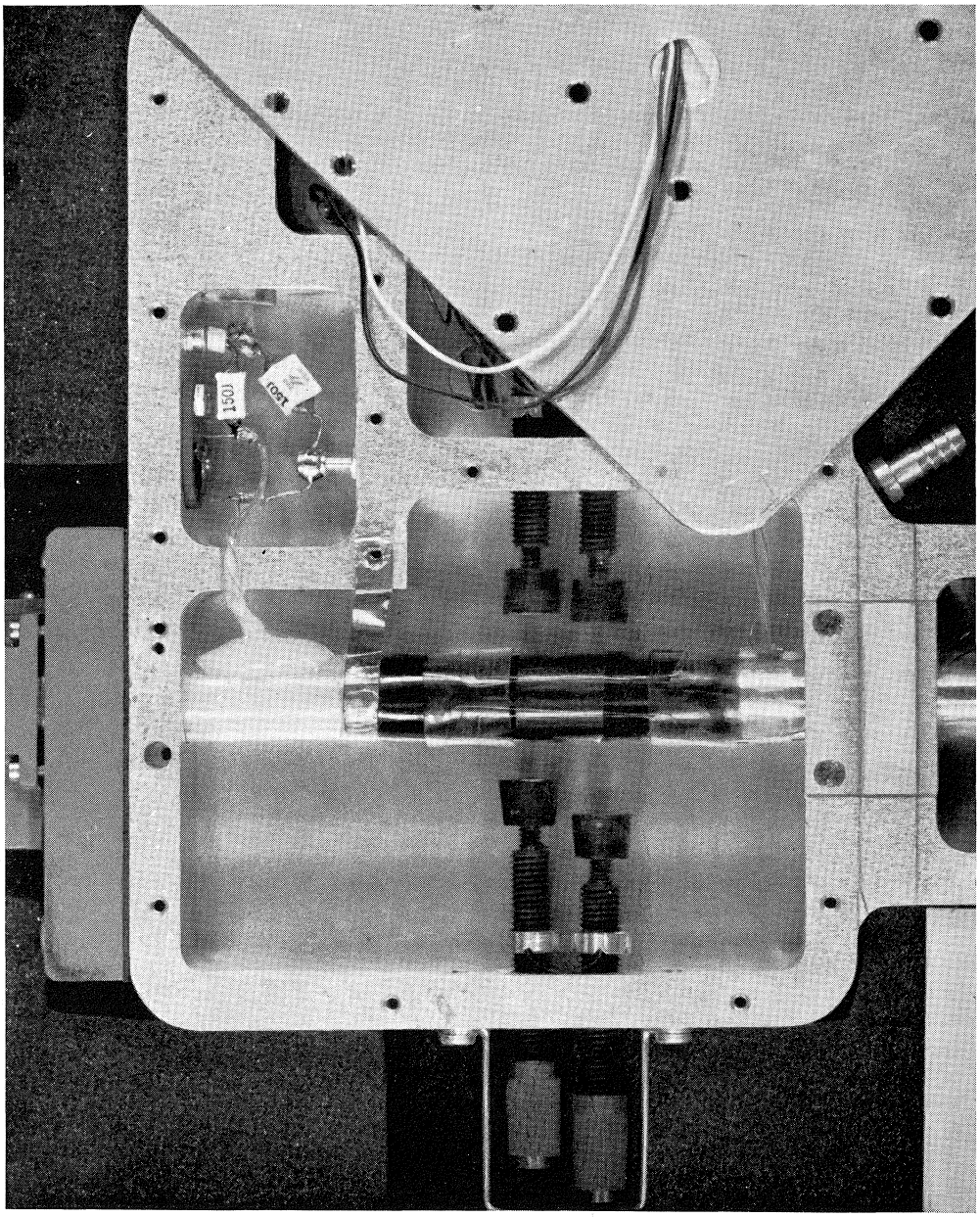

FIG. 4. Varian V-4333 probe (40.5 MHz) modified for double-resonance experiments by the addition of a second transmitter-coil.

Can. J. Chem. Downloaded from www.nrcresearchpress.com by 210.87.254.6 on 09/05/12
For personal use only.

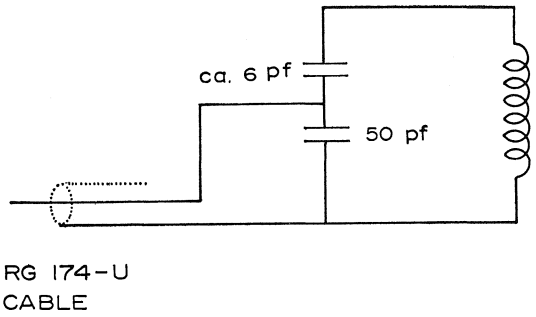

FIG. 5. Tuning network for the second transmitter-coil attached to the Varian V-4333 probe for ^{31}P - {^{1}H} experiments.

homogeneity after removal of the probe. The set-up-time interval between Figs. 6*A* and 6*B* was ca. 1 min.

The spectra shown in Fig. 7 are of a solution of trimethyl phosphite in deuterochloroform solution, and serve to compare the effectiveness of c.w. decoupling with that of noise-modulated decoupling. In Fig. 7*A* the "normal" spectrum shows the ^{31}P - ^{1}H coupling of ca. 10.6 Hz. The series of spectra shown in Fig. 7*B* demonstrates the effect of c.w. irradiation on the phosphorus resonance, initially with the frequency centered on the ^{31}P resonance (40.486,570.0 MHz) and subsequently set "off-resonance". It is apparent that the effective bandwidth of the decoupling field is small. Figure 7*C* shows the increase in effective bandwidth following noise-modulation using the SONY tape recorder system and a tape with noise having a nominal high-frequency limit of 500 Hz; the power output of the frequency synthesizer was unaltered from that used for the c.w. experiments. Further increases in decoupling bandwidth are observed when "noise" up to 1000 Hz (Fig. 7*D*) and up to 2000 Hz (Fig. 7*E*) is used. The final spectra (Fig. 7*F*) were obtained using our version of a pseudo-random sequence generator; its specifications were as close to those used by Ernst (4) as we could achieve. [12]

It is noteworthy that under the (less than optimum) conditions used to measure these spectra, the tape-recorder system introduces slightly more random noise than does the pseudo-random sequence generator. However, this noise does not in normal practice hinder the measure-

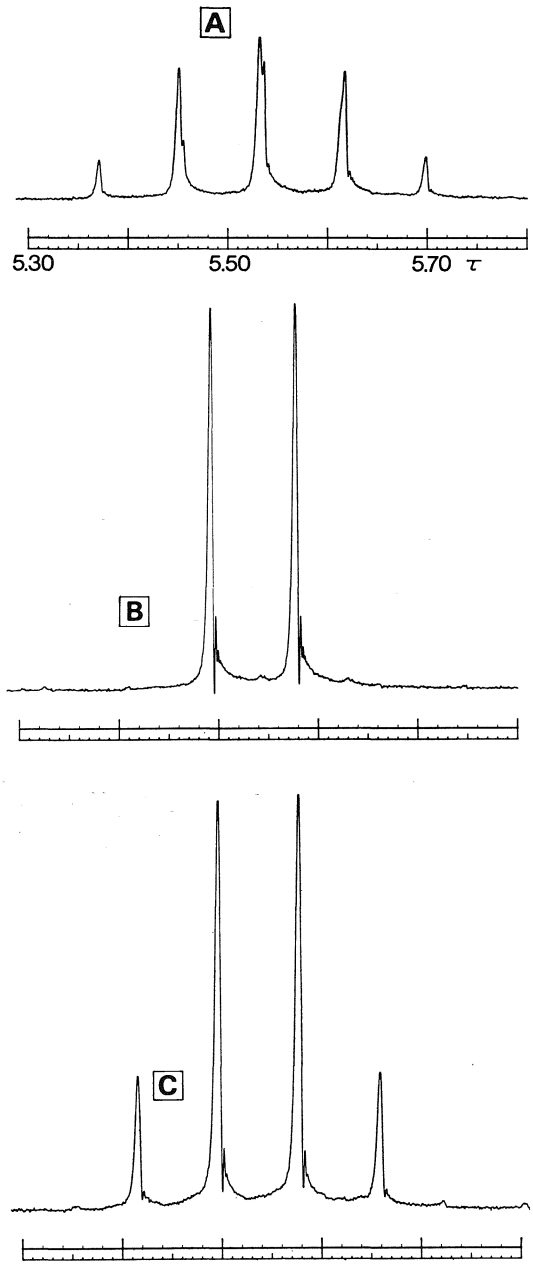

FIG. 6. Partial p.m.r. spectra (100 MHz) of a deuterochloroform solution of diphenyl (1,1,1-trifluoroethyl) phosphate. [A], normal spectrum; [B], spectrum obtained with continuous-wave irradiation of the fluorine substituent (94.087, 140.0 MHz); [C], spectrum obtained with c.w. irradiation of phosphorus (40.480, 340.0 MHz). All spectra were recorded with the same spectrometer settings; the sweep-rate was 0.2 Hz/s.

[12]Ernst gave no experimental details of his unit, beyond the number of "bits" used and the clock frequency.

Can. J. Chem. Downloaded from www.nrcresearchpress.com by 210.87.254.6 on 09/05/12
For personal use only.

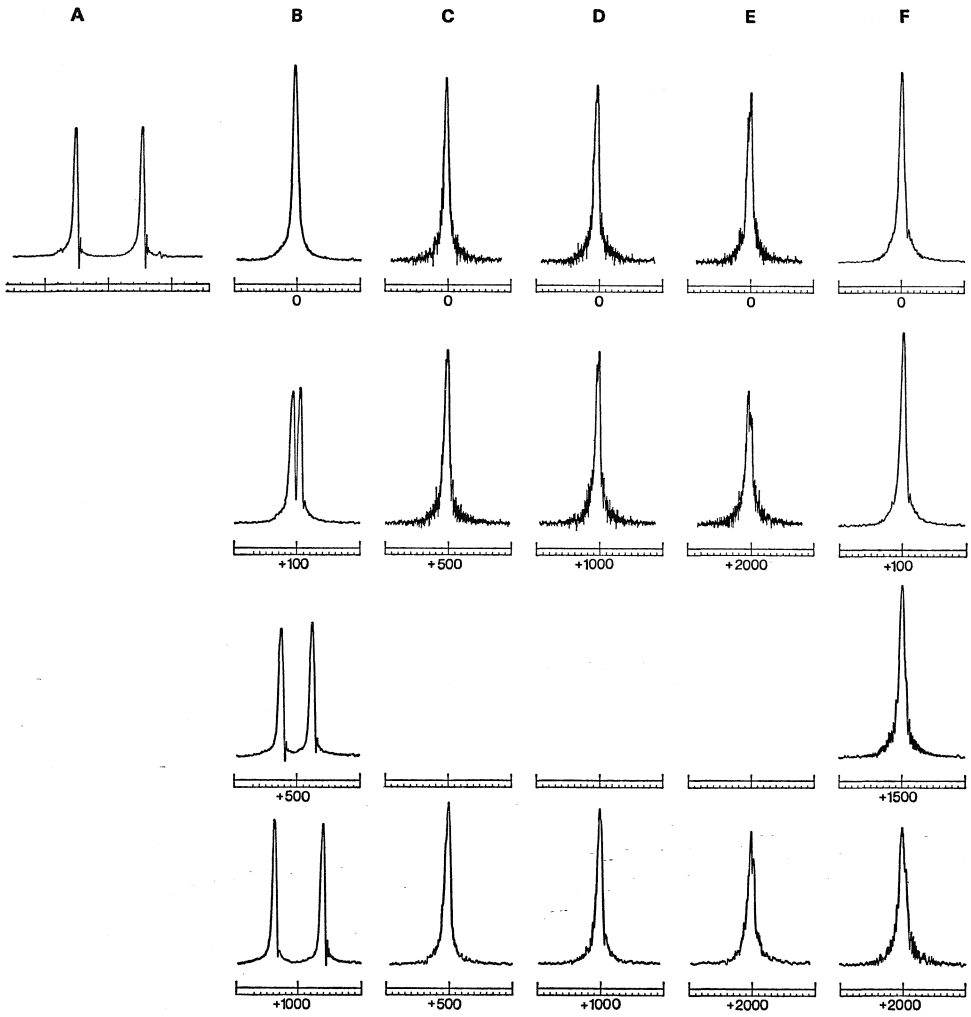

FIG. 7. Proton magnetic resonance spectra (100 MHz) of a deuterochloroform solution of trimethylphosphite. (*A*) Normal spectrum. (*B*) Spectra obtained with c.w. irradiation at 40.486,570.0 MHz and with subsequent offsets from that frequency. (*C*) Spectra obtained using the tape-recorder system for noise-modulation with a nominal high-frequency cut-off of 500 Hz. (*D*) As for (*C*) but using a 1000 Hz tape. (*E*) As for (*C*) but using a 2000 Hz tape. (*F*) Spectra obtained with noise-modulation derived from a pseudo-random sequence generator. The lower set of spectra in columns (*C*), (*D*), and (*E*) were run with increased filtering.

ment of adequately resolved n.m.r. spectra. The level of noise introduced is critically dependent upon the balance of the probe and is normally much less than that shown in Fig. 7; as we have already mentioned, *no* special attempts were made to optimize the conditions used for these particular measurements. Furthermore, the relatively high frequency of this noise means that it can be removed by application of a very moderate amount of filtering. The lower set of spectra in Fig. 7 illustrate this point; they were run with the "filter-bandwidth" control decreased to 0.5 Hz. In other applications which we shall discuss elsewhere, we have commonly achieved "natural" resolution using a 1 KHz noise-tape.

It is apparent from the spectra shown in Fig. 7 that a tape-recorder system can provide a convenient source of noise-modulation which is suitable for many heteronuclear-decoupling experiments. It is an inexpensive system available

Can. J. Chem. Downloaded from www.nrcresearchpress.com by 210.87.254.6 on 09/05/12
For personal use only.

to any n.m.r. laboratory having temporary access to a well-equipped audio-visual laboratory. We have already used this approach in several applications and have not, to date, detected any noteworthy limitations; for example, using a 1 KHz tape we (7) have successfully irradiated a series of ^{19}F resonances spread over ca. 2 KHz and removed all their couplings from a proton spectrum.

It should be stressed that the concepts which we have used as the basis of our decoupler have been available in the literature for some time. Nevertheless, we believe this account to be a useful addition to the literature because it should make heteronuclear-decoupling more widely available at the "application", rather than "research", level.

Clearly a number of variations and improvements are possible.[13] For example, a "cassette" tape-recorder might be more convenient than the more bulky tape-deck we use. Furthermore, a less expensive frequency generator would suffice for many applications of noise-modulated decouplings. For many such experiments it is unnecessary to use a unit having either an inherently high-frequency stability or a high "resetability"; for example, we have used a Hewlett–Packard v.h.f. signal generator (model 608D). It should also be noted that some laboratories may be able to use an additional Varian V-4311 radiofrequency unit to provide the basic decoupling-frequency.

Laboratories interested in a rather limited range of heteronuclear-decoupling experiments may find attractive the simplicity of adding a second transmitter coil to the Varian probe rather than effecting the more complex double-tuning. The modification we have made to our ^{31}P (40.5 MHz) probe, described in Experimental, has performed well for some time now.

Since we completed this work, details of the N.P.L. modification of the Varian probe have been published (8), as also has another modification (9).

We are indebted to the National Research Council of Canada for their generous financial support of this work; separate major equipment grants covered the initial cost of the Varian spectrometer and subsequently of the equipment purchased from Hewlett–Packard (Grant No. E 1338). It is also a pleasure to thank Professor C. A. McDowell for his interest in this study, and Mr. W. Griba of the Audio-Visual Department, Simon Fraser University, for providing the "white-noise" tape-recording.

1. R. A. HOFFMANN and S. FORSEN. *In* Progress in nuclear magnetic resonance spectroscopy. Vol. 1. J. W. Emsley, J. Feeney, and L. H. Sutcliffe (*Editors*). The Pergamon Press, Ltd., London, 1966, and references therein.
2. J. D. BALDESCHWIELER and E. W. RANDALL. Chem. Rev. **63**, 81 (1963), and references therein.
3. W. MCFARLANE. *In* Annual reviews of n.m.r. spectroscopy. E. F. Mooney (*Editor*). Academic Press, Inc., London. 1968, and references therein.
4. R. R. ERNST. J. Chem. Phys. **45**, 3845 (1966).
5. LEROY F. JOHNSON. Private communication.
6. F. A. L. ANET and A. J. R. BOURNE. J. Amer. Chem. Soc. **89**, 760 (1967), and other papers published by F. A. L. Anet in the same journal.
7. W. R. CULLEN, L. D. HALL, and R. N. JOHNSON. To be published.
8. A. CHARLES and W. MCFARLANE. Mol. Phys. **14**, 299 (1968).
9. G. J. LONG and A. G. MORITZ. Mol. Phys. **15**, 439 (1968).

[13]A referee suggested that . . . "At moderately high powers, ground loops and/or drifts of the probe balance can arise because of slight swaying of the double-tuned box." It was suggested that the adaptor be firmly bolted to the probe body.

We prefer to retain the flexibility of our approach and have never in the past 2 years encountered any instability of probe balance.

Can. J. Chem. Downloaded from www.nrcresearchpress.com by 210.87.254.6 on 09/05/12
For personal use only.

Chemical examination of the wax from needles of black spruce *(Picea mariana)* and balsam fir *(Abies balsamea)*

R. M. Beri and H. W. Lemon
Ontario Research Foundation, Sheridan Park, Ontario

Received July 18, 1969

A waxlike substance extracted from the needles of black spruce by means of petroleum ether gives, upon saponification, capric, lauric, myristic, pentadecanoic, palmitic, stearic, oleic, linoleic, linolenic, arachidic, behenic, lignoceric acids, and one acid not identified. Acids of the C-20 to C-24 series constitute approximately 38% of the total acids. The unsaturated acids present are mostly of the C-18 series. The acids were identified by the gas–liquid chromatography (g.l.c.) of their methyl esters.

The constituent acids of the waxlike substance from balsam fir needles are capric, lauric, myristic, pentadecanoic, palmitic, palmitoleic, heptadecanoic, stearic, oleic, linoleic, linolenic, arachidic, behenic, lignoceric, and about 7 more, not identified. The acids of the C-20 to C-24 series are present to the extent of ca. 20%. About 55% of the acids are of the C-18 series, which is mostly unsaturated. There are present certain unsaturated acids, ca. 5%, of the C-20 to C-22 series.

10-Nonacosanol has been isolated from the unsaponifiable matter remaining after saponification of the waxlike substances from black spruce and balsam fir foliage. Its identity has been established by infrared, nuclear magnetic resonance, and mass spectrometry.

Canadian Journal of Chemistry, **48**, 67 (1970)

Can. J. Chem. Downloaded from www.nrcresearchpress.com by 210.87.254.6 on 09/05/12
For personal use only.

Introduction

Black spruce (*Picea mariana* (Mill.) B.S.P.) and balsam fir (*Abies balsamea* (L.) Mill.) are widely distributed throughout Eastern Canada. Shaw (1, 2) has studied the chemical nature of the essential oil from foliage and twigs of these two trees. A number of references are in the literature referring to the utilization of conifer foliage as animal feed, as a source of vitamin C, for production of chlorophyll and water soluble chlorophyll derivatives, etc. Gagnon (3) has studied the free amino acid content in needles of *A. balsamea* and *P. mariana* growing on different sites. Bougault and Bourdier (4) investigated the wax constituents of several conifers and found that these waxes were largely mixtures of compounds belonging to a class of natural products having the properties of acids, alcohols, and esters, but more or less in the combined form. Watanabe (5) examined the leaf wax of 38 species of conifers and showed that many of these waxes are estolides of juniperic and sabinic acids. In his study the non-saponifiable matter, 1,12-dodecanediol, was found in many species including Chinese juniper, 'arbor vitae' (*Thuja standishii ?*), *Abies veitchii*, *Abies sachalinensis*, and *Picea jezoensis*; 1,16-hexadecanediol was found in Chinese juniper; melissyl alcohol in *Juniperus rigida*, *Cunninghamia lanceolata*, arbor-vitae, and a Japanese species of hemlock; 10-nonacosanol, found in Chinese juniper, *Abies sachalinensis*, and a Japanese species of hemlock, was believed to be more common in coniferal waxes than previously thought. Eglinton and Hamilton (6) reviewed the physiology, physical appearance, chemical constituents, chemotaxonomy, and biosynthesis of the surface waxes of plants, emphasizing leaf wax.

The present paper deals with a study of the chemical nature of the waxlike substance extracted from the needles of black spruce (*P. mariana*) and balsam fir (*A. balsamea*).

Experimental

Black Spruce Needle Extract

The source of needles was the branches of the top 10 ft of a 37 ft high tree. The tree was cut in May while still frozen. Needles were hand-picked on arrival and placed in cold storage (−5°C) until used.

The needles were first air-dried for 5–6 days and extracted with petroleum ether (30–60°C). On extraction a green product of a semi-solid consistency, acid no. 50.0, ester no. 131.7, was obtained in a yield of 1.60%. It was saponifiable with difficulty and was saponified by the method of Odham (7). After saponification, the saponifiable and the unsaponifiable matter were worked-up in the usual manner.

Saponifiable Matter

The saponifiable matter was methylated with boron trifluoride–methanol reagent according to the method of Metcalfe *et al.* (8). The methyl esters after isolation were submitted to g.l.c. on a column of 12% DEGS (diethylene glycol succinate) on Chromosorb W at 187°C. The relative position of the esters eluting from the column was determined by comparison with the elution times of known standards, which were passed through the gas–liquid chromatography (g.l.c.) column under identical experimental conditions. From the

Can. J. Chem. Downloaded from www.nrcresearchpress.com by 210.87.254.6 on 09/05/12
For personal use only.

TABLE 1

Component fatty acids of black spruce needle extract, before and after hydrogenation

No.	Common name of parent compound	Code†	Percentage* Before hydrogenation	Percentage* After hydrogenation
1	Capric	10:0	1.60	1.64
2	Lauric	12:0	8.15	9.16
3	Myristic	14:0	3.91	4.48
4	Pentadecanoic	15:0	0.78	1.09
5	Palmitic	16:0	10.19	11.00
6	Stearic	18:0	2.29	39.09
7	Oleic	18:1	9.44	
8	Linoleic	18:2	14.28	
9	Unknown		5.23	
10	Linolenic	18:3	5.73	
11	Arachidic	20:0	4.05	3.21
12	Behenic	22:0	13.45	13.08
13	Lignoceric	24:0	20.88	17.31

*Reported as area % of methyl ester of the total mixed esters.
†e.g. Saturated C-12 = 12:0; mono-unsaturated C-12 = 12:1.

chromatograms, the percentages of the esters were calculated. The percentages given in Table 1 are for the methyl esters and are reported as area percentage of the total area for the mixed esters, as determined from the g.l.c. curves of the chromatogram.

Methyl esters were hydrogenated in absolute ethanol by passing a slow current of hydrogen with platinum oxide as a catalyst. The hydrogenated methyl esters were chromatographed on a column of 12% DEGS at 187°C. From the chromatogram the approximate percentage of the hydrogenated methyl esters was calculated and is reported in Table 1.

From Table 1 it will be noticed that the black spruce needle extract contains ca. 38% acids of the C-20 to C-24 series and, of the unsaturated acids found, most are of the C-18 series.

Unsaponifiable Matter

The unsaponifiable matter was chromatographed over Brockman grade II alumina and eluted with petroleum ether, petroleum ether and chloroform in varying proportions, chloroform, and methanol. Eluates were chromatographed in a column of 2% SE-30 on Chromosorb W at 227°C. All the eluates, excepting those of petroleum ether:chloroform (1:1 by volume), gave a number of peaks. From the petroleum ether:chloroform (1:1 by volume) eluate, a substance, m.p. 83.5°C (Watanabe reports 78–81°C), was crystallized out. Its infrared (i.r.) spectrum showed strong absorption at 8.90 μ (1124 cm^{-1}) (an absorption at 1120 cm^{-1} is reported for an impure sample (9)), indicating it to be a saturated secondary or a highly symmetrical secondary alcohol. The nuclear magnetic resonance (n.m.r.) spectrum of the compound in $CDCl_3$ at 100 MHz showed an asymmetric triplet at 0.88 p.p.m. (terminal methyl groups), a singlet at 1.25 p.p.m., having $W_{1/2}$ = 3.2 Hz (CH_2 groups), and a broad peak at 3.5 p.p.m. (OH groups). Integrals gave the 0.88:3.5 p.p.m. peak ratio 6:1 and the 3.5:1.25 p.p.m. ratio 1:>45. All peak positions are reported with respect to internal TMS.

From i.r. and n.m.r. observations, the compound appeared to be a secondary aliphatic alcohol.

Mass spectra of the compound by direct insertion to the ion source gave the base peaks at *m/e* 297 with *m/e* 406 (23%) next in abundance. A very weak molecular ion peak appeared at *m/e* 424 (<1%), and other peaks at *m/e* 378, (2.3%), 278 (8.7%), 157 (15.5%), etc. Molecular weight of the compound is 424 and hence the molecular formula is $C_{29}H_{60}O$. The key fragmentation with respect to elucidating the position of hydroxyl is as follows

$424^+ \rightarrow 406^+ + H_2O$ (Typical of an alcohol)

$406^+ \rightarrow 378^+ + C_2H_4$

$424^+ \rightarrow 297^+ + C_9H_{19}$ $C_{19}H_{39}—\overset{+}{C}H—OH$ *m/e* 297

$297^+ \rightarrow 279^+ + H_2O$

$279^+ \rightarrow 278^+ + H$

$424^+ \rightarrow 157^+ + C_{19}H_{39}$ $C_9H_{19}—\overset{+}{C}H—OH$ *m/e* 157

Thus the hydroxyl is at position 10 and the structure of the compound is $C_{19}H_{39}CH(OH)C_9H_{19}$, i.e. 10-nonacosanol.

The compound was acetylated and the acetylated product melted at 44.5° (lit. 44.5–45.5°C (10)). The i.r. spectra of the acetate showed a strong absorption at 5.75 μ (1736 cm^{-1}).

Balsam Fir Needle Extract

The source of needles was the branches of the top 10 ft of a 24 ft high tree. The tree was cut in May while still frozen. Needles were hand-picked on arrival and placed in cold storage (−5°C) until used.

The needles were first air-dried for 5–6 days and

TABLE 2

Component fatty acids of balsam fir needle extract, before and after hydrogenation

No.	Common name of parent compound	Code	Percentage* Before hydrogenation	Percentage* After hydrogenation
1	Capric	10:0	0.55	0.30
2	Unknown		0.71	
3	Lauric	12:0	1.41	0.81
4	Unknown		0.86	
5	Myristic	14:0	3.46	3.36
6	Pentadecanoic	15:0	1.22	1.09
7	Palmitic	16:0	14.99	13.86
8	Palmitoleic	16:1	0.61	
9	Heptadecanoic	17:0	5.77	5.09
10	Stearic	18:0	2.14	55.15
11	Oleic	18:1	20.86	
12	Linoleic	18:2	12.63	
13	Unknown		2.84	
14	Linolenic	18:3	12.79	
15	Arachidic	20:0	2.51	6.80
16	Unknown		1.92	3.06
17	Unknown		1.92	
18	Unknown		0.65	
19	Behenic	22:0	3.47	3.84
20	Unknown		1.18	
21	Lignoceric	24:0	7.58	6.61

*Reported as area % of methyl ester of the total mixed esters.

extracted with petroleum ether (30–60°). A waxlike substance of semi-solid consistency, acid no. 43.6, ester no. 148.3, was obtained by petroleum ether extraction of the air-dried needles in 1.55% yield. It was separated into the saponifiable and the unsaponifiable matter.

Saponifiable Matter

The saponifiable matter was methylated and the methyl esters were chromatographed in a column of 12% DEGS on Chromosorb W at 187°C, before and after hydrogenation. The % of the component fatty acids before and after hydrogenation was calculated from the chromatograms and is reported in Table 2,

A review of Table 2 will show that balsam fir needle extract contains ca. 55% acids of C-18 series which are mostly unsaturated in nature. There are present certain unsaturated acids, ca. 5%, of C-20 to C-22 series. The acids of C-20 to C-24 series are present to the extent of ca. 20%.

Unsaponifiable Matter

From the unsaponifiable fraction by column chromatography over Brockman grade II alumina, 10-nonacosanol, m.p. 83.5°C, was isolated. This substance when admixed with a sample of 10-nonacosanol isolated earlier from black spruce needle extract, showed no difference when examined by g.l.c. and i.r. spectroscopy.

Nuclear magnetic resonance spectra were recorded by F. J. Hopton of Ontario Research Foundation, and mass spectra by Robert Schaffer of Morgan Schaffer Corporation, Montreal.

The authors are grateful to The Canadian International Development Agency for the provision of funds allowing R. M. Beri to carry out this work and to the Ontario Research Foundation for providing the necessary facilities and guidance.

The material was obtained through the courtesy of Mr. A. J. Carmichael of the Research Branch of the Ontario Department of Lands and Forests.

1. A. C. SHAW. Can. J. Res. **28B**, 268 (1950).
2. A. C. SHAW. Can. J. Chem. **31**, 193 (1953).
3. J. D. GAGNON. Nature, **212**, 844 (1966).
4. J. BOUGAULT and L. BOURDIER. Compt. Rend. **147**, 1311 (1908).
5. H. WATANABE. Yakugaku Zasshi, **73**, 176 (1953).
6. G. EGLINTON and R. J. HAMILTON. Sci. **156**, 1322 (1967).
7. G. ODHAM. Arkiv. Kemi, **21**, 379 (1963).
8. L. D. METCALFE, A. A. SCHMITZ, and J. R. PELKA. Anal. Chem. **38**, 514 (1966).
9. S. J. PURDY and E. V. TRUTER. Proc. Royal Soc. (London), Ser. B, **158**, 536 (1963).
10. H. R. BENTLEY *et al.* J. Chem. Soc. 596 (1955).

Can. J. Chem. Downloaded from www.nrcresearchpress.com by 210.87.254.6 on 09/05/12
For personal use only.

Can. J. Chem. Downloaded from www.nrcresearchpress.com by 210.87.254.105 on 09/05/12
For personal use only.

A Mössbauer study of adducts of triphenyltin chloride with oxygen-donor substances

R. W. J. WEDD AND J. R. SAMS
Department of Chemistry, University of British Columbia, Vancouver 8, British Columbia

Received June 12, 1969

Mössbauer parameters for triphenyltin chloride and a number of its adducts with oxygen-donating Lewis bases are reported. The isomer shifts for all the compounds reported are constant within experimental error (1.29 ± 0.03 mm s^{-1}, relative to SnO_2). An approximate correlation between quadrupole splitting and the shift in element–oxygen stretching frequency between neat and complexed base is noted. This suggests that in general for these adducts, larger quadrupole splittings are associated with stronger complexes.

Canadian Journal of Chemistry, **48**, 71 (1970)

Introduction

A considerable body of evidence has been presented recently showing that quadrupole splittings in the Mössbauer spectra of Sn(IV) compounds can be strongly influenced by asymmetry in the σ-bonding, contrary to earlier suggestions (1–4).

It was thought for some time that in compounds of the type R_3SnX, quadrupole splitting would be observed only if the group X possessed a nonbonding electron pair capable of π-bonding to the empty 5d or 6p orbitals on the tin atom, whereas no splitting would be observed for substituents with no available lone pairs (1). Indeed, Stöckler and Sano (4) have suggested recently that the splittings observed for a number of pentafluorophenyltin compounds were due primarily to polarization effects via p_π–p_π and p_π–d_π interactions, although ^{19}F nuclear magnetic resonance (n.m.r.) data (5) show that there is very little π-electron transfer from pentafluorophenyl to tin in $(CH_3)_3SnC_6F_5$. On the other hand, Parish and Platt (6) and Chivers and Sams (7, 8) have presented evidence showing that quadrupole splittings in a wide variety of tetraorganotin compounds can be induced by σ-bonding (electronegativity) effects only. More recent data to be published shortly further substantiate this view (9).

Greenwood and Ruddick (3) proposed a "rule" for quadrupole splittings in hexacoordinate tin compounds similar to that of Gibb and Greenwood (1) for tetracoordinate tin compounds, i.e., that splitting would be observed only if some (but not all) of the ligands attached to tin had a nonbonding p_π-electron pair. However, a study of hexacoordinate adducts of SnX_4 (X = Cl, Br) with various oxygen, nitrogen, and sulfur donor molecules (10) showed that splittings were observed in some cases. It appears that several different effects may be operative in these compounds (11), none have to do with π-bonding asymmetry.

This situation is somewhat different in the case of pentacoordinate tin compounds, since these will always show fairly large quadrupole splittings. Even here, however, differences in σ-bonding amongst the substituents on the tin atom can play an important role in determining the actual magnitude of the splitting observed. For example, a study of a number of trimethyltin haloacetates (which are linear polymers in the solid state with pentacoordinate tin atoms and bridging OCO groups) has yielded a linear correlation between the quadrupole splitting and the p*K* of the acid from which the compound was derived (12). It was these results which led to our interest in studying adducts of triphenyltin chloride with various O-donor substances. In particular, we hoped to determine if a relation existed between the quadrupole splitting and the nature of the Lewis base. Ligands having oxygen donor atoms were particularly chosen for the following reason. Philip *et al.* (10) found that adducts of $SnCl_4$ and $SnBr_4$ with nitrogen- and sulfur-donor ligands did not exhibit quadrupole splitting, whereas with oxygen-donor ligands splittings were sometimes, but not always, observed. It, therefore, appeared that larger variations in bonding were to be expected for the O-donor complexes.

Experimental

Triphenyltin chloride from M & T Chemicals was recrystallized from methanol and thoroughly dried prior

TABLE 1

Mössbauer parameters and element–oxygen stretching frequencies for $(C_6H_5)_3SnCl{\cdot}L$ complexes

Base	δ*†	Δ*	ν_{E-O_1}‡§	ν_{E-O_c}‡	$\Delta\nu_{E-O}$
Neat	1.31	2.55			
$(CH_3)_2SO$	1.26	3.25	1047	956, 946	91, 101
$(C_3H_7)_2SO$	1.28	3.08	1018	981, 969	37, 49
$(C_4H_9)_2SO$	1.30	3.20	1028	972, 962	56, 66
$(CH_2)_4SO$	1.29	3.18	1020	957, 949	63, 71
$(CH_3O)_3PO$	1.31	3.18	1281	1239	42
$(C_2H_5O)_3PO$	1.30	3.15	1263	1222	41
$(C_6H_5O)_3PO$	1.31	3.07	1295	1280	15
$(C_6H_5)_3PO$	1.29	3.14	1190	1159	31
$(C_6H_5)_3AsO$	1.29	3.09	880	871, 859	9, 21
C_5H_5NO	1.30	3.03	1244	1217, 1210	27, 34
$(CH_3)_2NCHO$	1.31	2.84	1670	1645	25

*In mm s^{-1}, ± 0.03 mm s^{-1}.
†Relative to SnO_2 at 80 °K.
‡In cm^{-1}, ± ~3 cm^{-1}.
§Uncomplexed base.

to use. The Lewis bases employed were obtained either from Aldrich Chemical Company or from Eastman Organic Chemicals and were used without further purification.

Two preparative procedures were employed. Where the donor substance was a solid at room temperature, stoichiometric quantities of triphenyltin chloride and base were separately dissolved in chloroform. The two solutions were mixed and the solvent subsequently removed under vacuum. In those cases where the donor substance was a liquid at room temperature, the complexes were prepared by adding an excess of base to a solution of triphenyltin chloride in chloroform and removing the solvent and unreacted base under vacuum. All the complexes appear to be air stable and offer no survival problems.

The Mössbauer spectrometer was of the constant acceleration type. All Mössbauer measurements were made with the absorbers at 80 ± 1 °K, and isomer shifts are reported relative to SnO_2 at this temperature. The velocity scale was calibrated against an NBS standard sodium nitroprusside absorber, using a value of 1.726 ± 0.002 mm s^{-1} for the quadrupole splitting of this compound. Frequent checks using metallic iron as calibrant have shown our drive system to be linear to within ± 0.01 mm s^{-1} over the velocity range reported here. We estimate the precision of the Mössbauer measurements as ± 0.03 mm s^{-1}. Infrared spectra were recorded on a Perkin–Elmer 457 instrument. The solids were dispersed in Nujol between CsI plates.

Results and Discussion

Mössbauer isomer shifts and quadrupole splittings of the complexes prepared and element–oxygen stretching frequencies of both neat and complexed bases are given in Table I. Also included are the Mössbauer parameters for neat triphenyltin chloride. The isomer shift is related to changes in s-electron density at the tin nucleus, while the quadrupole splitting gives a measure of the deviation from cubic symmetry of the electron distribution about the tin atom. Since pure s electrons will not contribute to the field gradient, the quadrupole splittings will be mainly affected by the distribution of p and d electron density in the various bonds to the tin atom.

As seen from Table I, the isomer shifts for all the adducts are constant within experimental error and furthermore, are essentially the same as that for neat triphenyltin chloride. This is perhaps not too surprising in view of other recent findings. Thus, it has been observed (7, 8) that in compounds of the general types $(CH_3)_3SnX$, $[(CH_3)_3Sn]_2X$, and $(CH_3)_2SnX_2$ (where X is an aryl group with other substituents), the isomer shifts are essentially constant (1.25 ± 0.07 mm s^{-1}), although the quadrupole splitting and ^{119}Sn—C—H coupling constants show marked variations. Moreover, the compounds $(CH_3)_3SnOCOCH_{3-n}X_n$ (X = halogen) also show effectively constant isomer shifts (12) which are, however, slightly higher than those for the tetraorganotin compounds mentioned above (1.39 ± 0.05 mm s^{-1}). On the other hand, it would clearly be erroneous to expect *any* series of compounds of a given general formula to exhibit constant isomer shifts, and it is fairly easy to find examples where this is not the case (see, for example, ref. 13). It is interesting that complexation has no effect upon the s-electron density at the tin nucleus. This may be due in part to the fact that R_3SnCl compounds are relatively weak Lewis acids, so that strong donor–acceptor interactions

Can. J. Chem. Downloaded from www.nrcresearchpress.com by 210.87.254.105 on 09/05/12
For personal use only.

Can. J. Chem. Downloaded from www.nrcresearchpress.com by 210.87.254.105 on 09/05/12
For personal use only.

are not likely. In this connection, it should be mentioned that attempts to prepare stable complexes of $(C_6H_5)_3SnCl$ with $Cl(C_2H_5O)_2PO$, $Cl_2(C_2H_5O)PO$, and Cl_3PO were not successful. Presumably, the replacement of one or more ethoxy groups by chlorine in $(C_2H_5O)_3PO$ reduces the basicity sufficiently to prevent complexation.

In a very recent paper which appeared during the course of the present study, Hill, Drago, and Herber (14) have reported Mössbauer results for 5 adducts of $(CH_3)_3SnCl$ with Lewis bases, and also find essentially constant isomer shifts. There was some uncertainty as to whether the slightly larger values observed by them for the pyridine and N,N-dimethylacetamide complexes were real or due to experimental errors (14).

The quadrupole splittings for the adducts reported in Table 1 are all larger than that for triphenyltin chloride itself, but only fairly small variations are shown amongst the complexes. The increase in quadrupole splitting on complexation can be interpreted as follows.

In triphenyltin chloride the tin atom is probably tetracoordinate, although the possibility of bridge bonding through chlorine cannot rigorously be excluded. Both the symmetric and asymmetric Sn—C stretching frequencies are observed (15) in the infrared, but details of the relative intensities are lacking. Chlorine bridging in $(CH_3)_3SnCl$ has been suggested (16), but Hill *et al.* (14) have argued that such association is very weak, if indeed present. The question is not really crucial, since in either case the microsymmetry about the tin atom will be C_{3v}, and the quadrupole splitting will depend only upon the z-component of the electric field gradient tensor, V_{zz}.

Upon adduct formation the tin atom is now pentacoordinate. In similar adducts of $(CH_3)_3SnBr$ (17), the absence of the $Sn—C_3$ symmetric stretch in the infrared points to a planar $(CH_3)_3Sn$ group, so that the geometry is presumably very close to a trigonal bipyramid. Hulme (18) has determined the X-ray structure of $(CH_3)_3SnCl\cdot C_5H_5N$ and reported "three methyl groups in the equitorial plane and an almost linear Cl—Sn—N arrangement perpendicular to it". It does not seem unreasonable to suppose that the $(C_6H_5)_3SnCl$ adducts reported here have closely similar structures, especially in view of the similarities between the structures of trimethyltin acetate and tribenzyltin acetate (19). If we assume, then, that local C_{3v} symmetry is maintained upon adduct formation, with the Cl—Sn—O bond angle close to 180°, the change in quadrupole splitting must be due almost entirely to a change in V_{zz}. This probably arises mainly from an increasing asymmetry in the electron distribution amongst the 5p-orbitals on the tin atom. Drago and co-workers (14, 20, 21) have offered a similar description of the bonding in adducts of $(CH_3)_3SnCl$ in terms of an increased imbalance in p_z and (p_x,p_y) orbital charge densities over that present in the neat parent compound.

Although the differences in quadrupole splittings amongst the adducts of $(C_6H_5)_3SnCl$ are not large, there appears to be an approximate correlation between Δ and the shift in element-oxygen stretching frequency for a given donor type. In all the ligands we have employed (of the general type R_nEO), the degree of E—O multiple bonding and hence the basicity of the ligand will be affected by the nature of R. This will then be reflected in observed E—O bond distances and stretching frequencies (22, 23). Since the interaction strength of $(C_6H_5)_3SnCl$ with the ligands will depend upon the basicity of the latter, one can use the negative shift of the element–oxygen stretching frequency upon complex formation as an indication of the strength of the donor–acceptor interaction (24, 25). With these ideas in mind, it appears in general from the results presented in Table 1 that the stronger the complexation, the larger the quadrupole splitting. Hill, Drago, and Herber (14) were unable to observe any trends in quadrupole splitting for the adducts of $(CH_3)_3SnCl$ which they studied. However, this may be due (26) to the fact that results for only 5 compounds, all of different donor types, were reported. It may well be that results similar to those observed here will be found if a broader spectrum of compounds is investigated. Work along these lines is currently underway in another laboratory (27).

Financial support from the National Research Council of Canada is gratefully acknowledged.

1. T. C. Gibb and N. N. Greenwood. J. Chem. Soc. A, 43 (1966).
2. R. H. Herber and G. I. Parisi. Inorg. Chem. **5**, 769 (1966).
3. N. N. Greenwood and J. N. Ruddick. J. Chem. Soc. A, 1679 (1967).

4. H. A. STÖCKLER and H. SANO. Trans. Faraday Soc. **64**, 577 (1968).
5. R. D. CHAMBERS and T. CHIVERS. J. Chem. Soc. A, 4782 (1964).
6. R. V. PARISH and R. H. PLATT. Chem. Commun. 1118 (1968).
7. T. CHIVERS and J. R. SAMS. Chem. Commun. 249 (1969).
8. T. CHIVERS and J. R. SAMS. J. Chem. Soc. A. In press.
9. M. C. WALDMAN and J. R. SAMS. To be published.
10. J. PHILIP, N. A. MULLINS, and C. CURRAN. Inorg. Chem. 7, 1895 (1968).
11. P. A. YATES, F. AUBKE, and J. R. SAMS. To be published.
12. C. PODER and J. R. SAMS. J. Organometal. Chem. Amsterdam, **19**, 67 (1969).
13. R. H. HERBER. Tech. Rep. Ser. 50, IAEA, 121 (1966). P. A. YATES, B. F. E. FORD, J. R. SAMS, and F. AUBKE. Chem. Commun. 791 (1969).
14. J. C. HILL, R. S. DRAGO, and R. H. HERBER. J. Amer. Chem. Soc. **91**, 1644 (1969).
15. R. C. POLLER. Spectrochim. Acta, **22**, 935 (1966).
16. V. H. KRIEGSMANN and S. PISCHTSCHAN. Z. Anorg. Allg. Chem. **308**, 212 (1961).
17. V. G. KUMAR DAS and W. KITCHING. J. Organometal. Chem. Amsterdam, **13**, 523 (1968).
18. R. HULME. J. Chem. Soc. 1524 (1963).
19. N. W. ALCOCK and R. E. TIMMS. J. Chem. Soc. A, 1873 (1968).
20. N. A. MATWIYOFF and R. S. DRAGO. Inorg. Chem. **3**, 337 (1964).
21. T. F. BOLLES and R. S. DRAGO. J. Amer. Chem. Soc. **88**, 5730 (1966).
22. D. W. CRUIKSHANK. J. Chem. Soc. 5486 (1961).
23. R. J. GILLESPIE and E. A. ROBINSON. Can. J. Chem. **41**, 2074 (1963).
24. D. M. L. GOODGAME and F. A. COTTON. J. Amer. Chem. Soc. **82**, 5774 (1960).
25. F. A. COTTON, R. FRANCIS, and W. D. HORROCKS. J. Phys. Chem. **64**, 1534 (1960).
26. R. H. HERBER. Private communication.
27. B. V. LIENGME. Private communication.

Can. J. Chem. Downloaded from www.nrcresearchpress.com by 210.87.254.105 on 09/05/12
For personal use only.

Preparation and characterization of some methyl cyanide complexes of Cu(I), Cu(II), and Zn(II) fluorosulfates

J. B. MILNE
Department of Chemistry, University of Ottawa, Ottawa 2, Canada
Received July 4, 1969

Tetrakis(methyl cyanide) complexes of Cu(I), Cu(II), and Zn(II) fluorosulfates have been prepared by reactions of anhydrous Cu(II) and Zn(II) fluorosulfates in methyl cyanide. The infrared spectra indicate a strong interaction between the fluorosulfate anion and the complex Cu(II) and Zn(II) cations. Conductivity measurements in methyl cyanide show strong association between the fluorosulfate anion and the dipositive cations. The Cu(I) compound is completely dissociated in methyl cyanide and, according to the infrared spectrum, shows no strong interaction with fluorosulfate anion.

Canadian Journal of Chemistry, **48**, 75 (1970)

Can. J. Chem. Downloaded from www.nrcresearchpress.com by 210.87.254.105 on 09/05/12
For personal use only.

The behavior in methyl cyanide of several cupric, zinc(II), and cuprous salts of strong acids and the properties of the complexes derived from such solutions has been the subject of several studies (1–5). Infrared spectra, conductivity studies, and ultraviolet and visible region spectrophotometry have shown that nitrate ion has the greatest tendency to bond to the cation but that tetrafluoroborate and perchlorate are distorted by dipositive cations, indicating bond formation also.

The fluorosulfate anion has been shown to be distorted by strongly polarizing cations (6, 7), suggesting that it forms bonds with some covalent character. The study of this interaction is now extended to the behavior of fluorosulfates in methyl cyanide.

Results and Discussion

Infrared Spectra

The infrared (i.r.) spectra of the complexes and, for comparison, that of methyl cyanide and the fluorosulfate anion are given in Table 1.

The absorptions of the fluorosulfate group can be clearly distinguished in the spectra. In the Cu(I) compound, the anion retains C_{3v} symmetry with the doubly degenerate asymmetric SO_3 stretching vibration and deformation, ν_4 and ν_5, respectively, remaining as single lines. No special attempt was made to observe the torsion, ν_6, which is infrared-active but which is normally very weak when the fluorosulfate anion retains C_{3v} symmetry (6). The fluorosulfate anion is distorted in the Cu(II) and Zn(II) complexes; the torsion, ν_6, appears strongly and the degeneracy of the asymmetric vibrations, ν_4 and ν_5, is lost, indicating anion symmetry lower than that of C_{3v}. In the Zn(II) complex the asymmetric SO_3 deformation, ν_5, is split into 3 absorptions, one more than expected for the C_s symmetry fluorosulfate anion. The additional absorption may arise from coupling with a lattice vibration. Such coupling has been observed for ν_5 in the spectrum of cesium fluorosulfate (7).

Interaction of the fluorosulfate anion with strongly polarizing cations results in an increase in the S—F stretching frequency, ν_2 (6, 8, 9). The formation of bonds through the oxygen atoms withdraws charge from the sulfur atom and causes an increase in the strength of the S—F bond. This effect is particularly striking where hydrogen bonding occurs. The S—F stretching vibration is 23 cm^{-1} higher in liquid fluorosulfuric acid than in the vapor (10), and ν_2 for aqueous solutions of fluorosulfate is more than 50 cm^{-1} higher than in ionic solids (ν_2: in solid $CsSO_3F$, 715 cm^{-1}; in solution, 786 cm^{-1}). No comparable shift in frequency is observed for the symmetric and asymmetric stretching vibrations in perchlorate and tetrafluoroborate (5, 11). In the methyl cyanide complexes, ν_2 increases in the order Cu(I) < Cu(II) < Zn(II), suggesting increased cation–anion interaction in that order. Cu(II) and Zn(II) methyl cyanide complex cations show a similar effect on the perchlorate and tetrafluoroborate anions (2, 3), while nitrate anion is coordinated to these cations (1, 4). The Cu(I)-complex perchlorates and tetrafluoroborates are ionic, but the nitrate shows evidence of some interaction (5).

The i.r. spectra of the complex cations have been assigned by comparison with the spectrum of methyl cyanide. No coupling of the vibrations of the ligands with each other is apparent in the

Can. J. Chem. Downloaded from www.nrcresearchpress.com by 210.87.254.105 on 09/05/12
For personal use only.

TABLE 1

Infrared spectral data of methyl cyanide complexes of Cu(I), Cu(II), and Zn(II) fluorosulfates*

(*a*) Anion part

	Frequency, cm^{-1}			
C_{3v} assignment	SO_3F^-† (aqueous solution)	$Zn(CH_3CN)_4(SO_3F)_2$	$Cu(CH_3CN)_4(SO_3F)_2$	$Cu(CH_3CN)_4SO_3F$
ν_6 (*e*) SF deformation	409	394 m	415 m	—
ν_3 (*a*) SO_3 symmetric deformation	566	557 m	555 m	552 wsh
ν_5 (*e*) SO_3 asymmetric deformation	592	575 m	585 s	570 s
		588 m	593 m	
		600 m		
ν_2 (*a*) SF stretch	786	778 s	725 vs	719 s
ν_1 (*a*) SO_3 asymmetric stretch	1082	1080 s	1070 s	1068 s
ν_4 (*e*) SO_3 symmetric stretch	1287	1240 vsb	1255 vsb	1280 sb
		1315 vsb	1302 vsb	

(*b*) Cation part

	Frequency, cm^{-1}			
C_{3v} assignment	CH_3CN‡	$Zn(CH_3CN)_4(SO_3F)_2$	$Cu(CH_3CN)_4(SO_3F)_2$	$Cu(CH_3CN)_4SO_3F$
ν_8 (*e*) CCN deformation	375 s	440 vwb	446 w	386 w
$2\times\nu_8$ (A_1)	750 m	865 vw	896 w	770 wsh
ν_4 (a_1) CC stretch	918 s	941 m	956 m	930 m
ν_7 (*e*) CH_3 rocking	1047 vs	1033 m	1040 m	1035 m
ν_3 (a_1) CH_3 symmetric deformation	1376 s	1366 w	1370 w	1360 w
ν_6 (*e*) CH_3 asymmetric deformation	1443 s	1400 wsh	1415 wb	1405 w
ν_2 (a_1) CN stretch	2251 vs	2286 m	2335 m	2263 m
$\nu_3+\nu_4$ (A_1)	2289 s	2305 w	2308 w	2295 w
ν_1 (a_1) CH_3 symmetric stretch	2944 s	2928 w	2945 w	2940 m
ν_5 (*e*) CH_3 asymmetric stretch	3002 s	2990 w	3007 w	3000 w

(*c*) Lattice and metal–ligand vibrations

Frequency, cm^{-1}		
$Zn(CH_3CN)_4(SO_3F)_2$	$Cu(CH_3CN)_4(SO_3F)_2$	$Cu(CH_3CN)_4SO_3F$
265 wb	215 mb	260 wb
	230 mb	
	325 mb	

*m = medium, s = strong, w = weak, b = broad, v = very, sh = shoulder.
†Reference 10.
‡Reference 5.

Can. J. Chem. Downloaded from www.nrcresearchpress.com by 210.87.254.105 on 09/05/12
For personal use only.

spectra. Where comparison can be made, the spectra are the same as those of the perchlorates and tetrafluoroborates. The CN stretching frequency lies 12 to 84 cm^{-1} higher in the complexes than in methyl cyanide itself. This increase in the frequency of ν_{CN} upon coordination has been the subject of considerable discussion (12, 13). Unlike other ligands where electron donation to an electron deficient center causes a weakening of the adjacent bond in the ligand, there is an increase in the CN bond strength upon coordination. A similar effect is observed when hydrogen cyanide and the halogen cyanides coordinate to antimony pentachloride (14).

In the spectrum of pure methyl cyanide and its complexes a second weaker absorption is observed 20–40 cm^{-1} higher than ν_{CN}. Venkateswarlu assigned this peak to the combination of the carbon–carbon stretching vibration, ν_4, and the symmetric CH_3 deformation, ν_3 (15). Since the combination is of the same symmetry type as ν_{CN}, it can steal intensity from this fundamental, thus accounting for the strength of this combination. For the same reason, Fermi resonance can take place between ν_2 and $\nu_3 + \nu_4$ if the 2 absorptions come close enough together. In this case the 2 absorptions will interact and the peaks will be shifted away from each other and their expected positions. In the spectra of the Zn(II) and Cu(II) complexes, the higher peak of the two is weaker and agrees well with the calculated position of $\nu_3 + \nu_4$. However, in the spectrum of the Cu(II) complex the weaker peak lies lower and is shifted some 18 cm^{-1} to lower frequency than that calculated from the fundamentals. In addition, the stronger peak lies some 80 cm^{-1} higher than ν_{CN} in methyl cyanide, which is exceptional compared to the other 2 complexes. The assignment of the 2 peaks which allows for Fermi resonance accounts for the observations very well.

Electrical Conductivity

The results of conductivity measurements in methyl cyanide are plotted as molar conductivity, Λ, vs. $C^{1/2}$ in Fig. 1. The conductivity of tetraethyl ammonium fluorosulfate is given for comparison. All of the plots are curved, but the slight curvature and high values for the 1:1 electrolytes suggest that a Kohlrausch extrapolation would give a fair approximation to Λ^0. For the 1:1 electrolytes, the conductivities are approximately the same as those of the perchlorates and tetrafluoroborates (2, 5). The anions have apparently similar mobilities in methyl cyanide. The 2:1 electrolyte fluorosulfates, unlike the perchlorates and tetrafluoroborates, have molar conductivities much lower than those of the 1:1 electrolytes in the concentration range studied. Inasmuch as the molar conductivity of a 2:1 electrolyte, capable of producing a dipositive cation and 2 fluorosulfate anions, is less than that of a 1:1 electrolyte, producing a unipositive cation and 1 fluorosulfate anion, the 2:1 complexes are strongly associated by comparison. This is not surprising when it is considered that triple ion formation probably becomes important in methyl cyanide at $C \sim 0.015$ ($C^{1/2} \sim 0.12$) (16) and such triple ions consist of a combination of a simple dipole and an ion, while in the present case a charged dipole and an anion are involved. The low conductivity of the 2:1 electrolyte fluorosulfates compared to the perchlorates and tetrafluoroborates must be due to the dipolar

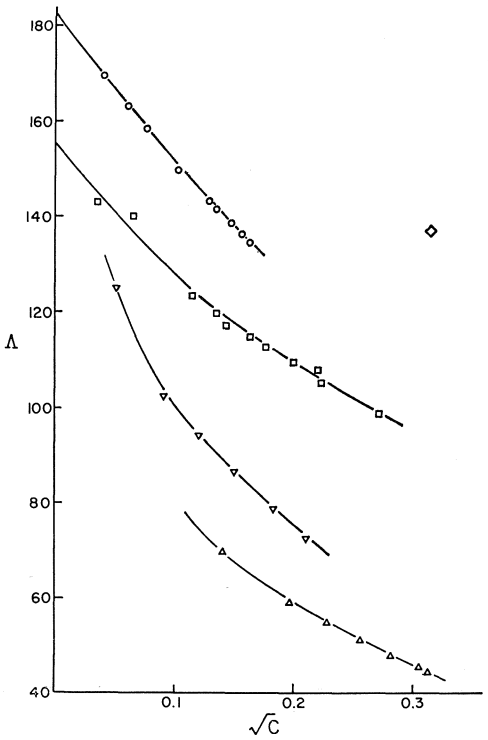

FIG. 1. Conductivity in methyl cyanide: ○, Et_4NSO_3F; □, $Cu(CH_3CN)_4SO_3F$; ▽, $Cu(CH_3CN)_4(SO_3F)_2$; △, $Zn(CH_3CN)_4(SO_3F)_2$; ◇, $Cu(CH_3CN)_4(BF_4)_2$ (3).

Can. J. Chem. Downloaded from www.nrcresearchpress.com by 210.87.254.105 on 09/05/12
For personal use only.

nature of the fluorosulfate anion which would favor pair formation. The lower molar conductivity of the Zn(II) complex compared to the Cu(II) complex probably results from 2 factors. First, Λ^0 for the Zn(II) complex cation may be lower than that of the Cu(II) case, as it is in water. This probably reflects the greater effective size of the solvation shell around the zinc cation as a result of the greater polarizing power of Zn^{2+} compared to Cu^{2+}. Second, ion pair formation is probably more extensive for the zinc complex for reason of greater polarizing power also.

Both the infrared spectra and conductivity give the same order of cation–anion interaction; Zn(II) > Cu(II) > Cu(I). Inasmuch as methyl cyanide is a stronger donor than the fluorosulfate anion, the ion pair formation in solution and the perturbation of the C_{3v} symmetry of the anion probably do not arise from direct metal–anion bonding but arise from interactions via hydrogen bonds. (In the solid cupric complex there is, however, the possibility of direct bonding as in the case of the ethylene diamine complex of cupric perchlorate (17) and tetrafluoroborate (18). Such direct bonding has been termed "semi-coordination".) The more acidic nature of the ligand protons in the Zn(II) cation, arising from greater polarization by Zn^{2+}, would give rise to strong hydrogen bonds which would account for the above order of cation–anion interaction.

Other Properties

The *d*-spacings for the X-ray powder photographs of the complexes are given in the Experimental section. Comparison of the photos of the Zn(II) and Cu(II) complexes with those of the corresponding tetrafluoroborates (3) shows that they are not iso-structural.

The ultraviolet (u.v.) and visible spectrum of the Cu(II) complex dissolved in methyl cyanide consists of a very strong absorption below 375 mμ and a broad peak at 758 mμ. The strong absorption at shorter wavelengths is probably due to the anion and the peak at 758 mμ is characteristic of Cu^{2+}. The λ_{max} and ε_{max} for several Cu(II) methyl cyanide complexes are given in Table 2. Both the position and the extinction coefficient of the Cu^{2+} absorption are similar to those of the corresponding perchlorate and tetrafluoroborate and different from that of the nitrate where there is covalent bonding. In the case of the fluorosulfate, the coordination of the cupric cation is apparently not affected by ion pair formation, suggesting that such pairing is electrostatic in nature in solution.

TABLE 2

λ_{max} and ε_{max} for some Cu(II) compounds in methyl cyanide

Compound	λ_{max} (mμ)	ε_{max}
$Cu(NO_3)_2$	850	47.0
$Cu(ClO_4)_2$	750	22.4
$Cu(BF_4)_2$	750	21.8
$Cu(SO_3F)_2$	758	19.8

Experimental

The Cu(II) and Zn(II) complexes were prepared by crystallization from a mixture of the anhydrous fluorosulfate (6) and methyl cyanide. For the Cu(I) complex, excess copper metal powder was added to a solution of cupric fluorosulfate. The copper metal was removed and the colorless solution evaporated to dryness. The tetraethyl ammonium fluorosulfate was prepared from a solution of the hydroxide and fluorosulfuric acid. The product was recrystallized from ethanol. Analysis of the 4 compounds appears in Table 3. All of the compounds had to be protected from moisture and all manipulations were carried out in a dry atmosphere. No hydrolysis of the complexes was evident as judged by the absence of any OH stretching vibrations in the infrared spectrum. Methyl cyanide was purified by refluxing over P_2O_5 followed by distillation.

The infrared spectra were taken in Nujol and Kel-F oil mulls with polyethylene, CsBr, KBr, and NaCl windows. Beckman 10 and 11 spectrometers were used.

X-Ray powder photographs were taken in Lindemann Tubes with Ni-filtered Cu K_α irradiation.

$Cu(NCCH_3)_4(SO_3F)_2$: 8.838(35), 8.036(65), 7.019(30), 6.366(20), 6.021(30), 5.535(65), 5.211(100), 4.844(10), 4.667(5), 4.149(45), 4.019(45), 3.798(80), 3.645(5), 3.545(80), 3.424(20), 3.336(45), 3.066(5), 2.794(5), 2.680(10), 2.635(5), 2.569(5).

$Cu(NCCH_3)_4SO_3F$: 7.929(5), 7.400(5), 6.411(5), 6.000(40), 5.417(5), 4.908(80), 4.227(30), 4.082(30), 3.864(10), 3.690(10), 3.587(5), 3.477(100), 3.235(5), 3.173(5), 3.000(10), 2.700(20), 2.540(20), 2.450(20), 2.199(20), 2.118(5), 2.056(5), 2.006(10), 1.812(10), 1.738(5).

$Zn(NCCH_3)_4(SO_3F)_2$: 9.063(10), 8.185(100), 7.431(10), 6.857(40), 6.276(5), 5.941(20), 5.690(80), 5.368(80), 4.207(10), 3.847(80), 3.645(80), 3.5517(50), 3.457(40), 3.324(65), 3.241(65), 3.085(20), 2.976(20), 2.919(50), 2.838(80), 2.769(30), 2.657(30), 2.590(5), 2.493(30), 2.366(40), 2.319(20), 2.247(40), 2.194(20), 2.120(30), 2.056(30), 2.039(5), 1.963(20), 1.922(50), 1.826(30), 1.796(40), 1.773(5), 1.754(5), 1.729(5), 1.685(20), 1.670(5), 1.617(40), 1.576(20), 1.541(20), 1.538(10), 1.524(5), 1.466(5), 1.422(5).

The u.v. and visible spectra were taken on a Beckman Model DK-2 spectrophotometer.

TABLE 3

Analysis of Cu(I), Cu(II), and Zn(II) complexes

Compound	% S		% metal	
	Found	Calcd.	Found	Calcd.
$Cu(CH_3CN)_4(SO_3F)_2$*	15.14	15.05	14.72	14.93
$Cu(CH_3CN)_4SO_3F$	—	—	19.71	19.46
$Zn(CH_3CN)_4(SO_3F)_2$	14.55	15.00	15.63	15.29
$(CH_3CH_2)_4NSO_3F$†	13.98	14.00	—	—

*% F: Found, 8.46; Calcd., 8.98.
†% C: Found, 41.59; Calcd., 41.90. % H: Found, 8.55; Calcd., 8.79.

1. C. C. ADDISSON, B. J. HATHAWAY, N. LOGAN, and A. WALKER. J. Chem. Soc. 4308 (1960).
2. B. J. HATHAWAY and A. E. UNDERHILL. J. Chem. Soc. 3705 (1960).
3. B. J. HATHAWAY, D. G. HOLAH, and A. E. UNDERHILL. J. Chem. Soc. 2444 (1962).
4. C. C. ADDISSON, D. W. AMOS, and D. SUTTON. J. Chem. Soc. 2285 (1968).
5. B. J. HATHAWAY, D. G. HOLAH, and J. D. POSTELTHWAITE. J. Chem. Soc. 3215 (1961).
6. J. GOUBEAU and J. B. MILNE. Can. J. Chem. **45**, 2321 (1967).
7. G. KAUFMANN, M. LEROY, J. B. MILNE, and A. RUOFF. Z. Anorg. Allg. Chem. In press.
8. D. W. A. SHARP. J. Chem. Soc. 3761 (1957).
9. D. A. EDWARDS, M. J. STIFF, and A. A. WOOLF. Inorg. Nucl. Chem. Lett. **3**, 427 (1967).
10. S. M. CHACKALACKAL and F. E. STAFFORD. J. Amer. Chem. Soc. **88**, 4815 (1966).
11. H. SIEBERT. Anwendungen der Schwingungsspektroskopie in der anorganischen Chemie. Springer-Verlag, New York. 1966.
12. R. A. WALTON. Quart. Rev. London, **19**, 126 (1965).
13. K. F. PURCELL and R. S. DRAGO. J. Amer. Chem. Soc. **88**, 919 (1966).
14. E. ALLENSTEIN and A. SCHMIDT. Chem. Ber. **97**, 1286 (1964); **97**, 1863 (1964).
15. P. VENKATESWARLU. J. Chem. Phys. **19**, 293 (1951).
16. R. M. FUOSS and F. ACCASCINA. Electrolytic conductance. Interscience Publishers, Inc., New York. 1959. p. 253.
17. A. PAJUNEN. Suom. Kem. **40B**, 32 (1967).
18. D. S. BROWN, J. D. LEE, B. G. A. MELSOM, B. J. HATHAWAY, I. M. PROCTER, and A. A. G. TOMLINSON. Chem. Commun. 369 (1967).

Can. J. Chem. Downloaded from www.nrcresearchpress.com by 210.87.254.105 on 09/05/12
For personal use only.

Can. J. Chem. Downloaded from www.nrcresearchpress.com by 210.87.254.40 on 09/05/12
For personal use only.

Rearrangement of the Diels–Alder adduct of azodibenzoyl and cyclopentadiene

DONALD MACKAY, J. A. CAMPBELL, AND C. P. R. JENNISON[1]
Department of Chemistry, University of Waterloo, Waterloo, Ontario

Received June 20, 1969

The product of the thermal isomerization of the Diels–Alder adduct **1** of azodibenzoyl and cyclopentadiene has been identified by degradation and nuclear magnetic resonance analysis as the *cis*-bicyclic oxadiazine **2***a*, the dihydro derivative of which has been synthesized. The isomerization is quantitative and is first order throughout in solution in a range of solvents; kinetic and other evidence point to it being a sigmatropic rearrangement.

Canadian Journal of Chemistry, **48**, 81 (1970)

In earlier work by one of us and co-workers (1) it was found that the Diels–Alder adduct **1** of azodibenzoyl and cyclopentadiene was labile, isomerizing irreversibly on heating either near its melting point (m.p.) or in solution to a substance $C_{19}H_{16}O_2N_2$, m.p. 130–131.5°. The latter had a carbon–carbon double bond (dibromide, m.p. 144.5–147°) and its infrared (i.r.) spectrum had absorptions at 1652 and 1630 cm^{-1} in the carbonyl region, but no NH absorption, while its 60 Mc.p.s. nuclear magnetic resonance (n.m.r.) spectrum showed two non-equivalent phenyl groups and two vinyl, two tertiary, and two methylene hydrogens, each pair being non-equivalent. This stable isomer, like **1**, was thus evidently a bicyclic compound.

Carpino and Rundberg (2) have recently concluded that this isomer is **2***a* or **2***b*, tentatively the former, by reducing it to **3**, the structure of which was inferred by Raney nickel cleavage to *cis*-2-benzoylaminocyclopentanol. We wish to show that the stable isomer is indeed **2***a*, to describe the rational synthesis of **3**, and to present evidence regarding the mechanism of the rearrangement.

Catalytic reduction of the stable isomer with Pd–H_2 in benzene or by catalytic hydrogen transfer with Pd in refluxing cyclohexene (3) gave a mixture of mainly a dihydro-derivative, m.p. 143–143.5°, and small amounts (5–10%) of a tetrahydro-derivative, m.p. 197–198°. The latter had amide NH and CO absorption in the i.r. and was shown to be 1,2-dibenzoyl-1-cyclopentylhydrazine (**4**), synthesized by reduction of cyclopentanone benzoylhydrazone with sodium borohydride followed by benzoylation of the resulting hydrazine. The formation of **4** showed that the integrity of the original azodibenzoyl skeleton and of the C-5 ring had been preserved in the isomerization, and that the stable isomer contained at least one C—N bond at a ring junction.

The dihydro-derivative, which could be more conveniently made, in nearly quantitative yield, by reaction with di-imide (hydrazine-oxygen in methanol or *p*-toluenesulfonylhydrazine in refluxing dioxane), arose from reduction of the carbon–carbon double bond (2); its n.m.r.

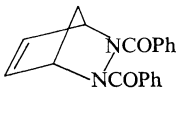

1

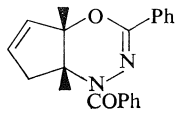

2*a*

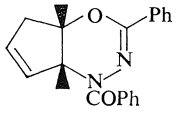

2*b*

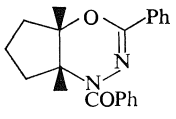

3

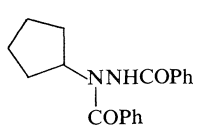

4

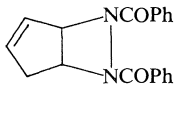

5

[1]Present address: Department of Chemistry, Ryerson Institute of Technology, Toronto, Ontario.

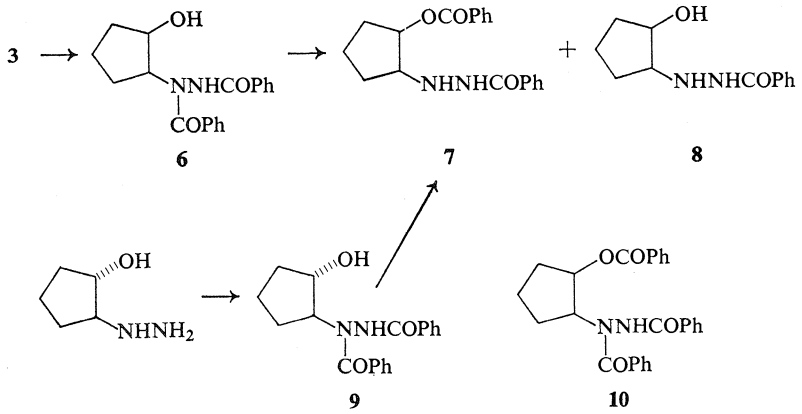

SCHEME 1

spectrum showed the phenyl groups and the tertiary hydrogens to be still non-equivalent. This ruled out the diazetidine **5** as a possible structure for the stable isomer and implied, therefore, a C—O link at the other ring junction which must have been the site of hydrogenolysis to **4**. The most plausible structures for the isomer and its dihydro-derivative were thus the bicyclic oxadiazines **2** and **3** or their epimers.

Confirmation of the structure and stereochemistry of **3** was obtained by hydrolyzing it with 0.8 *N* aqueous ethanolic hydrochloric acid (Scheme 1). Work-up gave the bases **7**, m.p. 88.5–89° (isolated directly as its hydrochloride in 37% yield), and **8**, m.p. 128–129° (11%), together with benzoic acid. The product expected from **3** was the *cis*-alcohol **6**, by analogy with the behavior of monocyclic 2-aryl-1,3,4-oxadiazines on hydrolysis (4). A control experiment, however, showed that **6** was efficiently converted into **7** under the conditions of the experiment, and its presence during the hydrolysis was indeed proven by thin-layer chromatography (t.l.c.).

The alternative *trans*-stereochemistry for **3** can be excluded since the hydrolysis would have given the *trans*-alcohol **9**; however, no **9** was detected, though it was independently shown to be stable to these conditions.

The synthesis of the hydrazine derivatives **6**–**10** was achieved as shown in Scheme 1. Cyclopentene oxide was cleaved with hydrazine to *trans*-2-hydrazinocyclopentanol, a dilute alkaline solution of which was shaken with two equivalents of benzoyl chloride, causing benzoylation at the nitrogens only to give the *trans*-*N*,*N*′-dibenzoyl alcohol **9**, m.p. 177.5–178°, in a good yield. Brief treatment of **9** with cold concentrated sulfuric acid, followed by neutralization, caused quantitative isomerization with inversion to the basic ester **7**, which was then hydrolyzed to **8** (80%) by 2 *N* aqueous methanolic sodium hydroxide. Benzoylation of **8** with an excess of benzoyl chloride in cold dilute alkali again occurred only at the nitrogen to give the *cis*-alcohol **6**, m.p. 170.5–171.5° in an excellent yield. The isomerization **9**→**7** is paralleled in cyclohexane chemistry (4).

The identity of the stereochemistries in **6**, **7**, and **8** followed from the fact that when treated with benzoyl chloride in pyridine they all gave the same tribenzoyl derivative **10**, m.p. 177.5–178.5°, which must have been *cis*, since it was different from the product, m.p. 139–140°, of benzoylation of the *trans*-compound **9**. Hydrolysis of **10** with alkali was hard to control to the dibenzoyl stage **6**, but proceeded smoothly, if allowed, to the monobenzoyl compound **8** in 90% yield; **8** could also be obtained from **7** under the conditions of hydrolysis of **3**, which probably accounted for its formation in that reaction.

The acid catalyzed intramolecular esterifications, under different conditions, of both epimeric alcohols **6** and **9** to the same benzoate **7** are part of a series of acyl transfer reactions of *cis*- and *trans*-2-hydrazinocyclopentanol derivatives presently being investigated.

In contrast to the degradation of the heterocyclic ring observed when **3** was heated with aqueous acid, reaction of **3** with hot concentrated sulfuric acid occurred only at the benzoyl substit-

Can. J. Chem. Downloaded from www.nrcresearchpress.com by 210.87.254.40 on 09/05/12
For personal use only.

uent, which was quantitatively removed to give, on neutralization, the oxadiazine **11** (Scheme 2), an oily base [λ_{max}(EtOH) 282 mμ; hydrochloride, m.p. 171–174° (decomposition)], from which **3** could be regenerated (>90%) by treating it with benzoyl chloride in pyridine.

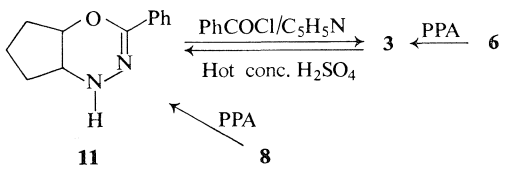

SCHEME 2

Conditions for the cyclodehydration of 2-acyl-1-(2-hydroxyalkyl)hydrazines to 1,3,4-oxadiazines have been worked out in some detail by Trepanier *et al.* (5–9). Application of these to the *cis*-alcohol **6** gave the best results with polyphosphoric acid (PPA) at 60° for 24 h; gas–liquid chromatography (g.l.c.) indicated a modest yield of **3** (40–60%), which was separated from acidic and basic products, and then gave a single peak in the gas–liquid chromatogram. The stereochemical purity was high since two crystallizations gave **3** of satisfactory m.p. Similarly PPA, or alternatively concentrated sulfuric acid, converted the monobenzoyl compound **8** into the base **11**.

The ring closures to **3** and to **11** constitute a rational proof of the structure of **3** though not of its stereochemistry, since inversion of configuration may accompany cyclization (7, 8). However, in the only recorded examples of oxadiazine formation from cyclic hydroxy-hydrazides, both *cis*- and *trans*-1,2-dibenzoyl-1-(2-hydroxycyclohexyl)hydrazines cyclized with retention of configuration (4). Attempts were made to cyclize the *trans*-alcohol **9** to the *trans*-isomer of **3**, or, if inversion occurred to **3** itself, using a variety of reagents; with acids (H_2SO_4, P_2O_5) the rearrangement to **7**, already noted, was observed, and with bases (NaOEt, KO*t*-Bu) the starting material was recovered.

The position of the carbon–carbon double bond in **2** could be inferred from the fact that while **2** could be converted into **4**, **3** could not, being indefinitely stable to the hydrogenation conditions. Thus in the path from **2** to **4**, hydrogenolysis must have preceded hydrogenation, suggesting the presence of an allylic oxygen, i.e. that the stable isomer was **2***a*.

A rigid proof was provided by the 60 Mc.p.s. n.m.r. analysis of the tertiary hydrogens in the base **11** and its dideuterio analogue. In **11** these were found centered at 5.5 and 6.8 τ (CCl_4), both essentially quartets, and must have been adjacent to oxygen and to basic nitrogen respectively since protonation by trifluoroacetic acid made the high-field absorption more complex (due to splitting by the extra proton on the adjacent nitrogen) and moved it down by 0.9 p.p.m., while it moved the other absorption correspondingly less (0.6 p.p.m.) (10). When **2** was reduced by *p*-toluenesulfonylhydrazine-d_3 in refluxing dioxane and the product was de-benzoylated with concentrated sulfuric acid to the base, only the absorption for the tertiary hydrogen next to the oxygen was affected, being simplified to a triplet. This located a deuterium in the methylene nearest the oxygen and so the stable isomer is (±)-*cis*-4-benzoyl-4,4*a*,5,7*a*-tetrahydro-2-phenylcyclopenta-1,3,4-oxadiazine (**2***a*).

The adduct **1** in the solid phase was stable for at least 15 h at 80°, but was completely isomerized in 10 h at 120°, and, in the molten state, in 10 min at 140°, the i.r. spectrum of the product being superimposable on that of purified **2***a*. The most striking demonstration of the completeness of the rearrangement was provided by the mass spectra of **1** and **2***a*, which were identical in every detail when run under the same conditions at an inlet temperature of 205°.

On heating in solution the rearrangement was again quantitative and could be conveniently followed by ultraviolet (u.v.) spectrometric analysis which showed first order kinetics throughout and one or more isosbestic points in a variety of solvents (Table 1). The log plot of the rate constants in 71% aqueous ethanol at various temperatures between 65° and 80° against $1/T$ gave a good straight line fit from which an energy of activation of 23.2 kcal mole^{-1} and an entropy of activation of about −9 e.u. (350 °K) were obtained (11). These values and the rather small solvent effect (12), together with the failure of added dienophiles to divert the reaction path (thus when **1** was refluxed with a 5-fold excess of maleic anhydride in iso-octane **2***a* was obtained quantitatively) strongly point to a concerted cyclic mechanism which can formally be interpreted as a [3,3]-sigmatropic shift **12**→**2***a*.

The rearrangement of the heterocycle **1** thus provides an exact parallel to the recently reported

Can. J. Chem. Downloaded from www.nrcresearchpress.com by 210.87.254.40 on 09/05/12
For personal use only.

TABLE 1

First order rate constants for the thermal isomerization of **1**

Solvent	Temperature (°C)	Isobestic points (mμ)	$k \times 10^4$ (s^{-1})
iso-Octane	77.5	231,253,335	1.82
Dioxane	77.0	232,258	1.96
Acetonitrile	77.0	230,259	0.60
29% Aqueous ethanol	77.5	228,259	4.50
48% Aqueous ethanol	77.5	228,258	3.67
71% Aqueous ethanol	77.5	227,258	2.54
	75.2	—	2.04
	73.5	—	1.77
	69.3	—	1.15

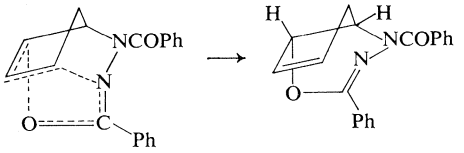

12 **2a**

(13) rearrangement of the carbocyclic Diels–Alder adducts of fulvenes and *cis*-hex-3-ene-2,5-dione.

A detailed study is now being made using a range of Diels–Alder adducts with structural variation both in the diene and in the azo components. A complete understanding of the mechanism must accommodate our observations to this point that **13** is stable indefinitely on heating, while **14** rearranges more slowly than **1** to give **15** only, and **16** rearranges rather faster than **1** to give both **17** and **18**. Steric factors may also play a role since the adduct **19** is extremely labile, having a transient existence at room temperature, detectable by n.m.r. analysis, when 1,4-dimethyl-2,3-diphenylcyclopentadiene (14) and azodibenzoyl are allowed to react: the product isolated is an oxadiazine, presumably **20**, whose structure has yet to be confirmed.

Experimental

Infrared spectra were taken on a Beckman IR9 or IR10 spectrophotometer. A Bausch and Lomb Spectronic 505 or a Coleman EPS-3T Hitachi spectrophotometer were used for measuring u.v. spectra. The n.m.r. analyses were done on a JEOL C60 or a Varian HA 100 spectrometer and absorptions are quoted in τ values against tetramethylsilane as standard; all values are from 60 Mc.p.s. spectra unless otherwise stated. The mass spectra were taken on a CEC 110 spectrometer.[2]

[2]We thank from this department, Dr. A. J. Carty for obtaining the 100 Mc.p.s. n.m.r. spectra and Dr. F. W. Karasek for obtaining the mass spectra.

Anhydrous magnesium sulfate was used as drying agent for solutions in organic solvents. Melting points are uncorrected.

1,2-Dibenzoyl-1-cyclopentylhydrazine(4)

Benzoylhydrazine and cyclopentanone (0.2 mole each) were refluxed in 70% aqueous acetic acid (100 ml) for ½ h and the solution was concentrated. The hydrazone separated out on cooling and was recrystallized from aqueous ethanol, m.p. 144–145°.

Cyclopentanone benzoylhydrazone (10 g, 50 mmole) and sodium borohydride (5 g, 130 mmole) were allowed to react in ethanol solution (100 ml) at room temperature for 3 days. The solvent was removed, the residue was decomposed with very dilute acetic acid, and the product was crystallized from aqueous ethanol giving an excellent yield of 2-benzoyl-1-cyclopentylhydrazine as needles, m.p. 101–101.5°.

The hydrazine (0.5 g, 2.5 mmole) was refluxed for 16 h with benzoyl chloride (0.35 ml, 3.0 mmole) in pyridine (5 ml). The addition of water precipitated a solid which after two crystallizations from benzene–petroleum ether (b.p. 60–80°) afforded **4** as fine needles, m.p. 197–198°; ν(Fluorolube) 3230 (NH), 1685, 1630 cm^{-1} (*sec, tert*-amide C=O); τ($CDCl_3$) 1.5(NH), 2.3–2.9(10 phenyl H), 5.4(*tert* H), 7.9–8.8 p.p.m. (8 methylene H).

Anal. Calcd. for $C_{19}H_{20}N_2O_2$: C, 74.00; H, 6.54; N, 9.09. Found: C, 74.42; H, 6.54; N, 9.08.

trans-2-Hydrazinocyclopentanol

Cyclopentene oxide (15) (80 g, 0.95 mole) was heated at 100° with an excess of 95% hydrazine for 20 h. Water and unreacted hydrazine were then removed at reduced pressure and the oily residue was distilled giving the hydroxyhydrazine as a colorless, viscous, hygroscopic liquid (96%), b.p. 105°/0.4 mm; τ($CDCl_3$) 5.7 sharp (OH, 3NH), 5.9(OC—H), 7.0(NC—H, $J_{1,2}$ = 3.5 c.p.s., determined by spin decoupling), 7.7–9.0 p.p.m. (6 methylene H).

Anal. Calcd. for $C_5H_{12}N_2O$: C, 51.69; H, 10.41. Found: C, 52.49; H, 10.68.

trans-1,2-Dibenzoyl-1-(2-hydroxycyclopentyl)-hydrazine (9)

A solution of benzoyl chloride (230 ml, 2.0 mole) in benzene (1.7 l) was added portionwise and with vigorous shaking to a solution of *trans*-2-hydrazinocyclopentanol (111 g, 0.96 mole) in 2 *N* sodium hydroxide (2.5 l). The

Can. J. Chem. Downloaded from www.nrcresearchpress.com by 210.87.254.40 on 09/05/12
For personal use only.

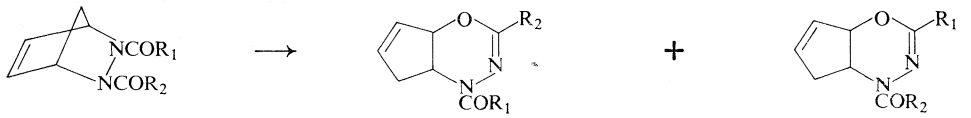

13 $R_1 = R_2 = OEt$
14 $R_1 = OEt$; $R_2 = Ph$
16 $R_1 = Ph$; $R_2 = p\text{-}BrC_6H_4$

15 $R_1 = OEt$; $R_2 = Ph$
17 $R_1 = Ph$; $R_2 = p\text{-}BrC_6H_4$

18 $R_1 = Ph$; $R_2 = p\text{-}BrC_6H_4$

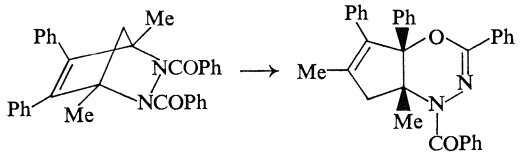

19 **20**

mixture was then stirred for 3 h and filtered to remove the product. The benzene layer was evaporated and the residue was combined with the filtered material. The whole was washed thoroughly with water and recrystallized from aqueous methanol to give **9** (80%) as prisms, m.p. 173–174°, raised to 177.5–178° on further recrystallization; ν($CHCl_3$) 3600–3200 (H-bonded OH, NH), 1685, 1655 cm^{-1} (*sec*, *tert*-amide C=O); τ($CDCl_3$) 1.2 (NH), 2.2–2.8 (10 phenyl H), 5.4–6.2 (2 *tert* H),[3] 6.4 (OH), 7.9–8.6 p.p.m. (6 methylene H).

Anal. Calcd. for $C_{19}H_{20}N_2O_3$: C, 70.35; H, 6.22; N, 8.64. Found: C, 70.40; H, 6.26; N, 8.71.

The *benzoate* was obtained as a gum, which slowly crystallized, by treating **9** (0.50 g, 1.5 mmole) in pyridine (5 ml) with benzoyl chloride (0.5 ml, 4 mmole) for 2 days at 5°, and then pouring the reaction mixture on ice. The solid (93%) was recrystallized from benzene–petroleum ether (b.p. 60–80°) as fine prisms, m.p. 139–140°; ν(CCl_4) 3365 (NH), 1702, 1672 cm^{-1} (ester, amide C=O); τ($CDCl_3$) 0.8 (NH), 1.8–3.0 (15 phenyl H), 4.6, 5.1 (2 *tert* H), 7.4–8.5 p.p.m. (6 methylene H).

Anal. Calcd. for $C_{26}H_{24}N_2O_4$: C, 72.88; H, 5.65; N, 6.54. Found: C, 73.15; H, 5.83; N, 6.71.

Compound **9** was unaffected when refluxed for 16 h with sodium ethoxide in ethanol or with potassium *t*-butoxide in *t*-butanol or benzene: the recovery was quantitative.

It was also stable when refluxed (0.50 g) for 17 h in a mixture of ethanol (7 ml), water (3 ml), and 12 *N* hydrochloric acid (0.6 ml), the conditions for hydrolysis of the oxadiazine **3**. Addition of an excess of potassium hydrogen carbonate, evaporation to dryness, and several extractions with ether led to a recovery of **9** (80%) in a pure state.

Anhydrous acidic conditions however, caused isomerization (see below).

Isomerization of ***9*** *to cis-2-Benzoyl-1-(2-benzoyloxycyclopentyl)hydrazine (****7****)*

Finely powdered **9** (1.00 g, 3.1 mmole) was dissolved in concentrated sulfuric acid (5 ml) at room temperature and after 5 min the solution was poured into an excess of ice-cold aqueous ammonia. The liberated oil readily crystallized and was extracted with methylene chloride; the extracts were dried and evaporated to give a quantitative yield of **7** which was twice crystallized from aqueous ethanol as prisms, m.p. 88.5–89°; ν(CCl_4) 3400, 3300 (NH), 1707, 1661 cm^{-1} (ester, amide C=O); τ(CCl_4) 1.5 (amide NH), 2.0–2.9 (10 phenyl H), 4.7 (C_2—H), 5.1 (amine NH), 6.7 (C_1—H), 7.8–8.7 p.p.m. (6 methylene H).

Anal. Calcd. for $C_{19}H_{20}N_2O_3$: C, 70.35; H, 6.22; N, 8.64. Found: C, 70.23; H, 6.24; N, 8.69.

The *hydrochloride* separated out in methanolic hydrochloric acid, and was recrystallized from the same solvent medium; it had m.p. 162–164°, with previous decomposition and loss of water.

Anal. Calcd. for $C_{19}H_{21}ClN_2O_3$: C, 63.24; H, 5.87; Cl, 9.83; N, 7.76. Found: C, 63.71; H, 5.99; Cl, 9.91; N, 7.83.

The *cis*-ester **7** could also be obtained by isomerization of **9** at room temperature either with thionyl chloride (5 h) or phosphoric oxide in methylene chloride (12 h). In each case the work-up entailed addition to aqueous alkali and extraction with methylene chloride.

*cis-2-Benzoyl-1-(2-hydroxycyclopentyl)hydrazine (****8****)*

A solution of the ester **7** (0.50 g, 1.55 mmole) in 2 *N* 50% aqueous methanolic sodium hydroxide (15 ml) was refluxed for ½ h and evaporated. Addition of an excess of dilute aqueous acetic acid and then of sodium hydrogen carbonate, followed by extraction with methylene chloride, gave the alcohol **8** (82%), the i.r. spectrum of which was identical with that of material recrystallized from aqueous methanol, m.p. 128–129°; ν(CCl_4) 3435, 3305, 3360 (OH, NH), 1662 cm^{-1} (amide C=O); τ($CDCl_3$) 1.2 (amide NH), 1.7–2.7(5 phenyl H), 5.3 one peak (OH, amine NH), 5.9 (C_2—H), 6.8 (C_1—H), 7.9–8.8 p.p.m. (6 methylene H).

Anal. Calcd. for $C_{12}H_{16}N_2O_2$: C, 65.43; H, 7.32; N, 12.72. Found: C, 65.34; H, 7.46; N, 12.47.

*cis-1,2-Dibenzoyl-1-(2-hydroxycyclopentyl)hydrazine (****6****)*

The alcohol **8** (0.20 g, 0.91 mmole) was dissolved with warming in 2 *N* sodium hydroxide (10 ml), ice was added followed by benzoyl chloride (0.21 ml, 1.82 mmole), and

[3]The tertiary hydrogens in all the *cis*- and *trans*-hydroxycyclopentylhydrazine derivatives studied, whether overlapping or distinguishable, showed little fine structure. The quoted τ values are the centers of the absorptions.

Can. J. Chem. Downloaded from www.nrcresearchpress.com by 210.87.254.40 on 09/05/12
For personal use only.

Can. J. Chem. Downloaded from www.nrcresearchpress.com by 210.87.254.40 on 09/05/12
For personal use only.

the whole was shaken vigorously until odorless. A small amount of precipitate was filtered off and the solution was treated in turn with an excess of dilute aqueous acetic acid and sodium hydrogen carbonate which brought down the crystalline dibenzoyl-derivative. Isolation with methylene chloride gave material (83%) of high purity (i.r.), which was twice recrystallized from aqueous methanol and afforded **6** as small prisms, m.p. 170.5–171.5°; $\nu(CHCl_3)$ 3395 broad (OH, NH), 1688, 1655 cm^{-1} (*sec*, *tert*-amide C=O); $\tau(CD_3SOCD_3)$ 2.0–2.7 (10 phenyl H), 5.3 overlapping (NH and *tert* H), 5.6 (*tert* H), 6.7 (OH), 7.8–8.6 p.p.m. (6 methylene H).

Anal. Calcd. for $C_{19}H_{20}N_2O_2$: C, 70.35; H, 6.22; N, 8.64. Found: C, 70.41; H, 6.24; N, 8.62.

*cis-1,2-Dibenzoyl-1-(2-benzoyloxycyclopentyl)-hydrazine (**10**)*

The *cis*-ester **7** (0.324 g, 1 mmole) was set aside in pyridine (3 ml) with benzoyl chloride (0.17 ml, 1.5 mmole) for 12 h at 5°. The solution was evaporated to remove most of the pyridine and was then made slightly acidic with dilute hydrochloric acid. Extraction of the precipitate with methylene chloride, removal of the solvent, and trituration of the residue with methanol gave the tribenzoyl derivative **10** (94%) directly pure (i.r.), recrystallized from aqueous methanol as fine needles, m.p. 178–179°; $\nu(CCl_4)$ 3420, 3310 (free, bonded NH), 1730, 1704, 1680 cm^{-1} (ester, *sec*-amide, *tert*-amide C=O); $\tau(CDCl_3)$ 1.7–2.9 (15 phenyl H, NH), 4.3, 5.0 (2 *tert* H), 7.4–8.5 p.p.m. (6 methylene H).

Anal. Calcd. for $C_{26}H_{24}N_2O_4$: C, 72.88; H, 5.65; N, 6.54. Found: C, 72.94; H, 5.70; N, 6.60.

Similar treatment of the monobenzoyl derivative **8** or the dibenzoyl derivative **6** with the appropriate amount of benzoyl chloride also gave **10** in excellent yields.

*Alkaline Hydrolysis of **10***

Attempts to hydrolyze only the ester group in **10** met with little success, even when cold very dilute alkali was used; the reaction usually proceeded further to give mixtures of **6** and **8**. Hydrolysis to **8** could be achieved in a high yield using hot alkali.

A solution of the ester **10** (1.00 g, 2.3 mmole) in 2 *N* 50% aqueous methanolic sodium hydroxide (30 ml) was refluxed for ½ h and then evaporated. The residue was dissolved in dilute aqueous acetic acid and an excess of sodium hydrogen carbonate was added to liberate the basic alcohol **8**, which was isolated with methylene chloride and obtained directly (90%) in a pure state.

*Labile Adduct **1***

A final crystallization of **1**(1) from aqueous acetone raised the m.p., which should be taken fairly rapidly, to 138–139°; $\nu(CCl_4)$ 1698, 1675 cm^{-1} (C=O doublet); λ_{max}(EtOH) 224 (ε 21 600), 255 mμ (ε 12 800); n.m.r. described previously (1); the mass spectrum was identical with that of **2***a*.

*Rearrangement to Stable Isomer **2a***

(a) Preparative Scale

A solution of **1** (3.0 g, 9.9 mmole) was refluxed in 80% aqueous methanol (50 ml) for 2 h and evaporated. The residue (quantitative) had an i.r. spectrum superimposable on that of purified **2***a*. Recrystallization from aqueous methanol gave prisms, m.p. 130–130.5°; $\nu(CCl_4)$ 1652 (C=O), 1635 cm^{-1} (C=N); λ_{max}(EtOH) 220 (ε 21 900), 290 mμ (ε 19 800); $\tau(CDCl_3$, 100 Mc.p.s.)[4] 2.1–2.9 (10 phenyl H), 3.71, 3.93 (C_7—H and C_6—H, AB quartet with further small splittings, $J_{6,7}$ = 7 c.p.s.), 5.05 (C_{4a}—H and C_{7a}—H overlapping, total width 33 c.p.s., $J_{4a,7a}$ at least 6 c.p.s.), 6.91, 7.64 p.p.m. (C-5 methylene H, AB quartet of doublets, further splittings, $J_{5A,5B}$ = 17.5, $J_{5A,4a} = J_{5B,4a}$ = 6 c.p.s.); mass spectrum 304(M^+, 30), 105 ($PhCO^+$, 100), 77 (Ph^+, 34).

(b) Direct Heating of Solid

The effect of temperature is qualitatively illustrated by the following: 80°, 15 h: no change; 120°, 5 h: mixture; 120°, 10 h: complete isomerization; 140° (melt), 10 min: complete isomerization.

(c) Kinetic Determinations

A Bausch and Lomb Spectronic 505 with a cell compartment heated by a constant temperature circulating pump was used. The spectra of dilute (ca. 5×10^{-5} *M*) solutions of **1** were run directly in 1 cm stoppered cells at suitable times (t) until there was no further change in absorbance (A_∞). Isosbestic points were observed throughout (Table 1). A plot of ln ($A_\infty - A_t$) against t gave a good straight line fit of slope $-k$, the first order rate constant; a Guggenheim first order plot (15) also gave the same value of k. The effect of temperature (T) on k was examined in 71% aqueous ethanol. Determinations were made at 6 temperatures between 65 and 80° and from the plot of log k against $1/T$ the energy of activation, ΔE^*, and entropy of activations, ΔS^*, were obtained as described by Foster *et al.* (11).

(d) Effect of Maleic Anhydride

The adduct **1** (100 mg, 0.33 mmole) and maleic anhydride (200 mg, 2.1 mmole) were refluxed together in a mixture of iso-octane (8 ml) and benzene (2 ml) for 1 day. The solvent was evaporated and the maleic anhydride allowed to sublime off at room temperature. The i.r. spectrum of the remaining crystalline material was that of analytically pure **2***a*.

*cis-4-Benzoyl-4,4a,5,6,7,7a-hexahydro-2-phenylcyclopenta-1,3,4-oxadiazine (**3**)*

(a) Hydrogenation

A solution of the stable isomer (**2***a*) (0.50 g, 1.7 mmole) in benzene (20 ml) in the presence of palladium black (25 mg) consumed slightly more than one equivalent of hydrogen at room temperature and atmospheric pressure. The mixture was heated and filtered, the cooled solution depositing crystalline 1,2-dibenzoyl-1-cyclopentylhydrazine (**4**) (<10%), m.p. and mixed m.p. 197–198°. The benzene soluble fraction, obtained by evaporation, was the dihydro-derivative (90%) which was crystallized 3 times from aqueous methanol to give an analytical sample as large prisms, m.p. 143–143.5° (lit. m.p. 143.5–145° (2)); $\nu(CCl_4)$ 1650 (C=O), 1646 cm^{-1} (C=N); λ_{max}(EtOH) 220 (ε 14 000), 290 mμ (ε 13 300); $\tau(CDCl_3$, 100 Mc.p.s.) 2.1–2.8 (10 phenyl H), 5.05 (C_{4a}—H, octet[5]

[4]For numbering of **2***a* see text. The splitting constants were determined by spin decoupling.

[5]A 4-line X portion of an ABX system split into 4 doublets. The determination of the $J_{4a,7a}$ and $J_{7a,7}$ values is possible in conjunction with the spectrum of the dideuteriated derivative (see (*d*)). The assignment of the correct values to the tertiary hydrogens follows from the spectrum of the de-benzoylated oxadiazine **11**.

Can. J. Chem. Downloaded from www.nrcresearchpress.com by 210.87.254.40 on 09/05/12
For personal use only.

$J_{4a,7a} = 3.6, |J_{4a,5A} + J_{4a,5B}| = 18$ c.p.s.), 5.55 (C_{7a}—H, triplet $J_{7a,7A} = 3, J_{7a,7B} < 0.5$ c.p.s.), 7.3–8.7 p.p.m. C-5, C-6, C-7 methylene H); mass spectrum 306 (M^+, 23), 105 ($PhCO^+$, 100), 77 (Ph^+, 29).

(b) Catalytic Hydrogen Transfer

2*a* (1.5 g, 5 mmole) was refluxed for 2 days in cyclohexene (15 ml) containing palladium black (50 mg). Work-up as described in (*a*) again gave **3** (90%) and a small amount of **4**.

(c) Di-imide

2*a* (1.0 g, 3.3 mmole) was dissolved in a mixture of methanol (3.60 ml), water (120 ml), and 95% hydrazine (2.5 ml), and the p*H* was adjusted to 9 using acetic acid. Air was bubbled through the solution for 2 days, evaporation losses being made up by the addition of methanol. Removal of the solvent gave a residue which after crystallization from aqueous methanol or benzene – petroleum ether (b.p. 60–80°) gave **3** (>90%), m.p. 143–143.5°.

The use of hydrogen peroxide in place of the air stream also proved successful.

(d) Dideuterio-di-imide

p-Toluenesulfonylhydrazine (5 g) was dissolved in tetrahydrofuran (10 ml) and D_2O (5 ml) was added. The solution was evaporated, the whole operation was repeated twice more, and the residue finally dried *in vacuo*.

The hydrazine-d_3 (0.19 g, 1.0 mmole) and **2***a* (0.18 g, 0.6 mmole) were refluxed in dry dioxane for 16 h. The solvent was removed and the resulting solid treated with ether and water. The ether layer was shaken out in turn with dilute sodium hydrogen carbonate and dilute hydrochloric acid and was then dried and evaporated. The residue showed an i.r. absorption at 1150 cm^{-1}, probably due to a sulfone by-product, which disappeared after one crystallization from aqueous methanol. A second crystallization gave the 6,7-dideuterio-derivative containing 1.5 atom D per molecule (determined by mass spectrometric analysis); the n.m.r. showed the expected differences in the methylene region and the C_{7a}—H at 5.5 τ as a doublet, $J_{4a,7a} = 3.6$ c.p.s.

*cis-4,4a,5,6,7,7a-Hexahydro-2-phenylcyclopenta-1,3,4-oxadiazine (**11**)*

The oxadiazine **3** (0.49 g, 1.6 mmole) was heated in concentrated sulfuric acid (10 ml) at 100° for 1 min, and set aside at room temperature for 3 h. The clear almost colorless solution was then poured into an ice-cold mixture of carbon tetrachloride and an excess of dilute sodium hydroxide. The organic layer and two carbon tetrachloride washings were combined, dried, and evaporated to give the oily base **11** (90%), which was directly pure (g.l.c.). An analytical sample was distilled at a bath temperature <200°/0.4 mm. pressure; ν(CCl_4) 3370 (NH weak, but very strong in Nujol), 1631 cm^{-1} (C=N); λ_{max}(EtOH) 282 mμ; τ(CCl_4) 2.0–2.9 (5 phenyl H), 4.7 (NH, sharp), 5.53 (C_{7a}—H, quartet), 6.80 (C_{4a}—H, quartet), 7.9—8.8 p.p.m. (C-5, C-6, C-7 methylene H); τ(CF_3CO_2H—CCl_4) 4.9 (C_{7a}—H), 5.9 p.p.m. (C_{4a}—H).

Anal. Calcd. for $C_{12}H_{14}N_2O$: C, 71.26; H, 6.98; N, 13.85. Found: C, 71.11; H, 6.95; N, 13.73.

The *hydrochloride*, prepared in ether by passage of hydrogen chloride, and crystallized from ether–methanol had m.p. 171–174° (decomposition).

Anal. Calcd. for $C_{12}H_{15}ClN_2O$: N, 11.70. Found: N, 11.88.

The 6,7-dideuterio analogue of **11** was prepared similarly from the deuteriated analogue of **3**; its n.m.r. spectrum (CCl_4) differed from that of the unlabelled isomer as expected in the methylene region and in the assignment: τ 5.5 p.p.m. (C_{7a}—H, triplet $J_{4a,7a} = J_{7a,7} = 4.5$ c.p.s.).

*Benzoylation of **11***

The base **11** (44 mg, 0.22 mmole) and benzoyl chloride (0.1 ml) were allowed to react in pyridine (2 ml) at room temperature for 18 h. The product was worked up by quenching with dilute hydrochloric acid and washing the precipitate (71%, 1 peak in g.l.c.) with aqueous ammonia. Two crystallizations from methanol gave **3**, m.p. 142–143° in admixture with material obtained by reduction of **2***a*.

*Acid Hydrolysis of **3***

A solution of **3** (1.45 g, 4.73 mmole) in a mixture of ethanol (20 ml), water (10 ml), and 12 *N* hydrochloric acid (2 ml) was refluxed for 17 h. The course of the reaction was monitored by removing and neutralizing small portions and subjecting them to t.l.c. In the early stages the starting material **3** and all three products **6**, **7**, and **8** were observed. As the reaction progressed **7** and **8** increased at the expense of **3**. The spot due to **6** was at all stages faint, indicating a low concentration of it (see control experiment below on isomerization of **6** to **7**).

When hydrolysis was complete the solution was cooled and a little 3 *N* hydrochloric acid added, causing the precipitation of the crystalline hydrochloride of **7** (0.64 g, 37%), directly pure. The mother liquor was basified with sodium carbonate, the solution was evaporated, and the residue extracted several times with ether. The combined extracts afforded a solid which was crystallized from aqueous ethanol to give the monobenzoyl derivative **8** (0.118 g, 11%). The ether insoluble fraction was acidified with dilute hydrochloric acid, taken to dryness, and again extracted with ether, from which benzoic acid (0.32 g, representing a total recovery of 71%) was obtained.

*Control Experiments Pertaining to Hydrolysis of **3***

*(a) Isomerization of cis-Alcohol **6** to Ester **7***

The alcohol **6** (20 mg, 0.06 mmole) was dissolved and refluxed in a mixture of ethanol (2 ml), water (1 ml), and 12 *N* hydrochloric acid (0.2 ml), the medium for the hydrolysis of the oxadiazine **3**. After 1 h (oxadiazine hydrolysis for 17 h) the solution was concentrated, made basic with aqueous sodium hydrogen carbonate, and extracted with methylene chloride. The dried extracts on evaporation gave a gum (95%) of i.r. spectrum identical with that of the ester **7**. Crystallization from aqueous methanol gave a pure product which did not depress the m.p. of authentic ester.

*(b) Hydrolysis of Ester **7** to Alcohol **8***

A solution of **7** (40 mg, 0.12 mmole) in ethanol (4 ml), water (2 ml), and 12 *N* hydrochloric acid (0.4 ml) was refluxed for 17 h (the conditions for the hydrolysis of the oxadiazine **3**). Addition of an excess of potassium carbonate, evaporation to dryness, and extraction with methylene chloride yielded a gum (33 mg), the i.r. spectrum of which showed it to be mainly starting material with a small amount of the product **8**. This mixture was

dissolved in methanol (5 ml) and a few drops of 12 *N* hydrochloric acid were added causing the hydrochloride of **7** to precipitate. The alcohol soluble fraction was basified with ammonia, evaporated, and extracted with methylene chloride giving a gum in which the i.r. absorption bands of the alcohol **8** were now predominant.

Synthesis of Oxadiazines by Ring Closure

(a) Oxadiazine 3

The *cis*-alcohol **6** (37 mg, 0.12 mmole) was mixed intimately with polyphosphoric acid (1 ml, K. and K. Laboratories) and heated for 24 h at 60°, and the clear mass was dissolved into a slight excess of ice-cold aqueous ammonia. Extraction with methylene chloride gave a gum (34 mg, two peaks of about equal area in g.l.c.) which was taken up in ether and then shaken in turn with dilute hydrochloric acid and dilute sodium hydroxide. The ether solution was then dried and evaporated to give a residue which crystallized and showed a single peak in its g.l.c. Two recrystallizations from aqueous methanol gave the oxadiazine **3**, m.p. 140.5–141.5°, alone or in admixture with material obtained by hydrogenation of **2***a*.

(b) Oxadiazine 11

The *cis*-alcohol **8** (245 mg, 1.1 mmole) was similarly heated in PPA (3 ml), and the reaction products worked up with aqueous sodium hydroxide and carbon tetrachloride. The n.m.r. spectrum of the carbon tetrachloride solution indicated the presence of **11** of at least 70% purity. Evaporation gave the oily oxadiazine (125 mg, corresponding to a 40% yield of **11**) which on benzoylation as described before gave the oxadiazine **3**, m.p. and mixed m.p. 142.5–143.5°, after crystallization from methanol.

The use of concentrated sulfuric acid in place of PPA also caused cyclodehydration of **8** to **11**. Heating at 100° for 5 min followed by treatment with ice and then aqueous sodium hydroxide gave an oil, isolated as before. Gas–liquid chromatography indicated a yield of about 50%.

We wish to thank the Province of Ontario for a Graduate Fellowship (to J.A.C.), and the National Research Council of Canada for support of this work and for a Scholarship (to J.A.C.).

1. D. MACKAY, U. F. MARX, and W. A. WATERS. J. Chem. Soc. 4793 (1964).
2. L. A. CARPINO and E. S. RUNDBERG, Jr. Chem. Commun. 1431 (1968).
3. E. A. BRAUDE, R. P. LINSTEAD, and P. W. D. MITCHELL. J. Chem. Soc. 3578 (1954).
4. T. TAGUCHI, J. ISHIBASHI, T. MATSUO, and M. KOJIMA. J. Org. Chem. **29**, 1097 (1964).
5. D. L. TREPANIER, V. SPRANCMANIS, and K. G. WIGGS. J. Org. Chem. **29**, 668 (1964).
6. D. L. TREPANIER and V. SPRANCMANIS. J. Org. Chem. **29**, 673 (1964).
7. D. L. TREPANIER and V. SPRANCMANIS. J. Org. Chem. **29**, 2151 (1964).
8. D. L. TREPANIER, V. SPRANCMANIS, D. S. THARPE, and P. E. KRIEGER. J. Het. Chem. **2**, 403 (1965).
9. D. L. TREPANIER, V. SPRANCMANIS, and J. N. EBLE. J. Med. Chem. **9**, 753 (1966).
10. J. L. SUDMEIER and C. N. REILLEY. Anal. Chem. **36**, 1698 (1964).
11. E. G. FOSTER, A. C. COPE, and F. DANIELS. J. Amer. Chem. Soc. **69**, 1893 (1947).
12. S. J. RHOADS. *In* Molecular rearrangements. *Edited by* P. de Mayo. Part. 1. Rearrangements through "no mechanism" pathways. Interscience Publishers, Inc., New York. 1963. Chap. 11.
13. M. T. HUGHES and R. O. WILLIAMS. Chem. Commun. 587 (1968).
14. P. BLADON, S. MCVEY, and P. L. PAUSON, and in part G. D. BROADHEAD and W. M. HORSPOOL. J. Chem. Soc. (C). 306 (1966).
15. E. A. GUGGENHEIM. Phil. Mag. **1**, 538 (1926).

Can. J. Chem. Downloaded from www.nrcresearchpress.com by 210.87.254.40 on 09/05/12
For personal use only.

Can. J. Chem. Downloaded from www.nrcresearchpress.com by 210.87.254.6 on 09/05/12
For personal use only.

Reaction of 3-aroylaziridines with diphenylcyclopropenone. Synthesis and properties of novel 4-aroyl-4-oxazolines

J. W. Lown, R. K. Smalley,[1] G. Dallas,[2] and T. W. Maloney
Department of Chemistry, University of Alberta, Edmonton, Alberta

Received July 16, 1969

3-Aroylaziridines and 3-acylaziridines react with diphenylcyclopropenone with the formation of novel 4-aroyl-4-oxazolines and 4-acyl-4-oxazolines respectively. The unusual physical and chemical properties of these reactive heterocycles are discussed.

Canadian Journal of Chemistry, **48**, 89 (1970)

4-Oxazolines represent an almost completely unexamined heterocyclic system, although they have been postulated as intermediates in several reactions, e.g. in the Lewis acid catalyzed rearrangement of 3-aroylaziridines leading to the formation of oxazoles (1) and in the synthesis of oxazoles by the addition of iminoethers to α-aminocarbonyl compounds (2). A 4-oxazoline structure **1** was suggested many years ago for a pyridinium ylid (3) but has since been rejected in favor of the enol betaine structure **2** (4).

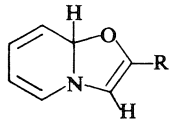

1

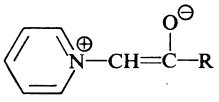

2 R = $C_6H_3(SC_2H_5)_2CH_3$

We recently described the preparation of 4-aroyl-4-oxazolines by the addition of azomethine ylids to diphenylcyclopropenone (5, 6). Very recently Baldwin *et al.* reported the preparation of 4-oxazolines of a different type by the valence rearrangement of isoxazolines via an acylaziridine intermediate (7), eq. [1]. The aziridine probably opens to an azomethine ylid which subsequently ring closes on the adjacent carbonyl group to give the 4-oxazoline. The 4-aroyl-4-oxazolines described in the present work show unusual physical and chemical properties and undergo a variety of [2 + 3] cycloadditions with activated multiple bonds.

Azomethine ylids may be conveniently prepared *in situ* by heating solutions of 3-aroylaziridines in inert solvents, eq. [2], and 1,3-dipolar addition products have been reported with dipolarophiles such as acetylenic esters, olefins, and aryl isothiocyanates (8–22). Their addition to carbonyl bonds has been reported only once (23). The carbonyl bond in diphenylcyclopropenone (DPP) (24) is highly polarizable owing to resonance of the type shown:

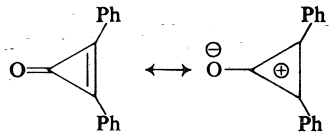

Consequently, DPP reacts readily with azomethine ylids derived from 3-aroylaziridines; however, the reaction takes a different course after the initial 1,3 dipolar addition.

Treatment of either *cis*- or *trans*-3-benzoyl-1-cyclohexyl-2-phenylaziridine (25) with one molar

[1]

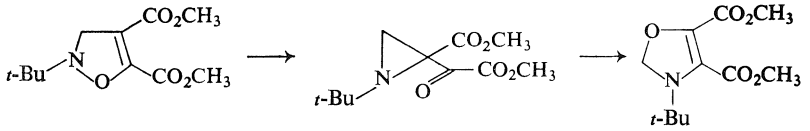

[2]

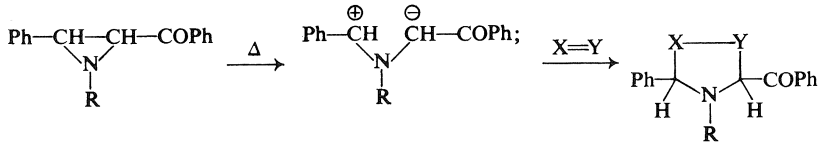

[1]N.R.C.C. Postdoctoral fellow 1967–1968.
[2]N.R.C.C. Studentship holder 1967–1969.

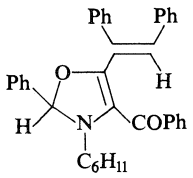

3

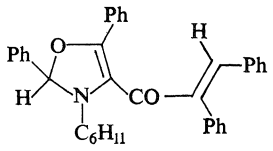

4

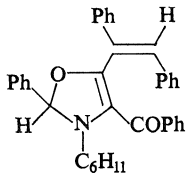

5

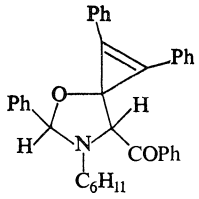

6

equivalent of DPP in refluxing benzene gives a deep-red solution and followed by chromatographic separation, affords a photochromic crystalline product m.p. 163° in 46.5% yield, which is assigned the 4-oxazoline structure **3**. The structural assignment rests on spectral evidence and the unusual chemical properties described below. The product exhibits an infrared (i.r.) band at 1695 cm^{-1} characteristic of an aromatic ketone (26*a*), consistent with **3** since space filling models indicate steric hindrance will prevent conjugation with the ring double bond.

The carbonyl frequency of **4** would represent an α,β unsaturated ketone and would absorb at 1665–1685 cm^{-1} (26*b*). In addition, in unsaturated ketones of this type the C=C stretch absorption at 1650–1600 (27) is of comparable intensity and no such band is visible in the spectrum of the product. Mass spectral evidence also supports **3** (see the following paper). For these reasons we reject **4**. Structure **5** is rejected on the basis of the known chemistry of DPP since nucleophile catalyzed ring opening proceeds in a *cis* fashion (24). Similarly **6** is rejected since there is no proton in the nuclear magnetic resonance (n.m.r.) spectrum corresponding to the 4 proton of the oxazolidine structure. Also, heating the product with deuterium oxide under base catalyzed conditions did not result in any deuterium incorporation. These facts together with the observed lack of dependence on the stereochemistry of the 3-aroylaziridine lend support to the rationalization shown in Scheme 1.

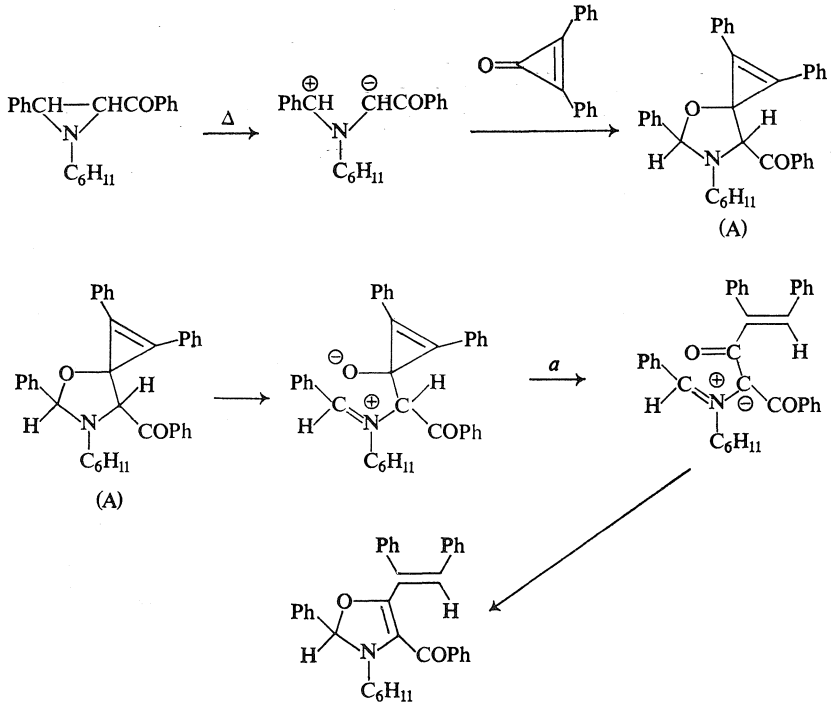

SCHEME 1

Can. J. Chem. Downloaded from www.nrcresearchpress.com by 210.87.254.6 on 09/05/12
For personal use only.

[3] 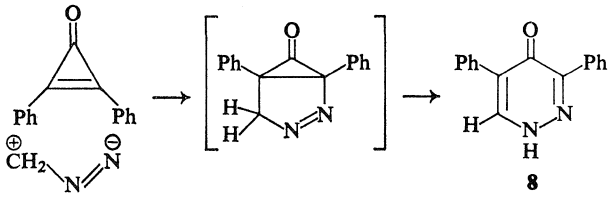

8

Experiments are currently underway with specifically 3-deuterated aziridines to examine the possibility of a concerted step for the ring opening *a*. The isolation of **7** in the analogous additions of iminocyclopropenes to azomethine ylids supports the intermediacy of the spiro-oxazolidine (A). This work will be reported in a subsequent publication.

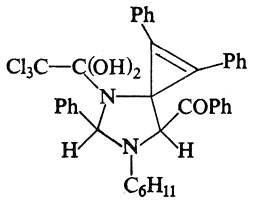

7

The observed reaction of DPP with azomethine ylids to produce 4-oxazolines is in marked contrast to that with other 1,3 dipoles e.g. diazomethane where primary addition occurs at the carbon–carbon double bond with the formation of a pyridazone **8** (28), eq. [3]. In view of the successful [2 + 3] cycloaddition of azomethine ylids to the carbonyl group in DPP described above, and to *p*-nitrobenzaldehyde (23), the obvious approach was made to confirm structure **3** i.e. via the reaction shown in eq. [4], so that the tetrahydro reduction product of **3** could be compared with the expected product **9**. There was no addition since the aliphatic aldehyde is not sufficiently reactive for 1,3 dipolar addition to the azomethine ylid.

A series of substituted 4-oxazolines was synthesized from DPP by this procedure. Best results were obtained by using highly purified aziridines in a molar ratio of 4:3, aziridine:DPP, at a temperature of about 80°. Contamination of the aziridine with a trace of amine hydrobromide and/or the presence of a greater proportion of DPP results in another reaction in which a furan predominates (see below). The choice of solvent is critical and we have examined (*a*) benzene, (*b*) acetonitrile, (*c*) methylene chloride, and (*d*) toluene. Solvents (*a*) and (*b*) give 4-oxazolines in good yield, (*d*) gives only furan, whilst (*c*) at the boiling point yields unreacted starting material in reduced yield. Having demonstrated that both *cis* and *trans* 3-aroylaziridines upon reaction with DPP give rise to 4-oxazolines, *cis–trans* mixtures of the aziridines were used for the general procedure. The analytical and spectral data on the 4-oxazolines are summarized in Tables 1 and 2. The scope of the synthesis is seen to extend to aroyl or acyl groups at position 4; biphenylyl or aryl (with either electron withdrawing or electron donating groups) at position 2, and with *N*-substituent of cyclohexyl, isopropyl, or methyl.

The numbering of substituents in Tables 1 and 2 refer to structure **10**.

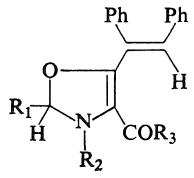

10

[4] 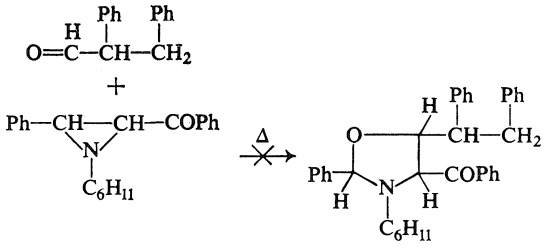

9

Can. J. Chem. Downloaded from www.nrcresearchpress.com by 210.87.254.6 on 09/05/12
For personal use only.

Can. J. Chem. Downloaded from www.nrcresearchpress.com by 210.87.254.6 on 09/05/12
For personal use only.

TABLE 1

4-Oxazolines

						Calculated				Found			
						%				%			
10	R_1	R_2	R_3	Melting point	Yield %	C	H	N	Molecular ion	C	H	N	Molecular ion
	C_6H_5	CH_3	C_6H_5	145°	20*	83.92	5.69	3.16	443.1885	83.80	5.60	3.25	443.1879
a	C_6H_5	$(CH_3)_2CH$	C_6H_5	175°	23.5*	84.05	6.20	2.97	471.2198	84.15	6.35	3.45	471.2192
b	C_6H_5	$(CH_3)_2CH$	$pCH_3C_6H_4$	165–166°	31*	84.10	6.44	2.89	485.2355	84.00	6.85	3.10	485.2358
c	C_6H_5	C_6H_{11}	C_6H_5	163°	65	84.50	6.51	2.74	511.2511	84.20	6.40	2.65	511.2510
d	$pCH_3OC_6H_4$	C_6H_{11}	C_6H_5	158–160°	23*	82.07	6.47	2.59	No molecular ion	82.02	6.45	2.62	—
e	$mNO_2C_6H_4$	C_6H_{11}	C_6H_5	165–166°	27*	77.70	5.76	5.04	556.2368	77.65	6.03	4.97	556.2362
f	$pNO_2C_6H_4$	C_6H_{11}	C_6H_5	180–182°	64	77.70	5.76	5.04	No molecular ion	77.46	5.75	5.19	—
g	$pC_6H_5C_6H_4$	C_6H_{11}	C_6H_5	122–123°	100	85.82	6.35	2.38	No molecular ion	85.64	6.28	2.32	—
h	C_6H_5	C_6H_{11}	$pCH_3OC_6H_4$	175.5–176.5°	79	82.07	6.47	2.59	541.2616	82.27	6.49	2.50	541.2614
i	C_6H_5	C_6H_{11}	$pCH_3C_6H_4$	176–176°	20*	84.53	6.72	2.67	525.2668	84.50	6.60	2.40	525.2665
j	C_6H_5	C_6H_{11}	$pNO_2C_6H_4$	191–192.5°	23	77.70	5.76	5.04	556.2362	77.56	6.03	4.76	556.2373
k	C_6H_5	C_6H_{11}	CH_3	80–82°	84	82.85	6.90	3.12	499.2355	82.65	7.04	3.03	449.2353
l	$pC_6H_5C_6H_4$	C_6H_{11}	CH_3	144–142°	59	84.53	6.72	2.67	525.2668	84.32	6.68	2.58	525.2675

*Indicates made by 1:1 aziridine: DPP; otherwise by 4:3 aziridine: DPP.

TABLE 2

Spectroscopic data of 4-oxazolines

					Nuclear magnetic resonance* (δ) ($CDCl_3$)				
10	R_1	R_2	R_3	Infrared cm^{-1} ($CHCl_3$)	2 Proton	Cyclohexyl CH_2 or $(CH_3)_2CH$— or CH_3	Cyclohexyl CH or $(CH_3)_2CH$—	Aryl + vinyl protons	Aryl substituent and acetyl protons
	C_6H_5	CH_3	C_6H_5	1700	4.3 (1) s	2.15 (3) s		6.75–8.0 (21) m	
a	C_6H_5	$(CH_3)_2CH$	C_6H_5	1700	4.95 (1) s	0.73 (3) d J = 6.5 Hz 0.81 (3) d J = 6.5 Hz	3.43 (1) m	6.75–8.15 (21) m	
b	C_6H_5	$(CH_3)_2CH$	$pCH_3C_6H_4$	1695	4.91 (1) s	0.72 (3) d J = 6.5 Hz 0.8 (3) d J = 6.5 Hz	3.39 (1) m	6.80–8.10 (20) m	2.42 (3) s CH_3
c	C_6H_5	C_6H_{11}	C_6H_5	1698	4.95 (1) s	0.35–1.75 (10) m	2.72–3.05 (1) m	6.8 –8.0 (21) m	
d	$pCH_3OC_6H_4$	C_6H_{11}	C_6H_5	1695	4.90 (1) s	0.50–1.66 (10) m	2.70–3.17 (1) m	6.75–8.08 (20) m	3.78 (3) s OCH_3
e	$mNO_2C_6H_4$	C_6H_{11}	C_6H_5	1696	4.96 (1) s	0.50–1.78 (10) m	2.67–3.24 (1) m	6.82–8.12 (20) m	
f	$pNO_2C_6H_4$	C_6H_{11}	C_6H_5	1696	5.03 (1) s	0.42–1.73 (10) m	2.70–3.15 (1) m	6.84–8.25 (20) m	
g	$pC_6H_5C_6H_4$	C_6H_{11}	C_6H_5	1700	5.10 (1) s	0.40–2.0 (10) m	2.30–3.30 (1) m	6.70–8.30 (25) m	
h	C_6H_5	C_6H_{11}	$pCH_3OC_6H_4$	1700	4.95 (1) s	0.38–1.95 (10) m	2.55–3.15 (1) m	6.78–8.10 (20) m	3.85 (3) s OCH_3
i	C_6H_5	C_6H_{11}	$pCH_3C_6H_4$	1695	4.96 (1) s	0.50–1.75 (10) m	2.65–3.0 (1) m	6.70–8.05 (20) m	2.42 (3) s CH_3
j	C_6H_5	C_6H_{11}	$pNO_2C_6H_4$	1699	5.05 (1) s	0.65–1.80 (10) m	2.54–2.94 (1) m	6.75–8.06 (19) m 8.16 (1) s	
k	C_6H_5	C_6H_{11}	CH_3	1703	5.14 (1) s	0.66–2.15 (10) m	3.10–3.56 (1) m	7.32–8.50 (16) m	2.02 (3) s CH_3
l	$pC_6H_5C_6H_4$	C_6H_{11}	CH_3	1700	4.86 (1) s	0.55–2.10 (10) m	2.80–3.55 (1) m	6.65–8.10 (20) m	1.90 (3) s CH_3

*s = singlet; m = multiplet; d = doublet.

Can. J. Chem. Downloaded from www.nrcresearchpress.com by 210.87.254.6 on 09/05/12
For personal use only.

Properties of 4-Aroyl-4-oxazolines

In view of their novelty and their marked reactivity in [2 + 3] cycloadditions (in this respect they resemble sydnones) the properties of these heterocycles have been examined in some detail.

The n.m.r. spectra summarized in Table 2 are consistent with the proposed structures. Those with an isopropyl group bonded to the nitrogen show non-equivalent methyl groups, indicating proximity to an asymmetric center in accordance with structure **10***a* for example.

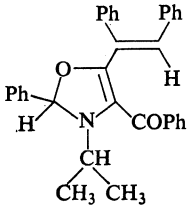

10*a*

The ultraviolet (u.v.) spectra are dominated by two intense absorption bands in the region (227.5–232) and (265–275.5) mμ (Table 3). The i.r. spectra show the characteristic aryl ketone absorption at 1695–1700 cm^{-1}. In the high resolution mass spectrum a common major mode of scission involves cleavage to the anil, a direct counterpart of the thermal cleavage involved in the [2 + 3] cycloaddition described below (see Table 4).

TABLE 3

Ultraviolet absorption spectra of 4-aroyl-4-oxazolines and their visible absorption on addition of *p*-toluene sulfonic acid

	Absorption spectrum		Acid added*	
Structure **10**	λ_{max} (CH_3CN) (mμ)	log ε	λ_{max}	λ_{max} (visible)
b	232	4.16	228	
	265	3.80	275	528
			317	
c	227	4.19	232	
	267	3.82	277	527
			311	
d	230	4.29	229	
	275	3.76	266	525
			316	
e	231	4.29	229	
	268	4.14	268	524
f	229	4.21	229	
	276	4.09	282	530
h	233	4.16	229	
	274	3.87	275	534
			326	
j	228	4.24	228	
	273	4.19	276	532
			350	
l	225	4.26	—	—
	260	4.31		
m	227	4.35	—	—
	260	4.38		

*Trace quantity of *p*-toluenesulfonic acid added, log ε was not determined since concentration of colored species is unknown.

TABLE 4

Principal fragmentations in the high resolution mass spectra of 4-aroyl-4-oxazolines*

Structure **10**	Molecular ion *m/e*	Relative abundance %	Anil *m/e*	Relative abundance %	M^+-Anil *m/e*	Relative abundance %
c	511	5	187	100	324	75
d	541	—	217	100	324	16
e	556	1	232	19	324	100
f	556	—	232	91	324	20
g	587	—	263	5	324	100
h	541	1	187	100	354	19
j	556	6	187	85	369	39
k	449	19	187	12	262	100
l	525	5	263	100	262	100

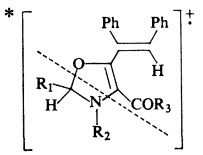

The dotted line shows the principal fragmentation mode.

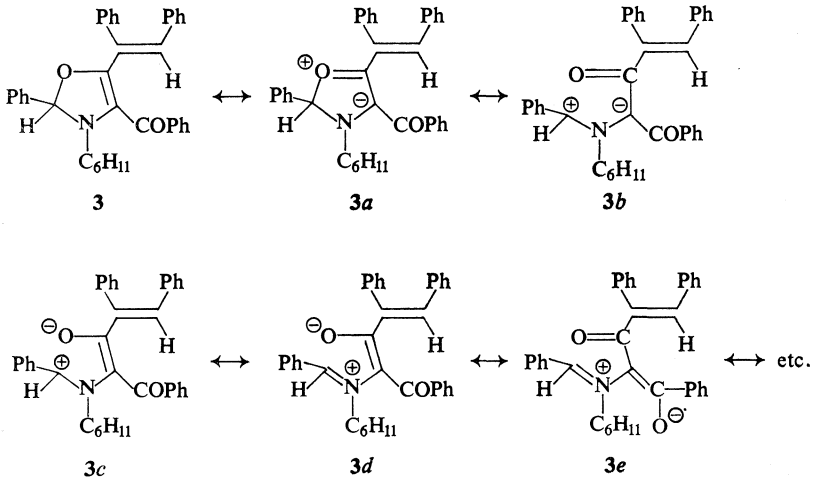

Another characteristic property of the 4-aroyl-4-oxazolines is their marked photochromism in the solid state where the white crystalline solids turn pinkish-red on exposure to light and revert to white in the dark. The phenomenon is reversible and no detectable decomposition occurs. In addition, all the oxazolines give bright red melts, and solutions in hot benzene, toluene, or xylene adopt a wine-red coloration. These phenomena may plausibly be associated with contributions from dipolar species. In the limit, substantial contributions from the canonical forms **3***b*, **3***c*, **3***d*, and **3***e* are equivalent to photochemical or thermal ring-chain valence isomerism to a new azomethine ylid. This situation exists in the case of **11** synthesized from the corresponding tricyclic aziridine **12** (21) and DPP. Compound **11** gives blood red crystals and behaves like a typically highly polar substance and has accordingly been assigned the zwitter ionic ylid structure.

Supporting evidence for these proposals is provided by the observed facile ring opening and [2 + 3] cycloaddition reactions described in this and in the accompanying paper.

The photochromism and thermochromism displayed by 4-aroyl-4-oxazolines is reminiscent of that shown by some 1,3 dipolar addition products of azomethine imines (29) and of the ring–chain isomerism exhibited by 2(biphenylyl)-3-acyl-(or 3-carbalkoxy)2,3-dihydro-1,3,4-oxadiazoles (30) e.g. eq. [5].

The appearance of the vivid red color of solutions of 4-oxazolines is enhanced by the addition of acids. Treatment with *p*-toluenesulfonic acid under mild conditions produces a strong visible absorption band at 530 mμ (see Table 3) and proved useful in substantially reducing the reaction time for various [2 + 3] cycloadditions of 4-oxazolines and evidently assists in the separation of the anil moiety (see accompanying paper). At room temperature the 4-oxazoline can be recovered in excellent yield from this acid treatment. The position of protonation on the 4-oxazolines (C, O, or N) unfortunately cannot be assigned with confidence

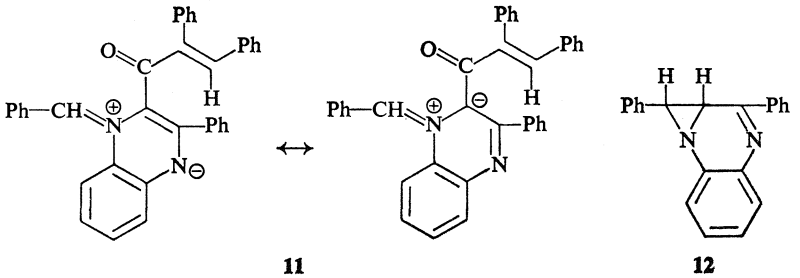

Can. J. Chem. Downloaded from www.nrcresearchpress.com by 210.87.254.6 on 09/05/12
For personal use only.

[5] 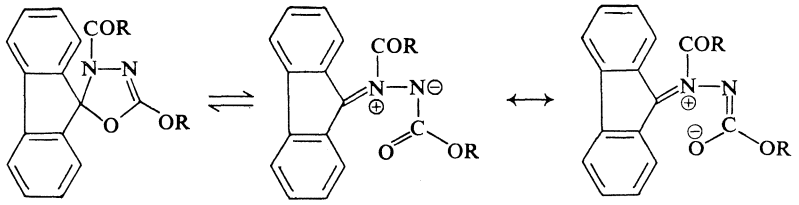

13

since addition of sufficient acid to affect the n.m.r. spectrum results in decomposition.

Benzaldehyde and benzoic acid were isolated from the controlled hydrolysis of **3** with hydrochloric acid, eq. [6]. A similar hydrolysis of **14**

[6] 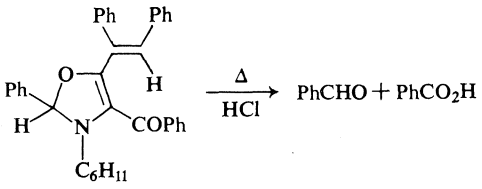

3

afforded *p*-nitrobenzaldehyde and benzoic acid, eq. [7].

The 4-aroyl-4-oxazolines are stable to alkali and to nucleophiles e.g. **3** was recovered unchanged after refluxing with (*a*) potassium carbonate in aqueous tetrahydrofuran, (*b*) potassium thiocyanate in acetone, and (*c*) sodium iodide in acetone. The solution turns red in the case of (*b*) and (*c*). A systematic study of the necessary structural features in the 4-oxazolines required for the photochromism and facile ring cleavage has been undertaken but is not yet complete. However a 2-aryl group and a 4-aroyl or acyl group seem to be essential. Baldwin *et al.* described the preparation of a 4-oxazoline via the valence rearrangement of an isoxazoline. The product lacked a 2-aryl group and has carbomethoxy groups at the 4 and 5 positions. No mention was made of any photochromism or tendency for [2 + 3] cycloadditions although it was remarked that the compound was unstable (7).

Chemical Reactions of 4-Aroyl-4-oxazolines

It was noted earlier that under certain conditions of the preparation of 4-aroyl-4-oxazolines that a common side reaction was formation of yellow crystalline furans of structure **15**. If the

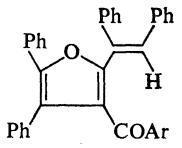

15

3-aroylaziridine is contaminated with some cyclohexylamine hydrobromide, or in the presence of excess DPP, furans like **15** are the only product of the reaction. While this type of reaction was found to have wider implications and its mechanism will be discussed more fully in the accompanying paper, we may represent the formation of furans under these conditions as shown schematically in Scheme 2.

Scheme 2 is supported by the following experiments. Treatment of **3** with one equivalent of DPP in refluxing toluene for 18 h, then chromatography on alumina gave furan **15** (Ar = Ph). The anil moiety is normally hydrolyzed to benzaldehyde in the work-up procedure and in this instance was characterized as the 2,4-dinitrophenylhydrazone. Occasionally however the anil is isolated intact. In a separate experiment **3** was allowed to react with diphenylacetylene (eq. [8]) and gave the same furan **15** in good yield, although the reaction was slower. However the possibility of thermal decarbonylation of DPP to diphenylacetylene under the

[7] 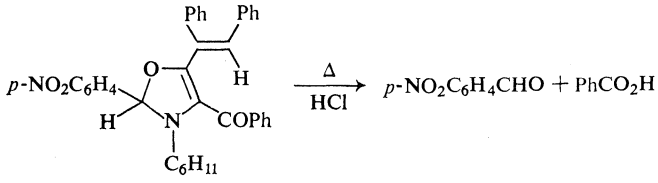

14

Can. J. Chem. Downloaded from www.nrcresearchpress.com by 210.87.254.6 on 09/05/12
For personal use only.

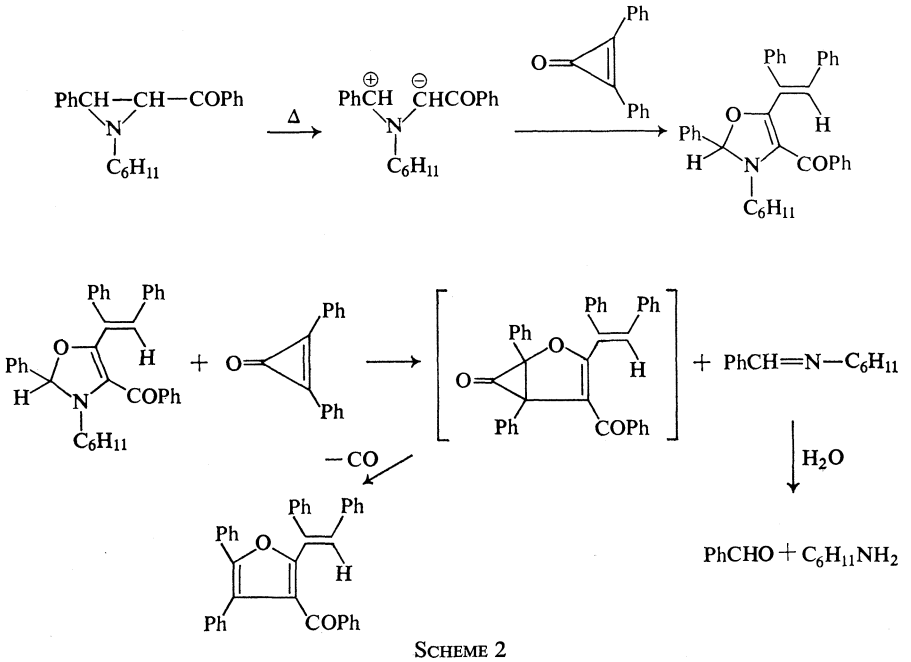

SCHEME 2

reaction conditions obtaining in the preparation of the 4-aroyl-4-oxazolines was discounted by a separate control reaction.

Another example in support of the reaction path in Scheme 2 is provided by the reaction of **3** with cycloheptenocyclopropenone (24) which gives the bicyclic furan **16**, eq. [9]. In this case, prior decarbonylation is even less likely.

Addition of DPP to 3-aroylaziridines via the azomethine ylid therefore involves competing 1:1 and 2:1 reactions to form **3** and **15** respectively. Other things being equal, higher reaction temperatures (e.g. refluxing toluene rather than benzene) and the presence of the amine hydrobromide favor the formation of the furans **15**. The amine hydrobromide is a by-product of the Gabriel synthesis of aziridines.

Experimental

Melting points were determined on a Fisher–Johns apparatus and are uncorrected. Infrared spectra were recorded on a Perkin–Elmer model 421 spectrophotometer, and only the principal, sharply defined peaks are reported. Nuclear magnetic resonance spectra were

[8] 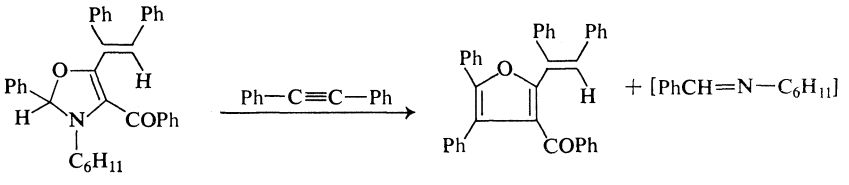

3

[9] 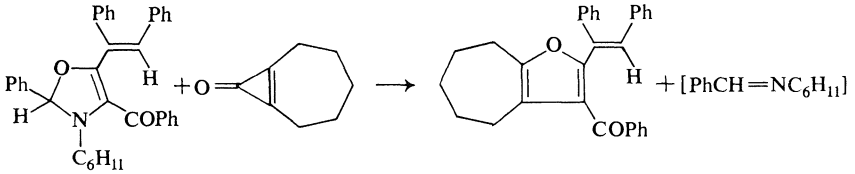

3 **16**

Can. J. Chem. Downloaded from www.nrcresearchpress.com by 210.87.254.6 on 09/05/12
For personal use only.

Can. J. Chem. Downloaded from www.nrcresearchpress.com by 210.87.254.6 on 09/05/12
For personal use only.

recorded on Varian A-60 and A-100 analytical spectrometers. The spectra were measured on approximately 10–15% (w/v) solutions in $CDCl_3$, with tetramethylsilane as a standard. Line positions are reported in parts per million (p.p.m.) from the reference. Absorption spectra were recorded in 'spectro'-grade solvents on a Beckman DB recording spectrophotometer. Mass spectra were determined on an Associated Electrical Industries MS-9 double focusing high resolution mass spectrometer. The ionization energy, in general, was 70 eV. Peak measurements were made by comparison with perfluorotributylamine at a resolving power of 15 000. Kieselgel DF-5 (Camag, Switzerland) and Eastman Kodak precoated sheets were used for thin-layer chromatography (t.l.c.). Microanalyses were carried out by Dr. C. Daesslé, Organic Microanalysis Ltd., Montreal, Quebec and by Mrs. D. Mahlow of this department.

General Preparation of 3-Aroylaziridines

The compounds required in this study were prepared by established methods involving Claisen–Schmidt condensations to form chalcones, then addition of bromine to form the dibromochalcones, and treatment of the latter with primary amines to provide 3-aroylaziridines (22 and references therein). The analytical and spectroscopic data on new aziridines prepared by this procedure are summarized in Tables 5 and 6.

Preparation of 4-Aroyl-4-oxazolines

General

The control experiments between diphenylcyclopropenone and isomerically pure samples of *cis* and *trans*-3-aroylaziridines employing a molar ratio of 1:1 are described in detail.

Thereafter 4-oxazolines and substituted furans were prepared using *cis–trans* mixtures of various aroylaziridines and in the case of the former, the improved technique using a 4:3 molar ratio of aziridine:DPP was used. Representative preparations are described in full and the analytical and spectroscopic data on the other 4-oxazolines prepared by similar procedures are summarized in Tables 1 and 2.

Control Experiments between Stereoisomerically Pure 3-Aroylaziridines and Diphenylcyclopropenone (1:1 Molar)

4-Benzoyl-3-cyclohexyl-5-(cis-1,2-diphenylvinyl)-2-phenyl-4-oxazoline

(*a*) A solution of 3.05 (0.01 mole) of *cis*-3-benzoyl-1-cyclohexyl-2-phenylaziridine (25) and 2.06 g (0.01 mole) of diphenylcyclopropenone (24) in 60 ml of dry benzene was heated under reflux for 24 h. Removal of the solvent *in vacuo* from the resulting deep red solution yielded an oily residue which was chromatographed on 200 g of alumina (B.D.H.). Elution with benzene caused the rapid separation of a pale orange band which was collected in 3 × 50 ml fractions. Removal of the solvent yielded an orange syrup which crystallized on trituration with heptane to give 4-benzoyl-3-cyclohexyl-5-(*cis*-1,2-diphenylvinyl)-2-phenyl-4-oxazoline as a pale pink solid 2.4 g, (46.5% yield); m.p. 162–163° (EtOH). The solid is strongly photochromic and the initially pink crystals become colorless when set aside in the dark.

Anal. Calcd. for $C_{36}H_{33}NO_2$: C, 84.50; H, 6.51; N, 2.74. Found: C, 84.2; H, 6.4; N, 2.65.

Mol. Wt. Calcd.: 511.2511. Found (mass spectrum): 511.2510.

The i.r. spectrum showed ν_{max} ($CHCl_3$), 1695 cm^{-1} (C=O); n.m.r., δ_{TMS} ($CDCl_3$), 2.7–3.05 (multiplet, 1H, cyclohexyl C*H*), 0.35–1.75 (multiplet 10H, cyclohexyl CH_2), 4.95 (singlet 1H, oxazoline 2 proton), 6.8–8.0 (multiplet, 21H, aromatic protons and vinyl proton).

Further elution of the column with benzene (200 ml) gave 0.25 g of unreacted 3-aroylaziridine, then elution with chloroform gave 0.6 g of a yellow oil consisting largely of benzaldehyde (identified as the 2,4-dinitrophenylhydrazone m.p. 238°; mixed m.p. undepressed on admixture with an authentic sample, and by the characteristic aldehyde absorption at 9.78 in the n.m.r. spectrum). Finally elution with ethanol yielded 0.5 g of unreacted diphenylcyclopropenone; m.p. 119°.

(*b*) A similar reaction was carried out between 2.44 g (0.008 mole) of *trans*-3-benzoyl-1-cyclohexyl-2-phenylaziridine (25) and 1.65 g (0.008 mole) of diphenylcyclopropenone in benzene and worked up as described above to yield 4-benzoyl-3-cyclohexyl-5-(*cis*-1,2-diphenylvinyl)-2-phenyl-4-oxazoline, 1.5 g (37% yield); m.p. 162–163° (EtOH) identical in all respects to that obtained with the *cis* stereomer of the 3-aroylaziridine described in (*a*) above.

Addition Reactions Employing Other Solvents with 1:1 Molar Ratio of 3-Aroylaziridine to Diphenylcyclopropenone

(*c*) A similar reaction between 1.5 g (0.005 mole) of *cis*-3-benzoyl-1-cyclohexyl-2-phenylaziridine and 1.03 g (0.005 mole) of diphenylcyclopropenone was carried out in refluxing acetonitrile. The reaction was worked up by a similar procedure to give 4-benzoyl-3-cyclohexyl-5-(*cis*-1,2-diphenylvinyl)-2-phenyl-4-oxazoline, 1.2 g (46.5% yield); m.p. 162–163° (EtOH).

(*d*) A similar reaction between 1.96 g (0.06 mole) of 1-benzyl-2-phenyl-3-toluoylaziridine and 1.24 g (0.06 mole) of diphenylcyclopropenone was performed in 60 ml of refluxing methylene chloride for 5 days followed by chromatography afforded unreacted starting materials in reduced yields.

(*e*) A solution of 3.05 (0.01 mole) of a mixture of *cis* and *trans*-3-benzoyl-1-cyclohexyl-2-phenylaziridine (25) and 2.06 g (0.01 mole) of diphenylcyclopropenone in 60 ml dry toluene was heated under reflux for 24 h. Removal of the solvent and chromatographic separation of the resulting oil on 300 g of alumina (B.D.H.) using benzene as eluent caused the rapid separation of a yellow band which was collected as 3 × 50 ml fractions. Removal of the solvent yielded a yellow oil which on trituration with heptane gave 3-benzoyl-4,5-diphenyl-2-(*cis*-1,2-diphenylvinyl)-furan as a pale yellow solid 1.45 g (28.9% yield). The product crystallized from ethanol as yellow crystals; m.p. 195–196°.

Anal. Calcd. for $C_{37}H_{26}O_2$: C, 88.41; H, 5.21; Found: C, 88.31; H, 5.18.

Mol. Wt. Calcd.: 502.1933. Found (mass spectrum): 502.1935.

The i.r. spectrum showed ν_{max} ($CHCl_3$), 1695 cm^{-1} (aryl C=O); n.m.r., δ_{TMS} ($CDCl_3$), 8.0–6.7 (multiplet, 25H, aromatic protons); 7.99 (singlet, 1H, vinyl proton).

Can. J. Chem. Downloaded from www.nrcresearchpress.com by 210.87.254.6 on 09/05/12
For personal use only.

TABLE 5

3-Acyl and 3-aroyl aziridines

R_1	R_2	R_3	Melting point	Yield %	Calculated % C	Calculated % H	Calculated % N	Calculated Molecular ion	Found % C	Found % H	Found % N	Found Molecular ion
$pC_6H_5C_6H_4$	C_6H_{11}	C_6H_5	127°	100	85.00	7.14	3.67	381.2093	84.90	7.23	3.64	381.1974
$mNO_2C_6H_4$	C_6H_{11}	C_6H_5	95°	88	72.00	6.29	8.00	350.1630	71.70	6.17	8.02	350.1634
C_6H_5	C_6H_{11}	$pCH_3OC_6H_4$	126–127°	75	78.81	7.46	4.18	335.1885	78.76	7.36	4.10	335.1888
C_6H_5	C_6H_{11}	CH_3	oil	85*	79.01	8.71	5.72	243.1623	78.90	8.83	5.75	243.1623

*For dibromochalcone see reference 33.

TABLE 6

Spectroscopic data on aziridines

R_1	R_2	R_3	Infrared cm^{-1} (O=C) ($CHCl_3$)	Nuclear magnetic resonance (δ) ($CDCl_3$)* Ring protons	Cyclohexyl CH_2 or $(CH_3)_2CH$	Cyclohexyl CH or $(CH_3)_2CH$	Aryl protons	Aryl substituent + acetyl protons
$pC_6H_5C_6H_4$	C_6H_{11}	C_6H_5	1680 (*cis*) 1665 (*trans*)	3.23 (2) s 3.53 (2) s	1.0–2.1 (10) m	2.2–3.0 (1) m	7.2–8.3 (14) m	
$mNO_2C_6H_4$	C_6H_{11}	C_6H_5	1681 (*cis*) 1667 (*trans*)	3.24 (1) $J = 7$ Hz 3.44 (1) $J = 7$ Hz 3.22 (2) s	0.83–2.06 (10) m	2.35–2.85 (1) m	7.30–8.30 (9) m	
C_6H_5	C_6H_{11}	$pCH_3OC_6H_4$	1658 (*trans*)	3.53 (2) s	0.85–2.00 (10) m	2.36–2.77 (1) m	6.83–8.14 (9) m	2.83 (3) s OCH_3
C_6H_5	C_6H_{11}	CH_3	1699	2.83 (1) s 2.88 (1) s 3.24–3.36 (2) d	1.00–2.00 (10) m	2.15–2.75 (1) m	7.26–7.46 (5) d	2.27 (3) s CH_3

*s = singlet; d = doublet; m = multiplet.

Can. J. Chem. Downloaded from www.nrcresearchpress.com by 210.87.254.6 on 09/05/12
For personal use only.

Further elution with benzene yielded an oil containing benzaldehyde and unreacted 3-aroylaziridine. Continued elution with chloroform and then ethanol gave unreacted diphenylcyclopropenone.

Control Attempted Deuterium Exchange of the 2-Proton of 4-Benzoyl-3-cyclohexyl-5-(cis-1,2-diphenylvinyl)-2-phenyl-4-oxazoline

A solution of 0.10 g of 4-benzoyl-3-cyclohexyl-5-(*cis*-1,2-diphenylvinyl)-2-phenyl-4-oxazoline in 25 ml of dry tetrahydrofuran was heated under reflux for 4 h with 2 ml of deuterium oxide and 0.05 g of anhydrous potassium carbonate. The solution was evaporated to dryness, and the process repeated with 25 ml of dry tetrahydrofuran, 0.05 g of potassium carbonate, and 1 ml of deuterium oxide. Examination of the n.m.r. spectrum of the product indicated that no exchange of the 2-proton had occurred. Accurate mass measurement (mass spectrum) also indicated no incorporation of deuterium had taken place.

Attempted Addition of 2,3-Diphenylpropanal to 3-Benzoyl-1-cyclohexyl-2-phenylaziridine

A solution of 0.05 g (0.005 mole) of 2,3-diphenylpropanal (31) and 1.05 g (0.005 mole) of 3-benzoyl-1-cyclohexyl-2-phenylaziridine in 60 ml of benzene was heated under reflux for 25 h, allowed to cool, and the solvent removed *in vacuo*. Chromatographic separation of the residual oil (2.05 g) afforded only unreacted starting materials and uncharacterized decomposition products.

Representative Improved Procedure for the Synthesis of 4-Aroyl-4-oxazolines Employing 4:3 Molar Ratio of 3-Aroylaziridine to Diphenylcyclopropenone

4-Anisoyl-3-cyclohexyl-5-(cis-1,2-diphenylvinyl)-2-phenyl-4-oxazoline

A solution of 0.62 g (0.00185 mole) of isomeric 3-anisoyl-1-cyclohexyl-2-phenylaziridine and 0.29 g (0.0014 mole) of diphenylcyclopropenone in 30 ml of benzene was heated under reflux for 24 h. The deep red solution was then cooled and the solvent removed *in vacuo*, yielding a red oil which was chromatographed on 40 g of alumina (B.D.H.). Elution with a 4:1 benzene:hexane mixture afforded a red oil which crystallized on trituration with ethanol to give 4-anisoyl-3-cyclohexyl-5-(*cis*-1,2-diphenylvinyl)-2-phenyl-4-oxazoline, 0.60 g (79% yield); m.p. 175–176.5° (from absolute ethanol).

Anal. Calcd. for $C_{37}H_{35}NO_3$: C, 82.07; H, 6.47; N, 2.59. Found: C, 82.27; H, 6.49; N, 2.50.

Mol. Wt. (mass spectrum) Calcd.: 541.2616. Found: 541.2614.

The i.r. spectrum showed ν_{max} ($CHCl_3$), 2850 (OCH_3), 1700 (C=O), 832 (1,4 disubst. ring) cm^{-1}; u.v., λ_{max} (CH_3CN), 233.5 mμ log ε 4.16, 274 mμ log ε 3.87; n.m.r. ($CDCl_3$), 0.38–1.95 (10H, multiplet cyclohexyl CH_2), 2.55–3.15 (multiplet, 1H, cyclohexyl CH), 3.85 (3H, singlet, methoxy protons), 4.95 (1H, singlet, 2 proton), 6.78–8.10 (multiplet, 20H, aryl protons plus vinyl proton).

Acid Hydrolysis of 4-Benzoyl-3-cyclohexyl-5-(cis-1,2-diphenylvinyl)-2-(p-nitrophenyl)-4-oxazoline

4-Benzoyl-3-cyclohexyl-5-(*cis*-1,2-diphenylvinyl)-2-(*p*-nitrophenyl)-4-oxazoline (0.30 g, 0.00054 mole) was heated under reflux in 25 ml of 2 *N* hydrochloric acid for a period of 3½ h. On cooling the orange mixture, a yellow residue appeared in the flask while a white sublimate was observed in the condenser and was isolated. The mixture was then extracted with ether (3 × 20 ml) to give an organic layer, an aqueous layer, and an insoluble yellow residue. (*i*) White sublimate: this was found to be benzoic acid 0.007 g, m.p. 116–118°, and was identified by spectral comparison with authentic material. (*ii*) Ether extract: this was dried ($MgSO_4$) and the ether removed *in vacuo* to yield a yellow oil 0.035 g which partly crystallized on standing. It was found to be *p*-nitrobenzaldehyde on the basis of its compatibility in i.r. and n.m.r. spectra with authentic material, and by its 2,4-dinitrophenylhydrazone derivative m.p. 317–318° (lit. 320° (32)) having an identical i.r. spectrum and undepressed mixed melting point with the same derivative of authentic *p*-nitrobenzaldehyde. (*iii*) Yellow residue: no structure could be assigned to this semi solid (0.02 g) which possessed a carbonyl stretching frequency in the i.r. spectrum (Nujol) of 1754 cm^{-1} and from the mass spectrum was seen to correspond to *m/e* 324 (i.e. parent oxazoline–anil moiety). (*iv*) Aqueous solution: this contained only cyclohexylamine hydrochloride.

Acid Hydrolysis of 3-Cyclohexyl-5-(cis-1,2-diphenylvinyl)-4-(p-nitrophenyl)-2-phenyl-4-oxazoline

0.40 g (0.00072 mole) of 3-cyclohexyl-5-(*cis*-1,2-diphenylvinyl)-4-(*p*-nitrophenyl)-2-phenyl-4-oxazoline was heated under reflux in 25 ml of 2 *N* hydrochloric acid for a period of 3½ h. From this reaction 4 products were isolated in the manner described above. The white sublimate (0.008 g) and the ether extract (0.050 g) were found to consist of benzoic acid (m.p. 119–120.5°), while the aqueous layer contained cyclohexylamine hydrochloride. As before, no structural assignment could be given to the brown residue (0.12 g, m.p. 85°) whose physical data was as follows. Mol. Wt. (mass spectrum): 369 (which corresponds to oxazoline–anil); the i.r. spectrum showed $\nu_{CHCl_3}^{max}$ 1766 (C=O) 1695 cm^{-1} (C=O); n.m.r. ($CDCl_3$), 6.7–8.5 (multiplet, aryl protons).

Acid Hydrolysis of 4-Benzoyl-3-cyclohexyl-5-(cis-1,2-diphenylvinyl)-2-phenyl-4-oxazoline

0.20 g (0.00039 mole) of 4-benzoyl-3-cyclohexyl-5-(*cis*-1,2-diphenylvinyl)-2-phenyl-4-oxazoline was heated under reflux in 25 ml of 50% (w/w) sulfuric acid for a period of 3 h. As in the procedure described above, benzoic acid was sublimed out in the condenser and benzaldehyde was obtained from the ether extract.

Reaction of 4-Benzoyl-3-cyclohexyl-5-(cis-1,2-diphenylvinyl)-2-phenyl-4-oxazoline with Nucleophiles and Bases.

(a) Potassium Thiocyanate

A solution of 0.064 g (0.125 mmole) of the title 4-oxazoline and 0.0032 g (0.025 mmole) of potassium thiocyanate in 10 ml of acetone was heated under reflux for 26 h; during which time it adopted a pink color. The solution was cooled, the solvent removed *in vacuo*, and the residue extracted with benzene affording 0.056 g (87.5% recovery) of unchanged 4-oxazoline; m.p. 158° (heptane), mixed m.p. 158° with authentic material.

Can. J. Chem. Downloaded from www.nrcresearchpress.com by 210.87.254.6 on 09/05/12
For personal use only.

(b) Sodium Iodide

Similarly, a solution of 0.064 g (0.125 mmoles) of the title 4-oxazoline and 0.005 g (0.025 mmoles) of sodium iodide in 10 ml of acetone was heated under reflux for 3 h, during which time it adopted a deep red color. The solution was allowed to cool when it reverted to the original straw color, the solvent removed *in vacuo*, and the organic material recovered by extraction with benzene affording 0.054 g (84.1% recovery) of unchanged 4-oxazoline; m.p. 156° (heptane) identical with authentic material.

(c) Dimethyl Sulfoxide

A solution of 0.511 g (0.001 mole) of the 4-oxazoline and 0.234 g (0.003 mole) of dimethyl sulfoxide in 30 ml of benzene was heated under reflux for 24 h. The solvent was removed *in vacuo* and the resulting red oil chromatographed on 30 g of Fisher alumina with a 1:1 mixture of heptane and benzene as eluant. The main fraction was a pink solid of the unchanged 4-oxazoline 0.408 g (80% recovery) m.p. 160°.

(d) Potassium Carbonate in Aqueous Tetrahydrofuran

As described above in the attempted deuterium exchange, the 4-oxazoline was completely inert to prolonged refluxing with potassium carbonate in tetrahydrofuran–deuterium oxide mixtures.

(e) Sodium Hydroxide

A suspension of 0.51 g of the 4-oxazoline in 25 ml of 10% aqueous sodium hydroxide was heated under reflux for 3 h. The mixture was then cooled and the solid material collected, washed with water, and dried, affording 0.47 g of the unchanged 4-oxazoline m.p. 161°, undepressed by admixture with the starting material.

3-Cyclohexyl-5-(cis-1,2-diphenylvinyl)-3-phenyl-4-(p-toluoyl)-4-oxazoline and 4,5-Diphenyl-2-(cis-1,2-diphenylvinyl)-3-(p-toluoyl) furan

A solution of 1.6 g (0.005 mole) 1-cyclohexyl-2-phenyl-3-(*p*-toluoyl)aziridine (25) and 1.03 g (0.005 mole) of diphenylcyclopropenone in 60 ml of dry benzene, was heated under reflux for 12 h. The residual oil obtained after removal of the solvent was chromatographed on 120 g alumina as in the previous experiments. The benzene eluants gave on evaporation, an orange oil which when dissolved in 20 ml heptane and cooled yielded, 4,5-diphenyl-2-(*cis*-1,2-diphenylvinyl)-3-(*p*-toluoyl) furan, m.p. 180 °C (0.3 g) which recrystallized from ethanol as pale yellow crystals, m.p. 186–187 °C, and which was identical (mixed m.p. undepressed, superimposable i.r. spectrum) with the product obtained from the reaction of 3-cyclohexyl-5-(*cis*-1,2-diphenyl)-3-phenyl-4-(*p*-toluoyl)-4-oxazoline with diphenylacetylene described below.

Anal. Calcd. for $C_{38}H_{28}O_2$: C, 88.34; H, 5.46. Found: C, 88.5; H, 5.4.

Mol. Wt. Calcd.: 516.2089. Found (mass spectrum): 516.2089.

The i.r. spectrum showed ν_{max} ($CHCl_3$), 1693 cm^{-1} (aryl C=O); n.m.r. spectrum δ_{TMS} ($CDCl_3$), 7.8–6.7 (multiplet, 24H, aromatic protons) 8.05 (singlet, 1H, vinyl proton) 2.35 (singlet, 3H, methyl protons).

Concentration and further cooling of the heptane solution yielded 3-cyclohexyl-4-(*cis*-1,2-diphenylvinyl)-2-phenyl-4-(*p*-toluoyl)-4-oxazoline, m.p. 168–170 °C, 0.65 g, (20% yield) pink crystals, m.p. 175–176 °C (EtOH) which slowly became colorless on standing in the dark.

Anal. Calcd. for $C_{37}H_{35}NO_2$; C, 84.53; H, 6.72; N, 2.67. Found: C, 84.5; H, 6.7; N, 2.6.

Mol. Wt. Calcd.: 525.2668. Found (mass spectrum): 525.2665.

The i.r. spectrum showed ν_{max} ($CHCl_3$), 1695 cm^{-1} (aryl C=O); δ_{TMS} ($CDCl_3$), 8.0–6.7 (multiplet, 20H, aromatic protons and vinyl proton); 4.96 (singlet, 1H, '2' proton); 2.42 (singlet, 3H, CH_3 protons); 2.65–3.0 (multiplet, 1H) and 1.8–0.4 (multiplet 10H, cyclohexyl protons).

4,5-Diphenyl-2-(cis-1,2-diphenylvinyl)-3-(p-toluoyl)-furan from Reaction of 4-Aroyl-4-oxazoline and Diphenylacetylene

A solution of 0.1 g (0.0002 mole) of 5-(*cis*-1,2-diphenylvinyl-3-isopropyl-2-phenyl-4-(*p*-toluoyl)-4-oxazoline and 0.05 g (0.00028 mole) of diphenylacetylene in 20 ml dry toluene was heated under reflux for 48 h. Treatment of the reaction mixture as in the previous experiments gave 4,5-diphenyl-2-(*cis*-1,2-diphenylvinyl)-3-(*p*-toluoyl)furan 0.075 g (70.5% yield) which crystallized from ethanol, m.p. 185–186 °C. The product was identical in all respects with the sample obtained from the reaction of 1-cyclohexyl-2-phenyl-3-(*p*-toluoyl)aziridine with diphenylcyclopropenone.

3-Benzoyl-4,5-diphenyl-2-(cis-1,2-diphenylvinyl)-furan from Reaction of 4-Aroyl-4-oxazoline with (a) Diphenylcyclopropenone and with (b) Diphenylacetylene

(*a*) A solution of 0.2 g (0.00039 mole) of 4-benzoyl-3-cyclohexyl-5-(*cis*-1,2-diphenylvinyl)-2-phenyl-4-oxazoline and 0.08 g (0.00039 mole) of diphenylcyclopropenone in 25 ml dry toluene was heated under reflux for 18 h. The resulting pale yellow solution was evaporated to a small volume and the residual oil chromatographed on 30 g alumina using benzene as eluent. A yellow band which rapidly separated, was evaporated to dryness and the residual semi-solid on trituration with cold heptane gave 3-benzoyl-4,5-diphenyl-2-(*cis*-1,2-diphenylvinyl)-furan as a yellow solid, which crystallized from ethanol m.p. 196 °C (0.04 g (20.5% yield)). The product obtained was identical in all respects to the furan previously isolated from the reaction of 3-benzoyl-1-cyclohexyl-2-phenyl-aziridine with diphenylcyclopropenone in toluene described above.

(*b*) A solution of 0.2 g (0.00039 mole) of 4-benzoyl-3-cyclohexyl-5-(*cis*-1,2-diphenylvinyl)-2-phenyl-4-oxazoline and 0.1 g (0.0056 mole) of diphenylacetylene in 25 ml dry toluene was heated under reflux for 18 h. Treatment of the reaction mixture as in the previous experiment gave 3-benzoyl-4,5-diphenyl-2-(*cis*-1,2-diphenylvinyl)-furan, 0.145 g (75.5% yield) m.p. 196 °C.

Control Attempted Thermal Decarbonylation of Diphenylcyclopropenone under the Reaction Conditions of Formation of 4-Aroyl-4-oxazolines and 3-Aroylfurans

A solution of 1 g of diphenylcyclopropenone and 50 mg of isopropylamine in 20 ml of dry benzene was heated under reflux for 24 h. Evaporation of the solvent gave unreacted diphenylcyclopropenone 0.95 g m.p. 118° (24).

Can. J. Chem. Downloaded from www.nrcresearchpress.com by 210.87.254.6 on 09/05/12
For personal use only.

A similar control experiment using toluene as solvent containing a trace of cyclohexylamine resulted in recovery of unchanged diphenylcyclopropenone.

Reaction of Cycloheptenocyclopropenone with 4-Benzoyl-3-cyclohexyl-5-(cis-1,2-diphenylvinyl)-2-phenyl-4-oxazoline

A solution of 0.061 g (0.005 mole) of cycloheptenocyclopropenone (24) and 0.25 g (0.005 mole) of 4-benzoyl-3-cyclohexyl-5-(*cis*-1,2-diphenylvinyl)-2-phenyl-4-oxazoline in 10 ml of toluene was heated under reflux for 27 h, allowed to cool, and solvent removed *in vacuo* leaving a yellow oil. Chromatography of the product on alumina (B.D.H.) with hexane/benzene (60:40) as eluant afforded 3-benzoyl-4,5-cycloheptено-2-(*cis*-1,2-diphenylvinyl)furan 0.067 g (32% yield) m.p. 160 °C (benzene/heptane).

Anal. Calcd. for $C_{30}H_{26}O_2$; C, 86.08; H, 6.27. Found: C, 84.83; H, 6.32.

Mol. Wt. Calcd.: 418.1933. Found (mass spectrum): 418.1935

The i.r. spectrum showed ν_{max} ($CHCl_3$), 1690 cm^{-1} (broad, arylketone); n.m.r. ($CDCl_3$), 1.8–2.3 (multiplet, 4H, 1,1′,5,5′-cycloheptenyl protons), 1.2–1.8 (multiplet, 6H, 2,2′,3,3′,4,4′-cycloheptenyl protons), 6.9–8.1 (multiplet, 10H, aryl protons and vinyl proton).

Reaction of 1,1a-Dihydro-1,2-diphenylazirino[1,2-a]-quinoxaline with Diphenylcyclopropenone

A solution of 2.08 g (0.007 mole) of 1,1*a*-dihydro-1,2-diphenylazirino[1,2-*a*]quinoxaline (21) and 1.45 g (0.007 mole) of diphenylcyclopropenone in 50 ml of dry benzene was heated under reflux for 24 h, during which time the solution adopted a blood red color. Evaporation of the solvent *in vacuo* left a red semi-solid which was subjected to chromatography on basic alumina in benzene. The main fraction appeared on the column as a deep red band and elution and evaporation of the solvent gave a red oil ca. 2.0 g. Trituration with hexane and chilling resulted in the deposition of small dark red crystals 0.43 g (12.7% yield) of 3-(*cis*-1,2-diphenylvinyl)-1-phenyl-4-phenyl-1H-oxazolo-[3,4-*a*]-quinoxaline, m.p. 101° (soften).

Anal. Calcd. for $C_{36}H_{26}N_2O$: C, 86.02; H, 5.22; N, 5.58. Found: C, 85.60; H, 5.65; N, 5.56.

Mol. Wt. Calcd.: 502.2045. Found (mass spectrum): 502.2040.

The i.r. spectrum showed ν_{max} ($CHCl_3$) 1625 cm^{-1}; n.m.r. spectrum, δ_{TMS} ($CDCl_3$), 6.05 (singlet, 1H, vinyl proton); 6.68–7.72 (multiplet, 24H, aromatic protons).

This research was supported by a National Research Council of Canada grant to J. W. Lown. We thank Mr. J. P. Moser for technical assistance and Mr. R. Swindlehurst and Dr. A. Hogg for the n.m.r. and mass spectra, respectively.

1. A. Padwa and L. Hamilton. Tetrahedron Letters, 1861 (1967).
2. J. W. Cornforth and H. T. Huang. J. Chem. Soc. 1960 (1948).
3. F. Krollpfeiffer and A. Müller. Ber. **66**, 739 (1933).
4. A. W. Johnson. 'Ylid chemistry' organic chemistry—a series of monographs, **7**, Academic Press, New York, 1966. p. 253.
5. J. W. Lown, R. K. Smalley, and G. Dallas. Chem. Commun. 1543 (1968).
6. J. W. Lown and R. K. Smalley. Tetrahedron Letters, 169 (1969).
7. J. E. Baldwin, R. G. Pudussery, A. K. Qureshi, and B. Sklartz. J. Amer. Chem. Soc. **90**, 5325 (1968).
8. P. B. Woller and N. H. Cromwell. J. Heterocycl. Chem. **5**, 579 (1968).
9. H. W. Heine and R. Peavy. Tetrahedron Letters 3123 (1965).
10. B. K. Campbell and K. N. Campbell. J. Org. Chem. **9**, 178 (1944).
11. R. Huisgen, W. Scheer, G. Szeimies, and H. Huber. Tetrahedron Letters, 397 (1966).
12. G. H. Coleman and G. P. Waugh. Proc. Iowa State Acad. Sci. **40**, 115 (1933); G. H. Coleman and G. P. Waugh. Proc. Iowa State Acad. Sci. **49**, 286 (1942).
13. A. Padwa and L. Hamilton. Tetrahedron Letters, 4363 (1963).
14. von R. V. Capeller, R. Griot, M. Haring and T. Wagner–Jauregg. Helv. Chim. Acta, **40**, 1652 (1957).
15. H. W. Heine, R. E. Peavy, and A. J. Durbetaki. J. Org. Chem. **31**, 3924 (1966).
16. H. W. Heine, A. B. Smith, and J. D. Bower. J. Org. Chem. **33**, 1097 (1968).
17. A. Padwa and L. Hamilton. J. Heterocycl. Chem. **4**, 118 (1967).
18. A. Padwa and W. Eisenhardt. Chem. Commun. **7**, 380 (1968).
19. R. Huisgen, W. Scheer, and H. Huber. J. Amer. Chem. Soc. **89**, 1753 (1967).
20. S. Oida and E. Ohki. Chem. Pharm. Bull. (Tokyo), **16**, 764 (1968).
21. H. W. Heine and R. Henzel. J. Org. Chem. **34**, 171 (1969).
22. J. W. Lown, G. Dallas, and T. W. Maloney. Can. J. Chem. **47**, 3557 (1969).
23. H. W. Heine and R. P. Henzel. J. Org. Chem. **34**, 171 (1969).
24. R. Breslow, T. Eicher, A. Krebs, R. A. Peterson, and J. Posner. J. Amer. Chem. Soc. **87**, 1320 (1965).
25. N. H. Cromwell, N. G. Barker, R. A. Wankel, P. J. Vanderhorst, F. W. Olson, and J. H. Anglin. J. Amer. Chem. Soc. **73**, 1044 (1951).
26. (*a*) L. J. Bellamy. The infrared spectra of complex molecules. Methuen, New York, 1958. p. 132; (*b*) p. 221.
27. K. Nakanishi. Infrared absorption spectroscopy-practical. Holden-Day Inc., San Francisco, 1962. p. 105.
28. P. T. Izzo and A. S. Kende. Chem. Ind. 839 (1964).
29. R. Huisgen. Angew. Chem. Int. Edn. **2**, 582, 584 (1963).
30. E. Fahr, K. Doppert, and F. Scheckenbach. Angew. Chem. **75**, 670 (1963).
31. H. Normant and T. Cuvigny. Bull. Soc. Chim. Fr. 1881 (1965).
32. N. D. Cheronis and J. B. Entriken. Semimicro qualitative analysis. Interscience Publishers, 1961. p. 586.
33. L. Claisen and A. Claparède. Ber. **14**, 2462 (1881).

Can. J. Chem. Downloaded from www.nrcresearchpress.com by 210.87.254.105 on 09/05/12
For personal use only.

Reactions of 4-aroyl-4-oxazolines and 3-aroyl-4,5-dihydrofurans

J. W. LOWN, R. K. SMALLEY,[1] G. DALLAS,[2] AND T. W. MALONEY
Department of Chemistry, University of Alberta, Edmonton, Alberta

Received July 16, 1969

4-Aroyl-4-oxazolines undergo stereospecific [2 + 3] cycloaddition to olefinic dipolarophiles with the formation of 3-aroyl-4,5-dihydrofurans. The latter are also found to be reactive towards further [2 + 3] cycloaddition reactions. Possible mechanisms for these reactions are discussed and the synthesis of several new furans and dihydrofurans reported.

Canadian Journal of Chemistry, **48**, 103 (1970)

In the preceding paper (1) we described the preparation and properties of 4-aroyl-4-oxazolines and their characteristic cycloaddition reactions with acetylenes and cyclopropenones to form furans. In this paper we consider possible mechanisms of these reactions and describe the remarkable stereospecific [2 + 3] cycloaddition of olefinic dipolarophiles to 4-aroyl-4-oxazolines with the formation of 3-aroyl-4,5-dihydrofurans. The latter are themselves found to be reactive towards [2 + 3] cycloaddition reactions.

The 4-aroyl-4-oxazolines are structurally similar to the 4-aroyloxazoles which Cornforth has shown undergo thermal isomerization (2). Dewar has interpreted this rearrangement in terms of an "open-chain zwitterion" *i.e.* a nitrogen ylid **2** (3) (see Scheme 1).

By analogy, our 4-aroyl-4-oxazolines could plausibly open to an ylid structure upon heating, eq. [1]. The isolation of a stable red crystalline 4-oxazoline in the quinoxaline series in the open chain form (structure **11** in the preceding paper (1)) supports this contention.

The very recent report by Takaku and coworkers of the synthesis of furans by the reaction of dimethyl sulfonium dibenzoyl methylide with acetylenes provides a direct analogy for our reaction of 4-aroyl-4-oxazolines with diphenylacetylene to give furans (4), eq. [2]. A similar

[1] 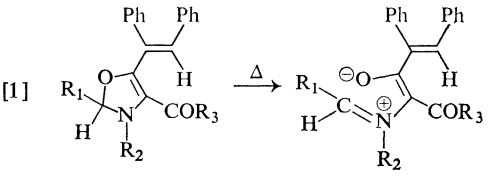

3 **4**

earlier example by Winterfeldt is shown in eq. [3] (5). A survey of the literature shows that information on the properties of diaroylammonium ylids and similar structures is virtually nonexistent, probably because of their poor nucleophilicity (4,6). However, species such as **4** are intrinsically interesting since they could conceivably react as C-nucleophiles, O-nucleophiles like the sulfur ylids described above, or could represent examples of 1,3-dipoles without internal octet stabilization (7) but with external octet stabilization provided by the anil moiety as shown in eq. [4]. If the latter interpretation were correct then the open-chain forms of the 4-aroyl-4-oxazolines such as **4** could be regarded as masked ketocarbenes and would be expected to undergo concerted [2 + 3] cycloadditions with reactive multiple bonds followed by expulsion of the anil. The observed reactions of **3** with acetylenes to form furans (8) does not distinguish between (*a*) behavior of **4** as an O-nucleophile and

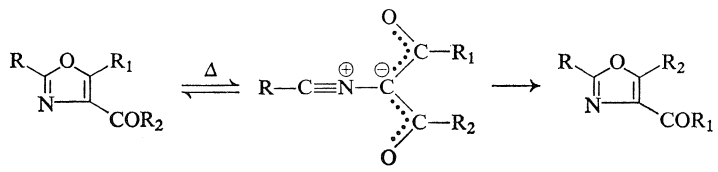

1 **2**

SCHEME 1

[1]N.R.C.C. Postdoctoral fellow 1967–1968.
[2]N.R.C.C. Studentship holder 1967–1969.

[2] 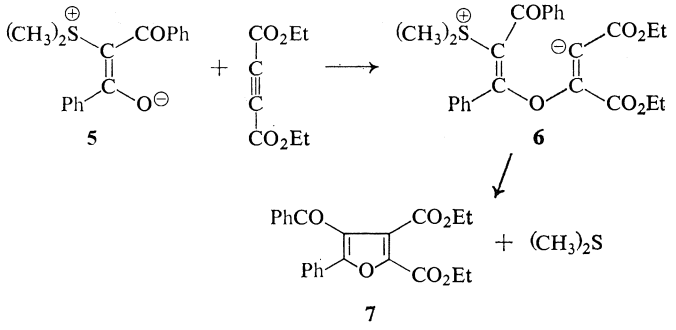

[3] 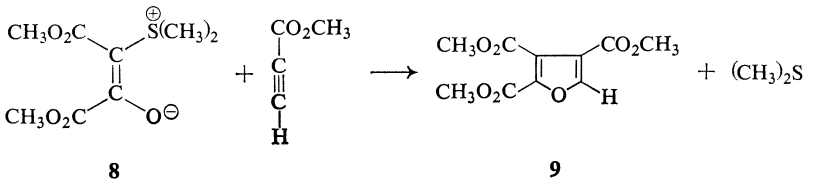

[4] 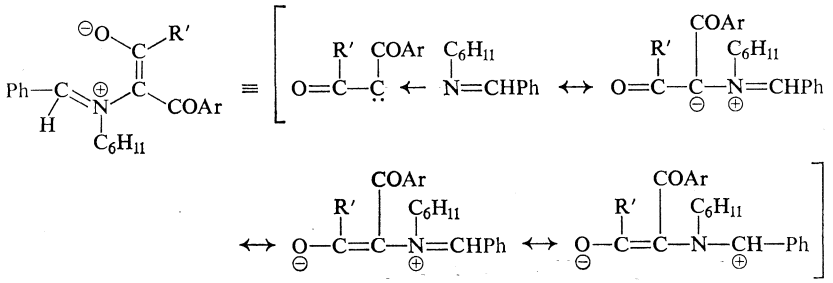

(*b*) behavior of **4** as a 1,3-dipole, but reaction with alkenes allows a distinction as will be shown.

Stereospecific [2 + 3] Cycloadditions of 4-Aroyl-4-oxazolines to Olefinic Dipolarophiles

Treatment of the 4-benzoyl-4-oxazoline **10** (R_1 = Ph) with one equivalent of diethyl maleate in refluxing toluene for 24 h, followed by chromatographic separation on alumina afforded the *cis*-3-aroyl-4,5-dihydrofuran (**11***b*) in 51% yield, as a white solid, m.p. 141–142°. The compound was assigned the *cis* geometry for the 4,5 protons because of the observation of an AB quartet in the nuclear magnetic resonance (n.m.r.) spectrum centered at 3.74 and 4.14 with a coupling constant of 11.5 Hz (9) (see Scheme 2).

Similarly, reaction of **10** (R_1 = Ph) with one equivalent of diethyl fumarate in refluxing toluene for 24 h, gave *trans*-**11***b* in 39% yield, m.p. 112–114°, which showed an AB quartet in the n.m.r. centered at 3.97 and 4.12 with a coupling constant of 3.7 Hz (9).

Similar stereospecific addition of **10** is observed with dimethyl maleate and dimethyl fumarate to form *cis*-**11***a* and *trans*-**11***a* respectively in yields of 66 and 73%. The addition of **10** to dimethyl maleate is particularly slow so that partial isomerization of the maleate occurs as had been observed previously by Huisgen *et al.* (10) in an attempt to observe stereospecific addition of a ketocarbene to maleate and fumarate. In the reaction described by Huisgen *et al.* complete isomerization of the maleate occurred, whereas in the present reaction partial isomerization resulted in an 80:20 *cis–trans* mixture.

The times required for completed addition of diethyl fumarate and diethyl maleate are cut dramatically to 75 min and 6 h, respectively, with no loss of stereospecificity, by the addition of *p*-toluenesulfonic acid in catalytic quantities (2–3 mg.). It was mentioned in the preceding

Can. J. Chem. Downloaded from www.nrcresearchpress.com by 210.87.254.105 on 09/05/12
For personal use only.

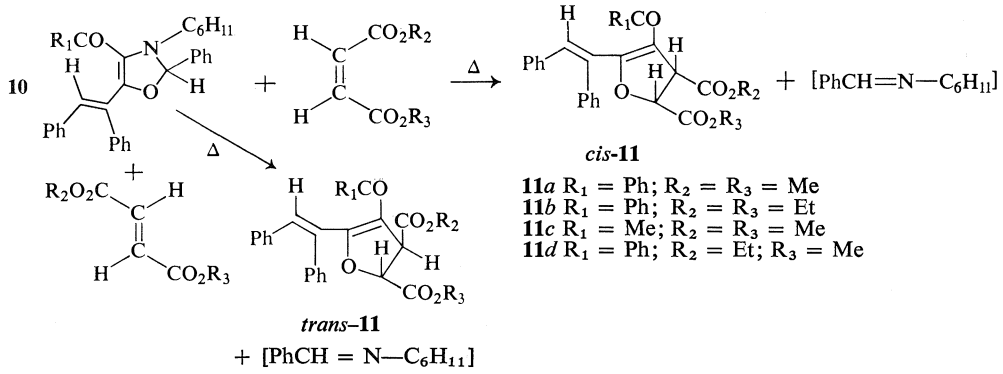

SCHEME 2

paper that the acid appears to assist in ring opening of the 4-oxazoline and the separation of the anil moiety.

The *cis* dihydrofurans may be epimerized with base to the thermodynamically more stable *trans* forms, eq. [5]. For example, treatment of *cis*-**11***b* with three equivalents of sodium methoxide in methanol for 3 h, afforded *trans*-**11***a*, m.p. 190°, in 40% yield. Reaction of *cis*-**11***b* with a catalytic quantity of sodium methoxide in methanol afforded the epimerized *trans* mixed methyl ethyl ester **11***d*, m.p. 164°. The structural assignment of *trans*-**11***d* was made on considerations of n.m.r. comparisons with *trans*-**11***a* and *trans*-**11***c*.

Further examples illustrating the generality of the observed stereospecific addition are provided by reactions with different types of 4-oxazolines **12** (R = CH_3 and C_6H_5) both of which react readily with dimethylfumarate to give **13***a* and **13***b*, exclusively possessing the *trans* configuration, eq. [6]. Compound **13***b* was identical to *trans* **11***a*. *N*-Phenylmaleimide is particularly reactive in [2 + 3] cycloadditions with 4-aroyl-4-oxazolines and 3-aroyl-4,5-dihydrofurans (see below) and reacts with **10** (R_1 = Ph) or **13***b* to give **15***a*, with **10** (R_1 = $pCH_3C_6H_4$) to give **15***b*, and with **13***a* to give **15***c* in which the bridgehead protons necessarily have a *cis* relationship.

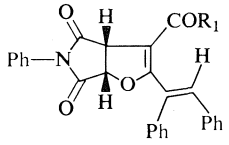

15

a R_1 = Ph
b R_1 = $pCH_3C_6H_4$
c R_1 = CH_3

Reaction of **10** (R_1 = Ph) with vinyl cyanide gave **16** and in this reaction the anil **17** was

[5]

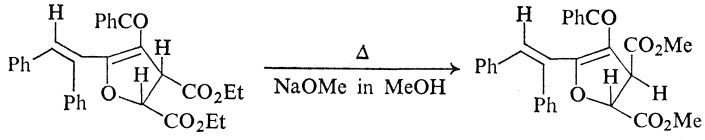

[6]

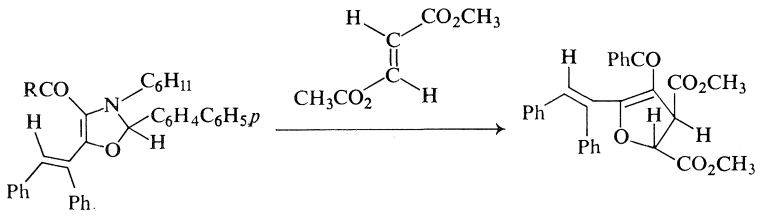

12*a* R = CH_3
12*b* R = C_6H_5

13*a* R = CH_3
13*b* R = C_6H_5

Can. J. Chem. Downloaded from www.nrcresearchpress.com by 210.87.254.105 on 09/05/12
For personal use only.

Can. J. Chem. Downloaded from www.nrcresearchpress.com by 210.87.254.105 on 09/05/12
For personal use only.

TABLE 1

3-Aroyl-4,5-dihydrofurans*

No.	R_1	R_2	R_3	R_4	R_5	Melting point	Yield %	Calculated % C	Calculated % H	Calculated % N	Calculated Molecular ion	Found % C	Found % H	Found % N	Found Molecular ion
trans-**11***a*	C_6H_5	H	CO_2CH_3	H	CO_2CH_3	188–190°	73	74.36	5.13	—	468.1572	74.24	5.43	—	468.1570
cis-**11***a*	C_6H_5	H	CO_2CH_3	CO_2CH_3	H	159–177°	66	74.36	5.13	—	468.1572	74.32	5.13	—	468.1575
trans-**11***b*	C_6H_5	H	$CO_2C_2H_5$	H	$CO_2C_2H_5$	114–115°	39	75.0	5.65	—	496.1886	74.86	5.68	—	496.1882
cis-**11***b*	C_6H_5	H	$CO_2C_2H_5$	$CO_2C_2H_5$	H	141–142°	60	75.0	5.65	—	496.1886	74.70	5.70	—	496.1883
trans-**11***c*	CH_3	H	CO_2CH_3	H	CO_2CH_3	144–145°	40	70.92	5.46	—	406.1416	70.80	5.38	—	406.1416
trans-**11***d*	C_6H_5	H	$CO_2C_2H_5$	H	CO_2CH_3	163–164°	46	74.69	5.39	—	482.1729	74.47	5.41	—	482.1724
16	C_6H_5	H	CN	H	H	184–186°	28	82.76	5.04	3.71	377.1416	82.61	5.05	4.0	377.1417
19	C_6H_5	H	COC_6H_5	H	COC_6H_5	189–191°	16	83.57	5.00	—	324.1150 236.0837	83.46	5.05	—	324.1151 236.0839
18	C_6H_5	H	COC_6H_5	COC_6H_5	H	125–128°	31	83.57	5.00	—	324.1150† 236.0837†	83.78	5.16	—	324.1154† 236.0839†
15*a*	C_6H_5	H	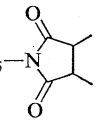		H	222–224°	65.5	79.64	4.85	2.81	497.1627	79.2	4.6	3.0	497.1621
15*b*	$C_6H_4CH_3p$	H	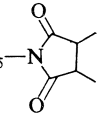		H	155–158°	64.5	79.84	4.89	2.74	511.1784	79.63	4.93	2.6	511.1783
15*c*	CH_3	H	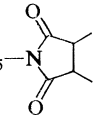		H	215–216°	34	77.23	4.87	3.22	435.1471	77.51	5.03	3.0	435.1473

*The compounds have the following general structure: 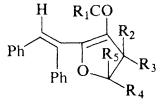

†Principal fragments measured; molecular ion too small to measure.

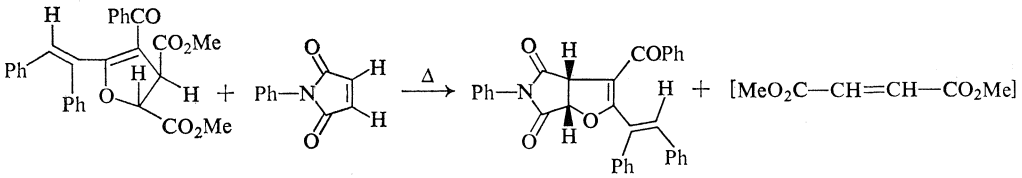

15*a*

SCHEME 3

isolated as such. Dibenzoylethylene reacted with **10** (R_1 = Ph) to give an approximately 2:1 mixture of the dihydrofurans **18** and **19**; however dibenzoylethylene is known to be susceptible to base addition (16) and in fact was shown to undergo a reaction with cyclohexylamine in a separate experiment. The analytical and spectral data on a series of *cis* and *trans* 3-aroyl-4,5-dihydrofurans prepared by this method are summarized in Tables 1 and 2.

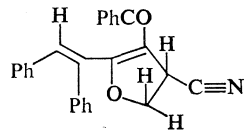

16

$C_6H_5CH{=}N{-}C_6H_{11}$

17

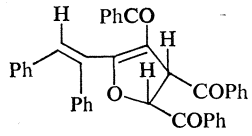

18

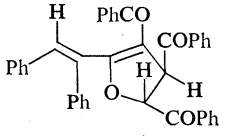

19

[2 + 3] Cycloadditions of 3-Aroyl-4,5-dihydrofurans

Significantly, the 3-aroyl-4,5-dihydrofurans described above give deep red melts and red solutions in hydrocarbon solvents at temperatures close to 175°, indicative of ring opening to charged species exactly like the 4-oxazolines (1).

Accordingly, treatment of *trans*-**11***a* with one equivalent of *N*-phenylmaleimide in refluxing *n*-butylbenzene for 2½ h gave the adduct *cis*-**15***a* (R_1 = Ph), m.p. 222°, in 27% yield identical in all respects to that obtained by direct reaction of *N*-phenylmaleimide with the 4-oxazoline as described above (see Scheme 3).

This represents a novel extension of the [2 + 3] cycloaddition reaction to the dihydrofuran series. Similarly, reaction of *trans*-**11***b* with one equivalent of *N*-phenylmaleimide in refluxing tetralin for 1½ h gave *cis*-**15***a* (15%). Successful reactions of the 3-aroyl-4,5-dihydrofurans, as in Scheme 3, in which a new 4,5-dihydrofuran is produced requires that the product have greater stability under the reaction conditions than the original dihydrofuran, otherwise the product will of course ring open in the same fashion. This limits the choice of reactive addends. While the reaction in Scheme 3 is stereoselective in that only *cis* dihydrofuran is formed from a *cis* olefin, a comparable reaction to confirm the complete stereospecificity of the reaction with a *trans* olefin has not so far been possible, because of the above thermodynamic limitations.

The Nature of the Reaction of 4-Aroyl-4-oxazolines with Alkenes and Cyclopropenones

We conclude from the evidence discussed above that 4-aroyl-4-oxazolines open thermally to give dipolar species which do not behave merely as oxygen nucleophiles. The observed stereospecificity of the reaction with alkenes demands that the dipolar species behave as externally stabilized ketocarbenes and consequently undergo concerted and stereospecific [2 + 3] cycloaddition to alkenes and is represented as shown in Scheme 4. Reactions of the product dihydrofurans are similarly envisaged as proceeding in a stepwise fashion via another ketocarbene 1,3 dipole with external octet stabilization (Scheme 5). Qualitatively, reaction of the 4-aroyl-4-oxazolines with fumarate to form the thermodynamically more stable *trans*-**11***a* or *trans*-**11***b* is faster than the comparable addition to maleate esters. Reaction rate studies will be undertaken to determine if this difference reflects activation energy or entropy differences and also to examine the marked rate enhancement by acid catalysis mentioned above.

Alternative Mechanisms for Reaction of 4-Aroyl-4-oxazolines with Alkenes and Alkynes

4-Oxazolines have been postulated as intermediates in the Lewis acid catalyzed rearrangement of 3-aroyl-aziridines leading to oxazoles (11)

Can. J. Chem. Downloaded from www.nrcresearchpress.com by 210.87.254.105 on 09/05/12
For personal use only.

Can. J. Chem. Downloaded from www.nrcresearchpress.com by 210.87.254.105 on 09/05/12
For personal use only.

TABLE 2

Spectroscopic data on 3-aroyl-4,5-dihydrofurans*

No.	R_1	R_2	R_3	R_4	R_5	$>=O$ Infrared cm^{-1} ($CHCl_3$)	Nuclear magnetic resonance $\delta_{TMS}(CDCl_3)$† Aryl + vinyl protons	Ring protons	4,5 Substituents + acetyl CH_3
trans-**11***a*	C_6H_5	H	CO_2CH_3	H	CO_2CH_3	1736 1701	7.18–7.90(16H)m	4.07 4.25 J = 3.7 Hz	3.02(3H)s 3.64(3H)s
cis-**11***a*	C_6H_5	H	CO_2CH_3	CO_2CH_3	H	1742 1699	7.17–7.83(16H)m	3.69 4.10 J = 11.5 Hz	3.57(6H)s
trans-**11***b*	C_6H_5	H	$CO_2C_2H_5$	H	$CO_2C_2H_5$	1735 1699	7.18–7.94(16H)m	3.97 4.12 J = 3.7 Hz	0.64(3H)t 3.48(2H)q 1.09(3H)t 4.07(2H)q
cis-**11***b*	C_6H_5	H	$CO_2C_2H_5$	$CO_2C_2H_5$	H	1735 1698	7.12–7.97(16H)m	3.74 4.14 J = 11.5 Hz	1.06–1.30(6H)t 3.90–4.24(4H)q
trans-**11***c*	CH_3	H	CO_2CH_3	H	CO_2CH_3	1730 1695	7.26–7.82(11H)m	3.72 4.21 J = 3.8 Hz	1.60(3H)s 3.64(3H)s 3.72(3H)s
trans-**11***d*	C_6H_5	H	$CO_2C_2H_5$	H	CO_2CH_3	1732 1701	7.20–7.93(16H)m	4.03 4.22 J = 3.5 Hz	0.75(3H)t 3.52(2H)q 3.71(3H)s
16	C_6H_5	H	CN	H	H	1704	7.23–7.80(16H)m	3.68 J_{AB} = 9.0 Hz 3.10 J_{BC} = 12.5 Hz 2.89 J_{AC} = 4.5 Hz	
19	C_6H_5	H	COC_6H_5	H	COC_6H_5	1705 1676	6.92–7.84(26H)m	4.89 5.42 J = 4.75 Hz	—
18	C_6H_5	H	COC_6H_5	COC_6H_5	H	1706 1685	6.90–7.88(26H)m	4.87 5.23 J = 7.1 Hz	—
15*a*	C_6H_5	H	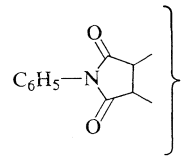		H	1780 1725–1695	6.80–8.10(21H)m	4.05 4.16 J = 9.2 Hz	—
15*b*	$C_6H_4CH_3p$	H			H	1780 1725 1705	6.80–8.00(20H)m	4.05 4.09 J = 9.25 Hz	2.38(3H)s
15*c*	CH_3	H			H	1715 1690	6.70–8.00(16H)m	3.62 4.05 J = 9 Hz	1.92(3H)s

*The compounds have the following general structure: 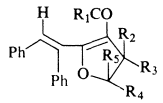

†s = singlet; d = doublet; q = quartet; t = triplet.

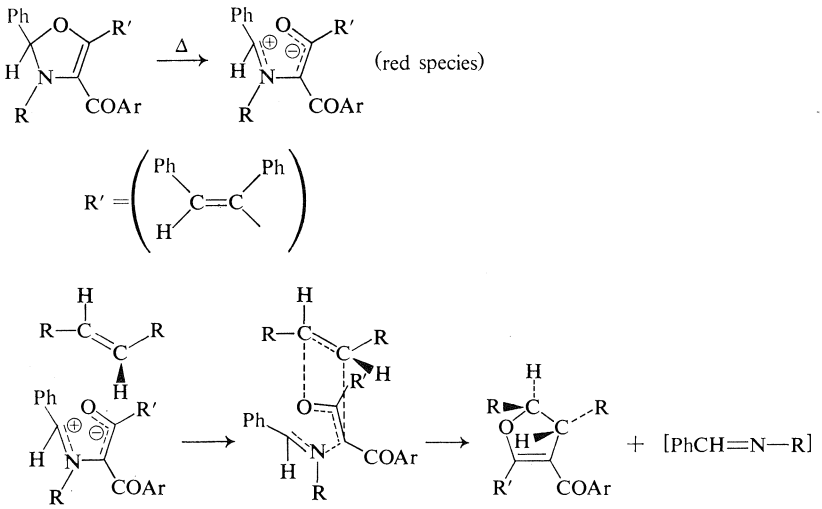

SCHEME 4

(see Scheme 6). The possibility existed therefore that the 4-oxazolines described in this paper in the thermally induced reactions with, for example, diphenylacetylene were decomposing to 4-aroyloxazoles prior to addition. The 4-aroyloxazoles could still give rise to zwitterionic intermediates by analogy with Dewar's mechanism for Cornforth's rearrangement in Scheme 1 discussed above. Such a reaction pathway (Scheme 7) may be discounted since (*a*) anils, or more often their hydrolysis products aromatic aldehydes, are detected in the products and not benzonitrile and (*b*) a deliberate thermal decomposition of 4-oxazoline **10** (R_1 = Ph) produced no evidence of cyclohexane formation. The elimination of cyclohexane in step (*i*) of Scheme 7 is also unlikely in view of Padwa's and Hamilton's results (11). Thermal decomposition of the 4-oxazoline **10** (R_1 = Ph) in refluxing toluene gave a mixture of products from which was isolated a yellow crystalline solid which is isomeric with and closely resembles the known α-pyrone **21** (12) and has tentatively been assigned structure **20**, eq. [7]. Compound **20** is also obtained in smaller yield by the photolysis of solutions of **10** in benzene. Other products are formed in minor amounts in these decompositions, but as yet no structures can be assigned with confidence. A parallel thermal decomposition of **10** (R_1 = Ph) in refluxing *n*-butanol also afforded

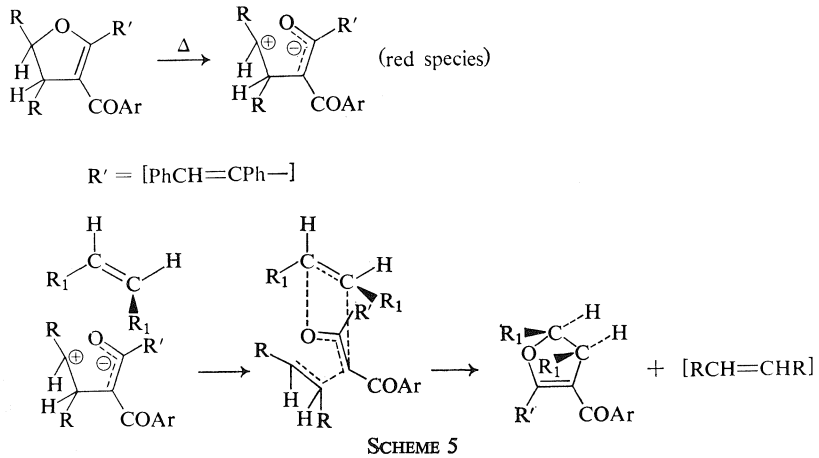

SCHEME 5

Can. J. Chem. Downloaded from www.nrcresearchpress.com by 210.87.254.105 on 09/05/12
For personal use only.

Can. J. Chem. Downloaded from www.nrcresearchpress.com by 210.87.254.105 on 09/05/12
For personal use only.

TABLE 3

3-Aroyl furans*

No.	R_1	R_2	R_3	Melting point	Yield %	Calculated % C	Calculated % H	Calculated Molecular ion	Found % C	Found % H	Found Molecular ion
—	C_6H_5	C_6H_5	C_6H_5	195–196°	74	88.41	5.21	502.1933	88.31	5.18	502.1935
—	$C_6H_4CH_3p$	C_6H_5	C_6H_5	186–187°	70.5	88.35	5.46	516.2089	88.53	5.41	516.2089
23*a*	C_6H_5	$CO_2C_2H_5$	$CO_2C_2H_5$	114–115°	54	75.30	5.30	494.1729	75.25	4.97	494.1716
23*b*	$C_6H_4CH_3p$	$CO_2C_2H_5$	$CO_2C_2H_5$	112–113°	57	75.58	5.55	508.1886	75.40	5.60	508.1875
28	C_6H_5	CO_2CH_3	CO_2CH_3	134–136°	43	74.68	4.72	466.1416	74.55	4.59	466.1415
27	C_6H_5	CO_2CH_3	CH_3†	73–74°	48.5	79.64	5.25	422.1518	79.35	4.90	422.1528
26	C_6H_5	CO_2CH_3	C_6H_5†	179–180°	59	81.79	4.99	484.1675	81.84	4.89	484.1678
—	CH_3	C_6H_5	C_6H_5	169–170°	44.5	87.22	5.49	440.1776	87.18	5.54	440.1774
29	C_6H_5	H	C_6H_5	163–165°	56	87.32	5.16	426.1620	87.06	5.41	426.1624
25	C_6H_5			83–85°	30	87.00	5.00	400.1463	86.51	5.12	400.1470

*The compounds have the following general structure:

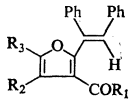

†Tentative assignments.

TABLE 4

Spectroscopic data on 3-aroylfurans

No.	R_1	R_2	R_3	Infrared cm^{-1} ($CHCl_3$)	Nuclear magnetic resonance $\delta_{TMS}(CDCl_3)$ Aryl protons	Vinyl proton	Tolyl CH_3 and ester
—	C_6H_5	C_6H_5	C_6H_5	1695	6.8–8.0(25H)m	7.99(1H)s	
—	$C_6H_5CH_3p$	C_6H_5	C_6H_5	1693	6.8–7.8(24H)m	8.05(1H)s	2.35(3H)s
23*a*	C_6H_5	$CO_2C_2H_5$	$CO_2C_2H_5$	1735 1700	7.2–7.9(15H)m	7.96(1H)s	1.11–1.16(6H)t 4.17 (4H)q
23*b*	$C_6H_4CH_3p$	$CO_2C_2H_5$	$CO_2C_2H_5$	1730–1695	7.0–7.8(14H)m	7.90(1H)s	2.37(3H)s 1.13–1.16(6H)t 4.16 (4H)q
28	C_6H_5	CO_2CH_3	CO_2CH_3	1744–1710	7.18–7.78(15H)m	7.86(1H)s	3.56(3H)s ester CH_3 3.61(3H)s ester CH_3
27	C_6H_5	CO_2CH_3	CH_3*	1730–1690	6.9–7.95(15H)m	8.05(1H)s	3.62(3H)s ester CH_3 2.70(3H)s ring CH_3
26	C_6H_5	CO_2CH_3	C_6H_5*	1730 1690	7.0–7.9(20H)m	8.15(1H)s	3.47(3H)s ester CH_3
—	CH_3	C_6H_5	C_6H_5	1690	6.6–7.9(21H)m	—	1.72(3H)s CH_3
29	C_6H_5	H	C_6H_5	1698	6.93–7.82(20H)m	8.17(1H)s	6.80(1H)s ring proton (5)
25	C_6H_5			1705	7.0–7.75(19H)m	7.84(1H)s	—

*Tentative assignments.

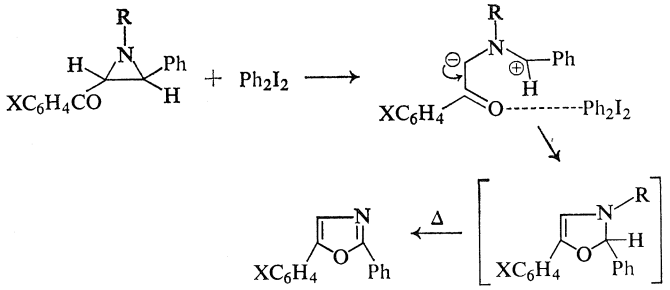

SCHEME 6

20 but no esters were detected which would have been expected if decomposition gave rise to a free ketocarbene followed by rearrangement to a ketene and subsequent reaction with the solvent.

[2 + 3] Cycloaddition of 4-Aroyl-4-oxazolines to Acetylenic Esters and to Benzyne

The 4-oxazolines (**10**) (R_1 = Ph and $pC_6H_4CH_3$) reacted readily with diethyl acetylenedicarboxylate in refluxing toluene to give furans **23***a* and *b* in 54 and 57% yields respectively. The orientation of the 2 and 3 groups in the furans is established by the observation of a characteristic aroyl ion R_1CO^+ in the mass spectrum which therefore excludes the alternative structure **24**. The orientation of these groups is therefore the same as in the parent 4-oxazolines and this applies to all [2 + 3] cycloaddition products described in this and in the preceding paper. This suggests that the dipolar species in Schemes 3 and 5 retain their configuration during the cycloaddition reactions or that structures such as **23** are intrinsically more stable than **24**.

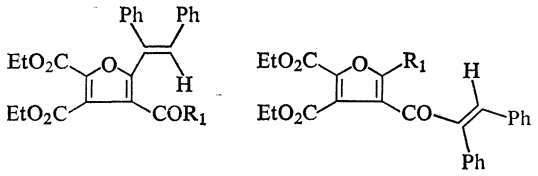

23 **24**

Similarly, substituted furans **26**–**29** are obtained in good yield by reaction of **10** (R_1 = Ph; $pC_6H_4CH_3$) with methyl phenylpropiolate, methyl methylpropiolate, dimethyl acetylenedicarboxylate, and phenyl acetylene.

Benzyne, generated *in situ* from diphenyliodonium carboxylate (15), reacts with **10** (R_1 = Ph) to give the benzofuran **25**, eq. [8]. The analytical and spectral data on these new furans are summarized in Tables 3 and 4.

Increasing interest is being shown in the 1,3-dipolar or [2 + 3] cycloaddition reaction (7). 1,3-Dipoles without octet stabilization (such as ketocarbenes, iminocarbenes, vinylcarbenes, iminoazenes, and ketoazenes) are particularly difficult to study owing to their short lifetime and high reactivity. Accordingly, further studies of

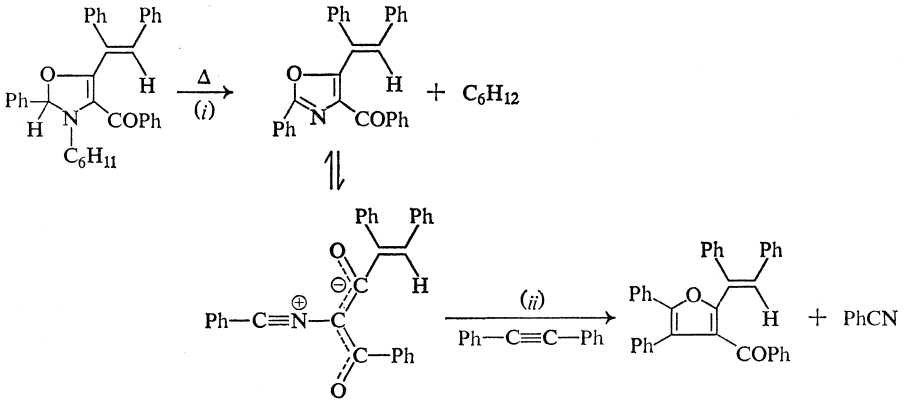

SCHEME 7

Can. J. Chem. Downloaded from www.nrcresearchpress.com by 210.87.254.105 on 09/05/12
For personal use only.

[7]

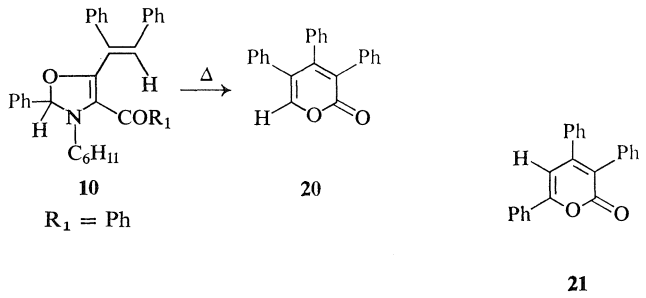

10
R_1 = Ph

20

21

[8]

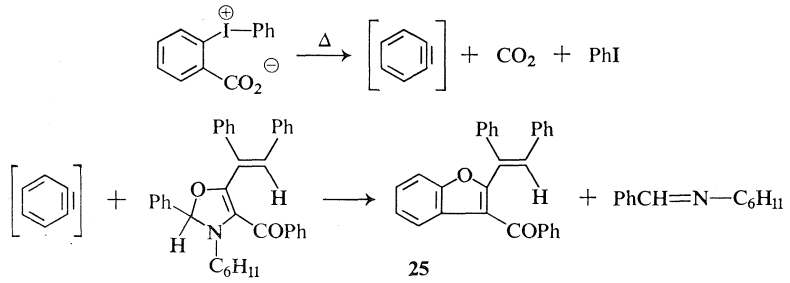

25

4-aroyl-4-oxazolines, 3-aroyl-4,5-dihydrofurans, 4-aroyl-4-thiazolines, and 4-aroyl-4-imidazolines are in progress with a view to providing new routes to "stabilized" or masked ketocarbenes, iminocarbenes, and related species.

Experimental

Melting points were determined on a Fisher–Johns apparatus and are uncorrected. Infrared (i.r.) spectra were recorded on a Perkin–Elmer model 421 spectrophotometer, and only the principal, sharply defined peaks are reported. Nuclear magnetic resonance (n.m.r.) spectra were recorded on Varian A-60 and A-100 analytical spectrometers. The spectra were measured on approximately 10–15% (w/v) solutions in $CDCl_3$, with tetramethylsilane as a standard. Line positions are reported in parts per million (p.p.m.) from the reference. Absorption spectra were recorded in 'spectro'-grade solvents on a Beckman DB recording spectrophotometer. Mass spectra were determined on an Associated Electrical Industries MS-9 double focusing, high resolution mass spectrometer. The ionization energy, in general, was 70 e*V*. Peak measurements were made by comparison with perfluorotributylamine at a resolving power of 15 000. Kieselgel DF-5 (Camag, Switzerland) and Eastman Kodak precoated sheets were used for thin layer chromatography (t.l.c.). Microanalyses were carried out by Dr. C. Daesslé, Organic Microanalysis Ltd., Montreal, Quebec and by Mrs. D. Mahlow of this department.

General Preparation of 3-Aroyl and 3-Acyl-4,5-dihydrofurans

These compounds were prepared by one of two methods; (*a*) under thermal conditions in high boiling solvents or (*b*) under acid catalysis in low boiling solvents. An example of each method is reported in detail after which the title, physical properties, and spectroscopic data are reported.

Reaction of 4-Benzoyl-3-cyclohexyl-5-(cis-1,2-diphenylvinyl)-2-phenyl-4-oxazoline with Dimethyl Fumarate

A solution of 0.511 g (0.001 mole) of 4-benzoyl-3-cyclohexyl-5-(*cis*-1,2-diphenylvinyl)-2-phenyl-4-oxazoline (1) and 0.144 g (0.001 mole) of dimethyl fumarate in 50 ml of toluene was heated under reflux for 18 h. The resulting yellow translucent solution was cooled, and the solvent removed *in vacuo*, giving a yellow oil which was subjected to chromatography on alumina (B.D.H.) with benzene as eluant. Removal of the solvent and trituration of the yellow syrup produced with heptane gave 3-benzoyl-4,5-*trans*-dicarbomethoxy-2-(*cis*-1,2-diphenylvinyl)-4,5-dihydrofuran as a white solid, 0.34 g (73% yield), m.p. 188–190° (absolute ethanol).

Anal. Calcd. for $C_{29}H_{24}O_6$: C, 74.36; H, 5.13. Found: C, 74.42; H, 5.16.

Mol. Wt. Calcd.: 468.1573. Found (mass spectrum): 468.1575.

The i.r. spectrum showed ν_{max}($CHCl_3$), 1736 (C=O) of ester, 1701 (C=O benzoyl) cm^{-1}, n.m.r. δ ($CDCl_3$), 3.02 (singlet, 3H, ester CH_3), 3.64 (singlet, 3H, ester CH_3), AB quartet centered at 4.07 and 4.25 (J = 3.7 Hz, 2H, 4,5 ring protons, *trans* coupled), 7.18–7.90 (multiplet, 16H, aryl protons and vinyl proton).

This same dihydrofuran was prepared in 75% yield by heating under reflux for 12 h, a solution of 0.587 g (0.001 mole) of 4-benzoyl-2-(*p*-biphenylyl)-3-cyclohexyl-5-(*cis*-1,2-diphenylvinyl)-4-oxazoline and 0.144 g (0.001 mole) of dimethyl fumarate in 40 ml of toluene. The product was isolated as described above and was identical to the dihydrofuran obtained from 4-benzoyl-3-cyclohexyl-5-(*cis*-1,2-diphenylvinyl)-2-phenyl-4-oxazoline and dimethyl fumarate.

Can. J. Chem. Downloaded from www.nrcresearchpress.com by 210.87.254.105 on 09/05/12
For personal use only.

Can. J. Chem. Downloaded from www.nrcresearchpress.com by 210.87.254.105 on 09/05/12
For personal use only.

Reaction of 4-Benzoyl-3-cyclohexyl-5-(cis-1,2-diphenylvinyl)-2-phenyl-4-oxazoline with Dimethyl Fumarate Under Conditions of Acid Catalysis

A solution of 0.08 g (0.00016 mole) of 4-benzoyl-3-cyclohexyl-5-(*cis*-1,2-diphenylvinyl)-2-phenyl-4-oxazoline in 20 ml of benzene containing 1 crystal of *p*-toluenesulfonic acid was prepared and shaken for a few moments till the characteristic wine red color was imparted to the solution. Dimethyl fumarate (0.023 g, 0.00016 mole) was added and the solution heated under reflux for 45 min. The yellow translucent solution obtained was concentrated *in vacuo* and the yellow oil produced was subjected to chromatography on alumina (B.D.H.) with benzene as eluant. Removal of the solvent and trituration of the product yellow syrup with heptane gave 3-benzoyl-4,5-*trans*-dicarbomethoxy-2-(*cis*-1,2-diphenylvinyl)-4-5-dihydrofuran as a white solid, 0.05 g (69% yield), m.p. 188–190° (absolute ethanol).

Anal. Calcd. for $C_{29}H_{24}O_6$: C, 74.36; H, 5.13. Found: C, 74.24; H, 5.43.

Mol. Wt. Calcd.: 468.1573. Found (mass spectrum): 468.1570.

The i.r. spectrum showed $\nu_{max}(CHCl_3)$, 1736 (broad C=O of ester), 1702 cm^{-1} (C=O benzoyl); n.m.r. δ ($CDCl_3$), 3.11 (singlet, 3H, ester CH_3), 3.72 (singlet, 3H, ester CH_3), AB quartet centered at 4.06 and 4.24 (J = 3.8 Hz; 2H, 4,5 ring protons *trans* coupled), 7.18–7.98 (multiplet, 16H, aryl protons and vinyl proton). This same dihydrofuran was prepared in 69% yield by heating under reflux for 50 min, a solution of 0.556 g (0.001 mole) of 4-benzoyl-3-cyclohexyl-5-(*cis*-1,2-diphenylvinyl)-2-(*p*-nitrophenyl)-4-oxazoline and 0.160 g (0.0011 mole) of dimethyl fumarate in 50 ml of toluene containing 2–3 mg of *p*-toluenesulfonic acid. The product was isolated as described above and was identical in all respects with that compound.

In a further experiment the above dihydrofuran was again prepared in 65% yield, by heating under reflux for 100 min, a solution of 0.556 (0.001 mole) of 4-benzoyl-3-cyclohexyl-5-(*cis*-1,2-diphenylvinyl)-2-(*m*-nitrophenyl)-4-oxazoline and 0.160 g (0.0011 mole) of dimethyl fumarate in 50 ml of toluene containing 2–3 mg of *p*-toluenesulfonic acid and isolating the product as described above.

Reaction of 4-Benzoyl-3-cyclohexyl-5-(cis-1,2-diphenylvinyl)-2-phenyl-4-oxazoline with Dimethyl Maleate

A solution of 0.511 g (0.001 mole) of 4-benzoyl-3-cyclohexyl-5-(*cis*-1,2-diphenylvinyl)-2-phenyl-4-oxazoline and 0.144 g (0.001 mole) of dimethyl maleate in 50 ml of toluene was heated under reflux for 22 h. The product was then isolated as previously described, to give a *cis–trans* mixture of 3-benzoyl-4,5-dicarbomethoxy-2-(*cis*-1,2-diphenylvinyl)-4,5-dihydrofuran as a white solid, 0.31 g (66% yield), m.p. 159–177° (absolute ethanol). This mixture was shown by n.m.r. to consist of a 78:22 *cis* to *trans* ratio but no separation could be performed.

Anal. Calcd. for $C_{29}H_{24}O_6$: C, 74.36; H, 5.13. Found: C, 74.32; H, 5.13.

Mol. Wt. Calcd.: 468.1572. Found (mass spectrum): 468.1575.

The i.r. spectrum showed $\nu_{max}(CHCl_3)$, 1742 (C=O of diester), 1699 cm^{-1} (C=O of benzoyl); n.m.r. δ ($CDCl_3$), 3.57 (singlet, 6H, ester CH_3), AB quartet centered at 3.69 and 4.10 (J = 11.5 Hz; 2H, 4,5 ring protons, *cis* coupled), 7.17–7.83 (multiplet, 16H, aryl protons and vinyl proton). This reaction was also performed under conditions of acid catalysis as follows.

A solution of 0.10 g (0.00017 mole) of 4-benzoyl-2-(*p*-biphenyl)-3-cyclohexyl-5-(*cis*-1,2-diphenylvinyl)-4-oxazoline and 0.03 g (0.0002 mole) of dimethyl maleate in 20 ml of toluene containing 0.008 g of *p*-toluenesulfonic acid was heated under reflux for 2¼ h, by which time the red solution had faded to a pale yellow color. The product was isolated as described above to give 3-benzoyl-4,5-dicarbomethoxy-2-(*cis*-1,2-diphenylvinyl)-4,5-dihydrofuran as a white solid, 0.037 g (47% yield), m.p. 169–178° (ethanol). Examination of this product by n.m.r. showed it to consist of a *cis–trans* mixture of which >90% was the *cis* isomer.

This reaction when repeated with the same molar quantities using 4-benzoyl-3-cyclohexyl-5-(*cis*-1,2-diphenylvinyl)-2-phenyl-4-oxazoline in benzene solution and under conditions of acid catalysis for a period of 20 h, gave the above isomeric dihydrofuran in 58% yield as an 82:18 *cis–trans* mixture as estimated by n.m.r.

3-Benzoyl-4,5-cis-dicarboethoxy-2-(cis-1,2-diphenylvinyl)-4,5-dihydrofuran

This compound was prepared in 51% yield as a white solid, m.p. 141–142° (absolute ethanol) by heating under reflux for 24 h a solution of 0.511 g (0.001 mole) of 4-benzoyl-3-cyclohexyl-5-(*cis*-1,2-diphenylvinyl)-2-phenyl-4-oxazoline and 0.172 g (0.001 mole) of diethyl maleate in 50 ml of toluene and employing the isolation procedure previously described.

Anal. Calcd. for $C_{31}H_{28}O_6$: C, 75.00; H, 5.65. Found: C, 74.70; H, 5.70.

Mol. Wt. Calcd.: 496.1886. Found (mass spectrum): 496.1883.

The i.r. spectrum showed $\nu_{max}(CHCl_3)$, 1735 (broad C=O of diester), 1698 cm^{-1} (C=O of benzoyl); n.m.r. δ ($CDCl_3$), 1.06–1.30 (two groups of overlapping triplets, 6H, ester CH_3), 3.90–4.24 (overlapping quartets, 4H, ester CH_2), AB quartet centered at 3.74 and 4.14 (J = 11.5 Hz; 2H, 4,5 ring protons, *cis* coupled), 7.12–7.97 (multiplet, 16H, aryl protons and vinyl proton).

This same dihydrofuran was prepared in 60% yield by heating under reflux for 25 h, a solution of 1.112 g (0.002 mole) of 4-benzoyl-3-cyclohexyl-5-(*cis*-1,2-diphenylvinyl)-2-(*p*-nitrophenyl)-4-oxazoline and 0.350 g (0.00203 mole) of diethyl maleate in 100 ml of toluene. The product was isolated as previously described.

A 39% yield of this same dihydrofuran was also obtained by the acid catalyzed procedure. A solution of 0.250 g (0.0005 mole) of 4-benzoyl-3-cyclohexyl-5-(*cis*-1,2-diphenylvinyl)-2-phenyl-4-oxazoline and 0.086 g (0.0005 mole) of diethyl maleate in 25 ml of benzene containing 1 crystal of *p*-toluene sulfonic acid was heated under reflux for 6 h. The product was isolated as described before.

3-Benzoyl-4,5-trans-dicarboethoxy-2-(cis-1,2-diphenylvinyl)-4,5-dihydrofuran

This compound was prepared in 39% yield as a white solid, m.p. 114–115° (absolute ethanol) by heating under reflux for 75 min, a solution of 0.511 g (0.001 mole) of 4-benzoyl-3-cyclohexyl-5-(*cis*-1,2-diphenylvinyl)-2-phenyl-4-oxazoline and 0.172 g (0.001 mole) of diethyl fumarate in 50 ml of benzene containing 1 crystal of

Can. J. Chem. Downloaded from www.nrcresearchpress.com by 210.87.254.105 on 09/05/12
For personal use only.

p-toluene sulfonic acid with subsequent work up as previously described.

Anal. Calcd. for $C_{31}H_{28}O_6$: C, 75.00; H, 5.65. Found: C, 74.86; H, 5.68.

Mol. Wt. Calcd.: 496.1886. Found (mass spectrum): 496.1882.

The i.r. spectrum showed ν_{max}($CHCl_3$), 1735 (C=O of ester), 1699 cm^{-1} (C=O of benzoyl); n.m.r. δ ($CDCl_3$), 0.64 (3H, triplet, ester CH_3), 1.09 (triplet, 3H, ester CH_3) 3.48 (quartet, 2H, ester CH_2), 4.07 (quartet, 2H, ester CH_2), AB quartet centred at 3.97 and 4.12 (J = 3.7 Hz); 2H, 4,5 ring protons, *trans* coupled), 7.18–7.94 (multiplet, 16H, aryl protons and vinyl proton).

3-Benzoyl-2-(cis-1,2-diphenylvinyl)-4,5-dihydrofurano-[4,5-c]-2′,5′-dioxo-N-phenylpyrrolidine

A solution of 0.25 g (0.0005 mole) of 4-benzoyl-3-cyclohexyl-5-(*cis*-1,2-diphenylvinyl)-2-phenyl-4-oxazoline and 0.10 g (0.00058 mole) of *N*-phenylmaleimide in 25 ml of toluene was heated under reflux for 48 h. The resulting pale yellow solution was evaporated to low bulk and the residual oil subjected to chromatography on 120 g of alumina (B.D.H.) with benzene as eluant. The first 3 × 50 ml fractions gave on evaporation a colorless oil which crystallized on trituration with heptane to give 3-benzoyl-2-(*cis*-1,2-diphenylvinyl)-4,5-dihydrofurano-[4,5-c]-2′,5′-dioxo-*N*-phenylpyrrolidine as a white solid, 0.16 g (65.8% yield), m.p. 222–224° (heptane-diglyme).

Anal. Calcd. for $C_{33}H_{23}NO_4$: C, 79.64; H, 4.85; N, 2.87. Found: C, 79.25; H, 4.60; N, 3.0.

Mol. Wt. Calcd.: 497.1627. Found (mass spectrum): 497.1621.

The i.r. spectrum showed ν_{max}($CHCl_3$), 1780 (cyclic imide) (14), 1725–1695 cm^{-1} (broad band); n.m.r. δ ($CDCl_3$), AB quartet centered at 4.05 and 4.16 (J = 9.2 Hz; 2H, ring junction protons, *cis* coupled), 6.80–8.10 (multiplet, 21H, aryl protons and vinyl proton).

2-(cis-1,2-Diphenylvinyl)-3-p-toluoyl-4,5-dihydrofurano-[4,5-c]-2′,5′-dioxo-N-phenylpyrrolidine

This compound was prepared in 64.5% yield as a white solid, m.p. 155–158° (heptane), by heating under reflux for 48 h, a solution of 0.25 g (0.0005 mole) of 5-(*cis*-1,2-diphenylvinyl)-3-isopropyl-2-phenyl-4-*p*-toluoyl-4-oxazoline and 0.10 g (0.00058 mole) of *N*-phenylmaleimide in 30 ml of toluene. The product was obtained by the work-up method previously described.

Anal. Calcd. for $C_{34}H_{25}NO_4$: C, 79.84; H, 4.89; N, 2.74. Found: C, 79.63; H, 4.93; N, 2.60.

Mol. Wt. Calcd.: 511.1784. Found (mass spectrum): 511.1783.

The i.r. spectrum showed ν_{max}($CHCl_3$), 1780 and 1725 (cyclic imide), 1705 cm^{-1} (C=O of toluoyl group); n.m.r. δ ($CDCl_3$), 2.38 (singlet, 3H, toluoyl CH_3), AB quartet centred at 4.05 and 4.09 (J = 9.25 Hz; 2H, ring junction protons, *cis* coupled), 6.80–8.00 (multiplet, 20H, aryl protons and vinyl proton).

3-Acetyl-2-(cis-1,2-diphenylvinyl)-4,5-dihydrofurano-[4,5-c]-2′,5′-dioxo-N-phenylpyrrolidine

This compound was prepared in 34% yield as a white solid, m.p. 215.5–216.5° (absolute ethanol) by heating under reflux for 3 h a solution of 0.263 g (0.0005 mole) of 4-acetyl-2-(*p*-biphenylyl)-3-cyclohexyl-5-(*cis*-1,2-diphenylvinyl)-4-oxazoline and 0.087 g (0.0005 mole) of *N*-phenylmaleimide in 20 ml of *o*-xylene. The product was isolated as previously described.

Anal. Calcd. for $C_{28}H_{21}NO_4$: C, 77.23; H, 4.87; N, 3.22. Found: C, 77.51; H, 5.03; N, 3.00.

Mol. Wt. Calcd.: 435.1471. Found (mass spectrum): 435.1473.

The i.r. spectrum showed ν_{max}($CHCl_3$), 1715 (imide C=O), 1690 cm^{-1} (C=O of acyl group); n.m.r. δ ($CDCl_3$), 1.92 (singlet, 3H, acyl CH_3), AB quartet centred at 3.62 and 4.05 (J = 9 Hz; 2H, 4,5 ring protons, *cis* coupled), 6.70–8.00 (multiplet, 16H, aryl protons and vinyl proton).

3-Acetyl-4,5-trans-dicarbomethoxy-2-(cis-1,2-diphenylvinyl)-4,5-dihydrofuran

This compound was prepared in 40% yield as a white solid, m.p. 144–145° (absolute ethanol) by heating under reflux for 4 h, a solution of 0.263 g (0.0005 mole) of 4-acetyl-2-(*p*-biphenylyl)-3-cyclohexyl-5-(*cis*-1,2-diphenylvinyl)-4-oxazoline and 0.072 g (0.0005 mole) of dimethyl fumarate in 20 ml of *o*-xylene. The product was isolated as described in the general method.

Anal. Calcd. for $C_{24}H_{22}O_6$: C, 70.92; H, 5.46. Found: C, 70.80; H, 5.38.

Mol. Wt. Calcd.: 406.1416. Found (mass spectrum): 406.1416.

The i.r. spectrum showed ν_{max}($CHCl_3$), 1730 (C=O of ester) 1695 cm^{-1} (C=O of acyl); n.m.r. δ ($CDCl_3$), 1.60 (singlet 3H, acyl CH_3), 3.64 (singlet 3H, ester CH_3), 3.72 (singlet, 3H, ester CH_3), AB quartet centred at 3.72 and 4.21 (J = 3.8 Hz; 2H, 4.5 ring protons, *trans* coupled), 7.26–7.82 (multiplet, 11H, aryl protons and vinyl proton).

This same dihydrofuran was also prepared in 25% yield by heating under reflux for 25 min, a solution of 0.449 g (0.001 mole) of 4-acetyl-3-cyclohexyl-5-(*cis*-1,2-diphenylvinyl)-2-phenyl-4-oxazoline and 0.144 g (0.001 mole) of dimethyl fumarate in 50 ml of *o*-xylene containing 1 crystal of *p*-toluenesulfonic acid. The product was isolated as before and was identical in all respects with the dihydrofuran prepared above.

Reaction of 4-Benzoyl-3-cyclohexyl-2-(cis-1,2-diphenylvinyl)-2-(p-nitrophenyl-4-oxazoline with Acrylonitrile

A solution of 0.556 g (0.001 mole) of 4-benzoyl-3-cyclohexyl-5-(*cis*-1,2-diphenylvinyl)-2-(*p*-nitrophenyl)-4-oxazoline and 0.060 g (0.00114 mole) of acrylonitrile in 50 ml of toluene was heated under reflux for 15 h. The cooled yellow solution was concentrated to low bulk and then subjected to chromatography on 30 g of basic alumina (B.D.H.). Elution with benzene afforded 2 fractions which on solvent removal *in vacuo* gave (*i*) a yellow oil (*ii*) a colorless oil.

Fraction (*i*): This yellow oil, 0.30 g, which could not be crystallized, was found by t.l.c. to consist of one major component contaminated by two minor ones from which it could not be separated. The main component was found to be *C*-(*p*-nitrophenyl)-*N*-cyclohexylmethylimine by compatibility of its spectral data with that of authentic material synthesized for comparison purposes. One of the minor components was *p*-nitrobenzaldehyde as deduced from the i.r., n.m.r., and mass spectra.

Mol. Wt. Calcd. for $C_{13}H_{16}N_2O_2$: 232.1211. Found (mass spectrum): 232.1209.

Can. J. Chem. Downloaded from www.nrcresearchpress.com by 210.87.254.105 on 09/05/12
For personal use only.

The i.r. spectrum showed ν_{max}($CHCl_3$), 1708 (C=O of aldehyde), 1640 (C=N), 1523 (NO_2), 850 cm^{-1} (1,4-disubstituted benzene ring); n.m.r. δ ($CDCl_3$), 1.05–2.20 (multiplet, 10H, cyclohexyl C*H*$_2$), 2.88–3.96 (multiplet, 1H, cyclohexyl C*H*), 7.44–8.30 (multiplet, 5H, aryl protons and imine C*H*). 9.97 (broad based singlet, 1H, aldehyde proton).

Fraction (ii): This consisted of a colorless oil which was induced to crystallize by trituration with heptane containing a little 95% ethanol to give 3-benzoyl-4-cyano-2-(*cis*-1,2-diphenylvinyl)-4,5-dihydrofuran as a white solid, 0.105 g (28% yield), m.p. 184–186° (pink melt) from absolute ethanol.

Anal. Calcd. for $C_{26}H_{19}NO_2$: C, 82.76; H, 5.04; N, 3.71. Found: C, 82.61; H, 5.05; N, 4.00.

Mol. Wt. Calcd.: 377.1416. Found (mass spectrum): 377.1417.

The i.r. spectrum showed ν_{max}($CHCl_3$), 2225 (C≡N), 1704 cm^{-1} (C=O); n.m.r. δ ($CDCl_3$), ABX spectrum centered at 3.68 (H_a), 3.10 (H_b), and 2.89 (H_c) respectively (J_{AB} = 9.0 Hz, J_{AC} = 4.5 Hz, J_{BC} = 12.5 Hz, 4 and 5 ring protons from first order treatment), 7.23–7.80 (multiplet, 16H, aryl protons and vinyl proton).

Reaction of 4-Benzoyl-3-cyclohexyl-5-(cis-1,2-diphenylvinyl)-2-phenyl-4-oxazoline with trans-1,2-Dibenzoylethylene

A solution of 1.022 g (0.002 mole) of 4-benzoyl-3-cyclohexyl-5-(*cis*-1,2-diphenylvinyl)-2-phenyl-4-oxazoline in 100 ml of toluene containing 0.009 g (0.00005 mole) of *p*-toluenesulfonic acid was prepared, and shaken for a few moments to allow the characteristic wine red color to develop. *trans*-1,2-Dibenzoylethylene (0.480 g, 0.00204 mole) was then added and the solution heated under reflux for 7 h. The resulting light orange solution was concentrated to low volume and the orange oil produced was subjected to chromatography on 75 g of alumina (B.D.H.). The main fraction, a pale yellow band, was obtained by elution with a 2:3 mixture of hexane and benzene. Removal of the solvent produced a pale yellow oil which was induced to crystallize by trituration with hexane containing a few drops of ethanol to give a *cis–trans* mixture of 3-benzoyl-4,5-dibenzoyl-2-(*cis*-1,2-diphenylvinyl)-4,5-dihydrofuran as a white solid, 0.527 g (47% yield), m.p. 188–189° (absolute ethanol). Examination by n.m.r. revealed a cis:trans ratio of 2:1. The isomers were separated (upper and lower bands) by preparative t.l.c. on silica plates with benzene as eluant. A total of 0.213 g of the isomeric mixture was separated in this way.

Upper band: A colorless oil obtained was induced to crystallize by trituration with hexane to give 3-benzoyl-*cis*-4,5-dibenzoyl-2-(*cis*-1,2-diphenylvinyl)-4,5-dihydrofuran as a white solid, m.p. 189.5–191.5° (red melt) from absolute ethanol.

Anal. Calcd. for $C_{39}H_{28}O_4$: C, 83.57; H, 5.00. Found: C, 83.78; H, 5.16.

Mol. Wt. Calcd.: 324.1150 and 236.0837. Found (mass spectrum; main fragments measured for molecular ion peak too small): 324.1151 and 236.0839.

The i.r. spectrum showed ν_{max}($CHCl_3$), 1706 (C=O of benzoyl group unconjugated), 1685 cm^{-1} (C=O of conjugated benzoyl group), n.m.r. δ ($CDCl_3$), AB quartet centered at 4.87 and 5.23 (J = 7.1 Hz; 2H, 4,5 ring protons, *cis* coupled), 6.90–7.88 (multiplet, 26H, aryl protons and vinyl proton).

Lower band: This consisted of a pale yellow oil which was crystallized in the manner described above to give 3-benzoyl-*trans*-4,5-dibenzoyl-2-(*cis*-1,2-diphenylvinyl)-4,5-dihydrofuran as a white solid, m.p. 125–128° (red melt) from absolute ethanol.

Anal. Calcd. for $C_{39}H_{28}O_4$: C, 83.57; H, 5.00. Found: C, 83.46; H, 5.05.

Mol. Wt. Calcd.: 324.1150 and 236.0837. Found (mass spectrum; main fragments measured for parent peaks too small). 324.1154 and 236.0839.

The i.r. spectrum showed ν_{max}($CHCl_3$), 1705 (C=O of dibenzoyl groups), 1676 cm^{-1} (C=O of conjugated benzoyl group); n.m.r. δ ($CDCl_3$), AB quartet centered at 4.89 and 5.42 (J = 4.75 Hz; 2H, 4,5 ring protons, *trans* coupled), 6.92–7.84 (multiplet, 26H, aryl protons and vinyl proton).

Reactions of 3-Aroyl-4,5-dihydrofurans

3-Benzoyl-4-carboethoxy-5-carbomethoxy-2-(cis-1,2-diphenylvinyl)-trans-4,5-dihydrofuran

3-Benzoyl-*cis*-4,5-dicarboethoxy-2-(*cis*-1,2-diphenylvinyl)-4,5-dihydrofuran (0.10 g, 0.0002 mole) was heated under reflux for 30 min in 10 ml of dry methanol containing ca 0.005 g of sodium methoxide. The cooled yellow solution was concentrated *in vacuo* and the yellow oil obtained was dissolved in benzene and washed with water and finally dried ($MgSO_4$). Following filtration and removal of the solvent *in vacuo* a yellow oil was obtained which crystallized on trituration with heptane to give 3-benzoyl-4-carboethoxy-5-carbomethoxy-2-(*cis*-1,2-diphenylvinyl)-*trans*-4,5-dihydrofuran as a white solid, 0.045 g (46% yield), m.p. 163–164° (red melt) from absolute ethanol.

Anal. Calcd. for $C_{30}H_{26}O_6$: C, 74.69; H, 5.39. Found: C, 74.47; H, 5.41.

Mol. Wt. Calcd.: 482.1729. Found (mass spectrum): 482.1724.

The i.r. spectrum showed ν_{max}($CHCl_3$), 1732 (C=O of ester), 1701 cm^{-1} (C=O of benzoyl group); n.m.r. δ ($CDCl_3$), 0.75 (triplet, 3H, ethyl ester C*H*$_3$), 3.52 (quartet, 2H, ethyl ester C*H*$_2$), 3.71 (singlet, 3H, methyl ester C*H*$_3$), AB quartet centered at 4.03 and 4.22 (J = 3.5 Hz; 2H, 4,5 ring protons, *trans* coupled), 7.20–7.93 (multiplet, 16H, aryl protons and vinyl proton).

3-Benzoyl-trans-4,5-dicarbomethoxy-2-(cis-1,2-diphenylvinyl)-4,5-dihydrofuran from 3-Benzoyl-cis-4,5-dicarboethoxy-2-(cis-1,2-diphenylvinyl)-4,5-dihydrofuran

3-Benzoyl-*cis*-4,5-dicarboethoxy-2-(*cis*-1,2-diphenylvinyl)-4,5-dihydrofuran (0.08 g, 0.00016 mole) was heated under reflux for 3 h in 15 ml of dry methanol containing 0.026 g (0.00048 mole) of sodium methoxide. The yellow solution obtained was cooled and the solvent removed *in vacuo* to yield an orange gum. The organic portion of this was taken up in benzene and washed with water and then dried over anhydrous sodium sulfate. Removal of the solvent *in vacuo* gave a pale yellow oil which crystallized on trituration with 95% ethanol to give 3-benzoyl-*trans*-4,5-dicarbomethoxy-2-(*cis*-1,2-diphenylvinyl)-4,5-dihydrofuran as a white solid 0.03 g (40% yield). This compound was identical in all respects with the dihydro-

Can. J. Chem. Downloaded from www.nrcresearchpress.com by 210.87.254.105 on 09/05/12
For personal use only.

furan obtained from the [2 + 3] cycloaddition reaction of a 4-oxazoline and dimethyl fumarate.

Reaction of 3-Benzoyl-4,5-trans-dicarbomethoxy-2-(cis-1,2-diphenylvinyl)-4,5-dihydrofuran with N-Phenylmaleimide

A solution of 0.161 g (0.00034 mole) of 3-benzoyl-4,5-*trans*-dicarbomethoxy-2-(*cis*-1,2-diphenylvinyl)-4,5-dihydrofuran and 0.060 g (0.00034 mole) of *N*-phenylmaleimide in 25 ml of *n*-butylbenzene was heated under reflux for 2½ h, by which time the red solution had faded to a straw color. The solution was cooled and the solvent removed *in vacuo* yielding a yellow syrup which was subjected to chromatography on 50 g of alumina (B.D.H.). The main fraction, a yellow band, was obtained by elution with benzene, the removal of which *in vacuo*, produced a yellow oil, which was induced to crystallize by trituration with 95% ethanol to give 3-benzoyl-2-(*cis*-1,2-diphenylvinyl)-4,5-*cis*-dihydrofurano-[4,5-c]-2′,5′-dioxo-*N*-phenylpyrrolidine, 0.046 g (27% yield), m.p. 218–220° (absolute ethanol). From its spectra data this compound was shown to be identical with that prepared from a 4-oxazoline and *N*-phenylmaleimide as reported in this paper.

Reaction of 3-Benzoyl-4,5-trans-dicarboethoxy-2-(cis-1,2-diphenylvinyl)-4,5-dihydrofuran with N-Phenylmaleimide

A solution of 0.10 g (0.0002 mole) of 3-benzoyl-4,5-*trans*-dicarboethoxy-2-(*cis*-1,2-diphenylvinyl)-4,5-dihydrofuran and 0.038 g (0.00022 mole) of *N*-phenylmaleimide in 25 ml of tetrahydronaphthalene was heated under reflux for 1¾ h, by which time the red solution had faded to a straw color. The product was isolated in the manner described above as a pale yellow oil which crystallized on trituration with heptane containing a few drops of 95% ethanol to give 3-benzoyl-2-(*cis*-1,2-diphenylvinyl)-4,5-*cis*-dihydrofurano-[4,5-c]-2′,5′-dioxo-*N*-phenylpyrrolidine as a white solid, 0.015 g (15% yield). As above, this compound was shown to be identical with authentic material synthesized from a 4-oxazoline and *N*-phenylmaleimide.

Thermal Decomposition of 4-Benzoyl-3-cyclohexyl-5-(cis-1,2-diphenylvinyl)-2-phenyl-4-oxazoline in Toluene

A solution of 0.767 g (0.0015 mole) of 4-benzoyl-3-cyclohexyl-5-(*cis*-1,2-diphenylvinyl)-2-phenyl-4-oxazoline in 60 ml of toluene was heated under reflux for 48 h. The deep red solution was allowed to cool overnight by which time the color had faded to yellow. The solution was concentrated *in vacuo* and the residue taken up in a small volume of benzene from which 0.02 g of a white solid (*i*) precipitated out, and was filtered off. The benzene solution was once again concentrated and subjected to chromatography on 50 g of basic alumina (B.D.H.) with benzene as eluant. Removal of the solvent *in vacuo* gave a yellow oil which solidified on standing. Recrystallization from ethanol gave a white solid (*ii*) 0.065 g, and a yellow filtrate which on concentration and cooling afforded a bright yellow solid (*iii*) 0.07 g, m.p. 144–146° (ethanol).

These compounds were:

(i) White insoluble compound. No structure could be assigned to this highly insoluble compound whose physical and spectral data are tabulated below. The m.p. was 278–280°. Anal. Found: C, 80.96; H, 5.14; N, 0.00. This gives an empirical formula of C_8H_6O or $C_{15}H_{12}O_2$. The principal fragments in the mass spectrum: *m/e* 235 and *m/e* 105 (C_6H_5CO). The i.r. spectrum showed ν_{max}(Nujol), 3083 (sharp C=CH), 1752, 1748 (C=O) cm^{-1}. No suitable solvent for n.m.r. could be found.

(ii) White compound from column. As above no structure could be assigned to this compound whose physical and spectral data are as follows. The m.p. was 180–181°. Anal. Found: C, 80.30; H, 4.76; N, 0.00 (empirical formula C_7H_5O). The principal peaks in the mass spectrum were the same as for the compound above *i.e. m/e* 235, 178, 105. Osmometric molecular wt.: 329. The i.r. spectrum showed ν_{max}($CHCl_3$), 1819, 1817, 1795 (C=O), 1680 cm^{-1}; n.m.r. δ ($CDCl_3$), 6.34 (broad based singlet), 7.10–7.94 (multiplet aryl protons), ratio ~ 1:19.

(iii) Yellow compound. This compound was assigned as an α-pyrone **20** on the basis of the compatibility of its physical and spectral properties with those of known α-pyrones. The m.p. was 144–146°. Anal. Calcd. for $C_{23}H_{16}O_2$: C, 85.19; H, 4.94. Found: C, 84.1; H, 5.01. Mol. Wt. Calcd.: 324.1150. Found (mass spectrum): 324.1157. The i.r. spectrum showed ν_{max}($CHCl_3$), 1719 (C=O of α-pyrone), 1701 cm^{-1} (shoulder C=O); u.v. ν_{max}($CHCl_3$), 243 mμ (log ε 4.07), 265 mμ (sh) (log ε 3.99), 361 mμ (log ε 4.09); n.m.r. δ ($CDCl_3$), 7.08–7.92 (multiplet, aryl protons and ring proton).

Thermal Decomposition of 4-Benzoyl-3-cyclohexyl-5-(cis-1,2-diphenylvinyl)-2-phenyl-4-oxazoline in n-Butanol

A solution of 0.256 g (0.0005 mole) of 4-benzoyl-3-cyclohexyl-5-(*cis*-1,2-diphenylvinyl)-2-phenyl-4-oxazoline in 20 ml of *n*-butanol was heated under reflux for 48 h. The cooled red solution was evaporated *in vacuo* and the residual red oil subjected to chromatography on 25 g of basic alumina (B.D.H.). The main fraction was a yellow band which on removal of the solvent and trituration of the resulting yellow oil with heptane gave a yellow solid, 0.029 g, m.p. 143–145° from ethanol. This product was found to be identical in all respects (superimposable i.r. spectrum, mass spectrum, and undepressed mixed melting point) with the α-pyrone obtained from the decomposition of the same 4-oxazoline in toluene. No other products were obtained from this reaction.

Photochemical Decomposition of 4-Benzoyl-3-cyclohexyl-5-(cis-1,2-diphenylvinyl)-2-phenyl-4-oxazoline in Presence of Dimethyl Fumarate

A solution of 0.102 g (0.0002 mole) of 4-benzoyl-3-cyclohexyl-5-(*cis*-1,2-diphenylvinyl)-2-phenyl-4-oxazoline and 0.029 g (0.0002 mole) of dimethyl fumarate in 10 ml of chloroform was subjected to photolysis for 1 h at room temperature using a Hanovia medium pressure mercury lamp (450 W) with a Vicor 7910 filter (> 2150 Å) and a quartz tube. At no time during the reaction did any red coloration appear in the solution. The reaction was monitored by following the disappearance of the 4-oxazoline carbonyl stretching frequency. The solvent was removed *in vacuo* and the yellow oil produced subjected to chromatography on 25 g of basic alumina (B.D.H.) with benzene as eluant. Removal of the solvent gave a yellow oil which crystallized on standing. This was a two

component mixture (t.l.c.) which was separated by crystallization from ethanol to give 0.005 g of a yellow solid, m.p. 141–142°, and a white solid which was found to be dimethyl fumarate. The yellow compound possessed identical spectral properties to the α-pyrone obtained from the thermal decomposition of the 4-oxazoline and it was concluded that both compounds were identical.

Thermal Decomposition of 4-Benzoyl-3-cyclohexyl-5-(cis-1,2-diphenylvinyl)-2-phenyl-4-oxazoline

A solution of 0.5 g of the title oxazoline in 20 ml of diphenylmethane (b.p. 261°) was added to 30 ml of boiling diphenylmethane and the deep red solution heated for 2 h at which time the color had faded. The solvent was distilled *in vacuo* and the distillate examined by gas–liquid chromatography (g.l.c.) and no evidence of cyclohexane was obtained.

Synthesis of Substituted Furans by Reaction of 4-Aroyl-4-oxazolines with Acetylenic Compounds and Diphenylcyclopropenone

3-Acetyl-2-(cis-1,2-diphenylvinyl)-4,5-diphenylfuran

A solution of 0.103 g (0.0005 mole) of diphenylcyclopropenone and 0.263 g (0.0005 mole) of 4-acetyl-2-(*p*-biphenylyl)-3-cyclohexyl-5-(*cis*-1,2-diphenylvinyl)-4-oxazoline in 20 ml of *o*-xylene was heated under reflux for 18 h. The solvent was evaporated *in vacuo* and the residual dark red gum was purified by chromatography on basic alumina (B.D.H.) using benzene as eluant. A yellow band was eluted, which on solvent removal *in vacuo* gave a yellow oil. Trituration of this residual oil with a small volume of hexane afforded 3-acetyl-2-(*cis*-1,2-diphenylvinyl)-4,5-diphenylfuran as a yellow solid, 0.098 g (44.5% yield), m.p. 169–170° (ethanol).

Anal. Calcd. for $C_{32}H_{24}O_2$: C, 87.22; H, 5.49. Found: C, 87.18; H, 5.54.

Mol. Wt. Calcd.: 440.1776. Found (mass spectrum): 440.1774.

The i.r. spectrum showed $\nu_{max}(CHCl_3)$, 1690 cm^{-1} (conjugated α,β unsaturated C=O) (13); n.m.r. δ ($CDCl_3$), 1.72 (singlet, 3H, acetyl CH_3), 6.6–7.9 (multiplet, 21H, aryl protons and vinyl proton).

3-Benzoyl-2-(cis-1,2-diphenylvinyl)-4,5-diphenylfuran

A solution of 0.587 g (0.001 mole) of 4-benzoyl-2-(*p*-biphenylyl)-3-cyclohexyl-5-(*cis*-1,2-diphenylvinyl)-4-oxazoline and 0.206 g (0.001 mole) of diphenylcyclopropenone in 40 ml of toluene was heated under reflux for 12 h during which time the deep red color at first produced faded to a yellow color. The solvent was removed *in vacuo* and the residual gum was purified by chromatography on basic alumina (B.D.H.) using benzene as eluant. A yellow band was eluted first, which after evaporation of the benzene and trituration of the residue with heptane, gave 3-benzoyl-2-(*cis*-1,2-diphenylvinyl)-4,5-diphenylfuran as a yellow solid, 0.448 g (89.2% yield). This material was identical in all respects to that reported by Lown and Smalley (lit. m.p. 195–196° (8)).

3-Benzoyl-4,5-dicarboethoxy-2-(cis-1,2-diphenylvinyl)-furan

A solution of 0.25 g (0.0005 mole) of 4-benzoyl-3-cyclohexyl-5-(*cis*-1,2-diphenylvinyl)-2-phenyl-4-oxazoline and 0.19 g (0.00058 mole) of diethyl acetylenedicarboxylate in 25 ml of toluene was heated under reflux for 24 h. The resulting pale yellow solution was evaporated to low bulk and subjected to chromatography on basic alumina (B.D.H.) with benzene as eluant. Evaporation of the benzene fractions gave 3-benzoyl-4,5-dicarboethoxy-2-(*cis*-1,2-diphenylvinyl)furan (0.13 g 54% yield) as a yellow oil which solidified on trituration with heptane, m.p. 114–115° (heptane).

Anal. Calcd. for $C_{31}H_{26}O_6$: C, 75.30; H, 5.30. Found: C, 75.25; H, 4.97.

Mol. Wt. Calcd.: 494.1729. Found (mass spectrum): 494.1716.

The i.r. spectrum showed $\nu_{max}(CHCl_3)$, 1735–1706 (ester C=O), 1700 cm^{-1} (C=O of benzoyl); n.m.r. δ ($CDCl_3$), 1.13–1.16 (overlapping triplets, 6H, ester CH_3), 4.17 (overlapping quartets, 4H, ester CH_2), 7.2–7.9 (multiplet, 15H, aryl protons) 7.96 (singlet, 1H, vinyl proton).

This same furan was also prepared in 47% yield, m.p. 112° (heptane) by heating under reflux for 10 min, a solution of 0.128 g (0.00025 mole) of 4-benzoyl-3-cyclohexyl-5-(*cis*-1,2-diphenylvinyl)-2-phenyl-4-oxazoline and 0.050 g (0.00029 mole) of diethyl acetylenedicarboxylate in 6 ml of benzene containing a trace of *p*-toluenesulfonic acid. The product was isolated as previously described and proved identical in all respects to the compound prepared by the above method.

3-Benzoyl-4,5-dicarbomethoxy-2-(cis-1,2-diphenylvinyl)-furan

This compound was prepared in 43% yield as a yellow solid, m.p. 134–136° (ethanol), by heating under reflux for 15 h, a solution of 0.256 g (0.0005 mole) of 4-benzoyl-3-cyclohexyl-5-(*cis*-1,2-diphenylvinyl)-2-phenyl-4-oxazoline and 0.072 g (0.0005 mole) of dimethyl acetylenedicarboxylate in 30 ml of toluene. The product was isolated, as previously described, as a yellow oil which slowly crystallized on trituration with heptane.

Anal. Calcd. for $C_{29}H_{22}O_6$: C, 74.68; H, 4.72. Found: C, 74.55; H, 4.59.

Mol. Wt. Calcd.: 466.1416. Found (mass spectrum): 466.1415.

The i.r. spectrum showed $\nu_{max}(CHCl_3)$, 1744–1710 cm^{-1} (C=O of diester); n.m.r. δ ($CDCl_3$), 3.56 (singlet, 3H, ester CH_3), 3.61 (singlet, 3H, ester CH_3), 7.18–7.78 (multiplet, 15H, aryl protons), 7.86 (singlet, 1H, vinyl proton).

4,5-Dicarboethoxy-2-(cis-1,2-diphenylvinyl)-3-(p-toluoyl)furan

This compound was prepared in 57% yield as a pale yellow solid, m.p. 112–113°, (heptane), by heating under reflux for 48 h a solution of 0.25 g (0.00051 mole) of 5-(*cis*-diphenylvinyl)-3-isopropyl-2-phenyl-4-(*p*-toluoyl)-4-oxazoline and 0.1 g (0.00058 mole) of diethyl acetylenedicarboxylate in 25 ml of toluene. The product was isolated as previously described.

Anal. Calcd. for $C_{32}H_{28}O_6$: C, 75.58; H, 5.55. Found: 75.40; H, 5.60.

Mol. Wt. Calcd.: 508.1886. Found (mass spectrum): 508.1875.

The i.r. spectrum showed $\nu_{max}(CHCl_3)$, 1730–1695 cm^{-1} (broad band, ester and ketone C=O); n.m.r. δ ($CDCl_3$), 1.13 and 1.16 (overlapping triplets, 6H, ester CH_3), 2.37 (singlet, 3H, methyl group), 4.16 (overlapping quartets,

Can. J. Chem. Downloaded from www.nrcresearchpress.com by 210.87.254.105 on 09/05/12
For personal use only.

Can. J. Chem. Downloaded from www.nrcresearchpress.com by 210.87.254.105 on 09/05/12
For personal use only.

4H, ester CH_2), 7.0–7.8 (multiplet, 14H, aryl protons), 7.9 (singlet, 1H, vinyl proton).

3-Benzoyl-4-carbomethoxy-2-(cis-1,2-diphenylvinyl)-5-phenylfuran

This compound was prepared as described above in 59% yield as a pale yellow solid, m.p. 178–180° (ethanol), by heating under reflux for 48 h a solution of 0.25 g (0.0005 mole) of 4-benzoyl-3-cyclohexyl-5-(*cis*-1,2-diphenylvinyl)-2-phenyl-4-oxazoline and 0.1 g (0.00062 mole) of methyl phenylpropiolate in 25 ml of toluene. The product was isolated as before.

Anal. Calcd. for $C_{33}H_{24}O_4$: C, 81.79; H, 4.99. Found: C, 81.84; H, 4.89.

Mol. Wt. Calcd.: 484.1675. Found (mass spectrum): 484.1678.

The i.r. spectrum showed $\nu_{max}(CHCl_3)$, 1730 (C=O of ester), 1690 cm^{-1} (aryl ketone); n.m.r. δ ($CDCl_3$), 3.47 (singlet 3H, ester CH_3), 7.0–7.9 (multiplet, 20H, aryl protons), 8.15 (singlet, 1H, vinyl proton).

3-Benzoyl-4-carbomethoxy-2-(cis-1,2-diphenylvinyl)-5-methylfuran

This compound was prepared as described above in 48.5% yield as a pale yellow solid, m.p. 73–74° (ethanol), by heating under reflux for 48 h a solution of 0.25 g (0.0005 mole) of 4-benzoyl-3-cyclohexyl-5-(*cis*-1,2-diphenylvinyl)-2-phenyl-4-oxazoline and 0.1 g (0.001 mole) of methyl methylpropiolate in 25 ml of toluene. The product was isolated by chromatography as previously described.

Anal. Calcd. for $C_{28}H_{22}O_4$: C, 79.64; H, 5.25. Found: C, 79.35; H, 4.90.

Mol. Wt. Calcd.: 422.1518. Found (mass spectrum): 422.1528.

The i.r. spectrum showed $\nu_{max}(CHCl_3)$, 1730–1690 cm^{-1} (ester carbonyl and aryl ketone carbonyl); n.m.r. δ ($CDCl_3$), 2.7 (singlet, 3H, ring methyl group), 3.62 (singlet, 3H, ester CH_3), 6.9–7.95 (multiplet, 15H, aryl protons), 8.05 (singlet, 1H, vinyl proton).

3-Benzoyl-2-(cis-1,2-diphenylvinyl)-5-phenylfuran

This compound was prepared in 56% yield, m.p. 163–165° (ethanol), by heating under reflux for 80 min a solution of 0.556 g (0.001 mole) of 4-benzoyl-3-cyclohexyl-5-(*cis*-1,2-diphenylvinyl)-2-(*m*-nitrophenyl)-4-oxazoline and 0.110 g (0.00108 mole) of phenylacetylene in 60 ml of xylene. The furan was isolated as previously described.

Anal. Calcd. for $C_{31}H_{22}O_2$: C, 87.32; H, 5.16. Found: C, 87.06; H, 5.41.

Mol. Wt. Calcd.: 426. Found (mass spectrum): 426.

The i.r. spectrum showed $\nu_{max}(CHCl_3)$, 1698 cm^{-1} (C=O of benzoyl group); n.m.r. δ ($CDCl_3$), 6.80 (singlet, 1H, ring proton), 6.93–7.82 (multiplet, 20H, aryl protons), 8.17 (singlet, 1H, vinyl proton).

3-Benzoyl-2-(cis-1,2-diphenylvinyl)benzofuran

A solution of 0.256 g (0.0005 mole) of 4-benzoyl-3-cyclohexyl-5-(*cis*-1,2-diphenylvinyl)-2-phenyl-4-oxazoline and 0.324 g (0.001 mole) of diphenyliodonium-2-carboxylate (15) in 50 ml of 1,3,5-trimethylbenzene (b.p. 165°) was heated under reflux for a period of 20 min. The yellow solution was cooled and the solvent removed *in vacuo* giving a yellow oil which was subjected to chromatography on basic alumina (B.D.H.). Elution with *n*-pentane removed aromatic byproducts from the intermediate benzyne while the main fraction, a yellow band was obtained by elution with benzene. Removal of the solvent *in vacuo* and trituration of the resulting yellow oil with 95% ethanol gave 3-benzoyl-2-(*cis*-1.2-diphenylvinyl)benzofuran as a pale yellow solid 0.060 g (30% yield). The t.l.c. showed a minor contaminant which was removed on recrystallization from ethanol, m.p. 83–85°.

Anal. Calcd. for $C_{29}H_{20}O_2$: C, 87.00; H, 5.00. Found: C, 86.51; H, 5.12.

Mol. Wt. Calcd.: 400.1463. Found (mass spectrum): 400.1470.

The i.r. spectrum showed $\nu_{max}(CHCl_3)$, 1705 (C=O of benzoyl group); n.m.r. δ ($CDCl_3$): 7.0–7.75 (multiplet, 19H, aryl protons), 7.84 (singlet, 1H, vinyl proton).

This research was supported by a National Research Council of Canada grant to J. W. Lown. We thank Mr. J. P. Moser for technical assistance and Mr. R. Swindlehurst and Dr. A. Hogg for the n.m.r. and mass spectra, respectively.

1. J. W. Lown, R. K. Smalley, G. Dallas, and T. W. Maloney. Can. J. Chem. Preceding paper.
2. J. W. Cornforth. *In* Heterocyclic compounds. Chapter 5, Volume 5. *Edited by* R. C. Elderfield, J. Wiley and Sons, 1957. p. 334.
3. M. J. S. Dewar. Electronic theory of organic chemistry. Oxford University Press, 1949. p. 87.
4. M. Takaku, Y. Hayasi, and H. Nozaki. Tetrahedron Letters, 2053 (1969).
5. E. Winterfeldt. Ber. **98**, 1581 (1965).
6. A. W. Johnson. Ylid chemistry. *In* Organic chemistry, Series of monographs. Vol. 7. Chapts. 7 and 9. Academic Press, Inc., New York, 1966.
7. R. Huisgen. Angew. Chem. Int. Ed. **2** [10], 565, 633 (1963).
8. J. W. Lown and R. K. Smalley. Tetrahedron Letters, 169 (1969).
9. H. W. Heine, R. E. Peavy, and A. J. Durbetaki. J. Org. Chem. **31**, 3924 (1966).
10. R. Huisgen, H. Konig, G. Binsch, and H. J. Sturm. Angew. Chem. **73**, 368 (1961).
11. A. Padwa and L. Hamilton. Tetrahedron Letters, 1861 (1967).
12. T. Eicher and A. Hansen. Tetrahedron Letters, 1169 (1967).
13. L. J. Bellamy. The infrared spectra of complex molecules. Methuen, New York, 1958. p. 132.
14. L. J. Bellamy. The infrared spectra of complex molecules. Methuen, New York, 1958. p. 221.
15. F. M. Beringer and S. J. Huang. J. Org. Chem. **29**, 445 (1964).
16. I. Kuwajima and T. Mukaiyama. J. Org. Chem. **29**, 1385 (1964).

Can. J. Chem. Downloaded from www.nrcresearchpress.com by 210.87.254.105 on 09/05/12
For personal use only.

Chemistry of metal hydrides. VII. An iridium(III) carbonyl cation and the formation of iridium(III) hydridocarbonyls

H. C. Clark and R. K. Mittal
Department of Chemistry, University of Western Ontario, London, Ontario

Received July 25, 1969

$IrCl_3(PEt_3)_3$ is readily converted to $IrHCl_2(CO)(PEt_3)_2$ by treatment with carbon monoxide in hot acetone, ethanol, or 2-methoxyethanol. Perchlorate, tetrafluoroborate, and tetraphenylborate salts containing the $[IrCl_2(CO)(PEt_3)_3]^+$ cation have been prepared, but attempts to obtain salts containing the $[IrHCl(CO)(PEt_3)_3]^+$ cation give only the neutral hydride, $IrHCl_2(CO)(PEt_3)_2$. The reactions of $[IrCl_2(CO)(PEt_3)_3]^+$ with ethanol, water, lithium aluminum hydride, aqueous potassium chloride solution, and sodium alkoxides are described.

Canadian Journal of Chemistry, **48**, 119 (1970)

Introduction

In previous papers (1–3), reactions leading to the insertion of unsaturated reactants in the Pt—H bond of Pt(II) 4-coordinate hydrides were described, as well as interconversion reactions (4) between such hydrides and cationic platinum(II) carbonyl salts. While the effects of different ligands on such reactions require further study (5), it is also clear that the square planar geometry of these hydrides may be a significant factor. A related study of the chemical behavior of some octahedral transition metal hydrides was therefore thought to be desirable, and for this purpose those of iridium(III) were chosen because of their stability and detailed characterization (6, 7 and refs. therein). The preparation of some cationic carbonyl iridium(III) derivatives, for comparison with their platinum(II) analogues, was also undertaken, and by using the neutral hydrido complexes of iridium(III) as starting materials, the possibility of obtaining hydridocarbonyl iridium(III) cations has also been explored.

Experimental

I. Reagents and Starting Materials

$IrCl_3[P(C_2H_5)_3]_3$ and $IrHCl_2[P(C_2H_5)_3]_3$ were prepared by the methods of Chatt *et al.* (7, 8). Alcohols and acetone were dried by the Grignard method, followed by distillation under nitrogen. Hydrocarbon solvents were dried over phosphorus pentoxide and distilled under nitrogen. Tetrahydrofuran was dried with lithium aluminum hydride and then distilled under nitrogen.

II. Conversions of $IrCl_3[P(C_2H_5)_3]_3$ to $IrHCl_2(CO)[P(C_2H_5)_3]_2$

Samples (approximately 0.20 g) of $IrCl_3[P(C_2H_5)_3]_3$ were taken in acetone, 2-methoxyethanol, or ethanol, and carbon monoxide was bubbled through the solution for about 60 h. During this time the acetone solution was kept at 65–70°, while for the other solvents the temperature was maintained at 140–150°.

Removal of solvent left yellow viscous products which were crystallized from petroleum ether (80–100°). The products obtained in the reactions in ethanol or 2-methoxyethanol were found to be solvates of $IrHCl_2(CO)[P(C_2H_5)_3]_2$ (see the analytical data in Table 1). Sublimation of these products under vacuum at 100° gave $IrHCl_2(CO)[P(C_2H_5)_3]_2$, this also being the product formed in acetone. Reaction of $IrCl_3[P(C_2H_5)_3]_3$ with ethanol for 60 h at 100 °C did not yield hydride.

III. Preparation of Salts $\{IrCl_2(CO)[P(C_2H_5)_3]_3\}^+X$

(*a*) Silver perchlorate (0.07 g, 0.337 mmole) was dissolved in dry acetone which was then saturated with carbon monoxide. An acetone solution containing an equimolar amount of $IrCl_3[P(C_2H_5)_3]_3$ (0.216 g, 0.331 mmole) was added to each sample. An immediate white turbidity or precipitate of silver chloride was observed and this increased in amount as carbon monoxide was bubbled through the refluxing mixture. The reaction mixture was filtered and acetone removed under reduced pressure. The residue was extracted with ethanol, the extract was filtered and petroleum ether (80–100°) was added to produce needle-like crystals of $\{IrCl_2(CO)[P(C_2H_5)_3]_3\}ClO_4$ (0.15 g, 60%) (see Table 1). A similar reaction of silver tetrafluoroborate (0.064 g, 0.328 mmole) and $IrCl_3[P(C_2H_5)_3]_3$ (0.217 g, 0.332 mmole) yielded (0.15 g, 62%) $\{IrCl_2(CO)[P(C_2H_5)_3]_2\}BF_4$.

Similarly the reaction in acetone of sodium tetraphenylborate (0.115 g, 0.336 mmole) with $IrCl_3[P(C_2H_5)_3]_3$ (0.216 g, 0.331 mmole) and carbon monoxide gave a crystalline product whose analyses were in reasonable agreement with those expected for $\{IrCl_2(CO)[P(C_2H_5)_3]_3\}B(C_6H_5)_4$ (0.16 g, 50%). However, the infrared spectrum of this product showed a peak at 1950 cm^{-1} corresponding to ν_{CO} for Ir(I) compounds (9). The following procedure was therefore used.

(*b*) Sodium tetraphenylborate (0.0685 g, 0.201 mmole) and $\{IrCl_2(CO)[P(C_2H_5)_3]_3\}ClO_4$ (0.1494 g, 0.20 mmole) in a 1:1 mole ratio were allowed to react in acetone. The mixture was stirred at 25° for about 2 h; it was then filtered and acetone was removed under reduced pressure. The residue was extracted with ethanol, the extract was filtered, and crystallization was induced by the addition of petroleum ether. The crystalline product showed only a

Can. J. Chem. Downloaded from www.nrcresearchpress.com by 210.87.254.105 on 09/05/12
For personal use only.

TABLE 1

Analytical data for products of $IrCl_3[P(C_2H_5)_3]_3$ reactions

Product	Analysis (%) Found C	H	Cl	P	Calculated C	H	Cl	P	Melting point (°C)
$IrHCl_2(CO)[P(C_2H_5)_3]_2$	29.9	6.97	13.12	11.55	29.56	5.8	13.43	11.73	70
$IrHCl_2(CO)[P(C_2H_5)_3]_2$.(2-methoxyethanol)	32.76	6.53	12.6	9.55	31.78	6.57	11.73	10.24	70–72
$IrHCl_2(CO)[P(C_2H_5)_3]_2.C_2H_5OH$	32.42	6.52	13.57	9.50	31.3	6.44	12.35	10.8	70–72
$\{IrCl_2(CO)[P(C_2H_5)_3]_3\}ClO_4$	30.41	6.14	—	11.90	30.6	6.04	—	12.4	145–148
$\{IrCl_2(CO)[P(C_2H_5)_3]_3\}BF_4$	30.83	6.17	8.63	12.27	31.1	6.14	9.7	12.7	130–135
$\{IrCl_2(CO)[P(C_2H_5)_3]_3\}B(C_6H_5)_4$	54.25	7.04	—	—	53.5	6.7	—	—	158–160

Can. J. Chem. Downloaded from www.nrcresearchpress.com by 210.87.254.105 on 09/05/12
For personal use only.

very weak infrared absorption at 1950 cm^{-1} and analyzed as $\{IrCl_2(CO)[P(C_2H_5)_3]_3\}B(C_6H_5)_4$ (0.11 g, 50%) (see Table 1).

(*c*) Attempts to prepare analogous salts (X = ClO_4, BF_4, or $B(C_6H_5)_4$) containing the $\{IrHCl(CO)[P(C_2H_5)_3]_3\}^+$ using carbon monoxide, the appropriate silver or sodium salt, and $IrHCl_2[P(C_2H_5)_3]_3$ gave only $IrHCl_2(CO)[P(C_2H_5)_3]_2$, which in each case was identified analytically and spectroscopically.

IV. Reactions with $\{IrCl_2(CO)[P(C_2H_5)_3]_3\}ClO_4$

(*a*) An acetone solution of silver perchlorate (0.041 g, 0.20 mmole) was saturated with carbon monoxide and an equimolar quantity of $\{IrCl_2(CO)[P(C_2H_5)_3]_3\}ClO_4$ (0.148 g, 0.20 mmole) was added. The solution was kept at 60–70° for 20 h while carbon monoxide was bubbled through. No precipitation occurred.

(*b*) $\{IrCl_2(CO)[P(C_2H_5)_3]_3\}ClO_4$ (0.155 g, 0.208 mmole) was refluxed in ethanol under a nitrogen atmosphere for 2 h. The ethanol was then removed under reduced pressure, and the product was isolated by extracting with pentane from which it eventually crystallized. The product was identified as $[IrHCl_2(CO)[P(C_2H_5)_3]_2].C_2H_5OH$.

Anal. Calcd. for $C_{15}H_{37}O_2Cl_2P_2Ir$: C, 31.3; H, 6.44. Found: C, 30.6; H, 6.40.

Sublimation under reduced pressure at 100° gave $IrHCl_2(CO)[P(C_2H_5)_3]_2$.

Anal. Calcd. for $C_{13}H_{14}OCl_2P_2Ir$: C, 30.05; H, 5.80. Found: C, 29.54; H, 5.80.

(*c*) $\{IrCl_2(CO)[P(C_2H_5)_3]_3\}ClO_4$ (0.150 g, 0.2 mmole) was placed in a Carius tube and a saturated solution of potassium chloride in degassed distilled water was added. The tube was sealed under vacuum and was shaken at 100° for 100 h.

On opening the tube and removing the solvent, a yellow viscous material was found from which a crystalline product was isolated by extraction with ethanol and slow addition of petroleum ether to the ethanol extract. The product was identified as $IrCl_3(CO)[P(C_2H_5)_3]_2$.

Anal. Calcd. for $C_{13}H_{30}OCl_3P_2Ir$: C, 27.7; H, 5.68. Found: C, 28.54; H, 5.17.

(*d*) $\{IrCl_2(CO)[P(C_2H_5)_3]_3\}ClO_4$ (0.156 g, 0.209 mmole) was dissolved in dry tetrahydrofuran and slightly more than an equimolar amount of lithium aluminum hydride (0.01 g, 0.26 mmole) was added slowly. After the addition was complete, the mixture was refluxed for 1 h under a nitrogen atmosphere. The mixture was hydrolyzed by the addition of aqueous tetrahydrofuran and the solution was then filtered. The solvents were removed by evaporation under reduced pressure and the residue was extracted with ethanol. The addition of petroleum ether caused crystallization and further purification was achieved by recrystallization from an ethanol – petroleum ether mixture. The product, $IrHCl_2(CO)[P(C_2H_5)_3]_2$, was identified spectroscopically.

(*e*) $\{IrCl_2(CO)[P(C_2H_5)_3]_3\}ClO_4$ (0.238 g, 0.32 mmole) was dissolved in dry ethanol and sodium metal (0.0082 g, 0.36 mmole) was added to the solution (slightly more than the equimolar amount required for $NaOC_2H_5$) under a nitrogen atmosphere. The solution was refluxed with magnetic stirring for about 2 h, then filtered to remove any turbidity, and the ethanol evaporated under reduced pressure. A yellow viscous compound was obtained which was extracted with dry benzene but could not be crystallized. Spectroscopically it was found to contain $IrCl_2(COOC_2H_5)[P(C_2H_5)_3]_3$ along with some $IrHCl_2(CO)[P(C_2H_5)_3]_2$.

The compound was hydrolyzed in dichloromethane solution with a saturated aqueous potassium chloride solution in a sealed Carius tube at 100 °C for 2 days with shaking. Ethanol was identified spectroscopically in the aqueous layer and hydride in the compound.

Attempts were also made using sodium methoxide and isopropoxide and by changing the reaction medium to acetone, benzene, and tetrahydrofuran. In the case of sodium methoxide no noticeable reaction took place, while with isopropoxide there was a slight reaction. In acetone some reaction took place and in benzene there was also some reduction of iridium(III) to iridium(I). In dry tetrahydrofuran, however, appreciable reduction of iridium(III) to iridium(I) took place and the product was stable either in vacuum or inert atmosphere but was oxidized in air.

Discussion

Our starting materials for these reactions, $IrCl_3(R_3P)_3$ and $IrHCl_2(R_3P)_3$ (where R = ethyl), were prepared by the methods of Chatt *et al.* (7) and have the configurations **1** and **2**, respectively

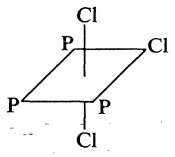

1

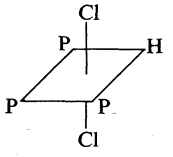

2

The trichloride complexes, $IrCl_3(R_3P)_3$, can be converted readily (10) to carbonyl complexes, $IrCl_3(CO)(R_3P)_2$, by treatment with carbon monoxide in an organic solvent, the products having configuration **3**

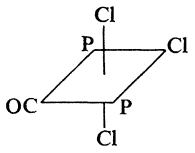

3

The trichloro-complex $IrCl_3(Et_2PhP)_3$ (configuration **1**) on treatment in ethanol with carbon monoxide also gives $IrHCl_2(CO)(Et_2PhP)_2$ of configuration **4**, but under more forcing conditions the product has configuration **5**.

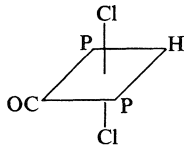

4

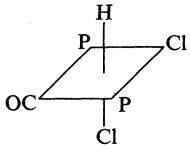

5

We have found that $IrCl_3(Et_3P)_3$, in acetone or 2-methoxyethanol at their boiling points, or in refluxing ethanol with the heating bath temperature at 140–150°, with the passage of carbon monoxide at approximately 1 atm pressure, gives good yields of the hydridocarbonyl, $IrHCl_2(CO)(PEt_3)_2$. This again has configuration **4** with carbon monoxide *trans* to hydride, confirmed by the low frequency (2105 cm^{-1}) of ν_{Ir-H}, together with the $\nu_{C=O}$ absorption at 2010 cm^{-1}, and the high field proton nuclear magnetic resonance (n.m.r.) absorption consisting of a 1:2:1 triplet at $\tau = 19.2$ with $J_{H-Ir-P} = 16.0$ c.p.s. Moreover, the infrared spectrum shows a band at 320 cm^{-1} which can be assigned to an Ir—Cl stretching vibration, whereas this frequency for chlorine *trans* to a phosphine or carbon monoxide is observed at 260–280 cm^{-1}.

Although numerous carbonyl and hydrido carbonyl neutral hexa-coordinated complexes of iridium(III) are known, few cationic species of these types have been reported. Malatesta *et al.* (11) reported that $IrH_3(PPh_3)_3$ readily evolves hydrogen on treatment with perchloric acid to give $[IrH_2(PPh_3)_3]ClO_4$. The resulting penta-coordinated cation, $[IrH_2(PPh_3)_3]^+$, is a good acceptor and readily adds another phosphine to give $[IrH_2(PPh_3)_4]^+$. Angoletta and Caglio (12) have also described the formation of two isomeric forms of $[IrH_2(CO)(PPh_3)_3]ClO_4$. We attempted to prepare the hexacoordinated cation $[IrHCl(CO)(PEt_3)_3]^+$ from carbon monoxide, $IrHCl_2(PEt_3)_3$, and silver perchlorate, silver tetrafluoroborate, or sodium tetraphenylborate, but in all cases the only iridium compound formed in good yield was $IrHCl_2(CO)(PEt_3)_2$ of configuration **4**. However, perchlorate and tetrafluoroborate salts containing the cation $[IrCl_2(CO)(PEt_3)_3]^+$ were readily obtained from similar reactions using $IrCl_3(PEt_3)_3$ instead of the hydrido complex. Their infrared spectra showed ν_{CO} at 2080 cm^{-1} for the perchlorate and 2070 cm^{-1} for the tetrafluoroborate, and also the expected strong peaks at 1000–1100 cm^{-1} and weaker peaks at 500–650 cm^{-1} associated with the anions (13). From a comparison of these carbonyl stretching frequencies with those of other iridium(III) carbonyl complexes (10), and also from the fact that one Ir—Cl stretching absorption was observed (at 320 cm^{-1} for the perchlorate and 330 cm^{-1} for the tetrafluoroborate), the cation has configuration **6** with *trans* chlorine atoms

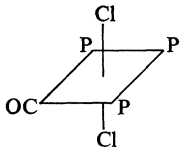

6

The product from the reaction of $IrCl_3(PEt_3)_3$ with carbon monoxide and sodium tetraphenylborate did not give reasonable analytical results for $[IrCl_2(CO)(PEt_3)_3]B(C_6H_5)_4$ and also the infrared spectrum showed, in addition to the carbonyl peak at 2075 cm^{-1}, a strong peak at 1945 cm^{-1} which is characteristic of iridium(I) carbonyls (9). Moreover, the integrated proton n.m.r. spectrum gave a ratio for ethyl:phenyl protons of 45:15 instead of the expected 45:20 ratio. Accordingly, the tetraphenylborate salt was best prepared by displacement from the perchlorate

$$[IrCl_2(CO)(P(C_2H_5)_3)_3]ClO_4 + NaB(C_6H_5)_4 \xrightarrow[25°]{\text{acetone}} [IrCl_2(CO)(P(C_2H_5)_3)_3]B(C_6H_5)_4 + NaClO_4$$

The product then gave reasonable analytical results and showed only one carbonyl absorption at 2075 cm^{-1} in the 1900–2100 cm^{-1} region.

In view of the interesting behavior of some of the platinum carbonyl cations, particularly towards alcohols and water (4), the chemistry of this iridium(III) carbonyl cation was worth further study. Unsuccessful attempts were made to displace more than one chloride from $IrCl_3(PEt_3)_3$ in the hope of obtaining more highly charged cationic species such as $[IrCl(CO)_2(PEt_3)_3]^{2+}$. This is not unexpected. The first chlorine which is readily displaced is *trans* to a phosphine with a high *trans* labilizing effect, but in the resulting cation, $[IrCl_2(CO)(PEt_3)_3]^+$,

Can. J. Chem. Downloaded from www.nrcresearchpress.com by 210.87.254.105 on 09/05/12
For personal use only.

Can. J. Chem. Downloaded from www.nrcresearchpress.com by 210.87.254.105 on 09/05/12
For personal use only.

the remaining chlorine atoms are *trans* to each other, and have little mutual labilizing effect.

The platinum carbonyl cations react with methanol and ethanol (4, 5) to give stable alkoxycarbonyls, $(R_3P)_2PtCl(COOR)$, and also the preparation of some alkoxycarbonyliridium(III) complexes has been described recently (14). These include compounds of the type $IrCl_2(COOR)(CO)L_2$ (R = CH_3, C_2H_5, or C_6H_5; L = PMe_2Ph or $AsMe_2Ph$) as well as carboxy complexes $IrCl_2(COOH)(CO)L_2$ which contain the carboxy group —COOH bound directly to a metal. It was hoped that reaction of $[IrCl_2(CO)(PEt_3)_3]^+$ with an alcohol would give $IrCl_2(COOR)(PEt_3)_3$ on analogy with the reactions of the platinum(II) cations; however, the only product obtained by refluxing the perchlorate salt with dry ethanol for 2 h was $IrHCl_2(CO)(PEt_3)_2$, obtained as a solvate with 1 molecule of ethanol. The latter was lost readily on sublimation to give the pure hydridocarbonyl. The reaction of the iridium(III) carbonyl perchlorate with water also differed substantially from that of the platinum(II) carbonyl cation which was converted to hydride (5). In the iridium(III) case, prolonged reaction of the perchlorate salt with water at 100° did not give a recognizable product, and no spectroscopic evidence could be obtained for hydride formation. Treatment with an aqueous potassium chloride solution gave only $IrCl_3(CO)(PEt_3)_2$, as might be expected from chloride ion interaction with the cation.

A further attempt was also made to obtain the hydridocarbonyl cation by treatment of the perchlorate salt with lithium aluminum hydride in refluxing tetrahydrofuran but the product was the neutral hydride $IrHCl_2(CO)(PEt_3)_2$.

The possibility of converting the carbonyl cation to an alkoxycarbonyl was further explored by investigating the reaction of the perchlorate salt with sodium ethoxide, where the following equation might apply

$$[IrCl_2(CO)(PEt_3)_3]ClO_4 + NaOEt \rightarrow IrCl_2(COOC_2H_5)(PEt_3)_3 + NaClO_4$$

This reaction produced a viscous material whose infrared spectrum showed a strong band at 1640 cm^{-1}, absorptions attributable to a

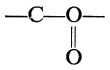

group, and to an iridium hydride. The product could not be crystallized, but on treatment with an aqueous potassium chloride gave ethanol and an unidentified hydrido compound. It appears that an alkoxy carbonyl may be formed but that other reactions, including that of the cation with ethanol, are also taking place. Similar reactions of the perchlorate with sodium methoxide, ethoxide, or isopropoxide in acetone or benzene were unsuccessful, although in benzene, and even more so in tetrahydrofuran, there appeared to be reaction leading to the formation of iridium(I) compounds.

It appears that the acceptor properties of the carbonyl iridium(III) cation determine its reactions with H^-, Cl^-, or OR^-, leading to the removal of a phosphine molecule from the coordination shell of iridium and formation of a neutral iridium(III) complex.

The financial support of the National Research Council of Canada is greatly appreciated.

1. H. C. Clark and W. S. Tsang. J. Amer. Chem. Soc. **89**, 529 (1967).
2. H. C. Clark and W. S. Tsang. J. Amer. Chem. Soc. **89**, 533 (1967).
3. H. C. Clark, K. R. Dixon, and W. J. Jacobs. J. Amer. Chem. Soc. **90**, 2259 (1968).
4. H. C. Clark, K. R. Dixon, and W. J. Jacobs. J. Amer. Chem. Soc. **91**, 1346 (1969).
5. W. J. Cherwinski and H. C. Clark. Can. J. Chem. In press.
6. L. Vaska. J. Amer. Chem. Soc. **83**, 756 (1961).
7. J. Chatt, R. S. Coffey, and B. L. Shaw. J. Chem. Soc. 7391 (1965).
8. J. Chatt, A. E. Field, and B. L. Shaw. J. Chem. Soc. 3371 (1963).
9. R. N. Scott, D. F. Shriver, and L. Vaska. J. Amer. Chem. Soc. **90**, 1079 (1968).
10. J. Chatt, N. P. Johnson, and B. L. Shaw. J. Chem. Soc. 1625 (1964).
11. L. Malatesta, M. Angoletta, A. Araneo, and F. Canziani. Angew. Chem. **73**, 273 (1961).
12. M. Angoletta and G. Caglio. Rend. Ist. Lomb. Sci. Lett. A, **97**, 823 (1963).
13. H. C. Clark and R. J. O'Brien. Inorg. Chem. **2**, 740 (1963) and refs. therein.
14. A. J. Deeming and B. L. Shaw. J. Chem. Soc. A, 443 (1969).

Isotope effect studies on elimination reactions.[1] VI. The mechanism of the bimolecular elimination reaction of 2-arylethylammonium ions[2]

P. J. SMITH[3] AND A. N. BOURNS
Department of Chemistry, McMaster University, Hamilton, Ontario
Received July 11, 1969

The mechanism of the elimination reaction of 2-arylethyltrimethylammonium ions with ethoxide ion in ethanol has been examined using tracer and kinetic isotope effect techniques. Absence of exchange with solvent of both 2-phenylethyltrimethylammonium-2,2-d_2 bromide and 2-(*p*-trifluoromethylphenyl)-ethyltrimethylammonium-2,2-d_2 bromide and the observation of nitrogen isotope effects of 1.3 and 0.9%, respectively, have eliminated a two-step process involving a freely-solvated carbanion intermediate for both salts. The observation of only a slight change in the magnitude of the nitrogen isotope effect when the solvent is changed from ethanol to water has also excluded a zwitterionic intermediate which is specifically hydrogen-bonded to the molecule of ethanol formed by removal of a β-hydrogen by ethoxide ion. Finally, tracer studies using α- and β-dideuterated substrates have eliminated the less probable reaction pathways involving ylide and carbene intermediates. It is concluded that the reaction of 2-arylethyltrimethylammonium salts with ethoxide ion is a concerted E2 process.

Canadian Journal of Chemistry, 48, 125 (1970)

Can. J. Chem. Downloaded from www.nrcresearchpress.com by 210.87.254.5 on 09/05/12
For personal use only.

Introduction

In a number of studies (1–5) in which kinetic isotope effect measurements have been used to determine transition state geometry in elimination processes, the reaction of ethoxide ion with 2-phenylethyltrimethylammonium ion producing styrene has been assumed to exemplify a typical E2 process. Considerable doubt, however, as to the validity of this assumption arose from the observation by Banthorpe and Ridd (6) that this reaction in ethanol-*O*-*d* appeared to be accompanied by isotopic exchange. They found that the unreacted quaternary salt, recovered as the tetraphenylborate after 25–30% reaction, had a deuterium content corresponding to 11.6% of that which would result from the complete exchange of one hydrogen atom per molecule. This result prompted the authors to draw the obvious conclusion that the elimination process is proceeding via the E1cb mechanism, eq. [1]

Assuming that the deuterium present in the tetraphenylborate salt is solely in the β-position and that exchange is not extraneous to the elimination reaction, it can be shown from Banthorpe's data that the ratio $k_2[\mathrm{EtOH}]/k_3$ in eq. [1] in the E1cb process would be approximately 0.35. On the other hand, work in these laboratories has shown that the nitrogen isotope effect, $(k^{14}/k^{15}-1)100$, under Banthorpe's reaction conditions, is 1.3% at 40 °C (7), showing that the C—N bond rupture is largely rate-determining. In fact, reaction by an E1cb mechanism giving rise to a nitrogen isotope effect of this magnitude and having a $k_2[\mathrm{EtOH}]/k_3$ ratio of only 0.35 would require an isotope effect for the carbon–nitrogen bond rupture step, $(k_3^{14}/k^{15}-1)100$, as large as 6%. Since the theoretical maximum isotope effect value for a C—N bond rupture process at 60 °C is about 3% (2) and since experimental values in a number of systems have all been less than 2% (2, 7–9), it would appear that there is a clear inconsistency in the isotopic exchange and the kinetic isotope effect results. Banthorpe recognized this and suggested that the transition state, for proton loss to give the carbanion, derives some stabilization from a partial breaking of the carbon–nitrogen bond.

Because of the discrepancy between Banthorpe's exchange results and the nitrogen isotope effect measurements, it was decided to reinvestigate the exchange process but with the deuterium label in the quaternary salt rather than in the solvent so as to establish the actual position of the exchange. Tests were carried out for exchange at each of the α- and β-positions by using as reactants 2-phenylethyltrimethylammonium-1,1-d_2 bromide and 2-phenylethyltrimethylammonium-2,2-d_2 bromide, respectively. In each case, the unreacted compound was isolated as the original bromide since this salt is more readily

[1]Part V: P. J. Smith and A. N. Bourns. (9).
[2]For a preliminary account of part of this study see reference 7.
[3]Holder of a N.R.C.C. studentship 1963–1964.

[1] $$PhCH_2CH_2\overset{+}{N}(CH_3)_3 + C_2H_5O^- \underset{k_2}{\overset{k_1}{\rightleftharpoons}} Ph\ddot{C}HCH_2\overset{+}{N}(CH_3)_3 + EtOH$$

$$\downarrow k_3$$

$$PhCH{=}CH_2 + N(CH_3)_3$$

[2] $$C_6H_5CH_2CH_2\overset{+}{N}(CH_3)_3 + \bar{O}Et \rightleftarrows C_6H_5CH_2\ddot{C}H\overset{+}{N}(CH_3)_3 + EtOH$$

$$C_6H_5CH_2\ddot{C}H\overset{+}{N}(CH_3)_3 \longrightarrow C_6H_5CH_2CH: + (CH_3)_3N$$

$$C_6H_5CH_2CH: \longrightarrow C_6H_5CH{=}CH_2$$

purified than the highly insoluble tetraphenylborate used by Banthorpe and Ridd.[4]

The exchange test was also carried out on 2-(*p*-trifluoromethylphenyl)-ethyltrimethylammonium-2,2-d_2 bromide since the strong electron-withdrawing substituent on the benzene ring might be expected to stabilize negative charge on the β-carbon and hence favor reaction by the E1cb mechanism.

Although the E2 and E1cb mechanisms are the most probable reaction pathways for the reaction, two other possible elimination processes have not been excluded in previous studies. One of these is the α-elimination or carbene mechanism, eq. [2], which has been observed in a few cases in which a very powerful base has been employed (11, 12). A test for this reaction pathway was carried out by determining the position of the deuterium label in the styrene formed from each of the labelled quaternary salts. 2-Phenylethyltrimethylammonium-1,1-d_2 bromide can be expected to form $C_6H_5CH{=}CD_2$ by β-elimination and $C_6H_5CH{=}CHD$ by the carbene process. On the other hand, 2-phenylethyltrimethylammonium-2,2-d_2 bromide will give $C_6H_5CD{=}CH_2$ by β-elimination and $C_6H_5CD{=}CHD$ by the α-elimination process. This test was applied to 2-(*p*-trifluoromethylphenyl)ethyltrimethylammonium-2,2-d_2 bromide as well.

A test was also carried out for reaction of the ylide (α′,β)-mechanism (13, 14) by the conventional method of examining for its deuterium content the trimethylamine formed in the reaction of the 2-phenylethyltrimethylammonium-2,2-d_2 salt, eq. [3].

[4]Subsequent to the completion of this work, Banthorpe and Ridd (10) reported on a reinvestigation of the exchange reaction and concluded that their earlier results were in error (*vide infra*).

Finally, a comparison was made of the nitrogen isotope effect in the elimination reaction with hydroxide ion in water and ethoxide ion in ethanol in an effort to distinguish between the concerted E2 process and an E1cb mechanism in which the intermediate zwitterion is specifically hydrogen-bonded to the molecule formed by abstraction of a β-hydrogen with base.

Results and Discussion

Deuterium Exchange at the β-*Carbon*

2-Phenylethyltrimethylammonium-2,2-d_2 bromide containing 1.88 atoms D/molecule was treated with 0.1 *M* ethoxide in anhydrous ethanol at 40 °C and the reaction was allowed to proceed half-way to completion. The unreacted salt was isolated and was found, within the limits of deuterium analysis by the falling-drop method (± 2%), to have the same deuterium content as the original reactant.

A nuclear magnetic resonance (n.m.r.) analysis of 1,2-dibromo-1-phenylethane formed from the styrene produced in the elimination reaction of the β-labelled salt showed signals corresponding to the phenyl- and the $-CH_2-Br$ hydrogens at 7.38 and 4.00 p.p.m. in the ratio or 5.00:2.04. There was no detectable signal at 5.15 p.p.m. which would result from the resonance of a hydrogen on the carbon adjacent to the benzene ring (β-carbon).

From these results, it can be concluded that there is no significant exchange of the hydrogens at the β-carbon. The E1cb mechanism involving a freely-solvated zwitterionic intermediate, $C_6H_5\ddot{C}HCH_2\overset{+}{N}(CH_3)_3$, in partial or complete equilibrium with reactant is therefore excluded.

Similar results were obtained in the reaction of 2-(*p*-trifluoromethylphenyl)ethyltrimethylammonium-2,2-d_2 bromide. The n.m.r. spectrum

Can. J. Chem. Downloaded from www.nrcresearchpress.com by 210.87.254.5 on 09/05/12
For personal use only.

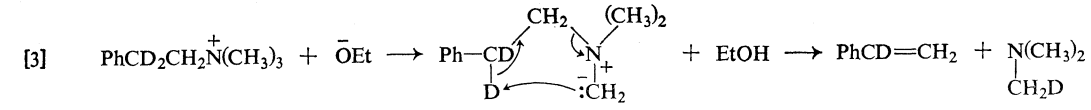

of 1,2-dibromo-1-*p*-trifluoromethylphenylethane showed peaks at 7.30 and 4.10 p.p.m. in the ratio of 4.00:1.99, with no absorption corresponding to the resonance of a hydrogen on the carbon adjacent to the benzene ring. The observation of no exchange, even when the phenyl group carries a strong electron-withdrawing substituent, agrees with the findings of Hodnett and Flynn (15) who have reported that no exchange occurred when 2-(*p*-nitrophenyl)ethyltrimethylammonium iodide is heated at 100° in tritiated water for one elimination reaction half-life.

Deuterium Exchange at the α-Carbon

An exchange test similar to that described for β-exchange was carried out with 2-phenylethyltrimethylammonium-1,1-d_2 bromide. The initial reactant analyzed for 1.94 atoms D/molecule and the salt recovered after 50% reaction showed 1.92 atoms D/molecule. These values are the same within the error of measurement and it is concluded that no significant exchange is occurring at the α-position.

In a communication accompanying a preliminary note (7) on the present investigation, Banthorpe and Ridd (10) reported that, subsequent to the publication of their initial paper (6), they had observed that the styrene formed from reaction of 2-phenylethyltrimethylammonium ion with base in deuterated solvent contained no detectable deuterium, the result expected for a reaction without exchange. They suggested that the presence of the label in the 2-phenylethyltrimethylammonium tetraphenylborate in their earlier experiments in deuterated solvent is the result of some co-precipitation of trimethylammonium tetraphenylborate, even under alkaline conditions. This contaminant would contain deuterium since the trimethylammonium ion would be formed from trimethylamine and the solvent C_2H_5OD.

Test for the Carbene (α-Elimination) Mechanism

Although the absence of exchange at the α-carbon shows that the zwitterion, $C_6H_5CH_2\ddot{\underset{\cdot\cdot}{C}}\overset{+}{H}N(CH_3)_3$, if formed, does not abstract a proton from the solvent under elimination reaction conditions, its intermediacy in an α-elimination process, eq. [2], is still a possibility provided that it were to be formed in the rate-determining step. If this were the case, however, it would be difficult to account for the nitrogen-isotope effect, unless the force constant for the carbon–nitrogen bond were to be considerably smaller in the zwitterion than in the quaternary salt.

Deuterium tracer studies provide an unequivocal test for this reaction pathway, since a β-elimination involves the loss of one hydrogen (or deuterium) from the β-carbon, while α-elimination involves the loss of a hydrogen atom (or deuterium atom) from the α-carbon and a migration of a hydrogen (or deuterium) from the β- to the α-position. This test was applied to the reaction of 2-phenylethyltrimethylammonium-1,1-d_2, 2-phenylethyltrimethylammonium-2,2-d_2, and 2-(*p*-trifluoromethylphenyl)ethyltrimethylammonium-2,2-d_2 by an n.m.r. analysis of the styrene dibromide and *p*-trifluoromethylstyrene dibromide formed in the reaction of the salts. The results are shown in Table 1 in which the absorption at 5.15 p.p.m., corresponding to the resonance of the $—CH_2Br$ hydrogens, is compared to that expected for the product from each of the two reaction pathways.

It is seen that the results clearly eliminate an α-elimination mechanism and are in complete accord with a β-elimination process for both the parent compound and the *p*-trifluoromethyl salt. This is further confirmed by the observation that the total deuterium content of the styrene dibromide formed from the 2-phenylethyltrimethylammonium-2,2-d_2, as determined by the falling-drop method, is precisely one-half that of the starting compound (0.94 compared to 1.88 atoms D/molecule).

Test for the Ylide (α′,β)-Mechanism

The reaction of 2-phenylethyltrimethylammonium-2,2-d_2 bromide with ethoxide ion in ethanol at 40° was allowed to proceed to completion and the trimethylamine, recovered as the hydrochloride, was analyzed for deuterium by the falling-drop method. No deuterium enrichment was found in this product, thus eliminating the α′,β-reaction pathway, which, as shown in eq. [3]

Can. J. Chem. Downloaded from www.nrcresearchpress.com by 210.87.254.5 on 09/05/12
For personal use only.

TABLE 1

A comparison of the number of hydrogen atoms found by n.m.r. analysis on the terminal carbon of styrene dibromide with the number predicted for the β- and α-elimination processes

	Atoms of hydrogen per molecule on the terminal carbon of the styrene dibromide		
	Predicted for		
Reactant	β-Elimination	α-Elimination	Found
$PhCD_2CH_2\overset{+}{N}(CH_3)_3$	2	1	2.04
p-CF_3—$PhCD_2CH_2\overset{+}{N}(CH_3)_3$	2	1	1.99
$PhCH_2CD_2\overset{+}{N}(CH_3)_3$	0	1	0.0

earlier, would involve the transfer of a deuterium atom on the β-carbon to a *N*-methyl carbon of the trimethylammonium group. This result is not unexpected since earlier work in this laboratory (16) has shown that α′,β-elimination is not involved in the *syn* elimination of *trans*-2-phenylcyclohexyltrimethylammonium ion with ethoxide under conditions which are more severe than those required for the elimination reaction of the acyclic salt.

The E2 Mechanism Versus an E1cb Pathway Involving a Specifically Solvated Zwitterion

Although the absence of hydrogen–deuterium exchange with solvent, coupled with a normal nitrogen isotope effect, excludes the usual E1cb mechanism, eq. [1], for the elimination reaction, there is a variant of this pathway which is not inconsistent with these observations. This is a process involving the formation of a zwitterionic intermediate which is specifically hydrogen-bonded to the molecule of ethanol formed by removal of the β-deuterium by ethoxide ion, eq. [4].

If in such a process $k_3 \gg k_4$, there would be no deuterium exchange with solvent ethanol, and if, at the same time, $k_3 \leq k_2$, the rate of elimination would be isotopically dependent on nitrogen since the step involving the rupture of the carbon–nitrogen bond would be wholly or partially rate-determining.

Such a specifically hydrogen-bonded species has been invoked by Cram *et al.* (17) to account for the very low or reverse hydrogen–deuterium isotope effects in certain isotopic exchange reactions. Formulating the isotopic exchange process by eq. [5], where DB is deuterated solvent, it is seen that the rate constant for exchange, $k_{obs.}{}^{H}$, is given by

$$\frac{k_1{}^{H} \cdot k_3{}^{H}}{k_2{}^{H} + k_3{}^{H}}.$$

Similarly, for exchange of the deuterated substrate with ordinary solvent,

$$k_{obs.}{}^{D} = \frac{k_1{}^{D} \cdot k_3{}^{D}}{k_2{}^{D} + k_3{}^{D}}.$$

It follows that the isotope effect for hydrogen–deuterium exchange, $(k^H/k^D)_{obs.}$, is equal to

$$\frac{k_1{}^{H} \cdot k_3{}^{H}}{k_1{}^{D} \cdot k_3{}^{D}} \cdot \frac{k_2{}^{D} + k_3{}^{D}}{k_2{}^{H} + k_3{}^{H}}.$$

When $k_3 \gg k_2$, this reduces to $(k^H/k^D)_{obs.} = k_1{}^{H}/k_1{}^{D}$ and a normal isotope effect favoring

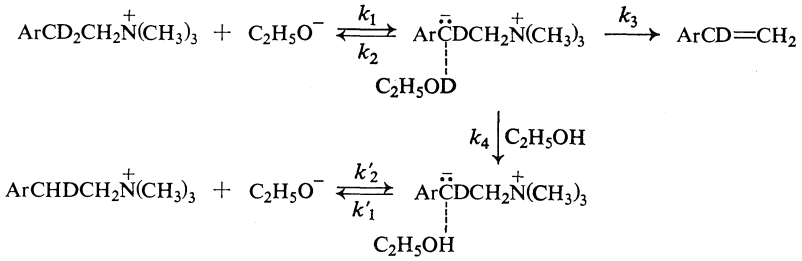

[4]

Can. J. Chem. Downloaded from www.nrcresearchpress.com by 210.87.254.5 on 09/05/12
For personal use only.

Can. J. Chem. Downloaded from www.nrcresearchpress.com by 210.87.254.5 on 09/05/12
For personal use only.

[5] $$-\overset{|}{\underset{|}{C}}-H + B \underset{k_2^H}{\overset{k_1^H}{\rightleftharpoons}} -\overset{|}{\underset{|}{C}}\overset{-}{:}\text{---}HB \xrightarrow[DB]{k_3^H} -\overset{|}{\underset{|}{C}}\overset{-}{:}\text{---}DB \longrightarrow -\overset{|}{\underset{|}{C}}-D + B$$

abstraction of hydrogen will result. This has been found, for example, in the hydrogen–deuterium exchange of toluene and $C_6H_5CD_3$ using lithium cyclohexylamide in cyclohexylamine (18). On the other hand, if $k_2 \gg k_3$, the equation for the ratio of the isotopic rate constants becomes

$$(k^H/k^D)_{obs.} = \frac{k_1^H k_2^D k_3^H}{k_1^D k_2^H k_3^D} = \frac{K^H}{K^D} \cdot \frac{k_3^H}{k_3^D}.$$

The hydrogen–deuterium isotope effect, k_3^H/k_3^D, for the second step of this process will be small since only hydrogen bonds are involved. The equilibrium isotope effect, K^H/K^D, will also be small, and may even favor the deuterated reactant, since the vibrational stretching frequency of the bond of hydrogen to either nitrogen or oxygen in the molecule HB will be greater than that of the original C—H bond. The overall isotope effect, $(k^H/k^D)_{obs.}$, therefore, will be small or less than unity. An example of this is the hydrogen–deuterium exchange reaction of toluene in dimethyl sulfoxide–potassium *tert*-butoxide, where $k^H/k^D \simeq 0.6$ was observed (19).

The β-hydrogen–deuterium isotope effect for the reaction of 2-phenylethyltrimethylammonium ion with ethoxide ion in ethanol has been measured by Saunders and Edison (1) and was found to have a value of 3.0 at 50 °C. Although this is relatively low compared to k^H/k^D values of six or more that are frequently observed in reactions in which a carbon–hydrogen bond is broken in a slow step, it is much larger than would be expected for a reaction proceeding by way of a specifically-solvated zwitterion which is in equilibrium with reactants, eq. [5]. On the other hand, the nitrogen isotope effect, $(k^{14}/k^{15}-1)100$ of 1% observed by Ayrey *et al.* at 60 °C (2) requires that the carbon–nitrogen bond be broken in a step which is at least partially rate-determining.

The only way in which both the hydrogen and nitrogen isotope effect can be accommodated by the mechanism of eq. [4] would be for the two steps, the formation and the decomposition of the specifically-solvated zwitterion, to be comparable in rate, i.e., $k_2 \simeq k_3$. Although such an equality might occur under a specific reaction condition, it would not be expected to be maintained if one were to modify the conditions, for example, by changing the solvent. The return of the intermediate to reactants involves the conversion of a zwitterion to oppositely charged ionic species, while its decomposition to product produces neutral molecules. If the rates of these two processes were to be about equal for reaction with ethoxide ion in ethanol, they should differ considerably for reaction with hydroxide ion in the much more polar solvent water. This difference would then be reflected in a large change in the magnitude of both the hydrogen and nitrogen isotope effects.

The nitrogen isotope effect for the reaction of 2-phenylethyltrimethylammonium ion has been remeasured for reaction with ethoxide ion in ethanol, this time at 40 °C, and has been determined as well for reaction with hydroxide ion in water at 97 °C. The results are shown in Table 2.

The effect of 0.8% for reaction in water at 97 °C would correspond to an effect of 1.1–1.2% at 40° (20, 21) and is therefore only slightly smaller than the 1.3% for the reaction in ethanol. A much larger difference than this would be anticipated for the two-step mechanism of eq. [4] if, as required by the isotope effect data, the rate of return of the zwitterion to reactants and the rate of its conversion to styrene are about equal in the reaction in ethanol. The E1cb mechanism involving a specifically-solvated zwitterion intermediate, therefore, would appear to have been eliminated as a reaction pathway.

A similar conclusion can be drawn from the hydrogen isotope effect data. Saunders and Edison (1) measured this effect for the reaction of the 2-phenylethyltrimethylammonium salt in ethanol and in 50% ethanol–water and obtained k^H/k^D ratios of 2.98 and 3.02, respectively, values which are identical within the limits of experimental error. Finally, the relatively small but systematic effect of *para*-substituents on the magnitude of both the hydrogen and nitrogen isotope effects in the reaction of 2-arylethyltrimethylammonium ion with ethoxide ion in ethanol (ref. 7 and unpublished results) is inconsistent with the mechanism of eq. [4].

It is concluded that no zwitterionic intermediate intervenes between reactants and products

TABLE 2

Nitrogen isotope effects in the E2 reaction of 2-phenylethyltrimethylammonium bromide

Experiment no.	Temperature	Extent of Reaction	$(k^{14}/k^{15}-1)100$
	A. Reagent: ethoxide ion in ethanol		
1	40	10	1.33
2	40	17	1.31
3	40	22	1.34
4	40	29	1.33
5	40	46	1.36
			Mean 1.33 ± 0.02*
	B. Reagent: hydroxide ion in water		
1	97	8.1	0.63
2	97	9.8	0.90
3	97	31.6	1.02
4	97	29.0	0.72
5	97	13.5	0.74
6	97	13.1	0.73
7	97	13.1	0.78
			Mean 0.78 ± 0.13*

*The error limits are given as the standard deviation.

in the elimination reaction of 2-arylethyltrimethylammonium salts and that the reaction is a simple one-step E2 process.

Experimental

Materials[5]

2-Phenylethyltrimethylammonium Bromide

This compound was synthesized using the procedure described by Saunders *et al.* (5). Tosylate ion was displaced from 2-phenylethyl tosylate by dimethylamine and the resulting dimethyl-2-phenylethylamine was quaternized by reaction with methyl bromide to give 2-phenylethyltrimethylammonium bromide; m.p. 237–238°; lit. m.p. 237.8–238.2° (5).

2-(p-Trifluoromethylphenyl)ethyltrimethylammonium Bromide

This compound was made by a reaction sequence starting with *p*-trifluoromethylbenzoic acid. This acid was converted to its ethyl ester via *p*-trifluoromethylbenzoyl chloride as an intermediate. The ethyl ester was reduced to the alcohol with lithium aluminum hydride. The alcohol was then converted to the bromide which was converted to the nitrile by a cyanide displacement. Reduction of the nitrile with lithium aluminum hydride and aluminum chloride produced the primary amine which was converted to dimethyl-2-(*p*-trifluoromethylphenyl)ethyl amine by the Escheweiler–Clarke reaction (22). Quaternization of the tertiary amine with methyl bromide yielded 2-(*p*-trifluoromethylphenyl)ethyltrimethylammonium bromide, m.p. 227.5–228°.

Anal.[6] Calcd. for $C_{12}H_{17}NBrF_3$: C, 46.18; H, 5.49; N, 4.49. Found: C, 46.18; H, 5.56; N, 4.56.

[5]All melting points are corrected.

[6]Elemental analyses were performed by Galbraith Laboratories Inc., Knoxville, Tennessee.

p-Trifluoromethylbenzoyl Chloride

To 88 g (0.46 mole) of *p*-trifluoromethylbenzoic acid was added 110 ml of thionyl chloride, purified by the method described in Fieser and Fieser (23), and the mixture was refluxed on the steam bath for 24 h. After removal of the excess thionyl chloride by distillation under reduced pressure, *p*-trifluoromethylbenzoyl chloride was distilled as a colorless liquid, 91.4 g (95%), b.p. 84–85°/20 mm; lit. b.p. 199–200°/750 mm. (24).

Ethyl p-Trifluoromethylbenzoate

Absolute (super-dry) ethanol, 72 g (1.57 mole), was added dropwise to a solution of 98.5 g (0.47 mole) of *p*-trifluoromethylbenzoyl chloride and 37.4 g (0.47 mole) of pyridine at 10°. The reaction mixture was refluxed for 3 h and was worked up using the procedure described by Haas and Bender (25), to produce 90.6 g (88%) of *p*-trifluoromethylbenzoate, b.p. 106–107°/24 mm; lit. b.p. 80.0–80.5°/5.5 mm. (25).

p-Trifluoromethylbenzyl Alcohol

Ethyl *p*-trifluoromethylbenzoate, 44 g (0.20 mole) was reduced with 5.7 g (0.15 mole) of lithium aluminum hydride in dry ether using the procedure described by Haas and Bender (25) to produce 34.3 g (97%) of product, b.p. 116–117°/27 mm; lit. b.p. 78.5–80°/4 mm. (25).

p-Trifluoromethylbenzyl Bromide

p-Trifluoromethylbenzyl alcohol, 35 g (0.20 mole), was added to 105 g (0.65 mole) of 48% hydrobromic acid using the procedure described by Haas and Bender (25) to give 35.7 g (73%) of *p*-trifluoromethylbenzyl bromide, b.p. 93.5–94°/20 mm.; lit. b.p. 65–66°/5 mm. (25).

p-Trifluoromethylbenzyl Cyanide

This compound was prepared by cyanide displacement on *p*-trifluoromethylbenzyl bromide by the method described in Vogel (26). Sodium cyanide 8.8 g in 9 ml of water was treated with 33 g (0.138 mole) of *p*-trifluoromethylbenzyl bromide in 40 ml of 95% ethanol to produce 18.6 g (73%) of *p*-trifluoromethylbenzyl cyanide, b.p. 131–132°/20 mm.

Can. J. Chem. Downloaded from www.nrcresearchpress.com by 210.87.254.5 on 09/05/12
For personal use only.

Can. J. Chem. Downloaded from www.nrcresearchpress.com by 210.87.254.5 on 09/05/12
For personal use only.

Anal. Calcd. for $C_9H_6NF_3$: C, 58.40; H, 3.26; N, 7.56. Found: C, 58.62; H, 3.42; N, 7.28.

2-(p-Trifluoromethylphenyl)ethylamine

This compound was prepared by the method described by Nystrom (27). A solution of 0.1 mole of lithium aluminum hydride and 0.1 mole of anhydrous aluminum chloride in 200 ml of anhydrous ether was treated with a solution of 0.1 mole of *p*-trifluoromethylbenzyl cyanide in 150 ml of dry ether to produce 15.1 g (80%) of product, b.p. 105.5–106°/22 mm.

Anal. Calcd. for $C_9H_{10}NF_3$: C, 57.20; H, 5.34; N, 7.40. Found: C, 55.59; H, 5.20; N, 7.18.

Dimethyl-2-(p-trifluoromethylphenyl)ethylamine

This compound was prepared from 2-(*p*-trifluoromethylphenyl)ethylamine by the method described in *Organic Syntheses* (22). To 20.5 g (0.4 mole) of ice-cooled 90% formic acid was added 15.1 g (0.08 mole) of 2-(*p*-trifluoromethylphenyl)ethylamine and 20.2 ml (0.24 mole) of 37% formalin. After completion of the reaction and work-up, 14.5 g (84%) of dimethyl-2-(*p*-trifluoromethylphenyl)ethylamine, b.p. 108–108.5°/23 mm. were recovered.

Anal. Calcd. for $C_{11}H_{14}NF_3$: C, 60.81; H, 6.50; N, 6.45. Found: C, 60.85; H, 6.67; N, 6.37.

2-Phenylethyltrimethylammonium-2,2-d_2 Bromide

This compound was prepared using the procedure described by Saunders and Edison (1). Ethyl phenylacetate-α,α-d_2 was synthesized and was found to contain 1.98 atoms D/molecule by a n.m.r. analysis. 2-Phenylethyltrimethylammonium-2,2-d_2 bromide, m.p. 238–239°; lit. m.p. 237.8–238.2° (5), prepared from the above ester in 4 steps, was found to contain 1.88 atoms D/molecule by the falling-drop method.[7]

2-(p-Trifluoromethylphenyl)ethyltrimethylammonium-2,2-d_2 Bromide

This compound was prepared by the method described for the corresponding undeuterated compound. Ethyl *p*-trifluoromethylbenzoate was reduced with lithium aluminum deuteride to produce *p*-trifluoromethylbenzyl alcohol-α,α-d_2. A n.m.r. analysis of this compound showed that it was better than 99% deuterated at the benzyl carbon. This alcohol was converted in 5 steps to 2-(*p*-trifluoromethylphenyl)ethyltrimethylammonium-2,2-d_2 bromide, m.p. 228–228.5°. A deuterium analysis by Nemeth indicated that this compound had 1.96 atoms D/molecule.

2-Phenylethyltrimethylammonium-1,1-d_2 Bromide

This compound was prepared from 2-phenylethanol-1,1-d_2 in 4 steps by the procedure of Saunders and Edison (1). Ethyl phenylacetate was reduced with lithium aluminum deuteride to produce 2-phenylethanol-1,1-d_2. A deuterium analysis by Nemeth showed this compound to contain 2.00 atoms D/molecule. This alcohol was converted to the tosylate. Tosylate ion was displaced with dimethylamine to form dimethyl-2-phenylethylamine-1,1-d_2 which was quaternized with methyl bromide to give 2-phenylethyltrimethylammonium-1,1-d_2 bromide, m.p. 237.5–238°; lit. m.p. 238–239° (5). A deuterium analysis by Nemeth indicated that this compound had 1.94 atoms D/molecule.

Deuterium Exchange Test

Exchange Tests Based on Deuterium Content of Recovered Reactant

2-Phenylethyltrimethylammonium-2,2-d_2 Bromide

The reaction of 2.1 g (0.17 mole) of quaternary salt with 0.23 *M* ethoxide in 100 ml of ethanol at 40 °C was allowed to proceed for about 1 half-life[8] and the exact extent of reaction was determined spectrophotometrically. The solution was then cooled in an ice-bath and the reaction quenched by the addition of a dilute solution of hydrobromic acid to the bromocresol green end-point. This solution was then extracted 3 times with 30 ml portions of benzene. The aqueous layer was taken to dryness under reduced pressure and the pale yellow residue was extracted 4 times with 50 ml amounts of hot acetone (Analar). The combined acetone extracts were taken to dryness under reduced pressure and the residue was recrystallized 3 times from ethanol–ether. The recovered salt, m.p. 237.5–238°, was analyzed for deuterium.

2-Phenylethyltrimethylammonium-1,1-d_2 Bromide

The procedure described in the previous paragraph was applied to the α-dideuterated salt. The recovered reactant, after 4 recrystallizations from ethanol–ether, melted at 238.8–239.4 °C.

Tracer Studies Based on Deuterium Content of Product Styrene

2-Phenylethyltrimethylammonium-2,2-d_2 Bromide

The reaction of 0.92 g (0.074 mole) of 2-phenylethyltrimethylammonium-2,2-d_2 bromide in 45 ml of 0.25 *M* sodium ethoxide in ethanol was allowed to proceed for a time corresponding to 10 half-lives. The reaction was quenched by cooling and then 20 ml of water were added and the solution extracted 3 times with 30 ml amounts of benzene. The combined benzene extracts were washed with water and then the benzene was removed by distillation under reduced pressure leaving a pale yellow liquid. To this residue was added 2 ml of dry chloroform followed by the dropwise addition of a solution of bromine in chloroform until the bromine color persisted. This solution was taken to dryness under reduced pressure leaving a white solid which was recrystallized 3 times from aqueous ethanol to give 1,2-dibromo-1-phenylethane, m.p. 77.0–77.4°; lit. m.p. 73–74° (28). A deuterium analysis was carried out on this compound using n.m.r.

2-Phenylethyltrimethylammonium-1,1-d_2 Bromide

The procedure used was that described in the previous paragraph. The isolated styrene dibromide, m.p. 77.5–78 °C, was analyzed for deuterium using n.m.r.

2-(p-Trifluoromethylphenyl)ethyltrimethylammonium-2,2-d_2 Bromide

A solution of sodium ethoxide in ethanol was added to the quaternary salt so that the concentration of each reactant was 0.0174 *M*. The reaction was allowed to proceed to completion (20 half-lives) at 40 °C and the product, *p*-trifluoromethylstyrene, was converted to its

[7]Deuterium analyses were performed by Mr. J. Nemeth, 303 W. Washington St., Urbana, Ill.

[8]The details of a kinetic study of the reaction of 2-arylethyltrimethylammonium ions with ethoxide in ethanol at 40° will be discussed in a subsequent paper.

dibromide by the method described for the parent compound. The white solid, 1,2-dibromo-1-*p*-trifluoromethylphenylethane, was recrystallized from ethanol–water to give white needles, m.p. 49–50 °C.

Anal. Calcd. for $C_9H_7Br_2F_3$: C, 32.53; H, 2.13; F, 17.17. Found: C, 32.41; H, 2.08; F, 17.16.

A deuterium analysis was carried out on this compound using n.m.r.

Test for the Ylide Mechanism Based on the Deuterium Content of Trimethylamine from the Reaction of 2-Phenylethyltrimethylammonium-2,2-d_2 Bromide

Quaternary salt, 1.07 g (0.087 mole), was treated with 50 ml of 0.113 *M* sodium ethoxide in ethanol at 40 °C in a sealed tube for one week. The trimethylamine was collected in 10 ml of 2 *N* hydrochloric acid, using the technique described by Ayrey, Bourns, and Vyas (2). The hydrochloric acid solution was taken to dryness under reduced pressure to give a white, hydroscopic salt. The trimethylamine hydrochloride was recrystallized 3 times from anhydrous ethanol, m.p. 276–277° (decomposition); lit. m.p. 277–278° (decomposition) (29). This compound was analyzed for deuterium.

Nitrogen Isotope Effects

The procedure was essentially that as described by Ayrey, *et al.* (2). Depending upon the reactivity of the compound under investigation, either of 2 methods was used to obtain the desired extent of reaction. For 2-phenylethyltrimethylammonium ion, a salt of relatively low reactivity, the reaction was stopped by rapid cooling in liquid nitrogen and the trimethylamine was then removed by distillation under reduced pressure at ice-bath temperature. For the more reactive compound, 2-(*p*-trifluoromethylphenyl)ethyltrimethylammonium ion, this method of quenching was unsatisfactory and the desired extent of reaction was achieved by adding the appropriate amount of base, corresponding to the extent of reaction required, and allowing the reaction to proceed for 20 half-lives. In these cases, the concentrations of the reactants were sufficiently low so that no more than 1% reaction occurred during the mixing of the reacting solutions.

The kinetic isotope effect was calculated as described previously (2).

This work was supported by the National Research Council of Canada.

1. W. H. Saunders Jr. and D. H. Edison. J. Amer. Chem. Soc. **82**, 138 (1960).
2. G. Ayrey, A. N. Bourns, and V. A. Vyas. Can. J. Chem. **41**, 1759 (1963).
3. H. Simon and G. Müllhofer. Chem. Ber. **97**, 2202 (1964).
4. L. J. Steffa and E. R. Thornton. J. Amer. Chem. Soc. **89**, 6149 (1967).
5. W. H. Saunders Jr., D. G. Bushman, and A. F. Cockerill. J. Amer. Chem. Soc. **90**, 1775 (1968).
6. D. V. Banthorpe and J. Ridd. Proc. Chem. Soc. 225 (1963).
7. A. N. Bourns and P. J. Smith. Proc. Chem. Soc. 366 (1964).
8. E. Buncel and A. N. Bourns. Can. J. Chem. **38**, 2457 (1960).
9. P. J. Smith and A. N. Bourns. Can. J. Chem. **44**, 2553 (1966).
10. D. V. Banthorpe and J. Ridd. Proc. Chem. Soc. 365 (1964).
11. W. Kirmse and W. von E. Doering. Tetrahedron **11**, 266 (1960).
12. V. Franzen, H. J. Schmidt, and C. Mertz. Chem. Ber. **94**, 2942 (1961).
13. G. Wittig and T. F. Burger. Ann. **632**, 85 (1960).
14. A. C. Cope and A. S. Mehta. J. Amer. Chem. Soc. **85**, 1949 (1963).
15. E. M. Hodnett and J. J. Flynn. J. Amer. Chem. Soc. **79**, 2300 (1957).
16. G. Ayrey, E. Buncel, and A. N. Bourns. Proc. Chem. Soc. 458 (1961).
17. D. J. Cram, D. A. Scott, and W. D. Nielson. J. Amer. Chem. Soc. **83**, 3696 (1961).
18. A. Streitwieser Jr., W. C. Langworthy, and D. E. Van Sickle. J. Amer. Chem. Soc. **84**, 251 (1962).
19. J. E. Hofman, A. Schriesheim, and R. E. Nichols. Private communication. Reported in Fundamentals of carbanion chemistry. *By* D. J. Cram. Academic Press, New York, 1965. p. 28.
20. J. Bigeleisen and M. G. Mayer. J. Chem. Phys. **15**, 261 (1947).
21. C. W. Young, J. S. Koehler, and D. S. McKinney. J. Amer. Chem. Soc. **69**, 1410 (1947).
22. R. N. Icke and B. B. Wisegarver. Organic synthesis. E. C. Horning, Ed. Coll. Vol. III. John Wiley and Sons, New York. p. 723.
23. C. F. Fieser. Experiments in organic chemistry. D. C. Heath and Company, Boston, Mass., 1957. p. 345.
24. R. G. Jones. J. Amer. Chem. Soc. **69**, 2346 (1947).
25. H. B. Haas and M. L. Bender. J. Amer. Chem. Soc. **71**, 1767 (1949).
26. A. I. Vogel. Practical organic chemistry. 3rd ed. Longman's Toronto. 1956. p. 761.
27. R. F. Nystrom. J. Amer. Chem. Soc. **77**, 2544 (1955).
28. W. J. Bailey and J. Bello. J. Org. Chem. **20**, 525 (1955).
29. C. D. Hodgman, ed. Handbook of chemistry and physics. 42nd ed. Chemical Rubber Publishing Co., Cleveland, 1960. p. 1262.

Can. J. Chem. Downloaded from www.nrcresearchpress.com by 210.87.254.5 on 09/05/12
For personal use only.

Can. J. Chem. Downloaded from www.nrcresearchpress.com by 210.87.254.42 on 09/05/12
For personal use only.

Isotope effect studies on elimination reactions. VII. The stereochemistry of elimination from 2-phenylethylammonium ions[1]

A. N. Bourns and A. C. Frosst[2]
Department of Chemistry, McMaster University, Hamilton, Ontario

Received July 11, 1969

The stereochemistry of the base-promoted elimination reactions of 2-phenylethyltrimethylammonium and 2-phenylethyldimethylanilinium ions has been investigated using both ethoxide ion in ethanol and *t*-butoxide in *t*-butyl alcohol as base–solvent systems. The proton magnetic resonance spectroscopic analysis of the deuterated styrene products formed from the reactions of the *threo*-2-phenylethylammonium-1,2-d_2 ions established that elimination proceeds more than 95% by an *anti* process.

Canadian Journal of Chemistry, **48**, 133 (1970)

Introduction

Base-promoted elimination reactions have generally been considered to proceed most readily via an *anti*-periplanar transition state. This geometric requirement has been regarded as arising out of the preference for the pair of electrons initially in the H—C_β bond to act on the α-carbon from one side, while the leaving group departs from the other side. Such an arrangement of atoms has been assumed in a number of studies, both in our laboratories (1–3) and elsewhere (4–6), in which kinetic isotope effects have been used to determine the effect of changes in substituents, base strength, and solvent on transition state structure in the elimination reactions of 2-arylethylammonium ions. Recently, however, it has been found that the elimination reactions of both open-chain (5, 7–12) and cyclic (13–19) quaternary ammonium ions proceed by a *syn* process more often than had previously been thought to be the case. Consequently, it seemed desirable to determine whether or not elimination in the 2-arylethylammonium system is in fact an *anti* process as has been assumed.

In the ground state, the preferred conformation for the 2-phenylethylammonium ion is undoubtedly **1**, which places the bulky groups in an *anti* relationship with one another. In order to achieve a transition state in which the departing groups are *anti* and coplanar, the bulky groups must move into staggered positions, conformation **2**, resulting in considerable steric retardation. Consequently, a normally less favored transition state geometry, which avoids this strong repulsive

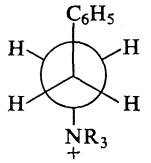

1

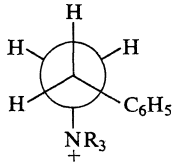

2

interaction between the two large groups, might be favored.

A study was therefore undertaken of the elimination behavior of 2-phenylethyltrimethylammonium and 2-phenylethyldimethylanilinium ions by determining, by means of proton magnetic resonance (p.m.r.) spectroscopy, the composition and configurations of the β-monodeuterated and α,β-dideuterated styrenes formed from the elimination reactions of *threo*-2-phenylethyltrimethylammonium ion (**3**) and *threo*-2-phenylethyldimethylanilinium ion (**4**). The products formed by *syn* and *anti* elimination of these ions are shown in eq. [1].

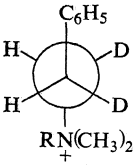

3 R = CH_3
4 R = C_6H_5

The stereochemical course of the elimination reactions has been investigated using both ethoxide ion in ethanol and *t*-butoxide ion in *t*-butyl alcohol as the base–solvent systems. The former has been used in our laboratories in most of the kinetic isotope effect studies on quaternary ammonium salt elimination reactions, while the latter has recently been shown (5, 8) to have the

[1]For Part VI in this series, see A. N. Bourns and P. J. Smith, preceding paper.
[2]McMaster University Postdoctoral Fellow, 1968–1969.

[1]

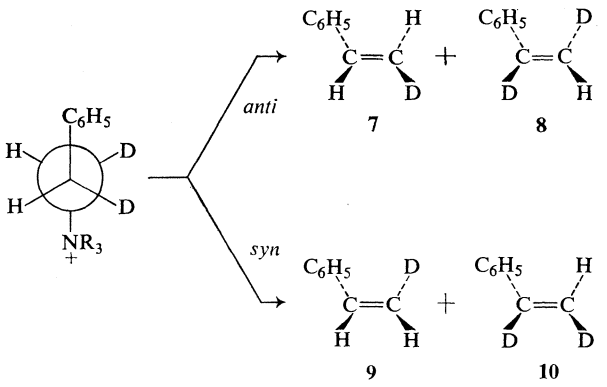

greater tendency to promote a *syn* elimination process.

The *threo*-2-phenylethyltrimethylammonium-1,2-d_2 bromide was obtained by quaternization of *threo*-2-phenylethyldimethylamine formed by nucleophilic displacement on *erythro*-2-phenylethyl-1,2-d_2 tosylate by dimethylamine. The tosylate was prepared from the corresponding alcohol which was obtained from *trans*-styrene-β-d_1 by Brown's method of hydroboration (20) using sodium borodeuteride. The *threo*-2-phenylethyldimethylanilinium-1,2-d_2 bromide was also prepared from *erythro*-2-phenylethyl-1,2-d_2 tosylate through nucleophilic displacement by *N*-methylaniline followed by quaternization with methyl bromide.

Experimental[3]

trans-Styrene-β-d_1

The *trans*-styrene-β-d_1 was supplied by Merck, Sharp and Dohme of Canada Limited, Montreal. From the p.m.r. spectrum of this material obtained using a Varian A-60 nuclear magnetic resonance (n.m.r.) spectrometer, as shown in Fig. 2*b*, and mass spectrometric analysis using a Hitachi Perkin–Elmer RMU-6A mass spectrometer, the isotopic purity of this material was found to be 89.0 ± 0.1%. The remaining 11% was determined to be undeuterated styrene.

erythro-2-Phenylethanol-1,2-d_2

This compound was prepared by the method of Brown and Zweifel (20). Sodium borodeuteride, 3.0 g (0.072 mole) (Merck, Sharp and Dohme), and 2-methyl-2-butene, 13.3 g (0.19 mole) (Eastern Chemical Corporation), in diglyme (80 ml) was treated with borontrifluoride etherate, 13.5 g (0.095 mole), in diglyme (30 ml). To the resulting solution, *trans*-styrene-β-d_1, 10.0 g (0.095 mole), in diglyme (30 ml) was added and the solution was stirred for 5 h at room temperature. Hydrolysis followed by alkaline oxidation was carried out in the usual manner with the temperature maintained below 45°C. Extraction of the product in ether and isolation by distillation gave 8.6 g (73%) of *erythro*-2-phenylethanol-1,2-d_2, b.p. 72–74°C/1 mm (undeuterated material, b.p. 77–78°C/2 mm).

erythro-2-Phenylethyl-1,2-d_2 p-Toluenesulfonate

The tosylate was prepared by the general procedure of Tipson (21). Treatment of *erythro*-2-phenylethanol-1,2-d_2, 8.6 g (0.069 mole), with *p*-toluenesulfonyl chloride, 16.4 g (0.086 mole), in dry pyridine (100 ml) gave the *p*-toluenesulfonate, 14 g (73%), m.p. 38–39°C (undeuterated material, m.p. 37.4–38°C (4); mixed m.p. 37.5–38.5°C).

threo-Dimethyl-2-phenylethylamine-1,2-d_2

The preparation of this material was performed by treating the *erythro*-2-phenylethyl-1,2-d_2 *p*-toluenesulfonate, 6.05 g (0.0217 mole), with anhydrous dimethylamine, 2.0 g (0.0453 mole), in anhydrous ether (4). Work-up of the reaction mixture gave 1.5 g (46%) of the product, b.p. 106°C/20 mm (lit. (4) b.p. 111°C/20 mm). Mass spectrometric analysis showed 0.89 atoms of deuterium on the α-carbon atom and 0.98 atoms of deuterium on the β-carbon atom.

threo-2-Phenylethyltrimethylammonium-1,2-d_2 Bromide

This compound was prepared by treating the tertiary amine, 1.3 g (0.0086 mole), with methyl bromide, 2 g (0.021 mole), in nitromethane (25 ml). The product was recrystallized from ethanol – ether to yield 1.9 g (90%), m.p. 238–238.5°C (undeuterated material, (4) m.p. 238–239.5°C).

threo-N,N-Methyl-2-phenylethylaniline-1,2-d_2

A solution of *erythro*-2-phenylethyl-1,2-d_2 *p*-toluenesulfonate, 8 g (0.0287 mole), and methylaniline, 3.4 g (0.0317 mole), in nitromethane (8 ml) was swept with dry nitrogen for 30 min. The flask was then stoppered securely and the reaction mixture was heated on the steam bath for 9 h. The nitromethane was removed under reduced pressure and then water (30 ml) and ether (20 ml) were added. The resulting solution was treated with sodium carbonate (3 g) and extracted with four 20 ml portions of ether. The combined ether layers were dried, evaporated under reduced pressure, and distilled to yield 3.5 g (57%) of the tertiary amine, b.p. 118–122°C/0.4 mm (undeuterated material, b.p. 133°C/1 mm).

[3]All melting points are corrected.

Can. J. Chem. Downloaded from www.nrcresearchpress.com by 210.87.254.42 on 09/05/12
For personal use only.

threo-2-Phenylethyldimethylanilinium-1,2-d_2 Bromide

Quaternization was carried out in the usual manner to yield 3.3 g (65%), m.p. 166–167°C (undeuterated material, m.p. 167–168°C; mixed m.p. 166–167°C).

Anal. Calcd. for $C_{16}H_{18}D_2NBr$: C, 62.34; H + D, 7.20; N, 4.55. Found: C, 62.24; H + D, 7.04; N, 4.51.

Materials for Elimination Reactions

Anhydrous ethanol was prepared by the method of Lund and Bjerrum (22). Anhydrous *t*-butyl alcohol was obtained by distilling Baker Reagent Grade material twice from sodium The standard solutions of alkoxides were obtained by dissolving the clean metal in the alcohol under a nitrogen atmosphere. Standardization of the alkoxide solutions was carried out just before use.

Elimination Reactions

The reactions were carried out in 50 ml volumetric flasks in a thermostatted bath at 60°C as described by Saunders and Williams (23). An accurately weighed amount (ca. 45 mmole) of the desired quaternary ammonium salt was dissolved in anhydrous alcohol (24 ml) in the reaction vessel and placed in the bath. After equilibration at the reaction temperature, an aliquot of standardized alkoxide solution was added to the reaction vessel and the solution made up to the standard volume with the addition of a little alcohol. After the reaction had proceeded for at least 20 half-lives, the solution was mixed with water (75 ml) and extracted with four 25 ml portions of pentane. The combined pentane layers were then washed with several aliquots of water and dried over anhydrous sodium sulfate. For reactions of the anilinium salt, it was necessary to extract the dimethylaniline out of the pentane layer with two 20 ml portions of 10% hydrochloric acid.

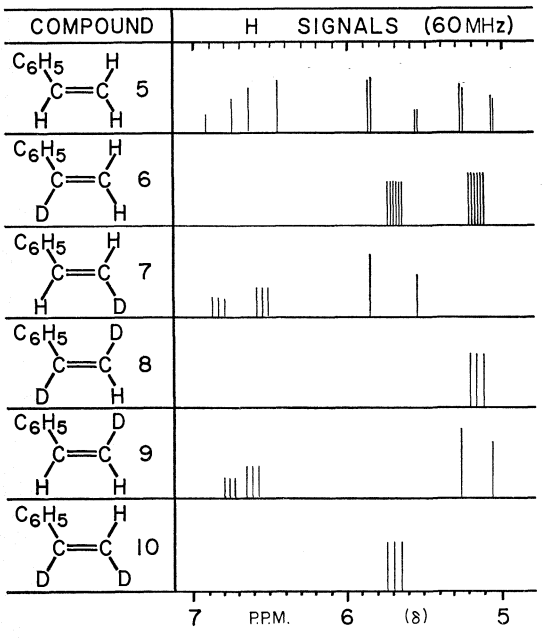

FIG. 1. Calculated signal patterns for the ethylenic protons of styrene and deuterated styrenes (24).

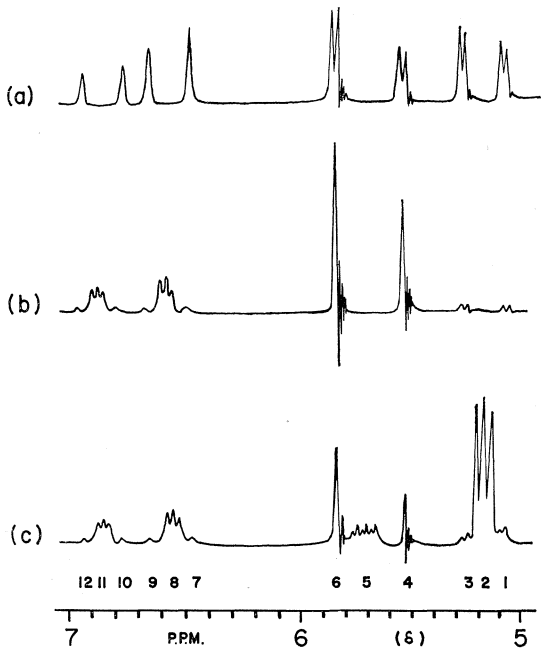

FIG. 2. Proton magnetic resonance spectra at 60 MHz of ethylenic protons for (*a*) styrene; (*b*) *trans*-styrene-β-d_1 supplied by MSD; (*c*) styrene products from reactions.

After the pentane had been removed by fractionation through a 6 in. column of glass helices, the residue styrene products were analyzed by n.m.r. spectroscopy using Varian A-60 and T-60 n.m.r. spectrometers.

Results and Discussion

Yoshino *et al.* (24) have calculated the signal patterns for the ethylenic protons of styrene and deuterated styrenes with the results as shown in Fig. 1. The spectra of styrene and the *trans*-styrene-β-d_1 supplied by Merck, Sharp and Dohme, Figs. 2*a* and 2*b*, respectively, were compared with the calculated patterns in order to confirm the signal patterns and the spin-coupling constants. The values determined from the spectra were found to be in complete agreement with the calculated values.

The styrene products recovered from the reactions all gave essentially identical spectra, of which a representative one is shown in Fig. 2*c*. These spectra were compared with the calculated patterns in order to determine the configurations of the products.

In Fig. 2*c*, the triplet 2 arises mainly from *trans*-styrene-α,β-d_2, formula **8**, the major product of *anti* elimination, with a small contribution

Can. J. Chem. Downloaded from www.nrcresearchpress.com by 210.87.254.42 on 09/05/12
For personal use only.

Can. J. Chem. Downloaded from www.nrcresearchpress.com by 210.87.254.42 on 09/05/12
For personal use only.

from styrene-α-d_1 (**6**) the major product resulting from elimination of the isotopic impurity, $C_6H_5CHDCH_2\overset{+}{N}R_3$, in the starting material. The two singlets 4 and 6 arise largely from *trans*-styrene-β-d_1 (**7**) the minor product of *anti* elimination, but will include a very small contribution from undeuterated styrene (**5**) the minor product from the isotopic impurity. The two triplets 8 and 11 also arise largely from *trans*-styrene-β-d_1 (**7**), but may include a contribution from *cis*-styrene-β-d_1 (**9**) the minor product of *syn* elimination. The two small doublets 1 and 3 and the signals 7, 9, 10, and 12 can arise from undeuterated styrene, the minor product resulting from elimination from the isotopic impurity, $C_6H_5CHDCH_2\overset{+}{N}R_3$, in the starting material, and from *cis*-styrene-β-d_1 (**9**) the minor product of *syn* elimination. The sextet 5 can arise from styrene-α-d_1 (**6**) the major product from the isotopic impurity, and from *cis*-styrene-α,β-d_2 (**10**) the major product of *syn* elimination.

For reaction exclusively by an *anti* process, the signals 5, 7, 9, 10, and 12 would arise solely from and would account completely for the elimination products, compounds **5** and **6**, formed from the 11% isotopic impurity, $C_6H_5CHDCH_2\overset{+}{N}R_3$, in the starting material. In the case of the trimethylammonium derivative, the total contributions of these peaks correspond to 14% of the product for reaction in ethoxide – ethanol and 12% for reaction in *t*-butoxide – *t*-butyl alcohol. The corresponding figures for the dimethylanilinium derivative were 12% for reaction in ethoxide – ethanol and 14% for reaction in *t*-butoxide – *t*-butyl alcohol. It can be concluded from these results that the amount of *syn* elimination in these reactions cannot exceed 4–5%.

On the other hand, there are good reasons for believing that the actual amount of *syn* elimination is much smaller than the n.m.r. data would suggest, at least for the reaction with ethoxide ion in ethanol. In the first place, there is no indication that a larger amount of the *syn* product is formed using *t*-butoxide in *t*-butyl alcohol, despite the fact that the tendency for this mode of elimination has been shown (5, 8) to be much greater in this base–solvent system. Secondly, in all cases, the ratio of the area of signal 5 to the area of the undeuterated styrene signals 7, 9, 10, and 12 is what would be predicted if signal 5 arose solely from styrene-α-d_1 (**6**) the major product from the isotopic impurity, $C_6H_5CHDCH_2\overset{+}{N}R_3$, without any contribution from *cis*-styrene-α,β-d_2 (**10**) the major product of *syn* elimination, and if there was the expected isotope effect for abstraction of hydrogen and deuterium from the β-carbon of the isotopic impurity.

These results show that the base-promoted elimination reactions of 2-phenylethyltrimethylammonium and 2-phenylethyldimethylanilinium ions do indeed proceed mainly, if not almost exclusively, via a transition state in which the departing groups occupy positions *anti* to one another. As was pointed out earlier, in order for these reactions to proceed via an *anti* elimination, the molecule must rotate about the C_α—C_β axis bringing the bulky groups into staggered positions and setting up large steric interactions between them. This transition state conformation, although sterically hindered, now has the participating orbitals coplanar. It must be concluded, therefore, that the molecule sacrifices the advantages of the less-encumbered transition state for the *anti*-periplanar transition state.

The observation of almost exclusive *anti* elimination from the 2-phenylethylammonium salts is consistent with the hypothesis offered by Bailey and Saunders (5) to account for the preference for *syn* elimination in the formation of *trans*-olefins from the reactions of salts of the type $R^1CH_2CH(R^2)\overset{+}{N}(CH_3)_3$ with bulky bases. In these systems, the β-hydrogen is shielded on both sides by the bulky alkyl groups in the conformation corresponding to **2**, mentioned earlier, whereas, in the 2-phenylethyl system, the β-hydrogen is readily accessible for attack by base.

This work was supported by the National Research Council of Canada.

1. G. Ayrey, A. N. Bourns, and V. A. Vyas. Can. J. Chem. **41**, 1759 (1963).
2. A. N. Bourns and P. J. Smith. Proc. Chem. Soc. 366 (1964).
3. A. N. Bourns and P. J. Smith. Preceding paper.
4. W. H. Saunders, Jr. and D. H. Edison. J. Amer. Chem. Soc. **82**, 138 (1960).
5. D. S. Bailey and W. H. Saunders, Jr. Chem. Commun. 1598 (1968).
6. W. H. Saunders, Jr., D. G. Bushman, and A. F. Cockerill. J. Amer. Chem. Soc. **90**, 1775 (1968).
7. J. Závada and J. Sicher. Proc. Chem. Soc. 96 (1963).
8. J. Závada and J. Sicher. Coll. Czech. Chem. Commun. **30**, 438 (1965).
9. M. Pánková, J. Sicher, and J. Závada. Chem. Commun. 394 (1967).
10. M. Pánková, J. Závada, and J. Sicher. Chem. Commun. 1142 (1968).

11. J. SICHER, J. ZÁVADA, and M. PÁNKOVÁ. Chem. Commun. 1147 (1968).
12. D. H. FROEMSDORF and H. R. PINNICK, JR. Chem. Commun. 1600 (1968).
13. J. SICHER, J. ZÁVADA, and J. KRUPICKA. Tetrahedron Lett. **15**, 1619 (1966).
14. J. ZÁVADA, M. SVOBODA, and J. SICHER. Tetrahedron Lett. **15**, 1627 (1966).
15. J. SICHER and J. ZÁVADA. Coll. Czech. Chem. Commun. **32**, 2122 (1967).
16. J. ZÁVADA and J. SICHER. Coll. Czech. Chem. Commun. **32**, 3701 (1967).
17. J. SICHER and J. ZÁVADA. Coll. Czech. Chem. Commun. **33**, 1278 (1968).
18. J. L. COKE, M. P. COOKE, JR., and M. C. MOURNING. Tetrahedron Lett. **18**, 2247 (1968).
19. J. L. COKE and M. P. COOKE, JR. Tetrahedron Lett. **18**, 2253 (1968).
20. H. C. BROWN and G. ZWEIFEL. J. Amer. Chem. Soc. **83**, 1241 (1961).
21. R. S. TIPSON. J. Org. Chem. **9**, 235 (1944).
22. H. LUND and J. BJERRUM. Chem. Ber. **64B**, 210 (1931).
23. W. H. SAUNDERS, JR. and R. A. WILLIAMS. J. Amer. Chem. Soc. **79**, 3712 (1957).
24. T. YOSHINO, Y. MANEEBE, and Y. KIKUCHI. J. Amer. Chem. Soc. **86**, 4670 (1964).

Can. J. Chem. Downloaded from www.nrcresearchpress.com by 210.87.254.42 on 09/05/12
For personal use only.

Can. J. Chem. Downloaded from www.nrcresearchpress.com by 210.87.254.42 on 09/05/12
For personal use only.

Reductive *C*-alkylation. II[1]

M. W. Roomi[2] and S. F. MacDonald
Biochemistry Laboratory, National Research Council, Ottawa, Canada

Received July 22, 1969

Methylpyrrole carboxylic esters generally are reductively methylated at 25–45°. Some are also reductively alkylated by aliphatic aldehydes generally to give, for example, 2,3(or 2,4)-dimethyl-4(or 3)-alkyl-5-carbethoxypyrroles, using hydriodic acid or HCl/AcOH–Zn/Hg respectively. An analogous alkylation by glyoxylic acid gave 5-carbethoxyhemopyrrole-dicarboxylic ester. Using HI, paraldehyde at 100° gave diethyl derivatives of dimethylpyrroles, and aminoacetal at 35° converted 2,4-dimethyl-3-acetylpyrrole into its 5-(2-amino-ethyl)-derivative. Reductive alkylations have been most useful with pyrroles but HI converted 2-biphenylcarbaldehyde into fluorene.

Canadian Journal of Chemistry, **48**, 139 (1970)

Introduction

In a further study of reductive *C*-alkylation, cf. (1), the most useful results have again been obtained with pyrroles. Attempts to methylate furans, thiophene, imidazole, and indoles have been unsuccessful, like those to ethylate benzene derivatives. However, hydriodic acid converted 2-biphenylcarbaldehyde or its acetal into fluorene.

Table 1 summarizes the pyrrole alkylations now carried out with various aldehydes and cyclopentanone using HI or HCl/AcOH–Zn/Hg. The products are coded in the table to conform to the numbers of the starting pyrroles but are distinguished by added decimal numbers; however recurring products retain their original designations. The methods of alkylation are indicated by letters A–F and *a-e*, which correspond to details in the Experimental. When the required pyrrole was obtained, no effort was made to improve the yield. The choice between methods A and B, as that between C and D, was arbitrary.

Tetramethylpyrrole (**2.1**) had been obtained from 2,4-dimethylpyrrole (**1**) and from some of its derivatives with paraformaldehyde and hydriodic acid at 100° (1). It has now been obtained in the same way from 2,3-dimethylpyrrole (**2**) from 2,5-dimethylpyrrole (**3**), from **10**, and from **13**. When paraldehyde was used instead of paraformaldehyde, the three dimethylpyrroles gave the corresponding dimethyl–diethylpyrroles (**1.1**, **2.2**, **3.1**). These latter alkylations are the first carried out with the more sensitive paraldehyde at 100°.

Reductive alkylations at 25–45°, retaining carbethoxy and acetyl groups, had been carried out on **9**, **11**, and particularly on **15** to show the variety of alkyl groups which could be introduced (1). These alkylations have been extended by the alkylation of **15** to **15.1** and to **15.2** with cyclopentanone and with aminoacetal, the latter introducing a ω-amino-ethyl group.

To find more useful applications of reductive alkylation, we studied that of pyrrole, 2-carbethoxypyrrole, and a representative series of methylpyrrole carboxylic esters at 25–45°, primarily with paraformaldehyde and paraldehyde. The results (Table 1) and earlier ones (1) separate the pyrroles into the following four groups. Presumably these define the applicability of the method to alkyl pyrrole carboxylic esters in general for, as will be reported later, the available homologues have behaved like the corresponding methyl derivatives.

(*i*) Not alkylated by paraformaldehyde: pyrrole and 2-carbethoxypyrrole,

(*ii*) Alkylated by paraformaldehyde but not by paraldehyde:

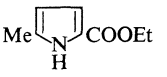

4

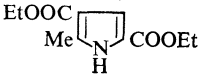

5

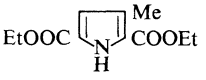

6

(*iii*) Alkylated by paraformaldehyde, paraldehyde and, presumably or in fact, higher aldehydes:

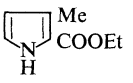

7

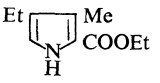

8

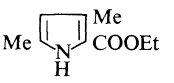

9

[1]Issued as NRCC No. 10957.
[2]NRCC Postdoctoral Fellow 1968-1970.

Can. J. Chem. Downloaded from www.nrcresearchpress.com by 210.87.254.42 on 09/05/12
For personal use only.

TABLE 1

Pyrroles and their alkylation products

Starting pyrrole	Alkylation method	Code	Substituents on pyrroles 2	3	4	5	% Yield	Melting point (°C) Found	Literature	Anal. Calcd. – Found C	H	N
		1	Me		Me							
1	B	**1.1**	"	Et	"	Et	56		(2*a*)	79.40 – 79.22	11.34 – 11.19	9.26 – 9.44
		2	Me	Me								
2	B	**2.1**	"	"	Me	Me	51	105–107	109–110(3)	77.99 – 77.81	10.64 – 10.32	11.37 – 11.45
2	B	**2.2**	"	"	Et	Et	48		(2*a*)	79.40 – 79.09	11.34 – 11.27	9.26 – 9.37
		3	Me			Me						
3	B	**2.1**	"	Me	Me	"	49	105–107				
3	B	**3.1**	"	Et	Et	"	46		(2*a*)	79.40 – 79.21	11.34 – 11.53	9.26 – 9.09
		4	COOEt			Me						
4	C*b*	**4.1**	"	Me	Me	"	50	127–129	128(2*b*)	66.27 – 66.42	8.34 – 8.40	7.73 – 7.89
		5	COOEt		COOEt	Me						
5	C($\frac{1}{2}$ h)*c*	**5.1**	"	Me	"	"	70	135	136(2*c*)	60.24 – 60.16	7.16 – 7.10	5.85 – 5.80
		6	COOEt	Me		COOEt						
6	C(45°, 3 h)*a*	**6.1**	"	"	Me	"	45	66–68	69–70(23)	60.24 – 59.93	7.16 – 7.21	5.85 – 6.06
		7	COOEt	Me								
7	C*b*	**4.1**	"	"	Me	Me	33	127–129		66.27 – 66.09	8.34 – 8.19	7.73 – 7.79
		8	COOEt	Me	Et							
8	C*b*	**8.1**	"	"	"	Me	53	91–92	95–96(2*d*)	67.66 – 67.69	8.78 – 8.72	7.17 – 7.19
8	C*b*	**8.2**	"	"	"	Et	64	71–73	73–74(4)	68.86 – 68.71	9.15 – 9.11	6.67 – 6.84
		9	COOEt	Me		Me						
9	F*b*	**9.1**	"	"	$CH_2CH_2CH_3$	"	48	99–99.5	98(5)	68.86 – 68.75	9.15 – 9.19	6.69 – 6.89
9	F*b*	**9.2**	"	"	$CHMe_2$	"	50	105–106.5		68.86 – 68.70	9.15 – 8.98	6.69 – 6.79
9	F*b*	**9.3**	"	"	$(CH_2)_3CH_3$	"	75	101–103	99(6)	69.92 – 69.84	9.48 – 9.37	6.27 – 6.37
9	F*c*	**9.4**	"	"	$(CH_2)_6CH_3$	"	51	47–49		72.41 – 72.60	10.26 – 10.11	5.28 – 5.23
9	F(25–30°, 1 h)*a*	**9.5**	"	"	$(CH_2)_{11}CH_3$	"	27	65–67		75.17 – 74.95	11.12 – 11.01	4.18 – 4.24
9	F(3 h)*d*	**9.6**	"	"	$(CH_2)_{17}CH_3$	"	40	76–78		77.27 – 77.11	11.77 – 11.71	3.34 – 3.27
		10	COOEt		Me	Me						
10	A	**2.1**	Me	Me	"	"	53	105–107				
10	C*b*	**4.1**	COOEt	Me	"	"	72	127–129		66.27 – 66.13	8.34 – 8.41	7.73 – 7.71
10	C*b*	**10.1**	"	Et	"	"	51	95–97	97(2*d*)	67.66 – 67.59	8.78 – 8.79	7.17 – 7.23
10	C(3 h)*d*	**10.2**	"	CH_2CHMe_2	"	"	45	109–111		69.92 – 70 23	9.48 – 9.79	6.27 – 6.27
10	C(3 h)*d*	**10.3**	"	$(CH_2)_6CH_3$	"	"	47	68–69		72.41 – 72.23	10.26 – 10.27	5.28 – 5.15
10	C(3 h)*b*	**10.4**	"	$(CH_2)_{11}CH_3$	"	"	35	70–71		75.17 – 75.08	11.12 – 11.04	4.18 – 4.30
10	C(3 h)*e*	**10.5**	"	$(CH_2)_{17}CH_3$	"	"	30	78–80		77.27 – 77.17	11.77 – 11.68	3.34 – 3.42
		12		COOEt	Me							
12	C*b*	**12.1**	Me	"	"	Me	70	103–105	104–105(2*e*)	66.27 – 66.11	8.34 – 8.18	7.73 – 7.65
12	C*e*	**12.2**	Et	"	"	Et	42	101–103		68.86 – 68.96	9.15 – 9.09	6.67 – 6.52
		13	Me	COOEt	Me							
13	A	**2.1**	"	Me	"	Me	53	105–107		77.99 – 77.96	10.64 – 10.43	11.37 – 11.47
13	C*b*	**12.1**	"	COOEt	"	Me	67	102–104		66.27 – 66.12	8.34 – 8.46	7.73 – 7.85
13	D*a*	**13.1**	"	"	"	Et	53	107–109	106–107(7)	67.66 – 67.31	8.78 – 8.72	7.17 – 7.08
		14	Me	COOEt		Me						
14	C*b*	**12.1**	"	"	Me	"	70	103–105		66.27 – 66.10	8.34 – 8.30	7.73 – 7.81
14	C*b*	**14.1**	"	"	Et	"	75	105–107	106–107(8)	67.66 – 67.54	8.78 – 8.69	7.17 – 7.28
14	C(1 h)*b*	**14.2**	"	"	$(CH_2)_4CH_3$	"	52	78–79		70.85 – 70.71	9.77 – 9.57	5.90 – 6.02
		15	Me	COMe	Me							
15	D*b*	**15.1**	"	"	"	$CH<(CH_2)_4$	95	167.5–168	164.5–165.5(9)	76.05 – 76.12	9.33 – 9.21	6.82 – 6.65
15	E	**15.2**	"	"	"	$CH_2CH_2NH_2$	29	106.5–107.5		66.63 – 66.51	8.95 – 8.89	15.54 – 15.62
		16	COOEt	CH_2CH_2COOEt		Me						
16	D*d*	**16.1**	"	"	Me	"	48	90.5–91.5	91(10)	62.90 – 63.06	7.92 – 8.03	5.24 – 5.19
16	D*c*	**16.2**	"	"	CH_2COOEt	"	75	66–66.5	66(11)	60.16 – 60.40	7.43 – 7.65	4.13 – 4.31
		17	COOEt	Me	Br	Me						
17	C*b*	**4.1**	"	"	Me	"	60	126–127		66.27 – 66.20	8.34 – 8.30	7.73 – 7.88

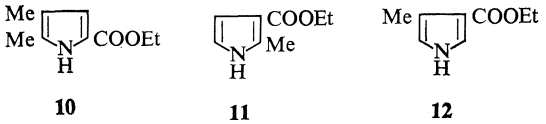

10 **11** **12**

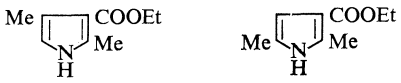

13 **14**

(*iv*) Alkylated by aldehydes and ketones:

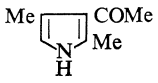

15

In the third group, the status of **7** is uncertain for its ethylation was not attempted. Some members of this group have been alkylated with higher aliphatic aldehydes to C-18 (cf. **9.1–9.6, 10.2–10.5, 14.2**) and, as no failures were encountered, the rest presumably could be. All that is known of their alkylation by ketones suggests that the results will be variable: **9** was alkylated to **9.2** by acetone but its alkylation by 2-butanone was incomplete. Alkylation by ketones will be less important because the alkyl groups in pyrroles from natural pigments are primary.

We normally used hydriodic acid, but hydrogen chloride in acetic acid with zinc amalgam was used in the alkylation of **9** by carbonyl compounds other than paraformaldehyde. Hydriodic acid was ineffective there and, in one case at least, gave the 3-(1-iodo-alkyl) derivative (1). There is no evidence that the zinc method is preferable in any other circumstances. It too failed in the ethylation of **4**, **5**, and **6** and, although an iodoalkyl derivative was again encountered in methylating **6** for only $\frac{1}{2}$ h using hydriodic acid, this was a transient intermediate.

Evidently the structural features making **9** more easily substituted than **10** (18) do not equally favor the reduction of its iodoalkyl derivatives with hydriodic acid. An analogous case is evident in the reduction of the methoxy-benzyl bromides by the same reagent, where the *m*-isomer is reduced fastest (12). As iodoacetic acid is reduced by hydriodic acid at room temperature (13), it was not surprising that **16**, though an analogue of **9**, was alkylated normally by glyoxylic acid and hydriodic acid.

The behavior of **4** with paraldehyde, in contrast to that of **9** and **10**, suggests that one factor limiting the generality of the method may be a difficulty in reducing complex intermediates from polydentate pyrroles at temperatures compatible with the retention of carbethoxy groups.

The more practical applications involved **5**, **9**, **10**, and **16**. Unfortunately, useful intermediates were not obtained from **5**. However, homologues of cryptopyrrole and hemopyrrole were obtained generally from **9** and **10** as 5-carbethoxy derivatives, and more complex hemopyrrole derivatives were obtained by alkylating **16** to **16.1** and **16.2** with paraformaldehyde or, as mentioned above, with glyoxylic acid.

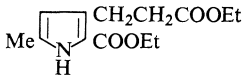

16

Finally, the displacement of halogen is illustrated by the methylation of 2,4-dimethyl-3-bromo-5-carbethoxypyrrole (**17**).

Experimental

Hydriodic acid (*d*, 1.94) and 50% hypophosphorus acid were used. The aldehydes were monomers except paraformaldehyde, paraldehyde, and stearaldehyde trimer. The sources of the starting pyrroles were as follows: **1**(2*f*); **2**(14); **3**, **5**, **10** (see below); **4**(15); **6**, **7**(16); **8**(2*g*); **9**(2*h*); **12**(17); **13**, **14**(2*i*); **15**(1); **16**(18); **17**(2*j*). Magnetic stirring was used. The m.p. are corrected. The nuclear magnetic resonance (n.m.r.) spectra of all the products were consistent with their assigned structures. The pyrroles gave positive Ehrlich reactions hot, and negative Beilstein tests for halogen.

2,5-Dimethylpyrrole (3)

Ammonium chloride (20 g) and ammonium carbonate (50 g) were dissolved in ammonium hydroxide (150 ml) by stirring at 35°. 2,5-Hexanedione (102.5 g) was added and the temperature rose to 60° over 5 min. The mixture was then heated and stirred for 10 min and the product (88%) was isolated as usual (19), b.p. 51.3–53.3°/6 mm.

2-Methyl-3,5-dicarbethoxypyrrole (5)

Phosgene (3 g) in toluene (15 ml) was added to 2-methyl-3-carbethoxypyrrole (4.59 g) in 20 ml of toluene and 3.63 g of dimethylaniline at room temperature. The mixture was allowed to stand overnight, then refluxed for 2 h. Dimethylaniline (3.63 g) in 20 ml of absolute ethanol was added at room temperature, the mixture was refluxed for 1 h, and the volatile material was removed in a rotary evaporator. The residue was added to 250 ml of 10% hydrochloric acid, and the precipitated solid was recrystallized from ethanol; yield, 70%; m.p. 129–131° (lit. (2*c*) 132°).

Anal. Calcd. for $C_{11}H_{15}O_4N$: C, 58.65; H, 6.71; N, 6.22. Found: C, 58.48; H, 6.42; N, 6.04.

Can. J. Chem. Downloaded from www.nrcresearchpress.com by 210.87.254.42 on 09/05/12
For personal use only.

Can. J. Chem. Downloaded from www.nrcresearchpress.com by 210.87.254.42 on 09/05/12
For personal use only.

*2,3-Dimethyl-5-carbethoxypyrrole (**10**)*

The carbethoxy group was introduced into 2,3-dimethylpyrrole exactly as into 2-methylpyrrole (15). The yield was 65%; m.p. 113–115° (lit. (*2h*) 114°).

Anal. Calcd. for $C_9H_{13}NO_2$: C, 64.65; H, 7.84; N, 8.38. Found: C, 64.55; H, 7.69; N, 8.49.

Methods of Alkylation Referred to in Table 1

A. The pyrrole (0.82 g) and paraformaldehyde (0.6 g) in 10 ml of acetic acid, 10 ml of hydriodic acid, and 2 ml of hypophosphorus acid were stirred for 3 h under nitrogen at 100°. The mixture was poured into water, made alkaline with ammonia, and extracted with ether. The ether was evaporated and the residue distilled (65°, 15 mm).

B. The pyrrole (2 g) and paraformaldehyde (1.2 g) in 50 ml of acetic acid, 50 ml of hydriodic acid, and 10 ml of hypophosphorus acid were treated as in method A. If paraldehyde (1.4 ml, an unintentional deficit) was used instead of paraformaldehyde, the product was distilled at ca. 50° (0.05 mm).

C. The pyrrole (4 mmoles) and 0.6 g of paraformaldehyde (or another aldehyde, for **10.4**, **10.5**, and **14.2** the theoretical amount, otherwise twice that) in 10 ml of acetic acid, 10 ml of hydriodic acid, and 2 ml of hypophosphorus acid were stirred at 25° (or as specified) for $2\frac{1}{2}$ h (or as specified). The solution (in the case of **5.1**, a suspension containing a labile and insoluble complex of this with iodine) was poured into water. The mixture was made alkaline with ammonia and the product was isolated by one of the following methods.

The solid was crystallized from (*a*) *n*-pentane, (*b*) ether – *n*-pentane, or (*c*) methanol.

The mixture was extracted with ether, the ether was evaporated, and the residue was distilled (1×10^{-4} mm) then crystallized from (*d*) *n*-pentane or (*e*) ether – *n*-pentane.

D. Hydriodic acid (10 ml) was stirred and cooled while 10 ml of acetic anhydride then 2 ml of hypophosphorus acid were added. The finely powdered pyrrole (4 mmoles) was added and stirred to solution, warming gently if necessary, then treated by one of the following methods.

(*a*) Paraldehyde (0.75 ml) was added and the solution was stirred for 5 min, decolorized with phosphonium iodide, and poured into 125 ml of ice-water. The cooled mixture was brought to p*H* 8 with ammonia and the solid was distilled (90–100°, 5×10^{-4} mm) then crystallized from *n*-hexane.

(*b*) Cyclopentanone (1.5 ml) was added in 3 portions over 45 min at 40°. After a further 30 min the solution was poured into ice-water and the solid was crystallized from *n*-hexane, from aqueous methanol, and again from *n*-hexane.

(*c*) Glyoxylic acid monohydrate (1.1 g) was added in 3 portions over 15 min at 40°. After a further 15 min the solution was evaporated (rotary, 25 then 35° bath, finally 0.5 mm). The residue was rubbed with 4 ml of water and left at 0° overnight. The solid was separated, washed with water (2 ml), dried, and warmed to solution in 5 ml of 7% hydrogen chloride in ethanol. After 6 h at 20° and some time at 0°, the product crystallized and more was obtained from the concentrated and cooled mother liquor. It was recrystallized from pentane.

(*d*) Paraformaldehyde (240 mg) was added, the solution was stirred 30 min, and the product was isolated as under (*c*).

E. Aminoacetaldehyde dimethyl acetal (0.75 ml) was dropped into a stirred solution of the pyrrole (548 mg) in 10 ml of hydriodic acid and 2 ml of hypophosphorus acid. The temperature rose to 50° then fell. After stirring for 4 h, finally at 35°, the mixture was evaporated in a shallow dish in a vacuum desiccator over KOH, finally at 0.1 mm. The residue was twice slurried and filtered with acetone. The clarified solution of the washed residue in water (5 ml) was made strongly alkaline with KOH, saturated with K_2CO_3, and extracted repeatedly with ether. The extract (125 ml) was boiled down, adding *n*-pentane toward the end to precipitate the product as pale yellow prisms.

Neut. Equiv. Calcd.: 180. Found: 182.

F. Acetic anhydride (20 ml) was stirred into 5 ml of cooled concentrated hydrochloric acid. The finely powdered pyrrole (4 mmoles) was dissolved in this and the carbonyl compound (8 mmoles) then added, followed by 10 g of zinc amalgam (20 mesh). The mixture was stirred at 20–25° (or as indicated) for 15 min (or as indicated), then decanted into ice-water. The product was isolated by one of the following methods.

The solid was distilled (1×10^{-4} mm) and either (*a*) distilled again or (*b*) crystallized from aqueous ethanol.

The mixture was extracted with ether, the washed and dried ether was evaporated, and the residue was either (*c*) distilled (100°, 1×10^{-4} mm) or (*d*) distilled (145–150°, 1×10^{-4} mm) then crystallized from pentane.

2-Biphenylcarbaldehyde Diethyl Acetal

An ethereal solution of the Grignard reagent from 2-iodobiphenyl and magnesium was treated with ethyl orthoformate, refluxed for 3 h, then worked up. The distilled product, which solidified at 0°, was drained on tile to give a crude product (ca. 80%) containing biphenyl. This was steam-distilled until about half had passed over, when the m.p. of the residue was constant and the vapor no longer smelt of biphenyl. The residue was distilled (ca. 85°, 1×10^{-3} mm) to give colorless prisms, m.p. 62–63°.

Anal. Calcd. for $C_{17}H_{20}O_2$: C, 79.65; H, 7.86. Found: C, 79.48; H, 7.84.

2-Biphenylcarbaldehyde (cf. 20–22)

The crude acetal (70 g) was hydrolyzed in 60 ml of water, 200 ml of acetic acid, and 10 ml of concentrated hydrochloric acid and the crude aldehyde, which resinified easily, was isolated and distilled, b.p. 148–151°/12 mm. Of this, 10 g was stirred for 2 days with saturated aqueous sodium metabisulfite (100 ml). The solid bisulfite complex was repeatedly washed with ether and with benzene, dissolved in water, and the p*H* of the solution was brought to 9. The aldehyde was isolated from this, using ether, as an oil (3.25 g) b.p. ca. 85°/0.1 mm, n_D^{26} 1.6200.

Anal. Calcd. for $C_{13}H_{10}O$: C, 85.69; H, 5.53. Found: C, 85.51; H, 5.40.

Fluorene

Hydriodic acid (10 ml) and 1 ml of hypophosphorus acid were stirred at 100° while 0.768 g of 2-biphenylcarbaldehyde (or 1.024 g of the acetal) in 5 ml of acetic acid were added. The mixture was stirred and slowly distilled

until the vapor reached 125° after 1 h. The combined distillate and residue were diluted with water and the product isolated using ether. It was sublimed (< 100°, 5×10^{-4} mm) and crystallized from methanol as colorless prisms (83%); Beilstein test for halogen was negative, m.p. 117.5–118° undepressed with authentic fluorene.

Anal. Calcd. for $C_{13}H_{10}$: C, 93.94; H, 6.06. Found: C, 93.67; H, 6.20.

1. B. V. GREGOROVICH, K. S. Y. LIANG, D. M. CLUGSTON, and S. F. MACDONALD. Can. J. Chem. **46**, 3291 (1968).
2. H. FISCHER and H. ORTH. Chemie des Pyrrols. Vol. I. Akademische Verlagsgesellschaft, Leipzig, 1934. (*a*) p. 58; (*b*) p. 239; (*c*) p. 255; (*d*) p. 242; (*e*) p. 248; (*f*) p. 42; (*g*) p. 241; (*h*) p. 238; (*i*) p. 247; (*j*) p. 92.
3. A. W. JOHNSON and R. PRICE. Org. Syn. **42**, 92 (1962).
4. S. F. MACDONALD and A. MARKOVAC. Can. J. Chem. **43**, 3247 (1965).
5. H. FISCHER, M. GOLDSCHMIDT, and W. NÜSSLER. Ann. Chem. **486**, 2 (1931).
6. H. FISCHER and M. BERTL. Z. Physiol. Chem. **229**, 37 (1934).
7. L. KNORR and K. HESS. Chem. Ber. **44**, 2762 (1911); **45**, 2626 (1912) (Note 1).
8. E. VECCHI. Gazz. Chim. Ital. **44**, I, 473 (1914).
9. Endo Laboratories, Inc. (by K. Schoen and I. J. Pachter), Belg. Pat. 670 796. C. A. **65**, 16943 (1966).
10. A. HAYES, G. W. KENNER, and N. R. WILLIAMS. J. Chem. Soc. 3779 (1958).
11. S. F. MACDONALD and R. J. STEDMAN. Can. J. Chem. **33**, 458 (1955).
12. A. LAPWORTH and J. S. SHOESMITH. J. Chem. Soc. 1391 (1922).
13. J. H. HOUBEN. Methoden der Organischen Chemie. Vol. II. 3rd ed. Georg Thieme Verlag, Leipzig. p. 358.
14. J. L. ARCHIBALD, D. M. WALKER, K. B. SHAW, A. MARKOVAC and S. F. MACDONALD. Can. J. Chem. **44**, 345 (1966).
15. A. TREIBS and W. OTT. Ann. Chem. **615**, 137 (1958).
16. A. H. CORWIN and J. L. STRAUGHN. J. Amer. Chem. Soc. **70**, 1416 (1948).
17. G. G. KLEINSPEHN and A. H. CORWIN. J. Amer. Chem. Soc. **75**, 5295 (1953).
18. S. F. MACDONALD. J. Chem. Soc. 4176 (1952).
19. D. M. YOUNG and C. F. H. ALLEN. Org. Syn. **16**, 25 (1936).
20. S. H. ZAHEER and S. A. FASEEH. J. Indian Chem. Soc. **21**, 381 (1944).
21. J. W. COOK, G. T. DICKSON, J. JACK, J. L. LOUDON, J. MCKEOWN, J. MACMILLAN, and W. F. WILLIAMSON. J. Chem. Soc. 139 (1950).
22. J. WIEMANN and J. J. GOTFROID. Compt. Rend. **255**, 2608 (1962).
23. U. EISNER, R. P. LINSTEAD, E. A. PARKS, and E. STEPHEN. J. Chem. Soc. 1655 (1956).

Can. J. Chem. Downloaded from www.nrcresearchpress.com by 210.87.254.42 on 09/05/12
For personal use only.

Can. J. Chem. Downloaded from www.nrcresearchpress.com by 210.87.254.5 on 09/05/12
For personal use only.

Dérivés du *tert*-butyl-3 cyclohexène. II. Les *tert*-butyl-3 cyclohexanediols-1,2

JEAN-CLAUDE RICHER ET CHRISTIAN FREPPEL
Département de Chimie, Université de Montréal, B. P. 6128, Montréal, Québec

Reçu le 11 août 1969

La stéréochimie de l'hydrolyse acide des époxydes dérivés du *tert*-butyl-3 cyclohexène est examinée. Pour fins de comparaisons les quatre *tert*-butyl-3 cyclohexanediols-1,2 ont été préparés et caractérisés.

Canadian Journal of Chemistry, **48**, 145 (1970)

Introduction

A la suite des travaux (1) qui nous ont amené à examiner la stéréochimie de la formation et de la réduction par $LiAlH_4$ des époxydes (**2** et **3**) du *tert*-butyl-3 cyclohexène (**1**), il nous est apparu intéressant, pour fins de comparaisons, d'étudier la stéréochimie de leur ouverture par l'acide formique (2, 3). Les résultats obtenus au cours de cette étude, ainsi que la caractérisation des quatre diols qui en dérivent, font l'objet de la présente communication.

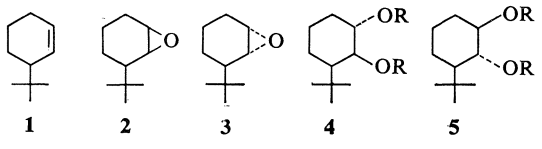

1 **2** **3** **4** **5**

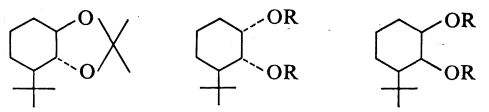

6 **7** **8**

a R = H *b* R = $Si(CH_3)_3$

Résultats et discussions

Les diols *trans* (**4***a* et **5***a*) sont obtenus avec un excellent rendement par hydroxylation directe (4, 5) du *tert*-butyl-3 cyclohexène (**1**); leur séparation a été effectuée en tirant partie du fait que seul le diol **5***a* est susceptible de former le dioxolane **6** (6–8) par réaction avec de l'acétone. L'action soit du tétroxyde d'osmium (6, 9, 10) soit du permanganate de potassium (11) sur l'alcène **1** conduit exclusivement au diol *cis*-**7***a* provenant d'une attaque de ces réactifs par la face opposée à celle du groupe *tert*-butyle. Par ailleurs, l'action conjuguée de l'iode et de l'acétate d'argent (10, 12, 13) sur l'alcène **1** conduit à un mélange contenant 57% du diol **7***a* et 43% de **8***a*; la séparation des deux isomères est réalisée par chromatographie sur gel de silice, des dérivés silylés (14, 15) **7***b* et **8***b*. Les propriétés des diols ainsi obtenus sont résumées dans le tableau 1. Les configurations relatives des diols, attribuées d'après leur mode respectif de formation sont en accord avec les déplacements chimiques observés pour les hydrogènes carbinoliques (16); l'absence de pont hydrogène intra-

TABLEAU 1

Propriétés des *tert*-butyl-3 cyclohexanediols-1,2

Produit	Point de fusion (°C)	Chromatographie en phase gazeuse*	Infrarouge† (cm^{-1})			Résonance magnétique nucléaire (p.p.m.)	
			OH libre	OH associé	Δν	C*H*—OH‡	
4*a*	98	5.2	3630			3.82	4.07
5*a*	54–56	8.1	3632	3589	43	3.30	
7*a*	69–70	6.5	3636	3582	54	3.50	3.82
8*a*	78–79	7.2	3627	3585	42	3.35	4.00

*Temps de rétention (min) des dérivés silylés correspondants utilisant une colonne de 6′ × 1/8″ maintenue à 170 °C et contenant 10% UCW 98 déposé sur du Diatoport S 80–100 mesh; le gaz porteur (40 ml/min) est l'azote.
†Pour des solutions ca. 3.5×10^{-3} *M* dans le CCl_4.
‡En solution dans le $CDCl_3$.

TABLEAU 2

Stéréochimie de l'hydrolyse des époxydes **2** et **3**

Epoxydes	Composition des diols*
(%) *cis*-**2**/(%) *trans*-**3**	(%) **4***a*/(%) **5***a*
0/100	47/53
10/90	53/47
74/26	85/15
84/16	91/9
(100)/(0)†	(100)/(0)

*Composition déterminées par c.p.g. et moyennes de 3 mesures. Incertitude ± 2%.
†Les valeurs entre parenthèses sont extrapolées.

moléculaire dans le spectre infra-rouge (i.r.) du diol **4***a* confirme aussi la configuration proposée.

A l'aide de ces produits de configuration établie sans ambiguités, il a été possible, utilisant la chromatographie en phase gazeuse (c.p.g.) des dérivés silylés comme méthode analytique, d'établir la stéréochimie de l'hydrolyse des époxydes **2** et **3** par l'acide formique; les résultats obtenus sont consignés dans le tableau 2.

Ces résultats qui peuvent être rapprochés de ceux obtenus lors de la réduction des époxydes **2** et **3** par $LiAlH_4$ permettent de confirmer que l'ouverture de l'époxyde *cis*-**2** s'effectue d'une façon normale (17) par fixation axiale en position 1 d'une molécule d'eau. Par ailleurs, l'ouverture *trans*-diaxiale de l'époxyde *trans*-**3** impliquant une attaque axiale, (*cis* par rapport au groupe *tert*-butyle en position adjacente) d'une molécule d'eau ne correspond qu'à environ 50% de la réaction; l'énergie d'activation de ce processus est telle qu'elle rend compétitive la réaction impliquant un état de transition comportant une forme croisée (18, 19) et conduisant à la formation du diol diéquatorial **5***a*.

Les résultats obtenus au cours du présent travail permettent de mettre en lumière l'influence de facteurs de nature stérique sur la stéréochimie de l'ouverture d'époxydes contenus dans des systèmes cyclohexaniques simples et peuvent être rapprochés de ceux obtenus en série stéroïdale par Barton *et al.* (20) et Lacoume et Levisalles (21).

Partie expérimentale

*1. Préparation des diols trans-**4a** et -**5a***

*1.1. Hydroxylation du tert-butyl-3 cyclohexène (**1**)*

A un mélange constitué par 35 ml d'acide formique à 88% et 12 ml d'eau oxygénée à 30%, on ajoute goutte à goutte et sous agitation énergique 5 g (36 mmoles) de *tert*-butyl-3 cyclohexène (**1**) fraichement distillé; lorsque l'addition est terminée, le mélange réactionnel est maintenu sous agitation tout d'abord à 40–50 °C pendant 1 h et ensuite à la température de la pièce pendant 1 nuit. L'excès d'acide formique est alors évaporé sous vide, la solution neutralisée au moyen d'une solution aqueuse de soude à 20% et les produits organiques (4.5 g de produit brut) extraits à l'éther de manière habituelle. La saponification des esters intermédiaires par de la soude conduit à 3.9 g (23 mmoles, 64% du rendement théorique) d'un produit qui d'après la c.p.g. des dérivés silylés serait composé de quantités équivalentes des diols **4***a* et **5***a*.

*1.2. Séparation des diols **4a** et **5a***

Un mélange formé de 12 g de diols, 500 ml d'acétone, et 70 g de sulfate cuivrique anhydre est chauffé à reflux durant 3 jours. Le produit est alors filtré sur de la terre diatomée, concentré sous vide, et chromatographié sur une colonne contenant 400 g de gel de silice. L'élution au moyen de 2 l d'un mélange acétate d'éthyle/cyclohexane, 20:80, conduit à 7 g de l'acétonide **6**; p.e.: 105 °C/17 mm Hg; i.r.: bandes à 1235, 1180, 1130, 1100, 1040, 870, 840, et 800 cm^{-1}; résonance magnétique nucléaire (r.m.n.): pics à 0.90 (*tert*-butyle), 1.27 (*gem* diméthyle), et massif centré à 3.0 p.p.m. (hydrogènes carbinoliques); spectre de masse: pic parent à *m/e* de 202 unités. L'élution au moyen d'un mélange acétate d'éthyle/cyclohexane, 40:60, permet de récupérer 5 g de diol **4***a* qui après recristallisation dans l'éther de pétrole présente les caractéristiques rapportées dans le tableau 1.

L'hydrolyse de 3 g d'acétonide **6** à 80 °C pendant 24 h au moyen d'un mélange acide acétique/eau, 50/50, fournit après évaporation de l'excès d'acide, neutralisation, et extraction à l'éther 2.4 g (98% du rendement théorique) du diol **5***a* dont les propriétés caractéristiques sont résumées dans le tableau 1.

*2. Préparation du diol cis-**7a***

A 1.2 g (8.7 mmoles) d'alcène **1** en solution dans 500 ml d'éther anhydre et maintenu à 0 °C dans l'obscurité, on ajoute goutte à goutte 2 g (7.8 mmoles) de tétroxyde d'osmium dissout dans 20 ml d'éther anhydre. Le mélange réactionnel est maintenu à l'obscurité à 0 °C durant 2 h et 3 jours à la température de la pièce. L'éther est alors évaporé puis on ajoute au résidu brunâtre 50 ml d'eau, 10 g de mannitol, 4 g de KOH, et 100 ml de chlorure de méthylène et l'on porte à reflux pendant 5 h. L'extraction au chloroforme conduit à un produit brut qui par analyse par c.p.g. (après silylation d'une fraction du tout) ne contiendrait que le diol **7***a*. La recristallisation de ce solide dans l'éther de pétrole fournit 1.1 g (80% du rendement théorique) du diol **7***a* dont les caractéristiques sont résumées dans le tableau 1.

*3. Préparation du diol **8a***

*3.1. Action de l'iode et de l'acétate d'argent sur le tert-butyl-3 cyclohexène (**1**)*

Dans un ballon à 3 tubulures muni d'un agitateur, on place 18 g (130 mmoles) d'alcène **1**, 600 ml d'acide acétique glacial, et 49.3 g (290 mmoles) d'acétate d'argent. Sous agitation énergique, on ajoute en 1.5 h 35 g (130 mmoles) d'iode. Une fois l'addition terminée, on maintient l'agitation pendant 1 h à la température de la pièce puis après avoir ajouté 59 ml d'acide acétique à 96% on chauffe à 90 °C pendant 4 h. Du chlorure de sodium (50 g) est alors ajouté; après avoir agité pendant 1 h

Can. J. Chem. Downloaded from www.nrcresearchpress.com by 210.87.254.5 on 09/05/12
For personal use only.

supplémentaire, le mélange réactionnel est filtré et le précipité lavé avec du benzène bouillant. Les solvants sont éliminés des fractions organiques réunies et la solution neutralisée à l'aide de soude à 30%. Les produits intermédiaires ainsi obtenus sont traités à la manière standard par 3 g de $LiAlH_4$ et conduisent à 17 g (75% du rendement théorique) d'un produit brut qui serait constitué d'après la c.p.g. (d'une petite fraction silylée) de 47% du diol **8***a* et 53% du diol **7***a*.

3.2. Séparation des diols 7a et 8a

Le mélange de diols (1.5 g) obtenu précédemment subit d'abord une purification préliminaire par chromatographie sur 200 g de gel de silice et élution à l'aide de 3 l d'un mélange acétage d'éthyle/cyclohexane, 30/70. Le liquide incolore ainsi obtenu est silylé quantitativement par traitement à 70 °C pendant 2 h avec 15 ml d'hexaméthyldisilazane, 7 ml de triméthylchlorosilane dans 20 ml de pyridine et conduit à 2.5 g d'un mélange des dérivés **7***b* et **8***b* qui est chromatographié sur 300 g de gel de silice. L'élution au moyen de 2 l d'éther de pétrole 30–60 et d'un l de cyclohexane fournit 1.3 g du dérivé **8***b* pur; l'élution par un mélange d'acétate d'éthyle/cyclohexane, 20:80, donne 1.5 g du dérivé **7***b* (contenant d'après la c.p.g. 10% de l'isomère **8***b*).

Le dérivé silylé **8***b* (1.3 g) dans 10 ml d'eau et 10 ml de méthanol est traité à reflux pendant 5 h par 3 g de soude. L'extraction à la manière habituelle conduit à 500 mg (70% du rendement théorique) du diol **8***a*, qui après recristallisation dans l'éther de pétrole présente les caractéristiques résumées dans le tableau 1.

4. Stéréochimie de l'hydrolyse des époxydes 3 et 4

La méthode générale utilisée consiste à ajouter à 5 g (32 mmoles) d'époxyde, 5 ml d'eau, et 20 ml d'acide formique à 85%, le mélange réactionnel étant agité à la température de la pièce. L'excès d'acide formique est alors éliminé et les produits extraits à la manière décrite dans la section 1.1. Les diols ainsi obtenus sont alors silylés d'après la technique décrite dans la section 3.2 et analysés par c.p.g. dans les conditions décrites au tableau 1.

Les auteurs remercient sincèrement le Conseil National de Recherches du Canada pour l'aide financière accordée sous forme de bourse et d'octrois de recherches. L'un de nous tient à exprimer sa reconnaissance au Dr. Pierre Maroni et Mademoiselle Marthe Benoit de la Faculté des Sciences de Toulouse pour l'acceuil et l'aide qui lui ont été accordés durant la préparation de ce manuscrit.

1. J. C. RICHER et C. FREPPEL. Can. J. Chem. **46**, 3709 (1968).
2. G. BERTI, B. MACCHIA, et F. MACCHIA. Tetrahedron Lett. 3421 (1965).
3. G. BERTI, B. MACCHIA, et F. MACCHIA. Tetrahedron, **24**, 1755 (1968).
4. N. A. LEBEL et G. G. ECKE. J. Org. Chem. **30**, 4316 (1965).
5. D. SWERN, G. N. BILDEN, J. W. FINDLEY, et J. T. SCANLAN. J. Amer. Chem. Soc. **67**, 1786 (1945).
6. R. B. WOODWARD, F. SONDHEIMER, D. TAUB, K. HEUSLER, et W. M. MCLAMORE. J. Amer. Chem. Soc. **74**, 4223 (1952).
7. J. CHUCHE, G. DANA, et M. R. MONOT. Bull. Soc. Chim. (France), 3300 (1967).
8. G. DANA, J. CHUCHE, et M. R. MONOT. Bull. Soc. Chim. (France), 3308 (1967).
9. H. F. VOGEL. *In* A textbook of practical organic chemistry. 3rd edition. Longmans, London, 1964. p. 895.
10. C. W. DAVEY, E. L. MCGENNIS, J. M. MCKEOWN, G. D. MEAKINS, M. W. PEMBERTON, et R. N. YOUNG. J. Chem. Soc. (C) 2674 (1968).
11. J. E. COLENAN, C. RICCIATI, et D. SWERN. J. Amer. Chem. Soc. **78**, 3342 (1956).
12. R. B. WOODWARD et F. V. BRUTCHER. J. Amer. Chem. Soc. **80**, 209 (1956).
13. D. GINSBURG. J. Amer. Chem. Soc. **75**, 5746 (1953).
14. E. J. HEDGLEY et W. G. OVEREND. Chem. Ind. 378 (1960).
15. C. SWEELEY, R. BENTLEY, M. MAKITA, et W. WELLS. J. Amer. Chem. Soc. **85**, 2497 (1963).
16. E. L. ELIEL, M. H. GIANNI, T. H. WILLIAMS, et J. B. STOTHERS. Tetrahedron Lett. 741 (1962).
17. A. FURST et A. PLATTNER. Helv. Chim. Acta, **32**, 275 (1949).
18. B. RICKBORN et S. Y. LWO. J. Org. Chem. **30**, 2212 (1965).
19. E. J. LANGSTAFF, R. Y. MOIR, R. A. B. BANNARD, et A. A. CASSELMAN. Can. J. Chem. **46**, 3649 (1968).
20. D. H. R. BARTON, D. A. LEWIS, et J. F. MCGHIE. J. Chem. Soc. 2907 (1957).
21. B. LACOUME et J. LEVISALLES. Bull. Soc. Chim. (France), 2245 (1964).

Can. J. Chem. Downloaded from www.nrcresearchpress.com by 210.87.254.5 on 09/05/12
For personal use only.

Can. J. Chem. Downloaded from www.nrcresearchpress.com by 210.87.254.40 on 09/05/12
For personal use only.

Phytochemical investigation of Manitoba plants. I. A new indole alkaloid and associated alkaloids from *Phalaris arundinacea*

R. C. S. AUDETTE, H. M. VIJAYANAGAR, AND J. BOLAN
School of Pharmacy, University of Manitoba, Winnipeg 19, Manitoba

AND

K. W. CLARK
Department of Plant Science, University of Manitoba, Winnipeg 19, Manitoba

Received May 8, 1969

Hordenine, gramine, and an unknown compound assigned the structure of 2,9-dimethyl-6-methoxy-1,2,3,4-tetrahydro-β-carboline and *n*-octacosanol were isolated from *Phalaris arundinacea* Var. Ottawa Synthetic C grown in Manitoba. The compounds were separated by a counter current distribution method followed by column chromatography on Woelm basic alumina, and were characterized by the use of infrared, ultraviolet, mass, and nuclear magnetic resonance spectroscopy.

Canadian Journal of Chemistry, **48**, 149 (1970)

Introduction

The acceptability of reed canary grass, *Phalaris arundinacea* L., as a livestock forage appears in part, to be related to differences in dry matter digestibility and dry matter intake. Low intake, rough haircoats, and profuse watering of the eyes of cattle on Michigan reed canary grass have been observed (1). Cattle feeding on forage which contained *P. arundinacea* as one grass species, in one locale of Manitoba, suffered from a reduction in milk production and liveweight gains. Postmortem examination revealed alkaloidal-type lesions in the livers of these cattle and prompted an investigation of the alkaloids of *P. arundinacea*.

Severe neurological disorders, called the "Phalaris staggers syndrome" and sudden deaths have occurred among livestock grazing on a related species, *P. tuberosa* L. in Australia (2–6). This species has been reported to contain several indolealkylamines, notably *N,N*-dimethyltryptamine and its 5-methoxy and 5-hydroxy derivatives (6). Small dosages of these compounds administered to sheep resulted in the formation of neurological disorders similar to those observed in sheep grazing on *P. tuberosa*. Higher doses resulted in cardiac arrest and were often fatal (3). Tryptamine derivatives are known to exert a strong action on the central nervous system and to interfere with some of the pharmacological effects of serotonin (**1**) (7).

In 1958, Wilkinson (8) reported the occurrence of hordenine (**2**) and 5-methoxy-*N*-methyltryptamine (**3**) in Australian *Phalaris arundinacea*. Culvenor *et al.* (9) reported gramine (**4**) as the major alkaloidal base (0.3% dry grass) in Australian *P. arundinacea*. We wish to report the isolation and identification of hordenine, gramine, *n*-octacosanol, and a previously unknown compound assigned the structure of 2,9-dimethyl-6-methoxy-1,2,3,4-tetrahydro-β-carboline. The total alkaloid contains a high proportion of

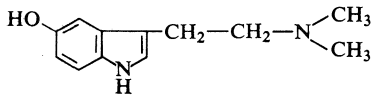

1

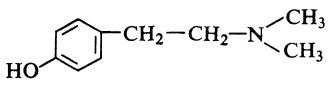

2

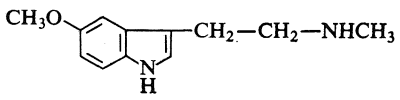

3

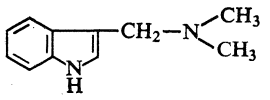

4

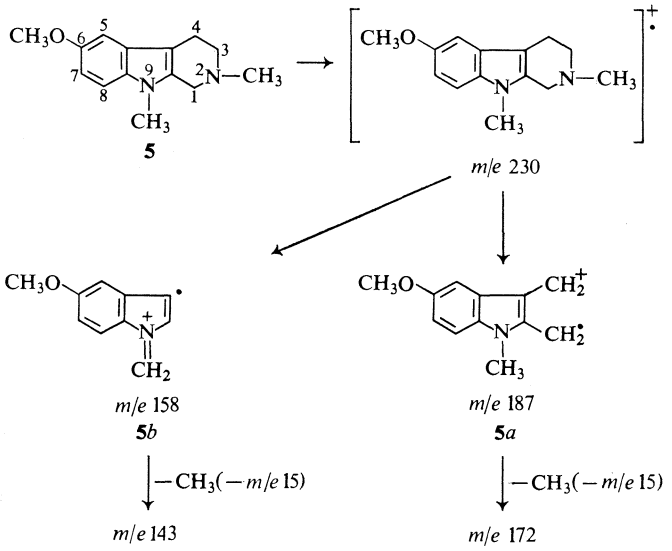

SCHEME 1

hordenine (0.009% on the weight of the dry grass) and a lesser proportion of some indole derivatives. The total alkaloid fraction from *P. arundinacea* gave a violet solution with *p*-dimethylaminobenzaldehyde in ethanol containing hydrochloric acid (Van Urk's reagent). The alkaloids were separated by a counter current distribution method followed by column chromatography on basic alumina.

Results and Discussion

Identification of Hordenine (2)

The ultraviolet (u.v.) (λ_{max} 279 mμ), infrared (i.r.), and mass spectra were identical with those of authentic hordenine. The nuclear magnetic resonance (n.m.r.) spectrum showed the expected A_2B_2 type of pattern with *ortho-* and *para-*couplings at 6.6 and 7.0 p.p.m. (a pair of doublets, $J = 9$ c.p.s.) integrating for 4 aromatic protons. A singlet at 8.1 p.p.m. was attributed to the phenolic—OH. An authentic sample gave similar signals.

Structure of 2,9-Dimethyl-6-methoxy-1,2,3,4-tetrahydro-β-carboline (5)

Thin-layer chromatography (t.l.c.) (R_f 0.3, blue with Van Urk's reagent) and gas–liquid chromatography (g.l.c.) (Fig. 1) (retention time, 25 min, 47 s) results were not comparable with any of the known indole alkaloids reported in *Phalaris* species. The u.v. spectrum showed absorption bands at λ_{max} 276, 297, and 309 mμ

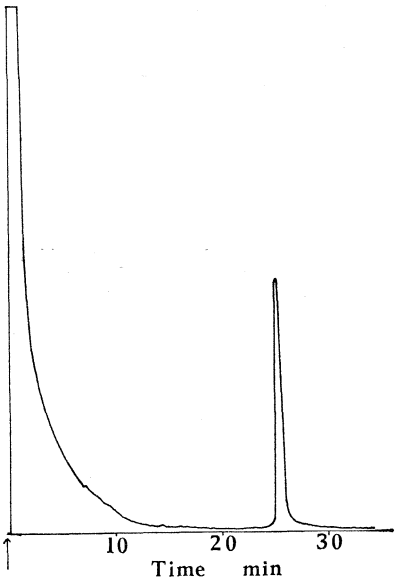

FIG. 1. Gas–liquid chromatogram of 2,9-dimethyl-6-methoxy-1,2,3,4-tetrahydro-β-carboline (**5**). Two μl of the sample were injected on a 6 ft, 1/8 in. i.d. Teflon 6 column, packed with 0.4% cyclohexanedimethanol succinate (CHDMS) on Chromosorb G, AW-DMCS 60/80. The column temperature was 195°. The helium flow rate was 100 ml/min. The hydrogen flame detector was kept at 260°, and the injection port at 230° (17). The retention time of **5** was 25 min 47 s.

which were similar to those of 5-methoxy-*N*,*N*-dimethyltryptamine. The i.r. spectrum had absorption bands at ν_{max} 2930, 2810, 1620, 1600,

Can. J. Chem. Downloaded from www.nrcresearchpress.com by 210.87.254.40 on 09/05/12
For personal use only.

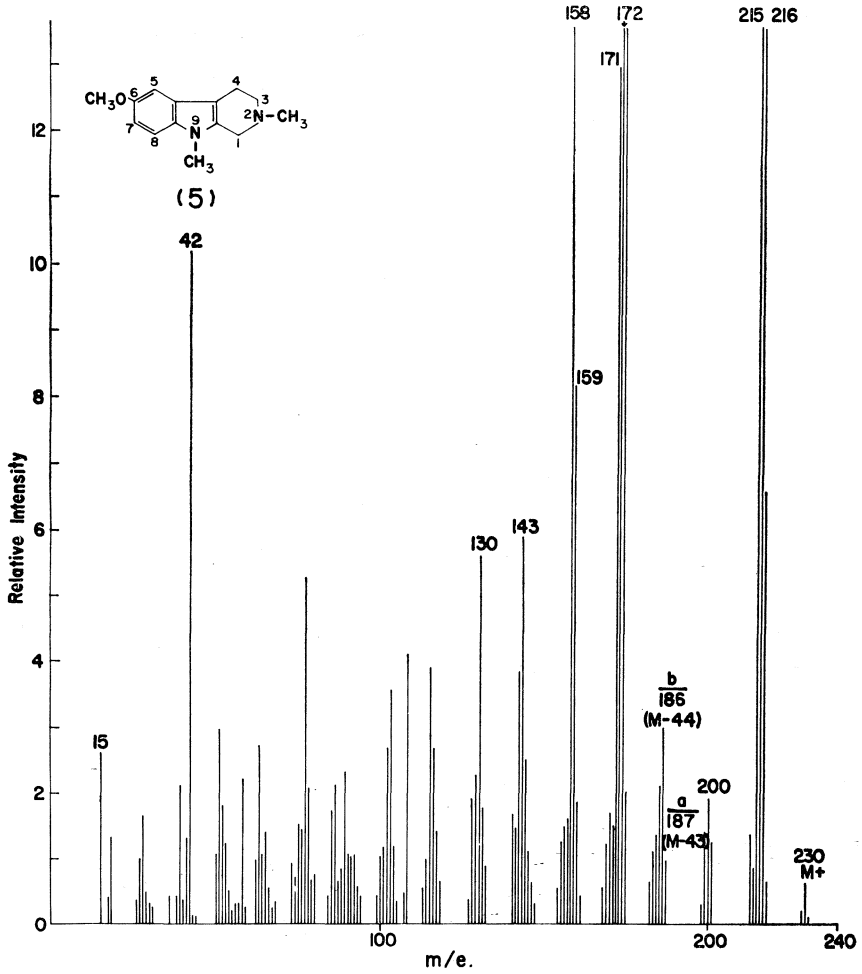

FIG. 2. Mass spectrum of 2,9-dimethyl-6-methoxy-1,2,3,4-tetrahydro-β-carboline (**5**).

1585, 1500, 1465, 1390, and 1300 cm^{-1}. Indolic —NH absorption (i.e. about 3250 cm^{-1}) seemed to be absent. The elemental analysis was consistent with the molecular formula $C_{14}H_{18}N_2O$ for the parent base. The molecular formula of the base was further verified with the aid of the mass spectrum reproduced in (Fig. 2) (M = 230). Aside from the molecular peak, it exhibited certain important peaks at *m/e* 216, 215, 200, 187, 186, 172, 171, 159, 158, 143, 130, 42, and 15. The fragmentation pattern of the compound (**5**) appeared to occur as shown in Scheme 1. The M-43 peak at *m/e* 187 can be ascribed to the ion (**5***a*) resulting from the loss of $CH_2{=}NCH_3$ at positions N-2 and C-3. The above peak seems to be characteristic of such cyclic systems (10–12). The peak at *m/e* 172 presumably arises from the loss of a methyl group of the methoxy from the fragment (**5***a*). The peak at *m/e* 158 could be ascribed to the ion (**5***b*) and the *m/e* 42 peak could be due to the formation of $CH{\equiv}\overset{+}{N}CH_3$.

The n.m.r. spectrum (Fig. 3) was also consistent with the tetrahydro-β-carboline derivative structure (**5**), with the two singlets at 2.38 and 3.73 p.p.m. which arise from the *N*-methyl of the basic nitrogen at position N-2 and the methoxy methyl at position C-6, respectively. The triplet (4H) centered at 2.69 p.p.m. represents the C-3 and C-4 saturated methylenes, while the singlet (2H) at 3.24 p.p.m. arises from the C-1 methylene

Can. J. Chem. Downloaded from www.nrcresearchpress.com by 210.87.254.40 on 09/05/12
For personal use only.

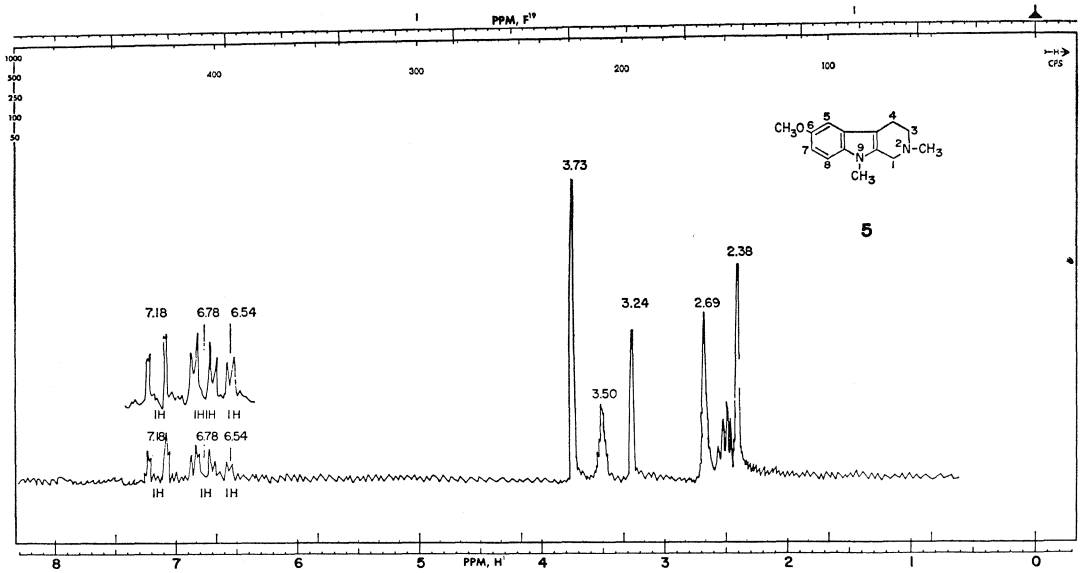

FIG. 3. Nuclear magnetic resonance spectrum of 2,9-dimethyl-6-methoxy-1,2,3,4-tetrahydro-β-carboline (**5**) in deuterodimethyl sulfoxide.

protons. The band at 3.50 p.p.m., however, is the methyl group attached to the non-basic indole methyl at position N-9. Methyls of this type have been found previously at around 3.58 p.p.m. (13). It is possible that the methyl at 3.50 p.p.m. is coupled with a very small coupling constant to the C-8 proton. In the aromatic region, the C-8 proton appeared as an AB-type doublet at 7.18 p.p.m. ($J_{7,8}$ = 8 c.p.s.), the C-5 proton *meta* coupled ($J_{5,7}$ = 2 c.p.s.) at 6.54, while the C-7 proton *ortho* coupled to C-8 ($J_{7,8}$ = 8 c.p.s.) and *meta* coupled to C-5 ($J_{5,7}$ = 2 c.p.s.) appeared at 6.78 p.p.m.

Identification of n-Octacosanol (6)

The elemental analysis of the compound is consistent with the molecular formula $C_{28}H_{58}O$. The above conformation was further verified by its mass spectrum (Fig. 4) (M = 410 − 18 (H_2O) = *m/e* 392 ion). The most characteristic fragmentation of the higher alcohols is associated with the elimination of water. Long chain aliphatic alcohols may therefore show a small or negligible molecular peak, but M-18 (M-H_2O) peaks will be discernible and the spectra of long chain aliphatic alcohols are therefore dominated by hydrocarbon peaks (14, 15).

$$\underset{\substack{(6)\\ m/e\ 410}}{CH_3(CH_2)_{26}CH_2OH} \xrightarrow{-H_2O} \underset{m/e\ 392}{\left[CH_2{=}CH{-}(CH_2)_{25}{-}CH_3\right]^+} + H_2O$$

A feature of the spectrum of most aliphatic alcohols is a mass peak formed by cleavage of the bond β to the oxygen atom (14). That is to say, in primary alcohols, an ion corresponding to the fragmentation to give (—CH_2OH)+ is prominent at *m/e* 31. Olefines are generally characterized by the mass number (C_nH_{2n}) of the parent peak (double bonds stabilize the parent ion and thus increase the possibility of its appearance) and by a series of peaks at *m/e* 41, 55, 69, 83, 97, 111, 125, and 139, each two mass units lower than the corresponding peak (*m/e* 43, 57, 71, and 85), which are also present in straight chain saturated compounds. These peaks result from the retention of charge on the unsaturated fragment. The base peak usually results from allylic cleavage and gives the resonance stabilized allylic carbonium ion, viz.

Can. J. Chem. Downloaded from www.nrcresearchpress.com by 210.87.254.40 on 09/05/12
For personal use only.

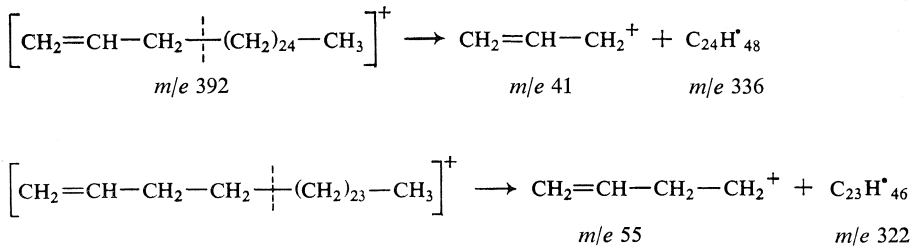

The above evidence together with the n.m.r. spectrum (Fig. 5), which showed a triplet at 0.85 p.p.m. integrating for 3 protons of a methyl group, overlapping triplets at 1.26 p.p.m. integrating for 52 protons of $(CH_2)_{26}$ groups, and a triplet at 3.62 p.p.m. due to a methylene group of $—CH_2OH$, strongly suggested the identity of this compound with *n*-octacosanol (**6**).

Experimental

Ultraviolet spectra were obtained with a Hilger and Watts Ultrascan recording spectrophotometer, using ethanol as a solvent. Infrared spectra were obtained on a Beckman Model 8 spectrophotometer using samples prepared either in KBr discs or in Nujol as a thin film on a sodium chloride block. Nuclear magnetic resonance spectra were measured on a Varian A-60 instrument, using a 10% solution of tetramethylsilane in carbon tetrachloride as an external reference (τ_{10}). Mass spectra were taken on an A.E.I. M.S.-9 mass spectrometer. A Beckman Model GC-5 gas chromatograph, equipped with a flame ionization detector and a Beckman 1 MV linear potentiometric recorder, was used for g.l.c. studies (17). Helium was used as the carrier gas.

Woelm basic alumina (Grade III) was used for column chromatography. Thin-layer chromatography was performed on Merck Kieselgel-G, using the solvent system chloroform:methanol (4:1 v/v) throughout the separation and the colors were developed with Van Urk's and Dragendroff's reagents (16). Microanalyses were carried out by Pascher, Mikroanalytisches Laboratorium, 53 Bonn, Buscstrasse54. Melting points are uncorrected.

Extraction and Fractionation

Dried ground grass (24.0 kg.) was extracted in a Soxhlet apparatus with ethanol (270 l). The ethanol was removed by distillation under reduced pressure and the resulting residue dissolved in chloroform. The chloroform solution was shaken with dilute sulfuric acid (0.6 *N*, 10 l) and the aqueous layer was then made alkaline with ammonium hydroxide (p*H* 9), saturated with sodium chloride, and extracted with chloroform until there was no color with Van Urk's reagent. The chloroform layer was dried over anhydrous potassium carbonate and removed by distillation under reduced pressure. The yield was (34.0 g, 1.5%) of crude bases.

The purification of the crude alkaloidal bases (24.0 g)

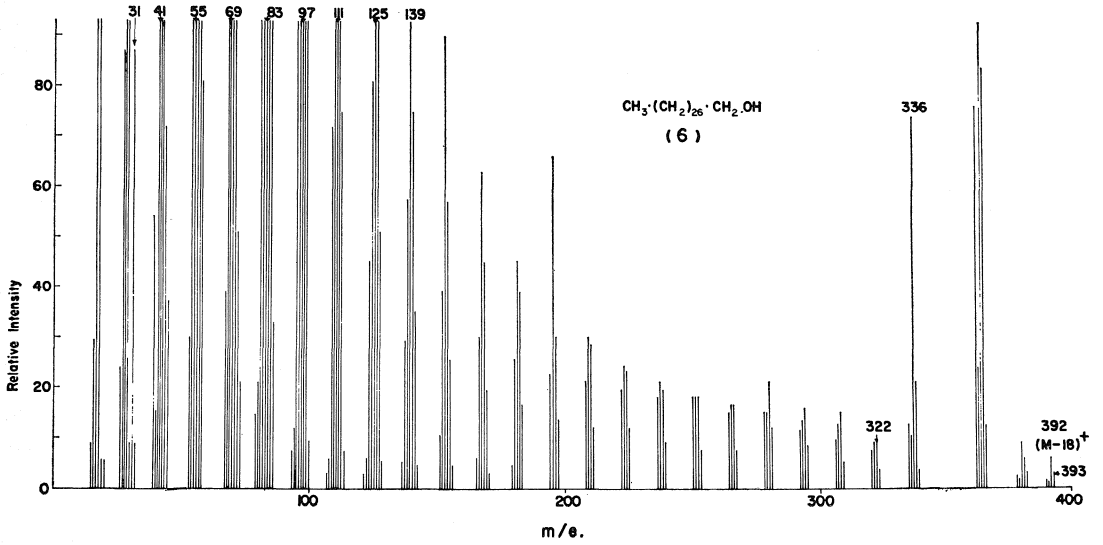

FIG. 4. Mass spectrum of *n*-octacosanol (**6**).

Can. J. Chem. Downloaded from www.nrcresearchpress.com by 210.87.254.40 on 09/05/12
For personal use only.

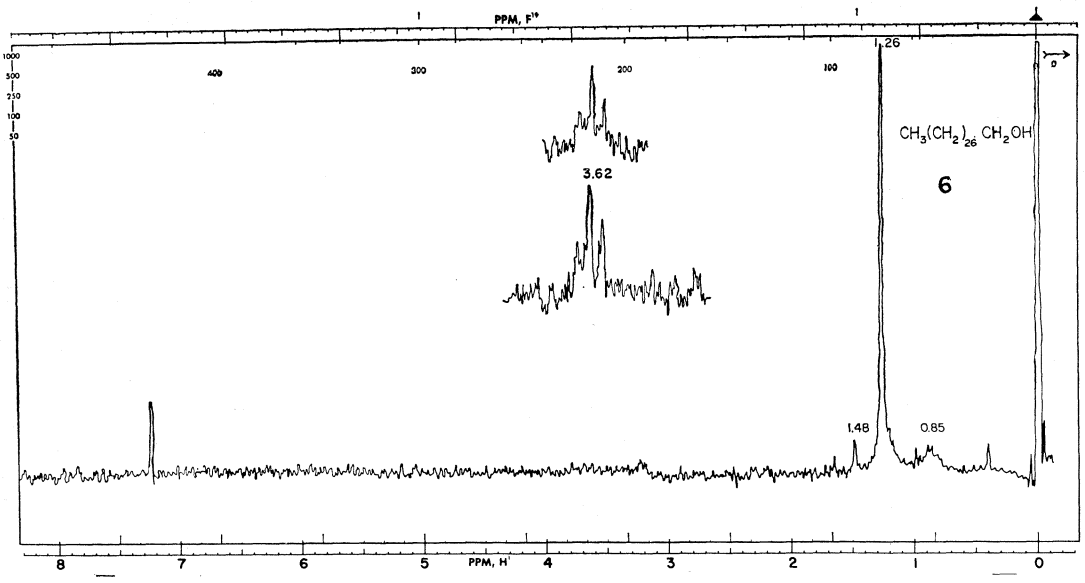

FIG. 5. Nuclear magnetic resonance spectrum of *n*-octacosanol (**6**) in deuterochloroform.

obtained from the above extraction procedure was carried out by counter current distribution between chloroform and hydrochloric acid (0.2 *N*, 100 ml phase, 44 tubes). Fraction 1 (6.5 g) gave hordenine (**2**) (1.5 g) along with some gramine (**4**) and other indole derivatives which possessed high R_f values when examined on t.l.c.

In fractions 2–15 (7.5 g) indole derivatives were obtained with the following R_f values and colors developed with Van Urk's reagent on t.l.c. (0.05, pink), (0.7 pink), and (0.9, blue); in fractions 16–30 (2.5 g), (0.05, pink), (0.15, blue), (0.25, pink), (0.7, pink), and (0.9, blue), and in fractions 30–44 (3.5 g), (0.7–0.9, brown) and (0.15, blue).

Fraction 1

Hordenine was isolated from the first fraction and on crystallization from benzene gave colorless needles m.p. 116–117°, mixed m.p. with authentic hordenine 117–118°. Thin-layer chromatography gave a red color (R_f 0.17) with Dragendroff's reagent; g.l.c. (17) on the CHDMS column showed a retention time of 58 s, corresponding to that of authentic hordenine.

Anal. Calcd. for $C_{10}H_{15}NO$: C, 72.7; H, 8.9; N, 8.7. Found: C, 72.7; H, 9.2; N, 8.5.

Fractions 2–15

Fractions 2–15 were combined, the solvent removed, and the residue was extracted with ether. The ether soluble portion was decanted and evaporated to dryness. The resulting residue on shaking with petroleum ether (b.p. 40–60°) gave colorless needles which were washed with methanol (1 ml) and filtered. The product was found to be 2,9-dimethyl-6-methoxy-1,2,3,4-tetrahydro-β-carboline (**5**), m.p. 214° (decomposed).

Anal. Calcd. for $C_{14}H_{18}N_2O$: C, 73.0; H, 7.8; N, 12.2. Found: C, 71.6; H, 7.5; N, 12.2.

Fractions 16–30

Fractions 16–30 were combined and the residue was shaken with ether. The ether was decanted and evaporated to dryness. The resulting residue when shaken with petroleum ether (b.p. 40–60°) gave a crystalline material (R_f 0.7, pink) which is under investigation. Thin-layer chromatography suggested that the ether soluble parts of the fractions 2–30 contain mainly indole derivatives with high R_f values except for some gramine (R_f 0.05).

All ether soluble fractions were combined and separated by column chromatography, using petroleum ether (b.p. 40–60°) and ether (1:1 v/v) as an eluent. In fractions 2–22, 23–38, and 39–44, indole derivatives were obtained with the following R_f values (0.05 and 0.7), (0.7 and 0.9), and (0.15, 0.7, and 0.9), respectively. Gramine was the major component of fractions 13–16 as indicated by g.l.c. (17) (retention time 51 s on CHDMS, similar to that of an authentic sample). A comparative study of the isolated compound and authentic gramine was done on t.l.c. under different eluent systems (chloroform:methanol, 4:1 v/v; ethyl acetate:isopropanol:ammonia, 9:7:4 v/v) and similar results were obtained.

The chloroform soluble parts of the ether extracted residues obtained from fractions 2–30 from the counter current distribution were combined and separated by column chromatography on alumina using chloroform as the eluent (5 ml fractions). The combined chloroform solutions of fractions 24–28 gave a non-alkaloidal compound, m.p. 79°, and fractions 36–40 yielded another non-alkaloidal material, m.p. 149°.

The non-alkaloidal compound (m.p. 79°, lit. (18) 83°) was identified as *n*-octacosanol (**6**). The i.r. spectrum showed absorption bands at ν_{max} 3285 (—OH), 2920, and 2850 cm^{-1}.

Anal. Calcd. for $C_{28}H_{58}O$: C, 81.9; H, 14.2. Found: C, 81.7; H, 14.3.

Can. J. Chem. Downloaded from www.nrcresearchpress.com by 210.87.254.40 on 09/05/12
For personal use only.

We wish to thank Dr. R. S. MacVicar, C.D.A. Research Station, Ottawa for a supply of seeds and clonal lines of *P. arundinacea* Var. Ottawa Synthetic C. Also, we wish to thank Dr. C. M. Wong, Department of Chemistry, University of Manitoba, for his assistance in interpretation of mass spectra and n.m.r. We wish to thank Miss Rosella Enns for her technical assistance. Financial assistance from the Canada Department of Agriculture, Northern Studies Committee, University of Manitoba, and the Faculty of Graduate Studies of the University of Manitoba is acknowledged with thanks.

1. W. J. VAN ARSDELL, G. A. BRANAMAN, C. M. HARRISON, and J. F. DAVIS. Quart. Bull. Mich. Ag. Exp. Stn. **37**, #1, 125 (1954).
2. I. W. MCDONALD. Aust. Vet. J. **18**, 182 (1942).
3. C. H. GALLAGHER, J. H. KOCH, R. M. MOORE, and J. D. STEEL. Nature, **204**, 542 (1964).
4. H. J. LEE and R. E. KUCHEL. Aust. J. Agr. Res. **4**, 88 (1953).
5. R. M. MOORE, G. W. ARNOLD, H. J. HUTCHINGS, and H. W. CHAPMAN. Aust. J. Sci. **24**, 89 (1961).
6. R. M. MOORE, J. D. WILLIAMS, and JOYCE CHIA. Aust. J. Biol. Sci. **20**, 1131 (1967).
7. V. ERSPAMER. Progr. Drug Res. **3**, 151 (1961).
8. S. WILKINSON. J. Chem. Soc. 2079 (1958).
9. C. C. J. CULVENOR, R. DALBON, and L. W. SMITH. Aust. J. Chem. **17**, 1301–1304 (1964).
10. A. M. DUFFIELD, H. BUDZIKIEWICZ, and C. DJERASSI. J. Amer. Chem. Soc. **86**, 5537 (1964).
11. H. BUDZIKIEWICZ, J. I. BRAUMAN, and C. DJERASSI. Tetrahedron, **21**, 1855 (1965).
12. S. AGURELL, B. HOLMSTEDT, and J. E. LINDGREN. Amer. J. Pharm. **140**, 148 (1968).
13. J. PECHER, R. H. MARTIN, N. DEFAY, M. KAISIN, J. PEETERS, and G. VAN BINST. Tetrahedron Lett. **8**, 270 (1961).
14. J. H. BEYNON. Mass spectrometry and its applications to organic chemistry. Elsevier Publishing Company, Amsterdam. 1960 p. 346.
15. K. BIEMANN. Mass spectrometry, organic chemical applications. McGraw-Hill, Book Co., Inc., New York. 1962. p. 109.
16. D. WALDI. *In* Thin-layer chromatography. A laboratory handbook. (*Edited by* Egon Stahl. Academic Press, Inc., New York. 1965. p. 491.
17. R. C. S. AUDETTE, J. BOLAN, H. M. VIJAYANAGAR, R. BILOUS, and K. W. CLARK. J. Chromatogr. **43**, 295 (1969).
18. The Merck index of chemicals and drugs. Merck and Co., Inc., New Jersey. 1960. p. 741.

Can. J. Chem. Downloaded from www.nrcresearchpress.com by 210.87.254.40 on 09/05/12
For personal use only.

Chelating polymers. I. The synthesis and acid dissociation behavior of several *N*-(*p*-vinylbenzenesulfonyl)-substituted diaminopolyacetic acid monomers, monomeric analogues, and related intermediates

R. M. GENIK-SAS-BEREZOWSKY AND I. H. SPINNER

Department of Chemical Engineering and Applied Chemistry, University of Toronto, Toronto 181, Ontario

Received June 24, 1969

Two new chelating monomers, *N*-(*p*-vinylbenzenesulfonyl)-1,2-diaminoethane-*N'*,*N'*-diacetic (SS-EDDA) and -*N*,*N'*,*N'*-triacetic (SS-ED3A) acids, as well as several monomeric analogues and related intermediates have been prepared. In addition, 2-oxo-1-piperazine acetic (S-KP), 3-oxo-1-piperazine acetic (U-KP), and 2-oxo-1,4-piperazine diacetic (3-KP) acids have been synthesized and the interconvertibility between these cyclic amides and their unsubstituted linear amino acid analogues, ethylenediamine-*N*,*N'*-diacetic (S-EDDA), -*N*,*N*-diacetic (U-EDDA), and -*N*,*N*,*N'*-triacetic (ED3A) acids respectively, was demonstrated.

The acid dissociation constants of the various amino acids were determined potentiometrically at 25° and $\mu = 0.1\ M(KNO_3)$ and the results were compared with the hydrogen ion affinities of related compounds. Dissociation schemes were proposed for all the compounds based on these results. Rationalizations of the linear amino acid and the cyclic amide dissociation constants were made in terms of the effects of cyclization and the inductive effects of neighboring groups. These rationalizations were found to be helpful in clarifying the dissociation schemes previously proposed for several of the linear amino acids.

Canadian Journal of Chemistry, **48**, 163 (1970)

Can. J. Chem. Downloaded from www.nrcresearchpress.com by 210.87.254.5 on 09/05/12
For personal use only.

Introduction

The applications of conventional cation exchange resins for the separation of metal ions are largely determined by their degree of selectivity. In the past three decades numerous attempts have been made to enhance the selectivity of these resins by incorporating into the polymer matrix functional groups capable of chelate formation. As a result, some 200 publications dealing with the synthesis and studies of such chelating ion exchange resins have appeared and several reviews and critical discussions are available (1–11).

An examination of this literature indicates that most chelating resins were prepared either by the condensation of aromatic amine or phenol derivatives with formaldehyde, or by the introduction of the functional groups into a preformed polymer matrix by classical reactions. Unfortunately, due to the possibility of various secondary reactions and lack of control over cross-linking, these products were usually heterogeneous and of poorly defined structure and were thus unsuitable for detailed chelation studies. The most successful method for preparing suitable products involves the polymerization under mild conditions, of pure vinyl-type monomers already possessing the chelating groups. However, because of the great difficulties in synthesizing such polymerizable substances, to date only a few have been described; namely, several unsaturated 1,3-diketones (12, 13) and vinylarylaminoacids (14, 15, 16–22).

The present study was undertaken to synthesize new monomers possessing chelating groups and capable of being homo- or co-polymerized to give polymers of well defined structure. It was decided to use a styrene derivative as the polymerizable portion of the compounds since exchange resins based on polystyrene possess favorable physical and chemical properties. Several diaminopolyacetic acids of the EDTA type were chosen as the functional groups due to the high range of selectivity available by means of p*H* manipulation. The compound *p*-(β-bromoethyl)benzenesulfonyl chloride, readily prepared in the laboratory in pure form, was selected as the intermediate for the polymerizable portion, since the amino acids could readily be joined to the aryl nucleus through a stable sulfonyl bridge, and subsequent dehydrobromination of the resultant products would yield the vinyl-type monomers. The polymers to be prepared by this procedure are shown in Chart 1.

The synthesis and study of suitably chosen monomeric analogues were also undertaken for use in attempts to predict the chelating properties of the proposed polymers.

Results and Discussion

(a) Organic Syntheses

The proposed method of synthesis of the monomers required the preparation of the di- and

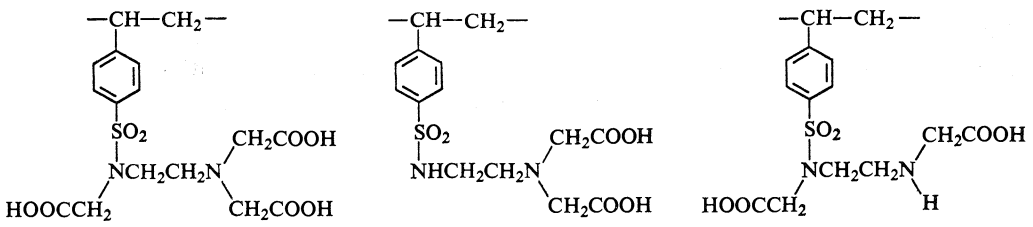

CHART 1

triacetic acids of ethylenediamine for coupling with *p*-(β-bromoethyl)benzenesulfonyl chloride (*p*-toluene- and benzenesulfonyl chlorides for the monomeric analogues) and subsequent dehydrobromination. This approach was undertaken in preference to the synthesis of the *N*-substituted arylsulfonylethylenediamines followed by carboxymethylation, because the conditions required for the latter step would undoubtedly result in the hydrolysis of the bromoethyl group.

The synthesis of the amino acids was attempted by both the alkaline condensation of chloroacetic acid with ethylenediamine and the carboxymethylation of the diamine with sodium cyanide and formaldehyde, but the most favorable results were obtained with the former method. The cyanide/formaldehyde method usually resulted in complex mixtures, especially in the attempted synthesis of the triacetic acid.

The symmetrical ethylenediamine-*N*,*N*′-diacetic acid (S-EDDA) was prepared by the cyanide/formaldehyde method. The unsymmetrical diacid, ethylenediamine-*N*,*N*-diacetic acid (U-EDDA), was obtained by the chloroacetate carboxymethylation of monoacetylated ethylenediamine followed by hydrolysis of the acetyl group. Attempts to prepare and recover pure ethylenediamine-*N*,*N*,*N*′-triacetic acid (ED3A) by the direct reaction of sodium chloroacetate with ethylenediamine at a 3:1 molar ratio resulted in complex mixtures of tetra-, tri-, and disubstituted products. Acidification of these alkaline reaction mixtures resulted in the removal of the major by-product, ethylenedinitrilotetraacetic acid (EDTA), by virtue of its low water solubility. However, this step also resulted in the cyclization of the non-fully substituted compounds. The recovery of the cyclic amide of ED3A, i.e. 2-oxo-1,4-piperazine diacetic acid (3-KP) in pure form from the remaining mixture of hydrochloride salts of amino acids and sodium chloride was possible because of the almost exclusive solubility of 3-KP in boiling dimethylformamide.

Doran (23) had investigated a considerable number of by-products and intermediates present as impurities in the preparation of EDTA by the cyanide/formaldehyde method, and had noted that cyclization of the non-fully substituted amino acids took place quite readily under acid conditions. Although she had been unable to isolate some of the amino acids in pure form, e.g. ED3A and 3-KP, she had nevertheless proposed (on the basis of paper electrophoresis studies) that these linear amino acids and their cyclic ketopiperazine counterparts were interconvertible. High p*H* (> 12) and high temperatures were said to result in decyclization.

Several of the compounds said to be interconvertible are shown in Scheme 1.

The results of some workers support the interconvertibility of S-EDDA/S-KP (24) but in the cases of ED3A/3-KP (25) and U-EDDA/U-KP (26), other workers have stated that they were

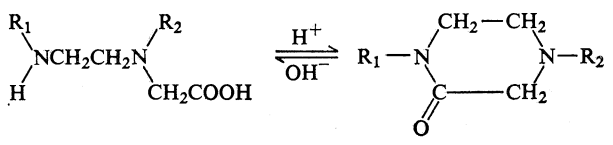

ED3A	($R_1 = R_2 = CH_2COOH$)	3-KP
U-EDDA	($R_1 = H$; $R_2 = CH_2COOH$)	U-KP
S-EDDA	($R_1 = CH_2COOH$; $R_2 = H$)	S-KP

SCHEME 1

Can. J. Chem. Downloaded from www.nrcresearchpress.com by 210.87.254.5 on 09/05/12
For personal use only.

Can. J. Chem. Downloaded from www.nrcresearchpress.com by 210.87.254.5 on 09/05/12
For personal use only.

unable to obtain the linear analogues from the cyclic amides.

The possibility of preparing the desired ED3A by cleaving the ring of 3-KP warranted a further investigation into the proposed interconvertibility. As a further aspect of this investigation, it was of interest to prepare the cyclic amide of U-EDDA, namely 3-oxo-1-piperazine acetic acid (U-KP) by treatment of the linear diacid in strong acid. In addition, 2-oxo-1-piperazine acetic acid (S-KP) was prepared in similar fashion and the dissociation properties of the latter two cyclic amides were studied for the first time and reported.

It was found that decyclization of both 3-KP and U-KP could be accomplished by refluxing in strongly alkaline aqueous medium (sodium hydroxide/amino acid molar ratio of 6:1).

The successful preparation and isolation in pure form of the arylsulfonyl derivatives of the inear amino acids by the reaction of the sulfonyl chlorides with the treated solutions of the cyclic amides, provided evidence of actual ring cleavage.

The reaction of the amino acids with the arylsulfonyl chlorides was accomplished by carrying out the coupling in a heterogeneous medium; contacting aqueous alkaline solutions of the amino acids with toluene solutions of the sulfonyl chlorides. Dehydrobromination of the bromoethyl compounds by refluxing in alcoholic potassium hydroxide solutions yielded the desired vinyl-type monomers.

The various amino acids prepared in this study were all white powdery materials, possessing indefinite decomposition points rather than sharp melting points. Further characterization of the products included elemental analysis, potentiometric studies, infrared (i.r.) spectroscopy, and where applicable, unsaturation tests.

(b) Potentiometric Study

A list of the various amino acids prepared in this study along with their dissociation constants obtained by potentiometric titrations at 25 ± 0.05 °C and an ionic strength of 0.1 *M* (KNO_3), is presented in Table 1. Several literature values are also given where applicable for comparison purposes. Good agreement of the results for U-EDDA, S-EDDA, and 3-KP with the literature values was obtained.

(i) Arylsulfonyl Amino Acids

The almost identical p*K* values obtained for the *p*-(β-bromoethyl)benzene-, *p*-toluene-, and benzenesulfonyl derivatives of the diamino diacids and also the triacids indicate that the dissociation of the amino acids is not influenced by the *p*-substituents on the benzene ring.

On examination of the dissociation constants of the diamino diacetic acids, the values of pK_1 (1.99–2.15) are attributed to a carboxyl proton. Further, those of pK_2 (7.8) are similar to the values of derivatives of iminodiacetic acid (30) and correspond to the dissociation of a proton of the ammonium nitrogen. The low p*K* values, as compared to the corresponding unsubstituted S-EDDA and U-EDDA indicate the strong electron attracting effect of the sulfone group on the acidities of the dissociable protons. (A similar effect is noted for the carbonyl group of *N*-acetyl-1,2-diaminoethane-*N'*,*N'*-diacetic acid (A-EDDA) and for the carbethoxy group of *N*-carbethoxy-β-aminoethyliminodiacetic acid (CE-EDDA) studied by Schwarzenbach *et al.* (27).) In the sulfone derivative of the symmetrical S-EDDA, the substituent is on the same nitrogen atom as the carboxyl group providing the first dissociable proton. Consequently, the pK_1 value has been lowered to a greater extent and to a lower value (6.51 → 1.99) than that of the derivative of the unsymmetrical U-EDDA (5.51 → 2.15). On the other hand, the ammonium proton should be influenced to an equal extent in both derivatives by the sulfone substituent, and this is shown by the identical values obtained for pK_2.

The titration curves (Figs. 1 and 2) of *N*-acetyl- and the *N*-arylsulfonyl-EDDA's in the free acid forms are similar to those of iminodiacetic (31) and *N*-benzyliminodiacetic (29) acids and one might thus expect them to display similar chelating behavior. The chelation curves with Cu(II) and Ni(II) obtained in some preliminary studies show this to be the case with the acetylated diacid. The sulfone derivative, however, displayed a different behavior. The indefinite second endpoint and the presence of a sharp inflection point at the third equivalent of added base suggest that competition with a hydroxy-complex has become important.

In the case of the *N*-arylsulfonyl substituted triacetic acids, the strong acidifying effect of the sulfone group is once again evident from a comparison of $pK_2 = 3.3$ and $pK_3 = 8.5$ with the values $pK_2 = 6.6$ and $pK_3 = 9.8 - 10.0$ reported

TABLE 1
Stoichiometric acid dissociation constants

Ligand	Formula	pK_1	pK_2	pK_3	Reference
BS-EDDA*	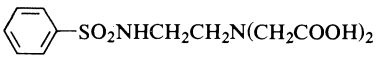	2.10	7.82	—	Present work, 25 °C, $\mu = 0.1$ (KNO_3)
TS-EDDA*	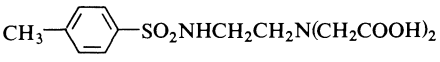	2.15	7.86	—	Present work, 25 °C, $\mu = 0.1$ (KNO_3)
BEBS-EDDA*	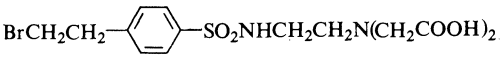	2.15	7.75	—	Present work, 25 °C, $\mu = 0.1$ (KNO_3)
TS-EDDA-sym.*	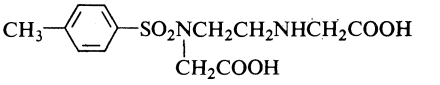	1.99	7.83	—	Present work, 25 °C, $\mu = 0.1$ (KNO_3)
A-EDDA*	$CH_3CONHCH_2CH_2N(CH_2COOH)_2$	1.94	8.17	—	Present work, 25 °C, $\mu = 0.1$ (KNO_3)
CE-EDDA	$C_2H_5OCONHCH_2CH_2N(CH_2COOH)_2$	2.2	8.57	—	(27), 20 °C, $\mu = 0.1$ (KCl)
BIMDA	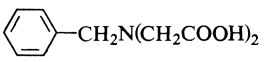	2.32	8.88	—	(29), 25 °C, $\mu = 0.1$ (KCl)
U-EDDA	$NH_2CH_2CH_2N(CH_2COOH)_2$	5.53	10.87	—	Present work, 25 °C, $\mu = 0.1$ (KNO_3)
		5.58	11.05	—	(27), 20 °C, $\mu = 0.1$ (KCl)
U-KP†	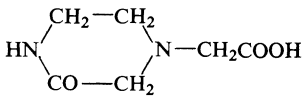	5.51	—	—	Present work, 25 °C, $\mu = 0.1$ (KNO_3)
S-EDDA	$HOOCCH_2NHCH_2CH_2NHCH_2COOH$	6.51	9.57	—	Present work, 25 °C, $\mu = 0.1$ (KNO_3)
		6.48	9.57	—	(28), 25 °C, $\mu = 0.1$ (KNO_3)
		6.42	9.46	—	(33), 30 °C, $\mu = 0.1$ (KCl)
S-KP†	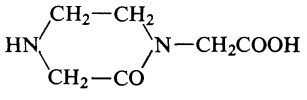	6.55	—	—	Present work, 25 °C, $\mu = 0.1$ (KNO_3)
3-KP	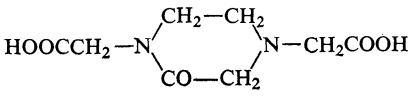	2.95	5.85	—	Present work, 25 °C, $\mu = 0.1$ (KNO_3)
		2.94	5.90	—	(25), 25 °C, $\mu = 0.1$ (KCl)
TS-ED3A*	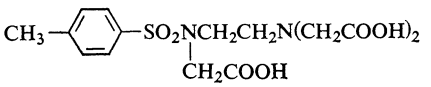	1.50	3.25	8.63	Present work, 25 °C, $\mu = 0.1$ (KNO_3)
BEBS-ED3A*	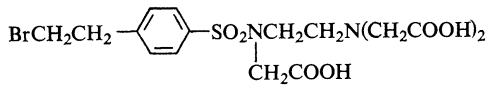	1.52	3.25	8.59	Present work, 25 °C, $\mu = 0.1$ (KNO_3)
B-ED3A	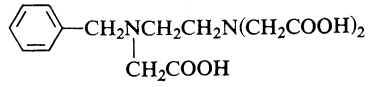	1.90	5.10	9.84	(32), 24 °C, $\mu = 0.1$ (KCl)

*Compounds not previously reported in literature.
†Dissociation constants not previously reported.

Can. J. Chem. Downloaded from www.nrcresearchpress.com by 210.87.254.5 on 09/05/12
For personal use only.

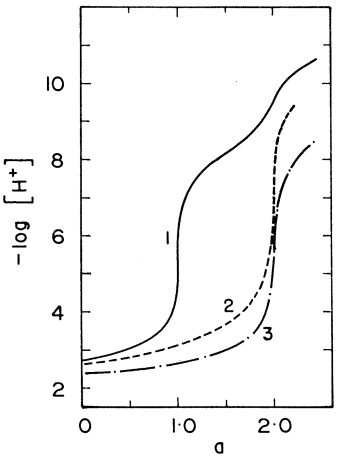

FIG. 1. Potentiometric titration curves of A-EDDA at 25 °C in 0.1 M KNO_3 (a = moles of KOH added per mole of amino acid). 1, free acid; 2, acid + Ni^{2+}; 3, acid + Cu^{2+}; $C_A = C_M = 2.0 \times 10^{-3}$ M.

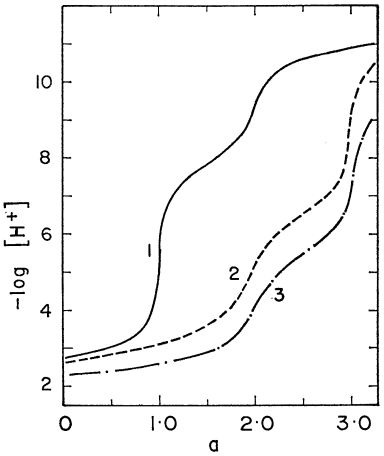

FIG. 2. Potentiometric titration curves of BS-EDDA at 25 °C in 0.1 M KNO_3. 1, free acid; 2, acid + Ni^{2+}; 3, acid + Cu^{2+}; $C_A = C_M = 2.0 \times 10^{-3}$ M.

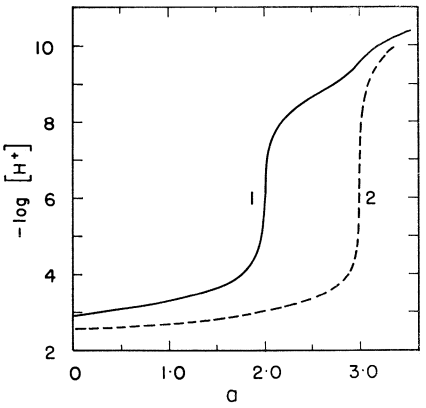

FIG. 3. Potentiometric titration curves of TS-ED3A at 25 °C in 0.1 M KNO_3. 1, free acid; 2, acid + Cu^{2+}; $C_A = C_M = 1.0 \times 10^{-3}$ M.

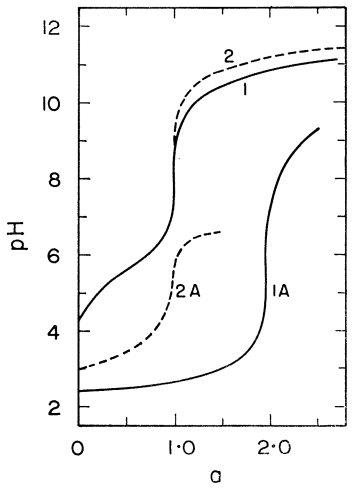

FIG. 4. pH titration curves at 25 °C in 0.1 M KNO_3. 1, U-EDDA; 1A, U-EDDA + Cu^{2+}; 2, U-KP; 2A, U-KP + Cu^{2+}; $C_A = C_M = 4.0 \times 10^{-3}$ M.

by Bruno *et al.* (32) for *N*-alkyl-ED3A's. The values of $pK_1 \simeq 1.5$ correspond to the dissociation of a proton of a carboxyl group attached to the sulfonamide nitrogen, $pK_2 = 3.3$ represents the dissociation of the second carboxyl, and $pK_3 = 8.5$ corresponds to the proton of the iminodiacetate nitrogen. The low values of pK_2 and pK_3 suggest a weaker chelating ability for these compounds as compared to those of the *N*-alkyl ED3A's. A qualitative verification of this comes from a comparison of some chelation curves obtained in a preliminary study (shown in Fig. 3) with those of the previously mentioned *N*-alkyl ED3A's (32).

(ii) Unsubstituted Amino Acids

1. Preliminary chelation studies. The curves obtained for the potentiometric titrations of U-EDDA, S-EDDA, and their cyclic amides in both free acid form and in the presence of equimolar amounts of Cu(II) are presented in Figs. 4 and 5. These results are used to provide further proof of the structure of the cyclic amides.

The chelating properties of U-EDDA and S-EDDA have already been discussed (27, 33)

Can. J. Chem. Downloaded from www.nrcresearchpress.com by 210.87.254.5 on 09/05/12
For personal use only.

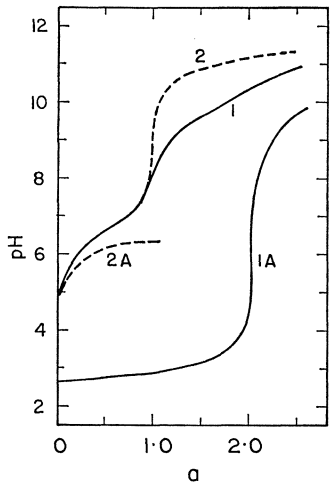

FIG. 5. pH titration curves at 25 °C in 0.1 M KNO_3. 1, S-EDDA; 1A, S-EDDA + Cu^{2+}; 2, S-KP; 2A, S-KP + Cu^{2+}; $C_A = C_M = 2.0 \times 10^{-3}$ M.

and they have been shown to be tetradentate ligands capable of forming very stable chelates. This is illustrated by the structures of the chelates (Chart 2) and is reflected by the considerable suppression of the titration curves in the presence of metal ion.[1]

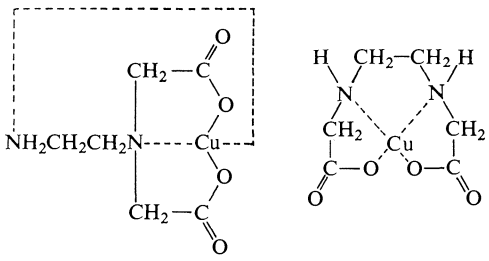

Cu(II) chelate of U-EDDA Cu(II) chelate of S-EDDA

CHART 2

The chelation curve for U-KP (Fig. 4) shows an end-point after the addition of one equivalent of base indicating the presence of only one carboxyl group (as opposed to two for U-EDDA). Furthermore, the results of Schwarzenbach *et al.* (27) with *N*-carbethoxy-β-aminoethyliminodiacetic and *N*-acetamidoiminodiacetic acid indicate that the inductive effect of the carbonyl group prevents the amide nitrogen atom from participating in the chelation. A similar effect is expected in the case of the cyclic amides of this work and thus U-KP can be expected to be bidentate (structure shown in Chart 3). These two facts account for the considerably lower stability of the U-KP chelate as compared to that of U-EDDA (chelation curves of Fig. 4).

The acetate group of S-KP is attached to an amide nitrogen atom which cannot coordinate with a metal. Coordination of a metal ion with the other nitrogen atom to form a chelate is also not expected to take place. This is confirmed by the titration curve of S-KP in the presence of Cu(II) (Fig. 5) which indicates negligible complex-formation and resembles very much the simple titration of $Cu(NO_3)_2$ with base.

The effects of refluxing 3-KP in a highly alkaline aqueous medium are illustrated by the titration curves of 3-KP before and after treatment (Fig. 6). For the free acids, there is little change in the first two buffer regions but beyond the second end-point, there is a significant suppression of the buffer region (compare with Figs. 4 and 5). In addition, in the titrations with Cu(II), there is a shift in the chelation end-point from 2.0 to approximately 2.5 for the treated 3-KP. These two observations suggest the presence of some additional weakly acidic functional group (in 3-KP)

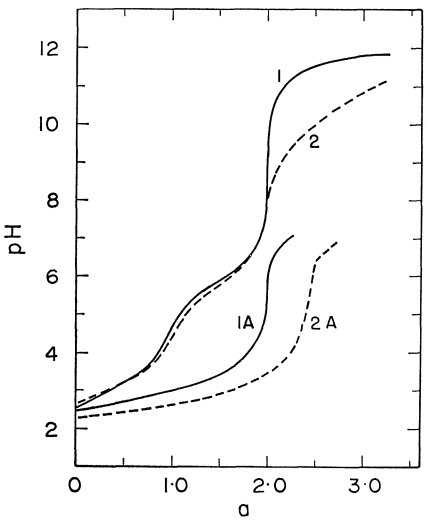

FIG. 6. pH titration for 3-KP before and after treatment with caustic. 1, 3-KP; 1A, 3-KP + Cu^{2+}; $C_A = C_M = 1.8 \times 10^{-3}$ M; 2, 3-KP after treatment; 2A, treated 3-KP + Cu^{2+}; $C_A = C_M = 1.1 \times 10^{-3}$ M.

[1]It should be noted that the presence of a second acetic acid group in the case of the diacids as compared to the monoacetic cyclic amides, is reflected by the lowering of the second buffer region in the titration curves of the free acids, and this is further indication of the structure of these compounds.

Can. J. Chem. Downloaded from www.nrcresearchpress.com by 210.87.254.5 on 09/05/12
For personal use only.

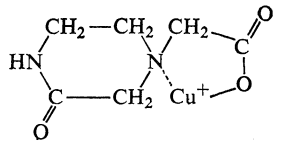

Cu(II) chelate of U-KP

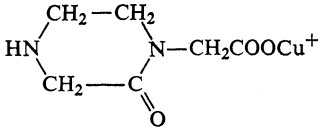

Cu(II) complex of S-KP

CHART 3

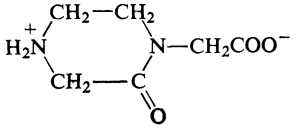

1

S-KP (pK_1 = 6.55)

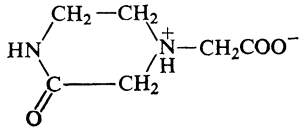

2

U-KP (pK_1 = 5.51)

CHART 4

capable of chelation, and were interpreted to indicate that cleavage of 3-KP had taken place. That ED3A was actually present was confirmed, as previously discussed, by the successful preparation of its arylsulfonyl derivatives from the treated 3-KP solution.

2. Dissociation schemes. Dissociation schemes are proposed for the cyclic amides of the diacetic acids as it was felt that the knowledge of the behavior of these simpler acids might lead to a better understanding of the behavior of 3-KP and some linear amino acids. It is proposed that both S-KP and U-KP exist as zwitterions with the dissociable protons migrating to the nitrogen atoms furthest from a carbonyl group (Chart 4).

The pK values may seem rather low for the dissociation of ammonium protons when compared to the customary values of pK 9–11 (30). However, an amide group is known to exert an appreciable inductive effect on the basicity of a nitrogen proton (27). In fact, preliminary results in this laboratory for 2-oxo-piperazine, where it is unequivocably a piperazinium proton which dissociates, indicate a value of p$K \simeq 6.5$ as compared to the corresponding value of 9.82 for piperazine (30). A similar decrease might therefore be expected in the pK values of S-KP and U-KP.[2]

An examination of the pK values and structures of S-KP and U-KP leaves little doubt that the pK for S-KP does indeed correspond to a nitrogen proton. If it were argued that the proton corresponded to a carboxyl, the greater proximity of the carbonyl group to the iminoacetate of S-KP would require that its pK be lower than that of U-KP (regardless of the location of the dissociable proton of U-KP) which is contrary to the observed values.

In the case of U-KP, several arguments can be put forth consistent with the observations and supporting the assumption that $pK_1 = 5.51$ corresponds to the dissociation of an ammonium proton.

A comparison of the pK values of S-KP and U-KP indicates a lower value ($\Delta pK = 1.0$) for the latter. Irving and Pettit (34) had noted that the introduction of an acetic acid substituent into a secondary nitrogen of a heterocyclic compound resulted in a decrease of the basicity of the nitrogen proton ($\Delta pK = 1$ for piperidine and $\Delta pK_1 = 1.2$ and $\Delta pK_2 = 1.1$ for piperazine).

In the case of S-KP, the proton (of a secondary nitrogen) which dissociates is much further removed from the acetate group than that of U-KP. Consequently, it could be expected that the COO^- group would affect the dissociation of the NH^+ group to a much greater extent in the case of the latter compound (35). The almost identical pK values obtained for S-KP and 2-oxo-piperazine suggest an almost negligible effect of the acetate group on the dissociable proton of the former compound, and the difference of 1.0 pK unit between U-KP and S-KP is therefore quite reasonable.

In addition, due to the minimal contribution of

[2]It is interesting to note the similarity between the pK_1 of S-KP and that of S-EDDA (pK_1 = 6.51) which has been attributed to the dissociation of an ammonium proton (33).

Can. J. Chem. Downloaded from www.nrcresearchpress.com by 210.87.254.5 on 09/05/12
For personal use only.

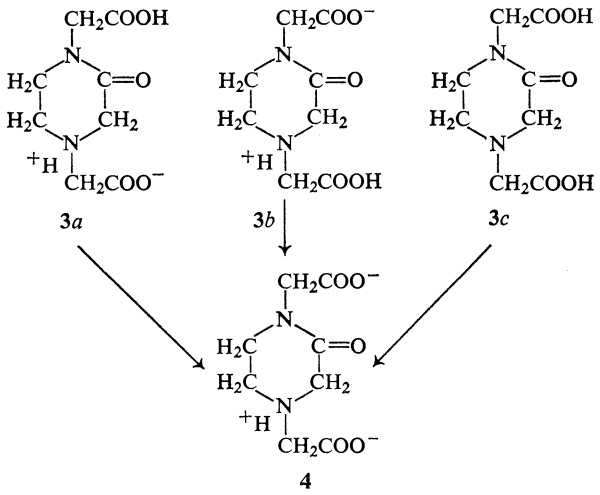

SCHEME 2

the acetate group to the overall lowering of the pK value to 6.55 in S-KP, the entire cyclic unsubstituted amide

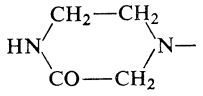

might be considered as an electron-withdrawing entity. Substitution of this group into an acetic acid molecule would therefore be expected to increase the acidity of the carboxyl proton to p$K < 4.76$. The resulting structure is in fact a U-KP molecule with an undissociated carboxyl proton. The observed value of p$K_1 = 5.51$ for U-KP is therefore seen to be inconsistent with the concept of a carboxyl proton but is quite consistent with the assumption that it is an ammonium proton which dissociates.

Although the acid dissociation constants for 3-KP have been reported (25) and compared with those of 1,4-piperazine diacetic acid, no dissociation schemes had been proposed. For the latter compound (p$K_1 = 4.46$ and p$K_2 = 8.70$) a neutral double betaine structure had been suggested (34).

The incorporation of a carbonyl group into the piperazine ring permits only one proton to exist in the ammonium form. The value p$K_1 = 2.94$ for 3-KP thus corresponds to the dissociation of a carboxyl proton, and 3 possible tautomers are considered for the neutral form of the molecule (Scheme 2). The structure **3***a* may be compared with monoprotonated glycylglycine (p$K_1 = 3.08$ (35)) where the increased acidity of the carboxyl proton (as compared to acetic acid) is also due mainly to the inductive effect of the amide group. In the cyclic 3-KP the closer proximity of the amide group might be expected to result in a value lower than 3.08. Thus **3***a* is consistent with the observed value of 2.94. Tautomer **3***b* appears less favorable since its structure at the ammonium end resembles monoprotonated glycine and because of this and the presence of the amide group in the ring, the pK value would be expected to be similar to or lower than p$K_1 = 2.34$ of glycine. The possibility of tautomer **3***c* where the second proton migrates to the nitrogen atom upon removal of the first proton from either of the carboxyl groups cannot be ruled out.

The mononegative anion of 3-KP (**4**) can be compared to the neutral form of U-KP. As expected, the pK_2 of 3-KP (5.85) is slightly higher than that of the analogous dissociation constant pK_1 of U-KP (5.51) because of the greater negative charge of the former compound (36).

Some conclusions may now be drawn with respect to some dissociation schemes proposed by other workers for several linear amino acids. There have been two different schemes proposed for the dissociation of the first proton of U-EDDA. Tillotson and Staveley (37) had argued that p$K_1 = 5.58$ corresponded to the dissociation of a carboxyl proton. To account for the high pK value, the structure

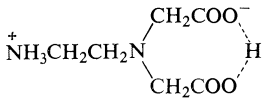

Can. J. Chem. Downloaded from www.nrcresearchpress.com by 210.87.254.5 on 09/05/12
For personal use only.

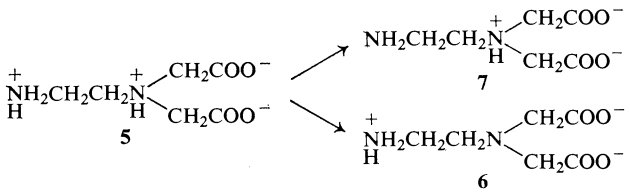

SCHEME 3

was proposed for the neutral molecule, on the grounds of increased stabilization of the zwitterion by internal hydrogen bond formation between the OH and COO^-. Such a structure is not possible in the case of the cyclic amide U-KP where an almost identical value of pK was obtained for the dissociation of an ammonium proton. It seems unnecessary therefore to postulate the existence of a carboxyl proton for U-EDDA. Schwarzenbach *et al.* (27) had proposed a different scheme (Scheme 3).

Both the nitrogen atoms of **5** were said to be equivalent, thus resulting in equal proportions of tautomers **6** and **7**. On the basis of the results and arguments presented here for S-KP/U-KP, the proton of the iminodiacetate nitrogen of **5** might be expected to be less basic than that of the ammonium nitrogen at the opposite end, leading to the route **5** → **6** as the preferred one. In addition, of the two tautomers, **6** would be expected to be more stable than **7** due to its greater charge separation.

The various schemes discussed thus far may be extended to provide additional information on the behavior of EDTA. There has been some controversy as to whether the value pK_3 = 6.16 corresponds to the dissociation of an ammonium proton (38) or of a carboxyl proton (37, 39). Support for the latter concept is based once again on the proposal of an internally bonded structure as shown previously for U-EDDA to account for the high pK value. However, the similarity between the pK_3 of EDTA and the pK values for the dissociation of the analogous protons in both S-EDDA and S-KP, where it is an ammonium proton which dissociates and where such an internally bonded structure is not likely, suggests that it is more probably an ammonium proton which corresponds to the pK_3 of EDTA.

Experimental

Potentiometric Titrations

The stoichiometric acid dissociation constants were calculated from potentiometric titrations of aqueous solutions of the amino acids with standard base.

Apparatus and Procedure

The titration vessel consisted of a 300 ml Berzelius beaker fitted with a Lucite cover containing holes for the electrodes, the tip of a 5 ml microburette, a thermometer, and gas inlet and outlet tubes. Stirring of the solutions was affected by means of an air-driven magnetic stirrer. The temperature was kept at 25.0 ± 0.05 °C by immersion of the vessel into a large constant-temperature water bath. Presaturated nitrogen was bubbled slowly through the solution to maintain an inert atmosphere. An ascarite tube was attached to the top of the microburette to prevent diffusion of CO_2 into the titrant.

The hydrogen-ion concentration was measured with the aid of a radiometer Model pHM4 meter equipped with a glass electrode and saturated calomel reference electrode, standardized with NBS buffer solutions over the pH range used in this study. Solutions were prepared from deionized water, which was made by passing laboratory distilled water through a mixed-bed ion exchanger. Carbonate-free potassium hydroxide (0.10 M in 0.10 M KNO_3) was prepared from a BDH concentrate and standardized potentiometrically against potassium acid phthalate. The exact end-point of these and subsequent titrations was determined by Gran's method (40).

The titrations were carried out with 200 ml of 1–2 × 10^{-3} M solutions of the ligands. Successive pH readings were taken after each addition of small increments of the base until the pH reached ≃11.0. The tip of the microburette was immersed in the solution only during the addition of the titrant, and during the measurements of pH, the stirrer and gas were shut off. Experimental data for several typical titrations are given in Figs. 1–5. The degree of neutralization of the ligand acid is designated by a.

Calculations

The pH meter was calibrated to serve as a concentration probe by titrating neutral 0.10 M KNO_3 solution with standard nitric acid and potassium hydroxide. The correction factors thus obtained for the conversion of pH to $-\log[H^+]$ found in the pH ranges 2–4 and 10–12 agreed very well and were assumed to be constant over the pH range employed in this study. The concentration of hydroxide ions was determined using a value of $K_c w$ = 1.628 × 10^{-14} determined experimentally by the method of Liberti and Light (41) (cf. 1.68 × 10^{-14} reported in refs. 42 and 43). The acid dissociation constants for the triacetic acids were calculated by the method outlined by Irving and Da Silva (44) and Da Silva (42). For those of

Can. J. Chem. Downloaded from www.nrcresearchpress.com by 210.87.254.5 on 09/05/12
For personal use only.

Can. J. Chem. Downloaded from www.nrcresearchpress.com by 210.87.254.5 on 09/05/12
For personal use only.

the remaining acids, the methods of Chaberek and Martell (31) were employed.

Organic Preparations[3]

p-(β-Bromoethyl)benzenesulfonyl Chloride

This compound was prepared by the procedures outlined by Metanomski (45) and Spinner *et al.* (46).

Ethylenediamine-N,N'-diacetic Acid (S-EDDA)

This compound was prepared by the reaction of ethylenediamine, sodium cyanide, and formaldehyde, essentially according to the procedure outlined in Bersworth's patents (47, 48). The alkaline reaction solution was acidified with 4 *N* hydrochloric acid to a p*H* of 4.4, in place of the sulfuric acid. Two recrystallizations of the crude product from alcohol–water mixtures gave the pure S-EDDA.

Anal. Calcd. for $C_6H_{12}N_2O_4$ (mol. wt. 176.17): C, 40.90; H, 6.87; N, 15.91; O, 36.32. Found (176.4): C, 40.92; H, 7.04; N, 15.72; O, 36.31.

2-Oxo-1-piperazine Acetic Acid (S-KP)

S-EDDA (17.62 g, 0.10 mole) was dissolved in 125 ml water containing 0.20 mole of hydrochloric acid. After refluxing for 2 h, cooling, and filtering, the hydrochloric acid was neutralized with an aqueous solution (50 ml) of the stoichiometric amount of sodium carbonate. The resulting solution was concentrated under reduced pressure to 50 ml of viscous liquid. Absolute alcohol (400 ml) was added, causing a thick yellow oil to separate out. Refrigeration for 5 days resulted in crystallization of the oil to give 11.5 g of crude product (75% S-KP). This material was dissolved in boiling dimethyl formamide (50 ml) and after removal of the insoluble solids by filtration, the product was reprecipitated with alcohol. Two such purifications yielded the pure white powdery product.

Anal. Calcd. for $C_6H_{10}N_2O_3$ (mol. wt. 158.16): C, 45.56; H, 6.37; N, 17.71; O, 30.35. Found (160.2): C, 45.33; H, 6.27; N, 17.53; O, 30.56.

N-Acetylethylenediamine (A-EDA)

The preparation of this compound was based on the procedure of Aspinall (49). The product (obtained in 72% yield) distilled at 119–123 °C (uncorrected) at 2–3 mm Hg (previously reported 125–130 °C at 5 mm Hg).

N-Acetyl-1,2-diaminoethane-N',N'-diacetic Acid (A-EDDA)

N-Acetylethylenediamine (83.5 g, 0.816 mole) in water (100 ml) was added with stirring to a solution of sodium chloroacetate (190 g, 1.63 mole) in water (800 ml) at 40–50° over a period of 2.5 h. The temperature was raised to 65–70° and heating and stirring was continued for 15 h, during which time a 33% aqueous solution of sodium hydroxide was added from time to time to maintain the p*H* at 9–11. The temperature was then increased to 100° for an additional 5 h during which time no appreciable change in p*H* occurred. After cooling, the mixture was acidified with the stoichiometric amount of concentrated hydrochloric acid to p*H* 1.8. Refrigeration of the solution overnight caused precipitation of crude (90% pure) A-EDDA (70.2 g, 38%).

Concentration of the mother liquor in stages under reduced pressure to 100 ml (removing the inorganic salts which had settled out at each stage by filtration) resulted in the precipitation of additional product (44.7 g, 16.2%) which proved to be 64% pure. The addition of 600 ml alcohol and refrigeration resulted in the precipitation of more crude (33% pure) product (12.9 g, 7.3%).

Near-pure product was obtained by dissolving the crude material in boiling dimethylformamide (1–2 ml DMF per g of pure organic material), filtering out the insoluble solids, and reprecipitating the A-EDDA from the cooled filtrate with alcohol. Further recrystallization from minimal amounts of boiling water gave a white crystalline product.

Anal. Calcd. for $C_8H_{14}N_2O_5$ (mol. wt. 218.21): C, 44.03; H, 6.47; N, 12.84; O, 36.66. Found (219.4): C, 44.59; H, 6.65; N, 12.49; O, 36.29.

Ethylenediamine-N,N-diacetic Acid (U-EDDA)

(*a*) A solution of A-EDDA (41.0 g, 0.187 mole) and sodium hydroxide (45.0 g, 1.12 mole) was made up in 600 ml water and refluxed gently for 7 h. After concentration under reduced pressure to 200 ml the solution was cooled, filtered, and acidified with concentrated hydrochloric acid (95.0 ml, 1.14 mole) which was added slowly (2 h) with stirring and cooling. Further concentration to 75 ml resulted in the precipitation of 14.57 g (44.0%) of almost pure U-EDDA (Mol. Wt. Calcd.: 176.2. Found: 175.8).

The mother liquor was treated with 200 ml acetone and refrigerated overnight, resulting in the precipitation of additional, 36% pure, U-EDDA (17.94 g, 19.5%).

Recrystallization from minimal amounts of boiling water gave a pure, white, crystalline product. Further attempts to recover more product from the mother liquor resulted in highly impure products and a viscous dark-yellow syrup which showed great reluctance to crystallize.

Anal. Calcd. for $C_6H_{12}N_2O_4$ (mol. wt. 176.17): C, 40.90; H, 6.87; N, 15.91; O, 36.32. Found (177.4): C, 40.76; H, 6.93; N, 15.50; O, 36.81.

(*b*) Another method of recovering greater yields of U-EDDA consisted of using the alkaline solution of the reaction mixture of A-EDDA as the starting material. This solution was treated with sufficient sodium hydroxide to give an overall sodium/amino acid molar ratio of 6:1 and refluxed. Recovery of the product was as above and usually resulted in yields of 65–75% of crude (60–70% pure) U-EDDA.

3-Oxo-1-piperazine Acetic Acid (U-KP)

The cyclic amide of U-EDDA was prepared from the diacid in a manner analogous to that of S-KP from S-EDDA.

Anal. Calcd. for $C_6H_{10}N_2O_3$ (mol. wt. 158.16): C, 45.57; H, 6.37; N, 17.72; O, 30.35. Found (159.6): C, 45.74; H, 6.59; N, 17.34; O, 30.61.

2-Oxo-1,4-piperazine Diacetic Acid (3-KP)

A solution of sodium chloroacetate (465 g, 4.0 equivalents) in 700 ml water was added at room temperature to a well-stirred solution of ethylenediamine (120 g, 2.0 mole) in 500 ml water, over a period of 8 h. During the first day of the reaction, 4.0 equivalents of sodium hydroxide solution (25% w/w) were added from time to time to maintain the p*H* at 10–12. The fifth and sixth equivalents

[3]Microanalyses were performed by Galbraith Laboratories, Inc., Knoxville, Tennessee 37921.

Can. J. Chem. Downloaded from www.nrcresearchpress.com by 210.87.254.5 on 09/05/12
For personal use only.

of chloroacetate (1.0 equivalent/175 ml water) were added during the next 2 days along with additional sodium hydroxide until a total of 5.5 equivalents of base had been added. After 8 days the p*H* remained unchanged and the solution was heated to boiling and concentrated to approximately 1800 ml. It was then filtered, cooled, and acidified with concentrated hydrochloric acid (500 ml, 6.0 equivalents) added over a period of 2 h. The resulting slurry was stirred for an additional 2 h and refrigerated overnight. The product was filtered, washed with water, and dried giving 99% pure ethylenediamine-*N*,*N*,*N*′,*N*′-tetra acetic acid (EDTA) (138 g, 0.47 mole).

The mother liquor was further acidified with concentrated hydrochloric acid (50 ml, 0.60 equivalents) and refluxed to ensure cyclization of the remaining non-fully substituted diamino acids. Concentration of the solution to 800 ml under reduced pressure resulted in the precipitation of solid which proved to be predominantly sodium chloride. The excess hydrochloric acid was neutralized with the stoichiometric amount of sodium hydroxide solution and the mixture was then reduced to 400 ml, resulting in another batch of sodium chloride. The viscous filtrate was diluted to 1000 ml with water and its acidity adjusted. (Note. Potentiometric titrations of samples of the solution were carried out at various stages and the acidity adjusted accordingly, as it was found that the presence of sodium salts of the amino acids or an excess of hydrochloride severely inhibited the crystallization of the free acid at later stages.)

Absolute ethanol (5 l) was added to the aqueous solution and the mixture was stirred for several hours resulting in the separation of a thick viscous syrup A. The alcohol–water solution was decanted from this syrup and was concentrated to 150 g of thick viscous syrup B. The first syrup (A) was leached with alcohol (4 × 1000 ml) resulting in a solid which was ground, filtered, washed with additional alcohol and dried, resulting in 163 g of 79% pure amino acids. The second syrup (B), containing approximately 0.5 mole of amino acids, was placed into 100 ml of boiling dimethylformamide, its acidity adjusted, and the mixture was boiled for 10–15 min. The insoluble materials were filtered out and the cooled filtrate was treated with alcohol. Refrigeration for several days resulted in the precipitation of 58.5 g of slightly hygroscopic product, containing 0.27 mole amino acid.

The crude products obtained from the two syrups A and B were then purified by dissolving in boiling DMF, filtering out and discarding the insoluble solids, and treating the cooled filtrate with large volumes of alcohol. This was followed by several days refrigeration to enable the syrups which separated out initially to solidify. Such treatments were found to be effective in isolating pure 3-KP and/or its monohydrate from inorganic salts and the hydrochloride salts of other amino acids. Total pure product obtained after 2 treatments with DMF was 0.46 mole (25%).

Anal. Calcd. for $C_8H_{12}N_2O_5$ (mol. wt. 216.19): i.e. 3-KP C, 44.44; H, 5.59; N, 12.96; O, 37.01. Found (215.8): C, 44.56; H, 5.91; N, 12.70; O, 35.94.

Ethylenediamine-N,N,N′-triacetic Acid (ED3A)

A solution of sodium hydroxide (60.0 g, 1.50 mole) in 300 ml water was added to 3-KP·H_2O (58.5 g, 0.25 mole) dissolved in 650 ml water and the resulting solution was strongly refluxed for 24 h. Potentiometric titrations of samples of the filtered, cooled solution with standard 0.10 *N* potassium hydroxide were carried out (the alkaline samples had been acidified with 0.10 *N* hydrochloric acid just prior to titration with base). The results (curves of Fig. 6) indicate a shift in the chelation end-point from 2.0 to approximately 2.5 equivalents for the treated solution. This, as mentioned previously, was interpreted as an indication of the presence of ED3A in the solution, from the cleavage of 3-KP.

N-{p-(β-Bromoethyl)benzenesulfonyl}-1,2-diaminoethane-N′,N′-diacetic Acid (BEBS-EDDA)

A solution of *p*-(β-bromoethyl)benzenesulfonyl chloride (56.7 g, 0.20 mole) in toluene (200 ml) was added slowly (3 h) to a well-stirred aqueous solution of U-EDDA (35.2 g, 0.20 equivalents) and sodium carbonate (10.6 g, 0.20 equivalents). Stirring was continued and after an additional 4 h, sodium carbonate (10.6 g, 0.20 equivalents) in 100 ml water was added to maintain the p*H* 8–10. Higher alkalinity was avoided to prevent the hydrolysis of the —CH_2CH_2Br group.

After a total of 2 days, the mixture was filtered, the small amount of insoluble material which had settled out discarded and the two layers were separated. The aqueous layer was allowed to stand overnight to clear up the murkiness, then treated with activated charcoal and filtered. Acidification with the stoichiometric amount of concentrated hydrochloric acid added over a period of 2 h resulted in the precipitation of the free acid as a slurry of fine white powder. The solid, after filtration, washing with water (5 × 200 ml) and drying, gave 37.5 g (44%) of crude product.

Anal. Found: Br, 18.62; S, 7.71.

Purification was accomplished by dissolving the product in acetone (20 ml/g solid), concentrating the solution to half its volume and then reprecipitating with water. The pure BEBS-EDDA was recovered as a white powdery material.

Anal. Calcd. for $C_{14}H_{19}N_2O_6SBr$ (mol. wt. 423.29): O, 22.69; S, 7.58; Br, 18.88. Found (420.7): O, 22.90; S, 7.60; Br, 18.80.

N-(p-Toluenesulfonyl)-1,2-diaminoethane-N′,N′-diacetic Acid (TS-EDDA)

This compound was prepared from *p*-toluenesulfonyl chloride and U-EDDA by a procedure similar to that of BEBS-EDDA. The alkaline aqueous layer was first concentrated to half its volume before acidification, resulting in yields of 65%. The crude product was recrystallized from boiling water (5 ml/g solid) to give white crystalline TS-EDDA.

Anal. Calcd. for $C_{13}H_{18}N_2O_6S$ (mol. wt. 330.36): C, 47.25; H, 5.49; N, 8.48; O, 29.05; S, 9.70. Found (333.3): C, 47.10; H, 5.44; N, 8.50; O, 28.94; S, 9.80.

The product was also obtained from the reaction of a toluene solution of *p*-toluenesulfonyl chloride with an alkaline aqueous solution of 3-oxo-1-piperazine acetic acid (U-KP) previously treated with sodium hydroxide in a manner similar to that of 3-KP except that refluxing was carried out for only 30 min.

N-(p-Toluenesulfonyl)-1,2-diaminoethane-N,N′-diacetic Acid (TS-EDDA-sym)

This compound was prepared by the same procedure

Can. J. Chem. Downloaded from www.nrcresearchpress.com by 210.87.254.5 on 09/05/12
For personal use only.

employed for TS-EDDA, substituting S-EDDA in place of U-EDDA.

Anal. Found (mol. wt. 334.9): N, 8.28; O, 29.73; S, 9.71.

N-(Benzenesulfonyl)-1,2-diaminoethane-N′,N′-diacetic Acid (BS-EDDA)

This compound was prepared from benzenesulfonyl chloride and U-EDDA by the procedure employed for TS-EDDA. The yield was considerably lower due to the appreciable water-solubility of the product.

Anal. Calcd. for $C_{12}H_{16}N_2O_6S$ (mol. wt. 316.33): C, 45.57; H, 5.10; N, 8.86; O, 30.35; S, 10.14. Found (318.9): C, 45.46; H, 5.10; N, 8.90; O, 30.30; S, 10.02.

N-{p-(β-Bromoethyl)benzenesulfonyl}-1,2-diaminoethane-N,N′,N′-triacetic Acid (BEBS-ED3A)

A highly alkaline solution (750 ml) initially containing 0.20 mole of 2-oxo-1,4-piperazine diacetic acid was refluxed with sodium hydroxide (48.0 g, 1.20 equivalents) as previously described. The excess base was partially neutralized to p*H* 11.8 with 1.2 *N* hydrochloric acid (0.50 equivalents). A small amount of material had precipitated out and was filtered off and discarded. A toluene solution (250 ml) of *p*-(β-bromoethyl)benzenesulfonyl chloride (34.10 g, 0.12 mole) was added (3 h) at room temperature to the well-stirred aqueous solution. Stirring of the heterogeneous mixture was continued for 3 days, after which time it was filtered and the layers separated. The aqueous solution was allowed to stand until the murkiness cleared up, then treated with activated charcoal and filtered. Acidification of the clear yellow solution with 1.2 *N* hydrochloric acid (500 ml) resulted in the precipitation of the desired product. (Approximately half-way through the acidification (p*H* $\simeq$ 4.6), a small amount (2.0 g) of extremely insoluble flocculent material had settled out and was filtered off. This solid, which proved very difficult to titrate, was discarded.) The product was filtered off, washed with water (4 × 250 ml) and dried, giving 17.82 g (18% yield based on the original amount of 3-KP) of white, powdery material.

Anal. Found: N, 5.78; S, 6.40; Br, 15.98.

The product showed very low water-solubility and was purified by stirring the crude material in large amounts of water and recovering by filtration. Three such treatments gave pure BEBS-ED3A.

Anal. Calcd. for $C_{16}H_{21}N_2O_8SBr$ (mol. wt. 481.33): C, 39.92; H, 4.40; N, 5.82; O, 26.60; S, 6.66; Br, 16.61. Found (492.1): C, —; H, —; N, 5.75; O, 26.44; S, 6.74; Br, 16.36.

N-(p-Toluenesulfonyl)-1,2-diaminoethane-N,N′,N′-triacetic Acid (TS-ED3A)

This compound was prepared from *p*-toluenesulfonyl chloride by the same procedure as employed for BEBS-ED3A.

Anal. Calcd. for $C_{15}H_{20}N_2O_8S$ (mol. wt. 388.39): N, 7.22; O, 32.96; S, 8.26. Found (395.6): N, 7.22; O, 33.10; S, 8.32.

N-(p-Vinylbenzenesulfonyl)-1,2-diaminoethane-N′,N′-diacetic Acid (SS-EDDA)

A solution of potassium hydroxide (7.41 g, 0.132 mole) in 170 ml 95% alcohol was added to a well-stirred slurry of BEBS-EDDA (16.93 g, 0.04 mole) in 450 ml alcohol at 60–70° over a period of 60 min, then refluxed for an additional 30 min. The excess base was neutralized with an alcoholic solution (50 ml) of hydrochloric acid (1.3 ml concentrated acid) added slowly to the alkaline alcoholic solution, previously cooled to 5–10°. After refrigeration for an additional 2 h, the mixture was filtered to remove the precipitated potassium halides and traces of *p-tert*-butylcatechol were added as polymerization inhibitor.

The filtrate was concentrated under reduced pressure to 100 ml of thick syrup which was dissolved in 100 ml water and acidified with hydrochloric acid (4.0 ml concentrated acid in 50 ml water). Refrigeration of the solution for 6 h, after decanting from the sticky sludge which had initially appeared during the acidification, resulted in the precipitation of white, flocculent material. The solid was recovered by filtration and dried, giving 4.43 g (32%) of crude product. A slurry of this solid in 40 ml water was stirred for 1 h and 3.36 g (25%) of pure SS-EDDA were recovered upon filtration and drying of the solid.

Anal. Calcd. for $C_{14}H_{18}N_2O_6S$ (mol. wt. 342.37): C, 49.11; H, 5.30; N, 8.18; O, 28.04; S, 9.37. Found: C, 48.96; H, 5.40; N, 7.96; O, 28.04; S, 9.57.

N-(p-Vinylbenzenesulfonyl)-1,2-diaminoethane-N,N′,N′-triacetic Acid (SS-ED3A)

BEBS-ED3A (17.8 g, 0.037 mole) was dissolved and neutralized in hot (50–60°) 95% ethanol (400 ml) containing the stoichiometric amount of potassium hydroxide. Additional potassium hydroxide (2.7 g, 0.048 mole) in 100 ml alcohol was added (15 min) with stirring, the temperature was raised, and the solution was refluxed 45 min. The excess base was neutralized with an alcoholic solution (50 ml) of hydrochloric acid (2.5 ml concentrated acid) added slowly to the alkaline solution, previously cooled in an ice-bath to 5–10°. Traces of *p-tert*-butylcatechol were added as polymerization inhibitor and the mixture was refrigerated for 3 h. A thick, oily residue settled out and after decanting and discarding the supernatant liquid, the oil was dissolved in 250 ml water. Acidification with the stoichiometric amount of 2 *N* hydrochloric acid precipitated white flocculent material. The product was removed by filtration, washed with water (5 × 50 ml), and dried, giving 5.98 g (40%) SS-ED3A.

Anal. Calcd. for $C_{16}H_{20}N_2O_8S$ (mol. wt. 400.42): C, 47.99; H, 5.04; N, 7.00; O, 31.97; S, 8.01. Found: C, 47.97; H, 5.08; N, 6.99; O, 32.07; S, 8.13.

Hydrogenation calculated for 1.000 double bond. Found: 0.993, 1.013.[4]

The authors which to express their appreciation to the National Research Council of Canada for financial assistance.

1. R. M. Wheaton and M. J. Hatch. *In* Ion exchange. Vol. 2. *Edited by* J. A. Marinsky. Marcel Dekker, Inc., New York. 1969. p. 211.
2. E. Blasius and B. Brozio. *In* Chelates in analytical chemistry. Vol. I. *Edited by* H. A. Flaschka and A. J. Barnard, Jr. Marcel Dekker, Inc., New York. 1967. p. 49.

[4]Double bond analyses by catalytic hydrogenation performed by Huffman Laboratories, Inc., Wheatbridge, Colorado 80 033.

3. P. TEYSSIÉ. Chim. **20**, 45 (1966).
4. R. HERING. J. Prakt. Chem. **31**, 320 (1966); Z. Chem. **5**, 402 (1965).
5. G. SCHMUCKLER. Talanta, **12**, 281 (1965).
6. R. ROSSET. Bull. Inform. Sci. Tech. (Paris) **85**, 13 (1964).
7. G. NICKLESS and G. R. MARSHALL. Chromatogr. Rev. **6**, 154 (1964).
8. V. V. RODE, E. G. RUKHADZE, and A. P. TERENT'EV. Russ. Chem. Rev. (Engl. Transl.) **32**, 666 (1963).
9. W. RIEMAN, III and A. C. BREYER. *In* Treatise on analytical chemistry, Part I. Theory and practice. Vol. 3. *Edited by* I. M. Kolthoff and P. J. Elving. Interscience Publishers, Inc., New York. 1961. p. 1583.
10. J. R. MILLAR. Chem. and Ind. (London), 606 (1957).
11. D. K. HALE. Res. **9**, 104 (1956).
12. R. C. DE GEISO, L. G. DONARUMA, and E. A. TOMIC. J. Appl. Polym. Sci. **7**, 1515 (1963).
13. A. R. DESPIĆ and D. J. KOSANOVIĆ. Makromol. Chem. **29**, 151 (1959).
14. G. F. D'ALELIO. U.S. Patent No. 3 214 413. Oct. 26, 1965.
15. G. F. D'ALELIO. U.S. Patent No. 3 090 771. May 21, 1963.
16. R. A. MOCK, R. C. CALKINS, and C. A. MARSHALL. U.S. Patent No. 3 089 079. 1961.
17. R. A. MOCK, R. C. CALKINS, and C. A. MARSHALL. U.S. Patent No. 2 980 607 Apr. 18, 1961.
18. R. A. MOCK, C. A. MARSHALL, and L. R. MORRIS. U.S. Patent No. 2 910 445. Oct. 27, 1959.
19. L. R. MORRIS. U.S. Patent No. 2 888 441. May 26, 1959.
20. L. R. MORRIS. U.S. Patent No. 2 875 162. Feb. 24, 1959.
21. R. A. MOCK and L. R. MORRIS. U.S. Patent No. 2 840 603. June 24, 1958.
22. L. R. MORRIS, R. A. MOCK, C. A. MARSHALL, and J. H. HOWE. J. Amer. Chem. Soc. **81**, 377 (1959).
23. M. A. DORAN. Anal. Chem. **33**, 1752 (1961).
24. D. G. HILL-COTTINGHAM. J. Chromatog. **8**, 261 (1962).
25. G. KÜHN, E. HOYER, and R. HERING. Z. Chem. **4**, 462 (1964).
26. R. B. LE BLANC. Anal. Chem. **31**, 1840 (1959).
27. G. SCHWARZENBACH, G. ANDEREGG, W. SCHNEIDER, and H. SENN. Helv. Chim. Acta, **38**, 1147 (1955).
28. L. C. THOMPSON. J. Inorg. Nucl. Chem. **24**, 1083 (1962).
29. C. EGER, W. M. ANSPACH, and J. A. MARINSKY. J. Inorg. Nucl. Chem. **30**, 1899 (1968).
30. L. G. SILLÉN and A. E. MARTELL. Stability Constants of Metal-Ion Complexes. Chem. Soc. Spec. Publ. No. 17. London. 1964.
31. S. CHABEREK, JR. and A. E. MARTELL. J. Amer. Chem. Soc. **74**, 5052 (1952).
32. A. J. BRUNO, S. CHABEREK, and A. E. MARTELL. J. Amer. Chem. Soc. **78**, 2723 (1956).
33. S. CHABEREK, JR. and A. E. MARTELL. J. Amer. Chem. Soc. **74**, 6228 (1952).
34. H. IRVING and L. D. PETTIT. J. Chem. Soc. 3051 (1963).
35. A. NEUBERGER. Proc. Roy. Soc. (London), Ser. A. **158**, 68 (1937).
36. N. E. OCKERBLOOM and A. E. MARTELL. J. Amer. Chem. Soc. **78**, 267 (1956).
37. M. J. L. TILLOTSON and L. A. K. STAVELEY. J. Chem. Soc. 3613 (1958).
38. A. NOVAK, M. COTRAIT, J. JOUSSOT-DUBIEN, and J. LASCOMBE. Inorg. Chem. **4**, 767 (1965).
39. D. CHAPMAN. J. Chem. Soc. 1766 (1955).
40. G. GRAN. Acta Chem. Scand. **4**, 559 (1950).
41. A. LIBERTI and T. S. LIGHT. J. Chem. Educ. **39**, 236 (1962).
42. J. J. R. F. DA SILVA. Rev. Port. Quim. **7**, 230 (1965).
43. J. J. R. F. DA SILVA and M. L. S. SIMÕES. Rev. Port. Quim. **7**, 137 (1965).
44. H. IRVING and J. J. R. F. DA SILVA. J. Chem. Soc. 448 (1963).
45. W. METANOMSKI. Ph.D. Thesis, University of Toronto, Toronto, Ontario. 1964.
46. I. H. SPINNER, J. YANNOPOULOS, and W. METANOMSKI. Can. J. Chem. **39**, 2529 (1961).
47. F. C. BERSWORTH. U.S. Patent No. 2 558 923. July 3, 1951.
48. F. C. BERSWORTH. U.S. Patent No. 2 387 735. Oct. 30, 1945.
49. S. R. ASPINALL. J. Amer. Chem. Soc. **63**, 852 (1941).

Can. J. Chem. Downloaded from www.nrcresearchpress.com by 210.87.254.5 on 09/05/12
For personal use only.

Can. J. Chem. Downloaded from www.nrcresearchpress.com by 210.87.254.6 on 09/05/12
For personal use only.

NOTES

Indoles and auxins. VII. Active esters and anhydrides of 3-indoleacetic acid[1]

JUDITH C. HART,[2] EILEEN M. MATHESON,[3] AND O. HUTZINGER
Atlantic Regional Laboratory, National Research Council of Canada, Halifax, Nova Scotia

Received April 15, 1969

The synthesis of activated esters and anhydrides of 3-indoleacetic acid is described. Their usefulness for the preparation of amino acid derivatives is shown by reaction with glycine methyl ester.

Canadian Journal of Chemistry, 48, 177 (1970)

3-Indoleacetic acid (IAA) is frequently found in conjugated and bound forms. For the preparation of these compounds and for introducing IAA into natural polymers, an "active" form of IAA is needed. 3-Indoleacetyl chloride is not convenient for this purpose. It has been prepared by standard methods (1–5) but it hydrolyzes and polymerizes readily and is therefore difficult to handle and store.

We have now investigated derivatives of IAA with groups normally used for carboxyl activation of amino acids in peptide synthesis: esters of IAA with *p*-nitrophenol, 2,4-dinitrophenol, pentachlorophenol, 8-hydroxyquinoline, and *N*-hydroxysuccinimide; mixed anhydrides of IAA and 3-indoleacetic anhydride. The mixed anhydride of IAA and ethyl chloroformate has been synthesized and used before (6–8). It is reactive but unstable and is prepared immediately before use. We found that the anhydride with isobutyl chloroformate (reported to give better yields in peptide synthesis (9)) has similar properties. The active esters were prepared by the dicyclohexylcarbodiimide or mixed anhydride methods. They are stable compounds, can be used for reactions in aqueous solutions and are hydrolyzed only slowly by *N*/10 sodium hydroxide at temperatures below 0°. 3-Indoleacetic anhydride is also stable on storage, it is slowly decomposed by moisture.

To show the usefulness of these derivatives for the synthesis of amino acid and peptide derivatives of IAA, the activated esters and 3-indoleacetic anhydride were allowed to react with glycine methyl ester (no racemization is expected in the amino component during this reaction; cf. 10). With exception of the 8-hydroxyquinoline derivative the reaction is complete after 10 h. The short reaction times required for completion of the reaction with 3-indoleacetic anhydride (30 min) and the 2,4-dinitrophenyl ester of IAA (1 h) are noteworthy.

The active forms of IAA mentioned above may also be useful for binding IAA chemically to proteins (11). 3-Indoleacetic anhydride and the mixed anhydrides react with phenolic hydroxy groups, the mixed anhydrides also provide a convenient route for the preparation of simple amides.

Experimental

Mixed Anhydride Method (A)

IAA (.01 *M*) in anhydrous tetrahydrofuran (THF; 30 ml) and triethylamine (1.4 ml) was treated with isobutyl chloroformate (method *A-1*) or ethyl chloroformate (*A-2*) (10 ml, 1 *M* solution in THF). For best results, the amino component should be added to the mixed anhydride after 3–5 min, or when the white paste becomes slightly yellow.

p-Nitro- or 2,4-dinitrophenol (.01 *M*) was added for the preparation of the activated nitrophenol esters. The mixture was stirred (10 min) at room temperature, ether (150 ml) added, and the solution carefully (to avoid hydrolysis) washed with *N*/10 sodium hydroxide and water. The ether solution was dried (Na_2SO_4), evaporated, and the residue recrystallized.

When ammonia gas was bubbled through the mixed anhydride solution at −10°, some THF removed, and water added, pure 3-indoleacetamide (m.p. 155°, yield 65–70%) precipitated from the reaction mixture.

Dicyclohexylcarbodiimide (DCC) Method (B)
Activated Esters (B-1)

DCC (.0105 *M*) was added to a solution of IAA (.01 *M*) and the hydroxy compound (.0105 *M*) in THF or ethyl acetate (30 ml) at 3°. The mixture was kept for 10 h at 3° and 4 h at 25°, the precipitate was removed, ether (150 ml) was added to the solution, and the ester worked up as before.

[1]Issued as NRCC No. 10956. For part VI see Anal. Biochem, in press.
[2]NRCC Summer Student (1968).
[3]NRCC Summer Student (1969).

Can. J. Chem. Downloaded from www.nrcresearchpress.com by 210.87.254.6 on 09/05/12
For personal use only.

TABLE 1

Properties of indoleacetic acid derivatives

3-Indoleacetic acid derivative*	Method	Yield (%) (recrystallized material)	Melting point (°C) (cryst. solvent)	Analysis								Time required for conversion into IAA glycine methyl ester†
				Calculated				Found				
				C	H	N	Cl	C	H	N	Cl	
1*a*	*A-1*	65	110 (methanol)	64.86	4.08	9.46	—	65.14	3.98	9.52	—	10 h
	B-1	78										
1*b*	*A-2*	58	150 (benzene)	56.31	3.25	12.31	—	56.24	3.26	11.96	—	1 h
1*c*	*B-1*	63	146 (ethyl acetate–chloroform)	61.76	4.44	10.29	—	62.19	4.46	10.01	—	8 h
1*d*	*B-1*	67	165 (ethanol)	45.37	1.90	3.31	41.86	45.37	1.86	3.27	41.70	5 h
1*e*	*B-1*	86	187 (benzene)	75.48	4.67	9.27	—	75.73	4.58	9.15	—	>2 days‡
1*f*§	*B-2*	88	145 (dioxane)	72.28	4.85	8.43	—	72.16	4.75	8.42	—	30 min

*Recently, the 2,4,5-trichlorophenyl ester of 3-indoleacetic acid has been prepared by a method similar to *B-1* (12).
†At the time indicated >90% of the active IAA derivative had been converted to the glycine methyl ester amide as shown by chromatography. For details see text.
‡Only 60–70% had reacted after 2 days.
§This compound has been mentioned in the literature (13, 14). However, no experimental or physical data were reported.

IAA Anhydride (B-2)

A solution of IAA (.02 *M*) and DCC (.0105 *M*) in anhydrous dioxane (30 ml) was kept at 25° for 3 h. The precipitate was removed, dioxane evaporated, the residue triturated with benzene and the solid recrystallized.

3-Indoleacetylglycine Methyl Ester

A solution of glycine methyl ester hydrochloride, the IAA-derivative (10^{-5} moles each), and triethylamine (0.01 ml) in dioxane (3 ml) was kept at room temperature for the time indicated in Table 1. The progress of the reaction was followed chromatographically using silica thin-layer plates, methanol–chloroform–carbon tetrachloride (1:5:4) as the developing solvent, and Ehrlich's reagent for visualization. For characterizing IAA glycine methyl ester, the combined reaction mixtures were chromatographed on silica thin-layer plates (1 mm thickness) in the same solvent. 3-Indoleacetylglycine methyl ester (R_F = 0.55) appears, after elution with methanol and evaporation of the solvent, as a colorless oil; mass spectrum, *m/e* 246 (M^+; 26%), 247 (4%), 157 (2.5%), 131 (12%), 130 (100%), 129 (5%).

Calcd. for $C_{13}H_{14}N_2O_3$: 246.10044. Found: 246.1000.

Data for all compounds are given in Table 1, their structures were ascertained by infrared (i.r.) and mass spectroscopy.[4]

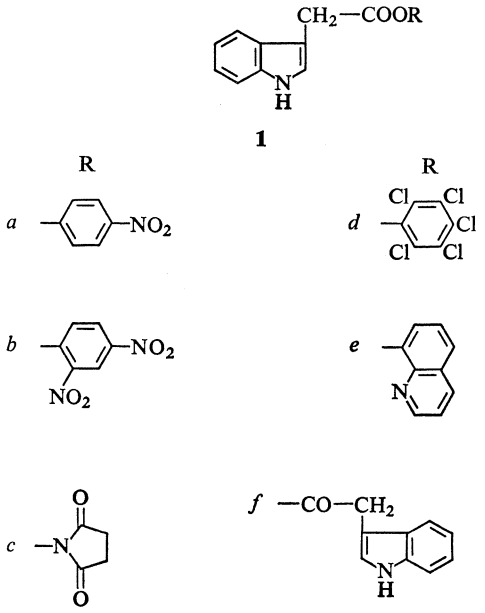

We thank Mr. D. J. Embree for recording the mass spectra and Dr. W. D. Jamieson for useful discussion of these.

1. E. Shaw and D. W. Woolley. J. Biol. Chem. **203**, 979 (1953).
2. K. N. F. Shaw, A. McMillan, A. G. Gudmundson, and M. D. Armstrong. J. Org. Chem. **23**, 1171 (1958).
3. L. E. Weller and H. M. Sell. J. Org. Chem. **23**, 1776 (1958).
4. M. Protiva, Z. J. Vejdelek, J. O. Jílek, and K. Macek. Collect. Czech. Chem. Commun. **24**, 3978 (1959).
5. D. G. Crosby, J. B. Boyd, and H. E. Johnson. J. Org. Chem. **25**, 1826 (1960).
6. T. Wieland and G. Hörlein. Ann. Chem. **591**, 192 (1955).
7. A. Patchornik, W. B. Lawson, E. Gross, and B. Witkop. J. Amer. Chem. Soc. **82**, 5923 (1960).
8. O. Hutzinger and T. Kosuge. Biochem. **7**, 601 (1968).
9. G. W. Anderson, J. E. Zimmerman, and F. M. Callahan. J. Amer. Chem. Soc. **89**, 5012 (1967).
10. F. Weygand, A. Prox, and W. König. Chem. Ber. **99**, 1451 (1966).
11. N. S. Ranadive and A. H. Sehon. Can. J. Biochem. **45**, 1681 (1967).
12. H. Gregory and J. S. Morley. J. Chem. Soc. (C), 910 (1968).
13. E. Seifert. German Patent 922 350 (1955); Chem. Abstr. **51**, 17 075 (1957).
14. W. Nagata, S. Hirai, K. Kawata, and T. Okumura. J. Amer. Chem. Soc. **89**, 5046 (1967).

[4]The mass spectrometry data are being deposited with the Mass Spectrometry Data Centre, AWRE Aldermaston, Berkshire, U.K.

Single bond radius of trigonal nitrogen and the C(sp²)—N(sp²) single bond

Arthur Camerman

Department of Biological Structure, University of Washington, Seattle, Washington 98105

Received September 8, 1969

Estimation of p-π character in nitrogen–carbon bonding is dependent on a knowledge of the trigonal nitrogen – trigonal carbon single bond length. Recent experimental results indicate a value of 1.470 ± 0.005 Å for this bond distance and a value of 0.720 ± 0.010 Å for the trigonal nitrogen single bond radius; these values are suggested as criteria for estimating p-π character in trigonal N – aromatic C bonds.

Canadian Journal of Chemistry, **48**, 179 (1970)

Estimations of interaction between p electrons of nitrogen and π electron clouds of aromatic systems, and therefore of the importance of resonance configurations for molecules such as amides, have been often dependent on the value one accepts for the single σ bond length between

Can. J. Chem. Downloaded from www.nrcresearchpress.com by 210.87.254.6 on 09/05/12
For personal use only.

IAA Anhydride (B-2)

A solution of IAA (.02 *M*) and DCC (.0105 *M*) in anhydrous dioxane (30 ml) was kept at 25° for 3 h. The precipitate was removed, dioxane evaporated, the residue triturated with benzene and the solid recrystallized.

3-Indoleacetylglycine Methyl Ester

A solution of glycine methyl ester hydrochloride, the IAA-derivative (10^{-5} moles each), and triethylamine (0.01 ml) in dioxane (3 ml) was kept at room temperature for the time indicated in Table 1. The progress of the reaction was followed chromatographically using silica thin-layer plates, methanol–chloroform–carbon tetrachloride (1:5:4) as the developing solvent, and Ehrlich's reagent for visualization. For characterizing IAA glycine methyl ester, the combined reaction mixtures were chromatographed on silica thin-layer plates (1 mm thickness) in the same solvent. 3-Indoleacetylglycine methyl ester (R_F = 0.55) appears, after elution with methanol and evaporation of the solvent, as a colorless oil; mass spectrum, *m/e* 246 (M^+; 26%), 247 (4%), 157 (2.5%), 131 (12%), 130 (100%), 129 (5%).

Calcd. for $C_{13}H_{14}N_2O_3$: 246.10044. Found: 246.1000.

Data for all compounds are given in Table 1, their structures were ascertained by infrared (i.r.) and mass spectroscopy.[4]

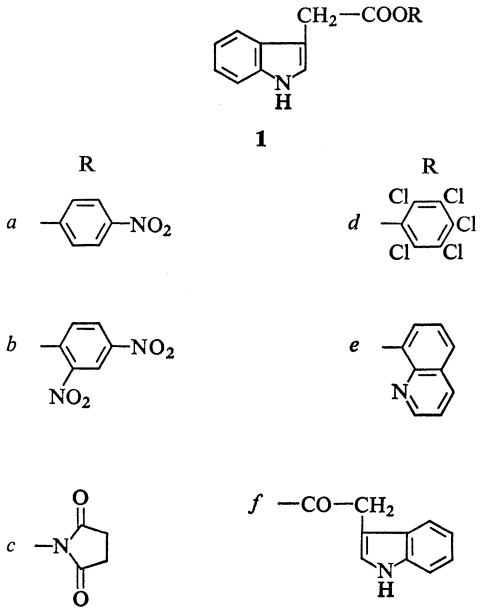

We thank Mr. D. J. Embree for recording the mass spectra and Dr. W. D. Jamieson for useful discussion of these.

1. E. Shaw and D. W. Woolley. J. Biol. Chem. **203**, 979 (1953).
2. K. N. F. Shaw, A. McMillan, A. G. Gudmundson, and M. D. Armstrong. J. Org. Chem. **23**, 1171 (1958).
3. L. E. Weller and H. M. Sell. J. Org. Chem. **23**, 1776 (1958).
4. M. Protiva, Z. J. Vejdelek, J. O. Jílek, and K. Macek. Collect. Czech. Chem. Commun. **24**, 3978 (1959).
5. D. G. Crosby, J. B. Boyd, and H. E. Johnson. J. Org. Chem. **25**, 1826 (1960).
6. T. Wieland and G. Hörlein. Ann. Chem. **591**, 192 (1955).
7. A. Patchornik, W. B. Lawson, E. Gross, and B. Witkop. J. Amer. Chem. Soc. **82**, 5923 (1960).
8. O. Hutzinger and T. Kosuge. Biochem. **7**, 601 (1968).
9. G. W. Anderson, J. E. Zimmerman, and F. M. Callahan. J. Amer. Chem. Soc. **89**, 5012 (1967).
10. F. Weygand, A. Prox, and W. König. Chem. Ber. **99**, 1451 (1966).
11. N. S. Ranadive and A. H. Sehon. Can. J. Biochem. **45**, 1681 (1967).
12. H. Gregory and J. S. Morley. J. Chem. Soc. (C), 910 (1968).
13. E. Seifert. German Patent 922 350 (1955); Chem. Abstr. **51**, 17 075 (1957).
14. W. Nagata, S. Hirai, K. Kawata, and T. Okumura. J. Amer. Chem. Soc. **89**, 5046 (1967).

[4]The mass spectrometry data are being deposited with the Mass Spectrometry Data Centre, AWRE Aldermaston, Berkshire, U.K.

Single bond radius of trigonal nitrogen and the C(sp^2)—N(sp^2) single bond

Arthur Camerman

Department of Biological Structure, University of Washington, Seattle, Washington 98105

Received September 8, 1969

Estimation of p-π character in nitrogen–carbon bonding is dependent on a knowledge of the trigonal nitrogen – trigonal carbon single bond length. Recent experimental results indicate a value of 1.470 ± 0.005 Å for this bond distance and a value of 0.720 ± 0.010 Å for the trigonal nitrogen single bond radius; these values are suggested as criteria for estimating p-π character in trigonal N – aromatic C bonds.

Canadian Journal of Chemistry, **48**, 179 (1970)

Estimations of interaction between p electrons of nitrogen and π electron clouds of aromatic systems, and therefore of the importance of resonance configurations for molecules such as amides, have been often dependent on the value one accepts for the single σ bond length between

Can. J. Chem. Downloaded from www.nrcresearchpress.com by 210.87.254.5 on 09/05/12
For personal use only.

Can. J. Chem. Downloaded from www.nrcresearchpress.com by 210.87.254.5 on 09/05/12
For personal use only.

trigonal carbon and trigonal nitrogen. No completely acceptable value for the $C(sp^2)$—$N(sp^2)$ single bond is in general use.

Truter (1), on the basis of bond lengths in thioacetamide, suggested 1.325 Å as the trigonal carbon – trigonal nitrogen single bond length and thus postulated that the value of 1.322 ± 0.003 Å found for the C—N bond in some amides is indicative of single bonded $C(sp^2)$—$N(sp^2)$.

Trueblood, Goldish, and Donohue (2) found the C—NH_2 bond length in *p*-nitroaniline to be 1.371 Å. The existence of resonance structures for this molecule necessitates a larger value for the C—N single bond, and they have estimated the σ bond between trigonal carbon and trigonal nitrogen to be 1.41 ± 0.02 Å on the basis of single bond radii of 0.735 ± 0.010 Å and 0.675 ± 0.015 Å for trigonal carbon and trigonal nitrogen, respectively. They suggest, however, that careful measurement of bond distances in an N-methyl pyridinium salt or related compound might give a better value for the latter radius. Trigonal nitrogen in N-substituted pyridinium salts has only one p electron which is delocalized in the pyridine π electron system and not available for π bond formation with substituent atoms. The bond formed between such a nitrogen atom and a substituent carbon is then truly a single bond. The length of such a bond provides a good basis for estimating multiple bond character and the importance of resonance configuration in other compounds containing sp^2 nitrogen atoms whose p electrons are available for p–p or p–π partial double bond formation.

The molecular structures of two such N-substituted compounds, N-phenyl-2,4,6-trimethylpyridinium perchlorate (3) (**1**) and N-methyl pyridoxal oxime (4) (**2**) have recently been elucidated in this laboratory and the results suggest values different from those cited above for the trigonal nitrogen bond radius and the trigonal carbon – trigonal nitrogen bond distance. The observed $C(sp^2)$—$N(sp^2)$ bond distance in (**1**) after correction for thermal motion is 1.470 ± 0.005 Å. Since the angle between the phenyl and pyridinium rings is 83.5°, there is essentially no electronic interaction between the π electron clouds of the two rings and the C—N distance is indicative of a $C(sp^2)$—$N(sp^2)$ single bond.[1]

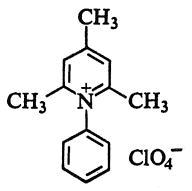

1

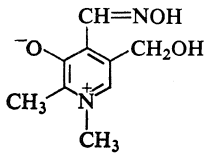

2

To deduce the value for the trigonal nitrogen single bond radius we must first find an acceptable trigonal carbon single bond radius. Estimates of this value in the literature (5) range from 0.73 to 0.76 Å. In a high-precision determination of the structure of 2-*p*-toluidinylnaphthalene sulfonate (6) the trigonal carbon – tetrahedral carbon bond distance was found to be 1.515 ± 0.003 Å. If one accepts the tetrahedral carbon single bond radius of 0.770 ± 0.010 Å, the trigonal carbon single bond radius is then 0.745 ± 0.010 Å, the value also obtained by assuming the covalent radius of carbon to be a linear function of its s character (7). The average of the six $C(sp^2)$—$C(sp^2)$ bond lengths in hexaphenylbenzene (8) is 1.499 ± 0.022 Å, suggesting 0.749 ± 0.011 for the $C(sp^2)$ single bond radius, well within the standard deviation of the figure derived above. When subtracted from the C—N single bond length of 1.470 Å, this results in the value of 0.725 ± 0.010 Å for the $N(sp^2)$ single bond radius.

The length of the $C(sp^3)$—$N(sp^2)$ bond in (**2**) is 1.485 ± 0.002 Å. Assuming the tetrahedral carbon single bond radius of 0.770 Å as before, this results in 0.715 Å for the $N(sp^2)$ single bond radius.

On this basis, an acceptable value for the trigonal nitrogen single bond radius is 0.720 ± 0.010 Å and an acceptable trigonal carbon – trigonal nitrogen single bond length is 1.470 ± 0.005 Å. Bond distances between sp^2 carbon and sp^2 nitrogen significantly shorter than 1.470 Å can reasonably be assumed to exhibit some added electronic interaction, other than the σ bond,

[1]The net positive charge on the pyridinium group is delocalized over the entire ring and the π electron density on the N atom is approximately the same as in pyrrole where the N atom donates two p electrons to the aromatic system. Furthermore, the lack of electronic interaction between the pyridinium and phenyl rings in **1** indicates that the net positive charge has no effect on the $N(sp^2)$—$C(sp^2)$ bond. An N-phenyl pyrrole derivative suitably substituted to ensure a large angle and hence no electronic resonance between the pyrrole and phenyl π systems would provide an equally useful model for the $N(sp^2)$—$C(sp^2)$ bond length.

between the atoms involved. The short C—N bond in amides, for example, has a highly significant amount of double bond character, emphasizing the importance of the charged resonance configuration to the amide structure.

The author thanks Professor L. H. Jensen for his encouragement and support. Acknowledgment is made of the financial support by USPHS Grant No. GM-13366 from the National Institutes of Health.

1. M. TRUTER. J. Chem. Soc. 997 (1960).
2. N. TRUEBLOOD, E. GOLDISH, and J. DONOHUE. Acta Cryst. **14**, 1009 (1961).
3. A. CAMERMAN, L. H. JENSEN, and A. T. BALABAN. In press.
4. A. C. BLOOMER and L. H. JENSEN. To be published.
5. M. J. S. DEWAR (*Editor*). Symposium on carbon bonds. Tetrahedron, **17**, 123–266 (1962).
6. A. CAMERMAN and L. H. JENSEN. Science, **165**, 493 (1969).
7. M. J. S. DEWAR and H. N. SCHMEISING. Tetrahedron, **5**, 166 (1959).
8. J. C. J. BART. Acta Cryst. **B24**, 1277 (1968).

Can. J. Chem. Downloaded from www.nrcresearchpress.com by 210.87.254.5 on 09/05/12
For personal use only.

Low frequency infrared and Raman spectra of the N,N,N′,N′-tetramethylethylenediamine adducts of the Group IIb dihalides

M. H. ABRAHAM
Department of Chemistry, University of Surrey, Guildford, Surrey, England

AND

F. W. PARRETT
Department of Chemistry, Royal Military College of Canada, Kingston, Ontario

Received September 16, 1969

A study of the low frequency vibrational spectra of the complexes MX_2.TMED (where M = Zn, Cd, Hg; X = Cl, Br, I; TMED = N,N,N′,N′-tetramethylethylenediamine suggests that in the solid state the zinc and mercury complexes are 4-coordinated but the cadmium complexes are all based on octahedral halogen bridged structures. Assignments of the vibrational bands are discussed.

Canadian Journal of Chemistry, **48**, 181 (1970)

Introduction

There have been many reports of the reactions between Lewis bases and the halides of the Group IIb metals (Zn, Cd, Hg). A recent publication by Houk and Dobson (1) lists the extensive literature on this topic. Generally 4-coordinated complexes of the type $MX_2.L_2$ (L = ligand) are formed with an approximately tetrahedral arrangement about the central metal atom. There is strong evidence, however, that in some cases polymeric 6-coordinated bridging structures are involved, e.g. in $CdCl_2(NH_3)_2$, $HgBr_2(NH_3)_2$, $CdBr_2(pyridine)_2$ (see literature in ref. 1), in CdX_2L_2 (where X = halogen, L = primary aromatic amine) (2), and in $CdCl_2$.TMED (3). We report here the infrared and laser Raman spectra of the complexes MX_2.TMED (M = Zn, Cd, Hg; X = Cl, Br, I).

Experimental

Preparation of the Complexes

A slight excess of the calculated quantity of TMED in a small amount of methanol was added to a solution of the metal halide in methanol. The resulting precipitate was dissolved on heating the mixture under reflux, additional methanol being added if necessary. The hot methanolic solution was filtered to remove insoluble matter and the filtrate allowed to stand at room temperature. The complex crystallized in good yield and was filtered and washed with methanol. All complexes were recrystallized from methanol.

Analyses

Analyses for metals were carried out by the standard EDTA method. In the analysis of the complex HgI_2.TMED it was not possible to obtain a satisfactory end point and no analytical figure for mercury was obtained. Analyses for C, H, N, and halogen were by A. Bernhardt of the Max-Planck Institüt, Mülheim, Germany. Details of the analyses of the complexes are given in Table 1. Infrared spectra (30–400 cm^{-1}) of the solid complexes were determined as Nujol mulls between polyethylene plates using a Research and Industrial Instruments Ltd. FS-720 Fourier Spectrophotometer, the transformation to a spectrum being carried out by a digital computer using a program described in detail elsewhere (4).

Raman spectra were determined on the Cary 81 Raman spectrometer using He–Ne laser excitation. All compounds were examined as powdered crystalline solids.

between the atoms involved. The short C—N bond in amides, for example, has a highly significant amount of double bond character, emphasizing the importance of the charged resonance configuration to the amide structure.

The author thanks Professor L. H. Jensen for his encouragement and support. Acknowledgment is made of the financial support by USPHS Grant No. GM-13366 from the National Institutes of Health.

1. M. TRUTER. J. Chem. Soc. 997 (1960).
2. N. TRUEBLOOD, E. GOLDISH, and J. DONOHUE. Acta Cryst. **14**, 1009 (1961).
3. A. CAMERMAN, L. H. JENSEN, and A. T. BALABAN. In press.
4. A. C. BLOOMER and L. H. JENSEN. To be published.
5. M. J. S. DEWAR (*Editor*). Symposium on carbon bonds. Tetrahedron, **17**, 123–266 (1962).
6. A. CAMERMAN and L. H. JENSEN. Science, **165**, 493 (1969).
7. M. J. S. DEWAR and H. N. SCHMEISING. Tetrahedron, **5**, 166 (1959).
8. J. C. J. BART. Acta Cryst. **B24**, 1277 (1968).

Low frequency infrared and Raman spectra of the N,N,N′,N′-tetramethylethylenediamine adducts of the Group IIb dihalides

M. H. ABRAHAM
Department of Chemistry, University of Surrey, Guildford, Surrey, England
AND
F. W. PARRETT
Department of Chemistry, Royal Military College of Canada, Kingston, Ontario

Received September 16, 1969

A study of the low frequency vibrational spectra of the complexes MX_2.TMED (where M = Zn, Cd, Hg; X = Cl, Br, I; TMED = N,N,N′,N′-tetramethylethylenediamine suggests that in the solid state the zinc and mercury complexes are 4-coordinated but the cadmium complexes are all based on octahedral halogen bridged structures. Assignments of the vibrational bands are discussed.

Canadian Journal of Chemistry, **48**, 181 (1970)

Introduction

There have been many reports of the reactions between Lewis bases and the halides of the Group IIb metals (Zn, Cd, Hg). A recent publication by Houk and Dobson (1) lists the extensive literature on this topic. Generally 4-coordinated complexes of the type $MX_2.L_2$ (L = ligand) are formed with an approximately tetrahedral arrangement about the central metal atom. There is strong evidence, however, that in some cases polymeric 6-coordinated bridging structures are involved, e.g. in $CdCl_2(NH_3)_2$, $HgBr_2(NH_3)_2$, $CdBr_2(pyridine)_2$ (see literature in ref. 1), in CdX_2L_2 (where X = halogen, L = primary aromatic amine) (2), and in $CdCl_2$.TMED (3). We report here the infrared and laser Raman spectra of the complexes MX_2.TMED (M = Zn, Cd, Hg; X = Cl, Br, I).

Experimental

Preparation of the Complexes

A slight excess of the calculated quantity of TMED in a small amount of methanol was added to a solution of the metal halide in methanol. The resulting precipitate was dissolved on heating the mixture under reflux, additional methanol being added if necessary. The hot methanolic solution was filtered to remove insoluble matter and the filtrate allowed to stand at room temperature. The complex crystallized in good yield and was filtered and washed with methanol. All complexes were recrystallized from methanol.

Analyses

Analyses for metals were carried out by the standard EDTA method. In the analysis of the complex HgI_2.TMED it was not possible to obtain a satisfactory end point and no analytical figure for mercury was obtained. Analyses for C, H, N, and halogen were by A. Bernhardt of the Max-Planck Institüt, Mülheim, Germany. Details of the analyses of the complexes are given in Table 1. Infrared spectra (30–400 cm^{-1}) of the solid complexes were determined as Nujol mulls between polyethylene plates using a Research and Industrial Instruments Ltd. FS-720 Fourier Spectrophotometer, the transformation to a spectrum being carried out by a digital computer using a program described in detail elsewhere (4).

Raman spectra were determined on the Cary 81 Raman spectrometer using He–Ne laser excitation. All compounds were examined as powdered crystalline solids.

Can. J. Chem. Downloaded from www.nrcresearchpress.com by 210.87.254.105 on 09/05/12
For personal use only.

Can. J. Chem. Downloaded from www.nrcresearchpress.com by 210.87.254.105 on 09/05/12
For personal use only.

TABLE 1
Analytical results

Complex	Melting point (°C)		Analyses (%)									
			C		H		N		Halogen		Metal	
	Exp.	Lit.	Found	Calcd.	Found	Calcd.	Found	Calcd.	Found	Calcd.	Found	Calcd.
$ZnCl_2$.TMED	178	177*	28.62	28.54	6.72	6.39	10.93	11.10	28.02	28.08	26.01	25.89
$ZnBr_2$.TMED	182	182†	21.30	21.11	4.85	4.72	8.30	8.21	46.88	46.81	19.25	19.15
ZnI_2.TMED	204	201‡	16.26	16.55	3.92	3.70	6.60	6.43	58.44	58.30	14.97	15.01
$CdCl_2$.TMED	257–258	254–255§	24.27	24.06	5.50	5.39	9.27	9.35	23.52	23.67	37.00	37.50
$CdBr_2$.TMED	245–247	—	18.42	18.55	4.08	4.15	7.41	7.21	41.01	41.15	28.57	28.94
CdI_2.TMED	210–211	—	14.78	14.94	3.06	3.34	5.97	5.81	53.05	52.61	23.01	23.30
$HgCl_2$.TMED	164	164*	18.70	18.59	4.50	4.16	7.34	7.23	18.10	18.29	51.86	51.74
$HgBr_2$.TMED	162	165*	15.25	15.12	3.31	3.38	6.00	5.88	33.42	33.53	42.02	42.09
HgI_2.TMED	162	—	12.75	12.63	2.57	2.83	5.05	4.91	45.20	44.48	—	35.15

*Reference 3.
†Reference 9.
‡Reference 10.
§Reference 11.

TABLE 2

Infrared and Raman spectra (30–400 cm^{-1}) of MX_2.N,N,N′,N′-tetramethylethylenediamine*

	Frequency (cm^{-1})					
	X = Cl		X = Br		X = I	
Assignments	Raman	i.r.	Raman	i.r.	Raman	i.r.
			M = Zn			
Molecular deformation and lattice modes		70 mbr		40 s	96 w	38 w
		98 w		72 m		
		112 mbr		84 w		
				94 m		
			169 w			
Bridged M—X stretching modes						
Free MX modes symmetric	307 s	310 mbr	233 m	238 s	142 s	136 m
assymmetric	339 vw	334 s		260 s	184 w	174 s
Skeletal vibrations	203 w	210 w	186 w			198 w
associated with stretching	215 w		197 vw	198 wsh		214 m
of metal–ligand bond	276 w			209 m	222 w	226 m
				252 wsh	265 vw	
	390 w			286 wsh	385 vw	
			M = Cd			
Molecular deformation and lattice modes				59 w		47 m
				89 s		58 m
				112 ms		
	155 m	155 s		126 ms		
Bridged M—X stretching modes	185 vw	160 wsh	142 s		130 s	132 w
	203 s	190 s		150 wsh		149 m
	227 m	224 w	175 m	160 s	170 m	170 w
Free MX modes symmetric						
assymmetric						
Skeletal vibrations			200 vw	195 s		
associated with stretching						194 s
of metal–ligand bond						206 wsh
	385 m		382 m		267 w	
			M = Hg			
Molecular deformation and lattice modes		50 w		46 wsh		46 m
		62 w		54 s		
		87 w				
				130 w		129 m
Bridged M—X stretching modes						
Free MX modes symmetric	267 s	266 sbr	177 s	179 s	138 vs	139 m
assymmetric	287 wsh	285, 292 sbr	214 w	212 vs	173 m	176 vs
Skeletal vibrations		254 wsh		200 wsh		160 wsh
associated with stretching				228 w	264 w	
of metal–ligand bond	377 w		377 w		374 w	

*s = strong, m = medium, w = weak, v = very, br = broad, sh = shoulder.

Results and Discussion

Nine complexes of the type MX_2.TMED (M = Zn, Cd, Hg; X = Cl, Br, I) were prepared and their vibrational spectra (infrared and Raman) examined (see Table 2). All complexes analyzed strictly for 1:1 complexes of the metal halide and TMED. It was observed that the cadmium halide complexes were much less soluble in methanol than were the complexes of the zinc and mercury halides. Our infrared spectra are in agreement with those reported by Coates and Ridley (3) for chloride and bromide adducts down to 200 cm^{-1}. For all the Zn and Hg adducts there are two bands for each complex, occurring in both the infrared and Raman spectra, which can be assigned to the two M—X

Can. J. Chem. Downloaded from www.nrcresearchpress.com by 210.87.254.105 on 09/05/12
For personal use only.

stretching modes expected for molecular C_{2v} units where the metal is tetrahedrally coordinated.

In all the CdX_2 complexes, the bands we assign as ν(M—X) are all at lower frequencies than expected by comparison with the tetrahedral Zn and Hg adducts, i.e. even lower than the corresponding M—X bands in the heavier HgX_2 adducts. This is indicative of octahedral halogen bridged structures and clearly occurs in all CdX_2.TMED adducts. Up to four M—X stretching modes would be expected in a halogen bridged structure. The cadmium bromide and iodide complexes are thus analogous in structure to the cadmium chloride complex; the structure of the latter complex was previously suggested (3) to involve a distorted octahedral symmetry.

It is possible that some of the low frequency modes are associated to some degree with a stretching of the metal–nitrogen donor bond. A number of authors have assigned absorptions to metal–nitrogen stretching modes at positions varying from, for example, 200 to 270 cm^{-1} (5, 6). This lack of agreement is not surprising when it is realized that in many cases there is a high degree of coupling between ligand and acceptor modes such that the assignment of any one absorption to a metal–donor atom mode can cease to have any meaning. Some vibrational analyses on similar metal complexes have been reported giving a more quantitative estimate of the extent of coupling of the metal–ligand modes (7, 8). In all our spectra, no one band in the region up to 400 cm^{-1} appears to be suitably assigned as due mainly to M—N stretching and we suggest that modes containing contributions of M—N stretching occur at a number of different frequencies.

1. L. W. Houk and G. R. Dobson. J. Chem. Soc. A, 1846 (1968).
2. J. M. Haigh, M. A. Van Dam, and D. A. Thornton. Inorg. Nucl. Chem. Lett. **3**, 7 (1967).
3. G. E. Coates and D. Ridley. J. Chem. Soc. 166 (1964).
4. F. W. Parrett. Laboratory practice. In press.
5. N. S. Gill and H. J. Kingdon. Aust. J. Chem. **19**, 2197 (1966).
6. C. W. Frank and L. B. Rogers. Inorg. Chem. **5**, 615 (1966).
7. I. R. Beattie and F. W. Parrett. J. Chem. Soc. A, 1784 (1966).
8. I. R. Beattie, M. Milne, M. Webster, H. E. Blayden, P. J. Jones, R. C. G. Killean, and J. L. Lawrence. J. Chem. Soc. A, 482 (1969).
9. J. G. Noltes and J. W. G. van den Hurk. J. Organometal. Chem. Amsterdam, **1**, 377 (1964).
10. M. H. Abraham and P. H. Rolfe. J. Organometal. Chem. Amsterdam, **7**, 35 (1967).
11. F. G. Mann and H. R. Watson. J. Chem. Soc. 2772 (1958).

Self-association of alcohols and phenols in nonpolar solvents

T. S. S. R. Murty[1]

Department of Chemistry, Rice University, Houston, Texas, 77001

Received August 25, 1969

A number of alcohols (primary, secondary, and tertiary) and phenols, covering a pK_a range from 9.4 to 19.0, gave on association a peak about 125 ± 5 cm^{-1} lower than the monomeric hydroxyl peak in the fundamental stretching region. Taken together with the extensive literature available on the association of alcohols and phenols in nonpolar solvents, this seems to indicate the presence of dimers.

Canadian Journal of Chemistry, **48**, 184 (1970)

The data in Table 1 show that the alcohols and phenols studied give in the hydroxyl fundamental region in carbon tetrachloride solutions a peak about 125 ± 5 cm^{-1} lower than the monomeric hydroxyl peak. The compounds listed include primary, secondary, and tertiary alcohols and phenols and cover a pK_a range from 9.4 (hexafluoro propanol) to 19.0 (triphenyl methanol). There seems to be good compensation of acidity and basicity so that the frequency shift, $\Delta\nu_{associated}$, defined as $\nu_{monomer} - \nu_{associated}$, is constant within experimental error (see Table 1).

Recently evidence was reported (1, 2) for only monomers and tetramers (both linear and cyclic) for the association of 1-octanol in *n*-decane; from 10^{-4} *m* in *n*-decane to neat 1-octanol over a 95 °C temperature range. Data evaluated from other workers for other alcohols in carbon

[1]Present address: Department of Chemistry, University of Calgary, Calgary, Alberta.

Can. J. Chem. Downloaded from www.nrcresearchpress.com by 210.87.254.105 on 09/05/12
For personal use only.

stretching modes expected for molecular C_{2v} units where the metal is tetrahedrally coordinated.

In all the CdX_2 complexes, the bands we assign as ν(M—X) are all at lower frequencies than expected by comparison with the tetrahedral Zn and Hg adducts, i.e. even lower than the corresponding M—X bands in the heavier HgX_2 adducts. This is indicative of octahedral halogen bridged structures and clearly occurs in all CdX_2.TMED adducts. Up to four M—X stretching modes would be expected in a halogen bridged structure. The cadmium bromide and iodide complexes are thus analogous in structure to the cadmium chloride complex; the structure of the latter complex was previously suggested (3) to involve a distorted octahedral symmetry.

It is possible that some of the low frequency modes are associated to some degree with a stretching of the metal–nitrogen donor bond. A number of authors have assigned absorptions to metal–nitrogen stretching modes at positions varying from, for example, 200 to 270 cm^{-1} (5, 6). This lack of agreement is not surprising when it is realized that in many cases there is a high degree of coupling between ligand and acceptor modes such that the assignment of any one absorption to a metal–donor atom mode can cease to have any meaning. Some vibrational analyses on similar metal complexes have been reported giving a more quantitative estimate of the extent of coupling of the metal–ligand modes (7, 8). In all our spectra, no one band in the region up to 400 cm^{-1} appears to be suitably assigned as due mainly to M—N stretching and we suggest that modes containing contributions of M—N stretching occur at a number of different frequencies.

1. L. W. Houk and G. R. Dobson. J. Chem. Soc. A, 1846 (1968).
2. J. M. Haigh, M. A. Van Dam, and D. A. Thornton. Inorg. Nucl. Chem. Lett. **3**, 7 (1967).
3. G. E. Coates and D. Ridley. J. Chem. Soc. 166 (1964).
4. F. W. Parrett. Laboratory practice. In press.
5. N. S. Gill and H. J. Kingdon. Aust. J. Chem. **19**, 2197 (1966).
6. C. W. Frank and L. B. Rogers. Inorg. Chem. **5**, 615 (1966).
7. I. R. Beattie and F. W. Parrett. J. Chem. Soc. A, 1784 (1966).
8. I. R. Beattie, M. Milne, M. Webster, H. E. Blayden, P. J. Jones, R. C. G. Killean, and J. L. Lawrence. J. Chem. Soc. A, 482 (1969).
9. J. G. Noltes and J. W. G. van den Hurk. J. Organometal. Chem. Amsterdam, **1**, 377 (1964).
10. M. H. Abraham and P. H. Rolfe. J. Organometal. Chem. Amsterdam, **7**, 35 (1967).
11. F. G. Mann and H. R. Watson. J. Chem. Soc. 2772 (1958).

Self-association of alcohols and phenols in nonpolar solvents

T. S. S. R. Murty[1]

Department of Chemistry, Rice University, Houston, Texas, 77001

Received August 25, 1969

A number of alcohols (primary, secondary, and tertiary) and phenols, covering a pK_a range from 9.4 to 19.0, gave on association a peak about 125 ± 5 cm^{-1} lower than the monomeric hydroxyl peak in the fundamental stretching region. Taken together with the extensive literature available on the association of alcohols and phenols in nonpolar solvents, this seems to indicate the presence of dimers.

Canadian Journal of Chemistry, **48**, 184 (1970)

The data in Table 1 show that the alcohols and phenols studied give in the hydroxyl fundamental region in carbon tetrachloride solutions a peak about 125 ± 5 cm^{-1} lower than the monomeric hydroxyl peak. The compounds listed include primary, secondary, and tertiary alcohols and phenols and cover a pK_a range from 9.4 (hexafluoro propanol) to 19.0 (triphenyl methanol). There seems to be good compensation of acidity and basicity so that the frequency shift, $\Delta\nu_{associated}$, defined as $\nu_{monomer} - \nu_{associated}$, is constant within experimental error (see Table 1).

Recently evidence was reported (1, 2) for only monomers and tetramers (both linear and cyclic) for the association of 1-octanol in *n*-decane; from 10^{-4} *m* in *n*-decane to neat 1-octanol over a 95 °C temperature range. Data evaluated from other workers for other alcohols in carbon

[1]Present address: Department of Chemistry, University of Calgary, Calgary, Alberta.

Can. J. Chem. Downloaded from www.nrcresearchpress.com by 210.87.254.6 on 09/05/12
For personal use only.

Can. J. Chem. Downloaded from www.nrcresearchpress.com by 210.87.254.6 on 09/05/12
For personal use only.

TABLE 1

Frequency shift on dimerisation ($\Delta\nu_{dimer}$) and frequency shift ($\Delta\nu$) on association with ether as base, of various alcohols and phenols in carbon tetrachloride*

No.	Alcohol or phenol	$\Delta\nu_{dimer}$ in cm^{-1}	$\Delta\nu$ in cm^{-1} with ether as base (20)	pK_a (19)
1	CH_3OH	132†, 137 (10), 108 (11), 113 (12), 115 (15), 121 (18)	147	16.2
2	CH_3CH_2OH	126†, 127 (12), 125 (15)	143	16.3
3	$CH_3CHOHCH_3$	130 (12)	134	17.2
4	$(CH_3)_3COH$	119 (10), 125 (12), 124 (15), 120 (21)	125	17.8
5	C_6H_5OH	128†, 136 (10), 130 (11), 134 (12), 129 (17)	275	9.95
6	CF_3CH_2OH	107 (16) –124 (18)	232 (18)	12.4
7	$CF_3CHOHCF_3$	118 (16)	—	9.4
8	$(CH_3)_3CCHOHC(CH_3)_3$	124 (13), 128 (13)	—	—
9	$CH_3CH_2CH_2OH$	124†	—	—
10	$CH_3(CH_2)_2CH_2OH$	126†, 128 (10)	150	—
11	$CH_3(CH_2)_3CH_2OH$	127†	—	—
12	$CH_3(CH_2)_6CH_2OH$	121†	—	—
13	$CH_3(CH_2)_8CH_2OH$	128†	—	—
14	$C_6H_5CH_2OH$	122†	155	—
15	$C_6H_{11}OH$	133 (12), 135 (14)	135	—
16	$CH_3CH_2CHOHCH_3$	129 (10)	134 (10)	—
17	$C_6H_5CHOHC_6H_5$	132 (18)	188	—
18	Adamantanol	125†	—	—
19	$(C_6H_5)_3COH$	120 (21)	—	19.0 (21)
20	p-$CH_3C_6H_4OH$	130†	—	10.26
21	p-$C_2H_5C_6H_4OH$	130†	—	—
22	3,4-$(CH_3)_2C_6H_3OH$	127†	—	10.36
23	2,4-$(CH_3)_2C_6H_3OH$	128†	—	10.60
24	3,5-$[(CH_3)_3.C]_2C_6H_3OH$	128†	—	—

*Numbers in parentheses are reference numbers.
†This work.

Can. J. Chem. Downloaded from www.nrcresearchpress.com by 210.87.254.6 on 09/05/12
For personal use only.

tetrachloride was found consistent with these assignments, and hope was expressed that "... experimental evidence will correct the widespread concept that self-association O—H---O—H dimer is present in appreciable quantities in nonpolar solutions". This is in dramatic contrast with the extensive literature available on the self-association of alcohols and phenols. Though there is considerable controversy over the shapes, sizes, and the thermodynamic constants, all the published data taken together seem to strongly indicate that a solution of an alcohol or phenol in a nonpolar solvent (carbon tetrachloride is the most used solvent for hydrogen bonding studies) consists of a mixture of hydrogen-bonded species along with the monomer, except, of course, in the case of hindered alcohols (3) and phenols (4), where, depending upon the extent of steric hindrance, either only dimers are possible or very little association is observed.

Though the authors (1) take very justifiable objection to *a priori* decision as to the stoichiometry of the self-association and designing mathematical analysis for this stoichiometry, it stands to reason that any quantitative study should successfully account for the qualitative facts observed. The qualitative facts are that in a nonpolar solvent a given alcohol or phenol shows three major absorption peaks in the fundamental hydroxyl stretching region: $\sim$3640 –3600 cm^{-1} (free hydroxyl), $\sim$3500 cm^{-1}, and $\sim$3300 cm^{-1}. The relative intensities of these absorption peaks depend in a predictable and understandable fashion (5) upon the nature of the alcohol or phenol, the concentration of the solute, the solvent being used, and the temperature.

Among the compounds listed in Table 1, it is known that some show association to a lesser degree and cannot form cyclic *n*-mers because of steric hindrance. Thus di-*t*-butyl carbinol (3) shows no bands in the infrared below 3500 cm^{-1} up to 3.0 *m*, and this band is shown as due to dimer. Moreover, the absorption bands near 3500 cm^{-1} and 3300 cm^{-1} in the fundamental stretching region cannot be due to open chain and cyclic tetramers, as the energy difference in terms of frequency shifts is much too large, whereas the reported (1) heat of hydrogen bond formation per hydrogen bond in 1-octanol is about 5.0 kcal in both the cases. Thus, the data presented in Table 1 and that available in the literature seems to indicate that the 3500 cm^{-1} band is due to dimers (linear or cyclic or both).

As early as 1951, Weltner and Pitzer (6) interpreted the heat capacity data on methanol vapor on the basis of tetramers, dimers, and monomers. The importance of the tetramers was emphasized, with a value for the heat of dissociation of 24.2 kcal/mole, which gives 6.05 kcal/mole per hydrogen bond if the tetramer is cyclic. It can easily be shown from spectroscopic (7, 8) and thermochemical data (9) that a hydrocarbon solvent approximates the vapor phase better than the so called "inert" solvents like carbon tetrachloride or basic solvents like benzene. The degree of solvation of the hydroxyl group decreases (7–9) in the order

gas phase < hydrocarbon solvent < carbon tetrachloride < benzene, etc.

The ν_{OH} values for phenol in various solvents, for example, are as follows (8): gas phase, 3654; perfluoro octane, 3644; hexane, 3621; carbon tetrachloride, 3611; benzene, 3557 cm^{-1}. Thus at a given concentration and temperature there will be more monomeric and open chain polymeric species in benzene than in carbon tetrachloride and more in carbon tetrachloride than in a hydrocarbon solvent (see ref. 5 for spectra). Thus it is not unreasonable that alcohols and phenols exist predominantly as higher polymers in nonpolar solvents if the nonpolar solvent is a hydrocarbon but not necessarily if the nonpolar solvent is carbon tetrachloride, carbon disulfide, or a host of other solvents.

Experimental

The spectra were measured using a Beckman IR-9 spectrophotometer. The path length of the cells varied depending upon experimental convenience. Beckman NIR silica cells of 10- and 1-cm path length, and 0–6 mm Beckman variable path length sodium chloride cells were used. The alcohols and phenols were used without further purification. The carbon tetrachloride was dried over phosphorous pentoxide and distilled over calcium hydride.

The author is grateful for the support of this work by a research grant (1967–68) from the Robert A. Welch Foundation. The valuable suggestions and critical comments of Professor Kenneth S. Pitzer during the course of this work are gratefully acknowledged.

1. A. N. Fletcher and C. A. Heller. J. Phys. Chem. **71**, 3742 (1967).

2. A. N. FLETCHER and C. A. HELLER. J. Phys. Chem. **72**, 1839 (1968).
3. R. M. HAMMAKER, R. M. CLEGG, L. K. PATTERSON, P. E. RIDER, and S. L. ROCK. J. Phys. Chem. **72**, 1837 (1968).
4. B. G. SOMERS and H. S. GUTOWSKY. J. Amer. Chem. Soc. **85**, 3065 (1963).
5. H. C. VAN NESS, J. VAN WINKLE, H. H. RICHTOL, and H. B. HOLLINGER. J. Phys. Chem. **71**, 1483 (1967).
6. W. WELTNER and K. S. PITZER. J. Amer. Chem. Soc. **73**, 2606 (1951).
7. T. S. S. R. MURTY and KENNETH S. PITZER. J. Phys. Chem. **73**, 1426 (1969).
8. A. ALLERHAND and P. V. R. SCHLEYER. J. Amer. Chem. Soc. **85**, 371 (1963).
9. T. S. S. R. MURTY. Doctoral Dissertation, University of Pittsburgh, Pittsburgh, Pa. 1967.
10. L. P. KUHN. J. Amer. Chem. Soc. **74**, 2492 (1952).
11. L. J. BELLAMY and R. J. PACE. Spectrochim. Acta, **22**, 525 (1966).
12. G. DUROCHER and C. SANDORFY. J. Mol. Spectrosc. **15**, 22 (1965).
13. L. K. PATTERSON and R. M. HAMMAKER. Spectrochim. Acta, **23A**, 2333 (1967).
14. W. MASSCHELEIN. Spectrochim. Acta, **18**, 1557 (1962).
15. U. LIDDEL and E. D. BECKER. Spectrochim. Acta, **10**, 70 (1957).
16. A. KIVINEN and J. MURTO. Suom. Kem. **B40**, 6 (1967).
17. B. B. WAYLAND and R. S. DRAGO. J. Amer. Chem. Soc. **86**, 5240 (1964).
18. K. F. PURCELL and S. T. WILSON. J. Mol. Spectrosc. **24**, 468 (1967).
19. L. LAMBERTS. J. Chim. Phys. **62**, 1404 (1965).
20. L. J. BELLAMY, K. J. MORGAN, and R. J. PACE. Spectrochim. Acta, **22**, 535 (1966).
21. G. L. BITMAN, V. G. ARISTOVA, K. K. POPKOV, I. I. SKOROKHADOV, and É. G. PEREVALOVA. Dokl. Phys. Chem. Sect. Engl. Transl. **176**, 702 (1967).

Thermolysis of bicyclo[4.2.2]deca-2,4,7,9-tetraene[1]

R. T. SEIDNER, N. NAKATSUKA, AND S. MASAMUNE
Department of Chemistry, University of Alberta, Edmonton, Alberta

Received July 7, 1969

This title compound has been shown to undergo thermal isomerizations, intramolecular Diels–Alder reaction, and rearrangement to *cis*-9,10-dihydronaphthalene. Evidence presented establishes that tetracyclo[4.4.0.0.^{2,10}0^{5,7}]deca-3,8-diene is the intermediate of these reactions.

Canadian Journal of Chemistry, **48**, 187 (1970)

We have recently shown that photolysis of some $(CH)_{10}$ hydrocarbons provides in high yield tetracyclo[4.4.0.0.^{2,10}0^{5,7}]deca-3,8-diene (**1**), an intermediate frequently proposed for many isomerizations of $(CH)_{10}$ isomers (1). We have also observed that **1** readily rearranged at room temperature to bicyclo[4.2.2]deca-2,4,7,9-tetraene (**2**) (1). We wish to show herein that **2** undergoes thermal isomerizations, intramolecular Diels–Alder reaction, and rearrangement to *cis*-9,10-dihydronaphthalene (**3**) and further to present evidence to demonstrate that **1** is indeed the intermediate of these reactions.

Figure 1 shows temperature dependent 100 MHz nuclear magnetic resonance (n.m.r.) spectra of **2** in *n*-dodecane.[2] The fine splitting of the signal at τ 6.96 (A) began to collapse even at 120° and the sharp quartet B (sextet with weak lines) at τ 4.60 then collapsed to a broad triplet at 140°, showing that splitting due to one of the smallest coupling (presumably $J \sim 1.0$) disappeared. Two sets of lines centered at τ 4.40 (C) and 4.60 (B) at room temperature nearly merged around 170° to 180° and the chemical shifts ($\Delta\nu \sim 21$ Hz) of these groups of protons (H-3,4,7,8,9, and 10) almost averaged. Above 180° the signals at τ 6.96 (A) and 4.05 (D) tended to merge, but due to other complications (conversion of **2** into **3**,

[1]The text portion of this note was originally submitted virtually in the same form to this Journal one year ago, July 15, 1968. Also, this work was presented as a part of "Chemistry of $(CH)_{10}$ Hydrocarbons" before IUPAC Symposium Valence Isomerization, Karlsruhe, Germany, September 9–12, 1968. Since then there have appeared four communications concerning the same or a similar subject [ref. (5, 10–12)]. A novel feature of the work has recently been emphasized [see ref. (13)]. Furthermore, some data reported in ref. (5) appear different from ours. Although, according to the Editor's previous suggestion we planned to publish this work in a full paper after the completion of the work on $(CH)_{10}$ hydrocarbons [see ref. (1)], we have decided to summarize this particular aspect of the chemistry as a note at this time.

[2]A preliminary analysis of a 100 MHz spectrum of **2** shows clearly that some signals of H-7 (B) and H-3 (C) overlap and the integration of these signals must be performed with extreme caution. Assignment of group C to H-3 and group D to H-2 is consistent with the size of the coupling constants and diamagnetic anisotropy of double bonds.

Can. J. Chem. Downloaded from www.nrcresearchpress.com by 210.87.254.6 on 09/05/12
For personal use only.

2. A. N. FLETCHER and C. A. HELLER. J. Phys. Chem. **72**, 1839 (1968).
3. R. M. HAMMAKER, R. M. CLEGG, L. K. PATTERSON, P. E. RIDER, and S. L. ROCK. J. Phys. Chem. **72**, 1837 (1968).
4. B. G. SOMERS and H. S. GUTOWSKY. J. Amer. Chem. Soc. **85**, 3065 (1963).
5. H. C. VAN NESS, J. VAN WINKLE, H. H. RICHTOL, and H. B. HOLLINGER. J. Phys. Chem. **71**, 1483 (1967).
6. W. WELTNER and K. S. PITZER. J. Amer. Chem. Soc. **73**, 2606 (1951).
7. T. S. S. R. MURTY and KENNETH S. PITZER. J. Phys. Chem. **73**, 1426 (1969).
8. A. ALLERHAND and P. V. R. SCHLEYER. J. Amer. Chem. Soc. **85**, 371 (1963).
9. T. S. S. R. MURTY. Doctoral Dissertation, University of Pittsburgh, Pittsburgh, Pa. 1967.
10. L. P. KUHN. J. Amer. Chem. Soc. **74**, 2492 (1952).
11. L. J. BELLAMY and R. J. PACE. Spectrochim. Acta, **22**, 525 (1966).
12. G. DUROCHER and C. SANDORFY. J. Mol. Spectrosc. **15**, 22 (1965).
13. L. K. PATTERSON and R. M. HAMMAKER. Spectrochim. Acta, **23A**, 2333 (1967).
14. W. MASSCHELEIN. Spectrochim. Acta, **18**, 1557 (1962).
15. U. LIDDEL and E. D. BECKER. Spectrochim. Acta, **10**, 70 (1957).
16. A. KIVINEN and J. MURTO. Suom. Kem. **B40**, 6 (1967).
17. B. B. WAYLAND and R. S. DRAGO. J. Amer. Chem. Soc. **86**, 5240 (1964).
18. K. F. PURCELL and S. T. WILSON. J. Mol. Spectrosc. **24**, 468 (1967).
19. L. LAMBERTS. J. Chim. Phys. **62**, 1404 (1965).
20. L. J. BELLAMY, K. J. MORGAN, and R. J. PACE. Spectrochim. Acta, **22**, 535 (1966).
21. G. L. BITMAN, V. G. ARISTOVA, K. K. POPKOV, I. I. SKOROKHADOV, and É. G. PEREVALOVA. Dokl. Phys. Chem. Sect. Engl. Transl. **176**, 702 (1967).

Thermolysis of bicyclo[4.2.2]deca-2,4,7,9-tetraene[1]

R. T. SEIDNER, N. NAKATSUKA, AND S. MASAMUNE
Department of Chemistry, University of Alberta, Edmonton, Alberta

Received July 7, 1969

This title compound has been shown to undergo thermal isomerizations, intramolecular Diels–Alder reaction, and rearrangement to *cis*-9,10-dihydronaphthalene. Evidence presented establishes that tetracyclo[4.4.0.0.^{2,10}0^{5,7}]deca-3,8-diene is the intermediate of these reactions.

Canadian Journal of Chemistry, **48**, 187 (1970)

We have recently shown that photolysis of some $(CH)_{10}$ hydrocarbons provides in high yield tetracyclo[4.4.0.0.^{2,10}0^{5,7}]deca-3,8-diene (**1**), an intermediate frequently proposed for many isomerizations of $(CH)_{10}$ isomers (1). We have also observed that **1** readily rearranged at room temperature to bicyclo[4.2.2]deca-2,4,7,9-tetraene (**2**) (1). We wish to show herein that **2** undergoes thermal isomerizations, intramolecular Diels–Alder reaction, and rearrangement to *cis*-9,10-dihydronaphthalene (**3**) and further to present evidence to demonstrate that **1** is indeed the intermediate of these reactions.

Figure 1 shows temperature dependent 100 MHz nuclear magnetic resonance (n.m.r.) spectra of **2** in *n*-dodecane.[2] The fine splitting of the signal at τ 6.96 (A) began to collapse even at 120° and the sharp quartet B (sextet with weak lines) at τ 4.60 then collapsed to a broad triplet at 140°, showing that splitting due to one of the smallest coupling (presumably $J \sim 1.0$) disappeared. Two sets of lines centered at τ 4.40 (C) and 4.60 (B) at room temperature nearly merged around 170° to 180° and the chemical shifts ($\Delta\nu \sim 21$ Hz) of these groups of protons (H-3,4,7,8,9, and 10) almost averaged. Above 180° the signals at τ 6.96 (A) and 4.05 (D) tended to merge, but due to other complications (conversion of **2** into **3**,

[1]The text portion of this note was originally submitted virtually in the same form to this Journal one year ago, July 15, 1968. Also, this work was presented as a part of "Chemistry of $(CH)_{10}$ Hydrocarbons" before IUPAC Symposium Valence Isomerization, Karlsruhe, Germany, September 9–12, 1968. Since then there have appeared four communications concerning the same or a similar subject [ref. (5, 10–12)]. A novel feature of the work has recently been emphasized [see ref. (13)]. Furthermore, some data reported in ref. (5) appear different from ours. Although, according to the Editor's previous suggestion we planned to publish this work in a full paper after the completion of the work on $(CH)_{10}$ hydrocarbons [see ref. (1)], we have decided to summarize this particular aspect of the chemistry as a note at this time.

[2]A preliminary analysis of a 100 MHz spectrum of **2** shows clearly that some signals of H-7 (B) and H-3 (C) overlap and the integration of these signals must be performed with extreme caution. Assignment of group C to H-3 and group D to H-2 is consistent with the size of the coupling constants and diamagnetic anisotropy of double bonds.

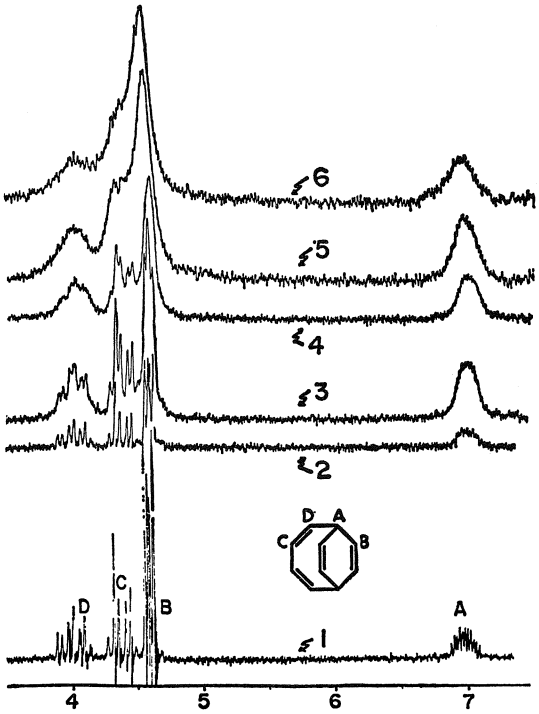

FIG. 1. 100 MHz n.m.r. spectra of **2** at 40° (1), 120° (2), 140° (3), 160° (4), 170° (5), and 180° (6).

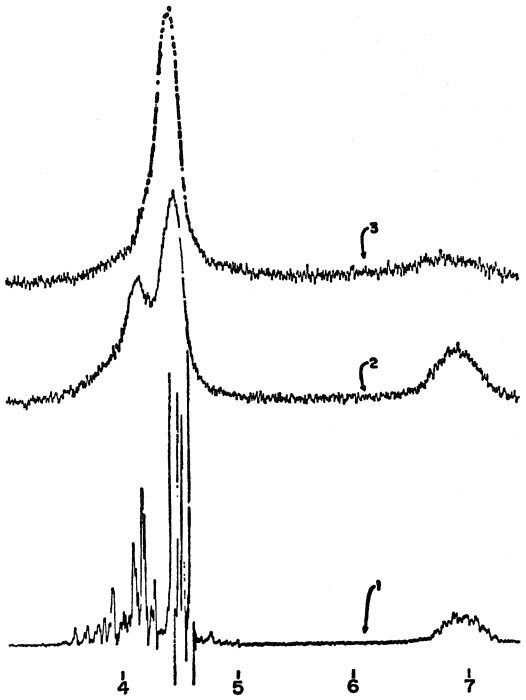

FIG. 2. 40 MHz n.m.r. spectra of **2** at 35° (1), 160° (2), and 180° (3).

vide infra) we were not able to confirm the actual coalescence of these peaks. Because of a large chemical shift difference ($\Delta\nu \sim 300$ Hz), we estimate signals A and D would coalesce above 210°. The half life time of **2** (conversion into **3**) is less than 43 min at 210° (*vide infra*). With a 40 MHz spectrometer at 180° (see Fig. 2), we could see that signals B and C ($\Delta\nu = 8 \sim 9$ Hz) coalesced and A and D tended to merge. The above spectral behavior is best interpreted by fast degenerate isomerization of **2** to **2'**. The approximate mean life times are of the order of 0.5 s at 140° and 0.025 s around 175°.[3]

In order to substantiate the above interpretation we have further investigated deuterium scrambling experiments. The synthetic methods reported for (non-deuterated) **2** (2, 3) were adopted with minor modification[4] for the

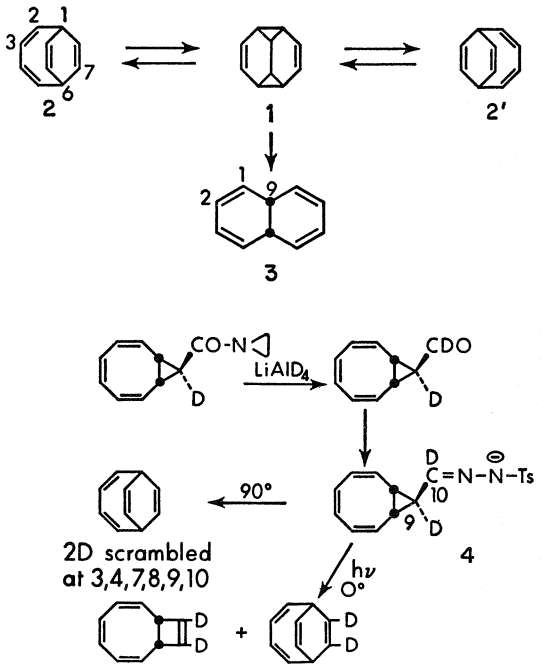

FIG. 3. Thermal reactions of **1** and **2** and synthesis of labelled **2**.

[3]A computer analysis of the kinetics is in progress in collaboration with Dr. J. F. Oth, European Research Associated, Brussels.

[4]Pyrolysis of the dry salt (**4**) similar to the Jones and Scott procedure provided in our hands only a 2% yield of **2**. However, if **4** was suspended in dry dioxane and heated at 95° the yield of **2** increased 4 to 5 times consistently. See Experimental.

introduction of deuterium atoms into **2**, as outlined in Fig. 3. Obviously, the spectral results indicate that specifically labelled **2** must be prepared under limited conditions (low temperature). In fact, when pyrolysis of the sodium salt (**4**) of the tosylhydrazone derived from 9,10-dideuterio-bicyclo[6.1.0]nonatriene-9-carboxaldehyde (>95% D at C-9, 99% D at C-10, n.m.r. analysis) was performed at 90 to 95° and followed by gas–liquid phase chromatography (g.l.p.c.) at 100° for ca. one h (2),[4] the resulting dideuterio-**2** contained 1.8 D/molecule[5] and the integral ratio of signal (A:B:C:D) in the spectrum was 2.0:2.8:1.5:2.0 (±0.1) and remained unchanged within experimental error upon further heating to 170°. The calculated value for the complete scrambling of 1.8 deuterium atoms at H-3,4,7,8,9,10 positions of **2** is 2.0:2.8:1.4:2.0. However, photolysis followed by alumina chromatography, both operations performed at 0°, provided deuterated-**2** (1.4 D/molecule)[5] and the integral ratio (A:B:C:D) was 2.0:2.7:1.9:2.0 (±0.1) showing that the 1.4 deuterium atoms were mainly located at H-7,8,9,10 (calculated: 2.0:2.6:2.0:2.0). The ratio changed to 2.0:3.0:1.6:2.0 after heating the sample at 80° for 1 h and this value remained constant on further heating. The calculated value for the complete scrambling is 2.0:3.07:1.53:2.0.[6] This result indicated that the deuterium scrambling was rapidly completed at 80° in accord with the results of temperature dependent n.m.r. spectra of **2**. Although Jones and Fairless reported (5) that thermolysis of 9-deuterio-**4** provided unscrambled 7-deuterio-**2** under conditions similar to ours and the data in the table indicated that the deuterium scrambled to approximately 50 and 100% completion by heating **2** at 170° for 1.25 h and 175° for 3.5 h, respectively, they intended, in the text, to make no claim concerning the rate of the deuterium scrambling. Our results are consistent with the observations by Grimme *et al.* (10) and the rapid scrambling is readily understandable in view of a small (negative or positive) entropy of activation expected for this reaction.

When **2** was pyrolyzed at 410° in a flow system,[7] compound **3** was obtained in 80% yield. Under the same conditions, dideuterio-**2** (1.8 D/molecule, *vide supra*) provided dideuterio-**3** and its n.m.r. spectrum revealed that deuterium was distributed at C-9,10 (0.6 D), and at C-2,3,6,7 (1.2 D) and that none was at C-1,4,5,8 within experimental error [calculated integral ratio of signals τ 4.14, 4.49, and 6.71 for the complete H-2,3,6,7,9,10 scrambling 1.4:2.0:0.7, found, 1.4:2.0:0.7 (±0.1)].

We have studied thermolysis of **2** at 178.7° ± 0.2° in *n*-dodecane. When the initial concentration of **2** was higher than 0.5 *M*, only a trace of **3** was found during the entire course of reaction and the product consisted of naphthalene, bicyclo-[4.2.2]deca-2,4,7-triene (**5**) (see Experimental for the structural assignment), tetrahydro-**2**, and some minor products. With a solution initially more dilute than 0.1 *M*, **3** was detected in addition to the products mentioned above and was obtained in as high as 7% yield when a 0.008 *M* solution of **2** was used. Plotting ln C_0/C [C = concentration of **2**] against t generated a curve with a steep (ca. $2k$) initial slope and an asymptotical approach to a straight line (k). In view of the pyrolysis results in a flow system and the known chemical behavior of **3** (which acts as a hydrogen donor or acceptor) (6),[8] we assumed that the first thermal reaction of **2** was

(A) **2** ⟶ **3**

[5]The intensity of M-1 (and M-2) peaks in the mass spectra of **2** was significantly high even at the lowest possible (10 eV) ionization potential for **2**. The lack of knowledge on the exact fragmentation pattern to produce the M-1 species and the degree of hydrogen-deuterium exchange at low electron energies, the mass spectra of dideuterio-**2** failed to provide the exact composition of a mixture of di-, mono-, and non-deuterio-**2**. Therefore, n.m.r. spectra of relatively concentrated solutions were employed to calculate the degree of deuteration of the product using spectra of the non-deuterated compound as a standard. The deuterium content (1.95 D/molecule for **4**) decreased during the pyrolysis (presumably at the stage of the intermediate, diazo compound) and photolysis despite care taken to avoid moisture. Compound **2**, obtained by pyrolysis, contained 1.8 D/molecule whereas photolysis provided **2** with 1.4 D/molecule. The rather significant loss of deuterium in the latter case is rationalized by a small amount of non-deuterated methanol which could not be excluded from the reaction mixture.

[6]This value is calculated for 1.4 deuterium atoms. Originally we performed a similar series of experiments using 7-monodeuterio-**2** and reached exactly the same conclusion as that described herein.

[7]A thermocouple was directly attached to a pyrolysis column. With this arrangement, bullvalene (**6**) decomposed at 505° (optimum temperature) into **3** (45%) and other products. Due to the temperature gradient of the system the temperatures indicated were not accurate. These experiments were performed by Dr. M. Wiesel of this laboratory (ref. 14).

[8]Thermolysis of *trans*-9,10-dihydronaphthalene is remarkably different from that of **3** (1).

followed by

(B) **3** + **2** ⟶ 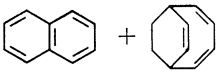 +

5

(C) **3** + **5** ⟶ 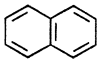 + tetrahydro-**2**

etc.,

Thus, the kinetics of this reaction in dodecane was very complex. In support of this assumption, use of *cyclooctene* as solvent and hydrogen acceptor replaced reactions (B) and (C) by reaction, **3** + cyclooctene → naphthalene + cyclooctane. The decrease of **2** in cyclooctene followed first order kinetics as shown in Fig. 4 [$k_{178.7°} = (2.15 \pm 0.08) \times 10^{-5}$ s^{-1}, $k_{201.8°} = (1.45 \pm 0.05) \times 10^{-4}$ s^{-1} (average deviations were employed)]. Therefore we can conclude that a process from **2** to **3** requires $\Delta H‡ = 34$ kcal, $\Delta S‡ = -5$ e.u.

All the evidence mentioned above is consistent with the view that both the degenerate isomerization (4 + 2) of **2** and thermal conversion (4 + 4) of **2** into **3** proceed through intermediate **1**. This mechanism is strongly supported by our previous findings (1) that **1** isomerized to **2** with great ease ($\Delta H‡ = 21$ kcal, $\Delta S‡ = 5$ e.u.). Obviously a pathway leading to bullvalene (**6**) from **1**, presumably via the diradical species proposed earlier (4) requires more energy than **1** to **2**. We found that thermal decomposition of **6** in *n*-dodecane proceeded as a first order reaction, because **6** did not accept hydrogen from **3** due

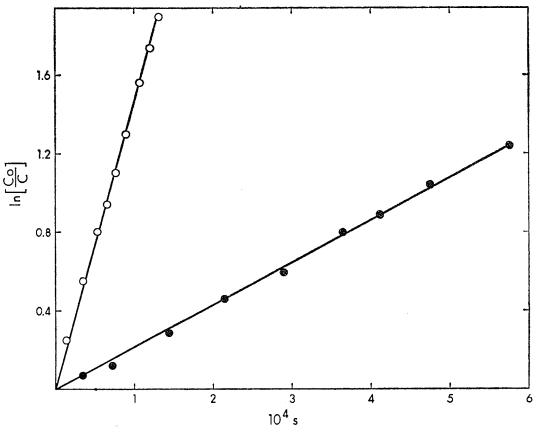

FIG. 4. Thermolysis of **2** in cyclooctene at 178.7° (●) and at 201.8° (○).

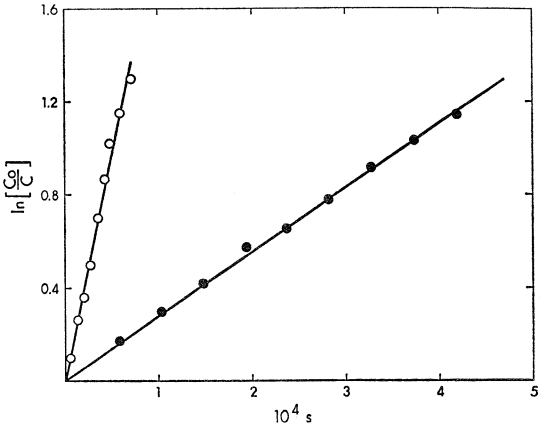

FIG. 5. Thermolysis of bullvalene in *n*-dodecane-d_{26} at 271.5° (●) and at 296.5° (○).

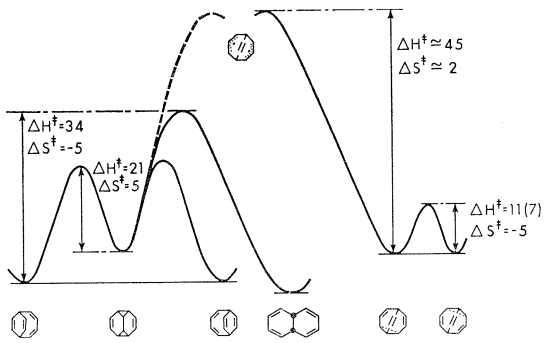

FIG. 6. Energy profile for thermal conversion of **1**, **2**, **3**, and **6**. $\Delta H‡$ is expressed in kcal/mol and $\Delta S‡$ in e.u.

to the unique stereochemistry of the molecule (**6**) in which the π orbitals were not oriented to overlap efficiently with those of another approaching molecule, [$k_{296.5°\pm0.5} = (1.89 \pm 0.2) \times 10^{-4}$ s^{-1}, $k_{271.5\pm0.5} = (2.09 \pm 0.2) \times 10^{-5}$ s^{-1}, $\Delta H‡ = 45$ kcal/mole, $\Delta S‡ = 2$ e.u. (see Fig. 5)]. If this thermolysis is the reverse process of **2** to **6**, then the difference in activation energy of the two processes, one from **6** and **2** and the other, the degenerate tautomerization of **6** (7), would approximately represent the amount of energy assistance by a concerted process in the latter case. Thus we may be allowed to draw an energy profile for these thermal processes as shown in Fig. 6. We would like to discuss this subject further when we have obtained adequate information including several heats of combustion and other activation energies.

Experimental

Temperature Dependent Nuclear Magnetic Resonance Spectra of Bicyclo[4.2.2.]deca-2,4,7,9-tetraene (2)

The spectra shown in Figs. 1 and 2 were measured with a Varian Associates HA-100 spectrometer equipped with a 15 in. magnet. The ambient sample temperatures were determined by means of a pre-calibrated ethylene glycol chemical shift. A Varian 4333 probe was employed for the operation at 40 MHz. For the 100 MHz spectra, a solution of 52 mg of **2** [synthesized by pyrolysis of **4** (2) (*vide infra*)] and 30 μl of hexamethyldisilane in 0.5 ml of *n*-dodecane was prepared and degassed by freeze-thaw cycles on a standard high vacuum rack and the sample tube sealed. For the 40 MHz spectra, a solution of 70 mg of **2** and 39 μl. of hexamethyldisilane in 0.25 ml of *n*-dodecane-d_{26} was employed.

Bicyclo[4.2.2]deca-2,4,7,9-tetraene (2)

(a) By Pyrolysis of Dry Sodium Salt of cis-Bicyclo[6.1.0]-nona-2,4,6-triene-exo-9-carboxaldehyde Tosylhydrazone[9]

A solution of the tosylhydrazone (1.7 g, 5.7 mmole) and sodium methoxide (440 mg, 8.2 mmole) in dry tetrahydrofuran (40 ml) and dry methanol (20 ml) was evaporated to dryness on a rotary evaporator. After drying the salt at room temperature under high vacuum, the salt was heated to 95° at 20 mm.[10] Collection of the generated hydrocarbons on a cold finger condenser (at 0°) yielded 40 mg of a light yellow liquid that contained **2** as the major product (40%) and a distribution of other hydrocarbons typified by the result reported (2). Preparative g.l.p.c. (100°, 10 ft × 3/8 in., 10% UCW98 on Chromosorb WAW) of this mixture gave pure **2** (15 mg, 2%). Compound **2** is now readily obtainable from bullvalene (9) but obviously this route (9) is not suitable for the deuterium labelling.

(b) Pyrolysis of 4 in Dioxane

The dry salt was prepared as above from the tosylhydrazone (1.7 g, 5.7 mmole) and sodium methoxide (440 mg, 8.2 mmole) and a stirred suspension of the salt in dry dioxane (50 ml) was heated at 95° until nitrogen evolution ceased (usually 30 min was sufficient). The cooled reaction mixture was treated with CO_2 and diluted with cold water (400 ml). The aqueous solution was then extracted with pentane (3 × 40 ml) and the combined extracts were washed with water and dried over $MgSO_4$. Distillation (to 100° at 20 mm) provided a C_{10} fraction (141 mg, 19% hydrocarbon yield) that contained **2** (51%) and 1,2-dihydronaphthalene (37%) as major products (n.m.r. and g.l.p.c.). Preparative g.l.p.c. of this hydrocarbon mixture gave pure **2** (60 mg, 8%).

9,10-Dideuterio-cis-bicyclo[6.1.0]nona-2,4,6-triene-exo-9-carboxaldehyde Tosylhydrazone

The deuterated compound was prepared from cyclooctatetraene by the same procedure as that applied for the corresponding non-deuterated compound except for those of deuterated reagents. Ethyl deuteriodiazoacetate (98% D) and lithium aluminum deuteride (99% D) were used to introduce the deuterium at C-9 and 10 positions of the aldehyde.

Deuterated Bicyclo[4.2.2]deca-2,4,7,9-tetraene

(a) Pyrolysis

The deuterated compound was obtained in exactly the same manner as described above for the non-deuterated compounds. The deuterium scrambling of the product is detailed in the Text.

(b) Photolysis

The tosylhydrazone (1.65 g) derived from dideuteriobicyclo[6.1.0]nonatriene-9-carboxaldehyde in 220 ml of dry tetrahydrofuran containing 450 mg of sodium methoxide was irradiated at 0° under conditions similar to those employed for the non-deuterated compound. The preparation of the hydrazone and photolysis conditions will be detailed in a separate paper (presumably entitled bicyclo[6.2.0]deca-2,4,6,9-tetraene) and experiments described herein are only modified parts of the work-up procedure to obtain bicyclo[4.2.2]-deca-2,4,7,9-tetraene without deuterium scrambling. Ten similar photolyses provided ca. 1.1 g of C_{10} hydrocarbons by distillation at 0°, 0.03 mm. Careful fractional distillation with a temperature controlled spiral column (15 cm) provided two main fractions, one (240 mg, −24 to −17° at 0.01 mm) containing bicyclo[6.2.0]deca-2,4,6,9-tetraene (70% purity) and the other (350 mg, −14° to −8° at 0.01 mm) containing **2** (30% purity). The latter fraction upon a second fractionation gave 250 mg of **2** of 40% purity which was chromatographed over 300 g of neutral alumina, Woelm grade II, at 0° twice, using pentane as eluent. Each fraction was examined by means of g.l.p.c. (F & M model 5750) and 40 mg of pure (>98%) deuterated-**2** was obtained.

Thermolysis of Bicyclo[4.2.2]deca-2,4,7,9-tetraene (2)

(a) Flow System

A column (o.d., 18 mm) was packed with glassbeads (d., 3 mm) to a height of 10 cm and wrapped with an electric heating tape and a thermocouple was attached directly to the outside wall of the column.[7] A nitrogen flow was maintained at 40 ml min^{-1} and a 10% ethereal solution of **2** was dropped into the heated column and the pyrolysate condensed at −80°. After several pyrolyses at various temperatures, the optimum temperature for the conversion of **2** into **3** was found to be 410° (80% yield). The pyrolysate obtained from 40 mg of dideuterio-**2** was distilled (b.p. ~0°, 0.01 mm) and chromatographed on 5 g of alumina (Woelm, netural, grade II, pentane). The fractions containing pure dideuterio-**3** (g.l.p.c. analysis) were combined and redistilled (0.01 mm) to afford ca. 25 mg of the product. The n.m.r. spectrum of this compound is discussed in the Text.

(b) Static Systems

Kinetic Measurement. Solutions of various concentrations of **2** (.8 *M*, .4 *M*, .08 *M*, .008 *M*) and cyclooctane

---

[9]Presently there are no official rules in existence to describe properly the stereochemistry of this compound. However, use of '*cis*' or '*trans*' for ring fusion and '*exo*' or '*endo*' for substituents is more appropriate than that employed before (4).

[10]Jones and Scott employed the pressure of 20–50 μ instead of 20 mm and did not use methanol to prepare the sodium salt of the tosylhydrazone (private communication August 15, 1969).

(standard) in *n*-dodecane was prepared. Samples in small vacuum sealed ampoules were removed from a constant temperature bath (the maximum temperature variation was 0.2° for a set temperature) at intervals and immediately cooled with liquid nitrogen before the product analysis. Two solutions of **2** (.64 *M* and .32 *M*) and *n*-dodecane (standard) in cyclooctene were also prepared for kinetic measurement. The course of the thermolysis was followed by g.l.p.c. (F and M model 5750, 6 ft × 3/16 in. column, 10% UCW98 on Chromosorb WAW, isothermal at 100°) and integration of the component peaks was carried out with a planimeter. Relative retention times of **2**, **3**, and **5** were 8.8, 7.5, and 9.6. Decrease of **2** (ln C_0/C) were determined by comparing the peak area of **2** with that of the standard. The rate reported in the text is the average of two runs with different initial concentrations at each temperature.

Thermolysis Products. After 10 h the g.l.p.c. analysis of the *n*-dodecane solution showed yields of **3** and **5** as indicated in Table 1 (not corrected for the relative sensitivity of the detector).

TABLE 1

Yields of **3** and **5** measured by g.l.p.c.

Initial concentration of **2** (*M*)	Yield of **3** (%)	Yield of **5** (%)
.008	7	3
.08	4	10
.4	1	15
.8	trace	16

The disappearance of **2** in cyclooctene was first order and the only products discernible were cyclooctane and naphthalene (see Fig. 4).

Bicyclo[4.2.2]deca-2,4,7-triene (5)

A 1.0 *M* solution of **2** (130 mg, 1.0 mmole) in *n*-dodecane (1.0 ml) was degassed, sealed in a small ampoule, and heated at 180° for 10 h. Chromatography of the product mixture over alumina (200 g, Woelm, neutral, grade I, pentane) yielded fractions of **5** that were free from **2** which was eluted later. Preparative g.l.p.c. (F and M model 700, 10 ft × 0.25 in., 10% SE30 on Chromasorb P, 100°) of these fractions produced pure **5** (10 mg, 7 ~ 8%): n.m.r. ($CDCl_3$) τ 3.8–4.4 (complex signals of two groups, 6H), 7.3 (broad, 2H) and 7.9–8.5 (complex, 4H); upon irradiation at signal τ 7.3, the olefinic protons exhibited a sharp singlet at τ 4.22 (2H) and a symmetrical signal (4H, τ 3.9–4.4), typical of an AA′XX′ system. (Therefore, the assignment of the double bonds to **5** as shown in the text is compatible with the n.m.r. spectrum and decoupling experiments. Principal fragments in mass spectrum, M^+, *m/e* 132.0939 (50) (calculated for $C_{10}H_{12}$: 132.0939), 117(67), 104(68), 91(100), 78(41). Catalytic hydrogenation (Pd/C, tetrahydrofuran) of **5** provided a fully saturated compound that was identical (g.l.p.c., infrared and mass spectrum) with material provided by catalytic hydrogenation of **2**.

Thermolysis of Bullvalene (6)

Bullvalene was prepared according to the procedure of Schröder (8). Pyrolysis of **6** in a flow system was performed in a manner similar to that for **2**. The optimum temperature for the conversion of **6** into **3** (45%) was 505° (6). A 0.33 *M* solution of **6** in *n*-dodecane-d_{26} containing *p*-di-*tert*-butylbenzene (internal standard) was prepared and distributed among several n.m.r. tubes which were degassed and sealed. The tubes were preheated to 250° immediately before immersion in a constant temperature bath and cooled with ice after removal. Analysis of the product mixture of each run was accomplished by n.m.r. spectral measurement performed at 100°. The peak area of the standard (τ 2.9) was compared to that of bullvalene (τ 5.9). The rate reported is an average value of three runs each temperature (see Fig. 5).

The authors are grateful to the National Research Council of Canada and the donors of the Petroleum Research Fund (American Chemical Society) for financial support, and Badische Anilin und Soda Fabrik A.G. for a generous gift of cyclooctatetraene.

1. S. Masamune, R. T. Seidner, H. Zenda, M. Wiesel, N. Nakatsuka, and G. Bigam. J. Amer. Chem. Soc. **90**, 5286 (1968). Leading references for the chemistry of $(CH)_{10}$ hydrocarbons are quoted therein. For the chemistry of [10] annulenes, see S. Masamune and R. T. Seidner. Chem. Commun. 542 (1969).
2. M. Jones, Jr. and L. T. Scott. J. Amer. Chem. Soc. **89**, 150 (1967).
3. S. Masamune, C. G. Chin, K. Hojo, and R. T. Seidner. J. Amer. Chem. Soc. **89**, 4804 (1967).
4. S. Masamune, H. Zenda, M. Wiesel, N. Nakatsuka, and G. Bigam. J. Amer. Chem. Soc. **90**, 2727 (1968).
5. M. Jones, Jr. and B. Fairless. Tetrahedron Letters, 4881 (1968).
6. W. von E. Doering and J. Rosenthal. J. Amer. Chem. Soc. **89**, 4534 (1967). Also see, M. Jones, Jr. J. Amer. Chem. Soc. **89**, 4236 (1967).
7. G. Schröder and J. F. Oth. Angew. Chem. int. Ed. **6**, 414 (1967).
8. G. Schröder. Chem. Ber. **97**, 3140 (1964).
9. H. P. Loffler and G. Schröder. Angew. Chem. int. Ed. **7**, 736 (1968). E. Vedejs. J. Amer. Chem. Soc. **90**, 4751 (1968).
10. W. Grimme, H. J. Riebel, and E. Vogel. Angew. Chem. Int. Ed. **7**, 823 (1968).
11. J. S. McConaghy, Jr. and J. J. Bloomfield. Tetrahedron Letters, 1121 (1969).
12. J. Altman, E. Babad, M. B. Rubin, and D. Ginsburg. Tetrahedron Letters, 1125 (1969).
13. D. Ginsburg. Accounts Chem. Res. **2**, 121 (1969).
14. W. von E. Doering, B. M. Ferrier, E. T. Fossel, J. H. Hartenstein, M. Jones, Jr., G Klumpp, R. M. Rubin, and M. Saunders. Tetrahedron, **23**, 3943 (1967).

The dimethyl formamide – acyl halide complex. II.[1] A synthesis of selected indole-3-aldehydes

D. E. HORNING AND J. M. MUCHOWSKI[2]
Bristol Laboratories of Canada Ltd., Candiac, Quebec

Received August 7, 1969

The synthesis of selected indole-3-aldehydes from the corresponding indoles and the DMF – acyl halide complex is described.

Canadian Journal of Chemistry, **48**, 193 (1970)

Can. J. Chem. Downloaded from www.nrcresearchpress.com by 210.87.254.42 on 09/05/12
For personal use only.

The equilibrium formation of a complex **1** on solution of an acyl halide in dimethyl formamide (DMF) was first recognized by Hall in 1956 (2). Bredereck *et al.* (3) subsequently showed that the isolable complexes obtained from certain acid bromides reacted with aniline to give the anilide and *N,N*-dimethyl-*N'*-phenylformamidine, i.e. the products of attack at the acyl and formyl carbons of **1**, respectively. We recently (1) described similar results for the nonisolable complexes derived from acid chlorides, and in addition, showed that sodium azide reacted by apparent exclusive attack at the acyl carbon of **1**, to give acyl azides in preparatively useful yields.

We now wish to describe the reaction that occurs between some 3-unsubstituted indoles and the DMF – acyl halide complex.

When indole was added to a solution of benzoyl

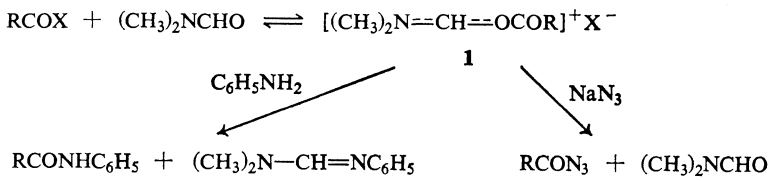

TABLE 1
Yields of indole-3-aldehydes

Starting indole	Acid halide	Reaction* time (h)	Product† yield (%)	Melting points (°C)‡	
				Observed	Reported
Indole	Acetyl chloride	49	48§	181–187 (194–196)§	196–197‖
Indole	Acetyl bromide	88	88.5	189–193 (194–196)§	196–197‖
Indole	Benzoyl chloride	49	85	183–189 (194–196)§	196–197‖
2-Methyl-indole	Benzoyl chloride	67	88	196–201 (200–202)**	202–203††
2-Phenyl-indole	Benzoyl chloride	71	96	240–248 (251–252)**	250–255‡‡

*The reaction times should not be regarded as definitive; 48 h would probably have been sufficient for those indoles which reacted.
†Unless stated otherwise, the yields refer to those of crude products.
‡The figures not in brackets refer to the melting point of the crude products; the values in parentheses represent the melting point observed after one crystallization.
§After one crystallization from benzene – ethanol.
‖See ref. 4.
**After one crystallization from ethanol.
††See ref. 5.
‡‡See ref. 6.

[1]For Part I, see ref. 1.
[2]To whom enquiries concerning this paper should be addressed.

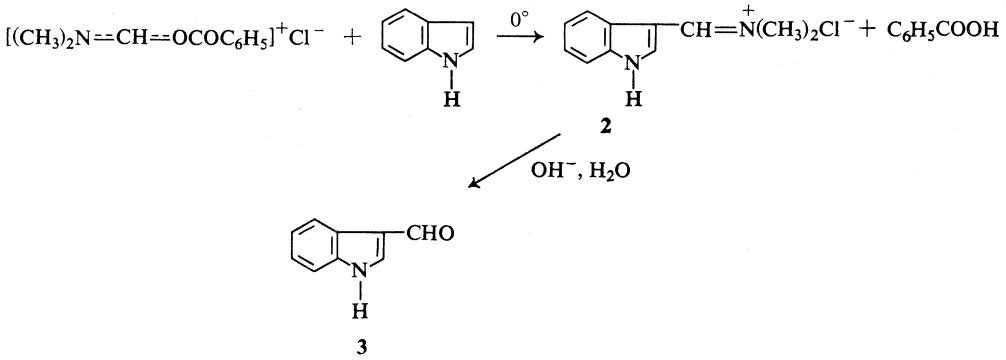

chloride in DMF at 0°, a hygroscopic crystalline solid slowly separated. This material, presumably the iminium salt **2**, gave a good yield of indole-3-aldehyde (**3**) upon alkaline hydrolysis. Acetyl bromide gave similar results, and even acetyl chloride[3] gave a modest yield of the aldehyde (see Table 1).

Under similar conditions, the benzoyl chloride–DMF complex reacted with 2-methyl and 2-phenylindole to give excellent yields of the corresponding 2-substituted indole-3-aldehydes. On the other hand, 2-methoxycarbonylindole and 4-cyanoindole did not react at all, the starting materials being recovered in 60–90% yield after 69 and 116 h, respectively. The inertness of the latter two compounds is probably explicable in terms of an electronic and a steric effect ("peri" cyano group) respectively.

Although the crude products had fairly wide melting point ranges, no contaminants could be detected by thin-layer chromatography (t.l.c.) on alumina, and their infrared (i.r.) spectra were almost identical (minor intensity differences for some of the absorption bands) to those of the authentic aldehydes prepared from the indoles and the DMF – phosphorous oxychloride adduct (4). It was, therefore, unnecessary to effect further purification of these materials before use in subsequent reactions. It should be noted, however, that one crystallization of the crude aldehydes was sufficient to provide samples whose physical properties (mixture melting points, t.l.c. behavior, and i.r. spectra) were indistinguishable from those of the purified authentic specimens.

In conclusion, the interaction of the DMF – acyl halide complexes with certain 3-unsubstituted indoles, provides a convenient, mild, but unhurried route, to the corresponding indole-3-aldehydes.

Experimental

The melting points were determined in a Gallenkamp melting point apparatus and are not corrected.

The acid chlorides were distilled before use; acetyl bromide was a commercial sample (technical grade) used as such. The starting indoles were obtained from commercial sources, or were prepared according to literature methods.

Synthesis of Indole-3-aldehydes

The following procedure was used throughout. A 100 ml three-necked flask containing a magnetic stirring bar, and fitted with a thermometer, a calcium chloride drying tube, and a nitrogen inlet, was flame dried. The apparatus was cooled to 0° in an ice bath and charged with 40 ml of dry DMF. A flow of purified, dry nitrogen through the apparatus was commenced, and when the DMF had reached 0°, 40 mmoles of the acid halide were added all at once from a hypodermic syringe (acetyl bromide was added dropwise to avoid a large temperature rise). The solution was stirred at 0° for 1 h, and then 15 mmoles of the indole were added all at once. After a further hour at 0°, the apparatus was tightly stoppered, affixed with a balloon filled with dry nitrogen, and stored at 0° for the length of time indicated in the table. During this time a crystalline solid separated from the solution. At the end of the specified reaction time the mixture was poured into 300 ml of ice-water, and a solution of 8.0 g of sodium hydroxide in 100 ml of water was added with stirring. The whole was placed in a preheated heating mantle and brought to reflux temperature as rapidly as possible. As soon as the boiling point was reached, heating was discontinued, and the clear solution was cooled with stirring to 0°. The precipitated solid was collected by filtration, washed well with water, and then dried *in vacuo*. The products obtained in this way had the melting points indicated in the Table. One crystallization from a suitable solvent gave materials identical in all respects to the

[3]Acetyl chloride was not examined in detail because it had previously been shown (1) that the apparent equilibrium concentration of the complex (**1**; R = CH_3; X = Cl) was much lower than that observed for benzoyl chloride or acetyl bromide.

Can. J. Chem. Downloaded from www.nrcresearchpress.com by 210.87.254.42 on 09/05/12
For personal use only.

corresponding authentic specimens, but the recovery of pure material from this operation usually did not exceed 80–85%; this behavior is typical for indole-3-aldehydes (e.g. see ref. 4).

1. D. E. HORNING and J. M. MUCHOWSKI. Can. J. Chem. **45**, 1247 (1967).
2. H. K. HALL, JR. J. Amer. Chem. Soc. **78**, 2717 (1956).
3. H. BREDERECK, R. GOMPER, K. KLEMM, and H. REMPERER. Chem. Ber. **92**, 837 (1959).
4. P. N. JONES and H. R. SNYDER. Organic Synthesis Vol. 39. John Wiley and Sons, Inc., New York. 1959. p. 30.
5. G. BARGER and A. J. EWINS. Biochem. J. II, 58 (1917).
6. H. R. SNYDER, S. SWAMINTHAN, and H. J. SIMS. J. Amer. Chem. Soc. **74**, 5110 (1952).

Preparation of 2,7-polymethylene-4,5-benzotropylium perchlorates

ROBERT E. HARMON, ROBERT SUDER, AND S. K. GUPTA
Department of Chemistry, Western Michigan University, Kalamazoo, Michigan 49001, U.S.A.

Received August 25, 1969

The first synthesis of 2,7-polymethylene-4,5-benzotropylium perchlorates has been achieved by reduction of the carbonyl function in 2,7-polymethylene-4,5-benzotropones and subsequent treatment with perchloric acid.

Canadian Journal of Chemistry, **48**, 195 (1970)

In this communication we wish to report the first synthesis of a new class of organic compounds; namely, 2,7-polymethylene-4,5-benzotropylium perchlorates (**3***a*–**3***b*). Prior to this work Eschenmoser et al. had reported the preparation of some simple benzotropylium perchlorates (1).

2,7-Polymethylene-4,5-benzotropones (**1***a*–**1***e*) were prepared by the reaction of phthalaldehyde (one mole) and cyclic ketones (one mole) (2). By infrared (i.r.) analysis, Kloster-Jensen and coworkers had postulated that the tropone ring system is planar if n is seven or larger (2). We have obtained substantiating evidence for this view from the nuclear magnetic resonance (n.m.r.) spectra of these compounds. For instance, when $n = 9$ (**1***c*), protons H_a resonate at 7.31 p.p.m., which is consistent with a conjugated ring system. However, when $n = 5$ (**1***a*), the protons resonate at 6.78 p.p.m. The downfield shift of the protons in the tropone ring system can be attributed to the increased planarity of the system as n is increased. This was further confirmed by the n.m.r. spectrum of **2***a* where the ring system is no longer planar and the H_a protons resonate at 6.25 p.p.m.

Lithium aluminium hydride reduction of the carbonyl function in **1***c*–**1***e* afforded the corresponding alcohols **2***a*–**2***c* in 60% yield. The 2,7-polymethylene-4,5-benzotropylium perchlorates (**3***a*–**3***b*) were prepared by treating **2***b*–**2***c* with a solution of 70% perchloric acid in ether. The n.m.r. spectra of **3***a*–**3***b* indicated a further downfield shift in the resonance due to the tropone ring protons H_a (9.2 p.p.m.).

Experimental

Melting points were determined with a Thomas-Hoover melting-point apparatus and are corrected. The elemental analyses were performed by Galbraith Laboratories, Inc., Knoxville, Tennessee 37921, U.S.A. A Beckman IR-8 spectrophotometer was used for recording the i.r. spectra. A Cary-14 spectrophotometer was used

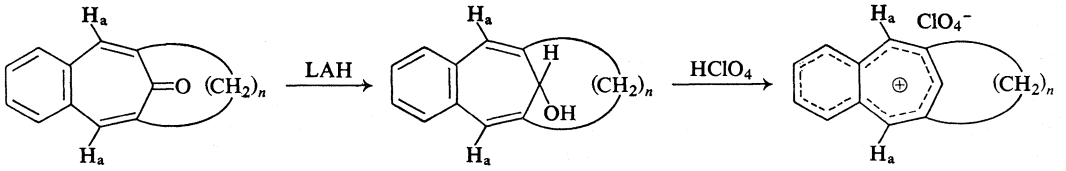

1*a* $n = 5$
1*b* $n = 7$
1*c* $n = 9$
1*d* $n = 10$
1*e* $n = 12$

2*a* $n = 9$
2*b* $n = 10$
2*c* $n = 12$

3*a* $n = 10$
3*b* $n = 12$

Can. J. Chem. Downloaded from www.nrcresearchpress.com by 210.87.254.42 on 09/05/12
For personal use only.

corresponding authentic specimens, but the recovery of pure material from this operation usually did not exceed 80–85%; this behavior is typical for indole-3-aldehydes (e.g. see ref. 4).

1. D. E. HORNING and J. M. MUCHOWSKI. Can. J. Chem. **45**, 1247 (1967).
2. H. K. HALL, JR. J. Amer. Chem. Soc. **78**, 2717 (1956).
3. H. BREDERECK, R. GOMPER, K. KLEMM, and H. REMPERER. Chem. Ber. **92**, 837 (1959).
4. P. N. JONES and H. R. SNYDER. Organic Synthesis Vol. 39. John Wiley and Sons, Inc., New York. 1959. p. 30.
5. G. BARGER and A. J. EWINS. Biochem. J. II, 58 (1917).
6. H. R. SNYDER, S. SWAMINTHAN, and H. J. SIMS. J. Amer. Chem. Soc. **74**, 5110 (1952).

Preparation of 2,7-polymethylene-4,5-benzotropylium perchlorates

ROBERT E. HARMON, ROBERT SUDER, AND S. K. GUPTA
Department of Chemistry, Western Michigan University, Kalamazoo, Michigan 49001, U.S.A.

Received August 25, 1969

The first synthesis of 2,7-polymethylene-4,5-benzotropylium perchlorates has been achieved by reduction of the carbonyl function in 2,7-polymethylene-4,5-benzotropones and subsequent treatment with perchloric acid.

Canadian Journal of Chemistry, **48**, 195 (1970)

In this communication we wish to report the first synthesis of a new class of organic compounds; namely, 2,7-polymethylene-4,5-benzotropylium perchlorates (**3***a*–**3***b*). Prior to this work Eschenmoser et al. had reported the preparation of some simple benzotropylium perchlorates (1).

2,7-Polymethylene-4,5-benzotropones (**1***a*–**1***e*) were prepared by the reaction of phthalaldehyde (one mole) and cyclic ketones (one mole) (2). By infrared (i.r.) analysis, Kloster-Jensen and coworkers had postulated that the tropone ring system is planar if n is seven or larger (2). We have obtained substantiating evidence for this view from the nuclear magnetic resonance (n.m.r.) spectra of these compounds. For instance, when $n = 9$ (**1***c*), protons H_a resonate at 7.31 p.p.m., which is consistent with a conjugated ring system. However, when $n = 5$ (**1***a*), the protons resonate at 6.78 p.p.m. The downfield shift of the protons in the tropone ring system can be attributed to the increased planarity of the system as n is increased. This was further confirmed by the n.m.r. spectrum of **2***a* where the ring system is no longer planar and the H_a protons resonate at 6.25 p.p.m.

Lithium aluminium hydride reduction of the carbonyl function in **1***c*–**1***e* afforded the corresponding alcohols **2***a*–**2***c* in 60% yield. The 2,7-polymethylene-4,5-benzotropylium perchlorates (**3***a*–**3***b*) were prepared by treating **2***b*–**2***c* with a solution of 70% perchloric acid in ether. The n.m.r. spectra of **3***a*–**3***b* indicated a further downfield shift in the resonance due to the tropone ring protons H_a (9.2 p.p.m.).

Experimental

Melting points were determined with a Thomas-Hoover melting-point apparatus and are corrected. The elemental analyses were performed by Galbraith Laboratories, Inc., Knoxville, Tennessee 37921, U.S.A. A Beckman IR-8 spectrophotometer was used for recording the i.r. spectra. A Cary-14 spectrophotometer was used

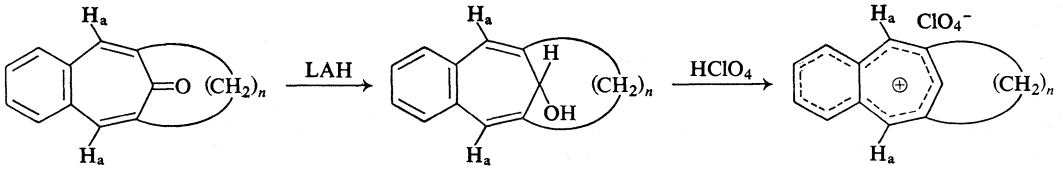

1*a* $n = 5$
1*b* $n = 7$
1*c* $n = 9$
1*d* $n = 10$
1*e* $n = 12$

2*a* $n = 9$
2*b* $n = 10$
2*c* $n = 12$

3*a* $n = 10$
3*b* $n = 12$

Can. J. Chem. Downloaded from www.nrcresearchpress.com by 210.87.254.5 on 09/05/12
For personal use only.

TABLE 1

Melting point and spectral data for compounds **1***a*–**1***e*

Compound **1**	Infrared (nujol) C=O(cm^{-1})	Melting point (°C)	Literature (2) melting point (°C)	Nuclear magnetic resonance ($CDCl_3$) δ
a	1679	166–168	168–169	0.9–2.3 (m, 10H, $(CH_2)_5$), 6.78 (d, 2H, J = 2 c.p.s. H_a), 7.05–7.60 (m, 4H, Ar*H*)
b	1609	109–110	110–111	1.0–3.7 (m, 14H, $(CH_2)_7$), 7.2 (s, 2H, H_a), 7.48 (d, 4H, J = 2 c.p.s., Ar*H*)
c	1610	115–116	116–117	0.9–3.8 (m, 18H, $(CH_2)_9$), 7.31 (d, 2H, J = 3 c.p.s., H_a), 7.48 (d, 4H, J = 3 c.p.s., Ar*H*)
d	1610	92–92.5		1.1–3.0 (m, 20H, $(CH_2)_{10}$), 7.27 (s, 2H, H_a), 7.44 (d, 4H, J = 2 c.p.s., Ar*H*)
e	1590	64–66	65–66	1.1–3.0 (m, 24H, $(CH_2)_{12}$), 7.52 (s, 2H, H_a), 7.6 (d, 4H, J = 4 c.p.s., Ar*H*)

to record the ultraviolet (u.v.) spectra. The n.m.r. spectra were obtained on a Varian A-60 spectrometer.

*Preparation of 2,7-polymethylene-4,5-benzotropones (**1***a*–**1***e*)*

These compounds were prepared by the procedure of Kloster-Jensen *et al.* (2). The melting points and i.r. spectra of the compounds **1***a*–**1***c* and **1***e* were in agreement with the literature values. 2,7-Decamethylene-4,5-benzotropone (**1***d*) a new compound, was analyzed for C and H.

Anal. Calcd. for $C_{21}H_{26}O$: C, 85.7; H, 8.85. Found: C, 85.76; H, 8.91.

We have obtained substantiating evidence for the structure of compounds **1***a*–**1***e* on the basis of their n.m.r. spectra. The results are summarized in Table 1.

*2,7-Polymethylene-4,5-benzo-2,6-cyclohepten-1-ols (**2***a*–**2***c*)*

The alcohols **2***a*–**2***c* were obtained by lithium aluminium hydride reduction of the corresponding benzotropones **1***c*–**1***e*. The appropriate benzotropone (3.6 mmole) was added to a suspension of lithium aluminium hydride (6.6 mmole) in anhydrous ether (50 ml) at 0°. The mixture was stirred at 0° for 3 h and then at room temperature for 1 h. Then an aqueous solution of ammonium chloride (10%) was added to it and the mixture stirred for about 30 min. The ether layer was separated, dried (anhyd. $MgSO_4$), and evaporated under diminished pressure to afford the corresponding alcohol in 50% yield. 2,7-Nonamethylene-4,5-benzo-2,6-cyclohepten-1-ol (**2***c*) was obtained as colorless crystals; m.p. 88–89.5°; n.m.r. ($CDCl_3$)δ 0.9–3.1 (m, 18H, $(CH_2)_9$), 4.1 (s, 1H, O*H*), 6.25 (s, 2H, H_a), 7.15 (s, 4H, Ar*H*); i.r. (nujol) 3580 (OH) and 1640 (C=C) cm^{-1}.

Anal. Calcd. for $C_{20}H_{26}O$: C, 85.1; H, 9.20. Found: C, 84.96; H, 9.15. The alcohols **2***d* and **2***e* were isolated only as oils and were used as such for the preparation of the compounds **3***a* and **3***b*.

*2,7-Decamethylene-4,5-benzotropylium Perchlorate (**3***a*)*

To a solution containing **2***d* (0.20 g, 1.5 mmole) in ether (50 ml) was added 70% perchloric acid (0.09 g, 1.0 mmole) dropwise. Crystals of **3***a* which separated out immediately were filtered and recrystallized from glacial acetic acid to afford 0.15 g (40%) crystals of **3***a*; m.p. 163–165°; n.m.r. (CD_3CN) δ 0.8–3.6 (m, 20H, $(CH_2)_{10}$), 8.36–9.30 (m, 4H, Ar*H*); 9.52–9.70 (m, 2H, H_a); i.r. (nujol) 1590 (C=C) cm^{-1}; u.v. (95% H_2SO_4) 291 (ε 55,000); 348 (ε 3900) and 440 (ε 2000) nm.

Anal. Calcd. for $C_{21}H_{27}ClO_4$: C, 66.8; H, 7.14; Cl, 9.83. Found: C, 66.62; H, 7.23; Cl, 9.65.

*2,7-Dodecamethylene-4,5-benzotropylium Perchlorate (**3***b*)*

It was prepared in 61% yield from the reaction of **2***c* with 70% perchloric acid by the above procedure; m.p. 170–171° (explodes); n.m.r. (CD_3CN) δ 0.8–3.6 (m, 24H, $(CH_2)_{12}$), 8.36–9.20 (m, 4H, Ar*H*). 9.64 (d, 2H, J = 4 cps, H_a); i.r. (nujol) 1590 (C=C) cm^{-1}; u.v. (95% H_2SO_4) 292 (ε 60,000), 349 (ε 5000), 450 (ε 1800) nm.

Anal. Calcd. for $C_{23}H_{31}ClO_4$: C, 67.9; H, 7.66; Cl, 8.73. Found: C, 68.02; H, 7.64; Cl, 9.01.

This work was supported by Grant CA-06140 from the National Cancer Institute.

1. A. Eschenmoser, E. Heilbronner, and H. H. Rennhard. Chem. Ind. (London) 415 (1955).
2. von Else Kloster-Jensen, N. Tarkoy, A. Eschenmoser, and E. Heilbronner. Helv. Chim. Acta, **39**, 786 (1956).

Can. J. Chem. Downloaded from www.nrcresearchpress.com by 210.87.254.5 on 09/05/12
For personal use only.

On the origin of peaks in the potentiostatic and potentiodynamic oxidation curves of ethylene glycol[1]

ASHOK K. VIJH
Institute of Research, Hydro-Quebec, 75, Dorchester Blvd. W., Montreal 1, Quebec

Received July 21, 1969

The peaks observed in the potentiostatic and potentiodynamic oxidation curves of ethylene glycol have been shown to be mainly kinetic inhibition inflections.
The manner in which this observation clarifies the significance of some previous work has been briefly pointed out.

Canadian Journal of Chemistry, **48**, 197 (1970)

Can. J. Chem. Downloaded from www.nrcresearchpress.com by 210.87.254.6 on 09/05/12
For personal use only.

Bagotskii and Vasile'v have reported some potentiodynamic studies on the electro-oxidation of ethylene glycol on smooth platinum in 1 *N* H_2SO_4 (1). The origin of potentiodynamic peaks observed by these authors is not clear, however, because complementary, steady-state, potentiostatic (point-by-point) studies were not carried out by them.

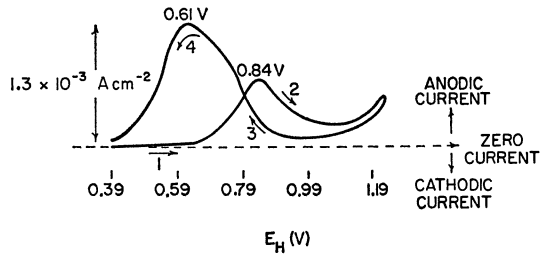

FIG. 1. A single-sweep potentiodynamic profile (16.8 mV s^{-1}) triggered from prior steady-state potential (0.39 V), corresponding to complete electrode coverage by ethylene glycol. System is smooth platinum in 1 *N* H_2SO_4 plus 2.5×10^{-1} *M* ethylene glycol. Helium atmosphere in the working compartment. Ascending peak (0.84 V) and descending peak (0.61 V) may be noted.

In our own recent work, the peaks observed in the single-sweep (from prior steady-state potential) potentiodynamic profiles (Fig. 1) in this system are closely similar to the current-reversal effects (2) observed in the steady-state (criterion of Wroblowa *et al.* (3)), point-by-point, potentiostatic current–potential relationships (Fig. 2). This would indicate that the potentiodynamic peaks at these sweep rates (16.8 to 336 mV s^{-1}) are *kinetic* in origin and are, in fact, inhibition inflections of the type reported by Gilroy and Conway (2). Further, when the potentiodynamic peaks are tested for pseudo-Faradaic nature (plot of peak current vs. scan rate) or for diffusion control (peak current vs. square root of scan rate) (4, 5), no linear relation is obtained, thus confirming our conclusion that the potentiodynamic peaks, both in the ascending and descending direction, are mainly kinetic in origin.

In Fig. 1, it is interesting to note that the anodic kinetic peak at 0.61 V appears instead of the cathodic oxide reduction peak on the descending (1.2 → 0.4 V) sweep. This would suggest recombinative removal of the oxide (or OH) by a heterogeneous reaction with ethylene glycol. For example, a reaction of the following general type may be involved

$$\mathrm{Pt.O} + \begin{matrix}\mathrm{CH_2OH}\\ |\\ \mathrm{CH_2OH}\end{matrix} + \mathrm{Pt} \rightarrow \mathrm{Pt.OH} + \mathrm{Pt} - \left[\begin{matrix}\mathrm{CHOH}\\ |\\ \mathrm{CH_2OH}\end{matrix}\right]$$

$$\mathrm{PtOH} + \mathrm{Pt} - \left[\begin{matrix}\mathrm{CHOH}\\ |\\ \mathrm{CH_2OH}\end{matrix}\right] \rightarrow \mathrm{Pt} + \mathrm{H_2O} + \mathrm{Pt} - \left[\begin{matrix}\mathrm{CHOH}\\ |\\ \mathrm{CHOH}\end{matrix}\right]$$

The *anodic* current associated with this peak would then arise by a normal Faradaic reaction of glycol oxidation on the bare surface sites available after reaction of adsorbed glycol species with the oxide.

In this respect, the potentiodynamic behavior would be somewhat similar to that of formic acid where a heterogeneous reaction between adsorbed HCOOH and OH· has been postulated.

It is believed that this brief note will resolve some points raised in connection with the origin of peaks observed in the potentiodynamic oxidation of some organics including ethylene glycol (6, 7), where it was concluded that the peaks (1) are pseudo-Faradaic in nature. Further, this

[1]This work was carried out in the Research and Development Laboratories of Sprague Electric Company, North Adams, Mass.

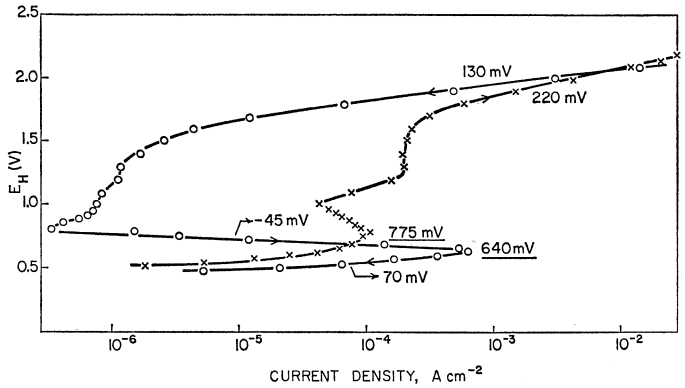

FIG. 2. A steady-state, potentiostatic (point-by-point), current–potential relationship on smooth platinum in 1 *N* H_2SO_4 plus 2.5×10^{-1} *M* ethylene glycol under helium atmosphere. ×, Ascending direction of potentials; ○, descending direction potentials. Ascending current reversal point (0.775 V) and descending current reversal point (0.640 V) may be noted.

example suggests that the indiscriminate use of potentiodynamic method for determining the electrode "coverage" does not always yield valid results. It is important that the *origin* of potentiodynamic peaks be established in such studies.

The author is grateful to the referees for helpful comments.

1. V. S. BAGOTSKII and Y. B. VASILE'V. Electrochim. Acta, **9**, 869 (1964).
2. D. GILROY and B. E. CONWAY. J. Phys. Chem. **69**, 1259 (1965).
3. H. WROBLOWA, B. PIERSMA, and J. O'M. BOCKRIS. J. Electroanal. Chem. **6**, 401 (1963).
4. A. K. VIJH. Ph.D. Thesis. University of Ottawa, Ottawa, Canada. 1966.
5. A. K. VIJH and B. E. CONWAY. J. Phys. Chem. **71**, 3655 (1967).
6. J. O'M. BOCKRIS. J. Electrochem. Soc. **113**, 1157 (1966).
7. B. E. CONWAY. J. Electrochem. Soc. **113**, 1157 (1966).

Evidence for a 'block-type' structure in the main chain of the cell-wall mannan from *Candida* species PRL 1S20[1]

P. A. J. GORIN AND J. F. T. SPENCER
Prairie Regional Laboratory, National Research Council, Saskatoon, Saskatchewan

Received August 8, 1969

Evidence for a 'block-type' structure involving α-(1→3)- and -(1→6)-D-mannopyranosyl units from the mannan in *Candida* species PRL 1S20 is presented.

Canadian Journal of Chemistry, **48**, 198 (1970)

In a previous publication the branched-chain mannan obtained from cells of *Candida* species PRL 1S20 by extraction with hot aqueous alkali has been shown to contain a main chain not previously found in other yeast mannans (1). The main chain was obtained from the mannan by a Smith degradation incorporating mild hydrolytic conditions. Methylation-fragmentation – gas–liquid chromatography (g.l.c.) analysis gave the methyl glycosides of 2,3,4,6-tetra-*O*-, 2,3,4-, and 2,4,6-tri-*O*-methylmannose. No methyl di-*O*-methyl-mannosides were detected. After corrections for the response of the g.l.c. detector are made, a respective 1:4.3:7.0 molar ratio of the fragments can be calculated. This ratio indicates a linear mannan with an average size of about 12 units and its specific rotation of +55° shows a preponderance of

[1]Issued as NRCC No. 10960

Can. J. Chem. Downloaded from www.nrcresearchpress.com by 210.87.254.6 on 09/05/12
For personal use only.

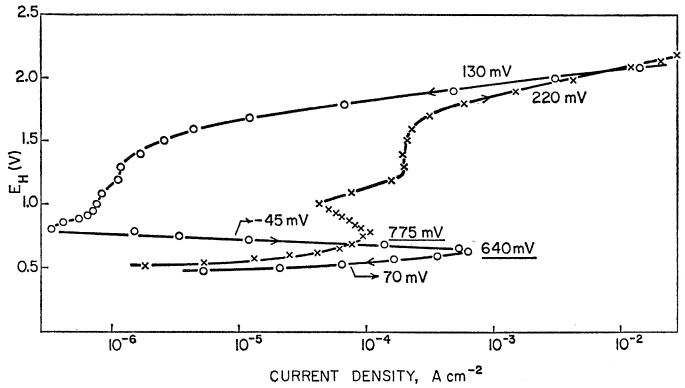

FIG. 2. A steady-state, potentiostatic (point-by-point), current–potential relationship on smooth platinum in 1 *N* H_2SO_4 plus 2.5×10^{-1} *M* ethylene glycol under helium atmosphere. ×, Ascending direction of potentials; ○, descending direction potentials. Ascending current reversal point (0.775 V) and descending current reversal point (0.640 V) may be noted.

example suggests that the indiscriminate use of potentiodynamic method for determining the electrode "coverage" does not always yield valid results. It is important that the *origin* of potentiodynamic peaks be established in such studies.

The author is grateful to the referees for helpful comments.

1. V. S. BAGOTSKII and Y. B. VASILE'V. Electrochim. Acta, **9**, 869 (1964).
2. D. GILROY and B. E. CONWAY. J. Phys. Chem. **69**, 1259 (1965).
3. H. WROBLOWA, B. PIERSMA, and J. O'M. BOCKRIS. J. Electroanal. Chem. **6**, 401 (1963).
4. A. K. VIJH. Ph.D. Thesis. University of Ottawa, Ottawa, Canada. 1966.
5. A. K. VIJH and B. E. CONWAY. J. Phys. Chem. **71**, 3655 (1967).
6. J. O'M. BOCKRIS. J. Electrochem. Soc. **113**, 1157 (1966).
7. B. E. CONWAY. J. Electrochem. Soc. **113**, 1157 (1966).

Evidence for a 'block-type' structure in the main chain of the cell-wall mannan from *Candida* species PRL 1S20[1]

P. A. J. GORIN AND J. F. T. SPENCER
Prairie Regional Laboratory, National Research Council, Saskatoon, Saskatchewan

Received August 8, 1969

Evidence for a 'block-type' structure involving α-(1→3)- and -(1→6)-D-mannopyranosyl units from the mannan in *Candida* species PRL 1S20 is presented.

Canadian Journal of Chemistry, **48**, 198 (1970)

In a previous publication the branched-chain mannan obtained from cells of *Candida* species PRL 1S20 by extraction with hot aqueous alkali has been shown to contain a main chain not previously found in other yeast mannans (1). The main chain was obtained from the mannan by a Smith degradation incorporating mild hydrolytic conditions. Methylation-fragmentation – gas–liquid chromatography (g.l.c.) analysis gave the methyl glycosides of 2,3,4,6-tetra-*O*-, 2,3,4-, and 2,4,6-tri-*O*-methylmannose. No methyl di-*O*-methyl-mannosides were detected. After corrections for the response of the g.l.c. detector are made, a respective 1:4.3:7.0 molar ratio of the fragments can be calculated. This ratio indicates a linear mannan with an average size of about 12 units and its specific rotation of +55° shows a preponderance of

[1]Issued as NRCC No. 10960

Can. J. Chem. Downloaded from www.nrcresearchpress.com by 210.87.254.6 on 09/05/12
For personal use only.

Can. J. Chem. Downloaded from www.nrcresearchpress.com by 210.87.254.6 on 09/05/12
For personal use only.

3-*O*-linked α-D-mannopyranose units, although the configurations of the 6-*O*- substituted units are uncertain. (It appears that the 3-*O*- and 6-*O*-substituted units occur in the same molecule since 2 successive Smith degradations of the *Candida* PRL 1S20 mannan gave a mannosyl glycerol (1).) This type of main-chain differs from those of the more common α-(1 → 6)-D-mannopyranose (1–6) and α-(1 → 3)-D-mannopyranose types (7, 8) and the linear mannan containing alternating β-(1 → 3)- and β-(1 → 4)-linked D-mannopyranose units (9).

In order to determine the sequence of (1 → 6)- and (1 → 3)- linkages in the *Candida* PRL 1S20 mannan main-chain, the polyalcohol derived by successive treatments of the undegraded mannan with sodium periodate and sodium borohydride was partially cleaved by acetolysis. This procedure splits (1 → 6)-linkages in mannans in preference to (1 → 2)- and (1 → 3)-linkages (10). Deacetylation of the products and paper chromatography showed mannose and oligosaccharides which appeared to have a maximum length of 5 units. These were isolated by cellulose column chromatography (yields in Table 1).

TABLE 1

Yields and specific rotations of fragments obtained following partial acetolysis of *C. Candida* PRL 1S20 mannan polyalcohol

Fragment obtained following partial acetolysis of *Candida* PRL 1S20 mannan polyalcohol	Yield (%) based on polyalcohol	Specific rotation (°), 0.1% solution at 25 °C
Mannose	2	—
Disaccharide	4	+61
Trisaccharide	3	+62
Tetrasaccharide	3	+79
Pentasaccharide	1	+88

Methylation-fragmentation – g.l.c. analysis of each oligosaccharide gave methyl 2,3,4,6-tetra-*O*- and methyl 2,4,6-tri-*O*-methylmannoside indicating 3-*O*-linked pyranose structures. The chain length of each oligosaccharide was found as follows. Their reducing ends were converted to 2-*O*-linked-D-arabinitol units by successive treatments with lead tetraacetate and sodium borohydride (11). The resulting polyols were oxidized with sodium periodate and the amounts of formaldehyde formed, as estimated by the chromotropic acid method, were in accord with the chain lengths suggested by the paper chromatographic mobility of the parent mannose oligosaccharides.

The specific rotations of the di-, tri-, tetra-, and pentasaccharide (Table 1) confirm that the 3-*O*-linkages have an α-configuration. Isolation of these fragments and comparison with the ratio of 3-*O*- to 6-*O*-linked D-mannopyranose units in the mannan shows that the main chain of *Candida* PRL 1S20 mannan does not contain 3-*O*-α- and 6-*O*-linked units evenly distributed along its length. Rather, a 'block-type' structure containing up to four consecutive α-(1 → 3)-linkages is indicated, which contrasts with the regular alternating structure of the β-(1 → 3)-, β-(1 → 4)-linked mannan (9).

Experimental

Conversion of Candida PRL 1S20 Mannan to its Polyalcohol

The mannan (1.50 g) was dissolved in water (25 ml) and sodium periodate (3.5 g) added, precautions being taken to prevent overheating. After 2 days, excess acetic acid (200 ml) was added and the precipitate of polyaldehyde which formed was removed by filtration; yield 1.38 g. The polyaldehyde was shaken in a solution of sodium borohydride (0.4 g) in water (50 ml) for 3 h. Excess reagent was then destroyed by addition of acetic acid, and the solution treated with a mixture of Amberlite IR120 (H^+ form) and Dowex 1 resin (bicarbonate form). The solution obtained after filtration was lyophilized to give a polyalcohol (1.21 g), which had the fluffy state required for the following partial acetolysis procedure.

Partial Acetolysis of Candida PRL 1S20 Polyalcohol

The polyalcohol (1.21 g) was partially acetolyzed (10) for 24 h with the reagent proportions used by Lee and Ballou (12). The product was deacetylated and the free sugars corresponded on a paper chromatogram (solvent: *n*-butanol – ethanol – water 3:2:2 v/v/v; spray: ammoniacal silver nitrate) to glycerol, mannose and 3-*O*-α-D-mannopyranosyl-D-mannose and higher oligosaccharides. The higher oligosaccharides had chromatographic rates, relative to lactose, of 1.1, 0.93, and 0.54, which were identical to those of α-(1 → 2)-linked D-mannopyranose tri-, tetra-, and pentasaccharides, respectively.

Isolation and Identification of Oligosaccharide Fragments

The product obtained by partial acetolysis of the *Candida* PRL 1S20 mannan polyalcohol was fractionated on a cellulose column using acetone–water mixtures in proportions described in a previous publication (1). The yields and specific rotations of the fragments are presented in Table 1. Hydrolysis of each fraction gave mannose only.

The di-, tri-, tetra-, and pentasaccharides were each partially methylated by the Haworth technique (13), care being taken to maintain the p*H* of the solution at 7–8 in the early stages of the reaction. After heating at 100° for 3 h, the alkali was neutralized and each solution extracted continuously with chloroform. The extracted products were completely methylated by the Kuhn procedure (14), each permethylated product showing an absence of O—H

absorption in the infrared at 3600 cm^{-1}. The methylated materials were converted to methyl *O*-methyl mannosides and their trimethylsilyl derivatives, which were analysed by g.l.c. using known standards (15). From each oligosaccharide, the methyl glycosides of only 2,3,4,6-tetra-*O*- and 2,4,6-tri-*O*-methylmannose could be detected.

Each oligosaccharide was successively treated with lead tetraacetate and excess sodium borohydride (11), converting their 3-*O*-linked D-mannopyranose reducing end-units to 2-*O*-linked D-arabinitol units. In a typical reaction the 3-*O*-linked D-mannopyranose oligosaccharide (10 mg) was dissolved in water (0.1 ml) and acetic acid (1 ml) added. Molar equivalents (1.2) of a 1% lead tetraacetate in acetic acid were added and after 10 min it was followed by 1.1 molar equivalents of oxalic acid in acetic acid. After 1 h the precipitate of lead oxalate was filtered off and the filtrate evaporated to dryness. Sodium borohydride (10 mg) was added and in 1 h the reagent was destroyed with excess acetic acid. The solution was shaken with Amberlite IR120 to remove cations and was then filtered and the filtrate evaporated to dryness. Repeated addition of methanol followed by evaporation removed boric acid. Traces of inorganic material were removed with an aqueous slurry of Amberlite IR120 (H^+ form) and Dowex 1-X8 (bicarbonate form). The slurry was filtered and the solution evaporated. The product gave a single spot on a paper chromatogram (solvent: *n*-butanol – ethanol – water 40:11:19 v/v/v spray ammoniacal silver nitrate). Each arabinitol derivative thus obtained was treated with excess sodium periodate for 1 h and the amounts of formaldehyde produced determined by a chromotropic acid method used for estimation of glycerol (16). The yields of formaldehyde in mole/mole were as follows: trisaccharide, 0.86; tetrasaccharide, 0.83; pentasaccharide, 0.88.

1. P. A. J. Gorin, J. F. T. Spencer, and R. J. Magus. Can. J. Chem. **47**, 3569 (1969).
2. G. H. Jones and C. E. Ballou. J. Biol. Chem. **244**, 1043 (1968).
3. G. H. Jones and C. E. Ballou. J. Biol. Chem. **244**, 1052 (1968).
4. P. A. J. Gorin and J. F. T. Spencer. Can. J. Chem. **46**, 2299 (1968).
5. P. A. J. Gorin, J. F. T. Spencer, and S. S. Bhattacharjee. Can. J. Chem. **47**, 1499 (1969).
6. P. A. J. Gorin, J. F. T. Spencer and D. E. Eveleigh. Carbohyd. Res. To be published.
7. P. A. J. Gorin and J. F. T. Spencer. Can. J. Chem. **45**, 1543 (1967).
8. P. A. J. Gorin and J. F. T. Spencer. Can. J. Chem. **46**, 3407 (1968).
9. P. A. J. Gorin, K. Horitsu, and J. F. T. Spencer. Can. J. Chem. **43**, 950 (1965).
10. P. A. J. Gorin and A. S. Perlin. Can. J. Chem. **34**, 1796 (1956).
11. A. J. Charlson and A. S. Perlin. Can. J. Chem. **34**, 1200 (1956).
12. Y.-C. Lee and C. E. Ballou. Biochem. **4**, 257 (1965).
13. W. N. Haworth. J. Chem. Soc. **8**, (1915).
14. R. Kuhn, H. Trischmann, and I. Low. Angew. Chem. **67**, 32 (1955).
15. S. S. Bhattacharjee and P. A. J. Gorin. Can. J. Chem. **47**, 1207 (1969).
16. M. Lambert and A. C. Neish. Can. J. Res. *B***28**, 83 (1950).

Can. J. Chem. Downloaded from www.nrcresearchpress.com by 210.87.254.6 on 09/05/12
For personal use only.

Can. J. Chem. Downloaded from www.nrcresearchpress.com by 210.87.254.5 on 09/05/12
For personal use only.

Molecular size distributions in multichain polymers: application of polymer theory to silicate melts[1]

C. R. MASSON, I. B. SMITH, AND S. G. WHITEWAY
Atlantic Regional Laboratory, National Research Council of Canada, Halifax, Nova Scotia

Received November 24, 1969

Expressions developed previously by Flory and by the authors for molecular size distributions in branched polymers were used to derive theoretical curves of activity vs. composition in binary silicate melts. In contrast with curves based on the Flory distribution those derived from our result were in good agreement with experiment over the entire range of compositions up to the maximum degree of polymerization allowed by the theory. The comparison is illustrated for the systems $PbO–SiO_2$ and $SnO–SiO_2$.

Canadian Journal of Chemistry, **48**, 201 (1970)

Introduction

In a recent paper (1) we derived a theoretical expression for N_x, the mole fraction of x-mers formed by self-condensation of multifunctional monomers, which differed from that of Flory (2).

On the basis of Flory's expression and ours, it is possible to derive theoretical curves of activity vs. composition for binary silicate melts $MO–SiO_2$. The purpose of this communication is to compare the results and show that our expression fits available data over the entire range of applicability of the theory whereas Flory's does not.

Calculation of Activities

The treatment is an extension of a previous approach (3, 4) which was limited to consideration of linear chains. Consider the equilibrium

[1] $$2SiO_4^{4-} \rightleftarrows Si_2O_7^{6-} + O^{2-}$$

Assuming ideal mixing of polyionic segments we may substitute ion fractions for activities in the expression for the equilibrium ratio

[2] $$k_{11} = N_2 N_{O^{2-}}/N_1^2$$

Substituting for N_1 and N_2 from each theory in eq. [2] and combining the result with the Temkin (5) equation

[3] $$a_{MO} = N_{M^{2+}} N_{O^{2-}}$$

where $N_{M^{2+}}$ is unity for a binary system, we obtain the activity of MO as a function of k_{11} and α, the fraction of functional groups that have condensed. The results are, for the Flory distribution

[4] $$\frac{a_{MO}}{1 - a_{MO}} = \frac{k_{11}(1 - \alpha)^2}{2\alpha(1 - 2\alpha)}$$

and, for our expression

[5] $$\frac{a_{MO}}{1 - a_{MO}} = \frac{k_{11}\left(1 - \frac{2\alpha}{3}\right)}{2\alpha}$$

In deriving these equations, both our expression and that of Flory were modified by inclusion of the term $(1 - N_{O^{2-}})$ to allow for the product of condensation, as described previously (1).

As will be shown in a subsequent publication (6), α may be expressed readily in terms of the mole fraction of SiO_2, yielding the equation

[6] $$\alpha = \frac{1 - (1 - a_{MO})\left(\frac{1}{N_{SiO_2}} - 2\right)}{2}$$

without additional assumptions.

Combination of eq. [6] with either eq. [4] or eq. [5] allows the activity of MO to be expressed as a function of the mole fraction of SiO_2 for selected values of k_{11}. Such curves are shown in Figs. 1 and 2.

Comparison with Experiment

In Fig. 1, curve *1* is based on our expression for the distribution, with $k_{11} = 0.196$; curve *2* was derived from Flory's expression with the

[1]NRCC No. 111 46.

same value of k_{11}. The experimental data are those of three independent groups of investigators (7–9). Both expressions yield activities in good agreement with experiment at low silica contents, but the curve based on the Flory distribution shows departure from the data when N_{SiO_2} exceeds about 0.3. It passes through a minimum at $N_{SiO_2} = 0.406$, $a_{PbO} = 0.282$. Substitution of these values in eq. [6] shows that the minimum occurs at $\alpha = 1/3$.

Similarly, in Fig. 2, curve *1* is based on our expression with $k_{11} = 2.55$ and curve *2* represents that of Flory with the same value of k_{11}. Curve *3* represents a further attempt to fit the data (10) by Flory's expression, using $k_{11} = 1.443$. The minima in curves *2* and *3* each correspond again to $\alpha = 1/3$.

The anomaly at $\alpha = 1/3$ predicted by Flory's expression was previously considered to represent the gel point, thought to occur at $\alpha = 1/(f - 1)$, where f is the functionality of the monomer. No such anomaly is predicted by our equation and none is observed in binary silicate melts. Activities based on our distributions vary smoothly with composition over the entire range

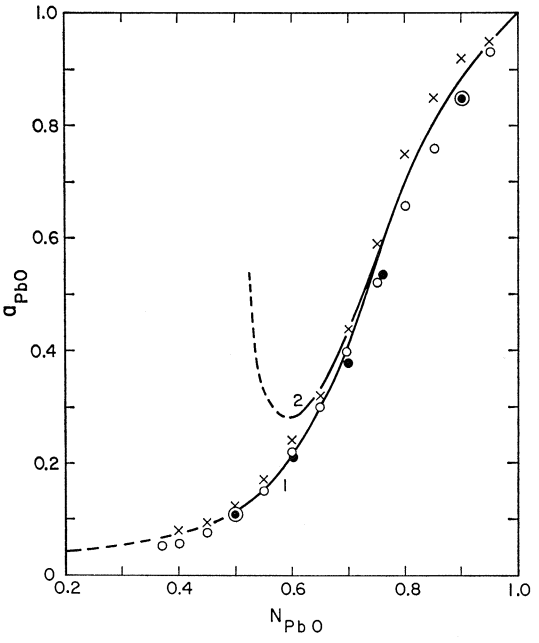

FIG. 1. Activity plotted against mole fraction of PbO for the system PbO–SiO_2 at 1000 °C. ○, Richardson and Webb (7); ●, Sridhar and Jeffes (8); ×, Charette and Flengas (9). The curves are theoretical, based on (*1*) our expression and (*2*) Flory's expression for the molecular size distribution, with $k_{11} = 0.196$.

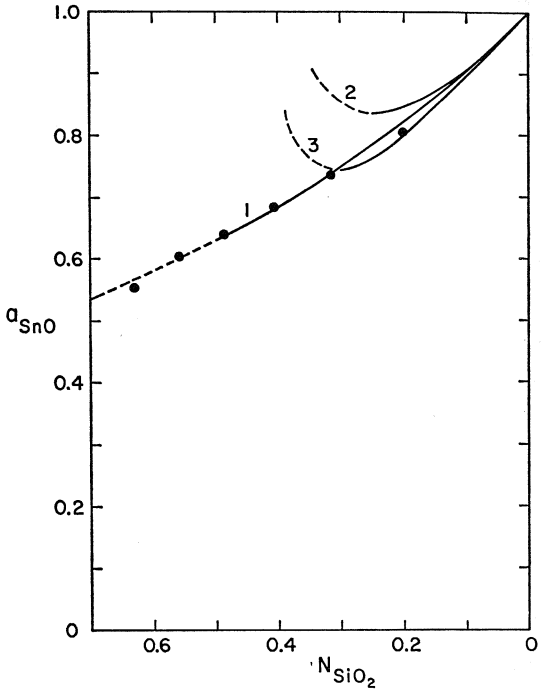

FIG. 2. Activity of SnO plotted against mole fraction of SiO_2 for the system SnO–SiO_2 at 1100 °C. ●, Kozuka, Siahaan, and Moriyama (10). The curves are theoretical, based on (*1*) our expression with $k_{11} = 2.55$, (*2*) Flory's expression with $k_{11} = 2.55$, and (*3*) Flory's expression with $k_{11} = 1.443$.

and are in good agreement with experiment at all compositions up to $\alpha_{max} = 1/2$, the maximum allowable value of α if intramolecular condensation is neglected. Similar good agreement is found (6) for other binary systems.

These results provide experimental support for the expressions we have derived for molecular size distributions in branched polymers.

1. S. G. WHITEWAY, I. B. SMITH, and C. R. MASSON Can. J. Chem. This issue.
2. P. J. FLORY. Principles of polymer chemistry. Cornell University Press, Ithaca, New York. 1953.
3. C. R. MASSON. Proc. Roy. Soc. London, **A287**, 201 (1965).
4. C. R. MASSON. J. Amer. Ceram. Soc. **51**, 134 (1968).
5. M. TEMKIN. Acta Physicochim. U.R.S.S. **20**, 411 (1945).
6. C. R. MASSON, I. B. SMITH, and S. G. WHITEWAY. To be published.
7. F. D. RICHARDSON and L. E. WEBB. Trans. Inst. Mining Met. **64**, 529 (1955).
8. R. SRIDHAR and J. H. E. JEFFES. Trans. Inst. Mining Met. **76**, C44 (1967).
9. G. G. CHARETTE and S. N. FLENGAS. Can. Met. Quart. **7**, 191 (1968).
10. Z. KOZUKA, O. P. SIAHAAN, and J. MORIYAMA. Trans. Jap. Inst. Metals, **9**, 200 (1968).

Can. J. Chem. Downloaded from www.nrcresearchpress.com by 210.87.254.5 on 09/05/12
For personal use only.

Can. J. Chem. Downloaded from www.nrcresearchpress.com by 210.87.254.6 on 09/05/12
For personal use only.

Canadian Journal of Chemistry

Published by THE NATIONAL RESEARCH COUNCIL OF CANADA

VOLUME 48 JANUARY 15, 1970 NUMBER 2

Volume changes in electrolytic hydrogen evolution at mercury in aqueous hydrochloric acid[1]

FRANK R. SMITH[2] AND HANS-ULRICH HEINTZE[3]

Chemistry Department, Memorial University of Newfoundland, St. John's, Newfoundland

Received June 5, 1969

Volume changes at a mercury cathode in hydrogen-saturated aqueous 0.1 *M* hydrochloric acid during electrolysis at 25 °C are less than those predicted by Faraday's Law

$$2H^+_{aq} + 2e^- \text{ (metal)} = H_2(g)$$

over a range of current densities from 0.4 to 83 μA mm^{-2}. Difficulties attributable to the anodic reaction of mercury were found using an apparatus similar to that of Müller (1) but constructed entirely of glass. A two-compartment cell proved to be advantageous in isolating the cathode reaction. Rates of volume change attributable to formation of $H_2(g)$ almost invariably increased with time of electrolysis but were always below expectation. In agreement with Müller, an increase of volume was observed after electrolysis. The evidence is consistent with formation and subsequent decomposition of a hydrogen amalgam. It suggests that, contrary to the usual assumptions (2), hydronium-ion discharge is not the slowest step in the overall hydrogen gas-producing reaction.

Canadian Journal of Chemistry, **48**, 203 (1970)

Introduction

The stoichiometry or non-stoichiometry of the electrolytic hydrogen evolution reaction (h.e.r.) is of importance for elucidating the mechanism. Volume measurements offer a comparatively simple method for determining the extent to which the process actually conforms to the equation

[1] $$2H_3O^+_{aq} + 2e^- \text{ (metal)} = 2H_2O + H_2(g)$$

However, few volumetric studies have been reported, so that the stoichiometry of the reaction must remain in doubt. Indeed, Lingane (3) reports that bright platinum electrodes used in sodium sulfate gas coulometers give less than theoretical yields of hydrogen and oxygen at <0.5 mA mm^{-2}, the error being about 4% at 0.1 mA mm^{-2}. Hydrogen peroxide formation is blamed for the decreased yield in these mixed systems.

Separate studies of hydrogen and oxygen evolution are needed. Two previous hydrogen studies have been made with mercury cathodes. Jofa's early study at up to 0.1 μA mm^{-2} with 3 *M* hydrochloric acid and other solutions remains unpublished, although it was reported by Frumkin (4) to give perfect agreement with electrical measurements over "a sufficiently long period of observation". Jofa evidently collected and measured the hydrogen itself. The irregular escape of bubbles from the metal surface makes this difficult and necessitates the "long period of observation" to average out irregularities. The alternative of measuring total volume changes offers the advantage that bubbles attached to the metal are included. This method used by Müller (1) resulted, however, in disagreement between volumetric and electrical measurements; only 40 to 50% of theoretical volume changes occurred during electrolysis, although subsequent changes brought the total to around 87%.

The present work was begun to clarify the disagreement between Jofa (4) and Müller (1). It forms part of a reinvestigation (5–7) of the hydrogen evolution reaction at mercury, the

[1]This research was supported, in part, by the Defence Research Board of Canada, Grant number 5401/09.

[2]To whom correspondence should be addressed.

[3]Present address: Chemistry Department, McGill University, Montreal, Quebec.

current–voltage curves having previously been carefully studied by Hiskey and Post (8) and others (9). Previous work by one of us (10, 11) suggests that atomic hydrogen dissolves in lead during cathodic electrolysis. The general similarity of mercury and lead in regard to the h.e.r. (12) reinforced the view that Müller's suggestion (1), following an earlier one by Heyrovsky (13), that hydrogen amalgam formation occurs at mercury, is quite reasonable. (Actually, Müller proposed hydronium amalgam formation (1).) Unfortunately, Müller's experimental approach was poor, for it involved rubber tubing and stoppers, pinchcocks, glass taps, and, in many experiments, dropping mercury electrodes which necessitated complicated corrections for mercury in- and out-flow. Improvements in technique, essential if the hypothesis were to be seriously tested, have been made and inherent difficulties in Müller's approach are overcome. In spite of these changes, hydrogen yields of less than theoretical have been consistently observed, over a wide range of current densities and charges. Hydrogen evolution rates, obtained from the slopes of volume–time curves, are also below those expected from current measurements.

Experimental

A one-compartment cell of volume 110 ml with a 1 ml pipette graduated in 0.01 ml was used for experiments 1 to 28, whereas a two-compartment cell of catholyte volume 8 ml and with a 0.2 ml pipette graduated in 0.001 ml was used in all later work. Both cells, shown diagrammatically in Fig. 1, were of Pyrex with Teflon-sleeved glass stoppers and platinum pinch seals (ref. 14, p. 106) for electrical contact. The resistance of the second cell was ca. 140 kohm when filled with 0.1 *M* HCl. Cathode areas and volumes used in the large and small cells were 60 mm^2 and ca 0.2 ml, and 50 mm^2 and ca. 0.8 ml, respectively.

Cell cleaning was with saturated NaOH, hot concentrated HNO_3, followed by water and steaming. The mercury cup was "Desicoted" (Beckman Instruments Inc.) and the cell recleaned omitting NaOH.

Shawinigan triple-distilled mercury was pipetted into the dry cell. 0.1 *M* HCl was prepared from a constant-boiling mixture and deionized, quadruple-distilled water. It was thoroughly hydrogen saturated (Matheson prepurified, Deoxo-treated) externally *and* in the cell (for some 4 to 12 h).

An air bath at 25.0 ± 0.1 °C was used, electrolysis only being commenced when the solution meniscus was steady (1 to 4 h after H_2 saturation). A Heath IP32 was used to supply constant currents, recorded to ±0.5% with a General Radio 100.00 ohm resistor and Heath EUW 20A recorder. Time intervals were measured with a Lab-chron 1400 and the voltage across the cell with a Heath EUW 24.

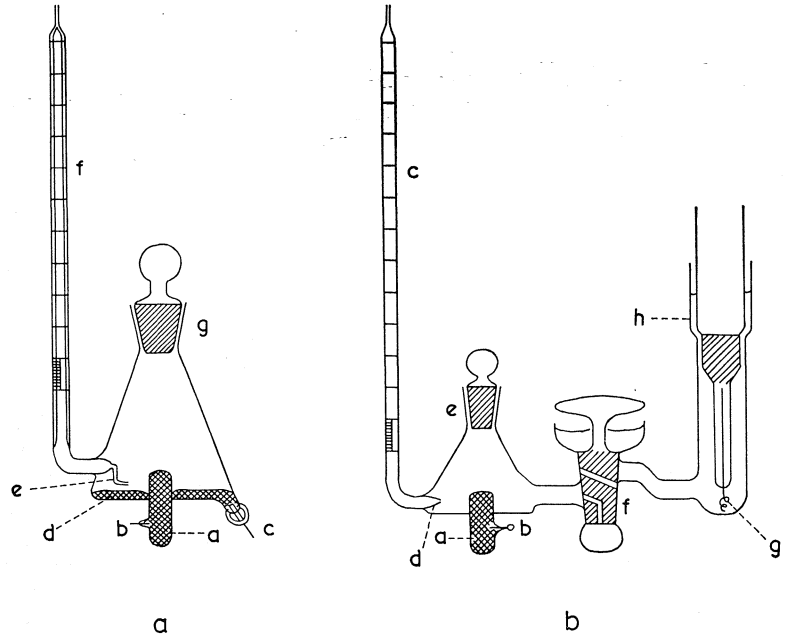

FIG. 1. (*a*) One-compartment cell: *a*, mercury cathode; *b*, platinum contact; *c*, platinum contact; *d*, mercury anode; *e*, gas inlet for saturation; *f*, 1 ml pipette, 0.01 ml graduations; *g*, Teflon-sleeved B19 stopper. (*b*) Two-compartment cell: *a*, mercury cathode; *b*, platinum contact; *c*, 0.2 ml pipette, 0.001 ml graduations; *d*, gas inlet for saturation; *e*, Teflon-sleeved B10 stopper; *f*, solution-sealed stopcock; *g*, platinum wire anode; *h*, C14 cone in grooved socket (Kontes, K25060).

Can. J. Chem. Downloaded from www.nrcresearchpress.com by 210.87.254.6 on 09/05/12
For personal use only.

Can. J. Chem. Downloaded from www.nrcresearchpress.com by 210.87.254.6 on 09/05/12
For personal use only.

Results

Over 40 experiments were carried out at current densities varying from 0.4 to 83 μA mm^{-2} and for periods from 30 min up to 24 h. Theoretical volumes and evolution rates range from 50 to nearly 800 μl, and from 2.5 nl s^{-1} to 0.65 μl s^{-1}, respectively. For calculation, the measured barometric pressure was corrected for the vapor pressure of water and the molar volume of molecular hydrogen at 25 °C, 760 Torr (24 479 ml) was computed with the aid of the second virial coefficient (15).

As Figs. 2 and 3 show, the volume–time plots were linear or gently curved. Rates were measured from the slopes of initial and final portions of these plots. The experimental points are not appreciably scattered but conform to the general trend for the experiment in question. Results for a representative group of experiments, mostly with the smaller cell, are given in Table 1. Reproducibility between duplicate experiments was poor, e.g. Exps. 30, 33, and 34 at ca. 2 μA mm^{-2} and Exps. 38 and 39 at ca. 50 μA mm^{-2}, probably because of variations in the condition of the mercury cathode.

Considering the consequences of using cells of radically different design, it is relevant to mention the results of 9 experiments at 0.100 mA, 4 with the small cell and 5 with the large one. The mean yield for the former group[4] was 76.2 ± 3.9%, as against an uncorrected mean of 62.0 ± 1.9% for the latter. The difference appears to be significant. Differences between the cells may arise because of (*a*) their leak rate, (*b*) their size, and (*c*) the reactions giving rise to volume changes in each case.

The small cell had the lower leak rate, 0.1 nl s^{-1} over a 24 h period in a blank experiment. Corrections might, therefore, be applied to the experimental yields and rates at low currents, e.g. +5% for Exps. 42 and 43 (c.f. Table 1), bringing their yields to 69.5 and 63% and the final rates to 0.0020 and 0.0018 μl s^{-1}, respectively. Corrections for other experiments (Exps. 29–41) are comparable with other estimated experimental errors of about ±1%.

Leak rates observed with the large cell, long after cessation of electrolysis, were between 0.2 and 0.8 nl s^{-1}. Taking the upper limit, this represents about 6% of expectations at 0.1 mA, which could partly account for the difference of 14% between the two cells. At 0.05 mA, a maximal correction of +12% could be applied, at 0.2 mA only +3%, while at 0.5 mA the known leak rate of 0.25 nl s^{-1} (Exp. 16) requires a negligible correction of only +½%. Clearly corrections are unnecessary at higher currents.

The large volume of the one-compartment cell could be responsible for three possible errors:

(*a*) Greater sensitivity of the measured volume to the precise temperature of the solution—it is in effect a water-plus-mercury thermometer; increased scatter of points only expected.

(*b*) Undersaturation with hydrogen initially, resulting in dissolution of desorbed hydrogen with consequent lower apparent yield; this must have occurred in Müller's work (1) for he used nitrogen only. Temperature dependence of hydrogen solubility is relevant: 100 ml of water dissolves 2.14 ml H_2 at 0 °C, 1.91 ml at 25 °C and 1.89 ml at 50 °C (16). Electromotive force measurements indicate (ref. 14, p. 95) that hydrogen saturation by bubbling is readily effected. Indeed, relief of supersaturation without stirring is said to be very slow.

(*c*) Supersaturation with hydrogen either before electrolysis (unlikely to be serious) or as a result of hydrogen desorption from mercury without bubble formation. The latter process appears probable at low currents but, at current densities of $\geqslant$10 μA mm^{-2}, bubble formation seems to occur very readily. This error is therefore likely to be large at low current densities only.

The above errors are unlikely to be serious for the small cell. Thus, a temperature change of 0.1 °C at 25 °C effects only a 0.3 μl volume change on 10 g water. The same temperature change could, at equilibrium, change the volume of hydrogen dissolved by 10 g water by at most 0.1 μl. Errors caused by supersaturation are difficult to assess quantitatively, but it should be noted that very often the volume of hydrogen evolved was comparable with that dissolved by the catholyte of the small cell at saturation (ca. 0.2 ml). It is difficult to believe that supersaturations as high as 50% could be achieved or maintained at about 30% for 20 h (c.f. Table 1, Exps. 38 and 39) particularly as the experiments in question were at 50 μA mm^{-2}. On the other hand, it is accepted that supersaturation is a serious problem with a cell volume of 110 ml, when anticipated hydrogen volumes are less than one third of the quantity dissolved at saturation.

The reactions occurring in the catholyte of the

[4]Standard deviation of the mean quoted in all cases.

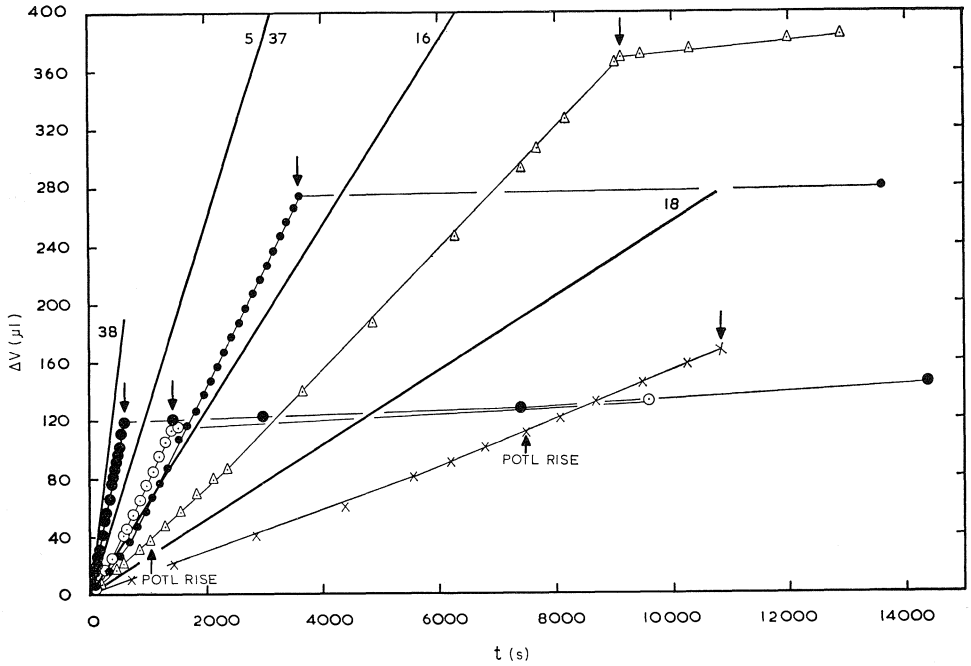

FIG. 2. Volume changes during and after electrolysis at 200 μA (crosses, Exp. 18), 500 μA (triangles, Exp. 16), 1.00 mA (open circles, Exp. 37; dots, Exp. 5), and 2.50 mA (shaded circles, Exp. 38). Arrows denote time of cessation of current or time of potential rise where indicated. Numbered lines indicate theoretical volume changes.

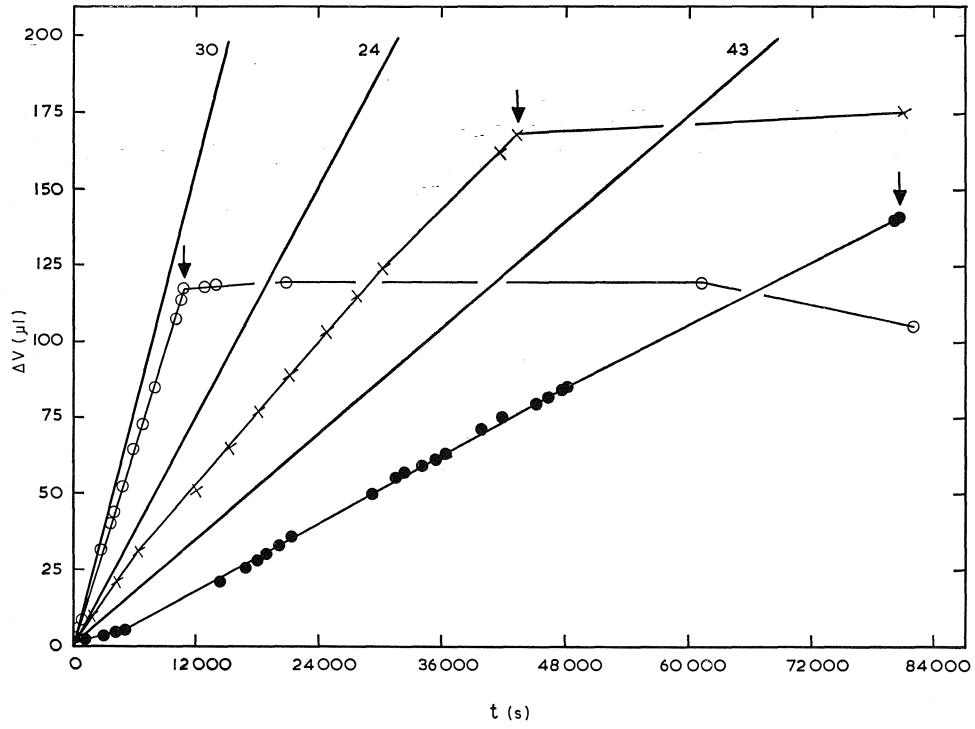

FIG. 3. Volume changes during and after electrolysis at 22.5 μA (shaded circles, Exp. 43), 50 μA (crosses, Exp. 24), and 100 μA (open circles, Exp. 30). Arrows denote time of cessation of current. Numbered lines indicate theoretical volume changes.

Can. J. Chem. Downloaded from www.nrcresearchpress.com by 210.87.254.6 on 09/05/12
For personal use only.

TABLE 1

Uncorrected hydrogen yields and evolution rates from volume measurements

Exp. No.	Current (mA)	Charge (C)	Theoretical volume (μl)	Percentage yield		Theoretical rate (μl s^{-1})	Observed rates (μl s^{-1})	
				To end of electrolysis	After electrolysis		Initial	Final
42	0.0200	0.385	51	64.5	—	0.00265	0.00065	0.0019
43	0.0225	1.81	243	58	—	0.0030	0.0011	0.0017
24	0.050	2.16	285	59	62(81 000 s)	0.0066	0.0050	0.0035
30	0.100	1.08	148	79	81(20 700 s)	0.0137	0.0100	0.0107
33	0.100	0.90	117	65	79(74 700 s)	0.0130	0.0083	0.0086
34	0.100	1.205	158	78.5	—	0.0131	0.0075	0.0115
18	0.200	2.16	287	58	—	0.0266	0.014	0.017
16	0.500	4.54	597	62	72.5(74 100 s)	0.0658	0.037	0.045
2*	1.00	2.275	301	105.5	139(50 500 s)	0.132	0.128	0.157
5	1.00	3.60	480	57.5	79(231 000 s)	0.133	0.055	0.093
37	1.00	1.40	184	61	71.5(9 600 s)	0.132	0.079	0.079
38	2.50	1.50	197	60.5	72.5(78 000 s)	0.328	0.197	0.197
39	2.50	1.75	227	50.5	67(14 800 s)	0.339	0.190	0.192
8†	5.00	6.06	789	40	ca. 190(86 400 s)	0.651	0.280	0.259

*Cell silicone greased.
†Mercury pretreated 600 s at 1 mA without volume recording.

two-compartment cell are different from those in the one-compartment cell. In the latter, reactions [2] and [3]

[2] $Hg(l) + 2H^+_{aq} + 2Cl^-_{aq} = H_2(g) + Hg_2Cl_2(c)$

[3] $2H^+_{aq} + 2Cl^-_{aq} = H_2(g) + Cl_2(g)$

may occur in parallel. Difficulties were encountered with the one-compartment cell which must have been more serious for Müller because of the very small area of the mercury anode in his "Prague vessel" (17). These difficulties were caused by the onset of reaction [3], indicated by a rise in the cell voltage (typically from 1.4 to 3.8 V at 0.2 mA and from 1.6 to 5.6 V at 1.0 mA), blocking of the calomel film, and, eventually, bubble formation on the anode. Chlorine evolution was expected to cause large positive errors but the formation of chlorine appears to be somewhat delayed (nucleation and growth of bubbles on the anode were observed *after* electrolysis) and volume changes during electrolysis were generally *less than theoretical for hydrogen alone*. Experiments 16 and 18 are examples of this, the voltage rise (c.f. Fig. 2) having no apparent effect on the shape of the volume–time plots. Volume changes after electrolysis were usually greater when reaction [3] was operative, as expected.

If only reaction [2] is operative, use of eq. [4] for theoretical volumes assumes that negligible volume changes occur in the condensed phases, a reasonable assumption. The true overall volume change is

$$[4]\quad \Delta \bar{V}_1 = \frac{Q}{2F}\left(\bar{V}_{H_2(g)}{}^{T,P-P_{H_2O}} + \bar{V}_{Hg_2Cl_2(c)}\right) - \frac{Q}{F}\left(\bar{V}_{HCl,0.1M} + \bar{V}_{Hg}\right)$$

where $\bar{V}$'s are molar or partial molar volumes as appropriate. Reaction [3] could, in principle, be avoided by use of a sufficiently large anode (3700 mm^2 used in present work) or by use of a two-compartment cell. Confinement of the volume changes to the cathode compartment involves assumptions of electroneutrality because of the transport effects which are presumed to occur. Then the overall reaction is much simplified to

[5] $2H^+_{aq} = H_2(g)$

and the volume change is

$$[6]\quad \Delta \bar{V}_2 = \frac{Q}{2F}\bar{V}_{H_2}{}^{T,P-P_{H_2O}} - 0.169\frac{Q}{F}\bar{V}_{HCl,0.1M}$$

where 0.169 is the transport number of chloride ion in 0.1 *M* HCl (18) at 25 °C.

Terms other than the first in eqs. [4] and [6] comprise only 0.1 and 0.025%, respectively, and will be disregarded.

Can. J. Chem. Downloaded from www.nrcresearchpress.com by 210.87.254.6 on 09/05/12
For personal use only.

Can. J. Chem. Downloaded from www.nrcresearchpress.com by 210.87.254.6 on 09/05/12
For personal use only.

Returning to the results, the mean corrected yield was found to be[5] 62.15 ± 2.45%, disregarding two experiments in which silicone grease had been applied to the stopper of the cell. In these experiments (Exp. 2 of Table 1 and one other), yields and rates close to the theoretical were obtained. Apparently the surface-active substance facilitated the formation of H_2, although an alternative possibility is provided by Cl_2 evolution which led to 139% yield in 13 h (Exp. 2).

The mean yield differs substantially from 100% and no single experiment was closer than 82.5% (in the absence of surfactants). The yields were plotted (not shown) as functions of current density and of charge. The mean yields appear to decrease as current density increases and, less obviously, as charge increases. Since most high charge experiments were performed with the larger cell, this conclusion is uncertain because of the disadvantages of this cell mentioned above. Mean corrected yields at different currents are: 66.25 ± 3.25% (0.021 mA), 64.6 ± 7.2% (0.05 mA), 68.3 ± 3.1% (0.1 mA), 54.65 ± 6.15% (0.2 mA), 61.8% (0.5 mA), 48.4 ± 4.5% (1.0 mA), 41.2% (1.25 mA), 56.3 ± 2.9% (2.5 mA), 40.0% (5.0 mA).

With regard to the dependence on charge, it may be noted that in several experiments the observed evolution rate increased (cf. Table 1, columns 8 and 9). This could imply increased yields as the charge increases and, in one experiment, repeated electrolysis of the same electrode and solution, only opening the tap to allow the pipette level to fall, resulted in a higher yield each time. On repetition, however, the opposite trend was found, thus no firm conclusion is possible.

A case therefore exists for the view that quantitative conversion of H^+_{aq} ions to H_2 gas does not keep pace with the passage of current across the interface. Because this conclusion is novel it is desirable to consider alternative explanations of the experimental findings. The most obvious possibility is that current was used in some competing cathodic reaction, such as the reduction of oxygen or foreign metal ions in solution or the reduction of calomel or dissolved mercurichloride complex ions (ref. 14, p. 149). Such processes would, of course, not result in volume changes comparable with those accompanying liberation of an equivalent quantity of hydrogen. It is conceivable that such processes as those mentioned above could account for increases in the rate of volume change as electrolysis proceeded, i.e., that they consumed a significant portion of the current initially. However, precautions were taken to ensure that the acid solution was relatively free from base metal ions and from oxygen. Only trace amounts of these could have been present and these would not be able to support a substantial fraction of the current, especially in an unstirred system. The view that alkali metal cations might be responsible can be discounted, for these, too, could not have been present in high concentration, and hydronium-ion discharge precedes that of alkali cations in acid solution. If any further argument is needed it may be pointed out that the excellent hydrogen overpotential data of Hiskey and Post (8) were obtained using 0.1 *M* HCl in *unstirred* solution. It is not credible that 20% of the charge could have been consumed by processes involving impurities. Finally, the observed growth of hydrogen yield must also be explained; this rules out large charge consumptions by oxygen, calomel, or mercuri-entities.

It is quite another matter to attempt a defence of Müller's experimental observations. This we cannot do, in particular, because of Müller's failure to saturate the solution initially with hydrogen, a matter of crucial importance in our view.

Discussion

Frumkin (2) has summarized the evidence for considering reaction [7] as the slowest stage in the h.e.r. at mercury in acid solution.

[7] $$H_3O^+_{aq} + e^-(\text{mercury}) + Hg(l) = H_2O(l) + Hg - H_{ads}$$

The argument rests largely on the absence of a measurable hydrogen coverage (θ_H) on mercury as evidenced by the lack of a pseudocapacity (2, 19). This means either that θ_H is very small or that it is potential-independent in the range of measurement. Assuming that the former is the case, the implications are that desorption of H_{ads} occurs at least as rapidly as step [7], probably by the ion-plus-atom reaction [8] or, less probably, by reaction [9]

[8] $$H_3O^+_{aq} + e^-(\text{mercury}) + Hg—H_{ads} = H_2O(l) + H_2(g) + Hg(l)$$

[9] $$2Hg—H_{ads} = 2Hg(l) + H_2(g)$$

[5] 66.75 ± 3.0% for 10 normal experiments with the small cell.

Can. J. Chem. Downloaded from www.nrcresearchpress.com by 210.87.254.6 on 09/05/12
For personal use only.

The present work indicates that hydrogen desorption does not keep pace with [7] under certain experimental conditions. The implication of the very slow volume increase after electrolysis is that step [9], the only purely chemical process, is very slow, as anticipated from knowledge about lead (20) as a recombination catalyst. It follows that hydrogen desorption as molecules occurs principally by [8] during current flow. The long-standing difficulty has been to reconcile an apparently low value of θ_H with an appreciable rate for [8], which would seem to depend linearly on θ_H. Gerischer has indicated (21) how favorable a low metal–hydrogen bond strength is to reaction [8]. The mercury–hydrogen bond is likely (2) to be weak, which helps to explain the paradox.

Weakly adsorbed hydrogen atoms, it is thought, could more readily escape from the surface, perhaps by evaporation (22) or by diffusion into the interior. The last suggestion is analogous to a hypothesis already proposed (10) for lead. The proposal of a hydrogen amalgam has been made earlier (13, 5) on the basis of incomplete evidence. Further work recently performed in this laboratory (6, 7) is in agreement with this idea. The slow growth of overpotential at mercury, already noted by Hiskey and Post (8), appears to be linked with saturation of the metal with atomic hydrogen. Detachment of hydrogen bubbles from a mercury surface under ultraclean conditions results in a potential shift (at constant current) opposite in sign to that of the slow growth; this is consistent with relief of surface supersaturation with atomic hydrogen, which otherwise accumulates continuously (6).

Diffusion of hydrogen atoms into mercury, step [10]

$$[10] \qquad Hg—H_{ads} = H_{abs}(\text{mercury}) + Hg(l)$$

competes with steps [8] and [9] and should be most rapid when θ_H is greatest, presumably at high current density. Its occurrence would result in a decreased H_2 yield, which seems to be observed most significantly at the highest current densities in the present work.

It is possible, with the aid of a fairly rapid equilibrium for step [10], to predict that conditions could be found in which θ_H is essentially potential-independent, being maintained constant by out-diffusion from the bulk metal. If this could occur, then the absence of a pseudocapacity would no longer imply a small θ_H and a major objection to step [8] as the predominant desorption step would be overcome.

Müller's discussion (1) of his results differs from the above, principally in that he envisaged the possibility of formation of hydronium amalgam or of a slowly decomposing aquated hydrogen molecule ion. We shall not discuss these possibilities further at this time, apart from remarking that we do not consider them very probable as explanations of the present results.

Thanks are due to the National Research Council of Canada and to the Defence Research Board for their generous support of this work.

1. O. H. Müller. *In* Polarography 1964. Vol. 1. *Edited by* G. J. Hills. Interscience Publishers, John Wiley and Sons, Inc., New York. 1966. p. 319.
2. A. N. Frumkin. *In* Advances in electrochemistry and electrochemical engineering. Vol. 1. Interscience Publishers, John Wiley and Sons, Inc., New York. 1961. p. 68.
3. J. J. Lingane. Electroanalytical chemistry. 2nd ed. Interscience Publishers, John Wiley and Sons, Inc., New York. 1958. pp. 452–457. J. A. Page and J. J. Lingane. Anal. Chim. Acta, **16**, 175 (1957).
4. A. N. Frumkin. Acta Physicochim. U.R.S.S., **18**, 23 (1943).
5. F. R. Smith and A. E. Wells. Nature, **215**, 1165 (1967).
6. S. N. Das and F. R. Smith. To be published.
7. F. R. Smith and S. N. Das. Unpublished results.
8. C. F. Hiskey and B. Post. J. Amer. Chem. Soc. **72**, 4203 (1950).
9. S. Jofa and K. Mikulin. Zh. Fiz. Khim. **18**, 137 (1944).
10. D. J. G. Ives and F. R. Smith. Trans. Faraday Soc. **63**, 217 (1967).
11. I. Cadersky, B. L. Muju, and F. R. Smith. Unpublished results.
12. A. N. Frumkin. *In* Advances in electrochemistry and Electrochemical Engineering. Vol. 3. *Edited by* P. Delahay. Interscience Publishers, John Wiley and Sons, Inc., New York. 1963. p. 297.
13. J. Heyrovsky. Trans Faraday Soc. **19**, 785 (1924).
14. G. J. Hills and D. J. G. Ives. *In* Reference electrodes. *Edited by* D. J. G. Ives and G. J. Janz. Academic Press, Inc., New York. 1961.
15. W. E. Deming and L. E. Shupe. Phys. Rev. **40**, 848 (1932).
16. Handbook of chemistry and physics. 45th ed. The Chemical Rubber Co., Cleveland, Ohio. 1964. p. B178.
17. E. H. Sargent and Co., Catalog No. S-29380.
18. G. M. Barrow. Physical chemistry. 2nd ed. McGraw-Hill Book Co., Inc., New York. 1966. p. 676.
19. B. E. Conway. Theory and principles of electrode processes. Ronald Press, New York. 1965. p. 173.
20. G. C. Bond. Catalysis by metals. Academic Press, Inc., New York. 1962. p. 175.
21. H. Gerischer. Z. Phys. Chem. Frankfurt, **8**, 137 (1956).
22. N. I. Kobosev. Zh. Fiz. Khim. **25**, 111 (1951); **26**, 112 (1952); **26**, 438 (1952).

Can. J. Chem. Downloaded from www.nrcresearchpress.com by 210.87.254.42 on 09/05/12
For personal use only.

Molar excess enthalpies and volumes of cyclohexane – isomeric decalin systems at 25 °C[1]

G. C. Benson, S. Murakami,[2] V. T. Lam,[3] and Jaswant Singh[4]
Division of Chemistry, National Research Council of Canada, Ottawa, Canada

Received September 4, 1969

The molar excess enthalpies and volumes of the systems cyclohexane – *cis*-decalin and cyclohexane – *trans*-decalin at 25 °C were determined by direct calorimetric and dilatometric measurements. The Flory theory of mixtures provides a useful basis for a qualitative interpretation of the results.

Canadian Journal of Chemistry, **48**, 211 (1970)

Introduction

The isothermal mixing of non-polar liquids is, in most cases, an endothermic process which can be explained semi-quantitatively in terms of differences in the dispersion forces between pairs of like and unlike molecules. In this regard, the systems cyclohexane – *cis*-decalin and cyclohexane – *trans*-decalin are of interest since they depart from the usual pattern. In particular, the formation (at 25 °C) of cyclohexane–decalin mixtures rich in cyclohexane leads to an evolution of heat, despite the fact that at lower concentrations the usual endothermic behavior is observed (1, 2).

Although the excess enthalpies and volumes of cyclohexane–decalin mixtures have been studied previously (1–4), further investigation of these interesting systems seems justified in view of the differences between the results reported and the doubts expressed regarding their reliability. The present paper describes measurements of the excess enthalpies and excess volumes of the two systems formed by mixing cyclohexane with the *cis* and *trans* isomers of decalin at 25 °C. Interpretation of the results in terms of the theory of Flory (5) is given in the Discussion section.

Experimental

Apparatus

Successive dilution techniques were used in determining both the heats and the volumes of mixing; all measurements were made at 25.00 °C. The isothermally jacketed calorimeter (6) employed for the enthalpy determinations contained a cooling module which facilitated the study of exothermic as well as endothermic processes. Over most of the concentration range the accuracy of the results is believed to be between 0.5 and 1.0 J mole^{-1}. The dilatometer of Pflug and Benson (7) was used for measuring the volume changes. In the case of equimolar mixtures, these could be determined with an accuracy estimated to lie between 1 and 2%. Further details of the equipment and operational procedures can be found in refs. 6 to 8.

Materials

The component liquids were purified in an F & M preparative gas chromatograph (Model 775). Spectro grade cyclohexane (Eastman Organic Chemicals) was passed through two 6 ft columns in series (both 3/4 in. diameter), one containing 18% Apiezon L on 30/60 Chromosorb W, and the other containing 20% squalane on the same solid support. The *cis* and *trans* isomers were separated from practical grade decalin (Matheson, Coleman and Bell decahydronaphthalene, containing approximately 57% of the *cis* and 43% of the *trans* isomers) using a 4 in. diameter column containing 20% Apiezon L on 30/60 Chromosorb W. Densities and refractive indices characterizing the final materials used for the enthalpy and volume measurements are given in Table 1, along with values from the literature (9, 10) for comparison.

Results

Our experimental results for the molar excess enthalpies (H^E, J mole^{-1}) and molar excess volumes (V^E, cm^3 mole) of the two systems cyclohexane (1) – *cis*-decalin (2) and cyclohexane (1) – *trans*-decalin (2) at 25.00 °C are listed in Table 2. These data are also presented graphically in Figs. 1 and 2.

The method of least squares was used to fit each set of results with an equation of the form

$$[1] \quad X^E = x_1 (1 - x_1) \sum_{p=1}^{n} c_p (1 - 2x_1)^{p-1}$$

where X^E represents either H^E or V^E, and x_1 is the mole fraction of cyclohexane. In each case, a minimum of 4 terms ($n = 4$ in eq. [1]) was needed

---

[1]NRCC No. 11 057.

[2]NRCC Postdoctorate Fellow, 1967–1969. Present address: Department of Chemistry, Faculty of Science, Osaka City University, Sumiyoshi-ku, Osaka, Japan.

[3]NRCC Postdoctorate Fellow, 1967–1969. Present address: Département de Chimie, Faculté des Sciences, Université de Sherbrooke, Sherbrooke, Quebec.

[4]NRCC Postdoctorate Fellow 1965–1967. Present address: Pollution Dynamics Corporation, 1190 Brooks Avenue, Rochester, New York.

TABLE 1

Properties characterizing the pure component liquids

Component	Density, d^{25} (g cm^{-3})			Refractive index, n_D^{20}		
	Experimental	Literature	Reference	Experimental	Literature	Reference
Cyclohexane	0.77385	0.77389	9	1.42626	1.42623	9
cis-Decalin	0.89288	0.89291	10	1.48090	1.48098	10
trans-Decalin	0.86596	0.86592	10	1.46949	1.46932	10

to represent the results adequately. The values adopted for the coefficients c_p, and the standard error of the estimate σ associated with the use of eq. [1] are summarized in Table 3; the curves in Figs. 1 and 2 were calculated from eq. [1] using these coefficients.

Results obtained in some of the previous investigations of cyclohexane–decalin mixtures are also shown in Figs. 1 and 2 for comparison with our results. Lundberg (1) reported excess enthalpies (at 25 °C) for 3 systems formed by mixing cyclohexane with isomeric decalin mixtures containing 10, 64, and 99% of the *cis* isomer, respectively. His results for the 10% *cis*-decalin mixture are quite close to our *trans*-decalin curve, but in general his values for the 64 and 99% *cis*-decalin mixtures lie above our *cis*-decalin curve. On the other hand, our *cis*-decalin curve is in good

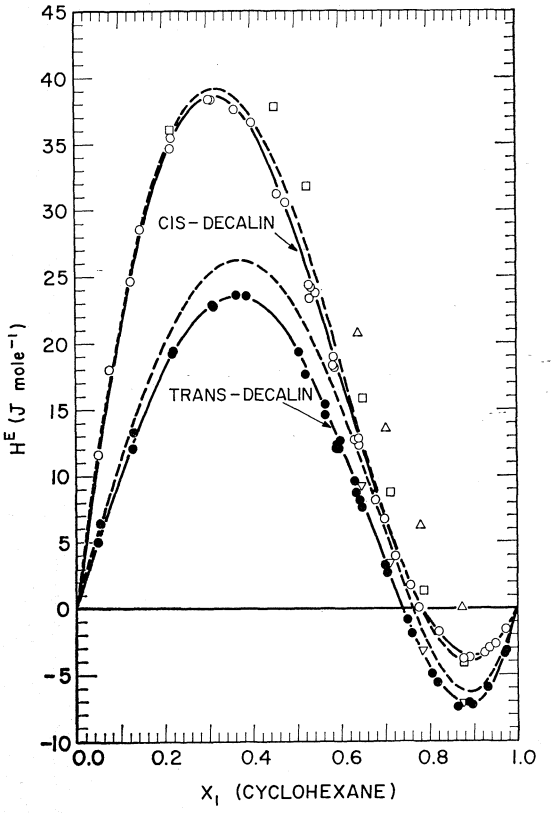

FIG. 1. Experimental molar excess enthalpies at 25 °C. Our results: ○, cyclohexane – *cis*-decalin; ●, cyclohexane – *trans*-decalin. Solid curves are least-squares representations by eq. [1]. Results of Lundberg for cyclohexane–decalin (mixture of isomers): △, 99% *cis*; □, 64% *cis*; ▽, 10% *cis*. Broken curves plotted from equations given in ref. 2 represent results of Sturtevant and Lyons.

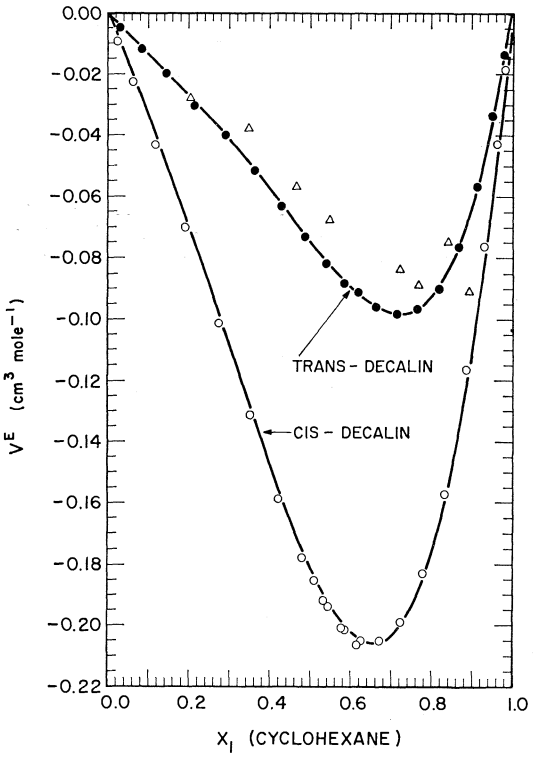

FIG. 2. Experimental molar excess volumes at 25 °C. Our results: ○, cyclohexane – *cis*-decalin; ●, cyclohexane – *trans*-decalin. Solid curves are least squares representations by eq. [1]. △, results of Gómez-Ibáñez and Wang (4) for cyclohexane – *trans*-decalin.

Can. J. Chem. Downloaded from www.nrcresearchpress.com by 210.87.254.42 on 09/05/12
For personal use only.

TABLE 2

Experimental values of the molar excess enthalpy H^E (J mole^{-1}) and molar excess volume V^E (cm^3 mole^{-1}) at 25 °C

Cyclohexane (1) – *cis*-decalin (2)				Cyclohexane (1) – *trans*-decalin (2)			
x_1	H^E	x_1	V^E	x_1	H^E	x_1	V^E
0.0536	11.69	0.0265	−0.0090	0.0508	5.15	0.0324	−0.0047
0.0803	18.07	0.0661	−0.0226	0.0601	6.50	0.0863	−0.0119
0.1282	24.76	0.1222	−0.0430	0.1323	12.13	0.1476	−0.0200
0.1495	28.60	0.1951	−0.0699	0.1340	13.35	0.2185	−0.0305
0.2188	34.67	0.2784	−0.1012	0.2226	19.22	0.2928	−0.0402
0.2219	35.55	0.3549	−0.1312	0.2277	19.45	0.3665	−0.0517
0.3071	38.44	0.4250	−0.1586	0.3123	23.01	0.4328	−0.0634
0.3101	38.30	0.4844	−0.1779	0.3153	22.98	0.4917	−0.0734
0.3662	37.63	0.5138	−0.1848	0.3689	23.70	0.5436	−0.0820
0.4056	36.65	0.5366	−0.1918	0.3941	23.66	0.5877	−0.0884
0.4614	31.25	0.5480	−0.1934	0.5091	19.32	0.6212	−0.0910
0.4816	30.60	0.5815	−0.2009	0.5262	17.63	0.6661	−0.0959
0.5324	24.39	0.5863	−0.2006	0.5697	14.57	0.7174	−0.0983
0.5356	23.45	0.6198	−0.2064	0.5705	15.35	0.7689	−0.0967
0.5367	24.22	0.6285	−0.2048	0.5967	12.44	0.8217	−0.0900
0.5465	23.88	0.6751	−0.2050	0.5980	12.13	0.8727	−0.0765
0.5862	18.34	0.7264	−0.1989	0.6033	12.04	0.9169	−0.0567
0.5877	19.00	0.7817	−0.1829	0.6039	12.69	0.9545	−0.0336
0.5899	18.02	0.8360	−0.1569	0.6363	9.59	0.9820	−0.0136
0.6350	12.70	0.8913	−0.1162	0.6395	8.74		
0.6413	12.47	0.9348	−0.0760	0.6475	8.20		
0.6438	12.84	0.9655	−0.0427	0.6524	7.65		
0.6828	8.22	0.9856	−0.0184	0.7035	3.34		
0.7024	6.78			0.7084	2.73		
0.7278	4.03			0.7525	−0.77		
0.7615	1.89			0.7633	−1.78		
0.7797	0.18			0.8088	−4.81		
0.8221	−1.69			0.8213	−5.50		
0.8805	−3.82			0.8674	−7.43		
0.8924	−3.68			0.8935	−7.06		
0.9290	−3.35			0.9003	−7.37		
0.9388	−2.98			0.9367	−5.92		
0.9529	−2.58			0.9742	−3.35		
0.9765	−1.54			0.9753	−3.10		

TABLE 3

Values of the coefficients for eq. [1] determined by the method of least squares*

System							
Component 1	Component 2	Function	c_1	c_2	c_3	c_4	σ
Cyclohexane	*cis*-Decalin	H^E	111.97	196.67	−26.60	−43.19	0.47
		V^E	−0.7280	0.5687	−0.1141	−0.0815	0.0007
Cyclohexane	*trans*-Decalin	H^E	78.37	112.43	−99.67	10.08	0.30
		V^E	−0.2980	0.3308	−0.2170	0.0344	0.0007

*Units: H^E, J mole^{-1}; V^E, cm^3 mole^{-1}.

agreement with that measured recently by Sturtevant and Lyons (2). The differences between our *trans*-decalin curve and that reported by the latter authors are larger in the endothermic region than can be attributed entirely to instrumental uncertainties. Possibly, differences in chemical purity have contributed to the discrepancy since Sturtevant and Lyons noted that, in some cases, their "results were extraordinarily sensitive to small amounts of impurities of unknown nature".

Our results for the excess volumes of cyclohexane – *trans*-decalin can be compared in Fig. 2 with those of Gómez-Ibáñez and Wang (4). The latter are more scattered but there is reasonable agreement between the two sets of data. It appears that the expansions reported by Danusso (3) for

Can. J. Chem. Downloaded from www.nrcresearchpress.com by 210.87.254.42 on 09/05/12
For personal use only.

TABLE 4
Parameters for the pure liquids at 25 °C

Component	v (cm³ mole⁻¹)	$10^3\,\alpha$ (deg⁻¹)	$10^6\,\beta$ (atm⁻¹)	v* (cm³ mole⁻¹)	T^* (°K)	p^* (J cm⁻³)	$\tilde{v}$
Cyclohexane	108.76	1.217†	115.5‡	84.27	4720	530.2	1.2906
cis-Decalin	154.84	0.851§	70.1‖	127.30	5739	542.6	1.2163
trans-Decalin	159.66	0.865§	77.0‖	130.93	5683	504.6	1.2194

†Based on density values from ref. 9.
‡Reference 19.
§Based on density values from ref. 10.
‖Calculated from the adiabatic compressibility (20*a*) and the heat capacity (20*b*).

cyclohexane–decalin (a mixture of isomers) at 30 °C are erroneous, although the conditions of that investigation are not strictly comparable with ours.

Discussion

Interpretation of the present results according to several different theories of mixtures was investigated. Neither the Scatchard–Hildebrand solubility parameter theory (11) nor the Barker quasi-lattice theory (12) appear to be very useful in providing an understanding of the results. In both of these theories, the quantity of primary interest is U_V^E, the molar excess energy at constant volume.

"Experimental" values of U_V^E were obtained from the excess enthalpies and volumes, using the thermodynamic relation

$$[2] \qquad U_V^E = H^E - T(\alpha/\beta)V^E$$

Values of α, the coefficient of thermal expansion, and of β, the isothermal compressibility, were estimated for the mixtures from data for the pure components (see Table 4) assuming additivity on a volume fraction basis. The volume term in eq. [2] is relatively large and is dominant at high concentrations of cyclohexane, completely eliminating the negative contribution from H^E, and leading to U_V^E vs. x_1 plots which for both systems are nearly symmetrical about the equimolar concentration. Thus it appears that identification of U_V^E and H^E as suggested in ref. 2 is not justified.

Values of U_V^E calculated from the Scatchard–Hildebrand theory, using solubility parameters estimated from latent heats of vaporization, are too small. They are approximately 1/3 and 1/6 of the experimental values for the *cis*- and *trans*-decalin systems, respectively.

Several Barker type models which approximately reproduced the experimental values of U^E were developed. However, none of these was satisfactory because the distinction between different kinds of contact areas in the decalin molecules was arbitrary, and it was impossible to give a reasonable interpretation of the contact interaction energies obtained for any of the different assignments.

The Flory theory (5) of mixtures provided the most interesting basis for the analysis of our results. In the remainder of this discussion, the Flory theory is reviewed briefly and its application to our results is described.

Flory Theory of Mixtures

Only the equations of the Flory theory needed for the present application are summarized here. The notation follows that of Flory closely and reference should be made to the original paper (5) for details of the derivations.

In order to deal with mixtures of molecules differing in size, a molecule is considered to be made up of r isometric portions or segments. Each segment has s intermolecular contact sites which can interact with neighboring sites. The molar volume v of a pure liquid can be written as

$$[3] \qquad \mathrm{v} = rv$$

where v is the volume of a mole of segments.

An asterisk is used to denote characteristic values of temperature, pressure, and volume. The characteristic volume is identified with the hard-core volume

$$[4] \qquad \mathrm{v}^* = rv^*$$

The reduced volume, defined by

$$[5] \qquad \tilde{v} = v/v^* = \mathrm{v}/\mathrm{v}^*$$

can be calculated from the expression

$$[6] \qquad \tilde{v} = [(1 + \tfrac{4}{3}\alpha T)/(1 + \alpha T)]^3$$

where α is the coefficient of thermal expansion.

Can. J. Chem. Downloaded from www.nrcresearchpress.com by 210.87.254.42 on 09/05/12
For personal use only.

Can. J. Chem. Downloaded from www.nrcresearchpress.com by 210.87.254.42 on 09/05/12
For personal use only.

The characteristic pressure p^* and temperature T^* are obtained from the relations

$$[7] \qquad p^* = (\alpha/\beta)T\tilde{v}^2$$

and

$$[8] \qquad T^* = T/\tilde{T}$$

where at zero pressure the reduced volume and temperature ($\tilde{T}$) satisfy the reduced equation of state

$$[9] \qquad \tilde{T} = (\tilde{v}^{1/3} - 1)/\tilde{v}^{4/3}$$

The reduced temperature appropriate for a mixture of two species of molecules (indicated by subscripts 1 and 2) at mole fraction x_1 is

$$[10] \quad \tilde{T} = (\phi_1 p_1^* \tilde{T}_1 + \phi_2 p_2^* \tilde{T}_2)/(\phi_1 p_1^* + \phi_2 p_2^* - \phi_1\theta_2 X_{12})$$

where X_{12} is a constant characterizing the difference in the energy of interaction between sites on neighboring molecules of species 1 and 2, from the average of the interactions in the pure component liquids. The segment fractions ϕ_1 and ϕ_2 are defined by

$$[11] \qquad \phi_2 = 1 - \phi_1 = x_2/(x_2 + x_1 r_1/r_2)$$

and the site fraction θ_2 by

$$[12] \qquad \theta_2 = \phi_2/(\phi_2 + \phi_1 s_1/s_2)$$

The formulae for the molar excess enthalpy and molar excess volume are

$$[13] \quad H^E = x_1 p_1^* v_1^* (\tilde{v}_1^{-1} - \tilde{v}^{-1}) + x_2 p_2^* v_2^* (\tilde{v}_2^{-1} - \tilde{v}^{-1}) + x_1 v_1^* \theta_2 X_{12} \tilde{v}^{-1}$$

and

$$[14] \qquad V^E = (x_1 v_1^* + x_2 v_2^*)(\tilde{v} - \tilde{v}^0)$$

where

$$[15] \qquad \tilde{v}^0 = \phi_1 \tilde{v}_1 + \phi_2 \tilde{v}_2$$

Exothermic heats of mixing are generally interpreted as indicating the formation of some kind of complex in the mixture. Such an interpretation is unrealistic for the present non-polar systems and it appears that their behavior is more analogous to that of systems of the *n*-alkanes, which are endothermic at room temperature, exothermic at higher temperatures, and at intermediate temperatures show a reversal of sign with composition (13, 14). Flory and co-workers (15, 16) have shown that this behavior follows qualitatively from eq. [13]. In this regard it is instructive to write eq. [13] in the form

$$[16] \quad H^E \cong x_1 v_1^* \theta_2 X_{12}/\tilde{v} + x_1 v_1^* \phi_2 [(\tilde{v}_1 - \tilde{v}_2)/\tilde{v}^0](p_2^*/\tilde{v}_2 - p_1/\tilde{v}_1) + [V^E/(\tilde{v}^0)^2](\phi_1 p_1^* + \phi_2 p_2^*)$$

which provides a good approximation for H^E when V^E is small. It is clear from eq. [16] that H^E is a sum of 3 contributions. The first term represents the contact interaction energy, the second term depends on the difference in the reduced volumes of the pure components, and the last term takes account of the effect of the volume change when the mixture is formed. For simple dispersion forces, the first term will usually be positive; the remaining terms may be of either sign, and when one or both of them is negative, the sign of H^E will depend on the relative magnitudes of the three contributions.

Values of the properties of the pure component liquids are given in Table 4, along with the corresponding values of the characteristic volumes, temperatures, and pressures, and of the reduced volumes. In order to calculate the excess properties of mixtures, the ratios r_1/r_2 and s_1/s_2 are required. Since the same hard core volume is adopted for the segments of both species

$$[17] \qquad r_1/r_2 = v_1^*/v_2^*$$

For small molecules which were approximately spherical, Abe and Flory (17) assumed that

$$[18] \qquad s_1/s_2 = (v_2^*/v_1^*)^{1/3}$$

In the present work, calculations were carried out using this assumption, and also treating the ratio s_1/s_2 as an adjustable parameter.

By definition, the square of the standard deviation between the experimental and theoretical values of H^E is given by the integral

$$[19] \quad \sigma_H^2(X_{12}, s_1/s_2) = \int_0^1 [H^E_{\text{expt}} - H^E_{\text{Flory}}(X_{12}, s_1/s_2)]^2 dx_1$$

where the dependence on X_{12} and s_1/s_2 has been indicated explicitly. The corresponding relation for the square of the standard deviation of the volumes is

$$[20] \quad \sigma_V^2(X_{12}, s_1/s_2) = \int_0^1 [V^E_{\text{expt}} - V^E_{\text{Flory}}(X_{12}, s_1/s_2)]^2 dx_1$$

Can. J. Chem. Downloaded from www.nrcresearchpress.com by 210.87.254.42 on 09/05/12
For personal use only.

TABLE 5

Summary of calculations using the Flory theory

System	Calculation	s_1/s_2	X_{12} (J cm^{-3})	σ_H (J mole^{-1})	H^E (0.5) (J mole^{-1})		σ_V (cm^3 mole^{-1})	V^E (0.5) (cm^3 mole^{-1})	
					Theory	Experimental		Theory	Experimental
Cyclohexane – *cis*-decalin	(*a*)	1.147	2.365	12.6	26.2	28.0	0.029	−0.2092	−0.1820
	(*b*)	4.60	5.351	3.1	25.3		0.024	−0.2099	
Cyclohexane – *trans*-decalin	(*a*)	1.158	1.791	8.4	15.5	19.6	0.021	−0.0713	−0.0745
	(*b*)	3.40	3.272	3.8	15.5		0.017	−0.0713	

Can. J. Chem. Downloaded from www.nrcresearchpress.com by 210.87.254.42 on 09/05/12
For personal use only.

The following calculations were carried out for each system: (*a*) s_1/s_2 was obtained from eq. [18] and the value of X_{12} which minimized σ_H^2 was determined; (*b*) s_1/s_2 and X_{12} were treated as variable parameters and their values chosen to minimize σ_H^2. In both calculations, the corresponding values of V^E and σ_V were computed from eqs. [14] and [20].

The results of the calculations are summarized in Table 5 and Figs. 3–5. It can be seen from these that the Flory theory provides reasonable estimates of V^E in both calculations; thus this function apparently is not sensitive to the method adopted in fitting H^E. On the other hand, it was not possible to adjust X_{12} to give a good fit of H^E when the value of s_1/s_2 was derived from eq. [18]. Much better fits of H^E were obtained when s_1/s_2 was treated as an adjustable parameter, but even then the exothermic parts of the curves were

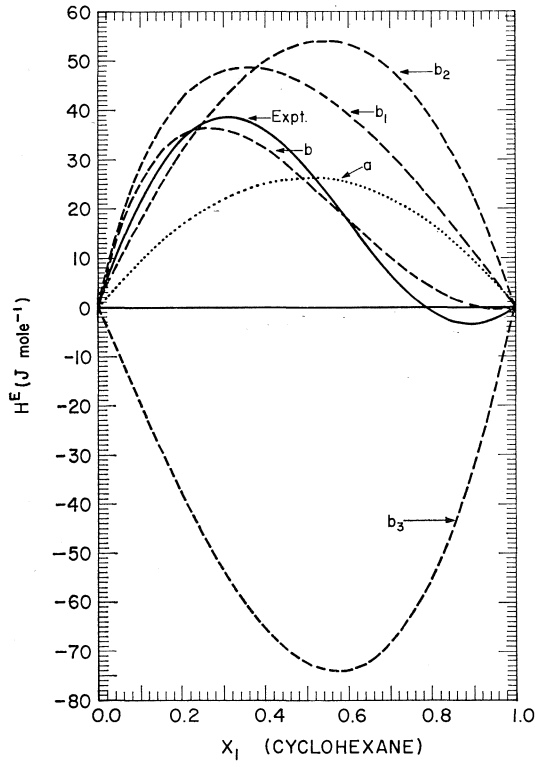

FIG. 3. Molar excess enthalpies calculated for cyclohexane – *cis*-decalin at 25 °C by the Flory theory. Curves *a* and *b*, H^E_{Flory} for calculations (*a*) and (*b*) described in text. In calculation (*b*), individual contributions for the three terms of eq. [16] are labelled b_1, b_2, and b_3, respectively. For comparison, solid curve represents our smoothed experimental results.

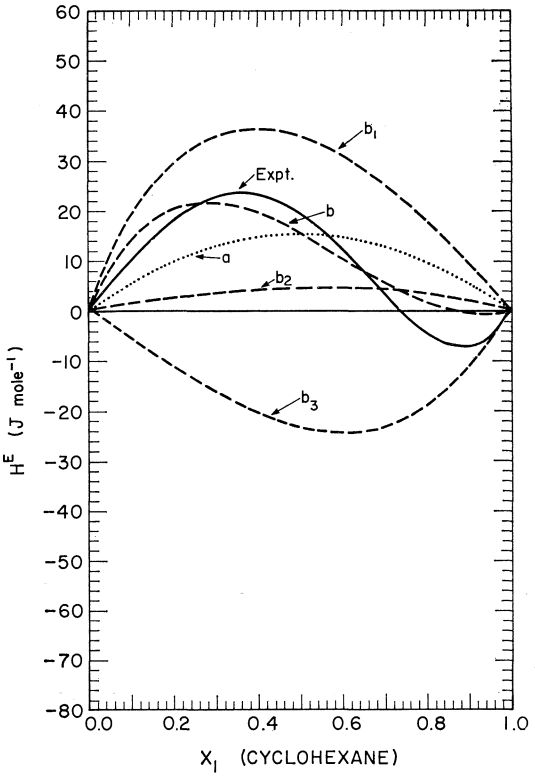

FIG. 4. Molar excess enthalpies calculated for cyclohexane – *trans*-decalin at 25 °C by the Flory theory. Curves *a* and *b*, H^E_{Flory} for calculations (*a*) and (*b*) described in text. In calculation (*b*), individual contributions of the three terms of eq. [16] are labelled b_1, b_2, and b_3, respectively. For comparison, solid curve represents our smoothed experimental results.

underestimated quite significantly. However, it is clear that explanation of the sigmoid shape of the excess enthalpy curve requires abandoning the assumption of spherical shape.

The values (4.6 and 3.4) obtained for s_1/s_2 in calculation (*b*) are considerably larger than might be expected from geometric considerations (i.e. measurements of the shadows cast by CPK (Ealing Scientific Ltd.) molecular models as described by Eichinger and Flory (18)). It can be seen from Table 5 that the values of the ratio s_{trans}/s_{cis} corresponding to calculations (*a*) and (*b*) are, respectively, less than unity and greater than unity. The latter result seems more reasonable in view of the more extended shape of the *trans*-decalin molecule as compared to the folded form of the *cis*-decalin molecule. Nevertheless, the strict interpretation of s_1/s_2 as a ratio of segment surface areas is

unrealistic in calculation (*b*), and this quantity must be considered to be a purely empirical parameter.

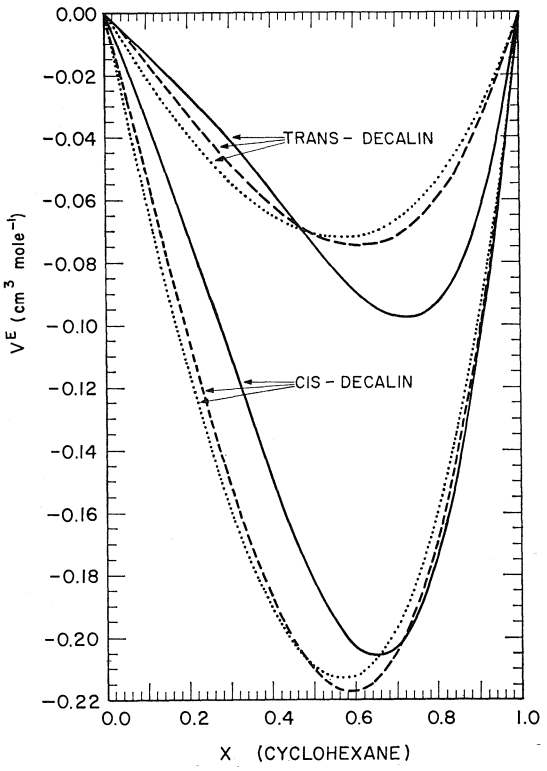

FIG. 5. Molar excess volumes at 25 °C calculated by the Flory theory. V^E_{Flory} for calculations (*a*) and (*b*) described in text are indicated by the dotted and broken curves, respectively. For comparison, solid curves represent our smoothed experimental results.

We are indebted to Dr. T. Boublík and Dr. J. Polák for helpful discussions of the thermodynamics of cyclohexane–decalin systems. We also wish to thank Mr. P. J. D'Arcy and Mr. C. J. Halpin for valuable technical assistance during the experimental measurements.

1. G. W. LUNDBERG. J. Chem. Eng. Data, **9**, 193 (1964).
2. J. M. STURTEVANT and P. A. LYONS. J. Chem. Thermodyn. **1**, 201 (1969).
3. F. DANUSSO. Atti Accad. Naz. Lincei, Rend. **13**, 131 (1952).
4. J. D. GÓMEZ-IBÁÑEZ and T. C. WANG. J. Phys. Chem. **70**, 391 (1966).
5. P. J. FLORY. J. Amer. Chem. Soc. **87**, 1833 (1965).
6. S. MURAKAMI and G. C. BENSON. J. Chem. Thermodyn. In press.
7. H. D. PFLUG and G. C. BENSON. Can. J. Chem. **46**, 287 (1968).
8. A. E. POPE, H. D. PFLUG, B. DACRE, and G. C. BENSON. Can. J. Chem. **45**, 2665 (1967).
9. American Petroleum Institute. Research Project 44. Selected values of properties of hydrocarbons and related compounds. Chemical Thermodynamic Properties Center, A. and M. College of Texas, College Station, Texas. Loose-leaf data sheets October 31, 1952.
10. D. L. CAMIN and F. D. ROSSINI. J. Phys. Chem. **57**, 1173 (1955).
11. J. H. HILDEBRAND and R. L. SCOTT. Regular solutions. Prentice-Hall Inc., Englewood Cliffs, New Jersey. 1962. Chap. 7.
12. J. A. BARKER. J. Chem. Phys. **20**, 1526 (1952).
13. M. L. MCGLASHAN and K. W. MORCOM. Trans. Faraday Soc. **57**, 581 (1961).
14. TH. HOLLEMAN. Phys. **31**, 49 (1965); see also Ph.D. thesis, University of Amsterdam, 1964.
15. P. J. FLORY, R. A. ORWOLL, and A. VRIJ. J. Amer. Chem. Soc. **86**, 3515 (1964).
16. R. A. ORWOLL and P. J. FLORY. J. Amer. Chem. Soc. **89**, 6822 (1967).
17. A. ABE and P. J. FLORY. J. Amer. Chem. Soc. **87**, 1838 (1965).
18. B. E. EICHINGER and P. J. FLORY. Trans. Faraday Soc. **64**, 2035 (1968).
19. G. A. HOLDER and E. WHALLEY. Trans. Faraday Soc. **58**, 2095 (1962).
20. (*a*) M. BACCAREDDA. Ricerca Sci. Ricostruz. **16**, 662 (1946). (*b*) J. P. MCCULLOUGH, H. L. FINKE, J. F. MESSERLY, S. S. TODD, T. C. KINCHELOE, and G. WADDINGTON. J. Phys. Chem. **61**, 1105 (1957).

Can. J. Chem. Downloaded from www.nrcresearchpress.com by 210.87.254.42 on 09/05/12
For personal use only.

Can. J. Chem. Downloaded from www.nrcresearchpress.com by 210.87.254.6 on 09/05/12
For personal use only.

Studies of rhenium–carboxylate complexes. III. The crystal and molecular structure of tetra-μ-*n*-butyratodirhenium(III) diperrhenate

C. Calvo, N. C. Jayadevan, C. J. L. Lock,[1] and R. Restivo

Institute for Materials Research and Department of Chemistry, McMaster University, Hamilton, Ontario

Received October 1, 1969

One of the compounds obtained by the reaction of rhenium(III) chloride with *n*-butyric acid while exposed to oxygen has been shown by single crystal X-ray diffraction to be tetra-μ-*n*-butyratodirhenium(III) diperrhenate. The crystals are triclinic with lattice parameters $a = 7.836(8)$ Å, $b = 10.746(8)$ Å, $c = 8.773(8)$ Å, $\alpha = 88.9(1)°$, $\beta = 106.5(1)°$, and $\gamma = 98.0(1)°$. The space group is $P\bar{1}$ and there is one formula unit per cell. A total of 1593 independent reflections were examined and the structure was refined by full 3-dimensional least-squares to an *R* value of 0.123. Two rhenium environments are found, one consisting of a dimer unit bridged by 4 carboxylate groups and the other a perrhenate group. This latter group, showing a mean Re—O distance of 1.75 Å, shares an oxygen atom with a rhenium atom in the dimer unit, and this Re—O bond length is 2.18 Å long. The structure results from packing of short chains, consisting of the dimer unit and the 2 perrhenate groups, running roughly parallel to the [111] direction.

Canadian Journal of Chemistry, **48**, 219 (1970)

Introduction

Taha and Wilkinson (1) prepared a novel series of carboxylato-complexes of rhenium which were postulated to have the molecular structures shown as **1** to **3**

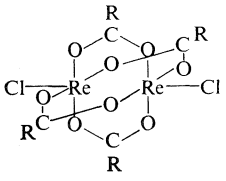

1

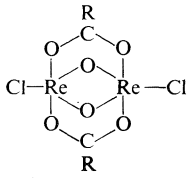

2

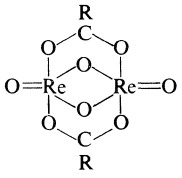

3

The molecular structure of **1** has been shown to be basically correct (2, 3), although the Re—Re distance is very short, implying a very strong rhenium–rhenium bond. Calvo *et al.* (4) have shown that the compound prepared by Taha and Wilkinson's method for **2** does not have the structure suggested, but is a chain structure consisting of alternate dimer units containing 2 rhenium atoms with a very short Re—Re distance and perrhenate groups. The dimeric rhenium(III) unit is bridged by 3 carboxylate groups and each rhenium has a chlorine atom attached forming nearly a square-planar array with the carboxylate oxygen atoms. Rouschias and Wilkinson (5) have since prepared other carboxylate complexes in which the bridging arrangement was postulated to be **4** and **5**. Cotton and Foxman (6) have shown that **5** is basically correct but that the unexpectedly short Re–Re distance of 2.522(2) Å implies a strong metal–metal bond. It was of interest to see

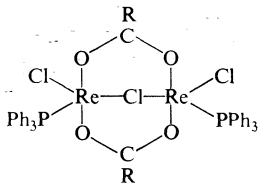

4

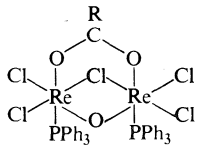

5

whether **3** was correct, whether the structure was basically correct but contained a strong Re—Re bond, or whether the structure, like **2**, was incorrect and contained a mixture of tightly bonded dimer Re(III) units together with groups containing rhenium in other formal oxidation states. We now report the correct structure for **3**.

Experiments

Rhenium(III) chloride[2] (2 g) was heated with *n*-butyric acid (25 ml) for 4 days at just below the boiling point in a slow stream of oxygen which was dried by bubbling

[1]To whom correspondence should be addressed.

[2]Obtained from the Shattuck Chemical Company Denver, Colorado.

Can. J. Chem. Downloaded from www.nrcresearchpress.com by 210.87.254.6 on 09/05/12
For personal use only.

through concentrated sulfuric acid. The small amount of purple crystals formed were filtered from the hot solution. The filtrate on cooling deposited orange crystals (1 g). They were washed repeatedly with ethanol to remove any impurities. Single crystals suitable for X-ray analysis were obtained by recrystallization from boiling butyric acid. The crystals were washed with petroleum ether until acid-free and dried in vacuo. Carbon and hydrogen analyses were done by Galbraith Laboratories, Knoxville, Tennessee.

Anal. Calcd. for $C_8H_{14}O_8Re_2$: C, 15.7; H, 2.3. Found: C, 15.9; H, 2.25.

The infrared spectrum was recorded on a Perkin–Elmer 337B spectrophotometer using powder samples suspended in a Nujol mull between sodium chloride plates. The spectrum was identical to that reported for oxorhenium(V)-μ-dioxo-μ-di(*n*-butyrato) oxorhenium(V) (1).

Crystallography

A single crystal of dimensions 0.08 × 0.08 × 0.08 mm³, which showed complete extinction every 90° when viewed through a polarizing microscope was used for X-ray studies. A Weissenberg photograph taken of the [100] zone with Cu Kα radiation and calibrated with the diffraction pattern from a single crystal of TiO_2 (a = 4.5929(5) Å, c = 2.9591(3) (7)) was used to calculate accurate reciprocal axes lengths b^* and c^* and the angle α^*. Precession photographs of the [001] and [010] zones obtained using Mo Kα radiation were also calibrated with a TiO_2 diffraction pattern and permitted a determination of all of the lattice parameters. The crystal data are shown in Table 1.

TABLE 1

Crystal data for $[Re_2(n\text{-}C_4H_7O_2)_4](ReO_4)_2$

Parameter	Unit	Value
a	Å	7.836(8)
b	Å	10.746(8)
c	Å	8.773(8)
α	degree	88.9(1)
β	degree	106.5(1)
γ	degree	98.0(1)
Volume	Å³	701.3
M		1220.8
D_{expt}	g/cm³	2.82(3)
D_{calcd}	g/cm³	2.88
Z		1
Systematic absences		none
Space group		$P\bar{1}$

The density of a few single crystals was measured by flotation in a diiodomethane–tetrachloromethane mixture whose density was subsequently determined with a pycnometer. The measured density of 2.82(3) g cm^{-3} implied that there were 2 molecular units of $[Re_2O_4(n\text{-}C_3H_7CO_2)_2]$ per unit cell.

The first 4 layers containing nkl (n = 0–3) were photographed by the multiple film technique and the equi-inclination Weissenberg method using Cu Kα radiation. Layers $hk0$ and $h0l$ were recorded on a precession camera using Mo Kα radiation.

The intensities of the reflections were estimated visually, and then corrected for Lorentz and polarization effects. All data collected using Cu Kα radiation were corrected for absorption assuming the crystal was a sphere of radius equal to 0.04 mm, since otherwise errors of 10–15% would have been introduced into the structure factors (μR = 1.27 for Cu Kα and 0.07 for Mo Kα).

Standard errors, σ, were assigned to each intensity and weights $w = 1/\sigma^2$ were used throughout the refinement. Greater weights were given to reflections which could be measured on all 3 films than to those which could be measured only on 1 or 2 films.[3] For unobserved reflections, weights calculated from $\sigma = 0.5F_{min}$ were used only when the calculated structure factor $|F_c| > 0.8F_{min}$, where F_{min} was the local minimum of the observed structure factor; otherwise they were given zero weight.

Solution of the Structure

The unit cell was triclinic with space group $P1$ or $P\bar{1}$. Patterson maps were calculated using the data from [010], [100], and [001] zones separately. Each one of these projections had 4 strong peaks per asymmetric unit of the projections, 2 of which had peak heights approximately double those of the other 2. This is characteristic of 4 rhenium atoms in the unit cell, related in pairs by a center of inversion, thereby indicating that the space group is $P\bar{1}$. This choice was confirmed by the successful structure analysis.

The Patterson solution of the 2 independent rhenium atoms of the asymmetric unit of the unit cell was determined. Structure factor calculation using the Re(0) scattering factors and an isotropic temperature coefficient B_i = 2.0 (Å)² gave R_1 indices of 0.20 for [010] data and 0.26 for [001] data.[4] The Re–Re distances were Re(1)–Re(1)$_i$ = 2.2 Å, Re(1)–Re(2) = 3.8 Å, and Re(2)–Re(2)$_i$ = 4.60 Å where the subscript i is used to indicate a centrosymmetrically related atom. This situation was similar to that observed in the structure of $[Re_2Cl_2(i\text{-}C_3H_7CO_2)_3](ReO_4)$ (4). Thus the cell contains a dimer unit with a very short Re–Re distance and 2 monomeric rhenium atoms. Moreover, the strongly-bonded rhenium dimer has a rigorous center of symmetry and hence can have only an even number of carboxylate groups coordinated to it.

Repeated structure factor calculation followed by difference synthesis located all non-hydrogen atoms. The Re(0) scattering curve of Cromer and

[3]Thus $\sigma = 0.1F_o$ if $50 < F_o < 200$, $\sigma = 0.15F_o$ if $20 < F_o < 50$ or $F_o > 200$, and $\sigma = 0.25\ F_o$ if $F_o < 20$.

[4] $R_1 = \dfrac{\Sigma|F_o - F_c|}{\Sigma|F_o|}$, $\quad R_2 = \left[\dfrac{\Sigma W(|F_o|^2 - |F_c|^2)}{\Sigma W|F_o|^2}\right]^{1/2}$

TABLE 2

Atomic parameters for $[Re_2(n\text{-}C_4H_7O_2)_2](ReO_4)_2$*

Atom	Coordinates			B (Å)^2
	x	y	z	
Re(1)	0.37718(84)	0.44523(16)	0.41665(17)	†
Re(2)	−0.08308(38)	0.32351(20)	0.13000(20)	†
O(1)	0.5232(54)	0.3026(25)	0.4209(33)	4.44(63)
O(2)	0.3110(44)	0.3651(20)	0.6003(25)	2.85(60)
O(3)	0.2292(52)	0.5899(26)	0.4047(33)	4.57(74)
O(4)	0.4556(52)	0.5250(25)	0.2353(32)	4.29(75)
O(21)	0.1521(52)	0.3407(25)	0.2398(31)	4.57(82)
O(22)	−0.2109(62)	0.4162(32)	0.2181(39)	6.32(93)
O(23)	−0.0831(60)	0.3871(32)	−0.0479(40)	6.44(97)
O(24)	−0.1348(62)	0.1656(30)	0.1479(38)	6.04(98)
C(21)	0.6019(90)	0.6051(46)	0.2669(56)	5.5(14)
C(22)	0.6486(98)	0.6790(49)	0.1176(62)	6.1(14)
C(23)	0.6524(96)	0.8125(48)	0.1172(62)	6.1(17)
C(24)	0.6633(108)	0.8769(58)	−0.0396(71)	7.6(17)
C(31)	0.3273(100)	0.6960(48)	0.5011(63)	6.0(13)
C(32)	0.1763(99)	0.7832(52)	0.4811(64)	6.6(14)
C(33)	0.2047(94)	0.8946(51)	0.3631(61)	6.3(17)
C(34)	0.1247(98)	−0.0034(51)	0.3735(63)	6.4(17)

Atom	U_{11}‡	U_{22}	U_{33}	U_{12}	U_{13}	U_{23}
Re(1)	464(24)	515(10)	344(8)	61(12)	21(11)	45(7)
Re(2)	549(28)	735(14)	474(11)	58(16)	31(16)	103(9)

*Estimated standard deviation in parentheses.
†Anisotropic thermal parameters used for rhenium atoms (Å)$^2 \times 10^4$.
‡These values were obtained from $\beta_{ij} = 2\pi^2 b_i b_j U_{ij}$ where β_{ij}'s appear as a temperature effect through exp $[-(\beta_{11}h^2 + 2\beta hk + ...)]$ in the structure factor expression and b_i are the reciprocal lattice vectors.

Waber (8) was used (initially without the anomalous dispersion corrections) to refine the scale factors, positional parameters, and the initial isotropic temperature factors of 3.0 (Å)^2 for oxygen atoms and 4.0 (Å)^2 for carbon atoms. The anomalous dispersion effects tabulated by Cromer (9) show a significantly different value for Mo Kα from that for Cu Kα data. After 2 cycles of refinement the molybdenum data were modified to obtain pseudo observed structure factors that would have been obtained if copper radiation were employed. Since the atomic positions of rhenium atoms significantly changed in 2 cycles of refinement, the new coordinates were used to correct the data once again. The rhenium atom positions used to obtain pseudo-copper data did not shift significantly in further cycles of refinement. The atomic scattering factors of carbon and oxygen atoms were taken from the "International tables for X-ray crystallography" (10).

Of the 1593 independent reflections used, 1173 were strong enough to be measured and were given non-zero weights in the last cycle of least-squares refinement where convergence occurred at $R_1 = 0.123$ and $R_2 = 0.133$. The positional parameters are given in Table 2 and the observed structure factors compared with those calculated[5] in Table 3. A difference Fourier map calculated using these structure factors had no residual peaks greater than 1.4 e/Å^3 or less than −1.5 e/Å^3. Further, no parameter shifted by more than ~ 1/3 of its estimated standard deviation in the last few cycles of refinement.

Results and Discussion

The structure which is shown in Fig. 1 consists of a carboxylato-bridged dimeric rhenium unit, $[Re_2(n\text{-}C_3H_7CO_2)_4]$ and two ReO_4 units, one at each end of the dimer unit. Thus the correct name of the compound is tetra-μ-*n*-butyratodirhenium(III) diperrhenate. The compound is the second of a series of compounds containing the strongly bonded Re_2 unit in addition to non-dimerized rhenium atoms (4). The method of preparation, analyses, average oxidation number

[5]Table 3 has been placed in the Depository of Unpublished Data. Photocopies may be obtained free of charge, upon request, from: Depository of Unpublished Data, National Science Library, National Research Council of Canada, Ottawa, Canada.

Can. J. Chem. Downloaded from www.nrcresearchpress.com by 210.87.254.6 on 09/05/12
For personal use only.

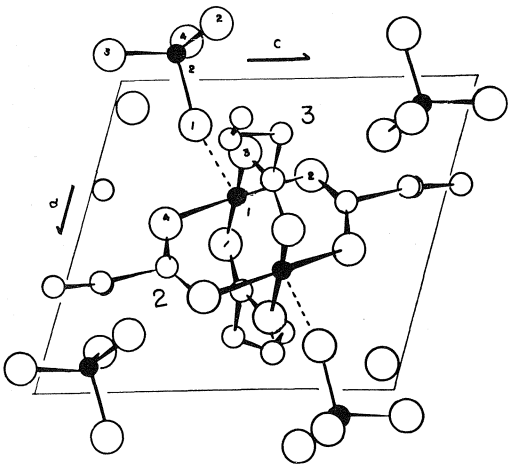

FIG. 1. Projection [010] of the compound $Re_2(n\text{-}C_3H_7CO_2)_4(ReO_4)_2$.

of V for the rhenium atoms, and infrared spectra of our compound are identical to those reported by Taha and Wilkinson (1) for oxorhenium(V)-μ-dioxo-μ-di-*n*-butyrato-oxorhenium(V) and it is clear that their compound must now be reformulated. The bond distances and bond angles are listed in Table 4. The numbering of atoms refers to that used in Fig. 2, and the subscript *i* in this table refers to the related atom generated by the center of symmetry. Each rhenium atom of the dimeric unit has an oxygen atom bonded at a distance of 2.18(3) Å along the Re–Re axis. This oxygen atom is shared with the perrhenate unit. Although large errors in the Re—O distances do not allow unambiguous conclusions to be drawn, the Re(dimer)—O(perrhenate) distance appears to be longer than the mean Re—O(carboxylate) distance of 2.02(3) Å ($\sim 5\sigma$). We feel, however, that the Re—O(perrhenate) bond is not abnormally long and should be considered as a

TABLE 4

Bond distances and bond angles in $[Re_2(n\text{-}C_3H_7CO_2)_4](ReO_4)_2$*

Bonded atoms	Distance (Å)	Bonded atoms	Distance (Å)
Re(1)—Re(1)$_i$	2.251(2)	Re(2)—O(21)	1.81(3)
—O(1)	2.03(3)	—O(22)	1.82(4)
—O(2)	1.98(2)	—O(23)	1.69(3)
—O(3)	2.05(3)	—O(24)	1.70(3)
—O(4)	2.00(2)		
—O(21)	2.18(3)		
C(31)—O(1)	1.17(7)	C(21)—O(2)	1.20(3)
—O(3)	1.41(5)	—O(4)	1.30(7)
—C(32)	1.58(9)	—C(22)	1.64(5)
C(33)—C(32)	1.60(6)	C(23)—C(22)	1.43(7)
—C(34)	1.39(9)	—C(24)	1.56(5)

Bonded atoms	Angle (°)	Bonded atoms	Angle (°)
Re(1)$_i$—Re(1)—O(1)	88.3(9)	O(3)—C(31)—O(1)$_i$	122(4)
—O(2)	89.9(7)	—O(32)	102(4)
—O(3)	92.4(9)	O(1)$_i$—C(31)—C(32)	125(5)
—O(4)	88.2(9)	O(4)—C(21)—O(2)$_i$	123(4)
—O(21)	175.0(14)	—C(22)	117(4)
O(1)—Re(1)—O(2)	86.6(13)	O(2)$_i$—C(21)—C(22)	120(4)
—O(3)	178.1(23)	C(11)—C(12)—C(13)	109(5)
—O(4)	91.6(14)	C(12)—C(13)—C(14)	115(5)
—O(21)	89.8(12)	C(21)—C(22)—C(23)	117(5)
O(2)—Re(1)—O(3)	95.1(13)	C(22)—C(23)—C(24)	115(5)
—O(4)	177.4(16)		
—O(21)	94.4(11)	O(21)—Re(2)—O(22)	112(2)
O(3)—Re(1)—O(4)	86.7(14)	—O(23)	104(2)
—O(21)	89.5(12)	—O(24)	100(2)
O(4)—Re(1)—O(21)	87.2(12)	O(22)—Re(2)—O(23)	107(2)
		—O(24)	113(2)
Re(1)—O(1)—C(31)$_i$	123(3)	O(23)—Re(2)—O(24)	120(2)
—O(3)—C(31)	114(3)		
—O(2)—C(21)	121(3)	Re(1)—O(21)—Re(2)	148(1)
—O(4)—C(21)	119(3)		

*Subscript *i* refers to the atom related by a center of symmetry to the corresponding atom listed in Table 2. Estimated standard deviations in parentheses.

Can. J. Chem. Downloaded from www.nrcresearchpress.com by 210.87.254.6 on 09/05/12
For personal use only.

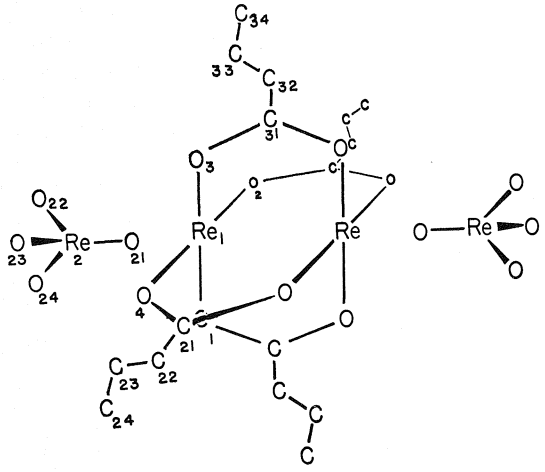

FIG. 2. The basic structural units of $Re_2(n\text{-}C_3H_7\text{-}CO_2)_4(ReO_4)_2$.

normal Re—O single bond. The errors involved preclude any conclusion that this bond is significantly longer than normal, a conclusion which has been drawn for the related axial Re—Cl bond distance in compounds of the type $Re_2(RCO_2)_4Cl_2$ (2, 3). However, the non-bonded distances between the oxygen atom (perrhenate) bonded to the dimer rhenium atom and the nearest neighbor oxygen atoms of the carboxylate atoms are 2.95(3)–3.05(3) Å, significantly greater than the sum of the van der Waals radii, 2.8 Å (11), so the difference in the rhenium–oxygen distances in this case cannot be caused by non-bonded interactions of the type we have discussed previously (4). The perrhenate groups have close to tetrahedral symmetry, although there appears to be a slight distortion, corresponding to squashing the tetrahedron along the tetrahedral 2-fold axis bisecting O(21)—Re—O(22) and O(23)—Re—O(24). The differences in the O(21), O(22) and O(23), O(24) distances (4σ) may not be significant but there appear to be differences between the O(23)—Re(2)—O(24) and O(21)—Re—O(24), O(21)—Re—O(23), O(22)—Re—O(24), O(22)—Re—O(23) angles (~7σ).

The perrhenate ion in tris(μ-*i*-butyrato)di-(chlororhenium(III)) perrhenate also showed a mean ReO bond length of 1.75 Å where 2 oxygen atoms are shared at a Re(dimer)—O distance of 2.28 Å. In this case the distortion of the tetrahedron is angular and can be pictured as a repulsion of the 2 oxygen atoms not shared between the perrhenate group and the dimer.

There are 4 bridging carboxylate groups in the dimer unit, and apart from the substitution of the chloride ligands in the axial positions by perrhenate groups, the dimeric unit has the same features as those shown by $Re_2(n\text{-}C_3H_7\text{-}CO_2)_4Cl_2$ (3) and $Re_2(C_6H_5CO_2)_4Cl_2 \cdot 2CHCl_3$ (2) and it is a complex of rhenium(III). Although crystallographically the unit possesses only a center of symmetry, the dimer has an eclipsed rotomeric configuration of approximate symmetry D_{4h}. Each rhenium atom is thus at the center of an approximately square set of oxygen atoms, with the other rhenium atom and an axial oxygen atom of an ReO_4 unit completing an axially distorted octahedral coordination about the metal atom as shown in Fig. 2.

The Re—Re distance of 2.251(2) Å is consistent with a bond order of 4 on the basis of the arguments of Cotton (12). Within the dimeric unit the rhenium-to-carboxylate oxygen bond lengths average 2.01(3) Å, and the 4 smallest O—Re—O angles are close to 90° within the uncertainties estimated. The planes calculated using the program PALS and giving individual atoms weights according to

$$\left[\frac{1}{a.b.c.\sigma(x).\sigma(y).\sigma(z)}\right]^{2/3}$$

where a, b, c are cell constants and $\sigma(x)$, $\sigma(y)$, and $\sigma(z)$ are standard deviations of the atomic coordinates, are shown in Table 5. The 4 carboxylate groups form 2 planes (planes *2* and *3*) which are orthogonal to each other and to the plane formed by each rhenium atom and the 4 carboxylic oxygen atoms coordinated to it. The planes show that the eclipsed rotomeric configuration is retained.

The C—O and C—C bond lengths and corresponding angles are similar to those observed in other carboxylato-bridged dimeric complexes and are in agreement with those found in $Re_2(n\text{-}C_3H_7CO_2)_4Cl_2$ (2) in this laboratory.

The structure results from packing short chains consisting of the dimer unit and the 2 perrhenate groups. These rods roughly parallel the [111] direction in the crystal. The tetra-μ-*n*-butyrato-dirhenium groups pack like mounted bicycle tires with the perrhenate groups acting as the protruding axle. The molecules pack with these axles coparallel and tilted with the chain direction defined by the line of extention of these groups.

Can. J. Chem. Downloaded from www.nrcresearchpress.com by 210.87.254.6 on 09/05/12
For personal use only.

TABLE 5

Weighted least-squares molecular planes*

Type of plane	No.	Equation
ReO_4	*1*	$0.5946x + 0.4651y + 0.6558z = 5.6642$
$Re_2O_2C(1)$	*2*	$-0.4946x - 0.3257y + 0.8057z = 0.3172$
$Re_2O_2C(2)$	*3*	$0.6253x - 0.7802y - 0.0181z = -2.5972$
$Re_2O_4C_2(1)$	*4*	$-0.4947x - 0.3257y + 0.8057z = 0.3165$
$Re_2O_4C_2(2)$	*5*	$0.6253x - 0.7801y - 0.0181z = -2.5966$

*The orthogonal coordinate system corresponds to the crystallographic *a*, *b*, *c** axes.

The nearest approach of 2 molecules in the chain is determined by the van der Waals contact of centrosymmetrically related perrhenate groups involving O(1) and O(3). The hydrocarbon forms the rim of this tire and limits the closest approach of parallel chains, with interaction between the hydrocarbon and perrhenate groups defining the length of the ***a*** axis.

Conclusions

We conclude that the compound formerly formulated as oxorhenium(V)-μ-dioxo-μ-di-*n*-butyrato-oxorhenium(V) is really tetra-μ-*n*-butyratorhenium(III) diperrhenate and is another in the series of rhenium(III) compounds containing the remarkably stable Re_2 unit. In addition it is the second compound in this series which contains perrhenate groups.

We wish to thank the National Research Council of Canada for financial support and one of us (N.C.J.) acknowledges the receipt of a Commonwealth Scholarship.

1. F. Taha and G. Wilkinson. J. Chem. Soc. 5406 (1963).
2. M. J. Bennett, W. K. Bratton, F. A. Cotton, and W. R. Robinson. Inorg. Chem. **7**, 1570 (1968).
3. C. Calvo, C. J. L. Lock, and R. Restivo. Part II, this series. To be published.
4. C. Calvo, N. C. Jayadevan, C. J. L. Lock. Can. J. Chem. **47**, 4213 (1969).
5. G. Rouschias and G. Wilkinson. J. Chem. Soc. A, 465 (1966).
6. F. A. Cotton and B. M. Foxman. Inorg. Chem. **7**, 1784 (1968).
7. D. T. Cromer and K. Herrington. J. Amer. Chem. Soc. **77**, 4708 (1955).
8. D.T. Cromer and J. T. Waber. Acta Cryst. **18**, 104 (1965).
9. D. T. Cromer. Acta Cryst. **18**, 17 (1965).
10. International tables for X-ray crystallography. Vol. III. Kynoch Press, Birmingham. 1962. Table 3.3.1A.
11. L. Pauling. The nature of the chemical bond. Cornell University Press, Ithaca, New York. 1942. p. 189.
12. F. A. Cotton. Inorg. Chem. **4**, 334 (1965).

Can. J. Chem. Downloaded from www.nrcresearchpress.com by 210.87.254.6 on 09/05/12
For personal use only.

Photochemical synthesis 29.[1,2,3] Photoannelation and cyclohexenone

P. DE MAYO, A. A. NICHOLSON, AND M. F. TCHIR
Department of Chemistry, University of Western Ontario, London, Ontario
Received July 8, 1969

Values of 1.7×10^8 s^{-1} and 2.5×10^7 M^{-1} s^{-1} for k_d, the unimolecular rate constant for decay, and k_r, the rate constant for addition to cyclohexene, have been obtained for cyclohexenone. These indicate that this cyclenone decays somewhat faster and reacts significantly slower with the same substrate (in the same solvent) than does cyclopentenone. Evidence is adduced, from sensitization experiments and the phosphorescence quenching of a range of carbonyl compounds, that the reactive triplet and lowest triplet of cyclohexenone lie close together, if they are indeed not identical, and the energy of this triplet is in the region of 66–68 kcal/mole. This is higher than that indicated by photostationary state measurements. This latter method, applied to cyclenones, may be suspect, and triplet energies so derived subject to doubt (that of cyclopentenone included) or have a different significance from those obtained by other methods. Further attempts to demonstrate the existence of a lower, cycloadditively unreactive, triplet in cyclopentenone have been negative. It now seems far more likely that the original interpretation was in error, that the lowest energy triplet is near 73 kcal/mole, and that a special mechanism for quenching benzophenone triplets by ground state cyclopentenone exists. The evidence for other multiple reactive triplets is re-examined as is the evidence for the nature of the states involved.

Canadian Journal of Chemistry, **48**, 225 (1970)

Can. J. Chem. Downloaded from www.nrcresearchpress.com by 210.87.254.5 on 09/05/12
For personal use only.

In an earlier publication (1) we discussed the mechanism of cyclopentenone photoannelation. We found, as had Eaton and co-worker (2) and, subsequently, Ruhlen and Leermakers (3) that the reaction proceeded through a triplet. We also found that the yield of this triplet, that is the intersystem crossing efficiency from the singlet, was 100%. The available evidence suggested that the photoannelation was a rapid reaction which was not stereospecific, but which did not allow complete stereochemical equilibration to occur. In subsequent work we showed that an intermediate complex was formed, as was originally suggested by Corey *et al.* (6), a fraction of which continued on to give products. The remainder collapsed to form molecules in the ground state (4), and led us to conclude that the partitioning of this intermediate was the most important factor in determining the quantum yield of photoannelation. Because the rate constant for formation of this complex, even at $-70°$, was close to 10^9 M^{-1} s^{-1} (4, 5) it seemed likely that this was some form of exciplex rather than a biradical, and that the formation of such a biradical, if an intermediate and not on a divergent pathway, was a subsequent step.[4] Similar conclusions with regard to the dimerization of cyclopentenone were reached by Wagner and Bucheck (8).

Two other features were discussed: the energy of the reactive state and its nature. Since it was found that sensitizers above 73 kcal/mole could induce photoannelation, but that nonetheless cyclopentenone quenched benzophenone triplets at a near diffusion controlled rate, it was suggested that T_2 was the reactive state and that T_1 (presumably below 68 kcal/mole) was inert in the photoannelation process. That the lowest triplet of cyclopentenone was below 68 kcal/mole was in accord with Leermaker's finding, from photoequilibration experiments, of a value of 62 kcal/mole (3, 19).

A later study with constrained cyclopentenones which had the advantage of showing phosphorescent emission, did not give as clear-cut results and required that the interpretation be re-examined (9).

Simultaneously with the above studies we have been making parallel investigations with cyclohexenone. Before and during the progress of our work there were valuable reports from other workers which suggested the existence of both parallels and divergences in behavior between these two ketones. Thus, although the yield of cyclopentenone reactive triplets was near unity that of cyclohexenone appeared to be less. There was also evidence (10, 11) that cyclohexenones reacted through two triplets apparently capable of being differentially quenched.

We report here the results obtained with cyclohexenone, and follow with a discussion

[1]For Part 28, see reference 9.
[2]Publication Number 1 from the Photochemistry Unit.
[3]This paper constitutes part of the thesis by P. DE MAYO, University of Paris, Faculty of Science, Orsay, France.
[4]That a biradical is formed at all seems very probable because of the unsaturated products, first noted by Corey *et al.* (6), which frequently accompany photoannelation. The lack of stereospecificity in the addition can be so construed (7) but involves more complex arguments. This point will be returned to later.

concerning the photoannelation process as it concerns cyclopentenone and cyclohexenone.

Experimental

Materials

Cyclohexenone was prepared from the corresponding ethylene ketal (12) by hydrolysis with aqueous (0.05 *N*) hydrochloric acid at room temperature. After distillation (60°/10 mm) the product had two impurities as indicated by gas–liquid chromatography (g.l.c.) on a 5% FFAP column (8′ × 1/8″) on Diatoport S at 50°. One had a shorter retention time (0.1%) and one (0.6%) somewhat longer than that of cyclohexenone. For the purest material the main impurity was removed by preparative g.l.c. This was used for the Beer's Law measurements: for the remainder the material of 99.3% purity was used.

Cyclopentene, *cyclopentenone*, and *cyclohexene* were purified as previously described (1). *Benzene* (Philips Research Grade) was used without further purification as was *cyclohexane* (Fisher spectroanalysed) and anhydrous *ether* (Mallinckrodt). *Isopropanol* was distilled from calcium hydride.

The calibrating compounds in g.l.c. analysis were *benzophenone*, *naphthalene*, *2-methylnaphthalene*, and *octacosane*. The first three were crystallized from 95% ethanol and the last (Aldrich) was used without further purification.

The diene *2,5-dimethyl-2,4-hexadiene* (Aldrich) was distilled under nitrogen (18″ spinning band) and stored at −20 °C under nitrogen. It was passed through a short column of alumina (Woelm, neutral) immediately before use. *trans-Piperylene* (Aldrich) was distilled and passed through a column of neutral alumina before use.

Sensitizers

Recrystallized *benzophenone* (4 times from 95% ethanol) was dried: $\varepsilon_{366} = 72$. *Acetophenone* was fractionally distilled: $\varepsilon_{313} = 39$. *p-Bromoacetophenone* was recrystallized from cyclohexane and sublimed. *p-Trifluoromethylacetophenone* (Eastman) showed no detectable impurities on g.l.c.; $\varepsilon_{313} = 35$. *p,p′-Dichlorobenzophenone* was prepared by the method of Dittrich (13). The final product was chromatographed on silicic acid (eluant: ethyl acetate – light petroleum (60–80°); 1:9) and recrystallized 5 times from ethanol, m.p. 144–145°, and shown to be greater than 99.9% pure by g.l.c. *p-Cyanobenzophenone* was prepared by the method of Aziz *et al.* (14). The final product was chromatographed on silicic acid (eluant: benzene) and after 4 recrystallizations (95% ethanol) had m.p. 113.5–115° [lit. value 113–114° (15)]. *4-Methyl-4-trichloromethylcyclohexadienone*, prepared by the method of Newman and Pinkus (16) had m.p. 104–105°. *4-Benzoylpyridine* (Aldrich) was recrystallized from light petroleum (60–80°) and g.l.c. showed greater than 99% purity. *Ethyl pyruvate* (Aldrich) was distilled and showed greater than 99% purity by g.l.c. *Triphenylamine* (Eastman) was purified by crystallization from ethyl acetate and had a m.p. of 127.5°.

Preparation of Adducts

A typical preparation was as follows. Cyclohexenone (2.045 g) in 25 ml cyclohexene was degassed by bubbling nitrogen through the solution. The solution was irradiated with a Hanovia 450 W medium-pressure mercury arc through a Pyrex filter for 30 min. The cyclohexenone was completely consumed as shown by thin-layer chromatography (t.l.c.). After removal of solvent the product was isolated and separated from low boiling material by g.l.c. (10% FFAP on Chromosorb P, 8′ × 3/8″ run at 160°). The dimers were prepared by irradiating cyclohexenone (1 g) in benzene (25 ml) in a similar fashion for 2 h. Separation was achieved on the same column at 220°. Four dimers (2 major; 2 minor) were observed in agreement with Hammond's observations (17).

Quantum Yields

The optical bench system has been described previously (1). Analysis was carried out with an Aerograph Hy-Fi-600-C gas chromatograph with flame detector, using a 5′ × 1/8″, 2.5% Carbowax 20 M on Diatoport S column at 160° (dimers) or 120° (adducts). An alternative column was a 5% FFAP 6′ × 1/8″ on Diatoport S at 135° (adducts) and 185° (dimers). The purified adducts were calibrated against naphthalene or 2-methylnaphthalene whilst the dimers were calibrated against benzophenone or octacosane. The 313 and 366 nm lines were isolated using the filters B and C described by Kasha (18). Irradiations were carried to between 1–5% conversion. (Reproducibility was ±0.01 in determinations of quantum yields in single determinations.) Values quoted are averages of 2–3 determinations.

Sensitized Reactions

The proportion of light absorbed by the components of the mixture was calculated from the absorbances at the wavelengths indicated and not from the integrated absorption over the band width passed by the filter. A small error is thus involved. The calibrating compound used for each sensitizer is indicated in Table 1. The validity of Beer's Law with regard to cyclohexenone was checked over 4 orders of magnitude in concentration using path lengths from 0.01 to 10 cm and no deviation was found. Irradiation in sensitized reactions was effected at the wavelength (see Table 1) in the 300–370 nm region at which the sensitizer absorbed most light. The results are plotted in Fig. 1.

Phosphorescence Quenching

The samples contained in Suprasil quartz tubes were irradiated with a 200 W Osram super-pressure mercury arc after passage through a Bausch and Lomb 0.5 m #33-86-07 monochromater. The emitted light from the sample in the nitrogen dewar was monitored at right angles to the irradiating beam with a Jarrel Ash scanning monochromater equipped with an EMI 6256 phototube and an Eldorado Model 201 Universal Photometer.

A standard solution of 2.497 g cyclohexenone in 25 ml EPA (Aminco: ether, isopentane, alcohol; 5:5:2) was prepared. Two 5 ml solutions containing 100 mg of sensitizer, one with and one without 2 ml of the cyclohexenone solution were made up in EPA.

Both samples were degassed by the freeze–thaw method, and one was the control for the other. The percentage quenching was measured as the average of 4 determinations. Benzophenone, acetophenone, 4-benzoylpyridine, 4-trifluoromethylacetophenone, *p,p′*-dichlorobenzophenone, and *p*-cyanobenzophenone were irradiated

Can. J. Chem. Downloaded from www.nrcresearchpress.com by 210.87.254.5 on 09/05/12
For personal use only.

TABLE 1

Quantum yields of sensitized addition and dimerization of cyclohexenone

Sensitizer	E_T (sens)*	Φ_{add_1}†‡§	Φ_{add_2}§‖	Φ_{dim}¶**	Φ_s/Φ_{add_1}	Φ_s/Φ_{add_2}	Wavelength (nm)
——	—	0.48	0.22	0.096	—	—	366
Acetophenone	73.6	0.33	0.22	—	0.69	1.0	313
p-Trifluoromethyl-acetophenone	70.8	0.10	—	—	0.208	—	313
Benzophenone	68.8	0.03	0.077	0.086	0.064	0.34	366
4,4′-Dichlorobenzophenone	68.0	—	0.03	0.095	—	0.14	366
4-Cyanobenzophenone	66.4	—	0.002	0.04	—	0.005	366

*Triplet energy in kcal/mole^{-1} (hydrocarbon matrix) given by Arnold (20).
†Addition in neat cyclohexene. Cyclohexenone concentration = 0.25 *M*.
‡Φ_{add_1} at 313 nm = 0.48.
§For the acetophenone and *p*-trifluoromethylacetophenone sensitized additions the calibrating compound was 2-methylnaphthalene, for the ther experiments naphthalene was used.
‖Addition in 1.96 *M* cyclohexene in benzene; concentration cyclohexenone = 0.45 *M*.
¶Concentration of cyclohexenone = 0.8 *M*.
**For the direct and benzophenone sensitized addition the calibrating compound was octacosane, for the rest benzophenone was used.

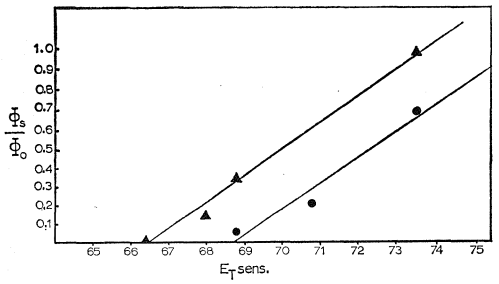

FIG. 1. Sensitized addition of cyclohexenone to cyclohexene. (—○—) In neat cyclohexene, (—△—) in benzene.

at 254 nm. Ethyl pyruvate and the dienone were irradiated at 366 nm and correction made for the fraction of light absorbed by the cyclohexenone. The results are listed in Table 2 and plotted in Fig. 2.

Quenching of Benzophenone Reduction in Isopropanol

The procedure was as described previously for cyclopentenone (1) except that a copper sulfate (saturated, 1 cm path length) – Pyrex filter system was used to cut off light below 313 nm. The results are plotted in Fig. 3. Curves in Figs. 3–8 were fitted by the least squares method.

Variation of Quantum Yield of Annelation with Substrate Concentration

A merry-go-round apparatus (19) was used (maintained at 20° ± 1° in a water bath). The 366 nm line was isolated with a combination of Corning filter 0-52 and 7-60. This combination had less than 1% transmittance at 395 and 342 nm. At 366 nm the absorbance was 0.37. The concentration of cyclohexenone in each tube was 0.104 *M* and care was taken to ensure the concentration was identical since not all the light was absorbed. Varying concentrations of cyclohexene were added and the mixture diluted with cyclohexane. Degassing was by the freeze–thaw method, and irradiation (450 W) was for 2 h. The calibration compound (2-methylnaphthalene) was

TABLE 2

Phosphorescence quenching of various sensitizers by cyclohexenone*

	Sensitizer	E_T†	E_T‡
1	Acetophenone‖	74.2	74.0
2	4-Trifluoromethylacetophenone‖	71.4§	71.5
3	Benzophenone‖	69.2	69.2
4	4,4′-Dichlorobenzophenone‖	—	68.5
5	4-Benzoyl pyridine‖	67.2§	67.5
6	4-Methyl-4-trichloromethyl-2,5-cyclohexadien-1-one¶	67.1§	67.0
7	4-Cyanobenzophenone‖	—	66.5
8	Ethyl pyruvate¶	65.0	65.0

*Cyclohexenone concentration = 0.44 *M*.
†Energies given by Dr. D. R. Arnold (20).
‡The O—O band, from which the triplet energy was calculated was the first well-defined peak in the phosphorescence spectrum.
§Solvent: ethanol–methanol (4:1).
‖Irradiated at 254 nm.
¶Irradiated at 366 nm and corrected for the amount of light absorbed by the cyclohexenone.

then added and the mixture analyzed by g.l.c. Two concentrations were checked on the optical bench (Fig. 4).

Stern–Volmer plots (Fig. 5) were performed in essentially the same manner, and checked on the optical bench. Viscosities were measured with an Ostwald viscometer calibrated with hexane, cyclohexane, and cyclohexene. At 1 *M* cyclohexene in cyclohexane the viscosity was 8.84 × 10^{-3} and at 3.39 *M* cyclohexene the

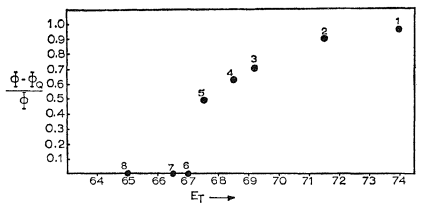

FIG. 2. Quenching of ketone phosphorescence by cyclohexenone. For the identification of the ketones, see Table 2.

Can. J. Chem. Downloaded from www.nrcresearchpress.com by 210.87.254.5 on 09/05/12
For personal use only.

Can. J. Chem. Downloaded from www.nrcresearchpress.com by 210.87.254.5 on 09/05/12
For personal use only.

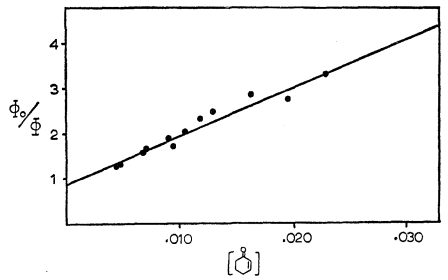

FIG. 3. Stern–Volmer plot for quenching of benzophenone reduction by isopropanol using cyclohexenone.

viscosity was 8.11×10^{-3} poise. The diffusion rates, calculated from the Debye equation were 7.36×10^9 and 8.03×10^9 M^{-1} s^{-1} at 1.0 M and 3.39 M respectively.

The densities were measured in the usual way using a picnometer.

Quantum Yield of Cyclohexenone Triplet Formation

Cyclohexenone (0.58 M) and the appropriate weight of *trans*-piperylene were dissolved in 10.0 ml of benzene. Five ml of the mixture were then transferred to the cell, degassed, and irradiated at 313 nm. The irradiated solution was distilled to remove the cyclohexenone and the ratio of *cis* to *trans* isomers was determined using a 15% β,β′-oxydipropionitrile on Diatoport S column (25′ × 1/8″) at 25°. The amount of *cis* isomer formed was 1.1–3.7%. No isomerization of the diene occurred on passage through neutral alumina or on distillation. A plot of $C/\Phi_{t\rightarrow c}$ against [*trans*-piperylene]$^{-1}$ is shown in Fig. 6. For comparison a similar plot of cyclopentenone (1) is included.

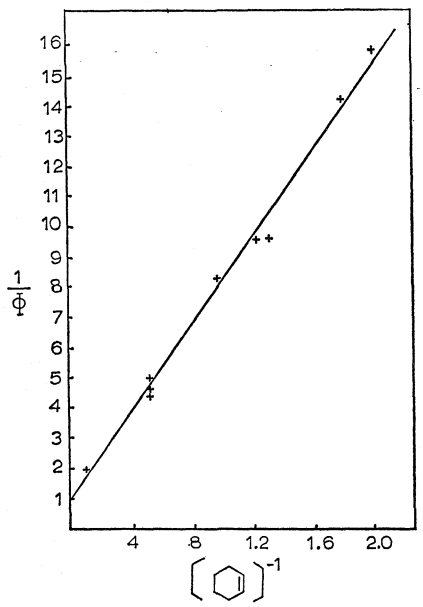

FIG. 4. Dilution curve for the addition of cyclohexenone to cyclohexene.

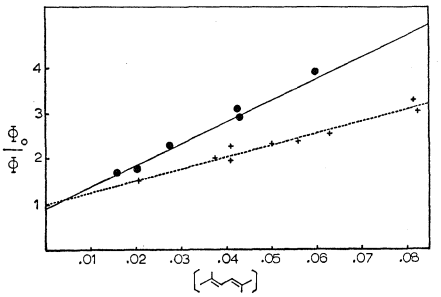

FIG. 5. Stern–Volmer plots for cyclohexenone addition to cyclohexene (—) 0.978 M, (- - -) 3.39 M.

Quenching of the Formation of the Tertiary Alcohol with Cyclopentene

The isopropanol addition product **2** was prepared by the method of Pfau *et al.* (30) and purified by chromatography on alumina (Woelm neutral, activity 4, eluant: 5% ether in carbon tetrachloride).

It was noted that the alcohol decomposed on the g.l.c., (Aerograph Hy-Fi-600-C-column: 5% FFAP on Diatoport S, 5′ × 1/8″) to give the same products as were obtained upon acid hydrolysis (30). The extent of decomposition depended both on the temperature of the column and the temperature of the injector. At temperatures above 200° the dehydration was virtually quantitative, while below 140° little decomposition was detected (CS_2 was used as solvent for these investigations). Acenaphthene was used as the calibrating compound for both the cyclopentene adduct and the tertiary alcohol **2**. The area ratio for the alcohol calibration was not as reproducible as that for the cyclopentene adduct, probably because of slight decomposition.

The quantum yields of addition were determined at 313 nm in a 5.0 cm cell and the cyclopentenone concentration was 0.01 M. A standard solution of cyclopentene

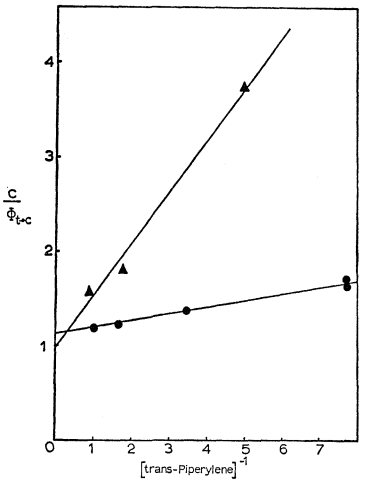

FIG. 6. Isomerization of *trans*-piperylene sensitized by (—○—) cyclopentenone and (—△—) cyclohexenone.

Can. J. Chem. Downloaded from www.nrcresearchpress.com by 210.87.254.5 on 09/05/12
For personal use only.

was prepared and the appropriate amount was introduced by pipette. The results are plotted in Figs. 7 and 8.

Attempted Quenching of Triphenylamine Phosphorescence by Cyclopentenone and Naphthalene

The spectra were recorded in the same manner as described above, but a Xenon light source (200 W) was used in place of the mercury source.

The samples were prepared by dissolving a weighed amount of triphenylamine in 10 ml of solvent and then transferring half to a volumetric flask into which quencher had been weighed. Both samples were degassed by two freeze–thaw cycles and then distilled bulb-to-bulb (twice) at 10^{-4} mm.

Results and Discussion

Intersystem Crossing Efficiency

In the case of cyclohexenone it was not found possible to achieve a limiting value in the quenching with piperylene as was the case (1) with cyclopentenone. In addition, at high quencher concentration, a number of unidentified products were formed, presumably by addition of cyclohexenone to piperylene and by the dimerization of piperylene. The sensitization of the isomerization may be represented by an equation of the form:

$$\frac{C}{\Phi_{t\rightarrow c}} = \frac{1}{\Phi_{ic}}\left(1 + \frac{k_d}{k_d + k_q[Q]}\right)$$

where k_d is the unimolecular rate constant for decay of the cyclenone triplet, [Q] is the piperylene concentration, k_q is the rate constant for energy transfer, C is the quantum yield of *cis*-piperylene from piperylene triplets (21) and Φ_{ic} is the intersystem crossing triplet yield for the cyclenone. A plot of $C/\Phi_{t\rightarrow c}$ against the reciprocal piperylene concentration (Fig. 6) gave intercepts (Φ_{ic}^{-1}) of close to unity for both ketones, the value for cyclopentenone already having been reported (1). From the slopes, k_d may be derived and it would appear, as was implicit in our earlier

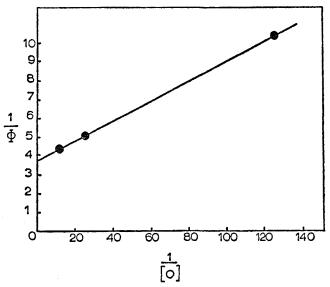

FIG. 7. Dilution curve for the addition of cyclopentenone to cyclopentene in isopropanol.

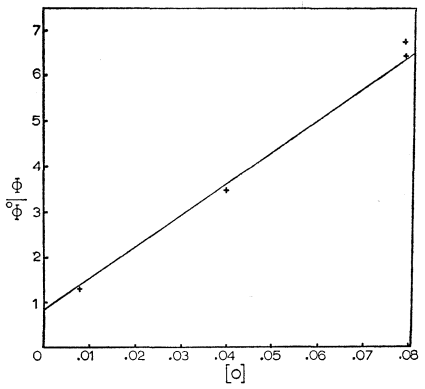

FIG. 8. Stern–Volmer plot. Quenching of alcohol **3** formation by cyclopentene.

discussion of cyclopentenone (1), that the triplet being quenched in the piperylene isomerization is the same as that involved in photoannelation. This is in agreement, in the case of cyclohexenone dimerization, with the work of Hammond and co-workers (22) who attempted to intercept a second triplet without success.

It thus seems probable that the yield of triplets in the case of isophorone and 4,4-dimethylcyclohexenone is near unity also, and the earlier low yield of reactive triplets recorded (11, see, however, reference 22) was a reflection of the partitioning of the first-formed exciplex (4).

Energy of the Cyclohexenone Triplet

The energy of the cyclohexenone triplet has been placed, by the photostationary state technique using 3 hydrocarbons, at 61 ± 1 kcal/mole (22). This contrasts with the results obtained on more rigid cyclohexenones by Kearns *et al.* (23, 24) which indicate lowest π,π triplets in the range 67–73 kcal/mole. Since cyclohexenone itself does not phosphoresce[5] we have attempted to locate the lowest triplet by the cruder chemical probe. In Table 1 are shown the ratio quantum yields of addition to cyclohexene and of dimerization induced by various sensitizers, to that yield obtained by direct irradiation. Since the cyclohexenone triplet is very short-lived (see below) complications due to back transfer of energy from the sensitizer are not expected. Slower Schenck quenching of the sensitizer (9, 25) by the

[5]Weak emission (at 61 ± 1 kcal/mole) from cyclohexenone has been reported but was, apparently, not reproducible (22).

Can. J. Chem. Downloaded from www.nrcresearchpress.com by 210.87.254.5 on 09/05/12
For personal use only.

alkene has not been corrected for and may be responsible for the lower ratios obtained for Φ_s/Φ_{add} in neat hydrocarbon. The 3 series of experiments (dimerization, addition to cyclohexene in benzene solvent, and addition in cyclohexene solvent) were not performed, for reasons associated with relative absorptivity, at the same cyclohexenone concentration. Correction could be made for this and adjustment made to 0.45 *M* cyclohexenone; it has the effect of moving the plot for addition in neat cyclohexene closer to that for addition in benzene solvent. However, since the effect is small and the method crude this has not been done here. The efficiencies for the addition to cyclohexene are plotted in Fig. 1.[6]

The results suggest, therefore, that a value in the region of 66–68 kcal/mole would be more appropriate for the triplet energy of cyclohexenone, significantly higher than that obtained from the photostationary state method.

As a further control the efficiency of energy transfer from the sensitizers to cyclohexenone was investigated by observing the degree of phosphorescence quenching of the various sensitizers by cyclohexenone. The results are listed in Table 2 and plotted graphically in Fig. 2. It will be observed that quenching drops from about 50% to zero over 0.5 kcal/mole. A sharper cut-off was, of course, to be expected as compared with the chemical processes, since the former is performed at 77 °K.[7] The energy of the ketone triplet below which quenching by cyclohexenone appears not detectable is the same as that determined by the sensitization experiments. It is noteworthy that Zimmerman and Hancock have observed weak emission in this region from 4,4-diphenylcyclohexenone (27).

A further conclusion to be drawn is that since the first set of experiments measured the energy of the *reactive* triplet, and since the phosphorescence quenching measured the energy, presumably, of the *lowest* triplet then, since these appear to be in the same region, the reactive triplet has a very similar energy to the lowest triplet, if it is, indeed not identical with it.[8]

The conclusion appears to be that the photostationary state technique of measuring triplet energies is susceptible to error arising from the chemical nature of the species involved. This may be associated with inefficient transfer which may, again, be associated with the twisted nature of the donor.

In any event the removal of this evidence as an indication of the position of the lower state of cyclohexenone also implies that the similarly determined energy of cyclopentenone T_1 is also suspect (3).

Decay and Reaction Rate Constants

With the tentative scheme already suggested (5), modified to include the possibility of direct product formation from the complex, the expression

$$[1] \qquad \Phi = \Phi_{ic} \cdot K \cdot \left(\frac{k_r[O]}{k_r[O] + k_d} \right)$$

may be derived. Here k_r is the rate constant for complex formation, and [O] is the concentration of olefin (cyclohexene). K is a composite constant and gives the fraction of complex that leads, eventually, to product, and is equal to:

$$\frac{k_5}{k_2 + k_5 + k_1} + \frac{k_2}{k_2 + k_5 + k_1} \cdot \frac{k_4}{k_4 + k_3}$$

where the rate constants have the significance indicated in Scheme 1.

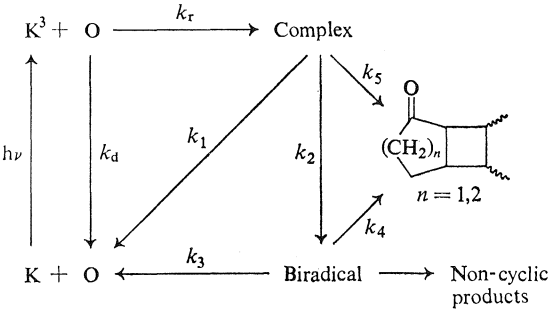

SCHEME 1

[6]It has been suggested that cyclohexenone exists in solution in aggregates. We have not (see Experimental) been able to confirm this (17).

[7]Using the usual Stern–Volmer expressions and the steady state assumption one obtains the formula:

$$\frac{\Phi_p - \Phi_q}{\Phi_p} = \frac{k_t[C]}{k_p/\Phi_p + k_t[C]}$$

where Φ_p is the quantum yield of phosphorescence of the donor, Φ_q the quantum yield in the presence of the quencher, k_d is the rate constant for decay of the donor and k_t is the energy transfer rate constant to the quencher. Since the ratio Φ_p/k_d is not known for most of the molecules used as donors, Fig. 2 has no significance other than to show the cut-off for sensitization.

[8]The report (22) that the dimerization of cyclohexenone may be sensitized by naphthalene (E_T = 61 kcal/mole) appears to contradict this. However, it is possible that this is singlet sensitization as has been found for cyclopentenone (26).

Can. J. Chem. Downloaded from www.nrcresearchpress.com by 210.87.254.5 on 09/05/12
For personal use only.

At the moment no way has been found to analyze K. From equation [1] the usual Stern–Volmer expression may be derived

$$\frac{\Phi_0}{\Phi} = 1 + \frac{k_q[Q]}{k_d + k_r[O]}$$

where k_q is the rate constant for quenching (with 2,5-dimethyl-2,4-hexadiene) and [Q] the concentration thereof. The value of k_q cannot be accurately assessed (28) but a diffusion controlled value in cyclohexane solvent was assumed; $k_q = 7.4$ and $8.1 \times 10^9\ M^{-1}\ s^{-1}$ at 0.98 and 3.4 M cyclohexene and is likely to be within a factor of 2 of the correct value. Such plots at 2 different concentrations in cyclohexane solvent are represented in Fig. 5, the slopes of which give the sum of k_d and k_r. A plot of the reciprocal of the quantum yield against the reciprocal of the olefin (cyclohexene) concentration (the reciprocal of eq. [1]) gives, from the slope, the ratio of k_d and k_r. The unimolecular decay rate constant was evaluated at $1.7 \times 10^8\ s^{-1}$, and bimolecular rate constant for annelation at $2.5 \times 10^7\ M^{-1}\ s^{-1}$. The value of k_d previously reported (10) for isophorone is much lower, but this figure requires modification to accord with eq. [1]. From the published data a value of 1.3 and $1.4 \times 10^8\ s^{-1}$ may be obtained in good agreement with our value.[9] A further value, that for 4,4-diarylcyclohexenones, of near $10^9\ s^{-1}$ has recently been recorded (29). The more rigid phenanthrone (**1**) has a maximum value of k_d at $4 \times 10^7\ s^{-1}$, but

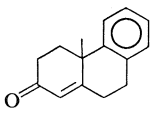

1

since lifetime appears to be associated with the rigidity of the system (2), the longer lifetime of **1** is not surprising.

A comparison may also be made with cyclopentenone. The value we have obtained in ether solvent (for the study of variation of decay and reaction rate constants with temperature) was $1.5 \times 10^8\ s^{-1}$ (5). Because of the errors inherent in k_q, assessment comparisons should be effected in the same type of solvent system. The value for cyclopentenone (determined in the addition to *trans*-hex-3-ene) using pentane as solvent, and a k_q value of $2.5 \times 10^{10}\ M^{-1}\ s^{-1}$ (4), was $\sim 8.5 \times 10^7\ s^{-1}$, that is, somewhat slower. Wagner and Bucheck[9] (8) have obtained a value of about half this from their study of cyclopentenone dimerization in acetonitrile (using $k_q = 10^{10}\ M^{-1}\ s^{-1}$).[10]

The value of k_r obtained for addition to cyclohexene cannot be compared exactly with values obtained for cyclopentenone.[11] The latter using ether as solvent has $k_r = 10.3 \times 10^8\ M^{-1}\ s^{-1}$. The values obtained previously (1) using acenaphthene as quencher and cyclohexane as solvent in the Stern–Volmer plot, recalculated on the assumption of complex formation, give $k_r = 7.8 \times 10^8\ M^{-1}\ s^{-1}$, whilst piperylene in neat cyclohexene gave $7.5 \times 10^8\ M^{-1}\ s^{-1}$. There is no question, therefore, that there is almost an order of magnitude difference in the value of the rate constants for addition to cyclohexene between cyclopentenone and cyclohexenone. If k_d for cycloheptenone were no lower than that for cyclohexenone, k_r need only drop by the same proportion again for decay to be fully competitive with annelation. That is, a change in the rate constant for addition as well as a possibly increased unimolecular decay rate constant is probably responsible for the reported lack of photochemical addition of cycloheptenone to olefins, in agreement with previous suggestions (7).

The Case for Multiple Reactive Triplets

We shall first consider the situation as regards cyclopentenone. Some time ago we reported (26) that sensitizers of ca. 73 kcal/mole were required to induce annelation, but that nonetheless cyclopentenone quenched benzophenone at a near diffusion controlled rate. This, despite the fact that in the presence of alkene no annelation occurred. Products of alcohol addition were observed as noted first by Pfau *et al.* (30). It was also found that although in moderate concentration in isopropanol, dimerization occurred, at below concentrations of 0.12 M the same tertiary alcohol was obtained in the absence of sensitizer

[9]Professor Wagner (personal communication) has obtained a value of $k_d = 3 \times 10^8\ s^{-1}$ in acetonitrile. His value for cyclopentenone in the same solvent is $4 \times 10^7\ s^{-1}$. We wish to thank Professor Wagner for his amiable exchange of information.

[10]These variations emphasize the need for making comparisons in the same type of solvent system. Aside from the questionable values for k_q, the solvent has an effect on the quantum yield of dimerization (10), and may conceivably have a specific effect on k_d.

[11]Such values will shortly be available at 2 temperatures.

Can. J. Chem. Downloaded from www.nrcresearchpress.com by 210.87.254.5 on 09/05/12
For personal use only.

by a chain process (1). This was believed to have been initiated by hydrogen abstraction by the triplet ketone. On this basis it was suggested that T_2 was the reactive species, and that T_1 merely abstracted hydrogen from the medium. That the 2 processes occur from 2 different species is a permissible interpretation, but is not necessarily required. A plot of the reciprocal of the quantum yield of addition of cyclopentenone to cyclopentene in isopropanol against the reciprocal of cyclopentene concentration (reciprocal of eq. [1]) has a slope (k_d/Kk_r) of .053 M^{-1} (Fig. 7) and an intercept ($1/K$) of 3.7. Hence $k_r/k_d \sim 70$. With the assumption that the *same* triplet is responsible for hydrogen abstraction (k_i), and that the triplet reacts only with the olefin the following Stern–Volmer relationship may be derived

$$\frac{\Phi_A^0}{\Phi_A} = 1 + \frac{k_r[O]}{k_i[I] + k_d}$$

where [I] is the concentration of isopropanol and Φ_A is the quantum yield of tertiary alcohol **2**. A plot of Φ_A^0/Φ_A against olefin concentration (Fig. 8) gave a slope of 69, whence $k_d + k_i[I] \approx k_d$, and, since $k_d \sim 10^8$, $k_i < 10^7$, which is acceptable.

If, on the other hand, two triplets are assumed with rate constant $T_2 \rightarrow T_1$ of k_1, and $T_2 \rightarrow T_0$ (k_2) then the annelation now requires the expression:

$$\frac{1}{\Phi} = \frac{1}{K} \cdot \left(1 + \frac{k_1 + k_2}{k_r[O]}\right)$$

and the value of 70 M^{-1} of the slope now refers to the quotient ($k_r/k_1 + k_2$). The Stern–Volmer expression is now:

$$\frac{\Phi_A^0}{\Phi} = 1 + \frac{k_r[O]}{k_1 + k_2}$$

and the value of 69 M^{-1} is in accord with this. No distinction can therefore be made.

Since the products obtained by Pfau may also be formed by the addition of isopropyl ketyl radicals produced by the reaction of unquenched benzophenone triplets with isopropanol, such arguments are inadmissible for proof of the chemical intervention of T_2. *This*, since the independent determination of the triplet energy of T_1 by the photostationary state method has now been shown to be suspect, *must depend essentially on the fact of the fast rate of quenching of benzophenone triplets by cyclopentenone.*

For purposes of comparison with cyclopentenone the quenching of benzophenone triplets in isopropanol by cyclohexenone was investigated. A linear Stern–Volmer plot (31–35) was obtained with a slope of 105 M^{-1} (Fig. 3). The Stern–Volmer plot of the quenching of the reduction by naphthalene (33) gave a slope of 192 M^{-1}. The ratio of the quenching rate of cyclohexenone to that of naphthalene (presumably diffusion controlled) is 0.54, as compared to 0.35 for cyclopentenone. The efficiency of phosphorescence quenching of benzophenone could possibly not have led to the expectation of so effective a process, but the situation, in view of the lower energy of the reactive triplet of cyclohexenone is somewhat ambiguous and certainly cannot be construed as indicating the existence of a very low cycloadditively unreactive triplet in cyclohexenone.

Further evidence accumulated from studies on constrained cyclopentenones showing phosphorescent emission did not resolve the problem (9), and the situation remained that either there was a cyclopentenone triplet below 69 kcal/mole, or a special quenching mechanism in cyclopentenone interaction with benzophenone was required.

We have shown earlier (9) that triphenylamine (E_T = 71 kcal/mole) (36) does not sensitize any chemical reaction in cyclopentenone. We have now observed that the phosphorescence of the amine is not quenched even by molar cyclopentenone, whereas 0.112 M naphthalene quenches 75% of the emission. This is surely clear evidence against the existence of a low triplet. On the other hand it is hard to provide an adequate interpretation of the quenching rate observed of benzophenone. Schenck-type quenching (9, 25) seems improbable since with alkenes it is already slow and deactivation of the bond should decrease the rate. A possibility has been indicated (9) wherein a complex formation occurs between the two ketones in the same way as in annelation, but now between the carbonyl group of benzophenone and the conjugated ethylenic linkage. If the decay of this exciplex were fast as compared with combination to give products then an explanation would be at hand. To examine this possibility, the α,β-unsaturated ketone cholestenone ($E_T \sim$ 73 kcal/mole) (24) was tested as a quencher for triplet benzophenone. At 0.026 M concentration, no quenching whatsoever of benzophenone reduction by isopropanol was detected. At this concentration Φ_0/Φ using cyclo-

Can. J. Chem. Downloaded from www.nrcresearchpress.com by 210.87.254.5 on 09/05/12
For personal use only.

hexenone as a quencher is 3.6 and for cyclopentenone the value is 2.7. There exists the possibility of chemical quenching of benzophenone triplets by reversible hydrogen atom transfer (37).[12] This would have to occur at such a rate that calculated as "energy transfer" it would seem to be near diffusion controlled both for cyclohexenone and cyclopentenone. This seems unlikely. The problem rests, therefore, without definitive solution, but we feel that our evidence for a reactive T_2 state in cyclopentenone is now inadequate. Observations by Chapman and his colleagues may be relevant to the quenching problem.

Chapman has suggested the presence of 2 reactive triplets following the excitation of certain cyclohexenone derivatives. The suggestion is based on 2 sets of experimental evidence. The first (10) depends on the observation that different proportions of head-to-head and head-to-tail dimers of isophorone were obtained by direct irradiation and by sensitization with benzophenone. The possibility of a complex of isophorone with benzophenone was considered unlikely by these authors, the remaining possibility then being the existence of 2 reactive triplets formed by selective excitation. If this explicit assumption were unfounded, then this same complexation could be responsible for the surprisingly efficient quenching of benzophenone by cyclohexenone and, *a fortiori* by cyclopentenone. This would remove the only remaining evidence for a reactive T_2 state.

The second set of experiments concerns the differential quenching of the addition of 4,4-dimethylcyclohexenone to 1,1-dimethoxyethylene by di-*tert*-butyl nitroxide which led to variation in the ratio of *cis* and *trans* adducts (10). There appears no doubt that differential quenching is occurring, but the possibility exists that the species being quenched are not the primary triplets. Since exciplexes seem likely as intermediates (4, 8) it is probable that 2 different exciplexes lead to the 2 different isomers, through the different biradicals, and that the radical quencher may be able to intervene in the transformation and decay of these where the energy transfer-type quencher cannot.[13] If the postulate of 2 reactive primary triplets in this reaction be unnecessary, then the isophorone case is correspondingly weakened, and the likelihood of a complex between benzophenone and cyclohexenone strengthened.

At the moment there is little evidence available to indicate the nature and properties of the complex, nor is it certain that the biradical derived from it is the only source of cyclobutane derivatives.

Relative Triplet Levels and Reactive States

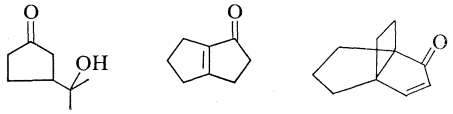

2 **3** **4**

The ketone **3** undergoes photoannelation, but the emission is without the structure so far found for authentic unmixed $^3(n,\pi)$ emission (9). On the other hand the ketone **4** shows such structure, although perhaps ambiguously, suggesting $^3(n,\pi)$ or mixed emission; it also cycloadds. Steroid Δ^4-3 ketones have been shown to add to ethylene (38) and excitation–emission studies (23, 24) may indicate a probable lowest $^3(\pi,\pi)$ state.

The calculations of Zimmerman *et al.* (39) suggest a similar charge difference across the ethylenic linkage in both states for enones, but in the $^3(\pi,\pi)$ state both positions are electron deficient. This would imply that cycloaddition should be an electrophilic process. It was at one time thought so based on competition experiments (6) and quantum yields of addition. Since it is known that both these interpretations are invalidated by the intervention of a complex an assured conclusion cannot be drawn.

The charge distribution calculated by Zimmerman *et al.* (39) refers to a flat molecule with bond lengths equal to those of the ground state. It is by no means certain whether the excited molecule reacts in this condition or in a relaxed state.[14]

---

[12]We are indebted to Professor P. J. Wagner, who suggested this possibility, for a discussion of this point.

[13]In Scheme 1 only one exciplex is shown. If two should be possible these may be interconvertible, in thermodynamic equilibrium depending on the solvent, or separated by a barrier which, under the conditions of the experiment may not interconvert. The second situation seems the most likely.

[14]It appears that the π,π triplet relaxes by rotation of the terminal carbon atom. We wish to thank Dr. J. Wasson, Professors D. P. Santry and J. J. McCullough, and Professor N. C. Baird (who have performed independent calculations establishing this fact) for informing us of their results. Further, Professor Baird has informed us that his calculations indicate the n,π triplet of the enone system may relax significantly by bond stretching. It also appears to be a general conclusion that a finite barrier to $^3(\pi,\pi)$ relaxation exists.

Can. J. Chem. Downloaded from www.nrcresearchpress.com by 210.87.254.5 on 09/05/12
For personal use only.

The energy levels of the two important excited states which, of course, change from their Franck–Condon values on relaxation may also, on relaxation, change their relative positions with regard to the ground state. Since distortion in the $(\pi,\pi)^*$ triplet may be very considerable, the O—O band in the emission or S → T absorption spectra, important methods of determining the state and energy of the lowest triplet, may be very far removed from the main emission (40). A misleading impression of the spectroscopic triplet energy involved may be gained which, in turn, may lead to an incorrect assignment of relative energy levels of triplets.

The energy measured by energy-transfer experiments is more confusing yet to interpret. Energy (triplet–triplet) transfer to give the relaxed triplet may not be efficient (40), but since important Franck–Condon factors are involved as well as energies it would seem that more data involving transfer from semi-flexible donor systems is required before the situation becomes clearer. In any event it is possible for a higher energy sensitizer to be required for the efficient generation of a relaxed triplet, or, conversely, that the energy of a chemically reactive triplet be significantly below that of the sensitizer required to generate it, a point germane to the issue under discussion.

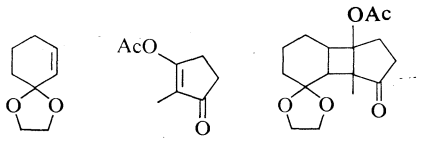

5 **6** **7**

It does seem clear that whatever the electron distribution in the reacting triplet its demands are not overwhelming since the overall dipole of the substrate molecule, not merely that of the chromophore, is important in determining orientation. This has been shown in cyclopentenone dimerization (1, 7, 41) where dipole–dipole stabilization with ionic solvents follows the Kirkwood–Onsager relationship. The addition of **5** to **6** shows this in a striking manner, **7** being formed to the extent of 98% in hydrocarbons and 45% in methanol (42). Whether the dipole of the substrate molecule as a whole or merely that of the olefinic chromophore is the more important has yet to be established. This fact, which has important implications for synthesis should be ascertainable from substrate molecules in which these factors are opposed.[15]

1. P. DE MAYO, J.-P. PETE, and M. F. TCHIR. Can. J. Chem. **46**, 2535 (1968).
2. (*a*) P. E. EATON. J. Amer. Chem. Soc. **84**, 2454 (1962); (*b*) P. E. EATON and W. S. HURT. J. Amer. Chem. Soc. **88**, 5038 (1966).
3. J. L. RUHLEN and P. A. LEERMAKERS. J. Amer. Chem. Soc. **89**, 4944 (1967).
4. P. DE MAYO, A. A. NICHOLSON, and M. F. TCHIR. Can. J. Chem. **47**, 711 (1969).
5. R. O. LOUTFY, P. DE MAYO, and M. F. TCHIR. J. Amer. Chem. Soc. **91**, 3984 (1969).
6. E. J. COREY, J. D. BASS, R. LE MAHIEU, and R. B. MITRA. J. Amer. Chem. Soc. **86**, 5570 (1964).
7. P. E. EATON. Account Chem. Res. **1**, 50 (1968).
8. P. J. WAGNER and D. J. BUCHECK. Can. J. Chem. **47**, 713 (1969).
9. R. L. CARGILL, P. DE MAYO, A. C. MILLER, K. R. NEUBERGER, D. M. POND, J. SALTIEL, and M. F. TCHIR. Mol. Photochem. **1**, 301 (1969).
10. O. L. CHAPMAN, P. J. NELSON, R. W. KING, D. J. TRECKER, and A. A. GRISWOLD. Rec. Chem. Progr. Kresge-Hooker Sci. Libr. **28**, 167 (1967).
11. O. L. CHAPMAN, T. H. KOCH, F. KLEIN, P. J. NELSON, and E. L. BROWN. J. Amer. Chem. Soc. **90**, 1657 (1968).
12. B. D. CHALLAND. Ph.D. Thesis. University of Western Ontario, 1968.
13. M. DITTRICH. Ann. **264**, 174 (1891).
14. W. TADROS, Y. AKHNOOKH, and G. AZIZ. J. Chem. Soc. 186 (1953).
15. S. PASYNKIEWICZ, W. DAHLIG, T. WOJNAROWSKI, and T. RADZIWONKA. Roczniki Chem. **37**, 293 (1963).
16. M. S. NEWMAN and A. G. PINKUS. J. Org. Chem. **19**, 978 (1956).
17. E. Y. LAM, D. VALENTINE, and G. S. HAMMOND. J. Amer. Chem. Soc. **89**, 3482 (1967).
18. M. KASHA. J. Opt. Soc. Amer. **38**, 929 (1948).
19. A. A. LAMOLA, and G. S. HAMMOND. J. Chem. Phys. **43**, 2129 (1965).
20. D. R. ARNOLD. Advances in Photochemistry, Vol. 6. Ed. W. A. Noyes, G. S. Hammond and J. N. Pitts, Jr. Interscience, New York, 1968, p. 301.
21. A. A. LAMOLA and G. S. HAMMOND. J. Chem. Phys. **43**, 2129 (1965).
22. E. Y. Y. LAM, D. VALENTINE and G. S. HAMMOND. J. Amer. Chem. Soc. **89**, 3482 (1967).
23. D. R. KEARNS, A. MARSH, and K. SCHAFFNER. J. Chem. Phys. **49**, 3316 (1968).
24. D. R. KEARNS, A. MARSH, and K. SCHAFFNER. Helv. Chim. Acta, **51**, 1890 (1968).
25. J. SALTIEL and K. R. NEUBERGER. J. Amer. Chem. Soc. **91**, 3658 (1969).
26. P. DE MAYO, J.-P. PETE, and M. F. TCHIR. J. Amer. Chem. Soc. **89**, 5712 (1967).
27. H. E. ZIMMERMAN and K. G. HANCOCK. J. Amer. Chem. Soc. **90**, 3749 (1968).
28. P. J. WAGNER and I. KOCHEVAR. J. Amer. Chem. Soc. **90**, 2232 (1968).

[15]A possible complexity which may arise in the case of close lying triplets is that polar solvents may affect the energies of these states such that, as was found by Porter and Suppan (43) with aromatic ketones, $^3(n,\pi)$ and $^3(\pi,\pi)$ may reverse relative positions. Such a phenomenon may explain the observation of oxetane formation (11) during photoannelation.

29. H. E. ZIMMERMAN and N. LEWIN. J. Amer. Chem. Soc. **91**, 879 (1969).
30. M. PFAU, R. DULOV, and M. VILKAS. C. R. 1817 (1962).
31. W. M. MOORE, G. S. HAMMOND, and R. P. FOSS. J. Amer. Chem. Soc. **83**, 2789 (1961).
32. G. S. HAMMOND, W. P. BAKER, and W. M. MOORE. J. Amer. Chem. Soc. **83**, 2795 (1961).
33. A. BECKETT and G. PORTER. Trans. Faraday Soc. **59**, 2038, 2051 (1963).
34. J. N. PITTS, H. W. JOHNSON, and T. KUWANA. J. Phys. Chem. **66**, 2456 (1962).
35. G. PORTER and G. WILKINSON. Trans. Faraday Soc. **57**, 1686 (1961).
36. N. J. TURRO. Molecular photochemistry. Benjamin, New York, 1967, p. 132.
37. B. M. MONROE and S. A. WEINER. J. Amer. Chem. Soc. **91**, 450 (1969).
38. J. FRIED. Tetrahedron Lett., 3451 (1966).
39. H. E. ZIMMERMAN, R. W. BINKLEY, J. J. MCCULLOUGH, and G. A. ZIMMERMAN. J. Amer. Chem. Soc. **89**, 6589 (1967).
40. A. BYLINA. Chem. Phys. Lett., **1**, 509 (1968).
41. G. MARK, F. MARK, and O. E. POLANSKY. Ann. **719**, 151 (1968).
42. B. D. CHALLAND and P. DE MAYO. Chem. Comm. 982 (1968).
43. G. PORTER and P. SUPPAN. Trans. Faraday Soc. **62**, 3375 (1966).

Can. J. Chem. Downloaded from www.nrcresearchpress.com by 210.87.254.5 on 09/05/12
For personal use only.

Can. J. Chem. Downloaded from www.nrcresearchpress.com by 210.87.254.42 on 09/05/12
For personal use only.

On the mechanism of ring opening in 2-pyrone irradiations[1]

J. P. GUTHRIE, C. L. MCINTOSH, AND P. DE MAYO
Department of Chemistry, University of Western Ontario, London, Ontario

Received August 12, 1969

The irradiation of 2-pyrone in benzene followed by pyrolysis gives a poor yield of cyclooctatetraene. The irradiation of 4-methoxy-6-methyl-2-pyrone in water gives *cis*-β-methyl glutaconic half ester and the corresponding diacid. Irradiation in benzene followed by the addition of water gives a mixture of the *cis* and *trans* glutaconic derivatives. It is believed that these substances derive from the β-lactone formed by irradiation, and support for this view is obtained from low temperature irradiations. An oligomeric intermediate (**16**) is suggested as a second intermediate in the irradiation in benzene, and a hemiketal (**20**) in the aqueous irradiation.

Canadian Journal of Chemistry, 48, 237 (1970)

About 10 years ago (1), it was reported that the irradiation of 4,6-dimethyl 2-pyrone (**1**) in methanol resulted in the formation of a methyl 3-acetonylcrotonate (**3**). It was suggested at that time, largely by analogy with the behavior of cyclic dienones (2), that a ketene (**2**) was involved as an intermediate. Subsequently it was found (3) that irradiation of a concentrated solution of the pyrone in benzene produced dimers, the pyrolysis of which gave a useful yield of tetramethylcyclooctatetraene (3, 4).

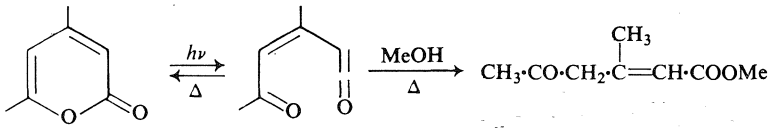

1 **2** **3**

Since the route to cyclooctatetraenes appeared promising we undertook a brief study of the irradiation of other, easily accessible, pyrones. Regrettably, aside from the poor yield of cyclooctatetraene itself (obtained from the pyrolysis of mixed 2-pyrone dimers) reported herein we have not, as yet, been able to extend the scope of the reaction. It may be that in the few cases tried, (2 + 2) or (2 + 4) dimers were formed rather than the desired (4 + 4). Orbital symmetry considerations may not apply since the reaction apparently proceeds through a triplet (5).

During this time Corey and Streith (6) reported that irradiation of 2-pyrone (**4**) at −10 to −20° resulted in isomerization to bicyclo[2.2.0]pyran-2-one (**5**), and commented that this strained β-lactone was a possible, alternative, precursor of the acetonylcrotonate obtained, in the case of **1**, by irradiation in methanol.

Finally, Pirkle and McKendry have very recently (7) attempted to resolve the problem of the nature of the acetonylcrotonate precursor. They reported that the irradiation of 2-pyrone (**4**) in methanol produced methyl *trans*-4-formyl-3-butenoate (**6**), a reaction analogous to the conversion of **1** to **2**. In addition they also observed that the thermal reaction of **5** with methanol gave the methoxypentadienoic acid (**7**) and not **6**. This appears to substantiate the correctness of the original surmise (1), and to exclude **5** as the precursor of **6** in any ground state process. Although these authors found that irradiation of **5** in methanol through Vycor did produce **6** (irradiation through Corex did not) they concluded that this was most probably due to the reversion of **5** to **4**. Since **4** is converted to **6** by irradiation through Pyrex, a direct route is required.

The authors also observed that the irradiation of 2-pyrone through Corex at −190° resulted in a steady state concentration (~ 5%) of a substance having an absorption band at 2128 cm^{-1} which was attributed to a ketene, **8**. On addition of methanol to the glass, the ester **6** was produced (0.3% yield) in a dark reaction. No absorption corresponding to **5** was, apparently, observed.

The formation of **7** was explained in terms of a zwitterionic intermediate. Since this is relevant to our own observations the subject will be returned

[1]Photochemical synthesis, Part 30. For Part 29 see reference 18. Publication No. 2 from the Photochemistry Unit.

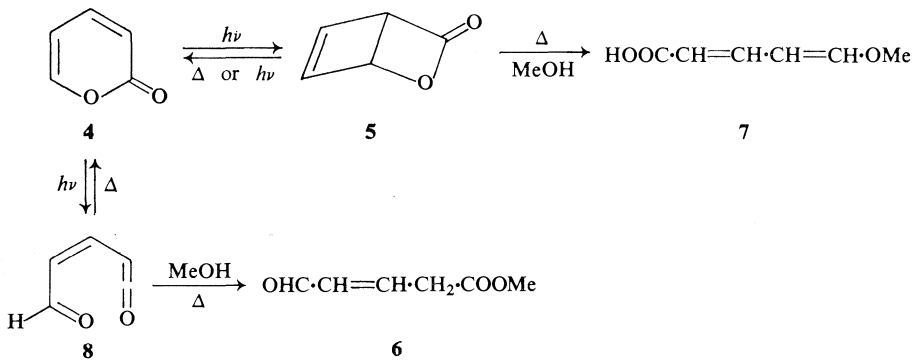

SCHEME 1

to later. The scheme arrived at by Pirkle and McKendry may, therefore, be summarized in Scheme 1, and corresponds largely to that which we have arrived at independently over the past few years (8).[2]

Irradiation of 4-methoxy-6-methyl-2-pyrone (**9**) in benzene did not result in significant dimer formation. The infrared (i.r.) spectrum showed the presence of carbonyl absorption at 1740 and 1645 cm^{-1} indicating the absence of both β-lactone and ketene. Nonetheless hydrolysis of the material in solution by the addition of aqueous dioxan or aqueous methanol at 50° gave a mixture of *cis*-(**10**) and *trans*-(**11**) β-methylglutaconic half esters and their corresponding diacids. The i.r. and nuclear magnetic resonance (n.m.r.) spectra of this mixture were identical with those reported by Jackman and Wiley (9). The acids and half-esters were converted into the diesters with diazomethane and separated by gas–liquid chromatography (g.l.c.), and identified separately (9).

The position of the double bond in the half-esters, not shown by these measurements, was proven by ozonolysis to give methyl acetoacetate characterized as its 2,4-dinitrophenylhydrazone (10).

It has appeared that the benzene solution contained a readily hydrolyzable species which was not one of the reactive intermediates so far identified. A clue that a simple molecular species was not involved was obtained when osmometric molecular weight determination revealed an average molecular weight 5 times that of the starting material.

It appeared that the most economical interpretation of these results was that indicated in Scheme 2. It was presumed that the fastest photochemical reaction was ketene (**12**) formation, and that the fastest thermal process was the reversal of this. The next, slower, photochemical process was presumed to be conversion to the β-lactone (**13**).

The rapid reversal of the lactone to pyrone appeared to be the normal reaction in the case of **1** and **4**, and, since any other reaction of the pyrone appeared slow (11), the overall reaction in methanol or water as solvent is the slow conversion of the ketene to the corresponding acid or ester. However, in the case of **9** the presence of the methoxyl group facilitates the cleavage of the carbon–oxygen bond of the β-lactone and instead of reversal of **13** to **9**, the system is drained in the direction of the zwitterion **14**. This type of ion, but less the stabilization from the methoxyl group, has been invoked by Corey and Pirkle (11) in the formation of tricyclo[$2^{3,6}$.1.1.0]pyran-2-one (**15**), and, as already mentioned, by Pirkle and McKendry in the formation of **7**, thermally, from **5**. The intermolecular addition of the carboxylate ion of one molecule to the cation of another then leads to the formation of a series of oligomers **16** which, as reported, has the average molecularity of 5.

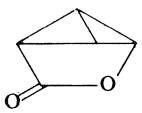

15

[2]Professor T. Money (University of British Columbia) has also arrived at a similar modified scheme from his study of triacetic acid lactone. We cordially thank Professor Money for a preprint of his forthcoming publication and for a free exchange of views.

Can. J. Chem. Downloaded from www.nrcresearchpress.com by 210.87.254.42 on 09/05/12
For personal use only.

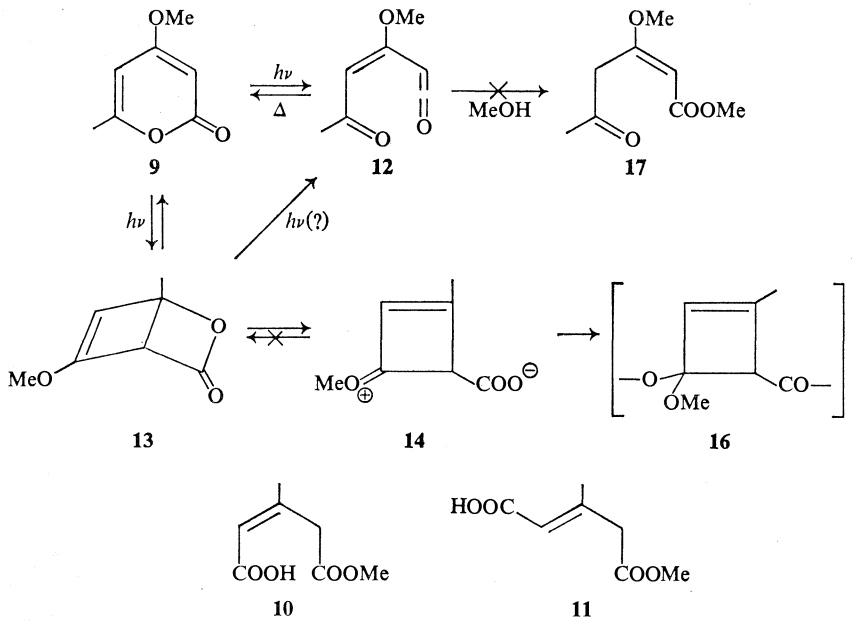

SCHEME 2

It appears in this system that the draining of product in the direction of **14** is sufficiently effective that the concentration of ketene is too low for normal ketoester formation. We have found that, in contrast with the alkyl pyrones, the irradiation of **9** in water gives the *cis*-half ester (**10**) and the corresponding diacid; no ketoester **17** (or isomer) was detected. Conceivably the methoxyl group may, by slightly increasing the basicity of the ketonic oxygen in **12**, increase the rate of reversal to **9**.

This general mechanism is supported by the results obtained by irradiation of **9** through Pyrex or quartz at $-190°$. Such a procedure produces a substance having i.r. absorption at 1807 and 1600 cm^{-1} in accord with expectation for the β-lactone **13** (6). No peaks were observed in the 2100–2120 cm^{-1} region as expected for a ketene, suggesting that either no ketene has been formed or, as we presently prefer, the reverse reaction with **12** even at this temperature is fast. When allowed to warm to $-100°$ the new peaks receded with the concurrent growth of peaks attributable to **9**.

Similar results were obtained in the low temperature irradiation of **1**. In that case irradiation through quartz did produce a band at 2118 cm^{-1} (in addition to the bands at 1809 and 1628 cm^{-1}) possibly to be attributed to a ketene. Irradiation at $-190°$ in the presence of methanol also did not give **3**, but this may merely reflect the rapidity of recyclization.

In principle it was possible to envisage the reclosure of ion **14** in the opposite sense from that of its formation. This would give the β-lactone **18**, which could then form the pyrone **19** in a thermal reaction. This pyrone, the methyl ether of β-methylglutaconic anhydride, could hydrolyze to the half-ester (**10**). However, no evidence for the presence of this pyrone could be found in the i.r. spectrum of irradiated **9** in benzene. This is in agreement with Pirkle and McKendry's recent finding that the zwitterion from deuterated **4** does not close back on the symmetrical allylic position (7), and leads one to consider the conversion of **13** to **14** as an essentially irreversible process. In addition we have found that the pyrone **19** is converted on standing in ethanol to a mixture of *cis*- and *trans*-β-methylglutaconic acid ethyl methyl esters. Addition of methanol to the benzene solution of the irradiation product did not produce any diester. Furthermore, the irradiated benzene solution of **19** did not show (osmometer) the presence of oligomeric material.

The different stereochemical consequences observed, depending on whether water was available or not, suggest the participation of 2 reactive species in the conversion of **14** to the final products. In the irradiation in the presence of water,

Can. J. Chem. Downloaded from www.nrcresearchpress.com by 210.87.254.42 on 09/05/12
For personal use only.

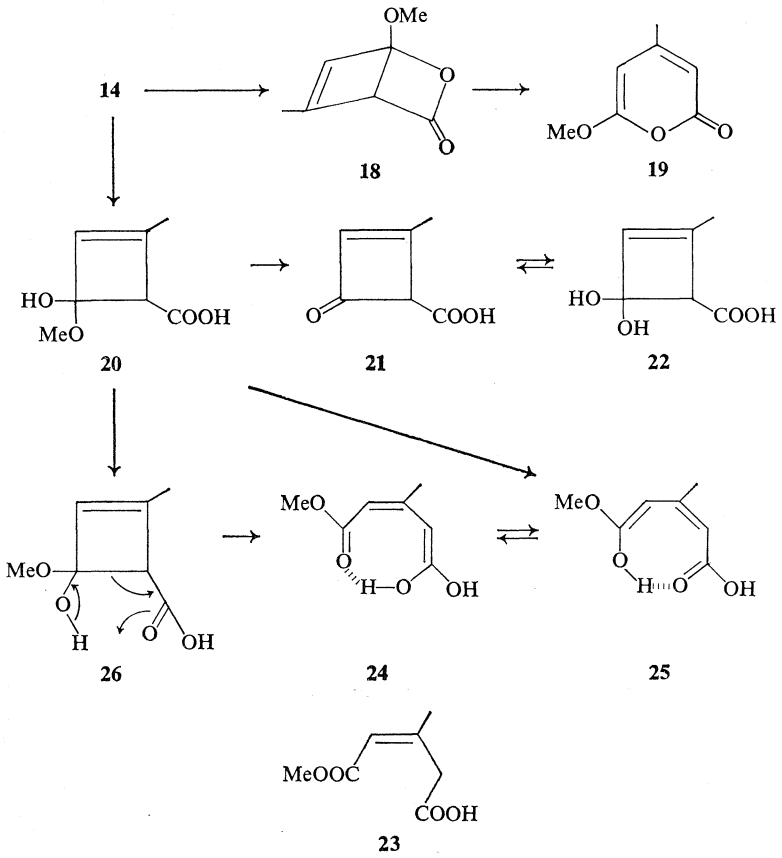

14 would be expected to be hydrated to give the hemiketal **20**, and this in turn could be converted to the ketone **21**, which would be in equilibrium with the ketone hydrate **22**. Two obvious pathways are open for the further transformation of these substances.

Dealdolization of **20**, most probably occurring by an intramolecular process, **26**, could lead to **24**, which should be in rapid tautomeric equilibrium with **25**. Rotation about the vinyl bonds in **24** or **25** gives a series of rotamers. It is not possible to predict the relative rates of protonation at carbon to give **10** as against *s-cis* – *s-trans* interconversion, yet exclusive formation of **10** requires that either protonation occur faster than rotation, or that protonation be much faster in the *s-cis* conformer. Furthermore, protonation of the carbon atom γ to the developing carboxyl group must be strongly preferred over protonation at the α carbon since no **23** was observed. Preferential intramolecular proton transfer from the carboxylic acid function is compatible with these requirements.

In an alternative pathway the cyclobutene (**20**) might undergo a thermal electrocyclic ring opening to **25** or rotamer thereof. This electrocyclic process would seem to be taking place under very mild conditions, but such transformations under not much more severe conditions have already been noted (7, 12, 13). Since one cannot be certain that rotational isomerization is not rapid relative to protonation on carbon, the stereochemistry of the final product reveals nothing about the stereochemistry of the ring opening.

Formation of both **10** and **11** when the reaction proceeds through the oligomer **16** may reflect a change in mechanism. It may also merely indicate a change in relative rates of the possible proton transfers in the absence of a neighboring carboxylic acid.

Experimental

Irradiation and Pyrolysis of 2-Pyrone

Coumalic acid was decarboxylated over a copper catalyst at 650° as described by Zimmerman *et al.* (14) to give 2-pyrone, b.p. 94°/15 mm; λ_{max}(EtOH) 217, 289

Can. J. Chem. Downloaded from www.nrcresearchpress.com by 210.87.254.42 on 09/05/12
For personal use only.

Can. J. Chem. Downloaded from www.nrcresearchpress.com by 210.87.254.42 on 09/05/12
For personal use only.

nm (ε 2700, 7500). The pyrone (3.2 g) was dissolved in 5 ml of dry benzene in a 9 mm Pyrex tube, the solution was degassed for 1/2 h with oxygen-free nitrogen, the tube sealed, then strapped to the outside of a water-cooled immersion well containing a Pyrex filter and a 450 W Hanovia medium-pressure arc lamp. The whole apparatus was immersed in a water-filled 4 l beaker and wrapped with aluminum foil, which acted as a reflector. The solution was irradiated for 120 h, then the crystalline precipitate filtered, (1.28 g, 40%). The i.r. absorption of the solid showed little if any absorption at 1560 cm^{-1} due to 2-pyrone. Attempted separation of the crystalline products by fractional recrystallization was unsuccessful.

The crystals, 300 mg, were pyrolyzed in a Pyrex distillation apparatus with a free flame by heating to above their melting point for 10 min. The resultant material was distilled under water pump vacuum into a dry ice – acetone cooled receiver. The products were a mixture of cyclooctatetraene, identified by i.r. and vapor-phase chromatographic (v.p.c.) retention time, and 2-pyrone, identified by i.r. and n.m.r.

The cyclooctatetraene was determined by adding a known weight of cyclohexanol to the distillate in chloroform. The mixture was then analyzed by v.p.c. (20% Carbowax 20M on Chromosorb P, 6′ × 1/4″, 120°, 40 cc/min of helium) and the ratio of the peaks determined by integration. The yield calculated was 2.4%.

The amount of 2-pyrone produced by reverse cleavage of the dimers was calculated by making the distillate to a specific volume with chloroform and measuring the areas of the i.r. absorption at 1546 and 1626 cm^{-1} on a Beckman IR7 using 0.1 mm cells. The amount of 2-pyrone was obtained by comparison with a graph of area vs. concentration prepared by using pure 2-pyrone. The yield calculated was 36.6%.

Cyclooctatetraene (83.3 mg) was pyrolyzed under similar conditions and distilled to give back 83.0 mg (99.5%) of the starting material.

Low Temperature Irradiation of 4,6-Dimethyl 2-Pyrone

(*a*) A thin film of the 4,6-dimethyl 2-pyrone was irradiated (15) with a focussed 850 W mercury arc through Pyrex at −190°. After 484 min, the i.r. absorption of the starting material had virtually disappeared. New bands appeared in their place with principal bands at 1809 and 1628 cm^{-1} attributed to the 4,6-dimethyl bicylo[2.2.0]-pyran-2-one. Further irradiation through quartz at −190° resulted in the appearance of 2 new i.r. bands at 2343 cm^{-1}, attributable to carbon dioxide, and at 2118 cm^{-1}, possibly due to a ketene.

(*b*) A sample of the 2-pyrone (10%) in a 1/1 mixture of methanol/tetrahydrofuran was irradiated as above through Pyrex at −190° with the assumed resultant formation of the bicyclo[2.2.0]pyran-2-one. The sample was allowed to warm while the i.r. absorption was monitored. At approximately −100°, the bicyclo[2.2.0]pyran-2-one bands disappeared with reformation of the starting material peaks. No new bands attributable to the keto ester were observed.

(*c*) Irradiation of a sample in methanol/tetrahydrofuran as above using quartz gave the same results. Again in this case no band was observed at 2118 cm^{-1}.

Irradiation of 4-Methoxy-6-methyl-2-pyrone

The pyrone (16) (100–300 mg), sublimed before use, was dissolved in 5 ml of dry benzene (distilled from calcium hydride and stored over sodium wire) in a 9 mm Pyrex tube which had been flamed out. The solution was degassed and irradiated as before. The reaction was followed by taking aliquots with a hypodermic needle through the septum and observing the disappearance of the ultraviolet (u.v.) absorption at 280 nm, (approximately 24 h).

The irradiated solution was transferred to a 100 ml flask, and either (*i*) an equal volume of water with enough dioxane to make a homogeneous solution, or (*ii*) aqueous methanol was added. After standing at 50° for 12 h, the solvent was removed under reduced pressure and the products separated by thin-layer chromatography (t.l.c.) using 50/50 ether/benzene to give a mixture, R_f = 0.6, (36%) of *cis*- and *trans*-β-methylglutaconic acid monomethyl esters and, R_f = 0.3 (50%), a mixture of *cis*- and *trans*-β-methylglutaconic acids (9).

Treatment of either of these mixtures with ethereal diazomethane gave a mixture of *cis*- and *trans*-β-methylglutaconic acids dimethyl esters, which were separated by v.p.c. (10% Carbowax 20M on Chromosorb P, 20′ × 1/4″, 150°, 60 cc/min) to give dimethyl *cis*-β-methylglutaconate, δ (CCl_4), 1.97 (3H, s), 3.70 (6H, s), 3.75 (2H, s), 5.83 (1H, s), and dimethyl *trans*-β-methylglutaconate, δ (CCl_4), 2.22 (3H, s), 3.12 (2H, s), 3.70 (6H, s), 5.80 (1H, s). Both these compounds gave i.r. and n.m.r. spectra identical with those reported by Jackman and Wiley (9).

In another experiment 387 mg of 4-methoxy-6-methyl-2-pyrone were dissolved in anhydrous benzene, which had been passed through active neutral alumina, and the solution placed in a 10 mm Pyrex tube. After degassing by the freeze–thaw method on a high vacuum pump, the tube was strapped to an immersion well and irradiated as described above. The solvent was then removed at room temperature under reduced pressure to yield a polymeric material whose average molecular weight was 510 (vapor pressure osmometer in benzene); ν_{max}(CCl_4), 1740 (C=O), 1645 (C=C) cm^{-1}; δ (CCl_4), 1.75 (3H, m),3.30 (1H, m), 3.65 (3H, m), 5.30 (1/5H, m), 6.00 (1/5H, m), 6.55 (8.5/10H, m).

Irradiation of 4-Methoxy-6-methyl-2-pyrone in Water

A solution of 100 mg of the 2-pyrone was dissolved in 200 ml of water and irradiated in an immersion apparatus with a 450 W medium-pressure mercury arc through Pyrex after degassing with oxygen-free nitrogen. The reaction was followed by the disappearance of the u.v. absorption at 280 nm (3.5 h). Solvent was removed under vacuum and the products separated by t.l.c. using 50/50 ether/benzene to give:

(*a*) *cis*-β-Methyl glutaconic acid monomethyl ester; R_f, 0.6; 50%; m.p. 77–78°; ν_{max}(CCl_4) 1747, 1698 (C=O), 1651 (C=C) cm^{-1}; δ(CCl_4), 2.00 (3H, d, J = 1.5 c.p.s.), 3.67 (2H, s), 3.71 (3H, s), 5.87 (1H, m), 11.71 (1H, s); λ_{max}(EtOH), 217 nm (ε 8000).

Anal. Calcd. for $C_7H_{10}O_4$: C, 53.16; H, 6.37; OMe, 19.62. Found: C, 53.08; H, 6.36; OMe, 19.12.

(*b*) *cis*-β-Methylglutaconic acid; R_f = 0.3; 50%; m.p. 152–153°; ν_{max}(Nujol), 1715; 1688 (C=O), 1642 (C=C) cm^{-1}; δ(CF_3COOH), 2.13 (3H, d, J = 2 c.p.s.), 3.90 (2H, s), 6.11 (1H, m); λ_{max}(EtOH), 217 nm (ε 13 100), identical with that reported by Jackman and Wiley (9).

A solution of the 2-pyrone was dissolved in water for 24 h at room temperature. The water was then removed under vacuum to give back the 2-pyrone unchanged, as shown by i.r. absorption.

Can. J. Chem. Downloaded from www.nrcresearchpress.com by 210.87.254.42 on 09/05/12
For personal use only.

Ozonolysis of cis-β-Methylglutaconic Acid Monomethyl Ester

Twenty mg of *cis*-β-methylglutaconic acid monomethyl ester from the water irradiation were ozonized at −70° in chloroform for 1/2 h. The excess ozone was removed with a stream of nitrogen and the reaction mixture hydrogenated at −70° for 5 min over 5% Pd/C catalyst. The catalyst was filtered off and the products treated with an excess of 2,4-dinitrophenylhydrazine-hydrochloride, then separated by t.l.c., using 5% ethyl acetate in benzene, to give 10 mg of methyl acetoacetate 2,4-dinitrophenylhydrazone, m.p. 120–121° (mixed m.p. 119.0–119.5° with an authentic sample (10), m.p. 119–120°).

Preparation of 6-Methoxy-4-methyl-2-pyrone

β-Methylglutaconic acid was prepared as described by Wiley and Smith (17) via the base catalyzed hydrolysis of ethyl isodehydroacetate. The anhydride was then formed by heating with acetic anhydride to give β-methylglutaconic anhydride. The anhydride was treated with ethereal diazomethane and the products recrystallized from ether – petrol (35–60°) to give 6-methoxy-4-methyl-2-pyrone, m.p. 53.0–53.5°; $\nu_{max}(CCl_4)$, 1755 (C=O), 1640, 1595, 1560 (C=C) cm^{-1}, δ (CCl_4), 2.07 (3H, s), 3.84 (3H, s), 5.14 (1H, m), 5.44 (1H, m); λ_{max}(EtOH), 281 nm (ε 4200), 315 nm (ε 4150).

Anal. Calcd. for $C_7H_8O_3$: C, 59.99; H, 5.75. Found: C, 59.45; H, 5.29.

Irradiation of 6-Methoxy-4-methyl-2-pyrone

This 2-pyrone (140 mg) was irradiated in dry benzene for 24 h under conditions identical to those used for 4-methoxy-6-methyl-2-pyrone. The solvent was evaporated to give material of average molecular weight 152 (vapor pressure osmometer in benzene). Examination of this material by n.m.r. showed only peaks attributable to starting material, *cis*- and *trans*-β-methylglutaconic acids and their monomethyl esters, formed by hydrolysis.

Hydrolysis of 6-Methoxy-4-methyl-2-pyrone

The pyrone (150 mg) was dissolved in 40 ml of 95% ethanol and left at room temperature for 24 h. The solvent was then removed under reduced pressure and the products separated by t.l.c. with 50/50 ether/benzene to give a mixture of *cis*- and *trans*-β-methylglutaconic acids ethyl methyl esters, $\nu_{max}(CCl_4)$, 1740, 1720 (C=O), 1660 (C=C) cm^{-1}; δ (CCl_4), 1.24 (3H, t, J = 7 c.p.s.), 1.92 (3/2H, d, J = 1.5 c.p.s.), 2.20 (3/2H, d, J = 1.5 c.p.s.), 3.07 (2/2H, s), 3.62 (3H, s), 3.78 (2/2H, s), 4.09 (2H, q, J = 7 c.p.s.), 5.75 (1H, m).

Anal. Calcd. for $C_9H_{14}O_4$: C, 58.05; H, 7.58. Found: C, 58.15; H, 7.22.

Low Temperature Irradiation of 4-Methoxy-6-methyl-2-pyrone

(*a*) A thin film of this pyrone was irradiated at −190° as above through Pyrex. New bands appeared in the i.r. at 1807 and 1600 cm^{-1} attributable to the 4-methoxy-6-methyl bicyclo[2.2.0]pyran-2-one. No bands in the region 2100–2120 cm^{-1} were observed.

(*b*) A similar irradiation through quartz produced the same results, but more rapidly.

1. P. DE MAYO. *In* Advances in Organic Chemistry. R. A. Raphael, E. C. Taylor and H. Wynberg (*Editors*). Interscience Publishers, Inc., New York. 1960. p. 394. The details are reported in the present paper.
2. D. H. R. BARTON. Helv. Chim. Acta, **42**, 2604 (1959).
3. P. DE MAYO and R. W. J. YIP. Proc. Chem. Soc. 84 (1964).
4. C. L. MCINTOSH, P. DE MAYO, and R. W. YIP. Photochemical syntheses. R. Srinivasan, *Editor*. Interscience Publishers, Inc., New York. To be published.
5. W. H. PIRKLE and L. H. MCKENDRY. Tetrahedron Lett. 5279 (1968).
6. E. J. COREY and J. STREITH. J. Amer. Chem. Soc. **86**, 950 (1964).
7. W. H. PIRKLE and L. H. MCKENDRY. J. Amer. Chem. Soc. **91**, 1179 (1969).
8. C. L. MCINTOSH. Ph.D. Thesis, University of Western Ontario, London, Ontario. 1969.
9. L. M. JACKMAN and R. H. WILEY. J. Chem. Soc. 2886 (1960).
10. G. D. JOHNSON. J. Amer. Chem. Soc. **73**, 5888 (1951).
11. E. J. COREY and W. H. PIRKLE. Tetrahedron Lett. 5255 (1967).
12. J. E. BALDWIN and M. C. MCDANIEL. J. Amer. Chem. Soc. **90**, 6118 (1968).
13. G. B. GILL. Quart. Rev. **22**, 346 (1968). See also, H. H. FREEDMAN, G. A. DOORAKIAN, and V. R. SANDE. J. Amer. Chem. Soc. **87**, 3019 (1965).
14. H. E. ZIMMERMAN, G. L. GRUNEWALD, and R. M. PAUFLER. Org. Syn. **46**, 101 (1966).
15. N. R. SMITH and R. H. WILEY. Org. Syn. **32**, 57, 76 (1952).
16. J. D. BU'LOCK and H. G. SMITH. J. Chem. Soc. 502 (1960).
17. R. H. WILEY and N. R. SMITH. J. Amer. Chem. Soc. **74**, 3893 (1952).
18. P. DE MAYO, A. A. NICHOLSON, and M. F. TCHIR. Can. J. Chem. This issue.

Can. J. Chem. Downloaded from www.nrcresearchpress.com by 210.87.254.40 on 09/05/12
For personal use only.

The proton relaxation and Overhauser effect in the nuclear magnetic resonance spectra of some amides[1,2]

S. BROWNSTEIN AND V. BYSTROV[3]
Division of Applied Chemistry, National Research Council, Ottawa, Ontario, Canada

Received June 19, 1969

The relaxation behavior of some amides was investigated in their high resolution spectra by the direct saturation–recovery and Overhauser effect methods. The recovery curves and steady-state Overhauser effects were obtained for solutions of dimethylformamide with double- and triple-resonance irradiations. The results were analyzed for 3- and 4-spin systems and the values of relaxation parameters were calculated. It was shown that for dimethylformamide the one-exponential recovery curve approximation gives the T_1 values with a precision better than experimental error ($\pm 2\%$). The observed difference in relaxation times for methyl group protons was explained by different correlation times and more restricted rotation of 1 of the groups. The correlation times for dipole–dipole interactions of methyl groups with the formyl proton were also evaluated with some reasonable assumptions.

The change of the relaxation rate of *N*-methyl protons in C_6H_6 and C_6D_6 solutions was explained by formation of the collision complex with amide molecules and specific intermolecular dipole–dipole proton interaction. This effect could be useful for determination of the *cis*- and *trans*-conformations in *N*-methyl substituted amides and peptides as an absolute method because it does not require measurements on both isomers.

Canadian Journal of Chemistry, **48**, 243 (1970)

Introduction

High resolution nuclear magnetic resonance (n.m.r.) spectroscopy based mainly on chemical shift and indirect spin–spin coupling data are now extensively used in the determination of molecular structure (1) and in the investigation of the intermolecular interactions of organic compounds in solution (2). The other very important parameters of the n.m.r. signal, the relaxation times, are used much less widely in high resolution n.m.r. spectroscopy. Most relaxation studies have been performed by pulse techniques and adiabatic rapid passage and so far have only limited applicability to the study of systems with several non-equivalent spins (3). More promising methods for measuring the relaxation parameters in high resolution n.m.r. spectra are the saturation–recovery technique (4) and the observation of dynamic and steady-state Overhauser effects (5). These techniques have been successfully used for spin systems coupled by indirect spin–spin coupling (6, 7) and for uncoupled spin systems (8–10). Investigations in this field may provide very valuable information on the relative contribution of various relaxation mechanisms and probabilities of the relaxation transitions and, therefore, about molecular motion, chemical exchange, and inter- and intramolecular interactions. Recently it was shown that the changes of the proton relaxation rates in high resolution n.m.r. spectra can be used to identify the portions of molecules directly involved in the formation of the substrate–enzyme complexes in solution (the binding interaction) (11, 12).

This paper is concerned with dependence of relaxation behavior on conformation of molecules and molecular interaction in solutions of some *N*-methyl substituted amides. One of the most difficult problems in the saturation-recovery method applied to systems with several non-equivalent spins is the general possibility that the recovery curves are represented by the sum of a number of exponential terms with different coefficients, even in the absence of spin–spin coupling (8, 13, 14). Therefore it is necessary to divide these curves into separate exponential terms or to prove by special experiments and calculations that the experimental curves depend mostly on only one exponential term, i.e., the coefficients of other terms are negligible.

Theory

If the sample under investigation contains more than one non-equivalent interacting spin system,

[1]A preliminary communication of these results was given at the 10th Experimental NMR Conference, Pittsburgh, February 27 – March 1, 1969.
[2]NRCC No. 11021.
[3]NRCC Postdoctoral Fellow, 1968–69. Permanent address: Institute for Chemistry of Natural Products, Academy of Sciences of U.S.S.R., Moscow.

Can. J. Chem. Downloaded from www.nrcresearchpress.com by 210.87.254.40 on 09/05/12
For personal use only.

then (in the absence of saturation effects and indirect spin–spin coupling) the longitudinal magnetization $M_z{}^i$ of the i-system may be given by a generalization of Solomon's equations (13).

$$[1] \quad \frac{dM_z{}^i}{dt} = -\sum_{j=1}^{n} \frac{M_z{}^j - M_0{}^j}{T_{1(ji)}} \qquad i = 1, \ldots, n$$

where n is the number of interacting spin systems, $M_0{}^j$ is the static z-magnetization at the j site

$$M_0{}^j = I_j(I_j + 1)N_j\hbar^2\gamma_j{}^2H_0/3kT$$

N_j is the number of equivalent nuclei in the group j and $T_{1(ji)}$ are the longitudinal relaxation parameters.

To simplify notations for the remainder of this paper, T with subscripts will be used to represent T_1 parameters.

If there is chemical exchange of spins between sites i and q with the residence times τ_i and τ_q, respectively, it is necessary to add to the right-hand side of eq. [1] the McConnell terms (15)

$$-M_z{}^i/\tau_i + M_z{}^q/\tau_q$$

By use of the equilibrium condition

$$M_0{}^i/\tau_i = M_0{}^q/\tau_q$$

eq. [1] may be rewritten as

$$[1a] \quad \frac{dM_z{}^i}{dt} = -\sum_{j\neq i,q} \frac{M_z{}^j - M_0{}^j}{T_{ji}} - \sum_{k=i,q} \frac{M_z{}^k - M_0{}^k}{T_{ki}{}^*}$$

where (8)

$$[2] \quad 1/T_{ii}{}^* = 1/T_{ii} + 1/\tau_i$$

$$[3] \quad 1/T_{qi}{}^* = 1/T_{qi} - 1/\tau_q$$

The solution of eq. [1] may be written in the form

$$[4] \quad M_z{}^i = \sum_{j=1}^{n} a_{ij} \exp(-b_j t) + c_i$$

if there are no degenerate roots b_j of the determinant

$$[5] \quad \begin{vmatrix} 1/T_{11} + b & 1/T_{21} & \ldots & 1/T_{n1} \\ 1/T_{12} & 1/T_{22} + b & \ldots & 1/T_{n2} \\ \vdots & \vdots & & \vdots \\ 1/T_{1n} & 1/T_{2n} & \ldots & 1/T_{nn} + b \end{vmatrix} = 0$$

It is obvious from the equations developed by Van Geet and Hume (16) and Van Geet (17) that the recovery of the absorption signal v follows the time dependence of M_z and therefore, in general, is represented by a multi-exponential function similar to eq. [4]. Usually it is difficult to recognize such behavior in the direct saturation–recovery experiments if there exists even minor instabilities in the working conditions of the n.m.r. spectrometer. For this reason in order to evaluate T_{ji} and b_j it is more convenient to use the Overhauser effect and continuous irradiation by strong radiofrequency (r.f.) fields of other than the investigated signals (8). If all signals $j \neq i$ are saturated ($M_z{}^j = 0$), then from eq. [1]

$$[6] \quad \frac{dM_z{}^i}{dt} = -\frac{M_z{}^i - M_0{}^i}{T_{ii}} + \sum_{j\neq i} \frac{M_0{}^j}{T_{ji}}$$

and the recovery after saturation of the i signal will be purely exponential

$$M_z{}^i = (M_0{}^i + T_{ii}\sum_{j\neq i} M_0{}^j/T_{ji}) \times [1 - \exp(-t/T_{ii})]$$

Such experiments provide the values of T_{ii}. The Overhauser effect

$$[7] \quad h_i = (M_{z(t\to\infty)}{}^i - M_0{}^i)/M_0{}^i$$

in this case is given by

$$[8] \quad h_i{}^{(j\neq i)} = \frac{T_{ii}}{M_0{}^i}\sum_{j\neq i} \frac{M_0{}^j}{T_{ji}}$$

The superscripts in parentheses on h designate the saturated spin sites.

If only one s signal is saturated ($M_z{}^s = 0$, double resonance conditions) then the Overhauser effect for the i signal may be written

$$[9] \quad h_i{}^{(s)} = \frac{M_0{}^s}{M_0{}^i}\frac{T_{ii}}{T_{si}} - \sum_{j\neq s, j\neq i} h_j{}^{(s)} \frac{M_0{}^j}{M_0{}^i}\frac{T_{ii}}{T_{ji}}$$

The solution of the system of these equations ($i = 1, \ldots, n; s = 1, \ldots, n; i \neq s$) if all possible $h_i{}^{(s)}$ are known gives only the ratios T_{ii}/T_{ji} of the relaxation parameters. It is quite understandable that the steady-state experiments cannot give the value in the time domain. To obtain such values it is necessary to conduct some appropriate dynamic experiments on, for example, saturation–recovery or Overhauser effect under multiple irradiation conditions (eq. [6]).

It is interesting to note that from eq. [9] it

Can. J. Chem. Downloaded from www.nrcresearchpress.com by 210.87.254.40 on 09/05/12
For personal use only.

follows that the steady-state Overhauser effects $h_i^{(s)}$ and $h_s^{(i)}$ may be observed even if there is no interaction between i and s spins, i.e., $1/T_{si}$ and $1/T_{is} = 0$. This indirect Overhauser effect can be positive or negative depending on the signs and magnitudes of the remaining T_{ji} in the system. Conceivably, some of the observed negative nuclear Overhauser effects (n.O.e.) (18, 19) may be explained by eq. [9]. Reduced to a 3-spin system this effect corresponds to the "three spin effect" (20), discovered in dynamic polarization experiments.

The expressions for the time constant T_{ji} for 2 interacting spins (13) in terms of level populations has been derived by Hoffman and Forsen (8). By generalization of those equations for the system of several interacting non-equivalent spins one may write the following expressions for the time constants T_{ii} and T_{ji} (21)

$$1/T_{ii} = W_{ii} + \sum_{j\neq i} W_{ij}'$$

$$1/T_{ji} = W_{ji}$$

where the transition probabilities W correspond to dipole–dipole interactions between like spins (22)

$$W_{ii} = (3/2)\gamma_i^4\hbar^2 I_i(I_i + 1)\sum^{N_i} \times [J_1(\omega_i) + J_2(2\omega_i)]$$

and between unlike spins (22)

$$W_{ij}' = \gamma_i^2\gamma_j^2\hbar^2 \sum^{N_j} I_j(I_j + 1)[(1/12)J_0(\omega_i - \omega_j) + (3/2)J_1(\omega_i) + (3/4)J_2(\omega_i + \omega_j)]$$

$$W_{ji} = \gamma_i^2\gamma_j^2\hbar^2 \sum^{N_i} I_i(I_i + 1)[(-1/12)J_0 \times (\omega_i - \omega_j) + (3/4)J_2(\omega_i + \omega_j)]$$

In the limit of extreme narrowing these equations may be simplified to (21)

[10] $$1/T_{ii}^* = W_{ii} + 2\sum_{j\neq i} W_{ij} + W_i + 1/\tau_i$$

[11] $$1/T_{ji}^* = W_{ji} - 1/\tau_j$$

where W_i corresponds to the magnetic interactions between i spins and random fluctuating fields, the "lattice". These fluctuating fields may be caused by interactions of the i spins with some spins which have very efficient relaxation mechanisms of their own, for example, with dissolved paramagnetic impurities (usually oxygen) and also with quadrupole nuclei. In the same manner the term W_i may also include the spin–rotation interactions and a relaxation mechanism caused by molecular motion modulation of anisotropic shielding.

The transition probabilities may be considered as containing the contributions from the intra- and intermolecular interactions

$$W_{ii} = W_{ii}^{\text{intra}} + W_{ii}^{\text{inter}}$$

$$W_{ij} = W_{ij}^{\text{intra}} + W_{ij}^{\text{inter}}$$

The intramolecular dipole–dipole contributions in the limit of extreme narrowing may be derived from Solomon's equations (13, 22) by generalization to the many spin case (21)

[12] $$W_{ii}^{\text{intra}} = 2I_i(I_i + 1)\gamma_i^4\hbar^2 \sum^{N_i} \tau_{ii} r_{ii}^{-6}$$

[13] $$W_{ij}^{\text{intra}} = (2/3)I_j(I_j + 1)\gamma_i^2\gamma_j^2\hbar^2 \times \sum^{N_j} \tau_{ij} r_{ij}^{-6}$$

where τ_{ii} and τ_{ij} are the correlation times for dipole–dipole interaction between the like and unlike spins, correspondingly, and r_{ii} and r_{ij} are the distances between the like and unlike spins.

Because the intermolecular contributions W_{ii}^{inter} and W_{ij}^{intra} are proportional to the number of spins in the volume unit (22) the following relationships (Onsager reciprocity relations) hold

[14] $$N_i I_i(I_i + 1)/T_{ij} = N_j I_j(I_j + 1)/T_{ji}$$

Experimental

The experiments were performed with a Varian HR-100 high resolution nuclear magnetic resonance spectrometer. The signals were recorded employing audio phase detection by operating the Varian V-3521A Integrator in the lower 2515 c.p.s. sideband mode. The radio- and audiofrequency phases were adjusted for an absorption signal on the sideband and zero signal on the central band (ν_{RF}, $\Theta = 0°$ mode (23)). An attenuation of 30 db of the r.f. power output from the 100 Mc.p.s. transmitter was used. The change of the H_1 field strength from the saturated to the unsaturated value was performed by switching the amplitude of the audiofrequency modulation furnished by the V-3521A Integrator to a properly adjusted value.

In order to obtain the necessary stability an internal phase-sensitive lock system on the audiofrequency sideband was used (24). This sideband was furnished by a Wavetek M-111 Voltage Controlled Generator. The frequency was measured by a Hewlett–Packard Electronic Counter 521C with 0.1 c.p.s. precision. To avoid undesirable interference with the transient processes, which arise when the signal is saturated, a Rhode and Schwartz Tunable Amplifier sharply tuned on the stabilization channel frequency was used on the input of the phase-sensitive detector. The output of the detector was fed to

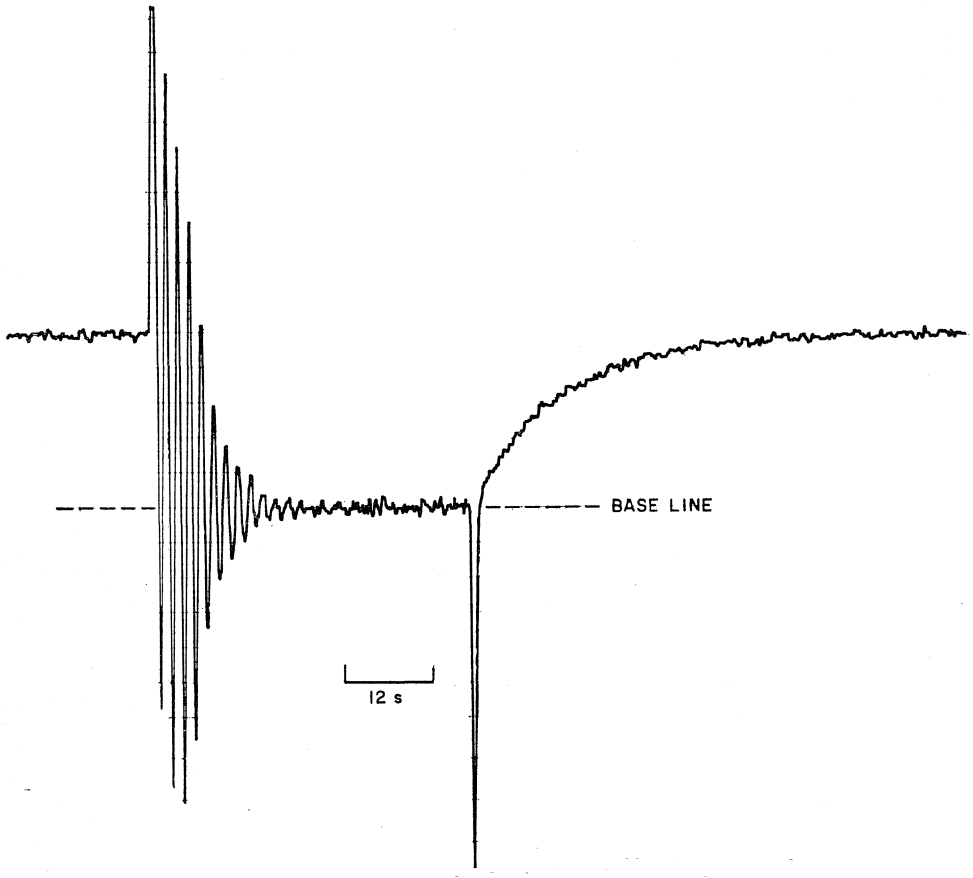

FIG. 1. A typical saturation recovery experimental result for the high-field *N*-methyl signal in the n.m.r. spectra of a 7.5% v/v solution of *N*,*N*-dimethylformamide in carbon disulfide (3% TMS as internal standard). $\Delta\nu^* = 3$ c.p.s., $\gamma H_{1(\text{sat.})}/2\pi = 0.6$ c.p.s., $H_{1(\text{sat.})}/H_{1(\text{rec.})} = 300$, $T_1 = 12.8$ s.

the input of the galvanometer in parallel to the pickup coils of the Varian V-K3506 Super Stabilizer.

The saturation–recovery technique developed by Van Geet (16, 17) was used. Several experiments, especially for the Overhauser effect, were performed with repeated scanning of the magnetic field ("sampling" method) (6, 8, 25). The advantage of Van Geet's technique is the possibility of observing the whole recovery curve and measuring shorter relaxation times.

As had been previously reported, in order to avoid a distortion of the recovery curves the following conditions are required:

1. The shape of the investigated line under recovery conditions has to be determined by the inhomogeneity of the magnetic field

$$\Delta\nu^* \gg 1/\pi T_2,\ 1/\pi T_1$$

where $\Delta\nu^*$ is the linewidth, T_1 and T_2 are the longitudinal and transverse relaxation times, respectively.

2. The strength of the saturating r.f. field $H_{1(\text{sat.})}$ has to be high enough to satisfy the conditions of saturation

$$\gamma H_{1(\text{sat.})} \gg 1/T_1$$

3. The shape of the saturated line has to be determined by the inhomogeneity

$$\Delta\nu^* \gg \gamma H_{1(\text{sat.})}/\pi$$

or by the saturating r.f. field

$$\Delta\nu^* \ll \gamma H_{1(\text{sat.})}/\pi$$

In the present work the following values of parameters were used: $\Delta\nu^* = 3$–5 c.p.s. (0.7–1.2 mOe) and $H_{1(\text{sat.})} =$ 0.1–0.3 mOe. A reasonably symmetric broadened peak without "spikes" and "bumps" was obtained by adjusting the homogeneity shim controls without spinning the sample.

A typical result by the saturation–recovery method is shown in Fig. 1. The magnetic field was adjusted by means of the frequency of the lock-in system for the resonance condition, so that the recorder is on the top of the peak. (Chemical shifts, thus obtained, are presented in Tables 7 and 8.) Then the amplitude of the r.f. field H_1 is increased to the saturation magnitude, $H_{1(\text{sat.})}$. At this moment the transient nutation (26) is started. After these nutations are damped the line is completely saturated ($M_z = 0$). When

Can. J. Chem. Downloaded from www.nrcresearchpress.com by 210.87.254.40 on 09/05/12
For personal use only.

Can. J. Chem. Downloaded from www.nrcresearchpress.com by 210.87.254.40 on 09/05/12
For personal use only.

H_1 is suddenly reduced to the non-saturation value $H_{1(\text{rec.})}$ a large negative transient pulse lasting 1–2 s is usually observed and then the n.m.r. signal recovers to the steady-state peak height.

The vertical range of the recorder employed was 7.5–8.0 inches. The points on the recovery curves could be estimated within ± 0.01 in. The experimental recovery curves (7–10 for each experiment) were digitized and fitted by an IBM-360/60 computer to the equation

$$Y = \Sigma_n W_n(\exp K_n X) + U$$

with 1 ($n = 1$, three parameters) or 2 ($n = 2$, five parameters) exponential terms by a Davidson–Fletcher–Powell minimization method.

The frequency of the transient nutation (in the resonance condition) directly corresponds to the amplitude $H_{1(\text{sat.})}$ of the saturation r.f. field (26).

$$\Omega = \gamma H_{1(\text{sat.})}$$

It is convenient to use this relation for calibrating the effective r.f. field. For the first sideband the effective r.f. field is (23)

$$H_{1(\text{eff.})} = J_1(\gamma H_m/\omega_m)H_1$$

where $J_1(\beta)$ is the first-order Bessel function, H_m and ω_m are the amplitude and frequency of the audiofrequency modulation, respectively, and H_1 is the amplitude of the r.f. field. If we assume that

$$\gamma H_m/\omega_m = KV_m$$

where V_m is the voltage across the modulation coils, then measuring the voltage V_m^0, which corresponds to disappearance of the first sideband in the u_{RF}, $\Theta = 90°$ mode ($\beta = 1.84$), the coefficient K can be found

$$K = 1.84/V_m^0$$

The ratio

$$H_{1(\text{rec.})}/H_{1(\text{sat.})} = J_1(KV_m^{(\text{rec.})})/J_1(KV_m^{(\text{sat.})}) \simeq V_m^{(\text{rec.})}/V_m^{(\text{sat.})}$$

was used for evaluating $H_{1(\text{rec.})}$.

To obtain reliable data for relaxation times it is very important that the $H_{1(\text{rec.})}$ value will be well below the saturation level (17). In Fig. 2 the dependence of $T_1/T_{1(\text{app.})}$ upon $\gamma H_{1(\text{rec.})}T_1$ is shown. Here T_1 is the limiting time of the recovery as $H_{1(\text{rec.})} \to 0$ in the benzene sample. (External TMS in a capillary was used for the lock-in system.) The apparent recovery time, $T_{1(\text{app.})}$, is measured with a particular $H_{1(\text{rec.})}$. Those experimental results are fitted quite well by the equation proposed by Van Geet (17) on a semi-theoretical basis

$$T_{1(\text{app.})}/T_1 = (Z)^{1/8}$$

where the saturation factor $Z = (1 + \gamma^2 H_1^2 T_1 T_2)^{-1}$, and assuming $T_1 = T_2$. The dependence corresponding to this equation is shown in Fig. 2 by the solid curve. A safe enough limit for measuring T_1 is

$$\gamma H_{1(\text{rec.})}T_1 < (0.3\text{–}0.5)$$

The longitudinal relaxation times measured in this work were corrected, if needed, in accordance with Fig. 2.

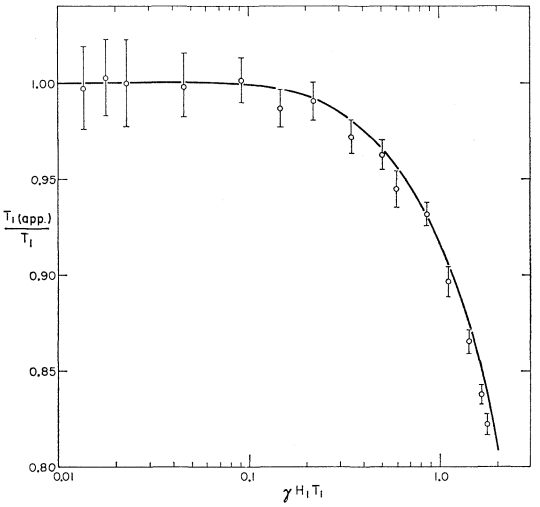

FIG. 2. The dependence of the ratio $T_{1(\text{app.})}/T_1$ upon $\gamma H_{1(\text{rec.})}T_1$ for the direct saturation–recovery experiments. $H_{1(\text{rec.})}$ is the amplitude of the r.f. field in the recovery period, $T_{1(\text{app.})}$ is the apparent relaxation time measured for a particular magnitude of $H_{1(\text{rec.})}$, T_1 is the relaxation time for $H_1 \to 0$.

On the other hand, the sensitivity is diminished when H_1 is decreased and this can become a difficult problem for dilute solutions with long T_1. In this case the accumulation of several recovery curves by a time-averaging technique might be very helpful. A preliminary attempt at this employing a Fabri-Tek computer of average transients was successful.

The dynamic Overhauser effect was observed under conditions of double and triple resonance. The irradiating r.f. fields were supplied by audiofrequency modulation with Hewlett-Packard 200J and 200A oscillators. The amplitudes of the modulation were chosen to correspond to $H_2 = H_3 \simeq 0.2$–0.3 mOe. A typical result is shown in Fig. 3 for the CH proton signal of pure dimethylformamide. The vertical line with upward arrow corresponds to switching off, and the downward to switching on the irradiating r.f. field H_2 applied on the low-field *N*-methyl signal. The horizontal lines show the unperturbed peak height. For the H_2-on period this height was obtained by shifting the H_2 frequency about 50 c.p.s. from the resonance value. The observing signal was scanned periodically by sweeping the frequency of the Wavetek M-111 VCG in the internal lock stabilization system.

The v/v solutions were prepared from commercially available compounds using the syringe technique. The samples in the usual 5 mm o.d. sample tubes were degassed by multiple (3–4 times) freeze–pump–thaw cycles and sealed under vacuum (5×10^{-5} mm Hg). As internal standards (3% v/v) tetramethylsilane (TMS), cyclohexane (for pure dimethylformamide), and sodium 2,2-dimethyl-2-silapentane sulfonate (DSS, for water solutions) were employed. All measurements were performed at room temperature, 25 ± 1 °C.

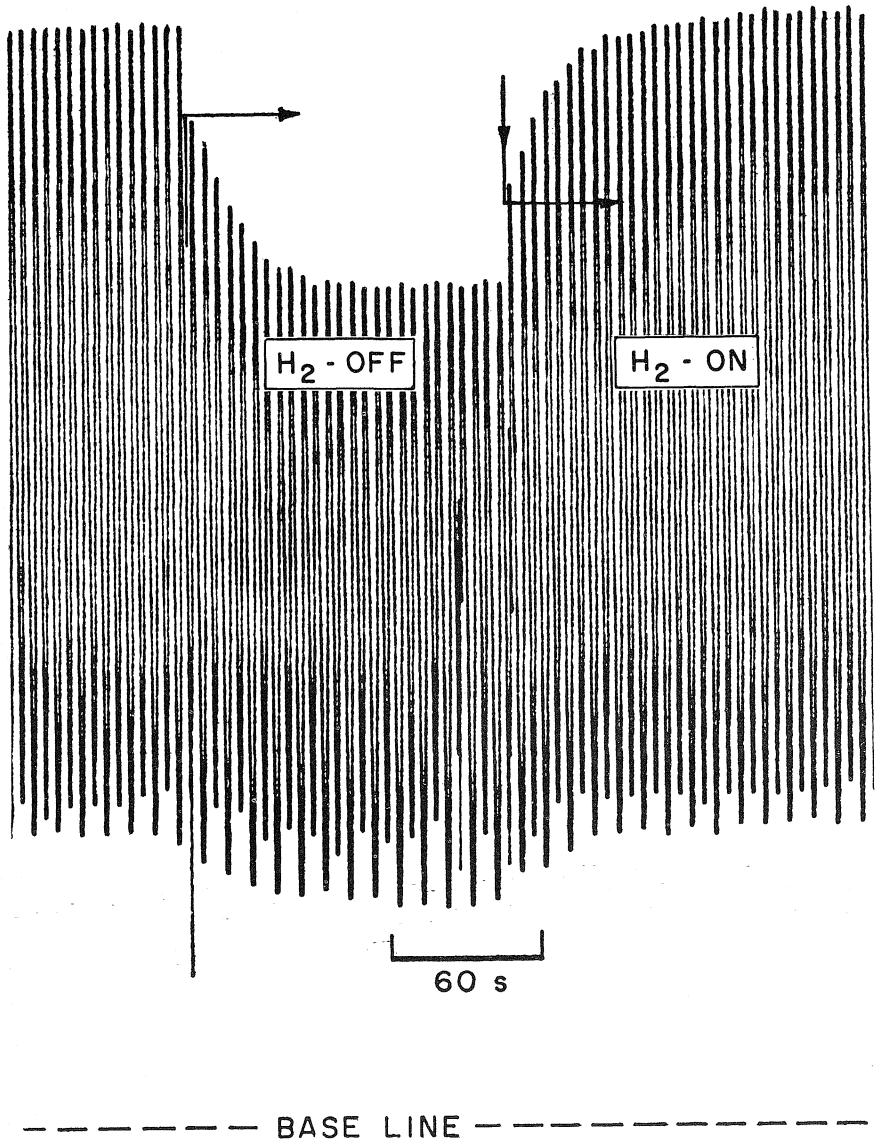

FIG. 3. A typical dynamic Overhauser experiment. The CH signal of *N,N*-dimethylformamide (pure liquid, 3% cyclohexane) was observed while the low-field N—CH_3 signal was irradiated by a r.f. field $H_2 \simeq 0.3$ mOe.

Results

In the general case, as follows from eqs. [1] and [4], the recovery curves might be very complicated and a straightforward approach for extracting the longitudinal relaxation time can lead to erroneous results. For that reason it seems to be necessary to use multiple resonance techniques and the Overhauser effect. This approach was performed for the 2-spin systems in formic acid and acetaldehyde (8). Here it will be extended to the 3-spin system in dimethylformamide.

Of course, dimethylformamide presents a much more complicated case than the 3-spin system: there are 8 spins in the molecule. But the ^{14}N relaxation time is determined mostly by the quadrupole relaxation mechanism and is much shorter than for protons and therefore the changes in the proton magnetization do not influence the

Can. J. Chem. Downloaded from www.nrcresearchpress.com by 210.87.254.40 on 09/05/12
For personal use only.

TABLE 1

The Overhauser effects (in %) for solutions of *N,N*-dimethylformamide (DMF)

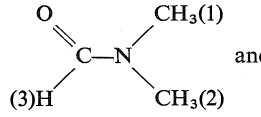

and *N,N*-dimethyldeuteroformamide (DMDF)

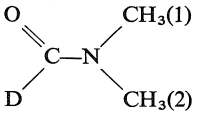

Compound	Solution	$h_1^{(2)}$	$h_1^{(3)}$	$h_2^{(1)}$	$h_2^{(3)}$	$h_3^{(1)}$	$h_3^{(2)}$	$h_1^{(2,3)}$	$h_2^{(1,3)}$	$h_3^{(1,2)}$
DMDF	Pure liquid (10% benzene)	3.2±0.3	—	2.3±0.4	—	—	—	—	—	—
DMF	Pure liquid (3% cyclohexane)	3.0±0.3	2.1±0.2	2.4±0.3	2.8±0.3	11.0±0.5	19±1	5.4±0.3	5.5±0.4	32±2
	15% v/v in CS_2 (3% TMS)	−5.4±0.4	1.5±0.2	−4.0±0.3	2.3±0.3	8.5±0.6	20±1	−3.7±0.3	−1.5±0.2	26±2
	5% v/v in D_2O (3% DSS)	2.2±0.2	1.2±0.2	2.0±0.3	2.5±0.2	7.8±0.6	22±2	4.0±0.4	4.9±0.3	29±2
								$h_1^{(solv.)}$	$h_2^{(solv.)}$	$h_3^{(solv.)}$
	5% v/v in H_2O (3% DSS)	1.5±0.3	1.0±0.3	1.0±0.3	2.0±0.3	3.0±0.4	9±1	11±1	7.0±0.7	20±2
	30% v/v in C_6H_6 (3% TMS)	−5.2±0.4	2.0±0.4	−4.2±0.3	2.9±0.3	10±1	17±1	9.7±0.5	6.0±0.4	15±1
	5% v/v in C_6H_6 (3% TMS)	−5.0±0.4	1.5±0.3	−4.1±0.3	2.0±0.3	*	*	20±2	8±1	*

*Not measured because the wings of the benzene signal cover the CH signal.

^{14}N magnetization (scalar relaxation of the second kind (ref. 22, p. 309)). A group of equivalent spins has, to a very good approximation, only 1 longitudinal relaxation time (ref. 22, p. 293) and therefore it is possible to consider the methyl protons as 1 spin with a corresponding relative steady-state magnetization (8).

In Table 1 are shown the experimental values of the Overhauser effect defined by eq. [7] for *N,N*-dimethyldeuteroformamide and some solutions of dimethylformamide. Most values are positive which corresponds to enhancement of the signal during the irradiation of another one.

The value of $h_3^{(2)}$ for heavy water solutions agrees well with the result of Anet and Bourn (18) for an 8% solution (18 ± 1%), but the $h_3^{(1)}$ is in significant divergence (−2 ± 1%).

For a 3-spin system, the Overhauser effects with 1 irradiating field $h_i^{(j)}$ and with 2 irradiating fields $h_i^{(j,k)}$ are, according to eqs. [8] and [9], related by the equation

$$h_i^{(j,k)} = \frac{h_i^{(k)}(1 + h_k^{(j)}) + h_i^{(j)}(1 + h_j^{(k)})}{1 - h_j^{(k)}h_k^{(j)}}$$

If the magnitudes of the single Overhauser effects are much less than 1, then the double Overhauser effect might be written as the sum of corresponding single effects

$$h_i^{(jk)} \simeq h_i^{(j)} + h_i^{(k)}$$

This simple rule is obeyed within the error limit for the data listed in Table 1.

Solving the system of eq. [9] for the 3- and 4-spin system, the ratio of relaxation parameters may be written as

$$[15] \qquad \frac{T_{ii}}{T_{ji}} = \frac{M_0{}^i}{M_0{}^j}\frac{h_i^{(j)} + h_i^{(k)}h_k^{(j)}}{1 - h_j^{(k)}h_k^{(j)}}$$

where $i, j, k = 1, 2, 3$, and

$$[16] \qquad \frac{T_{ii}}{T_{ji}} = \frac{M_0{}^i}{M_0{}^j} \times \frac{\begin{aligned} &h_i^{(j)}(1 - h_k^{(l)}h_l^{(k)}) + h_i^{(k)}(h_k^{(j)} + h_k^{(l)} \\ &\quad \times h_l^{(j)}) + h_i^{(l)}(h_l^{(j)} + h_l^{(k)}h_k^{(j)}) \end{aligned}}{\begin{aligned} &1 - h_k^{(l)}h_l^{(k)} - h_j^{(k)}(h_k^{(j)} + h_l^{(j)}h_k^{(l)}) \\ &\quad - h_j^{(l)}(h_l^{(j)} + h_k^{(j)}h_l^{(k)}) \end{aligned}}$$

where $i, j, k, l = 1, 2, 3, 4$. In the case $h \ll 1$ both of these equations reduce to

$$T_{ii}/T_{ji} \simeq h_i^{(j)}M_0{}^i/M_0{}^j$$

which corresponds to the equation for the 2-spin system (8).

For calculating the relaxation parameters T_{ji} it is necessary to know the value of T_{ii}. These values may be obtained by measuring the recovery curves under conditions of multiple irradiation. Such experiments were done for the 2- and 3-spin

Can. J. Chem. Downloaded from www.nrcresearchpress.com by 210.87.254.40 on 09/05/12
For personal use only.

TABLE 2

The longitudinal relaxation parameters T_{ji} (s) for solutions of *N,N*-dimethylformamide (DMF) 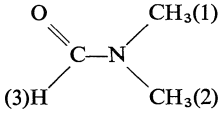 and *N,N*-dimethyldeuteroformamide (DMDF) 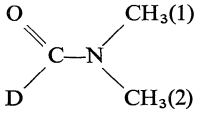

Compound	Solution	i	T_{ji}*,† $j=1$	$j=2$	$j=3$	$j=4$§
DMDF	Pure liquid	1	8.7	270		
	(13% benzene)	2	280	6.8		
DMF	Pure liquid	1	8.2	240	125	
	(3% cyclohexane)	2	230	6.3	73	
		3	390	230	15.0	
	15% v/v in CS_2	1	16.9	−330	410	
	(3% TMS)	2	−310	11.9	180	
		3	1300	530	34.6	
	5% v/v in D_2O	1	9.6	390	200	
	(3% DSS)	2	400	5.6	74	
		3	620	230	16.9	
	5% v/v in H_2O	1	5.8	370	190	2800
	(3% DSS)	2	390	4.2	70	3000
		3	600	200	6.2	4800
		4	(50)	(60)	(30)	
	30% v/v in C_6H_6	1	10.7	−200	210	440
	(3% TMS)	2	−200	7.8	130	650
		3	690	390	21.6	600
		4	(110)	(160)	(130)	17.4
	5% v/v in C_6H_6	1	13.3	−270	330	2200
	(3% TMS)	2	−260	10.6	190	4400
		3	(990)	(570)	(26.2)‡	
		4	(67)	(130)		20.2

*Underlined values were obtained for T_{ii}.
†The values of T_{ji} in parentheses are estimated from the relationship given in eq. [15].
‡Extrapolated from the concentration dependence (Fig. 6).
§Solvent.

systems listed first in Table 2, and the underlined figures were obtained for T_{ii}. The off-diagonal elements of the relaxation parameter matrix were then calculated from the ratios obtained using eq. [15]. From these data it is then possible to calculate the expected shape of the recovery curves without irradiation (the monoresonance recovery) in accordance with eq. [4]. The coefficients a_{ij} and the inverse values of the roots b_j of the determinant eq. [5] are listed in Table 3 for the 3-spin systems. It is seen that the contribution to the recovery shape from the main exponential term is more than 95%, so it is quite safe to suppose that the recovery curves for solutions of dimethylformamide are adequately fitted by 1-exponential equations. The 3-exponential curves with coefficients and roots listed in Table 3 were simulated and fitted by the computer with the 1-exponential equation. The resultant characteristic times $1/B_i$ are listed in the last column of Table 3. It is seen that these values are very close to the T_{ii} obtained from double Overhauser effect experiments (Table 2) and the differences between them are well below the experimental error (±2%). Indeed, there was no difference (within the experimental error) between results for triple and monoresonance recovery curves, obtained by fitting to a 1-exponential

Can. J. Chem. Downloaded from www.nrcresearchpress.com by 210.87.254.40 on 09/05/12
For personal use only.

TABLE 3

Calculated parameters for the equations

$M_0^i - M_z^i = \Sigma_j a_{ij} \exp(-b_j t) \simeq A \exp(-B_i t)$

Compound	Solution	i	a_{ij} $j=1$	$j=2$	$j=3$	$j=4$	$1/b_j$ (s^{-1})	$1/B_i$ (s^{-1})	T_{1i} (s)
DMDF	Pure liquid	1	0.990	0.010			8.73	8.71	8.7
	(13% benzene)	2	0.016	0.984			6.78	6.81	6.8
		1	0.979	0.011	0.010		8.22	8.24	8.2
DMF	Pure liquid	2	0.021	0.964	0.015		6.25	6.36	6.3
	(3% cyclohexane)	3	0.002	0.003	0.995		15.22	15.17	15.0
		1	0.985	0.010	0.005		16.98	16.98	16.9
	15% v/v in CS_2	2	0.019	0.970	0.011		11.82	12.00	11.9
	(3% TMS)	3	0.002	0.001	0.997		34.92	34.87	34.6
		1	0.993	0.001	0.006		9.59	9.62	9.6
	5% v/v in D_2O	2	0.003	0.985	0.012		5.58	5.65	5.9
	(3% DSS)	3	0.002	0.001	0.997		17.09	17.06	16.9
		1	0.952	0.012	0.004	0.032	10.68	10.83	10.7
	30% v/v in C_6H_6	2	0.019	0.966	0.007	0.008	7.74	7.88	7.8
	(3% TMS)	3	0.002	0.001	0.981	0.016	21.92	21.82	21.6
		4	0.012	0.001	0.029	0.958	17.56	17.59	17.4

TABLE 4

Longitudinal relaxation times T_{1i} (s) for some amides in 5% v/v solutions

Compound	Solvent	T_{1i} *trans*-NCH_3	*cis*-NCH_3	CH
Dimethylformamide	H_2O	5.8±0.2	4.2±0.2	6.2±0.3
	D_2O	9.6±0.3	5.6±0.2	16.9±0.8
	CH_3COOH	5.0±0.2	3.6±0.1	—
	CD_3COOD	6.9±0.2	4.4±0.2	—
	C_5H_5N	11.5±0.3	8.4±0.3	19.7±1
	C_5D_5N	16.5±0.4	10.6±0.3	36.0±1
	$CHCl_3$	9.4±0.3	6.4±0.2	—
	$CDCl_3$	10.0±0.4	7.0±0.2	—
	C_6H_6	13.3±0.4	10.6±0.4	—
	C_6D_6	18.3±0.5	11.9±0.4	—
N-Butyl-*N*-methylformamide	C_6H_6	7.8±0.2	6.6±0.2	—
	C_6D_6	9.3±0.3	6.9±0.2	16.8±1‡ 18.6±1§
N-Methyl-2-pyrrolidone	C_6H_6	8.4±0.2*	—	—
	C_6D_6	10.2±0.3	—	—
N-Methyl-2-piperidone	C_6H_6	8.4±0.3*	—	—
	C_6D_6	10.7±0.4*	—	—
1,4-Dimethyl-2,5-piperazinedione	C_6H_6	6.3±0.2	4.3±0.1†	—
	C_6D_6	7.3±0.2	4.5±0.1†	—

*These measurements were done with irradiation of the C—CH_2—C multiplet to decouple the N—CH_2 triplet to remove partial coincidence with the N—CH_3 signal.
†N—CH_2—CO.
‡*Trans*.
§*Cis*.

Can. J. Chem. Downloaded from www.nrcresearchpress.com by 210.87.254.40 on 09/05/12
For personal use only.

Can. J. Chem. Downloaded from www.nrcresearchpress.com by 210.87.254.40 on 09/05/12
For personal use only.

equation.[4] The attempts to fit double resonance experimental recovery curves (which are expected to be 2-exponential) with a 2-exponential equation were not successful, apparently because of the very small contribution from 1 of the exponential terms. Because the above is true for the pure liquid, a solution in an inert solvent (CS_2), and in a highly associated solvent (D_2O), we assume that for solutions of dimethylformamide and other simple amides with similar structure the direct saturation–recovery method will give a relaxation time very close to the diagonal term T_{ii} of the relaxation parameter matrix. This approach was used for 4-spin systems to calculate the nondiagonal T_{ji}, listed in Table 2, and for other solutions and amides in obtaining T_{ii} (Table 4 and Figs. 4–6).

As opposed to the recovery curves, the dynamic Overhauser effect curves are determined, as usual, by several experimental terms with coefficients of the same order of magnitude. Because of the small amplitude of the Overhauser effect and comparatively large error we did not try to fit these curves to an exponential-type equation and used only the steady-state effects. The calculated shapes of the dynamic Overhauser effect agree qualitatively with the experimental.

Almost all values of T_{ji} have a positive sign. Only the T_{21} and T_{12} for CS_2 and C_6H_6 solutions have a negative sign. Presumably, this corresponds to the hindered internal rotation around the C—N amide bond, which causes a change of relative position of the *N*-methyl groups. The upper limit for the life time τ_{CH_3} (eqs. [2] and [1]) is $16 \leqslant \tau_{CH_3} \leqslant 330$ s at 25 °C, which corresponds to a free energy of rotation of $19.7 \leqslant \Delta G^{\neq} \leqslant 21.5$ kcal/mole. Assuming that the order of magnitudes of T_{21} and τ are the same for pure liquid and solutions of dimethylformamide, we obtain $\Delta G^{\neq} \simeq 20.5$ kcal/mole which is in good agreement with the results of recent investigation of internal rotation in dimethylformamide by various methods (28).

Discussion

The experimental results on T_{ji} (Table 2) allow a few conclusions to be drawn on the relaxation processes in the samples investigated. The mutual dipole–dipole interactions between the nonequivalent protons is more important for CH proton relaxation than for CH_3 protons. Apparently, the most important mechanism for CH_3 relaxation is the interaction within this group of protons. It is also possible that the effect of internal rotation ($-1/\tau_i$) partly compensates the contribution from the dipole–dipole interactions, in accordance with eqs. [2] and [3]. Within the experimental error the ratios T_{ij}/T_{ji} are close to the theoretical values expected from eq. [14].

The T_{11} time constant for the *trans*-methyl group is always longer than T_{22} for the *cis*-methyl. From eq. [10] one may expect that with some reasonable assumptions the time constants for methyl protons of *N*,*N*-dimethyldeuteroformamide and *N*,*N*-dimethylformamide are connected by the equation

$$(1/T_{ii})_{DMDF} = (1/T_{ii})_{DMF} - 2(1/T_{i3})_{DMF}$$

where *i* is 1 or 2. From the data for the pure liquid *N*,*N*-dimethylformamide sample (Table 2) this equation gives

$$(T_{11})_{DMDF} = 8.55 \quad \text{s}$$

and

$$(T_{22})_{DMDF} = 6.78 \quad \text{s}$$

These figures almost exactly coincide with the data for the *N*,*N*-dimethyldeuteroformamide sample (Table 2).

If for the 15% v/v solution of *N*,*N*-dimethylformamide in CS_2 one neglects the intermolecular contribution to the W_{ij} terms, then one may calculate the correlations times τ_{13} and τ_{23} for dipole–dipole interactions between the CH proton and the methyl group by eqs. [11] and [13], assuming, naturally, that $1/\tau_3 = 0$

$$\tau_{i3} = 2/3\gamma^4\hbar^2 T_{3i}\langle r_{i3}^{-6}\rangle_{av}$$

The values of $\langle r_{i3}^{-6}\rangle_{av}$ were calculated by computer for 3 models of rotation around the *N*-methyl bond (see Fig. 7 in ref. 29): 1 free rotation, 2 eclipsed methyl C—H and N—CH_3 bonds (the conventional angles in peptide conformational studies are $\phi = 0°$, 120°, and 240° (30)), and 3 eclipsed methyl C—H and N—CHO bonds ($\phi = 60°$, 180°, and 360°). The results are

$$\tau_{13} = (9.7 \pm 1.5)10^{-12} \quad \text{s}$$

for all 3 models

$$\tau_{23} = (2.5 \pm 0.3)10^{-12} \quad \text{s}$$

[4]The saturation recovery of all signals *i* will be near-exponential with time constants T_{ii} when the matrix of $1/T_{ij}$ is near-diagonal, as may be seen from the characteristic eq. [5]. In other words, the saturation recovery of nucleus *i* will be near-exponential with time constant T_{ii} unless there exists at least 1 group *j* such that the mutual influence of M_z^i on M_z^j and vice-versa is non-negligible. A mathematical treatment may be found in ref. 27.

Can. J. Chem. Downloaded from www.nrcresearchpress.com by 210.87.254.40 on 09/05/12
For personal use only.

for 1st model

$$\tau_{23} = (3.5 \pm 0.5)10^{-12} \quad \text{s}$$

for 2nd model, and

$$\tau_{23} = (2.2 \pm 0.3)10^{-12} \quad \text{s}$$

for 3rd model. That the τ_{23} is shorter than τ_{13} corresponds to faster rotation of the *N,N*-dimethylformamide molecule around the longer axis, which is parallel to the C—N amide bond, than around the perpendicular axis.

Assuming that in inert solvents, such as CS_2,

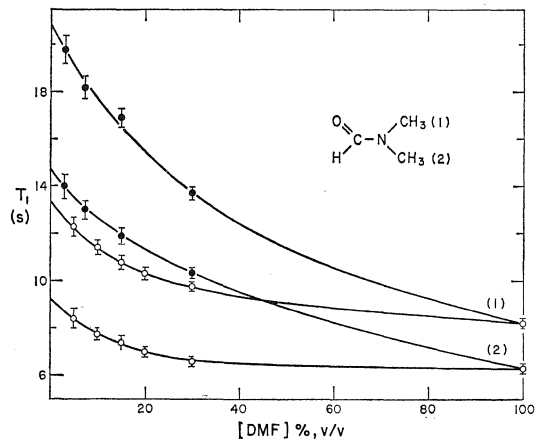

FIG. 4. The concentration dependence of the longitudinal relaxation time of the *N*-methyl groups of *N,N*-dimethylformamide in CS_2 (●) and CCl_4 (○) solutions.

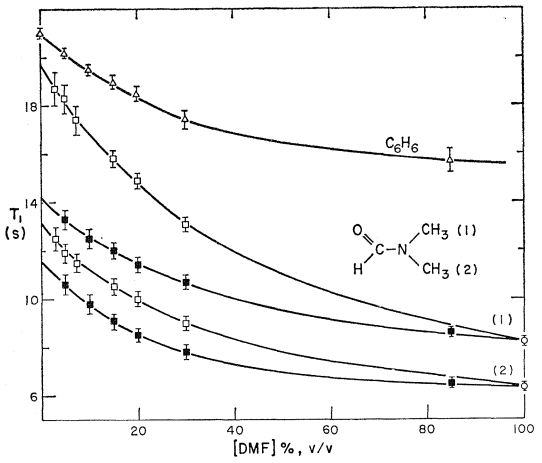

FIG. 5. The concentration dependence of the longitudinal relaxation time of the *N*-methyl groups of *N,N*-dimethylformamide in C_6H_6 (■) and C_6D_6 (□) solutions, as well as T_1 for the solvent C_6H_6 (△) protons.

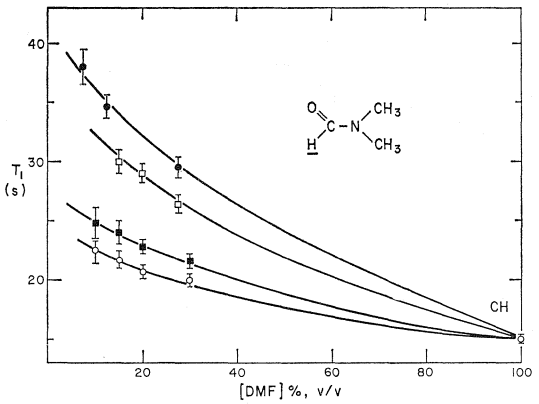

FIG. 6. The concentration dependence of the longitudinal relaxation time of the CH proton of *N,N*-dimethylformamide in CS_2 (●), CCl_4 (○), C_6H_6 (■), and C_6D_6 (□) solutions.

the "lattice" contributions W_i and the intermolecular contributions W_{ii}^{inter} are the same for both types of *N*-methyl groups (*cis* and *trans*), the difference in time constants T_{11} and T_{22} for *N,N*-dimethyldeuteroformamide can only be explained by the difference in correlation times τ_{11} and τ_{22}. (The contribution to $1/T_{ii}$ from the interaction with nitrogen by a dipole–dipole mechanism and a scalar mechanism of the second kind must be very small because of the small magnitudes of γ_N and the indirect spin–spin coupling constants (31), and also because of the relatively fast relaxation of the nitrogen spin.) Then following eqs. [10], [11], and [12] we can calculate

$$\tau_{22} - \tau_{11} = [T_{22}^{-1} - T_{11}^{-1} - 2(T_{23}^{-1} - T_{13}^{-1})]/3\gamma^4\hbar^2 r_{\text{HH}}^{-6}$$

where r_{HH} is the interproton distance within a methyl group. For the 15% v/v solution of *N,N*-dimethylformamide in CS_2 we obtain

$$\tau_{22} - \tau_{11} = 0.5 \times 10^{-12} \quad \text{s}$$

i.e., the correlation time of dipole–dipole interaction within the group of equivalent protons is longer for the *cis*-methyl group, which apparently means that the rotation of this group is more restricted than the *trans*-methyl.

For rough evaluation of the τ_{11} and τ_{22} magnitudes we assume $\tau_1 = \tau_2 = 100$ s, which corresponds to $\Delta G^{\ddagger} = 20.8$ kcal/mole (28), and that the "lattice" contribution W_1 and W_2 are the

TABLE 5

Intramolecular and solute–solvent intermolecular contributions to the longitudinal relaxation times of *N,N*-dimethylformamide

Solvent	$T_{1(intra)}^{-1}$ (s^{-1})			$T_{1(inter)}^{-1}$ (s^{-1})		
	trans-CH_3	*cis*-CH_3	CH	*trans*-CH_3	*cis*-CH_3	CH
Benzene*	0.049	0.075	0.027	0.021	0.011	0.009
Water†	0.107	0.182	0.073	0.065	0.056	0.098
Acetic acid†	0.146	0.229	—	0.054	0.049	—
Pyridine†	0.072	0.095	0.029	0.025	0.024	0.022
Chloroform†	0.100	0.143	—	0.006	0.013	—

*For extrapolated data in infinitely dilute solutions.
†For 5% v/v solutions.

same as for the CH proton

$$W_{33}^{inter} + W_3 = T_{33}^{-1} - 2(T_{31}^{-1} + T_{32}^{-1})$$

Then from eqs. [10]–[12] we can get

$$\tau_{11} \sim 0.4 \times 10^{-12} \text{ s}$$

$$\tau_{22} \sim 0.9 \times 10^{-12} \text{ s}$$

The extrapolated values of T_1 for solutions of *N,N*-dimethylformamide (Figs. 4–6) in general increases with decreasing viscosity of the solutions. An exception is the CCl_4 solution where T_1 are longer than in the pure liquid although the viscosity of CCl_4 (0.97 cP) is higher than *N,N*-dimethylformamide (0.80 cP). Probably this is an effect arising from some degree of self-association in the pure liquid because of electric dipole–dipole interaction between the molecules (32). The extrapolated differences of the relaxation rates for *cis*- and *trans*-methyl protons $(1/T_1)_2 - (1/T_1)_1$ are also roughly proportional to the viscosity with the same exception (in CCl_4 this difference is smaller than in pure liquid).

It is important to compare the change of longitudinal relaxation rates $1/T_1$ in undeuterated and deuterated solvents (33). Deuterons have a much smaller magnetic moment than protons and their effectiveness in relaxation is a factor 24 smaller than that of protons (33). It is a reasonable assumption that the interactions within the same molecules (intramolecular interactions, $1/T_{1(intra)}$) and interactions between nuclei in different molecules (intermolecular interactions, $1/T_{(inter)}$) contribute independently to the total probability $(1/T_1)$ (33). These interactions for a solution can be separated by comparing the relaxation times, extrapolated to zero concentration of the compound in deuterated and undeuterated solvents, or, less precise, obtained for dilute solutions. The extrapolated longitudinal relaxation times are given by

$$(1/T_1)_{undeuter.\ solv.} = 1/T_{1(intra)} + 1/T_{1(inter)}$$

$$(1/T_1)_{deuter.\ solv.} = 1/T_{1(intra)} + 1/24T_{1(inter)}$$

The calculated values of $T_{1(intra)}^{-1}$ and $T_{1(inter)}^{-1}$ for some solutions of *N,N*-dimethylformamide are shown in Table 5. In the approximation of the isotropic interactions of spherical molecules the $T_{1(inter)}$ correspond to $T_{i,\ solv.}$ time constants in eqs. [10] and [11] and in Table 2.

It is seen that for the benzene solution (Table 5) the intermolecular interaction is larger for the *trans*-methyl group than for *cis*-methyl. This is in agreement with the structure of the well-known collision complex between amide and benzene molecules, which was developed by studying the chemical shifts (2, 35). In this complex the benzene molecule is coplanar with the amide, and the axis of symmetry of the benzene molecule is very close to the position of the *cis*-methyl group

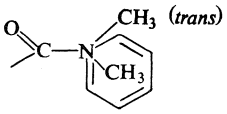

This means that the protons of benzene are closer to the *trans*-methyl group protons and therefore the mutual solute–solvent dipole–dipole intermolecular interaction for these protons is stronger than for the *cis*-methyl protons.

The T_1 measurements for some other amides (Tables 4 and 6) in benzene solutions confirms this assumption.

For the *cis N*-methyl groups the difference $(1/T_1)C_6H_6 - (1/T_1)C_6D_6$ is about 0.01 s^{-1} or less and for *trans N*-methyl groups, 0.02 s^{-1} or greater.

It seems quite probable that such an approach of comparing the change of relaxation rates of

Can. J. Chem. Downloaded from www.nrcresearchpress.com by 210.87.254.40 on 09/05/12
For personal use only.

TABLE 6

The difference between relaxation times for amides in 5% v/v benzene and deuterobenzene solutions

Compound	$(1/T_1)_{C_6H_6} - (1/T_1)_{C_6D_6}$ (± 0.003 s^{-1})	
	trans-NCH_3	*cis*-NCH_3
N,*N*-Dimethylformamide	0.020	0.010
N-Butyl-*N*-methylformamide*	0.020	0.007
N-Methyl-2-pyrrolidone	0.021	—
N-Methyl-2-piperidone	0.027	—
1,4-Dimethyl-2,5-piperazinedione†	0.022	0.010‡

*The equilibrium mixture of the *cis*- and *trans*-conformations (34).
†2% w/v solution.
‡For N—CH_2—C protons.

N-methyl groups could be useful for assignment of *cis–trans* isomerism about the amide bond in *N*-methyl substituted amides and peptides. It might be an absolute method, because it does not require both isomers to be available.

Surprisingly, for all other pairs of undeuterated and deuterated solvents except water (Tables 4 and 5) there are almost no specific differences (within the experimental error) in changing of relaxation rates $1/T_1$. There are at least 2 possible explanations: the solvent molecules are acting as a bulk surrounding, or there are several binding sites for specific solute–solvent interaction, over which the intermolecular contributions are effectively averaged. For the water solutions of *N*,*N*-dimethylformamide the largest solute–solvent intermolecular interaction is observed for the CH proton. This may correspond to the hydrogen bonding of water molecules to the C=O oxygen.

The authors wish to thank Dr. R. F. Henry and Mr. R. F. Trushel for developing the computer program for the fitting of the recovery curves. The authors are very grateful to Prof. L. W. Reeves for lending the *N*,*N*-dimethyldeuteroformamide sample and to Dr. T. N. Khazanovich (Institute of Chemical Physics, Academy of Sciences of the U.S.S.R., Moscow) for a very valuable discussion.

TABLE 7

Chemical shifts (c.p.s., ±1 Hz) of the v/v solutions of dimethylformamide (TMS as internal standard)

% formamide	Solvent	Chemical shift		
		trans-NCH_3	*cis*-NCH_3	CH
97	(Cyclohexane)	279	296	804
85	Benzene	275	286	799
30		258	245	788
20		252	233	781
15		249	225	777
10		246	217	773
7.5		245	213	773
5		245	211	—
3		243	205	—
30	CCl_4	280	295	792
20		279	294	787
15		278	294	786
10		278	294	786
5		278	294	786
30	CS_2	272	288	783
20		273	288	783
15		273	289	782
7.5		274	289	780
5		275	290	—
5	Water (3% DSS)	285	301	793
5	Acetic acid	288	301	—
5	Pyridine	271	263	805
5	Chloroform	288	297	—

1. Annual review of NMR spectroscopy. *Edited by* E. F. Mooney. Academic Press, Inc., London and New York. 1968.
2. P. Laszlo. *In* Progress in nuclear magnetic resonance spectroscopy. Vol. 3. *Edited by* J. W. Emsley, J. Feeney, and L. H. Sutcliffe. Pergamon Press, Inc., Oxford. 1967. Chap. 6.
3. J. Jonas and H. S. Gutowsky. *In* Annual review of physical chemistry. Vol. 19. *Edited by* H. Eyring, C. J. Christensen, and H. S. Johnston. Annual Reviews, Inc., Palo Alto, California. 1968. p. 447.
4. N. Bloembergen, E. M. Purcell, and R. V. Pound. Phys. Rev. **73**, 679 (1948).
5. A. W. Overhauser. Phys. Rev. **92**, 411 (1953).
6. E. L. Mackor and C. MacLean. *In* Progress in nuclear magnetic resonance spectroscopy. Vol. 3. *Edited by* J. W. Emsley, J. Feeney, and L. H. Sutcliffe. Pergamon Press, Inc., Oxford. 1967. Chap. 4.
7. V. Sinivee. Eesti NSV Tead. Akad. Toim., Teh. Fuus. Mat. Tead. Seeria, **15**, 182 (1966); E. Lippmaa and J. Puskar. Eesti NSV Tead. Akad. Toim., Teh. Fuus. Mat. Tead. Seeria, **17**, 130 (1968) and references cited therein.
8. R. A. Hoffman and S. Forsén. J. Chem. Phys. **45**, 2049 (1966).

TABLE 8

Chemical shifts (±1 Hz) of the v/v solutions of amides in benzene (TMS as internal standard)

Compound	N—CH_3	N—CH_2	CO—CH_2	C—CH_2—C
N-Methyl-2-pyrrolidone	250	259	197	128
N-Methyl-2-piperidone	270	259	215	120
1,4-Dimethyl-2,5-piperazinedione	233	318		—

	trans-NCH_3	*cis*-NCH_3	*trans*-CH	*cis*-CH
N-Butyl-*N*-methylformamide	250	211	786	778

Can. J. Chem. Downloaded from www.nrcresearchpress.com by 210.87.254.40 on 09/05/12
For personal use only.

9. P. A. HART and J. P. DAVIS. J. Amer. Chem. Soc. **91**, 512 (1969) and references cited therein.
10. E. LIPPMAA and M. ALLA. Eesti NSV Tead. Acad. Toim., Teh. Fuus. Mat. Tead. Seeria, **17**, 117 (1968) and references cited therein.
11. J. C. METCALF, A. S. V. BURGEN, and O. JARDETZKY. *In* Molecular associations in biology. *Edited by* B. Pullman. Academic Press, New York and London. 1968. p. 487.
12. J. T. GERIG. J. Amer. Chem. Soc. **90**, 2681 (1968) and references cited therein.
13. I. SOLOMON. Phys. Rev. **99**, 559 (1955).
14. A. A. BROOKS, J. D. CUTNELL, E. O. STEJSKAL, and V. W. WEISS. J. Chem. Phys. **49**, 1571 (1968).
15. H. M. MCCONNELL. J. Chem. Phys. **28**, 430 (1958).
16. A. L. VAN GEET and D. N. HUME. Anal. Chem. **37**, 983 (1965).
17. A. L. VAN GEET. Anal. Chem. **40**, 304 (1968).
18. F. A. L. ANET and A. J. R. BOURN. J. Amer. Chem. Soc. **87**, 5250 (1965).
19. M. C. WOODS. Report at the 10th Experimental NMR Conference, Pittsburgh, February 27–March 1, 1969.
20. D. F. S. NATUSCH, R. E. RICHARDS, and D. TAYLOR. Mol. Phys. **11**, 421 (1966).
21. T. N. KHAZANOVICH. Institute of Chemical Physics, Academy of Sciences of the U.S.S.R., Moscow. Private communication.
22. A. ABRAGAM. The principles of nuclear magnetism. Clarendon Press, Oxford. 1962. pp. 295–302.
23. O. HAWORTH and R. E. RICHARDS. *In* Progress in nuclear magnetic resonance spectroscopy. Vol. 1. *Edited by* J. W. Emsley, J. Feeney, and L. H. Sutcliffe. Pergamon Press, Inc., Oxford. 1966. Chap. 1.
24. R. A. FREEMAN and W. A. ANDERSON. J. Chem. Phys. **37**, 2053 (1962).
25. J. G. POWLES and D. J. NEALE. Proc. Phys. Soc. London, **77**, 737 (1961).
26. H. C. TORREY. Phys. Rev. **76**, 1059 (1949).
27. S. FORSÉN and R. A. HOFFMAN. J. Chem. Phys. **39**, 2892 (1963).
28. P. I. INGLEFIELD, E. KRAKOWER, L. W. REEVES, and R. STEWART. Mol. Phys. **15**, 65 (1968).
29. V. F. BYSTROV, S. L. PORTNOVA, V. I. TSETLIN, V T. IVANOV, and YU. A. OVCHINNIKOV. Tetrahedron, **25**, 493 (1969).
30. J. T. EDSALL, P. J. FLORY, J. C. KENDREW, A. M. LIGOURY, G. NEMETHY, C. RAMAKRISHNAN, and H. A. SHERAGA. Biopolym. **4**, 421 (1966).
31. A. J. R. BOURN and E. W. RANDALL. J. Mol. Spectrosc. **13**, 29 (1964); Mol. Phys. **8**, 567 (1965).
32. R. C. NEWMAN, JR., W. SNIDER, and V. JONAS. J. Phys. Chem. **72**, 2469 (1968).
33. J. G. POWLES and R. FIGGINS. Mol. Phys. **10**, 155 (1966).
34. L. A. LAPLANCHE and M. T. ROGERS. J. Amer. Chem. Soc. **85**, 3728 (1963).
35. J. V. HATTON and R. E. RICHARDS. Mol. Phys. **5**, 139 (1962).

Can. J. Chem. Downloaded from www.nrcresearchpress.com by 210.87.254.40 on 09/05/12
For personal use only.

Can. J. Chem. Downloaded from www.nrcresearchpress.com by 210.87.254.105 on 09/05/12
For personal use only.

New method for the synthesis of 6-amino-6-deoxy-α-D-glucopyranosides

T. L. NAGABHUSHAN
R & L Molecular Research Ltd., 8045 Argyll Road, Edmonton 82, Alberta

Received August 1, 1969

A general method for the synthesis of 6-amino-6-deoxy-α-D-glucopyranosides from 3,4-di-*O*-acetyl-1,2-dideoxy-6-*O*-*p*-tolylsulfonyl-D-*arabino*-hex-1-enopyranose (3,4-di-*O*-acetyl-6-*O*-*p*-tolylsulfonyl-D-glucal) is described. The key steps in the synthesis are addition of nitrosyl chloride to the above glycal, condensation of the resulting nitroso–chloro adduct with alcohols or phenols to provide α-glycosides of 3,4-di-*O*-acetyl-2-oximino-6-*O*-*p*-tolylsulfonyl-D-*arabino*-hexopyranose, and conversion of the α-oximinoglycosides to α-glucoside derivatives. Propyl, isopropyl, phenyl, and L-menthyl 2,3,4-tri-*O*-acetyl-6-*O*-*p*-tolylsulfonyl-α-D-glucopyranosides are thus prepared and the last compound is converted to L-menthyl 6-amino-6-deoxy-α-D-glucopyranoside.

Canadian Journal of Chemistry, **48**, 257 (1970)

Introduction

The natural occurrence of 6-amino-6-deoxy-D-glucose as an α-glycoside in the antibiotic Kanamycin-A (1) has created new interest in synthetic methods for establishing the α-glycosidic linkage between 6-amino-6-deoxy-D-glucose and the hydroxyl group of a desired aglycon. Although little has been reported in the literature along these lines, publications by two Japanese groups (2, 3) have provided evidence that Koenigs–Knorr type condensations can be employed for this purpose and indeed, Kanamycin-A has been synthesized by an application of these procedures (4, 5).

It is now established that the nitrosyl chloride adduct of 3,4,6-tri-*O*-acetyl-1,2-dideoxy-D-*arabino*-hex-1-enopyranose (3,4,6-tri-*O*-acetyl-D-glucal) reacts with alcohols to give α-glycosides of acetylated 2-oximino-D-*arabino*-hexopyranose (6). The oximinoglycosides are readily converted to α-glucosides by way of the corresponding ketoglycosides (7). The high degree of stereospecificity observed both in the glycosidation of the nitrosyl chloride adduct and in the borohydride reduction of the ketoglycoside prompted us to examine the possibility of applying the above method for a direct synthesis of acetylated 6-*O*-*p*-tolylsulfonyl-α-D-glucopyranosides, since such compounds would be excellent precursors of 6-amino-6-deoxy-α-D-glucopyranosides.

This paper is, therefore, concerned with the preparation of 3,4-di-*O*-acetyl-1,2-dideoxy-6-*O*-*p*-tolylsulfonyl-D-*arabino*-hex-1-enopyranose (**3**) and its conversion to 2,3,4-tri-*O*-acetyl-6-*O*-*p*-tolylsulfonyl-α-D-glucopyranosides (**5** to **8**) by way of dimeric 3,4-di-*O*-acetyl-2-deoxy-2-nitroso-6-*O*-*p*-tolylsulfonyl-α-D-glucopyranosyl chloride (**4**).

Results and Discussion

The readily available 1,2,3,4-tetra-*O*-acetyl-6-*O*-*p*-tolylsulfonyl-β-D-glucopyranose (**1**) (8) was converted to 2,3,4-tri-*O*-acetyl-6-*O*-*p*-tolylsulfonyl-α-D-glucopyranosyl bromide (**2**) by a slight modification of the published method (9). Reduction of **2** with zinc dust in aqueous acetic acid provided, as expected, 3,4-di-*O*-acetyl-1,2-dideoxy-6-*O*-*p*-tolylsulfonyl-D-*arabino*-hex-1-enopyranose (**3**).[1]

Reaction of **3** with nitrosyl chloride as in the preparation of dimeric 3,4,6-tri-*O*-acetyl-2-deoxy-2-nitroso-α-D-glucopyranosyl chloride (10, 11) afforded a mixture of two crystalline compounds from which the desired 3,4-di-*O*-acetyl-2-deoxy-2-nitroso-6-*O*-*p*-tolylsulfonyl-α-D-glucopyranosyl chloride (**4**) could be obtained only in low yields by repeated recrystallizations. The structure of the by-product which contains no nitrogen and analyses for $C_{17}H_{20}Cl_2O_8S$ is being investigated and will be discussed in a subsequent paper. However, when **3** was reacted with two equivalents of nitrosyl chloride at 0° for 3 h the nitrosyl chloride adduct **4** was formed in high yield. Structural evidence for **4** was obtained from its infrared (i.r.) and nuclear magnetic resonance (n.m.r.) spectra and a first order analysis of the n.m.r. signals shown by H-1, H-2, and H-3 also permitted the assignment of α-*gluco* configuration to **4** (11). Physical and chemical properties of **4** such as the colorless nature of the crystals, the ability to produce light blue colored solutions and to react spontaneously with triethylamine to give triethylamine hydrochloride

[1]During the course of this work the preparation of 3,4-di-*O*-acetyl-1,2-dideoxy-6-*O*-*p*-tolylsulfonyl-D-*arabino*-hex-1-enopyranose (**3**) by a different route was published (13).

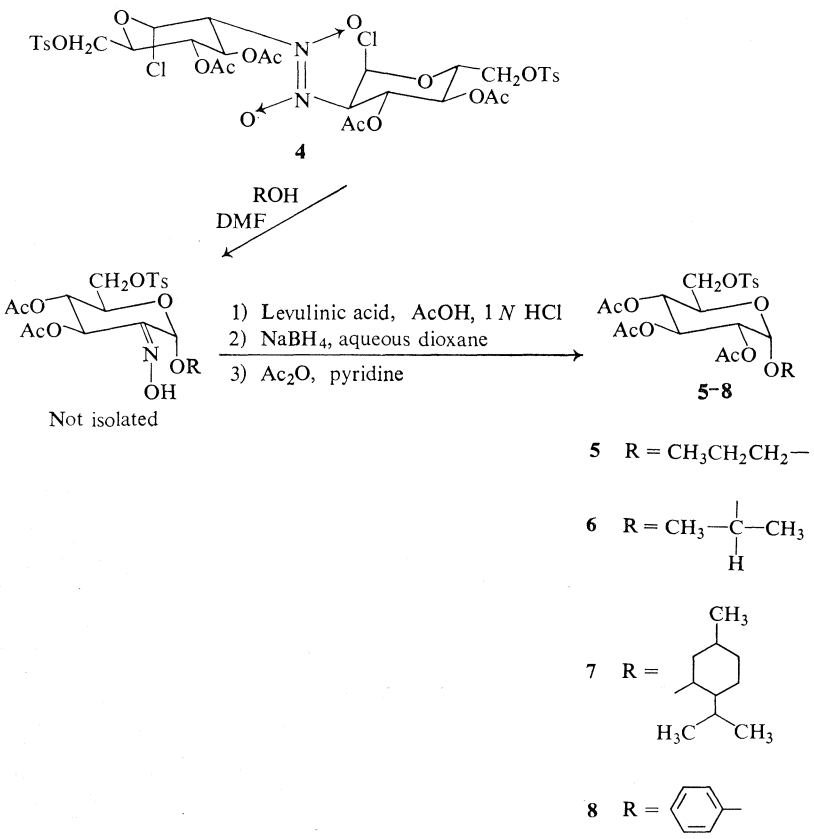

SCHEME 1

with simultaneous formation of a deep blue coloration characteristic of acetylated 2-nitrosoglycals suggested that the compound existed as a dimer in the crystalline state (11). The observed α-*gluco* configuration in **4** seems to offer further evidence for a four-center type addition mechanism as proposed by Lemieux and co-workers (10, 11).

Conversion of **4** into 2,3,4-tri-*O*-acetyl-6-*O*-*p*-tolylsulfonyl-α-D-glucopyranosides was accomplished by general procedures (6, 7) and is illustrated in Scheme 1.[2] Structures of compounds **5–8** thus prepared are shown in Table 1 with overall yields from **4**, physical constants, and n.m.r. parameters. The assignment of the α-*gluco* configuration is apparent from these n.m.r. parameters.

Conversion of L-menthyl 2,3,4-tri-*O*-acetyl-6-*O*-*p*-tolylsulfonyl-α-D-glucopyranoside (**7**) to L-menthyl 6-amino-6-deoxy-α-D-glucopyranoside hydrochloride (**11**) by replacement of the tosyl group by azide followed by *O*-deacetylation and catalytic reduction of the azido group was performed by standard procedures well established in the literature (12). The structure of **11** was proved by i.r. and n.m.r. spectroscopy and by conversion to the crystalline *N*-acetate **12**.

Experimental

Melting points are uncorrected. Infrared spectra were measured with a Perkin–Elmer Model 137 "Infracord" spectrophotometer. Nuclear magnetic resonance spectra were measured at 60 Mc.p.s. with a Varian A-60 spectrometer. Chemical shifts are given in τ values and refer,

[2]Although the oximino glycosides were not purified, in at least one case n.m.r. spectral analysis of the crude reaction product indicated the purity of the compound to be greater than 90%. Thus, the spectrum of crude isopropyl 3,4-di-*O*-acetyl-2-oximino-6-*O*-*p*-tolylsulfonyl-α-D-*arabino*-hexopyranoside showed the following signal pattern, characteristic of acetylated 2-oximino-α-D-*arabino*-hexopyranosides (6); τ 4.03 (singlet, H-1), τ 4.16 (doublet, H-2, $J_{2,3}$ = 9.0 c.p.s.) and τ 4.98 (triplet, H-3, $J_{3,4}$ = 9.0 c.p.s.).

Can. J. Chem. Downloaded from www.nrcresearchpress.com by 210.87.254.105 on 09/05/12
For personal use only.

TABLE 1

2,3,4-Tri-*O*-acetyl-6-*O*-*p*-tolylsulfonyl-α-D-glucopyranosides

Aglycon	Structure	Melting point °C	$[\alpha]_D^{24}$ ° in chloroform (concentration)	Overall yield based on **4** %	Chemical shifts (τ values) and spacings (c.p.s.)					
					H_1	H_2	H_3	$J_{1,2}$	$J_{2,3}$	$J_{3,4}$
$CH_3CH_2CH_2$—	**5**	123–125	+113.5 (1.93)	55	5.09	5.33	4.61	3.75	9.5	10.0
CH_3–CH(–CH_3)–	**6**	103–105	+128.3 (2.51)	56	4.96	5.36	4.63	3.75	9.75	10.05
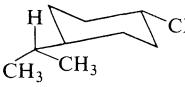	**7**	120–122	+76.3 (3.75)	60	4.93	5.28	4.53	3.75	9.0	10.05
	8	101–108	+109.9 (2.85)	55	4.45	5.13	4.40	4.0	9.0	10.0

unless otherwise stated, to spectra measured in deuteriochloroform with tetramethylsilane as the internal standard. Optical rotations were determined using a Carl–Zeiss Circular Polarimeter Model 0.01°. Thin-layer chromatography (t.l.c.) was performed on silica gel using ethyl acetate – *n*-hexane (1:1, 2:1) as the solvent system and 25% sulfuric acid as the detector. Anhydrous sodium sulfate was used for drying solutions and solvents were removed *in vacuo* at 40–45 °C.

Physical constants and n.m.r. parameters for compounds **5**–**8** are given in Table 1 along with the overall yields from **4**.

*3,4-Di-O-acetyl-1,2-dideoxy-6-O-p-tolylsulfonyl-*D-*arabino-hex-1-enopyranose (3)*

1,2,3,4-Tetra-*O*-acetyl-6-*O*-*p*-tolylsulfonyl-β-D-glucopyranose (**1**, 50 g) (8) was added in one portion to a solution of hydrogen bromide in glacial acetic acid (30–33%, 650 ml) at 4 °C and the mixture was shaken for 1.5 h without external cooling. The clear solution was poured on to crushed ice (2.5 kg) with stirring. The semicrystalline precipitate was collected by filtration and dissolved in ether (400 ml). Any insoluble material was separated by filtration and the filtrate freed from acids by appropriate washings, dried, and concentrated. (Should it become necessary to leave the solution over sodium sulfate overnight, a little methylene chloride is added to inhibit crystallization. Methylene chloride or chloroform is not recommended for the extraction). The residue (46.5 g) was used as such for the zinc reduction.

A mixture of acetic acid (257 ml), water (172 ml), and zinc dust (86 g) was stirred vigorously at 2–5 °C. A solution of the above compound (**2**, 92.9 g from two runs) in acetic acid (534 ml) and water (172 ml) was added dropwise during 1.5 h at such a rate that the temperature did not exceed 5 °C. The stirring was continued for additional 2.5 h. The reaction mixture was saturated with sodium chloride and work-up in the usual manner using ether as the extractant gave a residue which was crystallized from ethanol to give 57.4 g (86.7%) of pure **3** with m.p. 103 °C and $[\alpha]_D^{24}$ + 30° (*c*, 1.064 in chloroform). $\nu_{max}^{(Nujol)}$ 1730–1740 (carbonyl), 1640 (glycal double bond), 1585 (phenyl), 1165, and 1180 cm^{-1} (tosyl). The n.m.r. data, τ 7.93 (2 *O*-acetyl groups), 7.50 (CH_3), 3.52 (H-1, $J_{1,2}$ = 6.5 c.p.s., $J_{1,3}$ = 1.0 c.p.s.), 5.1 (H-2, $J_{2,3}$ = 3.5 c.p.s.), A_2B_2 type quartet at low field for 4 aromatic protons.

Anal. Calcd. for $C_{17}H_{20}O_8S$: C, 53.12; H, 5.20; S, 8.33. Found: C, 52.99; H, 5.22; S, 8.29.

*3,4-Di-O-acetyl-2-deoxy-2-nitroso-6-O-p-tolylsulfonyl-α-*D-*glucopyranosyl Chloride Dimer (4)*

A stock solution of nitrosyl chloride (10.4 g) (Matheson of Canada Ltd., Whitby, Ontario) in reagent grade methylene chloride (520 ml) was prepared at 0 °C under anhydrous conditions. To this solution (260 ml) maintained at 0 °C was added, with stirring, **3** (30 g) and the solution stirred for 2 h. The remaining portion of the stock solution was now added and the mixture stirred for an additional 1 h at 0 °C. After removal of the solvent the residual product was crystallized from chloroform (150 ml) and *n*-hexane (600 ml). Recrystallization in a similar manner afforded 24.9 g (71%) of pure **4**, m.p. 131–133 °C, $[\alpha]_D^{24}$ + 146.73° (*c*, 2.14 in chloroform). $\nu_{max}^{(Nujol)}$ 1740 (carbonyl), 1585 (phenyl), 1165 and 1180 cm^{-1} (tosyl). The n.m.r. data, τ 8.02 (2 *O*-acetyl groups), 7.57 (CH_3), 3.52 (H-1, $J_{1,2}$ = 3.75 c.p.s.), 4.71 (H-2, $J_{2,3}$ = 10 c.p.s.), 4.07 (H-3, $J_{3,4}$ = 9.5 c.p.s.), 4.88 (H-4) and an A_2B_2 type quartet at low field for the 4 aromatic protons.

Anal. Calcd. for $(C_{17}H_{20}ClNO_9S)_2$: C, 45.40; H, 4.44; Cl, 7.88; N, 3.11. Found: C, 45.23; H, 4.85; Cl, 8.10; N, 3.05.

*General Method for the Synthesis of Alkyl or Aryl 2,3,4-Tri-O-acetyl-6-O-p-tolylsulfonyl-α-*D-*glucopyranosides. Preparation of Isopropyl 2,3,4-Tri-O-acetyl-6-O-p-tolylsulfonyl-α-*D-*glucopyranoside (6)*

The procedure illustrated here is applicable in general for the synthesis of compounds **5**–**8**. Any modification in the work-up of individual compounds is described under separate headings.

A solution of **4** (5 mmole monomer) and isopropanol (7.5 mmole) in dry *N*,*N*′-dimethylformamide (8 ml) was

Can. J. Chem. Downloaded from www.nrcresearchpress.com by 210.87.254.105 on 09/05/12
For personal use only.

Can. J. Chem. Downloaded from www.nrcresearchpress.com by 210.87.254.105 on 09/05/12
For personal use only.

set aside at room temperature, under anhydrous conditions, for 60 h. The solvent was removed and a solution of the residue in methylene chloride (75 ml) was washed with water (5 × 50 ml), dried, and concentrated. The crude sirupy product (2.4 g) was dissolved in glacial acetic acid (17 ml) together with levulinic acid (2.95 g) and 1.12 *N* hydrochloric acid (5.1 ml). After stirring the mixture for 18 h at room temperature, it was diluted with methylene chloride (100 ml) and the resulting solution washed free of acids. After drying, the solvent was removed and the crude sirupy residue (2.1 g) dissolved in dioxane (23 ml). Water (2 ml) was added to the solution and the mixture was cooled with stirring to 5 °C. A solution of sodium borohydride (0.133 g) in dioxane (2 ml) and water (4 ml) was added dropwise maintaining the temperature at 5 °C. After the addition was complete, the mixture was stirred for 0.5 h at that temperature and for 1 h at room temperature. Excess borohydride was destroyed by the addition of acetic acid (2 ml) and the solvents were removed. The residual sirup was dried and acetylated at room temperature for 18 h with pyridine (10 ml) and acetic anhydride (6.6 ml). The sirupy residue obtained after usual work-up was crystallized from hot isopropanol (8 ml). $\nu_{max}^{(Nujol)}$ 1725 (carbonyl), 1580 (phenyl), 1165 cm^{-1} (tosyl). Additional n.m.r. data (Table 1), τ 7.59 (CH_3).

Anal. Calcd. for $C_{22}H_{30}O_{11}S$: C, 52.60; H, 5.97; S, 6.38. Found: C, 52.87; H, 6.17; S, 6.30.

n-Propyl 2,3,4-Tri-O-acetyl-6-O-p-tolylsulfonyl-α-D-glucopyranoside (5)

This compound was prepared by the general method described above with the difference that 22 ml acetic acid was used for the hydrolysis of the oxime. $\nu_{max}^{(Nujol)}$ 1725 (carbonyl), 1580 (phenyl), 1160 cm^{-1} (tosyl). Additional n.m.r. data (Table 1), τ 8.05, 8.0 (3 *O*-acetyl groups), 7.59 (CH_3), 9.1 (CH_3 of the *n*-propyl group), 8.1 – 8.9, and 6.2 – 6.9 (CH_2—CH_2 of the *n*-propyl group).

Anal. Calcd. for $C_{22}H_{30}O_{11}S$: C, 52.60; H, 5.97; S, 6.38. Found: C, 52.57; H, 6.21; S, 6.20.

L-*Menthyl 2,3,4-Tri-O-acetyl-6-O-p-tolylsulfonyl-α-D-glucopyranoside (7)*

The crude sirupy product obtained after the condensation of **4** with L-menthol as mentioned in the general method, was washed with *n*-hexane (2 × 3 ml) to remove excess L-menthol before subjecting it to hydrolysis. $\nu_{max}^{(Nujol)}$ 1725 (carbonyl), 1580 (phenyl), 1170 cm^{-1} (tosyl). Additional n.m.r. data, (Table 1), τ 9.06 – 9.39 (superimposed signals of the CH_3 groups), 7.55 (CH_3).

Anal. Calcd. for $C_{29}H_{42}O_{11}S$: C, 58.20; H, 7.01; S, 5.35. Found: C, 57.95; H, 6.71; S, 5.65.

Phenyl 2,3,4-Tri-O-acetyl-6-O-p-tolylsulfonyl-α-D-glucopyranoside (8)

The procedure was essentially the same as for **6**, except, after removal of *N,N'*-dimethylformamide the methylene chloride solution was washed with 0.05 *N* sodium hydroxide solution to remove excess phenol. For the hydrolysis, acetic acid (9 ml), levulinic acid (3.2 g), and 1.12 *N* hydrochloric acid (5.1 ml) were used. $\nu_{max}^{(Nujol)}$ 1725 (carbonyl), 1580 (phenyl), 1165 cm^{-1} (tosyl). Additional n.m.r. data (Table 1), τ 8.03, 7.99 (3 *O*-acetyl groups), 7.95 (CH_3), 2.2 – 3.2 (9 aromatic hydrogens).

Anal. Calcd. for $C_{25}H_{28}O_{11}S$: C, 55.98; H, 5.22; S, 5.97. Found: C, 55.78; H, 5.13; S, 6.65.

L-*Menthyl 6-Azido-6-deoxy-α-D-glucopyranoside (10)*

A solution of **7** (2.99 g, 5 mmole) and sodium azide (1.63 g, 25 mmole) in a mixture of *N,N'*-dimethylformamide (15 ml) and water (2 ml) was refluxed. The reaction was followed by t.l.c. and was complete after 2.15 h. The residue obtained after usual work-up was *O*-deacetylated in solution in methanol (18 ml), water (5 ml), and triethylamine (2 ml) at room temperature for 20 h. The solvents were removed and the product dried over P_2O_5 and crystallized from hot *n*-hexane (6 ml). The yield of pure **10**, m.p. 88–90 °C, $[\alpha]_D^{24}$ + 16.94° (*c*, 1.18 in methanol), was 82%. $\nu_{max}^{(Nujol)}$ 2100 (azide), 3350 cm^{-1} (OH).

Anal. Calcd. for $C_{16}H_{29}N_3O_5$: C, 55.97; H, 15.1; N, 12.24. Found: C, 55.71; H, 15.32; N, 12.14.

L-*Menthyl 6-Amino-6-deoxy-α-D-glucopyranoside Hydrochloride (11)*

Hydrogen was bubbled through a well stirred solution of **10** (0.686 g, 2 mmole) in methanol (10 ml) and 0.5 *N* hydrochloric acid (4 ml) in the presence of 10% palladium-on-carbon (0.1 g). The reduction was followed by i.r. spectroscopy (disappearance of the azide band at 2100 cm^{-1}) and was complete in 2.5 h. Work-up in the usual manner afforded a residue (600 mg) which was recrystallized from methanol (5 ml) and ether (50 ml) to give 0.597 g (84.4%) of pure **11**, m.p. 230° (d), $[\alpha]_D^{24}$ + 56.49° (*c*, 1.54 in water). $\nu_{max}^{(Nujol)}$ 1600 cm^{-1} ($NH_3^{\oplus}$). The n.m.r. data, τ 4.95 (doublet for H-1, $J_{1,2}$ = 3.0 c.p.s.), 9.16 (superimposed signals of the CH_3 groups of the aglycon moiety).

Anal. Calcd. for $C_{16}H_{32}ClNO_5$: C, 54.31; H, 9.05; N, 3.96. Found: C, 54.19; H, 9.15; N, 3.99.

L-*Menthyl 6-Acetamido-6-deoxy-α-D-glucopyranoside (12)*

To a stirred solution of **11** (0.265 g) in a mixture of methanol (10 ml) and water (3 ml) was added aqueous sodium hydroxide solution (30 mg in 2 ml water) followed by acetic anhydride (0.15 ml). After 0.5 h at room temperature work-up in the usual manner yielded 0.25 g (90.9%) of pure **12**, m.p. 216 °C. $[\alpha]_D^{24}$ + 54.71° (*c*, 1.59 in methanol). $\nu_{max}^{(Nujol)}$ 1640 (amide I), 1540 (amide II), 3350–3500 cm^{-1} (OH and NH).

Anal. Calcd. for $C_{18}H_{33}NO_6$: C, 60.16; H, 8.91; N, 3.89. Found: C, 60.24; H, 8.62; N, 3.70.

The author thanks Professor R. U. Lemieux, Director of Research for his advice and encouragement in the conduct of this research and Messrs. J. M. Brouwer, W. Merlo, and B. Baechler for their excellent technical assistance.

1. M. J. Cron, D. L. Evans, F. M. Palermiti, D. F. Whitehead, I. R. Hooper, P. Chu, and R. U. Lemieux. J. Amer. Chem. Soc. **80**, 4741 (1958).
2. S. Umezawa, S. Koto, and Y. Ito. Bull. Chem. Soc. Japan, **36**, No. 2, 183 (1963).
3. T. Ueno, N. Karihara, S. Hashimoto, and M. Nakajima. Agr. Biol. Chem. **31**, No. 11, 1346 (1967).

4. M. NAKAJIMA, A. HASEGAWA, N. KARIHARA, H. SHIBATA, T. UENO, and D. NISHIMURA. Tetrahedron Lett. No. **5**, 623 (1968).
5. S. UMEZAWA, K. TATSUTA, and S. KOTO. Bull. Chem. Soc. Japan, **42**, No. 2, 533 (1969).
6. R. U. LEMIEUX, T. L. NAGABHUSHAN, and S. W. GUNNER. Can. J. Chem. **46**, 405 (1968).
7. R. U. LEMIEUX, R. SUEMITSU, and S. W. GUNNER. Can. J. Chem. **46**, 1040 (1968).
8. J. STANĚK and L. TAJMR. Chem. Listy **52**, 551 (1958).
9. H. OHLE and L. VON VARGHA. Ber. **61**, 1203 (1928).
10. R. U. LEMIEUX, T. L. NAGABHUSHAN, and I. K. O'NEILL. Can. J. Chem. **46**, 413 (1968).
11. R. U. LEMIEUX, T. L. NAGABHUSHAN, and I. K. O'NEILL. Tetrahedron Lett. **29**, 1909 (1964).
12. S. UMEZAWA and K. TATSUTA. Bull. Chem. Soc. Japan, **41**, No. 2464 (1968).
13. T. MAKI and S. TEJIMA. Chem. Pharm. Bull. (Tokyo), **15**, 255 (1967).

Can. J. Chem. Downloaded from www.nrcresearchpress.com by 210.87.254.105 on 09/05/12
For personal use only.

Can. J. Chem. Downloaded from www.nrcresearchpress.com by 210.87.254.105 on 09/05/12
For personal use only.

Deuterium exchange of *C*-methyl protons in lumazine derivatives[1]

J. M. McAndless[2] and Ross Stewart
Department of Chemistry, University of British Columbia, Vancouver, British Columbia

Received August 7, 1969

Proton magnetic resonance spectroscopy has been used to examine the deuterium exchange of the methyl protons in two lumazine derivatives. The exchange occurs at the C-7 methyl group in 6,7,8-trimethyllumazine (**2**) and at the C-6 methyl group in 1,7-dihydro-6,7,8-trimethyllumazine (**3**). The former reaction is subject to both general acid- and general base-catalysis but the latter only to general acid-catalysis. Plausible mechanisms for the reactions of both compounds are advanced, involving in the case of **3**, acid-catalyzed addition of water across the C_6—N_5 double bond.

Canadian Journal of Chemistry **48**, 263 (1970)

Riboflavin (**1**, R = ribityl) and other flavin nucleotides occupy a central position in the reaction chain that is responsible for oxidation in living systems (1). 6,7,8-Trimethyllumazine (**2**) and its derivatives are simple compounds that are structurally related to the flavins and might serve as models for these co-enzymes. Furthermore, as pteridines they are examples of a biologically important class of compounds in their own right.

We have begun a study of alkyllumazines and their dihydro derivatives with a view to elucidating the mechanism of the redox processes that bring about their interconversion. As part of the program the dihydro derivative of **2** was prepared and was found to have the structure **3** resulting from a 1,6-type addition of hydrogen rather than the 1,4-type addition that riboflavin (**1**) undergoes. It soon became apparent that both **2** and **3** undergo an interesting exchange of the protons in certain of their methyl groups and we describe these reactions herein.[3]

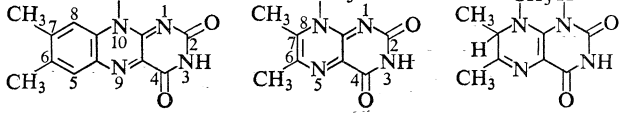

1 **2** **3**

Experimental

A Varian A-60 60 MHz spectrometer was used to record the overall spectra of the prepared compounds. Chemical shifts (Table 1) are quoted as δ values with tetramethyl silane as external reference. For kinetic measurements, a Varian HA-100 100 MHz spectrometer was employed and the solvent peak (HOD) was used as internal reference and lock signal. (The technical help of Mr. R. Burton is gratefully acknowledged.) Sodium phosphate buffer solutions (0.10 *M*) in D_2O were adjusted to the desired acidity with D_2SO_4, with the ionic strength maintained at 0.42 by the addition of sodium chloride. (Measurements of acidity were not corrected to give the corresponding p*D* values.[4]) Solvent systems at $H_0 = -0.37$ and p*H* = 8.2 were prepared from the appropriate mixture of D_2O – anhydrous trifluoroacetic acid (2) and D_2O–pyridine respectively. The exchange took place in 0.07 *M* D_2O solutions of the lumazine dissolved in the appropriate nitrogen-flushed phosphate buffer. Since the *N*-methyl protons did not exchange under the reaction conditions, peaks from these groups were used as reference and the exchange was followed by the measurement of area under the *C*-methyl peak. Before and after each measurement, the samples of **3** were thermostatted at 30.0° in a water bath. The exchange of **2** occurred at such a rate that the reaction was monitored in its entirety in the spectrometer probe, the temperature of which was 31.4°.

[1]Taken in part from the Ph.D. thesis of J. M. McAndless, University of British Columbia, 1969.

[2]Holder of a NRCC Studentship.

[3]As this paper was being prepared, a communication appeared which reported the exchange of the 7-methyl protons in **2** and some of its derivatives (9). Although no kinetic work was reported, these authors advance, as we do, a mechanism for the exchange in alkaline solution which involves the ion shown in Scheme 1. A related reaction is the exchange of the 7-methyl protons in riboflavin 5′-phosphate (10).

[4]It has been shown that a glass–calomel p*H* assembly is useful for measurements of p*D* in heavy water through the application of a scale-factor of about 0.4 unit (11). Since a similar change occurs in the p*K* values of phosphoric acid in going to D_2O (6), the general shape of the rate profile (Fig. 3) would not be radically altered were the appropriate p*D* and $pK_{\text{phosphoric acid}}(D_2O)$ values to be used in its construction.

Can. J. Chem. Downloaded from www.nrcresearchpress.com by 210.87.254.105 on 09/05/12
For personal use only.

TABLE 1

Proton magnetic resonance data (s, d, q — singlet, doublet, quartet)

Compound	Protons	δ(p.p.m.) D_2O	δ(p.p.m.) TFAA*	J(c.p.s.)
2	C-6 Methyl (s)	2.61		
	C-7 Methyl (s)	2.75	—	—
	N-8 Methyl (s)	4.02		
3	C-7 Methyl (d)	1.19	1.36	6.5
	C-6 Methyl (s)	2.01	2.38	
	N-8 Methyl (s)	3.03	3.10	
	C-7 Proton (q)†	—	4.57	6.5

*Trifluoroacetic acid.
†In D_2O, the quartet resonance is partially masked by the HOD solvent peak.

The exchange followed first-order kinetics for most of the reaction. In the case of **3** however, the reactions in the more acidic media were characterized by an initial fast rate of undetermined order, followed by first-order kinetics.

6,7,8-Trimethyllumazine (**2**) was prepared by published methods (3).

1,7-Dihydro-6,7,8-trimethyllumazine (3)[5]

Since this compound proved to be susceptible to aerial oxidation in solution, all solvents used in work-up and recrystallization were flushed thoroughly with nitrogen before use. A 1.5 g sample of **2** in 50 ml 5 *M* acetic acid was hydrogenated over platinum oxide at ambient temperature and atmospheric pressure. The dihydro product was purified by recrystallization from hot aqueous ethanol to yield 0.75 g (49%) of **3** as pale yellow needles (hygroscopic), m.p. 298–300° (decomposed, uncorrected).

Anal. Calcd. for $C_9H_{12}N_4O_2$: C, 51.92; H, 5.81; N, 26.91. Found: C, 52.11; H, 5.60; N, 26.72.

Spectroscopic and ionization data for **2** and **3** are collected in Tables 2 and 3.

TABLE 2

Spectroscopic data*

Compound	Ion	λ_{max}(mμ)	$\log_{10}\varepsilon$	p*H*
2	0	256, 277, 404	4.13, 4.00, 4.08	7.0
	−	244, (268), 313	4.26, (3.77), 4.28	12.0
		362	3.84	
3	+	236, 274, 352	4.01, 4.17, 3.66	1.0
	0	280, 316	4.19, 3.79	5.0
	−	230, 284, 318	4.33, 4.05, 3.75	10.0

*Determined at 25.0° in aqueous media; ( ), shoulder.

[5]An analogous compound containing a β-hydroxyethyl group instead of a methyl group at the 8-position has been given the name 8-(β-hydroxyethyl)-6,7-dimethyl-7,8-dihydrolumazine (12). We prefer the name given above because it reveals the positions of the hydrogens in the compound.

TABLE 3

Ionization constants in water at 25.0°*

Compound	pK_a	pK_{BH+}
2	9.85 ± 0.06	0.85 ± 0.1†
3	7.29 ± 0.03	2.86 ± 0.05

*Ionization constants are thermodynamic values determined from spectral changes accompanying ionization; p*H* measurements made with a radiometer instrument, Model 26.
†(12).

Results and Discussion

Assignment of Exchanging Groups

The typical exchange pattern of **2** is illustrated in Fig. 1, the selective decrease in amplitude of the downfield methyl peak being attributed to exchange of the C-7 methyl group protons with solvent. This assignment is made on the following grounds.

(*i*) In trifluoroacetic acid with external TMS as reference, the downfield *C*-methyl peak in a series of closely related pteridine derivatives, including 6,7,8-trimethyl-2-amino-4-hydroxypteridine, has consistently been assigned to the C-7 methyl group (4). The relative positions are consistent with the proton magnetic resonance (p.m.r.) spectrum of pteridine itself (5) and the known polarization of bonds in pteridines.

(*ii*) 1,7-Dihydro-6-d_3-7,8-trimethyllumazine, formed by the exchange of the C-6 methyl protons of **3** (see later) can be oxidized by D_2O_2 in unbuffered D_2O to 6-d_3-7,8-trimethyllumazine. Comparison of the p.m.r. spectra of this latter compound and **2** confirms the C-7 methyl group assignment.

(*iii*) Only the C-7 methyl group of **2** can produce a charge-delocalized anion by proton loss (Scheme 1).

Figure 2 illustrates the exchange pattern of **3**. The amplitude decrease of the downfield *C*-methyl singlet is attributed to exchange of the C-6 methyl group protons with solvent through the intermediacy of **4**. The assignment is supported by the following.

(*i*) The p.m.r. spectrum of **3** exhibits a non-exchanging doublet resonance which must be due to the C-7 methyl group.

(*ii*) Only the C-6 methyl group of **3** can produce a low-energy methylene intermediate (Scheme 2).

Can. J. Chem. Downloaded from www.nrcresearchpress.com by 210.87.254.105 on 09/05/12
For personal use only.

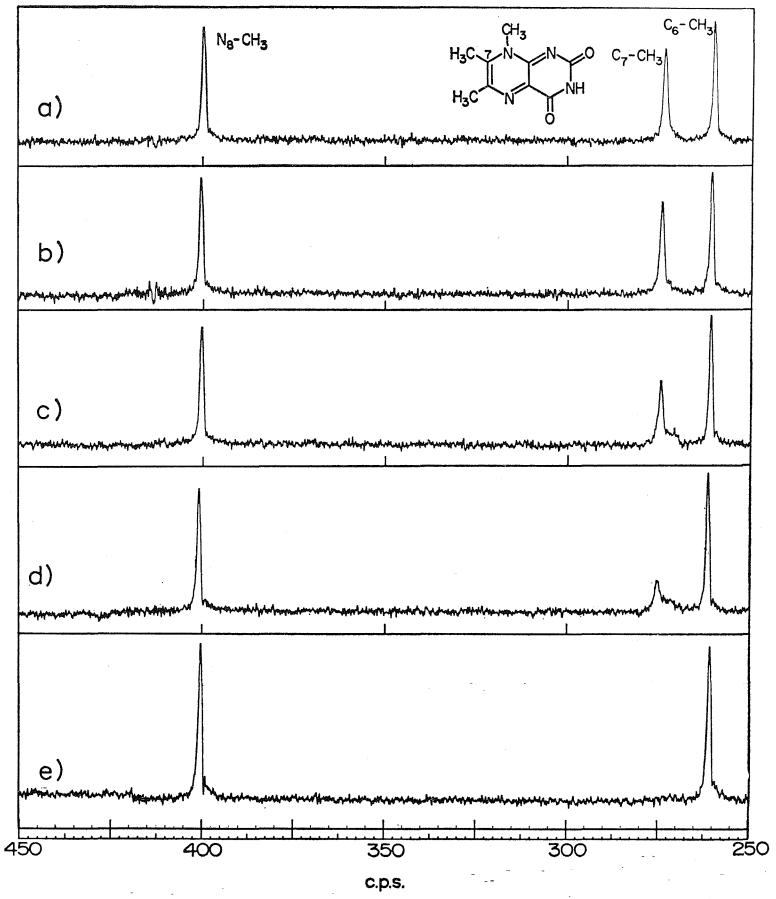

FIG. 1. Proton magnetic resonance spectrum of 6,7,8-trimethyllumazine (**2**); (*a*) in unbuffered D_2O (HOD solvent peak at δ 4.68); (*b*) after 2.5 min in p*H* 2.0, 0.10 *M* Na_2DPO_4 at 31.4°; (*c*) after 13 min; (*d*) after 27 min; (*e*) after 75 min.

Mechanism

(a) 6,7,8-Trimethyllumazine (2)

The exchange was examined in the p*H* range −0.37 to 8.0; over most of this range the substrate is predominantly in the neutral form. The variation of k_1 with p*H* (Fig. 3) shows the exchange is subject to both acid- and base-catalysis. In the present case, the results of experiments examining the dependence of the rate upon buffer concentration at two p*H* values (Fig. 4) show the reaction is subject to general catalysis by the phosphate buffer species as well as by hydronium ion (H_3O^+). The observed k_1 at a given p*H* value within the range examined is a composite value as indicated by eq. [1].

$$[1] \quad k_1 = k_0 + k_{H_3O^+}[H_3O^+] + k_{HA}[HA] + k_{A^-}[A^-] + k_{A^{2-}}[A^{2-}]$$

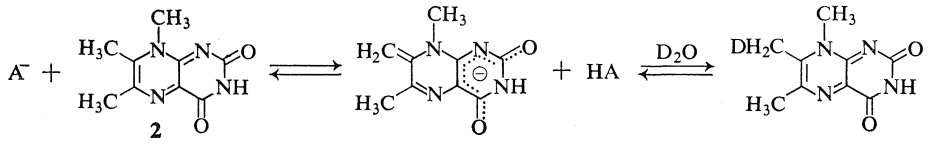

2

Base-catalyzed exchange of 6,7,8-trimethyllumazine (**2**)

SCHEME 1

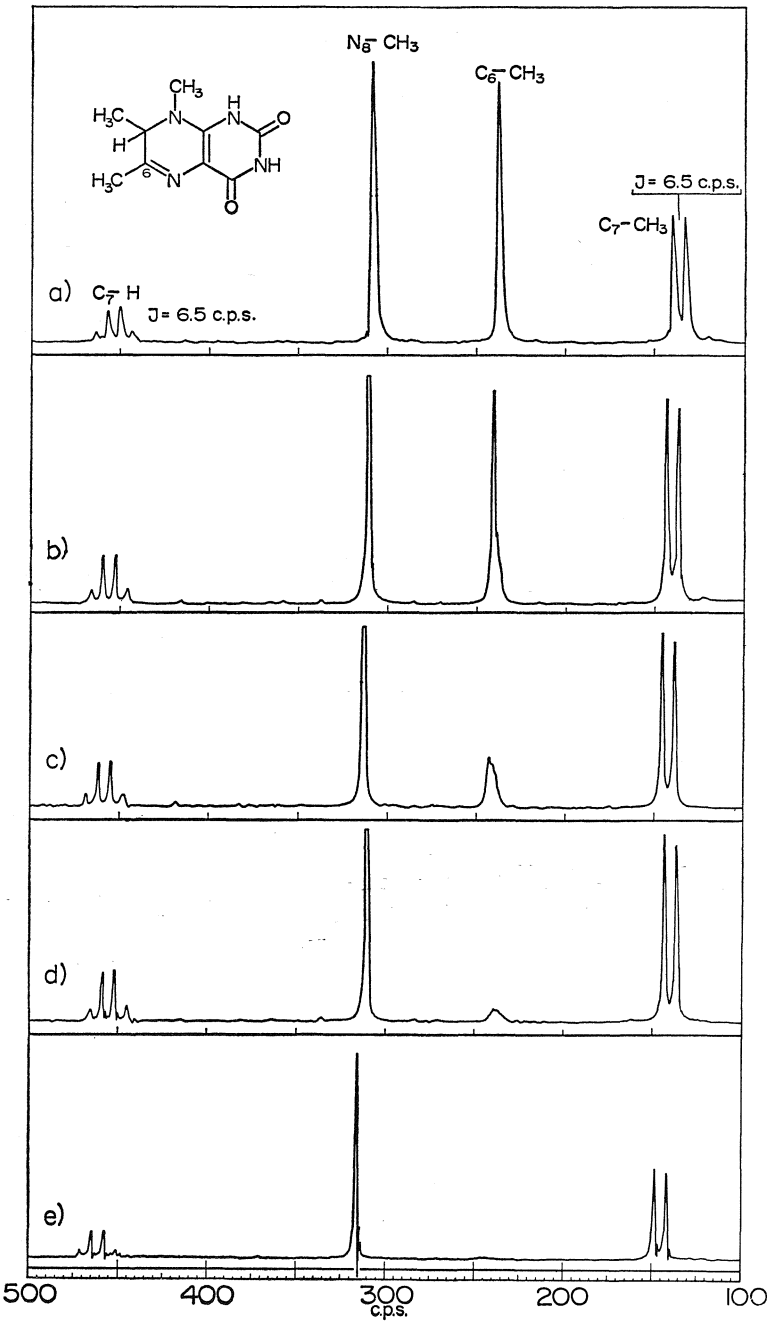

FIG. 2. Proton magnetic resonance spectrum of dihydro-6,7,8-trimethyllumazine (3); (*a*) in trifluoroacetic acid – D_2O ($H_0 = -0.37$), $T = 30.0°$, 7 min after start of exchange; (*b*) after 4 h; (*c*) after 22 h; (*d*) after 54 h; (*e*) after 80 h.

where k_0 is the uncatalyzed exchange rate constant, $k_{H_3O^+}$, k_{HA}, etc. are specific rate constants referring to the species indicated by the subscripts, and $HA = H_3PO_4$, $A^- = H_2PO_4^-$, and $A^{2-} = HPO_4^{2-}$. The value of $k_{H_3O^+}$ may be obtained by extrapolation of the line at pH 2 in Fig. 4 to zero buffer concentration. Using the known dissociation constants of phosphoric acid

Can. J. Chem. Downloaded from www.nrcresearchpress.com by 210.87.254.105 on 09/05/12
For personal use only.

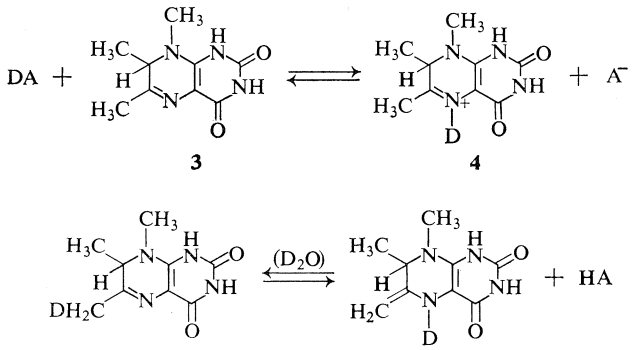

Acid-catalyzed exchange of **3**

SCHEME 2

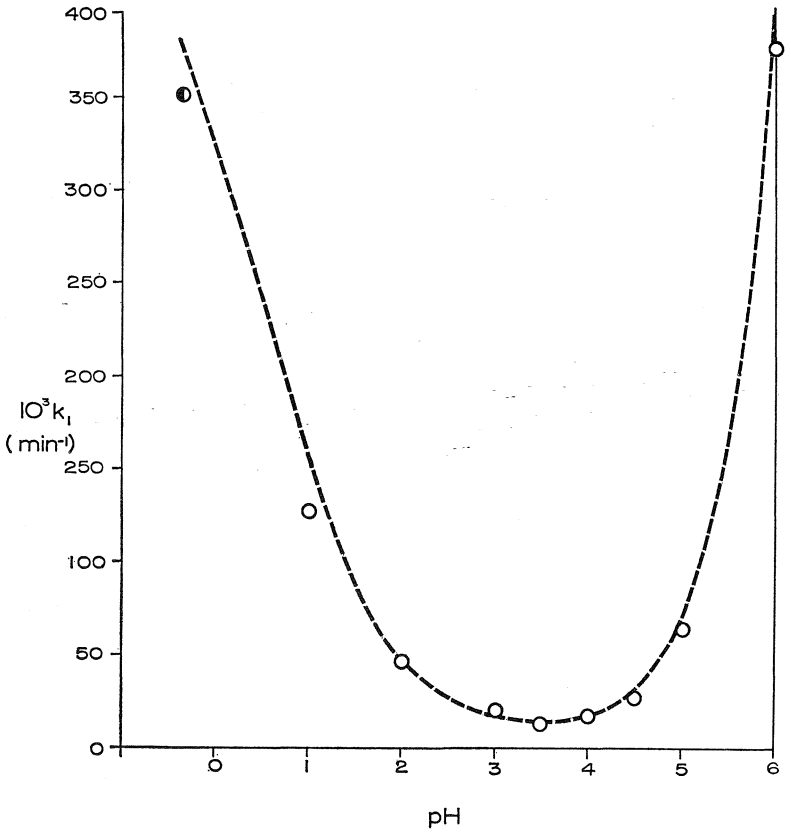

FIG. 3. Effect of acidity on rate of exchange of the C-7 methyl protons of **2**; ○, 0.1 *M* phosphate buffer, $\mu = 0.42$, $T = 31.4°$; ◐, trifluoroacetic acid – D_2O, $H_0 = -0.37$. Dotted line is calculated curve using eq. [1].

(6), the values of the specific catalytic constants are obtained from the experimentally determined values of k_1 and application of eq. [1] at various p*H* values. The values (in l mole^{-1} min^{-1}) calculated for the specific constants are as follows

$k_{H_3O^+} = 1.2$, $k_{HA} = 0.41$, $k_{A^-} = 0.14$,

$k_{A^{2-}} = 52.9$

Can. J. Chem. Downloaded from www.nrcresearchpress.com by 210.87.254.105 on 09/05/12
For personal use only.

Can. J. Chem. Downloaded from www.nrcresearchpress.com by 210.87.254.105 on 09/05/12
For personal use only.

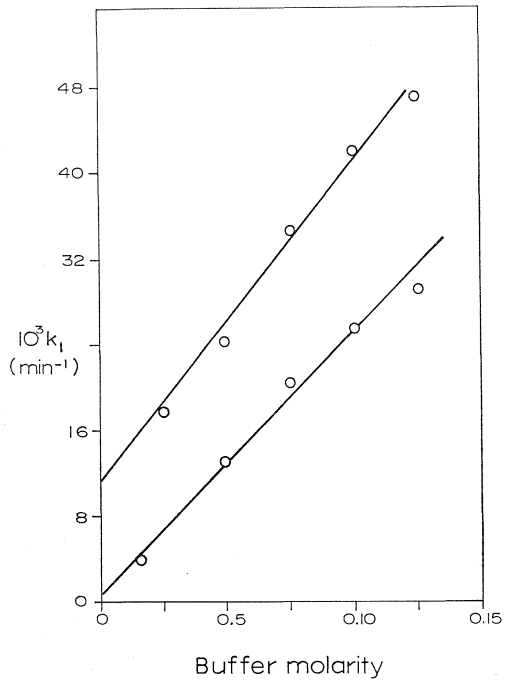

FIG. 4. Relation between phosphate buffer concentrations and rate of exchange of the C-7 methyl protons of **2** at 31.4°; upper curve, pH 2.0 (slope = 0.29 min^{-1} M^{-1}); lower curve pH 4.5 (slope = 0.24 min^{-1} M^{-1}).

Using these values the smooth curve in Fig. 3 was constructed.[6] In all calculations, the value of the uncatalyzed rate constant, k_0, is assumed to be small in comparison to the other constants. This is a reasonable assumption in view of the very slow rate of exchange observed for **2** in unbuffered D_2O at pH 6.5 ($t_{1/2} \sim 1.5$ weeks).

A mechanism for the acid-catalyzed exchange of **2** is shown in Scheme 3. (Protonation at the 4-position oxygen is a trivial variation of this scheme.) Above pH 4 the general base-catalyzed exchange becomes more important. The mechanism of the exchange in the more basic pH range is illustrated by the reversible pathway shown in Scheme 1. The facile exchange observed for the C-7 methyl group protons is doubtless due to the long conjugated bonding arrangement and extensive charge delocalization in the intermediates leading to exchanged product.

(b) 1,7-Dihydro-6,7,8-trimethyllumazine (3)

The exchange was examined in the pH range −0.37 to 8.2 (Fig. 5). In general the rates are

[6]Catalysis by HA (H_3PO_4) and A^{2-} (HPO_4^{2-}) is undoubtedly acid- and base-catalysis, respectively. Further work will be required however, to determine whether A^- ($H_2PO_4^-$) is acting as an acid or as a base.

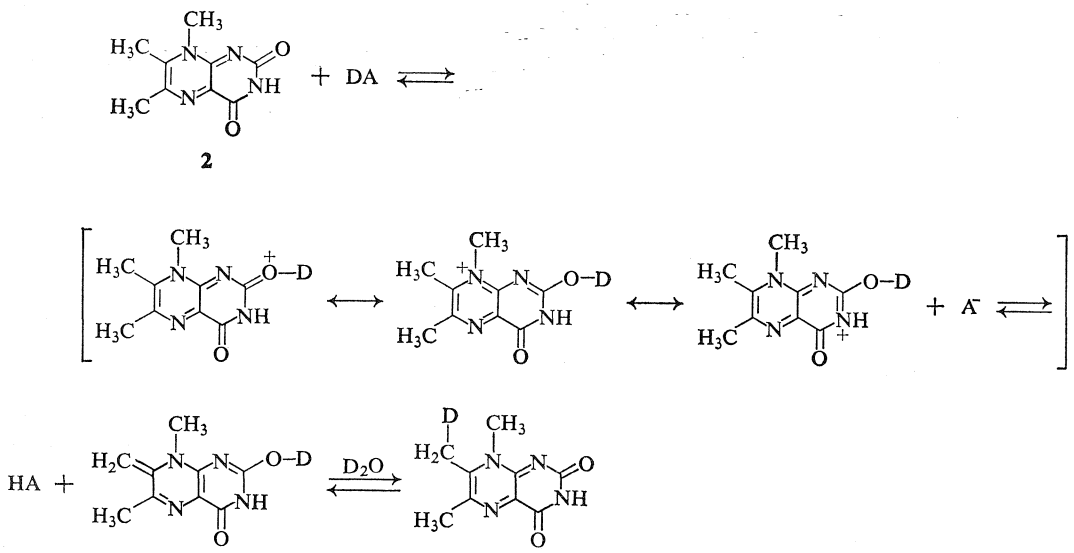

Acid-catalyzed exchange of 6,7,8-trimethyllumazine(**2**)

SCHEME 3

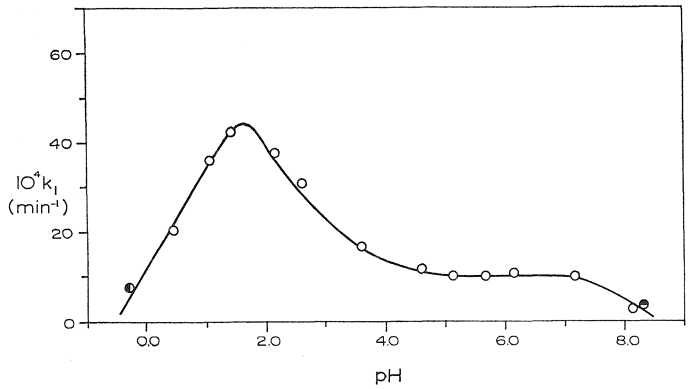

FIG. 5. Effect of acidity on rate of exchange of the C-6 methyl protons of **3**; ○, 0.1 *M* phosphate buffer, $\mu = 0.42$, $T = 30.0°$; ◐, trifluoroacetic acid – D_2O, $H_0 = -0.37$; ◓, pyridine–D_2O, p*H* = 8.2.

much lower than those of the oxidized form, **2**. (The half-life for the exchange of **2** at p*H* 6 in 0.1 *M* phosphate is 1.8 min at 31.4° compared to a value of 677 min for **3** under essentially the same conditions.)

The acid-catalysis observed in solutions more acidic than p*H* 4 is attributed to the reaction path shown in Scheme 2.[7]

The pK_{HA} of **3** has been found to be 7.29 (Table 3) and the decrease in the rate of exchange beyond p*H* 7 presumably reflects the difficulty of proton loss from the anion, **5**.

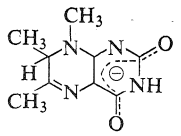

5

Reaction of 3 in Acid Solution

In solutions more acidic than p*H* 2, a fast initial reaction followed by a slower reaction of precisely first order accounts for the greater part of the exchange that took place. The spectra of **3** in this region (except for $H_0 = -0.37$) were characterized by the appearance of a small peak adjacent to the C-6 methyl resonance which increased in size, but did not shift in position, with increasing acidity of the medium. The possibility arises that acid-catalyzed addition of the elements of water across the C_6—N_5 bond to form a hydrated cation of **3** is responsible for the decrease in exchange rate. A possible hydration scheme is shown in Scheme 4. Protonation of the primary amino group will shift the equilibrium toward the ring-opened form in the more strongly acidic solutions.

Pteridines are known to undergo acid-catalyzed hydrations. Indeed, pteridine itself rapidly adds a molecule of water to form "hydrated pteridine", 3,4-dihydro-4-hydroxypteridine (as the cation) (7). This compound slowly undergoes fission of the dihydropyrimidine ring to form the cation of 2-aminomethyleneamino-3-formylpyrazine. Similar behavior is shown for 2-, 4-, and 7-methylpteridine, the rate of the ring-opening reaction varying linearly with hydrogen ion activity (8).

For **3**, a bathochromic shift of 34 mμ was observed in going from the neutral species to the cation. The change from pteridine to its protonated hydrate is similarly accompanied by a bathochromic shift of about 20 mμ (7*b*).

The financial support of the National Research Council of Canada is gratefully acknowledged.

[7]Although *O*-protonation predominates in some analogous cases (13) recent work with pteridine derivatives analogous to **3** (14) suggests that protonation occurs at the N-5 position, as in **4**. Although both kinds of cation are undoubtedly present in acid solution, only **4** has a facile exchange route open to it.

1. (*a*) R. STEWART. Oxidation mechanisms: application to organic chemistry, W. A. Benjamin, Inc., New York. 1964. Chapter 11. (*b*) G. R. PENZER and G. K. RADDA. Quart Rev. (London), **21**, 43 (1967). (*c*) P. HEMMERICH, C. VEEGER, and H. C. S. WOOD. Angew. Chem. **77**, 1 (1965). (*d*) H. BEINERT. *In*

Can. J. Chem. Downloaded from www.nrcresearchpress.com by 210.87.254.105 on 09/05/12
For personal use only.

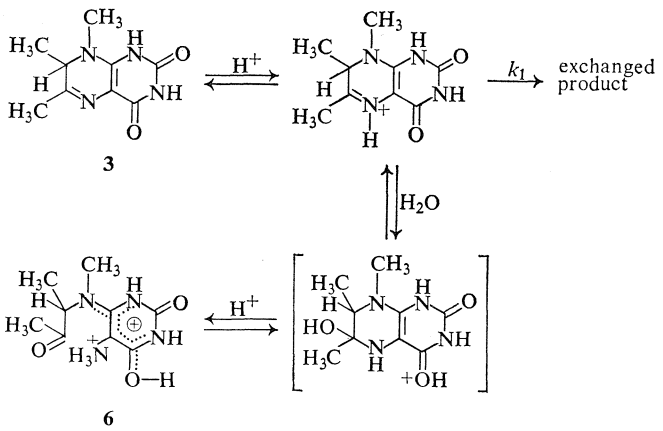

3 6

Hydration of **3** in acidic media

SCHEME 4

The enzymes. Vol. 2. P. D. Boyer, H. Lardy, and K. Myrback (*Editors*). Academic Press, Inc., New York. 1960. Chapter 10.
2. J. E. B. RANDLES and J. M. TEDDER. J. Chem. Soc. 1218 (1955).
3. A. J. BIRCH and C. J. MOYE. J. Chem. Soc. 2622 (1958).
4. A. DIEFFENBACHER, R. MONDELLI, and W. VON PHILIPSBORN. Helv. Chim. Acta, **49**, 1355 (1966).
5. S. MATSUURA and T. GOTO. J. Chem. Soc. 1773 (1963); 623 (1965).
6. C. K. RULE and V. K. LA MER. J. Amer. Chem. Soc. **60**, 1974 (1938).
7. (*a*) D. D. PERRIN and Y. INOUE. Proc. Chem. Soc. (London), 342 (1960); J. Chem. Soc. 2600 (1962). (*b*) D. D. PERRIN. J. Chem. Soc. 645 (1962).
8. Y. INOUE and D. D. PERRIN. J. Chem. Soc. 2648 (1963).
9. T. PATERSON and H. C. S. WOOD. Chem. Commun. 290 (1969).
10. F. J. BULLOCK and O. JARDETZKY. J. Org. Chem. **30**, 2056 (1965).
11. (*a*) K. MIKKELSEN and S. O. NEILSEN. J. Phys. Chem. **64**, 632 (1960); (*b*) M. PAABO and R. G. BATES. Anal. Chem. Abstr. **87**, 155th Nat. A.C.S. Conference, San Francisco, 1968.
12. W. PFLEIDERER, J. W. BUNTING, D. D. PERRIN, and G. NUBEL. Chem. Ber. **99**, 3503 (1966).
13. (*a*) H. E. A. KRAMER and R. GOMPPER. Tetrahedron Lett. **15**, 969 (1963); (*b*) N. J. LEONARD and J. A. ADAMIK. J. Amer. Chem. Soc. **81**, 595 (1959).
14. A. BOBST. Helv. Chim. Acta, **50**, 1480 (1967).

Can. J. Chem. Downloaded from www.nrcresearchpress.com by 210.87.254.105 on 09/05/12
For personal use only.

Radiolysis of aqueous chloroform solutions

B. J. REZANSOFF,[1] K. J. MCCALLUM, AND R. J. WOODS
Department of Chemistry and Chemical Engineering, University of Saskatchewan, Saskatoon, Saskatchewan
Received June 13, 1969

Saturated aqueous chloroform solutions (0.07 *M*) with p*H* ranging from 0.8 to 12.6 have been irradiated with ^{60}Co γ-radiation in the presence and absence of air. $G(Cl^- + ClO^-)$ increases with increasing p*H* in the p*H* range 1–3 (aerated solutions) or 3–6 (deaerated solutions) and again at p*H* greater than 10.5. The variation in yield from aerated solutions in the region p*H* 1–3 is attributed to competition between chloroform and hydrogen ions for hydrated electrons. However, such competition cannot account for the p*H* effect observed in deaerated solutions between p*H* 3 and 6. Increased yields from both aerated and deaerated solutions at high p*H* are attributed to the formation of O^- by reaction of hydroxyl radicals and hydroxide ions. Formic acid and oxalic acid have been identified as minor products when aerated chloroform solutions are irradiated.

Canadian Journal of Chemistry, **48**, 271 (1970)

Can. J. Chem. Downloaded from www.nrcresearchpress.com by 210.87.254.5 on 09/05/12
For personal use only.

Introduction

Hydrogen chloride is a major product when chlorinated hydrocarbons are exposed to ionizing radiation and the ease with which it can be detected and estimated has led to the use of chlorinated organic compounds, generally in the presence of oxygen and water, as radiation dosimeters (1). One of the simplest dosimeters of this type is an aerated, saturated, aqueous solution of chloroform. The yield of hydrogen chloride from such a solution is linear with absorbed energy up to about 2×10^{18} eV g^{-1}; above this the yield falls due to oxygen depletion in the solution.

The radiation chemistry of near-neutral (p*H* 6) aqueous chloroform solutions has been investigated by Teplý and Bednář (2) and Teplý (3) who identified hydrogen chloride as the major radiolysis product and carbon dioxide and hydrogen peroxide as secondary products. *G*(HCl) for saturated chloroform solutions[2] was found to be about 26 for 150 kVp X-rays and ^{60}Co γ-rays in the presence of oxygen, falling to 6.3 in oxygen-free solutions, and decreasing as the concentration of chloroform was reduced. The relatively high yield of hydrogen chloride from aerated solutions was attributed to a mechanism such that the yield of chloride would probably be dependent upon dose rate. However, no dose rate dependence was observed by Teplý and Bednář (2) or by Woods and Spinks (4). The present experiments were carried out to clarify the radiolysis mechanism.

Experimental

Materials

The distilled water used was redistilled from alkaline permanganate and acid dichromate solutions and then stored in Pyrex bottles.

Chloroform (Fisher Certified Reagent) was washed with water (×10) and distilled water (×4) and then distilled, collecting the fraction b.p. 59–62 °C. The purified chloroform was stored under the triply-distilled water in the dark.

Chloroform-^{14}C (New England Nuclear Corporation) was used as supplied after dilution with inactive chloroform purified as described above. The activity of the diluted material was determined using a Nuclear Chicago Unilux scintillation counter (Model 6850) and the channels-ratio counting technique (6).

Irradiation Procedure

Irradiations were carried out in an Atomic Energy of Canada "Gammacell" containing a nominal 5000 curies ^{60}Co. Dose rates were measured using the ferrous sulfate dosimeter (7), assuming a *G* value for ferric ion of 15.5, and were of the order of 5×10^{15} eV g^{-1} s^{-1}.

Chloroform solutions for irradiation were prepared by shaking purified chloroform with triply-distilled water to give a saturated solution (0.070 ± 0.002 *M* at room temperature) which was diluted to give the less concentrated solutions. The p*H* of the solution was adjusted using reagent grade sulfuric acid or sodium hydroxide as required, and was measured using a Beckman p*H* meter (Model 76). Air-saturated solutions (5–8 ml) were irradiated in screw-capped Pyrex vials having a Tygon liner in the cap. Oxygen-free (nitrogen-saturated) solutions were irradiated in similar vials sealed with rubber serum bottle caps. Oxygen was displaced by passing a stream of pure nitrogen, saturated with water vapor and chloroform, through the solution for 15 min prior to irradiation by means of hypodermic needles inserted through the rubber cap.

The absorbed dose was varied between $(0.3–2) \times 10^{18}$

[1]Present address: Nutana Collegiate, Saskatoon, Saskatchewan.

[2]The *G* value is defined as the number of molecules of product formed per 100 eV of energy absorbed from the radiation.

Can. J. Chem. Downloaded from www.nrcresearchpress.com by 210.87.254.5 on 09/05/12
For personal use only.

eV g^{-1}; the latter dose was insufficient to wholly deplete the oxygen originally present in air-saturated samples.

Analysis

Chloride ion was determined by titration with 0.05 *M* mercuric nitrate solution using bromophenol blue – diphenylcarbazone indicator after the addition of sulfuric acid or sodium hydroxide solution to bring the p*H* of the irradiated solution to between 3.0 and 3.6 (8). Hypochlorous acid titrated as chloride. Blank determinations were carried out on unirradiated chloroform solutions and the appropriate correction made. The blank was most significant at high p*H* (11–12.6), where hydrolysis of the chloroform was sufficiently fast to yield appreciable amounts of chloride ion. The hydrolysis is temperature dependent and samples irradiated at a p*H* greater than 10 were kept in a constant temperature bath at 36.2 °C (the temperature in the Gammacell at the time that these samples were being irradiated) before and after irradiation. All samples, irradiated and blank, were subsequently acidified at the same time and then analyzed.

Total acid produced upon irradiation was only determined for samples irradiated at near-neutral p*H* and was estimated by titration with standard sodium hydroxide solution using methyl red as indicator. With this indicator, formic and oxalic acids are titrated, the latter as a dibasic acid, but carbonic acid reacts to only a small extent and hypochlorous acid to an insignificant extent.

Total oxidizing product was estimated by adding 1.0 ml 0.015 *M* ferrous sulfate solution to 10.0 ml irradiated solution and estimating the ferric ion produced from the increase in optical density at 304 mμ. A calibration curve was prepared using hydrogen peroxide as a standard. "Non-volatile" oxidizing product was estimated in the same way after passing a stream of purified nitrogen through the acidified irradiated solution for 10 min.

The quantity of chloride ion, total acid, and oxidizing material produced was determined at various absorbed doses and the quantity plotted against absorbed dose. Linear plots were obtained and used to calculate the appropriate *G* values. Induction periods were observed in some instances but the length of the induction period was not reproducible; the *G* values are based on the slope of the linear portion of the plots.

Formic and oxalic acids were estimated using a tracer method. Samples of saturated chloroform solution (25 or 50 ml containing about 4 microcurie $^{14}CHCl_3$) were irradiated and subsequently added to a weighed quantity (about 100 mg) of non-radioactive sodium formate or oxalic acid. The formic acid was subsequently isolated as the *p*-bromophenacyl ester and oxalic acid as the calcium salt. Samples of the formate ester, purified by crystallization from aqueous ethanol, were dissolved in toluene containing 7.0 g PPO (2,5-diphenyloxazole) and 50 mg POPOP (1,4-bis-2-(5-phenyloxazolyl)benzene) per l and counted using a Unilux scintillation counter and the channels-ratio technique of counting (6). The precipitated calcium oxalate was thoroughly washed with water, carefully dried, and oxidized with perchloric acid to liberate the carbon content as carbon dioxide. The ^{14}C content was estimated by counting the carbon dioxide in an ionization chamber using a Dynacon 600 electrometer. Both formate ester and carbon dioxide were counted for a sufficient time to give a statistical counting accuracy of about 3%.

Results

$G(Cl^- + ClO^-)$ values for 0.07 *M* chloroform solutions are plotted as a function of the p*H* of the solution for air-saturated and for nitrogen-saturated (oxygen-free) solutions in Figs. 1 and 2, respectively. The *G* values appeared to be independent of the build-up of chloride ion during radiolysis (10^{-3} *M* Cl^- was produced by the highest doses absorbed by the air-saturated solutions and 2×10^{-4} *M* Cl^- by the highest absorbed dose in the nitrogen-saturated solutions). The linearity of the plots of $Cl^- + ClO^-$ against absorbed dose indicates that the yields are independent of the oxygen concentration until the oxygen is very nearly exhausted. The yields were found to be independent of temperature from 25 to 37 °C. In near-neutral 0.07 *M* chloroform solutions, *G*(total acid) was 30.1 ± 1.1 for aerated and 7.2 ± 0.25 for oxygen-free solutions; the corresponding $G(Cl^- + ClO^-)$ values are 28.4 ± 1.0 and 6.45 ± 0.25, respectively. For similar solutions irradiated at rather lower dose rates, Teplý and Bednář (2, 3) found $G(Cl^-) = 6.3 \pm 0.3$ for nitrogen-saturated solutions irradiated with 150 kVp X-rays and $G(Cl^-) = 25.8 \pm 1.3$ and 26.6 ± 1.3 for solutions irradiated in the presence of oxygen with ^{60}Co γ-rays and 150 kVp X-rays, respectively; the yields were independent of the concentration of oxygen to low oxygen concentrations. These authors determined chloride by several methods and the quoted $G(Cl^-)$ values probably include any ClO^- formed.

Yields of oxidizing products determined for air-saturated 0.07 *M* solutions over a range of p*H* are shown in Fig. 1. The "non-volatile" oxidizing product is most probably hydrogen peroxide since organic peroxides formed in this system will readily hydrolyze. Teplý and Bednář (2) found $G(H_2O_2) = 2.03 \pm 0.01$ for 150 kVp X-rays at p*H* 6 by polarography, corresponding to our value for non-volatile oxidizing product of 1.7 ± 0.3. The "volatile" oxidizing product is almost certainly chlorine, which we titrate as HCl + HClO. The low yield of volatile oxidizing product compared with $G(Cl^- + ClO^-)$ shows that the major part of the latter product is chloride ion; we have therefore condensed

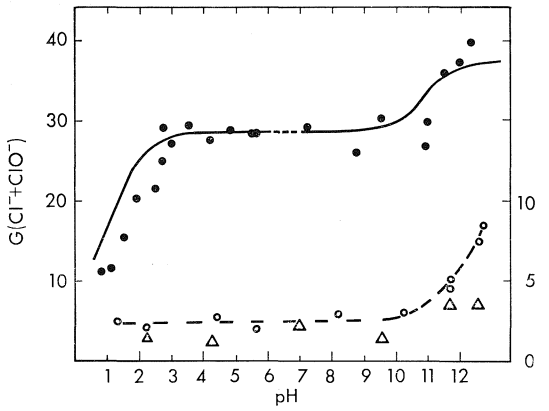

FIG. 1. Variation with pH of $G(Cl^- + ClO^-)$ (●), G(total oxidizing product) (○), and G("non-volatile" oxidizing product) (△) from aerated 0.07 M chloroform solution upon γ-irradiation. The solid lines are calculated responses.

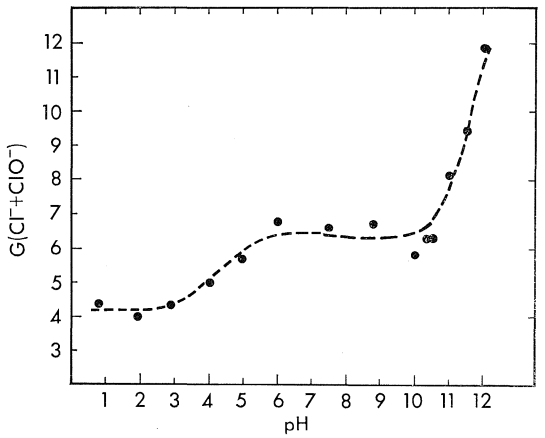

FIG. 2. Variation with pH of $G(Cl^- + ClO^-)$ from nitrogen-saturated 0.07 M chloroform solution upon γ-irradiation.

$G(Cl^- + ClO^-)$ to $G(Cl^-)$ in the following discussion.

The effect of chloroform concentration and of added ferrous sulfate upon $G(Cl^- + ClO^-)$ is shown in Table 1.

Yields of oxalic and formic acids from air-saturated 0.07 M chloroform solutions were $G(C_2H_2O_4) = 0.21 \pm 0.01$ (pH 3.7), $G(CH_2O_2) = 0.23 \pm 0.02$ (pH 1.0), and $G(CH_2O_2) = 0.73 \pm 0.06$ (pH 4.8).

Discussion

Rate constants are from ref. 5 and are for aqueous solutions unless otherwise indicated.

Air-Saturated Chloroform Solutions

The reactive species produced in water by γ-irradiation are hydrated electrons, hydrogen atoms, and hydroxyl radicals. Hydrogen and hydrogen peroxide are also formed, but will probably be protected against radical attack in the present systems by the relatively high concentration of chloroform present. Reactions of the reactive species in acid and neutral chloroform solutions are

[1] $e_{aq}^- + H^+ \rightarrow H$
$k_1 = 2.3 \times 10^{10}\ M^{-1}\ s^{-1}$

[2] $e_{aq}^- + CHCl_3 \rightarrow Cl^- + CHCl_2$
$k_2 = 2.0 \times 10^{10}\ M^{-1}\ s^{-1}$

[3] $H + CHCl_3 \rightarrow HCl + CHCl_2$
$k_3 = 1.6 \times 10^{9}\ M^{-1}\ s^{-1}$ (in hexane)

[4] $H + CHCl_3 \rightarrow H_2 + CCl_3$
$k_4 = 2.2 \times 10^{8}\ M^{-1}\ s^{-1}$ (in hexane)

[5] $OH + CHCl_3 \rightarrow H_2O + CCl_3$
$k_5 = 5 \times 10^{6}\ M^{-1}\ s^{-1}$ (estimated below)

[6] $OH + Cl^- + H^+ \rightarrow H_2O + Cl$
$k_6 = 7.6 \times 10^{9}\ M^{-2}\ s^{-1}$ (9)

TABLE 1

$G(Cl^- + ClO^-)$ from γ-irradiated aqueous chloroform solutions

Chloroform concentration (M)	Other solute	Atmosphere during irradiation	Initial pH	$G(Cl^- + ClO^-)$
7×10^{-2}	None	Air	4–10	28.4 ±1.0
		Nitrogen	1–2	4.25±0.20
		Nitrogen	6–10	6.45±0.25
7×10^{-3}	None	Air	0.5–1.5	10.5 ±0.3
		Air	4–10	21.2 ±0.7
7×10^{-4}	None	Air	4–10	10.1 ±1.6
7×10^{-2}	10^{-2} M $FeSO_4$	Air	5.8	10.9 ±0.7
	10^{-3} M $FeSO_4$	Air	5.5	19.1 ±0.7

Can. J. Chem. Downloaded from www.nrcresearchpress.com by 210.87.254.5 on 09/05/12
For personal use only.

Can. J. Chem. Downloaded from www.nrcresearchpress.com by 210.87.254.5 on 09/05/12
For personal use only.

Reaction [6] will not be significant when near-neutral 0.07 M chloroform solutions are irradiated since the highest chloride concentrations produced were about 10^{-3} M, but it may compete successfully with reaction [5] at low pH and when more dilute chloroform solutions are irradiated. The chlorine atoms formed will probably dimerize (9)

[7] $2Cl \rightarrow Cl_2$ $(+H_2O \rightleftarrows HCl + HClO)$

In the presence of oxygen, additional reactions include

[8] $e_{aq}^- + O_2 \rightarrow O_2^-$
$k_8 = 2 \times 10^{10}\ M^{-1}\ s^{-1}$

[9] $H + O_2 \rightarrow HO_2$
$k_9 = 2 \times 10^{10}\ M^{-1}\ s^{-1}$

[10] $2HO_2 \rightarrow H_2O_2 + O_2$
$k_{10} = 2.2 \times 10^{6}\ M^{-1}\ s^{-1}$ (10)

[11] $CHCl_2 + O_2 \rightarrow O_2CHCl_2$

[12] $CCl_3 + O_2 \rightarrow O_2CCl_3$

The concentration of oxygen in air-saturated chloroform solutions is approximately 2.5×10^{-4} M and reaction [8] will compete with reaction [2] at low chloroform concentrations but not to a significant extent with 0.07 M $CHCl_3$. The ion O_2^- is also formed by dissociation of HO_2

[13] $HO_2 \rightleftarrows H^+ + O_2^-$ $\quad pK_a = 4.5$ (11)

and will probably be the predominant form of this species in solutions with pH greater than 4.5. However, in the absence of a pH effect in the region pH 3–6 that can be attributed to dissociation of HO_2, this will be treated throughout as the neutral radical. The reduction in chloride yield with decreasing pH between pH 3–1 is consistent with competition between hydrogen ions (reaction [1]) and chloroform (reaction [2]) for hydrated electrons if the hydrogen atoms formed do not react with chloroform. This implies that the rate constants shown for reactions [3] and [4], which were determined in hexane by competition between solvent and solute for radiation-produced hydrogen atoms (12), are both high by about two orders of magnitude when applied to the reaction of hydrogen atoms with chloroform in aqueous solution. Differences of this magnitude have been reported previously (5) between rate constants for hydrogen atom reaction with acetic acid, ethyl acetate, and acetone, measured in hexane by the competition technique and determined independently in aqueous solution. The probable reaction of hydrogen atoms in the presence of oxygen is reaction [9].

Yields of hydrated electrons, hydrogen atoms, hydroxyl radicals, and hydrogen peroxide in γ-irradiated, neutral, 0.07 M chloroform solution are estimated (13) to be $G_{e_{aq}^-} = 2.99$, $G_H = 0.55$, $G_{OH} = 2.88$, and $G_{H_2O_2} = 0.71$ when allowance is made for scavenging of hydrated electrons in the spurs by chloroform (14). These yields are small compared with the experimental yield of chloride in the presence of oxygen. Absence of a dose-rate effect upon $G(Cl^-)$ implies that this product is not the result of a chain reaction and we attribute the relatively large chloride yields to hydrolysis of the intermediate, chlorine-containing, organic radicals as represented by the stoichiometric equations

[14] $O_2CHCl_2 + H_2O \rightarrow OH + CO_2 + 2HCl$

[15] $O_2CCl_3 + 2H_2O \rightarrow HO_2 + CO_2 + 3HCl$

[16] $CHCl_2 + H_2O \rightarrow CHO + 2HCl$

[17] $CCl_3 + 2H_2O \rightarrow COOH + 3HCl$

Oxygen is an efficient radical scavenger and in the presence of oxygen the predominant hydrolysis reactions are expected to be [14] and [15]. By analogy with the hydrolysis of organic compounds containing the groups C(Cl)O and CCl, reactions [14] and [15] are expected to be considerably faster than [16] and [17]. However, the minor products, formic acid and oxalic acid, are probably formed via the latter reactions

[18] $2COOH \rightarrow HOOC—COOH$
$(2COO^- \rightarrow {}^-OOC—COO^-)$

[19] $2COOH \rightarrow HCOOH + CO_2$

[20] $CHO + CHCl_2 + H_2O \rightarrow$
$CHCl_2 + HCOOH + HCl$

Since reaction [18] predominates in near-neutral solutions and [19] at low pH (15), reaction [20] is included to account for the decrease in G(HCOOH) from chloroform solutions from pH 4.8 to 1; the decrease in G(HCOOH) is proportional to the decrease in the number of hydrated electrons reacting with chloroform predicted from the rate constants for reactions [1] and [2].

The radiolysis of 0.07 M chloroform solutions in the presence of oxygen can be represented by a mechanism made up of reactions [1], [2], [5],

Can. J. Chem. Downloaded from www.nrcresearchpress.com by 210.87.254.5 on 09/05/12
For personal use only.

and [9] to [20]. With the exception of reactions [16] and [20], which make a minor contribution to the radiolysis, the mechanism is not a chain reaction and the product yields would be expected to be independent of dose rate, as observed by Teplý and Bednář (2) and by Woods and Spinks (4). The mechanism predicts the following relationships for neutral solutions where formic acid is formed only by reaction [20]

[21] $$G(Cl^-) = 6G_{e_{aq}^-} + 3G_{OH} + 3G(HCOOH) = 28.77$$
(Found, 28.4 ± 1.0)

[22] $$G(\text{total acid}) = G(Cl^-) + G(HCOOH) + 2G(C_2H_2O_4) = 29.92$$
(Found, 30.1 ± 1.1)

[23] $$G(CO_2) = 2G_{e_{aq}^-} + G_{OH} - 2G(C_2H_2O_4) = 8.44$$
(Found, 8.4)(2, 3)

[24] $$G(H_2O_2) = G_{H_2O_2} + \tfrac{1}{2}(G_{e_{aq}^-} + G_H + G_{OH}) - G(C_2H_2O_4) = 3.71$$
(Found, 2.03 ± 0.01)(2)

The product yields are predicted using the estimated yields of radicals and H_2O_2 from water radiolysis and the experimental yields of formic acid and oxalic acid. The mechanism predicts a higher yield of hydrogen peroxide than that found, suggesting some reaction of H_2O_2, or its precursor HO_2, with the organic radicals produced.

The effect of pH on $G(Cl^-)$ from 0.07 M air-saturated chloroform solutions is shown in Fig. 1. The solid curve between pH 0.5 and 6 was derived (eq. [25]) from the proposed mechanism assuming competition between hydrogen ions and chloroform for hydrated electrons, and an average yield of 6.73 chloride ions ($6 + 3G(HCOOH)/G_{e_{aq}^-}$ at pH 7) from each hydrated electron reacting with chloroform. Allowance was made for the slight increase in $G_{e_{aq}^-}$ and

[25] $$G(Cl^-) = 3G_{OH} + 6.73G_{e_{aq}^-} \times \left\{\frac{k_2[CHCl_3]}{k_1[H^+] + k_2[CHCl_3]}\right\}$$

G_{OH} in the system at low pH (13).

At pH higher than 10, the yield of chloride for air-saturated 0.07 M chloroform solutions increases (Fig. 1). In this region hydroxide ions may compete with chloroform for hydroxyl radicals

[26] $$OH + OH^- \rightarrow O^- + H_2O \qquad k_{26} = 3.6 \times 10^8\ M^{-1}\ s^{-1}$$

The rate constant for the reaction between hydroxyl radicals and chloroform (reaction [5]) is estimated approximately to be $\sim 5 \times 10^6\ M^{-1}\ s^{-1}$ from the effect of ferrous ion upon $G(Cl^-)$ from aerated chloroform solution (Table 1) (published rate constants (5) indicate that ferrous ions will react with hydroxyl radicals in competition with reaction [5] but that they will not react to a significant extent with hydrated electrons or hydrogen atoms at concentrations of 10^{-2} to 10^{-3} M Fe^{2+}). The solid curve in Fig. 1 between pH 7 and 13 depicts the effect upon $G(Cl^-)$ of competition between reactions [5] and [26] assuming $k_5 = 5 \times 10^6\ M^{-1}\ s^{-1}$ and a yield of 6 ions (Cl^- or ClO^-) for each O^- reacting with chloroform. At high pH, the yield of "volatile" oxidizing product, which we have tentatively identified as chlorine (or HCl + HOCl), increases, suggesting that O^- reacts with chloroform in a similar manner to the hydrated electron

[27] $$O^- + CHCl_3 \rightarrow ClO^- + CHCl_2$$

Each O^- would then give $ClO^- + 5Cl^-$. The calculated curve becomes level above pH 12.5 at $G(Cl^-) \sim 38$; however, a chain reaction producing chloride is possible if reaction [27] is followed by reactions [11] and [14]. We find no evidence of a chain reaction up to pH 12; above this, thermal hydrolysis of the chloroform renders the radiolysis results unreliable.

Nitrogen-Saturated Chloroform Solutions

In the absence of oxygen, $G(Cl^-)$ is independent of pH below pH = 3, where competition between hydrogen ions and chloroform for hydrated electrons will be significant. The increase in $G(Cl^-)$ between pH 3 and 6 (Fig. 2) cannot be attributed to competition between these reactions and appears to be due to a pH-dependent reaction of the organic radicals present. At high pH, the increase in $G(Cl^-)$ is consistent with competition between hydroxide ions and chloroform for hydroxyl radicals.

The authors are grateful to the National Research Council of Canada for financial assistance.

1. H. FRICKE and E. J. HART. *In* Radiation dosimetry. Vol. 2. *Edited by* F. H. Attix and W. C. Roesch. 2nd ed. Academic Press, Inc. New York. 1966. p. 210.
2. J. TEPLÝ and J. BEDNÁŘ. Proc. 2nd Intern. Conf. Peaceful Uses At. Energ. United Nations, Geneva, **29**, 71 (1958).
3. J. TEPLÝ. Coll. Czech. Chem. Commun. **24**, 1933 (1959); **25**, 24 (1960).
4. R. J. WOODS and J. W. T. SPINKS. Can. J. Chem. **38**, 77 (1960).
5. M. ANBAR and P. NETA. Intern. J. Appl. Radiat. Isotop. **16**, 227 (1965).
6. L. A. BAILLIE. Intern. J. Appl. Radiat. Isotop. **8**, 1 (1960).
7. J. WEISS, A. O. ALLEN, and H. A. SCHWARZ. Proc. Intern. Conf. Peaceful Uses At. Energ. United Nations, New York, **14**, 179 (1956).
8. F. E. CLARKE. Anal. Chem. **22**, 553 (1950).
9. J. F. WARD and L. S. MYERS. Radiat. Res. **26**, 483 (1965).
10. H. A. SCHWARZ. Radiat. Res. Suppl. 4, 89 (1964).
11. G. CZAPSKI and L. M. DORFMAN. J. Phys. Chem. **68**, 1169 (1964).
12. T. J. HARDWICK. J. Phys. Chem. **66**, 2246 (1962).
13. E. HAYON. Trans. Faraday Soc. **61**, 734 (1965).
14. E. HAYON. J. Phys. Chem. **68**, 1242 (1964).
15. E. J. HART, J. K. THOMAS, and S. GORDON. Radiat. Res. Suppl. 4, 74 (1964).

Can. J. Chem. Downloaded from www.nrcresearchpress.com by 210.87.254.5 on 09/05/12
For personal use only.

Can. J. Chem. Downloaded from www.nrcresearchpress.com by 210.87.254.40 on 09/05/12
For personal use only.

Vapor–liquid equilibria in the system acetone–benzene

A. N. CAMPBELL AND R. M. CHATTERJEE[1]
Department of Chemistry, University of Manitoba, Winnipeg, Manitoba

Received June 2, 1969

The saturation pressures and vapor–liquid compositions of 7 mixtures of the system acetone–benzene have been determined from a temperature of 100 °C and a pressure of about 2 atm up to the highest temperatures and pressures at which liquid and vapor coexist. The critical temperatures were determined by the disappearance-of-meniscus method.

The *P–T–X* relations at the liquid–vapor phase boundaries, as obtained by the determination of the bubble-point pressure vs. temperature curves of a series of mixtures of known composition, do not indicate the existence of an azeotrope in the range of temperature and pressure of this research. The binary data have been treated thermodynamically to yield the liquid-phase activity coefficients. The partial molal volumes in the liquid mixture required for the Poynting correction (effect of pressure on liquid phase properties) for liquid-phase activity coefficients have also been obtained. The fugacity coefficient of a component in the vapor mixture has been obtained by a modified Redlich–Kwong equation, as suggested by Chueh and Prausnitz. Following their modification of the van Laar equation, several binary liquid phase parameters, such as the binary interaction constant, Henry's constant and dilation constant, as required for the solution model for excess Gibbs energy, have been calculated.

Canadian Journal of Chemistry, **48**, 277 (1970)

The equilibrium properties of liquid mixtures at high pressure are required for engineering calculations e.g., design of apparatus for separation of components, etc. They are also of interest for the physico-chemical understanding of the interactions between the solute and solvent molecules. There is no satisfactory method available for predicting such properties from theory of solutions alone. Sometimes, analytical equations of state with constants related to the composition and the critical properties of the pure components are used for estimating the *P–V–T* properties of mixtures, provided some information on the properties of the mixtures is available. Although experimental *P–V–T* data at high pressure for mixtures of hydrocarbons are plentiful, they are not so common for mixtures containing a polar liquid. In a previous paper (1), we have determined the requisite data for the pure components, acetone and benzene. This paper reports the measurements of saturation pressures and vapor–liquid compositions of the binary system acetone–benzene, and also the treatment of experimental equilibrium data to derive thermodynamic functions.

The method of correlating vapor–liquid equilibrium data in this study is based on the separate description of the deviations occurring in the vapor phase and liquid phase. The vapor-phase nonideality is calculated from the modified Redlich–Kwong equation of state (2); the liquid nonideality is calculated with reference to the pure liquid components and the deviations from ideal solution laws. However, for the component whose critical temperature is below the temperature of the solution, pure liquid cannot be used as a reference state. Therefore, Henry's constant and the ideal dilute solution laws are used for a supercritical component, thus avoiding any hypothetical standard states. The effect of pressure and composition, respectively, on the liquid-phase activity coefficients has been calculated.

Experimental

The purification of materials has been previously described (1). The compositions of liquid and of vapor phases were determined refractometrically. When analyzing the vapor phase, the small amount of material required for a determination of refractive index was an advantage. An uncertainty of ± 0.0001 in refractive index corresponded to an uncertainty of 0.001 in mole-fraction.

The determination of critical temperature has been described previously as has also the determination of vapor pressure (1). In the static method of pressure measurement it was necessary to keep the vapor space as small as possible so that the whole system could be kept at a uniform temperature and that the volume and the composition of the liquid were not changed appreciably by evaporation as the temperature was raised. The true liquid-phase composition was therefore essentially the same as the charged composition. It would have been easy to apply corrections for changes in liquid composition due to vaporization. However, they were so small that it was not considered necessary.

The direct experimental determination of vapor–liquid equilibrium entails the separation of samples of the liquid

[1]Present address: Department of Chemical Engineering, University of Toronto, Toronto 181, Ontario.

Can. J. Chem. Downloaded from www.nrcresearchpress.com by 210.87.254.40 on 09/05/12
For personal use only.

and vapor which are in true equilibrium and determination of the concentrations of both phases. The high pressure bomb used in our research was made of glass, contained in a metal cylinder placed in a thermostat. The apparatus is shown in Fig. 1. This simple apparatus worked surprisingly well; the operation is therefore described in some detail.

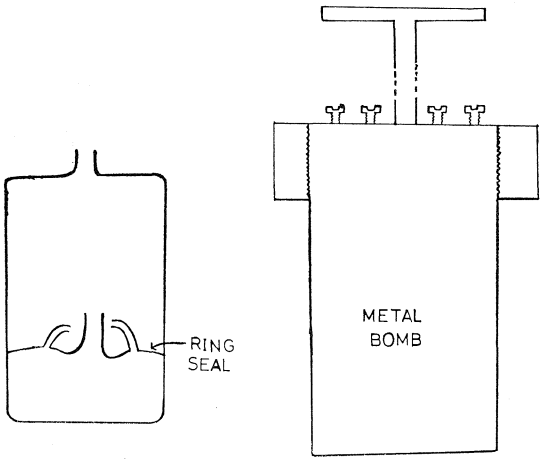

FIG. 1. Cross-sectional view of the glass and metal bombs for vapor–liquid equilibrium determination.

The bomb was made of 70 mm Pyrex standard wall tubing and was divided into two compartments by a ring seal, such that the upper chamber was $\frac{2}{3}$ the whole volume. The total volume of the bomb was approximately 450 ml. The liquid mixture was charged through a 7 mm filling tube sealed to the center of the ring. Around the central tube there were four vapor-escape tubes communicating with both compartments and extending 4 mm above the ring seal. These vents were bent downwards towards the central tube to prevent the escape of condensed vapor to the lower chamber. The cell was evacuated after freezing the charged liquid in the bottom compartment. At the end of an experiment, the equilibrium liquid was sampled through the central hole by means of a hypodermic syringe.

The sealed bomb was placed within a metal cylinder, which also contained liquid mixture of the same composition as that in the glass bomb. This was done to create an approximately equal pressure, within and without the bomb. The metal cylinder was of the usual pressure bomb type. The metal bomb and its contents were shaken in the thermostat by means of an eccentric shaker.

After equilibrating for 24 h, the bomb was removed from the thermostat and cooled in ice–water. The glass bomb was then opened and the liquid and condensed vapor phases sampled. It will be seen from the diagram that the condensed vapor accumulates in the central ring. At the lower temperatures, the amount of condensed vapor was small, but it was sufficient for the determination of refractive index.

It must be noted that in this procedure of vapor–liquid composition determination, one has to choose the amount of liquid charged in such a way that the following condition is satisfied

$$\frac{\text{Density of vapor at the temperature of measurement}}{\text{Density of liquid at room temperature}} = \frac{\text{Volume of liquid used}}{\text{Volume of the container}}$$

Above this temperature, there will be a single vapor space with no liquid. This will be the highest temperature up to which liquid and vapor will coexist for a particular filling.[2] Our liquid volume was chosen in such a way that this condition was fulfilled even at the highest temperatures.

Results

The gas–liquid critical temperatures have been measured for the binary mixture acetone–benzene over the whole concentration range, and are reproduced in Table 1. The surface fraction is given by

$$\theta_i = \frac{x_i v_{ci}^{2/3}}{\sum x_i v_{ci}^{2/3}}$$

The uncertainty of measurement is ± 0.1 °C.

TABLE 1

Gas–liquid critical temperatures of the system acetone–benzene*

Concentration of acetone		Experimental critical temperature (°C)
Mole fraction	Surface fraction	
0.0925	0.0997	283.95
0.1580	0.1690	279.70
0.2160	0.2300	276.75
0.3290	0.3480	270.20
0.4410	0.4620	264.00
0.5440	0.5640	258.90
0.6530	0.6720	252.95
0.7640	0.7790	247.35
0.8250	0.8366	244.10
0.8690	0.8781	241.55
0.9370	0.9410	238.20

*Value of the correlating parameter τ_{12} selected $= -0.0096$.

For a binary mixture, the critical temperature is given by

$$T_c = \theta_1 T_{c_1} + \theta_2 T_{c_2} + 2\theta_1\theta_2\tau_{12}$$

Where τ_{12} is a parameter characteristic of the 1–2 interaction (4). By expressing the critical temperature of the mixture as a function of surface

[2]We are indebted to Dr. R. L. Scott of the University of California, Los Angeles (3), for drawing our attention to this fact.

Can. J. Chem. Downloaded from www.nrcresearchpress.com by 210.87.254.40 on 09/05/12
For personal use only.

TABLE 2

Experimental bubble-point pressures of the system acetone–benzene

Temperature (°C)	Saturated pressure (atm)
0.093 mole fraction acetone	
99.85	2.083
110.05	2.808
117.45	3.243
127.35	3.983
134.60	4.610
143.35	5.427
152.70	6.634
161.55	7.842
173.30	9.780
185.75	12.30
194.05	14.18
207.30	17.36
216.65	20.08
223.50	22.39
231.65	25.18
243.30	29.70
251.55	33.08
258.10	35.92
263.15	38.19
269.25	40.92
271.50	41.89
0.151 mole fraction acetone	
261.70	39.11
263.35	39.84
265.80	40.88
267.65	41.77
269.30	42.50
270.80	43.29
271.55	43.63
0.209 mole fraction acetone	
99.95	2.275
108.50	2.846
116.25	3.368
125.30	4.052
135.55	5.246
145.50	6.368
154.45	7.645
161.05	8.683
170.50	10.42
182.35	12.79
192.55	15.26
203.70	18.04
210.50	20.26
217.65	22.60
225.50	25.28
233.85	28.49
241.90	31.76
248.45	34.54
255.60	37.78
259.55	39.69
265.30	42.39
268.35	43.81
270.10	44.79
0.332 mole fraction acetone	
100.05	2.481
108.55	3.170
114.60	3.625
123.50	4.395
132.35	5.390
140.65	6.402
149.85	7.635
157.65	8.946
168.50	10.98
175.95	12.44
183.50	14.18
190.45	15.92
196.70	17.80
204.50	20.24
211.35	22.48
218.60	25.17
224.75	27.43
231.55	30.34
238.30	33.19
246.65	36.89
254.85	40.70
259.05	42.64
261.40	43.78
0.438 mole fraction acetone	
99.90	2.645
105.60	3.096
112.45	3.763
119.85	4.398
125.60	4.947
132.65	5.886
140.10	6.823
149.90	8.250
157.55	9.621
165.40	11.22
173.95	13.08
178.50	14.19
187.05	16.26
193.60	18.14
199.75	20.11
207.35	22.74
216.00	25.99
222.95	28.90
230.50	32.18
238.55	35.88
244.70	38.67
249.85	41.18
257.60	44.71
260.10	45.95
0.657 mole fraction acetone	
99.85	2.996
107.50	3.605
115.30	4.421
122.55	5.220
127.65	5.923
134.70	6.907
143.15	8.285
149.60	9.496
157.55	11.19
165.85	12.96
174.80	15.20
179.50	16.41
186.30	18.44
194.70	21.39
199.65	23.16
207.50	26.37
214.05	29.13
221.35	32.47
227.50	35.31
235.95	39.26
242.35	42.24
247.60	44.76
250.05	45.99
0.761 mole fraction acetone	
99.95	3.166
109.55	4.089
117.35	4.888
124.60	5.820
132.50	6.995
139.95	8.226
147.50	9.689
156.70	11.62
164.85	13.63
172.55	15.59
179.90	17.50
188.65	20.39
196.30	23.20
202.55	25.80
210.10	29.08
216.80	32.16
222.55	35.01
224.65	36.02
225.40	36.32
232.50	39.83
0.872 mole fraction acetone	
99.85	3.340
107.70	4.163
116.40	5.196
123.85	6.193
129.90	7.089
139.65	8.786
144.35	9.608
149.95	10.69
157.85	12.57
164.05	14.12
174.80	17.09
181.95	19.39
189.50	22.06
198.95	25.62
208.40	29.96
215.35	33.39
221.45	36.50
225.15	38.49

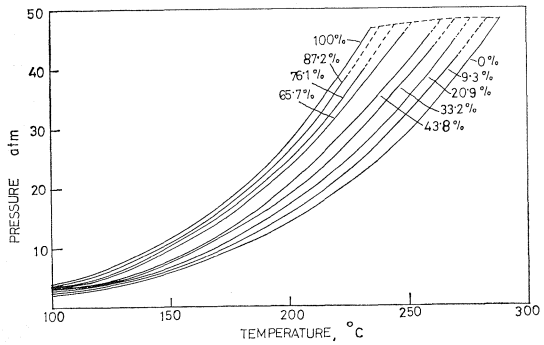

FIG. 2. Pressure as a function of temperature, for liquids of constant composition (in mole % acetone).

fraction, it is observed that the quadratic term $2\theta_1\theta_2\tau_{12}$ makes a comparatively small contribution. The critical temperatures are more linear when plotted against surface fraction than mole fraction. The correlating parameters τ_{12} for critical temperatures, and v_{12} for critical volumes are required for calculating critical pressures, and all these are required for the thermodynamic analysis of vapor–liquid equilibria in the critical region.

The experimental data for saturation vapor pressure (bubble-points) of 7 mixtures of the system acetone–benzene are given in Table 2. Pressure as a function of temperature, for various constant compositions of liquid phase, is expressed graphically in Fig. 2.

Equilibrium vapor and liquid compositions are given in Table 3.

Thermodynamic Analysis and Discussion

In order to understand and interpret the phase behavior of mixtures, experimental data are usually subjected to thermodynamic analysis. The statistical description of intermolecular forces in fluids is as yet incomplete and, therefore, until a satisfactory theoretical model of general

TABLE 3

Experimental vapor–liquid equilibria of the system acetone–benzene at different isotherms

Compositions mole fraction acetone		Compositions mole fraction acetone		Compositions mole fraction acetone	
In liquid	In vapor	In liquid	In vapor	In liquid	In vapor
T = 100 °C		0.188	0.301	T = 225 °C	
0.085	0.207	0.237	0.356	0.116	0.155
0.149	0.285	0.321	0.450	0.208	0.308
0.177	0.325	0.429	0.559	0.260	0.360
0.222	0.387	0.534	0.655	0.320	0.403
0.284	0.421	0.622	0.729	0.432	0.513
0.371	0.543	0.732	0.810	0.576	0.661
0.378	0.558	0.789	0.850	0.700	0.764
0.439	0.609	0.860	0.903	0.822	0.860
0.510	0.667	T = 175 °C		0.899	0.920
0.548	0.699	0.086	0.144	T = 250 °C	
0.611	0.742	0.146	0.220	0.096	0.113
0.635	0.764	0.218	0.311	0.194	0.225
0.758	0.843	0.305	0.411	0.280	0.328
0.784	0.865	0.401	0.517	0.400	0.451
0.862	0.913	0.510	0.621	0.499	0.539
T = 125 °C		0.625	0.720	0.597	0.622
0.100	0.186	0.741	0.812	0.656	0.669
0.168	0.293	0.842	0.885	T = 260 °C	
0.247	0.393	0.885	0.913	0.066	0.073
0.364	0.518	T = 200 °C		0.162	0.184
0.456	0.611	0.105	0.154	0.261	0.289
0.575	0.707	0.236	0.312	0.360	0.385
0.704	0.799	0.348	0.445	0.427	0.442
0.816	0.875	0.413	0.507	T = 270 °C	
0.880	0.917	0.540	0.635	0.101	0.108
T = 150 °C		0.638	0.723	0.141	0.149
0.070	0.126	0.735	0.802	0.186	0.196
0.127	0.221	0.796	0.848	0.226	0.233
		0.892	0.918		

Can. J. Chem. Downloaded from www.nrcresearchpress.com by 210.87.254.40 on 09/05/12
For personal use only.

Can. J. Chem. Downloaded from www.nrcresearchpress.com by 210.87.254.40 on 09/05/12
For personal use only.

validity is devised to relate the properties of solutions to theoretically derived properties of the pure components, experimental data will continue to be represented by well-behaved mathematical functions arbitrarily chosen by the individual investigator. The data presented in Tables 2 and 3 have been treated thermodynamically to obtain the "nonidealities" in the vapor phase expressed as fugacity coefficients and in the liquid phase as activity coefficients by a numerical technique, initially described by Chueh and Prausnitz (5). The semiempirical technique based on molecular thermodynamics is briefly presented below.

The fundamental vapor–liquid equilibrium equation for any component i is

$$\phi_i y_i P = \gamma_i x_i f_i^0$$

where ϕ is the vapor phase fugacity coefficient, γ is the liquid-phase activity coefficient, x and y are, respectively, mole fractions in liquid and vapor, P is the total pressure, and f^0 is the standard state fugacity. Chueh and Prausnitz (2) have shown that the vapor-phase fugacity coefficients calculated with the Redlich–Kwong equation (6) are in excellent agreement with the experimental results when Redlich's original mixing rule for constant a is modified by inclusion of one binary interaction constant. This must be obtained from experimental data. The second virial coefficients of pure benzene and pure acetone are available in the literature (7) up to 335 and 150°, respectively. The cross coefficients have not been determined for this system beyond 90 °C (8) and no experimental information is available about the saturated liquid volumes of this binary system. Therefore, the binary constant k_{12} which represents the deviation from the geometric mean for $T_{c_{12}}$ was estimated from interpolation. The critical binary constant $2\tau_{12}/(T_{c_1} + T_{c_2})$ was obtained from the experimental data of the critical temperatures of the binary mixtures shown in Table 1. The critical volumes have not been measured experimentally for the binary mixture acetone–benzene. The correlating parameter for critical volumes was estimated from the generalized chart given in the monograph of Chueh and Prausnitz (9).

The calculated fugacity coefficients are shown in Tables 4 and 5. The dimensionless constants Ω_a and Ω_b which are universal in the original Redlich–Kwong equation have been reevaluated from the saturated volumetric properties of the vapor phase of each pure component (1). There are no experimental fugacity coefficients available for this system which can be compared with the calculated values, but in view of the agreement that Chueh and Prausnitz have obtained for other systems, it is reasonable to conclude that the numbers in Tables 4 and 5 represent the extent of nonideality of the vapor phase in this system.

The technique of calculating the activity coefficient is based on the fact that it depends on the liquid-phase composition and also on the total pressure. It is possible to write two pressure-independent activity coefficients which satisfy the isothermal, isobaric Gibbs–Duhem equation. van Laar developed an equation which is an integrated form of the Gibbs–Duhem equation for representing the activity coefficients as a function of composition; this makes possible the representation of high pressure vapor–liquid equilibria in a manner identical with that generally used for low-pressure data. Chueh *et al.* (10) modified the van Laar equation to take the dilation of liquid mixtures in the critical region into account; this was useful for representing activity coefficients of binary mixtures with only two parameters: the binary interaction constant $\alpha_{22(1)}$ (or α_{12}) and the dilation constant $\eta_{2(1)}$. In addition, Henry's constant[3] $H_{2(1)}^{(P0)}$ is required, since the excess Gibbs energy is defined with reference to a mixture which obeys Henry's law. These parameters are temperature-dependent and therefore to derive the thermodynamic functions, for each isotherm, P–X–Y data were read from large scale plots of vapor–liquid equilibrium compositions (Table 3) and of the lines of constant composition on the pressure–temperature diagram (Table 2). Calculations were made with an IBM 360/65 computer using the programs written by Prausnitz and Chueh (9). The results are shown in Tables 4 and 5. Also shown are the partial molal liquid volumes of each component in the mixture. They are calculated to show the effect of pressure on liquid phase properties. Saturated molal volumes of the binary mixtures are first calculated from the corresponding states correlation of Lyckman *et al.* (11),

[3]The symbol $H_{2(1)}^{(P0)}$ represents Henry's constant for solute 2 in solvent 1, as defied by

$$H = \lim_{x_i \to 0} f_i^L / x_i$$

The superscript P0 indicates that the reference pressure is zero.

Can. J. Chem. Downloaded from www.nrcresearchpress.com by 210.87.254.40 on 09/05/12
For personal use only.

TABLE 4

Thermodynamic analysis of the system benzene (1)–acetone (2) up to $T_{R_2} = 0.93$*†

Temperature (°C)	x_2	y_2	$\bar{V}_1^L$ (cc mole^{-1})	P (atm)	$\bar{V}_2^L$ (cc mole^{-1})	γ_1 Obsd.	γ_1 Calcd.	γ_2 Obsd.	γ_2 Calcd.	ϕ_1	ϕ_2
100‡	0.093	0.181	99.34	2.085	96.49	1.0571	1.0009	1.1148	1.1041	0.9527	0.9658
	0.209	0.368	98.38	2.277	94.41	1.0170	1.0046	1.0952	1.0816	0.9490	0.9608
	0.332	0.500	97.63	2.475	92.52	1.0311	1.0121	1.0130	1.0601	0.9454	0.9563
	0.438	0.607	97.19	2.648	91.14	1.0271	1.0219	0.9931	1.0439	0.9425	0.9525
	0.657	0.783	96.85	3.001	88.90	1.0457	1.0544	0.9596	1.0175	0.9371	0.9452
	0.761	0.847	96.94	3.169	88.12	1.1138	1.0767	0.9427	1.0088	0.9346	0.9420
	0.872	0.921	97.19	3.346	87.47	1.1302	1.1067	0.9407	1.0026	0.9322	0.9386
125§	0.093	0.176	103.33	3.657	102.45	0.9978	1.0009	1.0789	1.1075	0.9304	0.9501
	0.209	0.348	102.27	4.045	100.03	0.9933	1.0047	1.0403	1.0842	0.9240	0.9422
	0.332	0.493	101.47	4.459	97.84	1.0000	1.0124	1.0131	1.0620	0.9176	0.9344
	0.438	0.600	101.05	4.817	96.23	1.0064	1.0226	1.0019	1.0453	0.9124	0.9279
	0.657	0.762	100.94	5.554	93.69	1.1160	1.0561	0.9633	1.0180	0.9022	0.9155
	0.761	0.833	101.23	5.905	92.83	1.1876	1.0792	0.9597	1.0091	0.8977	0.9098
	0.872	0.919	101.79	6.279	92.17	1.1370	1.1101	0.9751	1.0027	0.8936	0.9037
150‖	0.093	0.170	107.98	6.284	109.82	1.0014	1.0008	1.1035	1.0944	0.8989	0.9283
	0.209	0.320	106.76	6.944	106.95	1.0268	1.0042	1.0077	1.0740	0.8894	0.9172
	0.332	0.458	105.89	7.649	104.35	1.0542	1.0110	0.9863	1.0546	0.8800	0.9060
	0.438	0.572	105.48	8.255	102.46	1.0571	1.0200	0.9958	1.0399	0.8727	0.8965
	0.657	0.754	105.65	9.507	99.52	1.1235	1.0494	0.9846	1.0159	0.8585	0.8783
	0.761	0.836	106.24	10.10	98.58	1.1319	1.0697	0.9905	1.0080	0.8525	0.8700
	0.872	0.918	107.25	10.74	97.91	1.1130	1.0967	0.9973	1.0024	0.8466	0.8614
175¶	0.093	0.154	113.41	10.18	119.10	1.0221	1.0006	1.0665	1.0768	0.8603	0.9027
	0.209	0.300	111.97	11.21	115.65	1.0493	1.0034	0.9990	1.0603	0.8477	0.8878
	0.332	0.442	110.99	12.31	112.54	1.0688	1.0090	0.9977	1.0446	0.8353	0.8724
	0.438	0.556	110.58	13.26	110.28	1.0730	1.0163	1.0075	1.0326	0.8255	0.8597
	0.657	0.750	111.15	15.22	106.86	1.1040	1.0403	1.0056	1.0130	0.8071	0.8350
	0.761	0.836	112.16	16.15	105.84	1.1021	1.0568	1.0085	1.0066	0.7993	0.8239
	0.872	0.916	113.85	17.15	105.22	1.0905	1.0787	1.0092	1.0020	0.7916	0.8124
200**	0.093	0.140	119.88	15.49	131.29	1.0288	1.0003	1.0252	1.0347	0.8176	0.8757
	0.209	0.279	118.15	17.06	127.11	1.0628	1.0016	0.9759	1.0273	0.8008	0.8563
	0.332	0.425	116.99	18.75	123.37	1.0753	1.0041	0.9999	1.0203	0.7844	0.8357
	0.438	0.535	116.58	20.19	120.69	1.0903	1.0075	1.0040	1.0149	0.7713	0.8189
	0.657	0.743	117.74	23.19	116.81	1.0880	1.0184	1.0171	1.0060	0.7474	0.7860
	0.761	0.835	119.43	24.61	115.82	1.0444	1.0257	1.0237	1.0030	0.7377	0.7711
	0.872	0.917	122.29	26.12	115.46	1.0202	1.0355	1.0166	1.0009	0.7274	0.7558

*x_2 = mole fraction acetone in liquid mixture; y_2 = mole fraction acetone in vapor phase; f_2 = fugacity of acetone; $\bar{V}_i^L$ = partial molal volume of component i; ϕ = fugacity coefficient in vapor phase; γ = activity coefficient in liquid phase; and $\bar{V}_i^\infty$ = partial molal volume of component i at infinite dilution.

†Correction to geometric mean, $T_{c_{12}} = 0.01$, $2\tau_{12}/(T_{c_1} + T_{c_2}) = -0.0096$, $2v_{12}/(V_{c_1} + V_{c_2}) = -0.0165$.

‡Reference fugacity (1) = 1.685 atm; reference fugacity (2) = 3.492 atm; $\alpha_{12} = 0.00054$ mole cc^{-1}.

§Reference fugacity (1) = 3.062 atm; reference fugacity (2) = 6.025 atm; $\alpha_{12} = 0.00056$ mole cc^{-1}.

‖Reference fugacity (1) = 5.062 atm; reference fugacity (2) = 9.472 atm; $\alpha_{12} = 0.00049$ mole cc^{-1}.

¶Reference fugacity (1) = 7.745 atm; reference fugacity (2) = 13.80 atm; $\alpha_{12} = 0.00040$ mole cc^{-1}.

**Reference fugacity (1) = 11.12 atm; reference fugacity (2) = 12.09 atm; $\alpha_{12} = 0.00019$ mole cc^{-1}.

Can. J. Chem. Downloaded from www.nrcresearchpress.com by 210.87.254.40 on 09/05/12
For personal use only.

TABLE 5

Thermodynamic analysis of the system benzene (1)–acetone (2) above $T_{R_2} = 0.93$*

Temperature (°C)	x_2	$\frac{f_2}{x_2}$ (atm)	y_2	P (atm)	Molal volume of saturated liquid mixture (cc mole^{-1})	ϕ_1	$\overline{V}_1^L$ (cc mole^{-1})	ϕ_2	$\overline{V}_2^L$ (cc mole^{-1})	γ_1 Obsd.	γ_1 Calcd.	γ_2 Obsd.	γ_2 Calcd.
225†	0.093	27.393	0.132	22.794	129.90	0.7679	127.96	0.8467	148.76	1.0286	0.9996	1.0687	1.0072
	0.209	30.500	0.310	25.107	129.53	0.74728	125.76	0.81901	143.80	1.9991	0.9982	1.1836	1.0156
	0.332	27.098	0.410	27.579	129.35	0.72489	124.31	0.79563	139.49	1.0707	0.9954	1.0455	1.0234
	0.438	27.548	0.525	29.706	129.42	0.70805	123.85	0.77368	136.56	1.0715	0.9920	1.0575	1.0289
	0.657	27.622	0.728	34.099	130.58	0.67599	125.83	0.73104	136.06	1.0853	0.9835	1.0478	1.0364
	0.761	27.852	0.823	36.186	131.91	0.66275	128.71	0.71128	132.91	1.0421	0.9799	1.0496	1.0380
	0.872	27.926	0.918	38.412	134.33	0.64891	134.11	0.69059	134.36	0.9283	0.9774	1.0434	1.0386
250‡	0.093	30.81	0.107	32.52	142.84	0.71103	139.09	0.82339	179.48	1.0350	0.9987	0.9923	1.0267
	0.209	32.25	0.240	35.35	144.09	0.68694	135.92	0.79446	175.01	1.0537	0.9948	1.0303	1.0506
	0.332	33.27	0.376	38.46	146.41	0.66228	133.40	0.76381	172.57	1.0665	0.9942	1.0517	1.0539
	0.438	33.68	0.485	41.20	149.86	0.64156	131.58	0.73820	173.31	1.0784	1.0080	1.0522	1.0319
	0.657	32.61	0.671	45.98	173.92	0.60808	98.43	0.69440	213.33	1.2192	1.1801	0.9574	0.9164
260§	0.093	34.05	0.105	36.82	150.57	0.68940	145.24	0.81900	202.53	1.0070	0.9975	1.0565	1.0538
	0.209	35.08	0.233	39.89	153.67	0.66375	141.00	0.78886	201.65	1.0358	0.9920	1.0742	1.0910
	0.332	35.14	0.356	43.20	159.80	0.63710	135.53	0.75869	208.63	1.0650	1.0056	1.0525	1.0566
	0.438	34.43	0.446	45.92	171.85	0.61514	119.78	0.73559	238.64	1.1256	1.0761	0.9863	0.9515
270‖	0.093	35.16	0.096	41.30	162.10	0.66823	153.30	0.82476	247.88	0.9999	0.9986	1.0227	1.0320
	0.151	36.60	0.158	43.12	165.65	0.65201	149.55	0.81121	256.23	1.0110	0.9976	1.0453	1.0395
	0.209	37.19	0.219	44.68	171.00	0.63923	143.68	0.79426	274.38	1.0231	0.9998	1.0336	1.0298

*For explanation of symbols, see footnote * of Table 4.

†Temperature = 225 °C; reference fugacity (1) = 15.164 atm; saturation pressure (1) = 20.921 atm; liquid partial molal volumes at infinite dilution: $\overline{V}_1^\infty = 130.28$ cc/mole, $\overline{V}_2^\infty = 153.38$ cc/mole; Henry's constant at the saturation pressure of the solvent determined graphically = 25.517 atm; $\alpha_{22(1)} = -0.00038$ mole/cc; $\eta_{2(1)}$ dilation constant of solute 2 in solvent 1 = −0.41834; Henry's constant at zero pressure = 23.58 atm.

‡Temperature = 250 °C; reference fugacity (1) = 19.796 atm; saturation pressure (1) = 29.470 atm; liquid partial molal volumes at infinite dilution: $\overline{V}_1^\infty = 142.27$ cc/mole, $\overline{V}_2^\infty = 184.34$ cc/mole; Henry's constant evaluated graphically = 30.756 atm; Henry's constant at zero pressure = 27.10 atm; $\alpha_{22(1)} = -0.00084$ mole/cc; $\eta_{2(1)} = -2.66938$.

§Temperature = 260 °C; reference fugacity (1) = 21.794 atm; saturation pressure (1) = 33.683 atm; liquid partial molal volumes at infinite dilution: $\overline{V}_1^\infty = 149.01$ cc/mole, $\overline{V}_2^\infty = 206.01$ cc/mole; Henry's constant at zero pressure = 27.174 atm; Henry's constant at saturation pressure (1) obtained graphically from $\ln f_2/x_2$ vs. x_2 plot = 31.845 atm; $\alpha_{22(1)} = -0.0017$ mole/cc; $\eta_{2(1)} = -4.47296$.

‖Temperature = 270 °C; reference fugacity (1) = 23.865 atm; saturation pressure = 37.921 atm; liquid partial molal volumes at infinite dilution: $\overline{V}_1^\infty = 158.31$ cc/mole, $\overline{V}_2^\infty = 243.40$ cc/mole; Henry's constant at zero pressure = 27.325 atm; Henry's constant at P_1^s (the saturation pressure of solvent) determined from a plot of $\ln f_2/x_2$ vs. $x_2 = 33.62$ atm; $\alpha_{22(1)} = -0.0011$ mole/cc; $\eta_{2(1)} = -10.10114$.

Can. J. Chem. Downloaded from www.nrcresearchpress.com by 210.87.254.40 on 09/05/12
For personal use only.

and these are then used in the modified Redlich–Kwong equation to give the partial molal volumes. The constants Ω_a and Ω_b in the Redlich–Kwong equation were reevaluated for the liquid state from the volumetric properties presented in a previous paper (1). These were different from those obtained for the vapor phase. Again, experimental partial molal volume data for this system are not available for comparison, but in view of the results of Chueh and Prausnitz, (12) it can be safely assumed that the calculated values in Tables 4 and 5 correctly represent the pressure dependence of the activity coefficients. It has been mentioned earlier that the choice of arbitrary hypothetical standard state fugacity of the noncondensable component has been avoided; this is done by using Henry's ideal dilute solution law. Figure 3 illustrates how Henry's constants are obtained from experimental data for several isotherms.

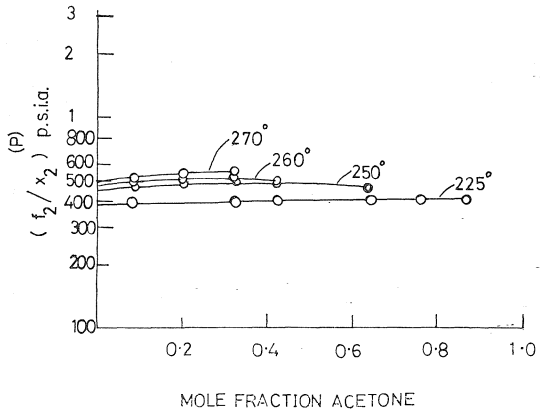

FIG. 3. Plot to obtain Henry's constant $H_{2(1)}^{(P_1S)}$ for acetone (2) in benzene (1) at 225, 250, 260, and 270 °C. ($\ln f_2^{(P)}/x_2$ is plotted against x_2 to evaluate Henry's constant, $H_{2(1)}^{(P_1S)}$, by extrapolation to $x_2 = 0$. The absolute pressure has not been converted to atmospheres, since $H_{2(1)}^{(P_1S)}$ must be in p.s.i.a. for the fitting program).

The composition dependences of the liquid phase activity coefficients are also shown in Tables 4 and 5. The thermodynamic analysis of binary mixtures, where both components can exist in the pure liquid state, has been performed using the symmetric convention for normalization of activity coefficients. For mixtures which contain one noncondensable component, an unsymmetric convention for normalization of activity coefficients has been used. The details of the rather involved calculations and the computer programs used are to be found in the book by Prausnitz and Chueh (9) and need not be reproduced here. The results for the system at temperatures less than $T_R = 0.93$ of the lighter component, where a one-parameter model for the excess Gibbs energy with $\eta_{2(1)} = 0$ can be used, are given in Table 4. Mixtures at reduced temperatures greater than 0.93 of the lighter component, i.e. in the acetone–benzene system isotherms above 218.5 °C, must be analyzed with the two-parameter model for the excess Gibbs energy. The results of these calculations are to be found in Table 5. The experimental data for the acetone–benzene system for all isotherms reported in Tables 4 and 5 have been tested extensively for thermodynamic consistency by the method of Chueh *et al.* (10) who extended to high pressures the integral (area) test for isothermal low-pressure data given by Herington (13) and by Redlich and Kister (14).

Table 4 shows that the one-parameter model of the van Laar equation is fairly successful in reproducing activity coefficients below $T_R = 0.93$ of acetone, i.e. those temperatures where both components can exist as pure liquids. The two-parameter model applied at temperatures where one of the components (acetone) is supercritical is apparently not very successful, as shown by the results in Table 5. According to Chueh and Prausnitz (5), a negative $\eta_{2(1)}$ is not permitted by the solution model. Disturbingly enough, the values for $\alpha_{22(1)}$ as obtained from our experimental data are also negative. This may not be significant, since it is in principle possible that α's can be negative as is explained later. The dilated van Laar model of Chueh *et al.* is based on the assumption that the nonideality of liquid mixtures is due to the interaction of solute molecules with each other in the environment of the solvent molecules and not to interactions between the solute and solvent molecules. It is not quite clear whether such a model can be applied to acetone–benzene mixtures where predominant interaction between the π electrons of benzene and the dipole of the polar acetone molecule is believed to exist. In addition, the solution model of Chueh *et al.* has several adjustable parameters which must be determined from experimental data; for example, Henry's constant is somewhat subjective since this must be obtained by extrapolation. Also, the calculations based on Chueh and Prausnitz's technique involve certain assumptions, for

example, $\overline{V}_1^L$ is taken as independent of pressure. This approximation becomes increasingly inaccurate as the temperature approaches the critical point and P becomes very different from P^r, which is arbitrarily chosen as zero. Moreover, this choice of $P^r = 0$ as a reference state also becomes increasingly hypothetical as the temperature increases and the calculations of γ(PO) at the highest temperatures are affected by this uncertainty. In view of the uncertainties in Henry's constant and in the partial molar volumes, the negative $\alpha_{22(1)}$ and $\eta_{2(1)}$ shown in Table 5 are probably not noteworthy.[4] Since certain simplifying assumptions must be made in all theories of liquid mixtures as a consequence of insufficient knowledge about intermolecular forces, and also because of lack of extensive experimental data, any general theory must await accurate and extensive experimental data on equilibrium properties of mixtures, especially those containing polar components. Chueh and Prausnitz's solution model gives consistently good results for mixtures of nonpolar (or slightly polar) components with no association, as reported in their publication (5); but since the simplifying assumptions are restricted for one type of mixture, an extension of their treatment must be made to polar components to make it more general, especially where the systems are strongly nonideal. The system reported in this paper is too close to ideality and hence cannot be regarded as providing the necessary physico-chemical measurements required to test the strain on the dilated van Laar model when applied to polar components in general. Additional study on other strongly nonideal systems is necessary to test the model.

[4]We are indebted to one of the referees for this suggestion.

1. A. N. Campbell and R. M. Chatterjee. Can. J. Chem. **47**, 3893 (1969).
2. P. L. Chueh and J. M. Prausnitz. Ind. Eng. Chem. Fundam. **6**, 492 (1967). G. M. Wilson, Advan. Cryog. Eng. **9**, 168 (1964).
3. R. L. Scott. Private communication.
4. P. L. Chueh and J. M. Prausnitz. A.I.Ch.E.J. **13**, 1107 (1967).
5. P. L. Chueh and J. M. Prausnitz. Ind. Eng. Chem. **60**, 34 (1968).
6. O. Redlich and J. N. S. Kwong. Chem. Rev. **44**, 233 (1949).
7. G. A. Bottomley and T. H. Spurling. Aust. J. Chem. **20**, 1789 (1967); **19**, 1331 (1966).
8. M. M. Abbott. Ph.D. Thesis Rensselaer Polytechnic Institute, Troy, New York. 1965.
9. J. M. Prausnitz and P. L. Chueh. Computer calculations for high pressure vapor–liquid equilibria. Prentice-Hall, Englewood Cliffs, New Jersey. 1968.
10. P. L. Chueh, N. K. Muirbrook, and J. M. Prausnitz. A.E.Ch.E.J. **11**, 1097 (1965).
11. E. W. Lyckman, C. A. Eckert, and J. M. Prausnitz. Chem. Eng. Sci. **20**, 703 (1965).
12. P. L. Chueh and J. M. Prausnitz. A.I.Ch.E.J. **13**, 1099 (1967).
13. E. F. G. Herington. Nature, **160**, 610 (1947).
14. O. Redlich and A. T. Kister. Ind. Eng. Chem. **40**, 345 (1948).

Can. J. Chem. Downloaded from www.nrcresearchpress.com by 210.87.254.40 on 09/05/12
For personal use only.

Length change – adsorption relations for the water – porous glass system to −40 °C[1]

R. F. FELDMAN
Division of Building Research, National Research Council of Canada, Ottawa, Canada

Received August 19, 1969

Adsorption of water has been studied extensively above 0 °C, but the problem of the phase transition of adsorbates in porous materials is presented at temperatures below 0 °C. Experiments that show how phase transitions modify length change – adsorption relationships are described.

Adsorption – length change measurements from −40 to −0.5 and isotherms at −20 and −0.5 °C were obtained. In another group of experiments different forms of isosteres were also obtained; the principle that water should be allowed to enter the sample at the low temperature was usually followed.

Isotherms and length change – adsorption characteristics below 0 °C are qualitatively similar to those above 0 °C, but a decrease in adsorptive capacity and length change was observed. These results and those obtained from the isosteres lead to the conclusion that capillary condensation and menisci theories are operative and that a solid meniscus exists. It follows therefore that the saturated vapor pressure of frozen adsorbate is greater than that of bulk ice and that its volumetric expansion on freezing is similar to the bulk phase transition. It is shown how these phenomena can predict migration of water and generation of pressure within the porous body when it is subjected to cooling and warming cycles.

Canadian Journal of Chemistry, **48**, 287 (1970)

Can. J. Chem. Downloaded from www.nrcresearchpress.com by 210.87.254.105 on 09/05/12
For personal use only.

Adsorption of water and corresponding length change by a number of porous materials (1) have been studied at the Division of Building Research, National Research Council. All previous work was done at normal room temperature conditions. Experiments at temperatures below the bulk freezing point are now described.

Adsorption of water at temperatures below 0 °C introduces the problem of the phase transition of adsorbates in porous materials. Understanding of these phenomena can be improved by considering experiments that show how phase transitions modify length change – adsorption relations.

Studies of the freezing of adsorbates (2, 3) present evidence both for and against the theory of capillary condensation and thus for and against explanations of the hysteresis exhibited by adsorption isotherms and the features of expansion isotherms (4) based on capillary condensation theory. Other workers (2, 5–8) have measured length change during cooling and warming of porous bodies containing different adsorbates and some (7, 8), mainly with water as adsorbate, have correlated these length changes with specific heat measurements.

The present experiments include adsorption – length change measurements from −40 to −0.5 °C and isotherms at −20 and −0.5 °C. In another group of experiments, different forms of isosteres were obtained; in most of these, the water was allowed to adsorb into the sample at the low temperature because it was thought that an equilibrium state might be obtained in this way and that other effects, such as migration of water and stresses during freezing, were more likely to occur when cooling had taken place after water had been allowed to enter the sample.

[1]NRCC No. 11 087.

Experimental

Apparatus

A gravimetric adsorption apparatus with metal valves and neoprene O-rings was used. The spiral had a sensitivity of 30 cm/g; the extensometer was a modified Tuckerman gauge (7) of sensitivity 2×10^{-6}, as calibrated by the manufacturer. This particular instrument was made of Invar of low thermal expansion, 0.9×10^{-6} deg^{-1}. This value was taken into account in the calculation of results.

The volume of the separate cell in which the extensometer was placed was approximately 200 ml. Pressure was measured by means of a Texas Instruments Bourdon type gauge sensitive to 1 μ. Temperature control of the alcohol baths was maintained to ±0.02 °C by proportional controllers.

Material

Porous glass (No. 7930) was supplied by Corning Glass Works in the form of 2.5 cm diameter tubes of 0.2 cm thickness. Adjoining samples were cut from the tube for the extensometer and spiral and were thus 0.2 cm thick. The surface area determined by water adsorption was 162 m^2/g assuming that each water molecule occupies 10.8 Å^2; water was purified by freezing and thawing during degassing.

Procedure

The samples both on the extensometer and the spiral were degassed at 150 °C for 24 h before each run. In addition to the sample mounted on the extensometer, 8 g of sample were included in the cell during determination

of isosteres, so that any adsorbate taken up or given off in the space could be considered as negligible.

Isothermal length change – adsorption curves were determined at −0.5, −20, −31.5, and −40 °C. The samples on the extensometer and spiral were exposed simultaneously to water vapor and allowed to come to equilibrium. At low temperatures more than a week was sometimes allowed; at higher temperatures from 2 to 24 h were allowed. Complete adsorption isotherms were determined at −0.5 and −20 °C, and a partial one at −31.5 °C.

Two other experiments somewhat unique in nature might come under the classification of isosteric determinations. One allowed the maximum amount of adsorbate to enter a sample at a particular temperature. When it was certain that no excess adsorbate had deposited in the extensometer cell, the valve was shut and the extensometer was warmed; in general, 2 to 24 h were allowed for equilibrium per point. The second experiment involved determining curves for maximum adsorption and maximum expansion as a function of temperature, commencing at the low temperature; at each temperature the samples were allowed to come to equilibrium with bulk ice at that same temperature. Great care was taken to ensure that deposition did not occur on the wire holding the sample to the spiral, or on the outer surface of the sample; after each temperature change was effected, the sample was pumped slightly and was then allowed to return to equilibrium. A "cooling–warming" isostere was also measured, in the same manner as other workers (5–8). This experiment served as a useful comparison especially since the samples used in this work had different surface areas and porosities to the samples of other workers.

Results

(1) Isothermal Length Change – Sorption Curves

These curves for −0.5, −20, −31.5, and −40 °C are shown on Fig. 1 (*a*, *b*, *c*, and *d*), respectively. Their main feature is similarity of the curves. OA for all the curves is of similar slope, and all exhibit the flat feature along AB. Sections BC for −20, −31.5, and −40 are fairly similar, but that for −0.5 is much longer and the extent of adsorption is much higher, 23.35% compared to 22.15, 21.6, and 21.2% for the −20, −31.5, and −40 °C curves, respectively. Thus, the adsorptive capacity ("apparent saturation" at each temperature) decreases with decreasing temperature, as has been found (2, 9, 10) for other systems. Length change follows the same pattern as adsorptive capacity, and more detailed results of these features will be presented.

One of the reasons for this marked decrease in capacity is, probably, that the effective relative pressure experienced by the sample is less than

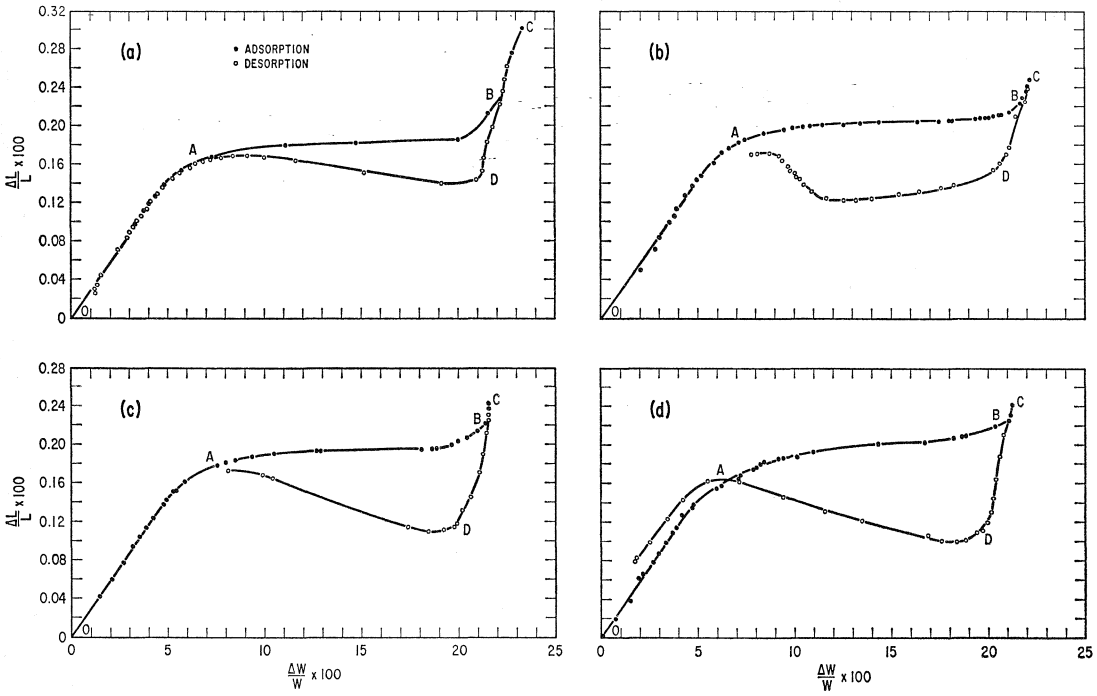

FIG. 1. Adsorption length change vs. weight change curves at (*a*) −0.5, (*b*) −20, (*c*) −31.5, (*d*) −40 °C.

Can. J. Chem. Downloaded from www.nrcresearchpress.com by 210.87.254.105 on 09/05/12
For personal use only.

Can. J. Chem. Downloaded from www.nrcresearchpress.com by 210.87.254.105 on 09/05/12
For personal use only.

unity. If the adsorbed matter retains the properties of a liquid below 0 °C, then the effective relative pressure experienced by the sample will be ($P_{0(BS)}/P_{0(SL)}$), the vapor pressure of bulk adsorbate divided by the vapor pressure of supercooled liquid at the temperature of the sample. This ratio will decrease from unity as the temperature decreases from the freezing point of bulk adsorbate. This explanation has been given by other workers (9, 10).

Another feature of the curves is the marked hysteresis: it is shallower in Fig. 1*a* than in the others. In Fig. 1*b* the hysteresis, which was obtained in two experiments, is an unfamiliar shape, and the loops shown in *b*, *c*, and *d* do not close. The hysteresis, together with AB and BC, was well explained above 0 °C by Amberg and McIntosh (4). The explanation involved the theory of capillary condensation with menisci producing a compressive force onto the substrate. If this is true, one must consider here a solid meniscus with the appropriate forces, since both Antoniou (7) and Litvan (8) have shown that at −40 °C all but two molecular layers (8.9%) of adsorbed water are in a frozen state. This has also been observed for other systems (11, 12). The vertical portion BC of curves of this type has been attributed to the flattening of menisci (4). The maximum weight adsorbed at −40 °C (Fig. 1*d*) is 21.2%. When 21.2% is adsorbed at −0.5, −20, and −31.5 °C (Fig. 1*a*, *b*, and *c*), the vertical portion BC has not been attained. In Fig. 1, however, the amount adsorbed is recorded as weight, not as volume occupied in the sample, and whereas the pore volume of the sample may be regarded as constant, the average specific volume of the adsorbate may not. Thus at −0.5 °C, 21.2% has not filled the pores sufficiently to cause flattening of the menisci, while at −40 °C it has. This implies that a change in specific volume of adsorbate may have occurred between these temperatures. If this is due to a phase change of the adsorbate involving an increase in volume, as for bulk water to ice transition, this effect can be explained.

One might expect the length change along BC in Fig. 1 (*b*, *c*, and *d*) to approach that of BC in Fig. 1*a*, if the adsorbate is frozen and equivalent to bulk ice, since $P_{0(BS)}/P_{0(Ads.S)}$ will equal unity. ($P_{0(BS)}$ is the vapor pressure of bulk solid and $P_{0(Ads.S)}$ the "saturated" vapor pressure of adsorbed solid at the same temperature.) Data derived from X-ray (13) and calorimetry (7, 8) have suggested, however, that the frozen adsorbate does not have the properties of bulk ice. In fact Hodgson and McIntosh (6) have made vapor pressure measurements indicating that $P_{0(Ads.S)} > P_{0(BS)}$ for the water system but that $P_{0(BS)} > P_{0(Ads.S)}$ for the benzene system. These latter results can explain the adsorption isotherms obtained for benzene (6) below its bulk freezing point.

(2) Adsorption Isotherms

Figure 2*a* illustrates an adsorption isotherm obtained at −20 °C and a partial one at −31.5 °C. Both are plotted using $P_{0(BS)}$ as the saturated vapor pressure at the temperature of the sample. The isotherm at −31.5 °C was experimentally determined by allowing a sample at −31.5 °C to come into equilibrium with an ice source held consecutively at different temperatures, up to −31.5 °C. The isotherm, although not complete, shows clearly a large hysteresis loop. Since a large portion of the adsorbate is frozen at this temperature, the implication is that a solid meniscus is responsible.

Figure 2*b* shows an isotherm obtained at −0.5 °C and one obtained at −20 °C replotted,

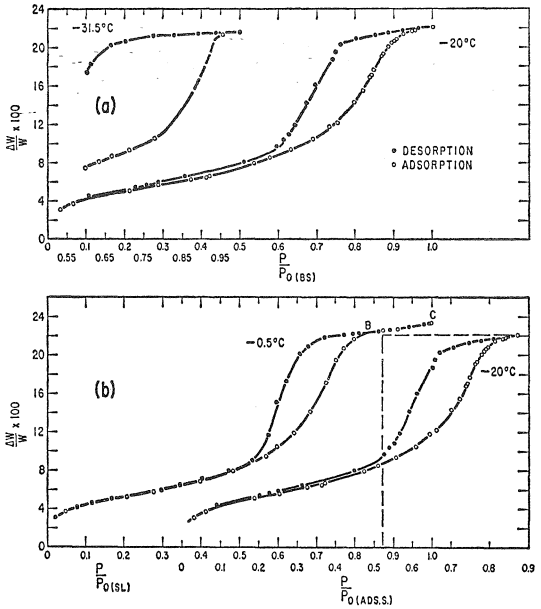

FIG. 2. Adsorption isotherms (*a*) at −31.5 and −20 °C plotted using $P_{0(BS)}$; (*b*) at −0.5 and −20 °C plotted using $P_{0(SL)}$ and $P_{0(Ads.S)}$, respectively.

Can. J. Chem. Downloaded from www.nrcresearchpress.com by 210.87.254.105 on 09/05/12
For personal use only.

using a different P_0 as described below. On superimposing the isotherm obtained at -20 °C (Fig. 2*a*) on the isotherm obtained at -0.5 °C, it was observed that the former was considerably distorted to the right. In addition, the primary hysteresis at the low pressure end opened at a higher relative pressure (0.6 to 0.53), and at the high pressure end closed at a higher relative pressure (0.96 to 0.84). The flat part of the isotherm approaching saturation is also considerably shortened for the -20 °C isotherm. P_0 was changed by trial and error until the main characterestics of the two curves shifted into position; the value used for P_0 was 0.879 mm of Hg where $P_{0(BS)}$ would be 0.776 mm; 0.879 mm is approximately midway between the supercooled and bulk–solid vapor pressure curve. With this value for $P_{0(Ads.S)}$ the isotherm can only attain a relative pressure of 0.873 (see Fig. 3). At this relative pressure on the -0.5 °C isotherm 0.35% more water is adsorbed. Again, one can explain these facts by the arguments used above and the assumption that freezing of the adsorbate occurred with an increase in the specific volume.

(*a*) The argument based on that of previous workers (9, 10), but using $P_{0(Ads.S)} > P_{0(BS)}$ as, in fact, it has been observed (6), the sample at -20 °C can attain only 0.873 P/P_0, and this is one explanation for a decreased adsorptive capacity. It is possible that this concept could also provide an explanation for the drastic change observed in xenon isotherms below the normal freezing point (2). Care must be taken, however, in assessing the vapor pressure measurements of an adsorbed solid. If the solid has a concave interface, i.e., concave meniscus, when the measurements are made, then a vapor pressure lower than $P_{0(Ads.S)}$ will result. The results from benzene isotherms (6), however, can be explained by assuming $P_{0(Ads.S)} < P_{0(BS)}$.

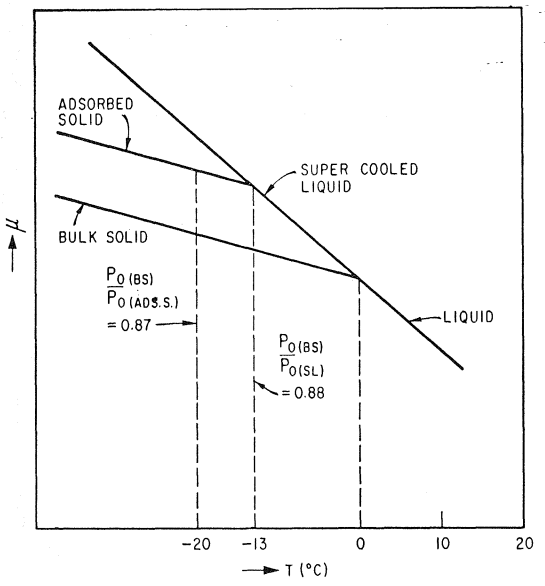

FIG. 3. Schematic of chemical potential vs. temperature illustrating adsorbed solid.

(*b*) When the equilibrium vapor pressure of the sample is controlled by a meniscus, it is largely the degree of filling of the capillary, and thus the volume adsorbed, that governs its shape. When freezing has occurred, therefore, and if it involves an increase in volume of adsorbate, one must expect a decrease in the weight adsorbed if the relative vapor pressure remains approximately constant; that this in fact occurs, will be shown in the following sections. This is the second explanation for a decreased adsorptive capacity. Figure 3 is a schematic diagram of chemical potential vs. temperature for water; a curve for "adsorbed solid" is drawn in at a constant difference of chemical potential to the bulk solid. There will be further discussion of Fig. 3 in Section *3* of the results.

If it is assumed that two molecular layers will not freeze (7, 8) and that any increase in adsorption in these layers as the temperature is lowered is negligible (Fig. 2*b*), then the total amount of adsorbate that can freeze or is frozen is 22.15 (maximum adsorbed at $-20°$) $-$ 8.9 (2 molecular layers) = 13.25%. Using the value 0.35 ml per 100 g of sample as the volume change of adsorbate due to freezing, then 13.25 $-$ (0.35/y) ml is the volume of unfrozen water at -20 °C for 100 g of adsorbent. This assumes that the density of the unfrozen water that can freeze is 1 g/cc. The specific volume increase on freezing is "y". These values will be referred to again in Section *3a*.

(3) Maximum Adsorption and Maximum Extension Isosteres

The maximum water adsorbed at various temperatures when the sample is in equilibrium with bulk ice at the same temperature, is presented in Fig. 4. The points are obtained from two experiments, illustrating reproducibility. At -36.4 °C, 21.23%, and at 0 °C, 23.35%, of water is adsorbed. This increase in adsorptive capacity is

Can. J. Chem. Downloaded from www.nrcresearchpress.com by 210.87.254.105 on 09/05/12
For personal use only.

most probably due to the two effects discussed above. To learn more about the phenomenon and to provide more convincing evidence for the explanations, however, the two effects should be separated. This can be done with the help of the maximum length change vs. temperature curve presented on Fig. 5, curve I. The change in maximum length, using that at −40 °C as reference, vs. the maximum water adsorbed at each temperature is plotted on Fig. 6. This curve is corrected for the thermal expansion of the dry sample.

One may observe two distinct regions on Fig. 6. The last point on the lower-slope linear section AB is −13 °C. The slope of this section is 0.0095% length change per 1% weight change. Using Fig. 1*a*, the length change from 9% (approximately 2 molecular layers) to saturation (23.35%) is 0.126%; thus, the average length change is 0.0089% per 1% weight change. The similarity in slope is the basis for assuming that between −36.4 and −13 °C, expansion occurs mainly by

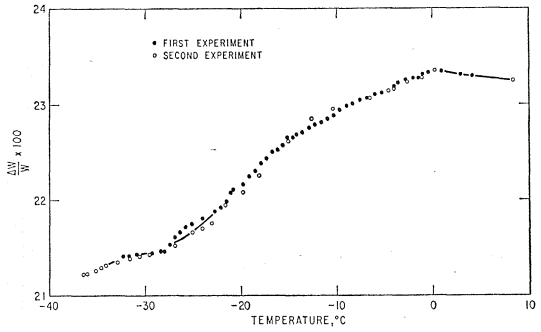

FIG. 4. Maximum water adsorbed vs. temperature.

added water adsorption without much change in the shape or position of the meniscus; this is given by the linear part AB of the curve, and is a manifestation of the decrease of volume of adsorbate on thawing which was discussed in Section *2b* of Results.

To illustrate further (although the following procedure is not possible experimentally), starting at B, with a solid meniscus, further cooling causes more freezing; an increase in volume of the adsorbate also occurs. To maintain the same relative pressure, some water is desorbed to reduce the volume, resulting in a contraction (an increase in Gibb's surface free energy) as defined by line BA or as discussed above with regard to the length change – adsorption characteristics on Fig. 1*a*. Reference to the characteristics of Fig. 1*a* is only

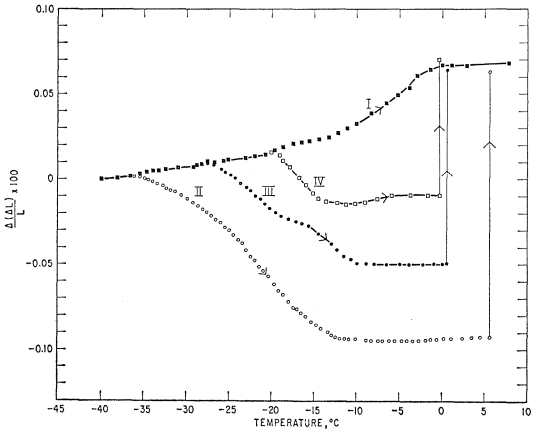

FIG. 5. Maximum length change curve (I) and warming isosteres; curves II, III, and IV.

an approximation because it is only for −0.5 °C, but the slopes OA on the other curves, Fig. 1 (*b*, *c*, and *d*), are very similar, so that this approximation is a good one, as the results show.

By assuming constant relative pressure, one assumes that the difference in chemical potential between solid adsorbate and bulk ice is approximately constant between −13 and −40 °C. (The change in temperature, −13 to −40 °C, will alter the difference in chemical potential by 10%.) If −13 °C is the point where no adsorbed solid meniscus remains in the small pores, then $P_{0(SL)}$ at this temperature should be equal to $P_{0(Ads.S)}$; $P_{0(BS)}/P_{0(SL)}$ at −13 °C should be equal to $P_{0(BS)}/P_{0(Ads.S)}$ for lower temperatures such as −20 °C. This is approximately correct, as is shown on Fig. 3. Also, above −13 °C the relative vapor pressure $P_{0(BS)}/P_{0(SL)}$, will increase as the temperature increases and the length change and

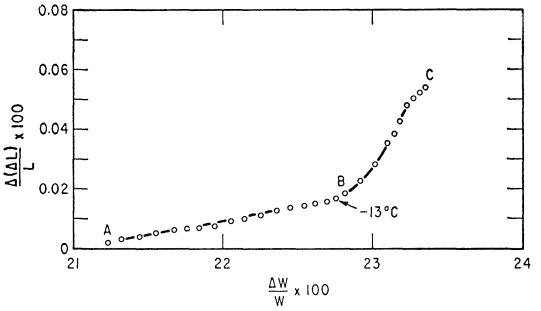

FIG. 6. Maximum length change vs. maximum weight change from −36.4 to 0 °C. (Corrected for thermal expansion of dry glass.)

Can. J. Chem. Downloaded from www.nrcresearchpress.com by 210.87.254.105 on 09/05/12
For personal use only.

adsorption should be the result of flattening of menisci. This is shown below.

Before considering BC in Fig. 6, however, one can use some of the data discussed above to calculate volume expansion when adsorbed water changes to solid adsorbate. This can be done in two ways

(*a*) Using the data at the end of Section (*2*), at -20 °C $13.25 - (0.35/y)$ ml is the volume of freezable water per 100 g of adsorbent. The assumption that the difference in the maximum adsorbed between -20 and -36.4 °C is due to and equal to the volume expansion on freezing, and thus that any increase in the amount adsorbed into the two layers owing to lower temperatures is negligible, is still maintained. The value for the difference is equal to 0.92. The specific volume expansion on freezing "y", is therefore equal to $0.92/\{13.25 - (0.35/y)\}$. "$y$" $= 0.0959$.

(*b*) Recognizing that -13 °C on Figs. 4 and 6 separates the two effects leading to increased adsorption with temperature, the weight change between A and B on Fig. 6 is taken and is 1.53%. At B (-13 °C) the maximum adsorbed is 22.76%. Subtracting the two molecular layers and accepting the assumptions of (*a*) above and that all the adsorbate is liquid at -13 °C, gives a value of 0.110 for the specific volume expansion.

These calculations have similar weaknesses. If the assumptions concerning the two molecular layers are not correct, the value may differ in either direction. If less than two molecular layers remain unfrozen, the value for the expansion on freezing will be lower. On the other hand, if the amount adsorbed in the two molecular layers increases with decrease in temperature, then the value will be greater. Constancy of relative pressure between -13 and -40 °C also might not be completely correct. The significance of these calculations, however, lies in the fact that both values are not far removed from that for normal water–ice transition. This is in contrast with Antoniou's calculations (7), which give a value 1/40 of the value for freezing to bulk ice. Antoniou concluded that the solid adsorbate was very different from bulk ice. Whereas some properties of the solid adsorbate and bulk ice do differ, it is now clear that the volume expansion of adsorbed water during transition to adsorbed solid is not too different from that of the bulk transition. Further discussion of the results obtained by earlier workers (6–8) will be made later.

Referring again to Fig. 6, the total $\Delta(\Delta L/L)$ per unit weight change from B to C is 0.0635. The slope of the top portion of BC on Fig. 1*a* is 0.0558. This comparison strongly suggests that BC on Fig. 6 or from -13 to 0 °C on Fig. 5 is due to an increase of the relative pressure on warming as $P_{0(BS)}/P_{0(SL)}$ approaches unity. Within the context of the capillary condensation theory, expansion is due to the flattening curvature of the menisci. Using the same argument as above and the same assumptions, one should be able to predict approximately, from the data on Fig. 4, the region BC of the isotherm at -0.5 °C on Fig. 2*b*. Thus, at -13 °C, where $P_{0(BS)}/P_{0(SL)}$ is 0.881, the Δw vs. T plot on Fig. 4 would predict adsorption to be 22.76, whereas on the isotherm it is 22.54%. This assumes that there is no ice in the small pores at -13 °C; and that the Δw vs. T curve is the point on the isotherm at each temperature; so that in referring to the -0.5 isotherm one would not expect exact agreement.

(4) "Warming" Length Change Isosteres

The role of the volume change when the adsorbate freezes is thus very important. It would be instructive to observe the length changes that occur during the transition. This has been attempted (6–8), but most of this work involved "loading" samples at the warm condition and then performing "cooling and warming" cycles (referred to later as "cooling–warming" isosteres). It is expected that some undesirable features can occur during this experiment: (*a*) movement of water out and back in the sample, since the sample at 0 °C contains more water than it would at lower temperatures; (*b*) stress in the sample as a result of expansion and freezing. The result would leave the sample in an undefined state and the length changes would be difficult to interpret. This will be referred to again in Section (*5*).

To avoid this, it was decided to load the samples at the low temperature and warm them. The transition would result in a decrease in volume of adsorbate and an increase in adsorptive capacity. These samples should thus remain well defined with respect to the $\Delta L/L$ vs. $\Delta W/W$ plots on Fig. 1.

Figure 5 shows warming isosteres, curves II, III, and IV. They contain, as is evident from the graph, the maximum amount that can be adsorbed at -36.2, -27.6, and -20.1 °C; that is, 21.23, 21.52, and 22.15%, respectively. The three

Can. J. Chem. Downloaded from www.nrcresearchpress.com by 210.87.254.105 on 09/05/12
For personal use only.

curves show very large shrinkages starting directly as warming proceeds, although for curve II the initial rate of shrinkage is very low. Shrinkage is complete at approximately −12, −10, and −11.5 °C for curves II, III, and IV, respectively. This is not too far off the temperature obtained from Fig. 6, especially for curves II and IV. If shrinkage is a result of transition, and this is shown at the end of the section, then the transition for this sample occurs between approximately −36.2 and −12 °C. Calorimetric data on other samples by Antoniou (7) suggest that it occurs between −32 and −5.5 °C, and by Litvan (8), between −22 and −7 °C. The maxima for heat curves for both were about −12 °C. These results were obtained on the basis of the "cooling–warming" isosteres and, as shown by Antoniou (7), samples from the same batch show considerable variation. Results in the previous section and those on Fig. 5 suggest that the transition range for the sample used here occurs at lower temperatures than the samples of the above workers.

When transition was completed, the three curves were continued to approximately 0 °C and beyond for curve II. At this point, the extensometer cell was opened and the samples were exposed to water vapor at saturation conditions, resulting in an expansion back to the "maximum length change vs. temperature" curve. This expansion amounted to 0.15% for curve II. Its magnitude, together with the fact that the sample contained 21.23% water, leads one to suspect that the expansion is related to BC on the length change – sorption characteristics of Fig. 1*a* and that shrinkage of curves II, III, and IV is related to the volume effect on thawing of the adsorbate and menisci.

Assuming that this is the case, an explanation can be given that agrees with other data. As temperature is increased, thawing occurs even at −35.5 °C, and a decrease in volume of adsorbate takes place. Unlike the "maximum length change" isostere, curve I, Fig. 5, where more adsorbate is available, none is available in this experiment and the adsorbate recedes in the capillary, leading to a change curvature and contraction. Thus, as curves II, III, and IV move toward higher temperatures, they are, in fact, travelling on the desorption part of an isotherm. The actual details, even on a macroscale, of how the change of the solid meniscus takes place are difficult to conceive. Even though it seems reasonable to assume that thawing first occurs near the adsorbent surfaces, what occurs when there is a mixture of both liquid and solid adsorbate in an adsorbent is difficult to say. It is possible that the strange nature of the desorption of Fig. 1*b* is a result of this. Nevertheless, Fig. 7 illustrates what occurs when the "warming isosteres" are measured.

On the left of the figure is the length–weight change plot at −40 °C, curve V, and on the right the same plot at −0.5 °C, curve VI. Figure 5 is

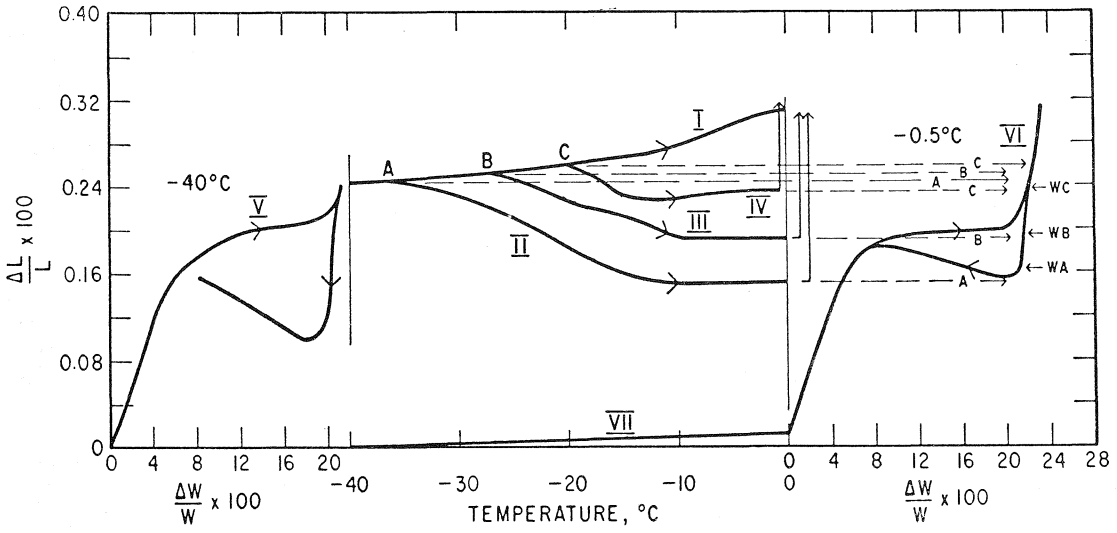

FIG. 7. Explanation for warming isosteres. I is maximum length change curve; II, III, and IV warming isosteres; V and VI length vs. weight change curves; and VII thermal expansion of dry glass.

Can. J. Chem. Downloaded from www.nrcresearchpress.com by 210.87.254.105 on 09/05/12
For personal use only.

reproduced in the middle, and the thermal expansion of the dried sample is below. The latter curve, corrected for the Invar extensometer, gives a thermal coefficient of 4.3×10^{-6} deg^{-1} compared with the value of 5.0×10^{-6} deg^{-1} obtained by Antoniou. Note that curve VI commences at the end of this thermal expansion curve. A, B, and C are marked at the beginning of curves II, III, and IV, and where they would be at the top of the length-to-weight change curve, curve VI. A, B, and C are also drawn over from the end of curves II, III, and IV to the desorption part of curve VI. These are again marked A, B, and C, so that length change AA, BB, and CC marked adjacent to curve VI represent the actual contraction that occurred during the warming isosteres. An independent confirmation of the fact that the contraction is, in fact, movement on the desorption curve can be obtained from prior knowledge of water content of the sample at A, B, and C, respectively, before the start of the experiment. These are marked on curve VI as WA, WB, and WC; as can be seen, they predict approximately the positions of A, B, and C after contraction. The actual values are given in Table 1.

TABLE 1

Comparison of contraction from warming isosteres and isotherms

Maximum saturation °C	Weight put on %	Actual contraction %	Contraction determined from isotherm data %
−20	22.15	0.025	0.022
−27.6	21.52	0.059	0.056
−36.2	21.23	0.081	0.096

It is clear from these results that the observed shrinkages are a result of the recession of menisci owing to decrease in volume of adsorbate with melting in the small pores.

(5) "Cooling–Warming" Length Change Isosteres

As stated previously, this experiment probably leaves a saturated porous system in an undefined state, but because of its practical importance (it is the kind of treatment a material will receive in nature) and because many measurements of this type have been made previously (2, 5–8) and have been correlated with calorimetric measurements (7, 8), it was deemed necessary to perform this experiment to provide comparison with previous results and to compare present results with those of experiments of Sections (1–4). It is thought that a satisfactory explanation can now be provided for the "cooling–warming" isosteres.

The "maximum length change" isostere is plotted on Fig. 8, curve I (see also curve I on Fig. 5). Curve II is the "cooling–warming" isostere; for convenience it is divided in characteristic regions similar to those of Antoniou (7) and will be discussed accordingly. Curve III is the thermal expansion of the dry glass.

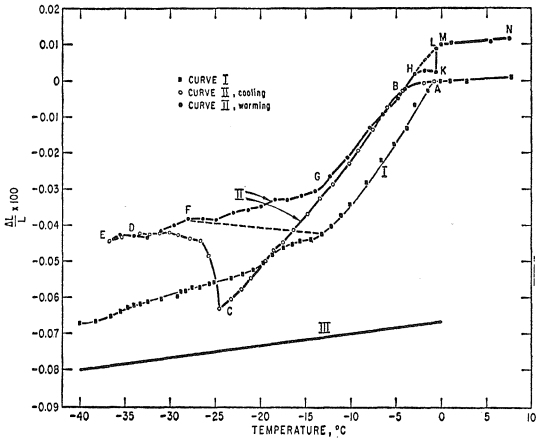

FIG. 8. "Warming–cooling" isostere (II) and maximum length change (I) curves. Curve III is thermal expansion of dry glass.

The isostere is very similar to Antoniou's second one (7); most of the features are present, the difference being that they are displaced to lower temperatures. The expansion on the cooling (CD) curve (attributed to freezing) is displaced from the range −13 to −17 °C to the range −25 to −34.5 °C. The shifting of effects to lower temperatures for this sample has already been mentioned, and variation within one batch has been noted by Antoniou (7).

Region A–B

This region of low contraction is similar to the thermal contraction of the material. No hump was observed at B, as it was by other workers (2, 7), but it is thought that some freezing commences at this point (−4.5 °C) in larger pores of the sample.

Regions B–C and C–D

A linear contraction is observed down to −25.0 °C; this curve is parallel to that of the

Can. J. Chem. Downloaded from www.nrcresearchpress.com by 210.87.254.105 on 09/05/12
For personal use only.

"maximum length change" isostere, curve I, down to −13 °C. The reason for expansion in the latter curve has been shown to be due to readsorption of water and flattening of menisci. Conversely, contraction BC is considered to be due to removal of water from the pores after ice has formed in larger pores at −4.5 °C; this effective decrease in relative pressure is the same as was previously discussed in Section (*3*) of Results.

Two further pieces of evidence prove conclusively that water migrates from the sample on cooling: (*a*) "cooling–warming" isosteres observed by Litvan (8) on a sample containing different water contents have shown BC very prominently at saturation; at all other water contents lower than saturation, region BC had vanished; (*b*) during the measurement of the isostere in the present work, it was observed, on the warming part of the cycle just beyond F, that the intensity of the image in the optical lever of the extensometer had dimmed somewhat; closer examination showed some hemispherical drops of ice on the mirrors; beyond G, the image became gradually brighter until at −3 °C, ice had disappeared. This point will be referred to again in this section, but it appears that the effect was not previously recorded because length measurements had been made either in a calorimeter, where no visual observation could be made, or in an enclosed cell containing a capacitance type extensometer.

The results of curve I were obtained by always bringing the sample into equilibrium with bulk ice at the same temperature. For the present experiment, curve II (cooling), the ice formed at −4.5 °C is not necessarily bulk ice but ice at a higher chemical potential produced either by pressure caused by the walls of the larger capillary or by a convex curvature of the ice, as discussed by Everett (14). This would explain why curve BC is displaced from curve I, and will also be discussed again. The fact that curve II (cooling), continues down to −25 °C without apparent freezing in the small pores is probably due to supercooling. It has been established in previous sections that thawing in the small pores took place between −36 to −13 °C. The cross-over with curve I seems to confirm supercooling. Other work (15) indicates that one form of ice will not necessarily nucleate another form from supercooled liquid. This can explain the fact that along CD, where freezing occurs, each point represents an apparent equilibrium; the frozen adsorbate might exist in domains, each with different properties. The expansion along CD, however, should not be used for a calculation of the volume change on freezing. As much water has moved into bigger pores or out of the sample, it is not known how much water has frozen along CD and some expansion of the frozen adsorbate could have taken place along the spaces vacated by water. In addition, the high stress against the pore walls resulting from freezing has probably caused some damage to the sample. It is also possible that in this region, CD, some readsorption of the expelled water into the small pores can take place because $(P_{0(BS)}/P_{0(SL)})_T < (P_{0(BS)}/P_{0(Ads.S)})_T$; i.e., the effective relative vapor pressure has increased.

Region D–E

It appears that from D at −34.5 °C to E at −36.6 °C no more freezing takes place because the sample now shrinks at the same rate as curve III.

Region E–F

At first the cooling curve, DE, is followed, but there is later deviation. Previous experiments suggest that some thawing and readsorption of adsorbate that had left the samples has taken place, but because of the stressed state of the sample and the frozen adsorbate one cannot tell from the isostere what is occurring.

Region F–G

A slight contraction is first observed, followed by an expansion in excess of the thermal expansion of the dry material. FG approaches close to BC without any contraction. It is believed that further thawing takes place along FG, and that at G, which is at −13 °C, thawing of the adsorbate in the small pores is complete. The location of G and the slope of GH to follow confirms this in relation to the other isosteres discussed. Further reference to FG and the hysteresis will be made.

Region G–H

It has a slope very similar to the same region of curve I, and the conclusion is that the water expelled on cooling re-enters the sample, owing to a permissible increase in the relative vapor pressure of the adsorbate in the sample and a flattening of the menisci. The sample is now in equilibrium with bulk ice, which was observed to be present but disappeared completely at the end of this region between −4 and −3 °C. As the system is now governed by the vapor pressure of

Can. J. Chem. Downloaded from www.nrcresearchpress.com by 210.87.254.105 on 09/05/12
For personal use only.

bulk ice, GH should be coincident with curve I in this temperature range. Discussion of regions HK and KL will show that it would be if no irreversible damage occurred to the sample. The point H is already above that of region AB, indicating damage.

Regions HK, KL, HL, and LMN

HK might first indicate that AB is being reproduced, but if the sample is in equilibrium with bulk ice, curve I should be followed and HK, a region of low expansion, does not conform to curve I. If damage to the sample did occur, however, its porosity might increase and all the water available might re-enter it at −3 °C. Further expansion along HK is the thermal effect only. This was checked by allowing the sample at −0.5 °C to be exposed to saturation conditions. As it had already been saturated at the beginning of the experiment, no expansion should occur. Expansion KL did occur, however, so that if more adsorbate had been available GH would have extended along HL and LM.

The curve GHLM is very similar to curve I. If it were brought down by an amount due to irreversible damage, i.e., from L to curve I, the point G would almost meet curve I at −13 °C, as is expected. If a line is drawn between F and this new point for G, it can be seen that there should have been a contraction in this region where thawing took place. A few further points can be elaborated in view of the above explanations:

(*a*) region AB on the cooling cycle is not reproduced on warming; it is probably the result of a supercooling effect followed by the formation of strained or curved ice in large pores;

(*b*) it is possible that there were no obvious heat effects between −5 and 0 °C in the calorimetric results (7, 8) because (*i*) all the bulk ice that vacated the sample had re-entered (in this case at −3 °C) the pores before 0 °C owing to increased porosity resulting from damage to the sample; and (*ii*) re-entrace takes place almost linearly between −5 and 0 °C, as is shown in Fig. 4;

(*c*) the hysteresis between the cooling and warming cycle can be attributed to supercooling and damage to the sample; if no damage occurred, the hysteresis effect would still be evident due to supercooling;

(*d*) it is now thought that irreversibilities observed in Fig. 1 (*b*, *c*, and *d*) are due to damage occurring during desorption;

(*e*) a comparison of "cooling–warming" isosteres obtained by various authors would be helpful in throwing light on some of the phenomena associated with this isostere.

Table 2 gives the temperature ranges of the various regions, as labelled by Antoniou (7) and referred to in Fig. 8. Examination of Table 2 reveals a variation in all ranges for all samples. For example, in some cases it appears that the two effects of thawing, i.e., thawing in small pores and thawing outside, leading to readsorption, may be partially overlapped. It seems especially true for samples 1 and 3. If this is the case, it will partly explain why the calorimetric heat maxima for different water contents do not shift as they appear to for benzene (6). It is surprising for two conditions, saturation, and moderately undersaturated. For other samples this may not be the case.

Discussion

Most of the observations in the present and related experiments could be explained by the capillary condensation theory extended to the solid adsorbate. It does not mean, however, that the Kelvin equation can be applied quantitatively in this region, and it is not suggested. Similarly, the fact that the Clausius–Clapeyron extension of the Kelvin equation does not predict freezing in small pores does not mean that the assumptions

TABLE 2

Temperature range of regions from several samples

Sample source	Temperature range of regions			
	BC	CD	FG	GH
Reference 6	−7 to −20	−20 to −26	−15 to −9	−9 to −6
Reference 6	−1 to −14	−14 to −16	−15 to −9	−9 to −1
Reference 7	−7 to −16	−16 to −18	−18 to −8	−8 to −4
Reference 5*	—	−24 to −29	−24 to −10	—
This work	−4 to −25	−25 to −34	−28 to −13	−13 to −3

*Not saturated.

Can. J. Chem. Downloaded from www.nrcresearchpress.com by 210.87.254.105 on 09/05/12
For personal use only.

made for the Kelvin equation above freezing are invalid. As discussed by several authors (7, 16), adsorbate, even 50 Å from the surface, is affected by surface forces; but whereas this effect may be negligible after two molecular layers with regard to vapor pressure as a function of radius of meniscus predictions, it is not negligible with regard to the freezing phenomenon.

The results for the length change isotherms of xenon (2) and benzene (6) were not readily explained. The behavior of xenon may be regarded as an exception; above freezing it stands apart from many other absorbates with regard to the relation of Gibbs free energy and length change (17). It has been concluded that it is not satisfactory to assume that γ (the change in surface energy) is generally approximately equal to π (spreading pressure) for all adsorbates and temperatures (18). The explanation for xenon does not seem applicable to benzene; the expansion for the first two molecular layers of the isotherm, as with water, is similar at all temperatures.

Any clarification that these experiments give of the adsorption-extension phenomenon below 0 °C is helpful in understanding the deterioration of building materials from exposure to temperatures below 0 °C. It appears that the mechanism of the movement of water from small pores to large ones, causing large pressures, is valid. This has been discussed by Everett (14) in thermodynamic terms, by Penner (19) in relation to soils, and by Powers (20) in relation to hydrated cement and concrete. These mechanisms should be especially pertinent when thick samples are used. The movement of water out of small pores will not be as easy and ice will more readily accumulate in the large pores, causing great pressure. As may be seen in these experiments, water can come out of a thin sample, or onto its surface, where it forms bulk ice and stress will be avoided. This occurred down to −25 °C. A solution to the problem is to prevent large amounts of water that may be held by capillary condensation from entering the material. There is evidence that surface coatings that change the contact angle may be helpful.

Conclusions

(*1*) The isothermal length change – adsorption curves can be explained below 0 °C by the capillary condensation and menisci theory. Because of these and other results a solid meniscus is postulated.

(*2*) A decrease in adsorption capacity is observed with decrease in temperature owing to two effects: (*a*) a reduction in the effective relative vapor pressure to which the sample is exposed due to the fact that $P_{0(SL)}$, the saturated vapor pressure of the unfrozen adsorbate in the sample is greater that $P_{0(BS)}$ at the same temperature; and (*b*) a volumetric expansion of adsorbate on freezing that is quantitatively similar to the bulk water – bulk ice transition.

(*3*) The higher vapor pressures of sample with respect to bulk ice are due to (*a*) supercooled liquid vapor pressures; and (*b*) vapor pressure of frozen adsorbate greater than that of bulk ice.

(*4*) The effects in (*2*) above cause length changes during measurement of isosteres owing to movement of water out of and back into the sample, and to the development of pressure when adsorbate freezes.

The author wishes to acknowledge many helpful discussions with Mr. P. J. Sereda and Dr. G. G. Litvan. Thanks are also due to Mr. S. Dods and Mr. H. Slade for help with the experimental work.

1. P. J. Sereda and R. F. Feldman. Appl. Chem. **13**, 150 (1963).
2. G. Litvan and R. McIntosh. Can. J. Chem. **41**, 3095 (1963).
3. B. R. Puri, Y. P. Myer, and D. D. Singh. Trans. Faraday Soc. **53**, 539 (1957).
4. C. H. Amberg and R. McIntosh. Can. J. Chem. **30**, 1012 (1952).
5. C. Hodgson and R. McIntosh. Can. J. Chem. **37**, 1280 (1959).
6. C. Hodgson and R. McIntosh. Can. J. Chem. **38**, 958 (1960).
7. A. A. Antoniou. J. Phys. Chem. **68**, 2754 (1964).
8. G. G. Litvan. Can. J. Chem. **44**, 2617 (1966).
9. C. H. Amberg, D. H. Everett, L. H. Ruiter, and F. W. Smith. Proc. 2nd Intern. Conf. of Surface Activity. Butterworth Scientific Publications, London, 1957.
10. A. V. Kiselev and V. V. Kulichenko. Zh. Fiz. Khim. **29**, 663 (1955).
11. J. A. Morrison and L. E. Drain. J. Chem. Phys. **19**, 1063 (1951).
12. J. A. Morrison, L. E. Drain, and J. S. Dugdale. Can. J. Chem. **30**, 890 (1952).
13. V. S. Brazhan. Kolloid. Zh. **21**, 645 (1959).
14. D. H. Everett. Trans. Faraday Soc. **57**, 1541 (1961).
15. G. Karagounis. Helv. Chim. Acta, **36**, 282, 1681 (1953); Helv. Chim. Acta, **37**, 805 (1954).
16. D. M. Anderson. J. Colloid Interface Sci., **25**, 174 (1967).
17. P. J. Sereda and R. F. Feldman. The solid-gas interface. Vol. 2. *By* E. A. Flood. Marcel Dekker, New York. 1967. Chap. 24. p. 729.
18. J. C. Eriksson. Surface Sc. **14**, 221–246 (1969).
19. E. Penner. Proc. Intern. Conf. on Low Temp. Sci. Sapporo Japan, 1966; Vol. 1, Part 2, 1401 (1967).
20. T. C. Powers. J. Amer. Conc. Inst. **16**, 245 (1944).

Dipole moments, charge-transfer parameters, and ionization potentials of the methyl-substituted benzene–tetracyanoethylene complexes

R. K. CHAN AND S. C. LIAO
Department of Chemistry, University of Western Ontario, London, Ontario
Received September 22, 1969

The dipole moments of a series of charge-transfer complexes of methylbenzenes with tetracyanoethylene in carbon tetrachloride solutions at 25 °C and the various parameters derived from Mulliken's theory have been evaluated. The energies of various states of the complexes were calculated via their relationships with the parameters, charge-transfer transition energies, and heats of formation of the complexes by means of the variation principle. Vertical ionization potentials of the donors were obtained from the calculated energies of the dative structures of the complexes. The dipole moments contributed from the charge-transfer interaction can also be reasonably interpreted as charge-transfer energies in terms of vertical ionization potentials of the donors.

Canadian Journal of Chemistry, 48, 299 (1970)

Can. J. Chem. Downloaded from www.nrcresearchpress.com by 210.87.254.6 on 09/05/12
For personal use only.

Introduction

It is worthwhile to investigate the characteristic relationships among various parameters of a molecular complex in accordance with the existing Mulliken theory (1), primarily among the dipole moment, heat of formation, and charge-transfer transition energy. The dipole moments and energy states of the iodine complexes with several aliphatic amines and with some oxygen, sulfur-containing donors have been determined by Kobinata and Nagakura (2) and by Bhat and Rao (3), respectively. The former assume that the dipole moment of the no-bond structure, μ_0, is negligibly small compared with that of the dative structure, μ_1. In both papers the authors apply the results of the variation method with the assumption that the energy of the ground state is small compared to that of the dative state, $W_G \ll W_1$, and is approximately equal to the energy of the no-bond state, $W_G \approx W_0$; energy of the excited state is also assumed approximately equal to that of the dative state, $W_E \approx W_1$ (4).

In the present study tetracyanoethylene complexes with a series of methylbenzenes have been investigated. Dipole moments of the complexes have been determined in carbon tetrachloride solutions at 25 °C. Calculations for various charge-transfer parameters and energies of the different states are carried out according to Mulliken's theory and the variation method without assuming $W_G \ll W_1$, $W_G \approx W_0$, and $W_E \approx W_1$. Vertical ionization potentials of the donors obtained in this work are in satisfactory agreement with the literature values.

Experimental

Materials

Tetracyanoethylene (TCNE) supplied by Eastman was recrystallized from chlorobenzene and purified twice by sublimation; m.p. 199–200 °C in a sealed tube. The liquid methylbenzenes and carbon tetrachloride were purified and dried over calcium hydride by fractional distillation and their purity was checked by gas chromatography. The solid methylbenzenes (1,2,4,5-tetramethylbenzene, pentamethylbenzene, and hexamethylbenzene) were recrystallized in alcohol and dried in a vacuum desiccator; their purity was checked by gas chromatography.

Procedure

The solutions for the dielectric-constant determinations were prepared by adding increments of TCNE to carbon tetrachloride solvent containing the methylbenzene in a dried atmosphere. The concentration ratio of methylbenzene to TCNE in the solution was of the order of 100:1. The dielectric constants of the solutions were measured by the WTW DM01 Dipole Meter, based upon the superposition principle, using a cylindrical gold-plated condenser cell, Type DFL1. Densities of the mixed solvents were measured by the use of a bicapillary pycnometer with scales on both stems, and some densities were calculated directly from the weights and densities of pure components. The refractive indices were determined by the use of a Bausch and Lomb Abbe-3L refractometer. All measurements were made at a constant temperature of 25 ± 0.05 °C.

The dipole moments of the complexes were evaluated by the Guggenheim method (5, 6)

$$[1] \qquad \mu^2 = \frac{27\,kT}{4\pi N_0}\frac{M_2}{d_1(\varepsilon_1 + 2)^2}(a_\varepsilon - a_n)$$

where k is Boltzmann's constant; N_0, Avogadro's number; M_2, the molecular weight of the complex; d_1 and ε_1 represent the density and dielectric constant of the mixed solvent at temperature T, respectively; a_ε and a_n represent the slopes of a plot of dielectric constant and

square of refractive index, respectively, against weight fraction of the complex in the solution.

Values of the dipole moments of the donors were selected from McClellan's book (7).

Charge-transfer spectra of the complexes in CCl_4 solutions were measured by a Cary 14 recording spectrophotometer from 1 to 50 °C at 5-to-10-degree intervals. The temperature was maintained to $\pm 0.5°$ by circulation of water from a thermostat and was measured by means of a copper–constantan thermocouple with a Hewlett Packard 7100 B recorder.

Since there was no absorption except by the complex itself in the visible region, the Benesi–Hildebrand equation (8)

$$[2] \qquad \frac{[\mathrm{TCNE}]l}{A} = \left(\frac{1}{K_x\varepsilon_{DA}}\right)\frac{1}{N_D} + \frac{1}{\varepsilon_{DA}}$$

was used for calculating the equilibrium constant K_x, in terms of mole fraction, where [TCNE] is the initial molar concentration of TCNE and N_D refers to the donor concentration in mole fraction, l represents the thickness of the cell in cm, A is the absorbance, and ε_{DA} is the extinction coefficient of the complex. The heat of complex formation, ΔH, calculated from the temperature dependence of the equilibrium constant, is constant within experimental errors.

Results

According to the Mulliken theory, the ground state and excited state wave functions of a charge-transfer complex with 1:1 stoichiometric ratio may be described by the resonance wave functions

$$[3] \quad \psi_G = a\psi_0(\mathrm{D}\cdots\mathrm{A}) + b\psi_1(\mathrm{D}^+\cdots\mathrm{A}^-)$$

$$[4] \quad \psi_E = a^*\psi_1(\mathrm{D}^+\cdots\mathrm{A}^-) - b^*\psi_0(\mathrm{D}\cdots\mathrm{A})$$

where D and A represent the donor and acceptor molecules, respectively; a, b, a^*, and b^* are coefficients defining the participation of corresponding no-bond structure (D · · · A) described by wave function ψ_0 and dative structure ($D^+ \cdots A^-$) described by ψ_1. The dipole moment of the complex at the ground state, μ_G, which is experimentally determined, can be expressed by

$$[5] \quad \boldsymbol{\mu}_G = -e\int\psi_G \sum \boldsymbol{r}_i\psi_G \, d\tau = (a^2 + abS)\boldsymbol{\mu}_0 + (b^2 + abS)\boldsymbol{\mu}_1$$

where $\boldsymbol{r}_i$ is the vector distance of the ith electron from any convenient origin and S is the overlap integral between ψ_0 and ψ_1, which is taken as 0.1 for most weak complexes (3, 9); $\boldsymbol{\mu}_0$ and $\boldsymbol{\mu}_1$ refer to the dipole moments of the no-bond and dative structures, respectively. On the basis of data from the X-ray structure investigation of aπ–bπ molecular complexes formed by TCNE with naphthalene (10) and perylene (11) in which the 2 planar components are parallel to one another with an intermolecular distance of 3.3 Å, the dipole moment of the dative structure is thus perpendicular to that of the no-bond structure. Therefore, in terms of magnitude, eq. [5] can be written in the following form

$$[6] \quad \mu_G^2 = (a^2 + abS)^2\mu_0^2 + (b^2 + abS)^2\mu_1^2$$

By substituting the experimental value of μ_G and known values of μ_0, μ_1, and S into eq. [6] with the aid of the normalization condition $a^2 + b^2 + 2abS = 1$, we may evaluate a and b. The percentage of charge-transfer, $b^2 + abS$, from the donor to the acceptor of the complex and the dipole moment contributed from the charge-transfer interaction in the complex, $\mu_{CT} = \mu_1(b^2 + abS)$, were also evaluated.

It is possible to calculate the energies of the various states of the complex through the relationships of the ground state energy, W_G, excited state energy, W_E, charge-transfer transition energy at maximum wavelength, $h\nu$, and the heat of formation, ΔH, obtained from spectroscopic data. Starting with the variation principle for the energies of the ground and excited states, the following equations are derived (4)

$$[7] \quad a(W_0 - W_G) + b(H_{01} - W_GS) = 0$$

$$[8] \quad a(H_{01} - W_GS) + b(W_1 - W_G) = 0$$

$$[9] \quad (W_G - W_0)(W_G - W_1) = (H_{01} - W_GS)^2$$

$$[10] \quad a^*(W_1 - W_E) - b^*(H_{01} - W_ES) = 0$$

$$[11] \quad a^*(H_{01} - W_ES) - b^*(W_0 - W_E) = 0$$

$$[12] \quad (W_1 - W_E)(W_0 - W_E) = (H_{01} - W_ES)^2$$

where W_0 and W_1 are the energies of the no-bond and dative states, respectively; H_{01} is the resonance integral between these states. Equations [9] and [12] are obtained by elimination of a,b and a^*, b^* from eqs. [7], [8] and [10], [11], respectively. For the purpose of convenience, let β_G and β_E represent the two quantities $(H_{01} - W_GS)$ and $(H_{01} - W_ES)$, respectively. Therefore, the energies of various states can be calculated without approximation from the charge-transfer spectra and dipole moment determination using the following equations

$$[13] \quad \beta_G = [(a^*S - b^*)ah\nu]/(aa^* + bb^*)$$

$$[14] \quad \beta_E = \beta_G - Sh\nu$$

Can. J. Chem. Downloaded from www.nrcresearchpress.com by 210.87.254.6 on 09/05/12
For personal use only.

Can. J. Chem. Downloaded from www.nrcresearchpress.com by 210.87.254.6 on 09/05/12
For personal use only.

TABLE 1

Dipole moments, charge–transfer parameters, and various energies of TCNE–methylbenzene complexes*

No.	Donor	μ_0	μ_G	μ_{CT}	a	b	$(b^2+abS)\%$	$h\nu$	$-\beta_G$	$-\beta_E$	$-\Delta H$	W_E	$-W_0$	W_1	$-R_G$	R_E
1	C_6H_6	0	0.75	0.75	0.967	0.175	4.74	74.5	12.4	19.9	2.7	71.8	0.5	66.3	2.3	5.5
2	$C_6H_5CH_3$	0.37	0.90	0.83	0.965	0.185	5.23	71.0	12.6	19.7	3.0	68.1	0.6	62.4	2.4	5.6
3	$1,2\text{-}(CH_3)_2C_6H_4$	0.52	1.06	0.94	0.960	0.200	5.94	67.3	12.8	19.6	3.4	63.9	0.7	58.0	2.7	5.9
4	$1,3\text{-}(CH_3)_2C_6H_4$	0.37	1.01	0.95	0.960	0.201	5.99	66.7	12.7	19.4	3.3	63.4	0.7	57.5	2.7	5.9
5	$1,4\text{-}(CH_3)_2C_6H_4$	0	0.96	0.96	0.959	0.203	6.06	66.4	12.8	19.5	3.6	62.9	0.8	56.9	2.7	5.9
6	$1,2,3\text{-}(CH_3)_3C_6H_3$	0.56	1.23	1.12	0.953	0.222	7.04	63.0	13.2	19.5	4.2	58.8	1.1	52.8	3.1	6.3
7	$1,2,4\text{-}(CH_3)_3C_6H_3$	0.37	1.16	1.11	0.954	0.221	7.00	63.2	13.2	19.5	4.1	59.1	1.0	52.8	3.1	6.3
8	$1,3,5\text{-}(CH_3)_3C_6H_3$	0	1.12	1.12	0.953	0.222	7.07	63.0	13.2	19.5	4.1	58.8	1.0	52.5	3.1	6.4
9	$1,2,3,4\text{-}(CH_3)_4C_6H_2$	0.52	1.38	1.30	0.946	0.243	8.17	59.5	13.5	19.5	4.6	54.9	1.1	48.2	3.5	6.8
10	$1,2,3,5\text{-}(CH_3)_4C_6H_2$	0.37	1.33	1.28	0.947	0.241	8.09	60.0	13.5	19.5	4.5	55.5	1.1	48.7	3.5	6.8
11	$1,2,4,5\text{-}(CH_3)_4C_6H_2$	0	1.32	1.32	0.945	0.245	8.33	58.8	13.5	19.4	4.8	54.0	1.2	47.3	3.5	6.8
12	$C_6H(CH_3)_5$	0.37	1.51	1.47	0.939	0.261	9.29	56.0	13.7	19.2	5.5	50.6	1.7	43.5	3.8	7.1
13	$C_6(CH_3)_6$	0	1.64	1.64	0.933	0.279	10.35	53.5	13.8	19.1	6.4	47.1	2.3	39.7	4.1	7.4

*All dipole moments are given in Debye units and energies in kcal per mole.

Can. J. Chem. Downloaded from www.nrcresearchpress.com by 210.87.254.6 on 09/05/12
For personal use only.

$$[15] \quad R_G = \tfrac{1}{2}\{(S^2h\nu - 2\beta_G S - h\nu) + [(S^2h\nu - 2\beta_G S - h\nu)^2 - 4\beta_G{}^2]^{\frac{1}{2}}\}$$

$$[16] \quad W_G = \Delta H$$

$$[17] \quad W_0 = \Delta H - R_G$$

$$[18] \quad W_E = \Delta H + h\nu$$

$$[19] \quad R_E = \beta_E{}^2/(W_E - W_0)$$

$$[20] \quad W_1 = W_E - R_E$$

where R_G and R_E refer to the resonance energies between the dative and no-bond structure for the ground and excited states, respectively. The results for the complete series of TCNE–methylbenzene complexes are summarized in Table 1. The energy diagrams of benzene and hexamethylbenzene complexes are also shown in Fig. 1.

According to Fig. 1

$$[21] \quad h\nu = W_1 - W_0 + R_E - R_G$$

$$[22] \quad W_1 = I_D - E_A - G_1$$

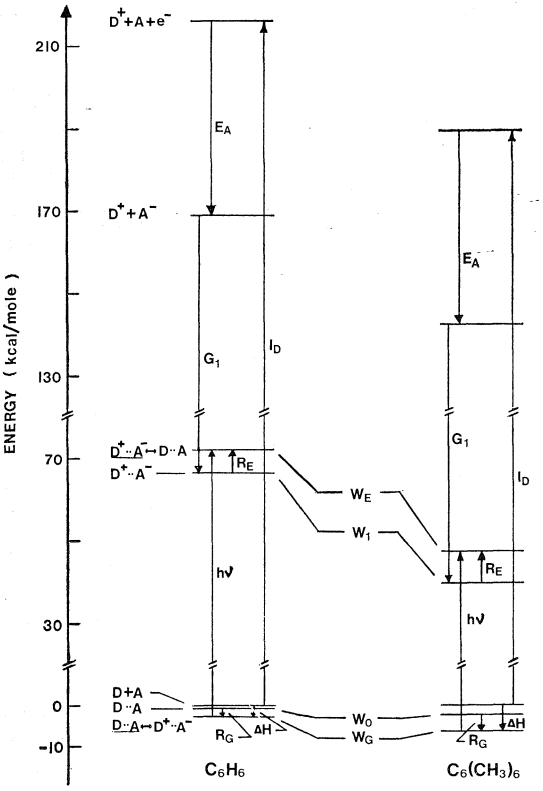

FIG. 1. Energy diagrams of TCNE complexes with benzene and hexamethylbenzene.

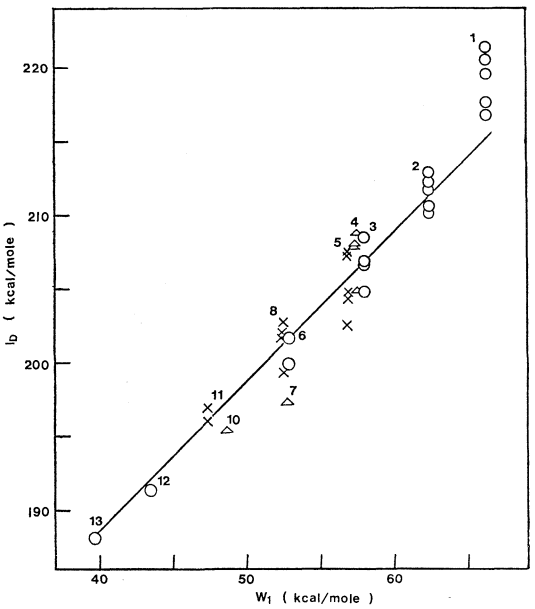

FIG. 2. Plot of vertical ionization potentials of donors vs. dative state energies of TCNE–methylbenzene complexes. Numbers refer to the donors as shown in Table 1.

where I_D refers to the vertical ionization potential of the donor, E_A is the electron affinity of the acceptor, G_1 represents the interaction energy between donor and acceptor at the dative state. G_1 is the sum of the Coulombic interaction at a separation of 3.3 Å and the energy, X, due to the polarization of the $D^+ \cdots A^-$ bond at the dative state

$$[23] \quad G_1 = (e^2/r) + X$$

The value of X, which is expected to be a few kcal/mole (9, 12), was evaluated by plotting the literature values of the vertical ionization potentials against the energies of the dative states as shown in Fig. 2. It was found to be 2 kcal/mole for the TCNE–methylbenzene complexes. The electron affinity of TCNE is taken as 2.04 eV or 47.1 kcal/mole from Trotter (13). Therefore, it is possible to evaluate the vertical ionization potentials of donors directly from eq. [22] with the aid of the energy of the dative state. The results are listed in Table 2.

Discussion

The dipole moment of the no-bond structure of the complex can be taken as that of the donor due to the nonpolar nature of the acceptor,

TABLE 2
Vertical ionization potentials of methylbenzenes in kcal/mole

No.	Compound	Ionization potential								
			Literature							
		Calcd.	(14)	(15)	(16)	(17)	(18)	(19)	(20)	(22)
1	C_6H_6	216.0	221.4	219.6	220.5		216.8	217.6		
2	$C_6H_5CH_3$	212.1	212.9	212.9	211.7	212.2	210.6		210.1*	
3	$1,2\text{-}(CH_3)_2C_6H_4$	207.6	204.8	206.9	208.5	206.6				
4	$1,3\text{-}(CH_3)_2C_6H_4$	207.2	204.8	208.0	208.7	207.8				
5	$1,4\text{-}(CH_3)_2C_6H_4$	206.4	202.5	204.8	207.3	204.3			207.3	
6	$1,2,3\text{-}(CH_3)_3C_6H_3$	202.5	200.0	201.8						
7	$1,2,4\text{-}(CH_3)_3C_6H_3$	202.5	197.2							
8	$1,3,5\text{-}(CH_3)_3C_6H_3$	202.2	199.3	202.7	201.6	202.0				
9	$1,2,3,4\text{-}(CH_3)_4C_6H_2$	197.8								
10	$1,2,3,5\text{-}(CH_3)_4C_6H_2$	198.3	195.4							
11	$1,2,4,5\text{-}(CH_3)_4C_6H_2$	196.9	196.0							197
12	$C_6H(CH_3)_5$	193.2	191.4							
13	$C_6(CH_3)_6$	189.3								188

*Also ref. 21.

TCNE; for the nonpolar donor it can be considered as zero. Thus eq. [6] is reduced to

$$[24] \qquad \mu_G = (b^2 + abS)\mu_1$$

This means that the dipole moment of the complex is due to the partial charge-transfer interaction from the donor to the acceptor. The value of μ_1, caused by the charge transfer of one electron to the acceptor from the donor, with the intermolecular distance 3.3 Å, is taken as 15.8 D for all complexes in this series. A change of 0.1 Å in distance causes a change of only 0.001 in the parameter a, 0.004 in b, 0.2 in $100(b^2 + abS)$, and 0.2 kcal/mole in most energy terms, which are within the experimental errors. For some of the donors, such as 1,2,3,4-tetramethylbenzene, which do not have appropriate literature values of dipole moment, the values of μ_0 derived from vector-summation of bond moments are chosen. A variation of 0.07 D in μ_0 due to the different literature data corresponds to a change of 0.001 in a, 0.002 in b, 0.1 in $100(b^2 + abS)$, and 0.1 kcal/mole in energy terms. The values of a and b found are relatively insensitive to the dipole moment of the complex, as are the quantities derived from a and b. For instance, there is only a change of 0.004 in a, 0.01 in b, 0.6 in $100(b^2 + abS)$, and 0.4 kcal/mole in energy when the dipole moment of the complex is varied by 0.1 D, which is approximately equal to the experimental scatter of the data.

In the calculation of the dipole moment of the complex, we assume that all of the acceptor in the solution is in the form of the complex, since the concentration ratio of donor to acceptor is of the order of 100:1; the complete complexation (23) is shown by the linear relationship of the increment of the dielectric constant of solution with the weight fraction of acceptor for a given amount of donor.

For those complexes having two maxima in the absorption spectra, such as 1,4-dimethylbenzene, 1,2,4-trimethylbenzene, and 1,2,4,5-tetramethylbenzene complexes, the wavelength of the maximum absorption without splitting is calculated according to Briegleb's empirical half-widths relationship (24, 25)

$$[25] \qquad \frac{\nu_h - \nu_1}{2(\nu_{max} - \nu_1)} \approx 1.2$$

where ν_h and ν_1 refer to the frequency at half the maximum intensity on the high- and low-energy sides of the peak located at ν_{max}. Several values of ν_{max} at different intensities are used to obtain an average value of ν_{max}. For instance, transition energies of 1,2-dimethylbenzene and 1,3-dimethylbenzene complexes are 67.3 and 66.7 kcal/mole, respectively. The lower-energy band of the 1,4-dimethylbenzene complex, 62.3 kcal/mole, is close to the energies of the unsplit charge-transfer bands of the trimethylbenzene complexes, whereas the higher-energy band, 72.0 kcal/mole, is higher than the unsplit charge-transfer band of the methylbenzene complex. Using eq. [25], the average value of $h\nu_{max}$ for the

Can. J. Chem. Downloaded from www.nrcresearchpress.com by 210.87.254.6 on 09/05/12
For personal use only.

1,4-dimethylbenzene complex was calculated to be 66.4 kcal/mole which is comparable and consistent with the unsplit spectra of 1,2- and 1,3-dimethylbenzene complexes (see Table 1).

The energy of the no-bond state, W_0, including the sum of the electrostatic energy and van der Waals energy, is expected to be small, ranging from -0.5 kcal/mole for the benzene complex to -2.3 kcal/mole for hexamethylbenzene. Thus, such complexes are formed under weak interaction. The resonance energy of interaction between the no-bond and dative structures in the ground state, R_G, is larger in magnitude than W_0, indicating that the resonance with the dative structure in the ground state is a major force for stabilizing the complex. It is shown in Table 1 that the contribution of resonance energy to the formation of the complex, ΔH or W_G, is by no means equal or nearly equal to W_0, and the forces leading to complex formation are not primarily electrostatic. On the contrary, the main contribution of the excited state energy, W_E, is largely due to the dative structure energy, W_1: 92% for benzene and 84% for hexamethylbenzene; the rest is contribution from the resonance energy, R_E.

The values of the estimated ionization potentials are in agreement with the literature data. The vertical ionization potential of 1,2,3,4-tetramethylbenzene, which is not available in the literature, is given in Table 2.

According to Matsen and co-workers (26), the relationship between charge-transfer energy and vertical ionization potential can be written as

$$[26] \quad h\nu = I_D - C_1 + \frac{C_2}{I_D - C_1}$$

where

$$[27] \quad C_1 = E_A + \frac{e^2}{r} + X + W_0$$

$$[28] \quad C_2 = (H_{01} - SW_G)^2 + (H_{01} - SW_E)^2 = \beta_G{}^2 + \beta_E{}^2$$

Obviously, the coefficients C_1 and C_2, which vary with the donor, are really not constants. However, they may be calculated and the values obtained are approximately 151 kcal/mole for C_1 and 552 (kcal/mole)^2 for C_2. The values of C_1 and C_2 obtained from Fig. 3 are 150 kcal/mole and 557 (kcal/mole)^2, respectively, in good agreement

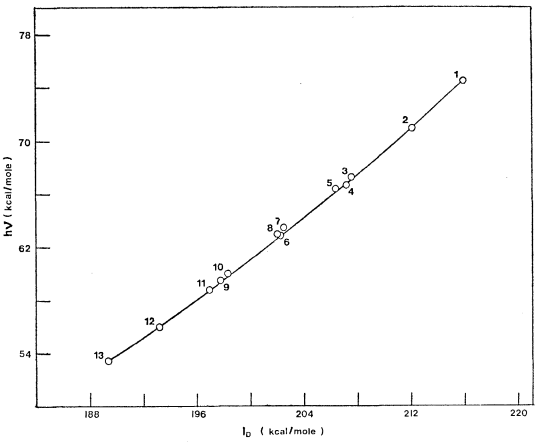

FIG. 3. Plot of charge-transfer energies of TCNE–methylbenzene complexes vs. vertical ionization potentials of donors. Numbers refer to the donors as shown in Table 1.

with the calculated values. The approximate linear relationship of these quantities can be expressed in terms of kcal/mole as

$$[29] \quad h\nu = 0.79\, I_D - 96$$

The values of the constants in the linear equation have no immediate theoretical significance; the fact that the slope is less than unity is a result of the non-zero resonance interaction (27). A similar equation was obtained by Voigt and Reid (25).

With increasing number of methyl substituents on the benzene ring, the dipole moment of the complex is increased. For the same number of methyl substituents, the more polar donor gives rise to higher dipole moment of the complex. The following relationship can be established between the dipole moments caused by the charge-transfer interaction, μ_{CT}, and vertical ionization potentials of the methylbenzenes as shown in Fig. 4.

$$[30] \quad \mu_{CT} = 28.9 - 0.24\, I_D + 5.08 \times 10^{-4}\, I_D{}^2$$

where μ_{CT} is in Debye units and I_D in kcal/mole. It can also be shown that

$$[31] \quad (b^2 + abS) = \frac{1}{2}\left[1 - \frac{1}{1 - aS}\frac{(I_D - C_1)^2}{(I_D - C_1)^2 + C_2}\right]$$

the lower the ionization potential of the donor for a given acceptor, the higher the degree of charge-transfer, i.e., the higher the dipole moment contribution from the charge-transfer interaction.

FOR ERRATA SEE
V. 49 #1 1971 P. 163

Can. J. Chem. Downloaded from www.nrcresearchpress.com by 210.87.254.6 on 09/05/12
For personal use only.

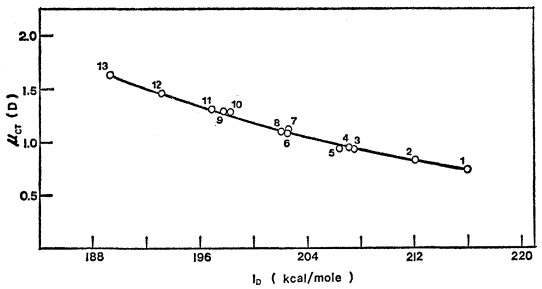

FIG. 4. Plot of dipole moments caused by charge-transfer interaction vs. ionization potentials of donors for TCNE–methylbenzene complexes. Numbers refer to the donors as shown in Table 1.

The authors are indebted to the National Research Council of Canada for financial support of this work.

1. R. S. MULLIKEN. J. Amer. Chem. Soc. **74**, 811 (1952).
2. S. KOBINATA and S. NAGAKURA. J. Amer. Chem. Soc. **88**, 3905 (1966).
3. S. N. BHAT and C. N. R. RAO. J. Amer. Chem. Soc. **90**, 6008 (1968).
4. G. BRIEGLEB. Elektronen-Donator-Acceptor-Komplexe. Springer-Verlag, Berlin. 1961. p. 12.
5. E. A. GUGGENHEIM. Trans. Faraday Soc. **45**, 714 (1949).
6. J. W. SMITH. Trans. Faraday Soc. **46**, 394 (1950).
7. A. L. MCCLELLAN. Table of experimental dipole moments. W. H. Freeman and Co., San Francisco. 1963.
8. H. A. BENESI and J. H. HILDEBRAND. J. Amer. Chem. Soc. **71**, 2703 (1949).
9. W. B. PERSON. J. Chem. Phys. **38**, 109 (1963).
10. R. M. WILLIAMS and S. C. WALLWORK. Acta Cryst. **22**, 899 (1967).
11. I. IKEMOTO and H. KURODA. Bull. Chem. Soc. Jap. **40**, 2009 (1967).
12. T. M. CROMWELL and R. L. SCOTT. J. Amer. Chem. Soc. **72**, 3825 (1950).
13. P. J. TROTTER. J. Chem. Phys. **48**, 2736 (1968).
14. F. MEYER and A. G. HARRISON. Can. J. Chem. **42**, 2256 (1964).
15. F. H. FIELD and J. L. FRANKLIN. J. Chem. Phys. **22**, 1895 (1954).
16. G. F. CRABLE and G. L. KEARNS. J. Phys. Chem. **66**, 436 (1962).
17. H. BABA, I. OMURA, and K. HIGASI. Bull. Chem. Soc. Jap. **29**, 521 (1956).
18. A. D. BAKER, D. P. MAY, and D. W. TURNER. J. Chem. Soc. B, 22 (1968).
19. R. E. HONIG. J. Chem. Phys. **16**, 105 (1949).
20. B. CANTONE, F. CRASSO, and S. PIGNATRARO. Mol. Phys. **11**, 221 (1966).
21. V. K. POTAPOV, D. N. SHIGORIN, A. D. FILYUGINA, and V. V. SOROKIN. Russ. J. Phys. Chem. Engl. Transl. **40**, 1256 (1966).
22. G. BRIEGLEB, J. CZEKALLA, and G. REUSS. Z. Phys. Chem. Frankfurt, **30**, 333 (1961).
23. M. DAVIS. J. Chem. Educ. **46**, 17 (1969).
24. G. BRIEGLEB and J. CZEKALLA. Z. Phys. Chem. Frankfurt, **24**, 37 (1960).
25. E. M. VOIGT and C. REID. J. Amer. Chem. Soc. **86**, 3930 (1964).
26. S. H. HASTINGS, J. L. FRANKLIN, J. C. SCHILLER, and F. A. MATSEN. J. Amer. Chem. Soc. **75**, 2900 (1953).
27. R. S. MULLIKEN and W. B. PERSON. Ann. Rev. Phys. Chem. **13**, 107 (1962).

Can. J. Chem. Downloaded from www.nrcresearchpress.com by 210.87.254.6 on 09/05/12
For personal use only.

Crystal and molecular structure of the *m*-bromobenzoate derivative of bisnorquassin

H. LYNTON
Department of Chemistry, University of New Brunswick, Fredericton, New Brunswick
Received July 4, 1969

The molecular structure of the *m*-bromobenzoate derivative of bisnorquassin, $C_{27}H_{27}O_7Br$, has been determined by the heavy atom method. The compound crystallizes in the orthorhombic system, space group $P2_12_12_1$, with unit cell dimensions $a = 20.09 \pm 0.02$ Å, $b = 14.63 \pm 0.02$ Å, $c = 8.06 \pm 0.01$ Å and 4 molecules in the unit cell. Final atomic parameters have been obtained from a block-diagonal least-squares refinement using anisotropic temperature parameters. The final agreement residual for 1665 observed reflections is $R = 0.107$.

The structure of bisnorquassin previously proposed by Findlay and Cropp, on the basis of spectroscopic and chemical evidence, is shown to be essentially correct.

Canadian Journal of Chemistry, **48**, 307 (1970)

Can. J. Chem. Downloaded from www.nrcresearchpress.com by 210.87.254.6 on 09/05/12
For personal use only.

Introduction

Bisnorquassin, $C_{20}H_{24}O_6$, was first prepared by Robertson *et al.* (1, 2) by the treatment of both quassin and norquassin with a warm mixture of concentrated hydrochloric and acetic acids. The complete structure and relative stereochemistry of quassin, a bitter principle from *Quassia amara*, has been established by Valenta *et al.* (3, 4). Early studies showed that bisnorquassin was not a simple bis-demethylated quassin, but in view of its ultraviolet (u.v.) absorption spectrum, possessed an extended system of conjugation.

A structure for bisnorquassin has been given by Findlay and Cropp (5) which is adequately supported by spectroscopic and chemical evidence. This structure is not complete in that the stereochemical configuration about certain carbon centers is not established. This X-ray analysis was undertaken to provide the complete stereochemical structure of this interesting compound.

Crystallographic and Intensity Data

The specimen of the *m*-bromobenzoate derivative of bisnorquassin used in the structure analysis was supplied by J. A. Findlay and J. S. Tandon.

The crystal data are given in Table 1. The compound is orthorhombic and the systematic absences establish the space group as $P2_12_12_1$. Unit cell dimensions were measured from oscillation and Weissenberg photographs. The density measurements indicate 4 molecules of $C_{27}H_{27}O_7Br$ in the unit cell.

All intensity data were collected from a needle shaped crystal of average length 0.25 mm and average cross section 0.15 mm. As the linear absorption coefficient for CuKα radiation is 29.7 cm^{-1}, no absorption corrections were made. Using the multiple film pack technique, equi-inclination Weissenberg photographs were obtained of layers *hk0* - - *hk6*. The total number of independent reflections with intensities above the minimum intensity limit for observation was 1665.

TABLE 1
Crystal data

System	Orthorhombic
Space group	$P2_12_12_1$
Systematic absences	$h00$: $h = 2n + 1$ $0k0$: $k = 2n + 1$ $00l$: $l = 2n + 1$
Molecular weight	543.4
Unit cell dimensions	
a	20.09 ± 0.02 Å
b	14.63 ± 0.02 Å
c	8.06 ± 0.01 Å
Volume	2370 Å^3
Measured density (by flotation)	1.50 g cm^{-3}
Calculated density (assuming 4 molecules in the unit cell)	1.52 g cm^{-3}

The intensities of all reflections were estimated by visual comparison with a calibrated strip prepared using a suitable reflection from the intensity crystal. Lorentz-polarization factors were applied to all data.

Structure Analysis

A 3-dimensional Patterson synthesis established the positions of the bromine atoms. Subsequent 3-dimensional Fourier syntheses then gave the coordinates of all the carbon and oxygen atoms.

The refinement was by successive cycles of

TABLE 2

Fractional atomic coordinates, and e.s.d. in parentheses*

Atom	x/a	y/b	z/c
Br	−3662(2)	−6170(2)	−0415(5)
O-1	−0936(9)	0165(12)	2771(24)
O-2	−0977(9)	−2708(11)	−2065(22)
O-3	−1499(9)	0010(13)	5173(22)
O-4	0438(13)	−3346(15)	−3466(32)
O-5	−0370(9)	−1998(13)	−4144(22)
O-6	−2359(8)	−3047(11)	−1378(23)
O-7	−2729(9)	−2385(13)	−3770(25)
C-1	0440(13)	−2406(17)	0575(37)
C-2	0354(13)	−3220(16)	−0476(39)
C-3	0162(13)	−3011(19)	−2179(37)
C-4	−0375(13)	−2284(16)	−2460(31)
C-5	−0331(10)	−1463(14)	−1267(29)
C-6	−0207(10)	−1805(15)	0503(34)
C-7	−0203(12)	−1006(16)	1727(28)
C-8	−0748(10)	−0285(14)	1249(28)
C-9	−1314(11)	−0642(13)	0283(29)
C-10	−1070(11)	−1100(16)	−1343(30)
C-11	−1473(10)	−1954(15)	−1953(27)
C-12	−2012(10)	−2266(15)	−0806(26)
C-13	−2138(11)	−1994(15)	0713(27)
C-14	−1723(10)	−1280(13)	1403(28)
C-15	−1723(14)	−1104(17)	3091(33)
C-16	−1392(12)	−0311(13)	3780(25)
C-17	0587(15)	−2702(22)	2521(42)
C-18	0176(13)	−0778(17)	−1954(37)
C-19	−1790(13)	0144(17)	−0303(40)
C-20	−2701(13)	−2388(22)	1793(38)
C-21	−2694(13)	−3035(18)	−2808(36)
C-22	−3024(12)	−3957(16)	−3196(32)
C-23	−3133(13)	−4524(16)	−1907(32)
C-24	−3463(13)	−5367(18)	−2120(45)
C-25	−3642(16)	−5627(20)	−3805(43)
C-26	−3510(15)	−5003(21)	−5078(37)
C-27	−3232(13)	−4135(17)	−4758(32)

*All values have been multiplied by 10^4.

block-diagonal least-squares,[1] employing only the observed reflections. The quantity minimized was $\Sigma\omega(F_o - F_c)^2$. The matrices used were 3 × 3 for the positional parameters and 6 × 6 for the anisotropic thermal parameters of each atom. The weighting scheme $\omega = 1/[a + |F_o| + c|F_o|^2]$ was employed with the following values: $a = 16.00$ and $c = 0.012$. Scattering factor curves used were those given in International Tables (7). During the structure refinement the scale factor for each layer was adjusted by comparison of observed and calculated F_o's.

The positions of the hydrogen atoms could not be deduced from a difference synthesis. No corrections were made for extinction, and in the last cycle, no parameter shift exceeded 0.2 times the estimated standard deviation. The final agreement residual, $R = \Sigma|F_o - F_c|/|\Sigma|F_o|$, for observed reflections was $R = 0.107$.

Results and Discussion

The final atomic coordinates are given together with their estimated standard deviations (e.s.d.) in Table 2. The temperature parameters are given in Table 3. Figures 1 and 2 give the intramolecular bond lengths and angles, and Fig. 3 shows the general stereochemistry of the molecule. Some bond angles are omitted from Fig. 2 and are given

[1]All computations were done on an I.B.M. 360/50 computer using programs by Ahmed *et al.* (6).

TABLE 3

Anisotropic temperature parameters*

Atom	β_{11}	β_{22}	β_{33}	β_{23}	β_{13}	β_{12}
Br	249	380	1983	656	−16	−123
O-1	220	332	477	−616	263	−110
O-2	212	312	114	−392	260	15
O-3	268	451	60	−112	213	−76
O-4	445	455	1485	−496	392	463
O-5	214	511	17	−127	291	−26
O-6	196	255	357	26	−250	−157
O-7	218	447	573	688	−359	−144
C-1	186	345	619	−180	98	160
C-2	207	296	546	−211	202	101
C-3	192	438	580	−537	429	−35
C-4	245	250	79	−2	219	71
C-5	96	271	3	99	−4	−95
C-6	59	316	314	43	−9	36
C-7	185	357	12	56	82	91
C-8	107	226	77	−4	−136	32
C-9	145	236	18	242	108	−92
C-10	154	276	37	30	−22	127
C-11	132	324	27	28	6	−95
C-12	122	277	53	−182	−98	−74
C-13	159	270	67	248	−376	−40

Can. J. Chem. Downloaded from www.nrcresearchpress.com by 210.87.254.6 on 09/05/12
For personal use only.

TABLE 3 *(Concluded)*

Atom	β_{11}	β_{22}	β_{33}	β_{23}	β_{13}	β_{12}
C-14	70	162	134	−271	66	28
C-15	245	279	337	−115	350	−5
C-16	172	360	568	−1057	446	−288
C-17	226	549	1055	−428	−127	135
C-18	197	262	916	−48	434	−202
C-19	152	372	1125	−260	46	231
C-20	150	648	426	−403	459	−452
C-21	191	359	478	−475	−134	−326
C-22	145	245	467	42	−74	−121
C-23	212	240	15	197	−1	−19
C-24	178	249	1721	307	−48	−161
C-25	247	432	1281	−101	−341	69
C-26	276	489	524	110	−491	−98
C-27	240	378	74	−2	−278	−123

*All values have been multiplied by 10^5; $T = \exp - [h^2\beta_{11} + k^2\beta_{22} + l^2\beta_{33} + kl\beta_{23} + hl\beta_{13} + hk\beta_{12}]$.

TABLE 4

Bond angles omitted from Fig. 2

Atoms	Angle (°)
O_2—C_4—C_3	106
O_5—C_4—C_5	111
C_4—C_5—C_{10}	101
C_6—C_5—C_{18}	116
C_8—C_9—C_{19}	112
C_{10}—C_9—C_{14}	114

in Table 4. A final set of structure factors has been placed in the Depository of Unpublished Data.[2]

The estimated standard deviations for all bonds are 0.03–0.04 Å except for C_1—C_{17} and C_{24}—C_{25} where the e.s.d. are 0.05 Å. The e.s.d. for all bond angles are 2–3°. Nothing can be established about

[2]Photocopies may be obtained, upon request, from: Depository of Unpublished Data, National Science Library, National Research Council of Canada, Ottawa, Canada.

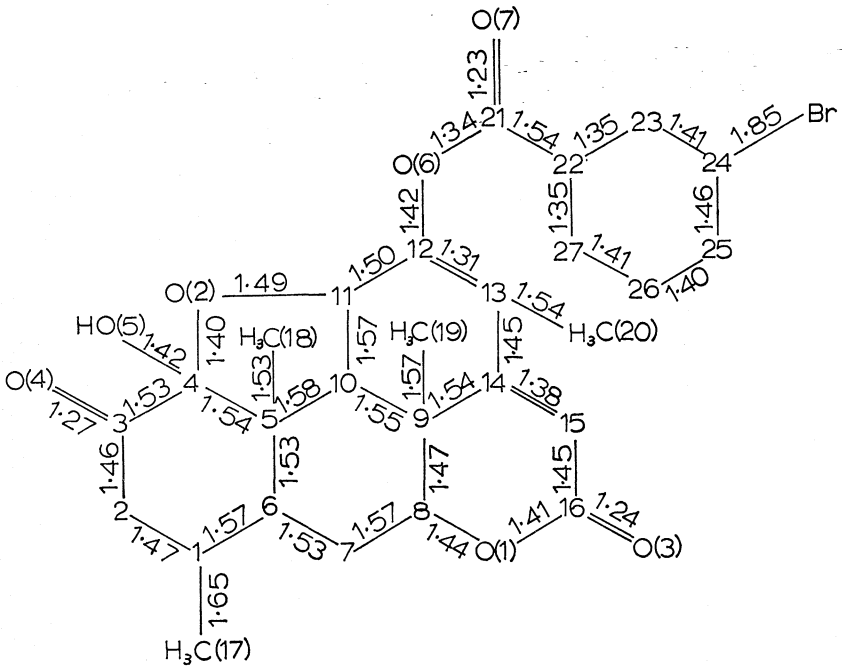

FIG. 1. Intramolecular bond distances.

Can. J. Chem. Downloaded from www.nrcresearchpress.com by 210.87.254.6 on 09/05/12
For personal use only.

Can. J. Chem. Downloaded from www.nrcresearchpress.com by 210.87.254.6 on 09/05/12
For personal use only.

TABLE 5
Best mean planes

Atom	Distance from plane (Å)
Benzene ring	
Equation $0.895x - 0.419y - 0.154z + 2.639 = 0$	
C-22	0.02
C-23	0.02
C-24	−0.03
C-25	0.01
C-26	0.03
C-27	−0.05
Chromophore	
Equation $-0.695x + 0.661y - 0.284z - 0.811 = 0$	
O-3	0.10
C-12	−0.01
C-13	0.08
C-14	0.04
C-15	−0.18
C-16	−0.03
Benzene ring and chromophore	
Equation $0.875x - 0.484y - 0.030z + 2.337 = 0$	
O-3	−0.42
O-6	0.38
C-12	0.42
C-13	−0.03
C-14	0.18
C-15	0.01
C-16	0.02
C-21	−0.18
C-22	−0.10
C-23	0.08
C-24	0.10
C-25	0.01
C-26	−0.17
C-27	−0.30

possible hydrogen bonding as no intermolecular distances were found to be shorter than the usual van der Waals separation values.

The gross structure proposed by Findlay and Cropp (5) is confirmed. The molecule has a cage conformation in which all substituent groups, except the hydrogen attached to C-6, point away from the center of the molecule. The hydrogens attached to C-10 and C-11 must be *cis* and not *trans* as suggested by Findlay and Cropp. They lie on the outward side of the 5-membered ring as does the methyl group attached to C-5 and the hydroxyl group attached to C-4. The hydrogen atom attached to C-1 is *cis* to the OH group at C-4.

The chromophore extending from O-3 through C-16, C-15, C-14, C-13 to C-12 is essentially planar and is coupled with the planar *m*-bromobenzoate substituent at C-12, the whole forming a large conjugated planar array in which no atom is more than 0.5 Å out of the best mean plane (see Table 5).

I wish to acknowledge the support of the National Research Council of Canada for this work, and I thank Mrs. Brenda Leffen for the estimation of the intensity data used in this analysis.

1. E. London, A. Robertson, and H. Worthington. J. Chem. Soc. 3431 (1950).
2. K. R. Hansen, D. B. Jaquiss, J. A. Lamberton, A. Robertson, and W. E. Savige. J. Chem. Soc. 4238 (1954).

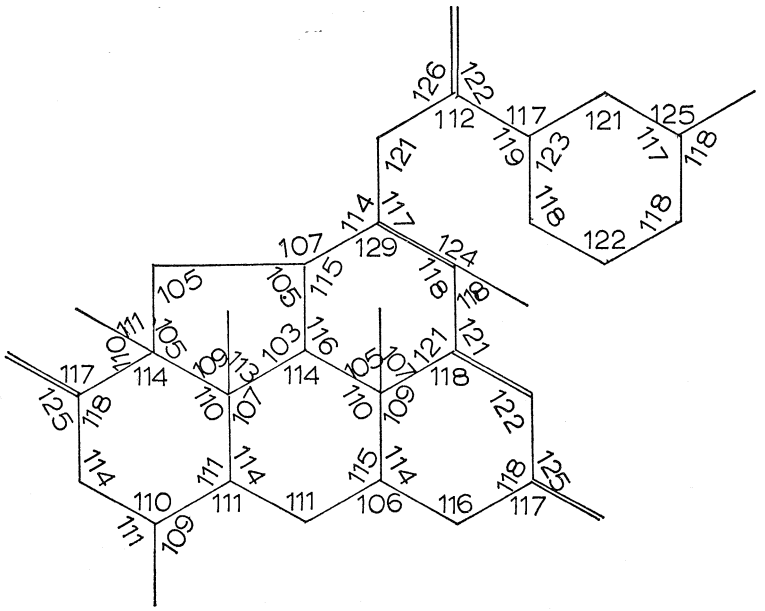

FIG. 2. Intramolecular bond angles.

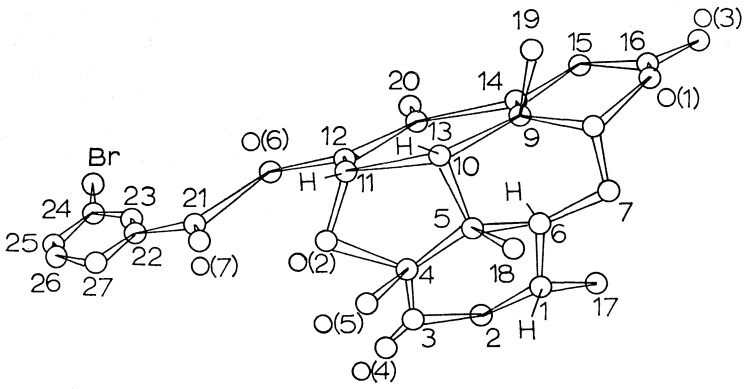

FIG. 3. General shape of the bisnorquassin molecule.

3. Z. VALENTA, S. PAPADOPOULOUS, and C. PODESVA. Tetrahedron, **15**, 100 (1961).
4. Z. VALENTA, A. H. GRAY, D. E. ORR, S. PAPADOPOULOUS, and C. PODESVA. Tetrahedron, **18**, 1433 (1962).
5. J. A. FINDLAY and D. T. CROPP. Can. J. Chem. **46**, 3765 (1968).
6. F. R. AHMED, S. R. HALL, C. P. HUBER, and M. E. PIPPY. N.R.C.C. Crystallographic Programs for the I.B.M./360 System, Divisions of Pure Physics and Pure Chemistry, National Research Council of Canada, Ottawa, Canada.
7. International Tables for X-ray Crystallography, Vol. III. The Kynoch Press, Birmingham, England, 1962. Table 3.3.1.A.

Can. J. Chem. Downloaded from www.nrcresearchpress.com by 210.87.254.6 on 09/05/12
For personal use only.

Can. J. Chem. Downloaded from www.nrcresearchpress.com by 210.87.254.40 on 09/05/12
For personal use only.

Study of some bisnorquassin derivatives

J. A. FINDLAY, R. F. LANGLER, AND J. S. TANDON
Department of Chemistry, University of New Brunswick, Fredericton, New Brunswick, Canada

Received July 4, 1969

The structures of several derivatives of bisnorquassin (**2***a*) are clarified. Chemical support for the mechanism of formation of this novel demethylation product of quassin (**1***a*) is provided, which together with the recent X-ray diffraction study of bisnorquassin *m*-bromobenzoate (**2***d*) offers an independent corroboration of the structure and stereochemistry of **1***a* deduced by Valenta.

Canadian Journal of Chemistry, **48**, 313 (1970)

The complete structure and stereochemistry of quassin $C_{22}H_{28}O_6$ (**1***a*) a bitter principle from *Quassia amara*, was deduced by Valenta and coworkers (1) in 1962. It had been known for some time that quassin produced an abnormal demethylation product $C_{20}H_{24}O_6$ named bisnorquassin (2, 3) when treated with a mixture of concentrated hydrochloric and acetic acid. Recently we proposed structure **2***a* for this novel product and outlined a likely transformation mechanism (4). At that time the configuration of centers C-1, C-4, C-10, and C-11 remained unassigned. The X-ray diffraction study of Lynton (5) on bisnorquassin *m*-bromobenzoate **2***d* has now clarified the remaining stereochemistry and has corroborated in detail our proposal **2***a* for bisnorquassin.

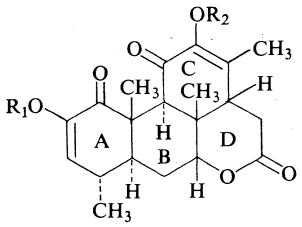

1

a $R_1 = R_2 = CH_3$
b $R_1 = R_2 = H$

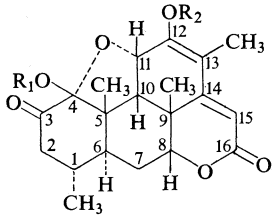

2

a $R_1 = R_2 = H$
b $R_1 = H$; $R_2 = COCH_3$
c $R_1 = H$; $R_2 = COC_6H_5$
d $R_1 = H$; $R_2 = COC_6H_5Br$ (*m*)

Prior to the conclusion of the X-ray study (5) we were seeking corroborative chemical evidence for structure **2***a* with a view also to determining additional stereochemical features of the molecule. This involved, in part, reexamining some of the derivatives of **2***a* reported by Robertson's group (2, 3). We now report our findings.

In one approach we have treated quassin (**1***a*) with concentrated DCl and CH_3COOD and obtained a polydeuterated bisnorquassin containing up to 7 deuterium atoms as evidenced by the mass spectrum which displayed ions of *m/e* 367, 366, 365, and 364, the latter two being the more abundant species. Examination of the nuclear magnetic resonance (n.m.r.) spectrum of this product indicated the absence of signals due to hydrogens at C-2, C-10, and C-11, all of which are clearly discernible in the corresponding spectrum of bisnorquassin at τ 7.7 (a multiplet, 2H), 7.4 (a doublet, 1H, J = 10 c.p.s.), and 5.0 (a doublet, 1H, J = 10 c.p.s.), respectively. In addition, the signal for the methyl group at C-13 (τ 8.1) is grossly diminished in the deuterated bisnorquassin spectrum. This result clearly supports structure **2***a* and the mechanism of formation proposed by us earlier (4) since all the hydrogens involved are potentially exchangeable via ketone-enol equilibria during the transformation of **1***a* to **2***a*.

An important feature of the n.m.r. spectrum of the polydeuterated bisnorquassin is that it displays a doublet at τ 9.1 (J = 5 c.p.s.) for the C-1 methyl group; a clear indication that C-1 has not epimerized in the quassin–bisnorquassin transformation. It follows then that the methyl group at C-1 must be α in bisnorquassin (**2***a*) corresponding to the same configuration at that site in quassin (**1***a*). This result, together with the X-ray solution of bisnorquassin *m*-bromobenzoate (**2***d*) allows for a complete and independent corroboration of the structure and stereochemistry

Can. J. Chem. Downloaded from www.nrcresearchpress.com by 210.87.254.40 on 09/05/12
For personal use only.

of quassin **1***a* (1) except for the centers C-10 and C-14.

It is noteworthy that the coupling constant *J* for the mutual splitting of hydrogens at C-10 and C-11 in **2***a* and a number of derivatives, including the *m*-bromobenzoate **2***d*, is of the order of 9–10 c.p.s. The magnitude of this coupling constant suggests a *trans* relationship of the C-10 and C-11 hydrogens but this is clearly misleading in the light of the X-ray diffraction studies on **2***d* which show these hydrogens to be *cis* and β. From inspection of models it is evident that this *cis* arrangement confers greater strain-free planarity on the chromophoric system in rings C and D in **2***a* and also provides for a less strained 5-membered hemi-ketal ring than do alternate *trans* C-10, C-11 configurations.

In attempts to gain chemical insight to the configuration of the hydroxyl group at C-4 in **2***a* we have examined the n.m.r. spectra of a number of bisnorquassin derivatives some of which were first reported in Robertson's papers (2, 3).

In the n.m.r. spectrum of bisnorquassin itself the signal for the C-5 methyl is found at τ 9.1, while the C-9 methyl shows at τ 8.6, the low field position of the latter can be ascribed to deshielding caused by the adjacent extended chromophoric system. We have attempted to prepare derivatives of **2***a* in which the C-4 hydroxyl was acetylated or benzoylated with the expectation that the n.m.r. spectra of such might show shifts in the field position for signals due to protons at C-10, C-11 or for the methyl protons at C-5, should these hydrogens be *cis* to the introduced acetoxy or benzoyloxy group at C-4. Since earlier studies reported (3) the preparation of *O,O*-diacetyl bisnorquassin (m.p. 232°), our initial efforts were directed at obtaining this compound. While we had no difficulty in preparing a monoacetate **2***b* (m.p. 231–233°) by the procedure described for preparation of the presumed diacetate, the only diacetate we were able to prepare proved to be an anhydrodiacetate (m.p. 232–234°) and this was obtained by treatment of bisnorquassin with acetic anhydride and fused sodium acetate.

The n.m.r. spectrum of the monoacetate **2***b* differs little from that of **2***a* apart from the additional singlet (3H) at τ 7.74 (CH_3CO). Since the ultraviolet (u.v.) spectrum (λ_{max} 275 mμ, ε 20 000 in alcohol) of **2***b* displays a slow time dependent shift (to λ_{max} 373 mμ ε, > 25 000) in basic media there is no doubt that the acetoxy group is attached to C-12. The corresponding monobenzoate **2***c* is readily prepared by treatment of bisnorquassin with benzoyl chloride and pyridine.

We formulate the anhydrodiacetate of bisnorquassin as **3***a*. In the n.m.r. spectrum of this compound the signal for the C-1 methyl appears as a singlet near τ 8.2. Singlets (3H each) at τ 7.75 and 7.9 are assigned to the two acetate methyl groups. A slightly broadened singlet at τ 4.5 (1H) (C_2—H) attests to the location of a double bond between C-1 and C-2, while a broad multiplet (1H) at τ 7.4 is assigned to the C_6—H. The other features of the spectrum are unexceptional. Further support for formulation **3***a* comes from its infrared (i.r.) spectrum (KBr) which shows bands at 1780 (enol acetate), 1710 (lactone), 1650 and 1605 cm^{-1} (conjugated double bonds) and no hydroxylic absorption.

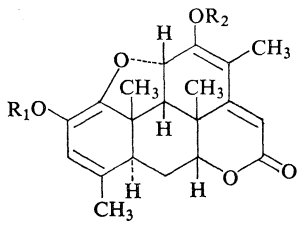

3

a $R_1 = R_2 = COCH_3$
b $R_1 = R_2 = COC_6H_5$

Formation of **3***a* can be visualized as occurring by 1,4-elimination via an intermediate enol acetate generated in the A ring. In attempting to obtain a dibenzoate of bisnorquassin we have encountered a parallel transformation leading to **3***b* which displays similar spectroscopic features to **3***a*.

Another interesting compound described (2, 3) earlier was obtained by prolonged treatment of bisnorquassin with diazomethane. This compound named α-*O*-methyl bisnorquassin (m.p. 210°) was initially believed to have the constitution $C_{21}H_{23}O_5 \cdot OMe$ (2) but was later amended to conform with $C_{20}H_{23}O_5 \cdot OMe$ (3). It displayed λ_{max} 315 mμ (ε 22 600) and did not appear to contain a hydroxyl group in view of the reported absence of hydroxylic bands in the i.r. spectrum and negative Zerewitinoff reaction.

In several attempts to prepare this compound with all the properties described we have been unsuccessful. However, by the same prolonged treatment of bisnorquassin with diazomethane

Can. J. Chem. Downloaded from www.nrcresearchpress.com by 210.87.254.40 on 09/05/12
For personal use only.

we have obtained a product with similar melting point (m.p. 206–208°) and u.v. spectrum (λ_{max} 312 mμ, ε 19 800). While the n.m.r. spectrum (*vide infra*) shows it to be a monomethyl ether, the mass spectrum displays a strong molecular ion of *m/e* 388, indicating a composition $C_{22}H_{28}O_6$. In addition this derivative displays hydroxylic absorption in the i.r. at 3600 cm^{-1} and responds positively to a Zerewitinoff determination and therefore does not appear to be identical with α-*O*-methyl bisnorquassin reported by Robertson and co-workers. We formulate this new derivative as **4** in the light of the following data. Its i.r. spectrum shows only one strong carbonyl band at 1700 cm^{-1} attributed to the enol lactone carbonyl. The n.m.r. spectrum displays a singlet (1H) at τ 4.3 (C_{15}—H), a doublet (1H) at 4.9 (J = 8 c.p.s.) (C_{11}—H), a triplet (1H) at 5.5 (J = 6 c.p.s.) (C_8—H) and a doublet (1H) centered at 7.5 (J = 8 c.p.s.) (C_{10}—H). The pattern of the low field signals is essentially the same as that in the bisnorquassin spectrum. The major difference is the appearance in the spectrum of **4** of a singlet (3H) at τ 6.15 (CH_3O) and a pair of doublets (1H each) at τ 7.0 and 7.5 (J = 4 c.p.s.), assigned to the hydrogens on the oxide bridge.

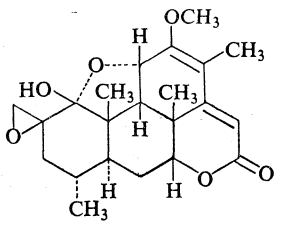

4

As chemical corroboration of structure **4** for the product of prolonged diazomethane treatment of bisnorquassin we have subjected it to treatment with concentrated hydrochloric acid and obtained the corresponding chlorohydrin (*m/e* 424) which on treatment with potassium carbonate solution refurnished the original oxide **4** in accord with expectation.

It should be noted that the simple bis demethylated quassin **1***b* can be prepared by treatment of quassin with aluminum chloride in hot nitrobenzene. The product **1***b* (m.p. 196–200°) is obtained in good yield and can be converted into quassin by treatment with ethereal diazomethane.[1] We have also succeeded in converting **1***b* into bisnorquassin (**2***a*) thus demonstrating the intermediacy of **1***b* in the quassin–bisnorquassin transformation as proposed by us recently (4).

[1]These two reactions were first carried out at the University of Liverpool. See ref. (6).

Experimental

General

The i.r. spectra were recorded on a Perkin–Elmer model 237B spectrophotometer. The mass spectra were determined on a Hitachi Perkin–Elmer model RMU-6D spectrometer. The n.m.r. spectra were recorded with a Varian 56.4 Mc/s instrument using tetramethylsilane as internal standard. A Köfler hot stage apparatus was employed to determine the melting points which are uncorrected.

Preparation of Bisnorquassin (2a)

Bisnorquassin was prepared from quassin (**1***a*) by the procedure described by London *et al.* (2) and was recrystallized to constant m.p. (250–253°) from 95% ethanol.

Preparation of Polydeuterated Bisnorquassin

A mixture of quassin (250 mg), CH_3COOD (2.5 ml) and concentrated DCl (0.75 ml) was heated on a steam bath for 1 h. The solution was concentrated, diluted with water, and cooled. A crystalline solid (180 mg) separated and was filtered off. After recrystallization from ethanol this material (m.p. 250–253°) showed no depression of melting point when admixed with bisnorquassin. The n.m.r. spectrum shows signals at τ 4.2 (singlet, 1H), 5.5 (multiplet, 1H), 8.2 (multiplet, 4H), 8.6 (singlet, 3H), 8.95 (singlet, 3H), and 9.1 (doublet, 3H, J = 5 c.p.s.). The mass spectrum displays abundant ions at *m/e* 367, 366, 365, and 364.

Preparation of Bisnorquassin Acetate (2b)

Bisnorquassin (100 mg) in dry pyridine (10 ml) was treated with acetic anhydride (10 ml) for 18 h at room temperature. After evaporation of the solution to dryness *in vacuo*, the residue was dissolved in glacial acetic acid (3 ml) from which the product (65 mg) crystallized on standing. After filtration and washing with water the product **2***b* was recrystallized from benzene and displayed m.p. 231–233°. The i.r. spectrum (CCl_4) shows bands at 3500, 1775, 1725, 1680, and 1600 cm^{-1}; λ_{max} (ethanol) 275 mμ (ε 20 000) shifts slowly in basic media to 373 (ε > 25 000). The mass spectrum displays a molecular ion of *m/e* 402 corresponding to $[C_{22}H_{26}O_7]^+$.

Preparation of Bisnorquassin Anhydrodiacetate (3a)

Bisnorquassin (1 g) in acetic anhydride (100 ml) was treated with sodium acetate (460 mg) and the solution was refluxed for 24 h. Evaporation *in vacuo* yielded a dark brown semi-solid mass which was taken up in hot ethanol. The cooled ethanolic solution yielded bisnorquassin anhydrodiacetate **3***a* (0.55 mg) which was recrystallized to constant melting point (232–234°) from ethanol. The i.r. spectrum (KBr) shows bands at 1780, 1710, 1650, and 1605 cm^{-1}; λ_{max} (ethanol) 268 mμ (ε 13 400) changes slowly on addition of base to λ_{max} 244 (ε 5600) and 380 mμ (ε 17 000). The n.m.r. spectrum displays signals at τ 4.1 (singlet, 1H), 4.5 (broad singlet, 1H) partly superimposed on a doublet centered near τ 4.6 (1H), 5.65 (multiplet, 1H), 7.4 (broad singlet, 1H), 7.75

Can. J. Chem. Downloaded from www.nrcresearchpress.com by 210.87.254.40 on 09/05/12
For personal use only.

(singlet, 3H), 7.9 (singlet, 3H), 8.2 and 8.25 (2 coalesced singlets, 6H), 8.7 (singlet, 3H) and 8.95 (singlet, 3H). The mass spectrum displays a molecular ion of *m/e* 426 corresponding to $[C_{24}H_{26}O_7]^+$.

*Preparation of Bisnorquassin Anhydrodibenzoate (**3b**)*

A mixture of bisnorquassin (1 g), dry pyridine (5 ml), and benzoyl chloride (2.5 ml) was heated at 70° for 24 h. The solution was evaporated to dryness and the residue taken up in ethyl acetate/ether (2:1). After washing this solution with dilute aqueous HCl it was dried over anhydrous magnesium sulfate and evaporated. The residue crystallized from ether/methanol yielding **3***b*, a crystalline solid (0.4 g) m.p. 243–244°. The i.r. spectrum (CCl_4) displays bands at 1750 (broad) and 1660 cm^{-1}; λ_{max} (ethanol) 231 (ε 12 900) and 267 mμ (ε 13 200) shifts slowly on addition of base to λ_{max} 380 mμ (ε 15 000). The n.m.r. spectrum shows signals at τ 1.93–3.30 (multiplets, 10H), 4.08 (singlet, 1H), 4.36 (singlet, 1H) partly superimposed on a doublet centered near τ 4.4, 5.45 (multiplet, 1H), 7.35 (broad based singlet, 1H), 7.7 (doublet, 1H, J = 7.4 c.p.s.), 8.1 (singlet, 3H), 8.2 (singlet, 3H), 8.5 (singlet, 1H) and 8.8 (singlet, 1H).

Anal. Calcd. for $C_{34}H_{30}O_7$: C, 74.30; H, 5.46; O, 20.19. Found: C, 74.22; H, 5.41; O, 20.29.

*Preparation of Bisnorquassin m-Bromobenzoate (**2d**)*

Bisnorquassin (0.2 g) in dry pyridine (3 ml) was treated with *m*-bromobenzoyl chloride (1.5 ml). After standing at room temperature for 18 h, the solution was evaporated to dryness. The crude product (0.23 g) was treated with carbon tetrachloride (10 ml) and the soluble portion was evaporated to dryness and chromatographed on a silica gel column. Bisnorquassin *m*-bromobenzoate **2***d* was eluted with $CCl_4/CHCl_3$ (1:1). The white crystalline product (40 mg) was recrystallized from ethanol to constant melting point (262–265°). The i.r. spectrum ($CHCl_3$) shows bands at 3600, 1750, 1725 (broad), 1670, 1600, and 1580 cm^{-1}. The mass spectrum displays a pair of molecular ions of approximately equal intensity at *m/e* 544 and 542 corresponding to $[C_{27}H_{27}O_7Br]^+$. The u.v. absorption spectrum displays λ_{max} 238 (ε 12 200) and 273 mμ (ε 18 700). The n.m.r. spectrum shows signals at τ 1.80–2.9 (multiplet, 4H), 4.0 (singlet, 1H), 4.9 (doublet, 1H, J = 9.6 c.p.s.), 5.4 (triplet, 1H, J = 6 c.p.s.), 7.4 (doublet, 1H, J = 9.6 c.p.s.), 7.65 (multiplet, 2H), 8.15 (singlet, 3H), 8.5 (singlet, 3H), 9.0 (singlet, 3H) and 9.1 (doublet, 3H, J = 5 c.p.s.).

*Preparation of **4***

Bisnorquassin (130 mg) in chloroform (5 ml) was treated with a large excess of ethereal diazomethane for a period of 12 h. After evaporation of solvent, the crude product was recrystallized from ethanol to furnish **4** (70 mg), m.p. 208–210°. The i.r. spectrum ($CHCl_3$) shows absorption maxima at 3600, 1700, 1640, and 1600 cm^{-1}; λ_{max} 312 mμ (ε 19 800). The mass spectrum displays a strong molecular ion of *m/e* 388 corresponding to $[C_{22}H_{28}O_6]^+$. The n.m.r. spectrum shows signals at τ 4.3 (singlet, 1H), 4.9 (doublet, 1H, J = 8 c.p.s.), 5.5 (triplet, 1H, J = 6 c.p.s.), 6.15 (singlet, 3H), 7.0 (doublet, 1H, J = 4 c.p.s.), 7.5 (doublet, 1H, J = 4 c.p.s.) superimposed on a signal at τ 7.6 (doublet, 1H, J = 8 c.p.s.), 8.2 (singlet, 3H), 8.7 (singlet, 3H), 8.9 (singlet, 3H) and 9.3 (doublet, 3H, J = 4 c.p.s.).

*Chlorohydrin of **4***

Compound **4** (79 mg) in anhydrous ether (5 ml) was treated with gaseous hydrochloric acid by bubbling a steady stream of gas through the solution for 1 h. The flask was then stoppered and the solution stirred for 18 h. Evaporation of the solvent gave a residue (89 mg) which was purified by preparative thin-layer chromatography on silica gel. The i.r. spectrum ($CHCl_3$) of the resulting chlorohydrin displays bands at 3680, 3520, 1695, and 1630 cm^{-1}. The n.m.r. spectrum shows signals at τ 4.35 (singlet, 1H), 4.9 (doublet, 1H, J = 10 c.p.s.), 5.45 (triplet, 1H, J = 7 c.p.s.), 6.1 (singlet, 3H), 6.45 (singlet, 1H), 6.7 (multiplet, 2H), 7.45 (doublet, 1H, J = 10 c.p.s.), 8.2 (singlet, 3H), 8.7 (singlet, 3H), 8.8 (singlet, 3H), and 9.25 (doublet, 3H, J = 5 c.p.s.). The mass spectrum displays a molecular ion of *m/e* 424 corresponding to $[C_{22}H_{29}O_6Cl]^+$. This compound was readily converted back to **4** by treatment with a solution of potassium carbonate in methanol/water.

*Preparation of **1b***

Aluminum chloride (1 g) was added to a solution of quassin (1 g) in nitrobenzene (25 ml) and the mixture was heated at 90° for 4 h. The solvent was removed by steam distillation and the residue taken up in chloroform. Crystallization of the chloroform soluble fraction from ethanol afforded **1***b* (650 mg), m.p. 196–200°. The mass spectrum displays a strong molecular ion of *m/e* 360 corresponding to $[C_{20}H_{24}O_6]^+$. The i.r. spectrum ($CHCl_3$) displays bands at 3500, 1740, 1690, and 1660 cm^{-1}; λ_{max} (ethanol) 273 mμ (ε 12 000) shifts in base to 315 mμ (ε 10 000).

*Conversion of **1b** to Bisnorquassin (**2a**)*

A mixture of **1***b* (100 mg), acetic acid (10 ml), and concentrated hydrochloric acid (3 ml) was heated on a steam bath for 1 h. The hot solution was diluted with water and on cooling yielded white crystalline needles (80 mg) which after recrystallization from ethanol proved to be identical with bisnorquassin (**2***a*) by m.p., mixed m.p., i.r., n.m.r., and mass spectra.

*Conversion of **1b** to Quassin (**1a**)*

Compound **1***b* (100 mg) in ether was treated with an excess of ethereal diazomethane for 1 h. After evaporation of ether the residue was recrystallized from acetone and ethanol to yield a product (55 mg) identical by m.p., mixed m.p., i.r., and u.v. spectrum with quassin **1***a*.

This work was supported in part by a grant from the National Research Council of Canada.

1. Z. Valenta, A. H. Gray, D. E. Orr, S. Papadopoulos, and C. Podesva. Tetrahedron **18**, 1433 (1962); Z. Valenta, S. Papadopoulos, and C. Podesva. Tetrahedron **15**, 100 (1961).
2. E. London, Alexander Robertson, and H. Worthington. J. Chem. Soc. 3431 (1950).
3. K. R. Hansen, D. B. Jaquiss, J. A. Lamberton, Alexander Robertson, and W. E. Savige. J. Chem. Soc. 4238 (1954).
4. J. A. Findlay and D. T. Cropp. Can. J. Chem. **46**, 3765 (1968).
5. H. Lynton. The crystal and molecular structure of the *m*-bromobenzoate derivative of bisnorquassin. (Submitted to Can. J. Chem.).
6. R. Henderson. Ph.D. Thesis, Liverpool, 1957. p. 132–134.

(Ref.: Can. J. Chem. 48, 317 (1970))

Canadian Journal of Chemistry, 48, 1174 (1970)

The ordinates of Figs. 1, 3, and 4 should be multiplied by 10^9, and that of Fig. 2 should be multiplied by 10^8.

Kinetics of the pyrolysis of propylene. Part I

M. SIMON AND M. H. BACK

Chemistry Department, University of Ottawa, Ottawa, Canada

Received August 25, 1969

The kinetics of the pyrolysis of propylene have been studied over the temperature range 743–873 °K and the pressure range 200–600 Torr. At the lower temperatures initial rates of formation of methane, propane, and C_6 products were measured and shown to be formed by a radical process of very short chain length. The orders and activation energies of the rates were consistent with the occurrence of the bimolecular initiation step

$$2C_3H_6 \rightarrow C_3H_5 + C_3H_7$$

Measurement of the pressure change showed that products of molecular weight higher than C_7 and not measured by the analysis were formed in the initial stages of the reaction at the lower temperatures. As these higher molecular weight compounds, which are more unstable than propylene, accumulated in the system their dissociation increased the concentration of radicals and caused a sharp increase in the rates of formation of the lower molecular weight stable products.

Canadian Journal of Chemistry, 48, 317 (1970)

Introduction

Mechanisms for the thermal reactions of olefins have generally been less detailed and more general than mechanisms for similar systems involving paraffins (1). Studies of the pyrolysis of olefins, for example, have rarely yielded the direct measurement of an elementary rate constant. There are two main features of the thermal reactions of olefins which make such quantitative measurements difficult. First, a wide range and variety of products is generally formed even in the initial stages, making separation, identification, and measurement difficult. Secondly, the formation of the products is preceded by an induction period and, until this induction period can be accounted for kinetically, a complete steady state solution of a proposed mechanism is not possible.

Results of previous studies of the pyrolysis of propylene in the temperature range 500–700 °C have been discussed by Kallend, Purnell, and Shurlock (2). They show that the mechanisms which have been suggested (3, 4) explain only the general features of the reaction and do not provide an exact description in terms of elementary reactions. In their study, Kallend, Purnell, and Shurlock identified 26 products and measured their rates of formation under a variety of conditions. Their main interest was in the role of the allyl radical and they proposed that various reactions of the C_6H_{11} radical, formed by addition of an allyl radical to propylene, accounted for the formation of most of the products of molecular weight greater than propylene. They also suggested that the main termination reaction was the combination of methyl and allyl radicals. The explanation of the induction period remained vague, however, and deductions about the initiation and termination steps from the kinetics in the region of maximum rate are not very convincing.

Results from a study of the pyrolysis of ethylene under similar conditions (5) were interpreted to show that the reaction was initiated by the bimolecular reaction of two ethylene molecules to form a vinyl and an ethyl radical. Such an initiation step appeared probable with propylene as well and indeed this reaction was shown by Marshall, Purnell, and Shurlock (6) to be faster under their conditions than the unimolecular dissociation of propylene. Nevertheless, the kinetics of the reaction led them to believe that the unimolecular dissociation was the initiation reaction in their system. It is, however, difficult to deduce the initiation step from the overall kinetics. In an attempt to clarify the system we have studied the pyrolysis at somewhat lower temperatures, where some simplicity in the number of products was achieved and the initial rates of formation of a few of the products were measurable before being obscured by rapid secondary reactions. These initial rate measurements helped to describe the mechanism in its initial stages and the results obtained were compatible with the occurrence of the bimolecular initiation reaction.

Pyrolysis of propylene in a shock tube (7) at temperatures of 1300 °K was shown to be initiated

FOR ERRATA SEE V. 48 NO. 7 1970 PAGE 1174

Can. J. Chem. Downloaded from www.nrcresearchpress.com by 210.87.254.42 on 09/05/12
For personal use only.

Can. J. Chem. Downloaded from www.nrcresearchpress.com by 210.87.254.42 on 09/05/12
For personal use only.

by the unimolecular fission of the C—C bond to give a methyl and a vinyl radical. Under these conditions of high temperature and low pressure, the unimolecular dissociation would indeed be expected to be faster than the bimolecular reaction.

Experimental

Propylene was pyrolyzed in a static system, the details of which have been described (5), over the temperature range 743–873 °K and the pressure range 200–600 Torr. Most of the experiments were done in the unpacked vessel with the S/V ratio of 1.0 cm^{-1}, but two series were done in the packed vessel with the S/V ratio of 8.5 cm^{-1}. The total amount of products and reactant from each experiment was analyzed on an F & M temperature-programmed gas chromatograph, using a 3 ft column of silica gel and alumina. This analysis resolved saturated and unsaturated hydrocarbons but not isomers of each group beyond C_4. The C_4 and C_6 peaks were collected separately and analyzed by isothermal operation on a 9 ft column of 30% tricresyl phosphate on chromosorb P (60–80 mesh). The column was maintained at 30 °C and the flow rate was 70 cc/min. Three other columns were used to check the number and separation of the main peaks. These were: (*a*) 12 ft of 20% Nujol on chromosorb P (60–80 mesh), (*b*) 6 ft of 30% Nujol on chromosorb P (60–80 mesh), (*c*) 12 ft of 18.5% squalane on chromosorb W (60–80 mesh). These columns showed the same number of major peaks with varying numbers of minor peaks, but the best separation was obtained with the column finally used. Products were identified by comparison of the mass spectrum and the retention time of the chromatographic peak with authentic samples.

The procedure for purification of propylene was identical to that described for ethylene (5). Analysis of a sample of propylene on the silica gel – alumina column showed a propane impurity of 0.007 mole%. A correction for this was applied to the yield of propane. No other impurities were observed by this analysis.

The pressure change of the reaction was followed with a Texas instrument fused quartz spiral gauge, Model 145. The reaction vessel was connected to the system with a Hoke diaphragm seal stainless steel valve. This eliminated a small drop in pressure in the initial stages of the reaction caused by absorption of propylene in the stopcock grease.

Results

In the very early stages of the reaction linear yield–time plots were observed for methane, ethylene, propane, and a C_6 fraction. After a short period of time the rates of methane, ethylene, and propane increased rapidly while the yields of the C_6 products approached a maximum value. Thus methane, ethylene, and propane could be classified as both primary and secondary products while the C_6 products were primary. As the rates of formation of the main products increased several other products appeared, the main ones being a C_4 fraction, composed of 1,3-butadiene, butene-1, and butene-2 in the approximate ratio 2:1:1, a C_5 fraction consisting mainly of 1,3-pentadiene, ethane, benzene, toluene, and hydrogen. The yield of butene-1 includes any isobutene produced, since these two isomers were not resolved. The C_4 fraction was a minor product at 743 °K and appeared to be secondary, but at 873 °K had become a major product with a well-defined initial rate. Methyl acetylene, *n*-hexane, and allene were shown to be absent. The latter compound may have been formed in trace amounts at 873 °K. Figures 1 and 2 show typical yields as a function of time for the main products. For simplicity the total C_4, C_5, and C_6 yields have been plotted, since the components show similar behavior. Yields of the C_6 compounds in the initial stages are shown in Figs. 3 and 4.

Since our analysis of the C_6 compounds differed in some respects from previous analyses, some details of the results are given. At the

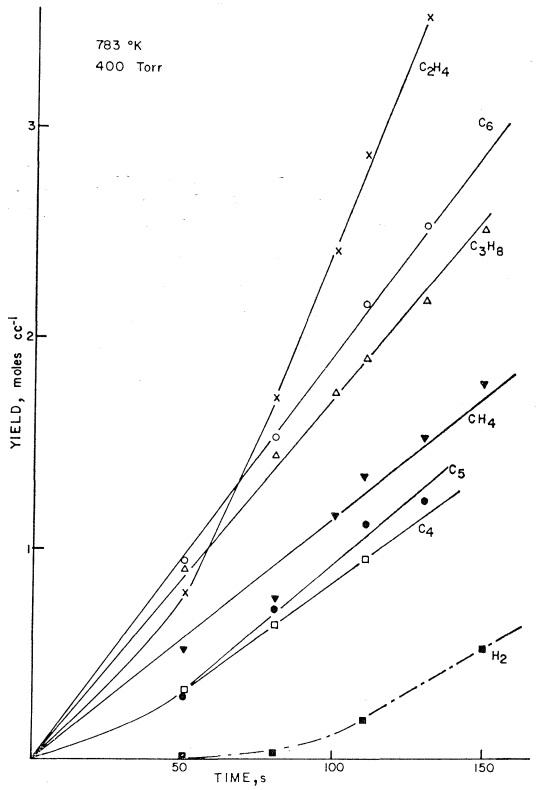

FIG. 1. Yield of products as a function of time; $T = 783$ °K; $P = 400$ Torr.

Can. J. Chem. Downloaded from www.nrcresearchpress.com by 210.87.254.42 on 09/05/12
For personal use only.

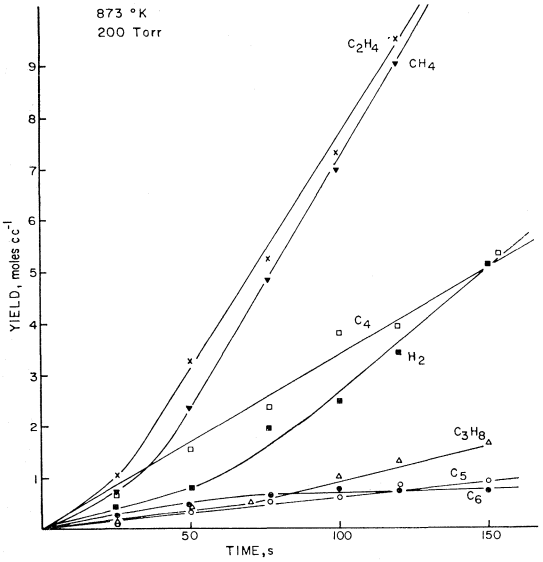

FIG. 2. Yield of products as a function of time; $T = 873$ °K; $P = 200$ Torr.

lowest temperature of the reaction, 743 °K, the two main peaks were 2-hexene (*cis* or *trans*) and 1-methylcyclopentene. The latter was well separated from any other peak and the mass spectrum was identical to that of the known sample. One possible alternative might be methylene cyclopentane, since the mass spectra of these two compounds differ at one peak only. The mass spectrum of the 2-hexene peak suggested that small amounts of 3-methylpentene-1, 2-ethylbutene-1, or 3-hexene might be present. A major peak appearing on the tail of the 2-hexene peak was identified as 3-methylcyclopentene. At low temperatures of reaction, where the 2-hexene peak was large, the amount of 3-methylcyclopentene was difficult to measure and may have been overestimated. Other peaks were very minor at the lowest temperature. As the reaction temperature was increased, the yield of 2-hexene decreased until at 873 °K, its yield was barely measurable. At the same time another peak became evident with retention time slightly shorter than 2-hexene, which had been present in small quantities at 743 °K and been masked by the large 2-hexene peak. This peak and the 3-methylcyclopentene peak were now clearly separated and the new peak was identified as cyclopentadiene. Two other peaks became more prominent at a reaction temperature of 873 °K. One was identified as 1,3-pentadiene, and the other was probably cyclopentene but was not positively identified. An additional small peak remained unidentified.

No evidence was found for the formation of hexadienes. 1,3-hexadiene was eluted at approximately the same time as 1-methylcyclopentene,

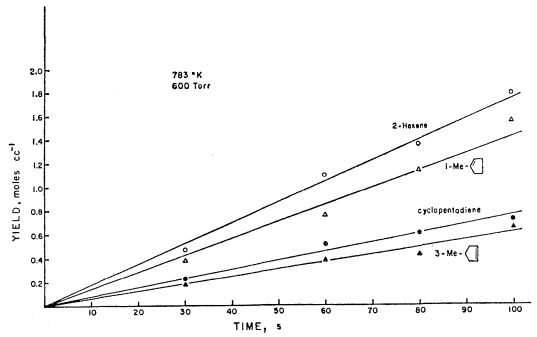

FIG. 3. Yield of products as a function of time; $T = 783$ °K; $P = 600$ Torr.

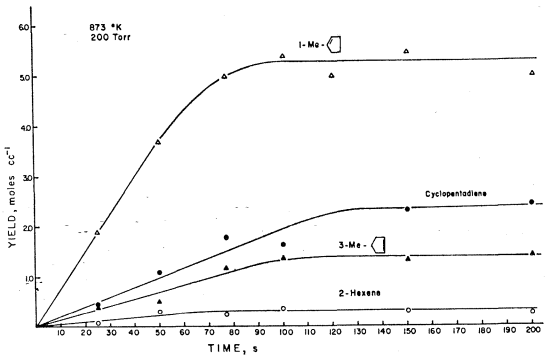

FIG. 4. Yield of products as a function of time; $T = 873$ °K; $P = 200$ Torr.

but the mass spectra are quite different and there was no indication of the presence of even small amounts of 1,3-hexadiene. 1,5-hexadiene was eluted between cyclopentadiene and 2-hexene, but again the mass spectra of both of these peaks gave no indication of the presence of the diene. 1,4-hexadiene was not checked on the column and it is possible it could have been one of the minor peaks, but our analysis indicated that hexadienes are not important products in the initial stages of the reaction below 873 °K.

The measurement of the initial rates depended on a sufficient period of time being available over which linear yield–time plots of the products

TABLE 1
Summary of the initial rates measured

T (°K)	$P^0_{C_3H_6}$ (Torr)	Initial rate (moles cc^{-1} s^{-1} × 10^{12})*							
		CH_4	C_3H_8	C_4H_8	C_4H_6	1-Me-	3-Me-	2-Hexene	
743	200	1.15	0.73	—	—	0.41	0.26	0.58	0.30
	400	2.95	4.14	—	—	2.26	1.01	2.44	1.01
	600	3.76	—	—	—	3.8	1.99	5.56	2.76
783	200	4.32	3.10	0.94	0.94	1.8	0.87	1.6	0.87
	400	11.3	17.3	3.76	3.76	7.75	3.69	8.16	3.2
		30.9P	37.1P	16.5P	16.5P	20.6P	12.9P	8.25P	5.15P
	600	18.8	—	6.0	5.87	15.2	6.50	17.5	8.01
803	200	20.7	11.3	4.7	5.5	8.46	4.0	2.11	3.38
823	200	—	13.2	29.3	25.9	16.9	2.8	2.8	3.76
			56.5P	40.2P	40.2P	16.7P	13.1P	4.12P	17.6P
	400	—	60.1	113.0	—	—	—	—	—
873	200	—	42.1	154	195	73.7	15.8	4.51	21.8

*P indicates experiment in packed reaction vessel.

were observed. This period of time decreased as the temperature was increased and as the pressure was increased. For example, the rapid increase in rates of methane and propane occurred after about 1000 s at 743 °K and after about 100 s at 823 °K. In each case only about 0.2% decomposition of propylene (calculated from the products measured) had occurred in this period. Furthermore, the rapid increase in rates occurred at different times for different products. The secondary production of ethylene was observed at very short times and the initial rate could not be measured with confidence at any temperature. The rate of formation of propane, on the other hand, was constant over a longer time interval. Consequently initial rates of formation of all the primary products were not measurable over the whole pressure range at each temperature. For minor products the distinction between primary and secondary was often difficult and there was considerable doubt about the initial rates when the yields were small. A summary of the initial rates measured is given in Table 1.

The orders of the rates with respect to propylene concentration were determined from the slopes of the plots of the log of the initial rates against the log of the pressure. Such plots for the products methane, propane, 2-hexene, butadiene 1-methylcyclopentene, 3-methylcyclopentene, and cyclopentadiene are shown in Figs. 5 and 6. The C_6 compounds were all second order in propylene. The order of the rate of propane formation was between 2 and 3 while that of methane formation was between 1 and 2. The rate of formation of the C_4 compounds appeared to be second order at low pressure but decreased toward first order at higher pressures. The rates of formation of 1-methylcyclopentene, 2-hexene, and butadiene as a function of temperature are shown in Fig. 7. The activation energies for the rates of formation of 1-methylcyclopentene, 3-methylcyclopentene, cyclopentadiene, and propane were all constant over the range of temperature studied. The activation energy for

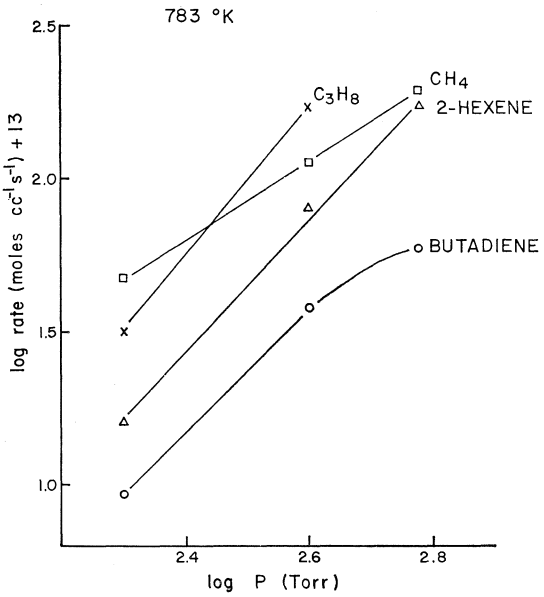

FIG. 5. Plot of log rate vs. log P.

Can. J. Chem. Downloaded from www.nrcresearchpress.com by 210.87.254.42 on 09/05/12
For personal use only.

Can. J. Chem. Downloaded from www.nrcresearchpress.com by 210.87.254.42 on 09/05/12
For personal use only.

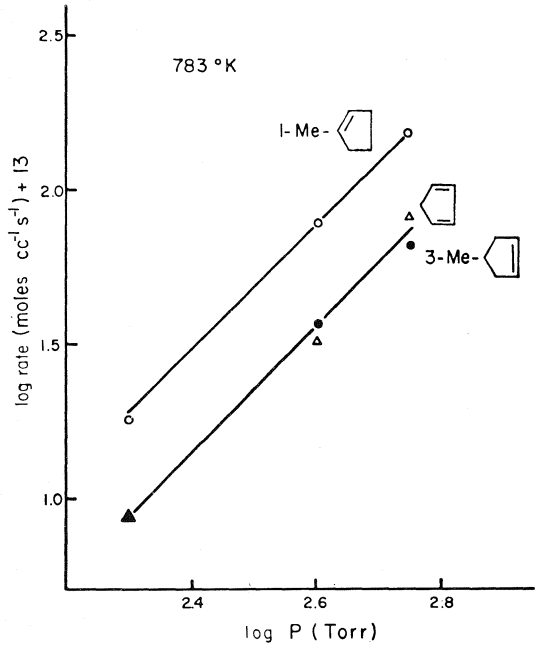

FIG. 6. Plot of log rate vs. log P.

2-hexene was much lower than for the other C_6 compounds and decreased at higher temperatures. The activation energy for butene and butadiene was higher than for the other products but also appeared to decrease at the higher temperature. In the case of the C_4 products this decrease may be linked to the changing order observed for their rates of formation at the lower temperature. A summary of the orders and activation energies measured is given in Table 2.

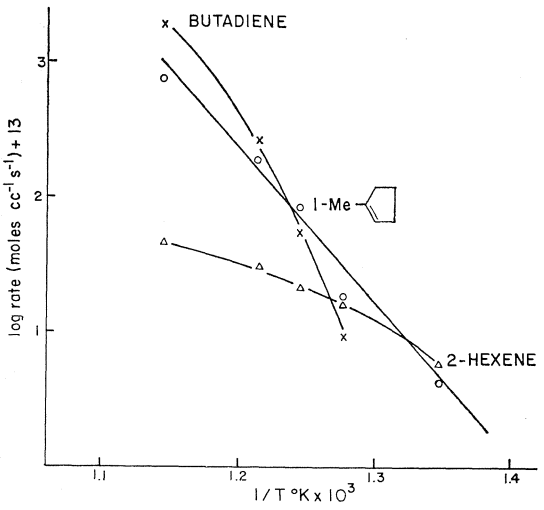

FIG. 7. Plot of log rate vs. $1/T$: ×, butadiene; ○, 1-Me- ; △, 2-hexene.

TABLE 2
Summary of reaction orders and activation energies

Product	Order at 743 °K	Order at 783 °K	Activation energy at 200 Torr (kcal/mole)
CH_4	1.2	1.3	—
C_3H_8	2.5	2.4	41
C_4H_8	—	—	80
C_4H_6	—	—	80
2-Hexene	2.0	2.1	—
1-Me-	2.0	2.0	51.9
3-Me-	2.0	2.0	42.5
	2.0	2.0	46.5

The change in pressure accompanying the reaction was measured over a range of pressure at each temperature. An initial decrease in pressure was observed at each temperature, but at 783 °K and higher, the pressure went through a minimum value and then increased. The maximum rate of pressure increase measured at 100 Torr and 873 °K is compared with results of previous workers in Table 3. It is clear that reproducible rate data for the pyrolysis of propylene can be obtained.

At the lower temperatures the measured change in pressure was greater than that calculated from the products analyzed. The difference was greatest at the lowest temperature while at 873 °K the measured and calculated curves were identical.

TABLE 3
Comparison of rate data

Maximum rate at 873 °K, 100 Torr (Torr $s^{-1} \times 10^2$)	Range of study: Temperature (°K)	Range of study: Pressure (Torr)	Reference
2.88	828–913	7–300	2
2.95	828–913	7–300	2
1.82	853–913	80–500	3
3.54	843–923	50–500	8
2.08	743–873	200–600	This work

Can. J. Chem. Downloaded from www.nrcresearchpress.com by 210.87.254.42 on 09/05/12
For personal use only.

At the lower temperatures, then, the measured products, which include those up to C_7, do not account for the total disappearance of propylene and there must be higher molecular weight products formed even in the initial stages of the reaction. Analysis for these higher molecular weight products is presently being attempted and the results show that the main components are C_8 and C_9 hydrocarbons. Quantitative measurements of these products together with an analysis of the change in pressure as a function of time will be described in Part II of this series.

Results from the experiments in the packed vessel are included in Table 1. The rate of formation of most of the products showed a significant increase in the packed vessel. The increase in the rates of formation of the light and heavy products largely balanced each other with the result that the change in pressure accompanying the reaction was not very different in the two vessels. This explains why measurements of the pressure change from different laboratories appear reasonably reproducible even though heterogeneous reactions may be important. At the same time the minor differences observed may be, to some extent, accounted for by variations in the extent of the contribution of heterogeneous reaction to the rate in the different studies.

Discussion

The products of the reaction have been separated into those which showed a constant, measurable initial rate and may be called primary, and those whose rates increased continuously from immeasurably small initial values. Of the primary products the more stable ones of low molecular weight showed a rapid increase in rate beyond the initial linear stage while the yields of the C_6 products approached maximum values. The decomposition thus appears to start off slowly, but as products more unstable than propylene build up, their rate of dissociation finally exceeds the rate of initiation by propylene itself and the overall rate increases. The more unstable products gradually reach a steady-state concentration as they are converted to the more stable saturated compounds. The induction period is therefore caused by the attainment of the steady-state concentration of these C_6 products. At the lower temperatures the higher molecular weight products, which were produced in appreciable quantities, may also contribute to the secondary initiation.

The initial rates of formation of the C_6 products were second order with respect to propylene. This suggests a second order initiation step and the most reasonable one is the bimolecular reaction of propylene to give an allyl and a propyl radical.

[1] $$2C_3H_6 \rightarrow C_3H_5 + C_3H_7$$

Addition, abstraction, and decomposition reactions of the radicals will then lead to the formation of the products. Indeed, Kallend, Purnell, and Shurlock (2) showed that the bimolecular reaction was faster than the unimolecular dissociation under their conditions of pyrolysis, but did not believe a bimolecular initiation process was compatible with the kinetics of the decomposition. The order of the decomposition which they measured, however, was not based on the initial rate but on the maximum rate where initiation must be largely from decomposition of the more unstable products.

The rate constant for the bimolecular reaction of propylene was calculated by Marshall, Purnell, and Shurlock (6) and was given by the following expression

$$\log k(\text{cc mole}^{-1}\ \text{s}^{-1}) = 14.4 - 51000/2.3RT$$

In this calculation the heat of formation of the allyl radical was taken to be 38.2 kcal/mole and the ratio of disproportionation to combination for the allyl and *n*-propyl radicals was assumed to be the same as that measured for allyl and ethyl radicals at 150 °C, viz. 0.12 (9). Using this expression, the rate of reaction [1] is compared with the initial rates of formation of propane, methane, and the C_6 products in Table 4. The initial rates of formation of the main products are less than the calculated rate of initiation, and even allowing a rather large uncertainty in this value, it is clear that the products measured in this initial region are not formed by a long chain process.

At low temperatures the main products were methane, ethylene, propane, and C_6 products and some higher molecular weight compounds not analyzed. This suggests a simple scheme of addition, abstraction, and decomposition following the bimolecular initiation.

TABLE 4
Comparison of the initial rate with the rate of product formation

T (°K)	$P^0_{C_3H_6}$ (Torr)	Rate (moles cc^{-1} s^{-1} × 10^{12}) $k_1[C_3H_6]^2$	$k_{1a}[C_3H_6]$	CH_4	C_3H_8	C_6 + pentadiene	$C_4H_8 + C_4H_6$
743	200	4.64	6.9×10^{-4}	1.15	0.73	1.55	—
823	200	101	0.28	—	13.2	26.3	55.2
873	200	541	7.0	—	42.1	116	349

Can. J. Chem. Downloaded from www.nrcresearchpress.com by 210.87.254.42 on 09/05/12
For personal use only.

[1] $2C_3H_6 \longrightarrow C_3H_5 + C_3H_7$
[2] $C_3H_7 + C_3H_6 \longrightarrow C_3H_8 + C_3H_5$
[3] $C_3H_7 + C_3H_6 \longrightarrow C_6H_{13}$
[4] $C_3H_7 \longrightarrow CH_3 + C_2H_4$
[5] $CH_3 + C_3H_6 \longrightarrow CH_4 + C_3H_5$
[6] $C_3H_5 + C_3H_6 \longrightarrow C_6H_{11}$
[7] $C_6H_{11} + C_3H_6 \longrightarrow C_6H_{10} + C_3H_7$
[8] $C_6H_{11} + C_3H_6 \longrightarrow C_6H_{12} + C_3H_5$
[9] $C_6H_{11} + C_3H_6 \longrightarrow C_9H_{17}$
[10] $C_6H_{11} \longrightarrow C_6H_{10} + H$
[11] $C_6H_{11} \longrightarrow CH_3$–
[12] CH_3– $\longrightarrow CH_3$– $+ H$
[13] CH_3– $\longrightarrow$ $+ CH_3 + H_2$
[14] CH_3– $+ C_3H_6 \longrightarrow CH_3$– $+ C_3H_7$
[15] CH_3– $+ C_3H_6 \longrightarrow C_9H_{17}$

This set of reactions is not intended to be complete but to give a general picture of the main types of reactions occurring in the initial stages. Termination reactions have not been included because our results do not provide positive evidence on this point. Some indirect evidence is discussed later. Transfer reactions such as [7] were suggested in the analogous polymerization of ethylene to account for the low activation energy observed for the rate of formation of products. They may also be important in the propylene system although there is no direct evidence for their occurrence.

Propane and Methane

Because of the competition between reactions [2] and [4] the order of the rate of formation of propane should be greater by one than that of the rate of formation of methane. This was observed within the limits of error (Table 2) and, in addition, the fractional orders show that k_4 and $(k_2 + k_3)$ $[C_3H_6]$ are of comparable magnitude. At lower temperatures the sum of the rate of formation of propane and methane was smaller than the calculated rate of formation of propyl radicals, but because of the large drop in pressure, it is reasonable to expect some of the propyl radicals may be lost by addition to propylene to form higher molecular weight products.

Because the chain length must be very short the activation energy for formation of the products would be expected to be close to E_1. The activation energy for formation of propane should be somewhat less because of the competition of reaction [4] and the observed value of 41 kcal/mole is reasonable. On the other hand, because of reaction [4], the activation energy for formation of methane should be greater than that of propane. The activation energy for the initial rate of formation of methane was about equal to that of propane over the range 743–783 °K. At higher temperatures a reliable initial rate could not be determined. Nevertheless, the yield of methane always exceeded that of any other product except ethylene and therefore its initial rate was probably at least equal to that of the C_4 products. Hence the activation energy for its formation probably increased at the higher temperatures to a value close to that observed for butene and butadiene.

The C_6 Products

The rates of formation of the C_6 compounds and cyclopentadiene were second order with respect to propylene at the two lowest temperatures. Within the framework of the reactions outlined there are two main mechanisms which allow for a second order dependence of the rates on propylene: (*a*) The C_6 products are formed

Can. J. Chem. Downloaded from www.nrcresearchpress.com by 210.87.254.42 on 09/05/12
For personal use only.

mainly by the transfer reaction [14] and the C_6H_{11} radical largely disappears by the cyclization reaction [11]. (*b*) The products are formed by the decomposition reactions [12] and [13] and, as above, the C_6H_{11} radical reacts mainly by reaction [11].

Of these two mechanisms (*a*) does not account for cyclopentadiene, which must involve a decomposition of the C_6H_{11} radical. Because of the similarity in the kinetics of the formation of cyclopentadiene and the methylcyclopentenes, mechanism (*b*) is preferred. The activation energy for formation of 1-methylcyclopentene was very close to E_1 while the activation energies for formation of 3-methylcyclopentene and cyclopentadiene were somewhat lower, indicating the contribution of some competing decomposition processes.

The reactions leading to the formation of hexene are more complex. The most obvious means to account for the low activation energy for hexene formation is by competitive decomposition reactions of a radical precursor to hexene. This radical could not, therefore, be C_6H_{11} but may be C_6H_{13} or a higher molecular weight radical formed by addition reactions. Such decomposition reactions may be written as follows

(*a*) (d′) $C_6H_{13} \rightarrow C_6H_{12} + H$

(d″) $C_6H_{13} \rightarrow$ products

(*b*) (d′) $C_9H_{19} \rightarrow C_6H_{12} + C_3H_7$

(d″) $C_9H_{19} \rightarrow$ products

The expressions for the rate of formation of hexene are

(*a*) Rate (hexene)

$$= \frac{k_{d'}k_3[C_3H_6]}{k_{d'} + k_{d''} + k_b[C_3H_6]}[C_3H_7]$$

(*b*) Rate (hexene)

$$= \frac{k_{d'}k_a[C_3H_6]}{k_{d'} + k_{d''} + k_b[C_3H_6]}[C_3H_7]$$

where k_a represents the process of addition of C_6H_{13} to propylene and k_b represents the bimolecular modes of disappearance of the appropriate radicals. When d′ is the important mode of dissociation of the radical, the activation energy for formation of hexene will be similar to that for the other C_6 products. As process d″ competes effectively at higher temperatures less hexene is formed. The activation energy for formation of hexene is reduced by the occurrence of $k_{d''}$ in the denominator. Thus $E_{d''}$ must be greater than $E_{d'}$, a condition which seems unlikely for case (*a*). A similar expression may be obtained by considering the decomposition of a radical formed by the addition of C_3H_5 radicals. A radical of molecular weight corresponding to C_9 or higher thus seems to be the most probable precursor for hexene.

The Butenes and Butadiene

The distribution of the butenes and butadiene was remarkably constant over the whole range of pressure and temperature, in agreement with the results of Kallend, Purnell, and Shurlock (2). The rate of the C_4 products was strongly temperature dependent and although the activation energy quoted is only approximate, it must be well in excess of that of the C_6 products. Thus a rate constant with an activation energy associated with it of about 30 kcal/mole must appear in the numerator of the rate expression. If such a rate constant is one relating to the decomposition of a radical then, within the present scheme, this decomposition process must be very minor compared to the other loss processes of the radical, otherwise the rate constant will appear in both numerator and denominator. This condition could be met at the lower temperatures where the C_4 products are indeed minor, but at the higher temperatures, the yields of these products exceed those of the C_6 products.

An additional source of methyl radicals would contribute to the formation of butene and methane but not the C_6 products. Such a source would be the initiation process suggested by Kallend, Purnell, and Shurlock (2).

[1*a*] $C_3H_6 \rightarrow CH_3 + C_2H_3$

[5] $CH_3 + C_3H_6 \rightarrow CH_4 + C_3H_5$

[17] $CH_3 + C_3H_6 \rightarrow C_4H_9$

[18] $C_4H_9 \rightarrow$ butene-1

[19] $C_4H_9 \rightarrow$ butene-2

[20] $C_4H_9 \rightarrow$ butadiene

[21] $C_2H_3 + C_3H_6 \rightarrow C_2H_4 + C_3H_5$

The activation energy for the rate of formation of butene would be somewhat less than E_{1a}, which is about 94 kcal/mole. This additional initiation step would also account for the fact that the yields of methane and ethylene always exceeded

that of the butenes. The rate of reaction [1*a*] (calculated using the data of Marshall, Purnell, and Shurlock) is, however, too small by at least a factor of 20 to account for the yields of butene and butadiene observed. Values of this calculated rate are included in Table 4. Furthermore, the dissociation of the *n*-butyl radical probably does not yield the ratios of butene-1, butene-2, and butadiene observed.

Kallend, Purnell, and Shurlock (2) suggested that the main source of butene-1 was the combination of methyl and allyl radicals.

[22] $$CH_3 + C_3H_5 \rightarrow C_4H_8^*$$
$$C_4H_8^* \rightarrow \text{butene-1}$$
$$C_4H_8^* \rightarrow \text{butene-2}$$
$$C_4H_8^* \rightarrow \text{butadiene}$$

An approximate steady-state solution of these equations and those involving methyl and allyl radicals leads to an expression for the rate of formation of butene which contains $(k_1)^2$ in the numerator. This predicts an activation energy of the order of 100 kcal/mole. In obtaining the activation energy for the rate of formation of butene as with butadiene, the best straight line was drawn through the four points, giving a value of 80 kcal/mole. These points might be interpreted as showing curvature, with a high activation energy of 106 kcal/mole over the range 783–823 °K, falling to about 56 kcal/mole between 823 and 873 °K. Thus over the range where the high activation energy was observed the combination of methyl and allyl radicals would be a reasonable source of the butenes. It may also be argued that the combination reaction with its large quantity of energy would reasonably be expected to lead to the formation of the butene isomers and of butadiene. The present results are probably not sufficiently precise to decide unambiguously on the source of the C_4 products, but it seems very unlikely that they arise from alternative modes of decomposition of the C_6 radical.

The Surface Reaction

A significant increase in rates of the main products was observed from the experiments in the packed vessel. An exception to this was hexene, whose rate was not altered appreciably. Some of the reactions leading to the formation of the products probably occur to a significant extent on the surface even in the unpacked vessel. At this stage it is not possible to measure the rate constants for the various elementary reactions and hence we cannot decide which reactions may be heterogeneous. By comparison with similar systems involving hydrocarbons, the reactions most likely to occur on the surface are the propagation reactions of radicals, where reaction occurs between an adsorbed radical and a molecule in the gas phase. In hydrocarbon systems radicals probably show more reactivity towards the surface than do the hydrocarbon molecules. Because the initiation step appears to be bimolecular we think it likely, but not shown conclusively, that this step is homogeneous and further studies designed to measure the rate constant for this reaction may provide the evidence on this point.

In summary, it is suggested that the initial step in the pyrolysis of propylene is the bimolecular reaction of propylene to give an allyl and a propyl radical. Subsequent reactions of abstraction, addition, and decomposition of the radicals give the products observed in the initial stages. An appreciable fraction of the radicals produced form high molecular weight products by addition to propylene. As products of molecular weight higher than propylene build up in the system, their rate of dissociation soon exceeds that of propylene and rates of formation of the lower molecular weight products increases rapidly. At the highest temperature studied, 873 °K, the secondary dissociation is so rapid that the build up of high molecular weight products cannot be detected.

The authors thank the National Research Council of Canada for generous financial support. They also thank Dr. J. L. Holmes for the mass spectrometric analyses.

1. E. W. R. Steacie. Atomic and free radical reactions. 2nd ed. Vol. I. Reinhold Publishing Corp., New York. 1954. p. 183.
2. A. S. Kallend, J. H. Purnell, and B. C. Shurlock. Proc. Roy. Soc. Ser. A, **300**, 120 (1967).
3. K. J. Laidler and B. W. Wojciechowski. Proc. Roy. Soc. Ser. A, **259**, 257 (1960).
4. A. Amano and M. Uchiyama. J. Phys. Chem. **68**, 1133 (1964).
5. M. L. Boyd, T. M. Wu, and M. H. Back. Can. J. Chem. **46**, 2415 (1968).
6. R. M. Marshall, J. H. Purnell, and B. C. Shurlock. Can. J. Chem. **44**, 2778 (1966).
7. G. A. Chappell and H. Shaw. J. Phys. Chem. **72**, 4672 (1968).
8. K. U. Ingold and F. J. Stubbs. J. Chem. Soc. 1794 (1951).
9. D. G. L. James and G. E. Troughton. Trans. Faraday Soc. **62**, 145 (1966).

Can. J. Chem. Downloaded from www.nrcresearchpress.com by 210.87.254.42 on 09/05/12
For personal use only.

Can. J. Chem. Downloaded from www.nrcresearchpress.com by 210.87.254.5 on 09/05/12
For personal use only.

Novel cycloaddition reactions with alkyl substituted nitrogen heterocycles

J. W. LOWN, R. WESTWOOD,[1] AND A. S. K. AIDOO
Department of Chemistry, University of Alberta, Edmonton, Alberta
Received August 20, 1969

2-Methylquinoxaline reacted with two molar equivalents of tetrachloro-1,2-benzoquinone to give two products (*a*) a colored polycyclic heterocycle structurally related to quinoxaline orange and (*b*) 2-(2-quinoxalino)-4,5,6,7-tetrachlorobenzo-1,3-dioxole. 2,6-Dimethylquinoline, 2-methylquinoline, and 1-methylisoquinoline react with the quinone to give products of type (*a*) whilst, 2,3-dimethylquinoxaline, 2,3-dibenzylquinoxaline, and 2-benzylpyridine react with the quinone to give products of type (*b*). Thermal decomposition of 2-quinoxalinylmethyltrimethylammonium hydroxides results in cycloaddition to form the new 5,8,13,16-tetraazadibenz[*a,h*]anthracene system. Similar thermal decomposition of 2-quinolinylmethyltrimethylammonium hydroxide produced the new 8,16-diazadibenz[*a,h*]anthracene ring system.

Canadian Journal of Chemistry, **48**, 327 (1970)

The reaction of 2,3-disubstituted quinoxalines with benzoquinone, originally thought to consist of a Diels–Alder addition (1, 2) to form polycyclic heterocycles, has recently been shown to lead only to charge transfer complexes (3, 4). An interest in the reactions of high potential quinones led us to consider the use of a more reactive quinone, namely tetrachloro-1,2-benzoquinone as a reagent in such reactions, which represent potential routes to new heterocycles.

We report the reaction of tetrachloro-1,2-benzoquinone with alkylquinoxalines, alkylquinolines, and alkylpyridines, which gave rise to products of two types, polycyclic heterocycles related structurally to quinoxaline orange, and substituted benzodioxole derivatives. The thermal decomposition of quinoxaline and quinoline quaternary ammonium salts, which was mechanistically related to the formation of the latter products, resulted in novel cycloaddition reactions with the formation of new tetraaza- and diazadibenzanthracenes.

2-Methylquinoxaline reacted with two molar equivalents of tetrachloro-1,2-benzoquinone in refluxing benzene and when followed by chromatographic separation, two products were isolated (*a*) a yellow crystalline solid m.p. 282° $C_{21}H_5N_2O_3Cl_7$ isolated in 23% yield which was assigned structure **1** and (*b*) a white solid $C_{15}H_6N_2Cl_4O_2$ m.p. 225–226° in 8% yield to which structure **2** has been assigned. Compound **1** showed bands in the infrared (i.r.) spectrum characteristic of a cyclic ether derived from tetrachloro-1,2-benzoquinone at 1430 cm^{-1} (5, 6) and of conjugated carbonyl at 1685 cm^{-1}. The mass spectrum revealed the presence of seven chlorine atoms in the molecular ion. Successive loss of one chlorine (giving a peak with a characteristic pattern for six chlorine atoms (7)) then carbon monoxide and then a tetrachloro-1,2-benzoquinone unit were observed. The nuclear magnetic resonance (n.m.r.) spectra of compounds similar to **1** described below confirmed that the methyl substituent had taken part in the reaction in accordance with the proposed structure. Significantly, compound **1** and similar structures derived from the quinoline and isoquinoline series are strongly colored, either deep yellow or orange, and bear a structural similarity to quinoxaline orange, recently assigned the new structure **3** by Cheeseman and Tuck (8). The

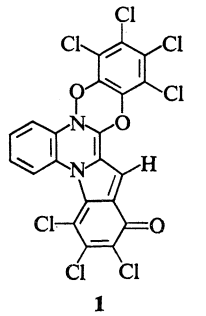

1

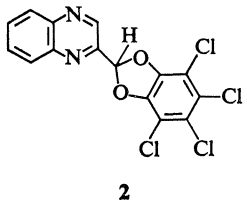

2

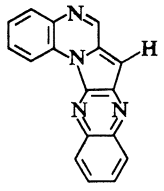

3

formation of compound **1** in this reaction is rationalized as shown in Scheme 1. In support of the suggested steps *a* and *b* in Scheme 1, it may be noted that (*i*) the chlorine atom adjacent to the

[1]NRCC Postdoctoral Fellow 1967–1969.

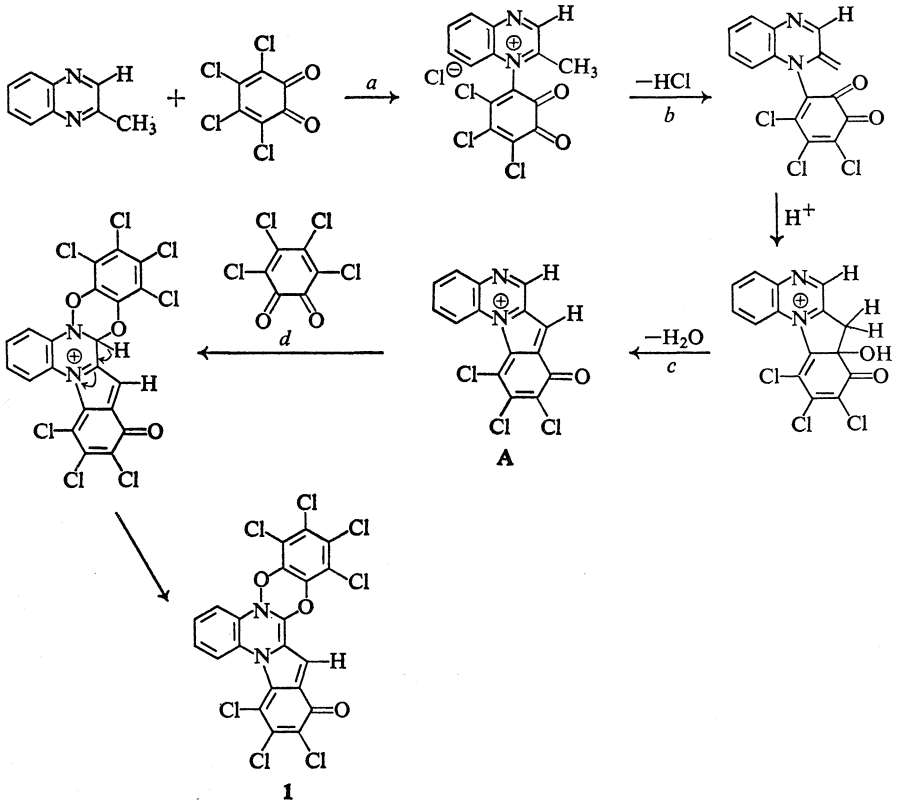

SCHEME 1

carbonyl group in tetrachloroquinones is notoriously susceptible to nucleophilic displacement (9) and (*ii*) the protons of 2-methyl substituents in quaternized quinoxalines have been shown to be very labile and to take part in tautomeric shifts (10) (see also Scheme 3). In step *a* the analogous nucleophilic attack by the 4-quinoxaline nitrogen, while sterically more favorable, would stop at the quaternary salt stage and not lead to the isolation of a product of the composition $C_{21}H_5N_2O_3Cl_7$.

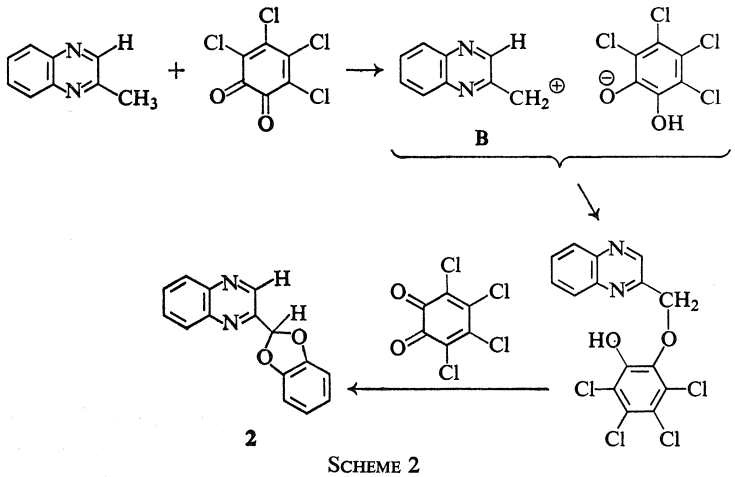

SCHEME 2

Can. J. Chem. Downloaded from www.nrcresearchpress.com by 210.87.254.5 on 09/05/12
For personal use only.

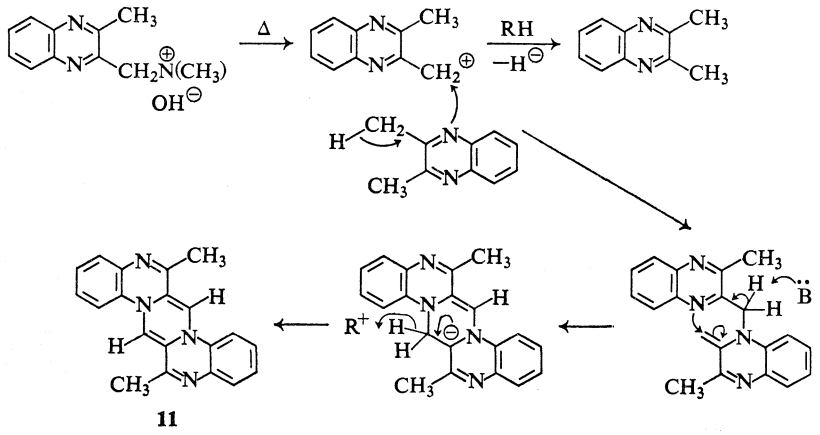

11

SCHEME 3

Compound **2** and similar compounds in this series showed in the i.r. spectrum a strong band at 1450 cm^{-1} typical of a cyclic ether derived from tetrachloro-1,2-benzoquinone (5, 6) and no carbonyl absorption. The n.m.r. spectrum showed a singlet for the acetal proton at 7.32 δ comparing favorably with a value of (7.22–7.52 δ) predicted for a proton in this type of environment by Shoolery's chemical shift rules (11). The formation of **2** is rationalized as shown in Scheme 2. This type of structure was also produced in the reaction of a series of model dimethylnaphthalenes with tetrachloro-1,2-benzoquinone to give for example **4** (eq. [1]). Brady's reagent under strongly acid conditions gave a positive test with the precipitation of the orange methylnapthaldehyde-2,4-dinitrophenylhydrazone (eq. [2]). A similar tetrachlorobenzodioxole derivative **5** has been obtained from a tetralone derivative recently (12). In addition, several methyl substituted

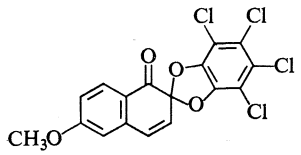

5

unsaturated hydrocarbons have been oxidized directly to unsaturated aldehydes **6** with 2,3-dichloro-5,6-dicyanobenzoquinone (DDQ) (13) (eq. [3]). The proposed mechanism via a stabilized

[3] $Ph-CH=CH-CH_3 \xrightarrow{DDQ} Ph-CH=CH-CHO$

6

carbonium ion, thence to an acetal is analogous to our reaction outlined in Scheme 2.

[1]

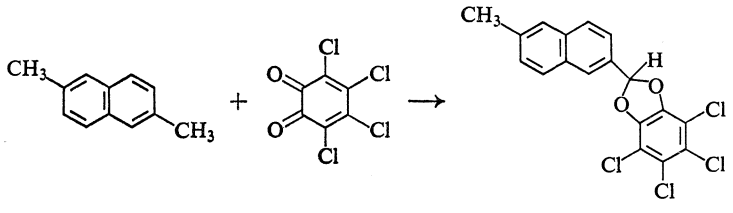

4

[2]

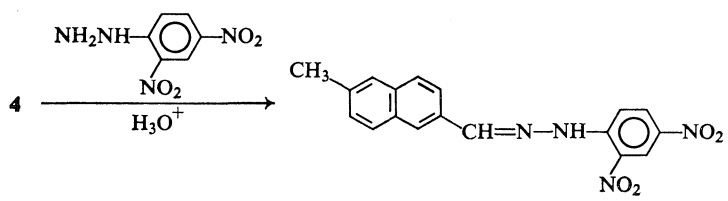

Can. J. Chem. Downloaded from www.nrcresearchpress.com by 210.87.254.5 on 09/05/12
For personal use only.

Can. J. Chem. Downloaded from www.nrcresearchpress.com by 210.87.254.5 on 09/05/12
For personal use only.

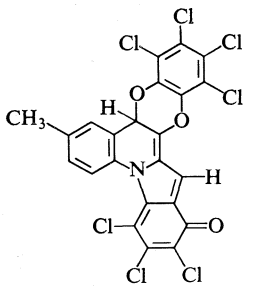

7

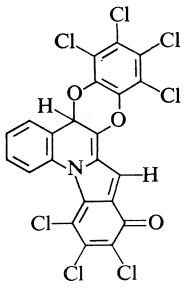

8

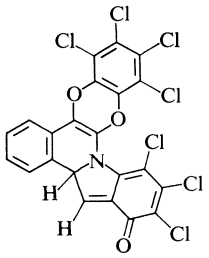

9

2,6-Dimethylquinoline, 2-methylquinoline, and 1-methylisoquinoline all reacted with tetrachloro-1,2-benzoquinone to give adducts **7**, **8**, and **9** i.e. similar in type to that proposed for compound **1**. All were highly colored crystalline solids. These compounds resisted attempts at chemical degradation but in step *d*, Scheme 1 the second molecule of quinone adds in a Diels–Alder reaction to stabilise the intermediate ion **A** by proton loss. If this addition of the quinone were prevented by steric hindrance, products of the type **1**, **7**, **8**, and **9** could not be formed. Accordingly 2,3-dimethylquinoxaline and 2,3-dibenzylquinoxaline reacted with tetrachloro-1, 2-benzoquinone but only products similar to structure **2** were isolated.

In the reaction of 2-benzylpyridine with tetrachloro-1,2-benzoquinone, resistance to loss of aromaticity in the pyridine ring dictates isolation of only **10**.

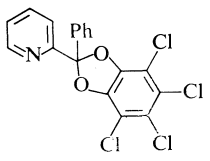

10

The properties of the intermediate quinoxalinyl cation (**B** in Scheme 2) now attracted our attention. The combination of a highly electrophilic cationic center with a nucleophilic ring nitrogen makes this type of species ideally suited to cycloaddition or dimerization reactions, provided it could be generated in the absence of the strongly nucleophilic quinol anion. Accordingly we examined the thermal decomposition of the trimethylammonium hydroxide salt derived from 2-bromomethyl-3-methylquinoxaline in refluxing toluene. Chromatographic separation of the reaction mixture afforded some 2,3-dimethylquinoxaline and a product $C_{20}H_{16}N_4$ which was assigned structure **11**. The formation of these two products is rationalized in Scheme 3. The very simple n.m.r. spectrum of **11** (see Fig. 1) consisting of an aryl methyl singlet, vinyl singlet, and aromatic ABCD pattern is in accordance with the symmetry of the structure. Owing to the high reactivity of the species concerned, as expected the reaction is quite complex and polymerization also occurs. Compound **11** represents the first reported example, as far as we are aware, of the 5,8,13,16-tetraazadibenz[*a*,*h*]anthracene ring system, the parent compound of which was obtained by a similar thermal decomposition of 2-quinoxalinylmethyl trimethylammonium hydroxide. Compound **12** also has a characteristically simple n.m.r. spectrum owing to its symmetry. Thermal decomposition of 2-quinolinylmethyl trimethylammonium hydroxide afforded 8,16-diazadibenz[*a*,*h*]anthracene (**13**), together with an unidentified trimer $C_{30}H_{21}N_3$.

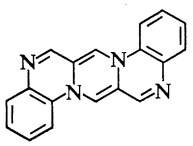

12

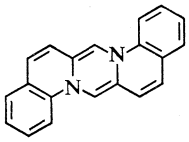

13

In view of the accessibility of the starting quaternary ammonium salts, their thermal decomposition promises to provide a convenient and direct route to polynuclear heterocycles which are otherwise difficult to prepare. The yields in these one step reactions are competitive with the overall yields of multistage syntheses which are normally employed to prepare structures of this complexity.

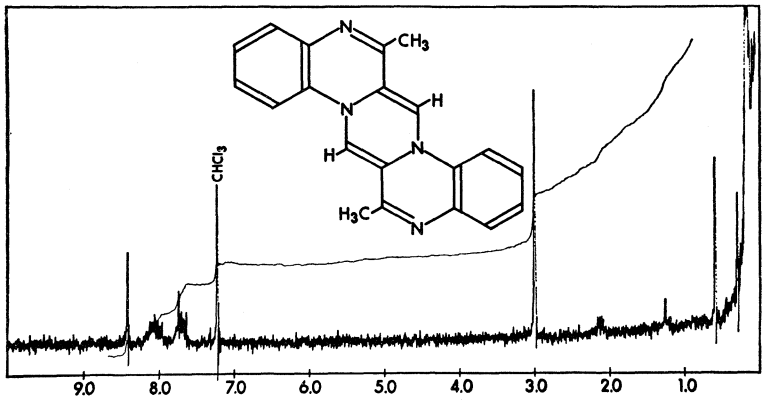

FIG. 1. The n.m.r. spectrum in $CDCl_3$ of 6,14-dimethyl-5,8,13,16-tetraazadibenz[*a*,*h*]anthracene.

Experimental

Melting points were determined on a Fisher–Johns apparatus and are uncorrected. Infrared spectra were recorded on a Perkin–Elmer model 421 spectrophotometer, and only the principal, sharply defined peaks are reported. Nuclear magnetic resonance spectra were recorded on Varian A-60 and A-100 analytical spectrometers. The spectra were measured on approximately 10–15% (w/v) solutions in $CDCl_3$, with tetramethylsilane as a standard. Line positions are reported in parts per million from the reference. Absorption spectra were recorded in 'spectro'-grade solvents on a Beckman DB recording spectrophotometer. Mass spectra were determined on an Associated Electrical Industries MS-9 double focusing high resolution mass spectrometer. The ionization energy, in general, was 70 eV. Peak measurements were made by comparison with perfluorotributylamine at a resolving power of 15 000. Kieselgel DF-5 (Camag, Switzerland) and Eastman Kodak precoated sheets were used for thin-layer chromatography (t.l.c.). Microanalyses were carried out by Dr. C. Daessle, Organic Microanalysis Ltd., Montreal, Quebec and by Mrs. D. Mahlow of this department.

2-Methylquinoxaline

2-Methylquinoxaline was prepared by the condensation of *iso*-nitrosoacetone (14) with *o*-phenylenediamine according to the method of Bennet and Willis (15) and had b.p. 60–63°/0.5 mm (lit. b.p. 118°/16 mm (15)).

Reaction between 2-Methylquinoxaline and Tetrachloro-1,2-benzoquinone

A solution of 2.88 g (0.02 mole) of 2-methylquinoxaline and 9.84 g (0.04 mole) of tetrachloro-1,2-benzoquinone in 200 ml of sodium dried benzene was heated under reflux for 24 h. The resulting dark brown solution was concentrated to ca. 20 ml and passed down a column of B.D.H. alumina, using benzene as eluant. Evaporation of the first eluant gave 0.064 g (8% yield) of 2-(2-quinoxalino)-4,5,6,7-tetrachlorobenzo-1,3-dioxole m.p. 213–214° (from benzene).

Anal. Calcd. for $C_{15}H_6Cl_4N_2O_2$: C, 46.45; H, 1.55; N, 7.29. Found: C, 46.50; H, 1.60; N, 7.30.

Mol. wt. calcd.: 385.9185. Found (mass spectrum): 385.9186, 33%; M—CHO 357, 100%; M—$C_8H_5N_2$, 257, 15%; M—$C_7HCl_4O_2$, 129, 33%. The n.m.r. spectrum $\delta_{TMS}(CDCl_3)$: 7.32 (1H, singlet, acetal hydrogen); 7.75–8.25 (4H, ABCD, aromatic protons); 9.1 (1H, singlet, aromatic proton adjacent to nitrogen).

Further elution with benzene gave 0.261 g (22.4% yield) of a yellow solid m.p. 265°, which upon repeated recrystallization from benzene gave bright yellow needles of **1**, m.p. 282–292 (decomposition to a bright red melt).

Anal. Calcd. for $C_{21}H_5Cl_7N_2O_3$: C, 43.35; H, 0.85; N, 4.80. Found: C, 43.16; H, 0.40; N, 5.60.

Mol. wt. calcd.: 577.8121. Found (mass spectrum): 577.8123, 10%; M—Cl, 543, 100%; M—$C_7Cl_5O_3$, 270.9821, 66% calcd. for $C_{14}H_5{}^{35}Cl_2N_2$, 270.9831. The i.r. spectrum ν_{max} ($CHCl_3$): 1685 (conjugated C=O); 1430 cm^{-1} (C—O—C stretch (5, 6)).

Reaction between Dimethylnaphthalenes and Tetrachloro-1,2-benzoquinone. General Procedure.

A solution of 4.0 g (0.025 mole) of a dimethylnaphthalene in 20 ml of dry chlorobenzene was added to a solution of 10 g (0.041 mole) of tetrachloro-1,2-benzoquinone in 130 ml. of dry chlorobenzene. The mixture was heated under reflux in an atmosphere of nitrogen for 48 h, allowed to cool, and the solvents removed *in vacuo*. The residue was subjected to chromatography on B.D.H. alumina using 1:1 benzene/hexane mixtures as eluant. The principal fraction consisted of a white microcrystalline solid after washing with hot hexane to remove some unreacted dimethylnaphthalene, and was purified by sublimation at ca. 200°/0.3 mm giving the pure 2-(methylnaphthyl)-4,5,6,7-tretrachlorobenzo-1,3-dioxole.

The analytical and spectral data on these new compounds are listed in Tables 1 and 2.

Treatment of these dioxole derivatives with 2,4-dinitrophenyl hydrazine in sulfuric acid in methanol/dioxane solutions gave immediate orange precipitates of the corresponding methylnaphthaldehyde 2,4-dinitrophenylhydrazones.

Can. J. Chem. Downloaded from www.nrcresearchpress.com by 210.87.254.5 on 09/05/12
For personal use only.

TABLE 1

2-(R_1-Methyl-R_2-naphthyl)-4,5,6,7-tetrachlorobenzo-1,3-dioxoles

No.	R_1	R_2	Melting point (°C)	Yield (%)	Observed C	Observed H	Observed Cl	Molecular* ion	Calculated C	Calculated H	Calculated Cl	Molecular ion
1	4	1	183–185	12	54.03	2.40	35.90	397.9438	54.00	2.52	35.46	397.9437
2	5	1	210	29	53.92	2.25	35.53	397.9434	54.00	2.52	35.46	397.9437
3	6	2	179–181	33	54.00	2.48	35.50	397.9438	54.00	2.52	35.46	397.9437
4	3	2	172–174	29	53.85	2.76	33.59	397.9434	54.00	2.52	35.46	397.9437

*Corresponds to $C_{18}H_{10}{}^{35}Cl_4O_2$.

TABLE 2

Spectroscopic properties of 2-(R_1-methyl-R_2-naphthyl)-4,5,6,7-tetrachlorobenzo-1,3-dioxoles

No.	R_1	R_2	Infrared spectrum ($CHCl_3$) (—O—C—O—)		Nuclear magnetic resonance spectrum* Aryl methyl	Aromatic protons
1	4	1	1450	1420	2.70 (s, 3H)	7.25–8.30 (m, 7H)
2	5	1	1445	1415	2.72 (s, 3H)	7.25–8.25 (m, 7H)
3	6	2	1450	1415	2.55 (s, 3H)	7.25–8.20 (m, 7H)
4	3	2	1450	1440	2.60 (s, 3H)	7.20–8.20 (m, 7H)

*S = Singlet; m = multiplet.

Reaction between 2,3-Dimethylquinoxaline and Tetrachloro-1,2-benzoquinone

A solution of 3.95 g (0.025 mole) of 2,3-dimethylquinoxaline and 12.3 g (0.05 mole) of tetrachloro-1,2-benzoquinone in 250 ml of sodium dried benzene was heated to reflux under nitrogen for 20 h. The dark reaction mixture was then cooled and filtered to remove a small amount of dark material. The filtrate was concentrated *in vacuo* to ca. 20 ml and passed down a column of B.D.H. alumina, using 1:1 benzene/skelly B as eluant. The second 700 ml collected was evaporated to give 0.225 g (22% yield) of crude material which was dissolved in benzene and rechromatographed on Woelm neutral alumina using benzene as the eluant. From this column was obtained 0.079 g of 2-(3-methyl-2-quinoxalino)-4,5,6,7-tetrachlorobenzo-1,3-dioxole as white needles m.p. 225–226° (from benzene).

Anal. Calcd. for $C_{16}H_8Cl_4N_2O_2$: C, 47.8; H, 2.00; N, 6.95. Found: C, 48.00; H, 1.88; N, 6.95.

Mol. wt. calcd.: 399.9342. Found (mass spectrum): 399.9341, 28%; M—CHO, 371, 100%, M—$C_9H_7N_2$, 257, 11%; M—$C_7HCl_4O_2$, 143, 4.5%.

The i.r. spectrum ν_{max} (Nujol mull): 1450 cm^{-1} (characteristic of tetrachlorobenzodioxole —O—C—O stretch (5, 6). The n.m.r. spectrum $\delta_{TMS}(CDCl_3)$: 2.78 (3H, singlet, CH_3); 7.40 (1H, singlet, acetal proton); 7.76–8.10 (4H, A_2B_2, aromatic protons).

Reaction Between 2-Methylquinoline and Tetrachloro-1,2-benzoquinone

A solution of 1.43 g (0.001 mole) of 2-methylquinoline and 4.92 g (0.002 mole) of tetrachloro-1,2-benzoquinone in 200 ml of sodium-dried benzene was heated to reflux under nitrogen for 24 h. The resulting dark brown solution was evaporated to ca. 50 ml and placed on a column of B.D.H. alumina made up in benzene. Elution with benzene gave a dark brown oil which on rechromatography on alumina gave 0.791 g (14% yield) of an orange solid **6**. Crystallization of this solid from benzene gave bright orange leaves m.p. 209–212° (decomposition).

Anal. Calcd. for $C_{22}H_6Cl_7NO_3$: C, 45.50; H, 1.08; N, 2.40; Cl, 42.80. Found: C, 45.50; H, 1.30; N, 2.55; Cl, 42.7.

Mol. wt. calcd.: 576.8171. Found (mass spectrum): 576.8190 (8%); M—$C_7Cl_5O_3$, 269.9874 (48%); calcd. for $C_{15}H_6{}^{35}Cl_2N$, 269.9878; M—Cl, 542, (100%). The i.r. spectrum: ν_{max} (Nujol mull) 1680 cm^{-1} (C=O str). The n.m.r. spectrum: $\delta_{TMS}(CDCl_3)$ 7.8–8.40 (multiplet, aromatic protons).

Reaction between 2,6-Dimethylquinoline and Tetrachloro-1,2-benzoquinone

A solution of 3.14 g (0.002 mole) of 2,6-dimethylquinoline and 9.76 g (0.004 mole) of tetrachloro-1,2-benzoquinone in 250 ml of sodium dried benzene was heated to reflux under nitrogen for 24 h. The resulting dark red solution was evaporated to ca. 25 ml and placed on a column of B.D.H. alumina made up in benzene. Elution with benzene gave as the main fraction an orange solution, evaporation of which gave 1.06 g (10% yield) of **5** as a bright orange solid m.p. 300° (decomposition).

Anal. Calcd. for $C_{23}H_8Cl_7NO_3$: C, 46.45; H, 1.35; N, 2.35. Found: C, 46.50; H, 1.30; N, 2.35.

Mol. wt. calcd. for $C_{23}H_8{}^{35}Cl_7NO_3$: 590.8327. Found (mass spectrum): 590 8330 (9%); M—Cl; 556 (100%); M—$C_7{}^{35}Cl_5O_3$ 284.0028 (45%), calcd. for $C_{16}H_8Cl_2N$, 284.0033. The i.r. spectrum: $\nu_{max}(CHCl_3)$: 1680 cm^{-1} (conjugated C=O).

Can. J. Chem. Downloaded from www.nrcresearchpress.com by 210.87.254.5 on 09/05/12
For personal use only.

Can. J. Chem. Downloaded from www.nrcresearchpress.com by 210.87.254.5 on 09/05/12
For personal use only.

Reaction between 1-Methylisoquinoline and Tetrachloro-1,2-benzoquinone

A solution of 1.43 g (0.001 mole) of 1-methylisoquinoline and 4.88 g (0.002 mole) of tetrachloro-1,2-benzoquinone in 200 ml of sodium dried benzene was heated under reflux under nitrogen for 24 h. The resulting dark brown solution was evaporated to ca. 25 ml and placed on a column of B.D.H. alumina made up in benzene. Elution with benzene resulted in the collection of an orange solution, evaporation of which gave 0.21 g (4% yield) of a bright orange solid **7** m.p. 270° (decomposition).

Anal. Calcd. for $C_{22}H_6Cl_7NO_3$: C, 45.50; H, 1.05; N, 2.40. Found: 45.38; H, 1.02; N, 2.75.

Mol. wt. calcd. for $C_{22}H_6{}^{35}Cl_7NO_3$: 576.8170. Found (mass spectrum): 576.8157 (10%); M—Cl 542 (100%); M—$C_7Cl_5O_3$, 269.9874 (42%) calcd. for $C_{15}H_6{}^{35}Cl_2N$ 269.9878. The i.r. spectrum ν_{max} (Nujol mull): 1680 cm^{-1} (C=O stretch).

2,3-Dibenzylquinoxaline

2,3-Dibenzylquinoxaline was prepared by the condensation of dibenzylglyoxal (16) with *o*-phenylenediamine, and had m.p. 117–118° (lit. (16) m.p. 118°).

Reaction between 2,3-Dibenzylquinoxaline and Tetrachloro-1,2-benzoquinone

A solution of 1.55 g (0.005 mole) of 2,3-dibenzylquinoxaline and 2.46 g (0.001 mole) of tetrachloro-1,2-benzoquinone in 150 ml of sodium dried benzene was heated to reflux under nitrogen for 20 h. The dark red solution was concentrated to 15 ml under reduced pressure and subjected to chromatography on a B.D.H. alumina column made up with benzene. Elution with benzene gave 0.234 g (9% yield) of 2-(3-benzyl-2-quinoxalino)-2-phenyl-4,5,6,7-tetrachlorobenzo-1,3-dioxole; m.p. 191–2° (from hexane).

Anal. Calcd. for $C_{28}H_{16}Cl_4N_2O_2$: C, 60.70; H, 2.93; N, 5.05. Found: C, 60.63; H, 3.08; N, 5.18.

Mol. wt. calcd. for $C_{28}H_{16}Cl_4N_2O_2$: 551.9968, (25%). Found (mass spectrum): 551.9966 (25%); M—C_6H_5CO, 447 (100%); M—$C_{15}H_{11}N_2$, 333 (80%). The i.r. spectrum ν_{max} (Nujol mull): 1450 cm^{-1}(s) (—O—C—O— stretch). The n.m.r. spectrum $\delta_{TMS}(CDCl_3)$: 5.6 (2H, singlet, $CH_2C_6H_5$); 7.0–8.4 (15H, multiplet, aromatic protons and acetal proton).

Reaction between 2-Benzylpyridine and Tetrachloro-1,2-benzoquinone

A solution of 1.69 g (0.002 mole) of 2-benzylpyridine and 9.76 g (0.004 mole) of tetrachloro-1,2-benzoquinone in 150 ml of sodium dried benzene was heated under reflux under a stream of nitrogen for 20 h. The resulting solution was concentrated *in vacuo* to 50 ml and subjected to chromatography on alumina in benzene. Elution with benzene gave as the main fraction 0.6 g (14.5% yield) of a brown solid which recrystallized from benzene as pale yellow needles of **8** 2-(2-pyridyl)-2-phenyl-4,5,6,7-tetrachlorobenzo-1,3-dioxole, m.p. > 300°.

Anal. Calcd. for $C_{18}H_9Cl_4NO_2$: C, 52.35; H, 2.20; N, 3.40. Found: C, 52.22; H, 2.40; N, 3.39.

Mol. wt. calcd.: 410.9389. Found (mass spectrum): 410.9394 (14%); M—C_6H_5CO, 306 (100%); M—C_5H_4N, 333 (9%). The i.r. spectrum $\nu_{max}(CHCl_3)$: 1450 cm^{-1} (—O—C—O— stretch). The n.m.r. spectrum $\delta_{TMS}(CDCl_3)$: 7.0–8.4 (multiplet, aromatic protons and acetal proton).

Preparation and Thermal Decomposition of Heteroaromatic Quaternary Ammonium Hydroxides

1-Bromo-2,3-butanedione

1-Bromo-2,3-butanedione was prepared by the method of Doerner (17).

2-Bromomethyl-3-methylquinoxaline

1-Bromo-2,3-butanedione (2.06 g, 0.001 mole) was added dropwise over a period of 1 h. to a stirred solution of 1.35 g (0.001 mole) of freshly recrystallized *o*-phenylenediamine in 150 ml of ether at room temperature. The solution was stirred for 1 h, washed with water, and dried ($MgSO_4$). Evaporation of the solvent gave 1.704 g (59% yield) of the required 2-bromomethyl-3-methylquinoxaline m.p. 119–120° (from hexane) (lit. (18) m.p. 119–120°.

2-(3-Methylquinoxalinyl)methyltrimethylammonium Bromide

A solution (25 ml) of 100 g of trimethylamine in 500 ml of dry benzene was added dropwise to a solution of 10 g of 2-bromomethyl-3-methylquinoxaline in 75 ml of dry benzene. The solid quaternary ammonium bromide which precipitated was collected, dried, and recrystallized from ethanol, 12.0 g (96% yield). A sample recrystallized from dry ethanol for analysis had m.p. 241–245° (decomposition).

Anal. Calcd. for $C_{13}H_{18}BrN_3$: C, 52.70; H, 6.20; N, 14.2. Found: C, 52.89; H, 6.54; N, 13.90.

The n.m.r. spectrum δ_{TMS} (D_2O); 2.6 (3H, singlet, aromatic methyl); 3.3 (9H, singlet, $N(CH_3)_3$); 4.8 (2H, singlet, methylene); 7.4–7.9 (4H, multiplet, aromatic protons).

Preparation and Decomposition of 2-(3-Methylquinoxalinyl)trimethylammonium Hydroxide

Freshly prepared silver oxide (5.33 g) was added to a solution of 4.93 g of 2-(3-methylquinoxolinyl)trimethylammonium bromide in 30 ml of distilled water and the resulting mixture was stirred under nitrogen for 2 h. The aqueous solution was filtered to remove the silver bromide and excess silver oxide and was then evaporated to dryness under reduced pressure at room temperature. Dry xylene (100 ml) was then added to the solid hydroxide obtained and the mixture heated under reflux for 2 h in an atmosphere of dry nitrogen. The reaction mixture was filtered to remove some dark polymeric material, concentrated to ca. 20 ml, and chromatographed on a column of B.D.H. alumina in benzene. Elution with benzene gave firstly 52 mg of 2,3-dimethylquinoxaline m.p. 108–109°, identified by comparison with an authentic sample (lit. m.p. 108–109° (19)). Further elution with benzene gave 0.55 g (1% yield) of 6,14-dimethyl-5,8,13,16-tetraazadibenz[*a,h*]-anthracene as pale yellow needles, m.p. 278–279° (from benzene).

Anal. Calcd. for $C_{20}H_{16}N_4$: C, 76.9; H, 5.15; N, 17.95. Found: C, 76.52; H, 5.35; N, 18.02.

Mol. wt. calcd.: 312.1375. Found (mass spectrum):

Can. J. Chem. Downloaded from www.nrcresearchpress.com by 210.87.254.5 on 09/05/12
For personal use only.

312.1376; M—CH_3 297 (92%); M—$C_9H_7N_2$, 169 (61%); M—$C_{10}H_8N_2$, 156 (27%). The n.m.r. spectrum δ ($CDCl_3$), 3.0 (6H, singlet, 6,14,CH_3); 7.6–8.2 (8H, ABCD, aromatic protons); 8.4 (2H, singlet, 7,15 protons).

2-Quinoxalinylmethyltrimethylammonium Bromide

N-Bromosuccinimide (1.78 g, 0.01 mole) was added to a boiling solution of 1.44 g (0.01 mole) of 2-methylquinoxaline (13) and 0.005 g of dry dibenzoyl peroxide in 100 ml of dry carbon tetrachloride. The mixture was heated under reflux for 2 h before being cooled, filtered to remove the succinimide, and evaporated to dryness. A solution (20 ml) of trimethylamine in dry benzene was added to the dark red oil and the mixture was allowed to stand in the refrigerator overnight. The precipitated 2-quinoxolinyl bromide 0.9 g (32% yield) was collected and recrystallized from dry methanol and ether m.p. 225–228° (decomposition).

Anal. Calcd. for $C_{12}H_{16}BrN_3$: C, 51.10; H, 5.70; N, 14.90. Found: C, 50.85; H, 6.0; N, 14.6.

The n.m.r. spectrum δ (D_2O): 3.25 (9H, singlet, *N*-methyls); 4.8 (2H, singlet, methylene protons); 7.9 (4H, multiplet, aromatic protons); 8.3 (1H, singlet, 3 quinoxoline proton).

Preparation and Decomposition of 2-quinoxalinylmethyltrimethylammonium Hydroxide

Freshly prepared silver oxide (1.32 g) was added to a solution of 0.8 g (0.003 mole) of 2-quinoxolinyltrimethylammonium bromide in 10 ml of distilled water and the resulting mixture stirred under nitrogen for 2 h. The resulting aqueous suspension was then filtered to remove the silver bromide and excess silver oxide and the filtrate evaporated to dryness under reduced pressure at room temperature. Dry xylene (50 ml) was then added to the solid quaternary hydroxide obtained and the mixture was heated under reflux for 2 h in an atmosphere of nitrogen. The dark reaction mixture was then filtered, evaporated to ca. 20 ml and placed on a column of B.D.H. alumina made up in dry benzene. Elution with a 1:1 mixture of benzene/chloroform gave a dark brown oil, trituration of which with benzene gave 0.046 g (5.5% yield) of 5,8,13,16-tetraazadibenz[*a,h*]anthracene m.p. 242–243° (from benzene).

Anal. Calcd. for $C_{18}H_{12}N_4$: C, 76.35; H, 3.90; N, 19.80. Found: C, 76.25; H, 3.91; N, 19.8.

Mol. wt. calcd.: 284.1062. Found (mass spectrum): 284.1061; M—$C_8H_5N_2$, 155 (14%); M—$C_9H_6N_2$, 142 (14%). The n.m.r. spectrum δ_{TMS}($CDCl_3$): 7.6–8.2 (8H, A_2B_2 aromatic protons); 8.2 (2H, singlet, 7,15 protons); 9.3 (2H, singlet, 6,14 protons).

2-Quinolinylmethyltrimethylammonium Bromide

N-Bromosuccinimide (17.8 g, 0.1 mole) was added in small portions to a boiling solution of 14.3 g (0.1 mole) of 2-methylquinoline and 0.5 g of dry dibenzoylperoxide in 250 ml of dry carbon tetrachloride. The resulting mixture was heated under reflux for 90 min then allowed to cool to room temperature, filtered to remove the succinimide 9.5 g (theory 9.8 g), and evaporated to dryness. The dark red oil obtained was dissolved in 50 ml of dry benzene and 30 ml of a 20% (w/v) solution of trimethylamine in dry benzene was added. The quaternary salt which precipitated from the benzene solution was collected and recrystallized from dry methanol and ether, 16.5 g (59% yield) m.p. 196–198° (decomposition).

Anal. Calcd. for $C_{13}H_{17}BrN_2$: C, 55.50; H, 6.16; N, 9.95. Found: C, 55.35; H, 6.35; N, 9.85.

The n.m.r. spectrum δ (D_2O): 3.1 (9H, singlet, N(CH_3)$_3$); 4.55 (2H, singlet, CH_2N protons); 7.5–8.3 (6H, multiplet, aromatic protons).

Preparation and Decomposition of 2-Quinolinylmethyltrimethylammonium Hydroxide

Silver oxide (6.96 g) was added to a solution of 5.62 g (0.02 mole) of 2-quinolinylmethyltrimethylammonium bromide in 75 ml of distilled water and the mixture was stirred under nitrogen at room temperature for 2 h. The excess silver oxide and silver bromide were filtered off and the filtrate evaporated to dryness at room temperature under reduced pressure. Dry xylene was then added to the residual solid and the stirred mixture was heated under reflux in a Dean–Stark apparatus until the decomposition was complete (ca. 6 h after which no more trimethylamine was given off). The dark brown solution obtained was evaporated to dryness and the residual brown oil subjected to chromatography on B.D.H. alumina with benzene. Elution of the column with methylene chloride gave as the major fraction 1.142 g of dark oil which upon trituration with benzene/hexane gave 0.604 g of a white solid, which was shown by t.l.c. to contain two components. Repeated recrystallization of this solid from benzene gave 8,16-diazadibenz[*a,h*]anthracene as a white crystalline solid m.p. 195–198°.

Anal. Calcd. for $C_{20}H_{14}N_2$: C, 85.1; H, 5.02; N, 9.95. Found: C, 85.09; H, 5.18; N, 9.61.

Mol. wt. calcd. for $C_{20}H_{14}N_2$: 282.1157. Found (mass spectrum): 282.1160 (98%); M—H (100%); M—C_9H_6N, 154 (25%). M—141,141 (12%); M—154, 128 (23%). The n.m.r. spectrum δ_{TMS}($CDCl_3$): 7.0–8.2 (multiplet, aromatic protons).

Careful crystallization of the mother liquors yielded a second component as a white crystalline solid m.p. 169–9° to which no structure has yet been assigned. Mol. wt. calcd. for $C_{30}H_{21}N_3$: 423.1736. Found: 423.1735. The n.m.r. spectrum δ_{TMS}($CDCl_3$): 3.91 (2H, doublet J = 3 Hz), 4.35 (1H, triplet, J = 3 Hz); 7.4–8.20 (18H, multiplet, aromatic protons).

This research was supported by a National Research Council of Canada grant to J. W. Lown. We thank Mr. J. P. Moser for technical assistance and Mr. R. Swindlehurst and Dr. A. Hogg for the n.m.r. and mass spectra, respectively.

1. A. Schonberg and A. Mustafa. J. Chem. Soc. 654 (1943).
2. A. Mustafa and M. Kamel. J. Amer. Chem. Soc. **77**, 1828 (1955).
3. C. W. Bird and G. W. H. Cheeseman. J. Chem. Soc. 3037 (1962).
4. E. C. Taylor and E. S. Hand. J. Org. Chem. **27**, 3734 (1962).
5. J. W. Lown and A. S. K. Aidoo. Can. J. Chem. **44**, 2507 (1966).
6. E. A. Braude, L. M. Jackman, R. P. Linstead, and G. Lowe. J. Chem. Soc. 3123 (1960).

7. K. BIEMANN. Mass spectrometry – organic chemical applications. McGraw-Hill Book Company, New York, 1962. p. 66.
8. G. W. H. CHEESEMAN and B. TUCK. Tetrahedron Lett. 4851 (1968).
9. D. BUCKLEY and H. B. HENBEST. Chem. Ind. (London), 1096 (1956).
10. M. J. HADDADIN and C. H. ISSODORIDES. Tetrahedron Lett. 4609 (1968).
11. A. J. BAKER and T. CAIRNS. Spectroscopic techniques in organic chemistry. Heyden and Sons Ltd., Publishers, 1965. p. 45.
12. T. R. KASTURI and T. ARUNACHALAM. Can. J. Chem. **46**, 3625 (1968).
13. I. H. SADLER and J. A. G. STEWART. Chem. Commun. 773 (1969).
14. G. CHARRIER. Chem. Zentralbl. **78** (II), 1231 (1907).
15. G. M. BENNET and G. H. WILLIS. J. Chem. Soc. 1960 (1928).
16. P. RUGGLI and P. ZELLER. Helv. Chim. Acta, **28**, 741 (1945).
17. M. P. DOERNER. U.S. Patent 2 821 555, Chem. Abstr. **52**, 9198*i*.
18. H. SIMON, G. HEUBACK, W. BETTERLICH, and H. GLEINIG. Ber. **98** 3692 (1965).
19. R. A. OGG and F. W. BERGSTROM. J. Amer. Chem. Soc. **53**, 1846 (1931).

Can. J. Chem. Downloaded from www.nrcresearchpress.com by 210.87.254.5 on 09/05/12
For personal use only.

N-Ammonium-*S*-thiosulfate zwitterions from alkaloids and tertiary amines

JOHN T. EDWARD AND JOSEPHINE WHITING[1]
Department of Chemistry, McGill University, Montreal, Quebec

Received July 18, 1969

The compounds prepared by Tercinet (1) from the reaction of various alkaloids with silver sodium thiosulfate have been shown to have *N*-ammonium-*S*-thiosulfate structures; they are better prepared by reaction of the alkaloids with sodium tetrathionate.

Les composés préparés par Tercinet (1) par la réaction de différentes alcaloïdes avec la thiosulfate mixte d'argent et de soude sont montrés d'avoir la structure des *N*-ammonium-*S*-thiosulfates. Une meilleure méthode de préparation se fait par la réaction des alcaloïdes avec la tetrathionate de soude.

Canadian Journal of Chemistry, **48**, 337 (1970)

Can. J. Chem. Downloaded from www.nrcresearchpress.com by 210.87.254.105 on 09/05/12
For personal use only.

In 1944 André Tercinet (1) described the reaction of silver sodium thiosulfate ($Ag_2S_2O_3$.-$2Na_2S_2O_3$) with strychnine, brucine, quinine, and harmine to give crystalline solids. He formulated these compounds as *S*-thiosulfate esters, the compound from strychnine, for example, being assigned the structure **1**. Such a compound

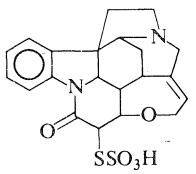

1

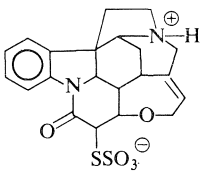

2

would be more plausibly formulated as **2**, a zwitterionic Bunte salt (2, 3). Silver ion is reduced to metallic silver in the reaction, and the overall reaction finds analogy in the formation of a zwitterionic Bunte salt from the oxidation of a mixture of *N*,*N*-dimethyl-1,4-phenylene diamine and sodium thiosulfate with dichromate (4, 5).

We were led to reinvestigate Tercinet's reaction because of the great usefulness of Bunte salts in synthesis (5), and because of the potential use of such compounds as anti-radiation agents (6, 7). However, while we obtained products having the composition and physical properties reported by Tercinet, we observed them to have, in many cases, different reactions, and in all cases we have shown his structures to be incorrect.

Tercinet obtained the same products, although in smaller yields, by heating the alkaloids with sodium thiosulfate and hydrogen peroxide; we have obtained them by substituting ferric chloride, mercuric oxide, or iodine for hydrogen peroxide. All of these oxidizing agents convert thiosulphate ion ($^{\ominus}S—SO_3^{\ominus}$) to tetrathionate ion ($^{\ominus}O_3S—S—S—SO_3^{\ominus}$), presumably via the radical $\cdot S—SO_3^{\ominus}$ (8*a*), and Tercinet's compounds are obtained most simply by reaction of the alkaloids with sodium tetrathionate, which was probably the effective reagent in his reactions. When a stream of oxygen is bubbled through a mixture of an alkaloid and silver sodium thiosulfate, little or none of Tercinet's product is obtained, the oxygen acting as a scavenger for $\cdot S—SO_3^{\ominus}$; however, the stream of oxygen has no effect on the yield of product from the alkaloid and sodium tetrathionate.

Sodium tetrathionate is the reagent of choice. It reacted with strychnidine to give a compound $C_{21}H_{24}N_2O_4S_2$ whose structure is discussed below. Tercinet failed to obtain any product from the reaction of strychnidine with silver sodium thiosulfate, perhaps because of the known sensitivity of strychnidine to oxidizing agents (9).

Tercinet's products do not behave like Bunte salts. Thus they do not react with iodine, known to convert Bunte salts to disulfides (10). Furthermore, Tercinet reported that his compound $C_{21}H_{22}N_2O_5S_2$ from strychnine was converted by sodium amalgam in alkaline solution back to strychnine, and not to a thiol, which would be expected. A thiol, along with sulfate ion, would also be expected from the acid hydrolysis of a Bunte salt. Instead, we have found that the hydrolysis of the strychnine product with 6 *N* hydrochloric acid yields strychnine, sulfur, and sulfate ion in essentially quantitative yields. All

[1]Née Josephine Jaworska, holder of NRCC Studentship, 1967–1969.

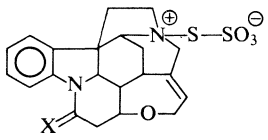

3

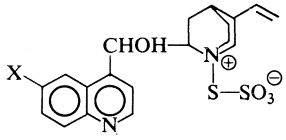

4

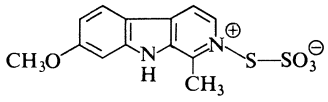

5

of this evidence points to a linkage of the $S—SO_3^{\ominus}$ group to nitrogen and not to carbon, since an N—S linkage can be broken by hydrolysis (11), so that the acid-catalyzed hydrolysis is represented by eq. [1].

$$[1] \quad R_3\overset{+}{N}—S—SO_3^- + H_2O \rightarrow R_3N + S + H_2SO_4$$

Bunte salts are hydrolyzed by alkali to mixtures of sulfite ion, disulfides, sulfinates, and other products (5). However, Tercinet reported that his compound $C_{21}H_{22}N_2O_5S_2$ from strychnine was converted by one equivalent of sodium hydroxide into "hydroxystrychnine", a compound for which no characteristics were reported. We have found that addition of one equivalent of sodium hydroxide to $C_{21}H_{22}N_2O_5S_2$ gave immediately a quantitative precipitation of strychnine, and not "hydroxystrychnine". This also points to the presence of a hydrolyzable $\diagdown\overset{+}{N}—S—SO_3^-\diagup$ group.

The facile recovery of the strychnine by acid or alkaline treatment of Tercinet's product could be explained if the latter were merely the thiosulfate salt of strychnine ($C_{21}N_{24}N_2O_5S_2$). However, this possibility was excluded by preparation of the salt, which proved to be quite different. Treatment of an aqueous solution of the thiosulfate with sodium bicarbonate resulted in an immediate precipitation of strychnine, whereas Tercinet's product was unaffected under these conditions. Furthermore, molecular weight measurements (by vapor pressure osmometry) showed that the thiosulfate was dissociated into ions, whereas Tercinet's product had approximately the molecular weight expected for its formula $C_{21}H_{22}N_2O_5S_2$ (see Table 5).

In summary, the evidence presented is best accommodated by the *N*-ammonium-*S*-thiosulfate zwitterion structure **3** (X = O) for the compound $C_{21}H_{22}N_2O_5S_2$ from strychnine, and by similar structures for analogous compounds obtained from brucine (1) and from dihydrostrychnine. Neostrychnine (pK_a 3.8; ref. 12) and pseudostrychnine (pK_a 5.6) did not react with sodium tetrathionate to give crystalline products. These amines are considerably less basic than strychnine, brucine, and dihydrostrychnine, all of which have $pK_a \simeq 7.4$ (15), and it seems likely that the *N*-ammonium-*S*-thiosulfate structure is formed by a reaction, as shown in eq. [2], for

[2]

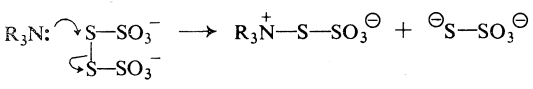

which their amino centers are insufficiently nucleophilic.[2] Reaction [2] has parallels in the reactions of several other nucleophiles (e.g. thiosulfate (13), cyanide (8*b*), azide (8*b*)) with tetrathionate ion.

On grounds of nucleophilicity, it might be expected that strychnidine would react at its more basic amino center (12) with tetrathionate to give the compound **3** (X = H_2). This was confirmed by its ultraviolet (u.v.) spectrum (Table 1), which was the same as that of strychnidine. Quaternization of the amino nitrogen joined to the aromatic ring would have resulted in a marked change of spectrum (14).

The question of reaction site also arises with respect to Tercinet's product $C_{20}H_{24}N_2O_5S_2$ from quinine, and to the similar derivatives obtained from cinchonine and cinchonidine.[3] Again, these compounds are hydrolyzed by acid

[2]The steric congestion about the basic nitrogen atom of the strychnine bases may hinder reaction, and may furnish an additional reason for the failure of neostrychnine and of pseudostrychnine to react. It has been pointed out by a referee that neostrychnine and pseudostrychnine are stronger bases than the less hindered quinoline and 6-methoxyquinoline, which do react.

[3]Tercinet failed to obtain derivatives from cinchonine and cinchonidine, and hence concluded erroneously that the methoxyl group of quinine was necessary for reaction.

Can. J. Chem. Downloaded from www.nrcresearchpress.com by 210.87.254.105 on 09/05/12
For personal use only.

TABLE 1

Ultraviolet spectra in ethanolic solution

Compound	$\lambda\lambda_{max}$(nm) and $\varepsilon\varepsilon$*
Strychnine	254(17 800), 280(6 100), 288(4 810)
3, X = O	254(17 800), 280(6 100), 288(4 800)
Strychnidine	254(17 700), 303(2 500),
3, X = H_2	254(17 700), 303(2 500),
Brucine	254(17 800), 280(6 100), 288(4 800)
N_b-Brucinium-*S*-thiosulfate	254(17 800), 280(6 100), 288(4 800)
Quinine	232(74 400), 279(8 740), 332(11 100)
4, X = OCH_3	232(74 400), 279(8 750), 332(11 100)
Cinchonine	227(47 000), 284(7 790), 314(4 850)
4, X = H	227(47 000), 284(7 790), 314(4 860)
Harmine	242(24 100), 307(10 200),
Harmine hydrochloride	249(18 000), 325(10 600),
5	249(18 000), 325(10 600),
6-Methyoxyquinoline	229(27 000), 269(2 830), 327(4 000)
6-Methoxyquinoline hydrochloride	250(27 700), 312(4 100), 340(4 100)
7, X = OCH_3	250(27 700), 312(4 100), 340(4 100)
2-Phenyl[1,2-*a*]imidazopyridine	245(34 500), 322(8 830)
2-Phenyl[1,2-*a*]imidazopyridine hydrochloride	239(20 700), 303(15 200)
8	239(20 700), 303(15 200)

*In parentheses.

or alkali to the parent alkaloids, and so must have the thiosulfate group attached to nitrogen; this formulation is supported by molecular weight determinations, which exclude the possibility of thiosulfate salts. Attachment of $\cdot S—SO_3^{\ominus}$ to the more basic quinuclidine nitrogen, as shown in **4** (X = H or OMe) would be expected and is indicated by the u.v. spectra of these products, which are very similar to those of the parent alkaloids. Quaternization of the aromatic nitrogen would have caused significant shifts in the spectra, as shown by the spectrum of 6-methoxyquinoline hydrochloride recorded in Table 1. In addition, the nuclear magnetic resonance (n.m.r.) spectra of the products are identical in the aromatic regions with the spectra of the parent compounds; quaternization of the aromatic nitrogen causes a downfield shift of peaks in this region, as shown in Table 2 for harmine, 6-methoxyquinoline and 2-phenyl-(1,2-*a*)imidazopyridine.

The chemical reactions of the product obtained by Tercinet from harmine indicate again *N*-thiosulfonation. The n.m.r. spectrum of the

TABLE 2

Selected n.m.r. signals

Compound in DMSO-d_6	Signals (δ, p.p.m.)
Cinchonine	7.6–8.9 (m, 6H)*
4, X = H	7.6–8.9 (m, 6H)*
Quinine	7.75–9.1 (m, 5H)*
4, X = OMe	7.75–9.1 (m, 5H)*
Harmine	6.7–7.1 (m, 2H), 7.7–8.25 (m, 3H), 7.3 (s, 1H)†
Harmine·CF_3CO_2H	6.8–7.15 (m, 2H), 8.2–8.55 (m, 3H), 12.3 (s, 1H)†
5	6.9–7.2 (m, 2H), 8.2–8.55 (m, 3H), 12.3 (s, 1H)†
6-Methoxyquinoline§	8.71‡ (d of d, 1H), 7.9–8.1 (two d, 2H)
6-Methoxyquinoline·CF_3CO_2H	9.14‡ (d of d, 1H), 8.7–8.9 (two d, 2H)
7, X = OMe	9.14‡ (d of d, 1H), 8.7–8.9 (two d, 2H)
2-Phenyl(1,2-*a*)imidazopyridine	8.30 (s, 1H), 8.38 (d, 1H)
2-Phenyl(1,2-*a*)imidazopyridine ·CF_3CO_2H	8.55 (s, 1H), 8.78 (d, 1H)
8	8.55 (s, 1H), 8.78 (d, 1H)

*Aromatic H.
†Indole NH.
‡Proton at 2-position (22); $J_{2,3}$ = 5 c.p.s.; $J_{2,4}$ = 1.5 c.p.s.
§Solvent: $CDCl_3$.

Can. J. Chem. Downloaded from www.nrcresearchpress.com by 210.87.254.105 on 09/05/12
For personal use only.

Can. J. Chem. Downloaded from www.nrcresearchpress.com by 210.87.254.105 on 09/05/12
For personal use only.

TABLE 3

Infrared peaks (cm^{-1}) of *N*-ammonium-*S*-thiosulfate derivatives in KBr

Parent amine	$\nu_{asym}(SO_3)$	$\nu_{sym}(SO_3)$	ν(S—N)	$\delta(SO_3)$
Strychnine	1250	1020	705	610
Brucine	1250	1020	705	610
Harmine	1240	1020	732	610
Quinine	1250	1020	705	615
Cinchonine	1250	1015	705	610
Cinchonidine	1250	1015	690	610
Strychnidine	1250	1015	705	610
Dihydrostrychnine	1250	1020	705	610
6-Methoxyquinoline	1250	1020	755	615
Quinoline	1240	1020	760	610
Juolidine	1260	1010	725	600
2-Phenyl[1,2-*a*] imidazopyridine	1250	1012	750	600

product (Table 2) shows a deshielding of the α- and β-protons of the pyridine portion of the molecule, similar to the deshielding in the trifluoroacetate salt. Furthermore, no N—H protons other than the original indole N—H proton were detected, indicating that the product was not a thiosulfate salt; this result was substantiated by vapor pressure osmometry, which showed that the compound $C_{13}H_{12}N_2O_4S_2$ was not dissociated. The u.v. spectrum of the product resembled very closely the spectrum of the hydrochloride of harmine (Table 1). All of this diverse evidence supports the structure **5** for the product obtained by Tercinet from harmine, a structure expected from the fact that harmine quaternizes easily at the pyridine nitrogen (15).

If the Tercinet products are formed by the action of tetrathionate according to equation 2, it might be expected that products having the grouping $-\overset{\oplus}{N}-S-SO_3^{\ominus}$ would be formed from other tertiary amines, but that quaternary ammonium ions would be unreactive. The latter supposition was supported by the failure of *N*-methylstrychninium chloride and of methylstrychnine (16) to react with tetrathionate. However, not all tertiary amines were found to react with sodium tetrathionate to give crystalline *N*-ammonium-*S*-thiosulfates. Amines giving crystalline products, and the structural formulae of the latter, are: juolidine (**6**); quinoline (**7**; X = H); 6-methoxyquinoline (**7**; X = OCH_3); and 2-phenyl-[1,2-*a*]imidazopyridine (**8**). 3-Quinuclidinol gave a crystalline product in small yield for which no satisfactory analysis could be obtained. The structures shown are supported by the combustion analysis of the compounds, their molecular weights in ionizing solvents, and their ready hydrolysis in acid or alkali to regenerate the parent amine. The possibility of their being thiosulfate salts is excluded by their apparent molecular weights in solution and by their infrared (i.r.) spectra, recorded in Table 3.[4] The structure **7** (X = OCH_3) for the product from 6-methoxyquinoline is in accord with its u.v. (Table 1) and n.m.r. (Table 2) spectra, both of which indicate quaternization of the ring nitrogen.

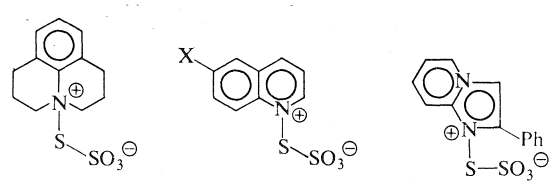

6 **7** **8**

Tertiary amines which failed to give any crystalline product with tetrathionate could be recovered after the reaction in high yield by extraction of the aqueous solution with ether. This suggests that the reaction represented by eq. [2] is an equilibrium which does not always proceed far to the right, and that formation of *N*-ammonium-*S*-thiosulfate derivatives in good yields occurs only when the zwitterions have low solubility in the reaction medium and hence crystallize out during the reaction. In harmony with this idea, it was found that addition of

[4]Thiosulfates show significantly different spectra. Thus the thiosulfate of strychnine shows peaks (KBr) at 1150, 990, 750, and 550 cm^{-1}.

TABLE 4
Physical properties of *N*-ammonium-*S*-thiosulfates

Parent amine	Melting point °C*	Yield %
Strychnine	242–245**	90
Brucine	192–195†	90
Harmine	170–175‡	75
Quinine	187–189§	85
Cinchonine	180–185	50
Cinchonidine	192–195	50
6-Methoxyquinoline	185–187	60
Quinoline	255–260	20
Juolidine	178–180	50–60
2-Phenyl[1,2-*a*]imidazopyridine	205–210	80–85
Strychnidine	235–240	40–50
Dihydrostrychnine	290–295	75

*All melting points involved decomposition of sample.
**Found: $[\alpha]_D$ − 52.5° (EtOH); reported, −50° (1).
†Found: $[\alpha]_D$ −66° (H_2O); reported, −64° (1).
‡Found: $[\alpha]_D$ +19.7° (EtOH); reported +19.5° (1).
§Found: $[\alpha]_D$ −155° (EtOH); reported, −151.7° (1).

thiosulfate to the reaction mixture of strychnine and tetrathionate depressed the yield of **3** (X = O); however, it also caused the formation of sulfur in increasing amounts. The genesis of the sulfur is obscure; it does not come from the acid hydrolysis of **3** (X = O), because the p*H* of the solution remains near neutrality throughout the reaction.

Compounds **3** (X = O), **4** (X = OCH_3), **7** (X = OCH_3), and **8** gave some protection to female mice (Swiss strain) against γ-radiation, but not enough to make them of interest as radioprotective agents.[5]

Experimental

The i.r. spectra were recorded with a Perkin–Elmer Model 337 spectrophotometer, n.m.r. spectra with a Varian A-60 spectrophotometer, and u.v. spectra with a Unicam SP 800 spectrophotometer. Optical rotations were determined using a Carl Zeiss polarimeter, and molecular weights using a Mechrolab Model 301A osmometer. All melting points are uncorrected. Analyses were done by Dr. C. Daessle of Montreal and Dr. Alfred Bernhardt of Elbach über Engelskirchen, West Germany.

Materials

Strychnidine (17), dihydrostrychnine (18), and neostrychnine (19) were prepared by methods in the literature, and had the correct physical constants; the other alkaloids and bases were commercial products, and were used without purification. Sodium tetrathionate was made according to Partington's method (20) by adding a saturated solution of sodium thiosulfate to a solution of iodine in alcohol at 10°. Potassium tetrathionate was obtained from K & K Rare Fine Chemicals.

[5]We are grateful to Dr. G. A. Grant, D.C.B.R.E., Shirley Bay, Ontario, for these tests.

Preparation of N-Ammonium-S-thiosulfate Derivatives

(a) By a Modification of Tercinet's Method

Strychnine (1 g) and 12% sodium thiosulfate solution (80 ml) were heated on a steam bath with stirring. 10% silver nitrate solution (90 ml) was added slowly (20 min). The mixture was heated for approximately 5 h, by which time fumes of SO_2 and H_2S became evident. A black precipitate was deposited and a silver mirror formed on the walls of the flask. The reaction mixture was filtered hot. The filtrate on cooling deposited fluffy white crystals, which were washed with chloroform to remove unreacted strychnine, and recrystallized from ethanol to give white needles (1.23 g, 90% yield), m.p. 242–245° decomposition (lit. 245° decomposition (1)).

Brucine (70% yield), quinine (60%), cinchonine (15%), and harmine (50%) reacted by this method to give *N*-ammonium-*S*-thiosulfate products. However, strychnine methiodide, methyl betaine strychnine, benzyl strychnine, benzylstrychninium sulfate, 6-methoxyquinoline, isoquinoline, indole, 2-methylindole, and 1,2-dimethylindole did not give crystalline products, and could be recovered unchanged after the reaction by extraction with organic solvents or by crystallization from the reaction liquors.

(b) By Reaction with Sodium or Potassium Tetrathionate

Strychnine (1 g) and potassium tetrathionate (4 g) were heated on a steam bath in water (125 ml) for 2 h; the mixture was then filtered hot. White crystals separated from the filtrate when cool, and were collected and washed with chloroform. They were recrystallized from ethanol to give pure N_b-strychninium-*S*-thiosulfate (1.3 g, 95%), m.p. 242–245° decomposition. Addition of a small amount of acetic acid reduced the reaction time to 1½ h, but the yield was only 75%. Excess acetic acid lowered the reaction time to 15 min, but the yield was only 30%.

Separate experiments showed that use of a smaller amount of tetrathionate, or of a shorter reaction time, led to lowered yields.

Compounds giving *N*-ammonium-*S*-thiosulfate derivatives and yields of the latter are shown in Table 4. 6-Methoxyquinoline, quinoline, and juolidine were used in

Can. J. Chem. Downloaded from www.nrcresearchpress.com by 210.87.254.105 on 09/05/12
For personal use only.

TABLE 5

Analyses of *N*-ammonium-*S*-thiosulfates

Parent amine	Product empirical formula	Analyses Calcd.% Found% C	H	N	S	Molecular weight*
Strychnine	$C_{21}H_{22}N_2O_5S_2$	56.48	4.96	6.27	14.36	446.5
		56.41	4.90	6.31	14.45	440±10 (EtOH, H_2O, MeOH)
Brucine	$C_{23}H_{26}N_2O_7S_2$	54.75	5.19	5.55	12.71	504.5
		55.00	5.28	5.43	12.81	505±10 (EtOH)
Harmine	$C_{13}H_{12}N_2O_4S_2$	48.14	3.76	8.64	19.77	324.3
		48.33	3.86	8.88	20.01	320±10 (MeOH)
Quinine	$C_{19}H_{24}N_2O_5S_2$	55.03	5.54	6.42	14.69	436.5
		55.05	5.52	6.32	14.48	425±10 (H_2O)
Cinchonine	$C_{18}H_{22}N_2O_4S_2$	56.14	5.45	6.89	15.76	406.5
		56.30	5.36	6.93	15.83	395±10 (MeOH)
Cinchonidine	$C_{18}H_{22}N_2O_4S_2$	56.14	5.45	6.89	15.76	406.5
		56.25	5.57	6.78	15.90	
6-Methoxy-quinoline	$C_{10}H_9NO_4S_2$	44.29	3.35	5.17	23.60	271.1
		44.39	3.60	5.31	23.34	270±10 (H_2O)
Quinoline	$C_9H_7NO_3S$	44.82	2.93	5.81	26.54	241.1
		44.70	2.95	5.69	26.64	240±10 (MeOH)
Juolidine	$C_{12}H_5NO_3S$	50.52	5.30	4.91	22.43	285.2
		50.39	5.28	4.77	22.56	285±10 (H_2O)
2-Phenyl[1,2-*a*] imidazopyridine	$C_{12}H_{10}N_2O_3S$	50.98	3.29	9.15	20.89	306.2
		50.69	3.57	8.93	20.64	300±10 (EtOH)
Strychnidine	$C_{21}H_{24}N_2O_4S_2$	55.99	5.82	6.22	14.20	432.4
		55.89	5.67	6.48	14.38	
Dihydrostrychnine	$C_{21}H_{24}N_2O_5S_2$	56.24	5.39	6.25	14.28	448.5
		56.29	5.41	6.50	14.49	

*By vapor pressure osmometry in the solvents indicated.

the form of their sulfate salts, to solubilize them in the aqueous medium; the sulfate salt of strychnine also reacted to give the *N*-ammonium-*S*-thiosulfate. However, the following amines did not react: neostrychnine, pseudostrychnine, benzimidazole, imidazole, benzothiazole, pyridine, *N*-methylpiperidine, hexamethylenetetramine, 4-phenylpyridine, 2-anilinopyridine, tetrahydroisoquinoline, triethylamine, and triamylamine. 3-Quinuclidinol gave a crystalline compound (ν_{max}(KBr) 1230, 1035, 690, 610 cm^{-1}) which had a bad combustion analysis.

Hydrolysis of N_b-Strychninium-S-thiosulfate in 6 N Hydrochloric Acid

N_b-Strychninium-*S*-thiosulfate (2.63 g) was stirred at room temperature for a few min with 6 *N* hydrochloric acid (50 ml). The yellow solution was extracted 4 times with chloroform to remove the color. The chloroform extracts, when dried over magnesium sulfate and evaporated to dryness, left a solid residue (0.18 g, 99%) which was identified as sulfur (no i.r. absorption between 4000 and 400 cm^{-1}, u.v. absorption at 264 mμ in ethanol (log ε 3.0) with a shoulder at 275 mμ (21). Barium chloride (few mls of 10% solution) was added to the aqueous layer. Barium sulfate precipitated, was removed by filtration, and dried to constant weight (1.30 g, 98.5%). The aqueous layer was neutralized with sodium bicarbonate. A white precipitate (1.877 g, 99.3%) separated which was identified as strychnine, m.p. 285–288° decomposition (lit. 286–288° decomposition), by an i.r. spectrum identical to that of an authentic sample of strychnine.

Hydrolysis of N_b-Strychninium-S-thiosulfate in Sodium Hydroxide

N_b-Strychninium-*S*-thiosulfate (1.578 g, 3.537 mequiv.) was exactly neutralized by addition of sodium hydroxide (22.15 ml, 0.1597 *N*, 3.535 mequiv.). A white precipitate of strychnine (1.18 g, 3.533 mequiv., m.p. 286–288° decomposition) identified by i.r. spectrum, was formed during the titration. The aqueous solution gave a positive test for sulfite (a precipitate with barium chloride that was soluble in acid; iodine was decolorized by the solution). No sulfur could be detected.

The same hydrolysis took place with aqueous ammonia or sodium carbonate, but not with sodium bicarbonate. The compound was somewhat soluble in warm bicarbonate solution, but could be recovered unchanged on cooling. An aqueous solution of the thiosulfate salt of strychnine, prepared by mixing warm aqueous solutions of the hydrochloride of the alkaloid and of sodium thiosulfate and filtering off the precipitate, gave strychnine immediately on treatment with sodium bicarbonate.

Reaction of Strychnine with Sodium Tetrathionate in the Presence of Sodium Thiosulfate

Strychnine (0.50 g) and sodium tetrathionate (1.66 g) in water (50 ml) were heated on a steam bath at 100° for 2 h. The solution was cooled to 0°, and the crystals that

Can. J. Chem. Downloaded from www.nrcresearchpress.com by 210.87.254.105 on 09/05/12
For personal use only.

formed were collected. The crystals were extracted with chloroform, leaving a residue of zwitterion **3** (X = O) (580 mg, 87%). The chloroform extract was dried over magnesium sulfate, and evaporated. The residue (140 mg) from the chloroform extract was boiled in water (100 ml) to dissolve a small amount of strychnine, leaving insoluble sulfur (75 mg), identified as above. The aqueous extract was evaporated to give strychnine (65 mg, 13%).

A similar reaction with 0.585 g of sodium thiosulfate added gave **3** (X = O) (386 mg, 57.5%), strychnine (204 mg, 40.5%), and sulfur (185 mg). When the amount of thiosulfate was increased to 2.51 g, the yields were: **3** (X = O) (203 mg, 30%), strychnine (355 mg, 67%), and sulfur (310 mg).

In separate experiments it was shown that in water at 100° the solubility of strychnine was 7.9×10^{-4} *M*, and of **3** (X = O), 1.5×10^{-2} *M*, so that both compounds were present in the first experiment above in amounts greater than required for saturation.

We acknowledge gratefully the financial support of Abbott Laboratories and of the National Research Council of Canada. We are indebted to Mr. Anwer Mehkeri for bringing the problem to our attention, and for a preliminary experiment.

1. ANDRE TERCINET. Bull. Soc. Chim. Fr. **11**, 500 (1944).
2. J. M. SWAN. Nature, **180**, 643 (1957).
3. J. M. SWAN. Aust. J. Chem. **14**, 69 (1961).
4. A. BERNTHSEN. Ann. **251**, 1 (1889).
5. B. MILLIGAN and J. M. SWAN. Rev. Pure Appl. Chem. **12**, 72 (1962).
6. L. BAUER and T. L. WELSH. J. Org. Chem. **27**, 4382 (1962).
7. J. M. BARTON and L. BAUER. Can. J. Chem. **47**, 1233 (1969).
8. R. C. BRASTED. Comprehensive inorganic chemistry. Vol. 8. D. van Nostrand, Princeton, N.J., 1961. (*a*) p. 164; (*b*) p. 171–173.
9. H. WIELAND, F. CALVET, and W. W. MOYER. Ann. **491**, 107 (1931).
10. H. E. WESTLAKE and G. DOUGHERTY. J. Amer. Chem. Soc. **64**, 149 (1942).
11. J. H. BILLMAN and E. O'MAHONEY. J. Amer. Chem. Soc. **61**, 2340 (1939).
12. H. L. HOLMES. The Alkaloids. vol. II. *Edited by* R. H. F. Manske and H. L. Holmes, Academic Press, Inc., New York, 1952. p. 539.
13. A. FAVA. Gazz. Chim. Ital. **83**, 87 (1953).
14. L. P. HAMMETT. Physical organic chemistry. McGraw-Hill, New York, 1940. p. 60.
15. V. V. S. IYER and R. ROBINSON. J. Chem. Soc. 1635 (1934).
16. J. T. EDWARD and R. ROBINSON. J. Chem. Soc. 1080 (1952).
17. P. KARRER, C. A. EUGSTER, and P. WASER. Helv. Chim. Acta, **32**, 2381 (1949).
18. A. E. OXFORD, W. H. PERKIN, and R. ROBINSON. J. Chem. Soc. 2389 (1927).
19. R. N. CHAKRAVARTI and R. ROBINSON. J. Chem. Soc. 78 (1947).
20. J. R. PARTINGTON. A textbook of inorganic chemistry. 6th edn., Macmillan and Co., London, 1957. p. 493.
21. P. D. BARTLETT, G. LOHAUS, and C. D. WEIS. J. Amer. Chem. Soc. **80**, 5064 (1958).
22. N. S. BHACCA, L. F. JOHNSON, and J. M. SHOOLERY. High resolution n.m.r. spectra catalog. Vol. 1. Varian, 1962.

Can. J. Chem. Downloaded from www.nrcresearchpress.com by 210.87.254.105 on 09/05/12
For personal use only.

Can. J. Chem. Downloaded from www.nrcresearchpress.com by 210.87.254.6 on 09/05/12
For personal use only.

Orientation of azide addition to homoconjugated dienes

R. S. McDaniel and A. C. Oehlschlager[1]
Department of Chemistry, Simon Fraser University, Burnaby 2, B.C., Canada

Received July 21, 1969

The 1,3-dipolarcycloaddition of phenyl azide to bicyclic dienes **8–10** proceeds readily at the angle strained double bond to give both 1,2,3-Δ^2-triazoline isomers which would result from the two possible orientations of addition. The major triazoline isomer in each case is that resulting from stabilization of the dipolar transition state by the neighboring unreactive double bond. The structures of the triazolines were deduced from their nuclear magnetic resonance spectra in CCl_4, $CDCl_3$, and C_6H_6.

Canadian Journal of Chemistry, **48**, 345 (1970)

The 1,3-dipolarcycloaddition of organic azides to alkenes to give 1,2,3-Δ^2-triazolines has been the object of continued interest for nearly four decades. The investigations of Huisgen and co-workers have established the stereospecifically *cis* nature of the addition as well as the principle electronic factors influencing the direction of addition (1). Thus, *p*-nitrophenyl azide (**1**) reacts

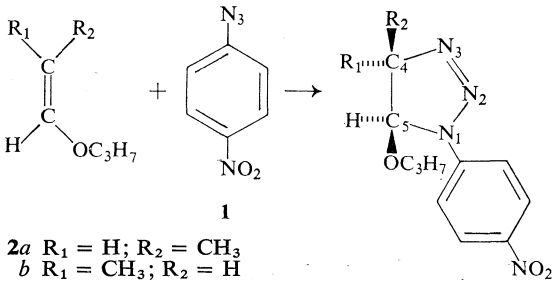

1

2*a* $R_1 = H; R_2 = CH_3$
b $R_1 = CH_3; R_2 = H$

3*a* $R_1 = H; R_2 = CH_3$
b $R_1 = CH_3; R_2 = H$

stereospecifically with the *cis* and *trans* enol ethers, **2***a* and **2***b*, to give the corresponding *cis* and *trans* 4,5-disubstituted triazolines, **3***a* and **3***b* respectively (2). Addition of phenyl azide to styrene occurs in only one direction giving **4** in high yield (3). Likewise 1,3-cyclohexadiene and 1-hexene are reported to yield **5** and **6** respectively upon reaction with *p*-bromophenyl azide (4).

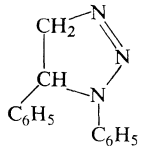

4

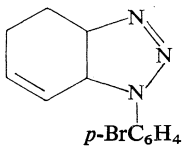

5

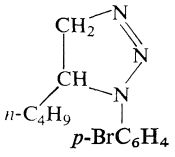

6

Although the 1,3-dipolarcycloaddition of azides to alkenes is formally classified as a concerted addition, the distinct preference for the orientation of addition noted above has been interpreted in terms of a transition state in which there is charge imbalance. Thus, the formation of bond *a* is considered to proceed more rapidly than bond *b* in the cycloaddition. Substituents on C_5 which stabilize the incipient positive charge at this position should not only facilitate addition but cause the particular orientation of azide addition noted above to be favored (transition state **7**). Except in cases where overriding steric effects operate, azide addition to alkenes has always been observed to take place in a Markownikoff fashion initiated by electrophilic attack by the terminal azide nitrogen on the alkene (2, 4). The dipolar nature of the addition process is also reflected by the observed substituent effect ($\rho = +0.84$) for the addition of substituted phenyl azides to norbornene (5).

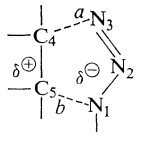

7

The electronic effects of the alkene substituents on the orientation of azide addition in all cases reported to date has been quite pronounced. In order to gain an insight into the effect of more remote alkene substituents on the orientation of azide addition we have determined the orientation

[1]To whom inquiries should be addressed.

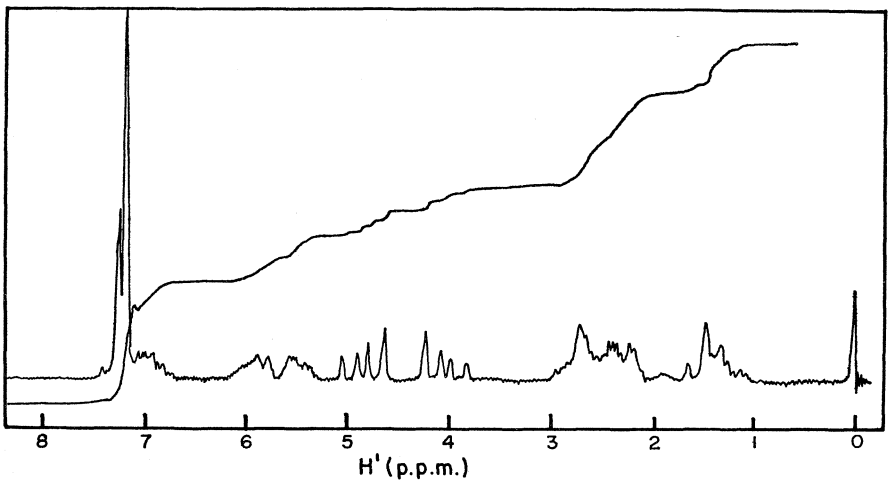

FIG. 1. Nuclear magnetic resonance spectrum of product **11** from reaction of phenyl azide and bicyclo(3.2.1)octa-2, 6-diene.

of addition to bicyclic homoconjugated dienes **8–10**. All of these dienes have one alkene bond which is highly strained and therefore should react rapidly with azide (1, 6). In each case only *exo* approach to the π cloud of the reactive alkene bond is sterically feasible (7). Furthermore, there

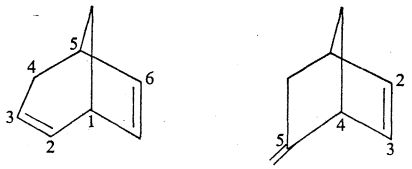

8 **9**

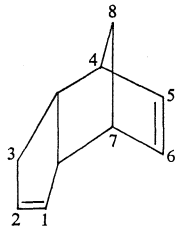

10

are no steric interactions which would favor either of the two possible orientations for addition of an azide to the *exo* side of the reactive double bonds of these dienes. Any preference for one orientation of *exo* addition of azide would therefore be a measure of the extent to which the distant, unreactive double bond of each diene provided stabilization to the dipolar transition state, **7**.

The reaction of excess phenyl azide with bicyclo(3.2.1)octa-2,6-diene (**8**) in inert solvent, at room temperature, leads to the formation of a monoaddition product, **11**. The nuclear magnetic resonance (n.m.r.) spectrum of **11** is reproduced in Fig. 1. The signals appearing in the δ 3.6–5.1 region are due to the hydrogens attached to the carbons bearing the nitrogens of the triazoline ring and definitely indicate the presence of more than one isomer. The presence of absorptions due to two olefinic hydrogens in the n.m.r. spectrum of **11** can, *a priori*, have two interpretations. First, **11** could be a mixture of triazoline adducts resulting from addition of azide to *both* the Δ^2 and Δ^6 double bonds of **8**. On the other hand, addition could have occurred *only* to the more strained Δ^6 double bond, but in two orientations. Since under the conditions of this reaction phenyl azide addition to bicyclo(3.2.1)oct-2-ene does not occur (8) but addition to bicyclo(2.2.1)hept-2-ene is facile, azide reaction with the Δ^6 and not the Δ^2 double bond of **8** is the correct interpretation. The mixture of isomers obtained is thus **11***a* and **11***b*.

Assignment of n.m.r. signals to H_2 and H_6 in **11***a* and **11***b* was made by comparison of the position of these signals with those due to similar hydrogens in **12** (9) and other triazolines (4). Huisgen *et al.* (9) report that signals due to H_2 and H_6 in **12** and its aryl-substituted derivatives are doublets (9.2–9.5 Hz) appearing at δ 3.64–3.68 and δ 4.51–4.58 respectively. Scheiner reports (4) hydrogens attached to C_5 of monocyclic triazo-

Can. J. Chem. Downloaded from www.nrcresearchpress.com by 210.87.254.6 on 09/05/12
For personal use only.

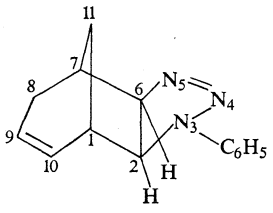

11*a*

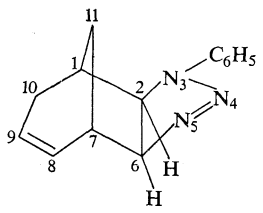

11*b*

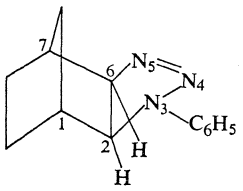

12

lines give n.m.r. signals between δ 3.6 and 4.0 whereas C_4 hydrogens resonate between δ 4.1 and 4.7. The two pairs of doublets (9.2 Hz) centered at δ 3.91 and 4.17 in the n.m.r. spectrum of **11** were thus assigned to H_2 of the isomers. Since H_2 of **11*a*** is sterically situated in the shielding portion of the π-cloud of the Δ^9 double bond, the n.m.r. signal due to this hydrogen would be expected at higher field than H_2 of **11*b***. Thus the doublet centered at δ 3.91 is assigned to H_2 in **11*a*** and the δ 4.17 doublet to H_2 in **11*b***. In a similar manner the doublets (9.2 Hz) centered at δ 4.74 and 4.98 were assigned to H_6 of **11*b*** and **11*a*** respectively. The above assignment is substantiated by the appearance of the doublets at δ 4.17 and 4.74 (**11*b***) which show strong perturbations causing the inside signal of each doublet to be significantly more intense than the outside signal. These perturbations are much less pronounced in the δ 3.91 and 4.98 doublets (**11*a***) as they should be . Integration also shows the pairs of doublets assigned to **11*a*** and **11*b*** to be correctly assigned. Integration of the AB quartets assigned to H_2 and H_6 of **11*a*** and **11*b*** showed **11*a*:11*b*** was 1.3:1.

Using benzene as an n.m.r. solvent had the effect of causing all hydrogens to resonate at higher field (10). That the effect is not uniform is evident from Table 1. The shielding experienced by H_2 of both **11*a*** and **11*b*** is considerably more (0.30–0.40 p.p.m.) than that experienced by H_6 (0.18–0.23 p.p.m.) in these isomers. We consider this to be due to unsymmetrical complexation of the benzene with **11*a*** and with **11*b***.

Ledaal (10) has summarized evidence for the formation of collision complexes between benzene and many different solutes. The model he proposed was one in which the dipole axis of the solute molecule coincided with the 6-fold symmetry axis of the benzene nucleus with the positive end of the dipole nearest to the benzene. For solutes with a dipole the solvent shift of different hydrogens of the solute increased as their proximity to the positive end of the dipole increased (i.e. the hydrogen lying in the diamagnetic shielding cone of the benzene nucleus was solvent-shifted the greatest amount). The larger the dipole moment, the larger the solvent shift for solutes of similar type.

Using the above model and the observed changes in chemical shift in **11*a*** and **11*b*** it is possible to designate the form of the **11*a***–benzene and **11*b***–benzene collision complexes. In both cases the benzene nucleus appears to lie below the solute molecule and to the side near the phenyl substituted nitrogen. The possibility that the benzene nucleus is situated at the end of the phenyl substituent of **11** as well as its location above the bicyclic ring system may be discounted because of the shifts observed *vide infra* (11).

The addition of phenyl azide to **9** gave a mixture of triazolines **13*a*** and **13*b***. That addition occurred to only the highly strained Δ^2 double bond was evident from the appearance of signals due to the C_{11} methylene hydrogens at δ 4.75 and 5.05. The hydrogens at C_2 and C_6 of **13*a*** and **13*b*** have an orientation with respect to the methylene bond

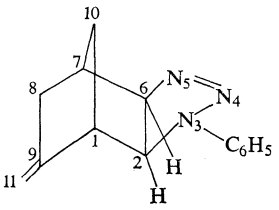

13*a*

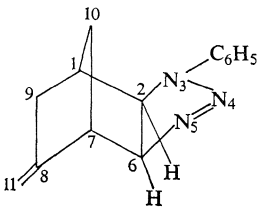

13*b*

similar to that of H_2 and H_6 in **11*a*** and **11*b*** with respect to the nuclear double bond in those triazolines. Thus, although in CCl_4, H_2 and H_6 in **13*a*** and **13*b*** were exhibited as a single AB quartet for both isomers, in benzene the two sets of AB quartets were sufficiently resolved to allow the assignment specified in Table 1. The **13*a*:13*b*** ratio was calculated in this case from integration of H_1 and H_7 signals in the benzene spectrum of these isomers to be 1.3:1. The bridgehead signal

Can. J. Chem. Downloaded from www.nrcresearchpress.com by 210.87.254.6 on 09/05/12
For personal use only.

TABLE 1
Chemical shifts of H_1, H_7, H_2, and H_6 of triazoline adducts

Sample	Solvent	Isomer *a*					Isomer *b*				
		H_1	H_7	H_2	H_6	$J_{2,6}$(Hz)	H_1	H_7	H_2	H_6	$J_{2,6}$(Hz)
	CCl_4	2.63	2.76	3.66	4.53	9.2	—	—	—	—	—
12	C_6H_6	2.23	2.50	3.12	4.17	9.2	—	—	—	—	—
	$\delta_{CCl} - \delta_{C_6H_6}$	0.40	0.26	0.54	0.36	—	—	—	—	—	—
	$CDCl_3$	—	—	3.91	4.98	9.2	—	—	4.17	4.74	9.2
11	C_6H_6	—	—	3.51	4.80	9.2	—	—	3.87	4.51	9.2
	$\delta_{CDCl_3} - \delta_{C_6H_6}$	—	—	0.40	0.18	—	—	—	0.30	0.23	—
p-NO_2**11**	C_5H_5N	—	—	4.00	5.15	9.0	—	—	4.25	4.99	9.0
	CCl_4	2.98	2.79	3.64	4.51	9.0	2.69	3.10	3.64	4.51	9.0
	C_6H_6	2.80	2.59	3.29	4.41	9.0	2.36	3.01	3.41	4.29	9.0
13	$\delta_{CCl_4} - \delta_{C_6H_6}$	0.18	0.20	0.35	0.10	—	0.33	0.9	0.23	0.22	—
	C_6F_6	2.97	2.71	3.59	4.46	9.0	2.71	2.97	3.59	4.46	9.0
	$\delta_{CCl_4} - \delta_{C_6F_6}$	0.01	0.08	0.05	0.05	—	−0.02	0.13	0.05	0.05	—
	CCl_4	—	—	3.56	4.37	9.0	—	—	3.56	4.43	9.0
	C_6H_6	—	—	3.27	4.27	9.0	—	—	3.27	4.26	9.0
14	$\delta_{CCl_4} - \delta_{C_6H_6}$	—	—	0.19	0.10	—	—	—	0.29	0.16	—
	$CDCl_3$	—	—	3.65	4.48	9.5	—	—	3.65	4.53	9.5
	$\delta_{CCl_4} - \delta_{CDCl_3}$	—	—	−0.09	−0.11	—	—	—	−0.09	−0.10	—

occurring at highest field in the benzene spectrum of the isomer mixture was assigned to H_1 of **13***b* because of its similarity in chemical shift to H_1 of **12**. Likewise, the signal at δ 2.79 was assigned to H_7 of **13***a*. Since the lowest field bridgehead hydrogen (δ 3.10) should be H_7 of **13***b*, the signal at δ 2.98 is deduced to be due to H_1 of **13***a*.

Addition of phenyl azide to *endo*-dicyclopentadiene has been reported several times (12, 13) but no evidence as to the homogeneity of the product has been available. Indeed the rather sharp melting range of the product could be construed as evidence for formation of a single triazoline adduct (14).

The n.m.r. spectrum of the addition product, **14**, revealed the presence of two olefinic hydrogens. Since phenyl azide addition proceeds readily with *exo*-1,2-dihydro-**10** (13, 15) but not with *exo*-5,6-dihydro-**10** (15) addition in the present case must have occurred to the Δ^5-double bond of **10**. Inspection of the δ 3.5–4.5 region of the n.m.r. spectrum of **14** revealed the presence of two isomeric triazolines. The AB quartet patterns of H_2 and H_6 in **14** were assigned to **14***a* and **14***b* as given in Table 1. Integration of the AB quartets due to H_2 and H_6 in **14***a* and **14***b* showed **14***a*:**14***b* to be 1.3:1.

The observation that there is a higher proportion of the "*a*" isomers than the "*b*" isomers in **11**, **13**, and **14** is interpreted in terms of stabilization of the positive charge generated at C_2 in the transition state leading to the "*a*" isomers. In each case (**8**–**10**) studied the π-cloud of the unreacting double bond is favorably situated for such homoconjugative stabilization. It is noteworthy that the addition of formic acid to **8** gives over 90% **15**, the result of homoconjugative participation by the Δ^2 double bond (16). Likewise **9** is reported to give a high proportion of **16** with formic acid (17). The orientation effect of the unreacting double bond in the dienes studied is significantly less in the azide reaction than in the formic acid addition. The

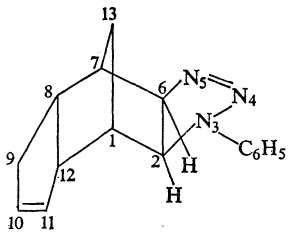

14*a*

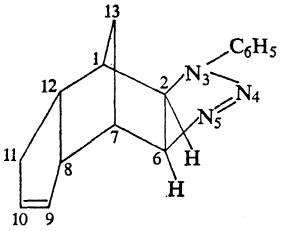

14*b*

Can. J. Chem. Downloaded from www.nrcresearchpress.com by 210.87.254.6 on 09/05/12
For personal use only.

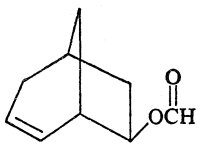

15

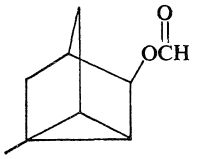

16

origin of this difference presumably lies in the amount of electron deficiency generated at C_2 in each type of reaction. The greater the electron deficiency the greater the orientation effect. Pursuing this reasoning one might expect (5) that substitution of an electron-withdrawing group (e.g. *p*-NO_2) on the aryl azide would introduce greater dipolar character into the transition state (**7**) for addition and thereby produce a greater orientational preference. The addition of *p*-nitrophenyl azide to **8** gave a mixture of *p*-nitrophenyl substituted **11***a* and **11***b*. The ratio of "isomer *a*" to "isomer *b*" was 1.5:1.

Calculation of the isomer ratio resulting from the *p*-nitrophenyl azide addition to **9** and **10** was unsuccessful because of the insolubility of the adducts in solvents in which the necessary signals could be resolved.

NOTE ADDED IN PROOF — Since the submission of this paper a report of *exo* and *endo* addition of phenyl azide to bicyclo(2.2.1)-2,5-heptadiene (**17**) has appeared (20). The ratio of *exo* to *endo* addition for monoaddition was 11:1. These workers observed a coupling of 3.5–4.5 Hz between the bridgehead hydrogens and the *exo* hydrogens attached to the *endo* triazoline adduct (**18**). Since the degree of steric hindrance on the *endo* side of **17** is less than in either **8**, **9**, or **10** one would expect an even higher proportion of *exo* addition in the present cases. The fact that no coupling of hydrogens attached to the triazoline rings in any of the adducts revealed any appreciable coupling with adjacent bridgehead hydrogens indicates all of the adducts presently investigated were *exo*.

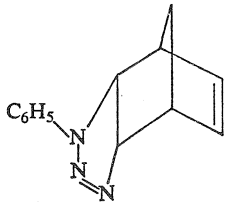

18

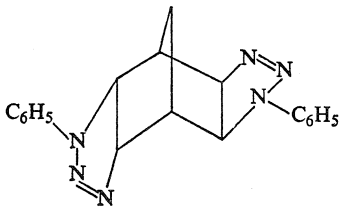

19

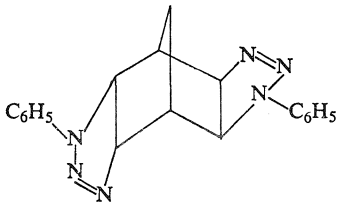

20

Finally, in agreement with the above discussion, the addition of phenyl azide to **18** gave a mixture of **19** and **20** in which **19** predominated (**19**:**20** was 1:5).

Experimental

Melting points were determined using a Fisher–Johns melting point apparatus and are uncorrected.

Nuclear magnetic resonance spectra were recorded on a Varian Model A56/60 spectrometer using tetramethylsilane as an internal standard.

Mass spectra were recorded on a Hitachi Perkin–Elmer RU-6 mass spectrometer.

Preparation of 3-Phenyl-3,4,5-triazotricyclo(5.2.1.0^{2,6})dec-4-ene (12)

The phenyl azide adduct of bicyclo(2.2.1)hept-2-ene was prepared in the usual manner (18) and had m.p. 99–100 °C (lit. (5) m.p. 101–102 °C). The n.m.r. spectra (18) confirmed the structure and purity of the adduct (Table 1).

Preparation of 3-Phenyl-3,4,5-triazotricyclo(5.3.1.0^{2,6})undec-4,8(9)-dienes (11)

A solution of 0.5 g of phenyl azide and 0.5 g of bicyclo-(3.2.1)octa-2,6-diene (19) in 25 ml of petroleum ether (b.p. 60–110°) was allowed to stand for several days. The excess phenyl azide was removed under vacuum and the crystalline sample was analyzed by n.m.r. Recrystallization from $CHCl_3$ – petroleum ether (b.p. 30–60°) gave a white solid in 85% yield, m.p. 67.5–69 °C. The n.m.r. analysis of the recrystallized product (Fig. 1) revealed no detectable change in **11***a*:**11***b* had occurred during the recrystallization.

Anal. Calcd. for $C_{14}H_{15}N_3$: $(M)^+$ 225. Found (mass spectrometry): $(M)^+$ 225; $(M\text{-}28)^+$ 197.

The *p*-nitrophenyl derivative of **11** had m.p. 168–90°; n.m.r. (pyridine) δ 1–2 (m, 4H), 2–3 (m, 8H), 4.0–5.2 (m, 2H Table 1) and 5.35–6.3 (m, 2H).

Can. J. Chem. Downloaded from www.nrcresearchpress.com by 210.87.254.6 on 09/05/12
For personal use only.

*Preparation of 3-Phenyl-8(9)-methylene-3,4,5-triazotricyclo(5.2.1.0^{2,6})dec-4-enes (**13**)*

The phenyl azide adduct of 5-methylene-2-norbornene (K and K Laboratories, Inc.) was prepared in the usual manner by reaction at room temperature for several days. The crude product showed the same **13***a*:**13***b* as that (70%) recrystallized from $CHCl_3$ – petroleum ether (b.p. 30–60°) m.p. 60.5–62°.

Anal. Calcd. for $C_{14}H_{15}N_3$: $(M)^+$ 225. Found (mass spectrometry): $(M)^+$ 225; $(M\text{-}28)^+$ 197.

The *p*-nitrophenyl derivative of **13** had m.p. 159–160 °C (decomposition) n.m.r. (pyridine) δ 1.14 (AB, J = 11Hz, $2H_{10}$), 1.83–2.35 (b, $2H_{8(9)}$), 2.42–2.92 (m, $2H_{BH}$), 3.12 (m, $1H_2$), 3.82 (d, J = 9Hz, $1H_6$), 4.80, and 5.08 ($H_2C{=}C\langle$). The AB quartets due to H_2 and H_6 of isomers *a* and *b* were also uncompletely resolved in benzene, chloroform.

*Preparation of **14***

The phenyl azide adduct of *endo*-dicyclopentadiene (Aldrich Chemical Co.) was prepared by reaction at room temperature for several days. Recrystallization of the crude product gave 75% **14**, m.p. 117–118° (lit. (13) 127–128 °C (MeOH); for n.m.r. see Table 1.

Anal. Calcd. for $C_{13}H_{17}N_3$: $(M)^+$ 251. Found (mass spectrometry): $(M)^+$ 251; $(M\text{-}28)^+$ 223.

The *p*-nitrophenyl derivative of **14** had m.p. 183–184 °C (decomposition); n.m.r. ($CHCl_3$) δ 1.28 (AB, J = 11Hz, $2H_{13}$), 2.2–2.8 (m, 4H), 2.8–3.5 (m, $2H_{BH}$), 3.72 (d, J = 9.2 Hz, $1H_2$), 4.62 (d, J = 9.2 Hz, H_{6b}), 4.67 (d, J = 9.2 Hz, H_{6a}), and 5.72 (s, 2H).

We wish to thank the N.R.C.C. and the S.F.U. Research Fund for financial support of this work. R.S.M. wishes to thank the N.R.C.C. for a 1967–1968 Bursary.

1. R. Huisgen. Angew. Chem. Int. Ed. Engl. **2**, 565 (1963).
2. R. Huisgen and G. Szeimies. Chem. Ber. **98**, 1153 (1965).
3. G. D. Buckley. J. Chem. Soc. 1850 (1954).
4. P. Scheiner. Tetrahedron, **24**, 349 (1967).
5. P. Scheiner, J. H. Schomaker, S. Deming, W. J. Libbey, and G. P. Nowack. J. Amer. Chem. Soc. **87**, 306 (1965).
6. K. Alder and G. Stein. Ann. **515**, 165 (1935).
7. K. Alder and G. Stein. Ann. **515**, 185 (1935).
8. K. Alder, H. Krieger, and H. Weiss. Chem. Ber. **88**, 144 (1955).
9. R. Huisgen, L. Moebius, G. Mueller, H. Stangl, G. Szeimies, and J. M. Vernon. Chem. Ber. **98**, 3992 (1965).
10. T. Ledaal. Tetrahedron Letters, 1683 (1968).
11. P. Laszlo and P. von R. Schleyer. J. Amer. Chem. Soc. **86**, 1171 (1964).
12. K. Alder and G. Stein. Ann. **504**, 216 (1933).
13. E. Fumakubo, I. Maritani, H. Taniguchi, T. Yamamoto, and S. Tuchiya. Chem. Ber. **96**, 2035 (1963).
14. H. E. Simmons, E. P. Blanchard, and R. D. Smith. J. Amer. Chem. Soc. **86**, 1347 (1964); especially ref. 48.
15. P. Wilder, Jr. and G. T. Youngblood. J. Amer. Chem. Soc. **78**, 5706 (1956); J. Org. Chem. **21**, 1436 (1956).
16. R. A. Appelton, J. C. Fairlie, R. McCrindle, and W. Parker. J. Chem. Soc. C, 1716 (1968).
17. P. von R. Schleyer and R. E. O'Connor, 134th Amer. Chem. Soc. Meeting, Chicago, Ill., September, 1958; Abstracts, 39P.
18. R. S. McDaniel and A. C. Oehlschlager. Tetrahedron, **25**, 1381 (1969).
19. J. M. Brown and J. L. Occolowitz. J. Chem. Soc. 411 (1968).
20. S. McLean and D. M. Findlay. Tetrahedron Letters, 2219 (1969).

Can. J. Chem. Downloaded from www.nrcresearchpress.com by 210.87.254.6 on 09/05/12
For personal use only.

Some reactions of hydrazine with ruthenium compounds

F. BOTTOMLEY[1]
Lash Miller Chemical Laboratories, University of Toronto, Toronto 181, Ontario
Received July 21, 1969

Some reactions of hydrazine with pentachloroaquoruthenite(III) and ammine complexes of ruthenium(II) and ruthenium(III) have been investigated in acid, neutral, and alkaline solution. In neutral solution it has been shown that hydrazine monohydrochloride oxidized hexaammineruthenium(II) to hexaammineruthenium(III). In alkaline solution nitrogenpentaammineruthenium(II) was formed, and a mechanism for this reaction is postulated.

Canadian Journal of Chemistry, **48**, 351 (1970)

Can. J. Chem. Downloaded from www.nrcresearchpress.com by 210.87.254.5 on 09/05/12
For personal use only.

Introduction

Goremykin and Avtokratora reported that addition of potassium pentachloroaquoruthenite, $K_2[Ru^{III}Cl_5H_2O]$, to a saturated solution of hydrazine hydrochloride, N_2H_5Cl, at room temperature yielded a compound formulated as $[Ru_2(N_2H_5)_4N_2H_4Cl_6]Cl_4.HCl$ (1). By heating an aqueous solution of this complex, or by heating a saturated aqueous solution of N_2H_5Cl with $K_2[RuCl_5H_2O]$, a second compound formulated as $[Ru_2Cl_2(N_2H_5)_5]Cl_4$ was obtained. Powell and Prout prepared $[Ru_2Cl_2(N_2H_5)_5]Cl_4$ from N_2H_5Cl and $K_2[Ru^{III}Cl_5H_2O]$ and by X-ray crystallography and chemical analysis showed that it was in fact chloropentaammineruthenium(III) dichloride, $[Ru^{III}(NH_3)_5Cl]Cl_2$ (2). These workers did not investigate the complex $[Ru_2(N_2H_5)_4N_2H_4Cl_6]Cl_4.HCl$.

Allen and co-workers reported that the reaction of hydrazine hydrate, $N_2H_4.H_2O$, with either ruthenium trichloride,[2] $RuCl_3$, ammonium hexachlororuthenate(IV), $(NH_4)_2[Ru^{IV}Cl_6]$, or $K_2[Ru^{III}Cl_5H_2O]$ yielded a mixture of nitrogenpentaammineruthenium(II), $[Ru^{II}(NH_3)_5N_2]^{2+}$, and hexaammineruthenium(II), $[Ru^{II}(NH_3)_6]^{2+}$, isolated with a variety of monoanions (3, 4). Fergusson and Love (5) reported that at -23 °C this reaction gave a mixture containing hydrazine and dinitrogen complexes of ruthenium(II).

Because of the variety of products obtained the reactions of hydrazine with ruthenium complexes have been investigated in more detail.

Results

Reaction in Acid Solution

The reported preparation of the compound $[Ru_2(N_2H_5)_4N_2H_4Cl_6]Cl_4.HCl$ (1) could not be repeated. At room temperature there was no apparent reaction between $K_2[Ru^{III}Cl_5H_2O]$ and N_2H_5Cl, though on heating $[Ru^{III}(NH_3)_5Cl]Cl_2$ was obtained, as described by Powell and Prout (2). A red compound having similar analytical, magnetic, and explosive properties to those described by the Russian workers was obtained using hydrazine dihydrochloride, $N_2H_6Cl_2$, instead of N_2H_5Cl. The infrared spectrum showed the compound contained hydrazine. Ion exchange showed that the compound was composed of a red anion and a colorless hydrazine-containing cation. In aqueous solution $N_2H_6Cl_2$ is completely dissociated

$$H_2O + N_2H_6Cl_2 \rightarrow N_2H_5^+ + H_3O^+ + 2Cl^-$$

The resultant high chloride ion concentration of a saturated solution of $N_2H_6Cl_2$ would appear to preclude loss of chloride ligand from $[Ru^{III}Cl_5H_2O]^{2-}$. Hence the compound has been reformulated as $N_2H_5[Ru^{III}Cl_5N_2H_5]\cdot\frac{1}{2}N_2H_5Cl$. The decomposition of the complex in all solvents except 6 *M* hydrochloric acid prevented further investigation.

Reactions in Neutral Solution

When an aqueous solution of $[Ru^{II}(NH_3)_6]^{2+}$ or $[Ru^{II}(NH_3)_5N_2]^{2+}$ was heated with N_2H_5Cl, in air or under argon, hexaammineruthenium(III), $[Ru^{III}(NH_3)_6]^{3+}$, isolated as iodide and tetrafluoroborate salts, was obtained. Slow decomposition to the blue solutions characteristic of aquochloro complexes of ruthenium(II) (6) took place when either starting material was heated in aqueous solution not containing N_2H_5Cl, a

[1]Present address: Department of Chemistry, University of New Brunswick, Fredericton, New Brunswick.

[2]Ruthenium trichloride as used in this work is a mixture of aquochlororuthenium-(III) and -(IV). All references to $RuCl_3$ are to this material.

Can. J. Chem. Downloaded from www.nrcresearchpress.com by 210.87.254.5 on 09/05/12
For personal use only.

result in qualitative agreement with those of Taube and co-workers (7). In aqueous solution containing excess chloride ion, slow decomposition took place in the case of $[Ru^{II}(NH_3)_5N_2]^{2+}$ and much more rapid decomposition in the case of $[Ru^{II}(NH_3)_6]^{2+}$. In hydrochloric acid solution the decomposition was considerably accelerated. Heating a solution of N_2H_5Cl and $[Ru^{II}(NH_3)_6]^{2+}$ or $[Ru^{II}(NH_3)_5N_2]^{2+}$ containing excess chloride ion gave $[Ru^{III}(NH_3)_6]^{3+}$ initially, but moderately rapid substitution of ammonia by chloride took place to form $[Ru^{III}(NH_3)_5Cl]Cl_2$, which was isolated and identified. The reaction

$$[Ru^{III}(NH_3)_6]^{3+} + Cl^- \rightarrow [Ru^{III}(NH_3)_5Cl]^{2+}$$

has been investigated previously (8).

Heating an aqueous solution of $[Ru^{III}(NH_3)_5Cl]Cl_2$ with N_2H_5Cl also yielded $[Ru^{III}(NH_3)_6]^{3+}$.

Allen and co-workers reported that addition of concentrated hydrochloric acid to a mixture of $N_2H_4.H_2O$ and $RuCl_3$ yielded on refluxing $[Ru^{III}(NH_3)_5Cl]Cl_2$ (4). In the present work when hydrochloric acid was added to a mixture of $RuCl_3$ and $N_2H_4.H_2O$, there was no apparent reaction until the solution became neutral, when, with vigorous gas evolution, the solution rapidly turned from red to pale yellow. The electronic spectrum of this solution showed absorption bands attributable to $[Ru^{III}(NH_3)_6]^{3+}$ and $[Ru^{III}(NH_3)_5Cl]^{2+}$ (8–10). Further addition of hydrochloric acid to the hot solution resulted in complete conversion to $[Ru^{III}(NH_3)_5Cl]Cl_2$, which was isolated and identified. The reaction proceeded in the same manner in argon or in air.

Because of the above results, the reaction between N_2H_5Cl and $K_2[Ru^{III}Cl_5H_2O]$ (2) was reinvestigated. The electronic spectrum of the reaction solution showed the presence of both $[Ru^{III}(NH_3)_6]^{3+}$ and $[Ru^{III}(NH_3)_5Cl]^{2+}$. Because of the substitution reaction only the latter could be isolated pure. The major product of the reaction, as reported by Powell and Prout (2), was $[Ru^{III}(NH_3)_5Cl]Cl_2$. A further product trichlorotrisammineruthenium(III), $[Ru^{III}(NH_3)_3Cl_3]$ (approximately 10% of product), was also isolated as an insoluble residue on recrystallization.

Reactions in Alkaline Solution

When $N_2H_4.H_2O$ was reacted with $RuCl_3$, $K_2[Ru^{III}Cl_5H_2O]$, or $(NH_4)_2[Ru^{IV}Cl_6]$ there was an exothermic reaction, vigorous gas evolution, and rapid formation of a red color. On cooling in air the red color slowly faded. When potassium iodide was added at any time after formation of the red color, a pale yellow mixture of $[Ru^{II}(NH_3)_5N_2]I_2$ and $[Ru^{II}(NH_3)_6]I_2$ was obtained (identified by spectroscopy (4)). At 0 °C in ethanol, under argon, $RuCl_3$ and $N_2H_4.H_2O$ yielded a red insoluble solid, recrystallized by dissolving in water and adding potassium iodide. The infrared spectrum indicated that the product contained hydrazine, molecular nitrogen, and ammonia. This material could not be purified further.

When an aqueous solution of $[Ru^{II}(NH_3)_6]^{2+}$ was heated with $N_2H_4.H_2O$ under argon the solution became red with evolution of hydrogen and nitrogen. The electronic spectra of the reaction solution over a period of time are shown in Fig. 1. On cooling under argon the red color did not fade, but on passing oxygen into the solution it rapidly became pale yellow and addition of potassium iodide yielded a mixture of $[Ru^{II}(NH_3)_5N_2]I_2$ and $[Ru^{II}(NH_3)_6]I_2$. Addition of potassium iodide to the cooled red solution under argon yielded a red solid. The infrared spectrum of this solid showed a weak absorption

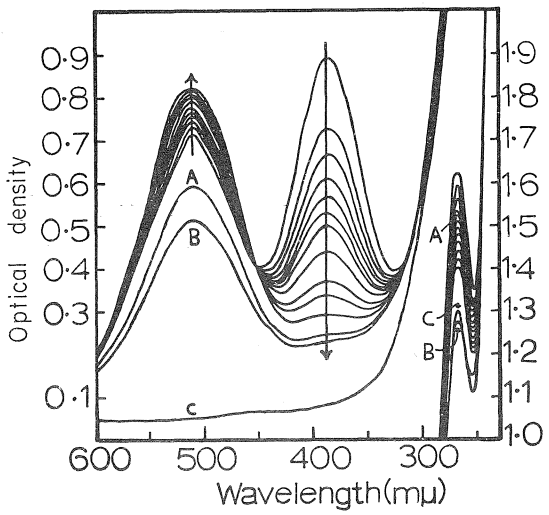

FIG. 1. Electronic spectra of the reaction between $[Ru^{II}(NH_3)_6]^{2+}$ and $N_2H_4.H_2O$. Spectra are plotted at intervals of 15 min. Spectra labelled *A*, *B*, and *C* were taken 6, 12, and 24 h, respectively, after opening cell to air. Concentration of $[Ru^{II}(NH_3)_6]^{2+}$: 7.5×10^{-4} moles per l.

band at 2129 cm^{-1} (νN_2 of $[Ru^{II}(NH_3)_5N_2]I_2$ (4)), strong absorption bands attributable to coordinated ammonia, but no other absorption bands. The solid was diamagnetic. This material was never obtained free from $[Ru^{II}(NH_3)_5N_2]I_2$, and it is probable that it contained $[Ru^{II}(NH_3)_6]I_2$ as well.

Similar results were obtained using $[Ru^{III}(NH_3)_6]^{3+}$ or $[Ru^{III}(NH_3)_5Cl]Cl_2$ as starting material.

Discussion

Reaction in Acid Solution

Although $N_2H_5^+$ is known as a ligand and as a cation (11, 12), the formulation $N_2H_5[Ru^{III}Cl_5N_2H_5]\frac{1}{2}N_2H_5Cl$ is not satisfactory, and a crystal structure analysis is planned to confirm the nature of the complex.

Reactions in Neutral Solution

The results indicate that in reactions of ruthenium(III) complexes with N_2H_5Cl, the hydrazine first reduces the ruthenium to a ruthenium(II) complex. In aqueous solution ammonia reacts with ruthenium(III) to give hydroxy complexes or polymers, but with ruthenium(II) ammine complexes are formed (6, 13). Therefore substitution by ammonia takes place after reduction to ruthenium(II) when aquochloro complexes of ruthenium(III) are used as starting material. The first identifiable product appears to be $[Ru^{II}(NH_3)_6]^{2+}$. This is then oxidized to $[Ru^{III}(NH_3)_6]^{3+}$. The mechanism of this reaction is unknown, but is under investigation and will be reported later. If excess chloride ion is present, substitution occurs, yielding $[Ru^{III}(NH_3)_5Cl^{2+}$.

Reaction of hydrochloric acid with a hydrazine hydrate – ruthenium trichloride mixture yields N_2H_5Cl from excess $N_2H_4.H_2O$. The solution contains $[Ru^{II}(NH_3)_5N_2]^{2+}$ and $[Ru^{II}(NH_3)_6]^{2+}$ (4). Oxidation by N_2H_5Cl yields $[Ru^{III}(NH_3)_6]^{3+}$ and further addition of chloride ion finally yields insoluble $[Ru^{III}(NH_3)_5Cl]Cl_2$. The oxidizing agent is N_2H_5Cl, not air or hydrochloric acid.

The reactions are summarized below

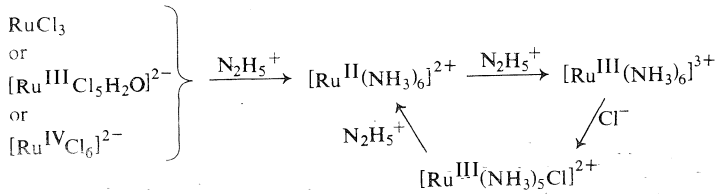

Oxidation by hydrazine (other than autoxidation), although proposed from consideration of electrode potentials (14), has rarely been observed. Titanium(III) (15) and chromium(II) (16) complexes are oxidized to titanium(IV) and chromium(III), respectively, by hydrazine in acid solution and Chatt *et al.* (17) have reported the reaction

$$(Et_2PhP)_3Re^{III}Cl_3 + N_2H_6Cl_2 \rightarrow (Et_2PhP)_2Re^{IV}Cl_4$$

These appear to be the only other well-documented oxidations of transition-metal complexes by hydrazine.

Powell and Prout noted that the crystals of $[Ru^{III}(NH_3)_5Cl]Cl_2$ which they investigated appeared to be disordered or contain impurity (2). In the light of the results presented here it is possible that either $[Ru^{III}(NH_3)_6]Cl_3$ or $[Ru^{III}(NH_3)_3Cl_3]$ was present in their sample.

Reactions in Alkaline Solution

As with the reactions in neutral solution, the initial product of the reaction between $N_2H_4.H_2O$ and aquochlororuthenium-(III) or -(IV) complexes is probably $[Ru^{II}(NH_3)_6]^{2+}$. From the results of the reaction between $N_2H_4.H_2O$ and $[Ru^{II}(NH_3)_6]^{2+}$, the following mechanism for the reaction is proposed based on the results of the reactions in neutral solution. The electronic spectra of the various intermediates are included

$$\underset{267\ m\mu\ (20)}{[Ru^{II}(NH_3)_6]^{2+}} + N_2H_4 \rightarrow \underset{276\ m\mu\ (11)}{[Ru^{III}(NH_3)_6]^{3+}}$$

$$\underset{276\ m\mu}{[Ru^{III}(NH_3)_6]^{3+}} + N_2H_4 \rightarrow \underset{380\ m\mu}{[Ru^{III}(NH_3)_5N_2H_4]^{3+}}$$

$$\underset{380\ m\mu}{[Ru^{III}(NH_3)_5N_2H_4]^{3+}} \xrightarrow{\text{fast}} \underset{510\ m\mu}{[Ru^{II}(NH_3)_5(NH{=}NH)]^{2+}} + \tfrac{1}{2}H_2$$

$$\underset{510\ m\mu}{[Ru^{II}(NH_3)_5(NH{=}NH)^{2+}} + O_2 \rightarrow \underset{221\ m\mu\ (4)}{[Ru^{II}(NH_3)_5N_2]^{2+}}$$

Because none of the proposed intermediates has been identified, this mechanism must be regarded

Can. J. Chem. Downloaded from www.nrcresearchpress.com by 210.87.254.5 on 09/05/12
For personal use only.

Can. J. Chem. Downloaded from www.nrcresearchpress.com by 210.87.254.5 on 09/05/12
For personal use only.

as speculative. In view of the solution reaction with oxygen it appears reasonable to formulate the red compound which was isolated as a diimide complex. It is unfortunate that in the infrared spectrum of such a complex the band due to the N=N stretching vibration would be obscured by the NH_3 degenerate deformation band at around 1600 cm^{-1}. A similar problem has been noted before (18, 19). Therefore, no *positive* evidence is available for the formulation given. The possibility that the observed changes are due to minor side products (e.g., the formation of intensely colored polymeric species such as ruthenium red (13)) is discounted because of the observed reaction with oxygen. It was found that molecular N_2 reacts very slowly, if at all, with $[Ru^{II}(NH_3)_6]^{2+}$, in agreement with the observations of Taube and co-workers (7). Hence this is not the source of $[Ru^{II}(NH_3)_5N_2]^{2+}$. The presence of $[Ru^{II}(NH_3)_6]^{2+}$ in the product may be explained either as unreacted starting material, or, when aquochlororuthenium-(III) or -(IV) complexes were used as starting material, by the replacement of coordinated N_2 by NH_3 in the highly ammoniacal solution, a reaction reported earlier (3, 4).

Experimental

Ruthenium trichloride and potassium pentachloroaquoruthenite(III) were purchased from Johnson, Matthey, and Mallory Limited and used as received. All other chemicals were reagent grade.

Nitrogenpentaammineruthenium(II)dichloride

This was prepared by a modification of Method 3 of ref. 4. A slurry of chloropentaammineruthenium(III) dichloride (1.0 g) in water (10 ml) was heated to 60 °C. Concentrated ammonia was added, dropwise, until the yellow complex dissolved to yield a wine-red solution. This was cooled in ice and methanesulfonic acid added dropwise, with stirring, until the p*H* of the solution was 4. Sodium azide (5 g) was added and the solution stirred at room temperature with frequent additions of methanesulfonic acid until the orange solution became pale yellow. Sodium chloride was added, and the resultant precipitate removed by filtration. The crude product was recrystallized 3 times by dissolving in water and adding sufficient sodium chloride to reprecipitate. The final product was washed with acetone and air dried. Yield: 0.5 g (50%).

Anal. Calcd. for $Cl_2H_{15}N_7Ru$: Cl, 24.86; H, 5.30; N, 34.38. Found: Cl, 25.38; H, 5.39; N, 34.10.

Chloropentaammineruthenium(III)dichloride

This was prepared by literature methods (4, 21).

Anal. Calcd. for $Cl_3H_{15}N_5Ru$: Cl, 36.35; H, 5.19; N, 23.93. Found: Cl, 34.84; H, 5.30; N, 23.90.

Hexaammineruthenium(II)chlorozincate

This was prepared by the method of Lever (6).

Anal. Calcd. for $Cl_4H_{18}N_6RuZn$: Cl, 34.55; H, 4.42; N, 20.47. Found: Cl, 34.93; H, 4.47; N, 20.86.

Hexaammineruthenium(III)triiodide

Hexaammineruthenium(II)chlorozincate (0.5 g) was dissolved in deoxygenated water (15 ml) and drops of ammonia added until no further precipitation of zinc hydroxide was observed. The zinc hydroxide was removed by filtration, the filtrate was neutralized with dilute hydrochloric acid, and to the solution a deoxygenated solution of hydrazine monohydrochloride (5 g) in water (10 ml) was added. The solution was boiled gently under argon until it became colorless, cooled, and a saturated, filtered, deoxygenated solution of potassium iodide added. The product was collected by filtration, washed quickly with deoxygenated water, alcohol, and ether, and dried under argon. Yield: 0.5 g, 70%.

Anal. Calcd. for $H_{18}I_3N_6Ru$: H, 3.11; I, 65.19; N, 14.48. Found: H, 3.06; I, 65.01; N, 14.48.

The electronic and infrared spectra and magnetism of the product agreed closely with those reported in the literature (10, 22–24). The above preparation is very rapid and convenient and provides an improved synthesis of hexaammineruthenium(III). For preparative purposes the reaction proceeds equally well in air. The same product was obtained when chloropentaammineruthenium(III)-dichloride (0.5 g) or nitrogenpentaammineruthenium(II)-dichloride (0.5 g) was used as starting material.

Reaction between Potassium Pentachloroaquoruthenite(III) and Hydrazine Monohydrochloride.

Potassium pentachloroaquoruthenite(III) (1.0 g) was dissolved in water (20 ml) and hydrazine monohydrochloride (10 g) added. The solution was boiled vigorously, precipitating a yellow-orange solid. The mixture was cooled and the precipitate collected by filtration. A slurry of the precipitate in water (10 ml) was heated to 60° and concentrated ammonia added dropwise, yielding a wine-red solution and an orange insoluble solid. The mixture was filtered, the filtrate cooled, and concentrated hydrochloric acid added. The yellow precipitate was collected by filtration, washed with water, alcohol, and ether, and air dried. Yield: 0.65 g, 75%. The product, $[Ru^{III}(NH_3)_5Cl]Cl_2$, was spectroscopically identical to that prepared by methods described above.

The orange residue was insoluble in dilute ammonia, water, and ethanol. From the infrared spectrum, chemical properties, and analysis it appeared to be trichlorotrisammineruthenium(III).

Anal. Calcd. for $Cl_3H_9N_3Ru$: Cl, 41.14; H, 3.51; N, 16.25. Found: Cl, 40.37; H, 3.51; N, 16.20.

Reaction Between Hydrazine Dihydrochloride and Potassium Pentachloroaquoruthenite(III)

Potassium pentachloroaquoruthenite(III) (0.5 g) was carefully added to a saturated solution of hydrazine dihydrochloride (25 ml). The solution became red-orange and after a few minutes red-orange crystals began to separate. The mixture was allowed to stand overnight at 5 °C, the crystals collected by filtration, washed with alcohol and ether, and air dried.

Anal. Calcd. for $(N_2H_5)[Ru^{III}Cl_5N_2H_5].\frac{1}{2}N_2H_5Cl$: Cl, 51.48; H, 3.33; N, 18.49; Ru, 26.70. Found (this work): Cl, 51.49; H, 2.65; N, 18.49. Found (ref. 1): Cl, 51.50; N, 18.63; Ru, 26.27.

The magnetic properties of the complex were identical to those found by the Russian workers if the different formulae are taken into account. The infrared spectrum showed bands at 1076, 1167, and 1209 cm^{-1}, attributable to hydrazine.

Reaction of Hydrazine Hydrate with Hexaammineruthenium(II)

All operations were carried out in an argon atmosphere and all solvents were deoxygenated with argon before use. Hexaammineruthenium(II)chlorozincate (0.5 g) was dissolved in water (15 ml), ammonia added dropwise, and the resultant precipitate of zinc hydroxide removed by filtration. To the solution was added hydrazine hydrate (5 ml) (85% aqueous solution) and the solution heated gently until it became deep red. It was cooled and a saturated, filtered solution of potassium iodide added. The precipitate was washed well with water, alcohol, and ether and dried. The ratio of N:I for the complex was approximately 3.3:1 by microanalyses, but was not reproducible from one preparation to another.

Electronic spectra were measured with a Bausch and Lomb Spectronic 505 instrument, infrared spectra with a Perkin–Elmer Model 521 spectrophotometer, using Nujol or hexachlorobutadiene mulls between potassium chloride plates. Magnetic moments were measured by the Gouy method. Gaseous reaction products were analyzed on a Fisher gas partitioner chromatograph. *p*-Dimethylaminobenzaldehyde was used to test for hydrazine (25). Microanalyses were by A. B. Gygli, Toronto.

The author wishes to thank the National Research Council of Canada for financial assistance during this work, Professor A. D. Allen for extremely helpful discussions, and a referee for valuable comments.

1. V. I. Goremykin and T. D. Avtokratora. Izv. Akad. Nauk SSSR, Otd. Khim. Nauk, 427 (1947).
2. H. M. Powell and C. K. Prout. J. Chem. Soc. 137 (1962).
3. A. D. Allen and C. V. Senoff. Chem. Commun. 621 (1965).
4. A. D. Allen, F. Bottomley, R. O. Harris, V. P. Reinsalu, and C. V. Senoff. J. Amer. Chem. Soc. **89**, 5595 (1967).
5. J. E. Fergusson and J. L. Love. Chem. Commun. 399 (1969).
6. F. M. Lever and A. R. Powell. Chem. Soc. London, Spec. Publ. **13**, 135 (1959).
7. P. C. Ford, J. R. Kuempel, and H. Taube. Inorg. Chem. **7**, 1976 (1968).
8. T. E. Eliades. Ph.D. Thesis, University of Toronto, Toronto, Ontario. 1968.
9. J. A. Broomhead, F. Basolo, and R. G. Pearson. Inorg. Chem. **3**, 826 (1964).
10. H. Hartmann and C. Buschbeck. Z. Phys. Chem. Frankfurt, **11**, 120 (1957).
11. C. K. Prout and H. M. Powell. J. Chem. Soc. 4177 (1961).
12. A. Braibanti, A. M. M. Lanfredi, and A. Tripicchio. Z. Krist. **124**, 335 (1967).
13. J. M. Fletcher, B. F. Greenfield, C. J. Hardy, D. Scargill, and J. L. Woodhead. J. Chem. Soc. 2000 (1961).
14. W. M. Latimer. Oxidation potentials. 2nd ed. Prentice–Hall Inc., Englewood Cliffs, New Jersey. 1952. p. 99.
15. D. Nicholls and R. Swindells. J. Chem. Soc. 4204 (1964).
16. C. F. Wells and M. A. Salam. J. Chem. Soc. A, 1568 (1968).
17. J. Chatt, J. D. Garforth, N. P. Johnson, and G. A. Rowe. J. Chem. Soc. 601 (1964).
18. R. B. King and M. B. Bisnette. Inorg. Chem. **5**, 300 (1966).
19. G. W. Parshall. J. Amer. Chem. Soc. **87**, 2133 (1965).
20. C. V. Senoff. Ph.D. Thesis, University of Toronto, Toronto, Ontario. 1965.
21. K. Gleu and K. Rehm. Z. Anorg. Allg. Chem. 227 (1936); 237 (1936).
22. A. D. Allen and C. V. Senoff. Can. J. Chem. **45**, 1337 (1967).
23. M. B. Fairey and R. J. Irving. Spectrochim. Acta, **22**, 359 (1966).
24. L. H. Vogt, J. L. Katz, and S. E. Wibberley. Inorg. Chem. **4**, 1157 (1965).
25. M. Pesez and A. Petit. Bull. Soc. Chim. France, **14**, 122 (1947).

Can. J. Chem. Downloaded from www.nrcresearchpress.com by 210.87.254.5 on 09/05/12
For personal use only.

Use of zero-intensity extrapolations in photochemistry

F. R. CALA, S-L. CHONG, H. P. SPERLING, AND S. TOBY
School of Chemistry, Rutgers University, New Brunswick, New Jersey 08903

Received June 30, 1969

In many photochemical systems it is possible to determine the quantum yield of one of several primary processes by measuring the overall quantum yield of a suitable product and extrapolating to zero incident light intensity. This technique is examined for some generalized mechanisms and for some particular examples.

Canadian Journal of Chemistry, **48**, 357 (1970)

Can. J. Chem. Downloaded from www.nrcresearchpress.com by 210.87.254.5 on 09/05/12
For personal use only.

Introduction

A simple method for the investigation of primary processes in photochemistry is the extrapolation to zero incident intensity of the quantum yield of a suitable product which is formed in a primary process. This "zero-intensity method" has been used in a study by Toby and Nimoy of the intramolecular formation of ethane in the photolysis of azomethane (1). The method is applicable to some other systems and the purpose of this paper is to discuss the use of the method for some generalized photochemical reaction mechanisms and to show, using specific examples, how information on both primary and secondary processes may be obtained.

Generalized Mechanisms

If a product is formed uniquely in one of several primary processes, then the quantum yield of that primary process may be directly measured. More often, the same product is formed by more than one path. As a first example, the main steps in the photolysis of some symmetrical ketones or azo compounds may be represented by

Mechanism I

$$A + h\nu \rightarrow M_1 + M_2 \quad (\phi_m)$$
$$A + h\nu \rightarrow 2R_1 + M_2 \quad (\phi_r)$$
$$2R_1 \xrightarrow{1} M_1$$
$$R_1 + A \xrightarrow{2} M_3 + R_2$$
$$2R_2 \xrightarrow{3} M_4$$
$$R_1 + R_2 \xrightarrow{4} M_5$$

where M_i are molecules and R_i are free radicals. The occurrence of the molecular split (ϕ_m) in addition to the radical split (ϕ_r) may be established as follows. Setting up steady-state equations for the radicals and assuming (2) $k_4/(k_1^{1/2} k_3^{1/2}) = 2$, it follows that

$$\Phi_{M_1} = \phi_m + 4\phi_r^2 k_1 I_a/(k_2[A] + 2k_1^{1/2}\phi_r^{1/2} I_a^{1/2})^2$$

Whence

$$\lim_{I_0 \rightarrow 0} \Phi_{M_1} = \phi_m$$

where I_a and I_0 represent absorbed and incident light intensity, respectively. Thus the presence of a positive intercept in a plot of Φ_{M_1} against I_0 at constant [A] establishes the occurrence of the molecular split. The use of the limiting slope in addition to the intercept enables us to obtain ratios of primary quantum yields without measuring absolute values of the incident intensity, as shown in the Appendix. Individual values of the primary quantum yields may then be obtained assuming $\phi_m + \phi_r = 1$.

The second example is that of a molecule which undergoes a symmetrical radical split and an unsymmetrical molecular split, such as certain peroxides and hydrocarbons.

A simplified scheme follows

Mechanism II

$$A + h\nu \rightarrow M_1 + M_2 \quad (\phi_m)$$
$$A + h\nu \rightarrow 2R_1 \quad (\phi_i)$$
$$2R_1 \xrightarrow{1} A$$
$$R_1 + A \xrightarrow{2} M_1 + R_2$$

We have omitted subsequent reactions of R_1 and R_2 or other steps involving M_2. These steps do not appreciably affect the rate of formation of M_1 at low intensities. Utilizing this low-intensity mechanism, we obtain

$$\Phi_{M_1} = \phi_m + k_2[A]\,[(k_2^2[A]^2 + 16k_1\phi_r I_a)^{1/2} - k_2[A]]/4k_1 I_a$$

The application of L'Hospital's theorem yields

$$\lim_{I_0 \to 0} \Phi_{M_1} = \phi_m + 2\phi_r$$
$$= 2 - \phi_m, \text{ provided } \phi_m + \phi_r = 1$$

Finally a case where the zero-intensity method does *not* work will be given. A typical photo-initiated chain reaction (3) may be represented by

$$A + h\nu \rightarrow M_1 + M_2 \quad (\phi_m)$$
$$A + h\nu \rightarrow R_1 + R_2 \quad (\phi_r)$$
[1] $$R_1 + A \xrightarrow{1} M_1 + R_3$$
[2] $$R_3 \xrightarrow{2} R_1 + M_2$$
$$R_1 + R_2 \xrightarrow{3} A$$
$$2R_1 \xrightarrow{4} M_3$$
$$2R_2 \xrightarrow{5} M_4$$

We take (2) $k_3/k_4^{1/2}k_5^{1/2} = 2$ and obtain

$$\Phi_{M_1} = \phi_m + k_1[A](1 - \phi_m)^{1/2}/2k_4^{1/2}I_a^{1/2}$$

Clearly, at low intensities the right-hand term will predominate, corresponding to long chains of reactions [1] and [2]. It should then be possible to plot Φ_{M_1} against I_0 and use the "infinite-intensity" extrapolation

$$\lim_{I_0 \to \infty} \Phi_{M_1} = \phi_m$$

Applications of Zero-intensity Method

Zero-intensity extrapolations yield information on both primary and secondary processes. In the following 4 examples, data were obtained from photolyses carried out in conventional systems which have been described previously (4, 5). All analyses were carried out by gas chromatography using a silica gel column. For convenience, quantum yields were plotted against the absorbed, rather than the incident, intensity at constant pressure. This does not affect the value of the intercept.

Azomethane

The low-intensity photolysis of azomethane may be represented by steps ϕ_m, ϕ_r, and *2* of Mechanism I together with the addition reaction

$$CH_3 + CH_3N_2CH_3 \xrightarrow{5} (CH_3)_2N_2CH_3$$

Thus

$$\lim_{I_0 \to 0} \Phi_{CH_4} = 2\phi_r k_2/(k_2 + k_5)$$
$$\lim_{I_0 \to 0} \Phi_{C_2H_6} = \phi_m$$

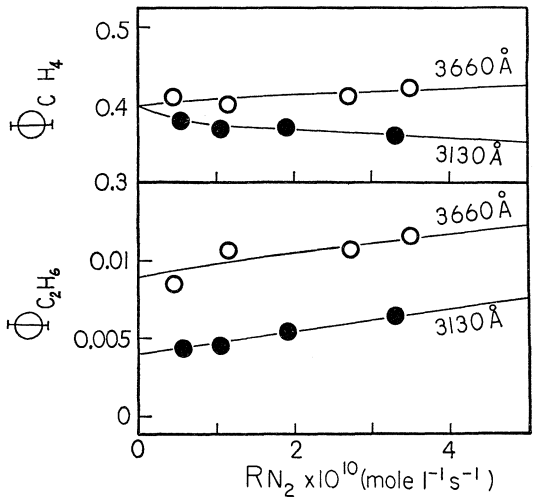

FIG. 1. Zero-intensity extrapolations from the photolysis of azomethane at 135 °C, 71 Torr, and the wavelengths indicated.

Assuming Φ_{N_2} equals unity (6), plots of the quantum yields of methane and ethane have shown clearly (5) that the limiting values of Φ_{CH_4} and $\Phi_{C_2H_6}$ are 0.5 and 0.01, respectively, at 180 °C. New data varying the wavelength at 135 °C is shown in Fig. 1. Lim Φ_{CH_4} is seen to be independent of wavelength in the range studied. This is expected since $\phi_r \simeq 1$ and the rate constants for thermolyzed radical reactions should not be wavelength-dependent. On the other hand, the wavelength dependence of $\phi_{C_2H_6}$ is explicable since a primary process is involved.

Hexafluoroazomethane

There is no evidence in published work (7–10) on the photolysis of gaseous hexafluoroazomethane for the existence of any primary process other than the radical split and the present study confirms this. As seen in Fig. 2, a plot of $\Phi_{C_2F_6}$ against intensity shows no intercept (at the low pressures used, Φ_{N_2} equals unity (10)). There is no abstraction reaction to give CF_4 as a product, and CF_3 radicals which do not dimerize undergo addition reactions in the photolysis at room temperature (9). At higher temperatures, CO_2 is formed, presumably in a heterogeneous reaction between CF_3 and the silica photolysis cell (8). We found traces of CO_2 at 100 °C and a large increase in Φ_{CO_2} at low intensities at 201 °C, shown in Fig. 2.

Can. J. Chem. Downloaded from www.nrcresearchpress.com by 210.87.254.5 on 09/05/12
For personal use only.

Can. J. Chem. Downloaded from www.nrcresearchpress.com by 210.87.254.5 on 09/05/12
For personal use only.

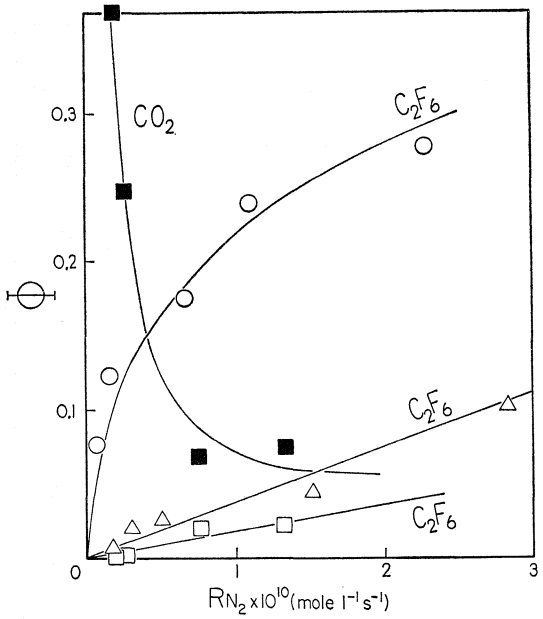

FIG. 2. Zero-intensity extrapolations from the photolysis of hexafluoroazomethane at 1.0 Torr and 3660 Å. Temperatures: ○, 31 °C; △, 100 °C; □, ■, 201 °C.

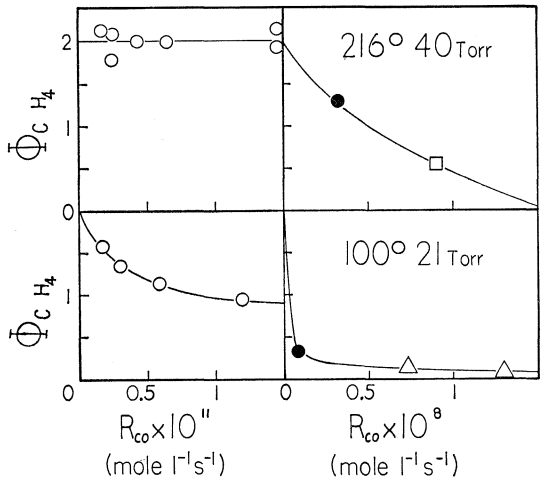

FIG. 3. Zero-intensity extrapolations from the photolysis of acetone at 3130 Å and temperatures and pressures shown. Symbols: △, Mandelcorn and Steacie, ref. 11; □, Darwent *et al.*, ref. 12; ●, Shaw and Toby, ref. 4; ○, this work. Literature points have been corrected, where necessary, to conditions shown.

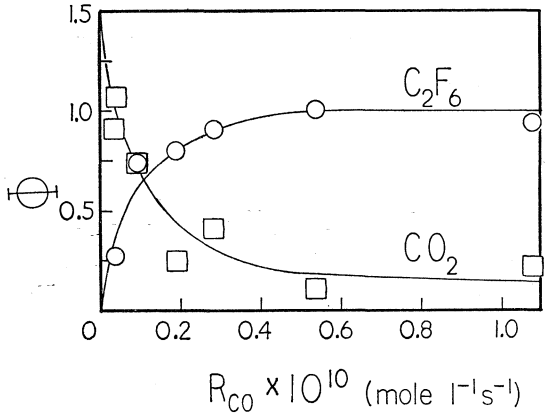

FIG. 4. Zero-intensity extrapolations from the photolysis of hexafluoroacetone at 3130 Å, 200 °C, and 7.5 Torr.

Acetone

The literature on the photolysis of gaseous acetone is very extensive (see citations in ref. 4). It is clear that ethane is formed entirely by methyl dimerization, but recent work (4) confirmed earlier observations that not all the observed methane could be accounted for by a gas-phase abstraction reaction. Shaw and Toby (4) suggested that some methane was formed either in a primary process or by a heterogeneous abstraction reaction. Any primary methane would result in lim $\Phi_{CH_4} < 2$ and our data in Fig. 3 show that this is not the case at 216 °C and presumably not at other temperatures. Figure 3 also includes previously published data to emphasize that zero-intensity extrapolations are of little use at the higher intensities normally employed.

Hexafluoroacetone (13)

Quantum yields from the photolysis of hexafluoroacetone at 3130 Å are given in Fig. 4, taking Φ_{CO} as unity under the conditions employed (14, 15). Although no conclusion may be drawn regarding lim $\Phi_{C_2F_6}$ it is interesting to note the increase in Φ_{CO_2} as $\Phi_{C_2F_6}$ decreases[1]. In fact, lim $\Phi_{CO_2} > 1$ and $\frac{1}{2}\Phi_{CO_2} + \Phi_{C_2F_6} = 1$. This implies that at the lowest intensities each CF_3 radical gives rise to a CO_2 molecule, possibly by $CF_3 + SiO_2 \rightarrow CO_2 + SiF_3$.

[1]Gordon (16) found no CO_2 at 350 °C, but used high ntensities.

We are grateful to the U.S. National Science Foundation and the Rutgers University Research Council for the support of this work.

1. S. TOBY and J. NIMOY. J. Phys. Chem. **70**, 867 (1966).
2. J. A. KERR and A. F. TROTMAN-DICKENSON. Progr. React. Kinet. **1**, 105 (1961).

3. For examples see K. J. Laidler. Chemical kinetics. 2nd ed. McGraw–Hill Book Co., Inc., New York. 1965. Chap. 8.
4. H. Shaw and S. Toby. J. Phys. Chem. **72**, 2337 (1968).
5. S-L. Cheng, J. Nimoy, and S. Toby. J. Phys. Chem. **71**, 3075 (1967).
6. M. H. Jones and E. W. R. Steacie. J. Chem. Phys. **21**, 1018 (1953).
7. J. R. Dacey and D. M. Young. J. Chem. Phys. **23**, 1302 (1955).
8. G. O. Pritchard, H. O. Pritchard, H. I. Schiff, and A. F. Trotman-Dickenson. Trans. Faraday Soc. **52**, 849 (1956).
9. J. R. Dacey, R. F. Mann, and G. O. Pritchard. Can. J. Chem. **43**, 3215 (1965).
10. E. C. Wu and O. K. Rice. J. Phys. Chem. **72**, 542 (1968).
11. L. Mandelcorn and E. W. R. Steacie. Can. J. Chem. **32**, 79 (1954).
12. B. de B. Darwent, M. J. Allard, M. F. Hartman, and L. J. Lange. J. Phys. Chem. **64**, 1847 (1960).
13. For recent work see N. C. Lang and K. O. Kutschke. Can. J. Chem. **46**, 1031 (1968).
14. P. B. Ayscough and E. W. R. Steacie. Proc. Roy. Soc. London. Ser. A, **234**, 476 (1956).
15. G. B. Porter. J. Phys. Chem. **70**, 4079 (1966).
16. A. S. Gordon. J. Chem. Phys. **36**, 1330 (1962).

Appendix

It is possible to obtain ratios of primary quantum yields by the zero-intensity method without measuring absolute intensities for a system of known mechanism.

Suppose the absolute intensity is given by $I_a = bi$, where the proportionality constant b is governed by geometrical factors and i is the measured current from a photocell. Then for Mechanism I, a plot of relative quantum yield ($= d[M_1]/dti$) against relative absorbed intensity will have a measured intercept of $b\phi_m$ and a measured limiting slope of $4b^2\phi_r^2k_1/k_2^2[A]^2$. Then

$$\frac{\text{limiting slope}}{(\text{intercept})^2} = \frac{4k_1\phi_r^2}{\phi_m^2k_2^2[A]^2}$$

This expression enables us to obtain the value of ϕ_r/ϕ_m in terms of measurable quantities.

In the case of Mechanism II a similar treatment yields

$$\frac{\text{limiting slope}}{(\text{intercept})^2} = \frac{-8k_1}{k_2^2[A]^2}\left(\frac{\phi_m}{\phi_r} + 2\right)^{-2}$$

If for these mechanisms we make the assumption that $\phi_m + \phi_r = 1$, then the systems serve as actinometers and we may obtain individual values of ϕ_m and ϕ_r by the above procedure.

Can. J. Chem. Downloaded from www.nrcresearchpress.com by 210.87.254.5 on 09/05/12
For personal use only.

Favorsky rearrangements of α-halogenated acetyl cycloalkanes. Part II[1,2,3,4]

CH. R. ENGEL, S. K. ROY, J. CAPITAINE, J. BILODEAU, C. MCPHERSON-FOUCAR, AND P. LACHANCE[5]
Department of Chemistry, Laval University, Quebec, Quebec, and Departments of Medical Research and Chemistry, University of Western Ontario, London, Ontario

Received June 12, 1969

On the basis of a study of the rearrangement with alkali of various α-halogenated 20-keto steroids in a variety of media, and in accord with data from the literature, a unifying explanation of the complex results obtained in Favorsky rearrangements of α-halogenated acetyl cycloalkanes is put forward.

Canadian Journal of Chemistry, **48**, 361 (1970)

Can. J. Chem. Downloaded from www.nrcresearchpress.com by 210.87.254.5 on 09/05/12
For personal use only.

Introduction

Since the discovery of the rearrangement with alkali of α-halogenated and α,α′-dihalogenated ketones by Al. Favorsky and his collaborators (3), an impressive number of mechanisms has been advanced for the explanation of the complex results obtained when various α-halogenated ketones are treated with various bases under various conditions (4, 5). The mechanism proposed by Loftfield (5) in 1951 and which was based on experiments with 1,2-C^{14}-2-chlorocyclohexanone, received wide acceptance (6) since it seemed to eliminate, at least for the case under investigation, all other mechanisms previously considered. According to Loftfield's theory (Scheme 1*a*), a proton is abstracted in the first, generally rate-determining step, from the α′-position, the resulting mesomeric anion closes, with a concerted expulsion of the halogen substituent, to an unstable cyclopropanone derivative, which is immediately opened by the base to the actual rearrangement products.[6] Burr and Dewar (8) put forward a basically related mechanism which differs from that of Loftfield insofar as it suggests that the mesomeric anion is transformed to a cyclopropanone derivative via a delocalized intermediate (Scheme 1*b*).

It will be apparent in the sequel that neither of these mechanisms, each taken by itself, nor any other single mechanism proposed up to date, can account for the experimental results obtained with α-halogenated acetyl cycloalkanes, such as α-halogenated 20-keto steroids.

Favorsky rearrangements of α-halogenated acetyl cycloalkanes have gained a certain prominence in the steroid field since they were used, with halogenated or tosylated 20-keto steroids as substrates, for the introduction of a 17-methyl substituent into steroids with a side chain in position 17, and thus for the synthesis of 17-methyl derivatives of C_{21}-steroid hormones, their analogues, and 17-epimers (9–15), some of which present considerable biological interest.

The rearrangement of 21-halogenated or tosylated 20-keto steroids, (compare **1**) (9*b*, 12*a*) with alkali methoxide in absolute methanol leads to a mixture of 17-epimeric 17-methyl etio esters (cf. **2** and **3**). This seemed to be in good agreement both with Loftfield's and Dewar's mechanisms since it appeared quite reasonable to assume that in either case the mesomeric anion, planar in positions 17 and 20, would afford both 17-epimers (compare Scheme 2). It even seemed plausible that the 17α-methyl etio ester should predominate because of the presence of the 18-methyl group which could be considered to hinder the concerted as well as the non-concerted ring closure to the cyclopropanone derivative with a β-configuration of the 20-methylene group.

However, according to the earlier literature, the products of the Favorsky rearrangements of 17α-halogenated 20-keto steroids, which had been carried out with alkali bicarbonate in aqueous methanol, consisted either entirely or at least predominantly of 17α-methyl etio acid

[1]For part I of this series cf. ref. 1.
[2]The present paper represents also part XXIX of the series on Steroids and Related Products. For part XXVIII cf. ref. 55.
[3]For preliminary accounts of the work described in this paper, cf. ref. 1 and 2; certain results were reported previously at the 43rd Annual Conference of the Chemical Institute of Canada, Ottawa, June 1960; cf. also footnote 4.
[4]Abbreviated from the B.Sc. theses of C. Foucar (Mrs. McPherson-Foucar), the University of Western Ontario, London, Ontario (1954), and of J. Bilodeau, Laval University, Quebec, Canada (1960), and from a portion of the D.Sc. thesis of P. Lachance, Laval University (1967).
[5]Holder of NRCC Scholarships 1961–1965.
[6]Tchoubar and Sackur (7) had already tentatively suggested such a mechanism for certain Favorsky rearrangements.

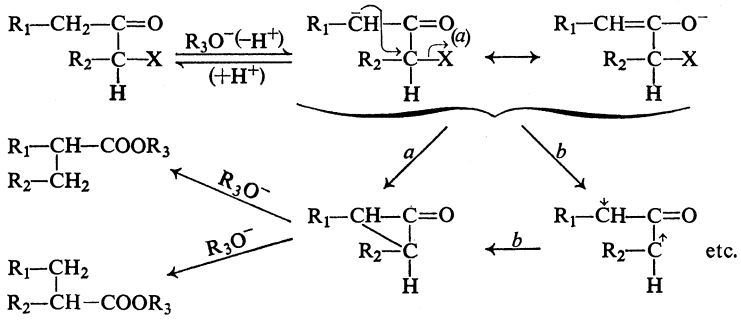

SCHEME 1

derivatives (compare **2**) (9*b*, 11*a*, 14, 16, 17).[7, 8] Neither Loftfield's nor Dewar's mechanism seemed to satisfy these results. Indeed, in the case of a reaction according to the mechanism suggested by Loftfield, the concerted formation of a cyclopropanone from a 17α-bromide should occur with inversion in position 17 and thus lead, stereospecifically, to a 17β-methyl 17-iso etio ester (Scheme 3) and not, as it does in fact, predominantly to the 17α-methyl epimer. In the case of Dewar's mechanism, the rearrangement should proceed through the same delocalized intermediate as in the case of the rearrangement of a 21-halogenated 20-keto steroid (cf. Scheme 2) and should thus afford the epimeric rearrangement products in the same proportion as in that instance. This again does not correspond to the experimental facts.[9]

[7]Marker and Wagner (16), who were the first to investigate the Favorsky rearrangement in the steroid field, did not assign a configuration to the rearrangement products they obtained from the 17α-bromo-3α-acetoxy- and 3β-acetoxy-5β-pregnan-20-ones; in each case they isolated a single epimer, but, according to present evidence, a 17α-methyl configuration has to be assigned to these rearrangement products (18*a*, *b*).

[8]In our previous article dealing with the synthesis of 11-keto 17α-methyl etio acids and their derivatives (14*b*), we reported the isolation of an isomer of the acetoxy ester **2** (R_1 = α-AcO, $R_2 = R_4 = R_6$ = H, R_3 = β-H, R_5 = O, $R_7 = CH_3$) and referred to a subsequent paper for the discussion of its structure. In the Experimental of the present communication we record its further characterization by the conversion of this epimer (**3**, R_1 = α-AcO, $R_2 = R_4 = R_6$ = H, R_3 = β-H, R_5 = O, $R_7 = CH_3$) to the hydroxy ester (**3**, R_1 = α-OH, $R_2 = R_4 = R_6$ = H, R_3 = β-H, R_5 = O, $R_7 = CH_3$) and to the hydroxy acid (**3**, R_1 = α-OH, $R_2 = R_4 = R_6 = R_7$ = H, R_3 = β-H, R_5 = O) which was readily remethylated to the methyl ester which, in turn, gave upon acetylation the original acetoxy methyl ester. These experiments were first described in the B.Sc. thesis of C. Foucar (Mrs. C. McPherson-Foucar) University of Western Ontario, May 1954. Subsequently, we had the occasion to compare our acetoxy ester with the product prepared by Wendler *et al.* (18*a*, *b*) and could establish the identity of both samples by the determination of a mixture melting point and the comparison of the infrared spectra. We wish to thank Dr. N. L. Wendler sincerely for kindly providing us with the comparison sample.

[9]The stereochemistry in position 17 of 17-brominated 20-keto steroids, previously inferred on the grounds of Fieser and Fieser's rule of rear attack (19), was rigorously established by Wendler *et al.* (18*a*, *b*) who also confirmed by chemical means the configuration of the epimeric 17-methyl etio acids and esters, previously assigned on the grounds of rotational differences, chromatographic mobility, and the biological activity of derived hormone analogues (10, 11*a*, 12, 13, 14*b*, 15).[10]

[10]The limited value of the comparison of chromatographic mobilities for the establishment of the configuration in position 17 is demonstrated by the fact that in contradistinction to the situation in the series of Δ^5-3β-hydroxy etienic esters and Δ^4-3-keto etienic esters (10, 12, 13), methyl 3α-acetoxy-11-oxo-17β-methyl-17-isoetianate (**3**, R_1 = α-AcO, $R_2 = R_4 = R_6$ = H, R_3 = β-H, R_5 = O, $R_7 = CH_3$) is eluted prior to methyl 3α-acetoxy-11-oxo-17α-methyletianate (**2**, R_1 = α-AcO, $R_2 = R_4 = R_6$ = H, R_3 = β-H, R_5 = O, $R_7 = CH_3$) from an aluminum oxide column (14*b*, 18*b*).

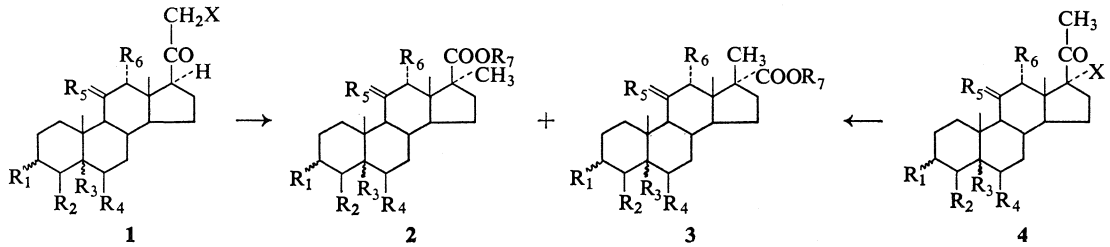

1 **2** **3** **4**

Can. J. Chem. Downloaded from www.nrcresearchpress.com by 210.87.254.5 on 09/05/12
For personal use only.

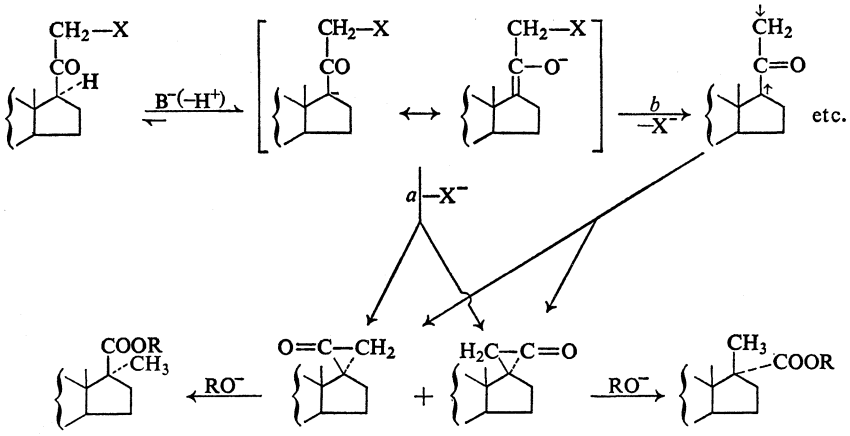

SCHEME 2

Wendler and his colleagues (18*a*, *b*) repeated the rearrangement of 17α-bromo-3α-acetoxy-5β-pregnane-11,20-dione (**4**, R_1 = α-AcO, R_2 = R_4 = R_6 = H, R_3 = β-H, R_5 = O, X = Br) which we had carried out with bicarbonate in aqueous methanol (14), but used sodium methoxide as base and methanol as solvent and obtained, qualitatively, results analogous to ours; they suggested, in order to reconcile these results with Loftfield's theory, that prior to the actual Favorsky rearrangement a transfer of halogen from position 17 to position 21 occurred and that the reaction should therefore afford the same products as the analogous reaction of a 21-halogenated 20-ketone.

Such a halide transfer had been previously suggested by Richard (20) in the case of Favorsky rearrangements of 1-chloro-1-phenylpropanone and of 2-chloro-1-phenylbutan-3-one but seems improbable in the present instance. It would imply the isomerization of an ion with the partial character of a primary carbanion to an ion with the partial character of a tertiary carbanion, without obvious energetic causes.[11] While the suggestion of Wendler *et al.* would agree qualitatively with their experimental results (they isolated the 17α- and 17β-methyl etio esters, according to their published papers (18*a*, *b*) in a proportion of 3:2, according to a subsequent private communication (18*c*) in a proportion of 1:1), it remains in opposition with the results obtained by us in the case of the rearrangement of the same 17α-bromo 11,20-diketone with potassium bicarbonate in aqueous methanol in which the 17α- and 17β-methyl etio acid derivatives were obtained in a proportion of 5:1 (14*b*), and especially with the results of the rearrangements of 17α-bromo 20-ketones devoid of an 11-oxygen substituent, carried out with bicarbonate in aqueous methanol (9*b*, 11, 16, 17), in which the 17α-methyl etio acid derivatives were practically the sole rearrangement products.

Hence, neither Dewar's nor Loftfield's mechanism, the latter not even with the additional refinement proposed by Wendler, could explain satisfactorily the stereochemical results of Favorsky rearrangements of α-halogenated 20-keto steroids; neither could any of the other mechanisms suggested for Favorsky rearrangements explain these results. Thus, the "semibenzilic acid mechanism" proposed by Tchoubar and Sackur (7) would correspond, from a stereochemical point of view, in its original

[11]Experiments by House and Gilmore (21) also seem to militate against such an assumption.

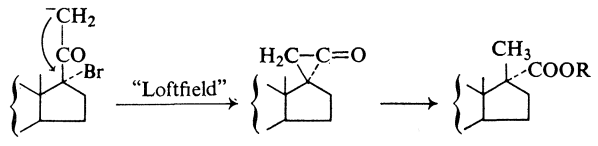

SCHEME 3

Can. J. Chem. Downloaded from www.nrcresearchpress.com by 210.87.254.5 on 09/05/12
For personal use only.

Can. J. Chem. Downloaded from www.nrcresearchpress.com by 210.87.254.5 on 09/05/12
For personal use only.

non-concerted version (7) to Dewar's mechanism, whereas in its concerted form (cf. 22) the stereochemical situation would resemble that of Loftfield's mechanism. Of course, the "semibenzilic acid mechanism" had to be excluded *a priori* in the case of the rearrangement of 21-halogenated 20-keto steroids, since in that instance not 17-methylated etio acid derivatives but 20-pregnanoic acid derivatives should be formed. Recently, Deghenghi *et al.* (23) have eliminated elegantly this type of mechanism also for 17-halogenated 20-keto steroids, on the basis of an investigation with deuterated derivatives.

Dependency of the Stereochemistry on the Medium

This situation warranted a re-evaluation of the problem. An examination of the results on hand suggested to us that the stereochemical differences observed were not due, as previously intimated,[12] to differences in the location of the halogen substituent (position 21 vs. position 17), but rather to the nature of the medium. Indeed, the rearrangements of the 11-non-ketonic 17α-bromo 20-keto steroids which seemed to be highly stereoselective (9*b*, 11, 16, 17) and the (somewhat less) stereoselective rearrangement of the 17α-bromo 11,20-diketone (14) had all been carried out with alkali bicarbonate in aqueous methanol whereas the non-stereoselective rearrangements of 21-halogenated 20-keto steroids (9*a*, *b*, 12*a*), as well as the non-stereoselective rearrangement of the 17α-bromo 11,20-diketone reported by Wendler *et al.* (18), had been carried out with alkali methoxide in absolute methanol.

In order to substantiate the assumption of a determining influence of the medium on the stereochemistry of the reaction, we at first confirmed that the rearrangement of 17α-bromopregnenolone acetate (**4**, R_1 = β-AcO, R_2 = R_6 = H, R_3 = R_4 = double bond, R_5 = H_2, X = Br) with potassium bicarbonate in aqueous methanol led almost exclusively to the "anti-Loftfield"[13] 17α-methyl etio ester, isolated after acetylation as the acetoxy ester **2** (R_1 = β-AcO, R_2 = R_6 = H, R_3 = R_4 = double bond, R_5 = H_2, R_7 = CH_3) in 92.5% yield (the "Loftfield"[13] 17β-methyl ester **3** [R_1 = 3β-AcO, R_2 = R_6 = H, R_3 = R_4 = double bond, R_5 = H_2, R_7 = CH_3] being isolated only in 4% yield).[14,15]

Furthermore, we subjected 17α-bromopregnenolone acetate (**4**, R_1 = β-AcO, R_2 = R_6 = H, R_3 = R_4 = double bond, R_5 = H_2, X = Br) and crude and amorphous[16] 17α-bromo-3α,12α-diacetoxy-5β-pregnan-20-one (**4**, R_1 = α-AcO, R_2 = R_4 = H, R_3 = β-H, R_5 = H_2, R_6 = AcO, X = Br), which had given with potassium bicarbonate in aqueous methanol only 17α-methyl etio acid derivatives (11), to the action of potassium methoxide in absolute methanol, under the conditions used for rearrangements of 21-halogenated 20-keto steroids (cf. 9*b*), and obtained the 17α-methyl and 17β-methyl rearrangement products in proportions of 1.8:1 and 3.4:1, respectively. The 3-hydroxy 5-etienic acid methyl esters were isolated as 3-acetates (**2** and **3**, R_1 = β-AcO, R_2 = R_6 = H, R_3 = R_4 = double bond, R_5 = H_2, R_7 = CH_3); the 17α-methylated rearrangement product of the 3,12-diacetoxy 17-bromo 20-ketone as the 3,12-diacetoxy etianate (**2**, R_1 = α-AcO, R_2 = R_4 = H, R_3 = β-H, R_5 = H_2, R_6 = AcO, R_7 = CH_3), the 17-epimeric product as the 20 → 12-lactone **5***a* which shows in the infrared (i.r.) (KBr) the characteristic band of a γ-lactone at 1775 cm^{-1}.

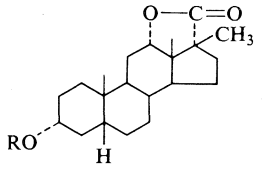

5 R = H
5*a* R = Ac

[12]Such an assumption is, for instance, implied in the articles of Wendler *et al.* (18*a*, *b*).

[13]The terms "Loftfield ester" and "anti-Loftfield ester" merely indicate that their stereochemistry would correspond, respectively not correspond, to a reaction following Loftfield's mechanism. We engage in no way the responsibility of Dr. Loftfield for our assignments and suggestions.

[14]The previously published data (9*b*) was based on an experiment carried out with very small amounts of material and were therefore open to question. On the other hand, the experiments of Marker and Wagner (16) could not be considered entirely convincing from a stereochemical point of view since these authors had not investigated the mother liquors of their rearrangement products. Neither were the results of Plattner *et al.* (17) beyond question, from a stereochemical standpoint, since an impure tribromide had been employed and since the 17-methylated rearrangement product had been isolated only in very low yield.

[15]In parallel experiments, Deghenghi *et al.* (23) had arrived at a similar conclusion.

[16]We were unable to obtain this bromide in the crystalline form (cf. 11) and could, therefore, purify it only to a certain extent by chromatography on silica gel.

TABLE 1

Proportion of 17α- and 17β-methyl etio acid derivatives in relation to starting materials and media

Substrate	Medium	Proportion of 17α- and 17β-methyl etio acid derivatives	Literature*
17α-Bromo-3β-acetoxy-5-pregnen-20-one	$KHCO_3$, CH_3OH, H_2O	23:1	P†
	$KOCH_3$, CH_3OH	1.8:1	P
	$NaOCH_3$, $CH_3O(CH_2)_2OCH_3$	1:19	P
17α-Bromo-3α,12α-diacetoxy-5β-pregnan-20-one	$KHCO_3$, CH_3OH, H_2O	1:≃0	11
	$KOCH_3$, CH_3OH	3.4:1	P
17α-Bromo-3α-acetoxy-5β-pregnane-11,20-dione	$KHCO_3$, CH_3OH, H_2O	5:1	14*b*, P
	$NaOCH_3$, CH_3OH	1:1	18*c*
21-Bromo-3β-acetoxy-5-pregnen-20-one	$KHCO_3$, CH_3OH, H_2O	1:≃0	P
21-Bromo-3β-hydroxy-5-pregnen-20-one	$KOCH_3$, CH_3OH	2:1	9*b*‡

*The letter "P" refers to experiments described in this publication.
†Cf. also ref. 23.
‡Heusser *et al.* discussed in their publication (9*b*) the rearrangement of 21-chloropregnenolone (**1**, R_1 = β-OH, $R_2 = R_6$ = H, $R_3 = R_4$ = double bond, $R_5 = H_2$, X = Cl) but obtained analogous results also when using the corresponding bromide.

We were not able to obtain, by hydrolysis of this lactone with alkali, the free acid **3** (R_1 = α-OH, $R_2 = R_4 = R_7$ = H, R_3 = β-H, $R_5 = H_2$, R_6 = OH) in the pure form since, upon the attempt to crystallize the product, it lactonized again. However, the i.r. spectrum of the crude acid fraction corresponded to the structure of the free acid.[17]

On the other hand, 21-bromopregnenolone acetate (**1**, R_1 = β-AcO, $R_2 = R_6$ = H, $R_3 = R_4$ = double bond, $R_5 = H_2$, X = Br)[18] gave with potassium bicarbonate in aqueous methanol, as the sole 17-methylated rearrangement products, an etio acid and an etio ester, isolated as the acetoxy methyl ester **2** (R_1 = β-AcO, $R_2 = R_6$ = H, $R_3 = R_4$ = double bond, $R_5 = H_2$, $R_7 = CH_3$), the 17-methyl group of which has the α-("anti-Loftfield") configuration. Apart from these rearrangement products (isolated in approximately 40% yield), we obtained in 18% yield 21-hydroxypregnenolone (**1**, R_1 = β-OH, $R_2 = R_6$ = H, $R_3 = R_4$ = double bond, $R_5 = H_2$, X = OH), isolated as the diacetate (**1**, R_1 = β-AcO, $R_2 = R_6$ = H, $R_3 = R_4$ = double bond, $R_5 = H_2$, X = AcO), as well as two minor products, which do not represent 17-methylated rearrangement products, and which were not further investigated.

In summary (cf. Table 1), the rearrangement of α-halogenated 20-keto steroids with alkali bicarbonate in aqueous methanol is highly stereoselective, whereas the rearrangement of such products with alkali methoxide in absolute methanol leads to mixtures of epimeric 17-methyl etio esters in which the 17α-methylated products predominate; the stereochemical composition of the rearrangement products does not depend decisively on the position of the halogen substituent in the starting material. These results can in no way be reconciled with Wendler's proposal (18*a*, *b*), not only because it implies the formation of the same mixture of epimers both from 17- and 21-halogenated 20-keto steroids (which is, *grosso modo*, correct only if one adheres to the same medium) but also because it does not foresee a marked stereochemical difference of the reaction as a consequence of a change in the medium.

[17]The ease of lactonization of this acid represents an additional proof of its stereochemistry in position 17.

[18]This acetate of 21-bromopregnenolone (24) was prepared from pregnenolone acetate (**4**, R_1 = β-AcO, $R_2 = R_6$ = X = H, $R_3 = R_4$ = double bond, $R_5 = H_2$) via the 20,21-enol acetate **i** (25, 26) by treating the latter with *N*-bromosuccinimide in dilute sulfuric acid (27). The structure of the desired 21-bromopregnenolone acetate (**1**, R_1 = β-AcO, $R_2 = R_6$ = H, $R_3 = R_4$ = double bond, $R_5 = H_2$, X = Br) was confirmed by its conversion, through the 21-iodide (**1**, R_1 = β-AcO, $R_2 = R_6$ = H, $R_3 = R_4$ = double bond, $R_5 = H_2$, X = I) to 3β,21-diacetoxy-5-pregnen-20-one (**1**, R_1 = β-AcO, $R_2 = R_6$ = H, $R_3 = R_4$ = double bond, $R_5 = H_2$, X = AcO) (28) which was hydrolyzed with perchloric acid in aqueous methanol (29) to the dihydroxy derivative (**1**, R_1 = β-OH, $R_2 = R_6$ = H, $R_3 = R_4$ = double bond, $R_5 = H_2$, X = OH) (30).

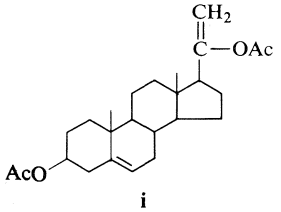

i

Can. J. Chem. Downloaded from www.nrcresearchpress.com by 210.87.254.5 on 09/05/12
For personal use only.

Can. J. Chem. Downloaded from www.nrcresearchpress.com by 210.87.254.5 on 09/05/12
For personal use only.

In independent and parallel experiments, House and Gilmore (21) have shown, in continuation of an earlier study by Stork and Borowitz (31), a similar dependency of the stereochemistry of Favorsky rearrangements on the nature of the medium in the case of α-halogenated 1-acetyl 2-methylcyclohexanes; they correlated the stereochemistry of their reaction product to the polarity of the solvent employed. As a "non-polar" solvent they used 1,2-dimethoxyethane and employed sodium methoxide as the base. In order to substantiate both our findings and those of the authors from the Massachusetts Institute of Technology (M.I.T.), we subjected 17α-bromopregnenolone acetate (**4**, R_1 = β-AcO, $R_2 = R_6$ = H, $R_3 = R_4$ = double bond, $R_5 = H_2$, X = Br) to the action of sodium methoxide in absolute dimethoxyethane. We obtained a mixture of the 17α- and 17β-methyl etio esters in a proportion of 1:19, which corresponds to a highly stereospecific reaction, leading predominantly to the "Loftfield product". We were also able to isolate, in very low yield (0.2%), methyl Δ^5-3β-acetoxy-21-pregnenoate (**6**), the formation of which can readily be visualized by the alternative opening by base of the major (17β-methylene) cyclopropanone intermediate. Up to this date, rearrangement products of this kind were never isolated from reactions of α-halogenated or α-tosylated 20-keto steroids with base.

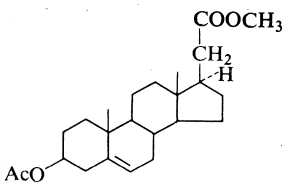

6

Discussion

Our experiments clearly demonstrate a dependence of the stereochemistry of the Favorsky rearrangements of α-halogenated 20-keto steroids on the nature of the medium and are, in this respect, in good agreement with those obtained by House and Gilmore (21) in the monocyclic series. However, the authors from the M.I.T. suggested that "the rearrangement in a non-polar medium was stereospecific but became non-stereospecific in a polar medium", which seems in contradiction with some of our results since we observed a high stereoselectivity in the polar medium, bicarbonate–methanol–water, and non-stereospecificity in the less polar medium, methoxide–methanol.

In order to explain the experimental facts, both those of the monocyclic series and those of the rearrangements of α-halogenated 20-keto steroids, we propose the following hypothesis (cf. 1, 2).

It is suggested that in a medium which is not inducive to the formation of a delocalized intermediate (compare Scheme 1), the reaction proceeds stereospecifically, according to Loftfield's mechanism, with inversion on the carbon atom carrying the halogen substituent; that in a medium which favors the formation of a delocalized intermediate, the geometry of which is planar in the area involved in the rearrangement, the reaction is non-stereospecific in the case of systems where no serious steric hindrance is exerted by groups in the neighborhood of the centers concerned [such a situation prevails in the case of the system studied by Stork and Borowitz (31) and House and Gilmore (21)]. We propose however, that if the starting material, and therefore also the delocalized intermediate, presents on one side of the molecule, in the neighborhood of the centers involved in the rearrangement, a structural feature exerting serious steric hindrance, the reaction becomes stereoselective, to the degree of the steric hindrance. In such a case the reaction may well lead predominantly, even exclusively, to a rearrangement product the stereochemistry of which is the opposite of that which would correspond to a product obtained by the concerted mechanism of Loftfield. We finally propose that in a medium in which the rate of the formation of the delocalized intermediate would be of the same order of magnitude as the rate of the concerted formation of the cyclopropanone intermediate, both pathways would be followed simultaneously, which would result in a mixture of epimers.

These proposals satisfy completely the results obtained by House and Gilmore (21), which is not surprising because for the systems they investigated it resembles their own. However, while their hypothesis is in contradiction with the results obtained with α-halogenated 20-keto steroids, our suggestion explains them satisfactorily. Indeed, in a medium not favoring the formation of a delocalized intermediate, such as methoxide in dimethoxyethane, the reaction leads predominantly to the 17β-etio ester, the formation of which should be expected in the case of the concerted mechanism of Loftfield. In the case of a

Can. J. Chem. Downloaded from www.nrcresearchpress.com by 210.87.254.5 on 09/05/12
For personal use only.

medium favoring the formation of a delocalized intermediate, such as bicarbonate in aqueous methanol, in which, according to the theory of House and Gilmore (21), one would expect the formation of a mixture of epimers in an approximate proportion of 1:1, our hypothesis predicts, because of the hindrance on the β-face of the steroid molecule, the predominant formation of the "anti-Loftfield product", the 17α-methyl etio acid derivative, which corresponds to the facts. Finally, in a medium, such as methoxide in absolute methanol, whose ability to promote the formation of a delocalized intermediate should lie between those of the media just mentioned (cf. below), in which the formation of the delocalized intermediate and the direct concerted ring formation could be considered to proceed at comparable rates, we should obtain a mixture of epimers, which agrees again with the experimental findings.

The fact that the β-face of the steroid molecule is hindered and that this hindrance is felt in the neighborhood of the centers involved in the Favorsky rearrangements under consideration, is experimentally well established. It is thus known that the bromination and chlorination of 20-keto steroids, or of their enol acetates, proceeds stereoselectively (9*b*, 11, 14, 16, 17, 18*a*,*b*, 27*a*, 32–34) and this in contradistinction to the non-stereoselective chlorination of 1-acetyl-2-methylcyclohexane study by House and Gilmore (21). It is also well-known that 17,20- and 16,17-double bonds are selectively epoxidized (cf. 35, 36) and dihydroxylated (cf. 37–39) from the α-face, etc. If one now assumes that this steric hindrance in the neighborhood of positions 17 and 20 is due in part to the presence of the 18-methyl group,[19] one could possibly explain the "special" results of the Favorsky rearrangements of the 17α-brominated 11,20-diketone (**4**, R_1 = α-AcO, $R_2 = R_4 = R_6$ = H, R_3 = β-H, R_5 = O, X = Br). Indeed (compare Table 1), the rearrangement of this product with potassium bicarbonate in aqueous methanol was less stereoselective than the rearrangement of 17α-bromo 20-ketones without an 11-keto function and the proportion of the 17β-methyl etio ester obtained by rearrangement with sodium methoxide in absolute methanol was also higher in the case of this 11,20-diketone than in the case of α-halogenated 20-ketones devoid of an 11-keto function (18*c*). While these results could be explained by the assumption of a long-range inductive effect unfavorable for the formation of a delocalized intermediate, they could also be rationalized, in part at least, on steric grounds. Indeed, inspection of models shows that when carbon atom 11 is trigonal, the 18-methyl group is bent away from the "upper" side of the side chain (the side corresponding to the β-face of the steroid nucleus) and that it should therefore hinder reactions on this side of the molecule less than the 18-methyl group of a steroid with a tetrahedral carbon atom in position 11.

The stereochemical outcome of the reaction of 21-halogenated 20-keto steroids with methoxide in absolute methanol needs, however, further comment. Indeed, the mesomeric ion formed by abstraction of a proton in position 17 of a 21-halogenated 20-keto steroid is planar (compare Scheme 2) and one could consider that our hypothesis should therefore predict, even in a medium not favoring the formation of a delocalized intermediate, the stereoselective formation of a cyclopropanone derivative with an α-configuration of its methylene group, which would be contrary to the facts, since in the medium methoxide–methanol an epimeric mixture of 17-methylated etio esters is obtained. We suggest however that also in this case there exists a significant stereochemical difference between the concerted and not concerted cyclopropanone formation. In the first instance the halogen substituent is expelled during ring closure, in the second it has already been abstracted. It can now be easily seen from an observation of models that in the formation of a cyclopropanone with an α-configuration of its methylene group, the expulsion of the 21-halogen substituent is hindered by the 18-methyl group, if one assumes the most probable conformation of the side chain, but that this is not true in the case of the formation of the 17-epimeric cyclopropanone derivative. Consequently, the free energy of the transition state leading to the cyclopropanone with an α-configuration of the methylene group is, in the case of this concerted ring closure, not significantly lower, possibly even higher, than the level of free energy of the transition state leading to the epimeric cyclopropanone. Under these circumstances, the stereoselective formation of 17α-methylated rearrangement products is not to be

[19]In part only, because it is known that even in the absence of an 18-methyl group, certain reactions in the region under consideration remain stereoselective, for instance the hydrogenation of the 16,17-double bond (40).

Can. J. Chem. Downloaded from www.nrcresearchpress.com by 210.87.254.5 on 09/05/12
For personal use only.

expected anymore; as a matter of fact, the experimental results point to a definite stereoselectivity towards the formation of the 17β-methylated products, if one considers, on the basis of the experiments with 17α-bromopregnenolone acetate, the ratio of the Dewar and Loftfield pathways to be approximately 1.8:1 in the specific medium.

The determining role of the medium on the steric course of this kind of Favorsky rearrangements was attributed by House and Gilmore (21) to the polarity of the solvent, a polar solvent favoring the rupture of the carbon–halogen bond and thus the formation of a delocalized intermediate. This might indeed be one of the factors involved, but Tchoubar and collaborators (41) suggested shortly after our preliminary communication (2) that the influence of the solvent was due to the association of protic solvents with the oxygen of the mesomeric anion, which would thus resemble primarily the canonical form in which the negative charge is localized on the oxygen atom and which should therefore not lend itself readily to a concerted ring closure. The French authors, who like Stork and House were working on rearrangements of a 1-halogenated 1-acetyl-2-methylcyclohexane, were able to further substantiate their hypothesis by a study on the influence of the concentration of the base and of the addition of "drying salts" (42). We consider that this mode of action of the medium may represent an important factor but suggest that a protic solvent may also exert its action by helping in the abstraction of the halogen anion through electrical attractive forces.

In summary, the hypothesis which we propose explains the stereochemistry of all the known Favorsky rearrangements of α-halogenated acetyl cycloalkanes. It is, however, important to emphasize that in the case of other Favorsky rearrangements, other mechanisms may and must be operative, for instance in that of the rearrangement of 2-bromocyclobutanone studied by Conia and Salaün (43).

The reality of a cyclopropanone intermediate in the case of certain Favorsky rearrangements has been strongly supported by the important experiments of Breslow *et al.* (44) and Turro and Hammond (45) and, more recently, by those of Pazos and Greene (46). For the intervention of a delocalized intermediate in some Favorsky rearrangements, Fort (8*b*) and Cookson and Nye (47) have put forward convincing evidence.

Fort now suggested (8*b*) that the delocalized intermediate postulated for certain Favorsky rearrangements may also be an intermediate for the non-rearranged products which often accompany the rearrangement products (cf. 4*b*). This, as a *major* pathway, seems improbable and can be excluded in a number of cases. For instance, we report in this paper the formation both of a substitution product and of a Favorsky rearrangement product in the reaction of 21-bromo-3β-acetoxy-5-pregnen-20-one (**1**, R_1 = β-AcO, $R_2 = R_6 = H$, $R_3 = R_4$ = double bond, $R_5 = H_2$, X = Br). As discussed above, a delocalized intermediate for the Favorsky rearrangement seems probable in such a medium. However, the same delocalized intermediate would have to be postulated in the case of the rearrangement of the isomeric 17α-bromide, 17α-bromo-3β-acetoxy-5-pregnen-20-one (**4**, R_1 = β-AcO, $R_2 = R_6 = H$, $R_3 = R_4$ = double bond, $R_5 = H_2$, X = Br) and, if the assumption of a common intermediate for substitution and Favorsky products were correct, one would have to expect in that case also the formation of the same substitution product, namely the 21-hydroxy derivative (**1**, R_1 = β-OH, $R_2 = R_6 = H$, $R_3 = R_4$ = double bond, $R_5 = H_2$, X = OH), which does not correspond to the facts (cf. Experimental and 23). The reaction affords in over 95% yield rearrangement products and, in very low yield, as the sole "substitution product", the 17α-methoxy derivative (**4**, R_1 = β-OH, $R_2 = R_6 = H$, $R_3 = R_4$ = double bond, $R_5 = H_2$, X = OCH_3) (23).[20] It would seem more reasonable to suggest that the "substitution products" arise, as originally proposed by Favorsky (3*c*), via an epoxy derivative for which considerable evidence is on hand (cf. 4*b*), and that the Favorsky rearrangement products are formed by different pathways.

On the other hand, Smissman and co-workers (49) suggested on the basis of a study on Favorsky rearrangements of α-halogenated 2-decalones that a delocalized intermediate must be excluded in Favorsky rearrangements since, in their series, under conditions which should, theoretically, be favorable for the formation of such intermediates,

[20]Another piece of evidence against the assumption of a common delocalized intermediate in the formation of both substitution and rearrangement products is due to House and Frank (48) who showed that the composition of the products, including the substitution products, obtained upon treatment of 9-epimeric 9-chloro-1-decalones with base depended on the stereochemistry of the halogen substituent.

Can. J. Chem. Downloaded from www.nrcresearchpress.com by 210.87.254.5 on 09/05/12
For personal use only.

no rearrangement products were isolated. Confronted with the stereochemical problems which were the basis of our work, as well as of that of House and Gilmore and of Tchoubar *et al.*, they reverted to Wendler's hypothesis.

House and co-workers now seem to favor (48) the idea, which they had already previously taken into consideration (21), that the stereochemical differences of Favorsky rearrangements in various media would not be due to the influence of the medium on the choice between the concerted and non-concerted cyclopropanone formation, but rather to the epimerization of one cyclopropanone derivative to the other. They possibly favor this explanation in consideration of the fact that no rearrangement products were obtained when the epimeric 9-chloro-1-decalones were treated with methoxide in absolute methanol while such products were formed in good yield when the reaction was carried out with methoxide in dimethoxyethane (48).

We prefer the explanation of the stereochemical situation involving both concerted and non-concerted pathways, in view of the probability of a delocalized intermediate in certain Favorsky rearrangements (see above). Furthermore, since Turro and Hammond (45) found that in the medium methoxide–methanol a cyclopropanone is converted extremely fast, almost quantitatively (and, of course, irreversibly) to rearrangement products, one would have to postulate in relatively polar and protic media an even faster equilibration of the epimeric cyclopropanones. In the case of the rearrangement of 11-non-ketonic 17α-bromo 20-keto steroids, the equilibration to the cyclopropanone with an α-configuration of its methylene group would have to proceed so fast as to virtually exclude any competitive opening of the originally formed cyclopropanone to rearrangement products. We hope that some experiments in progress in our laboratory on the stereochemistry of rearrangements of 21-halogenated 20-keto steroids in an aprotic medium should shed some light on the situation.

The fact that in the experiments of Smissman and co-workers (49) and House and Frank (48) the proportion of non-Favorsky products was found significantly higher (up to quasi-exclusion of Favorsky products) in media which should favor, *per se*, the formation of a delocalized intermediate than in media favoring a concerted cyclopropanone formation, corresponds well to established data from the literature (4*b*) and agrees with the finding reported in this paper that the reaction of 21-bromo-3β-acetoxy-5-pregnen-20-one (**1**, R_1 = β-AcO, $R_2 = R_6 = H$, $R_3 = R_4$ = double bond, $R_5 = H_2$, X = Br) with bicarbonate in aqueous methanol leads to an appreciable extent to substitution in position 21, whereas the rearrangement of the same product with methoxide in absolute methanol leads practically exclusively to Favorsky rearrangement products. The question arises why the proportion of substitution and rearrangement products varies not only with the nature of the medium but also with the nature of the α-halogenated ketone. We suggest that at least in part steric factors may be responsible for these variations. Thus, the practically exclusive formation of Favorsky rearrangement products in the case of the rearrangement of 17α-bromo-3β-acetoxy-5-pregnen-20-one (**4**, R_1 = β-AcO, $R_2 = R_6 = H$, $R_3 = R_4$ = double bond, $R_5 = H_2$, X = Br) with bicarbonate in aqueous methanol, a medium which should also favor the formation of non-Favorsky products, may be explained on steric grounds, the 18-methyl group impeding the formation of epoxy derivatives. We shall discuss this question and its experimental basis in a following paper of this series.

In conclusion we may point out that our interpretation of the Favorsky rearrangement seems in agreement with a recent publication by Warnhoff *et al.* (50) and with two articles by Bordwell and Scamehorn (51) which appeared after the preparation of this manuscript.

Experimental[21]

*Methyl 3α-Acetoxy-11-oxo-17β-methyl-17α-etianate (**3**, R_1 = α-AcO, $R_2 = R_4 = R_6 = H$, R_3 = β-H, $R_5 = O$, $R_7 = CH_3$) from 17α-Bromo-3α-acetoxy-5β-pregnane-11,20-dione*

For further characterization, the isomer of methyl 3α-acetoxy-11-oxo-17α-methyletianate (**2**, R_1 = α-AcO, $R_2 = R_4 = R_6 = H$, R_3 = β-H, $R_5 = O$, $R_7 = CH_3$)

[21]The melting points were taken in evacuated capillaries and the temperatures were corrected. If not otherwise stated, the aluminum oxide used for chromatography was prepared, from Merck's alkaline aluminum oxide, as described in footnote 31 of ref. 11*a*, and showed activity II–III. For chromatography on silica gel, Davison's silica gel 923 was employed. Thin-layer chromatography was performed with Merck-Darmstadt silica gel. The i.r. spectra were recorded on a Beckman IR-4 spectrophotometer and the u.v. spectra on a Beckman DK-1A spectrophotometer. The microanalyses were performed by Mr. J. F. Alicino, Metuchen, New Jersey, the late Mr. A. Bernhardt, Mülheim (Ruhr), and Dr. C. Daesslé, Montreal, to whom much appreciation is due. We express sincere thanks to Merck & Company, Montreal, for the generous gift of their aluminum oxide.

Can. J. Chem. Downloaded from www.nrcresearchpress.com by 210.87.254.5 on 09/05/12
For personal use only.

(14*b*), which had been eluted with petroleum ether – benzene (4:1) from aluminum oxide prior to this 17α-methyl ester **2** (R_1 = α-AcO, $R_2 = R_4 = R_6$ = H, R_3 = β-H, R_5 = O, $R_7 = CH_3$), was isolated in larger amounts by repeated chromatography and recrystallizations of mixtures containing both esters **2** and **3**. A sample of ester **3** (R_1 = α-AcO, $R_2 = R_4 = R_6$ = H, R_3 = β-H, R_5 = O, $R_7 = CH_3$) was recrystallized for analysis from methanol; needles, m.p. 155°;[22] $[\alpha]_D^{22}$ + 39.3° (*c*, 1.064 in $CHCl_3$); no ultraviolet (u.v.) absorption maximum between 215 and 250 mμ; ν_{max}(nujol) 1721 (acetate), 1704 (methyl ester and 11-ketone), 1255 (acetate), 1165 (methyl ester), and 1037 cm^{-1} (acetate).[23]

Anal. Calcd. for $C_{24}H_{36}O_5$: C, 71.25; H, 8.97; OCH_3, 7.67. Found: C, 71.27; H, 9.08; OCH_3, 7.59.

Methyl 3α-Hydroxy-11-oxo-17β-methyl-17α-etianate
*(**3**, R_1 = α-OH, $R_2 = R_4 = R_6$ = H, R_3 = β-H, R_5 = O, $R_7 = CH_3$)*

A solution of 267 mg of the above described acetoxy ester **3** (R_1 = α-AcO, $R_2 = R_4 = R_6$ = H, R_3 = β-H, R_5 = O, $R_7 = CH_3$) in 40 ml of 5% methanolic potassium hydroxide was refluxed for 2 h under nitrogen. The usual work-up gave 229 mg (95% yield) of crude hydroxy ester **3** (R_1 = α-OH, $R_2 = R_4 = R_6$ = H, R_3 = β-H, R_5 = O, $R_7 = CH_3$) and 50 mg of a crude acid fraction. The neutral fraction was recrystallized 3 times from ether–hexane for analysis; fine needles, m.p. 153°; depressed upon admixture of the hydroxy ester **2** (R_1 = α-OH, $R_2 = R_4 = R_6$ = H, R_3 = β-H, R_5 = O, $R_7 = CH_3$); $[\alpha]_D^{22}$ + 25.2° (*c*, 1.032 in $CHCl_3$) ν_{max}($CHCl_3$) 3610 (hydroxyl), 1714, 1708 (broad band, methyl ester, 11-ketone), 1435 (12-CH_2), 1165 (methyl ester), and 1035 cm^{-1} (hydroxyl).[23]

Anal. Calcd. for $C_{22}H_{34}O_4$: C, 72.89; H, 9.45. Found: C, 72.69; H, 9.55.

Recrystallization of the acid fraction from acetone gave only unsatisfactory results; very small quantities of impure acid **3** (R_1 = α-OH, $R_2 = R_4 = R_6 = R_7$ = H, R_3 = β-H, R_5 = O) were obtained; m.p. 168–170°.

Reacetylation

A solution of 85 mg of the above mentioned hydroxy ester **3** (R_1 = α-OH, $R_2 = R_4 = R_6$ = H, R_3 = β-H, R_5 = O, $R_7 = CH_3$) in 3 ml of pyridine was treated at room temperature with 2 ml of acetic anhydride for 16 h. The usual work-up afforded a crude product which was chromatographed on 6 g of aluminum oxide. Petroleum ether – benzene (4:1 and 1:1) eluted 94 mg of crystalline acetoxy ester **3** (R_1 = α-AcO, $R_2 = R_4 = R_6$ = H, R_3 = β-H, R_5 = O, $R_7 = CH_3$), m.p. 140–150°. Recrystallization from methanol gave the pure product, identified by a mixture melting point and the comparison of the i.r. spectrum with that of an authentic sample.

3α-Hydroxy-11-oxo-17β-methyl-17α-etianic Acid
*(**3**, R_1 = α-OH, $R_2 = R_4 = R_6 = R_7$ = H, R_3 = β-H, R_5 = O)*

In a sealed tube, 418 mg of acetoxy keto ester **3** (R_1 = α-AcO, $R_2 = R_4 = R_6$ = H, R_3 = β-H, R_5 = O, $R_7 = CH_3$) was heated for 48 h with 20 ml of 7% methanolic potassium hydroxide to 170°. The crude acid fraction (474 mg) was separated from the acetone insoluble material to give 401 mg (96% yield) of crystalline acid **3** (R_1 = α-OH, $R_2 = R_4 = R_6 = R_7$ = H, R_3 = β-H, R_5 = O), m.p. 246.5–250.5°. Recrystallization from acetone raised the melting point to 257–259°. A sample was recrystallized twice from acetone for analysis; small cubes, m.p. 260°, not depressed upon admixture of the crude acid isolated after partial saponification (see above) but upon admixture of the isomeric acid **2** (R_1 = α-OH, $R_2 = R_4 = R_6 = R_7$ = H, R_3 = β-H, R_5 = O); $[\alpha]_D^{22}$ + 24.8° (*c*, 1.025 in dioxane); ν_{max}($CHCl_3$) 3545 (very broad, multiple associated hydroxyl band), 1707, 1703 (broad band, carboxyl and 11-ketone), 1435 (12-CH_2), and 1035 and 1020 cm^{-1} (hydroxyl bands).[23]

Anal. Calcd. for $C_{21}H_{32}O_4$: C, 72.38; H, 9.26. Found: C, 72.40; H, 9.13.

Methylation

To a solution of 87 mg of the hydroxy keto acid **3** (R_1 = α-OH, $R_2 = R_4 = R_6 = R_7$ = H, R_3 = β-H, R_5 = O) in absolute methanol, was added, at 0°, a large excess of a 1.8% ethereal diazomethane solution. The reaction mixture was maintained for 6 h at 0°, and then allowed to warm to 20° and kept for another 6 h at that temperature. The excess reagent was destroyed with acetic acid and the product was taken to dryness. Recrystallization of the residue (111 mg) gave 85 mg (94% yield) of pure hydroxy keto methyl ester **3** (R_1 = α-OH, $R_2 = R_4 = R_6$ = H, R_3 = β-H, R_5 = O, $R_7 = CH_3$), m.p. 147–149.5°, not depressed upon admixture of an authentic sample.

Rearrangement of 17α-Bromo-3β-acetoxy-5-pregnen-20-one
*(**4**, R_1 = β-AcO, $R_2 = R_6$ = H, $R_3 = R_4$ = double bond, $R_5 = H_2$, X = Br) with Potassium Bicarbonate in Aqueous Methanol*

To a solution of 9 g of analytically pure 17α-bromo-3β-acetoxy-5-pregnen-20-one (**4**, R_1 = β-AcO, $R_2 = R_6$ = H, $R_3 = R_4$ = double bond, $R_5 = H_2$, X = Br) (9*b*, 52, 53) in 405 ml of methanol, 20.291 g of potassium bicarbonate in 80.8 ml of water was added. The mixture was refluxed for 4 h, cooled, and poured into ice water. The product was extracted with ether, the ethereal solution was washed with water and dried over sodium sulfate. Evaporation of the solvent gave 6.0 g of a residue which crystallized upon addition of methanol, representing the *neutral fraction*. The alkaline aqueous solution remaining after the ether extraction was combined with the first water washings and acidified with 2 *N* sulfuric acid to p*H* 3. The product was extracted with dichloromethane and the organic solution was washed to neutral with water and dried over sodium sulfate. Evaporation of the solvent left 1.226 g of a crystalline product, m.p. 233–239°, representing the *acid fraction*.

The *neutral fraction* was acetylated in the usual fashion with 18 ml of acetic anhydride in 35 ml of pyridine. The reaction product was dissolved in a small quantity of dichloromethane, and methanol was added. The crystalline product was separated, washed, and dried, thus affording 4.358 g of *methyl* Δ^5*-3β-acetoxy-17α-methyl-etienate* (**2**, R_1 = β-AcO, $R_2 = R_6$ = H, $R_3 = R_4$ = double bond, $R_5 = H_2$, $R_7 = CH_3$), m.p. 164–165°,

[22]Upon admixture with a comparison sample kindly provided by Dr. N. L. Wendler, the melting point was not depressed. We express sincere thanks to Dr. Wendler for providing us with this sample.

[23]This spectrum was kindly taken by Prof. Hans H. Günthard, Swiss Federal Institute of Technology, Zurich, Switzerland, to whom we express our sincere appreciation.

Can. J. Chem. Downloaded from www.nrcresearchpress.com by 210.87.254.5 on 09/05/12
For personal use only.

$[\alpha]_D^{23}$ − 56.4° (*c*, 1.000 in $CHCl_3$). The mother liquors were taken to dryness and the residue was recrystallized in the same fashion to give another batch of 1.268 g of the same material. For analysis, a sample was recrystallized 3 times from methanol; pellets, m.p. 166–166.5°; $[\alpha]_D^{23}$ − 57.1° (*c*, 1.000 in $CHCl_3$) [lit. (*9b*): m.p. 163°; $[\alpha]_D^{23}$ − 58.7°]; ν_{max}(KBr) 1740 (acetate and 20-ester), 1250 cm^{-1} (acetate).

Anal. Calcd. for $C_{24}H_{36}O_4$: C, 74.19; H, 9.34. Found: C, 74.18; H, 9.46.

Chromatography of the remaining mother liquors gave 209 mg of the same ester and 147 mg of crude crystalline *methyl* Δ⁵-*3β-acetoxy-17β-methyl-17α-etienate* (**3**, R_1 = β-AcO, $R_2 = R_6 = H$, $R_3 = R_4$ = double bond, $R_5 = H_2$, $R_7 = CH_3$), m.p. 146–147°, eluted with petroleum ether – benzene (1:1 and 1:4). Two recrystallizations gave 73 mg of the pure product which was recrystallized once more for analysis; m.p. 151–152°; $[\alpha]_D^{23}$ − 72.0° (*c*, 1.000 in $CHCl_3$); the m.p. was not depressed upon admixture of an authentic sample (*9b*).

Anal. Calcd. for $C_{24}H_{36}O_4$: C, 74.19; H, 9.34. Found: C, 74.07; H, 9.29.

Chromatography of the mother liquors gave another 100 mg of the 17α-methyl ester, m.p. 163–165°, and 77 mg of the 17β-methyl ester, m.p. 146–147°. The identity of these products was established by the determination of mixture melting points and by comparison of the i.r. spectra with those of authentic samples.

The *acid fraction* was dissolved in 22 ml of absolute ether and 22 ml of absolute methanol. At −10°, a 3% ethereal diazomethane solution (85 ml) was added. The mixture was allowed to come to room temperature and was stored for 16 h. The usual work-up gave 1.371 g of a crystalline product which was acetylated with 6 ml of acetic anhydride in 12 ml of pyridine. The resulting crystalline product (1.306 g), m.p. 150–154°, was recrystallized from dichloromethane – methanol. Thus, 951 mg of the *17α-methyl etio ester* **2** (R_1 = β-AcO, $R_2 = R_6 = H$, $R_3 = R_4$ = double bond, $R_5 = H_2$, $R_7 = CH_3$), m.p. 162–163°, was obtained. Chromatography of the mother liquors and of certain fractions from the purification of the neutral part gave another 137 mg of *17α-methyl etio ester* **2** (R_1 = β-AcO, $R_2 = R_6 = H$, $R_3 = R_4$ = double bond, $R_5 = H_2$, $R_7 = CH_3$), m.p. 158–160°, and 71 mg of the *17β-methyl etio ester* **3** (R_1 = β-AcO, $R_2 = R_6 = H$, $R_3 = R_4$ = double bond, $R_5 = H_2$, $R_7 = CH_3$), m.p. 144–148°.

In toto 7.304 g of 17α-methyl etio ester **2** (R_1 = β-AcO, $R_2 = R_6 = H$, $R_3 = R_4$ = double bond, $R_5 = H_2$, $R_7 = CH_3$) (92.5%) and 335 mg of the 17β-methyl etio ester **3** (R_1 = β-AcO, $R_2 = R_6 = H$, $R_3 = R_4$ = double bond, $R_5 = H_2$, $R_7 = CH_3$) (4% yield) were isolated. A quantity of 60 mg (0.4%) of a mixture of both esters was not further separated and an oily fraction (196 mg, 2.7%) was not further investigated.

*Rearrangement of 17α-Bromo-3β-acetoxy-5-pregnen-20-one (**4**, R_1 = β-AcO, $R_2 = R_6 = H$, $R_3 = R_4$ = double bond, $R_5 = H_2$, X = Br) with Potassium Methoxide in Absolute Methanol*

To a solution of 700 mg of potassium in 85 ml of absolute methanol was added, portionwise, 3.591 g of analytically pure 17α-bromo-3β-acetoxy-5-pregnen-20-one (**4**, R_1 = β-AcO, $R_2 = R_6 = H$, $R_3 = R_4$ = double bond, $R_5 = H_2$, X = Br), m.p. 146–147°, over a period of 20 min. Subsequently, 20 ml of absolute methanol was added and the mixture was refluxed for another 20 min. The volume of the solution was reduced to 50 ml and the mixture was poured into ice water and the precipitate was extracted with ether. The ethereal solution was washed with iced 2 *N* sulfuric acid, with cold sodium bicarbonate solution, and with water and was dried over sodium sulfate. The evaporation of the solvent gave 2.957 g of a crystalline product, m.p. 135–136°, representing the *neutral fraction*. The aqueous, alkaline phase of the extraction was combined with the first sulfuric acid washings and acidified with sulfuric acid to p*H* 3. Extraction with dichloromethane gave 12 mg of an amorphous *acidic product* which was not further investigated.

The *neutral fraction* (2.957 g) was acetylated with 18 ml of acetic anhydride in 50 ml of pyridine and was worked up in the usual fashion to give 3.25 g of a crystalline product, m.p. 120–144°. Recrystallization from methanol gave 136 mg of *methyl* Δ⁵-*3β-acetoxy-17α-methyletienate* (**2**, R_1 = β-AcO, $R_2 = R_6 = H$, $R_3 = R_4$ = double bond, $R_5 = H_2$, $R_7 = CH_3$), m.p. 163–165°. The mother liquors were chromatographed on 75 g of aluminum oxide, activity III. Elutions with petroleum ether – benzene (9:1) afforded various fractions melting between 145 and 150° which, upon recrystallization from methanol, gave 346 mg of the *17α-methyl ester* **2**, m.p. 162–163°. Petroleum ether – benzene (4:1) gave fractions which, upon recrystallization from methanol, afforded 104 mg of *methyl* Δ⁵-*3β-acetoxy-17β-methyl-17α-etienate* (**3**, R_1 = β-AcO, $R_2 = R_6 = H$, $R_3 = R_4$ = double bond, $R_5 = H_2$, $R_7 = CH_3$), m.p. 149–150°. The remainder of the petroleum ether – benzene fractions was combined, as were the mother liquors of the previous crystallizations. Repeated chromatography on aluminum oxide and recrystallizations from methanol gave 634 mg of *17α-methyl ester* **2** (R_1 = β-AcO, $R_2 = R_6 = H$, $R_3 = R_4$ = double bond, $R_5 = H_2$, $R_7 = CH_3$), m.p. 160–164°, and 678 mg of the *17β-methyl 17-iso-ester* **3** (R_1 = β-AcO, $R_2 = R_6 = H$, $R_3 = R_4$ = double bond, $R_5 = H_2$, $R_7 = CH_3$), m.p. 146–150°.

The identity of the 2 isomeric esters isolated was established on the grounds of mixture m.p. with authentic samples and by comparison of the i.r. spectra.

In summary, 1.8 g (56.5%) of *methyl* Δ⁵-*3β-acetoxy-17α-methyletienate* (**2**, R_1 = β-AcO, $R_2 = R_6 = H$, $R_3 = R_4$ = double bond, $R_5 = H_2$, $R_7 = CH_3$) and 1.025 g (32.2%) of *methyl* Δ⁵-*3β-acetoxy-17β-methyl-17α-etienate* (**3**, R_1 = β-AcO, $R_2 = R_6 = H$, $R_3 = R_4$ = double bond, $R_5 = H_2$, $R_7 = CH_3$) were isolated in the pure state. There remained 0.36 g (10.9%) of an oily product which was not further investigated.

*Rearrangement of 17α-Bromo-3β-acetoxy-5-pregnen-20-one (**4**, R_1 = β-AcO, $R_2 = R_6 = H$, $R_3 = R_4$ = double bond, $R_5 = H_2$, X = Br) with Sodium Methoxide in 1,2-Dimethoxyethane*

A solution of 1.654 g of sodium in 30 ml of absolute methanol was taken to dryness. The dried residue was suspended, by the use of a vibro-stirrer, in 185 ml of 1,2-dimethoxyethane and there was added 8.0 g of analytically pure 17α-bromo-3β-acetoxy-5-pregnen-20-one (**4**, R_1 = β-AcO, $R_2 = R_6 = H$, $R_3 = R_4$ = double bond, $R_5 = H_2$, X = Br), m.p. 147–148°, in 85 ml of 1,2-dimethoxyethane. The mixture was refluxed with

Can. J. Chem. Downloaded from www.nrcresearchpress.com by 210.87.254.5 on 05/05/12
For personal use only.

stirring for 2 h, the product was cooled and poured into ice water. The precipitate was extracted with ether, the ethereal layer was washed with iced 2 *N* sulfuric acid and with cold sodium bicarbonate solution, and was dried over sodium sulfate. Evaporation of the solvent gave 6.1 g of a yellowish residue, representing the *neutral fraction*. The alkaline, aqueous phase of the extraction was combined with the first sulfuric acid washings and acidified to p*H* 3, with sulfuric acid. Extraction with dichloromethane gave 183 mg of an oily acidic product.

The *neutral fraction* (6.1 g) was acetylated with 30 ml of acetic anhydride in 60 ml of pyridine and worked up in the usual fashion. Two recrystallizations of the reaction product from methanol gave 2.798 g of *methyl* Δ^5*-3*β*-acetoxy-17*β*-methyl-17*α*-etienate* (**3**, R_1 = β-AcO, R_2 = R_6 = H, R_3 = R_4 = double bond, R_5 = H_2, R_7 = CH_3), m.p. 147–148°, $[\alpha]_D^{23}$ − 69.8° (*c*, 1.000 in $CHCl_3$). Triangle crystallization of the mother liquors gave another 1.467 g of the same product, m.p. 147–148°.

Repeated chromatography and recrystallizations of the remaining mother liquors gave 330 mg (4.5%) of *17*α*-methyl etio ester* **2**, m.p. 158–163°, and 1.452 g of *17*β*-methyl ester* **3**, m.p. 144–148°, which raised the yield of this ester to 80.5%.

From the chromatogram fractions which followed those which had given pure 17β-methyl ester **3**, 16 mg of *methyl* Δ^5*-3*β*-acetoxy-21-pregnenoate* (**6**), m.p. 121–123°, was obtained. This product was identified by a mixture m.p. and by the comparison of its i.r. spectrum with that of an authentic sample, and was recrystallized for analysis; m.p. 127–128°; $[\alpha]_D^{23}$ − 54.4° (*c*, 1.000 in $CHCl_3$) [lit. (54) m.p. 128–129°, $[\alpha]_D$ − 57°]; ν_{max}(KBr) 1740 (methyl ester and acetate), 1675 (double bond), and 1245 cm^{-1} (ester).

Anal. Calcd. for $C_{24}H_{36}O_4$: C, 74.19; H, 9.34. Found: C, 74.34; H, 9.20.

There remained 61 mg (0.8%) of a non-separated mixture of the 17-methylated etio esters, 101 mg (1.4%) of a mixture of the 17β-methyl 17-iso etio ester **3** and the 21-methyl ester **6**, 675 mg (9.5%) of amorphous products, and 183 mg (2.5%) of an acid fraction which were not further investigated.

*Rearrangement of 17*α*-Bromo-3*α*,12*α*-diacetoxy-5*β*-pregnan-20-one (**4**, R_1 = α-AcO, R_2 = R_4 = H, R_3 = β-H, R_5 = H_2, R_6 = AcO, X = Br) with Potassium Methoxide in Absolute Methanol*

To a solution of potassium methoxide prepared from 2.21 g of potassium and 200 ml of absolute methanol, was added, at reflux temperature, a solution of 12.9 g of purified, amorphous 17α-bromo-3α,12α-diacetoxy-5β-pregnan-20-one (**4**, R_1 = α-AcO, R_2 = R_4 = H, R_3 = β-H, R_5 = H_2, R_6 = AcO, X = Br) (11) in 70 ml of absolute methanol, dropwise within 20 min. The mixture was refluxed for 2 h, the volume of the solution was reduced to 100 ml and the product was poured into ice water. The precipitate was extracted with ether, the ethereal solution was washed with water, cold dilute sulfuric acid, iced potassium bicarbonate solution, a cold dilute sodium thiosulfate solution, and with water, and was dried over sodium sulfate. Evaporation of the solvent gave 9.08 g of a dark, oily product, representing the *neutral fraction*.

The aqueous phase of the original extraction was combined with the first sulfuric acid washings, acidified with 2 *N* sulfuric acid to p*H* 3, and the mixture was extracted with dichloromethane. The organic phase was washed with water and dried over sodium sulfate. Evaporation of the solvent gave 100 mg of an amorphous product, representing the *acid fraction* which was not further investigated.

The *neutral fraction* was dissolved in 120 ml of acetic acid and 12 ml of water and debrominated at 80°, for 1 h, with 12 g of zinc dust. After cooling, the product was extracted with ether, the ethereal solution was washed with dilute hydrochloric acid, with a saturated sodium bicarbonate solution, and with water, and was dried over sodium sulfate. Removal of the solvent gave 8.94 g of a dark, oily product, which was acetylated in 45 ml of pyridine with 23 ml of acetic anhydride. The usual work-up gave 9.04 g of a partially crystalline product which was dissolved in a mixture (1:1) of petroleum ether and benzene and absorbed on 270 g of aluminum oxide, activity III. Elutions with petroleum ether – benzene (4:1) gave 2.406 g of crystals, m.p. 127–130°. Recrystallization from ether–hexane gave 956 mg of *methyl 3*α*,12*α*-diacetoxy-17*α*-methyl-5*β*-etianate* (**2**, R_1 = α-AcO, R_2 = R_4 = H, R_3 = β-H, R_5 = H_2, R_6 = AcO, R_7 = CH_3), m.p. 156–158°. The identity of the product was established by a mixture m.p. and by the comparison of the i.r. spectrum with that of an authentic sample.

The mother liquors of this recrystallization were taken to dryness and recrystallized from pure hexane to give 172 mg of *3*α*-acetoxy-12*α*-hydroxy-17*β*-methyl-17*α*-etianic acid lactone (20 → 12)* (**5***a*), m.p. 144–145°. A sample was recrystallized 4 times from hexane for analysis; m.p. 138–140°; $[\alpha]_D^{23}$ + 141.5° (*c*, 1.000 in $CHCl_3$); ν_{max}(KBr) 1775 (γ-lactone), 1730, 1210 cm^{-1} (acetate); nuclear magnetic resonance (n.m.r.) at 60 MHz [TMS, 0 p.p.m., $CDCl_3$] δ 0.85 (18-CH_3), 0.97 (19-CH_3), 1.11 (17-CH_3), 2.01 (acetyl), 4.36 (doublet at 260 and 263 Hz, 12β-H), 4.7 p.p.m. (3β-H).[24]

Anal. Calcd. for $C_{23}H_{34}O_4$: C, 73.75; H, 9.15. Found: C, 73.84; H, 9.05.

The remaining mother liquors (1.246 g) were chromatographed on 35 g of aluminum oxide, activity III. Petroleum ether – benzene mixtures (9:1, 4:1, and 1:1) eluted 648 mg of a product crystallizing from hexane, m.p. 142–144°. Recrystallization from hexane gave 145 mg of the *lactone* **5***a*.

The mother liquors of this crystallization were again chromatographed on 15 g of aluminum oxide, but no crystalline product could be obtained. In the original chromatogram of the *neutral fraction*, further elutions with petroleum ether – benzene (4:1) gave 1.068 g of a crystalline material, m.p. 114–116°. Recrystallization from ether–hexane gave 170 mg of the *17*α*-methyl etio ester* (**2**, R_1 = α-AcO, R_2 = R_4 = H, R_3 = β-H, R_5 = H_2, R_6 = AcO, R_7 = CH_3). Recrystallization of the mother liquors from hexane gave 41 mg of *lactone* **5***a*. The mother liquors of these recrystallizations were rechromatographed on 25 g of aluminum oxide, activity III. Petroleum ether – benzene (4:1) eluted 310 mg of a product, melting between 106 and 116°. Recrystallization from hexane gave 113 mg of *lactone* **5***a*. Petroleum ether – benzene

[24]The spectrum was recorded on a Varian A60 instrument.

Can. J. Chem. Downloaded from www.nrcresearchpress.com by 210.87.254.5 on 09/05/12
For personal use only.

mixtures (1:1 and 1:4) eluted 187 mg of *3α,12α-diacetoxy-5β-pregnan-20-one* (**4**, R_1 = α-AcO, $R_2 = R_4$ = H, R_3 = β-H, $R_5 = H_2$, R_6 = AcO, X = H). The identity of this product was established by the determination of a mixture m.p. and the comparison of its i.r. spectrum with that of an authentic sample.

In the original chromatogram of the *neutral fraction*, petroleum ether – benzene (1:4), pure benzene, benzene–ether (1:1), and pure ether gave 1.451 g of an oily product. The i.r. spectrum revealed a hydroxy group (ν_{max}(KBr) 3400 cm^{-1}). The material was reacetylated in the usual fashion and chromatographed on aluminum oxide but no crystalline product could be obtained.

Taking into account the recovery of the debrominated starting material, 3α,12α-diacetoxy-5β-pregnan-20-one, 17.3% (1.518 g) of pure *methyl 3α,12α-diacetoxy-17α-methyl-5β-etienate* (**2**, R_1 = α-AcO, $R_2 = R_4$ = H, R_3 = β-H, $R_5 = H_2$, R_6 = AcO, $R_7 = CH_3$) and 6.7% (471 mg) of *lactone* **5***a* were obtained; there remained 3.554 g (39%) of a mixture of the lactone and the 17α-methyl etio ester. According to an i.r. analysis of this mixture, the total yield of the 17α-methyl etio ester amounted to approximately 31%, that of the lactone to approximately 9%. Further untractable mixtures still contained these two products so that this proportion is only an approximation.

Hydrolysis of 3α-Acetoxy-12α-hydroxy-17β-methyl-5β,17α-etianic Acid Lactone (20 → 12) (5a)

(*a*) A solution of 250 mg of the acetoxy lactone **5***a*, m.p. 144–145°, in 8 ml of methanol was refluxed with a solution of 120 mg of potassium carbonate in 3.6 ml of methanol and 1.4 ml of water for 5 h and was subsequently allowed to stand for another 12 h. The mixture was poured into ice water and the precipitate was extracted with ether. The ethereal solution was washed with water and dried over sodium sulfate. Evaporation of the solvent gave 214 mg of a *neutral fraction*. The aqueous phase of the extraction, together with the first water washings, was acidified to the Congo-blue reaction with sulfuric acid and the mixture was extracted with dichloromethane. The organic solution was washed with water, dried over sodium sulfate, and taken to dryness. There remained 9 mg of an amorphous *acid fraction*.

The *neutral fraction* was chromatographed on 9 g of aluminum oxide, activity III. Petroleum ether – benzene (1:4), pure benzene, and benzene–ether (1:1) eluted 90 mg of *3α,12α-dihydroxy-17β-methyl-5β,17α-etianic acid lactone (20 → 12)* (**5**), m.p. 169–173°. A sample was recrystallized 3 times from hexane for analysis; m.p. 174.5–175.5°; $[\alpha]_D^{22}$ + 11° (*c*, 0.862 in $CHCl_3$); ν_{max}(KBr) 3265 (hydroxyl), 1775 cm^{-1} (γ-lactone).

Anal. Calcd. for $C_{21}H_{32}O_3$: C, 75.90; H, 9.70. Found: C, 75.97; H, 9.65.

(*b*) A solution of 103 mg of lactone **5***a*, m.p. 144–145°, in 3.1 ml of a 5.6% methanolic potassium hydroxide solution was refluxed for 4 h. After cooling, the product was poured into ice water and the precipitate was extracted with ether. The ethereal layer was washed with dilute sulfuric acid, with sodium bicarbonate solution, and with water. Evaporation of the solvent gave 59 mg of *lactone* **5**.

The aqueous phase and the first acid washings were combined and acidified with sulfuric acid to the Congo-blue reaction. The product was extracted with dichloromethane, the organic solution was washed with water and dried over sodium sulfate. Evaporation of the solvent gave 62 mg of a crystalline product, m.p. 162–164°, which showed in the i.r. a typical absorption of a hydroxy acid. Recrystallization from hexane gave, however, as the only pure product, 22 mg of *lactone* **5**, m.p. 174–175°, not depressed upon admixture of an authentic sample (see above); ν_{max}(KBr) 3265 and 1775 cm^{-1}.

3β,20-Diacetoxy-5,20-pregnadiene (i)

From a solution of 20 g of 3β-acetoxy-5-pregnen-20-one (**4**, R_1 = β-AcO, $R_2 = R_6$ = X = H, $R_3 = R_4$ = double bond, $R_5 = H_2$) and of 3 g of *p*-toluenesulfonic acid in 336 ml of isopropenyl acetate the solvent was removed, in the course of 10 h, through a Vigreux column, by slow distillation, the volume of the solution being maintained at approximately 200 ml by occasional additions of isopropenyl acetate. After cooling, the residue was poured into ice water and the mixture was extracted with ether. The ethereal solution was washed with cold water, iced saturated sodium bicarbonate solution, and with water, and was dried over a sodium sulfate. Removal of the solvent gave 24.3 g of a dark-brown product which crystallized upon addition of methanol; m.p. 97–105°. Recrystallization from methanol gave 11.7 g (52.4%) of pure 3β,20-diacetoxy-5,20-pregnadiene (**i**), m.p. 119–120°. A sample was recrystallized 3 times from ether–methanol for analysis; pellets, m.p. 121–122°, $[\alpha]_D^{23}$ − 44.4° (*c*, 1.000 in $CHCl_3$) [lit. (25): m.p. 122–123°; $[\alpha]_D$ − 45.8°]; ν_{max}(KBr) 1740 (acetates), 1665 (20-methylene), and 1240 cm^{-1} (acetates).

Anal. Calcd. for $C_{25}H_{36}O_4$: C, 74.96; H, 9.06. Found: C, 74.83; H, 8.80.

21-Bromo-3β-acetoxy-5-pregnen-20-one (1, R_1 = β-AcO, $R_2 = R_6 = H$, $R_3 = R_4$ = double bond, $R_5 = H_2$, X = Br) (24)

To a mixture of 5.3 g of *N*-bromosuccinimide in 495 ml of *t*-butyl alcohol and of 11.7 g of 3β,20-diacetoxy-5,20-pregnadiene (**i**), there were added 10.1 ml of water and, with vigorous stirring, dropwise, in the course of 35 min, 59.7 ml of 1 *N* sulfuric acid. The mixture was stirred for 1 h at room temperature and then precipitated in 3 l of ice water. The product was extracted with ether, the organic solution was washed with a cold 10% sodium bisulfite solution, with an iced sodium bicarbonate solution, and with water, and was dried over sodium sulfate. Removal of the solvent gave 13.7 g of a yellowish crystalline product, m.p. 137–140°. Several recrystallizations from methanol gave 8.5 g of pure 21-bromo-3β-acetoxy-5-pregnen-20-one (**1**, R_1 = β-AcO, $R_2 = R_6 = H$, $R_3 = R_4$ = double bond, $R_5 = H_2$, X = Br), m.p. 144–145°. The product was recrystallized from methanol for analysis, giving 6.96 g of colorless needles, m.p. 145.5–146°; $[\alpha]_D^{22}$ + 46.2° (*c*, 1.000 in $CHCl_3$) [lit. (24): m.p. 143–144.5°; $[\alpha]_D$ + 35° (dioxane)]; ν_{max}(KBr) 1730 (acetate), 1705 (ketone), and 1250 cm^{-1} (acetate).

Anal. Calcd. for $C_{23}H_{33}O_3Br$: C, 63.15; H, 7.60; Br, 18.27. Found: C, 63.42; H, 7.50; Br, 18.01.

3β,21-Diacetoxy-5-pregnen-20-one (1, R_1 = β-AcO, $R_2 = R_6 = H$, $R_3 = R_4$ = double bond, $R_5 = H_2$, X = AcO)

To a solution of 100 mg of 21-bromopregnenolone

Can. J. Chem. Downloaded from www.nrcresearchpress.com by 210.87.254.5 on 09/05/12
For personal use only.

acetate (**1**, R_1 = β-AcO, $R_2 = R_6$ = H, $R_3 = R_4$ = double bond, $R_5 = H_2$, X = Br), m.p. 141–143°, in 10 ml of absolute acetone, 40 mg of dry sodium iodide in 10 ml of absolute acetone was added. The mixture was refluxed for 15 min; a slightly yellowish precipitate formed. Dry potassium acetate (125 mg) in 0.5 ml of acetic acid was added and the mixture was refluxed for 12 h. The cooled product was concentrated *in vacuo* and extracted with ether. The organic solution was washed with water and dried over sodium sulfate. Removal of the solvent *in vacuo* gave 104 mg of colorless crystals, m.p. 161–163°. A sample was recrystallized twice from ether–methanol for analysis; m.p. 166–167°; ν_{max}(KBr) 1760 and 1740 (21-acetoxy-20-keto doublet), and 1245 cm^{-1} (acetate).

Anal. Calcd. for $C_{25}H_{36}O_5$: C, 72.08; H, 8.71. Found: C, 71.80; H, 8.48.

*Rearrangement of 21-Bromo-3β-acetoxy-5-pregnen-20-one (**1**, R_1 = β-AcO, $R_2 = R_6$ = H, $R_3 = R_4$ = double bond, $R_5 = H_2$, X = Br) with Potassium Bicarbonate in Aqueous Methanol*

To a solution of 10.0 g of analytically pure 21-bromopregnenolone acetate (**1**, R_1 = β-AcO, $R_2 = R_6$ = H, $R_3 = R_4$ = double bond, $R_5 = H_2$, X = Br), m.p. 145.5–146°, in 438 ml of methanol, 21.9 g of potassium bicarbonate in 87.4 ml of water was added. The mixture was heated for 4 h; the precipitate which formed during the addition of the potassium bicarbonate solution dissolved after a few minutes of heating.

The cooled solution was poured into ice water, and the precipitate was extracted with ether. The ethereal solution was washed with water and dried over sodium sulfate. Evaporation of the solvent gave 7.6 g of an oily product, representing the *neutral fraction*. The alkaline aqueous phase remaining after the ether extraction was combined with the first water washings and acidified with 2 *N* sulfuric acid to the Congo-blue reaction. The product was extracted with dichloromethane, the organic phase was washed with water and dried over sodium sulfate. Removal of the solvent gave 592 mg of a crystalline *acid fraction* which was recrystallized from methanol to give 177 mg of *3β-hydroxy-17α-methyl-5-etienic acid* (**2**, R_1 = β-OH, $R_2 = R_6$ = H, $R_3 = R_4$ = double bond, $R_5 = H_2$, R_7 = H), m.p. 245–246°. The m.p. was not depressed upon admixture of an authentic product. A sample was recrystallized from methanol for analysis; needles, m.p. 244–245°; $[\alpha]_D^{22}$ − 55.4° (*c*, 1.000 in ethanol); ν_{max}(KBr) 3400 (alc. hydroxyl), 2675 (broad associated acid band), and 1704 cm^{-1} (carboxyl).

Anal. Calcd. for $C_{21}H_{32}O_3$: C, 75.90; H, 9.63. Found: C, 75.67; H, 9.80.

The *neutral fraction* was acetylated in the usual fashion with 19 ml of acetic anhydride in 38 ml of pyridine. The amorphous product obtained (8.9 g) was chromatographed on 270 g of aluminum oxide, activity II. Elutions with petroleum ether – benzene (1:1) gave 2.356 g of *methyl Δ⁵-3β-acetoxy-17α-methyletienate* (**2**, R_1 = β-AcO, $R_2 = R_6$ = H, $R_3 = R_4$ = double bond, $R_5 = H_2$, $R_7 = CH_3$), m.p. 165–166°. The identity of the product was established by a mixture m.p. and the comparison of the i.r. spectrum with that of an authentic sample. The following chromatogram fractions (766 mg) melted between 145 and 150°. They were rechromatographed on 300 g of silica gel deactivated with methanol (4 ml of methanol for 10 g of silica gel). Petroleum ether saturated with methanol eluted 423 mg of a product melting at 158–160°. Subsequent elutions with the same solvent gave 214 mg of crystals, m.p. 159–160°. These products gave no m.p. depression upon admixture. They were combined and recrystallized with methanol to give 211 mg of *3β,21-diacetoxy-5-pregnen-20-one* (**1**, R_1 = β-AcO, $R_2 = R_6$ = H, $R_3 = R_4$ = double bond, $R_5 = H_2$, X = AcO), m.p. 160–161°. A sample was recrystallized 3 times from methanol for analysis; pellets, m.p. 165.5–166°; $[\alpha]_D^{23}$ + 20.4° (*c*, 1.000 in $CHCl_3$) [lit. (27*d*): m.p. 165–166°; $[\alpha]_D^{22}$ + 28°]; ν_{max}(KBr) 1758 and 1738 (21-acetoxy-20-keto doublet), and 1250 cm^{-1} (acetate).

Anal. Calcd. for $C_{25}H_{36}O_5$: C, 72.08; H, 8.71. Found: C, 72.36; H, 8.47.

The structure of this product was confirmed by comparison with an authentic sample.

The following fractions of the original aluminum oxide chromatogram which had been eluted with benzene–ether mixtures (863 mg) were rechromatographed on 26 g of aluminum oxide, activity II. Petroleum ether – benzene (1:1) eluted 115 mg of *17α-methyl etio ester* **2** (R_1 = β-AcO, $R_2 = R_6$ = H, $R_3 = R_4$ = double bond, $R_5 = H_2$, $R_7 = CH_3$), m.p. 153–155°. The identity of this product was established by comparison of the i.r. spectrum and by a mixture m.p. with an authentic sample. Further elutions with the same solvent mixture gave 286 mg of a crystalline product ("substance A"), m.p. 98–100°. A sample was recrystallized from methanol for analysis; m.p. 102–103°; $[\alpha]_D^{23}$ − 179.5° (*c*, 0.875 in $CHCl_3$); ν_{max}(KBr) 1739, 1250 cm^{-1}.

Anal. Found: C, 74.32; H, 9.06.

The product was not further investigated.

Another portion of the chromatogram fractions of the original aluminum oxide chromatogram on the neutral reaction product, eluted with benzene–ether (4:1 and 1:1) mixtures (171 mg) was rechromatographed on 7 g of aluminum oxide, activity III. Elutions with petroleum ether – benzene (4:1) gave 37 mg of a product melting between 102 and 137°, representing, according to thin-layer analysis, a mixture which, according to the i.r. spectra, contained some 3β,21-diacetoxy-5-pregnen-20-one. This product was not further investigated.

The chromatogram fractions of the original aluminum oxide chromatogram on the *neutral fraction*, which had been eluted with petroleum ether – benzene (1:4) (888 mg) were rechromatographed on 30 g of aluminum oxide, activity III. Elutions with petroleum ether – benzene gave 386 mg of a product melting between 124 and 132°. Further elutions with the same solvent gave another 156 mg of the same product, m p. 128–136°. Recrystallization from methanol afforded 83 mg of *3β,21-diacetoxy-5-pregnen-20-one* (**1**, R_1 = β-AcO, $R_2 = R_6$ = H, $R_3 = R_4$ = double bond, $R_5 = H_2$, X = AcO), m.p. 159–161°.

The mother liquors were rechromatographed on florisil, deactivated with aqueous methanol. Elutions with petroleum ether saturated with methanol gave 560 mg of a crystalline product, m.p. 130–136°, representing a mixture. This material was rechromatographed on 12 g of aluminum oxide, activity III. Elutions with petroleum ether – benzene (1:1) gave 287 mg of *3β,21-diacetoxy-5-pregnen-20-one* (**1**, R_1 = β-AcO, $R_2 = R_6$ = H, R_3 =

Can. J. Chem. Downloaded from www.nrcresearchpress.com by 210.87.254.5 on 09/05/12
For personal use only.

R_4 = double bond, $R_5 = H_2$, X = AcO), m.p. 147–152°. Elutions with petroleum ether – benzene (1:4) gave 74 mg of "substance A", m.p. 100–101°.

All the amorphous fractions of the various chromatograms were reacetylated in the usual fashion, and the product (1.425 g) was rechromatographed on 42 g of aluminum oxide, activity III. Elutions with petroleum ether – benzene (1:1) gave another 263 mg of *3β,21-diacetoxy-5-pregnen-20-one* (**1**, R_1 = β-AcO, $R_2 = R_6$ = H, $R_3 = R_4$ = double bond, $R_5 = H_2$, X = AcO), m.p. 149–151°.

Methanol containing 2% of acetic acid eluted 521 mg of a partially crystalline product, the i.r. spectrum of which revealed that it was an acid [ν_{max}(KBr) 2675 (broad) and 1710 cm^{-1}]. The product was dissolved in 10 ml of absolute methanol and 10 ml of absolute ether and methylated with 24 ml of a 1.6% ethereal diazomethane solution for a period of 15 h. The usual work-up gave 370 mg of an oily product which was filtered through silica gel. Thus 220 mg of a product, crystallizing from acetone–hexane, was obtained; m.p. 173–175°. A sample was recrystallized 3 times from acetone–hexane for analysis; m.p. 178–179°; $[\alpha]_D^{23}$ – 50.4° (*c*, 1.000 in $CHCl_3$); ν_{max}(KBr) 3250 (alc. OH), and 1740 and 1710 cm^{-1}.

Anal. Found: C, 76.53; H, 8.92.

The mother liquors of the crystallization were acetylated with acetic anhydride in pyridine in the usual fashion. Crystallization of the reaction product from methanol gave 26 mg of crystals, m.p. 161–162°; $[\alpha]_D^{23}$ – 32.5° (*c*, 1.000 in $CHCl_3$), ν_{max}(KBr) 1740 and 1240 cm^{-1}.

Anal. Found: C, 74.22; H, 9.07.

This product, "substance B", was not further investigated.

Methylation of the Acid Fraction

The mother liquors of the Δ^5-3β-hydroxy-17α-methyletienic acid (**2**, R_1 = β-OH, $R_2 = R_6$ = H, $R_3 = R_4$ = double bond, $R_5 = H_2$, R_7 = H) were taken to dryness (433 mg) and methylated in the course of 15 h in 9 ml of absolute methanol and 9 ml of absolute ether with 42 ml of a 1.3% ethereal diazomethane solution. The usual work-up gave 445 mg of crude *methyl Δ^5-3β-hydroxy-17α-methyletienate* (**2**, R_1 = β-OH, $R_2 = R_6$ = H, $R_3 = R_4$ = double bond, $R_5 = H_2$, $R_7 = CH_3$), m.p. 138–139°. The product was chromatographed on silica gel (40 g). Elutions with benzene – ethyl acetate (96:4) eluted 61 mg of pure *hydroxy 17α-methyl etio ester* **2** (R_1 = β-OH, $R_2 = R_6$ = H, $R_3 = R_4$ = double bond, $R_5 = H_2$, $R_7 = CH_3$), m.p. 137–138°. A sample was recrystallized for analysis from methanol; m.p. 142–143°; $[\alpha]_D^{23}$ – 52.8° (*c*, 1.000 in $CHCl_3$); ν_{max}(KBr) 3450 and 1715 cm^{-1}.

Anal. Calcd. for $C_{22}H_{34}O_3$: C, 76.30; H, 9.83. Found: C, 76.12; H, 9.68.

The identity of the product was confirmed by the determination of a mixture m.p. and by comparison of the i.r. spectrum with that of an authentic sample.

The mother liquors of the crystallizations were taken to dryness and were acetylated in the usual fashion. The resulting product was crystallized from methanol to give 204 mg of *methyl Δ^5-3β-acetoxy-17α-methyletienate* (**2**, R_1 = β-AcO, $R_2 = R_6$ = H, $R_3 = R_4$ = double bond, $R_5 = H_2$, $R_7 = CH_3$), m.p. 160–162°. The identity of the product was established by the determination of a mixture m.p. and by comparison of the i.r. spectrum with that of an authentic sample. From the mother liquors of the crystallization another 130 mg of the same product could be obtained by chromatography on 5 g of aluminum oxide, activity II.

In toto, the reaction of the bromide with potassium bicarbonate gave, after the usual acetylation and methylation, 3.279 g (37.3%) of *methyl Δ^5-3β-acetoxy-17α-methyletienate* (**2**, R_1 = β-AcO, $R_2 = R_6$ = H, $R_3 = R_4$ = double bond, $R_5 = H_2$, $R_7 = CH_3$), and 1.577 g (17.5%) of *3β,21-diacetoxy-5-pregnen-20-one* (**1**, R_1 = β-AcO, $R_2 = R_6$ = H, $R_3 = R_4$ = double bond, $R_5 = H_2$, X = AcO). No other identifiable products were isolated, in particular no 17β-methyl 17-iso etio ester or etio acid **3**.

In another experiment, carried out on 24 g of 21-bromo-3β-acetoxy-5-pregnen-20-one (**1**, R_1 = β-AcO, $R_2 = R_6$ = H, $R_3 = R_4$ = double bond, $R_5 = H_2$, X = Br), a 36% yield of the 17α-methyl etio ester and a 16% yield of 3β,21-diacetoxy-5-pregnen-20-one were realized.

We wish to pay homage to the memory of the late Dean J. B. Collip in whose Department this work was started and whose inspiring example and constant encouragement helped us decisively. Sincere thanks are expressed to Professor J. A. Gunton, the former Head of the Chemistry Department of the University of Western Ontario, for kindly putting one of his laboratories at our disposal, and to Mr. D. Capitaine, Mrs. G. Pelletier, and Mrs. K. Hausen for technical assistance. Financial support from the National Research Council of Canada and the award of NRCC scholarships to one of us (P. L.) are gratefully acknowledged.

1. CH. R. ENGEL. Chim. **19**, 507 (1965).
2. CH. R. ENGEL, S. K. ROY, J. BILODEAU, and P. LACHANCE. Abstr. XIXth Int. Congr. Pure Appl. Chem. London, 1963. p. 53.
3. Cf. *inter alia*: (*a*) AL. FAVORSKY. J. Russ. Phys. Chem. Soc. **26**, 590 (1894); (*b*) H. SSEMENOV. J. Russ. Phys. Chem. Soc. **43**, 693 (1911); (*c*) AL. FAVORSKY. J. Prak. Chem. [2] **88**, 658 (1913); (*d*) AL. FAVORSKY and W. BOSKOWSKY. J. Russ. Phys. Chem. Soc. **46**, 1097 (1914).
4. For review articles compare: (*a*) R. JACQUIER. Bull. Soc. Chim. France **D35** (1950); (*b*) A. S. KENDE. The Favorsky rearrangement of halo ketones. *In* Organic reactions. Vol. **11**. J. Wiley and Sons, New York, 1960. p. 261.
5. R. B. LOFTFIELD. J. Amer. Chem. Soc. **73**, 4707 (1951).
6. Cf. (*a*)L. F. FIESER and M. FIESER. Advanced organic chemistry. Reinhold Publishing Corp., New York, 1961. pp. 414–415; (*b*) J. W. WHELAND. Advanced organic chemistry. John Wiley and Sons, Inc., New York–London, 1960. pp. 555–556; R. C. FUSON. Reactions of organic compounds. John Wiley and Sons Inc., New York–London, 1962. pp. 265–266.
7. B. TCHOUBAR and O. SACKUR. C. R. Acad. Sci. **208**, 1020 (1939).
8. (*a*) J. G. BURR and M. J. S. DEWAR. J. Chem. Soc. 1201 (1954); (*b*) compare also A. W. FORT. J. Amer. Chem. Soc. **84**, 2620, 2625 (1962).

9. (*a*) PL. A. PLATTNER, H. HEUSSER, and P. TH. HERZIG. Helv. Chim. Acta, **32**, 270 (1949); (*b*) H. HEUSSER, CH. R. ENGEL, P. TH. HERZIG, and PL. A. PLATTNER. Helv. Chim. Acta, **33**, 2229 (1950); (*c*) HS. H. GÜNTHARD, E. BERIGER, CH. R. ENGEL, and H. HEUSSER. Helv. Chim. Acta, **35**, 2437 (1952); (*d*) R. DEGHENGHI and R. GAUDRY. J. Amer. Chem. Soc. **83**, 4668 (1961).
10. H. HEUSSER, CH. R. ENGEL, and PL. A. PLATTNER. Helv. Chim. Acta, **33**, 2237 (1950).
11. (*a*) CH. R. ENGEL, K. F. JENNINGS, and G. JUST. J. Amer. Chem. Soc. **78**, 6153 (1956); (*b*) CH. R. ENGEL, G. JUST, and R. BUTTERY. Can. J. Chem. **39**, 1805 (1961).
12. (*a*) CH. R. ENGEL and G. JUST. J. Amer. Chem. Soc. **76**, 4909 (1954); (*b*) H. HEUSSER, E. BERIGER, and CH. R. ENGEL. Helv. Chim. Acta, **37**, 2166 (1954).
13. CH. R. ENGEL and G. JUST. Can. J. Chem. **33**, 1515 (1955).
14. (*a*) CH. R. ENGEL. J. Amer. Chem. Soc. **77**, 1064 (1955); (*b*) CH. R. ENGEL. J. Amer. Chem. Soc. **78**, 4728 (1956).
15. CH. R. ENGEL. Can. J. Chem. **35**, 131 (1957).
16. R. E. MARKER and R. B. WAGNER. J. Amer. Chem. Soc. **64**, 216 (1942).
17. PL. A. PLATTNER, H. HEUSSER, and S. F. BOYCE. Helv. Chim. Acta, **31**, 603 (1948).
18. (*a*) N. L. WENDLER, R. P. GRABER, and J. J. HAZEN. Chem. Ind. (London), 847 (1956); (*b*) N. L. WENDLER, R. P. GRABER, and J. J. HAZEN. Tetrahedron **3**, 144 (1958); (*c*) N. L. WENDLER. Personal communication.
19. L. F. FIESER and M. FIESER. Experientia, **4**, 285 (1948).
20. G. RICHARD. C. R. Acad. Sci. **200**, 1944 (1935).
21. H. O. HOUSE and F. GILMORE. J. Amer. Chem. Soc. **83**, 3980 (1961).
22. C. W. SHOPPEE. Helv. Chim. Acta, **27**, 11 (1944).
23. R. DEGHENGHI, G. SCHILLING, and G. PAPINEAU-COUTURE. Can. J. Chem. **44**, 789 (1966).
24. A. MARQUET and J. JACQUES. Bull. Soc. Chim. France, 30 (1962).
25. R. B. MOFFETT and D. I. WEISBLAT. J. Amer. Chem. Soc. **74**, 2183 (1952).
26. H. VAN DER HAIGHE, E. R. KATZENELLENBOGEN, K. DOBRINER, and T. F. GALLAGHER. J. Amer. Chem. Soc. **74**, 2810 (1952).
27. Cf. (*a*) H. V. ANDERSON, E. R. GARRETT, F. H. LINCOLN, JR., H. A. NATHAN, and J. E. HOGG. J. Amer. Chem. Soc. **76**, 743 (1954); (*b*) R. B. MOFFETT and H. V. ANDERSON. J. Amer. Chem. Soc. **76**, 747 (1954); (*c*) D. A. LYTTLE and R. H. LEVIN. U. S. Patent. 2 705 720 (1955); (*d*) see also C. DJERASSI and C. T. LENK. J. Amer. Chem. Soc. **75**, 3493 (1953).
28. T. REICHSTEIN and C. MONTIGEL. Helv. Chim. Acta, **22**, 1212 (1939).
29. J. FRIED and F. SABO. J. Amer. Chem. Soc. **79**, 1130 (1957).
30. H. REICH and T. REICHSTEIN. Helv. Chim. Acta, **22**, 1124 (1939).
31. G. STORK and I. J. BOROWITZ. J. Amer. Chem. Soc. **82**, 4307 (1960).
32. Cf. also R. U. SHOCK and W. Y. KARPEL. U. S. Patent, 2 684 963 (1954).
33. CH. R. ENGEL, R. M. HOEGERLE, and R. DEGHENGHI. Can. J. Chem. **38**, 1199 (1960).
34. (*a*) D. G. MARSHALL and R. GAUDRY. Can. J. Chem. **38**, 1945 (1960); (*b*) J. S. MILLS, O. Kandiani, and C. DJERASSI. J. Org. Chem. **24**, 1056 (1960).
35. T. H. KRITCHEVSKY and T. F. GALLAGHER. J. Amer. Chem. Soc. **73**, 184 (1951).
36. P. L. JULIAN, E. W. MEYER, W. J. KARPEL, and I. R. WALLER. J. Amer. Chem. Soc. **72**, 5145 (1950).
37. H. REICH, M. SUTTER, and T. REICHSTEIN. Helv. Chim. Acta, **23**, 170 (1940).
38. H. HIRSCHMAN. J. Biol. Chem. **140**, 797 (1941).
39. S. BERNSTEIN, R. H. LENHARD, W. S. ALLEN, M. HELLER, R. LITTELL, S. M. STOLAR, L. I. FELDMAN, and R. H. BLANK. J. Amer. Chem. Soc. **78**, 5693 (1956).
40. G. STORK, H. N. KHASTGIR, and A. J. SOLO. J. Amer. Chem. Soc. **80**, 6457 (1958).
41. A. GAUDEMER, J. PARELLO, A. SKROBEK, and B. TCHOUBAR. Bull. Soc. Chim. France, 2405 (1965).
42. A. SKROBEK and B. TCHOUBAR. C. R. Acad. Sci. **263**, 80 (1966).
43. J. H. CONIA and J. SALAÜN. Tetrahedron Lett., 1175 (1963).
44. R. BRESLOW, J. POSNER, and A. KREBS. J. Amer. Chem. Soc. **85**, 234 (1963).
45. N. J. TURRO and W. B. HAMMOND. J. Amer. Chem. Soc. **87**, 3258 (1965).
46. J. F. PAZOS and C. D. GREENE. J. Amer. Chem. Soc. **89**, 1030 (1967).
47. (*a*) R. C. COOKSON and M. J. NYE. Proc. Chem. Soc. 129 (1963). (*b*) R. C. COOKSON and M. J. NYE. J. Chem. Soc. 2009 (1965).
48. H. O. HOUSE and G. A. FRANK. J. Org. Chem. **30**, 2948 (1965).
49. E. E. SMISSMAN, T. L. LEMKE, and O. KRISTIANSEN. J. Amer. Chem. Soc. **88**, 334 (1966).
50. E. W. WARNHOFF, C. M. WONG, and W. T. TAI. J. Amer. Chem. Soc. **90**, 514 (1968).
51. F. G. BORDWELL and R. G. SCAMEHORN. J. Amer. Chem. Soc. **90**, 6749, 6751 (1968).
52. P. L. JULIAN and W. J. KARPEL. J. Amer. Chem. Soc. **72**, 362 (1950).
53. CH. R. ENGEL and H. JAHNKE. Can. J. Biochem. Physiol. **35**, 1047 (1957).
54. A. L. WILDS and C. DJERASSI. J. Amer. Chem. Soc. **68**, 2125 (1946).
55. R. BOUCHARD and CH. R. ENGEL. Can. J. Chem. **46**, 2201 (1968).

Can. J. Chem. Downloaded from www.nrcresearchpress.com by 210.87.254.5 on 09/05/12
For personal use only.

Can. J. Chem. Downloaded from www.nrcresearchpress.com by 210.87.254.5 on 09/05/12
For personal use only.

Study of the Wallach rearrangement and related processes in the 100% sulfuric acid region[1]

E. BUNCEL AND W. M. J. STRACHAN
Department of Chemistry, Queen's University, Kingston, Ontario

Received July 28, 1969

Study of the acid-catalyzed Wallach rearrangement of azoxybenzene is extended into the 100% H_2SO_4 region. The rate of formation of 4-hydroxyazobenzene can be followed spectrally in a straight-forward manner until close to 99% H_2SO_4, but in higher acidities sulfonation of this product becomes kinetically important. The advent of second equilibrium protonations of 4-hydroxyazobenzene and of 4-hydroxyazobenzene-4′-sulfonic acid further complicate the azoxybenzene rearrangement as followed spectrally. Above 100% H_2SO_4 a second sulfonation is also observed. A method is given for dissecting the rate data for the primary rearrangement process from the first of the sulfonation reactions.

The rate of the azoxybenzene rearrangement is observed to increase continuously up to 99.99% H_2SO_4 (the upper limit of the present kinetic method). This suggests that the second proton transfer step to azoxybenzene is rate-determining and not an equilibrium process. These results permit a clarification of a previously proposed mechanism (1).

Canadian Journal of Chemistry, **48**, 377 (1970)

Previously we reported (1) on the kinetics of the acid catalyzed Wallach rearrangement (2) of azoxybenzene to 4-hydroxyazobenzene. The advisability of extending the kinetic studies to the 100% H_2SO_4 region was pointed out (1). Since then the results of two other kinetic studies on the Wallach rearrangement have appeared (3, 4) and have included examination of substituted azoxybenzenes. Different mechanisms have been proposed by the authors (3, 4) for the rearrangement process (see also ref. 2).

Results

The rate of rearrangement of azoxybenzene to 4-hydroxyazobenzene was followed spectrally, in aqueous sulfuric acid at 25°. The spectral behavior in a kinetic run with azoxybenzene varies with the acid concentration as described below. Azoxybenzene, with a pK_a of -5.15 (1) is half protonated in 65% H_2SO_4 and 99.9% protonated in 85% H_2SO_4. Hence in the acid media of this study (>90% H_2SO_4), virtually complete monoprotonation can safely be assumed and reaction can be followed (up to ca. 98% H_2SO_4) by the decrease in the 390 mμ absorption due to the conjugate acid of azoxybenzene. 4-Hydroxyazobenzene ($pK_a^1 = -1.0$) is likewise fully protonated in these media and its formation from azoxybenzene is accompanied by a growth of the 460 mμ absorption ascribed to the conjugate acid of 4-hydroxyazobenzene (6). A kinetic run in 96.0% H_2SO_4 (Fig. 1) illustrates these spectral changes. A fairly sharp isosbestic point[2] characterizes the interconversion between the two absorbing species.

Above 98% H_2SO_4 a second equilibrium protonation of 4-hydroxyazobenzene becomes effective ($pK_a^2 = -10.2$), the probable site of the second protonation being the phenolic oxygen (6). The diprotonated species has maximum absorption at 424 mμ, so that in a kinetic run with azoxybenzene in >98% H_2SO_4 the product absorption will be shifted to progressively shorter wavelengths as the acid concentration is increased from 98 to 100% H_2SO_4.

A kinetic run with azoxybenzene in 99.59% H_2SO_4 is shown in Fig. 2. In this experiment the first 5 spectral runs were taken at intervals of 1 min after mixing and thereafter at intervals of 5–10 min, with the last scan taken after 50 min. In the early stages the formation of a peak at ca. 434 mμ is apparent (rearrangement is ~50% complete with the fifth scan, *vide infra*) and in accord with the above discussion, this is ascribed to formation of partly diprotonated 4-hydroxyazobenzene. Subsequently there is a gradual shift

[1]Part VIII in a series on the Wallach rearrangement. Presented in part at the 50th Annual Conference of the Chemical Institute of Canada, Toronto, June 1967, and communicated in preliminary form: Chem. Commun. 765 (1969).

[2]As the acid concentration is increased, the "isosbestic point" becomes progressively more diffuse and it is not clear which is the lower limit of acid concentration where isosbestic point behavior is still completely valid. A kinetic run in 92.7% H_2SO_4 gave a very sharp isosbestic point.

Can. J. Chem. Downloaded from www.nrcresearchpress.com by 210.87.254.5 on 09/05/12
For personal use only.

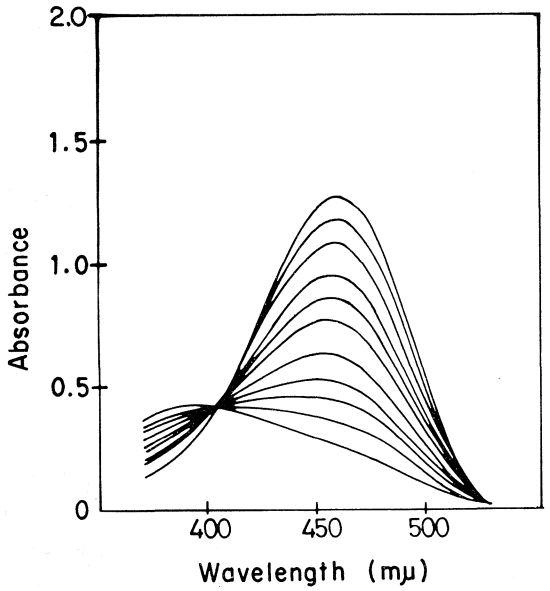

FIG. 1. Azoxybenzene (3.39×10^{-5} *M*, 1 cm pathlength cell) in 96.0% H_2SO_4 at 25°. First 3 spectra correspond to reaction times of 11, 18, and 24 min; the last spectrum to 320 min.

in absorption to the 460 mμ region, which is ascribed to the advent of a sulfonation reaction, secondary to the rearrangement, to form 4-hydroxyazobenzene-4′-sulfonic acid.[3] The two consecutive processes, rearrangement followed by sulfonation, account for the absence of an isosbestic point in this system. Kinetic data for the sulfonation of 4-hydroxyazobenzene for 91.7–100.07% H_2SO_4 were reported earlier (5). The absorption due to 4-hydroxyazobenzene-4′-sulfonic acid occurs at 465 mμ in the less concentrated acid media where this product is present in monoprotonated form ($pK_a^1 = -1.45$ (7)) but above 100% H_2SO_4, a second equilibrium protonation takes place ($pK_a^2 = -11.1$) and absorption shifts to 420 mμ, being λ_{max} for the second conjugate acid of 4-hydroxyazobenzene-4′-sulfonic acid (6).

The procedure adopted in order to evaluate the rate constant for the azoxybenzene → 4-hydroxyazobenzene reaction in sulfuric acid media where the consecutive 4-hydroxyazobenzene → 4-hydroxyazobenzene-4′-sulfonic acid reaction has comparable rate was as follows. Using 4-hydroxyazobenzene as the substrate the sulfonation process was followed spectrally by repeated scanning over the region of interest (ca. 350–500 mμ) and the isosbestic point (λ) was noted. The kinetic run with azoxybenzene was then performed under identical conditions (acid and substrate concentration) but following the reaction at constant wavelength, the isosbestic λ for the 4-hydroxyazobenzene → 4-hydroxyazobenzene-4′-sulfonic acid reaction. At this isosbestic λ, the primary rearrangement process can be followed without interference from the consecutive sulfonation reaction. For the 99.59% H_2SO_4 system the isosbestic λ was 430 mμ and when the kinetic run was performed with azoxybenzene a typical exponential curve resulted and gave a rate constant for rearrangement of 227×10^{-5} s^{-1}. A similar procedure was used for 99.09 and 99.90% H_2SO_4. On the other hand, in 99.97 and 99.99% H_2SO_4, where the rate of the initial rearrangement was more rapid so that this process was virtually complete after a few minutes, the isosbestic λ (as well as the rate constant) for the subsequent sulfonation could readily be obtained using azoxybenzene itself as substrate. In these acid media azoxybenzene showed initial absorption (ca. 1 min) in the 420–426 mμ region and the

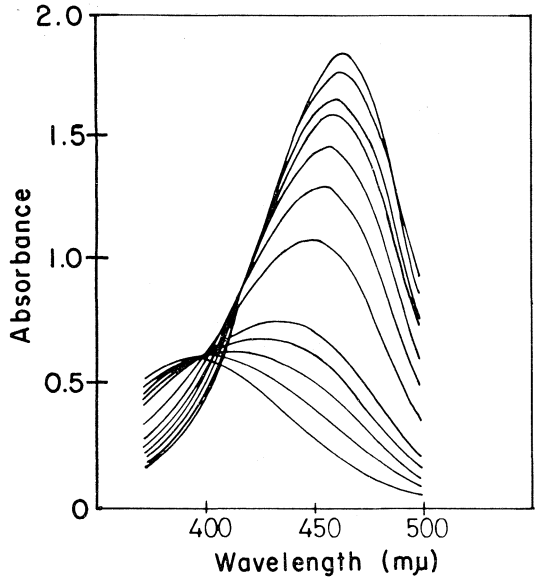

FIG. 2. Azoxybenzene (1.03×10^{-5} *M*, 4 cm cell) in 99.59% H_2SO_4 at 25°. The first 3 spectra correspond to reaction times of 1, 2, and 3 min; last spectrum to 50 min.

[3]In 99.59% H_2SO_4 the rate constants of the two consecutive processes, rearrangement and sulfonation, are 230×10^{-5} and 80×10^{-5} s^{-1} respectively. Hence the above discussion, by considering the two processes as separate, is a simplifying one.

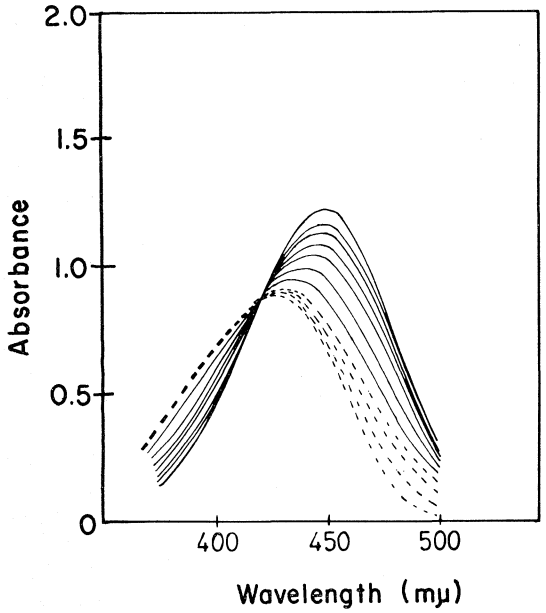

FIG. 3. Azoxybenzene (2.84×10^{-5} *M*, 1 cm cell) in 100.01% H_2SO_4 at 25°. Dashed curves cover first 30 min reaction time; full curves the following 140 h.

isosbestic λ was between 424 and 430 mμ. The 99.99% H_2SO_4 system represented the limit of this kinetic method ($T_{1/2} \sim 20$ s) for evaluating the rate of the azoxybenzene rearrangement.

A kinetic run with azoxybenzene in 100.01% H_2SO_4 is shown in Fig. 3. The spectral behavior in this system appears identical in all respects to that exhibited by 4-hydroxyazobenzene as substrate under identical reaction conditions (cf. Fig. 4 in ref. 5). The initial fast process (dashed lines, $T_{1/2} \sim 5$ min) is identified as sulfonation of 4-hydroxyazobenzene, formed virtually completely by the time the first scan is taken (2 min), and the subsequent slow process (full lines, $T_{1/2} \sim 28$ h) is ascribed (5) to a further sulfonation of 4-hydroxyazobenzene-4′-sulfonic acid. The second sulfonation process was also reported previously, as observed with 4-hydroxyazobenzene or 4-hydroxyazobenzene-4′-sulfonic acid (5). In an analogous manner (see also Experimental), kinetic runs carried out with azoxybenzene in the 100% H_2SO_4 region could be used to generate rate constants for the first and second sulfonations of the initially formed 4-hydroxyazobenzene. These rate data are given in Tables 2 and 3 respectively. In Table 1 are presented the kinetic data for the primary rearrangement, while all three rate processes are shown in the $\log k - H_0$ (8) plot of Fig. 4.

Discussion

The measurements described above show that spectral examination of azoxybenzene in the 100% H_2SO_4 region is complicated as a result of

TABLE 1

Kinetic data for rearrangement of azoxybenzene to 4-hydroxyazobenzene in aqueous H_2SO_4 at 25°

Weight (%) H_2SO_4	H_0	$10^5 \times k_{obs}$ (s^{-1})	λ mμ
92.7 §	−8.58	13.4	460*
94.73	−8.83	18.0	463‡
94.73	−8.83	14.8	390‡
96.0 §	−9.01	29.0	460*
96.0 §	−9.01	24.4	390*
96.18	−9.03	26.0	463‡
96.18	−9.03	25.1	390‡
97.78	−9.31	43.8	463‡
97.78	−9.31	39.8	390‡
98.3 §	−9.45	59.6	460*
98.8 §	−9.62	77.0	460*
99.00	−9.74	76.8	463‡
99.00	−9.74	70.2	463*
99.09	−9.78	84	430†
99.59	−10.10	227	430†
99.90	−10.59	860	430†
99.97	−10.99	2310	428†
99.99	−11.06	4160	424†
99.99	−11.06	4520	424†
99.99	−11.06	3800	424†

*Reaction followed by periodic scanning. Rate constant calculated from absorbance changes at wavelength indicated by Guggenheim method.

†Reaction followed at constant wavelength shown (the isosbestic λ for the consecutive sulfonation). Rate constant calculated from $\log (A_\infty - A_t)$ vs. *t* plot or by Guggenheim method.

‡Reaction followed at constant wavelength shown (not the isosbestic λ). Rate constant calculated by Guggenheim method.

§Acid concentrations determined by titration (remainder by conductivity method).

TABLE 2

Kinetic data for conversion of 4-hydroxyazobenzene to 4-hydroxyazobenzene-4′-sulfonic acid, observed with azoxybenzene as substrate in aqueous H_2SO_4 at 25°

Weight (%) H_2SO_4	H_0	$10^5 \times k_{obs}$ (s^{-1})	λ mμ
99.96	−10.94	287	463‡
99.97	−10.99	224	480‡
99.99	−11.06	251	480‡
99.99	−11.06	253	460†‡
99.99	−11.06	251	460‡
100.00	−11.09	254	480†*
100.03	−11.17	252	480‡
100.06	−11.23	239	480‡
100.07	−11.25	222	480†*

*As in Table 1.

†Rate constant calculated using $A_\infty - A_t$ plot. Data obtained either as indicated under footnote * or as in footnote ‡.

‡Reaction followed at constant wavelength shown. Rate constant calculated by Guggenheim method.

Can. J. Chem. Downloaded from www.nrcresearchpress.com by 210.87.254.5 on 09/05/12
For personal use only.

TABLE 3

Kinetic data for sulfonation of 4-hydroxyazobenzene-4′-sulfonic acid, observed with azoxybenzene as substrate in aqueous H_2SO_4 at 25°

Weight (%) H_2SO_4	H_0	$10^5 \times k_{obs}$ (s^{-1})	λ mμ
99.99	−11.06	0.560	460‡
100.00	−11.09	0.651	460‡
100.01	−11.12	0.840	460‡
100.01	−11.12	0.647	460*
100.07	−11.25	1.31	460*
100.14	−11.36	1.36	460*
100.32	−11.53	2.33	460*
100.51	−11.66	3.08	460*

*‡As in Table 2.

the consecutive sulfonation of the initially formed 4-hydroxyazobenzene and the second equilibrium protonations of the reaction products, 4-hydroxyazobenzene and the 4′-sulfonic acid. Since several species are absorbing in the spectral region corresponding to the rate measurements, dissection of the various kinetic and equilibrium processes is essential for a meaningful interpretation of the measurements. The dissection of the three rate processes, as detailed in the preceding sections, yields the data of Fig. 4. Curves 2 and 3 of this figure show that the kinetic measurements obtained with azoxybenzene as substrate yield rate data which are continuous and in full agreement

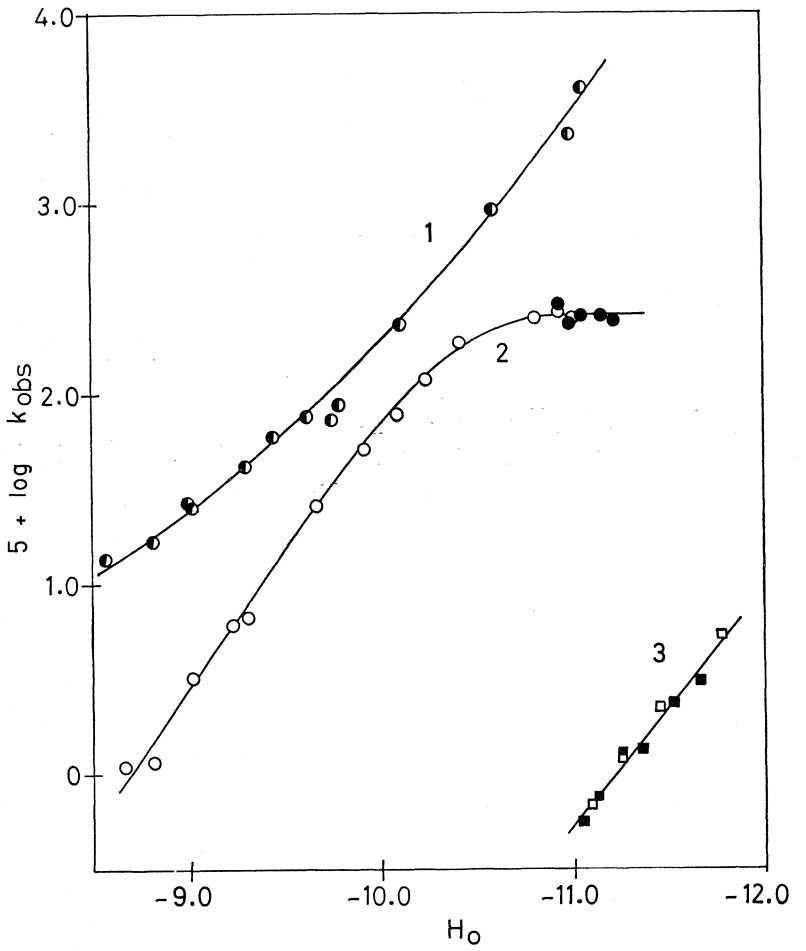

FIG. 4. The $\log k - H_0$ plots for rearrangement of azoxybenzene to 4-hydroxyazobenzene (curve 1); the conversion of 4-hydroxyazobenzene to 4-hydroxyazobenzene-4′-sulfonic acid (curve 2); and a further sulfonation of 4-hydroxyazobenzene-4′-sulfonic acid (curve 3). On curve 2 the open circles (○) are data reproduced from ref. 5, while the shaded circles (●) are the new data from Table 2. On curve 3 the open squares (□) are data reproduced from ref. 5, while the shaded squares (■) are the data of Table 3.

Can. J. Chem. Downloaded from www.nrcresearchpress.com by 210.87.254.5 on 09/05/12
For personal use only.

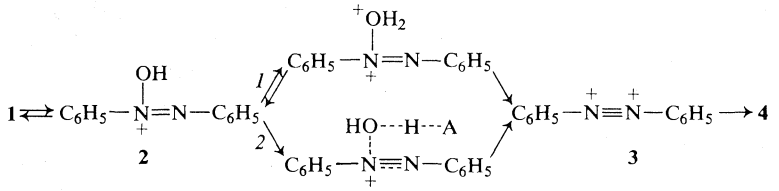

SCHEME 1

with kinetic data previously obtained (5) in the study of the sulfonation processes of 4-hydroxyazobenzene and of 4-hydroxyazobenzene-4′-sulfonic acid. This overall agreement between the two studies adds confidence to the interpretation of the measurements.

Our present data on the primary rearrangement process (curve 1 of Fig. 4) allow an improved interpretation of the mechanism which was proposed (1, 9) on the basis of a kinetic study in less concentrated acid. That mechanism is summarized in Scheme 1 and is based on the continued kinetic dependence on acidity beyond the stage of complete monoprotonation. Following the first equilibrium protonation of azoxybenzene (**1** + H^+ ⇄ **2**), path *1* (9) shows a possible second equilibrium protonation which is followed by rate-determining loss of H_2O to give the resonance-stabilized dicationic intermediate **3** (10, 11). Reaction of **3** with H_2O of the medium,[4] in accord with the demonstrated intermolecularity of the reaction (12, 13), followed by deprotonation would yield the 4-hydroxyazobenzene product, **4**. Subsequently (1) we considered an alternative route to the dication **3**, involving rate-determining proton-transfer and concurrent heterolysis of the N—O bond (path *2* in Scheme 1), but differentiation between the two routes could not be made on the basis of available evidence, including correlations between rate and acidity functions. The measurements with azoxybenzene over the region 92.3–99.99% H_2SO_4 show a monotonic increase in the rate of rearrangement, with no evidence for a spectrally detectable intermediate (**3**). However, the continued sensitivity of the rate of rearrangement to acid concentration up to the 100% H_2SO_4 region argues against appreciable diprotonation of azoxybenzene in these media.[5] On this basis the continued involvement of acid in the azoxybenzene rearrangement is consistent with a rate-determining proton-transfer mechanism. The reaction path given by path *2* of Scheme 1 is hence consistent with the facts currently known on the azoxybenzene rearrangement in the aqueous sulfuric acid system.

Experimental

Materials

Azoxybenzene was purified and had physical properties as described previously (1). Sulfuric acid solutions were analyzed titrimetrically or conductimetrically (15) and are given in per cent by weight.

Kinetic Measurements

The instrumentation and kinetic methods were essentially as described previously (5), though only the "direct method" was used in this work. In addition, in the 99–100% H_2SO_4 region the following method was generally used. The azoxybenzene solution (0.01 ml of ca. 1×10^{-2} *M* solution in ethanol) was placed by means of a Hamilton syringe into a 4.00 cm cuvette, evaporated to dryness, and sulfuric acid added from a 10 ml fast delivery pipette. In these cases a first observation was generally obtained by 0.7 min. In the "isosbestic point" runs absorbance was recorded by means of a Unicam Scale Expansion Accessory SP 250 and a Beckman 1005 Recorder. All kinetic data were obtained at 25°.

The rate of rearrangement of azoxybenzene to 4-hydroxyazobenzene was computed from absorbance changes at 390, 460/463, or 424–430 mμ, the significance of these wavelengths being given in the text. A few runs were performed at wavelengths close to the isosbestic λ, giving the following data: 99.09% H_2SO_4, $k = 112\ s^{-1}$ (426 mμ); 99.59% H_2SO_4, $k = 240\ s^{-1}$ (425 mμ); 99.90% H_2SO_4, $k = 990\ s^{-1}$ (428 mμ). These values appear to be in approximate agreement with the data of Table 1. However, following absorbance changes at 460 mμ for the above acids gave apparent rate constants of 88, 160, and 420 s^{-1} respectively, indicating increasing deviation from the data of Table 1 with increasing acidity.

The sulfonation reactions were followed at 460/463 or 480 mμ for reasons given previously (5). Azoxybenzene

[4]For a discussion of H_2O or HSO_4^- as the nucleophilic species, see ref. 14, which also reports pertinent data (4) on the acid-catalyzed hydrolysis of azobenzene-4-hydrogen sulfate.

[5]This discussion does not necessarily extend to the ethanolic medium employed by Hahn *et al.* (3) in which system a levelling off in rate was actually observed.

Can. J. Chem. Downloaded from www.nrcresearchpress.com by 210.87.254.5 on 09/05/12
For personal use only.

concentrations were in the range 10^{-5} to 10^{-4} M, the higher concentrations being generally used in the runs followed at 390 mμ (see Fig. 1).

We thank the National Research Council of Canada for financial support, and the Department of University Affairs for the award of an Ontario Graduate Fellowship to W. M. J. S.

1. E. BUNCEL and B. T. LAWTON. Can. J. Chem. **43**, 862 (1965).
2. E. BUNCEL. *In* Mechanisms of molecular migrations. *Edited by* B. S. Thyagarajan. Interscience—John Wiley and Sons, Inc., New York. 1968.
3. C. S. HAHN, K. W. LEE, and H. H. JAFFÉ. J. Amer. Chem. Soc. **89**, 4975 (1967).
4. D. DUFFEY and E. C. HENDLEY. J. Org. Chem. **33**, 1918 (1968).
5. W. M. J. STRACHAN and E. BUNCEL. Can. J. Chem. **47**, 4011 (1969).
6. W. M. J. STRACHAN, A. DOLENKO, and E. BUNCEL. Can. J. Chem. **47**, 3631 (1969).
7. R. L. REEVES. J. Amer. Chem. Soc. **88**, 2240 (1966).
8. M. A. PAUL and F. A. LONG. Chem. Rev. **57**, 1 (1957).
9. E. BUNCEL and B. T. LAWTON. Chem. Ind. (London), 1835 (1963).
10. P. H. GORE. Chem. Ind. (London), 191 (1959).
11. E. BUNCEL, A. DOLENKO, I. G. CSIZMADIA, J. PINCOCK, and K. YATES. Tetrahedron, **24**, 6671 (1968).
12. M. M. SHEMYAKIN and V. I. MAIMIND. *In* Chemistry of natural and synthetic coloring matters. *Edited by* T. S. Gore. Academic Press, Inc., New York. 1962; M. M. SHEMYAKIN, V. I. MAIMIND, and B. K. VAICHUNAITE. Chem. Ind. (London), 755 (1958).
13. S. OAE, T. FUKUMOTO, and M. YAMAGAMI. Bull. Chem. Soc. Japan, **36**, 601 (1963).
14. E. BUNCEL and W. M. J. STRACHAN. Can. J. Chem. **47**, 911 (1969).
15. R. J. GILLESPIE and S. WASIF. J. Chem. Soc. 204 (1953); R. J. GILLESPIE, J. V. OUBRIDGE, and C. SOLOMONS. J. Chem. Soc. 1804 (1957); D. M. LICHTY. J. Amer. Chem. Soc. **30**, 1834 (1908).

Can. J. Chem. Downloaded from www.nrcresearchpress.com by 210.87.254.5 on 09/05/12
For personal use only.

Can. J. Chem. Downloaded from www.nrcresearchpress.com by 210.87.254.40 on 09/05/12
For personal use only.

NOTES

New synthesis of (±)-cyclohexene-1,3/2,4-tetrol (conduritol-B)

T. L. NAGABHUSHAN
R & L Molecular Research Ltd., 8045 Argyll Road, Edmonton 82, Alberta

Received August 1, 1969

1,4,5,6-Tetra-*O*-acetyl-myoinositol is reacted with *N,N'*-thiocarbonyl diimidazole to give 1,4,5,6-tetra-*O*-acetyl-myoinositol-2,3-thionocarbonate. This is desulfurized with trimethyl phosphite to yield tetra-*O*-acetyl-(±)-cyclohexene-1,3/2,4-tetrol (tetra-*O*-acetyl-conduritol-B).

Canadian Journal of Chemistry, **48**, 383 (1970)

Although a method for the preparation of tetra-*O*-acetyl-(±)-cyclohexene-1,3/2,4-tetrol (tetra-*O*-acetyl-conduritol-B, **4**) from myoinositol has been described (1), the low yields of the intermediate bromoquercitol-A pentaacetates obtained in our laboratory, especially in large scale preparations, prompted us to examine the possibility of synthesizing the compound by the method of Corey and Winter (2).

The readily available 1,4,5,6-tetra-*O*-acetyl-myoinositol (**1**) (3) was reacted with *N,N'*-thiocarbonyl diimidazole (**2**) (4) to give 1,4,5,6-tetra-*O*-acetyl-myoinositol-2,3-thionocarbonate (**3**). Treatment of **3** with trimethyl phosphite provided tetra-*O*-acetyl-(±)-cyclohexene-1,3/2,4-tetrol (**4**) which was characterized both by nuclear magnetic resonance (n.m.r.) spectroscopy and *O*-deacetylation to conduritol-B (**5**).

Experimental

Melting points were determined on a heating stage and are uncorrected. Infrared spectra were measured with a Perkin–Elmer Model 137 "Infracord" infrared spectrophotometer. Nuclear magnetic resonance spectra were measured at 60 Mc.p.s. with a Varian A60 n.m.r. spectrometer. Chemical shifts are given in τ values and refer to spectra measured in deuteriochloroform, with tetramethylsilane as the internal standard.

1,4,5,6-Tetra-O-acetyl-myoinositol-2,3-thionocarbonate (3)

1,4,5,6-Tetra-*O*-acetyl-myoinositol (**1**) (3) was prepared as a monohydrate. The compound was dried over phosphorus pentoxide and further dehydrated by dissolving in tetrahydrofuran and drying over phosphorus pentoxide. The amorphous solid obtained after removal of the solvent *in vacuo* was again dried.

Thiophosgene (14.6 ml, 0.191 mole) was added dropwise to a stirred solution of freshly dried imidazole (52.0 g, 0.764 mole) in anhydrous acetone (1040 ml) under anhydrous conditions. The temperature of the mixture was maintained at 25–28°. After 90 min the precipitated imidazole hydrochloride was collected by filtration and in the filtrate was dissolved the previously dried 1,4,5,6-tetra-*O*-acetyl-myoinositol (**1**, 66.4 g, 0.19 mole). The mixture was refluxed under anhydrous conditions for 2 h. The solvent was removed and the residual yellow solid dissolved in ethyl acetate. The solution was extracted with 3.6 *N* hydrochloric acid (106.4 ml) in order to remove imidazole. The organic phase was washed successively with water, a saturated solution of sodium bicarbonate, and water. After drying the solution over anhydrous sodium sulfate, the solvent was removed and the crystalline residue recrystallized from hot ethanol. The colorless crystals were isolated, washed with cold

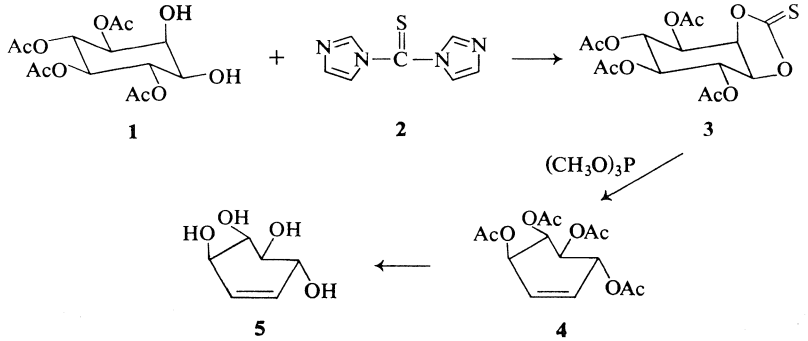

ethanol, and dried. The yield of **3** was 32.05 g (40%), m.p. 166–168°; ν_{max}(Nujol) 1750 (C=O), 1160 cm^{-1} (C=S); n.m.r. data: τ 7.84–7.91, 4 *O*-acetyl groups, 4.53–5.03, 6 ring hydrogens.

Anal. Calcd. for $C_{15}H_{18}O_{10}S$: C, 46.14; H, 4.65; S, 8.21. Found: C, 46.66; H, 4.58; S, 8.09.

*Conduritol-B Tetraacetate (**4**)*

A solution of 1,4,5,6-tetra-*O*-acetyl-myoinositol-2,3-thionocarbonate (**3**, 27.65 g, 0.071 mole) in trimethyl phosphite (200 ml) was refluxed under nitrogen for 5 h. The solvent was removed and to the clear oily residue was added water (200 ml). After seeding, the mixture was set aside a few minutes when crystallization started. The mixture was refrigerated overnight. The crystals were collected, washed with water, and dried. The product still smelled of trimethyl phosphite and, therefore, was washed thoroughly with *n*-hexane and recrystallized from ethanol–water. The compound, m.p. 85–85.5°, was obtained in a yield of 81% (18.02 g) (reported (1) m.p. 91–92.5°, corrected); ν_{max}(Nujol) 1750 cm^{-1} (C=O); n.m.r. data: τ 7.95–7.99, 4 *O*-acetyl groups, 4.34–4.83, 6 protons, multiplets.

*Conduritol-B (**5**)*

Triethylamine (4 ml) was added to a solution of conduritol-B tetraacetate (**4**, 5 g, 15.92 mmole) dissolved in 70% aqueous methanol (50 ml) and the mixture was set aside 6 h with occasional shaking. The solvents were removed and the residual white solid dried over phosphorus pentoxide. Recrystallization from hot methanol and benzene afforded colorless crystals of **5** (74%), m.p. 199.5–201° (reported (1) m.p. 204.5–205°, corrected).

The author thanks Professor R. U. Lemieux, Director of Research, for his guidance and encouragement in the conduct of this research and Mr. B. Baechler and Mr. W. Merlo for technical assistance.

1. G. E. McCasland and E. C. Horswill. J. Amer. Chem. Soc. **75**, 4020 (1953).
2. E. J. Corey and R. A. E. Winter. J. Amer. Chem. Soc. **85**, 2677 (1963).
3. S. J. Angyal, M. E. Tate, and S. D. Gero. J. Chem. Soc. 4116 (1961).
4. H. A. Staab and G. Walther. Ann. Chem. **657**, 98 (1962).

The heat of formation of the norbornyl cation

H. Spencer[1] and Y. K. Mo

Department of Chemistry and Chemical Engineering, University of Saskatchewan, Saskatoon, Saskatchewan

Received July 7, 1969

The heat of formation of the norbornyl ion has been evaluated from experimental data. This was compared to the heats of formation of various formulations of the norbornyl ion computed by quantum mechanical methods.

Canadian Journal of Chemistry, **48**, 384 (1970)

A recent report on the heats of formation of several possible formulations for the norbornyl ion calculated by quantum mechanical methods (1) prompts us to report an evaluation of the enthalpy of formation of the $C_7H_{11}^+$ ion, which occurs in the mass spectrum of norbornyl bromide (2).

This ion was presumed to be the norbornyl cation and its appearance potential in the mass spectrometer was observed to be 10.26 ± 0.05 eV (2). The appearance potential of an ion is related to its heat of formation by eq. [1].

$$[1] \quad \text{A.P.} = \Delta H_f(C_7H_{11}^+) + \Delta H_f(Br) - \Delta H_f(C_7H_{11}Br)$$

For ΔH_f(Br) we have adopted the value +26.73 ± 0.11 kcal/mole found in the literature (3). There does not appear to be any direct measurement of ΔH_f for norbornyl bromide but Bedford *et al.* have reported a value of −22.01 ± 0.65 kcal/mole for ΔH_f^0 of bicyclo[2,2,1]heptane (cryst) (4) which, combined with the value of 13 ± 2 kcal/mole for $\Delta H_{sublimation}$ reported by Chiang *et al.* (5), leads to ΔH_f for bicyclo[2,2,1]heptane (gas) = −9.91 ± 2.65 kcal/mole. Using bond dissociation data from the literature (3, 6, 7), we have computed the heat of reaction for the bromination of bicyclo-[2,2,1]heptane via the process outlined in reaction [2]

$$[2] \quad C_7H_{12} + Br_2 \rightarrow C_7H_{11}Br + HBr$$

In computing this heat of reaction we have assumed the dissociation energies of the C—H and C—Br bonds at C-2 in the norbornyl system to be the same as those reported for $(CH_3)_2$-CH—H and $(CH_3)_2$CH—Br, viz. 94.5 ± 1 and

[1]Present address: Imperial Chemical Industries Limited, Pharmaceutical Division, Mereside, Alderley Park, Macclesfield, Cheshire, SK10 4TG, England.

Can. J. Chem. Downloaded from www.nrcresearchpress.com by 210.87.254.40 on 09/05/12
For personal use only.

ethanol, and dried. The yield of **3** was 32.05 g (40%), m.p. 166–168°; ν_{max}(Nujol) 1750 (C=O), 1160 cm^{-1} (C=S); n.m.r. data: τ 7.84–7.91, 4 *O*-acetyl groups, 4.53–5.03, 6 ring hydrogens.

Anal. Calcd. for $C_{15}H_{18}O_{10}S$: C, 46.14; H, 4.65; S, 8.21. Found: C, 46.66; H, 4.58; S, 8.09.

*Conduritol-B Tetraacetate (**4**)*

A solution of 1,4,5,6-tetra-*O*-acetyl-myoinositol-2,3-thionocarbonate (**3**, 27.65 g, 0.071 mole) in trimethyl phosphite (200 ml) was refluxed under nitrogen for 5 h. The solvent was removed and to the clear oily residue was added water (200 ml). After seeding, the mixture was set aside a few minutes when crystallization started. The mixture was refrigerated overnight. The crystals were collected, washed with water, and dried. The product still smelled of trimethyl phosphite and, therefore, was washed thoroughly with *n*-hexane and recrystallized from ethanol–water. The compound, m.p. 85–85.5°, was obtained in a yield of 81% (18.02 g) (reported (1) m.p. 91–92.5°, corrected); ν_{max}(Nujol) 1750 cm^{-1} (C=O); n.m.r. data: τ 7.95–7.99, 4 *O*-acetyl groups, 4.34–4.83, 6 protons, multiplets.

*Conduritol-B (**5**)*

Triethylamine (4 ml) was added to a solution of conduritol-B tetraacetate (**4**, 5 g, 15.92 mmole) dissolved in 70% aqueous methanol (50 ml) and the mixture was set aside 6 h with occasional shaking. The solvents were removed and the residual white solid dried over phosphorus pentoxide. Recrystallization from hot methanol and benzene afforded colorless crystals of **5** (74%), m.p. 199.5–201° (reported (1) m.p. 204.5–205°, corrected).

The author thanks Professor R. U. Lemieux, Director of Research, for his guidance and encouragement in the conduct of this research and Mr. B. Baechler and Mr. W. Merlo for technical assistance.

1. G. E. McCasland and E. C. Horswill. J. Amer. Chem. Soc. **75**, 4020 (1953).
2. E. J. Corey and R. A. E. Winter. J. Amer. Chem. Soc. **85**, 2677 (1963).
3. S. J. Angyal, M. E. Tate, and S. D. Gero. J. Chem. Soc. 4116 (1961).
4. H. A. Staab and G. Walther. Ann. Chem. **657**, 98 (1962).

The heat of formation of the norbornyl cation

H. Spencer[1] and Y. K. Mo

Department of Chemistry and Chemical Engineering, University of Saskatchewan, Saskatoon, Saskatchewan

Received July 7, 1969

The heat of formation of the norbornyl ion has been evaluated from experimental data. This was compared to the heats of formation of various formulations of the norbornyl ion computed by quantum mechanical methods.

Canadian Journal of Chemistry, **48**, 384 (1970)

A recent report on the heats of formation of several possible formulations for the norbornyl ion calculated by quantum mechanical methods (1) prompts us to report an evaluation of the enthalpy of formation of the $C_7H_{11}^+$ ion, which occurs in the mass spectrum of norbornyl bromide (2).

This ion was presumed to be the norbornyl cation and its appearance potential in the mass spectrometer was observed to be 10.26 ± 0.05 eV (2). The appearance potential of an ion is related to its heat of formation by eq. [1].

$$[1] \quad \text{A.P.} = \Delta H_f(C_7H_{11}^+) + \Delta H_f(Br) - \Delta H_f(C_7H_{11}Br)$$

For ΔH_f(Br) we have adopted the value +26.73 ± 0.11 kcal/mole found in the literature (3). There does not appear to be any direct measurement of ΔH_f for norbornyl bromide but Bedford *et al.* have reported a value of −22.01 ± 0.65 kcal/mole for ΔH_f^0 of bicyclo[2,2,1]heptane (cryst) (4) which, combined with the value of 13 ± 2 kcal/mole for $\Delta H_{sublimation}$ reported by Chiang *et al.* (5), leads to ΔH_f for bicyclo[2,2,1]heptane (gas) = −9.91 ± 2.65 kcal/mole. Using bond dissociation data from the literature (3, 6, 7), we have computed the heat of reaction for the bromination of bicyclo-[2,2,1]heptane via the process outlined in reaction [2]

$$[2] \quad C_7H_{12} + Br_2 \rightarrow C_7H_{11}Br + HBr$$

In computing this heat of reaction we have assumed the dissociation energies of the C—H and C—Br bonds at C-2 in the norbornyl system to be the same as those reported for $(CH_3)_2$-CH—H and $(CH_3)_2$CH—Br, viz. 94.5 ± 1 and

[1]Present address: Imperial Chemical Industries Limited, Pharmaceutical Division, Mereside, Alderley Park, Macclesfield, Cheshire, SK10 4TG, England.

Can. J. Chem. Downloaded from www.nrcresearchpress.com by 210.87.254.5 on 09/05/12
For personal use only.

67.6 ± 2.4 kcal/mole, respectively. For D(Br—Br) and D(H—Br) we have used the values 46.1 ± 0.03 and 87.6 ± 0.13 kcal/mole. The heat of reaction calculated from this data is $+14.6 \pm 3.5$ kcal/mole.

The heat of formation of norbornyl bromide could now be obtained from eq. [3]

$$[3]\quad \Delta H_f(C_7H_{12})_{gas} + \Delta H_f(Br_2)_{gas} = \Delta H_f(C_7H_{11}Br)_{gas} + \Delta H_f{}^0(HBr)_{gas} + \Delta H_{reaction}$$

For $\Delta H_f(Br_2)_{gas}$ and $\Delta H_f{}^0$(HBr) we have used the established values of $+7.34 \pm 0.18$ kcal/mole and -8.66 ± 0.33 kcal/mole (8), and for ΔH_f of bicyclo[2,2,1]heptane and the heat of reaction we have used the quantities calculated above. From this data we have calculated ΔH_f(norbornyl bromide) $= -9.63 \pm 6.66$ kcal/mole.

Using this last value in eq. [1] gives ΔH_f (norbornyl ion)$_{gas} = +200 \pm 7.9$ kcal/mole. The agreement between this value and the values calculated by Klopman is excellent and seems to support the validity of the method and assumptions used by him in the quantum mechanical treatment. We understand that the value for the heat of formation of the "classical" norbornyl cation has recently been recalculated using different C—C bond lengths and revised (9), and because of the relatively large errors attendant upon this method of deriving the experimental heat of formation, it is, unfortunately, not possible to conclude that there is significantly better agreement with the quantum mechanically calculated value of the heat of formation for any one particular formulation of the norbornyl ion.

1. G. KLOPMAN. J. Amer. Chem. Soc. **91**, 89 (1969).
2. D. C. DEJONG and S. R. SHRADER. J. Amer. Chem. Soc. **88**, 3881 (1966).
3. V. I. VEDENEYEV, L. V. GURVICH, V. N. KONDRAT'YEV, V. A. MEDVEDEV, and YE. L. FRANKEVICH. Bond energies, ionisation potentials and electron affinities. St. Martins Press, New York. 1966.
4. A. F. BEDFORD, A. E. BEEZER, C. T. MORTIMER, and H. D. SPRINGALL. J. Chem. Soc. 3823 (1963).
5. J. F. CHIANG, C. F. WILCOX, JR., and S. H. BAUER. J. Amer. Chem. Soc. **90**, 3149 (1968).
6. PRAKASH S. NANGIA and SIDNEY W. BENSON. J. Amer. Chem. Soc. **86**, 2773 (1964).
7. C. F. MORTIMER, H. O. PRITCHARD, and H. A. SKINNER. Trans. Faraday Soc. **48**, 220 (1952).
8. F. D. ROSSINI, D. D. WAGMAN, W. H. EVANS, S. LEVINE, and I. JAFFE. Selected values of chemical thermodynamic properties. National Bureau of Standards, Washington, D.C. 1952.
9. G. KLOPMAN. Private communication.

Esterification of ε-*N*-carbobenzoxy-L-lysine with boron trifluoride – alcohol[1]

JOHN COGGINS, RUTH DEMAYO, AND N. LEO BENOITON[2]

Department of Biochemistry, University of Ottawa, Ottawa 2, Ontario

Received August 18, 1969

The esterification of ε-*N*-carbobenzoxy-L-lysine with various boron trifluoride – alcohol mixtures at 80 °C leads to some deprotection, which increases as the chain length of the alcohol increases. A convenient synthesis of ε-*N*-carbobenzoxy-L-lysine methyl ester in 58% yield from ε-*N*-carbobenzoxy-L-lysine and boron trifluoride – methanol has been developed.

Canadian Journal of Chemistry, **48**, 385 (1970)

ε-*N*-Carbobenzoxy-L-lysine esters are usually prepared from ε-*N*-carbobenzoxy-L-lysine α-*N*-carboxy anhydride and the pertinent alcohol (1). Our dissatisfaction with the use of this method for preparing the methyl ester (1, 2) has prompted an investigation of the feasibility of obtaining this ester directly from ε-*N*-carbobenzoxy-L-lysine. The latter has been achieved (3) using the thionyl chloride method (4), however the product obtained had a melting point 4° lower than that previously reported (1, 2).

This paper presents the results of a study of the esterification of ε-*N*-carbobenzoxy and other mono-*N*-substituted lysines with boron trifluoride – alcohol mixtures which are reagents used for the synthesis of aliphatic (5) and aromatic (6)

[1]Supported by a grant from the Medical Research Council of Canada.

[2]Associate of the Medical Research Council of Canada.

Can. J. Chem. Downloaded from www.nrcresearchpress.com by 210.87.254.5 on 09/05/12
For personal use only.

67.6 ± 2.4 kcal/mole, respectively. For D(Br—Br) and D(H—Br) we have used the values 46.1 ± 0.03 and 87.6 ± 0.13 kcal/mole. The heat of reaction calculated from this data is $+14.6 \pm 3.5$ kcal/mole.

The heat of formation of norbornyl bromide could now be obtained from eq. [3]

$$[3] \quad \Delta H_f(C_7H_{12})_{gas} + \Delta H_f(Br_2)_{gas} = \Delta H_f(C_7H_{11}Br)_{gas} + \Delta H_f{}^0(HBr)_{gas} + \Delta H_{reaction}$$

For $\Delta H_f(Br_2)_{gas}$ and $\Delta H_f{}^0$(HBr) we have used the established values of $+7.34 \pm 0.18$ kcal/mole and -8.66 ± 0.33 kcal/mole (8), and for ΔH_f of bicyclo[2,2,1]heptane and the heat of reaction we have used the quantities calculated above. From this data we have calculated ΔH_f(norbornyl bromide) $= -9.63 \pm 6.66$ kcal/mole.

Using this last value in eq. [1] gives ΔH_f (norbornyl ion)$_{gas} = +200 \pm 7.9$ kcal/mole. The agreement between this value and the values calculated by Klopman is excellent and seems to support the validity of the method and assumptions used by him in the quantum mechanical treatment. We understand that the value for the heat of formation of the "classical" norbornyl cation has recently been recalculated using different C—C bond lengths and revised (9), and because of the relatively large errors attendant upon this method of deriving the experimental heat of formation, it is, unfortunately, not possible to conclude that there is significantly better agreement with the quantum mechanically calculated value of the heat of formation for any one particular formulation of the norbornyl ion.

1. G. KLOPMAN. J. Amer. Chem. Soc. **91**, 89 (1969).
2. D. C. DEJONG and S. R. SHRADER. J. Amer. Chem. Soc. **88**, 3881 (1966).
3. V. I. VEDENEYEV, L. V. GURVICH, V. N. KONDRAT'YEV, V. A. MEDVEDEV, and YE. L. FRANKEVICH. Bond energies, ionisation potentials and electron affinities. St. Martins Press, New York. 1966.
4. A. F. BEDFORD, A. E. BEEZER, C. T. MORTIMER, and H. D. SPRINGALL. J. Chem. Soc. 3823 (1963).
5. J. F. CHIANG, C. F. WILCOX, JR., and S. H. BAUER. J. Amer. Chem. Soc. **90**, 3149 (1968).
6. PRAKASH S. NANGIA and SIDNEY W. BENSON. J. Amer. Chem. Soc. **86**, 2773 (1964).
7. C. F. MORTIMER, H. O. PRITCHARD, and H. A. SKINNER. Trans. Faraday Soc. **48**, 220 (1952).
8. F. D. ROSSINI, D. D. WAGMAN, W. H. EVANS, S. LEVINE, and I. JAFFE. Selected values of chemical thermodynamic properties. National Bureau of Standards, Washington, D.C. 1952.
9. G. KLOPMAN. Private communication.

Esterification of ε-*N*-carbobenzoxy-L-lysine with boron trifluoride – alcohol[1]

JOHN COGGINS, RUTH DEMAYO, AND N. LEO BENOITON[2]

Department of Biochemistry, University of Ottawa, Ottawa 2, Ontario

Received August 18, 1969

The esterification of ε-*N*-carbobenzoxy-L-lysine with various boron trifluoride – alcohol mixtures at 80 °C leads to some deprotection, which increases as the chain length of the alcohol increases. A convenient synthesis of ε-*N*-carbobenzoxy-L-lysine methyl ester in 58% yield from ε-*N*-carbobenzoxy-L-lysine and boron trifluoride – methanol has been developed.

Canadian Journal of Chemistry, **48**, 385 (1970)

ε-*N*-Carbobenzoxy-L-lysine esters are usually prepared from ε-*N*-carbobenzoxy-L-lysine α-*N*-carboxy anhydride and the pertinent alcohol (1). Our dissatisfaction with the use of this method for preparing the methyl ester (1, 2) has prompted an investigation of the feasibility of obtaining this ester directly from ε-*N*-carbobenzoxy-L-lysine. The latter has been achieved (3) using the thionyl chloride method (4), however the product obtained had a melting point 4° lower than that previously reported (1, 2).

This paper presents the results of a study of the esterification of ε-*N*-carbobenzoxy and other mono-*N*-substituted lysines with boron trifluoride – alcohol mixtures which are reagents used for the synthesis of aliphatic (5) and aromatic (6)

[1]Supported by a grant from the Medical Research Council of Canada.

[2]Associate of the Medical Research Council of Canada.

Can. J. Chem. Downloaded from www.nrcresearchpress.com by 210.87.254.105 on 09/05/12
For personal use only.

TABLE 1

Esterification of ε-*N*-substituted-L-lysines*

Reactants		Yield of products (%)				
R	R_1	H·Lys(R)·OH	H·Lys(R)·OR_1	H·Lys·OH	H·Lys·OR_1	Total
Z†	methyl	4.8	92.0	0.4	5.8	103.0
Z	ethyl	28.8	66.5	2.4	5.3	103.0
Z	propyl	13.9	67.5	3.2	15.0	99.6
Z	butyl	6.7	48.4	5.9	27.0	88.0
Z	benzyl	15.7	32.3	24.6	16.0	88.6
Z‡	methyl	1.4	94.3	<0.1	1.2	96.9
Ac	methyl	12.4	76.3	1.6	9.1	99.4
For	methyl	0	0	2.7	93.3	96.0
Z	*iso*-propyl	81.8	12.7	6.8	1.2	102.5
Bz	*tert*-butyl	83.9	5.9	0.2	0	90.0

*H · Lys (R) · OH (2.5 mmoles) + $BF_3 \cdot O(C_2H_5)_2$ (12.5 mmoles) + R_1OH (25 ml) $\xrightarrow[24\ h]{80°}$ H · Lys (R) · OR_1.

†Z = carbobenzoxy; Ac = acetyl; For = formyl; Bz = benzoyl.
‡α-*N*-carbobenzoxy.

carboxylic acid esters, and describes a convenient synthesis of ε-*N*-carbobenzoxy-L-lysine methyl ester from ε-*N*-carbobenzoxy-L-lysine.

ε-*N*-Carbobenzoxy-L-lysine in excess methanol was heated in the presence of different amounts of boron trifluoride ethyl ether at 80 °C. Aliquots of the reaction mixtures were then analyzed for starting material, deprotected starting material, desired ester, and ester of the deprotected starting material. The time course of the reaction is illustrated in Fig. 1. In the presence of 5 moles of catalyst, the reaction was first order with respect to ε-*N*-carbobenzoxy-L-lysine and essentially complete after 24 h. When only 2 moles of catalyst were used, the reaction had proceeded to only 80% after 32 h. In a 16 h experiment, water (0.9% v/v) was added, with no apparent effect on the reaction.

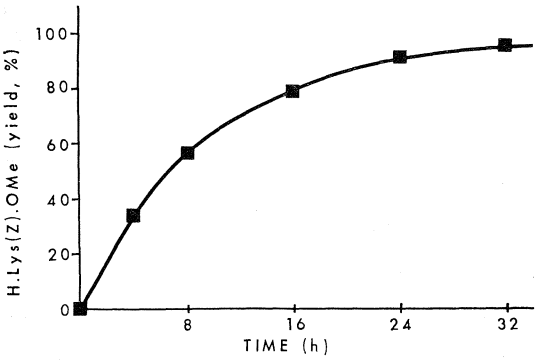

FIG. 1. Esterification of ε-*N*-carbobenzoxy-L-lysine in boron trifluoride – methanol at reflux temperature; 5 moles of $BF_3 \cdot O(C_2H_5)_2$ per mole of H·Lys(Z)·OH.

The results of the analyses for the different components when the mono-*N*-substituted lysines were heated at 80 °C in various boron trifluoride – alcohol mixtures for 24 h appear in Table 1. It is seen that the yields of esters of ε-*N*-carbobenzoxy-L-lysine decreased from 92 to 32% in going from the methyl to the butyl, and then the benzyl ester. This was accompanied by a parallel increase in the extent of cleavage of the carbobenzoxy group from about 6 to 40% (H·Lys·OH + H·Lys·OR_1). Since the same amount (5–15%) of starting material was recovered regardless of the primary alcohol used except for ethanol, and the extent of esterification (H·Lys(R)·OR_1 + H·Lys·OR_1) was over 70% in all cases except for the benzyl ester, the differences in the yields obtained reflect a difference in the susceptibility to cleavage of the urethane group by the various boron trifluoride – alcohol mixtures rather than a difference in the reactivity of the alcohols. The apparently anomolous result obtained with ethyl alcohol, when more starting material was recovered than in the other cases, was confirmed by a duplicate experiment.

The lack of esterification observed when *iso*-propyl and *tert*-butyl alcohol were used is in agreement with the demonstration that these alcohols are dehydrated to give water – boron trifluoride complex and the corresponding polyolefin in the presence of boron trifluoride (7). The resistance to cleavage of the *N*-acyl and *N*-carbobenzoxy groups to boron trifluoride etherate – methanol under our conditions stands

Can. J. Chem. Downloaded from www.nrcresearchpress.com by 210.87.254.105 on 09/05/12
For personal use only.

Can. J. Chem. Downloaded from www.nrcresearchpress.com by 210.87.254.105 on 09/05/12
For personal use only.

in striking contrast to the reported cleavage of amides to methyl esters by hot boron trifluoride – methanol (8, 9). That this apparent difference was not due to the fortuitous use by us of the etherate instead of gaseous boron trifluoride was demonstrated when results identical with those recorded in Table 1 were obtained for the esterification of ε-*N*-carbobenzoxy-L-lysine using boron trifluoride dissolved in methanol as the reagent.

In a preparative run, a yield of 58% of ε-*N*-carbobenzoxy-L-lysine methyl ester was obtained.[3] A simple and efficient purification of the product was achieved by the expedience of extracting it into an organic solvent from an aqueous solution at a p*H* (9.0) intermediate between the pK_a' of the α-amino group of the ester[4] and the much higher pK_a' of the ε-amino group of the lysine ester. At this p*H*, lysine, lysine methyl ester, and ε-*N*-carbobenzoxy-lysine remain in the aqueous phase, with most of the latter precipitating out. The product obtained with this procedure requires no recrystallization.

Experimental

Materials

Boron trifluoride ethyl ether (product No. 4272) was obtained from Distillation Product Industries, Rochester, New York, and was used without purification. ε-*N*-Carbobenzoxy-L-lysine was purchased from Pierce Chemical Company, Rockford, Illinois. Sources for the other lysine derivatives have been reported (10). The reagent grade alcohols were kept over anhydrous magnesium sulfate for 12 h, then over anhydrous calcium sulfate for 12 h, and filtered.

Method

A mixture of mono-*N*-substituted lysine (2.5 mmoles) and boron trifluoride ethyl ether (1.52 ml; 12.5 mmoles) in the alcohol (25 ml) was heated in an 80 °C oil-bath. The solution was made up to 50 ml with the alcohol (with ethanol for the butyl and benzyl esters) and a sample was diluted with p*H* 2.2 citrate buffer. An aliquot was placed on the 0.9 × 7 cm column of a Beckman model 120B amino acid analyzer and 0.35 *N* sodium citrate, p*H* 5.28, was pumped through for 40 min for the determination of lysine and starting material. The esters, which remained on the column, were then saponified by removing the buffer from the column head and forcing 0.2 *N* sodium hydroxide (1.3 ml) half-way down the resin column. After 20 min (at 57 °C) the column head was filled with sodium hydroxide (8.5 ml), the p*H* 5.28 buffer line was attached to the column, buffer was pumped through and the effluent from the column was collected for 20 min. The effluent was acidified, diluted to a known volume, and analyzed for lysine and mono-*N*-substituted derivative on the same column as described above. A control experiment had indicated that saponification of the methyl ester was complete without the 20 min delay period, but that it was required for complete saponification of the ethyl and benzyl esters. The *tert*-butyl esters were determined by difference after analyzing for the amino acid before and after cleavage of the ester with hydrogen bromide in acetic acid.

Preparation of ε-N-Carbobenzoxy-L-lysine Ester·HCl

A mixture of ε-*N*-carbobenzozy-L-lysine (7.0 g; 0.025 mole) and boron trifluoride ethyl ether (15.2 ml; 0.125 mole) in methanol (100 ml) in a flask fitted with a condenser was heated in a 80 °C oil-bath for 24 h. The cooled mixture was filtered through Celite, the solvent was removed *in vacuo* (bath temperature 40 °C), the residual oil was dissolved in water (50 ml) and extracted with ether (2 × 25 ml). 4 *N* NaOH was added to the cooled stirred solution until the p*H* was 9.0. The solution was saturated with NaCl, ethyl acetate (100 ml) was added, and the mixture was filtered to remove the ε-*N*-carbobenzoxy-L-lysine. The organic layer was separated and the aqueous layer was extracted again with ethyl acetate (2 × 100 ml). The combined extracts were dried ($MgSO_4$ followed by $CaSO_4$), the solvent was evaporated off, methanol (20 ml) was added to the residue, followed by 8 *N* HCl in methanol (3 ml). Ether (300 ml) was then added slowly while cooling the solution and ε-*N*-carbobenzoxy-L-lysine methyl ester·HCl (4.9 g; 58%) separated as white crystals with m.p. 117–118°, $[\alpha]_D^{25}$ +15.5° ±0.1° (*c*, 2 in H_2O), (lit. m.p. 117° (1); 117°, $[\alpha]_D^{21}$ +15.0° (2), 113–114°, sintered 111° (3)). On analysis with the amino acid analyzer the product was found to contain 0.1% of starting material, but no detectable amounts of lysine or lysine methyl ester.

[3]Carbobenzoxy-phenylalanine ester has been obtained in 70% yield from carbobenzoxy-phenylalanine, and phenylalanine ethyl ester in 40% yield from phenylalanine, using the same conditions.

[4]The pK_1' of lysine ethyl ester is 7.54. Unpublished results of J. H. Seely and N. L. Benoiton.

1. M. Bergmann, L. Zervas, and W. F. Ross. J. Biol. Chem. **111**, 245 (1935).
2. R. A. Boissonas, S. Guttmann, R. L. Huguenin, P. A. Jaquenod, and E. Sandrin. Helv. Chim. Acta, **41**, 1867 (1958).
3. T. Shiba and T. Kaneko. Bull. Chem. Soc. Japan, **33**, 1721 (1960).
4. M. Brenner and W. Huber. Helv. Chim. Acta, **36**, 1109 (1953).
5. H. D. Hinton and J. A. Nieuwland. J. Amer. Chem. Soc. **54**, 2017 (1932).
6. G. Hallas. J. Chem. Soc. 5770 (1965).
7. E. F. Mooney and M. A. Qaseem. Chem. Commun. 230 (1967).
8. D. J. Hamilton and M. J. Price. J. Chem. Soc. (D), 414 (1969).
9. S. G. Toole and F. J. Sowa. J. Amer. Chem. Soc., **59**, 1971 (1937).
10. J. Leclerc and L. Benoiton. Can. J. Chem. **46**, 1047 (1968).

Crystallographic studies of cobalt arsenates. IV. Crystal parameters of cobalt diarsenate

J. OZOG, N. KRISHNAMACHARI, AND C. CALVO
Institute for Materials Research and Department of Chemistry, McMaster University, Hamilton, Ontario

Received June 20, 1969

The crystal structure of cobalt diarsenate has been shown to be a new member of a series of structures closely related to that of the mineral thortveitite. The triclinic unit cell parameters are: $a = 6.55$ Å, $b = 8.52$ Å, $c = 4.76$ Å, $\alpha = 91.0°$, $\beta = 104.0°$, $\gamma = 91.3°$. There are 2 molecules per unit cell with a symmetry $C1$ or $C\bar{1}$ and a measured density 5.01 g/cm^3. The single crystal patterns show nearly the $C2/m$ symmetry characteristic of the mineral thortveitite and its analogues.

Canadian Journal of Chemistry, **48**, 388 (1970)

Can. J. Chem. Downloaded from www.nrcresearchpress.com by 210.87.254.6 on 09/05/12
For personal use only.

Taylor and Heyding (1) reported the Debye–Scherrer pattern of $2CoO.As_2O_5$ obtained by reacting 2 moles of CoO with 1 mole of As_2O_5 at 800 °C. The pattern obtained was poorly defined since the sample appeared to be contaminated with other cobalt arsenates and silica from the container. Despite these difficulties probable lines for $2CoO.As_2O_5$ were selected and an indexing attempted with an orthorhombic cell defined by $a = 8.16$ Å, $b = 8.56$ Å, and $c = 9.19$ Å.

It was felt important that either $Co_2As_2O_7$ or its apparent isomorph $Ni_2As_2O_7$ (1) be examined in single crystal form since this cell seemed to be at variance with the otherwise perfect correlation between cationic radius and structure type. Table 1 shows that the diphosphates, divanadates, and diarsenates invariably showed the thortveitite structure (2) for one of its polymorphs for cations whose radii were less than about 1 Å. The results of the present study are included in Table 1. The situation among the silicates has been summarized by Ito and Johnson (3). Furthermore, the volume of the cell reported by Taylor and Heyding (1), when compared with that of $Mg_2As_2O_7$ (4), suggested that their unit cell would contain 5 formula units, if the packing efficiencies were similar.

TABLE 1

Structure types for $X_2Y_2O_7$ compounds with $X \leq 1.0$ Å*,†

X	Radius (Å)	$P_2O_7^{4-}$	$As_2O_7^{4-}$	$V_2O_7^{4-}$
Mg^{2+}	0.69	{α,β}	{β}	‡
Ni^{2+}	0.66	{α,β}		‡
Co^{2+}	0.71	{α,β}	{α}	‡
Zn^{2+}	0.71	{α,β}	{β}	‡
Mn^{2+}	0.79	{β}	‡	{β}
Cu^{2+}		{α,β}	‡	‡
Cd^{2+}	0.97		{β}	{β}
Ca^{2+}	1.01		New	New

*α = polymorph of the thortveitite structure.
†β = thortveitite structure.
‡Unknown.

In previous studies in the $CoO–As_2O_5$ system (5–7) it was apparent that single crystals could be produced from stoichiometric samples heated in open containers but that the products had unpredictable compositions. Thus $Co_2As_2O_7$ was precipitated from a solution containing $CoCl_2$ and $Na_4As_2O_7$. The solid was dried at 500 °C, sealed in an evacuated quartz tube, and heated in stages until it melted. The melting temperature found was 1125 ± 25 °C using an uncalibrated thermocouple. The sample was cooled slowly and upon cooling the tube cracked, probably because of the differential coefficient of the expansion between quartz and $Co_2As_2O_7$ and the fact that the container had been wetted by the liquid. The actual chemical attack, however, was modest.

Crystals could easily be aligned so as to rotate about the [110] axis, making use of the fact that the (001) and (11$\bar{0}$) faces gave excellent optical reflections. This feature is generally common to this family of compounds. The zero level Weissenberg photograph was nearly superimposable upon a photograph from a similarly oriented crystal of $Mn_2P_2O_7$. Further photographs taken to see if $Co_2As_2O_7$ was a polymorph of the thortveitite structure, as is the case for the diphosphates, showed that it was in fact triclinic. Although the photographs show nearly the $C2/m$ symmetry anticipated, the α and γ angles deviate significantly from 90°. In addition, intensity differences were apparent between reflections that would be identical if the crystal were monoclinic. The density was measured by

pycnometer and is reported with lattice parameters determined from an uncalibrated set of films in Table 2 both for the centered cell analogous to that of the mineral and for a primitive cell.

The crystals obtained always showed a pattern arising from two unequal sized crystals misoriented by about 4°. Two additional trials, starting with the precipitation, resulted in similar crystals. The Debye–Scherrer pattern from the bulk of the sample rather than from grinding selected single crystals was similar to that obtained by Taylor and Heyding (1). The pattern obtained from a powder of selected crystals had substantially fewer lines than that reported by these authors.

From the crystal chemistry of the other members of this series it is expected that $Co_2As_2O_7$ will transform to the $C2/m$ symmetry and become isostructural to thortveitite at some high temperature. A structure resolution of this phase would be of interest since the As—O—As may not be constrained, at least on the average, to be linear.

TABLE 2

Crystal data for $Co_2As_2O_7$

Lattice parameter	$Co_2As_2O_7$	Primitive triclinic space group
a (Å)	6.55	5.31
b (Å)	8.52	5.44
c (Å)	4.76	4.76
α (°)	91.0	96.2
β (°)	104.0	96.4
γ (°)	91.3	105.5
Systematic absences		hkl, $h+k$ = odd
Density (g/cm^3), calcd. for $Z = 2$		4.91
Density (g/cm^3), exp.		5.01
Space group		$C1$ or $C\bar{1}$

NOTE ADDED IN PROOF. A further preparation of $Co_2As_2O_7$ has yielded crystals nearly the same as reported here but showing superstructure reflections parallel to $(1\bar{1}1)$. These are such that reflections appear at one-fifth the normal spacing.

This research has been supported by a grant from the National Research Council of Canada.

1. J. B. TAYLOR and R. D. HEYDING. Can. J. Chem. **36**, 597 (1958).
2. D. W. J. CRUICKSHANK, H. LYNTON, and G. A. BARCLAY. Acta Cryst. **15**, 491 (1962).
3. J. ITO and H. JOHNSON. Amer. Mineral. **53**, 1940 (1968).
4. C. CALVO and K. NEELAKANTAN. To be published.
5. N. KRISHNAMACHARI and C. CALVO. To be published.
6. N. KRISHNAMACHARI and C. CALVO. To be published.
7. N. KRISHNAMACHARI and C. CALVO. To be published.

Erratum: Signs of spin–spin coupling constants between aldehydic and ring protons in 2,6-dinitrobenzaldehyde. Evidence for a hyperconjugative contribution to $J_p^{H,CHO}$

C. L. BELL, S. S. DANYLUK, AND T. SCHAEFER
Argonne National Laboratory, Argonne, Illinois 60439

Received October 16, 1969
(Ref.: Can. J. Chem. **47**, 3529 (1969))

Canadian Journal of Chemistry, **48**, 389 (1970)

On page 3531, line 13 of the right-hand column should read $|J_{AX}| = J_o^{H,CHO} < 0.10$ Hz and not $|J_{AX}| = J_o^{H,CHO} = 0.10$ Hz.

Can. J. Chem. Downloaded from www.nrcresearchpress.com by 210.87.254.6 on 09/05/12
For personal use only.

Erratum: Hydrogen bonding in lidocaine salts. I. The $\overset{+}{N}H$ stretching band and its dependence on the associated anion

GEORGE A. NEVILLE AND ZEPHYR R. REGNIER
Research Laboratories, Food and Drug Directorate, Department of National Health and Welfare, Ottawa, Canada
Received December 1, 1969

(Ref.: Can. J. Chem. **47**, 4229 (1969))

Canadian Journal of Chemistry, **48**, 390 (1970)

Figure 1 on p. 4231 should be as follows.

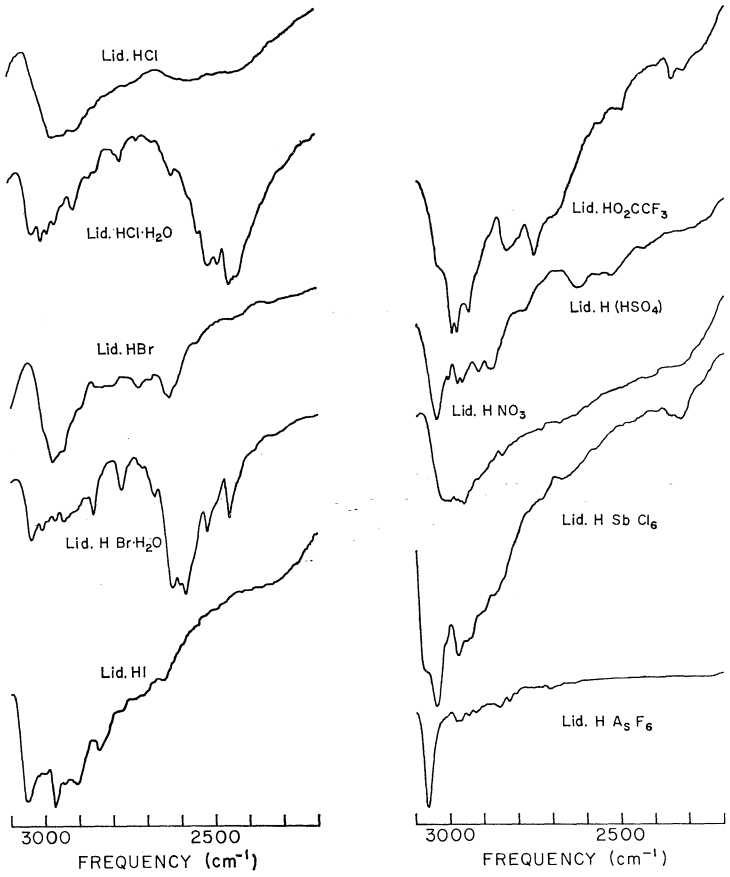

FIG. 1. Infrared spectra of lidocaine salts from 3100 to 2200 cm^{-1}.

Erratum: Long-range spin–spin coupling constants between ring protons and aldehydic protons in some *para*-substituted benzaldehydes

S. S. DANYLUK, C. L. BELL, AND T. SCHAEFER
Division of Biological & Medical Research, Argonne National Laboratory, Argonne, Illinois, U.S.A.

Received November 20, 1969

(Ref.: Can. J. Chem. **47**, 4005 (1969))

Canadian Journal of Chemistry, **48**, 391 (1970)

On page 4007, right-hand column, Fig. 2 should be shown as below and not as printed.

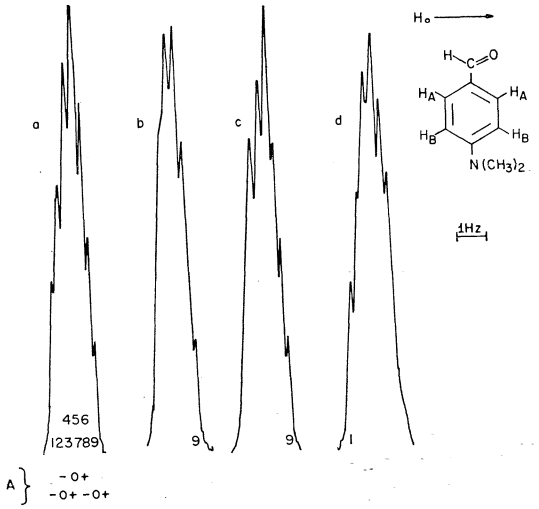

FIG. 2. In (*a*), the single proton resonance spectrum of the aldehydic proton in *p*-dimethylaminobenzaldehyde is shown. In (*b*), (*c*), (*d*), double resonance spectra are recorded under conditions described in the text.

Can. J. Chem. Downloaded from www.nrcresearchpress.com by 210.87.254.42 on 09/05/12
For personal use only.

Pulse radiolysis of nitric oxide in aqueous solution[1]

W. A. SEDDON AND M. J. YOUNG
Physical Chemistry Branch, Atomic Energy of Canada Limited, Chalk River Nuclear Laboratories, Chalk River, Ontario

Received November 3, 1969

Pulse radiolysis of aqueous solutions of nitric oxide at neutral p*H* shows that the reaction initiated by the hydrated electron, $e^-(aq)$, proceeds via NO^- and a new transient thought to be $(N_2O_2)^-$, and not HNO as indicated previously by steady state radiolysis.

Canadian Journal of Chemistry, 48, 393 (1970)

Earlier studies (1–3), on the radiation chemistry of nitric oxide solutions indicated that the products of γ radiolysis, HNO_2 and N_2O, were explicable by a fairly simple mechanism

$$[1] \qquad e^-(aq) + NO \rightarrow NO^- \left(\xrightarrow{H^+} HNO\right)$$

$$[2] \qquad H + NO \rightarrow HNO$$

$$[3] \qquad OH + NO \rightarrow HNO_2$$

$$[4] \qquad HNO + 2NO \rightarrow HNO_2 + N_2O$$

While the above reaction sequence is stoichiometrically correct the pulse radiolysis results demonstrate that the detailed mechanism is more complex at neutral p*H*, particularly with respect to reactions involving anionic species generated via $e^-(aq)$.

Figure 1 (open circles), shows the transient spectrum with absorption maxima at 250 and 380 mμ, observed from 1.7 m*M* NO solutions 120 μs after a 2–3 krads, 0.5 μs pulse of electrons from a 2 MeV Van de Graaff accelerator. The spectrum 2 μs after the pulse appears identical and is about 20% lower in intensity at 380 mμ. Addition of OH radical scavengers, 10^{-1} *M* methanol or 2×10^{-2} *M* KSCN, did not remove the transient. The absorption is not observed in 1.7 m*M* NO solutions containing 0.4 *M* H_2SO_4 as electron scavenger. Similarly, it is reduced by a factor of about 10 in solutions containing a 20-fold excess of N_2O, indicating that a precursor of this species is $e^-(aq)$.

The permanent product absorption (closed circles) is due to the formation of nitrite (reaction [3]), which absorbs intensely at 210 mμ (4).

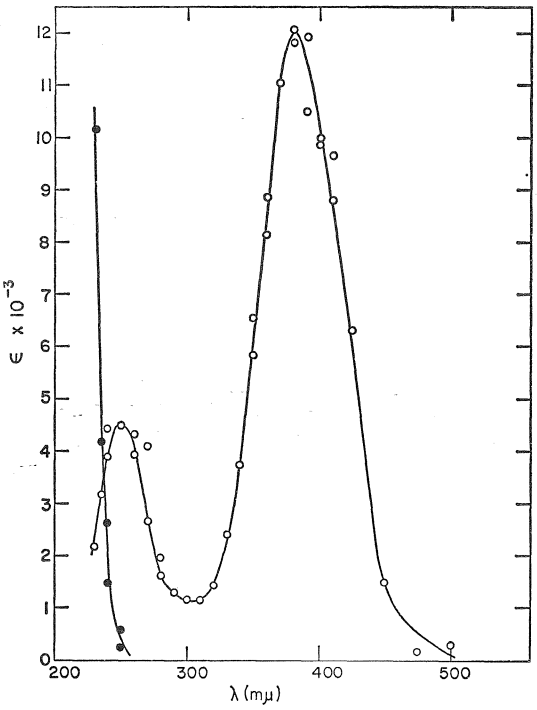

FIG. 1. Absorption spectra of species produced in the pulse radiolysis of 1.7 m*M* NO in aqueous solution at neutral p*H*. ○, transient species observed 120 μs after the pulse; ●, permanent product absorption due to NO_2^-.

The rate of decay of $e^-(aq)$ was found to be pseudo first order and the half life, $t_{\frac{1}{2}}$, inversely proportional to the NO concentration from which we derive $k(e^-(aq) + NO) = 2.3 \pm 0.4 \times 10^{10}\ M^{-1}\ s^{-1}$. This value is lower than an earlier reported figure (5) of $3.1 \pm 0.2 \times 10^{10}\ M^{-1}\ s^{-1}$, but is in good agreement with the relative rate

[1]A.E.C.L. No. 3491.

constant ratios (1–3); $k(e^-(aq) + NO)/k(e^-(aq) + N_2O) = 2.5 \pm 0.2$, $k(e^-(aq) + NO)/k(e^-(aq) + NO_2^-) = 5.4 \pm 0.7$, and the absolute rate constants (5, 6), $k(e^-(aq) + N_2O) = 8.7 \pm 0.6 \times 10^9$ and $k(e^-(aq) + NO_2^-) = 4.1 \pm 0.6 \times 10^9$ M^{-1} s^{-1}, respectively.

The build up of the transient absorption (monitored at 380 mμ) occurs with two distinct rates. Initially there is a rapid pseudo first order increase, the rate of which is about seven times slower than the rate of decay of $e^-(aq)$ observed in the same solution. This indicates that NO^-, presumably produced in reaction [5], does not absorb strongly at this wavelength but is the precursor of the initial absorbing species. This species we suggest is the radical anion $(N_2O_2)^-$ formed in a subsequent slower reaction [6].

[5] $$e^-(aq) + NO \rightarrow NO^-$$

[6] $$NO^- + NO \rightarrow (N_2O_2)^-$$

It was found that $t_{\frac{1}{2}}$ for the formation of $(N_2O_2)^-$ was inversely proportional to NO concentration and that $k_6 = 3.3 \pm 0.7 \times 10^9$ M^{-1} s^{-1}. Both NO^- and $(N_2O_2)^-$, formed by negative ion molecule reactions in N_2O have been identified in the gas phase by mass spectrometry (7).

Following the initial rapid build up of absorption a slow additional increase is observed which reaches its maximum intensity about 150 μs after the pulse in 1 mM solutions of NO. The kinetics of its formation are a function of NO concentration but are complicated by its subsequent decay which is first order and markedly pH dependent. Additional $(N_2O_2)^-$ might be formed at a rate which depends upon the dissociative equilibrium [7], for HNO formed directly via reaction [2].

[7] $$HNO \rightleftarrows H^+ + NO^-$$

This possibility should depend markedly on pH and the relative rates of reactions [6] and [4], with reaction [4] becoming more important in acid solution (1, 3). When the pH is decreased from 7.1 (buffered solution) to 3.5, it is found that the transient still builds up in two distinct stages but the overall intensity decreases by about 75%; an amount greater than explicable simply in terms of a competition between reactions [5] and [8]

[8] $$e^-(aq) + H^+ \rightarrow H$$

Protonation of NO^- and/or $(N_2O_2)^-$ could account for this effect with the relative equilibrium concentrations and rates of formation of each being a function of the respective pK values for HNO and HN_2O_2. If the pK values for these species are greater than about 3.5 (i.e. weaker acids than HNO_2), then an alternative explanation, conversion of $(N_2O_2)^-$ to yet another species, must be considered.

The final absorption eventually decays by an acid catalyzed process, the half life of which decreases from $t_{\frac{1}{2}} = 2.1$ ms at pH 7.1 to $t_{\frac{1}{2}} = 191$ μs at pH 3.5, the corresponding first order rate constants being $0.33 \pm 0.02 \times 10^3$ and $3.6 \pm 0.2 \times 10^3$ s^{-1}, respectively.

A complete kinetic analysis as a function of NO concentration, pH, and ionic strength is required to elucidate the mechanism in further detail.

It is a pleasure to thank Drs. F. Wilkinson, B. Michael, and Professor J. W. Hunt for their advice on the design of pulse radiolysis equipment. We also thank Dr. Hunt for the use of his apparatus to confirm our preliminary observations and our colleagues for many helpful discussions.

1. W. A. Seddon and H. C. Sutton. Trans. Faraday Soc. **59**, 2323 (1963).
2. T. W. Woodward and H. C. Sutton. Trans. Faraday Soc. **62**, 70 (1966).
3. R. J. Knight and H. C. Sutton. Trans. Faraday Soc. **63**, 1 (1967).
4. H. L. Friedman. J. Chem. Phys. **21**, 319 (1963).
5. S. Gordon, E. J. Hart, M. S. Matheson, J. Rabani, and J. K. Thomas. Discuss. Faraday Soc. **36**, 193 (1963).
6. M. Anbar and P. Neta. Int. J. Appl. Radiation Isotopes, **18**, 493 (1967).
7. J. L. Moruzzi and J. T. Dakin. J. Chem. Phys. **49**, 5000 (1968).

Can. J. Chem. Downloaded from www.nrcresearchpress.com by 210.87.254.42 on 09/05/12
For personal use only.

Canadian Journal of Chemistry

Published by THE NATIONAL RESEARCH COUNCIL OF CANADA

VOLUME 48 FEBRUARY 1, 1970 NUMBER 3

Heats of formation of some alkylthio radicals

D. H. FINE[1] AND J. B. WESTMORE

Chemistry Department, University of Manitoba, Winnipeg, Manitoba

Received August 29, 1969

From a comparison of the dissociation energies of carbon–oxygen and carbon–sulfur bonds in alcohols, thioalcohols, ethers, and thioethers, a self-consistent set of values for the heats of formation of the methylthio-, ethylthio-, *n*-butylthio-, *iso*-butylthio-, *sec*-butylthio-, *t*-butylthio-, phenylthio-, and benzylthio-radicals is derived.

Canadian Journal of Chemistry, **48**, 395 (1970)

Introduction

An understanding of sulfur chemistry would be enhanced by the availability of reliable thermochemical data. In this paper we derive values for the heats of formation of the alkylthio radicals by comparing the few reliable (1) carbon–sulfur bond dissociation energies with the carbon–oxygen values obtained from the relatively well-studied alkoxy radicals (2, 3).

The principal path towards the heats of formation of free radicals is by the union of thermodynamic and kinetic data. This method combines heats of formation determined calorimetrically with activation energies, derived from kinetic measurements, which are identified with dissociation energies of particular bonds. For many ethers and thioethers, represented by RXR′, the dissociation energy of the R—XR′ bond is too large to be determined directly by the kinetic method. It may nevertheless be evaluated indirectly from the relationship

$$D(\mathrm{R—XR'}) = \Delta H_f^0(\mathrm{R}\cdot, \mathrm{g}) + \Delta H_f^0(\cdot\mathrm{XR'}, \mathrm{g}) - \Delta H_f^0(\mathrm{RXR'}, \mathrm{g})$$

provided that the heats of formation of the radicals R· and ·XR′ and of the parent molecule RXR′ are known. Heats of combustion of compounds containing carbon, hydrogen, oxygen, or sulfur can be measured to high precision by combustion calorimetry. Evaluation of the heat of formation of the gaseous compounds also requires knowledge of the heat of sublimation or vaporization of RXR′ at 25 °C.

Source of Data

Available experimental values for the standard heats of formation of the alkyl-, aryl-, oxy-, and thio-radicals (3, 4) are listed in Table 1.

The heats of formation of the parent oxygen- and sulfur-compounds in the gas phase at 25 °C are given in Table 2. Experimental values are available for only some of the ethers and thioethers, and it is therefore necessary to make use of estimated values. Pilcher, Pell, and Coleman (17) calculated the heats of formation of the ethers by using the same Allen-type (25) equation that Skinner (26) had derived for the alcohols. The correlation was not good for *iso*-propyl-*t*-butyl ether (error 2.5 kcal/mole) and for di-*t*-butyl ether (error 10.6 kcal mole). We ascribe this discrepancy to steric interference when alkyl groups are attached to both carbon atoms of the C—O—C grouping, i.e. the hydrogen atom of an α methyl group interferes sterically with the hydrogen atom of the opposite α′ carbon atom. The interference is small and we take account of it by adding 0.91 kcal/mole for every 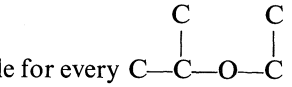

[1]Present address: Chemical Engineering Department, Massachusetts Institute of Technology, Cambridge, Mass. 02139.

TABLE 1

Standard heats of formation of alkyl-, aryl-, oxy-, and thio-radicals at 25 °C

Radical	Heat of formation (kcal/mole)	Reference
$CH_3\cdot$	34.0 ±1	4
$C_2H_5\cdot$	25.7 ±1	4
n-$C_3H_7\cdot$	21 ±2	4
iso-$C_3H_7\cdot$	17.6 ±1	4
n-$C_4H_9\cdot$	17 ±2	4
sec-$C_4H_9\cdot$	12.4 ±1	4
iso-$C_4H_9\cdot$	14 ±2	4
t-$C_4H_9\cdot$	6.8 ±1	4
$C_6H_5CH_2\cdot$	45 ±1	4
$C_6H_5\cdot$	80 ±1	5
$H\cdot$	52.09±0.06	6
$CH_3O\cdot$	2 ±2	3
$C_2H_5O\cdot$	−4.4 ±1	7
n-$C_3H_7O\cdot$	−13 ±2	3
iso-$C_3H_7O\cdot$	−13 ±2	3
n-$C_4H_9O\cdot$	−16 ±2	3
sec-$C_4H_9O\cdot$	−18 ±2	3
iso-$C_4H_9O\cdot$	−18 ±2	3
t-$C_4H_9O\cdot$	−22 ±2	3
$C_6H_5CH_2O\cdot$	25 ±5	2
$C_6H_5O\cdot$	13 ±3	1, 8, 9
$HO\cdot$	9.3 ±1	10
$CH_3S\cdot$	29	1, 11, 12
$C_2H_5S\cdot$	25	1, 13
$C_6H_5S\cdot$	50	4
$HS\cdot$	33 ±3	4

interaction. The equations (17, 23) we use are

$$\Delta H_f^0(\mathrm{ROR}) = (-39.28 - 2.35a - 2.58b - 5.66c + 0.55d + 1.43e + 0.91f) \text{ kcal/mole}$$

$$\Delta H_f^0(\mathrm{RSR}) = (-4.10 - 2.35a - 2.58b - 3.30c' + 0.65d + 1.20e') \text{ kcal/mole}$$

where a is the number of C atoms, b the number of C—C—C interactions, c and c' the number of C—C—O and C—C—S interactions, respectively, d the number of 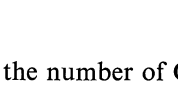 interactions, e and e' the number of 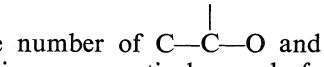 interactions, respectively, and f the number of 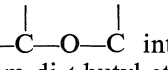 interactions. The ethers, apart from di-*t*-butyl ether, give an average deviation between the experimental and calculated values of ±0.21 kcal/mole, which is considerably less than the average experimental uncertainty interval of ±0.35 kcal/mole. Di-*t*-butyl ether is difficult to prepare and Smutny and Bondi (18) have shown that the strain due to overcrowding is about 7.6 kcal/mole, which agrees well with the 7.0 kcal/mole deviation between experimental and calculated values which we obtain here (see Table 2). For the thioethers, McCullough and Good's (23) scheme gives an average deviation between the experimental and calculated values of ±0.28 kcal/mole, which is again less than the average experimental uncertainty interval of ±0.35 kcal/mole. Since the carbon–sulfur bond is longer than the carbon–oxygen bond (1.82 Å compared with 1.42 Å), steric interference is negligible in the thioethers and no correction is applied.

Paucity of experimental data makes it difficult to extend the correlation to aryl ethers or aryl thioethers.

Discussion

The ROR′ and RSR′ bond dissociation energies, calculated from the data in Tables 1 and 2 are listed in Table 3. Comparisons (1) of bond dissociation energies have been made between corresponding oxygen- and sulfur-compounds and lead to heats of formation for $HS\cdot$, $C_6H_5S\cdot$, $CH_3S\cdot$, and $C_2H_5S\cdot$ radicals believed to be reliable to ±3 kcal/mole.

From Table 3 certain trends are immediately obvious. The alkoxy–alkyl bond dissociation energies are almost independent of the nature of the alkoxy or alkyl groups: the average dissociation energies for the methoxy–, ethoxy–, *n*-propoxy–, *iso*-propoxy–, *n*-butoxy–, *sec*-butoxy–, *iso*-butoxy–, and *t*-butoxy–alkyl bonds are 80, 82, 78, 81, 80, 81, 80, and 81 kcal/mole, respectively. Only for compounds containing the *n*-propoxy group are the bond dissociation energies seen to be out of line. The experimental values, based on pyrolyses of *n*-propyl nitrite (2), nitrate (2), and peroxide (28) are −15.1, −12.0, and −10.7 kcal/mole, respectively. Kerr (4) decided that, in keeping with the heat of formation of the methoxy- and ethoxy-radicals, the value based on the peroxide data was likely to be the more reliable. We support this argument as there is no reason why $D(n\text{-}C_3H_7O\text{—R})$ should be 2 kcal/mole less than that for other alkoxy–alkyl bonds.

Apart from the methylthio- and ethylthio-containing alkylthio ethers, neither the heat of formation of the alkylthio radical nor the alkyl-

Can. J. Chem. Downloaded from www.nrcresearchpress.com by 210.87.254.42 on 09/05/12
For personal use only.

TABLE 2

Heats of formation (kcal/mole) of the parent oxygen- and sulfur-compounds, in the gas phase at 25 °C

	X = oxygen			X = sulfur		
Compound	$-\Delta H_f^0$	Obsd. − calcd.†	Reference	$-\Delta H_f^0$	Obsd. − calcd.†	Reference
H_2X	57.7989		6	4.82±0.10		22
CH_3XH	48.08±0.05		14	5.46±0.14		22
C_2H_5XH	56.24±0.12		14	10.99±0.12		22
n-C_3H_7XH	61.85±0.26		14	16.19±0.16		22
iso-C_3H_7XH	65.42		14	18.19±0.16		22
n-C_4H_9XH	65.81±0.14		15	21.02±0.28		22
sec-C_4H_9XH	70.1 ±0.25		14	23.12±0.19		22
iso-C_4H_9XH	67.9 ±0.26		14	23.21±0.21		22
t-C_4H_9XH	74.9 ±0.25		14	26.21±0.21		22
$C_6H_5CH_2XH$	25.0 ±0.8		14, 16	−21.9 ±0.6		22
C_6H_5XH	23.05±0.15		14	−26.66±0.28		22
CH_3XCH_3	43.99±0.12	−0.01	17	8.94±0.10	−0.14	22, 23
$CH_3XC_2H_5$	51.73±0.16	+0.26	17	14.22±0.27	+0.23	22, 23
CH_3X*n*-C_3H_7	56.82±0.26	+0.10	17	19.51±0.23	−0.13	22, 24
CH_3X*iso*-C_3H_7	60.24±0.23	0.00	17	21.58±0.18	−0.10	22, 23
CH_3X*n*-C_4H_9	61.85*		17	24.2 ±0.6	+0.11	22, 23
CH_3X*sec*-C_4H_9	65.17*		17	26.41*		23
CH_3X*iso*-C_4H_9	63.88*		17	26.24*		23
CH_3X*t*-C_4H_9	70.00±1.2	−0.91	17, 18	28.93±0.19	+0.31	22, 23
$CH_3XCH_2C_6H_5$				−19.0 ±0.7		22
$CH_3XC_6H_5$	19.1 ±0.8		14, 16	−23.5 ±0.7		22
$C_2H_5XC_2H_5$	60.28±0.18	−0.28	17, 19	19.92±0.19	+0.18	22, 23
C_2H_5X*n*-C_3H_7	65.15*		17	24.97±0.18	+0.06	22, 23
C_2H_5X*iso*-C_3H_7	68.25*		17	28.0 ±0.6	−0.87	22, 23
C_2H_5X*n*-C_4H_9	69.86*		17	30.3 ±0.6	−0.34	22, 23
C_2H_5X*sec*-C_4H_9	73.18*		17	32.06*		23
C_2H_5X*iso*-C_4H_9	71.89*		17	31.89*		23
C_2H_5X*t*-C_4H_9	77.10*		17	35.3 ±0.6	+0.41	22, 23
$C_2H_5XCH_2C_6H_5$				−12.4 ±0.7		22
$C_2H_5XC_6H_5$	26.6 ±0.8		14, 16	−18.4 ±0.7		22
n-C_3H_7X*n*-C_3H_7	69.99±0.5	−0.13	17, 20	29.93±0.21	+0.03	22, 23
n-C_3H_7X*iso*-C_3H_7	73.18*		17	32.06*		23
n-C_3H_7X*n*-C_4H_9	74.79*		17	34.89*		23
n-C_3H_7X*sec*-C_4H_9	78.11*		17	36.99*		23
n-C_3H_7X*iso*-C_4H_9	76.82*		17	36.82*		23
n-C_3H_7X*t*-C_4H_9	82.03*		17	39.82*		23
iso-C_3H_7X*iso*-C_3H_7	76.1 ±0.6	+0.10	17, 20	33.84±0.23	+0.32	22, 23
iso-C_3H_7X*n*-C_4H_9	78.11*		17	36.99*		23
iso-C_3H_7X*sec*-C_4H_9	81.43*		17	39.09*		23
iso-C_3H_7X*iso*-C_4H_9	80.14*		17	38.92*		23
iso-C_3H_7X*t*-C_4H_9	85.6 ±0.6	−0.25	17, 18	41.92*		23
n-C_4H_9X*n*-C_4H_9	79.8 ±0.5	−0.08	17, 20	39.96±0.35	−0.41	22, 23
n-C_4H_9X*sec*-C_4H_9	81.75*		17	41.75*		23
n-C_4H_9X*iso*-C_4H_9	81.75*		17	41.92*		23
n-C_4H_9X*t*-C_4H_9	86.96*		17	44.75*		23
sec-C_4H_9X*sec*-C_4H_9	86.2 ±0.5	+0.16	17, 20	44.02*		23
sec-C_4H_9X*iso*-C_4H_9	85.07*		17	43.85*		23
sec-C_4H_9X*t*-C_4H_9	90.28*		17	46.85*		23
iso-C_4H_9X*iso*-C_4H_9	83.78*		17	42.9 ±0.5	+0.78	22, 23
iso-C_4H_9X*t*-C_4H_9	88.99*		17	46.68*		23
t-C_4H_9X*t*-C_4H_9	87.2 ±0.2	+7.0	17, 18	49.6 ±0.5	+0.08	22, 23
$C_6H_5CH_2XCH_2C_6H_5$				−46.1 ±1.0		22
$C_6H_5XC_6H_5$	−6.1		16, 21	−55.3 ±0.7		22

*Calculated values.
†Difference between observed and calculated values of ΔH_f^0.

thio–alkyl bond dissociation energies are known. However, the data for the methylthio- and ethylthio-ethers closely parallel the data for the ethers. Thus, whereas the dissociation energy of the alkoxy–alkyl bond is 80 ± 2 kcal/mole, that of the alkylthio–alkyl bond is 11 ± 3 kcal/mole lower, at least for the methylthio- and ethylthio-ethers. As we may reasonably expect the relationship between the dissociation energies of the oxygen- and sulfur-compounds to persist for

Can. J. Chem. Downloaded from www.nrcresearchpress.com by 210.87.254.42 on 09/05/12
For personal use only.

Can. J. Chem. Downloaded from www.nrcresearchpress.com by 210.87.254.42 on 09/05/12
For personal use only.

TABLE 3

Bond dissociation energies (kcal/mole) in ROR′ and RSR′ compounds

	Bond dissociation energy†, R =										
Bond broken	$CH_3\cdot$	$C_2H_5\cdot$	*n*-$C_3H_7\cdot$	*iso*-$C_3H_7\cdot$	*n*-$C_4H_9\cdot$	*sec*-$C_4H_9\cdot$	*iso*-$C_4H_9\cdot$	*t*-$C_4H_9\cdot$	$C_6H_5CH_2\cdot$	$C_6H_5\cdot$	$H\cdot$
HO—R	91	91	92	92	92	92	91	91	79	112	119
HS—R	72	70	70	69	71	69	70	66	56	86	90
C_6H_5O—R	66	65								87	88
C_6H_5S—R	60	57								74	75
CH_3O—R	80	79	80	80	81*	80*	80	79	66‡	101	102
CH_3S—R	72	69	70	68	70	68*	69*	65	55	86	86
C_2H_5O—R	82	82	82*	82*	83*	82*	82*	80*		103	104
C_2H_5S—R	73	71	71	71	72	70*	71*	67	58	87	88
n-C_3H_7O—R	78	78*	78	78*	79*	78*	78*	76*			101
n-C_3H_7S—R	(71)	(69)	(69)	(68)*	(70)*	(67)*	(69)*	(65)*			(86)
iso-C_3H_7O—R	81	81*	81*	81	82*	81*	81*	79*			104
iso-C_3H_7S—R	(73)	(71)	(70)*	(69)	(71)*	(69)*	(70)*	(66)*			(87)
n-C_4H_9O—R	80*	80*	80*	80*	81	78*	80*	78*			102
n-C_4H_9S—R	(71)	(69)	(69)*	(68)*	(70)	(67)*	(69)*	(65)*			(86)
sec-C_4H_9O—R	81*	81*	81*	81*	81*	81	81*	79*			104
sec-C_4H_9S—R	(72)*	(70)*	(70)*	(69)*	(71)*	(68)*	(70)*	(66)*			(87)
iso-C_4H_9O—R	80*	80*	80*	80*	81*	80*	80*	78*			102
iso-C_4H_9S—R	(71)*	(69)*	(69)*	(68)*	(70)*	(67)*	(68)	(65)*			(86)
t-C_4H_9O—R	82	81*	81*	81	82*	81*	81*	72			105
t-C_4H_9S—R	(72)	(70)	(70)*	(69)*	(71)*	(68)*	(70)*	(65)			(87)
$C_6H_5CH_2O$—R											102
$C_6H_5CH_2S$—R	(70)	(68)							(54)		(85)

*Based on calculated values for the heat of formation of the parent compound.
†Numbers in parentheses were derived here using "best fit" values.
‡Estimated value, see ref. 27.

Can. J. Chem. Downloaded from www.nrcresearchpress.com by 210.87.254.42 on 09/05/12
For personal use only.

other alkyl ethers and alkylthioethers we are able to derive "best fit" values for the bond dissociation energies D(R'S—R) (see the values in parentheses in Table 3). From these "best fit" bond dissociation energies we derive the heats of formation of the remaining alkylthio radicals (see Table 4).

TABLE 4

Standard heats of formation of the alkylthio radicals derived in this work

Radical	Heat of formation (kcal/mole) This work*	Literature†
$CH_3S\cdot$	29 ± 3	30 (1, 11, 12)
$C_2H_5S\cdot$	25 ± 3	25 (1, 13)
n-$C_3H_7S\cdot$	18 ± 3	20 (13)
iso-$C_3H_7S\cdot$	17 ± 3	18 (13)
n-$C_4H_9S\cdot$	13 ± 3	15 (13)
sec-$C_4H_9S\cdot$	12 ± 3	—
iso-$C_4H_9S\cdot$	11 ± 3	—
t-$C_4H_9S\cdot$	9 ± 3	11 (13)
$C_6H_5CH_2S\cdot$	55 ± 5	—
$C_6H_5S\cdot$	50 ± 3	50 (4)

*Derived in this work from "best fit" bond dissociation energies.
†Reference numbers in parentheses.

A knowledge of the relevant bond dissociation energies in the asymmetrical ethers and thioethers enables one to predict which bond is the weakest and hence where the molecule will split on pyrolysis. For example, the pyrolysis of methyl phenyl ether (29) in quartz tubes at 500–600 °C yields phenol as the major product. The decomposition is readily explained if the first step is

$$CH_3OC_6H_5 \rightarrow CH_3\cdot + \cdot OC_6H_5$$

This is to be expected, as the methyl–oxygen bond is 34 kcal/mole weaker than the phenyl–oxygen bond, viz. $D(CH_3—OC_6H_5) = 67$ and $D(CH_3O—C_6H_5) = 101$ kcal/mole. The thermal decompositions of methyl phenyl sulfide (30) and methyl benzyl sulfide (11) have been investigated in a toluene flow system at 470–700 °C. For methyl phenyl sulfide the main products are methane, benzenethiol, and bibenzyl (from the toluene). Back and Sehon (30) ascribed the primary mode of reaction to the methyl–sulfur bond rupture

$$CH_3SC_6H_5 \rightarrow CH_3\cdot + \cdot SC_6H_5$$

The activation energy of 60 kcal/mole which they measured was ascribed to this process and they were hence able to derive a value for the heat of formation of the phenylthio radical. The weakest bond was broken, since

$$D(CH_3—SC_6H_5) = 60 < D(CH_3S—C_6H_5) = 87 \text{ kcal/mole}$$

For methyl benzyl sulfide, the principal pyrolysis products, methanethiol and bibenzyl, are formed at the rame rate. The decomposition is most readily explained by the reactions

$$C_6H_5CH_2SCH_3 \rightarrow C_6H_5CH_2\cdot + \cdot SCH_3$$

$$C_6H_5CH_3 \text{ (carrier gas)} + \cdot SCH_3 \rightarrow C_6H_5CH_2\cdot + HSCH_3$$

$$2C_6H_5CH_2\cdot \rightarrow C_2H_5CH_2CH_2C_6H_5$$

The sulfur atom remains attached to the methyl group to give the methylthio radical, because

$$D(C_6H_5CH_2—SCH_3) = 55 < D(C_6H_5CH_2S—CH_3) = 70 \text{ kcal/mole}$$

In methanethiol and ethanethiol the carbon–sulfur bond is weaker than the sulfur–hydrogen bond

$$D(CH_3—SH) = 73 \text{ kcal/mole}$$

$$D(CH_3S—H) = 87 \text{ kcal/mole}$$

$$D(C_2H_5—SH) = 70 \text{ kcal/mole}$$

and

$$D(C_2H_5S—H) = 88 \text{ kcal/mole}$$

Sehon and Darwent (31) have shown that the first step in the pyrolysis of methanethiol is

$$CH_3SH \rightarrow CH_3\cdot + \cdot SH$$

For ethanethiol the decomposition is more complex, being predominantly a molecular rearrangement at low temperature

$$C_2H_5SH \rightarrow C_2H_4 + H_2S$$

and a free-radical process at higher temperatures

$$C_2H_5SH \rightarrow C_2H_5\cdot + \cdot SH$$

On pyrolysis, benzenethiol (31) and 2-methyl-2-propanethiol (32) also split predominantly at the carbon–sulfur bond.

The results listed in Table 4 depend upon a comparison of bond dissociation energies in many analogous pairs of compounds. Since a significant body of independently obtained data is involved, this would suggest that most values are within the error limits given of ±3 kcal/mole. The reliability

of the data depend upon the reliability of the gas-phase heats of formation of (*i*) the parent compounds, (*ii*) the alkyl- and alkoxy-radicals, and (*iii*) the mercapto-, methylthio-, and ethylthio-radicals. Although the experimental heat of formation data for the parent compounds have been supplemented by calculated values, we have shown the uncertainties to be less than ± 0.5 kcal/mole. The uncertainties in the heats of formation of the alkyl and alkoxy radicals are generally about 1 to 2 kcal/mole. The largest uncertainties (± 3 kcal/mole) are associated with the mercapto-, methylthio-, and ethylthio-radicals (1). The heats of formation of the alkylthio radicals presented here are self-consistent. If subsequent data suggest a revision of the values for the mercapto-, methylthio-, or ethylthio-radicals, it should only be necessary to adjust the values for the other sulfur-containing radicals by a similar amount.

We thank the National Research Council of Canada and the Faculty of Graduate Studies, University of Manitoba for financial assistance.

1. D. H. Fine and J. B. Westmore. Chem. Commun. 273 (1969).
2. P. Gray and A. Williams. Chem. Rev. **59**, 239 (1959).
3. P. Gray, R. Shaw, and J. C. J. Thynne. Progr. React. Kinet. **4**, 63 (1967).
4. J. A. Kerr. Chem. Rev. **66**, 465 (1966).
5. A. S. Rodgers, D. M. Golden, and S. W. Benson. J. Amer. Chem. Soc. **89**, 4578 (1967).
6. Natl. Bur. Stand. Circ. 500. Washington, D.C. (1952).
7. C. Leggett and J. C. J. Thynne. Trans. Faraday Soc. **63**, 2504 (1967).
8. S. W. Benson. J. Amer. Chem. Soc. **87**, 972 (1965).
9. Peter Gray. Personal communication. (1968).
10. B. A. Thrush. Progr. React. Kinet. **3**, 64 (1965).
11. E. H. Braye, A. H. Sehon, and B. de B. Darwent. J. Amer. Chem. Soc. **77**, 5282 (1955).
12. T. F. Palmer and F. P. Lossing. J. Amer. Chem. Soc. **84**, 4661 (1962).
13. H. Mackle. Tetrahedron, **19**, 1159 (1963).
14. J. H. S. Green. Quart. Rev. **15**, 125 (1961).
15. H. A. Gundry, A. J. Head, and G. B. Lewis. Trans. Faraday Soc. **58**, 1309 (1962).
16. D. R. Stull. Ind. Eng. Chem. **39**, 517 (1947).
17. G. Pilcher, A. S. Pell, and D. J. Coleman. Trans. Faraday Soc. **60**, 499 (1964).
18. E. J. Smutny and A. Bondi. J. Phys. Chem. **65**, 546 (1961).
19. G. Pilcher, H. A. Skinner, A. S. Pell, and A. E. Pope. Trans. Faraday Soc. **59**, 316 (1963).
20. M. Colomina, A. S. Pell, H. A. Skinner, and D. J. Coleman. Trans. Faraday Soc. **61**, 2641 (1965).
21. G. T. Furukawa, D. C. Ginnings, P. E. McCoskey, and R. A. Nelson. J. Res. Natl. Bur. Stand. **46**, 195 (1951).
22. H. Mackle and P. A. G. O'Hare. Tetrahedron, **19**, 961 (1963).
23. J. P. McCullough and W. D. Good. J. Phys. Chem. **65**, 1430 (1961).
24. M. J. S. Dewar and H. N. Schmeising. Tetrahedron, **5**, 166 (1959); **11**, 96 (1960).
25. T. L. Allen. J. Chem. Phys. **31**, 1039 (1959).
26. H. A. Skinner. J. Chem. Soc. 4396 (1962).
27. S. W. Benson. J. Chem. Educ. **42**, 502 (1965).
28. E. J. Harris. Proc. Roy. Soc. London, Ser. A, **173**, 126 (1939).
29. Yu. K. Shaposhnikov and L. V. Kosyukova. Khim. Pererab. Drev. Ref. Inform. No. 3, 6–9 (1965). Chem. Abstr. **66**, 37557*a*.
30. M. H. Back and A. H. Sehon. Can. J. Chem. **38**, 1076 (1960).
31. A. H. Sehon and B. de B. Darwent. J. Amer. Chem. Soc. **76**, 4806 (1956).
32. C. J. Thompson, R. A. Meyer, and J. S. Bell. J. Amer. Chem. Soc. **74**, 3287 (1952).

Can. J. Chem. Downloaded from www.nrcresearchpress.com by 210.87.254.42 on 09/05/12
For personal use only.

Can. J. Chem. Downloaded from www.nrcresearchpress.com by 210.87.254.105 on 09/05/12
For personal use only.

Phosphinohydrazines. Part IV. Coordination compounds of N,N-dimethyl,N′-diphenylphosphinohydrazine and N,N-dimethyl-N′-diphenylthiophosphinatohydrazine[1]

E. W. AINSCOUGH, L. K. PETERSON[2], AND D. E. SABOURIN
Department of Chemistry, Simon Fraser University, Burnaby 2, British Columbia

Received June 16, 1969

A study of complexes of (*a*) N,N-dimethyl,N′-diphenylphosphinohydrazine, DPH, viz., $Pd(DPH)Cl_2$, $Pd(DPH)_2Cl_2$, $[Pd(DPH)_2Cl]ClO_4$, $Pt(DPH)_2Cl_2$, $Pt(DPH)Cl_4$, $Hg(DPH)Cl_2$; (*b*) N,N-dimethyl,N′-diphenylthiophosphinatohydrazine, DPS, viz., $Pd(DPS)Cl_2$, $Pt(DPS)Cl_4$, $Ag(DPS)NO_3$, $Zn(DPS)Cl_2$, $Cd(DPS)Cl_2$, and $Hg(DPS)Cl_2$, and (*c*) N,N-dimethylhydrazine, DMH, viz., $Zn(DMH)_2Cl_2$ and $Cd(DMH)Cl_2$, has been carried out using conductivity, molecular weight, infrared, and nuclear magnetic resonance measurements. DPH functions mostly as a unidentate ligand, with the phosphorus atom as the preferred donor site. Thus $Pd(DPH)Cl_2$ is a chlorobridged dimer in solution in weakly polar solvents, while the monomeric form in polar solvents is of uncertain structure. A *trans*, four-coordinate structure is consistent for $Pd(DPH)_2Cl_2$. For $[Pd(DPH)_2Cl]ClO_4$, however, one DPH ligand is chelating through the phosphorus and terminal nitrogen atoms, while the second ligand is unidentate; the compound is a monomeric uni–univalent electrolyte in nitrobenzene. The ligand DPS appears to chelate via the sulfur and central nitrogen atoms, giving four-membered ring structures; a *cis* configuration is suggested for $Pd(DPS)Cl_2$. $Zn(DMH)_2Cl_2$ is monomeric in solution, with the Me_2N group coordinated to the metal.

Canadian Journal of Chemistry, **48**, 401 (1970)

Discussion

The ligand N,N-dimethyl,N′-diphenylphosphinohydrazine, $Me_2NNHP\Phi_2$, DPH, has three potential donor sites in the P–N–N skeleton, affording a variety of possible modes of unidentate function, as well as bidentate behavior, as a chelating or bridging ligand (1). While chelation requires a four-membered ring structure via the phosphorus and terminal nitrogen atoms, there are two possible bridging modes: the formation of six-atom rings, using P and central N atoms, or eight-atom rings, using P and terminal N atoms. With N,N-dimethyl,N′-diphenylthiophosphinatohydrazine, $Me_2NNHP(S)\Phi_2$, DPS, the three donor sites of the S=P—N—N skeleton are the S and the two N atoms. Possible chelate complexes may exhibit four- or five-membered cyclic structures, depending on the alternative usage of the central or the terminal nitrogen atoms; and there also exists the possibility of bridged, polynuclear complex formation. The "mixed" character of the donor sites, in the sense that P and S are so-called "soft" bases whereas the N atom is "hard" (2), should play a significant role with respect to the nature of the complexes formed.

The synthesis of complexes of DPH and DPS has been reported (1). The DPH molecule is more sensitive to solvolysis than DPS; thus reactions between salts of Zn(II) or Cd(II) and DPH in methanolic solution yield complexes of N,N-dimethylhydrazine, DMH, viz., $Zn(DMH)_2Cl_2$ and $Cd(DMH)Cl_2$. In general, the DPS complexes are much less soluble than the corresponding DPH ones; many physicochemical measurements could not be made because of low solubilities. Molecular weight data given in Table 1 indicate that the complexes $M(DPH)Cl_2$ and $M(DPH)_2Cl_2$ (M = Pd, Pt, Hg) are essentially monomeric in acetone solution. In dibromomethane, two of the complexes, $Pd(DPH)Cl_2$ and $Hg(DPH)Cl_2$, show extensive dimerization.

Assuming a preference for four-coordination for Pd(II) and Pt(II) (3), then the complexes $M(DPH)_2Cl_2$, which are monomeric non-electrolytes in solution, require only monodentate DPH; the possible ligand sites being P, central N, or terminal N. The preferred site may be deduced from the infrared spectra and the chemical shift data pertaining to the free and the complexed ligand. In the free ligand, the N—H stretching vibration occurs at 3190 cm^{-1}; in complexes, the value (3230 cm^{-1}) indicates the absence of coordination by the central nitrogen atom. The Me_2N protons are not deshielded in the complexes (7.8 and 7.9 τ) relative to the value for the free ligand (7.6), indicating the absence of coordination by that site (4). Thus, by elimination, the P atom must be the donor site, a conclusion in agreement with the findings of Nielsen

[1]Presented at the Annual Conference, Chemical Institute of Canada, Montreal, Quebec, May, 1969.
[2]To whom correspondence should be addressed.

TABLE 1

Molecular weight data* for complexes of DPH, DPS, and DMH

Compound†	Molecular weight: Observed: Acetone solution	Molecular weight: Observed: Dibromomethane solution	Molecular weight: Calculated
DPH	248	—	244
DPS	279	—	276
$Pd(DPH)Cl_2$	418	805	421
$Pd(DPH)_2Cl_2$	580	677	666
$[Pd(DPH)_2Cl]ClO_4$	—	390	730
$Pt(DPH)_2Cl_2$	695	—	755
$Hg(DPH)Cl_2$	540	860	516
$Pd(DPS)Cl_2$	448	—	453
$Hg(DPS)Cl_2$	380	447	538
$Zn(DMH)_2Cl_2$	245	—	256

*Measurements were made using a Hitachi Perkin–Elmer Osmometer, Model 115.
†$Pt(DPH)Cl_4$, $Pt(DPS)Cl_4$, $Ag(DPS)NO_3$, $Zn(DPS)Cl_2$, $Cd(DPS)Cl_2$, and $Cd(DMH)Cl_2$ were insoluble. DPH = $Me_2NNHP\Phi_2$; DPS = $Me_2NNHP(S)\Phi_2$; DMH = Me_2NNH_2.

et al. (5) that the P atom is the most basic of the three donor sites of DPH. The appearance of a single ν(Pd—Cl) vibration at 350 cm^{-1} is indicative of a *trans* configuration for $Pd(DPH)_2Cl_2$ (6).

Complexes of the stoichiometry $M(DPH)Cl_2$ (M = Pd, Hg) may maintain four-coordinate metal centers in several ways: (*a*) by the use of chelating DPH; (*b*) by dimerization via bridging DPH, in six-atom (**1**) or eight-atom (**2**) ring structures; and (*c*) by dimerization, via bridging Cl (**3**)

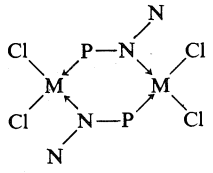

1

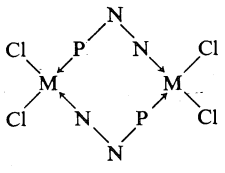

2

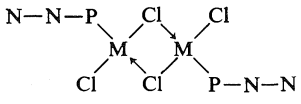

3

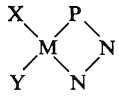

4

where P—N—N = $\Phi_2PNHNMe_2$ = DPH. The complexes $M(DPH)Cl_2$ (M = Pd, Hg) exhibit solvent dependent molecular weights, being monomeric in acetone and dimeric in weakly polar dibromomethane solution. The proton magnetic resonance (p.m.r.) absorptions of monomeric $Pd(DPH)Cl_2$ in acetone or deuterated acetone could not be measured. However, the structure probably involves DPH as a chelating ligand, giving a strained, four-membered cyclic system (**4**, X = Y = Cl), although coordination by a molecule of acetone in a non-chelated complex cannot be discounted entirely. In deuterochloroform and in nitrobenzene, where dimerization is expected to predominate, the chemical shifts for the Me_2N protons of the complex are identical with those for free ligand. The DPH ligand must therefore be monodentate, with dimerization of $M(DPH)Cl_2$ occurring via a chloro-bridging mechanism. Experiments with Fisher–Hirschfelder models indicate that chloro-bridged dimers are readily constructed, whereas bridging by DPH is sterically unfavorable. As described above for the $M(DPH)_2Cl_2$ complexes, the P atom is again the preferred donor site, and the absorptions at 3218 cm^{-1} (M = Pd) and 3250 cm^{-1} (M = Hg) must be due to the uncoordinated N—H grouping.

The compound $[Pd(DPH)_2Cl]ClO_4$ is a uni–univalent electrolyte in solution in nitrobenzene (Table 2), and the observed molecular weight (Calcd., 730, obsd., 390) is consistent with the dissociation of such a monomeric 1:1 electrolyte. For the palladium atom to remain four-coordinate in $[Pd(DPH)_2Cl]^+$, the structure must involve one chelated DPH and one unidentate DPH ligand (**4**, M = Pd, X = DPH, Y = Cl). The p.m.r. absorptions are consistent with this requirement: two bands (at 6.8 and 7.8 τ) are observed, indicating two different functions for the terminal Me_2N groups; the lower field resonance must correspond to the Me_2N group of the chelating DPH ligand. A model of the ion $[Pd(DPH)_2Cl]^+$ can be constructed, although

Can. J. Chem. Downloaded from www.nrcresearchpress.com by 210.87.254.105 on 09/05/12
For personal use only.

TABLE 2

Molar conductivities* of complexes of DPH, DPS, and DMH

Compound	Λ, ohm^{-1} cm^2	Compound	Λ, ohm^{-1} cm^2
$Pd(DPH)Cl_2$	2.0	$Pd(DPS)Cl_2$	3.0
$Pd(DPH)_2Cl_2$	2.5	$Pt(DPS)Cl_4$	Insoluble
$Pt(DPH)_2Cl_2$	2.0	$Ag(DPS)NO_3$	40†
$[Pd(DPH)_2Cl]ClO_4$	27	$Zn(DPS)Cl_2$	1.0
$Hg(DPH)Cl_2$	1.0	$Cd(DPS)Cl_2$	Insoluble
$Pt(DPH)Cl_4$	Insoluble	$Hg(DPS)Cl_2$	3.0
		$Zn(DMH)_2Cl_2$	10.0

*Measured with a radiometer conductivity meter, type CDM2d, using a cell with polished platinum electrodes. Solution concentrations were 10^{-3} *M* in nitrobenzene at 25 °C, unless otherwise specified. The apparatus was standardized using Et_4NClO_4 (Λ, 33 ohm^{-2} cm^2, lit. 33 ohm^{-1} cm^2 (12)).
†In nitromethane solution; the conductivity for a 1:1 electrolyte is 70–100 ohm^{-1} cm^2 (12, 13).

minor bond strain in the four-membered ring is indicated for this structure.

The investigation of complexes of DPS is limited by problems of solubility, hence data on solution properties is quite sparse. Molecular weight data were obtained for two members, thus $Pd(DPS)Cl_2$ is a stable monomer in solution in acetone, whereas $Hg(DPS)Cl_2$ undergoes considerable dissociation in that solvent. The weakening of the P═S bond, in complexes (598–603 cm^{-1}, Table 3) relative to the value in DPS (640 cm^{-1}) is indicative of coordination by the sulfur atom (7). The weakening of the N—H bond (from 3228 cm^{-1} in DPS to 3090–3180 cm^{-1} in complexes) may be indicative of coordination by the central nitrogen (8), in marked contrast to the behavior of DPH, where the central N atom does not coordinate. This bonding arrangement implies chelation by DPS to form a four-membered cyclic structure. Experiments with Fisher–Hirschfelder models show that both four-membered and five-membered chelate complexes may be constructed; the latter involves the terminal N atom (of the Me_2N group) as donor. Unfortunately, the p.m.r. absorptions, which would distinguish the site of coordination, could not be observed. The appearance of two ν(Pd–Cl) vibrations (at 335 and 315 cm^{-1}, Table 3) confirms the *cis* arrangement for the chloro groups (refs. 6*a*, *b*, and pp. 44, 75 of 6*c*) as required by the chelated complex.

The silver complex, $Ag(DPS)NO_3$, exhibits infrared bands at 3160 and 603 cm^{-1}, indicative of coordination by the central N and terminal S atoms, while bands at 1370 and 825 cm^{-1} (9) are evidence for an ionic nitrate grouping. The conductivity (40 ohm^{-1} cm^2, Table 2) is quite low for a simple 1:1 electrolyte; this may be due to ion-pairing effects, or to the formation of a polymeric, two-coordinate silver complex. The latter characteristic may also account for the low solubility of the compound. Molecular weight and p.m.r. data could not be obtained, leaving the problem of the function of the DPS ligand as an open question.

$Zn(DMH)_2Cl_2$ may have a structure similar to that of its cobalt(II) analogue (10). That the NH_2 group is not involved in coordination is shown by the similarity of the infrared spectra (Table 4) of DMH (3228 cm^{-1}) and the complex

TABLE 3

Infrared spectra of complexes of DPS

Compound	ν(N—H), cm^{-1}	ν(P═S), cm^{-1}
DPS	3228(m)	640 s)
$Pd(DPS)Cl_2$	3090(w)	600(s)
$Pt(DPS)Cl_4$	3160(m)	603(s)
$Ag(DPS)NO_3$	3160(m)	600(s)
$Zn(DPS)Cl_2$	3180(m)	603(s)
$Cd(DPS)Cl_2$	3120(m)	600(s)
$Hg(DPS)Cl_2$	3140(w)	598(s)

TABLE 4

Infrared spectra* of complexes of DPH and DMH

Compound	ν(N—H)
DPH	3190(m)
$Pd(DPH)Cl_2$	3218(m)
$Pd(DPH)_2Cl_2$	3230(w)
$Pt(DPH)_2Cl_2$	3230(w)
$[Pd(DPH)_2Cl]ClO_4$	3230(w)
$Hg(DPH)Cl_2$	3250(w)
$Pt(DPH)Cl_4$	3200(w)
Me_2NNH_2, DMH	3228(m)
$Zn(DMH)_2Cl_2$	3245(s), 3175(w)
$Cd(DMH)Cl_2$	3250(m), 3199(w)

*s = strong; m = medium; w = weak; b = broad. Infrared spectra were obtained using a Perkin–Elmer 457 spectrometer fitted with an NaCl prism. The region (600–250) cm^{-1} was scanned using polyethylene film. The substances were examined as mulls in Nujol.

Can. J. Chem. Downloaded from www.nrcresearchpress.com by 210.87.254.105 on 09/05/12
For personal use only.

TABLE 5

Proton magnetic resonance absorption spectra* for N-methyl protons in complexes of DPH and DMH

Compound	$\tau(CDCl_3)$	$\tau(\Phi NO_2)$	Compound	$\tau(CDCl_3)$	$\tau(\Phi NO_2)$
DPH	7.6	7.6	$[Pd(DPH)_2Cl]ClO_4$	6.8, 7.8	6.7, 7.8
$Pd(DPH)Cl_2$	7.9	7.6	$Hg(DPH)Cl_2$	7.6	—
$Pd(DPH)_2Cl_2$	7.8	7.8	Me_2NNH_2, DMH	7.6	7.6
$Pt(DPH)_2Cl_2$	7.9	—	$Zn(DMH)_2Cl_2$	—	6.7

*The spectra were observed in solution in $CDCl_3$ or in ΦNO_2, with $SiMe_4$ as internal standard, using a Varian A56/60 instrument. The N—H protons could not be detected because of the low solubilities of the above compounds.

TABLE 6

Infrared spectra of DMH complexes in Nujol*

Complex	Frequency (cm^{-1})				
$Zn(DMH)_2Cl_2$	3240 (s)	3175 (m)	1588 (s)	1296 (m)	1147 (s)
	1086 (w)	1010 (m)	803 (m)	718 (m)	707 (m)
	555 (w)	412 (s)	295 (s)		
$Cd(DMH)Cl_2$	3255 (s)	3195 (m)	1605 (m)	1590 (s)	1260 (w)
	1224 (w)	1210 (w)	1130 (s)	1115 (s)	1082 (w)
	1008 (m)	980 (w)	950 (w)	820 (s)	720 (m)
	525 (w,b)	440 (s)			

*m = medium, s = strong, w = weak, b = broad.

(3245 and 3175 cm^{-1}) in the ν(N—H) region. Preferential coordination by the Me_2N group has been rationalized as a result of the inductively enhanced basicity of this nitrogen atom (10). Our p.m.r. measurements are consistent with coordination by the Me_2N group, as shown by the deshielding effect in $Zn(DMH)_2Cl_2$ (6.7 τ) relative to the free ligand (7.6 τ, Table 5). The complex is monomeric in solution in acetone and probably has a tetrahedral structure.

Notably, the cadmium complex $Cd(DMH)Cl_2$ has 1:1 metal:ligand stoichiometry; the 1:2 complex analogous to $Cd(N_2H_4)_2Cl_2$ (11) was not obtained in our preparation. $Cd(DMH)Cl_2$ is insoluble, and probably has a polymeric structure. The infrared spectra of the DMH complexes of Zn(II) and Cd(II) are given in Table 6.

The authors are grateful to one of the referees for pointing out an error in our earlier assignment of P=S absorption bands. The financial support of the National Research Council of Canada is acknowledged.

1. E. W. Ainscough, L. K. Peterson, K. I. Thé, and G. L. Wilson. Can. J. Chem. **47**, 3405 (1969).
2. S. Ahrland, J. Chatt, and N. R. Davies. Quart. Rev. London, **12**, 265 (1958).
3. F. A. Cotton and G. Wilkinson. Advanced inorganic chemistry. 2nd ed. Interscience, J. Wiley and Sons, Inc., New York. 1966. p. 1023.
4. (*a*) C. W. Heitsch. Inorg. Chem. **4**, 1019 (1965). (*b*) T. D. Coyle and F. G. A. Stone. J. Amer. Chem. Soc. **83**, 4138 (1961). (*c*) J. M. Miller and M. Onyszchuk. Can. J. Chem. **43**, 1518 (1964).
5. R. P. Nielsen, J. F. Vincent, and H. H. Sisler. Inorg. Chem. **2**, 760 (1963).
6. (*a*) R. J. H. Clark and C. S. Williams. Inorg. Chem. **4**, 350 (1965). (*b*) D. M. Adams, J. Chatt, J. Gerratt and A. D. Westland. J. Chem. Soc. 434 (1964). (*c*) D. M. Adams. Metal–ligand and related vibrations. E. Arnold Ltd., London. 1967. pp. 44, 74.
7. (*a*) M. G. King and G. P. McQuillan. J. Chem. Soc. A 898 (1967). (*b*) P. Nicpon and D. W. Meek. Inorg. Chem. **6**, 145 (1967).
8. (*a*) I. S. Ahuja and P. Rastogi. Inorg. Nucl. Chem. Lett. **5**, 255 (1969). (*b*) G. W. A. Fowles, R. A. Hoodless, and R. A. Walton. J. Chem. Soc. 5873 (1963).
9. (*a*) B. O. Field and C. J. Hardy. Quart. Rev. **18**, 383 (1964). (*b*) C. C. Addison and D. Sutton. Progress in Inorganic Chemistry. *Edited by* F. A. Cotton, Interscience, J. Wiley and Sons, Inc., New York. 1967. Vol. 8, p. 195.
10. D. Nicholls, M. Rowley, and R. Swindells. J. Chem. Soc. A 950 (1966).
11. (*a*) H. Franzen and O. von Mayer. Z. Anorg. Chem. **60**, 247 (1908). (*b*) L. Sacconi and A. Sabatini. J. Inorg. Nucl. Chem. **25**, 1389 (1963).
12. J. R. Hall, M. R. Litzow, and R. A. Plowman. Aust. J. Chem. **18**, 1331 (1965).
13. F. A. Cotton and J. A. McCleverty. Inorg. Chem. **6**, 229 (1967).

Can. J. Chem. Downloaded from www.nrcresearchpress.com by 210.87.254.105 on 09/05/12
For personal use only.

The crystal and molecular structure of $NaBF_3OH$

M. J. R. Clark and H. Lynton
Department of Chemistry, University of New Brunswick, Fredericton, New Brunswick
Received September 15, 1969

The crystal and molecular structure of sodium hydroxytrifluoborate, $NaBF_3OH$, has been established by X-ray analysis. This compound crystallizes in the hexagonal system, space group $P6_3$ with cell parameters $a = 8.08_4$ Å and $c = 7.95_8$ Å. There are 6 molecules in the unit cell. Atomic parameters have been obtained from a block-diagonal least-squares refinement using anisotropic temperature parameters for boron and fluorine, and isotropic temperature parameters for sodium. The final agreement residual for 195 observed reflections is $R = 0.090$.

The $[BF_3OH]^-$ anions are distorted tetrahedra. It was not possible to distinguish between the positions of the fluorine atoms and the isoelectronic hydroxyl group.

Canadian Journal of Chemistry, **48**, 405 (1970)

Can. J. Chem. Downloaded from www.nrcresearchpress.com by 210.87.254.40 on 09/05/12
For personal use only.

Introduction

Sodium hydroxytrifluoborate, $NaBF_3OH$, was first reported to have been prepared by Meerwein and Pannwitz (1) by the reaction of boron trifluoride etherate with an ether suspension of sodium hydroxide. Klinkenberg (2) reported the preparation of the same material by the slow addition of water to a solution of boron trifluoride in absolute ether, the solution containing sodium pellets. Klinkenberg states that the compound he obtained gives an X-ray powder diffraction pattern identical with that given by $NaBF_4$. Klinkenberg further reports that $NaBF_4$ (and by inference, $NaBF_3OH$) crystallizes in the orthorhombic system, space group *Cmcm* and is isomorphous with $NaClO_4$. This result for $NaBF_4$ has since been verified (3–6).

Ryss and Slutskaya (7) more recently have prepared a material with the formula $NaBF_3OH$ by mixing $NaHF_2$ and H_3BO_3 in cold aqueous solution. Since this material has somewhat different properties to those reported by Meerwein and Pannwitz (1) and by Klinkenberg (2), Ryss and Slutskaya have questioned whether the previous investigators had in fact prepared $NaBF_3OH$. Ryss and Slutskaya (7) and Wamser (8) have found that the $[BF_3OH]^-$ ion is rapidly hydrolyzed in the presence of alkali whereas the $[BF_4]^-$ ion is more stable. As Meerwein and Pannwitz and also Klinkenberg prepared their samples under basic conditions, this suggests that these earlier workers must have obtained impure $NaBF_4$.

Aknmanova and Kurilchikova (9) have examined the infrared spectrum of $NaBF_3OH$ as prepared by Ryss and Slutskaya. By comparison with other materials, they have associated certain absorption bands with B—OH, with B—F, and with possible hydrogen bonding.

Experimental

The procedures reported by Meerwein and Pannwitz and by Klinkenberg for the preparation of $NaBF_3OH$ were repeated. In both cases the compound obtained gave an instantaneous precipitate with nitron acetate as do all tetrafluoborate salts (10), and showed the typical infrared absorption bands of tetrafluoborate salts (11). The X-ray powder diffraction patterns of both products corresponded with those of a mixture of $NaBF_4$, H_3BO_3, and NaF.

The procedure of Ryss and Slutskaya was repeated and gave a material which, on analysis, was found to be compatible with the formula $NaBF_3OH$. This material reacted very slowly with nitron acetate and gave an infrared absorption spectrum identical to that reported by Aknmanova and Kurilchikova (9) for $NaBF_3OH$. X-ray examination showed this material to have hexagonal symmetry.

The sodium content of $NaBF_3OH$ was analyzed by use of the anion exchange resin Dowex 2-X and titration with standard HCl solution to a methyl orange end point. The fluorine and boron contents were analyzed by use of the cation exchange resin Dowex 50-X and titration with standard NaOH solution to a first phenolphthalein end point for the fluorine content, and to a second phenolphthalein end point after the addition of mannitol for the boron content. Wamser (12) has described this latter reaction in aqueous solution as

$$HBF_3OH + 2H_2O \rightleftarrows [HBF_2(OH)_2, HBF(OH)_3] \rightleftarrows 3HF + H_3BO_3$$

The boron content was also determined using a Zeiss flame spectrophotometer, the emission line at 521 mμ being examined. The theoretical results for $NaBF_3OH$ (in meq. per g) are: Na, 9.276; F, 27.828; and B, 9.276. The experimental results are: Na, 9.25; F, 27.73; B (volumetric), 9.25; and B (emission), 9.27.

Can. J. Chem. Downloaded from www.nrcresearchpress.com by 210.87.254.40 on 09/05/12
For personal use only.

Crystallographic and Intensity Data

The crystals of $NaBF_3OH$ are needle shaped. Examination with a polarizing microscope establishes the crystals as uniaxial negative with the unique direction along the needle axis.

The crystal data are listed in Table 1. $NaBF_3OH$ shows hexagonal symmetry and the observed systematic absences are compatible with the space groups $P6_3$, $P6_3/m$, and $P6_322$. The crystals of $NaBF_3OH$ show an observable pyroelectric effect on being cooled, eliminating the centrosymmetric space group $P6_3/m$. The results of the structure analysis confirm the assignment of the space group as $P6_3$. Precise cell dimensions were determined from Weissenberg photographs calibrated with aluminum powder.

TABLE 1
Crystal data for $NaBF_3OH$

System	Hexagonal
Space group	$P6_3$
Systematic absences	$00l$: $l = 2n + 1$
Molecular weight	107.8
Unit cell dimensions	
a	8.08_4 Å
c	7.95_8 Å
Volume	450.4 Å^3
Measured density (by flotation)	2.38 g cm^{-3}
Calculated density (assuming 6 molecules in the unit cell)	2.38_5g cm^{-3}
Absorption coefficient (Cu Kα)	40.5 cm^{-1}

Intensity data were collected by the multiple filmpack technique. Equi-inclination Weissenberg photographs were taken of all layers accessible on the c axis and also of the zero layer on the a axis. The crystal used for collection of the c axis data was needle shaped with cross-section 0.2 mm and length 0.8 mm, and the crystal used to collect the a axis data was approximately cube shaped with dimensions 0.2 mm by 0.2 mm by 0.3 mm. The optimum size, $2/\mu$, was calculated to be 0.49 mm. Absorption corrections were made assuming cylindrical shape for the c axis crystal and spherical shape for the for the a axis crystal.

The number of permitted independent reflections for Cu Kα radiation was calculated to be 373 overall and 328 within the range of photographs taken. The number of reflections with intensities above the minimum required for observation was found to be 195. The intensities for all observed reflections were estimated by visual comparison with a calibrated strip prepared using a suitable reflection from the intensity crystals. Lorentz polarization factors were applied to all intensity data. The $0kl$ data was used to put the $hk0$ to $hk6$ data on a common scale.

Structure Determination

Sufficient information for the solution of the projection of the structure on the xy plane was obtained from the following inequality (13)

$$|\hat{F}_{hkl}|^2 \leq \tfrac{1}{6} + \tfrac{1}{6}(-1)^l \hat{F}_{2h,2k,0} + \tfrac{1}{3}\hat{F}_{h-k,h+2k,0} + \tfrac{1}{3}(-1)^l \hat{F}_{h,k,0}$$

The two-dimensional, and then the three-dimensional structures, were refined by Fourier and least-squares techniques[1]. For the refinement by successive cycles of block-diagonal least-squares, only the observed reflections were employed. The quantity minimized was $\sum w(F_o\text{-}F_c)^2$. The weighting scheme $w = 1/[a + |F_o| + c|F_o|^2]$ was used, with $a = 10.0$ and $c = 0.025$. The matrices used were 9×9 for the positional and thermal parameters for the fluorine and boron atoms, and 4×4 for the sodium atoms. For the space group $P6_3$ the anisotropic temperature parameters of an atom lying either on the six-fold or on one of the three-fold axes are interrelated (15): $\beta_{11} = \beta_{12} = \beta_{22} \neq \beta_{33}$; $\beta_{13} = \beta_{23} = 0$. Since the sodium atoms are situated on the six-fold and three-fold axes and because the programs of Ahmed *et al.* (14) do not handle interrelated parameters, it was found convenient to treat the sodium atoms as isotropic.

Since the hydroxyl group could not be distinguished from the isoelectronic fluorine atoms

TABLE 2
Fractional atomic coordinates*

Atom	Fractional atomic coordinates		
	x	y	z
B	3485(22)	3086(21)	2607(34)
F(1)	1539(14)	2268(13)	2380(29)
F(2)	4108(17)	2357(17)	3781(18)
F(3)	3789(17)	2384(17)	0946(18)
F(4)	4379(14)	5117(15)	2563(30)
Na(1)	3333	6667	4495(19)
Na(2)	3333	6667	0581(20)
Na(3)	0000	0000	0000

*All values have been multiplied by 10^4. Estimated standard deviations in parentheses.

[1]All computations were done on an I.B.M. 360/50 computer using programs by Ahmed *et al.* (14).

TABLE 3
Temperature parameters

Atom	Anisotropic* β_{11}	β_{22}	β_{33}	β_{23}	β_{13}	β_{12}	Isotropic, B(Å)^2
B	703	231	265	−997	−732	744	
F(1)	232	372	1449	−246	−613	21	
F(2)	1006	711	679	73	−862	1202	
F(3)	989	640	737	−97	275	539	
F(4)	997	791	1103	−26	435	828	
Na(1)							1.236
Na(2)							0.915
Na(3)							2.884

*Anisotropic values have been multiplied by 10^5. $T = \exp -(h^2\beta_{11} + k^2\beta_{22} + l^2\beta_{33} + kl\beta_{23} + hl\beta_{13} + hk\beta_{12})$.

on the basis of peak heights in an electron density synthesis or from the vibrational amplitudes, the refinement was carried out using the fluorine atomic scattering factor curve only. The atomic scattering factor curve for $F^{-\frac{1}{4}}$ was obtained by interpolation between the curves for F^0 and F^- given in International Tables (16). The atomic scattering factor curves for Na^+ and B^0 were obtained from the same source.

The refinement was taken to be completed when no parameter shift exceeded 0.3 times the estimated standard deviation. The final agreement residual, $R = \sum||F_o| - |F_c||/\sum|F_o|$, for the observed reflections was $R = 0.090$. No correction was made for extinction. A final set of structure factors has been placed in the Depository of Unpublished Data.[2]

Results and Discussion

There are six molecules of $NaBF_3OH$ in the unit cell. Two Na^+ cations lie on the six-fold axis and two on each of the three-fold axes. The atoms composing the $[BF_3OH]^-$ anions all lie in general positions. Three fluorine atoms and a hydroxyl group occupy the apices of a distorted tetrahedron about each boron. Since the hydroxyl group could not positively be distinguished from the fluorine atoms, all positions are called fluorine atoms in the accompanying tables and figure. If the $[BF_3OH]^-$ anions are taken to be spherical, then the structure of $NaBF_3OH$ is a hexagonal close-pack, with Na^+ cations in all the octahedral holes (Fig. 1).

[2]Photocopies may be obtained, free of charge, upon request to: Depository of Unpublished Data, National Science Library, National Research Council of Canada, Ottawa, Canada.

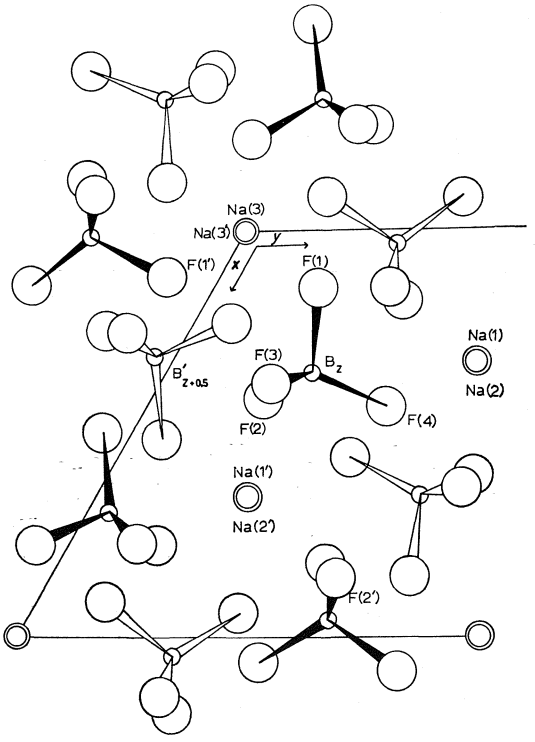

FIG. 1. Illustration of the structure of $NaBF_3OH$ viewed along the c direction.

The final atomic coordinates are given in Table 2, along with their estimated standard deviations. The temperature parameters are shown in Table 3. A detailed analysis of the agreement of individual reflections is summarized in Table 4. Tables 5, 6, and 7 give the important intramolecular and intermolecular distances and angles.

Previous investigators have reported that the difference between the atomic scattering factor

Can. J. Chem. Downloaded from www.nrcresearchpress.com by 210.87.254.40 on 09/05/12
For personal use only.

Can. J. Chem. Downloaded from www.nrcresearchpress.com by 210.87.254.40 on 09/05/12
For personal use only.

TABLE 4

Agreement summary

Category	Limits	Number
Observed reflections		
1	$\|\Delta F\| \leq 1.0\|F_{th}\|$*, or $\|\Delta F\|/\|F_o\| \leq 0.20$	191
2	$\|\Delta F\| \leq 2.0\|F_{th}\|$, or $\|\Delta F\|/\|F_o\| \leq 0.30$	4
3	$\|\Delta F\| \leq 3.0\|F_{th}\|$, or $\|\Delta F\|/\|F_o\| \leq 0.40$	0
4	$\|\Delta F\| > 3.0\|F_{th}\|$, or $\|\Delta F\|/\|F_o\| > 0.40$	0
Total observed reflections		195
	$\|F_o\|_{min}$	4.18
	$\|F_o\|_{max}$	74.41
Unobserved reflections		
1	$\|F_c\| \leq 1.0\|F_{th}\|$	109
2	$\|F_c\| \leq 1.5\|F_{th}\|$	22
3	$\|F_c\| \leq 2.0\|F_{th}\|$	2
4	$\|F_c\| > 2.0\|F_{th}\|$	0
Total unobserved reflections		133
	$\|F_c\|_{max}$	14.88
	$\|F_{th}\|_{min}$	3.22
	$\|F_{th}\|_{max}$	8.99

*$|F_{th}|$ = threshold amplitude.

TABLE 5

Intramolecular distances in the $[BF_3OH]^-$ anion*

Atoms	Distance (Å)
B—F(1)	1.38(2)
B—F(2)	1.33(3)
B—F(3)	1.51(3)
B—F(4)	1.43(2)
F(1)—F(2)	2.33(2)
F(1)—F(3)	2.11(2)
F(1)—F(4)	2.30(2)
F(2)—F(3)	2.27(2)
F(2)—F(4)	2.34(2)
F(3)—F(4)	2.39(2)

*Estimated standard deviations in parentheses.

TABLE 6

Bond angles in the $[BF_3OH]^-$ anion*

Atoms	Angle (degrees)
F(1)—B—F(2)	118.2(1.8)
F(1)—B—F(3)	93.8(1.5)
F(1)—B—F(4)	110.4(1.7)
F(2)—B—F(3)	106.3(1.6)
F(2)—B—F(4)	116.2(1.8)
F(3)—B—F(4)	109.1(1.6)

*Estimated standard deviations in parentheses.

TABLE 7

Nearest intermolecular neighbors*

Atoms	Distance (Å)
F(1) ... Na(3)	2.49(2)
Na(3′)	2.64(2)
F(1′)	2.81(2)
F(2) ... Na(2′)	2.31(2)
F(4′)	3.03(2)
Na(3′)	3.05(1)
F(3) ... Na(1′)	2.36(2)
Na(3)	2.79(1)
F(1′)	3.10(2)
F(4) ... Na(1)	2.39(2)
Na(2)	2.42(1)
F(2′)	3.03(2)

*See Fig. 1. Estimated standard deviations in parentheses.

curves for oxygen and fluorine is insufficient to distinguish between the two species of atoms when eye-estimated data is used (17, 18). Similarly, Burns, Ellison, and Levy (19) were unable to distinguish between the isoelectronic F^- and Na^+ ions even with diffractometer collected data (final agreement residual $R = 0.027$) but resorted to neutron diffraction in order to identify the two species.

The structure obtained for $NaBF_3OH$ was examined for additional information which might locate the hydroxyl group. Examination for evidence of hydrogen bonding was inconclusive. Table 7 shows that only one F—F intermolecular distance is less than 3 Å; this distance is the 2.81 Å between F(1) and F(1′) atoms. This is an acceptable distance for hydrogen bonding, falling within the range of 2.65–3.14 Å reported by Zachariasen (20) for O---H---O in several borates. Nevertheless, similar F—F non-bonding approach distances are found in structures where no hydrogen bonding occurs: $NaBF_4$(6), 2.847 Å and K_3SiF_7(21), 2.84 Å.

An examination of bond lengths in structures containing BF_3X tetrahedra, Table 8, suggests the following order of magnitude for bonds: B—N > B—O > B—F. On this basis, F(3) might be the hydroxyl group. However, least squares refinement of a model with F(3) as the hydroxyl and F(1), F(2), and F(4) as fluorine atoms yielded an agreement residual of $R = 0.127$, compared with $R = 0.090$ for the model where all were taken to be fluorine. By application of the statistical theory of linear hypotheses as described by Hamilton (22), the model with F(3) a hydroxyl group, when compared with the model having

TABLE 8
Boron–fluorine and boron–X bond lengths in some BF_3X tetrahedra*

Compound	Method	Atoms	Bond length (Å)	Reference
$NaBF_4$	X-Ray	B—F	1.366(2) –1.392(2)	6
KBF_4	"	B—F	1.353(11)–1.402(7)	23
$RbBF_4$	"	B—F	1.332(20)–1.427(21)	23
$CsBF_4$	"	B—F	1.294(21)–1.421(12)	23
NH_4BF_4	"	B—F	1.379(7) –1.404(4)	23
$NaBF_4$	n.m.r.	B—F	1.412(15)	24
KBF_4	"	B—F	1.410(15)	24
$RbBF_4$	"	B—F	1.432(15)	24
$CsBF_4$	"	B—F	1.445(15)	24
NH_4BF_4	"	B—F	1.382(6)	24
$Cu(pyO)_4(BF_4)_2$	X-Ray	B—F	1.30 –1.40	25
$Cu(en)_2(BF_4)_2$	"	B—F	1.30(3) –1.41(3)	26
$H_3N{\cdot}BF_3$	"	B—F	1.36(2) –1.39(2)	27
		B—N	1.60(2)	
$H_3CN_2N{\cdot}BF_3$	"	B—F	1.37(2) –1.38(2)	28
		B—N	1.58(2)	
$(H_3C)_3N{\cdot}BF_3$	"	B—F	1.39(3)	29
		B—N	1.585(30)	
$H_3CCN{\cdot}BF_3$	"	B—F	1.32(2)	30,31
		B—N	1.64(2)	
$BF_3{\cdot}2H_2O$	"	B—F	1.340(10)–1.402(10)	17
		B—O	1.565(10)	17
$(CH_3)_2O{\cdot}BF_3$	Electron diffraction	B—F	1.43(3)	32
		B—O	1.50(6)	

*Estimated standard deviations in parentheses.

all fluorine, was found to be rejected at a confidence level better than 99.5%. Models involving the other possible hydroxyl group positions were similarly examined, but were neither significantly favored nor disfavored when compared with the model having all fluorine. The possibility of a random structure cannot be discounted.

We acknowledge the financial support of the National Research Council of Canada for this work.

1. H. Meerwein and W. Pannwitz. J. Prakt. Chem. **141**, 123 (1934).
2. K. J. Klinkenberg. Rec. Trav. Chim. **56**, 36 (1937).
3. A. Bellanca. Rend. Soc. Mineral. Ital. **3**, 20 (1946).
4. Von E. Höhne and L. Kutschabsky. Z. Anorg. Allgem. Chem. **344**, 279 (1966).
5. A. Weiss and K. Zohner. Phys. Stat. Sol. **21**, 257 (1967).
6. G. Brunton. Acta Cryst. **B24**, 1703 (1968).
7. I. G. Ryss and M. M. Slutskaya. J. Gen. Chem. U.S.S.R. **22**, 45 (1952).
8. C. A. Wamser. J. Amer. Chem. Soc. **70**, 1209 (1948).
9. M. V. Aknmanova and G. E. Kurilchikova. Opt. Spectrosc. **8**, 498 (1960).
10. D. R. Martin and J. K. Riecke. J. Amer. Chem. Soc. **73**, 5895 (1951).
11. G. L. Coté and H. W. Thompson. Proc. Roy. Soc. London, **210**, 217 (1951).
12. C. A. Wamser. J. Amer. Chem. Soc. **69**, 409 (1947).
13. D. Harker and J. S. Kasper. Acta Cryst. **1**, 70 (1948).
14. F. R. Ahmed, S. R. Hall, C. P. Huber, and M. E. Pippy. N.R.C. Crystallographic programs for the I.B.M./360 system. Division of Pure Physics and Pure Chemistry, National Research Council, Ottawa, Canada.
15. W. J. A. M. Peterse and J. H. Palm. Acta Cryst. **20**, 147 (1966).
16. International tables for X-ray crystallography. Vol. III. The Kynoch Press, Birmingham, England. 1962. Table 3.3.1.A.
17. W. B. Bang and G. B. Carpenter. Acta Cryst. **17**, 742 (1964).
18. S. Anderson and J. Galy. Acta Cryst. **B25**, 847 (1969).
19. J. H. Burns, R. D. Ellison, and H. A. Levy. Acta Cryst. **B24**, 230 (1968).
20. W. H. Zachariasen. Acta Cryst. **16**, 385 (1963).
21. D. L. Deadmore and W. F. Bradley. Acta Cryst. **15**, 186 (1962).
22. W. C. Hamilton. Acta Cryst. **18**, 502 (1965).
23. M. J. R. Clark and H. Lynton. Can. J. Chem. **47**, 2579 (1969).
24. H. J. C. Yeh and J. L. Ragle. J. Phys. Chem. **72**, 3688 (1968).
25. D. S. Brown, J. D. Lee, and B. G. A. Melsom. Chem. Commun. 852 (1968).
26. D. S. Brown, J. D. Lee, and B. G. A. Melsom. Acta Cryst. **B24**, 730 (1968).
27. J. L. Hoard, S. Geller, and W. M. Cashin. Acta Cryst. **4**, 396 (1951).
28. S. Geller and J. L. Hoard. Acta Cryst. **3**, 121 (1950).
29. S. Geller and J. L. Hoard. Acta Cryst. **4**, 399 (1951).
30. J. L. Hoard, T. B. Owen, A. Buzzell, and O. N. Salmon. Acta Cryst. **3**, 130 (1950).
31. J. L. Hoard, S. Geller, and T. B. Owen. Acta Cryst. **4**, 405 (1951).
32. S. H. Bauer, G. R. Finlay, and A. W. Laubengayer. J. Amer. Chem. Soc. **67**, 339 (1945).

Can. J. Chem. Downloaded from www.nrcresearchpress.com by 210.87.254.40 on 09/05/12
For personal use only.

Can. J. Chem. Downloaded from www.nrcresearchpress.com by 210.87.254.105 on 09/05/12
For personal use only.

Infrared and Raman spectra of liquid and crystalline silicon tetrafluoride[1]

F. BESSETTE[2] AND A. CABANA
Département de chimie, Université de Sherbrooke, Sherbrooke, Québec

AND

R. P. FOURNIER AND R. SAVOIE
Département de chimie, Université Laval, Québec 10, Québec

Received August 29, 1969

The Raman and infrared spectra of liquid and crystalline SiF_4 have been recorded. The assignment of some of the Raman bands of the crystal to longitudinal modes has been confirmed by the infrared reflection spectrum. These indicate that the crystal structure is not centrosymmetric. In other respects the spectra are also more complicated than is expected on the basis of the previously reported T_d^3 structure. Possible explanations are discussed.

On a enregistré les spectres Raman et infrarouges de SiF_4 dans ses états condensés. Certaines bandes Raman du cristal, attribuées à des modes longitudinaux de par le spectre de réflexion infrarouge, indiquent que la structure du cristal n'est pas centrosymétrique. Les spectres sont par ailleurs plus compliqués que ceux prédits d'après la structure cristalline T_d^3 proposée antérieurement. On apporte quelques explications à ces anomalies.

Canadian Journal of Chemistry, **48**, 410 (1970)

Introduction

The SiF_4 molecule has a tetrahedral structure, as indicated by the number of observed fundamentals in the Raman (1) and infrared (1–4) spectra of the gas. Only early Raman studies of the liquid are available (5, 6). This silicon halide is interesting because the large difference in electronegativities of Si (1.8 in the Pauling scale) and of F (4.0) makes it one of the most nearly ionic volatile compounds. At 1 atm pressure, SiF_4 sublimes at -95.7 °C: its triple point is at -90.2 °C and 1318 mm Hg (6).

A compression study of silicon tetrafluoride has shown that no phase transition occurs in the solid above -175 °C (7). X-Ray diffraction studies of the crystalline powder (8) and of a single crystal (9) indicate a body-centered cubic lattice of space group T_d^3 ($I\bar{4}3m$), with the molecules on sites of T_d symmetry. No splitting of the vibrational fundamentals is predicted for this structure because of the high local symmetry and the presence of only 1 molecule per primitive cell. However, Hexter (10) has observed a splitting of the infrared ν_3 band of this solid (unpublished results). This is inconsistent with the T_d^3 structure, but Fox and Hexter (11) suggested that a crystal shape effect could be responsible for this unexpected splitting. The present study was aimed at clarifying this point and also at comparing the spectra of SiF_4 with those of CF_4, a similar compound recently studied by us (12).

Experimental

The silicon tetrafluoride used in these experiments was obtained from Matheson of Canada Ltd. The gas, stated to be 99.6% pure, contained traces of SO_2, CO_2, and $SiOF_2$. These impurities were partly removed by trap-to-trap distillations and did not interfere with the present spectra.

The infrared spectra were recorded on Perkin–Elmer Models 621 and 125 spectrometers. These instruments were calibrated with standard gas samples and the frequency accuracy ranged from ± 0.5 to ± 2 cm^{-1}, depending on the sharpness of the bands. Two different techniques were used for the preparations of the samples. The ν_1 region was studied with a variable-thickness cell equipped with Irtran-2 windows spaced 0.3 or 1 mm apart. The gas was first condensed to a liquid from which the crystal was slowly grown. The spectra of the ν_3 and ν_4 regions could not be obtained with the closed cell, since the pressure necessary to condense the gas was sufficient to push the windows apart to such an extent that complete absorption occurred. For that reason the spray-on technique had to be used, but great care was taken to properly anneal the microcrystals thus obtained. The spectra were recorded at -175 °C, liquid nitrogen, and liquid helium temperatures using a helium Dewar of conventional design. The temperatures were measured with a carbon resistor or copper–constantan thermocouple embedded in the sample cell.

[1]Work supported, in part, by the Defence Research Board of Canada (Grant No. 9511-67).

[2]Present address: Department of Chemistry, University of Reading, Reading, England.

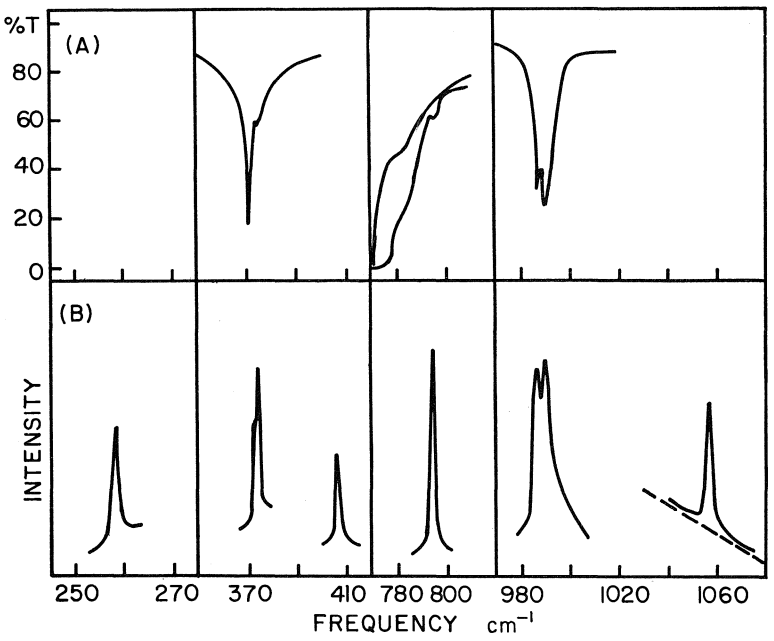

FIG. 1. Infrared (*A*) and Raman (*B*) spectra of crystalline SiF_4 at liquid-nitrogen temperature (77 °K). The infrared spectrum of the ν_1 region (795 cm^{-1}) was recorded with samples 0.3 and 1 mm thick.

The reflection spectra were recorded using a Perkin–Elmer Model 621 spectrometer equipped with additional optics as previously described (13). In the ν_3 region identical results were obtained from solids prepared either by the spray technique or in the closed cell. The ν_4 region could only be studied with samples prepared by the first method because of the strong reflectivity of the Irtran-6 windows. Difficulties were also experienced in trying to determine the exact reflection intensity; since an absolute scale was not necessary in this study, only relative figures were obtained.

The Raman spectra were recorded on a Cary Model 81 spectrometer equipped with a Toronto arc source. The instrument was carefully calibrated with various discharge lamps and the frequencies reported in this paper should be accurate to ± 1 cm^{-1} for sharp peaks. The crystalline samples were obtained by slowly cooling the liquid in a 20 mm o.d. Pyrex cell. This cell, containing a ~50 mm long polycrystalline mass, was sealed and placed in the tail section of a L-shaped Dewar for the spectra at liquid nitrogen temperature. The spectrum of the liquid was obtained with a straight Dewar (14), the temperature and the pressure being carefully monitored by a copper–constantan thermocouple and a monel Bourdon pressure gauge. Cold nitrogen gas was used to maintain the temperature at about −85 °C, which led to a sample pressure of about 2 atm.

The rather peculiar way in which SiF_4 was (visually) observed to crystallize from the melt in the preparation of our samples is worth mentioning. The first solid to be formed was usually quite transparent but cracked shortly thereafter, possibly as a result of thermal strains. On the other hand, it is also possible that SiF_4 first crystallizes as a disordered solid and that a phase transition occurs in the solid at a temperature very close (a fraction of a degree) to the melting point. We were unable to obtain spectroscopic evidence for the existence of this disordered phase which would make SiF_4 similar in its behavior to other related molecules (e.g. CF_4).

Results and Discussion

A. Infrared and Raman Spectra of Crystalline SiF_4

The Raman and the infrared absorption spectra of crystalline SiF_4 at liquid nitrogen temperature are shown in Fig. 1. Observed frequencies at maximum intensity are summarized in Table 1. The ν_2 region was not investigated in the infrared for lack of suitable windows for the closed cell. Fortunately, this band will not prove useful in the discussion that follows. The ν_1 infrared band at 795 cm^{-1} is seen as a very weak shoulder on the high-frequency side of the overtone $2\nu_4$ which absorbs strongly with a crystal 1 mm thick. The splitting of ν_3, first reported by Hexter (10), is clearly observed in both the infrared and Raman spectra at 987.7 and 991.2 cm^{-1}. The ν_4 band is also split (370.3/373.7 cm^{-1}) and it is clear (see Table 1) that these doublets have essentially identical frequencies in the two

Can. J. Chem. Downloaded from www.nrcresearchpress.com by 210.87.254.105 on 09/05/12
For personal use only.

TABLE 1

Vibrational frequencies (cm^{-1}) of gaseous, liquid, and solid SiF_4

Gas (ref. 1)		Liquid	Solid		
Infrared	Raman	Raman	Infrared	Raman	Assignment
—	268	269	—	258.3	ν_2
391	390	384	370.3 373.7	370.6 373.3	ν_4 transverse
—	—	—	~407	407.5	ν_4 longitudinal
—	800	799	795	795.3	ν_1
1031	1010	1006	987.7 991.2	987.8 991.3	ν_3 transverse
—	—	—	~1055	1057.3	ν_3 longitudinal

types of spectra. On the other hand, ν_1 and ν_2 give rise to very sharp Raman singlets. Finally, two unexpected bands which have no infrared counterparts are observed in the Raman spectrum at 407 and 1057 cm^{-1}.

The infrared and Raman bands of solid SiF_4 are narrow and thus characteristic of an ordered crystal. However, there is some disagreement between the observed splittings and the reported crystal structure. In particular, the splitting of the triply degenerate fundamentals normally indicates that the molecules are located on sites of symmetry lower than T_d or that the primitive cell of the crystal contains more than one molecule (15, 16). We will now briefly consider other possible causes for these discrepancies.

Fox and Hexter (11) explained the splitting of ν_3 in solid SiF_4 as a "crystal-shape splitting". Their calculations based on the transition-dipole–transition-dipole interaction model showed that the sample shape could influence the multiciplicity of a vibrational band in molecular crystals, when the particle size is much greater than the lattice parameters but much smaller than the wavelength of the exciting radiation. It is known that crystallites prepared by the spray technique might be of appropriate size for this effect to be felt, whereas crystals grown slowly from the liquid would not, especially not in the Raman effect where the wavelength of the exciting radiation (4358 Å) is 20 times smaller than in the infrared. The fact that the infrared spectrum of a sample prepared by the spray technique is very similar to the Raman spectrum of a crystal grown from the melt argues against the explanation given above for the splitting of the ν_3 and ν_4 bands of solid SiF_4.

In a discussion of the effect of lattice vibrations on the internal modes of molecular crystals, Hornig (15) has pointed out that the local symmetry in a crystal may be reduced when the molecules are displaced from their equilibrium positions during the cycle of a lattice vibration. This may lead to a splitting of the degenerate vibrational modes. Specifically, in the case of a site symmetry T_d, the F_2 internal modes are predicted to be split through anharmonic coupling with translational modes, whereas the E mode should not be split, which is exactly what is observed in the present spectra. However, the magnitude of such splitting should be linear in the amplitude of the lattice vibrations and should, therefore, be reduced as the temperature is lowered. The fact that the splitting of ν_3 remained unchanged in infrared spectra recorded at liquid nitrogen and helium temperatures indicates that such an effect is not responsible for the splittings observed in the spectra of crystalline SiF_4.

B. Piezoelectric Nature of Crystalline SiF_4

We have mentioned previously that two unexpected peaks have appeared in the Raman spectrum of the solid: one at 1057.3 cm^{-1}, located about 67 cm^{-1} on the high-frequency side of ν_3 and one at 407.5 cm^{-1}, about 35 cm^{-1} away from ν_4. Given the large frequency difference, it is very unlikely that these features result from crystal field effects and they are most probably longitudinal components associated with each of the two F_2 modes. Longitudinal and transverse waves propagate with different frequencies in cubic or uniaxial crystals, the longitudinal component having the higher frequency

Can. J. Chem. Downloaded from www.nrcresearchpress.com by 210.87.254.105 on 09/05/12
For personal use only.

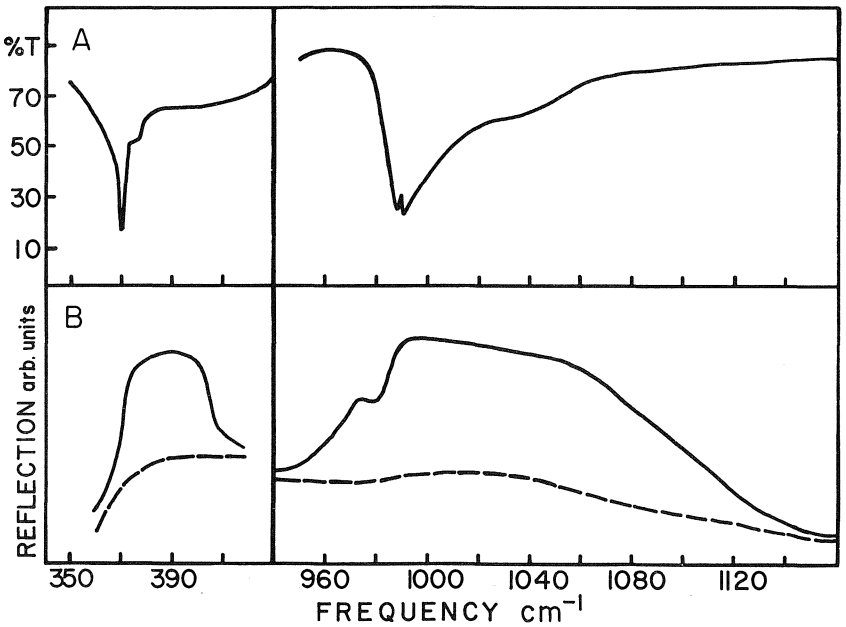

FIG. 2. Infrared absorption and reflection spectra of thick layers of SiF_4 in the ν_3 and ν_4 regions.

(17, 18). Only transverse modes should be seen in infrared absorption spectra at normal incidence, but both may be observed in Raman spectra (17, 19).

The foregoing interpretation can easily be verified, since strong infrared absorption bands are usually complicated by a reflection shoulder extending to the longitudinal frequency ν_l (20, 21), a phenomenon which, however, should not be observed if the sample thickness is less than one wavelength of the incident radiation (22). This behavior is well illustrated in Fig. 1 where a sample less than 1 μ thick was used. When the thickness is increased, reflection shoulders appear on the high-frequency side of ν_3 and ν_4 (see Fig. 2*A*). This has been confirmed by the pure reflection spectrum (Fig. 2*B*) in which it is seen that the reflection bands are approximately limited by the transverse (ν_t) and longitudinal (ν_l) frequencies.

The direct observation of longitudinal modes in Raman spectra is of interest since the frequency difference $\nu_l - \nu_t$ is related (21) to the dipole derivative $\delta\mu/\delta Q$ by the equation

$$\frac{\delta\mu}{\delta Q} = \pm \frac{3n_0}{n_0^2 + 2}\left(\frac{\pi(\nu_l^2 - \nu_t^2)}{N}\right)^{\frac{1}{2}}$$

in which n_0 is the refractive index at higher frequencies and N the number of oscillators per cm^3. From this equation, using the results of X-ray diffraction studies (8, 9) to determine N and setting n_0 at an estimated value of 1.4, we calculate $\delta\mu/\delta Q_3 = \pm 186.6$ and $\delta\mu/\delta Q_4 = \pm 83.3$ ($cm^{3/2}\ s^{-1}$). These values are quite close to those obtained for gaseous SiF_4 (23) (± 167.4 and $\pm 73.4\ cm^{3/2}\ s^{-1}$), considering that the above formula is only approximate (24). Perhaps more significant is the fact that the ratio $\delta\mu/\delta Q_3 / \delta\mu/\delta Q_4$ obtained by us (2.24) is almost identical to that for the gas phase (2.29).

The presence of longitudinal components in the Raman spectrum of crystalline SiF_4 has important implications as to the crystal structure of this compound. Since $\nu_l \neq \nu_t$ only if $\delta\mu/\delta Q \neq 0$, i.e. if the band is also infrared-active, the crystal has to be noncentrosymmetric and thus piezoelectric. It is clear that the infrared and Raman bands would then have identical frequencies since they correspond to identical vibrations. This is shown to be the case in Table 1.

C. Possible Structures of Crystalline SiF_4

We now search for space groups consistent with our spectroscopic data. It is unlikely that the structure deduced from X-ray scattering experiments could be seriously in error and thus it is

Can. J. Chem. Downloaded from www.nrcresearchpress.com by 210.87.254.105 on 09/05/12
For personal use only.

TABLE 2

Correlation diagrams for site and factor groups consistent with the vibrational spectra of crystalline SiF_4

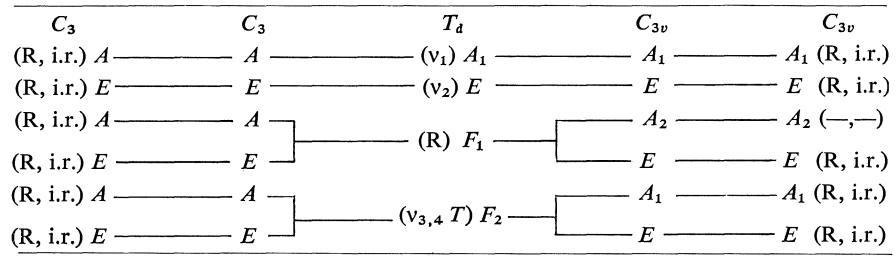

expected that these space groups would be somewhat related to T_d^3. The spectra of SiF_4 bear some resemblance with those of CF_4, which we have recently studied (12). Working along the same line, we search for possible combinations of site and factor groups (15, 16) yielding two active Raman components for the F_2 modes and only one for the A_1 and E modes. This procedure is somewhat simplified since only noncentrosymmetric structures need be considered. Only two sets of groups predict the observed Raman spectrum; these are the C_3 and C_{3v} factor groups with C_3 and C_{3v} site groups, respectively. The correlation diagrams for both combinations (Table 2) also indicate that the infrared spectrum should consist of doublets for ν_3 and ν_4 and that the ν_1 band should be active in the solid, in agreement with our results. The observation of two infrared and Raman lattice modes would point to a C_3 structure since only one band is predicted for the more symmetrical C_{3v} lattice. Unfortunately, these low frequency modes are expected to be extremely weak and have not been detected.

The availability of C_3 and C_{3v} sites in the various space groups of the C_3 and C_{3v} crystallographic classes (25) leaves only 5 possible space groups: C_3^1, C_3^4, C_{3v}^1, C_{3v}^2, and C_{3v}^5. We can go one step further in our deductions by assuming that the actual structure is close to the *bcc* structure deduced from X-ray diffraction studies (8, 9). It should then be possible to transform the C_3 or C_{3v} lattice into a *bcc* structure by a particular choice of parameters. This can be easily done, for example by choosing a rhombohedral unit cell with an angle of 109° 28′, in which case the side dimension of the cubic cell obtained is $2/\sqrt{3}$ that of the rhombohedron. However, such a transformation would require the molecules to occupy 3 inequivalent sets of sites in the C_3^1, C_{3v}^1, and C_{3v}^2 unit cells (25) and these space groups are therefore rejected.

Although our discussion is becoming more and more speculative, we can compare the molecular packing in the remaining C_3^4 and C_{3v}^5 space groups. Again, trying to reconcile our results and those obtained from X-ray studies, the trigonal structures can be obtained from the *bcc* lattice either by distorting the crystal along a given C_3 axis or by rotating the individual molecules about such an axis. This latter possibility is interesting since the silicon atoms are then left in their *bcc* positions. The variations of some characteristic intermolecular F . . . F distances with the angle of rotation are shown in Fig. 3. It is seen that many curves meet at 2.99 Å in the T_d^3 structure. The packing in the C_{3v}^5 structure obtained by rotating the molecules by 60° looks as good as in T_d^3, although it seems surprising that X-ray studies could have failed to distinguish between these two structures. Molecular rotations through any angle different than 0 or 60° leads to C_3^4 structures which are not very stable, except near 0 and 60°, in view of some rather short F . . . F distances.

In brief, the present results could be interpreted on the basis of a C_3^4 or C_{3v}^5 crystal structure which could be very similar to the cubic structure found after X-ray studies. However, it seems that a significant departure from cubic symmetry would be needed to account for the splittings in the infrared and Raman spectra. Nevertheless the possibility of an erroneous X-ray crystal structure is considered to be a more likely

Can. J. Chem. Downloaded from www.nrcresearchpress.com by 210.87.254.105 on 09/05/12
For personal use only.

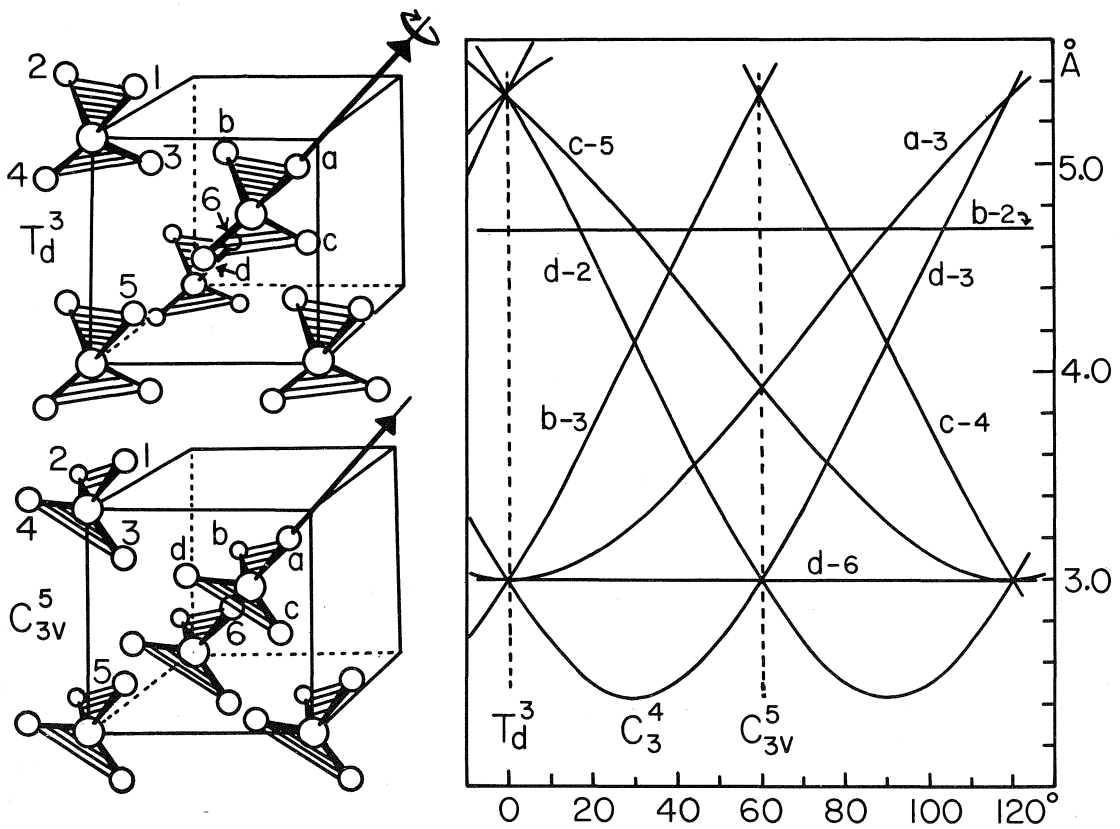

FIG. 3. Variation of F . . . F distances of SiF_4 molecules as a function of rotation about a C_3 axis in a *bcc* unit cell.

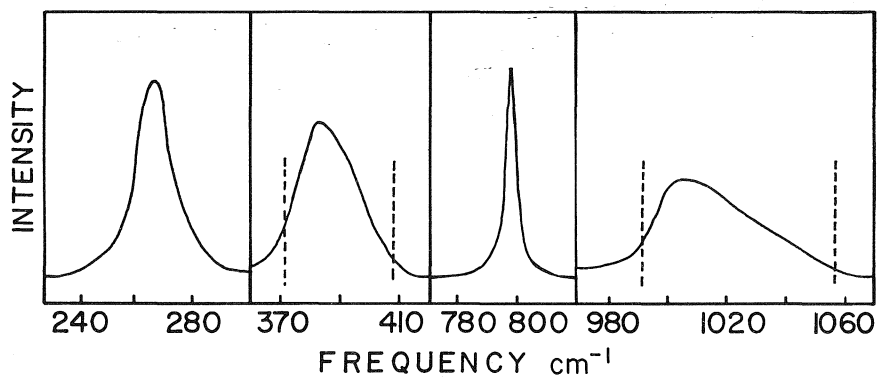

FIG. 4. Raman spectrum of liquid SiF_4 at −85 °C. The dotted lines indicate the transverse (ν_t) and longitudinal (ν_l) frequencies in the crystal.

explanation than those discussed in section A. A careful reinvestigation of the crystal structure of solid SiF_4 is therefore suggested.

D. Raman Spectrum of Liquid SiF_4

The Raman spectrum of liquid SiF_4 at −85 °C is reproduced in Fig. 4. Frequencies at maximum intensity are presented in Table 1. The bands are of course much broader than in the solid, except for ν_1 which is only slightly influenced by the physical state.

With such a spectrum, one is tempted to try to

Can. J. Chem. Downloaded from www.nrcresearchpress.com by 210.87.254.105 on 09/05/12
For personal use only.

relate band shapes and widths to the degree of free molecular rotation in the liquid. Although these properties are closely related, it is clear that another effect is playing a very important role in this case. The spectrum shows that each of the ν_3 and ν_4 bands is unsymmetrical, with a high-frequency tail extending approximately to the longitudinal frequency of the solid. In fact, the bands in the liquid are seen to be limited by the ν_t and ν_l frequencies observed in the spectrum of the crystal. A similar phenomenon has been observed in the case of ν_3 of CF_4 (12). This behavior ought to be frequent in Raman spectra of liquids, although it is directly observable only when $\delta\mu/\delta Q$ is sufficiently large to produce a noticeable asymmetry in band shapes. It should be pointed out that great care should be exercised when rotational correlation functions are calculated from infrared or Raman bands of pure liquids. In the infrared, it is obvious that one should correct for the reflection superimposed on the absorption spectrum; fortunately that type of correction is easily carried out. In the Raman, one should correct for the influence of the liquid structure on the scattering, such as that described above. To our knowledge, no mention of this difficulty has been presented previously and evidently no way of overcoming it has been suggested.

The authors wish to thank the National Research Council of Canada for grants in support of research and for the award of post-graduate scholarships to two of us (F.B. and R.P.F.).

1. E. A. JONES, J. S. KIRBY-SMITH, P. J. H. WOLTZ, and A. H. NIELSEN. J. Chem. Phys. **19**, 242 (1951).
2. C. R. BAILEY, J. B. HALE, and J. W. THOMPSON. Proc. Roy. Soc. London, Ser. A, **167**, 555 (1938).
3. P. J. H. WOLTZ, E. A. JONES, and A. H. NIELSEN. Phys. Rev. **79**, 416 (1950).
4. J. HEICKLEN and V. KNIGHT. Spectrochim. Acta, **20**, 295 (1964).
5. D. M. YOST, E. N. LASSETTRE, and S. T. GROSS. J. Chem. Phys. **4**, 325 (1936). Unpublished results of Best and Trampe, as reported by D. M. Yost, Proc. Indian Acad. Sci. Sect. A, **8**, 333 (1938).
6. W. I. PATNODE and J. PAPISH. J. Phys. Chem. **34**, 1494 (1930).
7. J. W. STEWART. J. Chem. Phys. **33**, 128 (1960).
8. G. NATTA. Gazz. Chim. Ital. **60**, 911 (1930).
9. M. ATOJI and W. N. LIPSCOMB. Acta Cryst. **7**, 597 (1954).
10. R. M. HEXTER. J. Chem. Phys. **37**, 1347 (1962).
11. D. Fox and R. M. HEXTER. J. Chem. Phys. **41**, 1125 (1964).
12. R. P. FOURNIER, R. SAVOIE, F. BESSETTE, and A. CABANA. J. Chem. Phys. **49**, 1159 (1968).
13. F. BESSETTE and A. CABANA. Spectrochim. Acta, **25A**, 157 (1969).
14. J. S. KITTELBERGER and D. F. HORNIG. J. Chem. Phys. **46**, 3099 (1967). R. SAVOIE and M. PÉZOLET. Can. J. Chem. **45**, 1677 (1967).
15. D. F. HORNIG. J. Chem. Phys. **16**, 1063 (1948).
16. R. S. HALFORD. J. Chem. Phys. **14**, 8 (1946). H. WINSTON and R. S. HALFORD. J. Chem. Phys. **17**, 607 (1949).
17. L. COUTURE-MATHIEU, H. POULET, and J. P. MATHIEU. C. R. **234**, 1761 (1952).
18. L. COUTURE-MATHIEU and J. P. MATHIEU. C. R. **235**, 371 (1953).
19. C. HAAS. Spectrochim. Acta, **8**, 19 (1956).
20. J. A. A. KETELAAR, C. HAAS, and J. FAHRENFORT. Physica, **20**, 1259 (1954).
21. C. HAAS and D. F. HORNIG. J. Chem. Phys. **26**, 707 (1957).
22. C. KITTEL. Introduction to solid state physics. 3rd ed. John Wiley and Sons, Inc., New York. 1966.
23. P. N. SCHATZ and D. F. HORNIG. J. Chem. Phys. **21**, 1516 (1953).
24. G. A. ANDERMANN and D. A. DOWS. J. Phys. Chem. Solids, **28**, 1307 (1967).
25. International tables for X-ray crystallography. Vol. 1. *Edited by* N. F. M. Henry and K. Lonsdale. Kynoch Press, Birmingham, England. 1952.

Can. J. Chem. Downloaded from www.nrcresearchpress.com by 210.87.254.105 on 09/05/12
For personal use only.

^{60}Co γ-radiolysis of oxygenated aqueous solutions of cysteine at p*H* 7

J. E. PACKER AND R. V. WINCHESTER[1]
Department of Chemistry, University of Auckland, Auckland, New Zealand

Received August 5, 1969

In the radiolysis of oxygenated aqueous solutions of cysteine (RSH) at p*H* 7, short chain reactions occur yielding cystine (RSSR) and hydrogen peroxide. Two competing reaction paths involving reaction of the thiyl radical (RS·) with oxygen or thiol anion (RS^-) are postulated to explain the results.

Canadian Journal of Chemistry, **48**, 417 (1970)

Can. J. Chem. Downloaded from www.nrcresearchpress.com by 210.87.254.40 on 09/05/12
For personal use only.

Introduction

Recently comprehensive studies (1, 2) have elucidated the radiation chemistry of oxygen-free aqueous solutions of cysteine. In view of the great interest in the role of this compound in biological systems and as a radiation protecting agent it is surprising that so little has been reported on oxygenated solutions (3, 4). The main reported effect of oxygen is an enhanced loss of thiol. This paper gives our results of a more extensive investigation at the physiologically interesting p*H* of 7, and our findings have caused us to extend our studies to other p*H*'s, this latter work now being in progress.

Results and Discussion

In the absence of oxygen, reactions [1]–[5] account for the reported results from steady-state radiolysis (1, 2) and reaction [6] has been shown to occur by pulsed radiolysis techniques.[2]

[1] $$RSH + \cdot OH \rightarrow RS\cdot + H_2O$$

[2] $$RSH + e_{aq}^- \rightarrow R\cdot + HS^-$$

[3a] $$RSH + H\cdot \nearrow RS\cdot + H_2$$

[3b] $$RSH + H\cdot \searrow R\cdot + H_2S$$

[4] $$R\cdot + RSH \rightarrow RH + RS\cdot$$

[5] $$2RS\cdot \rightarrow RSSR$$

[6] $$RS\cdot + RS^- \rightleftarrows RSSR^-$$

The transient $RSSR^-$ disappears by reactions [−6] and [5]. A detailed study of the kinetic behavior of this transient for cysteamine has been reported (4), and the authors indicate that the cysteine (RSH) system behaves in a similar manner.[3]

At p*H* 7, in the presence of oxygen, we find a decrease in $G(H_2S)$ which is explained in terms of oxygen competing for e_{aq}^-

[7] $$e_{aq}^- + O_2 \rightarrow O_2^-$$

A plot of $1/G(H_2S)$ vs. $[O_2]/[RSH]$ is linear, with intercept of 0.36 and slope 1.36, from which $G_{e_{aq}^-} = 2.8$ and $k_7/k_2 = 3.8$. As $k_7 = 1.88 \times 10^{10}$ $M^{-1}\,s^{-1}$ (ref. 6), we find $k_2 = 4.9 \times 10^9$ $M^{-1}\,s^{-1}$, which may be compared with 4.4×10^9 and 5.4×10^9 found by Trumbore and co-workers (2) using nitrate and acetone, respectively, in place of oxygen, 1.1×10^{10} found by Armstrong and co-workers (1) using H^+ as competing scavenger, and 8.7×10^9 $M^{-1}\,s^{-1}$ found by Braams (7) using pulse radiolysis.

The data in Table 1 illustrate the main features of the system at p*H* 7.

The presence of oxygen causes a marked increase in G(—RSH), G(RSSR), and $G(H_2O_2)$. At lower initial oxygen concentrations and higher initial cysteine concentrations, G(—RSH) = $2G$(RSSR) + $G(H_2S)$, showing that no other sulfur-containing products are formed. Where this sulfur balance holds, G(—RSH) is almost independent of oxygen concentration but decreases with decreasing cysteine concentration. At lower cysteine and higher oxygen concentrations the above sulfur balance is lost, G(—RSH) being greater than $2G$(RSSR) + $G(H_2S)$, implying the formation of products with sulfur in a higher oxidation state. G(—RSH) also decreases under these conditions.

In an unbuffered solution of 4.4×10^{-3} M cysteine hydrochloride, it was previously found

[1]Present address: Division of Biology, National Research Council of Canada, Ottawa 7, Canada, where requests for reprints should be sent.

[2]G. S. McNaughton, private communication.

[3]G. E. Adams and G. S. McNaughton, private communication.

TABLE 1

Yields from ^{60}Co γ-irradiated cysteine solutions at pH 7

[RSH] (moles/l)	[O_2] (moles/l)	Yield (molecules/100 eV)			
		G(—RSH)	G(RSSR)	$G(H_2S)$	$G(H_2O_2)$
3×10^{-3}	0	8.6±0.3	2.8±0.2	3.0 ±0.1	0.74
	9.75×10^{-5}	36.3±1	15.5±3	2.35±0.1	—
	2.2×10^{-4}	37.1±1*	17.7±1	2.0 ±0.1	9.9±0.3
1×10^{-3}	9.75×10^{-5}	30.1±1†	14.2±1	2.05±0.1	6.7±0.3
	4.8×10^{-4}	28.8±1	10.1±1	0.93±0.05	—
	1.16×10^{-3}	19.1±1.5	7.5±0.5	0.56±0.05	6.7±0.3
5×10^{-4}	9.75×10^{-5}	22.9±1.5‡	9.3±0.5	1.6 ±0.1	4.7±0.3
	4.8×10^{-4}	15.4±1	3.9±0.3	0.57±0.06	—
	1.16×10^{-3}	14.4±1	3.1±0.5	0.24±0.04	—
1×10^{-4}	9.75×10^{-5}	—	4.9±1.6	—	2.7±0.7

*Result *a*.
†Result *b*.
‡Result *c*.

(5) that G(—RSH) = 13.4 and that $G(H_2O_2)$ = 4.4 (= $G_{H_2O_2} + G_{e_{aq}} + G_H$) and that these values were independent of oxygen concentration. The following reaction scheme was postulated, involving a short chain reaction producing an intermediate peroxide which reacted with cysteine to give cystine

[8] $RSH + O_2^- \text{ or } HOO\cdot \rightarrow RS\cdot + HO_2^- \text{ or } H_2O_2$

[9] $RS\cdot + O_2 \rightarrow RSOO\cdot$

[10] $RSOO\cdot + RSH \rightarrow RSOOH + RS\cdot$

[11] $RSOOH + 3RSH \rightarrow 2RSSR + 2H_2O$

At the higher pH used in this work, both G(—RSH) and $G(H_2O_2)$ are greater, showing that the chain length has increased and that H_2O_2 is produced in the chain reaction. $G(\text{—RSH})_{nc}$ and $G(H_2O_2)_{nc}$, the yields produced in the initiation reactions [1]–[4] and [8] (in the presence of oxygen reaction [4] may be replaced by reactions [12] and [13]) may be calculated from the relationships

[12] $R\cdot + O_2 \rightarrow ROO\cdot$

[13] $ROO\cdot + RSH \rightarrow ROOH + RS\cdot$

$$G(\text{—RSH})_{nc} = G_{OH} + G_H + G_{e_{aq}^-} + G(H_2S)$$

and

$$G(H_2O_2)_{nc} = G_{H_2O_2} + G_H + G_{e_{aq}^-} - G(H_2S)$$

The former equation holds because each alanyl radical produced by loss of HS^- abstracts a further hydrogen atom from cysteine, and the latter holds because a reducing radical reacting directly with cysteine (to give HS^-) rather than with oxygen does not yield hydrogen peroxide. The latter expression is slightly high, as the very minor contribution of reaction [3*a*] is excluded for simplicity. The values of G_{OH}, G_H, $G_{e_{aq}^-}$, and $G_{H_2O_2}$ were taken from ref. 8, and $G(H_2S)$ values are those measured experimentally. Assuming no H_2O_2 is produced or additional thiol lost in chain termination steps, $G(\text{—RSH})_c$ and $G(H_2O_2)_c$, the yields produced by the chain reaction, may be determined by subtracting these G_{nc} values from the G values measured experimentally. Thus in Table 2, determination *a*, $G(\text{—RSH})_c$ is equal to G(—RSH) from Table 1, result *a* less 7.9, the value of $G(\text{—RSH})_{nc}$. These figures are given in Table 2 (determinations *a*, *b*, and *c*) for corresponding results labelled *a*, *b*, and *c* in Table 1 where H_2S and RSSR are virtually the only sulfur-containing products.

A slow reaction between cysteine and hydrogen peroxide occurs at pH 7, but by determining yields immediately after removal of the solutions from the source its effects were minimized. Small corrections, slightly increasing the true value of $G(H_2O_2)$ and decreasing that of G(—RSH), would not affect the conclusions drawn from the data.

Reactions [9]–[11] cannot account for the enhanced hydrogen peroxide yields at pH 7. In our preliminary report (9) we suggested that reaction [14] may occur at the higher pH

[14] $RSOOH + RSH \rightarrow RSSR + H_2O_2$

We now think that this is unlikely because of the

Can. J. Chem. Downloaded from www.nrcresearchpress.com by 210.87.254.40 on 09/05/12
For personal use only.

TABLE 2

Yields from chain reaction for ^{60}Co γ-irradiated cysteine solutions at pH 7

Determination* [RSH] (moles/l)	Yield (molecules/100 eV) $G(—RSH)_{nc}$	$G(H_2O_2)_{nc}$	$G(—RSH)_c$	$G(H_2O_2)_c$	$\frac{G(H_2O_2)_c}{G(—RSH)_c}$	$G(—RSH)_c$'†
a 3×10^{-3}	7.9	2.2	29.2	7.7	0.36	13.8
b 1×10^{-3}	7.9	2.15	22.2	4.55	0.20	13.1
c 5×10^{-4}	7.5	2.6	15.4	2.1	0.135	11.2

*Results a, b, and c from Table 1 were used in calculation of $G(—RSH)_c$ for determinations a, b, and c, respectively (see text).
†Amount of cysteine lost by reaction sequence [9]–[11] ($G(—RSH)_c - 2G(H_2O_2)_c$), molecules/100 eV.

change in the ratio, $G(H_2O_2)_c/G(—RSH)_c$, with cysteine concentration. Even if RS^- reacted as in reaction [14] and RSH as in reaction [11], this ratio should not change with cysteine concentration at a fixed pH, as the ratio $[RS^-]/[RSH]$ would remain constant. Another possible reaction producing H_2O_2 is

[15] $RSOO\cdot + RSH \text{ or } RS^- \rightarrow RSSR + HOO\cdot \text{ or } O_2^-$

This reaction alone cannot account for the experimental data, as $G(—RSH)_c$ should equal $2G(H_2O_2)_c$. The possibility of RSH reacting as in reaction [10] and RS^- as in reaction [15] is unlikely for the reasons outlined for reaction [14].

A more plausible explanation for the enhanced yields at both higher pH and higher cysteine concentration and the changing ratio $G(H_2O_2)_c/G(—RSH)_c$ is a competition between RS^- (about 4% of cysteine is in the mercaptide form at pH 7) and O_2 for the thiyl radical

[6] $RS\cdot + RS^- \rightarrow RSSR^-$

[9] $RS\cdot + O_2 \rightarrow RSOO\cdot$

The cystine–electron adduct, $RSSR^-$, could react with oxygen

[16] $RSSR^- + O_2 \rightarrow RSSR + O_2^-$

and the chain would be propagated by reaction [8] which produces a further RS·. Propagation by reactions [6], [16], and [8] removes two molecules of cysteine and produces one molecule of H_2O_2. At a fixed pH, $[RS^-]$ is proportional to the initial cysteine concentration and thus a larger proportion of thiyl radicals (RS·) react by this pathway, accounting for the variation in $G(H_2O_2)_c/G(—RSH)_c$ shown. The amount of cysteine lost by reaction sequence [9]–[11], i.e. $G(—RSH)_c - 2G(H_2O_2)_c$ is shown in the last column of Table 2. The slight variation with concentration is not inconsistent with this model because, although the fraction of thiyl radicals reacting via the reaction sequence [9]–[11] is less at the higher cysteine concentrations, this higher concentration of RSH molecules enhances the rate of reaction [10] which is presumed to be the slow step in that chain reaction. The greater number of thiyl radicals reacting via reaction sequence [6], [16], and [8] with increasing thiol concentration is a major factor in the cysteine concentration-dependence of $G(—RSH)$ and $G(H_2O_2)$ overall[4]. If this explanation is correct, one would predict decreasing $G(—RSH)_c$- and $G(H_2O_2)_c/G(—RSH)_c$-values at a fixed cysteine concentration as the pH is lowered. This problem is currently being investigated.

The above discussion is based on the assumption that no thiol molecules are consumed or H_2O_2 produced in the chain termination step. As reactions [10] and [16] are likely to be the slow chain propagating steps, and as reaction [6] is reversible, RSOO· is the only radical whose concentration would build up appreciably, and which may disappear by reaction [17]

[17] $2\ RSOO\cdot \rightarrow RSSR + 2O_2$

[18] $RS\cdot + O_2^- \xrightarrow{H^+} RSOOH$

Reaction [18], which would invalidate the assumption, is unlikely to occur because RS· and O_2^- radicals should react fast with oxygen and cysteine, respectively, which are present in much higher relative concentration. It is possible that RSOO· radicals at higher oxygen concentrations may rearrange or react with oxygen, accounting for the formation of products with sulfur in a higher oxidation state, and for lower values of

[4]Pulse-radiolysis studies by one of us have very recently provided direct evidence for reactions [9] and [16].

Can. J. Chem. Downloaded from www.nrcresearchpress.com by 210.87.254.40 on 09/05/12
For personal use only.

TABLE 3

Yields from ^{60}Co γ-irradiated cysteine solutions with scavengers

Scavenger	G(—RSH)		$G(H_2O_2)$	
	1×10^{-3}§	3×10^{-3}§	1×10^{-3}§	3×10^{-3}§
Nil*	29±1	37±1	6.7	9.9
Acetone†	17±1	17±1	4.2	6.0
N_2O‡	29±1	39±3	3.3	6.4
N_2O‡ + 2.5×10^{-4} M Tl^+	23±1	—	5.8	—
N_2O‡ + 5×10^{-4} M Tl^+	16±1	—	3.1	—

*$[O_2] = 2.2 \times 10^{-4}$ M.
†[Acetone] $= 2 \times 10^{-2}$ M, $[O_2] = 2.6 \times 10^{-4}$ M.
‡$[N_2O] = 2.1 \times 10^{-2}$ M, $[O_2] = 2.1 \times 10^{-4}$ M.
§[RSH] values, in moles/l.

G(—RSH). The relatively low value of G(—RSH) in acidic solution indicates that reaction [10] is slow and that a reaction proceeding through reactions [16], [8], and [6] provides a faster pathway. The decrease in G(—RSH) and loss of material sulfur balance at lower $[RSH]/[O_2]$ may be caused by a further reaction between RSOO· and oxygen.

The effects of scavengers on G(—RSH) and $G(H_2O_2)$ for oxygenated solutions at pH 7 are shown in Table 3.

Nitrous oxide competes for e_{aq}^- by reaction

[19] $$e_{aq}^- + N_2O \rightarrow N_2 + \cdot OH$$

but should not alter the yield of thiyl radicals because all e_{aq}^-, however they react in this system, yield, overall, one thiyl radical. Thus N_2O should have no effect on $G(\text{—RSH})_c$ and $G(H_2O_2)_c$. Overall G(—RSH) should decrease only by an amount equal to the decrease in $G(H_2S)$, while $G(H_2O_2)$ overall should decrease by $G_{e_{aq}^-} - G(H_2S)$. Within experimental error this is observed for G(—RSH), but $G(H_2O_2)$ decreases by more than expected. Acetone also competes for e_{aq}^-, but it has been shown (ref. 1*c*) that the isopropanol radical formed abstracts a hydrogen atom from cysteine (reaction [20]). The appreciable reduction in G(—RSH) found is probably due to oxygen reacting with the isopropanol radical and thus preventing reaction [20]. Reaction [21] could also contribute to this decrease

[20] $$CH_3COCH_3^- + RSH \xrightarrow{H^+} CH_3CHOHCH_3 + RS\cdot$$

[21] $$RSSR^- + CH_3COCH_3 \rightarrow RSSR + CH_3COCH_3^-$$

Thallous ions, in the presence of excess N_2O will compete with cysteine for hydroxyl radicals by reaction [22] and cause a decrease in RS· yield.

[22] $$Tl^+ + \cdot OH \rightarrow Tl^{2+} + OH^-$$

Thus G(—RSH) should decrease with increasing thallous-ion concentration. Again this is observed. The oxygenated acetone and thallous systems are too complex for meaningful interpretation of hydrogen peroxide yields in their presence.

Experimental

Materials

L-Cysteine hydrochloride (Reidel-de-Hae), oxygen and nitrous oxide (medical grade) (N.Z. Industrial Gases) were used as supplied. A.R. Sodium dihydrogen phosphate and A.R. sodium hydroxide were used to prepare 0.02 M buffer solutions at pH 7. Where H_2O_2 was to be determined, phosphate buffer could not be used and the pH of the cysteine hydrochloride solution was adjusted to 7 with the sodium hydroxide. Triply-distilled water was used throughout.

Irradiations

Samples (10 ml) were irradiated in a 200-Curie ^{60}Co source at a dose rate of approximately 8×10^{17} eV/min.

Analysis

Free thiol, after removal of H_2S, was determined spectrophotometrically at 412 mμ by reaction with 5,5′-dithiobis(2-nitrobenzoic acid) (10) at pH 8. Cystine was determined spectrophotometrically by its absorption in acid solution at 248 mμ. H_2S was determined by the methylene blue method (11) and H_2O_2 by the titanium sulfate method (12).

This research was sponsored by the Air Force Office of Scientific Research, Office of Aerospace Research, United States Air Force, under A.F.O.S.R. Grant No. 950–65. We thank the New Zealand Universities Grants Committee for a Postgraduate scholarship to R.V.W.

1. (*a*) D. A. Armstrong and V. G. Wilkening. Can. J. Chem. **42**, 2361 (1964). (*b*) V. G. Wilkening, M. Lal, M. Arends, and D. A. Armstrong. Can. J. Chem. **45**, 1209 (1967). (*c*) V. G. Wilkening, M.

Can. J. Chem. Downloaded from www.nrcresearchpress.com by 210.87.254.40 on 09/05/12
For personal use only.

LAL, M. ARENDS, and D. A. ARMSTRONG. J. Phys. Chem. **72**, 185 (1968).
2. (*a*) A. EL. SAMAHY, H. L. WHITE, and C. N. TRUMBORE. J. Amer. Chem. Soc. **86**, 3177 (1964). (*b*) A. AL-THANNON, R. M. PETERSON, and C. N. TRUMBORE. J. Phys. Chem. **72**, 2395 (1968).
3. (*a*) W. M. DALE and J. V. DAVIES. Biochem. J. **48**, 129 (1951). (*b*) A. J. SWALLOW. J. Chem. Soc. 1334 (1952). (*c*) S. L. WHITCHER, M. ROTHERHAM, and N. TODD. Nucleonics. **11**, 30 (1953). (*d*) P. MARKAKIS and A. L. TAPPEL. J. Amer. Chem. Soc. **82**, 1613 (1960).
4. G. E. ADAMS, G. S. MCNAUGHTON, and B. D. MICHAEL. *In* Chemistry of ionization and excitation (Proc. Newcastle Conf. 1966). *Edited by* G. R. A. Johnson and G. Scholes. Taylor and Francis, Ltd., London. 1967. p. 281.
5. J. E. PACKER. J. Chem. Soc. 2320 (1963).
6. L. F. DORFMAN and M. S. MATHESON. Prog. React. Kinet. **3**, 65 (1965).
7. R. BRAAMS. Radiat. Res. **27**, 319 (1966).
8. D. C. WALKER. Quart. Rev. **21**, 79 (1967).
9. J. E. PACKER and R. V. WINCHESTER. Chem. Commun. 826 (1968).
10. G. L. ELLMAN. Arch. Biochem. Biophys. **82**, 70 (1959).
11. J. K. FOGO and M. POPOWSKY. Anal. Chem. **21**, 732 (1949).
12. G. M. EISENBERG. Anal. Ed. Ind. Eng. Chem. **15**, 327 (1943).

Can. J. Chem. Downloaded from www.nrcresearchpress.com by 210.87.254.40 on 09/05/12
For personal use only.

Can. J. Chem. Downloaded from www.nrcresearchpress.com by 210.87.254.6 on 09/05/12
For personal use only.

Chlorination of some indole derivatives with ethyl *N,N*-dichlorocarbamate

J. M. MUCHOWSKI
Bristol Laboratories of Canada, Candiac, Quebec

Received August 14, 1969

The sole product obtained from the reaction of indole-2-carboxylic acid and ethyl *N,N*-dichlorocarbamate was 3,3,5-trichlorooxindole (**7**). In contrast, methyl indole-2-carboxylate gave a mixture of methyl-3,5-dichlorooxindole-3-carboxylate (**10**) and methyl-3,5,7-trichlorooxindole-3-carboxylate (**11**), the same products as obtained from the chlorination of methyl indole-3-carboxylate. The structures of these products were confirmed by degradation to known compounds and/or by synthesis, and mechanisms for their formation were suggested.

Canadian Journal of Chemistry, **48**, 422 (1970)

Introduction

In connection with an extensive investigation of the reactions of *N*-monochloro- and *N,N*-dichlorocarbamates, Chabrier reported (1) that a slight excess of methyl *N,N*-dichlorocarbamate, in aqueous acetic acid, converted indole-2-carboxylic acid (**1**) and methyl indole-2-carboxylate (**4**) to the trichloro compounds **2** and **5** respectively. In warm acetic acid, compounds **5** and **2** liberated one mole and two moles of iodine respectively from potassium iodide, corresponding to one and two labile chlorine atoms. The reduction products thus obtained were assigned structures **6** and **3**, with the juxtaposition of one hydrogen, and one chlorine atom in compound **6** being unspecified.

We considered structures **2**, **3**, **5**, and **6** to be unlikely on several counts. Firstly, the epoxide **2** bears both α-amino and α-halo substituents, which together might be expected to impart it with a considerable degree of instability (2, 3, and references therein). Secondly, **5** contains an α-halo alcohol and an α-halo amine moiety, neither of which would be likely to survive the hydrolytic reaction conditions (aqueous acetic acid). Finally, in aqueous medium, *N,N*-dichlorocarbamates generate hypochlorous acid (Chabrier himself recognized this), and consequently, they would be expected to effect reactions similar to those observed with other positive halogen sources.

A consideration of the plausible mechanisms for the chlorination of indole-2-carboxylic acid (see below) led us to suspect that the structures of compounds **2** and **3** would be correctly represented by 3,3,5-trichlorooxindole (**7**) and 5-chlorooxindole (**8**). Indeed, the melting point (192°) reported by Chabrier for the reduction product **3**, was close to the literature value (195–196°; (4)) for 5-chlorooxindole. We did not have any preconceived structure for the chlorination product of methyl indole-2-carboxylate.

Recently, Foglia and Swern (5) reexamined Chabrier's work and showed that compounds **2** and **3** in fact did possess the oxindole structures **7** and **8**. Further, on the basis of spectral and degradative studies, they suggested that the

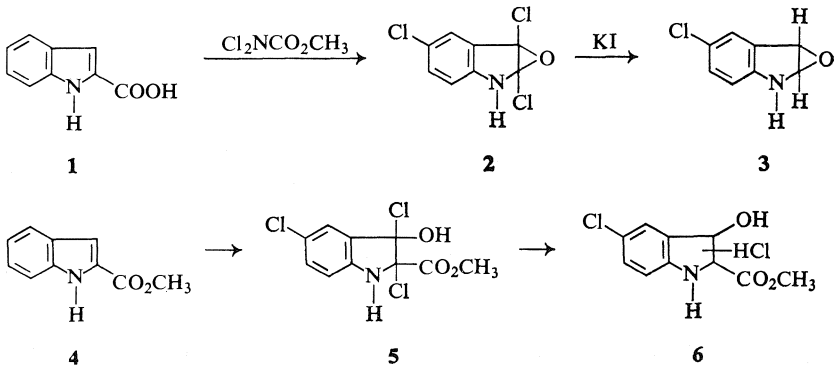

TABLE 1

Ultraviolet and infrared spectra of some substituted oxindoles

Substituents (compound no.)	Ultraviolet spectra* $\frac{\lambda_{max}\ (m\mu)}{\log \varepsilon}$					Infrared spectra† (cm^{-1})
5-Chloro- (**8**)	212 4.00	253 4.12	288 3.11			3448, 3220, 1742, 1712
5,7-Dichloro- (**15**)	217 4.12	253 4.13	295 3.20	304 3.14		3148 (b)‡, 1724, 1697§
3,3,5-Trichloro- (**7**)	223 4.37	263 3.73	327 3.08			3435, 3225 (b), 1752
3-Methoxycarbonyl-3,5-dichloro- (**10**)	220 4.36	263 3.82	318 3.10			3444, 3218 (b), 1763, 1743 (sh)
3-Methoxycarbonyl-3,5,7-trichloro- (**11**)	225 4.35	264 3.81	322 3.22			3424, 1766
3-Methoxycarbonyl-5-chloro- (**13**)	221 4.45	234 4.29	261 4.24	286 3.90	291.5 3.81	3450, 3240 (b), 1757, 1725, 1717 (sh), 1662, 1652 (sh), 1637, 1570, 1561 (sh)
		233 4.48	258 4.13	290 4.25	311 (sh)‖ 3.99	

*Measured in 95% ethanol on a Unicam SP 800 u.v. spectrophotometer.
†Recorded in chloroform (unless specified otherwise) with a Perkin–Elmer 237B grating spectrophotometer or a Unicam SP-200G i.r. spectrophotometer.
‡b = Broad; sh = shoulder.
§Recorded as a Nujol mull.
‖Measured in 0.04 *N* sodium hydroxide (95% ethanol).

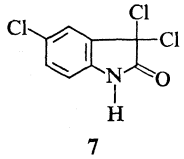

7

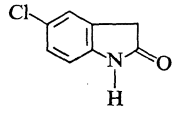

8

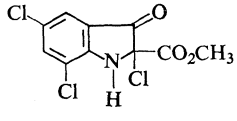

9

trichloro compound **5**, obtained from methyl indole-2-carboxylate, had the indoxylic ester structure **9**.

We had also repeated Chabrier's experiments; inasmuch as our observations and conclusions differed in several important aspects from those of Foglia and Swern, we have chosen to publish our results in their entirety.

Results and Discussion

A solution of indole-2-carboxylic acid, in aqueous acetic acid, when treated with 2 moles of ethyl *N*,*N*-dichlorocarbamate (Chabrier used methyl *N*,*N*-dichlorocarbamate) gave a trichloro compound with physical properties in agreement with those reported by Chabrier for **2**. The structure of this compound was conclusively established as 3,3,5-trichlorooxindole (**7**) on the basis of its infrared (i.r.) (see Table 1), ultraviolet (u.v.) (see Table 1), and nuclear magnetic resonance (n.m.r.) (see Table 2) spectra, as well as by iodide ion reduction to 5-chlorooxindole (**8**, Chabrier's monochloro compound **3**).

Under conditions similar to those used for indole-2-carboxylic acid, ethyl *N*,*N*-dichlorocarbamate (EDC) converted methyl indole-2-carboxylate to a mixture which could be separated by column chromatography on silica gel into approximately equal amounts of a dichloro ($C_{10}H_7NO_3Cl_2$) and a trichloro compound ($C_{10}H_6NO_3Cl_3$). The n.m.r. spectrum of the former was indicative of a 1,2,4-trisubstituted benzene system, whereas the latter had resonances attributable to a 1,2,4,6-tetrasubstituted benzenoid system. Both compounds also possessed n.m.r. absorptions for NH and methoxycarbonyl moieties. The u.v. spectra of these two compounds were, perhaps, the most revealing of all of their spectral properties. Not only were they nearly identical with one another, but they were also

Can. J. Chem. Downloaded from www.nrcresearchpress.com by 210.87.254.6 on 09/05/12
For personal use only.

TABLE 2

Nuclear magnetic resonance spectra* of some substituted oxindoles

Substituents (compound no.)	Aromatic 4	Aromatic 6	Aromatic 7	Coupling constants (c.p.s.) J_{ortho}	Coupling constants (c.p.s.) J_{meta}	CH_2	OCH_3	NH
3,3,5-Trichloro- (7)†	7.52 (d)‡	7.29 (q)	6.87 (d)	8.4	2.3	—	—	11.02
5-Chloro- (8)	7.30 (d)§	7.20 (q)§	6.91 (d)	8.6	2.0	3.52	—	10.47
5,7-Dichloro- (15)	7.34 (m)‖	7.26 (m)‖	—	—	—	3.63	—	10.91
3-Methoxycarbonyl-3,5-dichloro- (10)	7.43 (d)	7.42 (q)	7.02 (d)	8.9	2.4	—	3.80	11.33
3-Methoxycarbonyl-3,5,7-trichloro- (11)	7.48 (d)‖	7.37 (d)‖	—	—	2.0	—	3.70	11.63
3-Methoxycarbonyl-5-chloro- (13)	7.75 (d)	7.05 (q)	7.30 (q)	8.4	1.9	—¶	3.87	11.78

*Unless specified otherwise, n.m.r. spectra were recorded with a Varian A-60A spectrometer in perdeuteriodimethylsulfoxide and are expressed in p.p.m. (δ) from internal tetramethylsilane.
†Measured in deuteriochloroform containing 30% perdeuteriodimethylsulfoxide.
‡d = Doublet; q = quartet; m = multiplet.
§This multiplicity was observed only after base catalyzed (triethylamine) exchange of the methylene protons at C-3. D_2O alone exchanged the NH proton, but this did not remove the above small (ca. 0.4 c.p.s.), long range coupling.
‖This assignment could be reversed.
¶The methine proton resonates over a 50 c.p.s. region centered at δ 8.57.

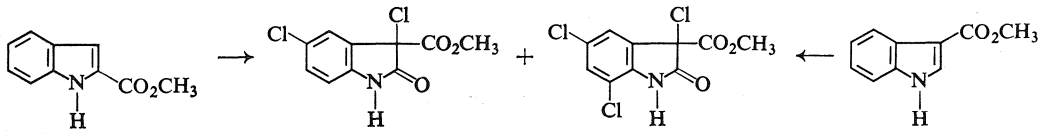

4 10 11 12

almost the same as that of 3,3,5-trichlorooxindole. On the basis of the elemental analyses and the spectral properties, we assigned the oxindole formulations **10** and **11** to the di- and trichloro compounds respectively. Strong support for these structures, the formation of which at some stage required a 1,2-migration of the methoxycarbonyl group, was derived from the observation that chlorination of methyl indole-3-carboxylate (**12**), also gave **10** and **11**, but in a 6:1 ratio. In addition, we have accumulated degradative and synthetic evidence (see below) which rigorously established the correctness of **10** and **11**.

Reduction of the dichloro ester **10** with potassium iodide in aqueous acetic acid, gave the monochloro derivative **13**, which was reconverted to **10** on treatment with EDC. This monochloro ester, which gave a blue–black color with methanolic ferric chloride, underwent rapid hydrolysis and decarboxylation to 5-chlorooxindole, in hot acetic acid containing hydrobromic acid. A similar series of reactions beginning with

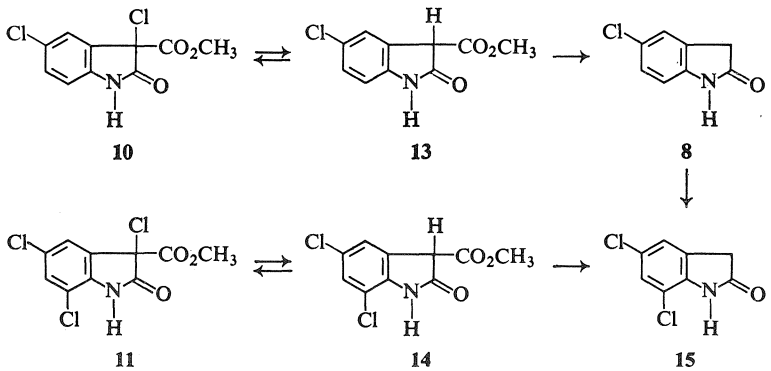

10 13 8

11 14 15

Can. J. Chem. Downloaded from www.nrcresearchpress.com by 210.87.254.6 on 09/05/12
For personal use only.

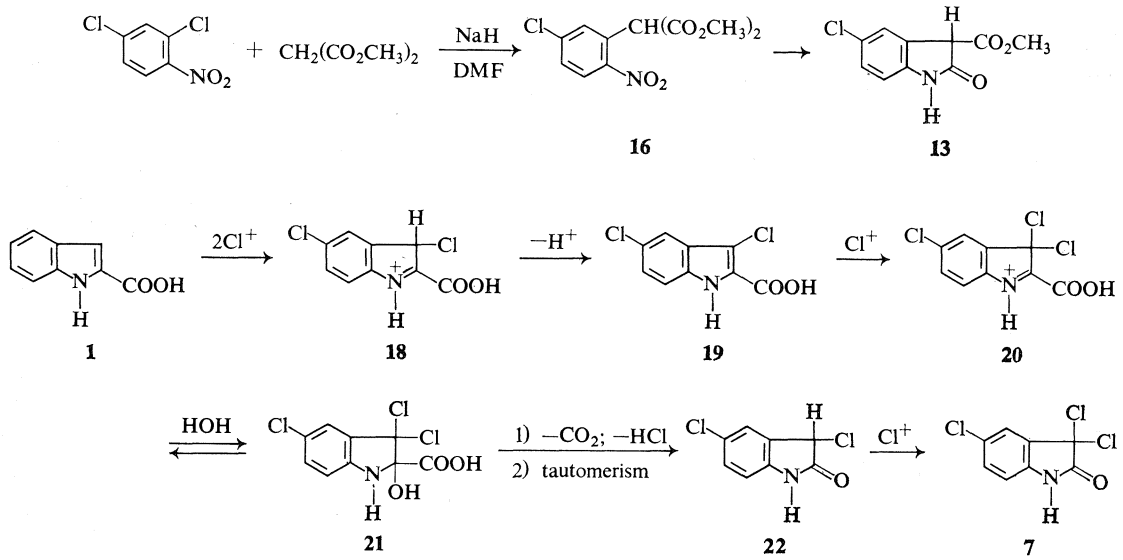

11 gave **14** which, by chlorination with EDC gave back **11**, or on hydrolytic decarboxylation produced 5,7-dichlorooxindole.

Finally, the monochloro ester **13**, and hence also **10**, was synthesized in an unambiguous manner by the reductive cyclization of dimethyl-2-nitro-5-chlorophenylmalonate (**16**), which in turn had been prepared from 2,4-dichloronitrobenzene and dimethylmalonate anion.

The chlorination of oxindole was also studied. Treatment of this compound with an excess of EDC at room temperature gave, after iodide ion reduction of the crude polychlorinated product, 5-chlorooxindole contaminated with two minor components (as indicated by thin-layer chromatography (t.l.c.)), one of which was probably 5,7-dichlorooxindole. Further chlorination of this mixture occurred slowly at room temperature, but rapidly at reflux temperature, and after reductive dechlorination, the sole product was 5,7-dichlorooxindole.

The question now arises concerning the nature of the trichloro compound(s) obtained from methyl indole-2-carboxylate, by Chabrier, Foglia and Swern, and ourselves. Inasmuch as the experimental details given by Chabrier were meagre, there was no way of being certain of reproducibility. We have, however, repeated the chlorination precisely as described by Foglia and Swern; the main products were nevertheless still the dichloro- and trichlorooxindole derivatives **10** and **11**, respectively. Finally, the melting points of the trichloro ester **11** (m.p. 208–210°) and 5,7-dichlorooxindole (**15**) obtained therefrom (m.p. 246–247°), agreed well with those reported by Foglia and Swern for the supposed indoxylic ester **9** (m.p. 203–204°) and its degradation product, "5,7-dichloroindoxyl" (m.p. 242–243°). Professor Swern has graciously provided us with the n.m.r. and i.r. spectra of these compounds.[1] The n.m.r. spectra of **9** and the assumed 5,7-dichloroindoxyl were identical to those observed by us for **11** and **15** respectively, and the i.r. spectra were, with the exception of a few minor intensity differences, superimposable. It is therefore concluded that, for these compounds, the assignment of indoxyl structures should be revised to the isomeric oxindole formulations.

We regard the chlorination of indole-2-carboxylic acid with EDC as proceeding by a mechanism similar to that suggested by Hinman and Bauman (6) for the oxidative halogenation of 3-alkylindoles with positive halogen sources. In this case, however, it is suggested that oxindole functionality is introduced by the elimination of the elements of carbon dioxide and hydrogen chloride from **21**.[2] Further chlorination of **22**

[1]The unstinting cooperation of Professor Swern in this matter is gratefully acknowledged.

[2]The introduction of chlorine at C_5 at some stage prior to the generation of oxindole functionality, is based on the tenuous argument that no trace of a 5,7-dichlorinated product analogous to **7** was observed in this reaction, whereas the chlorination of oxindole did give this product.

Can. J. Chem. Downloaded from www.nrcresearchpress.com by 210.87.254.6 on 09/05/12
For personal use only.

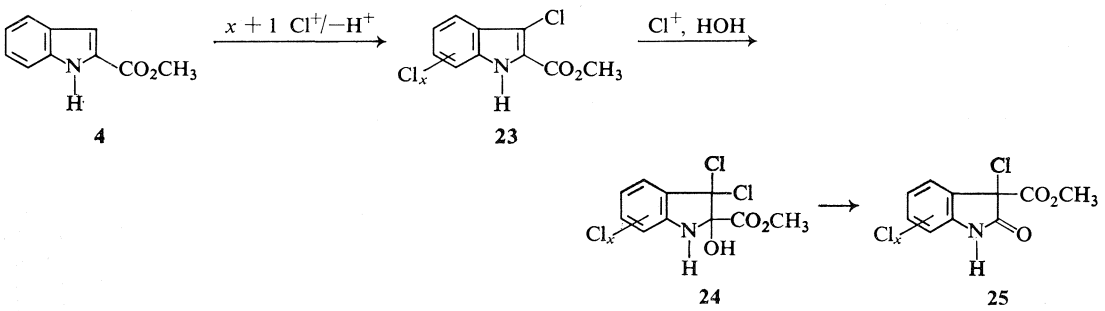

thus produced, would then give the observed product **7**.

An intermediate **24** analogous to **21** must be involved in the chlorination of methyl indole-2-carboxylate, except that here, the loss of the elements of hydrogen chloride is accompanied by a 1,2-shift of the methoxycarbonyl group. An identical mechanism has been proposed by Acheson *et al.* (7) to explain the formation of trimethyl-1-methyl-5-bromooxindole-3,3,4-tricarboxylate from trimethyl-1-methylindole-2,3,4-tricarboxylate and bromine in aqueous acetic acid.

Experimental

The melting points were determined in a Gallenkamp melting point apparatus and are not corrected.

The thin-layer chromatograms were performed on microscope slides coated with silica gel containing calcium sulfate as a binder. The spots were rendered visible by spraying the hot slides with 1% aqueous permanganate solution. The column chromatographic separations were carried out by the method of Loev and Snader (8) using J. T. Baker silica gel containing ca. 4% water.

Ethyl *N,N*-dichlorocarbamate was prepared from ethyl carbamate by the method of Foglia and Swern (9). Indole-2-carboxylic acid, indole-3-carboxylic acid, and the corresponding methyl esters were purchased from commercial sources or were prepared according to literature procedures.

3,3,5-Trichlorooxindole

A stirred solution of indole-2-carboxylic acid (1.000 g, 6.21 mmoles) in 50 ml of 90% acetic acid was treated dropwise with ethyl *N,N*-dichlorocarbamate (EDC, 1.96 g, 12.42 mmoles) at a rate such that the reaction temperature did not exceed 30° (cooling was necessary). When the addition was completed, stirring at room temperature was continued for 1.5 h. The solution was then poured with stirring into a large volume of ice-water, and after ca. 10 min the white solid was collected by filtration, washed well with water, and dried *in vacuo*. This material (1.164 g) was homogeneous by t.l.c. [2% methanol in dichloromethane (v/v)] and had m.p. 184–186°. Crystallization of this solid from benzene–cyclohexane gave two crops (65.7%) of the product, m.p. 186–188° (777 mg) and m.p. 184–187° (188 mg). Chabrier (1) reported m.p. 188° for this compound.

5-Chlorooxindole

3,3,5-Trichlorooxindole (473 mg, 2 mmoles) was dissolved in 10 ml of acetic acid and placed in a water bath at 80°. 3 *M* KI solution (7 ml) was added and the brown iodine color was discharged by the dropwise addition of saturated aqueous sodium sulfite solution. After a few min the brown color reappeared; it was discharged again in the same way. This process was repeated until the solution remained clear yellow in color. The hot solution was then diluted with a large volume of ice-water, and the product was extracted into ethyl acetate. The extract was washed with water, dried over sodium sulfate, and evaporated *in vacuo* to give 302 mg of a solid which was homogeneous by t.l.c. (2% methanol in methylene chloride). On crystallization from alcohol, 5-chlorooxindole was obtained in two crops (68.7%) weighing 198 mg, m.p. 194–196° (lit. (4), m.p. 195–196°), and 33 mg, m.p. 193–195°, respectively.

Chlorination of Methyl Indole-2-carboxylate

Methyl indole-2-carboxylate (3.500 g, 20 mmoles) in 100 ml of 90% acetic acid, was treated as above with 5.22 g (33 mmoles) of EDC. The crude product weighed 3.968 g and had m.p. 160–170° (softening at 150°). The t.l.c. (10% acetonitrile in methylene chloride) showed the presence of two closely spaced (0.15 R_f difference) major components as well as traces of a less and a more polar moving component. The above mixture (1.000 g) was taken up in the minimum amount of a solution of 10% acetonitrile in 1,2-dichloroethane and placed on a dry packed column of silica gel (300 g). The column was developed with the same solvent; twelve 50 ml fractions were collected and monitored by t.l.c.

Fractions 3 to 5 were evaporated *in vacuo* and the residue was crystallized from benzene to give 251 mg of a solid m.p. 207–210° which was homogeneous by t.l.c. After three more crystallizations from benzene–cyclohexane (2:1) it had m.p. 208–210°.

Anal. Calcd. for $C_{10}H_6NO_3Cl_3$: C, 40.79; H, 2.05; N, 4.76; Cl, 36.13. Found: C, 41.04; H, 2.08; N, 5.04; Cl, 36.38.

Fractions 8–12 were evaporated *in vacuo* and the residue was crystallized from benzene to give 247 mg of a solid which was homogeneous by t.l.c. and had m.p. 188–189°. Three more crystallizations of this material from benzene gave a solid with m.p. 192–194°.

Can. J. Chem. Downloaded from www.nrcresearchpress.com by 210.87.254.6 on 09/05/12
For personal use only.

Can. J. Chem. Downloaded from www.nrcresearchpress.com by 210.87.254.6 on 09/05/12
For personal use only.

Anal. Calcd. for $C_{10}H_7NO_3Cl_2$: C, 46.17; H, 2.71; N, 5.39; Cl, 27.27. Found: C, 46.44; H, 2.70; N, 5.37; Cl, 26.96.

When the chlorination was repeated under conditions identical to those described by Foglia and Swern (5) (80% acetic acid, 2 moles of EDC/mole of ester) the majority of the mixture still consisted of the above di- and trichloro compounds in a 3:1 ratio, but the chromatographic separation was now more difficult to achieve, since the proportion of the more and less polar impurities mentioned above was greater.

Chlorination of Methyl Indole-3-carboxylate

Methyl indole-3-carboxylate (2.628 g, 15 mmoles) was dissolved in 75 ml of 90% acetic acid and treated as above with 4.74 g (30 mmoles) of EDC. The usual workup gave 3.57 g of a powder which on crystallization from benzene gave 2.20 g of a solid which was homogeneous by t.l.c. and had m.p. 188–193°. Recrystallization from benzene gave a solid with m.p. 190–192° (mixture m.p. 190–193°) with spectral characteristics identical to those of the dichloro compound prepared from methyl indole-2-carboxylate.

The mother liquor from the first crystallization, on standing deposited 316 mg of a solid m.p. 197–203° which was shown by t.l.c. to be mainly the trichloro compound contaminated with the dichloro compound. The mother liquor from this crystallization was evaporated and the residue (834 mg) was chromatographed on a dry packed column of 300 g of silica gel using 10% acetonitrile in chloroform as the eluent (50 ml fractions). Fractions 3 to 7 contained the trichloro compound (227 mg) which was combined with the 197–203° material from above. Two crystallizations of this mixture from benzene gave 330 mg of the trichloro compound m.p. 205–207°, mixture m.p. 205–208°, with identical t.l.c. behavior, and spectral characteristics as the trichloro compound obtained from methyl indole-2-carboxylate.

Preparation of Methyl-5-chlorooxindole-3-carboxylate by Reductive Dechlorination of Methyl-3,5-dichlorooxindole-3-carboxylate

Methyl-3,5-dichlorooxindole-3-carboxylate (2.20 g, 8.47 mmoles) in 100 ml of acetic acid, was reduced with 35 ml of 3 *M* KI solution, in the same way as 3,3,5-trichlorooxindole, but at room temperature. After pouring the reaction mixture into water, the crude product was collected by filtration, washed well with water, and dried *in vacuo*. The white solid thus obtained had m.p. 143–144° and weighed 1.628 g (85.2%). It gave a deep blue–black color with methanolic ferric chloride. The melting point depended very much on the mode of handling. For example, solution in hot benzene, followed by the addition of 1/2 the volume of cyclohexane, and very slow cooling gave needles, m.p. 145–147°. Sublimation of this solid at 100°/0.001 mm gave a sublimate with m.p. 138–143°. The solution i.r. spectra were, however, identical.

Anal. Calcd. for $C_{10}H_8O_3NCl$: C, 53.22; H, 3.57; N, 6.21; Cl, 15.71. Found: C, 53.31; H, 3.71; N, 6.17; Cl, 15.71.

Chlorination of Methyl-5-chlorooxindole-3-carboxylate

The above monochloro compound, in 90% acetic acid, was treated with an equimolar amount of EDC in the usual manner. The reaction solution was worked up as before except that the product was extracted into dichloromethane. The material obtained therefrom was crystallized from benzene to give 77.7% of a solid m.p. 194–195°, mixture m.p. with methyl-3,5-dichlorooxindole-3-carboxylate undepressed.

Hydrolysis and Decarboxylation of Methyl-5-chlorooxindole-3-carboxylate

The monochloro compound (226 mg, 1 mmole) was dissolved in a solution made up of 9 ml of acetic acid and 1 ml of 48% hydrobromic acid and heated on a steam bath for 25 min (the enol test of a small aliquot worked up after 15 min, was negative). The solution was poured into water and extracted with ethyl acetate. The extract was washed with water, dried over sodium sulfate, and evaporated *in vacuo*. The residue on crystallization from benzene gave 108 mg (64.3%) of 5-chlorooxindole, m.p. 191–193°, identical to an authentic specimen prepared in the same way from synthetic methyl-5-chlorooxindole-3-carboxylate.

Preparation of Methyl-5,7-dichlorooxindole-3-carboxylate

The trichloro compound (590 mg, 2 mmoles) dissolved in 50 ml of acetic acid, was reduced in the usual manner (but at 80° for solubility reasons). After isolation by extraction with ethyl acetate, etc., the crude product weighed 490 mg, had m.p. 218–220°; and gave a blue–black enol test with methanolic ferric chloride. It was not further characterized.

Chlorination of Methyl-5,7-dichlorooxindole-3-carboxylate

The crude 5,7-dichloro ester was chlorinated with an equimolar amount of EDC in the same way as described for the monochloro ester. After 5 h at room temperature, workup of the reaction provided a mixture which was crystallized from benzene to give methyl-3,5,7-trichlorooxindole-3-carboxylate in 48.5% yield. It had m.p. 203–206°, and was identical to a specimen prepared by the previous methods.

Hydrolysis and Decarboxylation of Methyl-5,7-dichlorooxindole-3-carboxylate

The crude dichloro ester from above (200 mg, 0.269 mmole) was hydrolyzed in the same manner as described for the monochloro ester (35 min). Crystallization of the crude product from alcohol gave two crops (75.9%) of 5,7-dichlorooxindole weighing 102 mg (m.p. 244–246°) and 16 mg (m.p. 239–241°), identical to a specimen obtained from the chlorination of 5-chlorooxindole.

Synthesis of Methyl-5-chlorooxindole-3-carboxylate from 2,4-Dichloronitrobenzene and Dimethyl Malonate

2.64 g of a 55% suspension of sodium hydride in mineral oil was freed of the carrier by washing with hexane in a nitrogen atmosphere, and then it was layered with 150 ml of anhydrous dimethyl formamide, and cooled with stirring in an ice bath. Dimethyl malonate (7.26 g, 6.3 ml, 55 mmoles) was added dropwise at a rate such that hydrogen evolution was not too vigorous. When the addition was completed and hydrogen evolution was slow, 9.6 g (50 mmoles) of solid 2,4-dichloronitrobenzene was added all at once. The reaction vessel (under a slight positive pressure of nitrogen) was placed in an oil bath

maintained at 70 ± 5° for 24 h. The cooled, deep red solution was poured onto a mixture of ice and 50 ml of 10% hydrochloric acid. The product was extracted into benzene, the extract was washed with water, dried over sodium sulfate, and evaporated *in vacuo*. The excess of dimethyl malonate was removed at 80°/0.03 mm leaving 11.82 g of a thick oil. This was taken up in 100 ml of glacial acetic acid containing 1.1 g of 10% palladium on charcoal, and hydrogenated at room temperature and an initial hydrogen pressure of 63 p.s.i.g. Hydrogen absorption ceased in 15 min and after 1/2 h the catalyst was removed by filtration, the filtrate was evaporated *in vacuo*, the residue was diluted with water and extracted with ethyl acetate. The organic phase was then shaken alternately with 1 *N* sodium hydroxide (3 × 50 ml) and water (3 × 50 ml). The combined alkali and water phases were washed with ethyl acetate and then made acidic with 150 ml of 10% hydrochloric acid. The crystalline product was extracted into ethyl acetate, the extract was washed well with water, dried over sodium sulfate, and evaporated *in vacuo*. The residue was twice crystallized from benzene–cyclohexane (charcoal) as described previously, to give a crystalline solid (1.581 g) m.p. and mixture m.p. 145–147°, identical in all its spectral properties to the compound obtained by iodide ion reduction of methyl-3,5-dichlorooxindole-3-carboxylate. Workup of the mother liquor gave a further 576 mg of product m.p. 142–144°. The yield was 2.157 g or 19.1% based on starting 2,4-dichloronitrobenzene.

Chlorination of Oxindole

A stirred solution of 1.33 g (10 mmoles) of oxindole in 60 ml of 80% acetic acid was treated with 4.74 g (30 mmoles) of EDC, as described previously. After 15 h at room temperature, the solution was poured into water, and the products were extracted into ethyl acetate. The usual manipulations gave a solid which was directly reduced with KI in acetic acid at 80°. Workup of the reaction solution, as described previously for the reduction of 3,3,5-trichlorooxindole, gave 1.11 g of a crude product which was shown by t.l.c. to consist of 5-chlorooxindole contaminated with two minor less polar substances (one of the spots had the same R_f value as 5,7-dichlorooxindole).

Chlorination of 5-Chlorooxindole

5-Chlorooxindole (3.046 g, 18.2 mmoles) and 75 ml of 80% acetic acid containing 7.2 g (45.6 mmoles) of EDC was heated at reflux temperature for 2 h. The solution was diluted with a large volume of cold water, the precipitated solid was collected by filtration, and then dissolved in 100 ml of acetic acid. The reduction with iodide solution (70 ml) was carried out at 80° as for 3,3,5-trichlorooxindole. After dilution of this solution with water, the product was extracted into ethyl acetate, and after the usual manipulations the crude product was crystallized giving 759 mg of a solid, m.p. 241–243°. Workup of the mother liquor (charcoal) gave a further 45 mg of product m.p. 242–244°. Total yield, 804 mg (21.9%). After three crystallizations from alcohol and sublimation at 125°/0.001 mm, it had m.p. 246–247°.

Anal. Calcd. for $C_8H_5NOCl_2$: C, 47.55; H, 2.49; N, 6.93; Cl, 35.10. Found: C, 47.69; H, 2.52; N, 6.91; Cl, 35.04.

1. (*a*) J. Bougault and P. Chabrier. C. R. **213**, 487 (1941). (*b*) P. Chabrier. Ann. Chim. **17**, 353 (1942).
2. C. L. Stevens and P. M. Pillai. J. Amer. Chem. Soc. **89**, 3084 (1967).
3. R. N. McDonald and T. E. Tabor. J. Org. Chem. **33**, 2934 (1968).
4. W. B. Wright and K. H. Collins. J. Amer. Chem. Soc. **78**. 221 (1956).
5. T. A. Foglia and D. Swern. J. Org. Chem. **33**, 4440 (1968).
6. R. L. Hinman and C. P. Bauman. J. Org. Chem. **29**, 1206 (1964).
7. (*a*) R. M. Acheson and R. W. Snaith. Proc. Chem. Soc. 344 (1963). (*b*) R. M. Acheson, R. W. Snaith, and J. M. Vernon. J. Chem. Soc. 3229 (1964).
8. B. Loev and K. M. Snader. Chem. Ind. 15 (1965).
9. T. A. Foglia and D. Swern. J. Org. Chem. **31**, 3625 (1966).

Can. J. Chem. Downloaded from www.nrcresearchpress.com by 210.87.254.6 on 09/05/12
For personal use only.

Can. J. Chem. Downloaded from www.nrcresearchpress.com by 210.87.254.40 on 09/05/12
For personal use only.

Crystal structure of di-*p*-tolyl mercury

M. MATHEW[1] AND N. R. KUNCHUR[2]

Chemistry Department, University of Western Ontario, London, Ontario

Received[3] April 25, 1967

Di-*p*-tolyl mercury crystallizes in space group $P2_1/c$ with cell constants $a = 10.12$, $b = 5.07$, $c = 11.65$ Å, $\beta = 91.8°$, $Z = 2$. The structure was solved by mercury-phased three-dimensional electron density Fourier synthesis and refined by least-squares. The final *R*-index was 0.085 for all reflections. The molecule of di-*p*-tolyl mercury is found to be planar having linear carbon–mercury–carbon bonds. There are no significant intermolecular close approaches, the structure is, therefore, of molecular type.

Canadian Journal of Chemistry, **47**, 429 (1969)

Introduction

This work forms part of a program of studying the crystal structures of coordination compounds of mercury. The stereochemistry of mercury differs considerably from that of zinc and cadmium, which are in the same group as mercury in the periodic table. Orgel (1) has attributed this to the much smaller d–s separation in the Hg ion as compared with that of zinc and cadmium ions. The structures of the coordination compounds of mercury can best be classified on the basis of difference in the electronegativity of mercury and the ligand, $[x(\mathrm{Hg}) - x(\mathrm{L})]$. The value of $x(\mathrm{L})$ is critical, because for $x(\mathrm{L}) > 2.5$, the characteristic coordination of mercury is diagonal and for $x(\mathrm{L}) < 2.5$, it is tetrahedral. Sulfur and carbon atoms occupy a transition position, $x(\mathrm{L}) = 2.5$ and hence the stereochemistry of mercury–carbon and mercury–sulfur compounds is particularly interesting.

Based on dipole moment measurement, structures have been proposed for organomercuric compounds containing C—Hg—C bonds. High dipole moments of these compounds have been attributed to the nonlinearity of these bonds by Horning and Wright (2). Preliminary work on di-*p*-tolyl mercury indicated a linearity of the two bonds. Further investigation of these compounds was undertaken, since a complete X-ray analysis on mercury aryl compounds does not exist.

Experimental

Some physical constants of di-*p*-tolyl mercury, $Hg(C_6H_4.CH_3)_2$ are summarized in Table 1.

TABLE 1

Some physical constants of di-*p*-tolyl

Molecular weight	382.86
Crystal type	Monoclinic
Space group	$P2_1/C$
Cell dimensions*	$a = 10.12 \pm 0.01$ Å
	$b = 5.07 \pm 0.01$ Å
	$c = 11.65 \pm 0.02$ Å
	$\beta = 91.8 \pm 0.3$
Volume of unit cell	597.4 Å^3
D_{calcd}†	2.13 g cm^{-3}
D_{obsd}	2.15 g cm^{-3}
Absorption coefficient for X-rays with $\lambda = 1.542$ Å	$\mu = 247$ cm^{-1}
Total number of electrons in the unit cell $F(000) = 356$.	

*Cell dimensions were determined from rotation and Weissenberg photographs.
†With $Z = 2$.

For collecting intensity data, needles of di-*p*-tolyl mercury of the size $0.15 \times 0.15 \times 0.50$ mm^3 were employed for taking Weissenberg photographs using multiple film technique. Intensity data were recorded from layers $k = 0 \rightarrow 3$ and $l = 0$ with nickel filtered Cu Kα radiation. Intensities were measured visually by comparison with a standard scale. A total of 760 out of the 886 reflections in the range of observation had nonzero intensities. Absorption corrections were applied assuming the crystal to be needle of diameter 0.15 mm ($\mu r = 1.9$) and also the usual Lorentz and polarization corrections were applied. Values for absolute scale for each layer were obtained from Wilson plots. The scale factors were improved by comparing the overlapping reflections of the set *hkl* with $k = 0 \rightarrow 3$ with *hk*0 reflections in the other set.

Structure Determination

Since the symmetry of the general position is 4-fold and there are two molecules in the unit cell, it follows that mercury has to occupy one of the four sets of special positions. All these positions are equivalent, so mercury atom was placed at $0,0,0; 0,\frac{1}{2},\frac{1}{2}$. All reflections which have contributions from mercury were used to compute a

[1]Present address: Department of Chemistry, University of Waterloo, Waterloo, Ontario.
[2]Present address: Department of Physics, University of Poona, Poona, India.
[3]Revision received September 2, 1969.

TABLE 2
Final coordinates with standard deviations

Atom	x/a	$\sigma(x)$, Å	y/b	$\sigma(y)$, Å	z/c	$\sigma(z)$, Å
Hg	0.0000		0.50000		0.50000	
C_1	0.1297	0.017	0.7923	0.016	0.4480	0.018
C_2	0.2305	0.016	0.8906	0.024	0.5246	0.017
C_3	0.3195	0.019	0.0871	0.024	0.4846	0.018
C_4	0.3139	0.014	0.1914	0.014	0.3740	0.015
C_5	0.2207	0.020	0.0805	0.024	0.2973	0.018
C_6	0.1259	0.017	0.8897	0.024	0.3367	0.018
C_7	0.4146	0.018	0.3957	0.022	0.3366	0.018

three-dimensional electron density Fourier synthesis. Since mercury does not contribute to reflections hkl with $k = 2n + 1$, the mercury-phased electron density map has an additional mirror plane of symmetry perpendicular to the b axis at $y = 0$. This pseudo-symmetry was destroyed by the following procedure. Carbon atoms of the *p*-tolyl ring were located in the electron density map. Structure factors were calculated for all atoms (excluding hydrogens) and the signs they gave were assigned to all reflections. A second cycle of three-dimensional electron density Fourier synthesis was then carried out to give improved coordinates for all carbon atoms. The structure was further refined by a third cycle of mercury-difference electron density Fourier synthesis. *R*-index at this stage was 0.12 for all observed reflections.

Further refinement was carried out by the full matrix least-squares methods. The scattering factors for Hg and C were those reported by Ibers (3) and Freeman (4), respectively. Anomalous dispersion corrections for the scattering of mercury were incorporated in the program of Busing and Levy. The values for $\Delta f'$ for Hg with Cu Kα radiation were taken from ref. (5). The following weighting scheme was used for the refinement.

$$\omega^{-\frac{1}{2}} = \sigma|F| = 0.1|F_{obsd}| \quad \text{for } |F_{obsd}| \geqslant 30$$

$$\omega^{-\frac{1}{2}} = \sigma|F| = 3.0 \quad \text{for } |F_{obsd}| < 30$$

The unobserved reflections were excluded during the refinement. After 6 cycles of refinement, the shifts for all positional parameters were less than 1/10 of their estimated standard deviations and hence the refinement was assumed to be complete. The final agreement *R*-index was 0.085 for all, including the unobserved reflections (for unobserved reflections, a value of $\frac{1}{2}$ of the minimum observed intensity was assumed). The *R*-index for mercury alone was 0.12. The scattering for all hydrogen atoms was neglected in all calculations. The final positional parameters and their estimated standard deviations are given in Table 2 and the thermal parameters in Table 3. The standard deviations were calculated by inverting the matrix in the final least-squares cycle. A listing of observed and calculated structure factors is given in Table 4. The final mercury-difference three-dimensional electron density map along the b axis is shown in Fig. 1.

Description and Discussion of the Structure

A diagramatic representation of the structure in (010) and (100) projections is shown in Figs. 2 and 3, respectively. The various bond lengths and bond angles are shown in Fig. 4. The standard deviations are 0.02 Å and 1.4° for distances and angles involving mercury–carbon atoms and

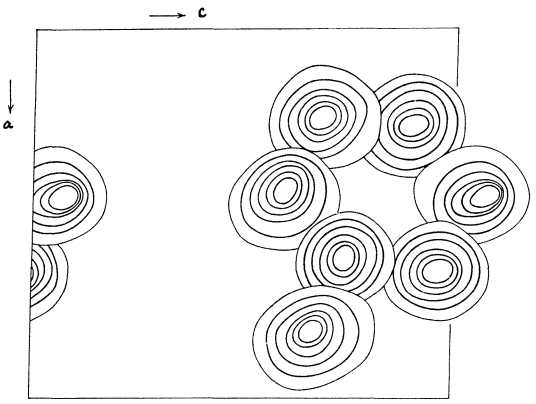

FIG. 1. Mercury-difference three-dimensional electron density map along the b axis. Contours are at intervals of 1e/Å^3.

Can. J. Chem. Downloaded from www.nrcresearchpress.com by 210.87.254.40 on 09/05/12
For personal use only.

TABLE 3

Anisotropic thermal parameters, B_{ij}*

Atom	B_{11}	B_{22}	B_{33}	B_{12}	B_{13}	B_{23}
Hg	71 (1)	443 (19)	77 (1)	4 (1)	10 (1)	4 (1)
C_1	119 (19)	155 (113)	148 (19)	24 (26)	20 (16)	58 (29)
C_2	70 (15)	437 (93)	101 (14)	−16 (30)	23 (13)	−4 (34)
C_3	95 (17)	497 (88)	75 (13)	−33 (12)	−13 (12)	−8 (33)
C_4	88 (16)	203 (108)	98 (14)	−8 (22)	10 (12)	−3 (23)
C_5	99 (19)	483 (91)	78 (13)	−41 (39)	−12 (13)	18 (33)
C_6	98 (18)	378 (102)	112 (17)	−25 (34)	−23 (15)	−13 (39)
C_7	145 (21)	247 (86)	116 (16)	12 (39)	23 (15)	17 (38)

*All values have been multiplied by 10^4. Estimated standard deviations are written in parentheses. The expression for calculating the temperature factor is

$$T = \exp - (h^2B_{11} + k^2B_{22} + l^2B_{33} + 2hkB_{12} + 2hlB_{13} + 2klB_{23})$$

0.03 Å and 1.8° for those involving carbon–carbon atoms. The two Hg—C bonds are exactly linear since mercury lies on a center of symmetry. The mean plane through the mercury and carbon atoms and that through the carbon atoms alone are given in Table 5. The deviations of the atoms from the least-squares planes are of the same magnitude as the estimated standard deviations in the distances between various atoms and so the molecule may be described as approximately planar.

The mercury–carbon distance is 2.08 ± 0.02 Å. The lengths of the carbon–carbon bonds vary from 1.39 to 1.44 Å and the angles from 116.5 to 123.9°. The deviations from the dimensions of a regular hexagon, as in benzene (C—C bond length = 1.39 Å, ∠ C—C—C = 120°), are not significant and so no conclusions can be drawn regarding the distortions in the geometry of the molecule.

There are a number of intermolecular contacts at distances varying between 3.70 and 4.00 Å. The shortest contact is that between two methyl groups. This is slightly less than the van der Waals diameter of a methyl group (4.00 Å). All other contacts are between the methyl groups and are

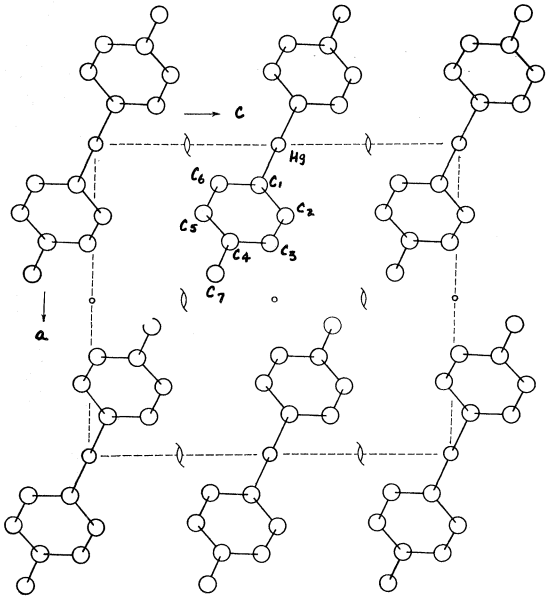

FIG. 2. Projection of the structure of di-*p*-tolyl mercury along the *b* axis.

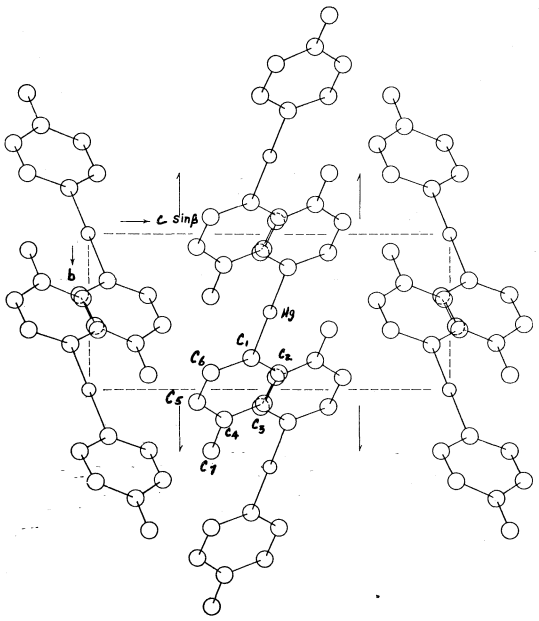

FIG. 3. Projection of the structure of di-*p*-tolyl mercury along the *a* axis.

Can. J. Chem. Downloaded from www.nrcresearchpress.com by 210.87.254.40 on 09/05/12
For personal use only.

TABLE 4

Observed and calculated structure factors*

H	K	L	FO	FC	H	K	L	FO	FC	H	K	L	FO	FC	H	K	L	FO	FC
0	0	2	145.7	157.9	-6	0	6	54.3	58.0	6	1	11	27.9	24.6	1	1	6	2.8*	-2.3
1	0	2	182.1	193.6	-7	0	6	56.5	56.0	5	1	11	22.8	22.8	2	1	6	2.8*	4.7
2	0	2	94.2	109.3	-8	0	6	50.4	45.7	6	1	11	19.1	18.0	3	1	6	2.8*	-5.2
3	0	2	130.6	144.1	-9	0	6	39.5	41.8	7	1	11	15.9	15.1	4	1	6	2.8*	5.9
4	0	2	93.7	105.9	-10	0	6	40.3	34.5	0	1	13	25.8	21.5	0	1	8	2.8*	1.5
5	0	2	59.4	58.3	-11	0	6	23.0	22.6	1	1	13	25.4	19.9	1	1	8	10.9	-10.3
6	0	2	73.5	72.7	-1	0	8	54.2	55.8	2	1	13	22.2	18.3	2	1	8	2.8*	-0.3
7	0	2	63.6	66.7	-2	0	8	58.9	61.2	3	1	13	12.9	15.5	3	1	8	6.4	2.9
8	0	2	56.5	56.4	-3	0	8	68.0	58.3	4	1	13	14.0	14.6	4	1	8	2.8*	-3.6
9	0	2	45.3	47.1	-4	0	8	64.9	55.3	5	1	13	17.4	17.4	0	1	10	2.8*	5.9
10	0	2	46.4	44.2	-5	0	8	56.5	53.7	-1	1	1	159.8	142.9	1	1	10	2.8*	-3.1
11	0	2	30.5	30.8	-6	0	8	61.5	58.9	-2	1	1	160.3	172.5	2	1	10	8.9	-7.4
12	0	2	21.5	23.8	-7	0	8	34.2	39.5	-3	1	1	79.3	103.4	-1	1	2	47.5	-43.8
0	0	4	118.2	118.1	-8	0	8	23.6	26.9	-4	1	1	99.6	103.9	-2	1	2	35.3	-25.1
1	0	4	103.7	96.1	-9	0	8	35.5	33.7	-5	1	1	106.6	94.5	-3	1	2	31.1	23.2
2	0	4	90.2	88.3	-10	0	8	27.3	27.3	-6	1	1	79.6	73.1	-4	1	2	34.2	25.9
3	0	4	96.3	99.4	-11	0	8	21.1	20.7	-7	1	1	83.9	71.1	-5	1	2	2.8*	-1.4
4	0	4	108.6	114.5	-1	0	10	46.1	41.5	-8	1	1	61.3	52.2	-6	1	2	2.8*	-4.0
5	0	4	66.7	71.2	-2	0	10	43.6	42.8	-9	1	1	48.5	43.0	-7	1	2	2.8*	4.3
6	0	4	48.9	58.4	-3	0	10	50.1	45.5	-10	1	1	45.0	43.0	-8	1	2	2.8*	-6.0
7	0	4	53.4	55.8	-4	0	10	39.0	37.4	-11	1	1	41.5	39.3	-9	1	2	2.8*	-1.1
8	0	4	53.4	51.9	-5	0	10	41.3	41.4	-12	1	1	26.8	25.2	-10	1	2	2.8*	0.2
9	0	4	50.7	42.5	-6	0	10	37.5	36.8	-1	1	3	138.0	131.1	-1	1	4	4.6	-9.4
10	0	4	27.4	27.1	-7	0	10	18.7	20.8	-2	1	3	109.4	106.6	-2	1	4	2.8*	4.7
11	0	4	24.6	23.9	-8	0	10	25.0	24.8	-3	1	3	101.5	103.8	-3	1	4	11.6	8.9
12	0	4	22.3	23.2	-9	0	10	36.0	26.3	-4	1	3	103.6	102.4	-4	1	4	7.8	5.2
0	0	6	130.6	114.6	-1	0	12	31.3	26.8	-5	1	3	65.9	72.0	-5	1	4	2.8*	-5.3
1	0	6	96.4	82.7	-2	0	12	36.7	33.0	-6	1	3	70.7	69.9	-6	1	4	2.8*	2.2
2	0	6	92.8	81.6	-3	0	12	31.7	27.4	-7	1	3	73.9	67.5	-1	1	6	2.8*	2.3
3	0	6	84.5	76.8	-4	0	12	21.3	21.4	-8	1	3	70.7	60.7	-2	1	6	9.2	-10.9
4	0	6	57.6	59.6	-5	0	12	27.9	25.8	-9	1	3	50.3	44.6	-3	1	6	2.8*	0.5
5	0	6	55.1	57.0	-6	0	12	21.3	22.2	-10	1	3	39.9	37.8	-4	1	6	7.8	9.1
6	0	6	46.1	52.4	-7	0	12	25.1	19.8	-11	1	3	34.3	33.4	-5	1	6	2.8*	7.5
7	0	6	41.2	45.8	-1	0	14	20.8	17.8	-12	1	3	22.4	23.5	-1	1	8	2.8*	-0.3
8	0	6	38.1	36.3	-2	0	14	19.9	17.8	-1	1	5	91.4	86.2	-2	1	8	2.8*	-1.8
9	0	6	37.7	36.7	-3	0	14	15.6	14.6	-2	1	5	107.0	95.7	-3	1	8	2.8*	5.7
10	0	6	33.2	27.6	-4	0	14	16.9	15.6	-3	1	5	105.4	95.7	-4	1	8	8.9	9.7
11	0	6	17.1	17.2	0	1	1	77.5	87.7	-4	1	5	71.0	71.5	-5	1	8	2.8*	-2.9
0	0	8	66.1	63.1	1	1	1	109.0	99.0	-5	1	5	71.0	70.6	-1	1	10	2.8*	4.0
1	0	8	58.8	57.1	2	1	1	126.1	131.8	-6	1	5	60.4	64.7	-2	1	10	2.8*	-1.5
2	0	8	52.2	51.6	3	1	1	117.5	121.6	-7	1	5	58.1	62.5	0	2	2	111.8	90.9
3	0	8	78.9	76.2	4	1	1	90.1	96.3	-8	1	5	46.5	49.7	1	2	2	110.4	82.6
4	0	8	53.6	54.8	5	1	1	111.4	101.8	-9	1	5	35.1	33.4	2	2	2	98.1	91.5
5	0	8	26.7	30.4	6	1	1	89.7	75.1	-10	1	5	34.5	33.6	3	2	2	82.0	96.5
6	0	8	31.9	34.6	7	1	1	75.5	68.8	-11	1	5	31.6	30.5	4	2	2	64.5	74.7
7	0	8	28.0	34.5	8	1	1	66.8	59.6	-12	1	5	21.4	24.4	5	2	2	66.9	74.1
8	0	8	25.8	26.2	9	1	1	42.0	37.7	-1	1	7	73.5	70.9	6	2	2	65.7	68.9
9	0	8	25.3	22.4	10	1	1	40.6	34.8	-2	1	7	80.8	76.5	7	2	2	50.1	47.9
10	0	8	22.7	20.9	11	1	1	35.3	33.9	-3	1	7	67.2	61.8	8	2	2	43.1	40.2
0	0	10	48.4	43.0	12	1	1	25.7	26.4	-4	1	7	65.2	55.9	9	2	2	37.5	37.2
1	0	10	40.3	41.0	0	1	3	114.9	105.3	-5	1	7	54.0	57.9	10	2	2	32.7	29.9
2	0	10	25.1	29.3	1	1	3	154.7	137.4	-6	1	7	41.0	43.7	11	2	2	23.9	24.7
3	0	10	34.5	35.8	2	1	3	117.9	112.6	-7	1	7	44.0	46.0	12	2	2	16.3	22.1
4	0	10	44.2	44.2	3	1	3	81.1	79.8	-8	1	7	37.4	39.5	0	2	4	93.6	94.5
5	0	10	27.1	29.0	4	1	3	75.8	78.4	-9	1	7	33.7	33.1	1	2	4	75.9	68.8
6	0	10	23.4	25.2	5	1	3	77.3	83.4	-10	1	7	31.8	28.1	2	2	4	61.9	50.7
7	0	10	24.1	23.7	6	1	3	78.5	76.5	-11	1	7	24.8	25.3	3	2	4	79.4	78.9
8	0	10	16.9	16.2	7	1	3	57.5	54.6	-1	1	9	58.2	52.3	4	2	4	69.1	74.0
9	0	10	15.9	14.5	8	1	3	55.3	50.9	-2	1	9	51.5	48.5	5	2	4	44.2	56.3
0	0	12	31.0	26.2	9	1	3	47.3	42.3	-3	1	9	47.3	47.5	6	2	4	52.4	57.1
1	0	12	28.4	26.3	10	1	3	36.8	34.6	-4	1	9	50.9	48.3	7	2	4	49.9	47.2
2	0	12	27.8	26.0	11	1	3	29.7	28.4	-5	1	9	34.0	34.4	8	2	4	36.8	35.5
3	0	12	24.1	22.4	12	1	3	15.2	18.6	-6	1	9	33.3	34.0	9	2	4	35.4	32.4
4	0	12	21.0	20.0	0	1	5	84.1	74.1	-7	1	9	34.0	37.7	10	2	4	29.7	24.7
5	0	12	16.9	16.7	1	1	5	98.6	89.0	-8	1	9	38.2	34.1	11	2	4	20.2	18.3
6	0	12	17.5	16.7	2	1	5	115.2	113.1	-9	1	9	27.2	23.6	0	2	6	68.2	74.6
7	0	12	20.1	18.4	3	1	5	84.1	78.1	-10	1	9	19.3	19.9	1	2	6	69.1	69.8
0	0	14	19.2	16.8	4	1	5	64.5	68.6	-1	1	11	35.9	35.4	2	2	6	50.8	53.9
1	0	14	14.2	15.1	5	1	5	58.6	63.1	-2	1	11	30.1	29.5	3	2	6	48.3	51.7
2	0	14	14.3	13.4	6	1	5	51.8	54.9	-3	1	11	32.4	31.3	4	2	6	51.8	53.8
3	0	14	18.8	15.4	7	1	5	52.3	49.9	-4	1	11	29.5	30.8	5	2	6	38.9	46.6
-1	0	2	82.5	83.8	8	1	5	38.8	37.8	-5	1	11	26.5	28.6	6	2	6	38.0	42.5
-2	0	2	103.5	112.0	9	1	5	33.9	31.0	-6	1	11	22.6	25.6	7	2	6	39.0	39.2
-3	0	2	96.1	111.4	10	1	5	26.5	28.6	-7	1	11	26.2	25.6	8	2	6	31.2	28.7
-4	0	2	87.2	105.6	11	1	5	23.3	26.7	-8	1	11	23.5	21.5	9	2	6	28.7	24.8
-5	0	2	89.9	93.8	0	1	7	69.1	67.4	-1	1	13	17.2	19.3	10	2	6	25.2	22.1
-6	0	2	109.7	101.4	1	1	7	67.2	55.0	-2	1	13	18.7	19.3	0	2	8	45.3	48.5
-7	0	2	73.3	70.9	2	1	7	60.4	61.5	-3	1	13	18.2	20.9	1	2	8	47.4	48.4
-8	0	2	61.7	59.0	3	1	7	50.5	54.3	-4	1	13	20.4	22.3	2	2	8	45.8	44.8
-9	0	2	64.5	56.8	4	1	7	49.2	54.6	-5	1	13	16.1	17.8	3	2	8	47.7	42.7
-10	0	2	31.8	32.7	5	1	7	52.7	50.4	-6	1	13	11.8	14.6	4	2	8	35.4	37.8
-11	0	2	29.3	28.4	6	1	7	37.8	41.1	0	1	2	21.9	15.6	5	2	8	31.4	32.8
-12	0	2	28.8	30.6	7	1	7	28.5	33.4	1	1	2	15.9	-9.7	6	2	8	27.6	29.3
-1	0	4	138.7	139.1	8	1	7	29.5	32.5	2	1	2	2.8*	-0.2	7	2	8	29.3	27.8
-2	0	4	97.2	91.9	9	1	7	20.7	24.0	3	1	2	14.5	17.1	8	2	8	29.3	23.8
-3	0	4	99.6	92.6	10	1	7	17.9	19.5	4	1	2	2.8*	-1.8	9	2	8	23.4	17.7
-4	0	4	89.3	90.9	0	1	9	42.5	44.4	5	1	2	7.8	9.9	0	2	10	42.2	36.7
-5	0	4	88.1	101.9	1	1	9	56.1	54.2	6	1	2	2.8*	4.1	1	2	10	34.3	32.9
-6	0	4	72.3	81.2	2	1	9	50.0	51.0	7	1	2	12.5	-9.7	2	2	10	30.7	29.6
-7	0	4	48.0	49.5	3	1	9	28.7	34.7	8	1	2	12.8	-10.4	3	2	10	32.7	28.6
-8	0	4	61.0	54.8	4	1	9	24.3	30.0	9	1	2	2.8*	2.8	4	2	10	28.1	25.3
-9	0	4	54.6	49.1	5	1	9	28.7	37.0	10	1	2	2.8*	4.5	5	2	10	26.0	23.2
-10	0	4	40.3	39.9	6	1	9	27.6	34.3	0	1	4	13.7	-9.4	6	2	10	25.4	21.7
-11	0	4	33.4	30.4	7	1	9	22.2	24.2	1	1	4	13.3	9.9	7	2	10	23.1	17.3
-12	0	4	23.0	24.2	8	1	9	22.6	23.1	2	1	4	11.3	-9.5	8	2	10	17.9	15.0
-1	0	6	91.1	79.9	9	1	9	14.7	18.5	3	1	4	2.8*	1.7	0	2	12	25.2	23.3
-2	0	6	85.7	68.7	0	1	11	33.4	32.2	4	1	4	7.8	3.6	1	2	12	23.1	21.7
-3	0	6	80.9	78.7	1	1	11	34.1	28.6	5	1	4	2.8*	-1.4	2	2	12	22.4	20.0
-4	0	6	74.2	77.0	2	1	11	35.3	33.9	6	1	4	2.8*	1.8	3	2	12	21.3	19.8
-5	0	6	73.2	73.3	3	1	11	32.2	28.5	0	1	6	7.7	-2.7	4	2	12	17.8	16.4

Can. J. Chem. Downloaded from www.nrcresearchpress.com by 210.87.254.40 on 09/05/12
For personal use only.

TABLE 4 (*Concluded*)

H	K	L	FO	FC	H	K	L	FO	FC	H	K	L	FO	FC	H	K	L	FO	FC
5	2	12	13.6	12.9	-1	2	1	7.8	6.2	-10	3	1	25.7	24.0	7	0	0	66.6	76.1
0	2	14	12.8	13.8	-2	2	1	44.3	36.8	-11	3	1	14.1	17.0	8	0	0	64.0	51.9
-1	2	2	109.2	97.4	-3	2	1	2.7*	1.4	-1	3	3	77.3	59.3	9	0	0	66.4	64.5
-2	2	2	113.8	94.2	-4	2	1	33.7	-32.7	-2	3	3	70.3	54.5	10	0	0	48.1	44.0
-3	2	2	99.4	97.8	-5	2	1	2.7*	5.1	-3	3	3	50.9	54.9	11	0	0	21.3	21.1
-4	2	2	77.0	92.3	-6	2	1	2.7*	-1.3	-4	3	3	48.9	53.7	12	0	0	23.7	25.5
-5	2	2	64.7	66.8	-7	2	1	2.7*	-2.8	-5	3	3	51.4	59.7	0	2	0	103.2	132.6
-6	2	2	54.3	61.5	-8	2	1	6.4	4.9	-6	3	3	46.8	45.4	1	2	0	93.4	96.6
-7	2	2	61.4	56.6	-9	2	1	2.7*	4.3	-7	3	3	39.1	38.4	2	2	0	101.7	96.5
-8	2	2	47.4	44.8	-10	2	1	2.7*	1.7	-8	3	3	40.3	36.7	3	2	0	93.4	91.2
-9	2	2	42.1	39.0	-1	2	3	7.8	9.0	-9	3	3	33.2	29.8	4	2	0	92.4	92.1
-10	2	2	33.5	34.8	-2	2	3	18.7	13.5	-10	3	3	21.8	22.1	5	2	0	85.9	84.3
-11	2	2	26.6	28.5	-3	2	3	36.9	-30.8	-11	3	3	18.1	19.5	6	2	0	58.8	60.1
-12	2	2	15.6	22.0	-4	2	3	2.7*	-5.1	-1	3	5	65.0	61.0	7	2	0	46.3	50.6
-1	2	4	90.5	90.7	-5	2	3	14.1	11.1	-2	3	5	57.2	51.9	8	2	0	46.9	47.8
-2	2	4	100.0	81.1	-6	2	3	8.9	7.1	-3	3	5	39.3	42.3	9	2	0	41.6	41.7
-3	2	4	100.3	88.4	-1	2	5	2.7*	3.9	-4	3	5	46.8	52.3	10	2	0	32.7	32.8
-4	2	4	68.6	70.5	-2	2	5	2.7*	2.3	-5	3	5	38.2	46.6	11	2	0	27.4	27.2
-5	2	4	50.3	60.7	-3	2	5	11.6	7.8	-6	3	5	35.2	38.8	12	2	0	21.4	22.6
-6	2	4	49.9	59.9	-4	2	5	2.7*	-0.9	-7	3	5	36.1	36.4	0	4	0	44.6	34.8
-7	2	4	46.0	45.4	-5	2	5	2.7*	-3.7	-8	3	5	33.9	31.1	1	4	0	55.1	49.7
-8	2	4	42.5	39.5	-1	2	7	2.7*	2.8	-9	3	5	28.6	25.5	2	4	0	51.4	48.9
-9	2	4	42.5	41.0	-2	2	7	13.9	12.1	-10	3	5	21.7	22.1	3	4	0	46.7	44.2
-10	2	4	36.2	34.7	-3	2	7	2.7*	-0.2	-1	3	7	46.8	43.7	4	4	0	41.6	39.2
-11	2	4	23.7	24.2	-4	2	7	17.0	-17.5	-2	3	7	30.1	33.6	5	4	0	35.3	32.3
-1	2	6	61.6	62.9	-5	2	7	2.7*	2.3	-3	3	7	36.1	40.3	6	4	0	29.8	35.5
-2	2	6	80.6	71.1	-1	2	9	2.7*	-5.0	-4	3	7	37.3	40.8	7	4	0	23.7	28.5
-3	2	6	71.1	67.8	-2	2	9	2.7*	4.3	-5	3	7	29.5	36.0	8	4	0	21.8	24.3
-4	2	6	49.1	5..7	-3	2	9	5.5	-6.8	-6	3	7	29.8	34.8	9	4	0	17.4	18.4
-5	2	6	47.4	51.6	-4	2	9	2.7*	-1.6	-7	3	7	29.8	29.4	10	4	0	14.3	16.9
-6	2	6	38.3	47.0	-1	2	11	2.7*	0.5	-8	3	7	27.1	23.4	0	6	0	11.7	11.7
-7	2	6	34.5	39.8	-2	2	11	2.7*	3.3	-9	3	7	22.3	21.0	1	6	0	16.3	15.4
-8	2	6	39.5	38.8	0	3	1	93.7	87.3	-1	3	9	26.5	26.8	2	6	0	17.0	14.7
-9	2	6	38.0	36.0	1	3	1	88.9	81.9	-2	3	9	28.1	31.0	3	6	0	16.0	15.7
-10	2	6	28.1	26.1	2	3	1	70.3	63.9	-3	3	9	30.3	32.1	4	6	0	12.8	13.3
-11	2	6	17.7	20.9	3	3	1	57.5	62.5	-4	3	9	24.7	27.5	1	1	0	8.4	-6.3
-1	2	8	45.1	52.6	4	3	1	70.1	61.4	-5	3	9	24.7	28.5	2	1	0	51.6	53.2
-2	2	8	54.1	53.3	5	3	1	50.7	42.5	-6	3	9	22.3	25.4	3	1	0	10.8	13.2
-3	2	8	43.7	42.2	6	3	1	49.3	44.9	-7	3	9	19.8	20.2	4	1	0	10.2	-12.4
-4	2	8	38.3	40.4	7	3	1	56.0	45.9	-8	3	9	15.9	16.5	5	1	0	5.3	-4.5
-5	2	8	38.3	41.6	8	3	1	43.3	36.0	-1	3	11	20.6	21.2	6	1	0	6.7	-4.5
-6	2	8	33.5	38.1	9	3	1	36.3	31.7	-2	3	11	24.7	23.4	7	1	0	12.3	-12.9
-7	2	8	34.1	33.0	10	3	1	26.8	25.0	-3	3	11	18.2	19.5	8	1	0	2.7*	-0.7
-8	2	8	32.4	30.2	11	3	1	16.1	18.2	-4	3	11	16.7	19.5	9	1	0	10.0	10.2
-9	2	8	27.6	25.9	0	3	3	86.9	67.4	-5	3	11	15.5	20.0	10	1	0	2.7*	0.1
-10	2	8	19.3	20.9	1	3	3	84.3	71.0	-6	3	11	13.0	17.0	1	3	0	4.7	-6.6
-1	2	10	42.0	36.1	2	3	3	76.1	63.6	-1	3	13	14.3	14.5	2	3	0	8.6	7.1
-2	2	10	34.1	30.9	3	3	3	55.9	55.7	0	3	2	11.8	7.6	3	3	0	8.4	-5.1
-3	2	10	33.3	31.9	4	3	3	57.8	58.0	1	3	2	2.7*	-3.2	4	3	0	2.7*	3.1
-4	2	10	34.7	31.9	5	3	3	48.4	48.5	2	3	2	2.7*	-2.2	5	3	0	2.7*	-3.3
-5	2	10	28.3	28.8	6	3	3	36.6	33.9	3	3	2	13.7	-11.1	6	3	0	2.7*	-1.6
-6	2	10	24.8	26.8	7	3	3	44.4	37.6	4	3	2	9.6	-9.1	7	3	0	2.7*	-2.1
-7	2	10	24.1	24.5	8	3	3	39.4	34.0	5	3	2	18.5	18.1	8	3	0	1.8*	-1.8
-8	2	10	23.9	22.0	9	3	3	29.4	25.5	6	3	2	2.7*	4.5	9	3	0	2.7*	2.2
-1	2	12	22.4	20.7	10	3	3	21.4	22.5	7	3	2	-5.8	-5.9	10	3	0	2.7*	-1.7
-2	2	12	21.8	22.1	11	3	3	14.3	18.3	8	3	2	2.6*	-3.2	1	5	0	2.7*	-1.2
-3	2	12	23.5	22.9	0	3	5	61.0	53.7	9	3	2	2.7*	0.1	2	5	0	2.7*	-3.9
-4	2	12	16.6	18.8	1	3	5	61.8	54.6	10	3	2	2.7*	-3.6	3	5	0	2.7*	1.9
-5	2	12	14.8	18.8	2	3	5	63.0	53.9	0	3	4	7.1	3.7	4	5	0	2.7*	0.8
-6	2	12	20.0	19.7	3	3	5	51.0	48.4	1	3	4	2.7*	2.2	5	5	0	2.7*	-1.4
-1	2	14	12.2	12.8	4	3	5	44.1	41.5	2	3	4	2.7*	-1.5					
0	2	1	4.4	4.2	5	3	5	40.3	40.7	3	3	4	2.7*	-1.3					
1	2	1	7.9	-5.6	6	3	5	34.5	34.1	4	3	4	14.5	-14.2					
2	2	1	2.7*	-1.2	7	3	5	30.0	28.7	5	3	4	2.7*	-2.9					
3	2	1	16.6	-15.9	8	3	5	30.5	29.0	6	3	4	5.9	7.6					
4	2	1	2.7*	-0.0	9	3	5	21.7	22.0	7	3	4	2.7*	-1.5					
5	2	1	8.3	-6.6	10	3	5	13.9	16.4	0	3	6	15.5	12.9					
6	2	1	8.7	-5.6	0	3	7	44.2	45.5	1	3	6	2.7*	1.7					
7	2	1	20.3	19.3	1	3	7	42.7	40.0	2	3	6	2.7*	1.5					
8	2	1	2.7*	2.9	2	3	7	42.7	42.2	3	3	6	2.7*	-1.0					
9	2	1	8.5	-8.1	3	3	7	40.3	41.3	4	3	6	2.7*	0.7					
10	2	1	2.7*	-3.0	4	3	7	34.8	33.8	5	3	6	2.7*	-2.6					
0	2	3	2.7*	-1.5	5	3	7	26.5	25.3	-1	3	2	8.1	-5.9					
2	2	3	2.7*	-4.5	6	3	7	27.3	26.0	-2	3	2	2.7*	1.8					
3	2	3	10.6	11.3	7	3	7	21.8	22.6	-3	3	2	5.0	5.3					
4	2	3	2.7*	0.3	8	3	7	19.3	20.0	-4	3	2	13.5	12.6					
5	2	3	2.7*	-4.8	9	3	7	17.7	18.8	-5	3	2	2.2*	-2.5					
6	2	3	12.6	-11.6	0	3	9	29.0	30.9	-6	3	2	12.0	-14.2					
0	2	5	12.3	-12.9	1	3	9	28.2	28.7	-7	3	2	2.7*	3.4					
1	2	5	2.7*	1.7	2	3	9	26.0	27.4	-8	3	2	2.7*	3.5					
2	2	5	2.7*	-0.5	3	3	9	28.1	29.9	-9	3	2	2.7*	1.7					
3	2	5	2.7*	-2.0	4	3	9	25.6	27.5	-10	3	2	2.7*	-0.0					
4	2	5	2.7*	3.1	5	3	9	20.8	20.7	-1	3	4	18.0	13.6					
5	2	5	2.7*	-3.5	6	3	9	17.4	17.5	-2	3	4	2.7*	-1.4					
0	2	7	2.7*	2.3	7	3	9	16.6	17.1	-3	3	4	2.7*	-2.9					
1	2	7	2.7*	-2.4	0	3	11	19.5	18.9	-4	3	4	2.7*	3.7					
2	2	7	2.7*	3.9	1	3	11	19.1	20.5	-5	3	4	11.1	-14.0					
3	2	7	2.7*	-2.6	2	3	11	16.0	17.9	-6	3	4	2.7*	-1.3					
4	2	7	2.7*	-0.4	3	3	11	16.0	17.3	-7	3	4	8.1	7.2					
5	2	7	5.5	-7.1	4	3	11	15.0	17.8	-1	3	6	2.7*	2.0					
6	2	7	2.7*	-3.2	5	3	11	12.8	15.1	-2	3	6	14.7	-18.8					
7	2	7	11.6	10.5	-1	3	1	77.3	70.4	-3	3	6	2.7*	0.4					
0	2	9	2.7*	-2.3	-2	3	1	53.3	58.5	-4	3	6	2.7*	2.5					
1	2	9	9.5	9.3	-3	3	1	57.1	64.2	-5	3	6	2.7*	1.0					
2	2	9	2.7*	2.0	-4	3	1	56.7	52.8	1	0	0	133.2	147.0					
3	2	9	2.7*	-2.0	-5	3	1	59.6	54.0	2	0	0	76.9	83.6					
4	2	9	2.7*	-0.3	-6	3	1	57.1	55.5	3	0	0	108.5	118.1					
0	2	11	10.0	-8.7	-7	3	1	45.9	42.0	4	0	0	99.6	98.7					
1	2	11	2.7*	1.1	-8	3	1	43.3	37.5	5	0	0	107.2	90.0					
2	2	11	2.7*	4.6	-9	3	1	36.6	33.6	6	0	0	95.2	82.6					

* Reflections indicated by asterisks are the accidentally unobserved reflections

Can. J. Chem. Downloaded from www.nrcresearchpress.com by 210.87.254.40 on 09/05/12
For personal use only.

TABLE 5

(*a*) Least-squares planes through Hg and C atoms

Designation	No. of atoms defining plane	Equation*	Atoms included
Plane 1	7	$-0.6368X + 0.7208Y + 0.2738Z - 3.5789 = 0$	C_1, C_2, C_3, C_4, C_5, C_6, C_7
Plane 2	8	$-0.6403X + 0.7172Y + 0.2753Z - 3.5561 = 0$	Hg, C_1, C_2, C_3, C_4, C_5, C_6, C_7

*X, Y, and Z are orthogonal coordinates in Å.

(*b*) Deviations of atoms from the planes

Plane	Deviations, Å							
	Hg	C_1	C_2	C_3	C_4	C_5	C_6	C_7
1	−0.041	0.013	−0.015	−0.007	0.031	−0.036	0.013	0.001
2	−0.018	0.025	−0.007	−0.006	0.029	−0.035	0.021	−0.010

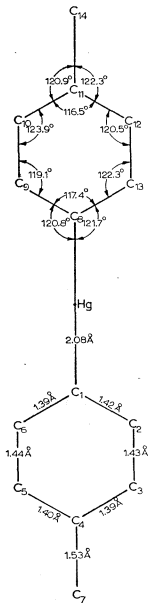

FIG. 4. Bond lengths and angles of di-*p*-tolyl mercury.

greater than van der Waals diameter of a methyl group.

The linearity of the C—Hg—C bonds has been confirmed by the present work and it would be reasonable to assume that in all mercury aryls, the C—Hg—C bonds are linear. This eliminates the possibility that the apparent moments of these compounds are due to the non-linearity of the mercury–carbon bonds.

The authors wish to thank Mr. Wyne Wilson of the Computing Centre of this university for writing the various programs for crystallographic calculations, Dr. C. Calvo of McMaster University for supplying the least-squares refinement program, and the National Research Council of Canada for financial support.

1. L. E. ORGEL. J. Chem. Soc. 4186 (1958).
2. W. C. HORNING and G. F. WRIGHT. Can. J. Chem. **42**, 2065 (1966).
3. J. A. IBERS. Acta Cryst. **11**, 447 (1958).
4. A. J. FREEMAN. Acta Cryst. **12**, 261 (1959).
5. International tables for X-ray crystallography. Vol. III. Kynoch Press. 1962. p. 215.

Can. J. Chem. Downloaded from www.nrcresearchpress.com by 210.87.254.40 on 09/05/12
For personal use only.

Etude par résonance paramagnétique électronique de la radiolyse en phase solide de composés cycliques perfluorés

CLAUDE CHACHATY, ALAIN FORCHIONI ET MASARU SHIOTANI

Service de Chimie physique, Centre d'Études Nucléaires de Saclay, Boîte Postale N°. 2,91Gif-sur-Yvette, France

Reçu le 11 septembre 1969

Le perfluorocyclohexane (PFCH) et le perfluorométhylcyclohexane (PFMCH) ont été irradiés en phase solide par les rayons γ du ^{60}Co. Le spectre de résonance paramagnétique électronique du PFCH irradié à 77 °K correspond essentiellement aux radicaux

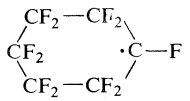

qui se réorientent dans la matrice au-dessus de 160 °K et se recombinent au point de transition situé à 180 °K. Lorsque l'irradiation est effectuée à 200 °K, $C_6F_{11}\cdot$ se forme également mais réagit sur le PFCH en donnant un radical que nous pensons être $CF_3-(CF_2)_5-$

Le spectre du PFMCH irradié à 77 °K n'a pas été identifié, il pourrait correspondre en partie à $(\cdot C_6F_{11}CF_3)^-$. A partir de 160–170 °K le spectre correspond uniquement à

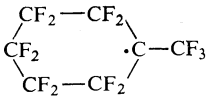

L'équivalence des quatre fluors γ ainsi que l'intensité relative 1:4:1 des trois principaux groupes de raies observés au-dessus de 210 °K suggèrent que le cycle effectue des mouvements rapides d'inversion.

Nous avons également étudié les radicaux

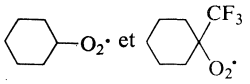

formés par irradiation en présence d'oxygène. La variation de leur spectre avec la température, en particulier au voisinage des points de transition permet de caractériser aisément les mouvements moléculaires mis en jeux.

Perfluorocyclohexane (PFCH) and perfluoromethylcyclohexane (PFMCH) have been irradiated in the solid state by γ rays of ^{60}Co. The electron spin resonance (e.s.r.) spectrum of PFCH irradiated at 77 °K corresponds mainly to

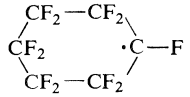

which is tumbling in the matrix above 160 °K and disappears at the transition point (180 °K). When γ irradiation is carried out at 200 °K, $C_6F_{11}\cdot$ is also produced, but reacts with PFCH giving a radical supposed to be $CF_3-(CF_2)_5-$

The e.s.r. spectrum of PFMCH γ irradiated at 77 °K has not been identified; it might be attributable in part to $(\cdot C_6F_{11}CF_3)^-$. Above 160–170 °K, the e.s.r. spectrum corresponds only to

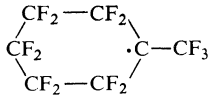

The equal coupling of the four γ fluorines and also the relative intensity 1:4:1 of the three main groups of lines observed above 210 °K suggest that ring inversion occurs with a high rate.

We have also studied the radicals

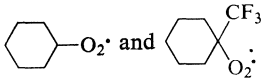

produced by γ irradiation in the presence of oxygen. The variation of their spectra with temperature, particularly near the transition points, is very characteristic of the motion involved.

Can. J. Chem. Downloaded from www.nrcresearchpress.com by 210.87.254.5 on 09/05/12
For personal use only.

Can. J. Chem. Downloaded from www.nrcresearchpress.com by 210.87.254.5 on 09/05/12
For personal use only.

Introduction

L'étude des radicaux fluorocarbonés a été abordée récemment par les physico-chimistes, en particulier dans le domaine de la résonance paramagnétique électronique (r.p.e.). Le problème du couplage hyperfin des fluors n'est pas complétement élucidé, malgré des progrès récents (1–4), car les données expérimentales sont assez restreintes, surtout celles relatives aux fluors β.

Par ailleurs, les mécanismes de formation de ces radicaux par radiolyse diffèrent notablement de ceux des radicaux hydrogénés sur lesquels portent la plupart des travaux, du fait que l'énergie de la liaison C—F (105 kcal/mole) est plus élevée que celle de la liaison F—F (38 kcal/mole) (5), alors que celle de H—H est généralement plus élevée que celle de C—H et que, de plus, le fluor possède une affinité électronique appréciable (85 kc/mole) (6).

Pour apporter une nouvelle contribution à ce domaine, nous nous sommes proposés d'étudier par r.p.e. la radiolyse en phase solide du perfluorocyclohexane (PFCH) et du perfluorométhylcyclohexane (PFMCH).

Ces composés ont été choisis en raison des nombreux travaux effectués sur leurs homologues hydrogénés (voir par exemple réfs. 7–10) qui peuvent amener des comparaisons intéressantes, et du fait également qu'ils constituent des matrices inertes susceptibles de piéger des radicaux très réactifs (11).

De plus, les produits de radiolyse en phase gazeuse du perfluorocyclohexane ont été identifiés par chromatographie (12) et par spectrométrie de masse (13) ce qui permet de recouper certains résultats que nous avons obtenus.

Partie expérimentale

Les expériences ont été effectuées sur des produits "Imperial Smelting". Le perfluorométhylcyclohexane a été utilisé tel quel, une analyse par spectrométrie de masse ayant indiqué la présence de moins de 1% d'impuretés, constituées essentiellement de perfluorotoluène. Le perfluorocyclohexane a été purifié par sublimations répétées. Les échantillons étaient dégazés sous une pression résiduelle de 10^{-4} Torr dans des ampoules en silice "Spectrosil". Quelques uns ont été irradiés en présence d'oxygène pour étudier les radicaux péroxydes. Les irradiations ont été effectuées à l'aide d'une source de 20 KCi de ^{60}Co avec des doses de 6 à 12 Mrads, en général à −196 °C, parfois également à −80 et à 0 °C.

Le spectromètre r.p.e. est un Varian V 4502 fonctionnant à 9200–9300 MHz avec une fréquence de modulation de 100 KHz. On déterminait le facteur g des radicaux fluorés en enregistrant leur spectre simultanément à celui d'un échantillon de brai, résonant à $g = 2.0029$ et placé dans un compartiment d'une double cavité V 4532. Le champ magnétique était mesuré à l'aide d'un magnétomètre à résonance nucléaire Varian F8 relié à un fréquencemètre Rochar A 1149.

Les mesures étaient effectuées en maintenant les échantillons à la température d'irradiation, puis en les réchauffant progressivement à l'intérieur de la cavité, dans un cryostat réglable entre −180 °C et la température ambiante.

Résultats et Discussion

Perfluorocyclohexane

Le PFCH est solide à température ambiante, son point de sublimation étant de 50 °C. Il possède un point de transition de phases à −93 °C (180 °K) mis en évidence par résonance magnétique nucléaire (r.m.n.) (14).

Le spectre r.p.e. du PFCH irradié à 77 °K a une largeur totale de 440 G. Nous n'avons pu analyser sa structure hyperfine, trop mal résolue au voisinage de cette température. Cette mauvaise résolution est essentiellement due aux couplages hyperfins très anisotropes des fluors[1].

A partir de 150 °K, on observe la croissance progressive d'un spectre "isotrope" centré à $g = 2.0039 \pm 0.0001$, comportant quatre groupes de raies bien résolues.

Comme nous l'avons indiqué dans une note préliminaire (15), ce spectre, qui devient prédominant au voisinage du point de transition est attribuable à $\dot{C}_6F_{11}$, les constantes de couplages des fluors étant $a_1 = 70.5$ G (1F), $a_2 = 61.25$ G (2F), $a_3 = 7.2$ G (4F). On peut constater sur la Fig. 2 le bon accord entre le spectre expérimental et celui calculé à partir de ces constantes.

a_1 et a_2 sont respectivement attribuables au fluor α et à deux fluors liés aux deux carbones β de $C_6F_{11}^{\cdot}$, a_3 peut correspondre aux quatre fluors γ, le couplage des deux autres fluors β étant inférieur à la largeur de raie (4–5 G) ou à deux fluors γ et à deux fluors β. Il est probable que dans le cas d'une structure rigide du cycle, deux fluors γ_1 et γ_2 ayant des positions inéquivalentes par rapport à l'orbitale de l'électron non apparié aient des couplages a_{γ_1} et a_{γ_2} différents (Fig. 3).

Un même couplage des quatre fluors γ impliquerait donc l'échange, par inversion du cycle,

[1]Dans ce texte, nous appellerons parfois "spectres anisotropes" les spectres de radicaux bloqués, par opposition aux "spectres isotropes" de radicaux en libre réorientation, pour lesquels l'anisotropie du tenseur g et du couplage hyperfin est annulée en moyenne.

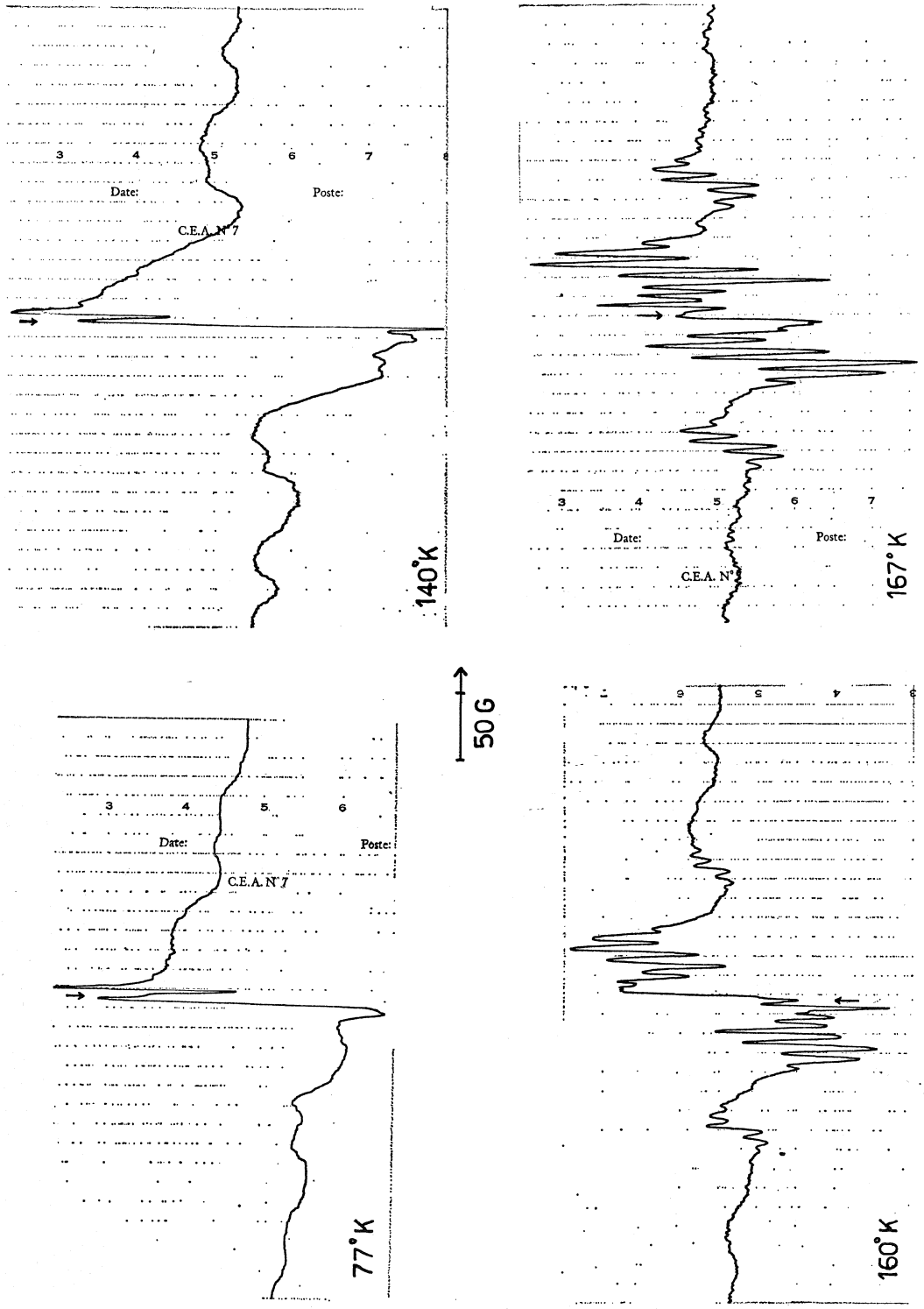

FIG. 1. Spectre du perfluorocyclohexane irradié à 77 °K puis réchauffé. Dans cette figure et les suivantes, les flèches verticales correspondent à $g = 2.0029$.

Can. J. Chem. Downloaded from www.nrcresearchpress.com by 210.87.254.5 on 09/05/12
For personal use only.

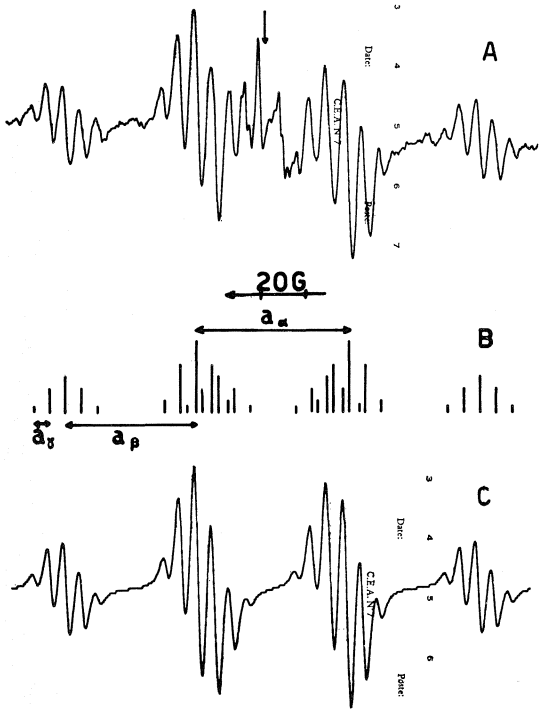

FIG. 2. Spectres du radical perfluorocyclohexyle. *A*, expérimental à 160 °K; *B*, spectre théorique correspondant à $a_F^{\alpha} = 70.5$ G, $a_F^{\beta_1} = 61$ G, $a_F^{\gamma_1} = a_F^{\gamma_2}$ ou $a_F^{\beta_2} = 7$ G (voir texte); *C*, spectre obtenu par calcul électronique en prenant $a_F^{\alpha} = 70$ G, $a_F^{\beta_1} = 61$ G, $a_F^{\gamma} = 7.2$ G pour une largeur de raie. $\Delta H_{1/2} = 6$ G (lorentziennes). La partie centrale du spectre *A* correspond au pic de la silice et à un autre radical non identifié.

de deux fluors γ portés par un même carbone, à une fréquence supérieure à $a_{\gamma_1} - a_{\gamma_2}$. L'exemple du cyclohexyle (9, 10) et du perfluorométhylcyclohexyle (15) dont il sera question plus loin, indique que l'on devrait observer alors l'élargissement de certaines raies qui peuvent même devenir indétectables quand la fréquence d'inversion augmente.

Dans le domaine où l'on a observé le spectre "isotrope" de $C_6F_{11}^{\cdot}$ (150–200 °K), toutes les raies ont la même largeur, pratiquement invariante avec la température. L'intensité relative 1–3–3–1 des quatre groupes de raies indique d'autre part qu'il n'y a pas disparition de certaines raies par échange rapide de fluors liés à un même carbone. L'attribution de a_3 à deux fluors β et deux fluors γ nous paraît donc plus plausible qu'à quatre fluors γ.

La variation avec la température du spectre r.p.e. du PFCH irradié à 77 °K est réversible

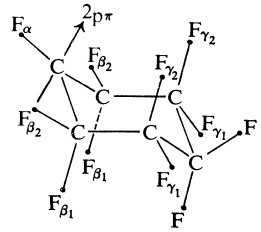

FIG. 3. Diagramme représentant la forme "chaise", configuration la plus stable, du radical perfluorocyclohexyle. On constate que les fluors γ_1 et γ_2 occupent des positions très différentes par rapport à l'axe de l'orbitale $2p\pi$ de l'électron non apparié qui fait un angle d'environ 90° avec la liaison $C_\gamma—F_{\gamma_1}$ et de 30° avec la liaison $C_\gamma—F_{\gamma_2}$.

pour l'essentiel; par conséquent $C_6F_{11}^{\cdot}$ est formé d'une manière prédominante sous irradiation γ. Cependant deux bandes extrêmes écartées de 440 G disparaissent définitivement au cours du réchauffement. Un tel écart est caractéristique d'un groupe $—CF_2^{\cdot}$ et correspond à la somme des valeurs principales $A_{\parallel}^{F}$ du tenseur hyperfins des fluors α (16, 17). Il est donc possible qu'il y ait formation d'une faible proportion de radicaux linéaires selon les réactions

[1] 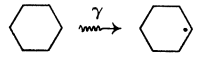

[2] 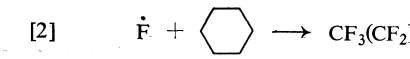

postulées par McKenzie *et al.* (12).

Lorsque le PFCH est irradié en présence d'oxygène, la peroxydation des radicaux fluorés s'effectue à partir de 140 °K. Malgré l'absence de structure hyperfine des spectres des peroxydes, il est certain, d'après ce qu'on a vu plus haut, que le radical prédominant est $C_6F_{11}O_2^{\cdot}$.

Entre 77 et 160 ± 5 °K, le spectre de $C_6F_{11}O_2^{\cdot}$ présente la structure caractéristique de radicaux péroxydes bloqués, avec deux pics dont les maxima donnent les valeurs principales de *g*: $g_{\parallel} = 2.0403 \pm 0.0002$ selon l'axe O—O, $g_{\perp} = 2.0043 \pm 0.0002$ dans le plan perpendiculaire à cette liaison d'où l'on déduit

[3] $g_i = \frac{1}{3}(g_{\parallel} + 2g_{\perp}) = 2.0163 \pm 0.0002$

A partir de 160 °K environ apparaît une raie unique dont l'intensité relative croît avec la température et qui est superposée au spectre anisotrope des radicaux péroxydes. Cette raie est centrée à $g \simeq 2.016$ et correspond donc aux

Can. J. Chem. Downloaded from www.nrcresearchpress.com by 210.87.254.5 on 09/05/12
For personal use only.

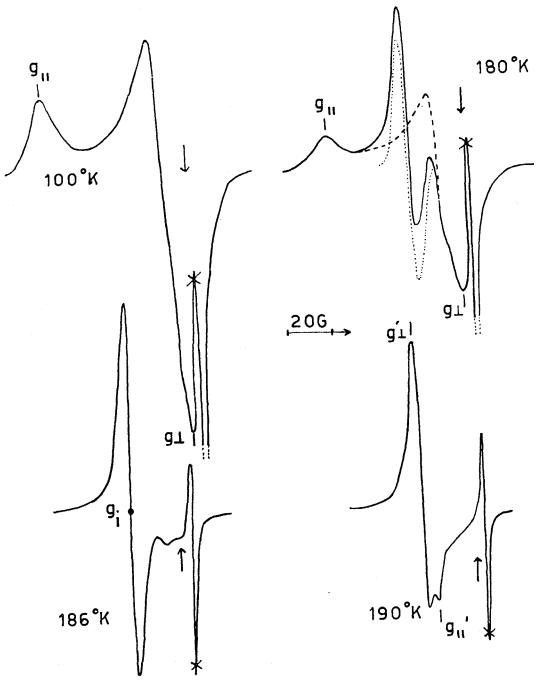

FIG. 4. Spectre du radical $C_6F_{11}O_2^{\cdot}$, les pics marqués d'une croix sont dûs à la silice de l'ampoule.

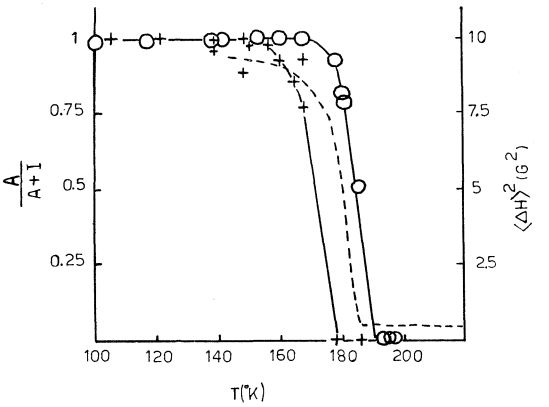

FIG. 5. Concentration relative, en fonction de la température, des radicaux $C_6F_{11}^{\cdot}$ (+) et $C_6F_{11}O_2^{\cdot}$ (○) bloqués. En pointillés: courbe du second moment du spectre r.m.n. du perfluorocyclohexane d'après la réf. 14 (A = anisotrope, I = isotrope).

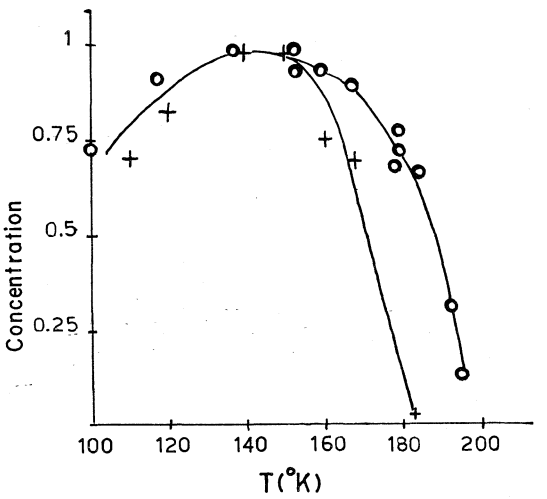

FIG. 6. Concentration (unités arbitraires) des radicaux $C_6F_{11}^{\cdot}$ (+) et $C_6F_{11}O_2^{\cdot}$ (○) en fonction de la température.

radicaux $C_6F_{11}O_2^{\cdot}$ en réorientation isotrope. Elle décroît rapidement au voisinage du point de transition (180 °K) du fait de la recombinaison de ces radicaux et l'on peut parfois observer avant leur disparition complète un autre spectre caractérisé par $g_{\parallel}' = 2.0123 \pm 0.0002$, $g_{\perp}' = 2.0182 \pm 0.0002$, $g_i \simeq 2.0162 \pm 0.0002$. Ce dernier est attribuable à des radicaux $C_6F_{11}O_2^{\cdot}$ pour lesquels le cycle est bloqué tandis que le groupe O—O tourne autour de la liaison C—O.

La relation

$$[4] \qquad \frac{g_{\parallel}' - g_{\perp}'}{g_{\parallel} - g_{\perp}} = 1 - \tfrac{3}{2}\sin^2\alpha$$

donnée par Toriyama et Iwasaki (18), où α est le demi angle au sommet du cône décrit par O—O, indique que l'angle C—O—O est égal à 118 ± 2°.

Nous avons déterminé par ailleurs en fonction de la température, le rapport $A/(A + I)$ de l'intensité des spectres anisotropes (radicaux bloqués), à celle des spectres globaux des radicaux $C_6F_{11}^{\cdot}$ et $C_6F_{11}O_2^{\cdot}$.

On peut constater sur la Fig. 5 que la décroissance de ce rapport, au voisinage du point de transition, est similaire à celle du second moment du spectre r.m.n. du PFCH (14) et donc que la réorientation des radicaux est en corrélation avec celle des molécules de la matrice. La recombinaison des radicaux s'effectue également au point de transition, les radicaux péroxydes étant un peu plus stables que les radicaux $C_6F_{11}^{\cdot}$ (Fig. 6).

Nous avons effectué aussi une série d'expériences en recuisant des échantillons dégazés ou non à 160–170 °K pendant 45 min avant de les irradier à 77 °K, afin d'éviter le piégeage éventuel de la phase "hautes températures" au-dessous de

Can. J. Chem. Downloaded from www.nrcresearchpress.com by 210.87.254.5 on 09/05/12
For personal use only.

Can. J. Chem. Downloaded from www.nrcresearchpress.com by 210.87.254.5 on 09/05/12
For personal use only.

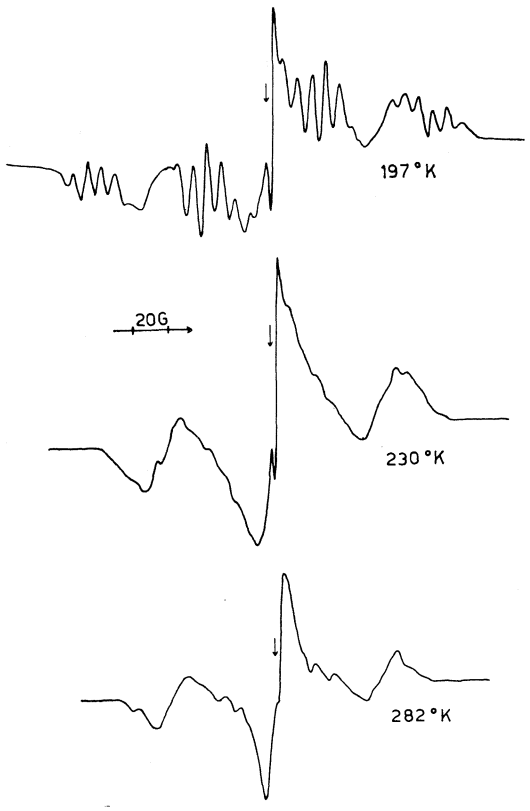

FIG. 7. Spectres du perfluorocyclohexane irradié à 195 °K puis réchauffé.

180 °K. Le comportement des radicaux en fonction de la température ne diffère pas essentiellement de celui observé pour les échantillons trempés directement à 77 °K.

L'irradiation à 200 °K du PFCH dégazé, donc en sa phase "hautes températures", conduit également au radical $C_6F_{11}^{\cdot}$ mais celui-ci disparaît rapidement (demi vie d'environ 1 h à 200 °K) en donnant un nouveau radical dont le spectre est un triplet 1:2:1 d'écart hyperfin 60 ± 1 G (Fig. 7). La largeur de ce triplet varie peu entre 77 et 300 °K, il ne présente donc pas l'anisotropie caractéristique d'un groupe $—CF_2^{\cdot}$, pour lequel, on l'a vu, cette largeur peut atteindre 400 G environ.

La constante de couplage observée pour ce nouveau spectre est proche de celle des deux fluors β les plus fortement couplés des radicaux $^{\cdot}C_6F_{11}$ et $^{\cdot}C_6F_{10}CF_3$. La stabilité du radical correspondant, qui ne disparaît que par sublimation du PFCH, indique par ailleurs que la valence libre est localisée sur un carbone tertiaire, comme le suggère l'exemple de $^{\cdot}C_6F_{10}CF_3$ dont il sera question plus loin. Il s'agirait donc d'un radical

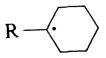

où R est un groupement que l'on ne peut identifier par r.p.e. en raison de la résolution insuffisante des spectres. Nous suggérons sous toutes réserves que le radical en question est

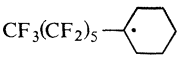

formé par la réaction

[5] 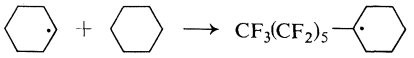

trop lente pour être observée dans la phase "basses températures". McKenzie *et coll.* (12) ont en effet détecté

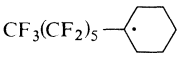

parmi les produits de radiolyse du PFCH, mais ils supposent que ce produit résulte de la recombinaison du radical $CF_3(CF_2)_5^{\cdot}$ et du perfluorocyclohexyle.

Perfluorométhylcyclohexane

Le PFMCH fond à 234 °K et possède deux points de transition de phase, l'un à 226.6 °K, l'autre à 172.8 °K, qui ont été mis en évidence par des mesures de chaleur spécifique (19). Ces mesures indiquent que si le PFMCH est solidifié rapidement à 77 °K, la phase intermédiaire est piégée au-dessous de 173 °K et redonne la phase "basses températures" vers 150 °K. Nos pré-

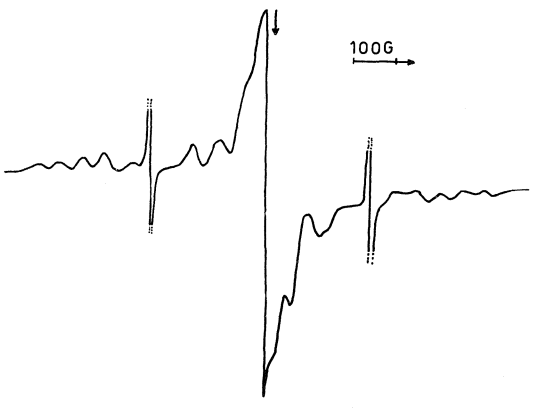

FIG. 8. Spectre à 77–110 °K du perfluorométhyl cyclohexane irradié à 77 °K. Les deux raies écartées de 500 G sont dues aux atomes $H^{\cdot}$ piégés dans la silice de l'ampoule.

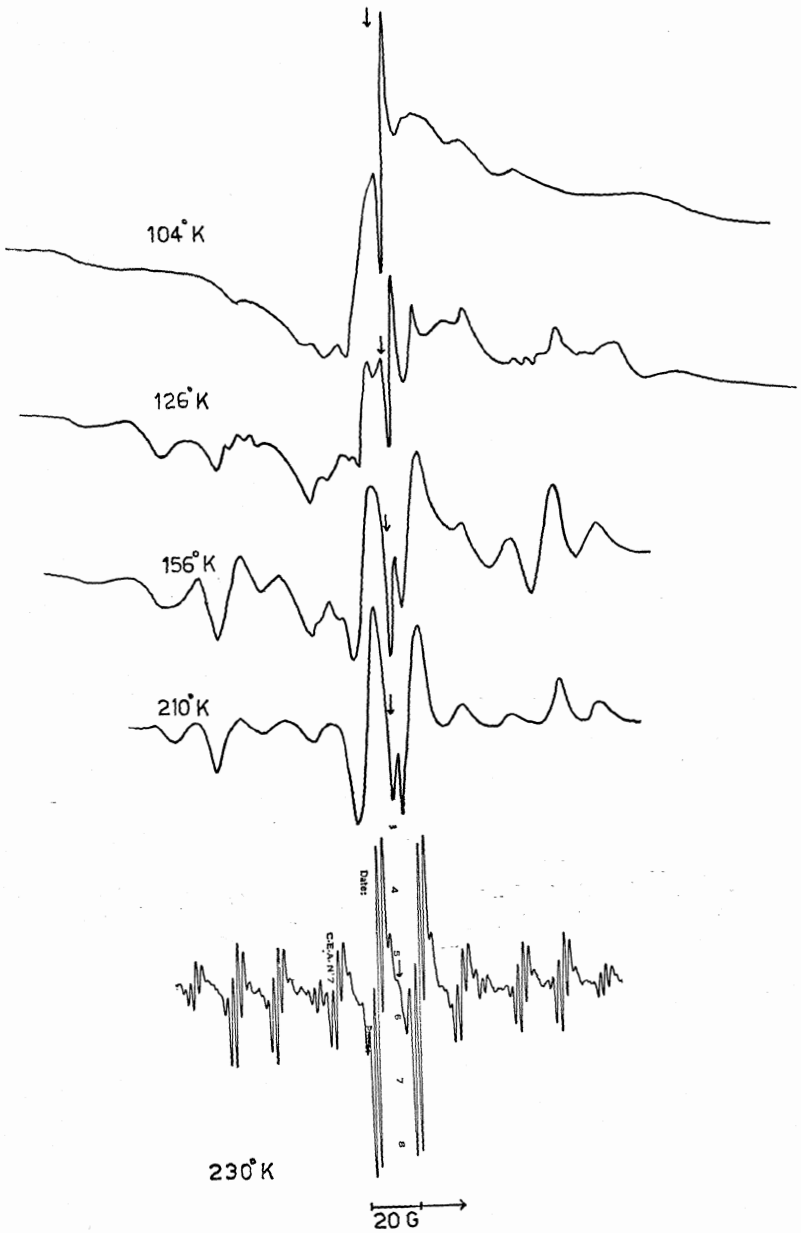

FIG. 9. Evolution en fonction de la température, du spectre du radical (échantillon non recuit).

mières expériences ont été effectuées sur des échantillons solidifiés directement à 77 °K avant irradiation. Par la suite les échantillons ont été préalablement recuits à 160 °K pendant 45 min pour n'obtenir que la phase stable au-dessous de 173 °K.

Le spectre obtenu après irradiation γ à 77 °K a une largeur totale de 1080 G. Les bandes extrêmes sont résolues, mais la partie centrale est masquée sur 200 G par un autre spectre dépourvu de structure hyperfine qui n'est certainement pas celui de $\dot{C}_6F_{10}CF_3$. Il est possible que le spectre répartie sur un millier de gauss soit dû au radical anion $(\dot{C}_6F_{11}CF_3)^-$ pour lequel l'électron non apparié aurait une densité appréciable dans l'orbitale 3s des fluors. En effet

Can. J. Chem. Downloaded from www.nrcresearchpress.com by 210.87.254.5 on 09/05/12
For personal use only.

Can. J. Chem. Downloaded from www.nrcresearchpress.com by 210.87.254.5 on 09/05/12
For personal use only.

dans le cas, par exemple, du radical ion $\cdot F_2^-$, pour lequel la densité de spin est principalement localisée dans cette orbitale, le couplage hyperfin des fluors est de 760 G (20). Une autre hypothèse que nous avons envisagée pour ce spectre très étendu, est son attribution à la transition $\Delta M_S = \pm 1$ du spin électronique total d'une paire de radicaux piégés à quelques angströms l'un de l'autre. Cette seconde possibilité nous paraît moins plausible car nous n'avons pas observé la transition $\Delta M_S = \pm 2$, qui en serait caractéristique.

Dans le cas des échantillons non recuits, le spectre représenté sur le Fig. 8 disparaît vers 120 °K pour faire place à celui du radical

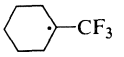

Cette transformation se produit vers 170 °K pour les échantillons recuits. Notons qu'aucun spectre attribuable à $\cdot C_6F_{12}^-$ n'a été observé dans le cas du perfluorocyclohexane.

La résolution du spectre de

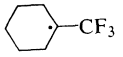

s'améliore considérablement quand la température s'élève (Fig. 9), l'anisotropie du couplage des fluors β disparaissant vers 150 °K par suite de la réorientation isotrope des radicaux. Le spectre devient alors un triplet 1:2:1 de quartets 1:3:3:1 centré à $g = 2.0027 \pm 0.0001$ dû au couplage prédominant de deux fluors β du cycle ($a_1' = 59 \pm 0.5$ G), et des fluors équivalents du groupe CF_3 ($a_2 = 18 \pm 0.5$ G). Ces attributions ont été vérifiées en reconstituant le spectre à l'aide d'un calculateur électronique JEOL JRA1, en essayant différentes largeurs de raies lorentziennes et gaussiennes, cette dernière forme de raie donnant la meilleure analogie entre les spectres théoriques et expérimentaux sans toutefois permettre une parfaite équivalence (Fig. 10).

A partir de 210 °K, donc au voisinage du deuxième point de transition, chaque bande du spectre de $\cdot C_6F_{10}CF_3$ se divise en un quintet binômial (Figs. 9 et 11). La structure de ce

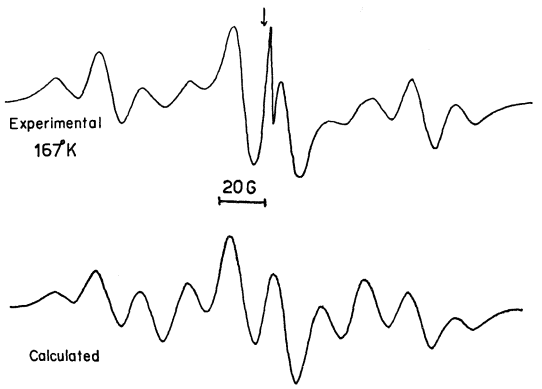

FIG. 10. Spectre du radical 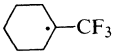 piégé dans la phase "basses températures" du PFMCH, comparé au spectre calculé avec $a_1' = 59$ G, $a_2 = 18$ G, pour une largeur de raie $\Delta H_{1/2} = 15$ G (gaussiennes).

spectre correspond alors à $a_1 = 61.55 \pm 0.05$ G (triplet), $a_2 = 17.81 \pm 0.05$ G (quartets 1:3:3:1), $a_3 = 2.23 \pm 0.05$ G (quintets 1:4:6:4:1). La largeur moyenne entre points de pente maximum des lorentziennes qui constituent alors ce spectre passe de 1.8 G à 210 °K, à 1.1 G à 234 °K. L'intensité relative des composants du triplet d'écart hyperfin a_1 est 1:3:1 (Fig. 11, *B*) d'après la hauteur des raies et non 1:2:1 comme on pourrait s'y attendre s'il correspondait seulement à deux fluors β (Fig. 11, *C*). Le rapport effectif 1:4:1 de l'intensité des composants du triplet apparaît si l'on égalise la largeur des raies par surmodulation (Fig. 11, *A*) ou si l'on effectue la double intégration du spectre expérimental (dérivée première de l'absorption).

Un fait analogue a été observé par Fessenden et Schuler (9) pour le radical cyclohexyle et attribué à l'inversion du cycle qui intervertit la position de deux protons β inéquivalents liés à un même carbone.

La contribution à la structure hyperfine globale du spectre de $\cdot C_6F_{10}CF_3$, de deux paires inéquivalentes de fluors dont les constantes de couplage sont a_1' et a_1'' ($a_1' > a_1''$) est un multiplet 1:2:1:2:4:2:1:2:1. Cette structure apparaitrait si le cycle était rigide ou s'inversait à

FIG. 11. Spectres du radical 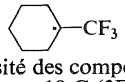 à 230 °K. *A*: surmodulé pour égaliser la largeur des raies et faire apparaître le rapport 1:4:1 de l'intensité des composants du triplet principal; *B*: enregistré dans les conditions optimales de résolution; *C*: calculé avec $a_F^{CF_3} = 18$ G (3F), $a_F^{\beta_1} = 61.5$ G (2F), $a_F^{\gamma} = 2.2$ G (4F), $\Delta H_{1/2} = 1.2$ G (lorentziennes), sans tenir compte de la contribution de $a_F^{\beta_2}$, ce qui donne par conséquent un rapport 1:2:1 pour les composants du triplet principal.

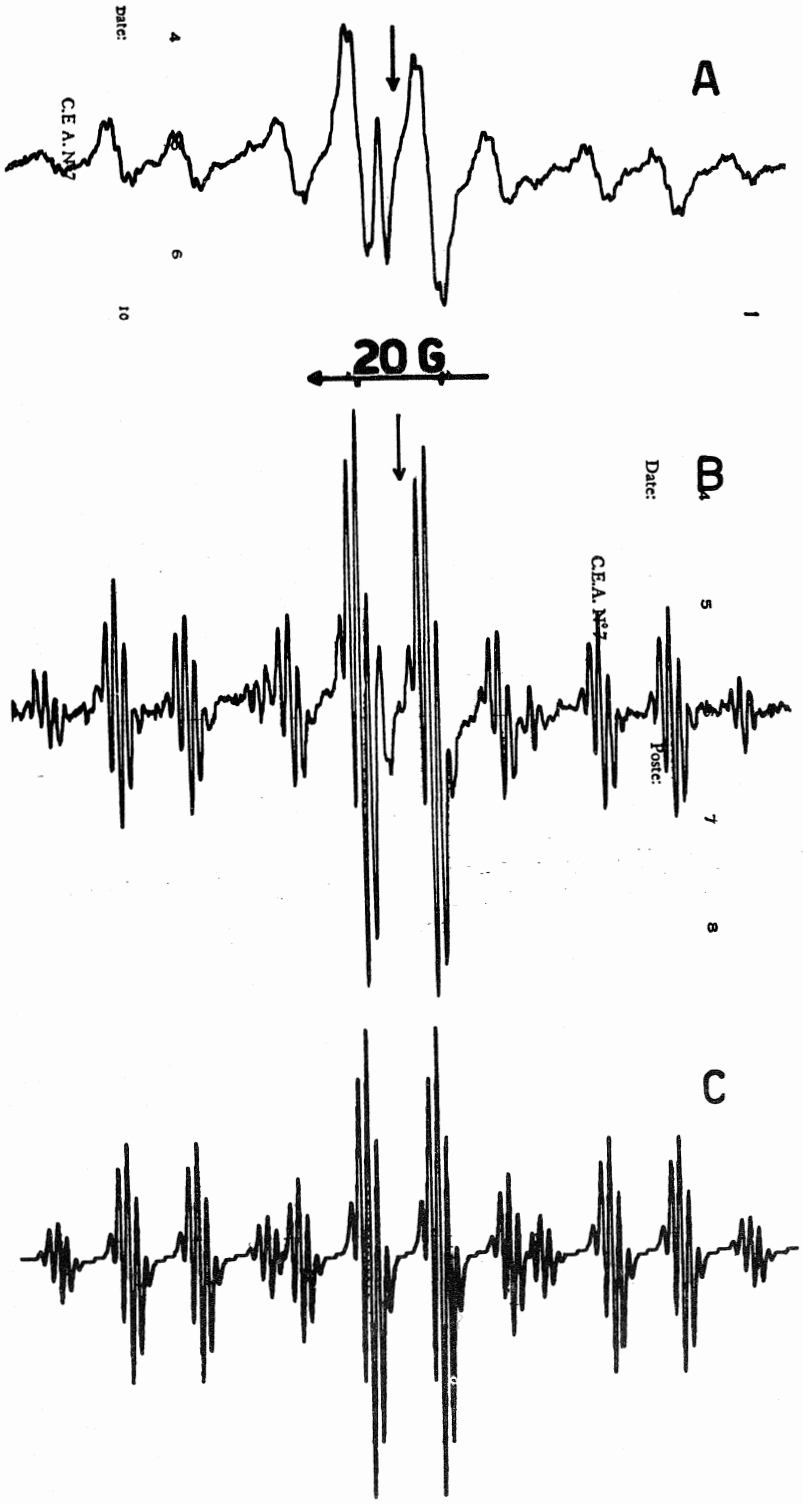

Can. J. Chem. Downloaded from www.nrcresearchpress.com by 210.87.254.5 on 09/05/12
For personal use only.

Can. J. Chem. Downloaded from www.nrcresearchpress.com by 210.87.254.5 on 09/05/12
For personal use only.

une fréquence très inférieure à $a_1' - a_1''$. Si au contraire l'inversion s'effectuait à une fréquence très supérieure à $a_1' - a_1''$, les quatre fluors β apparaitraient équivalents et donneraient un quintet 1:4:6:4:1 d'écart hyperfin $(a_1' + a_1'')/2$. Soient M_β' et M_β'' les nombres quantiques nucléaires totaux des deux paires de fluors β. Si l'inversion s'effectue à une fréquence de l'ordre de $a_1' - a_1''$ (soit $\simeq$ 150 MHz), sans changement des spins nucléaires, les raies correspondant à $M_\beta' = M_\beta'' = \pm 1$, $M_\beta' = M_\beta'' = 0$ demeurent étroites, tandis que celles correspondant à $M_\beta' \neq M_\beta''$ s'élargissent jusqu'à devenir indétectables. La contribution des fluors β au spectre global est alors le triplet 1:4:1 d'écart hyperfin $a_1' + a_1''$ que nous avons observé.

La structure hyperfine due aux fluors β dont le couplage est le plus faible est inobservable au-dessus de 210 °K pour les raisons que nous venons d'exposer et au-dessous de cette température, parce que masquée par la largeur des raies. Il est cependant probable que leur constante de couplage a_1'' soit la différence de 2.5 ± 0.5 G entre les écarts hyperfins a_1 et a_1' que l'on observe de part et d'autre de 210 °K pour le triplet principal. a_2 correspond, comme déjà indiqué, aux fluors de CF_3 en rotation libre et a_3 aux quatre fluors γ devenant équivalents par suite de l'inversion suffisamment rapide du cycle.

Lorsque cette inversion se produit le rapport apparent de l'intensité des composants du triplet principal est, on l'a vu, de 1:3:1, alors que le rapport effectif est 1:4:1. Ce fait nous paraît explicable par l'effet du deuxième ordre (9, 21), dû aux termes non diagonaux de l'hamiltonien de spin, qui divise chaque raie correspondant à $M_\beta' = M_\beta'' = 0$ en un triplet 1:2:1 d'écart hyperfin $(a_1' + a_1'')^2/2H \simeq 0.5$ G. Nous avons effectivement vérifié par calcul électronique des spectres que, pour une largeur de raies lorentziennes de 1.1 G, la structure hyperfine non résolue de trois raies séparées par 0.5 G provoque un élargissement qui diminue leur hauteur de 30%.

La configuration géométrique des radicaux hydrocarbonés à électron π peut en partie être déterminée à partir des constantes de couplage des protons β données par la relation

$$[6] \qquad a_H^\beta = B_0 + B\cos^2\theta$$

avec $B \simeq 50$ à 60 G pour une densité de spin de 1 sur le carbone α, $B_0 < 5$ G, θ étant l'angle entre le plan C_α—C_β—H et l'axe de l'orbitale $2p\pi$ de l'électron non apparié.

Récemment Iwasaki (4) a établi théoriquement les relations

$$[7] \qquad A_\parallel^F = 15.6 + 68.7\cos^2\theta \quad \text{G}$$

$$[8] \qquad A_\perp^F = 5.3 + 23.3\cos^2\theta \quad \text{G}$$

pour les valeurs principales du tenseur hyperfin d'un fluor β, ce qui donne une constante de couplage

$$[9] \qquad a_F^\beta = 8.7 + 34.8\cos^2\theta$$

Ces relations sont partiellement basées sur les résultats expérimentaux de Rogers et Whiffen (2) relatifs au radical $^-CO_2$—CF_2—$\dot{C}F$—CO_2^-. Pour ce radical, les constantes de couplage des fluors β sont de 34.8 et 40.4 G, soit en moyenne $a_F^\beta = 37.6$ G pour un angle θ de l'ordre de 30° (4).

La relation [9] n'étant pas compatible avec nos résultats expérimentaux, nous avons également cherché à établir une relation de la forme $a_F^\beta = B_0 + B\cos^2\theta$ à partir des constantes de couplage

$$[10] \qquad |a_1'| = |B_0 + B\cos^2\theta| = 59 \text{ G}$$

$$[11] \qquad |a_2| = |B_0 + B\cos^2(\theta \pm 2\pi/3)| = 2.5 \text{ G}$$

$$[12] \qquad |a_3| = |B_0 + B/2| = 18 \text{ G} \quad \text{(rotation libre de } CF_3\text{)}$$

Parmi les multiples solutions que donne ce système, compte tenu des combinaisons possibles entre les signes de a_1', a_2 et a_3, celle qui nous paraît la plus plausible est

$$\theta_1 = 4°, \theta_2 = -116°$$
$$|B| = 82 \text{ G}$$
$$|B_0| = 23 \text{ G}$$

a_1', a_2 et a_3 étant de même signe tandis que B et B_0 sont de signes contraires. Ces valeurs de θ_1 et θ_2 sont en effet très proches de celles que nous avons obtenues (22) pour le radical méthylcyclohexyle

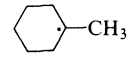

De plus la relation

$$[13] \qquad |a_F^\beta| = |-23 + 82\cos^2\theta| \quad \text{(G)}$$

est compatible avec les résultats de Rogers et

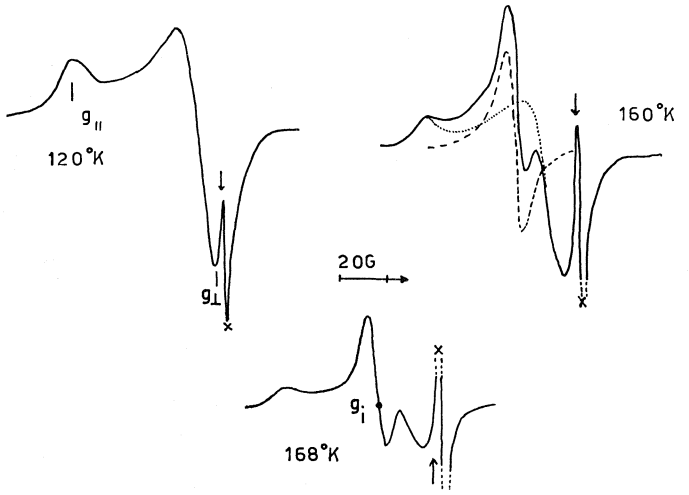

FIG. 12. Spectres attribués au radical 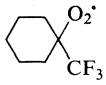 les pics marqués d'une croix sont dûs à la silice de l'ampoule.

Whiffen (2) pour le radical

$$^{-}CO_2—CF_2—{}^{\cdot}CF—CO_2{}^{-}$$

puisqu'en prenant $\theta = 30°$ on obtient $|a_F^{\beta}| = 38.5$ G.

Lorsque le PFMCH est irradié en présence d'oxygène, la formation de radicaux péroxydes, vraisemblablement

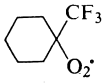

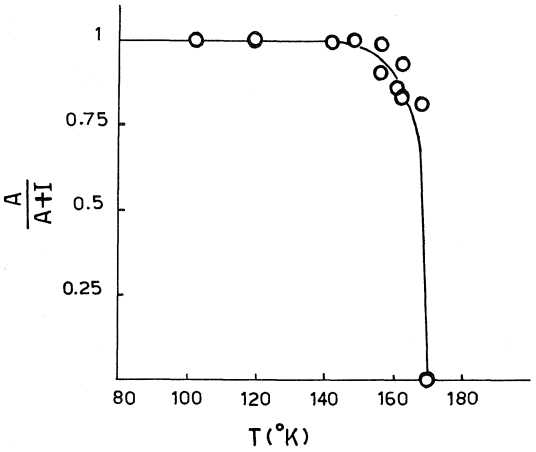

FIG. 13. Concentration relative, en fonction de la température, des radicaux 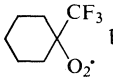 bloqués.

se manifeste dès 120 °K. Leur spectre est très semblable à celui de

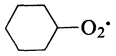

et, comme celui-ci, dépourvu de structure hyperfine.

Les valeurs principales du tenseur g sont, pour les radicaux bloqués, $g_{\|} = 2.0393 \pm 0.0002$ et $g_{\perp} = 2.0039 \pm 0.0002$, ce qui donne $g_1 = 2.0157 \pm 0.0002$.

Au cours du réchauffement apparaît une raie centrée à $g \simeq 2.016$ dont l'intensité s'accroît aux dépends du spectre anisotrope comme le montre les Figs. 12 et 13. Cette raie correspond aux radicaux péroxydes en réorientation isotrope, au voisinage du point de transition situé à 173 °K.

On a comparé sur la Fig. 14, la décroissance en fonction de la température de la concentration de

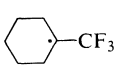 et de 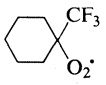

La concentration des radicaux perfluoro-méthyl–cyclohexyle diminue au voisinage du point de transition le plus bas ($T = 173$ °K) puis demeure constante jusqu'à la fusion ($T = 234$ °K). La grande stabilité du radical

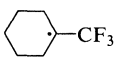

qui a une demi durée de vie de 10 min à 230 °K, est explicable par l'encombrement stérique du

Can. J. Chem. Downloaded from www.nrcresearchpress.com by 210.87.254.5 on 09/05/12
For personal use only.

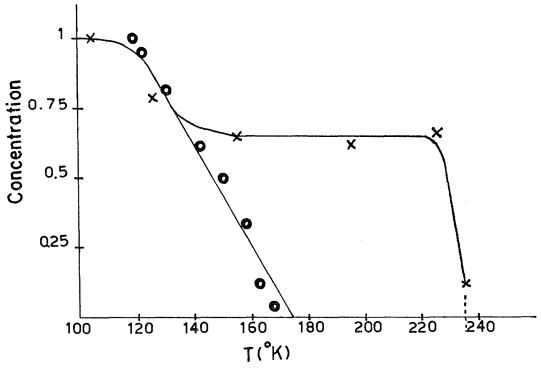

FIG. 14. Concentration (unités arbitraires) des radicaux 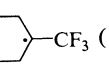 (×) et 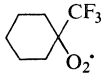 (○) en fonction de la température.

groupe CF_3 et des fluors β du cycle qui entourent le carbone porteur de la valence libre. En effet, le radical

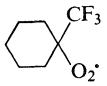

pour lequel l'électron célibataire est localisé sur l'oxygène se recombine à partir de 140–150 °K pour disparaître complètement au premier point de transition (173 °K).

Conclusion

Les études par r.p.e. des radicaux perfluorés en phase solide amorphe ou polycristalline sont en général difficiles en raison de la résolution insuffisante des spectres. Dans le cas des radicaux $\cdot C_6F_{11}$ et $\cdot C_6F_{10}CF_3$, étudiés ici, leur réorientation dans la matrice est assez rapide pour annuler en moyenne le couplage dipolaire et obtenir des spectres bien résolus dont on déduit des valeurs précises des constantes de couplages, en particulier celles des fluors γ que l'on n'observe généralement pas en phase solide. Ce couplage hyperfin à longue distance, indique que l'électron non apparié est délocalisé sur toute la molécule par conjugaison de son orbitale $2p\pi$ centrée sur le carbone et celles des fluors (23–25).

D'autres travaux paraissent nécessaires pour relier la structure des radicaux fluorés au couplage hyperfin des fluors β. Cependant la valeur de la constante de couplage du fluor α du radical $C_6F_{11}\cdot$ suggère que le site du carbone porteur de la valence libre est plan (voir par exemple réf. 3) et il en est probablement de même pour le radical $\cdot C_6F_{10}CF_3$ étant donné la similitude des résultats obtenus.

1. R. J. COOK, J. R. ROWLANDS et D. H. WHIFFEN. Mol. Phys. **7**, 31 (1963–64).
2. M. T. ROGERS et D. H. WHIFFEN. J. Chem. Phys. **40**, 2662 (1964).
3. R. W. FESSENDEN et R. H. SCHULER. J. Chem. Phys. **43**, 2704 (1965).
4. M. IWASAKI. Actes du 7e Congrès de r.p.e., Sapporo. 1968. p. 31.
5. J. A. KERR. Chem. Rev. **5**, 465 (1966).
6. V. I. VENEDEYEV. Bond energies, ionization potentials and electron affinities. Ed. Arnold, Londres.
7. N. YA. CHERNIAK, N. N. BUBNOV, L. S. POLIAK, YU. D. TSVETKOV et V. V. VOEVODSKI. Opt. i Spektrosk. **6**, 564 (1959).
8. K. LEIBLER et H. SZWARC. J. Chim. Phys. **57**, 1109 (1960).
9. R. W. FESSENDEN et R. H. SCHULER. J. Chem. Phys. **39**, 2147 (1963).
10. S. OGAWA et R. W. FESSENDEN. J. Chem. Phys. **41**, 994 (1964).
11. C. CHACHATY et A. FORCHIONI, C. R. **268***C*, 300 (1969).
12. D. R. MCKENZIE, F. W. BLOCH et R. H. WISWALL. J. Phys. Chem. **69**, 2526 (1965).
13. M. B. FALLGATTER et R. J. HANRAHAN. J. Phys. Chem. **69**, 2059 (1965).
14. A. FRATIELLO et D. C. DOUGLASS. J. Chem. Phys. **41**, 974 (1964).
15. C. CHACHATY, A. FORCHIONI et M. SHIOTANI. C. R. **268***C*, 1181 (1969).
16. M. IWASAKI, K. TORIYAMA et B. EDA. J. Chem. Phys. **42**, 63 (1965).
17. R. J. LONTZ. J. Chem. Phys. **45**, 1339 (1966).
18. K. TORIYAMA et M. IWASAKI. Actes du 6e Congrès de r.p.e., Kyoto. 1966. p. 96.
19. A. DWORKIN. C. R. **269***C*, 473 (1969).
20. Z. ŠRONBEK, L. NOVÁK et K. ŽEĎANSKY. Solid State Phys. Suppl. **6**, 173 (1964).
21. R. W. FESSENDEN. J. Chem. Phys. **37**, 747 (1962).
22. C. CHACHATY. J. Chim. Phys. **64**, 614 (1967).
23. D. R. EATON, A. D. JOSEY, W. D. PHILLIPS et R. E. BENSON. Mol. Phys. **5**, 407 (1962).
24. P. J. SCHEIDLER et J. R. BOLTON. J. Amer. Chem. Soc. **88**, 371 (1966).
25. J. L. GERLOCK et E. G. JANZEN. J. Phys. Chem. **72**, 1832 (1967).

Can. J. Chem. Downloaded from www.nrcresearchpress.com by 210.87.254.5 on 09/05/12
For personal use only.

Can. J. Chem. Downloaded from www.nrcresearchpress.com by 210.87.254.105 on 09/05/12
For personal use only.

Electron spin resonance study of γ-irradiated dipotassium difluoromalonate monohydrate

F. G. Herring, W. C. Lin, and M. R. Mustafa
Department of Chemistry, University of British Columbia, Vancouver 8, British Columbia

Received October 8, 1969

The γ-irradiation of dipotassium difluoromalonate monohydrate led to the formation of two molecular configurations of the $\dot{C}F_2CO_2^-$ radical in addition to the previously identified $\dot{C}F(CO_2^-)_2$ radical. A comparison of the α-fluorine coupling in the two forms of the $\dot{C}F_2CO_2^-$ radical indicates that loss of a carboxylate group nearly coplanar with the C—C—C plane in the undamaged molecule is favored.

Canadian Journal of Chemistry, **48**, 447 (1970)

Introduction

The effect of irradiating a material with low energy X-rays (40 kV) is to produce tracks (overlapping of spurs) (1) in the crystal lattice. This high linear energy transfer (l.e.t.) thus causes a high density of radicals which in turn causes a broadening of electron spin resonance (e.s.r.) lines (2). As a consequence of this, only the dominant species formed by X-irradiation may be observed by e.s.r. On the other hand, radiation of low l.e.t., such as γ-rays from a ^{60}Co source, will give e.s.r. lines of much narrower line width. This fact, together with the fact that low l.e.t. radiation will cause well separated spurs and therefore less reaction between the radical species formed, means that additional radical species may be identified after γ-irradiation.

Such is the case in the study of irradiation damage in dipotassium difluoromalonate monohydrate ($CF_2(CO_2K)_2 . H_2O$). Previous low energy X-irradiation led to the formation of the fluoromalonyl radical (3). It was apparent from this work that other radicals were present but could not be identified. The subsequent irradiation of the difluoromalonate with γ-rays led to a sample in which two forms of the $\dot{C}F_2CO_2^-$ radical were shown to be present. These two forms correspond to the loss of one or other of the carboxylate groups which, our previous study (3) indicated, are at roughly 85° to each other.

Experimental

The γ-irradiation was carried out at room temperature in a ^{60}Co gammacell. The dose rate was 4000 rads min^{-1} and the duration of irradiation was 20 min. The e.s.r. techniques were the same as described previously (3) and the same axis system was used.

Results

Figure 1 shows an example of the spectra obtained in this work. The four strong lines (marked A) are due to the radical $\dot{C}F(CO_2^-)_2$, which occupies two symmetry related sites (3). In addition to these lines, two other sets of lines marked B and C are seen, one set (B) being more intense than the other. The lines B may be assigned to two $\dot{C}F_2CO_2^-$ radicals of the same configuration occupying two symmetry related sites. Previous work (4, 5) has shown that the fluorine coupling tensors in $\dot{C}F_2CO_2^-$ are nearly axially symmetric and have their unique principal axes parallel to each other. Consequently two such radicals occupying two symmetry related sites will give rise to a five-line pattern with intensity ratios 1:1:4:1:1. Thus the lines B can be interpreted as the outer lines of such a pattern and half the splitting between two corresponding outer lines should be a reasonable measure of the fluorine hyperfine splitting.

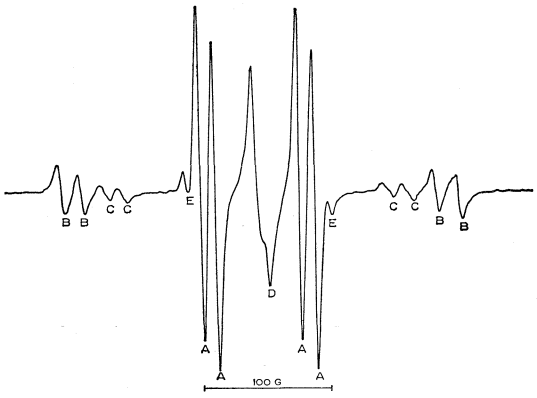

FIG. 1. Electron spin resonance spectrum of γ-irradiated dipotassium difluoromalonate monohydrate.

The formation of the $\dot{C}F_2CO_2^-$ radical requires the loss of a CO_2^- group. Our previous work (3) on the $\dot{C}F(CO_2^-)_2$ suggested that the two carboxylate groups are not coplanar in the

Can. J. Chem. Downloaded from www.nrcresearchpress.com by 210.87.254.105 on 09/05/12
For personal use only.

radical and consequently are not expected to be coplanar in the parent molecule. This situation then leads to the possibility of the formation of $\dot{C}F_2CO_2$ radicals in which either the CO_2^- group is coplanar with the FCF fragment or out of plane. This situation has been observed by Horsfield, Morton, and Whiffen (6) in their studies in the radiation damage in malonic acid. We suggest therefore that the lines denoted by C in Fig. 1 are due to a second $\dot{C}F_2CO_2^-$ radical with a different molecular configuration. This interpretation is confirmed by the results.

The broad resonance marked D in Fig. 1 is no doubt due to (*i*) overlapping of the central lines of the two types of $\dot{C}F_2CO_2^-$ radicals, (*ii*) the resonance due to CO_2^- radicals produced by the homolytic fission of the $F_2C—CO_2^-$ bond, (*iii*) forbidden transitions from the main radical species $\dot{C}F(CO_2^-)_2$. The two very weak lines marked E in Fig. 1 which could be observed only in some orientations were not identified.

It is now necessary to describe in some detail the analysis of the spectra observed for the $\dot{C}F_2CO_2^-$ radicals. The more intense of these radicals will be called radical **1** and the less intense, radical **2**. The method of obtaining the tensor elements from the experimental data was described in our previous study (3). For radical **2** it was possible to observe the outer lines of the 1:1:4:1:1 pattern at most of the orientations in the *ab*, *bc*, and *ca* planes. Consequently both the hyperfine coupling tensor and the **g**-tensor were obtained readily. However, for radical **1** overlapping of lines of the main species ($\dot{C}F(CO_2^-)_2$) prevented the measurement of its hyperfine splitting for all orientations in the *ca* plane. The complete tensor for this radical was obtained by fitting the experimental data in the *ab* and *bc* planes using a trial and error procedure. This method led to an agreement between the experimental and the calculated data that is quite acceptable.

The results of the measurements on radicals **1** and **2** are displayed in Figs. 2, 3, and 4 in which the calculated values, using the final tensors, are given as solid lines for radical **1** and broken lines for radical **2**. The experimental points are shown

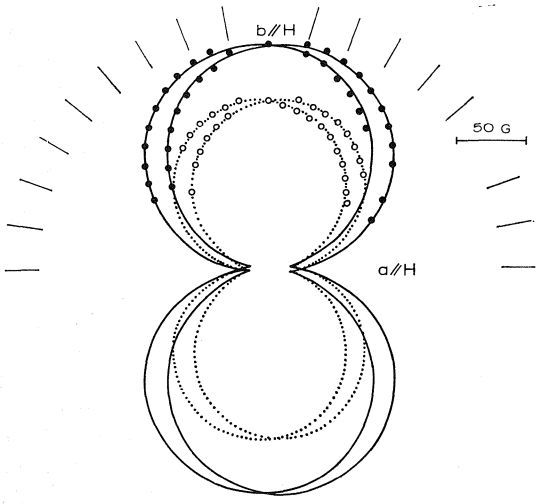

FIG. 2. Angular variation of the hyperfine splitting of the two forms of $\dot{C}F_2CO_2^-$ both in two nonequivalent sites with H in the *ab* plane.

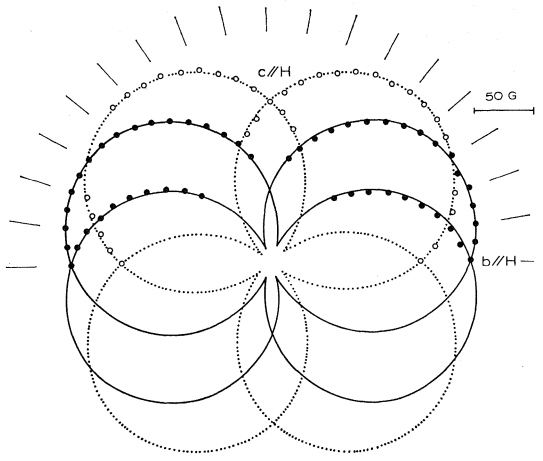

FIG. 3. Angular variation of the hyperfine splitting of the two forms of $\dot{C}F_2CO_2^-$ both in two nonequivalent sites with H in the *bc* plane.

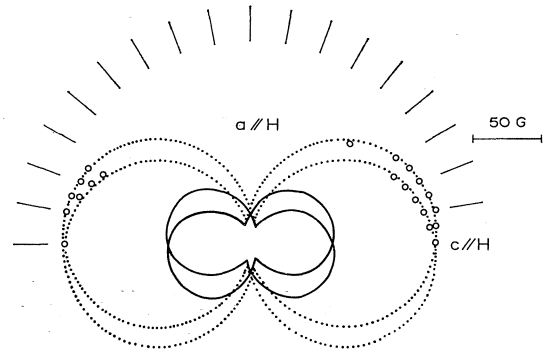

FIG. 4. Angular variation of the hyperfine splitting of the two forms of $\dot{C}F_2CO_2^-$ both in two nonequivalent sites with H in the *ac* plane.

Can. J. Chem. Downloaded from www.nrcresearchpress.com by 210.87.254.105 on 09/05/12
For personal use only.

as open circles (radical **2**) and solid circles (radical **1**). The diagonalized hyperfine coupling tensors are given in Tables 1 and 2 together with the direction cosines for one crystallographic site. The crystal is orthorhombic so that the direction cosines of the remaining three sites can be obtained by sign changes (3).

The **g**-tensors were also measured. This was done including a second order correction as described previously (3). The results are given in Tables 3 and 4 together with the direction cosines of the principal axes.

To conclude this section we may say that the fluorine hyperfine coupling tensors are sufficiently similar to those of $\dot{C}F_2CONH_2$ (4) and $\dot{C}F_2COONH_4$ (5) to confirm our interpretation that the resonance lines observed in addition to those from the $\dot{C}F(CO_2^-)_2$ radical are from the $\dot{C}F_2CO_2^-$ radicals.

Discussion

The previous work on the $\dot{C}F(CO_2^-)_2$ radical (3) showed that the principal axis of the largest principal value of the fluorine hyperfine coupling tensor is nearly perpendicular to the crystallographic *b* axis and makes equal angles with the *a*- and the *c*-axes, the direction cosines for one crystallographic site being 0.705, 0.075, 0.706. This direction can reasonably be taken as the normal to the C—C—C plane in the undamaged molecule ($CF_2(CO_2^-)_2$). The e.s.r. studies and molecular orbital calculations (3) indicated, as in the case of malonic acid (7), that the two carboxylate groups in the fluoromalonyl radical are not coplanar. One of the groups is thought to be in the C—C—C plane and the other rotated by roughly 85°.

If the $\dot{C}F_2CO_2^-$ radical is completely planar, a study of the angles between the largest principal values of the fluorine coupling tensors for the two $\dot{C}F_2CO_2^-$ radicals and the $\dot{C}F(CO_2^-)_2$ radical should yield information about the angles between the C—C—C plane and the two CO_2 planes. From the foregoing we would expect that the direction cosines of the unique principal axes of one of the $\dot{C}F_2CO_2^-$ radicals would be parallel to that of the $\dot{C}F(CO_2^-)_2$ radical and the other roughly perpendicular to it. This situation could arise by the rotation of the CF_2 group into the plane of the CO_2^- group after the loss of one or other of the CO_2^- groups.

Calculations showed that none of the possible sign combinations for the direction cosines of the principal axes for the four crystallographic sites corresponded to the above situation.

The work of Horsfield, Morton, and Whiffen (6) on γ-irradiated malonic acid showed that in the radical $\dot{C}H_2CO_2^-$, the CH_2 group is nearly perpendicular to the plane of the carboxylate group. They suggested that forces in the crystal prevented rotation about the Ċ—C axis. A similar situation may occur in the present case

TABLE 1

The fluorine hyperfine coupling tensor for radical **1**

Principal values (G)	Direction cosines of principal axes w.r.t.		
	a	*b*	*c*
181 ± 2	0.091	0.940	0.328
13 ± 2	0.757	0.149	−0.637
11 ± 2	0.647	−0.306	0.698

TABLE 2

The fluorine hyperfine coupling tensor for radical **2**

Principal values (G)	Direction cosines of principal axes w.r.t.		
	a	*b*	*c*
188 ± 2	0.078	0.678	0.730
19 ± 2	0.965	−0.234	0.114
7 ± 2	0.249	0.696	−0.673

TABLE 3

The **g**-tensor for radical **1**

Principal values	Direction cosines of principal axes w.r.t.		
	a	*b*	*c*
2.008 ± 0.001	0.598	−0.299	0.743
2.006 ± 0.001	0.801	0.239	−0.548
1.998 ± 0.001	−0.014	0.924	0.383

TABLE 4

The **g**-tensor for radical **2**

Principal values	Direction cosines of principal axes w.r.t.		
	a	*b*	*c*
2.008 ± 0.001	0.572	0.576	−0.584
2.007 ± 0.001	0.816	−0.470	0.335
1.998 ± 0.001	0.081	0.669	0.739

and, if so, the angle between the unique principal axis of the two $\dot{C}F_2CO_2^-$ radicals would correspond to the C—C—C angle in the parent molecule. We found that one choice of signs of the principal axes gave an angle of 113 ± 3°. This angle is not far from the tetrahedral angle. Consistent with this choice, we also found that the angle between the unique principal axis of $\dot{C}F(CO_2^-)_2$ and radical **1** is 84 ± 3° and, between $\dot{C}F(CO_2^-)_2$ and radical **2**, an angle of 59 ± 3° was calculated. Both these angles would be expected to be 90° if one carboxyl group is strictly parallel and the other strictly perpendicular to the C—C—C plane in the undamaged molecule. The deviation from 90° is most probably due to the fact that the parent molecule does not have this idealized geometry and that partial rotation about the Ċ—C bond occurs when the radicals are formed.

The dependence of α-fluorine hyperfine coupling tensors upon delocalization has been discussed previously (3). On the basis of the fact that $\mathbf{A}_{\|}$ for radical **1** is less than that for radical **2**, we might suggest that radical **1** would have its CO_2^- group more in plane with the CF_2 than radical **2**. Consequently the more likely radical to be produced appears to be the one which corresponds to the loss of a carboxylate group more in the C—C—C plane of the parent molecule.

The authors wish to thank the National Research Council of Canada for financial support.

1. J. CUNNINGHAM. Radical ions. *Edited by* E. T. Kaiser and L. Kevan, Interscience Publishers Inc., New York. 1968. p. 475.
2. R. C. SMITH and S. J. WYARD. Nature, **191**, 897 (1961).
3. F. G. HERRING, W. C. LIN, and M. R. MUSTAFA. In press.
4. R. J. LONTZ and W. GORDY. J. Chem. Phys. **37**, 357 (1962).
5. F. D. SRYGLEY and W. GORDY. J. Chem. Phys. **46**, 2245 (1967).
6. A. HORSFIELD, J. R. MORTON, and D. H. WHIFFEN. Mol. Phys. **4**, 327 (1961).
7. J. A. GOEDKOOP and C. H. MACGILLAVRY. Acta Cryst. **10**, 125 (1957).

Can. J. Chem. Downloaded from www.nrcresearchpress.com by 210.87.254.105 on 09/05/12
For personal use only.

Can. J. Chem. Downloaded from www.nrcresearchpress.com by 210.87.254.42 on 09/05/12
For personal use only.

Studies of specifically fluorinated carbohydrates. Part V.[1] Derivatives of 3,6-anhydro-5-deoxy-5-fluoro-1,2-*O*-isopropylidene-α-L-idofuranose

L. D. HALL AND P. R. STEINER[2]

Department of Chemistry, The University of British Columbia, Vancouver 8, British Columbia

Received June 23, 1969

The facile synthesis of 3,6-anhydro-5-deoxy-5-fluoro-1,2-*O*-isopropylidene-α-L-idofuranose (**4**) from readily available precursors is described. The ^1H and ^{19}F nuclear magnetic resonance spectra of this derivative have been analyzed. Interestingly, the fluorine substituent exhibits detectable spin coupling with all ring protons except H-2. Both of the anomeric 1,2-di-*O*-acetyl derivatives of (**4**) have also been studied.

Canadian Journal of Chemistry, **48**, 451 (1970)

Introduction

We have previously described (2, 3) studies of pyranosyl fluoride derivatives which illustrate the potential which fluorine nuclear magnetic resonance (^{19}F n.m.r.) spectroscopy has as a sensitive "probe" for studying pyranose derivatives. In order to apply the ^{19}F n.m.r. technique to the more difficult problems associated with furanose systems, it was felt necessary to have previously studied some derivatives having reasonably defined conformations. The 3,6-anhydro-1,2-*O*-isopropylidene–hexofuranose system (**1**, **2**) seemed admirably suited for this purpose. Earlier proton magnetic resonance (p.m.r.) studies (4) had shown the conformation of this system to be relatively insensitive to changes in the nature of the ring substituents. Thus, as far as is possible for a furanose derivative, this would appear to be a conformationally "rigid" system.

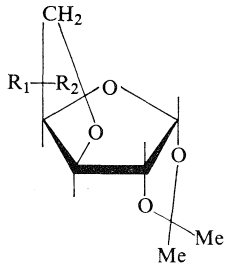

1 R_1 = OH; R_2 = H
2 R_1 = H; R_2 = OH

Discussion

It is well known that sulfonate esters can undergo S_N2 displacement reactions with fluoride ions (5–8). In a preliminary study we found that the reaction of 3-*O*-acetyl-1,2-*O*-isopropylidene-5,6-di-*O*-mesyl-α-D-glucofuranose (**3**) with anhydrous potassium fluoride, in anhydrous ethylene glycol, afforded a crystalline product in ca. 48% yield. Although p.m.r. spectroscopy showed that both the single acetate group and the two mesyl groups had been removed, ^{19}F n.m.r. indicated that only one fluorine substituent had been introduced. The elemental analysis suggested that the product was a mono-fluoro,

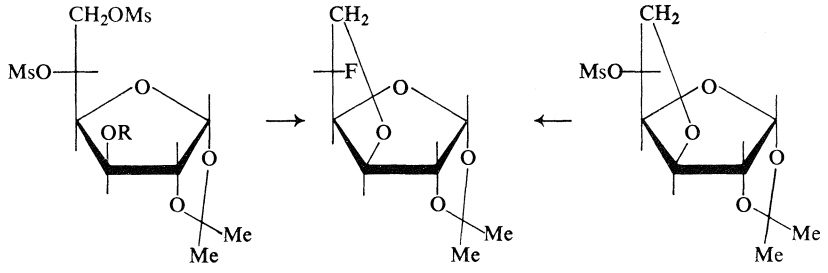

3 R = $COCH_3$
6 R = $CH_2C_6H_5$

4

5

[1]For Part IV, see ref. 1.
[2]Recipient of an NRCC Studentship, 1968–1969.

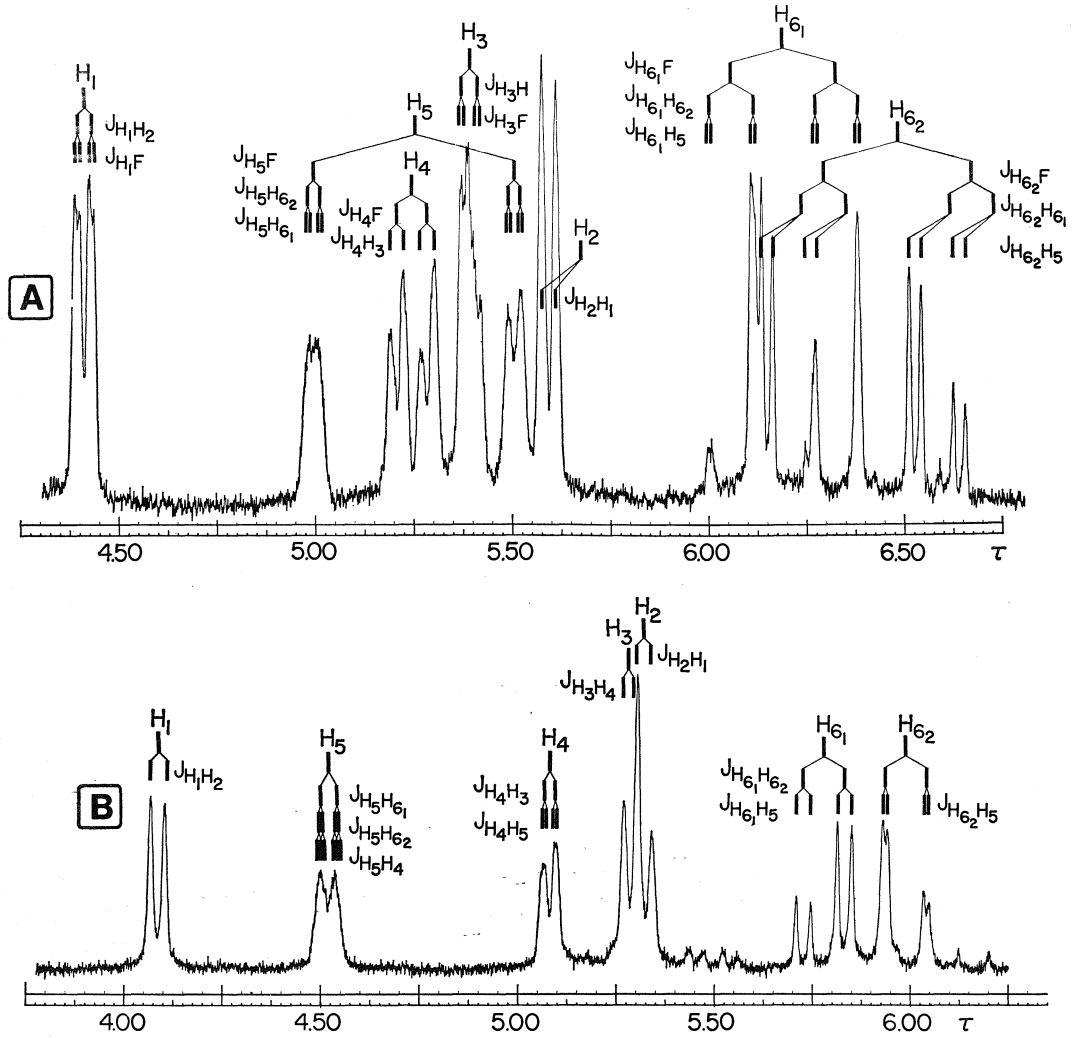

FIG. 1. Partial 100 MHz proton magnetic resonance spectra of: (*A*) 3,6-anhydro-5-deoxy-5-fluoro-1,2-*O*-isopropylidene-α-L-idofuranose (**4**) in benzene-d_6 solution; (*B*) 3,6-anhydro-5-*O*-benzoyl-1,2-*O*-isopropylidene-α-L-idofuranose in chloroform-*d* solution. The first-order assignments are as indicated. The small peaks at τ 5.50 and 6.15 in the lower spectrum are due to residual impurities.

mono-anhydro, mono-isopropylidene hexose derivative. This same derivative was subsequently obtained in significantly higher (75%) yield from 3,6-anhydro-1,2-*O*-isopropylidene-5-*O*-mesyl-α-D-glucofuranose (**5**) under conditions similar to those used previously for **3**. On this basis, and the known (9) stereo-specificity of displacement reactions in this system, this derivative appeared to be the desired 3,6-anhydro-5-deoxy-5-fluoro-1,2-*O*-isopropylidene-α-L-idofuranose (**4**). Further evidence favoring this formulation followed from a comparison (*vide infra*) of the p.m.r. parameters found for **4** with those of related derivatives of the D-gluco (**1**) and L-ido (**2**) systems.

The attempted formation of a 5,6-difluoro-L-idofuranose derivative by the action of potassium fluoride on 3-*O*-benzyl-1,2-*O*-isopropylidene-5,6-di-*O*-mesyl-α-D-glucofuranose (**6**), afforded a significant yield (45%) of **4**. This indicated that the benzyl group was labile under the rather vigorous conditions used in this reaction, which

Can. J. Chem. Downloaded from www.nrcresearchpress.com by 210.87.254.42 on 09/05/12
For personal use only.

Can. J. Chem. Downloaded from www.nrcresearchpress.com by 210.87.254.42 on 09/05/12
For personal use only.

was a novel observation at the time this work was completed. Since then evidence has been adducted for the ability of benzyl ethers to provide anchimeric assistance in solvolysis reactions (10), and for their lability during certain nucleophilic displacement reactions (11).

Subsequently, attempts were made to obtain the D-gluco analogue of **4** starting from 3,6-anhydro-1,2-*O*-isopropylidene-5-*O*-mesyl-α-L-idofuranose (**8**). Although an intractable mass resulted from reactions with anhydrous potassium fluoride in ethylene glycol, the observation of a ^{19}F resonance at ϕ +207.6 showed that a small amount of the desired product had probably been formed; unfortunately, a pure sample could not be isolated. The greater facility of displacement reactions going from the D to L configuration at C-5 of the 3,6-anhydro-1,2-*O*-isopropylidene-D-*xylo*-hexofuranose system, reflects the fact that the nucleophile now attacks C-5 from the *exo* position; inversions from the L to D configuration require approach from the more-hindered, *endo* side. This is strictly analogous to the situation which pertains in the 1,4;3,6-dianhydrohexitol system (12).

The assignment of the p.m.r. spectrum of **4** (Fig. 1*A*) was greatly simplified by the previous assignment of that of the corresponding benzoate (**7**) (Fig. 1*B*). The doublet at lowest field (τ 4.41) in Fig. 1*A* was conventionally assigned to H-1. Irradiation of this resonance (τ 4.41) resulted in the collapse of the doublet at τ 5.68 which was thus identified as H-2. The doublets at τ 5.0 and 5.5, each of which integrated for 0.5 proton, were together assigned to H-5; their separation (50.1 Hz) is within the range characteristic (2, 3) of geminal ^{19}F–^{1}H couplings. The assignments of the H-3 (τ 5.41) and H-4 (τ 5.29) resonances follow from the knowledge that $J_{2,3}$ is very small and that H-2 should thus be a narrower resonance than H-4, which should be coupled with H-3, H-5, and F-5.

It should then have been possible to complete the assignment of the H-6 resonances by finding the geminal ^{1}H–^{1}H coupling, which should have been repeated 8 times. However, the assignment was complicated by the overlap of the two H-6 resonances due to the large vicinal ^{19}F–^{1}H couplings; the (initially tentative) first-order assignment is indicated in Fig. 1*A*. At this stage it would have been logical to have performed an iterative computer analysis of the whole spectrum. Unfortunately, this possibility was precluded by the fact that our computer-program would solve only a 6-spin case. Nevertheless, a complete analysis of the H-6 resonances was accomplished; an expanded sweep-width of the resonances is shown in Fig. 2. Three iterations using the "mode C" part of the TWØSUM program (see Experimental) were sufficient to give a histogram plot in excellent agreement with the experimental spectrum (Fig. 2). The corresponding parameters are listed in Table 1, together with the first-order values.

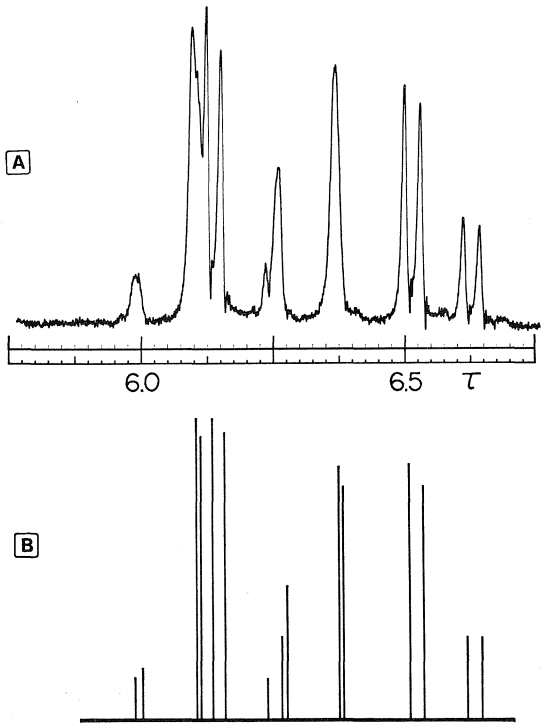

FIG. 2. (*A*) (100 MHz) p.m.r. spectrum of the H-6 resonances of 3,6-anhydro-5-deoxy-5-fluoro-1,2-*O*-isopropylidene-α-L-idofuranose (**4**) in benzene-d_6 solution; (*B*) histogram of this region corresponding to the data obtained from "mode C".

The fluorine spectrum of **4**, shown in Fig. 3 consists of 46 transitions which can be readily assigned on a first-order basis using the coupling constants listed in Table 2. The spectrum simulated using a plot-routine (SMASH) in conjunction with LAØCØØN III is in excellent agreement with the experimental spectrum, showing that the parameters listed for **4** in the table are reasonably accurate, in spite of the poor "resolution" of the p.m.r. spectrum. The sole

TABLE 1

Comparison of the coupling constants and chemical shifts obtained by first-order and computer analysis of the H-5 and H-6 resonances of **4**

	$J_{5,6_1}$ (Hz)	$J_{5,6_2}$ (Hz)	$J_{6_1,6_2}$ (Hz)	$J_{5,F}$ (Hz)	$J_{6_1,F}$ (Hz)	$J_{6_2,F}$ (Hz)	τ(H-5)	τ(H-6_1)	τ(H-6_2)
First order values	2.9	1.1	−11.3	50.1	26.5	37.6	5.30	6.22	6.48
TWØSUM* values	2.8	0.8	−11.1	50.4	26.1	38.3	5.30	6.25	6.41

*See Experimental.

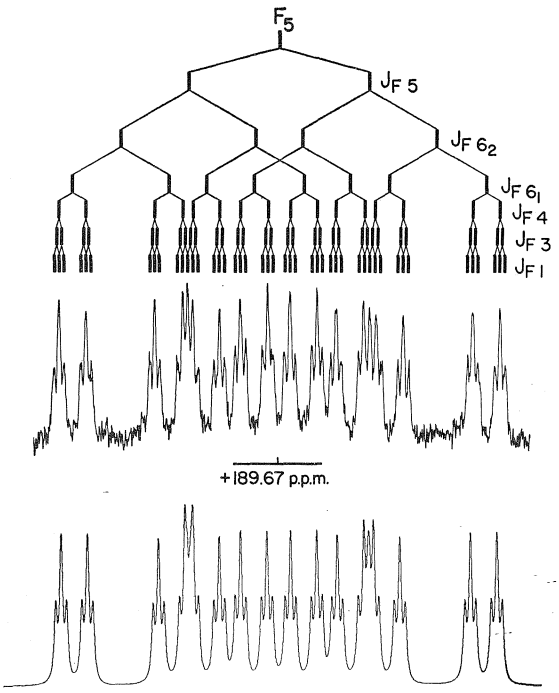

FIG. 3. ^{19}F n.m.r. spectrum of 3,6-anhydro-5-deoxy-5-fluoro-1,2-*O*-isopropylidene-α-L-idofuranose (**4**) in benzene-d_6 solution. The simulated (lower) spectrum was obtained from the parameters listed in Tables 2 and 3 using the LAØCØØN III program and the SMASH plot routine.

discrepancy is in the low-field quintet. That this discrepancy is observed in the low-field portion of the F-5 resonance is anticipated. Since the signs of all the ^1H–^1H and ^{19}F–^1H couplings are known (13), it is possible to construct a spin-state assignment table for the spectrum and to show that the low-field ^{19}F transitions should be more susceptible to second-order effects than the high-field transitions. We shall not give the details of this argument, which has been used previously by Hooper *et al.* (14).

The 1,2-*O*-isopropylidene group was removed from **4** by standard methods and the free sugar was converted to a mixture of the anomeric 1,2-diacetates with acetic anhydride–pyridine. Pure samples of the α- (**10**) and β- (**11**) anomers were obtained by gas–liquid chromatography (g.l.c.) of the crude reaction mixture.

Assignment of the anomeric configurations of these two derivatives was made on the basis of their $J_{1,2}$ values (4, 15); the α- configuration was assigned to the derivative having $J_{1,2} = 4.4$ Hz while the compound assigned to the β- configuration had $J_{1,2} < 0.5$ Hz.

Although the H-1, H-5, and H-6 resonances of both **10** and **11** could be unequivocally assigned, the remaining resonances were so overlapped that an incisive assignment was not possible. Thus, although the parameters for **10** and **11** are sufficiently accurate to give a fair description of the spectra of these derivatives, their accuracy is lower than that of the other derivatives discussed in this paper.

The parameters obtained from the n.m.r. spectra of **4**, **10**, and **11** and from the p.m.r. spectra of related derivatives are listed in Tables 2 and 3. Comparison of the ^1H–^1H couplings of these derivatives suggests that they all favor closely similar conformations. We see no compelling reason at this time to change our previous (4) conformational assignment, that the furanose ring favors the $^3T_2$ conformation, while the 3,6-anhydro rings exist in the V_4 conformation. However, as we have discussed elsewhere (16) it is very difficult to distinguish one particular furanose conformer from its next nearest neighbors in the pseudorotational cycle.

It is of some interest to note that **11** has 4 sets of vicinal ^1H–^1H couplings which are ca. 0.5 Hz. Even allowing for the fact that such small couplings do not unequivocally indicate a dihedral separation of 90° (16, 17), this set of couplings provides a reasonably precise conformational evaluation.

Can. J. Chem. Downloaded from www.nrcresearchpress.com by 210.87.254.42 on 09/05/12
For personal use only.

TABLE 2

Coupling constants (Hz) for derivatives of the 3,6-anhydro-D-*xylo*-hexafuranose system

Compounds		H_1–H_2	H_2–H_3	H_3–H_4	H_4–H_5	H_5–H_{6_1}	H_5–H_{6_2}	H_{6_1}–H_{6_2}
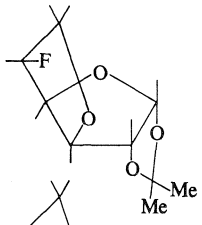		3.5	<0.5	3.2	<0.5	2.8	0.8	−11.1
	4†	1,F 1.5	2,F <0.5	3,F 1.5	4,F 7.5	5,F 50.4	6_1,F 38.3	6_2,F 26.1
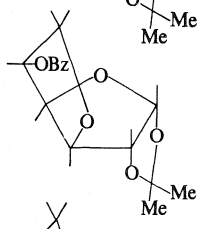	**7**‡	3.6	<0.5	3.2	0.8	3.6	1.1	−10.4
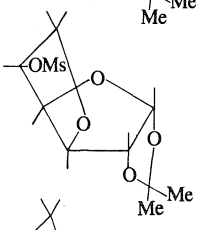	**8***	3.5	<0.5	3.4	0.8	2.4	1.4	−10.6
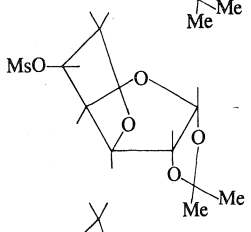	**5**‡	3.7	<0.5	3.5	4.4	6.7	7.4	−8.2
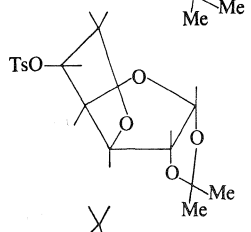	**9**‡	3.3	<0.5	3.6	3.8	6.3	8.2	−8.8
	9*§	3.5	<0.5	3.7	4.1	6.5	8.1	−8.8
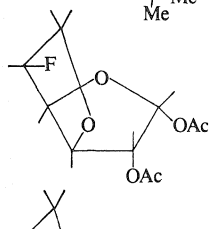		4.4	<0.5	3.3	<0.5	2.8	0.8	−11.6
	10*‖	1,F 2.0	2,F <0.5	3,F <1.0	4,F 8.1	5,F 50.6	6_1,F 38.1	6_2,F 22.3
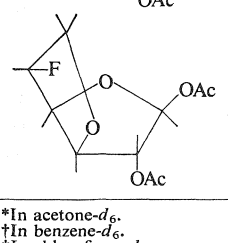		<0.5	<0.5	4.6	<0.5	3.0	~1.0	−11.4
	11*	1,F 2.7	2,F <0.5	3,F ~1.0	4,F 10.8	5,F 50.6	6_1,F 39.8	6_2,F 25.5

*In acetone-d_6.
†In benzene-d_6.
‡In chloroform-*d*.
§60 MHz Data from ref. 4.
‖The parameters pertaining to the H-2, H-3, and H-4 resonances are less accurate than those of the H-1, H-5, and H-6 resonances.

Can. J. Chem. Downloaded from www.nrcresearchpress.com by 210.87.254.42 on 09/05/12
For personal use only.

TABLE 3

Chemical shifts (τ-values, ϕ_c-values) for derivatives of the 3,6-anhydro-D-*xylo*-hexofuranose system

Compounds		F	H-1	H-2	H-3	H-4	H-5	H-6_1	H-6_2	R
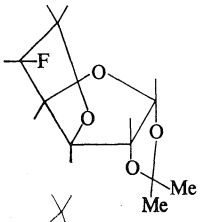	**4**†	+189.7	4.41	5.68	5.41	5.29	5.30	6.41	6.25	—
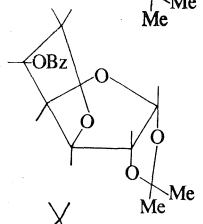	**7**‡	—	4.10	5.34	5.29	5.09	4.53	5.79	6.01	1.9–2.9 (OBz)
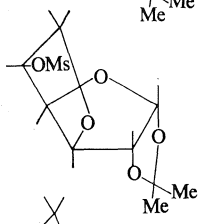	**8***	—	4.12	5.41	5.38	5.12	4.92	5.90	5.96	6.97 (OMs)
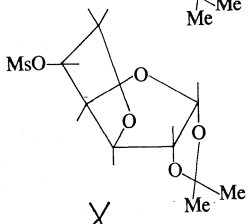	**5**‡	—	4.02	5.38	5.43	5.03	4.95	5.92	6.20	6.92 (OMs)
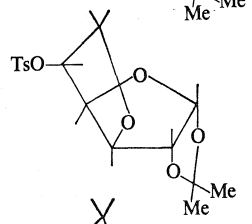	**9**‡	—	4.12	5.48	5.56	5.33	5.18	6.08	6.31	7.57 (OTs)
	9*§	—	4.06	5.45	5.54	5.27	4.98	6.37	6.90	7.51
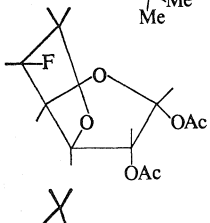	**10***‖	+190.8	3.66	5.06	5.12	5.03	4.92	6.09	5.92	7.97 8.01 (OAc)
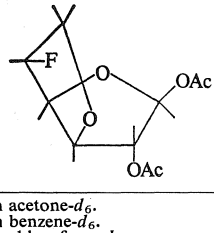	**11***	+186.7	3.88	4.90	5.32	5.07	4.86	5.72	6.00	7.96 7.98 (OAc)

*In acetone-d_6.
†In benzene-d_6.
‡In chloroform-*d*.
§60 MHz Data from ref. 4.
‖The shifts for H-2, H-3, and H-4 are not accurate.

Can. J. Chem. Downloaded from www.nrcresearchpress.com by 210.87.254.42 on 09/05/12
For personal use only.

Can. J. Chem. Downloaded from www.nrcresearchpress.com by 210.87.254.42 on 09/05/12
For personal use only.

It seems reasonably well established that the magnitude of a geminal ^1H–^1H coupling depends upon the relative orientation of an oxygen substituent attached to an adjacent carbon (2, 3, 18–22). It is thus of relevance that the $6_1,6_2$ couplings of the D-gluco derivatives are larger (less negative) than those of the L-ido derivatives. This is in accord with the proposed (4) conformation for the 3,6-anhydro ring. The *O*-5 substituent is "*anti—trans*" with respect to H-6, in the L-ido series, but is "*gauche*" with respect to both H-6_1 and H-6_2 in the D-gluco series.

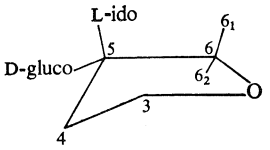

We had already (23) determined the F_1–H_2 couplings of the 2-deoxy-α-D-*arabino*-hexopyranosyl fluoride (**12**); $J_{F,2a}$ = 38.0 Hz and $J_{F,2e}$ = 5.0 Hz. Insofar that the total electronegativity of the substituents associated with the C-1, C-2 fragment of **12** is the same as that of the C-5, C-6 fragment of derivatives **4**, **10**, and **11**, we had anticipated that there might be some coherent relationship between the two sets of vicinal ^{19}F–^1H couplings. The value of $J_{F,6_2}$ of **4** is close to that of $J_{F,2a}$ of **12**; however, the value of $J_{F,6_1}$ is over 5 times that of $J_{F,2e}$. It may be that comparisons between couplings of different sizes of cyclic systems are not permissible; alternatively, it could arise from a configurational dependence (24, 25).

Besides the 3 vicinal ^{19}F–^1H couplings, compound **4** evidenced several *long-range* ^{19}F–^1H couplings. Since we are accumulating further data from other classes of fluorinated furanose derivatives, we shall delay a discussion of these couplings until later.

Our experience with the analysis of the spectra of compound **4** indicates that anything less than a complete analysis of a spectrum of this complexity may leave some subtle features unaccounted for. Nevertheless, it is satisfying to note that in this, and probably a number of other instances, the first-order parameters are within 5% of the true values. It is questionable therefore, whether the very considerable amount of work associated with an iterative-analysis procedure is totally justified if the resultant parameters are to be used for a semi-quantitative conformational evaluation. It does, however, seem most worthwhile to use, as a matter of course, a computer program to simulate a histogram plot of the spectrum, using as input data the first-order parameters. This plot will provide a check on the validity of the first-order analysis and possibly provide an incentive to obtain more clearly resolved spectra.

Experimental

All solutions were concentrated under reduced pressure. All melting points were measured on a Fisher–Johns heating stage and are uncorrected. All optical rotations were measured with a Bendix ETL-NPL automatic polarimeter (model 143A) using either a 4.0 or 0.5 cm cell; chloroform solutions were used throughout. Microanalyses were performed by Mr. P. Borda of this Department.

All ^1H n.m.r. spectra were measured with a modified Varian HA-100 spectrometer operating in the "locked" frequency-sweep or field-sweep mode, using tetramethylsilane as internal reference. All ^{19}F n.m.r. spectra were recorded at 94.071 MHz with the same spectrometer operating in the locked field-sweep mode. ^{19}F Shifts are quoted as "ϕ_c" values and were obtained for chloroform solution with ca. 20% trichlorofluoromethane as internal reference.

The computer analyses of n.m.r. spectra were performed with an I.B.M. 7044 computer in the Computer Center at U.B.C. Two basic programs were used; the TWØSUM[3] and LAØCØØN III[4] programs. The plot routine (SMASH) used in conjunction with the LAØCØØN III program and a CALCOMP plotter, was written for us by John Coulthart of the U.B.C. Computer Center. The TWØSUM program which we used has two stages: "mode-B", which gives a histogram plot corresponding to the parameters given; and in "mode-C", the experimentally determined transition energies are compared with those of the mode-B histogram and after a number of iterations, the accurate shifts and couplings are obtained.

3,6-Anhydro-5-deoxy-5-fluoro-1,2-O-isopropylidene-α-L-idofuranose (4)

(a) From 3-O-Acetyl-1,2-O-isopropylidene-5,6-di-O-mesyl-α-D-glucofuranose (3)

A dried sample of **3** (5 g, m.p. 135° (5)) and anhydrous potassium fluoride (5 g), in anhydrous ethylene glycol (50 ml), were heated under reflux for 2.0 h. During this time white crystals sublimed onto the condenser walls. The discolored solution was poured into ice-water and the whole extracted with chloroform. The combined chloroform extracts were dried (Na_2SO_4) and concentrated to give crude **4**. This crude product, together with the sublimed crystals from the condenser, was purified by sublimation to give fine, needle-like crystals of (**4**) (1.21 g, 48%), m.p. 96.5–97.5°, $[\alpha]_D^{22}$ +15.4° (*c*, 1.97).

[3]Kindly provided by Dr. John Martin, Chemistry Department, University of Alberta, Edmonton, Alberta.
[4]Kindly provided by Dr. A. A. Bothner-By, Chemistry Department, Mellon Institute, Pittsburgh, Pa.

Can. J. Chem. Downloaded from www.nrcresearchpress.com by 210.87.254.42 on 09/05/12
For personal use only.

Anal. Calcd. for $C_9H_{13}O_4F$: C, 52.94; H, 6.37; F, 9.11. Found: C, 53.12; H, 6.21; F, 9.31.

(b) From 3,6-Anhydro-1,2-O-isopropylidene-5-O-mesyl-α-D-glucofuranose (5)

A dried sample of **5** (1 g, m.p. 114° (4)) and anhydrous potassium fluoride (1 g) in anhydrous ethylene glycol (25 ml) were heated under reflux for 1.0 h. Treatment of the reaction mixture as described in (*a*) above gave pure crystals of **4** (0.55 g, 75.3%).

(c) From 3-O-Benzyl-1,2-O-isopropylidene-5,6-di-O-mesyl-α-D-glucofuranose (6)

A non-crystalline sample of **6** (1.5 g, (26)) and anhydrous potassium fluoride (1.5 g) in anhydrous ethylene glycol (30 ml) were heated under reflux for 1.0 h. Treatment of the resulting discolored solution in the same manner as (*a*) above afforded crystals of **4** (0.25 g, 45.5%). The ^{19}F n.m.r. spectrum of the mother liquors revealed a further resonance (a broad triplet) at ϕ_c +234, in addition to that observed for **4**. The ^1H n.m.r. spectrum showed that one mesyl group (τ 6.2), the isopropylidene moiety (τ 8.0–8.2), and the benzyl group (τ 1.9–2.8) remained on this minor secondary product. The large fluorine shift is indicative of a primary fluoride, thus suggesting this (non-isolated) product to be 5-*O*-benzyl-6-deoxy-6-fluoro-1,2-*O*-isopropylidene-α-D-glucofuranose.

(d) Other Methods

Reaction between **1** and a mixture of anhydrous potassium fluoride and anhydrous potassium hydrogen fluoride led to extensive charring.

Reaction between 1,2-*O*-isopropylidene-5,6-di-*O*-mesyl-α-D-glucofuranose and tetra *n*-butylammonium fluoride in acetonitrile solution afforded **5**, m.p. and mixed m.p. 114–115°.

1,2-di-O-Acetyl-3,6-anhydro-5-deoxy-5-fluoro-1,2-O-isopropylidene-L-idofuranose (9, 10)

A solution of **4** (500 mg) in aqueous acetic acid (30%, 25 ml) was kept on a steam-bath. After 3 h, thin-layer chromatography indicated that the hydrolysis was complete. Concentration gave a colorless syrup; p.m.r. confirmed that the isopropylidene group had been completely removed.

A solution of this product (300 mg) in dry pyridine (10 ml) and acetic anhydride (2 ml), was kept at room temperature overnight. This solution was then poured into ice-water, which was subsequently extracted with chloroform. Concentration of the combined chloroform extracts afforded a pale-yellow syrup.

Two separate multiplets at ϕ_c +176.1 and ϕ_c +180.0 p.p.m. were observed in the ^{19}F n.m.r. spectrum of this syrup. Separation of part of the anomeric mixture was achieved by g.l.c. (5% butanediol succinate on 60–80 Diaport S). On the basis of ^1H and ^{19}F n.m.r., together with fluorine heteronuclear double resonance, the products were assigned to the α- (**10**) and β- (**11**) anomers of 1,2-*O*-acetyl-3,6-anhydro-5-deoxy-5-fluoro-1,2-*O*-isopropylidene-L-idofuranose, with the former comprising 65% and the latter 35% of the mixture. The samples were not subject to any further chemical evaluations.

It is a pleasure to thank the National Research Council of Canada for their generous financial support of this work, especially for the equipment used in the heteronuclear decoupling experiments (Grant E 1338).

1. L. D. Hall and J. F. Manville. Can. J. Chem. **47**, 379 (1969).
2. L. D. Hall and J. F. Manville. Can. J. Chem. **47**, 1 (1969).
3. L. D. Hall and J. F. Manville. Can. J. Chem. **47**, 19 (1969).
4. R. J. Abraham, L. D. Hall, L. Hough, and K. A. McLauchlan. J. Chem. Soc. 3699 (1962).
5. F. Micheel and A. Klemer. Advan. Carbohyd. Chem. **16**, 85 (1961) and references therein.
6. J. E. G. Barnett. Advan. Carbohyd. Chem. **22**, 177 (1967) and references therein.
7. A. B. Foster, R. Hems, and J. M. Webber. Carbohyd. Res. **5**, 292 (1967), and references therein.
8. L. Evelyn and L. D. Hall. Chem. Ind. (London), 183 (1968).
9. D. H. Buss, L. D. Hall, and L. Hough. J. Chem. Soc. 1616 (1965).
10. G. R. Gray, F. E. Hartman, and R. Barker. J. Org. Chem. **30**, 2020 (1965).
11. J. S. Brimacombe and O. A. Ching. Carbohyd. Res. **5**, 234 (1967); **8**, 82 (1968).
12. A. C. Cope and T. Y. Shen. J. Amer. Chem. Soc. **78**, 5912 (1956). M. Jackson and L. D. Hayward. Can. J. Chem. **37**, 1048 (1959) and references therein.
13. L. D. Hall and J. F. Manville. Carbohyd. Res. **9**, 11 (1969).
14. D. L. Hooper, N. Sheppard, and C. M. Woodman. J. Chem. Phys. **45**, 398 (1966).
15. J. D. Stevens and H. G. Fletcher. J. Org. Chem. **33**, 1799 (1968) and references therein to earlier studies.
16. P. R. Steiner. M.Sc. Thesis, University of British Columbia, Vancouver 8, British Columbia. 1969.
17. B. Coxon. Carbohyd. Res. **8**, 125 (1968).
18. J. A. Pople and A. A. Bothner-By. J. Chem. Phys. **42**, 1339 (1965).
19. A. A. Bothner-By. Advan. Magn. Res. **1**, 195 (1965).
20. R. C. Cookson, T. A. Crabb, J. J. Frankel, and J. Hudek. Tetrahedron Suppl. **7**, 355 (1966).
21. B. Coxon. Tetrahedron, **22**, 2281 (1966).
22. L. D. Hall and J. F. Manville. *In* Deoxy sugars. Advan. Chem. Ser. **74**, 228 (1968).
23. L. D. Hall and J. F. Manville. Can. J. Chem. **45**, 1299 (1967).
24. H. Booth. Tetrahedron Letters, 411 (1965).
25. L. D. Hall and J. F. Manville. Chem. Commun. 37 (1968).
26. N. Prentice, L. S. Cuendet, and F. Smith. J. Amer. Chem. Soc. **78**, 4436 (1956).

Can. J. Chem. Downloaded from www.nrcresearchpress.com by 210.87.254.42 on 09/05/12
For personal use only.

N-Chlorination of secondary amides. III. Kinetics of dechlorination of *N*-chloroamides

M. WAYMAN AND E. W. C. W. THOMM
Department of Chemical Engineering and Applied Chemistry, University of Toronto, Toronto, Ontario

Received July 15, 1969

Several *N*-chlorinated secondary amides have been dechlorinated in aqueous or aqueous methanol solutions of phenol. The dechlorinating agents were found to be OH^- and $C_6H_5O^-$, with the rate expression

$$-\frac{d[R_1\overset{\overset{\displaystyle O}{\|}}{C}\text{—}NClR_2]}{dt} = \{k'_{OH^-}[OH^-] + k'_{C_6H_5O^-}[C_6H_5O^-]\}[R_1\overset{\overset{\displaystyle O}{\|}}{C}\text{—}NClR_2]$$

The substituent groups R_1 and R_2 of the *N*-chloroamide $R_1\overset{\overset{\displaystyle O}{\|}}{C}\text{—}NClR_2$ influence the dechlorination reactions through induction and resonance effects. The reactivity of the *N*-chloroamides was found to be in the order

$$H\overset{\overset{\displaystyle O}{\|}}{C}\text{—}NClCH_3 > CH_3\overset{\overset{\displaystyle O}{\|}}{C}\text{—}NClCH_3 \simeq CH_3CH_2\overset{\overset{\displaystyle O}{\|}}{C}\text{—}NClCH_3 > CH_3NH\overset{\overset{\displaystyle O}{\|}}{C}\text{—}NClCH_3$$

and

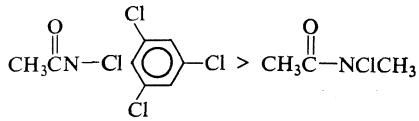

These results are discussed and reaction mechanisms proposed.

Canadian Journal of Chemistry, 48, 459 (1970)

Introduction

The kinetics of the *N*-chlorination of secondary amides has been studied and elementary reactions have been proposed (1, 2). However, these reactions are reversible and the combined positive chlorine can be released, especially in a medium where the chlorine demand is high (3). The present work investigated the kinetics of the reverse reaction, that is, of chlorine-releasing. In order to create an artificial chlorine demand in the reaction medium, phenol was added in excess. Phenol was used by Hurst and Soper (4), who studied the reaction of *N*-chloroacetamide with phenols, and who reported that the *N*-chloroacetamide reacts partly by hydrolysis and partly by direct chlorination of the phenoxide ion. They found that the rate of hydrolysis was proportional to the hydroxide ion concentration and calculated an equilibrium hydrolysis constant. Their work was carried out with different phenols in the p*H* range of 6.4 to 9.3.

In the present work, the reaction of phenol with 5 *N*-chlorinated secondary amides has been studied at p*H* values at which their rates of reaction were conveniently measured, the total p*H* range employed being 4.3 to 11.0. The chlorination kinetics of 4 of these amides have been reported (1, 2), while *N*,2,4,6-tetrachloroacetanilide is being investigated here for the first time. This last-named compound is much more reactive than the others, and was therefore studied in a mildly acidic aqueous methanol medium, while the others were reacted in alkaline aqueous solution.

Experimental

(a) Reagents

The *N*-chloroamides were synthesized by reacting the respective amides with hypochlorous acid in an acidic medium, using the procedure outlined in our previous communication (1). The amides used were purchased from Eastman Kodak Company, and were of the purest commercial grades. Since in our previous work (1, 2), purification by distillation or recrystallization had no noticeable effect on the rate of *N*-chlorination, they were used as purchased. Hypochlorous acid was obtained by acidifying sodium hypochlorite solutions (Fisher Scientific Company) to the appropriate p*H*. The reactions were allowed to proceed until about 95% of the hypochlorous acid had been consumed. A 5% excess of each amide was used. *N*,2,4,6-Tetrachloroacetanilide was isolated and recrystallized from methanol. It was found to be 99.5% pure based

Can. J. Chem. Downloaded from www.nrcresearchpress.com by 210.87.254.42 on 09/05/12
For personal use only.

on positive chlorine content. The other amides were left in dilute solutions. These solutions contained about 5×10^{-3} *M* chloride ions. At this low concentration, the chloride ion was found to have only negligible effects on the rate of the reaction (5).

Phenol was purchased from BDH. The "AnalaR" grade was used without further purification.

(b) Experimental Procedure

Kinetic runs were carried out according to Hurst and Soper (4). A brief outline is presented below.

Freshly prepared *N*-chloroamide and phenol solutions (containing 10 to 50 fold excess of phenol) of twice the required concentration were made up in acetate buffer (low p*H* range) or in sodium hydroxide solution (high p*H* range). At high p*H*, NaOH and C_6H_5OH form a buffer system. Water was used as the solvent for all *N*-chloroamides except *N*,2,4,6-tetrachloroacetanilide, for which the solvent was water–methanol mixtures.

When both solutions had attained the thermostat temperature, the buffered phenol solution was added to an equal volume of chloroamide solution. The p*H* of the reaction medium was periodically checked during the course of the reaction. No change of p*H* was observed in all systems studied.

The *N*-chloroamide content of the reaction mixture was determined at suitable intervals by iodometry. There was no free hypochlorous acid or hypochlorite in the solution as any would be immediately consumed by the phenol which reacts much faster than the free unchlorinated amides.

The reaction was allowed to proceed until 50–80% of the *N*-chloroamides had been dechlorinated.

The results of a typical run for $CH_3\overset{\overset{O}{\|}}{C}—NClCH_3$ are given in Table 1.

From the *N*,2,4,6-tetrachloroacetanilide–H_2O–CH_3OH system, a precipitate was obtained by addition of water to the solution after dechlorination. This was analyzed for its elemental composition.

(c) Treatment of Data

All results fit the following pseudo first order rate expression:

$$-\frac{d[R_1\overset{\overset{O}{\|}}{C}NClR_2]}{dt} = k'_{obs}[R_1\overset{\overset{O}{\|}}{C}NClR_2]$$

where $R_1\overset{\overset{O}{\|}}{C}NClR_2$ denotes the *N*-chloroamide. The observed rate constant, k'_{obs}, was calculated from the best straight line of the plot of log $[R_1\overset{\overset{O}{\|}}{C}NClR_2]$ vs. time.

Results

Typical observed rate constants, k'_{obs}, plotted against initial phenol concentration $[C_6H_5OH]_0$ are presented in Fig. 1. It is evident from the plots, that k'_{obs} is a linear function of $[C_6H_5OH]_0$ at constant p*H*. However, the slopes of these lines are dependent on the p*H* of each amide. Furthermore, by extrapolating k'_{obs} to zero phenol concentration, rate constants k'_0 are obtained. Typical values of k'_0 are represented in Fig. 2, plotted against $[OH^-]$. As can be seen, log k'_0 is a linear function of log $[OH^-]$ with a slope of 1. We may then consider that the rate constant k'_0 is the contribution to the total rate constant k'_{obs} by hydroxide ion.

When log k'_{obs} is plotted against log $[OH^-]$ for solutions containing a fixed amount of phenol in excess, no linearity was found (Fig. 3). However,

TABLE 1

A typical run* for *N*-chloroacetamide

Time (min)	Titre of N—Cl for 5 ml of reaction mixture (ml)	p*H*
0	24.9	10.01
20	20.8	
40	17.6	10.01
60	15.0	
90	11.9	10.01
120	9.2	

*Reaction conditions: 25 °C; $[C_6H_5OH]_0$ = 0.05 *M*; $[Na_2S_2O_3]$ = 0.0020 *N*.

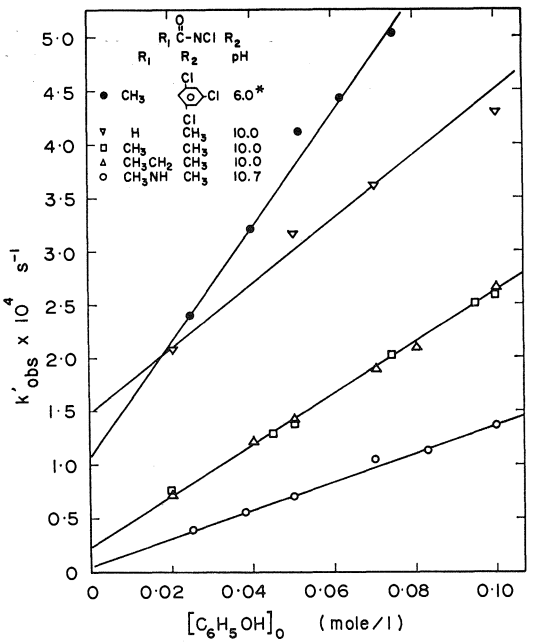

FIG. 1. Observed rate constants as a function of total phenol concentration, at 25 °C. (*1:1/H_2O:MeOH)

TABLE 2

Rate constant as a function of the hydrogen ion and initial phenol concentrations (*N*,2,4,6-tetrachloroacetanilide in 1:1/H_2O:CH_3OH (v:v) at 25 °C)

p*H*	$\frac{\Delta k'_{obs}}{\Delta[C_6H_5OH]_0}$ $l\ mole^{-1}\ s^{-1}$	$\frac{[H^+]\Delta k'_{obs}}{\Delta[C_6H_5OH]_0}$ s^{-1}
4.30	1.08×10^{-4}	5.40×10^{-9}
5.00	5.67×10^{-4}	5.67×10^{-9}
5.32	1.08×10^{-3}	5.30×10^{-9}
5.61	2.28×10^{-3}	5.70×10^{-9}
6.00	5.40×10^{-3}	5.40×10^{-9}
	mean	5.50×10^{-9}

when the slopes of the lines of Fig. 1, i.e. $\Delta k'_{obs}/\Delta[C_6H_5OH]_0$, were multiplied by the hydrogen ion concentration, $[H^+]$, constant values were obtained for each *N*-chloroamide. Typical data are listed in Table 2. This suggests the participation in the reaction of the phenoxide ion rather than the unionized phenol, from the following consideration:

$$C_6H_5OH \rightleftharpoons H^+ + C_6H_5O^-$$

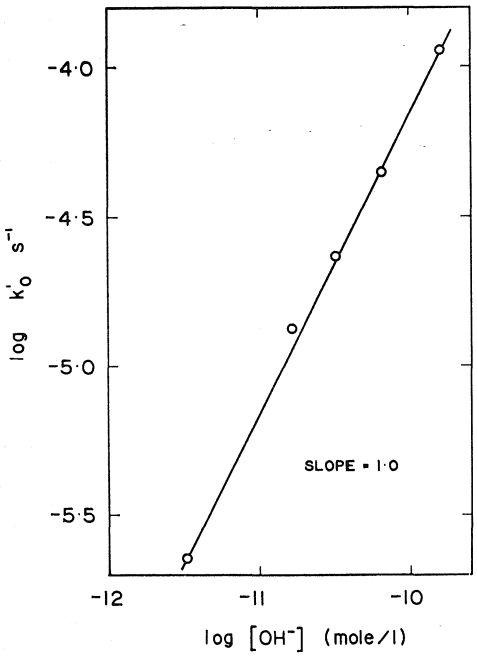

FIG. 2. Extrapolated rate constants as a function of hydroxide ion concentration: *N*,2,4,6-tetrachloroacetanilide in 1:1/H_2O:CH_3OH(v:v) at 25 °C.

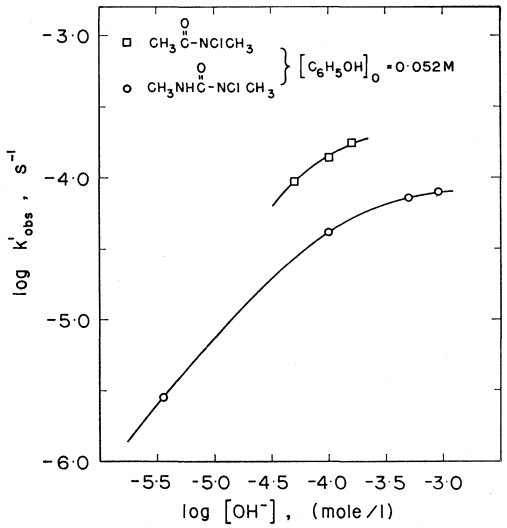

FIG. 3. Observed rate constants as a function of hydroxide ion concentration, 25 °C.

with the equilibrium constant

$$K_{C_6H_5OH} = \frac{[H^+][C_6H_5O^-]}{[C_6H_5OH]},$$

$$\therefore \frac{\Delta k'_{obs}}{\Delta[C_6H_5OH]_0} = \frac{\Delta k'_{obs} K_{C_6H_5OH}}{[H^+]\Delta[C_6H_5O^-]_0}$$

and

$$\frac{[H^+]\Delta k'_{obs}}{\Delta[C_6H_5OH]_0} = \frac{\Delta k'_{obs} K_{C_6H_5OH}}{\Delta[C_6H_5O^-]_0}$$

This was found to be a constant, as shown in Table 2. Thus, $\Delta k'_{obs}/\Delta[C_6H_5O^-]_0$ is a constant value, which indicates a reaction involving $C_6H_5O^-$

Thus the total observed rate constant can be broken into two components: (*i*) the contribution of the hydroxide ion; and (*ii*) the contribution of the phenoxide ion.

$$k'_{obs} = k'_{OH^-}[OH^-] + k'_{C_6H_5O^-}[C_6H_5O^-]$$

where

$$k'_{OH^-}[OH^-] = k'_0$$

Our formulation of k'_{obs} confirms that of Hurst and Soper (4).

By rearranging, k'_{obs} can be expressed as:

$$k'_{obs} = \left[k'_{OH^-} + k'_{C_6H_5O^-}\frac{K_{C_6H_5OH}}{K_w}[C_6H_5OH]\right] \times [OH^-]$$

Can. J. Chem. Downloaded from www.nrcresearchpress.com by 210.87.254.42 on 09/05/12
For personal use only.

where K_w is the ion product of water. For solutions with a fixed amount of total phenol, k'_{obs} is not a linear function of the hydroxide ion concentration, especially at pH higher than 9 where the dissociation of phenol becomes appreciable. The higher the pH, the smaller the $[C_6H_5OH]$; thus the flatter the slope $\Delta k'_{obs}/\Delta[OH^-]$. This explains the curvature of the lines in Fig. 3.

The values of k'_{OH^-} and $k'_{C_6H_5O^-}$ at different pH have been calculated, and are shown in Table 3. They exhibit good consistency over a wide range of pH, and thus furnish further support for the formulation of k'_{obs}.

In these experiments, as the pH increased the buffer concentration also increased. It can be seen from Table 3 that the specific rate constants were independent of the pH, and thus the buffer concentration. It follows that ionic strength does not affect the specific rate constants in this range.

In Fig. 4, the specific rate constants of *N*,2,4,6-tetrachloroacetanilide are plotted against the solvent composition and the reciprocal of the dielectric constant of the solvent. For both hydroxide and phenoxide ions, the reaction proceeds more rapidly in a less polar solvent (methanol-rich) than in a highly polar solvent (water-rich). Both k'_{OH^-} and $k'_{C_6H_5O^-}$ exhibit linearity with the reciprocal of the dielectric constant D of the solvent. However, the solvent composition has a greater effect on k'_{OH^-} than on $k'_{C_6H_5O^-}$.

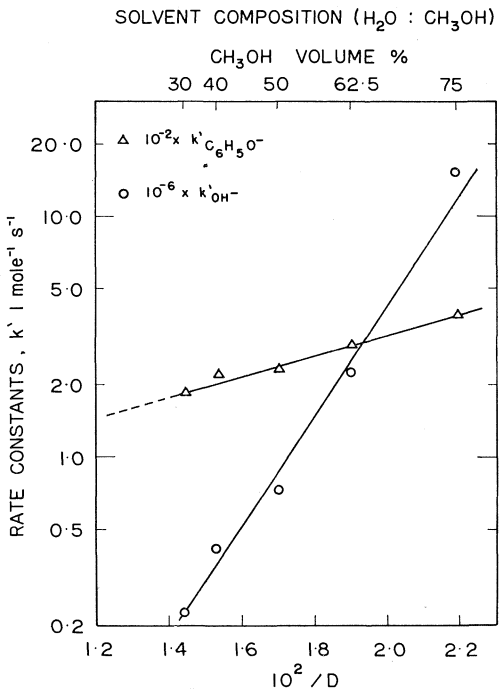

FIG. 4. Effects of solvent on the rate of dechlorination: *N*,2,4,6-tetrachloroacetanilide in H_2O–CH_3OH at 25 °C.

TABLE 3

Rate constants at various hydroxide ion concentrations at 25 °C*

	N-Chloroamide§			
	$10^{-5} \times k'_{OH^-}$† l mole^{-1} s^{-1}	$10^3 \times k'_{C_6H_5O^-}$‡ l mole^{-1} s^{-1}		
p*OH*	I	I	II	III
11.49	6.95	2.30×10^5	—	—
10.79	8.20	2.37×10^5	—	—
10.49	7.20	2.30×10^5	—	—
10.19	6.85	2.37×10^5	—	—
9.79	7.00	2.23×10^5	—	—
5.45	—	—	—	1.55
4.30	—	—	4.52	—
4.00	—	—	4.50	1.50
3.80	—	—	4.50	—
3.30	—	—	—	1.43
3.00	—	—	—	1.50
mean	7.24	2.31×10^5	4.51	1.49

*$[CH_3COOH]$ in buffer = 0.05 *M*; $[C_6H_5OH]_0 = 0.05 - 0.25$ *M*; $[C_6H_5OH]_0 = 0.05 - 0.25$ *M*.
†$K_{H_2O} = 5.9 \times 10^{-18}$ mole l^{-1} in 1:1/H_2O:CH_3OH (15).
‡$K_{C_6H_5OH} = 1.05 \times 10^{-10}$ mole l^{-1} in water (16); $K_{C_6H_5OH} \simeq 2.4 \times 10^{-11}$ mole l^{-1} in 1:1/H_2O:CH_3OH (17).

§I: 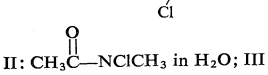 in 1:1/H_2O:CH_3OH(v:v);

II: $CH_3C(=O)$—$NClCH_3$ in H_2O; III: $CH_3NHC(=O)$—$NClCH_3$ in H_2O.

TABLE 4

Rate constants of *N*-chloroamides in water at 25 °C

N-chloroamide			
R_1	R_2	$k'_{C_6H_5O^-}$ (l mole^{-1} s^{-1})	k'_{OH^-} (l mole^{-1} s^{-1})
CH_3NH	CH_3	1.53×10^{-3}	0.012
CH_3CH_2	CH_3	4.4×10^{-3}	0.28
CH_3	CH_3	4.5×10^{-3}	0.28
H	CH_3	5.87×10^{-3}	1.50
CH_3*	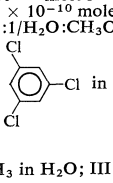	1.5×10^2	7.7×10^4

*Values extrapolated from methanol–water solutions to pure water.

Can. J. Chem. Downloaded from www.nrcresearchpress.com by 210.87.254.42 on 09/05/12
For personal use only.

Can. J. Chem. Downloaded from www.nrcresearchpress.com by 210.87.254.42 on 09/05/12
For personal use only.

The specific rate constants are listed in Table 4. The hydroxide ion is a more reactive reagent than the phenoxide ion. The order of reactivity of the various *N*-chloroamides is the same as that of the *N*-chlorination of the amides by the negatively charged hypochlorite ion (2).

The hydrolysis constants, K_h, where,

$$K_h = \frac{[R_1C(=O)—NHR_2][HOCl]}{[R_1C(=O)—NClR_2]}$$

of *N*-chloroamides are generally low. These can be calculated from the following equilibrium:

$$R_1C(=O)—NClR_2 + OH^- \underset{k_{OCl^-}}{\overset{k'_{OH^-}}{\rightleftharpoons}} R_1C(=O)—NHR_2 + OCl^-$$

such that

$$\frac{k'_{OH^-}}{k'_{OCl^-}} = \frac{[R_1C(=O)—NHR_2][OCl^-]}{[R_1C(=O)—NClR_2][OH^-]} = K_h \frac{K_{HOCl}}{K_w}$$

where

$$K_{HOCl} = \frac{[H^+][OCl^-]}{[HOCl]}$$
$$= 5.6 \times 10^{-8} \text{ mole/l at } 25\ ^\circ\text{C (6)}$$

and

$$K_w = [H^+][OH^-]$$
$$= 1.0 \times 10^{-14} \text{ mole/l}^2 \text{ at } 25\ ^\circ\text{C}.$$

The K_h values at 25 °C have been calculated from k'_{OH^-} (present data) and k'_{OCl^-} (2) and they are tabulated in Table 5. These hydrolysis constants fall within the general range of values reported for other *N*-chlorinated amines and amides (7).

The activation energies of the *N*-chloroacetamide series are presented in Table 6. The activation energy for the phenoxide reaction is about twice that for the hydroxide reaction.

TABLE 5
Hydrolysis constants

N-chloroamide $R_1C(=O)—NClR_2$		
R_1	R_2	K_h at 25 °C
CH_3NH	CH_3	$<1.2 \times 10^{-7}$
CH_3CH_2	CH_3	3.3×10^{-6}
CH_3	CH_3	1.6×10^{-6}
H	CH_3	7.0×10^{-6}
CH_3	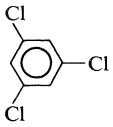	$\sim 1 \times 10^{-4}$

TABLE 6
Variation of rate constants with temperature*

$CH_3—C(=O)—NClCH_3 + HO^-$ or $C_6H_5O^-$

T °C	$k'_{C_6H_5O^-} \times 10^2$ (l mole^{-1} s^{-1})	k'_{OH^-} (l mole^{-1} s^{-1})
15	0.195	0.187
25	0.45	0.28
35	1.16	0.413
ΔE_a(kcal/mole)	16.2	7.4

*$K_{C_6H_5OH} = 1.05 \times 10^{-10}$ mole l^{-1} (16); $\Delta H^0_{C_6H_5OH \rightleftharpoons H^+ + C_6H_5O^-} = 5.65$ kcal/mole (16).

Discussion

1. The Molecular Nature of the Reactants

In the conditions of these experiments, the specific rate constants k'_{OH^-} and $k'_{C_6H_5O^-}$ were found to be independent of p*H*, and since the buffer systems employed varied in ionic strength, it can safely be deduced that ionic strength has no noticeable effect on the specific rate constants. If we assume, following Brönsted (8), that dependence of specific rate constants upon ionic strength requires that the reacting species be charged, that is, ions, then we may deduce that at least one of the *N*-chloroamide and the dechlorinating species is uncharged. The reaction rates are functions of hydroxide and phenoxide ion concentrations; hence, the *N*-chloroamide reacts as a molecule, and not as an ion.

2. Dechlorination

(a) Phenoxide–Hydroxide Dechlorination

This work suggests that the phenoxide ion takes part in the dechlorination of the chlorinated amides, which may be represented as follows:

$$R_1C(=O)—N(Cl)R_2 + C_6H_5O^- \xrightarrow{k'_{C_6H_5O^-}} R_1C(=O)—NHR_2 + C_6H_4ClO^-$$

Soper and Smith (9) reported that the phenoxide is much more reactive than the undissociated phenol molecule. Similarly, the dependence of k'_0 on the hydroxide ion concentration clearly indicates the following reaction:

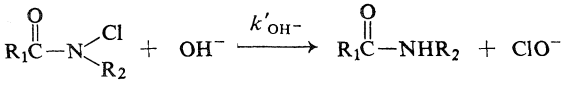

(b) Dechlorination Product

The dechlorination reactions proposed above require that the *N*-chloroamides revert to their corresponding amides. The elemental analysis of the dechlorination product isolated from the *N*,2,4,6-tetrachloroacetanilide system is presented in Table 7.

TABLE 7

Analysis of dechlorination product from *N*,2,4,6-tetrachloroacetanilide

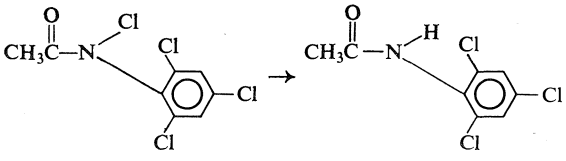

Element	C	H	N	O	Cl
Theoretical (wt%)	40.27	2.66	5.73	6.70	44.52
Found (wt%)	40.3	2.52	5.86	6.67	44.6

The good agreement between the theoretical values and observed values lends support to the proposed reactions.

(c) Solvent Effects

We suggest that the dechlorination processes of *N*-chloroamides involve the interaction of a molecular species B (the *N*-chloroamide) and the charged dechlorinating agent A having a charge of Z_A (HO^- or $C_6H_5O^-$), to form an intermediate M* that also has the charge Z_A.

$$A^{Z_A} + B^0 \rightarrow M^{*Z_A} \rightarrow \text{products}$$

For this type of reaction the reaction rate is markedly solvent dependent (10). In solvents with a high solvating power (or polarity), the charged species A^{Z_A} is surrounded by the solvent molecules, and its rate of reaction with B^0 is reduced. Conversely, the charge Z_A, which is localized to a single ion before reaction, becomes dispersed over a larger volume in the transition state. Since the charge density has been diminished, the intermediate involves less solvation than the reactant, and its formation is facilitated in a less polar solvent. This has been confirmed in the present work. Both phenoxide and hydroxide ions react faster in methanol-rich than in water-rich media.

The solvent effect can be expressed by the Laidler–Eyring equation in terms of the dielectric constant, D, of the medium (11):

$$\ln k = a + \frac{Z_A^2 E^2}{2hT}\left(\frac{1}{D}\right)\left(\frac{1}{r_A} - \frac{1}{r_{M^*}}\right)$$

where k is the specific rate constant; a, a constant at constant temperature T; Z_A, the charge of A or M*; E, the electronic charge; h, the Boltzmann gas constant; and r_i, the radius of the species i. The slopes of the log k vs. $1/D$ plots in Fig. 4 are equal to

$$\frac{(Z_A E)^2}{4.606\,hT}\left(\frac{1}{r_A} - \frac{1}{r_{M^*}}\right)$$

Since the phenoxide ion is larger than the hydroxide ion, the equation would lead to the expectation that the dielectric constant of the medium would have a greater effect on the hydroxide reaction than on the phenoxide reaction, as demonstrated in Fig. 4.

3. Effects of Substituent Groups

For the *N*-chloroamide series, $R_1C(=O)-NClR_2$, the higher the electron-withdrawing power of R_1 and R_2, the faster the reaction. The electron-withdrawing power of the substituents is in the following order:

$$C_6H_2Cl_3 > H > CH_3 \simeq CH_3CH_2 > CH_3NH$$

the reactivity of the corresponding *N*-chloroamides is in exactly the same sequence; namely

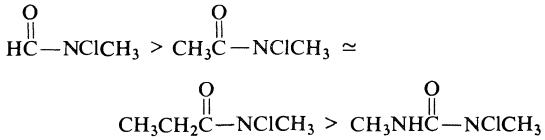

and

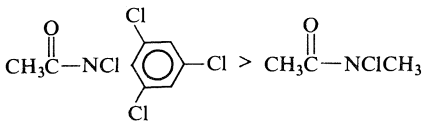

Can. J. Chem. Downloaded from www.nrcresearchpress.com by 210.87.254.42 on 09/05/12
For personal use only.

Can. J. Chem. Downloaded from www.nrcresearchpress.com by 210.87.254.42 on 09/05/12
For personal use only.

The primary reaction between the *N*-chloroamide and the dechlorinating species XO^- may be represented by the formation of the following intermediate:

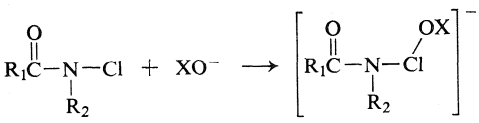

with decomposition taking the following path

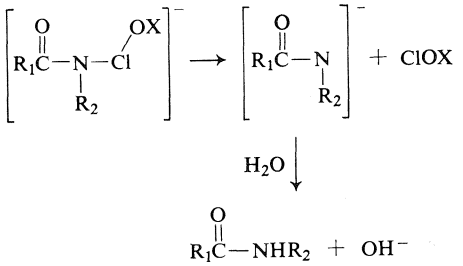

where if X = H, then

$$ClOH \rightleftharpoons H^+ + OCl^- ;$$

if X = C_6H_5, then

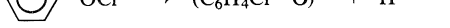

The formation of the first intermediate is the rate-limiting step. It is easily seen that the higher the residual positive charge on the amido nitrogen, the weaker the N—Cl bond, Cl being positive, and the more ready the formation of the intermediate. It follows, then, a higher electron-withdrawing power of the substituent groups R_1 and R_2 would facilitate the dechlorination reactions, as found.

In a recent paper Burstall *et al.* (12) suggested a somewhat similar mechanism for the reaction of OH^- and *p*-NO_2—$C_6H_5O^-$ with *N*-chlorinated secondary aromatic amides. They proposed, as we do, that the primary reaction is between the *N*-chlorinated molecule and the ions. They suggested, however, that the primary addition compound of the OH^- and the *N*-chlorinated molecule involved a bond between the amide carbon and the hydroxyl oxygen. Since the next step suggested in both their mechanism and ours is the splitting of HOCl, we prefer our representation. In the representation of the phenoxide reactions, Burstall *et al.* (12) represented the amido chlorine atom as moving directly to the *ortho* position of the phenoxide ring, but make no attempt to show a structure for the intermediate. Again, at least in the case of unsubstituted phenoxide, we prefer to stay with the same mechanism as proposed for the hydroxide reaction.

Because of the bulkiness of the phenoxide ion, the formation of its intermediate with the *N*-chloroamide is expected to be slower than that with the hydroxide ion due to steric hindrance. This has been confirmed in the present work.

Resonance effects probably influence the dechlorination reactions. Pauling (13) suggested that amides have two main resonance structures. It is reasonable to consider that the *N*-chloroamides have analogous structures:

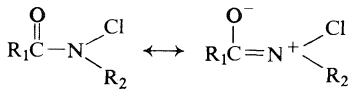

The combined inductive effect of the substituents and the resonance of the amides can be summarized if we can extend the Hammett equation to the present systems:

$$\log (k/k_0) = \sigma\rho$$

where k is the specific rate constant, k_0 is a reference rate constant, σ is the substituent constant independent of the reaction, and ρ is the reaction proportionality constant. A positive ρ value indicates that the reaction is facilitated by electron-withdrawing substituents and a negative ρ value would indicate electron-releasing substituents. Taft (14) proposed that σ is made up of two components: σ_I, the inductive effect; and σ_R, the resonance effect:

$$\sigma_p = \sigma_I + \sigma_R$$

where σ_p is the σ value for *p*-substituted benzene rings. It is reasonable to consider that there are similar inductive and resonance effects on the structures of the *N*-chloroamides as on the benzene rings.

Figure 5 plots the rate constants of the two reaction series of the *N*-chlorinated amides $R_1C(=O)NClCH_3$ with HO^- and $C_6H_5O^-$ against σ_p of the substituents. The positive slopes clearly indicate facilitation of reaction by electron-withdrawal by the substituent groups. Furthermore, the linearity of the plots lends indirect support to the hypothesis that both inductive and resonance effects come into play in the reaction.

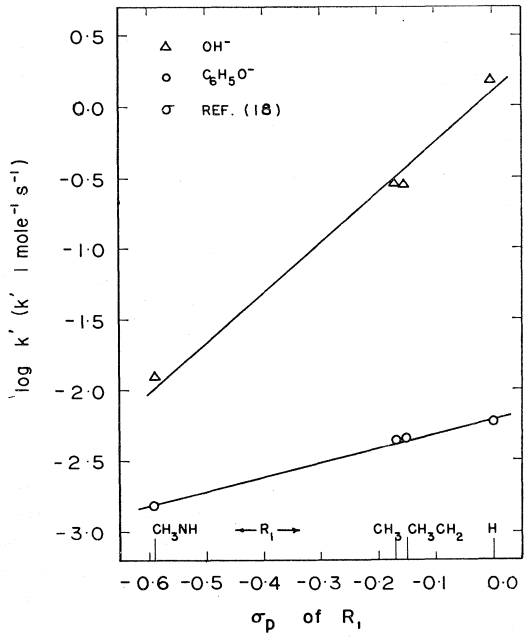

FIG. 5. Effects of the substituents of the *N*-chloroamides, $R_1C(=O)—NClCH_3$, on the reaction rates.

Our studies of chlorination of these amides (1, 2) have suggested that the primary mechanism is different in acid medium from that in alkaline medium, whereas the present studies suggest that the mechanism of dechlorination is independent of p*H*, at least in the range studied, p*H* 4 to 11.

This work was supported in part by the Defence Research Board of Canada (Grant No. 2075-05). One of us, E. W. C. W. Thomm, would like to thank the National Research Council of Canada for a Scholarship awarded from 1967.

1. M. WAYMAN and E. W. C. W. THOMM. Can. J. Chem. **47**, 2561 (1969).
2. E. W. C. W. THOMM and M. WAYMAN. Can. J. Chem. **47**, 3289 (1969).
3. M. WAYMAN, H. SALAMAT, and E. J. DEWAR. Can. J. Chem. Eng. **46**, 282 (1968).
4. F. B. HURST and F. G. SOPER. J. Chem. Soc. 107 (1949).
5. E. W. C. W. THOMM. Ph.D. Thesis. University of Toronto, Toronto, Canada (1969).
6. A. SKRABAL and A. BERGER. Monatsh. **70**, 168 (1937).
7. F. G. SOPER. J. Chem. Soc. **125**, 1899 (1924).
8. J. N. BRÖNSTED. Z. Phys. Chem. **102**, 169 (1922); **115**, 337 (1925).
9. F. G. SOPER and G. F. SMITH. J. Chem. Soc. 1852 (1926).
10. E. S. AMIS. Solvent effects on reaction rates and mechanisms. Academic Press, N.Y. 1966. Chapter II.
11. K. J. LAIDLER and H. EYRING. Ann. N.Y. Acad. Sci. **39**, 303 (1940).
12. M. L. BURSTALL, M. S. GIBSON, J. S. GREIG, B. MCGHEE, and D. G. STEWART. J. Chem. Soc. 3717 (1960).
13. L. PAULING. The nature of the chemical bond. 3rd ed. Cornell University Press, Ithaca, N.Y. 1960. p. 281.
14. R. W. TAFT, JR. J. Amer. Chem. Soc. **79**, 1045 (1957).
15. D. J. GLOVER. J. Amer. Chem. Soc. **87**, 5275, 5279 (1963).
16. L. P. FERNANDEZ and L. G. HEPLER. J. Amer. Chem. Soc. **81**, 1783 (1959).
17. J. M. VANDENBELT, C. H. SPURLOCK, M. GIFFELS, and M. W. EASH. Science **121**, 646 (1955).
18. H. H. JAFFE. Chem. Rev. **53**, 191 (1953).

Can. J. Chem. Downloaded from www.nrcresearchpress.com by 210.87.254.42 on 09/05/12
For personal use only.

Studies in isoxazole chemistry. II.[1] Isoxazoles from the Δ^2-isoxazolin-5-ols and their acetates

R. G. MICETICH
R & L Molecular Research Ltd., 8045 Argyll Road, Edmonton 82, Alberta
Received August 6, 1969

Various 3-substituted-5-acetoxy-Δ^2-isoxazolines were made by the 1,3-dipolar cycloaddition of nitrile oxides to vinyl acetate or isopropenyl acetate. These compounds were readily converted in high yield to 3-substituted isoxazoles or 3-substituted-5-methylisoxazoles respectively, on heating. Treatment of the 3-substituted-5-acetoxy-Δ^2-isoxazolines with sodium hydroxide in methanol gave rise to the stable Δ^2-isoxazolin-5-ols after acidification. These compounds could also be converted to 3-substituted isoxazoles by heating alone, or better, in the presence of thionyl chloride. The nuclear magnetic resonance spectra of these compounds are discussed.

Canadian Journal of Chemistry, 48, 467 (1970)

In a continuation of our work on isoxazoles, we had occasion to require various 3-substituted isoxazoles. It is reported that 3-substituted isoxazoles can be made by the action of hydroxylamine on β-ketoaldehydes (1, 2) or β-chlorovinylketones (3). In the last two instances, the preparation is complicated by the fact that a mixture of the 3- and 5-substituted isoxazoles usually results. It appeared to us, that a much more convenient, unambiguous synthesis, suitable for the preparation of relatively large amounts of various 3-substituted isoxazoles was via the relatively neglected Δ^2-isoxazolines. The isoxazolines are readily obtained by the 1,3-dipolar cycloaddition of nitrile oxides to olefins (4, 5).

It has been noted (6, 7, 8) that isoxazolines of structure **1**, with R″ = Cl or NO_2, readily eliminate HR″ to give isoxazoles **3**; and a similar elimination occurs with isoxazolines of structure **2**, when R″ = Cl, Br, alkoxy, or amine (9–14). This area has not been utilized sufficiently for the specific purpose of preparing isoxazoles. It has been shown that other groups can also be eliminated in this manner from Δ^2-isoxazolines to give rise to the more stable aromatic isoxazole ring. Thus Quilico and Speroni (15) found that benzonitrile oxide reacted with β-diketones, only in presence of base, forming isoxazoles **5**. They suggested that the reaction involved a 1,3-dipolar cycloaddition of the nitrile oxide to the enol form of the β-diketone, with subsequent dehydration of the resulting Δ^2-isoxazolin-5-ol **4**, which could not be isolated.

D'Alcontres and Grünanger (16) obtained 3-phenylisoxazole by heating 3-phenyl-5-acetoxy-Δ^2-isoxazoline for several hours with methanolic hydrogen chloride and assumed that it was formed by dehydration of the intermediate alcohol (which was not isolated). Various isoxazoles have been obtained in a similar manner

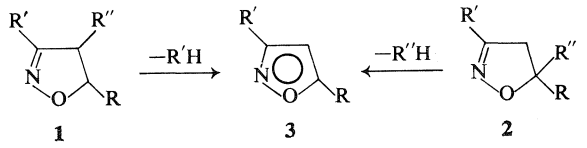

1 **3** **2**

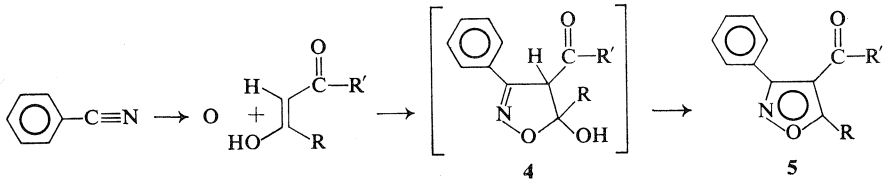

4 **5**

[1]See ref. 32.

by heating 5-acetoxy-Δ^2-isoxazolines with alcoholic acid (17–20), or by treating the Δ^2-isoxazoline-5-boronic acids with sodium hydroxide (21).

The nitrile oxides (either isolated or formed *in situ*) reacted readily with vinyl acetate to form the 3-substituted-5-acetoxy-Δ^2-isoxazolines (**8**) – (Table 1), the other product of the reaction in some cases, being the respective nitrile oxide dimer, the furoxan. The yields could be further increased by using the "dilution technique" of Huisgen (4), or the "reverse addition" method of Kanō and co-workers (22). The 3-substituted-5-acetoxy-Δ^2-isoxazolines (**8**) thus obtained, were found to eliminate acetic acid readily on heating above 160–190 °C, to give excellent yields of the 3-substituted isoxazoles **11** (Table 3). Since it is not necessary to isolate the 5-acetoxyisoxazoline, this method forms a simple, essentially 1-step synthesis of 3-substituted isoxazoles. Thus, 3-*o*-chlorophenylisoxazole **11***b* was obtained in a 60% overall yield without isolation of the intermediate isoxazoline. This compound was identical (boiling point (b.p.), infrared (i.r.), and nuclear magnetic resonance (n.m.r.) spectra) with a sample obtained in 30% yield by the action of *o*-chlorobenzonitrile oxide on acetylene. The 3-carbethoxy isoxazole **11***f* prepared by this method (90%) was identical (b.p., i.r. and n.m.r. spectra) with a sample obtained in 23% yield by the action of carbethoxynitrile oxide on vinyl bromide.

This method can also be utilized for the preparation of 3,5-disubstituted isoxazoles. Thus, 3-phenyl-5-methylisoxazole (**11***g*) (23) was obtained in 28% overall yield by the reaction of benzonitrile oxide with isopropenyl acetate and distillation of the crude isoxazoline **8***g*, which was not characterized. 3-Carbomethoxy-5-methylisoxazole (**11***h*) was obtained in 27% overall yield by this method.

The scope of this reaction has not been further investigated. The use of other substituted vinyl acetates, e.g. β-phenylvinyl acetate (24), could lead to 3-substituted-5-phenylisoxazoles.

3-Phenyl-5-acetoxy-Δ^2-isoxazoline (**8***a*) (16, 17, 19) underwent an extremely smooth immediate reaction with sodium hydroxide in methanol to give the sodio-derivative of 3-phenyl-Δ^2-isoxazolin-5-ol (**9***a*) in 96% yield. Small amounts (ca. 0.4%) of 3-phenylisoxazole were also isolated from this reaction. The sodio-salt **9***a*, on acidification, gave 3-phenyl-Δ^2-isoxazolin-5-ol (**10***a*) in quantitative yield. This same compound has recently been reported in a preliminary paper by Bianchi and co-workers (25) and was obtained by the hydrolysis of 3-phenyl-Δ^2-isoxazolin-5-boronic acid. This compound, contrary to expectation, was a stable, crystalline solid with a m.p. of 120–121 °C. On heating to ca. 200 °C, or better, on heating under reflux with thionyl chloride, it was converted to 3-phenylisoxazole (**11***a*) in excellent yields. Table 2 lists the 3-substituted-Δ^2-isoxazolin-5-ols (**10**) made in this manner. The sodio-salt **9***a*, on acidification with deuteriosulfuric acid in D_2O, gave the deuterated 3-phenyl-Δ^2-isoxazolin-5-ol (**10***a*(D)). This compound was also obtained by crystallizing 3-phenyl-Δ^2-isoxazolin-5-ol (**10***a*) repeatedly from D_2O.

Nuclear Magnetic Resonance Spectra

Although n.m.r. spectroscopy has been used to differentiate between isomeric *cis*- and *trans*-3,4,5 - trisubstituted - Δ^2 - isoxazolines (26), the n.m.r. spectra of 3,5-disubstituted-Δ^2-isoxazolines have not been commented upon so far. Figure 1 shows the n.m.r. spectra of the 3-phenyl compounds in this series and the 3-carbethoxy-5-acetoxy-Δ^2-isoxazoline **8***f* prepared by us. As expected, the isoxazolines **8***a*, **8***f*, and **10***a*(D) exhibit resonances characteristic of ABX spin systems (27, 28). The spectrum of **10***a* is further complicated by geminal coupling of H_x to the hydroxyl proton (29). The hydroxyl proton appears as a doublet centered at τ 2.90, with a spacing of 7 c.p.s. and H_x shows a multiplet centered at τ 4.03. In the case of the deuterated compound **10***a*(D), as expected, the H_x multiplet collapses to a quartet, thus reducing the four proton system to an ABX type spin system.

The 3-carbethoxy-5-acetoxy-Δ^2-isoxazoline (**8***f*), 3-carbethoxyisoxazole (**11***f*), and 3-carbomethoxyisoxazole (**11***e*) prepared by this route were found to be pure from the n.m.r. spectra and analysis. Quilico and Panizzi (30) have reported the preparation of 3-carbethoxyisoxazole by the reaction of carbethoxychloraldoxime on disodium acetylene, but the product was not characterized except by conversion to the acid.

The n.m.r. spectrum ($CDCl_3$) of 3-carbomethoxy-5-methylisoxazole (**11***h*) m.p. 92–93°, showed a sharp singlet at τ 6.05 (—$COOCH_3$), a singlet at 7.51 (C_5—CH_3), and a singlet at 3.58 (isoxazole C_4—H). The n.m.r. spectrum ($CDCl_3$)

TABLE 1

3-Substituted-5-acetoxy-Δ^2-isoxazolines

Compound 8*	R′	Melting point or boiling point (°C)	Yield (%)	Recrystallization solvent	Infrared spectrum ν_{max} (cm^{-1})	Analysis					
						Calculated (%)			Found (%)		
						C	H	N	C	H	N
a		90–91†	70	CCl_4	3020 (shoulder) 1730 (strong) 1600, 1550 (weak)	64.40	5.36	6.83	64.11	5.60	6.59
c	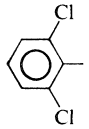	136–138	82	CCl_4	3050 (shoulder) 1720 (strong) 1570, 1540 (medium)	48.18	3.28	5.11	48.27	3.10	4.96
d	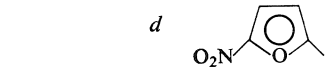	104–105	38	CCl_4	3100 (sharp) 1750 (strong) 1550, 1520, 1490 (medium)	45.00	3.33	11.66	45.22	3.13	11.41
f	$-COOC_2H_5$	127/1.2mm m.p. 35–37	83		1740, 1730 (strong) 1590 (medium)	47.77	5.46	6.96	47.53	5.72	7.10

*Compound 8 has the following structure: 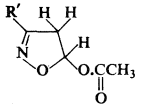

†Reported m.p. 88–89° (16); 90–90.5° (17). The compound melts at 90–91°, solidifies and remelts at 107–108° (see ref. 19).

TABLE 2

3-Substituted-5-hydroxy-Δ^2-isoxazolines

Compound 10*	R′	Melting point (°C)	Yield (%)	Recrystallization solvent	Infrared spectrum ν_{max} (cm^{-1})	Analysis					
						Calculated (%)			Found (%)		
						C	H	N	C	H	N
a		120–122†	96	benzene	3200 (broad) 1590 (weak)	66.25	5.52	8.58	65.98	5.43	8.87
a (D)		120–121	90	D_2O	2380 (strong) 1590 (weak)						
c	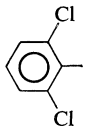	125–127	55	benzene–hexane	3300 (broad) 1600 (weak) 1570, 1550 (medium)	46.80	2.99	6.34	46.54	3.01	6.03
d	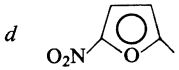	164–168	86	ethyl acetate–hexane	3500, 3100 (sharp) 1550 (weak) 1500, 1490 (medium)	42.57	3.01	14.40	42.42	3.03	14.15

*Compound 10 has the following structure: 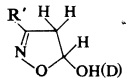

†Reported m.p. 120–121° (25).

TABLE 3

3-Substituted isoxazoles

Compound 11*	R′	R	Melting point or boiling point (°C)	Yield (%)	Temperature for preparation	Infrared spectrum ν_{max} (cm^{-1})	Analysis: Calculated (%) C	H	N	Found (%) C	H	N
a		H	124/12mm†	83	160	1500 (weak) 3120, 3080 (medium) 1550 (sharp, strong)						
b		H	85/0.3mm 90/0.5mm	60‡ 30§	170	3100, 3030 (medium) 1590, 1560 (medium, sharp) 1540 (strong, sharp) 1490 (medium)	60.15	3.34	7.80	60.41	3.51	7.60
c	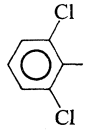	H	160/1mm 61–62	90	175	3150 (weak) 1580, 1550 (medium) 3100 (sharp, medium)	50.50	2.33	6.54	50.35	2.20	6.30
e	—$COOCH_3$	H	93/14mm	85‡	190	1740 (sharp, strong) 1540 (sharp, weak)	47.25	3.94	11.02	47.35	4.10	11.15
f	—$COOC_2H_5$	H	60/1mm	90‡ 23‖	180	3100 (sharp, medium) 1740 (sharp, strong) 1540 (sharp, weak)	51.06	4.96	9.93	51.00	4.65	10.22
g		—CH_3	41–42¶	28‡	160	3020 (weak) 1600 (sharp, strong) 1570 (sharp, medium)						
h	—$COOCH_3$	—CH_3	92–93	27	160	3100 (weak) 1710 (broad, strong) 1590 (sharp, medium)	51.06	4.96	9.92	51.04	5.15	9.91

*Compound **11** has the following structure: 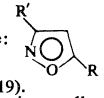

†Reported b.p. 75°/2 mm, m.p. 12–14 °C (19).
‡Made without isolation of the intermediate isoxazoline.
§Made by reaction of *o*-chlorobenzonitrile oxide on acetylene.
‖Made by reaction of carbethoxynitrile oxide on vinyl bromide.
¶Reported m.p. 42–43 °C (23).

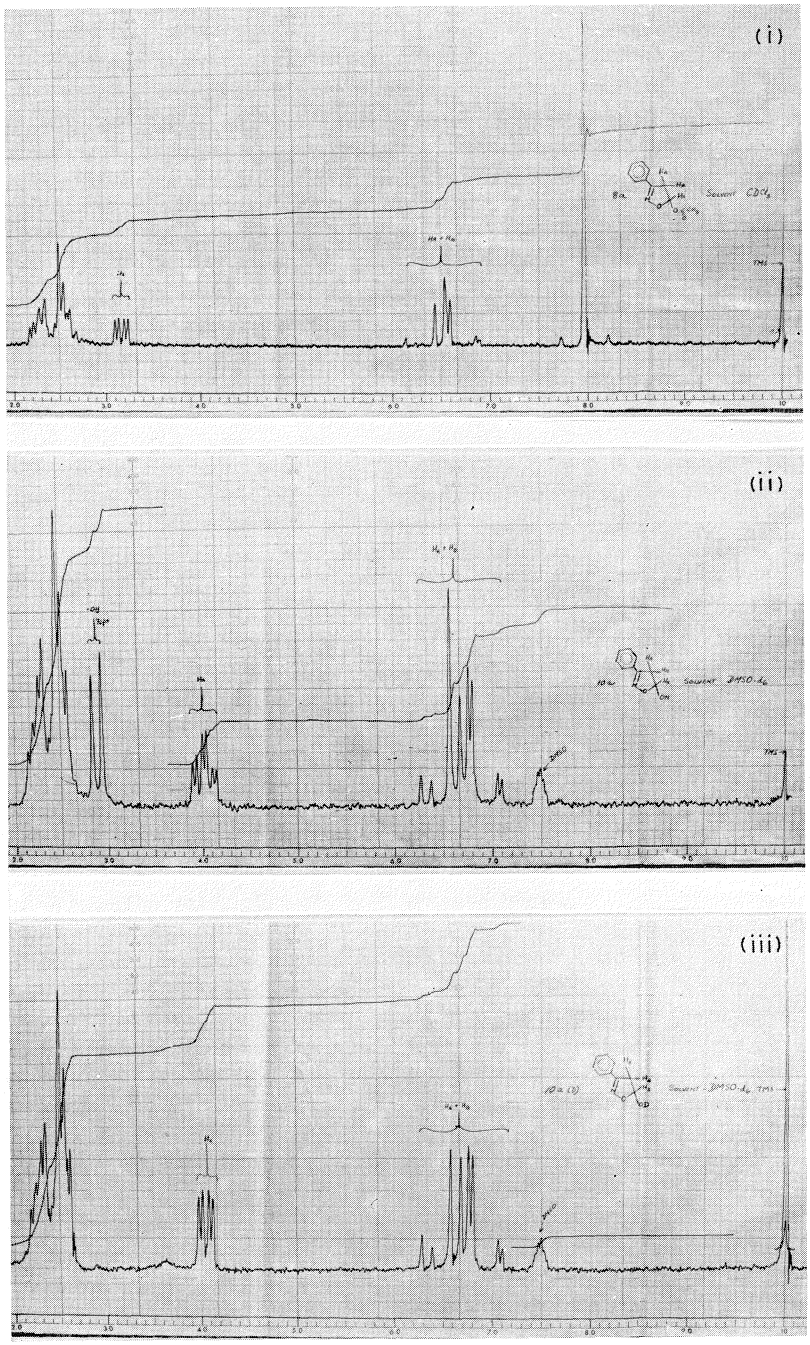

FIG. 1. The n.m.r. spectra of the 3,5-disubstituted-Δ^2-isoxazolines: (*i*) **8***a*; (*ii*) **10***a*; (*iii*) **10***a*(D).

of the isomeric 3-methyl-5-carbomethoxyisoxazole, m.p. 103–105°, made in a similar way to that described for the ethyl ester (31), showed 3 sharp singlets at τ 3.19 (isoxazole C_4—*H*), 6.05 (—COOCH_3), and 7.63 (C_3—CH_3). This is in agreement with our findings on the methyl nitrofuryl isoxazole isomers (32).

Experimental

All melting points were taken on a Fisher–Johns apparatus and are uncorrected. Infrared spectra were measured on a Perkin–Elmer model 137 Spectrophotometer. All solids were measured as Nujol mulls and liquids as films. Nuclear magnetic resonance spectra were measured on a Varian model A-60, using tetramethylsilane as an internal reference in the solvents specified.

*3-(2′,6′-Dichlorophenyl)-5-acetoxy-Δ²-isoxazoline (**8c**)*

Vinyl acetate (43 g, 0.5 mole) was added slowly with shaking to 2,6-dichlorobenzonitrile oxide (33) (15.5 g, 0.082 mole) in an ice-bath. There was an immediate exothermic reaction. The reaction mixture was left overnight at room temperature and the excess vinyl acetate removed under vacuum. The resulting solid crystallized from carbon tetrachloride as white crystals, m.p. 136–138°. Yield 18.4 g (82%).

*3-(5-Nitrofur-2-yl)-5-acetoxy-Δ²-isoxazoline (**8d**)*

5-Nitrofuryl-2-chloraldoxime (32, 34) (34 g, 0.178 mole) and vinyl acetate (22.4 g, 0.26 mole) were dissolved in ether (200 ml), and the solution heated under reflux with efficient stirring. Triethylamine (20.2 g, 0.2 mole) dissolved in ether (50 ml) was added slowly down the condenser over a period of ca. 1 h. After the addition, water (75 ml) was added to the dark reaction mixture which was then stirred and filtered. The solid thus obtained was shaken with ethyl acetate (500 ml) and water (500 ml) and the ethyl acetate layer combined with the ether layer from the original mixture. The combined organic layers were dried over magnesium sulfate, filtered, and solvent removed when 39.5 g, of a black semi-solid mass was obtained. The residue was heated with carbon tetrachloride (1.5 l), decolorizing charcoal and Celite added, and filtered hot, when 16.0 g (38%) of a yellow solid m.p. 100–103°, separated on cooling. Recrystallization from carbon tetrachloride raised the melting point to 104–105 °C.

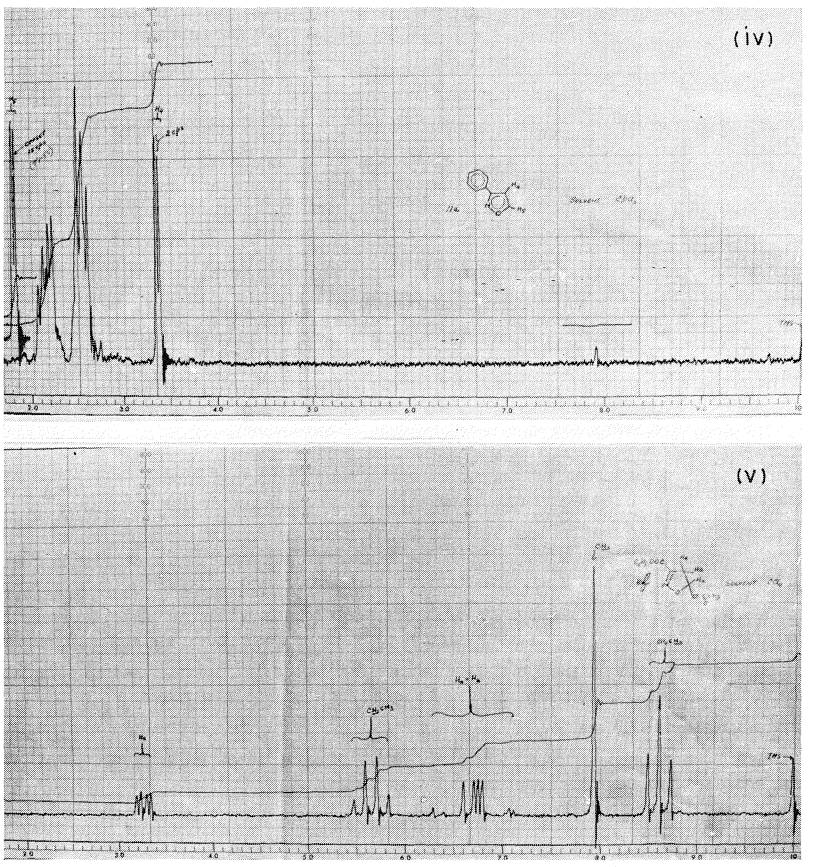

FIG. 1 (cont.). The n.m.r. spectra of the 3,5-disubstituted-Δ²-isoxazolines: (*iv*) **11***a*; (*v*) **8** *f*.

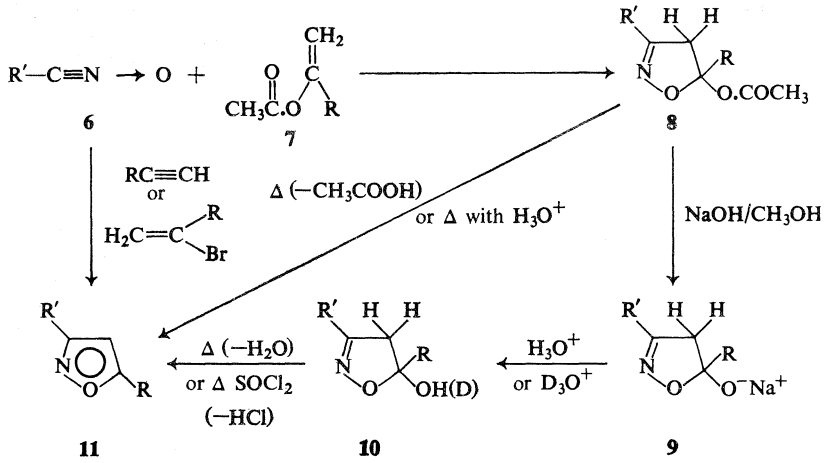

	R′	R
a		H
b		H
c	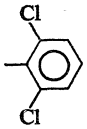	H
d	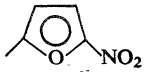	H
e	$-COOCH_3$	H
f	$-COOC_2H_5$	H
g		$-CH_3$
h	$-COOCH_3$	$-CH_3$

SCHEME 1

3-Carbethoxy-5-acetoxy-Δ²-isoxazoline (8f)

A solution of carbethoxychloraldoxime (35) (15 g, 0.1 mole) and vinyl acetate (86 g, 1 mole) in ether (200 ml) was stirred vigorously and heated under reflux on a water bath and a solution of triethylamine (12 g, 0.12 mole) in ether (100 ml) added slowly down the condenser. After the complete addition, heating was continued for another h, water (150 ml) added and the layers separated. The ether layer was dried over magnesium sulfate, filtered, solvent removed, and the residue distilled under reduced pressure, when 16.7 g (83%) of a colorless oil, b.p. 127.5°/1.2 mm was obtained. The compound crystallized on standing, m.p. 35–37 °C (ether).

3-Phenyl-Δ²-isoxazolin-5-ol (10a)

A solution of sodium hydroxide in methanol (30 ml of a 3 *M* solution 0.09 mole) was added to a stirred mixture of 3-phenyl-5-acetoxy-Δ²-isoxazoline (21.6 g, 0.088 mole) in methanol (150 ml). A clear solution resulted. After ca. 5 min the solvent was removed under reduced pressure and the resulting solid dried under vacuum. The solid was stirred with ether, filtered, washed well with ether, and dried to give the sodio-salt. The ether washings on concentration gave 0.5 g (0.4°) of an oil whose i.r. spectrum and n.m.r. spectrum were identical with those of 3-phenylisoxazole.

The sodio-salt was dissolved in water (50 ml) and concentrated hydrochloric acid (10 ml) added, when an oil separated. The mixture was extracted with ethyl acetate (3 × 50 ml) and the combined ethyl acetate layers dried over magnesium sulfate, filtered, and solvent removed. A white solid, (16.3 g, 96%) m.p. 120–122° was obtained.

Recrystallization from benzene did not change the m.p.

Recrystallization (6 times) from D_2O gave the deuterated 3-phenyl-Δ^2-isoxazolin-5-ol, m.p. 120–121°. This compound was also made by the action of deuteriosulfuric acid in D_2O on the dried sodio-salt.

*3-(2′,6′-Dichlorophenyl)-Δ^2-isoxazolin-5-ol (**10c**)*

Melting point 125–127 °C was obtained by the same procedure.

*3-(5-Nitrofur-2-yl)-Δ^2-isoxazolin-5-ol (**10d**)*

A solution of sodium hydroxide in methanol (20 ml of a 1 *M* solution, 0.02 mole) was added *dropwise* to a well stirred, ice cold suspension of 3-(5-nitrofur-2-yl)-5-acetoxy-Δ^2-isoxazoline (4.8 g, 0.02 mole) in methanol (60 ml). After ca. 5 min stirring in an ice-bath, dilute hydrochloric acid (6.7 ml of a 3 *M* solution) was added to the yellow solution. The solution became clear and after a few minutes a white solid separated. Water (100 ml) was added and the mixture concentrated under reduced pressure. Ethyl acetate (500 ml) was added, the mixture shaken well and the layers separated. The ethyl acetate layer was dried over magnesium sulfate, filtered, and solvent removed, when 4.3 g, (86%) of a faint yellow solid, m.p. 164–168° was obtained. Recrystallization from ethyl acetate–hexane raised the m.p. to 170–172 °C.

*3-Phenylisoxazole (**11a**)*

3-Phenyl-5-acetoxy-Δ^2-isoxazoline **8***a* (16, 17, 19) (25 g, 0.122 mole) was heated with stirring on an oil bath at 160°. When most of the acetic acid had distilled over, water-pump vacuum was applied and a light yellow oil, b.p. 128°/15 mm was collected. Redistillation of this oil gave 14.7 g, (83%) of a colorless oil, b.p. 124°/12 mm.

*3-o-Chlorophenylisoxazole (**11b**)*

From Vinyl Acetate

Nitrosyl chloride (68 ml) was added to an ice cold solution of *o*-chlorobenzaldoxime (138 g, 0.88 mole) in ether (2.4 l), the mixture left overnight at room temperature, filtered, and concentrated. The resulting yellow oil and vinyl acetate (95 g, 1.1 mole) dissolved in ether (2.5 ml) was stirred in an ice-bath and triethylamine (92 g, 0.9 mole) added slowly. After the complete addition, the mixture was heated under reflux, with stirring for 2 h, water (300 ml) added, and the layers separated. The ether layer was dried over magnesium sulfate, filtered, and solvent removed. The resulting thick brown oil was heated with stirring on an oil bath at 170° for 1/2 h, by which time most of the acetic acid had distilled over. The residue was then distilled under a water-pump vacuum (to remove all the acetic acid) and then under 0.5 mm pressure, and the fraction b.p. 71–90°/0.5 mm, (104 g) collected. On redistillation 3-*o*-chlorophenylisoxazole, b.p. 90°/0.5 mm or 85°/0.3 mm, was obtained as a clear liquid.

From Acetylene

A solution of *o*-chlorobenzchloraldoxime (18.8 g, 0.012 mole) in tetrahydrofuran (250 ml) was heated under reflux with vigorous stirring and kept saturated with acetylene, while a solution of triethylamine (10.2 g, 0.011 mole) in tetrahydrofuran (30 ml) was added slowly down the condenser. After 4 h, water (200 ml) was added, and the mixture concentrated under reduced pressure. The mixture was extracted with ether (3 × 200 ml) and the combined ether extracts dried, filtered, and solvent removed. The residue was distilled under reduced pressure and the fraction, b.p. 90°/0.5 mm, weight 5.3 g (30%) collected. It was a colorless oil, whose spectra (i.r. and n.m.r.) were identical with that of the sample made from vinyl acetate.

*3-(2′,6′-Dichlorophenyl)isoxazole (**11c**)*

3-(2′,6-Dichlorophenyl)-5-acetoxy-Δ^2-isoxazoline (8.0 g, 0.03 mole) was stirred and heated on an oil bath at 175° for ca. 2 h by which time the acetic acid had distilled over. The residue was distilled under reduced pressure and gave 5.8 g, (90%) of a clear oil b.p. 160°/1 mm, m.p. 61–62° (hexane).

*3-Carbethoxyisoxazole (**11f**)*

From the Isoxazoline

3-Carbethoxy-5-acetoxy-Δ^2-isoxazoline (40 g, 0.2 mole) was heated on an oil bath at 180° for 1/2 h by which time ca. 11 g of acetic acid had distilled over. Distillation of the residue under reduced pressure gave 25.1 g, (90%) of a clear oil b.p. 60°/1 mm.

From Vinyl Bromide

Triethylamine (6 g, 0.055 mole) was added slowly to a stirred solution of carbethoxychloraldoxime (7.5 g, 0.05 mole) and vinyl bromide (6 g, 0.055 mole) in ether (150 ml), at room temperature. The mixture was left overnight at room temperature and then stirred with water and the ether layer separated. The aqueous layer was extracted with ether (2 × 50 ml). The combined ether layers were dried over magnesium sulfate and solvent removed. Distillation of the residue gave 1.6 g, (23%) of 3-carbethoxyisoxazole b.p. 60°/1 mm and 3.0 g, (70%) of 3,4-dicarbethoxy-furoxan b.p. 105°/0.5 mm.

*3-Carbomethoxyisoxazole (**11e**)*

Boiling point 93°/14 mm was obtained in 85% yield from the crude isoxazoline using the same procedure as for the ethyl ester.

*3-Carbomethoxy-5-methylisoxazole (**11h**)*

A solution of carbomethoxychloroaldoxime (27.5 g, 0.2 mole), [m.p. 62–64°, obtained in 50% yield by the same method as described for the ethyl ester (35)], and *iso*propenyl acetate (40 g, 0.4 mole) in ether (500 ml) was stirred vigorously and heated under reflux, while a solution of triethylamine (20.2 g, 0.2 mole) in ether (50 ml) was added slowly down the condenser. There was the immediate precipitation of triethylamine hydrochloride. An i.r. spectrum of the mixture showed the reaction to be complete after the addition of triethylamine. Water (150 ml) was added with stirring and the ether layer separated, dried over magnesium sulfate, filtered, and concentrated. The residue was heated on an oil bath at 165° and after ca. 20 min subjected to a water-pump vacuum and the fraction boiling at ca. 150°/12 mm collected. This fraction was redistilled when three fractions were obtained.

Fraction 1 weight 7.2 g (27%) b.p. 120–130°/11 mm, solidified and crystallized from carbon tetrachloride as white flakes, m.p. 92–93° and was 3-carbomethoxy-5-methylisoxazole.

Fraction 2 weight 1.5 g, b.p. 132–145°/11 mm was discarded.

Fraction 3 weight 8.0 g (40%), b.p. 147–150°/11 mm

was 3.4-dicarbomethoxyfuroxan and showed two sharp singlets at τ 5.97 and 6.00, in its n.m.r. spectrum.

*3-Phenyl-5-methylisoxazole (**11g**)*

Boiling point 142–144°/15 mm, m.p. 41–42° was obtained in 28% yield by using the same procedure as above.

3-Methyl-5-carbomethoxyisoxazole

This compound was made in the same way as the ethyl ester (31) in 80% yield and had m.p. 103–105°.

Anal. Calcd. for $C_6H_7NO_3$: C, 51.06; H, 4.96; N, 9.92. Found: C, 51.04; H, 5.15; N, 9.91.

The author thanks Professor R. U. Lemieux for his advice and interest, Messrs. R. A. Fortier and R. Thomas for their capable technical assistance, and Drs. T. Nagabhushan, R. Raap, and C. Chin for fruitful discussion on this work.

1. N. K. Kochetkov, E. E. Nifantjev, and A. N. Nesmeyanov. Izv. Akad. Nauk S.S.S.R., Otd. Khim. Nauk, 949 (1957).
2. K. von Auwers and H. Wunderling. Ber. **69**, 638 (1934).
3. N. K. Kochetkov. Usp. Khim. **24**, 32 (1955); N. K. Kochetkov. Chem. Tech. (Berlin) **7**, 578 (1955).
4. R. Huisgen. Angew. Chem. (Int.), **2**, 565 (1963).
5. N. K. Kochetkov and S. D. Sokolov. *In* Advances in heterocyclic chemistry. Vol. 2. Academic Press, New York, 1963. p. 375.
6. P. Grünanger. Gazz. Chim. Ital. **84**, 359 (1954); Atti accad. nazl. Lincei, Rend. Classe sci. fis. mat. e nat., **16**, 726 (1954).
7. P. Grünanger and S. Mangiapan. Gazz. Chim. Ital. **88**, 149 (1958).
8. P. Vita Finzi and M. Arbasino. Ann. Chim. (Rome), **54**, 1165 (1964).
9. R. G. Micetich. Paper under preparation.
10. S. Minami and J. Matsumoto. Chem. Pharm. Bull. (Japan), 15 (3), 366 (1967).
11. P. Rajogopalan and C. N. Talaty. Tetrahedron Lett. **38**, 4537 (1966).
12. L. Birkoffer and A. Widdig. Tetrahedron Lett. **48**, 4299 (1965).
13. G. Bianchi, A. Cogoli, and R. Gandolfi. Gazz. Chim. Ital. **98**, 74 (1968).
14. I. Adachi and H. Kano. Chem. Pharm. Bull. (Japan), **16**, (1), 117 (1968).
15. A. Quilico and G. Speroni. Gazz. Chim. Ital. **76**, 148 (1946).
16. G. S. D'Alcontres and P. Grünanger. Gazz. Chim. Ital. **80**, 741 (1950).
17. G. Just and K. Dahl. Tetrahedron Lett. **22**, 2441 (1966).
18. G. S. D'Alcontres and G. Mollica. Atti accad. nazl. Lincei, Rend., Classe sci. fis. mat. e nat. **10**, 52 (1951); Chem. Abstr. **46**, 495g (1952).
19. R. Paul and S. Tchelitcheff. Bull. Soc. Chim. (France), 2215 (1962).
20. M. R. Langella and P. Vita Fiuzi. Chim. Ind. (Milan), **47**, 996 (1965); Chem. Abstr. **63**, 16324h (1965).
21. G. Bianchi, A. Cogoli, and P. Grünanger. J. Organometal. Chem. **6**, 598 (1966); Chem. Abstr. **66**, 18735 (1967).
22. H. Kanō, I. Adachi, R. Kido, and K. Hirose. J. Med. Chem. **10**, 411 (1967).
23. G. Desimoni and P. Grünanger. Gazz. Chim. Ital. **97**, 25 (1967).
24. G. S. D'Alcontres and P. Grünanger. Gazz. Chim. Ital. **80**, 831 (1950).
25. G. Bianchi, A. Cogoli, and P. Grünanger. Ric. Sci. **36**, 132 (1966); Chem. Abstr. **64**, 19650e (1966).
26. M. C. Aversa, G. Cum, and M. Crisafulli. Gazz. Chim. Ital. **98**, 42 (1968).
27. R. J. Abraham and H. J. Bernstein. Can. J. Chem. **39**, 216 (1961).
28. E. W. Garbisch, Jr. J. Chem. Ed. **45**, 402 (1968).
29. O. L. Chapman and R. W. King. J. Amer. Chem. Soc. **86**, 1256 (1964).
30. A. Quilico and L. Panizzi. Gazz. Chim. Ital. **72**, 458 (1942).
31. K. Nakagawa and S. Sumimoto. Shionogi & Co. Ltd., Japan, 22 283, Oct. 21st 1963; Chem. Abstr. **60**, 4154b (1964).
32. R. G. Micetich. J. Med. Chem. **12**, 611 (1969).
33. G. Grundman and J. M. Dean. J. Org. Chem. **30**, 2809 (1965).
34. R. Lenaers and F. Eloy. Helv. Chim. Acta, **117**, 1069 (1963).
35. G. S. Skinner. J. Amer. Chem. Soc. **46**, 731 (1924).

Can. J. Chem. Downloaded from www.nrcresearchpress.com by 210.87.254.6 on 09/05/12
For personal use only.

Lignin and related compounds. II. Studies using ruthenium and Raney nickel as catalysts for lignin hydrogenolysis

J. M. Pepper and Y. W. Lee

Department of Chemistry and Chemical Engineering, University of Saskatchewan, Saskatoon, Saskatchewan

Received August 18, 1969

Five cyclohexyl compounds, derived from lignin, have been isolated and identified from the products of the catalytic hydrogenolysis of spruce wood over ruthenium and Raney nickel catalysts. One of these, 3-(4-hydroxy-3-methoxycyclohexyl)-1-propanol, a previously unreported compound, has been synthesized and characterized.

Canadian Journal of Chemistry, **48**, 477 (1970)

In a previous communication (1), the gas-liquid chromatograms of spruce lignin hydrogenolysis products obtained using excess Raney nickel, ruthenium on charcoal, and ruthenium on alumina as catalysts were illustrated. Of the 9 compounds represented as distinct peaks in these chromatograms, 4, labelled C, D, E, and F in Fig. 1, were identified as aromatic derivatives whereas the other 5 compounds, labelled 1 through 5, were reported as cyclohexyl derivatives but their structures had not been determined. This paper deals with the identification of these 5 compounds, the quantitative estimation of all 9 lignin derivatives, and suggestions as to their origin as a result of the hydrogenolysis process.

The chromatograms reproduced in the previous paper and that shown herein as Fig. 1, are of the ether-soluble fraction of the chloroform-soluble fraction obtained from the products of the catalytic hydrogenolysis of spruce lignin. Details of the hydrogenolysis, isolation, separation, and chromatography were given in the previous publication (1). Subsequent to the chromatographic work reported earlier, it was found that a better separation, for quantitative analytical purposes, could be obtained using a column packed with 10% SE-30 on Chromosorb W (80/100 mesh, DMCS treated, acid washed), operated under identical conditions. A pure sample of each compound was collected from the gas chromatograph and identified by comparison of its relative retention time and its mass, infrared (i.r.), and nuclear magnetic resonance (n.m.r.) spectra with similar spectra of an authentic sample.

Using dihydrosinapyl alcohol as the internal standard, the relative abundance of each of these 9 lignin degradation products was determined for each of the 3 catalyst systems under study and is given in Table 1 in terms of the percentage, by weight, of the total ether-soluble fraction; along with the total yield of all such products based on the original Klason lignin. Such values are recorded as obtained by the use of both a planimeter and the triangulation method; with the average of such values considered to be most suitable.

The results of the experiments reported in

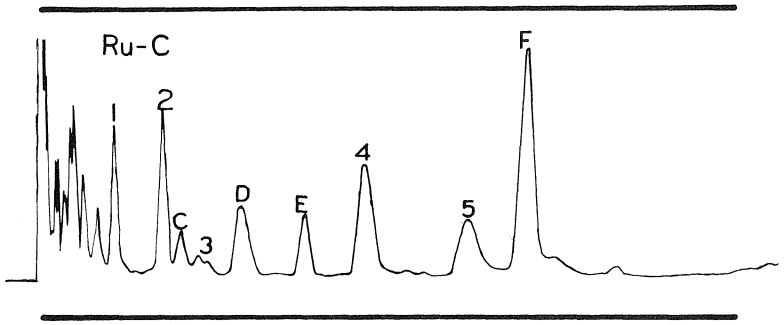

Fig. 1. Gas–liquid chromatogram of spruce lignin hydrogenolysis products: 1, 4-ethylcyclohexanol; 2, 4-*n*-propylcyclohexanol; C, 4-methylguaiacol; 3, 3-cyclohexyl-1-propanol; D, 4-ethylguaiacol; E, 4-*n*-propylguaiacol; 4, 3-(4-hydroxycyclohexyl)-1-propanol; 5, 3-(4-hydroxy-3-methoxycyclohexyl)-1-propanol; F, dihydroconiferyl alcohol.

TABLE 1

Gas–liquid chromatographic analysis of ether-soluble spruce lignin hydrogenolysis products*

	Abundance of chromatographable products†,‡										
Catalyst	1	2	C	3	D	E	4	5	F	Total	Yield of recovered lignin§
Raney-Ni (10 g)	0.66	0.83	1.00	1.69	1.00	0.87	40.9	12.6	6.32	65.9	16.5
Ru-C	1.56	3.49	1.39	0.32	2.70	1.61	6.95	4.52	10.3	32.8	11.8
Ru-alumina	0.67	1.72	0.97	1.05	2.02	2.51	19.8	12.2	15.2	56.1	14.6

*For details of isolation refer to reference 1.
†Percent of total ether-soluble fraction as calculated subsequent to the measurement of average peak areas as obtained using the planimeter and the triangulation methods.
‡Product identity: C, 4-methylguaiacol; D, 4-ethylguaiacol; E, 4-*n*-propylguaiacol; F, dihydroconiferyl alcohol; 1, 4-ethylcyclohexanol; 2, 4-*n*-propylcyclohexanol; 3, 3-cyclohexyl-1-propanol; 4, 3-(4-hydroxycyclohexyl)-1-propanol; 5, 3-(4-hydroxy-3-methoxycyclohexyl)-1-propanol.
§Percent of original Klason lignin.

Table 1 support the conclusion made in the previous publication (1), that the use of any of the catalyst systems (excess Raney nickel, ruthenium-on-charcoal, and ruthenium-on-alumina) results in a more extensive degradation of the lignin fraction along with a significant amount of ring reduction to the corresponding cyclohexyl derivatives. It may be of some significance that of the various compounds obtained, the major amount is represented by those of the 1-substituted-3-propanol structure. In this way, these 3 catalyst systems resemble more closely that of palladium-on-charcoal (1).

Authentic samples of each of the identified compounds were available or were synthesized as reported in the Experimental section. 1-(4-Hydroxycyclohexyl)-3-propanol and 1-(4-hydroxy-3-methoxycyclohexyl)-3-propanol (peaks 4 and 5, Fig. 1) were prepared by the hydrogenation of dihydroconiferyl alcohol over ruthenium-on-alumina (5%) catalyst. As part of this synthetic study, it was of interest to note that a marked difference in the nature of the products was obtained depending on the conditions of the reaction. Under the conditions indicated in Table 2, negligible reaction occurred at a temperature below 120°. For hydrogenations carried out at 160, 175, and 195°, the nature of the products obtained is indicated in Table 2, with the approximate relative abundance as indicated by the relative ratio of peak areas, as observed by gas chromatography. The main reactions appear to be an initial ring saturation, followed by a reductive loss of methoxyl, followed by a reduction of the propyl alcoholic function and/or side chain cleavage of carbon–carbon bonds.

The suggestion that was made in the earlier publication (1), that two types of ether linkage may exist in the lignin is supported by the observations recorded in this paper. All the compounds identified in Fig. 1 may be reasonably expected to be derived from either *n*-propylguaiacol (peak E) or dihydroconiferyl alcohol (peak F). That *n*-propylguaiacol should be considered as a primary lignin cleavage product along with dihydroconiferyl alcohol, and not a reduction product of the latter, is indicated in 2 ways. The production of the cyclohexyl derivatives is more readily explained as arising from the further reduction of each of these 2 compounds resulting in decreased yields of the 2 aromatic compounds relative to the total yield of recovered substances. In the second place, the Ru-alumina catalytic hydrogenolysis of pure dihydroconiferyl alcohol (Table 2) gave rise to no *n*-propylguaiacol suggesting that this secondary reaction is not the source of *n*-propylguaiacol found in the lignin products of a similar treatment of spruce wood.

This paper records the isolation, for the first time, of 3-(4-hydroxy-3-methoxycyclohexyl)-1-propanol as a hydrogenolysis product of lignin; and also of its synthesis and characterization. The other cyclohexanols have been reported previously as lignin products (2).

Experimental

The ether-soluble spruce lignin hydrogenolysis products used in this study were those whose isolation and yields were recorded in the previous publication (1). They had been obtained by the hydrogenolysis of preextracted wood meal (10 g), in dioxane–water (1:1 v/v, 150 ml) at an initial hydrogen pressure of 500 p.s.i.g. at a temperature of 195° for 5 h over the appropriate catalyst (1 g for ruthenium-charcoal (5%) and ruthenium-alumina (5%) and 10 g for Raney nickel). For the study using Raney

Can. J. Chem. Downloaded from www.nrcresearchpress.com by 210.87.254.6 on 09/05/12
For personal use only.

TABLE 2

Hydrogenolysis of dihydroconiferyl alcohol*

Dihydroconiferyl alcohol (g)	Ru-alumina (5%) (g)	Temperature (°C)	Time (h)	Ratio of peak areas of cyclohexyl derivatives and starting material†,‡					
				1	2	3	4	5	F
0.40	0.20	160	1	—	—	—	1	1	1.5
0.50	0.50	175	0.5	10	2.5	0.3	8	6	1
0.52	1.05	195	5	10	4	0.1	—	—	—

*Solvent: dioxane–water (1:1 v/v, 50 ml); hydrogen (initial pressure, 500 p.s.i.g.).
†Product identity: 1, 4-ethylcyclohexanol; 2, 4-*n*-propylcyclohexanol; 3, 3-cyclohexyl-1-propanol; 4, 3-(4-hydroxycyclohexyl)-1-propanol; 5, 3-(4-hydroxy-3-methoxycyclohexyl)-1-propanol; F, dihydroconiferyl alcohol (starting material).
‡Other peaks appeared in the chromatogram but represented compounds that were not identified.

nickel (10 g), the ether-soluble fractions of the 2 runs recorded in Table 1 of the previous paper were combined, while for the study using Ru-alumina catalyst the run was used which had yielded 0.68 g of ether-soluble material. Chromatographic separation of the components of the ether-soluble fractions was made using an F & M Chromatograph, model 5750 with hydrogen flame detector and temperature programming. The column (1/8 in. × 6 ft) was packed with 10% SE-30 on Chromosorb W (80–100 mesh, DMCS treated, acid washed). The chromatograms were obtained at a helium flow rate of 40 ml/min; temperature programmed from 100 to 250 °C at 4°/min; injection temperature 260°; detector temperature 270°; recorder chart speed 0.5 in./min.

The quantitative analytical data reported in Table 1 were obtained by a method similar to that reported earlier (1) but using 1-(4-hydroxy-3,5-dimethoxyphenyl)-3-propanol (dihydrosinapyl alcohol) as the internal standard. Each of the cyclohexyl derivatives obtained as lignin hydrogenolysis products was identified by comparison of its relative retention time with that of an authentic sample and by i.r., n.m.r., and mass spectra.

Source of Reference Compounds

Authentic samples of each of the cyclohexyl derivatives were obtained as indicated below. For analytical purposes, a fraction was obtained by gas–liquid chromatography (g.l.c.) using an Aerograph A90P machine, fitted with a column (1/4 in. × 6 ft) packed with 15% SE-30 on Chromosorb W (80–100 mesh, DMCS treated, acid washed); column, detector, and injector temperatures of 190, 230, and 210° respectively; and a helium flow rate of 40 ml/min. In each case the identity of the compound was checked by means of its mass, i.r. and n.m.r. spectra. For 3-(4-hydroxy-3-methoxycyclohexyl)-1-propanol, details of its preparation and characterization are given because it is a previously unreported compound.

4-Ethylcyclohexanol

This alcohol was commercially available from Aldrich Chemical Company Inc.

4-n-Propylcyclohexanol

This hexanol was prepared by the catalytic hydrogenation (5% Rh-alumina, 175°) of eugenol or dihydroconiferyl alcohol; α-naphthylurethane derivative, m.p. 133–134°; reported (3) m.p. 134–135°.

3-Cyclohexyl-1-propanol

This propanol was prepared by the catalytic hydrogenation (5% Rh-charcoal, 100°) of 3-phenyl-1-propanol.

3-(4-Hydroxycyclohexyl)-1-propanol

This propanol was prepared by the catalytic hydrogenation (5% Rh-alumina, 160°) of dihydroconiferyl alcohol (see Table 2).

3-(4-Hydroxy-3-methoxycyclohexyl)-1-propanol

This propanol was prepared by the catalytic hydrogenation of dihydroconiferyl alcohol (0.5 g) in dioxane (50 ml) over 5% Ru-alumina (0.25 g) at an initial pressure of hydrogen of 500 p.s.i.g. for 1 h at 160°. By g.l.c. of the chloroform-soluble fraction a compound was obtained which had the same retention time (on two different columns) as compound 5 isolated from the products of lignin hydrogenolysis. This compound (as a mixture of its diastereoisomers) was shown to be 3-(4-hydroxy-3-methoxycyclohexyl)-1-propanol as follows: *m/e* 188 (M^+ 1.7), 170 (0.7, loss of water), 129 (100, characteristic loss of side chain (4)), 111 (27.2, loss of water from *m/e* 129 fragment), 98 (16.3), 97 (27.2, loss of methanol from *m/e* 129 fragment), 81 (27.2), 71 (22.2), 69 (27.2), 67 (28.4), 59 (7.2, side chain), 58 (22.2), 57 (20.8, characteristic of cyclohexanols (4)), 55 (27.2), 45 (53.1), 41 (50.7) and 31 (23.5); i.r. spectrum (KBr disc): 3380, 2910, 2840, 1440, 1180, 1075, 1050, 970 cm^{-1}; n.m.r. spectrum ($CDCl_3$): CH_2OH, τ 6.4 (t, 2H); OCH_3, τ 6.6 (s, 3H); 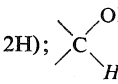 OH, 7.7 (s, 2H); , τ 5.9 (narrow m, 1/2H (equatorial)); τ 6.4 (broad m, 1/2H (axial)); 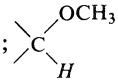 , τ 6.7 (m, 1H); remaining protons as a broad m from ca. τ 7.9 to ca. τ 9. The n.m.r. spectrum of the diacetate of this compound confirmed the above assignments.

The authors are grateful for the support provided by a grant from the Department of Forestry of Canada, and for financial assistance received from the National Research Council of Canada.

1. J. M. Pepper and Y. W. Lee. Can. J. Chem. **47**, 723 (1969).
2. I. A. Pearl. The chemistry of lignin. Marcel Dekker Inc., New York, 1967.
3. E. E. Harris, J. D'Ianni, and H. Adkins. J. Amer. Chem. Soc. **60**, 1467 (1938).
4. H. Budzikiewicz, C. Djerassi, and D. H. Williams. Interpretation of mass spectra of organic compounds. Holden-Day, Inc., San Francisco 1964.

Can. J. Chem. Downloaded from www.nrcresearchpress.com by 210.87.254.6 on 09/05/12
For personal use only.

Can. J. Chem. Downloaded from www.nrcresearchpress.com by 210.87.254.40 on 09/05/12
For personal use only.

Electron paramagnetic resonance spectroscopic study of radicals derived from glycine, *dl*-α-alanine, and β-alanine in aqueous solution[1]

P. SMITH, W. M. FOX, D. J. MCGINTY[2], AND R. D. STEVENS
Department of Chemistry, Duke University, Durham, North Carolina, 27706

Received June 16, 1969

The substrates glycine, *dl*-α-alanine, and β-alanine have been examined in turn within an aqueous continuous-flow system using the titanous chloride – hydrogen peroxide radical-generating method. The temperature was 25 ± 2 °C and the p*H* of the reaction mixture was varied within the range of values ca. 2 to ca. 5 by addition of sulfuric acid. The electron paramagnetic resonance spectra of the following transient radicals were observed: from glycine, $\cdot CH(NH_2)COOH$; from *dl*-α-alanine, $CH_3\dot{C}(NH_2)COOH$ and $\cdot CH_2CH(NH_3^+)COOH$; and from β-alanine, $CH_2(NH_3^+)\dot{C}HCOOH$. The structure of the radical from glycine has been established as $\cdot CH(NH_2)COOH$, not $\cdot CH(NH_3^+)COO^-$; in clarification of conflicting analyses by earlier workers, who employed reaction conditions similar to those of this present study but who did not obtain spectra as well resolved as those reported here. One group of these earlier workers claimed that glycine gave the radicals $\cdot CH(NH_3^+)COO^-$ and $\cdot CH_2COO^-$ and the other group postulated correctly that the radical formed was $\cdot CH(NH_2)COOH$. The structural assignment $\cdot CH(NH_2)COOH$ is confirmed by the observation in the present investigation of a similarly-structured radical, $CH_3\dot{C}(NH_2)COOH$, from *dl*-α-alanine. This latter radical was not found by the earlier workers. An additional, small, previously unreported proton hyperfine coupling has been observed in the spectrum from $\cdot CH(NH_2)COOH$ when no sulfuric acid is added to the reaction mixture, i.e. p*H* ca. 4. It has been assigned to the carboxyl-group proton in the above radical. This appears to be the first time such an assignment has been made, and hence, arguments have been cited for its justification. The coupling-constant data obtained for the $\cdot CH(NH_2)COOH$ radical are markedly different from those for the radicals $\cdot CH(NH_3^+)COO^-$ and $\cdot CH(NH_2)COO^-$ reported by other investigators to be formed from glycine under reaction conditions clearly unlike those employed in this present study, even though all three formulas differ only with respect to protonation. These differences are discussed.

Canadian Journal of Chemistry, **48**, 480 (1970)

Introduction

The reaction between titanous chloride and hydrogen peroxide in the presence of a reactive organic substrate within an aqueous continuous-flow system has been shown (1) to be an effective method for the generation of transient free radicals for the purpose of electron paramagnetic resonance (e.p.r.) spectroscopic observations. The basic reactions taking place may be represented by the equations

[1] $\quad Ti(III) + H_2O_2 \rightarrow Ti(IV) + OH^- + \cdot OH$

[2] $\quad \cdot OH + SH \rightarrow H_2O + S\cdot$

or

[3] $\quad \cdot OH + SH \rightarrow \cdot SHOH$

where SH denotes the organic substrate, and the details of the mechanism of this radical-generating system have attracted recent attention (2–7).

A number of investigations using this radical-generating method have already been reported from this laboratory (8–12), and the present work concerns the extension of this method to the three simple amino acids, glycine, *dl*-α-alanine, and β-alanine in acidic solution. As expected from the results of earlier studies in this laboratory with similar saturated aliphatic substrates such as carboxylic acids (9) and primary amines[3], these amino acids were not highly reactive. Nevertheless, it proved possible to detect hydrogen-atom abstraction products in all three cases.

Recently, the results of two related studies of these same substrates in acidic solution with the use of this radical-generating method have been published (13, 14). The present report extends and clarifies this previous work. In particular, the present investigation establishes conclusively the analysis of the e.p.r. spectrum produced with the use of the substrate glycine in acidic solution, and identifies the radical which is formed as $\cdot CH(NH_2)COOH$. Our results for glycine conflict with those given by one group of the earlier

[1]This work was supported by National Science Foundation Grant GP 7534.

[2]In partial fulfillment of the requirements for graduation with distinction, National Science Foundation Undergraduate Research Participant.

[3]P. Smith and P. B. Wood. Unpublished work.

Can. J. Chem. Downloaded from www.nrcresearchpress.com by 210.87.254.40 on 09/05/12
For personal use only.

workers (13) but are in essential agreement with those of the other group (14). Our assignment was rendered more convincing by the identification in this present investigation of a similar species, $CH_3\dot{C}(NH_2)COOH$, as one of the hydrogen-atom abstraction products formed from the substrate *dl*-α-alanine. This radical was not observed in the previous studies with α-alanine (13, 14).

Experimental

The experimental arrangement and procedures were essentially as described before (11). Spectra were recorded as the first derivative and *g*-values were taken as before against peroxylamine disulfonate (11). All substrates were Eastman White-Label grade and were used without further purification, for all gave spectra free of unassignable lines.

Unless specified otherwise, the following reaction conditions were employed: total flow rate, 2–8 ml s^{-1} divided equally between the two streams; the reaction temperature, 25 ± 2 °C; the titanous chloride concentration in the reducing stream, 0.01–0.001 *M*; the hydrogen peroxide concentration in the oxidizing stream, 0.04–0.3 *M*; the sulfuric acid was added only to the oxidizing stream, the concentration being 0.0–0.7 *M*, which corresponds to a p*H* range in the reaction mixture of ca. 4–5 to ca. 2–3. With the oxidizing stream 2 *M* in amino acid, the approximate p*H* ranges were 3.9–2.3, 5.0–2.4, and 5.2–3.3 for glycine, *dl*-α-alanine, and β-alanine, respectively; if the glycine concentration was ca. 2.5 *M*, the approximate p*H* range was 4.2–2.6. Similarly, because the presence of amino acid in the reducing stream tended to result in the formation of a precipitate, amino acids were included usually only in the oxidizing stream. As mentioned above, these substrates proved to be relatively unreactive and the concentrations in the oxidizing stream found to be necessary were 2–3 *M* for glycine and 2 *M* for the alanines.

As expected from our previous work with the use of titanous chloride – hydrogen peroxide radical-generating system, the best resolved spectra were obtained when the titanous chloride concentration was as low as practicable (8). The spectroscopic results for glycine and seemingly for *dl*-α-alanine were dependent on the sulfuric acid concentration, and consequently this dependence was carefully studied. Apart from these two phenomena, no quantitative studies of the effects of changing the reaction conditions were carried out, for these effects were shown to be small.

Results

Glycine, $CH_2(NH_2)COOH$

This substrate gave a completely symmetrical spectrum which varied with the acidity of the medium but was clearly due to only one radical. When the peroxide stream was 0.5 *M* in sulfuric acid, i.e. when the reaction mixture was of p*H* ca. 2.5, the spectrum contained 14 visible lines in 7 groups. This is essentially the same observation that has been reported by earlier workers (13, 14) who employed comparable reaction conditions. However, the spectra of these earlier workers were of greater line width and smaller signal-to-noise ratio than those of this present study. Armstrong and Humphreys (13) included sulfuric acid in both reaction streams at a concentration of 0.03 *M*, the p*H* of the reaction mixture being 2.6. They noticed only the basic 7 groups of lines. Taniguchi *et al.* (14) worked with reaction mixtures, dilute with respect to sulfuric acid, but did not specify numerically the sulfuric acid concentration or the p*H*. These workers observed all 14 lines but only with partial resolution. The present work resulted in virtually complete resolution of these 14 lines so that their relative amplitudes could be measured meaningfully and with reliability. A typical spectrum observed in this present investigation and taken under conditions of low p*H* is shown in Fig. 1. When the p*H* of the reaction mixture was increased by reducing the amount of sulfuric acid added to the oxidizing stream without changing the concentration of the other components, the resolution of the spectrum initially decreased, but at the highest p*H* value which could be so attained, i.e. 4, a well-resolved spectrum was again observed, as illustrated in Fig. 2. The same 7 groups of lines were observed as before, but the total number of resolved lines increased from 14 to at least 21. This change could be accounted for if a small 1:1 doublet interaction was added to those giving rise to the first spectrum. This observation was not made by earlier workers who worked either at p*H* values lower than 4 (13, 14) or at p*H* values considerably greater than 4, viz., ca. 10–11 (15).

Two possible interpretations have been suggested already for the spectrum of the glycine-derived radical in acidic solution. The first is due to Armstrong and Humphreys (13). They postulated that this species might be the $\cdot CH(NH_3^+)COO^-$ radical in which a_H^{CH}, $a_H^{NH_3+}$, and a_N are nearly equal, i.e. $a_H^{CH} = a_H^{NH_3+} = 6.0$ G and $a_N = 5.8$ G; and that, under their resolution conditions, this combination of coupling constants yield 7 lines of theoretical relative intensity 1:5:11:14:11:5:1. They called attention to the fact that in one respect this analysis did not accord with their observed spectrum, viz. the intensity of the outermost wing lines relative

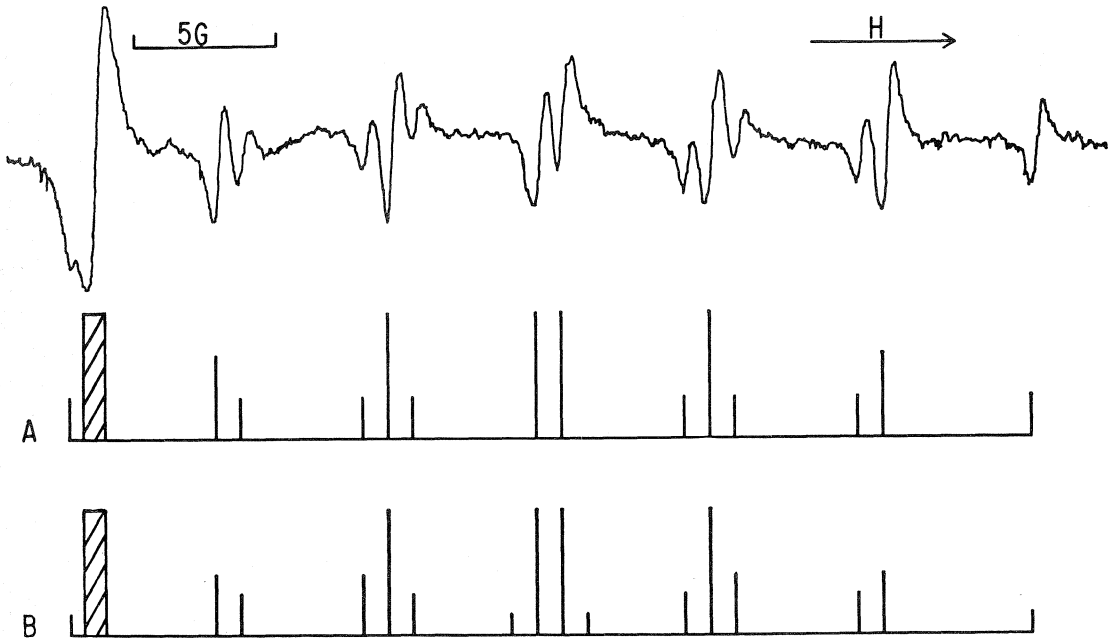

FIG. 1. First-derivative plot of the e.p.r. spectrum for hydrogen-atom abstraction from the substrate glycine in the presence of added sulfuric acid: temperature, 25 °C; [$TiCl_3$] in the reducing stream, 0.005 *M*; [H_2O_2], [glycine], and [H_2SO_4] in the oxidizing stream, 0.04, 2, and 0.7 *M*, respectively; p*H* of the mixed streams, ca. 2.3; total flow rate, 5 ml s^{-1} equally divided between the two streams. Stick plot (*A*) shows the theoretical positions and relative intensity distribution of the lines for a doublet (1:1) of triplets (1:1:1) of triplets (1:2:1); stick plot (*B*), those for a quartet (1:2:2:1) of quartets (1:3:3:1). The shaded block in these two diagrams corresponds to one or more paramagnetic inorganic species produced even in the absence of an organic substrate (2–7). Analysis (*A*) is favored over analysis (*B*), see the text under Results. The former is consistent with the radical ·$CH(NH_2)COOH$ (a_H^{CH} = 11.6 G, a_N = 6.3 G, and $a_H^{NH_2}$ = 5.4 G); the latter, with the radical ·$CH(NH_3^+)COO^-$ ($a_H^{CH} = a_N > a_N^{NH_3^+}$).

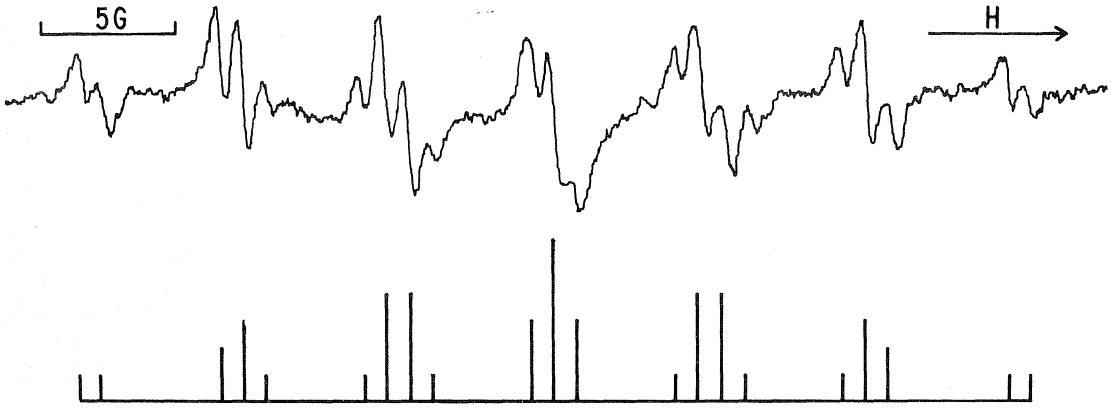

FIG. 2. First-derivative plot of the e.p.r. spectrum for hydrogen-atom abstraction from the substrate glycine: temperature, 25 °C; [$TiCl_3$] in the reducing stream, 0.005 *M*; [H_2O_2] and [glycine] in the oxidizing stream, 0.04 and 2 *M*, respectively; no sulfuric acid was added to either stream; p*H* of the mixed streams, ca. 3.9; total flow rate, 5 ml s^{-1} equally divided between the two streams. The stick plot shows the theoretical positions and intensity distribution of the lines for the radical ·$CH(NH_2)COOH$, a doublet (1:1) of triplets (1:1:1) of triplets (1:2:1) of doublets (1:1) (a_H^{CH} = 11.6 G, a_N = 6.3 G, $a_H^{NH_2}$ = 5.4 G, and a_H^{COOH} = 0.8 G).

Can. J. Chem. Downloaded from www.nrcresearchpress.com by 210.87.254.40 on 09/05/12
For personal use only.

Can. J. Chem. Downloaded from www.nrcresearchpress.com by 210.87.254.40 on 09/05/12
For personal use only.

to the center line in their spectrum was approximately 1:5, not the predicted 1:14. To explain this observation, they postulated that a second radical, $\cdot CH_2COO^-$, was also present; and that this second radical gave a triplet spectrum (1:2:1), $a_H^{CH_2} = 17.2$ G, whose lines coincided with the center line and two outermost wing lines of the spectrum from the $\cdot CH(NH_3^+)COO^-$ radical, altering their relative intensities. We have checked this idea experimentally by making one of the streams of the flow system 0.3 *M* with respect to acetic acid in addition to including glycine and sulfuric acid in the oxidizing stream. By so doing, the $\cdot CH_2COOH$ radical was made unambiguously in the presence of the glycine-derived radical with $a_H^{CH_2}(\cdot CH_2COOH)$ being found equal to 21.3 G as reported (9) already in earlier studies in this laboratory (the formulation $\cdot CH_2COOH$ is possibly more appropriate than $\cdot CH_2COO^-$ in acidic solution). The spectra of the glycine-derived radical and the $\cdot CH_2COOH$ radical were seen superimposed, and it was found that none of the 3 lines (9) in the $\cdot CH_2COOH$ spectrum coincided with the appropriate lines in that from the glycine-derived radical. However, Armstrong and Humphreys' problem is somewhat alleviated if all 3 hyperfine couplings a_N, $a_H^{NH_3^+}$, and a_H^{CH} are not nearly equal. The stick plot (*B*) in Fig. 1 illustrates this point. This plot shows the theoretical positions and relative intensities of lines for $a_H^{CH} = a_N > a_H^{NH_3^+}$, i.e. $a_H^{CH} = a_N = 6.3$ G and $a_H^{NH_3^+} = 5.4$ G. These hyperfine couplings combine to give 16 lines of relative intensity (1):(3:2):(3:6:2):(1:6:6:1):(2:6:3):(2:3):(1), these lines being arranged in 7 groups as indicated by the parentheses. This seems to be the most suitable analysis based on the zwitterionic formula $\cdot CH(NH_3^+)COO^-$, but as pointed out below, it does not match the spectrum observed in this present investigation as well as that based on the formula $\cdot CH(NH_2)COOH$.

The second interpretation of the glycine-derived radical in acidic solution is that of Taniguchi *et al.* (14) who, as noted above, observed with the use of glycine a 7-line spectrum bearing evidence of a further 7 lines which were only partly resolved. On the basis of this partially resolved spectrum, they postulated that the radical present had the structure $\cdot CH(NH_2)COOH$. To obtain a theoretical 14-line spectrum they assumed a_H^{CH}, $2a_N$, and $2a_H^{NH_2}$ were roughly equal, i.e. $a_H^{CH} = 12.4$, $a_N = 6.6$, and $a_H^{NH_2} = 5.5$ G. This analysis was achieved by matching their experimental spectrum with a computer-simulated spectrum generated on the assumption that the line width was 1.5 G (in our investigations with this same substrate, the line widths were 0.4 G). The stick plot (*A*) in Fig. 1 shows the theoretical positions and relative intensities of the lines for this analysis using the coupling-constant values found to give the best fit with our spectra (a_H^{CH}, a_N, and $a_N^{NH_2}$ equal to 11.6, 6.3, and 5.4 G, respectively). This combination of hyperfine couplings yields 14 lines of relative intensity (1):(2:1):(1:3:1):(3:3):(1:3:1):(1:2):(1) arranged in 7 groups. As argued below, the analysis by Taniguchi *et al.* (14) happens to be correct.

The difference between the stick plots for the two interpretations outlined above is small. The upper plot (*A*) contains 14 lines; the lower plot (*B*) has lines of comparable intensity in all 14 positions, but, in addition, has two lines of equal, low intensity located symmetrically one on either side of the doublet (1:1) postulated to occur in the center of the spectrum. This is a small difference which would probably be obliterated in an incompletely resolved spectrum. Thus, it is felt that in the absence of a well-resolved spectrum, and in a situation where there are two rather similar alternative analyses, even a computer simulation such as was carried out by Taniguchi *et al.* (14) to justify their interpretation may not be a definitive link between one of these analyses and the experimental spectrum. As clearly evidenced in Fig. 1, our spectroscopic results show the central group of lines to be only a 1:1-doublet, as predicted for the radical $\cdot CH(NH_2)COOH$, although the resolution and intensity of the spectrum should be sufficient to identify the 1:6:6:1 quartet predicted for the radical $\cdot CH(NH_3^+)COO^-$ if it were present. Also, we find that the measured relative intensities of the lines are in better agreement with those predicted for the radical $\cdot CH(NH_2)COOH$ rather than $\cdot CH(NH_3^+)COO^-$.

Analysis of the glycine-derived radical as $\cdot CH(NH_2)COOH$ is clearly confirmed by the study of the spectrum of the minor radical product from *dl*-α-alanine (see later in this section). By analogy with the treatment of the results found

Can. J. Chem. Downloaded from www.nrcresearchpress.com by 210.87.254.40 on 09/05/12
For personal use only.

for glycine, this minor radical might be postulated to be either $CH_3\dot{C}(NH_2)COOH$ or $CH_3\dot{C}(NH_3^+)COO^-$. However, its spectrum can be unambiguously analyzed and is found to be consistent with the formulation $CH_3\dot{C}(NH_2)COOH$ only. It is reasonable to assume that the radical formed from glycine must exist in a like tautomeric form, and hence, must be $\cdot CH(NH_2)COOH$. In support of this view, it is found that there is a great similarity in the sets of coupling constants assigned to these two similar radicals from glycine and *dl*-α-alanine, whereas the coupling constants which were assumed (13) to result from the radical $\cdot CH(NH_3^+)COO^-$ are inconsistent with those observed for other radicals containing the same functional group $-\dot{C}HNH_3^+$, as evidenced, for example, by the results of single-crystal studies of the radicals $\cdot CH(NH_3^+)COO^-$ (16–19) and $\cdot CH_2NH_3^+$ (20)[4].

For the above reasons we consider the structure of the radical produced from glycine in acidic solution with the use of the titanous chloride – hydrogen peroxide radical-generating system to be $\cdot CH(NH_2)COOH$[5]. Hence, the additional doublet observed (Fig. 2) when no sulfuric acid is added to the reaction mixture can be assigned only to the carboxyl group proton, as it is the only unidentified proton in this formulation. The stick plot in Fig. 2 gives the theoretical positions and relative intensities of the lines for the coupling constants found in this present study to give the best fit, viz. a_H^{CH}, a_N, $a_H^{NH_2}$, and a_H^{COOH} equal to 11.6, 6.3, 5.4, and 0.8 G, respectively.

dl-α-*Alanine*, $CH_3CH(NH_2)COOH$

This compound gave an unsymmetrical spectrum due to two radicals whose spectra are centered on different *g*-values. This is illustrated in Fig. 3. The dominant spectrum, a doublet (1:1) of triplets (1:2:1) of triplets (1:1:1), was readily assignable to the radical $\cdot CH_2CH(NH_3^+)COOH$, with a_H^{CH}, $a_H^{CH_2}$, and a_N equal 26.0, 22.3, and 3.6 G, respectively. As expected (13, 14), no hyperfine interaction was observed from the $(-NH_3^+)$ group protons. The less intense component of the spectrum was more complex and partially obscured by the major one, but could be satisfactorily analyzed in terms of hyperfine couplings which are consistent with the radical $CH_3\dot{C}(NH_2)COOH$, viz. a quartet (1:3:3:1) of triplets (1:1:1) of triplets (1:2:1) with $a_H^{CH_3}$, a_N, and $a_H^{NH_2}$ equal to 11.4, 5.4, and 3.9 G, respectively. The former spectrum was observed by earlier workers using similar reaction conditions (13, 14) and analyzed in the manner outlined above. The minor spectrum, however, was not observed during these earlier investigations (13, 14), possibly because of the low radical concentrations obtained.

In the absence of added sulfuric acid the minor spectrum became more complex but, on account of the accompanying reduction in the signal-to-noise ratio, it could not be readily analyzed. Possibly an additional doublet was partially resolved as was found in the spectrum from the glycine-derived radical under similar conditions.

β-*Alanine*, $CH_2(NH_2)CH_2COOH$

Hydrogen-atom abstraction from carbon in this compound could give rise to either of the radicals, $\cdot CH(NH_3^+)CH_2COOH$ (or $\cdot CH(NH_2)CH_2COOH$, by analogy with the result for glycine) or $CH_2(NH_3^+)\dot{C}HCOOH$. However, on the basis of earlier experience in this laboratory of the relative ease of hydrogen-atom abstraction from saturated aliphatic carboxylic acids (9) and primary amines[3] with the use of the titanous chloride radical-generating system, e.g. acetic acid and methylamine, the radical $CH_2(NH_3^+)\dot{C}HCOOH$ was considered more likely to be observed than the radical $\cdot CH(NH_2)CH_2COOH$. The spectrum of a single radical was observed and readily analyzed in terms of a triplet (1:2:1) of doublets (1:1) of triplets (1:1:1) with coupling constants 24.5, 20.9, and 3.6 G, respectively. These couplings are very similar in size to those from the α-alanine-derived radical $\cdot CH_2CH(NH_3^+)COOH$ which bears a $(-NH_3^+)$ group on the β-C atom, i.e. a doublet (1:1) of triplets (1:2:1) of triplets (1:1:1) with coupling constants,

[4]For example, ref. 20 reports for $\cdot CH_2NH_3^+$ that the isotropic values of a_H^{CH}, $a_H^{NH_3^+}$, and a_N are 25.0, 19.2, and 4.1 G, respectively; and, for $\cdot CH(NH_3^+)COO^-$, 22.1, 15.7, and 3.1 G, respectively.

[5]Of course, this position is somewhat arbitrary, for the $(-COO^-)$ structure and the (—COOH) structure must exist together in aqueous solution, the proportion of the former with respect to the latter being smaller the higher the p*H* of the solution. The observed p*H* dependence of the e.p.r. spectrum is an indication of the rate of the proton-exchange reactions involving such structures. Similar considerations must apply also to the other related species described in the main text, e.g. the $\cdot CH_2COOH$ radical.

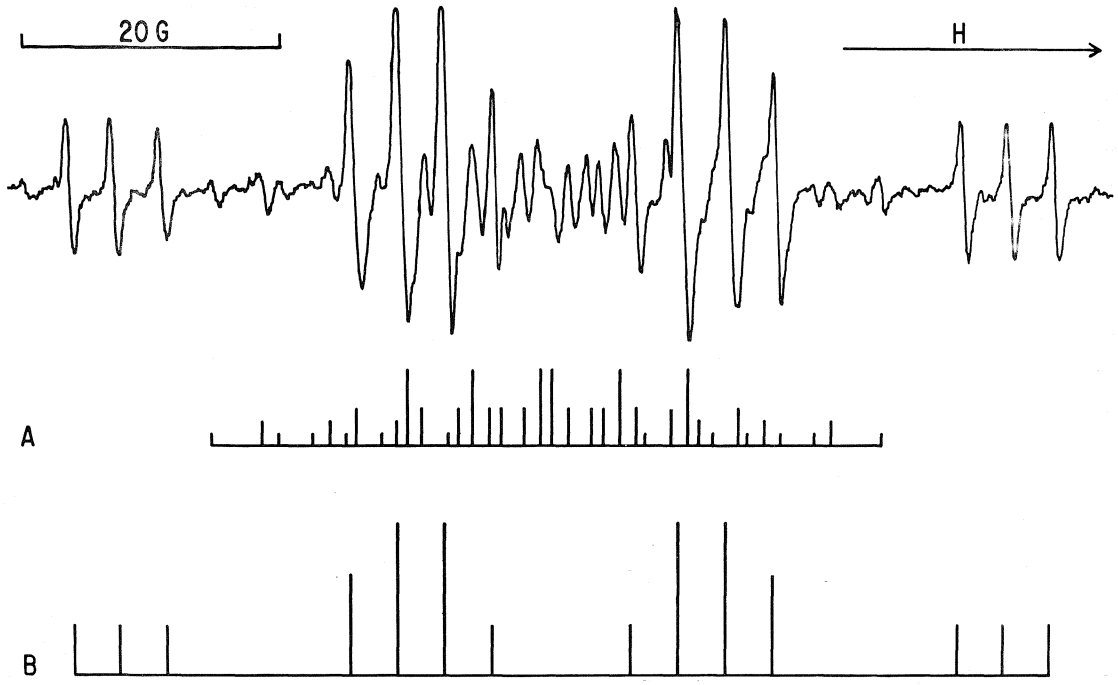

FIG. 3. First-derivative plot of the e.p.r. spectrum for hydrogen-atom abstraction from the substrate *dl*-α-alanine in an acidic medium: temperature, 25 °C; [$TiCl_3$] in the reducing stream, 0.005 *M*; [H_2O_2], [α-alanine], and [H_2SO_4] in the oxidizing stream, 0.04, 2, and 0.5 *M*, respectively; p*H* of the mixed stream, ca. 2.5; total flow rate, 5 ml s^{-1} equally divided between the two streams. Stick plot (*A*) shows the theoretical positions and relative intensity distribution of the lines from the radical $CH_3\dot{C}(NH_2)COOH$, a quartet (1:3:3:1) of triplets (1:1:1) of triplets (1:2:1) ($a_H^{CH_3}$ = 11.4 G, a_N = 5.4 G, and $a_H^{NH_2}$ = 3.9 G); stick plot (*B*) shows similar data for the radical $\cdot CH_2CH(NH_3^+)COOH$, a doublet (1:1) of triplets (1:2:1) of triplets (1:1:1) ($a_{\beta-H}^{CH}$ = 26.0 G, $a_H^{CH_2}$ = 22.3 G, and a_N = 3.6 G).

respectively, 26.0, 22.3, and 3.6 G, and hence were assigned to the latter radical, $CH_2(NH_3^+)\dot{C}HCOOH$, which also has a ($—NH_3^+$) group on β-C. The other product of hydrogen-atom abstraction, $\cdot CH(NH_2)CH_2COOH$, would be expected to be magnetically similar to the radical formed from glycine, $\cdot CH(NH_2)COOH$, and to have hyperfine interactions very different from those actually observed. These results agree with those of previous studies with this same substrate (13, 14).

The coupling constants and *g*-values for the radicals observed for all 3 amino acids are presented in Table 1 together with comparable data reported by previous workers (13, 14, 21). As far as these data may be directly compared, they are in reasonable agreement. As shown in Table 1, the *g*-value for the hitherto unreported $CH_3\dot{C}(NH_2)COOH$ radical is in line with expectation, for it is about the same size as the *g*-values for the other two radicals which bear one or two strongly delocalizing α-substituents, $\cdot CH(NH_2)COOH$ and $CH_2(NH_3^+)\dot{C}HCOOH$, and it is appreciably larger than the *g*-value of the one radical which does not bear such a substituent, $\cdot CH_2CH(NH_3^+)COOH$ (see Table 1).

Discussion

Recently, while this present investigation was well underway, three reports have presented the results of e.p.r. studies of the transient radicals formed during the reaction between titanous chloride and hydrogen peroxide in the presence of amino acids within an aqueous, continuous-flow system. The work was performed either in acidic solution (13, 14) or at p*H* values of ca. 10–11 in the presence of ethylenediaminetetraacetic acid (EDTA) as a complexing agent (15). In the present report we are concerned with the substrates glycine, *dl*-α-alanine, and β-alanine in acidic solution, for which we have been able to determine the products of reaction more

Can. J. Chem. Downloaded from www.nrcresearchpress.com by 210.87.254.40 on 09/05/12
For personal use only.

TABLE 1

Hyperfine coupling constants and g-values for radicals derived from amino-acids

Radical	Coupling constants, G				g-Value	Reference
	a_N	a_H^{NH}	$a_{\alpha\text{-}H}^{CH}$	$a_{\beta\text{-}H}^{CH}$		
$\cdot CH(NH_2)COOH$	6.26	5.38	11.64	—	2.0035	—[a,b]
	(5.8)	(6.0)	(6.0)	—	2.0031	(13)[c]
	6.6	5.5	12.4	—	—	(14)
$CH_3\dot{C}(NH_2)COOH$	5.39	3.87	—	11.37	2.0034	—[a]
$\cdot CH_2CH(NH_3^+)COOH$	3.61	—	22.27	25.96	2.0026	—[a]
	3.5	—	22.2	26.8	2.0024	(13)
	3.6	—	22.8	26.6	—	(14)
$CH_2(NH_3^+)\dot{C}HCOOH$	3.59	—	20.89	24.46	2.0034	—[a]
	3.7	—	21.7	24.3	2.0029	(13)
	3.3	—	21.4	24.5	—	(14)
	3.40	—	21.17	25.03	—	(21)[d]

[a]These are the results of this present investigation, the data being taken at 25 ± 2 °C. In this present investigation, a-values and g-values are judged to have a maximum uncertainty of ca. 0.05 G and ca. 0.0002, respectively; and the signs of a- and Q-values are omitted.
[b]$a_{\gamma-H}^{COOH} = 0.8$ G at pH ca. 4.0.
[c]These couplings are for the radical $\cdot CH(NH_3^+)COO^-$.
[d]Obtained by adding amino-radicals to acrylic acid with the use of the $TiCl_3 - NH_2OH$ radical-generating system (21).

precisely than have previous workers (13, 14) (Section I) and to clarify their discordant interpretation of the spectrum of the radical formed from glycine (Section II). Spin-density calculations and the McConnell Q-parameters and Fischer Δ-functions calculated from them are discussed in Section III.

I. Products of Hydrogen-Atom Abstraction

The present work confirms the results of the earlier investigations with these same amino acids (13, 14) that hydrogen-atom abstraction is observed to take place only from carbon; and, where there are two hydrogen-bearing carbon atoms in the same amino-acid molecule, the major radical product observed is that formed by hydrogen-atom abstraction from the carbon more distant from the amino group. The carboxyl group would be expected to exert a similar deactivating effect as found, for example, in the case of simple aliphatic carboxylic acids (9). However, the deactivating effect of the amino group overrides that of the carboxyl group, e.g. β-alanine forms $CH_2(NH_3^+)\dot{C}HCOOH$ and no detectable quantities of $\cdot CH(NH_2)CH_2COOH$, in agreement with the results of previous workers (13, 14); and it also overrides the expected (9) preference for hydrogen-atom abstraction to occur at a secondary rather than a primary carbon atom, e.g. α-alanine forms more $\cdot CH_2$-$CH(NH_3^+)COOH$ than $CH_3\dot{C}(NH_2)COOH$. In this latter case, the formation of the radical $CH_3\dot{C}(NH_2)COOH$ observed in the present investigation was not reported by the previous workers (13, 14). Furthermore, as would be expected on the basis of the known deactivating influence of carboxyl and protonated amino groups (9, 13, 14, 22, 23)[6] in reactions with the use of the titanous chloride – hydrogen peroxide radical-generating system, these amino acids were only moderately reactive to attack.

These results are qualitatively consistent with the basic reaction mechanism given in reactions [1]–[3], where the attacking species is a simple hydroxyl radical which would be expected to be an electrophilic reagent (9, 22, 23, 26). There is considerable evidence to show that the titanous chloride – hydrogen peroxide radical-generating system has a mechanism more complicated than that given by reactions [1]–[3], for example, on account of the presence of radical-titanium-ion complexes (2–7). Nevertheless, the latest evidence would allow reaction [2] to be used to represent what is observed to occur here, i.e. that both the effective attacking species and the effective substrate attacked may be regarded as not being complexed with titanium ion. Consequently, it is relevant to point out that these results are in line with expectation for hydroxyl-radical attack. However, it should be emphasized that as implied already (see Experimental), the kinetic aspects of this investigation were explored only in a qualitative fashion.

[6]Under our experimental conditions, the acidity-constant data (24, 25) suggest the amino groups are essentially all protonated and the carboxyl groups are at least about half dissociated for all three substrates.

Can. J. Chem. Downloaded from www.nrcresearchpress.com by 210.87.254.40 on 09/05/12
For personal use only.

Can. J. Chem. Downloaded from www.nrcresearchpress.com by 210.87.254.40 on 09/05/12
For personal use only.

II. The Structure of Radicals Formed from Glycine

The radical $\cdot CH(NH_3^+)COO^-$ has been postulated as one of the two positively identified products of the X- or γ-irradiation of solid crystalline glycine at room temperature, the other being the radical $\cdot CH_2COO^-$ (16–19). The radical $\cdot CH(NH_2)COO^-$ has also been postulated as the species produced from glycine (15) by the reaction between titanous chloride and hydrogen peroxide in aqueous solution of p*H* ca. 10–11 in the presence of EDTA as a complexing agent. In the present work we have confirmed the conclusions of Taniguchi *et al.* (14) that the radical $\cdot CH(NH_2)COOH$ is formed in acidic aqueous solution by the reaction between titanous chloride and hydrogen peroxide in the presence of glycine. This final formulation contrasts with results for the irradiation of solid crystalline glycine with ionizing radiation at room temperature (16–19), as there seems to be no immediately obvious reason for the existence of one tautomer, $\cdot CH(NH_2)COOH$, in acidic aqueous solution and the other, $\cdot CH(NH_3^+)COO^-$, in the solid state. Glycine in the solid crystalline state exists as a dipolar zwitterion $CH_2(NH_3^+)COO^-$ (27) and, consequently, it is not altogether surprising that irradiation with ionizing radiation gives a similar zwitterionic radical, $\cdot CH(NH_3^+)COO^-$. However, proton exchange to form the structure $\cdot CH(NH_2)COOH$ should readily occur if it were energetically favorable (17). A possible explanation of the stability of the $\cdot CH(NH_3^+)COO^-$ radical in a crystal of the parent glycine molecule is that the radical is forced to conform to the requirements of the ambient glycine lattice, i.e. the hydrogen bonding between the ($-NH_3^+$) and ($-COO^-$) groups (27).

The stability of the $\cdot CH(NH_2)COOH$ tautomeric form in acidic aqueous solution can be rationalized, as it allows a single π-system to encompass the whole radical and so results in delocalization of the unpaired spin onto nitrogen. There is clear evidence for this sort of delocalization which is discussed below (Section III).

Delocalization of unpaired spin onto nitrogen also gives rise to a partial positive charge on nitrogen

[4] $\cdot CH(\ddot{N}H_2)COOH \leftrightarrow {}^-{:}CH(\dot{N}H_2^+)COOH$

which should tend to inhibit further protonation of the amino group. The above separation of charges predicts an overall negative charge on the carboxyl-group end of the radical, which will tend to oppose the ionization of the carboxyl-group proton. This makes more certain the assignment of the observed 0.8 G single-proton interaction (Fig. 2) to the carboxyl-group proton in radical $\cdot CH(NH_2)COOH$. There appear to be no previous reports of hyperfine interactions from carboxyl-group protons which, under most conditions are expected to exchange too rapidly to be observed in an e.p.r. spectrum (28, 29).

The magnitude of the above carboxyl-group proton doublet coupling is consistent with those of the methoxyl-proton hyperfine interactions observed for similar radicals such as $CH_3\dot{C}HCOOCH_3$ (9) and $(CH_3)_2\dot{C}COOCH_3$ (9), i.e. 1.3 and 1.4 G, respectively. This assumes that Q_H^{OH} and $Q_H^{OCH_3}$ are approximately equal, although there is considerable uncertainty about the sizes of these *Q*-parameters (30). The assignment is strengthened by the observation that the size of the doublet behaves in the manner expected for an interaction with an exchangeable proton, i.e. the addition of sulfuric acid initially broadens the lines of the spectrum containing the doublet, but further additions sharpen the lines to give a spectrum in which the doublet is not observed (31). However, the measurements carried out were not extensive enough to enable a reliable estimate of the kinetic parameters of the exchange to be made.

It is interesting to note that the radical observed by Poupko *et al.* to be formed from glycine in basic solution and postulated to be $\cdot CH(NH_2)COO^-$ (15) is attributed a set of hyperfine coupling constants which are distinct from those of the radical $\cdot CH(NH_2)COOH$ (Table 1). The values for a_H^{CH} and a_N of $\cdot CH(NH_2)COO^-$ (15) are 13.6 and 6.0 G, respectively, and are similar to those assigned by us to the radical $\cdot CH(NH_2)COOH$, for which a_H^{CH} is 11.6 G and a_N is 6.3 G. However, we find $a_H^{NH_2}(\cdot CH(NH_2)COOH)$ is 5.4 G, whereas $a_H^{NH_2}(\cdot CH(NH_2)COO^-)$ is reported to be 3.2 G for one proton and 2.8 G for the other (15). These latter couplings in the anion form of the radical are unequal and about half the size of the symmetrical coupling in the neutral species. This seems an unexpectedly large perturbation to be accounted for merely by the state of protonation of the ($-CO-O^-$) group.

The restricted rotation of the amino group is consistent with both sets of hyperfine couplings.

Can. J. Chem. Downloaded from www.nrcresearchpress.com by 210.87.254.40 on 09/05/12
For personal use only.

However, it is difficult to predict whether the (—ĊH—CO—OH) group or the (—ĊH—CO—O^-) group should couple unsymmetrically to the amino group protons under these circumstances. Clearly, unsymmetrical coupling is possible for both, as they are unsymmetrical groups, but there is little experimental guide to their properties. There are a variety of examples of methyl radicals bearing a single α-carbonyl substituent, i.e. of functional structure

$$\cdot CH_2—CO—$$

1

to show that the coupling of the unpaired spin to the α-protons may be symmetrical or unsymmetrical, as illustrated by the radical $\cdot CH_2—CO—CH_3$ (29), where the α-proton couplings are unequal[7], and the radical $\cdot CH_2—CO—NH_2$ (11, 32), where they are equal. In addition, the analogous coupling to the protons in the aromatic ring in radical anions from many aromatic ketones, such as that from acetophenone

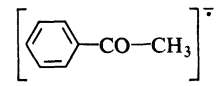

2

is unsymmetrical (33).

More relevantly, it is known that the unpaired spin in groups such as —ĊH—OH and —NH—O· couples unsymmetrically to the aromatic protons in radicals such as $C_6H_5—ĊH—OH$ (34, 35) and $C_6H_5—NH—O\cdot$ (36). Unfortunately there seems to be little data on the magnetic properties of either of the groups —ĊH—CO—O^- or —ĊH—CO—OH. The spectrum of the radical $C_6H_5—ĊH—CO—OH$ would probably give a measure of the asymmetry of the hyperfine couplings induced by the latter group, but it does not appear to have been reported up to this time (37). Thus, the possibility of an appreciable difference in the magnetic properties of the radicals $\cdot CH(NH_2)COO^-$ and $\cdot CH(NH_2)COOH$ cannot be ruled out, especially as the alternative protonation

[5] $\cdot CH(NH_2)COO^- + H^+ \rightarrow \cdot CH(NH_3^+)COO^-$

has been shown to drastically redistribute the unpaired spin and revamp the pattern of hyperfine couplings (16–19).

III. Spin Densities, McConnell Q-Parameters, and Fischer Δ-Functions

The results of molecular orbital (m.o.) π-electron spin-density, ρ^π, calculations from this and previous investigations (14, 15) on glycine- and α-alanine-derived radicals are listed in Table 2. Poupko *et al.* (15) performed a closed-shell self-consistent field – molecular orbital (s.c.f.m.o.) calculation on the radical $\cdot CH(NH_2)COO^-$ by way of the Pariser–Parr–Pople method (ref. 38, chap. 16). Taniguchi *et al.* (14) carried out a simple Hückel (H.m.o.) calculation on the radical $\cdot CH(NH_2)COOH$, using the m.o. parameters generally recommended by Pullman and Pullman (ref. 38, chap. 4; ref. 39). We have carried out H.m.o. calculations on the $\cdot CH(NH_2)COOH$ and $CH_3Ċ(NH_2)COOH$ radicals similar to that done by Taniguchi *et al.* (14). In addition, because the radicals $\cdot CH(NH_2)COO^-$ and $CH_3Ċ(NH_2)COO^-$ are of possible importance, we have made H.m.o. calculations on these radicals as well. For our calculations, the H.m.o. parameters used were those which earlier work[8] has shown to best fit the e.p.r. results obtained for a series of radicals similar to the amino-acid-derived radicals of this present work, e.g. radicals produced from simple aliphatic carboxylic acids (9) and related esters (9) and amides[9].

As shown in Table 2, the four sets of m.o. calculations for the glycine-derived radicals yield similar results, e.g. $\rho_{\alpha\text{-}C}^\pi = 0.53$–$0.63$ and $\rho_N^\pi = 0.22$–0.26. Also, these results are like those from our H.m.o. calculations for the α-alanine-derived radicals, e.g. $\rho_{\alpha\text{-}C}^\pi$ and ρ_N^π are found to be 0.54–0.55 and 0.18, respectively. In particular, the four sets of H.m.o. spin-density data from this present work seem in reasonable accord; also, these data show that the state of protonation of the (—CO—O^-) group has little effect on the spin-density distribution except at the oxygen atoms. In order to better evaluate these spin-density data, we have used them to calculate the

[7]This inequality, first observed in liquid acetone solution at −49.5 °C by Zeldes and Livingston (29), has now been discerned with the use of the substrate acetone and the aqueous titanous chloride – hydrogen peroxide radical-generating system at 25 °C (P. Smith and D. J. McGinty. Unpublished work).

[8]P. Smith and D. J. McGinty. Unpublished work. These H.m.o. parameters are distinct from those employed in previously published work from this laboratory (9).

[9]P. Smith and P. B. Wood, unpublished work, and ref. 11.

TABLE 2

Comparison of π-electron spin densities calculated by m.o. methods for radicals derived from amino acids

Radical	Calculated spin density α-C	N	O	C_β^{CO}	CH_3	Reference
$\cdot CH(NH_2)COO^-$	0.63	0.225	0.07	0.002	—	(15)[a]
	0.58	0.22	0.06	0.07	—	—[b,c,d]
$\cdot CH(NH_2)COOH$	0.53	0.26	—	—	—	(14)[e]
	0.55	0.22	0.14[f]	0.07	—	—
	—	—	0.02[g]	—	—	—[b,d,h]
$CH_3\dot{C}(NH_2)COO^-$	0.55	0.18	0.07	0.08	0.05	—[b,i,j]
$CH_3\dot{C}(NH_2)COOH$	0.54	0.18	0.13[f]	0.085	0.05	—
	—	—	0.02[g]	—	—	—[b,j,k]

[a]Calculated by the closed-shell s.c.f.m.o. method of Pariser, Parr, and Pople (ref. 38, chap. 16).
[b]This work.
[c]Calculated by the H.m.o. method with the use of the following parameters: $h(C) = 0$, $k(C—C) = 0.9$; $h(\overset{1.5}{O}) = 1.3$, $k(C{=}O) = 1.5$; $h(\ddot{N}) = 1.2$, $k(C—N) = 0.9$. The notation followed is that of Streitweiser (39), so that $\alpha(X) = \alpha_0 + h(X)\beta_0$ and $\beta(C—X) = k(C—X)\beta_0$, where α_0 and β_0 are, respectively, the Coulomb integral and resonance integral for benzene. These parameters were those found by other[8] H.m.o. calculations to best fit e.p.r. data on a series of radicals similar to those in this table, e.g., radicals from simple aliphatic carboxylic acids (9) and related esters (9) and amides[9].
[d]On the assumption that $\rho_{\alpha-C}^{\pi}$ ($CH_3\dot{C}(NH_2)COOH$) equals 0.388 (see footnote (*j*)) and that $\Delta(—CH_3)$ equals 0.081 (41, 42), the experimental value of $\rho_{\alpha-C}^{\pi}$ is found to be 0.388/0.919 or 0.422. On the assumption that Q_N^N equals 23.0 G (30), the experimental value of ρ_N^{π} is found to be 0.272.
[e]Calculated by the H.m.o. method with the use of the parameters of Pullman and Pullman (39).
[f]O(C=O).
[g]O(C—O—H).
[h]Calculated by the H.m.o. method with the use of the parameters listed in footnote (*c*) except that those of oxygen were: $h(\dot{O}) = 1.1$, $k(C{=}O) = 1.8$; $h(\ddot{O}) = 1.5$, $k(C—O) = 0.9$.
[i]Calculated by the H.m.o. method with the use of the parameters listed in footnote (*c*) and two additional parameters derived by the method described in footnote (*c*): $h(CH_3) = 1.9$, $k(C—CH_3) = 0.7$, i.e. treating $—CH_3$ as a hetero-atom.
[j]On the assumption that $Q_H^{CCH_3}$ equals 29.3 G (41, 42), the experimental value of $\rho_{\alpha-C}^{\pi}$ is found to be 0.388. On the assumption that Q_N^N equals 23.0 G (30), the experimental value of ρ_N^{π} is found to be 0.234.
[k]Calculated by the H.m.o. method with the use of the parameters specified in footnote (*i*) except that those for oxygen were as in footnote (*h*).

TABLE 3

McConnell Q-parameter values[a] for radicals derived from amino acids

Radical	Q_H^{CH}	$Q_H^{CCH_3}$	Q_N^N	$Q_H^{NH_2}$	Reference[b]
$\cdot CH(NH_2)COOH$	22	—	24	21	(14)
	21	—	28	24	This work
$CH_3\dot{C}(NH_2)COOH$	—	21	30	22	This work

[a]Calculated with the use of eqs. [6]–[9]. The *a*-values used are those of the present investigation and are listed in Table 1. The ρ^{π}-values used are from the present investigation and from that of other workers (14).
[b]For the source of the ρ^{π}-values used. These values are given in Table 2.

McConnell Q-parameter values Q_H^{CH}, $Q_H^{CCH_3}$, Q_N^N, and $Q_H^{NH_2}$ shown in Table 3, calculated with the use of the following equations

$$[6] \qquad a_H^{CH} = Q_H^{CH}\rho_{\alpha-C}^{\pi}$$

$$[7] \qquad a_H^{CH_3} = Q_H^{CCH_3}\rho_{\alpha-C}^{\pi}$$

$$[8] \qquad a_N^N = Q_N^N\rho_N^{\pi}$$

$$[9] \qquad a_H^{NH_2} = Q_H^{NH_2}\rho_N^{\pi}$$

The Q-parameter values listed in Table 3 are in the range obtained for aliphatic radicals (9, 30, 40, 41). However, the results for Q_H^{CH} and $Q_H^{CCH_3}$ are lower than those usually found for aliphatic radicals for which Q_H^{CH} equals ca. 23–26 G and $Q_H^{CCH_3}$ equals ca. 29 G (9, 30, 40, 41). In other words, the calculated $\rho_{\alpha-C}^{\pi}$ values in Table 2 are higher than might be expected, the value obtained via the more sophisticated m.o. method (15) being the highest. The values of Q_N^N and $Q_H^{NH_2}$ are in the usual range, which is ca. 20–35 G for Q_N^N and ca. 21–36 G for Q_N^{NH} (30), but commonly Q_H^{NH} is greater than Q_N^N rather than the reverse observed here (30). By way of the equation

$$[10] \qquad a_H^{OH} = Q_H^{OH}\rho_O^{\pi}$$

the calculated value of ρ_O^{π} can be used to estimate an extremely rough value of Q_H^{OH} equal to ca. 40 G for the OH proton in $\cdot CH(NH_2)COOH$.

Can. J. Chem. Downloaded from www.nrcresearchpress.com by 210.87.254.40 on 09/05/12
For personal use only.

This value is not within the range which has been reported already for this parameter, i.e., ca. 7–21 G (30). This difference is not surprising in view of the crudity of the H.m.o. method for calculating ρ^{π} values in hetero-atom radicals (see, e.g., ref. 42).

The π-electron spin density at α-C calculated in the present work for the radicals $\cdot CH(NH_2)COOH$ and $CH_3\dot{C}(NH_2)COOH$ can be used to calculate Fischer Δ-functions from the equation

$$[11] \qquad \rho_{\alpha\text{-}C}{}^{\pi} = \Pi_{i=1}^{i=3}(1 - \Delta(\text{—}X_i))$$

where $\Delta(\text{—}X_i)$ is the Fischer Δ-function of substituent $\text{—}X_i$ at the sp^2 carbon atom on which the unpaired spin is localized in the radical $\cdot CX_1X_2X_3$ (41). It is usually assumed (40) that $\Delta(\text{—}H)$ and $\Delta(\text{—}CH_3)$ equal 0 and 0.081, respectively, and, in this case, a value of Δ(—COOH) between 0.072 and 0.121 is also assumed, as this corresponds to the range of values calculated from other radicals[10]. These assumptions give a value of $\Delta(\text{—}NH_2)$ equal to about 0.39 for the $\cdot CH(NH_2)COOH$ radical and about 0.35 for the $CH_3\dot{C}(NH_2)COOH$ radical. As far as we are aware, this is easily the highest Δ-function of any substituent yet reported and corresponds to a substituent which delocalizes the unpaired spin to the greatest extent[11]. There are insufficient data to test the basic assumption (40) that the numerical value of a given Δ-function is independent of environment, i.e. $\Delta(\text{—}NH_2)$ remains constant for a variety of amino-substituted methyl radicals.

The hydrogen peroxide used in this work was kindly provided by FMC Corporation, Inorganic Chemical Division. The experimental assistance of Peter B. Wood is also gratefully acknowledged.

1. W. T. Dixon and R. O. C. Norman. J. Chem. Soc. 3119 (1963).
2. K. Takakura and B. Rånby. J. Phys. Chem. **72**, 164 (1968).
3. H. Fischer. Ber. Bunsenges. Phys. Chem. **71**, 685 (1967).
4. R. E. Florin, F. Sicilio, and L. A. Wall. J. Phys. Chem. **72**, 3154 (1968).
5. Y. S. Chiang, J. Craddock, D. Michewich, and J. Turkevich. J. Phys. Chem. **70**, 3509 (1966).
6. R. O. C. Norman. Proc. Roy. Soc. Ser. A, **302**, 315 (1968).
7. M. S. Bains, J. C. Arthur, Jr., and O. Hinojosa. J. Phys. Chem. **72**, 2250 (1968).
8. (*a*) P. Smith and P. B. Wood. Can. J. Chem. **45**, 649 (1967). (*b*) P. Smith and P. B. Wood. 151st Meeting, Amer. Chem. Soc., Pittsburgh, Pa., 1966. Abstr. No90.
9. P. Smith, J. T. Pearson, P. B. Wood, and T. C. Smith. J. Chem. Phys. **43**, 1535 (1965).
10. J. T. Pearson, P. Smith, and T. C. Smith. Can. J. Chem. **42**, 2022 (1964).
11. P. Smith and P. B. Wood. Can. J. Chem. **44**, 3085 (1966).
12. P. Smith, J. T. Pearson, and R. V. Tsina. Can. J. Chem. **44**, 753 (1966).
13. W. A. Armstrong and W. G. Humphreys. Can. J. Chem. **45**, 2589 (1967).
14. H. Taniguchi, K. Fukui, S. Ohnishi, H. Hatano, H. Hasegawa, and T. Maruyama. J. Phys. Chem. **72**, 1926 (1968).
15. R. Poupko, B. L. Silver, and A. Lowenstein. Chem. Commun. 453 (1968).
16. J. R. Morton. J. Amer. Chem. Soc. **86**, 2325 (1964).
17. M. A. Collins and D. H. Whiffen. Mol. Phys. **10**, 317 (1966).
18. A. Hedberg and A. Ehrenberg. J. Chem. Phys. **48**, 4822 (1968).
19. P. B. Ayscough and A. K. Roy. Trans. Faraday Soc. **64**, 582 (1968).
20. R. P. Kohin and P. G. Nadeau. J. Chem. Phys. **44**, 691 (1966).
21. C. Corvaja, H. Fischer, and G. Giacometti. Z. Phys. Chem. Frankfurt, **45**, 1 (1965).
22. W. T. Dixon, R. O. C. Norman, and A. L. Buley. J. Chem. Soc. 3625 (1964).
23. R. O. C. Norman and B. C. Gilbert. Advan. Phys. Org. Chem. **5**, 53 (1967).
24. H. R. Mahler and E. H. Cordes. Biological chemistry. Harper and Row, Publishers, New York, 1966. Chaps. 2 and 5.
25. M. May and W. A. Felsing. J. Amer. Chem. Soc. **73**, 406 (1951).
26. G. E. Adams, J. W. Boag, J. Currant, and B. D. Michael. *In* Pulse radiolysis. M. Ebert, J. P. Keene, A. J. Swallow, and J. H. Baxendale (*Editors*). Academic Press, Inc., New York. 1965. p. 131.
27. R. E. Marsh. Acta. Crystalogr. **11**, 654 (1958).
28. H. Fischer. Mol. Phys. **9**, 149 (1965).
29. H. Zeldes and R. Livingston. J. Chem. Phys. **45**, 1946 (1966).
30. P. Smith and W. M. Fox. Can. J. Chem. **47**, 2227 (1969).
31. J. A. Pople, W. G. Schneider, and H. J. Bernstein. High-resolution nuclear magnetic resonance. McGraw-Hill Book Co. Inc., New York. 1959. Chap. 10.
32. R. Livingston and H. Zeldes. J. Chem. Phys. **47**, 4173 (1967).
33. (*a*) N. Steinberger and G. K. Fraenkel. J. Chem. Phys. **40**, 723 (1964). (*b*) P. H. Rieger and G. K. Fraenkel. J. Chem. Phys. **37**, 2811 (1962).
34. R. Livingston and H. Zeldes. J. Chem. Phys. **44**, 1245 (1966).
35. H. Fischer. Z. Naturforsch. **20***a*, 488 (1965).
36. Th. A. J. W. Wajer, A. Mackor, Th. J. de Boer, and J. D. W. van Voorst. Tetrahedron Lett. 1941 (1967).

[10]W. M. Fox, P. Smith, and P. B. Wood. Unpublished work.

[11]A still higher estimate for $\Delta(\text{—}NH_2)$, equal to about 0.53, can be calculated from the $a_H^{CH_3}$ ($CH_3\dot{C}H(NH_2)COOH$) value of 11.37 G in Table 1, on the assumption that $Q_{\beta\text{-}H}^{CCH_3}$ equals 29.3 G (40, 41) together with the assumption that Δ(—H), $\Delta(\text{—}CH_3)$, and Δ(—COOH) equal 0, 0.081, and 0.072–0.121, respectively.

Can. J. Chem. Downloaded from www.nrcresearchpress.com by 210.87.254.40 on 09/05/12
For personal use only.

37. R. O. C. NORMAN and R. J. PRITCHETT. J. Chem. Soc. *B*, 926 (1967).
38. A. STREITWEISER. Molecular orbital theory for organic chemists. John Wiley and Sons, Inc., New York. 1961.
39. B. PULLMAN and A. PULLMAN. Quantum biochemistry. Interscience Publishers, Inc., New York. 1963. pp. 104–110.
40. H. FISCHER. Z. Naturforsch. **20***a*, 428 (1965).
41. R. W. FESSENDEN and R. H. SCHULER. J. Chem. Phys. **39**, 2147 (1963).
42. G. VINCOW. J. Chem. Phys. **38**, 917 (1963).

Can. J. Chem. Downloaded from www.nrcresearchpress.com by 210.87.254.40 on 09/05/12
For personal use only.

Can. J. Chem. Downloaded from www.nrcresearchpress.com by 210.87.254.105 on 09/05/12
For personal use only.

Coordination complexes of gallium(III) and indium(III) halides. IV.[1] Infrared spectra, Raman spectra, and structures of complexes with dimethylsulfoxide and dimethylsulfoxide-d_6

A. J. Carty and H. A. Patel
Chemistry Department, University of Waterloo, Waterloo, Ontario

AND

P. M. Boorman
Chemistry Department, University of Calgary, Calgary, Alberta

Received September 8, 1969

The preparation and characterization by far-infrared and Raman spectroscopy of dimethylsulfoxide (dmso) and dimethylsulfoxide-d_6 (dmso-d_6) complexes of gallium trihalides are reported. The compounds $GaX_3(dmso)_6$ (X = Br, I) have ionic structures containing the hexacoordinate cation $Ga(dmso)_6^{3+}$. Reaction of gallium trichloride with dmso gives $GaCl_3(dmso)_{1.5}$. This compound appears to be identical with $GaCl_3(dmso)_2$ described by other workers and has been shown to have the structure $[Ga(dmso)_6][GaCl_4]_3$. Some new vibrational data are presented for $InX_3(dmso)_3$ (X = Cl, Br) and $InI_3(dmso)_2$.

Canadian Journal of Chemistry, **48**, 492 (1970)

Introduction

Current interest in the coordination chemistry of the Group III halides centers on the elucidation of molecular structure by vibrational spectroscopy (1–3) and X-ray crystallography (4, 5). Although recent far-infrared (6) and X-ray (5) studies have demonstrated the presence of six-coordinate gallium(III) in the ionic complexes $GaCl_3(bipy)$, $GaBr_3(bipy)_2MeCN$, $GaI_3(bipy)$ (bipy = 2,2′-bipyridyl) and five-coordinate gallium in $GaCl_3(NMe_3)_2$ (7), there is still little structural information on gallium(III) halide complexes of coordination number greater than four. Since dimethylsulfoxide (dmso) is well known to be a σ donor capable of producing complexes of high coordination number (8 and references therein), we have investigated in detail the vibrational spectra of adducts with gallium(III) chloride, bromide, and iodide. A brief report that gallium(III) chloride reacts with dmso to give $GaCl_3(dmso)_2$ (9) has appeared. This was of special interest in view of the possibility of five coordination in this compound and the reported $InCl_3(dmso)_3$ (10) and $TlCl_3(dmso)_2$ (2) stoichiometries for the corresponding indium trichloride and thallium trichloride complexes. This paper also includes some new data for dmso and dmso-d_6 complexes of the type InX_3L_3 (X = Cl, Br; L = dmso, dmso-d_6) and InI_3L_2.

[1]For part III of the series, see ref. 6.

Experimental

Gallium trihalides (99.99% purity) were purchased from Fluka, A. G., Buchs, Switzerland in sealed ampoules which were attached to a vacuum line before use. Indium trihalides were prepared as previously described (10). All solvents used were Spectroscopic Grade and were stored over molecular sieves (Linde Type 4A) prior to distillation. Dimethylsulfoxide-d_6 was obtained in 1 g ampoules from Stohler Isotope Chemicals.

Preparation of Complexes

Gallium Trihalide Complexes

Approximately 25 ml of anhydrous ethanol or acetone was added in a drybox to a reaction vessel equipped with a magnetic stirring bar. The vessel was then cooled to liquid nitrogen temperature on the vacuum line and gallium trihalide (ca. 1.0 g) sublimed into the vessel under high vacuum. The trihalide dissolved in the solvent on raising the temperature slowly. All stopcocks were then closed and a slight excess of dmso or dmso-d_6 added in a drybox. With ethanol as solvent an immediate white precipitate of the complex was produced. The complexes could be recrystallized as colorless prisms from 4:1 ethanol/acetone. Analytical data for the complexes are given in Table 1.

Tetrafluoroborate derivatives of the cations $Ga(dmso)_6^{3+}$, $Ga(dmso\text{-}d_6)_6^{3+}$ were prepared by reacting hot solutions of the gallium trihalide complexes in acetone with solutions containing an excess of sodium tetrafluoroborate in hot ethanol/acetone. On cooling, colorless crystals of the desired tetrafluoroborates were obtained. Melting points and gallium analyses showed that the same derivative $[Ga(dmso)_6](BF_4)_3$ was produced from each of the three halide complexes.

$[Ga(dmso)_6][GaCl_4]_3$ (0.55 g) in acetone (25 ml) was reacted with tetraphenylarsonium chloride (0.85 g) in acetone (25 ml). The colorless product was identified as $Ph_4As[GaCl_4]$ by microanalysis and comparison with an

Can. J. Chem. Downloaded from www.nrcresearchpress.com by 210.87.254.105 on 09/05/12
For personal use only.

TABLE 1

Analytical data for gallium trihalide complexes

Compound	Melting point (°C)	Analysis (%) C Found	C Calcd.	H Found	H Calcd.	S Found	S Calcd.	Halogen Found	Halogen Calcd.	Ga Found	Ga Calcd.
$[Ga(dmso)_6][GaCl_4]_3$	271	12.47 12.28	12.28	3.16 3.17	3.09	16.44	16.40	36.35	36.28	23.63	23.81
$[Ga(dmso)_6]Br_3$	148	18.30 18.40	18.52	4.76 4.55	4.66	24.46	24.73	31.01	30.82	8.70	8.90
$[Ga(dmso)_6]I_3$	189	15.75 15.76	15.68	4.39 4.40	3.90	21.25	20.9	42.91	41.42	7.56	7.57
$[Ga(dmso)_6](BF_4)_3$	>350	18.12	18.04	4.48	4.53					8.70	8.72
$[Ph_4As][GaCl_4]$	178	47.21	48.10	3.86	3.30						

authentic sample of the same compound prepared from gallium trichloride and tetraphenylarsonium chloride.

Indium Complexes

These were prepared as previously described (10). A minimum of solvent was used in the preparation of the dmso-d_6 complexes.

Infrared and Raman Spectra

Infrared spectra above 650 cm^{-1} were measured on a Beckman IR-9 spectrophotometer as Nujol mulls between sodium chloride plates. In the 650–200 cm^{-1} region an IR-12 spectrophotometer was employed. Samples were run as Nujol mulls between cesium iodide windows. Frequencies were accurate to $\pm$ 2 cm^{-1}.

Analyses

Microanalyses were carried out by A. B. Gygli, Toronto; Alfred Bernhardt, Elsbach uber Engelskirchen, Germany; and Chemalytics, Inc., Tempe, Arizona. Gallium was determined by titration with EDTA using 1-(2-pyridylazo)-2 napthol as an indicator (11).

Results and Discussion

Gallium Complexes

The analytical data for the product of the reaction between gallium trichloride and dmso in solution clearly show that the correct empirical formula for this compound is $GaCl_3(dmso)_{1.5}$. This and the similarity of the far-infrared spectrum of our product to that reported previously for $GaCl_3(dmso)_2$ (9*a* and results quoted from ref. 9*b*) raises doubts as to the authenticity of the latter compound. The reactions of $GaCl_3(dmso)_{1.5}$ with tetraphenylarsonium chloride to give $Ph_4As[GaCl_4]$ and with sodium tetrafluoroborate to give $[Ga(dmso)_6](BF_4)_3$ strongly indicate that the most probable formulation for this compound is $[Ga(dmso)_6][GaCl_4]_3$. Gallium tribromide and triiodide, on the other hand, form complexes analyzing as $GaX_3(dmso)_6$ (X = Br, I), for which the simple ionic structures $[Ga(dmso)_6]X_3$ seem appropriate in view of the ready synthesis of $[Ga(dmso)_6](BF_4)_3$ in each case by replacement reactions with sodium tetrafluoroborate.

Infrared Spectra (2000–650 cm^{-1})

A thorough vibrational analysis of dimethylsulfoxide and dimethylsulfoxide-d_6 has been published by Cotton and Horrocks (12). Provided that ν(S—O) can be assigned in the dmso complexes, it is possible to determine whether the ligand is S or O bonded on the basis of an increase or decrease in this frequency on complexing (13). Unequivocal ν(S—O) assignments are sometimes not possible, however, when dmso-d_6 compounds are unavailable, since CH_3 rocking modes occur in the same spectral region as ν(S—O) (8). On occasion this has led to reversal of assignments for ν(S—O) and $\delta_{rock}(CH_3)$ in complexed dmso and hence to differences in the magnitude of the shift Δν in ν(S—O) (13, 14). With the aid of the deuterated complexes prepared here, an assignment[2] of ν(S—O) was possible for each compound. Table 1 lists ν(S—O) and $\delta_{rock}(CH_3)$ modes for the dmso and dmso-d_6 complexes. The decrease of ca. 100 cm^{-1} in ν(S—O) in each case is clearly consistent with oxygen-bonded dmso, as expected. Although the magnitude of these shifts is comparable to those occurring in transition-metal complexes (15) it would be unwise to draw any conclusions regarding the relative Ga—O or In—O bond strengths in these compounds from Δν values, since the vibrational analysis (12) clearly demonstrates that the vibration labelled ν(S—O) is not a pure stretch but involves a considerable proportion of methyl rocking. It is, however, worth noting that for the three gallium complexes, Δν is virtually identical. This is further evidence for the presence of the same cation in each case.

Far-Infrared and Raman Spectra (550–200 cm^{-1})

Recent data for the free ligands dmso and dmso-d_6 in this region (16) are in good agreement with the earlier work of Cotton and Horrocks (12). We have not, therefore, attempted to remeasure these spectra. The molecule dmso has C_s symmetry, thus making all normal modes infrared and Raman active. This should also be the case in the complexes where the ligand molecules can at most retain their C_s symmetry. Moreover, internal vibrations of the ligand should be readily assignable by comparison with the deuterated species. The far-infrared and Raman spectra of the dmso and dmso-d_6 complexes are given in Table 2 together with an assignment.

The spectra of $[Ga(dmso)_6]Br_3$, $[Ga(dmso)_6]I_3$, and $[Ga(dmso)_6](BF_4)_3$ between 300 and 500 cm^{-1} are very similar to those of other hexakis(dmso) complexes (15) and are readily interpreted. The very strong band at ca. 490 cm^{-1} in all the spectra does not correspond to any internal vibration of the ligand. Metal–oxygen stretching modes have been found in this region by other

[2]Since ν (S—O) and δ_{rock} (CH_3) are coupled in dmso (8), neither vibration is "pure". The terms serve as convenient labels for following frequency changes.

Can. J. Chem. Downloaded from www.nrcresearchpress.com by 210.87.254.105 on 09/05/12
For personal use only.

Can. J. Chem. Downloaded from www.nrcresearchpress.com by 210.87.254.105 on 09/05/12
For personal use only.

TABLE 2

Far-infrared, Raman frequencies and assignments for dmso and dmso-d_6 complexes*

Frequencies (cm^{-1})										
$[Ga(dmso)_6][GaCl_4]_3$		$[Ga(dmso\text{-}d_6)_6][GaCl_4]_3$		$[Ga(dmso)_6]Br_3$		$[Ga(dmso\text{-}d_6)_6]Br_3$		$[Ga(dmso)_6]I_3$		$[Ga(dmso\text{-}d_6)_6]I_3$		Assignments
Infrared	Raman	Infrared	Raman	Infrared	Raman	Infrared	Raman	Infrared	Raman	Infrared	Raman	
			483 m						492 w		467 w	ν(Ga—O)
502 (18)	498 m	470 (13)	458 w	493 (20)	493 w	469 m	469 m	429 (20)	458 w	467 (20)	442 w	
380 (20)	381 m	380 (20)	383 m									ν_3 (Ga—Cl)
358 (17)		335 (10)		353 (18)	353 s	333 (19)	—	353 (18)	345 m	332 (20)		δ_s(C—S—O)
	347 vs		348 vs									ν_1 (Ga—Cl)
347 (16)		320 (8)	320 m	333 (17)	333 m	323 (18)	321 s	328 (16)	323 m	320 (18)	320 m	δ_a (C—S—O)
324 (12)	314 m	286 (3)		309 (5)	309 w	295 (16)	289 s	303 (2)		291 (15)		δ (C—S—C)
263 (15)	263 w	240 (6)		258 (12)		245 (17)	222 m	275 (7)		240 (17)		δ(O—Ga—O)
				245 (16)		225 (11)	209 m	252 (14)		230 (14)		or
				215 (15)		209 (11)		242 (12)		210 (10)		δ(Ga—O—S)
								212 (14)				

Frequency (cm^{-1})									
$[Ga(dmso)_6](BF_4)_3$	$[(Ga(dmso\text{-}d_6)_6](BF_4)_3$	$In(dmso)_3Cl_3$		$In(dmso\text{-}d_6)_3Cl_3$		$In(dmso)_3Br_3$		$In(dmso\text{-}d_6)_3Br_3$		Assignments
Infrared	Infrared	Infrared	Raman	Infrared	Raman	Infrared	Raman	Infrared	Raman	
										ν (Ga—O)
495 (20)	470 (20)									
		451 (20)	449 m	426 (20)	423 m	452 (20)	456 m	425 (20)	426 m	ν (In—O)
		442 (19)	441 sh	412 (18)	409 sh	sh443 (19)	453 m	415 (19)	415 m	
		350 (12)		322 (12)		344 (15)	346 s	318 (17)	318 s	δ_s(C—S—O)
357 (20)	335 (19)	341 (6)	346 m	312 (5)	332 s	sh336 (11)	—	310 (10)		δ_a(C—S—O)
348 (16)	330 (18)	317 (7)	310 m	282 (17)		318 (9)	315 s	275 (7)	274 s	δ (C—S—C)
330 (17)	292 (15)	284 (12)	267 vs	282 (17)	280 vs	208 (20)	186 vs		186 s	ν (In—X)
		259 (18)		257 (18)			158 m		150 m	
										δ(O—Ga—O
										or
263 (15)	242 (18)									δ(Ga—O—S)
246 sh	233 sh									
212 (16)	212 (12)									

Frequency (cm^{-1})				
$In(dmso)_2I_3$		$In(dmso\text{-}d_6)_2I_3$		Assignments
Infrared	Raman	Infrared	Raman	
456 (20)	458 m	426 (20)	432 m	ν(In—O)
442 (19)	444 m	410 (18)	410 m	
344 (18)	344 s	320 (17)	321 m	δ_s (C—S—O)
310 (10)	310 s	298 (10)	297 w	δ (C—S—C)
	198 sh		197 w	
	192 m		191 w	ν (In—X)
	183 m		183 m	
	141 vs		141 vs	

*Numbers in parentheses indicate intensity; the highest intensity band is assigned an arbitrary value of 20; s = strong, m = medium, w = weak, v = very, sh = shoulder.

Can. J. Chem. Downloaded from www.nrcresearchpress.com by 210.87.254.105 on 09/05/12
For personal use only.

workers for dimethylsulfoxide, pyridine N-oxide, phosphine oxide, and acetylacetonate complexes (23). If the 490 cm^{-1} band is a pure gallium–oxygen stretching mode, the ratio of the frequencies ((Ga—O)dmso)/((Ga—O)dmso-d_6) would equal $(M_{dmso\text{-}d_6}/M_{dmso})^{\frac{1}{2}}$ (M = molecular weight). Inspection of the spectra shows that the frequency ratio is 1.051, close to the calculated ratio of 1.035. This provides some confirmation for the validity of the assignment and also suggests that the vibration in question is not significantly coupled with C—S—O or C—S—C deformations. Some caution is necessary here,[3] however, since a frequency of 490 cm^{-1} for a pure ν(Ga—dmso) mode predicts a Ga—O force constant in excess of the 2.60 mdyn $Å^{-1}$ found for Ga—Cl in $GaCl_4^-$ (20). In other non-transition-metal complexes, the ratio $k_{M-ligand}/k_{M-Cl}$ (k = stretching force constant) is usually assumed to lie between 0.5 and 0.75 (26). Clearly, normal-coordinate calculations on oxo-complexes will be necessary before assignments of ν(M—O) modes in the region 350–500 cm^{-1} can be theoretically justified.

The symmetric and antisymmetric C—S—O deformations ν_{11} and ν_{23} occur as a pair of strong bands at ca. 350 and 330 cm^{-1}, respectively.[4] As expected, on deuteration these bands move to lower frequency, with the symmetric mode showing the larger decrease. The C—S—C angle deformation at 308 cm^{-1} in dmso (16) occurs slightly lower in the complexes and shifts 14–18 cm^{-1} on deuteration.

There are three or four bands occurring in the 200–300 cm^{-1} region of the spectra of these compounds which are not due to internal ligand vibrations. These shift to varying degrees on deuteration and cannot, therefore, arise from metal–halogen modes. They are almost certainly attributable to δ(O—Ga—O) and δ(S—O—Ga) vibrations. Although less is known about ligand–metal–ligand deformation modes these are often found at frequencies approximately 1/2 of those of the corresponding stretches (17). A complete assignment of these bands is, however, impossible at the present time without a full normal-coordinate analysis of the cation.

The far-infrared and Raman spectra of $GaCl_3(dmso)_{1.5}$ prove conclusively that this compound should be formulated as $[Ga(dmso)_6][GaCl_4]_3$. As in the bromide and iodide complexes, ν(Ga—O) appears as a strong band near 500 cm^{-1} in the infrared. The similarity of ν(Ga—O) frequencies in $GaCl_3(dmso)_{1.5}$ and $[Ga(dmso)_6]X_3$ (X = Br, I, BF_4) is also evidence for the presence of the cation $Ga(dmso)_6^{3+}$ in the former. The ligand vibrations $\nu_{11}\delta_s$(C—S—O), $\nu_{23}\delta_a$(C—S—O), and $\nu_{12}\delta$(C—S—C) occur at 353, 347, and 324 cm^{-1} in $[Ga(dmso)_6][GaCl_4]_3$ and move to 335, 320, and 286 cm^{-1} on deuteration. The ν_{11} and ν_{23} modes actually appear as shoulders on the very strong infrared absorption at 380 cm^{-1} in $[Ga(dmso)_6][GaCl_4]_3$ due to ν_3 of the tetrahedral anion $GaCl_4^-$. The $\nu_3(t_2)$ vibration of $GaCl_4^-$ has previously been found at 380 cm^{-1} in $Ph_4As[GaCl_4]$ (18) and at similar frequencies for other tetrachlorogallates (19). The presence of the ion $GaCl_4^-$ is nicely illustrated by a comparison of the infrared spectra of $[Ga(dmso)_6][GaCl_4]_3$ and $[Ga(dmso\text{-}d_6)_6][GaCl_4]_3$ with the Raman spectrum of $[Ga(dmso)_6][GaCl_4]_3$ (Fig. 1). ν_1 of $GaCl_4^-$, which is infrared inactive, shows up as the strongest band in the Raman spectra, while the t_2 mode is weaker. The frequencies[5] of ν_3 and ν_1 from the Raman, 381 and 347 cm^{-1}, are almost identical with the values reported by Woodward for aqueous solutions of this ion (20). We were, however, unable to trace the two bending modes ν_2 and ν_4 for $GaCl_4^-$, owing to increased background noise below 200 cm^{-1}. As expected, the far-infrared spectra of $[Ga(dmso)_6](BF_4)_3$ and $[Ga(dmso\text{-}d_6)_6](BF_4)_3$ prepared from the chlorides agree with the above conclusions on the structure of $Ga(dmso)_{1.5}Cl_3$. ν_3 of $GaCl_4^-$ is completely absent from the spectra.

It is of interest to examine the spectra of the cation $[Ga(dmso)_6]^{3+}$ present in all of the halide complexes, since the nature of the vibrational modes associated particularly with the MO_6 skeleton might provide information on the point group of the cation and possible distortion from octahedral symmetry. The data in Table 2 illustrate two important features. Firstly, it is clear that bands attributed to ν(Ga—O) are coincident

[3]We thank a referee for bringing this point to our attention.

[4]Since the cation point group is probably C_3 (see later) and there is no plane of symmetry which bisects the C—S—C angle, the two angle deformations have separate symmetry coordinates. We retain the terms symmetric and antisymmetric solely to show the relationship to the free ligand modes.

[5]In acetone solution the 347 cm^{-1} band is polarized (ρ = 0.09), thus confirming the proposed assignment.

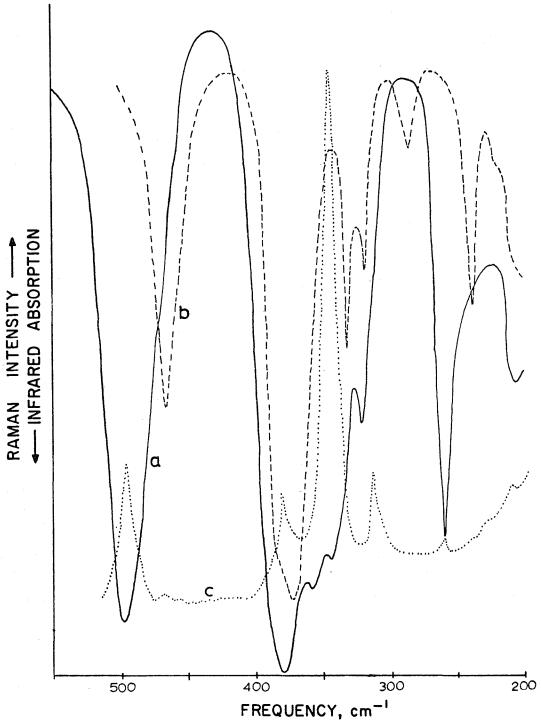

FIG. 1. Far-infrared spectra of *a*, $[Ga(dmso)_6][GaCl_4]_3$; *b*, $[Ga(dmso\text{-}d_6)_6][GaCl_4]_3$; and *c*, Raman spectrum of $[Ga(dmso)_6][Gacl_4]_3$.

in the infrared and the Raman. The large half-widths of ca. 45 cm^{-1} of the ν(Ga—O) bands in the infrared and the weakness of ν(Ga—O) absorptions in the Raman are also evident. The first observation suggests that the cation cannot belong to the point group O_h as there are no coincidences in this group. Moreover a lowering of symmetry from $O_h \rightarrow D_{3d} \rightarrow S_6$ as shown in the correlation table (Table 3) does not solve the problem, although the degeneracy of the T_{1u} mode is removed as the symmetry is lowered. Other workers have suggested on the basis of infrared evidence alone that transition-metal hexakis(dmso) complexes have S_0 symmetry (16). Further symmetry lowering to C_3 would not remove any further degeneracies but could cause all vibrations to be infrared and Raman active. While we could not identify all infrared bands in the Raman owing to background noise, the coincidences of the ν(Ga—O) frequencies are striking. We conclude, therefore, that the Ga(dmso)$_6^{3+}$ and Ga(dmso-d_6)$_6^{3+}$ cations have, at most, C_3 symmetry in the solid state. Molecular models show that with C_3 symmetry, effective packing of six dmso molecules around the Ga^{3+} ion is possible.

TABLE 3

Correlation table showing the effect of symmetry lowering on the $A_{1g}(\nu_1)$ and $T_{1u}(\nu_3)$ ν(M—O) stretching modes of a regular octahedral MO_6 species

Symmetry	Mode	
O_h	T_{1u}(i.r.)	A_{1g}(R)
D_{3d}	A_{2u}(i.r.) + E_u(i.r.)	A_{1g}(R)
S_6	A_u(i.r.) E_u(i.r.)	A_g(R)
C_3	A(R, i.r.) E(R, i.r.)	A(R, i.r.)

Indium Complexes

Infrared data for $InX_3(dmso)_3$, $InX_3(dmso\text{-}d_6)_3$ (X = Cl, Br) and $InI_3(dmso\text{-}d_6)_2$ in the ν(S—O) region are included in Table 4. The spectra of the deuterated complexes confirm the previous tentative assignments for ν(S—O) in these compounds (10). The far-infrared spectra of these adducts have been reported previously but opinions differ as to whether the compounds $InX_3(dmso)_3$ (X = Cl, Br) have *cis*-C_{3v} octahedral or *trans*-C_{2v} octahedral structures, since three metal–halogen bands were identified in one case (21) and only two in the other (22). Comparison of the spectra of $InCl_3(dmso)_3$ and $InCl_3(dmso\text{-}d_6)_3$ between 200 and 400 cm^{-1} suggests that ν(In—Cl) vibrations appear as a medium intensity sharp band at 284 cm^{-1} and a broad, incompletely resolved doublet centered at 262 cm^{-1}.

The Raman spectra of $InCl_3(dmso)_3$ and $InCl_3(dmso\text{-}d_6)_3$ show only a single intense Raman line at 267 and 282 cm^{-1}, respectively. For an MX_3L_3 *cis*-C_{3v} model, two ν(M—Cl) modes are expected ($a_1 + e$) in the infrared and Raman compared with three ν(M—Cl) modes ($2a_1 + b_2$) for the *trans* isomer. Although the infrared data might be considered as pointing to a *cis* configuration, this assignment does not seem justified in view of the appearance of only one Raman band for each complex in the region of In—Cl stretching. Owing to low solubility in

Can. J. Chem. Downloaded from www.nrcresearchpress.com by 210.87.254.105 on 09/05/12
For personal use only.

Can. J. Chem. Downloaded from www.nrcresearchpress.com by 210.87.254.105 on 09/05/12
For personal use only.

TABLE 4

Infrared frequencies and assignments in the ν(S—O) region for dmso and dmso-d_6 complexes*

Frequency (cm^{-1})						
$[Ga(dmso)_6][GaCl_4]_3$	$[Ga(dmso\text{-}d_6)_6][GaCl_4]_3$	$[Ga(dmso)_6]Br_3$	$[Ga(dmso\text{-}d_6)_6]Br_3$	$[Ga(dmso)_6]I_3$	$[Ga(dmso\text{-}d_6)_6]I_3$	Assignments
	835 (18)	1059 (8)	842 (15)	1057 (5)	842 (13)	
1035 (15)	792 (4)	1003 (15)	801 (10)	1000 (13)	803 (9)	δ_{rock} $(CH_3)CD_3$
990 (18)	772 (12)	969 (16)	777 (14)	963 (17)	780 (15)	
941 (20)	945 (20)	938 (20)	940 (20)	943 (20)	945 (20)	ν (S—O)
Frequency (cm^{-1})						
$In(dmso)_3Cl_3$	$In(dmso\text{-}d_6)_3Cl_3$	$In(dmso)_3Br_3$	$In(dmso\text{-}d_6)_3Br_3$	$In(dmso)_2I_3$	$In(dmso\text{-}d_6)_2I_3$	Assignments
1038 (13)	831 (11)	1034 (13)	833 (10)	1035 (13)	834 (10)	
1009 (10)	788 (3)	1010 (9)	790 (2)	1010 (10)	788 (2)	δ_{rock} $(CH_3)CD_3$
993 (20)	764 (10)	987 (20)	766 (9)	990 (20)	765 (9)	
938 (20)	942 (20)	950 (20)	948 (20)	940 (20)	941 (20)	ν(S—O)
950 (20)	960 (20)	941 (20)	962 (20)	950 (20)	955 (20)	

*Numbers in parentheses indicate intensity; the highest intensity band is assigned an arbitrary intensity of 20.

Can. J. Chem. Downloaded from www.nrcresearchpress.com by 210.87.254.105 on 09/05/12
For personal use only.

suitable solvents, we were also unable to obtain Raman polarization measurements on the bands in question. However, Beattie, Ozin, and Gilson (26) have recently shown that for the species MX_3L_3 (L = pyridine), a single intense line due to equatorial M—X stretching is observed in the Raman. While this may only be valid for light metal atoms, the Raman spectra of $InCl_3(dmso)_3$ and $InCl_3(dmso\text{-}d_6)_3$ resemble that for $SiCl_3(py)_3^+$ (26). On this basis, a *trans* assignment could be made. Thus, in view of the ambiguity in the solid state infrared and Raman results, we do not consider a stereochemical assignment for $InCl_3(dmso)_3$ justifiable at this stage. This may be due in part to the coalescence of ν(In—Cl) modes as a result of the large mass of indium, although other workers (26) have pointed out the inadequacies of vibrational spectra in predicting a *cis* or *trans* geometry for $SiCl_4(py)_2$ (26).

Solid $InBr_3(dmso)_3$ shows two bands at 189 and 158 cm^{-1} in the Raman, with the former very intense. The 158 cm^{-1} band moves to 150 cm^{-1} on deuteration and may not be due to a pure ν(In—Br) mode. In solution, only the higher band appears and this is polarized ($\rho = 0.09$), indicating that this is an a_1 mode. In this case a *cis* configuration seems more reasonable although again the assignment is tentative and must await confirmation from X-ray work.

For $InI_3(dmso)_2$ and $InI_3(dmso\text{-}d_6)_2$, the Raman spectra are more complex. However, it is clear that the very strong Raman band at 141 cm^{-1} and the weaker band at 183 cm^{-1} arise from ν_1 and ν_3 of InI_4^-, since these differ by only 2 cm^{-1} from the frequencies found for the same modes in a previous investigation (24). Moreover, in acetone solution the 141 cm^{-1} band is polarized ($\rho = 0.12$ for $InI_3(dmso)_2$; $\rho = 0$ for $InI_3(dmso\text{-}d_6)_2$), while the 183 cm^{-1} band is depolarized. The complex can therefore be formulated as $[In(dmso)_4I_2][InI_4]$, with the band at 193 cm^{-1} and shoulder at 198 cm^{-1} in the Raman arising from the cation. We were, however, unable to determine depolarization ratios in this case due to the low intensities of the bands. It is interesting that the cation frequencies are higher than those of InI_4^-; ν(M—X) usually decreases in frequency with increasing coordination number. However, a recent X-ray study of $InI_3(dmso)_2$ has confirmed the ionic dimer structure in the solid state (25) and shown the cation to have a *trans* configuration.

Conclusions

This work establishes that the dmso complexes of gallium trihalides have structures $[Ga(dmso)_6][GaCl_4]_3$, $[Ga(dmso)_6]Br_3$, and $[Ga(dmso)_6]I_3$. Unequivocal structural assignments for $InCl_3(dmso)_3$ and $InBr_3(dmso)_3$ are not possible with far-infrared and Raman data alone. $InI_3(dmso)_2$ has the structure $[InI_2(dmso)_4][InI_4]$. For both metals there appears to be a tendency to octahedral coordination when dmso is the donor molecule. In the gallium complexes, this occurs by complete replacement of halide ion from the coordination sphere. It is worth noting that gallium apparently resembles aluminum in this respect rather than the later metals in the group, since reaction of anhydrous $AlCl_3$ with dmso gives $[Al(dmso)_6]Cl_3$ (9) whereas thallium trichloride gives the non-ionic, five-coordinate $TlCl_3(dmso)_2$ (2). Two further observations can also be made. First of all it is becoming increasingly obvious that the formation of ionic dimers is a general feature of the coordination chemistry of gallium and indium (1, 5), particularly when the complex stoichiometry is such that the anion is the tetrahalometallate ion. Secondly, this and previous work (6) illustrate that six-coordinate gallium complexes are readily prepared, provided suitable ligands are chosen.

We thank the National Research Council of Canada and the Ontario Government, Department of University Affairs for financial support. We are grateful to Dr. A. Walker, University of Toronto for the use of the IR-12 spectrometer.

1. A. J. Carty. Coord. Chem. Rev. **4**, 29 (1969).
2. R. A. Walton. Inorg. Chem. **7**, 640 (1968).
3. I. R. Beattie and G. A. Ozin. J. Chem. Soc. 2373 (1968).
4. M. V. Veidis and G. J. Palenik. Chem. Commun. 586 (1969).
5. R. Restivo and G. J. Palenik. Chem. Commun. 867 (1969).
6. A. J. Carty. Can. J. Chem. **46**, 3779 (1968).
7. I. R. Beattie, T. R. Gilson, and G. A. Ozin. J. Chem. Soc. 1092 (1968).
8. W. F. Currier and J. H. Weber. Inorg. Chem. **6**, 1539 (1967).
9. (*a*) B. F. G. Johnson and R. A. Walton. Spectrochim Acta, **22**, 1853 (1966). (*b*) R. L. Richards. Ph.D. thesis. University of Manchester, Manchester, England. 1964.
10. A. J. Carty and D. G. Tuck. J. Chem. Soc. A, 1081 (1966).
11. E. P. Cocozza. Chem. Anal. **49**, 46 (1960).
12. W. D. Horrocks, Jr. and F. A. Cotton. Spectrochim. Acta, **17**, 134 (1961).
13. F. A. Cotton and R. Francis. J. Amer. Chem. Soc. **82**, 2986 (1960).

14. R. S. DRAGO and D. MEEK. J. Phys. Chem. **65**, 1446 (1961).
15. F. A. COTTON, R. FRANCIS, and W. D. HORROCKS, JR. J. Amer. Chem. Soc. **64**, 1534 (1960).
16. C. V. BERNEY and J. H. WEBER. Inorg. Chem. **7**, 283 (1968).
17. N. N. GREENWOOD, T. S. SRIVASTAVA, and B. P. STRAUGHAN. J. Chem. Soc. A, 699 (1966).
18. A. J. CARTY. Can. J. Chem. **45**, 3187 (1967).
19. P. L. GOGGIN and T. G. BUICK. Chem. Commun. 290 (1967).
20. L. A. WOODWARD and A. A. NORD. J. Chem. Soc. 3721 (1956).
21. D. M. ADAMS, A. J. CARTY, P. CARTY, and D. G. TUCK. J. Chem. Soc. A, 162 (1968).
22. R. A. WALTON. J. Chem. Soc. A, 1487 (1967).
23. D. M. ADAMS. Metal–ligand and related vibrations. E. Arnold, London. 1968, pp. 102–103.
24. L. A. WOODWARD and G. H. SINGER. J. Chem. Soc. 716 (1958).
25. F. EINSTEIN and D. G. TUCK. Unpublished work.
26. I. R. BEATTIE, T. R. GILSON, and G. A. OZIN. J. Chem. Soc. A, 2772 (1968).

Can. J. Chem. Downloaded from www.nrcresearchpress.com by 210.87.254.105 on 09/05/12
For personal use only.

Can. J. Chem. Downloaded from www.nrcresearchpress.com by 210.87.254.40 on 05/05/12
For personal use only.

NOTES

Radiolysis of cyclohexane with perfluorocyclohexane at very high dose rates[1]

N. H. SAGERT[2]

Physical Chemistry Branch, Chalk River Nuclear Laboratories, Atomic Energy of Canada Ltd., Chalk River, Ontario

Received October 14, 1969

The radiolysis of liquid cyclohexane using perfluorocyclohexane as an electron scavenger has been examined at very high dose rates. The dose rates, 10^{27} to 10^{28} eV/g s, were such that geminate recombination of ions is essentially unaffected by dose rate, but high concentrations of radicals are produced, leading to radical–radical reactions. Up to 0.7 G units of the mixed dimer, $C_6F_{11}\cdot C_6H_{11}$, were produced indicating that large concentrations of C_6F_{11} radicals are formed in the neutralization process. Thus, at conventional dose rates (10^{16} eV/g s), $C_6F_{11}H$ is probably produced by reactions of C_6F_{11} radicals rather than by proton transfer to a perfluorocyclohexane or perfluorocyclohexyl anion.

Canadian Journal of Chemistry, **48**, 501 (1970)

Introduction

Perfluorocyclohexane (PCH) has been used as an electron scavenger in the radiolysis of hydrocarbons (1–3). It scavenges electrons efficiently and one C—F bond is broken for every electron scavenged (2–4). Because dissociation of the PCH anion is prohibitively endothermic (5), C—F bond breaking probably occurs in the neutralization step (4, 6). The mechanism for this bond breaking has been the subject of some speculation and several mechanisms have been proposed (2, 3, 6). They may be summarized, omitting intermediate steps, as

$$[1a]\quad C_6F_{12}^- + C_6H_{12}^+ \rightarrow C_6F_{11} + C_6H_{11} + HF$$

$$[1b]\quad \rightarrow C_6F_{11}H + C_6H_{11} + F$$

where reaction [1*a*] involves a free C_6F_{11} radical and reaction [1*b*] involves proton transfer to an anion.

The radiolysis of cyclohexane at very high dose rates (10^{24} to 10^{28} eV/g s) has been described and, compared to γ-radiolysis at $\sim 10^{16}$ eV/g s, significant changes in the yields of the major products, hydrogen, cyclohexene, and dicyclohexyl were noted (7). These changes were ascribed to radical–radical interactions. The work reported here was undertaken to identify the radicals produced in the radiolysis of cyclohexane with PCH by examining yields of products, particularly that of the dimers, at high dose rates. It was hoped that this would allow a distinction to be made between reactions of type [1*a*] and [1*b*].

Experimental

Sources and purification of cyclohexane and PCH have been described (4). Irradiations were carried out in metal cells of the type described by Boyd *et al.* (7). These cells were irradiated with a Febetron 705 pulsed electron source (Field Emission Corp.), and the adsorbed dose was determined by adiabatic calorimetry (8).

Analytical techniques have been described (4, 9). In the absence of authentic standards, the area sensitivity of the hydrogen flame detector for $C_6F_{11}\cdot C_6H_{11}$ was taken as half the sensitivity for dicyclohexyl plus half the sensitivity for perfluorodicyclohexyl.

Results

The yields of the major products, as well as $C_6F_{11}H$ and $C_6F_{11}\cdot C_6H_{11}$, are shown in Figs. 1 and 2 for the radiolysis of cyclohexane in the presence of PCH. The open symbols are for a dose rate of 6×10^{27} eV/g s and a dose of $4.2_2 \times 10^{20}$ eV/g. The closed symbols are for a dose rate of 3.7×10^{27} eV/g s and a dose of $2.6_0 \times 10^{20}$ eV/g. Hydrogen yields were reduced on adding PCH much as they were on adding N_2O to cyclohexane under similar conditions (7), but cyclohexene and dicyclohexyl were also reduced. Undecafluorocyclohexane was produced, although in smaller yields than at conventional dose rates (4), and a new product, $C_6F_{11}\cdot C_6H_{11}$, was produced in measurable yield. The ratio of $C_6F_{11}\cdot C_6H_{11}$ to $C_6F_{11}H$ was constant over the range of scavenger concentrations used. Perfluorodicyclohexyl was produced with a yield of

[1]A.E.C.L. No. 3496.

[2]Present address: Materials Science Branch, Whiteshell Nuclear Research Establishment, Pinawa, Manitoba.

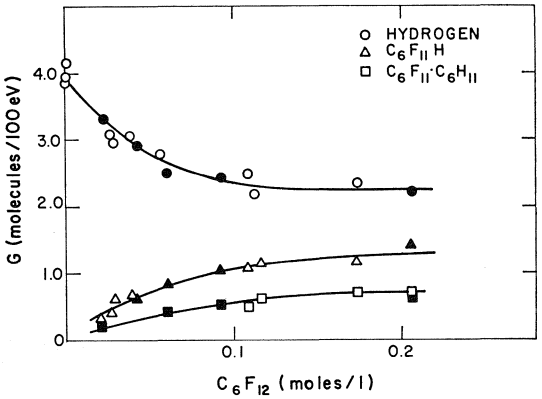

FIG. 1. Hydrogen, $C_6F_{11}H$, and $C_6F_{11}\cdot C_6H_{11}$ yields from the radiolysis of cyclohexane with PCH. Open symbols for a dose rate of 6×10^{27} eV/g s and a dose of $4.2_2 \times 10^{20}$ eV/g, filled symbols for a dose rate of 3.7×10^{27} eV/g s and a dose of $2.6_0 \times 10^{20}$ eV/g.

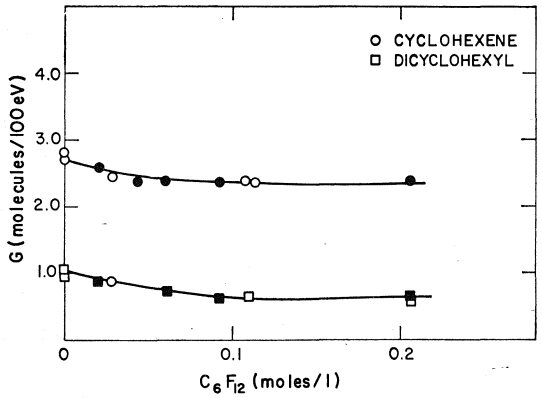

FIG. 2. Cyclohexene and dicyclohexyl yields from the radiolysis of cyclohexene with PCH. The filled and open symbols have the same significance as in Fig. 1.

$\sim$ 0.05 G units at 0.2 *M* PCH. Perfluorocyclohexene could not be determined as it was not separated from PCH on our column.

Discussion

No $C_6F_{11}\cdot C_6H_{11}$ is produced at low dose rates (4), demonstrating that neutralization does not give this product directly. At Febetron dose rates (10^{27}–10^{28} eV/g s) $C_6F_{11}\cdot C_6H_{11}$ is produced. This might occur either by a change in the neutralization process or by radical combination.

At high scavenger concentrations we are dealing with electron scavenging which affects geminate recombination (6). Boyd *et al.* have assumed that geminate recombination is unaffected by high dose rates (7). If a dose of 5×10^{20} eV/g is delivered in an infinitesimally small time, and, if the concept of spurs has any validity in hydrocarbons, then spur centers will be separated by 50 Å at $t = 0$, assuming that the average energy per spur is 50 eV. However, the pulse has a half-width of 25 ns and a total width of 100 ns. Hunt and Thomas (10) have shown that most geminate ions recombine in a few ns. More recently, Rzad *et al.* (11), using the data of Thomas *et al.* (12), have calculated that 50% of the biphenyl anions formed in dilute solutions of biphenyl in cyclohexane decay in $\frac{1}{2}$ ns. The other 50% decay somewhat more slowly, but only 4% of the ions survive at 170 ns. Therefore, our interaction centers or spurs are separated, on the average, by at least 100 Å, which is of the order of the effective thermalization distance in *n*-hexane (13). Thus, at Febetron dose rates, neutralization processes are unaffected by the high dose rate. Therefore, all the dose rate effects reported are assumed to be due to radical–radical interactions, and the large yield of $C_6F_{11}\cdot C_6H_{11}$ is taken as evidence that C_6F_{11} is produced as a product of the neutralization process.

The production of C_6F_{11} takes place in reactions summarized by [1*a*]. This might occur by reaction [1*a*] directly, or by dissociation of an excited state of PCH as suggested by Warman *et al.* (6).

$$[2] \qquad C_6F_{12}^- + C_6H_{12}^+ \rightarrow C_6F_{12}^* + C_6H_{12}$$

$$[3] \qquad C_6F_{12}^* \rightarrow C_6F_{11}\cdot + F\cdot$$

Rajbenbach (3) has suggested that a possible reaction sequence is

$$[4] \qquad C_6F_{12}^- + C_6H_{12} \rightarrow C_6F_{11}^- + C_6H_{11}\cdot + HF$$

$$[5] \qquad C_6F_{11}^- + C_6H_{12}^+ \rightarrow C_6F_{11}H + C_6H_{11}\cdot$$

Our results suggest that if reaction [4] occurs, it is followed by simple neutralization, reaction [6], rather than by reaction [5].

$$[6] \qquad C_6F_{11}^- + C_6H_{12}^+ \rightarrow C_6F_{11}\cdot + C_6H_{12}$$

A complete analysis of the data is not possible at the present time because of the lack of rate constant data and because the yields from the radiolysis of pure cyclohexane at Febetron dose rates could only be accounted for to within 15% (7). However, it was noted that the C_6F_{11} yield, measured as $G(C_6F_{11}H)$ plus $G(C_6F_{11}\cdot C_6H_{11})$,

Can. J. Chem. Downloaded from www.nrcresearchpress.com by 210.87.254.40 on 09/05/12
For personal use only.

is 1.9 G units with 0.2 *M* PCH, which is a smaller yield than the 3.2 G units obtained at $\sim 10^{16}$ eV/g s with 0.2 *M* PCH. This smaller yield may be explained if some radical–radical reactions possible at high dose rates are considered

[7*a*] $H\cdot + C_6F_{11}\cdot \rightarrow HF + C_6F_{10}$

[7*b*] $\rightarrow C_6F_{11}H$

[8*a*] $C_6H_{11}\cdot + C_6F_{11}\cdot \rightarrow C_6F_{11}\cdot C_6H_{11}$

[8*b*] $\rightarrow C_6H_{11}F + C_6F_{10}$

[8*c*] $\rightarrow C_6F_{11}H + C_6H_{10}$

[9*a*] $C_6F_{11}\cdot + C_6F_{11}\cdot \rightarrow C_6F_{11}\cdot C_6F_{11}$

[9*b*] $\rightarrow C_6F_{12} + C_6F_{10}$

The normal abstraction reaction of C_6F_{11}, reaction [10] may also occur to some extent, although

[10] $C_6F_{11} + C_6H_{12} \rightarrow C_6F_{11}H + C_6H_{11}$

if an analogy may be drawn with C_2F_5 radicals (14), it probably has an activation energy of 5 to 7 kcal/mole and hence will be slow compared with reactions [7] to [9]. Fluorine atoms are known to react very rapidly with hydrocarbons (15), so radical–radical reactions involving them have not been considered. Furthermore, the reaction analogous to reaction [8*b*] has not been observed for the reaction of C_2F_5 radicals with C_2H_5 radicals (14) so it is probably of minor importance. Reaction [9*a*] has a yield of 0.05 G units at 0.2 *M* PCH and thus accounts for only 0.1 G units of C_6F_{11}. The ratio k_{9b}/k_{9a} is unknown, but it is unlikely that reaction [9*a*] accounts for more than a few tenths of a G unit of C_6F_{11}. Hence most of the smaller measured C_6F_{11} yield is likely due to reaction [7*a*].

The advice and assistance of A. W. Boyd, C. Willis, and D. A. Armstrong, particularly with regard to dosimetry, and comments on this manuscript by A. W. Boyd, D. R. Smith, and C. Willis are gratefully acknowledged.

1. L. A. Rajbenbach. J. Amer. Chem. Soc. **88**, 4275 (1966).
2. N. H. Sagert. Can. J. Chem. **46**, 95 (1968).
3. L. A. Rajbenbach. J. Phys. Chem. **73**, 356 (1969).
4. N. H. Sagert, J. A. Reid, and R. W. Robinson. Can. J. Chem. **47**, 2655 (1969).
5. M. M. Bibby and G. Carter. Trans. Faraday Soc. **59**, 2455 (1963).
6. J. M. Warman, K.-D. Asmus, and R. H. Schuler. Advan. Chem. Ser. **82**, 25 (1968).
7. A. W. Boyd, C. Willis, O. A. Miller, and A. E. Rothwell. Advan. Chem. Ser. **82**, 456 (1968).
8. C. Willis, O. A. Miller, A. E. Rothwell, and A. W. Boyd. Radiation Res. **35**, 428 (1968).
9. N. H. Sagert and A. S. Blair. Can. J. Chem. **46**, 3284 (1968).
10. J. W. Hunt and J. K. Thomas. J. Chem. Phys. **46**, 2954 (1967).
11. S. J. Rzad, P. P. Infelta, J. M. Warman, and R. H. Schuler. J. Chem. Phys. **50**, 5034 (1969).
12. J. K. Thomas, K. Johnson, T. Klippert, and R. Lowers. J. Chem. Phys. **48**, 1608 (1968).
13. A. Mozumder and J. L. Magee. J. Chem. Phys. **47**, 939 (1967).
14. R. L. Thommarson and G. O. Pritchard. J. Phys. Chem. **76**, 2307 (1966).
15. G. C. Fettis and J. H. Knox. Progr. Reaction Kinetics, **2**, 1 (1964).

Erratum: The critical constants and orthobaric densities of acetone, chloroform, benzene, and carbon tetrachloride

A. N. Campbell and R. M. Chatterjee
Department of Chemistry, University of Manitoba, Winnipeg, Manitoba

Received October 27, 1969

Canadian Journal of Chemistry, **48**, 503 (1970)

On p. 3897, the constants *A*, *B*, *C*, and *D* for the Cragoe equation given in Table V should be, respectively, $+2.217305$, -7.035734×10^2, $+1.005633 \times 10^{-2}$, and -6.508827×10^{-6} for benzene and $+1.062382 \times 10$, -2.033738×10^3, -7.418258×10^{-3}, and $+5.463349 \times 10^{-6}$ for carbon tetrachloride.

On p. 3898, line 15 in the left hand column should read $x = (2T - (T_{max} + T_{min}))/(T_{max} - T_{min})$.

Can. J. Chem. Downloaded from www.nrcresearchpress.com by 210.87.254.40 on 09/05/12
For personal use only.

is 1.9 G units with 0.2 *M* PCH, which is a smaller yield than the 3.2 G units obtained at $\sim 10^{16}$ eV/g s with 0.2 *M* PCH. This smaller yield may be explained if some radical–radical reactions possible at high dose rates are considered

[7*a*] $H\cdot + C_6F_{11}\cdot \rightarrow HF + C_6F_{10}$

[7*b*] $\rightarrow C_6F_{11}H$

[8*a*] $C_6H_{11}\cdot + C_6F_{11}\cdot \rightarrow C_6F_{11}\cdot C_6H_{11}$

[8*b*] $\rightarrow C_6H_{11}F + C_6F_{10}$

[8*c*] $\rightarrow C_6F_{11}H + C_6H_{10}$

[9*a*] $C_6F_{11}\cdot + C_6F_{11}\cdot \rightarrow C_6F_{11}\cdot C_6F_{11}$

[9*b*] $\rightarrow C_6F_{12} + C_6F_{10}$

The normal abstraction reaction of C_6F_{11}, reaction [10] may also occur to some extent, although

[10] $C_6F_{11} + C_6H_{12} \rightarrow C_6F_{11}H + C_6H_{11}$

if an analogy may be drawn with C_2F_5 radicals (14), it probably has an activation energy of 5 to 7 kcal/mole and hence will be slow compared with reactions [7] to [9]. Fluorine atoms are known to react very rapidly with hydrocarbons (15), so radical–radical reactions involving them have not been considered. Furthermore, the reaction analogous to reaction [8*b*] has not been observed for the reaction of C_2F_5 radicals with C_2H_5 radicals (14) so it is probably of minor importance. Reaction [9*a*] has a yield of 0.05 G units at 0.2 *M* PCH and thus accounts for only 0.1 G units of C_6F_{11}. The ratio k_{9b}/k_{9a} is unknown, but it is unlikely that reaction [9*a*] accounts for more than a few tenths of a G unit of C_6F_{11}. Hence most of the smaller measured C_6F_{11} yield is likely due to reaction [7*a*].

The advice and assistance of A. W. Boyd, C. Willis, and D. A. Armstrong, particularly with regard to dosimetry, and comments on this manuscript by A. W. Boyd, D. R. Smith, and C. Willis are gratefully acknowledged.

1. L. A. Rajbenbach. J. Amer. Chem. Soc. **88**, 4275 (1966).
2. N. H. Sagert. Can. J. Chem. **46**, 95 (1968).
3. L. A. Rajbenbach. J. Phys. Chem. **73**, 356 (1969).
4. N. H. Sagert, J. A. Reid, and R. W. Robinson. Can. J. Chem. **47**, 2655 (1969).
5. M. M. Bibby and G. Carter. Trans. Faraday Soc. **59**, 2455 (1963).
6. J. M. Warman, K.-D. Asmus, and R. H. Schuler. Advan. Chem. Ser. **82**, 25 (1968).
7. A. W. Boyd, C. Willis, O. A. Miller, and A. E. Rothwell. Advan. Chem. Ser. **82**, 456 (1968).
8. C. Willis, O. A. Miller, A. E. Rothwell, and A. W. Boyd. Radiation Res. **35**, 428 (1968).
9. N. H. Sagert and A. S. Blair. Can. J. Chem. **46**, 3284 (1968).
10. J. W. Hunt and J. K. Thomas. J. Chem. Phys. **46**, 2954 (1967).
11. S. J. Rzad, P. P. Infelta, J. M. Warman, and R. H. Schuler. J. Chem. Phys. **50**, 5034 (1969).
12. J. K. Thomas, K. Johnson, T. Klippert, and R. Lowers. J. Chem. Phys. **48**, 1608 (1968).
13. A. Mozumder and J. L. Magee. J. Chem. Phys. **47**, 939 (1967).
14. R. L. Thommarson and G. O. Pritchard. J. Phys. Chem. **76**, 2307 (1966).
15. G. C. Fettis and J. H. Knox. Progr. Reaction Kinetics, **2**, 1 (1964).

Erratum: The critical constants and orthobaric densities of acetone, chloroform, benzene, and carbon tetrachloride

A. N. Campbell and R. M. Chatterjee
Department of Chemistry, University of Manitoba, Winnipeg, Manitoba

Received October 27, 1969

Canadian Journal of Chemistry, **48**, 503 (1970)

On p. 3897, the constants *A*, *B*, *C*, and *D* for the Cragoe equation given in Table V should be, respectively, $+2.217305$, -7.035734×10^2, $+1.005633 \times 10^{-2}$, and -6.508827×10^{-6} for benzene and $+1.062382 \times 10$, -2.033738×10^3, -7.418258×10^{-3}, and $+5.463349 \times 10^{-6}$ for carbon tetrachloride.

On p. 3898, line 15 in the left hand column should read $x = (2T - (T_{max} + T_{min}))/(T_{max} - T_{min})$.

Can. J. Chem. Downloaded from www.nrcresearchpress.com by 210.87.254.6 on 09/05/12
For personal use only.

Electron spin resonance study of trapped electrons in irradiated organic glasses at 4.2 °K

HIROSHI YOSHIDA[1] AND TAKENOBU HIGASHIMURA

Research Reactor Institute, Kyoto University, Kumatori-cho, Sennan-gun, Osaka, Japan

Received June 23, 1969

Electron spin resonance of electrons trapped in organic glasses, ethanol, 2-methyltetrahydrofuran, and 3-methylhexane were studied at the four different conditions (combination of irradiation with γ-rays and measurement at both 77 and 4.2 °K). It was evident that the spectral width, ΔH_{ms}, changes irreversibly when the glasses are warmed up to 77 °K after the irradiation at 4.2 °K: from 6.7, 5.6, and 4.5 to 14, 4.4, and 4.0 G for ethanol, 2-methyltetrahydrofuran, and 3-methylhexane, respectively. These observations strongly support Smith and Pieroni's (4) suggestion that the molecular orientation is not a necessary condition for electrons to be trapped in the irradiated organic glasses.

Canadian Journal of Chemistry, **48**, 504 (1970)

Can. J. Chem. Downloaded from www.nrcresearchpress.com by 210.87.254.5 on 09/05/12
For personal use only.

Introduction

Electrons trapped in organic glasses irradiated by ionizing radiations have been extensively studied by means of the electron spin resonance (e.s.r.) technique as well as by optical absorption measurements. Although the reactions of the electrons with several solutes added to the glasses have now been comprehended (see, for example, ref. 1), the trapping mechanism of the electrons has not yet been fully elucidated. Recently, Ekstrom and Willard reported the dependence of both e.s.r. spectral width and optical absorption maximum of the trapped electrons upon the polarity of the matrix molecules, inferring that the electrons are trapped in pre-existing cavities in the glasses at 77 °K (2). Yoshida and co-workers suggested, as a result of an e.s.r. study, that it is possible for the electron trapping (due to the electronic polarization of the matrix molecules) to occur also in the non-polar glass of 3-methylpentane (3).

When the organic glasses are irradiated at a temperature so low that the molecular rearrangement is restricted, the mechanism of the electron trapping might be further clarified from the observed e.s.r. spectra and optical absorption. Smith and Pieroni carried out an e.s.r. investigation by irradiating at 4.2 °K and by measuring at the same temperature, and found the spectral widths of the trapped electrons to be different from those observed by both irradiating and measuring at 77 °K (4). From the results, they suggested that the molecular orientation is not a necessary condition for the electrons to be trapped in the glasses. However, evidence seems to be needed to show that the difference in the spectral widths is not due to their reversible dependence upon temperature but due to the irreversible change of the surroundings by the raising temperature.

In the present investigation, the e.s.r. spectra of the trapped electrons in polar glasses of ethanol and 2-methyltetrahydrofuran and in non-polar glass of 3-methylhexane were studied with irradiation and measurement both at 4.2 and 77 °K. In addition to the reconfirmation of the difference in the spectral widths, it was proved that the difference actually resulted from the irreversible change of the surroundings.

Experimental

2-Methyltetrahydrofuran and 3-methylhexane were purified by the procedure described before (5). After the usual purification treatments, ethanol was dried by BaO in the final stage. The dried samples were transferred to the e.s.r. sample tubes of pure quartz by trap-to-trap distillation, sealed under vacuum at better than 10^{-4} mm Hg, and irradiated by ^{60}Co γ-rays in the dark.

The cryostats were of two different types, the cavity-in-Dewar type (JEOL Co. Model JES-LHC-1X) and the Dewar-in-cavity type designed by the authors (6). The irradiation at 4.2 °K was carried out with the former cryostat containing the sample, followed by the measurements at 4.2 °K and then at 77 °K, the change of temperature being achieved by replacing liquid helium with liquid nitrogen. For measurements at 4.2 °K after irradiation at 77 °K, the samples were quickly transferred from a liquid nitrogen Dewar vessel to the latter cryostat without getting warmed.

The e.s.r. measurements were carried out with a conventional X-band spectrometer using 100 kc.p.s. magnetic field modulation when the Dewar-in-cavity type cryostat was used, and 80 c.p.s. modulation when the cavity-in-Dewar type cryostat was used. Distortion of the signal by fast passage effect was looked for by making observations, especially at 4.2 °K, at several values of the

[1]Present address: Faculty of Engineering, Hokkaido University, Sapporo, Japan.

TABLE 1

Line width of the e.s.r. singlet spectrum of the trapped electrons in γ-irradiated organic glasses in different temperature conditions

Glasses	Irradiation at 77 °K, measurement at		Irradiation at 4.2 °K, measurement at	
	77 °K	4.2 °K	4.2 °K	77 °K
Ethanol*	14.3	14 ±1	—	—
2-Methyltetrahydrofuran*	4.4±0.1	4.6±0.1	5.6	4.4
3-Methylhexane*	4.0	3.9±0.2	4.5	4.0
Ethanol†	14	—	6.7	—
2-Methyltetrahydrofuran†	4.5	—	6.3	—
3-Methylpentane†	3.7	—	4.9	—

*This work.
†Reference 4.

modulation amplitude (H_m) and microwave power incident on the resonance cavity. Under the conditions used ($H_m = 1.0 \sim 0.2$ G, microwave power of 1 and 10 μW for the 80 c.p s. and 100 kc.p.s. modulation), no effects of fast passage on spectral width appeared to occur.

Results and Discussion

Observed e.s.r. spectra for 2-methyltetrahydrofuran are shown representatively in Fig. 1. In all conditions examined, the sharp singlet spectra due to the trapped electrons are observable at the central portion of the recorded signals. The width of a singlet spectrum is determined as that between the maximum and the minimum points of the recorded derivative curves (peak-to-peak width, ΔH_{ms}). Similar spectra of the trapped electrons are also observed from the glasses of ethanol and 3-methylhexane. The observed values of ΔH_{ms} are listed in Table 1, values reported by Smith and Pieroni (4) are cited for comparison.

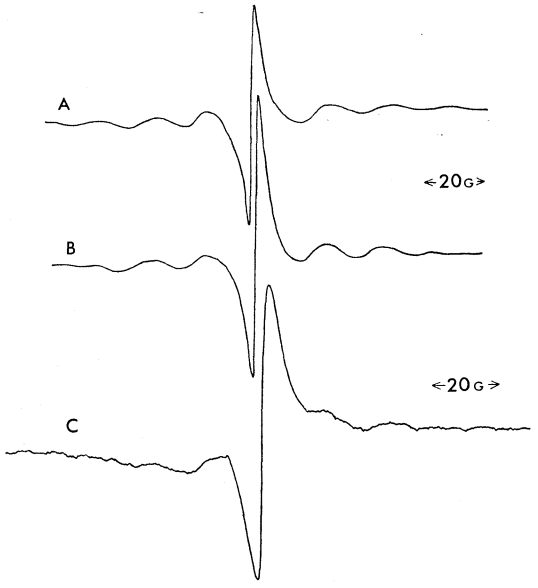

FIG. 1. The e.s.r. spectra of 2-methyltetrahydrofuran glass irradiated with γ-rays up to the dose of 1.7×10^5 rads. Irradiated at 77 °K and measured with the modulation frequency of 100 Kc.p.s. (*A*) at 77 °K and (*B*) at 4.2 °K, (*C*) irradiated and measured at 4.2 °K with the modulation frequency of 80 c.p.s.

According to previous report (4), electrons in the ethanol glass give spectrum of width 6.7 G at 4.2 °K, in contrast to 14 G when examined at 77 °K. In the present investigation, lowering the temperature of the glass to 4.2 °K after the irradiation at 77 °K does not cause the change in the width. These two observations, independent of each other, lead to the following conclusions; (*a*) the trapped electrons in the glass once warmed to 77 °K, show a width of 14 G which is independent of the measuring temperature, and (*b*) the surroundings of the trapped electrons in the glass irradiated at 4.2 °K change during the course of warming to 77 °K. Conclusion (*b*), already suggested in ref. 4, is further supported by conclusion (*a*). The change of the surroundings has probably resulted from the orientation of the ethanol molecules induced by the electrons themselves, so that the H atoms of the hydroxyl groups come closer to the electrons, giving the stronger hyperfine interaction and the wider e.s.r. spectrum.

If one supposes a fairly continuous distribution of trap depths in the glass, an alternative interpretation may be possible. The electrons generated at 4.2 °K may then populate some shallow

Can. J. Chem. Downloaded from www.nrcresearchpress.com by 210.87.254.5 on 09/05/12
For personal use only.

Can. J. Chem. Downloaded from www.nrcresearchpress.com by 210.87.254.5 on 09/05/12
For personal use only.

traps. When the temperature is raised to 77 °K, these shallow traps can be irreversibly depopulated as the electrons move to deeper traps. As a matter of fact, Dainton *et al.* (7), Ershov *et al.* (8), and Hase (9) demonstrated, from optical experiments, the irreversible change in the electron environment when the electrons were partially bleached, suggesting the distribution of the trap depths. If this is also the case here, the number of the traps available for the electrons at 4.2 °K should be larger than the number at 77 °K. However, no sign of increase of the trapped electrons yield by irradiation at the lower temperature is observed. Therefore, the irreversible change in the surroundings of the trapped electrons seems to be due to the orientation of the matrix molecules rather than to the migration of the electrons to the deeper traps.

As reported previously (2, 10), the trapped electrons in the irradiated 2-methyltetrahydrofuran glass give the width of 4.4 G when examined at 77 °K. However, a somewhat broader spectrum (ΔH_{ms} = 5.6 G) is observed by both irradiating and measuring at 4.2 °K. Raising the temperature to 77 °K causes a narrowing of the width to 4.4 G, which is in agreement with the width observed with the irradiation at 77 °K. On the other hand, lowering the temperature from 77 °K causes no change of width. Therefore, the change in the width is attributed to the irreversible orientation of the matrix molecules when the molecules acquire their mobility.

When the 3-methylhexane glass is irradiated at 77 °K, the electrons are stably trapped and give rise to spectrum of width 4.0 G. This value agrees with the previously reported one (11). Here too, a larger value of ΔH_{ms}, 4.5 G, is obtained by both irradiating and measuring at 4.2 °K. The variation of width with temperature is qualitatively the same as that for the 2-methyltetrahydrofuran glass.

In contrast to the broadening of the spectrum width for the ethanol glass, narrowing of the width is observed for the 2-methyltetrahydrofuran and 3-methylhexane glasses when the irradiated samples are warmed from 4.2 to 77 °K. This is reasonably interpreted by the bond moment of the matrix molecule; the sign of the bond moment $\overrightarrow{C—H}$ (−0.4 D) is opposite to that of $\overrightarrow{O—H}$ (1.5 D) (see, for example, ref. 12). Hence, the H atoms in the methylene groups tend to depart from the trapped electrons, because of their slight but excess negative charge, resulting in weaker hyperfine interaction and the broader e.s.r. spectra.

According to the results so far mentioned, it is concluded that, not only in non-polar glass but also in polar glass, the electrons liberated from the matrix molecules by ionizing radiations may be trapped with or without molecular orientation. Smith and Pieroni reached a similar conclusion (4). The results also lead to the conclusion that the width of the e.s.r. spectra of the trapped electrons is independent of measuring temperature, after completion of molecular orientation.

Smith and Pieroni suggested that the yield of the trapped electrons was independent of the irradiation temperature (4). In the present investigation, the yield at 4.2 °K was found to be smaller (1/2 ~ 1/3) than that at 77 °K. However, this result should be examined further, before being considered conclusive, because of the experimental difficulties of measuring the absolute intensity of the spectra at 4.2 °K.

The authors express their sincere thanks to Dr. T. Iwai of Ube Industries Ltd. for the use of experimental facilities in FAPIG Laboratory, where a part of the investigation with the irradiation at 4.2 °K was carried out.

1. W. H. Hamill. Radical ions. Kaiser and Kevan (*Editors*). Interscience Publishers Inc., New York. 1968. p. 321. H. Yoshida and K. Hayashi. Advan. Polym. Sci. **6**, 401 (1969). D. R. Smith, F. Okenka, and J. J. Pieroni. Can. J. Chem. **45**, 833 (1967).
2. A. Ekstrom and J. E. Willard. J. Phys. Chem. **72**, 4599 (1968).
3. M. Irie, K. Hayashi, S. Okamura and H. Yoshida. J. Chem. Phys. **48**, 922 (1968).
4. D. R. Smith and J. J. Pieroni. Can. J. Chem. **45**, 2723 (1967).
5. M. Irie, K. Hayashi, S. Okamura, and H. Yoshida. Int. J. Radiat. Phys. Chem. **1**, 279 (1969).
6. H. Yoshida, T. Warashina, Y. Maeda, and T. Higashimura. Rev. Sci. Instrum. **39**, 1967 (1968).
7. E. S. Dainton, G. A. Salmon, and U. F. Zucker. J. Chem. Soc. (C), 1794 (1966).
8. B. G. Ershov, I. E. Makarov, and A. K. Pikaev. High Energy Chem. **1**, 472 (1967).
9. H. Hase. J. Phys. Soc. Jap. **24**, 589 (1968).
10. D. R. Smith and J. J. Pieroni. Can. J. Chem. **43**, 876 (1965).
11. J. Lin, K. Tsuji, and Ff. Williams. J. Amer. Chem. Soc. **90**, 2766 (1968).
12. R. Daudel, R. Lefebvre, and C. Moser. Quantum chemistry. Interscience Publishers Inc., New York. 1959. p. 206.

Kinetics of the reaction of glycine with *N*-ethylmaleimide

JAMES LESLIE
Department of Pharmaceutical Chemistry, School of Pharmacy, University of Maryland, Baltimore, Maryland 21201

Received August 11, 1969

The rate law for the reaction of glycine with *N*-ethylmaleimide (NEM) has been determined to be $-\mathrm{d(NEM)}/\mathrm{d}t = k\mathrm{(NEM)(glycine)}/a_{H^+}$, which is consistent with a rate-controlling reaction of an unprotonated amino group with the *N*-ethylmaleimide. The rate constant, k, has the value 3.7×10^{-11} min^{-1} at 25°.

Canadian Journal of Chemistry, **48**, 507 (1970)

Can. J. Chem. Downloaded from www.nrcresearchpress.com by 210.87.254.40 on 09/05/12
For personal use only.

The reaction of *N*-ethylmaleimide with sulfhydryl compounds is frequently used for the chemical modification of proteins and in the quantitative determination of sulfhydryl groups (1). However, *N*-ethylmaleimide can also react with amino groups and imidazole derivatives (2–6) at a rate which may be comparable to the rate of reaction of this reagent with the sulfhydryl groups in proteins (4). We have been interested in the rate of reaction of *N*-ethylmaleimide with sulfhydryl groups in proteins, and so we examined the kinetics of the reaction of *N*-ethylmaleimide with glycine. We wish to report the results since few quantitative studies have been made on this reaction.

Experimental

The reaction of *N*-ethylmaleimide with glycine, both used as obtained from Nutritional Biochemicals Corporation, was followed by measuring the rate of decrease in absorbance of the maleimide at 300 mμ. All absorbance measurements were made in 1 cm cells at 25 ± 1° in a Beckman DU-2 spectrophotometer with a slit width fixed at 0.5 mm. Measurements of p*H* were made on the reaction mixture using a Beckman Zeromatic p*H* meter fitted with a thin combination electrode and standardized with commercial buffers. Solutions of glycine (in 0.1 *M* phosphate buffer with KCl added to maintain an approximate constant ionic strength) and *N*-ethylmaleimide were mixed in volumetric flasks, diluted to volume with buffer-KCl, and samples transferred to the spectrophotometer cells where the absorbance was measured at appropriate time intervals.

Results and Discussion

In all experiments glycine was present in much higher concentrations than the *N*-ethylmaleimide. Linear plots were obtained when the logarithm of the absorbance of the *N*-ethylmaleimide was plotted vs. time, and the slope of the lines obtained remained constant when the initial concentration of *N*-ethylmaleimide was varied 4-fold, indicating a first-order disappearance of the reagent. The rate constant was calculated from the slopes of the lines. These pseudo first-order rate constants were determined for a series of glycine concentrations and hydrogen ion activities, when it was observed that the first-order rate constant was directly proportional to the glycine concentration and inversely proportional to the hydrogen ion activity. These observations suggest the rate law in eq. [1], in which a_{H^+} is the hydrogen ion activity, and (NEM) is the concentration of

$$[1] \quad -\mathrm{d(NEM)}/\mathrm{d}t = k_2\mathrm{(NEM)(glycine)}/a_{H^+}$$

N-ethylmaleimide. However, in addition to reacting with glycine, *N*-ethylmaleimide undergoes hydrolysis at a rate which may be expressed by eq. [2]. The overall disappearance of *N*-ethylmaleimide is then described by eq. [3]. At

$$[2] \quad -\mathrm{d(NEM)}/\mathrm{d}t = k_3\mathrm{(NEM)}/a_{H^+}$$

$$[3] \quad -\mathrm{d(NEM)}/\mathrm{d}t = k_2\mathrm{(NEM)(glycine)}/a_{H^+} + k_3\mathrm{(NEM)}/a_{H^+}$$

constant glycine concentration and hydrogen ion activity eq. [3] reduces to a first-order rate equation with an observed rate constant k_1. This first-order rate constant is related to the hydrogen ion activity and the glycine concentration by eq. [4]. Interpolation of the data of Gregory (7)

$$[4] \quad k_1 = k_3/a_{H^+} + k_2\mathrm{(glycine)}/a_{H^+}$$

yields a value of 2.0×10^{-11} min^{-1} for k_3. Table 1 shows typical results obtained for the reaction over a range of glycine concentrations and hydrogen ion activities. The constancy of the values for k_2, 36.95 ± 1.36 (standard deviation), shows that eq. [1] describes the kinetics of the reaction of glycine with *N*-ethylmaleimide.

TABLE 1

Rate constants for the reaction of glycine with *N*-ethylmaleimide*

Hydrogen ion activity $a_{H^+} \times 10^7$	Glycine (*M*)	KCl (*M*)	$k_1 \times 10^3$ (min^{-1})	$k_2 \times 10^{10}$ (min^{-1})
1.55	0.16	0.26	3.76	35.2
1.59	0.32	0.13	7.66	37.4
1.59	0.48	—	10.86	35.5
4.47	0.40	—	3.40	37.4
2.04	0.40	—	7.71	38.8
1.12	0.40	—	13.50	37.4

*All measurements were made in 0.1 *M* phosphate. The initial *N*-ethylmaleimide concentration was about 7.5×10^{-4} *M*. Temperature 25 ± 1°.

The observed rate law can be explained by a rate-controlling reaction of the unprotonated amino group with the *N*-ethylmaleimide. The dependency on the hydrogen ion activity is thus explained since this would determine the amount of the amino group present in the unprotonated form. The rate law is consistent with a mechanism in which there is a nucleophilic attack of the amino group on the *N*-ethylmaleimide (2). Analogous reactions would indicate that the product would be *N*-(1-ethyl-2,5-dioxopyrrolidine-3-yl)glycine (4), although in this work the product was not isolated and identified.

The rate constants were determined for glycine but it is unlikely that the amino groups of other amino acids would differ greatly from the value observed for glycine. This was not determined in the present work but it is indicated by the less quantitative studies of Riggs (8) which showed that histidine, valine, serine, and glycine reacted with *N*-ethylmaleimide at similar rates. However, constants cannot be calculated from his data as presented. At p*H* 7 and 0.1 *M* glycine one can calculate a rate constant of 3.7×10^{-3} min^{-1} for the disappearance of *N*-ethylmaleimide, whereas it would be 9.2×10^5 min^{-1} under similar conditions for the reaction with the sulfhydryl group of cysteine (9).

1. J. L. WEBB. Enzyme and metabolic inhibitors. Vol. III. Academic Press, New York, 1966. p. 337.
2. D. G. SMYTH, A. NAGAMATSU, and J. S. FRUTON. J. Amer. Chem. Soc. **82**, 4600 (1960).
3. C. F. BREWER and J. P. RIEHM. Anal. Biochem. **18**, 248 (1967).
4. D. G. SMYTH, O. O. BLUMENFELD, and W. H. KONIGSBERG. Biochem. J. **91**, 589 (1964).
5. D. G. SMYTH and D. F. ELLIOTT. Analyst **89**, 81 (1964).
6. G. GUIDOTTI and W. KONIGSBERG. J. Biol. Chem. **239**, 1474 (1964).
7. J. D. GREGORY. J. Amer. Chem. Soc. **77**, 3922 (1955).
8. A. RIGGS. J. Biol. Chem. **236**, 1948 (1961).
9. G. GORIN, P. A. MARTIC, and G. DOUGHTY. Arch. Biochem. Biophys. **115**, 593 (1966).

Photoreaction of nitroso compounds in solution.[1] XIII. Photo-oxidation of alkyl nitrites

Y. L. CHOW, T. HAYASAKA, AND J. N. S. TAM
Department of Chemistry, Simon Fraser University, Burnaby 2, British Columbia

Received August 14, 1969

Photolysis of 1-pentyl and menthyl nitrites in the presence of oxygen were shown to give mainly the oxidized *rearrangement* products 4-nitratopentyl and 10-nitratomenthyl derivatives in disagreement with the published report (2). Under the photo-oxidation conditions, menthyl nitrite also gave 10-nitrosomenthyl derivatives which were also shown to be photo-oxidized to 10-nitratomenthyl derivatives. The photo-oxidation products were conveniently reduced to the corresponding diols and were, in turn, identified as bisbenzoate.

Canadian Journal of Chemistry, **48**, 508 (1970)

It has been reported that photolysis of 1-octyl nitrite in the presence of oxygen gave 1-octyl nitrate as the major product but no rearranged product such as the dimer of 4-nitrosooctanol or the oxidation product therefrom (2). The report implies that bimolecular oxidation processes leading to 1-octyl nitrate are far faster (by 100 times at minimum) than the intramolecular hydrogen-nitroso group exchange reaction (3) which is the major reaction in the absence of oxygen. In contrast we have demonstrated (1)

[1]For the preceding paper (Part XII) in this series, see ref. 1.

Can. J. Chem. Downloaded from www.nrcresearchpress.com by 210.87.254.40 on 09/05/12
For personal use only.

TABLE 1

Rate constants for the reaction of glycine with *N*-ethylmaleimide*

Hydrogen ion activity $a_{H^+} \times 10^7$	Glycine (*M*)	KCl (*M*)	$k_1 \times 10^3$ (min^{-1})	$k_2 \times 10^{10}$ (min^{-1})
1.55	0.16	0.26	3.76	35.2
1.59	0.32	0.13	7.66	37.4
1.59	0.48	—	10.86	35.5
4.47	0.40	—	3.40	37.4
2.04	0.40	—	7.71	38.8
1.12	0.40	—	13.50	37.4

*All measurements were made in 0.1 *M* phosphate. The initial *N*-ethylmaleimide concentration was about 7.5×10^{-4} *M*. Temperature 25 ± 1°.

The observed rate law can be explained by a rate-controlling reaction of the unprotonated amino group with the *N*-ethylmaleimide. The dependency on the hydrogen ion activity is thus explained since this would determine the amount of the amino group present in the unprotonated form. The rate law is consistent with a mechanism in which there is a nucleophilic attack of the amino group on the *N*-ethylmaleimide (2). Analogous reactions would indicate that the product would be *N*-(1-ethyl-2,5-dioxopyrrolidine-3-yl)glycine (4), although in this work the product was not isolated and identified.

The rate constants were determined for glycine but it is unlikely that the amino groups of other amino acids would differ greatly from the value observed for glycine. This was not determined in the present work but it is indicated by the less quantitative studies of Riggs (8) which showed that histidine, valine, serine, and glycine reacted with *N*-ethylmaleimide at similar rates. However, constants cannot be calculated from his data as presented. At p*H* 7 and 0.1 *M* glycine one can calculate a rate constant of 3.7×10^{-3} min^{-1} for the disappearance of *N*-ethylmaleimide, whereas it would be 9.2×10^5 min^{-1} under similar conditions for the reaction with the sulfhydryl group of cysteine (9).

1. J. L. WEBB. Enzyme and metabolic inhibitors. Vol. III. Academic Press, New York, 1966. p. 337.
2. D. G. SMYTH, A. NAGAMATSU, and J. S. FRUTON. J. Amer. Chem. Soc. **82**, 4600 (1960).
3. C. F. BREWER and J. P. RIEHM. Anal. Biochem. **18**, 248 (1967).
4. D. G. SMYTH, O. O. BLUMENFELD, and W. H. KONIGSBERG. Biochem. J. **91**, 589 (1964).
5. D. G. SMYTH and D. F. ELLIOTT. Analyst **89**, 81 (1964).
6. G. GUIDOTTI and W. KONIGSBERG. J. Biol. Chem. **239**, 1474 (1964).
7. J. D. GREGORY. J. Amer. Chem. Soc. **77**, 3922 (1955).
8. A. RIGGS. J. Biol. Chem. **236**, 1948 (1961).
9. G. GORIN, P. A. MARTIC, and G. DOUGHTY. Arch. Biochem. Biophys. **115**, 593 (1966).

Photoreaction of nitroso compounds in solution.[1] XIII. Photo-oxidation of alkyl nitrites

Y. L. CHOW, T. HAYASAKA, AND J. N. S. TAM
Department of Chemistry, Simon Fraser University, Burnaby 2, British Columbia

Received August 14, 1969

Photolysis of 1-pentyl and menthyl nitrites in the presence of oxygen were shown to give mainly the oxidized *rearrangement* products 4-nitratopentyl and 10-nitratomenthyl derivatives in disagreement with the published report (2). Under the photo-oxidation conditions, menthyl nitrite also gave 10-nitrosomenthyl derivatives which were also shown to be photo-oxidized to 10-nitratomenthyl derivatives. The photo-oxidation products were conveniently reduced to the corresponding diols and were, in turn, identified as bisbenzoate.

Canadian Journal of Chemistry, **48**, 508 (1970)

It has been reported that photolysis of 1-octyl nitrite in the presence of oxygen gave 1-octyl nitrate as the major product but no rearranged product such as the dimer of 4-nitrosooctanol or the oxidation product therefrom (2). The report implies that bimolecular oxidation processes leading to 1-octyl nitrate are far faster (by 100 times at minimum) than the intramolecular hydrogen-nitroso group exchange reaction (3) which is the major reaction in the absence of oxygen. In contrast we have demonstrated (1)

[1]For the preceding paper (Part XII) in this series, see ref. 1.

Can. J. Chem. Downloaded from www.nrcresearchpress.com by 210.87.254.105 on 09/05/12
For personal use only.

Can. J. Chem. Downloaded from www.nrcresearchpress.com by 210.87.254.105 on 09/05/12
For personal use only.

that the intramolecular hydrogen-nitroso group exchange reaction is much faster than oxidation processes in the photo-oxidation of *N*-nitroso-*N*-hexylacetamide yielding 4-nitratohexylacetamide in good yield. It has been well established that, in both photoreactions in the absence of oxygen, the formations of alkoxy and amido radicals are the primary step followed by an intramolecular hydrogen transfer (3, 4). As there was very little reason to believe that the hydrogen transfer to an alkoxy radical should be slower than that to an amido radical, photolyses of 1-pentyl and menthyl nitrites (**1***a*, *b*) in the presence of oxygen were therefore investigated.

In the presence of oxygen, 1-pentyl nitrite (**1***a*) was slowly photolyzed to a mixture showing strong absorption for a nitrate group (1620, 1280, and 870 cm^{-1}). The major part of the product consisted of highly polar compounds and could not be separated on a silicic acid column. Less polar fractions were, however, partially separated to give semi-pure 1,4-pentandiol dinitrate (**2**, 9.5%), 4-nitratopentanal (**3**, 5.5%), and 4-nitratopentanol (**4**, 12.5%). Due to the instability of these oily nitrates, attempted purification by various methods failed. The nuclear magnetic resonance (n.m.r.) spectra, however, show the terminal methyl signals as doublets indicating that the nitrate group is located at C-4 in **2**, **3**, and **4**. The crude photolysate was therefore reduced with lithium aluminum hydride and benzoylated to give pentan-1,4-diol bisbenzoate (**5**).

Photolysis of menthyl nitrite (**1***b*) under the same conditions turned out to be less amenable giving a complex mixture probably due to formation of stereoisomers. Only 10-nitratomenthone (**6**) could be obtained after extensive purification of less polar fractions. Reduction with lithium aluminum hydride of the crude product and subsequent benzoylation gave 10-benzoyloxymenthyl benzoate (**7**) and 10-benzamidomenthyl benzoate (**8**) in addition to two impure fractions. The last two impure fractions are assumed to be epimers of **7** since the infrared (i.r.), n.m.r., and mass spectra are very similar to those of **7**. The isolation of **6**–**8** clearly demonstrated that the 10-methyl group had been functionalized as the nitrosomethyl (—CH_2NO) and nitratomethyl (—CH_2ONO_2) group as the result of the photolysis. It should be pointed out that the 10-hydrogen atom nitroso (or nitrato) group exchange reaction in **1***b* could lead to two epimers, the preference of which is *a priori* not predictable since the nature of the transition state of hydrogen transfer is not precisely known (3, 5). The stereochemistry of **6**, **7**, and **8** is therefore unknown.

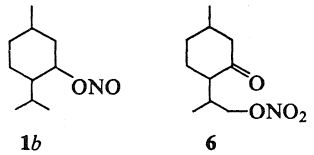

1*b* **6**

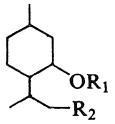

7 R_1 = C_6H_5CO—; R_2 = $C_6H_5CO_2$—
8 R_1 = C_6H_5CO—; R_2 = C_6H_5CONH—

The results prove that alkoxy radicals, as generated in the photolysis, also readily undergo 1,5-hydrogen transfer to give a *C*-radical prior to oxidation processes. It is well known that nitric oxide is readily oxidized to nitrogen oxides of higher oxidation levels. Radical recombination of a *C*-radical with nitric oxide and $\cdot NO_3$ leads to a *C*-nitroso compound (such as **9**) and a nitrate (such as **10**). These results are in agreement with the results observed in the photolysis of nitrosamides. The formation of oxidation products **3** and **6** could be due to ozone generated during photolysis of nitrites (6).

Thus the photolyses produce not only the 4-nitrato compound **10** but also the 4-nitroso compound **9** as can be seen by the isolation of benzamido derivative **8**, although the corresponding amide is not isolated in the photolysis of 1-pentyl nitrite. A *C*-nitroso compound is generally in equilibrium with the corresponding dimer (7) and photolabile when irradiated in Pyrex apparatus (8, 9). In analogy to the photooxidation of 4-nitrosohexylacetamide (1), **9** is expected to be transformed to **10** efficiently under the photolysis conditions. This is proven in the following manner. When **1***b* was photolyzed with

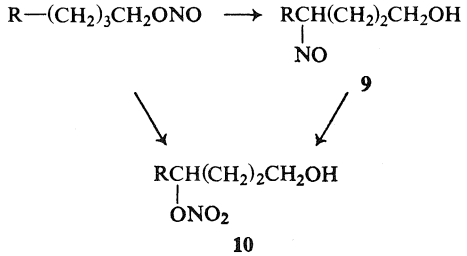

10

Can. J. Chem. Downloaded from www.nrcresearchpress.com by 210.87.254.105 on 09/05/12
For personal use only.

a light source of > 330 mμ under nitrogen, intense absorption at 295 mμ emerged rapidly as the nitrite absorption at 340 mμ faded away. The former peak corresponds to well established absorption of a nitroso dimer (7, 8). The crude product showed no nitrate i.r. absorption but did show a strong 1180 cm^{-1} band typical of *trans*-dimer (6, 7) of *C*-nitroso compound **9**. On further irradiation of the crude product with a light source of > 280 mμ under oxygen atmosphere, the ultraviolet (u.v.) absorption at 295 mμ disappeared. The crude product showed intense nitrate i.r. absorption and was worked up in the same way to afford **6** and **7**.

Experimental

Infrared spectra were determined as liquid films or nujol mulls. The n.m.r. spectra were determined with a Varian A-56/60 spectrometer in CCl_4 with internal TMS reference. Mass spectra were determined at 80 eV on a heated inlet with Hitachi RMU-6E. The microanalyses were made by Dr. A. Bernhardt, West Germany.

Synthesis of Nitrites

1-Pentyl nitrite was prepared from 1-pentanol according to known procedures (10). The yellow oil was distilled at 18°/12 mm; i.r. 1640, 1460, 1050, 980, and 800 cm^{-1}; n.m.r. τ 9.1 (3H, t, J = 6 Hz), 8.57 (6H), and 5.33 (2H, m). A solution of *l*-menthol (m.p. 40–43°) in pyridine was treated with nitrosyl chloride (11) to give an oil which was chromatographed on a silicic acid column to give oily menthyl nitrite; i.r. 1635, 1450, 800, and 765 cm^{-1}; n.m.r. τ 4.90 (1H, m).

Photolysis of 1-Pentyl Nitrite

(*A*) A solution of 1-pentyl nitrite (2.2 g) in benzene (100 ml) was placed in a flat-bottom flask (Pyrex) and irradiated with a G. E. Par 38 lamp for 12 h. A slow stream of oxygen was introduced during the irradiation. The progress of the reaction was followed by monitoring the decrease of the nitrite absorption at 371, 357, 345, and 333 mμ. Evaporation of benzene gave an oil showing i.r. absorption at 1730 (m), 1620, 1280, and 870 cm^{-1}. The oil was chromatographed on a silicic acid column to give the following fractions. With pure chloroform, the first fraction contains 1,4-pentanediol dinitrate (**2**, 350 mg) slightly contaminated with 4-nitratopentanal (**3**, 150 mg), and the second fraction contains nearly pure **3**. Preparative thin-layer chromatography (t.l.c.) separation did not effect an analytically pure sample. The impure dinitrate **2** shows i.r. 1620, 1280, and 870 cm^{-1}; n.m.r. τ 4.83 (1H, m), 5.55 (2H, m), 8.56 and 8.61 (3H, two sets of d, J = 6 Hz); *m/e* (at 15 eV) 147, 132, 115, 101, 86, and 85. The pentanal **3** shows i.r. 2740, 1730, 1620, 1280, and 870 cm^{-1}; n.m.r. τ 8.64 (3H, d, J = 6 Hz), 7.97 (2H, m), 7.47 (2H, m), 4.91 (1H, m), and 0.33 (1H, t, J = 1.5 Hz).

A mixture of chloroform–methanol (95:5) elutes a fraction (1.14 g), a part of which (500 mg) was separated by preparative t.l.c. to give the major component, 4-nitratopentanol, (**4**, 347 mg); i.r. 3400, 1620, 1275, 1060, 1010, and 865 cm^{-1}; n.m.r. τ 8.7 (3H, d, J = 7 Hz), 6.50 (2H, m), 4.95 (1H, m); *m/e*, 132, 115, 101, and 85.

A 2,4-DNPH derivative of pentanal **3** was prepared but could not be purified by chromatography or recrystallization. The best 2,4-DNPH derivative has m.p. 85–90°; n.m.r. τ 4.81 (1H, sextet, J = 6 Hz), 7.45 (2H), 7.90 (2H), 8.52 (3H, d, J = 6.5 Hz), 2.49 (1H, t, J = 4 Hz); *m/e* (direct insertion) 327, 281, 265, 167, and 182.

(*B*) The crude photolysate (500 mg) was stirred with lithium aluminum hydride (600 mg) in anhydrous ether overnight. A sodium hydroxide solution (10%) was added to decompose the reaction mixture. The crude product (150 mg) shows no nitrate absorption. This oil was treated with benzoyl chloride in pyridine. The benzoylation product was chromatographed on a basic alumina column twice to afford 1-pentyl benzoate (80 mg) and 1,4-pentandiol bisbenzoate (**5**, 80 mg). Bisbenzoate **5** was distilled to afford an analytical sample; i.r. 1720, 1280, and 1100 cm^{-1}; n.m.r. τ 8.62 (3H, d, J = 6 Hz), 8.13 (4H), 5.65 (2H), and 4.81 (1H); *m/e* 312, 227, 207, 190, 149, 105, and 85.

Anal. Calcd. for $C_{19}H_{20}O_4$: C, 73.06; H, 6.45. Found: C, 73.15; H, 6.22.

*Photolysis of Menthyl Nitrite (**1b**)*

(*A*) The photolysis of **1***b* (1.5 g) was carried out in the same manner as above except that air was substituted for oxygen. The crude product showed i.r. absorption at 1710 (weak), 1630, 1280, and 870 cm^{-1} and a long streak on a t.l.c. plate. Chromatography of the crude product on a silicic acid column did not afford any separation except the first fraction (150 mg) eluted with pure chloroform. This fraction was purified by preparative t.l.c. to give 10-nitratomenthone (**6**, 75 mg); i.r. 1710, 1625, 1280, and 870 cm^{-1}; n.m.r. τ 5.20 (2H, m), 9.1 (6H, m); *m/e* 169, 153, 139, 127, 112, and 98.

The crude product (1.5 g) was reduced with lithium aluminum hydride followed by benzoylation. Alumina chromatography of the crude material gave fractions containing (*i*) menthyl benzoate (186 mg), (*ii*) bisbenzoate **7** (656 mg), and (*iii*) other (700 mg). The first fraction was shown to be identical by t.l.c., i.r., and n.m.r. spectra with an authentic menthyl benzoate. The second fraction was further purified by preparative t.l.c. to give 10-benzoyloxymenthyl benzoate **7** as a thick resin; i.r. 1730, 1600, 1270, and 1120 cm^{-1}; n.m.r. τ 2.07 (4H), 2.65 (6H), 5.05 (1H), 5.84 (2H, AB part of ABX system), 9.03 (3H, J = 5 Hz) and 9.08 (3H, J = 7 Hz); *m/e* 275, 258, 244, 169, 153, 138, 124, 119, 105, and 95.

Anal. Calcd. for $C_{24}H_{28}O_4$: C, 75.76; H, 7.42. Found: C, 75.48; H, 7.35.

The third fraction was rechromatographed (silicic acid) to afford more bisbenzoate **7** and two fractions (340 mg) both of which showed very similar i.r. and n.m.r. spectral patterns but different t.l.c. behaviors from those of **7**. Both fractions were oil and decomposed on vacuum distillation. The fraction (230 mg) eluted with benzene–ethyl acetate (9:1) was further purified by preparative t.l.c. to give crystalline 10-benzamidomenthol benzoate **8**; m.p. 162–163°; i.r. 3340, 1710, 1640, 1535, and 1275 cm^{-1}; n.m.r. τ 2.1 (2H), 2.36 (2H), 2.65 (6H), 5.12 (1H, m), 6.70 (2H, broad d, J = 6.5); *m/e* 379, 274, 257, 186, 174, 162, 161 (100%), 134, 122.

Anal. Calcd. for $C_{24}H_{29}NO_3$: C, 75.96; H, 7.70; N, 3.69. Found: C, 75.77; H, 7.64; N, 3.51.

(*B*) Menthyl nitrite (1.5 g) was photolyzed in the same manner except that purified nitrogen was substituted for oxygen and the light was filtered through a 0.01% solution of 2,7-dimethyl-3,6-diazacyclohepta-1,6-diene perchlorate. This filter solution cuts off the incident light below 330 mμ. After 6.5 h, the absorption in the 375 mμ region decreased to nil but very intense absorption appeared at 295 mμ which tailed to 330 mμ. The crude product shows 7 major spots on a t.l.c. plate. Small amounts of menthol (132 mg) and menthone (35 mg) were removed by alumina chromatography. Other components could not be separated by repeated chromatography.

The same photolysis was repeated as above. When the nitrite had disappeared, the photolysate was further irradiated under condition *A* until the u.v. absorption at 295 mμ had disappeared. The reaction mixture was worked up in a manner similar to that of *A* to afford menthyl benzoate (150 mg) and bisbenzoate **7** (980 mg).

We are grateful to the Defence Research Board and the National Research Council of Canada for generous support of this project.

1. Y. L. Chow and J. N. S. Tam. Chem. Commun. 747 (1969).
2. P. Kabasakalian and E. R. Townley. J. Amer. Chem. Soc. **84**, 2711 (1962).
3. M. Akhtar. *In* Advances in photochemistry. Vol. II. W. A. Noyes, Jr., G. S. Hammond, and J. N. Pitts, Jr., Editors. Interscience Publishers, New York, N.Y., 1963. p. 263.
4. Y. L. Chow, J. N. S. Tam, and A. C. H. Lee. Can. J. Chem. **47**, 2441 (1969).
5. C. Walling and A. Padwa. J. Amer. Chem. Soc. **85**, 1959 (1963).
6. P. L. Hanst and J. G. Calvert. J. Phys. Chem. **63**, 2071 (1959).
7. B. G. Gowenlock and W. Lüttke. Quart. Rev. **12**, 321 (1958).
8. A. Mackor, Th. A. J. W. Wajer, and Th. J. de Boer. Tetrahedron Lett. 2757 (1967).
9. A. Mackor, Th. A. J. W. Wajer, and Th. J. de Boer. Tetrahedron, **24**, 1623 (1968).
10. L. Hunter, and J. A. Marriott. J. Chem. Soc. 285 (1936).
11. D. H. R. Barton, J. M. Beaton, L. E. Geller, and M. M. Pechet. J. Amer. Chem. Soc. **82**, 2640 (1960).

Erratum: Structure of didehydrochelidonine

M. H. Benn and R. E. Mitchell
Department of Chemistry, The University, Calgary 44, Alberta

Received November 14, 1969

(Ref.: Can. J. Chem. **47**, 3701 (1969))

Canadian Journal of Chemistry, **48**, 511 (1970)

On page 3703, in footnote 5, an R_f is given as 0.41.
This line should read "... respectively 0.57 and 0.14 in methanol–benzene (5:95, v/v), ..."

Can. J. Chem. Downloaded from www.nrcresearchpress.com by 210.87.254.105 on 09/05/12
For personal use only.

Can. J. Chem. Downloaded from www.nrcresearchpress.com by 210.87.254.40 on 09/05/12
For personal use only.

Variation of the nuclear Overhauser effect in dimethylformamide with temperature

J. K. SAUNDERS AND R. A. BELL
Department of Chemistry, McMaster University, Hamilton, Ontario

Received November 20, 1969

The nuclear Overhauser effects at the formyl proton of dimethylformamide have been measured at and above room temperature. At 90° separate irradiation of the high field and low field methyl signals results in equal nuclear Overhauser effects from both methyls.

Canadian Journal of Chemistry, **48**, 512 (1970)

The intramolecular nuclear Overhauser effect (n.O.e.) has been used with telling results in nuclear magnetic resonance (n.m.r.) spectral assignments and in molecular structure determinations (1). The power of the method lies in its ability to locate spatially proximate nuclei in a molecule and, to date, the majority of studies have been concerned with substrates of fairly rigid structure. A limited number of n.O.e. have been observed in conformationally mobile groups such as aromatic methoxy ethers (2) and comment has been made on the conformational preferences of some mononucleotides (3) and vitamin D (4). However, no study has yet been reported on the temperature dependence of the n.O.e. in a simple conformationally mobile molecule. We report here the variation with temperature of the n.O.e. observed in dimethylformamide (DMF).

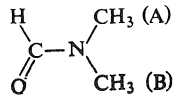

The n.O.e. results obtained for a 2.5% solution of DMF in dimethylsulfoxide-d_6 are shown in Table 1. Saturation of the low field methyl absorption (assigned site A adjacent to the formyl proton (5)) shows an essentially constant n.O.e. of 28% for the formyl proton from 30 to 90°. However, the high field methyl absorption (assigned site B) shows an n.O.e. varying from almost zero (0–3%) at 31° to 28% at 90°. Most significantly, the temperature at which the two methyl groups show identical n.O.e. is far below the coalescence temperature of the two lines and their absorptions are still 15.5 Hz apart (at 100 MHz). The reason for this, of course, lies in the differing time scales of the n.O.e. and coalescence phenomena. In the n.O.e. case the time scale is based on the relaxation time T_1 of the methyl groups whereas in the case of coalescence the time scale is formed by the frequency difference of the two methyl absorptions.

TABLE 1
Variable temperature nuclear Overhauser effects in dimethylformamide

	Nuclear Overhauser effect of formyl proton (%)†	
Temperature*	Irradiate CH_3(A)	Irradiate CH_3(B)
31	28	3
40	—	6
50	28	9
55	—	13
60	28	18
70	28	24
80	28	26
90	28	27–28

*$T = \pm 3°$.
†The n.O.e. = ±1%.

The temperature variation of the n.O.e. on irradiation of the high field absorption is a result of transfer of spin saturation by the methyl group at site B to site A as the rate of rotation about the C—N bond changes. Low rotation rates (room temperature or lower) cause no effective transfer of saturation whereas higher rotation rates cause an increasingly efficient transfer of saturation. The general process of transfer of spin saturation amongst different chemical sites, which may be either intramolecular or intermolecular, can be examined by measurements of a transient

response (6) or a steady-state response (7); the latter being followed in the present work. A quantitative study of the n.O.e. variation requires a knowledge of both rotation rates about the C—N bond and methyl group relaxation times and will be developed in the full paper.

The consequence of the present results is exceedingly important when n.O.e. data is being applied to conformational and structural studies on unknown substrates. Clearly, the mere occurrence of an n.O.e. in an unknown substrate is not sufficient evidence for the time independent spatial proximity of two nuclei. Neither can the existence of such an n.O.e., measured at a single temperature, in a known or suspected, conformationally mobile system be taken as sufficient evidence to infer a *conformational preference*. The sole inference which may be made from single temperature n.O.e. data is that two nuclei (or groups of nuclei) can be located in each other's neighborhood for some period of time. The extent of this time period for which an n.O.e. will be observable will be dependent on the relaxation times of the irradiated nuclei. Therefore, to be more exact in structural deductions additional information is required which may be provided by variable temperature n.O.e. measurements or by some alternative physical measurement.

The magnitude of the n.O.e. in DMF observed in this study (28%) is significantly greater than the previously published report (1*a*) of 18% obtained for DMF in D_2O solution. The reason for this discrepancy is not entirely clear and we have therefore remeasured the n.O.e. of a very carefully degassed, 2.6% solution of DMF in 99.7% D_2O containing 3% DSS as an internal lock. At 31°, the low field methyl gives rise to a 27% n.O.e. at the formyl hydrogen which is consistent with the value found in DMSO-d_6 solution. It is of interest to note that both D_2O and DMSO are behaving as magnetically inert solvents and also that DMF is monomeric in both solvents (5*b*).

We wish to thank the National Research Council of Canada for generous financial assistance and for the award of a Fellowship to J. K. Saunders.

1. (*a*) F. A. L. Anet and A. R. J. Bourn. J. Amer. Chem. Soc. **87**, 5250 (1965); (*b*) K. Tori, M. Ohtsuru, I. Horibe, and K. Takeda. Chem. Commun. 943 (1968); (*c*) D. J. Aberhart, K. H. Overton, and S. Hunek. Chem. Commun. 162 (1969); (*d*) T. Tomimatsu, H. Hashimoto, T. Shingu, and K. Tori. Chem. Commun. 551 (1969); (*e*) G. R. Newkome and N. S. Bhacca. Chem. Commun. 385 (1969); (*f*) R. A. Bell and M. B. Gravestock. Can. J. Chem. **47**, 3661 (1969) and references cited therein.
2. J. K. Saunders, R. A. Bell, C.-Y. Chen, D. B. MacLean, and R. H. F. Manske. Can. J. Chem. **46**, 2876 (1968); E. L. Eliel and F. Nader. J. Amer. Chem. Soc. **91**, 536 (1969); M. C. Woods, S. Ebine, M. Hoshino, K. Takahashi, and I. Miura. Tetrahedron Lett. 2879 (1969); J. Lugtenburg and E. Havinga. Tetrahedron Lett. 1505 (1969).
3. P. A. Hart and J. P. Davis. J. Amer. Chem. Soc. **91**, 512 (1969); P. A. Hart and J. P. Davis. Biochem. Biophys. Res. Commun. **34**, 733 (1969).
4. J. Lugtenburg and E. Havinga. Tetrahedron Lett. 2391 (1969).
5. (*a*) B. B. Wayland, R. S. Drago, and H. F. Henneike. J. Amer. Chem. Soc. **88**, 2455 (1966); (*b*) M. Rabinovitz and A. Pines. J. Amer. Chem. Soc. **91**, 1585 (1969).
6. R. A. Hoffman and S. Forsén. J. Chem. Phys. **45**, 2049 (1966); F. A. L. Anet and A. R. J. Bourn. J. Amer. Chem. Soc. **89**, 760 (1967).
7. B. M. Fung. J. Chem. Phys. **49**, 2973 (1968); B. M. Fung and R. D. Stolow. Chem. Commun. 257 (1967).

Can. J. Chem. Downloaded from www.nrcresearchpress.com by 210.87.254.40 on 09/05/12
For personal use only.

Canadian Journal of Chemistry

Published by THE NATIONAL RESEARCH COUNCIL OF CANADA

VOLUME 48 FEBRUARY 15, 1970 NUMBER 4

Can. J. Chem. Downloaded from www.nrcresearchpress.com by 210.87.254.6 on 09/05/12
For personal use only.

Molecular motion in solid complexes of trimethylamine with boron trihalides and borane

C. T. YIM AND D. F. R. GILSON

Department of Chemistry, McGill University, Montreal, Quebec

Received October 14, 1969

Wide line nuclear magnetic resonance studies of trimethylamine complexes of BF_3, BCl_3, BBr_3, and BH_3 show that rotation of methyl groups and rotation about the B—N axes occur in the solid phases. The complex between ammonia and boron trifluoride has also been studied.

Canadian Journal of Chemistry, **48**, 515 (1970)

Introduction

Crystals of highly symmetrical molecules often undergo solid–solid phase transitions which are associated with changes in molecular rotational freedom. The application of nuclear magnetic resonance (n.m.r.) methods to the study of rotational motions of such molecules was first reported by Powles and Gutowsky (1), for a series of tetrasubstituted methanes. They observed that rotation of methyl groups about their C_3 axes, a more complex internal motion, isotropic rotation, and finally lattice diffusion could occur with increasing temperature. More recently the series $M(CH_3)_4$, where M = Si, Ge, Sn, and Pb, has been studied by Smith (2). Methyl group rotation occurred below 77 °K in all four cases but general molecular reorientation occurred for only the silicon and germanium compounds. The tetramethylammonium ion rotates isotropically in the bromide salt about 300 °K but line width and second moment data were not reported for temperatures below 120 °K (3). In tetramethylammonium chloride and iodide (4), isotropic rotation leads to line width and second moment transitions over the temperature ranges 265–300 and 210–250 °K, respectively. The resonances became very easily saturated at lower temperatures and this prevented further studies. The transition temperatures for methyl group rotation are not known for this series of compounds.

This paper reports wide line n.m.r. studies on solid complexes of the type $(CH_3)_3N.BX_3$, where X = F, Cl, Br, and H. These compounds possess high dipole moments and deviate from "spherical" shape as X changes from H to Br. A study of the solid ammonia – boron trifluoride complex is also reported.

Experimental

Proton and fluorine resonances were measured using a Varian DP60 Spectrometer operating at 56.4 MHz for both nuclei. Second moment calculations were performed on an IBM360/75 using programs written in this laboratory. Complexes were prepared by standard methods (5).

Results and Discussion

Trimethylamine – Boron Trifluoride Complex

The experimental line widths and second moments are plotted vs. temperature in Fig. 1. The proton second moment decreases sharply from 18.0 G^2 at 77 °K to about 8.0 G^2 at 110 °K, followed by a slower decrease to 2.2 G^2 at 160 °K. It is evident that two partially overlapping transitions are involved. Over the same temperature range the fluorine second moment decreases from 7.4 to 3.2 G^2. Above 160 °K both the fluorine and the proton second moments remain constant up to the melting point. The results are in general agreement with those of Dunell *et al.* (6) except that no evidence was found for the premelting transition at 390 °K.

The trimethylamine – boron trifluoride complex crystallizes with a rhombohedral unit cell, one molecule per unit cell, and the crystallog-

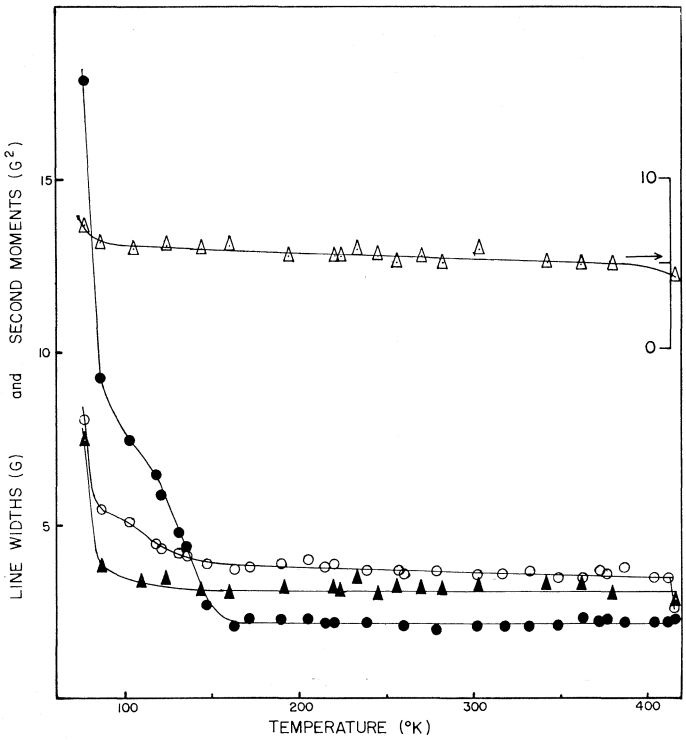

FIG. 1. The temperature dependence of the line widths (open symbols) and second moments (solid symbols) of the proton (circles) and fluorine resonances (triangles) of the trimethylamine – boron trifluoride complex, left hand scale applied to upper curve only.

raphic positions of all the nuclei except hydrogen have been determined (7). In order to calculate a rigid lattice second moment it is necessary to know the proton positions. If the methyl group protons are situated in symmetrical positions in the rigid molecule there are only two possible orientations of the methyl groups consistent with C_{3v} symmetry (it is assumed here that no change occurs in crystal structure at low temperature). One of the possible orientations can be eliminated since it requires a distance between adjacent protons of different methyl groups of less than the sum of the van der Waals radii. The theoretical proton and fluorine second moments for the other configuration were computed for the rigid structure and for different modes of reorientation and are given in Table 1. The calculated values for a motion in which the methyl groups and the BF_3 group reorient about their threefold axes and the whole molecule rotates about the B—N axis are 2.5 and 3.4 G^2 for proton and fluorine, respectively. These values are in excellent agreement with the experimental second moments above 160 °K, 2.2 G^2 (^1H) and 3.2 G^2 (^{19}F).

The comparison between theoretical and experimental second moments reveals the nature of the two transitions below 150 °K; the higher temperature transition involves a rotation about the B—N axis and the low temperature transition is associated with the methyl group rotation. The latter is not complete at 77 °K. In the neighborhood of 77 °K, the fluorine second moment shows a sharp upward trend due to the cessation of the BF_3 rotation.

Trimethylamine – Boron Trichloride and Tribromide Complexes

The temperature dependence of the proton second moments and line widths of the complexes of boron trichloride and tribromide are shown in Figs. 2 and 3. The behavior is similar in both complexes. As the temperature is increased from

Can. J. Chem. Downloaded from www.nrcresearchpress.com by 210.87.254.6 on 09/05/12
For personal use only.

TABLE 1

Calculated second moments for the trimethylamine – boron trifluoride complex

Group			Second moment (G^2)		
CH_3	$(CH_3)_3N$	BF_3	Intramolecular	Intermolecular	Total
^1H resonance					
Static	Static	Static	25.9	6.1	32.0
Rotating	Static	Static	7.4	3.1	10.5
Rotating	Static	Rotating	7.3	2.9	10.2
Rotating	Rotating	Static	1.3	1.3	2.6
Rotating	Rotating	Rotating	1.3	1.2	2.5
	Isotropic		0	1.1	1.1
^{19}F resonance					
Static	Static	Static	21.9	4.0	25.9
Rotating	Static	Static	16.2	2.6	18.8
Rotating	Static	Rotating	3.0	1.6	4.6
Rotating	Rotating	Static	15.3	1.5	16.8
Rotating	Rotating	Rotating	2.4	1.1	3.4
	Isotropic		0	0.7	0.7

77 °K, the second moments decrease rapidly and reach a plateau value of about 7.6 G^2. At higher temperatures, around 210 °K for $(CH_3)_3NBCl_3$ and 230 °K for $(CH_3)_3NBBr_3$, a second transition reduces the proton second moments to 1.25 G^2, after which the second moments remain constant. Measurements above 200 °C were not made because the samples showed discoloration on prolonged heating in the n.m.r. probe.

The detailed crystal structures of these complexes have not been reported, and estimates of the theoretical second moments, Table 2, were based on the values for the boron trifluoride complex. The experimental second moments at about 300 °K lie between the values calculated for isotropic rotation and simultaneous rotation of the CH_3 groups about their C—N axes and the $(CH_3)_3N$ group about the B—N axis. The latter mode is the preferred explanation in view of the conclusions drawn for the boron tri-

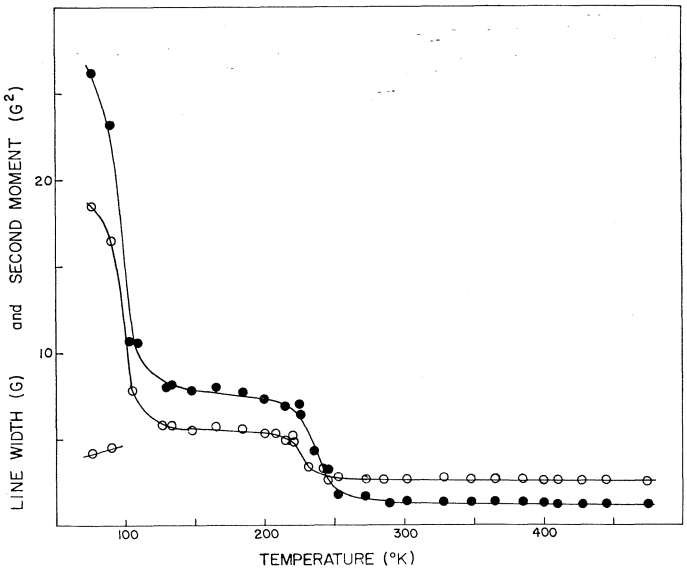

FIG. 2. Line width (open circles) and second moments (solid circles) of proton resonance of the trimethylamine – boron trichloride complex as a function of temperature.

Can. J. Chem. Downloaded from www.nrcresearchpress.com by 210.87.254.6 on 09/05/12
For personal use only.

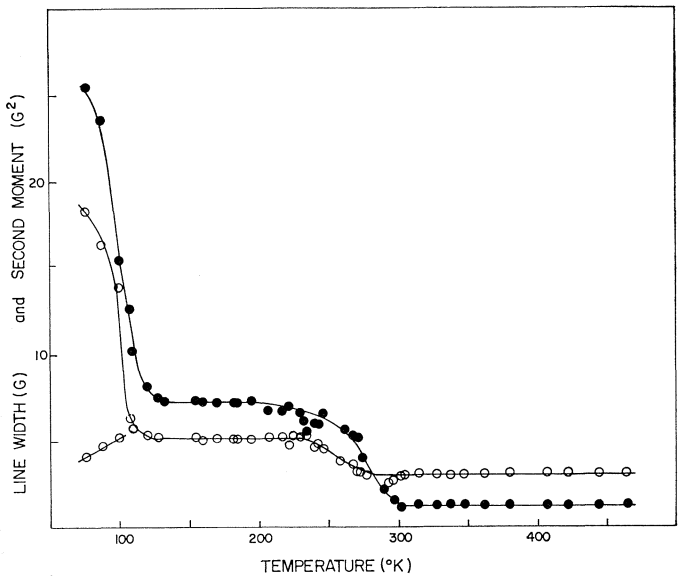

FIG. 3. Line width (open circles) and second moments (solid circles) of the proton resonance of the trimethylamine – boron tribromide complex as a function of temperature.

fluoride complex.[1] The transitions at 210 and 230 °K are due to the onset of rotation about the B—N axes. The agreement between experimental and calculated values is only fair, which may be due to differences between the assumed and the actual structure. The transition below 100 °K involves methyl group reorientation.

TABLE 2
Calculated second moments for the trimethylamine complexes of boron trichloride and tribromide

Group		Second moment
CH_3	$(CH_3)_3N$	(G^2)
Static	Static	30.2
Rotating	Static	9.5
Rotating	Rotating	1.8
	Isotropic	0.7

Trimethylamine – Borane Complex

The proton second moment and line width are plotted vs. temperature in Fig. 4. The behavior of this complex is similar to the others at low temperatures, but at 325 °K there are steady decreases in the line width and second moment until 358 °K where abrupt *increases* occur. The second moment changes from 1.8 to 2.7 G^2.

Unit cell dimensions and the space group have been determined by X-ray diffraction (8) and partial molecular structure data have been obtained by gas phase electron diffraction (9). Calculated second moments are given in Table 3. The lattice is almost rigid at 77 °K. From 200 °K to room temperature, the observed second moment, 3.1 G^2, is compatible with simultaneous rotation of the CH_3 and BH_3 groups about their C_3 axes plus rotation about the B—N axis. The second moment at 120 °K of 8.5 G^2 can be interpreted as corresponding to either of two different composite motions: (*a*) rotation of both the CH_3

TABLE 3
Calculated second moments for the trimethylamine–borane complex

Group			Second moment
CH_3	$(CH_3)_3N$	BH_3	(G^2)
Static	Static	Static	37.0
Rotating	Static	Static	19.3
Rotating	Static	Rotating	11.8
Rotating	Rotating	Static	12.2
Rotating	Rotating	Rotating	4.0
	Isotropic		1.4

[1]A ^{35}Cl nuclear quadrupole resonance study is in progress to examine possible motion of the BCl_3 group.

Can. J. Chem. Downloaded from www.nrcresearchpress.com by 210.87.254.6 on 09/05/12
For personal use only.

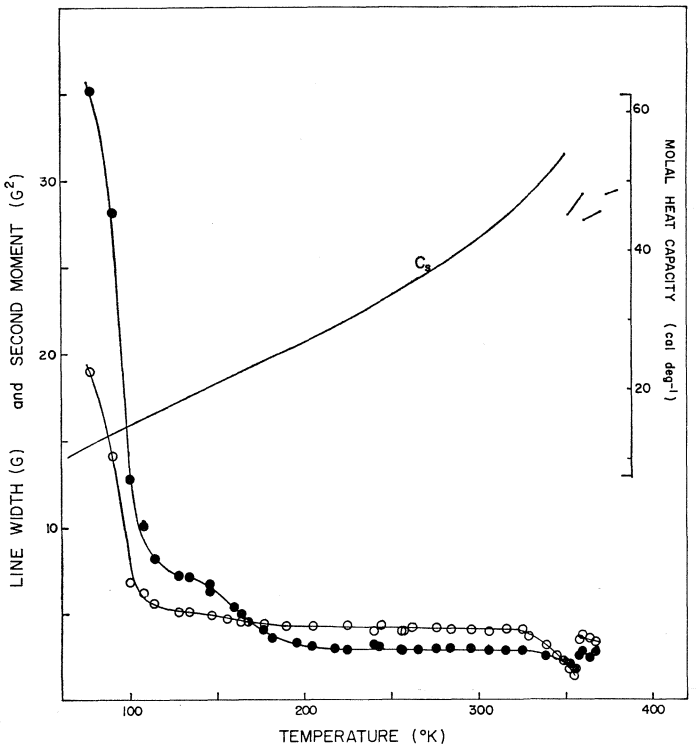

FIG. 4. Line width (open circles) and second moment (solid circles) of the proton resonance of the trimethylamine – borane complex as a function of temperature. Molal heat capacity data taken from Good *et al.* (13).

and the BH_3 groups or (*b*) rotation of the methyl groups plus rotation of the $(CH_3)_3N$ moiety but with the BH_3 group stationary. Merchant and Fung have reported that the quadrupole splitting of the deuterium resonance in $(CH_3)_3N.BD_3$ is rotationally averaged at 130 °K (10). The discrepancy between calculated and experimental second moments indicates that some further motion occurs, possibly a torsional oscillation about the B—N axis.

The decrease in second moment at about 320 °K can be explained by the gradual onset of isotropic rotational motion or by a "wobbling" of the B—N axis about its equilibrium direction. This latter motion, although it occurs about a preferred axis, nonetheless represents a mode of attack upon the barrier to isotropic rotation. The increase in second moment and line width at 358 °K is unusual, but similar increases have been reported previously for cyclopentane (11) and some methyl cyclosiloxanes (12). The heat capacity of the trimethylamine borane complex has been measured from 11 °K to the melting point by Good *et al.* (13). Thermal transitions were observed at 350.1 and 360.4 °K and are shown in Fig. 4. This latter transition may coincide with a change in crystal structure which is responsible for the second moment increase. The entropy change on fusion is 3.21 cal deg^{-1} $mole^{-1}$ and indicates the presence of orientational disorder in the high temperature phase, although the trimethylamine–borane complex is not typical of a true plastic crystal because the second moment just below the melting point is too high for isotropic rotation or lattice diffusion. The heat capacity data show no marked changes at the same temperatures as the earlier n.m.r. transitions. Darmon and Brot have discussed the relationship between thermal and n.m.r. transitions (14) and concluded that a thermal transition and a line-narrowing transition will both occur if the molecule has lower symmetry than that of its allowed orientations. If reorientation occurs to indistinguishable positions then no disorder is introduced and a thermal transition is not observed.

Can. J. Chem. Downloaded from www.nrcresearchpress.com by 210.87.254.6 on 09/05/12
For personal use only.

TABLE 4
Activation energies from line width data

Group	Line width (G) Below transition	Above transition	E_a (kcal mole^{-1})	$\alpha\ \nu_0$ (s^{-1})
CH_3 rotation				
—BH_3*	20.0–22.0	5.4–5.8	1.7–2.3	2.0×10^9–5.1×10^{10}
—BF_3	20.0	5.6	1.7	1.0×10^{10}
—BCl_3	19.5–21.0	5.5	1.6–1.9	4.7×10^8–2.0×10^9
—BBr_3	19.2–20.8	5.3	1.7–2.0	8.6×10^8–3.7×10^9
$(CH_3)_3N$ rotation				
—BH_3	5.4–5.8	4.3	1.9–2.2	1.9×10^7–3.2×10^7
—BF_3	5.4–5.7	3.8	1.6–1.8	3.2×10^7–6.7×10^7
—BCl_3	5.5	2.7	9.3	2.7×10^{13}
—BBr_3	5.3	2.5	9.1	1.4×10^{12}

*Includes rotations of both CH_3 and BH_3 groups

Barriers to Rotation

Line width data can be used to calculate the activation energies necessary for reorientation using the modified B.P.P. equation (15). Smith (16) has discussed the validity of the modified B.P.P. equation and the values of E and ν_0 calculated from the equation. With the approximations and assumptions that are involved, the error in the activation energy should be no worse than 15–20%. The transitions involving methyl group rotation are not complete at 77 °K and therefore the limiting line widths have to be estimated from the experimental data for similar systems, $(CH_3)_3CCl$ and $(CH_3)_3CBr$ (1) and $(CH_3)_3N$ (17). Values of 20 to 22 G seem to be appropriate and computations of barrier heights and pre-exponential factors were made for line widths in this range. The methyl group motion in the boron trifluoride and borane complexes is followed immediately by rotation about the B—N axis, and the lower limiting line width has also to be estimated. In fact, the barrier heights are not too sensitive to the actual values (Table 4). The activation energy for methyl group rotation is essentially the same for each compound, about 2 kcal mole^{-1}. By comparison, the line width transitions for the tetramethyl compounds studied by Smith (2) all occur below 77 °K, and spin–lattice relaxation time measurements gave barriers of less than 1 kcal mole^{-1} for methyl group rotation in the

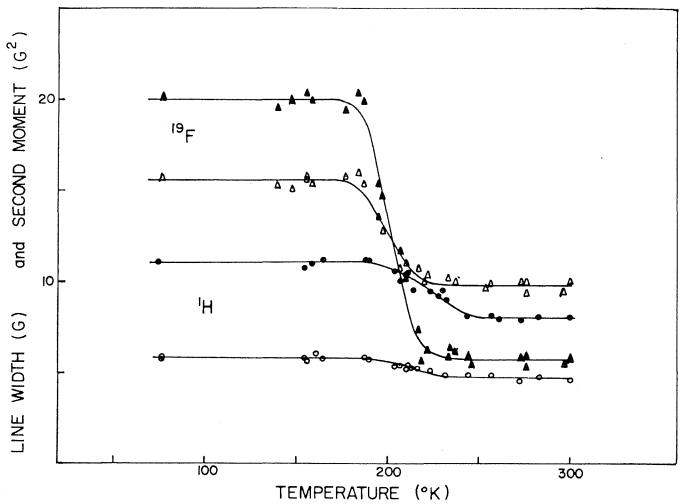

FIG. 5. The temperature dependence of the line widths (open symbols) and second moments (solid symbols) of the proton and fluorine resonances of the ammonia – boron trifluoride complex.

Can. J. Chem. Downloaded from www.nrcresearchpress.com by 210.87.254.6 on 09/05/12
For personal use only.

germanium, tin, and lead compounds. Stejskal *et al.* (18) obtained 2.6 to 3.0 kcal mole^{-1} for neopentane. In trimethylamine itself, the transition occurs from 105 to 135 °K and the calculated activation energy was 5.75 kcal mole^{-1} (16). However, the second moment above the transition is too low and some additional motion is undoubtedly occurring. The activation energies for rotation about the B—N axis are also given in Table 4. The values for the BCl_3 and BBr_3 complexes, are much higher than those of the BF_3 and BH_3 complexes which is expected as a result of the increased size of the BX_3 group.

Isotropic rotation does not occur for these complexes, with the possible exception of trimethylamine–borane. The complexes have high dipole moments, ranging from 4.04 D for the BF_3 complex to 5.57 D for the tribromide (19), and the electrostatic interactions prevent disordering of the molecular dipoles. This is not the case for *t*-butyl chloride and bromide, where isotropic rotation does occur (1).

The wide line n.m.r. spectra of trimethylamine complexes with bromine, iodine, and iodine monochloride have been studied by Fyfe (20). The behavior is similar to the boron trihalide and borane complexes in that methyl group reorientation occurs and is followed by rotation about the nitrogen–halogen axis.

Ammonia – Boron Trifluoride Complex

The proton and fluorine line widths and second moments are shown in Fig. 5 as a function of temperature. The experimental second moments at 77 °K are in agreement with the values calculated, based on the known crystal structure (21), for a rotating NH_3 group and a stationary BF_3 group. Above the transition the second moments reduce to values in agreement with the rotation of both groups about the molecular axis. The ^{19}F line width data lead to an activation energy of 5.7 ± 0.9 kcal mole^{-1}, $\nu_0 = 1.07 \times 10^{11}$ s^{-1}, for reorientation of the BF_3 group.

This complex has been studied previously by Leane and Richards (22) and by Dunell *et al.* (6). The results obtained by these groups differed considerably. The present work confirms the results of Dunell *et al.*

This work was supported by grants from the National Research Council of Canada. C.T.Y. acknowledges a McConnell Memorial Fellowship of McGill University. We thank Dr. B. A. Dunell and Dr. C. A. Fyfe for communication of results prior to publication.

1. J. G. Powles and H. S. Gutowsky. J. Chem. Phys. **21**, 1695 (1953).
2. G. W. Smith. J. Chem. Phys. **42**, 4229 (1965).
3. D. J. Blears, S. S. Danyluk, and E. Bock. J. Phys. Chem. **72**, 2269 (1968).
4. D. F. R. Gilson and J. Tsau. Unpublished results.
5. N. N. Greenwood and R. L. Martin. Quart. Rev. **8**, 1 (1954).
6. B. A. Dunell, C. A. Fyfe, C. A. McDowell, and J. Ripmeester. Trans. Faraday Soc. **65**, 1153 (1969).
7. S. Geller and J. L. Hoard. Acta Cryst. **4**, 399 (1951).
8. S. Geller, R. E. Hughes, and J. L. Hoard. Acta Cryst. **4**, 380 (1951).
9. S. H. Bauer. J. Amer. Chem. Soc. **59**, 1804 (1937).
10. S. Z. Merchant and B. M. Fung. J. Chem. Phys. **50**, 2265 (1969).
11. F. A. Rushworth. Proc. Roy. Soc. Ser. A, **222**, 526 (1954).
12. E. G. Rochow and H. G. LeClair. J. Inorg. Nucl. Chem. **1**, 92 (1955).
13. W. D. Good, H. L. Finke, S. S. Todd, and D. R. Douslin. U.S. Bureau of Mines, Bartlesville, Technical Report AD635296. 1966.
14. I. Darmon and C. Brot. Molec. Cryst. **2**, 301 (1967).
15. H. S. Gutowsky and G. E. Pake. J. Chem. Phys. **18**, 162 (1950).
16. G. W. Smith. J. Chem. Phys. **50**, 3595 (1969).
17. P. J. Haigh, P. C. Canepa, G. A. Matzkamin, and T. A. Scott. J. Chem. Phys. **48**, 4234 (1968).
18. E. O. Stejskal, D. E. Woessner, T. C. Farrar, and H. S. Gutowsky. J. Chem. Phys. **31**, 55 (1959).
19. C. M. Bax, A. R. Katritsky, and L. E. Sutton. J. Chem. Soc. 1258 (1958).
20. C. A. Fyfe. Private communication.
21. J. L. Hoard, S. Geller, and W. M. Cashin. Acta Cryst. **A**, 396 (1951).
22. J. B. Leane and R. E. Richards. Spectrochim. Acta, **10**, 154 (1957).

Can. J. Chem. Downloaded from www.nrcresearchpress.com by 210.87.254.6 on 09/05/12
For personal use only.

Kinetics of the hydrolysis of thiochloroformate esters in pure water

A. Queen, T. A. Nour,[1] M. N. Paddon-Row,[2] and K. Preston[3]
Parker Chemistry Laboratory, University of Manitoba, Winnipeg, Manitoba
Received[4] December 2, 1968

The effects of structural changes on the rates of hydrolysis of a series of thiochloroformate esters in water have been investigated. The reactivity is enhanced by increased electron donation by the hydrocarbon group. These results, the activation parameters for the hydrolysis of methyl thiochloroformate and the solvent deuterium isotope effect, are shown to be consistent with the operation of the S_N1 mechanism.

Canadian Journal of Chemistry, **48**, 522 (1970)

Can. J. Chem. Downloaded from www.nrcresearchpress.com by 210.87.254.6 on 09/05/12
For personal use only.

Introduction

It is well known that alkyl chloroformates (**1**; X = O) undergo solvolytic reactions much more slowly than other acid chlorides (1, 2) and also seem to find the S_N1 mechanism unfavorable. Two factors are responsible for these characteristics.

(*i*) The initial states are stabilized by conjugation (**2**; X = O) and the effect is enhanced by structural changes that increase electron donation by the alkyl group. This is shown by the rate sequence

$$ClC_2H_4O(CO)Cl > CH_3O(CO)Cl > C_2H_5O(CO)Cl > i\text{-}C_3H_7O(CO)Cl$$

for bimolecular methanolysis (3).

(*ii*) The energies of the acylium ions and the transition states leading to them are raised by the powerful inductive electron withdrawal of the alkoxy group in the contributing structures (**3**; X = O). This opposes the mesomeric stabilization associated with the forms (**4**; X = O) which, in any case, is partly nullified by the initial state conjugation. It follows from these arguments that the S_N1 mechanism will only be likely for those chloroformates having strongly electron donating substituents. Thus the rate sequence

$$C_6H_5O(CO)Cl > CH_3O(CO)Cl > C_2H_5O(CO)Cl \approx n\text{-}C_3H_7O(CO)Cl < i\text{-}C_3H_7O(CO)Cl$$

for hydrolysis (1) reflects the operation of a bimolecular mechanism for the first four compounds and probably the S_N1 pathway for isopropyl chloroformate. Indeed, a careful study of the hydrolysis of this compound (1) has led us to conclude that two distinct mechanisms operate concurrently. Dimethylcarbamyl chloride reacts entirely by the S_N1 pathway, a conclusion supported (4, 5) by our recent observation that the corresponding fluoride reacts about a million times more slowly with water (6).

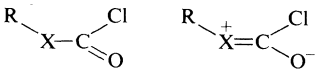

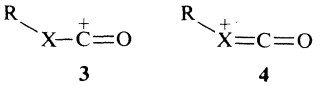

As an extension of our earlier studies, we have now determined the rates of hydrolysis of the corresponding thiochloroformate esters (**1**; X = S) in pure water. There have been no previously reported studies of the rates of solvolysis of these compounds, probably because it has been assumed that they would behave quite analogously to the oxygen compounds. We have found that this assumption is not entirely correct.

Results

The rate data for the hydrolysis of the thiochloroformate esters in water at 4.62 °C. are given in Table 1. The hydrolysis of the *t*-butyl compound was too fast to be followed by our equipment. For purposes of comparison, rate constants for the hydrolysis of acetyl chloride (7) and the corresponding chloroformate esters, calculated from earlier data (1), are included in this table. Table 2 lists rate constants for the hydrolysis of methyl thiochloroformate at different temperatures, the figures representing

[1]University of Manitoba Postdoctoral Fellow, 1967–1969.
[2]University of Manitoba Postdoctoral Fellow, 1968–1969.
[3]Summer research student, 1968.
[4]Revision received September 26, 1969.

TABLE 1

Rate constants for the hydrolysis of acyl chlorides in water at 4.616 °C

Structure	k ($\times 10^4$ s^{-1}) C_6H_5	CH_3	C_2H_5	n-C_3H_7	i-C_3H_7	t-C_4H_9	Reference
R—S—(C=O)—Cl	1.060	4.733	26.69	29.64	116.9	Fast	This work
R—O—(C=O)—Cl	20.55	0.6738	0.4110	0.4498	1.015	—	(1)
CH_3—(C=O)—Cl		2.9×10^6*					(7)

*In 75% water/dioxane at 27 °C.

TABLE 2

The effect of temperature on the rate of hydrolysis of methyl thiochloroformate in water and the derived thermodynamic parameters for 25 °C*

Temperature (°C)	k ($\times 10^4$ s^{-1})	Temperature (°C)	k ($\times 10^4$ s^{-1})
0.227	2.307±0.002	9.534	10.11±0.024
1.562	2.867±0.003	10.881	12.48±0.040
1.773	2.995±0.005	11.830	14.32±0.037
2.565	3.383±0.005	13.605	18.47±0.026
3.916	4.225±0.004	14.245	20.33±0.041
4.616	4.733±0.007	15.410	24.18±0.051
5.788	5.702±0.008	16.498	28.00±0.038
6.884	6.717±0.012	18.148	35.31±0.060
7.021	6.909±0.012	20.053	45.78±0.073
8.689	8.901±0.020		

*Empirical constants for eq. [1]: $A = -10419.721$, $B = -42.06539$, $C = 136.9811$; values derived are: $\Delta F^{\ddagger} = 20\,509 \pm 3$ cal/mole, $\Delta H^{\ddagger} = 22\,161 \pm 125$ cal/mole, $\Delta S^{\ddagger} = 6.4 \pm 0.4$ cal/mole deg, $\Delta C_p^{\ddagger} = -86 \pm 8$ cal/mole deg.

average values of several independent experiments. These data were fitted by a least-squares method (8) to the equation

$$[1] \qquad \log k = A/T + B \log T + C$$

where T is the absolute temperature. Table 2 footnote also gives the constants calculated for eq. [1] and the derived parameters $\Delta H^{\ddagger}$, $\Delta S^{\ddagger}$, and $\Delta C_p^{\ddagger}$ at 25 °C.

Discussion

The data given in Table 1 show that thiochloroformate esters also react less rapidly with water than other acid chlorides. Hence, the reactivities of these compounds are, like those of the chloroformates, affected by initial state conjugation. Consistent with the fact that sulfur is less electronegative than oxygen and also shows less tendency to use its lone pair electrons for π bond formation (9, 10), the alkyl thiochloroformates are more reactive than the oxygen analogues. However, two features of the data given in Table 1 require explanation. First, phenyl thiochloroformate is much less reactive than phenyl chloroformate. Secondly, the rate sequence

$$C_6H_5S(CO)Cl < CH_3S(CO)Cl < C_2H_5S(CO)Cl \approx n\text{-}C_3H_7S(CO)Cl < i\text{-}C_3H_7S(CO)Cl < t\text{-}C_4H_9S(CO)Cl$$

contrasts with

$$C_6H_5O(CO)Cl > CH_3O(CO)Cl > C_2H_5O(CO)Cl \approx n\text{-}C_3H_7O(CO)Cl < i\text{-}C_3H_7O(CO)Cl$$

Since dipole moment measurements have shown that the preferred configurations for both chloroformate (11) and thiochloroformate esters (12) are those in which the halogen atom and the hydrocarbon group are *cis* to each other (**1**) rather than *trans*, the differences noted above do not seem to stem from initial state conformational differences. On the other hand, the dipole moment data indicate that inductive electron release by the RS— groups in the thiochloroformate esters is modified by a secondary effect which decreases as R changes in the order

$$C_6H_5 > CH_3 > C_2H_5 \approx n\text{-}C_3H_7 > i\text{-}C_3H_7 > t\text{-}C_4H_9$$

It has, therefore, been suggested (12) that conjugative electron release by aryl groups (**5**) and hyperconjugative release by alkyl groups (**6**) to the d orbitals of sulfur occurs in these compounds.

Can. J. Chem. Downloaded from www.nrcresearchpress.com by 210.87.254.6 on 09/05/12
For personal use only.

Can. J. Chem. Downloaded from www.nrcresearchpress.com by 210.87.254.6 on 09/05/12
For personal use only.

It might be expected that similar effects would operate to stabilize the initial states for hydrolysis, so that the rates should increase across the series from R = C_6H_5 to R = t-C_4H_9, as we have found. However, it is not safe to correlate the dipole moment and kinetic data without also considering the mechanism of the reaction in more detail.

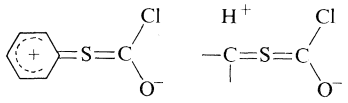

5 6

The Mechanism of the Hydrolysis of Thiochloroformate Esters

Bond breaking can occur at more than one position. Alkyl–sulfur bond fission would yield either an alcohol as a product of substitution or an alkene as a product of elimination. The second alternative is not possible for methyl thiochloroformate and vapor phase chromatography of the hydrolysate did not indicate methanol as a product of the reaction. However, methanethiol was identified as a volatile product by preparation of 2,4-dinitrophenyl methyl sulfide. The infrared spectrum of the volatile products showed no significant light absorption at 859 cm^{-1}, indicating that carbonyl sulfide was not formed. These results show that no cleavage of the alkyl–sulfur bond occurs during hydrolysis. The formation of methanethiol shows that the carbonyl–sulfur bond is ruptured at some stage in the reaction but it is most likely that this occurs after rate determining cleavage of the carbon–chlorine bond. In the light of these conclusions, the activation parameters given in Table 2 are very interesting, in particular the positive value of the entropy of activation. The corresponding figures for the hydrolysis of methyl chloroformate are $\Delta H^{\neq}$ = 16.199 kcal/mole, $\Delta S^{\neq}$ = −19.07 cal/mole deg, $\Delta C_p{}^{\neq}$ = −36.0 cal/mole deg and for the hydrolysis of isopropyl chloroformate the figures are 24.102 kcal/mole, 10.12 cal/mole deg and −9.1 cal/mole deg, respectively (1). Buncel (13) has suggested that solvolytic fragmentation processes are indicated when the entropies of activation are more positive than would be expected on the basis of data for similar reactions where fragmentation is not possible. Thus, he considers the hydrolyses of alkyl chlorosulfates to involve concurrent rupture of the alkyl–oxygen and the sulfur–halogen bonds and the corresponding reaction of isopropyl chloroformate to probably involve similar changes at the alkyl–oxygen and carbon–chlorine bonds (14). We have interpreted our data for the latter case somewhat differently in terms of two simultaneous reactions, one of them being a unimolecular process in which heterolysis of the carbon–chlorine bond occurs (1). The present investigations show that fragmentation of the kind suggested by Buncel does not occur in the hydrolysis of methyl thiochloroformate and the positive entropy of activation must be accounted for in some other way.

[2]

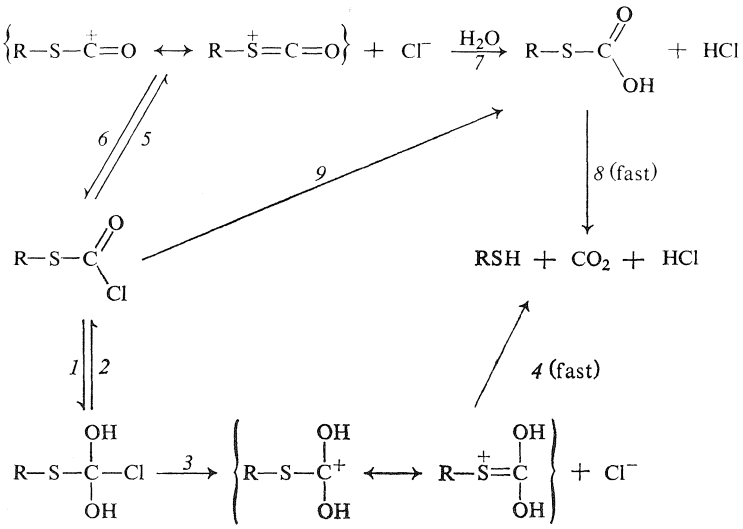

Can. J. Chem. Downloaded from www.nrcresearchpress.com by 210.87.254.6 on 09/05/12
For personal use only.

Examination of the products of the hydrolysis of isopropyl thiochloroformate indicated that no appreciable amounts of isopropyl alcohol, propene, or carbonyl sulfide were formed in the reaction, but 2-propanethiol was identified by preparing its 2,4-dinitrophenyl derivative. The reaction is thus subject to the same considerations as that of the methyl analogue. This must also be the case for phenyl thiochloroformate, since heterolysis of the aryl–sulfur bond is unlikely under the reaction conditions used.

Three different mechanisms could lead to rate determining carbon–halogen bond rupture, as shown in [2].

Since the rate of the direct displacement reaction would be determined by step **9** and thus with an increase of order during the activation process, the positive entropy of activation found for the hydrolysis of methyl thiochloroformate indicates that this mechanism is unlikely for the present reactions. This conclusion is reinforced by the fact that methyl and ethyl thiofluoroformates hydrolyze slightly more quickly than the chlorides (6). We have previously analyzed the alternative bimolecular mechanism (steps *1*, *2*, *3*, and *4*) for the corresponding reactions of chloroformate esters and shown (1) that, by assuming the steady state approximation for the tetrahedral intermediate, the observed rate constant is given by eq. [3]. The simplified equations [4] and [5] apply under the special conditions indicated

$$[3] \quad k_{obsd} = \frac{k_1}{1 + k_2/k_3}$$

$$[4] \quad k_{obsd} = k_1 \quad \text{when} \quad k_2 \ll k_3$$

$$[5] \quad k_{obsd} = \frac{k_1}{k_2} \cdot k_3 = Kk_3 \quad \text{when} \quad k_2 \gg k_3$$

$$[6] \quad \Delta S^{\ddagger}_{obsd} = \Delta S_E{}^0 + \Delta S_3{}^{\ddagger} + F$$

The observed entropy of activation for the general case, eq. [3], can be expressed in the form of eq. [6], where F is a function lying between the limits $F = 0$ when $k_3 \ll k_2$ and $F = \Delta S_2{}^{\ddagger} - \Delta S_3{}^{\ddagger}$ when $k_3 \gg k_2$. It is generally agreed that an entropy change of about -16 cal/mole deg should be associated with processes involving the covalent attachment of a molecule of water (15) and this figure should be a minimum value for $\Delta S_E{}^0$. Hence, in the present case, $\Delta S_3{}^{\ddagger}$ must be at least 22 cal/mole deg, an unrealistically large value. It could be argued that steps *3* and *4*, which together involve the rupture of four bonds, are essentially concerted and that the resulting highly disordered transition state would cause an increase in the entropy of activation. However, in the absence of any analogous examples, this must be regarded as a highly tenuous and unlikely proposal and the addition–elimination mechanism seems to be excluded for the present reactions.

In the light of these arguments, the S_N1 pathway (steps *5*, *6*, *7*, and *8*) is the most likely mechanism for the hydrolyses of thiochloroformates. Only one observation, namely that the corresponding thiofluoroformates show enhanced solvolytic reactivity (see discussion above), is not in accord with this mechanism. These results are similar to some we have obtained with alkyl haloformates (6), which undoubtedly react with water by the addition–elimination mechanism (1). However, it is possible that the thiochloroformates and thiofluoroformates hydrolyze by different mechanisms[5], so that the leaving group effect does not necessarily preclude the unimolecular mechanism for the solvolyses of the chlorides. If this is so, the other data are entirely in accord with the operation of the S_N1 mechanism. Thus, the effects of the structural changes on the rates of reaction simply reflect the different inductive effects of the hydrocarbon groups. The activation parameters for the hydrolysis of methyl thiochloroformate are very similar to those found for S_N1 hydrolysis of alkyl halides (16, 17, 18) and dimethylcarbamyl chloride (1) in water. In particular, the large negative heat capacity of activation is persuasive evidence for this mechanism, since smaller values of about -30 to -50 cal/mole deg seem to characterize bimolecular hydrolysis in water (1, 17). In agreement with this view, the solvent isotope effect, $k(D_2O)/k(H_2O) = 0.69$ at 4.62 °C, is similar to that found for the hydrolysis of *t*-butyl chloride (19) and is much smaller than the values of about 0.55 reported for the hydrolyses of alkyl chloroformates (1).

It is worthwhile considering further why the S_N1 mechanism should be a favorable route for the hydrolysis of thiochloroformates and carbamyl chlorides but not chloroformates. In the solvolytic addition–elimination mechanism [reaction [2], steps *1*, *2*, *3*, and *4*], it is reasonable

[5]The authors thank a referee for this suggestion.

Can. J. Chem. Downloaded from www.nrcresearchpress.com by 210.87.254.6 on 09/05/12
For personal use only.

to assume that the nucleophile will be supplied by the solvent cage surrounding the molecule. Hence, for a given compound, the initial state energies will be the same for unimolecular and bimolecular hydrolysis and the mechanism will be decided by the differences in the transition state energies. In the series of compounds (R—(CO)—Cl; R = R′O, R′$_2$N, or R′S), the inductive effect of the hetero atom is opposed by its mesomeric effect, when this can operate. Consider first of all the case of the chloroformate esters. The powerful mesomeric electron donation of the oxygen atom, which acts to stabilize a forming acylium ion, is largely offset by a strong inductive withdrawal which has the opposite effect. On the other hand, mesomerism is much reduced in the bimolecular process leading to a tetrahedral intermediate and the inductive effect dominates in stabilizing the transition state. In consequence, the S_N1 mechanism is not favored for the reaction of chloroformates. In the case of dimethylcarbamyl chloride, the weak inductive effect of the nitrogen atom is further reduced by the two methyl groups so that the energies of the transition states for unimolecular and bimolecular hydrolysis are only slightly affected by this effect. However, mesomeric electron donation is particularly large for nitrogen, leading to considerable stabilization of the incipient acylium ion. Nevertheless, the activation energy for bimolecular solvolysis might still be less than for that for ionization. In this case, the favorable entropy of activation for the unimolecular mechanism and the unfavorable value for the bimolecular one are both sufficiently large to dictate that hydrolysis should follow the S_N1 pathway. For thiochloroformates, the inductive effect of the sulfur atom is weak, like that of nitrogen, but the tendency for mesomeric electron release is smaller than those for either nitrogen or oxygen. The balancing of the two effects for the unimolecular and bimolecular mechanisms leads to the situation where the activation energies for these alternatives are closer together than for the hydrolysis of chloroformates but further apart than for the corresponding carbamyl chlorides. Once again, it would seem that the entropy terms for the alternative mechanisms are sufficiently different to favor reaction by the S_N1 mechanism. In agreement with these proposals, the enthalpy of activation for the hydrolysis of methyl thiochloroformate is larger than the value of 20.26 kcal/mole for the solvolysis of dimethylcarbamyl chloride in water at 25 °C (1). A recent comparison (20) of the stabilization energies of acylium ions and carbonium ions, relative to the formyl and methyl cations, respectively, shows that the methoxy group has only a small effect for the acylium ion (6 kcal/mole) but a large effect for the carbonium ion (66 kcal/mole). Moreover, the differences in the changes of reactivity on replacing chlorine by fluorine in methyl chloroformate, methyl thiochloroformate, and dimethylcarbamyl chloride (see previous discussion) provide qualitative support for this analysis, as follows. The activation energy is usually lower and the entropy of activation more negative for bimolecular solvolysis of acid fluorides than for acid chlorides (21). These compensating differences cause only fairly small changes in reactivity for the haloformates. For unimolecular solvolysis, the activation energies are significantly larger for fluorides than chlorides, so that the change in reactivity should be large, as we have observed for the dimethylcarbamyl halides. Apparently, the increase in the activation energy is not sufficient in this case to favor reaction by the bimolecular mechanism whereas this change seems to occur for the hydrolyses of the thiohaloformates.

Experimental

Material

The preparation and purification of the thiochloroformate esters have been previously described (12). The hydrolyzable chloride content of the compounds was never less than 99.5% of the theoretical amount.

Conductivity water was prepared by passing distilled water through a column of Rexyn AG 501 ion-exchange resin.

Measurement of Rates

The methods used in these studies have been previously described as have the methods of calculating the rate constants and the activation parameters (1, 8).

Products of Hydrolysis

Methyl thiochloroformate (5 ml) was added dropwise to water (100 ml) in a flask fitted with a stirrer and a reflux condenser. A tube passed from the top of the condenser to a trap containing anhydrous magnesium sulfate and immersed in an acetone – dry ice bath. After the reaction had finished, the volatile contents of the trap were allowed to evaporate through a short column maintained at 20 °C. and were collected in a second trap. Part of the contents of this trap were slowly passed into a mixture of ethanol (4.5 ml) and aqueous sodium hydroxide (10%; 0.5 ml) at 0 °C and the solution then treated with 2,4-dinitrofluorobenzene (0.5 ml) in ethanol

(5 ml). The resulting yellow solid was filtered and recrystallized from ethanol to yield 2,4-dinitrophenyl methyl sulfide, m.p. and mixed m.p. with an authentic sample 126 °C. (lit. 127 °C, ref. 22). The infrared spectrum of the contents of the trap were examined in the gaseous state using a sodium bromide cell. Strong absorption at 2350 cm^{-1} was attributed to carbon dioxide while the absence of significant absorption at 859 cm^{-1} showed the absence of carbonyl sulfide. The aqueous reaction mixture was examined for methanol, with negative results, by injecting samples (20 μl) into an 8 ft Poropak column attached to a Varian Aerograph Model 1520 gas chromatograph. Trial experiments showed that this apparatus was capable of detecting less than 0.01% of methanol in the samples used.

Similar experiments with isopropyl thiochloroformate led to the isolation of 2,4-dinitrophenyl-2′-propyl sulfide, m.p. and mixed m.p. with an authentic sample, 95 °C (lit. 94.5 °C ref. 22). No isopropanol or propene were detected by means of vapor phase chromatography.

The authors gratefully acknowledge the award of a grant by the National Research Council of Canada and financial support by the Graduate and Post-Doctoral Support Committee of the University of Manitoba Research Board.

1. A. Queen. Can. J. Chem. **45**, 1619 (1967).
2. E. W. Crunden and R. F. Hudson. J. Chem. Soc. 3748 (1961).
3. R. Leimu. Ber. **70**, 1040 (1937).
4. R. E. Parker. Advan. Fluorine Chem. **3**, 63 (1963).
5. C. G. Swain and C. B. Scott. J. Amer. Chem. Soc. **75**, 246 (1953).
6. A. Queen, T. A. Nour, and Helen Gyulai. Unpublished results.
7. R. F. Hudson and G. E. Moss. J. Chem. Soc. 5157 (1962).
8. R. L. Heppolette and R. E. Robertson. J. Amer. Chem. Soc. **83**, 1834 (1961). E. C. W. Clarke and D. N. Glew. Trans. Faraday Soc. **62**, 539 (1966).
9. H. Bohme, H. Fisher, and R. Frank. Ann. **563**, 54 (1949).
10. F. G. Bordwell, G. D. Cooper, and H. Morita. J. Amer. Chem. Soc. **79**, 376 (1957).
11. E. Bock and D. Iwacha. Can. J. Chem. **45**, 3177 (1967).
12. A. Queen, T. A. Nour, and E. Bock. Can. J. Chem. **47**, 343 (1969).
13. E. Buncel and J. P. Millington. Can. J. Chem. **43**, 556 (1965).
14. E. Buncel. Private communication.
15. L. L. Schaleger and F. A. Long. Advan. Phys. Org. Chem. **1**, 1 (1963).
16. R. E. Robertson. Soum. Kem. **A33**, 63 (1960).
17. R. E. Robertson. Progr. Phys. Org. Chem. **4**, 213 (1967).
18. R. E. Robertson. Can. J. Chem. **42**, 1707 (1964).
19. P. M. Laughton and R. E. Robertson. Can. J. Chem. **34**, 1714 (1956). W. J. Albery and B. H. Robinson. Trans. Faraday Soc. **65**, 1623 (1969).
20. P. R. Briggs and T. W. Shannon. J. Amer. Chem. Soc. **91**, 4307 (1969).
21. C. A. Bunton and J. H. Fendler. J. Org. Chem. **31**, 2307 (1966). B. L. Archer, R. F. Hudson, and J. E. Wardhill. J. Chem. Soc. 888 (1953).
22. R. W. Bost, J. O. Turner, and R. D. Norton. J. Amer. Chem. Soc. **54**, 1985 (1932).

Can. J. Chem. Downloaded from www.nrcresearchpress.com by 210.87.254.6 on 09/05/12
For personal use only.

Effect of pressure on the rate of solvolysis of *t*-butyl chloride in ethanol–water mixtures[1]

B. T. BALIGA and E. WHALLEY
Division of Chemistry, National Research Council of Canada, Ottawa, Canada

Received July 30, 1969

The effect of pressure on the rate of spontaneous solvolysis of *t*-butyl chloride in ethanol–water mixtures in the range 0 to 40% v/v ethanol at 0 °C has been measured up to a maximum pressure of 3 kbar. The results have been examined from several points of view and the conclusions are briefly described in the summary.

Canadian Journal of Chemistry, **48**, 528 (1970)

Can. J. Chem. Downloaded from www.nrcresearchpress.com by 210.87.254.5 on 09/05/12
For personal use only.

1. Introduction

Several reactions are now known (1–3) for which the constant-volume parameters of activation vary in a simpler manner with solvent composition than the constant-pressure parameters. One of the strongest variations of the constant-pressure parameters with solvent com position occurs for the solvolysis of *t*-butyl chloride in ethanol–water mixtures (4), and a study of the constant-volume parameters for this system is clearly required.

Furthermore, the constant-pressure entropy of activation in water is 12 cal deg^{-1} $mole^{-1}$ at 25 °C. The mechanism is undoubtedly S_N1

$$t\text{-BuCl} \rightarrow t\text{-Bu}^+ + \text{Cl}^-$$

and the transition state has presumably an appreciably higher dipole moment than the initial state. This implies an appreciable loss of entropy when the transition state is formed due to dipole–solvent interaction. The observed positive entropy of activation presumably implies that the *t*-Bu and Cl are well separated in the transition state so that the gain in entropy due to their looser attachment to one another more than compensates the loss of entropy due to increased interaction with the solvent. A relatively large separation of the *t*-Bu and Cl might affect the activation volume.

Consequently, the solvolysis of *t*-butyl chloride in ethanol–water at 0 °C has been followed to a maximum pressure of 3 kbar.

2. Experimental

Reagents

t-Butyl chloride was prepared (5) from Eastman Kodak White Label *t*-butanol. The final fraction boiling at 50.0 to 50.5 °C was > 99.5% pure by gas chromatographic analysis, and was used. Pure dry ethanol was prepared from commercial absolute ethanol (5) and used for preparing ethanol–water mixtures by volume. Distilled water was degassed by boiling and was stored out of contact with air.

Kinetics

The rate of hydrolysis at various pressures was measured using the conductance technique described previously (6). The thermostat bath was a vigorously stirred mixture of ice and water, whose temperature was constant to ±0.02 °C. In order to prevent water from coming into contact with the leads, the top of the pressure vessel was fitted with a sliding brass cylinder sealed with an O-ring at the bottom to keep the water out. The cylinder normally protruded above the water level, and the empty space inside it was filled with cotton wool for thermal insulation.

The vessel with mercury, the conductance cell and its associated parts, hydraulic oil, and the solvent (~100 ml in a volumetric flask) were kept in a refrigerator at −5 °C. 20 μl of *t*-butyl chloride was quickly added to the solvent and the solution stirred. The cell was rinsed, filled with the solution, and assembled with the cooled vessel, mercury, oil, etc. The vessel was lowered to the thermostat bath and pressurized slowly. The assembly was carried out as quickly as possible, and with experience the time taken from adding the *t*-butyl chloride to pressurizing the vessel was 7 min. In highly aqueous ethanol–water at high pressure, the reaction becomes too fast for the use of this technique and the runs, therefore, had to be restricted to lower pressures.

The time for thermal equilibrium was checked by pressurizing aqueous 0.002 *M* hydrogen chloride to 1000 bars in the kinetics apparatus. The conductance reached a constant value in 12 to 15 min after pressurizing. In all the runs the first reading was taken a minimum of 20 min after pressurizing.

3. Results

For the accuracy desired in this work, there was no need to correct the conductances for the change in equivalent conductance with concentration. The rate constants were obtained by the

[1] NRCC No. 11081.

TABLE 1

Rate constants for the solvolysis of *t*-butyl chloride in water–ethanol at 0 °C and various pressures

	$10^6\ k/s^{-1}$ at % v/v ethanol in water			
p/bar	0	10	25	40
50	712	481	266.0	60.8
100				63.6
249		501	295.4	72.1
348				78.3
496	745	545	328.7	87.6
595				92.2
741		576	359.5	99.3
987	771	605	385.6	110.5
1480	808	665	434	131.8
1973				144.7
2472				155.4
2955				163.8

Guggenheim method of analysis using least-squares on an IBM-360 computer as in the earlier work (6). The rate constants are given in Table 1 and are reproducible to about 0.5%, except in 0 and 10% v/v ethanol where the reproducibility, since the reaction is fast, is about 1%. These errors were estimated from the standard deviations, the agreement between a few duplicated runs, the deviations of the rate constants at various pressures from fitted lines as described in section (4.5), and the deviations from a smooth line in Fig. 2.

Graphical plots of ln *k* vs *p* are given in Fig. 1. The rate constants extrapolated to zero pressure

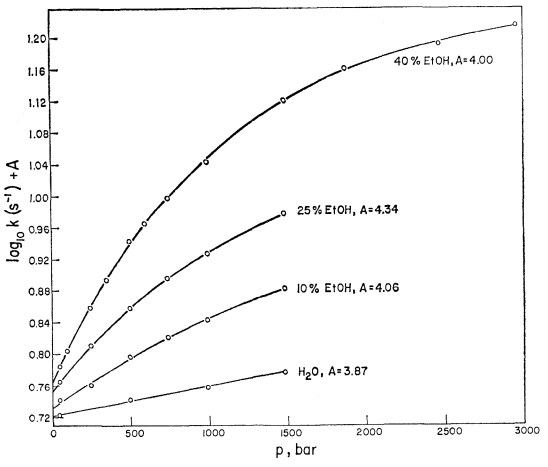

FIG. 1. Rate constants for the solvolysis of *t*-butyl chloride in water–ethanol at 0 °C. The numbers on the curves are the % v/v ethanol.

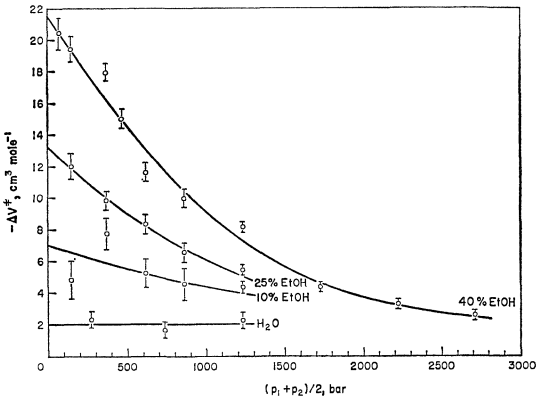

FIG. 2. Mean volumes of activation for the solvolysis of *t*-butyl chloride in water–ethanol at 0 °C. The numbers on the curves are the % v/v ethanol.

are compared with those of Winstein and Fainberg (4) in Table 2. The agreement is good.

Mean volumes of activation $\Delta V^{\ddagger}_{mean}$ calculated between adjacent pressures p_1 and p_2 from the relation

$$[1] \qquad \Delta V^{\ddagger}_{mean} = \frac{-RT}{(p_1 - p_2)} \ln \frac{k_1}{k_2}$$

are plotted against the mean pressure $(p_1 + p_2)/2$ for the various solvents in Fig. 2. The zero-pressure intercepts are the volumes of activation at zero pressure.

The difference in $\Delta V^{\ddagger}$ between solvents can be expressed as

$$[2] \qquad -\Delta\Delta V^{\ddagger} = RT \frac{\partial \ln k_1/k_2}{\partial p}$$

where k_1 and k_2 are now the rate constants in solvents 1 and 2 at the same pressure. Plots of $\ln k_1/k_2$ against p are shown in Fig. 3 and the slopes at zero pressure give the difference $\Delta\Delta V^{\ddagger}$ of activation volume for the various solvent pairs as follows

$$\Delta\Delta V^{\ddagger}\ (0\text{–}10) = 5.0 \pm \sim 0.4$$
$$\Delta\Delta V^{\ddagger}\ (0\text{–}25) = 10.7 \pm \sim 0.5$$
$$\Delta\Delta V^{\ddagger}\ (0\text{–}40) = 19.9 \pm \sim 0.5$$
$$\Delta\Delta V^{\ddagger}\ (10\text{–}25) = 6.7 \pm \sim 0.6$$
$$\Delta\Delta V^{\ddagger}\ (10\text{–}40) = 15.0 \pm \sim 0.8$$
$$\Delta\Delta V^{\ddagger}\ (25\text{–}40) = 8.2 \pm \sim 0.6$$

Since ln *k* vs. *p* for water (see Fig. 1) is essentially linear, the volume of activation in water is −2.0

Can. J. Chem. Downloaded from www.nrcresearchpress.com by 210.87.254.5 on 09/05/12
For personal use only.

TABLE 2

Comparison of rate constants at 1 bar for the solvolysis of *t*-butyl chloride in water–ethanol at 0 °C

% v/v ethanol in water	$10^6\ k/s^{-1}$ This work	$10^6\ k/s^{-1}$ Reference 4
0	712	727
10	469	475
25	258	259
40	57.9	57.6

$\pm$ 0.5 cm^3 mole^{-1} which is consistent with the value extrapolated from the plot in Fig. 2. From this value and the first three relations above, the volume of activation in the mixed solvents can be obtained. The last three relations are included as a check. The activation volumes obtained are consistent with those obtained from Fig. 2, and with the limiting slopes in Fig. 1. They are summarized in Table 3, which also gives the thermal expansivities α and compressibilities κ for the solvents obtained from the literature (7, 8). The only other measurements of the effect of pressure on the rate of solvolysis of *t*-butyl chloride are rough values of Buchanan and Hamann (9) in 80% aqueous ethanol at 25 °C which yield a volume of activation of about -21 cm^3 mole^{-1}, and those of Hyne, Golinkin, and Laidlaw (10) in 80% v/v aqueous ethanol at 30 °C, which by least-squares gives a value of -22.2 ± 0.9 cm^3 mole^{-1} (10) and by a graphical reanalysis $-20 \pm \sim 1.5$ cm^3 mole^{-1}. Olavi and Virtanen (11) have measured the activation volume for the solvolysis of *t*-butyl bromide in several organic or largely organic solvents and obtained values in the range -20.6 to -41.7 cm^3 mole^{-1}. Because the solvents were quite different, these values cannot be compared with ours.

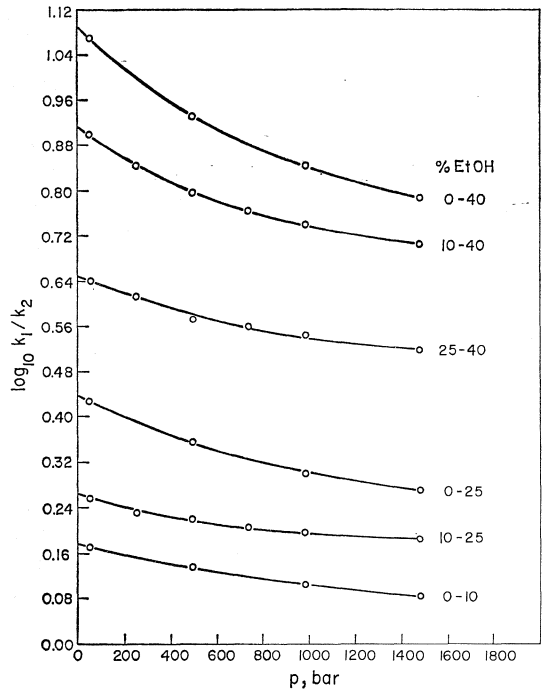

FIG. 3. Ratio of rate constants in different solvents for the solvolysis of *t*-butyl chloride. The numbers attached to the curves are the % v/v ethanol of the solvent.

The activation enthalpy and entropy at constant pressure according to Winstein and Fainberg (4) are given in Table 4. Since their enthalpies and entropies refer to 12.5 °C, they were adjusted to 0 °C using heat capacities of activation graphically interpolated from those recently measured by Martin and Robertson (12). The data in the last column of Table 3 were used to obtain the constant-volume energy and entropy of activation by means of the expressions

$$\Delta U_V^{\ddagger} = \Delta H_P^{\ddagger} - T\alpha\Delta V^{\ddagger}/\kappa$$

$$\Delta S_V^{\ddagger} = \Delta S_P^{\ddagger} - \alpha\Delta V^{\ddagger}/\kappa,$$

and they are given in the last two columns of Table 4. The change of activation parameters with solvent composition are plotted in Fig. 4.

4. Discussion

1. Volume of Activation in Water

It is well established (13) that the solvolysis of *t*-butyl chloride occurs in two steps, the first being the slow ionization of the halide and the second a fast combination of the *t*-butyl carbonium ion with the solvent. Presumably, the transition state is

$$(CH_3)_3C^{\delta+} - - - - - Cl^{\delta-}$$

in which the C—Cl bond is stretched and partial charges have appeared on the separating fragments. Two factors contribute essentially to the volume change of this reaction (14, 15); (*i*) the change of volume of the substrate and (*ii*), the change of volume due to changes in the interaction of the solvent with the substrate.

A rough estimate by Evans (16) suggested that the C—Cl bond is stretched by about 0.7 Å to form the transition state, and this multiplied by

Can. J. Chem. Downloaded from www.nrcresearchpress.com by 210.87.254.5 on 09/05/12
For personal use only.

TABLE 3

Thermal expansivity and compressibility of water–ethanol mixtures, and volumes of activation for the solvolysis of *t*-butyl chloride in these mixtures at 0 °C

% v/v ethanol in water	$10^6\,\alpha$ / deg^{-1}*	$10^6\,\kappa$ / bar^{-1}*	$\Delta V^{\neq}$ / cm^3 mole^{-1}	$T\alpha\Delta V^{\neq}/\kappa$ / cal mole^{-1}
0	−68.1	50.3	−2.0± ~0.5	18± ~ 5
10	25.3	44.1	−7.0± ~1.0	−26± ~ 5
25	241	38.1	−13.2± ~0.6	−545± ~ 50
40	625	44.3	−21.5± ~1.0	−1979± ~100

*Values of α and κ for water are from ref. 7, and for other solvents, from ref. 8.

TABLE 4

The activation parameters for the hydrolysis of *t*-butyl chloride in water–ethanol mixtures at 0 °C

% v/v ethanol in water	$\Delta G_p^{\neq}$ / cal mole^{-1}	$\Delta H_p^{\neq}$ / cal mole^{-1} ± 150	$T\Delta S_p^{\neq}$ / cal mole^{-1} ± 150	$\Delta U_V^{\neq}$ / cal mole^{-1} ± ~200	$T\Delta S_V^{\neq}$ / cal mole^{-1} ± ~200
0	19 864	24 258	4 394	24 240	4 376
10	20 095	24 555	4 460	24 581	4 486
25	20 424	22 700	2 276	23 245	2 821
40	21 240	20 858	−382	22 837	1 597

the cross section of the molecule yields a volume expansion of about 12 cm^3 mole^{-1}. This estimate compares favorably with the observed values listed in Table 5 for several unimolecular decompositions in which large changes in the interaction with the solvent probably do not occur. Hamann (17) has reviewed a number of free-radical decompositions which have similar volumes of activation.

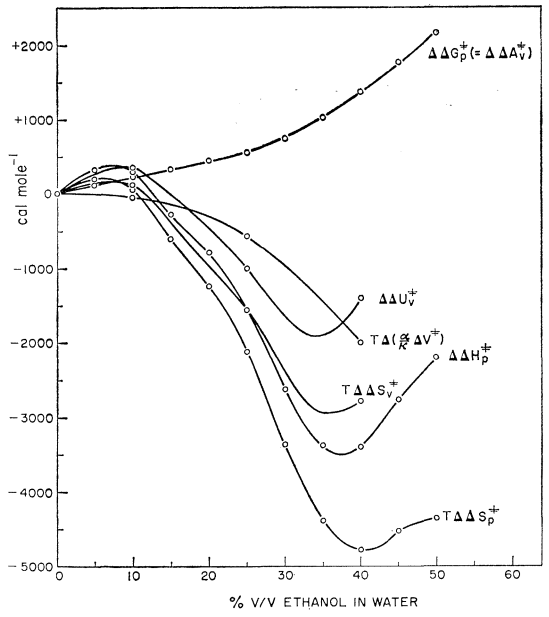

FIG. 4. Changes in the activation parameters for the solvolysis of *t*-butyl chloride with composition in ethanol–water at 0 °C.

The transfer of charge from Cl to *t*-Bu will tend to make the Cl part expand due to the decreased nucleus–electron attraction and the *t*-Bu part contract due to the increased nucleus–electron attraction (18). The two effects will tend to compensate one another, and for lack of knowledge they are neglected.

The increased electrostatic interaction with the solvent when the transition state is formed causes a volume decrease. This might be expected to be similar to the volume decrease accompanying the formation of zwitter-ions of α-amino acids

[3] $$NH_2CHRCO_2H \rightleftharpoons \overset{+}{N}H_3CHRCO_2^-$$

but probably somewhat smaller because the charges will not be so well separated in the transition state. According to density measurements of Cohn and others (19, 20*a*), the volumes of formation of zwitter-ions from the unionized amino acids are in the range −13 to −18 cm^3 mole^{-1}.

If the charges are almost fully developed in the transition state for the solvolysis of *t*-butyl chloride, the expansion due to the stretching of the

Can. J. Chem. Downloaded from www.nrcresearchpress.com by 210.87.254.5 on 09/05/12
For personal use only.

TABLE 5

Volumes of activation for several unimolecular decompositions in which large changes in the interaction with the solvent are not expected

Reaction	Temperature °C	Solvent	$\Delta V^{\ddagger}$/cm^3 mole^{-1}	Reference
$CHCl_3 + OH^- \rightarrow H_2O + [CCl_2\text{---}Cl]^{\ddagger -}$	25	H_2O	16	34
$CCl_3CO_2^- \rightarrow [CCl_3\text{---}CO_2]^{\ddagger -}$	85	H_2O	13	35
	163	H_2O	10	36*
$t\text{-Bu}\overset{+}{S}Me_2 \rightarrow [t\text{-Bu---}SMe_2]^{\ddagger +}$	61.4	EtOH	10	
$t\text{-Bu}\overset{+}{S}Me_2 \rightarrow [t\text{-Bu---}SMe_2]^{\ddagger +}$	71	H_2O	9	36,37
$t\text{-Am}\overset{+}{S}Me_2 \rightarrow [t\text{-Am---}SMe_2]^{\ddagger +}$	53.8	80% v/v EtOH in H_2O	14	37
$ArN_2^+ \rightarrow [Ar\text{---}N_2]^{\ddagger +}$	Various 21–71	H_2O	10	37
$EtHg^+ \rightarrow [Et\text{---}Hg]^{\ddagger +}$	114	H_2O	6	36
$iso\text{-}PrHg^+ \rightarrow [iso\text{-}Pr\text{---}Hg]^{\ddagger +}$	46.4	H_2O	9	36

*Several others decarboxylations are also reported.

bond and the contraction due to the electrostatic interaction are therefore expected to be of a similar magnitude, and the experimental activation volume of -2 cm^3 mole^{-1} can be qualitatively understood. The large separation of charge was derived by Scatchard (21) from the large effect of solvent composition on the rate.

2. Origin of the Volume of Formation of Zwitter-ions

The cause of the contraction in reaction [3] is worth a brief discussion. Gucker, Klotz, and Allen (22) and Gucker, Lamb, Marsh, and Haag (23) have discussed the solvation of zwitter-ions based on a model in which the zwitter-ion is represented as an incompressible dipolar sphere (24) of radius a and the solvent as a continuous dielectric of permittivity ε. A model (15) in which the zwitter-ion is compressible, or alternatively is in a compressible cavity in the solvent, is more realistic and is adopted here. The contribution to the volume of reaction [3] due to the interaction of the zwitter-ion with the solvent is (15), on the basis of this model when electric saturation of the dielectric is ignored,

$$[4] \quad \Delta V_{es} = \frac{3}{2} N \frac{\mu^2}{a^3} \times \left\{ \frac{1}{2} \frac{\partial \varepsilon^{-1}}{\partial p} + \left(1 - \frac{3}{2\varepsilon}\right) \frac{\partial \ln a}{\partial p} \right\}$$

where μ is the dipole moment of the zwitter-ion.

For glycine the volume of zwitter-ion formation is (19)

$$\Delta V = -13 \quad \text{cm}^3 \text{ mole}^{-1}$$

and the dipole moment (20*b*) is

$$[5] \qquad \mu = \sim 15 \quad \text{D}$$

The molar volume of crystalline glycine is 46.6 cm^3 mole^{-1} (25), and so, taking glycine to be spherical, $a^3 = 77$ Å^3. Then

$$[6] \quad \tfrac{3}{2} N \frac{\mu^2}{a^3} = 2.6 \times 10^6 \quad \text{cm}^3 \text{ bar mole}^{-1}$$

and so from eqs. [4]–[6]

$$[7] \quad \left\{ \frac{1}{2} \frac{\partial \varepsilon^{-1}}{\partial p} + \left(1 - \frac{2}{3\varepsilon}\right) \frac{\partial \ln a}{\partial p} \right\} = -5.0 \times 10^{-6} \quad \text{bar}^{-1}$$

For water

$$[8] \quad \frac{1}{2} \frac{\partial \varepsilon^{-1}}{\partial p} = -0.30 \times 10^{-6} \quad \text{bar}^{-1}$$

If the model is a reasonable representation of glycine in water, it follows from eqs. [7] and [8] that little of the volume of zwitter-ion formation is an electrostriction of the solvent as described by eq. [8]. Almost all of it, which is described by the second term on the right-hand side of eq. [4] or on the left-hand side of eq. [7], is a compression of the zwitter-ion due to the ion–solvent interaction, and the correct volume change is predicted by eq. [4] if

$$\partial \ln a / \partial p = -4.6 \times 10^{-6} \quad \text{bar}^{-1}$$

which is at least not unreasonable.

The model will of course fail in so far as other interactions contribute to the volume of ionization, and if saturation of the dielectric occurs.

Can. J. Chem. Downloaded from www.nrcresearchpress.com by 210.87.254.5 on 09/05/12
For personal use only.

Can. J. Chem. Downloaded from www.nrcresearchpress.com by 210.87.254.5 on 09/05/12
For personal use only.

It seems likely, however, that the conclusion that electrostriction of the solvent is relatively small and the compression of the ion contributes the major part of the volume of ionization will not be changed by a more elaborate analysis. The density of crystalline (zwitter-ionic) glycine of 1.61 g cm^{-3} (25) is appreciably higher than that expected for a molecular crystal of glycine. This confirms that there is a considerable contraction of the molecule when the zwitter-ion is formed in a condensed phase. The compression of the ion is also an important part of the volume of solvation of ordinary ions (18).

3. Effect of Solvent on the Activation Volume

The activation volume in 40% v/v ethanol–water is ten times its value in water (see Table 3). The extra contraction is of course due to the change in the interaction with the solvent when the transition state is produced. It is possible that this interaction causes the breaking C---Cl bond to be less elongated in the transition state in the mixed solvents; but this seems unlikely to contribute more than a small fraction of the observed effect.

In water, the contraction due to the interaction with the solvent seems to be about -14 cm^3 $mole^{-1}$ according to section (4.1). If we assume that the intrinsic volume of the transition state is independent of the solvent composition, then the contraction due to interaction with the solvent appears to become about -19, -25, and -34 cm^3 $mole^{-1}$ in 10, 25, and 40% v/v ethanol–water.

The detailed cause of the large variation in the contribution of the interaction with the solvent to the volume of activation is not directly known, although it is not unprecedented experimentally. There is, for example, an appreciable increase in the value of $-\Delta V^{\neq}$ for the spontaneous solvolysis of benzyl chloride in ethanol–water mixtures (10) as the concentration of ethanol increases. Furthermore, there is a definite increase in $-\Delta V^{\neq}$ even for the acid-catalyzed hydrolysis (2) of methyl acetate and ethylene oxide in acetone–water mixtures as the concentration of acetone increases, and a similar change in $-\Delta V^{\neq}$ for the acid-catalyzed iodination of acetone and of acetophenone (1) in ethanol–water mixtures, although these reactions are not usually thought of as occurring with large changes in the interaction with the solvent. These effects, as was pointed out earlier (1), cannot be described by eq. [4] if the dielectric constant ε of the mixture is given by Oster's (26) equation in the form suitable for high dielectric constants

$$[9] \qquad \varepsilon = \sum_i \varepsilon_i \phi_i$$

where ε_i and ϕ_i are the dielectric constants of the pure components and their volume fractions in the mixture. According to this equation, $\partial\varepsilon^{-1}/\partial p$ changes little in the range 0 to 40% v/v ethanol–water (1). It is possible, of course, that eq. [9] does not give the correct pressure variation of the dielectric constant, and a verification is desirable. It seems likely, however, as was concluded earlier for some other reactions (1, 2), that the effect of solvent on the volume of activation cannot be accounted for by dielectric theory, unless saturation occurs.

Arnett and co-workers (27) have shown that a large part of the solvent effect on the activation enthalpy and entropy for this reaction (and for others also) is in fact an effect on the enthalpy and entropy of solution of the initial state. Following this lead, Golinkin, Lee, and Hyne (28) have shown that the solvent variation of the activation volume for the solvolysis of benzyl chloride in water–ethanol is largely caused by a variation with solvent of the partial volume of the initial state benzyl chloride. It is quite possible that the solvolysis of *t*-butyl chloride behaves in a similar way, and so causes at least a part of the observed effect. However, the partial volume of *t*-butyl chloride would have to change by about -20 cm^3 $mole^{-1}$ in the composition range studied if all the change in the activation volume were caused in this way, and this is about 20% of the molar volume of the pure liquid.

The effect of solvent on the activation volume under pressure is quite different. At 1230 bar the activation volumes are (Fig. 2) -2.0, -3.9, -5.0, and -7.2 cm^3 $mole^{-1}$ in 0, 10, 25, and 40% v/v ethanol–water, and if the curves in Fig. 2 for 0, 10, and 25% v/v can be extrapolated to 3 kbar, the activation volume appears to become almost independent of solvent. No other reaction appears to have been reported for which the effect of solvent on the activation volume is so sensitive to the pressure. The effect of solvent on the rate constants is also sensitive to the pressure, but much less so than the activation volume. For example, the ratio of rate constants in 0 and 40% v/v ethanol–water is 117 at 50 bar and 61.3 at

Can. J. Chem. Downloaded from www.nrcresearchpress.com by 210.87.254.5 on 09/05/12
For personal use only.

1480 bar. The only comparable measurements of the effect of solvent and pressure on the activation volume are those on the solvolysis of benzyl chloride at 50 °C in ethanol–water mixtures by Hyne, Golinkin, and Laidlaw (10) and in glycerol–water by Gay and Whalley (29), and there is a partial analogy with the acid-catalyzed enolization of acetone and acetophenone in ethanol–water mixtures (1), and with the acid-catalyzed hydrolysis of methyl acetate and ethylene oxide in acetone–water mixtures (2). Spectacular effects of the kind described here occurred in none of these measurements.

It is possible to speculate that part of the explanation is that the partial volume of *t*-butyl chloride is less dependent on solvent composition at 3 kbar than it is at zero pressure. It appears very difficult to check this speculation experimentally.

4. Activation Parameters at Constant Volume

By transforming to constant-volume conditions, the large minima in the activation enthalpy and entropy at constant pressure cannot be entirely transformed away, but are approximately halved. For two other reactions, the acid-catalyzed hydrolysis of methyl acetate in acetone–water (2) and the neutral solvolysis of benzyl chloride in ethanol–water (3), the minima in the constant-pressure parameters disappears when transformed to constant volume. Clearly, only about a half of the minimum in the constant-pressure parameters for the solvolysis of *t*-butyl chloride can be ascribed to the use of constant-pressure conditions. The minimum in the constant-volume parameters presumably reflects fundamental processes that occur in the solution.

5. Representation of the Rate Constant as a Function of Pressure

Sometimes (30–32) rate constants are fitted to a function of pressure by least squares, either for interpolation or for calculating the activation volume. The function most commonly used is a power series, no doubt because it is linear in the parameters and so is relatively easy to fit. A power series is probably useful for small departures of $\ln k$ from linearity in the pressure, but might not be useful for large departures such as shown by the present results in 40% v/v ethanol.

According to Fig. 2, the activation volume in 40% v/v ethanol–water seems to be approaching asymptotically a value near zero, and to represent it by a power series in the pressure requires at least three terms

$$\Delta V^{\ddagger} = a + bp + cp^2$$

If the rate constant is represented by a power series, at least a cubic is required, and since power series of second and higher order might have extrema for real values of the pressure, all power series must fail at high enough pressures unless the extrema occur at imaginary pressures. This suggests that the equation

$$[10] \qquad \log_{10} k = \frac{a + bp}{1 + cp}$$

might be a better representation than a power series with the same number of parameters. This equation implies that at zero pressure

$$\ln k\,(p = 0) = a$$

$$\Delta V^{\ddagger}\,(p = 0) = -RT(b\text{-}ac)$$

and in the limit of high pressure

$$\lim_{p\to\infty} \ln k = b/c$$

$$\lim_{p\to\infty} \Delta V^{\ddagger} = 0$$

and k has no extrema. When fitted by least squares, this equation yielded

$$a = 1.7560 \pm 0.002$$

$$b = (1.8534 \pm 0.05) \times 10^{-3} \quad \text{bar}^{-1}$$

$$c = (764.4 \pm 20) \times 10^{-6} \quad \text{bar}^{-1}$$

and the standard deviation of the points about the curve was 0.0022.

For comparison, a quadratic

$$[11] \qquad \log_{10} k = a + bp + cp^2$$

yielded

$$a = 1.7834$$

$$b = 319 \times 10^{-6} \quad \text{bar}^{-1}$$

$$c = 60.6 \times 10^{-9} \quad \text{bar}^{-2}$$

with a standard deviation of 0.012 and a highly non-random S-shaped curve of deviations against the pressure. A cubic equation was fitted with the following parameters

$$a = 1.7649 \pm 0.003$$

$$b = (413 \pm 9) \times 10^{-6} \quad \text{bar}^{-1}$$

$$c = -(146 \pm 8) \times 10^{-9} \quad \text{bar}^{-2}$$

$$d = (19.7 \pm 2) \times 10^{-12} \quad \text{bar}^{-3}$$

with a standard deviation of 0.0028.

The quadratic eq. [11] is clearly not useful. The cubic equation with four parameters fits about as well as eq. [10] with three parameters, and might have slightly more nearly random deviations. Equations [10] and [11] and the cubic equation yield activation volumes of −26.7, −16.7, and −21.6 cm^3 $mole^{-1}$, respectively. The last value is the only one that is even close to the value of $-21.5 \pm \sim 1$ cm^3 $mole^{-1}$ determined from Fig. 2. The large difference in the values obtained from eq. [10] and the cubic, although both equations are moderately good fits to the original data, cautions against too great reliance on fitted equations. An attempt (33) to use another empirical equation does not give reliable volumes of activation at zero pressure (17).

It is concluded, therefore, that while the power series is not as good as eq. [10] in fitting log k against pressure for the reaction considered provided the same number of parameters is used, it gives a better activation volume if a larger number of parameters is used. It seems likely that the method used in Fig. 2 is the most reliable way of obtaining the activation volume.

Summary

1. The activation volumes for the spontaneous solvolysis of *t*-butyl chloride in 0, 10, 25, and 40% v/v ethanol in water at 0 °C are −2.0, −7.0, −13.2, and −21.5 cm^3 $mole^{-1}$. In pure water, the small value is a result of the expansion in the transition state due to the lengthening of the C—Cl bond and the opposing contraction due to the changing interaction with the solvent when the transition state is produced. Analogy with the activation volumes for the unimolecular decomposition of ions, and with the volume of formation of zwitter-ions of glycine and other amino acids supports this view.

2. Most of the volume of formation of glycine zwitter-ion, which is −14 cm^3 $mole^{-1}$, appears to be due to the compression of the zwitter-ion by the dipole–solvent interaction. Electrostriction of the solvent contributes only a small part.

3. The effect of solvent on the activation volume is of course largely caused by the changing interaction with solvent when the transition state is produced. It cannot be accounted for by the solvation of the transition state on the basis of the usual dipole-in-dielectric theory. It is possibly due in part to the effect of solvent on the partial volume of *t*-butyl chloride, by analogy with Golinkin, Lee, and Hyne's analysis of similar effects of solvent on the activation volume for the solvolysis of benzyl chloride. Unfortunately, experimental verification of this speculation will not be easy.

4. At 3 kbar, the activation volume appears to be little dependent on the pressure. The cause of this is not known, although it is possible to speculate that the partial volume of the initial state *t*-butyl chloride depends little on the solvent at this pressure.

5. The minimum in the constant-pressure activation enthalpy and entropy as a function of solvent composition is approximately halved if the constant-volume activation energy and entropy are considered. The minima here do not appear to be entirely an artifact of using constant-pressure conditions, as they do for several other reactions.

6. The rate constant as a function of pressure cannot be represented by a power series of less than third order. If an empirical equation is required, a rational function of the form $\ln k = (a + bp)/(1 + cp)$ appears to be more suitable than a power series with the same number of parameters. However, the rational function gives a poor value of the activation volume at zero pressure. It is concluded that graphical methods are the best for extracting activation volumes from the rate constants.

We are grateful to A. Lavergne for help with the high-pressure apparatus and to M. E. Bednas for the gas chromatographic analysis.

1. B. T. BALIGA and E. WHALLEY. Can. J. Chem. **42**, 1835 (1964).
2. B. T. BALIGA, R. J. WITHEY, D. POULTON, and E. WHALLEY. Trans. Faraday Soc. **61**, 517 (1965).
3. B. T. BALIGA and E. WHALLEY. J. Phys. Chem. **71**, 1166 (1967).
4. S. WINSTEIN and A. H. FAINBERG. J. Amer. Chem. Soc. **79**, 5937 (1957).
5. A. I. VOGEL. Textbook of practical organic chemistry. 3rd ed. Longmans, Green and Co., London. 1956.
6. B. T. BALIGA and E. WHALLEY. J. Phys. Chem. **73**, 654 (1969).
7. G. S. KELL and E. WHALLEY. Phil. Trans. Roy. Soc. London, Ser. A, **258**, 565 (1965).
8. J. TIMMERMANS, The physico-chemical constants of binary systems in concentrated solutions. Vol. 4. Interscience Publishers Inc., New York. 1960.

Can. J. Chem. Downloaded from www.nrcresearchpress.com by 210.87.254.5 on 09/05/12
For personal use only.

9. J. BUCHANAN and S. D. HAMANN. Trans. Faraday Soc. **49**, 1425 (1953).
10. J. B. HYNE, H. S. GOLINKIN, and W. G. LAIDLAW. J. Amer. Chem. Soc. **88**, 2104 (1966).
11. P. OLAVI and I. VIRTANEN. Suom. Kem. **B 40**, 178 (1967).
12. J. G. MARTIN and R. E. ROBERTSON. J. Amer. Chem. Soc. **88**, 5353 (1966).
13. C. K. INGOLD. Structure and mechanism in organic chemistry. Bell and Sons, London. pp. 308–418.
14. E. WHALLEY. Advan. Phys. Org. Chem. **2**, 93 (1964).
15. E WHALLEY. J. Chem. Phys. **38**, 1400 (1963).
16. A. G. EVANS. Trans. Faraday Soc. **42**, 719 (1946).
17. S. D. HAMANN. *In* High pressure physics and chemistry. Vol. 2. *Edited by* R. S. Bradley. Academic Press, Inc., London. 1963. p. 163.
18. E. WHALLEY. Ber. Bunsenges. Phys. Chem. **70**, 958 (1966).
19. E. J. COHN, T. L. MCMEEKIN, J. T. EDSALL, and M. H. BLANCHARD. J. Amer. Chem. Soc. **56**, 784 (1934).
20. E. J. COHN and J. T. EDSALL. Proteins, amino acids and peptides. Reinhold Publishing Corp., New York. 1943. (*a*) Chap. 7, (*b*) Chap. 6.
21. G. SCATCHARD. J. Chem. Phys. **7**, 657 (1939).
22. F. T. GUCKER, I. M. KLOTZ, and T. W. ALLEN. Chem. Rev. **30**, 191 (1942).
23. F. T. GUCKER, I. M. KLOTZ, G. A. MARSH, and R. M. HAAG. J. Amer. Chem. Soc. **72**, 310 (1950).
24. J. G. KIRKWOOD. J. Chem. Phys. **2**, 351 (1934).
25. R. E. MARSH. Acta Cryst. **11**, 654 (1958) and references therein.
26. G. OSTER. J. Amer. Chem. Soc. **66**, 2036 (1946).
27. E. M. ARNETT, P. MCC. DUGGLEBY, and J. J. BURKE. J. Amer. Chem. Soc. **85**, 1350 (1963). E. M. ARNETT, W. G. BENTRUDE, J. J. BURKE, and P. MCC. DUGGLEBY. J. Amer. Chem. Soc. **87**, 1541 (1965). E. M. ARNETT, W. G. BENTRUDE, and P. MCC. DUGGLEBY, J. Amer. Chem. Soc. **87**, 2048 (1965).
28. H. S. GOLINKIN, I. LEE, and J. B. HYNE. J. Amer. Chem. Soc. **89**, 1307 (1967).
29. D. L. GAY and E. WHALLEY. To be published.
30. J. KOSKIKALLIO and E. WHALLEY. Trans. Faraday Soc. **55**, 815 (1959).
31. H. S. GOLINKIN, W. G. LAIDLAW, and J. B. HYNE. Can. J. Chem. **44**, 2193 (1966).
32. W. J. LE NOBLE. Progr. Phys. Org. Chem. **5**, 207 (1967).
33. S. W. BENSON and J. A. BERSON. J. Amer. Chem. Soc. **84**, 152 (1962).
34. W. J. LE NOBLE and M. DUFFY. J. Amer. Chem. Soc. **86**, 4512 (1964).
35. A. PHILLIPS and E. WHALLEY. Unpublished work.
36. K. R. BROWER, B. GAY, and T. L. KONKOL. J. Amer. Chem. Soc. **88**, 1681 (1966).
37. K. R. BROWER. J. Amer. Chem. Soc. **85**, 1401 (1963).
38. K. R. BROWER. J. Amer. Chem. Soc. **82**, 4535 (1960).

Can. J. Chem. Downloaded from www.nrcresearchpress.com by 210.87.254.5 on 09/05/12
For personal use only.

Crystal structure of triclinic rubidium dichromate, $Rb_2Cr_2O_7$

N. Ch. Panagiotopoulos and I. D. Brown
Department of Physics, McMaster University, Hamilton, Ontario

Received July 17, 1969

The crystal structure of triclinic rubidium dichromate has been determined by single crystal X-ray diffraction. The crystal belongs to space group $P\bar{1}$ with $a = 13.554$, $b = 7.640$, $c = 7.735$ Å, $\alpha = 93.64°$, $\beta = 98.52°$, $\gamma = 88.80°$ and has four $Rb_2Cr_2O_7$ units in the unit cell. The final weighted agreement index after refinement by least-squares analysis is 0.058. The configuration of the dichromate ions is similar to that found in most other dichromate structures (Cr—O (bridging) = 1.78 Å, Cr—O (terminal) = 1.62 Å). The two non-equivalent Cr—O—Cr angles are 123 and 137°. The rubidium ions are surrounded by either 8 or 9 oxygen atoms at distances ranging from 2.86 to 3.31 Å. The structure of triclinic $Rb_2Cr_2O_7$ is similar, but not identical, to that of triclinic $K_2Cr_2O_7$.

Canadian Journal of Chemistry, **48**, 537 (1970)

Can. J. Chem. Downloaded from www.nrcresearchpress.com by 210.87.254.6 on 09/05/12
For personal use only.

Introduction

The alkali metal dichromates are probably all polymorphic (1, 2). A knowledge of the structure of the various polymorphs is necessary in order to understand the nature of the phase transitions between them. Up to the present only two such structures have been reported, those of $(NH_4)_2Cr_2O_7$ (3) and triclinic $K_2Cr_2O_7$ (4, 5). However, the lattice parameters of many of the crystalline phases are known and are very similar, implying a series of related structures. For example, both $Rb_2Cr_2O_7$ and $K_2Cr_2O_7$ have triclinic forms, stable at room temperature, with cell constants similar enough to suggest that the structures are closely related, but sufficiently different to show that it is unlikely that they are identical.

Experimental

Single crystals of triclinic $Rb_2Cr_2O_7$ were obtained by slow evaporation at 42 °C of an aqueous solution which was prepared from $Na_2Cr_2O_7$ using an ion exchange column in Rb salt form.

The cell constants which are listed in Table 1 were measured from Weissenberg photographs calibrated with rutile ($a = 4.59369$, $c = 2.95814$ Å (6)). The density of 3.12 g cm^{-3} (7) corresponds to four $Rb_2Cr_2O_7$ units per unit cell.

Integrated Weissenberg photographs were taken of the layers $k = 0$, 1, 2, 3, 4 with Cu Kα radiation using a crystal with dimensions 0.06 × 0.20 × 0.06 mm, and integrated precession photographs of the layers $l = 0$, 1, and 2, and $h = 0$, 1, and 2, with Mo Kα radiation using a second crystal with dimensions 0.09 × 0.03 × 0.09 mm.

The intensities, which were measured with a microdensitometer, were corrected for Lorentz and polarization effects but not for absorption which was considered negligible. A standard error (σ) was estimated for each intensity measurement for use in weighting the observed structure factors during the least-squares refinement, and each unobserved reflection was assigned the value of the local minimum observable intensity. In all, 3221 measurements were made of 2881 independent reflections, of which 1263 were unobserved.

It was assumed that the structure of triclinic $Rb_2Cr_2O_7$ would be related to that of triclinic $K_2Cr_2O_7$ (5) and such a model, using space group $P\bar{1}$, was prepared from the [010] and [001] Patterson projections. The positions of the oxygen atoms were determined from difference syntheses. The coordinates and anisotropic temperature factors of each atom and a scale factor for each of the 11 independently measured layers were refined with a full matrix least-squares program, using the International tables (8) scattering factors for Rb^+, Cr^{2+}, O (bridging oxygen atoms), and O^- (terminal oxygen atoms). The scattering factors were corrected for dispersion using the mean value of the real parts of the corrections for Cu Kα and Mo Kα radiations (8). In this refinement, the weight (W) used was $1/\sigma^2$, except for two reflections which were believed to suffer extinction, for all unobserved reflections for which $F_c < F_o$ and for 43 other reflections for which the intensity measurements were judged *a priori* to be

TABLE 1
Crystal Data for Triclinic $Rb_2Cr_2O_7$*

System	Triclinic
Space group	$P\bar{1}(C_i^1)$
Cell constants	
a	13.554±0.001 Å
b	7.640±0.003 Å
c	7.735±0.002 Å
α	93.64 ±0.20°
β	98.52 ±0.01°
γ	88.80 ±0.04°
Unit cell volume	790 Å^3
Formula weight	386.9
Density measured	3.12 g cm^{-3}
calculated	3.25 g cm^{-3}
Number of $Rb_2Cr_2O_7$ units per unit cell	4
X-Ray absorption coefficient	
Mo Kα	157.8 cm^{-1}
Cu Kα	404.4 cm^{-1}

*The cell constants for triclinic $K_2Cr_2O_7$ (5) are: $a = 13.367$, $b = 7.376$, $c = 7.445$ Å, $\alpha = 90.75°$, $\beta = 96.21°$, $\gamma = 97.96°$.

Can. J. Chem. Downloaded from www.nrcresearchpress.com by 210.87.254.6 on 09/05/12
For personal use only.

TABLE 2

Observed (F_o) and calculated (F_c) structure factors of the hk0, 0kl, and h0l layers*

H	K	L	Fo	Fc	σ	H	K	L	Fo	Fc	σ	H	K	L	Fo	Fc	σ	H	K	L	Fo	Fc	σ	H	K	L	Fo	Fc	σ
-8	-9	0	15	-9	3	-7	-4	0	23-	0	11	-8	0	0	64	66	4	0	-7	-5	44	42	3	-12	0	4	16-	12	8
-7	-9	0	16*	-0***		-6	-4	0	68	66	5	-7	0	0	19-	19	9	0	-7	-6	17-	-5	8	-11	0	4	16-	-16	8
-6	-9	0	27	35	5	-5	-4	0	108	107	5	-6	0	0	51	54	4	0	-7	-7	15-	-0	7	-10	0	4	16-	15	8
-5	-9	0	24-	-13	12	-4	-4	0	47	-49	5	-5	0	0	15-	6	7	0	-8	6	29	29	4	-9	0	4	32	-31	4
-4	-9	0	25-	-13	12	-3	-4	0	15	21	3	-4	0	0	305	-332	41	0	-8	5	17-	-18	8	-8	0	4	26	-32	4
-3	-9	0	25-	13	12	-2	-4	0	45	-44	3	-3	0	0	12-	-7	6	0	-8	4	44	-44	3	-7	0	4	68	-65	3
-2	-9	0	25-	1	12	-1	-4	0	78	-75	7	-1	0	0	7-	-0	3	0	-8	3	33	34	4	-6	0	4	39	40	4
-1	-9	0	28	20	5	0	-4	0	18	28	18	0	0	2	169	-164	9	0	-8	2	21	20	9	-5	0	4	98	98	2
0	-9	0	36	37	6	1	-4	0	21-	13	10	0	0	3	11	-17	11	0	-8	1	18-	2	9	-4	0	4	74	72	3
1	-9	0	25-	-3	12	2	-4	0	21-	2	10	0	0	4	47	-46	2	0	-8	0	18-	-16	9	-3	0	4	168	171	4
2	-9	0	22	-20	7	3	-4	0	21-	10	10	0	0	5	14-	-4	7	0	-8	-1	18-	12	9	-2	0	4	78	-77	3
3	-9	0	25-	-11	12	4	-4	0	21-	3	10	0	0	6	16-	-7	8	0	-8	-2	46	49	3	-1	0	4	46	-47	3
4	-9	0	25	-32	9	5	-4	0	53	-50	3	0	0	7	30	26	5	0	-8	-3	45	-45	3	0	0	4	45	-46	3
5	-9	0	24-	-3	12	6	-4	0	22-	-6	11	0	0	8	41	41	4	0	-8	-4	30	-25	5	1	0	4	161	-161	9
6	-9	0	24	19	6	7	-4	0	23-	21	11	0	0	9	26	-26	3	0	-8	-5	16-	-1	8	2	0	4	99	101	3
7	-9	0	23-	7	11	8	-4	0	24-	-4	12	0	-1	9	24	-21	3	0	-9	4	20	-20	6	3	0	4	63	61	2
8	-9	0	21-	15	10	9	-4	0	24-	7	12	0	-1	8	54	57	3	0	-9	3	21	-20	7	4	0	4	13-	17	6
-11	-8	0	22-	1	11	10	-4	0	25-	10	12	0	-1	7	33	34	4	0	-9	2	17-	-0	8	5	0	4	124	126	3
-10	-8	0	24-	-7	12	11	-4	0	26-	-10	13	0	-1	6	48	-50	2	0	-9	1	25	24	6	6	0	4	69	-68	3
-9	-8	0	25-	4	12	12	-4	0	26-	-6	13	0	-1	5	27	-27	3	0	-9	0	37	37	4	7	0	4	51	-51	2
-8	-8	0	25-	19	12	13	-4	0	26-	10	13	0	-1	4	31	-27	2	0	-9	-1	17-	6	8	8	0	4	16-	-2	8
-7	-8	0	18	18	4	14	-4	0	18	-21	4	0	-1	3	23	-25	2	0	-9	-2	24	-27	6	9	0	4	29	-34	4
-6	-8	0	32	20	16	15	-4	0	30	-24	7	0	-1	2	9-	1	4	0	-9	-3	16-	-2	8	10	0	4	26	23	5
-5	-8	0	43	-27	17	16	-4	0	24*	6***		0	-1	0	7-	1	3	0	-9	-4	21	-22	5	11	0	4	22	24	5
-4	-8	0	26-	-9	13	-17	-3	0	23-	-3	11	0	-1	-2	10-	-12	5	1	0	0	4-	-0	2	12	0	4	14	-17	14
-3	-8	0	60	-56	8	-16	-3	0	18	-24	9	0	-1	-3	107	104	5	2	0	0	20	16	8	13	0	4	12-	-9	6
-2	-8	0	43	-44	5	-15	-3	0	23	-26	7	0	-1	-4	13-	-7	6	3	0	0	7-	-7	3	14	0	4	9-	-8	4
-1	-8	0	39	33	6	-14	-3	0	30	-26	6	0	-1	-5	42	-42	2	4	0	0	268X	-332***		-14	0	5	37	-34	2
0	-8	0	26-	-16	13	-13	-3	0	26-	2	13	0	-1	-6	16-	-13	8	5	0	0	13	6	13	-13	0	5	14	-18	14
1	-8	0	60	57	7	-12	-3	0	88	91	6	0	-1	-7	17-	-12	8	6	0	0	59	54	2	-12	0	5	42	44	3
2	-8	0	29	28	8	-11	-3	0	25-	14	12	0	-1	-8	18-	14	9	7	0	0	12-	19	6	-11	0	5	16-	-0	8
3	-8	0	41	-39	6	-10	-3	0	72	73	3	0	-1	-9	37	40	4	8	0	0	70	66	3	-10	0	5	16-	-7	8
4	-8	0	26-	16	13	-9	-3	0	23-	-6	11	0	-2	10	23	-27	5	9	0	0	14-	-4	7	-9	0	5	16	20	16
5	-8	0	26-	-14	13	-8	-3	0	161	-164	8	0	-2	9	18-	11	9	10	0	0	59	-59	4	-8	0	5	57	-57	4
6	-8	0	26-	-11	13	-7	-3	0	21-	-5	10	0	-2	8	18-	-7	9	11	0	0	16-	-12	8	-7	0	5	15-	-7	7
7	-8	0	31	33	2	-6	-3	0	78	-80	7	0	-2	7	17-	9	8	12	0	0	16-	4	8	-6	0	5	34	34	3
8	-8	0	25-	-8	12	-5	-3	0	20-	13	10	0	-2	6	16-	-18	8	13	0	0	16-	9	8	-5	0	5	21	-22	5
9	-8	0	24-	-21	12	-4	-3	0	142	137	5	0	-2	5	79	82	5	14	0	0	44	31	5	-4	0	5	38	36	2
10	-8	0	23-	-4	11	-3	-3	0	19-	2	9	0	-2	4	101	100	5	15	0	0	14-	8	7	-3	0	5	14	19	14
11	-8	0	21-	-11	10	-2	-3	0	101	-97	6	0	-2	3	198	-197	9	16	0	0	16	-22	16	-2	0	5	31	-18	4
-13	-7	0	52	-58	4	-1	-3	0	22*	-17***		0	-2	2	87	-87	5	-16	0	1	43	-39	1	-1	0	5	14	17	7
-12	-7	0	24-	17	12	0	-3	0	76	-71	11	0	-2	1	10-	-7	5	-15	0	1	20	17	5	0	0	5	14-	-4	7
-11	-7	0	36	-27	4	1	-3	0	45	41	4	0	-2	0	116	-114	6	-14	0	1	48	46	2	1	0	5	10	21	10
-10	-7	0	43	40	3	2	-3	0	170	155	15	0	-2	-1	228	206	11	-13	0	1	16-	-15	8	2	0	5	33	-38	3
-9	-7	0	49	53	3	3	-3	0	19-	1	9	0	-2	-2	97	99	10	-12	0	1	29	28	4	3	0	5	10	-18	10
-8	-7	0	27	-26	13	4	-3	0	65	-64	5	0	-2	-3	60	-60	3	-11	0	1	16-	1	8	4	0	5	11	-18	11
-7	-7	0	26-	12	13	5	-3	0	27	-26	2	0	-2	-4	14-	-7	7	-10	0	1	34	-29	3	5	0	5	67	-74	5
-6	-7	0	26-	-9	13	6	-3	0	167	-153	15	0	-2	-5	15-	-17	7	-9	0	1	32	30	3	6	0	5	50	51	8
-5	-7	0	41	-36	4	7	-3	0	21-	8	10	0	-2	-6	25	19	5	-8	0	1	51	53	3	7	0	5	16-	6	8
-4	-7	0	32	31	2	8	-3	0	104	100	4	0	-2	-7	60	-61	5	-7	0	1	31	-31	2	8	0	5	16-	8	8
-3	-7	0	26-	18	13	9	-3	0	23-	12	11	0	-2	-8	29	-34	2	-6	0	1	24	22	2	9	0	5	40	38	3
-2	-7	0	26-	-3	13	10	-3	0	105	105	5	0	-2	-9	55	54	3	-5	0	1	29	-28	1	10	0	5	26	-28	4
-1	-7	0	26-	18	13	11	-3	0	25-	10	12	0	-3	10	25	-33	7	-4	0	1	85	-84	2	11	0	5	14-	-2	7
0	-7	0	26-	-17	13	12	-3	0	59	-50	7	0	-3	9	18-	-7	9	-3	0	1	43	41	2	12	0	5	12-	9	6
1	-7	0	26-	-21	13	13	-3	0	26-	-12	13	0	-3	8	18-	5	9	-2	0	1	15	13	15	13	0	5	9-	-8	4
2	-7	0	26-	-2	13	14	-3	0	27-	-13	13	0	-3	7	45	45	7	-1	0	1	5-	-4	2	-14	0	6	15	20	15
3	-7	0	26-	-7	13	15	-3	0	26-	0	13	0	-3	6	35	37	3	0	0	1	18	-14	18	-13	0	6	13-	-12	6
4	-7	0	26-	14	13	16	-3	0	25-	21	12	0	-3	5	27	-28	4	1	0	1	20	22	0	-12	0	6	35	-24	5
5	-7	0	26-	-6	13	17	-3	0	23-	12	11	0	-3	4	36	-33	3	2	0	1	9	20	9	-11	0	6	15-	8	7
6	-7	0	26-	17	13	-17	-2	0	25-	-11	12	0	-3	3	13-	-3	6	3	0	1	8	11	8	-10	0	6	16-	-9	8
7	-7	0	26-	17	13	-16	-2	0	26-	-17	13	0	-3	2	13-	8	6	4	0	1	58	62	2	-9	0	6	16	25	16
8	-7	0	26-	1	13	-15	-2	0	27-	13	13	0	-3	1	45	-43	2	5	0	1	49	-53	4	-8	0	6	16-	-5	8
9	-7	0	50	45	6	-14	-2	0	26-	2	13	0	-3	0	72	-71	3	6	0	1	22	-20	2	-7	0	6	33	-37	4
10	-7	0	25-	-21	12	-13	-2	0	26-	-6	13	0	-3	-1	34	-34	2	7	0	1	12-	3	6	-6	0	6	80	-80	3
11	-7	0	25-	-6	12	-12	-2	0	25-	17	12	0	-3	-2	25	26	3	8	0	1	70	-71	6	-5	0	6	16	-26	16
12	-7	0	24-	-1	12	-11	-2	0	24-	7	12	0	-3	-3	14-	8	7	9	0	1	36	33	3	-4	0	6	16	20	16
13	-7	0	34	-37	5	-10	-2	0	26	16	5	0	-3	-4	37	38	4	10	0	1	16	-20	16	-3	0	6	16	20	8

Can. J. Chem. Downloaded from www.nrcresearchpress.com by 210.87.254.6 on 09/05/12
For personal use only.

TABLE 2 (Concluded)

-14	-6	0	24-	9	12	-9	-2	0	22-	7	11	0	-3	-5	16	20	4	11	0	1	16	-18	16	-2	0	6	178	180	7
-13	-6	0	25-	-5	12	-8	-2	0	21-	-15	10	0	-3	-6	78	-80	4	12	0	1	16-	4	8	-1	0	6	16-	-1	7
-12	-6	0	26-	-5	13	-7	-2	0	32	29	4	0	-3	-7	18-	-10	9	13	0	1	16-	-2	8	0	0	6	16-	-7	8
-11	-6	0	26-	17	13	-6	-2	0	19-	3	9	0	-3	-8	18-	21	9	14	0	1	15-	-13	7	1	0	6	16-	-9	8
-10	-6	0	39	39	4	-5	-2	0	67	67	4	0	-3	-9	17-	-20	8	15	0	1	26	28	3	2	0	6	160	-154	4
-9	-6	0	26-	17	13	-4	-2	0	66	63	4	0	-4	9	17-	-3	8	-15	0	2	24	-33	8	3	0	6	16-	5	8
-8	-6	0	26-	-11	13	-3	-2	0	119	-57	59	0	-4	8	18-	-8	9	-14	0	2	15-	-9	7	4	0	6	29	27	29
-7	-6	0	25	-25	12	-2	-2	0	29	29	6	0	-4	7	40	-41	4	-13	0	2	16-	13	8	5	0	6	16-	-3	8
-6	-6	0	113	-115	7	-1	-2	0	213	-178	19	0	-4	6	27	25	5	-12	0	2	16-	-15	8	6	0	6	75	75	3
-5	-6	0	28	-34	5	0	-2	0	127	-114	18	0	-4	5	16-	-5	8	-11	0	2	16-	22	8	7	0	6	16	-17	16
-4	-6	0	43	44	5	1	-2	0	75	68	11	0	-4	4	15-	-0	7	-10	0	2	15-	-3	7	8	0	6	44	-42	2
-3	-6	0	25-	11	12	2	-2	0	97	-90	9	0	-4	3	232	230	6	-9	0	2	67	-63	3	9	0	6	14-	-9	7
-2	-6	0	187	178	14	3	-2	0	218	196	15	0	-4	2	48	-50	2	-8	0	2	45	-38	6	10	0	6	12	-20	12
-1	-6	0	24-	-6	12	4	-2	0	109	104	13	0	-4	1	154	-152	8	-7	0	2	68	68	3	11	0	6	10	10	9
0	-6	0	44	-39	12	5	-2	0	69	-69	6	0	-4	0	27	28	1	-6	0	2	19	19	6	-13	0	7	9	-15	9
1	-6	0	24-	-7	12	6	-2	0	36	36	3	0	-4	-1	14-	9	7	-5	0	2	99	94	4	-12	0	7	32	-33	2
2	-6	0	147	-138	10	7	-2	0	64	-65	5	0	-4	-2	15-	1	7	-4	0	2	123	118	7	-11	0	7	33	35	2
3	-6	0	25-	6	12	8	-2	0	30	-34	3	0	-4	-3	22	-20	5	-3	0	2	256	-250	12	-10	0	7	14-	3	7
4	-6	0	30	31	2	9	-2	0	53	57	4	0	-4	-4	38	33	3	-2	0	2	125	-121	5	-9	0	7	15-	-6	7
5	-6	0	25-	-7	12	10	-2	0	23-	-1	11	0	-4	-5	90	90	8	-1	0	2	63	-64	3	-8	0	7	19	28	19
6	-6	0	36	33	4	11	-2	0	24-	-20	12	0	-4	-6	41	-43	3	0	0	2	153	-164	6	-7	0	7	20	-27	6
7	-6	0	25-	-4	12	12	-2	0	25-	-11	12	0	-4	-7	18-	-5	9	1	0	2	279X	336***		-6	0	7	20	-28	6
8	-6	0	43	-49	5	13	-2	0	26	-25	6	0	-4	-8	18-	-10	9	2	0	2	87	92	3	-5	0	7	20	15	20
9	-6	0	26-	-4	13	14	-2	0	19	-17	4	0	-4	-9	44	-46	3	3	0	2	73	77	3	-4	0	7	20	-26	6
10	-6	0	26-	6	13	15	-2	0	48	49	5	0	-5	9	37	-39	3	4	0	2	92	100	4	-3	0	7	20	16	20
11	-6	0	26-	7	13	16	-2	0	26-	9	13	0	-5	8	18-	-21	9	5	0	2	201	-208	9	-2	0	7	16-	-0	8
12	-6	0	34	32	2	17	-2	0	25-	7	12	0	-5	7	18-	13	9	6	0	2	45	-49	3	-1	0	7	16-	-1	8
13	-6	0	25-	2	12	-17	-1	0	18	-25	4	0	-5	6	17-	18	8	7	0	2	36	-35	2	0	0	7	23	26	6
14	-6	0	23-	-9	11	-16	-1	0	40	36	4	0	-5	5	24	20	6	8	0	2	25	-29	4	1	0	7	16-	0	8
-16	-5	0	20-	-7	10	-15	-1	0	52	52	5	0	-5	4	16-	1	8	9	0	2	52	54	4	2	0	7	59	57	2
-15	-5	0	24-	11	12	-14	-1	0	26-	-0	13	0	-5	3	16-	7	8	10	0	2	16-	27	8	3	0	7	16-	-3	8
-14	-5	0	26-	-21	13	-13	-1	0	63	79	12	0	-5	2	16-	9	8	11	0	2	33	-38	8	4	0	7	16-	-12	8
-13	-5	0	26-	20	13	-12	-1	0	68	-74	5	0	-5	1	27	-30	4	12	0	2	16-	-17	8	5	0	7	15-	0	7
-12	-5	0	26-	-7	13	-11	-1	0	119	-123	7	0	-5	0	16-	2	7	13	0	2	15-	-8	7	6	0	7	64	-64	3
-11	-5	0	26-	-17	13	-10	-1	0	23-	19	11	0	-5	-1	54	-55	4	14	0	2	14-	1	7	7	0	7	14	24	14
-10	-5	0	26-	6	13	-9	-1	0	132	-127	13	0	-5	-2	16-	-2	8	15	0	2	23	27	5	8	0	7	12-	-2	6
-9	-5	0	25-	5	12	-8	-1	0	90	92	7	0	-5	-3	49	50	2	16	0	2	16	18	16	9	0	7	10-	-1	5
-8	-5	0	25-	-2	12	-7	-1	0	114	123	5	0	-5	-4	29	31	4	-15	0	3	55	-56	3	10	0	7	30	32	4
-7	-5	0	24-	2	12	-6	-1	0	28	-29	4	0	-5	-5	17-	-1	8	-14	0	3	15-	-5	7	-11	0	8	14	-26	7
-6	-5	0	24-	19	12	-5	-1	0	45	50	6	0	-5	-6	22	23	-0	-13	0	3	57	52	4	-10	0	8	11	15	11
-5	-5	0	29	-31	2	-4	-1	0	55	-56	5	0	-5	-7	40	-40	4	-12	0	3	16	-22	16	-9	0	8	13	-8	6
-4	-5	0	23-	7	11	-3	-1	0	54	-58	8	0	-5	-8	17-	-13	8	-11	0	3	16-	2	8	-8	0	8	14-	12	7
-3	-5	0	23-	24	11	-2	-1	0	12-	4	6	0	-5	-9	25	25	4	-10	0	3	16-	5	8	-7	0	8	46	45	7
-2	-5	0	23-	-4	11	-1	-1	0	11-	-5	5	0	-6	8	17-	10	8	-9	0	3	59	-58	3	-6	0	8	15-	4	7
-1	-5	0	23-	-0	11	0	-1	0	10-	1	5	0	-6	7	22	23	7	-8	0	3	20	24	5	-5	0	8	41	-36	5
0	-5	0	23-	2	11	1	-1	0	11-	1	5	0	-6	6	76	-76	4	-7	0	3	42	44	4	-4	0	8	31	-32	3
1	-5	0	40	-37	5	2	-1	0	21	-23	5	0	-6	5	28	-26	5	-6	0	3	12	2	6	-3	0	8	35	-35	3
2	-5	0	38	-41	7	3	-1	0	37	-42	3	0	-6	4	57	56	2	-5	0	3	16	16	4	-2	0	8	27	-25	4
3	-5	0	91	93	7	4	-1	0	15-	2	7	0	-6	3	17-	-11	8	-4	0	3	11-	-6	5	-1	0	8	102	95	4
4	-5	0	41	36	5	5	-1	0	32	-29	5	0	-6	2	64	68	3	-3	0	3	49	-48	3	0	0	8	41	41	3
5	-5	0	68	69	8	6	-1	0	23	24	3	0	-6	1	17-	6	8	-2	0	3	20	18	2	1	0	8	31	29	3
6	-5	0	79	77	7	7	-1	0	19-	-5	9	0	-6	0	42	-39	3	-1	0	3	7	-9	7	2	0	8	28	32	4
7	-5	0	121	-123	6	8	-1	0	20-	14	10	0	-6	-1	21	15	7	0	0	3	17	-17	2	3	0	8	97	-91	4
8	-5	0	25-	-15	12	9	-1	0	22-	0	11	0	-6	-2	17-	-22	8	1	0	3	10-	-9	5	4	0	8	19	-22	4
9	-5	0	65	-66	5	10	-1	0	23-	-9	11	0	-6	-3	17-	7	8	2	0	3	10-	2	5	5	0	8	12-	0	6
10	-5	0	53	-50	4	11	-1	0	64	65	4	0	-6	-4	55	-53	2	3	0	3	8	-15	8	6	0	8	16	-16	16
11	-5	0	77	79	6	12	-1	0	45	-34	10	0	-6	-5	18-	-2	9	4	0	3	12-	7	6	7	0	8	37	43	3
12	-5	0	26-	1	13	13	-1	0	26-	4	13	0	-6	-6	84	86	4	5	0	3	78	81	4	-7	0	9	15	26	15
13	-5	0	26	24	6	14	-1	0	26-	-8	13	0	-6	-7	17-	2	8	6	0	3	13-	-4	6	-6	0	9	11-	-5	5
14	-5	0	22	27	7	15	-1	0	52	-49	12	0	-7	-7	17-	-12	8	7	0	3	29	33	3	-5	0	9	17	-19	17
15	-5	0	29	-28	4	16	-1	0	19	17	4	0	-7	6	18-	0	9	8	0	3	27	38	5	-4	0	9	17	15	17
16	-5	0	20-	-1	10	17	-1	0	25-	8	12	0	-7	5	18-	-2	9	9	0	3	57	-61	4	-3	0	9	18	-22	18
-16	-4	0	24	-24	9	-17	0	0	25-	-14	12	0	-7	4	18-	-10	9	10	0	3	16-	11	8	-2	0	9	12-	-0	6
-15	-4	0	26-	-16	13	-16	0	0	23	-22	7	0	-7	3	18-	5	9	11	0	3	16-	1	8	-1	0	9	12-	-4	6
-14	-4	0	26-	12	13	-15	0	0	27-	8	13	0	-7	2	17-	20	8	12	0	3	16-	-16	8	0	0	9	17	-26	17
-13	-4	0	26-	-6	13	-14	0	0	23	31	7	0	-7	1	17-	6	8	13	0	3	14-	-0	7	1	0	9	11-	5	5
-12	-4	0	26-	11	13	-13	0	0	26-	9	13	0	-7	0	17-	-17	8	14	0	3	12-	-2	6	2	0	9	11-	-3	5
-11	-4	0	25-	19	12	-12	0	0	25-	4	12	0	-7	-1	17-	-13	8	15	0	3	13	-18	13	3	0	9	35	34	2
-10	-4	0	38	-44	4	-11	0	0	24-	-12	12	0	-7	-2	22	-22	7	-15	0	4	12	16	12						
-9	-4	0	50	-53	4	-10	0	0	58	-59	5	0	-7	-3	46	-43	3	-14	0	4	14	-26	14						
-8	-4	0	24-	17	12	-9	0	0	21-	-4	10	0	-7	-4	25	19	3	-13	0	4	16	-20	16						

* σ is the estimated standard error of F_o. A minus sign after F_o indicates an unobserved reflection, an asterisk indicates an unreliable measurement of F_o which was given zero weight during refinements, a cross indicates a reflection believed to show extinction effects and omitted from the final refinement.

TABLE 3

Coordinates and temperature factors of the atoms in triclinic $Rb_2Cr_2O_7$*

	Coordinates			Temperature factor components					
Atom	x	y	z	β_{11}	β_{22}	β_{33}	β_{12}	β_{13}	β_{23}
Rb1	0.13528	0.11118	0.87628	37	91	106	−12	20	−18
Rb2	−0.15303	0.22589	0.62431	32	122	73	−8	6	16
Rb3	0.34205	0.55555	0.80287	24	102	88	−2	8	12
Rb4	0.62878	0.78601	0.70265	37	131	86	−7	14	6
σ(Rb)	0.00011	0.00019	0.00016	1	4	3	2	1	3
Cr1	0.1107	0.2853	0.3915	24	73	73	−16	4	−7
Cr2	−0.0853	0.3531	0.1361	26	71	79	−2	13	7
Cr3	0.3883	0.0613	0.7559	28	93	84	−8	13	1
Cr4	0.5826	0.3022	0.7157	26	85	78	−12	13	−0
σ(Cr)	0.0002	0.0003	0.0003	2	6	4	3	2	4
OB1	0.0238	0.4283	0.2734	50	59	105	0	10	−10
O11	0.1994	0.4025	0.4953	23	117	193	9	−13	−67
O12	0.1543	0.1463	0.2571	46	168	93	28	11	−27
O13	0.0546	0.1833	0.5225	40	267	122	2	25	49
O21	−0.1478	0.5180	0.0506	21	73	192	15	15	54
O22	−0.1528	0.2493	0.2534	44	91	80	−20	13	−2
O23	−0.0546	0.2166	−0.0158	46	128	80	23	14	−13
OB3	0.4712	0.1857	0.6530	37	111	127	−41	15	32
O31	0.2966	0.0102	0.6072	35	135	142	−5	16	24
O32	0.3496	0.1818	0.9121	29	151	97	8	21	−22
O33	0.4430	−0.1138	0.8289	48	140	156	−7	−14	4
O41	0.6197	0.3717	0.5466	69	115	103	1	55	31
O42	0.6678	0.1800	0.8150	34	129	191	16	27	39
O43	0.5604	0.4666	0.8438	48	118	104	6	34	−17
σ(O)	0.0007	0.0013	0.0012	8	26	20	11	10	17

*The standard errors are those indicated by the least-squares refinement. The temperature factors appear in the structure factor calculation as $\exp(-10^{-4}(\beta_{11}h^2 + \beta_{22}k^2 + \beta_{33}l^2 + 2\beta_{12}hk + 2\beta_{13}hl + 2\beta_{23}kl))$.

particularly unreliable. In each of these latter cases the weight was set to zero. After several rounds of refinement, the weighted agreement index

$$R_2 = [\sum W(|F_o| - |F_c|)^2/\sum W|F_o|^2]^{1/2}$$

had fallen to 0.058 and the unweighted agreement index

$$R_1 = \sum(|F_o| - |F_c|)/\sum|F_o|$$

had fallen to 0.063. The values of $W(|F_o| - |F_c|)^2$ showed no systematic variation which would indicate that the weighting scheme was inadequate.

The observed and final calculated structure factors for the $0kl$, $h0l$, $hk0$ layers are given in Table 2. (The complete set of structure factors is in the Depository for Unpublished Data.[1]) The final atomic coordinates and temperature factors are given in Table 3. The temperature factors suggest that the $Cr_2O_7^{2-}$ ions are librating around Cr—Cr axis with a root-mean-square amplitude of 6°. Interatomic distances and angles are given in Table 4. The Cr—O distances are given both before and after correction for the apparent shortening caused by $Cr_2O_7^{2-}$ libration.

[1]Copies may be obtained free of charge, upon request, from the Depository of Unpublished Data, National Science Library, National Research Council of Canada, Ottawa, Canada.

Discussion

Triclinic $Rb_2Cr_2O_7$ and triclinic $K_2Cr_2O_7$ are similar although, as suspected, the crystals are not isostructural. Both contain sheets in which pairs of dichromate ions related by centers of symmetry are repeated in the b and c directions at the corners of an almost square net. In both structures, two crystallographically distinct sheets alternate along the a direction, with adjacent sheets aligned, not parallel to each other, but related by a rotation of 90° about the sheet normal (see Fig. 1).

The presence of the centers of symmetry in each sheet results in the opposite sides of the sheet being enantiomorphically related to each other. Thus, it is possible to identify one side of each sheet as right-handed and the other as left-handed. In $K_2Cr_2O_7$, the sheets pack with right-handed and left-handed sides in contact. In $Rb_2Cr_2O_7$, the sheets pack with sides of the same handedness in contact, an arrangement which corresponds to a structure of type VIII in the scheme proposed by Brown and Calvo (9).

Can. J. Chem. Downloaded from www.nrcresearchpress.com by 210.87.254.6 on 09/05/12
For personal use only.

TABLE 4
Interatomic distances and angles in triclinic $Rb_2Cr_2O_7$*

Atom pair	Distance (Å) Uncorrected	Thermally corrected	Atom pair	Distance (Å) Uncorrected	Thermally corrected
Cr1—Cr2	3.122	3.122	Cr3—Cr4	3.307	3.307
Cr1—OB1	1.780	1.787	Cr3—OB3	1.789	1.799
Cr2—OB1	1.772	1.776	Cr4—OB3	1.759	1.768
	Mean corrected Cr—O (bridge) = 1.782				
Cr1—O11	1.600	1.614	Cr3—O31	1.600	1.607
O12	1.604	1.622	O32	1.615	1.624
O13	1.602	1.624	O33	1.609	1.624
Cr2—O21	1.624	1.636	Cr4—O41	1.593	1.611
O22	1.630	1.636	O42	1.606	1.622
O23	1.616	1.629	O43	1.602	1.613
	Mean corrected Cr—O (terminal) = 1.622				
OB1—O11	2.73		OB3—O31	2.71	
O12	2.77		O32	2.78	
O13	2.75		O33	2.80	
O21	2.78		O41	2.74	
O22	2.76		O42	2.77	
O23	2.77		O43	2.72	
O11—O12	2.62		O31—O32	2.63	
O13	2.65		O33	2.63	
O12—O13	2.62		O32—O33	2.66	
O21—O22	2.67		O41—O42	2.61	
O23	2.66		O43	2.60	
O22—O23	2.63		O42—O43	2.62	
O12—O23	3.33		O32—O43	3.75	
O13—O22	3.29		O33—O42	3.84	

Atoms	Angle (deg)	Atoms	Angle (deg)
Cr1—OB1—Cr2	123.0	Cr3—OB3—Cr4	137.5
OB1—Cr1—O11	107.7	OB3—Cr3—O31	106.1
OB1—Cr1—O12	109.6	OB3—Cr3—O32	109.3
O13	108.8	O33	110.6
O11—Cr1—O12	109.7	O31—Cr3—O32	110.0
O13	111.5	O33	109.8
O12—Cr1—O13	109.4	O32—Cr3—O33	110.9
OB1—Cr2—O21	110.0	OB3—Cr4—O41	109.6
O22	108.5	O42	110.9
O23	109.4	O43	108.2
O21—Cr2—O22	110.2	O41—Cr4—O42	109.5
O23	110.4	O43	109.0
O22—Cr2—O23	108.2	O42—Cr4—O43	109.5

Rb—O distances less than 3.31 Å

Atom pair	Distance (Å)	Atom pair	Distance (Å)	Atom pair	Distance (Å)	Atom pair	Distance (Å)
Rb1—O12c	2.91	Rb2—O22	2.89	Rb3—O32	3.02	Rb4—O42b	3.11
O13	2.87	O23c	2.91	O33b	2.88	O43	2.96
O23c	2.90	O13	3.04	O43	3.00	O33b	2.90
O21′$\bar{a}$	2.86	O11′$\bar{a}$	3.07	O41′	2.92	O31′	3.23
O22′d	2.89	O12′d	3.04	O42′c	†	O32′c	2.94
O23′d	3.07	O13′d	†	O43′c	2.87	O33′c	†
OB1′$\bar{a}$	†	OB1′$\bar{a}$	3.19	OB3′	†	OB3′	2.90
O11	†	O21c	†	O31b	†	O41	3.31
O32	2.93	O42$\bar{a}$	3.06	O22′$\bar{a}$	2.93	O12′	2.96
O31	3.28	O41$\bar{a}$	3.24	O21′$\bar{a}$	3.09	O11′	3.24
		O31′d	2.99	O11	3.02		

*The standard errors derived from the errors in the cell constants and the errors indicated by the least-squares refinement are: Cr—Cr, 0.004 Å; Cr—O, 0.010 Å; O—O, 0.014 Å; angles, 1.0°. Symmetry transformations from the atom coordinates in Table 3 are indicated by $a = [100]$, $b = [010]$, $c = [001]$, $d = [\bar{1}\bar{1}0]$, $\bar{a} = [\bar{1}00]$. The prime denotes a prior inversion of the coordinates through the center of symmetry at (1/2, 1/2, 1/2).
†Distance greater than 3.31 Å.

Can. J. Chem. Downloaded from www.nrcresearchpress.com by 210.87.254.6 on 09/05/12
For personal use only.

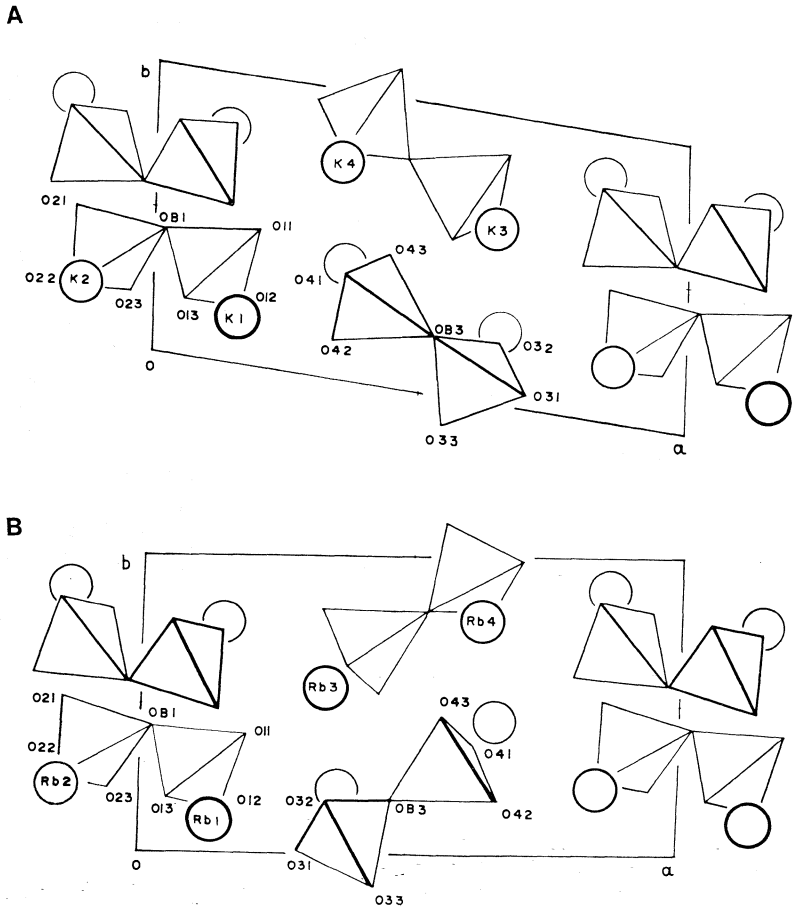

FIG. 1. A, structure of triclinic $K_2Cr_2O_7$ viewed down the *c* axis. B, structure of triclinic $Rb_2Cr_2O_7$ viewed down the *c* axis. Oxygen atoms lie at the apices of the tetrahedra, chromium atoms lie at the centers.

TABLE 5

A comparison of bond lengths and angles in triclinic $K_2Cr_2O_7$ and triclinic $Rb_2Cr_2O_7$*

	$K_2Cr_2O_7$		$Rb_2Cr_2O_7$	
	I	II	I	II
Cr—O bridging	1.78 Å	1.78 Å	1.78 Å	1.78 Å
Cr—O terminal	1.63 Å	1.60 Å	1.63 Å	1.62 Å
OB1—Cr1—O11 OB3—Cr3—O31	106.1°	106.6°	107.7°	106.1°
O—Cr—O (all others)	109.8°	109.7°	109.6°	109.7°
Cr—OB—Cr	124.0°	127.6°	123.0°	137.5°
Twist angle	5°	10°	1°	9°
Root-mean square angle of libration about Cr—Cr	6°		6°	

*The crystallographically non-equivalent sheets are designated by I and II.

Can. J. Chem. Downloaded from www.nrcresearchpress.com by 210.87.254.6 on 09/05/12
For personal use only.

Because of the 90° rotation between adjacent sheets, the role of *b* and *c* translations is interchanged between one sheet and the next. The slight inequalities in the lengths of *b* and *c* necessarily result in a distortion of the second sheet compared to the first, The first sheets in both $K_2Cr_2O_7$ and $Rb_2Cr_2O_7$ (Cr1, Cr2) are virtually identical. The second sheets (Cr3, Cr4) differ from the first sheets in a similar way in both structures but the effect is more pronounced in $Rb_2Cr_2O_7$. The small differences in environment of the dichromate ions result in differences of the angle at the bridging oxygen atom and the twist angle[2] as is shown in Table 5. However, apart from these two angles, both crystallographically distinct dichromate groups found in triclinic $Rb_2Cr_2O_7$ are identical, and are, in addition, identical to the two found in triclinic $K_2Cr_2O_7$ (5).

The rubidum atoms are surrounded by between 8 and 9 oxygen atoms at distances varying between 2.86 and 3.31 Å, leading to an average Rb—O distance of 3.00 Å. In $K_2Cr_2O_7$, the K atoms are also surrounded by 7, 8, or 9 atoms, but at the rather smaller average distance of 2.85 Å.

[2]This angle is calculated by taking the average of the three smallest angles occurring between the projections of opposite Cr—O bonds onto the plane perpendicular to Cr—Cr.

We wish to thank the National Research Council of Canada for financial support and one of us (N.Ch.P.) wishes to thank the Province of Ontario for an Ontario Graduate Fellowship.

1. U. KLEMENT and G. SCHWAB. Z. Kristallogr. **114**, 170 (1960).
2. Y. I. VESNIN and L. A. KHRIPIN. Zh. Neorg. Khim. **11**, 2216 (1966).
3. A. BYSTRÖM and K. WILHELMI. Acta Chem. Scand. **5**, 1003 (1951).
4. E. A. KUZ'MIN, V. V. ILYUKHIN, and N. V. BELOV. Dokl. Akad. Nauk. SSSR, **173**, 1068 (1967).
5. J. K. BRANDON and I. D. BROWN. Can. J. Chem. **46**, 933 (1968).
6. M. E. STRAUMANIS, T. EJIMA, and W. J. JAMES. Acta Crystallogr. **14**, 493 (1961).
7. Handbook of Chemistry and Physics. 48th ed. The Chemical Rubber Co. 1967. p. B-215.
8. International tables for X-ray crystallography. Vol. III. Kynoch Press, Birmingham. 1962. Tables 3.3.1A, 3.3.2B, 3.3.2C.
9. I. D. BROWN and C. CALVO. J. Solid State Chem. In press.

Can. J. Chem. Downloaded from www.nrcresearchpress.com by 210.87.254.6 on 09/05/12
For personal use only.

Can. J. Chem. Downloaded from www.nrcresearchpress.com by 210.87.254.6 on 09/05/12
For personal use only.

Metal ion initiated halogenation reaction of *N*-haloamines

F. Minisci and G. P. Gardini
Istituto di Chimica Organica, Università di Parma, Parma, Italy

AND

F. Bertini
Istituto di Chimica, Politecnico di Milano, Milano, Italy

Received June 17, 1969

The metal ion catalyzed chlorination of 1-chlorobutane, 1-chlorohexane, methyl-pentanoate, and methyl-heptanoate by protonated *N*-chloroamines proceeds by a free radical chain mechanism and the chain carrying species was shown not to be a chlorine atom, but an amino radical cation.

Canadian Journal of Chemistry, **48**, 544 (1970)

Recently Tanner and Mosher (1) reported as the conclusion of their investigations that the metal ion catalyzed chlorination of hydrocarbon substrates by *N*-chloroamines proceeds by a free radical chain mechanism. The chain carrying species in these halogenations is the chlorine atom.

This conclusion is in contrast with what we have reported with many substrates, which unambiguously show that a chlorine atom is not the chain carrying species under our experimental conditions, but it is an amino radical cation which determines a unique, synthetically useful and theoretically interesting reaction (2) owing to its high sensitivity to the polar effects, whether in hydrogen abstraction or in addition to unsaturated systems (alkenes, alkynes, and arenes) (3).

To avoid every possibility of confusion here we report the results obtained with 1-chlorobutane, 1-chlorohexane, methyl-pentanoate, and -heptanoate following the scheme described by Tanner and Mosher. These results are shown in Table 1 and are so eloquent in confirming our mechanism that comments are superfluous.

A more complete study on the subject will be published in an Italian journal.

Experimental

Materials

N-Chloro- and *N*-bromo-dimethylamine were prepared according to the method previously reported (2). The other substrates were commercially available. Gas–liquid chromatographic (g.l.c.) analyses were carried out as previously reported (2).

TABLE 1
Halogenation with *N*-haloamines

Reaction No.	Reaction conditions	Isomer distribution* (%)					
		Cl—CH_2—CH_2—CH_2—CH_3					
1	$(CH_3)_2\overset{+}{N}HCl/Fe^{++}$	Traces	6.6	87.8	5.4		
2	$Cl_2,H_2SO_4/HOAc$	4.3	17.8	48.8	29.1		
3†	$Cl_2,H_2SO_4/HOAc$	5.4	20.9	52.0	21.6		
		Cl—CH_2—CH_2—CH_2—CH_2—CH_2—CH_3					
4	$(CH_3)_2\overset{+}{N}HCl/Fe^{++}$	—	Traces	6.8	19.4	71.6	2.2
5	$(CH_3)_2\overset{+}{N}HBr/Fe^{++}$	—	Traces	4.7	19.8	73.0	2.2
		CH_3OCO—CH_2—CH_2—CH_2—CH_3					
6	$(CH_3)_2\overset{+}{N}HCl/Fe^{++}$	—	13.3	79.9	6.7		
7	Cl_2/CCl_4	3.5	26.9	42.5	26.7		
8‡	$H_2SO_4/HOAc$	3.4	29.4	40.4	26.8		
		CH_3OCO—CH_2—CH_2—CH_2—CH_2—CH_2—CH_3					
9	$(CH_3)_2\overset{+}{N}HCl/Fe^{++}$	—	0.9	4.7	19.2	72.2	2.9
10§	Cl_2	1.8	9.4	21.3	23.9	26.5	17.2

*Values are the averages of the results of three independent experiments. The values agreed to within ±4%.
†Taken from ref. 1.
‡Chloroesters of the reaction 7 placed in $H_2SO_4/HOAc$.
§Chloroesters obtained in CCl_4 placed in $H_2SO_4/HOAc$.

Chlorination and Bromination with N-Chloro- and N-Bromo-dimethylamine (Reaction 1,4,5,6,9; Table 1)

The procedure was identical for all substrates. To a solution of *N*-halodimethylamine (0.037 moles) in 21.3 ml of sulfuric acid were added 3.7 ml of acetic acid and 0.05 moles of substrate. The reaction mixture was stirred rapidly and 0.025 moles of finely powdered ferrous sulfate heptahydrate were added with external cooling; temperature 20–30°. The reaction was completed within 8 min. The mixture was then poured on ice and extracted with *n*-hexane. The solution was washed with sodium bicarbonate solution and examined by g.l.c. Not even traces of dichlorinated products were present.

Photoinitiated Chlorination of 1-Chlorobutane with Chlorine in Sulfuric/Acetic Acid (Reaction 2; Table 1)

The use of the same concentrations of the previous procedure led to the formation of considerable amount of trichloro-butanes. The reaction was then carried out by irradiating at room temperature for 20 min, a mixture of 0.05 moles of 1-chloro-butane, 21.3 ml of sulfuric acid, 3.7 ml of acetic acid, and 0.005 moles of chlorine.

The mixture was then worked-up according to the previous procedure.

Effect of Sulfuric–Acetic Acid upon Chlorinated Methylpentanoate and Heptanoate (Reactions 7,8,10; Table 1)

Methylesters (0.1 moles) in carbon tetrachloride were added to a solution of chlorine (0.01 moles) in carbon tetrachloride and irradiated at room temperature until the chlorine color had disappeared. A sample of the solution was analyzed by g.l.c. (reaction 7). The solvent was carefully removed and the mixture of chlorinated esters was placed with stirring in 21.3 ml of sulfuric acid, 3.7 ml of acetic acid, and 0.025 moles of powdered ferrous sulfate heptahydrate for 8 min at 20–30°. The mixture was then worked-up as described in the chlorination with *N*-chloroamine (reactions 8, 10). No product different from the chloroester isomers was present; that was a further confirmation of the stability of the chloroesters.

1. D. D. Tanner and M. W. Mosher. Can. J. Chem. **47**, 715 (1969).
2. R. Bernardi, R. Galli, and F. Minisci. J. Chem. Soc. (B) 324 (1967); Chim. Ind. (Milan), **49**, 594 (1967); F. Minisci, R. Galli, M. Cecere, and R. Bernardi, Chim. Ind. (Milan), **49**, 946 (1967); F. Minisci, R. Galli, and M. A. Rossetti. Chim. Ind. (Milan), **49**, 947 (1967); F. Minisci, R. Galli, R. Bernardi, and M. Perchinunno. Chim. Ind. (Milan), **50**, 328, 453 (1968); **51**, 280 (1969).
3. F. Minisci. Chim. Ind. (Milan), **49**, 705 (1967); F. Minisci and M. Cecere. Chim. Ind. (Milan), **49**, 1333 (1967).

Can. J. Chem. Downloaded from www.nrcresearchpress.com by 210.87.254.6 on 09/05/12
For personal use only.

Can. J. Chem. Downloaded from www.nrcresearchpress.com by 210.87.254.105 on 09/05/12
For personal use only.

Halogenation with *N*-haloamines in strong acids. I. The nature of the chain propagating radical[1]

J. SPANSWICK[2] AND K. U. INGOLD
Division of Chemistry, National Research Council of Canada, Ottawa, Canada

Received September 8, 1969

The *N*-haloamine halogenation of 1-chlorobutane in 4 *M* sulfuric acid in acetic acid as solvent is a radical chain process in which aminium radicals are the principal hydrogen atom abstracting species. With *N*-chloroamines, a concurrent chlorine atom chain is promoted by impurities such as molecular chlorine, hydrogen chloride, and chloride ion.

Canadian Journal of Chemistry, **48**, 546 (1970)

Introduction

The halogenation of organic substrates with *N*-chloroamines and *N*-bromoamines in strong acids[3] is a free radical chain process. The intramolecular reaction, which is the well known Hoffman–Löffler reaction (1) gives predominantly δ-halogenated amines.[4] The halogenation can be initiated both photochemically and by the addition of one electron reducing agent, such as ferrous ion. There is abundant evidence (1–4) that the reaction involves intramolecular hydrogen atom abstraction by an aminium radical, i.e. by a protonated amino radical $H-\overset{+}{N}\cdot$. The reaction can be represented by Scheme 1.

The intermolecular halogenation with *N*-haloamines in strong acids has usually been assumed to involve a similar series of reactions, i.e.

$$H-\overset{+}{N}-X \xrightarrow{(-X\cdot)} H-\overset{+}{N}\cdot \xrightarrow{RH} H-\overset{+}{N}-H + R\cdot$$

$$R\cdot + H-\overset{+}{N}-X \longrightarrow H-\overset{+}{N}\cdot + RX$$

These reactions have been extensively investigated during the past 4 or 5 years by Minisci and co-workers in Italy (5) and by Neale and co-workers in the United States (6). In addition to the analogy that can be drawn with the Hoffman–Löffler reaction, the evidence favoring the participation of aminium radicals in the intermolecular halogenations include the following observations.

(*i*) Halogenation is highly selective. In particular, chloroamine chlorinations are much more selective than free radical chlorinations which involve chlorine atoms as the hydrogen atom abstracting species (5*d*–5*i*).

(*ii*) Chlorinations with an *N*-chloroamine and

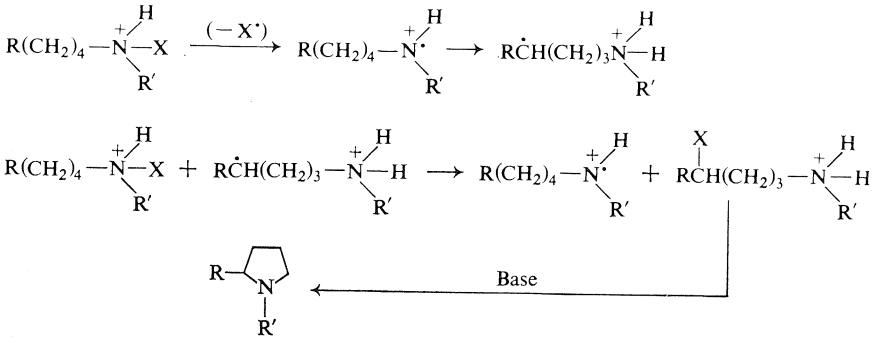

SCHEME 1

[1]Issued as NRCC No. 11058.
[2]NRCC Fellow 1968–1969.
[3]Among the acids which are generally employed in these reactions are sulfuric acid, various mixtures of sulfuric acid and acetic acid, and trifluoroacetic acid.
[4]These are usually subsequently cyclized to pyrrolidines by treatment with base.

Can. J. Chem. Downloaded from www.nrcresearchpress.com by 210.87.254.105 on 09/05/12
For personal use only.

brominations with the same *N*-bromoamine show the same selectivity. For example, the isomer distributions for the chlorination and bromination of methyl hexanoate are practically identical (*5e*, *5i*).

(*iii*) The relative reactivities of ring substituted toluenes towards chlorination by the piperidinium radical, $(CH_2)_5\overset{+}{N}\cdot H$, can be correlated by means of the Hammett equation using σ^+ constants (6). The ρ value of -1.36 is comparable to that for bromination with $Br^\cdot$ (-1.46) but is much greater than for chlorination with $Cl^\cdot$ (-0.66).

(*iv*) Further evidence that aminium radicals are probably present in these systems is provided by the facile free radical chain addition of chloroamines to olefins (*5a–c*, 7).

$$R_2NCl + \diagup C{=}C \diagdown \xrightarrow[\text{radical chain}]{H^+} R_2N{-}\overset{|}{C}{-}\overset{|}{C}{-}Cl$$

Our interest in the kinetics and absolute rate constants for free radical reactions in solution was stimulated by the information outlined above. Intermolecular halogenations with *N*-haloamines in strong acids appeared suitable for studying the absolute reactivities of nitrogen cation radicals, about which there is little information presently available. After the completion of a kinetic study on some of these reactions, which is described in the following paper, a report by Tanner and Mosher (8) appeared which suggested that these intermolecular halogenations actually involved the halogen atom as the chain propagating radical. These authors found

$$X^\cdot + RH \longrightarrow HX + R^\cdot$$

$$R_2'\overset{+}{N}H + HX \longrightarrow X_2 + R_2'\overset{+}{N}H_2$$
$$\quad\;\; |$$
$$\quad\;\; X$$

$$R^\cdot + X_2 \longrightarrow RX + X^\cdot$$

no significant experimental differences in the isomer distribution from the cuprous chloride, ferrous sulfate, and ferrous chloride initiated chlorination of 1-chloropropane with four different *N*-chloroamines. Furthermore, an identical isomer distribution was obtained for the photochemically initiated chlorination of 1-chloropropane using molecular chlorine as the chlorinating agent — a reaction that must involve chlorine atoms as the chain propagating species. Similar results were obtained for the relative rates of reaction of a number of different hydrocarbons towards *N*-chloroamines and molecular chlorine. In addition, the bromination of 1-chloropropane with *N*-bromodiethylamine (Cu^+ initiated) and with molecular bromine (photoinitiated) gave the same isomer distribution of brominated products but a distribution that was distinctly different from that for the chlorinations.

Since our kinetic studies could not distinguish unequivocally between an aminium radical chain and a chlorine atom chain, we undertook a reinvestigation into the nature of the radical involved in these reactions. The isomer distribution for the halogenation of 1-chlorobutane was chosen as the most suitable diagnostic tool for distinguishing between the two radicals. The results of this work are reported in the present paper. These results show unequivocally that for *pure* chloroamines the aminium radical is the principal species propagating the chain in intermolecular halogenations,[5] the change to a chlorine atom chain being promoted by impurities such as molecular chlorine, hydrogen chloride, and, under certain circumstances, chloride ion.

Experimental

Preparation of N-Haloamines

N-Chlorodimethylamine

It was prepared by the chlorination of 0.5 *M* aqueous dimethylamine with 0.5 *M* sodium hypochlorite solution (9). The chloroamine was extracted with ether, washed, and carefully dried over sodium sulfate. *N*-Chlorodimethylamine hydrosulfate was precipitated as a crystalline salt by the addition of 90% of the calculated volume of concentrated sulfuric acid from a syringe to the stirred solution, which was cooled to 0°. In order to obtain a product pure enough for kinetic work, it is important that the salt should be precipitated in a crystalline form. The white prismatic crystals were quickly washed with cold anhydrous ether, and the ether was removed by vacuum pumping for 15 min in the dark. The still crystalline product was dissolved in the solvent of choice and stored at $-78°$ in the dark.

N-Chloropiperidine

It was prepared by the same method but the dry ethereal solution was concentrated at room temperature and the residue distilled. The chloroamine was immediately redistilled and stored at liquid nitrogen temperature in the dark.

Our kinetic studies showed that when the chloroamines were prepared and stored in this way, their rate of reaction with the substrate being chlorinated (decanoic acid)

[5]Further support for this view is contained in the preceding paper of this issue by F. Minisci *et al.* (*5j*).

Can. J. Chem. Downloaded from www.nrcresearchpress.com by 210.87.254.105 on 09/05/12
For personal use only.

in the dark at 30° was extremely small. Furthermore, in the absence of added photo-initiators the reaction was initiated only very slowly by light of 3650 Å wavelength. However, when the fullest precautions were not taken, both the background thermally initiated reaction and the photo-initiated reaction could become quite large.

N-Bromodimethylamine

It was prepared in the same way by the bromination of 0.5 *M* aqueous dimethylamine with 0.5 *M* sodium hypobromite solution. The colorless crystalline hydrosulfate was dissolved in the solvent of choice and stored at liquid nitrogen temperature in the dark. *N*-Bromodimethylamine can be stored in this way for at least 2 weeks but at room temperature the formation of bromine is discernible after several hours.

Chain Initiation

α,α′-Azo-bis-cyclohexylnitrile (ACHN) was employed as photo-initiator and α,α′-azo-bis-isobutyronitrile (AIBN) as the thermal initiator.[6] The reactions were carried out in sealed ampoules which had been degassed by the freeze–thaw method. The photo-reactions were initiated by light from a 200–250 V, 250 W ME/D B.T.H. ultraviolet lamp. The light beam was passed through a Corning C.S. No. 7-51 filter (maximum transmittance 3650 Å). The thermal reactions were kept in the dark in a thermostatted water bath for the required period of time. At the end of the reaction period the ampoules were opened, the clear reaction mixture poured into ice/water and extracted with carbon tetrachloride, and the extract analyzed by gas–liquid chromatography (g.l.c.).

Other reactions were initiated by the addition of electron reducing agents (Cu^+, Fe^{2+}, Co^{2+}, Ce^{3+}). The finely powdered metal salts were added in one lot to the stirred solution of the reagents and stirring was continued through the reaction period. The slurry was poured into ice/water and extracted with carbon tetrachloride for g.l.c. analysis.

Analysis

The *N*-haloamines were analyzed for positive halogen by reaction with potassium iodide and titration of the liberated iodine (3). It was necessary to buffer the saturated potassium iodide solution (30% acetic acid, 70% isopropanol) with sodium acetate in order to obtain reproducible titrations.

The chlorinated and brominated isomers of 1-chlorobutane were analyzed by g.l.c. using a 12 ft by 1/8 in. column (20% methyl silicone gum rubber on an 80–100 mesh silanized diatomaceous earth support) and a flame-ionization gauge detector. We are indebted to Dr. Tanner for authentic samples of the various isomers. All analyses are averages of not less than three separate determinations.

All reactions were run to completion, that is, they were continued until the *N*-haloamine was completely consumed. For the *N*-chloroamines this means that both chloroamine and any free chlorine were consumed but for *N*-bromodimethylamine, a certain amount of molecular bromine remained in the reaction mixture at the point where it was worked-up for analysis. Because all the halochlorobutane isomers are stable under the reaction conditions, no serious attempt was made to determine the overall efficiency with which the halogen is transferred from the *N*-haloamine to the 1-chlorobutane, since this can have no bearing whatever on the nature of the radical halogenating agent which yields the observed mixture of isomers. A few, rather rough, quantitative measurements with equimolar *N*-chloroamine and 1-chlorobutane indicated a 50% or greater yield of dichlorobutanes with relatively little trichlorobutanes. Whether the true yield of chlorinated 1-chlorobutanes was 100% based on chloroamine or whether some chlorine was lost as HCl, or by chlorinating the amine itself or the acetic acid solvent was not determined. For *N*-bromodimethylamine the yield of bromochlorobutanes also appeared to be ~ 50% or greater.

All the work described in this paper was carried out at 30°. The solvent was 4 *M* sulfuric acid in acetic acid except for a few experiments with the molecular halogens in CCl_4 and $CFCl_3$.

Results and Discussion

The isomer distributions listed in Table 1 for the chlorination of 1-chlorobutane with molecular chlorine show no significant solvent effect on change from the non-polar solvents, CCl_4 and $CFCl_3$, to the sulfuric acid/acetic acid medium. The same isomer distribution is produced by photo and by thermal initiation. The individual isomers were shown to be stable in the acid medium for at least 24 h, as has been previously reported by Tanner and Mosher. Similar results, but with the different isomer ratios that characterize a bromine atom chain, are given in Table 2 for brominations with molecular bromine.

Chlorination with *N*-chlorodimethylamine (Table 3) and *N*-chloropiperidine (Table 4) gave isomer distributions which are quite different from that obtained from a chlorine atom chain. Both of the AIBN initiated reactions and also the ACHN photo-initiated *N*-chloropiperidine reaction gave very similar isomer distributions. This isomer distribution[7] (4.7, 10.3, 77.9, 7.1) is the most different from that for chlorine atoms (5.1, 23.5, 45.6, 25.8), and probably most nearly represents the isomer distribution of a pure unhindered aminium radical reaction in this particular solvent.[8] The isomer distributions for the

[6]A number of other potential thermal initiators which were tested proved unsatisfactory in the sulfuric–acetic acid solvent. Di-*t*-butylperoxyoxalate and *t*-butylhyponitrite decomposed too rapidly and 2,2,3,3-tetraphenylbutane was insoluble. Azo-isopropane was an ineffective photo-initiator.

[7]That is, the mean of runs 16–19 and 27–30.

[8]The higher selectivity observed in more acidic solvents (see e.g. experiment 26 and various papers by Minisci *et al.*) probably represents a real effect of acidity on selectivity. The possibility that there is some chlorine atom chain in 4 *M* H_2SO_4/AcOH even with AIBN initiation which does not occur in 16 *M* H_2SO_4(85%)/AcOH cannot, however, be entirely ruled out.

TABLE 1

The isomer distribution for the chlorination of 1-chlorobutane with molecular chlorine (initial 1-chlorobutane ~ 0.25 *M*)

Experiment no.	Solvent	Initiation	Duration of experiment	Cl—CH_2—	—CH_2—	—CH_2—	—CH_3
1	CCl_4	*hν*	5 min	5.8	24.5	45.1	24.6
2	$CFCl_3$	*hν*	5 min	6.2	23.4	44.7	25.7
3	$CFCl_3$	*hν*	5 min	6.0	24.3	43.7	26.0
4*	4 *M* H_2SO_4/AcOH	—	6 h	4.4	22.4	45.9	27.3
5*	4 *M* H_2SO_4/AcOH	—	24 h	4.9	22.9	46.9	25.3
6	4 *M* H_2SO_4/AcOH	*hν*	5 min	4.0	24.1	46.2	25.7
7†	4 *M* H_2SO_4/AcOH	—	24 h	4.7	23.4	46.3	25.6
8	4 *M* H_2SO_4/AcOH	AIBN	12 h	4.7	22.9	46.3	26.1
—‡	CCl_4	*hν*	—	10.5	27.6	45.3	13.7
—‡	85% H_2SO_4/15% AcOH	*hν*	—	5.4	20.9	52.0	21.6

*Products of experiment 3 stored in 4 *M* H_2SO_4/AcOH.
†Products of experiment 6 after 24 h.
‡Results of Tanner and Mosher (8).

TABLE 2

The isomer distribution for the bromination of 1-chlorobutane with molecular bromine (initial 1-chlorobutane ~ 0.25 *M*)

Experiment no.	Solvent	Initiation	Duration of experiment	Cl—CH_2—	—CH_2—	—CH_2—	—CH_3
9	CCl_4	*hν*	10 min	25.2	26.0	48.8	Trace
10	CCl_4	*hν*	10 min	24.4	27.5	48.1	Trace
11*	CCl_4	*hν*	10 min	21.4	26.2	48.6	3.8
12	4 *M* H_2SO_4/AcOH	*hν*	1 h	23.6	23.6	52.8	Trace
13†	4 *M* H_2SO_4/AcOH	—	24 h	23.7	26.7	49.6	Trace
14	4 *M* H_2SO_4/AcOH	*hν*	1 h	23.0	28.0	49.0	Trace
15‡	4 *M* H_2SO_4/AcOH	—	48 h	23.8	26.8	49.4	Trace

*Flushed continuously with N_2.
†Products of experiment 12.
‡Products of experiment 14.

photo-initiated *N*-chlorodimethylamine reaction diverge slightly from that of an aminium radical towards that of a chlorine atom, which implies that chlorine atoms may play a small role in this reaction. Presumably some chlorine atoms are generated either by the direct photolysis of the chloroamine or, more probably, by photolysis of the corresponding *N*,*N*-dichloroamine.[9]

Initiation of the Me_2NCl reaction with ferrous sulfate gives an isomer distribution that is somewhat closer to that of chlorine atoms than the photolytic reaction. This implies that chlorine atoms can play a more important role in the $FeSO_4$ initiated reaction. It is worth noting that molecular chlorine was formed in these $FeSO_4$ initiated reactions in sufficient concentration to escape from the solvent so that its characteristic odor became unpleasantly easily detected. In contrast to the Me_2NCl reaction, the initiation of the *N*-chloropiperidine reaction with ferrous sulfate, ferrous chloride, cuprous chloride, and cerous sulfate gave isomer distributions which are essentially identical to that which we believe corresponds to an unhindered aminium radical in this solvent. It would appear that molecular chlorine is obtained considerably less readily from *N*-chloropiperidine than from *N*-chlorodimethylamine. However, isomer ratios characteristic of a chlorine atom chain were obtained with *N*-chloropiperidine when the reaction was initiated with cobaltous chloride, and cerous chloride, and with cerous sulfate in the presence of chloride ion. The odor of chlorine in the presence of these three catalysts was unmistakable.

The addition to *N*-chloropiperidine of anhydrous hydrogen chloride (Table 5), or the addition of chloride ion (experiment 47), incline the

[9]Neale and Walsh (4*a*) have shown that *N*-chlorodi-*n*-butylamine undergoes a non-radical disproportionation to yield *N*,*N*-dichloro-*n*-butylamine. In the absence of an externally added initiator, the dichloroamine is believed to be the important photo-initiator in the Hoffman–Löffler rearrangement of the chloroamine. Such a disproportionation is less likely to occur with *N*-chloropiperidine than with Me_2NCl.

Can. J. Chem. Downloaded from www.nrcresearchpress.com by 210.87.254.105 on 09/05/12
For personal use only.

TABLE 3

The isomer distribution for the chlorination of 1-chlorobutane with *N*-chlorodimethylamine in 4 *M* H_2SO_4/AcOH (initial 1-chlorobutane ~ 0.25 *M*; *N*-chloroamine ~ 0.25 *M*)

Experiment no.	Initiation	[Initiator]*M*	Duration of experiment (h)	Cl—CH_2—	—CH_2—	—CH_2—	—CH_3
16	AIBN	0.01	20	4.5	11.1	74.5	9.8
17	AIBN	0.01	24	4.8	10.6	78.8	5.8
18	AIBN	0.01	44	4.3	9.8	77.5	8.4
19	AIBN	0.01	68	4.0	9.8	78.8	7.4
20	ACHN/*hν*	0.015	2	4.5	14.4	70.4	10.7
21	ACHN/*hν*	0.015	3	4.4	14.8	69.6	11.2
22	*hν*	—	20	4.7	14.8	67.9	12.6
23	$FeSO_4$	1.0	2	4.5	17.6	63.6	14.3
24*	$FeSO_4$	1.0	3	4.7	18.1	63.6	13.6
25*	$FeSO_4$	1.0	24	4.5	17.6	63.7	14.2
26†	$FeSO_4$	1.0	0.5	1.2	6.1	87.3	5.4
—†‡	$FeSO_4$	—	—	Trace	6.6	87.8	5.4
1–8§	—	—	—	5.1	23.5	45.6	25.8

*Molecular chlorine was formed in these reactions.
†In 85% H_2SO_4/AcOH.
‡Results of Minisci *et al.* (5*j*).
§Average value of experiments 1–8, i.e. chlorine atom chlorination.

TABLE 4

The isomer distribution for the chlorination of 1-chlorobutane with *N*-chloropiperidine in 4 *M* H_2SO_4/AcOH (initial 1-chlorobutane ~ 0.25 *M*; *N*-chloroamine ~ 0.25 *M*)

Experiment no.	Initiation	[Initiator]*M*	Duration of experiment (h)	Cl—CH_2—	—CH_2—	—CH_2—	—CH_3
27	AIBN	0.01	24	5.3	10.3	78.0	6.4
28	AIBN	0.01	24	4.9	10.1	78.6	6.4
29	ACHN/*hν*	0.015	3	5.1	10.4	78.3	6.2
30	ACHN/*hν*	0.015	3	5.3	10.3	78.1	6.3
31	*hν*	—	20	6.6	14.2	69.8	9.4
32	$FeSO_4$	1.0	2	6.5	10.3	76.9	6.3
33	$FeSO_4$	1.0	2	5.4	10.0	78.9	5.7
34	$FeCl_2$	1.0	2	5.3	9.6	78.7	6.4
35	$FeCl_2$	0.06	20	5.1	9.3	79.6	6.0
36	CuCl	0.06	2	7.0	10.2	75.9	6.9
37	CuCl	0.06	2	4.7	9.4	76.2	9.7
38	CuCl	0.06	16	5.1	9.3	79.5	6.1
39	CuCl	0.06	16	4.2	9.8	79.5	6.5
40	CuCl	0.06	20	7.5	8.8	78.1	5.6
41	$Ce_2(SO_4)_3$	0.06	20	4.9	10.3	79.2	5.6
42	$Ce_2(SO_4)_3$	0.06	20	4.8	9.7	79.1	6.4
43*	$CoCl_2$	0.06	22	5.6	25.9	48.5	20.0
44*	$CeCl_3$	0.06	3	4.6	19.5	54.8	21.1
45*	$CeCl_3$	0.06	20	5.6	22.8	52.7	18.9
46*	$CeCl_3$	0.06	20	5.8	23.3	45.9	25.0
47*	$Ce_2(SO_4)_3$/NaCl	0.06/0.06	20	6.5	25.6	48.4	19.5
1–8†	—	—	—	5.1	23.5	45.6	25.8

*Molecular chlorine was formed in these reactions.
†Chlorine atom chain.

isomer distribution towards that for a chlorine atom chain. Hydrogen chloride must therefore be able to react with the chloroamine to generate molecular chlorine (10) as was previously claimed by Tanner and Mosher (8). However, in contrast to Tanner, we must agree with Minisci *et al.* (5*d*) that hydrogen chloride is not formed in sufficient quantity under the conditions employed in these chlorinations for its reaction with chloroamine to significantly affect the isomer distribution.

The complete conversion of an aminium radical chain to a chlorine atom chain is not accomplished by the addition of small amounts of molecular chlorine (Table 5). For example, the addition to the *N*-chlorodimethylamine reaction of 10 mole % of chlorine (based on *N*-chlorodimethylamine) gives an isomer distribution

Can. J. Chem. Downloaded from www.nrcresearchpress.com by 210.87.254.105 on 09/05/12
For personal use only.

TABLE 5

The influence of chlorine and hydrogen chloride on the isomer distribution for the chlorination of 1-chlorobutane with chloroamines in 4 *M* H_2SO_4/AcOH (Initial 1-chlorobutane ~ 0.25 *M*; *N*-chloroamine ~ 0.25 *M*; reaction initiated with 0.01 *M* AIBN and run for 12 h)

Experiment no.	Chloroamine	% Cl_2 or HCl*	Cl—CH_2—	—CH_2—	—CH_2—	—CH_3
16–19†	Me_2NCl	0	4.4	10.3	77.4	7.9
48	Me_2NCl	2% Cl_2	4.8	12.3	72.3	10.6
49	Me_2NCl	10% Cl_2	4.3	14.6	66.1	15.0
1–8†	—	100% Cl_2	5.1	23.5	45.6	25.8
27–30†	$(CH_2)_5NCl$	0	5.1	10.3	78.3	6.3
50	$(CH_2)_5NCl$	2% HCl	4.9	8.3	80.7	6.1
51	$(CH_2)_5NCl$	8% HCl	4.0	12.9	72.4	10.7

*Approximate mole % based on added chloroamine concentration.
†Average isomer distribution for these experiments.

TABLE 6

The isomer distribution for the bromination of 1-chlorobutane with *N*-bromodimethylamine in 4 *M* H_2SO_4/AcOH (initial 1-chlorobutane ~ 0.25 *M*; *N*-bromoamine ~ 0.15 *M*)

Experiment no.	Initiation	[Initiator]*M*	Duration of experiment (h)	Cl—CH_2—	—CH_2—	—CH_2—	—CH_3
52	AIBN	0.01	30	4.6	8.8	77.3	9.3
53*	ACHN/*hν*	0.015	1	4.2	8.5	80.3	7.0
54*	ACHN/*hν*	0.015	2	4.2	8.3	80.3	7.2
55	$FeSO_4$	1.0	2	5.4	10.2	78.4	6.0
56	$FeSO_4$	1.0	3	5.1	11.6	76.6	6.7
16–19†	—	—	—	4.4	10.3	77.4	7.9
9–15‡	—	—	—	23.6	26.4	49.5	0.5

*Considerable amounts of Br_2 formed during the reaction.
†Dimethylaminium radical chain.
‡Bromine atom chain.

which roughly corresponds to a one-third chlorine atom chain and a two-thirds aminium radical chain. This must mean that chlorine atoms and aminium radicals are of roughly equal importance as hydrogen atom abstracting agents in this particular system. Provided the HCl–chloroamine reaction is fast, the alkyl radicals derived from 1-chlorobutane must attack molecular chlorine and the protonated chloroamine at very roughly comparable rates.

The most conclusive proof that the aminium radical is involved in these systems is the similarity of the isomer distribution for the bromination of 1-chlorobutane by *N*-bromodimethylamine (Table 6) with the isomer distribution already assigned to the aminium radical. Perhaps the most interesting result in these particular experiments was the fact that although considerable amounts of molecular bromine were formed in the photo and thermal initiated reactions, the isomer distributions did not change from that due to an aminium radical. The bromine atom isomer distribution is of course distinctly different from that for the aminium radical. The lack of influence of the bromine is most readily accounted for by the fact that hydrogen atom abstraction from 1-chlorobutane by a bromine atom will be an endothermic process and will therefore occur rather slowly. The molecular bromine may play a role in brominating the alkyl radicals

$$R^{\cdot} + Br_2 \rightarrow RBr + Br^{\cdot}$$

but the resulting bromine atom does not continue the chain by attacking the 1-chlorobutane.

In the absence of ACHN, the photo-initiated reactions with *N*-chlorodimethylamine (experiment 22) and *N*-chloropiperidine (experiment 31) give isomer distributions which are intermediate between those for an aminium radical and for a chlorine atom. The experimental conditions normally employed in the Hoffman–Löffler reaction involve the direct photolysis of the chloroamine. The present results suggest that direct photolysis leads to both chlorine atom and aminium radical chain reactions. Since a chlorine atom is less selective in hydrogen atom abstraction

Can. J. Chem. Downloaded from www.nrcresearchpress.com by 210.87.254.105 on 09/05/12
For personal use only.

TABLE 7

Summary of isomer distribution for the chlorination and bromination of 1-chlorobutane in 4 M H_2SO_4/AcOH

Experiment no.	Reactant	Initiation	Radical	Cl—CH_2—	—CH_2—	—CH_2—	—CH_3
16–19	Me_2NCl	AIBN	$Me_2\overset{+\cdot}{N}H$	4.4	10.3	77.4	7.9
27–30	$(CH_2)_5NCl$	AIBN, ACHN/$h\nu$	$(CH_2)_5\overset{+\cdot}{N}H$	5.1	10.3	78.3	6.3
32–42	$(CH_2)_5NCl$	$FeSO_4$, $FeCl_2$, CuCl, $Ce_2(SO_4)_3$	$(CH_2)_5\overset{+\cdot}{N}H$	5.5	9.7	78.3	6.5
52–56	Me_2NBr	AIBN, ACHN/$h\nu$ $FeSO_4$	$Me_2\overset{+\cdot}{N}H$	4.7	9.5	78.6	7.2
1–8	Cl_2	$h\nu$, AIBN	$Cl^{\cdot}$	5.1	23.5	45.6	25.8
43–47	$(CH_2)_5NCl$	$CoCl_2$, $CeCl_3$, $Ce_2(SO_4)_3$/NaCl	$Cl^{\cdot}$	5.6	23.4	50.1	20.9
9–15	Br_2	$h\nu$	$Br^{\cdot}$	23.6	26.4	49.5	0.5

than an aminium radical and since, in the Hoffman–Löffler reaction, chlorine abstracts intermolecularly while the aminium radical abstracts intramolecularly, we should expect that the yield of the desired cyclized product will be increased by all procedures that reduce the importance of the chlorine atom chain. It is therefore not surprising to find that the procedures that Neale and Walsh (4*a*) have reported increase the yield of cyclized product from the photoinitiated Hoffman–Löffler reaction of *N*-chlorodi-*n*-butylamine are all consistent with a decrease in the importance of the chlorine atom chain. These procedures include (*i*) increasing the chloroamine purity, (*ii*) rapid flushing of the system with nitrogen (this will remove HCl and Cl_2), (*iii*) increasing the light intensity and decreasing its wavelength. (This will increase the rate of radical reactions relative to non-radical reactions. Presumably some HCl or Cl_2 is formed by non-radical pathways.)

Neale and Walsh have also reported (4*a*) that for chloroamines for which intramolecular abstraction (Hoffman–Löffler reaction) is possible, this process occurs more slowly than the addition of the aminium radical to 1,3-dienes but more rapidly than their addition to simple olefins. Minisci *et al.* have reported (5*h*) that intermolecular abstraction from methyl hexanoate is competitive with intramolecular abstraction for both *N*-chloro-*n*-butylamine and *N*-chlorodi-*n*-butylamine. Similarly, 12% of benzyl chloride is formed from toluene and *N*-chlorodi-*n*-butylamine (5*b*). However, in the reaction of *N*-chlorodi-*n*-butylamine with 1-chlorobutane in 4 M H_2SO_4/AcOH (initiation, ACHN/$h\nu$, and $FeSO_4$) and in 85% H_2SO_4/AcOH (initiation $FeSO_4$) we could detect no trace of any dichlorobutanes. Presumably 1-chlorobutane is considerably less reactive towards aminium radicals than methyl hexanoate or toluene. From the relative concentrations of chloroamine and 1-chlorobutane, we estimate that for these particular reagents $k_{inter}/k_{intra} < 10^{-3}\ M^{-1}$.

Conclusion

The isomer distributions obtained in the present work are summarized in Table 7. There can be little doubt that *N*-haloamines yield aminium radicals and that under carefully controlled conditions, aminium radicals are by far the most important hydrogen atom abstracting agents in these systems. Furthermore, although a chlorine atom chain is promoted by the hydrogen chloride – chloroamine reaction, small amounts of chlorine or hydrogen chloride do not have a very important effect on the dichlorobutane isomer distribution. The negligible effect of bromine on the isomer distribution in the presence of bromoamine is probably due to the low rate of hydrogen atom abstraction by bromine atoms.

1. M. E. Wolff. Chem. Rev. **63**, 55 (1963), and references cited therein.
2. S. Wawzonek and P. J. Thelen. J. Amer. Chem. Soc. **72**, 2118 (1950). S. Wawzonek and T. P. Culbertson. J. Amer. Chem. Soc. **81**, 3367 (1959).

Can. J. Chem. Downloaded from www.nrcresearchpress.com by 210.87.254.105 on 09/05/12
For personal use only.

3. E. J. COREY and W. J. HERTLER. J. Amer. Chem. Soc. **82**, 1657 (1960).
4. (*a*) R. S. NEALE and M. R. WALSH. J. Amer. Chem. Soc. **87**, 1255 (1965). (*b*) R. S. NEALE, M. R. WALSH, and N. L. MARCUS. J. Org. Chem. **30**, 3683 (1965).
5. (*a*) F. MINISCI, R. GALLI, and M. CECERE. Tetrahedron Lett. 4663 (1965). (*b*) F. MINISCI, R. GALLI, and R. BERNARDI. Tetrahedron Lett. 699 (1966). (*c*) F. MINISCI, R. GALLI, and M. CECERE. Tetrahedron Lett. 3163 (1966). (*d*) F. MINISCI, R. GALLI, A. GALLI, and R. BERNARDI. Tetrahedron Lett. 2207 (1967). (*e*) F. MINISCI, R. GALLI, and R. BERNARDI. Chem. Commun. 903 (1967). (*f*) F. MINISCI, R. GALLI, and R. BERNARDI. Chim. Ind. (Milan), **49**, 594 (1967). (*g*) F. MINISCI, R. GALLI, and R. BERNARDI. J. Chem. Soc. 324 (1968). (*h*) F. MINISCI, R. GALLI, R. BERNARDI, and M. PERCHINUMNO. Chim. Ind. (Milan), **50**, 453 (1968). (*i*) F. MINISCI. Private communication. (*j*) F. MINISCI, G. P. GARDINI, and F. BERTINI. Can. J. Chem. This issue.
6. R. S. NEALE and E. GROSS. J. Amer. Chem. Soc. **89**, 6579 (1967).
7. (*a*) R. S. NEALE and R. L. HINMAN. J. Amer. Chem. Soc. **85**, 2666 (1963). (*b*) R. S. NEALE. J. Amer. Chem. Soc. **86**, 5340 (1964). (*c*) R. S. NEALE. Tetrahedron Lett. 483 (1966). (*d*) R. S. NEALE. J. Org. Chem. **32**, 3263 (1967). (*e*) R. S. NEALE and N. L. MARCUS. J. Org. Chem. **32**, 3273 (1967). (*f*) R. S. NEALE and N. L. MARCUS. J. Org. Chem. **33**, 3457 (1968).
8. D. D. TANNER and M. W. MOSHER. Can. J. Chem. **47**, 715 (1969).
9. G. H. COLEMAN. J. Amer. Chem. Soc. **55**, 3001 (1933). H. BOCK and K. L. KOMPA. Chem. Ber. **99**, 1347 (1966).
10. S. KOMORI, M. OKAHARA, and Y. HORADA. Kogyo Kagaku Zasshi, **66**, 1850 (1963).

Can. J. Chem. Downloaded from www.nrcresearchpress.com by 210.87.254.105 on 09/05/12
For personal use only.

Can. J. Chem. Downloaded from www.nrcresearchpress.com by 210.87.254.42 on 09/05/12
For personal use only.

Halogenation with *N*-haloamines in strong acids. II. Kinetics and rate constants[1]

J. SPANSWICK[2] AND K. U. INGOLD
Division of Chemistry, National Research Council of Canada, Ottawa, Canada

Received September 8, 1969

The kinetics of the radical chain chlorination of decanoic acid by *N*-chlorodimethylamine and *N*-chloropiperidine in 2 and 4 *M* H_2SO_4 in acetic acid have been examined at 30°. The rate of reaction is proportional to the decanoic acid concentration and to the square root of the rate of chain initiation. The rate controlling step for propagation involves the attack of an aminium radical on decanoic acid, and termination involves the self-reaction of two aminium radicals. The latter reaction may involve the prior, rapid deprotonation of one or both radicals. The propagation rate constant has been estimated to be in the range 7×10^2 to 1×10^4 M^{-1} s^{-1} and the termination rate constant to be in the range 6×10^6 to 5×10^7 M^{-1} s^{-1}.

Canadian Journal of Chemistry, **48**, 554 (1970)

Introduction

In the preceding paper (1), it was shown that the halogenation of 1-chlorobutane in 4 *M* sulfuric acid in acetic acid by *N*-haloamines is a free radical chain process in which the principal hydrogen atom abstracting species is an aminium radical. The present paper reports on the kinetics of the reaction of *N*-chlorodimethylamine and *N*-chloropiperidine with decanoic acid in sulfuric–acetic acid solvents. These reactions have been found to be suitable for the application of the rotating sector method, and the absolute rate constants for chain propagation and termination have been estimated.

Experimental

Materials

The preparation and storage of the *N*-chloroamines were described in the previous paper (1). Eastman "white label" decanoic acid was purified by vacuum distillation. This compound proved a more suitable substrate than a number of others that were examined. For example, cyclohexane was too volatile, and there was a slow dark (thermal) reaction with toluene and *p*-xylene. Reagent grade sulfuric and acetic acids were used as solvents without purification.

Apparatus and Procedure

The general features of the apparatus and the general experimental procedure have been described previously (2, 3). The reaction was initiated with the light from a 200–250 V, 250 W ME/D B.T.H. lamp filtered through a Corning C.S. No. 7-51 filter (maximum transmittance 3650 Å). α,α′-Azo-bis-cyclohexylnitrile (ACHN) was employed as a photo-initiator, generally at a concentration of 1.5×10^{-2} *M*. In the absence of this compound, a photo-initiated reaction did not take place during the first 10 min of the irradiation of carefully purified and degassed reagents. This result contrasts with the experience of most previous workers who have reported that reaction occurs in the dark and that its rate is increased by ultraviolet irradiation. This difference probably reflects differences in the purity of the chloroamines. However, it is worth noting that all our *N*-chlorodi-*n*-butylamine samples exhibited a dark reaction (even in the absence of decanoic acid). Kinetic work with this chloroamine was not possible.

For most kinetic purposes the rate of the photo-initiated reaction was followed by measuring the heat evolved in the exothermic chain process with a thermocouple placed at the center of a cylindrical Pyrex cell 1.5 cm long and 3 cm in diameter. These measurements of heat evolution were calibrated in terms of true rates of reaction by titration for active chlorine (1). The measured rate of temperature rise together with the reaction rate determined by titration yielded a mean value of 38.5 ± 4.0 kcal/mole for the actual heat of the overall reaction, i.e.

$$\text{HN}^{+}\text{Cl} + \text{RH} \longrightarrow \text{HN}^{+}\text{H} + \text{RCl}$$

$$\Delta H = -38.5 \pm 4.0 \text{ kcal/mole}$$

Reactions were also initiated thermally with α,α′-azo-bis-isobutyronitrile (AIBN). The reactants were sealed in ampoules under vacuum. There was little dead space in these ampoules and so it proved possible to make some measurements on cyclohexane even though this hydrocarbon was too volatile for use in the photo-apparatus which had a large dead space. The rates were estimated by titration for active chlorine.

The kinetic work described in this paper was done at 30° in 2 *M* H_2SO_4/AcOH and 4 *M* H_2SO_4/AcOH as solvents. Two other more acidic sulfuric–acetic acid mixtures (1 *M* H_2SO_4/AcOH with 30% volume Ac_2O ($-H_0 > 12$ (6), $\eta = 2.6$ cp), and 85% (16 *M*) H_2SO_4/AcOH ($-H_0 = 9.9$, $\eta = 28$ cp)) were also examined. Both proved unsatisfactory as solvents for absolute rate studies by our procedure because a thermally initiated reaction between chloroamine and decanoic acid occurred spontaneously in the dark at a quite appreciable rate. Trifluoroacetic acid was also unsatisfactory as a solvent for absolute rate studies because there was a large contribution to termination from a kinetically first order process.

Estimation of the Rate of Chain Initiation

The determination of absolute rate constants by the

[1]Issued as NRCC No. 11059.
[2]NRCC Fellow 1968–1969.

TABLE 1

Rate constants for nitrogen evolution from the azo-initiators at 30° ([AIBN] = 1.0×10^{-2} *M*; [ACHN] = 1.5×10^{-2} *M*, the light intensity was the same in all ACHN experiments)

Initiator	AIBN	ACHN/*hν*	ACHN/*hν*
Solvent	4 *M* H_2SO_4/AcOH	2 *M* H_2SO_4/AcOH	4 *M* H_2SO_4/AcOH
$k \times 10^{-5}(s^{-1})$	0.02*	17†	17†
e ($e/(1-e) \propto 1/\eta^{\frac{1}{2}}$)	0.16	0.26	0.16
e ($e/(1-e) \propto 1/\eta$)	0.02	0.06	0.02
Viscosity (cp)	18.3	5.6	18.3
Acidity‡ ($-H_0$)	4.4	3.4	4.4

*In non-acidic solvents of low viscosity, such as chlorobenzene ($\eta = 0.7$ cp), $k = 9 \times 10^{-8}$ s^{-1} (4).
†In chlorobenzene $k = 17 \times 10^{-5}$ s^{-1} under similar experimental conditions.
‡Reference 5.

rotating sector technique requires a knowledge of the rate of chain initiation, R_i. Unfortunately, the usual induction period method (2, 3) could not be used because no suitable inhibitor of the chain reaction could be found. The free radicals, galvinoxyl, 2,2,6,6-tetramethyl-4-pyridone nitroxide, and 2,2-diphenyl-1-picrylhydrazyl were immediately converted to non-radical products on solution in sulfuric–acetic acid solvents, and their products did not inhibit the chlorination. 4,4′-Dimethoxydiphenyl nitroxide was stable for a limited period in the solvent but the solution was too intensely colored for R_i to be measured in a photochemically initiated reaction. Although 2,6-di-*t*-butyl-4-methoxyphenol (BMeOP) produced a slight reduction in the initial rate, the reaction was not retarded by 2,6-di-*t*-butyl-4-methylphenol, 2-*t*-butyl-4-methoxyphenol, and hydroquinone. The unique behavior of BMeOP aroused questions as to the mechanism and radical trapping efficiency of this retarder which invalidated its use to determine R_i.

Faced with this situation, we were forced to estimate R_i from the measured rates of decomposition of ACHN and AIBN. These were determined by measuring the rates of nitrogen evolution under conditions comparable to those of the kinetic experiments. The results are given in Table 1 together with the viscosities and acidities ($-H_0$ function) of the solvents. The rate of chain initiation is given by $R_i = 2ek$ [azo compound], where e is the efficiency of chain generation. An absolute maximum value can be put on R_i by assuming that each molecule of azo compound decomposed generates two radicals ($e = 1.0$). However, this maximum value is undoubtedly much too large because even in low viscosity solvents (such as, say, chlorobenzene with $\eta = 0.7$ cp) $e = 0.5 \pm 0.2$ both for the thermal decomposition of AIBN (7, 8) and for the photo-decomposition of ACHN (9). A number of workers (see e.g. 10–17) have shown that e is significantly lower in solvents with viscosities in the range of interest (i.e. 5.6 cp for 2 *M* H_2SO_4 and 18.3 cp for 4 *M* H_2SO_4, Table 1) than in low viscosity solvents. The ratio ($e/(1-e)$) has been reported to be proportional both to $1/\eta^{1/2}$ (11, 13) and to $1/\eta$ (15–17). These relations allow rough maximum and minimum values to be placed on e in the solvents used in this work. A reasonable value for the chain initiation efficiency is 0.5 in a solvent with $\eta = 0.7$ cp. Assuming $e = 0$ when $\eta = \infty$, the dependence of ($e/(1-e)$) on $1/\eta^{1/2}$ gives efficiencies of 0.26 in 2 *M* H_2SO_4 and 0.16 in 4 *M* H_2SO_4, while the dependence on $1/\eta$ gives $e = 0.06$ and 0.02. These values of e are listed in Table 1 and have been used to calculate the rates of chain initiation given in Table 4. Although this procedure for estimating probable maximum and minimum rates of chain initiation is unsatisfactory, it is difficult to see how it can be improved upon until a suitable inhibitor of the reaction is discovered.

Results and Discussion

Kinetics

The overall rates of reaction of *N*-chlorodimethylamine and *N*-chloropiperidine with decanoic acid are proportional to the square root of the rate of chain initiation. Thus, for the thermal reactions the rate is proportional to the square root of the AIBN concentration (Fig. 1), and for

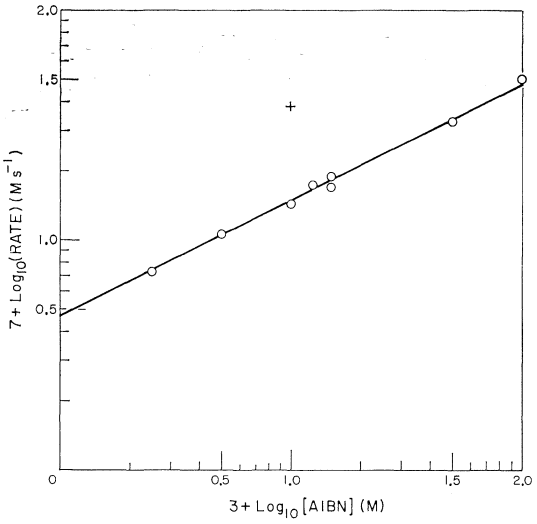

FIG. 1. Rate of consumption of *N*-chlorodimethylamine as a function of [AIBN] at 30° in 4 *M* H_2SO_4/AcOH. Initial concentrations, [$(CH_3)_2NCl$] = 0.20 *M*, [decanoic acid] = 0.25 *M*. Rates by titration after 6–20 h. The conversion of RH was kept as low as was consistent with accurate titrations. The straight line drawn has a slope of 0.5. The point X is the average of 3 experiments with 0.20 *M* [cyclohexane].

Can. J. Chem. Downloaded from www.nrcresearchpress.com by 210.87.254.42 on 09/05/12
For personal use only.

TABLE 2

The photochemically initiated reaction of *N*-chlorodimethylamine and *N*-chloropiperidine with decanoic acid in 4 *M* H_2SO_4/AcOH (ACHN = 1.5×10^{-2} *M*, estimated $R_i = 80 \times 10^{-8}$ *M* s^{-1})

[Chloroamine] (*M*)	[Decanoic acid] = [RH] (*M*)	$\frac{[RH]}{[>NCl]}$	Rate $\times 10^5$ (*M* s^{-1})	$\frac{\text{Rate}}{[RH]} \times 10^5$ (s^{-1})
Me_2NCl				
0.05	0.25	5.0	7.28	29.1
0.15	0.25	1.7	7.6	30.4
0.45	0.50	1.1	10.7	21.4
0.25	0.25	1.0	7.6	30.4
0.37	0.25	0.67	9.27	37.1
0.45	0.25	0.55	7.83	31.3
0.45	0.15	0.33	4.63	30.9
0.45	0.12	0.26	4.36	36.3
0.45	0.06	0.13	2.41	40.1
$(CH_2)_5NCl$				
0.40	0.25	0.63	10.9*	43.6*
0.40	0.14	0.35	6.2	44.3
0.40	0.07	0.18	3.34	47.7

*Mean of three experiments.

the photo reactions under steady illumination the rate is proportional to $[ACHN]^{0.5}$ (in the range 2×10^{-3} to 3×10^{-2} *M*). At any particular ACHN concentration the rate is proportional to the square root of the light intensity. These results indicate that the chains are terminated by the bimolecular reactions of two radicals.

The reaction rate is directly proportional to the decanoic acid concentration but is independent of the chloroamine concentration. Some typical results are given in Table 2 for reactions in 4 *M* H_2SO_4/AcOH. Confirmation that the rate was independent of the chloroamine concentration was provided by the fact that during the course of any single experiment the rate (measured by heat evolution or chloroamine titration) remained constant for more than 90% of the reaction.

The kinetics are consistent with the reaction scheme [1]–[4].

[1] Initiation: Production of R$^\cdot$ (Rate R_i)

[2] Propagation:

$$R^\cdot + HN^+Cl \longrightarrow RCl + HN^{+\cdot}$$

[3] $$HN^{+\cdot} + RH \xrightarrow{k_p} HN^+H + R^\cdot$$

[4] Termination: $$HN^{+\cdot} + HN^{+\cdot} \xrightarrow{2k_t}$$

Inactive products

The overall rate of reaction is given by

$$\frac{-d[>NCl]}{dt} = \frac{k_p[RH]R_i^{1/2}}{(2k_t)^{1/2}}$$

That is, the rate controlling step for chain propagation involves hydrogen atom abstraction by an aminium radical and termination predominantly involves the self reaction of two aminium radicals.

Strong evidence that *N*-chloroamine chlorination of 1-chlorobutane involves aminium radicals rather than chlorine atoms as the principal hydrogen atom abstracting agents was provided in the previous paper (1). Support for a similar aminium radical chain reaction with decanoic acid as the substrate is provided by the isomer distributions for its chlorination by chloroamines and by molecular chlorine, which are given in Table 3. The data in this table were obtained for reactions run to completion. The yields of chlorodecanoic acids from the *N*-chloroamine chlorinations were greater than 80%, based on the initial chloroamine concentrations.

Absolute Rate Constants

The rotating sector technique (2, 3, 9) was applied to the reactions of *N*-chlorodimethylamine and *N*-chloropiperidine both in 2 *M* H_2SO_4 and in 4 *M* H_2SO_4 in acetic acid. From 3–6 individual experiments at various reactant concentrations were carried out for each chloroamine in the two solvents. In each of these indi-

Can. J. Chem. Downloaded from www.nrcresearchpress.com by 210.87.254.42 on 09/05/12
For personal use only.

TABLE 3

The isomer distribution for the chlorination of decanoic acid in 4 M H_2SO_4/AcOH*

Chlorinating agent	Initiation	HOOC—CH_2—	—CH_2—	—CH_2—	—CH_2—	—CH_2—	—CH_2—	—CH_2—	—CH_2—	—CH_3
Me_2NCl†	ACHN/$h\nu$	—	—	1.7	6.1	12.6	16.2	23.4	39.0	1.0
Me_2NCl	AIBN	—	1.1	2.4	7.5	14.1	18.0	15.9	40.8	Trace
Me_2NCl‡	$FeSO_4$	—	—	0.5	4.1	10.7	17.5	21.6	44.4	1.1
$(CH_2)_5NCl$	ACHN/$h\nu$	—	Trace	1.3	6.7	13.2	17.9	18.4	40.9	1.1
Cl_2	$h\nu$	Trace	7.0	9.6	10.8	11.6	12.9	16.0	20.8	11.3

*Analyzed by gas–liquid chromatography after conversion to the methyl esters. We are indebted to Mr. M. Bednas of these laboratories for most of the analyses.
†Analysis kindly performed by Professor Minisci.
‡Chlorination of methyl decanoate in concentrated H_2SO_4 (R. Bernardi *et al.* (29)).

vidual experiments, from 5–20 measurements were made of the rate under steady illumination, $-d[\gtrdot NCl]/dt$, and of the ratio of this rate to the rate under the optimum frequency (9) of intermittent illumination. From this ratio the quantity $2k_tR_i$ is derived. These results are summarized in Table 4.

For both assumptions regarding chain initiation efficiency the values of

$$k_p/(2k_t)^{1/2} = \frac{-d[\gtrdot NCl]}{dt} \Big/ [RH]R_i^{1/2},$$

appear to be essentially independent of chloroamine and of acid strength.[3] This suggests that the propagation and termination rate constants are not significantly affected by the change in chloroamine and solvent since it is unlikely that they would change by large, but comparable, amounts. Although the values of $2k_tR_i$ appear to be greater in 2 M H_2SO_4 than in 4 M H_2SO_4, the estimated maximum termination rate constants ($e/(1 - e)$ assumed $\propto 1/\eta$) are approximately equal in the two solvents and so are the estimated minimum termination rate constants ($e/(1 - e)$ assumed $\propto 1/\eta^{1/2}$).

The termination rate constants have about 1/10–1/100 of the values calculated for bimolecular diffusion controlled reactions from the relation (20):

[I] $$k_{diffusion} = 8RT/(3 \times 10^3)\eta \ M^{-1}\,s^{-1}$$

The significance of the difference between measured and calculated termination rate constants is hard to assess in the absence of an accurate value of R_i. A measured value smaller than calculated seems not unreasonable for two positively charged aminium radicals, since electrostatic repulsion may reduce the frequency of close encounters. On the other hand, all our experimental rate constants for radical–radical reactions which have been obtained in the present apparatus by the same general procedure, have been smaller than the diffusion controlled values calculated from eq. [I] by a factor of at least 4 and sometimes of 10 or more. The radicals investigated include *t*-butoxy (2), a number of alkyl and trialkyltin radicals (3), and the trichloromethyl radical (21). Although the low measured values may reflect an inherent error in our procedure, our results have generally been in good agreement with the rate constants found by other workers using different experimental methods. It seems likely, therefore, that eq. [I] may overestimate diffusion controlled rate constants (22). However, the fact that by either calculation $2k_t$ for both chloroamines is about the same in both acids, whereas the viscosity in 2 M H_2SO_4 is only about 1/3 the viscosity in 4 M H_2SO_4, indicates that the self reaction of aminium radicals is somewhat slower than diffusion controlled.

In considering termination it is important to realize that deprotonation (like protonation) is an extremely rapid process and that the kinetics do not distinguish between the three possible processes outlined below, all of which may contribute to termination.

The aminium radical pair in the box represents two radicals in close proximity to one another, one or both of which may be deprotonated immediately prior to, or during the course of, reaction with the other radical. It is unfortunate that the absolute rate constants could not be measured over a wider range of acid strengths

[3]Previous workers have reported that the rate of the intramolecular (Hoffman–Löffler) reaction is increased (18) and decreased (19) by an increase in solvent acidity. However, in neither piece of work was the rate of initiation in the different solvents estimated.

Can. J. Chem. Downloaded from www.nrcresearchpress.com by 210.87.254.42 on 09/05/12
For personal use only.

Can. J. Chem. Downloaded from www.nrcresearchpress.com by 210.87.254.42 on 09/05/12
For personal use only.

TABLE 4

Summary of rates and rate constants for the chloroamine chlorination of decanoic acid at 30°

Chloroamine	Initiator	Solvent	$\frac{-d[>NCl]}{dt}/[RH] \times 10^4$ (Mean value) (s^{-1})	$2k_tR_i$ (Mean value)(s^{-2})	Estimated $R_i \times 10^8$ ($M\ s^{-1}$)	$\frac{k_p}{(2k_t)^{\frac{1}{2}}}$ ($M^{-\frac{1}{2}}\ s^{-\frac{1}{2}}$)	$2k_t \times 10^{-8}$ ($M^{-1}\ s^{-1}$)	$k_{diffusion} \times 10^{-8}$ ($M^{-1}\ s^{-1}$)	$k_p \times 10^3$ ($M^{-1}\ s^{-1}$)
$(CH_3)_2NCl$	AIBN	4 M H_2SO_4/AcOH	0.04	—	0.029*	0.23	—	—	—
					0.0036†	0.67	—	—	—
$(CH_3)_2NCl$	ACHN/$h\nu$	4 M H_2SO_4/AcOH	3.2	5.4	80*	0.36	0.07	3.7	0.9
					10†	1.0	0.5	3.7	7
$(CH_3)_2NCl$	ACHN/$h\nu$	2 M H_2SO_4/AcOH	3.1	15	130*	0.27	0.1	12	0.9
					30†	0.56	0.5	12	4
$(CH_2)_5NCl$	ACHN/$h\nu$	4 M H_2SO_4/AcOH	4.4	5.0	80*	0.49	0.06	3.7	1
					10†	1.4	0.5	3.7	10
$(CH_2)_5NCl$	ACHN/$h\nu$	2 M H_2SO_4/AcOH	2.7	10	130*	0.24	0.08	12	0.7
					30†	0.49	0.3	12	3

*Assuming $e/(1-e)$ is proportional to $1/\eta^{\frac{1}{2}}$.
†Assuming $e/1-e)$ is proportional to $1/\eta$.

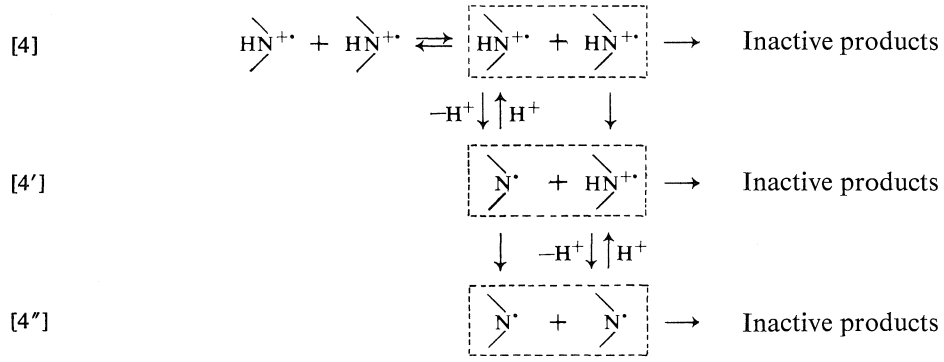

since very strong acids might be expected to produce some decrease in $2k_t$ if processes [4′] and [4″] play an important role in termination. In this connection, Corey and Hertler concluded that an increase in acid strength decreased the rate of chain termination in the Hoffman–Löffler reaction (18). They suggested that this resulted from the fact that the self-reaction of two protonated, positively charged nitrogen radicals was far slower than the self-reaction of the neutral radicals which were assumed to be the species actually responsible for termination. However, as Neale and Walsh have pointed out (19), this requires that the basicity of the amino radical be less than that of the corresponding chloroamine, since the latter is protonated even in the most weakly acidic solutions used. The available evidence (19, 23) suggests that the radical is a much stronger base than the chloroamine. Corey and Hertler's suggestion that the coupling of two charged radicals is disfavored relative to the neutral radicals may well apply to two "free" radicals though it is by no means certain that it applies to geminate pairs of radicals formed in a solvent cage.[4] Our own results show that reaction [4] is rapid but is probably not as fast as the reaction of two uncharged radicals.

The estimated maximum rate constants for chain propagation are in the range 3–10 $\times$ 10^3 M^{-1} s^{-1} and the minimum rate constants are in the range 0.7–1.0 $\times$ 10^3 M^{-1} s^{-1}. Assuming a normal pre-exponential factor of $\sim 10^{8.5}$ M^{-1} s^{-1} (26) for hydrogen atom abstraction, the activation energy for abstraction will be in the range 6–8 kcal/mole.

The propagation rate constants indicate that aminium radicals have a reactivity towards unactivated secondary hydrogens which is somewhat smaller than that of the *t*-butoxy radical ($k_{\mathrm{ButO}\cdot + \mathrm{C_6H_{12}}} = 3 \times 10^4$ (2), 5×10^5 M^{-1} s^{-1} (8)[5]). It is interesting to note that the heats of chlorination of saturated hydrocarbons by *t*-butyl hypochlorite and chloroamine are rather similar, viz. $\Delta H_{\mathrm{ButO}\cdot + \mathrm{C_6H_{12}}} = -42.4 \pm 1$ kcal/mole (27), and $\Delta H_{\mathrm{HN}^{+\cdot} + \text{decanoic acid}} = -38.5 \pm 4$ kcal/mole. However, in respect to selectivity the *t*-butoxy and aminium radicals behave quite differently. *t*-Butoxy is a relatively unselective radical (28) but aminium radicals are highly selective (1 and references cited therein). The high selectivity of the aminium radical is presumably due to the fact that a radical cation is much more sensitive to both inductive and field effects than is even the most highly electrophilic neutral radical of similar absolute reactivity.

1. J. Spanswick and K. U. Ingold. Can. J. Chem. Preceding paper, this issue.
2. D. J. Carlsson and K. U. Ingold. J. Amer. Chem. Soc. **89**, 4885 (1967).
3. D. J. Carlsson and K. U. Ingold. J. Amer. Chem. Soc. **90**, 7047 (1968).
4. G. Henrici-Olivé and S. Olivé. Makromol. Chem. **58**, 188 (1962).
5. N. F. Hall and W. F. Spengeman. J. Amer. Chem. Soc. **62**, 2487 (1940).
6. J. Russel and A. E. Cameron. J. Amer. Chem. Soc. **60**, 1345 (1938).

[4]Staples and co-workers (24) have found that the rate constant for the dimerization of radical anions of 1,1-diphenylethylene in hexamethylphosphoramide is $\sim 10^5$ M^{-1} s^{-1}, considerably less than the diffusion controlled limit, whereas Hammond and Newman (25) have reported that the extent of recombination of *geminate* radical pairs is only slightly affected by whether the two radicals are charged or neutral.

[5]$k_{\mathrm{Me_2NH}^{+\cdot} + \mathrm{C_6H_{12}}}$ appears to be about 2.5 times as great as $k_{\mathrm{Me_2NH}^{+\cdot} + \text{decanoic acid}}$ (see Fig. 1).

Can. J. Chem. Downloaded from www.nrcresearchpress.com by 210.87.254.42 on 09/05/12
For personal use only.

7. G. S. HAMMOND, J. N. SEN, and C. E. BOOZER. J. Amer. Chem. Soc. **77**, 3244 (1955).
8. C. WALLING and V. P. KURKOV. J. Amer. Chem. Soc. **89**, 4895 (1967).
9. J. A. HOWARD and K. U. INGOLD. Can. J. Chem. **43**, 2729 (1965).
10. H. KIEFER and T. G. TRAYLOR. J. Amer. Chem. Soc. **89**, 6667 (1967).
11. T. KOENIG and M. DEINZER. J. Amer. Chem. Soc. **90**, 7014 (1968).
12. T. KOENIG and R. WIELESEK. J. Amer. Chem. Soc. **91**, 2551 (1969).
13. T. KOENIG. J. Amer. Chem. Soc. **91**, 2558 (1969).
14. W. A. PRYOR and A. SMITH. J. Amer. Chem. Soc. **89**, 1741 (1967).
15. A. P. STEFANI, G. F. THROWER, and C. V. JORDAN. J. Phys. Chem. **73**, 1257 (1969).
16. O. DOBIS, J. M. PEARSON, and M. SZWARC. J. Amer. Chem. Soc. **90**, 278 (1968). K. CHAKRAVORTY, J. M. PEARSON, and M. SZWARC. J. Amer. Chem. Soc. **90**, 283 (1968).
17. F. E. HERKES, J. FRIEDMAN, and P. D. BARTLETT. Intern. J. Chem. Kinet. **1**, 193 (1969).
18. E. J. COREY and W. R. HERTLER. J. Amer. Chem. Soc. **82**, 1657 (1960).
19. R. S. NEALE and M. R. WALSH. J. Amer. Chem. Soc. **87**, 1255 (1965).
20. A. M. NORTH. Quart. Rev. (London), **20**, 421 (1966).
21. D. J. CARLSSON, K. U. INGOLD, and L. C. BRAY. Intern. J. Chem. Kinet. **1**, 315 (1969).
22. W. A. PRYOR. Private communication.
23. E. J. LAND and G. PORTER. J. Chem. Soc. 3540 (1961).
24. T. L. STAPLES, J. JAGUR-GOODZINSKI, and M. SZWARC. J. Amer. Chem. Soc. **91**, 3721 (1969).
25. G. S. HAMMOND and R. C. NEWMAN, JR. J. Amer. Chem. Soc. **85**, 1501 (1963).
26. S. W. BENSON. Thermochemical kinet. J. Wiley and Sons, Inc., New York. 1968.
27. C. WALLING and C. G. PAPAIOANNOU. J. Phys. Chem. **72**, 2260 (1968).
28. C. WALLING and B. B. JACKNOW. J. Amer. Chem. Soc. **82**, 6108 (1960).
29. R. BERNARDI, R. GALLI, and F. MINISCI. J. Chem. Soc. *B* 324 (1968).

Can. J. Chem. Downloaded from www.nrcresearchpress.com by 210.87.254.42 on 09/05/12
For personal use only.

Can. J. Chem. Downloaded from www.nrcresearchpress.com by 210.87.254.42 on 09/05/12
For personal use only.

Preparation and reactions of triarylsilylmethylmetallic reagents

A. G. Brook, J. M. Duff,[1] and D. G. Anderson[2]
Department of Chemistry, University of Toronto, Toronto 181, Ontario

Received August 5, 1969

Triarylsilylmethylmetallic reagents have been prepared by several routes: metalation; addition of phenyllithium to vinyltriphenylsilane; direct synthesis; and by halogen–metal exchange. The latter method is highly superior as regards both generality of application and yields. Dibromomethylsilanes undergo halogen–metal exchange at −78°, and reaction of the product with hydrogen bromide serves as a valuable way of converting geminal dibromides to monobromides. The organometallic reagents have been characterized in several ways, in particular by carbonation to give the related carboxylic acid.

Canadian Journal of Chemistry, **48**, 561 (1970)

Much is known about the preparation and reactions of trialkylsilylmethylmetallic reagents (1, 2, 3) (Alk_3SiCH_2M, M = Li or MgX), which have been shown to be of great value in the synthesis of β-functional organosilicon compounds (4). However, little has been reported regarding the related triarylsilylmethylmetallics (Ar_3SiCH_2M). We wished to employ these reagents for the synthesis of β-ketosilanes and silylacetic acids and hence we have investigated, at least briefly, the following possible routes to these reagents: metalation; addition of an organolithium reagent to a vinylsilane; direct synthesis from a triarylsilylmethyl halide and metal; and halogen–metal exchange of the halide with *n*-butyllithium. All of these routes could be used to provide certain triarylsilylmethylmetallic reagents once appropriate conditions had been established, but the halogen–metal exchange route at low temperature was the most widely applicable reaction and gave the best yields of products as will be seen below. For derivatizing the organometallic reagents, their reactions with several reagents (H_2O, D_2O, CO_2, Me_3SiCl, MeI, and benzoic anhydride) were investigated.

Metalation

It has been reported that tetramethylsilane is metalated by *n*-butyllithium-tetramethylethylenediamine (TMEDA) complex to give trimethylsilylmethyllithium in reasonable yield (5) and Gornowicz and West (6) have shown that a wide variety of trimethylsilyl derivatives (Me_3SiX, X = Cl, OAC, $OSiMe_3$, etc.) can undergo a similar reaction. These results infer that the carbanion may be stabilized to some extent by the neighboring silicon atom, but other effects may be important as well since neither methyltriphenylsilane nor bis(triphenylsilyl)methane could be metalated to any appreciable extent by this reagent. However, it is possible to metalate a methyl group to which one or more phenyl groups is directly attached and Gilman and coworkers have shown that benzyltriphenylsilane (7), benzhydryltriphenylsilane (8) and 9-fluorenyltrimethylsilane (9) undergo the metalation reaction. In our re-investigation we found that virtually quantitative metalation of benzhydryltriphenylsilane could be effected at room temperature using *n*-butyllithium in tetrahydrofuran and, as shown in Table 1, the resulting organometallic was deuterated or methylated in greater than 80% yield. Carbonation to give the expected triphenylsilyldiphenylacetic acid gave only a mixture of diphenylacetoxytriphenylsilane, triphenylsilanol, and diphenylacetic acid. These products were those expected from the base-catalyzed rearrangement of triphenylsilyldiphenylacetic acid, a reaction which has been shown to occur readily with silylacetic acids under mild conditions (10). Metalation of benzyltriphenylsilane using *n*-butyllithium in ether gave the lithium reagent in good yield; it was derivatized by methylation, trimethylsilylation, and by carbonation.

Addition of Phenyllithium to Vinyltriphenylsilane

Cason and Brooks have shown that a variety of organolithium reagents add to the double bond of vinyltriphenylsilane to give substituted 1-triphenylsilylethyllithium reagents (11, 12)

$$Ph_3SiCH{=}CH_2 + RLi \rightarrow Ph_3SiCHLiCH_2R$$

[1]NRCC Postgraduate Scholarship Holder, 1967–1969.
[2]Postdoctoral Fellow, 1966–1968.

TABLE 1

Triphenylsilylmethylmetallic reagents and their reactions

Reagent	Method of preparation	Reactant	Product	Yield (%)	Melting point (°C)
1) Ph_3SiCPh_2Li	RH + *n*-BuLi in THF 3–4 h	D_2O	Ph_3SiCPh_2D	88	160–161*
		MeI	Ph_3SiCPh_2Me	81	207–208†
		CO_2	$Ph_3SiOCOCHPh_2$ + Ph_3SiOH + Ph_2CHCO_2H		104–105‡
2) $Ph_3SiCHPhLi$	RH + *n*-BuLi in Et_2O 18 h	MeI	$Ph_3SiCHPhMe$	79	127–128§
		Me_3SiCl	$Ph_3SiCHPhSiMe_3$	76	123–124
		CO_2	$Ph_3SiCHPhCO_2H$	60	157–162‖
3) $Ph_3SiCHLiCH_2Ph$	$Ph_3SiCH{=}CH_2$ + PhLi in Et_2O 16–24 h	H_2O	$Ph_3SiCH_2CH_2Ph$	75	146.5–148¶
		D_2O	$Ph_3SiCHDCH_2Ph$	78	146.5–148[a]
		Me_3SiCl	$Ph_3SiCH(SiMe_3)CH_2Ph$	38	85–86
		CO_2	$Ph_3SiCH(CO_2H)CH_2Ph$	67	214–216[b]
4) Ph_3SiCH_2Li	Ph_3SiCH_2Br + *n*-BuLi in Et_2O	H_2O	Ph_3SiCH_3	85	64–66[c,d]
		D_2O	Ph_3SiCH_2D	78	64–66[c,e]
		PhCHO	$Ph_3SiCH_2CH(OH)Ph$	81	135–137[c,d]
		$(PhCO)_2O$	Ph_3SiCH_2COPh	86	87.5–89[d,f]
		CO_2	$Ph_3SiCH_2CO_2H$	78	173–175[f,g]

*The n.m.r. showed 100% monodeuterated: mixed m.p. with undeuterated compound, m.p. 160–161°, not depressed.
†Mixed m.p. with sample provided by Dr. H. Gilman, not depressed.
‡Compounds identified by mixed m.p. and spectra. The expected carboxylic acid, as its lithium salt, would be expected to very readily rearrange (10).
§The n.m.r. of crude product showed little recovered benzylsilane. Mixed m.p. with authentic sample not depressed.
‖Wide m.p. range due to thermal decomposition of the acid (10).
¶Mixed m.p. with authentic sample, m.p. 146–148° (12) undepressed.
[a]Compound contained 91% deuterium (n.m.r.). Mixed m.p. with undeuterated sample not depressed.
[b]Melting point varies between 210–220° because of thermal decomposition. Treatment of this acid with diazomethane gave methyl ester m.p. 77–78°, in 67% yield.
[c]Halogen–metal exchange done at 25°.
[d]Identified by mixed m.p. with authentic sample.
[e]Compound contained 81% deuterium (n.m.r.). Mixed m.p. with undeuterated sample not depressed.
[f]Halogen–metal exchange done at −78°.
[g]Literature m.p. 175.5–177.5 (23).

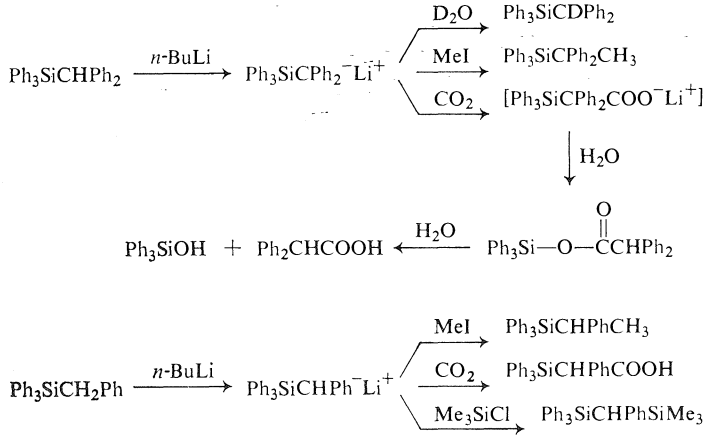

Reinvestigation of the reaction using phenyllithium in ether showed that the reaction was complete in less than 16 h (workup after 6 h revealed unreacted vinylsilane). Deuterolysis of the clear red solution gave 78% of deuterium labelled 1-phenyl-2-triphenylsilylethane ($Ph_3SiCHDCH_2Ph$), estimated by nuclear magnetic resonance (n.m.r.) to be 91% monodeuterated on the carbon adjacent to silicon. If the reagent was allowed to stand for 4 days prior to deuteration the product contained only 28% deuterium, indicating some reaction with the ether solvent. The original workers failed to isolate any acid on carbonation, obtaining instead 47% of the

Can. J. Chem. Downloaded from www.nrcresearchpress.com by 210.87.254.42 on 09/05/12
For personal use only.

TABLE 2

Carboxylic acids from bromomethylsilanes and bromomethylgermanes*

Bromide	Exchange conditions† Temperature (°C)	Exchange conditions† Time (min)	Acid	Yield (%)	Melting point (°C)
Ph_3SiCH_2Br	−78	20	Ph_3SiCH_2COOH	78	174–176
Me_3SiCH_2Br	−23	60	Me_3SiCH_2COOH	60	37–39‡
1-NpPhMeSiCH_2Br	−78	30	1-NpPhMeSiCH_2COOH	80	120–121.5
$Ph_3SiCHBrCH_3$	−78	15	$Ph_3SiCH(COOH)CH_3$	24	186–187
$Ph_3SiCBr{=}CH_2$	−23	60	$Ph_3SiC(COOH){=}CH_2$	71	200–201
$Ph_3SiCBr{=}CHPh$	25	20	$Ph_3SiC(COOH){=}CHPh$	77	225–228
Ph_3GeCH_2Br	25	5	Ph_3GeCH_2COOH	85	168–169.5
1-NpPhMeGeCH_2Br	25	5	1-NpPhMeGeCH_2COOH	63	116.5–118.5

*The general reaction scheme is: $R_3MCR'R''Br + n\text{-BuLi} \rightarrow R_3MCR'R''Li \xrightarrow{CO_2} R_3MCR'R''CO_2H$.
†Exchange reactions carried out in diethyl ether – hexane solvent at −78° (Dry Ice – acetone bath) or −23° (Dry Ice – CCl_4 bath) or at room temperature.
‡Literature m.p. 40° (24).

hydrolysis product, 1-phenyl-2-triphenylsilylethane. Since their short reaction time of 6 h precludes complete reaction with the ether solvent it appears possible that they employed wet Dry Ice since carbonation in our hands gave 67% of the expected acid. The suggestion that decarboxylation had occurred (12) seems unlikely since this behavior has not been observed with any of several silylacetic acids investigated (10).

Reaction of Bromomethyltriphenylsilane with Lithium and Magnesium

Chloromethyltriphenylsilane was reported to react with magnesium by Huang and co-worker (13) and the same Grignard reagent has been reported more recently (14) but this work was not reproducible in our hands. Using bromomethyltriphenylsilane (prepared by reaction of triphenylsilylmethanol with phosphorus tribromide, (15)) we were able to obtain reaction with magnesium in THF or with lithium in refluxing ether but treatment of the resulting mixtures with trimethyl- or triphenylchlorosilane or with carbon dioxide afforded methyltriphenylsilane and 1,2-bis(triphenylsilyl)ethane as major products. For example, on one occasion, reaction of the intermediate organolithium solution with carbon dioxide gave a 5% yield of triphenylsilylacetic acid in addition to 45% of methyltriphenylsilane and 40% of 1,2-bistriphenylsilylethane. Direct synthesis, therefore, does not seem particularly useful.

Halogen–Metal Exchange Reactions

Halogen–metal exchange is a well established type of reaction (16) which to date has had little application in organosilicon chemistry. We have found as shown in Table 1 that bromomethyltriphenylsilane readily undergoes exchange with *n*-butyllithium in ether. Deuteration studies (using n.m.r. spectroscopy) revealed that the yield of Ph_3SiCH_2Li from the reaction at room temperature was about 80%. Other products found were *n*-pentyltriphenylsilane, obtained in low yield from coupling of butyllithium with the bromide, and methyltriphenylsilane obtained in about 15% yield, which probably arose from a reduction reaction of the type proposed by Eastham (17). When samples of the reagent in ether were hydrolyzed in D_2O after various time intervals, it was found that the reaction of the organolithium reagent with the solvent was surprisingly rapid, and within 8 h at room temperature no deuterium was incorporated in the resulting methyltriphenylsilane. This rapid reaction with the solvent indicates that the reagent must be used immediately or stored at a low temperature and provides a reasonable explanation for the lack of success previously found in preparing it, or the corresponding Grignard reagent, in refluxing ether or the even more reactive THF. Halogen–metal exchange also occurs rapidly at lower temperatures and side reactions appear to be minimized at −78°. The reactions of the reagent with benzaldehyde, carbon dioxide, and benzoic anhydride were found to occur in good yield as is shown in Table 1.

Since the halogen–metal exchange occurred so efficiently investigations were made to determine the scope of the reaction. Although chloromethyltriphenylsilane gave only a very low yield of

Can. J. Chem. Downloaded from www.nrcresearchpress.com by 210.87.254.42 on 09/05/12
For personal use only.

Can. J. Chem. Downloaded from www.nrcresearchpress.com by 210.87.254.42 on 09/05/12
For personal use only.

Ph_3SiCH_2Li using this method, it was found, using similar experimental conditions to those described above for Ph_3SiCH_2Br, that bromine–lithium exchange appears to be general for compounds containing the Si—C—Br linkage and, although the number of compounds studied is somewhat small, it seems likely that many α-bromogermanes also undergo this reaction. Thus each of the bromides shown in Table 2 was successfully converted via halogen–metal exchange to the β-carboxymetalloid by carbonation of the organolithium reagent prepared by halogen–metal exchange.

The results indicate that the reaction is successful with either aryl or alkyl groups attached to silicon. The organolithium derivative of 1-bromoethyltriphenylsilane would be expected to be destabilized relative to those of the first three bromides of Table 2 and it therefore is not surprising that the bromine–metal exchange occurred in much lower yield in this case. The n.m.r. spectrum of the crude product from this reaction showed absorptions due to vinyltriphenylsilane (from dehydrobromination) and broad absorptions from $\delta = 0.7$ to 2.7 p.p.m. indicating that other unknown side-reactions were occurring. The yield of anion was found to be higher when exchange was carried out at low temperature.

Previous investigators have found that vinyl bromides only undergo efficient halogen–metal exchange when there is a phenyl group available to stabilize the resulting carbanion. Thus Curtin and Crump (18) have shown that both *cis*- and *trans*-bromostilbene react with *n*-butyllithium to form stilbenyllithium in high yield, but where no phenyl group is attached to the bromine-bearing carbon, exchange is accompanied by other reactions. It has now been found that α-bromovinylsilanes undergo the halogen–metal exchange reaction with high efficiency. The success of this reaction implies substantially enhanced rates of exchange or significant stabilization of the carbanion by the adjacent metalloid atom.

Geminal halogeno–lithium compounds (X—C—Li) can be prepared by halogen–metal exchange of dihalides at low temperatures (19). We have found that α,α-dibromosilanes and -germanes also readily react with *n*-butyllithium at −78° to form these species. Since these intermediates appeared to be reasonably stable at the low temperature used, the reaction allowed a convenient synthesis of monobromo compounds from the dibromides by bubbling gaseous HBr into the cold solution.

$$R_3MCBr_2R \xrightarrow[-78^\circ]{n\text{-BuLi}} R_3M{-}CBr(Li){-}R \xrightarrow[-78^\circ]{HBr} R_3M{-}CHBr{-}R$$

This reaction has considerable synthetic potential since in many cases dibromides are more readily synthesized than the monobromo compounds. For example, 1-bromoethyltriphenylsilane has been prepared in these laboratories by the bromination of 1-triphenylsilylethanol (20) using PBr_3 in carbon tetrachloride but the yield of bromide was low, and the starting carbinol itself is not easily prepared. However, it was found that ethyltriphenylsilane would react with *N*-bromosuccinimide with ultraviolet (u.v.) irradiation to give 1,1-dibromoethyltriphenylsilane in good yield. Using the halogen–metal exchange procedure the dibromide was converted to the monobromide in 83% yield.

$$Ph_3SiLi + CH_3CHO \xrightarrow[50\%]{} Ph_3SiCHOHCH_3$$

$$Ph_3SiCHOHCH_3 \xrightarrow[24\%]{PBr_3} Ph_3SiCHBrCH_3$$

$$Ph_3SiCH_2CH_3 \xrightarrow[73\%]{2NBS} Ph_3SiCBr_2CH_3 \xrightarrow[2)\ HBr\ -78^\circ \quad 83\%]{1)\ n\text{-BuLi}\ -78^\circ} Ph_3SiCHBrCH_3$$

Can. J. Chem. Downloaded from www.nrcresearchpress.com by 210.87.254.42 on 09/05/12
For personal use only.

TABLE 3

Preparation and reduction of dibromomethylsilanes and -germanes*

Dibromide	Method of preparation	Yield (%)	Melting point (°C)	Monobromide	Yield (%)	Melting point (°C)
$Ph_3SiCBr_2CH_3$	$Ph_3SiCH_2CH_3$ + 2 NBS	73	162.5–163.5	$Ph_3SiCHBrCH_3$	83	126–127.5
$Ph_3SiCHBr_2$	Ph_3SiH + $PhHgCBr_3$	65	154–156†	Ph_3SiCH_2Br	83	121–122‡
1-NpPhMeSiCHBr$_2$	R_3SiH + $PhHgCBr_3$	47	oil	R_3SiCH_2Br	76	63.5–64.5
$Ph_3GeCHBr_2$	Ph_3GeH + $PhHgCBr_3$	51	146.5–147.5	Ph_3GeCH_2Br	74	120.5–122
	Ph_3GeH + $CHBr_3$ + KO-*t*-Bu	78	146.5–147.5			
1-NpPhMeGeCHBr$_2$	R_3GeH + $PhHgCBr_3$	66	oil	R_3GeCH_2Br§	80	59.5–60.5

*Reaction conditions for halogen–metal exchange reactions were diethyl ether – hexane solvent for 5–10 min at −78° for silanes and − 120° for germanes.
†Literature m.p. 154–156° (21).
‡Identified by mixed m.p. with an authentic sample.
§Reaction conditions were ether–THF, 1:1, 10 min reaction time at about −120° (methylcyclohexane cooled to its freezing point with liquid nitrogen was used as coolant).

Further, dihalocarbenes generated from the phenyltrihalomethylmercury reagent will insert into an Si—H or Ge—H bond to give reasonable yields of dihalomethylsilanes or -germanes (21). In our hands the use of equimolar amounts of phenyldibromomethylmercury and arylsilanes (Ph_3SiH and R_3Si^*H) at 80° gave poor yields of the monobromomethylsilanes. Seyferth *et al.* have reported similar results (22) although the use of higher temperatures (130°) led to significantly improved yields in many cases of aliphatic (but not aromatic) silanes. Consequently, a preferred method of synthesis of monobromomethylsilanes and -germanes involves the preparation of the dibromo compound followed by its reduction using the bromine–metal exchange reaction at low temperatures as shown in Table 3. Within the limitations of this study it is quite apparent that, if appropriately handled, triarylsilylmethyllithium reagents are quite readily prepared, are quite stable, and can serve as exceedingly valuable synthetic reagents.

$$R_3MH + :CBr_2 \longrightarrow R_3MCHBr_2 \xrightarrow[2)\ HBr]{1)\ n\text{-BuLi}} R_3MCH_2Br \xrightarrow[2)\ CO_2]{1)\ n\text{-BuLi}} R_3MCH_2COOH$$

M = Si, Ge

Experimental

Some typical experimental procedures are outlined below; other pertinent information is given in Tables 1 to 3. Analytical data and the important spectral features of all new compounds are given in Tables 4 and 5. All reactions involving organometallic reagents were carried out under an atmosphere of dry, oxygen-free nitrogen. Diethyl ether was freshly distilled from sodium ribbon which showed the color of benzophenone ketyl and tetrahydrofuran was freshly distilled from lithium aluminum hydride. The *n*-butyllithium was purchased from Foote Mineral Co. and was approximately 1.6 *M*, as analyzed by the double titration method (25). Nuclear magnetic resonance spectra were recorded on a Varian A-60 Spectrometer and chemical shift values are reported in p.p.m. (δ units) below internal tetramethylsilane in carbon tetrachloride or deuterochloroform solution. Infrared (i.r.) spectra were recorded on a Perkin–Elmer 237B Spectrometer in carbon tetrachloride unless otherwise specified. Melting points were determined on a Fisher–Johns apparatus and are uncorrected.

Metalation Reactions

Triphenylsilyldiphenylmethyllithium (Ph_3SiCPh_2Li)

A solution of 2.13 g (0.005 mole) of benzhydryltriphenylsilane in 50 ml of tetrahydrofuran was treated with 12.5 ml (0.02 mole) of a 1.6 *M* solution of *n*-butyllithium in hexane. A deep red solution resulted instantly. After 3 h at room temperature excess methyl iodide was added, causing the color to disappear instantly. After stirring for 2 h the solution was worked up with dilute hydrochloric acid, several volumes of ether being added to facilitate separation of the layers. The organic layer was dried with magnesium sulfate. Removal of solvent on a rotary evaporator gave a brownish solid which was recrystallized from 1-propanol-ethyl acetate to give 1.78 g (81%) of pure 1,1-diphenylethyltriphenylsilane; m.p. 207–208°; n.m.r. (carbon tetrachloride): 7–7.6 (25 H, m), 2.05 p.p.m. (3 H, s). The previously reported m.p. of 194–195° (8) is now considered to be erroneous (26).

A similarly prepared solution of the anion from 0.86 g of benzhydryltriphenylsilane was poured into a well-stirred slurry of Dry Ice in ether and the resulting cloudy suspension was worked up with dilute hydrochloric acid or saturated aqueous ammonium chloride as soon as the excess carbon dioxide had sublimed. An i.r. spectrum of the resulting oil showed a silanol band at 2.70 μ, a wide strong carbonyl peak at 5.79 μ, and a series of broad bands from 7–9 μ, consistent with the presence in the mixture of a considerable amount of diphenylacetoxytriphenylsilane.

The n.m.r. spectrum (deuterochloroform) also indicated the presence of diphenylacetoxytriphenylsilane (5.17 p.p.m., s) together with diphenylacetic acid (5.02 p.p.m., s) and starting benzhydrylsilane (4.50 p.p.m., s) in the ratio 19:11:10, respectively. Attempts to crystallize the acetoxysilane were unsuccessful and chromatography on silica gel gave only the hydrolysis products, triphenylsilanol and diphenylacetic acid.

Pure diphenylacetoxysilane was prepared by stirring a suspension of silver diphenylacetate and triphenylchlorosilane in benzene for 36 h in the dark. Recrystallization from pentane of the product obtained after filtration of silver chloride and removal of the benzene gave a 78% yield of diphenylacetoxytriphenylsilane, m.p. 104–105°. This compound had identical n.m.r. and i.r. spectral bands to those described above for the acetoxysilane from the carbonation reactions.

Triphenylsilylphenylmethyllithium ($Ph_3SiCHPhLi$)

A solution of 7.0 g (0.020 mole) of benzyltriphenylsilane in 100 ml of ether was treated with 0.070 mole of *n*-butyllithium in hexane. Stirring for 18 h at room temperature gave a clear yellow solution to which was added, all at once, 19.3 ml (0.15 mole) of trimethylchlorosilane. After stirring for 1 h work-up gave an oil which was crystallized from 95% ethanol to give 6.40 g (70%) of (α-trimethylsilylbenzyl)triphenylsilane, m.p. 123–124°.

Triphenylsilylbenzylmethyllithium ($Ph_3SiCHLiCH_2Ph$)

A solution of 19.3 g (0.0675 mole) of vinyltriphenylsilane and 0.084 mole of freshly prepared phenyllithium in 300 ml of diethyl ether was stirred at room temperature

Can. J. Chem. Downloaded from www.nrcresearchpress.com by 210.87.254.42 on 09/05/12
For personal use only.

TABLE 4
Spectral and analytical data for new compounds

Compound	Nuclear magnetic resonance (No. of H, multiplicity)*	Analysis			
		Calculated		Found	
		C	H	C	H
$Ph_3SiCHPh(SiMe_3)$	7–8 (20, m), 2.49 (1, s) −0.18 (9, s)†	79.56	7.14	79.55	7.02
$Ph_3SiCH(SiMe_3)CH_2Ph$	7–8 (20, m), 2–4 (3, ABC) −0.20 (9, s)†	79.75	7.39	80.08	7.35
$Ph_3SiCBr_2CH_3$	7–7.7 (15, m), 2.71 (3, s)‡	53.83	4.06	53.81	4.07
1-NpPhMeSiCH_2Br	7.2–8.1 (12, m), 3.10 (2, s) 0.87 (3, s)†	63.34	5.02	63.35	5.09
1-NpPhMeSi$CHBr_2$	7–7.9 (12, m), 5.48 (1, s) 0.80 (3, s)†	51.46	3.84	51.45	3.90
Ph_3GeCH_2Br	7.2–7.7 (15, m), 3.23 (2, s)‡	57.36	4.31	57.40	4.30
$Ph_3GeCHBr_2$	7.2–8.0 (15, m), 5.79 (1, s)‡	47.86	3.38	47.83	3.36
1-NpPhMeGeCH_2Br	7.2–8.0 (12, m), 3.17 (2, s) 0.94 (3, s)‡	56.06	4.04	56.19	4.40
1-NpPhMeGe$CHBr_2$	7.1–7.9 (12, m), 5.85 (1, s) 1.09 (3, s)‡	46.52	3.47	46.82	3.53

*The n.m.r. positions in p.p.m. (δ) below TMS.
†Carbon tetrachloride solvent.
‡Deuterochloroform solvent.

TABLE 5
Spectral and analytical data for new compounds

Compound	Infrared* (μ)	Analysis			
		Calculated		Found	
		C	H	C	H
$Ph_3SiOCOCHPh_2$	5.79	81.66	5.57	81.47	5.41
$Ph_3SiCHPhCO_2H$	5.90	79.15	5.62	78.68	5.47
$Ph_3SiCH(CO_2H)CH_2Ph$	5.80 (w), 5.90†	79.04	5.93	79.43	6.25
$Ph_3SiCH(CO_2Me)CH_2Ph$	5.80	79.58	6.20	79.98	6.11
1-NpPhMeSiCH_2CO_2H	5.91	74.47	5.92	74.46	5.89
$Ph_3SiCH(CO_2H)CH_3$	5.92	75.86	6.06	75.86	6.15
$Ph_3SiC(CO_2H)=CH_2$	5.92, 6.01	76.33	5.49	76.20	5.35
$Ph_3SiC(CO_2H)=CHPh$	5.93	79.76	5.46	79.56	5.47
$Ph_3GeCH_2CO_2H$	5.92	66.19	4.94	66.20	4.98
1-NpPhMeGeCH_2CO_2H	5.93	65.08	5.17	65.01	5.13

*In carbon tetrachloride.
†In chloroform solvent, w = weak.

for 19 h. The resulting clear red solution was poured into a rapidly stirred slurry of 150 g of crushed dry ice in ether. The cloudy suspension was worked up with 200 ml of 3% hydrochloric acid. A small amount of tetrahydrofuran had to be added during work-up to dissolve the product. Removal of solvent at reduced pressure gave a white solid which was recrystallized from methylene chloride – pentane to give 18.4 g (67%) of 2-triphenylsilyl-3-phenylpropanoic acid, m.p. 200–209°. Recrystallization from the same solvent gave m.p. 214–216°. The structure of this compound was confirmed by alkaline hydrolysis.

A solution of 2.00 g of the acid in aqueous ethanolic dioxane, containing 0.6 g of potassium hydroxide, was stirred at room temperature for 3 days. Work-up gave 0.45 g (61%) of pure hydrocinnamic acid, m.p. 47–48°, identified by mixed m.p. Removal of solvent from the initial organic layer gave 1.29 g of crude triphenylsilanol which on recrystallization from carbon tetrachloride gave 1.10 g (81%) of pure material, m.p. 154–155°, identified by mixed m.p.

Diazomethane in ether was added to a solution of 1.50 g of the original acid in 25 ml of dry tetrahydrofuran. Removal of solvent gave an oil which was crystallized from methanol to give 1.02 g (67%) of methyl 2-triphenylsilyl-3-phenylpropionate; m.p. 77–78°; n.m.r. (carbon tetrachloride): 7–8 (20 H, m), 3.09 (3 H, s), 2.7–3.4 p.p.m. (3 H, ABC system).

Bromomethyltriphenylsilane

Triphenylsilylmethanol was prepared by passing dry formaldehyde over a rapidly stirred solution of triphenylsilyllithium in tetrahydrofuran. The product was purified by several recrystallizations from petroleum ether

Can. J. Chem. Downloaded from www.nrcresearchpress.com by 210.87.254.42 on 09/05/12
For personal use only.

Can. J. Chem. Downloaded from www.nrcresearchpress.com by 210.87.254.42 on 09/05/12
For personal use only.

(60–70°) to give white crystals of m.p. 108–110° (27). Reaction of a solution of this carbinol in carbon tetrachloride with 1/3 mole of phosphorous tribromide for 19 h at room temperature, followed by work-up with dilute hydrochloric acid and extraction of the organic layer with 5% sodium bicarbonate to remove phosphites, gave a 75% yield of bromomethyltriphenylsilane, m.p. 121–122° (15). This compound may also be readily prepared by reduction of the dibromide (see Table 3).

Reaction of Bromomethyltriphenylsilane with Magnesium (15)

A mixture of 1.0 g (0.0028 mole) of bromomethyltriphenylsilane and 0.08 g (0.0033 g atom) of purified magnesium in 10 ml of tetrahydrofuran was stirred for 2 h at room temperature. A white precipitate formed and most of the magnesium dissolved but at no time was the Gilman Color Test I (28) positive. The reaction mixture was added to a slurry of Dry Ice in ether and following normal acid work-up 0.65 g (89%) of methyltriphenylsilane, m.p. 67–68°, was obtained by recrystallization from ethanol. The i.r. spectrum of the crude reaction product indicated that no carboxylic acid was present. Several additional experiments in ethyl ether and tetrahydrofuran gave similar results.

Reaction of Bromomethyltriphenylsilane with Lithium (15)

A solution of 2.0 g (0.0057 mole) of bromomethyltriphenylsilane in 25 ml of ethyl ether and 0.10 g (0.014 g atom) of lithium was refluxed for 20 h. A precipitate formed and a double titration indicated that a 17% yield of triphenylsilylmethyllithium was present. After refluxing for an additional 12 h the Color Test I was still positive but a double titration indicated that the yield of lithium reagent had dropped to 5%. The purple reaction mixture was added to a slurry of Dry Ice in ether and, following normal acid work-up, 0.52 g (45%) of 1,2-bistriphenylsilylethane, m.p. 204–209° (lit. m.p. 209–211° (29)), was obtained by crystallization from ethanol. Chromatography of the mother liquor on silica gel gave 0.44 g (38%) of methyltriphenylsilane, m.p. 64–68°, and 0.07 g (5%) of triphenylsilylacetic acid, m.p. 165–168°.

In a similar experiment chloromethyltriphenylsilane was recovered unchanged after refluxing for 72 h with lithium in ethyl ether.

Halogen–Metal Exchange Reactions

Triphenylsilylacetic Acid

A solution of 4.10 g (0.0116 mole) of bromomethyltriphenylsilane in 100 ml of ether was cooled to −78° and was treated with 8.0 ml (0.0128 mole) of *n*-butyllithium in hexane. After 20 min, 20 g of crushed Dry Ice were added. The reaction was worked-up with 2% hydrochloric acid before it had reached 0° to give a white solid which was recrystallized from methylene chloride – pentane to give 2.85 g (78%) of triphenylsilylacetic acid, m.p. 173–175°.

Phenacyltriphenylsilane

To the organolithium reagent, similarly prepared from 0.700 g (0.0020 mole) of bromomethyltriphenylsilane in ether at −78°, was added, all at once, 0.30 g (0.0022 mole) of benzoic anhydride. The resulting suspension was stirred for 15 min and then was allowed to warm up to room temperature. Work-up with saturated aqueous sodium bicarbonate removed benzoic acid and removal of the solvents gave a white solid. Recrystallization from 30 ml of dry *n*-hexane at −20° gave 0.65 g (86%) of phenacyltriphenylsilane, m.p. 87.5–89°, identified by mixed m.p. with material obtained by oxidation of 2-hydroxy-2-phenylethyltriphenylsilane (30).

2-Triphenylsilylpropenoic Acid

Dehydrobromination in refluxing pyridine of 1,2-dibromoethyltriphenylsilane, m.p. 106–107°, (obtained in high yield from the u.v. bromination of vinyltriphenylsilane) gave α-bromovinyltriphenylsilane in 80% yield, m.p. 131–132° (20).

A solution of 0.50 g (0.00137 mole) of this compound in 10 ml of dry ether at −23° was treated with 0.00163 mole of *n*-butyllithium. The solution turned yellow immediately and a white precipitate formed. After 1 h powdered Dry Ice was added and the reaction was worked-up with dilute acid while cold to give a white solid. Recrystallization from benzene–pentane gave 0.32 (71%) of 2-triphenylsilylpropenoic acid, m.p. 198–200°. Recrystallization from benzene gave m.p. 200–201°; n.m.r. (deuterochloroform): δ 7–7.6 (15 H, m), 6.22, 7.25 p.p.m. (AB system, J = 2.5 Hz).

Triphenylgermylacetic Acid

To a solution of 0.65 g (0.00163 mole) of bromomethyltriphenylgermane in 10 ml of ether at room temperature was added 0.00175 mole of *n*-butyllithium. The solution was carbonated after 5 min and acidic work-up gave 0.57 g (96%) of crude triphenylgermylacetic acid, m.p. 142–149°. Recrystallization from *n*-hexane – cyclohexane gave 0.50 g (85%); m.p. 168–169.5°; n.m.r. (deuterochloroform): 7.2–7.5 (15 H, m), 2.18 (2 H, s), 10.75 p.p.m. (1 H, s).

Preparation and Reduction of α,α-Dibromosilanes and -germanes

1,1-Dibromoethyltriphenylsilane

Ethyltriphenylsilane (1.44 g, 0.050 mole) and *N*-bromosuccinimide (1.95 g, 0.011 mole) were stirred at reflux in 20 ml of carbon tetrachloride. Addition of benzoyl peroxide failed to initiate bromination but irradiation[3] of the reaction mixture for 30 min resulted in complete consumption of the NBS. The mixture was cooled to 0° and was filtered to remove succinimide. Removal of solvent at reduced pressure gave a solid which was recrystallized from methylene chloride – methanol to give 1.63 g (73%) of 1,1-dibromoethyltriphenylsilane, m.p. 159–162°. Recrystallization from *n*-hexane gave the analytical sample, m.p. 162.5–163.5°.

When a solution of 4.46 g (0.010 mole) of this dibromide in 90 ml of ether was cooled to −78° a considerable amount of precipitate formed. Addition of 6.9 ml (0.011 mole) of *n*-butyllithium in hexane gave a yellow color immediately and the precipitated dibromide dissolved as the halogen–metal exchange proceeded. After 5 min anhydrous hydrogen bromide was bubbled into the solution until the yellow color disappeared. A white precipitate formed at this stage. The mixture was allowed to warm up to room temperature and then was worked up with water. The crude product, a white solid, was shown by n.m.r. to be largely 1-bromoethyltriphenyl-

[3]Westinghouse "PAR 38" 100 W, Clear Mercury Lamp, ASA Code H38-4GS.

Can. J. Chem. Downloaded from www.nrcresearchpress.com by 210.87.254.42 on 09/05/12
For personal use only.

silane along with a minor amount of α-bromovinyltriphenylsilane (from dehydrobromination). Recrystallization from methylene chloride – methanol gave 3.05 g (83%) of 1-bromoethyltriphenylsilane, m.p. 121–122°, identified by mixed m.p. with material prepared by bromination of 1-triphenylsilylethanol (20).

1-Naphthylphenylmethyl(dibromomethyl)silane

A solution of 24.8 g (0.100 mole) of 1-naphthylphenylmethylsilane in 500 ml of dry benzene was heated at 65–70° for 6 days with 68 g (0.128 mole) of phenyltribromomethylmercury. The reaction mixture was filtered to give 44.2 g (97%) of phenylmercuric bromide and the solvent was removed at reduced pressure to give 38 g of thick oil. Chromatography on silica gel gave the desired product (19.6 g, 47%) as a thick oil which could not be crystallized under a variety of conditions.

A solution of 7.55 g (0.018 mole) of the above oil in 300 ml of diethyl ether was cooled to −78° and was treated with 12 ml (0.0193 mole) of *n*-butyllithium in hexane. After 10 min hydrogen bromide was bubbled in and the solution was allowed to warm up to room temperature. Work-up gave 5.8 g of brown oil which was chromatographed on silica gel to give 4.40 g (76%) of 1-naphthylphenylmethyl(bromomethyl)silane, m.p. 60–62°. Recrystallization from *n*-hexane gave the analytical sample, m.p. 63.5–64.5°.

Triphenyldibromomethylgermane

(*a*) A mixture of 5.0 g (0.0164 mole) of triphenylgermane and 9.0 g (0.017 mole) of phenyltribromomethylmercury in 50 ml of dry benzene was heated at reflux for 2 h. Work-up gave 8 g of oil which was chromatographed on alumina to give 4.0 g (51%) of triphenyldibromomethylgermane, m.p. 144–146°. Recrystallization from *n*-heptane – cyclohexane raised the m.p. to 146.5–147.5°.

(*b*) Triphenylgermane (0.95 g, 0.00312 mole) was dissolved in 15 ml of benzene and 13 g of bromoform and the solution was stirred rapidly under nitrogen. Solid potassium *t*-butoxide–*t*-butanol (1:1 complex) was added in small portions over 1 h and the mixture was stirred for an additional 1/4 h. Aqueous work-up gave 1.32 g of crude solid product which was recrystallized from *n*-heptane–cyclohexane to give 1.15 g (78%) of triphenyldibromomethylgermane, m.p. 144–146.5°, identified by mixed m.p. with the above material.

When this reaction was carried out in *t*-butanol solution the yield was significantly reduced.

1-Naphthylphenylmethyldibromomethylgermane

A solution of 4.40 g (0.015 mole) of 1-naphthylphenylmethylgermane and 8.75 g (0.0165 mole) of phenyltribromomethylmercury in 100 ml of dry benzene was heated at reflux for 2 h. Filtration gave 5.5 g (93%) of phenylmercuric bromide. Removal of the solvent followed by chromatography of the resulting oil on silica gel, eluting with carbon tetrachloride, gave 4.60 g (66%) of the desired dibromide as an oil. Further chromatography gave the analysis sample.

A solution of 4.04 g (0.0087 mole) of the dibromide in 240 ml of a 1:1 mixture of ether and tetrahydrofuran, cooled to −120°, was treated with 0.0095 mole of *n*-butyllithium in 6.0 ml of hexane. The solution turned yellow instantly and the color deepened over 10 min. Hydrogen bromide gas was then bubbled through the solution. The cooling bath was removed and addition of HBr was continued until all the yellow color had gone. Work-up, followed by chromatography on silica gel, gave 3.23 g of solid, m.p. 42–47°, which was recrystallized from hexane to give 2.65 g (81%) of 1-naphthylphenylmethyl(bromomethyl)germane, m.p. 55.5–57.5°. Further recrystallization from hexane gave the analysis sample, m.p. 59.5–60.5°.

This research was supported by the National Research Council of Canada.

1. F. C. Whitmore and L. H. Sommer. J. Amer. Chem. Soc. **68**, 481 (1946).
2. C. R. Hauser and C. R. Hance. J. Amer. Chem. Soc. **74**, 5091 (1952).
3. L. H. Sommer, R. M. Murch, and F. A. Hitch. J. Amer. Chem. Soc. **76**, 1619 (1954).
4. C. Eaborn. Organosilicon compounds. Butterworths Scientific Publications, 1960. p. 399 ff.; D. J. Peterson. J. Org. Chem. **33**, 780 (1968).
5. D. J. Peterson. J. Organometal. Chem. **9**, 373 (1967).
6. A. Gornowicz and R. West. J. Amer. Chem. Soc. **90**, 4478 (1968).
7. H. Gilman and H. Harzfeld. J. Amer. Chem. Soc. **73**, 5878 (1951).
8. T. C. Wu, D. Wittenberg, and H. Gilman. J. Org. Chem. **25**, 596 (1960).
9. H. Gilman, R. A. Benkeser, and G. E. Dunn. J. Amer. Chem. Soc. **72**, 1689 (1950).
10. A. G. Brook, D. G. Anderson, and J. M. Duff. J. Amer. Chem. Soc. **90**, 3876 (1968).
11. L. F. Cason and H. G. Brooks. J. Amer. Chem. Soc. **74**, 4582 (1952).
12. L. F. Cason and H. G. Brooks. J. Org. Chem. **19**, 1278 (1954).
13. C. T. Huang and P. T. Wang. Acta Chim. Sinica, **25**, 341 (1959).
14. J. F. Lutsenko, Yu. I. Baukov, O. V. Dudukina, and E. N. Kramarova. J. Organometal. Chem. **11**, 35 (1968).
15. G. J. D. Peddle. M.A. Thesis, University of Toronto, Toronto, Ontario, 1961.
16. R. G. Jones and H. Gilman. Organic reactions. Vol. VI. J. Wiley and Sons, New York, 1951. Chapter 7.
17. J. F. Eastham. J. Org. Chem. **28**, 280 (1963).
18. D. Y. Curtin and J. W. Crump. J. Amer. Chem. Soc. **80**, 1922 (1958).
19. D. Seyferth and R. B. King. Annual surveys on organometallic chemistry. Vol. I. Elsevier Publishing Co., 1964. p. 8.
20. G. E. Legrow. M.A. Thesis, University of Toronto, Toronto, Ontario, 1962.
21. D. Seyferth and J. M. Burlitch. J. Amer. Chem. Soc. **85**, 2667 (1963).
22. D. Seyferth, S. B. Andrews, and H. D. Simmons. J. Organometal. Chem. **17**, 9 (1969).
23. D. Wittenberg, P. B. Talukdar, and H. Gilman. J. Amer. Chem. Soc. **82**, 3608 (1960).
24. L. H. Sommer, J. R. Gold, G. M. Goldberg, and N. S. Marans. J. Amer. Chem. Soc. **71**, 1509 (1949).
25. H. Gilman and J. W. Norton. Organic reactions. Vol. VIII. J. Wiley and Sons, 1954. p. 286.
26. H. Gilman. Private communication, 1966.
27. B. Iachia. M.A. Thesis, University of Toronto, Toronto, Ontario, 1959.
28. H. Gilman and F. Schulze. J. Amer. Chem. Soc. **47**, 2002 (1925).
29. D. Wittenberg, D. Aoki, and H. Gilman. J. Amer. Chem. Soc. **80**, 5933 (1958).
30. A. G. Brook and J. B. Pierce. Can. J. Chem. **42**, 298 (1964).

Can. J. Chem. Downloaded from www.nrcresearchpress.com by 210.87.254.5 on 09/05/12
For personal use only.

Equilibration d'imines cyclaniques[1]

JEAN-CLAUDE RICHER ET DAVID PERELMAN[2]
Département de Chimie, Université de Montréal, B.P. 6128, Montréal, P.Q.

Reçu[3] le 26 mars 1968

La synthèse et les propriétés d'imines cyclaniques sont rapportées; les spectres infrarouge, ultraviolet, de résonance magnétique nucléaire, et de masse ont été déterminés. Les cétimines et les aldimines isomères ont été équilibrées en utilisant des agents basiques comme l'hydroxyde de sodium fondu, l'hydrure de sodium dans le tétrahydrofuranne, et le *tert*-butylate de potassium dans le DMSO. Le ΔF du groupe benzaldimino (—N=CH—C_6H_5) a été établi par équilibration directe des dérivés de la serie *tert*-butyl-4-cyclohexyle et par la technique de la résonance magnétique nucléaire.

Canadian Journal of Chemistry, **48**, 570 (1970)

Introduction

Les premiers résultats sur l'isomérisation des imines ou selon leur terminologie sur la mobilité prototropique du système méthylène–azométhine, ont été rapportés par Ingold et Shoppee (1). Tel que le démontre la revue de Cram (2), ce sujet a depuis fait l'objet d'un grand nombre de travaux. En ce qui concerne l'application de ces réactions aux cétones cycliques, Ingold et Shoppee (1) ont mentionné que l'imine formée par condensation de la cyclohexanone avec la *p*-nitrobenzylamine peut être transformée d'une manière irréversible en *N*-(*p*-nitrobenzylidène)cyclohexylamine; le fait que cette transformation serait irréversible a été confirmé par Baddar (3).

Ces résultats nous ont incités à examiner les possibilités de transformer des cétones cycliques (**1**) en amines (**5**) correspondantes en utilisant les étapes décrites dans le schéma réactionnel 1. Les problèmes stéréochimiques qui se présentent lors de la transformation d'une cétone telle que la *tert*-butyl-4 cyclohexanone (**9**) en amines isomères (**13** et **14**) ont aussi été examinés. Les résultats obtenus au cours de cette étude font l'objet de la présente communication.

Résultats et discussion

Synthèse et propriétés des imines

La préparation de ces dérivés s'effectue à partir de produits carbonylés et aminés appropriés d'après la réaction I du schéma 1. Les rendements, la pureté chromatographique, et les propriétés physiques des imines ainsi obtenues sont résumées dans le tableau 1.

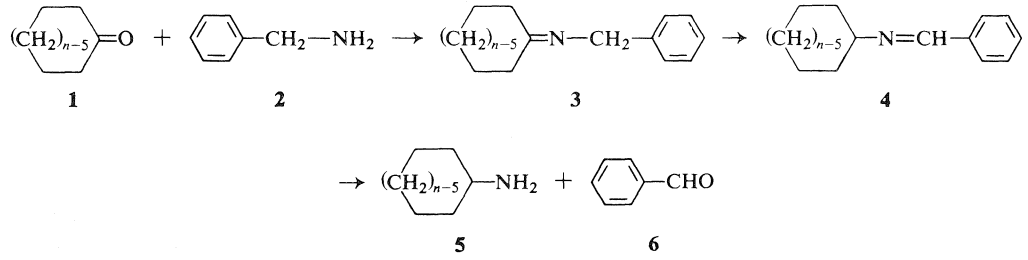

1 **2** **3** **4** **5** **6**

a, $n = 5$; *b*, n, $= 6$; *c*, $n = 7$

SCHÉMA 1

Les spectres de résonance magnétique nucléaire (r.m.n.) des imines dérivées de cyclanones et de la benzylamine sont rapportées dans le tableau 2; ces spectres sont conformes aux structures proposées. L'absence dans chaque cas de protons vinyliques permet d'exclure l'existence de dérivés

[1]Les résultats rapportés dans le présent travail ont été présentés en partie devant la XXXVIeme réunion de l'ACFAS, Sherbrooke, novembre 1967.

[2]Les résultats rapportés dans la présente communication sont tirés de la thèse de doctorat de D. Perelman, Faculté des Sciences, Université de Montréal, décembre 1967.

[3]Revision reçue le 6 octobre 1969.

TABLEAU 1
Caractéristiques des imines

Produit	Rendement (%)	Point d'ébullition (°C/mm Hg)	n_D^{25}	c.p.g. T_r (min)	Pureté (%)	Spectre infrarouge (cm^{-1})	Spectre ultraviolet λ_{max}	Spectre ultraviolet ε
3*a****	72	104–106/0.085	1.5448	12.2¶	97**	1672		
3*b*	76	104–112/0.3†	1.5440	8.0	98	1650		
3*c**	60	104–106/0.07	1.5419	14.4	>99	1645		
4*a**	83	90–92/0.1	1.5518	5.5¶	99	1645	248	16300
4*b*	82	98/1.1‡	1.5500	5.0	>99	1640	248	17200
4*c**	91	100–102/0.07	1.5470	7.5	99	1640	248	18100
7*a**	80	90–91/20	1.4901	2.0		1680		
7*b*	78	92–98/0.1§	1.4973	3.5	98	1655		
7*c**	81	184/20	1.5032	7.0				
8	87	113/0.4‖	1.5978	15.0	100	1640		
10*	50	130/0.03	1.5298	23	90–95**	1653		
11*	67	126–128/0.7	1.5270	10.4	100	1640	248	16800
12*	51	p.f. 78–78.5		16.8	100	1640	248	14200
16*a**	60	105–107/0.7	1.5278	10.0	99	1655		
16*b**	78	118–120/1.0	1.5224	12.7	99	1657		
17*a**	79	96–97/0.1	1.5335	6.5	>99	1643	248	16700
17*b**	78	102–104/0.3		11.0	>99	1640	248	17200
19*	43	104/0.13	1.5428	6.0	100	1631	248	12000

*Produit nouveau caractérisé par des méthodes physiques; le spectre de masse présente un pic parent à la valeur de *m/e* attendue.
†Litt. (4) 125–128/1 mm Hg, n_D^{25} 1.5452.
‡Litt. (5) 136/16 mm Hg.
§Litt. (6) 113–116/9 mm Hg, n_D^{20} 1.4996.
‖Litt. (7) 116–117/0.1 mm Hg, n_D^{20} 1.6017.
¶Analyses effectuées à 183 °C.
**Pureté évaluée par r.m.n.

TABLEAU 2
Spectres r.m.n. des cétimines*

Produits	Types de protons: Méthylènes†	Benzyliques	Divers
3*a*	2.18 (m)	4.28 (s)	1.70 (alicycliques)
3*b*	2.24 (m)	4.39 (s)	1.58 (alicycliques)
3*c*	2.36 (m)	4.28 (s)	1.55 (alicycliques)
10	2.06 (m)	4.39 (s)	0.85 (*tert*-butyle)
16*a*	2.04 (s) et 2.12 (m)	4.38 (s) et 4.41 (s)	0.87 et 0.88 (*gem*-diméthyles)
16*b*	2.04 (s) et 2.12 (s)	4.52 (s)	0.92 et 0.98 (*gem*-diméthyles)

*Déplacements chimiques, $-\delta$, en p.p.m.
†Méthylènes adjacents à la liaison C=N.

du type énamine. Les spectres des *N*-(diméthyl-3,3 cyclohexylidène) (**16***a*) et *N*-(tétraméthyl-3,3,5,5 cyclohexylidène) (**16***b*) benzylamines présentent des aspects caractéristiques; d'une part alors que les protons benzyliques du second composé apparaissent sous forme de singulet ceux du premier se présentent sous la forme de deux singulets indiquant ainsi la présence des isomères *syn* et *anti*; d'autre part le fait que les protons des groupes méthyles de ces deux imines apparaissent sous forme de deux singulets alors que les spectres r.m.n. des cétones correspondantes ne montrent dans chaque cas qu'un singulet confirme la présence de l'isomère géométrique dans l'imine **16***a* et suggère que la liaison iminobenzyle a une influence à longue distance.

Les spectres des aldimines dérivées de cycloalkylamines et du benzaldéhyde sont résumés dans le tableau 3; d'une façon générale seuls les pics correspondants aux protons aldiminiques et aux protons attachés au carbone portant le groupe aldimino sont rapportés. Ces dérivés pourraient exister dans deux formes isomères *syn* et *anti*; la présence d'un seul singulet aldiminique suggérerait toutefois qu'un seul isomère

Can. J. Chem. Downloaded from www.nrcresearchpress.com by 210.87.254.5 on 09/05/12
For personal use only.

TABLEAU 3

Spectres r.m.n. des aldimines*

Produits	Types de protons		
	C*H*—N=CH—	—N=C*H*—	Divers
4*a*	3.65 (m)	8.09 (s)	
4*b*	3.04 (m)	8.14 (s)	
4*c*	3.28 (m)	8.10 (s)	
7*a*	3.63 (m)		
7*b*	3.25 (m)		
7*c*	3.40 (m)		
8	4.62 (s)	8.14 (s)	
11	3.42 (m)	8.20 (s)	
12	3.00 (m)	8.12 (s)	
17*a*	3.25 (m)	8.15 (s)	0.96 (*gem*-diméthyle)
17*b*	3.54 (m)	8.41 (s)	0.97 et 1.08 (*gem*-diméthyles)
19	3.42 (m)		2.10 (—N=C(CH$_3$)—)

*Déplacements chimiques, — δ, en p.p.m.

est présent dans chaque cas. Cette hypothèse est compatible avec les résultats de Hine et Yeh (8) qui ont proposé que les aldimines dans lesquelles la liaison imine est conjuguée avec un noyau aromatique existeraient préférentiellement dans la configuration *anti*. La r.m.n. peut se prêter à l'analyse conformationnelle des composés cyclohexaniques. Il est possible à partir des résultats rapportés dans le tableau 3 et utilisant l'équation proposée par Eliel (9) de calculer la constante pour l'équilibre conformationnel de l'aldimine **4***b*; cette constante d'équilibre s'établirait à 4 et correspondrait à une différence d'énergie libre de 0.83 kcal/mole. Cette valeur est en accord avec celle (0.68 kcal/mole) obtenue par Eliel (10) en utilisant la même méthode.

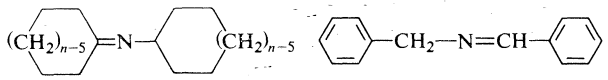

7 **8**

a, $n=5$; *b*, $n=6$; *c*, $n=7$

Afin de s'assurer que la chromatographie en phase gazeuse (c.p.g.) pouvait être utilisée pour analyser les cétimines et leurs aldimines isomères un mélange équimoléculaire de **3***b* et **4***b* a été examiné; le chromatogramme indiquait la présence de quatre produits **7***b*, **4***b*, **3***b*, et **8** de temps de rétention respectifs de 3.5, 5, 8, et 15 minutes; ces identifications ont été effectuées par superposition de pics avec des substances authentiques. La formation des produits mineurs **8** et **7***b* ne provient pas d'une décomposition dans le chromatographe puisque le spectre de r.m.n. du mélange **3***b* et **4***b*, montre la présence du proton aldiminique et des protons benzyliques attendus pour la *N*-benzylidènebenzylamine (**8**). Il a été établi que cette réaction de transfert (appelée transchiffisation (11)) est générale et qu'elle peut être représentée par l'équation **3** + **4** → **7** + **8**. Les résultats obtenus lors de la c.p.g. de divers mélanges d'imines isomères sont résumés dans le tableau 4. La formation des composés présents en quantité mineure peut être rationnalisée d'après la série de réactions suivantes, possible si les imines utilisées contiennent à l'état d'impureté des traces d'amines **2** et/ou **5**. Le système d'équation est le suivant: **2** + **4** → **8** + **5** et **5** + **3** → **2** + **7**. Quoique les auteurs (12) aient proposé un autre mécanisme réactionnel pour expliquer de tels résultats une réaction analogue a été signalée récemment.

Can. J. Chem. Downloaded from www.nrcresearchpress.com by 210.87.254.5 on 09/05/12
For personal use only.

TABLEAU 4
Analyses chromatographiques de mélanges d'imines

Mélange	Temps de rétention des imines			
3*a* + **4***a**	**8***a* (2.8)	**4***a* (5.5)	**3***a* (12.2)	**8** (16.5)
3*b* + **4***b*	**8***b* (3.5)	**4***b* (5.0)	**3***b* (8.0)	**8** (15.0)
3*c* + **4***c*	**8***c* (6.2)	**4***c* (7.5)	**3***c* + **8** (14.4)†	

*Analyse effectuée à 183 °C.
†Inséparables dans les conditions utilisées.

Equilibrations des imines par le tert-butylate de potassium dans le DMSO

L'utilisation du *tert*-butylate de potassium dans le DMSO comme milieu basique pouvant promouvoir les réactions qui procèdent par l'intermédiaire de carbanions a été bien établie (2, 13). L'isomérisation d'aldimines provenant de la condensation de cycloalkylamines et du benzaldéhyde et de cétimines provenant de la condensation de cycloalcanones sur le benzylamine a été examinée dans ce milieu réactionnel; les résultats obtenus sont résumés dans le tableau 5. La position de l'équilibre entre les aldimines (**4**) et les cétimines (**3**), dérivés cyclaniques comportant respectivement des carbones sp^3 et sp^2, a été évaluée d'une manière directe grâce à une équation du type: $k_n = (\mathbf{4} + \mathbf{7})/(\mathbf{3} + \mathbf{8})$. L'analyse chromatographique des amines obtenues après hydrolyse acide des mélanges réactionnels a permis de calculer cet équilibre par l'équation équivalente: k_n = cycloalkylamine/benzylamine. Dans chacun des cas examinés, ces deux méthodes conduisent aux mêmes résultats. Le tableau 5 comporte aussi les constantes d'équilibre pour la formation des cyanohydrines des cyclanones correspondantes (14). Il est évident d'après ce tableau que la position de l'équilibre aldimine/cétimine est tout à fait parallèle. Les résultats obtenus avec les cétimines cyclaniques non substituées sont très bien expliqués à l'aide de l'hypothèse de la tension interne (I-strain) proposée par Brown et Gerstein (15), alors que la tendance observée lorsqu'on examine les résultats des tétraméthyl-3,3,5,5, de la diméthyl-3,3, et de la cyclohexanone non substituée est en accord avec le concept de l'encombrement axial proposé par Wheeler et Zabicky (14) pour expliquer la stabilité relative des cyanohydrines correspondantes.

L'application de cette méthode à l'équilibration de la cétimine **10** qui donne lieu à la formation de deux aldimines épimères **11** et **12** a aussi été examinée. Les résultats obtenus sont consignés dans le tableau 6 et permettent de mettre en évidence que l'équilibre conformationnel pour le groupe benzaldimino se situe à 12.3% de l'isomère *cis* (**11**) et 87.7% de l'isomère *trans* (**12**) ce qui équivaut à 25° à une valeur *A* de 1.16 kcal/mole. Cette valeur diffère toutefois de la valeur de 0.83 kcal/mole évaluée d'après la méthode de la r.m.n. développée par Eliel (9). Malgré sa validité apparente et en dépit de son application répandue (16), cette méthode est d'une part expérimentalement peu précise et d'autre part basée sur l'hypothèse que le groupe *tert*-butyle n'exerce aucun effet sur le noyau cyclohexanique. Cette dernière hypothèse a récemment été très sévèrement critiquée par Kwart et Takeshita (17), Mateos *et al.* (18), Shah-Malak et Utley (19), et Wolfe et Campbell (20).

Les résultats rapportés par ces auteurs indiquent clairement que le noyau cyclohexanique est déformé par le groupe *tert*-butyle; il n'est donc pas étonnant que la différence d'énergie

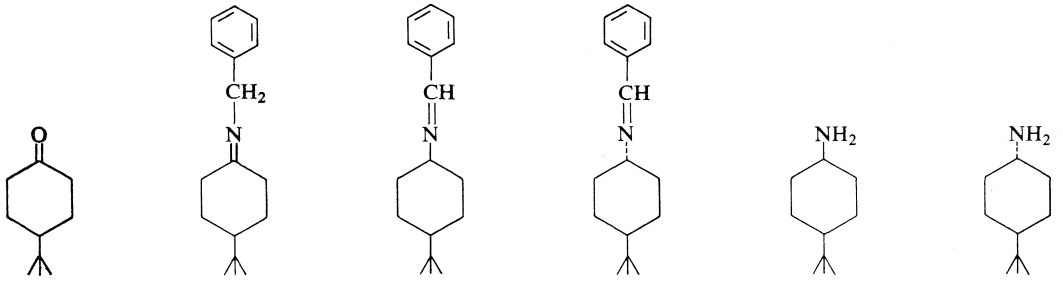

9 **10** **11** **12** **13** **14**

Can. J. Chem. Downloaded from www.nrcresearchpress.com by 210.87.254.5 on 09/05/12
For personal use only.

TABLEAU 5

Isomérisation d'imines en présence de *tert*-butylate de potassium

Imine	Temps de réaction (h)	Imine/ Base	Pourcentages à l'équilibre				K_N	$R_N^{REL.}$	K_{CYANO}
3*b*	1	4/1	**7***b* (1)	**4***b* (93)		**3***b* (traces) **8** (6)			
	1.25	2/1	**7***b* (1)	**4***b* (91)	**19** (5)	**3***b* (traces) **8** (3)			
4*b*	1.25	4/1	**7***b* (traces)	**4***b* (99)		**3***b* (traces) **8** (1)	28.4	1.00	1.00†
	3	2/1	**7***b* (traces)	**4***b* (91)	**19** (8)	**3***b* (traces) **8** (1)			
3*c*	1	4/1	**7***c* (12.5)	**4***c* (38.2)		**3***c* + **8** (49.3)			
4*c*	1	4/1	**7***c* (13.5)	**4***c* (35.2)		**3***c* + **8** (51.3)	0.97	0.03	0.008*
16*a*	4	2.5/1	**23***a* (2.2)	**17***a* (88.5)		**16***a* (traces) **8** (9.3)			
17*a*	3	4/1	**23***a* (5.6)	**17***a* (87.4)		**16***a* (traces) **8** (7.0)	12.0	0.4	0.033†
16*b*	6	2/1	**23***b* (3.8)	**17***b* (71.7)		**16***b* (21.8) **8** (2.7)			
17*b*	5	2.2/1	**23***b* (2.0)	**17***b* (76.3)		**16***b* (20.2) **8** (1.5)	3.3	0.1	0.0013‡

*Constantes d'équilibre relatives pour la formation des cyanohydrines.
†Valeurs utilisées par Brown (25).
‡Valeurs tirées de la référence 14.

TABLEAU 6

Isomérisation de la *N*-(4-*tert*-butylcyclohexylidène) benzylamine (**10**) et des aldimines **11** et **12**

Imines	Temps de réaction (h)	Imine/Base	Aldimine *cis*/ Aldimine *trans*
10	4	10/1	12.4/87.6
	19	10/1	12.7/87.3
	20	10/1	12.4/87.6
11	21	2/1	12.8/87.2
12	20	2/1	11.1/88.9

libre pour le groupe benzaldimino obtenue par cette méthode diffère de ceux obtenus par équilibration directe des aldimines *cis* (**11**) et *trans* (**12**).

Il a été observé lors de l'équilibration de la *N*-cyclohexylidène benzylamine (**3***b*) que le produit de la réaction contient en plus de la *N*-benzylidène cyclohexylamine (**4***b*) et des produits de "transamination" (**7***b*) et (**8**), la *N*-(phényl-1 éthylidène)cyclohexylamine (**19**) lorsque le rapport de concentration base/imine est augmenté. Les propriétés physiques et spectrales de ce composé sont absolument identiques aux propriétés correspondantes d'un échantillon authentique; de plus l'acétophénone obtenue par hydrolyse a pu être mise en évidence. Cette réaction de méthylation (par l'intermédiaire du diméthylsulfoxide) peut-être rapprochée de celle obtenue par Russel et Weiner (21), par Nozaki, *et al.* (22), et par Hunter et Cram (23), qui ont décrits récemment la méthylation de divers composés par l'anion diméthylsulphynyl (**20**) dans le DMSO; ce résultat est toutefois inattendu si l'on considère que Corey et Chaykovsky (24) ont rapporté que l'action de l'anion diméthylsulphynyl sur la *N*-benzylidène aniline (**21**) conduit avec un rendement de 92% au produit d'addition (**22**) de cet anion sur l'imine. Afin de confirmer que la *N*-(phényl-1 éthylidène)cyclohexylamine (**19**) se forme bien d'après cette réaction, une solution de l'anion diméthylsulphynyle (**20**) dans le DMSO a été préparée suivant les indications de Corey et Chaykovsky (24) et l'action de cet anion sur la cétimine (**3***b*) d'une part et sur son aldimine

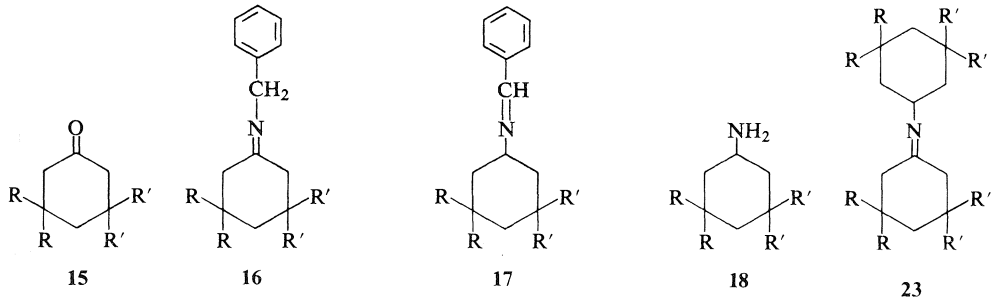

15 **16** **17** **18** **23**

a, R′=CH$_3$; R=H; *b*, R=R′=CH$_3$

Can. J. Chem. Downloaded from www.nrcresearchpress.com by 210.87.254.5 on 09/05/12
For personal use only.

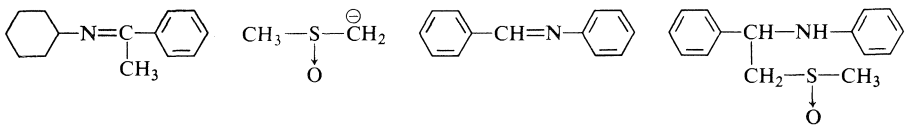

19 20 21 22

isomère (**4***b*) d'autre part a été examinée; il a été observé que le produit de méthylation (**19**) se forme avec de bons rendements quelle que soit l'imine utilisée. Pour expliquer ces résultats il est préconisé que la cétimine **3***b* est d'abord isomérisée en aldimine **4***b*; l'application à ce composé du mécanisme de méthylation proposée par Russel et Weiner (21) repris par Hunter et Cram (23) permet alors d'expliquer la formation des produits.

Equilibrations avec de la potasse

La distillation de la *N*-cyclohexylidènebenzylamine (**3***b*) sur du KOH en fusion, en suivant les indications de Campbell *et al.* (26) qui ont rapporté que la distillation d'imines est plus efficace lorsqu'elle est effectuée dans ces conditions, a conduit à un mélange contenant principalement l'aldimine **4***b*; d'après le spectre ultraviolet (u.v.) le produit de la distillation contiendrait environ 80% de **4***b*; ce résultat indique que la cétimine de départ (**3***b*) est facilement isomérisée lors de sa distillation en présence de KOH. Il a été possible au point de vue préparatif d'effectuer sur la cyclohexanone la transformation décrite dans le schéma réactionnel 1 avec un rendement global de 75%; la cyclohexylamine obtenue est pure à 99%. Ce résultat indique que dans des conditions appropriées la méthode décrite peut s'avérer d'une grande utilité pour la synthèse d'amines à partir de la cétone correspondante.

TABLEAU 7

Equilibrations d'imines de la série *tert*-butyl-4 cyclohexyle en présence d'hydroxyde de potassium

Imine	Temps de contact (h)	Rapport **11**/**12***
10	Distillation	37/63
	4	27/73
	19	22.5/77.5
	71	21.8/78.2
12	18	5.9/94.1
	77	13.2/86.8
	163	20.5/79.5

*Les valeurs rapportées sont des moyennes d'au moins trois mesures.

Au point de vue conformationnel, la stéréochimie de la réaction d'isomérisation a été effectuée à partir de la *N*-(*tert*-butyl-4 cyclohexylidène) benzylamine **10**; l'équilibre a aussi été atteint à partir de l'aldimine *trans* **12**. Les résultats obtenus sont rapportés dans le tableau 7; ils démontrent que le produit du controle cinétique de l'isomérisation des cétimines en aldimines contient une quantité appréciable de l'aldimine instable (axiale). De plus il ressort de l'examen de ces résultats que la position de l'équilibre *cis*/*trans* des groupes benzaldimino dans la série *tert*-butyl-4 cyclohexyle se situe à une valeur moyenne de 21.2% de *cis* **11** et 78.8% de *trans* **12**; cette valeur correspond à une différence d'énergie libre de 1.02 kcal/mole pour le groupe —N=CH—C_6H_5 à 140 °C. Cette valeur est en accord avec celle trouvée précédemment pour le même équilibre en présence de *tert*-butylate de potassium dans le DMSO à 25 °C.

En se basant sur le fait que les aldimines peuvent être isomérisées il est donc possible d'affirmer que la transformation des *N*-cycloalkylidène benzylamines en aldimines correspondantes est une réaction d'équilibre; cette conclusion est en opposition avec celle présentée par Ingold et Shoppee (1) et Baddar (3).

Equilibrations avec de l'hydrure de sodium

L'hydrure de sodium dans le tétrahydrofuranne (ou dans la diméthylformamide) permet d'isomériser rapidement (moins de 5 heures) la *N*-cyclohexylidènebenzylamine (**3***b*) en aldimine (**4***b*); l'évolution de grandes quantités d'hydrogène (correspondant à au moins 80% de l'hydrure mis en réaction) lors de l'addition d'eau à la fin de la réaction démontre que des quantités catalytiques d'hydrure de sodium sont utilisées au cours de cette transformation. Il est de plus noté que l'isomérisation de la cétimine (**3***b*) en aldimine (**4***b*) est accompagnée par la formation de *N*-benzylcyclohexylamine (**26**); la formation d'amine secondaire au cours des équilibrations en présence d'hydrure de sodium ne nous permet pas d'utiliser cette méthode pour établir directement le ΔF du groupe benzaldimino dans ces

Can. J. Chem. Downloaded from www.nrcresearchpress.com by 210.87.254.5 on 09/05/12
For personal use only.

conditions. Pour fins de comparaisons, les amines secondaires **24** et **25** ont toutefois été préparées; de plus il a été établi que la réduction de la cétimine **10** par l'hydrure double de lithium et d'aluminium conduit à un mélange d'amines secondaires contenant 22% de l'amine *cis* (**24**). Ce résultat comme ceux obtenus par Cabaret *et al.* (27) lors de la réduction de sels d'immonium peut être rationalisé en se basant sur les hypothèses complètement stériques proposées récemment (28, 29).

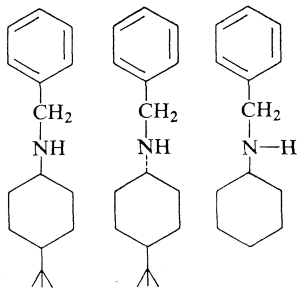

24 **25** **26**

Les résultats obtenus au cours de ce travail permettent donc de mettre en évidence que l'équilibration cétimine–aldimine peut être réalisée relativement facilement; à cause des réactions secondaires qui peuvent se produire, le milieu basique utilisé doit être choisi en fonction des particularités du système examiné.

Partie expérimentale

Les points de fusion sont déterminés sur un "Hot Stage Apparatus" de la compagnie Reichert (Autriche) muni d'un thermomètre calibré. Les indices de réfraction sont mesurés sur un réfractomètre du type Abbe de la compagnie Karl Zeiss. Les spectres infrarouges (i.r.) ont été déterminés à l'aide d'un spectrophotomètre "Beckmann" modèle IR-8 à double faisceau entre deux plaques de NaCl. Les spectres u.v. sont pris dans l'éthanol sur un spectrophotomètre "Bausch et Lomb" modèle Spectronic 505. Les spectres de r.m.n. ont été mesurés sur un spectromètre "Varian" modèle A-60, pour des solutions dans le tétrachlorure de carbone; les déplacements chimiques ($-\delta$) sont exprimés en p.p.m. et se réfèrent au tétraméthylsilane utilisé comme standard interne.

Les spectres de masse sont déterminés sur un spectromètre "Hitachi" modèle R.M.U. 6D, à 25°. L'énergie du faisceau d'électrons ionisants est de 20 eV. La chambre à ionisation est maintenue à 250°. Les analyses par c.p.g. ont été effectuées sur un appareil de la compagnie F et M, modèle 810 à l'aide d'une colonne de cuivre de 2.5 m contenant 10% de Versamid absorbée sur du Chromosorb W.

1. Synthèse et caractéristiques des imines

*1.1 Synthèse de la N-cyclohexylidènebenzylamine (**4***b*)*

Une solution contenant 98 g (1 mole) de cyclohexanone (**1***b*) et 107 g (1 mole) de benzylamine (**2**) dans 500 ml de benzène anhydre est chauffée à reflux sous atmosphère d'azote dans un montage muni d'un séparateur d'eau Dean-Stark. Le mélange est refroidi une fois que le volume théorique (18 ml) d'eau est recueilli. Le benzène est distillé sous pression normale et le résidu, purifié par distillation sous vide fournit 142 g (76% du rendement théorique) de l'imine **4***b* qui se présente sous forme d'un liquide jaune, p.e. 104–112 °C/0.3 mm Hg et qui doit être conservé à -5 °C afin d'éviter sa décomposition.

Cette procédure expérimentale a été utilisée pour la préparation des autres imines qui sont rapportées dans le tableau 1.

*1.2 N-(benzylidène) diméthyl-3,3 cyclohexylamine (**16***a*)*

L'oxime de la diméthyl-3,3 cyclohexanone (**15***a*) est préparée en chauffant à reflux (pendant 18 h) un mélange pyridinique de 7 g (0.055 mole) de diméthyl-3,3 cyclohexanone (**15***a*) et de 16.7 g (0.24 mole) de chlorhydrate d'hydroxylamine. Le mélange est refroidi et versé dans de l'eau glacée. L'oxime est extraite à l'éther; la phase organique est lavée avec de l'acide chlorhydrique dilué, de l'eau, et séchée sur du sulfate de sodium anhydre. L'évaporation du solvant laisse 7.5 g (96% de rendement) d'un résidu visqueux qui n'a pas été purifié. Une solution éthérée de l'oxime brute est ajoutée à une suspension de 4 g (105 mmoles) de $LiAlH_4$ dans l'éther. Le mélange est chauffé à reflux pendant 2 h puis agité à la température de la pièce pendant 12 h. L'amine **18***a* (2.77 g, 40% de rendement global) extraite et distillée se présente sous forme d'un liquide incolore: p.e. 62 °C/20 mm; n_D^{20}: 1.4520; c.p.g.: à 140 °C, un seul pic à 3.8 min; r.m.n.: 0.88 et 0.90 p.p.m. (groupes méthyles), 2.66 p.p.m. (*H*—C^{NH2}); i.r.: bandes de vibration de valence N—H à 3380, 3300, et 3200 cm^{-1}, bande de vibration de déformation N—H à 1600 cm^{-1}.

La condensation de cette amine (**18***a*) avec le benzaldéhyde (**6**) suivant le processus expérimental décrit dans la section 1 conduit à l'aldimine attendue (**17***a*) avec un rendement de 79%. Les propriétés physiques sont rapportées dans la partie théorique.

*1.3 N-(benzylidène) tétraméthyl-3,3,5,5 cyclohexylamine (**17***b*)*

*1.3.1 Oxime de la tétraméthyl-3,3,5,5 cyclohexanone (**15***b*)*

A une solution aqueuse contenant 16.4 g de (0.1 mole) de sulfate d'hydroxylamine, on ajoute 15.4 g (0.1 mole) de tétraméthyl-3,3,5,5 cyclohexanone (**15***b*). Le mélange est rendu alcalin par addition d'hydroxyde de sodium aqueux et agité pendant 12 h à la température de la pièce. Le précipité blanc est filtré, lavé avec de l'eau, séché, et recristallisé dans du benzène pour fournir 30 g (70% du rendement théorique) de l'oxime désirée qui se présente sous forme de cristaux blancs, p.f.: 147.5–148°; r.m.n.: 0.98 p.p.m. (groupes méthyles), 1.33 p.p.m. (méthylène en position 4), 1.97 p.p.m. (méthylène *anti*), 2.24 p.p.m. (méthylène *syn*) et 9.50 p.p.m. (OH).

*1.3.2 Tétraméthyl-3,3,5,5 cyclohexylamine (**18***b*)*

Une solution éthérée contenant 11.8 g (70 mmoles) d'oxime est ajoutée à une suspension de 5.32 g (140 mmoles) de $LiAlH_4$ dans l'éther. Le mélange est chauffé à reflux pendant 12 h et l'amine **18***b* (30 g soit 44% du

Can. J. Chem. Downloaded from www.nrcresearchpress.com by 210.87.254.5 on 09/05/12
For personal use only.

Can. J. Chem. Downloaded from www.nrcresearchpress.com by 210.87.254.5 on 09/05/12
For personal use only.

rendement théorique) isolée de la façon habituelle se présente sous forme d'un liquide incolore, p.e. 86–88 °C/17 mm Hg; n_D^{26} 1.4569; i.r.: bandes de vibration de valence N—H à 3380, 3300, et 3220 cm^{-1}, bande de vibration de déformation N—H à 1600 cm^{-1}; c.p.g.: à 160 °C un seul pic à 4.0 min et r.m.n.: pics à 0.98 et 0.89 p.p.m. (méthyles) et à 2.87 p.p.m. $H—\underset{\displaystyle NH_2}{\overset{\displaystyle |}{\underset{\displaystyle |}{C}}}—$.

1.3.3 Condensation de l'amine ***18b***

La condensation de cette amine (**18***b*) avec le benzaldéhyde (**6**) conduit à l'aldimine **17***b* dont les propriétés sont décrites dans le tableau 1.

2. Isomérisation des imines

2.1 Isomérisation préparative de la N-cyclohexylidène benzylamine (3b)

Une solution de 28.0 g (0.15 mole) de cétimine (**3***b*) brute dans 35 ml de DMSO est ajoutée à une solution de 2.25 g (0.02 mole) de *tert*-butylate de potassium dans 175 ml de DMSO. Le mélange est agité à la température de la pièce pendant 6 h. Le produit de l'isomérisation (24.7 g, 88% de récupération) est hydrolysé par chauffage en milieu acide dilué et 8.2 g (55% de rendement global) de cyclohexylamine **5***b* pure sont obtenus.

2.2 Equilibration des cétimines et des aldimines

D'une manière générale une solution contenant 0.566 g (0.5 mmole) de *tert*-butylate de potassium dans 80 ml de DMSO est préparée dans une boite à gants (atmosphère de N_2) et placée dans un ballon à une tubulure surmonté d'une ampoule à additionner contenant 50 mmoles de la cétimine à isomériser dans 20 ml de DMSO. Cette solution de cétimine est additionnée à la solution de base qui devient alors rouge. Le mélange réactionnel est alors agité à la température de la pièce pendant 12 h, et décomposé par addition d'eau glacée (la coloration du milieu devient alors jaune). Ces équilibrations permettent d'isoler, par extractions à la manière habituelle, les imines brutes avec des rendements pratiquement quantitatifs.

Cette procédure a été utilisée pour l'équilibration de toutes les imines étudiées et les résultats obtenues ont été résumées dans les tableaux 5 et 6.

3. Méthylation des imines

3.1 Méthylation de la cétimine (3b)

Une suspension de 50 mmoles de NaH dans le DMSO anhydre est chauffée à 75° durant 2 h; le dégagement d'hydrogène est alors de 1190 ml (calculé 1280 ml). La solution est ramenée à la température de la pièce et 7.15 g (40 mmoles) de la cétimine (**3***b*) dans le DMSO sont alors ajoutés lentement. Le mélange réactionnel, rouge foncé, est agité pendant 2 h et l'addition d'eau glacée ne cause aucun dégagement de gaz. Le produit de la réaction (rendement: 62%) est isolé par extraction à l'éther et purifié par distillation à 82 °C sous 0.1 mm Hg. Les spectres i.r. et r.m.n. de ce produit sont absolument identiques aux spectres correspondants de la *N*-(phényl-1 éthylidène)cyclohexylamine (**19**) authentique. La c.p.g. de ce produit révèle la présence d'un pic majeur (99% du total) dont le temps de rétention est de 6 min.

3.2 Méthylation de l'aldimine (4)

L'application à l'aldimine **4** de la réaction décrite dans la section précédente conduit au même produit avec un rendement de 76%.

4. Equilibrations en présence de potasse

4.1 Distillation de la N-cyclohexylidènebenzylamine sur de l'hydroxyde de potassium

Un échantillon de la cétimine **3***b* brute, préparée suivant les indications décrites dans la section 1.1, est distillé sous vide en présence de pastilles d'hydroxyde de potassium. Le mélange devient rouge-orange quand la température atteint 110 °C. A 120–125 °C l'hydroxyde de potassium est en état de fusion. La fraction principale receuillie, est un liquide jaune pâle qui présente les caractéristiques suivantes: p.e.: 139 °C/8 mm Hg; i.r.: 1640 cm^{-1} (imine conjuguée; bande principale) et 1650 cm^{-1} (imine non-conjuguée; bande faible); u.v.: λ_{max} dans l'éthanol: 248 mμ avec ε de 13500.

4.2 Isomérisation préparative

La cétimine **3***b* brute, préparée à partir de 9.8 g (0.1 mole) de cyclohexanone et de 10.7 g (0.1 mole) de benzylamine, est chauffée pendant 4 h en présence d'un poids égal d'hydroxyde de potassium. Les imines sont isolées par extraction à l'éther et hydrolysées en milieu acide chlorhydrique aqueux. Les produits neutres sont éliminés par extraction à l'éther et les amines sont régénérées par addition d'hydroxyde de potassium à la solution aqueuse refroidie. Les amines sont extraites à l'éther et la phase organique est lavée avec de l'eau, séchée sur du sulfate de sodium anhydre, et évaporée. Le liquide résiduel (7.3 g, 75% de rendement) est analysé par c.p.g. à 120 °C sur une colonne de Carbowax-Hyprose 10% absorbé sur Chromosorb W lavé avec du KOH en solution aqueuse. Le chromatogramme révèle la présence de la cyclohexylamine (**5***b*, 86%) et de la benzylamine (**2**, 14%). La distillation du mélange d'amines fournit la cyclohexylamine **5***b* pure; p.e.: 132–138 °C à pression atmosphérique et n_D^{26}: 1.4598.

4.3 Etudes stéréochimiques

Les isomérisations de la cétimine **10** et de l'aldimine **12** sont effectuées en utilisant un processus expérimental similaire à celui décrit dans la section 4.2. Les imines brutes sont hydrolysées en présence d'acide chlorhydrique et les amines obtenues analysées par c.p.g. Les résultats obtenus sont rapportés dans le tableau 7.

5. Isomérisation des imines par l'hydrure de sodium dans le tétrahydrofuranne

5.1 Procédure générale

Une suspension de 2.49 g (50 mmoles) d'hydrure de sodium à 50% dans l'huile minérale est ajoutée à 200 ml de tétrahydrofuranne anhydre dans un ballon à trois tubulures muni d'un réfrigérant et d'une ampoule à addition contenant 9.35 g (50 mmoles) de *N*-cyclohexylidènebenzylamine (**3***b*) dans 25 ml de THF; cette solution est ajoutée lentement à la suspension et aucune réaction apparente n'est notée. Une fois l'addition terminée, le mélange réactionnel est chauffé à 75 °C; après 2 h, le mélange est rouge vif. La suspension est refroidie après 21 h de chauffage et de l'eau est alors ajoutée; les premières gouttes d'eau décolorent le mélange et un dégagement rapide de gaz suit. Un excès d'eau est ajouté et le mélange est extrait à l'éther. La phase organique est lavée avec de l'eau et séchée sur sulfate de sodium. L'éther est évaporé et le THF est distillé sous vide. Le spectre i.r. du résidu est pratiquement superposable au spectre de la *N*-benzylidènecyclohexylamine **4***b* pure. Le produit de la

réaction est distillé et un liquide légèrement teinté est receuilli avec un rendement de 65%. La c.p.g. du produit ne montre qu'un pic de temps de rétention de 5 min. Le spectre r.m.n. de ce produit est pratiquement superposable au spectre de l'imine **4***b*; il révèle toutefois la présence d'un faible singulet à 3.67 p.p.m. Ce produit est alors hydrolysé en milieu acide aqueux et la fraction aminée est isolée selon la méthode habituelle. L'analyse par c.p.g. sur une colonne de Versamid 10% dans les conditions suivantes: 8 min à 108 °C puis programmation de température au rythme de 50 °C/min puis 10 min à 195 °C révèle la présence de deux composés aminés: la cyclohexylamine **5***b* de temps de rétention de 3.6 min qui représente 88% du total et la *N*-cyclohexylbenzylamine **26** de temps de rétention 18 min et formant 12% du total. L'amine secondaire est identifiée par comparaison avec du produit pur dont la préparation est décrite dans la section 5.2.

*5.2 Préparation et propriétés des N-cyclohexylbenzylamines **24**, **25**, et **26***

*5.2.1 N-cyclohexylbenzylamine **26***

Préparée selon la méthode de Mousseron *et al.* (30), cette amine montre dans son spectre r.m.n. un pic à 2.39 p.p.m. correspondant à l'hydrogène en position 1 sur le cyclohexane. Sa phénylurée font à 128–130 °C (litt. (30); 127–128 °C). Sa c.p.g. sur une colonne de Versamid à 10% à 205 °C montre un pic après 5 min; ce composé est inséparable de la *N*-benzylidènecyclohexylamine **4***b*.

*5.2.2 N-(tert-butyl-4 cyclohexyl) benzylamine cis (**24**)*

Cette amine est préparée à partir de la *N*-benzylidène *tert*-butyl-4 cyclohexylamine *cis* (**11**) par réduction avec $LiAlH_4$ d'après la procédure habituelle. Le produit receuilli avec un rendement de 63% se présente sous forme de liquide incolore ayant les caractéristiques suivantes: p.e.: 110–111 °C/0.2 mm Hg; n_D^{26}: 1.5123; r.m.n.: pic à 2.80 p.p.m. correspondant à un hydrogène en position 1 du noyau cyclohexanique; c.p.g.: sur une colonne de Versamid 10% à 205 °C, un pic à 11.8 min; spectre de masse: pic parent à *m*/*e* de 245 unités.

*5.2.3 N-(tert-butyl-4 cyclohexyl) benzylamine trans (**25**)*

Une solution éthérée de 1.33 g (5.5 mmoles) de la *N*-benzylidène *tert*-butyl-4 cyclohexylamine *trans* (**12**) est ajoutée à une suspension de 0.8 g (22 mmoles) de $LiAlH_4$ dans l'éther. Le mélange est chauffé à reflux pendant 7 h et l'amine secondaire **25** est isolée à la manière habituelle et purifiée par distillation. Le produit receuilli avec un rendement de 73% se présente sous forme d'un liquide incolore ayant les caractéristiques suivantes: p.e.: 112–114 °C/0.2 mm Hg; n_D^{26}: 1.5127; r.m.n.: pic à 2.28 p.p.m. correspondant à l'hydrogène en position 1 du noyau cyclohexanique; c.p.g.: sur une colonne de Versamid 10% à 205 °C, un pic à 17 min; spectre de masse: pic parent à *m*/*e* de 245 unités.

*5.3 Réduction de la N-(tert-butyl-4 cyclohexylidène) benzylamine (**10**)*

Une solution éthérée de 2.44 g (10 mmoles) de la cétimine **10** est ajoutée à une suspension de 0.59 g (15.5 mmoles) de $LiAlH_4$ dans l'éther. Le mélange est chauffé à reflux pendant 4 h et les amines **24** et **25** isolées selon les méthodes habituelles sont analysées par c.p.g. à l'aide d'une colonne de Versamid à 10% maintenue à 205 °C. Le chromatogramme montre la présence de 22% de l'amine *cis* (**24**) et 78% de l'amine *trans* (**25**) qui sont identifiées par superposition de pics à l'aide de produits purs.

Les auteurs remercient vivement le Conseil National de Recherche du Canada et le Ministère de l'Education de la Province de Québec pour l'aide financière apportée sous forme d'octrois de Recherches et de bourses d'études.

Les auteurs remercient aussi vivement Mlle Thérèse Madaule et M Gilles Audet et Denis Paquette pour l'aide technique apportée.

Les auteurs tiennent aussi à remercier la Compagnie Dow Chemicals du Canada qui a gracieusement fourni la *tert*-butyl-4 cyclohexanone utilisée au cours de ce travail.

L'un de nous (J. C. R.) tient à exprimer sa profonde gratitude au Dr. Pierre Maroni et à Mlle Marthe Benoit de la Faculté des Sciences de Toulouse pour l'accueil et l'aide qui lui ont été accordés durant la préparation de ce manuscrit.

1. C. K. Ingold et C. W. Shoppee. J. Chem. Soc. 1199 (1929).
2. D. J. Cram. Fundamentals of carbanion chemistry. Academic Press, Inc., New York. 1965. p. 186 et suivantes.
3. F. G. Baddar. J. Chem. Soc. 136 (1950).
4. R. Baltzly et O. Kander. J. Org. Chem. **16**, 173 (1951).
5. A. Skita et C. Wulff. Chem. Ber. **59**, 2683 (1926).
6. H. L. Wehrmeister. J. Org. Chem. **25**, 2132 (1960).
7. P. A. S. Smith et R. N. Loepphy. J. Amer. Chem. Soc. **89**, 1147 (1967).
8. J. Hine et C. Y. Yeh. J. Amer. Chem. Soc. **89**, 2669 (1967).
9. E. L. Eliel. Chem. Ind. (London), 568 (1959).
10. E. L. Eliel. Communication personnelle.
11. R. Kuhn, P. Zilliken, et H. Trischmann. Chem. Ber. **83**, 304 (1950).
12. A. Lawson et J. O. Stevens. J. Chem. Soc. (C), 1514 (1968).
13. C. Agami. Bull. Soc. Chim. France, 1021 (1965).
14. O. H. Wheeler et S. Z. Zabicky. Can. J. Chem. **36**, 656 (1958).
15. H. C. Brown et M. Gerstein. J. Amer. Chem. Soc. **72**, 2926 (1950).
16. E. L. Eliel et R. J. L. Martin. J. Amer. Chem. Soc. **90**, 682 (1968).
17. H. Kwart et T. Takeshita. J. Amer. Chem. Soc. **86**, 1161 (1964).
18. J. L. Mateos, C. Perez, et H. Kwart. Chem. Commun. 125 (1967).
19. F. Shak-Malak et J. H. P. Utley. Chem. Commun. 69 (1967).
20. S. Wolfe et J. R. Campbell. Chem. Commun. 872 (1967).
21. G. A. Russel et S. A. Weiner. J. Org. Chem. **31**, 248 (1966).
22. H. Nozaki, Y. Yamamoto, et R. Noyori. Tetrahedron Lett. 1123 (1966).
23. D. H. Hunter et D. J. Cram. J. Amer. Chem. Soc. **88**, 5765 (1966).
24. E. J. Corey et M. Chaykovsky. J. Amer. Chem. Soc. **87**, 1745 (1965).
25. H. C. Brown. Bull. Soc. Chim. France, 980 (1956).
26. K. N. Campbell, A. H. Sommers, et B. K. Campbell. J. Amer. Chem. Soc. **66**, 82 (1945).
27. D. Cabaret, G. Chauvière, et Z. Welvart. Tetrahedron Lett. 4109 (1966).
28. J. C. Richer. J. Org. Chem. **30**, 324 (1965).
29. A. V. Kamernitzky et A. A. Akhrem. Tetrahedron, **18**, 705 (1962).
30. M. Mousseron, R. Jacquier, M. Mousseron-Canet, et R. Zagdoun. Bull. Soc. Chim. France, 1042 (1952).

Can. J. Chem. Downloaded from www.nrcresearchpress.com by 210.87.254.5 on 09/05/12
For personal use only.

Can. J. Chem. Downloaded from www.nrcresearchpress.com by 210.87.254.105 on 09/05/12
For personal use only.

Condensation of some substituted phenols and anilines with formaldehyde. Formation of 2-phenyl-1,3-benzoxazines and *N*-(2-hydroxybenzyl)-anilines[1]

E. C. Horswill, D. A. Lindsay, and K. U. Ingold
Division of Chemistry, National Research Council of Canada, Ottawa, Ontario
Received September 18, 1969

The formalin condensation of 2,4-di-*t*-butylphenol and 2,4-di-*t*-butylaniline yields the benzoxazine **2** which, on hydrolysis, gives the hydroxybenzylaniline **3***a*. In contrast to a report by Kuliev *et al.* (2, 3) the condensation of equimolar quantities of 4-*t*-butylphenol, *o*-toluidine, and formaldehyde yields *N*-(2-hydroxy-5-*t*-butylbenzyl)-*o*-toluidine (**4**), rather than 2-amino-3-methyl-2′-hydroxy-5′-*t*-butyldiphenylmethane (**5**).

Canadian Journal of Chemistry, **48**, 579 (1970)

Butylated phenols and aromatic primary and secondary amines are among the most commonly employed oxidation inhibitors (1). Bis-phenols such as 2,2′-methylene-bis(4,6-di-*t*-butylphenol) are particularly useful in certain applications and we therefore attempted to prepare the analogous aminophenol in which one of the OH groups was replaced by NH_2, i.e., 2-amino-2′-hydroxy - 3,3′,5,5′ - tetra - *t* - butyldiphenylmethane (**1**).

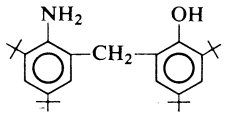

1

A promising approach to the synthesis of **1** was suggested by the work of Kuliev *et al.* who reported that 2-amino-2′-hydroxydiphenylmethanes were formed by the alkaline condensation of a variety of phenols with formaldehyde and aniline (2) or *ortho*-toluidine (3).

There is an extensive literature on the self-condensation of phenols and anilines using alkaline or acid formalin solutions. Phenols condense through their *ortho* and *para* positions while anilines condense through their nitrogen atom. Kuliev *et al.*'s procedures therefore appeared most useful as a preparative method. However, when we applied their reaction conditions to mixtures of 2,4-di-*t*-butylphenol and 2,4-di-*t*-butylaniline, the crystalline product which separated was found to have the benzoxazine structure, **2**. This structure was readily deduced from the molecular weight (mass spectrometry) and from the absence of absorption in the O—H and N—H stretching region of the infrared (i.r.) spectrum (3700–3100 cm^{-1}).

[1]NRCC No. 11077.

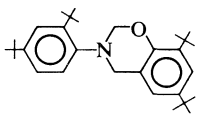

2

Treatment of the benzoxazine **2** with hydrogen chloride opened the ring to give the hydrochloride of *N*-(2-hydroxy-3,5-di-*t*-butylbenzyl)-2,4-di-*t*-butylaniline (**3***a*).

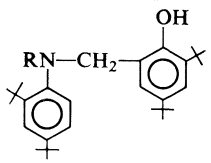

3*a* R = H
3*b* R = CH_3

This behavior is closely analogous to that reported by Burke for formalin condensations of *p*-substituted phenols and aliphatic amines (4). That is, condensations using phenol, formaldehyde, amine molar ratios of 1:2:1 gave benzoxazines which could be hydrolyzed by acid to *o*-alkylaminomethylphenols. The latter compounds could also be formed directly by reacting equimolar quantities of the three reagents. In our own case, the use of one mole of formaldehyde gave half a mole of the benzoxazine (together with unchanged dibutylphenol and dibutylaniline) rather than one mole of **3***a*.

To prevent benzoxazine formation, *N*-methyl-2,4-di-*t*-butylaniline was condensed with 2,4-di-*t*-butylphenol and formaldehyde. The product was **3***b* rather than a diphenylmethane (i.e. it was not *N*-methyl **1**) since *N*-methyl-2,4-di-*t*-butylaniline was regenerated by hydrolysis with hot alcoholic hydrochloric acid.

Can. J. Chem. Downloaded from www.nrcresearchpress.com by 210.87.254.105 on 09/05/12
For personal use only.

In order to learn more about these reactions, Kuliev *et al.*'s condensation of equimolar quantities of 4-*t*-butylphenol, *o*-toluidine, and formaldehyde was repeated (3). The principal product was *N*-(2-hydroxy-5-*t*-butylbenzyl)-*o*-toluidine **4**. None of the minor products appeared

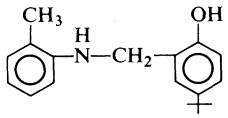

4

likely to be the anticipated aminodiphenylmethane, **5**. Analysis by thin-layer chromatography (t.l.c.) during the course of the reaction showed that the corresponding benzoxazine is

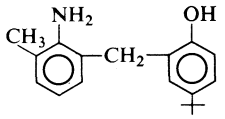

5

initially formed in much higher yield than **4**. That is, **4** reacts more rapidly with formaldehyde than the starting phenol and toluidine. Once the free formaldehyde is consumed, the benzoxazine serves as a source of formaldehyde so that **4** is formed in high yield from the equimolar mixture of reactants. The benzoxazine is readily purified by crystallization, its hydrolysis provides a convenient route to pure **4**. The structure of **4** was confirmed by its synthesis from 2-hydroxy-5-*t*-butylbenzaldehyde and *o*-toluidine via the benzylidene.

The possibility that **4** was an intermediate in the formation of **5** was suggested by Kuliev *et al.* We therefore attempted to rearrange **4** (and **3***a*) with acid (HCl) and base (sodium *t*-butoxide). In all cases the *N*-benzylaniline hydrolyzed before there was any detectable rearrangement.

Since Kuliev *et al.*'s product was not crystalline it is difficult to be absolutely certain that we have obtained the same compound. Their principal physical evidence for structure **5** appears to be the identification of a primary amino group from the i.r. spectrum in the 3300–3500 cm^{-1} region. Our own compound, **4**, has such a broad, strong absorption in the 3200–3400 cm^{-1} region (resulting from intramolecular hydrogen bonding) that a specific N—H vibration band was not detectable.[2] Chemical evidence for the existence of a primary amine group in their compounds consists of the purported reactions of these compounds with nitrous acid, benzaldehyde, and phthalic anhydride. No experimental details of these reactions are given. In particular, it is not stated whether nitrogen was evolved in the nitrous acid reaction. The reaction of **4** with nitrous acid gives the *N*-nitroso derivative in high yield. In our hands, **4** reacted very slowly with benzaldehyde even under quite drastic conditions and we were unable to identify the reaction products. The reaction with phthalic anhydride probably involved the initial formation of a phthalamic acid with subsequent dehydration to the amide ester, **6**. This compound, like the phthalamide, **7**, formed from a primary amine, would be insoluble in alkali and the reaction with anhydride would not, therefore, serve to distinguish a 2-hydroxybenzylaniline from a primary amine.

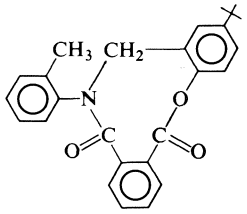

6

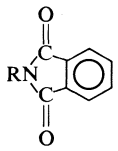

7

It must be concluded that Kuliev *et al.*'s structural assignments are incorrect and that their products are all *N*-benzylanilines. These compounds are of relatively little interest as oxidation inhibitors.

Experimental

All melting points were determined on a Kofler hot stage using factory-calibrated thermometers. Thin-layer chromatograms were run on Eastman Chromagram Sheet Type 6060 (silica gel with indicator) unless otherwise stated. Spots were detected by ultraviolet (u.v.) light and a spray reagent (*p*-nitrobenzenediazonium fluoborate, ninhydrin, or Fast Blue Salt B). The nuclear magnetic resonance (n.m.r.) spectra were obtained on a "Varian Associates" HR 100 spectrometer in carbon tetrachloride at 100 MHz using TMS as internal standard. The mass spectra were determined in an Atlas CH 4

[2]The *N*-acetamide derivative of **4** also showed only an intramolecularly bonded hydrogen band maxima at 3260 cm^{-1}.

Can. J. Chem. Downloaded from www.nrcresearchpress.com by 210.87.254.105 on 09/05/12
For personal use only.

spectrometer. The microanalyses were carried out by Mr. J. R. H. Seguin.

Preparation of 2,4-di-t-Butylaniline

3,5-Di-*t*-butylbromobenzene was prepared from 1,3,5-tri-*t*-butylbenzene by the method of Bartlett *et al.* (5) but with the addition of a vacuum pumping over fresh paraffin of the main distillate. This step cleanly removes a troublesome oily impurity and facilitates the subsequent recrystallization from pentane. Nitration of the bromo compound by the method of Rundel (6) yields 2-nitro-3,5-di-*t*-butyl-1-bromobenzene. To a solution of 2 g of this nitro compound in 150 ml methanol was added 0.2 g of magnesium oxide and 1.0 g 5% Pd/C and the mixture hydrogenated at 3 atm pressure. After concentration the product was dissolved in benzene, washed with water, dried, and reconcentrated to a pale yellow syrup. The yield was 1.0 g (78%). This aniline was prepared from the nitro compound as required in order to prevent its oxidative discoloration.

Acetamide derivative, m.p. 155.1–155.7 °C (without recrystallization) (lit. 153–154 °C (6), 153.5–154.5 °C (7)).

*Attempted Preparation of 2-Amino-2'-hydroxy-3,3',5,5'-tetra-tert-butyldiphenylmethane (**1**)*

Heating at 96 °C (bath) and stirring together 96 mg of 2,4-di-*tert*-butylaniline, 96 mg of 2,4-di-*tert*-butylphenol, 0.035 ml of formalin, and 1 mg of barium hydroxide octahydrate for 3 h gave a soft solid on cooling, which could readily be separated from the aqueous layer. After drying the solid weighed 141 mg. Thin-layer chromatography of this mixture showed it to contain the benzoxazine **2** with lesser amounts of the substituted *N*-benzylaniline **3***a* and of the starting aniline. None of the other spots, which were only present as traces on the t.l.c., showed the blue color usually given by a primary amine with ninhydrin spray and were therefore unlikely to be compound **1**. A sample of the solid reaction mixture recrystallized from ethanol gave colorless needles, m.p. 174–175.5 °C, which were identified as the benzoxazine **2** by comparison of their Debye–Scherrer pattern with that of an authentic sample (8). Other experiments in which the amount of catalyst was varied showed no new spots on the t.l.c.

Preparation of N-(3,5-Di-tert-butyl-2-hydroxybenzyl)-2,4-di-tert-butylaniline (3a)

Bubbling hydrogen chloride gas into a solution of 0.77 g of the benzoxazine **2** in 20 ml of ether and then cooling to −15 °C produced sheaves of colorless microscopic needles weighing 0.19 g, m.p. 135–159 °C. After several recrystallizations from ethanol–water the compound melted from 146–150 °C and gave a negative Beilstein copper wire test for halogen, showing that the salt had hydrolyzed completely to the free base **3***a*.

Anal. Calcd. for $C_{29}H_{45}NO$ (mol. wt., 423): C, 82.21; H, 10.71; N, 3.31. Found (mass spectroscopy, 423): C, 82.52; H, 10.71; N, 3.59.

N-Benzylidene-2,4-di-tert-butylaniline

A neat mixture of 0.22 g of freshly distilled benzaldehyde and 0.40 g of 2,4-di-*tert*-butylaniline rapidly reacted to produce water. The water was later removed as the benzene azeotrope. Vacuum removal of the benzene left 0.54 g of oil which soon crystallized completely, m.p. 88–95 °C. Recrystallization from methanol gave 0.46 g of colorless product, m.p. 95–97.5 °C.

N-Benzyl-2,4-di-tert-butylaniline

A solution of 0.46 g of the *N*-benzylidene 2,4-di-*tert*-butylaniline in 50 ml of purified cyclohexane was selectively hydrogenated at 1 atm with 0.10 g of 5% platinum on carbon catalyst to give, after catalyst and solvent removal, 0.38 g of the *N*-benzyl compound, m.p. 77–84 °C. Thin-layer chromatography showed that negligible hydrogenolysis had occurred. Recrystallization from a small volume of 95% ethanol gave only 0.19 g of product, m.p. 86.2–87.2 °C. Reductive alkylation of 2,4-di-*tert*-butylaniline and benzaldehyde using the same solvent and catalyst was very much slower and did not go to completion presumably because the condensation is much slower in solution.

N-Methyl-N-benzyl-2,4-di-tert-butylaniline

A solution of 0.24 g of *N*-benzyl-2,4-di-*tert*-butylaniline and 0.080 ml of formalin in 40 ml of cyclohexane with 0.03 g of 5% platinum on carbon catalyst was hydrogenated at 1 atm. After filtration, concentration, and crystallization from 95% ethanol, the dry crystals weighed 0.23 g, m.p. 74–77 °C. Recrystallization from 95% ethanol with centrifugal filtration gave 0.21 g of material, m.p. 74.6–76.5 °C.

Preparation of N-Methyl-2,4-di-tert-butylaniline

Hydrogenolysis of a solution of 1.00 g of *N*-methyl-*N*-benzyl-2,4-di-*tert*-butylaniline in 50 ml of purified cyclohexane with 0.10 g of 5% palladium on carbon at 1 atm, then removal of catalyst and solvent produced 0.69 g of colorless syrup, η_D^{25} 1.5169 (lit. η_D^{25} 1.5200 (9)) which crystallized to the solid, m.p. 21.8–24.2 °C.

Preparation of N-(3,5-Di-tert-butyl-2-hydroxybenzyl)-N-methyl-2,4-di-tert-butylaniline (3b)

Heating and stirring 0.11 g of *N*-methyl-2,4-di-*tert*-butylaniline, 0.14 g of 2,4-di-*tert*-butylphenol, and a solution of 0.10 g of barium hydroxide in 3.0 ml of formalin for 2.5 h at 93° (bath) produced 0.22 g of a colorless crystalline compound of m.p. 125–175 °C. Thin-layer chromatography of the crude material showed a little 2,4-di-*tert*-butylphenol (an excess was used) as the only impurity. Recrystallization from isopropyl alcohol yielded 0.11 g of microscopic needles, m.p. 174.8–177.0 °C. Although this melting point is close to that of the benzoxazine **2**, the i.r. spectra of the two compounds showed that they are quite different. The benzoxazine spectrum shows no absorption in the 3700–3100 cm^{-1} region (8). The spectrum of the *N*-methyl product (2% in CCl_4) has a small sharp peak at 3600 cm^{-1} (free OH) and a large broad absorption band centered ~ 3200 cm^{-1} (hydrogen-bonded OH). This region of the spectrum is similar to that of the substituted *N*-benzyl compounds, **3***a* and **4**. The n.m.r. spectrum shows a slightly broadened peak at 7.47 τ due to the methyl group attached to nitrogen which the benzoxazine spectrum does not show. Finally, hydrolysis for 5 h of a suspension of 23 mg of **3***b* in 7 ml of boiling ethanolic hydrochloric acid (6:1, v/v) gave two products, one of which was identified by t.l.c. as *N*-methyl-2,4-di-*tert*-butylaniline.

Mol. Wt. Calcd. for $C_{30}H_{47}NO$: 437.36576. Found (by Dr. Jamieson) (mass spectroscopy): 437.3658.

Can. J. Chem. Downloaded from www.nrcresearchpress.com by 210.87.254.105 on 09/05/12
For personal use only.

Preparation of N-(5-tert-Butyl-2-hydroxybenzyl)-o-toluidine (4)

(a) Kuliev's Method

When 3.03 g of 4-*tert*-butylphenol, 2.16 g of *o*-toluidine, and a solution of 0.15 g of barium hydroxide octahydrate in 1.60 ml (1.05 mole/mole) of formalin were stirred at room temperature, heat was evolved. After 20 min, t.l.c. analysis of the reaction mixture showed 6-*t*-butyl-3,4-dihydro-3-*o*-tolyl-2*H*-1,3-benzoxazine (8) as the only product along with unused starting amine and phenol. The mixture was stirred and heated at 96 °C (bath) for 2.5 h, dissolved in benzene, washed, dried, and the solvent distilled to give 5.93 g of orange syrup, η_D^{20} 1.5730 (lit. η_D^{20} 1.5688 (3)). Thin-layer chromatographic analysis showed *mostly* the toluidine derivative **4** (see below). On standing, the syrup slowly crystallized. Trituration with pentane left 2.28 g of cream colored crystals, m.p. 62–80 °C which were identified as compound **4** by comparison of their Debye–Scherrer pattern with those obtained from the compound isolated in parts (*b*) and (*c*) below.

Thin-layer chromatographic analysis of the crude reaction mixture on acidic alumina (Eastman Chromagram sheet 6063) revealed three fast running (in benzene–hexane, 1:2) impurities designated α, β, and γ in order of decreasing R_f values. The γ-impurity was scraped from the t.l.c. and introduced directly into the mass spectrometer. It gave a molecular weight of 222 (mol. wt. calculated for $C_{18}H_{23}NO$: 269). This method was not applicable to the α and β compounds, one of which was weighed as follows. A 0.95 g sample of a similar reaction mixture was refluxed for 48 h with 200 ml of ethanol – 36% hydrochloric acid (1:1 v/v). A small amount of polymer was filtered from the cooled hydrolyzate (t.l.c. analysis showed none of the impurities present in the polymer) and the filtrate concentrated to dryness, then reconcentrated with ethanol several times to remove excess hydrochloric acid. This mixture of hydrochloride salts was extracted with a total of 6.0 ml of water. The t.l.c. analysis of the aqueous solution after regeneration of the free bases showed a large amount of *o*-toluidine with none of the fastest running compound α. When the insoluble residue was regenerated with liquid ammonia and extracted with benzene the t.l.c. showed mostly compound α with traces of the other impurities. Evaporation of the benzene left 5.0 mg of solids. Since this impure sample contained all of the compound α from 0.95 g of reaction mixture we conclude that compound α comprises not more than 0.5% of the original mixture. On the basis of spot size and color we can estimate that compound β constitutes considerably less than 0.5% of the original mixture.

(b) From the Benzoxazine

The preferred preparation of **4** is the following, which uses the easily purified 6-*tert*-butyl-3,4-dihydro-3-*o*-tolyl-2*H*-1,3-benzoxazine (8).

Three ml of concentrated hydrochloric acid were added dropwise but rapidly to a cooled, vigorously stirred solution of 5.00 g of the benzoxazine in 30 ml of ether. The colorless crystals of the *N*-benzyl hydrochloride were filtered, washed with ether, briefly air dried, then shaken with benzene and 10 ml of concentrated ammonium hydroxide. The benzene layer was separated, washed, and dried (Na_2SO_4). When concentrated, it left a syrup which was redissolved in 10 ml of pentane. Fine colorless needles came out, weight 3.91 g, m.p. 88–93 °C. Recrystallization from hexane gave 3.57 g of compound **4**, m.p. 89.5–92.8 °C. A sample recrystallized for analysis melts at 92.7–94.0 °C. Its i.r. spectra showed strong intramolecular hydrogen bonding of the phenolic hydroxyl group. The use of gaseous hydrogen chloride and dry ether for the above preparation gave a mixture of the benzoxazine and *N*-benzyl hydrochlorides which was difficult to purify.

Anal. Calcd. for $C_{18}H_{23}NO$: C, 80.26; H, 8.61; N, 5.20. Found: C, 80.45; H, 8.60; N, 5.10.

N-Acetyl derivative of **4**, m.p. 103–104.7 °C (80% ethanol/water).

Anal. Calcd. for $C_{20}H_{25}NO_2$: C, 77.14; H, 8.09; N, 4.50. Found: C, 76.83; H, 8.07; N, 4.30.

Hydrochloride salt of **4**, m.p. 145–164 °C (decomposition).

Anal. Calcd. for $C_{18}H_{24}NOCl$: C, 70.69; H, 7.91; N, 4.58; Cl, 11.59. Found: C, 70.64; H, 7.80; N, 4.39; Cl, 11.72.

(c) From 2-Hydroxy-5-tert-butylbenzaldehyde

2-Hydroxy-5-*tert*-butylbenzaldehyde was prepared by condensing formaldehyde with 4-*tert*-butylphenol and oxidizing with acidified *p*-nitroso-dimethylaniline (10). It was purified by recrystallization of its phenylhydrazone from 95% ethanol to m.p. of 183.5–186.8 °C then recovered by steam distillation of its suspension in dilute acid (11).

A mixture of 1.94 g of this aldehyde and 1.17 g of *o*-toluidine was stirred at room temperature (22 °C) for 0.5 h at which time t.l.c. showed that the reaction was complete. The product was diluted with benzene, washed with 1 *N* hydrochloric acid and water, then dried. Removal of solvent afforded 2.51 g of the syrupy aldimine which was hydrogenated in 100 ml of ethanol with 0.25 g of 5% palladium-on-carbon at room temperature. The crude product (2.34 g) was crystallized from 7 ml of hexane and furnished 1.46 g of needles, m.p. 90.8–94.0 °C, identified with the compound isolated in parts (*a*) and (*b*) above by their common Debye–Scherrer pattern. Its structure was deduced to be that of compound **4** by its method of synthesis and confirmed by its n.m.r. spectrum which showed chemical shifts (in p.p.m. to low field) of 1.24 for *t*-butyl protons, of 2.15 for methyl, and 4.30 for methylene protons at room temperature. Sharp peaks for OH and NH protons at 8.25 and 3.67 respectively were only visible at low temperatures (in CS_2) presumably because of rapid exchange at room temperature.

Reaction of 4 with Nitrous Acid

The *N*-(5-*tert*-butyl-2-hydroxybenzyl)-*o*-toluidine hydrochloride prepared from 2.00 g of the benzoxazine as in part (*b*) above was stirred with a mixture of dilute hydrochloric acid and ice while 5.5 ml of 10% sodium nitrite solution was added dropwise. No gas was evolved. After standing 24 h at room temperature, the mixture was filtered and the yellow solid washed and dried, giving 1.92 g of material melting from 121–128 °C. Recrystallization from heptane gave 1.52 g of yellow crystals, m.p. 126–133 °C. A sample for analysis, after further purification melts at 132.0–134.5 °C.

Anal. Calcd. for $C_{18}H_{22}N_2O_2$ (mol. wt., 298): C,

72.46; H, 7.43; N, 9.39. Found (mass spectroscopy, 298): C, 72.40; H, 7.54; N, 9.54.

The authors wish to thank Dr. D. Jamieson of the Atlantic Regional Laboratories for the mass spectroscopic data on compound **3***b*. Our thanks are also due to Dr. R. F. Pottie and Mr. R. L. Sander for the other mass spectra, to Mr. R. Ironside for the i.r. spectra and to Dr. S. Brownstein for the n.m.r. spectra.

1. K. U. INGOLD. Chem. Rev. **61**, 563 (1961); Advan. Chem. Ser. **75**, 296 (1968).
2. A. M. KULIEV, M. A. RASULOVA, and G. A. ZEINALOVA. Azerb. Khim. Zhur. 3 (1964). Chem. Abstr. **63**, 13116*g* (1965). Available as an N.R.C.C. technical translation.
3. A. M. KULIEV, M. A. RASULOVA, and G. A. ZEINALOVA. Azerb. Khim. Zhur. 3 (1965). Chem. Abstr. **63**, 17944*c* (1965). Available as an N.R.C.C. technical translation.
4. W. J. BURKE. J. Amer. Chem. Soc. **71**, 609 (1949).
5. P. D. BARTLETT, M. ROHA, and R. M. STILES. J. Amer. Chem. Soc. **76**, 2349 (1954).
6. W. RUNDEL. Chem. Ber. **96**, 636 (1963).
7. J. BURGERS, W. VAN HARTINGSVELDT, J. VAN KEULEN, P. E. VERKADE, H. VISSER, and B. M. WEPSTER. Rec. trav. chim. **75**, 1341 (1956).
8. S. BROWNSTEIN, E. C. HORSWILL, and K. U. INGOLD. Can. J. Chem. **47**, 3243 (1969).
9. J. BURGERS, M. A. HOEFNAGEL, P. E. VERKADE, H. VISSER, and B. M. WEPSTER. Rec. trav. chim. **77**, 520 (1958).
10. British Patent 161 679 (1920).
11. F. B. DAINS and I. R. ROTHROCK. Amer. Chem. J. (Baltimore), **16**, 637 (1894).

Can. J. Chem. Downloaded from www.nrcresearchpress.com by 210.87.254.105 on 09/05/12
For personal use only.

Can. J. Chem. Downloaded from www.nrcresearchpress.com by 210.87.254.42 on 09/05/12
For personal use only.

Reactions of diphenylcyclopropenone with 1,3-dipoles

J. W. LOWN, T. W. MALONEY, and G. DALLAS[1]
Department of Chemistry, University of Alberta, Edmonton, Alberta

Received July 31, 1969

Diphenylcyclopropenone reacts with 1,3-diphenylisobenzofuran to give a benzotropone derivative **5**, with 3-carboalkoxyaziridines to give *trans*-3-pyrrolines (e.g. **10**), and with a 3-cyanoaziridine to give the pyrrole **20**. Possible mechanisms of these reactions are considered and compared with previous 1,3-dipolar additions to cyclopropenones.

Canadian Journal of Chemistry, **48**, 584 (1970)

Diphenylcyclopropenone reacts with 3-aroylaziridines to form 4-aroyl-4-oxazolines (1). This reaction is most plausibly interpreted as proceeding by an initial [2 + 3] cycloaddition of an azomethine ylide (derived from thermal cleavage of the aziridine) to the carbonyl bond of the diphenylcyclopropenone, followed by rearrangement, eq. [1]. In the parallel addition of 3-aroylaziridines to iminocyclopropenes, the intermediate [2 + 3] cycloaddition product **3** was isolated directly (2), eq. [2]. Another [2 + 3] cycloaddition to a cyclopropenone is that reported by Izzo and Kende in which, by contrast, addition of the diazomethane takes place to the carbon–carbon double bond (3, 4), eq. [3]. Information on the reaction of cyclopropenones and their derivatives with 1,3-dipoles, apart from the examples above, is non-existent (5).

Accordingly, we here report further examples of the reaction of diphenylcyclopropenone, with some 1,3-dipoles.

1,3-Diphenylisobenzofuran may be regarded as a potential 1,3-dipole of the carbonyl ylide type (6). It was found to react readily with diphenylcyclopropenone (eq. [4]) to give a crystalline adduct which was assigned structure **5** on the basis of its elemental analysis for $C_{35}H_{24}O_2$ and spectral properties. The product shows a

[1]

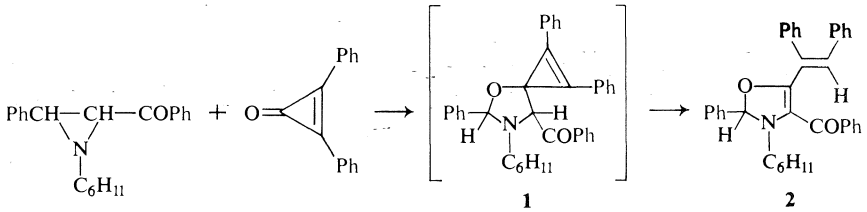

1 **2**

[2]

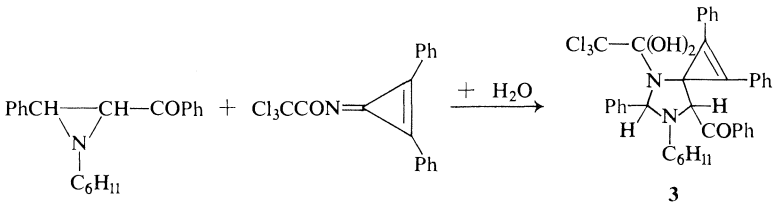

3

[3]

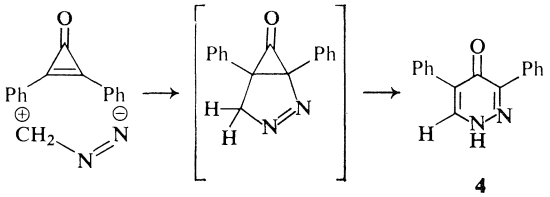

4

[1] NRCC Studentship holder, 1967–1969.

[4]

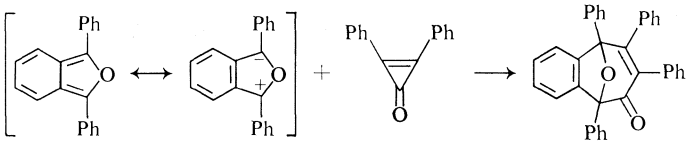

5

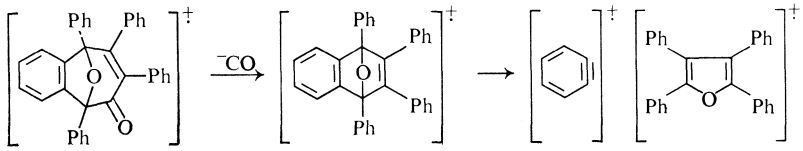

m/e 476 *m/e* 448 *m/e* 76 *m/e* 372

SCHEME 1

[5]

$$R_1CH{=}CH \cdot COOR_2 + Br_2 \rightarrow R_1CHBr{-}CHBrCOOR_2$$

$$R_1CHBr{-}CHBrCOOR_2 + 3C_6H_{11}NH_2 \rightarrow R_1{-}CH(N(C_6H_{11}))-CH-COOR_2$$

6 $R_1 = pC_6H_5{-}C_6H_4$; $R_2 = CH_3$
7 $R_1 = C_6H_5$; $R_2 = CH_3$
8 $R_1 = C_6H_5$; $R_2 = CH_3CH_2$
9 $R_1 = C_6H_5$; $R_2 = CH(CH_3)_2$

carbonyl band in the infrared (i.r.) at 1680 cm^{-1} and absorption in the ultraviolet (u.v.) at 337 (log ε 3.90), 296 (log ε 3.96), and 248 mμ (log ε 4.58). The high resolution mass spectrum shows the fragmentation pattern shown in Scheme 1. The reaction is plausibly interpreted as another [2 + 3] cycloaddition to the carbonyl bond of the cyclopropenone followed by rearrangement. In the case of 1,3-diphenylisobenzofuran, of course, one cannot distinguish formally between a [2 + 3] cycloaddition of a carbonyl ylide and a Diels–Alder addition of the diene system to the carbonyl bond.

Thermal cleavage of substituted aziridines provides a method of generating azomethine ylides *in situ* (7–11). As mentioned above we had examined 3-aroylaziridines and 3-acylaziridines previously, and we now examined a series of aziridines bearing other substituents with surprising results.

Some new 3-carboalkoxyaziridines were prepared by the Gabriel method (12), eq. [5]. 3-Carbomethoxy-1-cyclohexyl-2-phenylaziridine **7** reacted with diphenylcyclopropenone in refluxing toluene to give the *trans*-3-pyrroline **10**. This reaction is rationalized as a [2 + 3] cycloaddition of the azomethine ylide to the carbon–carbon double bond of the diphenylcyclopropenone, followed by decarbonylation as shown in Scheme 2. In support of Scheme 2, diphenylacetylene reacted readily with aziridine **7** to give **10** (eq. [6]) but, as has been observed previously, diphenylcyclopropenone is more reactive and gives better yields than diphenylacetylene (13). Such reactions of aziridines with alkynes (via azomethine ylides) are now firmly established and have produced 3-pyrrolines (10, 14, 16), 2-pyrrolines (11), and mixtures of both (15). Especially relevant to this work are the 3-pyrrolines **11** and **12** recently

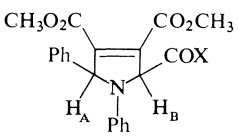

11

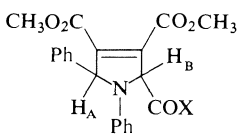

12

a X = OC_2H_5
b X = $N(C_2H_5)_2$

cis a J_{AB} = 3.5 Hz *trans a* J_{AB} = 7.5 Hz
cis b J_{AB} = 4 Hz *trans b* J_{AB} = 7 Hz

Can. J. Chem. Downloaded from www.nrcresearchpress.com by 210.87.254.42 on 09/05/12
For personal use only.

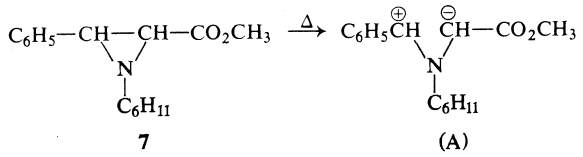

7 (A)

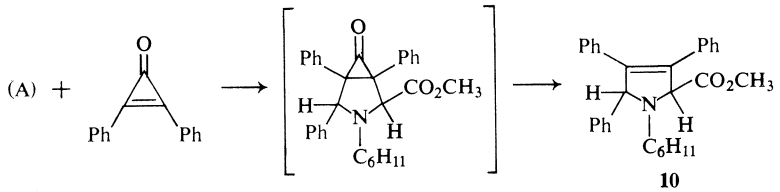

10

SCHEME 2

[6]

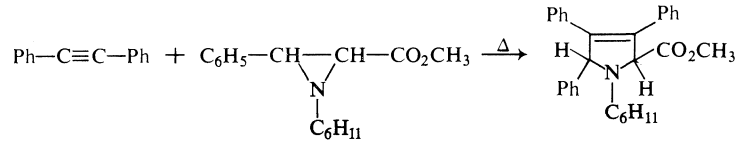

7 10

[7]

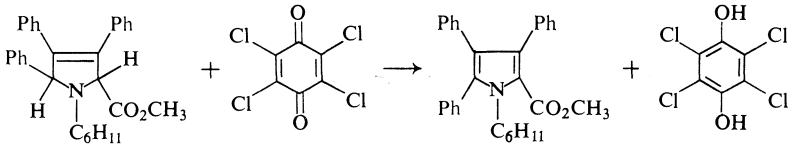

10 13

obtained by Deyrup by the addition of stereoisomeric *cis*- and *trans*-3-aziridine carboxylic acid derivatives to dimethylacetylenedicarboxylate (16). An unusual feature of the nuclear magnetic resonance (n.m.r.) spectra of these compounds is the magnitude of the long range coupling constants J_{AB}. (Deyrup mentioned that Huisgen has observed similar long range coupling constants in 3-pyrrolines.) The observed stereospecificity of the 1,3-dipolar additions to form **11** and **12** suggested that the initial adduct had not undergone 1,3 hydride migration to the 2-pyrroline isomer as is sometimes observed (11). Compounds **11** and **12** show u.v. absorptions at 284 (log ε 3.27), 240 (log ε 4.37), 288 (log ε 3.25), and 242 mμ (log ε 4.35) respectively.

In our work compound **10** was accordingly assigned the *trans*-3-pyrroline structure because the n.m.r. spectrum showed an AB quartet, $J = 6$ Hz, assigned to *trans* long range coupling. The chemical shifts are closely comparable to those in **11***a*. Unfortunately **12***a* was not fully characterized by Deyrup for a closer comparison (16). The i.r. spectrum of **10** shows an ester carbonyl at 1725 cm^{-1} indicative of a saturated ester, whereas the corresponding ester carbonyl in the pyrrole **13** absorbs at 1698 cm^{-1} closely comparable with values observed in other carboalkoxy pyrroles (17). The absorption spectrum of **10** showed maxima at 284 (log ε 4.13) and 250 mμ (log ε 4.34) comparable with **11** and **12** and therefore compatible with structure **10**. Deyrup observed stereospecific addition to form **11***a*, **11***b*, and **12***b* in refluxing carbon tetrachloride but observed post-isomerization of **11***a* to **12***a* when the reaction was carried out in refluxing toluene. It is not surprising therefore that in our reactions only *trans*-3-pyrrolines like **10** were isolated since toluene or *o*-xylene were used as solvents for the additions.

The 3-pyrroline structure for **10** was confirmed by the ready dehydrogenation with tetrachloro-1,4-benzoquinone to the pyrrole **13** in good yield, eq. [7]. Surprisingly, the apparently closely

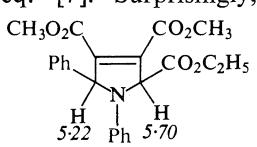

11*a*

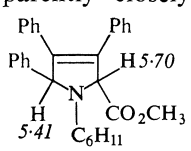

10

Can. J. Chem. Downloaded from www.nrcresearchpress.com by 210.87.254.42 on 09/05/12
For personal use only.

Can. J. Chem. Downloaded from www.nrcresearchpress.com by 210.87.254.42 on 09/05/12
For personal use only.

[8] 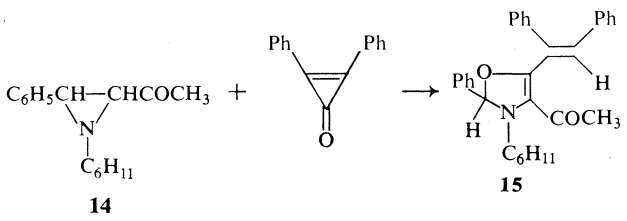

14 15

[9] 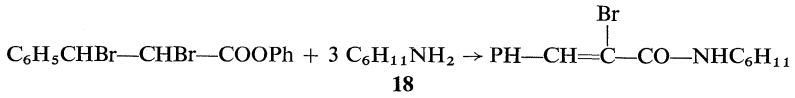

18

[10] 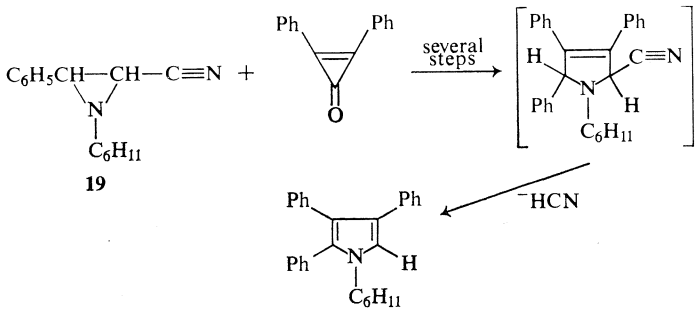

19 20

related 3-acetyl-1-cyclohexyl-2-phenylaziridine **14** reacted with diphenylcyclopropenone to give a 4-acyl-4-oxazoline **15** (13), eq. [8]. Similar results were obtained in the reaction of carboalkoxyaziridines **6**, **8**, and **9** with the cyclopropenone, i.e. *trans*-3-pyrrolines like **10** were the only products isolated. All showed AB quartets in the n.m.r. spectra with coupling constants of 6 Hz. The i.r., n.m.r., u.v., and mass spectra of the *trans*-3-pyrrolines together with the corresponding pyrroles were compatible with their assigned structures and are reported in full in the Experimental section. Suitable model polysubstituted pyrroles for comparison of the u.v. spectra were found to be scarce in the literature. However, the spectra of **16** and **17** (18) are convincingly similar when allowance is made for the effects of aryl groups on the intensities of the absorptions.

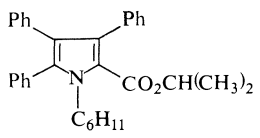

16

λ_{max} 254 (ε 15 760)
λ_{max} 281 (ε 19 320)

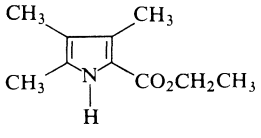

17

λ_{max} 253 (ε 6800)
λ_{max} 285 (ε 15 800)

The corresponding 3-carbophenoxyaziridine could not be prepared for comparison because of the lability of the phenoxy group towards cyclohexylamine. The product of the attempted Gabriel synthesis was the amide **18**, eq. [9].

The observed behavior of diphenylcyclopropenone with 3-carboalkoxyaziridines is analogous to its reaction with 4-aroyl-4-oxazolines (13). In the latter reactions carbon monoxide is also lost and furans are formed.

3-Cyano-1-cyclohexyl-2-phenylaziridine **19** was synthesized and reacted readily with diphenylcyclopropenone by [2 + 3] cycloaddition to the carbon–carbon double bond and the product was the pyrrole **20**, eq. [10]. In this reaction, the intermediate pyrroline was not isolated, since hydrocyanic acid is eliminated under the reaction conditions to give the pyrrole directly. By utilizing 3-cyanoaziridines with acetylenic compounds, the latter reaction provides a route to substituted pyrroles bearing a hydrogen at the 2-position.

Diphenylcyclopropenone is quite basic because of substantial contributions from the following valence forms (4, 5). However, we may rule out the unlikely prior *O*-nucleophilic attack

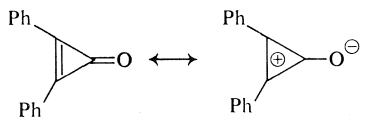

TABLE 1
Site of attack in cyclopropenones by 1,3-dipoles

Substrate	Reactant	1,3-Dipole type	Product type	Site of attack
DPP*	1,3-Diphenylisobenzofuran	Carbonyl ylide	3,4-Benzotropone	C=O
DPP	3-Aroylaziridines	Azomethine ylide	4-Aroyl-4-oxazoline	C=O
DPP	3-Acylaziridines	Azomethine ylide	4-Acyl-4-oxazoline	C=O
DPP	3-Carboalkoxyaziridines	Azomethine ylide	*trans*-3-pyrroline	C=C
DPP	3-Cyanoaziridine	Azomethine ylide	Pyrrole	C=C
DPP	4-Aroyl-4-oxazoline	Externally§ stabilized ketocarbene	Furan	C=C
DPP	4-Acyl-4-oxazoline	Externally§ stabilized ketocarbene	Furan	C=C
DPP	Diazomethane‡	Diazoniumbetaine	4-Pyridazone	C=C
CCP†	4-Aroyl-4-oxazoline	Externally§ stabilized ketocarbene	Furan	C=C

*DPP = Diphenylcyclopropenone.
†CCP = Cycloheptenocyclopropenone.
‡Reference 3.
§Reference 13.

of diphenylcyclopropenone on aziridines in the reactions which lead to 4-oxazolines. Reactions of good nucleophiles, with aziridines result in 1,2 bond cleavage rather than 2,3 bond cleavage (19). Therefore we may reasonably claim that all the reactions between cyclopropenones and substituted aziridines discussed above are of the [2 + 3] cycloaddition type.

Table 1 summarizes the results obtained and shows clearly that small differences in structure of the 1,3-dipole result in exclusive attack at either the carbonyl bond or at the carbon–carbon double bond of the cyclopropenone. In no instance has a mixture of products been obtained corresponding to both possible modes of addition. Our view of these reactions is that they reflect the very close similarity in dipolarophilic reactivity of the carbon–carbon double bond and the carbonyl bond in cyclopropenone owing to its unusual electronic structure. In contrast, normal alkenes are much better 1,3-dipolarophiles than the sluggish ketones and aldehydes (16). Thus small differences due to steric hinrance effects or differences in product stability will dictate the site of attack, rather than any intrinsic differences in the properties of the 1,3-dipoles themselves.

In conclusion it may be stated that cyclopropenones are reactive towards a variety of 1,3-dipoles and thus provide useful synthetic routes to 4-oxazolines, oxobenzotropones, 3-pyrrolines, pyrroles, and furans.

Experimental

Melting points were determined on a Fisher–Johns apparatus and are uncorrected. Infrared spectra were recorded on a Perkin–Elmer model 421 spectrophotometer, and only the principal, sharply defined peaks are reported. Nuclear magnetic resonance spectra were recorded on Varian A-60 and A-100 analytical spectrometers. The spectra were measured on approximately 10–15% (w/v) solutions in $CDCl_3$, with tetramethylsilane as a standard. Line positions are reported in parts per million from the reference. Absorption spectra were recorded in 'spectro'-grade solvents on a Beckman DB recording spectrophotometer. Mass spectra were determined on an Associated Electrical Industries MS-9 double focusing high resolution mass spectrometer. The ionization energy, in general, was 70 eV. Peak measurements were made by comparison with perfluorotributylamine at a resolving power of 15 000. Kieselgel DF-5 (Camag, Switzerland) and Eastman Kodak precoated sheets were used for thin-layer chromatography (t.l.c.). Microanalyses were carried out by Dr. C. Daesslé, Organic Microanalysis Ltd., Montreal, Quebec and by Mrs. D. Mahlow of this department.

Reaction of 1,3-Diphenylisobenzofuran with Diphenylcyclopropenone

A solution of 1.35 g (0.005 mole) of 1,3-diphenylisobenzofuran and 1.03 g (0.0005 mole) of diphenylcyclopropenone (4) in 30 ml of toluene was heated under reflux for 24 h during which time the solution turned yellow–orange. Evaporation of the solvent afforded a yellow gum which was chromatographed on basic alumina with benzene as eluant and afforded as a main fraction a pale

Can. J. Chem. Downloaded from www.nrcresearchpress.com by 210.87.254.42 on 09/05/12
For personal use only.

Can. J. Chem. Downloaded from www.nrcresearchpress.com by 210.87.254.42 on 09/05/12
For personal use only.

yellow gum which crystallized from heptane as a white crystalline solid of 2,5,6,7-tetraphenyl-3,4-benzotropone-2,5-oxide 0.635 g (27% yield), m.p. 215°.

Anal. Calcd. for $C_{35}H_{24}O_2$: C, 88.21; H, 5.08. Found: C, 88.27; H, 5.17.

The i.r. spectrum $\nu_{max}(CHCl_3)$: 1680 cm^{-1} (C=O); n.m.r. spectrum $\delta_{TMS}CDCl_3$: 6.7 (multiplet, 24H, aromatic protons); absorption spectrum ($CHCl_3$): 337 (log ε 3.90), 296 (log ε 3.96), 248 mμ (log ε 4.58).

Mass spectrum: [*m/e*, relative abundance, ion formula, calcd. and observed peak measurements on principal fragments given] 476 (6%), $C_{35}H_{24}O_2$; 476.1776; 476.1776; 448 (1%), $C_{34}H_{24}O$, 448.1827, 448.1818; 372 (100%), $C_{28}H_{20}O$, 372.1514, 372.1516; 76 (3%), C_6H_4, 76.0313, 76.0313.

1. Synthesis of Aziridines

2-(p-Biphenyl)-1-cyclohexyl-substituted Aziridines

These compounds were prepared by the following general method. Condensation of biphenyl-4-aldehyde with the appropriate active methylene compound afforded the corresponding α,β-unsaturated carbonyl compound. Bromination in chloroform solution, followed by treatment of the dibromo derivative with cyclohexylamine in benzene solution yielded the desired aziridine. Some of the aziridines synthesized were oils which decomposed upon attempted distillation, consequently their microanalyses were unsatisfactory. However, they were adequately characterized by spectral data and by the formation of crystalline cycloaddition adducts.

Biphenyl-4-aldehyde

This compound was prepared according to the procedure described by Cromwell and Cahoy (20). The product crystallized from methanol as a white solid (59% yield), m.p. 57–58° (lit. m.p. 58–59°).

4-Phenylstyryl-phenyl Ketone

This ketone was prepared using the Kohler–Chadwell procedure for the preparation of phenylstyryl ketone. The product was recrystallized from methanol as a yellow solid (53% yield), m.p. 110.5–112° (lit. m.p. 111.5–112.5° (21)).

3-p-Biphenyl-2,3-dibromo-1-phenylpropanone

To a solution of 22 g (0.0775 mole) of 4-phenylstyryl phenyl ketone in 100 ml of chloroform was added, during 20 min with stirring, a solution of 12.4 g (0.0775 mole) of bromine in 50 ml of chloroform. The bromine color was discharged very rapidly and after the addition was completed, the resultant pale yellow solution was stirred for 15 min. The solvent was removed by distillation under reduced pressure, leaving the product as a pale yellow solid (34.2 g, 100% yield) which was purified by recrystallization from benzene/hexane affording 3-(*p*-biphenyl)-2,3-dibromo-1-phenylpropanone as a white solid m.p 185.5–186°.

Anal. Calcd. for $C_{21}H_{16}Br_2O$: C, 57.75; H, 3.63; Br, 35.99. Found: C, 57.66; H, 3.56; Br, 36.22.

The i.r. spectrum $\nu_{max}(CHCl_3)$: 1690 cm^{-1} (aromatic C=O); n.m.r. spectrum $\delta_{TMS}(CDCl_3)$: AB quartet centered at 5.7 and 6.0, J_{AB} = 11 Hz (2H, 2, 3 protons); 7.25–8.3 (multiplets, 14H, aryl protons).

3-Benzoyl-2-(p-biphenyl)-1-cyclohexylaziridine

To a solution of 22.2 g (0.05 mole) of 3-*p*-biphenyl-2,3-dibromo-1-phenylpropanone in 300 ml of benzene, were added 54.5 g (0.55 mole) of cyclohexylamine and the mixture was stirred at room temperature for 24 h. The cyclohexylamine hydrobromide which had separated was removed by filtration, the filtrate washed with water (2 × 100 ml) and dried ($MgSO_4$). The benzene and most of the cyclohexylamine was removed by distillation under reduced pressure to leave a pale yellow oil, 20 g (100% yield) which when triturated with hexane gave the desired aziridine as a white solid m.p. 127° from methanol.

Anal. Calcd. for $C_{27}H_{27}NO$ (381.2094): C, 85.00; H, 7.14; N, 3.67. Found (381.1974 (mass spectrum)): C, 84.90; H, 7.23; N, 3.64.

The i.r. spectrum $\nu_{max}(CHCl_3)$: 1680 cm^{-1} (aromatic C=O); n.m.r. spectrum $\delta_{TMS}(CDCl_3)$: 1.0–3.0 (multiplet, 11H, cyclohexyl protons); 3.23 and 3.63 (singlets, 2H, aziridine ring protons); 7.2–8.3 (multiplet, 14H, aromatic protons).

3-Acetyl-2-(p-biphenyl)-1-cyclohexylaziridine

This compound was synthesized according to the method of Cromwell and Cahoy (20). Recrystallization from ether afforded a *cis–trans* mixture of the product in 65% yield m.p. 84–89° (lit. m.p. for two isomers 82–83° and 102–103° (20)).

2-(p-Biphenyl)-3-carbomethoxy-1-cyclohexylaziridine

This compound was synthesized according to the method of Woller and Cromwell (22) and was purified by recrystallization from hexane as a white solid in 97% yield, m.p. 69–72° (lit. m.p. 72°) and was used in subsequent reactions as a *cis–trans* mixture.

3-Carboalkoxy-1-cyclohexyl-2-phenylaziridines

These aziridines were synthesized from the appropriate cinnamic acid esters.

3-Carboisopropoxy-1-cyclohexyl-2-phenylaziridine

(i) Isopropyl cinnamate was prepared by the Fischer Speier procedure, using sulfuric acid as catalyst, as a colorless oil in 62% yield, b.p. 109–110°/4 mm (lit. b.p. 107.5–108°/2 mm (23)).

(ii) Isopropyl-2,3-dibromo-3-phenylpropionate. To a solution of 9.5 g (0.05 mole) of isopropyl cinnamate in 100 ml of chloroform, a solution of 8 g (0.05 mole) of bromine in 50 ml of chloroform was added dropwise with stirring over a period of 45 min. The resulting solution was stirred for a further 3 h and then evaporated *in vacuo* to yield the crude dibromide 17.3 g (100% yield) as a pale yellow oil, which slowly crystallized on cooling. The product was purified by recrystallization from hexane as a white solid, m.p. 52.5–53°.

Anal. Calcd. for $C_{12}H_{14}Br_2O$: C, 41.16; H, 4.03; Br, 45.67. Found: C, 41.10; H, 3.99; Br, 45.49.

The i.r. spectrum $\nu_{max}(CHCl_3)$: 1730 cm^{-1} (ester C=O); n.m.r. spectrum $\delta_{TMS}(CDCl_3)$: 1.33 (doublet, J = 6 Hz, 6H, (CH_3)2CH—); AB quartet centered at 4.76 and 5.29 J = 12 Hz (2H, —C*H*Br—C*H*Br—); 4.93–5.4 (septet, 1H, $(CH_3)_2CH$); 7.33 (singlet, 5H, aryl protons).

(iii) 3-Carboisopropoxy-1-cyclohexyl-2-phenylaziridine. To a solution of 7 g (0.02 mole) of isopropyl 2,3-dibromo-3-phenylpropionate in 100 ml of benzene were added 21.8 g (0.22 mole), of cyclohexylamine and the mixture was stirred at room temperature for 24 h. The cyclohexylamine hydrobromide which had separated was removed by filtration, and the filtrate washed with water

Can. J. Chem. Downloaded from www.nrcresearchpress.com by 210.87.254.42 on 09/05/12
For personal use only.

(2 × 50 ml) and dried ($MgSO_4$). The solvent and most of the cyclohexylamine was removed *in vacuo* (at temperatures < 50°) leaving the aziridine as a yellow oil which was purified by chromatography on B. D. H. grade I alumina using benzene as eluant. The desired aziridine was thus isolated as a pale yellow oil 5.2 g (91% yield) as a mixture of *cis* and *trans* isomers.

Anal. Calcd. for $C_{18}H_{25}NO_2$ (287.1885): C, 75.21; H, 8.77; N, 4.87. Found (287.1881 (mass spectrum)): C, 74.62; H, 8.90; N, 5.05.

The i.r. spectrum $\nu_{max}(CHCl_3)$: 1710, 1730 cm^{-1} (ester C=O in *cis* and *trans* isomers); n.m.r. spectrum $\delta_{TMS}(CDCl_3)$: 0.66–2.0 (multiplet, 10H, cyclohexyl protons); 0.93 and 1.26 (doublets, J = 12 Hz, 6H, $(CH_3)_2CH$—), 2.25–3.3 (multiplet, 3H, $C_5H_{10}CH$—N and aziridine ring protons), 4.55–5.20 (septet, 1H, $(CH_3)_2CH$—); 7.0–7.6 (multiplet, 5H, aryl protons).

3-Carbomethoxy-1-cyclohexyl-2-phenylaziridine

Methyl 2,3-dibromo-3-phenylpropionate was prepared by bromination of methyl cinnamate. The crude product, a pale yellow solid was recrystallized from ethanol as a white solid in 87.3% yield, m.p. 118–119° (lit. m.p. 115° (24)).

The desired aziridine was then prepared and purified by an exactly similar procedure to that described for the corresponding isopropyl ester aziridine. The product, a pale yellow oil (95% yield) was isolated as a mixture of *cis* and *trans* lsomers.

Anal. Calcd. for $C_{16}H_{21}NO_2$ (259.1572): C, 74.08; H, 8.17; N, 5.40. Found (259.1568 (mass spectrum)): C, 75.12; H, 8.22; N, 5.59.

The i.r. spectrum $\nu_{max}(CHCl_3)$: 1725, 1740 cm^{-1} (ester C=O); n.m.r. spectrum $\delta_{TMS}(CDCl_3)$: 0.9–2.1 (multiplet, 10H, cyclohexyl protons); 2.35–3.3 (multiplet, 3H, $C_5H_{10}CH$—N and aziridine ring protons); 3.45 and 3.75 (singlets $COOCH_3$ of *cis* and *trans* isomer); 7.0–7.7 (multiplet, 5H, aryl protons).

3-Carbethoxy-1-cyclohexyl-2-phenylaziridine

Ethyl 2,3-dibromo-3-phenylpropionate was prepared by bromination of ethyl cinnamate, by a similar procedure to that described for the corresponding isopropyl ester. The crude dibromide was purified by recrystallization from hexane as a white crystalline solid in 91% yield, m.p. 76–76.5° (lit. m.p. 74–75° (25)).

The 3-carbethoxy substituted aziridine was prepared from the dibromide by an analogous procedure to that described for other aziridines in this series and was isolated as a *cis–trans* mixture as a pale yellow oil in 74% yield.

Anal. Calcd. for $C_{17}H_{23}NO_2$ (273.1729): N, 5.12. Found (273.1729 (mass spectrum)): N, 4.88.

The i.r. spectrum $\nu_{max}(CHCl_3)$: 1715 and 1738 cm^{-1} (ester C=O); n.m.r. spectrum $\delta_{TMS}(CDCl_3)$: 0.7–2.0 (multiplet, 13H, cyclohexyl protons and CH_3—CH_2) 2.35–3.35 (multiplet, 3H, $C_5H_{10}CH$N— and aziridine ring protons) 4.22 (quartet, J = 7 Hz, CH_2—CH_3); 7.20–8.0 (multiplet, 5H, aryl protons).

Attempted Synthesis of 3-Carbophenoxy-1-cyclohexyl-2-phenylaziridine

This synthesis was attempted in the same manner as previously described for 3-carboalkoxy substituted aziridines. The product proved to be 2-bromo-*N*-cyclohexyl-3-phenylpropenoic acid amide.

Phenyl 2,3-Dibromo-3-phenylpropionate

This compound was prepared by bromination of phenyl cinnamate by a similar procedure to that described previously. The crude product was purified by recrystallization from benzene–hexane as a white crystalline solid, m.p. 130–135° (lit. m.p. 127° (26)).

Reaction of Phenyl 2,3-Dibromo-3-phenylpropionate with Cyclohexylamine

To a solution of 7.7 g (0.02 mole) of phenyl 2,3-dibromo-3-phenylpropionate in 150 ml of benzene were added 21.8 g (0.22 mole) of cyclohexylamine and the resultant mixture was stirred for 24 h. The cyclohexylamine hydrobromide which had separated was removed by filtration and the filtrate washed with water (2 × 100 ml) and dried ($MgSO_4$). The benzene and excess base were removed *in vacuo*, and trituration of the residue with hexane afforded 2-bromo-*N*-cyclohexyl-3-phenylpropenoic acid amide 5 g (82% yield), m.p. 95–97°. An analytical sample was prepared by recrystallization from hexane m.p. 110–111°.

Anal. Calcd. for $C_{15}H_{18}BrNO$ (307.0570): C, 58.42; H, 5.89; N, 4.54. Found (307.0571 (mass spectrum)): C, 58.49; H, 5.95; N, 4.80.

The i.r. spectrum $\nu_{max}(CHCl_3)$: 1650 (α,β unsaturated amide C=O), 3408 cm^{-1} (NH stretch); n.m.r. spectrum $\delta_{TMS}(CDCl_3)$: 0.7–2.26 (multiplet, 10H, cyclohexyl protons), 3.55–4.2 (multiplet 1H, $C_5H_{10}CH$N) 6.55–6.95 (broad singlet, 1H, NH); 7.22–7.92 (multiplet, 5H, aromatic protons); 8.33 (singlet, 1H, vinyl proton).

A similar experiment carried out with 3 molar equivalents of cyclohexylamine gave the same product in 67% yield. Phenol was also isolated in 62% yield and characterized by comparison with an authentic sample.

2. Reaction of Carboalkoxy Substituted Aziridines with Diphenylcyclopropenone and Diphenylacetylene

5-(p-Biphenyl)-2-carbomethoxy-1-cyclohexyl-trans-2,5-dihydro-3,4-diphenylpyrrole

(*a*) A solution of 1.03 g (0.005 mole) of diphenylcyclopropenone and 1.675 g (0.005 mole) of 2-(*p*-biphenyl)-3-carbomethoxy-1-cyclohexylaziridine in 40 ml of benzene was heated under reflux for 20 h. Removal of the solvent *in vacuo*, followed by trituration of the residual orange oil with a small volume of heptane gave the crude dihydropyrrole as a yellow solid 1.38 g (50% yield). The product was purified by recrystallization from ethanol m.p. 174°.

Anal. Calcd. for $C_{36}H_{35}NO_2$: C, 84.16; H, 6.87; N, 2.73. Found: C, 84.01; H, 6.74; N, 2.83.

Mass spectrum: base peak at M-2 (dehydrogenation to pyrrole ion under electron impact). Calcd. for $C_{36}H_{33}NO_2$: 511.2511. Found: 511.2510. The i.r. spectrum $\nu_{max}(CHCl_3)$: 1725 cm^{-1} (ester C=O); n.m.r. resonance spectrum $\delta_{TMS}(CDCl_3)$: 0.75–2.90 (multiplet, 11H, cyclohexyl protons); 3.57 (singlet, 3H, methyl protons); AB quartet centered at 5.41 and 5.70, J = 6 Hz) (2H, 5,2 pyrrole protons respectively, 6.90–7.70 (multiplet, 19H, aryl protons); absorption spectrum ($CHCl_3$): 246 (log ε 4.41), 251 (log ε 4.47), 263 (log ε 4.51), 287 mμ (log ε 4.35).

(*b*) A solution of 0.356 g (0.002 mole) of diphenylacetylene and 0.67 g (0.002 mole) of 2-(*p*-biphenyl)-3-carbomethoxy-1-cyclohexylaziridine in 16 ml of toluene

Can. J. Chem. Downloaded from www.nrcresearchpress.com by 210.87.254.42 on 09/05/12
For personal use only.

was heated under reflux for 89 h. The solvent was removed *in vacuo* and the residual gum was dissolved in heptane and the resulting solution chilled. The solid which separated was collected and recrystallized from ethanol 0.016 g (2% yield), m.p. 174°; 5-(*p*-biphenyl)-2-carbomethoxy-1-cyclohexyl-2,5-dihydro-3,4-diphenylpyrrole, identical in all respects with the product obtained in the above experiment (*a*).

2-Carbomethoxy-1-cyclohexyl-trans-2,5-dihydro-3,4,5-triphenylpyrrole

(*a*) A solution of 1.03 g (0.005 mole) of diphenylcyclopropenone and 1.3 g (0.005 mole) of 3-carbomethoxy-1-cyclohexyl-2-phenylaziridine in 20 ml of toluene was heated under reflux for 20 h. The solvent was removed *in vacuo* and the residual gum triturated with a small volume of hexane to yield the product as a pale yellow solid, 2 g (86% yield). Recrystallization from ethanol afforded the pure 2,5-dihydropyrrole as a white crystalline solid, m.p. 149.5–150°.

Anal. Calcd. for $C_{30}H_{31}NO_2$: C, 82.33; H, 7.15; N, 3.20. Found: C, 82.37; H, 7.11; N, 3.50.

Mass spectrum: base peak at M-2 (dehydrogenation to pyrrole ion under electron impact). Calcd. for $C_{30}H_{29}NO_2$: 437.2355. Found: 437.2350. The i.r. spectrum $\nu_{max}(CHCl_3)$: 1725 cm^{-1} (ester C=O); n.m.r. spectrum $\delta_{TMS}(CDCl_3)$: 0.8–2.3 (multiplet, 10H, cyclohexyl protons); 2.42–3.0 (multiplet, 1H, $C_5H_{10}CHN$); 3.57 (singlet, 3H, $COOCH_3$); AB quartet centered at 5.43 and 5.70, J = 6 Hz (2H, 5,2 pyrrole protons respectively), 6.83–7.5 (multiplet, 15H, aryl protons); absorption spectrum ($CHCl_3$): 250 (log ε 4.34), 284 mμ (log ε 4.13).

(*b*) A solution of 0.9 g (0.005 mole) of diphenylacetylene and 1.3 g (0.005 mole) of 3-carbomethoxy-1-cyclohexyl-2-phenylaziridine in 15 ml of toluene was heated under reflux for 5 days. The toluene was evaporated *in vacuo* and the residual gum purified by chromatography on basic alumina using benzene as eluant. Evaporation of the main fraction gave 2-carbomethoxy-1-cyclohexyl-*trans*-2,5-dihydro-3,4,5-triphenylpyrrole as a yellow solid 0.582 g (26% yield). Recrystallization from ethanol afforded the white solid product m.p. 148–149° which was identical in all respects to the product described in (*a*) above.

2-Carbethoxy-1-cyclohexyl-trans-2,5-dihydro-3,4,5-triphenylpyrrole

A solution of 0.687 g (0.003 mole) of diphenylcyclopropenone and 0.910 g (0.0033 mole) of 3-carbethoxy-1-cyclohexyl-2-phenylaziridine in 20 ml of toluene was heated under reflux for 14 h. The solvent was removed *in vacuo* and the residual orange oil triturated with a small volume of hexane to yield the crude 2,5-dihydropyrrole 0.872 g (52% yield) as a pale yellow solid from ethanol m.p. 115–116°.

Anal Calcd. for $C_{31}H_{33}NO_2$: C, 82.41; H, 7.37; N, 3.10. Found: C, 82.69; H, 7.53; N, 3.01.

Mass spectrum: base peak at M-2 (dehydrogenation to pyrrole ion under electron impact). Calcd. for $C_{31}H_{31}NO_2$: 449.2362. Found: 449.2355. The i.r. spectrum $\nu_{max}(CHCl_3)$: 1717 cm^{-1} (ester C=O); n.m.r. spectrum $\delta_{TMS}(CDCl_3)$: 0.7–2.2 (multiplet, 13H, cyclohexyl protons and CH_2CH_3); 2.4–3.0 (multiplet, 1H, $C_5H_{10}CHN$); 4.03 (quartet, J = 7 Hz, 2H, CH_2CH_3); AB quartet centered at 5.37 and 5.67, J = 6 Hz (2H, 5,2 pyrrole protons); 6.8–7.46 (multiplet, 15H, aromatic protons); absorption spectrum ($CHCl_3$): 2.44 (log ε 4.49), 250 (log ε 4.51), 254 (log ε 4.63), 284 mμ (log ε 4.46).

2-Carboisopropoxy-1-cyclohexyl-trans-2,5-dihydro-3,4,5-triphenylpyrrole

A solution of 1.03 g (0.005 mole) of diphenylcyclopropenone and 1.44 g (0.005 mole) of 3-carboisopropoxy-1-cyclohexyl-2-phenylaziridine in 40 ml of *o*-xylene was heated under reflux for 16 h. The solvent was removed by distillation under reduced pressure and the resultant orange gum crystallized upon cooling to a yellow solid 0.952 g (41% yield), recrystallization from ethanol gave the pure dihydropyrrole in m.p. 122–123°.

Anal. Calcd. for $C_{32}H_{35}NO_2$: C, 82.49; H, 7.58; N, 3.01. Found: C, 82.49; H, 7.62; N, 2.82.

Mass spectrum: base peak at M-2. Calcd. for $C_{32}H_{33}NO_2$: 463.2511. Found: 463.2512. The i.r. spectrum $\nu_{max}(CHCl_3)$: 1710 cm^{-1} (ester C=O); the n.m.r. spectrum $\delta_{TMS}(CDCl_3)$: 0.67–2.3 (multiplet, 16H, cyclohexyl protons and $(CH_3)_2CH$); 2.4–3.0 (multiplet, 1H, $C_5H_{10}CHNH$); 4.52–5.2 (multiplet, 1H, $(CH_3)_2CH$); AB quartet centered at 5.36 and 5.67, J = 6 Hz (2H, 5,2 pyrrole protons respectively); 6.7–7.5 (multiplet, 15H, aryl protons; absorption spectrum ($CHCl_3$): 249 (log ε 4.24, 253 (log ε 4.24), 279 mμ (log ε 4.25).

5-(p-Biphenyl)-2-carbomethoxy-1-cyclohexyl-3,4-diphenylpyrrole

A solution of 0.170 g (0.33 mmole) of 5-(*p*-biphenyl)-2-carbomethoxy-1-cyclohexyl-*trans*-2,5-dihydro-3,4-diphenylpyrrole and 0.164 g (0.66 mmole) of *p*-chloranil in 10 ml of dry chlorobenzene was heated under reflux for 24 h. The resultant solution was cooled, diluted by addition with 25 ml of ether, and washed with (*i*) 25 ml of 4% sodium hydroxide solution containing 1% sodium bisulfite; (*ii*) 2 × 25 ml portions of water. The ether layer was removed and dried ($MgSO_4$). Evaporation of the solvent gave the pyrrole as a tan solid 0.132 g (78% yield), m.p. 178–179°. An analytical sample was prepared by recrystallization from ethanol m.p. 186–186.5°.

Anal. Calcd. for $C_{36}H_{33}NO_2$ (511.2511): N, 2.74. Found (511.2510): N, 2.92.

The i.r. spectrum $\nu_{max}(CHCl_3)$: 1698 cm^{-1} (α,β unsaturated ester C=O); n.m.r. spectrum $\delta_{TMS}(CDCl_3)$: 0.9–2.4 (multiplet; 11H, cyclohexyl protons); 3.53 (singlet, 3H, $COOCH_3$) 6.7–7.7 (multiplet, 19H, aryl protons); absorption spectrum ($CHCl_3$): 2.53 (log ε 4.71), 295 mμ (log ε 4.41).

2-Carboisopropoxy-1-cyclohexyl-3,4,5-triphenylpyrrole

A solution of 0.233 g (0.5 mmole) of 2-carboisopropoxy-1-cyclohexyl-*trans*-2,5-dihydro-3,4,5-triphenylpyrrole and 0.123 g (0.5 mmole) of *p*-chloranil in 13 ml of dry chlorobenzene was heated under reflux for 20 h. The reaction mixture was worked up as described in the preceding experiment. The product after recrystallization from ethanol was a white solid 0.180 g (78% yield) m.p. 176°.

Anal. Calcd. for $C_{32}H_{33}NO_2$ (463.2511): C, 82.87; H, 7.18; N, 3.02. Found (463.2512 (mass spectrum)): C, 83.13; H, 7.13; N, 3.21.

The i.r. spectrum $\nu_{max}(CHCl_3)$: 1683 cm^{-1} (α,β unsaturated ester C=O); n.m.r. spectrum $\delta_{TMS}(CDCl_3)$: 0.9 (doublet, J = 6.2 Hz, 6H, $CH(CH_3)_2$); 0.77–2.46 (multiplet, 11H, cyclohexyl protons); 4.0–5.17 (multiplet, 1H,

Can. J. Chem. Downloaded from www.nrcresearchpress.com by 210.87.254.42 on 09/05/12
For personal use only.

$CH(CH_3)_2$); 6.6–7.4 (multiplet, 15H, aromatic protons); absorption spectrum ($CHCl_3$): 254 (log ε 4.20), 281 mμ (log ε 4.29).

1,2-Dibromo-1-cyano-phenylethane

This compound was prepared from cinnamonitrile in 85% yield by the method of Birks and Wright m.p. 88–89° (lit. 92°) (27).

3-Cyano-1-cyclohexyl-2-phenylaziridine

To a solution of 2.89 g (0.01 mole) of 1,2-dibromo-1-cyano-2-phenylethane in 150 ml of benzene stirred at 0°, was added dropwise a solution of 9.0 g (0.09 mole) of cyclohexylamine in 30 ml of benzene. The solution was then stirred at room temperature for a period of about 14 days when the theoretical quantity 3.6 g of cyclohexylamine hydrobromide was filtered off. The yellow filtrate was concentrated *in vacuo* and subjected to chromatography on 120 g of basic alumina (BDH) with benzene as eluant. Removal of the solvent gave 3-cyano-1-cyclohexyl-2-phenylaziridine as a buff colored solid 2.07 g (92% yield), m.p. 108.5°–110.5° from heptane.

Anal. Calcd. for $C_{15}H_{18}N_2$ (226.1470): C, 79.64; H, 7.96; N, 12.39. Found (226.1470 (mass spectrum)): C, 79.42; H, 8.00; N, 12.44.

The i.r. spectrum ν_{max}($CHCl_3$): 2253 (C≡N), (C≡N of *trans* isomer) 2200 cm^{-1}; n.m.r. spectrum δ ($CDCl_3$): 1.00–2.08 (multiplet, 11H, cyclohexyl C*H* and CH_2), AB quartet centered at 2.90 and 2.31 (J = 6.3 Hz, 2H, 2,3 ring protons), 7.27–7.58 (multiplet, 5H, aryl protons).

Reaction of 3-Cyano-1-cyclohexyl-2-phenylaziridine with Diphenylcyclopropenone in Xylene as Solvent

A solution of 0.452 g (0.002 mole) of 3-cyano-1-cyclohexyl-2-phenylaziridine and 0.406 g (0.002 mole) of diphenylcyclopropenone was heated under reflux in 35 ml of *o*-xylene for 24 h. The yellow solution was cooled and the xylene removed *in vacuo* giving a yellow oil which solidified on standing. Recrystallization from ethanol gave a white solid 0.55 g (73% yield) m.p. 165–166° of 1-cyclohexyl-2,3,4-triphenylpyrrole.

Anal. Calcd. for $C_{28}H_{27}N$ (377.2143): C, 89.12; H, 7.16; N, 3.71. Found (377.2144 (mass spectrum)): C, 89.17; H, 7.34; N, 3.78.

The i.r. spectrum ν_{max}($CHCl_3$): 1602 cm^{-1} (aromatic C=C) (there was *no* C≡N stretching frequency present in spectrum); n.m.r. spectrum ($CDCl_3$): 0.83–2.28 (multiplet, 10H, cyclohexyl CH_2), 3.57–4.13 (multiplet, 1H, cyclohexyl C*H*), 7.00–7.42 (multiplet, 16H, aryl protons and ring C_5 proton); absorption spectrum ($CHCl_3$): 247 (log ε 4.38), 253 (log ε 4.37), 286 mμ (log ε 4.10).

This same pyrrole was also obtained in 61% yield m.p. 164–165° by heating under reflux for 24 h a solution of 0.226 g (0.001 mole) of 3-cyano-1-cyclohexyl-2-phenylaziridine and 0.206 g (0.001 mole) of diphenylcyclopropenone in 25 ml of toluene. The product was isolated in the manner described above and was identical in all respects with the above mentioned pyrrole.

This research was supported by a National Research Council of Canada grant to J. W. Lown. We thank Mr. J. P. Moser for technical assistance and Mr. R. Swindlehurst and Dr. A. Hogg for the n.m.r. and mass spectra, respectively.

1. J. W. Lown, R. K. Smalley, and G. Dallas. Chem. Commun. 1543 (1968).
2. J. W. Lown, R. Westwood, and J. P. Moser. Can. J. Chem. In press.
3. P. T. Izzo and A. S. Kende. Chem. Ind. 839 (1964).
4. R. Breslow, T. Eicher, A. Krebs, R. A. Peterson, and J. Posner. J. Amer. Chem. Soc. **87**, 1320 (1965).
5. For reviews of cyclopropenone chemistry see: (*a*) A. Krebs. Angew. Chem. Intern. Ed. **4**, 10 (1965); (*b*) G. L. Closs. *In* Advances in alicyclic chemistry. Vol. 1. H. Hart and G. J. Karabatsos, *Editors*, Academic Press Inc., New York, N.Y., 1966. pp. 114–121.
6. R. Huisgen. Angew. Chem. Int. Ed. **2**, 565 (1963).
7. H. W. Heine, R. E. Peavy, and A. J. Durbetaki. J. Org. Chem. **31**, 3924 (1966).
8. von R. v. Capeller, R. Griot, M. Haring, and T. Wagner–Jauregg. Helv. Chim. Acta, **40**, 1652 (1957).
9. H. W. Heine, A. B. Smith, and J. D. Bower. J. Org. Chem. **33**, 1097 (1968).
10. R. Huisgen, W. Scheer, and H. Huber. J. Amer. Chem. Soc. **89**, 1753 (1967).
11. A. Padwa and L. Hamilton. J. Heterocycl. Chem. **4**, 118 (1967).
12. S. Gabriel. Chem. Ber. **21**, 1049 (1888); S. Gabriel and R. Stelzner. Chem. Ber. **28**, 2929 (1895).
13. J. W. Lown and R. K. Smalley. Tetrahedron Lett. 169 (1969); J. W. Lown, R. K. Smalley, G. Dallas, and T. W. Maloney. Can. J. Chem. In press.
14. H. W. Heine and R. E. Peavy. Tetrahedron Lett. 3123 (1965).
15. R. Huisgen, W. Scheer, G. Szeimies, and H. Huber. Tetrahedron Lett. 397 (1966).
16. J. A. Deyrup. J. Org. Chem. **34**, 2724 (1969).
17. Physical methods in organic chemistry. Vol. **2**. *Editor*, A. R. Katritzky, Academic Press (New York), 1963. p. 311.
18. U. Eisner and P. H. Gore. J. Chem. Soc. 922 (1958).
19. P. E. Fanta. *In* Heterocyclic Compounds. Part 1. *Editor*, A. Weissberger, Interscience Publishers, 1964. p. 551.
20. N. H. Cromwell and R. P. Cahoy. J. Amer. Chem. Soc. **80**, 5524 (1958).
21. R. H. Wiley, C. H. Jarboe, F. N. Hayes, E. Hansbury, J. T. Neilsen, P. X. Callahan, and M. C. Sellers. J. Org. Chem. **23**, 732 (1958).
22. P. B. Woller and N. H. Cromwell. J. Heterocycl. Chem. **5**, 579 (1968).
23. W. J. Svirbely, W. M. Eareckson, K. Matsuda, H. B. Pickard, I. S. Solet, and W. B. Tuemmler. J. Amer. Chem. Soc. **71**, 507 (1949).
24. R. Anschutz and L. P. Kinnicutt. Ber. **11**, 1220 (1878).
25. J. J. Sudborough and K. J. Thompson. J. Chem. Soc. **83**, 671 (1903).
26. C. Liebermann and A. Hartmann. Ber. **25**, 958 (1892).
27. A. M. Birks and G F. Wright. J. Amer. Chem. Soc. **62**, 2412 (1940).

Can. J. Chem. Downloaded from www.nrcresearchpress.com by 210.87.254.105 on 09/05/12
For personal use only.

Mass spectrometric study of the thermal decomposition of dimanganese decacarbonyl and dicobalt octacarbonyl

D. R. BIDINOSTI AND N. S. MCINTYRE
Department of Chemistry, University of Western Ontario, London, Ontario

Received October 3, 1969

The free radicals $\cdot Mn(CO)_5$ and $\cdot Co(CO)_4$ have been produced by the pyrolysis of $Mn_2(CO)_{10}$ and $Co_2(CO)_8$ in graphite flow reactors. The effusing molecular beams from these reactors were analyzed mass spectrometrically. Evidence is presented for the following equilibria

$$Mn_2(CO)_{10} \rightleftharpoons 2 \cdot Mn(CO)_5$$
$$Co_2(CO)_8 \rightleftharpoons 2 \cdot Co(CO)_4$$

From the temperature dependence of the equilibrium constants, enthalpy changes of 24.9 ± 2 and 14.5 ± 2 kcal/mole, respectively, have been obtained. These enthalpy changes give D(Mn—Mn) = 21 ± 3 kcal/mole and D(Co—Co) = 13 ± 3 kcal/mole, which substantiate the earlier literature values based on electron impact measurements.

Canadian Journal of Chemistry, **48**, 593 (1970)

Introduction

In two earlier communications we reported the metal–metal bond dissociation energies in dimanganese decacarbonyl (1) and dicobalt octacarbonyl (2). These values were obtained from the measured ionization potentials of the free radicals, $\cdot Mn(CO)_5$ and $\cdot Co(CO)_4$, and the appearance potentials of $Mn(CO)_5^+$ and $Co(CO)_4^+$ from $Mn_2(CO)_{10}$ and $Co_2(CO)_8$. Although the value of 18.9 kcal/mole for D(Mn—Mn) was surprisingly low, it was compatible with the $\Delta H = 34 \pm 13$ kcal/mole estimated by Cotton and Monchamp (3) for the reaction

[1] $$Mn_2(CO)_{10} \rightleftharpoons 2 \cdot Mn(CO)_5$$

Since then, Hopgood and Poë (5) have reported an activation energy of 37 kcal/mole for Mn—Mn bond fission, whereas Svec and Junk (6) have reported D(Mn—Mn) = 22 kcal/mole. On the other hand, our value of 11.5 kcal/mole for D(Co—Co) was in sharp contrast to the 76 kcal/mole reported by Winters and Kiser (4).

In the present work, the thermal decompositions of manganese decacarbonyl and cobalt octacarbonyl have been examined in the attempt to produce the free radicals $\cdot Mn(CO)_5$ and $\cdot Co(CO)_4$ under equilibrium conditions in a molecular-flow reactor. The enthalpy changes accompanying these equilibria, reactions [1] and [2]

[2] $$Co_2(CO)_8 \rightleftharpoons 2 \cdot Co(CO)_4$$

have been obtained by thermodynamic methods and provide an alternative method to the electron impact studies (1, 2, 6) for determining the metal–metal bond dissociation energies.

Experimental

The general features of the mass spectrometer have been described previously (7). For the present study the Knudsen effusion cell (see Fig. 2 in ref. 7) was replaced by a cylindrical molecular-flow reactor (8, 9). The reactor R (see Fig. 1) with its integral vapor inlet tube I and base was machined from a solid rod of spectroscopic grade graphite. It was provided with a snug-fitting graphite cap which contained an 0.8 mm diameter effusion orifice having a knife-edge profile. The interior dimensions of the reactors were 22 mm × 12.7 mm diameter, which gave a ratio of interior surface to effusion orifice area greater than 2400:1. The graphite inlet tube I was 29 mm long × 1.5 mm interior diameter. The reactor was held by a force fit onto a 5 mm diameter Pyrex inlet tube GT, which passes through the mounting plate M and is joined to the main source flange by means of a kovar–glass seal. A second kovar–glass seal is attached to the exterior of the flange and immediately terminates in a 10/18 joint. The sample reservoir was a 20 ml Pyrex bulb on one arm of a greaseless teflon-plug stopcock which uses Viton O-rings for sealing. On the other arm was a ground-glass joint for direct connection to the bottom joint of the inlet tube. A hood H made from a section of a thin-walled Pyrex bubble was placed over the inlet to deflect incoming molecules and prevent direct line of sight transmission through the effusion orifice. Two thermocouple wells T were drilled into the base and top of each reactor to accommodate chromel P/alumel thermocouples which were calibrated at the melting point of Sn. The main reactor body was wound with a tight helix of Thermocoax heating wire, type INcAc10. This is a fine nichrome wire surrounded by compressed magnesia and encased in flexible inconel tubing having an outside diameter of 1 mm. The ends of the inconel tubing were brought out of the mass spectrometer vacuum chamber through the main source flange to which they were brazed. The inner

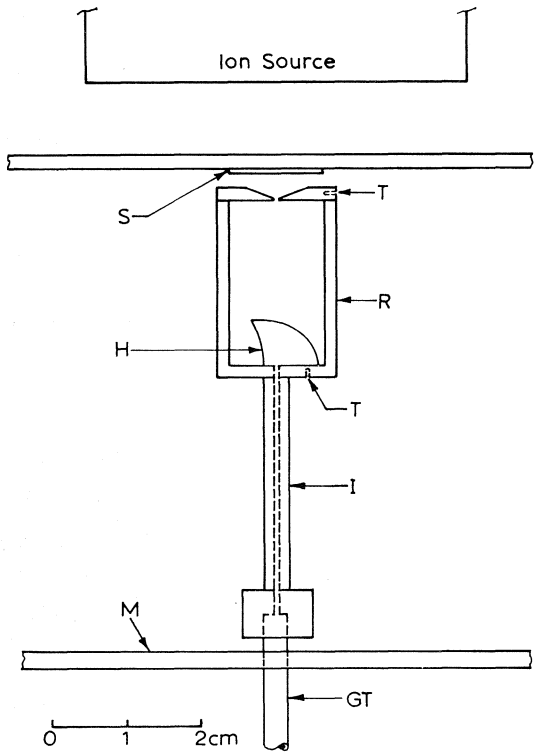

FIG. 1. Molecular-flow reactor.

heating wire and magnesia insulation were therefore outside the vacuum wall. Currents in the range 0–2.5 A, as supplied by a regulated d.c. power supply, gave reactor temperatures in the range 300–800 °K. The maximum temperature difference recorded by the two thermocouples was at the higher temperature, where the top of the cell was 2.5° hotter than the bottom. During each run the temperatures at the two thermocouple wells remained constant to within 1°. Radiation shields were not required for the temperatures used in this study.

Before each pyrolysis the reactor was outgassed at 800 °K. The pressure in the ion chamber housing in the absence of sample introduction was 2×10^{-7} Torr. Under conditions of maximum gas flow into the hot reactor, this pressure reached a maximum value of 2×10^{-6} Torr. The maximum pressure of the carbonyl vapor inside the reactor was established by calibrating the mass spectrometer detection sensitivity for manganese and cobalt carbonyls. A known weight of metal carbonyl was allowed to effuse at constant temperature from a Knudsen effusion cell having identical interior and orifice dimensions with the flow reactor. From the weight loss over a given period of time and the orifice dimensions, the pressure of the carbonyl vapor under molecular-flow conditions was calculated and compared with the observed ion current of the parent metal carbonyl ion. Comparison of these ion currents with those produced by the effusing vapors from the reactors gave the pressure of metal carbonyl vapor in the reactor. For each of the pyrolyses reported herein, the total gas pressure in the reactor was always less than 10^{-3} Torr. Hence molecular flow conditions are maintained. Different reactor pressures below 10^{-3} Torr were obtained by cooling the sample reservoir.

The shutter S was used to distinguish between ion current intensities from molecules in the effusing molecular beam and those from background molecules in the ion source region. All ion intensities reported herein have been corrected for small contributions from background vapors.

The carbonyls were obtained from Alfa Inorganics. Dicobalt octacarbonyl was sublimed in vacuo and transferred under nitrogen into one of the sample reservoirs. The bulb was then evacuated and put on the reactor inlet system. Dimanganese decacarbonyl was used directly as provided. No impurities could be detected in the mass spectrometer.

Results

Dimanganese Decacarbonyl

With the reactor at room temperature, the mass spectrum of the effusing $Mn_2(CO)_{10}$ beam was taken. The ionization potential of $Mn_2(CO)_{10}$ and the appearance potential of $Mn(CO)_5^+$ were found to be 8.42 ± 0.1 and 9.26 ± 0.1 eV, respectively. The reactor temperature was then slowly increased. Above 210 °C an ion current of $Mn(CO_5)^+$ could be observed at electron accelerating voltages below 9.26 V. As previously reported (1), the appearance potential of $Mn(CO)_5^+$ for reactor temperatures in the range 210–310 °C was 8.44 ± 0.10 eV. This decrease in appearance potential was taken as evidence for the production of the $\cdot Mn(CO)_5$ radical in the reactor, and the value 8.44 eV is therefore the ionization potential of the $\cdot Mn(CO)_5$ radical. Furthermore, over this same temperature range, the ion current intensity ratios $Mn(CO)_5^+/Mn_2(CO)_{10}^+$ and $Mn(CO)_4^+/Mn_2(CO)_{10}^+$ increased with temperature, whereas the ratios $Mn_2(CO)_9^+/Mn_2(CO)_{10}^+$ and $Mn_2(CO)_8^+/Mn_2(CO)_{10}^+$ remained constant. All of these observations are consistent with the assumption that the only molecular source of $Mn(CO)_5^+$, other than fragmentation of $Mn_2(CO)_{10}$, is $\cdot Mn(CO)_5$. The temperature variation of the ion intensity ratio of $Mn(CO)_5^+/Mn_2(CO)_{10}^+$, taken at 50 eV, is shown in Fig. 2.

Under conditions of molecular flow, the partial pressure P_i of a gaseous species in an effusion reactor can be related to the observed ion current I_{i^+} by

$$P_i = C_i I_{i^+} T \qquad [3]$$

Can. J. Chem. Downloaded from www.nrcresearchpress.com by 210.87.254.105 on 09/05/12
For personal use only.

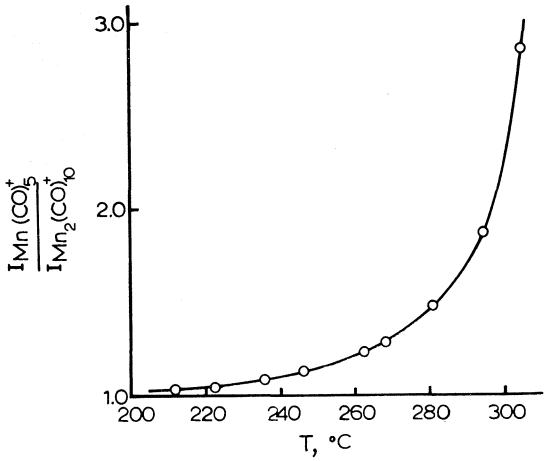

FIG. 2. Dependence of the ion intensity ratio of $Mn(CO)_5^+/Mn_2(CO)_{10}^+$ on the reactor temperature, for 50 eV electrons.

where T is the temperature of the gas in the reactor (10). The constant C_i contains a number of terms which depend on the geometry of both the reactor and ion source, the ion transmission characteristics of the mass spectrometer, the electron multiplier detection efficiency for the ion i^+, and the partial ionization cross section of the ith molecular species. All of these terms were kept constant throughout each experiment except the last, which is assumed to be temperature independent. At electron energies below 9.26 eV, it was therefore possible to relate through eq. [3] the ion current of $Mn(CO)_5^+$ exclusively to the partial pressure of $\cdot Mn(CO)_5$ in the reactor, and the ion current of $Mn_2(CO)_{10}^+$ to the partial pressure of $Mn_2(CO)_{10}$. Unfortunately, at electron energies below 9.26 V, the ion currents of $Mn(CO)_5^+$ and $Mn_2(CO)_{10}^+$ were too small for quantitative study since the energy is within 1 eV of their ionization thresholds. By operating at 10.3 V, the ion currents of $Mn(CO)_5^+$ and $Mn_2(CO)_{10}^+$ were considerably enhanced since the slopes of both ionization efficiency curves increase sharply in this region. Whereas the source of the $Mn_2(CO)_{10}^+$ remained unambiguous under these new conditions, that for $Mn(CO)_5^+$ was due to two processes, ionization of $\cdot Mn(CO)_5$ and dissociative ionization of $Mn_2(CO)_{10}$. Examination of the ionization efficiency curve for $Mn(CO)_5^+$ from $Mn_2(CO)_{10}$ showed that at this energy, which is 1 V above the appearance potential, less than 2% of the observed $Mn(CO)_5^+$ ion current was due to fragmentation. At the higher reactor temperatures, where the ratio $\cdot Mn(CO)_5/Mn_2(CO)_{10}$ is larger, this contribution was even less.

The equilibrium constant for an equilibrium of the type $A \rightleftharpoons 2B$ can be written in terms of ion current intensities using eq. [3]

$$K_p = \frac{CI_{B^+}{}^2 T}{I_{A^+}}$$

Substitution into the Van't Hoff equation gives

$$\log \frac{I_{B^+}{}^2 T}{I_{A^+}} = \frac{-\Delta H^0}{2.303RT} + C'$$

where C' is a temperature independent constant. Van't Hoff plots of ion currents taken at 10.3 eV for two different reactor pressures are shown in Fig. 3. Least-squares calculations for the slopes give $\Delta H = 25.3$ and 24.6 kcal/mole, with an average $\Delta H = 24.9 \pm 2$ kcal/mole for reaction [1].

Cobalt Octacarbonyl

The procedure followed was identical to that for $Mn_2(CO)_{10}$. The ionization potential of $Co_2(CO)_8$ and the appearance potential of $Co(CO)_4^+$ were initially found to be 8.26 ± 0.1 and 8.80 ± 0.1 eV, respectively. The reactor

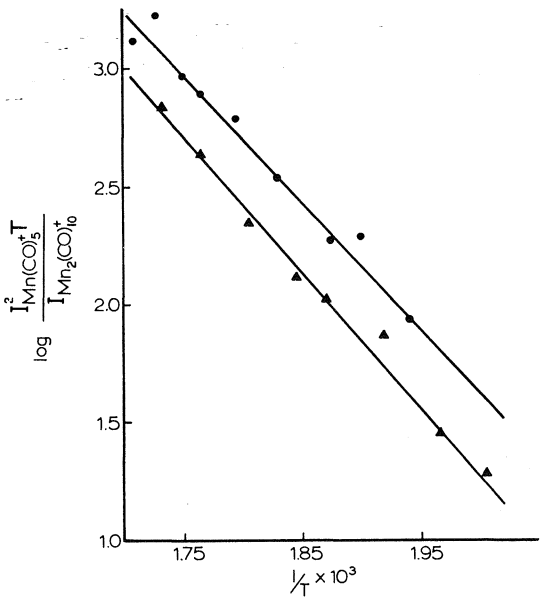

FIG. 3. Van't Hoff plots for the equilibrium $Mn_2(CO)_{10} \rightleftharpoons 2 \cdot Mn(CO)_5$.

Can. J. Chem. Downloaded from www.nrcresearchpress.com by 210.87.254.105 on 09/05/12
For personal use only.

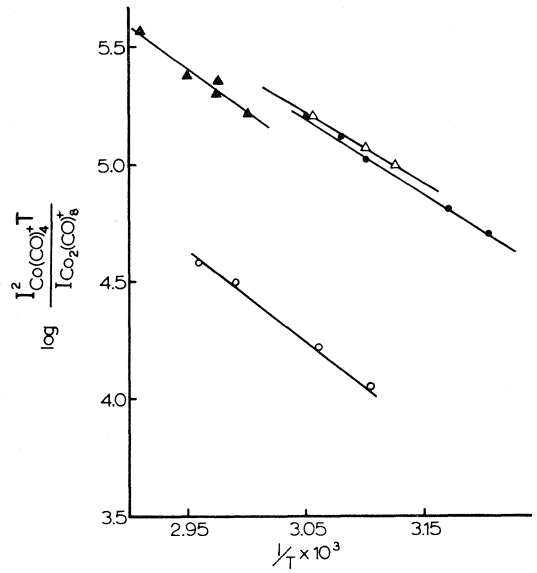

FIG. 4. Van't Hoff plots for the equilibrium $Co_2(CO)_8 \rightleftharpoons 2 \cdot Co(CO)_4$.

temperature was then slowly raised while the mass spectrum was repeatedly scanned. With cell temperatures in the range 35–85 °C, $Co(CO)_4^+$ was observed at electron accelerating voltages below 8.80 V and the threshold voltage measured to be 8.30 eV (2). Once again the ratios $Co(CO)_4^+/Co_2(CO)_8^+$ and $Co(CO)_3^+/Co_2(CO)_8^+$ increased with reactor temperature, whereas $Co_2(CO)_7^+/Co_2(CO)_8^+$ and $Co_2(CO)_6^+/Co_2(CO)_8^+$ remained constant, which is consistent with the production of the $\cdot Co(CO)_4$ radical. Above 85 °C, the composition of the effusing beam was exclusively CO.

Optimum enhancement of ion current of $Co(CO)_4^+$ produced by ionization of the radical relative to the dissociative ionization of $Co_2(CO)_8$ was obtained by using an electron accelerating voltage of 9.8 V, which is 1 V above the dissociative ionization onset. Van't Hoff plots of ion currents taken at 9.8 V for four different reactor pressures are shown in Fig. 4. Least-squares calculations for the slopes give ΔH = 14.9, 13.4, 14.0, and 15.6 kcal/mole, with an average $\Delta H = 14.5 \pm 2$ kcal/mole for reaction [2].

Discussion

The value $\Delta H = 24.9 \pm 2$ kcal/mole for reaction [1] falls within the very broad limits of Cotton's $\Delta H = 34 \pm 13$ kcal/mole (3).

The bond dissociation energies, D(Mn—Mn) and D(Co—Co), for these carbonyls are the standard internal energy changes at 0 °K for reactions [1] and [2]. These can be calculated in the following way using Kirchoff's equation

$$\Delta E_0^0 = \Delta E_T^0 - \Delta C_v T = \Delta H_T^0 - RT - \Delta C_v T$$

For reaction [1], the average temperature of the range from which ΔH was determined was 540 °K and for reaction [2], the average temperature was 330 °K.

We can estimate ΔC_v for reaction [1] by considering (11) the creation of six new degrees of freedom, three translational and three rotational, and the loss of six vibrational modes. If we now assume that at T = 540 °K there is complete contribution by the rotational and translational modes but no contribution by the vibrational modes, then $\Delta C_v = 6(\frac{1}{2}R) - 0(\frac{1}{2}R) = 3R$. This gives D(Mn—Mn) = $\Delta E_0^0 = \Delta H_T^0 - 4RT$ = 20.6 kcal/mole. Since the assumption of no vibrational heat capacity contribution from the six lost modes is certainly an over simplification, the $4RT$ correction may be too large by as much as $2RT$. Consequently, a reasonable value for D(Mn—Mn) is 21 ± 3 kcal/mole, which is in excellent agreement with the values obtained by electron impact (1, 6). The relatively large energy of activation reported by Hopgood and Poë (5) for reaction [1] in solution is most probably due to the stabilization of $Mn_2(CO)_{10}$ by solvation.

The weaker metal–metal bond in $Co_2(CO)_8$ makes the assumption of no contribution to the heat capacity of this molecule by the six lost vibrations even more tenuous. When applied, the $4RT$ correction, which is certainly too large, gives D(Co—Co) = 11.9 kcal/mole. The correction of $2RT$ is probably more realistic and gives D(Co—Co) = 13 ± 3 kcal/mole. This value is in excellent agreement with D(Co—Co) = 11.5 ± 4.6 kcal/mole based on the ionization potential of $\cdot Co(CO)_4$ (2). The discrepancy between these values and the D(Co—Co) = 76 kcal/mole reported by Winters and Kiser (4) is immense. This figure was arrived at by estimating $\Delta H_f(Co_2(CO)_8)$ and measuring the appearance potential of Co^+, which is assumed to occur by the process

$$Co_2(CO)_8 + e \rightarrow Co^+ + Co(CO)_4 + 4CO + 2e$$

This method is susceptible to two very significant errors. First, the value which one estimates for

Can. J. Chem. Downloaded from www.nrcresearchpress.com by 210.87.254.105 on 09/05/12
For personal use only.

$\Delta H_f(Co_2(CO)_8)$ is very sensitive to the energy contribution which is assigned to the Co—CO bond, since both this value and its uncertainty are multiplied by eight. Second, the ionization efficiency curve for Co^+ has a very long tail, due to the complex nature of this ionization process, which makes it very difficult to accurately measure the appearance potential. Furthermore, the assignment of the measured appearance potential to the above process is questionable since competing processes not involving the production of $Co(CO)_4$ are possible.

This research was sponsored by the Air Force Office of Scientific Research, Office of Aerospace Research, United States Air Force, under AFOSR Grant No. 1356–68.

1. D. R. BIDINOSTI and N. S. MCINTYRE. Chem. Commun. 555 (1966).
2. D. R. BIDINOSTI and N. S. MCINTYRE. Chem. Commun. 1 (1967).
3. F. A. COTTON and R. R. MONCHAMP. J. Chem. Soc. 533 (1960).
4. R. E. WINTERS and R. W. KISER. J. Phys. Chem. **69**, 1618 (1965).
5. D. HOPGOOD and A. J. POË. Chem. Commun. 831 (1966).
6. H. J. SVEC and G. A. JUNK. J. Amer. Chem. Soc. **89**, 2836 (1967).
7. D. R. BIDINOSTI and N. S. MCINTYRE. Can. J. Chem. **45**, 641 (1967).
8. D. R. BIDINOSTI and R. F. PORTER. J. Amer. Chem. Soc. **83**, 3737 (1961).
9. A. B. BAYLIS, G. A. PRESSLEY, and F. E. STAFFORD. J. Amer. Chem. Soc. **88**, 2428 (1966).
10. P. GOLDFINGER. *In* Mass spectrometry. *Edited by* R. I. Reed. Academic Press, Inc., London. 1965. p. 270.
11. T. L. COTTRELL. The strengths of chemical bonds. Butterworths Scientific Publications, London. 1958. p. 13.

Can. J. Chem. Downloaded from www.nrcresearchpress.com by 210.87.254.105 on 09/05/12
For personal use only.

Ion neutralization reactions in irradiated hydrogen chloride, hydrogen bromide, and nitrous oxide

D. E. WILSON AND D. A. ARMSTRONG
Department of Chemistry, The University of Calgary, Calgary, Alberta
Received October 10, 1969

Rates of ion neutralization have been measured in hydrogen chloride, hydrogen bromide, and nitrous oxide by collecting the ions remaining in a defined volume at various times after ionization by a pulse of 120 k.v.p. X-rays. Values of the total homogeneous ion–ion recombination coefficient, α, have been obtained for each gas over a range of pressures in the region 50 to 650 Torr. From a study of the effects of pressure and ion density, the relative rates of wall diffusion, mutual neutralization, and three-body neutralization have been deduced.

Canadian Journal of Chemistry, **48**, 598 (1970)

Can. J. Chem. Downloaded from www.nrcresearchpress.com by 210.87.254.40 on 09/05/12
For personal use only.

Introduction

The neutralization of ions in an irradiated gas may take place by any one or a combination of the following three different reactions

(*a*) Diffusion to the cell wall, where neutralization occurs with an adsorbed ion of opposite sign

[1] $\left.\begin{matrix} X^+ \rightarrow X^+_{\text{on wall}} \\ Y^- \rightarrow Y^-_{\text{on wall}} \end{matrix}\right\} (X^+ + Y^-)_{\text{on wall}} \rightarrow \text{neutral products}$

(*b*) Homogeneous mutual neutralization

[2] $X^+ + Y^- \rightarrow \text{neutral products}$

(*c*) Homogeneous neutralization stabilized by collisions with a third body

[3] $X^+ + Y^- + M \rightarrow \text{neutral products} + M$

The products derived from these three reactions may differ (see, for example, ref. 1), and a complete understanding of the radiolysis of any given system, therefore, requires a knowledge of the relative rates of these three reactions.

The basic kinetic features of the three reactions are as follows. Reaction [1] is generally controlled by the rate of wall diffusion. Therefore, its rate varies inversely with pressure, and, to a good approximation, is first order in the ion concentration. The rate of reaction [2] is pressure independent and proportional to the square of the ion concentration. Reaction [3] has the same concentration dependence as [2], but its rate increases with increasing pressure up to a maximum at about 1 atm. The three processes are, therefore, kinetically distinguishable, and it is possible to obtain a reasonably clear picture of their relative importance by measuring the rate of ion decay under varying conditions of pressure and initial ion density. Few gases of interest to radiation chemists have been subjected to this type of investigation. Indeed, most of the experimental work on ion recombination has thus far been confined to air and oxygen, which are used in ionization chambers and have special importance in the ionosphere (2, 3). The purpose of all of these studies has been to measure the total homogeneous recombination coefficient, α, which is equal to the sum of the rate constants of reactions [2] and [3], corrections being made when necessary for the rate of ion loss by reaction [1].

The purpose of the present work was to measure the rate constants of the homogeneous ion neutralization reactions in nitrous oxide and the hydrogen halides, and to estimate the rate of reaction [1], under typical radiolysis conditions. Nitrous oxide is frequently used as a dosimeter (4) for gas-phase radiolysis, and for this reason it is essential that its mechanism of radiolysis be fully understood. The radiolysis of the hydrogen halides is under investigation in this laboratory and further progress requires quantitative data for the rates of the ion neutralization reactions. A few experiments to check the reliability of our method were carried out in oxygen, which has been studied rather extensively in other laboratories.

Experimental

Apparatus

Pulses of 120 k.v.p. X-rays were produced by a 12 in. diameter rotating lead sector with a single 180° open slit. The sector was housed in a 3/8 in. thick steel box located in a fixed position directly beneath the tube of the Müller MG150 X-ray unit. After passing through the slit and an opening in the steel housing, the diameter of the X-ray beam was larger than that of the irradiation cells. Thus the entire cell volumes were irradiated, as in a typical X-ray or γ-ray radiolysis. Initial ion concentrations were

Can. J. Chem. Downloaded from www.nrcresearchpress.com by 210.87.254.40 on 09/05/12
For personal use only.

varied by altering the distance between the cell and the X-ray tube.

At a set delay time after each ionizing pulse, a high voltage was applied to an electrode within the cell, and the charge due to the ions remaining in the calibrated volume of the cell was collected on a second electrode connected to the input of a dynamic capacitor electrometer (Victoreen 475A). The time constant of the electrometer was long relative to the time of one sector revolution. Thus the charge collected for each revolution was given by the steady electrometer current divided by the frequency of rotation of the sector. The design of the electronic system was essentially as used by McGowan (2), with certain simplifications made possible by recent improvements in electronic components. A crystal timer system was used to set the variable delay time and the duration of the high voltage pulse, the high voltage being switched directly through a reed relay capable of switching up to 5000 V.

All of the experiments reported here were performed with the sector rotating at 1000 r.p.m., which gives an ionizing pulse of 30 ms. This relatively long duration had the advantage that the ion distribution existing at the cessation of the pulse approached rather closely to that occurring in a steady-state radiolysis at the same dose rate. Hence, our initial rates of ion neutralization should be similar to those which obtain during continuous irradiation. Furthermore, we do not observe the effects of ion ageing and initial inhomogeneity in the ion distribution which are seen with short pulse experiments (2, 3).

Attempts to use cells with metal electrodes proved unsatisfactory because of perturbations of the dose rate and chemical reactions with the hydrogen halides. Graphite coated electrodes were therefore employed, the cells being baked under vacuum at 250 °C for 12 h prior to each experiment. Most experiments were performed in cells similar to those previously described (1, 5). The cylindrical collecting surface was 40 mm long and 33 mm in diameter with a coaxially mounted 7 mm tube serving as the high voltage electrode. Some experiments were also carried out using cylindrical cells 33 mm in diameter with graphite coated ends serving as plane-parallel electrodes 14 mm apart.

All experiments were performed at room temperature.

Material

Hydrogen chloride and hydrogen bromide were purified as described previously (6). Nitrous oxide, obtained from the Matheson Co., was thoroughly deaerated and purified by repeated distillations from a trap at −120 °C to a trap at liquid nitrogen temperature, retaining only the middle fraction of the distillate.

In the experiments with oxygen, the gas was taken from a cylinder of Matheson Extra Dry Grade and passed slowly through three cold traps at −140 °C at approximately 1 Torr-l s^{-1}, and then into the irradiation cell.

Calculations

When reactions [2] and [3] are the only processes leading to ion loss in a uniformly ionized gas, the total homogeneous ion–ion recombination coefficient, α, is given by the equation

$$[4] \qquad \frac{dn_+}{dt} = \frac{dn_-}{dt} = -\alpha n_+ n_-$$

With the present technique, if the ion densities of the positive and negative ions are equal ($n_+ = n_- = n$), the integrated form of this equation (2) becomes

$$[5] \qquad \alpha = \frac{d(1/n)}{dt} = evV\frac{d(1/I)}{dt}$$

where the charge collected per second is measured as a steady electrometer current, I, e is the electronic charge, ν the frequency of rotation of the sector, and V is the calibrated volume between the electrodes. A value of α can therefore be calculated from the slope of a plot of the reciprocal of the current vs. the delay time. However, this derivation takes no account of ion losses by process [1] (i.e. diffusion to the walls of the cell), and a correction must be applied in order to obtain accurate values of α from the measured values, α_m.

A correction factor to the recombination coefficient can be calculated approximately by considering diffusion and recombination separately. For short decay times, t, this gives

$$[6] \qquad \frac{\alpha_m}{\alpha} - 1 = \frac{k_1}{\alpha n}$$

The magnitude of k_1 is equal to (D/Λ^2), where D is the diffusion coefficient (assumed equal for positive and negative ions) and Λ is a characteristic diffusion length depending on the geometry and dimensions of the cell (7). A rigorous analysis requires the solution of the differential equation

$$[7] \qquad \frac{\partial n}{\partial t} = -\alpha n^2 + D\nabla^2 n$$

McGowan has obtained computer solutions of this expression for the simplest case of one dimensional diffusional loss of ions between infinite plane-parallel electrodes (8). These calculations show that expression [8] holds for values of αnt

$$[8] \qquad \frac{\alpha_m}{\alpha} - 1 = \frac{K}{\alpha n}\left(\frac{D}{\Lambda^2 t}\right)^{\frac{1}{2}}$$

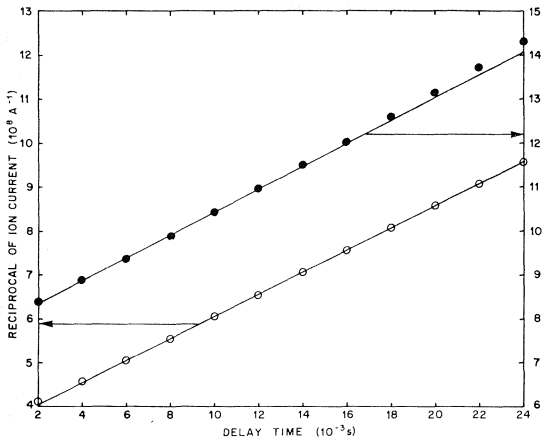

FIG. 1. Plots of the reciprocal of the electrometer current vs. delay time for oxygen at 300 Torr at two different initial ion densities.

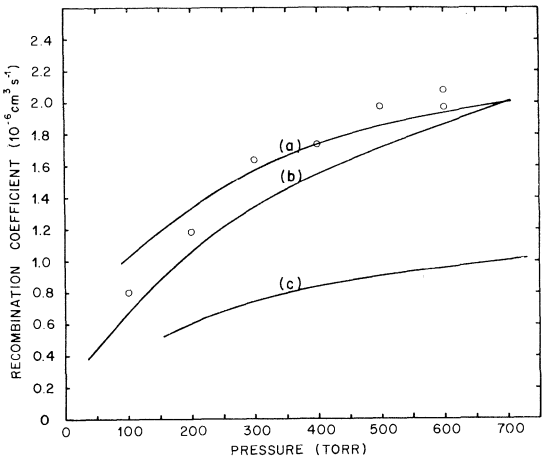

FIG. 2. Plots of the recombination coefficient vs. pressure for oxygen. (*a*) Gardner (9); (*b*) McGowan (2); (*c*) Ebert *et al.* (3); (○) present results.

less than 10^{-1} and $\alpha n\Lambda^2/D$ greater than 10^2. At constant decay time this equation reduces to [9]

$$[9] \qquad \frac{\alpha_m}{\alpha} - 1 = \frac{K'}{\alpha n}$$

Differences in cell geometry should largely be accounted for by the parameter Λ, and one would expect a relationship of the same form to apply in cylindrical cells. Formally this is similar to eq. [6].

In the present experiments, α_m was measured at each gas pressure for different initial ion densities. Values of α were calculated using eq. [9], within the limiting conditions given above. With ion densities of the order of 10^7 cm^{-3} and greater, the diffusion loss was of the order of a few % at pressures above 300 Torr. Below this pressure it increased, being most serious in oxygen.

Results

Values of α_m were determined at each gas pressure from plots of the reciprocal of the electrometer current vs. the delay time. Figure 1 shows plots of this type for oxygen at 300 Torr. For the conditions applying to the lower curve in Fig. 1, α_m is 10% larger than α. At 100 Torr, wall diffusion became the predominant mechanism of ion loss in oxygen, and at even lower pressures the diffusion loss in our cells was too large for accurate values of α to be determined. Our measurements of α in oxygen are compared with other reported values in Fig. 2.

For both hydrogen chloride and hydrogen bromide at pressures above 300 Torr, plots of $1/I$ vs. delay time were found to give excellent linearity over several half-lives. Moreover, at all pressures, the diffusion correction was considerably smaller than that required for oxygen. The values of α in these gases are shown in Fig. 3. The two cells used for measurements in HCl required different corrections for diffusion, but gave values of α which were identical within experimental error.

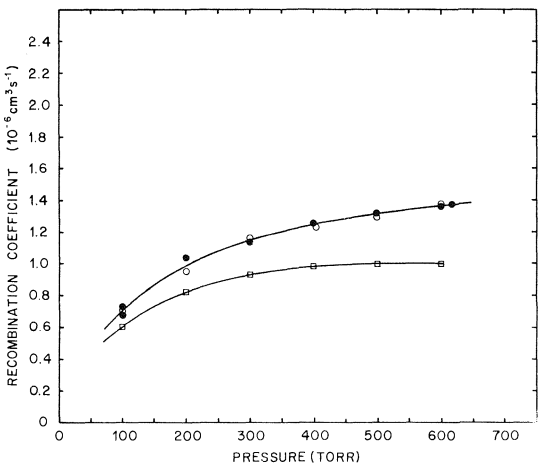

FIG. 3. Plots of the recombination coefficient vs. pressure for hydrogen chloride and hydrogen bromide: (○) HCl using cell with concentric electrodes; (●) HCl using cell with plane parallel electrodes; (□) HBr using cell with concentric electrodes.

Can. J. Chem. Downloaded from www.nrcresearchpress.com by 210.87.254.40 on 09/05/12
For personal use only.

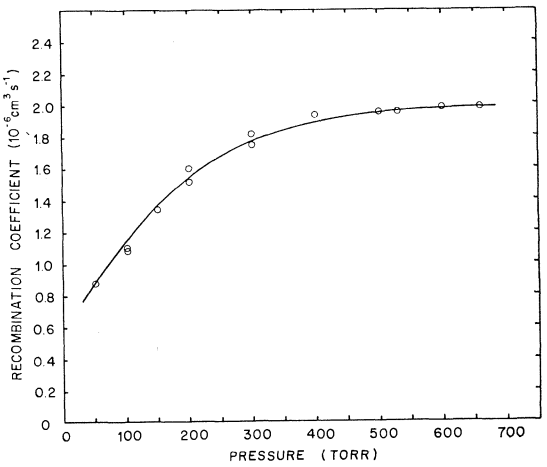

FIG. 4. Plot of the recombination coefficient vs. pressure for nitrous oxide.

Additional measurements were carried out for hydrogen chloride to which small amounts of sulfur hexafluoride (2 mole % SF_6) had been added. Previous measurements showed no significant change in α when this electron scavenger was present (5). We have confirmed this result.

Wall diffusion in nitrous oxide was again found to be considerably less important than in oxygen, and it was possible to make measurements of α down to pressures as low as 50 Torr, before diffusion became the predominant process. The corrected values of α are shown in Fig. 4.

Discussion

Our values of α for oxygen are seen to be in good agreement with those of McGowan and Gardner (see Fig. 2, curves *a* and *b*). The results of Ebert, Booz, and Koepp gave much smaller values of α, and would appear to be in error. It has been suggested that this may be due to impurities in their oxygen (2).

Mass spectrometric evidence has demonstrated that O_4^+ will be the predominant positive ion in irradiated oxygen (10). The negative ions O_2^- and O_4^- will also be present in the initial stages of the radiolysis, but once the ozone concentration has risen to 10 p.p.m., O_3^- will predominate as a result of reaction [10] (11)

$$[10] \qquad O_2^- + O_3 \rightarrow O_2 + O_3^-$$

Hence O_3^- and O_4^+ will be the main species undergoing neutralization. The situation in nitrous oxide is somewhat more complex. The main products are nitrogen, nitric oxide, and oxygen (12), and the latter two may undergo charge transfer reactions with N_2O^- and N_2O^+. In this case there is insufficient information on electron affinities and on rate constants to make a definite assignment of the recombining ions. Physical and chemical evidence favors H_2X^+ and HX_2^- as the most stable ionic species in the hydrogen halides (13), both ions being heavily clustered at normal temperatures and pressures. Hence the average ion masses will be much greater in the hydrogen halides than in oxygen. This is reflected in the much lower mobilities of the ions in hydrogen chloride than in oxygen. Clustering would also be expected to occur to some extent in nitrous oxide.

We may now consider the relative magnitudes of the rate constants of reactions [1], [2], and [3] in the four gases. As stated earlier, k_1 is given by D/Λ^2, and for our cells Λ is about 0.2 cm. This is consistent with the fact that at 200 Torr, reaction [1] was estimated to contribute 25, 12, 8, and 10% of the total ion loss in oxygen, hydrogen chloride, hydrogen bromide, and nitrous oxide, respectively, with ion densities of 2×10^7 cm^{-3}. The smaller contributions of reaction [1] in the polar gases are consistent with the increased masses of the ions. In steady state X- or γ- radiolysis, much larger cells are used and for typical dose rates, reaction [1] should not be significant at pressures above 200 Torr, even in oxygen.

Measurements of α at low pressures in oxygen lead to a value of $k_2 = 2 \times 10^{-7}$ cm^3 s^{-1} (2), k_2 being the low pressure limit of α. From Fig. 3, the values of k_2 in the hydrogen halides also appear to be of this order of magnitude. If k_2 is taken to be independent of pressure, it is then evident that at pressures approaching 1 atm the values of k_3 in the hydrogen halides are much less than in oxygen. The most extensive theoretical calculations on ion neutralization have been carried out on reaction [3] (14), and while quantitative calculations are not possible except for the simplest systems, certain general observations may be made. One factor which has been demonstrated both theoretically (15) and experimentally (16) is that when the masses of the ions and neutral molecules are very different, energy transfer to the third body will be inefficient, and this will lead to a decrease in the magnitude of k_3. This may account for the relatively low values of

Can. J. Chem. Downloaded from www.nrcresearchpress.com by 210.87.254.40 on 09/05/12
For personal use only.

k_3 for the clustered ions in the hydrogen halides. The high value of $\alpha = 3.0 \times 10^{-6}$ cm^3 s^{-1} (constant over the pressure range 250 to 650 Torr), calculated by Armstrong and Back from their measurements of ion lifetimes in gaseous hydrogen chloride (5), is contrary to our present observations. However, the technique employed by them was not primarily designed for determining accurate values of α (17).

The low pressure limit of α in nitrous oxide appears to be significantly higher than 2×10^{-7} cm^3 s^{-1} (see Fig. 4), extrapolation to zero pressure giving $k_2 = (6 \pm 1) \times 10^{-7}$ cm^3 s^{-1}. If $k_3 = \alpha - k_2$, then at the higher pressures k_3 in nitrous oxide (1.4×10^{-6} s^{-1} at 600 Torr) is also lower than that in oxygen. It should, however, be noted that the analysis of α at the higher pressures is complicated by the fact that k_2 may change with pressure due to increased clustering. The assumption of a constant value of k_2 is then most serious in nitrous oxide, where k_2 is a significant fraction of α.

The relatively high value of k_2 in nitrous oxide at low pressures may account for certain results which have been obtained in steady-state radiolysis experiments. The results of Burtt and Kircher (12) imply that there is an increase in the yield of products from neutralization reactions at pressures below 100 Torr. This increase is not due to the increased rate of reaction [1], as wall diffusion would have been negligible under their conditions. However, it could correspond to an increase in the fraction of ions being neutralized by reaction [2], which evidently may lead to product formation, while reaction [3] does not.

1. T. W. Woodward and R. A. Back. Can. J. Chem. **41**, 1463 (1963).
2. S. McGowan. Phys. Med. Biol. **10**, 25 (1965); Can. J. Phys. **45**, 439 (1967).
3. H. J. Ebert, J. Booz, and R. Koepp. Z. Phys. **181**, 187 (1964).
4. F. T. Jones and T. J. Sworski. J. Phys. Chem. **70** 1546 (1966).
5. D. A. Armstrong and R. A. Back. Can. J. Chem. **45**, 3079 (1967).
6. R. A. Lee, R. S. Davidow, and D. A. Armstrong. Can. J. Chem. **42**, 1906 (1964).
7. M. A. Biondi and S. C. Brown. Phys. Rev. **75**, 1700 (1949).
8. S. McGowan. Can. J. Phys. **45**, 429 (1967).
9. M. E. Gardner. Phys. Rev. **53**, 75 (1938).
10. D. A. Durden, P. Kebarle, and A. Good. J. Chem. Phys. **50**, 805 (1969).
11. W. A. Boyd, C. Willis, R. Cyr, and D. A. Armstrong. To be published.
12. B. P. Burtt and J. F. Kircher. Radiat. Res. **9**, 1 (1958).
13. R. S. Davidow and D. A. Armstrong. J. Chem. Phys. **48**, 1235 (1968).
14. E. W. McDaniel. Collision phenomena in ionized gases. John Wiley and Sons, Inc., New York. 1964.
15. D. R. Bates and M. R. Flannery. Proc. Roy. Soc. London, Ser. A, **302**, 367 (1968). B. H. Mahan. J. Chem. Phys. **48**, 2629 (1968).
16. B. H. Mahan and J. C. Person. J. Chem. Phys. **40**, 392 (1964). G. H. Fisk, B. H. Mahan, and E. K. Parks. J. Chem. Phys. **48**, 2649 (1967).
17. C. J. Wood, R. A. Back, and D. H. Dawes. Can. J. Chem. **45**, 3071 (1967).

Can. J. Chem. Downloaded from www.nrcresearchpress.com by 210.87.254.40 on 09/05/12
For personal use only.

Can. J. Chem. Downloaded from www.nrcresearchpress.com by 210.87.254.6 on 09/05/12
For personal use only.

Competitive chlorination reactions with ICl. II. CH_4, C_2H_6, C_3H_8, and C_2H_5Cl

CAROL C. KELLY, W. H. S. YU, AND M. H. J. WIJNEN
Hunter College of the City University of New York, 695 Park Avenue, New York, New York 10021

Received August 5, 1969

The H atom abstraction from CH_4, C_2H_6, C_3H_8, and C_2H_5Cl by Cl atoms produced by photolysis of ICl in daylight has been studied. Relative rates for the abstractions from CH_4, C_2H_6, primary and secondary hydrogens from propane, and for the abstraction from the CH_3 and CH_2Cl sides of C_2H_5Cl have been obtained at room temperature. These data are compared with other literature values.

Canadian Journal of Chemistry, **48**, 603 (1970)

Introduction

Recently (1) we have reported that the photolysis of ICl at room temperature is an excellent source of Cl atoms. Quantitative data are available in the literature regarding H atom abstractions from methane, ethane, propane, and ethyl chloride by Cl atoms. It seemed interesting to study these reactions by this technique in order to compare the data.

Experimental

The experimental technique is extremely simple. The experiments were carried out in a 1 l flask attached to a vacuum system. The ICl was admitted from a reservoir, separated from the reaction flask by a teflon stopcock, and frozen in a cold finger of the reaction flask. Although no attempt was made to measure the amount of ICl admitted, care was taken to admit sufficient ICl so that its maximum vapor pressure of about 30 Torr would be reached upon evaporation. Immediately after the flask was saturated with ICl vapor, the mixture of gases to be studied was admitted. Total pressure in the reaction flask varied from about 60 to 120 Torr. The photolysis of ICl was carried out in daylight since the reaction proceeded rapidly enough to make use of other light sources superfluous.

It was always necessary to carry out one preliminary experiment to establish the approximate reaction time. The reaction time is, obviously, dependent upon the compounds to be studied: the number of H atoms available for abstraction, and the ease by which they can be abstracted. The reaction time also depends upon the pressure of the hydrocarbons in the reaction flask since there are two competing reactions

$$Cl + RH \rightarrow R + HCl$$

$$Cl + ICl \rightarrow Cl_2 + I$$

As an example, it may be mentioned that we used reaction times of 15 to 30 min for ICl–C_2H_5Cl mixtures and of about 5 min for ICl–C_2H_6–C_3H_8 mixtures. It was necessary to keep the conversions of the hydrocarbons below 2%. At large conversions, iodine atoms or molecules built up to an extent that they started acting as scavengers, thus complicating the reaction mechanism. The reaction products were analyzed by gas chromatography. A 12 ft long column containing 20% silicon grease (by weight) was used for analysis.

The ICl was obtained from Eastman Organic Chemicals, Distillation Products Industries and was degassed for about 2 h at Dry Ice temperature to remove traces of molecular chlorine. Short degassings were repeated each day before starting the experiments.

Results and Discussion

If the necessary precautions are taken to avoid overexposure, the reaction mechanism of the photolysis of ICl in the presence of a mixture of hydrocarbons may be represented by

$$[1] \qquad ICl + h\nu \rightarrow I + Cl$$

$$[2] \qquad Cl + RH \rightarrow R + HCl$$

$$[3] \qquad Cl + R'H \rightarrow R' + HCl$$

$$[4] \qquad Cl + ICl \rightarrow Cl_2 + I$$

$$[5] \qquad R(R') + ICl \rightarrow RCl(R'Cl) + I$$

This mechanism is essentially identical to that proposed by Hofer and Wiig (2) for the photochemical reaction of ICl with H_2. There is no doubt that ICl as a photochemical source of Cl atoms is, kinetically speaking, much simpler than ICl as a thermal source of Cl atoms (3). The use of the photochemical system, as discussed earlier (1), is, however, limited to a very narrow temperature range and cannot, therefore, be used for activation energy studies.

In Table 1, we give the results obtained in the photolysis of ICl in the presence of various hydrocarbon mixtures. Columns 1 and 2 give the relative amounts of RCl and R'Cl produced; columns 3 and 4 give the relative amounts of RCl and R'Cl per available hydrogen atom. Preliminary data indicated that ethane was much more readily attacked by Cl atoms than methane

TABLE 1

Photolysis of ICl in the presence of various hydrocarbon mixtures

(*A*) $C_2H_6 + CH_4 + ICl$; $[CH_4]/[C_2H_6] = 6.25$

Products in relative amounts		Relative amounts per available H	
CH_3Cl	C_2H_5Cl	CH_3Cl	C_2H_5Cl
39	400	9.75	66.7
33	371	8.25	61.8
32	430	8.00	71.7
24	300	6.00	50.0
26	306	6.50	51.0

(*B*) $C_2H_6 + C_3H_8 + ICl$; $[C_2H_6]/[C_3H_8] = 1.81$

Products in relative amounts			Relative amounts per available H		
C_2H_5Cl	2-C_3H_7Cl	1-C_3H_7Cl	C_2H_5Cl	2-C_3H_7Cl	1-C_3H_7Cl
129	123	85	21.5	61.5	14.2
229	187	137	38.2	93.5	22.8
67	59	40	11.1	29.5	6.7
120	103	69	20.0	51.5	11.5

(*C*) $C_2H_5Cl + ICl$

Products in relative amounts		Relative amounts per available H	
1,1-$C_2H_4Cl_2$	1,2-$C_2H_4Cl_2$	1,1-$C_2H_4Cl_2$	1,2-$C_2H_4Cl_2$
352	88.0	176	29.3
18	4.8	9	1.6
36	8.8	18	2.9

(*D*) $C_2H_5Cl + C_3H_8 + ICl$; $[C_2H_5Cl]/[C_3H_8] = 2.05$

Products in relative amounts		Relative amounts per available H	
1-C_3H_7Cl	1,1-$C_2H_4Cl_2$	1-C_3H_7Cl	1,1-$C_2H_4Cl_2$
40	10.5	6.7	5.2
122	31.0	20.3	15.5
81	25.3	13.5	14.6
37	10.0	6.2	5.0

was. Therefore, a ratio $[CH_4]/[C_2H_6] = 6.25$ was used as indicated in section *A* of Table 1. In the case of ethane–propane mixtures, three products were observed: C_2H_5Cl originating from Cl atom reacting with ethane and 1- and 2-chloropropane caused by Cl atom reacting with primary and secondary hydrogens in propane. In section *C* we give the data for reactions of Cl atoms with H atoms from the CH_2Cl and from the CH_3 group in CH_3CH_2Cl, thus forming 1,1- and 1,2-dichloroethane. In order to relate reactions of Cl atom with C_2H_5Cl to those with ethane, methane, and propane, we studied a mixture of C_2H_5Cl and C_3H_8 reported in section *D*. In these experiments, 4 products were produced: 1- and 2-chloropropane and 1,1- and 1,2-$C_2H_4Cl_2$. We have reported in section *D* only 1-C_3H_7Cl and 1,1-$C_2H_4Cl_2$. Our analytical technique was such that we could not separate 2-chloropropane sufficiently from the excess C_2H_5Cl used as starting material. The 1,2-$C_2H_4Cl_2$ produced was too small to be measured in the first and in the last experiment reported in section *D*. In the other experiments the ratio 1,2-$C_2H_4Cl_2$/1,1-$C_2H_4Cl_2$ was identical to the ratio obtained with C_2H_5Cl alone given in section *C*. From the data reported in Table 1, the relative reaction rates of Cl atoms with CH_4, C_2H_6, C_3H_8 (to produce $\dot{C}H_2CH_2CH_3$ and $CH_3\dot{C}HCH_3$ radicals), and with C_2H_5Cl (to produce $CH_3\dot{C}HCl$ and $\dot{C}H_2CH_2Cl$ radicals) may be calculated. These data are summarized in Table 2, where we placed the rate constant for

Can. J. Chem. Downloaded from www.nrcresearchpress.com by 210.87.254.6 on 09/05/12
For personal use only.

TABLE 2

Relative rates per available H atom for reaction
$Cl + RH \rightarrow R + HCl$ at 25 °C

RH	Source of H	Relative rates		
		This work	Literature	
			Value	Reference
CH_4		2.0± 0.2	0.4	(4)
C_2H_6	(Standard)	100	100	
C_3H_8	Primary	110 ±10	120	(4)
C_3H_8	Secondary	480 ±20	444	(4)
C_2H_5Cl	CH_3	7.4± 0.4	12	(9)
C_2H_5Cl	CH_2Cl	44.0± 4	61	(9)

Cl with ethane equal to 100. It should be mentioned that these calculations are based upon the assumption that the reaction

$$R + ICl \rightarrow RCl + I$$

will not require an activation energy. This assumption seems quite reasonable considering the fact that the R—Cl bond is considerably stronger than the I—Cl bond. Furthermore, if ICl were not an efficient free-radical scavenger, we should have observed recombination or disproportionation products of the radicals produced.

Possible complications could also arise if the reaction

$$R + ICl \rightarrow RI + Cl$$

would occur. However, we have not been able to observe any positive evidence for this reaction. Limiting, temporarily, the discussion to the data for methane, ethane, and propane given in Table 2, the following conclusions may be drawn. The abstraction of a secondary hydrogen predominates over the abstraction of a primary hydrogen in propane. The H atom abstraction of a primary hydrogen from propane and ethane is about 50 times faster than the H atom abstraction from methane. In column 2 of Table 2, we give the corresponding values calculated from data by Knox and Nelson (4). We have used ethane as a reference since in both investigations the reaction rates of Cl with CH_4 and with C_3H_8 were compared to the rate of Cl with ethane. The agreement is excellent in regard to H atom abstraction from propane. Our data indicate, however, that methane is 5 times more reactive than previously reported. We should point out that, having observed this discrepancy, we repeated the experiments of ICl with a mixture of methane and ethane using a different $[CH_4]/[C_2H_6]$ ratio. The data were in agreement with those reported in Table 2. The ratio of preexponential factors in the Arrhenius equation for methane and ethane has been reported as $A_M/A_E = 0.39$ (5). However, the ratios of A factors for the abstraction of a primary hydrogen from, respectively, propane, butane, and isobutane over the A factor for H atom abstraction from ethane are all, within experimental error, reported to be equal to unity (4). If we would accept that A_M/A_E also may be equal to unity, the data for methane would agree much better. This suggestion is, furthermore, supported through calculations by Fettis and Knox (6) which indicate that the ratio A_{exp}/A_{calcd} shows a much larger deviation for the reaction $Cl + CH_4$ than for any other abstraction reaction by Cl atoms. Accepting $A_M/A_E = 1.0$ and accepting as collision diameters $\sigma_{Cl} = 2$, $\sigma_{CH_4} = 3.5$, and $\sigma_{C_2H_6} = 5.3$Å, we obtain an activation energy difference of 2.2 kcal/mole between H atom abstraction from methane and ethane by Cl atoms. This value is comparable to $E_M - E_E = 2.8$ kcal/mole reported in the literature (4, 7).

It should be mentioned that Goldfinger *et al.* (8) obtained for the H atom abstraction from CH_4 by Cl atoms a relative value of 0.8, intermediate between those reported by us and by Knox and Nelson.

Two reactions must be considered for H atom abstractions from C_2H_5Cl

[A] $Cl + CH_3CH_2Cl \rightarrow CH_2CH_2Cl + HCl$

[B] $Cl + CH_3CH_2Cl \rightarrow CH_3CHCl + HCl$

Our value $k_A/k_B = 0.17 \pm 0.02$ is in excellent agreement with previous data by Goldfinger and

Can. J. Chem. Downloaded from www.nrcresearchpress.com by 210.87.254.6 on 09/05/12
For personal use only.

co-workers, $k_A/k_B = 0.20$ (9). Comparisons with the rate of abstraction from ethane (see Table 2) are not so good but, nevertheless, quite reasonable.

To some extent it is of course possible to consider C_2H_5Cl as a substituted propane where the methyl group has been replaced by a Cl atom. Thus, the hydrogens of the CH_2Cl group in C_2H_5Cl are comparable to the secondary hydrogens in propane. Indeed, the data for primary and "secondary" H atom abstractions from propane and C_2H_5Cl are quite similar. Alternately, the difference in reactivity between the H atoms in C_2H_5Cl may be explained by the electron withdrawing power of the highly electronegative Cl atom. The electrons are drawn toward the Cl atom, thus weakening the C—H bonds in the CH_2Cl group. This is in complete agreement with observations regarding the C—H bond strengths in CH_4 and CH_3Cl. Hydrogen atom abstractions from CH_4 and CH_3Cl by Cl (10) atoms and by Br (11) atoms indicate that the C—H bond is weaker in CH_3Cl than in CH_4.

Surprising is the fact that the rate of H atom abstraction from C_2H_5Cl is considerably slower than that from C_2H_6. A priori it might have been expected that the rates per available H atom should be equal for the methyl groups in C_2H_6 and in C_2H_5Cl. In reality the ratio is about 15 in favor of H atom abstraction from ethane. An explanation for this observation cannot, in our opinion, be sought in a steric effect caused by the bulky Cl atom. The CH_3 group is larger than the Cl atom but, nevertheless, the rate of secondary H atom abstraction from propane is about 11 times faster than the rate of H atom abstraction from the CH_2Cl side in C_2H_5Cl. It seems more plausible that the low rates for H atom abstraction from C_2H_5Cl may be caused through a repulsion of the approaching Cl atom by the Cl atom in C_2H_5Cl. It might be expected that such an effect would be larger for the H atoms on the CH_2Cl side than for those in the CH_3 group of C_2H_5Cl. In spite of this, H atom abstraction from the CH_2Cl group occurs much faster than from the CH_3 group in C_2H_5Cl. This indicates that there should be a noticeable difference in bond strengths between the C—H bonds in the CH_3 and those in the CH_2Cl group of C_2H_5Cl. This observation is confirmed through recent estimates by Franklin and Huybrechts (12) which yield $D(CH_3CHCl—H) = 96.7$ and $D(CH_2ClCH_2—H) = 98.0$ kcal/mole.

Finally, we would like to mention that the H atom abstraction from C_2H_5Cl by Cl atoms has been studied in this laboratory by a different method. Cl atoms produced by photolysis of CCl_4 were allowed to react with C_2H_5Cl (13). By summation of all the products originating from CH_2CH_2Cl and from CH_3CHCl radicals, a value of $k_A/k_B = 0.11 \pm 0.02$ was obtained to be compared with 0.17 ± 0.02 from this study. Although these data are outside the experimental error limit, they both confirm the marked difference in reactivity between the H atoms in the CH_3 and those in the CH_2Cl group of C_2H_5Cl. The authors are of the opinion that the method discussed in this paper provides a more direct approach to the determination of k_A/k_B than the photolysis of CCl_4 in the presence of C_2H_5Cl. The value $k_A/k_B = 0.17 \pm 0.02$ should, therefore, be given preference.

The authors express their appreciation to the National Science Foundation for supporting this work.

1. Carol C. Kelly and M. H. J. Wijnen. J. Phys. Chem. **73**, 2447 (1969).
2. L. J. E. Hofer and E. O. Wiig. J. Amer. Chem. Soc. **67**, 1441 (1945).
3. S. W. Benson, F. J. Cruickshank, and R. Shaw. Int. J. Chem. Kinetics, **1**, 29 (1969).
4. J. H. Knox and R. L. Nelson. Trans. Faraday Soc. **55**, 937 (1959).
5. J. H. Knox. Chem. Ind. 1631 (1955).
6. G. C. Fettis and J. H. Knox. Progress in reaction kinetics. Vol. 2. The Pergamon Press Ltd., New York. 1964. pp. 34, 35.
7. G. C. Fettis, J. H. Knox, and A. F. Trotman-Dickenson. Can. J. Chem. **38**, 1643 (1960).
8. P. Goldfinger, G. Huybrechts, and G. Martens. Trans. Faraday Soc. **57**, 2210 (1961).
9. C. Cillien, P. Goldfinger, G. Huybrechts, and G. Martens. Trans. Faraday Soc. **63**, 1631 (1967).
10. J. H. Knox. Trans. Faraday Soc. **58**, 275 (1962).
11. G. C. Fettis, J. H. Knox, and A. F. Trotman-Dickenson. J. Chem. Soc. 4177 (1960).
12. J. L. Franklin and G. Huybrechts. Int. J. Chem. Kinetics, **1**, 3 (1969).
13. W. H. S. Yu. Ph.D. Thesis. Hunter College of the City University of New York, New York. July 1969.

Can. J. Chem. Downloaded from www.nrcresearchpress.com by 210.87.254.6 on 09/05/12
For personal use only.

Can. J. Chem. Downloaded from www.nrcresearchpress.com by 210.87.254.40 on 09/05/12
For personal use only.

Infrared spectrum of HDO in water and in NaCl solution[1]

HANS R. WYSS[2] AND MICHAEL FALK[3]
Atlantic Regional Laboratory, National Research Council of Canada, Halifax, Nova Scotia

Received July 11, 1969

The molar absorptivity of dilute HDO in water and in aqueous NaCl solutions was determined at temperatures between 10 and 85° in the spectral region from 4000 to 2000 cm^{-1}. The infrared band profiles for the OH and OD stretching fundamentals are single-peaked and devoid of shoulders, in contrast to the high-frequency shoulders recently observed in the Raman spectrum. It is shown that such shoulders do not contradict a single-peaked distribution of OH oscillators with respect to intermolecular geometry. Absence of resolvable sub-bands in the spectrum of HDO in concentrated salt solutions indicates a wide distribution of ion–H_2O interactions, akin to the distribution of H_2O–H_2O interactions in water.

Canadian Journal of Chemistry, **48**, 607 (1970)

Introduction

The infrared (i.r.) absorption bands of isotopically dilute solutions of HDO in H_2O or D_2O provide an important probe of hydrogen bonding in water and in aqueous solutions. Earlier i.r. studies of HDO in water (1–7) and in electrolyte solutions (1, 5) were limited to narrow portions of the spectrum, and did not provide accurate band profiles as a function of temperature. Hence, an improved, quantitative measurement seemed in order. We have now measured the i.r. spectrum of H_2O–HDO–D_2O and H_2O–HDO–D_2O–NaCl solutions as a function of temperature and HDO concentration. From these measurements we have calculated accurate molar absorptivities of HDO in water and in NaCl solution at each temperature at 10 or 20 cm^{-1} intervals between 4000 and 2000 cm^{-1}.

Experimental

Samples

Mixtures of H_2O (doubly distilled) and D_2O (supplied by Merck, Sharp and Dohme of Canada Ltd.) were prepared by weighing. A series of seven D_2O-rich solutions and a series of seven H_2O-rich solutions were used, with isotopic contents of approximately 0, 0.5, 1, 2, 4, 8, and 15% of the less abundant component.

For the salt spectra, we prepared stock solutions containing 1 mole of NaCl in 11.0 moles of H_2O or of D_2O. Starting from these two stock solutions, two series of H_2O–D_2O mixtures were made up as before. The approximate isotopic contents were chosen to be 0, 0.4, 0.8, 1.5, 3, 6, and 10% of the less abundant component.

Accurate values of the isotopic contents of the D_2O-rich solutions were computed by an iterative least-squares fit to the absorbance data, assuming Beer's law. This procedure also yielded the spectrum of isotopically pure D_2O, and the isotopic purity of commercial D_2O, 99.81 ± 0.04%.

Except for the weighings, all manipulations with the D_2O solutions were carried out in an improvised dry-box under nitrogen, to minimize hydrogen exchange with atmospheric water.

Spectroscopic Measurements

The spectrometer and the thermostatic chamber were described before (6). The solutions were contained in a CaF_2 cell. Its optical path (approximately 0.05 mm) was determined by the fringe method at every temperature. To increase the accuracy, the spectra were recorded single-beam, i.e. without any reference cell. The measurements for H_2O–D_2O solutions were carried out at 10, 35, 60, and 85° and those for H_2O–D_2O-salt solutions at 10 and 85°. Typical spectra recorded in this manner are shown in Fig. 1. The absorbances at each of the four temperatures were tabulated at 10 or 20 cm^{-1} intervals. These digital data were then processed to eliminate the contributions from the absorption of H_2O and D_2O, and the reflection losses. The spectral range examined was 4000 to 2000 cm^{-1}.

Calculation of the Concentrations

The concentrations of H_2O, HDO, and D_2O in mole/l were calculated from the weighed amounts of H_2O and D_2O. The equilibrium constant of the process $H_2O + D_2O \rightleftharpoons 2$ HDO was assumed to be 3.80 (8) for all solutions and temperatures. The densities of H_2O (9) and D_2O (10) at the temperatures of the experiment were also required. The densities of H_2O–D_2O solutions were calculated assuming additivity of the molar volumes of H_2O and D_2O. For the NaCl solutions we assumed that the molar volume of NaCl is the same in D_2O as in H_2O, and that the ratio of densities at two temperatures is the same for water and for NaCl solutions.

Calculation of HDO Absorptivities

Three H_2O–HDO–D_2O mixtures were chosen at every temperature and frequency. The application of Beer's law provided three equations of the type

$$A = A_0 + d\cdot(\varepsilon_{H_2O}\cdot C_{H_2O} + \varepsilon_{HDO}\cdot C_{HDO} + \varepsilon_{D_2O}\cdot C_{D_2O})$$

[1]NRCC No. 11083.

[2]NRCC Postdoctoral Fellow 1966–1967. Present address: Department of Physical Chemistry, Hoffmann–LaRoche, Inc., Nutley, New Jersey.

[3]To whom requests for reprints should be addressed.

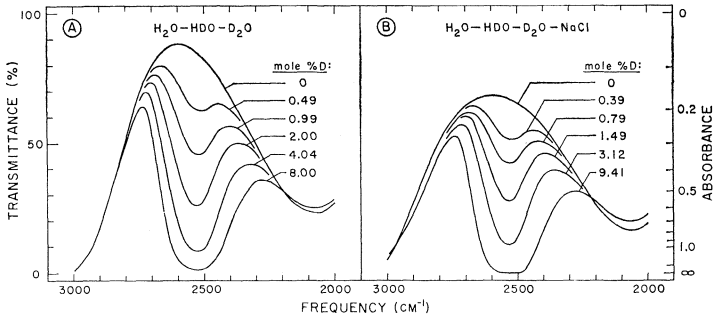

FIG. 1. Typical spectra of H_2O–HDO–D_2O and of H_2O–HDO–D_2O–NaCl solutions used in the calculation of the HDO absorptivity between 3000 and 2000 cm^{-1}.

where A is the measured absorbance, A_0 is the base line, d is the optical path, ε is molar absorptivity and C is concentration in mole/l. From these three equations we eliminated A_0 and ε_{H_2O} (or ε_{D_2O}, if D_2O was the less abundant component). The value of ε_{HDO} was then obtained by inserting the value of ε_{D_2O} (or ε_{H_2O}, if H_2O was the more abundant component) which was derived from the spectra of pure H_2O or D_2O at the appropriate temperature. Corrections were made for the losses due to reflection at the two CaF_2/air interfaces and the two CaF_2/water interfaces. The former loss was measured with a single CaF_2 window, while the latter was calculated from the mean refractive indices of water and CaF_2 (the dispersion was neglected). The total absorbance correction thus obtained was -0.027, about 5% of the peak absorbances which were of the order of 0.5.

The H_2O-rich solutions were used in the regions of strong D_2O absorption, and vice versa. Data from the two solutions with highest HDO concentrations were used only in areas outside the main HDO absorption bands.

Results

Because of the importance of good spectral data in the evaluation of structural models for water and aqueous solutions, we are presenting in Table 1 our complete set of absorptivities of HDO. The absorptivities at 10 and 85° have been plotted in Fig. 2. The spectrum of dilute HDO in the region of 4000 to 2000 cm^{-1} contains three bands which correspond to the OH stretching vibration, ν_3, the OD stretching vibration, ν_1, and $2\nu_2$, an overtone of the bending vibration. In addition, the high-frequency side of ν_3 and the low-frequency side of ν_1 are overlapped slightly by adjacent bands. An important advantage of the HDO spectra over those of H_2O and D_2O is the separation of the stretching fundamentals. The spectrum gives the band profiles of ν_3 and ν_1 almost directly; the "tails" of the bands can be freed from overlapping combination bands by simple extrapolation. To calculate band areas the extrapolation was done with model functions fitted to the nonoverlapped part of the band tails. A Gauss function (11) was used for the high-frequency tails and a Cauchy function (11) for the low-frequency tails.

The observed band parameters for the ν_3 and ν_1 bands of HDO in water and in NaCl solution are plotted in Fig. 3 as a function of temperature.

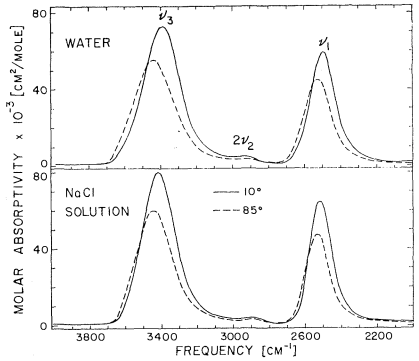

FIG. 2. Molar absorptivity of HDO in the region of 4000 to 2000 cm^{-1} at 10 and 85° in water and in aqueous NaCl solutions.

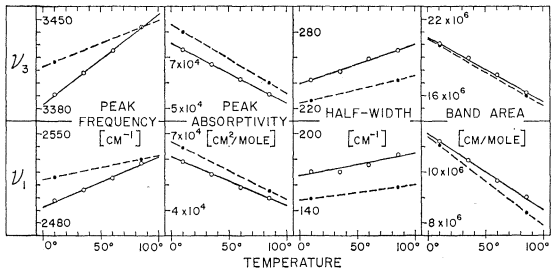

FIG. 3. Effect of temperature on the parameters of ν_3 and ν_1 bands of HDO in water (full lines) and in aqueous NaCl solutions (broken lines).

Can. J. Chem. Downloaded from www.nrcresearchpress.com by 210.87.254.40 on 09/05/12
For personal use only.

TABLE 1

Molar absorptivity (10^3 cm^2/mole) of HDO in water and in 9.1 mole % NaCl solution

Frequency (cm^{-1})	Water					NaCl solution	
	10°	25°*	35°	60°	85°	10°	85°
4000	0.93	0.91	0.89	0.89	0.91	0.85	0.85
3900	0.80	0.82	0.83	0.87	0.91	0.85	0.85
3800	0.88	0.89	0.90	0.93	0.95	0.85	0.85
3780	0.91	0.93	0.95	0.99	1.02	0.85	0.85
3760	1.03	1.06	1.08	1.13	1.18	0.85	0.85
3740	1.15	1.18	1.20	1.24	1.31	0.86	0.91
3720	1.21	1.28	1.33	1.42	1.56	0.95	1.07
3700	1.44	1.55	1.63	1.87	2.20	1.14	1.32
3680	2.23	2.41	2.54	2.97	3.63	1.50	1.77
3660	3.97	4.23	4.40	5.38	6.81	2.35	3.19
3640	6.67	7.02	7.25	8.63	10.4	3.90	6.07
3620	9.51	10.2	10.7	13.0	15.4	7.30	11.0
3600	13.1	14.5	15.4	18.6	21.3	11.7	17.5
3580	17.0	18.8	20.0	23.5	25.2	17.8	23.8
3560	22.0	24.3	25.8	28.8	30.9	25.4	30.8
3540	27.8	29.8	31.2	33.8	36.5	33.6	37.1
3520	34.2	36.5	38.0	40.5	42.2	43.5	42.8
3500	42.5	44.7	46.2	46.9	47.2	53.6	50.6
3490	46.3	48.5	50.0	50.0	49.2	57.9	53.5
3480	50.7	52.3	53.3	53.2	51.2	62.1	55.9
3470	54.3	55.6	56.4	55.7	52.8	67.0	57.6
3460	58.2	59.1	59.7	57.8	54.3	71.4	59.0
3450	61.7	61.8	61.8	59.4	55.3	74.5	59.8
3440	65.3	64.4	63.8	60.7	55.5	77.4	60.2
3430	68.0	66.6	65.6	61.4	55.2	79.1	59.8
3420	70.0	68.1	66.8	61.4	54.2	80.1	58.8
3410	71.8	69.1	67.3	60.8	52.9	80.1	56.7
3400	72.9	69.4	67.1	59.3	51.0	78.6	53.8
3390	73.0	68.9	66.1	57.4	49.0	76.3	51.5
3380	72.6	67.7	64.5	55.0	46.8	73.0	48.4
3370	71.5	66.1	62.5	52.5	44.5	69.5	45.4
3360	70.0	63.4	59.0	50.1	42.3	65.7	42.8
3350	67.3	60.5	56.0	46.7	39.8	61.2	39.3
3340	63.5	57.1	52.8	43.5	37.3	56.4	36.5
3330	59.4	53.3	49.2	40.5	34.7	52.4	33.2
3320	56.0	49.8	45.7	37.8	31.8	48.1	30.1
3310	51.5	45.7	41.8	35.0	29.4	43.1	27.1
3300	47.5	41.9	38.2	32.4	27.0	38.1	24.1
3280	39.5	35.2	32.4	27.2	21.8	30.0	19.0
3260	31.7	28.9	27.0	21.8	18.3	23.6	15.8
3240	24.8	22.8	21.5	18.2	14.8	18.8	12.9
3220	19.4	18.0	17.1	14.7	12.3	14.8	10.7
3200	16.0	14.9	14.2	12.2	10.5	12.2	9.30
3180	13.4	12.4	11.7	9.80	8.00	10.2	8.00
3160	11.6	10.6	10.0	8.50	7.20	8.50	6.70
3140	9.50	8.84	8.40	7.50	6.50	7.10	5.70
3120	8.19	7.68	7.35	6.50	5.68	6.00	5.00
3100	7.06	6.66	6.40	5.72	5.02	5.20	4.40
3080	6.22	5.89	5.67	5.07	4.51	4.70	3.70
3060	5.72	5.36	5.13	4.56	4.02	4.20	3.40
3040	5.16	4.82	4.60	4.18	3.80	4.00	3.10
3020	4.93	4.61	4.40	3.98	3.60	3.60	2.80
3000	4.83	4.49	4.26	3.85	3.45	3.40	2.60
2980	4.87	4.54	4.33	3.88	3.47	3.40	2.50
2960	4.99	4.69	4.50	3.98	3.62	3.60	2.60
2950	5.08	4.78	4.58	4.08	3.69	3.75	2.75
2940	5.15	4.84	4.63	4.16	3.77	3.90	2.90
2930	5.13	4.81	4.60	4.19	3.79	4.00	3.15
2920	4.98	4.65	4.44	4.10	3.72	4.10	3.40
2900	4.46	4.21	4.04	3.76	3.49	4.20	3.50
2880	3.82	3.65	3.54	3.34	3.13	4.00	3.30
2860	3.10	3.00	2.94	2.80	2.68	3.70	2.90

Can. J. Chem. Downloaded from www.nrcresearchpress.com by 210.87.254.40 on 09/05/12
For personal use only.

TABLE 1 (*concluded*)

Frequency (cm^{-1})	Water					NaCl solution	
	10°	25°*	35°	60°	85°	10°	85°
2840	2.63	2.54	2.49	2.36	2.24	3.10	2.30
2820	2.06	2.04	2.02	1.95	1.91	2.30	1.90
2800	1.57	1.59	1.61	1.65	1.74	1.50	1.50
2780	1.34	1.40	1.45	1.57	1.69	1.20	1.40
2760	1.32	1.39	1.44	1.61	1.76	0.80	1.30
2740	1.41	1.50	1.57	1.72	1.92	0.80	1.40
2720	1.64	1.72	1.78	1.96	2.18	1.10	1.60
2700	2.12	2.26	2.36	2.80	3.48	1.50	2.20
2680	3.95	4.16	4.30	5.02	6.01	2.20	3.50
2660	6.50	6.94	7.24	8.41	10.2	4.10	6.20
2640	9.90	10.5	10.9	12.3	15.1	7.00	11.2
2620	15.2	16.0	16.6	18.0	21.0	13.2	19.6
2600	21.7	22.7	23.4	25.2	28.0	25.3	28.0
2580	29.4	30.4	31.1	32.7	34.7	37.4	36.7
2570	33.0	34.6	35.7	36.8	38.0	45.0	40.1
2560	38.2	39.3	40.0	41.0	40.8	50.2	43.1
2550	44.3	44.1	44.0	44.3	43.1	55.3	45.6
2540	49.6	48.9	48.4	46.8	44.5	60.5	47.2
2530	53.6	52.5	51.7	48.3	44.9	63.4	47.6
2520	56.3	54.4	53.2	49.0	44.8	64.5	47.1
2510	58.3	55.8	54.1	49.0	44.0	64.4	45.5
2500	59.3	56.2	54.1	48.1	42.6	62.7	42.4
2490	58.9	55.4	53.1	46.6	40.5	59.4	38.3
2480	57.3	53.6	51.1	43.6	37.2	55.2	33.7
2470	53.3	49.9	47.6	40.0	33.8	50.0	29.2
2460	49.2	45.7	43.4	35.9	30.0	44.1	25.8
2440	39.9	36.4	34.0	27.8	22.5	32.9	19.0
2420	30.6	27.2	25.0	20.3	17.2	23.2	13.6
2400	22.1	20.2	18.9	15.8	13.0	16.0	10.8
2380	16.6	15.3	14.4	12.3	10.4	11.9	8.40
2360	13.2	12.3	11.7	10.1	8.60	9.10	6.80
2340	10.3	9.63	9.18	8.06	6.92	7.20	5.70
2320	8.38	7.82	7.45	6.52	5.62	5.70	4.60
2300	6.95	6.50	6.20	5.46	4.70	4.60	3.70
2280	5.76	5.37	5.11	4.50	3.91	3.80	3.10
2260	4.70	4.41	4.22	3.75	3.30	3.40	2.80
2240	3.97	3.75	3.60	3.21	2.85	3.20	2.60
2220	3.40	3.21	3.08	2.80	2.54	2.95	2.50
2200	2.91	2.80	2.72	2.50	2.21	2.75	2.35
2180	2.58	2.47	2.40	2.21	2.02	2.65	2.20
2160	2.27	2.18	2.13	2.00	1.80	2.50	2.05
2140	2.02	1.93	1.87	1.77	1.60	2.42	1.95
2120	1.87	1.78	1.73	1.60	1.45	2.38	1.80
2100	1.81	1.73	1.68	1.53	1.35	2.25	1.70
2080	1.84	1.73	1.66	1.47	1.27	2.20	1.60
2060	1.92	1.77	1.67	1.44	1.21	2.15	1.50
2040	2.02	1.86	1.75	1.43	1.18	2.10	1.40
2020	2.17	1.98	1.86	1.52	1.19	2.10	1.30
2000	2.30	2.11	1.99	1.62	1.23	2.10	1.20

*Estimated by interpolation.

The peak frequency was determined by fitting a least-squares cubic polynomial through the observed values of absorptivity in the region of 50 to 70 cm^{-1} about the maximum (12). The band areas were obtained by integration between 3800 and 2760 cm^{-1} for ν_3, and between 2760 and 2000 cm^{-1} for ν_1. The absorptivity values at the integration limits are negligible. The temperature variation of all four band parameters of HDO in water was found to be linear within experimental error [over a temperature range greater than 100° small deviations from linearity have been observed for ν_1 (7)]. The solid lines in Fig. 3 represent least-squares straight lines through the four experimental points at 10, 35, 60, and 85°. The temperature variation of the band parameters of the NaCl solution was assumed also to be linear (broken lines in Fig. 2).

Can. J. Chem. Downloaded from www.nrcresearchpress.com by 210.87.254.40 on 09/05/12
For personal use only.

TABLE 2

Comparison of measured band parameters for ν_3 and ν_1 of HDO in water with earlier measurements

Peak frequency (cm^{-1})	Peak absorptivity $\times 10^{-3}$ (cm^2/mole)	Half-width (cm^{-1})	Area $\times 10^{-6}$ (cm/mole)	Temperature	Authors
ν_3 3404	69.6	247	19.3	25°*	This work
3404	64	255		25°*	Falk and Ford (6)
3388		246		24°	van Eck *et al.* (2)
3405		240		25°	Waldron (1)
3410	62.5	265		25°	Bayly *et al.* (3)
3390		260	21.3	27°	Swenson (4)
3405				25°	Hartman (5)
ν_1 2502	56.4	172	10.7	25°*	This work
2503	42	160		25°*	Falk and Ford (6)
2502		160		24°	van Eck *et al.* (2)
2520		165		25°	Waldron (1)
2500	41.4	185		25°	Bayly *et al.* (3)
2512		175	9.8	27°	Swenson (4)
2507	55	168	9.9	30°	Franck and Roth (7)

*Values for this temperature were obtained by interpolation.

Our measured band parameters for HDO in water are compared in Table 2 with those reported by earlier workers. The spread of the reported frequencies is probably largely due to the subjective factor in the visual location of the maxima of very broad bands (12). The main causes of the spread of values obtained for the other band parameters are the errors in the HDO concentration, base-line errors, use of different ranges of integration, and the difficulties inherent in the measurement of absolute intensities (13). The spread of the values in Table 2 is indicative of the probable absolute error in our determination of the band parameters, with the exception of the peak absorptivity of ν_1, where the spread of values reported appears larger than our probable error. An independent redetermination of the peak absorptivity of ν_1 would be of interest.

The profiles of ν_3 and ν_1 bands are nearly identical. They are single-peaked, devoid of shoulders, and slightly asymmetric. These observations agree with those of earlier workers (1–7, 14). The deviation from symmetry can be described by the asymmetry index which we define as $(A - B)/(A + B)$, where A and B are the areas under the band *above* and *below* the peak frequency. This index for our bands varies from about -0.04 at 10° to about -0.08 at 85°. The profiles of the ν_3 and ν_1 bands in NaCl solutions are qualitatively similar to those in water, as has been observed by Waldron (1) and Hartman (5).

Figure 4 shows the comparison of the observed band profiles of ν_3 and ν_1 with the Gauss and Cauchy functions fitted to the observed values of band amplitude, half-width, and peak frequency. The observed band profiles are intermediate between the Gauss and Cauchy functions at low frequencies, but more closely approach the Gauss function at high frequencies.

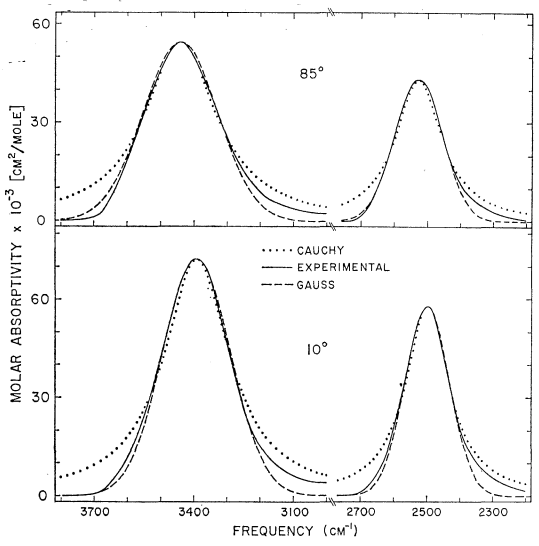

FIG. 4. Comparison of measured absorptivity profiles of HDO in water at 10 and 85° with Gauss and Cauchy functions.

Can. J. Chem. Downloaded from www.nrcresearchpress.com by 210.87.254.40 on 09/05/12
For personal use only.

Can. J. Chem. Downloaded from www.nrcresearchpress.com by 210.87.254.40 on 09/05/12
For personal use only.

Discussion

Possible Interpretation of Shoulders in the Raman Bands of HDO

Recently published Raman spectra of HDO in water (15–17) show shoulders at 3640 and 2660 cm^{-1}, i.e. on the high-frequency side of the ν_3 and ν_1 bands. The origin of these shoulders, not detectable in the i.r. spectrum, is of considerable interest. The shoulders have been assigned to distinct non-bonded OH and OD groups (15–17). This assignment implies a *two-peaked* distribution of OH groups with respect to intermolecular geometry, one peak corresponding to the "bonded" and the other to "non-bonded" groups. We wish to point out, however, that an alternate explanation of the Raman shoulders is possible, and that vibrational band profiles with a shoulder or a secondary maximum may also arise in the case of a *single-peaked* distribution of OH oscillators with respect to intermolecular geometry.

The environment of an OH oscillator in liquid water can be described by a set of geometric parameters. The most important of these parameters are the nearest-neighbor O · · · O distance R, the nearest-neighbor O—H · · · O angle, the angle describing the orientation of the lone pair of electrons on the nearest-neighbor oxygen atom, and parameters measuring the orientation with respect to additional neighbors (18). For the sake of simplicity let us *at first* retain only the parameter R. Let us further assume that:

(*i*) An oscillator is characterized by a wavenumber shift s caused by hydrogen bonding, an i.r. intensity f, and a Raman intensity f', all of which are functions of R.

(*ii*) As the geometry around the oscillator approaches the non-bonded structure, e.g. for large R values, the functions f, f', and s approach asymptotically their non-bonded values.

(*iii*) The distribution p of oscillators as a function of R has a single peak.

All oscillators with geometries between R and $R + dR$ will contribute to the band envelope between s and $s - ds$. This leads to the following expression for the i.r. band envelope $e(s)$ as a function of the wavenumber shift:

$$e(s) = p \cdot f \cdot dR/ds$$

In the corresponding expression for the Raman band envelope $e'(s)$, f' replaces f.

Of the three factors on the right only the distribution p reflects the water structure at a given temperature and is the same for all vibrational bands. The derivative dR/ds reflects the dependence of vibrational frequency on geometry and is different for every vibrational transition, as are f and f'. We must thus expect that different vibrational bands of HDO will have different envelopes and that each band will have different Raman and i.r. envelopes.

Because of the asymptotic behavior of s for large R, dR/ds diverges at $s = 0$. It thus depends on the functions p and f (or f') whether $e(s)$ [or $e'(s)$] also diverges. If it does, then our simplest model predicts a sharp secondary maximum at $s = 0$.

The outcome of this qualitative argument is not affected by the replacement of a single geometric parameter R by a set of six parameters which would completely define the orientation of a nearest-neighbor H_2O molecule with respect to a given OH group. We still expect an asymptotic behavior of s for large values of some of these parameters, hence a sharp secondary maximum at $s = 0$ is still possible. This sharp maximum, together with the rest of the $e(s)$ envelope, would be broadened and shifted away from the vapor frequency by the interactions of an OH · · · OH_2 system with farther molecular neighbors, hitherto neglected in our model. We may expect these farther-neighbor interactions to have an approximately Gaussian distribution, and to be independent of the OH · · · OH_2 configuration. The final $e(s)$ envelope will then be the convolution of this Gaussian with the original $e(s)$ distribution. The convolution would result in a curve with a broad secondary maximum or a shoulder, qualitatively corresponding to the observed Raman band profiles of HDO.

For the OH and OD stretching band, the relative intensity of the feature would be 10 to 20 times smaller in the i.r. spectrum than in the Raman spectrum and may be undetectable. This is because of the steep increase of the i.r. intensity f with increasing strength of hydrogen bonding (19), in contrast to the Raman intensity f', which is thought to be nearly independent of the hydrogen-bond geometry (14). The difference between f and f' also causes an overall displacement of the i.r. band envelope toward lower wavenumbers with respect to the Raman envelope. This displacement was experimentally observed (Fig. 5). The experimental ratio of the i.r. intensity to the Raman intensity, $e(s)/e'(s)$, which should equal f/f' according to our equation, varies by a factor

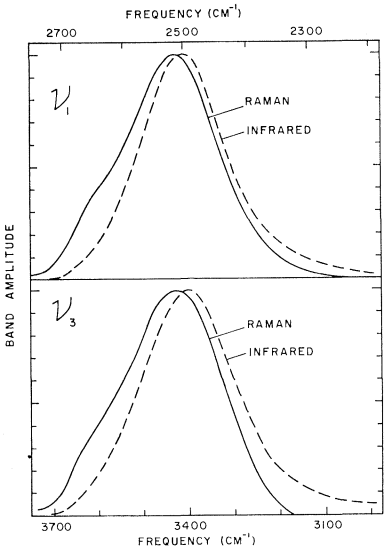

FIG. 5. Comparison of i.r. band envelopes (this work) with Raman band envelopes for ν_1 (ref. 15) and for ν_3 (ref. 17) of HDO in water at 25°.

of about 10 between the vapor frequency (3705 cm^{-1} for ν_3 and 2519 cm^{-1} for ν_1) and the ice frequency (3300 cm^{-1} for ν_3 and 2440 cm^{-1} for ν_1).

Increasing temperature will shift the maximum of $p(R)$ toward higher values of R, i.e. toward the asymptotic part of $s(R)$. Thus the feature near $s = 0$ will grow at the expense of the main peak. Its frequency will remain constant, in contrast to that of the main peak which will move toward $s = 0$. This agrees with the temperature dependence of the 2660 cm^{-1} shoulder in the Raman spectrum of HDO (15, 16). At sufficiently high temperatures the main peak should coalesce with the secondary feature.

We conclude that the Raman shoulders at 3640 and 2660 cm^{-1} *may be* due to the asymptotic behavior of frequency as a function of geometry. The shoulders thus do not contradict a single-peaked distribution of intermolecular hydrogen-bond geometries in liquid water.

The intensity of such features may be taken as a measure of "non-bonded" or "weakly bonded" OH groups, but if there exists a continuum of geometries of OH oscillators in water, then all divisions of the continuum into "bonded" and "non-bonded" are arbitrary (6). The asymptotic region may be different for different vibrational transitions, depending on the form of $s(R)$. Estimates of concentrations of "bonded" and "non-bonded" OH groups derived from different vibrational bands may therefore differ, particularly if the bands differ widely in their shape as in the overtone region (20, 21).

Effect of NaCl on the Spectrum and Structure of Water

Comparison of the lower and upper parts of Fig. 2 shows that no new features appear in the HDO spectrum when NaCl is added to water. The effect of NaCl on the OH and OD stretching bands of HDO near room temperature is to increase the peak absorptivity, to decrease the band width, and to shift the peak frequency upward. These observations agree with those of Waldron (1) and Hartman (5). Hartman's results show that the band parameters vary almost linearly with the solute concentration, indicating that the nature of the ion-water interactions is not drastically altered at higher concentrations (22). Thus the present conclusions based on data from concentrated solutions of NaCl should also be applicable to more dilute solutions. As the temperature increases, the upward shift of the peak frequency caused by the addition of NaCl decreases. Extrapolation shows that above 90 or 100° the peak frequency will be shifted downward.

The lack of any new features in the spectrum of HDO in NaCl solutions is an important clue to the structure of water around the Na^+ and Cl^- ions. The OH (and OD) groups in NaCl solutions can have as their nearest-neighbor *either* an oxygen atom of another water molecule *or* a chloride ion. This gives rise to two classes of OH groups, OH · · · O and OH · · · Cl^-, which could be expected *a priori* to produce two distinct sets of sub-bands in the spectrum. The peak frequencies and half-widths of these sub-bands should correspond to the distributions of the OH · · · O and OH · · · Cl^- interaction energies. If the OH · · · Cl^- groups in solution are so strongly ordered by the anion as to form a regular structure with a narrow spread of interaction energies and geometries, then a narrow sub-band would result. The half-widths of the OH and OD stretching bands of HDO in the crystalline hydrate $NaCl \cdot 2H_2O$ are of the order of 5 cm^{-1} (23, 24). Such narrow sub-bands would be easily resolved as secondary peaks or shoulders in the spectra. We have examined the HDO band shapes in NaCl solutions for the presence of such secondary peaks or shoulders. Even in spectra of solutions supercooled to −30° (which might be expected to show

Can. J. Chem. Downloaded from www.nrcresearchpress.com by 210.87.254.40 on 09/05/12
For personal use only.

a greater resolution of existing sub-bands than those at higher temperatures) *no new features appear*. This shows that the $OH \cdots Cl^-$ groups must have a distribution of frequencies similar to that of the $OH \cdots O$ groups, with a half-width of the order of 100 or 200 cm^{-1}. A large band width indicates that the $OH \cdots Cl^-$ groups have a variety of interaction energies in aqueous solution. It appears therefore that the water molecules surrounding the chloride ion assume a variety of instantaneous orientations, and have no strong preference for any single, well-defined configuration. The OH and OD stretching band profiles offer no direct information on the water $\cdots Na^+$ interactions, but it seems likely that they also give rise to a wide distribution of distances, orientations, and energies.

The highly irregular and flexible structure of water around ions is in line with the flexibility of hydrogen bonds in crystalline hydrates (25, 26). Such irregular structure has also been postulated by Vaslow (27) on the basis of theoretical calculations, and by Brady and co-worker (28, 29) on the basis of X-ray diffraction studies of aqueous solutions. A wide distribution of ion-water distances and orientations would render arbitrary the division of the ionic hydration "spheres" into definite concentric structural regions (30).

The addition of NaCl to water seems to decrease the incidence of very strong hydrogen bonds (shown by a decrease of the intensity of ν_3 below about 3350 cm^{-1}) *and* of very weak hydrogen bonds (shown by a decrease of intensity of ν_3 above 3600 cm^{-1}), while increasing the incidence of intermediate hydrogen bonds, with maximal increase for those corresponding to the ν_3 frequency near 3450 cm^{-1}. This leads to an upward shift of the peak frequency at low temperatures, a downward shift at higher temperatures, and a narrowing of the band at all temperatures. It should be stressed that the effect of NaCl on the spectrum of water does *not* correspond to the effect of changing the temperature, showing that the concept of "structural temperature" for ionic solutions, introduced by Bernal and Fowler (31), is not strictly applicable.

The present conclusions on the structure of concentrated solutions of NaCl are similar to those recently reached by Wall and Hornig (32) on the basis of their Raman study of solutions of the halides of potassium and of some divalent and trivalent metals. The i.r. technique offers much better resolution and higher signal-to-noise ratio. Our findings for NaCl solutions therefore complement and confirm those of Wall and Hornig.

We are indebted to Mr. Ping Seto for technical help in the measurements and computations.

1. R. D. Waldron. J. Chem. Phys. **26**, 809 (1957).
2. E. L. van P. van Eck, H. Mendel, and J. Fahrenfort. Proc. Roy. Soc. (London), Ser. A, 247, 472 (1958).
3. J. G. Bayly, V. B. Kartha, and W. H. Stevens. Infrared Phys. **3**, 211 (1963).
4. C. A. Swenson. Spectrochim. Acta, **21**, 987 (1965).
5. K. A. Hartman. J. Phys. Chem. **70**, 270 (1966).
6. M. Falk and T. A. Ford. Can. J. Chem. **14**, 1699 (1966).
7. E. U. Franck and K. Roth. Discuss. Faraday Soc. **43**, 108 (1967).
8. I. Kirshenbaum. Physical properties and analysis of heavy water. McGraw-Hill, New York, 1951. p. 54.
9. Handbook of chemistry and physics. 39th edition. Chemical Rubber Publishing Company, Cleveland, 1957. p. 1994.
10. R. Schrader and K. Wirtz. Z. Naturforsch. Pt. A, 6, 220 (1951).
11. R. N. Jones, K. S. Seshadri, N. B. W. Jonathan, and J. W. Hopkins. Can. J. Chem. **41**, 750 (1963).
12. R. N. Jones, K. S. Seshadri, and J. W. Hopkins. Can. J. Chem. **40**, 334 (1962).
13. K. S. Seshadri and R. N. Jones. Spectrochim. Acta, **19**, 1013 (1963).
14. T. T. Wall and D. F. Hornig. J. Chem. Phys. **43**, 2079 (1965).
15. G. E. Walrafen. J. Chem. Phys. **48**, 244 (1968).
16. G. E. Walrafen. *In* Hydrogen-bonded systems. *Edited by* A. K. Covington. Taylor and Francis Ltd., London, 1968. p. 9.
17. H. J. Bernstein. Personal communication, to be published, 1969.
18. J. A. Pople. Proc. Roy. Soc. (London), Ser. A, 205, 163 (1951).
19. G. C. Pimentel and A. L. McClellan. The hydrogen bond. Freeman and Co., San Francisco, 1960. p. 88 and 102.
20. W. Luck. Discuss. Faraday Soc. **43**, 133 (1967).
21. W. Luck and W. Ditter. J. Mol. Struct. **1**, 339 (1967–68).
22. O. Ya. Samoilov. Structure of aqueous electrolyte solutions and the hydration of ions. *Translated by* D. J. G. Ives. Consultants Bureau, New York, 1965. pp. 144–148.
23. J. Schiffer. Ph.D. Thesis, Princeton University, N.J. 1963.
24. T. A. Ford and M. Falk. J. Mol. Struct. **3**, 445 (1969).
25. W. H. Baur. Acta Cryst. **19**, 909 (1965).
26. W. C. Hamilton. *In* Structural chemistry and molecular biology. *Edited by* A. Rich and N. Davidson. W. H. Freeman, San Francisco, 1968. p. 466.
27. F. Vaslow. J. Phys. Chem. **67**, 2773 (1963).
28. G. W. Brady and J. T. Krause. J. Chem. Phys. **27**, 304 (1957).
29. G. W. Brady. J. Chem. Phys. **28**, 464 (1958).
30. H. S. Frank and W. Y. Wen. Discuss. Faraday Soc. **24**, 133 (1957).
31. J. D. Bernal and R. H. Fowler. J. Chem. Phys. **1**, 515 (1933).
32. T. T. Wall and D. F. Hornig. J. Chem. Phys. **47**, 784 (1967).

Can. J. Chem. Downloaded from www.nrcresearchpress.com by 210.87.254.40 on 09/05/12
For personal use only.

Can. J. Chem. Downloaded from www.nrcresearchpress.com by 210.87.254.40 on 09/05/12
For personal use only.

Homolytic decomposition of di-*sec*-butyl peroxide[1]

R. HIATT AND SANDOR SZILAGYI[2]
Department of Chemistry, Brock University, St. Catharines, Ontario

Received August 19, 1969

Rates and products have been determined for the thermal decomposition of *sec*-butyl peroxide at 110–150 °C in several solvents.

The decomposition was shown to be unimolecular with energies of activation in toluene, benzene, and cyclohexane of 35.5 ± 1.0, 33.2 ± 1.0, 33.8 ± 1.0 kcal/mole respectively. The activation energy of thermal decomposition for the deuterated peroxide was found to be 37.2 + 1.0 kcal/mole in toluene.

About 70–80% of the products could be explained by known reactions of free alkoxy radicals, and very little, if any, disproportionation of two *sec*-butoxy radicals in the solvent cage could be detected.

The other 20–30% of the peroxide yielded H_2 and methyl ethyl ketone. The yield of H_2 was unaffected by the nature or the viscosity of the solvent, but H_2 was not formed when *s*-Bu_2O_2 was photolyzed in toluene at 35 °C nor when the peroxide was thermally decomposed in the gas phase.

α,α′-Dideutero-*sec*-butyl peroxide was prepared and decomposed in toluene at 110–150 °C. The yield of D_2 was about the same as the yield of H_2 from *s*-Bu_2O_2, but the rate of decomposition (at 135 °C) was only $^1/_{1.55}$ as fast.

Mechanisms for hydrogen production are discussed, but none satisfactorily explains all the evidence.

Canadian Journal of Chemistry, **48**, 615 (1970)

Introduction

The decomposition of dialkyl peroxides has received less attention than that of other peroxidic species, partly, because being rather more stable, they have been less utilized for commercial purposes (i.e., initiation of free radical chain reactions); partly, because being less easily reduced, they are harder to analyze quantitatively. But perhaps too, because dialkyl peroxides have the reputation of being "well behaved" they have been regarded as uninteresting species. Dialkyl peroxides are commonly supposed to cleave on heating at the O—O bond by an exclusively homolytic process, relatively uncomplicated by other types of decomposition either radical or molecular in nature.

[1] $$\mathrm{ROOR} \rightarrow 2\ \mathrm{RO}\cdot$$

Yet most of the evidence for this belief is based on the studies of one member of the series, *tert*-butyl peroxide. Some recent evidence (1, 2) has indicated that decomposition of di-secondary alkyl peroxides might be more complex. Thus while Pryor and co-workers (1) found that *sec*-butyl peroxide initiated the polymerization of styrene at the same rate that *tert*-butyl peroxide did, Hiatt *et al.* (2), showed that the former underwent thermal decomposition about four times as fast as the latter. Moreover it was found (2*b*) that molecular hydrogen formed a significant fraction of the products from the thermal decomposition of *s*-Bu_2O_2.

Apart from the novelty of intensive study on a nontertiary peroxide, this project has been concerned with the mechanism of hydrogen formation and with the behavior of two secondary alkoxy radicals generated in a solvent cage.

The reaction of alkoxy radicals with each other has considerable implications for hydrocarbon autoxidation, a free radical chain reaction of which the termination step is generally written

[2] $$2\ \mathrm{RO_2}\cdot \rightarrow \text{non-radical products.}$$

Studies on the induced decomposition of hydroperoxides (3), the formation of O^{16}–O^{18} from autoxidation in the presence of $O_2{}^{16}$–$O_2{}^{18}$ mixtures (4), and the formation of tetroxides (5) have shown that when "R" is tertiary, the reaction proceeds as follows:

[3] $$2\ \mathrm{RO_2}\cdot \rightarrow \mathrm{ROOOOR}$$

[4] $$\mathrm{ROOOOR} \rightarrow 2\ \mathrm{RO}\cdot + \mathrm{O_2}$$

[5] $$2\ \mathrm{RO}\cdot \longrightarrow \begin{matrix}\mathrm{ROOR} \\ \mathrm{RO}\cdot + \mathrm{RO}\cdot\end{matrix}$$

The last reaction indicates the two possibilities open to *tert*-alkoxy radicals generated in close proximity, i.e., within a "solvent cage", either to react with each other by coupling or to diffuse apart and initiate new radical chains. Since the radical–radical coupling is usually assumed to be collision-controlled ($E_a = 0$), diffusion apart controls the number of alkoxy radicals which

[1]This work is taken, in part, from the M.Sc. thesis of S. Szilagyi.

[2]NRCC Predoctoral Scholarship holder, 1968–1969. Present address: Department of Chemistry, University of British Columbia, Vancouver, British Columbia.

Can. J. Chem. Downloaded from www.nrcresearchpress.com by 210.87.254.40 on 09/05/12
For personal use only.

become free. For *tert*-butoxy in benzene, about 90% diffuse apart at 30 °C and greater than 95% at 100 °C, in rough correlation with solvent viscosity (3).

For secondary peroxy radicals, the situation is much less clear. Studies of induced decomposition of secondary hydroperoxides have indicated that interaction of two secondary peroxy radicals at 45 °C in benzene always leads to nonradical products; yet at 100 °C and above, there seems to be some chain character to the induced decomposition (2*c*).

Two explanations seem possible: (*i*) the tetroxide may decompose in a manner first advanced by Russell (6), not available to the tertiaries (eq. [6]); (*ii*) two *sec*-alkoxy radicals generated in a solvent cage might undergo facile disproportionation (eq. [7]). The ease of this reaction should be shown by the study of the decomposition of di-*sec*-alkylperoxides.

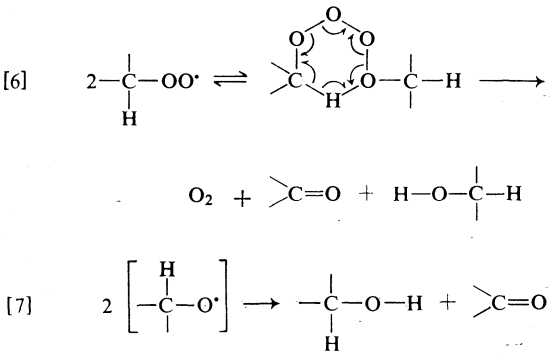

The formation of H_2 has been frequently noted in the decomposition of peroxy hemiacetals (7, 8, 9, 10, 11), and a concerted mechanism involving a cyclic transition state proposed (eq. [8]). However, the applicability of this reaction for dialkyl peroxides has not been established.

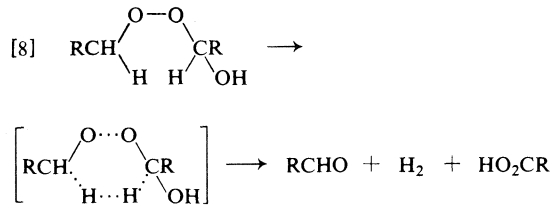

The following study of decomposition of *sec*-butyl peroxide has been made possible by development of gas–liquid chromatography (g.l.c.) techniques for peroxide analysis.

Experimental

1. Materials

Di-*sec*-butyl peroxide was prepared from *sec*-butyl methane sulfanate by the method of Welch *et al.* (12). The 11–12% yields of crude peroxide (distilling at 58–62°/0.5 mm Hg) were not appreciably improved by using the modification of Pryor and co-workers (1*c*). Two successive redistillations gave peroxide containing no impurities detectable by infrared (i.r.), nuclear magnetic resonance (n.m.r.), or g.l.c. analysis.

α,α′-Dideutero-di-*sec*-butyl peroxide was obtained in the same manner uisng 2-butanol-2-*d* prepared by the reduction of 2-butanone with $LiAlD_4$ (Merck, Sharp and Dohme, 99% isotopic purity). Analysis of this peroxide by n.m.r. showed it to contain 1.6 ± 0.1% of

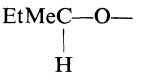

Assuming a statistical distribution of H and D on the α-carbons, the peroxide was calculated to be a mixture of ~96.7% dideutero, ~3.2% of monodeutero and no more than 0.025% of non-deuterated material.

Solvents for the peroxide decompositions were either reagent or "chromatograde", fractionally redistilled through a 3 ft spinning band column to reduce impurities to the point where they no longer interfered with the g.l.c. analyses of products.

sec-Butyl peroxydicarbonate was donated by the Lucidol Division of the Wallace and Tiernan Corporation. It titrated 97+% and was used without further purification.

2. Procedures

For measurements of the rate of thermal decomposition a set of 8–10 pyrex ampoules was filled with peroxide solution, degassed, sealed under vacuum, placed in a constant temperature bath, and withdrawn at suitable intervals for analysis of residual peroxide.

The contents of these ampoules also served for preliminary product studies, but for analyses of evolved gases and more precise determinations of liquid and solid products, 20–30 ml of a peroxide solution was degassed and sealed in 100 ml flask equipped with a break-seal. After heating for a time equivalent to at least 10 half-lives, the bulb was cooled and opened on a calibrated vacuum line.

Photolyses of peroxide solutions were carried out in an apparatus modelled on that described by Kieffer and Traylor (13) in which ampoules are placed in a rotating frame surrounding a mercury arc lamp. In all, the solutions were shielded from the source by 3 approximately 1 mm thicknesses of pyrex. Without this protection, 2-butanone, (a product of the decomposition) also underwent photolysis.

3. Analyses

Most of the analyses were performed by g.l.c. using an F & M model 700 chromatograph equipped with a disc integrator. Most satisfactory for *s*-Bu_2O_2 analysis was of 1/8″ × 6′ stainless steel "Hi-Pak" column supplied prepacked with silicone rubber Se-30 by the F & M Company. At a column temperature of 70 °C, injection port, 35–40 °C, and helium flowrate of 44 ml/min, the peroxide was eluted undecomposed in 6.0 min. Under

TABLE 1
Rate constants for the thermal decomposition of s-Bu_2O_2

Solvent	$[s\text{-}Bu_2O_2]_0$	Temperature °C	10^3 k, min^{-1}	E_a kcal
Toluene	0.302	110	0.536	
	0.149	110	0.560	
	0.302	120	1.77	
	0.149	120	1.79	
	0.216	130	3.48	
	0.122	130	3.47	35.5±1.0
	0.0160	130	3.70	
	0.358	135	9.30	
	0.0820	140	14.7	
	0.149	150	45.6	
	0.121	150	46.2	
Benzene	0.110	115	0.72	
	0.245	135	6.5	33.2±1.0
	0.117	140	14.5	
	0.123	150	40.4	
Cyclohexane	0.088	115	0.505	
	0.163	135	4.70	33.8±1.0
	0.099	150	30.8	

these conditions retention times for other compounds were as follows: cyclohexane, 1.6 min; benzene, 2.0 min; toluene, 3.0 min. Unfortunately, this column did not separate 2-butanol from 2-butanone.

The liquid products of decomposition were analyzed on a 6 ft × 1/4″ copper column packed with 20% Ethofat on chromosorb W. s-Bu_2O_2 could be eluted undecomposed from this column as well, but its retention time coincided with that of toluene.

A third column which did not decompose the peroxide and which did separate *all* the liquid components was 6′ × 1/4″ copper packed with 15% Ethofat plus 15% di-isodecyl phthalate on chromosorb W. Because of the high loading, however, elution times were inordinately long, and the peak for s-Bu_2O_2, especially, was too flat at low concentrations to permit accurate integration.

For solid components, a 6′ × 1/4″ copper column packed with Apriezon N on chromosorb P was used.

Gaseous products were analyzed on the following columns: hydrogen, activated charcoal; methane and carbon monoxide, molecular sieve 13X; ethane, de-activated silica gel; butane, 20% squalane on chromosorb W.

With the helium carrier gas, the hydrogen peak areas did not increase linearly with concentration, and it was necessary to plot calibration curves.

For all g.l.c. determinations, results were taken as the average obtained from three separate injections. Deviations from the average value were typically ± 3–5%.

Determination of deuterium content in the products of decomposition of the deuterated peroxide was performed mass spectrophotometrically by West Coast Technical Services.

sec-Butyl peroxydicarbonate was analyzed by iodometric titration.

Results

1. *Rates of Decomposition of sec-Butyl Peroxide*

First order rate constants, obtained from the linear plots of log $[s\text{-}Bu_2O_2]$ vs. t (time), for the thermal decomposition of s-Bu_2O_2 in toluene, benzene, and cyclohexane at 110–150° are shown in Table 1. Plots of log $[P_\infty - P_t]$ vs. t (where P refers to any one of the major products: acetaldehyde, *sec*-butanol, 2-butanone, or bibenzyl) were also linear and had slopes agreeing closely with those obtained from log $[s\text{-}Bu_2O_2]$ vs. t plots. The rate constants, though subject to some scatter, particularly at low initial concentrations of peroxide, did not vary in any systematic way with $[s\text{-}Bu_2O_2]_0$, thus suggesting that radical induced decomposition of the peroxide was not a serious factor.

As a further check that the peroxide was not being attacked by radicals of the type produced by its decomposition, toluene solutions containing 0.1228 M s-Bu_2O_2 and 0.0394 M *sec*-butyl peroxydicarbonate were heated at 80 °C for 4 h and at 100 °C for 3 h. This treatment completely decomposed the peroxydicarbonate but the concentration of s-Bu_2O_2 was not changed. (The peroxydicarbonate was shown to give freeradical type products when thermally decomposed alone in toluene but did not *yield* any s-Bu_2O_2 (see below)).

As shown in Table 1, rates and activation energies for thermal decomposition were very nearly the same in the three solvents.

2. *Rates of Decomposition of α,α′-Dideutero-sec-butyl Peroxide*

α,α′-Dideutero-*sec*-butyl peroxide was prepared by first reducing butanone with $LiAlD_4$ to yield 2-deutero-2-butanol. The dialkyl peroxide

Can. J. Chem. Downloaded from www.nrcresearchpress.com by 210.87.254.40 on 09/05/12
For personal use only.

TABLE 2

Rate constants for the thermal decomposition of α,α′-dideutero-*sec*-butyl peroxide in toluene

$[s\text{-}Bu_2O_2\text{-}d_2]_0$	Temperature °C	$10^3\ k_1\ min^{-1}$	E_a kcal
0.350	110	0.304	
0.210	135	6.10	37.2±1
0.210	150	29.5	

resulted from the treatment of the alcohol methanesulfonate with H_2O_2 (see Experimental).

The deuterated peroxide was decomposed in toluene at 110, 135, and 150 °C. The first order rate constants are shown in Table 2. Values for k_H/k_D (here defined as the rate constant for the non-deuterated species divided by that for the deutero compound) were respectively 1.83, 1.53, and 1.56 at the 3 temperatures. The activation energy of decomposition in toluene was found to be 37.2 kcal/mole.

3. *Products of Decomposition of sec-Butyl Peroxide in the Liquid Phase*

3.1. *Decompositions in Toluene, Benzene, and Cyclohexane*

Both gaseous and liquid products of the thermal decomposition were analyzed by g.l.c. Preliminary results were obtained by analysis of the contents of the ampoules used for rate studies but more precise measurements were obtained by decomposing larger samples in 100 ml bulbs (heated for a time equal to at least 10 half-lives). Analysis of the rate study samples showed that the nature of the products did not change, either qualitatively or quantitatively[3] during the course of reaction, so that the products after complete decomposition could be considered valid.

Most work was done on the products of decomposition in toluene. These, as shown in Table 3, were *sec*-BuOH, acetaldehyde, methyl ethyl ketone, bibenzyl, methane, ethane, and carbon monoxide.

Analysis of methane and ethane were hampered by the solubility of these gases in the liquid phase. The yield of ethane seems particularly low (see Discussion). More accurate results could have been obtained, no doubt, with further work, but it was felt that these were less relevant to the main argument than other information.

Butane (not shown in Table 3) was found in trace amounts and another relatively small unidentified peak on the gas chromatogram was tentatively ascribed to alkylated biphenyls. Xylenes were not formed, nor apparently were any other substances not tabulated or mentioned here.

Those products of decomposition in benzene and in cyclohexane which could be measured accurately are shown in Tables 4 and 5. Biphenyl was formed when $s\text{-}Bu_2O_2$ was decomposed in benzene, but was not readily determined quantitatively since it appeared in the tail of the toluene peak in g.l.c. analyses. Decompositions in cyclohexane produced several materials (appearing

[3]This was only approximately true for acetaldehyde, a small fraction of which underwent radical attack yielding CH_4 + CO.

TABLE 3

Products of the decomposition of *sec*-butyl peroxide in toluene at 110–150 °C

Temperature °C	Concentration*	H_2† (%)	CH_4‡ (%)	CO‡ (%)	C_2H_6‡ (%)	Acetaldehyde‡ (%)	Methyl ethyl ketone‡ (%)	*sec*-Butanol‡ (%)	Bibenzyl† (%)
110	0.1860	29.5	4.2	5.6	8.8	22.0	42.0	31.6	33.4
120	0.1754	24.7	4.8	6.4	7.8	30.7	35.7	30.7	34.2
130	0.1754	22.9	5.9	7.8	9.5	27.9	33.6	29.1	35.2
140	0.1754	21.1	6.7	8.7	11.6	36.5	32.0	27.6	36.0
150	0.1754	19.9	6.6	8.3	13.1	38.6	29.0	26.1	38.2

*Initial concentration of $s\text{-}Bu_2O_2$ mole/l.
†% yield based on decomposed peroxide, assuming 1 mole peroxide gives 1 mole of product.
‡% yield based on decomposed peroxide, assuming 1 mole peroxide gives 2 moles of product.

Can. J. Chem. Downloaded from www.nrcresearchpress.com by 210.87.254.40 on 09/05/12
For personal use only.

Can. J. Chem. Downloaded from www.nrcresearchpress.com by 210.87.254.40 on 09/05/12
For personal use only.

TABLE 4

Products of the decomposition of *sec*-butyl peroxide in benzene at 130–150 °C

Temperature (°C)	Concentration* (mole/l)	H_2† (%)	CH_4‡ (%)	CO‡ (%)	C_2H_6‡ (%)	Acetaldehyde‡ (%)	Methyl ethyl ketone‡ (%)	*sec*-Butanol‡ (%)	Toluene‡ (%)	Ethyl benzene‡ (%)
130	0.2521	28.2	9.8	17.6	—	29.7	31.5	19.1	3.6	0.99
145	0.2521	19.8	10.3	20.3	—	41.0	29.7	17.9	4.2	0.96
150	0.2521	18.4	14.9	23.2	13.7	34.3	25.9	15.9	4.2	1.0

*Initial concentration of *s*-Bu_2O_2 mole/l.
†% yield based on decomposed peroxide, assuming 1 mole peroxide gives 1 mole of product.
‡% yield based on decomposed peroxide, assuming 1 mole peroxide gives 2 moles of product.

TABLE 5

Products of the decomposition of *sec*-butyl peroxide in cyclohexane at 140 and 150 °C

Temperature (°C)	Concentration* (mole/l)	Acetaldehyde† (%)	Methyl ethyl ketone† (%)	*sec*-Butanol† (%)
140	0.1709	2.5	22.3	52
150	0.1709	4.5	19.9	47

*Initial concentration of *s*-Bu_2O_2 in mole/l.
†% yield based on decomposed peroxide assuming 1 mole peroxide gives 2 moles product.

as peaks in g.l.c. analyses) which were not identified. Hydrogen, methane, carbon monoxide, and ethane were products in amounts which seemed roughly comparable to yields in other solvents, but were not analyzed quantitatively.

3.2. Decompositions in Mineral Oil

A 0.1974 *M* solution of *sec*-butyl peroxide in mineral oil was heated at 130 °C for about 4 days (complete decomposition). The analysis of the gas phase showed yields of 22.5% H_2, 6.8% CH_4, and 7.5% CO, based on decomposed peroxide.

3.3. Decompositions of α,α'-Dideutero-sec-butyl Peroxide in Toluene

Gaseous products and the amount of $PhCH_2D$ formed in the decomposition of the deuterated peroxide were analyzed mass-spectrographically by West Coast Technical Service (Table 6). Bibenzyl was analyzed by g.l.c. The other products were not analyzed quantitatively, but appeared not to differ qualitatively from those from non-deuterated peroxide.

3.4. Photolytic Decompositions of sec-Butyl Peroxide

Solutions of *s*-Bu_2O_2 in toluene were photolyzed by irradiation with an AH-3 mercury vapor lamp, (temperature, 35 °C), following the method used by Kieffer and Traylor (13) for the photolysis of *t*-Bu_2O_2. A possible complication was found to obscure interpretation of the products in that methyl ethyl ketone could be readily photolyzed under these conditions. Insertion of 3 approximately 1 mm layers of pyrex glass (including the lamp jacket) appeared to minimize this complication; i.e., photolysis of solutions of methyl ethyl ketone in toluene under these conditions gave no products involving solvent.

As a further precaution, photolyses were carried to only a small fraction of total peroxide decomposition.

The products of photolysis, shown in Table 7, consisted of methyl ethyl ketone, *s*-BuOH, acetaldehyde, and bibenzyl.

No gaseous products were detected even when 30 ml of 0.2 *M* solution of *sec*-butyl peroxide in toluene was photolyzed for 5 h, (90% decomposition of *s*-Bu_2O_2).

While the yield of bibenzyl seems to be easily interpretable (see Discussion) the difference in acetaldehyde yields is puzzling.

TABLE 6

Products from thermal decomposition of 5.08 mmole of dideutero-*sec*-butyl peroxide in 20 g of toluene at 130 °C

Product*	mmole	(%)
D_2	.943	19.9†
HD	.066	
CH_4	.256	2.6‡
CH_3D	.0183	
C_2H_6	1.26	12.9‡
C_2H_5D	.048	
$PhCH_2D$	1.56	39.1†
$(PhCH_2)_2$		

*Analysis of gaseous products and $PhCH_2D$ by West Coast Technical Service.
†% yield based on 1 mole peroxide gives 1 mole product.
‡% yield based on 1 mole peroxide gives 2 moles product.

4. Products of Decomposition of sec-Butyl Peroxide in the Gas Phase

An ampoule containing 0.11296 g of *s*-Bu_2O_2 was broken inside an evacuated 500 ml bulb and heated at 130 °C for 4 days. (At this temperature all the peroxide appeared to be in the gas phase.) Gas analysis showed a bare trace of hydrogen estimated to be no more than 0.03% (based on decomposed peroxide). Yields of CH_4 and CO were 0.3 and 0.4% respectively.

The vapors of 0.28064 g toluene and 0.17944 g *s*-Bu_2O_2 were decomposed in identical manner. Again a bare trace of hydrogen was produced together with 0.7 of CH_4 and 1.1% of CO.

No attempts were made to detect or determine the other products of decomposition.

Can. J. Chem. Downloaded from www.nrcresearchpress.com by 210.87.254.40 on 09/05/12
For personal use only.

TABLE 7

Products of photolytic decomposition of *sec*-Bu_2O_2

	Run 1	Run 2
Concentration of *s*-Bu_2O_2 ($t = 0$) [*M*]	0.192	0.1105
($t = \infty$) [*M*]		
Concentration of *s*-Bu_2O_2	0.123	0.0445
Decomposed *s*-Bu_2O_2 [*M*]	0.069	0.0660
Acetaldehyde* (%)	10	17.1
Methyl ethyl ketone* (%)	22.6	26.0
sec-Butanol* (%)	74.0	53.0
Bibenzyl† (%)	42.0	33.5

*% yield based on 1 mole peroxide gives 2 moles product.
†% yield based on 1 mole peroxide gives 1 mole product.

TABLE 8

Products of decomposition of *sec*-butyl peroxydicarbonate in toluene

Temperature (°C)	Concentration* ($\times 10^{-2}$ *M*)	Acetaldehyde† (%)	Methyl ethyl ketone† (%)	*sec*-Butanol† (%)	*s*-Bu_2O_2‡ (%)	Bibenzyl‡ (%)
35	6.10	0	5.8	87.5	0	72.0
46	7.83	Trace	14.3	85.4	0	65.4
110	7.83	1.7	10.8	78.5	0	54.0

*Initial peroxydicarbonate concentration.
†% yield based on 1 mole peroxide gives 2 moles product.
‡% yield based on 1 mole peroxide gives 1 mole product.

5. Decomposition of Di-sec-butyl Peroxydicarbonate

Since the photolysis of *s*-Bu_2O_2 gave less certain results than had been expected, several thermal decompositions of di-*sec*-butyl peroxydicarbonate were carried out in the hope that these would demonstrate the behavior of *sec*-butoxy radicals at room temperature. (Table 8).

Its decomposition in toluene gave rather high yields of bibenzyl, but no hydrogen or other gases apart from CO_2, and no *s*-Bu_2O_2. Among the decomposition products were 3 unidentified compounds, but their concentrations were very small.

Discussion

1. Induced Decomposition of s-Bu_2O_2

The thermal decomposition of *t*-Bu_2O_2 appears uncomplicated by radical-induced decomposition (14), and chain transfer experiments in polymerizing styrene (1) have shown that *s*-Bu_2O_2 is no more readily attacked by free radicals than *t*-Bu_2O_2 is. However, radical-induced decomposition has been suggested to explain why *s*-Bu_2O_2 decomposes about 7 times as fast in solution as in the gas phase (where initial peroxide concentrations were much lower) (2*b*).

The fact that thermal decomposition of *s*-Bu_2O_2 in solution shows true first-order kinetics is not sufficient to rule out induced decomposition (2*e*), but the additional evidence reported here is fairly convincing. Most important is the imperviousness of the peroxide to radicals produced from decomposition of *sec*-butyl peroxydicarbonate. But it may be noted as well that the products of decomposition include substantial amounts of solvent dimer (Table 3) and that the rate of decomposition in alkane solvents is the same as in benzene or toluene.[4] A more precise evaluation of the rate of decomposition in the vapor phase is needed, but the reaction in solution, if indeed much faster, cannot be attributed to induced decomposition. Published E_a's and *A* factors for thermal decomposition of other dialkyl peroxides in the vapor phase agree quite well with those for *s*-Bu_2O_2 in solution (Table 9, Table 1).

2. The Mechanism of Hydrogen Formation

Formation of molecular hydrogen from the thermal decomposition of α-hydroxy peroxides

[4]For hydroperoxides at least, alkane solvents promote the radical-induced reaction and give much faster decomposition rates (2*e*).

Can. J. Chem. Downloaded from www.nrcresearchpress.com by 210.87.254.40 on 09/05/12
For personal use only.

TABLE 9

Rate parameters for thermal decomposition of dialkyl peroxides in the vapor phase

Peroxide	E_a kcal/mole	A s^{-1}	Reference
Me_2O_2	36.9	4.1×10^{15}	15
Me_2O_2	35.2±2.5	1.6×10^{15}	16
Pr_2O_2	36.5	2.5×10^{15}	17
t-Bu_2O_2	36.0	4.0×10^{14}	18
t-Bu_2O_2	39.1	3.2×10^{16}	19
t-Bu_2O_2	37.4±0.5	2.5×10^{16}	20

[9] $RO_2H + R'CHO \longrightarrow RO_2CHR'(OH) \rightarrow RCHO + R'CO_2H + H_2$ + other products

is well documented. First detected by Blank and Finkenbeiner (8) in the reaction of hydrogen peroxide with formaldehyde in basic solution, the generation of hydrogen was traced to the bis(hydroxymethyl) peroxide intermediate and later shown to be general for peroxy hemiacetals (eq. [9]) (7, 9–11). Pyrolysis of solid bis(hydroxymethyl) peroxide yields 60–85% of H_2 (21); a 40–60% yield is obtained from thermal decomposition of n-BuO_2CHPr(OH) in α-methylstyrene solution (10). Vapor phase decomposition of bis(hydroxymethyl) peroxide produces only 1–4% of H_2 however, (11*a*).

A concerted mechanism involving a cyclic 6-membered ring transition state (eq. [10]), originally proposed by Wieland and Wingler (21) has gained general acceptance as a result of a series of elegant papers by Durham and coworkers (7, 10) on the thermal decomposition of primary alkyl hydroperoxides. As would be expected for such a mechanism, very low A factors were obtained, consistent with a sterically constrained transition state; replacement of the relevant hydrogens by deuterium resulted in the production of D_2 with a kinetic isotope effect of 3.2–3.9 (10*b*).

[10] 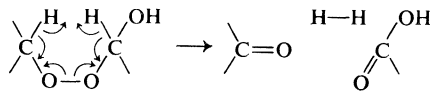

At the outset we expected that hydrogen generation in the decomposition of s-Bu_2O_2 would exhibit the same characteristics; it did not.

Treating the decomposition as the sum of two separate reactions; $k_d = k_H$ (hydrogen formation) + k_r (O—O homolysis to radicals), and combining the data of Tables 1 and 3, we obtain:

$$k_H = 10^{12}e^{-31.0/RT}$$

$$k_r = 10^{15}e^{-35.2/RT}$$

While hydrogen formation thus does exhibit a lower activation energy than the homolysis reaction and the A factor is lower by 10^3, this is barely below the range of "normal" A factors for unimolecular reactions and not very convincing for severe constraint in the transition state.

α,α′-Dideuterated peroxide decomposed somewhat slower than the non-deuterated species, and did produce D_2 (together with a little H—D consistent with the small percentage of monodeuterated impurity present (Experimental)). But the yield of D_2 (+HD) differed little from the H_2 yield from the non-deuterated compound. Again treating the system as two separate reactions, eq. [11], at 135 °C in toluene, $k_{r(H)} = 7.32 \times 10^{-3}$ min^{-1}, $k_{H(H)} = 1.95 \times 10^{-3}$ min^{-1}, $k_{r(D)} = 5.95 \times 10^{-3}$ min^{-1}, and $k_{H(D)} = 1.16 \times 10^{-3}$ min^{-1}, (where (H) and (D) refer to the non-deuterated and deuterated species respectively).

[11] s-$Bu_2O_2 \xrightarrow{k_H} H_2 + 2\ EtC(=O)Me$; s-$Bu_2O_2 \xrightarrow{k_r} 2\ s$-$BuO\cdot$

If k_r refers to simple homolysis, its isotope rate effect can be termed "secondary" and if k_H is a

Can. J. Chem. Downloaded from www.nrcresearchpress.com by 210.87.254.40 on 09/05/12
For personal use only.

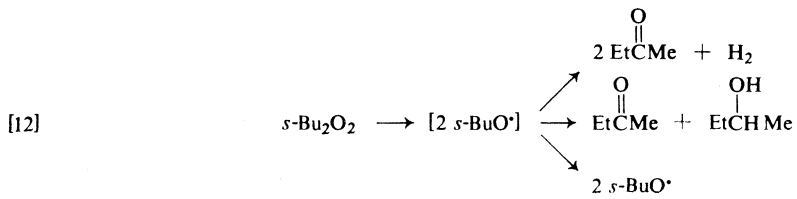

[12] $s\text{-}Bu_2O_2 \longrightarrow [2\ s\text{-}BuO\cdot] \longrightarrow 2\ EtC(=O)Me + H_2$; $[2\ s\text{-}BuO\cdot] \longrightarrow EtC(=O)Me + EtCH(OH)Me$; $[2\ s\text{-}BuO\cdot] \longrightarrow 2\ s\text{-}BuO\cdot$

concerted molecular reaction, the effect would be "primary". Thus the secondary isotope effect is 1.47 and the primary 1.68. While it is difficult to say what these effects *should* be, the "secondary" effect seems rather high[5] and the primary effect, quite low.

A more critical appraisal of the results of Mosher and Durham (10) in the light of these findings leads to a heightened appreciation of these authors' own reservations. The "first-order" rate constants for overall decomposition, and for H_2 evolution (and H_2 yields) vary considerably with changes of initial concentration of peroxy hemiacetal. It seems quite possible that even at low concentrations, the decomposition was not unimolecular, thereby making *A* factors calculated on an assumed first-order reaction highly questionable. The determination of deuterium isotope rate effects was complicated by not having isotopically pure compounds. While the assumptions necessitated, *re* composition of the mixture, in order to calculate k_H/k_D values seem reasonable, the relative amounts of H_2, HD, and D_2 actually produced did not agree with the k_H/k_D ratios so obtained, as Durham and Mosher themselves point out (10*b*).

In short, it appears that kinetic isotope effects and *A* factors for decomposition (insofar as these have been measured) do not give convincing support for a cyclic concerted mechanism, nor do they disprove it.

The strongest evidence against the cyclic mechanism is the drastic diminution of hydrogen yield when the peroxides are decomposed in the vapor phase.[6] Conceivably solvents could stabilize *cis* conformation of the peroxide, supposing that the vapor conformation was skew, an explanation that, while it would also rationalize the normal *A* factors, doesn't seem very plausible.

A much more obvious possibility is that the hydrogen is formed in a solvent cage after the initial O—O homolysis (eq. [12]). However, this is not tenable in the light of other evidence: (*i*) increasing the solvent viscosity substantially by using mineral oil instead of toluene or benzene produced no increase in H_2 yield; (*ii*) photolyses of *s*-Bu_2O_2 at 35°, which presumably at some stage produces two *s*-BuO. radicals in a solvent cage,[7] gave no H_2. Furthermore, for such a mechanism, the decomposition rate differences between deuterated and non-deuterated peroxide would be entirely secondary effects on O—O

[5]Secondary deuterium isotope rate effects for radical reactions can be cited for comparison:

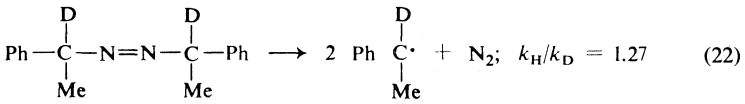

$Ph(D)(Me)C{-}N{=}N{-}C(D)(Me)Ph \longrightarrow 2\ Ph(D)(Me)C\cdot + N_2;\ k_H/k_D = 1.27$ (22)

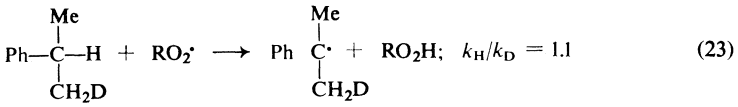

$Ph(Me)(H)C{-}CH_2D + RO_2\cdot \longrightarrow Ph(Me)C\cdot{-}CH_2D + RO_2H;\ k_H/k_D = 1.1$ (23)

[6]The H_2 yield may in fact be zero. Neither our own experiments with *s*-Bu_2O_2 nor those of Jenkins and Style (11*a*) with $(HOCH_2{-}O{-})_2$ were so sophisticated as to rule out a small amount of decomposition of liquid or solid peroxide on the reaction chamber walls. Unfortunately Durham and Mosher did not extend their work to vapor phase studies.

[7]We cannot be sure whether these photolyses were direct or sensitized by solvent and/or products such as 2-butanone, nor how nearly comparable these results are to a thermal reaction. Yields of cage products from thermal decompositions not infrequently differ from photolysis yields (25*a*, *b*) and the latter may differ from one sensitizer to another (25*b*, *c*, *d*). However, the differences are qualitative rather than absolute. For this reason we feel that our photolytic results do support the conclusion that hydrogen formation is not preceded by O—O homolysis.

Can. J. Chem. Downloaded from www.nrcresearchpress.com by 210.87.254.40 on 09/05/12
For personal use only.

cleavage.[8] The measured rate ratios, $k_{d(H)}/k_{d(H)}$, of 1.83, 1.55, and 1.56 at 110, 135, and 150 °C respectively, appear much too large for solely secondary effects.

A third alternative, suggested by the vapor phase results, is a polar, or perhaps even ionic, transition state leading to H_2 formation. To check this, *s*-Bu_2O_2 was decomposed at 140° in acetonitrile. The result, a yield of hydrogen the same as that obtained with toluene or benzene as solvents, dampened further speculation along this line.

Thus, in the end, our results seem to have disqualified all the available mechanisms, possibly excepting the concerted cyclic pathway if modified by as yet untested conformational effects.

3. Products from the sec-Butoxy Radicals. Escape from the Solvent Cage

Assuming that the reaction

[13] $$s\text{-}Bu_2O_2 \rightarrow H_2 + 2\ EtC(=O)Me$$

is at least a separate and distinct pathway for the decomposition, attention can be focussed on the other products. These, which account for about 80% of the thermal decomposition at 150°, 70% at 110°, and 100% for the photolytic decomposition at 35 °C, can be ascribed to *sec*-butoxy radicals with fair confidence since induced decomposition of the peroxide was negligible.

The alkoxy radicals would be initially formed within a solvent cage and could do any of three things: (*i*) diffuse apart and out of the cage; (*ii*) disproportionate to butanone plus 2-butanol within the cage; (*iii*) recombine to *s*-Bu_2O_2. (No estimation of *s*-Bu_2O_2 formed by recombination is possible from this work; it being indistinguishable from unreacted starting material).

[14] $$s\text{-}Bu_2O_2 \rightleftharpoons [2\ s\text{-}BuO\cdot] \rightarrow EtC(=O)Me + s\text{-}BuOH$$
$$[2\ s\text{-}BuO\cdot] \rightarrow 2\ s\text{-}BuO\cdot$$

A measure of the percent of *s*-BuO· escaping from the cage is the amount of solvent dimer formed, supposing the following reactions to be efficient.

[15] $$s\text{-}BuO\cdot + SH \rightarrow S\cdot + s\text{-}BuOH$$

[16] $$2\ S\cdot \rightarrow S{-}S$$

(where SH is solvent)

Thermal decomposition of *t*-Bu_2O_2 in toluene at 100 °C has been shown to yield 100% of the theoretical amount of bibenzyl (2*b*), and bibenzyl yield has been used to estimate the numbers of free radicals formed from thermal decomposition of hydroperoxides in toluene solution (2*e*, 24).

In other circumstances, however, the bibenzyl yield has been less than quantitative; thermal decomposition of *t*-Bu_2O_2 in toluene at 150 °C and above gives gradually decreasing bibenzyl yields as the temperature is varied (2*e*). We have found that pyrolyses of di-*t*-butyl peroxalate in toluene at 45–60° produces only ~ 80% of the expected amount of bibenzyl (26). Similar pyrolyses of *sec*-butyl peroxydicarbonate (Table 8) give low bibenzyl yields. Nevertheless, the yield of bibenzyl must represent a *lower limit* for the numbers of radicals escaping the cage.

In Table 10 the bibenzyl yield from decompositions of *s*-Bu_2O_2 in toluene is given as a percentage of the peroxide decomposing by the radical route, showing that nearly half (at least) of the *s*-BuO· radicals escape from the solvent cage. No more than half of the *s*-BuO· radicals then, disproportionate to butanone + butanol in the cage.

Other considerations, however, suggest that this is a gross exaggeration of cage disproportionation. Another method of computation which gives much smaller numbers is to assume that all the butanone is formed either in the cage or by the non-radical route (giving H_2). The fifth column of Table 10 has been calculated on this basis: cage disproportion = (MEK yield − H_2 yield) × 2 (to include the equivalent amount of *s*-BuOH formed). The values thus obtained decrease gradually with increasing temperature,

[8]This is not necessarily so if there is a competition,
$$s\text{-}Bu_2O_2 \rightleftharpoons [2\ s\text{-}BuO\cdot] \rightarrow 2\ MEK + H_2$$
However, if the observed isotope rate effects derived from this, the yield of H_2 should be substantially greater than the D_2 yield, which was not the case.

Can. J. Chem. Downloaded from www.nrcresearchpress.com by 210.87.254.40 on 09/05/12
For personal use only.

TABLE 10
Estimations of disproportion of *sec*-butoxy radicals in the solvent cage from products of thermal decomposition in toluene

Temperature (°C)	*s*-Bu_2O_2-H_2 yield (%)	Bibenzyl yield* (%)	Difference (%)	Cage disproportion† (%)
110	70.5	33.4	37.1	25.0
120	75.3	34.2	41.1	22.0
130	77.1	35.2	41.9	21.4
140	78.9	36.0	42.9	21.8
150	80.1	38.2	41.9	18.2
35	100.0	33–42	67–58	52.4–45.4

*Based on total peroxide decomposed, assuming 1 mole peroxide gives 1 mole bibenzyl.

†Calculated from yields of butanone; cage disproportion = 2[% Et C(=O) Me − % H_2]; values from Table 3.

paralleling the decrease in solvent viscosity, in a fashion similar to that measured for cage recombinations of 2 *t*-BuO·'s (2*b*, 27). They looked quite good in fact, until analysis of the products from decomposition of deuterated peroxide in toluene indicated that some butanone was formed by radical–radical reactions *outside* the cage.

As shown in Table 6, decomposition of 5.08 mmole of dideutero-*sec*-butyl peroxide in toluene produced 1.56 mmole of $PhCH_2D$. This could not have come from attack of benzyl radicals on the peroxide, since induced decomposition is negligible. Some probably resulted from benzyl radical abstracting from CH_3CDO, but the results (taking into account also the small amounts of CH_3D and C_2H_5D formed) indicate that about 1.3 mmoles must have arisen in some other way. The only other way that seems possible[9] is disproportionation between benzyl radicals and *sec*-butoxy radicals.

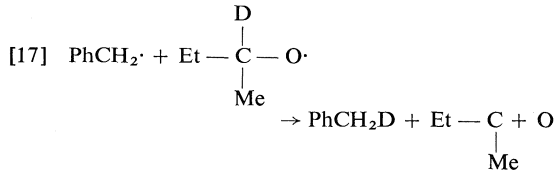

[17] $PhCH_2\cdot + Et-\underset{\displaystyle Me}{\overset{\displaystyle D}{\underset{|}{\overset{|}{C}}}}-O\cdot \rightarrow PhCH_2D + Et-\underset{\displaystyle Me}{\underset{|}{C}}+O$

Unfortunately the yield of MEK was not measured in this experiment. If it had been the same as for non-deuterated peroxide, there would have been 3.08 mmoles. About 2.02 mmoles of this would have been formed by the part of the decomposition leading to D_2 + 2 MEK, leaving 1.06 mmoles to be accounted for as a product of *sec*-butoxy radicals.

It has been suggested above that all of this arose via cage interactions of 2 *s*-BuO·. But it now appears that *more* than this amount can be accounted for from non-cage interactions of benzyl and *s*-BuO·.

These calculations are admittedly crude, but show, as a very real possibility, no cage disproportionation of *sec*-butoxy radicals to butanone plus *sec*-butyl alcohol at all. This is an uncomfortable conclusion and a little difficult to swallow in view of well established proclivities for alkyl–alkyl (25*a*, 29) and alkyl–alkoxy (30*a*) radical pairs to disproportionate as well as combine. We make it not as a pronouncement but as a spur to further research, there being, so far as we can tell, no unambiguous demonstration that disproportionation between two alkoxy radicals occurs with any degree of facility. The disproportionation/combination ratios quoted by Gray *et al.* (30*a*) for ethoxy (12/1) and methoxy (9.3/1) (31) are based on the assumption that two alkyl peroxy radicals initially yield two alkoxy radicals plus O_2. The one thing demonstrated conclusively by our work is that this supposition is untrue for other than tertiary peroxy radicals.

A referee has suggested De Sousa's work with dibenzyl hyponitrite (32) to be sufficient proof for cage disproportionation of alkoxy radicals. True enough, the virtually constant 50% yield of benzaldehyde over a 200-fold range of initial concentrations of hyponitrite in cyclohexane is impressive; the strong implication is that *all* the benzyloxy radical pairs disproportionate (32*b*). But a year later (32*c*) De Sousa blithely destroys

[9]The possibility that benzyl radicals attack the product, 2-deutero-2-butanol was considered but thought unlikely since the peroxide itself is not attacked. Russell and Brown (28) found that benzyl radicals would not even abstract deuterium from α-deuterotoluene.

Can. J. Chem. Downloaded from www.nrcresearchpress.com by 210.87.254.40 on 09/05/12
For personal use only.

TABLE 11
Yields of *s*-BuOH and acetaldehyde from *s*-BuO

Temperature (°C)	*s*-BuOH*		AcH§	AcH/*s*-BuOH*	
	a†	b‡		a†	b‡
110	19.1	31.6	27.6	1.44	0.87
120	19.7	30.7	37.1	1.88	1.21
130	18.4	29.1	35.8	1.94	1.23
140	16.7	27.6	44.3	2.65	1.60
150	17.0	26.1	47.0	2.76	1.80

*% yield of *s*-BuOH from decomposition of *s*-Bu_2O_2 in toluene.
†Neglecting *s*-BuOH assumed to result from cage reaction.
‡Total *s*-BuOH.
§Including that found as CH_4 + CO.

his argument, nonchalantly mentioning that decomposition of dibenzyl hyponitrite in toluene produces a "good" yield of bibenzyl. Unfortunately he does not divulge just how good the yield was.

4. Cleavage of sec-Butoxy Radicals and Subsequent Reactions

Consideration of the products of decomposition (Tables 3, 4, and 5) together with the preceding discussion suggests the following pattern for *s*-BuO· radicals which have escaped the solvent cage.

[18] *s*-BuO· + SH (solvent) → *s*-BuOH + S·

[19] *s*-BuO· → Et· + AcH

[20] *s*-BuO· + S· → SH + Et C(=O) Me

[21] AcH + R· (any radical) → Ac· + RH

[22] Ac· → Me· + CO

[23] Me· (Et·) + SH → S· + MeH (EtH)

The nearly equal yields of CH_4 and CO in all the analyses make acetaldehyde seem a reasonable precursor. *sec*-Butoxy radicals could also be a source of Me·, of course, but no trace of propionaldehyde was found, indicating that *s*-BuO· cleavage was solely to acetaldehyde and ethyl radicals.

The acetaldehyde vs. *s*-BuOH yields in toluene at different temperatures (Table 3) permit an estimation of the difference in activation energies for the competing cleavage and hydrogen abstraction reaction.

$$[24] \quad \frac{[\text{AcH}]}{[s\text{-BuOH}]} = \frac{k_1[s\text{-BuO}\cdot]}{k_2[\text{PhCH}_3][s\text{-BuO}\cdot]} = \frac{A_1}{A_2[\text{PhCH}_3]} - \frac{(E_2 - E_1)}{RT}$$

where AcH represents acetaldehyde, and k_1 and k_2 the rate constants for scission and abstraction, respectively.

$$[25] \quad \ln \frac{[\text{AcH}]}{[s\text{-BuOH}]} = \ln \frac{A_1}{A_2[\text{PhCH}_3]} + \frac{E_2 - E_1}{RT}$$

Plotting log [AcH]/[*s*-BuOH] vs. $1/T$ should give a straight line with slope equal to $(E_2 - E_1)/_{2.303\,R}$.

Acetaldehyde/*s*-BuOH ratios were calculated on two bases, (Table 11), (*a*) that all *s*-BuOH came from non-cage reaction of *s*-BuO·, (*b*) that some *s*-BuOH did come from cage reactions (as calculated for column 5, Table 10) and therefore should be subtracted from total *s*-BuOH.

Plots of log ([AcH]/[*s*-BuOH]) calculated on either basis vs. $1/T$ were linear and both gave $E_2 - E_1 = 5.2 - 5.4$ kcal. The value is considerably smaller than that measured for *t*-BuO· (11.3 kcal) (30*b*) but is comparable to the activation energy difference (6–7 kcal) for cleavage of *i*-PrO· vs. its abstraction from ethyl isobutyrate (30*b*).

5. The Fate of Ethyl and Methyl Radicals

Most methyl and ethyl radicals produced in toluene solution abstracted hydrogen from toluene, though as shown by the products from deuterated peroxide (Table 6) some attack on

AcD or Et C(O·) D Me

occurred. No xylenes or ethyl toluenes were produced, nor were any products of benzyl radical coupling with methyl or ethyl.

The poor product balances for methyl and particularly for ethyl seem largely associated with experimental difficulties in determining

Can. J. Chem. Downloaded from www.nrcresearchpress.com by 210.87.254.40 on 09/05/12
For personal use only.

methane and ethane, respectively. Decompositions in benzene produced both toluene and ethyl benzene but toluene accounted for less than half of the methyl radicals and ethyl benzene for less than 1/30 of the ethyls not found as methane or ethane, respectively.

We wish to acknowledge the financial support of the National Research Council of Canada under which this work was carried out, and further to express our appreciation to Dr. J. M. Miller and Mr. J. Fogelman for their assistance in the n.m.r. analyses, and to the Lucidol Division of Wallace & Tiernan Inc., for donation of peroxide samples.

Appreciation is also due to a number of former colleagues at Stanford Research Institute for helpful comments and discussion.

1. (*a*) W. A. PRYOR, A. LEE, and C. E. WITT. J. Amer. Chem. Soc. **86**, 4229 (1964); (*b*) W. A. PRYOR and G. E. L. KAPLAN. J. Amer. Chem. Soc. **86**, 4234 (1964); (*c*) W. A. PRYOR, D. M. HUSTON, T. R. FISKE, T. L. PICKERING, and E. CIUFFARIN. J. Amer. Chem. Soc. **86**, 4237 (1964).
2. (*a*) R. HIATT, T. MILL, and F. R. MAYO. J. Org. Chem. **33**, 1416 (1968); (*b*) R. HIATT, T. MILL, K. C. IRWIN, and F. K. CASTLEMAN. J. Org. Chem. **33**, 1421 (1968); (*c*) R. HIATT, T. MILL, K. C. IRWIN, and F. K. CASTLEMAN. J. Org. Chem. **33**, 1428 (1968); (*d*) R. HIATT, K. C. IRWIN, and C. W. GOULD. J. Org. Chem. **33**, 1430 (1968); (*e*) R. HIATT and K. C. IRWIN. J. Org. Chem. **33**, 1436 (1968).
3. (*a*) R. HIATT, J. CLIPSHAM, and T. VISSER. Can. J. Chem. **42**, 2754 (1964); (*b*) D. B. DENNY and J. D. ROSEN. Tetrahedron, **20**, 1137 (1962); (*c*) A. FACTOR, C. A. RUSSELL, and T. G. TRAYLOR. J. Amer. Chem. Soc. **87**, 3692 (1965).
4. P. D. BARTLETT and T. G. TRAYLOR. J. Amer. Chem. Soc. **85**, 2405, 2411 (1963).
5. P. D. BARTLETT and G. GUARALDI. J. Amer. Chem. Soc. **89**, 4799 (1967).
6. G. A. RUSSELL. J. Amer. Chem. Soc. **79**, 3871 (1957).
7. L. J. DURHAM, C. F. WURSTER, and H. S. MOSHER. J. Amer. Chem. Soc. **80**, 332 (1958).
8. O. BLANK and FINKENBEINER. Ber. **31**, 2979 (1898).
9. A. RIECHE and F. HITZ. Ber. **62**, 2458 (1929).
10. (*a*) L. J. DURHAM and H. S. MOSHER. J. Amer. Chem. Soc. **82**, 4537 (1960); (*b*) L. J. DURHAM and H. S. MOSHER. J. Amer. Chem. Soc. **84**, 2811 (1962).
11. (*a*) A. D. JENKINS and D. W. G. STYLE. J. Chem. Soc. 2337 (1953); (*b*) D. W. G. STYLE and D. SUMMERS. Trans. Faraday Soc. **42**, 338 (1946).
12. F. WELCH, H. R. WILLIAMS, and H. S. MOSHER. J. Amer. Chem. Soc. **77**, 551 (1955).
13. H. KIEFFER and T. G. TRAYLOR. J. Amer. Chem. Soc. **89**, 6667 (1967).
14. J. H. RALEY, F. F. RUST, and W. E. VAUGHAN. J. Amer. Chem. Soc. **70**, 1336 (1948).
15. Y. TAKEZAKI and C. TAKEUCHI. J. Chem. Phys. **22**, 1523 (1956).
16. P. L. HANST and J. G. CALVERT. J. Phys. Chem. **63**, 104 (1959).
17. E. J. HARRIS. Proc. Roy. Soc. **A173**, 176 (1939).
18. J. MURAWSKI, J. S. ROBERTS, and M. SZWARC. J. Chem. Phys. **19**, 698 (1951).
19. J. G. RALEY, F. F. RUST, and W. E. VAUGHAN. J. Amer. Chem. Soc. **70**, 88 (1948).
20. L. BATT and S. W. BENSON. J. Chem. Phys. **36**, 895 (1962).
21. H. WIELAND and A. WINGLER. Ann. **431**, 301 (1923).
22. S. SELTZER. J. Amer. Chem. Soc. **83**, 2625 (1961).
23. C. E. BOOZER, B. W. PONDER, J. C. TRISLER, and C. E. WIGHTMAN. J. Amer. Chem. Soc. **78**, 1506 (1956).
24. A. D. KIRK and J. H. KNOX. Trans. Faraday Soc. **56**, 1796 (1960).
25. (*a*) S. F. NELSON and P. D. BARTLETT. J. Amer. Chem. Soc. **88**, 143 (1966); (*b*) P. D. BARTLETT and N. A. PORTER. J. Amer. Chem. Soc. **90**, 5317 (1968); (*c*) P. D. BARTLETT and P. S. ENGEL. J. Amer. Chem. Soc. **90**, 2960 (1968); (*d*) J. R. Fox and G. S. HAMMOND. J. Amer. Chem. Soc. **86**, 4031 (1964).
26. Unpublished results in these laboratories.
27. R. HIATT and T. G. TRAYLOR. J. Amer. Chem. Soc. **87**, 3766 (1965).
28. G. A. RUSSELL and H. C. BROWN. J. Amer. Chem. Soc. **74**, 3995 (1952).
29. (*a*) W. A. PRYOR. Free radicals. McGraw-Hill, New York, 1966. p. 317; (*b*) W. E. MORGANROTH and J. G. CALVERT. J. Amer. Chem. Soc. **88**, 5387 (1966); (*c*) A. P. STEFANI. J. Amer. Chem. Soc. **90**, 1694 (1968).
30. (*a*) P. GRAY, R. SHAW, and J. C. J. THYNNE. Progress in reaction kinetics. Vol. 4. G. Porter, *Editor*, Pergamon Press, London, 1967. p. 88; (*b*) pp. 109–112.
31. J. HEICKLEN and H. S. JOHNSTON. J. Amer. Chem. Soc. **84**, 4030, 4394 (1962).
32. (*a*) J. B. DE SOUSA. Nature. **199**, 64 (1963); (*b*) S. K. HO and J. B. DE SOUSA. J. Chem. Soc. 1788 (1961); (*c*) S. NAIR and J. B. DE SOUSA. J. Chem. Soc. 4464 (1962).

Can. J. Chem. Downloaded from www.nrcresearchpress.com by 210.87.254.40 on 09/05/12
For personal use only.

Can. J. Chem. Downloaded from www.nrcresearchpress.com by 210.87.254.105 on 09/05/12
For personal use only.

Thermolysis of some 2,3-diazabicyclo[3.3.0]octene systems

MANFRED P. SCHNEIDER AND ROBERT J. CRAWFORD
Department of Chemistry, University of Alberta, Edmonton, Alberta

Received August 11, 1969

The kinetics and products of thermolysis of 2,3-diazabicyclo[3.3.0]oct-2-ene (**1**), 2,3-diazabicyclo-[3.3.0]octa-2,7-diene (**2**), and *exo*-4-methyl-2,3-diazabicyclo[3.3.0]octa-2,7-diene (**3**) are described and compared with previously studied pyrazolines. The secondary kinetic isotope effects of **1**-d_2 and **2**-d_2 have been measured. The synthesis and nuclear magnetic resonance spectra of these compounds and their thermolysis products are discussed.

Canadian Journal of Chemistry, **48**, 628 (1970)

Introduction

The thermolysis of simple alkyl-1-pyrazolines has been suggested to proceed via the formation of a trimethylene intermediate (1) having a 0,0 geometry (2). We wish to report further studies on the thermolysis of alkyl-1-pyrazolines in the gas phase, in particular a series of bicyclo azo compounds that do not readily achieve the desired 0,0 geometry. A comparison of products and kinetic parameters with previously studied pyrazolines is also reported.

Results and Discussion

The addition of diazomethane to cyclopentene produces 2,3-diazabicyclo[3.3.0]oct-2-ene (**1**) in good yield (3). Similarly the addition of diazomethane to cyclopentadiene produced 2,3-diazabicyclo[3.3.0]octa-2,7-diene (**2**). Preparation of diazomethane-d_2 and addition to cyclopentene and cyclopentadiene permitted the synthesis of **1**-d_2 and **2**-d_2. The nuclear magnetic resonance (n.m.r.) spectrum of the adduct **2** displayed a signal of integrated intensity corresponding to 3 protons in the vinyl proton region of the spectrum. The observation of a proton, other than the vinyl protons, at even lower field, δ 5.65, then the C-3 proton of 3-vinyl-1-pyrazoline at δ 4.80 (4*a*) rather than in the region of the tertiary proton on C-3 of *cis*, or *trans*-3,4-dimethyl-1-pyrazoline (δ 4.04 and 3.85 respectively) (4*b*) lead us to the assignment of structure **2** rather than **2***a* for the adduct of diazomethane to cyclopentadiene. This is the same mode of 1,3-dipolar addition as has been observed for diazomethane with 1,3-butadiene and 2,3-dimethyl-1,3-butadiene (**4***a*). The structure **2***a* would be expected to have only 2 protons at low field and to show protons at approximately δ 4.0. The *dideuterio* derivative **2**-d_2 gives rise to no signal in this region of the spectrum. These along with kinetic observations (see below) are compatible with **2** but not **2***a*.

The addition of diazoethane to cyclopentadiene produced, on purification, only the *exo*-4-methyl-2,3-diazabicyclo[3.3.0]octa-2,7-diene (**3**), with no evidence of the *endo* isomer. The methyl group was assigned the *exo* position on the basis of its 100 MHz n.m.r. spectrum (Table 1). The coupling constants between H-1, H-2, and H-3 in **2** serve to assist the assignment. The proton of the methylene group at C-3 that has the smaller coupling constant to H-3 was assigned to the position *trans* to H-1 (models indicate a dihedral angle of close to 90° for H-1 and H-3). The larger coupling of 8.8 Hz between H-2 and H-3 of **2** is not observed in **3**, and only the smaller coupling remains. On this basis, and on consideration of the importance of steric factors in 1,3-dipolar addition the methyl group is assigned to the *exo* configuration in **3**.

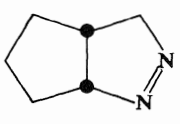

1

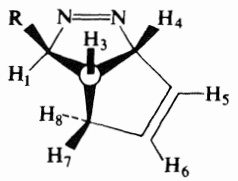

2 R = H_2–
3 R = CH_3–

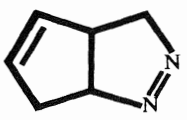

2*a*

Thermolysis of **3** at 200 Torr. and 145° produced two compounds **4** and **5** in 38 and 62% yields

TABLE 1

The 100 MHz n.m.r. spectrum of **2** and **3**

Proton	Chemical shift	Coupling constants (Hz)
	Compound **2**	
H-1	δ4.12	
		$J_{1,2} = 17.9$
H-2	4.59	
H-3	2.55	$J_{1,3} = 4.5$
H-4	5.65	$J_{1,4} = 2.2$
H-5	5.98	$J_{2,3} = 8.8$
H-6	5.68	
H-7	2.68	
H-8	2.07	
	Compound **3**	
H-1	τ4.22	
		$J_{1,3} = 4.9$
$-CH_3$	1.46	
H-3	2.63	$J_{1,4} = 2.3$
H-4	5.85	
H-5	6.03	
H-6	5.75	
H-7	2.24	
H-8	2.14	

respectively.[1] Compound **4** was assigned the *exo* structure and **5** the *endo* on the basis of their n.m.r. spectra (Table 2). Both isomers were observed to be stable under the reaction conditions. The coupling constant of the methinyl proton on C-6 to the other cyclopropyl hydrogens is 2.6 Hz for the *exo* compound **4** and 7.3 Hz for the *endo* isomer **5**. The thermolysis of **2** produced only **6** and **2**-d_2 produced **6**-d_2 having deuterium in the cyclopropyl methylene group. The assignments in Table 2 were assisted by the use of **2**-d_2 and **6**-d_2, and those assignments previously made by Corey and Dawson (5) and Meinwald and Mazzocchi (6).

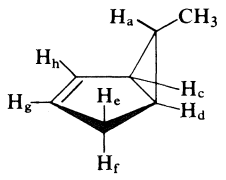

4

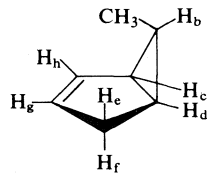

5

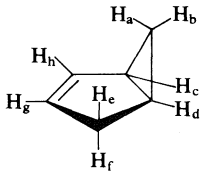

6

Kinetic data for the gas phase thermolysis of **1**, **2**, and **3** (at 100 to 200 Torr.) are recorded in Table 3. The deuterated compounds **1**-d_2 and **2**-d_2 used for the n.m.r. assignment are included as their kinetic isotope effects confirm those previously observed (4*a*) for 3-vinyl-1-pyrazoline and 1-pyrazoline (7). Seltzer has demonstrated that for the carbon–nitrogen bond undergoing cleavage in the rate-determining transition state that $\Delta\Delta G^{\ddagger}$ values of the magnitude of 80 to 110 cal mole^{-1} per deuterium are observed (8). The values of $\Delta\Delta G^{\ddagger}$ for **1**-d_2 and **2**-d_2 calculated using the expression $n\Delta\Delta G^{\ddagger} = -RT\ln k_H/k_D$, where n = the number of α-deuterium atoms, are 93

[1]Studies at 250° indicate that **4** and **5** are interconvertible, and that **4** is thermodynamically more stable than **5**, however conversions to other diene and bicyclic products prevent an exact measurement of stabilities from being determined.

TABLE 2

Coupling constants and chemical shifts for the products **4**, **5**, and **6**

Compound	Proton	Chemical shift (δ)	Proton	Chemical shift (δ)	Coupling constants (Hz)
6	H_a	−0.19	H_e	2.50	$J_{a,b} = 3.3$
	H_b	+0.74	H_f	2.25	$J_{a,c} = J_{a,d} = 4.1$
	H_c	1.70	H_g	5.88	$J_{b,c} = 7.0$
	H_d	1.50	H_h	5.28	$J_{b,d} = 7.8$ $J_{c,d} = 6.0$
4	H_a	0.23	H_c	2.50	$J_{a,c} = J_{a,d} = 2.6$
	CH_3	1.03	H_f		
	H_c	1.56	H_g	5.39	
	H_d	1.32	H_h	5.85	
5	CH_3	0.75	H_e	2.19	$J_{b,d} = J_{c,d} = J_{d,e} = 7.3$
	H_b	1.02	H_f	2.50	$J_{d,f} = 1.7$
	H_c	1.95	H_g	5.57 and 5.62	$J_{b,c} = 7.3$
	H_d	1.52	H_h		

Can. J. Chem. Downloaded from www.nrcresearchpress.com by 210.87.254.105 on 09/05/12
For personal use only.

TABLE 3
Kinetic parameters for thermolysis

Compound	Temperature (°C)	10^4 $k(s^{-1})$	
1	197.9±0.1	3.83±0.06	E_a = 38.5±0.5 kcal mole^{-1}
	210.6	11.6 ±0.2	log A = 14.45±0.3
	219.9	23.9 ±0.4	
			k_H/k_D = 1.21±0.04†
1-d_2	219.9	19.7 ±0.2	
2	136.2±0.1	3.90±0.06	E_a = 37.2±0.3 kcal mole^{-1}
	145.4	10.5 ±0.7	log A = 16.47±0.5
	155.9	31.4 ±0.5	
	160.0	48.5 ±0.6	
2-d_2	155.3	23.4 ±0.4	k_H/k_D = 1.23±0.04*†
3	145.4	35.7 ±0.8	

*Average of three runs 1.20, 1.26, and 1.20.
†Corrected for 5%-d_1

and 83 cal mole^{-1} respectively. These data along with the observation that **3** undergoes thermolysis 3.5 times faster than **2** indicates that both carbon–nitrogen bonds are breaking in the rate-determining transition state.

The products obtained from **1** were identified by their retention times on the gas chromatograph (g.c.) column and by their n.m.r. spectra on isolation. They are consistent with those expected from a trimethylene intermediate (1). The olefin yields, 32%, are larger in those cases wherein the migrating hydrogen atom is attached to a tertiary carbon. The failure of **2** and **3** to produce any detectable olefin is similar to that of 3-vinyl-1-pyrazoline. We consider the olefin forming process to be most definitive of the structure of the intermediate and the failure of **2** and **3** to produce olefins may in fact be due to alternative mechanisms. Roth and Martin (9) have recently suggested a radical displacement process which if applied to **3** would in fact predict the stereochemistry of the major product (Scheme 1). However, such a scheme is incapable of explaining the increase in the rate on going from **2** to **3** nor does it explain the decrease in rate on going from **2** to **2**-d_2. A concerted process of the type "$\sigma_s^2 + \sigma_a^2$" which is susceptible to a substituent effects in a manner analogous to homolytic cleavages is also capable of explaining the major products of thermolysis. A small decrease in the HC_5C_4 bond angle brings one very close to the appropriate geometry. Such being the case we would expect a conrotatory mode of ring closure to prevail (Scheme 2). An alternative route has recently been suggested by Allred and Smith (10) using trigonal radicals and is illustrated in Scheme 3. The initially formed trigonal center is inverted as a consequence of recoil associated with the breaking of the two CN bonds. The evidence presented is not such that one can discriminate between these two mechanisms.

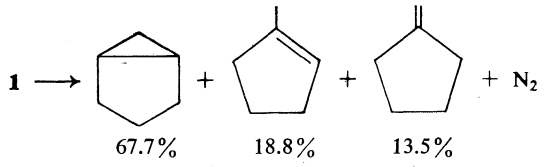

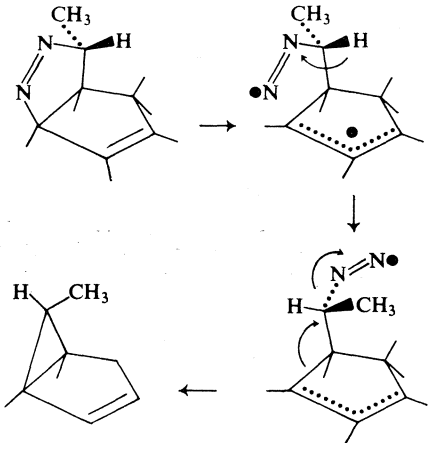

SCHEME 1

The activation energy for thermolysis of **2** is only 1.3 kcal mole^{-1} less than that of **1**, in contrast to the 8.8 kcal mole^{-1} decrease observed on

Can. J. Chem. Downloaded from www.nrcresearchpress.com by 210.87.254.105 on 09/05/12
For personal use only.

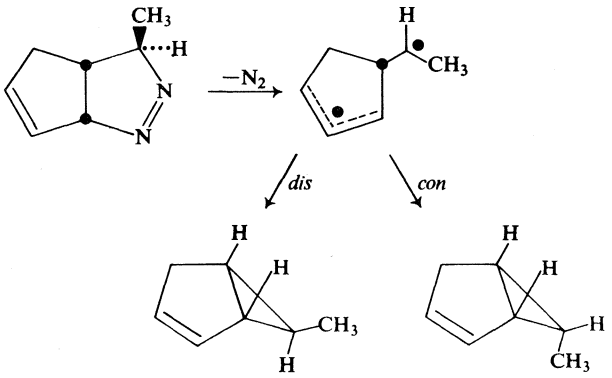

SCHEME 2

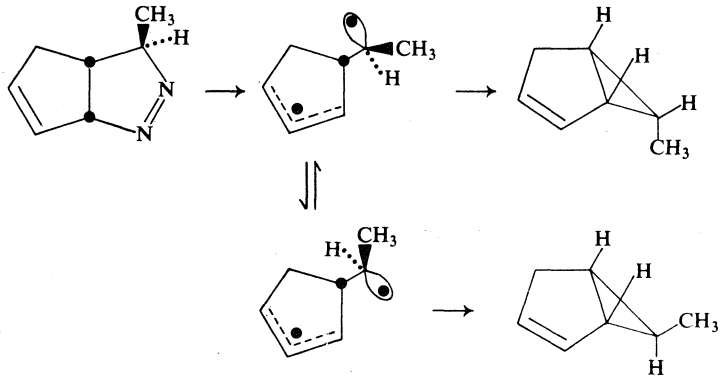

SCHEME 3

going from 3-methyl-1-pyrazoline (**7**) to 3-vinyl-1-pyrazoline (**8**). Table 4 contains a comparison of activation parameters for **1**, **2**, 3-methyl-1-pyrazoline, and 3-vinyl-1-pyrazoline. It is interesting to note the smaller log A value for **8** suggesting that the transition state involves a restriction of rotation about the C_3–vinyl bond. The change in free energy on going from **1** to **2** is similar to that found on going from **7** to **8**, however, this change is primarily in the activation energy for the last pair and mostly in the entropy, (or log A), term for the first pair, suggesting that considerably more bond breaking has to be achieved to reach the transition state for the bicyclic systems than for the simpler cyclic pair **7** and **8**.

TABLE 4

Comparison of saturated and vinyl-1-pyrazolines

Compound	log A	E_a (kcal mole^{-1})	k(s^{-1}) at 200 °C	$\Delta\Delta G^{\ddagger}$[a] (kcal mole^{-1})
1	14.24	39.7	6.17×10^{-4} [b]	
2	16.53	37.2	2.95×10^{-1}	−5.8
7	15.70[c]	41.0	5.02×10^{-4}	
8	14.50[d]	32.2	4.37×10^{-1} [b]	−6.6

a. Free energy change on going from saturated to the vinyl system.
b. Extrapolated from data at lower temperatures.
c. Reference 1.
d. Reference 4*a*.

Can. J. Chem. Downloaded from www.nrcresearchpress.com by 210.87.254.105 on 09/05/12
For personal use only.

Can. J. Chem. Downloaded from www.nrcresearchpress.com by 210.87.254.105 on 09/05/12
For personal use only.

Experimental

Preparation of 2,3-Diazabicyclo[3.3.0]octa-2,7-diene (2)

A concentrated ethereal solution of diazomethane was allowed to react, for 2 days, in a pressure bottle with a twofold excess of cyclopentadiene. The ether was removed under reduced pressure and the residue was distilled at 25 Torr., the whole fraction boiling up to 75° was collected. The separation of the dicyclopentadiene and **2** was achieved by chromatography on a Florisil column. The dicyclopentadiene was eluted with pentane after which **2** was eluted with ether. Vacuum distillation of the product gave a colorless liquid, b.p. 62° at 7 Torr., yield 45%, n_D^{27} 1.4993.

Anal. Calcd. for $C_6H_8N_2$: C, 66.64; H, 7.46; N, 25.91. Found: C, 66.49; H, 7.37; N, 26.43.

Ultraviolet (u.v.) absorption λ_{max} 323 mμ (ε 219, 95% C_2H_5OH), n.m.r. spectrum, see text.

2,3-Diazabicyclo[3.3.0]octa-2,7-diene-4,4-d_2 (2-d_2)

This was prepared in a manner analogous to that above only diazomethane-d_2 (11) was used. Thermolysis produced **6**-d_2 with all of its deuterium attached to C-7.

Preparation of exo-4-methyl-2,3-diazabicyclo[3.3.0]octa-2,7-diene (3)

An ethereal solution of diazoethane was allowed to react with cyclopentadiene in a manner analogous to that described above. Upon evaporation of the solvent the residue was chromatographed on Florisil, the dicyclopentadiene being eluted with pentane and the pyrazoline with ether. The product **3** was isolated by distillation at 6 Torr., b.p. 69°. Mass spectrum, parent peak calcd. for $C_7H_{10}N_2$: 122.0844. Found: 122.0845. The n.m.r. spectrum, see text.

Thermolysis of 1, 2, and 3 and Product Identification

A sample of **2** was placed in a pyrex break seal of approximately 18 ml volume, and heated for 10 half-lives at 160°. The break seal was then attached to a conventional vacuum system and the products distilled into a trap which was attached to g.c. system. The g.c. consisted of a 10 ft β,β′-oxydipropionitrile column, a Gow-Mac Model TR-11-B, thermal conductivity cell with a Gow-Mac Model 40-05C power supply in conjunction with a Sargent Model SR recorder. For larger samples a 250 ml break seal system was used and the product trapped in an ampoule. The various components were then separated using a Wilkens Autoprep and a 20 ft β,β′-oxydipropionitrile column. Thermolysis of **2** produced 98.5% of **6** and 0.5% of each of three minor products which were not identified. The products from the thermolysis of **1** and **3** are described in text.

The n.m.r. spectra were obtained on a Varian Associates HR-100. The mass spectra were obtained on an AEI MS-9.

Kinetic Measurements

The reactor system and procedures used have been described previously (1). The thermocouple used for the temperature measurements was a four-junction Chromel–Alumel type with an ice–water reference junction, and was calibrated against roll sulfur, tin (anal.), and lead (anal.).

Rates measured gave good first order plots to 90% completion, and the starting materials were not observed to isomerize under the reaction conditions.

The authors acknowledge support from the National Research Council of Canada and from the Petroleum Research Fund of the American Chemical Society.

1. R. J. Crawford and A. Mishra. J. Amer. Chem. Soc. **88**, 3963 (1966).
2. R. Hoffmann. J. Amer. Chem. Soc. **90**, 1475 (1968).
3. H. Paul, I. Lange, and A. Kausmann. Ber. **98**, 1789 (1965).
4. (*a*) R. J. Crawford and D. M. Cameron. Can. J. Chem. **45**, 691 (1967). (*b*) R. J. Crawford and L. Ali. J. Amer. Chem. Soc. **84**, 3908 (1967); L. Ali. M.Sc. Thesis. University of Alberta, Edmonton, Alberta. 1967.
5. E. J. Corey and R. L. Dawson. J. Amer. Chem. Soc. **85**, 1782 (1963).
6. J. Meinwald and P. H. Mazzocchi. J. Amer. Chem. Soc. **89**, 1755 (1967).
7. B. Al-Sader and R. J. Crawford. J. Amer. Chem. Soc. **46**, 3301 (1968).
8. S. Seltzer and S. G. Mylonakis. J. Amer. Chem. Soc. **89**, 6584 (1967); S. Seltzer and F. T. Dunne. J. Amer. Chem. Soc. **87**, 2628 (1965); S. Seltzer. J. Amer. Chem. Soc. **85**, 14 (1963).
9. W. R. Roth and M. Martin. Ann. **702**, 1 (1967).
10. E. L. Allred and R. L. Smith. J. Amer. Chem. Soc. **89**, 7133 (1967).
11. L. C. Leitch, P. E. Gagnon, and A. Cambron. Can. J. Res. **288**, 256 (1950).

Can. J. Chem. Downloaded from www.nrcresearchpress.com by 210.87.254.105 on 09/05/12
For personal use only.

Assignments of configuration by nuclear Overhauser effects in some dibenzthiepin derivatives

ROBERT R. FRASER AND FRANCIS J. SCHUBER
Department of Chemistry, University of Ottawa, Ottawa, Canada
Received September 2, 1969

The configuration of the benzylic protons responsible for each absorption in the nuclear magnetic resonance spectra of 1,11-dimethyl-5,7-dihydrodibenz(*c*,*e*)thiepin and its *S*-oxide and *S*-dioxide have been determined by nuclear Overhauser experiments. Successful application of the method was achieved by using partially deuterated derivatives for the purpose of removing undesirable relaxation mechanisms between protons. Triple irradiation of doublets was also usefully employed. The sulfoxide assignments arrived at herein reverse the tentative assignments put forth by us (1). It is noteworthy that all experiments on the sulfoxide failed when $CDCl_3$ was used as solvent. In DMSO normal nuclear Overhauser effects were seen, presumably since sulfoxide dimers are not formed in this solvent. The sulfonium perchlorate derivative of the thiepin was also synthesized. The remarkable similarity of its n.m.r. spectrum to that of the sulfoxide is interpreted as evidence that the effect of the sulfoxide group on the shifts of neighboring protons is due primarily to the "lone pair" on sulfur.

L'utilisation de l'effet Overhauser nucléaire a permis de déterminer la configuration des protons benzyliques dans la diméthyl-1,11 dihydro-5,7 dibenz(*c*,*e*)thiépine, aussi que dans le sulfoxyde et la sulfone dérivés. Les résultats obtenus pour le sulfoxyde inversent l'attribution de configuration précédemment publiée (1). Il est à noter que l'observation d'effets est liée à certaines conditions; (*a*) utilisation de composés partiellement deutériés afin d'éliminer des phénomènes de relaxation indésirables; (*b*) dans le cas du sulfoxyde les expériences ont été négatives dans $CDCl_3$ et positives dans DMSO-d_6, solvant dans lequel le sulfoxyde n'est vraisemblablement pas sous forme dimère. La triple irradiation de doublets a aussi été utilisée avec succès. Le perchlorate du méthyl sulfonium de la thiépine a été préparé. Son spectre de résonance magnétique nucléaire présente une grande analogie avec celui du sulfoxyde. Ceci tend a montrer que l'effet du sulfoxyde sur le déplacement chimique des protons adjacents est dû principalement au doublet libre du soufre.

Canadian Journal of Chemistry, **48**, 633 (1970)

We have recently determined the relative rates of base-catalyzed hydrogen–deuterium exchange of the diastereotopic protons in the *S*-oxide, **2** and *S*-dioxide **3** of 1,11-dimethyl-5,7-dihydrodibenz(*c*,*e*)thiepin (**1**) (1, 2). The three compounds are all conformationally frozen (3), a property which allows a correlation between the observed rates and configuration of the exchanging protons to be made. This paper describes the determination of configuration of each benzylic proton in **1**, **2**, and **3** by use of the nuclear Overhauser effect (n.O.e.) (4). Previously, in the rigid 7,12-dihydropleiadene system, n.O.e. experiments provided assignments of configuration to the benzylic protons therein (5). A second topic, that of the magnetically anisotropic shielding influence of a sulfoxide group, is discussed particularly with reference to the observed shifts in **1**, **2**, **3**, and in the derived sulfonium salt **4**.

Compounds **2**, **3**, and **4** were prepared from the thiepin **1** (3) by standard methods. The nuclear magnetic resonance (n.m.r.) spectra of compounds **1**–**4** were measured in deuterochloroform and in DMSO-d_6 (except for **4**). The chemical shifts in δ units and coupling constants in Hz were determined by exact analysis of the AB spectra and are presented in Table 1. The benzylic protons of each compound are numbered in order of their appearance from low to high field. See, for example the spectrum of **2**, (Fig. 1). Although the shifts will be discussed in detail later, the effect of changing solvent from $CDCl_3$ to DMSO-d_6 is seen to be very large for **1** and **3**, a result of considerable practical importance. This large shift separation between the benzylic protons in DMSO-d_6 allowed the n.O.e. studies to be easily carried out. It is interesting to note that in **3** the benzylic protons actually cross over from one solvent to the other. This was proven by a study of selectively deuterated **3** in both solvents.

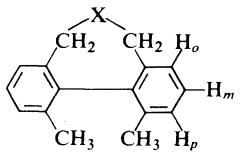

1 X = S
2 X = SO
3 X = SO_2
4 X = $\overset{+}{S}$—CH_3; ClO_4^-

TABLE 1
Nuclear magnetic resonance parameters for **1–4**

Compound	Solvent	Aromatic region*	Benzylic region*	CH_3 region*
1	$CDCl_3$	7.20 s	3.275 s	2.092 s
1 (H_m = D)	DMSO-d_6	7.246 and 7.200	H_1 = 3.410 $J_{1,2}$ = 12.4 H_2 = 3.016	2.022 s
2	$CDCl_3$	7.1–7.4 m	H_1 = 4.119 H_4 = 2.976 $J_{1,4}$ = 11.4 H_2 = 3.629 H_3 = 3.289 $J_{2,3}$ = 13.7	CH_{3_1} = 2.180 CH_{3_2} = 2.154
2 (H_m = D)	1% in† $CDCl_3$	H_o = 7.170, 7.230 H_p = 7.296, 7.346‡	Unchanged	CH_{3_1} = 2.170 CH_{3_2} = 2.150
2 (H_m = D)	DMSO-d_6	H_o = 7.11, 7.23 H_p = 7.26, 7.31	H_1 = 4.279 H_4 = 2.566 $J_{1,4}$ = 11.5 H_2 = 3.677 H_3 = 3.071 $J_{2,3}$ = 14.0	CH_{3_1} = 2.06 CH_{3_2} = 2.01
3	$CDCl_3$	7.340 s	H_1 = 3.943 H_2 = 3.857 $J_{1,2}$ = 13.3	2.155 s
3	DMSO-d_6	7.371 s	H_1 = 4.219 H_2 = 3.732 $J_{1,2}$ = 13.7	2.072 s
4 (H_m = D)	$CDCl_3$	7.374, 7.444 7.465, 7.489 Assignments unknown	H_1 = 4.842 H_4 = 3.172 $J_{1,4}$ = 11.6 H_2 = 4.371 H_3 = 3.822 $J_{2,3}$ = 14.5	CH_{3_1} = 2.146 CH_{3_2} = 2.127

*s = singlet; m = multiplet.
†Shifts did not change measurably compared with those of a 5% solution.
‡H_p assignments made from n.O.e. results.

Nuclear Overhauser Effects

It has been shown that enhancement of the signal intensity for a proton A occurs on irradiation of a proton B provided that the main relaxation mechanism for A is a direct dipole–dipole interaction with B (4). If this is the only mechanism a 50% enhancement (n.O.e.) will occur. Competing mechanisms for relaxation of A (other neighboring protons, solvent protons, oxygen, etc.) decrease this n.O.e. One method of removing undesired relaxation mechanisms is to replace the offending protons by deuterium atoms since the dipole–dipole contribution to T_1, the spin-lattice relaxation time, is given by $1/T_1^{AB} = \hbar^2\gamma_A^2\gamma_B^2\tau/d^6$ where γ_A represents the magnetogyric ratio of proton A, similarly γ_B for B, τ is the correlation time for random molecular motion and d is the internuclear distance between A and B. Thus a decrease in γ_B by deuterium substitution results in reduction of $1/T_1^{AB}$ to 1/42 its original value. The $1/d^6$ dependence of dipole–dipole relaxation is responsible for the fact that n.O.e.'s are not normally observed for protons separated by more than 3 Å (4, 6).

In compounds **1–3** one of each pair of diastereotopic protons (that with the *pro-S* configuration in the *R*-biphenyl) lies much closer to the *ortho* aromatic proton than the other, the distances measured from Dreiding models being 2.4 and 3.6 Å respectively. In these compounds it is obvious that the proton which gives the larger n.O.e. on irradiation of the *ortho* aromatic proton will have the *pro-S* configuration in the *R*-biphenyl.

A sample of **1** having deuterium in the *meta* positions of both rings was prepared to prevent

TABLE 2
Nuclear Overhauser effect results for **1** (H_m = D)

Proton irradiated	Nuclear Overhauser effect		
	H_1	H_2	H_o
H_o	8	−5	—
H_1*	—	60†	23
H_2*	40	—	−5

*Triple irradiation was performed by tuning an oscillator to each line of the doublet for H_1 (or H_2).
†A value of 47% was obtained on the same sample but using a different HA-100 by Dr. R. A. Bell and Mr. J. K. Saunders.

Can. J. Chem. Downloaded from www.nrcresearchpress.com by 210.87.254.105 on 09/05/12
For personal use only.

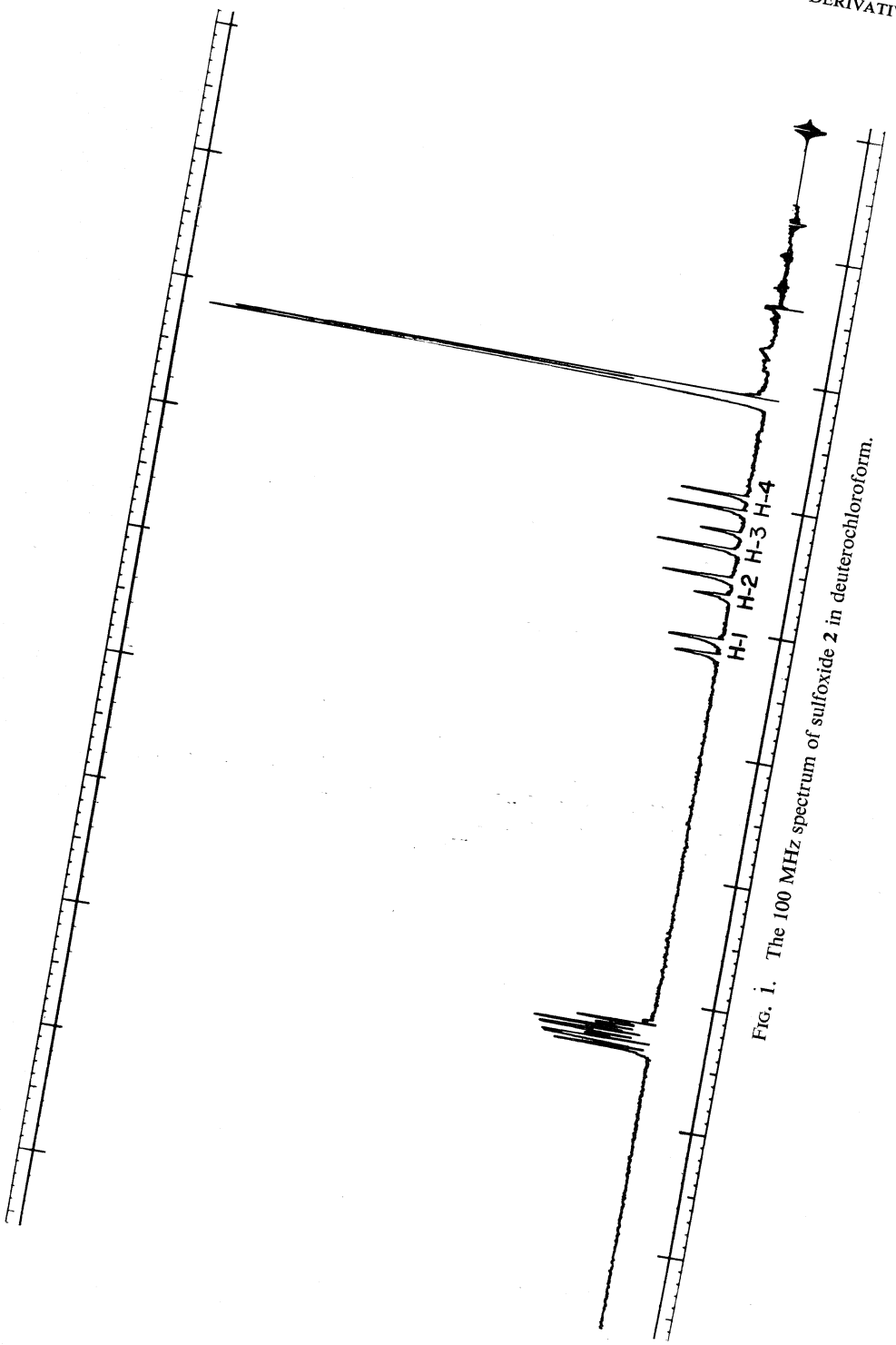

FIG. 1. The 100 MHz spectrum of sulfoxide **2** in deuterochloroform.

Can. J. Chem. Downloaded from www.nrcresearchpress.com by 210.87.254.105 on 09/05/12
For personal use only.

Can. J. Chem. Downloaded from www.nrcresearchpress.com by 210.87.254.105 on 09/05/12
For personal use only.

relaxation of the *ortho* protons by the *meta* protons. In addition it simplified the aromatic proton absorption into four singlets. This allowed irradiation of the *ortho* proton absorption to be performed. The results of n.O.e. experiments on **1** are given in Table 2. The observations are that there is a larger n.O.e. between H_o and H_1 than between H_2 and H_o both in experiments observing n.O.e.'s for H_o, and in observing n.O.e.'s for H_1 and H_2 on irradiation of H_o. We can conclude that H_1 is closer to H_o and therefore has the "*pro-S* in *R*" configuration. We wish to point out that this conclusion is confirmed by the n.O.e. results on **2** coupled with the chemical interrelation of **1** with **2**. The negative sign for the n.O.e. of H_2 on irradiation of H_o is not unusual and its origin has been discussed (7). The fact that the n.O.e. for H_1 on irradiation of H_o is smaller than that for H_o on irradiation of H_1 is a reflection of a dominating relaxation between H_1 and H_2. We determined the *geminal* n.O.e.'s between these protons and found them to be 40 and 60% for H_1 and H_2 respectively. Since the latter value exceeded the theoretical maximum of 50% and a similar value was also observed in experiments on **3**, we asked Dr. R. A. Bell and Mr. J. K. Saunders to check our results for **1** and **3** using their instrument. They found the *geminal* n.O.e.'s for H_2 in **1** and **3** to be 47 and 48% respectively. They obtained excellent agreement for all the other n.O.e.'s in Table 2 and for those for **3** (H_m = D) in Table 3. It would appear that we were using slightly too much r.f. power during triple irradiation, although this normally results in a decrease in the n.O.e. (4).

The n.O.e. experiments on the sulfone **3** were performed using three selectively deuterated samples. The results are recorded in Table 3. The

TABLE 3
Nuclear Overhauser effect results for **3**

Isotopic label	Proton irradiated	Nuclear Overhauser effect		
		H_1	H_2	H_o
H_m = D	H_o	10	−1	—
	H_1*	—	58†	21
	H_2*	30	—	0
H_1, H_m = D	H_o	—	6	—
	H_2	—	—	0
H_2 = D	H_o	0	—	—
	H_1	—	—	23

*Triple irradiation.
†A value of 48% was obtained by Bell and Saunders on the same sample but using a different HA-100.

observation of a 21 and a 23% n.O.e. for H_o when the low field benzylic absorption is irradiated establishes the "*pro-S* in *R*" configuration for H_1 (in a DMSO-d_6 solution of **3**). The smaller n.O.e. for H_1 on irradiation of H_o again reflects the strong interaction between the H_1 and H_2 dipoles. We were surprised to learn that we could not observe any n.O.e. for H_1 on irradiation of H_o in a sample in which H_m was not replaced by deuterium (in spite of the fact that H_2 was replaced by deuterium). We suspect that the failure to observe any n.O.e. is due to the near-degeneracy of all the aromatic protons. This would perhaps make it difficult to saturate H_o without overloading the spectrometer, or perhaps the tightly coupled 3-spin system acts to average the n.O.e.'s of all 3 protons.

The sulfoxide **2** possesses 4 magnetically non-equivalent benzylic protons, 2 non-equivalent methyl groups, and 6 non-equivalent aromatic protons, due to the presence of the pseudo-asymmetric sulfoxide group. The configurational assignments of all the benzylic protons can be achieved with the aid of the n.O.e. results in Table 4. A notable feature of the experiments on **2** (H_m = D) was the complete absence of an n.O.e. between H_1 or H_4 and the *ortho* aromatic protons, when deuterochloroform was used as solvent. Isolation of H_1 by replacing H_4 by deuterium and vice versa failed to produce any n.O.e. At this point the previously recognized tendency of sulfoxides towards dimerization was recalled (8) and a switch to DMSO-d_6 solvent produced the desired n.O.e.'s. The change in solvent also enhanced the n.O.e.'s observable in deuterochloroform. These results establish a *pro-S* configuration for H_1 and a *pro-R* configuration for H_4 in the *R*-biphenyl.

Chemical Interrelation of H_1 with H_2 in 2

The configurations of H_2 and H_3 have been established as *pro-S* and *pro-R* respectively in the *R*-biphenyl by a chemical inversion of the sulfoxide group in a sample of **2** containing deuteriums in place of H_2, H_3 and H_4. Treatment of this sulfoxide with Meerwein's reagent, then hydrolysis of the alkoxysulfonium salt yields a sulfoxide of inverted configuration (9). The n.m.r. of this sulfoxide in deuterochloroform showed a broad singlet at the position of H_2, and slight absorption for H_1 which is attributed to unreacted starting material.

TABLE 4
Nuclear Overhauser effect results for **2**

Isotopic label	Proton irradiated	Nuclear Overhauser effect*				
		H_o	H_1	H_4	H_p	$H_{p'}$
H_1H_m = D	H_o	—	—	5 (0)	—	—
	H_4	3	—	—	—	—
	CH_{3_1}	—	—	—	28	14
	CH_{3_2}	—	—	—	9	24
$H_2H_3H_4H_m$ = D	H_o	—	31 (0)	—	—	—
	H_1	33 (0)	—	—	—	—
H_m = D	H_1†	—	—	(28)	—	—
	H_4†	—	(24)	—	—	—
	CH_{3_1}	—	—	—	(10)	(16)
	CH_{3_2}	—	—	—	(11)	(10)

*Values in brackets were measured on solutions of **2** in deuterochloroform, others were measured in DMSO-d_6.
†Triple irradiation.

Stereochemical Assignments in Relation to the Sulfoxide Group

The last stereochemical assignment to be made concerns the orientation of each pair of *geminal* benzylic protons with respect to the adjacent sulfoxide group. A Dreiding model of **2** shows that one pair of *geminal* protons has the orientation present in axial thiane-*S*-oxide, the other that in equatorial thiane-*S*-oxide.[1] The alpha protons in equatorial thiane-*S*-oxide have been found to have the larger shift difference (0.87 p.p.m.) and smaller *geminal* coupling constant (11.7 Hz) in comparison with the axial conformer, (0.48 p.p.m. and 13.7 Hz respectively) (11). These effects of configuration at sulfur on both shifts and coupling constants have been confirmed by several other workers in related systems (12, 13). By using these correlations we can assign the wide-spaced AB quartet (J = 11.4 Hz) for H_1H_4 to the methylene group having the C—H_4 bond *trans* to the lone pair on sulfur as in equatorial thiane-*S*-oxide. The remaining AB pattern for H_2H_3 (J = 13.7 Hz) has the C—H_3 bond *trans* to the oxygen on sulfur. Figure 2 presents a 3-dimensional formula of **2** showing the completed assignments for H_1, H_2, H_3, and H_4.

These assignments *reverse* our earlier tentative assignments for the H_1H_4 and H_2H_3 pairs with respect to the adjacent aromatic rings (1). The change is of particular importance to the conclusions reached on the stabilities of *alpha*-sulfinyl carbanions. It was found that H_2 exchanged 1100 times as fast as H_1 and that H_4 exchanged 3 times as fast as H_3. Both observations are at odds with the theoretical predictions of Wolfe *et al.* (14) and the experimental work of Hutchinson *et al.* (15). We are currently studying the effects of solvent and structural changes on exchange rates in hopes of clarifying some of the existing differences.

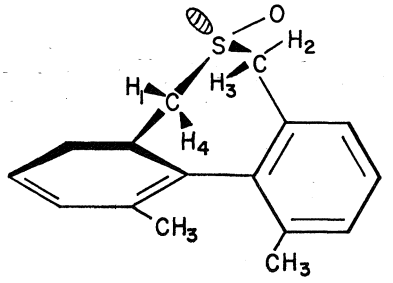

FIG. 2. A 3-dimensional formula of sulfoxide **2**.

Chemical Interrelations of Isotopically Labelled 1, 2, and 3

A sample of **2** containing 67% of deuterium label in place of H_2, H_3, and H_4 was reduced to **1** and a second sample oxidized to **3**. The n.m.r. spectra of both products in DMSO-d_6 showed absorptions for H_1 twice the intensity of that for H_2. These experiments show that the low field half of each AB spectrum in all 3 compounds is due to protons having the same configuration and thus provide confirmation of the internal consistency of the n.O.e. experiments.

[1]In the model of **2** there is a 15° deviation from the perfectly staggered arrangement, which is in the same direction as the slight but detectable deviation in thiane itself (10).

Can. J. Chem. Downloaded from www.nrcresearchpress.com by 210.87.254.105 on 09/05/12
For personal use only.

Can. J. Chem. Downloaded from www.nrcresearchpress.com by 210.87.254.105 on 09/05/12
For personal use only.

The Effect of a Sulfoxide Group on Chemical Shifts

In recent years, the influence of a sulfoxide group on the chemical shift of neighboring protons has been extensively studied. Early investigations proposed the anisotropy of the S—O bond to be similar either to that of the carbonyl group (16) or the acetylene group (17). More recently, closer examination by two sets of investigators (12, 18) has led each to propose that the group as a whole must be considered in any attempt to understand its magnetic anisotropic effect. The shifts observed for the conformationally rigid sulfoxide **2** reinforce this proposal. Furthermore, comparisons with the sulfonium salt, **4**, provide evidence that the dominant influence of the sulfoxide group is exerted not by the S—O bond but by the "*lone pair*" of electrons.

Two major influences of the sulfoxide group on chemical shifts are denoted by the data in Table 1. First, its introduction by conversion of one of the sulfide "lone pairs" into an S—O bond has caused the following changes in δ; $\Delta\delta_1 = +0.836$, $\Delta\delta_2 = +0.318$, $\Delta\delta_3 = +0.008$, $\Delta\delta_4 = -0.302$ p.p.m. The upfield shift of H_4 (which is *trans* to the "lone pair") is in the opposite direction to that predicted by an acetylene-like anisotropy for the S—O bond. It is of course, an effect analogous to that reported already (11, 12). It is obvious then that the shifts of protons *alpha* to a sulfoxide behave in a consistent fashion but not in accordance with acetylene-like anisotropy.

The second major shift comparison to be noticed in Table 1 is that of the S—O shielding to that of the $\overset{+}{S}$—CH_3 shielding. If the values for the protons adjacent to the $\overset{+}{S}$—CH_3 grouping are corrected by 0.8 p.p.m. for the effect of the positive charge on sulfur (δ CH_3 in benzylmethyl sulfide is 2.0 compared to 2.8 for S—CH_3 in **4**) then the influence of the S—CH_3 grouping on the δ values of the adjacent protons is $\Delta\delta_1 = +0.76$, $\Delta\delta_2 = +0.325$, $\Delta\delta_3 = -0.25$, and $\Delta\delta_4 = -0.87$ p.p.m. The assignments for these protons in the sulfonium salt were shown to be analogous to those in the sulfoxide by a chemical interrelation. Sulfoxide **2** containing 67% deuterium in place of H_2, H_3, and H_4 was reduced, then alkylated to give **4** whose n.m.r. spectrum in deuterochloroform showed 67% deuterium at H_3 and H_4 and only 33% deuterium at H_1 and H_2. The *geminal* coupling constants in **4** again are used to distinguish the two methylene groups as their *geminal* coupling constants differ by 2 Hz.[2]

We interpret the notable similarity in the effects of the $\overset{+}{S}$—O and $\overset{+}{S}$—CH_3 groups on the *alpha* protons as evidence that their common structural feature, the "lone pair" is exerting the dominant influence in both cases. In other words the shifts observed in the conversion of **1** to **2** and **1** to **4** are due mainly to removal of one of the "lone pairs" on sulfur. A logical alternate explanation of these shifts would be that the S—O and S—CH_3 groups possess similar anisotropies.

This explanation would require the methyl group to deshield H_1 and H_2 strongly. Methyl groups normally shield vicinal protons, and only in a few cases involving obvious steric compression they have exhibited deshielding of up to 0.3 p.p.m. (20, 21). In view of this we prefer the former rationalization that the "lone pair" exerts the dominant effect on the shifts of the *alpha* protons in **2** and **4**.

A further complication in general when dealing with the chemical shift data for sulfoxides is revealed by our difficulty in obtaining n.O.e.'s in deuterochloroform. This difficulty showed that intermolecular association of **2** is substantial in this solvent. For rigorous comparison, all shifts should represent the values obtained by extrapolation to infinite dilution. In view of these considerations the use of model compounds chosen for their similarity in geometry to the sulfoxide of interest appears to be the only reliable method by which stereochemical assignments in new sulfoxides can be made. Two recent alternative methods of assigning stereochemistry to protons in conformationally mobile sulfoxides have been reported (22, 23, 24) although one of these (22) fails for benzyl sulfoxides.

Experimental

All n.m.r. spectra were measured on a Varian HA-100 spectrometer which was modified to prevent overloading of the phase-sensitive detector. The modification con-

[2]The correlation of *geminal* coupling constants with configuration at sulfur should be the same for both **2** and **4** since experimental (13) and theoretical (19) evidence shows that a co-linear arrangement of an electron pair with an adjacent C—H bond causes a decrease in size of the coupling constant. (It actually causes an algebraic increase in J but J is negative in sign (19).)

TABLE 5
Preparation of selectively deuterated **2** and **3**

Product	Starting material	Concentration and solvent	Base (ml)*	Time (h)	Temperature (°C)
2 ($H_2H_3H_4$ = D)	**2**	40 mg/ml in *t*-BuOD	0.15 (A)	16	25
2 ($H_1H_2H_3H_4$ = D)	**2**	33 mg/ml in *t*-BuOD	1.0 (A)	16	25
2(H_1 = D)	**2** ($H_1H_2H_3H_4$ = D)	30 mg/ml in *t*-BuOH	0.1 (A)	16	25
3 (H_1 = D)	**3**	20 mg/ml in *t*-BuOD	0.13 (B)	2	80
3 (H_1, H_2 = D)	**3**	20 mg/ml in *t*-BuOD	0.13 (A)	0.25	80
3 (H_2 = D)	**3** (H_1H_2 = D)	20 mg/ml in *t*-BuOH	0.13 (B)	2	80

*Base A is 0.50 *M* potassium *t*-BuO$^-$ in *t*-BuOH or *t*-BuOD. Base B is 0.259 *M* sodium phenoxide in the same solvent.

sisted simply of replacing the 1 K resistor, R357 on the Varian schematic, with a 2.2 K resistor.

All n.O.e.'s were determined on samples having concentrations of 5% (w/v) or less. All samples were degassed by three freeze-thaw cycles on a vacuum line prior to sealing at 0.1 mm. All values reported for n.O.e.'s are the average of at least three determinations by at least two operators. One determination consisted of running five integrals with the oscillator tuned to the desired frequency and five integrals at twice the desired frequency. The power level of the oscillator was adjusted to 20 mV with the instrument in the spin-decoupling mode. Power levels much above or below this value invariably gave smaller n.O.e.'s. For each determination the standard deviation in the five integrals was always less than 3% and usually less than 2%. We therefore feel that the n.O.e.'s reported are accurate to better than ±5%.

*1,11-Dimethyl-5,7-dihydrodibenz(c,e)thiepin (**1**)*

The synthesis of **1** was carried out as described in the literature (3). Compound **1** (H_m = D) was synthesized from 2-amino-3-methyl-5-deuterobenzoic acid which was prepared as follows: a suspension of 3 g of 2-amino-3-methylbenzoic acid in 160 ml of heavy water containing 0.7 ml concentrated hydrochloric acid was heated under reflux for 16 h. Upon cooling the solution, 2 g of **1** (H_m = D) crystallized. After a second exchange with fresh heavy water the n.m.r. of the solid showed that less than 2% of protons remained in the 5-position.

*Preparation of Sulfoxide (**2**)*

Following the procedure of Leonard and Johnson (25) oxidation of **1** with sodium metaperiodate gave **2** in 90% yield. The product after recrystallization from cyclohexane melted from 137–138°.

Anal. Calcd. for $C_{16}H_{16}OS$: C, 74.98; H, 6.29. Found: C, 75.01; H, 6.41.

*Preparation of Sulfone (**3**)*

A solution of 240 mg of **1** in 10 ml of methylene chloride was treated slowly with a solution of 500 mg of *meta*-chloroperbenzoic acid in 5 ml of methylene chloride. After standing for 4 h, the reaction mixture was washed with a saturated solution of sodium bicarbonate, then with water. The organic layer was separated, dried over sodium sulfate, and concentrated. The compound **3**, obtained in 92% yield after recrystallization from acetone, melted from 221–222 °C.

Anal. Calcd. for $C_{16}H_{16}O_2S$: C, 70.39; H, 5.92. Found: C, 70.41; H, 5.98.

*Preparation of Sulfonium Perchlorate (**4**)*

To a solution of 15 mg of **1** in 7 ml of acetone were added a few drops of methyl iodide and 25 mg of silver perchlorate. After 3 h of stirring, a few drops of methanol were added and the silver iodide was filtered off. Evaporation of the filtrate left a residue which on trituration with ether gave a solid. Recrystallization from methanol/ether gave 30 mg (80% yield) of a solid, m.p. 189–191°.

Anal. Calcd. for $C_{17}H_{19}ClO_4S$: C, 57.54; H, 5.40. Found: C, 57.47; H, 5.07.

*Syntheses of Stereoselectively Deuterated **2** and **3***

All exchanges were conducted by dissolving the starting material in *t*-butanol (or *t*-butanol-*O*-D), treating with base, then quenching at a time determined by trial and error with hydrochloric acid. After addition of water, the product which crystallized was collected by filtration, washed, dried, and recrystallized. The specific conditions for the selectively deuterated samples of **2** and **3** are given in Table 5.

*Inversion of the Sulfoxide in **2** (H_2,H_3, H_4, H_m = D)*

Application of the procedure of Johnson and coworker (9) to the sample deuterated at H_2, H_3, and H_4 gave sulfoxide **2** whose n.m.r. showed 75% of one proton at δ 3.60 and 25% of a proton (unreacted starting material) at δ 4.09.

*Correlation of **2** with **3***

A sample of **2** containing 70% deuterium in place of H_2, H_3, and H_4 was oxidized by *meta*-chloroperbenzoic acid and worked up in the manner described above. The n.m.r. of product **3** in DMSO-d_6 showed absorption in the region δ 4.20 twice as intense as that at δ 3.71.

Can. J. Chem. Downloaded from www.nrcresearchpress.com by 210.87.254.105 on 09/05/12
For personal use only.

*Correlation of **1** with **2***

A solution of 40 mg of **2** (H_2, H_3, H_4 = D) in 3 ml of anhydrous tetrahydrofuran was treated with 3 ml of hydriodic acid (57%). After 10 min, the colored solution was added to 10 ml water, and the mixture was extracted with ether. The ether extracts were washed with thiosulfate, saturated bicarbonate, water, then dried and concentrated. The residue was crystallized from ethanol–water. An n.m.r. spectrum of the product in DMSO-d_6 showed the low field benzylic absorption to be twice as intense as the higher field absorption.

*Correlation of **2** with **4***

Conversion of a sample of **2** containing 70% deuterium in place of H_2, H_3, and H_4 was converted to the sulfide and sulfonium salts by the methods described above. The n.m.r. of the partially deuterated **4** in deuterochloroform showed only 35% deuterium content in place of H_1 and H_2 and still 70% deuterium label in place of H_3 and H_4.

The authors thank the National Research Council of Canada for generous financial assistance. The financial aid of Bristol Laboratories is also appreciated. The technical assistance of Mr. John Maxwell in determining n.O.e. values and Mr. Hector Seguin, who performed the microanalyses, is also gratefully acknowledged. We wish to thank Dr. R. A. Bell and Mr. J. K. Saunders for kindly checking some of our n.O.e.'s on their HA-100.

1. R. R. Fraser and F. J. Schuber. Chem. Commun. 397 (1969).
2. R. R. Fraser and F. J. Schuber. Chem. Commun. 1474 (1969).
3. K. Mislow, M. A. W. Glass, H. B. Hopps, E. Simon, and G. H. Wahl, Jr. J. Amer. Chem. Soc. **86**, 1710 (1964).
4. F. A. L. Anet and A. J. R. Bourn. J. Amer. Chem. Soc. **87**, 5250 (1965).
5. J. G. Colson, P. T. Lansbury, and F. D. Saeva. J. Amer. Chem. Soc. **89**, 4987 (1967).
6. R. A. Bell and E. N. C. Osakwe. Chem. Commun. 1093 (1968).
7. R. A. Bell and J. K. Saunders. Can. J. Chem. **46**, 3421 (1968).
8. (*a*) R. F. Watson and J. F. Eastham. J. Amer. Chem. Soc. **87**, 664 (1965). (*b*) K. Mislow, M. M. Green, P. Laur, and D. R. Chisholm. J. Amer. Chem. Soc. **87**, 665 (1965).
9. C. R. Johnson and D. McCants, Jr. **87**, 5406 (1965).
10. J. B. Lambert, R. G. Keske, and D. K. Weary. J. Amer. Chem. Soc. **89**, 5921 (1967).
11. J. B. Lambert and R. G. Keske. J. Org. Chem. **31**, 3429 (1966); see also J. B. Lambert and R. G. Keske. Tetrahedron Lett. 2023 (1969).
12. A. B. Foster, T. D. Inch, M. H. Qadir, and J. M. Webber. Chem. Commun. 1086 (1968).
13. R. C. Cookson and T. A. Crabb. Tetrahedron, **24**, 2385 (1968).
14. S. Wolfe, A. Rauk, and I. G. Csizmadia. Can. J. Chem. **47**, 113 (1969).
15. B. J. Hutchinson, K. K. Andersen, and A. R. Katritzky. J. Amer. Chem. Soc. **91**, 3839 (1969).
16. S. Wolfe and A. Rauk. Chem. Commun. 778 (1966).
17. J. G. Pritchard and P. C. Lauterbur. J. Amer. Chem. Soc. **83**, 2105 (1961).
18. R. D. G. Cooper, P. V. DeMarco, J. C. Cheng, and N. D. Jones. J. Amer. Chem. Soc. **91**, 1408 (1969).
19. J. A. Pople and A. A. Bothner-By. J. Chem. Phys. **42**, 1339 (1965).
20. A. Segre and J. I. Musher. J. Amer. Chem. Soc. **89**, 706 (1967).
21. E. L. Eliel, M. H. Gianni, T. H. Williams, and J. B. Stothers. Tetrahedron Lett. 741 (1962).
22. E. T. Strom, B. S. Snowden, Jr., and P. A. Toldan. Chem. Commun. 50 (1969).
23. M. Nishio. Chem. Commun. 51 (1969).
24. W. Amann and G. Kresze. Tetrahedron Lett. 4909 (1968).
25. N. J. Leonard and C. R. Johnson. J. Org. Chem. **27**, 282 (1962).

Can. J. Chem. Downloaded from www.nrcresearchpress.com by 210.87.254.105 on 09/05/12
For personal use only.

Cumulative yields in the 14 MeV neutron fission of ^{232}Th and ^{238}U in the symmetric region

L. H. GEVAERT[1] AND R. E. JERVIS

Department of Chemical Engineering and Applied Chemistry, University of Toronto, Toronto, Ontario

AND

H. D. SHARMA[2]

Department of Chemistry, University of Waterloo, Waterloo, Ontario

Received[3] October 28, 1968

The radiochemical yields of molybdenum-99, ruthenium-103 and -105, palladium-109 and -112, silver-111 and -113, cadmium-115, and tin-121 and -125 formed in the 14 MeV fission of thorium-232 and uranium-238 have been determined using a low background Geiger–Muller counter, NaI(Tl) crystal, and Ge(Li) detector. The absolute mass yield for molybdenum-99 has been obtained using a copper monitor for neutron flux and for the other nuclides using molybdenum-99 as an internal standard. The mass distribution curves derived from the chain yields, in the symmetric region show the presence of a third peak in thorium-232, and only the familiar two peaks for uranium-238 in the asymmetric region. By comparison of normalized cumulative mass yields from this study with prompt fission yield data, the average number of prompt neutrons emitted from fission fragments has been obtained as a function of mass in ^{238}U + n fission. It appears that there are two regions of enhanced neutron emission in the mass range 103–128, and that the heavy fragments emit more neutrons than the light ones.

Canadian Journal of Chemistry, **48**, 641 (1970)

Introduction

It is well known that the mass–yield curve for the fission of nuclei in the region of gold and bismuth is symmetric (1, 2), while in the low energy fission of uranium and other heavier elements the curve is asymmetric (3). In between, for several nuclei such as ^{226}Ra with charged particles (4–7) the mass distribution exhibits three peaks. Britt *et al.* (6) have further shown in many fissioning nuclei that in the symmetric region, the kinetic energy of the fission fragments is lower than for other fragments, which is attributed to a larger elongation of the fissioning nucleus at the scission point (8). In most fission processes the observed dip in the kinetic energy of the fragments has been explained on the basis of either the two mode hypothesis (t.m.h.) (6) or the fragment shell theory (f.s.t.) (9, 10). The two mode hypothesis (t.m.h.) in its simple form suggests that the shape of the mass–yield curves can be rationalized on the basis of superposition of mass yields due to two modes, each one having a fixed type and shape of distribution. Furthermore, the yields in the symmetric mode are expected to be enhanced as the excitation energy of the compound nucleus increases and thus the three-humped curve becomes more evident at moderate excitation energies (15–40 MeV). Even with relatively high energy protons (170 MeV), the mass–yield curve for ^{238}U has been interpreted on the basis of t.m.h. (11).

According to f.s.t., the yields of fission fragments are due to the shape of the fissioning nuclide at the point of scission, which is produced by minimization of potential energy due to the coulombic and surface energy resulting from deformation. The fissioning nuclide can therefore take many shapes and lead to a particular mass–yield curve, i.e. having one, two, or three peaks, even though the peak-to-trough ratio is low for the fissioning systems. On the basis of f.s.t., Ferguson and Read (10) have calculated the mass yields for the thermal neutron fission of ^{235}U, for which the yields are well established. They found a reasonable agreement between the experimental and calculated yields.

The radiochemical yields for most fissioning systems at moderate excitation energies are not well established in the symmetric region where the predictions due to t.m.h. and f.s.t. may differ. A reinvestigation of ^{232}Th with reactor neutrons (12, 13) has revealed a small third peak which supports t.m.h. However, similar studies of ^{227}Ac, ^{231}Pa, and ^{237}Np under identical conditions have shown the presence of the third peak in

[1]Present address: Consumers Glass Co. Ltd., Toronto 18, Ontario.

[2]To whom all correspondence should be addressed.

[3]Revision received July 28, 1969.

Can. J. Chem. Downloaded from www.nrcresearchpress.com by 210.87.254.105 on 09/05/12
For personal use only.

TABLE 1

Prominent β-particle and γ-ray energies and half-life of fission products*

Nuclide	β-Particle E_{max} (MeV)	β-Particle Abundance (%)	γ-Ray Energy (MeV)	γ-Ray Abundance (%)	$t_{1/2}$
^{99}Mo			0.740	12	67 h
	1.18	83	0.780	4.4	
	0.80	3			
	0.41	14			
^{103}Ru	0.217	99	0.497	88	39.6 days
^{105}Ru	1.87	11	0.67	18	4.44 h
	1.14	44	0.726	48	
	and others				
^{109}Pd	1.028	100	—	—	13.47 h
^{111}Ag	1.04	93	0.34	6	7.5 days
	0.8	1			
	0.69	6			
^{112}Pd–Ag	3.94	54	0.617	41	21 h
	3.35	22			
	1.96	10			
	and others				
^{113}Ag	~2.0		0.30		5.3 h
^{115}Cd–In	—		0.336	95	53.5 h
^{121}Sn	0.383	100	—		27 h
^{125}Sn	2.35		—		9.7 days

*Data from refs. 33, 46, and from γ-ray spectra of the nuclides.

^{227}Ac fission, while ^{231}Pa and ^{237}Np have only two peaks (14). Since these studies were done with reactor neutrons (low excitation energy) and with small amounts of material, it was not possible to draw any conclusions concerning the mechanism of fission.

While some mass yields in the symmetric region have been reported for ^{232}Th and ^{238}U with 14 MeV neutrons (15–24), a systematic study in these systems, in which a complete range of symmetrical yields are simultaneously obtained, is somewhat lacking. In the present study the yields of selected nuclides in the mass range of 103 to 125 have been determined to establish the shape of the mass–yield curve for both the nuclides.

Experimental

Uranyl nitrate and thorium nitrate were irradiated with 14.7 MeV neutrons from a Texas Nuclear Model 9900, Cockroft Walton type neutron generator having a total neutron output of ~10^{11} n/s produced by the $^{3}_{1}H(^{2}_{1}H,n)^{4}_{2}He$ reaction. The tritium target half-life in these irradiations was approximately 6 h and gave almost constant neutron output over a period of 3 h.

The materials were put in a stainless steel cassette lined with aluminum foil and wrapped with cadmium foil to absorb thermal neutrons which might be present in the target area. The cassette was sandwiched between copper foils and put against the target end of the generator for irradiation. Usually the irradiations were done for a period of 1–3 h depending on the half-life of the radioisotope to be isolated. Longer-lived fission products were not isolated, primarily due to the limitations of the tritium target lifetime.

The irradiated samples were dissolved in HCl or HNO_3, depending on the elements to be separated from them. A known amount of inactive carrier of an element was added to an aliquot of the solution and allowed to interchange with the fission product nuclides of the same element. After the interchange was completed, the element was separated and purified from the solution following standard radiochemical procedures taken from the literature (25, 27) after introducing appropriate modifications. The fission product nuclides were finally obtained as precipitates which were filtered using a lucite filter assembly. The precipitates were washed, dried, weighed, and mounted onto a sample holder for radiochemical assay.

The radiochemical assay was carried out by using three types of detectors, namely, a low background Geiger–Muller counter for β-counting, and a NaI(Tl) crystal 3 in. × 3 in. diameter and a 22 cc Ge(Li) detector, in conjunction with a 400 channel analyzer for γ-ray spectrometry. The efficiencies for the detection of nuclides were established as follows.

Can. J. Chem. Downloaded from www.nrcresearchpress.com by 210.87.254.105 on 09/05/12
For personal use only.

Can. J. Chem. Downloaded from www.nrcresearchpress.com by 210.87.254.105 on 09/05/12
For personal use only.

(i) Gamma Calibrations

Calibrated sources of ^{54}Mn, ^{60}Co, ^{137}Cs, and ^{203}Hg were obtained from the International Atomic Energy Agency (I.A.E.A.), Vienna. Aliquots of the sources were deposited onto filter papers maintaining an identical area of deposition for each sample. The photopeak efficiencies for these nuclides were estimated from the number of pulses accumulated in their respective photopeaks in γ-ray spectra using the NaI(Tl) crystal and the Ge(Li) detector. The detection efficiencies, ε_γ, for nuclides emitting γ-rays between 0.279 and 1.33 MeV were obtained by interpolation of the photopeak efficiencies and nuclear data as shown in Table 1.

(ii) Beta Calibrations

Aliquots of ^{60}Co and ^{137}Cs from I.A.E.A. were deposited onto thin gold-coated VYNS films. The calibration results with a 4π beta proportional counter gave 93 and 96% efficiencies for ^{60}Co and ^{137}Cs samples, respectively. These values were considered reasonable in view of the thickness of the plated samples and the thickness of the films. A sample of ^{46}Sc of high specific activity was prepared and calibrated by the γ-ray spectrometry method. The ε_β (beta efficiency) values of the low background counter were determined for the calibrated samples of ^{203}Hg, ^{60}Co, and ^{46}Sc containing known amounts of their respective inert carriers.[4] The values for ^{121}Sn were extrapolated from these curves and were further verified by directly calibrating a high specific-activity sample of ^{121}Sn by the 4π counter, and subsequently precipitating tin as phenyl arsonate, $(C_6H_5AsO_3)_2Sn.4H_2O$, from aliquots of the calibrated solution of ^{121}Sn containing a known amount of inert tin carrier, and assaying by the low background counter. The detection efficiencies of the low background counter for other nuclides of interest were determined in a similar manner.

The gravimetric methods of elemental estimations were checked by precipitating the elements from their respective calibrated samples containing known amounts of inert carriers, and subsequent determination of the activities by the γ-ray spectrometry or by the low background counter. Lastly, the methods of radiochemical assay for some nuclides were checked by determining their chain yields in thermal neutron fission of ^{235}U using ^{99}Mo as an internal monitor (Table 2).

The 14 MeV neutron flux was monitored by assaying ^{64}Cu produced by the ^{65}Cu(n,2n)^{64}Cu reaction. The variation of neutron flux over the entire area caused by fluctuations of the deuteron beam over the exposed area of the tritium target was examined. The total number of neutrons impinging on the copper foils over the entire area showed very little variation although there were radial variations in the ^{64}Cu activity in the foil.

[4]β-Ray spectra of these nuclides as well as ^{121}Sn have allowed shapes (46).

TABLE 2
Chain yields of fission products in thermal neutron fission of ^{235}U

Nuclide	Chain yield: Present work	Chain yield: Literature (7, 39)
^{103}Ru	3.1 ±0.13	2.9
^{105}Ru	0.95 ±0.04	0.9
^{112}Pd	0.012±0.0006	0.013
^{115}Cd	0.01 ±0.0006 (does not include ^{115m} Cd)	0.011
^{121}Sn	0.012±0.001	0.0125
^{125}Sn	0.012±0.0012	0.011

Results

The cumulative yields for selected nuclides ranging from mass number 103 to 125 are given in Tables 3 and 4 for ^{232}Th and ^{238}U, respectively, along with values obtained by others (15–24,

TABLE 3
Chain yields of nuclides in ^{232}Th with 14 MeV neutron fission

Nuclide	Chain yields (%): Lyle *et al.* 1964 (20)	Broom 1964 (21)	Ford and Leachmann 1965 (19)	Ganapathy and co-workers 1966 (22, 23)	Mo and Rao 1968 (24)	This work
^{99}Mo	1.84	1.96		2.0	2.0	2.0 ±0.08
^{103}Ru	1.21			0.75		0.83±0.05
^{105}Ru				0.92		1.00±0.09
^{106}Ru				1.07		
^{109}Pd			1.61	1.10		1.28±0.15
^{111}Ag	1.50	1.13	1.85	1.50		1.21±0.08
^{112}Pd			1.77			1.32±0.08
^{112}Ag	1.29	1.32				
^{113}Ag		1.10	1.34	1.20		1.26±0.08
^{115}Ag	1.26	1.72				
^{115}Cd				1.24	1.5	1.20±0.10
^{121}Sn					1.0	0.93±0.10
^{125}Sn (9.7 days)					0.58	0.52±0.04
^{129}Sb	1.19					
^{129}Te					1.6	

TABLE 4

Chain yields of nuclides in ^{238}U with 14 MeV neutron fission

Nuclide	Chain yields (%)						
	Ames *et al.* 1957 (15)	Cunninghame 1958 (16)	Broom 1962 (17)	James *et al.* 1964 (18)	Ford and Leachmann 1965 (19)	Gorman and Tomlinson 1968 (32)	This work
^{99}Mo	5.7			6.47		5.5	$5.6_0 \pm 0.14$
^{103}Ru						5.15	$4.4_4 \pm 0.15$
^{105}Ru	3.4			2.65			$3.0_0 \pm 0.1$
^{109}Pd				1.20	1.20		1.54 ± 0.15
^{111}Ag	0.87	0.81	0.6	0.98	1.08		1.10 ± 0.05
^{112}Pd				0.79	1.12		1.24 ± 0.05
^{113}Ag			0.6	0.87	0.66		0.88 ± 0.05
^{115}Cd	0.71	0.64		0.64			0.86 ± 0.09
^{121}Sn	0.73						1.14 ± 0.11
^{125}Sn (9.7 days)	0.83						0.85 ± 0.085

TABLE 5

14 MeV neutron fission mass yields

Mass number	^{232}Th		^{238}U	
	Yield (%)	Number of determinations	Yield (%)	Number of determinations
99	2.00 ± 0.085	11	5.6 ± 0.14	7
103	0.83 ± 0.05	4	4.4 ± 0.15	3
105	1.00 ± 0.08	4	3.0 ± 0.1	3
109	1.28 ± 0.15	3	1.54 ± 0.15	3
111	1.21 ± 0.08	2	1.11 ± 0.06	3
112	1.33 ± 0.09	3	1.25 ± 0.06	3
113	1.26 ± 0.085	2	0.88 ± 0.06	3
115	1.31 ± 0.14	4	0.93 ± 0.12	4
121	0.98 ± 0.13	6	1.2 ± 0.14	4
125	1.0 ± 0.4	6	1.5 ± 0.4	4

32). The yields are averages of 2 to 6 determinations as shown in Table 5. The yield of ^{99}Mo was determined by estimating the activities due to ^{99}Mo produced in the fissioning nuclei and monitoring total neutron dose from ^{64}Cu in the copper foil. Saturation activities A_s for the nuclides were calculated using the relationship

$$[1] \qquad A_s = \frac{A_0}{\varepsilon(1 - e^{-\lambda t_{irr}})}$$

where A_0 = observed count-rate after extrapolation to the time at the end of irradiation and correction for chemical yield, λ = decay constant, and t_{irr} = total time of irradiation. ε is counter efficiency.

$$[2] \qquad Y_{Mo} = \frac{A_s(Mo)\cdot\sigma_{Cu}n_{Cu}100}{A_s(Cu)\cdot\sigma_f n_f}$$

where σ_{Cu} = cross section for the $^{65}_{29}Cu(n,2n)^{64}_{29}Cu$ reaction, taken as 0.970 *b* (28); σ_f = cross section for fission for either ^{232}Th or ^{238}U, taken as 0.37 (29) or 1.17 *b* (29–31); n_{Cu} = number of ^{65}Cu atoms in the foil, and n_f = number of fissioning nuclei.

The yields of ^{99}Mo were estimated as 5.60 ± 0.14 and $2.00 \pm 0.05\%$ for ^{238}U and ^{232}Th, respectively, the former being in good agreement with the recent value of 5.50 ± 0.25 obtained by Gorman and Tomlinson (32). The yields for the other nuclides have been calculated by relating them to the ^{99}Mo yield in each irradiation taken as a monitor for total fissions.

Discussion

The cumulative yields reported in this work have been obtained using conventional radiochemical separations and counting methods, employing a low background counter for pure β-emitters and γ-ray spectrometry for others. The sources of error arise in many ways in their deter-

Can. J. Chem. Downloaded from www.nrcresearchpress.com by 210.87.254.105 on 09/05/12
For personal use only.

Can. J. Chem. Downloaded from www.nrcresearchpress.com by 210.87.254.105 on 09/05/12
For personal use only.

mination. The magnitudes of errors associated with the yields have been minimized experimentally and the resultant levels estimated as stated below.

The presence of thermal neutrons in the target area could cause ^{235}U in natural uranium to fission and thus enhance the yields in the asymmetric region, especially for ^{99}Mo used as an internal monitor. To check this, gold wire was included in the irradiation assembly. The neutron flux was estimated by assaying the activity due to ^{196}Au and ^{198}Au formed by the reactions ^{197}Au(n,2n)^{196}Au and ^{197}Au(n,γ)^{198}Au, respectively. The error due to the presence of thermal neutrons was estimated to be less than 0.1%.

Tritium target depletion and deuterium beam instability in the generator caused some fluctuations in the neutron flux during irradiations. Since the half-lives of the several nuclides determined differ from both those of ^{99}Mo and ^{64}Cu (external monitor), the errors in the calculation of fission yield by eqs. [1] and [2] were examined for each fission product nuclide by using a modified equation, wherein the neutron flux ϕ was allowed to vary by 40% during the irradiation time

$$A_s = k\sum_{i=1}^{m}(1\text{-}e^{-\lambda t/m})\,\phi_i\,[e^{-\lambda t(1-i/m)}]$$

where A_s = activity, k is directly proportional to the weight of target material and the cross section for the nuclide, t = irradiation time, m = total number of differential time periods, and ϕ_i = neutron flux during the ith time interval.

The value of A_s for each nuclide was then compared with the value obtained by the eqs. [1] and [2]. A maximum error of 0.5% was estimated in ^{105}Ru determination. It was further minimized by reducing the irradiation time to 1 h.

An estimate of errors in gravimetric estimations of the elements separated was arrived at by carrying out large numbers of determinations both for thermal neutron fission of ^{235}U and the 14 MeV fission of ^{232}Th and ^{238}U for elements such as tin. The reported yields for tin nuclides are the average of such determinations. For elements such as Ag the agreement among replicate samples was found to be good in all the irradiations, and thus fewer determinations were done.

The activities due to the nuclides after chemical separations were followed over a minimum period of four half-lives, taking care that a total of at least 1000 counts were accumulated during each counting period. In the case of ^{125}Sn this was achieved within a period of 1 h. In γ-ray spectrometry, the area under the photopeak due to selected γ-rays emitted by the nuclide was calculated and plotted against decay time. The data were subjected to a least-squares fitting program taking into account the known half-lives of the nuclides. The maximum counting error was 1% in the case of ^{125}Sn and 5% in the case of ^{109}Pd, although activity due to ^{121}Sn and ^{112}Pd had to be subtracted based on their respective decay curves.

The yields could have been increased if the activities were also produced from certain impurities by (n,p) or (n,2n) reactions. Elements such as tin and antimony, which could have been present in p.p.m. amounts in the target materials, were irradiated in pure form and the activities of the nuclides of interest estimated. From these data it was deduced that the contribution due to impurities towards the fission yields was less than 0.2%.

The yields are subject to changes if γ-ray abundance data quoted in Table 1 or the recent results of Macdonald and Sharma (33) on the γ-ray spectra resulting from the decay of ^{112}Ag are altered. The uncertainty due to such changes in γ-ray intensities is not likely to be more than 3%, as the spectra of nuclides of interest were taken with the Ge(Li) detector, and the relative intensities of the γ-rays examined. They were then compared with the counting data from the calibrated low background counter.

The derivation of mass yield from the experimentally determined chain yield for a particular nuclide requires some assumptions and deductions based on the charge-distribution hypotheses. There is no satisfactory recipe for obtaining fractional isobaric yields in fission at moderate excitation energies. The data on the independent yields of isobaric chains in 14 MeV neutron fission of ^{232}Th and ^{238}U are limited to some shielded nuclides. Recently, Rao *et al.* (34) have suggested that the experimentally determined yields, Y_i, of the shielded nuclides ^{124}Sb, ^{126}Sb, and ^{136}Cs give a better fit with the Gaussian curve (35)

$$Y_i = (c\pi)^{-\frac{1}{2}}\exp\,[-(Z-Z_p)^2/c]$$

where c = 1.7 and Z is the atomic number of the shielded nucleus, if a constant charge-to-mass ratio (c.c.r.) hypothesis is assumed for calculating

Can. J. Chem. Downloaded from www.nrcresearchpress.com by 210.87.254.105 on 09/05/12
For personal use only.

Z_p for nuclides in the symmetric region and equal-charge-displacement hypothesis (e.c.d.) for deriving Z_p for nuclides in the asymmetric region. Coryell *et al.* (36) earlier suggested a prescription for obtaining Z_p for various types of fission differing in compound nuclei and in excitation energy. The distribution curve for any isobaric sequence is assumed to be the same as found in thermal neutron fission of ^{235}U. The shift in Z_p, denoted as $\Delta Z_p(A)$, is given by

$$\Delta Z_p(A) = Z_p(A) - Z_p(A)\ [^{235}U]$$

$$\Delta Z_p(A) = \tfrac{1}{2}(Z_c - 92) - 0.19(A_c - 236) + 0.19(\upsilon_T - 2.5)$$

where Z_c and A_c are atomic number and mass number of the compound nucleus, respectively, and υ_T is the average number of neutrons emitted in fission. Wogman *et al.* (37) have somewhat modified Coryell's prescription to relate Z_p values in ^{241}Am and ^{243}Cm. It appears from the published results on $Z_p(A)$ that in fast fission it is possible to obtain only approximate values of $Z_p(A)$ for the nuclides under investigation. It may, however, be pointed out that Z_p values for 124 and 126 as obtained by Rao *et al.* (34) are very close to the ones obtained by Coryell's prescription if Z_p for these mass numbers in thermal neutron fission of ^{235}U are taken from the results reported by Aras and Gordon (38). The mass yields as calculated from the experimentally determined chain yields, and from the Gaussian curve using the calculated Z_p values from the hypothesis and $c = 1.7$, will have uncertainties of no more than 0.5% except for mass numbers between 125 and 129. The mass-spectrometric yields determined by Gorman and Tomlinson (32) have uncertainties of even less than 0.2% of the mass yields, i.e. the independent yields of isobars not included in the chain is $< 0.2\%$ of the total mass yield. The fractional cumulative yield at ^{129}Sb may be $\sim 90\%$ of the total yield.

The yields for 115, 121, and 125 need further consideration. ^{115}Cd, ^{121}Sn, and ^{125}Sn have metastable states for which the yields have not been determined. Z_p for 115 is ~ 45.5, and hence the ^{115}Cd isomers mainly result from the decay of their precursor, ^{115}Ag. The yield ratio of the isomers has been assumed to be the same as observed in β-decay of ^{115}Ag isomers (8% for ^{115m}Cd). Similarly, for 121, the yield of the long-lived isomer of ^{121}Sn is assumed to be 5%. This may introduce a maximum error of 3% in the mass yields. The mass yield of 125 merits further discussion. If $Z_p(125)$ is ~ 49 for both the fissioning systems, ^{125}In, ^{125m}In, ^{125}Sn, and ^{125m}Sn will have appreciable independent yields. The decay characteristics of the isomers of ^{125}In are not known and thus it is unrealistic to relate the mass yield for 125 to the yield of 9.7d ^{125}Sn. Ideally the chain yield at ^{125}Sb would represent the mass yield, but the half-life of ^{125}Sb is too long and therefore the count rate due to it was very low considering the limitation of irradiation times with a (T,D) neutron generator. An attempt was made to measure the yield of 9.5 min ^{125}Sn, but it has not yet been possible to obtain quantitative data. The results thus far indicate that the yield of ^{125}Sn is lower in both the systems compared to that obtained in the thermal neutron fission of ^{235}U recently measured by Erdahl (39). The yield of this isomer is also lower in the ^{232}Th fission with reactor neutrons, and qualitative yield measurements are indicative that the mass yield of this nuclide is about 1.0%. In ^{238}U fission it is about 1.5%. As a result of these uncertainties, the chain yields of mass 125 in Figs. 1 and 2 and Table 5 are considered uncertain to $\sim 30\%$.

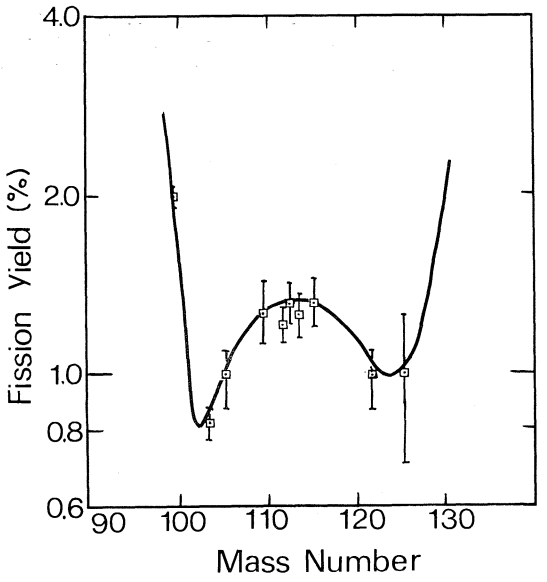

FIG. 1. Mass–yield curve in the 14 MeV neutron fission of ^{232}Th in the symmetric region.

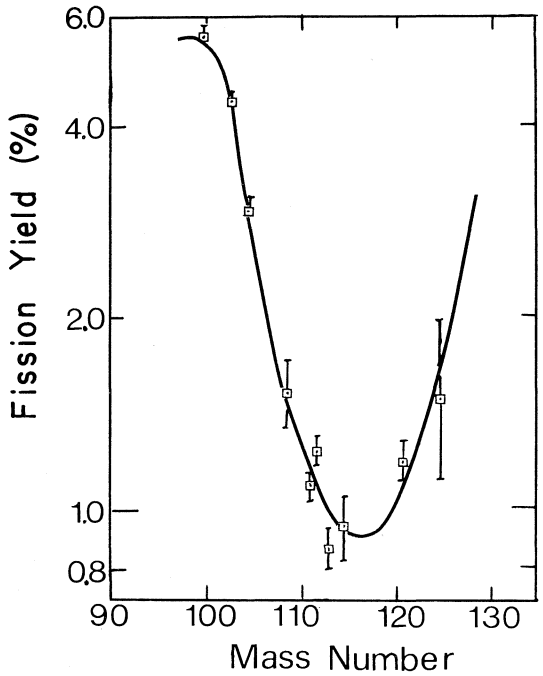

FIG. 2. Mass–yield curve in the 14 MeV neutron fission of ^{238}U in the symmetric region.

The cumulative yields are given in Table 5 along with the estimated errors.

The chain yields for ^{232}Th fission are in general agreement with others (Table 3). It is worthy of comment that in the recent results of Ganapathy and Kuroda, the yield for ^{103}Ru is slightly lower than the value reported here, whereas Mo and Rao, on the other hand, reported higher yields for ^{115}Cd. Ford and Leachman's values are consistently higher, which may be due to normalization, because they were interested in a comparative study of the yields of these nuclides produced at different excitation energies. The values are plotted against mass numbers as shown in Fig. 1. It is evident that a third peak is present in this fissioning system, similar to the one obtained by Iyer *et al.* for reactor neutron fission (12). It is not, however, as pronounced as is expected from the superposition of mass yields due to t.m.h.

Comments on the chain yields of ^{238}U are of a similar nature. There are variations among the yields when compared with those obtained by various investigators. James *et al.* report a lower value for ^{105}Ru, while Ames *et al.* obtained 0.73% for ^{121}Sn, compared to the value 1.14% obtained by us. The mass yields are plotted against mass number in Fig. 2.

The radiochemical yields at these excitation energies ($\sim$ 20 MeV) arise from multichance fission processes, viz. the (n,f), the (n,nf), and the (n,2nf) reactions, and from post-fission neutron emission from the fragments. To estimate the approximate contribution towards the mass yields in the symmetric region from each process, the ratios (s/a) of symmetric-to-asymmetric yield are plotted against $(E_{exc} - 5)^{-1/2}$, similar to the correlations given by Jones (40). The contribution due to each process, i.e. the (n,f), the (n,nf), and the (n,2nf), can be estimated by taking into account the excitation energy of the fissioning nuclei, and the cross section for each process. The maximum contribution towards the mass yields ($\sim$ 80%) in the symmetric region is from the first chance fission, i.e. from the compound nuclei ^{233}Th and ^{239}U.

Gonnenwein and Pfeiffer (41) have reported prompt mass yields for ^{232}Th and ^{238}U fissioned with 14 MeV neutrons from double energy measurements using solid-state detectors. In unfolding the prompt mass–yield curve, the average mass numbers of the compound nuclei are assumed to be 238 for ^{238}U and 231.7 for ^{232}Th. This assumption may not be strictly valid for obtaining prompt mass yields in the symmetric region. Moreover, Terrell's saw-tooth curve for prompt neutron emission (42) is used in arriving at the mass–yield curve. These two factors introduce uncertainties in the prompt yield data. Nevertheless, a comparison by means of cumulative distributions of the prompt yields and the radiochemical yields should permit an assessment of the average number of neutrons $\upsilon(A)$ as a function of the fragment mass (42). This procedure depends on the availability of accurate data, especially for the prompt yields obtained from time-of-flight measurements. Similarly, the radiochemical mass–yield curve should be well defined. These radiochemical and recently reported mass-spectrometric (32) yields for ^{238}U are the best measurements thus far for this fissioning system at these excitation energies. However, there are still uncertainties since some yields have been arrived at by interpolation. A derivation of the number of neutrons emitted at each mass can provide some potentially useful information concerning the fission process (43);

Can. J. Chem. Downloaded from www.nrcresearchpress.com by 210.87.254.105 on 09/05/12
For personal use only.

Can. J. Chem. Downloaded from www.nrcresearchpress.com by 210.87.254.105 on 09/05/12
For personal use only.

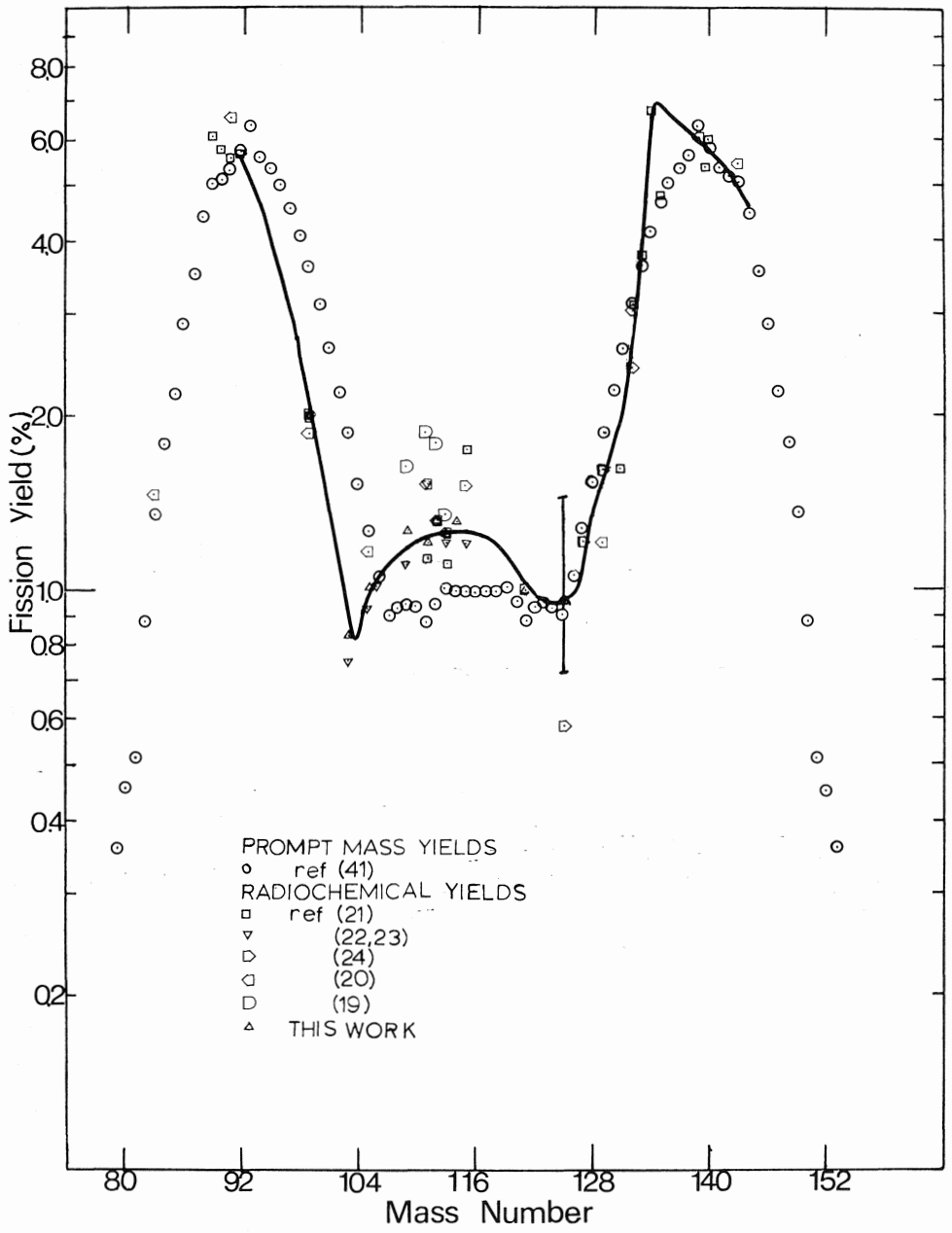

FIG. 3. Prompt and radiochemical mass yields in the 14 MeV neutron fission of ^{232}Th.

therefore the data represented in Figs. 3 and 4 have been compared, and the neutron–emission curve thus obtained is shown in Fig. 5. For ^{238}U, the radiochemical yields are normalized at A = 117 which give the average number of neutrons $\bar{\upsilon}$ = 3.65. The average number of post-fission neutrons in ^{238}U is taken as 3.7 by Gonnenwein and Pfeiffer (41), which is in agreement with υ_T = 4.7 (including prefission neutrons). It may be worth mentioning again that the prompt yields are normalized at A = 119, whereas it has been discussed earlier that the yields in the symmetric

Can. J. Chem. Downloaded from www.nrcresearchpress.com by 210.87.254.105 on 09/05/12
For personal use only.

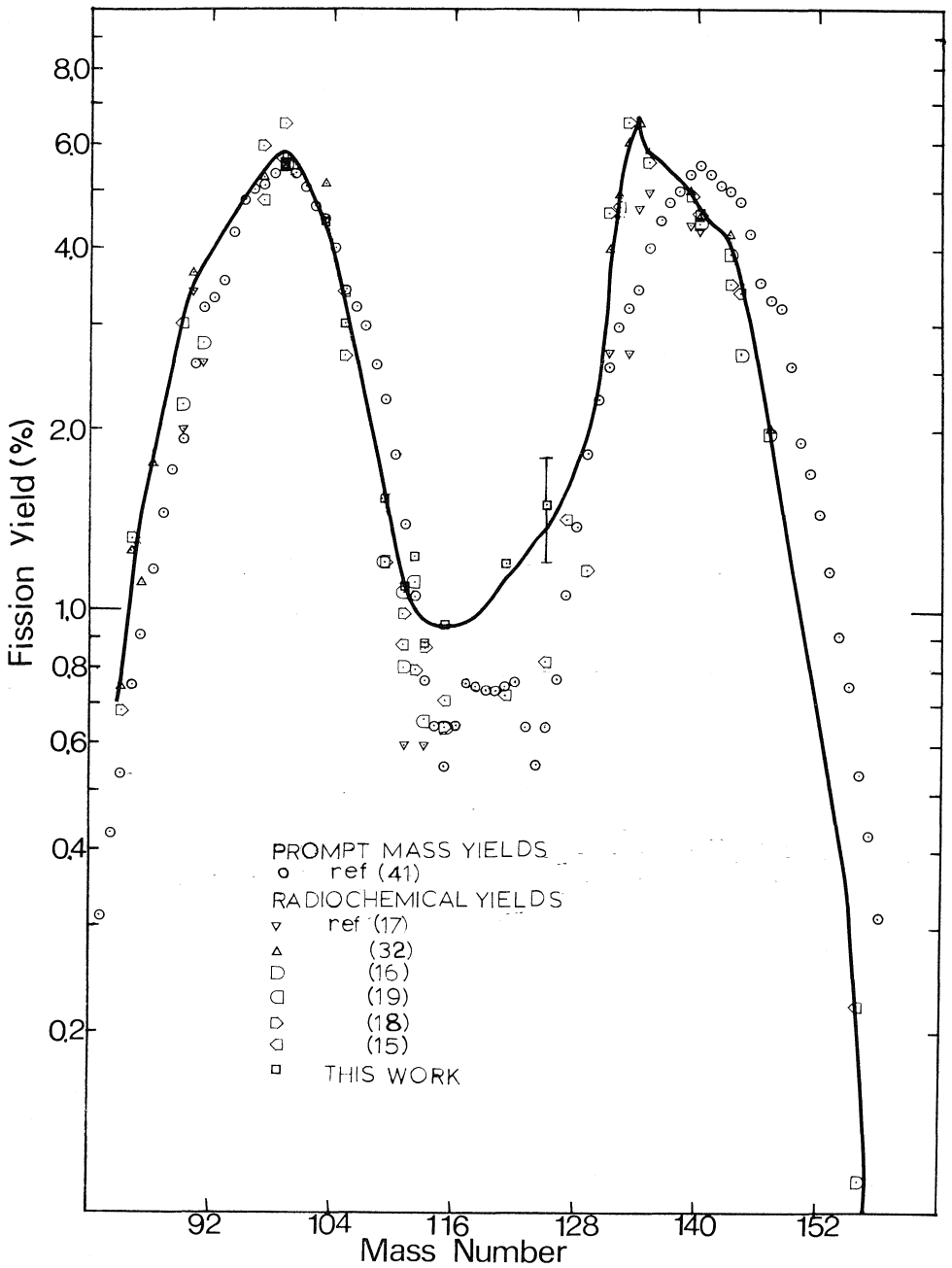

FIG. 4. Prompt and radiochemical mass yields in the 14 MeV neutron fission of ^{238}U.

region mainly arise due to the (n,f) process in the ^{239}U compound nucleus, and thus should be normalized at $A = 119.5$. The $\bar{\upsilon}(A)$ could be higher by 0.5 neutrons in the symmetric region. Similarly the neutron–emission curve for ^{232}Th has been derived by assuming that the radiochemical yields can be normalized at $A = 114$.

The shape of the $\upsilon(A)$ curve for ^{238}U is similar to that observed in low-excitation fission except that a sharp decrease occurs in the mass range

Can. J. Chem. Downloaded from www.nrcresearchpress.com by 210.87.254.105 on 09/05/12
For personal use only.

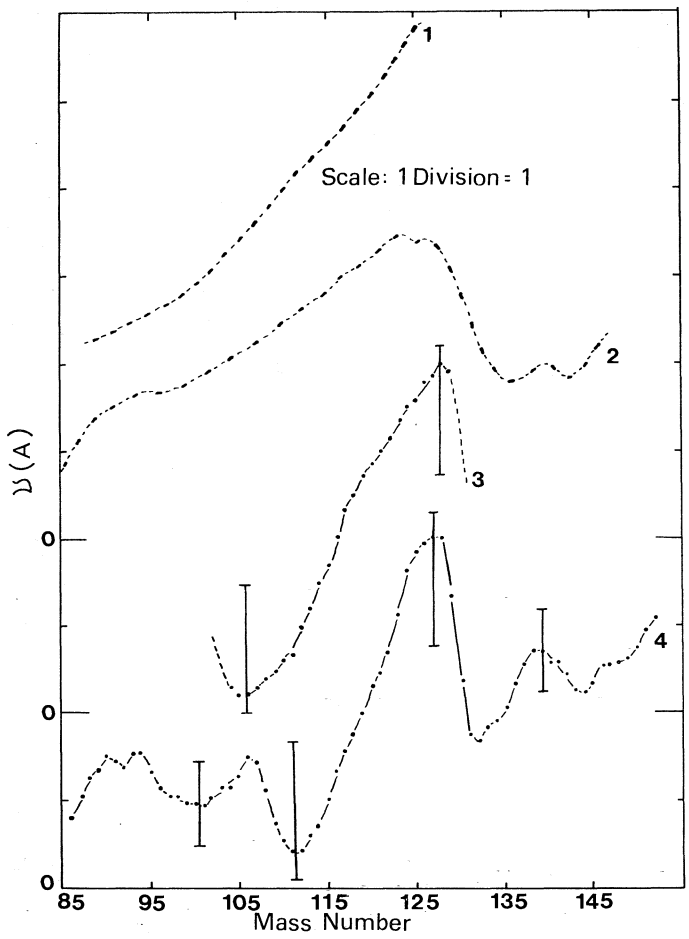

FIG. 5. Neutron emission curve as a function of fission-fragment mass; *1*, ^{209}Be + 53.25 MeV α-particles (45); *2*, ^{226}Ra + 13.0 MeV protons (44); *3*, ^{232}Th + 14 MeV neutrons; and *4* ^{238}U + 14 MeV neutrons.

125–132, and a less marked decrease in the range 106–112. Similar trends have been observed in the α-particle induced fission of ^{238}U (43), the 14 MeV neutron induced fission of ^{235}U (43), and the 13 MeV proton induced fission of ^{226}Ra (44). The $\upsilon(A)$ curve obtained in ^{226}Ra fission, wherein a prominent three-humped mass–yield distribution is found, is shown for comparison in Fig. 5. It is evident that additional small humps are present near masses of 95 and 140 in both systems. The general features of the $\bar{\upsilon}(A)$ curve for ^{226}Ra fission have been interpreted by Konecny and Schmitt (44) on the basis of two components of fission; namely, (*a*) one giving rise to fragments in the region of symmetric mass division that may be described in terms of a liquid drop model, and (*b*) the other described in terms of "fragment-structure fission" such as is observed in the low-excitation fission of heavy fissioning nuclides.

The recent results of Plasil, Ferguson, and Schmitt (45) for the α-particle induced fission of ^{209}Bi, which exhibits a mass distribution in the form of a single hump in the symmetric region, have also yielded a $\upsilon(A)$ curve with a similar shape in the symmetric region as obtained in this study for ^{238}U, and also for ^{232}Th.

It must be emphasized that there are uncertainties in both the prompt and secondary mass yields which give rise to corresponding uncertainties in the number of neutrons emitted. It is difficult to estimate the errors, but the arrow bars (Fig. 5) suggest possible uncertainty limits in the $\upsilon(A)$ values. It is therefore premature to speculate on any detailed mechanism from these curves.

Can. J. Chem. Downloaded from www.nrcresearchpress.com by 210.87.254.105 on 09/05/12
For personal use only.

However, from the general trend of the $\upsilon(A)$ curve, it can be inferred that there is a definite tendency for the heavy fission fragments to emit more neutrons than the corresponding light fragments. This conclusion, if substantiated by further measurements, seems to have some bearing on the applicability of charge distribution hypotheses. The c.c.r. hypothesis would *a priori* lead to the conclusion that the light fragments will have higher excitation energy and thus emit a larger number of neutrons, contrary to our finding. It is therefore of importance that some mass-spectrometric yields be determined in 14 MeV neutron induced fission of ^{232}Th and ^{238}U, along with time-of-flight measurements on the fragments. The comparison of these data will show whether there is, indeed, some fine structure in the $\upsilon(A)$ curve.

Financial support of the research through the provision of a National Research Council Fellowship (L.H.G.), and, in part, the Ford Foundation Research Fellowship (H.D.S.), and the provision of equipment by the National Research Council of Canada and the Ford Foundation, is gratefully acknowledged.

1. E. F. Neuzil and A. W. Fairhall. Phys. Rev. **129**, 2705 (1963).
2. A. W. Fairhall. Phys. Rev. **102**, 1335 (1956).
3. E. K. Hyde. Univ. Calif. Rad. Lab. Rep. UCRL-9036. 1960.
4. R. C. Jensen and A. W. Fairhall. Phys. Rev. **109**, 942 (1958).
5. R. C. Jensen and A. W. Fairhall. Phys. Rev. **118**, 771 (1960).
6. H. D. Britt, H. E. Wegner, and J. C. Gursky. Phys. Rev. **129**, 2239 (1963).
7. E. K. Hyde. The nuclear properties of the heavy elements iii fission phenomena. Prentice–Hall, Inc., New York. 1964.
8. H. C. Britt and S. L. Whetstone Jr. Phys. Rev. **133**, B603 (1964).
9. J. P. Unik and J. R. Huizenga. Phys. Rev. **134**, B90 (1964).
10. J. M. Ferguson and P. A. Read. Phys. Rev. **150**, 1018 (1966).
11. E. Hagebo, A. C. Pappas, and P. Aagaard. J. Inorg. Nucl. Chem. **26**, 1639 (1964).
12. R. A. Iyer, C. K. Mathews, N. Ravindran, K. Rengan, D. V. Singh, M. V. Ramaniah, and H. D. Sharma. J. Inorg. Nucl. Chem. **25**, 465 (1963).
13. A. Wyttenback and H. R. Von Gunten. *In* Physics and chemistry of fission. Vol. I. Int. At. Energy Ass., Vienna. 1965.
14. R. S. Iyer, H. D. Jain, M. N. Namboodiri, M. Rajagopalan Rajkishore, M. V. Ramaniah, C. L. Rao, N. Ravindran, and H. D. Sharma. *In* Physics and chemistry of fission. Vol. I. Int. At. Energy Ass., Vienna. 1965. p. 439.
15. D. P. Ames, J. P. Balagna, J. W. Barns, A. A. Comstock, G. A. Cowan, P. G. Elkin, G. P. Ford, J. S. Gilmore, D. C. Hoffman, G. W. Knobeloch, E. J. Lang, M. A. Melnick, C. D. Minkkinen, B. D. Pollock, J. E. Sattizhan, C. W. Stanley, and B. Warren. U.S. At. Energy Comm. Decl. Rep. LA 1997 (1956).
16. J. G. Cunninghame. J. Inorg. Nucl. Chem. **5**, 1 (1957).
17. K. M. Broom. Phys. Rev. **126**, 627 (1962).
18. R. H. James, G. R. Martin, and P. J. Silvester. Radiochim. Acta, **3**, 76 (1964).
19. G. P. Ford and R. B. Leachman. Phys. Rev. **137**, B826 (1965); Physics and chemistry of fission. Vol. I. Int. At. Energy Ass., Vienna. 333 (1965).
20. S. J. Lyle, G. R. Martin, and J. E. Whitley. Radiochim. Acta, **3**, 80 (1964).
21. K. M. Broom. Phys. Rev. **133**, B874 (1964).
22. R. Ganapathy and P. K. Kuroda. J. Inorg. Nucl. Chem. **28**, 2071 (1966).
23. R. Ganapathy and H. Ihochi. J. Inorg. Nucl. Chem. **28**, 3071 (1966).
24. T. Mo and M. N. Rao. J. Inorg. Nucl. Chem. **30**, 345 (1968).
25. C. D. Coryell and N. Sugarman (*Editors*). Radiochemical studies: the fission products, NNES, Div. IV, Vol. 9. McGraw-Hill Book Co., Inc., New York and London. 1951.
26. J. Kleinberg. U.S. At. Energy Comm. Decl. Rep. LA 1721. 1954.
27. M. Lindner. Univ. Calif. Rad. Lab. Rep. UCRL-4377. 1954.
28. J. T. Prud'homme. Texas nuclear neutron generator manual. Austin, Texas. 1962.
29. R. J. Howerton. Univ. Calif. Rad. Lab. Rep. UCRL-5226 (1969).
30. V. M. Pankratov. Atom. Energy USSR, **14**, 177 (1963).
31. W. D. Allen and R. L. Henkel. Progr. Nucl. Energy **2**, 38 (1958). D. J. Hughes, J. E. Sanders, and J. Horowitz. (*Editors*). The Pergamon Press, Ltd., New York.
32. D. J. Gorman and R. H. Tomlinson. Can. J. Chem. **46**, 1663 (1968); AECL Prog. Rept. PR-CMa-2.
33. J. A. Macdonald and H. D. Sharma. Private communication.
34. A. S. Rao, M. N. Rao, and P. K. Kuroda. J. Inorg. Nucl. Chem. **31**, 591 (1969).
35. A. C. Wahl, R. L. Ferguson, D. R. Nethaway, D. E. Troutner, and K. Wolfsberg. Phys. Rev. **126**, 1112 (1962).
36. C. D. Coryell, M. Kaplan, and R. D. Fink. Can. J. Chem. **39**, 646 (1961).
37. N. A. Wogman, J. A. Powers, and J. W. Cobble. Phys. Rev. **152**, 1088 (1966).
38. N. K. Aras and G. E. Gordon. J. Inorg. Nucl. Chem. **28**, 736 (1966).
39. B. R. Erdahl. Ph.D. Thesis, Washington University, St. Louis. 1966; University Microfilm No. 67–7035.
40. W. H. Jones, A. Timnick, J. H. Paehler, and T. H. Handley. Phys. Rev. **99**, 184 (1955).
41. F. Gonnenwein and E. Pfeiffer. Z. Phys. **207**, 209 (1967).
42. J. Terrell. Phys. Rev. **127**, 880 (1962).
43. S. L. Whetstone Jr. Phys. Rev. **133** B613 (1964).
44. E. Konecny and H. W. Schmitt. Phys. Rev. **172** 1213 (1968).
45. F. Plasil, R. L. Ferguson, and H. W. Schmitt. Proceedings of 1969 Int. At. Energy Ass. Symposium on physics and chemistry of fission, Vienna. Paper SM 122/124.
46. C. M. Lederer, J. M. Hollander, and I. Perlman. Table of isotopes. John Wiley and Sons, Inc., New York.

Can. J. Chem. Downloaded from www.nrcresearchpress.com by 210.87.254.42 on 09/05/12
For personal use only.

Cumulative yields in the photofission of ^{232}Th and ^{238}U in the symmetric region

L. H. GEVAERT,[1] R. E. JERVIS, AND S. C. SUBBARAO
Department of Chemical Engineering and Applied Chemistry, University of Toronto, Toronto, Ontario

AND

H. D. SHARMA[2]
Department of Chemistry, University of Waterloo, Waterloo, Ontario

Received[3] October 1968

Fission mass yields for molybdenum-99, ruthenium-103 and -105, palladium-109 and -112, silver-111, cadmium-115, and tin-121 and -125 in the 25 MeV bremsstrahlung beam fission of thorium-232 and uranium-238 have been determined using radiochemical methods. The mass–yield curve for thorium-232 shows a pronounced third peak in the symmetric region, contrary to the results of Hiller and Martin with 69 MeV brehmsstrahlung. In the case of uranium-238, the curve is flat between mass numbers 111 to 121 in contrast to the 14 MeV neutron fission of the nuclide which shows a valley in this region.

Canadian Journal of Chemistry, **48**, 652 (1970)

Introduction

Numerous studies exist on the determination of chain yields in the photofission of ^{232}Th and ^{238}U (1–10). Schmitt and Sugarman (1) determined the yields of 26 fission chains for ^{238}U fission with bremsstrahlung beams with maximum energy of 48, 100, and 300 MeV and some selected peak and trough yields at lower beam energy. Richter and Coryell (2), Katz *et al.* (3), and others (4–8) reported the yields for selected fission products in ^{238}U and ^{232}Th at various energies. The results of these studies indicate that the shapes of mass–yield curves are generally similar to those obtained in other fissioning systems, except that the yields for mass numbers ranging from 77 to 84 are substantially higher compared to those obtained in thermal neutron fission, and the yields in the symmetric region are also higher. In the photofission of ^{226}Ra, a three-peaked mass-distribution curve was observed (5), whereas in ^{232}Th, a two-peaked curve was observed (9, 10).

Our earlier study on 14 MeV neutron fission of ^{232}Th and ^{238}U indicated that the shapes of the mass–yield curve in the symmetric region are different (11). ^{232}Th has a three-humped curve while ^{238}U has a two-peaked one. It was of interest to determine the mass yields in the symmetric region in the photofission of ^{232}Th and ^{238}U to examine whether mass–yield distribution in this region is significantly different compared to that obtained from neutron-fissioned compound nuclei.

Experimental

Uranyl nitrate or thorium nitrate (2 g) was irradiated with a bremsstrahlung beam produced by 25 MeV electrons impinging on a thin, air-cooled tungsten target. The electrons escaping from the tungsten target were deflected by a magnet during the irradiation. The samples, wrapped in a cadmium foil, were placed about 2 ft away from the target. The irradiation time varied from 1 to 3 h.

The methods of chemical separation and radiochemical assay for the nuclides isolated from the irradiated materials were similar to those described in our study of 14 MeV neutron fission of these nuclides using calibrated detectors. The activities of the nuclides of interest were much higher compared to those obtained in the 14 MeV neutron fission (11). ^{99}Mo was arbitrarily chosen as an internal standard and was assayed in each irradiation.

Results

The chain yields for selected nuclides for mass numbers ranging from 103 to 125 are given in Tables 1 and 2 along with the ones obtained by others at different photon energy. These yields have been estimated based on arbitrary ^{99}Mo yields of 2 and 6.0% for ^{232}Th and ^{238}U, respectively. If any different ^{99}Mo yields are measured in the future, the other yields will need revision accordingly.

The errors associated with radiochemical assay have been discussed in the preceding paper (11), and are lower in these determinations since higher

[1]Present address: Consumers Glass Co. Ltd., Toronto 18, Ontario.
[2]To whom all correspondence should be addressed.
[3]Revision received July 28, 1969.

TABLE 1
Photofission yields of ^{232}Th

Mass chain	Total chain yield (%) This work (25 MeV)	Hiller *et al.* (9) (69 MeV)	Zysin *et al.* (10) (10 MeV)
83		1.89	1.8
89		6.7	
91		5.7	5.7
^{99}Mo	2.00	1.85	1.1
^{103}Ru	$0.54_0 \pm 0.074$		
^{105}Ru	$0.53_2 \pm 0.054$	0.83	
^{109}Pd	$0.65_5 \pm 0.13$		
^{111}Ag	$0.73_4 \pm 0.10$	0.9	
^{112}Pd	1.00 ± 0.057	0.68	
^{113}Ag		0.58	0.066
^{115}Cd	$0.80_6 \pm 0.092$		0.032
^{117}Cd		0.68	0.037
^{121}Sn	$0.41_8 \pm 0.047$		
^{125}Sn(9.7 days)	$0.28_9 \pm 0.025$		
129			0.50
131		2.25	
133			4.3
139			5.0
140		6.6	7.0
141		6.8	
143		4.8	9.5

TABLE 2
Photofission yields of ^{238}U

Mass chain	Total chain yield (%) This work (25 MeV)	Meason *et al.* (8) (17.5 MeV monoenergetic)	Schmitt and Sugarman (1)	Richter and Coryell (2)	Katz *et al.* (3)
77					0.05
83		0.24		0.288	
84		0.66		0.511	
89			2.6	3.67	4.0
91		4.3		4.22	
92		4.4		3.46	
93			5.29		
97					
^{99}Mo	6.00	5.6	6.6	6.06	5.3
^{103}Ru	$4.0_8 \pm 0.50$		3.0		3.0
^{105}Ru	$2.6_8 \pm 0.31$	2.5		3.61	2.0
^{106}Ru			2.1		
^{109}Pd	$0.63_5 \pm 0.060$			0.224	
^{111}Ag	$0.43_6 \pm 0.044$		0.43		0.27
^{112}Pd	$0.41_4 \pm 0.030$		0.26	0.110	
^{113}Ag		0.19		0.0627	
^{115}Cd	$0.40_6 \pm 0.055$		0.25	0.0522	0.33
^{121}Sn	$0.37_3 \pm 0.063$				
^{125}Sn(9.7 days)	$0.30_6 \pm 0.051$				
127					
131		2.2	4.1	4.43	
132		7.8	5.0	5.78	
133		5.5		7.06	
134		5.7			
135		2.6			
139		4.9		5.97	4.8
140		6.0	4.9	5.77	
143			4.0	5.32	4.4
144			3.8		

Can. J. Chem. Downloaded from www.nrcresearchpress.com by 210.87.254.42 on 09/05/12
For personal use only.

TABLE 3
Cumulative mass yields in photofission

Mass number	^{232}Th Yield (%)	^{232}Th Number of determinations	^{238}U Yield (%)	^{238}U Number of determinations
99	2.0	8	6.0	8
103	0.54 ± 0.07	6	$4.0_9 \pm 0.5$	6
105	$0.53_2 \pm 0.054$	8	$2.6_8 \pm 0.31$	6
109	$0.65_5 \pm 0.13$	2	$0.63_5 \pm 0.06$	2
111	$0.73_4 \pm 0.10$	2	$0.43_6 \pm 0.04$	2
112	$1.0_1 \pm 0.065$	2	$0.42_0 \pm 0.04$	2
115	0.87 ± 0.12	7	0.44 ± 0.06	5
121	0.44 ± 0.060	6	$0.39_3 \pm 0.072$	4
125*	0.70 ± 0.30	6	0.72 ± 0.3	6

*The error is large since the isomer yield is not known.

count rates were recorded for the nuclides under investigation. However, larger errors were introduced due to fluctuations of the electron beam from the accelerator during irradiations.

Discussion

The cumulative yields as shown in Table 3 are derived from the assumptions described in our preceding paper. The total yields of mass 125 similarly have large errors.

In addition to the photon beam from the tungsten target, neutrons are produced in the tungsten target by the (γ, n) reaction. The energy of these neutrons is variable, and sufficiently high to cause both ^{232}Th and ^{238}U to fission and enhance the yields. The neutron flux in the target zone was estimated by irradiating sulfur, gold wire, copper, and aluminum along with ^{232}Th and ^{238}U samples, all wrapped in cadmium foil. The absence of the activity due to ^{198}Au in the gold wire confirmed that the thermal neutron flux was below the detection limit as given in Table 4. Similarly, no measurable ^{24}Na was found in the aluminum samples, indicating that the flux of neutrons above 6 MeV was negligible.

^{32}P obtained in the sulfur monitor is produced by neutrons having energy >0.09 MeV. There was a sufficient amount of ^{32}P activity to warrant quantitative estimation of the neutron flux from the tungsten target. Sulfur was irradiated with 14 MeV neutrons along with copper foil as a neutron flux monitor. The ^{32}P activity was assayed in both the neutron and bremsstrahlung beam irradiations, and compared. From the distribution in energy of neutrons emitted from the tungsten target with a 25 MeV electron beam (12), the cross-section data for the ^{32}S(n,p)^{32}P reaction (13) and the fission cross sections for ^{232}Th and ^{238}U (11), it was estimated that the contribution from neutron fission to the ^{99}Mo yield in the photofission of ^{232}Th and ^{238}U was not more than 0.7 and 2%, respectively. For nuclides in the symmetric region, the yields due to 0.05 and 6 MeV neutrons (maxima at 2.25 MeV) are lower compared to photofission yields. An upper limit of 0.5% contribution to the yields from neutron fission was estimated. The mass yields are presented in Table 3, as well as the cumulative errors associated with the determination. The average number of neutrons emitted in these fissioning systems is taken as 3.5. The uncertainty based on the assumptions of charge distribution hypotheses is similar to 14 MeV neutron-fissioning systems if Coryell's prescription is followed for obtaining Z_p for these systems (14).

In the photofission of ^{232}Th and ^{238}U by a bremsstrahlung beam, the fissioning nuclei are mainly excited to about 15 MeV by dipole resonance absorption of photons even though the maximum energy of the bremsstrahlung beam may be higher (15). It is expected that the shape of the mass–yield curves will resemble those obtained with bremsstrahlung beams of 14 MeV and higher. The mass–yield curve for ^{232}Th as shown

TABLE 4
Monitor threshold and detection limits

Reaction	Threshold	Detection limit (n/cm^2 s)
^{27}Al(n,α)^{24}Na	6 MeV	1×10^5
^{32}S(n,p)^{32}P	0.09 MeV	3×10^6
^{197}Au(n,γ)^{198}Au	Thermal	5×10^4

Can. J. Chem. Downloaded from www.nrcresearchpress.com by 210.87.254.42 on 09/05/12
For personal use only.

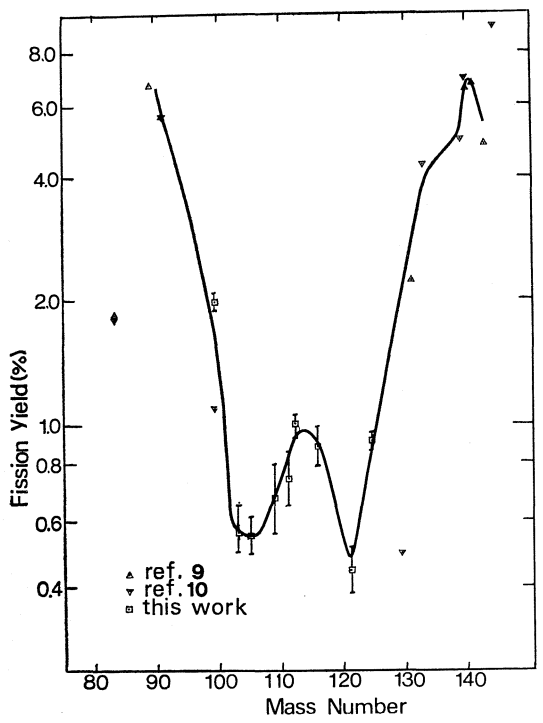

FIG. 1. Mass–yield curve in the 25 MeV photofission of ^{232}Th.

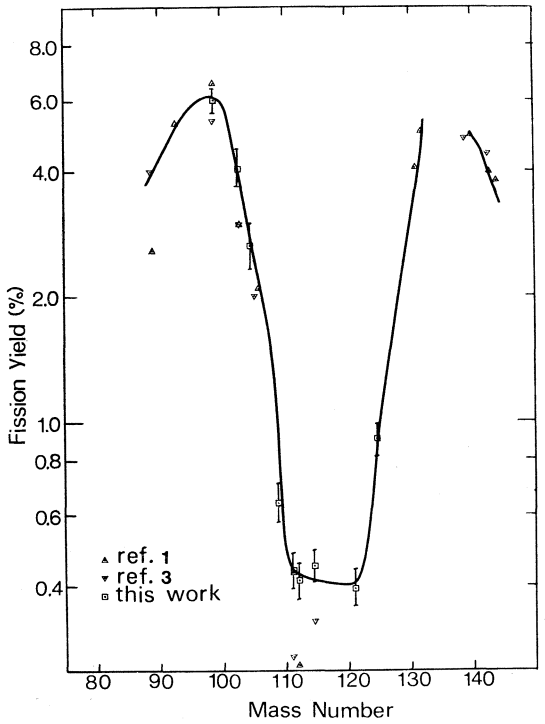

FIG. 2. Mass–yield curve in the 25 MeV photofission of ^{238}U.

in Fig. 1 has a pronounced third peak in the symmetric region, contrary to the results of Hiller and Martin (9) and Zysin *et al.* (10). The third peak is narrower compared to that in the 14 MeV neutron fission of ^{232}Th but similar to that obtained for ^{232}Th fissioned with reactor neutrons (16).

The mass–yield curve for ^{238}U as presented in Fig. 2 has almost the same yields from mass numbers 111 to 121. The mass yield for 111 is in good agreement with the one obtained by Schmitt and Sugarman at 21 MeV, whereas Katz reported a lower value. The mass yields for ^{112}Pd and ^{115}Cd are a little higher than those obtained by others (Table 2). The shape of the curve is slightly different compared to the one obtained in the 14 MeV neutron fission. The peak-to-trough ratio is about 14. The prompt mass yieldsreported by Hogg (17) are not precise enough to make a direct comparison with these radiochemical yields. However, from a comparison of the shapes of the prompt yield and radiochemical yield curves, it appears that the neutron emission as a function of primary fission fragments might be different from particle-induced fission. It will be of interest to obtain precise data on prompt yields along with some mass-spectrometric yields in photofission to derive the neutron-emission curve.

In summary, the mass–yield distribution for fission of ^{232}Th with 25 MeV bremhsstrahlung shows a three-humped curve whereas ^{238}U has the usual two-peaked curve.

Financial support of the research through the provision of a National Research Council of Canada Fellowship (LHG), and, in part, a Ford Foundation Research Fellowship (HDS), and the provision of equipment by the National Research Council of Canada and the Ford Foundation, is gratefully acknowledged.

1. R. A. SCHMITT and N. SUGARMAN. Phys. Rev. **95**, 1260 (1954).
2. H. G. RICHTER and C. D. CORYELL. Phys. Rev. **95**, 1550 (1954).
3. L. KATZ, T. M. KAVANAGH, A. G. W. CAMERON, E. C. BAILEY, and J. W. T. SPINKS. Phys. Rev. **99**, 98 (1958).
4. J. G. CUNNINGHAME, M. P. EDWARDS, G. P. KIH, and K. H. LOKAN. Nucl. Phys. **44**, 588 (1963).

Can. J. Chem. Downloaded from www.nrcresearchpress.com by 210.87.254.42 on 09/05/12
For personal use only.

5. R. B. DUFFIELD, R. A. SCHMITT, and R. A. SHARP. Proc. 2nd Int. Conf. Peaceful Uses At. Energy, Geneva, **15**, 202, paper 678 (1958).
6. A. P. KOMAR, B. A. BOCHAGOV, and V. I. FADEEV. Sov. Phys. Dokl. **7**, 913 (1963); **8**, 978 (1964).
7. B. A. BOCHAGOV, A. P. KOMAR, and G. E. SOLYAKIN. Sov. Phys. JETP, Engl. Transl. **11**, 889 (1960); **16**, 1135 (1963).
8. J. L. MEASON and P. K. KURODA. Phys. Rev. **142**, 691 (1966).
9. D. M. HILLER and D. S. MARTIN. Phys. Rev. **90**, 581 (1953).
10. Y. A. ZYSIN, A. A. LBOV, and L. I. SEL'DHENKOV. Fission product yields and their mass distribution. Engl. Transl. Consultants Bureau Enterprises Inc., New York. 1964.
11. L. H. GEVAERT, R. E. JERVIS, and H. D. SHARMA. This issue.
12. J. S. HEWITT, K. G. MCNEILL, and J. W. JURY. In Press.
13. P. JESSEN, M. BORMAN, F. DREYER, and H. NEUERT. Nucl. Data, **1**, 148 (1966); **1**, 117 (1966).
14. C. D. CORYELL, M. KAPLAN, and R. D. FINK. Can. J. Chem. **39**, 646 (1961).
15. R. A. SCHMITT and R. B. DUFFIELD. Phys. Rev. **105**, 1277 (1957).
16. R. H. IYER, C. K. MATHEWS, N. RAVINDRAN, K. RENGAN, D. V. SINGH, M. V. RAMANIAH, and H. D. SHARMA. J. Inorg. Nucl. Chem. **25**, 465 (1963).
17. G. R. HOGG. Nucl. Phys. **72**, 167 (1965).

For personal use only.

Selenium tetrafluoride adducts. II. Adducts with boron trifluoride and some pentafluorides

R. J. GILLESPIE AND A. WHITLA
Department of Chemistry, McMaster University, Hamilton, Ontario
Received October 3, 1969

Adducts of selenium tetrafluoride with SbF_5, AsF_5, NbF_5, TaF_5, and BF_3 have been investigated by means of infrared, Raman, and nuclear magnetic resonance spectroscopy and conductimetric and cryoscopic measurements. It is concluded that in the solid state these compounds are best formulated as having ionic structures $SeF_3^+MF_6^-(BF_4^-)$, although the ions interact rather strongly by fluorine bridging. This fluorine bridging apparently persists in the molten state and to some extent in solution in nitrobenzene.

Canadian Journal of Chemistry, **48**, 657 (1970)

Can. J. Chem. Downloaded from www.nrcresearchpress.com by 210.87.254.42 on 09/05/12
For personal use only.

It has been suggested that the adducts of SeF_4 with Lewis acids are in general ionic compounds of the SeF_3^+ ion (1). This suggestion has received support from the recent work of Evans and Long (2), who showed that the Raman spectra of the molten complexes $SeF_4 \cdot AsF_5$ and $SeF_4 \cdot SbF_5$ could be interpreted in terms of the ionic structures $SeF_3^+ \cdot AsF_6^-$ and $SeF_3^+ \cdot SbF_6^-$. Still more recently, Edwards and Jones (3) have determined the crystal structure of the complex $SeF_4 \cdot 2NbF_5$, which they showed to have a geometry consistent with the formulation $SeF_3^+Nb_2F_{11}^-$. There are fluorine bridges between the SeF_3^+ and the $Nb_2F_{11}^-$ ions, each SeF_3^+ forming three such bonds and thus achieving a distorted octahedral configuration with the lone pair of electrons on the selenium apparently occupying a seventh coordinate position in the face of the octahedron defined by the three fluorine bridge bonds.

In Part I (4) we showed that the adduct $SeF_4 \cdot SO_3$ can be only very approximately represented by the formulation $SeF_3^+ \cdot SO_3F^-$, as there is clear evidence that the SeF_3 groups are bound together quite strongly by bridging fluorosulfate groups, giving dimeric and higher polymeric structures which persist in the molten state and in solution. Presumably the bridge bonds have an appreciable amount of covalent character.

In this paper we report the results of our studies of the 1:1 adducts of SeF_4 with BF_3, SbF_5, AsF_5, NbF_5, TaF_5, and BiF_5.

Experimental Section

Selenium tetrafluoride was prepared as described in the previous paper (4). Boron trifluoride (Matheson) and arsenic pentafluoride (Ozark–Mahoning) were used directly from the cylinder, which was connected to the vacuum system. Antimony pentafluoride (Allied Chemicals) was distilled twice at atmospheric pressure, and the center fraction from the second distillation was distilled under vacuum into the reaction flask. Niobium and tantalum pentafluorides (Ozark–Mahoning) were sublimed into the reaction flask.

The adducts with boron trifluoride and arsenic pentafluoride were prepared by bubbling the gas through selenium tetrafluoride. The unreacted selenium tetrafluoride was removed under vacuum, leaving a fine white powder in both cases.

The adducts of SbF_5, NbF_5, and TaF_5 were prepared by distilling an excess of selenium tetrafluoride onto the pentafluoride in a trap, allowing the system to warm up slowly to ~0° until a clear solution was obtained, then pumping off the unreacted SeF_4 under vacuum, leaving the product as a fine white powder.

Anal. Calcd. for SeF_4BF_4: Se, 35.44; F, 59.70. Found: Se, 35.3; F, 54.5.

Anal. Calcd. for SeF_4SbF_5: Se, 21.24; F, 46.00; Sb, 32.76. Found: Se, 21.2; F, 46.3; Sb, 31.6.

Anal. Calcd. for SeF_4AsF_6: Se, 24.30; F, 52.64. Found: Se, 24.4; F, 52.3.

Anal. Calcd. for SeF_4NbF_5: Se, 23.03, F; 49.87; Nb, 27.10. Found: Se, 21.0; F, 50.8; Nb, 30.5.

Anal. Calcd. for SeF_4TaF_5: Se, 18.32; F, 39.68; Ta, 42.00. Found: Se, 17.9; F, 38.1; Ta, 45.2.

The experimental methods for the infrared, Raman, and nuclear magnetic resonance (n.m.r.) measurements have been described previously (4). The Raman spectrum of $SeF_4 \cdot BF_3$ was obtained using He/Ne laser excitation.

Results and Discussion

Infrared and Raman Spectra

The frequencies of the lines observed in the infrared and Raman spectra of the adducts of SeF_4 with the pentafluorides SbF_5, AsF_5, NbF_5, and TaF_5 are given in Tables 1 to 4.

A reasonable assignment of the observed lines for all these adducts can be made on the assumption that they are essentially ionic compounds which can be formulated as $SeF_3^+MF_6^-$. The

TABLE 1

Infrared and Raman spectra of SeF_3SbF_6*

Frequency, SeF_3SbF_6 (cm^{-1})					Frequency, SbF_6^- (5) (cm^{-1})	
	Raman					
Infrared	Melt†		Solid	Assignment	Infrared	Raman
269 s	276 s	(275)	264	ν_5 (T_{2g}) SbF_6^-		270
284 s			285			298
290 m	309 m	(290)		ν_4 SeF_3^+		
				ν_4 (T_{1u}) SbF_6^-	350	
374 m	373 m	(381)		ν_2 SeF_3^+		
451 m						
489 m						
538 m	522 s	(550)	516 m	ν_2 (E_g) SbF_6^-		583
562 m	561 s		560 m			
			600 w			
641 s	648 s	(645)	645 s	ν_1 (A_{1g}) SbF_6^-		664
683 s	663 m		675 m	ν_3 (T_{1u}) SbF_6^-	660	
			690 w			
738 m	742 s	(743)	746 s	ν_3 SeF_3^+		
765 m	775 s	(781)	774 s	ν_1 SeF_3^+		

*s = strong, m = medium, w = weak.
†Values in parentheses are from ref. 2.

TABLE 2

Infrared and Raman spectra of SeF_3AsF_6*

Frequency, SeF_3AsF_6 (cm^{-1})					Frequency, AsF_6^- (5) (cm^{-1})	
	Raman					
Infrared	Melt†		Solid	Assignment	Infrared	Raman
	239 w					
305 m	311 m	(277)		ν_4 SeF_3^+		
366 m	372 m	(366)		ν_2 SeF_3^+, ν_5 (T_{2g}) AsF_6^-		372
				ν_4 (T_{1u}) AsF_6^-	392	
547 m	530 m	(551)		ν_2 AsF_6^-		576
568 m	569 m					
653 m	675 s	(676)	645 s	ν_1 (A_{1g}) AsF_6^-		679, 685
712 s	691 w			ν_3 (T_{1u}) AsF_6^-	700	
728 s			721 m			
760 sh	754 sbr	(750)	753 m	ν_3 SeF_3^+		
781 w	784 vs	(778)	778 s	ν_1 SeF_3^+		

*w = weak, m = medium, s = strong, sh = shoulder, br = broad, v = very.
†Values in parentheses are from ref. 2.

MF_6^- ion belongs to the point group O_h and therefore has six normal modes of vibration, $\nu_1(A_{1g})$, $\nu_2(E_g)$, $\nu_3(T_{1u})$, $\nu_4(T_{1u})$, $\nu_5(T_{2g})$, and $\nu_6(T_{2u})$, of which ν_1, ν_2, and ν_5 are Raman active and ν_3 and ν_4 are infrared active. SeF_3^+ is expected to be pyramidal and would have four fundamentals, all active in both the infrared and Raman. The frequencies for SeF_3^+ are expected to be close to those for the isoelectronic molecule AsF_3. However, in every case the spectra have features which show that the compounds are not completely satisfactorily formulated as simple ionic compounds. Thus for $SeF_3 \cdot SbF_6$, ν_1, ν_2, and ν_5 for SbF_6^- appear in the infrared and ν_3 appears in the Raman. Thus the mutual exclusion rule is not obeyed either in the crystal

Can. J. Chem. Downloaded from www.nrcresearchpress.com by 210.87.254.42 on 09/05/12
For personal use only.

TABLE 3

Infrared and Raman spectra of SeF_3NbF_6*

Frequency, SeF_3NbF_6 (cm^{-1})				Frequency, NbF_6^- (6) (cm^{-1})	
	Raman				
Infrared	Melt	Solid	Assignment	Infrared	Raman
	256 s		ν_5 (T_{2g}) NbF_6^-		
	279 s				
	317 shm		ν_4 SeF_3^+		
370 m	372 m		ν_2 SeF_3^+		
472 sbr		450 m			
571 s		577 m	ν_2 (E_g) NbF_6^-		562
			ν_3 (T_{1u}) NbF_6^-	583	
657 s			ν_1 (A_1) NbF_6^-		683
715 s	724 sbr	712 m	$\nu_3SeF_3^+$		
		738 m			
766 s	769 vs	769 s	ν_1 SeF_3^+		

*s = strong, sh = shoulder, m = medium, br = broad, v = very.

TABLE 4

Infrared and Raman spectra of SeF_3TaF_6*

Frequency, SeF_3TaF_6 (cm^{-1})				Frequency, TaF_6^- (7), infrared (cm^{-1})
	Raman			
Infrared	Melt	Solid	Assignment	
			ν_4 (T_{1u}) TaF_6^-	220, 232, 245
304 w			ν_4 SeF_3^+	
357 w			ν_2 SeF_3^+	
493 s		472 w		480
511 s				
576 m		565 w	ν_3 (T_{1u}) TaF_6^-	582
635 s				
668 m				
728 m	721 m	720 s	ν_3 SeF_3^+	720
	740 m	742 s		
769 m	774 s	773 s	ν_1 SeF_3^+	

*w = weak, s = strong, m = medium.

or the melt and presumably, therefore, the center of symmetry of the octahedral ion has been removed. In addition, we note that the degenerate vibrations ν_2, ν_3, and ν_5 of SbF_6^- are split into doublets, which again shows that there must be a reduction in symmetry from the octahedral symmetry of an isolated SbF_6^- ion. The most reasonable way to account for this reduction in symmetry is to assume that the SbF_6^- ion forms fluorine bridges to neighboring SeF_3^+ ions.

It is tempting to suggest that each SbF_6^- ion forms two such bridges to give the following structure

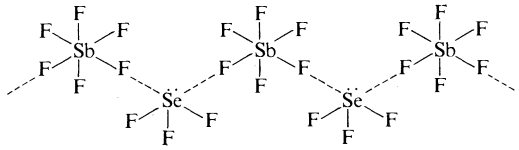

However, there is no real evidence that this is the case, and in view of Edwards and Jones' work (3), the actual structure may be more complex than this.

Agreement is generally good between our results for the Raman spectrum of the melt and the spectra obtained by Long and Evans (2),

Can. J. Chem. Downloaded from www.nrcresearchpress.com by 210.87.254.42 on 09/05/12
For personal use only.

TABLE 5
Vibrational frequencies for SeF_3^+ and AsF_3

	Frequency (cm^{-1})					
Assignment	SeF_3SbF_6	SeF_3AsF_6	SeF_3NbF_6	SeF_3TaF_6	SeF_3BF_4	AsF_3 (6)
$\nu_1(A_1)$	775	784	769	773	763	707
$\nu_2(A_1)$	373	372	372	357	382	341
$\nu_3(E)$	742	754	724	740	730	644
$\nu_4(E)$	309	311	317	304	325	274

although they did not observe the splittings of the degenerate vibrations. We are unable to assign two moderately strong lines in the infrared at 451 and 489 cm^{-1}. There is good agreement between the frequencies assigned to the SeF_3^+ ion and those observed in the other compounds studied and in the isoelectronic molecule AsF_3 (Table 5). Our assignment for SeF_3^+ agrees with that of Evans and Long (2), except in the case of ν_4, for which we prefer the observed frequency of 309 cm^{-1}. This assignment can be made consistently for all the other compounds studied (Table 5). The band observed at 600 cm^{-1} in the Raman of the solid cannot be assigned with certainty. It might arise from a crystal (factor-group) splitting of ν_2 of SbF_6^- or possibly it is the third component of the triply degenerate ν_3.

The spectrum of $SeF_3 \cdot AsF_6$ can be assigned in a quite similar manner (Table 2). We note the splitting of ν_2 and ν_3 of AsF_6^- and the occurrence of ν_1, ν_2, and ν_3 of AsF_6^- in both the infrared and Raman, again indicating reduced symmetry for both ions which can be most simply explained in terms of fluorine bridging between the ions. Our results for the melt agree quite well with those of Evans and Long (2) except that the sharp line that they report at 277 cm^{-1} we find at 311 cm^{-1} in the Raman spectrum of the melt and at 305 cm^{-1} in the infrared of the solid. We have assigned this line to ν_4 of SeF_3^+ and the frequency agrees quite well with that found in the other compounds studied.

Assignments cannot be made with such certainty for $SeF_3 \cdot NbF_6$ and $SeF_3 \cdot TaF_6$ because there is less complete information on the vibrational frequencies of the NbF_6^- and TaF_6^- ions, and because of the poorer quality of some of our data, particularly the Raman spectra of the crystalline material. However, the four characteristic frequencies of SeF_3^+ are observed in each case and the assignments that can be made are quite consistent with the ionic structure. We note again a removal of the degeneracies of $\nu_5(NbF_6^-)$ and of $\nu_3(SeF_3^+)$ which we take as evidence of fluorine bridging. A Raman spectrum of solid $SeF_3 \cdot BiF_6$ gave lines at 510, 530, 582, 592, 727, 742, and 769 cm^{-1}, of which the 727 and 742 cm^{-1} lines may be attributed to ν_3 of SeF_3^+ and the 769 cm^{-1} line to ν_1 of SeF_3^+.

Our general conclusion from the spectra of these complexes of SeF_4 with pentafluorides is that they are all to be regarded as ionic compounds of the type $SeF_3^+MF_6^-$ and that these ions are held together by relatively strong fluorine bridges.

The adduct $SeF_4 \cdot BF_3$ would be expected to have the ionic structure $SeF_3^+BF_4^-$. All four fundamental frequencies for the tetrahedral BF_4^- ion are allowed in the Raman, but only the asymmetric stretch and bend ν_3 and ν_4 are allowed in the infrared. A satisfactory assignment (Table 6) can be made on the basis of the ionic structure, the frequencies assigned to the SeF_3^+ ion being very close to those for this ion in the complexes with pentafluorides. There is, however, one unusual feature of the spectrum which we are not able to explain satisfactorily; that is, that the symmetrical stretching frequency ν_1 of the BF_4^- ion has an unusually low frequency. If, alternatively, one were to assume that the ν_1 band for BF_4^- is hidden under the strong ν_1 and ν_3 bands of SeF_3^+, then it is difficult to account for the moderately strong band at 683 cm^{-1} which at low temperatures in both the infrared and Raman appears to be split. This splitting might also suggest that this band should not be assigned to the non-degenerate vibration ν_1; unless, of course, this is to be regarded as a crystal (i.e., factor-grouping) splitting. We note that the forbidden bands ν_1 and ν_2 of BF_4^- are observed in the infrared, and a splitting of the ν_3 band of SeF_3^+ is observed in the Raman spectrum of the solid, which is very similar to the splitting observed in almost all the other complexes.

Can. J. Chem. Downloaded from www.nrcresearchpress.com by 210.87.254.42 on 09/05/12
For personal use only.

TABLE 6

Infrared and Raman spectra of SeF_3BF_4*

Frequency, SeF_3BF_4 (cm^{-1})				Frequency, BF_4^- (cm^{-1})	
	Raman				
Infrared	Melt	Solid	Assignment	Infrared	Raman
	163 vw				
	208 vw	230	Torsional and other modes of the polymeric chain		
	275 w				
	300 w	287			
	325 m	327	ν_4 SeF_3^+		
343 m	357 m	365	ν_2 (*E*) BF_4^-		369
379 w	382 m	387	ν_2 SeF_3^+		
519 s					
532 s	525 m	529	ν_4 (T_2) BF_4^-	521, 536	541
553 msh					
652 m		657	ν_1 (A_1) BF_4^-	772	786
668 m	678 msh	678			
		707			
725 s	730 sbr		ν_3 SeF_3^+		
		729			
746 ssh	763 vs	761	ν_1 SeF_3^+		
831 w					
975 s	974 sbr			1030	
1076 s	1050 wsh	1054	ν_3 (T_2) BF_4^-		1100
1149 msh				1059	

*v = very, w = weak, m = medium, s = strong, sh = shoulder, br = broad.

Nuclear Magnetic Resonance

The results obtained in the investigation of the ^{19}F resonance of these complexes in the molten state are summarized in Table 7. For $SeF_3 \cdot SbF_6$, two rather broad resonances were observed at 27.0 and −95.7 p.p.m. from CF_3CO_2H with relative areas of 2:1 which may be attributed to SbF_6^- and SeF_3^+, respectively. $KSbF_6$ in water has a ^{19}F chemical shift of +32.3 p.p.m. and liquid SeF_4 has a chemical shift of −141 p.p.m. from CF_3CO_2H (8). The breadth of the SbF_6^- signal could be due to collapse of the multiplet expected from Sb–F coupling as a result of quadrupole relaxation or alternatively it might be due to a slow fluorine exchange resulting, for example, from a slight dissociation of the adduct into its two components

$$SeF_3 \cdot SbF_6 \rightleftarrows SeF_4 + SbF_5$$

The width of the SeF_3^+ signal must also be attributed to this slow exchange and this is supported by the absence of satellites due to ^{77}Se–F coupling. The observation of only one signal for all the other molten complexes must also be attributed to such an exchange which, in these cases, occurs more rapidly so that the signals due to the two ions are collapsed into a single signal. Such exchange processes would be expected to be facilitated if the two ions are strongly bonded together by fluorine bridges as we have suggested above.

TABLE 7

^{19}F n.m.r. data for the molten complexes

Complex	δ(p.p.m. from CF_3CO_2H)*			
SeF_3SbF_6	+27.0	(360)	−95.7	(27)
SeF_3AsF_6		−52.5	(310)	
SeF_3NbF_6		−170	(260)	
SeF_3TaF_6		−56.4	(200)	

*Values in parentheses are the line widths in Hz.

Conductimetric and Cryoscopic Measurements

The results of the conductivity measurements on solutions of the adducts in nitrobenzene are given in Fig. 1. The compounds SeF_3SbF_6, SeF_3AsF_6, SeF_3NbF_6, and SeF_3TaF_6 all give conducting solutions and appear to be extensively ionized in dilute solution. The SeF_3BF_4 compound, on the other hand, gives a low conductivity comparable with that of the weak

Can. J. Chem. Downloaded from www.nrcresearchpress.com by 210.87.254.42 on 09/05/12
For personal use only.

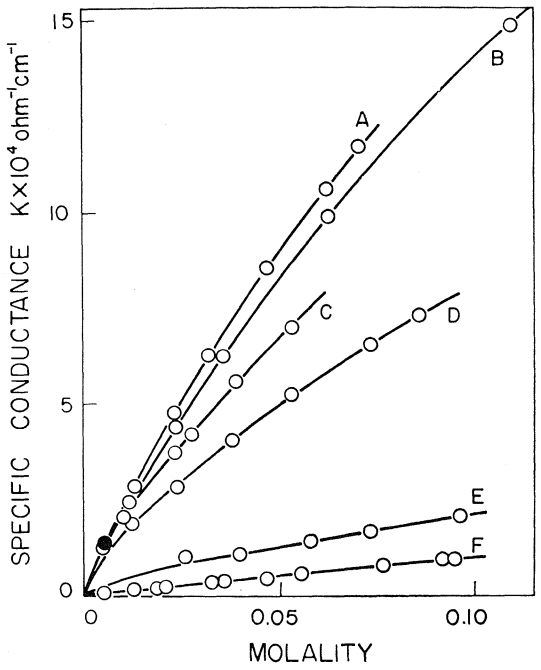

FIG. 1. Conductivities of solutions in nitrobenzene: *A*, SeF_3SbF_6; *B*, SeF_3AsF_6; *C*, SeF_3TaF_6; *D*, SeF_3NbF_6; *E*, SeF_3BF_4; *F*, SeF_3SO_3F; ●, tetramethylammonium picrate, ref. 10.

electrolyte $AlCl_3$ (9). The cryoscopic results for SeF_3AsF_6, SeF_3NbF_6, SeF_3TaF_6, and SeF_3BF_4 are given in Fig. 2. The freezing point depressions approach the depression expected for a binary electrolyte at low concentrations but indicate that dissociation is incomplete at higher concentrations. From both the cryoscopic and conductimetric results, it would appear that the extent of dissociation of these adducts in nitrobenzene decreases in the order

$$SeF_3SbF_6 > SeF_3AsF_6 > SeF_3TaF_6 > SeF_3NbF_6 > SeF_3BF_4$$

It seems reasonable to conclude that incomplete dissociation is due to fluorine bridging between the anion and the cation and that therefore the strength of the fluorine bridging increases along the above series.

The conductivities of the adducts SeF_3BF_4, SeF_3SbF_6, SeF_3AsF_6, SeF_3NbF_6, and SeF_3TaF_6 were measured in the molten state at temperatures just above their melting points. All the conductivities fell in the range 1.5 to 3.3 × 10^{-2} Ω^{-1} cm^{-1}, which is about 20 times greater than the conductivity of molten SeF_3SO_3F (4). It seems clear that in contrast to SeF_3SO_3F, the adducts of SeF_4 with BF_3 and the pentafluorides that we have investigated are appreciably, if not extensively, ionized in the molten state.

Conclusions

A consistent interpretation of all the above data can be given on the basis of a fluorine-bridged ionic structure for all the SeF_4 adducts studied, the degree of interaction between the ions increasing along the series SeF_3SbF_6, SeF_3AsF_6, SeF_3TaF_6, SeF_3NbF_6, SeF_3BF_4. All these compounds are more ionic than SeF_3SO_3F, which we have previously shown to be a largely-covalent compound (4). The fluorine bridging is sufficiently strong to be retained to a considerable extent in the molten state and to cause incomplete dissociation in the ionizing solvent nitrobenzene.

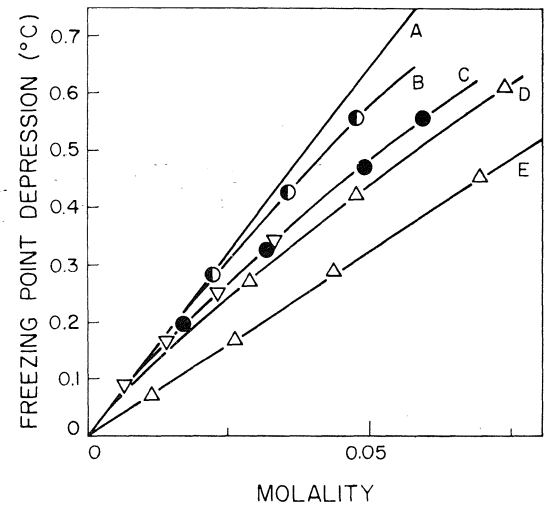

FIG. 2. Freezing point of solutions in nitrobenzene: *A*, ideal binary electrolyte; *B*, SF_3AsF_6; *C*, (▽) SeF_3TaF_6, (●) SeF_3NbF_6; *D*, $SeF_3{\cdot}BF_4$; *E*, 1,3,5 trinitrobenzene (non-electrolyte).

We thank the National Research Council of Canada for financial support of this work. We also thank the National Research Council of Canada and the International Nickel Company for the award of scholarships (to W.A.W.).

Can. J. Chem. Downloaded from www.nrcresearchpress.com by 210.87.254.42 on 09/05/12
For personal use only.

1. R. D. PEACOCK. Progr. Inorg. Chem. **2**, 237 (1960).
2. J. A. EVANS and D. A. LONG. J. Chem. Soc. A, 1688 (1968).
3. A. J. EDWARDS and G. R. JONES. Chem. Commun. 346 (1968).
4. R. J. GILLESPIE and A. WHITLA. Can. J. Chem. In press.
5. G. M. BEGUM and A. C. RUTENBERG. Inorg. Chem. **6**, 2212 (1967).
6. H. SIEBERT. Anwendungen der Schwingungsspektroskopie in der Anorganischen Chemie. Springer-Verlag, Berlin. 1966.
7. J. S. FORDYCE and R. L. BAUM. J. Chem. Phys. **44**, 1159 (1966).
8. E. L. MUETTERTIES and W. D. PHILLIPS. J. Amer. Chem. Soc. **81**, 1084 (1959).
9. R. E. VAN DYKE and H. E. CRAMFORD. J. Amer. Chem. Soc. **73**, 2018 (1951).
10. E. G. TAYLOR and C. A. KRAUS. J. Amer. Chem. Soc. **69**, 1731 (1947).

Can. J. Chem. Downloaded from www.nrcresearchpress.com by 210.87.254.42 on 09/05/12
For personal use only.

Ion–molecule reactions in carbonyl sulfide – hydrocarbon mixtures

I. DŽIDIĆ, A. GOOD, AND P. KEBARLE
Chemistry Department, University of Alberta, Edmonton, Alberta

Received August 28, 1969

The major ion–molecule reactions occurring in pure COS and in mixtures of COS with methane, methyl iodide, ethane, and ethylene were investigated in a Nier-type mass spectrometer. In cases where two or more reactions could be postulated to account for the observed product ions, appearance potential data and graphical analysis were used to evaluate the contributions of the individual reactions. Phenomenological cross sections were obtained for the reactions studied and approximate rate constants were then calculated.

An independent set of measurements were carried out in a high-pressure pulsed-beam mass spectrometer, in which the absolute rate constants for reactions occurring in COS were measured, using nitrogen as a carrier gas. The rate constants thus obtained were used to verify the validity of the rate constants calculated from the measured cross sections.

Canadian Journal of Chemistry, **48**, 664 (1970)

Can. J. Chem. Downloaded from www.nrcresearchpress.com by 210.87.254.6 on 09/05/12
For personal use only.

Introduction

Little work has been reported in the literature on the reactions of sulfur-containing ions. Several ion–molecule reactions occurring in H_2S/CH_4 mixtures have been reported (1), and a series of secondary ions were observed (2) as products of reactions of excited CS_2^+ ions with CS_2, I_2, and C_2H_4. Reactions involving S^+ precursors were not reported.

A great deal of work on the reactions of S atoms with hydrocarbons has been reported by Gunning *et al.* (3, 4), and it seemed desirable to complement these studies of neutral reactions with an investigation of those occurring between S^+ ions and hydrocarbons. In the present study, reactions occurring in mixtures of COS and hydrocarbons, and in COS alone, have been examined. COS was chosen for this purpose as it is a good source of S^+ ions, which are formed with an intensity equal to 33% of that of the parent ion at 70 eV.

Experimental

Cross-section Measurements

The reaction cross-section measurements were performed using a 90° Nier-type mass spectrometer with a 6 in. radius of curvature. The ion source had an electron beam entrance slit of dimensions 0.25 × 0.0075 cm and an ion exit slit of 0.8 × 0.0025 cm. The trap current was typically 0.2 μA. Inside the ion source, the repeller-ion exit slit distance was 0.45 cm, and the electron beam entrance slit was 0.16 cm above the plane of the ion exit slit. The effective electron beam distance from the ion exit slit, l, was obtained by measuring the ion source voltage $V_{i.s.}$ (relative to ground) required to focus the peak of the calibrating gas (Ar m/e 40) at constant magnetic field and variable repeller voltage V_r. Since under these conditions the total accelerating voltage V_{acc} (relative to ground) must remain constant, the relationship

$$V_{i.s.} = V_{acc} - E_r l$$

must hold, where E_r is the field strength obtained from the repeller voltage V_r and the repeller distance $d = 0.45$ cm. A plot of $V_{i.s.}$ vs. E_r gave a straight line with a negative slope equal to $l = 0.13$ cm. To make the determination more accurate, low V_{acc} were used (~ 300 V) and V_{acc} was measured with a digital voltmeter. The value $l = 0.13$ cm will be used in the further calculations involving the conversion of the cross sections to rate constants. The above method for determining the effective distance of the electron beam from the exit slit is simpler, although probably less accurate, than the method described by Stevenson (5). The electron accelerating voltage was measured by a potentiometer.

Total pressures of the order of a few microns were easily obtainable in the ion source because of the narrow slits and the high external pumping speed provided by a 4 in. (200 l/s) pumping system. A separate 1 in. pumping system was used to pump the mass-analyzer tube.

The gas handling plant contained two 2-l reservoirs, each with a set of two leaks. The pressures on the high pressure side were measured using two 0–20 and 0–200 Torr Wallace and Tiernan diaphragm-type manometers. The ion source pressures obtained with a given pressure in the reservoir and a given leak were first measured with a McLeod gauge attached directly to the ion source. These calibrations gave equations of the type

$$P_{(\text{ion source})} = \text{constant} \times P_{(\text{reservoir})}$$

where the constant depended on the leak used. In the further experiments only the reservoir pressure was determined and the ion source pressure then obtained with the appropriate conversion factor. The dual reservoir system allowed convenient handling of binary gas mixtures, the two gases being fed separately to the ion source. The ion currents were measured using a Faraday cup collector and a vibrating reed electrometer.

Absolute Rate Constant Measurements

The absolute rate constant values reported were measured using a pulsed electron beam and a delay pulsed ion collection system to obtain the variation of the ionic intensities with time. This system has recently been described in some detail (6). In the present work, total

Can. J. Chem. Downloaded from www.nrcresearchpress.com by 210.87.254.6 on 09/05/12
For personal use only.

pressures of 1 to 3 Torr were employed, and the ion intensities were measured up to 2000 μs delay time. An electron pulse of 10 μs duration, with a time interval of 3000 μs between pulses, was used and the ion collection pulse was also of 10 μs duration. The experiments were performed at room temperature (300 °K).

In order to slow down the rates of the reactions occurring, it was necessary to work with COS pressures of much less than the 1 Torr required for satisfactory ion sampling. The COS was therefore leaked into a stream of pure nitrogen through a capillary leak, and the partial pressure of COS could then be calculated either by measuring the relative COS^+ and N_2^+ peak heights using the quadrupole ion source (6), or by using the known conductance of the capillary leak to calculate the COS flow rate as a percentage of the flow rate through the ion source. This total flow rate was measured by a flow-meter connected to the exhaust of the rotary pump used to draw the gas stream through the ion source. In a typical run, the nitrogen pressure was ~ 2 Torr and the COS pressure ~ 5 μ. The COS pressure on the reservoir side of the capillary leak was controlled using appropriate slush baths.

Because of the extremely low pressures of COS used in this apparatus, it was not possible to study the reactions of S^+ and COS^+ ions with hydrocarbons, as the pressures of hydrocarbons required would be too low to measure accurately. However, the results obtained, using this system to study the reactions of S^+ and COS^+ with neutral COS molecules, were used to provide an independent check on the cross-section values produced as described above. Some additional reactions occurring in COS were also investigated.

Calculation of Cross Sections from Data

In cases where an observed product ion may be formed by more than one thermochemically allowed process, and where different precursor ions may be involved, the determination of the cross sections for the various possible processes is not straightforward. In such cases, it is necessary first of all to identify which ions are responsible for the observed products. Certain ions may be eliminated as precursors by a comparison of the observed appearance potentials of the product ion and the possible primary ions. If the appearance potential of the product ion is significantly higher than that of a particular primary ion, then this primary ion is ruled out as a precursor. In order to compare ionization efficiency curves for primary and secondary ions, these curves were normalized at 20 eV of electron accelerating voltage.

More reliable information, leading to the evaluation of the individual cross sections of two concurrent ion–molecule reactions which give the same product, may be obtained by the method of Hutchison and Pobo (7), which has been applied extensively by Harrison and coworkers (see, for example, ref. 8).

If we consider the two possible reactions

$$A^+ + M_1 \rightarrow P^+ + N_1$$
$$B^+ + M_2 \rightarrow P^+ + N_2$$

then we can say that the product ion current I_P arising from these two reactions can be expressed as the sum of the independent contributions of the two reactions. Thus we can write

$$[i] \qquad I_P = f_1 Q_1 d[M_1] I_A + f_2 Q_2 d[M_2] I_B$$

where f_n is the collision efficiency, Q_n is the phenomenological cross section, d is the distance, calculated as described above, from the electron beam to the ion exit slit, $[M_n]$ is the concentration of neutral reactant, and I_x is the ion-current of the ion x, assuming that the collection efficiencies were the same for the various ions. Equation [*i*] may be rearranged to give two other expressions

$$[ii] \qquad \frac{I_P}{I_A} = f_1 Q_1 d[M_1] + f_2 Q_2 d[M_2] \frac{I_B}{I_A}$$

$$[iii] \qquad \frac{I_P}{I_B} = f_1 Q_1 d[M_1] \frac{I_A}{I_B} + f_2 Q_2 d[M_2]$$

These equations predict that a plot of I_P/I_A vs. I_B/I_A should give a straight line with slope proportional to f_2Q_2 and intercept proportional to f_1Q_1, and that a plot of I_P/I_B vs. I_A/I_B should have slope proportional to f_1Q_1 and intercept proportional to f_2Q_2. If either the intercept or the gradient is found to be zero, then we can say that the corresponding reaction is not occurring to any detectable extent.

The ratio of secondary ion current to primary ion current was measured as a function of electron energy at constant ion-source pressure. An increase in this ratio with increasing electron energy was taken to indicate the occurrence of a second reaction involving a primary ion of higher appearance potential than that being plotted. Similarly, a decrease in ratio showed that an ion of lower appearance potential was involved. If such a change in ratio was observed, then the data were treated by means of eqs. [*ii*] and [*iii*].

The method depends upon the assumptions that the relative collection efficiencies and reaction cross sections of the various ions are independent of electron energy. All the present measurements were obtained at low electron voltages (below 20 eV) and at a low field strength of 1.65 V/cm. In order for the results to be meaningful, a plot of the ratio of the secondary and primary ion currents vs. the primary ion current should be a horizontal straight line in the case of an ion formed by one reaction only. In the application of this method by Harrison (8), it was found that straight line plots could not be obtained at repeller field strengths of less than 10 V/cm. The ability of the present apparatus to yield straight line plots at much lower field strengths, as shown in Fig. 1 for the formation of $C_2H_2S^+$ from COS^+ and C_2H_6, may be due to the much narrower ion exit slit, and the consequently reduced effect of field penetration from the electrodes below the ion source. The very low electron beam current used would also make electron space-charge trapping effects negligible (9).

Results and Discussion

Cross-section Measurements

Data were obtained for the reactions occurring in pure COS, and in binary mixtures of COS with methane, methyl iodide, ethane, and ethylene.

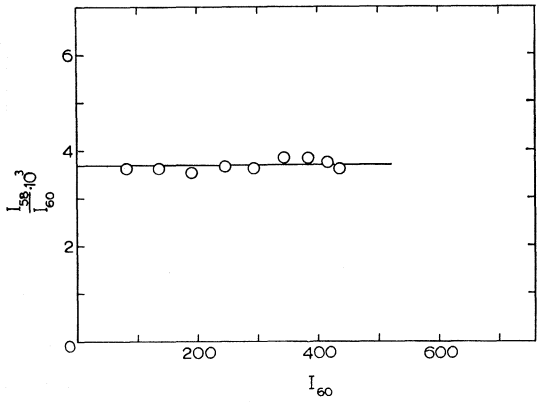

FIG. 1. Plot of $I_{C_2H_2S^+}/I_{COS^+}$ vs. I_{COS^+} at 1.65 V repeller potential in the COS/C_2H_6 system.

Pure COS

The ion S_2^+ (*m/e* 64) was observed when COS alone was present in the ion source at pressures of less than one micron. The appearance potential of S_2^+ coincided with the ionization potential of COS^+, indicating that reaction [1] was occurring

$$[1] \qquad COS^+ + COS \rightarrow S_2^+ + 2CO \qquad \Delta H = -19.6$$

The exothermicity, expressed in kcal $mole^{-1}$ here and subsequently, is calculated using the values for the ionization potentials, appearance potentials, and heats of formation which were obtained from the sources indicated in the Appendix.

The other possible, and thermochemically allowed, precursor for the S_2^+ ion is the S^+ ion

$$[2] \qquad S^+ + COS \rightarrow S_2^+ + CO \qquad \Delta H = -75$$

Both reactions [1] and [2] were observed. Figure 2 shows the ratio plot based on eq. [*ii*] for S_2^+ and the primary ions S^+ and COS^+. From the intercept and slope of Fig. 2 (3.0×10^{-3} and 6.67×16^{-4}, respectively) and the experimental concentration of COS (7.85×10^{12} molecules/cc), we obtain the values $Q_1 = 6.5 \times 10^{-16}$ and $Q_2 = 30.0 \times 10^{-16}$, both in cm^2 $molecule^{-1}$ units.

COS/Methane Mixtures

The secondary ions CH_3S^+, CH_2S^+, and CHS^+ were observed in COS/CH_4 mixtures and a number of thermochemically allowed reactions may be postulated, involving the precursor ions CH_3^+, S^+, COS^+, and CH_4^+. The observed appearance potentials (a.p.) of the secondary ions did not permit a positive assignment of precursors to the reactions, because they could have coincided either with S^+ (the a.p. of which was measured here as 13.6 eV, in good agreement with the value of Dibeler and Walker (10)) or CH_3^+ (a.p. = 14.2 eV). It was therefore decided to use methyl iodide in place of methane, in order to obtain CH_3^+ ions at a lower appearance potential (12.3 eV).

COS/Methyl Iodide Mixtures

In the COS/methyl iodide system, the same series of secondary ions, CH_3S^+, CH_2S^+, and CHS^+, were observed as in the COS/methane mixtures. A number of possible processes may be written to account for these products.

$$[3] \qquad CH_3^+ + COS \rightarrow CH_3S^+ + CO \qquad \Delta H = -33.3$$

$$[4] \qquad S^+ + CH_3I \rightarrow CH_3S^+ + I \qquad \Delta H = -61.8$$

$$[5] \qquad COS^+ + CH_3I \rightarrow CH_3S^+ + CO + I \qquad \Delta H = -6.1$$

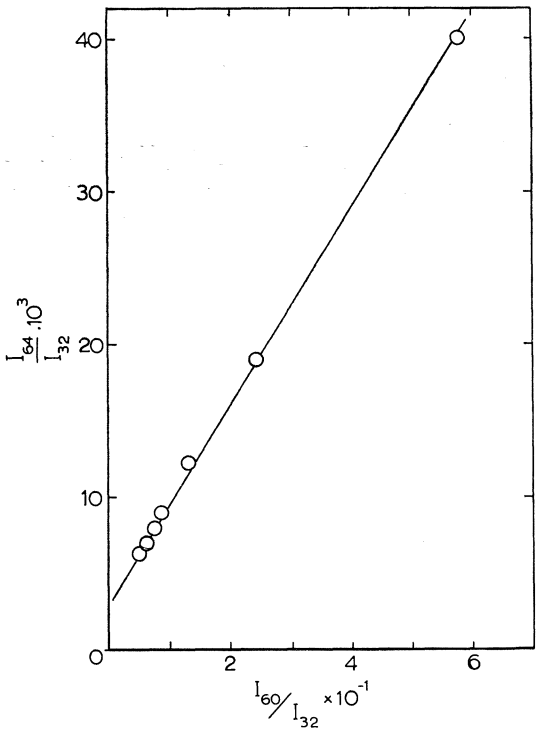

FIG. 2. Dependence of $I_{64}(S_2^+)$ on $I_{60}(COS^+)$ and $I_{32}(S^+)$ in pure COS.

Can. J. Chem. Downloaded from www.nrcresearchpress.com by 210.87.254.6 on 09/05/12
For personal use only.

Can. J. Chem. Downloaded from www.nrcresearchpress.com by 210.87.254.6 on 09/05/12
For personal use only.

[6] $CH_3^+ + COS \rightarrow CH_2S^+ + CO + H$ $\Delta H = +26.8$

[7] $S^+ + CH_3I \rightarrow CH_2S^+ + HI$ $\Delta H = -73.0$

[8] $COS^+ + CH_3I \rightarrow CH_2S^+ + CO + HI$ $\Delta H = -17.3$

[9] $CH_3^+ + COS \rightarrow CHS^+ + CO + H_2$ $\Delta H = +15.7$

[10] $S^+ + CH_3I \rightarrow CHS^+ + H_2 + I$ $\Delta H = -12.5$

[11] $COS^+ + CH_3I \rightarrow CHS^+ + CO + H_2 + I$ $\Delta H = +42.9$

The appearance potential of CH_3S^+ in this system was found to be intermediate between those of CH_3^+ and COS^+, indicating that either or both of these ions could have been the precursor to CH_3S^+ formation.

A plot of I_{47}/I_{32} vs. I_{15}/I_{32} was found to pass through the origin, as did a plot of I_{47}/I_{32} vs. I_{60}/I_{32}. These plots thus indicated that reaction [4] was not occurring, but no information about the cross sections of reactions [3] and [5] could be obtained in this way, as both reactions were contributing to the gradient in each case. However, a plot of I_{47}/I_{15} vs. I_{60}/I_{15} could be used, as shown in Fig. 3, to give values of 3.1×10^{-3} and 1.2×10^{-3} for the intercept and gradient, respectively, which, at the measured reservoir pressures of 1.0 Torr of COS and 1.6 Torr of CH_3I, led to values of 43.5×10^{-16} and 10.5×10^{-16} cm^2 molecule^{-1} for Q_3 and Q_5, respectively.

The appearance potential of CH_2S^+ (m/e 46) was found to coincide with that of CH_3^+. A

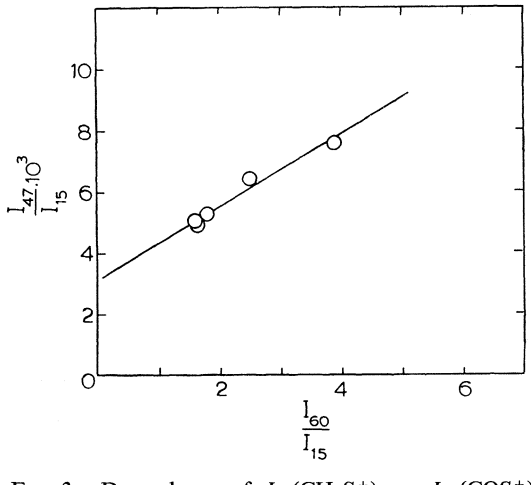

FIG. 3. Dependence of $I_{47}(CH_3S^+)$ on $I_{60}(COS^+)$ and $I_{15}(CH_3^+)$ in the COS/CH_3I system.

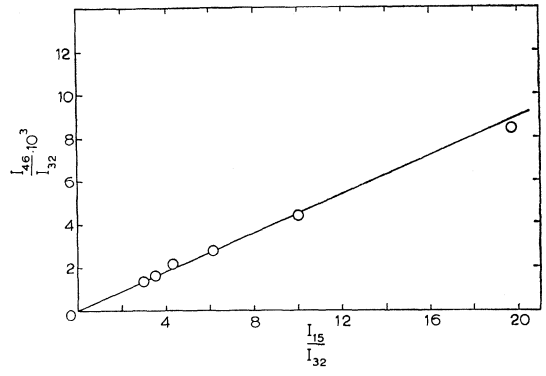

FIG. 4. Dependence of $I_{46}(CH_2S^+)$ on $I_{32}(S^+)$ and $I_{15}(CH_3^+)$ in the COS/CH_3I system.

plot of I_{46}/I_{32} vs. I_{15}/I_{32}, shown in Fig. 4, passed through the origin, and hence indicated that reaction [7] was not occurring. The gradient of the line was 4.5×10^{-4}. Similarly, a plot of I_{46}/I_{15} vs. I_{60}/I_{15}, not shown, was a horizontal line of intercept 4.4×10^{-4}, and thus showed that reaction [8] did not occur to any extent. Taking the mean of the above two values, 4.45×10^{-4}, a value of 6.25×10^{-16} cm^2 molecule^{-1} was calculated for Q_6.

The appearance potential of CHS^+ (m/e 45) was observed to be slightly higher than that of CH_3^+, suggesting that the S^+ ion might also be a precursor in this case. A plot of I_{45}/I_{32} vs. I_{15}/I_{32}, shown in Fig. 5, yielded values of 1.7×10^{-3} and 4.45×10^{-4} for the intercept and gradient, respectively, and hence values of 14.9×10^{-16} and 6.24×10^{-16} cm^2 molecule^{-1} were calculated for Q_{10} and Q_9, respectively.

It can be seen immediately that reactions [6] and [9] are found to occur despite their apparent

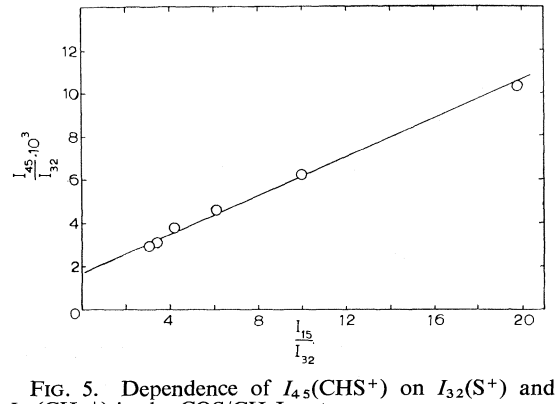

FIG. 5. Dependence of $I_{45}(CHS^+)$ on $I_{32}(S^+)$ and $I_{15}(CH_3^+)$ in the COS/CH_3I system.

Can. J. Chem. Downloaded from www.nrcresearchpress.com by 210.87.254.6 on 09/05/12
For personal use only.

endothermicity. The heats of formation of the CH_nS^+ ions appear to be the least well known of the terms involved in the calculations. Thus our data seem to suggest that the published heats of formation of these fragments (11) may be too large by as much as 30 kcal mole^{-1}. These values were obtained from the appearance potentials of the appropriate ions in the fragmentation of trimethylene sulfide and tetrahydrothiophene, and thus could possibly include some kinetic or vibrational energy possessed by the fragment ions.

Reactions [4] and [7], despite their high exothermicity, were not observed to occur. Assuming, once again, that the heats of formation of the CH_nS^+ ions may be too large, these reactions may be up to 100 kcal mole^{-1} exothermic, and hence it is possible that they do, in fact, occur, but that the exothermicity is sufficiently large to cause fragmentation of the product ions. The C—S bond dissociation energy in the CH_3S free radical, for example, has been calculated to be 68 kcal mole^{-1} (12).

COS/Ethane Mixtures

The secondary ions $C_2H_2S^+$ and $C_2H_6S^+$ were observed in the mass spectrum of mixtures of COS and ethane. We can suggest three possible reactions leading to the formation of the $C_2H_6S^+$ (*m/e* 62) ion

[12] $\quad COS^+ + C_2H_6 \rightarrow C_2H_6S^+ + CO \qquad \Delta H = -24.9$

[13] $\quad S^+ + C_2H_6 \rightarrow C_2H_6S^+ \qquad \Delta H = +1.5$

[14] $\quad C_2H_6^+ + COS \rightarrow C_2H_6S^+ + CO \qquad \Delta H = -39.1$

Because of the presence of the $CO^{34}S^+$ ion (also *m/e* 62) it was not possible to study the $C_2H_6S^+$ ion itself. Experiments were therefore carried out using C_2D_6 and studying the $C_2D_6S^+$ (*m/e* 68) ion. The reactions involving the deuterated ion should show slight variations in thermochemistry and in cross sections, but the results may be applied to the corresponding reactions, [12] to [14] above, with a fair degree of accuracy. The appearance potential of $C_2D_6S^+$ was found to correspond to that of COS^+, indicating that COS^+ was precursor ion in the formation of $C_2D_6S^+$.

Figure 6 shows a plot of I_{68}/I_{36} vs. I_{60}/I_{36}, and the data were found to yield a straight line passing through the origin. This confirmed that reaction [12*a*] was the only one to occur in the production

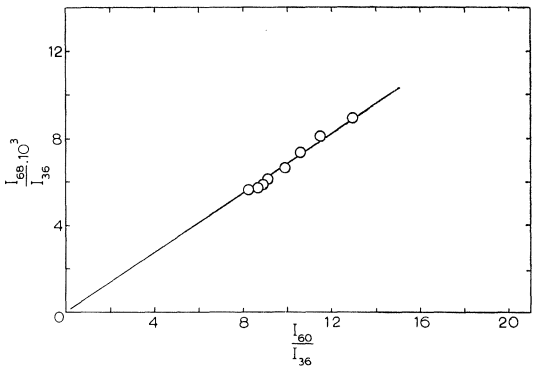

FIG. 6. Dependence of $I_{68}(C_2D_6S^+)$ on I_{60} (COS^+) and $I_{36}(C_2D_6^+)$ in the COS/C_2D_6 system.

[12*a*] $\quad COS^+ + C_2D_6 \rightarrow C_2D_6S^+ + CO$

of $C_2D_6S^+$. The line shown in Fig. 6 had a slope of 6.8×10^{-4}, at reservoir pressures of 1.1 Torr of COS and 1.7 Torr of C_2D_6. We can thus calculate that $Q_{12a} \approx Q_{12} = 5.6 \times 10^{-16}$ cm^2 molecule^{-1}.

We can write three possible reactions to account for the formation of the $C_2H_2S^+$ ion (*m/e* 58).

[15] $\quad COS^+ + C_2H_6 \rightarrow C_2H_2S^+ + 2H_2 + CO \qquad \Delta H = +36.9$

[16] $\quad S^+ + C_2H_6 \rightarrow C_2H_2S^+ + 2H_2 \qquad \Delta H = -18.8$

[17] $\quad C_2H_6^+ + COS \rightarrow C_2H_2S^+ + 2H_2 + CO \qquad \Delta H = +22.7$

The appearance potential of the $C_2H_2S^+$ ion was found to coincide with the ionization potential of COS^+. This indicated reaction [15] as the probable pathway for $C_2H_2S^+$ formation, but did not rule out the possibility of contributions from reactions [16] and [17], which involved precursors of higher appearance potential than that of COS^+. In order to investigate this possibility, plots of I_{58}/I_{32} vs. I_{60}/I_{32} and I_{58}/I_{30} vs. I_{60}/I_{30} were made. In both cases straight lines through the origin were obtained. Both sets of data are plotted in Fig. 7, and the straight line through the combined results has a gradient of 6.25×10^{-3}. These results were obtained with reservoir pressures of 1.1 Torr of COS and 1.7 Torr of C_2H_6, and thus we calculate that $Q_{15} = 51.6 \times 10^{-16}$ cm^2 molecule^{-1}.

Once again our results indicate that an apparently endothermic reaction has occurred. However, the value for $\Delta H_f^{298}(C_2H_2S^+)$ may be subject to the same errors as the values of ΔH_f^{298}

Can. J. Chem. Downloaded from www.nrcresearchpress.com by 210.87.254.6 on 09/05/12
For personal use only.

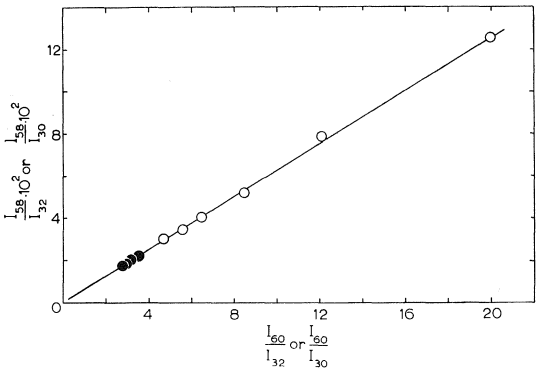

FIG. 7. Dependence of $I_{58}(C_2H_2S^+)$ on (*i*) I_{60} (COS^+) and $I_{32}(S^+)$, denoted by ○, and (*ii*) on $I_{32}(S^+)$ and $I_{30}(C_2H_6^+)$, denoted by ●, in the COS/C_2H_6 system.

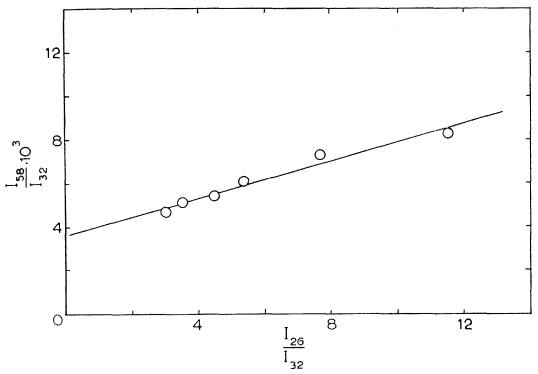

FIG. 8. Dependence of $I_{58}(C_2H_2S^+)$ on $I_{32}(S^+)$ and $I_{26}(C_2H_2^+)$ in the COS/C_2H_4 system.

(CH_nS^+) discussed above (11). In addition, as the heat of formation was calculated using the fragmentation of tetrahydrothiophene, the ion observed in that case may have had a different structure to that observed in our system. For example, in the heat of formation work, the ion may have contained a C—S—C chain, which is unlikely in the present system.

COS/Ethylene Mixtures

$C_2H_2S^+$ and $C_2H_3S^+$ were observed as secondary ions in the mass spectrum of mixtures of COS and ethylene. There are five possible reactions which may be written to account for the formation of $C_2H_2S^+$ (*m/e* 58)

[18] $COS^+ + C_2H_4 \rightarrow C_2H_2S^+ + H_2 + CO$ $\quad \Delta H = +4.2$

[19] $S^+ + C_2H_4 \rightarrow C_2H_2S^+ + H_2$ $\quad \Delta H = -51.5$

[20] $C_2H_2^+ + COS \rightarrow C_2H_2S^+ + CO$ $\quad \Delta H = -18.9$

[21] $C_2H_3^+ + COS \rightarrow C_2H_2S^+ + CO + H$ $\quad \Delta H = +43.8$

[22] $C_2H_4^+ + COS \rightarrow C_2H_2S^+ + H_2 + CO$ $\quad \Delta H = +16.7$

The appearance potential of $C_2H_2S^+$ coincided with that of S^+, indicating that reaction [19] was occurring. However, the possibility of $C_2H_2^+$ as a precursor could not be ruled out, as its appearance potential was very close to that of S^+. Accordingly, a plot of I_{58}/I_{32} vs. I_{26}/I_{32} was made, and this is shown in Fig. 8. Values of 3.7×10^{-3} and 4.25×10^{-4} were obtained for the intercept and the gradient, respectively. Reservoir pressures of 1.1 Torr of COS and 1.8 Torr of C_2H_4 were used, and hence the values $Q_{19} = 28.9 \times 10^{-16}$ and $Q_{20} = 5.42 \times 10^{-16}$ cm^2 molecule^{-1} were obtained.

There are also several possible pathways leading to the formation of the $C_2H_3S^+$ ion (*m/e* 59).

[23] $COS^+ + C_2H_4 \rightarrow C_2H_3S^+ + CO + H$ $\quad \Delta H = +39.3$

[24] $S^+ + C_2H_4 \rightarrow C_2H_3S^+ + H$ $\quad \Delta H = -16.4$

[25] $C_2H_3^+ + COS \rightarrow C_2H_3S^+ + CO + H$ $\quad \Delta H = -25.3$

[26] $C_2H_4^+ + COS \rightarrow C_2H_3S^+ + CO + H$ $\quad \Delta H = +51.8$

The observed appearance potential for the $C_2H_3S^+$ ion was found to correspond closely to that of $C_2H_3^+$, thus suggesting reaction [25] as a source of $C_2H_3S^+$ ions. Plots of I_{59}/I_{32} vs. I_{27}/I_{32} and I_{59}/I_{60} vs. I_{27}/I_{60} were made from the data, and these are shown combined in Fig. 9.

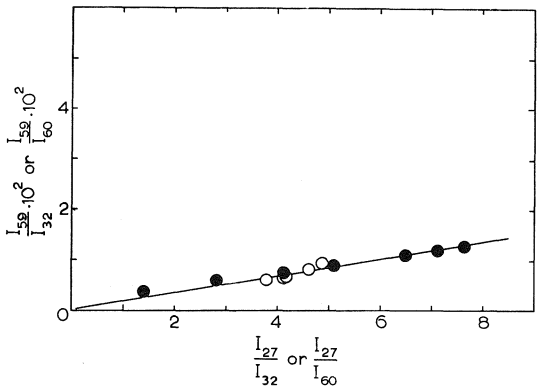

FIG. 9. Dependence of $I_{59}(C_2H_3S^+)$ on (*i*) $I_{32}(S^+)$ and $I_{27}(C_2H_3^+)$, denoted by ○, and (*ii*) on $I_{60}(COS^+)$ and $I_{27}(C_2H_3^+)$, denoted by ●, in the COS/C_2H_4 system.

TABLE 1

Observed reaction cross sections and calculated rate constants

Reaction	$FQ \times 10^{16}$* (cm^2 molecule^{-1})	k (molecule cc^{-1} s^{-1})
$S^+ + COS \rightarrow S_2^+ + CO$	30.0 ±1.1†	2.4×10^{-10}
$S^+ + COS \rightarrow S_2^+ + CO$		5.4×10^{-10} ‡
$S^+ + CH_3I \rightarrow CHS^+ + H_2 + I$	14.9 ±0.9	2.6×10^{-10}
$S^+ + C_2H_4 \rightarrow C_2H_2S^+ + H_2$	28.9 ±2.3	2.3×10^{-10}
$S_2^+ + COS \rightarrow S_3^+ + CO$		5.8×10^{-12} ‡
$COS^+ + COS \rightarrow S_2^+ + 2CO$	6.5 ±0.2	3.7×10^{-11}
$COS^+ + COS \rightarrow S_2^+ + 2CO$		3.23×10^{-10} ‡
$COS^+ + CH_3I \rightarrow CH_3S^+ + CO + I$	10.5 ±1.1	6.0×10^{-11}
$COS^+ + C_2H_6 \rightarrow C_2H_2S^+ + CO + 2H_2$	51.6 ±5.5	2.9×10^{-10}
$COS^+ + C_2D_6 \rightarrow C_2D_6S^+ + CO$	5.6 ±0.3	3.2×10^{-11}
$CH_3^+ + COS \rightarrow CH_3S^+ + CO$	43.5 ±4.2	5.0×10^{-10}
$CH_3^+ + COS \rightarrow CH_2S^+ + CO + H$	6.25±0.4	7.3×10^{-11}
$CH_3^+ + COS \rightarrow CHS^+ + CO + H_2$	6.24±0.2	7.2×10^{-11}
$C_2H_2^+ + COS \rightarrow C_2H_2S^+ + CO$	5.4 ±0.5	4.7×10^{-11}
$C_2H_3^+ + COS \rightarrow C_2H_3S^+ + CO$	21.7 ±1.2	1.8×10^{-10}
$CS^+ + COS \rightarrow SC_2^+ + CO$		7.7×10^{-10} ‡

*Cross sections determined at $Erl = 0.214$ V.
†Error limits correspond to standard deviation of least-square treatment of data.
‡Obtained by pulsing method.

It can be seen that neither reaction [23] nor reaction [24] occurs, as the intercept is zero within experimental error. The gradient was measured as 1.7×10^{-3} for the combined data. The reservoir pressures used were given above, and were used to calculate a value for Q_{25} of 21.7×10^{-16} cm^2 molecule^{-1}.

Calculation of Rate Constants from Cross-section Data

The cross sections given in Table 1 were converted to thermal rate constants k with use of the Stevenson and Gioumousis (13) equation

$$[iv] \qquad k = Q\left(\frac{Erle}{2m_p}\right)^{1/2}$$

where $Erl = 0.214$ V is the voltage difference from the electron beam to the ion exit slit, e is the electronic charge, and m_p the mass of the primary ion.

Absolute Rate Constants in Pure COS Using Delay Pulse Techniques.

COS^+ and S^+ ions were produced in the ion source of the pulsed system by charge exchange from nitrogen, as discussed above. In view of the high concentration of nitrogen relative to that of COS, the initial step in the system was the three-body association reaction [27] to give N_4^+. This was then followed by two second-order reactions [28] and [29] to give COS^+ and S^+, respectively.

[27] $N_2^+ + 2N_2 \rightarrow N_4^+ + N_2$

[28] $N_4^+ + COS \rightarrow COS^+ + 2N_2$

[29] $N_4^+ + COS \rightarrow S^+ + CO + 2N_2$

The rate constant for reaction [27] was obtained from the gradient of a plot of $\log I_{N_2^+}$ vs. t, using the equation

$$[v] \qquad k_{27} = \frac{2.3 \log\left[(I_{N_2^+})_{t_2}/(I_{N_2^+})_{t_1}\right]}{(t_2 - t_1) \times [N_2]^2}$$

A variety of runs was carried out, using pressures of from 1.2–3 Torr of nitrogen and from 1 to 30 μ of COS. A mean value of 6.2×10^{-29} molecule^{-2} cc^2 s^{-1} was obtained for k_{27}. This is in good agreement with the value of 8.5×10^{-29} which was previously reported (14), and with the value of 8.9×10^{-29} previously obtained in this laboratory (6). A similar investigation of the decay of the N_4^+ ion led to a value for $(k_{28} + k_{29})$ of 1.7×10^{-9}, which is a reasonable value for a process involving charge exchange, such as reaction [28].

The S^+ and COS^+ ions found in this way may then undergo the reactions already discussed for the pure COS system above

[1] $COS^+ + COS \rightarrow S_2^+ + 2CO$

[2] $S^+ + COS \rightarrow S_2^+ + CO$

An examination of the ion intensity curves for the N_4^+ and S^+ ions indicated that N_4^+ had essentially decayed to zero, i.e., reaction [29] had ceased to be significant, in the time region during which the S^+ ion was decaying by reaction [2].

Can. J. Chem. Downloaded from www.nrcresearchpress.com by 210.87.254.6 on 09/05/12
For personal use only.

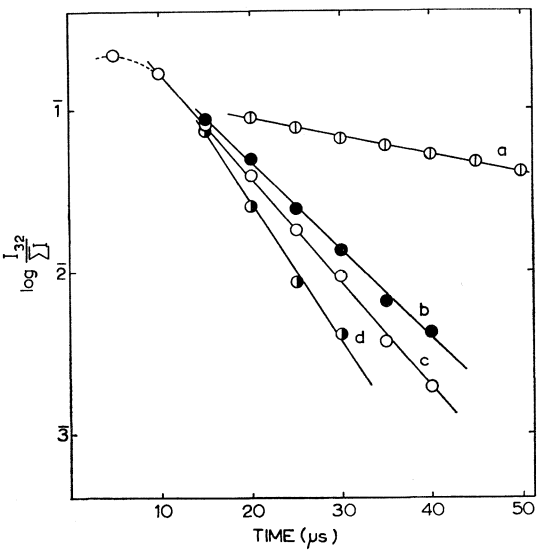

FIG. 10. Logarithmic plot of ion-intensity as a function of time for the ion S^+. Typical decay curves for $[N_2]$ and [COS] are (*a*) 6.44 × 10^{16}, 0.50 × 10^{14}; (*b*) 6.44 × 10^{16}, 2.68 × 10^{14}; (*c*) 6.44 × 10^{16}, 2.97 × 10^{14}; (*d*) 3.74 × 10^{16}, 4.12 × 10^{14} (all in molecules cc^{-1}), respectively.

Accordingly, the rate constant k_2 could be obtained by plotting log I_{S^+} vs. t and measuring the gradient. Figure 10 shows some of the S^+ data plotted in this way. Equation [*vi*] could then be applied.

$$[vi] \qquad k_2 = \frac{2.3 \log [(I_{s^+})_{t_2}/(I_{s^+})_{t_1}]}{(t_2 - t_1) \times [\mathrm{COS}]}$$

The rate of the reaction was found to be dependent on the first power of the COS concentration and to be independent of nitrogen concentration. A mean value for k_2 of 5.4 × 10^{-10} molecule^{-1} cc s^{-1} was obtained, with a scatter in the individual data of approximately ± 1 × 10^{-10}. This agrees, within a factor of 2, with the value of k_2 calculated from the measured cross section for reaction [2] (see Table 1). This degree of agreement is satisfactory in view of the simplifying assumptions which are made in such rate constant calculations, and in view of the fact that data were obtained on two different instruments.

Reaction [1] was studied in a similar fashion, but the results in this case were not so satisfactory. A value of 3.2 × 10^{-10} molecule^{-1} cc s^{-1} was obtained for k_1^{app} (for approximate value of k_1). This is approximately eight times larger than the value of k_1 calculated in Table 1. It is, however, possible to account for this apparently anomalous result by postulating the occurrence of reaction [30], the charge exchange reaction between the COS^+ ion and a molecule of H_2S

$$[30] \qquad COS^+ + H_2S \rightarrow H_2S^+ + COS$$

Hydrogen sulfide was present as an impurity in COS even after numerous trap-to-trap distillations.[1] In addition, COS reacts with water to give hydrogen sulfide, and it was observed in the mass spectrum that the small amount of water normally present in the high pressure spectrum of nitrogen had largely disappeared, suggesting that this reaction had taken place. Reaction [30] is calculated to be exothermic by about 15 kcal mole^{-1}. The corresponding reaction between S^+ and H_2S would not be expected on thermochemical grounds. If we assume a reasonable value of $\geqslant 1 \times 10^{-9}$ molecule^{-1} cc^2 s^{-1} for k_{30}, we can see that the presence of a few percent of hydrogen sulfide in the COS would be sufficient to explain this discrepancy between the two sets of data. The ion H_2S^+ (*m/e* 34) was observed to appear in high intensity in the spectra, which supports the view that it was acting as a "sink" for positive charge.

An ion at *m/e* 96, corresponding to S_3^+, was observed at long delay times. The appearance of this ion was accompanied by a decrease in the intensity of the S_2^+ ion, suggesting the occurrence of reaction [31]. The exothermicity of the reaction can be calculated, as the heat of formation of the S_3^+ ion is known (15)

$$[31] \qquad S_2^+ + COS \rightarrow S_3^+ + CO \qquad \Delta H = -40.5$$

and the reaction is shown to be energetically possible. Decay plots for the S_2^+ ion gave a mean value of 5.8 × 10^{-12} molecule^{-1} cc s^{-1} for k_{31}.

Another fragment ion formed by COS and observed in the present system is the CS^+ ion (*m/e* 44). This ion was found to undergo a rapid decay, the rate of which was proportional to the first power of the COS concentration. This suggests the occurrence of reaction [32]

[1]The pulsed electron beam determinations of the thermal rate constants were done only recently, while the cross-section determinations described in the previous section were made two years ago. Different supplies of COS gas were used in the two series of experiments and it is not known whether the COS used in the earlier experiments did contain H_2S as an impurity.

Can. J. Chem. Downloaded from www.nrcresearchpress.com by 210.87.254.6 on 09/05/12
For personal use only.

TABLE 2

Absolute rate constant data (T = 300 °K)

$[N_2] \times 10^{-16}$ (molecules cc^{-1})	$[COS] \times 10^{-14}$ (molecules cc^{-1})	$k_1^{app} \times 10^{10}$ (molecule^{-1} cc s^{-1})	$k_2 \times 10^{10}$ (molecule^{-1} cc s^{-1})	$k_{31} \times 10^{12}$ (molecule^{-1} cc s^{-1})	$k_{32} \times 10^{10}$ (molecule^{-1} cc s^{-1})
6.44	0.129	2.07	6.84	—	—
”	”	4.48	6.50	—	—
”	2.97	3.01	4.93	—	6.50
”	”	4.14	5.46	7.70	10.5
”	2.68	2.60	4.53	5.15	6.40
”	”	3.93	4.49	3.90	6.00
”	0.496	—	5.34	9.24	9.50
”	”	3.30	5.10	3.57	8.30
3.74	4.12	2.85	4.88	3.79	8.00
9.66	1.35	2.71	6.12	7.46	6.40
		Mean 3.23	Mean 5.42	Mean 5.83	Mean 7.70

[32] $$CS^+ + COS \rightarrow CS_2^+ + CO$$

which may be calculated to be exothermic by 32 kcal mole^{-1} if the CS_2^+ is formed in either the $^2\pi_{3/2g}$ or $^2\pi_{1/2g}$ states (16). Little CS_2^+ was observed in the spectrum, but we might expect CS_2^+ to charge-exchange with hydrogen sulfide. Such a reaction may be calculated to be thermoneutral for the $^2\pi_{3/2g}$ state, and slightly exothermic in the case of the $^2\pi_{1/2g}$ state.

If we assume that reaction [32], or some other reaction involving CS^+ and COS, does occur, then our decay plots for the CS^+ ion yield a value of 7.7×10^{-10} molecule^{-1} cc s^{-1} for k_{32}. This value may also include a contribution from the charge exchange reaction between CS^+ and hydrogen sulfide, which is $\sim$ 5 kcal mole^{-1} exothermic, and so our result probably represents an upper limit for k_{32}. The CS^+ ion was not studied in the cross-section work, as its reactions would not be expected to interfere with those under observation.

Other ions which were observed in the system included N^+ and N_3^+, the reactions of which were not considered in this study, together with traces of impurity ions NO^+ and NO_2^+, and the H_3S^+ ion, which was found to grow to large intensity at long delay times, and which presumably arose from the capture of a hydrogen atom from either water or hydrogen sulfide by the H_2S^+ ion. The ions H_2O^+ and H_3O^+ were also present in small amounts, together with an ion at m/e 53 which could have been $H^+.H_2O/H_2S$.

The absolute rate constant data obtained as described in this section are summarized in Tables 1 and 2. In comparing the rate constant data calculated by the Stevenson relationship from the cross-section measurements with the thermal rate constants obtained with the pulsed technique, one should consider that the Stevenson relationship is not valid for molecules with permanent dipoles. Thus, since COS has a permanent dipole, the cross-section conversions of reactions involving neutral COS might lead to rate constants which are easily in error by a factor of 2.

Comparison with Reactions of Sulfur Atoms and Neutral COS

It is interesting to compare the ion–molecule reactions discussed above with the reactions occurring under photolytic conditions. Such reactions have been extensively discussed in a review article (17).

The photolysis of pure COS leads to the formation of CO and of S atoms, of which 75% are formed in the $^1D_2$ state, and the remainder in the ^3P state. Both S species may then abstract a sulfur atom from a further molecule of COS

$$COS + h\nu \rightarrow CO + S^*$$

$$COS + S^* \rightarrow S_2 + CO$$

Collisional relaxation of excited S atoms, and the third-order combination of two triplet S atoms may also occur. S_2 is then thought to undergo a third-order polymerization reaction with S_2 to give S_4, which may in turn dimerize or undergo combination or disproportionation reactions with other species such as S_2. In view of the observation of S_2^+ and S_3^+ ions in our system, it seems reasonable to assume that higher polymers could have been obtained at higher ion

Can. J. Chem. Downloaded from www.nrcresearchpress.com by 210.87.254.6 on 09/05/12
For personal use only.

source pressures, especially as such reactions are thermochemically allowed.

S atoms react with paraffins solely by means of an insertion reaction to give the corresponding mercaptan

$$RH + S(^1D) \rightarrow RSH$$

which may, as in the case of methane, fragment in various ways, giving products such as $CH_3S + H$, $CH_3 + SH$, $CH_2 + H_2S$, and $CH_2S + H_2$.

The reaction of S^+ ions with ethane to give the mercaptan ion $C_2H_5SH^+$ was, however, calculated to be endothermic and was shown above not to occur. Instead, mercaptan ions appeared to be formed by reaction [12] involving COS^+ as precursor.

The reaction of S atoms with olefins has been shown to yield either an episulfide or a vinyl mercaptan.

$$S(^1D) + C_2H_4 \rightarrow \underset{\diagdown\ \diagup \atop S}{H_2C\text{———}CH_2} \text{ and } CH_2{=}CHSH$$

In the present study, however, the $C_2H_4S^+$ ion was not observed in COS/ethylene mixtures. We can calculate that the formation of such an ion from the reaction of S^+ ions with ethylene would be a highly exothermic process (11) and hence probably occurs in our system, but is followed by fragmentation of the $C_2H_4S^+$ ion which yields $C_2H_2S^+ + H_2$.

Appendix

Source of Thermochemical Data

Whenever possible, appearance potential and heat of formation data were obtained or calculated from Field and Franklin (18), or Vedeneyev, Gurvich, Kondrat'yev, Medvedev, and Frankevich (19). The ionization potential of COS (20), from which the value $\Delta H_f(COS^+)$ of 221.9 was calculated, and the heats of formation of the various $C_xH_yS^+$ ions (11) were taken from more recent results. Heats of formation of various neutral molecules and fragments were obtained from the series of papers on the thermochemistry of sulfur compounds published by Mackle and O'Hare (12, 21).

1. F. H. Field and F. W. Lampe. J. Amer. Chem. Soc. **80**, 5583 (1958).
2. A. Henglein. Z. Naturforsch. **17a**, 37 (1962).
3. A. R. Knight, O. P. Strausz, and H. E. Gunning. J. Amer. Chem. Soc. **85**, 2349 (1963).
4. H. A. Wiebe, A. R. Knight, O. P. Strausz, and H. E. Gunning. J. Amer. Chem. Soc. **87**, 1443 (1965).
5. D. P. Stevenson and D. O. Schissler. The chemical and biological action of radiations. Academic Press, Inc., London and New York. 1961. p. 260.
6. D. A. Durden, P. Kebarle, and A. Good. J. Chem. Phys. **50**, 805 (1969).
7. D. Hutchison and L. Pobo. Paper presented at ASTM E-14 meeting Chicago. June, 1961.
8. A. G. Harrison and J. M. S. Tait. Can. J. Chem. **40**, 1986 (1962).
9. A. G. Harrison and A. A. Herod. Presented at the Seventeenth Annual Conference on Mass Spectrometry and Allied Topics, Dallas, Texas. May, 1969.
10. V. H. Dibeler and J. A. Walker. *In* Advances in mass spectrometry, Vol. IV. International Publishing Co., London. 1968. p. 767.
11. E. J. Gallegos and R. W. Kiser. J. Phys. Chem. **66**, 136 (1962).
12. H. Mackle. Tetrahedron, **19**, 1159 (1963).
13. G. Gioumousis and D. P. Stevenson. J. Chem. Phys. **29**, 294 (1958).
14. (*a*) P. Warneck. J. Chem. Phys. **46**, 502 (1967). (*b*) P. F. Knewstubb. *In* Advances in mass spectrometry. Vol. IV. International Publishing Co., London. 1968.
15. J. Drowart, P. Goldfinger, D. Detry, H. Rickert, and H. Keller. *In* Advances in mass spectrometry. Vol. IV. International Publishing Co., London. 1968. p. 499.
16. J. L. Franklin, J. G. Dillard, H. M. Rosenstock, J. T. Herron, K. Draxl, and F. H. Field. N.S.R.D.S.-N.B.S. Publication No. 26, (1969).
17. O. P. Strausz. Organo-sulphur chemistry. *Edited by* M. J. Janssen. Interscience Publishers, Inc., New York. 1967. p. 11.
18. F. H. Field and J. L. Franklin. Electron impact phenomena. Academic Press, Inc., London and New York. 1961.
19. V. I. Vedeneyev, L. V. Burvich, V. N. Kondrat'yev. V. A. Medvedev, and Ye. L. Frankevich. Bond energies, ionization potentials and electron affinities. Edward Arnold and Co., London. 1966.
20. M. J. Al-Jaboury, D. P. May, and D. W. Turner. J. Chem. Soc. 6350 (1965).
21. H. Mackle and P. A. G. O'Hare. Tetrahedron, **19**, 961 (1963).

Can. J. Chem. Downloaded from www.nrcresearchpress.com by 210.87.254.6 on 09/05/12
For personal use only.

Can. J. Chem. Downloaded from www.nrcresearchpress.com by 210.87.254.40 on 09/05/12
For personal use only.

Réactions dans le sulfolane. V. Ions trihalogénures[1]

M. Deneux et R. L. Benoit
Département de Chimie, Université de Montréal, Montréal 101, Québec

Reçu le 18 septembre 1969

Les équilibres entre I_2 et I^-, Br^-, Cl^- dans le sulfolane ont été étudiés par potentiométrie et spectrophotométrie à 30 °C. Les stabilités de Br_3^- et Cl_3^- ont été déterminées. Les constantes de formation, à force ionique nulle, ont été calculées par programme: $\log K_{I_2Y^-} = 7.49$, 7.23 et 7.23 pour Y = I, Br et Cl; $\log K_{X_3^-} = 7.49$, 7.33 et 4.11 pour X = I, Br, Cl. L'équilibre de dismutation: $2I_2Y^- \rightleftarrows I_3^- + IY_2^-$ a été caractérisé: $\log K_d = -1.55$ et -0.64 pour Y = Br et Cl respectivement. Les stabilités et les spectres des ions trihalogénures, dans le sulfolane, sont comparés avec les résultats déjà connus pour d'autres solvants.

Equilibria between I_2 and I^-, Br^-, Cl^- in sulfolane were studied by potentiometry and spectrophotometry at 30 °C. The stabilities of Br_3^- and Cl_3^- were also determined. The stability constants at nil ionic strength were calculated by means of a program: $\log K_{I_2Y^-} = 7.49$, 7.23, and 7.23 for Y = I, Br, and Cl; $\log K_{X_3^-} = 7.49$, 7.33, and 4.11 for X = I, Br, and Cl. The disproportionation equilibria $2I_2Y^- \rightleftarrows I_3^- + IY_2^-$ were characterized by $\log K_d = -1.55$ (Y = Br) and -0.64 (Y = Cl). The stabilities and spectra of the trihalide ions in sulfolane are compared with similar data for other solvents.

Canadian Journal of Chemistry, **48**, 674 (1970)

Introduction

Les solvants polaires aprotiques, dont le sulfolane (TMS) fait partie, possèdent des propriétés solvatantes qui les différencient nettement des solvants protiques tels l'eau et le méthanol. Ces différences, qui apparaissent particulièrement dans le comportement des nucléophiles X^-, sont attribuées au rôle prépondérant des liaisons hydrogène entre solvant et X^- (1). Ainsi, les petits ions halogénures sont beaucoup plus fortement solvatés par les solvants protiques que par les solvants aprotiques. Pour évaluer les changements d'énergie de solvatation (énergie de transfert) des nucléophiles X^- d'un solvant à un autre, une hypothèse extrathermodynamique est nécessaire (2). En utilisant ainsi celle proposée par Strehlow (2), des déterminations de potentiel du système Ag^+/Ag et des produits de solubilité des sels AgX dans différents solvants, on a évalué précédemment les énergies de transfert des ions Cl^- et Br^- (3). Cependant, si l'on fait des comparaisons à l'intérieur de la série des solvants polaires aprotiques, les énergies de transfert des ions Ag^+ sont grandes et celles des halogénures trouvées petites, de telle sorte que la méthode précédente conduit à des résultats peu précis pour ces dernières (3). Nous nous sommes donc proposés d'utiliser une autre méthode qui implique la détermination des constantes de stabilité des ions I_2Y^-: $K_{I_2Y^-} = (I_2Y^-)/(I_2)(Y^-)$(Y = Cl, Br, I). Si l'on mesure par ailleurs les variations d'énergie de solvatation de I_2 d'un solvant à un autre, par exemple par détermination du coefficient de partage de I_2 avec un solvant immiscible, on obtient alors les variations des énergies de transfert des ions I_2Y^- et Y^-. Comme les anions I_2Y^- ont des "rayons ioniques" élevés et aussi peu differents lorsque Y passe de Cl à I, on pourra alors proposer comme nouvelle hypothèse extrathermodynamique que pour les solvants polaires aprotiques, les énergies de transfert de tous les ions I_2Y^- sont négligeables et calculer, à partir des variations observées, les énergies de transfert des ions Y^-. Nous avons donc commencé par déterminer les constantes de formation des ions I_2Y^- dans le TMS. Des résultats préliminaires ont déjà été communiqués (4), mais ils avaient été obtenus en milieu $LiClO_4$ 0.1 *M* et la formation de paires d'ions $Li^+ \cdot Cl^-$ et $Li^+ \cdot Br^-$ avait été négligée (3, 5). Pour cette même raison, nous avons aussi repris la détermination des constantes de stabilité des ions Br_3^- et Cl_3^-. De plus, il convenait d'examiner la possibilité d'existence dans le TMS d'équilibres de dismutation (6) tel

[1] $$2I_2Y^- \rightleftarrows I_3^- + IY_2^- \quad (K_d)$$

venant s'ajouter aux équilibres primaires tels:

[2] $$I_2 + Y^- \rightleftarrows I_2Y^- \quad (K_{I_2Y^-})$$

Tous les résultats ont été interprétés au moyen d'un programme.

[1]Article précédent (IV): voir réf. 3.

Can. J. Chem. Downloaded from www.nrcresearchpress.com by 210.87.254.40 on 09/05/12
For personal use only.

Partie Expérimentale

La purification du sulfolane, celle des chlorure, bromure et perchlorate de tétraéthylammonium ont été décrites précédemment (3). L'iodure de tétraéthylammonium a été recristallisé deux fois dans l'éthanol et séché sous vide à 40 °C. Le ferrocène a été recristallisé dans l'éthanol, puis sublimé. Les solutions de ferrocène-perchlorate de ferricinium dans le TMS ont été obtenues par oxydation in situ d'une partie du ferrocène par le perchlorate d'argent. Les valeurs des constantes de formation des ions I_2Y^- (Y = Br, Cl) ont été obtenues à partir des mesures de force électromotrice (f.é.m.) de la cellule

[3] $$\begin{matrix} \text{Pt/Et}_4\text{NI}(2 \times 10^{-2}\ M) \\ \text{I}_2(10^{-2}\ M) \end{matrix} \text{//Et}_4\text{NClO}_4(10^{-1}\ M)\text{//} \begin{matrix} \text{Et}_4\text{NI}(10^{-2}\text{–}10^{-3}\ M) \\ \text{Et}_4\text{NY}(a) \\ \text{I}_2(b) \end{matrix} \text{/Pt}$$

thermostatée à 30.0 ± 0.1 °C. En général, une solution d'iode dans le TMS était ajoutée à la solution contenant I^- et Y^-; dans le cas de I_2Cl^-, on a aussi réalisé une expérience sans Et_4NI, c'est-à-dire avec Et_4NCl seul présent au départ dans le compartiment de mesure, et un essai où la solution de chlorure était ajoutée à une solution contenant I^- et I_2 au départ. La cellule suivante a été utilisée pour X_3^- (X = I, Br, Cl)

[4] $$\begin{matrix} \text{Pt/Et}_4\text{NI}(2 \times 10^{-2}\ M) \\ \text{I}_2(10^{-2}\ M) \end{matrix} \text{//Et}_4\text{NClO}_4(10^{-1}\ M)\text{//} \begin{matrix} \text{Et}_4\text{NX}(10^{-2}\text{–}10^{-3}\ M) \\ \text{X}_2(c) \end{matrix} \text{/Pt}$$

Les solutions de Br_2 et Cl_2 ajoutées ont été préparées dans le tétrachlorure de carbone, afin de minimiser l'action directe de ces halogènes sur le TMS. Sauf pour I_3^- où deux expériences ont été faites par addition de I^- à I_2, les solutions d'halogène ont été ajoutées aux solutions d'halogénure correspondant. Pour la détermination d'un potentiel "normal apparent" du système I_2/I^-, la solution de référence a été remplacée par une solution de ferrocène 10^{-2} *M* – perchlorate de ferricinium 10^{-2} *M*. Les différences de potentiel lues sur un millivoltmètre numérique "Tacussel–Ariès 10000" s'établissaient en moins de deux minutes et restaient stables pendant plusieurs heures. La reproductibilité est estimée à ±2 mV. Les densités optiques des solutions d'iode dans le TMS auxquelles on a ajouté différentes quantités d'halogénure ont été enregistrées sur un appareil "Bausch and Lomb Spectronic 500". Les cellules avaient 1 mm d'épaisseur.

Calculs

Les valeurs expérimentales E de la f.é.m. des cellules (3) et (4) sont reliées aux concentrations libres de X^- et X_2 par l'équation de Nernst

[5] $$E = E^0 + \frac{RT}{2F} \log_e \frac{(X_2)}{(X^-)^2}$$

Des calculs approchés ou des comparaisons avec des valeurs publiées dans la littérature pour des solvants similaires nous permettent d'obtenir des valeurs approximatives pour E^0 et les constantes de formation K des ions trihalogénures. Les calculs ultérieurs sont effectués à l'aide du programme TIPOT, version améliorée de POTAG2 (3). Les courbes de dosage $A = f(v)$, A étant soit une mesure pH, soit un potentiel d'électrode répondant à un ion métallique ou à un système oxydo-réducteur et v le volume de la solution ajoutée, peuvent être traitées par TIPOT, en présence ou non d'un précipité. L'interprétation se fait par affinement possible d'un certain nombre de paramètres, tels que les constantes de formation, le potentiel normal apparent E^0 du système d'électrodes, les concentrations totales des réactifs présents au départ ou ajoutés lors du dosage. La force ionique I et les concentrations libres de toutes les espèces en solution sont calculées en chaque point.

Résultats

Les données expérimentales, ainsi que les tableaux de concentrations, pour chaque expérience sont consignés dans le dépôt du Conseil National de Recherches du Canada. Les résultats, le facteur $R = (\sum_i r_i^2/N - M)^{1/2}$ où N est le nombre total de mesures, M le nombre de constantes affinées et $r_i = |E_i - E_i^{cal}|$, ont été regroupés dans le Tableau 1. Les marges d'erreurs données sont égales à trois fois la déviation standard estimée à partir des éléments diagonaux de la matrice inverse correspondant au dernier cycle de l'affinement par moindres carrés non linéaires. Les courbes potentiométriques (Fig. 1)

TABLEAU 1

Constantes de formation d'ions trihalogénures, constantes d'équilibre de dismutation dans le sulfolane à 30 °C

X_2Y^-	log $K_{X_2Y^-}$*	log K_d'	log K_d	R (mV)
I_3^-	7.49±0.01			2.5
Br_3^-	7.33±0.02			3.6
Cl_3^-	4.11±0.02			2.9
I_2Br^-	7.23±0.02	5.42±0.1	−1.55±0.15	2.1
I_2Cl^-	7.23±0.03	6.33±0.04	−0.64±0.1	2.8

*Les valeurs publiées dans la Réf. 4 (log $K_{X_2Y^-}$ = 7.5, 6.4, 3.1, 6.5 et 4.8 pour X_2Y^- = I_3^-, Br_3^-, Cl_3^-, I_2Br^- et I_2Cl^- respectivement) ont été déterminées à 22 °C et en milieu $LiClO_4$ 0.1 *M*.

correspondant à l'addition de I^- à I_2 ou I_2 à I^- sont interprétées de manière satisfaisante en ne tenant compte que de l'équilibre

[6] $$I^- + I_2 \rightleftarrows I_3^-$$

Dans les parties de courbes où $C_{I_2} > C_{I^-}$, l'on a essayé de détecter la présence des ions I_5^-. La valeur de la constante cherchée décroit constamment au cours de l'affinement, alors que l'accord avec la courbe expérimentale n'est pas amélioré. Les tableaux de concentrations montrent aussi que cette espèce serait formée en quantité négligeable. Le potentiel normal apparent E^0 du couple I_2/I^- par rapport à la référence ferrocène-perchlorate de ferricinium est de -0.104 ± 0.004 V, ce qui conduit aux valeurs suivantes pour les systèmes I_2/I_3^- et I_3^-/I^-: 0.345 ± 0.005 V et -0.330 ± 0.005 V respectivement. Les courbes potentiométriques de Br_2–Br^- et Cl_2–Cl^- (Fig. 1) sont aussi expliquées par les seuls équilibres analogues à (6). Les valeurs de $K_{X_3^-}$ sont données dans le Tableau 1.

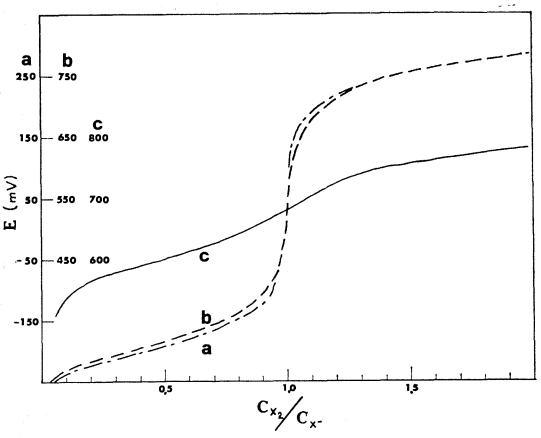

FIG. 1. Courbes potentiométriques des systèmes X_2–X^- dans le sulfolane ($C_{X^-} \simeq 10^{-2}$ *M*). (*a*), X = I; référence: ferricinium/ferrocène; (*b*), X = Br; référence: I_3^-/I^-; (*c*), X = Cl; référence: I_3^-/I^-.

Dans le cas des systèmes I^-–I_2–Y^- (Y = Br, Cl), les équilibres [1] et [2] doivent être considérés et on définit accessoirement, pour l'utilisation du programme, un nouvel équilibre

[7] $$2Y^- + I_2 \rightleftarrows IY_2^- + I^- \quad (K_d')$$

En effet, bien que les équilibres [6] et [2] conduisent à des valeurs affinées de $K_{I_3^-}$ et $K_{I_2Y^-}$ les valeurs trouvées diffèrent d'une courbe à l'autre. D'autre part, l'équilibre [2] seul explique mal le fonctionnement de l'électrode de platine dans une solution contenant uniquement Y^- et I_2. On a alors fixé E^0 et $K_{I_3^-}$ à leurs valeurs connues et effectué l'affinement pour $K_{I_2Y^-}$ et K_d'. Les valeurs des constantes sont dans le Tableau 1.

On a cherché à confirmer la présence des ions I_3^- et IY_2^- dans les solutions de I_2Y^- par spectrophotométrie (6): les spectres ultra-violet (u.v.) des différentes solutions contenant Y^- (Y = I, Br, Cl) et I_2 en proportions variables sont représentés sur les Fig. 2 et 3. Les spectres des solutions d'iodure et d'iode présentent deux pics d'absorption à 295 et 367 mμ. Ces longueurs d'onde λ_{max}, ainsi que les coefficients d'extinction molaire ε_{max} calculés en considérant la formation de I_3^- complète, restent constants pour des valeurs de $\rho = C_{Y^-}/C_{I_2}$ comprises entre 3.3 et 0.8. Pour le système I_2–Br^-, on observe une bande d'absorption assez large vers 280 mμ et un épaulement aux environs de 350 mμ; le maximum se déplace de 275 à 280 mμ en fonction des valeurs décroissantes de ρ (Y = Br). Pour le système I_2–Cl^-, quatre pics apparaissent à 232, 265, 291 et 367 mμ; seul le dernier pic semble posséder une position fixe.

Can. J. Chem. Downloaded from www.nrcresearchpress.com by 210.87.254.40 on 09/05/12
For personal use only.

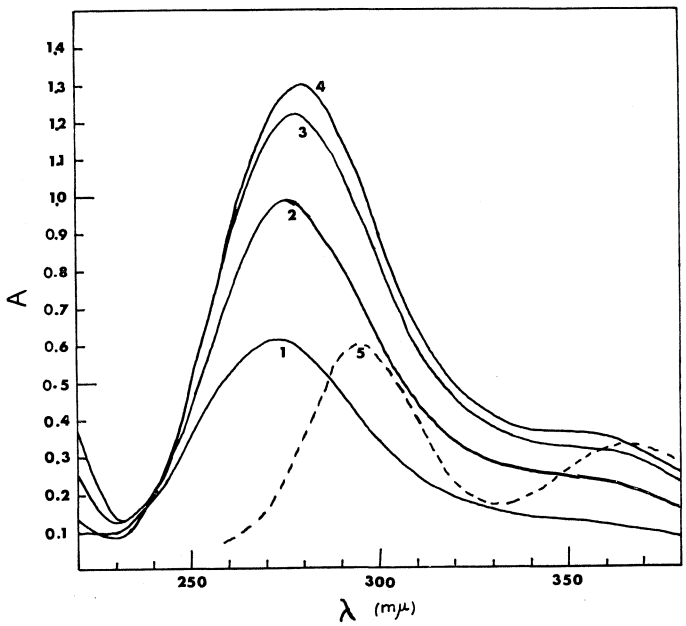

FIG. 2. Spectres d'absorption de solutions de I_2 et I^- ou Br^- dans le sulfolane. Cellule de 1 mm d'épaisseur; TMS en référence: *1*, $C_{I_2} = 1.57 \times 10^{-4}$ *M*, $C_{Br^-} = 5.78 \times 10^{-4}$ *M*; *2*, $C_{I_2} = 2.61 \times 10^{-4}$ *M*, $C_{Br^-} = 4.82 \times 10^{-4}$ *M*; *3*, $C_{I_2} = 3.36 \times 10^{-4}$ *M*, $C_{Br^-} = 4.13 \times 10^{-4}$ *M*; *4*, $C_{I_2} = 3.92 \times 10^{-4}$ *M*, $C_{Br^-} = 3.61 \times 10^{-4}$ *M*. Cellule de 2 mm d'épaisseur; TMS en référence; *5*, $C_{I_2} = 6.67 \times 10^{-5}$ *M*, $C_{I^-} = 6.04 \times 10^{-5}$ *M*.

Discussion

L'influence de la force ionique aux niveaux considérés ($3.3 \times 10^{-3} < I < 1.6 \times 10^{-2}$) sur des équilibres tels que [1] et [2] est faible, de telle sorte que les valeurs des constantes *K* dans le Tableau 1 sont très sensiblement valables à force ionique nulle. Il est mal aisé de comparer les valeurs de *K* trouvées à celles précédemment obtenues (4) étant donné les températures et milieux différents, toutefois les plus faibles stabilités à 22 °C et en milieu $LiClO_4$ 0.1 *M* paraissent principalement dues à la formation de paires d'ions entre Li^+ et Br^- et Cl^-.

Des calculs récents (7) ont montré qu'à "l'état libre" (gazeux) les énergies de formation des ions X_3^- correspondaient à l'ordre de stabilité $F_3^- \gg Cl_3^- > Br_3^-$. L'ordre différent observé dans le TMS, $I_3^- \sim Br_3^- \gg Cl_3^-$, est évidemment dû aux effets de solvatation sur les anions et les halogènes. On a déjà commenté la plus faible stabilité des ions Cl_3^- en milieu polaire aprotique aussi bien que aqueux (8). Par rapport au même acide de Lewis I_2, les basicités des halogénures Cl^-, Br^- et I^- dans le TMS sont trouvées être sensiblement les mêmes. Par ailleurs les stabilités des ions I_2Cl^-, I_2Br^- et I_2I^- sont voisines à "l'état libre" (7). Ce dernier fait, stabilités voisines de ces trois trihalogénures, dans le TMS et à "l'état libre", signifierait que les différences d'énergie de solvatation des ions I_2Y^- et Y^- sont faibles et donc, comme les énergies de solvatation des ions I_2Y^- sont probablement très voisines, que les énergies de solvatation de Cl^-, Br^- et I^- dans le TMS sont peu différentes. Toutefois, le peu de précision des calculs (2 kcal) (7) limite la valeur de la conclusion précédente et ne permet pas des comparaisons avec les chaleurs de solvatation des ions Cl^-, Br^- et I^- qui varient de 79.6 à 72.1 kcal (9). On pourrait aussi conclure que les différences des ordres de stabilité dans le TMS et à "l'état libre" sont surtout dues aux plus fortes interactions des plus petites molécules d'halogènes avec le solvant.

Etant donné le nombre de résultats, limités à I_3^-, sur la stabilité des ions I_2Y^- dans d'autres solvants polaires aprotiques, il n'est pas encore possible d'examiner les conséquences de la nouvelle hypothèse extrathermodynamique proposée, à savoir que les énergies de transfert des

Can. J. Chem. Downloaded from www.nrcresearchpress.com by 210.87.254.40 on 09/05/12
For personal use only.

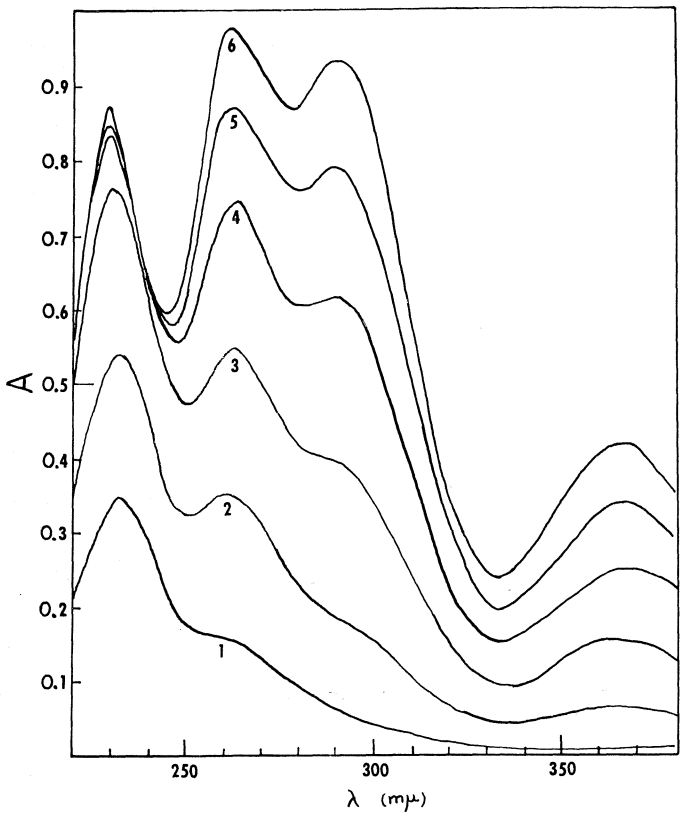

FIG. 3. Spectres d'absorption de solutions de I_2 et Cl^- dans le sulfolane. Cellule de 1 mm d'épaisseur; TMS en référence; *1*, $C_{I_2} = 8.78 \times 10^{-5}$ *M*, $C_{Cl^-} = 9.00 \times 10^{-4}$ *M*; *2*, $C_{I_2} = 1.61 \times 10^{-4}$ *M*, $C_{Cl^-} = 8.25 \times 10^{-4}$ *M*; *3*, $C_{I_2} = 2.76 \times 10^{-4}$ *M*, $C_{Cl^-} = 7.07 \times 10^{-4}$ *M*; *4*, $C_{I_2} = 3.62 \times 10^{-4}$ *M*, $C_{Cl^-} = 6.19 \times 10^{-4}$ *M*; *5*, $C_{I_2} = 4.29 \times 10^{-4}$ *M*, $C_{Cl^-} = 5.50 \times 10^{-4}$ *M*; *6*, $C_{I_2} = 4.83 \times 10^{-4}$ *M*, $C_{Cl^-} = 4.95 \times 10^{-4}$ *M*.

ions I_2Y^- sont négligeables dans les milieux polaires aprotiques. A noter cependant que l'hypothèse de Strehlow conduit à des énergies de transfert sensiblement nulles de I_3^- pour ces milieux (10). Les valeurs de $K_{I_3^-}$ connues sont trop imprécises pour aboutir à des résultats valables sur les énergies de transfert de I^- autres que les résultats approximatifs déjà déduits de l'hypothèse de Strehlow (10).

La dismutation des ions I_2Br^- et I_2Cl^- dans les solvants a déjà été étudiée qualitativement par Popov et Swensen (6). En comparant les spectres de solutions préparées à partir de sels de I_2Cl^-, I_3^- et ICl_2^-, la dismutation de I_2Cl^- dans l'acétonitrile a été mise en évidence par ces auteurs. Dans le TMS, pour les systèmes I_2–Br^- et I_2–Cl^-, si l'on suppose les espèces I_2Br^- et I_2Cl^- seules formées complètement, et si l'on calcule les coefficients d'extinction à différentes longueurs d'onde, on n'obtient pas de valeurs fixes lorsque la composition des solutions varie. Utilisant les constantes d'équilibre déterminées par potentiométrie, le programme TIPOT nous a permis de connaître les concentrations des différentes espèces dans chacune des solutions. Déduisant l'absorption due à I_3^-, les spectres de I_2Br^- et I_2Cl^- ont été calculés. La constance des ε de ces derniers ions à différentes longueurs d'onde est en accord avec le schéma réactionnel envisagé et les constantes calculées. Dans le TMS les λ_{max} et ε_{max} pour I_2Br^-, I_2Cl^- et ICl_2^- sont respectivement: 275 ± 3 mμ, 46 300 ± 1 900 cm^{-1} $mole^{-1}$ l; 263 ± 3, 36 500 ± 1 000; 232 ± 4, 66 000 ± 2 500. Bien que le système I_2–Br^- ne présente qu'un pic large aux environs de 280 mμ, ce dernier est en fait la superposition de plusieurs bandes: la faible dismutation de I_2Br^- ($K_d = 10^{-1.55}$) et le faible écart entre les

Can. J. Chem. Downloaded from www.nrcresearchpress.com by 210.87.254.40 on 09/05/12
For personal use only.

λ_{max} font que les bandes d'absorption de I_3^- (367 et 295 mμ), I_2Br^- (275 mμ) et IBr_2^- (non calculable) se confondent en un pic large. La dismutation de I_2Cl^- étant plus importante ($K_d = 10^{-0.64}$) et les λ_{max} plus éloignés (367, 295, 263 et 232 mμ pour I_3^-, I_2Cl^- et ICl_2^- respectivement) on peut distinguer les quatre bandes.

Les valeurs des λ_{max} des ions I_3^-, I_2Br^-, I_2Cl^- et ICl_2^- dans le TMS sont en bon accord avec les résultats de Popov et Swensen (6) dans l'acétonitrile. La bande de ICl_2^- à 336 mμ ($\varepsilon = 310$) n'a pu être observée dans les solutions de I_2Cl^- dans le TMS, à cause de sa faible intensité et de la proximité de la bande de I_3^- à 367 mμ ($\varepsilon = 26\,100$); les précédents auteurs avaient évité cette difficulté en utilisant un sel de ICl_2^-. En ce qui concerne les valeurs des ε_{max}, l'accord entre nos résultats et ceux de Popov et Swensen est bon dans les cas de I_3^- et I_2Br^-, à cause de la faible dismutation de ce dernier, mais mauvais pour I_2Cl^-, ces auteurs ne tenant pas compte de la dismutation importante. Pour ICl_2^-, les valeurs calculées à partir de la dismutation de I_2Cl^- sont $\lambda = 232 \pm 4$ et $\varepsilon = 66\,000 \pm 2\,500$ alors que les auteurs précités obtiennent 54 500 à 227 mμ avec un sel de ICl_2^-. En comparant les bandes d'absorption de I_3^-, I_2Br^- et I_2Cl^-, on note que la longueur d'onde de la bande la plus intense passe de 295 à 275 et 263 mμ. Par contre la deuxième bande de I_3^- à 367 mμ semble, ou ne pas avoir son équivalent dans I_2Br^- et I_2Cl^-, ou plus vraisemblablement être d'intensité nettement plus faible ($\varepsilon <$ 10 000).

Nous remercions le Conseil National de Recherches du Canada pour une bourse d'études (M.D.) et une subvention. Nous sommes reconnaissants au professeur A. L. Beauchamp d'avoir écrit le programme TIPOT et de nous avoir conseillés lors de son utilisation.

1. A. J. PARKER. Quart. Rev. **16**, 163 (1962).
2. R. G. BATES et H. STREHLOW. *Dans* The chemistry of non-aqueous solvents. *Edité par* J. J. Lagowski. Academic Press Inc., New York, N.Y., 1966. Chapitres 3 et 4.
3. R. L. BENOIT, A. L. BEAUCHAMP, and M. DENEUX. J. Phys. Chem. **73** (10), 3268 (1969).
4. R. L. BENOIT et M. GUAY. Inorg. Nucl. Chem. Lett. **4**, 215 (1968).
5. R. FERNÁNDEZ-PRINI and J. E. PRUE. Trans. Faraday Soc. **62**, 1257 (1966).
6. A. I. POPOV and R. F. SWENSEN. J. Amer. Chem. Soc. **77**, 3724 (1955).
7. E. H. WIENBENGA and D. KRACHT. Inorg. Chem. **8**, 738 (1969).
8. R. L. BENOIT, M. GUAY, et J. DESBARRES. Can. J. Chem. **46**, 1261 (1968).
9. G. CHOUX and R. L. BENOIT. J. Amer. Chem. Soc. **91**, 6221 (1969).
10. R. L. BENOIT. Inorg. Nucl. Chem. Lett. **4**, 723 (1968).

Can. J. Chem. Downloaded from www.nrcresearchpress.com by 210.87.254.40 on 09/05/12
For personal use only.

Can. J. Chem. Downloaded from www.nrcresearchpress.com by 210.87.254.40 on 09/05/12
For personal use only.

Acid-catalyzed cyclization of mangostin

PETER YATES AND H. B. BHAT
Lash Miller Chemical Laboratories, University of Toronto, Toronto, Ontario

Received November 25, 1968

The acid-catalyzed cyclization of mangostin is shown to give products in which one, but not both, of the isopentenyl side chains gives rise to dihydropyran rings. The presence of a methoxyl group at C-7 and thus the structure originally assigned to mangostin is thereby confirmed.

Canadian Journal of Chemistry, **48**, 680 (1970)

Mangostin, the major coloring matter from the fruit hulls, bark, and dried latex of *Garcinia mangostana*, was assigned structure **1** by Yates and Stout (1, 2) some years ago. A recent suggestion (3), based on benzene-induced solvent shifts in nuclear magnetic resonance (n.m.r.) spectra, that the position of the methoxyl group had been misassigned and that mangostin has structure **2**, has been shown to be unacceptable on several grounds (4). These included the results of a study of the acid-catalyzed cyclization of mangostin. We report here in detail on this study.

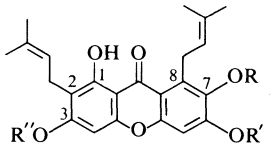

1 R = CH_3; R′ = R″ = H
2 R = R″ = H; R′ = CH_3
10 R = R′ = R″ = CH_3

Treatment of mangostin with hydrated *p*-toluenesulfonic acid in acetic acid at room temperature for 24 h gave 6 products, assigned structures **3**–**8**. Compound **3**, 1-isomangostin, is colorless, gives a negative test with ethanolic ferric chloride, and has the characteristic ultraviolet (u.v.) spectrum (Table 1) of mangostin derivatives with an ether linkage rather than a chelated hydroxyl group at C-1 (2, 5). Methylation of **3** gave dimethyl-1-isomangostin (**9**), which has been obtained previously by acid-catalyzed cyclization of dimethylmangostin (**10**) (5).

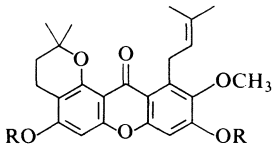

3 R = H
9 R = CH_3

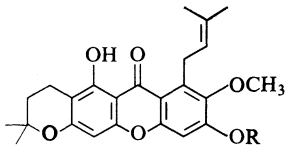

4 R = H
11 R = CH_3

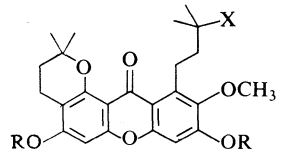

5 X = OH; R = H
6 X = $OCOCH_3$; R = H
12 X = OH; R = CH_3
13 X = $OCOCH_3$; R = CH_3

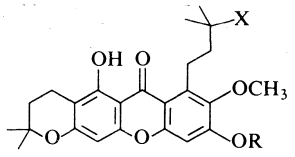

7 X = OH; R = H
8 X = $OCOCH_3$; R = H
14 X = OH; R = CH_3
15 X = $OCOCH_3$; R = CH_3

Compound **4**, 3-isomangostin, is pale yellow, gives a positive test with ethanolic ferric chloride, and has a u.v. spectrum (Table 1) characteristic of mangostin derivatives with a chelated hydroxyl group at C-1. Its n.m.r. spectrum confirmed the presence of this group and demonstrated the retention of a single isopentenyl side chain. On methylation with diazomethane or with dimethyl sulfate and potassium carbonate it gave a monomethyl ether, which is assigned structure **11**.

The colorless compounds **5** and **6** were shown to be members of the 1-isomangostin series by

TABLE 1

Ultraviolet spectra of the cyclization products from mangostin and their derivatives

Compound	λ_{max} (EtOH) mμ (log ε)			
1-Isomangostin series				
3	244 (4.58)	254 (4.52)	307 (4.39)	345 (4.03)
5	244 (4.51)	254 (4.44)	307 (4.18)	345 (3.97)*
6	244 (4.44)	254 (4.39)	307 (4.11)	345 (3.92)*
9†	245 (4.54)	255 (4.34)	302 (4.34)	336 (3.94)
12†	245 (4.54)	255 (4.55)	302 (4.36)	337 (4.00)
13	245 (4.44)	252 (4.43)	304 (4.22)	340 (3.87)
3-Isomangostin series				
4	243 (4.60)	257 (4.54)	319 (4.48)	355 (4.12)
7	243 (4.46)	253 (4.42)	319 (4.38)	355 (3.97)
8	243 (4.52)	257 (4.47)	319 (4.43)	355 (4.04)
11	243 (4.44)	252 (4.43)	317 (4.38)	355 (3.93)*
14	243 (4.52)	259 (4.54)	317 (4.42)	355 (3.94)
15	244 (4.44)	260 (4.49)	317 (4.38)	355 (3.93)

*Shoulder.
†Reference 5; A. Ault, unpublished results.

their u.v. spectra (Table 1) and by negative tests with ethanolic ferric chloride. The composition of **5** shows that its formation from mangostin involves the addition of the elements of water. That it results from hydration of the ethylenic double bond in the side chain at C-8 was demonstrated by its conversion to a dimethyl ether identical with compound **12**, previously obtained by the action of formic acid on dimethylmangostin (**10**) followed by basic hydrolysis (2), and by similar treatment of dimethyl-1-isomangostin (**9**) (5). Compound **5** is also formed when 1-isomangostin (**3**) is treated with hydrated *p*-toluenesulfonic acid in acetic acid. That compound **6**, whose composition shows that its formation involves the addition of the elements of acetic acid, results from addition of acetic acid to the C-8 side chain was shown by its conversion to a dimethyl ether, assigned structure **13**, that is identical with the product obtained when dimethyl-1-isomangostin (**9**) (5) is treated with anhydrous *p*-toluenesulfonic acid and acetic acid.

The yellow compounds **7** and **8** were shown to be members of the 3-isomangostin series by their u.v. (Table 1) and n.m.r. spectra and by positive tests with ethanolic ferric chloride. Their composition demonstrates that they are the 3-isomangostin analogues of **5** and **6**, respectively. On methylation they each give monomethyl ethers, assigned structures **14** and **15**, respectively.

When mangostin was treated with anhydrous *p*-toluenesulfonic acid in benzene at reflux for 30 min, it was converted to 1-isomangostin (**3**) and 3-isomangostin (**4**). The greater complexity of the product mixture when hydrated *p*-toluenesulfonic acid and acetic acid are used, results from the involvement of water and acetic acid in product formation.

The compounds **4**, **7**, **8**, **11**, **14**, and **15**, assigned to the 3-isomangostin series, might instead have been formulated in terms of the alternative structure **2** for mangostin as derivatives of **16**. However, in the cases of **4** and **11**, such structures can immediately be eliminated since the n.m.r. spectra of these compounds show 2-proton doublets at δ 4.12 and 4.16, respectively. These are assignable to the $ArCH_2C{=}C$ protons of an isopentenyl side chain at C-8 but not at C-2, for the methylene groups must have an *ortho* relationship to the carbonyl groups (6), which exert an anisotropic deshielding effect upon them (6*b*). A similar conclusion can be reached with respect to compounds **7**, **8**, **14**, and **15**. Each of these, like **4** and **11**, shows in its n.m.r. spectrum two 2-proton triplets at δ 1.7–1.85 and 2.7–2.75 with $J = 7$ Hz, which can be assigned to the two pairs of methylene protons of the dihydropyran ring on the basis of their splitting pattern (6*a*, 7). The position of the lower field triplet, assignable to the $ArCH_2$ protons, shows that this ring must be derived from the side chain at C-2 (7); were the ring formed from the side chain at C-8, the adjacent carbonyl group would be expected to shift the $ArCH_2$ proton signal to ca. δ 3.5 (6*a*) due to the anisotropic effect referred to above. Each of the compounds **7**, **8**, **14**, and **15**, but not **4** or **11**, shows in its spectrum a 2-proton multiplet at δ 3.4–3.8; this is assigned to the $ArCH_2$ protons in the uncyclized side chain;

Can. J. Chem. Downloaded from www.nrcresearchpress.com by 210.87.254.40 on 09/05/12
For personal use only.

Can. J. Chem. Downloaded from www.nrcresearchpress.com by 210.87.254.40 on 09/05/12
For personal use only.

the circumstance that this appears as a multiplet rather than a triplet is attributed to restricted rotation of the chain. The adjacent methylene protons, $ArCH_2CH_2CX(CH_3)_2$, give rise to a multiplet that appears in the δ 1.6–2.4 region. The position of the $ArCH_2$ proton signals confirms that the uncyclized side chain is adjacent to the carbonyl group at C-8, as in the structures assigned.

The failure to observe any products of type **16** in which the side chain at C-8 has undergone cyclization to give a dihydropyran ring, or any products in which both side chains of mangostin have undergone cyclization, i.e., compounds in the 1-isonormangostin (**17**) or 3-isonormangostin (**18**) series (2, 5), provides strong evidence that there is not a hydroxyl group at C-7.[1] This argument is particularly cogent with respect to the absence of a product in the 1-isonormangostin series, for closure at the *chelated* hydroxyl group at C-1 could hardly occur without concomitant closure at an *unchelated* hydroxyl group at C-7. Thus this position must be the site of the methoxyl group in mangostin, as originally proposed (1, 2).

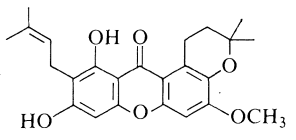

16

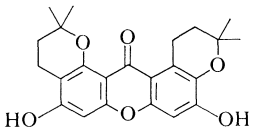

17

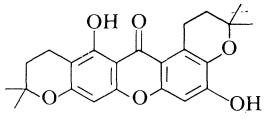

18

Experimental

Melting points were recorded in capillary tubes and are uncorrected. Chromatography was carried out on silica plates (1.25 mm thickness) containing a phosphor, unless otherwise specified.

*Cyclization of Mangostin (**1**) with Hydrated p-Toluenesulfonic Acid in Acetic Acid. Formation of Compounds **3–8***

A mixture of mangostin (1.00 g), *p*-toluenesulfonic acid hydrate (3.00 g), and acetic acid (50 ml) was stirred at room temperature for 24 h. The pale yellowish green solution was diluted with ethyl acetate, washed repeatedly with aqueous sodium bicarbonate, and dried with anhydrous sodium sulfate. The solvent was removed under reduced pressure, and the residual orange gum was dissolved in a small amount of acetone. The colorless crystalline material that separated in 2 h was collected and recrystallized from acetone to give compound **5** (80 mg), m.p. 261–263° (decomp.); λ_{max}(Nujol) 3.00, 6.20, and 6.35 μ; *m/e* 428; no color with ethanolic ferric chloride.

Anal. Calcd. for $C_{24}H_{28}O_7$: C, 67.27; H, 6.59. Found: C, 66.94; H, 6.60.

The mixture from the original acetone mother liquor was chromatographed on 10 plates with ethyl acetate – benzene (1:1 v/v) as eluent. The bands revealed by u.v. radiation had the following approximate R_f values: 0.4, 0.5, 0.7, and 0.9. The material from the band with R_f 0.4 was extracted with ethyl acetate and crystallized from this solvent to give compound **7** as lemon-yellow crystals (80 mg), m.p. 182–183° (decomp.); λ_{max}($CHCl_3$) 2.90, 3.20 (br), 6.10, and 6.30 μ; δ(CD_3COCD_3) 1.29 (s, 6 H), 1.35 (s, 6 H), 1.85 (t, J = 7 Hz, superimposed on m; 4 H), 2.68 (t, J = 7 Hz, 2 H), 3.5 (m, 2 H), 3.85 (s, 3 H), 6.21 (s, 1 H), and 6.84 (s, 1 H); δ(C_5D_5N/$CDCl_3$) 13.96 (s, 1 H); *m/e* 428; olive-green color with ethanolic ferric chloride.

Anal. Calcd. for $C_{24}H_{28}O_7$: C, 67.27; H, 6.59. Found: C, 67.26; H, 6.52.

The material from the band with R_f 0.5 was extracted with ethyl acetate to give a colorless crystalline product (50 mg), which was crystallized from acetone to give compound **6** as colorless crystals, m.p. 237–239° (decomp.); λ(Nujol) 3.30, 5.90, 6.20, and 6.35 μ; δ(CD_3OD) 1.40 (s, 6 H), 1.58 (s, 6 H), 1.82 (t, $J \sim 7$ Hz), 1.9 (m), 2.02 (s, 3 H), 2.66 (t, $J \sim 7$ Hz, 2 H), 3.8 (m), 3.81 (s, 3 H), 6.33 (s, 1 H), and 6.71 (s, 1 H); δ(C_5D_5N) 1.40 (s, 6 H), 1.70 (s superimposed on m; 8 H), 2.05 (s, 3 H), 2.2 (m, 2 H), 2.88 (t, J = 7 Hz, 2 H), 3.7 (m, 2 H), 3.93 (s, 3 H), 6.65 (s, 1 H), and 6.97 (s, 1 H); *m/e* 470; no color with ethanolic ferric chloride.

Anal. Calcd. for $C_{26}H_{30}O_8$: C, 66.37; H, 6.43. Found: C, 66.63; H, 6.63.

The material from the band with R_f 0.7 appeared to be a mixture and was re-chromatographed with ethyl acetate – benzene (1:7 v/v) as eluent. It was separated into 2 bands, of which the faster moving was extracted with ethyl acetate to provide a pale yellow crystalline product (60 mg) which was crystallized from ethyl acetate – ether to give compound **8** as pale yellow crystals, m.p. 188–189° (decomp.); λ_{max}($CHCl_3$) 2.90, 5.80, 6.05, 6.20, and 6.30 μ; δ(C_5D_5N) 1.27 (s, 6 H), 1.70 (s superimposed on m; 8 H), 2.04 (s, 3 H), 2.3 (m, 2 H), 2.73 (t, $J \sim 7$ Hz, 2 H), 3.65 (m, 2 H), 6.42 (s, 1 H), 7.07 (s, 1 H), and 14.43 (s, 1 H); *m/e* 470; olive-green color with ferric chloride.

Anal. Calcd. for $C_{26}H_{30}O_8$: C, 66.37; H, 6.43. Found: C, 66.31; H, 6.38.

The material from the slower-moving band from the re-chromatography was extracted with ethyl acetate and crystallized from benzene to give 1-isomangostin (**3**) as colorless crystals, m.p. 241–243° (decomp.) with initial melting at 154–155° and resolidification at 180°; λ_{max} (Nujol) 2.9, 3.20, 6.20, and 6.35 μ; δ(DMSO-d_6) 1.31

[1]Although the weight balance in the cyclization with hydrated *p*-toluenesulfonic acid was poor, and that with anhydrous *p*-toluenesulfonic acid was only 73%, the remainder of the product mixture in each case had an R_f value of zero and therefore could contain no compounds in the **16–18** series.

Can. J. Chem. Downloaded from www.nrcresearchpress.com by 210.87.254.40 on 09/05/12
For personal use only.

(s, 6 H), 3.62 (d, J = 1 Hz, 3 H), 3.77 (d, J = 1 Hz, superimposed on m; 5 H), 3.68 (s, 3 H), 3.98 (br d, J = 7 Hz, 2 H), 5.2 (m, 1 H), 6.35 (s, 1 H), 6.72 (s, 1 H), 10.45 (s, 1 H), and 10.54 (s, 1 H) (signals due to solvent at 2.5 (DMSO-d_5) and 3.35 (H_2O)); *m/e* 410; no color with ethanolic ferric chloride. An analytical sample heated at 80° *in vacuo* over P_2O_5 exhibited the same double melting point.

Anal. Calcd. for $C_{24}H_{26}O_6 \cdot \frac{1}{4}H_2O$: C, 69.46; H, 6.44. Found: C, 69.72; H, 6.50.

An analytical sample heated at 180° *in vacuo* over P_2O_5 had a single m.p. 241–243° (decomp.); its infrared (i.r.) spectrum (Nujol mull) was similar to that of the sample heated at 80°, but had weaker absorption in the 2.9 μ region; its n.m.r. spectrum (DMSO-d_6 containing H_2O (*vide supra*)) was closely similar to that of the sample heated at 80°; *m/e* 410.

Anal. Calcd. for $C_{24}H_{26}O_6$: C, 70.23; H, 6.39. Found: C, 70.30; H, 6.52.

The material from the band with R_f 0.9 in the original chromatogram was extracted with ethyl acetate to give an orange gum (100 mg) which was crystallized from petroleum ether (b.p. 70–80°) to give 3-isomangostin (**4**) as pale yellow needles, m.p. 154–155° (decomp.); λ_{max}(Nujol) 3.10, 6.15, 6.25, and 6.35 μ; δ($CDCl_3$) 1.35 (s, 6 H), 1.68 (d, $J \sim$ 1 Hz, 3 H), 1.82 (s superimposed on t, $J \sim$ 7 Hz, 5 H), 2.72 (t, J = 7 Hz, 2 H), 3.80 (s, 3 H), 4.12 (d, $J \sim$ 6 Hz, 2 H), 5.31 (m, 1 H), 6.26 (s, 1 H), 6.32 (br s, 1 H), 6.85 (s, 1 H), and 13.79 (s, 1 H); *m/e* 410; olive-green color with ethanolic ferric chloride.

Anal. Calcd. for $C_{24}H_{26}O_6$: C, 70.23; H, 6.39. Found: C, 70.05; H, 6.37.

*Cyclization of Mangostin (**1**) with Anhydrous p-Toluenesulfonic Acid in Benzene. Formation of **3** and **4***

p-Toluenesulfonic acid (125 mg) was treated with benzene (125 ml), and 35 ml of the latter were distilled to remove water. Mangostin (1.00 g) was added, and the mixture was boiled under gentle reflux for 30 min. The solution was cooled, diluted with ethyl acetate, washed twice with water, and dried over anhydrous sodium sulfate. Removal of the benzene gave a deep orange gum which was chromatographed on 10 plates with ethyl acetate – benzene (1:7 v/v) as eluent. The material from the faster-moving, major band (R_f 0.5) was extracted with ethyl acetate. The extract was stripped of solvent and the residue was crystallized from petroleum ether (b.p. 60–80°) to give 3-isomangostin (**4**) as pale yellow fluffy needles (582 mg), m.p. 154–155° (decomp.), shown by mixed m.p. and i.r. spectral comparison to be identical with the sample obtained from cyclization in acetic acid.

The material from the slower-moving band was extracted with ethyl acetate and crystallized from benzene to give 1-isomangostin (**3**), (146 mg) m.p. 241–243° (decomp.) with initial melting at 154–155° and resolidification at 180°, shown by mixed m.p. and i.r. spectral comparison to be identical with the sample obtained from cyclization in acetic acid.

*Methylation of 1-Isomangostin (**3**). Formation of Dimethyl-1-isomangostin (**9**)*

A solution of 1-isomangostin (**3**), m.p. 155° and 241–243°, (200 mg) in acetone (20 ml) was treated with potassium carbonate (200 mg) and dimethyl sulfate (1.0 ml), and the mixture was boiled under reflux for 5 h. It was then filtered and the filtrate was stripped of solvent. The residue was left in contact with water for 12 h and then extracted with ether. The ethereal extract was washed with water, dried, and stripped of solvent. The residue was crystallized from cyclohexane – petroleum ether to give dimethyl-1-isomangostin (**9**), m.p. 128–129°, shown by mixed m.p. and i.r. spectral comparison to be identical with a sample of **9** prepared by acid-catalyzed cyclization of dimethylmangostin (**10**) (5).

The same product was obtained on similar methylation of 1-isomangostin, m.p. 241–243°.

*Methylation of 3-Isomangostin (**4**). Formation of Methyl-3-isomangostin (**11**)*

A solution of 3-isomangostin (**4**) (100 mg) in ether (10 ml) was treated with excess ethereal diazomethane. After 24 h the solution was filtered and stripped of solvent; the residue was crystallized from ethanol to give methyl-3-isomangostin (**11**) (80 mg), m.p. 138–139°; λ_{max}(Nujol) 6.10, 6.30, and 6.35 μ; δ($CDCl_3$) 1.36 (s, 6 H), 1.67 (d, $J \sim$ 1 Hz, 3 H), 1.84 (s superimposed on t, $J \sim$ 7 Hz; 5 H), 2.72 (t, J = 7 Hz, 2 H), 3.79 (s, 3 H), 3.95 (s, 3 H), 4.16 (d, J = 7 Hz, 2 H), 5.29 (m, 1 H), 6.26 (s, 1 H), 6.77 (s, 1 H), and 13.84 (s, 1 H); *m/e* 424; olive-green color with ethanolic ferric chloride.

Anal. Calcd. for $C_{25}H_{28}O_6$: C, 70.74; H, 6.65. Found: C, 70.72; H, 6.64.

Methylation of **4** with dimethyl sulfate in acetone at reflux also gave the monomethyl ether **11**.

*Methylation of **5**. Formation of **12***

A solution of **5** (20 mg) in methanol (3 ml) was treated with excess ethereal diazomethane as before. Crystallization of the product from methanol gave colorless crystals of **12**, m.p. 201–203°. This was shown by mixed m.p. and i.r. spectral comparison to be identical with a sample of **12** prepared by reaction of dimethylmangostin (**10**) with formic acid followed by basic hydrolysis (2, 5).

*Reaction of 1-Isomangostin (**3**) with Hydrated p-Toluenesulfonic Acid in Acetic Acid. Formation of **5***

A solution of 1-isomangostin (**3**) (50 mg) and *p*-toluenesulfonic acid hydrate (150 mg) in acetic acid (0.3 ml) was kept at room temperature for 36 h. The resulting pale yellow crystalline mass was treated with aqueous sodium bicarbonate, and the mixture was extracted with ethyl acetate. The extract was washed with water, dried over anhydrous sodium sulfate, and stripped of solvent. The residue was crystallized from acetone to give **5** (30 mg), m.p. 262–263° (decomp.); this was shown by mixed m.p. and i.r. spectral comparison to be identical with the sample obtained directly from mangostin.

*Methylation of **6**. Formation of **13***

A solution of **6** (10 mg) in methanol (2 ml) was treated with excess ethereal diazomethane as above. Crystallization of the product from ethanol gave colorless crystals of **13**, m.p. 132–133°; λ_{max}(Nujol) 5.80, 6.05, and 6.30 μ; δ($CDCl_3$) 1.41 (s, 6 H), 1.60 (s, 6 H), 1.83 (t, J = 7 Hz, superimposed on m; 4 H), 2.04 (s, 3 H), 2.64 (t, J = 7 Hz, 2 H), 3.45 (m, 2 H), 3.83 (s, 3 H), 3.88 (s, 3 H), 3.92 (s, 3 H), 6.35 (s, 1 H), and 6.71 (s, 1 H); *m/e* 438 ($M - C_2H_4O_2$).

Anal. Calcd. for $C_{28}H_{34}O_8$: C, 67.45; H, 6.87. Found: C, 67.55; H, 6.62.

*Reaction of Dimethyl-1-isomangostin (**9**) with Anhydrous p-Toluenesulfonic Acid in Acetic Acid. Formation of **13***

p-Toluenesulfonic acid (300 mg) was treated with benzene (20 ml), and the benzene was distilled to remove water. Acetic acid (5 ml) and dimethyl-1-isomangostin (**9**) (50 mg) were added, and the solution was kept at room temperature for 24 h. It was then diluted with ethyl acetate, washed with aqueous sodium bicarbonate, dried over anhydrous sodium sulfate, and stripped of solvent. The residue was chromatographed on 3 Eastman chromatogram sheets (silica gel) with ethyl acetate – benzene (1:3 v/v) as eluent. The material from the band below that of unconsumed starting material was extracted with ethyl acetate and crystallized from methanol to give **13**, m.p. 132–133°; this was shown by mixed m.p. and i.r. spectral comparison to be identical with the sample obtained by methylation of **6**.

*Methylation of **7**. Formation of **14***

A solution of **7** (200 mg) in acetone (30 ml) was treated with potassium carbonate (1.0 g) and dimethyl sulfate (0.2 ml), and the mixture was boiled under reflux for 6 h. It was then filtered, and the filtrate was stripped of solvent. The residue was chromatographed on 2 plates with ethyl acetate – benzene (1:3 v/v) as eluent. The material from the major band was extracted with ethyl acetate and crystallized from acetone – petroleum ether to give **14** as long yellow needles, m.p. 151–153°; λ_{max}(Nujol) 2.95, 6.10, 6.25, and 6.35 μ; δ($CDCl_3$) 1.32 (s, 6 H), 1.39 (s, 6 H), 1.77 (t, $J \sim 7$ Hz, superimposed on m; 4 H), 2.70 (t, $J = 7$ Hz; 2 H), 3.5 (m, 2 H), 3.81 (s, 3 H), 3.87 (s, 3 H), 6.28 (s, 1 H), 6.72 (s, 1 H), and 13.86 (s, 1 H).

Anal. Calcd. for $C_{25}H_{30}O_7$: C, 67.85; H, 6.83. Found: C, 68.06; H, 6.91.

*Methylation of **8**. Formation of **15***

A solution of **8** (80 mg) in ether (10 ml) was treated with excess ethereal diazomethane as before. The product was chromatographed on one plate with ethyl acetate – benzene (1:8 v/v) as eluent. The material from the major band was extracted with ethyl acetate and crystallized from petroleum ether (b.p. 60–80°) to give **15**, m.p. 148–149° (decomp.); λ_{max}(Nujol) 5.80, 6.05, and 6.20 μ; δ($CDCl_3$) 1.36 (s, 6 H), 1.58 (s, 6 H), 1.83 (t, $J = 7$ Hz, 2 H), 2.02 (s superimposed on m; 5 H), 2.72 (t, $J = 7$ Hz, 2 H), 3.5 (m, 2 H), 3.84 (s, 3 H), 3.94 (s, 3 H), 6.25 (s, 1 H), 6.74 (s, 1 H), and 13.9 (br s, 1 H); δ(CD_3COCD_3) 1.35 (s, 6 H), 1.55 (s, 6 H), 1.85 (t, $J = 7$ Hz, 2 H), 1.96 (s, 3 H), 2.68 (t, $J = 7$ Hz, 2 H), 3.45 (m), 3.82 (s, 3 H), 4.02 (s, 3 H), 6.20 (s, 1 H), and 6.93 (s, 1 H); *m/e* 484.

Anal. Calcd. for $C_{27}H_{32}O_8$: C, 66.92; H, 6.66. Found: C, 66.93; H, 6.86.

We thank Professor G. H. Stout, University of Washington, for informing us of related work in his laboratory, and Mr. James Savage for technical assistance. Generous financial support of this research by the National Research Council is gratefully acknowledged.

1. P. Yates and G. H. Stout. Chem. Ind. (London), 1392 (1956).
2. P. Yates and G. H. Stout. J. Amer. Chem. Soc. **80**, 1691 (1958).
3. F. Scheinmann. Chem. Commun. 1015 (1967).
4. G. H. Stout, M. M. Krahn, P. Yates, and H. B. Bhat. Chem. Commun. 211 (1968).
5. P. Yates and A. Ault. Tetrahedron, **23**, 3307 (1967).
6. (*a*) G. H. Stout, V. F. Stout, and M. J. Welsh. Tetrahedron, **19**, 1667 (1963). (*b*) L. J. Haynes and D. R. Taylor. J. Chem. Soc. (C), 1685 (1966); B. Jackson, H. D. Locksley, and F. Scheinmann. J. Chem. Soc. (C), 785 (1967).
7. B. Jackson, H. D. Locksley, and F. Scheinmann. J. Chem. Soc. (C), 2500 (1967).

Can. J. Chem. Downloaded from www.nrcresearchpress.com by 210.87.254.40 on 09/05/12
For personal use only.

Can. J. Chem. Downloaded from www.nrcresearchpress.com by 210.87.254.42 on 09/05/12
For personal use only.

NOTES

Electrochemical studies of yttrium and yttrium–zinc alloys in fused LiCl–KCl eutectic

YOSHIO HOSHINO[1] AND JAMES A. PLAMBECK
Department of Chemistry, University of Alberta, Edmonton, Alberta

Received September 19, 1969

The electromotive force of cells of the type Y(s)/YCl_3 + LiCl–KCl (eutectic)/Y–Zn alloy (saturated liquid) has been measured over the temperature range 450–570 °C. Thermodynamic values for the limiting solid YZn_{12} existing in this region are: ΔG_f^0, −48.7 kcal/mole at 450 °C; ΔH_f^0, −74.9 kcal/mole; ΔS_f^0, −36 cal/deg mole. The standard molar potential of the Y(III)–Y(0) couple was determined to be −2.831 V against Pt(II)–Pt(0).

Canadian Journal of Chemistry, **48**, 685 (1970)

Introduction

Fused-salt electromotive force (e.m.f.) methods have been previously used in this laboratory to study the zinc-rich portion of the uranium–zinc (1) and lanthanum–zinc (2) systems, this work being of interest in the possible electrochemical separation of fission product impurities. The separation of lanthanum from uranium has been shown to become significantly less feasible on alloying with zinc (2). The present paper completes the work with a study of the yttrium–zinc system in the course of which the standard potential of the Y(III)–Y(0) couple was determined.

Experimental

Materials

The fused LiCl–KCl eutectic was prepared by the method of Laitinen *et al.* (3) and ampuled under argon for future use. The salt used for the yttrium–zinc cells was prepared by adding anhydrous YCl_3 (A. D. MacKay Inc., N.Y.) before purification of the melt, as previously (2). Reagent grade zinc shot (Allied Chemical, N.Y.) was cast into a small ingot under fused zinc chloride for future use. Yttrium rod or sheet (3 mm rod, 99.9%, A. D. MacKay Inc., N.Y.) was used as the yttrium electrode, attached to tantalum leads. Yttrium–zinc alloys were made up by melting together weighed amounts of the elements, either in situ using the apparatus previously employed for uranium (1) or prior to the experiment in a tantalum crucible (4).

Apparatus

The instruments, cell, and electrodes used were those previously used (1) to study uranium–zinc. Auxiliary reference electrodes were platinum (5) rather than silver as previously used (1).

Procedure

The procedure used in e.m.f. studies of the Y(III)–Y(0) couple was that employed by Laitinen and Plambeck (5) for rhodium and iridium. The procedure used in the e.m.f. studies of the Y–Zn alloy was that used previously for U–Zn (1). The solubility of yttrium in zinc (6) is much lower than the solubility of uranium in zinc and measurements in the unsaturated region were therefore not possible.

Results and Discussion

Yttrium(III)–Yttrium(0) Electrode

The Y(III)–Y(0) couple has previously been studied in the LiCl–KCl eutectic only by Yang and Hudson (7), from whose data Plambeck (8) calculated the standard molarity-scale potential of this couple to be −2.859 V against the standard molar platinum electrode (s.m.p.e.) of Laitinen and Liu (9). Inasmuch as this calculation involved extrapolation from data taken at temperatures higher than 450 °C and higher concentrations than those at which obedience to Henry's Law can be assumed, a redetermination of the standard potential of this couple appeared necessary.

A total of 19 concentration–potential data points were taken in two separate experiments at 450 ± 0.5 °C at concentrations of Y(III) between 5×10^{-3} and 8×10^{-2} M, using two different platinum reference electrodes. These data obeyed the Nernst equation as shown in Fig. 1. From the data given in Fig. 1, less the three points below 0.01 M which show systematic deviation, a least-squares calculation gave the molarity-scale standard potential E_M^0 as −2.831 ± 0.003 V against

[1]Present address: Department of Chemistry, Tokyo Institute of Technology, O-okayama, Meguro-ku, Tokyo, Japan.

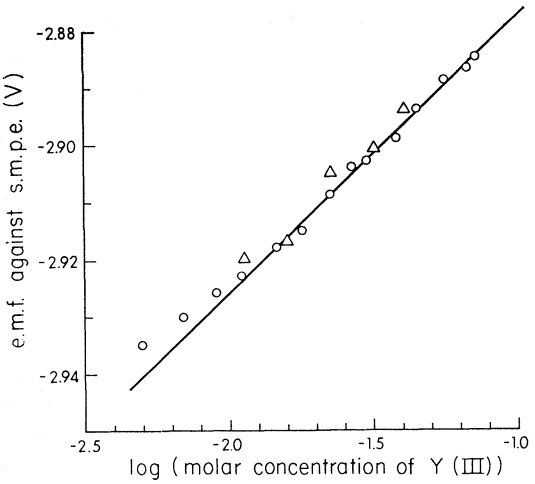

FIG. 1. Potential of Y(III)/Y electrode against s.m.p.e., in volts, as a function of the logarithm of the molar concentration of Y(III). Circles, run 1; triangles, run 2; line has slope corresponding to three electrons exactly.

s.m.p.e. The Nernst slope was 46.7 ± 1.6 mV/log unit, in excellent agreement with the value of 47.8 expected for a three-electron process at this temperature. This standard potential differs by 28 mV from the previous (8) value, the difference probably being primarily due to the extrapolation from higher temperatures. The present value is to be preferred. It corresponds to −2.836 and −2.866 V, with the same error, on the molality and mole fraction scales, respectively, against the appropriate standard platinum reference electrode.

The Yttrium–Zinc System

Two separate experiments using completely different electrodes and electrolyte charges were carried out. The yttrium–zinc pool was about 0.2 atom % yttrium and the cell potential was insensitive to addition of yttrium. The electrolyte was LiCl–KCl eutectic about 0.05 *M* in Y(III) and the cell potential was insensitive to addition of further Y(III) by anodization of the yttrium rod.

The cell temperature was randomly varied between 450 and 570 °C and the cell e.m.f. recorded. Several hours were needed to reach equilibrium, as before (1), and the potentials did not vary more than 0.1 mV/30 min once equilibrium had been reached. The (mean) potential values are given in Table 1. The cell e.m.f. is inversely proportional to temperature and this

TABLE 1

Temperature dependence of e.m.f. of the yttrium–zinc cell

Temperature (°C)	Electromotive force (mV)
472.0	695.7
494.6	683.2
520.75	668.5
545.75	654.6
569.75	641.9
456.0*	698.5
470.5*	690.5
496.5*	676.7
518.0*	664.3
547.0*	648.5

*Cell 2, otherwise cell 1.

dependence is described by the least-squares equation $E = 1.0831 - 5.252 \times 10^{-4} T$ V, where T is the temperature (°K), the standard errors on the intercept and slope being 1.6 and 5.5%, respectively.

The cell Y(s)/YCl_3 + LiCl–KCl (eutectic)/Y–Zn (saturated liquid) is nearly identical to the cells discussed previously (1, 2) and the thermodynamic discussions given earlier apply. The limiting solid phase whose thermodynamic properties are here determined is presumed to be YZn_{12} on the basis of the work of Veleckis, Schablaske, Johnson, and Feder (10), although Chiotti, Mason, and Gill (4) report it as YZn_{11}. The difference is not significant (1) for the present study. The enthalpy of formation ΔH_f^0 for this compound is then −74.94 ± 1.56 kcal/mole, and the entropy of formation ΔS_f^0 is −36.3 ± 2.0 cal/deg mole. The free energy of formation ΔG_f^0 is, at 500 °C, −46.8 ± 1.0 kcal/mole. All of these values correspond to the reaction

$$Y\,(s) + 12Zn\,(l) \rightarrow YZn_{12}\,(s)$$

The results of this study are not in agreement with the only previous data, that of Chiotti, Mason, and Gill (4), who report ΔG_f^0 as −53.43 ± 0.15 kcal/mole at 500 °C for the limiting Y–Zn compound. The discrepancy is even larger for enthalpy and entropy than for free energy. The present direct measurements should be preferred, at least within the temperature range employed here, over the indirect calculation from the vapor pressure of zinc above yttrium–zinc alloys (4), because such studies are least accurate for compounds of high zinc content. It must be noted, however, that the discrepancy between cell and

Can. J. Chem. Downloaded from www.nrcresearchpress.com by 210.87.254.42 on 09/05/12
For personal use only.

vapor pressure measurements is much less in the uranium–zinc system (1) than in the present yttrium–zinc study.

Conclusion

The free energy of formation of the limiting yttrium–zinc compound obtained in this study, −48.7 kcal/mole at 450 °C, is similar to that for the limiting lanthanum–zinc (2) compound, −58.8 kcal/mole; both are much larger than that for the limiting uranium–zinc compound, −26.1 kcal/mole. The effect of alloying with zinc is thus the same for yttrium as for lanthanum, i.e. to reduce the feasibility of electrochemically separating these elements from uranium by a significant factor.

The authors are grateful to the National Research Council of Canada for support of this research.

1. Y. Hoshino and J. A. Plambeck. Can. J. Chem. **47**, 965 (1969).
2. J.-B. Lesourd and J. A. Plambeck. Can. J. Chem. **47**, 3387 (1969).
3. H. A. Laitinen, W. S. Ferguson, and R. A. Osteryoung. J. Electrochem. Soc. **104**, 516 (1957).
4. P. Chiotti, J. T. Mason, and K. J. Gill. Trans. Met. Soc. A.I.M.E. **227**, 910 (1963).
5. H. A. Laitinen and J. A. Plambeck. J. Amer. Chem. Soc. **87**, 1202 (1965).
6. I. Johnson and I. G. Dillon. U.S. At. Energy Comm. Rep. ANL-7083. 1965. p. 106.
7. L. Yang and R. G. Hudson. Trans. Met. Soc. A.I.M.E. **215**, 589 (1959).
8. J. A. Plambeck. J. Chem. Eng. Data, **12**, 77 (1967).
9. H. A. Laitinen and C. H. Liu. J. Amer. Chem. Soc. **80**, 1015 (1958).
10. E. Veleckis, R. V. Schablaske, I. Johnson, and H. M. Feder. Trans. Met. Soc. A.I.M.E. **239**, 58 (1967).

Perfluoroalkyl vicinal dihypohalites[1]

A. F. Janzen and R. Pollitt
Department of Chemistry, University of Manitoba, Winnipeg, Manitoba

Received May 23, 1969

The preparation of perfluoroalkyl vicinal dihypohalites is described. The new compounds were characterized by ^{19}F nuclear magnetic resonance, infrared spectroscopy, and chemical reactions.

Canadian Journal of Chemistry, **48**, 687 (1970)

The synthesis of a number of perfluoroalkyl hypochlorites,[2] R_fOCl, has been described very recently (1, 2). We wish to report the synthesis of perfluoroalkyl vicinal dihypochlorites **1**, -bromites **2**, and -iodites **3**.

$$\begin{matrix}(CF_3)_2C{-}O{-}X\\ |\\ (CF_3)_2C{-}O{-}X\end{matrix}$$

1 X = Cl
2 X = Br
3 X = I

Compounds **1** and **2** were prepared by reaction of disodium perfluoropinacolate with chlorine and bromine, respectively (eq. [1]). Attempts to extend the reaction to iodine were unsuccessful.

[1] $(CF_3)_2C(O)C(CF_3)_2O{\cdot}2Na + 2X_2 \rightarrow (CF_3)_2C(OX)C(CF_3)_2OX + 2NaX$

1 X = Cl
2 X = Br

Compound **3** was prepared by reaction of disodium perfluoropinacolate with iodine monochloride or iodine monobromide (eq. [2]).

[2] $(CF_3)_2C(O)C(CF_3)_2O{\cdot}2Na + 2IX \rightarrow (CF_3)_2C(OI)C(CF_3)_2OI + 2NaX$

X = Cl,Br

The reactions were conveniently carried out in the solvent trichlorofluoromethane. Sodium halides were recovered in high yield, identified by their X-ray powder patterns and found to be consistent with reactions shown in eqs. [1] and [2].

The ^{19}F nuclear magnetic resonance (n.m.r.) spectra of the dihypohalites showed, in each case, a sharp single absorption peak, indicating

[1]Presented at the 52nd Canadian Chemical Conference and Exhibition, Montreal, May 25–28, 1969.
[2]These compounds may also be named chloroxyperfluoroalkanes (see reference 2).

Can. J. Chem. Downloaded from www.nrcresearchpress.com by 210.87.254.42 on 09/05/12
For personal use only.

vapor pressure measurements is much less in the uranium–zinc system (1) than in the present yttrium–zinc study.

Conclusion

The free energy of formation of the limiting yttrium–zinc compound obtained in this study, −48.7 kcal/mole at 450 °C, is similar to that for the limiting lanthanum–zinc (2) compound, −58.8 kcal/mole; both are much larger than that for the limiting uranium–zinc compound, −26.1 kcal/mole. The effect of alloying with zinc is thus the same for yttrium as for lanthanum, i.e. to reduce the feasibility of electrochemically separating these elements from uranium by a significant factor.

The authors are grateful to the National Research Council of Canada for support of this research.

1. Y. Hoshino and J. A. Plambeck. Can. J. Chem. **47**, 965 (1969).
2. J.-B. Lesourd and J. A. Plambeck. Can. J. Chem. **47**, 3387 (1969).
3. H. A. Laitinen, W. S. Ferguson, and R. A. Osteryoung. J. Electrochem. Soc. **104**, 516 (1957).
4. P. Chiotti, J. T. Mason, and K. J. Gill. Trans. Met. Soc. A.I.M.E. **227**, 910 (1963).
5. H. A. Laitinen and J. A. Plambeck. J. Amer. Chem. Soc. **87**, 1202 (1965).
6. I. Johnson and I. G. Dillon. U.S. At. Energy Comm. Rep. ANL-7083. 1965. p. 106.
7. L. Yang and R. G. Hudson. Trans. Met. Soc. A.I.M.E. **215**, 589 (1959).
8. J. A. Plambeck. J. Chem. Eng. Data, **12**, 77 (1967).
9. H. A. Laitinen and C. H. Liu. J. Amer. Chem. Soc. **80**, 1015 (1958).
10. E. Veleckis, R. V. Schablaske, I. Johnson, and H. M. Feder. Trans. Met. Soc. A.I.M.E. **239**, 58 (1967).

Perfluoroalkyl vicinal dihypohalites[1]

A. F. Janzen and R. Pollitt
Department of Chemistry, University of Manitoba, Winnipeg, Manitoba

Received May 23, 1969

The preparation of perfluoroalkyl vicinal dihypohalites is described. The new compounds were characterized by ^{19}F nuclear magnetic resonance, infrared spectroscopy, and chemical reactions.

Canadian Journal of Chemistry, **48**, 687 (1970)

The synthesis of a number of perfluoroalkyl hypochlorites,[2] R_fOCl, has been described very recently (1, 2). We wish to report the synthesis of perfluoroalkyl vicinal dihypochlorites **1**, -bromites **2**, and -iodites **3**.

$$\begin{matrix}(CF_3)_2C{-}O{-}X\\ |\\ (CF_3)_2C{-}O{-}X\end{matrix}$$

1 X = Cl
2 X = Br
3 X = I

Compounds **1** and **2** were prepared by reaction of disodium perfluoropinacolate with chlorine and bromine, respectively (eq. [1]). Attempts to extend the reaction to iodine were unsuccessful.

[1] $(CF_3)_2C(O)C(CF_3)_2O{\cdot}2Na + 2X_2 \rightarrow (CF_3)_2C(OX)C(CF_3)_2OX + 2NaX$

1 X = Cl
2 X = Br

Compound **3** was prepared by reaction of disodium perfluoropinacolate with iodine monochloride or iodine monobromide (eq. [2]).

[2] $(CF_3)_2C(O)C(CF_3)_2O{\cdot}2Na + 2IX \rightarrow (CF_3)_2C(OI)C(CF_3)_2OI + 2NaX$

X = Cl,Br

The reactions were conveniently carried out in the solvent trichlorofluoromethane. Sodium halides were recovered in high yield, identified by their X-ray powder patterns and found to be consistent with reactions shown in eqs. [1] and [2].

The ^{19}F nuclear magnetic resonance (n.m.r.) spectra of the dihypohalites showed, in each case, a sharp single absorption peak, indicating

[1]Presented at the 52nd Canadian Chemical Conference and Exhibition, Montreal, May 25–28, 1969.
[2]These compounds may also be named chloroxyperfluoroalkanes (see reference 2).

Can. J. Chem. Downloaded from www.nrcresearchpress.com by 210.87.254.6 on 09/05/12
For personal use only.

Can. J. Chem. Downloaded from www.nrcresearchpress.com by 210.87.254.6 on 09/05/12
For personal use only.

the equivalence of all 12 fluorine atoms. Chemical shifts relative to internal $CFCl_3$ are: **1**, + 70.1; **2**, +70.1; **3**, +70.8 p.p.m. This is the region to be expected for perfluoropinacol derivatives (3) and may be compared with perfluoropinacol itself, which has a sharp singlet at +70.7 p.p.m.

All the compounds had infrared (i.r.) spectra consistent with their proposed structures, the principal feature being strong absorption in the region 1260–1210 cm^{-1} associated with carbon–fluorine stretching frequencies. In particular, the i.r. spectra eliminated the possibility that C=C, C=O, or —OH groups were present.

The stability of dihypohalites was briefly investigated. They were found to be stable at 0 °C in $CFCl_3$ solution but decomposition occurred on standing at 25°. The rate of decomposition increased on heating or in the presence of ultraviolet (u.v.) light. Decomposition accompanied attempts to remove the last traces of solvent at reduced pressure in the vacuum system at room temperature and −22°. Compounds **1** and **2** were found to decompose if eq. [1] was carried out with excess chlorine or bromine. The ^{19}F n.m.r. proved very useful in checking the purity of solutions of dihypohalites since decomposition caused disappearance of the sharp singlet and appearance of complex multiplets.

Chemical reactions are entirely consistent with the formulation of the new compounds as dihypohalites. For example, when preparation of dihypohalites was carried out in tetrahydrofuran the final product was perfluoropinacol, indicating hydrogen abstraction from solvent. It is well known that the analogous reaction of *t*-butyl hypochlorite and hydrocarbon solvents gives *t*-butyl alcohol (4). If benzaldehyde is added to a solution of **1** in carbon tetrachloride the main products are benzoic acid and benzoyl chloride. These products are also found when *t*-butyl hypochlorite reacts with benzaldehyde in carbon tetrachloride (5).

The reaction of disodium perfluoropinacolate proceeds with $(C_6H_5)_2ICl$ and $C_6H_5ICl_2$ and characterization of these and similar reactions is now in progress.

One explanation for the relative stability of perfluoroalkyl vicinal dihypohalites, as compared to the unknown alkyl derivatives, may be decreased repulsion of non-bonded electrons on oxygen and halogen due to proximity of highly electronegative trifluoromethyl groups.

Experimental

General

A conventional vacuum system was used for handling volatile materials. Disodium perfluoropinacolate was prepared from hexafluoroacetone (Matheson of Canada Ltd.) and sodium in tetrahydrofuran, as described previously (3). When required, most of the tetrahydrofuran could be pumped off and replaced by the solvent trichlorofluoromethane ($CFCl_3$).

Halogens and interhalogen compounds were commercial samples and used without further purification. Sodium halides were recovered after completion of reaction and identified by their X-ray powder patterns.

Infrared spectra were determined on a Perkin–Elmer 377 spectrophotometer. Nuclear magnetic resonance spectra were determined on a Varian A-56/60A spectrometer, using 60 MHz and 56.4 MHz for proton and fluorine respectively. The ^{19}F chemical shifts are all relative to internal $CFCl_3$.

Reaction of Disodium Perfluoropinacolate with Chlorine

Disodium perfluoropinacolate (3.21 g, 8.50 mmoles), tetrahydrofuran (3 ml), and $CFCl_3$ (30 ml) were cooled to −22° and chlorine gas added to the solution. Immediate precipitation occurred and addition of chlorine was stopped when precipitation ceased. The precipitate was identified as sodium chloride (0.97 g, 17 mmoles).

The product, $(CF_3)_2C(OCl)C(CF_3)_2OCl$, was stable in solution for several weeks at −22° in the absence of light. Decomposition increased rapidly on heating or in the presence of u.v. light to give a black oil. Decomposition also occurred if the preparation was carried out using excess chlorine.

Reaction of Disodium Perfluoropinacolate with Bromine

Disodium perfluoropinacolate (3.60 g, 9.52 mmoles), tetrahydrofuran (2 ml), and $CFCl_3$ (30 ml) were cooled to 0° and bromine (3.0 g, 19 mmoles) added. Sodium bromide (1.84 g, 17.9 mmoles) was filtered off leaving the product, $(CF_3)_2C(OBr)C(CF_3)_2OBr$, in solution. Decomposition occurred in the presence of excess bromine.

Reaction of Disodium Perfluoropinacolate with Iodine Monochloride

Iodine monochloride (3.1 g, 19 mmoles) was added to a solution of disodium perfluoropinacolate (3.60 g, 9.52 mmoles), tetrahydrofuran (3 ml), and $CFCl_3$ (60 ml) at room temperature. Sodium chloride (0.70 g, 12 mmoles) was filtered off and the product, $(CF_3)_2C(OI)C(CF_3)_2OI$, remained in solution. Decomposition occurred on gently warming to give mainly hexafluoroacetone and iodine.

Reaction of Disodium Perfluoropinacolate with Iodine Monobromide

The reaction with iodine monobromide proceeded under conditions similar to those described for iodine monochloride to give $(CF_3)_2C(OI)C(CF_3)_2OI$ and sodium bromide.

Reaction with Tetrahydrofuran

When preparation of dihypohalites was carried out in tetrahydrofuran the major product was perfluoropinacol, identified by comparison of its i.r. and ^{19}F n.m.r. spectra with that of a known sample prepared by the reaction of hexafluoroacetone and triethyl phosphite (6). Fluorine

n.m.r. showed a single peak at +70.7 p.p.m. (literature value +4.54 p.p.m. relative to 1,2-difluorotetrachloroethane as external reference (7)).

Reaction with Benzaldehyde

A solution containing $(CF_3)_2C(OCl)C(CF_3)_2OCl$ (4 g, 10 mmoles) was prepared as described above and majority of solvent removed. Carbon tetrachloride (20 ml) and benzaldehyde (10.5 g) was added and the solution irradiated for 12 h using a Hanovia Utility u.v. quartz lamp situated 18 cm from the silica reaction vessel. The products were benzoic acid (1.0 g, 8.2 mmoles), identified by its i.r. spectrum, and a smaller amount of benzoyl chloride, identified by gas chromatographic analysis. The latter technique indicated additional products, which could be chlorine substituted fluorocarbons, but these were not identified.

The authors wish to thank Dr. C. J. Willis for his continuing interest in this work. The financial assistance of the National Research Council of Canada is gratefully acknowledged.

1. D. E. Gould, L. R. Anderson, D. E. Young, and W. B. Fox. J. Amer. Chem. Soc. **91**, 1310 (1969).
2. G. J. Schack and W. Maya. J. Amer. Chem. Soc. **91**, 2902 (1969).
3. M. Allan, A. F. Janzen, and C. J. Willis. Can. J. Chem. **46**, 3671 (1968).
4. C. Walling and P. J. Wagner. J. Amer. Chem. Soc. **86**, 3368 (1964).
5. D. Ginsburg. J. Amer. Chem. Soc. **73**, 702 (1951).
6. N. P. Gambaryan, Y. A. Cheburkov, and I. L. Knunyants. Izv. Akad. Nauk SSSR, Ser. Khim. 1526 (1964).
7. M. J. Middleton and R. V. Lindsey, Jr. J. Amer. Chem. Soc. **86**, 4948 (1964).

Some indoleninyl hydroperoxides

H. I. Kesswani[1]

Department of Chemistry, University of Birmingham, Birmingham, England

Received June 13, 1969

Exposure of 2,3-dimethyl-4-carbethoxy-7-ethylindole (**1**) and 2,3,5,7-tetramethylindole (**5**) to air yielded the corresponding indoleninyl hydroperoxides, **2** and **6** respectively. The decomposition of **2** under various conditions yielded *o*-acylaminoketone (**3**).

Canadian Journal of Chemistry, **48**, 689 (1970)

The formation of hydroperoxides is a property common to many 1,2,3,4-tetrahydrocarbazoles (1). Leete (2) in 1961 reported the formation of 2,3-diethyl-3-hydroperoxyindolenine in a quantitative yield by exposing a solution of 2,3-diethylindole in light petroleum (b.p. 60–80°), containing a trace of hydrogen peroxide, to air. Beer and his co-workers (3) have shown that the presence of an electron-releasing substituent in the benzene ring of indole derivatives facilitates peroxide formation. When the solution of 2,3-dimethyl-4-carbethoxy-7-ethylindole (**1**) (4) in light petroleum (b.p. 60–80°) containing a trace of hydrogen peroxide was exposed to the atmosphere for 24 h, it slowly deposited colorless needles of the corresponding 3-hydroperoxyindolenine (**2**) in 80% yield. Treatment of this peroxide with hot ethanol (50%) containing two drops of glacial acetic acid gave the expected 2-acetamidoacetophenone derivative (**3**) in 50% yield.

In order to see if such autoxidations occur in other indoles having electron-releasing group in the benzene ring, the 2,4-dimethylhydrazone (**4**) of ethyl methyl ketone was cyclized using boron trifluoride-etherate under the same conditions used for the preparation of the indole **1** (4). The

[1]Present address: Postdoctoral fellow, School of Pharmacy, University of Manitoba, Winnipeg 19, Manitoba.

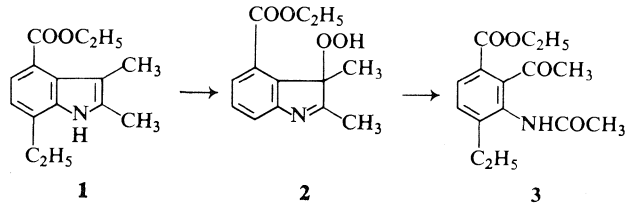

1 **2** **3**

Can. J. Chem. Downloaded from www.nrcresearchpress.com by 210.87.254.6 on 09/05/12
For personal use only.

n.m.r. showed a single peak at +70.7 p.p.m. (literature value +4.54 p.p.m. relative to 1,2-difluorotetrachloroethane as external reference (7)).

Reaction with Benzaldehyde

A solution containing $(CF_3)_2C(OCl)C(CF_3)_2OCl$ (4 g, 10 mmoles) was prepared as described above and majority of solvent removed. Carbon tetrachloride (20 ml) and benzaldehyde (10.5 g) was added and the solution irradiated for 12 h using a Hanovia Utility u.v. quartz lamp situated 18 cm from the silica reaction vessel. The products were benzoic acid (1.0 g, 8.2 mmoles), identified by its i.r. spectrum, and a smaller amount of benzoyl chloride, identified by gas chromatographic analysis. The latter technique indicated additional products, which could be chlorine substituted fluorocarbons, but these were not identified.

The authors wish to thank Dr. C. J. Willis for his continuing interest in this work. The financial assistance of the National Research Council of Canada is gratefully acknowledged.

1. D. E. Gould, L. R. Anderson, D. E. Young, and W. B. Fox. J. Amer. Chem. Soc. **91**, 1310 (1969).
2. G. J. Schack and W. Maya. J. Amer. Chem. Soc. **91**, 2902 (1969).
3. M. Allan, A. F. Janzen, and C. J. Willis. Can. J. Chem. **46**, 3671 (1968).
4. C. Walling and P. J. Wagner. J. Amer. Chem. Soc. **86**, 3368 (1964).
5. D. Ginsburg. J. Amer. Chem. Soc. **73**, 702 (1951).
6. N. P. Gambaryan, Y. A. Cheburkov, and I. L. Knunyants. Izv. Akad. Nauk SSSR, Ser. Khim. 1526 (1964).
7. M. J. Middleton and R. V. Lindsey, Jr. J. Amer. Chem. Soc. **86**, 4948 (1964).

Some indoleninyl hydroperoxides

H. I. Kesswani[1]

Department of Chemistry, University of Birmingham, Birmingham, England

Received June 13, 1969

Exposure of 2,3-dimethyl-4-carbethoxy-7-ethylindole (**1**) and 2,3,5,7-tetramethylindole (**5**) to air yielded the corresponding indoleninyl hydroperoxides, **2** and **6** respectively. The decomposition of **2** under various conditions yielded *o*-acylaminoketone (**3**).

Canadian Journal of Chemistry, **48**, 689 (1970)

The formation of hydroperoxides is a property common to many 1,2,3,4-tetrahydrocarbazoles (1). Leete (2) in 1961 reported the formation of 2,3-diethyl-3-hydroperoxyindolenine in a quantitative yield by exposing a solution of 2,3-diethylindole in light petroleum (b.p. 60–80°), containing a trace of hydrogen peroxide, to air. Beer and his co-workers (3) have shown that the presence of an electron-releasing substituent in the benzene ring of indole derivatives facilitates peroxide formation. When the solution of 2,3-dimethyl-4-carbethoxy-7-ethylindole (**1**) (4) in light petroleum (b.p. 60–80°) containing a trace of hydrogen peroxide was exposed to the atmosphere for 24 h, it slowly deposited colorless needles of the corresponding 3-hydroperoxyindolenine (**2**) in 80% yield. Treatment of this peroxide with hot ethanol (50%) containing two drops of glacial acetic acid gave the expected 2-acetamidoacetophenone derivative (**3**) in 50% yield.

In order to see if such autoxidations occur in other indoles having electron-releasing group in the benzene ring, the 2,4-dimethylhydrazone (**4**) of ethyl methyl ketone was cyclized using boron trifluoride-etherate under the same conditions used for the preparation of the indole **1** (4). The

[1]Present address: Postdoctoral fellow, School of Pharmacy, University of Manitoba, Winnipeg 19, Manitoba.

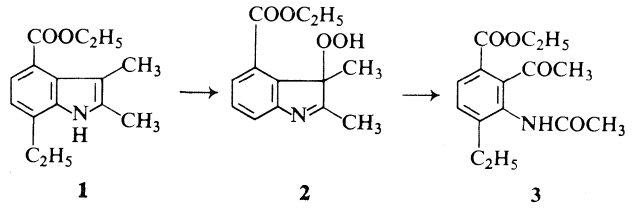

1 **2** **3**

Can. J. Chem. Downloaded from www.nrcresearchpress.com by 210.87.254.6 on 09/05/12
For personal use only.

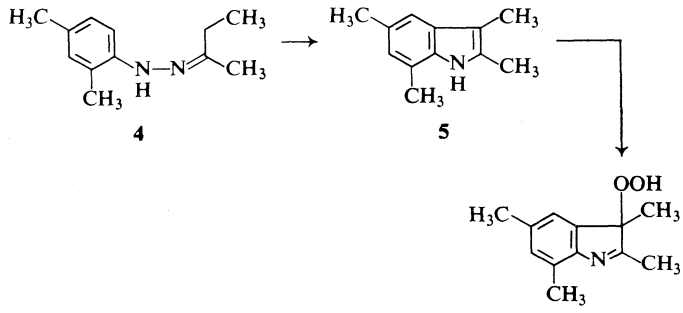

4 5 6

resulting product again appeared, from its nuclear magnetic resonance (n.m.r.) and infrared (i.r.) spectra, to be a mixture of an indole (**5**) and a corresponding 3-hydroperoxyindolenine (**6**). A solution of this crude product in light petroleum (b.p. 60–80°), when exposed to the atmosphere, slowly deposited the pure hydroperoxyindolenine which was characterized by its elemental analysis, n.m.r., and i.r. spectra. Attempts were made to oxidize ethyl 2,3-dimethylindole-5-carboxylate (**7**) and ethyl 3-(2′-ethoxycarbonylethyl)-2-methylindole-5-carboxylate (**8**) (5) to the corresponding peroxides, but 95% of the starting materials were recovered unchanged.

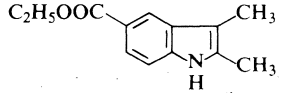

7

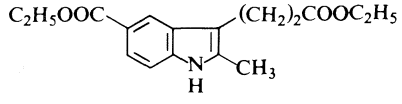

8

Experimental

The i.r. spectra were obtained with a Perkin–Elmer Model 125 Spectrophotometer. The ultraviolet (u.v.) spectra were taken in ethanol with a Unicam SP. 800 Spectrophotometer. The n.m.r. spectra were determined on Varian A-60 Spectrometer, using a 10% solution of tetramethylsilane in carbon tetrachloride as an external reference (τ_{10}). Microanalyses were performed by the staff of the Analytical Department. All melting points are uncorrected.

Ethyl 2,3-Dimethyl-7-ethyl-3-hydroperoxyindolenine-4-carboxylate (2)

Ethyl 2,3-dimethyl-7-ethylindole-4-carboxylate (**1**) (1.0 g) was dissolved in sufficient hot petroleum (b.p. 60–80°) to prevent rapid crystallization on cooling, and 30% hydrogen peroxide (2 ml) was added to the above solution, which was then exposed to air for 24 h. The resulting crystalline product on recrystallization from a mixture of ethyl acetate and light petroleum (b.p. 60–80°) gave colorless needles (0.9 g, 80%) of **2**, m.p. 125–126°. Infrared ν_{max} (CCl_4): 3375 (a very weak band, O—H) and 1718 cm^{-1} (aryl ester C—O); u.v. λ_{max}: 234 (ε 25 100) and 306 mμ (ε 1520, shoulder); n.m.r. ($CDCl_3$): δ 1.25 (6H, —O—CH_2—CH_3 and Ar—CH_2—CH_3, two overlapping triplets), 1.54 (3H, C-3 methyl, singlet), 2.18 (3H, C-2 methyl, singlet), 2.88 (2H, Ar—CH_2—CH_3, quartet), 4.19 (2H, —O—CH_2—CH_3, quartet), 7.12 and 7.57 (2H, J = 8 c.p.s., pair of doublets), and 10.26 (1H, —O—OH, singlet).

Anal. Calcd. for $C_{15}H_{19}NO_4$: C, 65.0; H, 6.9; N, 5.1. Found: C, 65.0; H, 6.7; N, 5.1.

Cleavage of Ethyl 2,3-Dimethyl-7-ethyl-3-hydroperoxyindolenine-4-carboxylate (2)

A solution of the 3-hydroperoxyindolenine (**2**) (0.45 g) in 50% aqueous ethanol (40 ml) containing glacial acetic acid (2 drops) was refluxed for 1/2 h. Ethanol was removed *in vacuo* and the product extracted with ether. The ether extracts after washing with water, brine and drying (anhydrous sodium sulfate) afforded, on evaporation, a white amorphous solid which on crystallization from a mixture of ethyl acetate and petroleum (b.p. 60–80°) gave white needles of 6-ethoxycarbonyl-3-ethyl-2-acetamidoacetophenone (**3**) (220 mg, 50%), m.p. 160–161°. Infrared ν_{max} (Nujol): 3300 (N—H), 1710 (a broad band, aryl ester and aryl ketone C—O combined), 1660 (amide I C—O), 1600 (C=C), and 1550 cm^{-1} (amide II C—O); u.v. λ_{max}: 241 (ε 23 500) and 276 mμ (ε 3800, shoulder); n.m.r. ($CDCl_3$): δ 1.22 (6H, —O—CH_2—CH_3 and Ar—CH_2—CH_3, two overlapping triplets), 2.08 (3H, —NH—CO—CH_3, singlet), 2.38 (5H, Ar—$COCH_3$ and Ar—CH_2—CH_3, quartet due to —CH_2— of ethyl and overlapping singlet of acetyl group), 4.29 (2H, —O—CH_2—CH_3, quartet), 7.15 and 7.76 (2H, J = 8 c.p.s., pair of doublets), and 8.12 (1H, —NH— of acetyl, singlet).

Anal. Calcd. for $C_{15}H_{19}NO_4$: C, 65.0; H, 6.9; N, 5.1. Found: C, 64.8; H, 7.2; N, 5.2.

2,3,5,7-Tetramethyl-3-hydroperoxyindolenine (6)

A solution of 2:4-dimethylhydrazine (2.0 g) and ethyl methyl ketone (1.6 g) in dry benzene (15 ml) was treated with glacial acetic acid (1 drop), and warmed on the water-bath for a few min. The solution was then dried

Can. J. Chem. Downloaded from www.nrcresearchpress.com by 210.87.254.6 on 09/05/12
For personal use only.

and evaporated *in vacuo* to give a red oil. The oily hydrazone was cyclized using boron trifluoride etherate in an analogous way to that used in the preparation of the indole **1** (4). Crystallization of the resulting red–brown gum (obtained after passing the material through a charcoal column) was attempted from polar solvents in order to avoid the autoxidation of the corresponding indole **5**, but failed. When the gum was extracted with light petroleum (b.p. 40–60°), the product was found to be a mixture of an indole **5** and its hydroperoxide **6**. Infrared ν_{max} (Nujol): 3350 (N—H) and 3150 cm^{-1} (a very weak band, O—H). A solution of this crude product in light petroleum (b.p. 60–80°), when exposed to the atmosphere, slowly deposited colorless needles of **6** (1.2 g, 40%), m.p. 115–116°. Infrared ν_{max} (Nujol): 3150 cm^{-1} (a very weak band, O—H); n.m.r. ($CDCl_3$): δ 1.39 (3H, C-3 methyl, singlet), 2.18 (3H, C-2 methyl, singlet), 2.24 (3H, Ar—CH_3, singlet), 2.36 (3H, Ar—CH_3, singlet), 6.92 (2H, J = 1 c.p.s. doublet, small splitting due to a very small chemical shift difference between the two aromatic protons), and 10.2 (1H, —O—OH, singlet).

Anal. Calcd. for $C_{12}H_{15}NO_2$: C, 70.24; H, 7.31; N, 6.83. Found: C, 70.1; H, 7.2; N, 6.9.

Grateful acknowledgment is made to the University of Birmingham for the award of a Research Studentship, and to Professor M. Stacey, F.R.S. for his interest in this work. Thanks are due to Dr. J. D. Hobson for his valuable suggestions in this work. Thanks are due also to Dr. J. R. Murray, School of Pharmacy, University of Manitoba for his financial support for this publication and to Dr. C. M. Wong, Department of Chemistry, University of Manitoba, for going through this manuscript.

1. R. J. S. Beer, T. Donavanik, and A. Robertson. J. Chem. Soc. 4946 (1952).
2. E. Leete. J. Amer. Chem. Soc. **83**, 3645 (1961).
3. R. J. S. Beer, T. Donavanik, and A. Robertson. J. Chem. Soc. 4139 (1954).
4. H. I. Kesswani. Ph.D. Thesis. University of Birmingham, Birmingham, England. 1967.
5. H. I. Kesswani. In preparation.

Rearrangement of a steroidal 14β-hydroperoxide. Cleavage of ring D

Adriano Afonso
Natural Products Research Department, Schering Corporation, Bloomfield, New Jersey 07003, U.S.A.

Received September 8, 1969

The rearrangement of 14β-hydroperoxy-Δ^{15}-androsten-3β-ol-17-one 3-acetate (**2**) with boron trifluoride etherate affords 3β,15-dihydroxy-14,15-seco-Δ^{15}-5α-androstene-14,17-dione 3-acetate (**4***a*). The decarbonylation of the rearrangement product was studied.

Canadian Journal of Chemistry, **48**, 691 (1970)

In connection with another problem, we had occasion to investigate the cleavage of the steroidal ring D between C-14 and C-16. A few methods for such a cleavage have been described in the literature (1); however, a simpler and more efficient degradative sequence was desired. It was observed previously that Δ^{14}-androsten-3β-ol-17-one acetate (**1**) is readily oxidized by oxygen into 14β-hydroperoxy-Δ^{15}-androsten-3β-ol-17-one acetate (**2**) (2). Since organic hydroperoxides are known to undergo acid catalyzed rearrangements involving C—C bond cleavage (3), the

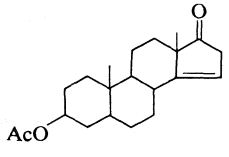

1

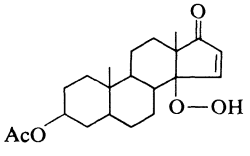

2

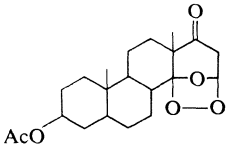

3

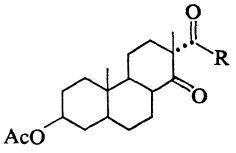

4

a R= 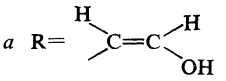

b R= 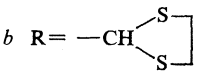

c R= $-CH_3$

rearrangement of **2** was studied. Treatment of **2** with boron trifluoride etherate in benzene led to the formation of an alkali-soluble product (20% yield) which was characterized as the 14,15-*seco*

Can. J. Chem. Downloaded from www.nrcresearchpress.com by 210.87.254.6 on 09/05/12
For personal use only.

and evaporated *in vacuo* to give a red oil. The oily hydrazone was cyclized using boron trifluoride etherate in an analogous way to that used in the preparation of the indole **1** (4). Crystallization of the resulting red–brown gum (obtained after passing the material through a charcoal column) was attempted from polar solvents in order to avoid the autoxidation of the corresponding indole **5**, but failed. When the gum was extracted with light petroleum (b.p. 40–60°), the product was found to be a mixture of an indole **5** and its hydroperoxide **6**. Infrared ν_{max} (Nujol): 3350 (N—H) and 3150 cm^{-1} (a very weak band, O—H). A solution of this crude product in light petroleum (b.p. 60–80°), when exposed to the atmosphere, slowly deposited colorless needles of **6** (1.2 g, 40%), m.p. 115–116°. Infrared ν_{max} (Nujol): 3150 cm^{-1} (a very weak band, O—H); n.m.r. ($CDCl_3$): δ 1.39 (3H, C-3 methyl, singlet), 2.18 (3H, C-2 methyl, singlet), 2.24 (3H, Ar—CH_3, singlet), 2.36 (3H, Ar—CH_3, singlet), 6.92 (2H, J = 1 c.p.s. doublet, small splitting due to a very small chemical shift difference between the two aromatic protons), and 10.2 (1H, —O—OH, singlet).

Anal. Calcd. for $C_{12}H_{15}NO_2$: C, 70.24; H, 7.31; N, 6.83. Found: C, 70.1; H, 7.2; N, 6.9.

Grateful acknowledgment is made to the University of Birmingham for the award of a Research Studentship, and to Professor M. Stacey, F.R.S. for his interest in this work. Thanks are due to Dr. J. D. Hobson for his valuable suggestions in this work. Thanks are due also to Dr. J. R. Murray, School of Pharmacy, University of Manitoba for his financial support for this publication and to Dr. C. M. Wong, Department of Chemistry, University of Manitoba, for going through this manuscript.

1. R. J. S. Beer, T. Donavanik, and A. Robertson. J. Chem. Soc. 4946 (1952).
2. E. Leete. J. Amer. Chem. Soc. **83**, 3645 (1961).
3. R. J. S. Beer, T. Donavanik, and A. Robertson. J. Chem. Soc. 4139 (1954).
4. H. I. Kesswani. Ph.D. Thesis. University of Birmingham, Birmingham, England. 1967.
5. H. I. Kesswani. In preparation.

Can. J. Chem. Downloaded from www.nrcresearchpress.com by 210.87.254.40 on 09/05/12
For personal use only.

Rearrangement of a steroidal 14β-hydroperoxide. Cleavage of ring D

Adriano Afonso
Natural Products Research Department, Schering Corporation, Bloomfield, New Jersey 07003, U.S.A.

Received September 8, 1969

The rearrangement of 14β-hydroperoxy-Δ^{15}-androsten-3β-ol-17-one 3-acetate (**2**) with boron trifluoride etherate affords 3β,15-dihydroxy-14,15-seco-Δ^{15}-5α-androstene-14,17-dione 3-acetate (**4***a*). The decarbonylation of the rearrangement product was studied.

Canadian Journal of Chemistry, **48**, 691 (1970)

In connection with another problem, we had occasion to investigate the cleavage of the steroidal ring D between C-14 and C-16. A few methods for such a cleavage have been described in the literature (1); however, a simpler and more efficient degradative sequence was desired. It was observed previously that Δ^{14}-androsten-3β-ol-17-one acetate (**1**) is readily oxidized by oxygen into 14β-hydroperoxy-Δ^{15}-androsten-3β-ol-17-one acetate (**2**) (2). Since organic hydroperoxides are known to undergo acid catalyzed rearrangements involving C—C bond cleavage (3), the rearrangement of **2** was studied. Treatment of **2** with boron trifluoride etherate in benzene led to the formation of an alkali-soluble product (20% yield) which was characterized as the 14,15-*seco*

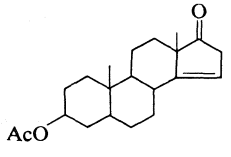

1

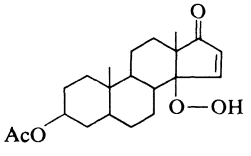

2

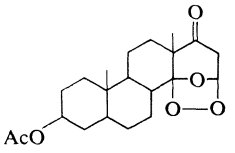

3

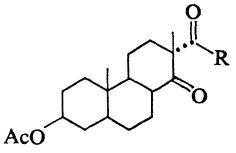

4

a R= 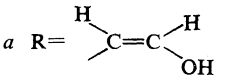

b R= 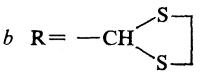

c R= $-CH_3$

androstane derivative **4***a*.[1] In agreement with the hydroxymethylene structure **4***a*, the product, gives a ferric chloride test, shows a chelated carbonyl absorption (4) in the infrared at 6.11–6.27 μ, its absorption maximum in the ultraviolet (u.v.) undergoes the characteristic bathochromic shift with alkali (4), and its nuclear magnetic resonance (n.m.r.) spectrum shows signals for two *cis*-olefinic protons (5). In another approach for ring D cleavage, ozonolysis of **1** afforded a crystalline ozonide **3** which on hydrogenolysis was converted into the same hydroxymethylene compound **4***a* in 31% yield.

Base treatment of **4***a* in order to cleave off C-15 would be expected to give non-specific cleavages. The desired selective decarbonylation at C-15 was achieved by treating **4***a* with ethylene *p*-toluenethiol sulfonate (6). The resulting thioketal **4***b* on desulfurization with Raney nickel afforded the methyl ketone **4***c*. Alternatively, **4***c* was obtained in one step from **4***a* by decarbonylation of the latter compound with tris-(triphenylphosphine)-chlororhodium (7). The presence of the new methyl group in **4***c* was evident from its n.m.r. spectrum. One of the above sequences for the degradation of ring D was applied in the synthesis of a resin acid (6*b*).

Experimental Section

Specific rotations were determined on 0.3% solutions in dioxane. The n.m.r. spectra in $CDCl_3$ using TMS as the internal standard were determined on a Varian A-60A spectrometer. The u.v. spectra were determined on a Cary 14 spectrophotometer. These measurements and microanalyses were performed by Mr. M. Yudis and his associates.

Ozonolysis of ***1***

A solution of 0.5 g of Δ^{14}-androsten-3β-ol-17-one acetate (**1**) (2) in 10 ml ethylacetate was cooled to −70° and a stream of ozonized oxygen was bubbled through it until the solution acquired a blue color. The reaction mixture was allowed to stand at −70° for 15 min and excess ozone was displaced by a stream of dry argon. The solution was evaporated under reduced pressure and the residue on crystallization from ethylacetate afforded 0.45 g (79%) of the ozonide **3** as colorless needles, m.p. 155–161° (decomposition); $[\alpha]_D^{26}$ − 89.3°; n.m.r., δ 0.82 (3H, s, 10—CH_3), 1.19 (3H, s, 13—CH_3), 2.00 (3H, s, —OC(=O)—CH_3) and an ABX splitting pattern for C-15, C-16 protons δ (H_A) 2.57, δ (H_B) 2.84 (2H, o, J_{AB} = 17, J_{AX} = 1.5, J_{BX} = 3.0 c.p.s.), δ (H_X) 5.96 (1H, m, J_{AX+BX} = 5.0 c.p.s.).

Anal. Calcd. for $C_{21}H_{30}O_6$: C, 66.64; H, 7.99. Found: C, 66.82; H, 7.78.

3β,15-Dihydroxy-14,15-seco-Δ^{15}*-5α-androstene-14,17-dione 3-acetate (****4a****)*

A. From Ozonide ***3***

A solution of 0.4 g of **3** in 10 ml of ethylacetate was hydrogenated in the presence of 0.2 g of 10% palladized carbon. The theoretical uptake of hydrogen was complete in 4 min. The catalyst was removed by filtration and the residue obtained upon evaporation of the filtrate was crystallized from ethylacetate–ether to afford 0.12 g (31%) of **4***a* as colorless plates, m.p. 142–147°; $[\alpha]_D^{26}$ − 30.6°; λ_{max}(MeOH) 258 mμ (ε 3480) → λ_{max}(MeOH/$OH^{\ominus}$) 300 mμ (ε 20,000); λ_{max}(Nujol) 5.76, 5.85, and 6.11–6.27 μ; n.m.r. δ 0.91 (3H, s, 10—CH_3), 1.40 (3H, s, 13—CH_3), 2.02 (3H, s, —O—C(=O)—CH_3), 5.57 (1H, d, —CO—C*H*=CHOH, J = 5 c.p.s.), 7.68 (1H, d, —CO—CH=C*H*OH, J = 5 c.p.s.).

Anal. Calcd. for $C_{21}H_{30}O_5$: C, 69.58; H, 8.34. Found: C, 69.86; H, 8.62.

B. From Hydroperoxide ***2***

A solution of 0.5 g of **2** (2) in 25 ml of dry benzene was treated with 1 ml of boron trifluoride etherate and the mixture was stirred at 60° for 15 min. During this period the mixture initially turned pale yellow in color then changed to dark brown and finally a brown oil material deposited on the walls of the flask. The reaction mixture was cooled and stirred for 5 min with 10 ml of cold 10% aqueous sodium acetate solution. The color changed to pale yellow. The mixture was diluted with ether and the organic phase was washed with 10% sodium bicarbonate solution, water, then was dried and evaporated. The pale brown residue was dissolved in ether and extracted rapidly with cold (0°) 2% sodium hydroxide solution. The aqueous extracts were rapidly acidified with cold (0°) 10% sulfuric acid and extracted with ether. The ether extract was washed with water, then dried and evaporated to afford 0.185 g of an oil which on crystallization from ethylacetate–ether afforded 0.105 g (20%) of **4***a* as colorless plates, m.p. 142–147°. The infrared (i.r.), u.v., and n.m.r. spectra are identical with **4***a* prepared as above from **3**.

Thioketal ***4b***

Crude hydroxymethylene ketone **4***a* obtained by the hydrogenation of 0.3 g of **3** was dissolved in 10 ml of methanol and the solution was treated with 0.32 g of ethylene *p*-toluenethiol sulfonate[2] and 0.4 g anhydrous potassium acetate. The mixture was then refluxed for 30 min under an argon blanket. The pale yellow solution

[1]The following mechanism may be suggested for this rearrangement:

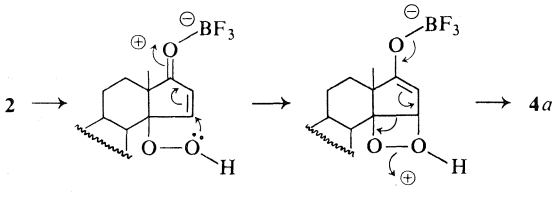

[2]Kindly supplied by D. I. Pachter of Endo Laboratories.

Can. J. Chem. Downloaded from www.nrcresearchpress.com by 210.87.254.40 on 09/05/12
For personal use only.

was then concentrated under reduced pressure, diluted with ice-water, and extracted with ethylacetate. The extract was washed with water, dried, and evaporated. The residue was applied on a 20 × 20 × 0.1 cm silica gel plate and developed with 20% ethylacetate–chloroform. The product was isolated from the major band and was crystallized from ethylacetate–hexane to afford 0.14 g (42%) of **4***b* as colorless plates, m.p. 136–137°; $[\alpha]_D^{26}$ − 35.2°; n.m.r., δ 0.89 (3H, s, 10—CH_3), 1.43 (3H, s, 13—CH_3), 2.00 (3H, s, —O—$\overset{\overset{O}{\|}}{C}$—C$H_3$), 3.35 (4H, m, —S—(C$H_2$)$_2$), 5.10 (1H, s, —S—C*H*—S—).

Anal. Calcd. for $C_{22}H_{32}O_4S_2$: C, 62.22; H, 7.59. Found: C, 62.27; H, 7.97.

Methyl Ketone **4***c*

A. From Thioketal **4***b*

A suspension of 0.3 g W-2 Raney nickel in a solution of 0.103 g of **4***b* in 65 ml of 95% ethanol was refluxed with stirring for 8 h. The mixture was then cooled and filtered. The filtrate was evaporated under reduced pressure and the residue on crystallization from hexane afforded 0.054 g (67%) of **4***c* as colorless prisms, m.p. 126–129°; $[\alpha]_D^{26}$ − 62.8°; n.m.r., δ 0.92 (3H, s, 10—CH_3), 1.40 (3H, s, 13—CH_3), 2.01 (3H, s, —O—$\overset{\overset{O}{\|}}{C}$—C$H_3$), 2.18 (3H, s, —$\overset{\overset{O}{\|}}{C}$—C$H_3$).

Anal. Calcd. for $C_{20}H_{30}O_4$: C, 71.82; H, 9.04. Found: C, 71.42; H, 8.98.

B. From the Hydroxymethylene Ketone **4***a*

Crude **4***a* obtained by the hydrogenation of 0.1 g of **3** was dissolved in 1 ml of benzene and the solution was added to 0.3 g of tris-(triphenyl-phosphine) chlororhodium in 6 ml of benzene. The reaction mixture was heated at 80° for 20 min. During this period the blood-red solution turned brown in color with the formation of a brown solid. The mixture was filtered hot and the filtrate was evaporated. The residue was suspended in ether and filtered. The residue obtained on evaporation of the ether filtrate was applied to a 10 × 20 × 0.1 cm silica gel plate which was then developed with 2% ethylacetate–chloroform. The material obtained by elution of the major band was crystallized from hexane to afford 0.035 g (40%) of colorless prisms, m.p. 126–129°, identical in all respects (i.r., thin-layer chromatography) with **4***c*.

1. (*a*) A. K. Bose and S. Harrison. Chem. Ind. (London), 254 (1963); (*b*) M. Fetizon and M. Golfier. Bull. Soc. Chim. (France), 167 (1963); (*c*) B. P. Johnston, R. C. Sheppard, C. E. Stehr, and S. Turner. J. Chem. Soc. (C), 1847 (1966).
2. A. Afonso. Can. J. Chem. **47**, 3693 (1969).
3. P. A. S. Smith. *In* Molecular rearrangements. Vol. I. P. de Mayo, *Editor*. Interscience Publishers, New York, N.Y., 1964. p. 568.
4. R. O. Clinton, A. J. Manson, F. W. Stonner, H. C. Neumann, R. G. Christiansen, R. L. Clarke, J. H. Ackerman, D. F. Page, J. W. Dean, W. B. Dickinson, and C. Carabateas. J. Amer. Chem. Soc. **83**, 1478 (1961).
5. N. S. Bhacca and D. H. Williams. Applications of nuclear magnetic resonance spectroscopy in organic chemistry. Holden-Day, Inc., San Francisco, Cal., 1964. p. 52.
6. (*a*) R. B. Woodward, A. A. Patchett, D. H. R. Barton, D. A. J. Ives, and R. B. Kelly. J. Chem. Soc. 1131 (1957); (*b*) A. Afonso, J. Amer. Chem. Soc. **90**, 7375 (1968).
7. D. J. Dawson and R. E. Ireland. Tetrahedron Lett. 1899 (1968).

Can. J. Chem. Downloaded from www.nrcresearchpress.com by 210.87.254.40 on 09/05/12
For personal use only.

Can. J. Chem. Downloaded from www.nrcresearchpress.com by 210.87.254.6 on 09/05/12
For personal use only.

Detection and chemistry of the triplet state of thymine[1]

A. G. SZABO
Division of Biology, National Research Council of Canada, Ottawa, Canada

AND

W. D. RIDDELL[2] AND R. W. YIP
Division of Chemistry, National Research Council of Canada, Ottawa, Canada

The transient produced on flash excitation of degassed solutions of thymine in acetonitrile has been characterized as the triplet excited state of thymine. This triplet state has a lifetime of 14 ± 1 μs and the associated dimerization rate was found to be 5.3 ± 0.3 × 10^8 M^{-1} s^{-1}. The triplet state of thymine could be quenched by 2,4-hexadien-1-ol with a rate constant of 8.1 ± 0.6 × 10^9 M^{-1} s^{-1}.

Canadian Journal of Chemistry, **48**, 694 (1970)

The photochemistry of thymine has been studied more intensively than the other bases which constitute DNA (1). This interest is stimulated by the isolation of a cyclobutane dimer of thymine from irradiated cellular systems and this dimer has been identified as one of the reparable lesions occurring in the DNA (2). The chemistry describing the photodimerization of thymine is another example of a photochemical cycloaddition reaction of α,β-unsaturated carbonyl compounds, for which mechanisms have been recently described by de Mayo (3) and Wagner (4) and their co-workers. Their studies have utilized the classical Stern–Volmer approach to obtain kinetic parameters associated with the cycloaddition reaction. In degassed aqueous solutions of thymine the quantum yield of thymine disappearance is 4.2 × 10^{-4} (5) and is apparently unaffected by oxygen. Lamola and Mittal (6) have found that the photodimerization of thymine in acetonitrile proceeds entirely via the triplet state, with a quantum yield of 5 × 10^{-3} (7 × 10^{-4} M thymine). Wagner estimated the lifetime, τ_0 (4.3 μs), of the triplet excited state of thymine by determining the factor $k_q\tau$ from Stern–Volmer kinetics and assuming the quenching rate, k_q, of triplet thymine by 1,3-pentadiene to be 1.1 × 10^{10} M^{-1} s^{-1} in acetonitrile. Considering the result for k_q of 3 × 10^9 M^{-1} s^{-1} obtained from the work of Riddell, Szabo, and Yip (7) on the flash photolysis of methyl orotate, we felt that the triplet state of thymine should be observable on the 0.8 μs flash apparatus in our laboratories.

When a degassed solution of thymine (5 × 10^{-5} M) in acetonitrile was flashed[3] a transient species with a $\tau_{1/2}$ of ca. 10 μs was observed which decayed by first order kinetics according to eq. [1]

$$[1] \quad 2.303 \log_{10} \text{O.D.} = k_{obs}\tau + \text{constant}$$

This transient could be characterized as the triplet excited state of thymine on the basis of the following consideration. Since the triplet state of thymine is the precursor of cyclobutane dimers, the observed rate of decay, k_{obs}, should vary with the thymine concentration consistent with a dimerization mechanism described by

$$[2] \quad k_{obs} = k_0 + k_{dim}[\text{thymine}] + k_q[\text{quencher}]$$

When solutions of varying thymine concentrations (1 × 10^{-5} – 2 × 10^{-4} M) in the absence of quencher were flash excited we observed excellent first order kinetics (Fig. 1) in agreement with the above scheme. The lifetime, $\tau_0 = 1/k_0$, obtained from the intercept of the kinetic plot (Fig. 1) was found to be 14 ± 1 μs. We conclude

[1]NRCC No. 11160.
[2]NRCC Postdoctoral Fellow, 1968–1969.

[3]The degassing and experimental techniques were identical to those described earlier (7). The flash apparatus was identical to the 5 μs dual beam photoelectric flash apparatus already described (8) except that a 0.16 μF, 40 kV capacitor was used. The photoflash was filtered through a 2 mm Vycor filter except as noted in the text. The transient was monitored at 330 mμ. The acetonitrile was "spectroquality", from Matheson, Coleman, and Bell and was used without further purification.

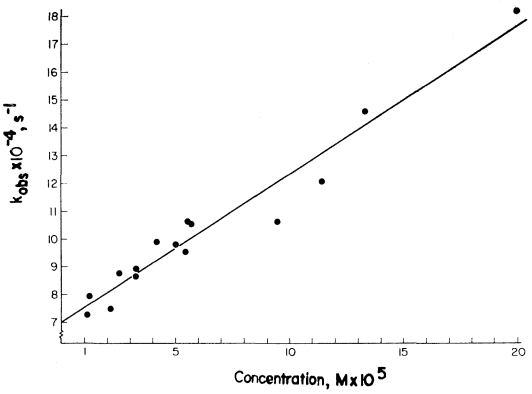

FIG. 1. Plot of k_{obs} vs. [thymine] in acetonitrile.

that the transient cannot be the singlet excited state of thymine. The value of k_{dim} was 5.3 ± 0.3 × 10^8 M^{-1} s^{-1} ruling out a radical intermediate. This value is in close agreement with the value reported by Wagner and Bucheck (4) of 7 × 10^8 M^{-1} s^{-1} and is of the same order as that found for the dimerization of the triplet state of methyl orotate in aqueous solution of 2.20 ± 0.05 × 10^9 M^{-1} s^{-1} (7). These results suggest that the dimerization reaction is less than diffusion controlled, the Debye treatment for the diffusion rate in acetonitrile predicting a value of 1.9 × 10^{10} M^{-1} at 25 °C. We confirmed the assignment of the triplet excited state by performing experiments with the known triplet quencher 2,4-hexadien-1-ol ($E_T \sim 56$ kcal M^{-1} (7)). When solutions of fixed concentration (4 × 10^{-5} M) of thymine and of varying concentrations of 2,4-hexadien-1-ol (0.25 × 10^{-5} – 1 × 10^{-5} M) were flash excited, we were able to quench the transient consistent with the kinetic expression [2] and obtained a value of k_q of 8.1 ± 0.6 × 10^9 M^{-1} s^{-1} (Fig. 2). Finally, when a solution of thymine (5 × 10^{-5} M) in acetonitrile was flash excited through a Pyrex filter no transient was observable. However, in a solution of thymine (5 × 10^{-5} M) and acetone (0.05 M) the same transient was present as had been observed when thymine had been flashed through a vycor filter.[4] No transient was observed when a solution of acetone in acetonitrile was flashed through a Pyrex filter. These sensitization experiments firmly establish the identity of the transient as the triplet excited state of thymine. Recently, Hayon (9) has observed a transient from the pulse radiolysis of thymine. No kinetic data were reported. He assigned the transient as the triplet excited state on the basis of the similarity between the ultraviolet absorption of the transient ($\lambda_{max} \sim 300$ mμ) and the spectrum he obtained for triplet uracil (λ_{max} 289 mμ). Our finding that there is no maximum above 310 mμ for the T–T absorption of thymine in acetonitrile is consistent with a triplet assignment for the transient observed in the system studied by Hayon. Typically[5] we find an optical density of 0.036 for the T–T absorption at 330 mμ.

We infer from the values of k_{dim} for the triplet state of thymine and methyl orotate (see Table 1) that steric factors are not as significant as Wagner (4) has suggested but perhaps electronic or other more subtle factors offer an explanation

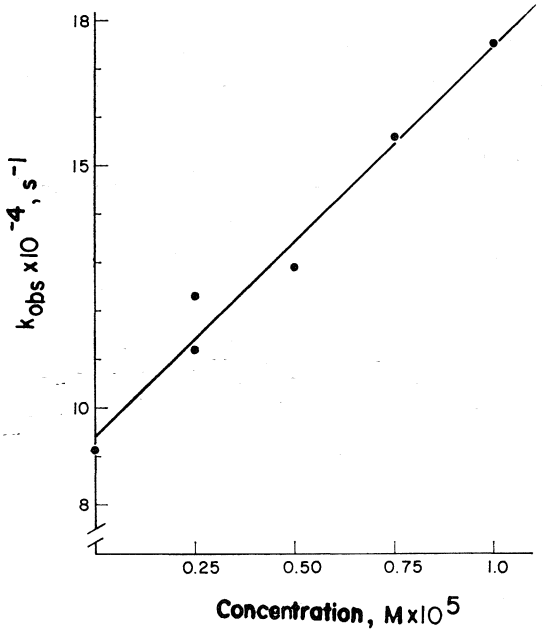

FIG. 2. Plot of k_{obs} vs. [2,4-hexadien-1-ol] for quenching studies of thymine in acetonitrile.

of the observed rate of differences between these two molecules. There is a discrepancy between our directly measured triplet lifetime of 14 μs and that estimated by Wagner and Bucheck (4) of 4.3 μs from his values of $k_q\tau_0$. Wagner and Bucheck's value reflects their choice of 1.1 × 10^{10}

[4]The transient was monitored at 340 mμ.

[5][thymine] = 5 × 10^{-5} M; photoflash energy, 82 J; filtered through Vycor glass, half bandwidth, 22 mμ; effective pathlength, 16 cm.

Can. J. Chem. Downloaded from www.nrcresearchpress.com by 210.87.254.6 on 09/05/12
For personal use only.

TABLE 1

Kinetic data associated with triplet excited states

Compound	$k_0 \times 10^{-4}$ (s^{-1})	τ_0 (μs)	$k_{dim} \times 10^{-8}$ ($M^{-1}\ s^{-1}$)	$k_q \times 10^{-9}$ ($M^{-1}\ s^{-1}$)
Thymine*	7.0 ± 0.3	14 ± 1	5.3 ± 0.3	8.1 ± 0.6
	(23)‡	(4.3)‡	(7.0)‡	(11.1)‡§
Methyl orotate†	0.35 ± 0.09	287 ± 72	22.0 ± 0.5	2.88 ± 0.15

*Acetonitrile solutions.
†Aqueous solutions, from ref. 7.
‡Results in parentheses are from ref. 4.
§Diffusion rate estimated for quenching by 1,3-pentadiene.

$M^{-1}\ s^{-1}$ for the k_q for 1,3-pentadiene in acetonitrile. If we insert our measured value of τ_0 into their value of $k_q\tau_0 = 4.73 \times 10^4\ M^{-1}$ at [thymine] = 0, the k_q for 1,3-pentadiene becomes $3.4 \times 10^9\ M^{-1}\ s^{-1}$. The difference between this value of k_q for 1,3-pentadiene and our measured k_q value of $8.1 \pm 0.6 \times 10^9\ M^{-1}\ s^{-1}$ for 2,4-hexadien-1-ol is likely due to a difference in quenching efficiencies of the two dienes (10, 11). It is felt that quenching by solvent impurity is a less likely alternative explanation for the lifetime discrepancy.

W.D.R. wishes to thank the National Research Council of Canada for the award of a Postdoctoral Fellowship. We are grateful to Mr. Peter Tolg and Mr. R. Lauzon for technical assistance.

1. J. G. BURR. *In* Advances in photochemistry. Vol. 6. *Edited by* W. A. Noyes, Jr., G. S. Hammond, and J. N. Pitts. Interscience Publishers, Inc., New York. 1968. p. 193.
2. J. K. SETLOW. *In* Comprehensive biochemistry. Vol. 27; Photobiology, ionizing radiations. *Edited by* M. Florkin and E. H. Stotz. Elsevier Publishing Co., Amsterdam. 1967. p. 157.
3. R. O. LOUTFY, P. DE MAYO, and M. F. TCHIR. J. Amer. Chem. Soc. **91**, 3986 (1969).
4. P. J. WAGNER and D. J. BUCHECK. J. Amer. Chem. Soc. **90**, 6530 (1968).
5. M. DANIELS and A. GRIMSON. Nature, **197**, 484 (1963).
6. A. A. LAMOLA and J. P. MITTAL. Science, **154**, 1560 (1966).
7. W. D. RIDDELL, A. G. SZABO, and R. W. YIP. In press.
8. R. W. YIP. Rev. Sci. Instr. **40**, 1035 (1969).
9. E. HAYON. J. Amer. Chem. Soc. **91**, 5397 (1969).
10. D. I. SCHUSTER, A. C. FABIAN, N. P. KONG, W. C. BARRINGER, W. V. CURRAN, and D. H. SUSSMAN. J. Amer. Chem. Soc. **90**, 5027 (1968).
11. A. J. FRY, R. S. H. LIU, and G. S. HAMMOND. J. Amer. Chem. Soc. **88**, 4781 (1966).

Can. J. Chem. Downloaded from www.nrcresearchpress.com by 210.87.254.6 on 09/05/12
For personal use only.

Can. J. Chem. Downloaded from www.nrcresearchpress.com by 210.87.254.42 on 09/05/12
For personal use only.

Canadian Journal of Chemistry

Published by THE NATIONAL RESEARCH COUNCIL OF CANADA

VOLUME 48 MARCH 1, 1970 NUMBER 5

The ^{35}Cl nuclear quadrupole resonance spectra of BCl_3 and several of its amine and nitrile complexes

M. KAPLANSKY AND M. A. WHITEHEAD

Radiofrequency Spectroscopy Laboratory, Chemistry Department, McGill University, Montreal, Quebec

Received May 7, 1969

The ^{35}Cl nuclear quadrupole resonance frequencies of BCl_3, two amine complexes, and five nitrile complexes of BCl_3 are reported for 77 °K. Two molecular orbital theories, BEEM-π and CNDO, are used to interpret the frequencies.

The temperature dependences of the ^{35}Cl nuclear quadrupole resonance frequencies of B-trichloroborazole are reported.

Canadian Journal of Chemistry, 48, 697 (1970)

Introduction

The ^{35}Cl nuclear quadrupole resonance (n.q.r.) of BCl_3 has previously been reported (1–3). The splitting of the two frequencies was related to the effect of the two boron isotopes on the internal vibrations of the molecule. Contradictory reports of the ^{35}Cl n.q.r. of B-trichloroborazole are in the literature: at 77 °K it is reported to give a single frequency (4), while at room temperature both a single frequency (4) and two frequencies (5) have been reported. A complete review of the ^{35}Cl n.q.r. of boron compounds has been published (6).

The chemistry of boron trihalide complexes is well established (7, 8). The compounds studied in this work are those in which BCl_3 complexes with organic nitrogen donors, either amine or nitrile. The ^{35}Cl n.q.r. frequencies of these BCl_3 complexes, and of the free BCl_3, are combined with BEEM-π (bond electronegativity equilization method - π) theory and with the CNDO (complete neglect of differential overlap) molecular orbital theory (23), in order to interpret the frequencies and relate them to the chemical bonding in the molecules.

A temperature dependence study of the ^{35}Cl n.q.r. of B-trichloroborazole is reported, and the origin of the line splitting analyzed, using the known crystal structure.

Experimental

Complexes of BCl_3 with the 19 amines and nitriles listed in Table 1 were prepared by dropwise addition of the amine to liquified boron trichloride in *n*-pentane at −78 °C (10), under dry nitrogen atmosphere; the solvents were dried over sodium wire. The precipitates were filtered, washed with solvent in a drybox, and dried in vacuo for several hours. In all cases, infrared (i.r.) spectra indicated boric acid impurities. The complexes were purified by crystallization from cold ethanol (30 °C) and again dried in vacuo; the boric acid i.r. peak disappeared. The i.r. spectrum of $(CH_3)_3NBCl_3$ in a pellet agreed with that reported in the literature (11). The i.r. spectra of the other amine complexes before and after recrystallization were compared to ensure that no reaction occurred between the complex and ethanol; a reaction was observed with the triethylamine complex and *hot* ethanol.

The nitrile complexes were prepared in an analogous fashion; because of their ease of hydrolysis and relative instability (12), no recrystallizations were carried out; they were purified by vacuum sublimation. In no case did this enhance the line intensities of the n.q.r. spectrum, nor did it allow previously unobserved lines to be detected. Complex formation was established by the shift of the nitrile stretching frequency relative to that in the uncomplexed molecule (13, 14).

The observed n.q.r. frequencies are listed in Table 1. Relative line intensities are reported for the compounds displaying multiple resonances.

Results and Discussions

Bonding in BCl_3 and its Complexes

(*i*) Two lines have been reported (3) for BCl_3 at 77 °K; 21.582 and 21.578 MHz. Valence bond

TABLE 1

^{35}Cl n.q.r. frequencies in boron trichloride complexes at 77 °K*

Compound	Frequencies (MHz)		Splitting (kHz)	Intensity ratio†	Average frequency (MHz)
$(CH_3)_3NBCl_3$§	21.352		427	1	21.565
	21.779			2	
$(C_2H_5)_3NBCl_3$	21.948		415	~1	22.225
	22.335	22.363		~2	
	22.392			~2	
CH_3CNBCl_3	22.254				
$C_2H_5CNBCl_3$	22.384				
$(CH_3)_2CHCNBCl_3$	22.332				
$C_4H_9CNBCl_3$	22.110		85	1	22.192
	22.195		77	1	
	22.272			1	
$CH_2{=}CHCNBCl_3$	22.308				

*Complexes of boron trichloride studied which did not give n.q.r. were: methyl amine, tripropyl amine, tributyl amine, pyridine, allyl cyanide, chloro acetonitrile, trichloro acetonitrile, phenyl cyanide, benzyl cyanide, para-methyl phenyl cyanide, para-chloro phenyl cyanide, and butyronitrile.

†These intensity ratios are only approximate; in $(C_2H_5)_3NBCl_3$ no simple integer ratio would actually fit the spectra.

§The ^{35}Cl n.q.r. temperature dependence of this molecule is to be published.

calculation (3), using an *assumed* 15% s-character in the chlorine σ-orbital, an arbitrary relationship between ionic character, i, and atomic electronegativity, predicted an asymmetry parameter η of 24%. The experimental result (3) for η of the Br in BBr_3 is 45%; it might be expected that η_{Cl} would be close to this value (29, 30), in view of the similarity in their crystal structures (31).

Therefore, the e^2Qq/h and η_{Cl} for BCl_3 were calculated by three methods which avoid the arbitrariness of the valence bond method (3): (*a*) CNDO (22), using Pople and Segal's parameters, which predict good charge distributions; (*b*) SAVE–CNDO (23), using Sichel and Whitehead's parameters, which predict good molecular energies; and (*c*) BEEM-π (15, 17), a charge density theory, which has proved successful in predicting the frequencies of n.q.r. lines in CCl double bonds.

The results are shown in Table 2. None of the theories predicts the correct frequency. The CNDO approaches closest with 23.56 MHz and an η_{Cl} of 52%; the BEEM-π is next with 23.72 MHz but an η_{Cl} of 16.6%, while the SAVE–CNDO gives 28.93 MHz and an η_{Cl} of 13%. Thus *if* η_{Cl} should resemble η_{Br}, the CNDO results are quite satisfactory. To give η_{Cl} as 45%, using (21)

$$\eta = \frac{1.5(2 - n)}{\rho\left/\left(1 + \frac{\eta^2}{3}\right)^{\frac{1}{2}}\right.}$$

in which n is the occupation number of the p_π orbital, namely, N_x, and ρ is the ratio of the ν_{BCl_3} to ν_{Cl}, n would have to be 1.8781 electrons. To lower the predicted frequency in the CNDO method and simultaneously lower η would require an increase in N_z toward the value predicted by BEEM-π.

Since neither the CNDO nor SAVE–CNDO theories differentiate between σ and π orbitals, all the orbital occupations on chlorine differ from their free atom values; in BEEM-π, which is a σ–π separation theory, only one π-orbital can bond, by symmetry, and the non-bonded π-orbital is doubly occupied.

Recent calculations (15) have shown BEEM-π to give excellent predictions of total charge densities and n.q.r. frequencies in molecules containing chlorine in which η_{Cl} is small. However (24), BEEM-π makes the relative charges in σ and π orbitals different from those predicted

Can. J. Chem. Downloaded from www.nrcresearchpress.com by 210.87.254.42 on 09/05/12
For personal use only.

TABLE 2
Orbital occupations of the chlorine atom of boron trichloride

Parameter	Method of calculation			Experimental
	CNDO*	SAVE–CNDO†	BEEM-π‡	
N_x (electrons)	1.8162	1.9244	2.0000	
N_y (electrons)	1.9590	1.9698	1.9523	
N_z (electrons)	1.4758	1.4198	1.5439	
Frequency ν (MHz)	23.59	28.93	23.72	21.58
e^2Qq/h (MHz)§	45.19	57.70	47.22	
η (%)	52	13	16.6	45
ionic character, i (%)			45	

*Reference 22.
†Reference 23.
‡Reference 9, 40% s-character assumed in the chlorine σ-orbital.
§$e^2Qq/h = 2\nu/(1 + \eta^2/3)^{1/2}$.

by ab initio calculations (25), so that its usefulness in predicting charge densities in specific orbitals is in doubt. Therefore the frequency predictions will be reliable, but the η predictions doubtful. The BEEM-π calculation assumes a 40% s-character in the chlorine σ-orbital as calculated by BEEM for the BCl_3 adducts (9).

The CNDO theory appears to be the most accurate theory for predicting ^{35}Cl n.q.r. in BCl_3, assuming that the η for ^{35}Cl in BCl_3 does resemble the η for Br in BBr_3. The orbital occupances for the boron in BCl_3 are also calculated; the π-orbital contains 0.6688 electron, the σ-orbital contains 0.2268 electron. Thus the frequency for the ^{11}B n.q.r. in BCl_3 should be 2.38 MHz, in good agreement with the recently published value of 2.54 MHz (32). A full discussion of the use of CNDO in predicting boron n.q.r. frequencies is under investigation (33).

(*ii*) The boron atom in the BCl_3 complexes is tetrahedrally hybridized, so that there is no π-orbital on the boron atom, and consequently no π-bond to the chlorine (16). In the case of a carbon atom bonded to chlorine, it has been shown that a change in the hybridization of the carbon atom from digonal to trigonal to tetrahedral causes a marked change in the ionic character of the carbon–chlorine bond, but has a very small effect on the hybridization (9) of the chlorine σ-orbital. Assuming this result to be valid for boron compounds, the change from a trigonal to a tetrahedral orbital on boron does not affect the s-character of the chlorine σ-orbital, which remains at about 40%.

The increased ionic character in the BCl bond should lower the ^{35}Cl n.q.r. frequency from that of BCl_3, the loss of π-bonding should raise the ^{35}Cl n.q.r. frequency. These opposing effects are responsible for the n.q.r. frequencies of BCl_3 and its complexes being approximately the same.

BEEM calculations on the complexes of BCl_3 have recently been published (9). The s-character of the chlorine σ-orbital in the amine complexes centers on 37% with an ionic character for the BCl bond of 37%; the nitrile complexes give an s-character of 41% and ionic character of 31%. For BCl_3 these are 40% s and 45% i, respectively, with 5% π-bond character (Table 2). Since increased ionic character, s-character, and π-bonding all lower the frequency (29), BCl_3 will have the lowest frequency, 21.58 MHz, the amine complexes the next lowest, 21.8 MHz, and the nitrile complexes the highest, 22.1 MHz.

Small changes in both i and s account for the different frequencies of molecules within each class.

The splitting of the lines about the average frequency in $(CH_3)_3NBCl_3$, $(C_2H_5)_3NBCl_3$, and $C_4H_9CNBCl_3$ must be due to crystallographic inequivalence of the chlorines, since the three chlorines are molecularly equivalent in each of these molecules. Crystallographic data are not available, but these molecules have all three chlorines equivalent in their lowest energy, completely staggered, conformation.

BEEM calculations of the chlorine s-hybridization and ionic character for the two amine complexes (9) showed that a change in the value of ρ has only a slight effect on the s-character predicted, so that an average value for the two compounds, 0.3689, is indicative of the s-character of chlorine.

The results for the nitrile complexes (9) show that the average s-character is 0.4094, an increase of 4% over the value for the amine complexes, due to the larger electronegativity of the nitrogen

Can. J. Chem. Downloaded from www.nrcresearchpress.com by 210.87.254.42 on 09/05/12
For personal use only.

TABLE 3

Comparison of inductive effects in boron–nitrogen compounds with analogous carbon–carbon compounds by the BEEM-π method

Compound	Chlorine ionic character	% increase*	Compound	Chlorine ionic character	% increase*
NH_3BCl_3	0.3543†		CH_3CCl_3	0.1357‡	
$CH_3NH_2BCl_3$	0.3593	1.43	$CH_3CH_3CCl_3$	0.1359	0.21
$(CH_3)_2NHBCl_3$	0.3637	2.67	$(CH_3)_2CHCCl_3$	0.1362	0.39
$(CH_3)_3NBCl_3$	0.3676	3.76	$(CH_3)_3CCCl_3$	0.1364	0.55
$(C_2H_5)_3NBCl_3$	0.3681	3.89	$(C_2H_5)_3CCCl_3$	0.1360	0.24
$(C_3H_7)_3NBCl_3$	0.3680	3.86	$(C_3H_7)_3CCCl_3$	0.1358	0.10
$(C_4H_9)_3NBCl_3$	0.3679	3.85	$(C_4H_9)_3CCCl_3$	0.1357	0.07
$HCNBCl_3$	0.3067§		$HC{\equiv}CCCl_3$	0.1000§	
CH_3CNBCl_3	0.3124	1.87	$CH_3C{\equiv}CCCl_3$	0.1025	2.41
$C_2H_5CNBCl_3$	0.3127	1.97	$C_2H_5C{\equiv}CCCl_3$	0.1025	2.45
$(CH_3)_2CHCNBCl_3$	0.3130	2.05	$(CH_3)_2CHC{\equiv}CCCl_3$	0.1025	2.48
$(CH_3)_3CCNBCl_3$	0.3132	2.13	$(CH_3)_3CC{\equiv}CCCl_3$	0.1026	2.51

*Relative to first compound of each group.
†Chlorine ionic character for s-character of 0.3689.
‡Chlorine ionic character for s-character of 0.4094.
§Chlorine ionic character for s-character of 0.20.

orbital bonded to boron in the nitrile complexes.

A comparison of the ionic characters of the CCl bond in nitrogen–boron compounds with those in carbon–carbon compounds is reported in Table 4. Substitution of methyl groups for hydrogens generally increases the ionic character to a maximum, after which substitution of further CH_3 has little effect. The relative ability of the boron and carbon atoms to transmit the inductive effect is clearly shown, a saturated boron atom is more efficient than even an unsaturated carbon atom.

The calculations on three typical compounds of the boron trihalide complexes by the SAVE–CNDO and CNDO methods do not predict the experimental frequencies at all well. The CNDO method requires the geometry to be put into the calculations; the calculations were performed assuming staggered conformations and bond lengths typical of the bonds present in the molecules (34). However, whereas BEEM is not geometry dependent, except with respect to the assumed hybridization of the atom, and consequently adjusts the s and i so as to generate ρ, the CNDO theories are completely dependent on the input geometry. Consequently, agreement between the experimental frequency and that predicted by the CNDO theories may signify the accuracy of the input information; disagreement, on the other hand, may be due to the inaccuracy of the input data or the parametrizations used in the theories.

The η predicted are due to the inequivalence of the p_x and p_y occupations predicted by the CNDO theories, this is to be expected in staggered conformations.

The previous agreement between the predicted and measured ^{11}B n.q.r. suggests the reliability of the CNDO theories; the disagreement in predicting the ^{35}Cl n.q.r. in BCl_3 and its complexes suggests the unreliability of CNDO theories in predicting n.q.r. frequencies (23). The temperature dependence of the ^{35}Cl n.q.r. frequencies of these complexes is being studied (38).

B-Trichloroborazole

The temperature dependence of the ^{35}Cl n.q.r. frequency in B-trichloroborazole (TCB) was investigated. Nakamura *et al.* (4) originally observed one line; 19.937 MHz at 77 °K and 19.639 MHz at 295 °K. They interpreted Coursen and Hoard's (19) crystallographic data to mean that there was only one type of chlorine atom in the crystal, and hence only one line to be expected. Smith and Tong (5) reported two lines at 19.638 and 19.958 MHz, at 295 °K. The results of Nakamura (4) and Smith and Tong (5), as well as those reported here, agree to within a few kHz at 295 °K. The lower frequency line is twice as intense as the higher one. This was explained (5) by assuming hydrogen bonding between the chlorine and hydrogen atoms of adjacent molecules with two different strength hydrogen bonds.

The lines were unobservable visually and had to be recorded. Nakamura (4) observed that the

Can. J. Chem. Downloaded from www.nrcresearchpress.com by 210.87.254.42 on 09/05/12
For personal use only.

TABLE 4

Calculation of the ^{35}Cl n q.r. frequencies and asymmetry parameters in three boron trichloride complexes by CNDO theories

Compound	SAVE–CNDO* Frequency (MHz)	SAVE–CNDO* η (%)	CNDO† Frequency (MHz)	CNDO† η (%)	Experimental (MHz)
CH_3CNBCl_3	29.91	8.2	27.39	4.0	22.25
$(CH_3)_3NBCl_3$	28.80	5.6	26.68	3.4	21.57
$(C_2H_5)_3NBCl_3$	24.04	12.3	25.62	13.3	22.23

*Reference 23.
†Reference 22.

line disappeared after storing the sample in a sealed tube for a month; no observable decomposition occurred in the sample used here; the resonance was detectable over a period of more than a year with no apparent loss of intensity.

In TCB the asymmetry parameter η should be appreciable due to π-bonding; no Zeeman studies have been performed so that η is unknown. However, by comparison of the structure of TCB with that of cyanuryl chloride and 1,3,5-trichlorobenzene, η should be at least 25%, so that the η dependent term in the librating effective field gradient (*efg*) must be included. For this reason the temperature dependence data was not analyzed by Bayer's method (35).

Table 5 lists the frequencies measured at ten different temperatures, along with the splitting of the lines. The data are plotted in Fig. 1; the lines are almost parallel, the splitting being constant to within the combined experimental errors. Therefore thermal motions are not responsible for the splitting of the lines, as they were in the metastable form of the tetrameric phosphonitrilic chloride (18).

TABLE 5

^{35}Cl n.q.r. frequencies in B-trichloroborazole as a function of temperature

Temperature (°K)	Frequency* (MHz) Line 1	Frequency* (MHz) Line 2	Splitting (kHz)
77	19.936	20.258	322
112	19.901	20.221	320
143	19.865	20.186	321
178	19.821	20.141	320
190	19.806	20.127	321
210	19.777	20.097	320
229	19.751	20.071	320
250	19.717	20.038	321
273	19.681	20.001	320
293	19.647	19.968	321

*Intensity ratio line 1: line 2 is 2:1.

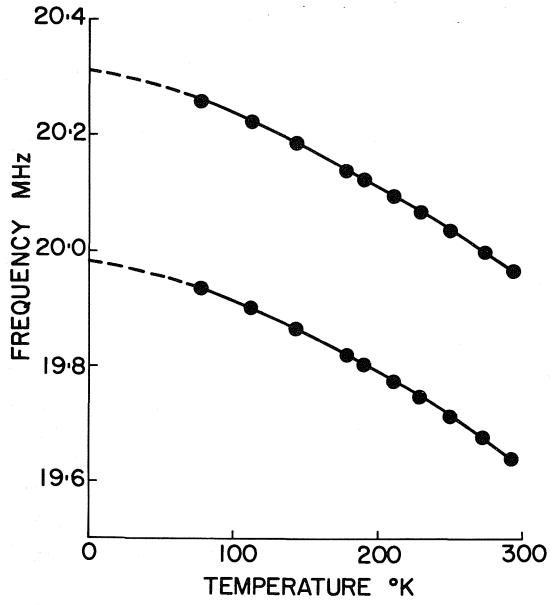

FIG. 1. Temperature dependence of the ^{35}Cl n.q.r. frequency in B-trichloride.

(a) The Frequency

Table 6 shows the results of molecular orbital calculations of the chlorine orbital occupations, frequencies, and asymmetry parameters for B-trichloroborazole, cyanuryl chloride, and 1,3,5-trichlorobenzene.

Both the CNDO theory and BEEM-π give good predictions of the frequency of 1,3,5-trichlorobenzene, while the CNDO successfully predicts the η. For cyanuryl chloride, both theories are incorrect for η and ν, as they are for B-trichloroborazole.

However, the η trends are reasonable; substitution of three nitrogens in a benzene ring increases the π-conjugation of substituents ortho and para, so that η should be increased in

Can. J. Chem. Downloaded from www.nrcresearchpress.com by 210.87.254.42 on 09/05/12
For personal use only.

Can. J. Chem. Downloaded from www.nrcresearchpress.com by 210.87.254.42 on 09/05/12
For personal use only.

TABLE 6

Electronic structures in trisubstituted derivatives using (*a*) CNDO and (*b*) BEEM-π

Compound		Chlorine orbital occupations			Frequency (MHz)		Asymmetry parameter (%)	
		N_z	N_x	N_y	Calculated	Experimental (77 °K)	Calculated	Experimental
B-trichloroborazole	(*a*)	1.4785	1.8770	1.9641	24.61	20.10	29.6	—
	(*b*)	1.6485	2.0000	1.9729	18.55§	20.10	29.0	—
Cyanuryl chloride	(*a*)	1.3255	1.9017	1.9783	33.92	36.77*	18.7	26*
	(*b*)	—	—	—	38.53	36.77	4	26
1,3,5-Trichlorobenzene	(*a*)	1.3076	1.9380	1.9876	36.03	ave. 35.29†	11	ave. 10.0
	(*b*)	—	—	—	35.34‡§	35.29	5	10.0

*Reference 36.
†Reference 37.
‡Reference 15.
§Reference 9, 20% s-character assumed for chlorine σ-bonded to carbon, 40% s-character for chlorine σ-orbital bonded to boron.

Can. J. Chem. Downloaded from www.nrcresearchpress.com by 210.87.254.42 on 09/05/12
For personal use only.

cyanuryl chloride relative to 1,3,5-trichlorobenzene; substitution of boron for carbon increases π-conjugation to the chlorines and raises η in B-trichloroborazole above the value in cyanuryl chloride. This is shown by the N_x results of the CNDO theory, and reflected in the η of both the CNDO and BEEM-π theories.

The frequency predictions are inconsistent, and since they are for free gaseous molecules, they are all approximately 10% too high. Allowing for this, the CNDO predicts B-trichloroborazole, and 1,3,5-trichlorobenzene, quite well, but not cyanuryl chloride; BEEM-π is best for cyanuryl chloride.

Thus neither theory is reliable, nor accurate, in predicting the n.q.r. frequencies.

(b) The Line Separation

The separation of 320 kHz between the two lines, 1.6% of the resonant frequency, is well within the limits for crystallographic splitting.

The possibility of hydrogen bonding being responsible is suggested by (*i*) the X-ray results (19), which show that within a molecule, 2 chlorines differ from the third, being 2.484 and 2.524 Å from hydrogens on adjacent molecules (20); and (*ii*) the i.r. spectra, which shows one band at 3440 ± 5 cm^{-1} in *n*-heptane (26), but two bands in the ratio 1:2 at 3470 and 3440 cm^{-1}, respectively, in the solid state in Nujol mull (27). This region is typical of the NH stretch, ν_{NH}. By analogy with the behavior of the i.r. of OH groups, in which decreasing ν_{OH} means increased hydrogen bonding, the 3470 line implies a weaker hydrogen bond, and the 3440 line a stronger hydrogen bond. This is substantiated by some recent i.r. work on amines (28).

In order to estimate the effect of the hydrogen atoms on the *efg* of chlorine, the following calculation was performed. Figure 2 shows a section of the *ab* plane of B-trichloroborazole (19). The between plane separation is large, and any effects on the chlorine *efg* due to hydrogens in other planes would be minimal. In addition to the difference in the chlorine–hydrogen distances, we must also consider the orientation of the hydrogens, relative to the chlorines. Because the free molecule contains two symmetry planes passing through each of the chlorines, the principal axis of the *efg* will coincide exactly with the boron–chlorine bond (the *z* axis). Distortion due to crystallographic effects would shift the *z* axis, but this effect will be assumed to be small.

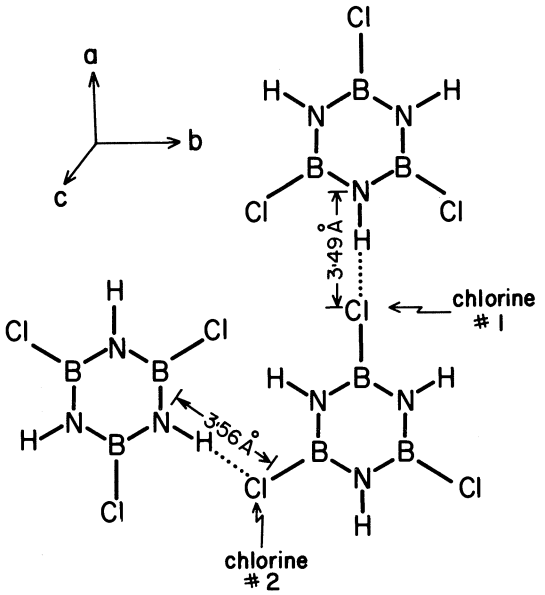

FIG. 2. Intermolecular bonding in B-trichloroborazole.

Assuming a point-charge model, the perturbations due to the hydrogens can be calculated.

The contribution to the field gradient of a point charge of magnitude *n* is

$$q = \frac{(3\cos^2\theta - 1)n}{r^3}$$

where θ is the angle between the principal axis (the *z* axis) and the point charge, and *r* is the distance between the resonant nucleus and the point charge. For chlorine atom #1 (Fig. 2), θ for the *z* axis is 180°, while for the *x* and *y* axes it is 90°. For chlorine atom #2, the angles for the *x*, *y*, and *z* axes are 90, 30, and 120°, respectively. Thus the following table may be constructed for the two chlorine atoms

Chlorine atom	*q*-values		
	q_{xx}	q_{yy}	q_{zz}
#1	$\frac{-n}{r^3}$	$\frac{-n}{r^3}$	$\frac{2n}{r^3}$
#2	$\frac{-n}{r^3}$	$\frac{1.25n}{r^3}$	$\frac{-.25n}{r^3}$

The effect of the proton on chlorine #1 will be to decrease the effective electron population along the *z* axis, and thus to increase the coupling

constant. Therefore, the frequency of chlorine atom #2 should decrease from the value in the free molecule. Since there are two chlorine atoms in position #2, the lower frequency line should be more intense, which is in agreement with experiment. This explains the direction of the frequency shift but does not explain its magnitude. The total field gradient change along the z axis between chlorine atoms #1 and #2, due to the electrostatic effect of the protons, is $2.25n/r^3$. For a charge of 0.20 electrons at a distance of 2.5 Å, the calculated total splitting is less than 20 kHz, compared to the observed value of 320 kHz. Hydrogen bonding can occur also at these distances. Charge in the σ-orbital is transfered from the lone pair σ-orbital on chlorine to the hydrogen. The field gradient at the chlorine is lowered, and the n.q.r. frequency decreased, the decrease is greater for chlorine at position #2. The combined effect of point charge and hydrogen bonding may account for the separation.

Thus the calculations from X-ray results and the i.r. measurements agree with a hydrogen bond interpretation of the n.q.r. results, since point charge alone cannot be responsible.

The authors are grateful to Mr. L. Krause for the calculations on BCl_3 and trichloroborazole by the BEEM and BEEM-π methods. This research was supported by the National Research Council of Canada, to whom M.K. is grateful for award of Scholarships (1966–1968), and partially by the Defence Research Board of Canada, Grant number 9530 – 55. The McGill Computing Centre provided facilities.

1. R. Livingston. J. Phys. Chem. **57**, 496 (1953).
2. D. C. Douglass. Ph.D. Thesis, Cornell University, Ithaca, N.Y. 1957. Quoted in J. Chem. Phys. **31**, 504 (1959).
3. T. Chiba. J. Phys. Soc. Jap. **13**, 860 (1958).
4. D. Nakamura, H. Watanabe, and M. Kubo. Bull. Chem. Soc. Jap. **34**, 142 (1961).
5. J. A. S. Smith and D. A. Tong. Chem. Commun. **1**, 3 (1965).
6. E. V. Bryukhova, V. I. Stanko, A. I. Klimova, N. S. Titova, and G. K. Semin. J. Struct. Chem. USSR, Engl. Transl. **9**, 31 (1968).
7. J. M. Miller and M. Onyszchuk. Can. J. Chem. **41**, 2898 (1963).
8. J. M. Miller and M. Onyszchuk. Can. J. Chem. **42**, 1518 (1964). B. A. Dunell, C. A. Fyfe, C. A. McDowell, and J. Ripmeester. Trans. Faraday Soc. **65**, 1153 (1969).
9. M. Kaplansky and M. A. Whitehead. Mol. Phys. **16**, 481 (1969).
10. W. Gerrard and M. F. Lappert. Chem. Rev. **58**, 1081 (1958).
11. R. L. Amster and R. C. Taylor. Spectrochim. Acta, **20**, 1487 (1964).
12. W. Gerrard, M. F. Lappert, and J. W. Wallis. J. Chem. Soc. 2178 (1960).
13. W. Gerrard, M. F. Lappert, H. Pyszora, and J. W. Wallis. J. Chem. Soc. 2182 (1960).
14. H. J. Coerver and C. Curran. J. Amer. Chem. Soc. **80**, 3522 (1958).
15. M. Kaplansky and M. A. Whitehead. Mol. Phys. **15**, 149 (1968).
16. J. L. Hoard, S. Geller, and T. B. Owen. Acta Cryst. **4**, 405 (1951).
17. N. C. Baird and M. A. Whitehead. Theoret. Chim. Acta, **6**, 167 (1966).
18. M. Kaplansky and M. A. Whitehead. Can. J. Chem. **45**, 1669 (1967).
19. D. L. Coursen and J. L. Hoard. J. Amer. Chem. Soc. **74**, 1742 (1952).
20. K. Lonsdale. Nature, **184**, 1060 (1959).
21. R. Bersohn. J. Chem. Phys. **22**, 2078 (1954).
22. J. A. Pople and G. A. Segal. J. Chem. Phys. **43**, S136 (1965).
23. J. M. Sichel and M. A. Whitehead. Theoret. Chim. Acta, **11**, 263 (1968).
24. R. J. Boyd, D. H. Lo, and M. A. Whitehead. Chem. Phys. Lett. **2**, 227 (1968).
25. E. Clementi. J. Chem. Phys. **46**, 4731 (1967).
26. R. M. Clipsham. Private communication.
27. J. D. Kittredge. Private communication.
28. E. L. Zhukova and I. I. Shmenko. Opt. Spectr. **25**, 279 (1968).
29. E. A. C. Lucken. Nuclear quadrupole coupling constants. Academic Press, Inc., New York. 1969. p. 260.
30. D. R. Armstrong and P. G. Perkins. J. Chem. Soc. A, 1218 (1967).
31. M. A. Rollier and A. Riva. Gazz. Chim. Ital. **77**, 361 (1947).
32. P. A. Casabella and T. Oja. J. Chem. Phys. **50**, 4814 (1969).
33. M. A. Whitehead. Unpublished data.
34. L. E. Sutton (*Editor*). Interatomic Distances. The Chemical Society, London. 1965.
35. T. Kushida, G. B. Benedek, and N. Bloembergen. Phys. Rev. **104**, 1364 (1956).
36. Y. Morino, T. Chiba, T. Shimozawa, and M. Yoyama. J. Phys. Soc. Jap. **13**, 869 (1958).
37. Y. Morino and M. Toyama. J. Phys. Soc. Jap. **15**, 288 (1960).
38. R. M. Hurt, D. F. R. Gilson, and M. A. Whitehead. To be published.

Can. J. Chem. Downloaded from www.nrcresearchpress.com by 210.87.254.42 on 09/05/12
For personal use only.

Can. J. Chem. Downloaded from www.nrcresearchpress.com by 210.87.254.40 on 09/05/12
For personal use only.

Volatilité du nitrate, chlorure et sulfure mercurique et préparation de sources radioactives de ^{203}Hg

JACQUES GROSSOLEIL ET J. C. ROY
Département de Chimie, Université Laval, Québec 10, Québec

Reçu le 15 septembre 1969

En utilisant le ^{203}Hg comme traceur, on a étudié la volatilité du $Hg(NO_3)_2$ et $HgCl_2$ en présence de HNO_3, HCl, H_2S, Na_2S, NaHS, $Na_2S_2O_3$ et NH_3. Les quantités de mercure ont varié de 1 à 50 μg et les autres conditions expérimentales ont été celles qu'on rencontre lors de la préparation de sources radioactives de référence, destinées aux mesures absolues du taux de désintégration. On a trouvé que les pertes étaient appréciables durant l'évaporation de solutions de $Hg(NO_3)_2$ dans HNO_3, qu'elles étaient nulles durant l'évaporation de solutions de $HgCl_2$ dans HCl, et qu'elles étaient de nouveau appréciables pour des sources solides issues de l'évaporation de chacune de ces solutions. En partant d'une solution de $Hg(NO_3)_2$ dans HNO_3, on a trouvé qu'il était très difficile d'éliminer complètement les pertes d'activité par précipitation du HgS; on n'y est arrivé seulement en ajoutant un grand excès d'ion sulfure sous forme de Na_2S et de NaHS ou de $Na_2S_2O_3$ en solution. La précipitation du HgS à partir d'une solution de $HgCl_2$ dans HCl est beaucoup plus facile que dans le cas précédent et élimine complètement les pertes d'activité.

On peut expliquer les résultats en admettant que la formation du complexe $HgCl_4^{2-}$ en milieu HCl stabilise l'ion mercurique et le rend non volatil, tandis que la formation de molécules volatiles de $Hg(NO_3)_2$ est favorisée en milieu HNO_3 où il n'y a pas de formation de complexe.

With ^{203}Hg as a tracer, the volatility of $Hg(NO_3)_2$ and $HgCl_2$ in the presence of HNO_3, HCl, H_2S, Na_2S, NaHS, $Na_2S_2O_3$, and NH_3 has been studied. The amounts of mercury varied between 1 and 50 μg and the other experimental conditions were those encountered in the preparation of radioactivity standards. We found that the losses of activity were large during the evaporation of solutions of $Hg(NO_3)_2$ in HNO_3, that they were nil during the evaporation of solutions of $HgCl_2$ in HCl, and that they were large again for the solid residues left after the evaporation of each one of these solutions. When using a solution of $Hg(NO_3)_2$ in HNO_3, we found it very difficult to eliminate completely the losses by a HgS precipitation; we stopped them completely only by addition of a large excess of sulfide ion as Na_2S and NaHS or of $Na_2S_2O_3$. The precipitation of HgS from a solution of $HgCl_2$ in HCl is much easier and stops the losses completely.

The results can be explained by saying that the formation of the $HgCl_4^{2-}$ complex in a HCl medium greatly stabilizes the mercuric ion and renders it nonvolatile, whereas the formation of volatile $Hg(NO_3)_2$ molecules is favored in a HNO_3 medium where no complex formation occurs.

Canadian Journal of Chemistry, **48**, 705 (1970)

Introduction

Lors de la préparation de sources solides de mercure radioactif pour en mesurer le taux de désintégration, les pertes de mercure, dues à la volatilité de plusieurs de ses sels, sont une cause possible d'erreur (1). Pour les enrayer, on précipite ordinairement le mercure sous forme de sulfure (2–4); plus précisément, dans un guide (4) sur la préparation de sources de référence on recommande de précipiter le sulfure mercurique à partir d'une solution diluée d'acide nitrique. Or nous avons trouvé des pertes substantielles en employant cette méthode au cours de travaux impliquant la préparation de sources de mercure (5). A la suite de cette observation, nous avons entrepris d'examiner le comportement du nitrate mercurique en solution dans l'acide nitrique diluée et du chlorure mercurique en solution dans l'acide chlorhydrique diluée pour finalement préciser les conditions pour une précipitation rapide et complète de sulfure mercurique en vue de préparer des sources de référence, destinées aux mesures absolues de taux de désintégration. Il est à noter que le choix du chlorure et du nitrate mercurique est basé sur le fait que les solutions radioactives de mercure sont ordinairement fournies sous l'une ou l'autre de ces formes.

Partie Expérimentale

Solutions Radioactives

Le mercure possède plusieurs isotopes radioactifs, dont deux sont utilisés pour la préparation de sources de référence; ce sont le ^{197}Hg et le ^{203}Hg. Dans le présent travail, nous avons utilisé le ^{203}Hg; sa période radioactive d'environ 47 jours et son schéma de désintégration simple (2) lui confèrent des propriétés nucléaires qui en font un excellent traceur.

Le mercure possède deux états d'oxydation, +1 et +2, correspondants aux sels mercureux et mercuriques. A cause de la forte tendance qu'ont les sels mercureux de

Can. J. Chem. Downloaded from www.nrcresearchpress.com by 210.87.254.40 on 09/05/12
For personal use only.

TABLEAU 1

Pertes de mercure pour des sources de ^{203}Hg, préparées à partir d'acide nitrique et de nitrate mercurique, durant l'évaporation à l'air ambiant, à la température ambiante et sous la lampe infrarouge

Fournisseur de la solution mère	Source no.	Masse de solution mg	Masse de Hg µg	Concentration initiale en HNO_3 M	Durée de l'évaporation min	$P_{évap}$ pertes de ^{203}Hg %	Pertes moyennes de Hg par min d'évaporation ng	Température
Produits commerciaux, Energie Atomique du Canada Ltée	*A*-1	132	3.9	0.05	150	24±3	6.3	
	A-2	22	7.1	0.5	110	4±2	2.5	
	A-3	51	16.5	0.5	100	4±2	6.5	
	A-4	108	18.6	0.05	30	2±1	2.9	
	A-5	98	32.3	0.15	120	2±1	5.5	
Dissolution dans HNO_3 de mercure électrodéposé sur films plastiques	*B*-1		4.7	0.01	170	33±3	8.8	
	B-2		10.0	0.5	150	5±2	3.3	
	B-3		17.0	0.5	30	1±1	3.4	
	B-4		18.0	0.01	180	14±3	14.0	
New England Nuclear Corp.	*C*-1	163	1.7	0.01	120	28±1	4.0	
	C-2	52	1.0	0.01	60	16±1	2.7	Ambiante, 20–25 °C
	C-3	53	1.0	0.015	45	18±1	4.0	
	C-4	56	1.6	0.02	60	20±1	5.3	
	C-5	18	2.4	0.05	120	23±1	4.6	
	C-6	10	1.3	0.10	95	15±1	2.1	
	C-7	16	2.2	0.10	85	14±1	3.7	
	C-8	19	2.5	0.10	110	6±1	1.4	
	C-9	23	3.0	0.10	105	19±1	5.5	
	C-10	29	3.7	0.10	120	10±1	3.1	
	C-11	9	1.2	1.7	70	37±1	6.5	
	C-12	19	1.2	3.5	140	30±1	2.6	
	C-13	13	1.2	4.8	140	37±1	3.2	
	C-14	35	1.4	8.6	180	38±1	3.0	
Produits commerciaux, Energie Atomique du Canada Ltée	*D*-1	212	2.5	0.08	100	64±4	16	
	D-2	153	3.9	0.04	40	26±4	25	
	D-3	192	7.6	0.06	55	22±3	30	Lampe infrarouge, ≈40 °C
	D-4	180	12.8	0.10	50	17±2	44	
	D-5	208	29.6	0.10	65	7±1	31	
	D-6	190	49.8	0.40	65	7±1	54	

Can. J. Chem. Downloaded from www.nrcresearchpress.com by 210.87.254.40 on 09/05/12
For personal use only.

se dismuter en sels mercuriques et en mercure, on emploie toujours les sels mercuriques pour la préparation de solutions radioactives de mercure.

Deux types de solutions radioactives de ^{203}Hg ont été utilisées: l'une, fournie par l'Agence Internationale de l'Energie Atomique, était du chlorure mercurique dissout dans une solution 0.1 *M* en HCl, l'autre était du nitrate mercurique dissout dans des solutions diluées d'acide nitrique. Cette dernière a été obtenue chez deux fournisseurs différents et préparée par nous par dissolution de mercure déposé électrochimiquement sur des films plastiques métallisés (5); les produits commerciaux de l'Energie Atomique du Canada ont fourni une solution 5 *M* en HNO_3, tandis que la firme New England Nuclear Corporation a fourni une solution 1 *M* en HNO_3. Les solutions mères reçues ont été, en général, diluées à l'aide de solutions qui permettent d'obtenir la molarité désirée en ions hydrogène, chlorure, nitrate et mercurique. Les solutions mères et diluées ont été stockées dans des pycnomètres en polyéthylène à ouvertures effilées (6) et conservées dans une enceinte contenant une solution de même nature que celle du pycnomètre, pour saturer l'atmosphère et éviter ainsi l'évaporation de la solution radioactive (7).

Les Méthodes de Comptage

Comme le ^{203}Hg émet des β ayant une énergie maximale de 210 keV en coïncidence avec des radiations γ de 279 keV (le rapport $\gamma/\beta = 0.816$), on peut suivre le comportement des sources en déterminant soit le taux d'émission des β ou des γ. Durant l'évaporation des solutions, on est conduit à détecter les γ parce que les β sont en grande partie absorbés dans la solution; à cette fin, on a utilisé un spectromètre formé d'un crystal de NaI (Tl), accouplé à une photomultiplicatrice, et relié, soit à un analyseur de 128 canaux (Modèle D-110, Nuclear Data) ou à un analyseur à simple canal. La source, une fois solide, on peut détecter soit les γ ou les β; ces derniers furent détectés avec un compteur 4π stéradians proportionnel à gaz, balayé avec du méthane à la pression atmosphérique. L'instrumentation électronique était formé de modules du type "NIM" provenant des compagnies Ortec et Canberra.

Les comptages ont été effectués en prenant les précautions suivantes: étalonnage fréquent des appareils, décontamination répétée du système de détection, mesures régulières de bruit de fond. On a également tenu compte de la variation des dimensions de la source durant le séchage pour des mesures au spectromètre γ. En comptage γ, l'imprécision des mesures était de l'ordre de ±0.5%, tandis qu'en comptage β, elle était beaucoup moindre.

Préparation et Étude d'une Source

Une goutte de solution radioactive est prélevée du pycnomètre, laquelle est pesée avant et après. Elle est alors déposée sur un film plastique mince supporté par un anneau d'aluminium; la préparation de ces films a été décrite en détail ailleurs (5, 8). On mesure immédiatement le taux d'émission des gammas pendant des périodes de 2 à 4 min, après quoi la source peut être traitée par une des méthodes de préparation énumérées plus loin ou ne subir aucun traitement spécial. Peu importe son sort, on reprend les mesures des taux d'émission gamma à intervalles réguliers pendant l'évaporation, en alternant avec des mesures du bruit de fond. Les taux d'émission trouvés sont alors corrigés de deux facteurs: le facteur de décroissance naturelle survenue pendant le séchage et le facteur de changement de géométrie de la goutte vis-à-vis du détecteur dû à l'évaporation de celle-ci. Lorsque la source est devenue solide, on mesure son taux d'émission β ou γ à divers intervalles au cours du temps pendant une période variant de 100 à 300 h et on corrige les taux d'émission pour la décroissance naturelle.

Résultats et Discussion

1. Comportement des Solutions de $Hg(NO_3)_2$ dans HNO_3

On a toujours observé que les solutions de nitrate mercurique dans l'acide nitrique évaporées telles quelles, de même que celles contenant un agent mouillant, présentent des pertes appréciables de mercure, lesquelles se manifestent d'ailleurs par une contamination prononcée des appareils de détection; cette contamination introduit un degré d'imprécision et rend les résultats plus difficiles à analyser. Le tableau 1 résume les observations expérimentales. Les valeurs dans la colonne identifiée par le sigle $P_{évap}$ donnent les pertes d'activité du ^{203}Hg pendant l'évaporation de la solution c'est-à-dire, à partir de la première mesure du taux d'émission de la source jusqu'à ce qu'elle devienne une source solide; elles sont exprimées en pourcents par rapport à l'activité initiale. Dans la colonne suivante, on les a exprimé en utilisant le système perte de mercure métallique par minute d'évaporation; ce système rend plus facile la comparaison des résultats puisqu'ils sont ramenés sur une base commune. Cette façon d'exprimer les résultats est acceptable en autant que le taux de pertes est à peu près constant au cours de l'évaporation, ce que nous avons trouvé expérimentalement. Ces taux d'évaporation s'appliquent pour des gouttes ayant des surfaces entre 0.5 et 1.0 cm^2 au moment de leurs dépositions sur le film.

Pour de tels systèmes, les résultats du tableau 1 montrent qu'à la température ambiante (20–25 °C) les pertes moyennes sont de l'ordre de 4 ng de mercure par min d'évaporation tandis qu'elles augmentent considérablement lorsque l'évaporation se fait sous une lampe infrarouge (≈40 °C) et deviennent alors de l'ordre de 30 ng de mercure par min d'évaporation. On doit s'attendre à ce qu'il en soit ainsi si les pertes sont dues à la volatilité du nitrate de mercure. Dans la mesure

Can. J. Chem. Downloaded from www.nrcresearchpress.com by 210.87.254.40 on 09/05/12
For personal use only.

où l'on peut comparer les résultats entre eux, la provenance de la solution, la molarité initiale en acide nitrique et la quantité de nitrate mercurique dans le domaine de concentration utilisée semblent avoir peu d'influence sur le taux des pertes. On peut expliquer, du moins en partie, ces pertes en admettant qu'elles se produisent par la volatilisation de molécules de $Hg(NO_3)_2$. Le nitrate mercurique est assez fortement dissocié dans l'eau pure, toutefois l'addition de HNO_3 destiné à enrayer l'hydrolyse provoque la régression de l'équilibre de dissociation et augmente le caractère covalent de la molécule et par conséquent sa volatilité.

2. Comportement de Solutions de $HgCl_2$ dans HCl

En se basant sur les mesures d'activité, les pertes, pour des solutions de $HgCl_2$ dans HCl évaporées telles quelles ou en présence d'agent mouillant, sont inférieures à la limite d'imprécision de nos mesures, soit $\pm 0.5\%$ pour une variété de conditions expérimentales, soit: (*a*) évaporation à l'obscurité dans une enceinte ventillée, (*b*) évaporation sous l'éclairage du laboratoire à l'air ambiant, (*c*) évaporation sous une lampe infrarouge à l'air ambiant, (*d*) évaporation sous pression réduite dans un dessicateur.

En fait, on peut dire que les pertes, s'il y en a, sont de beaucoup inférieures à 0.5% puisqu'il n'y a pas eu de contamination du système de détection durant l'évaporation; nous sommes portés à croire qu'elles sont nulles.

La molarité initiale des solutions était en général de 0.1 *M* en HCl et la quantité de mercure a varié entre 1 et 40 μg.

Nous croyons que la complexation de $HgCl_2$ par l'ion chlorure selon les réactions

$$HgCl_2 + Cl^- \rightarrow HgCl_3^-$$

et

$$HgCl_3^- + Cl^- \rightarrow HgCl_4^{2-}$$

donne des espèces nonvolatiles en solution et fait en sorte qu'il n'y a pas de pertes pendant l'évaporation. La constante d'équilibre pour la formation de $HgCl_4^{2-}$ est élevée et par ailleurs, nous savons par les travaux de Kraus et Nelson (9) que $HgCl_2$ donne des complexes très stables en milieu chlorhydrique puisque le mercure est fortement absorbé sur une résine échange d'anion sur un domaine très étendu de concentration en HCl.

3. Comportement des Sources Solides de Nitrate et Chlorure Mercurique

Les sources solides issues de l'évaporation de $Hg(NO_3)_2$ dans HNO_3 et de $HgCl_2$ dans HCl ont montré des pertes appréciables dans les conditions où nous les avons conservées. Quoique du même ordre de grandeur pour les deux sels, elles ont semblé plus élevées pour $Hg(NO_3)_2$ que pour $HgCl_2$; elles ont varié, en général, entre 10 et 20 ng de mercure par h pendant les 100 premières heures d'exposition à l'air ambiant à température ambiante; ce taux de perte a été de 4 à 5 fois plus élevé sous la lampe infrarouge. La surface apparente recouverte par la matière solide a pu varier entre 0.2 et 0.5 cm^2.

4. Précipitation du HgS à Partir de Solutions de $HgCl_2$ dans HCl

Comme précédemment, dans les autres conditions, il n'y a pas de pertes pendant l'évaporation lorsqu'on traite la goutte de solution radioactive de $HgCl_2$ dans HCl par H_2S gazeux en plaçant la source dans une enceinte où l'on fait circuler les gaz. Les sources solides de sulfure mercurique issues de la précipitation n'ont présenté aucune perte lorsqu'on les a gardées dans de petites boîtes fermées et individuelles pendant plusieurs mois; on a observé des pertes moyennes de 0.3% en les gardant sous pression réduite dans un dessiccateur pendant 25 h et de 1% en les plaçant sous une lampe infrarouge pendant la même période. Ces résultats indiquent que la précipitation du mercure en HgS a été complète mais qu'il faut éviter de placer le HgS solide dans des conditions qui favorisent sa décomposition ou sa volatilisation.

5. Précipitation de HgS à Partir de Solutions de $Hg(NO_3)_2$ dans HNO_3

En partant d'une solution de nitrate dans HNO_3, on a trouvé qu'il était très difficile d'éliminer complètement les pertes d'activité par précipitation du HgS; on y est arrivé qu'en ajoutant un grand excès d'ion sulfure sous forme de Na_2S et de NaHS ou de $Na_2S_2O_3$ en solution. Rappelons qu'il est possible de déceler de très faibles pertes d'activité pendant l'évaporation, disons de l'ordre de 0.1 à 0.2%, par la contamination qu'elles produisent dans le système de détection.

(a) Précipitation par Addition de H_2S

En utilisant seulement du gaz H_2S pour

précipiter le mercure, on a observé d'une part que la molarité initiale en HNO_3 devrait être inférieure à 0.1 *M* pour empêcher, semble-t-il, la dissolution du HgS fraîchement précipité dans l'acide qui se concentre à mesure que l'évaporation se poursuit; en effet, on a observé chez des sources solides issues de la précipitation de HgS à partir de solutions 0.5 *M* en HNO_3 des pertes du même ordre de grandeur que chez les sources solides de $Hg(NO_3)_2$. D'autre part, pendant l'évaporation de sources traitées au gaz H_2S seulement, on a observé des pertes d'activité de quelques pourcents chez la plupart d'entre elles; cette série de sources contenait quelques microgrammes en mercure en milieu 0.05 *M* de HNO_3. On a observé que ces pertes se produisaient au tout début de l'évaporation et sont dues, sans doute, à la volatilisation du $Hg(NO_3)_2$ qui n'est pas encore transformé en HgS. On a cherché à les éliminer en ajoutant un sulfure en solution sous forme de Na_2S et de NaHS ou une solution de $Na_2S_2O_3$ pour obtenir une précipitation plus rapide et plus complète du mercure en HgS au tout début de l'évaporation.

(b) Précipitation par Addition de Na_2S, NaHS ou $Na_2S_2O_3$ en solution

En précipitant le mercure au moyen d'un léger excès d'une solution de l'un ou de l'autre de ces trois réactifs, les résultats ont été plus satisfaisants qu'en employant le gaz H_2S seul. On a trouvé que les pertes moyennes étaient de l'ordre de 1% pour des solutions contenant quelques microgrammes de mercure dans des milieux de 0.01 à 0.05 *M* en HNO_3. Plusieurs des sources solides issues de l'évaporation des solutions ainsi traitées ont été conservées dans des petites boîtes fermées, à l'abri de la lumière et de l'air, et leurs taux d'émission ont été mesurés à divers intervalles; après 4, 14 et 21 jours, elles ont accusé des pertes moyennes égales respectivement à 0.6, 1.4 et 2.1% ce qui nous amènent à penser que des traces de nitrate mercurique ont subsistées et ont été responsables des pertes. Rappelons que les pertes étaient nulles pour les sources solides de HgS, issues de $HgCl_2$ et conservées dans les mêmes conditions.

En dernière analyse, nous devons conclure que, malgré tous les essais que nous avons effectués avec le $Hg(NO_3)_2$ en solution dans HNO_3 diluée, nous avons été incapable de trouver une méthode sûre permettant d'éliminer les pertes d'activité par une précipitation au HgS sans ajouter de grandes quantités de matières solides, ce qui n'est pas toujours souhaitable pour la préparation de sources de référence.

6. Préparation de Sources Solides de ^{203}Hg par Précipitation par NH_3 Gazeux

La précipitation des sels mercuriques par NH_3 gazeux ne conduit pas à l'hydroxyde, mais à la formation de complexes amoniés, dont la constitution dépend du pH de la solution et dont la nature est très controversée. On devine qu'il sera bien difficile de savoir quelle quantité de matières solides on obtiendra en fin de séchage sur le support.

Les sources obtenues avec le nitrate et le chlorure mercurique en solution dans l'acide correspondant, préparées par balayage pendant tout le séchage par NH_3 gazeux a fait ressortir les mêmes caractéristiques que les études précédentes: (*a*) pertes nulles au séchage pour les sources issues de $HgCl_2$, (*b*) faibles pertes au séchage pour les sources issues de $Hg(NO_3)_2$, (*c*) pertes très faibles après séchage pour les sources issues de $HgCl_2$, (*d*) fortes pertes après séchage pour les sources issues de $Hg(NO_3)_2$.

Nous n'avons pas poussé plus loin cette étude car dans tous les cas de dépôt de matières solides déposées étaient trop importantes. Cette méthode n'est pas recommandable.

Conclusion

En se basant sur nos observations expérimentales il découle qu'entre $HgCl_2$ en solution dans HCl et $Hg(NO_3)_2$ en solution dans HNO_3, il faut choisir le premier système d'abord pour éviter les pertes d'activité durant l'évaporation des solutions, ensuite, pour être sûr qu'il n'y a pas de pertes durant la précipitation du HgS. Même en choisissant le premier système, il faut prendre certaines précautions pour éviter la décomposition du HgS solide; on a trouvé qu'en gardant chaque source solide à l'abri de la lumière et de l'air dans une petite boîte fermée, les pertes ont été nulles pendant très longtemps.

Il semble qu'on ait favorisé l'utilisation de $Hg(NO_3)_2$ en solution dans HNO_3 dilué (4) pour que le mercure radioactif soit en milieu oxydant et ainsi éviter la réduction de l'ion mercurique. Il faut se rappeler que la formation de complexe dans HCl stabilise fortement l'ion mercurique

Can. J. Chem. Downloaded from www.nrcresearchpress.com by 210.87.254.40 on 09/05/12
For personal use only.

que les complexes $HgCl_4^{2-}$ n'a pas de tendance à être réduit, et de plus, on peut obtenir en milieu HCl, une précipitation complète en HgS sur un domaine beaucoup plus étendu de concentration qu'avec HNO_3.

Tous ces avantages militent en faveur de l'emploi de $HgCl_2$ dans HCl pour stocker les solutions radioactives de mercure et pour la préparation de sources de référence.

1. YOSHIMASA TANAKA, ZAZUTA KITAHARA et YOKO YOSHIDA. Yakugaku Zasshi, **84**, 687 (1964).
2. J. G. V. TAYLOR. Can. J. Phys. **40**, 383 (1962).
3. J. S. MERRITT, J. G. V. TAYLOR et P. J. CAMPION. Can. J. Chem. **37**, 1109 (1959).
4. B. KAHN, G. R. CHOPPIN et J. G. V. TAYLOR. Users guides for radioactivity standards. National Academy of Sciences, National Research Council, Washington, D.C. October 1967.
5. Y. UJIHIRA et J. C. ROY. Can. J. Chem. **46**, 1221 (1968).
6. J. S. MERRITT et J. G. V. TAYLOR. Gravimetric sampling in the standardization of solutions of radionuclides. Rapport de l'Energie Atomique du Canada, Chalk River, A.E.C.L. No. 2679. 1967.
7. A. P. BAERG. Metrologia, **2**, No. 1, 23 (1966).
8. J. C. ROY et J. TURCOTTE. Can. J. Chem. **45**, 1379 (1967).
9. K. A. KRAUS et F. NELSON. *Dans* Proceedings of the international conference on the peaceful uses of atomic energy. Vol. 7. Geneva, 1955. United Nations, New York. 1956. p. 113.

Can. J. Chem. Downloaded from www.nrcresearchpress.com by 210.87.254.40 on 09/05/12
For personal use only.

Can. J. Chem. Downloaded from www.nrcresearchpress.com by 210.87.254.42 on 09/05/12
For personal use only.

Methyltin trinitrate and a comparison of its properties with other methyltin nitrates

J. R. FERRARO
Chemistry Division, Argonne National Laboratory, Argonne, Illinois

AND

D. POTTS AND A. WALKER[1]
Department of Chemistry, Scarborough College, University of Toronto, Toronto 181, Ontario

Received September 30, 1969

Methyltin trinitrate has been prepared by the reaction of dinitrogen pentoxide on methyltin trichloride in carbon tetrachloride, followed by sublimation in vacuo at 60 °C. Conductivities and ultraviolet spectra of methyltin trinitrate in several solvents are reported. Vibrational spectra indicate that the three nitrato groups are all bonded in the same bidentate manner and the reactivity of the compound towards aliphatic hydrocarbons and diethyl ether shows that the compound is chemically similar to tin(IV) nitrate. The vibrational spectrum of methyltin trinitrate is compared with those for trimethyltin nitrate, dimethyltin dinitrate, and tin(IV) nitrate. Nuclear magnetic resonance spectra have been determined for the series $Me_nSn(NO_3)_{4-n}$ ($n = 1, \ldots, 4$), and a comparison of the ^{117}Sn– and ^{119}Sn–proton coupling constants for the series has been made showing that the tin atom becomes more electron deficient and has more s character in its bonding orbital to carbon as n decreases. The pyridine adduct $MeSn(NO_3)_3 \cdot 2py$ has been prepared and the infrared spectrum of this compound indicates that the nitrate groups are unidentate.

Canadian Journal of Chemistry, **48**, 711 (1970)

Recent work on organo-tin nitrate compounds has led to the preparation and characterization of the series Me_3SnNO_3 (1), $Me_2Sn(NO_3)_2$ (2), and $Sn(NO_3)_4$ (3). Attempts to prepare the missing member, $MeSn(NO_3)_3$, by reaction of dinitrogen pentoxide on dimethyltin dinitrate in chloroform (2) have failed. We have prepared methyltin trinitrate by the reaction of methyltin trichloride with dinitrogen pentoxide in carbon tetrachloride, followed, after removal of solvent in vacuo, by sublimation at 60 °C.

It has now become clear that in the reactions of the tetramethyl derivatives of lead (4), tin (2), and germanium (5) with dinitrogen pentoxide or tetroxide, the usual product is the dinitrate. Further nitrate substitution is impossible by this technique and it is also impossible to stop the reaction at the mononitrate stage. Monomethyl or dimethyl derivatives of these three metals may, therefore, in general be reacted with dinitrogen pentoxide without removal of methyl groups.

In addition to studying the properties of methyltin trinitrate, this paper also makes a comparison of the properties of the entire series $Me_nSn(NO_3)_{4-n}$ ($n = 0, \ldots, 4$).

Discussion and Results

Methyltin trinitrate is a white crystalline solid. It is extremely hygroscopic and fumes in the air. The compound reacts with Nujol in a manner similar to $Sn(NO_3)_4$ (3), and it reacts violently with diethyl ether liberating nitrogen dioxide. This chemical reactivity, in conjunction with infrared data, is taken to indicate that the nitrate groups in $MeSn(NO_3)_3$ are bidentate (3), and that the reactivity of the compound is due to the liberation of NO_3 radicals. In both chemical and physical properties methyltin trinitrate resembles tin(IV) nitrate more closely than the other two members of the series, whose nitrato groups are thought to be monodentate (1, 2).

Methyltin trinitrate sublimes in vacuo at 60 °C, and it is interesting to note the increase in volatility for the series $Me_nSn(NO_3)_{4-n}$ ($n = 0, \ldots, 3$) as n decreases. Thus, Me_3SnNO_3 sublimes in vacuo at 100 °C, $Me_2Sn(NO_3)_2$ at 85 °C, $MeSn(NO_3)_3$ at 60 °C, and $Sn(NO_3)_4$ at 40 °C. Like tin(IV) nitrate (3), methyltin trinitrate is not only soluble in water and in many polar organic solvents, but it is also appreciably soluble in chloroform and carbon tetrachloride. If the compound is heated gently, it first melts and then decomposes liberating nitrogen dioxide and leaving a yellow residue. If heated strongly, however, the compound decomposes explosively.

Ultraviolet Absorption Spectra

The spectra of methyltin trinitrate in water and

[1]To whom correspondence should be addressed.

Can. J. Chem. Downloaded from www.nrcresearchpress.com by 210.87.254.42 on 09/05/12
For personal use only.

TABLE 1

Molar conductivity values of $MeSn(NO_3)_3$ in various solvents at 25.0 °C

H_2O		DMSO		MeOH		MeCN		$MeNO_2$	
Concentration $M \times 10^3$	Conductance Ω^{-1} cm^2	Concentration $M \times 10^3$	Conductance Ω^{-1} cm^2	Concentration $M \times 10^3$	Conductance Ω^{-1} cm^2	Concentration $M \times 10^3$	Conductance Ω^{-1} cm^2	Concentration $M \times 10^2$	Conductance Ω^{-1} cm^2
0.409	891	0.507	102	1.06	176	1.19	0.731	1.62	0.555
0.697	913	0.775	108	1.98	149	3.14	3.11	4.78	1.49
2.97	923	2.82	98.5	4.13	114	7.39	6.62	6.37	2.16
4.52	920	4.39	94.0	8.00	89.1	10.4	6.06	7.95	2.39
7.68	906	7.06	86.8	11.4	77.4	13.1	5.73	9.58	2.32

Can. J. Chem. Downloaded from www.nrcresearchpress.com by 210.87.254.42 on 09/05/12
For personal use only.

dimethylsulfoxide (DMSO) are shown in Fig. 1 and the spectra in methyl cyanide, ethyl acetate, and methanol are shown in Fig. 2. In water, ε_{max} is 25.9 at 298 mμ and although this is indicative of full ionic dissociation, the value of ε is somewhat higher than expected for ionization producing three nitrate ions per mole of compound (ε = 7.1/nitrate ion at 302.5 mμ) (6). The peak maximum is also shifted to slightly lower wavelength than expected. These deviations may arise as a result of interference from a charge-transfer band of the hydrolyzed $(MeSn)^{3+}$ species. This also seems to be the case in DMSO since the usual maximum at 312.5 mμ (ε = 5.0/nitrate ion) (6) appears only as an inflection at 305 mμ (ε = 18.2). Since conductivity measurements in this solvent show essentially complete ionization, the interfering charge-transfer band may be attributed to the solvated $(MeSn)^{3+}$ species. The spectra in both H_2O and DMSO were not time dependent, nor was the spectrum of the aqueous solution changed upon boiling, as was the case for $Me_2Sn(NO_3)_2$ (2).

The spectra of methyltin trinitrate in methyl cyanide, ethyl acetate, and methanol are typical of solutions of anhydrous metal nitrates in these solvents (2, 3, 6), and indicate considerable metal–nitrate interaction (6). In ethyl acetate ε_{max} is 26.4 at 262.5 mμ and in methanol it is 20.5 at 272.5 mμ.

Conductivities

The molar conductivities of methyltin trinitrate in water, dimethylsulfoxide, methanol, methyl cyanide, and nitromethane are listed in Table 1. The low conductivity values of methyl cyanide and nitromethane solutions indicate that methyltin trinitrate is virtually a nonelectrolyte in these solvents (7). Aqueous solutions of methyltin trinitrate are quite acidic ($pH \sim 2$) and thus the very high conductivity values of these solutions are the result of hydrolysis as was the case with dimethyltin dinitrate (2). (The molar conductivity for $La(NO_3)_3$ in H_2O at 25 °C is $\sim 350\ \Omega^{-1}\ cm^2$ for a 0.0033 *M* solution (8).) The conductivity values of dimethylsulfoxide solutions are considerably higher than those expected for 1:2 electrolytes in this solvent. (Molar conductivity of $Me_2Sn(NO_3)_2$, a 1:2 electrolyte, is $59.7\ \Omega^{-1}\ cm^2$ at 0.0065 *M* (2).) The values obtained in methanol show concentration dependence typical of weak electrolyte behavior. Therefore, while in very dilute solutions (0.001 *M*) the conductivity indicates some degree of ionization ($AgNO_3$ in MeOH has a molar conductivity of $94.20\ \Omega^{-1}\ cm^2$ at a concentration of 0.00168 *M* (9)), at the concentration used for the ultraviolet (u.v.) spectrum (0.0167 *M*) there will be considerable association as the u.v. spectrum demonstrates.

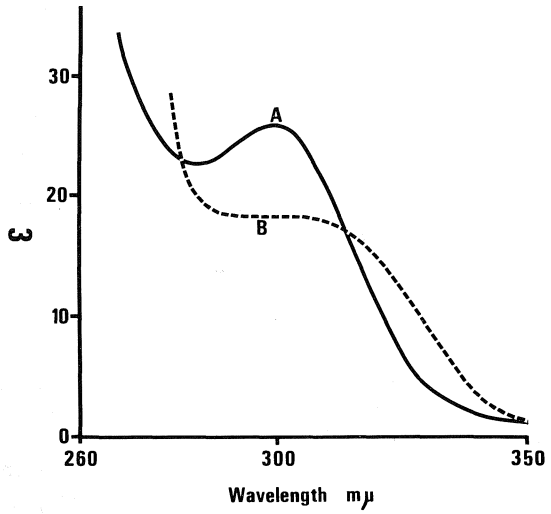

FIG. 1. Ultraviolet spectra of solutions of methyltin trinitrate at 25 °C. *A*, water; *B*, dimethylsulfoxide.

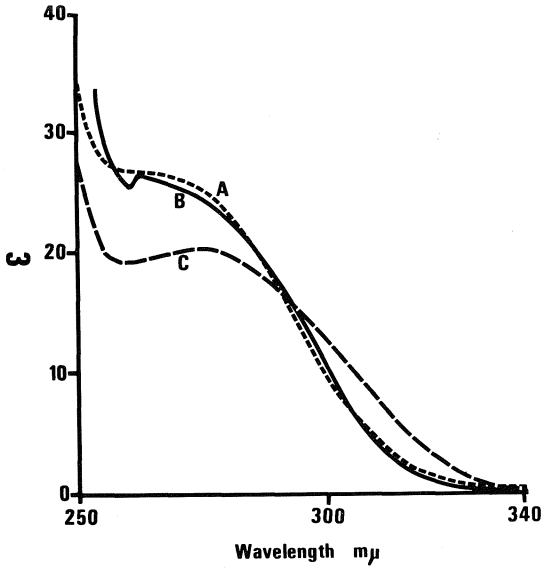

FIG. 2. Ultraviolet spectra of solutions of methyltin trinitrate at 25 °C. *A*, methyl cyanide; *B*, ethyl acetate; *C*, methyl alcohol.

Molecular Weight

The molecular weight of $MeSn(NO_3)_3$ was determined cryoscopically in nitrobenzene and

TABLE 2

Vibrational spectra of methyltin trinitrate*

Frequency, cm^{-1}		
Infrared	Raman	Assignment
3220 vw 3195 vw 3175 vw		C—H stretching
1630 s,sp 1605 s,sp 1575 m,sp	1630 m,p 1605 w,p 1515 s,p	Terminal N=O stretching
1240 s,sp 1210 m,sp	 1210 vw,dp	Asym. NO_2 stretching
974 s,sp	990 m,p	Sym. NO_2 stretching
786 m,sp		CH_3 rock
775 m,sp 770 m,sp	 800 s,p	NO_2 out-of-plane rock and sym. NO_2 bend
685 w		Asym. NO_2 bend
555 w	512 w,p	Sn—C stretch
304 s,sp 226 m,sp		Asym. Sn—O stretching Sym. Sn—O stretching

*s = strong, m = medium, w = weak, vw = very weak, sp = sharp, p = polarized, dp = depolarized.

found to be 291.3, indicating only slight dissociation from the monomeric value of 319.7.

Vibrational Spectra

The observed infrared and Raman bands of methyltin trinitrate and their assignments are listed in Table 2. The nitrato band assignments are based upon literature values (10) for titanium tetranitrate, tin tetranitrate, and vanadium(V) oxide trinitrate. The strong infrared bands in the 1600 cm^{-1} region are characteristic of the terminal N=O group stretching frequencies found in compounds containing bidentate nitrato groups. Likewise, the bands in the 1200 and 1000 cm^{-1} regions are typical for the asymmetric and symmetric NO_2 stretching modes, respectively, for such compounds. The observed sequence of Raman polarization for the 1600, 1200, and 1000 cm^{-1} regions is polarized, depolarized, and polarized, respectively. This order (10), together with the observed intensity sequence[2] (strong, very weak, medium), is conclusive evidence that the nitrato groups in methyltin trinitrate are all bidentate. It is difficult (10) to assign the bands in the 780 cm^{-1} region since the CH_3 rock, symmetric NO_2 bend, and NO_3 out-of-plane rock modes all occur in the same area. We have shown that the CH_3 rocking mode of methyltin trichloride in carbon disulfide occurs at 790 cm^{-1} and thus the infrared band at 786 cm^{-1} is assigned to the CH_3 rock for the nitrate. The asymmetric in-plane bending mode in tin(IV) nitrate occurs at 696 cm^{-1} (10) and this corresponds to the infrared band at 685 cm^{-1} in methyltin trinitrate. In tin(IV) nitrate the symmetric NO_2 in-plane bending mode occurs at 802 cm^{-1} and the out-of-plane rock occurs at 783 cm^{-1} (10). For methyltin trinitrate the infrared bands at 775 and 770 cm^{-1} are thus assigned to these two modes, while the strong polarized Raman band at 800 cm^{-1} must be assigned to the symmetric NO_2 bend. The bands observed at 555 cm^{-1} (infrared) and 512 cm^{-1} (Raman) are typical of Sn—C stretches, the Sn—C stretch in methyltin trichloride occurring at 547 cm^{-1} (infrared).

The splitting of the bands in the 1600 and 1200 cm^{-1} regions probably results from coupling of the vibrations of the three nitrato groups in the molecule. The fact that all the bands in the 1600 cm^{-1} region are all polarized suggests a very low order of symmetry for the molecule, probably C_1.

An interesting comparison can be made for the Sn—C and Sn—O stretching modes for the methyltin nitrate series $Me_nSn(NO_3)_{4-n}$ (n = 0, . . . , 4) as is shown in Table 3. It is seen that as the number of nitrate groups increases, both the Sn—C and Sn—O stretching frequencies increase, the latter to a greater extent. The increases in these frequencies can be explained by the greater positive charge on the tin atom with the introduction of the electronegative nitrato groups (2).

The presence of two Sn—O stretching frequencies for Me_3SnNO_3 might indicate a bidentate nitrato group in this compound. However, Raman polarization studies on this compound and the dinitrate, which would have determined this, were not possible due to lack of solubility in a suitable solvent. The exact nature of the metal–nitrato bonding in $(CH_3)_3SnNO_3$ and $(CH_3)_2Sn(NO_3)_2$ remains in doubt.

Nuclear magnetic resonance spectra

Data for the nuclear magnetic resonance (n.m.r.) spectra of tetramethyltin, trimethyltin nitrate, dimethyltin dinitrate, and methyltin trinitrate in dichloromethane at 37 °C are presented in Table 4.

[2]Paper presented by N. Logan at the Annual General Meeting of the Chemical Society, Nottingham, 1969.

Can. J. Chem. Downloaded from www.nrcresearchpress.com by 210.87.254.42 on 09/05/12
For personal use only.

TABLE 3

Sn—C and Sn—O stretching frequencies in cm^{-1} for the series $Me_nSn(NO_3)_{4-n}$ ($n = 0, \ldots, 4$)

Compound	Sn—C stretch		Sn—O stretch	
	Asymmetric	Symmetric	Asymmetric	Symmetric
Me_4Sn	524*	504*	—	—
Me_3SnNO_3	557†	520†	220	152
$Me_2Sn(NO_3)_2$	558‡	527‡	283	209
$MeSn(NO_3)_3$	—	555	304	226
$Sn(NO_3)_4$	—	—	344§	302§

*Reference 13.
†Reference 1.
‡Reference 2.
§Reference 3.

TABLE 4

Nuclear magnetic resonance spectra of $Me_nSn(NO_3)_{4-n}$ ($n = 1, \ldots, 4$) in dichloromethane at 37 °C

Compound	τ (p.p.m.)	$J(^{117}Sn—CH_3)$ (c.p.s.)	$J(^{119}Sn—CH_3)$ (c.p.s.)
$(CH_3)_4Sn$	9.92	51.4	53.4
$(CH_3)_3SnNO_3$	9.29	56.1	58.4
$(CH_3)_2Sn(NO_3)_2$	8.52	78.3	81.6
$(CH_3)Sn(NO_3)_3$	8.12	128.4	134.4

A plot of τ vs. n for the series $Me_nSn(NO_3)_{4-n}$ ($n = 1, \ldots, 4$) is virtually a straight line and the increase in chemical shift (decrease in τ values) to low field with decreasing values of n reflects the increase in electron deficiency of the tin atom as compared to its state in tetramethyltin. Furthermore, this effect is greater for the nitrato groups than that previously observed (11) for the methyltin chloride series and is consistent with the increased infrared stretching frequencies observed for the Sn—C and Sn—O bonds.

Holmes and Kaesz (12) have suggested that the tin–proton coupling constants in methyltin halides may be correlated to the percent of s-character in the tin orbital used in bonding to the carbon atom. If the coupling constants for the nitrate series (Table 4) are treated in a similar manner (12) to the chloride series, it is found that for the series of compounds $Me_nSn(NO_3)_{4-n}$ ($n = 1, \ldots, 4$) the percent of s-character for the tin bonding orbitals to carbon increases for decreasing n. This increase is largest for the nitrate series.

Brown and Morgan (13) have measured the infrared and n.m.r. spectra of several methyltin compounds, and have found that linear relationships exist between the observed $^{119}Sn—CH_3$ coupling constants and both the symmetric and asymmetric tin–carbon stretching frequencies. When our data for the methyltin nitrate series is compared to that obtained by Brown and Morgan, it is found that the methyltin nitrate results fit the same straight lines. As in the case of methyltin trichloride (13), the Sn—C stretching frequency for methyltin trinitrate lies on the extrapolated line for $\nu_{sym.}$ vs. $J(^{119}Sn—CH_3)$ plot. These relationships have been taken to indicate (13) that increasing percent of s-character of the tin orbital in the tin–carbon bond results in increasing tin–carbon stretching frequencies as are observed for the nitrate series.

Pyridine Adduct

Methyltin trinitrate forms a pyridine adduct $MeSn(NO_3)_3 \cdot 2py$ similar in nature to the one formed with $Sn(NO_3)_4$ (3). The adduct crystallizes from a solution of methyltin trinitrate and pyridine in chloroform. The compound is only slightly hygroscopic and does not react with either diethyl ether or Nujol. The infrared spectrum is indicative of unidentate nitrato groups (3), as is the loss of chemical reactivity. The principal nitrate bands in the infrared in cm^{-1} are as follows: 1512 s, br (asym. NO_2 stretch);

Can. J. Chem. Downloaded from www.nrcresearchpress.com by 210.87.254.42 on 09/05/12
For personal use only.

1300 s, br (sym. NO_2 stretch); 975 s (NO stretch); 805 m (out-of-plane rock).

Experimental

Methyltin trinitrate

Dinitrogen pentoxide was prepared by a gas-phase reaction between dinitrogen tetroxide and ozone. Methyltin trichloride (6.2 g) was dissolved in carbon tetrachloride (15 ml) and added to a solution containing N_2O_5 (23.3 g) in carbon tetrachloride (60 ml). Brown fumes were formed immediately upon mixing, with the production of a yellow oil. After 3–4 h stirring, the solvent and excess pentoxide were removed in vacuo, leaving a yellow solid. After double sublimation in vacuo at 60 °C, pure $MeSn(NO_3)_3$ (4.2 g) is obtained as white crystalline solid. Care was taken to exclude moisture at all times from the reaction.

Anal. Calcd. for $MeSn(NO_3)_3$: Sn, 37.12; C, 3.76; NO_3^-, 58.18. Found: Sn, 37.43; C, 3.98; NO_3^-, 57.54.

$MeSn(NO_3)_3 \cdot 2py$

Pyridine (5.0 ml, 0.062 mole) in chloroform (5 ml) was added to a solution containing methyltin trinitrate (1.51 g, 0.0047 mole) in chloroform (10 ml). After mixing, the solution turned light yellow and after 5–10 min fine transparent crystals were precipitated. After filtration and washing with petroleum ether, the yield of the resulting fine white powder was 1.10 g. Moisture was carefully excluded at all stages of the reaction.

Anal. Calcd. for $MeSn(NO_3)_3 \cdot 2py$: Sn, 24.83; C, 27.64; NO_3^-, 38.92. Found: Sn, 24.61; C, 27.35; NO_3^-, 38.57.

Tin analysis was carried out by igniting the compound, after first moistening with concentrated sulfuric acid and weighing as SnO_2. Nitrate was determined as nitron nitrate, and carbon was determined by the Van Slyke wet oxidation method.

All solvents were dried by standard techniques. Pyridine was dried by allowing analar pyridine to stand 24 h over calcium hydride, followed by distillation onto molecular sieves.

Infrared spectra were recorded using a Beckman I.R. 12 spectrophotometer. Spectra of $MeSn(NO_3)_3$ were taken in carbon tetrachloride and carbon disulfide using either variable path length cells with KRS-5 plates or sealed fixed path silver chloride cells with 0.1 mm teflon spacers. Far infrared spectra (200–400 cm^{-1}) were taken in carbon tetrachloride using 0.1 mm polyethylene liquid cells. All other spectra were obtained with Nujol or halocarbon mulls between either KRS-5 or high density polyethylene windows. Raman spectra were obtained in carbon disulfide using a Spex Raman Instrument and a Carson Argon ion laser.

Ultraviolet spectra were recorded using a Cary #14 spectrophotometer using fused silica cells and dried spectroscopic solvents.

Conductivities were recorded with a Beckman Model RC-18 bridge system, and a cell following the design of Greiner (14).

Nuclear magnetic resonance spectra were run on a Varian T-60 spectrophotometer. Spectra were run in dichloromethane with tetramethylsilane as an internal reference in the case of Me_3SnNO_3 and $Me_2Sn(NO_3)_2$. The proton peak from dichloromethane was used as a standard for Me_4Sn and $MeSn(NO_3)_3$. ($MeSn(NO_3)_3$ was found to react with $(CH_3)_4Si$.)

We wish to thank the National Research Council of Canada for supporting this work and for a Studentship to D.P.

1. H. C. Clark and R. J. O'Brien. Inorg. Chem. **2**, 740 (1963).
2. C. C. Addison, W. B. Simpson, and A. Walker. J. Chem. Soc. 2360 (1964).
3. C. C. Addison and W. B. Simpson. J. Chem. Soc. 598 (1965).
4. D. Potts and A. Walker. Can. J. Chem. **47**, 1621 (1969).
5. D. Potts and A. Walker. Unpublished results.
6. C. C. Addison and D. Sutton. J. Chem. Soc. A, 1524 (1966).
7. C. C. Addison, B. J. Hathaway, N. Logan, and A. Walker. J. Chem. Soc. 4308 (1960).
8. International critical tables of numerical data, physics, chemistry and technology. Vol. VI. McGraw-Hill Book Co., Inc., New York. 1929. p. 238.
9. R. E. Busby and V. S. Griffiths. J. Chem. Soc. 902 (1963).
10. C. C. Addison, D. W. Amos, and D. Sutton. J. Chem. Soc. A, 808 (1967).
11. M. P. Brown and D. E. Webster. J. Phys. Chem. **64**, 698 (1960).
12. J. R. Holmes and H. D. Kaesz. J. Amer. Chem. Soc. **83**, 3903 (1961).
13. T. L. Brown and G. L. Morgan. Inorg. Chem. **2**, 736 (1963).
14. R. H. Greiner. Fusion. Nov. 1960. p. 11.

Can. J. Chem. Downloaded from www.nrcresearchpress.com by 210.87.254.42 on 09/05/12
For personal use only.

Nuclear magnetic resonance studies of solid methylammonium halides

J. TSAU[1] AND D. F. R. GILSON
Department of Chemistry, McGill University, Montreal 110, Quebec
Received October 7, 1969

Wide-line nuclear magnetic resonance studies of methylammonium chloride, bromide, and iodide and their partially deuterated analogues show that second-moment and line-width transitions occur which can be interpreted as due to molecular reorientation about the C—N axes. In the bromide and iodide salts this motion persists below 77 °K.

Canadian Journal of Chemistry, **48**, 717 (1970)

Can. J. Chem. Downloaded from www.nrcresearchpress.com by 210.87.254.6 on 09/05/12
For personal use only.

Introduction

The room-temperature crystal structures of methylammonium chloride and bromide (1–3) are tetragonal and the C—N axes coincide with the fourfold *c* axes of the crystals. The lack of correspondence between the site symmetry and the point-group symmetry of the cation indicates that there must be either disordering of the proton positions or rotation about the C—N bond. The existence of low-temperature modifications of methylammonium chloride was shown by Aston and Ziemer (4) from heat capacity measurements. The room-temperature α-form changes irreversibly to the β-form at 220 °K. When this phase is heated to 220 °K it converts to the γ-form, which then changes to the α-form at 264 °K. Confirmation of the three different phases of methylammonium chloride was obtained from temperature-dependent infrared spectroscopic studies (5, 6). Cabana and Sandorfy (6) and Théorêt and Sandorfy (7) also demonstrated that, over the temperature range 12 to 470 °K, there were four phases present in methylammonium bromide, two for the iodide, and two (probably) for the fluoride. At low temperatures, the infrared absorptions, normally broad at room temperature, sharpen and split into several peaks as the degeneracy of the site symmetry is removed. The changes in heat capacity and entropy of the γ-to-α transition favor a positional disordering, although the transition is narrow (4 °C) for an order–disorder process. The disappearance of the torsional mode and the shape of the degenerate bands in the α-phase led Théorêt and Sandorfy to tentatively suggest that a one-dimensional hindered rotation occurs. Stammler (2) has examined X-ray powder diffraction patterns of methylammonium chloride at different temperatures and attributed the change in powder pattern to a decrease in symmetry from the tetragonal phase.

Wide-line nuclear magnetic resonance (n.m.r.) provides an excellent technique for studying molecular reorientation, and the present paper describes such a study of methylammonium chloride, bromide, and iodide and their deuterated analogues.

Experimental

Methylammonium halides were obtained from commercial sources, recrystallized from absolute ethanol three times, and dried in vacuo. All compounds analyzed satisfactorily. Deuteration on nitrogen was performed by repeated recrystallization from heavy water. Compounds deuterated on carbon were lent to us by Professor Sandorfy and were originally obtained from Merck, Sharp, and Dohme.

Proton magnetic resonance spectra were obtained using a Varian DP60 spectrometer with a modified "feed-through" low proton probe and associated temperature control equipment. Second moments were calculated from the experimental derivative curves using a computer program and corrected for finite modulation amplitude. The effects of incomplete isotopic exchange were neglected in the calculation of theoretical second moments.

Results

The temperature dependence of the experimental line widths and second moments is shown in Fig. 1 for methylammonium chloride and its deuterated species. At 77 °K the experimental second moment of CH_3NH_3Cl is 34.64 ± 0.35 G^2. The second moment decreases, commencing at about 110 °K, to a value of 7.50 ± 0.41 G^2 at 245 °K, followed by a gradual decrease from this temperature to 6.2 G^2 at 470 °K, the upper temperature limit of the apparatus. For CD_3NH_3Cl the limiting values of second moment are 31.8 ± 0.6 and 6.3 ± 0.5 G^2 at 212 °K, and the transition is narrower, occurring between 125 and

[1]NRCC Studentship holder, 1966–1969.

Can. J. Chem. Downloaded from www.nrcresearchpress.com by 210.87.254.6 on 09/05/12
For personal use only.

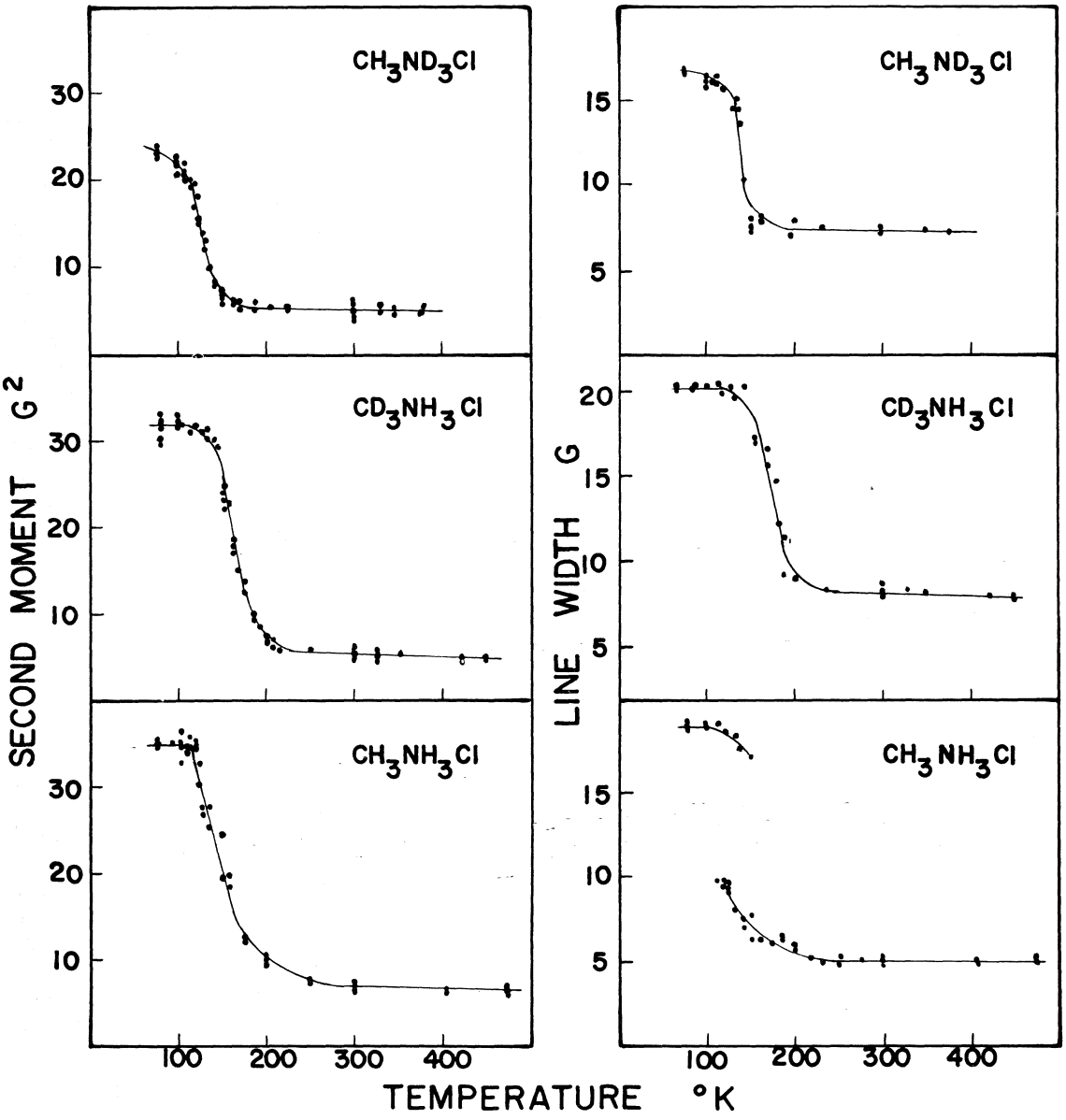

FIG. 1. Temperature dependence of second moments and line widths for methylammonium chlorides.

200 °K. For CH_3ND_3Cl the limiting values are 22.8 ± 0.7 and 5.0 ± 0.6 G^2 at 175 °K, but the transition is shifted to lower temperature and is not quite complete at 77 °K.

Experimental second moments for the bromide and iodide salts are listed in Table 1 for temperatures of 77 and 300 °K. The transition is in progress at 77 °K for the bromide but is complete below this temperature for the iodide.

Discussion

The application of the wide-line n.m.r. method involves, in most cases, a comparison of the experimentally determined second moments with values calculated from the van Vleck formula, which, in turn, requires a knowledge of the proton positions in the crystal. The crystal structures of the low-temperature phases of the methylammonium salts are unknown (but are probably

TABLE 1

Experimental second moments for methylammonium bromide and iodide

Molecule	Second moment, G^2	
	77 °K	300 °K
CH_3NH_3Br	24.5*	7.5
CH_3ND_3Br	10.8	5.8
CD_3NH_3Br	10.6	6.0
CH_3NH_3I	8.8	7.5
CH_3ND_3I	6.5	5.5

*High-temperature limit of transition 250 °K.

monoclinic). The crystals of methylammonium chloride shatter when cooled to liquid nitrogen temperature, which is a further indication that a change in crystal structure occurs. In cases where the structure is unknown (or not known in sufficient detail) it is usual to divide the theoretical second moment into *intra-* and *inter*-molecular contributions. The former can be calculated using reasonable values for the bond lengths and angles, while the intermolecular second moment is estimated by comparison with values obtained for crystals with similar structures. For the methylammonium salts an additional method can be used. In the deuterated molecules, the dominant dipolar interactions arise within the $-CH_3$ and $-\overset{+}{N}H_3$ groups alone and the shape of the proton resonance line provides further information. For the calculation of line shapes and second moments, all angles were assumed to be tetrahedral and a value of 1.096 Å was used for the C—H bond length. A readily acceptable value of the N—H bond length for a four-coordinate nitrogen atom is not available. Distances of 1.032 Å for the ammonium ion and 1.06 Å for the hydrazinium ion have been given (8). In the present study, a value of 1.045 Å has been used, which represents a compromise between the line shapes and second moments in CD_3NH_3Cl. The calculated intramolecular second moments for the species $CH_3\overset{+}{N}H_3$, $CH_3\overset{+}{N}D_3$, and $CD_3\overset{+}{N}H_3$ are given in Table 2 for the rigid ion and for rotation of the ion about the C—N axis. An accurate calculation of the intermolecular second moment (rigid lattice) cannot be made, and therefore an estimate was obtained from the high-temperature tetragonal structure by introducing a "disorder" in the proton positions. The carbon and nitrogen positions were fixed with the coordinates of the known structure, but over several unit cells. Different proton positions were generated by rotating different methylammonium ions through fixed angular increments. In this way a number of ordered structures were obtained and an average taken of the second moments of these different structures. Intermolecular second moments for the rotating cases were calculated using the Andrew and Eades formulae (9).

The total calculated second moments for the rigid lattice cases are larger than the experimental values at 77 °K, Table 2. The disagreement is due, in part, to an incorrect value for the intermolecular contributions, plus some residual torsional motion. The agreement is close enough, however, to show that the transitions are due to reorientation of the methylammonium ions about their C—N axes. This motion persists to below 77 °K for the bromide and iodide salts.

The theoretical line shapes for an isolated triangular configuration of nuclei have been calculated by Andrew and Bersohn (10). The presence of neighboring nuclear spins causes a broadening of the resonance line and loss of detail but this effect can be introduced into the calculation by including a Gaussian broadening function, β^2, as described by Pake for the two-spin system (11). The application of the line shape analysis to the species $CH_3\overset{+}{N}D_3$ and

TABLE 2

Second moments of methylammonium chloride

Species	Calculated second moment, G^2						Experimental second moment, G^2	
	Rigid lattice			Rotating methylammonium ions				
	Intra	Inter	Total	Intra	Inter*	Total	77 °K	245 °K
CH_3NH_3Cl	30.52	8.79*	39.31	7.62	1.60	9.22	34.6	7.3
CH_3ND_3Cl	21.98	4.83	26.81	5.50	0.79	6.29	22.8	4.9
CD_3NH_3Cl	30.79	3.24	34.03	7.46	0.62	8.08	31.8	6.3

*Based on structure given in ref. 1.

Can. J. Chem. Downloaded from www.nrcresearchpress.com by 210.87.254.6 on 09/05/12
For personal use only.

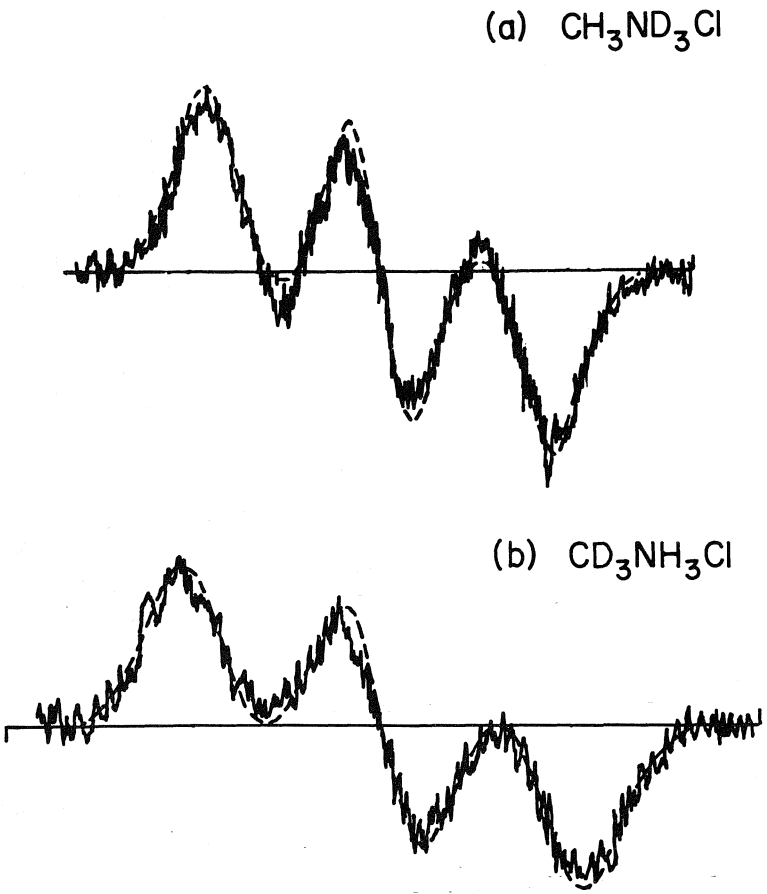

FIG. 2. Experimental derivative line shapes at 77 °K for (*a*) CH_3ND_3Cl, (*b*) CD_3NH_3Cl. Dashed curves are theoretical line shapes.

$CD_3\overset{+}{N}H_3$ involves approximations. In the first case the experimental second moment has not quite reached the limiting value at 77 °K, and, strictly speaking, the $-\overset{+}{N}H_3$ case is not an isolated three-spin system since the nitrogen atom should be included. The line shapes were computed for CH_3ND_3Cl for different values of β^2 with the same molecular geometry used for the intramolecular second moment calculation. The best agreement with the experimental curve at 77 °K was obtained with $\beta^2 = 2.25\ G^2$, Fig. 2*a*. The second moment of the calculated curve was $23.34\ G^2$. For CD_3NH_3Cl, line shapes were calculated for different values of β^2 and also for different N—H distances in the range 1.020 to 1.050 Å. The best fit for the line shape whose second moment agreed with the experimental value of $31.8\ G^2$, Fig. 2*b* was for an N—H distance of 1.045 Å and $\beta^2 = 2.61\ G^2$. This N—H value was then used in the calculation of the theoretical second moments of Table 2.

The line shapes were calculated for the rotating cases and are shown in Fig. 3. The curves shown by Powles and Gutowsky (12) do not include a flat, weak portion at their extrema. In the present study these regions were observed experimentally and appeared in the calculated line shapes. The gradual loss of these "tails" of the resonance signal is responsible for the decrease in second moment above the transition and may arise from additional molecular motion such as an oscillation of the molecular axis.

The correlation frequency, ν_c, responsible for line narrowing can be related to the line width by eq. [1] and then used in the Arrhenius expression

Can. J. Chem. Downloaded from www.nrcresearchpress.com by 210.87.254.6 on 09/05/12
For personal use only.

Can. J. Chem. Downloaded from www.nrcresearchpress.com by 210.87.254.6 on 09/05/12
For personal use only.

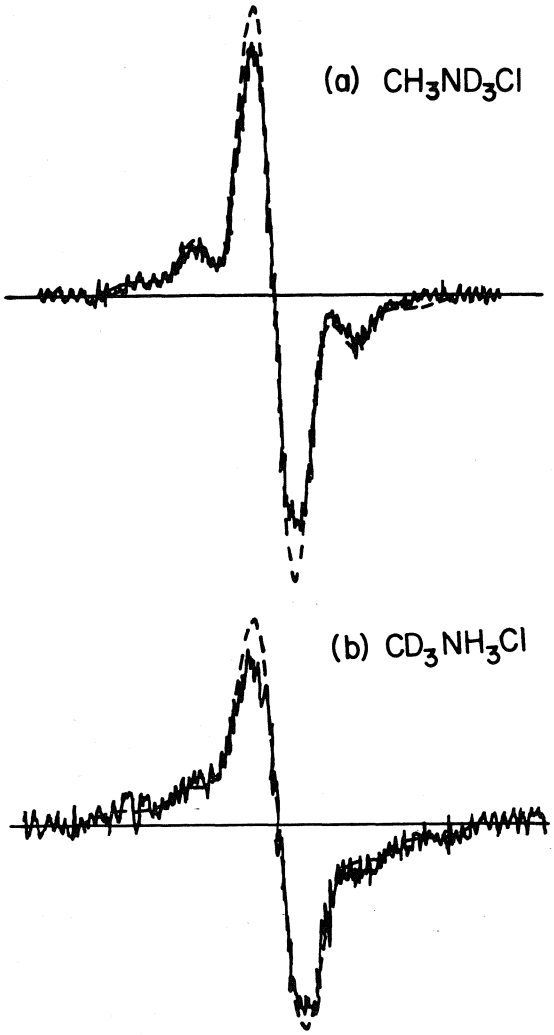

FIG. 3. Experimental and calculated line shapes: (*a*) CH_3ND_3Cl at 190 °K, $\beta^2 = 1.0\ G^2$; (*b*) CD_3NH_3Cl at 200 °K, $\beta^2 = 1.69\ G^2$.

to obtain an activation energy for molecular reorientation.

$$[1] \quad \nu_c = \frac{\alpha\gamma(\delta H)}{2\pi} \Big/ \tan\left[\frac{\pi}{2} \cdot \frac{(\delta H)^2 - B^2}{A^2 - B^2}\right]$$

where δH is the line width at temperature T, A is the value below, and B above, the transition, γ is the magnetogyric ratio, and α is a constant approximately equal to unity (13). The line-width transitions occur at different temperatures for CH_3ND_3Cl and CD_3NH_3Cl. If the potential barrier is unaltered by isotopic substitution, then the difference in transition temperature indicates that the methylammonium ion does not rotate as a whole and instead the motions of the two halves are independent. There are arguments against this conclusion. Line narrowing occurs when the correlation frequency approaches the frequency equivalent of the line width and, since the line widths are different in the two cases, this would result in different transition temperatures. Isotopic substitution will alter the moments of inertia, but for correlated motion of the ion this should shift the transitions to higher temperatures in both cases. In favor of uncorrelated motion is the fact that the temperature dependence of the second moment of CH_3NH_3Cl is not symmetrical about the midpoint of the transition and could be a composite of two transitions. Also the infrared spectroscopic studies of Théorêt and Sandorfy (7) showed that the torsional frequency shifted further on N-deuteration than on C-deuteration, leading to the conclusion that the torsional motion was mainly an $-\overset{+}{N}H_3$ group motion. The n.m.r. line-width analysis gives activation energies of 4.8 kcal mole^{-1} for methyl group reorientation and 6.1 kcal mole^{-1} for the $-\overset{+}{N}H_3$ group. The pre-exponential factors are 4.3×10^{13} and 1.4×10^{14} s^{-1}, respectively.

There is no apparent correspondence between the n.m.r. transitions and the transitions observed in the heat capacity measurements. The relationship between n.m.r. and thermal data has been discussed by Darmon and Brot (14). The line width is sensitive to any reorientational motion of sufficient frequency, but the thermodynamic functions are affected by the appearance of orientational disorder regardless of the time scale. Thus a hindered rotation in which the molecule moves between indistinguishable positions will not appear as a heat capacity transition. A change in crystal structure, such as occurs in the methylammonium halides, will be observed by thermodynamic measurements but will have only slight effects on the second moment since the reorientational motion has already exerted the major influence.

The financial assistance of the National Research Council of Canada is gratefully acknowledged. The authors thank Professor C. Sandorfy for the loan of the deuterated compounds.

1. E. W. HUGHES and W. N. LIPSCOMB. J. Amer. Chem. Soc. **68**, 1970 (1946).

2. M. STAMMLER. J. Inorg. Nucl. Chem. **29**, 2203 (1967).
3. E. J. GABE. Acta. Cryst. **14**, 1296 (1961).
4. J. C. ASTON and C. W. ZIEMER. J. Amer. Chem. Soc. **68**, 1405 (1946).
5. R. D. WALDRON. J. Chem. Phys. **21**, 734 (1953).
6. A. CABANA and C. SANDORFY. Spectrochim. Acta, **18**, 843 (1962).
7. A. THÉORÊT and C. SANDORFY. Spectrochim. Acta, **23A**, 519 (1967).
8. Interatomic distances. Chem. Soc., London, Spec. Publ. 18.
9. E. R. ANDREW and R. G. EADES. Proc. Roy. Soc. London, Ser. A, **216**, 398 (1953).
10. E. R. ANDREW and R. BERSOHN. J. Chem. Phys. **18**, 159 (1950).
11. G. E. PAKE. J. Chem. Phys. **16**, 327 (1948).
12. J. G. POWLES and H. S. GUTOWSKY. J. Chem. Phys. **21**, 1695 (1953).
13. H. S. GUTOWSKY and G. E. PAKE. J. Chem. Phys. **18**, 162 (1950).
14. I. DARMON and C. BROT. Mol. Cryst. **2**, 301 (1967).

Can. J. Chem. Downloaded from www.nrcresearchpress.com by 210.87.254.6 on 09/05/12
For personal use only.

Conditions in solution during the formation of gibbsite in dilute Al salt solutions. 4. Effect of Cl concentration and temperature and a proposed mechanism for gibbsite formation[1]

R. C. TURNER AND G. J. ROSS
Soil Research Institute, Canada Department of Agriculture, Ottawa, Canada
Received October 15, 1969

Experiments were made to determine the effect of conditions in chloride solution on the formation of gibbsite. It was found that the temperature of the systems and the chloride concentration in solution had a marked effect on the rate of all the reactions occurring. In all cases gibbsite was identified as the final product, except when the temperature was 10 °C and when the chloride concentration was about 0.6 *N*. When the temperature was 10 °C the reactions were very slow, and there was no reason to believe that gibbsite would not have been the final product if sufficient time had been allowed. In the system in which the chloride concentration was about 0.6 *N*, the final product was an aluminum hydroxychloride. In all systems the concentration of polynuclear hydroxyaluminum ions started at relatively low values, increased with time to a maximum, and then decreased, while with the solids the reverse was true. A mechanism for the formation of gibbsite is proposed.

Canadian Journal of Chemistry, 48, 723 (1970)

Can. J. Chem. Downloaded from www.nrcresearchpress.com by 210.87.254.105 on 09/05/12
For personal use only.

Introduction

It was shown in a previous publication (1) that when dilute solutions of aluminum salts were titrated with a base to about 80% neutralization, gibbsite formed after a number of weeks of reaction. It was concluded on the basis of the characteristics of the titration curves that polynuclear hydroxyaluminum cations were formed in the early stages, then gradually disappeared and gibbsite eventually crystallized. There was some indication that, even at chloride concentrations as low as 1.5×10^{-2} *M*, there was partial substitution of Cl for the OH ions in the amorphous solids which preceded the appearance of gibbsite. Later (2), it was shown that the Cl/Al mole ratio in the initial solid phase ranged from zero to 0.5, depending on the concentration of Cl ions in solution and the degree of neutralization. In the latter publication (2), it was shown that when the NaOH was added to either 10^{-2} or 10^{-3} *M* $AlCl_3$ solutions, polynuclear hydroxyaluminum cations were the main product of reactions with slow titrations, whereas the initial solid phase was the main product with fast titrations. Regardless of the rate of addition of the base, however, a solid was the only product when neutralization reached 100%.

The objectives of the work reported here were to determine the effect of (*a*) length of time of reaction on the concentrations of mononuclear and polynuclear hydroxyaluminum ions in solution, (*b*) temperature on the rate of reactions occurring, and (*c*) Cl ion concentration in solution on the formation of gibbsite in partially neutralized $AlCl_3$ solutions, when the time required to add the base was less than 15 min (fast titrations). A mechanism for the formation of gibbsite is proposed and discussed in the light of the results presented here and of other published results.

Experimental

The concentrations of $AlCl_3$ used in the experiments varied from 1.25×10^{-3} to 1.95×10^{-1} *M*. The solutions were titrated to the desired degree of neutralization by adding NaOH dropwise while NaOH–H_2SO_4–H_2O washed air was bubbled through the solutions, the time required to add the base being less than 15 min.

In the most dilute solutions the total Al concentration was 1.25×10^{-3} *M*. They were titrated to NaOH/Al mole ratios of 2.1 and allowed to react for a number of weeks in constant temperature water baths, while NaOH–H_2SO_4–H_2O washed air was bubbled slowly through the suspensions. The systems were studied at three temperatures, 26, 40, and 10 °C.

Two $AlCl_3$ concentrations were used in the systems in which the concentrations were relatively high and the systems were studied at 26 °C. The most concentrated solution was 1.95×10^{-1} *M* and it was titrated to a NaOH/Al ratio of 2.4. The other two systems used contained total Al concentrations of 5.85×10^{-2} *M*, one was titrated to a NaOH/Al ratio of 2.4 and the other to 1.5.

Samples were analyzed periodically for mononuclear and polynuclear Al ions by 8-quinolinolate extraction methods (3). The total Al in the systems less that measured as mono- plus polynuclear ions was assumed to be in the solid state. Evidence will be presented in the

[1]Contribution No. 317.

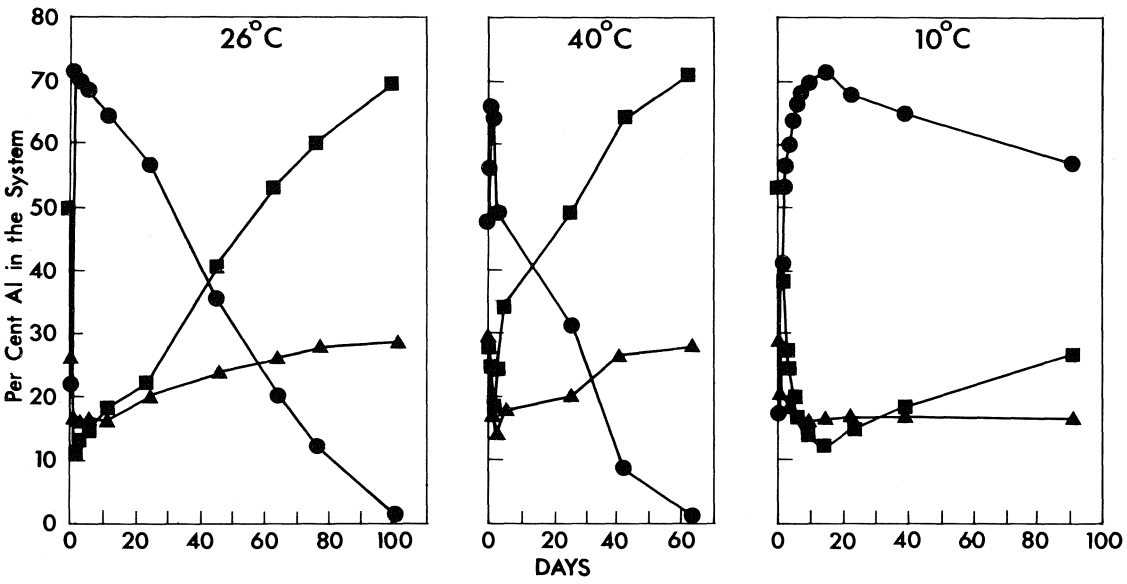

FIG. 1. Effect of temperature and length of time of aging on the concentrations of solid material, mononuclear ions, and polynuclear ions in 1.25×10^{-3} *M* solutions of $AlCl_3$ to which NaOH was added to make NaOH/Al mole ratios of 2.1. ▲, mononuclear ions; ●, polynuclear ions; ■, solids.

discussion to show that this assumption is justified at least to a good approximation.

The solids were separated from some of the solutions by filtering through 10 mμ Millipore filters under suction or by centrifugation. The solids were again suspended in H_2O (approximately 10 mg/ml) and 1 ml of suspension was placed and dried on a 37.5 by 25 mm glass slide. X-Ray analysis of these oriented samples was done with a Phillips diffractometer using Fe-filtered Co radiation (Co $K\alpha.\lambda = 1.7902$ Å).

Electron micrographs of some of the solids were also obtained. For this purpose a drop of suspension was placed on a copper grid coated with 0.25% Formvar. After 3 min, excess suspension was drawn off and the specimen was shadow-casted with platinum–iridium in an Edwards Hi Vacuum shadow caster coating unit. The specimen was then examined under a Siemens Elmiskop electron microscope.

Results

Figure 1 shows that the temperature at which the systems were maintained had a marked effect on the reactions occurring. At all three temperatures the % of the total Al in the systems that was in the form of polynuclear hydroxyaluminum ions started at relatively low values, increased with time to a maximum, and then decreased. With the solid material the reverse occurred, i.e., the amount of solid started at relatively high values, decreased to a minimum, and then increased. The effect of time on the concentrations of mononuclear Al ions was much less than with the other forms, the concentrations decreased at first to a minimum and then increased. At 26 °C the maximum and minimum for polynuclear ions and solids, respectively, was reached in from 2 to 3 days. The length of time required to reach these maxima and minima was reduced to less than one day by increasing the temperature to 40 °C, and increased to about 15 days by reducing it to 10 °C. During this stage of the reactions, i.e., until the minima in solids were reached, the solids were amorphous to X-rays. The effect of temperature was even more pronounced after these maxima and minima were reached. When the temperature was 26 °C the concentration of polynuclear hydroxyaluminum ions decreased to essentially zero in about 100 days. At this time the solid showed the X-ray pattern for gibbsite and the amount of solid, calculated from the % of total Al in the system in the solid form, accounted for essentially all of the base added, assuming that the solid could be represented by the formula $Al(OH)_3$. The results at 40 °C were the same as those at 26 °C, except that it required only 60 days for the concentration of polynuclear ions to reach essentially zero. At 10 °C, however, the concentration of polynuclear ions decreased much more slowly so that after 90 days the amount

Can. J. Chem. Downloaded from www.nrcresearchpress.com by 210.87.254.105 on 09/05/12
For personal use only.

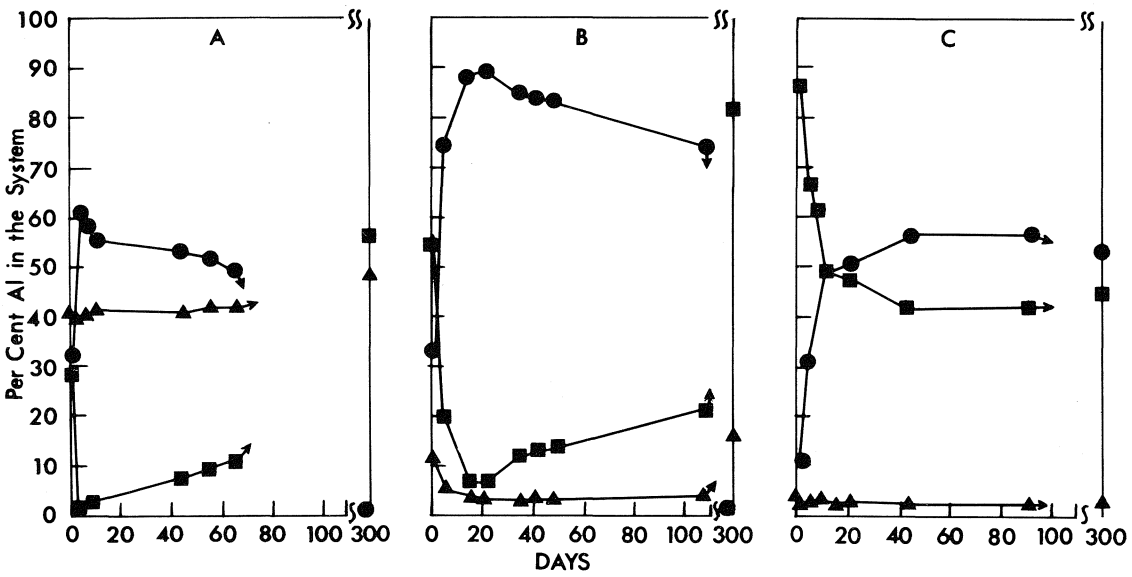

FIG. 2. Effect of Cl^- concentration in solution, NaOH/Al mole ratio, and length of time of aging on the concentration of solid material, mononuclear ions, and polynuclear ions in partially neutralized $AlCl_3$ solutions at 26 °C. Section *A*, total Al 5.85×10^{-2} *M*, NaOH/Al 1.5; *B*, total Al 5.85×10^{-2} *M*, NaOH/Al 2.4; *C*, total Al 1.95×10^{-1} *M*, NaOH/Al 2.4. ▲, mononuclear ions; ●, polynuclear ions; ■, solids.

of Al in the form of polynuclear ions was still much greater than in the solid form and the solid was amorphous to X-rays. It was obviously going to require a very long time at this low temperature for the formation of gibbsite.

When the total concentration of Al in the systems was 5.85×10^{-2} *M* and the systems were maintained at 26 °C (sections *A* and *B*, Fig. 2) the reactions were similar to those that occurred at the lower concentration with the same temperature (Fig. 1) but the length of time required for the reactions was greater. When the OH/Al mole ratio was 1.5 (section *A*),the % of total Al in the solid decreased to a minimum of less than 1, whereas when the OH/Al ratio was 2.4 (section *B*), the minimum for Al in the solid was about 6% of the total Al. After the minima and maxima were reached the % of total Al in the solid increased, while that in the form of polynuclear ions decreased very slowly, so that it required 300 days for the concentration of polynuclear ions to reach zero. At this time the solids showed distinct X-ray patterns of gibbsite and essentially all of the base added could be accounted for in the solids, assuming that they could be represented by the formula $Al(OH)_3$.

With the highest concentration of $AlCl_3$, 1.95×10^{-1} *M*, the reactions (section *C*, Fig. 2) were essentially different from those with the lower concentrations at the same temperature. Although the percentage of total Al of the system in the polynuclear ions and solid forms started at low and high values and then increased and decreased to maximum and minimum values, respectively, as they did at the lower concentrations, it required a long time to reach these maximum and minimum values. In fact, the rate of change of concentration of the two forms was so slow that it was impossible to determine the length of time required to reach the maximum and minimum but it was apparently between 40 and 90 days. The decrease in the concentration of polynuclear ions and increase in solids after the maximum and minimum were reached was very slow so that after 300 days, there was still more Al in the form of polynuclear ions than in the solids. Furthermore, although the solids present after 300 days were not amorphous to X-rays, they did not show the gibbsite pattern. The X-ray pattern from the oriented specimen of the solid showed a prominent symmetrical peak with the apex at 13.77 Å when the relative humidity of the atmosphere in contact with the sample was 95%. The position of the diffraction peak was very sensitive to the relative humidity, however, so that when the relative humidity was reduced to

Can. J. Chem. Downloaded from www.nrcresearchpress.com by 210.87.254.105 on 09/05/12
For personal use only.

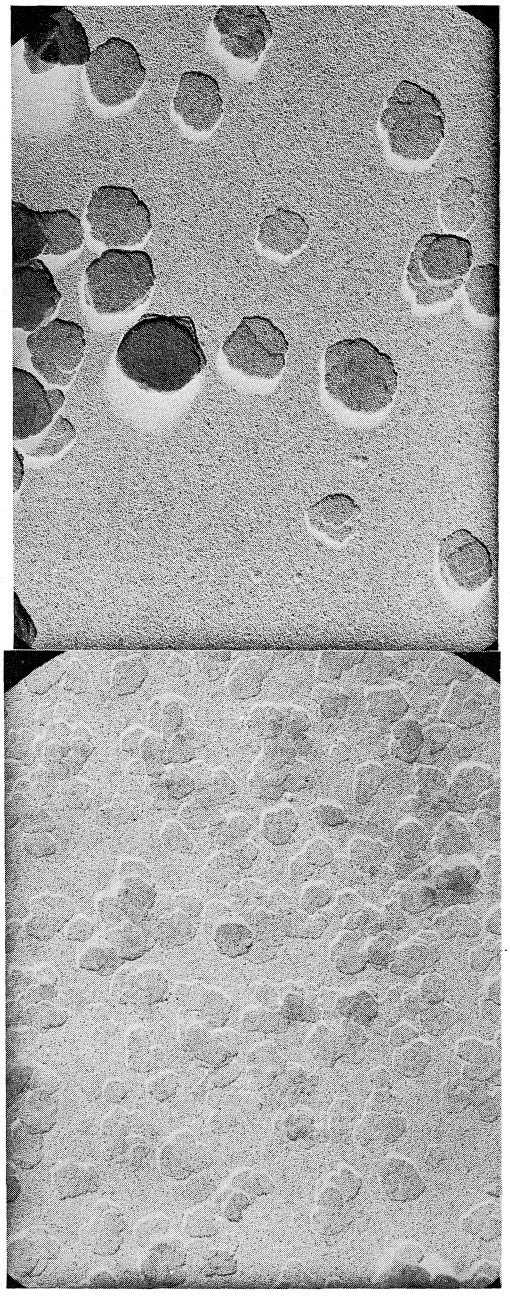

FIG. 3. Electronmicrographs of gibbsite crystals. Upper section, formed in a system with NaOH/Al 1.5; lower section, formed in a system with NaOH/Al 2.4.

15%, the peak shifted, making the apex appear at 10.69 Å. The Cl/Al mole ratio in the solid at this time was 0.4.

Electronmicrographs of the gibbsite crystals formed in the two systems with total Al concentration of 5.85×10^{-2} (Fig. 2) are shown in Fig. 3. They show that the gibbsite crystals from the system in which the NaOH/Al mole ratio was 1.5 (upper section) were much larger than those from the system in which this ratio was 2.4 (lower section). An estimate of the average volume of the crystals in each of the sections made from the area of the basal planes of individual crystals and the length of the shadows showed that the crystals in the upper section had approximately 2×10^6 unit cells while those in the lower section were about 1/10 this size.

Discussion

It has been shown (2) that, with unaged partially neutralized $AlCl_3$ where it was possible to measure the Al in the initial solid phase as well as in the mono- and polynuclear ions, the total Al in the system was equal to the sum of the Al in the three forms. In these unaged systems, however, the separation of the solids from the solution by filtration through 10 mμ Millipore filters was essentially quantitative, whereas after the systems were aged for a few hours or days, depending on conditions, a variable fraction of the solid passed through the filters. It was necessary, therefore, to have some other means of testing the assumption that the total Al in the systems less that measured in the mono- plus polynuclear ions was in the solids. This was done by comparing the amount calculated in this way with that which was non-dialyzable. It was found that the amount of Al in the solid form determined in the two ways agreed reasonably well. Consequently, the assumption that the total Al in the systems less that in the form of mono- and polynuclear ions was in the solids is correct to a good approximation, regardless of the length of time of aging. This conclusion is also in agreement with results of Smith (4).

It is obvious from the results just discussed and those presented in Figs. 1 and 2 that the initial solid phase consists of relatively large particles (greater than 10 mμ in diameter), and that the size of the particles as well as the quantity of solid present decreases in the early stages of aging. The decrease in particle size in the early stages of aging was also indicated by the results published by Fripiat and Pennequin (5). As indicated previously (3), it is only the initial solid phase that reacts fairly rapidly with 8-quinolinol.

Can. J. Chem. Downloaded from www.nrcresearchpress.com by 210.87.254.105 on 09/05/12
For personal use only.

Can. J. Chem. Downloaded from www.nrcresearchpress.com by 210.87.254.105 on 09/05/12
For personal use only.

It was pointed out there that only a fraction of the solid resulting from 24 h aging was destroyed by the 8-quinolinol in the time required to dissolve the unaged solid completely. It appears, therefore, that the properties of the solid begin to change immediately after it is formed.

The results presented above for relatively high salt concentrations are very enlightening. According to Gastuche and Herbillon (6) and Fripiat and Pennequin (5), the solid phase that forms first on the addition of a base to an $AlCl_3$ solution contains Cl substituting for OH ions and considerable H_2O which prevents or retards the crystallization of gibbsite. They found, however, that if the Cl ions are removed from the solution quickly enough after the addition of the base, gibbsite crystallizes fairly rapidly. This is obviously because the Cl ions must be replaced by the OH ions before gibbsite can result. It should be expected that the ease with which the Cl ions are eliminated from the particles would be a function of the Cl^- concentration in solution, and it is reasonable to assume that there should be a concentration above which this cannot occur. The results in sections *A* and *B* of Fig. 2 show that this elimination of Cl^- from the particles occurred even when the Cl^- concentration in solution was about 0.18 *M* because gibbsite was formed, but the process was much slower than at the lower concentrations (Fig. 1) and much slower than when Cl^- was removed by dialysis (5). When the Cl^- concentration was raised to 0.6 *M*, however, the chloride was not eliminated from the particles and a material containing chloride which was probably approaching crystalline aluminum hydroxychloride because it showed a strong X-ray diffraction band with peak at 13.77 Å (7), rather than gibbsite, resulted. Thus, these experimental results agree qualitatively with those of Gastuche and Herbillon (6) and Fripiat and Pennequin (5), but show in addition that gibbsite will form in acid aqueous chloride solutions even when the Cl^- concentration is as great as 0.18 *M*.

The hydroxyaluminum material in the form of polynuclear ions, unlike the solid material, seems always to be the same regardless of the conditions under which it is formed. In all of the experiments for which results are reported above and in special experiments in which Cl^- was replaced with I^-, NO_3^-, or ClO_4^- in the systems, the first order rate constant for the reaction between the polynuclear ions and the 8-quinolinol mixture (3) was determined at 26 °C. It was found that this rate constant was independent of the temperature at which the polynuclear ions were formed, length of time of aging after the first few hours, degree of neutralization, the kind of anion present, and whether the concentration of the ions was increasing or decreasing when the samples were taken, providing the composition and concentration of the 8-quinolinol reaction mixture was kept constant. From the work of Brosset (8) and Brosset *et al.* (9) it appears probable that a specific polynuclear hydroxyaluminum cationic species with formula $Al_6(OH)_{15}^{3+}$ is formed in partially neutralized aqueous solutions of Al salts, unless the anion present forms a strong complex with Al. The results of Matijevic *et al.* (10) agree with this except that they found that the cation had a charge of 4 with $Al_8(OH)_{20}^{4+}$ as the probable formula. Regardless of which of these species is the one that actually exists, providing only one exists, the rate constant for the reaction between the polynuclear ions and a specific 8-quinolinol reaction mixture should always be the same at constant temperature, which agrees with the results from the present investigation. If, on the other hand, the polynuclear ions had a variable composition and increased in size and OH/Al ratio as they progressed towards gibbsite, the rate constant for the reaction between them and 8-quinolinol should change with length of time of aging as well as with degree of neutralization, which is contrary to experimental results. Furthermore, Gastuche and Herbillon (6) and Fripiat and Pennequin (5) showed that gibbsite forms under conditions in which the polynuclear ions as well as Cl^- are removed by dialysis as fast as they are formed. Thus the theory that the mechanism by which gibbsite is formed is a polymerization process involving these hydroxyaluminum polynuclear cations (11–13) is not consistent with experimental facts. This brings up the question of a mechanism which is consistent with experimental facts.

Summarizing these results, it has been shown that there is an initial solid phase when a base is added to an $AlCl_3$ solution (3, 5, 6), which decreases in quantity (3) and size of particles (5) during the early stages of aging, while the concentration of hydroxyaluminum polynuclear ions increases. This is followed by an increase in

quantity and particle size of the solid and decrease in the concentration of polynuclear ions. In addition, rate of reaction determinations indicate a single species of polynuclear ions. Consequently, the following mechanism is proposed, in which it is assumed that the polynuclear ions have the formulae $Al_6(OH)_{15}^{3+}$ (9) and that Cl^- is the extraneous anion. The treatment would be essentially the same if it was assumed that the formula of the polynuclear ions was $Al_8(OH)_{20}^{4+}$ (10) or even $Al_{13}(OH)_{32}^{7+}$ (14).

The most rapid reaction that occurs when the base is added is

$$[1]\quad Al.6H_2O^{3+}Cl_3^- + n\text{NaOH} = \textit{Al(OH)}_n\textit{Cl}_{3-n}\textit{.3H}_2\textit{O} + n\text{NaCl} + 3H_2O$$

where italics denote solid. This initial solid phase contains considerable H_2O and Cl^-. It is much more soluble than gibbsite and is metastable relative to the hydroxyaluminum polynuclear cations, which form more slowly. Consequently, a competing but slower reaction

$$[2]\quad 6\,Al.6H_2O^{3+}Cl_3^- + 15\,\text{NaOH} = Al_6(OH)_{15}^{3+}Cl_3^- + 15\,\text{NaCl} + 36H_2O$$

occurs simultaneously. Because the polynuclear ions are stable with respect to the initial solid, reaction [1] goes to the left, i.e., the initial solid phase begins to dissolve as the formation of the polynuclear ions progresses. Besides these two competing reactions, there is another one which is a consecutive reaction with respect to reaction [1]. This third is a solid phase reaction in which the initial solid phase, through elimination of Cl^- and H_2O and rearrangements, eventually becomes gibbsite. Gibbsite, besides being much more insoluble than the initial solid phase, is also stable with respect to the polynuclear Al ions. The original reactant and final products are shown by the reaction

$$[3]\quad \textit{Al(OH)}_n\textit{Cl}_{3-n}\textit{3H}_2\textit{O} = \textit{Al(OH)}_3 + (3-n)\,\text{HCl} + nH_2O$$

where $Al(OH)_3$ represents gibbsite. This reaction does not go in a single step. It represents a gradual process with the solid becoming less and less soluble as Cl^- and H_2O are eliminated and rearrangements towards the gibbsite structure occur. At some stage in these processes the solid becomes stable with respect to the polynuclear ions and reaction [2] goes to the left, i.e., the concentration of the polynuclear ions begins to decrease as the solid particles begin to grow.

If this mechanism is correct, the maximum number of gibbsite crystals finally resulting in a system is determined by the number of solid particles present when the amount of solid in the system reaches a minimum (Figs. 1 and 2). It is possible, of course, unless all of the particles are exactly the same and grow at the same rate, that during aging some of the smaller particles might disappear in the aging process, which would result in a smaller number of gibbsite crystals than of solid particles at the time of minimum solid present. This decrease in particles through dissolution should be minimized and probably prevented as long as polynuclear ions, rather than the most soluble particles, control the ion activity product $(Al)(OH)^3$ in solution, which would be the case as long as these ions are present. It can be seen that when the NaOH/Al ratio of the 5.85×10^{-2} *M* Al systems was 1.5 (section *A*, Fig. 2), the minimum of solid present was less than 1%, whereas when the NaOH/Al ratio was 2.4 (section *B*, Fig. 2), the minimum of solid represented from 6 to 7% of the Al. Thus, if the number of gibbsite crystals present when the polynuclear ions became zero were greatly influenced by the amount of solid present at its lowest value, it would be expected that the gibbsite crystals would be less numerous and larger in the system with the lower NaOH/Al ratio than in the one with the higher ratio. This agrees with results shown in Fig. 3.

It is apparent that all of the results presented in this paper are consistent with the proposed mechanism. Gastuche and Herbillon (6) and Fripiat and Pennequin (5) showed that there is an initial solid phase which contains considerable H_2O and Cl^- ions and that when the dialyzable material was separated from the aqueous suspension, gibbsite resulted fairly rapidly. Frink and Sawhney (15) showed that the initial solid is much more soluble than gibbsite and this was supported by other published work (1). Brosset *et al.* (9) and Matijevic *et al.* (10) presented fairly strong evidence that there is only one species of hydroxyaluminum polynuclear cation. Furthermore, it is known that dilute solutions of $AlCl_3$ can be stored at room temperature without having gibbsite formed even though such solutions, at concentrations for instance, 10^{-4} to 10^{-2} *M*, are supersaturated with respect to

Can. J. Chem. Downloaded from www.nrcresearchpress.com by 210.87.254.105 on 09/05/12
For personal use only.

Can. J. Chem. Downloaded from www.nrcresearchpress.com by 210.87.254.105 on 09/05/12
For personal use only.

gibbsite (16). These solutions, however, are undersaturated with respect to the initial solid phase which forms when the ion activity product $(Al)(OH)^3$ is raised to about $10^{-31.7}$ (1, 15). Therefore, there is considerable experimental evidence in support of the proposed mechanism. It is necessary, however, to show that the mechanism also gives a logical explanation of experimental results that have been used to support other proposed mechanisms.

Ruff and Tyree (12) found by a light scattering technique that the average molecular weight of the products of hydrolysis increased with increasing NaOH/Al mole ratios. They filtered their solutions through fritted filters. As demonstrated by the fact that there was no loss of Al by the filtration, this did not remove the solid particles. They also showed that the turbidity at a given total Al concentration and NaOH/Al ratio decreased considerably with time of aging from 1 to 181 h. This means that the mean molecular weights calculated from these results must have decreased considerably with time for the first few days. Since the solid particles are much larger than the polynuclear cations, the average molecular weights would decrease as the ratio of solid to polynuclear ions decreases. Consequently, their results on the effect of aging can be interpreted to be consistent with those presented in Figs. 1 and 2, which show that the ratio of solid to polynuclear ions decreased with time for the first few days. In the same way, their results showing that the average molecular weights increased with increasing NaOH/Al ratios when the partially neutralized solutions were aged can be explained on the basis that as the NaOH/Al ratio is increased, the ratio of solid to polynuclear ions also increases (Fig. 2).

Finally, Hsu and Bates (11) proposed a system of polymerization of hydroxyaluminum cations for the formation of gibbsite which requires that the NaOH/Al mole ratio be increased to 3 in chloride solutions for gibbsite to form. Their theory requires that the polynuclear charged particles increase in size and that their OH/Al ratio increases as the NaOH/Al ratio is increased. These requirements are contrary to considerable experimental evidence: (*a*) the rate constant for the reaction between the polynuclear ions and 8-quinolinol is independent of the NaOH/Al ratio, (*b*) gibbsite forms even when the NaOH/Al mole ratio is as low as 1.5 (Fig. 2, section *B*), (*c*) Matijevic *et al.* (10) and Brosset *et al.* (9) concluded that a single species of polynuclear ions existed over a wide range of *pH* values. The fact that Hsu and Bates could not centrifuge any solid from their solutions, even with an ultracentrifuge, does not contradict the proposed mechanism because gibbsite did not form in these systems. It is quite possible that the techniques they used for partially neutralizing the $AlCl_3$ solutions resulted in reaction [1] going entirely to the left, i.e., that all of the Al in the system was in the form of mono- and polynuclear cations after a certain length of time of aging.

The authors thank N. M. Miles for the X-ray diffraction analysis, M. Jaakkamainen for the analysis of the solids for Cl^-, and S. Itz for the electronmicrographs of the gibbsite crystals.

1. R. C. Turner. Soil Sci. **106**, 338 (1968).
2. R. C. Turner and G. J. Ross. Can. J. Soil Sci. **49**, 389 (1969).
3. R. C. Turner. Can. J. Chem. **47**, 2521 (1969).
4. R. W. Smith. Ph.D. Thesis, Stanford University, Stanford, California. 1969.
5. J. J. Fripiat and M. Pennequin. Bull. Soc. Chim. Fr. 1655 (1965).
6. Marie-Claire Gastuche and A. Herbillon. Bull. Soc. Chim. France, 1404 (1962).
7. L. W. Levy and H. Breuil. C. R. **225**, 1744 (1962).
8. C. Brosset. Acta Chem. Scand. **6**, 910 (1952).
9. C. Brosset, G. Biedermann, and L. G. Sillen. Acta Chem. Scand. **8**, 1917 (1954).
10. E. Matijevic, K. G. Mathai, R. H. Ottewill, and M. Kerker. J. Phys. Chem. **65**, 826 (1961).
11. Pa Ho Hsu and T. F. Bates. Miner. Mag. **33**, 749 (1964).
12. J. K. Ruff and S. Y. Tyree. J. Amer. Chem. Soc. **80**, 1523 (1958).
13. F. G. R. Gimblett. Inorganic polymer chemistry. Butterworth and Co., London. 1963.
14. J. Aveston. J. Chem. Soc. 4438 (1965).
15. C. R. Frink and B. L. Sawhney. Soil Sci. **103**, 144 (1967).
16. C. R. Frink and M. Peech. Inorg. Chem. **2**, 473 (1963).

Can. J. Chem. Downloaded from www.nrcresearchpress.com by 210.87.254.6 on 09/05/12
For personal use only.

Perhaloketones. XX.[1] A monoenophilic perchlorinated cage ketone

EVERETT E. GILBERT
Specialty Chemicals Division, Allied Chemical Corporation, Morristown, N.J. 07960

Received July 31, 1969

Ketone **4** reacted thermally with a series of terminal alkenes, forming unsaturated alcohols of type-**1**. The failure of **4** to react with internal or cyclic alkenes, with some alkenes at multiple ratios, or to more than a limited extent with the pendant vinyl groups of polybutadiene, suggests a high degree of steric inhibition in this reaction compared with hexafluoroacetone. Several allyl ethers formed tetrahydrofuran derivatives (type-**2**). 4-Allylanisole uniquely formed a type-**1** product thermally convertible to type-**2**. Type-**2** derivatives could also be obtained from *sym*-tetrafluorodichloroacetone, but not from diethyl oxomalonate.

Canadian Journal of Chemistry, **48**, 730 (1970)

Ketones with highly electropositive carbonyl carbon atoms, such as carbonyl cyanide (1), diethyl oxomalonate (2, 3), hexafluoroacetone, and similar fluorinated ketones[2] (4, 5) react thermally with alkenes containing allylic hydrogen atoms forming tertiary alkenols of type-**1**. Tetrahydrofuran ring formation (type-**2**) has also been noted (4), and photochemical activation yields oxetanes (type-**3**) (2, 3, 6):

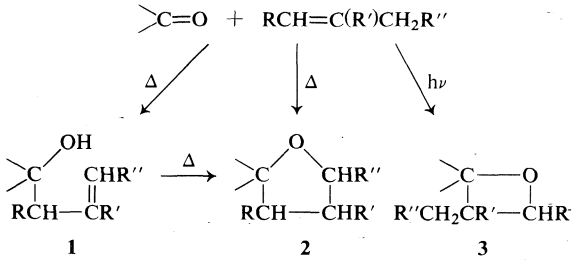

1 **2** **3**

Ketone **4** (1,1*a*,3,3*a*,4,5,5,5*a*,5*b*,6-decachlorooctahydro - 1,3,4 - metheno - 2H - cyclobuta[*cd*]-pentalen-2-one, also known as decachloropentacyclo[5.3.0.$0^{2,6}$.$0^{4,10}$.$0^{5,9}$]decan - 3 - one[3]) has been shown in work at this laboratory (7)

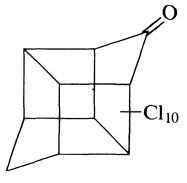

4

to have a highly electropositive carbonyl carbon atom, but one which, in the reactions studied, is considerably less electropositive than that in hexafluoroacetone. We have also found[4] that reaction with alkenes is progressively less facile as the fluorine atoms in hexafluoroacetone are replaced stepwise by chlorine. It has likewise been noted (8) that steric effects in this type of reaction are significant. These considerations suggested that the reactivity of **4** with alkenes might be quite limited; the present study was undertaken to explore this question.

It was in fact found that **4** reacts readily with terminal alkenes at 1:1 molar ratio, forming alkenols of type-**1** (R = H), as summarized in Table 1. The yields in many cases are good, and in the one case where the reaction rate was considered (α-methylstyrene), such was found to be quite rapid at the temperature used (ca. 140°). Of the substrates listed in Table 1, all are terminal alkenes except 1-methylcyclohexene and 1-methylcycloheptene. It is known, however, that 1-methylcycloalkenes are in equilibrium with the corresponding methylenecycloalkanes in the presence of acid (9). It seems possible that such an equilibrium could be induced in our case by the presence of the highly electrophilic carbonyl carbon atom of the perhaloketone, especially under the fairly drastic reaction conditions used. Ketone **4** was in fact found to form identical products from 1-methylcyclohexene and methylenecyclohexane, a result similar to that noted in another study at this laboratory using hexafluoroacetone[5] with the same alkenes. Others (5) have

[1]Perhaloketones. XIX. See ref. 13.
[2]Allied Chemical Corporation, unpublished research data.
[3]Sometimes referred to as "Kepone", which is a registered trademark of Allied Chemical Corporation applying to **4** only when used in insecticidal or acaricidal formulations.
[4]Allied Chemical Corporation, unpublished research data.
[5]Allied Chemical Corporation, unpublished research data.

Can. J. Chem. Downloaded from www.nrcresearchpress.com by 210.87.254.6 on 09/05/12
For personal use only.

TABLE 1

Reaction of **4** with alkenes

Substrate	Reaction time (h)*	Yield (%)†	Melting point (°C)	Product type	Calcd. (%)			Found (%)		
					C	H	Cl	C	H	Cl
1-Heptene	48	95	25	**1**	34.6	2.4	—	34.8	2.5	—
10-Undecenoic acid	24	82	138	**1**	37.4	3.0	—	37.5	3.0	—
Methyl 10-undecenoate	24	95	Oil‡	**1**	—	—	—	—	—	—
Methylenecyclohexane	20	20	125	**1**	34.8	2.0	—	34.7	2.2	—
1-Methylcyclohexene	24	7	—§	**1**	—	—	—	—	—	
1-Methylcycloheptene	20‖	95	108	**1**	36.0	2.5	59.1	36.2	2.5	59.2
Allylcyclohexane	96	90	190	**1**	37.2	2.6	57.8	37.5	2.5	57.7
Allylbenzene	24	75	174	**1**	37.5	1.7	58.4	37.1	1.7	58.1
α-Methylstyrene	1	75¶	248¶	**1**	—	—	58.4	—	—	58.6
1-Allyl-3,4-methylenedioxybenzene	24	62**	178	**1**	36.8	1.5	54.5	37.0	1.7	54.4
4-Allylanisole	24	86††	148	**1** and **2**	37.6	1.7	55.5	37.7	1.4	55.2
4-Allylanisole	72	95	173	**2**	37.6	1.7	55.5	37.7	1.9	55.5
Diallyl ether	24	39	95	**2**	32.6	1.7	60.3	32.7	1.7	60.1
Allyl phenyl ether	96	20‡‡	145	**2**	36.5	1.6	—	36.3	1.4	—
Allyl *o*-tolyl ether	120	75§§	—§§	**1** and **2**	37.6	1.9	—	37.8	1.8	—
Allyl *p*-tolyl ether	96	63	155	**2**	37.6	1.9	—	37.6	2.1	—
Allyl 2,4-dichlorophenyl ether	96	18	269	**1**	32.9	1.2	—	32.8	1.2	—
Polybutadiene‖ ‖	24	84	Rubber	**1**	—	—	—	—	—	33.5[a]
Polybutadiene¶¶	72	52	Rubber	**1**	—	—	—	—	—	48.4[b]

*All runs made in refluxing xylene (ca. 140°), except as indicated.
†Mole% crude product based on **4** used; in some cases unreacted **4** was recovered.
‡Saponified with alcoholic potassium hydroxide to the free acid, which was shown identical to that prepared directly from **4** and 10-undecenoic acid.
§Shown to be identical with the derivative of **4** with methylenecyclohexane.
‖Prepared in refluxing *o*-dichlorobenzene (ca. 180°).
¶The yield was 87% after 8, 24, and 44 h. The products were always intractable mixtures of hydroxy compounds, of which the highest melting point observed was that given.
**Yield 96% after 100 h.
††Obtained 45% type-**1** product, m.p. 148°, and 41% type-**2**. Type-**1** was converted to type-**2** after 24 h.
‡‡Yield 0% after 24 h.
§§Obtained 15% type-**1** product, m.p. 210°, and 60% type-**2**, m.p. 160°. Type-**1** could not be converted to type-**2** by heating 48 h at 180°.
‖ ‖Contains 20% pendant vinyl groups.
¶¶Contains over 95% pendant vinyl groups.
[a]Corresponds to reaction of **4** with about 50% of the pendant vinyl groups.
[b]Corresponds to reaction of **4** with about 22% of the pendant vinyl groups.

TABLE 2

Reaction of *sym*-tetrafluorodichloroacetone with allylic compounds

Substrate	Reaction time (h)*	Yield		Boiling point °C, (mm)	Structure type	Calcd. (%)		Found (%)	
		Crude	Distilled†			C	H	C	H
α-Methylstyrene	72	93	32	141–145 (10)	**1**‡	45.5	3.2	45.8	3.0
4-Allylanisole	144	91	—	122–124 (0.5)	**2**	45.0	3.5	45.3	3.4
Allyl phenyl ether	310	67	25	164–168 (20)	**2**	43.4	3.0	43.6	3.2
Diallyl ether	144	97	45	98–102 (10)	**2**	36.3	3.4	36.0	3.2

*Reaction temperature 45 to about 100°.
†Mole % based on substrate reacted.
‡Could not be converted to a type-2 compound by refluxing for 90 h in xylene (ca. 140 °C).

also noted alkene isomerization during reaction with hexafluoroacetone.

Internal open-chain alkenes and cycloalkenes react with hexafluoroacetone, but much less easily than terminal alkenes[5] (5, 8). It is therefore not surprising that **4** did not react with 3-heptene, even though it gave an excellent yield with 1-heptene. Cyclooctene and cyclododecene likewise did not react with **4**, in the latter case even when raising the reaction temperature from 140 to 180°.

Hexafluoroacetone and the related fluorochloroacetones will react with some alkenes at 2:1 or even 3:1 molar ratio[5] (5, 10). However, there was no evidence in the present study that **4** reacted at other than 1:1 molar ratio. Efforts to obtain such derivatives from α-methylstyrene and from diallyl ether were unsuccessful.

The reactivity of **4** with terminal alkenes in general, suggested that it might also combine with the pendant vinyl groups present in polybutadiene as the result of 1,2-diene addition. As shown in Table 1, about 50% of such groups reacted in 24 h in a polymer containing 20% pendant vinyl groups, compared with about 22% in 72 h for one containing over 95%. In contrast, hexafluoroacetone was found to react with all of the pendant groups, even at 100°, in a polybutadiene containing 75% of them[6] (11). This provides a graphic illustration of the lower reactivity and/or higher steric requirement in this reaction of **4** compared to hexafluoroacetone.

Products of structural type-**1** gave infrared (i.r.) spectra with the expected hydroxyl group at 3500 cm^{-1}, and with olefinic unsaturation at 1600 and 1650 cm^{-1}. The nuclear magnetic resonance (n.m.r.) spectra also agree with **1**. In several cases, however, **4** formed products in which both of these groups were absent. This was noted with four allyl ethers (cf. Table 1). 4-Allylanisole similarly gave a product of type-**2** after a reaction time of 72 h, but in 24 h formed one of type-**1** which could be converted to the other isomer on further heating.

Gambaryan *et al.* (4) suggested that one of the products they obtained from the reaction of methyl allyl ether with hexafluoroacetone contained a tetrahydrofuran ring of type-**2**, although they cite no experimental proof. Our n.m.r. spectra do indeed substantiate tetrahydrofuran ring formation, not only from **4**, but also from tetrafluorodichloroacetone, as shown in Table 2. The spectral data also rules out the formation of oxetane rings of type-**3**.

Those authors hypothesize the formation of the type-**2** product from type-**1**, although this was not demonstrated, and in fact, they were unable to isolate any type-**1** material from their reaction mixture. We have found that the type-**1** product from **4** and 4-allylanisole is converted to **2** upon further heating. However, the type-**1** derivative from **4** and allyl *o*-tolyl ether could not be converted to the ring compound even by heating at 180° for 48 h. Since both types of compounds appear in the reaction mixture obtained under milder conditions (cf. Table 1), it is concluded that in this case at least, **1** is not the precursor for **2**.

As indicated in Table 1, only type-**2** compounds were isolated from the reaction of **4** with three allyl ethers (diallyl ether, allyl phenyl ether, and allyl *p*-tolyl ether). On the other hand, allyl *o*-tolyl ether gave a 1:4 mixture of **1** and **2**, and allyl 2,4-dichlorophenyl ether gave only type-**1**. It therefore seems possible that increasing steric

[6]Allied Chemical Corporation, unpublished research data.

Can. J. Chem. Downloaded from www.nrcresearchpress.com by 210.87.254.6 on 09/05/12
For personal use only.

Can. J. Chem. Downloaded from www.nrcresearchpress.com by 210.87.254.6 on 09/05/12
For personal use only.

hindrance in the *ortho* position of the benzene ring may interfere with tetrahydrofuran ring formation. However, this conclusion should be taken with reservation, since the allyl ethers (unlike most of the other alkenes) gave product mixtures.

The fact that 4-allylanisole gave products of both types with **4** suggested that other allylbenzene derivatives might behave similarly. Only type-**1** products could be obtained, however, from allylbenzene or from 1-allyl-3,4-methylenedioxybenzene (safrole). The conditions used involved longer times of reaction (70 and 100 h, respectively) at the usual temperature, as well as heating the corresponding type-**1** products at 180° for 24 h. As noted in Table 2, 4-allylanisole also forms a type-**2** derivative with tetrafluorodichloroacetone. An unsuccessful effort was made to convert the only type-**1** derivative of this ketone (made from α-methylstyrene) to a type-**2** compound. It seems possible that facile formation of tetrahydrofuran rings uniquely from 4-allylanisole may result from unusual stabilization of the carbonium ion by conjugation of the ether oxygen with the benzene ring:

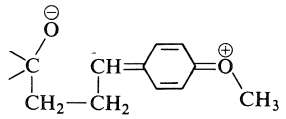

Baddeley *et al.* (12) have emphasized that the formation of such quinoid structures is quite responsive to the oxygen–carbon bond angle. Possibly for this reason safrole is unable to undergo conjugation and therefore to form a type-**2** product.

Since **4**, hexafluoroacetone and tetrafluorodichloroacetone can form type-**2** products, an effort was made to obtain such from diethyl oxomalonate. Only type-**1** derivatives of this compound have been reported in the studies made to date of its monoenophilic reactions (1, 2, 3). However, only type-**1** derivatives were obtained by us even after prolonged heating with 4-allylanisole, 1-allyl-3,4-methylenedioxybenzene, or α-methylstyrene. Unsuccessful efforts were also made to catalyze ring closure by heating in the presence of toluenesulfonic acid. No published reports were noted on the reaction of diethyl oxomalonate with allyl ethers, and an effort on our part to achieve this with allyl phenyl ether resulted in no reaction. A steric problem does not appear to be involved, since diethyl oxomalonate reacts easily with internal alkenes and cycloalkenes, and forms oxetanes (type-**3**) in good yields in the presence of light.

Experimental

Melting points were taken in capillary tubes on a Mel-Temp block and are uncorrected. The proton n.m.r. spectra were obtained on a Varian Associates Model A-60 Spectrometer with tetramethylsilane as internal reference. Infrared spectra were taken on a Perkin–Elmer Infracord. Tetrafluorodichloroacetone and hydrated ketone **4** were obtained from B & A Chemicals Dept., Allied Chemical Corporation, Morristown, N. J. Ketone **4** can be further purified by recrystallization from methanol (7).

General Procedure for Syntheses

The following general procedure was employed to prepare the compounds listed in Table 1. A mixture of purified **4** tetrahydrate (11.5 g, 0.02 mole) and xylene (75 ml) was heated to reflux and slowly distilled over about 30 min to remove 25 ml, including the water of hydration. The alkene (0.04 mole) was added to the resulting xylene solution of anhydrous **4**, and the mixture was refluxed for the stated time. The solution was then cooled to partially crystallize any unreacted **4**, which was filtered. (It is easily identified by its melting point, 355° (decomposition), its high solubility in methanol and in hot 3% aqueous sodium hydroxide, and its i.r. spectrum with carbonyl absorption at 1800 cm^{-1}.) The filtrate was evaporated to dryness *in vacuo* to remove solvent and excess alkene. The residue was next freed of any remaining **4** by trituration with cold methanol, or, in some cases by extraction with three successive 50 ml portions of boiling 3% aqueous sodium hydroxide. The product was finally recrystallized from methanol, hexane, or methylcyclohexane.

o-Dichlorobenzene (b.p. 180°) was substituted for xylene as the reaction solvent with cyclododecene and with 1-methylcycloheptene. The samples of polybutadiene were reacted with **4** in the usual manner with xylene as solvent, employing **4** equimolar with the pendant vinyl content of the polymer. Unreacted **4** was extracted from the reaction mixture with three 100 ml portions of boiling 3% aqueous sodium hydroxide. No solvent was employed when using tetrafluorodichloroacetone (b.p. 45°). Equimolar quantities of ketone and alkene were refluxed at gradually increasing temperature as the reaction proceeded (cf. Table 2), and the reaction mixture was then distilled *in vacuo*.

Spectral data on the type-**1** product from **4** and 4-allylanisole: n.m.r. ($(D_3C)_2CO$) δ 7.3 (d,2,aromatic), 6.85 (d,2,aromatic), 6.30 (m,2,CH=CH), 5.80 (s,1,OH), 3.75 (s,3,OCH_3), 2.60 (d,2,OCH_3); i.r. (KBr) 3510 (OH), 1630 (C=C), 1595 and 1498 (phenyl ring), 1350 (δ OH), and 965 cm^{-1} (δ CH *trans* configuration). The other type-**1** products similarly showed OH and C=C groups in the i.r. spectra. The type-**2** derivative from tetrafluorodichloroacetone and 4-allylanisole gave n.m.r. (CCl_4) δ 6.8–7.2 (quartet,4,aromatic), 5.2 (quartet,1,CH), 3.7 (s,3,OCH_3), 2.2–2.7 (m,4,—CH_2CH_2—). The type-**2**

derivative from **4** and 4-allylanisole similarly gave an n.m.r. spectrum showing the presence of the tetrahydrofuran ring. The i.r. spectra showing the absence of OH and C=C was noted with all the type-**2** compounds.

Diethyl Oxomalonate-alkene Reactions

Diethyl oxomalonate (3.5 g, 0.02 mole), 1-allyl-3,4-methylenedioxybenzene (safrole) (3.2 g, 0.02 mole), and xylene (25 ml) were refluxed for 72 h. Removal of the solvent *in vacuo* gave 4.5 g (67%) of a yellow oil which solidified on standing. Recrystallization from isopropanol gave diethyl 3-(3′,4′-methylenedioxyphenyl) allyl hydroxymalonate, m.p. 62°; i.r. (Nujol mull) 1600 (C=C), 1740 (ester CO), 3550 cm^{-1} (OH).

Anal. Calcd. for $C_{17}H_{20}O_7$: C, 60.7; H, 6.0. Found: C, 60.6; H, 6.1.

The hydroxymalonate ester (1.8 g, 5 mmoles) was converted to the diamide by stirring with concentrated ammonium hydroxide (10 ml) and methanol (20 ml) for 4 h at room temperature. The product (1.3 g, 87%) crystallized on standing overnight; m.p. 208° (from isopropanol); n.m.r. ($(CD_3)_2SO$) δ 7.48 (s,4,NH_2), 7.4–6.8 (quartet,2,aromatic), 6.82 (s,1,aromatic), 6.4 (d,1,CH=C—C), 6.2–5.6 (m,1,C=CH—C), 6.0 (s,1,-O—CH_2—O), 5.5 (s,1,OH), 2.7 (d,2,C=C—CH_2—).

Anal. Calcd. for $C_{13}H_{14}N_2O_5$: N, 10.1. Found: N, 10.0.

Diethyl oxomalonate was reacted similarly with α-methylstyrene by heating for 144 h. The yield of crude oily product was 93%. The ester has been prepared before (2, 3) using much shorter times of reaction. It was identified as diethyl 2-phenylallyl hydroxymalonate by conversion to the diamide; m.p. 152° (from benzene); n.m.r. ($(CD_3)_2SO$) δ 7.2–7.7 (m,5,aromatic), 7.5 (s,4,-NH_2), 5.4 (s,2,C=CH_2), 3.6 (s,1,OH), 3.1 (s,2,—CH_2—).

Anal. Calcd. for $C_{12}H_{14}N_2O$: N, 11.9. Found: N, 11.6.

4-Allylanisole similarly gave an oily 3-(4′-methoxyphenyl) allyl hydroxymalonate after 120 h. It was identified as the diamide; m.p. 212° (from isopropanol); n.m.r. ($(CD_3)_2SO$) δ 7.5 (s,4,NH_2), 7.4–6.8 (quartet,4,aromatic), 6.65 (d,1,CH=C—C), 5.5 (s,1,OH), 3.75 (s,3,-OCH_3), 2.75 (d,2,C=C—CH_2); i.r. (KBr) 3420–3150 (OH,NH), 1650 (amide I), 1565 (amide II), 1585 and 1495 (phenyl ring), 950 cm^{-1} (δ CH *trans* configuration).

Anal. Calcd. for $C_{13}H_{16}N_2O_4$: N, 10.6. Found: N, 10.7.

We are grateful to Dr. J. J. Murray and to Dr. J. O. Peterson for helpful discussions, to Dr. R. P. Hirschmann for spectral data and interpretations, and to Mr. G. E. Mohler for analytical data.

1. O. Achmatowicz and K. Belinak. Rocz. Chem. **39** (11), 1685 (1965); C. A. **64**, 17474 (1966).
2. O. Achmatowicz and O. Achmatowicz, Jr. Rocz. Chem. **36**, 1791 (1962); C. A. **59**, 8610 (1963).
3. M. Hara, Y. Odaira, and S. Tsutsumi. Tetrahedron Lett. **31**, 2981 (1967).
4. N. P. Gambaryan, E. M. Rokhlina, and Yu.V. Zeifman. Izv. Akad. Nauk SSSR. Ser. Khim. **8**, 1466 (1965); C. A. **63**, 16202 (1965).
5. W. H. Urry, J. H. Y. Niu, and L. G. Lundsted. J. Org. Chem. **33** (6), 2302 (1968).
6. J. F. Harris, Jr., and D. D. Coffman. J. Amer. Chem. Soc. **84**, 1553 (1962).
7. B. S. Farah, E. E. Gilbert, P. Lombardo, and A. C. Pierce. J. Chem. Eng. Data **11** (3), 409 (1966).
8. R. L. Adelman. J. Org. Chem. **33**, (4), 1400 (1968).
9. A. C. Cope, D. Ambros, E. Ciganek, C. F. Howell, and Z. Jacura. J. Amer. Chem. Soc. **82**, 1750 (1960).
10. P. Lombardo, and P. E. Newallis. J. Org. Chem. **30**, 3836 (1965).
11. W. J. Middleton. U.S. Patent 3 332 892 (July 25, 1967).
12. G. Baddeley, N. H. P. Smith, and M. A. Vickers. J. Chem. Soc. 2455 (1956).
13. Everett E. Gilbert. J. Het. Chem. **6**, 483 (1969).

Can. J. Chem. Downloaded from www.nrcresearchpress.com by 210.87.254.6 on 09/05/12
For personal use only.

Can. J. Chem. Downloaded from www.nrcresearchpress.com by 210.87.254.40 on 09/05/12
For personal use only.

Reductions with sulfurated borohydrides. IV. Reduction of oximes

J. M. LALANCETTE AND J. R. BRINDLE
Département de Chimie, Faculté des Sciences, Université de Sherbrooke, Sherbrooke, Québec

Received September 29, 1969

Sulfurated sodium borohydride can reduce oximes to the corresponding amine with yields depending on the steric requirement of the oxime. Intermediate hydroxylamine can be obtained predominantly under appropriate experimental conditions. A reaction mechanism taking into account the availability of only one hydrogen for reduction on the hydride and the production of intermediate hydroxylamine is proposed.

Canadian Journal of Chemistry, **48**, 735 (1970)

We have reported the reduction of aldehydes (1) with sulfurated borohydrides (2). Reductions were also observed with oximes derived from aldehydes and ketones. This paper reports reduction of typical oximes.

We have noted that aromatic and aliphatic oximes can be reduced by sodium sulfurated borohydride to the corresponding amines. The degree of reduction depends upon steric hindrance and reactivity of the reactant and also upon temperature and time of contact. Minimizing the two latter factors leads to the formation of an intermediate hydroxylamine. A mechanism for the reduction is suggested from the following observations: in contrast to $NaBH_4$, where all hydrogen atoms are available for reduction, only one hydrogen atom is available with $NaBH_2S_3$ for this type of reduction. This conclusion is confirmed by the yield of amine observed in the course of reduction of benzaldoxime; with a 2/1 molar ratio of sulfurated hydride and oxime, an almost quantitative yield of benzylamine was observed, while a 50% yield of benzylamine was obtained with a 1/1 molar ratio and a 25% yield was obtained with a 1/2 molar ratio.

Furthermore, the reduction must take place through a hydride shift from the boron atom to the positive carbon of the oxime group. This hypothesis has been confirmed by reduction of benzaldoxime with deuterated sulfurated hydride, deuterium being found on the methylene group of benzylamine.

Those observations are consistent with a mechanism where one mole of reducing agent would attack initially the double bond to give the boron derivative **1**. Then, a second molecule of the hydride contributes to the elimination of the hydroxyl groups of the oxime, giving compound **2**, eqs. [1] and [2].

Since the amine and the hydroxylamine must come from the hydrolysis of **2** and **1** respectively (eqs. [3] and [4]), at the end of the reaction, **2** must be in large excess over **1**, this explaining the 90% yield of benzylamine (**3**) and the 5% yield of benzylhydroxylamine (**4**).

The availability of only one hydrogen for reduction cannot be explained by the formation of a boric ester with the hydroxyl group of the oxime, since very little hydrogen is evolved from the reaction mixture in the course of the reduction.

With sterically hindered oximes and with *O*-methylbenzaldoxime, no intermediate hydroxylamine was observed.

The monoboric ester **1** has not been isolated but

[1] $$NaBH_4 + C_6H_5CH{=}NOH \rightarrow C_6H_5CH_2{-}N(OH)(BS_3^{\oplus}Na^{\oplus})(H)$$

[2] $$\mathbf{1} + NaBH_2S_3 \rightarrow \left[-CH_2{-}N(B{-}H)(O)(B)(H)\right] \rightarrow C_6H_5CH_2{-}N(H)(B{-}S_3^{\ominus}Na^{\oplus})(H)$$

2

[3] $$\mathbf{1} + H_2O \rightarrow C_6H_5CH_2{-}N\begin{matrix}OH\\H\end{matrix} + H_3BO_3 + \text{polysulfides}$$

[4] $$\mathbf{2} + H_2O \rightarrow C_6H_5CH_2{-}NH_2 + H_3BO_3 + \text{polysulfides}$$

its presence has been proved in the following manner: a reaction was performed in the usual way but at 10 °C and for only 6 h; at this point the reaction mixture was split into two equal parts, the first one being analyzed (i.e. hydrolysis, extraction, etc.) and found to give mainly $C_6H_5CH_2NHOH$ and the second part was refluxed for 24 h, after which it was analyzed and found to contain mainly $C_6H_5CH_2{-}NH_2$. These last observations seem to be a good justification for the existence of partial reduction where the intermediate still retains an OH group as in **1**.

These results clearly indicate that the second hydrogen on the sulfurated borohydride is very sensitive towards steric hindrance. A similar behavior has been noted with reduction of ketone where two levels of reducing capacity, for each hydrogen on boron, have been shown. This point will be reported in the following paper of this series.

Experimental

Nuclear magnetic resonance (n.m.r.) measurements were made with a Varian A-60 apparatus. Infrared (i.r.) measurements were made with a Perkin–Elmer apparatus, model 257 spectrophotometer. Vapor-phase chromatography (v.p.c.) measurements were made mostly with a Varian model 90-P apparatus using an Se 30, 5 ft column.

A. Optimal Conditions for Reduction. Reduction of Benzaldoxime

To a suspension of 0.20 mole (26.4 g) of $NaBH_2S_3$ in tetrahydrofuran (200 ml), 0.1 mole (12.1 g) of benzaldoxime in tetrahydrofuran (300 ml) was added dropwise. The reaction mixture was stirred and refluxed for 24 h. At this point the tetrahydrofuran was evaporated to dryness with a vacuum pump. The remaining yellow–brownish solid was covered with a layer of ethyl ether (250 ml) and hydrolyzed with a solution of 10% hydrochloric acid until p*H* 1. The precipitated sulfur was filtered off and the filtrate washed repeatedly with ethyl ether. The aqueous filtrate was neutralized to p*H* 11 with a solution of 20% sodium hydroxide after being covered with a layer of ethyl ether (200 ml). The resulting basic layer was repeatedly washed with ethyl ether and after drying over magnesium sulfate, the evaporation of ethyl ether gave a yield of 90% of reduction products. The i.r., v.p.c., and n.m.r. of these products, from comparison with authentic benzylamine and benzylhydroxylamine indicated the presence of 5% of benzylhydroxylamine and 95% of benzylamine.

Following the same procedure, a 50% yield of benzylamine was obtained with a 1/1 molar ratio and a 25% yield of benzylamine was obtained with 1/2 molar ratio of reducer and benzaldoxime.

B. Reduction of Typical Oximes

Following the procedure cited in section A, cyclohexanoxime, 4-*tert*-butyl cyclohexanoxime, 1,3-diphenyl 2-propanoxime, benzophenoxime, acetophenoxime, 1-camphoroxime, 1-heptanoxime, and *O*-methyl benzaldoxime were reduced to the corresponding amines. Results are reported in Table 1.

TABLE 1

Reduction of typical oximes with $NaBH_2S_3$

Reactants	Yield %	
	Amine	Hydroxylamine
Acetophenoxime	91	5
Benzaldoxime	90	5
Benzophenoxime	35	30
1-Camphoroxime	46	—
Cyclohexanoxime	25	22
4-*tert*-Butyl cyclohexanoxime	10	25
1,3-Diphenyl 2-propanoxime	50	nil
1-Heptanoxime	26	—
O-Methyl benzaldoxime	31	nil

The resulting amine and hydroxylamine of the benzaldoxime reduction were identified by comparison with i.r., n.m.r., and v.p.c. spectra. For the cyclohexanoxime reduction, the products were identified by separation (i.e. filtration of the solid hydroxylamine) and then individual analysis of the pure components.

The products obtained from all the other reductions of oximes were identified by analysis of v.p.c., i.r., and n.m.r. spectra, and also by their boiling and melting points when possible.

C. Reduction of Substituted Oximes

Following the procedure cited in section A, 0.05 mole of *O*-methyl benzaldoxime was submitted to reduction. A modest yield of 31% of benzylamine was detected in a state of great purity and positively identified with the aid of n.m.r., i.r., and v.p.c. spectra. Approximately 50% of starting oxime was recovered unreacted.

D. Reduction with Deuterated Hydride

The preparation of $NaBD_2S_3$ and the reduction procedure of benzaldoxime was identical with the procedure

Can. J. Chem. Downloaded from www.nrcresearchpress.com by 210.87.254.40 on 09/05/12
For personal use only.

cited in section A, the reaction being carried on a 2.50 g scale. The n.m.r. of the resulting products (i.e. 90% of $C_6H_5CHDNH_2$ and 5% of $C_6H_5CHDNHOH$) showed, as expected, a half decrease for the integration of the methylene of the amine at $\tau = 6.35$ and also a half decrease for the integration of the methylene of the hydroxylamine at $\tau = 6.15$, as compared with the integrations of the non-deuterated products.

E. Reduction of an Optically Active Oxime

Following the procedure cited in section A and using 1-camphoroxime as reactant, we obtained a 46% yield of a mixture of optical isomers, i.e. 1-isobornylamine and 1-bornylamine. The proportions were found to be about 50/50 for the two isomers, using two different methods of analysis.

The first method was a v.p.c. analysis made with a Micro-tek apparatus using a 12 ft silicon oil column at a constant temperature of 80°, giving a 50/50 ratio of isomers.

The second method was a polarimetric analysis made with a Rudolph polarimeter, model 80, No. 1240 and this method was performed on the crude amine mixture $[\alpha]_D^{26} - 4.48°$ (ethanol); 1-bornylamine $[\alpha]_D^{20} - 50.8°$; 1-isobornylamine $[\alpha]_D^{8} + 47.3°$, indicating a 47/53 isobornyl/bornylamine ratio.

F. Production of Hydroxylamine. Study of the Intermediate Hydroxylamines

Following the procedure cited in section D, except for the reaction temperature, which was maintained at 10 °C, and a time of contact of only 6 h, a white solid was obtained and recrystallized in ethyl ether and petroleum ether to give a m.p. of 57–57.5°. (Reported m.p.: 57°).

Anal. Calcd. for C_7H_9NO: C, 68.29; H, 7.32; N, 11.36 Found: C, 68.19; H, 7.36; N, 11.21.

In the case of the reduction of cyclohexanoxime, the procedure cited in section A was followed until it was time to neutralize the hydrochlorides with a 20% solution of NaOH. At this point, the caustic neutralization was made without an ethereal layer permitting the solid cyclohexylhydroxylamine to precipitate in the aqueous solution. It was then filtered, washed with H_2O and recrystallized in carbon tetrachloride. m.p. 140–142° (lit. m.p. 141–142°).

Anal. Calcd. for $C_6H_{11}NHOH$: C, 62.60; H, 11.31; N, 12.17. Found: C, 62.33; H, 11.52; N, 10.09.

Anal. Calcd. for cyclohexylsulfamic acid derivative, $C_6H_{13}NO_3S$: S, 17.86; N, 7.85. Found: S, 17.36; N, 7.70. Melting point 170–172° (lit. m.p. 169° (3)).

G. Reaction of the Hydroxylamines

Following exactly the same procedures as in section A, 0.0163 mole of $C_6H_5CH_2NHOH$ were added to 0.0163 mole of $NaBH_2S_3$. A 40% yield of benzylamine was isolated and positively identified by n.m.r. spectrum.

H. Evolution of Hydrogen in the Course of the Reduction

In the course of a reduction as in section A, the system was connected to a "Wet Test" meter through drying tubes filled with KOH pellets. It was noted that less than 5% of the hydrogen initially on boron was evolved as H_2 during the reduction.

1. J. M. LALANCETTE and A. FRECHE. Can. J. Chem. **47**, 739 (1969).
2. J. M. LALANCETTE, R. MONTEUX, and A. FRECHE. Can. J. Chem. **46**, 2754 (1968).
3. G. SODER and H. S. SCHNELL. C. A. **51**, 12970*a* (1957).

Can. J. Chem. Downloaded from www.nrcresearchpress.com by 210.87.254.40 on 09/05/12
For personal use only.

Can. J. Chem. Downloaded from www.nrcresearchpress.com by 210.87.254.42 on 09/05/12
For personal use only.

Mass spectra of some deuterium labelled dimethylquinolines

P. M. Draper and D. B. MacLean
Department of Chemistry, McMaster University, Hamilton, Ontario

Received July 15, 1969

The mass spectra of several dimethylquinolines, labelled in the methyl group with deuterium, have been examined. The results are in agreement with the formation of ring-expanded molecular ions prior to fragmentation to the M—H and M—CH_3 ions. Two ring-expanded ions may form since there are two methyl groups which can participate in the ring expansion process. Ring expansion through a methyl group located on the benzenoid ring is favored over ring expansion through a methyl group on the pyridine ring.

Canadian Journal of Chemistry, **48**, 738 (1970)

In an earlier study on alkylquinolines, we proposed (1) that dimethylquinolines fragment through the sequence M ⟶ M—H ⟶ M—(H + HCN) and M ⟶ M—CH_3 ⟶ M—(CH_3 + HCN). We postulated also that the loss of methyl occurs from a ring expanded molecular ion since the monomethylquinolines show little tendency to lose a methyl group (1, 2). Sample *et al.* (2) examined the spectra of 2,3- and 2,4-dimethylquinoline and suggested that they fragment by loss of H with ring expansion, followed by loss of CH_3CN or HCN.

The intervention of ring expanded ions in the fragmentation of aromatic and heteroaromatic systems is well documented. Ring expansion in the formation of tropylium ions has been reviewed by Grubb and Meyerson (3) and its mechanism studied by Meyer and Harrison (4*a*), by Meyerson *et al.* (4*b*) and by Rinehart *et al.* (5). In the case of toluene it has been shown that ring expansion occurs by random insertion of the methyl carbon into the 6 C—C bonds of the benzene nucleus (5). Ring expansion in methylisoquinolines, methyl indoles, and *N*-methylpyrrole has been reported by Marx and Djerassi (6) who studied ^{13}C labelled derivatives of these compounds. In the quinoline system we have proposed the intervention of a ring-expanded ion to account for our results on methylquinolines labelled with deuterium and ^{13}C (7). In an attempt to substantiate the ring expansion hypothesis for dimethylquinolines and to gain insight into the mechanism of the loss of the methyl groups from the molecular ion we have prepared and examined several deuterated dimethylquinolines.

The spectra of the labelled dimethylquinolines and their unlabelled analogues examined in this study are shown in Fig. 1 and partial spectra in relative ion intensities in Table 1. In Table 2, we have recorded the M—CH_3/M—CD_3 peak intensity ratios for the labelled compounds and the percent label retention in the M ⟶ M—H transformation. Label retention in this transformation was calculated by the procedure described earlier (7).

Preliminary examination of the results in Table 2 shows that the 2 methyl groups in the labelled compounds are not lost with equal facility, nor is the hydrogen loss in the transformation M ⟶ M—H a completely random process. Complete randomization of 3 deuteriums and 8 hydrogens in the molecule would result in 73% retention of the 3 deuteriums. That the 2 methyl groups are not lost equally is not surprising since the methyl groups in the molecule are not equivalent.

Comparison of the spectra of the undeuterated and deuterated dimethylquinolines (Fig. 1) shows that some scrambling occurs on loss of methyl from the labelled derivatives. In other words the methyl group lost does not consist entirely of the original methyl hydrogens. The extent of scrambling appears to vary among the isomers but a quantitative estimation is difficult because of contributions from peaks observed at M-16 and M-17 in the spectra of the unlabelled compounds. In all cases, the scrambling appears to be considerably less than that observed in the spectra of the labelled xylenes where the data indicated that one of the methyl hydrogens has a 50:50 chance of exchanging with a ring hydrogen before loss of methyl (8).

We have interpreted our labelling results on the dimethylquinolines by assuming that ring expansion may proceed by 2 pathways since there are 2 exocyclic methyl groups which may partici-

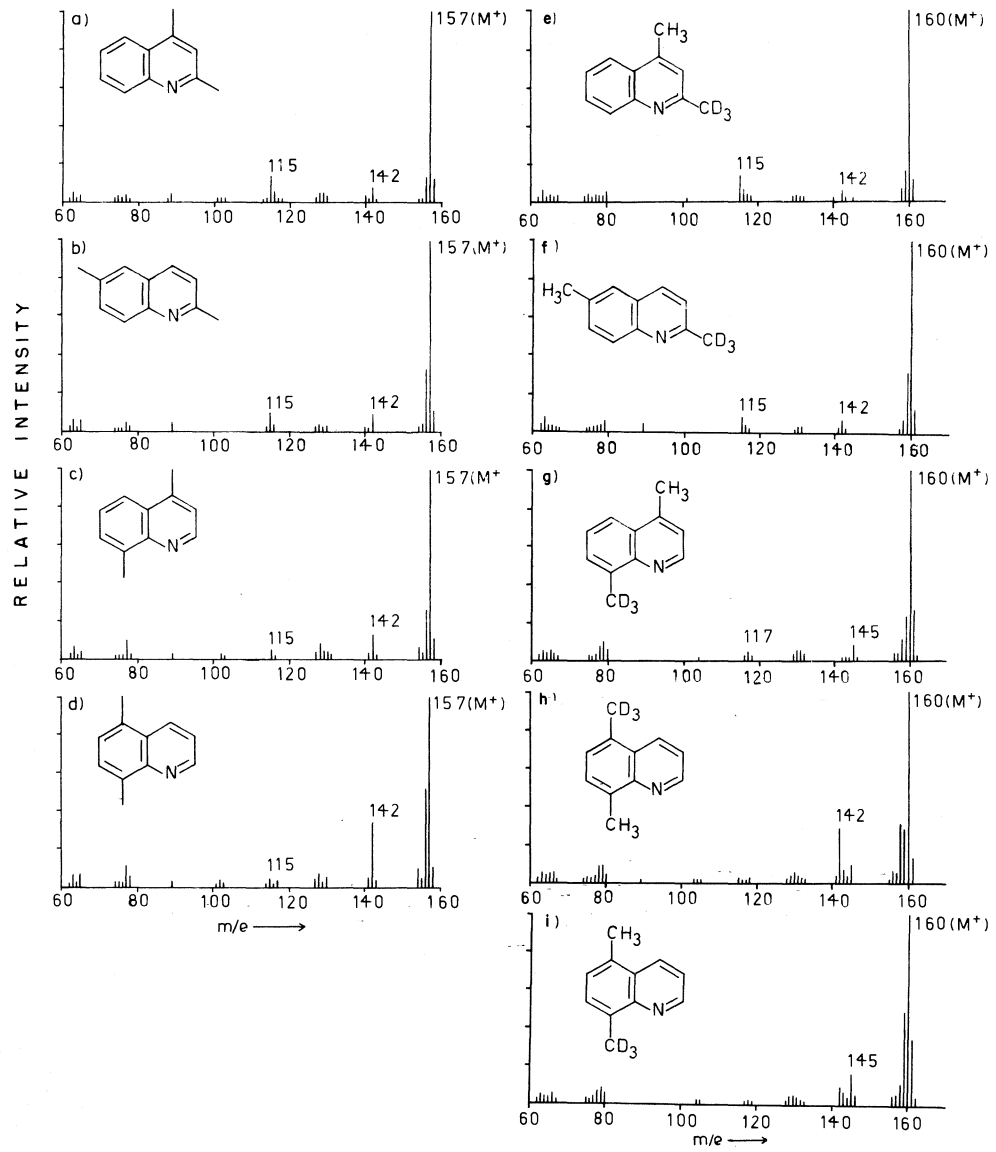

FIG. 1. Mass spectra of dimethylquinolines: (*a*) 2,4-dimethylquinoline, (*b*) 2,6-dimethylquinoline, (*c*) 4,8-dimethylquinoline, (*d*) 5,8-dimethylquinoline, (*e*) 2,4-dimethylquinoline-2-α-d_3, (*f*) 2,6-dimethylquinoline-2-α-d_3, (*g*) 4,8-dimethylquinoline-8-α-d_3, (*h*) 5,8-dimethylquinoline-5-α-d_3, (*i*) 5,8-dimethylquinoline-8-α-d_3.

pate in the ring expansion process. Thus, ions represented by structures **1** and **2** may be formed by ring expansion involving the C-2 and C-6 methyl groups, respectively, in 2,6-dimethylquinoline (Scheme 1). Since loss of methyl does not involve extensive scrambling of the methyl and side chain hydrogens, it would appear that an equilibrium between **1** and **2** is relatively unimportant. A simple phenyl–methyl cleavage is usually an unfavorable process so it is likely that further rearrangement of **1** and **2**, possibly to **3** and **4**, respectively, precedes loss of CH_3. Alternatively, the formation of **5** and **6** from **1** and **2**, respectively, (by a series of 1,2-hydrogen shifts) may be favored since less skeletal rearrangement is required than in the formation of **3** and **4**. In either case, loss of H or CH_3 from **3**–**6** may occur from a methylene position. The

Can. J. Chem. Downloaded from www.nrcresearchpress.com by 210.87.254.42 on 09/05/12
For personal use only.

Can. J. Chem. Downloaded from www.nrcresearchpress.com by 210.87.254.42 on 09/05/12
For personal use only.

TABLE 1

Partial spectra of the dimethylquinolines

m/e	2,4-Dimethyl	2,4-Dimethyl -2-α-d_3	2,6-Dimethyl	2,6-Dimethyl -2-α-d_3	4,8-Dimethyl	4,8-Dimethyl -8-α-d_3	5,8-Dimethyl	5,8-Dimethyl- 5-α-d_3	5,8-Dimethyl- 8-α-d_3
162						3.0			4.0
161		14.0		12.0		27.5		13.7	36.0
160		100.0		100.0		100.0		100.0	100.0
159		16.0		31.5		23.3		28.8	49.5
158	14.0	6.0	12.0	6.2	12.0	11.0	12.0	31.8	12.3
157	100.0	1.3	100.0	1.8	100.0	4.0	100.0	5.4	6.4
156	13.8	1.3	33.2	1.8	27.5	3.9	53.3	7.0	5.0
155	2.5		3.6		4.5	1.1	5.0	2.6	1.9
154	2.0		2.9		7.0		11.0		
153			0.4		0.5		1.0		
146						2.0		1.7	6.0
145		2.0		1.6		8.9		9.5	16.0
144		1.8		1.2		3.4		3.7	5.5
143	1.7	2.5	1.2	2.6	1.8	3.1	4.0	7.5	7.8
142	8.0	5.0	9.0	7.5	13.5	1.9	35.7	29.0	9.0
141	2.0	1.5	3.0	2.2	3.8	1.0	6.0	4.4	15.0
140	3.5	2.1	2.9	1.7	1.5	0.5	1.9		

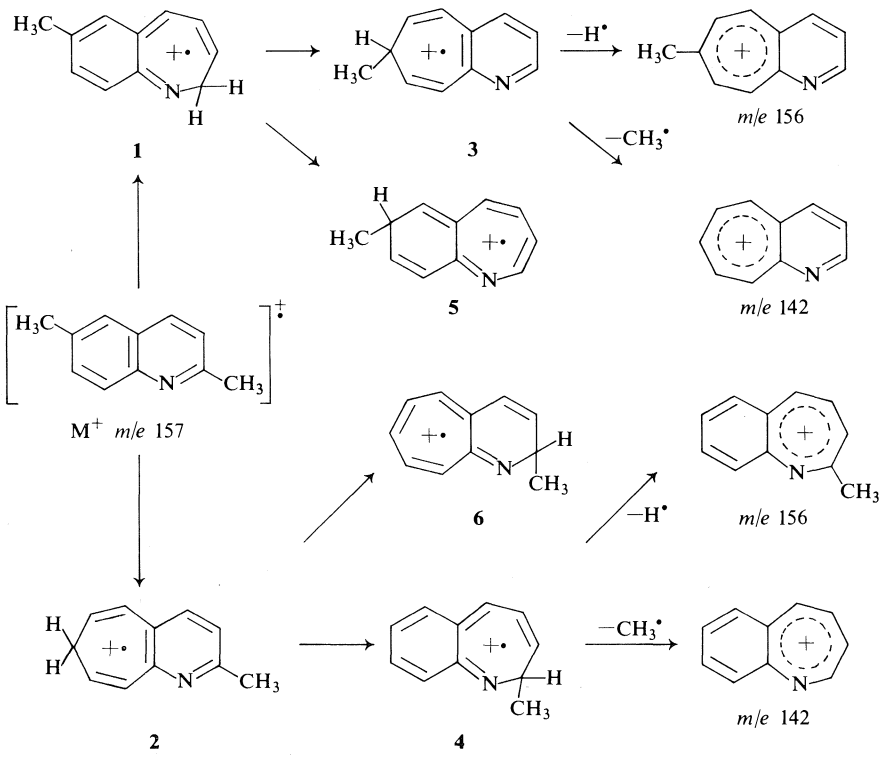

SCHEME 1

TABLE 2

Mass spectra of labelled dimethylquinolines

Compound	M—CH_3/ M—CD_3	% Retention (M → M—H)
2,4-Dimethylquinoline-2-α-d_3	1:2.5	77
2,6-Dimethylquinoline-2-α-d_3	1:5	91
4,8-Dimethylquinoline-8-α-d_3	4:1	64
5,8-Dimethylquinoline-5-α-d_3	1:3	40
5,8-Dimethylquinoline-8-α-d_3	2:1	86

extent to which H and CH_3 are lost from each of the rearranged ions would be difficult to estimate without a knowledge of the relative energies of the reactant and product ions.

The preferred loss of the C-2 methyl may be accounted for by assuming that ring expansion in the benzenoid ring is more favorable energetically than ring expansion in the pyridine ring. Therefore ion **2** would be more abundant than ion **1** and loss of the C-2 methyl favored over that at C-6. There are not, to our knowledge, any appearance potential studies to justify this assumption but there is indirect evidence. Sample *et al.* (2) and we (1) observed, in the case of monomethylquinolines, that the M-1 ion was more intense in those quinolines which carried a methyl group in the benzenoid ring than in those which have the methyl group in the pyridine ring. Moreover, it was shown (2) that the M—(H + HCN)/M—H ratio in monomethylquinolines substituted in the pyridine ring was greater than in those substituted in the benzene ring. This result is also compatible with our hypothesis since it would be expected that HCN would be lost more readily from the higher energy species. A less compelling argument, because it has never been proved that methyl pyridines undergo ring expansion before fragmentation (although it has been postulated (9)), arises from a comparison of the abundance of the M-1 ion relative to M^+ in toluene (3) and the methylpyridines (10). It is found that the M-1 ion is much more abundant in the former. Moreover, the appearance potential of the M-1 ion from toluene (3) is some 0.5 eV less than the M-1 ion from methyl pyridines (9). Thus the favored loss of methyl from C-2

Can. J. Chem. Downloaded from www.nrcresearchpress.com by 210.87.254.42 on 09/05/12
For personal use only.

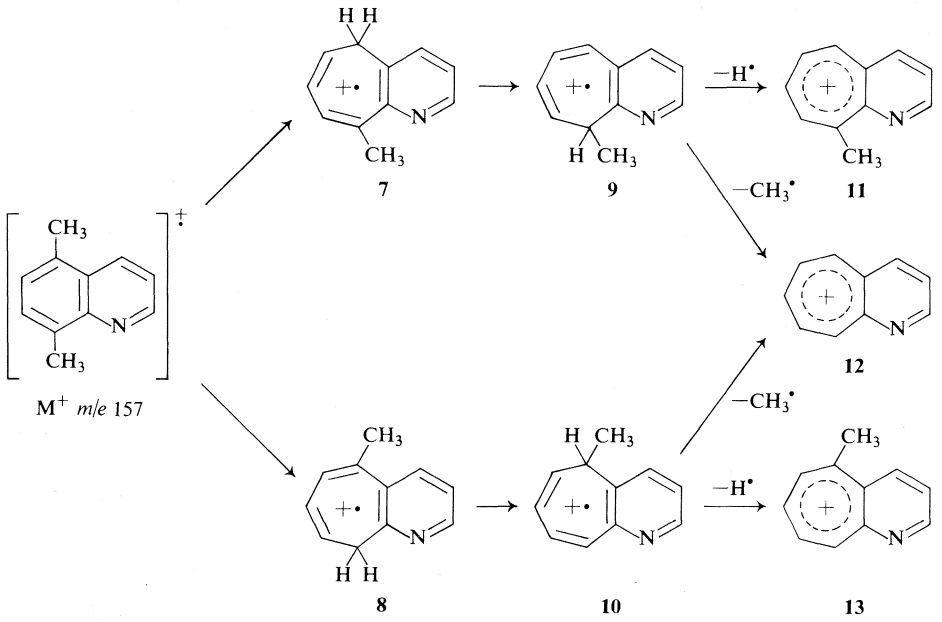

SCHEME 2

in the spectrum of 2,6-dimethylquinoline may be explained by assuming that there are two separate pathways one of which is favored energetically over the other.

A similar argument suffices for 4,8-dimethylquinoline-8-α-d_3 where loss of methyl at C-4 is favored over loss of methyl at C-8. Thus, ring expansion involving the C-8 methyl is favored over ring expansion involving the C-4 methyl. Similarly, loss of the C-2 methyl is preferred over loss of the C-4 methyl in the spectrum of 2,4-dimethylquinoline-2-α-d_3 which suggests that ring expansion involving the C-4 methyl may be favored over ring expansion involving the C-2 methyl. Simple α-cleavage of the 2-methyl group (in analogy with loss of CH_3 from 2-methylquinoline (1)) may also contribute to the preferred loss of the 2-methyl in the 2-substituted dimethylquinolines.

The spectra of the labelled 5,8-dimethylquinolines show that loss of the C-5 methyl occurs to a greater extent than loss of the C-8 methyl. This suggests that the two possible ring expanded ions, represented by structures **7** and **8** (Scheme 2), are not formed in equal abundance, or that loss of methyl from **10** occurs more readily than from **9**. The M—CH_3/M—CD_3 peak intensity ratios in the two labelled 5,8-dimethylquinolines are not the inverse of one another as might be expected. The difference could be attributed to a mass effect in which the heavier CD_3 is lost more readily than CH_3.

In Scheme 1 it is proposed that both H and CH_3 are lost from the same intermediates. A correlation should therefore be observed between the label retention in the M ⟶ M—H process and the M—CH_3/M—CD_3 ratios in the spectra of the deuterated compounds. In the spectra of the monomethylquinolines randomization of all 9 hydrogens in the molecule appears to occur before loss of H (7), while in the dimethylquinolines only the ring and side chain hydrogens participating in the ring expansion process will be randomized. The hydrogens in the remaining methyl group will be lost in the transformation M ⟶ M—CH_3. For example, in the spectrum of 2,6-dimethylquinoline-2-α-d_3, ring expansion and rearrangement by the sequence M^+ ⟶ **2** ⟶ **4** will result in 100% retention of label in the M ⟶ M—H process, while ring expansion through the C-2 methyl should result in a randomization of the 3 methyl deuteriums and the 5 ring hydrogens. Since the former sequence (in which 100% retention of deuterium is observed) appears to predominate, then a high retention of deuterium should be observed, and such is

Can. J. Chem. Downloaded from www.nrcresearchpress.com by 210.87.254.42 on 09/05/12
For personal use only.

Can. J. Chem. Downloaded from www.nrcresearchpress.com by 210.87.254.42 on 09/05/12
For personal use only.

actually the case. The results on 2,4-dimethylquinoline-2-α-d_3 are also roughly in accord with loss of H from 2 ring expanded intermediates.

In the spectrum of 4,8-dimethylquinoline-8-α-d_3, the M—CH_3/M—CD_3 peak intensity ratios suggest that ring expansion involving the C-8 methyl occurs to a greater extent than ring expansion through the C-4 methyl. Ring expansion at C-8 with randomization of the 3 deuteriums and 5 hydrogens should result in 62.5% retention of 3 deuteriums on loss of H, while ring expansion to the C-4 methyl results in 100% retention of label. For example, if 80% of the H lost originates through ring expansion in the benzene ring and 20% by ring expansion in the pyridine ring, then the expected label retention would be $0.8 \times 62.5 + 0.2 \times 100 = 70\%$. The 64% retention of label observed in the spectrum of 4,8-dimethylquinoline-8-α-d_3 is relatively close to this value. The approximate values for ring expansion in the benzene and pyridine rings (80% and 20%, respectively) were chosen from the observed M—CH_3/M—CD_3 ratio of 4:1.

Ionization and ring expansion of 5,8-dimethylquinoline may result in formation of two ring expanded ions **7** and **8** as shown in Scheme 2. It would be expected that ring expansion through the C-5 and C-8 methyls should occur to about the same extent since the spectra of 5- and 8-monomethylquinolines are nearly identical (1). However, **7** and **8** are not identical in structure and they are therefore not necessarily formed in equal abundance. Further rearrangement of **7** and **8**, possibly to **9** and **10**, respectively, is likely since the phenyl–methyl cleavage is an unfavorable process.

Since loss of the C-5 methyl is favored over loss of the C-8 methyl in the transformation M ⟶ M—15, it might be expected that ring expansion to **8** occurs more readily than ring expansion to **7**. However, if **8** is more abundant than **7**, then loss of a C-8 methyl hydrogen in the process M ⟶ M—H should occur to a greater extent than loss of a C-5 methyl hydrogen, and this is contrary to the labelling results. Alternatively, the position of the methyl group in the rearranged molecular ions **9** and **10**, and the relative stabilities of the fragment ions **11**–**13**, may influence the fragmentation of **9** and **10**. Thus ion **9** may fragment preferably by loss of H (some of which may originate from the C-5 methyl), while loss of the C-8 methyl may be less important. On the other hand, **10** may fragment mainly by loss of the C-5 methyl, while expulsion of H (which originates from the ring and C-8 methyl) may be less important.

From the above discussion, therefore, the favored loss of methyl from C-5 does not appear too unreasonable, nor is the 86% retention of label observed in the transformation M ⟶ M—H in the 8-α-d_3 derivative unreasonable. However, the low M—H/M—D peak intensity ratio in the 5-α-d_3 derivative cannot be explained by this mechanism. The result for this compound suggests that some loss of H from the C-5 methyl may occur before ring expansion, or H may be lost from the methylene position in the ring expanded ion **7** before complete randomization has occurred. A slight preference for loss of the methyl hydrogens over ring hydrogens has been observed in the spectrum of toluene (11), but it is much smaller than that observed in the 5-α-d_3 derivative. No explanation is offered to account for the anomalous behavior of this compound.

To account for the labelling results on the dimethylquinolines, we have suggested that loss of H and CH_3 may proceed from two possible ring expanded ions, and that one of these may be of lower energy than the other. If this is the case, then formation of the lower energy species should predominate to an even greater extent when the energy of the ionizing electrons (the ionization voltage) is decreased. In other words, the M—CH_3/M—CD_3 peak intensity ratios in the spectra of the labelled dimethylquinolines should depend on the ionization voltage. However, if methyl is lost from a single species, then the M—CH_3/M—CD_3 peak intensity ratios should be independent of the ionization voltage.

To show that loss of methyl may indeed originate from two species of different energy, the spectra of some of the deuterated compounds were determined at varying electron energies, and the results are shown in Table 3. The ionizing voltages shown in the table are those registered by the ionization gauge and do not necessarily represent the absolute values. The repeller voltages were maintained at a constant value (2 V) for all the readings.

The results in Table 3 show that the M—CH_3/M—CD_3 peak intensity ratios depend on the energy of the ionizing electrons in all the compounds examined. In the spectrum of 4,8-dimethylquinoline-8-α-d_3, the ratio increases

TABLE 3
Dependence of M—CH_3/M—CD_3 ratios on ionizing voltage

Ionizing voltage	M—CH_3/M—CD_3		
	4,8-Dimethylquinoline -8-α-d_3	5,8-Dimethylquinoline -5-α-d_3	5,8-Dimethylquinoline -8-α-d_3
80	4.5	0.33	1.8
20	6.3	0.34	2.0
16	8.4	0.33	2.2
14	9.1	0.31	2.3
12.5	9.1	0.29	2.4
11.5	9.1	0.27	2.5

from about 4.5 at 80 eV to 9.1 at 11.5 eV, and this is in accord with the lower energy process (ring expansion in the benzene ring with expulsion of the C-4 methyl) occurring to a greater extent relative to the higher energy process at lower ionizing voltages. The change in M—CH_3/M—CD_3 ratios in the labelled 5,8-dimethylquinolines is much smaller, but the results from both compounds suggest that expulsion of the C-5 methyl requires somewhat less energy than expulsion of the C-8 methyl.

Further fragmentation of the M-1 and M-15 ions in the spectra of the dimethylquinolines appears to proceed mainly by loss of HCN. The extent of hydrogen scrambling in the M—(H + HCN) and M—(CH_3 + HCN) ions in the deuterated compounds is difficult to estimate because of the adjacent peaks found in the spectra of the unlabelled compounds. The M—(CH_3 + HCN) peak (*m/e* 115) in the spectra of 2,4- and 2,6-dimethylquinoline is found mainly at *m/e* 115 in the spectra of the labelled derivatives since most of the label is lost as CD_3. In the spectrum of 4,8-dimethylquinoline-8-α-d_3 most of the methyl is lost as CH_3, and peaks at *m/e* 117 and 118 which may arise through loss of DCN and HCN, respectively, from M—CH_3 are observed. Therefore, little information regarding the fragmentation of the dimethylquinolines is obtained on examination of the M—(H + HCN) and M—(CH_3 + HCN) ions in the spectra of their deuterated analogues.

In summary of our work it appears that the labelling results on the mono- and dimethylquinolines are compatible with the formation of ring expanded ions in their fragmentation. It should be noted that the labelling results may be influenced by an isotope effect, and in some cases other fragmentation pathways may also contribute to the ion in question. Either of these factors could give anomalous results but they could also account for some of the differences between the observed and predicted results.

Experimental

Apparatus, Methods, and Materials

Mass spectra were determined on a Hitachi Perkin–Elmer RMU-6A mass spectrometer at an ionizing potential of 80 eV and an ionizing current of 50 μA. Samples were introduced through an all-glass inlet system maintained at 200 °C.

All samples for mass spectrometry (with the exception of alkylquinolines labelled with deuterium in the 2-α-position) were purified by gas chromatography on a 6 ft column of 20% Apiezon M on celite. The column temperature was maintained at 180 to 230° depending on the volatility of the material. Gas chromatography of alkylquinolines labelled in the 2-α-position caused back exchange; therefore, these compounds were purified by chromatography over alumina. It was also necessary to pump a small amount of CH_3OD through the mass spectrometer before introduction of these samples.

The isotopic composition of all the labelled compounds was determined by low voltage mass spectrometry.

Nuclear magnetic resonance (n.m.r.) spectra were determined in $CDCl_3$ solution on a Varian A-60 spectrometer. Chemical shifts are expressed in parts per million (δ) from tetramethylsilane used as an internal standard.

The CH_3OD (99 atom % D) and CD_3I (99 atom % D) were obtained from Merck, Sharp and Dohme of Canada Ltd. $LiAlD_4$ was obtained from Ventron Corporation, Metal Hydrides Division, Beverly, Massachusetts. The unlabelled quinolines used as reference compounds in this work were prepared by methods described in our previous paper (1).

2,4-Dimethylquinoline-2-α-d_3

The method used was similar to that described for the preparation of 2-methylquinoline-2-α-^{13}C (7); 4-methylquinoline-*N*-oxide was converted to 4-methyl-*N*-ethoxyquinolinium iodide (m.p. 119–121°) which was in turn reacted with CD_3MgI. The isotopic composition of the product was: d_2 6%, d_3 92%, d_4 2%. The n.m.r. spectrum of the labelled compound showed a singlet at 2.56 δ (3H) while the spectrum of the unlabelled analogue showed

Can. J. Chem. Downloaded from www.nrcresearchpress.com by 210.87.254.42 on 09/05/12
For personal use only.

Can. J. Chem. Downloaded from www.nrcresearchpress.com by 210.87.254.42 on 09/05/12
For personal use only.

singlets at 2.54 (3H) and 2.62 δ (3H) assigned to the methyl hydrogens at C-4 and C-2, respectively.

2,6-Dimethylquinoline-2-α-d_3

The procedure used was similar to that described above; 6-methylquinoline-*N*-oxide was converted to 6-methyl-*N*-ethoxyquinolinium iodide (m.p. 105–107°) which was in turn reacted with CD_3MgI. The composition of the product was: d_2 2.5 and d_3 97.5%. The n.m.r. spectrum of the deuterated compound showed a singlet at 2.43 δ (3H) while the spectrum of the unlabelled analogue showed singlets at 2.42 (3H) and 2.67 δ (3H) assigned to methyl hydrogens at C-6 and C-2, respectively.

4,8-Dimethylquinoline-8-α-d_3

Methyl-vinyl-ketone (18 ml) was added dropwise to a stirred solution (at 0°) of 10.2 g anthranilic acid in 30 ml conc. HCl. After 0.5 h, 8 g $ZnCl_2$ was added and the mixture boiled gently for 4 h. The mixture was cooled, poured on crushed ice, and washed twice with chloroform. The aqueous fraction was adjusted to p*H* 4 and extracted 5 times with chloroform. The residue from the chloroform extracts was recrystallized from methanol yielding 6.3 g (45%) 4-methylquinoline-8-carboxylic acid which melted at 167–181° (lit. 182–183° (12)).

Treatment of a methanolic solution of the acid with excess diazomethane at 0° yielded the corresponding methyl ester in 83% yield. This ester (1.03 g) was reduced with $LiAlD_4$ (120 mg) in ether at 0° yielding 0.43 g 4-methyl-8-hydroxymethylquinoline-8-α-d_2 (m.p. 112.5–114° after recrystallization from ethanol–petroleum ether). The deuterated alcohol was converted to its hydrochloride which was in turn converted to 4-methyl-8-chloromethylquinoline-8-α-d_2 (m.p. 43°) using the same conditions as those used for the preparation of the labelled 8-chloromethylquinoline (7). Treatment of the labelled chloromethylquinoline with zinc, deuteroacetic acid, and D_2O at room temperature for 6 h afforded the desired 4,8-dimethylquinoline-8-α-d_3 whose composition was: d_2 5, d_3 81, d_4 13, d_5 1%. The n.m.r. spectrum showed a singlet at 2.62 δ (3H) while the spectrum of the unlabelled compound gave singlets at 2.58 (3H) and 2.82 δ (3H) assigned to methyl protons at C-4 and C-8, respectively.

5,8-Dimethylquinoline-5-α-d_3

H_2SO_4 (7.5 ml) was added dropwise to a mixture of 5.1 g 3-amino-4-methylbenzoic acid, 3 ml nitrobenzene, and 10.5 ml glycerol. The mixture was heated under gentle reflux for 5 h, cooled, and poured on crushed ice. It was then basified with ammonia and extracted with ether to remove unreacted nitrobenzene. The aqueous layer was boiled with charcoal, filtered, and acetic acid added to the hot filtrate. 8-Methylquinoline-5-carboxylic acid (3.0 g, m.p. 272–277° with decomposition) crystallized from the cooled solution. This acid was converted to its methyl ester with excess diazomethane, and the ester reduced to 8-methyl-5-hydroxymethylquinoline-5-α-d_2 (m.p. 116–118°) with $LiAlD_4$ in the usual manner. The deuterated alcohol was converted to 8-methyl-5-chloromethylquinoline-5-α-d_2 (m.p. 86–87°) which was in turn reduced to the desired 5,8-dimethylquinoline-5-α-d_3 with zinc and deuteroacetic acid. The composition of the product was: d_2 7, d_3 90, and d_4 3%. The n.m.r. spectrum gave a singlet at 2.78 δ (3H) while singlets at 2.56 (3H) and 2.78 δ (3H) assigned to methyl hydrogens at C-5 and C-8, respectively, were observed in the spectrum of the unlabelled analogue. The picrate of the undeuterated compound prepared by the same series of reactions melted at 182–184° (lit. 186° (13)).

5,8-Dimethylquinoline-8-α-d_3

5-Methylquinoline-8-carboxylic acid [m.p. 173–175° (lit. 174° (14))] was prepared in 66% yield from 2-amino-4-methylbenzoic acid under Skraup conditions similar to those described by Campbell *et al.* (15) for the preparation of 8-quinolinecarboxylic acid. Treatment of the acid with excess diazomethane at 0° yielded the corresponding methyl ester which was in turn reduced to 5-methyl-8-hydroxymethylquinoline-8-α-d_2 (m.p. 71–72.5°) with $LiAlD_4$ at 0°. Reaction conditions similar to those described for the preparation of the labelled 8-methylquinoline (7) were used to convert the above alcohol to 5-methyl-8-chloromethylquinoline-8-α-d_2 (m.p. 65–68°) which was in turn reduced to 5,8-dimethylquinoline-8-α-d_3. The isotopic composition of the product was: d_2 4.5%, d_3 74.5%, d_4 21%. The n.m.r. spectrum showed a singlet at 2.56 δ (3H) while the spectrum of the unlabelled compound showed singlets at 2.56 (3H) and 2.78 δ (3H) assigned to the methyl hydrogens at C-5 and C-8, respectively.

The award of a bursary and studentships by the National Research Council of Canada to P. M. Draper is gratefully acknowledged. This work was supported through a grant from the National Research Council of Canada.

1. P. M. Draper and D. B. MacLean. Can. J. Chem. **46**, 1487 (1968).
2. S. D. Sample, D. A. Lightner, O. Buchardt, and C. Djerassi. J. Org. Chem. **32**, 997 (1967).
3. H. M. Grubb and S. Meyerson. *In* Mass spectrometry of organic ions. *Edited by* F. W. McLafferty. Academic Press Inc., New York. 1963. Chap. 10.
4. (*a*) F. Meyer and A. G. Harrison. J. Amer. Chem. Soc. **86**, 4757 (1964). (*b*) S. Meyerson, H. Hart, and L. C. Leitch. J. Amer. Chem. Soc. **90**, 3419 (1968).
5. K. L. Rinehart, Jr., A. C. Buchholz, G. E. Van Lear, and H. L. Cantrill. J. Amer. Chem. Soc. **90**, 2983 (1968).
6. M. Marx and C. Djerassi. J. Amer. Chem. Soc. **90**, 678 (1968).
7. P. M. Draper and D. B. MacLean. This issue.
8. S. Meyerson and P. N. Rylander. J. Phys. Chem. **62**, 2 (1958).
9. T. F. Palmer and F. P. Lossing. J. Amer. Chem. Soc. **85**, 1733 (1963).
10. W. G. Cole, D. H. Williams, and A. N. H. Yeo. J. Chem. Soc. B, 1284 (1968).
11. J. G. Burr and R. A. Meyer. J. Chem. Phys. **40**, 2046 (1964).
12. H. Arai, K. Saito, and N. Murata. Kogyo Kagaku Sasshi, **63**, 319 (1960). C. A. **59**, 6362*g* (1963).
13. R. H. F. Manske, L. Marion, and F. Leger. Can. J. Res. B, **20**, 133 (1942).
14. L. Bradford, T. J. Elliott, and F. M. Rowe. J. Chem. Soc. 437 (1947).
15. K. N. Campbell, J. F. Kerwin, R. A. LaForge, and B. K. Campbell. J. Amer. Chem. Soc. **68**, 1844 (1946).

Mass spectra of labelled methylquinolines

P. M. Draper and D. B. MacLean
Department of Chemistry, McMaster University, Hamilton, Ontario
Received July 15, 1969

The mass spectra of some labelled methylquinolines have been studied. Randomization of all nine hydrogens in the molecule appears to precede hydrogen loss in the fragmentation of the monomethylquinolines and the formation of ring expanded intermediates is proposed to account for the randomization. Possible mechanisms for the ring expansion are considered.

Canadian Journal of Chemistry, **48**, 746 (1970)

Can. J. Chem. Downloaded from www.nrcresearchpress.com by 210.87.254.42 on 09/05/12
For personal use only.

We have recently reported the mass spectra of the alkylquinolines, and we have presented preliminary labelling evidence for the formation of ring expanded ions in the fragmentation of these compounds (1). We now wish to report the results of additional labelling experiments which were undertaken in an attempt to clarify further the fragmentation mechanisms.

The evidence for tropylium ion formation in the spectra of the alkylbenzenes is summarized in a review by Grubb and Meyerson (2), while the mechanism of tropylium ion formation has been studied by Meyer and Harrison (3*a*), Meyerson *et al.* (3*b*), and Rinehart *et al.* (4). The latter workers showed that formation of the tropylium ion from toluene occurs by a random insertion of the methyl carbon into any carbon–carbon bond of the original ring rather than by a simple 1,2-insertion into adjacent carbon–carbon bonds of the ring. Labelling evidence to support formation of analogous ring expanded ions in the fragmentation of heteroaromatic compounds containing nitrogen was obtained by Marx and Djerassi (5) who recorded the spectra of some ^{13}C labelled methylisoquinolines, methylindoles, and methylpyrrole. They noted that their results were consistent with formation of ring expanded ions by insertion of the exocyclic alkyl carbon into adjacent carbon–carbon or carbon–nitrogen bonds of the original ring. However, a small percentage of the label could not be accounted for by this mechanism.

A recent study by Cole *et al.* (6) on deuterated methylpyridines indicated extensive scrambling of hydrogen in the M—H and M—HCN ions. Their results, however, do not confirm or refute the intermediacy of a ring-expanded species prior to the formation of these ions. As in the case of 2-methylquinoline (1) they found that the methyl pyridines lose methyl and that at 70 eV there is little scrambling of hydrogen in this process.

The first systematic investigation of the mass spectra of alkylquinolines was reported by Sample *et al.* (7) in 1967. In the spectra of the monomethylquinolines substituted in the pyridine ring, they postulated the formation of a benzazatropylium ion to account for the constant M—(H + HCN)/M—H peak intensity ratios. Analogous ions were similarly proposed to account for the spectra of monomethylquinolines substituted in the benzene ring. Since these authors did not prepare deuterated compounds they were unable to provide further evidence regarding the fragmentation mechanisms of the monomethylquinolines. In our work we reported the spectra of 3 deuterated monomethylquinolines (1). In these compounds randomization of all 9 hydrogens in the molecule appeared to precede formation of the M-1 ion and therefore an azatropylium type ion appeared to be an adequate representation of this ion. However, we did not propose structures for the rearranged molecular ion which would account for the hydrogen randomization.

The results of the spectra of the labelled monomethylquinolines that we have determined are summarized in Table 1. In the first column, the percent label retention in the M—H ion is listed. The label retention expected for statistical loss of a single hydrogen or deuterium from the ring containing the substituent is shown in the second column, and the calculated label retention for random loss of a single hydrogen or deuterium from the whole molecule in the third column. The label retention in the M—(H + HCN) ion is listed in the next column and finally the value calculated for random loss of H from the whole molecule in the formation of M—(H + HCN).

TABLE 1

Mass spectra of labelled monomethylquinolines

	% Retention (M—H)	Calculated for random loss of H from ring containing substituent	Calculated for random loss of H from molecule	% Retention [M—(H + HCN)]	Calculated for random loss from the molecule in the M—(H + HCN) process
2-Methylquinoline-2-α-d_3	74	40	67		
4-Methylquinoline-2-d_1	91	80	89	50	78
8-Methylquinoline-8-α-d_1	89	83	89	78	78
8-Methylquinoline-8-α-d_3	69	50	67		

TABLE 2

Partial spectra of the methylquinolines

m/e	2-Methyl	2-Methyl -2-α-d_3	4-Methyl	4-Methyl -2d_1	8-Methyl	8-Methyl -8-α-d_1	8-Methyl -8-α-d_3	2-Methyl -2-α-^{13}C
148		1					2	
147		11.8					19.5	
146		100.0		1.0		11.0	100.0	
145		11.5	0.8	13.5		12.3	32.5	13.0
144	11.3	5.5	12.1	100.0	11.0	100.0	20.0	100.0
143	100.0	1.5	100.0	23.2	100.0	41.5	5.0	84.0
142	10.2	1.2	17.1	5.2	42.3	14.2	2.5	10.1
141	2.5	0.5	3.3	2.1	9.5	3.9		4.0
140	2.5		2.2	1.0	2.7	1.0		2.2
120		1.0					2.3	
119		3.5				0.4	5.5	
118		7.0	0.5	4.0	0.6	3.5	10.0	2.0
117	3.9	8.0	5.0	6.5	5.4	5.6	9.0	9.0
116	7.0	2.8	9.2	15.0	6.3	12.4	3.5	18.0
115	16.0	1.0	25.5	15.0	14.0	5.5	1.8	15.1
114	2.0		2.7	2.0	3.2	2.2	1.0	3.1
113	1.3		1.8	1.0	1.9	1.0		1.0

The results shown in Table 1 are the average of two or more determinations. Partial spectra of the labelled and unlabelled compounds are given in Table 2.

Label retention in the transformation M ⟶ M—H was calculated from the peak intensities at M—H and M—D in the spectra of the labelled compounds by the equation (M—H)/(M—H) + (M—D) × 100. The peak intensities were first corrected for isotopic impurities (determined by low voltage mass spectrometry) and for naturally occurring ^{13}C. Peaks corresponding to M—2H ions were observed in the spectra of the unlabelled compounds, and corrections for the contributions of these ions at M—D (M-2) in the spectra of the labelled analogues were estimated as follows. The peak at *m/e* 140 (M—3H) in the spectrum of the undeuterated compound is found at *m/e* 140 [M—(D + 2H)] and 141 (M—3H) in the spectrum of a monodeuterated analogue, while the peak at *m/e* 141 (M—2H) in the undeuterated compound is observed at *m/e* 141 [M—(H + D)] and 142 (M—2H) in the labelled compound. Therefore, if the sum of the relative intensities of the peaks at *m/e* 140 and 141 in the deuterated compound is subtracted from the sum of the peak intensities at *m/e* 140 and 141 in the undeuterated compound, then the difference corresponds to M—2H ions contributing at M-2 in the labelled compound. The M—2H contribution may then be subtracted from the total M-2 peak intensity to give the M—D contribution. The correction for the compounds containing 3 deuteriums was similar to that described above, except that the peak at M-5 [M—(2D + H)] was also considered in the correction.

An alternative method of calculating label retention which does not require the above

Can. J. Chem. Downloaded from www.nrcresearchpress.com by 210.87.254.42 on 09/05/12
For personal use only.

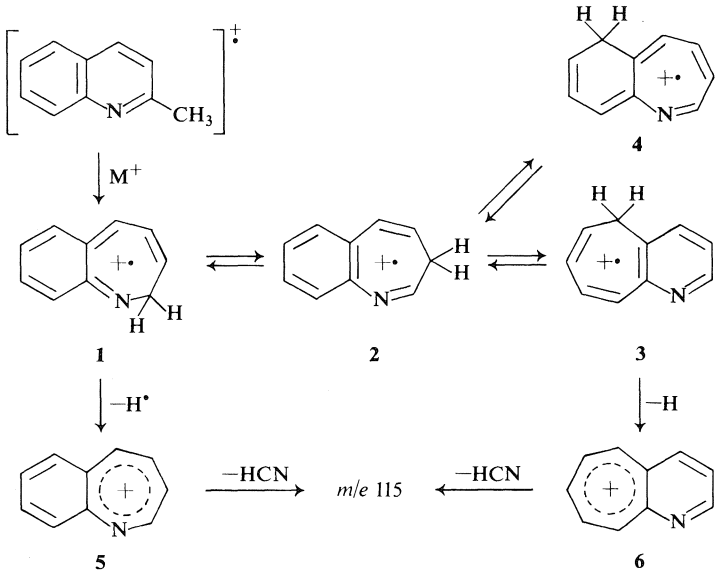

SCHEME 1

correction uses the ratio I_2/I_1 where I_2 is the intensity of the M—H peak in the spectrum of the labelled compound and I_1 is the M—H peak intensity in the spectrum of the unlabelled analogue. This method has been used to calculate label retention in the spectra of compounds where introduction of the label has no effect on the total yield of the fragment ion in question (8), but in the spectra of the labelled monomethylquinolines an apparent isotope effect results in the sum of the peak intensities at M—H and M—D being slightly less than the M—H peak intensity in the unlabelled analogue. Therefore, in this investigation the label retention was calculated from the observed peak intensities at M—H and M—D.

This isotope effect adds some uncertainty to the results since it is not certain whether the observed M—H to M—D peak intensity ratios actually represent the ratios in which hydrogens in various parts of the molecule would be lost in the absence of an isotope effect. If loss of hydrogen from the molecular ion is favored over loss of a chemically equivalent deuterium, then the observed M—H to M—D ratio will be greater than the ratio of equivalent hydrogens to deuteriums actually present in the molecular ion. Therefore, the label retention calculated from the M—H to M—D ratio would be higher than in the absence of such an effect. Alternatively, the isotope effect may be a consequence of the relative rates of hydrogen and deuterium transfers in the anticipated rearrangement process. The favored transfer of hydrogen over deuterium observed in the McLafferty rearrangement (9) may be interpreted in terms of the relative rates of hydrogen and deuterium transfer. A similar effect in the monomethylquinolines would result in a lower rate of rearrangement and fragmentation, and a consequent lowering of fragment ion intensity in the deuterated compounds. In any case the isotope effect observed in the methylquinolines is relatively small and therefore should not greatly affect the labelling results.

The peak at *m/e* 116 in the spectra of the monomethylquinolines labelled with a single deuterium (or ^{13}C) corresponds to retention of label in the M ⟶ M—(H + HCN) process, and the peak at *m/e* 115 corresponds to loss of label. Therefore, label retention in the M—(H + HCN) ion was calculated from the peak intensities at *m/e* 115 (I_1) and *m/e* 116 (I_2) by the equation $I_2/I_1 + I_2 \times 100$. Peaks of appreciable intensity at masses 113, 114, 116, and 117 as well as at 115 in the spectra of the unlabelled methylquinolines contribute to the *m/e* 115 and 116 peak intensities in the spectra of the labelled compounds, and corrections for these contributions were made in a manner similar to the procedure described for contributions of the M—2H ion at M—D. (In this case, the correction could be made only

Can. J. Chem. Downloaded from www.nrcresearchpress.com by 210.87.254.42 on 09/05/12
For personal use only.

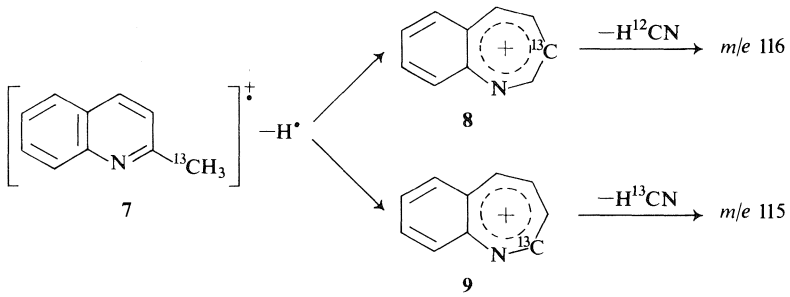

7 8 9

SCHEME 2

for those compounds containing a single heavy atom, and therefore we have not calculated the label retention in the M—(H + HCN) ion for the compounds containing 3 deuteriums).

It was found that the relative ion yields in this region of the spectra were about 10% lower in the labelled derivatives than in the unlabelled compounds because of the isotope effect. Therefore, the peak abundances in this region of the labelled derivatives were multiplied by a factor such that the relative intensities of the peaks became equivalent in both the unlabelled and labelled compounds.

The results listed in Table 1 are not compatible with formation of a simple benzyl ion by loss of a methyl hydrogen, nor are they compatible with a ring expansion and randomization of the hydrogens in the ring containing the substituent. They suggest that all 9 hydrogens in the molecule become randomized before or during formation of the M—H ion.

This hydrogen randomization is consistent with the formation of ring expanded intermediates in the fragmentation of methylquinolines, and a possible fragmentation mechanism (using 2-methylquinoline as an example) is outlined in Scheme 1. A methylquinoline substituted in the pyridine ring is first ionized and then undergoes ring expansion to a benzazacycloheptatriene ion **1**. The hydrogens may become randomized through a series of 1,2-hydrogen shifts (**1** ⟶ **2** etc). Rearrangement to ions of type **3** or, alternatively **4**, accounts for randomization and loss of hydrogen in the benzene ring. Loss of H (possible from the methylene position as suggested for the methylethylbenzenes (3*a*)) from any of the ring expanded molecular ions yields a benzazatropylium ion **5** or a tropylium type ion **6**. The results for the monomethylquinolines substituted in the benzene ring may be explained in a similar manner; in these compounds initial ionization and ring expansion may result in a cycloheptatriene ion **3**.

The label retention in the M—(H + HCN) ion also shows that hydrogen rearrangement precedes the loss of HCN. In the spectrum of 4-methylquinoline-2-*d*, about 50% of the deuterium is retained in the M—(H + HCN) ion while random loss from the molecule in the M ⟶ M—(H + HCN) process requires 78% retention. In the 8-α-d_1 derivative, the label retention is about 78% while random loss from the molecule in the M ⟶ M—(H + HCN) process also requires 78% retention. These results are in accord with randomization of the hydrogens in the molecule before loss of HCN, and show that hydrogens in the benzene ring participate in the loss of HCN.

The deuterium labelling results on the monomethylquinolines, therefore, are consistent with formation of ring expanded species before loss of H, but they do not suggest a mechanism for the ring expansion process. We felt that ring expansion could occur either by insertion of the exocyclic methyl carbon into adjacent carbon–carbon or carbon–nitrogen bonds, or by a random insertion of the methyl carbon into any carbon–carbon or carbon–nitrogen bonds in the molecule. The former mechanism is similar to that suggested by Marx and Djerassi (5) to account for their ^{13}C labelling results on 1-methylisoquinoline and the methylindoles, while the latter mechanism has precedence in the work of Rinehart *et al.* (4) who provided evidence for a tropylium ion formed by random insertion.

The ring expansion of labelled 2-methylquinoline by insertion of the 2-methyl carbon into adjacent carbon–carbon or carbon–nitrogen bonds is outlined in Scheme 2. Ring expansion of 2-methylquinoline-2-α^{13}C, **7**, results in **8** when

Can. J. Chem. Downloaded from www.nrcresearchpress.com by 210.87.254.42 on 09/05/12
For personal use only.

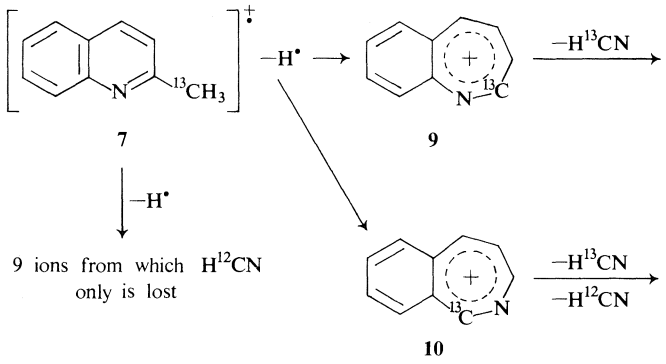

SCHEME 3

the methyl carbon is inserted between C-2 and C-3, and in **9** when inserted between N and C-2. Ion **8** will eliminate $H^{12}CN$ (unless further skeletal rearrangement occurs) while $H^{13}CN$ should be lost from **9**.

We determined the spectrum of **7** and observed 85% retention of ^{13}C after loss of HCN. This would suggest that the pathway to **8** (insertion of the methyl carbon into a carbon–carbon bond rather than a carbon–nitrogen bond) predominates if the ring expansion occurs by this mechanism. The examination of 2-methylquinoline-2-^{13}C would have provided further insight into this rearrangement but there did not seem to be a simple synthetic route to it.

It should be noted that the results from the spectrum of **7** are also consistent with the ring expansion occurring by a more random insertion of the methyl carbon. If ring expansion of **7** occurs by a random insertion into any of the carbon–carbon or carbon–nitrogen bonds of the molecule, then 11 possible ions can be formed. Of these, only 2 ions, **9** and **10**, (Scheme 3) can eliminate $H^{13}CN$. Ion **9** should eliminate $H^{13}CN$ only while **10** might eliminate $H^{13}CN$ and $H^{12}CN$ in approximately equal proportions. In ion **9** we assume that elimination will not occur toward the ring juncture. Therefore, if the ring expansion occurs in this manner one might expect $1\frac{1}{2}/11$ or 14% loss of ^{13}C (i.e. 86% retention) from **7** on expulsion of HCN. Similarly, if the ring expansion occurs by a random insertion of the methyl carbon into any carbon–carbon or carbon–nitrogen bond in the pyridine ring then $1\frac{1}{2}/6$ or 25% loss of ^{13}C (75% retention) from **7** would be predicted. The 85% retention of label observed in our experiment is therefore roughly in accord with the mechanisms shown, bearing in mind the fact that the various bonds in the quinoline system are not equivalent and thus a completely statistical insertion might not be expected.

The possible ring expansion mechanisms might be differentiated by examination of the spectra of labelled methylquinolines such as 4-methylquinoline-4-α-^{13}C and 5-methylquinoline-5-α-^{13}C. If a significant amount of ^{13}C is lost on elimination of HCN from the labelled 4-methylquinoline, then it is clear that the mechanism of ring expansion is more complicated than that outlined in Scheme 2. Similarly, the spectrum of the labelled 5-methylquinoline should indicate whether a methyl carbon on the benzene ring may be involved in the loss of HCN. Work along these lines is currently in progress.

Experimental

Apparatus, Methods, and Materials

Mass spectra were determined on a Hitachi Perkin–Elmer RMU-6A mass spectrometer at an ionizing potential of 80 eV and an ionizing current of 50 μA. Samples were introduced through an all-glass inlet system maintained at 200 °C.

All samples for mass spectrometry (with the exception of alkylquinolines labelled with deuterium in the 2-α-position) were purified by gas chromatography on a 6 ft column of 20% Apiezon M on celite. The column temperature was maintained at 180 to 230° depending on the volatility of the material. Gas chromatography of alkylquinolines labelled in the 2-α-position caused back exchange; therefore, these compounds were purified by chromatography over alumina. It was also necessary to pump a small amount of CH_3OD through the mass spectrometer before introduction of these samples.

The isotopic composition of all the labelled compounds was determined by low voltage mass spectrometry.

Nuclear magnetic resonance (n.m.r.) spectra were determined in $CDCl_3$ solution on a Varian A-60 spectrometer. Chemical shifts are expressed in parts per million (δ) from tetramethylsilane used as an internal standard.

CH_3OD (99 atom % D), and $^{13}CH_3I$ (57 atom % ^{13}C)

Can. J. Chem. Downloaded from www.nrcresearchpress.com by 210.87.254.42 on 09/05/12
For personal use only.

Can. J. Chem. Downloaded from www.nrcresearchpress.com by 210.87.254.42 on 09/05/12
For personal use only.

were obtained from Merck, Sharp and Dohme of Canada Ltd. $LiAlD_4$ was obtained from Ventron Corporation, Metal Hydrides Division, Beverly, Massachusetts.

Preparation of Alkylquinolines

The unlabelled quinolines used as reference compounds in this work were prepared by methods described in our previous paper (1) where we have also described the preparation of 2-methylquinoline-2-α-d_3, 4-methylquinoline-2-*d*, and 8-methylquinoline-8-α-d_1.

2-Methylquinoline-2-α-^{13}C

The labelled 2-methylquinoline was prepared from *N*-ethoxyquinolinium iodide and $^{13}CH_3MgI$ by the method of Červinka *et al.* (10). Its composition was: ^{12}C 45%, ^{13}C 55% (corrected for naturally occurring ^{13}C).

8-Methylquinoline-8-α-d_3

8-Quinolinecarboxylic acid was prepared by a Skraup reaction on anthranilic acid and was converted to its ethyl ester by the method of Campbell *et al.* (11). The ester was reduced to 8-hydroxymethylquinoline-8-α-d_2 [m.p. 72–73.5° (lit. 77–78° (12))] in 41% yield by adding an ether solution of the ester (0.6 g) to a suspension of $LiAlD_4$ (70 mg) in anhydrous ether at 0°, and stirring the mixture for 1 h.

The deuterated alcohol was separated from unreacted starting material by chromatography over alumina (the unreacted ester was eluted with benzene while chloroform was required to elute the alcohol from the column). Reduction of the ester in excess $LiAlD_4$ gave a nearly quantitative yield of alcohol but scrambling (probably in the 2-position) resulted.

HCl gas was bubbled into a benzene solution of the alcohol, and the resulting hydrochloride filtered off. The hydrochloride was then converted to 8-chloromethylquinoline-8-α-d_2 hydrochloride by treatment with thionyl chloride (using the conditions described by Kaslow and Schlatter (13)). The labelled chloromethylquinoline hydrochloride was treated with dilute NH_4OH, and the free base (m.p. 52–54°, lit. 53.5–54.5° (13)) was isolated by extracting the basic solution with ether. 8-Chloromethylquinoline-8-α-d_2 (0.24 g) was stirred with zinc (140 mg), deuteroacetic acid (2.5 ml) and D_2O (1 ml) for 6 h at room temperature, and then the mixture was refluxed for 1 h. The acid layer was basified with NH_3, extracted with ether and the ether layer dried over Na_2SO_4. Evaporation of the solvent gave 8-methylquinoline-8-α-d_3 in 67% yield. The composition of the product was: d_2 6.5%, d_3 86%, d_4 7.5%. A singlet at 2.76 δ (3H) in the n.m.r. spectrum of the unlabelled analogue was absent in the spectrum of the labelled compound.

The award of a bursary and studentships by the National Research Council of Canada to P. M. Draper is gratefully acknowledged. This work was supported through a grant from the National Research Council of Canada.

1. P. M. Draper and D. B. MacLean. Can. J. Chem. **46**, 1487 (1968).
2. H. M. Grubb and S. Meyerson. *In* Mass spectrometry of organic ions. *Edited by* F. W. McLafferty. Academic Press Inc., New York. 1963. Chap. 10.
3. (*a*) F. Meyer and A. G. Harrison. J. Amer. Chem. Soc. **86**, 4757 (1964). (*b*) S. Meyerson, H. Hart, and L. C. Leitch. J. Amer. Chem. Soc. **90**, 3419 (1968).
4. K. L. Rinehart, Jr., A. C. Buchholz, G. E. Van Lear, and H. L. Cantrill. J. Amer. Chem. Soc. **90**, 2983 (1968).
5. M. Marx and C. Djerassi. J. Amer. Chem. Soc. **90**, 678 (1968).
6. W. G. Cole, D. H. Williams, and A. N. H. Yeo. J. Chem. Soc. B, 1284 (1968).
7. S. D. Sample, D. A. Lightner, O. Buchardt, and C. Djerassi. J. Org. Chem. **32**, 997 (1967).
8. S. Meyerson and P. N. Rylander. J. Phys. Chem. **62**, 2 (1958).
9. J. K. MacLeod and C. Djerassi. J. Amer. Chem. Soc. **89**, 5182 (1967).
10. O. Červinka, A. Fabryova, and L. Matouchova. Collect. Czech. Chem. Commun. **28**, 535 (1963).
11. K. N. Campbell, J. F. Kerwin, R. A. LaForge, and B. K. Campbell. J. Amer. Chem. Soc. **68**, 1844 (1946).
12. C. E. Kaslow and W. R. Clark. J. Org. Chem. **18**, 55 (1953).
13. C. E. Kaslow and J. M. Schlatter. J. Amer. Chem. Soc. **77**, 1054 (1955).

An analytical solution of the Gibbs–Duhem equation in multicomponent systems

A. D. PELTON
Department of Metallurgy and Materials Science, University of Toronto, Toronto 181, Ontario
Received September 8, 1969

A general analytical power-series solution of the Gibbs–Duhem equation in multicomponent systems of any number of components has been developed. The simplicity and usefulness of the solution is made possible through the choice of a special set of composition variables.

Canadian Journal of Chemistry, **48**, 752 (1970)

Can. J. Chem. Downloaded from www.nrcresearchpress.com by 210.87.254.42 on 09/05/12
For personal use only.

Introduction

In a previous publication (1), an analytical power-series solution of the Gibbs–Duhem equation for ternary systems was developed. In the present investigation, the solution is expanded and generalized to apply to systems of any number of components.

The analytical solution shows the necessary thermodynamic relationships between the various solution properties which must be observed in any calculations, approximation techniques, and solution models concerned with multicomponent systems.

The solution may be used to calculate isothermal partial properties of mixing of all components from experimental values of this property for one component or from experimental values of the corresponding integral property of mixing. Such a calculation was done in the previous publication (1) for a ternary system with the aid of a digital computer. The method was shown to be faster and more accurate than the older graphical Gibbs–Duhem integration techniques. Although graphical techniques have been proposed for quaternary systems by Darken (2) and by Gokcen (3), these techniques would be extremely tedious and quite inaccurate. For quinary and higher-order systems, graphical techniques are virtually impossible.

In such calculations, endpoint or boundary values of the properties being calculated are always required. The analytical technique permits the easy utilization of endpoint values and points out clearly the minimum number of boundary values required in any calculation. Nikol'skii (4) has determined general relationships between the coefficients of series expansions for partial molar properties of mixing, using the mole fractions as composition variables. Nikol'skii's equations, however, do not lend themselves to use in calculations of the aforementioned type, since the utilization of boundary values is very difficult. Also, Nikol'skii's equations are in a form not easily fitted by standard surface-fitting techniques. To overcome these difficulties, it has been found necessary to use composition variables other than the mole fractions.

The relationships derived in the present study should prove useful in calculations aimed at approximating properties of multicomponent systems from available data for subsystems. They should also be of use in studies of interaction parameters in dilute systems and in other studies of solution behavior. The composition variables used permit an easy description of relationships in multicomponent systems and should provide the basis for a fruitful approach to such studies of solutions.

The Composition Variables

Consider a system of N components. Let X_i be the mole fraction of the ith component. A set of $(N-1)$ composition variables, y_i, may be defined as follows

$$y_1 = \frac{X_2 + X_3 + \cdots + X_N}{X_1 + X_2 + \cdots + X_N} = 1 - X_1$$

$$y_2 = \frac{X_3 + X_4 + \cdots + X_N}{X_2 + X_3 + X_4 + \cdots + X_N}$$

$$\cdot \quad \cdot \quad \cdot$$

$$\cdot \quad \cdot \quad \cdot \qquad [1]$$

$$\cdot \quad \cdot \quad \cdot$$

$$y_m = \frac{X_{m+1} + X_{m+2} + \cdots + X_N}{X_m + X_{m+1} + X_{m+2} + \cdots + X_N}$$

$$\cdot \quad \cdot \quad \cdot$$

$$\cdot \quad \cdot \quad \cdot$$

$$\cdot \quad \cdot \quad \cdot$$

$$y_{N-1} = \frac{X_N}{X_{N-1} + X_N}$$

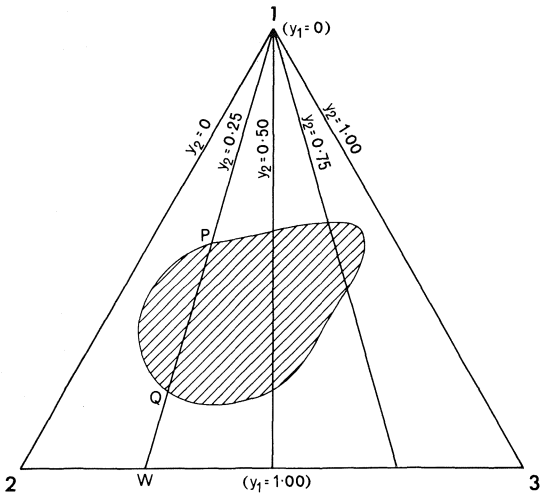

FIG. 1. Quasi-binary lines in a ternary system.

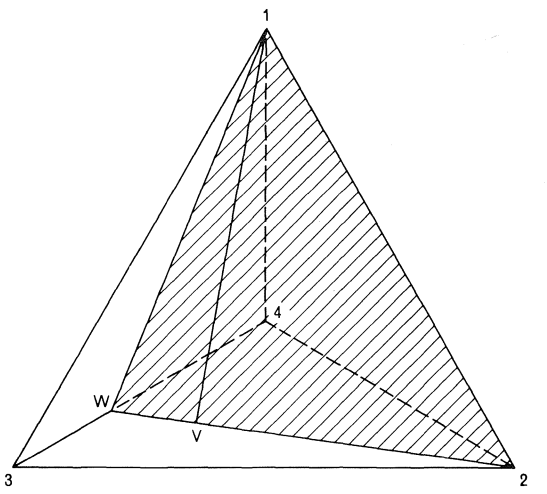

FIG. 2. Quasi-ternary plane and quasi-binary line in a quaternary system.

The inverse transformations are

$$X_1 = (1 - y_1)$$

$$X_2 = y_1(1 - y_2)$$

$$X_3 = y_1y_2(1 - y_3)$$

$$\cdot \quad \cdot \quad \cdot$$

[2] $$\cdot \quad \cdot \quad \cdot$$

$$\cdot \quad \cdot \quad \cdot$$

$$X_{N-1} = y_1y_2y_3 \cdots y_{N-2}(1 - y_{N-1})$$

$$X_N = y_1y_2y_3 \cdots y_{N-1}$$

Gokcen (3) used a similar set of composition variables in his proposed graphical integration technique for quaternary systems.

Note that all the variables y_i assume values between zero and unity.

For binary systems, only the one variable $y_1 = (1 - X_1) = X_2$ is required. For ternary systems, the two variables $y_1 = (1 - X_1)$ and $y_2 = X_3/(X_2 + X_3)$ are required. The variable y_2 is constant along a quasi-binary line of constant X_3/X_2 ratio as shown in Fig. 1. The variable can assume values from $y_2 = 0$ in the 1–2 binary system, to $y_2 = 1$ in the 1–3 binary system.

For quaternary systems, the three variables y_1, y_2, and y_3 are required. The variable y_3 is constant in a quasi-ternary plane of constant X_4/X_3 ratio such as the plane 1–2–W in Fig. 2. The variable can assume values from $y_3 = 0$ in the 1–2–3 ternary system to $y_3 = 1$ in the 1–2–4 ternary system. Within any quasi-ternary plane given by a constant value of y_3, the variable y_2 will also be constant along a quasi-binary line, such as the line 1–V in Fig. 2 which lies within the quasi-ternary plane.

In general, for an N-component system, y_{N-1} is constant along a quasi-$(N - 1)$-component surface which contains the 1, 2, 3, ···, and $(N - 2)$ corners of the composition polyhedron. For any constant value of y_{N-1}, the variable y_{N-2} will also be constant along a quasi-$(N - 2)$-component surface which lies within the previous quasi-$(N - 1)$-component surface and which contains the 1, 2, 3, ···, and $(N - 3)$ corners of the composition polyhedron. The variable y_{N-3} will then also be constant along a quasi-$(N - 3)$-component surface within the previous quasi-$(N - 2)$-component surface; etc.

Can. J. Chem. Downloaded from www.nrcresearchpress.com by 210.87.254.42 on 09/05/12
For personal use only.

It may also be seen that compositions lying within any subsystem of the N-component system may be easily described. Setting $y_m = 1$ automatically sets $X_m = 0$. Setting $y_m = 0$ sets

$$X_{m+1} = X_{m+2} = \cdots = X_N = 0$$

Thus, it may be seen that the variables y_i provide a simple, easily visualized description of a multicomponent system.

The Form of the Series Expansions

Let f_i be an isothermal partial molar property of mixing of the ith component in the system. Let f be the corresponding integral molar property of mixing.

Since series expansions are to be written for f_i and f in the composition variables, the properties and their derivatives must be continuous and finite functions in and on the boundaries of the entire composition range of the system. Certain total properties of mixing such as the total free energy of mixing or the total entropy of mixing do not satisfy these conditions, since the corresponding partial property of mixing of a component becomes infinite when the mole fraction of that component is zero. However, excess properties of mixing will always satisfy these conditions.

Consider first a binary system. For component 1, f_1 may be expanded as

$$f_1 = \sum_{j=2} a_j {y_1}^j \qquad [3]$$

It is well known that properties such as the partial molar excess free energy of mixing and enthalpy of mixing are well-fitted by such an expansion. That the expansion must start with the $j = 2$ term was proven in the previous publication (1). Such restrictions on coefficients in the general case will be discussed later.

For a ternary system, an expansion for f_1 as in eq. [3] will hold along any quasi-binary line, such as the line 1–W in Fig. 1, where y_2 is constant. It is for this reason that such lines are called "quasi-binary" lines. The values of the coefficients a_j will depend upon the particular quasi-binary line in question. The coefficients a_j may be written as expansions in y_2, so that for the ternary system

$$f_1 = \sum_{j=2} \sum_{k=0} a_{jk} {y_1}^j {y_2}^k \qquad [4]$$

If y_2 is constant, eq. [4] reduces to eq. [3]. It has been shown (1) that partial properties in ternary systems are well-fitted by such an expansion.

For a quaternary system, an expansion for f_1 as in eq. [4] will be valid along any quasi-ternary plane, such as the plane 1–2–W in Fig. 2, where y_3 is constant. It is for this reason that such planes are called "quasi-ternary" planes. In general, for a quaternary system, then

$$f_1 = \sum_{j=2} \sum_{k=0} \sum_{m=0} a_{jkm} {y_1}^j {y_2}^k {y_3}^m \qquad [5]$$

When y_3 is constant, eq. [5] reduces to eq. [4]. If y_2 is also constant, as it is along the quasi-binary line 1–V in Fig. 2, then eq. [5] reduces to eq. [3].

For an N-component system, adopting a more general notation, the expansion for f_1 may be written as follows

$$f_1 = \sum_{\substack{j_1=2,\\ j_m=0\\ (m=2,3,\cdots,N)}} {}^1a_{j_1 j_2 j_3 \cdots j_{N-1}} {y_1}^{j_1} {y_2}^{j_2} {y_3}^{j_3} \cdots {y_{N-1}}^{j_{N-1}} \qquad [6]$$

Similar expansions for the partial properties of all the other components and for the integral property may be written as follows

$$f_i = \sum_{\substack{j_m=0\\ (m=1,2,\cdots,N)}} {}^ia_{j_1 j_2 \cdots j_{N-1}} {y_1}^{j_1} {y_2}^{j_2} \cdots {y_{N-1}}^{j_{N-1}} \qquad (2 \leqslant i \leqslant N) \qquad [7]$$

Can. J. Chem. Downloaded from www.nrcresearchpress.com by 210.87.254.42 on 09/05/12
For personal use only.

[8] $$f = \sum_{\substack{j_1=1,\\ j_m=0\\ (m=2,3,\cdots,N)}} \phi_{j_1 j_2 \cdots j_{N-1}} y_1^{j_1} y_2^{j_2} \cdots y_{N-1}^{j_{N-1}}$$

where the coefficients ${}^i a_{j_1 j_2 \cdots j_{N-1}}$ are the expansion coefficients for the ith component.

The upper limits of the summations may be chosen in any manner suitable to describe a particular system.

The simplicity of these expansions may be seen to be a result of the use of the composition variables y_i. If other composition variables, such as the mole fractions, were used, the expansions would be much more complicated.

The expansion [6] for f_1 starts with the $j_1 = 2$ term. For $j_1 = 0$, the missing coefficients ${}^1 a_{0 j_2 j_3 \cdots}$ must be zero, since $f_1 = 0$ when $y_1 = 0$ ($X_1 = 1$). (Where the standard convention that $\lim y_1^{\,0} = 1$ as $y_1 \to 0$ has been adopted.) That the missing coefficients ${}^1 a_{1 j_2 j_3 \cdots}$ for $j_1 = 1$ must be zero follows from the relationships to be derived shortly. (However, it may be seen that this restriction is a result of Raoult's Law that $\lim \partial f_1 / \partial y_1 = 0$ as $y_1 \to 0$.)

In the expansion [8] for f, the missing coefficients $\phi_{0 j_2 j_3 \cdots}$ for $j_1 = 0$ must be zero, since $f = 0$ when $y_1 = 0$ ($X_1 = 1$).

Certain other restrictions on the expansion coefficients result from boundary conditions. Suppose that $y_k = 0$ (where $k = 2, 3, \cdots, N - 2$). This means that

$$X_{k+1} = X_{k+2} = \cdots = X_N = 0$$

That is, compositions along the 1–2– $\cdots$ $-k$ subsystem are described. In this case, it may be seen from eqs. [1] that the variables $y_{k+1}, y_{k+2}, \cdots$, and y_{N-1} are all undetermined. The properties f_i and f cannot be functions of these variables in this subsystem. For $j_k \neq 0$, there is no problem, since the factors $y_k^{j_k}$ in eqs. [6], [7], and [8] are all zero when $y_k = 0$. However, for $j_k = 0$, the factors $y_k^{j_k}$ equal unity when $y_k = 0$. In eqs. [6] and [7], then, terms such as

$${}^i a_{j_1 j_2 \cdots j_{k-1} 0 j_{k+1} \cdots j_{N-1}} y_1^{j_1} y_2^{j_2} \cdots y_{k-1}^{j_{k-1}} (1) y_{k+1}^{j_{k+1}} \cdots y_{N-1}^{j_{N-1}}$$

occur. In order that f_i not be a function of y_{k+1}, y_{k+2}, etc., the coefficients ${}^i a_{j_1 j_2 \cdots}$ must be zero when $j_k = 0$. The only exception occurs when $j_{k+1}, j_{k+2}, \cdots$, and j_{N-1} are also all zero. The same sort of restriction obviously applies to the expansion coefficients $\phi_{j_1 j_2 \cdots}$ in eq. [8]. The restrictions on the expansion coefficients may be summarized as

[9] $${}^i a_{j_1 j_2 \cdots} = 0 \quad (i = 1, 2, \cdots, N)$$

$$\phi_{j_1 j_2 \cdots} = 0$$

when

$$j_k = 0 \quad (k = 2, 3, \cdots, N - 2)$$

unless

$$j_{k+1} = j_{k+2} = \cdots = j_{N-1} = 0$$

Note that the above restriction does not apply when $k = N - 1$.

The restrictions [9] are illustrated for the case of a quinary system. In this case, the restrictions simply mean that all coefficients of the forms ${}^i a_{j_1 0 j_3 j_4}$ and ${}^i a_{j_1 j_2 0 j_4}$ are zero except for the coefficients ${}^i a_{j_1 000}$ and ${}^i a_{j_1 j_2 00}$, which need not be zero. (Note that the coefficients ${}^i a_{j_1 j_2 j_3 0}$ need not be zero.) The same sort of restrictions apply to the coefficients $\phi_{j_1 j_2 j_3 j_4}$.

There is one further set of restrictions which applies to the coefficients of f_1 and f. The discussion of these restrictions will be left until later.

All the restrictions mentioned above result from boundary conditions. If the series expansions are used only over a restricted composition range which does not contact the boundary of the composition polyhedron, these restrictions are not strictly necessary. However, in order for the equations to be generally applicable, the restrictions should be observed.

Can. J. Chem. Downloaded from www.nrcresearchpress.com by 210.87.254.42 on 09/05/12
For personal use only.

Can. J. Chem. Downloaded from www.nrcresearchpress.com by 210.87.254.42 on 09/05/12
For personal use only.

Relationships between Expansion Coefficients

By substituting the inverse variable transformations [2] into the equation

$$f = \sum_{i=1}^{N} X_i f_i \qquad [10]$$

and into the Gibbs–Duhem equation

$$\sum_{i=1}^{N} X_i \, \mathrm{d}f_i = 0 \qquad [11]$$

it may be shown (see Appendix I) that

$$f - f_1 = y_1 \left(\frac{\partial f}{\partial y_1}\right)_{y_m} \qquad [12]$$

By substituting the expansions [6] and [8] for f_1 and f into eq. [12] and equating coefficients of $({y_1}^{j_1} {y_2}^{j_2} \cdots)$ (see Appendix I), the following relationship may be shown

$${}^{1}a_{j_1 j_2 \cdots} = (1 - j_1)\phi_{j_1 j_2 \cdots} \qquad [13]$$

For $j_1 = 1$, the coefficients ${}^{1}a_{1 j_2 j_3 \cdots}$ must all be zero, since the coefficients $\phi_{1 j_2 j_3 \cdots}$ must be finite. This proves the assertion made previously.

If the expansion coefficients ${}^{1}a_{j_1 j_2 \cdots}$ for f_1 are known, then the expansion coefficients $\phi_{j_1 j_2 \cdots}$ for f are uniquely determined from eq. [13], except when $j_1 = 1$. These coefficients, $\phi_{1 j_2 j_3 \cdots}$, can be found from boundary conditions, as will be discussed shortly. Conversely, however, a knowledge of the coefficients $\phi_{j_1 j_2 \cdots}$ will give a complete expression for f_1.

By differentiating eq. [10] with respect to y_i and y_{i-1} (for $i = 2, 3, \cdots, N - 1$), it may be shown (see Appendix II) that

$$f_i - f_{i-1} = \frac{1}{y_1 y_2 \cdots y_{i-1}} \left(y_{i-1} \frac{\partial f}{\partial y_{i-1}} - y_i \frac{\partial f}{\partial y_i} \right) \qquad [14]$$

By substituting the expansions [6], [7], and [8] into eq. [14] and equating coefficients, it may be shown (see Appendix II) that

$${}^{i}a_{j_1 j_2 \cdots} = {}^{i-1}a_{j_1 j_2 \cdots} + (j_{i-1} + 1 - j_i) \cdot \phi_{(j_1+1)(j_2+1)\cdots(j_{i-1}+1) j_i j_{i+1} \cdots j_{N-1}} \quad (i \geqslant 2) \qquad [15]$$

Equation [14], and thus eq. [15], are only true for $i < N$, but it may easily be shown (see Appendix III) that eq. [15] also holds for $i = N$ if the simple convention that $j_N = 0$ is adopted.

If the expansion coefficients $\phi_{j_1 j_2 \cdots}$ of f are known, then, from eq. [13] and from the recursion relationship [15], the expansion coefficients for f_i ($i = 1, 2, \cdots, N$) are all uniquely determined.

Substitution of eq. [13] into eq. [15] yields the relationship

$${}^{i}a_{j_1 j_2 \cdots} = {}^{i-1}a_{j_1 j_2 \cdots} - \frac{(j_{i-1} + 1 - j_i)}{j_1} \cdot {}^{1}a_{(j_1+1)(j_2+1)\cdots(j_{i-1}+1) j_i j_{i+1} \cdots j_{N-1}} \qquad [16]$$

$$(i \geqslant 2, j_1 \neq 0)$$

The recursion relationship [16] permits the expansion coefficients ${}^{i}a_{j_1 j_2 \cdots}$ of f_i ($i = 2, 3, \cdots, N$) to be calculated if the expansion coefficients ${}^{1}a_{j_1 j_2 \cdots}$ for f_1 are known, except when $j_1 = 0$. These coefficients, ${}^{i}a_{0 j_2 j_3 \cdots}$, can be found from boundary values, as will be discussed later.

Further Restrictions on Coefficients

Because of the restrictions [9] on the coefficients ${}^{i}a_{j_1 j_2 \cdots}$, one further set of restrictions on the expansion coefficients of f and of f_1 is necessary.

Consider eq. [15]. Let $j_k = 0$, where $k < i$, and $k \neq N - 1$. In this case, because of the restrictions [9], the terms ${}^{i}a_{j_1 j_2 \cdots}$ and ${}^{i-1}a_{j_1 j_2 \cdots}$ are both zero unless $j_{k+1} = j_{k+2} = \cdots = j_{N-1} = 0$. For $k < i$, then, it may be seen from eq. [15] that if any subscript of the expansion coefficient ϕ is unity, the

coefficient must be zero; the only exception being coefficients of the form $\phi_{(j_1+1)\cdots 1111\cdots 10000\cdots 0}$, where the first 0 is in the ith subscript.

From eq. [16], it may be seen that exactly the same restriction applies to the coefficients ${}^1a_{j_1j_2\cdots}$ of f_1.

By considering this restriction for all values of i ($i = 2, 3, \cdots, N$), it may be seen that, in general

$$[17] \qquad \phi_{j_1j_2\cdots} = 0 \qquad {}^1a_{j_1j_2\cdots} = 0$$

when

$$j_k = 1 \quad (k = 2, 3, \cdots, N-2)$$

unless

$$j_{k+1} = j_{k+2} = \cdots = j_{m-1} = 1$$

and also

$$j_m = j_{m+1} = \cdots = j_{N-1} = 0$$

for all m where $k + 1 \leqslant m \leqslant N$.

(Note that the above restriction does not apply when $k = N - 1$.)

In words, this restriction simply means that if any subscript of a coefficient $\phi_{j_1j_2\cdots}$ or ${}^1a_{j_1j_2\cdots}$ is unity, the coefficient must be zero unless this subscript is followed by a string of 1's, followed by a string of 0's. For example, in a quinary system, all coefficients of the form $\phi_{j_11j_3j_4}$ are zero except for the coefficients ϕ_{j_1100}, ϕ_{j_1110}, and ϕ_{j_1111}. Also, all coefficients of the form $\phi_{j_1j_21j_4}$ are zero except for the coefficients $\phi_{j_1j_210}$ and $\phi_{j_1j_211}$. (The coefficients $\phi_{j_1j_2j_31}$ need not be zero.) The same sort of restrictions apply to the expansion coefficients ${}^1a_{j_1j_2j_3j_4}$ of f_1.

It should be stressed again that the restrictions [17] are a result of the restrictions [9], and one set of restrictions cannot be observed without the other.

Including Boundary Values

If the expansion coefficients ${}^1a_{j_1j_2\cdots}$ of f_1 are known, then all the coefficients ${}^ia_{j_1j_2\cdots}$ of f_i ($i = 2, 3, \cdots, N$) can be calculated from eq. [16] except when $j_1 = 0$. These coefficients ${}^ia_{0j_2j_3\cdots}$ can only be obtained from endpoint values of f_i in or on the boundary of the composition range under consideration.

Equation [7] for f_i ($i = 2, 3, \cdots$) may be expanded as

$$[18] \qquad f_i = \sum_{\substack{j_m=0 \\ (m=2,3,\cdots)}} {}^ia_{0j_2j_3\cdots}y_2{}^{j_2}y_3{}^{j_3}\cdots + \sum_{\substack{j_1=1, \\ j_m=0 \\ (m=2,3,\cdots)}} {}^ia_{j_1j_2\cdots}y_1{}^{j_1}y_2{}^{j_2}\cdots$$

The first term on the right-hand side of eq. [18] is constant along lines where $y_2, y_3, \cdots$, and y_{N-1} are constant. These lines are quasi-binary lines radiating from the "1-corner" of the composition polyhedron. In a ternary system as in Fig. 1, these are the lines 1–W. In a quaternary system as in Fig. 2, these are the lines 1–V. The knowledge of one endpoint value of f_i at some point along a quasi-binary line is thus sufficient to give values of f_i at any point on that line.

Let $f_{i(y_1{}^*y_2y_3\cdots)}$ be some known endpoint value of f_i at some point where $y_1 = y_1{}^*$ along a quasi-binary line where $y_2, y_3, \cdots$ and y_{N-1} are constant. Then

$$[18] \qquad f_{i(y_1{}^*y_2y_3\cdots)} = \sum_{\substack{j_m=0 \\ (m=2,3,\cdots)}} {}^ia_{0j_2j_3\cdots}y_2{}^{j_2}\,y_3{}^{j_3}\cdots + \sum_{\substack{j_1=1, \\ j_m=0 \\ (m=2,3,\cdots)}} {}^ia_{j_1j_2\cdots}y_1{}^{*j_1}y_2{}^{j_2}\cdots$$

Let $f_{i(y_1y_2\cdots)}$ be the value of f_i at any value of y_1 along the same quasi-binary line. Substitution of eq. [19] into eq. [18] then gives

$$[20] \qquad f_{i(y_1y_2\cdots)} = f_{i(y_1{}^*y_2y_3\cdots)} + \sum_{\substack{j_1=1, \\ j_m=0 \\ (m=2,3,\cdots)}} {}^ia_{j_1j_2\cdots}(y_1{}^{j_1} - y_1{}^{*j_1})y_2{}^{j_2}y_3{}^{j_3}\cdots$$

Can. J. Chem. Downloaded from www.nrcresearchpress.com by 210.87.254.42 on 09/05/12
For personal use only.

In Fig. 1, for example, if the coefficients ${}^1a_{j_1j_2}\ldots$ of f_1 are known over the shaded region, then values of f_2 and f_3 at any point along the quasi-binary line 1–W between P and Q would be given by eq. [16] and by the knowledge of the values of $f_{2(y_1{}^*y_2)}$ and $f_{3(y_1{}^*y_2)}$ at any point on this line, say at point Q, which could lie on a phase boundary such as a liquidus. In the quaternary system in Fig. 2, values of f_i at any point on the line 1–V are given by a knowledge of an endpoint value $f_{i(y_1{}^*y_2y_3)}$ at any point on this line (within the composition range where the equations apply).

Thus, it may be seen that the use of endpoint values permits the determination of f_i without the explicit determination of the coefficients ${}^ia_{0j_2j_3}\ldots$

If the 2–3– $\cdots$ –N subsystem forms a boundary of the region in which values of the coefficients of f_1 are known, then endpoint values of f_i in this subsystem may be used. In this case, $y_1{}^* = 1$, and eq. [20] takes a particularly simple form. The endpoint values used, $f_{i(1y_2\cdots)}$, are values of f_i at points such as point W in Fig. 1, or point V in Fig. 2. These endpoint values may be obtained from independent measurements, say of f_2, in the 2–3– $\cdots$ –N subsystem. If f_2 is known as a function of composition in this subsystem, then the terms $f_{i(1y_2y_3\cdots)}$ can be expressed as functions of $y_2, y_3, \cdots$, and y_{N-1}. The functional form of $f_{i(1y_2y_3\cdots)}$ would be as in eqs. [6] and [7], since when $y_1 = 1$, the variables $y_2 = (1 - X_2), y_3, y_4, \cdots$ are the proper variables for describing the 2–3– $\cdots$ –N subsystem using the present method.

Endpoint Values for the Integral Property

If it is desired to calculate f from a knowledge of the coefficients ${}^1a_{j_1j_2}\ldots$ for f_1, then eq. [13] will allow the calculation of all the coefficients $\phi_{j_1j_2}\ldots$ except when $j_1 = 1$. In order to get a complete expression for f, therefore, endpoint values are required.

Equation [8] may be expanded as

$$[21] \qquad f = y_1 \cdot \sum_{\substack{j_m=0 \\ (m=2,3,\cdots)}} \phi_{1j_2j_3\cdots} y_2{}^{j_2} y_3{}^{j_3} \cdots + \sum_{\substack{j_1=2, \\ j_m=0 \\ (m=2,3,\cdots)}} \phi_{j_1j_2\cdots} y_1{}^{j_1} y_2{}^{j_2} \cdots$$

If $f_{(y_1{}^*y_2y_3\cdots)}$ is some known endpoint value of f at a point where $y_1 = y_1{}^*$ along a quasi-binary line where $y_2, y_3, \cdots$, and y_{N-1} are constant, then

$$[22] \qquad f_{(y_1{}^*y_2\cdots)} = y_1{}^* \cdot \sum_{\substack{j_m=0 \\ (m=2,3,\cdots)}} \phi_{1j_2j_3\cdots} y_2{}^{j_2} y_3{}^{j_3} \cdots + \sum_{\substack{j_1=2, \\ j_m=0 \\ (m=2,3,\cdots)}} \phi_{j_1j_2\cdots} y_1{}^{*j_1} y_2{}^{j_2} \cdots$$

By substitution of eq. [22] into eq. [21], it may be seen that $f_{(y_1y_2\cdots)}$ at any point on the same quasi-binary line may then be calculated from the equation

$$[23] \qquad f_{(y_1y_2\cdots)} = (y_1/y_1{}^*) \cdot f_{(y_1{}^*y_2y_3\cdots)} + \sum_{\substack{j_1=2, \\ j_m=0 \\ (m=2,3,\cdots)}} \phi_{j_1j_2\cdots} (y_1{}^{j_1} - y_1 y_1{}^{*j_1-1}) y_2{}^{j_2} y_3{}^{j_3} \cdots$$

By the use of endpoint values, therefore, complete expressions for f may be found without the explicit determination of the coefficients $\phi_{1j_2j_3\ldots}$.

The Necessity of Using Boundary Values

Consider the quaternary system in Fig. 2. Suppose that f_1 has been measured along the 1–2 binary line. Values of f_2 along this binary line can then be calculated using the boundary condition that $f_2 = 0$ when $X_2 = 1$. The value of f_2 at $X_1 = 1$ ($y_1 = 0$) could thus be calculated. From Fig. 2 it may be seen that this value, $f_{2(0y_2y_3)}$, at the "1-corner" of the composition tetrahedron could then be used as an endpoint value along any quasi-binary line 1–V. No independent measurements of f_2 anywhere would then be required to give values of f_2 at any point in the quaternary system. For an N-component system, then, it would seem that the use of the condition that $f_i = 0$ when $X_i = 1$ obviates the necessity for measuring endpoint values.

In fact, as will be shown later, the use of these boundary conditions will give explicit expressions for the coefficients ${}^ia_{0j_2j_3\ldots}$.

Can. J. Chem. Downloaded from www.nrcresearchpress.com by 210.87.254.42 on 09/05/12
For personal use only.

This technique will not work, of course, if experimental measurements of f_1 have been made only over a restricted range of composition such as the shaded area in Fig. 1. The coefficients ${}^1a_{j_1j_2}\ldots$ of the expansion [6] for f_1 will then apply only over this region. Obviously, boundary conditions at the points $X_i = 1$ outside this region cannot be used. It is also obvious from the previous discussion that values of f_1 near $X_1 = 1$ are required, since, essentially, calculated endpoint values, $f_{i(0y_2y_3\cdots)}$, at the "1-corner" are being used.

However, even if values of f_1 in the required composition regions are known, the technique is still not applicable, since it requires that extremely accurate values of f_1 in the region near $X_1 = 1$ be known. Such accuracy is required since f_i is usually quite large in this region and, through the Gibbs–Duhem relation, is very sensitive to changes in the partial derivatives of f_1 with respect to the y_i. However, f_1 is very small in this region, and it is very difficult to determine the partial derivatives with any accuracy. Thus, in practice, endpoint values of f_i obtained from independent measurements are always required.

Similarly, in calculations of the integral property f, the use of the conditions that $f = 0$ at the corners of the composition polyhedron is, in practice, not possible for the same reasons.

Explicit Expressions for the Coefficients ${}^ia_{0j_2j_3}\ldots$ and $\phi_{1j_2j_3}\ldots$

In this section, explicit expressions for the coefficients ${}^ia_{0j_2j_3}\ldots$ ($i = 2, 3, \cdots$) and $\phi_{1j_2j_3\ldots}$ will be derived from the boundary conditions at the corners of the composition polyhedron. Such equations have just been shown to be not useful in calculations of f_i and f from experimental measurements of f_1. However, if the present method is used in approximation techniques, or in studies of solution behavior, etc., such explicit expressions should be useful.

In order to calculate the coefficients ${}^ia_{0j_2j_3\ldots}$, the restrictions [9] must be applied for $k = 1$. That is

$$[24] \qquad {}^ia_{0j_2j\ldots_3} = 0 \quad \text{unless} \quad j_2 = j_3 = \cdots = j_{N-1} = 0$$

This is a statement of the fact that f_i is single-valued when $y_1 = 0$ ($X_1 = 1$). Thus, for each value of i ($i = 2, 3, \cdots$), there is only one non-zero coefficient of the form ${}^ia_{0j_2j_3\ldots}$, namely, the coefficient ${}^ia_{000\cdots0}$.

To determine ${}^ia_{000\cdots0}$ ($i = 2, 3, \cdots$), the boundary condition that $f_i = 0$ when $X_i = 1$ is used. When $X_i = 1$, $y_1 = y_2 = \cdots = y_{i-1} = 1$, and $y_i = y_{i+1} = \cdots = y_{N-1} = 0$.

Therefore, when $X_i = 1$

$$[25] \qquad f_i = {}^ia_{000\cdots0} + \sum_{\substack{j_1=1,\\ j_m=0\\ (m=2,3,\cdots)}} {}^ia_{j_1j_2}\ldots(1)^{j_1}(1)^{j_2}\cdots(1)^{j_{i-1}}(0)^{j_i}(0)^{j_{i+1}}\cdots$$

$$= 0$$

All terms in the summation in eq. [25] are zero unless $j_i = j_{i+1} = \cdots = j_{N-1} = 0$. Therefore

$$[26] \qquad {}^ia_{000\cdots0} = -\sum_{\substack{j_1=1,\\ j_m=0\\ (m=2,3,\cdots)}} {}^ia_{j_1j_2\cdots j_{i-1}000\cdots0} \quad [i = 2, 3, \cdots]$$

In order to calculate the coefficients $\phi_{1j_2j_3}\ldots$, the restrictions [17] must be applied for $k = 1$. That is

$$[27] \qquad \phi_{1j_2j_3\ldots} = 0$$

unless

$$j_2 = j_3 = \cdots j_{m-1} = 1$$

and

$$j_m = j_{m+1} = \cdots j_{N-1} = 0$$

where $2 \leqslant m \leqslant N$. These coefficients may be found from the boundary conditions that $f = 0$ at the corners of the composition polyhedron.

Can. J. Chem. Downloaded from www.nrcresearchpress.com by 210.87.254.42 on 09/05/12
For personal use only.

Let $X_i = 1$ ($i = 2, 3, \cdots$). Then $y_1 = y_2 = \cdots = y_{i-1} = 1$ and $y_i = y_{i+1} = \cdots = y_{N-1} = 0$. Therefore, when $X_i = 1$

[28]
$$f = \sum_{\substack{j_1=1,\\ j_m=0\\ (m=2,3,\cdots)}} \phi_{j_1 j_2 \ldots}(1)^{j_1}(1)^{j_2}\cdots(1)^{j_{i-1}}(0)^{j_i}(0)^{j_{i+1}}\cdots$$
$$= \sum_{\substack{j_1=1,\\ j_m=0\\ (m=2,3,\cdots)}} \phi_{j_1 j_2 \cdots j_{i-1}000\cdots 0}$$
$$= 0$$

Taking i successively as $i = 2, 3, \cdots, N$ in eq. [28] and applying the restrictions [27]

[29]
$$\phi_{1000\cdots} = -\sum_{j_1=2} \phi_{j_1000\cdots}$$
$$\phi_{11000\cdots} = -\phi_{1000\cdots} - \sum_{\substack{j_1=2,\\ j_2=0}} \phi_{j_1 j_2 000\cdots}$$
$$\phi_{111000\cdots} = -\phi_{11000\cdots} - \phi_{1000\cdots} - \sum_{\substack{j_1=2,\\ j_2=0,\\ j_3=0}} \phi_{j_1 j_2 j_3 000\cdots}$$
$$\vdots$$

That is

[30]
$$\phi_{111\cdots 11000\cdots 0} = -\sum_{\substack{j_1=2,\\ j_m=0\\ (m=2,3,\cdots)}} (\phi_{j_1000\cdots} + \phi_{j_1 j_2 000\cdots} + \cdots + \phi_{j_1 j_2 \cdots j_{i-1}000\cdots})$$

where the first zero subscript on the left is the ith subscript.

Summary

In an N-component system, a set of $(N - 1)$ special composition variables, y_i, may be defined as in eqs. [1]. These variables assume constant values along various quasi-subsystems of the N-component system.

Isothermal partial molar properties of mixing, f_i, for each component, and the corresponding integral property of mixing, f, may be expressed as power series in the variables y_i as in eqs. [6]–[8].

In order that the expansions be consistent with certain boundary conditions, the expansion for f_1 for component 1 must start with the y_1^2 term, and the expansion for f must start with the y_1^1 term as shown in eqs. [6] and [8]. Also, the restrictions [9] on all the coefficients, and the restrictions [17] on the expansion coefficients for f_1 and f, must be observed if the properties are to be single-valued along the boundaries of the composition polyhedron. None of these restrictions need strictly be observed if the equations are to be applied over a restricted composition region which does not contact the edges of the composition polyhedron. However, in order that the equations be generally applicable, the restrictions should be observed.

The various coefficients are related by eq. [13] and by the recursion relationships of eqs. [15] and [16].

The relationships should prove useful in calculations aimed at approximating properties of multicomponent systems from available data for subsystems. They should also be of use in studies of interaction parameters in dilute systems and in other studies of solution behavior. In such cases, it will be

Can. J. Chem. Downloaded from www.nrcresearchpress.com by 210.87.254.42 on 09/05/12
For personal use only.

desirable for the expansions to be consistent with the boundary conditions that $f_i = 0$ when $X_i = 1$ and that $f = 0$ when $X_i = 1$ and also for all the properties to be single-valued when $X_1 = 1$. In this case, the restrictions [24] and [27] must be observed and also the relationships [26] and [30] must hold. All boundary conditions are then satisfied. When such complete expansions for f_i and f are written using eqs. [26] and [30], the expansion coefficients ${}^{i}a_{j_1 j_2}\ldots$ of f_i ($i = 2, 3, \cdots$) are not all linearly independent; nor are the expansion coefficients $\phi_{j_1 j_2}\ldots$ of f. The expansion coefficients ${}^{1}a_{j_1 j_2}\ldots$ of f_1, however, are all linearly independent.

The analytical method may be used to calculate the expansion coefficients of the properties f_i ($i = 2, 3, \cdots$) and f if the expansion coefficients of f_1 for component 1 may be found by a surface-fitting technique to measured values of f_1 over a composition range. The desired coefficients may be calculated from eqs. [13] and [16], except for the coefficients ${}^{i}a_{0 j_2 j_3}\ldots$ of f_i when $j_1 = 0$ and the coefficients $\phi_{1 j_2 j_3}\ldots$ of f when $j_1 = 1$. Complete solutions for f_i and f require the additional knowledge of endpoint values of f_i and f obtained from independent measurements on the boundary of the composition range studied. One endpoint value of f_i (or f) along a quasi-binary line emanating from the "1 corner" of the composition polyhedron is sufficient to fix values of f_i (or f) anywhere along that line (within the composition range where the equations are valid). Complete expansions for f_i and f are then given by eqs. [20] and [23]. Endpoint values may be obtained from known values of the properties f_i along phase boundaries, or, if the 2–3– $\cdots$ –N subsystem forms a boundary of the composition range studied, from independent measurements of a property f_i in this subsystem.

A completely worked example of this type of calculation for the Bi–Cd–Sn ternary system was done previously (1). All the steps in the method, including the use of endpoint data from independent measurements in the 2–3 subsystem were explicitly illustrated in this example.

The boundary conditions that f_i and f are zero when $X_i = 1$ (as in eqs. [26] and [30]) cannot be used in such calculations unless f_1 has been measured over the entire composition range of the N-component system and unless values of f_1 in the vicinity of $X_1 = 1$ are known with a degree of accuracy seldom attainable. In practice, endpoint values of f_i and f from independent measurements will almost always be required.

One of the advantages of the present method is that boundary value requirements are clearly pointed out and that the inclusion of boundary values in the calculations is a simple matter.

The analytical method may also be used to calculate the coefficients of the expansions for f_i ($i = 1, 2, 3, \cdots$) if the expansion coefficients $\phi_{j_1 j_2}\ldots$ of f may be obtained by a surface-fitting technique to measured values of f over a composition range. The relationships [13] and [15] may be used for this purpose. No endpoint values of the properties f_i from independent measurements are required in this case.

The author wishes to thank Professor S. N. Flengas of this department for his encouragement and for many helpful discussions. A maintenance grant from Shell Canada Ltd. and financial assistance from the National Research Council of Canada are also gratefully acknowledged.

1. A. D. Pelton and S. N. Flengas. Can. J. Chem. **47**, 2283 (1969).
2. L. S. Darken. J. Amer. Chem. Soc. **72**, 2909 (1950).
3. N. A. Gokcen. J. Phys. Chem. **64**, 401 (1960).
4. S. S. Nikol'skii. Russ. J. Phys. Chem. Engl. Transl. **39**, 1541 (1965).

Appendix I

Substitute eqs. [2] into eq. [10] and collect terms

$$[A\text{-}1] \quad f = (1 - y_1)f_1 + y_1(1 - y_2)f_2 + \cdots + y_1 y_2 \cdots y_{N-2}(1 - y_{N-1})f_{N-1} + y_1 y_2 \cdots y_{N-1} f_N$$

$$[A\text{-}2] \quad f = f_1 + y_1(f_2 - f_1) + y_1 y_2(f_3 - f_2) + \cdots + y_1 y_2 \cdots y_{N-1}(f_N - f_{N-1})$$

Can. J. Chem. Downloaded from www.nrcresearchpress.com by 210.87.254.42 on 09/05/12
For personal use only.

Differentiate eq. [A-2] with respect to y_1 at constant $y_2, y_3, \cdots, y_{N-1}$

$$[A\text{-}3]\quad \frac{\partial f}{\partial y_1} = \left[\frac{\partial f_1}{\partial y_1} + y_1 \cdot \frac{\partial(f_2 - f_1)}{\partial y_1} + \cdots + y_1 y_2 \cdots y_{N-1} \frac{\partial(f_N - f_{N-1})}{\partial y_1}\right] + [(f_2 - f_1) + y_2(f_3 - f_2) + y_2 y_3(f_4 - f_3) + \cdots + y_2 y_3 \cdots y_{N-1}(f_N - f_{N-1})]$$

Substitute eqs. [2] into eq. [11] and collect terms

$$[A\text{-}4]\quad (1 - y_1)\,df_1 + y_1(1 - y_2)\,df_2 + \cdots + y_1 y_2 \cdots y_{N-1}\,df_N = 0$$

$$[A\text{-}5]\quad df_1 + y_1\,d(f_2 - f_1) + y_1 y_2\,d(f_3 - f_2) + \cdots + y_1 y_2 \cdots y_{N-1}\,d(f_N - f_{N-1}) = 0$$

Since eq. [A-5] holds everywhere, it also holds along a line where $y_2, y_3, \cdots$, and y_{N-1} are constant. Thus, by eq. [A-5], the first term on the right-hand side of eq. [A-3] is zero. By substitution from eq. [A-2], the second term on the right of eq. [A-3] is given, with the result that

$$[A\text{-}6]\quad f - f_1 = y_1\left(\frac{\partial f}{\partial y_1}\right)_{y_m}$$

Substitute the expansions [6] and [8] for f_1 and f into eq. [A-6]

$$[A\text{-}7]\quad \sum_{\substack{j_1=1,\\ j_m=0\\ (m=2,3,\cdots)}} \phi_{j_1 j_2 \cdots} y_1^{j_1} y_2^{j_2} \cdots - \sum_{\substack{j_1=2,\\ j_m=0\\ (m=2,3,\cdots)}} {}^1a_{j_1 j_2 \cdots} y_1^{j_1} y_2^{j_2} \cdots = \sum_{\substack{j_1=1,\\ j_m=0\\ (m=2,3,\cdots)}} j_1 \cdot \phi_{j_1 j_2 \cdots} y_1^{j_1} y_2^{j_2} \cdots$$

Equate coefficients of $y_1^{j_1} y_2^{j_2} \cdots y_{N-1}^{j_{N-1}}$ on both sides of eq. [A-7]

$$[A\text{-}8]\quad \phi_{j_1 j_2 \cdots} - {}^1a_{j_1 j_2 \cdots} = j_1 \cdot \phi_{j_1 j_2 \cdots}$$

Eq. [A-8] may be rearranged to give eq. [13].

Appendix II

Differentiate eq. [A-2] with respect to y_i ($i = 2, 3, \cdots, N - 1$)

$$[A\text{-}9]\quad \frac{\partial f}{\partial y_i} = \left[\frac{\partial f_1}{\partial y_i} + y_1 \frac{\partial(f_2 - f_1)}{\partial y_i} + \cdots + y_1 y_2 \cdots y_{N-1} \frac{\partial(f_N - f_{N-1})}{\partial y_i}\right] + \frac{1}{y_i}[y_1 y_2 \cdots y_i(f_{i+1} - f_i) + y_1 y_2 \cdots y_{i+1}(f_{i+2} - f_{i+1}) + \cdots + y_1 y_2 \cdots y_{N-1}(f_N - f_{N-1})]$$

Differentiate eq. [A-2] with respect to y_{i-1} ($i = 2, 3, \cdots, N - 1$)

$$[A\text{-}10]\quad \frac{\partial f}{\partial y_{i-1}} = \left[\frac{\partial f_1}{\partial y_{i-1}} + y_1 \frac{\partial(f_2 - f_1)}{\partial y_{i-1}} + \cdots + y_1 y_2 \cdots y_{N-1} \frac{\partial(f_N - f_{N-1})}{\partial y_{i-1}}\right] + \frac{1}{y_{i-1}}[y_1 y_2 \cdots y_{i-1}(f_i - f_{i-1}) + y_1 y_2 \cdots y_i(f_{i+1} - f_i) + \cdots + y_1 y_2 \cdots y_{N-1}(f_N - f_{N-1})]$$

By eq. [A-5], the first terms on the right-hand sides of eqs. [A-9] and [A-10] are zero.

Multiply eqs. [A-9] and [A-10] by y_i and y_{i-1}, respectively, and subtract the resulting equations

$$[A\text{-}11]\quad y_{i-1}\frac{\partial f}{\partial y_{i-1}} - y_i \frac{\partial f}{\partial y_i} = y_1 y_2 \cdots y_{i-1}(f_i - f_{i-1})$$

Can. J. Chem. Downloaded from www.nrcresearchpress.com by 210.87.254.42 on 09/05/12
For personal use only.

Rearrange eq. [A-11] and substitute the expansions [7] and [8]

$$[A\text{-}12]\quad \sum_{\substack{j_m=0\\(m=1,2,\cdots)}} ({}^{i}a_{j_1j_2\cdots} - {}^{i-1}a_{j_1j_2\cdots})y_1^{j_1}y_2^{j_2}\cdots$$

$$= \frac{1}{y_1y_2\cdots y_{i-1}} \cdot \sum_{\substack{j_1=1,\\ j_m=0\\(m=2,3,\cdots)}} (j_{i-1}\cdot\phi_{j_1j_2\cdots} - j_i\cdot\phi_{j_1j_2\cdots})y_1^{j_1}y_2^{j_2}\cdots$$

$$= \sum_{\substack{j_1=1,\\ j_m=0\\(m=2,3,\cdots)}} (j_{i-1} - j_i)\cdot\phi_{j_1j_2\cdots}y_1^{j_1-1}y_2^{j_2-1}\cdots y_{i-1}^{j_{i-1}-1}y_i^{j_i}y_{i+1}^{j_{i+1}}\cdots$$

$$= \sum_{\substack{j_1=0,\\ j_m=-1\\(m=2,3,\cdots,i-1),\\ j_n=0\\(n=i,i+1,\cdots)}} (j_{i-1} + 1 - j_i)\cdot\phi_{(j_1+1)(j_2+1)\cdots(j_{i-1}+1)j_ij_{i+1}\cdots}y_1^{j_1}y_2^{j_2}\cdots$$

By equating coefficients of $y_1^{j_1}y_2^{j_2}\cdots y_{N-1}^{j_{N-1}}$ on both sides of eq. [A-12], it may be seen that

$$[A\text{-}13]\quad {}^{i}a_{j_1j_2\cdots} = {}^{i-1}a_{j_1j_2\cdots} + (j_{i-1} + 1 - j_i)\cdot\phi_{(j_1+1)(j_2+1)\cdots(j_{i-1}+1)j_ij_{i+1}\cdots}$$

The lower summation indices (-1) on the right-hand side of eq. [A-12] may be disregarded because of the restrictions [9], which state that the coefficients $\phi_{j_1j_2\cdots} = 0$ when any $j_k = 0$.

Appendix III

Take $i = (N - 1)$ in eq. [A-9]

$$[A\text{-}14]\quad y_{N-1}\left(\frac{\partial f}{\partial y_{N-1}}\right) = y_1y_2\cdots y_{N-1}(f_N - f_{N-1})$$

Substitute eq. [8] into eq. [A-14], simplify, and alter the summation indices in the same manner as in the derivation of eq. [A-12]

$$[A\text{-}15]\quad f_N - f_{N-1} = \sum_{\substack{j_1=0,\\ j_m=-1\\(m=2,3,\cdots)}} \phi_{(j_1+1)(j_2+1)\cdots(j_{N-1}+1)}\cdot(j_{N-1} + 1)\cdot y_1^{j_1}y_2^{j_2}\cdots$$

The lower summation indices (-1) may be disregarded, as before, because of the restrictions [9].

By substituting the expansions [7] for f_N and f_{N-1} into eq. [A-15] and equating coefficients, it is seen that

$$[A\text{-}16]\quad {}^{N}a_{j_1j_2\cdots} = {}^{N-1}a_{j_1j_2\cdots} + (j_{N-1} + 1)\cdot\phi_{(j_1+1)(j_2+1)\cdots(j_{N-1}+1)}$$

Eq. [A-16] may be taken as a case of the general eq. [15] if the convention that $j_N = 0$ is adopted.

Can. J. Chem. Downloaded from www.nrcresearchpress.com by 210.87.254.42 on 09/05/12
For personal use only.

Can. J. Chem. Downloaded from www.nrcresearchpress.com by 210.87.254.5 on 09/05/12
For personal use only.

Deuterium and hydrogen sulfides: vapor pressures, molar volumes, and thermodynamic properties[1]

E. C. W. Clarke and D. N. Glew
Exploratory Research Laboratory, Dow Chemical of Canada, Limited, Sarnia, Ontario

Received October 17, 1969

An apparatus is described in which deuterium and hydrogen sulfides have been prepared by the hydrolysis of aluminum sulfide. Liquid densities have been determined at −79 °C and give the molar volumes 34.811 ± 0.003 cm^3 for deuterium sulfide and 34.711 ± 0.003 for hydrogen sulfide. Vapor pressures of deuterium and hydrogen sulfides have been determined at −78 °C in a quartz–metal apparatus, and in the range −30 to +30 °C in a stainless steel apparatus. Equations are derived for the deuterium and hydrogen sulfide vapor pressures and for their ratio. An isotopic vapor pressure cross-over point is found at −48 °C, above which deuterium sulfide is more volatile than hydrogen sulfide. Gas and liquid molar volumes and enthalpy changes are evaluated for liquid vaporization at saturation. The deuterium and hydrogen sulfide vaporization standard thermodynamic function changes and their errors, together with the isotopic differences for these functions and their errors, are tabulated between −80 and +50 °C.

Canadian Journal of Chemistry, **48**, 764 (1970)

Introduction

Earliest vapor pressure measurements showed that deuterium sulfide was less volatile than hydrogen sulfide near its triple point temperature (1). This reduced deuterium compound volatility relative to that of the hydrogen compound is apparently normal for simple compounds at temperatures between the triple and normal boiling points (2). However, our early measurements of the deuterium sulfide vapor pressure at about 30 °C indicated that the deuterium sulfide vapor pressure was, in fact, higher than that interpolated for hydrogen sulfide (3, 4). This inversion of isotope effect for the vapor pressures of the simple deuterium and hydrogen sulfides was of sufficient interest that we prepared both compounds in the same manner and measured their vapor pressures in the same apparatus. From this first set of vapor pressure determinations for deuterium sulfide, we have evaluated the vaporization thermodynamic function changes together with their errors, and have made a detailed comparison with those for hydrogen sulfide.

In the evaluation of the thermodynamic function changes, the liquid molar volume of deuterium sulfide was required, and since this was unavailable, we determined the molar volumes of liquid hydrogen and deuterium sulfides in the same apparatus at −79 °C.

[1]Contribution No. 172.

Experimental

Materials

Water was laboratory distilled. Deuterium oxide contained 0.22 weight % protium oxide as supplied by Atomic Energy of Canada, Limited. Chemically pure grade aluminum sulfide was obtained from K and K Laboratories Incorporated.

The metal equipment was all of type-316 stainless steel which showed no attack by hydrogen sulfide over a six month period as assessed from vapor pressure determinations.

Preparation of Deuterium and Hydrogen Sulfides

Gaseous deuterium sulfide was prepared in the apparatus shown in Fig. 1 by the reaction of liquid deuterium oxide with aluminum sulfide according to the equation

$$Al_2S_3 + 6D_2O \rightarrow 2Al(OD)_3 + 3D_2S$$

Approximately 50 g of crushed aluminum sulfide was placed in the quartz reactor C and the whole apparatus was evacuated with gentle heating of C using a cool blue Bunsen flame. Bulb A was detached from the apparatus, approximately 1 g deuterium oxide was added, the bulb was replaced, and the deuterium oxide freeze-degassed. Bulb A was rotated and the liquid deuterium oxide flowed into vessel B. With taps 1, 2, 5, 8, and 11 closed and all others open, a few drops of deuterium oxide were admitted to the reactor via tap 2. As deuterium sulfide was generated, the pressure indicated by the Pyrex Bourdon gauge G was allowed to increase up to about 1 atm. The apparatus was left in this condition for about 30 min and then evacuated. This process was repeated twice more to replace exchangeable protium in the system by deuterium. The deuterium-conditioned system was then evacuated.

Bulb A was removed from the apparatus, filled to about one third of its capacity with 50 g deuterium oxide and replaced. The deuterium oxide was freeze-degassed three times and transferred to B by rotation of A. The deuterium oxide removal trap D and deuterium sulfide condensation

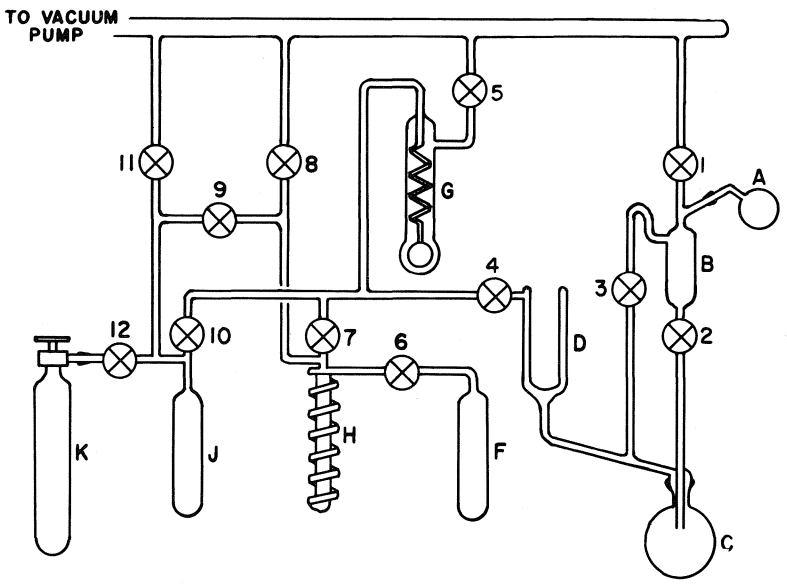

FIG. 1. Apparatus for preparation of deuterium and hydrogen sulfides.

bulb F were cooled to −80 °C by solid carbon dioxide – acetone mixtures. With taps 3, 4, 6, and 7 open and all others closed, tap 2 was opened to give a slow drip of deuterium oxide onto the aluminum sulfide in C. The deuterium oxide flow was controlled so that the generated pressure on gauge G did not exceed 500 Torr, while the gaseous deuterium sulfide was condensed in F. On completion of reaction, F was cooled by liquid nitrogen to condense deuterium sulfide from C, tap 4 was closed and F evacuated via 8 to remove any non-condensable gases, tap 8 was then closed.

The deuterium oxide condensation helix H and bulb F were cooled with solid carbon dioxide – acetone mixtures and bulb J was cooled with liquid nitrogen. Needle valve 9 was opened until the pressure at G was reduced to about 250 Torr, so that deuterium sulfide distilled into J leaving small quantities of the solid deuterium sulfide deuterate ($D_2S.5.75D_2O$) in F and H; these deuterate residues were pumped from F and H at room temperature. The deuterium sulfide was distilled twice more, in the same manner from J to F and back again from F to J, removing all deuterium oxide and non-condensable impurities; the purified liquid was distilled from J into the 316-type stainless steel storage cylinder K.

Hydrogen sulfide was prepared similarly in the same apparatus using distilled water in place of deuterium oxide.

The most probable impurities in the hydrogen sulfide were thought to be phosphine and arsine, which were found by the molybdenum blue method (5, 6) to be present at levels not exceeding 3 p.p.m. by weight. The deuterium sulfide prepared in the same way was assumed to be equally free from phosphorus and arsenic compounds. The fast irreversible reaction of deuterium oxide with aluminum sulfide was assumed to produce deuterium sulfide with the same isotopic composition as the deuterium oxide.

Density Measurement

The liquid densities of hydrogen and deuterium sulfides were determined in a 15 cm^3 quartz pyknometer having a 0.1 cm diameter capillary stem inscribed with two reference marks. The pyknometer volume at 25 °C was determined by weighing water, using the density compilation of Dorsey (7); the volume at −79 °C was evaluated using the coefficient of expansion of quartz. The pyknometer, totally immersed in a stirred acetone bath, was maintained at −79 °C with a precision of 0.003 °C as determined by platinum resistance thermometer.

The pyknometer was filled between the stem reference marks with deuterium sulfide by condensation at −79 °C of the vapor from a weighed stainless steel cylinder. The cylinder was detached and reweighed. A series of measurements were made of deuterium sulfide meniscus position and bath temperature, after which the deuterium sulfide was transferred into the cylinder which was reweighed. The weight of deuterium sulfide in the pyknometer was determined from the mean weight of the full cylinder minus the cylinder weight when the pyknometer contained deuterium sulfide. All weights were corrected for damp air buoyancy.

The density of liquid hydrogen sulfide was determined in the same way. The three independent sets of densities for both hydrogen and deuterium sulfides are recorded in Table 1.

Vapor Pressure Measurements

Below Atmospheric Pressure

Vapor pressure measurements were conducted using about 8 cm^3 of liquid deuterium sulfide in the quartz pyknometer bulb immersed in a stirred acetone thermostat bath, the temperature of which was controlled within 0.005 °C between −78 and −77 °C. Temperature was measured with a precision of 0.001 °C by a platinum resistance thermometer in conjunction with a Mueller

Can. J. Chem. Downloaded from www.nrcresearchpress.com by 210.87.254.5 on 09/05/12
For personal use only.

TABLE 1

Density of liquid hydrogen and deuterium sulfides

Hydrogen sulfide			Deuterium sulfide		
Mass (g)	Temperature (°C)	Density (g/cm³)	Mass (g)	Temperature (°C)	Density (g/cm³)
14.9745	−79.35	0.98249	15.8016	−79.18	1.03684
	−79.31	0.98246		−79.24	1.03684
	−79.58	0.98291		−79.12	1.03677
	−79.70	0.98311		−79.07	1.03671
	−79.67	0.98310		−79.03	1.03657
	−79.65	0.98306		−79.04	1.03662
14.9522	−79.00	0.98170	15.8130	−79.06	1.03696
	−79.00	0.98176		−79.02	1.03681
	−78.90	0.98162		−78.94	1.03667
	−78.77	0.98136		−78.97	1.03671
	−78.76	0.98129		−78.98	1.03674
	−78.77	0.98125		−78.93	1.03664
	−78.72	0.98122		−78.89	1.03656
15.3462	−79.21	0.98227	15.8170	−79.27	1.03714
	−79.33	0.98247		−79.18	1.03700
	−79.31	0.98210		−79.02	1.03678
				−79.01	1.03673
Ave.	−79.00	0.98180		−78.96	1.03669
		σ = 0.00007		−78.99	1.03667
				−78.92	1.03661
				−78.93	1.03658
				−78.92	1.03655
			Ave.	−79.00	1.03667
					σ = 0.00008

bridge, amplifier, and galvanometer. Pressure was measured with an accuracy of ±0.02 % by a 0–16 p.s.i. range Texas Instruments Incorporated fused quartz precision Bourdon gauge. The gauge was calibrated against a wide-bore mercury manometer, for which the column height difference was determined by cathetometer comparison against a meter standard. The hydrogen sulfide vapor pressure was determined similarly.

Above Atmospheric Pressure

Vapor pressure measurements were made using about 34 g of liquid deuterium sulfide in a 75 cm³ stainless steel reservoir immersed in a stirred water–glycol thermostat bath, the temperature of which was controlled within 0.002 °C between −30 and +30 °C. The liquid temperature was measured with a precision of 0.0003 °C by a platinum resistance thermometer in a copper thermowell strapped to the reservoir. Pressure was measured with an accuracy of 0.03% on a Texas Instruments Incorporated fused quartz precision gauge with ranges 0–200 and 0–500 p.s.i., calibrated against a Budenberg Ranger dead weight tester. The accuracy of the dead weight tester was stated by the manufacturer to be 0.03%, based on comparison with an instrument calibrated by the National Physical Laboratory. All entries in Table 2 for hydrogen sulfide and in Table 3 for deuterium sulfide, are mean values for sets of five pressure–temperature measurements taken over a 2 h period.

Standardization

The 25 ohm platinum resistance thermometer was calibrated and the Leeds and Northrup G-2 Mueller bridge was standardized before, during, and after our experimental measurements. The platinum resistance thermometer was calibrated at the water triple point using three-day-old mantles, in Jarrett cells, contained in a closed chest packed with melting ice (8).

All equations were derived by the method of least squares and all uncertainties shown are standard errors. The temperature scales are related by 0 °C ≡ 273.15 K, and the gas constant R is taken as 1.98717 thermochemical cal/mole deg (9).

Results and Discussion

Liquid Densities

The densities of liquid hydrogen sulfide presented in Table 1 are in excellent agreement with the extensive measurements of Klemenc and Bankowski (10), but do not agree with the measurements of Baxter, Burrage, and Tanner (11). The errors of our determinations arise mainly from the mass of liquid contained in the pyknometer, as determined from the mass difference of the liquid storage cylinder recorded in Table 1. The three mean densities, one for each mass of hydrogen sulfide, were adjusted to −79.00 °C using the coefficient of expansion (10), and these three temperature-adjusted means were averaged to give the final value. The deuterium

Can. J. Chem. Downloaded from www.nrcresearchpress.com by 210.87.254.5 on 09/05/12
For personal use only.

TABLE 2
Vapor pressure of hydrogen sulfide

Temperature (°C)	Pressure			Error on calculated pressure (%)
	Observed (atm)	Calculated (atm)	Difference (%)	
29.982	22.443	22.442	+0.006	0.014
29.963	22.436	22.432	+0.020	0.014
24.997	19.903	19.903	−0.001	0.010
24.990	19.891	19.900	−0.047	0.010
20.037	17.582	17.591	−0.048	0.008
14.975	15.440	15.438	+0.015	0.008
14.954	15.439	15.429	+0.061	0.008
14.935	15.430	15.422	+0.053	0.008
9.989	13.508	13.511	−0.020	0.008
9.988	13.511	13.511	+0.003	0.008
4.992	11.760	11.763	−0.025	0.008
4.955	11.747	11.751	−0.029	0.008
0.018	10.192	10.193	−0.009	0.008
− 0.004	10.186	10.187	−0.004	0.008
− 5.016	8.769	8.768	+0.012	0.008
− 9.901	7.532	7.531	+0.015	0.008
−14.868	6.412	6.411	+0.010	0.009
−19.996	5.390	5.391	−0.016	0.011
−24.974	4.523	4.522	+0.013	0.014
−28.515	3.972	3.972	−0.010	0.016
−77.080	0.3926	0.3926	+0.007	0.011
−77.260	0.3883	0.3883	+0.003	0.011
−77.422	0.3845	0.3844	+0.007	0.011
−77.568	0.3810	0.3810	+0.006	0.011
−77.741	0.3770	0.3770	−0.007	0.011
−77.873	0.3739	0.3739	−0.015	0.011

TABLE 3
Vapor pressure of deuterium sulfide

Temperature (°C)	Pressure			Error on calculated presssure (%)
	Observed (atm)	Calculated (atm)	Difference (%)	
30.023	22.789	22.795	−0.026	0.027
25.020	20.196	20.198	−0.010	0.018
20.024	17.827	17.826	+0.005	0.013
14.948	15.637	15.629	+0.052	0.011
14.899	15.613	15.609	+0.028	0.011
14.470	15.440	15.433	+0.043	0.011
9.996	13.688	13.683	+0.033	0.010
9.508	13.492	13.501	−0.070	0.011
5.014	11.905	11.910	−0.045	0.011
4.973	11.901	11.896	+0.038	0.011
4.943	11.884	11.886	−0.018	0.011
− 0.009	10.295	10.300	−0.047	0.011
− 0.013	10.303	10.298	+0.043	0.011
− 0.022	10.292	10.295	−0.031	0.011
− 5.034	8.850	8.855	−0.055	0.011
− 9.997	7.581	7.581	+0.010	0.011
−15.166	6.406	6.404	+0.036	0.013
−19.826	5.467	5.465	+0.023	0.015
−24.953	4.557	4.556	+0.017	0.019
−28.194	4.043	4.044	−0.030	0.022
−77.063	0.3872	0.3872	+0.001	0.016
−77.258	0.3827	0.3826	+0.016	0.016
−77.457	0.3779	0.3779	−0.011	0.016
−77.660	0.3732	0.3732	+0.017	0.017
−77.863	0.3684	0.3685	−0.023	0.017

Can. J. Chem. Downloaded from www.nrcresearchpress.com by 210.87.254.5 on 09/05/12
For personal use only.

sulfide densities were adjusted to −79.00 °C in the same way.

The literature contains no value to compare with our deuterium sulfide density measurements. At −79.00 °C the molar volume 34.8108 ± 0.0027 cm^3 for deuterium sulfide is found to be 0.29% larger than the 34.7112 ± 0 0026 cm^3 for hydrogen sulfide.

Vapor Pressures

New vapor pressure measurements for hydrogen sulfide between −78 and +30 °C are presented in Table 2, together with calculated values from the best (12) representative equation

$$[1]\quad \log_{10} P_H(\text{atm}) = 26.82579 - 1538.461/T - 9.00784 \log_{10} T + 0.0064481T$$

with P_H in normal atmosphere (9) and temperature T absolute. The percentage differences between observed and calculated pressures, shown in the fourth column, lead to a standard error of 0.026% on a single determination, which properly corresponds with the accuracy of pressure measurement. The percentage differences of the data from eq. [1] are plotted in Fig. 2, together with the results of other workers (1, 4, 13, 14). The greater scatter evident in our measurements at temperatures above 5 °C results from the greater variability of the 500 p.s.i. range of the quartz gauge. The final column of the table gives the percentage standard error on the vapor pressure evaluated from eq. [1].

Our new measurements represented by eq. [1] fall nearly in the middle of the range of earlier work. The single determination of the triple-point pressure by Kruis, Popp, and Clusius (1) is apparently too high, while the pressures and equation of Clark, Cockett, and Eisner (14) are too low. Our measurements are in good agreement with the lower temperature determinations of Giauque and Blue (13), while at their higher temperatures the reaction of hydrogen sulfide with mercury is probably responsible for their high values. The vapor pressures of Klemenc and Bankowski (10) are too high to be shown in Fig. 2. At high pressures our measurements are in good agreement with the tabulated values between 40 and 90 °F from Kay and Rambosek (4), but indicate that their value at 30 °F is too high.

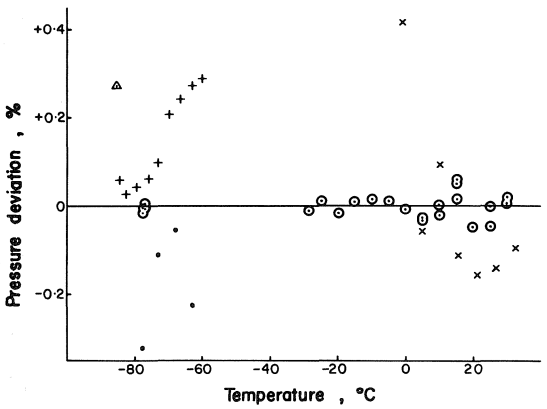

FIG. 2. Deviations of hydrogen sulfide vapor pressures from eq. [1]: △, Kruis, Popp, and Clusius; +, Giauque and Blue; ●, Clark, Cockett, and Eisner; ×, Kay and Rambosek; ○, this work.

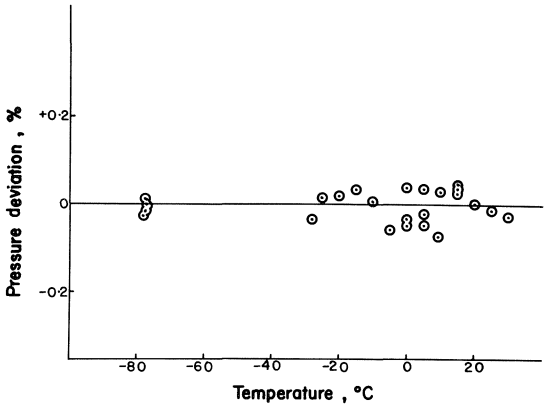

FIG. 3. Deviations of the deuterium sulfide vapor pressures from eq. [2].

Deuterium sulfide vapor pressures between −78 and +30 °C are presented in Table 3, together with calculated values from the best (12) representative equation

$$[2]\quad \log_{10} P_D(\text{atm}) = 29.06074 - 1601.543/T - 9.89939 \log_{10} T + 0.0070815T$$

The percentage differences of the measurements from eq. [2], plotted in Fig. 3, lead to a standard error of 0.037% on a single deuterium sulfide vapor pressure determination. This error is significantly larger than that of the hydrogen sulfide data, because of equipment failures in the course of the deuterium sulfide measurements. The only literature value, by Kruis, Popp, and Clusius (1), was for the triple-point pressure, which is 0.8% higher than predicted by eq. [2].

To eliminate systematic errors due to the apparatus prior to curve-fitting in order to

Can. J. Chem. Downloaded from www.nrcresearchpress.com by 210.87.254.5 on 09/05/12
For personal use only.

TABLE 4
Deuterium to hydrogen sulfide vapor pressure ratio

Temperature (°C)	Vapor pressure ratio P_D/P_H			Error on calculated ratio (%)
	Experimental	Calculated	Difference (%)	
30.023	1.0144	1.0147	−0.024	0.028
25.020	1.0141	1.0142	−0.005	0.019
20.024	1.0142	1.0137	+0.055	0.014
14.948	1.0135	1.0131	+0.037	0.011
14.899	1.0128	1.0131	−0.033	0.011
14.470	1.0130	1.0131	−0.010	0.011
9.996	1.0131	1.0125	+0.053	0.011
9.508	1.0117	1.0125	−0.074	0.011
5.014	1.0117	1.0119	−0.021	0.011
4.973	1.0126	1.0119	+0.064	0.011
4.943	1.0120	1.0119	+0.009	0.011
− 0.009	1.0108	1.0112	−0.040	0.012
− 0.013	1.0117	1.0112	+0.044	0.012
− 0.022	1.0110	1.0112	−0.026	0.012
− 5.034	1.0098	1.0105	−0.069	0.012
− 9.997	1.0096	1.0097	−0.007	0.012
−15.166	1.0090	1.0088	+0.024	0.013
−19.826	1.0082	1.0078	+0.038	0.016
−24.953	1.0068	1.0067	+0.005	0.021
−28.194	1.0058	1.0060	−0.019	0.024
−77.063	0.9853	0.9854	−0.007	0.017
−77.258	0.9854	0.9853	+0.012	0.017
−77.457	0.9850	0.9852	−0.019	0.017
−77.660	0.9852	0.9850	+0.023	0.018
−77.863	0.9848	0.9849	−0.009	0.018

obtain a realistic estimate of the random errors on the P_D/P_H ratio, the hydrogen sulfide data were adjusted to the temperatures of the nearest deuterium sulfide measurements using the temperature coefficients from eq. [1]. The resulting P_D/P_H ratios between −78 and +30 °C are presented in Table 4, together with calculated values from the best (12) representative equation

$$[3]\quad \log_{10}(P_D/P_H) = 2.01608 - 58.2986/T - 0.79967 \log_{10} T + 0.0005511T$$

which indicates a standard error of 0.039% on a single P_D/P_H ratio. It is found from eq. [3] that at −48.1 ± 1.1 °C, the vapor pressures of hydrogen and deuterium sulfides are equal, while at higher temperatures deuterium sulfide is the more volatile.

Equations of State

Equations of state for hydrogen and deuterium sulfides were required to evaluate the gaseous molar volumes from pressure–temperature measurements (3, 15). We chose to use the Redlich–Kwong equation (16)

$$[4]\quad \left[P + \frac{a}{T^{1/2}V(V+b)}\right](V-b) = RT$$

because it had been shown (17) to be a good representative function, and because its two adjustable constants made it a convenient smoothing function, readily fitted to the data. In Table 5 are shown the different values for a and b necessary to fit the low temperature (l.t.) measurements from −78 to −77 °C and the high temperature (h.t.) measurements from −30 to +30 °C.

Hydrogen Sulfide Vapor

The P–V–T measurements of Reamer, Sage, and Lacey (3) and of Wright and Maass (15) were fitted by least squares to give the values of $a(H_2S$, h.t.) and $b(H_2S$, h.t.) presented in Table 5. The standard error on a single pressure determination was 0.28%, which corresponded to an error on a of 0.372%, calculated assuming b to be error-free.

The second virial coefficient for hydrogen sulfide at the normal boiling point was evaluated from the calorimetric heat of vaporization and the vapor pressure measurements of Giauque and

Can. J. Chem. Downloaded from www.nrcresearchpress.com by 210.87.254.5 on 09/05/12
For personal use only.

TABLE 5
Constants for Redlich–Kwong eq. [4]

Conditions	a $(cm^2/g\text{-}mole)^2$ atm $(°K)^{1/2}$	b $(cm^3/g\text{-}mole)$
Low temperature		
(H_2S, l.t.)	9.726×10^7	33.92
(D_2S, l.t.)	9.744×10^7	33.92
High temperature		
(H_2S, h.t.)	11.072×10^7	57.96
(D_2S, h.t.)	11.048×10^7	57.96

TABLE 6
Hydrogen sulfide saturation properties

Temperature (°C)	Pressure (atm)	V_g $(cm^3/mole)$	V_l $(cm^3/mole)$	ΔH_{sat} (cal/mole)
−80.0	0.32746	47990	34.65	4640
−75.0	0.44504	36140	34.96	4596
−70.0	0.59463	27650	35.27	4552
−65.0	0.78214	21470	35.60	4507
−60.275	1.0000	17110	35.91	4464
−60.176	1.0050	17030	35.91	4463
−60.0	1.0140	16900	35.93	4461
−55.0	1.2972	13450	36.26	4413
−50.0	1.6391	10830	36.61	4363
−45.0	2.0476	8811	36.97	4310
−40.0	2.5310	7234	37.34	4256
−35.0	3.0979	5990	37.73	4199
−30.0	3.7572	4999	38.13	4140
−25.0	4.5182	4205	38.54	4081
−20.0	5.3903	3561	38.97	4020
−15.0	6.3834	3034	39.42	3957
−10.0	7.5072	2600	39.88	3891
− 5.0	8.7720	2239	40.36	3823
0.0	10.188	1938	40.86	3753
5.0	11.766	1685	41.38	3681
10.0	13.515	1471	41.93	3605
15.0	15.448	1289	42.50	3528
20.0	17.574	1134	43.11	3448
25.0	19.905	1000	43.76	3366
30.0	22.452	885.3	44.45	3282
35.0	25.225	785.9	45.20	3196
40.0	28.237	699.7	46.01	3109
45.0	31.500	624.9	46.91	3021
50.0	35.024	559.9	47.90	2932

Blue (13). The values for $a(H_2S$, l.t.) and $b(H_2S$, l.t.) consistent with this virial coefficient were calculated by a least squares fit of our low temperature vapor pressure data.

Deuterium Sulfide Vapor

For deuterium sulfide at low temperatures, the value of $b(D_2S$, l.t.) was taken equal to $b(H_2S$, l.t.) and a least squares fit made of our low temperature vapor pressures to determine $a(D_2S$, l.t.).

Since there are no direct P–V–T measurements available for deuterium sulfide at high temperatures, $a(D_2S$, h.t.) and $b(D_2S$, h.t.) were estimated as perturbations on the hydrogen sulfide values $a(H_2S$, h.t.) and $b(H_2S$, h.t.). The value of $b(D_2S$, h.t.) was taken to be equal to that of $b(H_2S$, h.t.), because our liquid molar volumes for hydrogen and deuterium sulfides were very nearly equal, and because the P–V–T properties derived for the vapor are not sensitively dependent on b. The value of $a(D_2S$, h.t.) was derived in the following manner. (*i*) From the vapor pressure of hydrogen sulfide between −30 and +30 °C (Table 2) and the liquid volume at 0 °C (Table 6)

Can. J. Chem. Downloaded from www.nrcresearchpress.com by 210.87.254.5 on 09/05/12
For personal use only.

TABLE 7
Deuterium sulfide saturation properties

Temperature (°C)	Pressure (atm)	V_g (cm³/mole)	V_l (cm³/mole)	ΔH_{sat} (cal/mole)
−80.0	0.32201	48810	34.75	4694
−75.0	0.43916	36630	35.07	4648
−70.0	0.58860	27940	35.38	4600
−65.0	0.77637	21630	35.71	4552
−60.275	0.99498	17200	36.02	4506
−60.176	1.0000	17120	36.03	4505
−60.0	1.0090	16980	36.04	4503
−55.0	1.2937	13470	36.38	4452
−50.0	1.6380	10840	36.73	4399
−45.0	2.0500	8801	37.09	4344
−40.0	2.5380	7213	37.47	4287
−35.0	3.1110	5964	37.86	4227
−30.0	3.7780	4970	38.26	4166
−25.0	4.5486	4175	38.68	4105
−20.0	5.4324	3532	39.11	4041
−15.0	6.4394	3006	39.56	3976
−10.0	7.5798	2573	40.03	3908
− 5.0	8.8639	2214	40.52	3838
0.0	10.302	1915	41.02	3765
5.0	11.906	1663	41.55	3690
10.0	13.685	1450	42.11	3613
15.0	15.651	1270	42.69	3533
20.0	17.815	1116	43.31	3451
25.0	20.188	983.4	43.96	3367
30.0	22.782	869.6	44.67	3281
35.0	25.609	771.2	45.43	3192
40.0	28.681	686.0	46.27	3103
45.0	32.009	612.1	47.18	3013
50.0	35.606	547.9	48.19	2922

we obtained the Redlich–Kwong constants $a_1 = 8.608 \times 10^7$ (cm²/g-mole)² atm (°K)$^{1/2}$ and $b_1 = 28.70$ cm³/g-mole. (*ii*) Assuming that b_2 for deuterium sulfide was equal to b_1, the deuterium sulfide vapor pressures between −30 and +30 °C (Table 3) were fitted to yield the Redlich–Kwong constants $a_2 = 8.590 \times 10^7$ (cm²/g-mole)² atm (°K)$^{1/2}$ and $b_2 = 28.70$ cm³/g-mole. (*iii*) Assuming that the a_2/a_1 ratio of the attractive constants in the Redlich–Kwong equation for deuterium to hydrogen sulfide was invariant and independent of the covolume b, the value of $a(D_2S$, h.t.) was then given by $a(H_2S, \text{h.t.}) \cdot (a_2/a_1)$.

The error on all a values was assumed to be the same, 0.372%, as for $a(H_2S$, h.t.).

Liquid Volumes

The liquid molar volumes for hydrogen sulfide, presented in Table 6, were evaluated from a sixth-order polynomial in temperature, which equation represented the measurements of Reamer, Sage, and Lacey (3), and of Klemenc and Bankowski (10) together with our value at −79 °C. The standard error on any calculated liquid volume is less than 0.005 cm³/mole.

The liquid deuterium sulfide molar volumes, presented in Table 7, were obtained as follows. Taking 373.07 and 372.07 °K, respectively, for the hydrogen and deuterium sulfide critical temperatures (4, 18), the factor, 1.00184, was found by which the hydrogen sulfide liquid molar volume at the same reduced temperature must be multiplied to obtain our deuterium sulfide liquid molar volume at −79 °C. This factor was assumed to be invariant, and was used to multiply all hydrogen sulfide liquid volumes to obtain the deuterium sulfide liquid volumes at the same reduced temperatures.

Saturation Properties

The hydrogen sulfide saturation vapor pressure P_H(atm) from eq. [1], vapor molar volume V_g (cm³) from eq. [4], liquid molar volume V_l (cm³), and enthalpy of vaporization ΔH_{sat} (cal) between −80 and +50 °C are presented in Table 6. This calorimetrically observable saturation molar enthalpy of evaporation ΔH_{sat} was

Can. J. Chem. Downloaded from www.nrcresearchpress.com by 210.87.254.5 on 09/05/12
For personal use only.

TABLE 8

Hydrogen sulfide vaporization standard thermodynamic function changes*

Temperature (°C)	$\Delta G°$ (cal/mole)		$\Delta H°$ (cal/mole)		$\Delta S°$ (cal/deg mole)		$\Delta C_p°$ (cal/deg mole)	
	Value	σ	Value	σ	Value	σ	Value	σ
−80.0	431.11	0.12	4642.3	9.1	21.803	0.047	− 8.04	0.50
−75.0	322.61	0.10	4601.9	6.8	21.596	0.035	− 8.12	0.45
−70.0	215.14	0.24	4561.1	4.7	21.393	0.024	− 8.21	0.40
−65.0	108.68	0.34	4519.8	2.8	21.192	0.015	− 8.29	0.35
−60.275	8.98	0.39	4480.5	1.4	21.005	0.008	− 8.37	0.31
−60.176	6.91	0.39	4479.6	1.4	21.001	0.008	− 8.38	0.31
−60.0	3.21	0.39	4478.2	1.3	20.994	0.008	− 8.38	0.31
−55.0	− 101.27	0.41	4436.0	0.8	20.799	0.004	− 8.46	0.26
−50.0	− 204.78	0.41	4393.5	1.6	20.606	0.006	− 8.55	0.21
−45.0	− 307.34	0.38	4350.6	2.5	20.416	0.010	− 8.63	0.16
−40.0	− 408.95	0.33	4307.2	3.2	20.228	0.012	− 8.72	0.12
−35.0	− 509.62	0.28	4263.4	3.6	20.042	0.014	− 8.80	0.08
−30.0	− 609.37	0.22	4219.1	3.8	19.858	0.015	− 8.89	0.05
−25.0	− 708.20	0.18	4174.5	3.8	19.676	0.015	− 8.98	0.06
−20.0	− 806.14	0.15	4129.4	3.6	19.496	0.014	− 9.06	0.10
−15.0	− 903.17	0.15	4083.9	3.2	19.318	0.013	− 9.15	0.14
−10.0	− 999.32	0.17	4037.9	2.7	19.142	0.011	− 9.23	0.19
− 5.0	−1094.59	0.19	3991.5	2.3	18.968	0.009	− 9.32	0.23
0.0	−1189.00	0.21	3944.8	2.3	18.795	0.008	− 9.40	0.28
5.0	−1282.54	0.21	3897.5	3.0	18.623	0.011	− 9.49	0.33
10.0	−1375.24	0.22	3849.9	4.4	18.454	0.016	− 9.57	0.37
15.0	−1467.08	0.24	3801.8	6.2	18.285	0.022	− 9.66	0.42
20.0	−1558.09	0.30	3753.3	8.3	18.118	0.029	− 9.74	0.47
25.0	−1648.27	0.42	3704.4	10.7	17.953	0.037	− 9.83	0.52
30.0	−1737.62	0.60	3655.1	13.3	17.789	0.046	− 9.91	0.57
35.0	−1826.16	0.83	3605.3	16.2	17.626	0.055	−10.00	0.61
40.0	−1913.88	1.12	3555.1	19.4	17.464	0.065	−10.08	0.66
45.0	−2000.81	1.46	3504.5	22.8	17.304	0.076	−10.17	0.71
50.0	−2086.93	1.86	3453.4	26.4	17.145	0.087	−10.25	0.76

*$d\Delta C_p°/dT = -0.0170 \pm 0.0096$ cal/deg² mole.

calculated from the Clapeyron relation

$$[5] \qquad \Delta H_{sat} = T\left(\frac{dP}{dT}\right)_{sat}(V_g - V_l)$$

where the value for $(dP/dT)_{sat}$ was derived from eq. [1]. The good agreement of our ΔH_{sat}, 4464 ± 1.4 cal at the normal boiling point -60.27_5 °C, with the calorimetric value, 4464 ± 4 cal (13), indicates the good agreement between the $(dP/dT)_{sat}$ slopes for the measurements of Giauque and Blue and for eq. [1].

The deuterium sulfide vapor pressure P_D (atm) from eq. [2] and other saturation properties are presented in Table 7. No literature data are available for comparison. At −80 °C the vaporization enthalpy for deuterium sulfide is 1.2% larger than for hydrogen sulfide, at 27 °C the enthalpies are equal, and at all higher temperatures deuterium sulfide has the smaller value.

Vaporization Standard Thermodynamic Function Changes

The vaporization equilibrium constant K (atm) at vapor pressure P and temperature T absolute is defined by the relation

$$[6] \qquad \ln K = \frac{\Delta G^0}{-RT} = \ln f - \frac{(P-1)}{RT} V_l$$

in which ΔG^0 is the vaporization standard free energy change for the transfer of one mole of liquid at 1 atm pressure to give vapor at 1 atm fugacity. The equilibrium vapor fugacity f in atmospheres is calculated from

$$[7] \qquad \ln f = \ln \frac{RT}{V-b} + \frac{b}{V-b} + \frac{a}{bRT^{3/2}} \ln \frac{V}{V+b} - \frac{a}{RT^{3/2}(V+b)}$$

as derived from the Redlich–Kwong equation of

Can. J. Chem. Downloaded from www.nrcresearchpress.com by 210.87.254.5 on 09/05/12
For personal use only.

TABLE 9

Deuterium sulfide vaporization standard thermodynamic function changes*

Temperature (°C)	$\Delta G°$ (cal/mole)		$\Delta H°$ (cal/mole)		$\Delta S°$ (cal/deg mole)		$\Delta C_p°$ (cal/deg mole)	
	Value	σ	Value	σ	Value	σ	Value	σ
−80.0	437.51	0.15	4697.3	9.9	22.054	0.051	− 8.71	0.53
−75.0	327.80	0.12	4653.6	7.4	21.831	0.038	− 8.77	0.48
−70.0	219.19	0.27	4609.5	5.1	21.611	0.027	− 8.83	0.43
−65.0	111.68	0.37	4565.2	3.2	21.396	0.017	− 8.89	0.38
−60.275	11.05	0.43	4523.1	1.6	21.196	0.009	− 8.95	0.33
−60.176	8.96	0.43	4522.2	1.6	21.191	0.009	− 8.95	0.33
−60.0	5.23	0.43	4520.6	1.6	21.184	0.009	− 8.95	0.33
−55.0	− 100.17	0.45	4475.7	0.9	20.976	0.004	− 9.01	0.28
−50.0	− 204.53	0.45	4430.5	1.7	20.771	0.006	− 9.07	0.23
−45.0	− 307.88	0.42	4384.9	2.6	20.569	0.010	− 9.13	0.18
−40.0	− 410.23	0.37	4339.1	3.4	20.370	0.013	− 9.19	0.13
−35.0	− 511.59	0.31	4293.0	3.8	20.175	0.015	− 9.25	0.09
−30.0	− 611.98	0.25	4246.6	4.1	19.982	0.016	− 9.31	0.06
−25.0	− 711.41	0.20	4199.9	4.1	19.792	0.016	− 9.37	0.07
−20.0	− 809.90	0.17	4152.8	3.9	19.604	0.015	− 9.43	0.10
−15.0	− 907.46	0.17	4105.5	3.5	19.419	0.014	− 9.49	0.15
−10.0	−1004.09	0.18	4057.9	3.0	19.236	0.012	− 9.56	0.20
− 5.0	−1099.82	0.20	4010.0	2.5	19.056	0.010	− 9.62	0.24
0.0	−1194.65	0.22	3961.7	2.5	18.877	0.009	− 9.68	0.29
5.0	−1288.60	0.22	3913.2	3.2	18.701	0.011	− 9.74	0.35
10.0	−1381.67	0.23	3864.4	4.6	18.527	0.016	− 9.80	0.40
15.0	−1473.88	0.25	3815.2	6.5	18.355	0.023	− 9.86	0.45
20.0	−1565.23	0.31	3765.8	8.7	18.185	0.030	− 9.92	0.50
25.0	−1655.73	0.44	3716.1	11.2	18.017	0.039	− 9.98	0.55
30.0	−1745.40	0.62	3666.1	14.0	17.851	0.048	−10.04	0.60
35.0	−1834.24	0.87	3615.7	17.1	17.686	0.058	−10.10	0.65
40.0	−1922.27	1.17	3565.1	20.4	17.523	0.069	−10.16	0.70
45.0	−2009.48	1.53	3514.2	24.0	17.362	0.080	−10.22	0.75
50.0	−2095.89	1.95	3462.9	27.8	17.202	0.092	−10.28	0.80

*$d\Delta C_p^0/dT = -0.0120 \pm 0.0102$ cal/deg² mole.

state, eq. [4]. The standard thermodynamic function changes for vaporization, the enthalpy ΔH^0, entropy ΔS^0, heat capacity ΔC_p^0, and its temperature derivative $d\Delta C_p^0/dT$, together with their errors, are evaluated by treating the $\ln K$ values from eq. [6] according to the method of Clarke and Glew (12).

Hydrogen Sulfide

The standard thermodynamic function changes for vaporization of hydrogen sulfide between −80 and +50 °C are presented in Table 8. The standard errors reported take into account experimental errors on the vapor pressures, errors on evaluation of the f/P ratio due to uncertainty of the Redlich–Kwong coefficient a, and errors on the estimation of the liquid molar volumes. The error due to uncertainty of the liquid molar volume contributes a very small part (~0.3%) of the total error at all temperatures. The error due to uncertainty of the vapor f/P ratio makes the largest contribution at all temperatures. The vapor pressure measurement error contributes a small proportion to the total error at high temperatures (14–22% at 30 °C), which proportion increases at low temperatures (25–45% at −75 °C).

An independent check on the consistency of our thermodynamic functions with other measurements is provided by a comparison of the hydrogen sulfide liquid heat capacities. We obtain the values 16.25 ± 0.48 cal/deg mole at −78° C and 16.07 ± 0.31 at the normal boiling point -60.27_5 °C from the ideal gas heat capacities (19) combined with our values for ΔC_p^0, with small corrections for change of the liquid from standard to saturation pressures. These values agree within their standard errors with the liquid heat capacities, 16.24 cal/deg mole at −78 °C and 16.32 at -60.27_5 °C, interpolated from calorimetric measurements (13).

Deuterium Sulfide

The standard thermodynamic function changes

Can. J. Chem. Downloaded from www.nrcresearchpress.com by 210.87.254.5 on 09/05/12
For personal use only.

TABLE 10
Isotope effect standard thermodynamic function changes*

Temperature (°C)	$\Delta\Delta G°$ (cal/mole)		$\Delta\Delta H°$ (cal/mole)		$\Delta\Delta S°$ (cal/deg mole)		$\Delta\Delta C_p°$ (cal/deg mole)	
	Value	σ	Value	σ	Value	σ	Value	σ
−80.0	6.40	0.09	54.9	3.8	0.251	0.020	−0.67	0.19
−75.0	5.19	0.07	51.6	2.9	0.234	0.015	−0.65	0.18
−70.0	4.06	0.11	48.4	2.1	0.218	0.011	−0.62	0.16
−65.0	3.00	0.15	45.4	1.4	0.204	0.007	−0.60	0.14
−60.275	2.07	0.17	42.6	0.8	0.190	0.005	−0.58	0.12
−60.176	2.05	0.17	42.5	0.8	0.190	0.005	−0.58	0.12
−60.0	2.02	0.18	42.4	0.8	0.190	0.004	−0.57	0.12
−55.0	1.10	0.19	39.6	0.4	0.177	0.002	−0.55	0.11
−50.0	0.25	0.19	37.0	0.6	0.164	0.002	−0.52	0.09
−45.0	−0.54	0.18	34.4	0.9	0.153	0.003	−0.50	0.07
−40.0	−1.28	0.17	32.0	1.1	0.143	0.004	−0.47	0.05
−35.0	−1.97	0.15	29.6	1.4	0.133	0.005	−0.45	0.04
−30.0	−2.61	0.12	27.5	1.5	0.124	0.006	−0.42	0.03
−25.0	−3.21	0.10	25.4	1.5	0.115	0.006	−0.40	0.02
−20.0	−3.76	0.08	23.5	1.5	0.108	0.006	−0.37	0.03
−15.0	−4.28	0.07	21.7	1.4	0.100	0.005	−0.35	0.04
−10.0	−4.77	0.06	20.0	1.2	0.094	0.005	−0.32	0.06
− 5.0	−5.23	0.06	18.4	1.0	0.088	0.004	−0.30	0.08
0.0	−5.65	0.06	17.0	0.9	0.083	0.003	−0.27	0.09
5.0	−6.05	0.06	15.7	1.0	0.078	0.003	−0.25	0.11
10.0	−6.43	0.06	14.5	1.3	0.074	0.005	−0.22	0.13
15.0	−6.79	0.06	13.4	1.8	0.070	0.006	−0.20	0.14
20.0	−7.14	0.08	12.5	2.5	0.067	0.009	−0.17	0.16
25.0	−7.46	0.12	11.7	3.3	0.064	0.011	−0.15	0.18
30.0	−7.78	0.17	11.0	4.2	0.062	0.014	−0.12	0.20
35.0	−8.08	0.24	10.4	5.2	0.060	0.018	−0.10	0.21
40.0	−8.38	0.34	10.0	6.3	0.059	0.021	−0.07	0.23
45.0	−8.67	0.45	9.7	7.5	0.058	0.025	−0.05	0.25
50.0	−8.96	0.58	9.5	8.8	0.057	0.029	−0.02	0.27

*$d\Delta\Delta C_p^0/dT = 0.0050 \pm 0.0035$ cal/deg² mole.

for vaporization of deuterium sulfide are presented in Table 9. The standard errors reported take into account the errors on determination of the vapor pressures, errors on the evaluation of the f/P ratio, and errors on the estimation of the liquid molar volumes. The standard thermodynamic function variance derived from the f/P ratio uncertainty for deuterium sulfide is equal to the sum of the variance from the f/P ratio uncertainty for hydrogen sulfide and the variance from the f/P difference uncertainty for deuterium and hydrogen sulfides. The standard thermodynamic function variance derived from the liquid molar volume uncertainty for deuterium sulfide is equal to the sum of the variance from the molar volume uncertainty for hydrogen sulfide and the variance from the molar volume difference uncertainty for deuterium and hydrogen sulfides. For deuterium sulfide the relative contributions of the components to the total error have the same distribution as that discussed for hydrogen sulfide.

Isotope Effect

The deuterium isotope effect for vaporization is defined by the equation

$$[8]\quad \ln\left(\frac{K_D}{K_H}\right) = \frac{\Delta\Delta G^0}{-RT} = \ln\left(\frac{P_D}{P_H}\right) + \ln\left(\frac{f_D/P_D}{f_H/P_H}\right) - \left(\frac{(P_D-1)V_{1D}}{RT} - \frac{(P_H-1)V_{1H}}{RT}\right)$$

in which the isotopic difference of standard free energy change, $\Delta\Delta G^0$, is related directly to the ratios of the vapor pressures and the f/P ratios, and to the differences of liquid molar volume terms. The isotopic difference of vaporization standard thermodynamic function changes, enthalpy $\Delta\Delta H^0$, entropy $\Delta\Delta S^0$, etc., together with their errors, are evaluated by treating the $\ln(K_D/K_H)$ values from eq. [8] according to the method of Clarke and Glew (12), and are presented in Table 10. The thermodynamic function errors derived from the uncertainty in the experimental vapor pressure ratio are determined direct-

Can. J. Chem. Downloaded from www.nrcresearchpress.com by 210.87.254.5 on 09/05/12
For personal use only.

ly from eq. [3] rather than from the difference between eqs. [2] and [1]. The thermodynamic function errors derived from the uncertainty of the ratio of the f/P values is a small percentage ($\sim$1.5%) of the error derived from the uncertainty of the separate f/P values, and are evaluated assuming that the Redlich–Kwong coefficient a for deuterium sulfide could be equal to that for hydrogen sulfide instead of the value in Table 5. Similarly, the errors on standard thermodynamic functions derived from the uncertainty of the liquid molar volume term are evaluated assuming that the molar volume for liquid deuterium sulfide could be the same as for hydrogen sulfide.

The deuterium and hydrogen sulfide vapor pressures show the well-known isotopic crossover effect which has been interpreted by Bigeleisen (20, 21). According to this theory at low temperatures the higher hydrogen sulfide vapor pressure arises mainly from the translational and rotational motions in the liquid. This should be accompanied by a larger liquid molar volume for hydrogen sulfide, in direct conflict with our volume measurements. This volume difference could be explained by hindered rotational (librational) motions in the liquid, on which the molar volume is more critically dependent than the vapor pressure.

This work was supported in part by a grant under the National Research Council of Canada Industrial Research Assistance Program, 1966.

1. A. Kruis, L. Popp, and K. Clusius. Z. Elektrochem. **43**, 664 (1937).
2. G. T. Armstrong. Nat. Bur. Std. Report 2306. 1953.
3. H. H. Reamer, B. H. Sage, and W. N. Lacey. Ind. Eng. Chem. **42**, 140 (1950).
4. W. B. Kay and G. M. Rambosek. Ind. Eng. Chem. **45**, 221 (1953).
5. A. I. Vogel. A textbook of quantitative inorganic analysis. 3rd ed. Longmans, Green and Co., Ltd., London. 1961. p. 810.
6. G. R. Kingsley and R. R. Schaffert. Anal. Chem. **23**, 914 (1951).
7. N. E. Dorsey. Properties of ordinary water-substance. Reinhold Publishing Corp., New York. 1940.
8. R. J. Berry. Can. J. Phys. **37**, 1230 (1959); E. H. McLaren and E. G. Murdock. Can. J. Phys. **44**, 2653 (1966).
9. Nat. Bur. Std. Tech. News Bull. October, 1963.
10. A. Klemenc and O. Bankowski. Z. Anorg. Chem. **208**, 348 (1932).
11. J. P. Baxter, L. J. Burrage, and C. C. Tanner. J. Soc. Chem. Ind. **53**, 410T (1934).
12. E. C. W. Clarke and D. N. Glew. Trans. Faraday Soc. **62**, 539 (1966).
13. W. F. Giauque and R. W. Blue. J. Amer. Chem. Soc. **58**, 831 (1936).
14. A. M. Clark, A. H. Cockett, and H. S. Eisner. Proc. Roy. Soc. London, Ser. A, **209**, 408 (1951).
15. R. H. Wright and O. Maass. Can. J. Res. **5B**, 442 (1931).
16. O. Redlich and J. N. S. Kwong. Chem. Rev. **44**, 233 (1949).
17. K. K. Shah and G. Thodos. Ind. Eng. Chem. **57**, 30 (1965).
18. H. Kopper. Z. Phys. Chem. Leipzig, **A175**, 469 (1936).
19. L. Haar, J. C. Bradley, and A. S. Friedman.
20. J. Bigeleisen. J. Chem. Phys. **34**, 1485 (1961).
21. J. Bigeleisen. J. Chim. Phys. **60**, 35 (1963).

Can. J. Chem. Downloaded from www.nrcresearchpress.com by 210.87.254.5 on 09/05/12
For personal use only.

Can. J. Chem. Downloaded from www.nrcresearchpress.com by 210.87.254.42 on 09/05/12
For personal use only.

Decomposition of aqueous dithionite. Part I. Kinetics of decomposition of aqueous sodium dithionite

W. J. LEM[1] AND M. WAYMAN

Department of Chemical Engineering and Applied Chemistry, University of Toronto, Toronto 181, Ontario

Received October 6, 1969

A rate equation for the total path of decomposition of aqueous $Na_2S_2O_4$ in the pH range 3.5–5.0 at 23 °C was determined, taking into account the rapid autocatalytic decomposition as well as the "induction" period. The kinetic data were determined by a continuous polarographic method. The form of the rate equation was found by studying the decomposition of aqueous $Na_2S_2O_4$ at various values of pH and at various initial concentrations. Rate constants were calculated from the data using the integrated form of the rate equation. The rate equation, with certain limitations, was found to be

$$\frac{-dC}{dt} = k_1[H^+]C + k_2[H^+]C(C_0 - C)$$

where $k_1 = 1.67 \times 10^{-1}$ l mole^{-1} s^{-1} and $k_2 = 5.83 \times 10^3$ l^2 mole^{-2} s^{-1} at 23 °C; C and C_0 being dithionite concentration at time t and initial concentration, respectively. The integrated form of the rate equation was used to generate decomposition curves, which are in reasonable agreement with the experimental data.

Canadian Journal of Chemistry, **48**, 776 (1970)

Introduction

Sodium dithionite, $Na_2S_2O_4$, is a strong reducing agent used in chemical industry and is unstable in aqueous solution. The kinetics and mechanism of the decomposition of aqueous dithionite are still in dispute. Little has been published about dithionite decomposition, and the published findings are contradictory. For example, the order of the decomposition reaction was reported to be first (1), three-halves (2), and second (3). The rate of decomposition of aqueous sodium dithionite is greatly affected by pH, being slow at high pH values and very rapid at low pH values. Decomposition takes place in stages, being slow during an "induction" period, the length of which depends on prevailing conditions, followed by a rapid autocatalytic reaction to completion. Most of the previous kinetic work on the decomposition of dithionite has been concerned with the induction period, where the reaction is still quite simple, and at high pH values, where the reaction is relatively slow. In the present work, the decomposition of sodium dithionite was investigated in aqueous solution at relatively low pH values, where the reaction is moderately rapid. The experiments were conducted in the absence of oxygen at room temperature. The objective was to determine a rate equation for the whole course of the reaction to complete decomposition.

[1]Present address: Imperial Oil Enterprises Limited, Sarnia, Ontario.

Experimental

Continuous polarographic analysis of dithionite as described by the authors (4) was modified for the present work. According to Furness (5), dithionite in 0.5 M $(NH_4)_2HPO_4$ and 0.5 M NH_4OH as supporting electrolyte produces a well-defined anodic curve with a half-wave potential of −0.43 V vs. standard calomel electrode (s.c.e.). In this study, a new supporting electrolyte suitable for the required pH range was found to be 0.1 M HOAc and 0.1 M NaOAc. This produced a similar anodic curve as shown in Fig. 1. In the polarographic analysis of dithionite, the applied voltage was kept constant at the plateau and the current was measured continuously against time. The voltage was kept constant at −0.2 V vs.

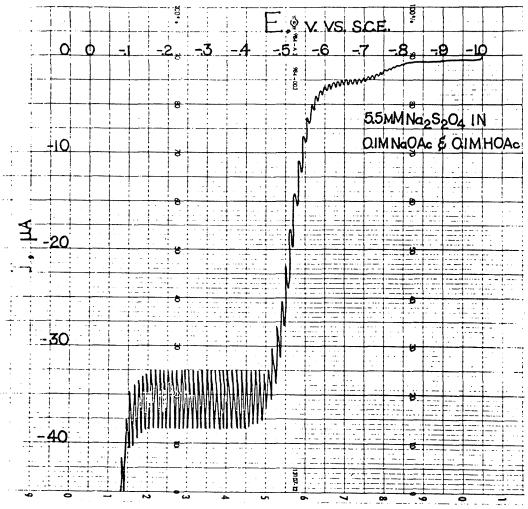

FIG. 1. Polarogram of 5.5 mM $Na_2S_2O_4$ in 0.1 M NaOAc and 0.1 M HOAc at m_d (rate of flow of Hg) = 1.215×10^{-3} g s^{-1}, t_d (drop time, i.e., time between drops of Hg) = 6 s per drop, T = 23 °C.

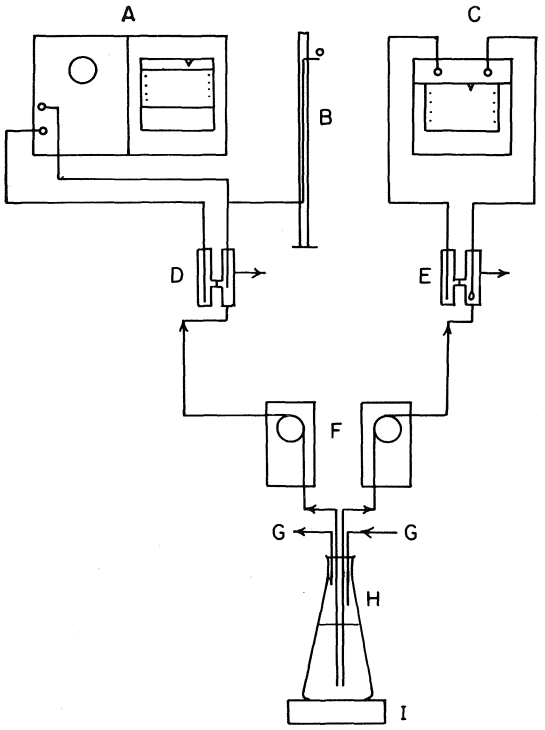

FIG. 2. Schematic diagram of the continuous polarographic analysis of buffered dithionite. The p*H* is also continuously recorded. *A*, Radiometer PO4 polarograph; *B*, Heathkit p*H* meter with recorder; *C*, dropping mercury electrode; *D*, continuous polarographic analysis H-cell; *E*, continuous p*H* H-cell; *F*, pumps; *G*, argon gas; *H*, dithionite solution containing acetate buffer; *I*, magnetic stirrer.

s.c.e. and the anodic current agreed with the Ilkovič equation, that is, the current was proportional to the concentration, other parameters being kept constant (6).

The apparatus used is shown in Fig. 2. The polarograph was a Radiometer PO4. A Heathkit Model EUW-301 meter was used for the continuous measurement of p*H*. The sodium dithionite, having a purity of 98%, was specially prepared and kindly provided by Associated Chemical Companies Ltd., of Harrogate, Yorkshire, England. The remaining impurities were mainly sodium carbonate, sodium sulfite, and sodium thiosulfate and it did not appear possible to increase the purity further for this work. All water used was distilled, de-ionized, deaerated by boiling, and swept with 99.997% argon gas which was also used to provide an inert atmosphere during the decomposition of dithionite.

In a 3 l flask with magnetic stirrer, a known weight of $Na_2S_2O_4$ was dissolved in the proper acetate buffer to give the required constant p*H* value. With argon gas providing the inert atmosphere, the solution was transferred from the flask to a modified polarographic H-cell with provision for the solution to come in from the bottom and go out at the top. An Aminco small-volume peristaltic-action pump was used with Tygon tubing having an outer diameter of $\frac{1}{8}$ in. to pump the solution at a rate of 3×10^{-4} l s^{-1}. The p*H* value was measured continuously.

The rate of decomposition of 5×10^{-3} *M* $Na_2S_2O_4$ at p*H* 4 was compared using NaOAc–HOAc buffer and, in a separate experiment, sodium hydrogen phosphate – citric acid buffer. They were found to be essentially identical, suggesting that acetate did not specifically affect the rate of decomposition of dithionite at constant p*H*.

Results and Discussion

In order to determine the rate equation of the decomposition of aqueous sodium dithionite, a series of experiments at different p*H* and different initial dithionite concentrations was performed. The buffer used was the sodium acetate – acetic acid system, at p*H* of 3.5, 4.0, 4.5, and 5.0, in which range the rate of decomposition was neither too fast nor too slow to be studied in this equipment, and at initial concentrations of $Na_2S_2O_4$ of 1, 2, 5, and 10×10^{-3} *M*. The decomposition of $Na_2S_2O_4$ under these conditions produced S-shaped concentration–time curves, three of which are shown in the irregular lines on Figs. 3, 4, and 5, and generalized in diagramatic form in Fig. 6. A rate equation which would produce this shape would have the form

$$[1] \quad \frac{-dC}{dt} = k_1[H^+]^m C^n + k_2[H^+]^p C^q (C_0 - C)^r$$

where C is the concentration of dithionite at time t (moles l^{-1}), C_0 is the initial concentration of dithionite (moles l^{-1}), $[H^+]$ is the concentration of the hydrogen ion (moles l^{-1}), k_1 and k_2 are rate constants, and m, n, p, q, and r are orders of reaction.

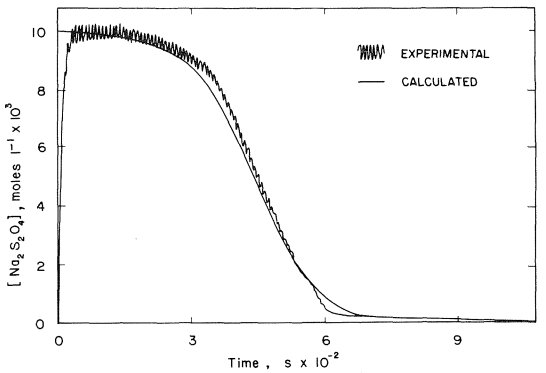

FIG. 3. Decomposition of 10 m*M* aqueous $Na_2S_2O_4$ at p*H* 4 using acetate buffer. The irregular curve is the polarograph recorder plot. The smooth curve was calculated from the integrated rate equation.

Can. J. Chem. Downloaded from www.nrcresearchpress.com by 210.87.254.42 on 09/05/12
For personal use only.

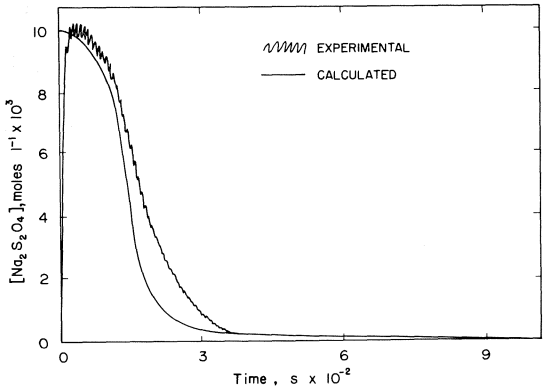

FIG. 4. Decomposition of 10 mM aqueous $Na_2S_2O_4$ at pH 3.5 using acetate buffer. The irregular curve is the polarograph recorder plot. The smooth curve was calculated from the integrated rate equation.

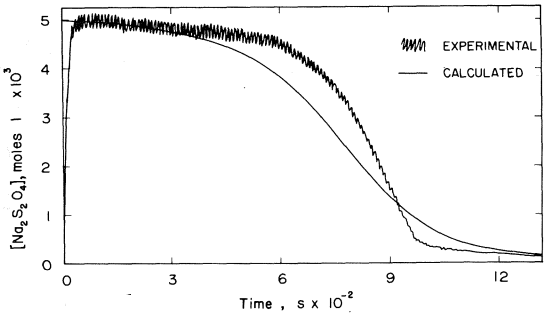

FIG. 5. Decomposition of 5 mM aqueous $Na_2S_2O_4$ at pH 4 using acetate buffer. The irregular curve is the polarograph recorder plot. The smooth curve was calculated from the integrated rate equation.

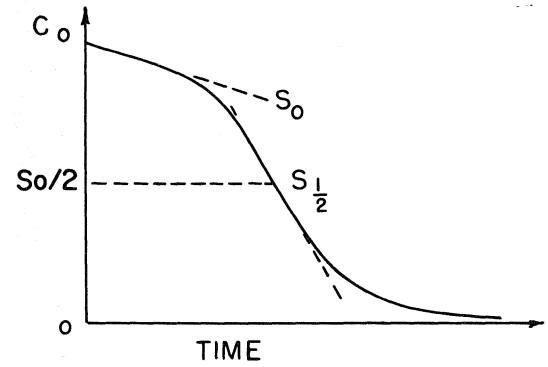

FIG. 6. Diagrammatic typical decomposition curve of aqueous sodium dithionite. S_0 = initial slope at $t = 0$ (moles s^{-1}), $S_{1/2}$ = slope at $C = C_0/2$.

In general, the first term on the right hand side of eq. [1] represents the intial rate of decomposition and thus, under these conditions, the rate during the induction period, while the second term represents the autocatalytic, rapid phase of the decomposition, $(C_0 - C)^r$ being a function of the concentration of a product of decomposition which is the catalyst.

At $t = 0$, $C = C_0$

$$[2] \qquad \left(\frac{dC}{dt}\right)_0 = S_0 = k_1[H^+]^m C_0{}^n$$

$$\therefore \log S_0 = n \log C_0 + \log k_1[H^+]^m$$

and

$$\log S_0 = m \log [H^+] + \log k_1 C_0{}^n$$

According to eq. [3], a plot of log S_0 vs. log C_0 at constant pH would give a slope equal to n, and an intercept equal to log k_1 $[H^+]^m$. A series of values of n were thus obtained at various pH values, as shown in Fig. 7. Similarly, from eq. [4], a plot of log S_0 vs. log $[H^+]$ at constant C_0 would give a slope equal to m and an intercept equal to log $k_1 C_0{}^n$. A series of values of m were obtained at various constant initial concentrations as shown in Fig. 8. Furthermore, knowing the values of m and n, the values of k_1 could be calculated from the intercepts. The values of m, n, and k_1 so obtained are shown in Table 1. The values of m and n were calculated from the least squares straight lines shown in Figs. 7 and 8. It is evident that the straight lines are only an approximation to the data, especially in Fig. 7 at the lower pH

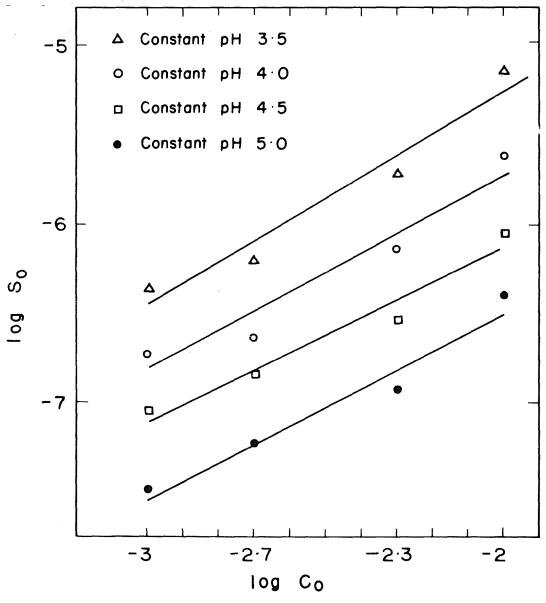

FIG. 7. Initial rates of decomposition of aqueous sodium dithionite solutions, plotted at constant pH.

Can. J. Chem. Downloaded from www.nrcresearchpress.com by 210.87.254.42 on 09/05/12
For personal use only.

Can. J. Chem. Downloaded from www.nrcresearchpress.com by 210.87.254.42 on 09/05/12
For personal use only.

TABLE 1

Summary of the results for the determination of the orders of reactions and rate constants for the decomposition of aqueous $Na_2S_2O_4$

pH*	n†	k_1† (l mole^{-1} s^{-1})	$(q + r)$‡	k_2‡ (l^2 mole^{-2} s^{-1})
3.5	1.23	1.08	1.36	3.50×10^4
4.0	1.10	1.48	1.74	2.81×10^4
4.5	0.99	2.23	1.82	3.00×10^4
5.0	1.08	2.70	1.44	4.62×10^4

C_0* (M)	m§	k_1§ (l mole^{-1} s^{-1})	p¶	k_2¶ (l^2 mole^{-2} s^{-1})
10×10^{-3}	0.84	5.92×10^{-1}	0.98	1.09×10^4
5×10^{-3}	0.90	5.94×10^{-1}	0.86	4.49×10^3
2×10^{-3}	0.80	2.23×10^{-1}	0.88	6.50×10^3
1×10^{-3}	0.80	3.13×10^{-1}	1.00	4.11×10^4

*Kept constant.
†From Fig. 7, plot of log S_0 vs. log C_0.
‡From Fig. 9, plot of log ΔS vs. log C_0.
§From Fig. 8, plot of log S_0 vs. log [H$^+$].
¶From Fig. 10, plot of log ΔS vs. log ([H$^+$].

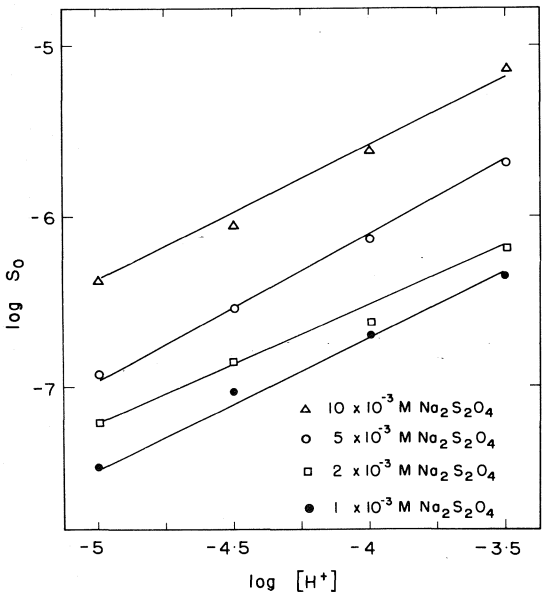

FIG. 8. Initial rates of decomposition of aqueous sodium dithionite solutions, plotted at constant initial dithionite concentrations.

values, where the slope appears to be increasing with concentration. Thus it is evident that n is a function of both pH and concentration. In spite of this variation, it is convenient and useful to round the values of m and n both to 1. Then eq. [1] may be written as

$$[5]\quad \frac{-dC}{dt} = k_1[H^+]C + k_2[H^+]^pC^q(C_0 - C)^r$$

This equation represents the reaction as somewhat more sensitive to pH than the experimental results warrant, and ignores a second order effect of dithionite concentration on the initial rate of decomposition at the lower pH values. While the addition of further terms to the equation would remedy these defects, the simplification represented by eq. [5] is valuable.

The values of k_1, shown in Table 1, vary too widely to be averaged, and will be calculated below by another method. From eq. [5], at $C = C_0/2$

$$[6]\quad -\left(\frac{dC}{dt}\right)_{1/2} = S_{1/2} = k_1[H^+]\frac{C_0}{2} + k_2[H^+]^p\left(\frac{C_0}{2}\right)^q\left(\frac{C_0}{2}\right)^r = \frac{S_0}{2} + k_2\frac{[H^+]^p}{2^{q+r}}C_0^{q+r}$$

Define $\Delta S \equiv S_{1/2} - S_0/2$

$$[7]\quad \Delta S = \frac{k_2[H^+]^p}{2^{q+r}}C_0^{q+r}$$

$$[8]\quad \log\Delta S = (q + r)\log C_0 + \log\frac{k_2[H^+]^p}{2^{q+r}}$$

and

$$[9]\quad \log\Delta S = p\log[H^+] + \log\frac{k_2C_0^{q+r}}{2^{q+r}}$$

According to eq. [8], a plot of log ΔS vs. log C_0 would give a slope equal to (q + r) at constant pH, and an intercept log $k_2[H^+]^p/2^{q+r}$. A series of values of $(q + r)$ were obtained at various values of constant pH as shown in Fig. 9. Similarly, according to eq. [9], a plot of log ΔS vs. log [H$^+$] would give a slope equal to p at constant C_0 and an intercept equal to log $k_2C_0^{q+r}/2^{q+r}$. A series of values of p were obtained at various constant initial concentrations as shown in Fig. 10. With the values of $(q+r)$ and p being known, the rate constant k_2 could be calculated from the intercepts. The values so obtained are shown in Table 1. The least squares straight lines in Figs. 9 and 10 are somewhat better than those in Figs. 7 and 8, although the pH = 3.5 line in Fig. 10 leaves much to be desired. As before, we shall assume that p = 1, recognizing that this ignores the concentration effect at low pH. The values of $(q + r)$ present a somewhat more serious problem since the points are

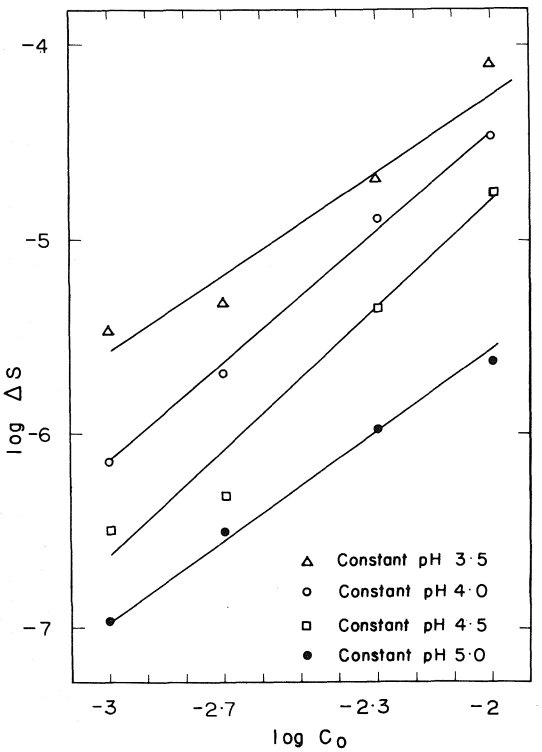

FIG. 9. Rates of decomposition of aqueous sodium dithionite solutions during the autocatalytic phase, plotted at constant p*H*.

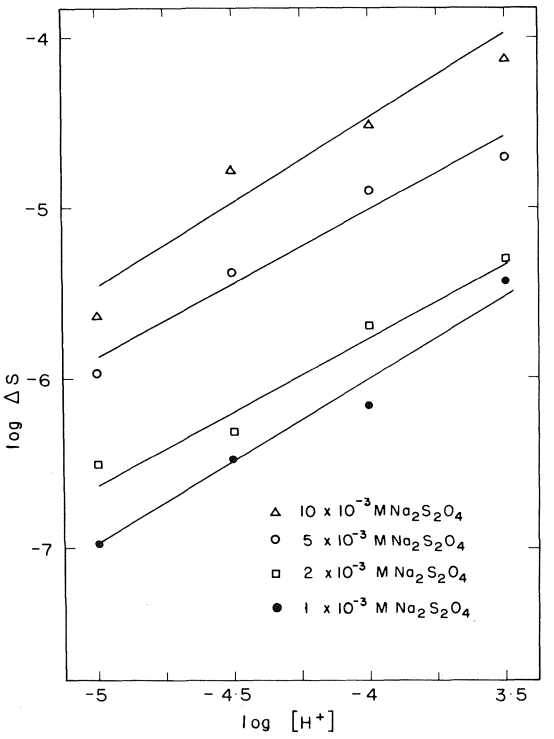

FIG. 10. Rates of decomposition of aqueous sodium dithionite solutions during the autocatalytic phase, plotted at constant initial dithionite concentrations.

scattered and the slopes vary from 1.36 to 1.82. For the purpose of approaching understanding of this reaction, we shall take $(q + r) = 2$, and assume that $q = r = 1$. These are bold assumptions, suggesting, for example, that the decomposition of each molecule of dithionite results in the formation of a molecule of catalyst, whereas there are undoubtedly a number of reactions proceeding simultaneously. However, making these approximations allows us to write eq. [1] in the form

$$[10] \quad \frac{-dC}{dt} = k_1[H^+]C + k_2[H^+]C(C_0 - C)$$

The variation in k_2, as that in k_1, was too great for averaging. The reason for this variation was, in part, the nature of the log–log plot. A small change in the slope changes the constants drastically. For example, at constant C_0 equals 10×10^{-3} M $Na_2S_2O_4$, the value of k_2 calculated based on p equals 1 was 4.11×10^4 l^2 mole^{-2} s^{-1}. If the value of p were taken as 0.9, k_2 would be equal to 1.50×10^4. Thus, the rate constants calculated this way were very sensitive to the values chosen for the reaction orders.

Another method for determining the rate constants used the integrated form of the rate equation [10] derived as follows. By rearranging eq. [10]

$$\frac{-dC}{dt} = (k_1[H^+] + k_2[H^+]C_0)C - k_2[H^+]C^2$$

and

$$[11] \quad -\int_{C_0}^{C} \frac{dC}{C\{(k_1[H^+] + k_2[H^+]C_0) - k_2[H^+]C\}} = \int_0^t dt$$

Since

$$\int \frac{dx}{x(a + bx)} = \frac{-1}{a} \log \frac{a + bx}{x}$$

Can. J. Chem. Downloaded from www.nrcresearchpress.com by 210.87.254.42 on 09/05/12
For personal use only.

$$[12] \qquad \left(\frac{1}{k_1[H^+] + k_2[H^+]C_0}\right)\left(\log\frac{k_1 + k_2C_0 - k_2C}{C} - \log\frac{k_1}{C_0}\right) = t$$

Equation [12] was used to generate C–t curves. By taking specified values of $[H^+]$ and C_0, the value of t was calculated at various concentrations. A plot of the calculated C–t curve was compared with the C–t curve obtained experimentally. The constants which best fitted the experimental data were taken as satisfactory values of k_1 and k_2. When k_1 and k_2 were taken as 1.67×10^{-1} l mole^{-1} s^{-1} and 5.83×10^3 l^2 mole^{-2} s^{-1}, respectively, at pH = 4 and $C_0 = 10 \times 10^{-3}$ M $Na_2S_2O_4$, the C–t curve calculated agreed reasonably well with that obtained experimentally; as shown in Fig. 3. Figures 4 and 5 similarly show decomposition curves generated using the integrated form of the rate equation and the same values of k_1 and k_2 at pH = 3.5 and $C_0 = 10 \times 10^{-3}$ M and at pH = 4.0 and $C_0 = 5 \times 10^{-3}$ M, respectively, and show reasonable agreement with the experimental decomposition curves.

Figure 11 shows a plot taken from Fig. 5 of the paper by Rinker *et al.* (2), the C–t curve at pH = 6.0 and $C_0 = 11.5 \times 10^{-3}$ M $Na_2S_2O_4$ at 60 °C. A C–t curve was generated using eq. [12] but the values for k_1 and k_2 had to be changed because the temperature was different. The curve so obtained using k_1 and k_2 as 5×10^{-2} l mole^{-1} s^{-1} and 1.67×10^5 l^2 mole^{-2} s^{-1}, respectively, is also shown in Fig. 11. There is reasonable agreement between these curves, suggesting some support for the general form of the rate equation and the approximations made.

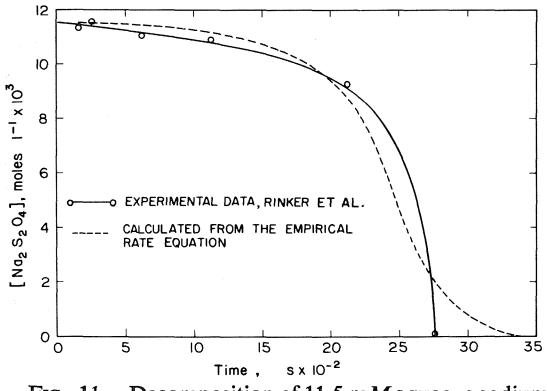

FIG. 11. Decomposition of 11.5 mM aqueous sodium dithionite at 60 °C: comparison of a curve generated using eq. [12] with the experimental data of Rinker *et al.* (2).

Conclusions

The rate of decomposition of aqueous $Na_2S_2O_4$ depends on its concentration, the concentration of a product of its decomposition, and the pH values, and may be represented by the following rate equation

$$\frac{-dC}{dt} = k_1[H^+]C + k_2[H^+]C(C_0 - C)$$

The values of k_1 and k_2 which best fit the experimental data at 23 °C are 1.67×10^{-1} l mole^{-1} s^{-1} and 5.83×10^3 l^2 mole^{-2} s^{-1}, respectively.

The rate equation shown here incorporates a number of approximations, the experimental data being somewhat less sensitive to pH and, at low pH, more sensitive to dithionite concentration than the equation implies. A better equation would have at least two more terms, one of which would reflect the sensitivity of the initial decomposition rates to dithionite concentration at low pH values and the other to reflect side reactions in which dithionite decomposition did not result uniquely in the autocatalyst.

The integrated form of the rate equation may be used to generate decomposition curves in reasonable agreement with experimental data.

This work was carried out at the University of Toronto, assisted by grants from the National Research Council of Canada and the Department of University Affairs of the Province of Ontario. One of us (W.J.L.) is grateful for an NRCC scholarship held during 1967–1969.

1. M. W. LISTER and R. C. GARVIE. Can. J. Chem. **37**, 1567 (1959).
2. R. G. RINKER, S. LYNN, D. M. MASON, and W. H. CORCORAN. Ind. Eng. Chem. Fundam. **4**, 282 (1965).
3. K. JELLINEK and E. JELLINEK. Z. Phys. Chem. Leipzig, **93**, 325 (1919).
4. W. J. LEM and M. WAYMAN. J. Soc. Dyers Colour. **83**, 277 (1967).
5. W. FURNESS. J. Soc. Dyers Colour. **66**, 270 (1950).
6. W. J. LEM. Ph.D. Thesis, Department of Chemical Engineering and Applied Chemistry, University of Toronto, Toronto, Ontario. 1969.

Can. J. Chem. Downloaded from www.nrcresearchpress.com by 210.87.254.42 on 09/05/12
For personal use only.

Can. J. Chem. Downloaded from www.nrcresearchpress.com by 210.87.254.5 on 09/05/12
For personal use only.

Decomposition of aqueous dithionite. Part II. A reaction mechanism for the decomposition of aqueous sodium dithionite

M. WAYMAN AND W. J. LEM[1]

Department of Chemical Engineering and Applied Chemistry, University of Toronto, Toronto 181, Ontario

Received October 6, 1969

The decomposition of dilute aqueous sodium dithionite has been studied in unbuffered solutions by means of continuous polarography, accompanied by recorded pH values. The decomposition–time curve began with a slow "induction" period followed by an S-shaped rapid phase. The pH values decreased slightly during the induction period and increased considerably during the rapid phase. The addition of a solution of fresh decomposition products eliminated the induction phase. The addition of sulfide also eliminated the induction period and catalyzed the reaction. The accepted stoichiometry (2) of the reaction was confirmed. The following sequence of reactions is proposed

$$S_2O_4^{2-} + H^+ \rightleftharpoons HS_2O_4^-$$

[4] $$HS_2O_4^- + H_2O \xrightarrow{k_4} HSO_2^- + HSO_3^- + H^+$$

[5] $$HS_2O_4^- + HSO_2^- \xrightarrow{k_5} S_2O_3^{2-} + HSO_3^- + H^+$$

In the presence of H_2S and possibly S formed in side reactions which consume H^+, reaction [5] is catalyzed and may be represented as

[9] $$HS_2O_4^- + HSO_2 \rightarrow S_2O_3^{2-} + HSO_3 + H^+$$

and

$$HSO_3 + e^- \rightarrow HSO_3^-$$

The rate equation is represented as

$$\frac{-d[S_2O_4^{2-}]}{dt} = k_4[H^+][S_2O_4^{2-}] + k_5[H^+][S_2O_4^{2-}][HSO_2^-]$$

Reaction [4] is rate limiting during the induction period and reaction [5] (catalyzed), during the rapid phase of decomposition.

Canadian Journal of Chemistry, 48, 782 (1970)

Introduction

Jellinek and Jellinek (1), in 1919, were probably the first to study the kinetics of the decomposition of aqueous $Na_2S_2O_4$. However, it was not until 1965 that Rinker *et al.* (2) proposed a stepwise mechanism. Decomposition of dithionite takes place in stages, being slow during an "induction" period, the length of which depends on the prevailing conditions, followed by a rapid autocatalytic reaction to completion. The mechanism proposed by Rinker *et al.* was in agreement with their experimental data for the induction period. They found that the initial reaction rate was three-halves order with respect to dithionite ion concentration and one-half order with respect to hydrogen ion concentration. However, they encountered difficulty in interpreting their results because the concentration data oscillated with time. They did not propose a rate equation or mechanism for the rapid reaction following the induction period. The object of the present study was to propose a mechanism for the whole course of the reaction of the decomposition of aqueous $Na_2S_2O_4$ in agreement with the rate equation derived in Part I (3) and with further experimental evidence. The rate equation, under conditions of an inert atmosphere, in the pH range of 3.5 to 5.0 in dilute aqueous solution at 23 °C could be represented, with certain qualifications, as

[1] $$\frac{-dC}{dt} = k_1[H^+]C + k_2[H^+]C(C_0 - C)$$

where C and C_0 are dithionite concentrations at time t and 0, respectively, $k_1 = 1.67 \times 10^{-1}$ l mole^{-1} s^{-1}, and $k_2 = 5.83 \times 10^3$ l^2 mole^{-2} s^{-1}.

[1]Present address: Imperial Oil Enterprises Limited, Sarnia, Ontario.

Can. J. Chem. Downloaded from www.nrcresearchpress.com by 210.87.254.5 on 09/05/12
For personal use only.

Experimental

Decomposition of Unbuffered Aqueous $Na_2S_2O_4$

Sodium dithionite of 98% purity (3) was dissolved in deaerated distilled water in concentrations from 1×10^{-3} to 10×10^{-3} *M*. The decomposition rate was determined from concentration–time curves obtained by continuous polarography (4) in the experimental arrangement shown in Fig. 1. The experiments were conducted in an argon atmosphere. Separate pumps were used to transfer the decomposing $Na_2S_2O_4$ solution and the acetate supporting electrolyte (3), the two streams being mixed in a T-tube before entering the analytical H-cell. The applied voltage between the dropping mercury electrode and the saturated calomel electrode was kept constant at −0.2 V. The current, which was proportional to the concentration of dithionite, was measured against time continuously. The p*H* value, which was changing during the decomposition, was also measured continuously.

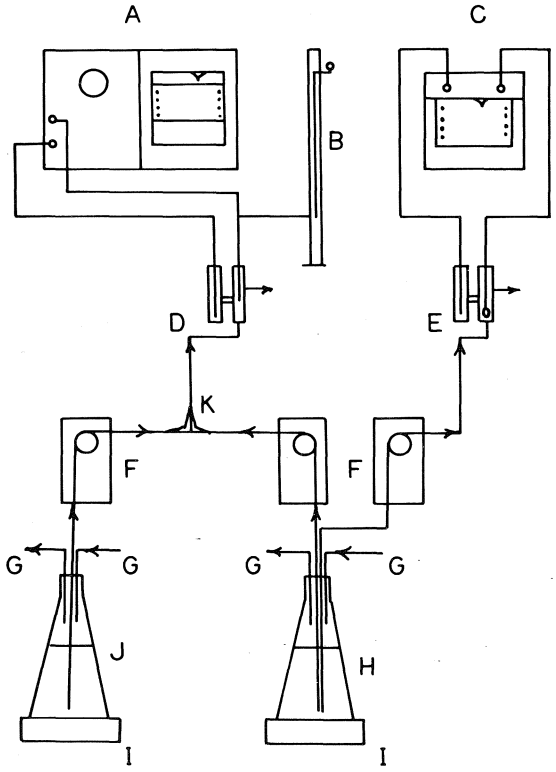

FIG. 1. Schematic diagram of continuous polarographic analysis of dithionite: *A*, Radiometer PO4 recording polarograph; *B*, dropping mercury electrode; *C*, Heathkit p*H* meter with recorder; *D*, continuous polarographic analysis H-cell; *E*, continuous p*H* H-cell; *F*, pump; *G*, argon; *H*, dithionite solution; *I*, magnetic stirrer; *J*, solution of supporting electrolyte; *K*, T-tube.

Two decomposition curves at 5×10^{-3} and 10×10^{-3} *M* $Na_2S_2O_4$ are shown in Figs. 2 and 3. The change of p*H* as the concentration of $Na_2S_2O_4$ decreased is also shown. The curves for p*H* vs. time are quite interesting in that the $Na_2S_2O_4$ solution was initially at p*H* of about 4, and the p*H* decreased slightly until the decomposition of dithionite began to accelerate, whereupon it increased rapidly. The increase in p*H* during the rapid decomposition of dithionite indicated that hydrogen ion was consumed in the reaction. Furthermore, the p*H*–time curves were also S-shaped, indicating a relationship between the rate of decomposition of dithionite and the hydrogen ion concentration. It is also seen that the p*H* value decreased after decomposition of $Na_2S_2O_4$ was complete, indicating continued reaction of decomposition products. Finally, sulfur, observed as a cloudy precipitate, disappeared if left over a period of about 24 h, again suggesting continuing reactions.

Addition of Fresh $Na_2S_2O_4$ to Newly-Decomposed $Na_2S_2O_4$

To study the effect of the products of newly-decomposed $Na_2S_2O_4$ on the rate of decomposition of $Na_2S_2O_4$, 2 l of 10×10^{-3} *M* $Na_2S_2O_4$ at constant p*H* was allowed to decompose. After the decomposition was complete, 10×10^{-3} mole of fresh solid $Na_2S_2O_4$ was added and the volume re-adjusted to 2 l. After the mixed solution was again decomposed, another 10×10^{-3} mole was added and the volume was again adjusted to 2 l. This process was repeated four times altogether at constant p*H* = 3.5, and in a separate experiment at p*H* = 4.0.

The log of the initial slope, S_0, was plotted against the number of additions, and, as can be seen in Fig. 4, the products of the decomposition of dithionite raised the initial rate of decomposition of dithionite by about 10 times. The induction period was eliminated. An increase in the amount of decomposition products did not increase the rate further, possibly due to the fact that some decomposition products tend to stabilize dithionite to some extent.

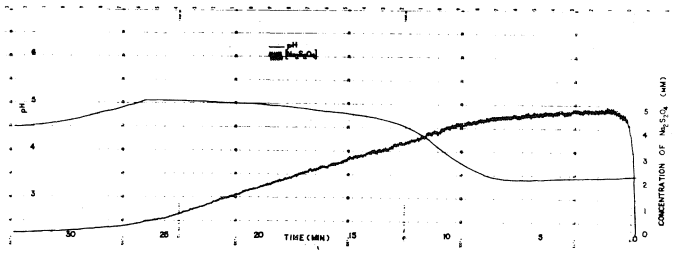

FIG. 2. Decomposition of 5 m*M* $Na_2S_2O_4$.

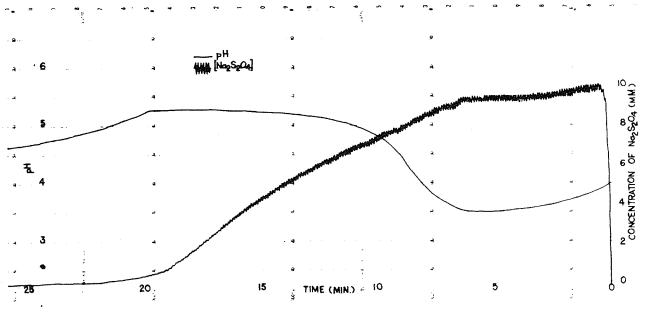

FIG. 3. Decomposition of 10 mM $Na_2S_2O_4$.

Effect of Possible Decomposition Products on the Rate of Decomposition of Aqueous $Na_2S_2O_4$

The effect of several possible products of the decomposition of aqueous $Na_2S_2O_4$ on its rate of decomposition was determined. As possible products, Na_2SO_3, $NaHSO_3$, $Na_2S_2O_3$, $Na_2S_2O_5$, and Na_2S at concentrations of 1, 5, and 10×10^{-3} M, were added to 10×10^{-3} M $Na_2S_2O_4$ at constant p$H = 4$. From the decomposition curves, plots of the logarithm of the concentration of the added possible product, log [X], was plotted against log S_0, the initial slope, as shown in Fig. 5, and against log ΔS, where $\Delta S = S_{1/2} - S_0/2$, $S_{1/2}$ being the slope when half of the dithionite was decomposed, as shown in Fig. 6. There was no definite trend in the initial rate of decomposition

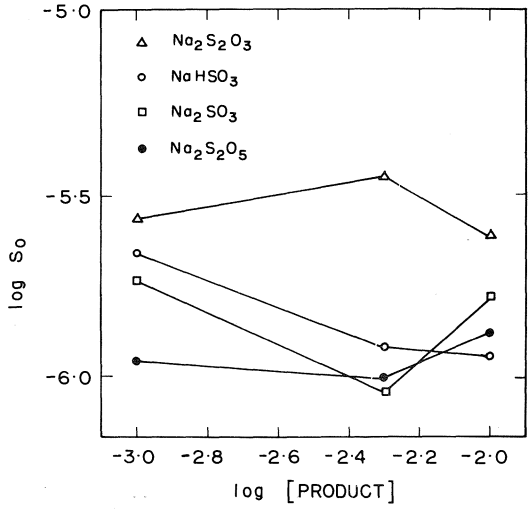

FIG. 5. Effect of some possible products on the initial rate of decomposition of 10 mM $Na_2S_2O_4$ at p$H = 4$.

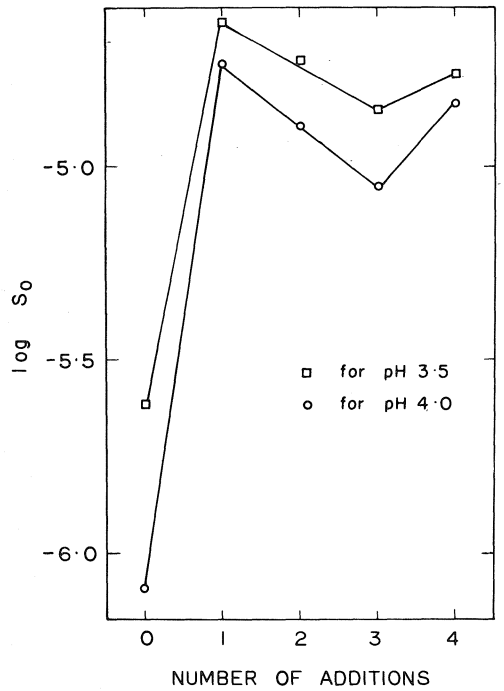

FIG. 4. Effect of successive additions of solutions of decomposition products of newly-decomposed $Na_2S_2O_4$ on the rate of decomposition of $Na_2S_2O_4$.

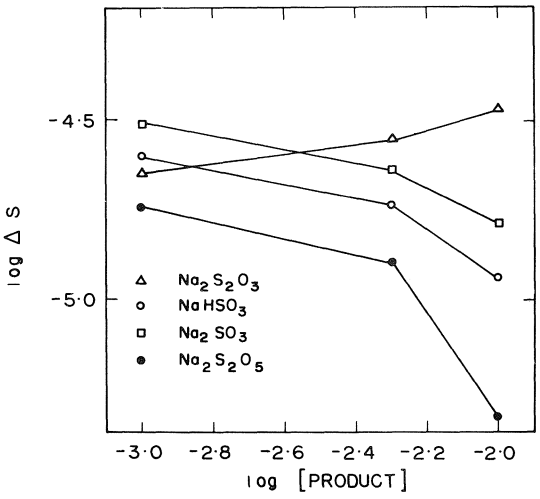

FIG. 6. Effect of some possible products on the autocatalytic rate of decomposition of 10 mM $Na_2S_2O_4$ at p$H = 4$.

Can. J. Chem. Downloaded from www.nrcresearchpress.com by 210.87.254.5 on 09/05/12
For personal use only.

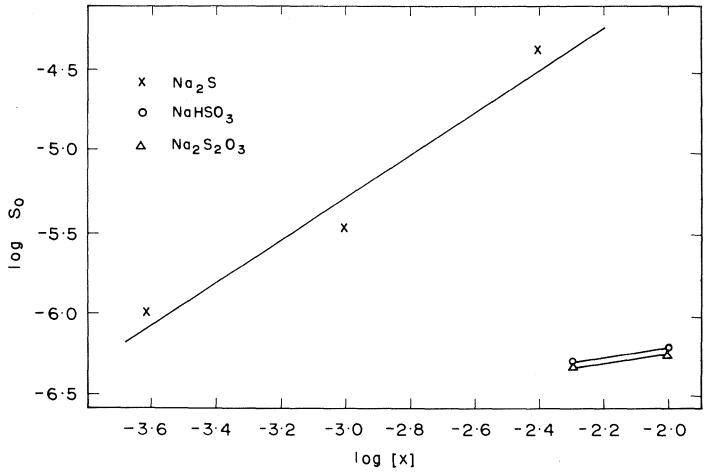

FIG. 7. Effect of Na_2S, $NaHSO_3$, and $Na_2S_2O_3$ on the initial rate of decomposition of 5 mM $Na_2S_2O_4$ at pH = 5.

attributable to the addition of these chemicals. However, in the case of log ΔS vs. log [X], $Na_2S_2O_3$ seemed to hasten somewhat the rate of decomposition, whereas Na_2SO_3, $NaHSO_3$, and $Na_2S_2O_5$ seemed to retard it.

These rate changes were small, however, compared to the effect of Na_2S. In the presence of these concentrations of Na_2S, the rate of decomposition was too great to be measured in this experimental arrangement at pH = 4, and the pH was raised to 5 where the $Na_2S_2O_4$ was more stable. A solution of 5×10^{-3} M $Na_2S_2O_4$ at pH = 5 was polarographically measured as usual for a few minutes and a known weight of Na_2S was introduced. The induction period was thereby eliminated. The rapid increase in the rate of decomposition was measured. The initial rate of decomposition after the addition of Na_2S was plotted for various added concentrations of Na_2S. For comparison, various concentrations of $Na_2S_2O_3$ and $NaHSO_3$ were added in the same manner to 5×10^{-3} M $Na_2S_2O_4$ at pH = 5. The results are shown in Fig. 7. The initial rate of decomposition of $Na_2S_2O_4$ was approximately proportional to added Na_2S on a log–log plot.

Determination of the Decomposition Products

In order to identify and determine the amounts of the major decomposition products, a polarographic method was used to analyze for $S_2O_3^{2-}$ and HSO_3^-. According to Kolthoff and Miller (5), HSO_3^- in 0.1 M HNO_3 produces a cathodic wave with a half-wave potential of −0.4 V vs. standard calomel electrode (s.c.e.). Thus, the amount of bisulfite could be determined without much difficulty, as shown in the polarogram Fig. 8. Although $S_2O_3^{2-}$ produced an anodic wave with a half-wave potential of −0.14 V vs. s.c.e. using 0.1 M KNO_3 as its supporting electrolyte, SO_3^{2-} produced an anodic wave with a half-wave potential of 0.01 V vs. s.c.e. in 0.1 M KNO_3. Thus, these two curves were too close to be analyzed quantitatively. However, when formaldehyde was added to the solution, it reacted with the sulfide but not with the thiosulfate, according to Furness (6). The resulting formaldehyde bisulfite did not interfere. Consequently, thiosulfate could be determined as shown in the polarogram in Fig. 9.

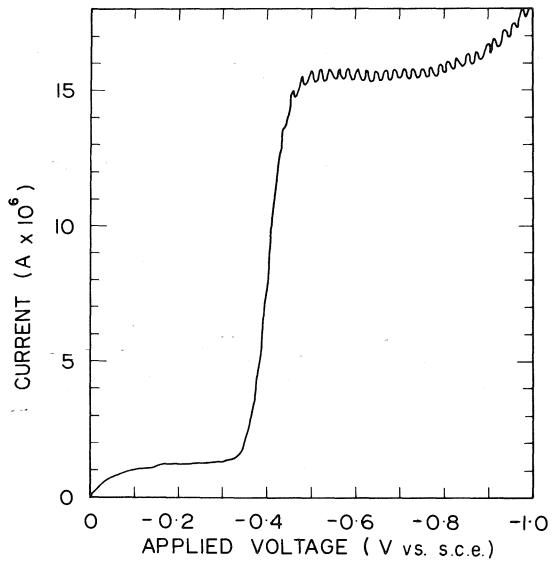

FIG. 8. Polarogram of 2 mM $NaHSO_3$ in 0.1 M HNO_3, at m_d (rate of flow of Hg) = 1.22×10^{-3} g s^{-1}, t_d (drop time) = 6 s per drop.

In this experiment, 4.00×10^{-3} M $Na_2S_2O_4$ was allowed to decompose completely. After two days, when no more $Na_2S_2O_4$ remained, $[S_2O_3^{2-}]$ and $[HSO_3^-]$ were polarographically determined. The concentrations were found to be 1.93×10^{-3} M for $S_2O_3^{2-}$ and 3.43×10^{-3} M for HSO_3^-. These results were approximately in accord with the following overall stoichiometry

$$[2] \qquad 2S_2O_4^{2-} + H_2O \rightarrow S_2O_3^{2-} + 2HSO_3^-$$

The deviations, especially in $[HSO_3^-]$, suggest that other products are also formed. It should be noted that the ions whose formulae are given are consistent with the dissociation constants, $H_2S_2O_3$, $HS_2O_3^-$, H_2SO_3, and

Can. J. Chem. Downloaded from www.nrcresearchpress.com by 210.87.254.5 on 09/05/12
For personal use only.

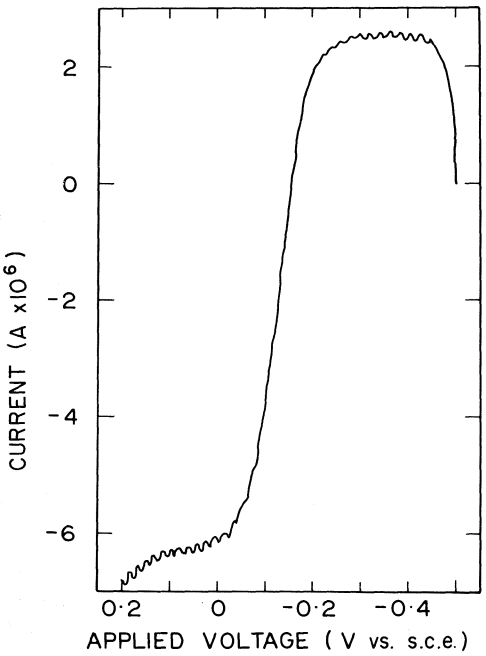

FIG. 9. Polarogram of 2 m*M* $Na_2S_2O_4$ in 0.1 *M* KNO_3 at $m_d = 1.22 \times 10^{-3}$ g s^{-1}, $t_d = 6$ s per drop.

SO_3^{2-} all being less than 2% of thiosulfate or bisulfite in this p*H* range. However, according to Jellinek's (7) value of $K_{a_2} = 3.6 \times 10^{-3}$ for dithionite, about 9% of the dithionite is in the form of $HS_2O_4^-$ at p*H* = 3.5, and about 0.28% at p*H* = 5.0.

Mechanism

A mechanism which describes the decomposition of aqueous $Na_2S_2O_4$ under the conditions used in these experiments should (*i*) be consistent with the previously determined rate eq. [1], (*ii*) identify the decomposition product in the second term of the rate equation, (*iii*) predict the overall stoichiometry of the reaction, and (*iv*) account for the catalytic behavior of H_2S. Regarding (*iii*), the observed stoichiometry did not balance perfectly, the sum of sulfur accounted for by thiosulfate and bisulfite amounting to only 91% of the sulfur in the starting dithionite, leaving 9% unaccounted for. Regarding (*iv*), we observed, as did Rinker and co-workers (2), the formation of a milky cloud, which we also took to be sulfur, and we noted that this milkiness formed just prior to the onset of the rapid phase of decomposition. We also noted that the cloud dissolved in the decomposition products over a longer period of time, i.e. overnight. Rinker *et al.* considered sulfur as a possible catalyst for the reaction.

The initial decomposition reactions of aqueous sodium dithionite may be represented as follows

$$S_2O_4^{2-} + H^+ \rightleftharpoons HS_2O_4^-$$

[3] $$S_2O_4^{2-} + H^+ \rightarrow HSO_2^- + SO_2$$

[4] $$HS_2O_4^- + H_2O \rightarrow HSO_2^- + HSO_3^- + H^+$$

As has been pointed out, the predominant dithionite ionic species is $S_2O_4^{2-}$, but the amount of $HS_2O_4^-$ present is not negligible in this range of p*H*. Bellobono (8) has demonstrated reaction [3] in the strongly acid decomposition of sodium dithionite accompanied by stripping and collection of SO_2. The presence of reaction [4] is consistent with the small decrease in p*H* during the induction period. Reaction [4] has the additional attraction of being an ion–molecule reaction, thereby satisfying one of the requirements of Rinker *et al.* (2), namely, rate independence of ionic strength.

Sulfoxylate is proposed as an intermediate by most workers in this field, including, for example, Lister and Garvie (9). The sulfoxylate formed in reactions [3] and [4] reacts with dithionite to form thiosulfate

[5] $$HS_2O_4^- + HSO_2^- \rightarrow S_2O_3^{2-} + HSO_3^- + H^+$$

The sum of reactions [4] and [5] accounts for the observed stoichiometry.

Reaction [5] is slow in the absence of a catalyst such as H_2S or possibly colloidal S. Several reactions of sulfoxylate have been proposed which may result in H_2S or S, such as

[6] $$H^+ + 3HSO_2^- \rightarrow H_2S + 2HSO_3^-$$

[7] $$H^+ + 2HSO_2^- \rightarrow S + HSO_3^- + H_2O$$

and H_2S may react with sulfoxylate to form S

[8] $$H^+ + HSO_2^- + H_2S \rightarrow 2S + 2H_2O$$

Reactions [6], [7], and [8] consume H^+ and may account for the rise in p*H* observed during the rapid phase of the decomposition of aqueous sodium dithionite.

The catalytic action of H_2S may be attributed to its ability to accept electrons, and its presence would therefore improve the ability of dithionite and sulfoxylate to react. We may regard such electron acceptance as furthering the formation

Can. J. Chem. Downloaded from www.nrcresearchpress.com by 210.87.254.5 on 09/05/12
For personal use only.

of free radicals such as HSO_2, giving rise to the more rapid reaction [9]

[9] $HSO_2 + HS_2O_4^- \rightarrow S_2O_3^{2-} + HSO_3 + H^+$

which differs from reaction [5] in that an electron has been removed from one of the reactants, and there is also a free radical product. It would be expected that this reaction would be much faster than reaction [5], which involves two negative ions. The equation of reaction [9] is a way of representing the catalyzed reaction [5]. The free radical product becomes the ion by re-acquiring the electron from the (temporarily negative) H_2S. It would be expected that polysulfides H_2S_x formed by the reaction of S and H_2S would be even more effective radical stabilizers. Collodial sulfur may behave similarly as a catalyst. The rate-controlling reaction proposed by Rinker and co-workers (2) is very similar to reaction [9].

This sequence of reactions may now be compared with the rate equation [1], which may be rewritten as

$$[10] \quad \frac{-d[S_2O_4^{2-}]}{dt} = k_4[H^+][S_2O_4^{2-}] + k_5[H^+][S_2O_4^{2-}][HSO_2^-]$$

The rate constants k_4 and k_5 have an integral relationship to k_1 and k_2, for which numerical values were derived in the previous paper (3).

Our satisfaction at the achievement of a representation of a formal relationship between the "observed" rate equation and a sequence of reasonable reactions is tempered by the awareness of the approximations involved in the formulation of the rate equation itself, the limited range of pH, temperature, and concentrations reported, and, furthermore, the interesting observation that while eq. [10] may have some merit in describing, however approximately, the decomposition of aqueous sodium dithionite, it fails completely with other dithionites such as the zinc salt (10).

This work was assisted by grants from the National Research Council and the Department of University Affairs of the Province of Ontario. One of us (W.J.L.) is grateful for an NRCC scholarship held during 1967–1969.

1. K. Jellinek and E. Jellinek. Z. Phys. Chem. Leipzig, **93**, 325 (1919).
2. R. G. Rinker, S. Lynn, D. M. Mason, and W. H. Corcoran. Ind. Eng. Chem. Fundam. **4**, 282 (1965).
3. W. J. Lem and M. Wayman. This issue.
4. W. J. Lem and M. Wayman. J. Soc. Dyers Colour. **83**, 277 (1967).
5. I. M. Kolthoff and C. S. Miller. J. Amer. Chem. Soc. **63**, 218 (1941).
6. W. Furness. J. Soc. Dyers Colour. **66**, 270 (1950).
7. K. Jellinek. Z. Phys. Chem. Leipzig, **76**, 257 (1911).
8. I. R. Bellobono. Congr. Intern. Soufre. Toulouse, May 1967.
9. M. W. Lister and R. C. Garvie. Can. J. Chem. **37**, 1567 (1959).
10. M. Wayman and W. J. Lem. To be published.

Can. J. Chem. Downloaded from www.nrcresearchpress.com by 210.87.254.5 on 09/05/12
For personal use only.

Can. J. Chem. Downloaded from www.nrcresearchpress.com by 210.87.254.42 on 09/05/12
For personal use only.

Cyclooctatetraenoquinones. I. The synthesis and structure of dibenzo[*a*,*e*]cyclooctene-5,6-dione

PETER YATES, ERROL G. LEWARS, AND PETER H. MCCABE
Lash Miller Chemical Laboratories, University of Toronto, Toronto 5, Ontario

Received September 11, 1969

Dibenzo[*a*,*e*]cyclooctene-5,6-dione (**18**), a derivative of 1,2-cyclooctatetraenoquinone (**4**), has been synthesized by selenium dioxide oxidation of dibenzo[*a*,*e*]cycloocten-5(6*H*)-one (**26**), itself obtained from the reaction of 5,11-dibromo-5,6,11,12-tetrahydrodibenzo[*a*,*e*]cyclooctene (**20**) with dimethyl sulfoxide and collidine. Infrared and proton magnetic resonance spectroscopic studies have shown that the 8-membered ring of **18** is not aromatic.

Canadian Journal of Chemistry, **48**, 788 (1970)

Introduction

Hückel's rule relating aromaticity to monocyclic $4n + 2$ (n integral) π-electron systems (1) and its empirical extension to polycyclic systems have stimulated studies of the synthesis and properties of a wide variety of cyclic π-electron systems (2). Prominent among these investigations are those of Katz and coworkers (3) on the dianion formed by reduction of cyclooctatetraene. It has been concluded (3, 4) that this dianion is a planar, aromatic species, **1**. This circumstance has been attributed in large part to the stabilization conferred by the 10 π-electron system ($4n + 2$), which more than offsets the angle-strain engendered by the assumption of the planar configuration. In contrast, cyclooctatetraene itself is non-planar and non-aromatic (**2**), since any stabilization conferred by the 8 π-electron system ($4n$) is small and insufficient to compensate for the angle-strain introduced in the planar configuration; indeed, the planar $4n$ π-electron system may be antiaromatic and actually destabilize this configuration (5).

Another $4n + 2$ π-electron system related to cyclooctatetraene is the dication that is formally derivable from it by removal of 2 π-electrons.

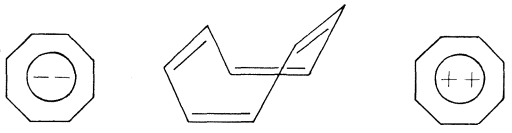

1 **2** **3**

This has not been observed directly (6), although the suggestion has been made that it may be an intermediate in the anodic oxidation of cyclooctatetraene (7). It is thus not known whether the dication exists as the planar aromatic species **3**, analogous to **1**, or adopts a non-planar, non-aromatic configuration.

A closely related problem concerns the possibility of the aromaticity of 1,2-cyclooctatetraenoquinone (**4**) and its 1,4 isomer (**5**). These will be aromatic if they exist as approximately planar species to which the canonical forms symbolized by **4***a* and **5***a*, which embody the cyclooctatetraene dication, make appreciable contributions. Additional factors that intrude in these

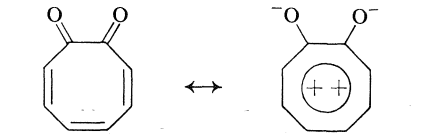

4 **4***a*

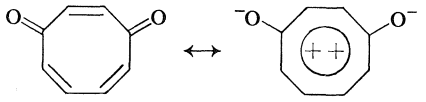

5 **5***a*

cases are the charge separation in the canonical forms represented by **4***a* and **5***a* and the Coulombic interaction between the negative charges on the oxygen atoms[1] in these forms. Both of these factors will tend to increase the energy of these structures and reduce their effectiveness in conferring aromaticity on the cyclooctatetraenoquinones. The related cyclobutadienoquinones (**6**) have been studied extensively by

[1]The Coulombic interaction between the two positive charges on the ring atoms is common to these structures and **3**.

Can. J. Chem. Downloaded from www.nrcresearchpress.com by 210.87.254.42 on 09/05/12
For personal use only.

Roberts and coworkers (8); their properties and unusual stability are in accord with substantial contributions from canonical forms symbolized by **6***a* (8*a*). However, the assumption of the

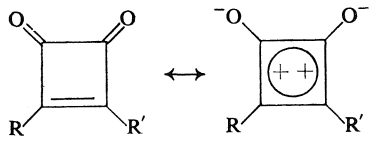

6 **6***a*

planar configuration implied by **6***a* requires no increased angle strain relative to nonplanar configurations, and these compounds are not precisely analogous to the cyclooctatetraenoquinones.[2] A more closely analogous case is that of tropone (**7**), where recent results suggest that there is only a minor contribution from structures symbolized by **7***a* (9, 10). Nevertheless, it is

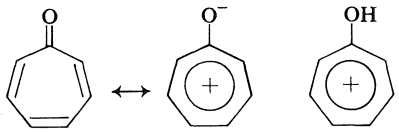

7 **7***a* **8**

probable that protonated tropone, i.e., the hydroxytropylium ion **8**, the formation of whose aromatic system does not require charge separation, has appreciable aromatic character (11),[3] and this suggests that although the cyclooctatetraenoquinones themselves may not be aromatic in character, protonated species derived from them, such as **9** and **10**, may be so. An

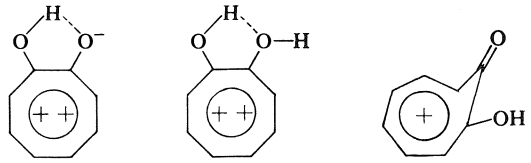

9 **10** **11**

alternative, but nonetheless interesting, possibility for the nature of the monoprotonated cyclooctatetraenoquinones is exemplified by the ion **11**, the analog of the homotropylium ion formed on protonation of 2,4,6-cyclooctatrienone (12).

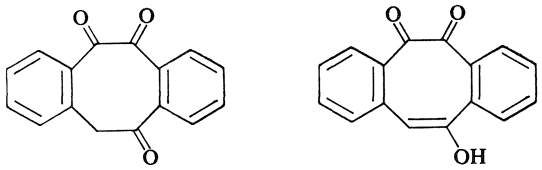

12 **13**

The first reference in the chemical literature to a potential cyclooctatetraenoquinone derivative appeared in 1940 when the preparation of a compound provisionally assigned structure **12** was reported (13). This would be converted by enolization to the hydroxydibenzo-1,2-cyclooctatetraenoquinone **13**. However, this compound has subsequently been shown to possess a different structure (14). Apparently, the first report of the preparation of cyclooctatetraenoquinone derivatives appeared in 1962 when Cava and Ratts (15) described the formation of the halodibenzo-1,4-cyclooctatetraenoquinones **14** and **15** on oxidation of the biphenylene derivatives **16** and **17**, respectively. The possible aromatic nature of the 8-membered ring was not alluded to. The first report of deliberate attempts to synthesize cyclooctatetraenoquinone derivatives seems to be that of McIntyre *et al.* (16); no such derivatives were obtained, however.

In the present work we have synthesized the 1,2-cyclooctatetraenoquinone derivative **18**, i.e., dibenzo[*a*,*e*]cyclooctene-5,6-dione,[4] and have examined its properties with especial reference to the possible aromaticity of the 8-membered ring.

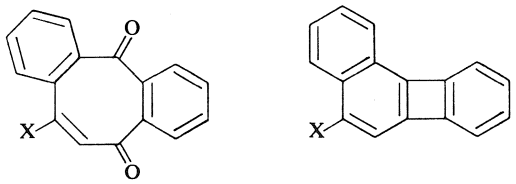

14 X = Br **16** X = Br
15 X = Cl **17** X = Cl

During the course of this work, Bendall and Neumer (17) have also reported the preparation of this compound, but by a different route.

[2]Another differentiating factor is the cross-ring interaction in the case of the cyclobutadienoquinones (8*a*).

[3]The very recent results of Bertelli and coworkers (10*b*), however, suggest that the aromaticity of **8** is less pronounced than has previously been considered.

[4]Dibenzo[*a*,*e*]cyclooctene is the *Chemical Abstracts* and *Ring Index* name for the hydrocarbon **19**.

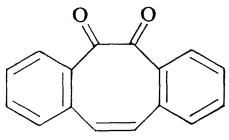

18

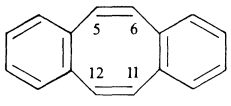

19

Synthesis of Dibenzo[a,e]cyclooctene-5,6-dione (18)

5,11-Dibromo-5,6,11,12-tetrahydrodibenzo-[*a*,*e*]cyclooctene (**20**) was prepared in 75% yield by bromination of the corresponding hydrocarbon (**21**) by the method of Cope and Fenton (18). The bromination is carried out with *N*-bromosuccinimide and is of interest since the 5,11-dibromo compound is formed with high selectivity. This may be due to the preferential formation of the bridged intermediate **22** in the course of the introduction of the second bromine atom (19).[5]

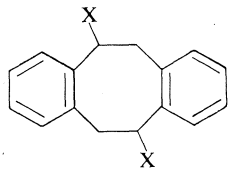

20 X = Br
21 X = H
25 X = OH

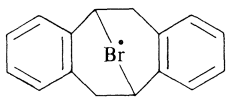

22

Treatment of the dibromo compound **20** with dimethyl sulfoxide and collidine (20) gave three products. The major product, obtained in ca. 40% yield, was dibenzo[*a*,*e*]cyclooctene-5,11-(6*H*,12*H*)-dione[6] (**23**), which has previously been prepared by a 6-step sequence from diphenylsuccinonitrile in an overall yield of 4% (13, 18). Another product was the hemiketal **24** (ca. 10%), which has previously been obtained by conversion of **20** to the diol **25** and oxidation of this with chromic acid, and also by Meerwein–Pondorff reduction of the dione **23** (18). The third product formed on treatment of **20** with dimethyl sulfoxide and collidine was dibenzo[*a*,*e*]cycloocten-5(6*H*)-one (**26**) (ca. 20%).

The ketone **26** has previously been prepared by oxidation of the corresponding alcohol, which was obtained from the dihydroanthracene derivative **27** (21). Since compound **26** was of crucial importance in the present investigation, it was necessary to confirm the structural assignment. Its structure was established by its spectra [λ_{max} (CCl_4) 5.98 μ; δ ($CDCl_3$) 4.02 (s, 2H), 6.88 (s, 2H),[7] 7.0–7.5 (m, 7H), and 8.25 (br d, 1H)]

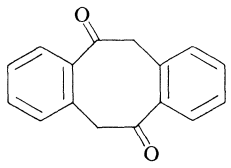

23

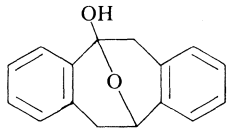

24

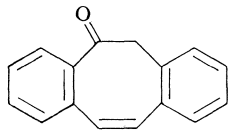

26

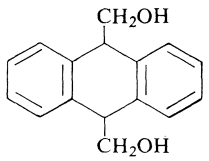

27

and the following reactions. Hydrogenation at atmospheric pressure over palladium–carbon gave 11,12-dihydrodibenzo[*a*,*e*]cycloocten-5-(6*H*)-one (**28**) (22, 23), identified by its spectra [λ_{max} (CCl_4) 5.97 μ; δ ($CDCl_3$) 3.20 (s, 4H), 4.05 (s, 2H), 6.75–7.20 (m, 7H), and 7.20–7.38 (m, 1H)] and its m.p. and that of its 2,4-dinitrophenylhydrazone (23). Wolff–Kishner reduction of **28** gave 5,6,11,12-tetrahydrodibenzo[*a*,*e*]cyclooctene (**21**), which was identified by comparison with an authentic sample (18). Wolff–Kishner reduction of **26** itself gave 5,6-dihydrodibenzo[*a*,*e*]cyclooctene (**29**) (22), identified by its proton magnetic resonance (p.m.r.) spectrum [δ ($CDCl_3$) 3.13 (s, 4H), 6.70 (s, 2H), and 7.05 (s, 8H)] and its m.p.

Oxidation of **26** with selenium dioxide in dioxane gave dibenzo[*a*,*e*]cyclooctene-5,6-dione

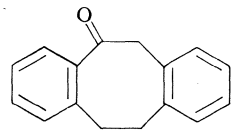

28

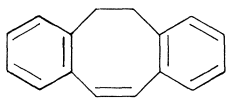

29

[5]This view implies that **20** is the *trans* stereoisomer; its stereochemistry has not been established, however.

[6]This name, the *Chemical Abstracts* term for **23**, is used with some reluctance, since it fails to indicate clearly that **23** and **18** are in different oxidation states; cf. footnote 4.

[7]That this single signal is a result of the accidental superimposition of the two vinyl proton signals was shown by examination of the corresponding ^{13}C satellites (*vide infra*).

Can. J. Chem. Downloaded from www.nrcresearchpress.com by 210.87.254.42 on 09/05/12
For personal use only.

Can. J. Chem. Downloaded from www.nrcresearchpress.com by 210.87.254.42 on 09/05/12
For personal use only.

(**18**) in 24% yield. The structure of this product was established by its spectra [λ_{max} (CCl_4) 5.83 and 6.00 μ; δ ($CDCl_3$) 6.83 (s, 2H), and 7.0–7.7 (m, 8H)], which will be discussed in detail subsequently, and its conversion on hydrogenation over palladium–carbon to 11,12-dihydrodibenzo[*a,e*]cyclooctene-5,6-dione (**31**), identified by direct comparison with an authentic sample prepared from **28** via the α-oximino derivative **30** (23). The melting point of **18** was undepressed on admixture with a sample of the product obtained by Bendall and Neumer (17) by oxidation of **32**, itself prepared by a benzoin condensation.[8] The infrared (i.r.) spectra of the two samples were identical.

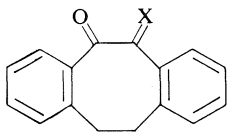

30 X = NOH
31 X = O

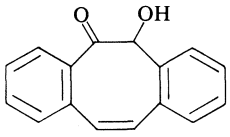

32

Properties of Dibenzo[a,e]cyclooctene-5,6-dione (18)

The i.r. spectrum of **18** shows two strong bands in the carbonyl-stretching region [λ_{max} (CCl_4) 5.83 and 6.00 μ]. In analogy with the spectra of many other α-diketones (24), these can be attributed to the antisymmetrical and symmetrical coupled stretching vibrations of the two carbonyl groups. Models suggest that the dihedral angle between the carbonyl groups is in the range 0–40°. This is consistent with the occurrence of strong coupling between the stretching vibrations of these groups; were the dihedral angle close to 90°, little or no coupling would be expected (25). The case of **18** may be contrasted with that of its dihydro derivative **31**, whose i.r. spectrum shows a strong carbonyl-stretching band at 5.97 μ (CCl_4) with a shoulder at 5.88 μ. It has previously been concluded on the basis of ultraviolet (u.v.) spectroscopic measurements that **31** exists in a crown-type conformation in which the intercarbonyl angle approaches 90° (23). Such a conformation would account for the weakness of the vibrational coupling. Davison (24*b*) has suggested that the mean of the 2 frequencies may be taken as the unperturbed frequency of the individual carbonyl groups. We consider that this is an acceptable approximation in a case such as **18** where the two bands are of comparable intensity, but is of dubious applicability in a case such as **31** where one band is very much stronger than the other. The estimate thus obtained for the approximate unperturbed position of the carbonyl-stretching band in **18** is 5.91 μ. For **31** the unperturbed position is taken as lying in the range between the mean frequency and that of the strong band, i.e., 5.92–5.97 μ. Comparison of these positions with each other and with the positions of the single carbonyl-stretching bands in the i.r. spectra of compounds **23** (5.95 μ), **26** (5.98 μ), and **28** (5.97 μ) shows that the position in the case of **18** is at shorter wavelength than in the other cases. Now, were the 8-membered ring of **18** aromatic in character, this would require, as discussed earlier, substantial contributions from canonical forms symbolized by **33**. If such contributions were important, it would be expected that the unperturbed carbonyl-stretching band of **18** would lie at an appreciably *longer* wavelength than the bands of **23**, **26**, **28**, and **31**. This would result from both the increased single bond character of the carbonyl bonds in **33** (26), and from the increased C—C—C angle at the carbonyl

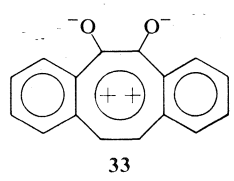

33

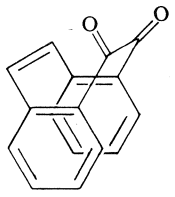

34

group (27). The fact that the band of **18** lies at *shorter* wavelength than the bands of the other compounds strongly contraindicates the aromaticity of the 8-membered ring.[9]

Additional evidence for this lack of aromaticity comes from p.m.r. studies. The two protons on the 8-membered ring of **18** give rise to a singlet at δ 6.83. The signals due to the corresponding protons in the enone **26** and the hydrocarbon **29** appear at δ 6.88 and 6.70 μ, respectively. Had the

[8]We thank Dr. J. F. Neumer, E. I. du Pont de Nemours and Co., for generously providing us with a sample of his product.

[9]The shift to shorter wavelength may be attributed to dipole–dipole interaction between the carbonyl groups, exacerbated by a relatively small dihedral angle between them.

Can. J. Chem. Downloaded from www.nrcresearchpress.com by 210.87.254.42 on 09/05/12
For personal use only.

8-membered ring of **18** been aromatic in character, it would have been expected to support a diamagnetic ring current that would lead to a significant deshielding of the protons attached to this ring (28). The fact that the signals that arise from these protons are closely similar in position to the vinylic proton signals of **26** and **29** again shows that the 8-membered ring of **18** is not aromatic. This is confirmed by the magnitude of the coupling constant between the protons on the 8-membered ring of **18**. This could not be measured directly because these protons have identical chemical shifts, but was obtained from observation of the upfield ^{13}C satellite signals, which gave $J_{H,H} = 12.8$ and $J_{H,^{13}C} = 160$ Hz. For comparison, the coupling constant between the corresponding protons in the enone **26** was measured. Resort again was had to the ^{13}C satellite signals because of the accidental identity of the chemical shifts of these protons in **26**. Observations of the upfield satellite signals gave $J_{H,H} = 12.6$ Hz; interestingly the two protons had different values of $J_{H,^{13}C}$, viz., 155 and 160 Hz.[10] The essential identity of $J_{H,H}$ for **18** and **26** demonstrates that in the former, like the latter, the protons on the 8-membered ring are olefinic rather than aromatic. Had those of **18** been aromatic in character, their coupling constant would have been significantly smaller than that observed (29), which falls within the range expected for *cis*-olefinic protons on medium-sized rings (30).

All of the evidence obtained thus shows that the 8-membered ring of **18** is not aromatic, and can be interpreted in terms of the nonplanar conformation **34** for this compound.[11]

Compound **18** is insoluble in concentrated hydrochloric acid and cannot be extracted from carbon tetrachloride with 50% sulfuric acid. The p.m.r. spectrum of **18** in trifluoroacetic acid is essentially identical with that in deuteriochloroform. Thus there is no indication of any special stability of the mono- or diprotonated forms of **18** attributable to structures of type **9**, **10**, or **11**.[12] The p.m.r. spectrum of the enone **26** in trifluoroacetic acid was also essentially identical to its spectrum in deuteriochloroform. This colorless compound gave a bright yellow solution in trifluoroacetic acid from which it could be recovered unchanged, perhaps indicating the formation of a small amount of protonated species, but the p.m.r. spectrum showed no sign of the dibenzo derivative of the homotropylium ion (33).

That the 8-membered rings of **18** and its protonated derivatives are nonaromatic does not rule out the possibility that the monocyclic compounds **4** and **5** or their protonated derivatives are aromatic. The fusion of the two benzene rings to the 8-membered ring in **18** could damp the aromaticity of this ring because of their tendency to appropriate π-electrons for their individual aromatic systems (34). Whether this is the origin of the failure to observe an aromatic 8-membered ring in the present work will not be known until the more challenging synthetic problem of preparing analogous compounds in the monocyclic series has been solved.

Experimental

Melting points were determined in capillary tubes with a Thomas-Hoover "Uni-Melt" apparatus and are uncorrected.

Infrared spectra were recorded in carbon tetrachloride solutions, unless otherwise stated, and were calibrated with the 3.51, 6.24, and 9.72 μ bands of polystyrene film. Proton magnetic resonance spectra were recorded in deuteriochloroform solutions, unless otherwise stated. The band positions are reported in parts per million downfield from tetramethylsilane as internal reference (δ scale).

Analytical thin-layer chromatography (t.l.c.) was carried out with thin layers of silica gel (Merck) on microscope slides. Preparative t.l.c. was carried out with 1.0 mm thick layers of silica gel (Merck) on 20 × 20 cm square glass plates. Analytical chromatograms were made visible with iodine vapor, and preparative chromatograms by the quenching of an u.v. phosphor added to the silica gel.

Solutions in organic solvents were dried over anhydrous magnesium sulfate and stripped of solvent with a rotary evaporator in conjunction with a water aspirator.

5,6,11,12-Tetrahydrodibenzo[a,e]cyclooctene (21)

Compound **21** was prepared from α,α′-dibromo-*o*-xylene according to the method of Cope and Fenton (18). The isolation of the compound was greatly facilitated by the use of a combined steam-distillation–extraction unit.[13] After 4 days, the chloroform solution was dried and evaporated, giving **21** as a colorless solid, m.p. 103–108°,

[10]We thank Professor W. F. Reynolds, University of Toronto, for a helpful discussion of these spectra.

[11]Dr. J. F. Neumer has kindly informed us that he and Dr. V. I. Bendall have reached the same conclusion regarding the non-planar (non-aromatic) character of **18** (31).

[12]Cf. the low basicity of 5*H*-dibenzo[*a*,*d*]cyclohepten-5-one (2,3,6,7-dibenzotropone) (32).

[13]Designed and constructed by Dr. A. C. Mackay.

Can. J. Chem. Downloaded from www.nrcresearchpress.com by 210.87.254.42 on 09/05/12
For personal use only.

which was consistently obtained in a yield of 33–40%. A sample recrystallized from 95% ethanol had m.p. 107.5–108.5° [lit. (18) m.p. 108.5–109°]; δ 3.03 (s, 8H) and 6.96 (s, 8H).

*5,11-Dibromo-5,6,11,12-tetrahydrodibenzo[a,e]cyclooctene (**20**)*

Compound **20** was prepared by treating **21** (recrystallized once from 95% ethanol) with *N*-bromosuccinimide as described by Cope and Fenton (18). The crude product, which was consistently obtained in ca. 75% yield, had m.p. 184–188° and was used without further purification. A sample recrystallized from 95% ethanol had m.p. 185–186° [lit. (18) m.p. 188.1–189°]; δ 3.62 (A part of ABX system, $J_{AB} \sim 14$, $J_{AX} \sim 8$ Hz, 2H), 4.32 (B part of ABX system, $J_{AB} \sim 14$, $J_{BX} \sim 11$ Hz, 2H), 5.35 (X part of ABX system $J_{AX} = 8$, $J_{BX} = 11$ Hz, 2H), and 6.9–7.2 (m, 8H).

The dibromo compound **20** was also formed when the hydrocarbon **21** was treated with bromine in carbon tetrachloride.

*Treatment of Compound **20** with Dimethyl Sulfoxide and Collidine. Formation of Dibenzo[a,e]cyclooctene-5,11(6H,12H)-dione (**23**), Dibenzo[a,e]cycloocten-5(6H)-one (**26**), and the Hemiketal **24***

In a 500 ml round-bottomed flask equipped with a condenser fitted with a drying tube were placed collidine (22 ml, 0.17 mole) and a solution of **20** (20.0 g, 0.055 mole) in dimethyl sulfoxide [Fisher Certified from a freshly opened bottle or from a previously opened bottle to which molecular sieves (Linde type 4A) had been added after opening; 300 ml]. The mixture was magnetically stirred and heated at 130° for 1.3 h. The solution was then allowed to cool to ca. 25° and poured into 1.5 l of cold water. The resulting suspension was filtered to give an off-white solid that was dried in a vacuum desiccator over phosphorus pentoxide, when it weighed 10.5 g. On t.l.c. it showed only 3 spots, corresponding to the starting material (**20**), the dione **23**, and the enone **26**. A 9.49 g portion of this mixture was chromatographed on a column of silica gel (470 g, 58 × 4 cm); fractions were combined on the basis of t.l.c. (with dichloromethane as developer) and i.r. spectra. Elution with benzene gave starting material (0.90 g), followed by the enone **26** (2.55 g). Elution with dichloromethane and with dichloromethane containing 0.5% of methanol gave the dione **23** (5.72 g).

The enone **26** was recrystallized from dichloromethane–hexane to give colorless needles (1.65 g, 15%), m.p. 114–115° [lit. (21) m.p. 114–116°]; λ_{max} 5.98 μ; δ 4.02 (s, 2H), 6.88 (s, 2H), 7.0–7.5 (m, 7H), and 8.25 (d, each component broad, J = ca. 8 Hz, 1H); δ (CF_3CO_2H) 3.98 (s, 2H), 7.02 (s, 2H), 7.1–7.6 (m, 7H), and 8.20 (d, 1H); a p.m.r. spectrum recorded at 100 MHz with high spectrum amplitude on a concentrated solution (160 mg in 0.3 ml of $CDCl_3$) showed the upfield ^{13}C satellites of the δ 6.88 signal as a pair of overlapping doublets; $J_{H,H'} = J_{H',H} = 12.6$, $J_{H,^{13}C} = 155$, $J_{H',^{13}C} = 160$ Hz.

Anal. Calcd. for $C_{16}H_{12}O$ (mol. wt. 220): C, 87.24; H, 5.45. Found (*m/e* 220): C, 87.24; H, 5.53.

The dione **23** was recrystallized from dichloromethane–hexane to give colorless needles (4.12 g, 35%), m.p. 203–204° [lit. (13) m.p. 203.5–204.5°]; λ_{max} 5.95 μ; δ 4.42 (s, 4H), 7.06–7.46 (m, 6H), and 7.61–7.85 (m, 2H).

Mol. Wt. Calcd. for $C_{16}H_{12}O_2$: 236. Found: *m/e* 236.

The original aqueous filtrate was extracted twice with chloroform, and the chloroform solution was washed once with dilute hydrochloric acid, twice with water, and once with aqueous sodium bicarbonate. The chloroform solution was then dried and stripped of solvent to give a sticky solid (1.29 g). This was recrystallized from dichloromethane–hexane to give the hemiacetal **24** as colorless prisms (0.53 g, 4.5%), m.p. 171–174°. This material was recrystallized from 95% ethanol to give colorless prisms, m.p. 177.5–178.5°; λ_{max} 3.03 (wm), 9.19, and 9.28 μ; δ 2.3–3.6 (m, 4H), 4.33 (s, 1H, absent after treatment with D_2O), 5.38 (d, J = 5 Hz, each component broad, 1H), 6.7–7.35 (m, 7H), and 7.35–7.65 (m, 1H). A mixture with authentic **24**, m.p. 178.5–180°, prepared by Meerwein–Ponndorf reduction of the dione **23** (18), had m.p. 177.5–179°; the i.r. spectra and t.l.c. behavior of the two samples were identical.

*Hydrogenation of **26**. Formation of 11,12-Dihydrodibenzo[a,e]cycloocten-5(6H)-one (**28**)*

The enone **26** (45 mg) in ethyl acetate (8 ml) was stirred with 10% palladium-on-charcoal (5 mg) at 15° under hydrogen at atmospheric pressure. During 45 min 1.05 molar equivalents of hydrogen were absorbed, after which the rate of uptake of hydrogen became very slow. The mixture was filtered, and the filtrate was evaporated to give the ketone **28** (44 mg, 97%) as colorless needles, m.p. 83–88°. This material was recrystallized from aqueous methanol to give colorless needles, m.p. 93.5–94° [lit. m.p. 95.2–96.5° (22), 93–94° (23)]; λ_{max} 5.97 μ; δ 3.20 (s, 4H), 4.05 (s, 2H), 6.75–7.20 (m with spike at δ 6.87, 7H), and 7.20–7.38 (m, 1H).

Mol. Wt. Calcd. for $C_{16}H_{14}O$: 222. Found: *m/e* 222.

The hydrogenation product gave a 2,4-dinitrophenylhydrazone, m.p. 194–197° [lit. (13) m.p. 196–197°].

*Wolff–Kishner Reduction of **28**. Formation of 5,6,11,12-Tetrahydrodibenzo[a,e]cyclooctene (**21**)*

In a 5 ml round-bottomed flask equipped with a condenser were placed the ketone **28** (20 mg, 0.089 mmole), potassium hydroxide (100 mg, ca. 2 mmoles), 85% hydrazine (0.2 ml, 3 mmoles), and diethylene glycol (1 ml). The mixture was heated at reflux for 2 h, the condenser was removed, and the temperature was allowed to rise to 200°; the condenser was then replaced, and the mixture was heated at reflux for a further 3 h. It was poured into dilute hydrochloric acid, and the organic products were extracted 3 times with dichloromethane. The extracts were washed twice with water, and the organic layer was dried and evaporated to give a colorless solid, which was recrystallized from 95% ethanol to give **21** as colorless prisms, m.p. 108–108.5°. A mixture with authentic **21** (*vide supra*) had m.p. 108–109°; the i.r. spectra of the two samples were identical.

*Wolff–Kishner Reduction of **26**. Formation of 5,6-Dihydrodibenzo[a,e]cyclooctene (**29**)*

This reduction of **26** (49 mg, 0.223 mmole) was carried out as described for **28**. The crude product was a colorless oil, which was sublimed at 90° (10^{-2} mm) to give **29** as a

colorless solid, m.p. 47–50°, which on recrystallization from 95% ethanol gave colorless prisms, m.p. 53.5–54.5° [lit. (22) m.p. 53.6–54.6°]; δ 3.13 (s, 4H), 6.70 (s, 2H), and 7.05 (s, 8H).

Mol. Wt. Calcd. for $C_{16}H_{14}$: 206. Found: *m/e* 206.

Oxidation of ***26*** *with Selenium Dioxide. Formation of Dibenzo[a,e]cyclooctene-5,6-dione (****18****)*

The enone **26** (500 mg, 2.27 mmoles), selenium dioxide (B.D.H.; 295 mg, 2.33 mmoles), dioxane (Fisher Certified, freshly refluxed and distilled over sodium under nitrogen, 8.3 ml), and water (0.7 ml) were heated at reflux for 127 h. The reaction was monitored by t.l.c. with hexane–acetone (1:1) as developer. The reaction mixture was poured into about 3 times its volume of water and extracted 3 times with dichloromethane. The extracts were combined and washed 3 times with water, dried, and stripped of solvent to give a bright yellow gum (587 mg). Preparative t.l.c. with hexane–acetone (1:1) as developer gave 4 fractions. The most mobile was a colorless solid (65 mg), which was shown to be the starting material **26** by mixture m.p. and i.r. spectral comparison. The next most mobile fraction was the major component (190 mg) of the mixture: on sublimation at 90° (10^{-2} mm) it gave **18** as a bright yellow powder (130 mg, 24%), m.p. 96–101°. Recrystallization from dichloromethane–hexane followed by resublimation at 85–90° (10^{-2} mm) gave yellow microprisms, m.p. 101–102°; λ_{max} 5.83 and 6.00 μ; λ_{max} (C_6H_{12}) 245 (log ε 4.30), 318 (log ε 3.41), 385 (log ε 2.18), and 407 mμ (log ε 2.00); δ 6.83 (s, 2H) and 7.0–7.7 (m, 8H); δ (CF_3CO_2H) 6.90 (s, 2H) and 7.1–7.7 (m, 8H); a p.m.r. spectrum recorded at 100 MHz with high spectrum amplitude on a concentrated solution (135 mg in 0.3 ml of $CDCl_3$) showed the upfield ^{13}C satellite of the δ 6.83 signal as a doublet; $J_{H,H} = 12.8$ and $J_{H,^{13}C} = 160$ Hz. A mixture with a sample[8] of the product obtained by Bendall and Neumer (17, 31) had m.p. 101–102°; the i.r. spectra of the two samples were identical.

Anal. Calcd. for $C_{16}H_{10}O_2$: C, 82.04; H, 4.30. Found: C, 82.18; H, 4.04.

Compound **18** was insoluble in cold or boiling concentrated hydrochloric acid; it was rapidly destroyed by concentrated sulfuric acid. When a solution of **18** in carbon tetrachloride was shaken with 50% sulfuric acid, the yellow color of the organic solution persisted and the aqueous solution remained colorless.

Hydrogenation of ***18****. Formation of 11,12-Dihydrodibenzo[a,e]cyclooctene-5,6-dione (****31****)*

Compound **18** (46 mg) in ethyl acetate (6 ml) was stirred with 10% palladium-on-charcoal (5 mg) at room temperature under hydrogen at atmospheric pressure. After 45 min 1.14 molar equivalents of hydrogen had been absorbed, the rate of uptake of hydrogen had greatly diminished, and the yellow color of the solution had been discharged. Filtration and removal of solvent gave an almost colorless oil, which slowly solidified on standing. This was subjected to preparative t.l.c. with acetone–hexane (3:7) as developer; elution of the major band with dichloromethane–chloroform (1:1) gave **31** as a colorless solid (36 mg, 78%); crystallization from methanol gave colorless plates, m.p. 131–132° [lit. (23) m.p. 131–132°]; λ_{max} 5.88 (sh, m) and 5.97 μ; δ 3.25 (s, 4H), 7.07–7.53 (m, 6H), and 7.60–7.85 (m, 2H).

Authentic **31** was prepared following the method of Leonard and coworkers (23) by treatment of the ketone **29** with isoamyl nitrite and sodium ethoxide to give the α-oximino derivative **30**, followed by reaction of this with aqueous formaldehyde. Recrystallization from aqueous ethanol gave colorless plates, m.p. 131–132°. A mixture with the hydrogenation product from **18** had m.p. 131–132°; the i.r. and p.m.r. spectra of the two samples were identical.

We thank the National Research Council of Canada for generous support of this work. One of us (E.G.L.) gratefully acknowledges the awards of an Alcan Jamaica Independence Overseas Scholarship, a Shell Canada Fellowship, a Special Open University of Toronto Fellowship, and an NRCC Scholarship.

1. E. Hückel. Z. Phys. **70**, 204 (1931); Z. Elektrochem. **43**, 751 (1937); Grundzüge der Theorie ungesättiger und aromatischer Verbindungen. Verlag Chemie, Berlin. 1938.
2. (*a*) D. Ginsburg, *editor*. Non-benzenoid aromatic compounds. Interscience Publishers, Inc., New York, 1959. (*b*) D. M. G. Lloyd. Carbocyclic non-benzenoid aromatic compounds. Elsevier, New York, 1966. (*c*) M. P. Cava and M. J. Mitchell. Cyclobutadiene and related compounds. Academic Press, Inc., New York. 1962.
3. T. J. Katz. J. Amer. Chem. Soc. **82**, 3784, 3785 (1960); T. J. Katz and H. L. Strauss. J. Chem. Phys. **32**, 1973 (1960); T. J. Katz, W. H. Reinmuth, and D. E. Smith. J. Amer. Chem. Soc. **84**, 802 (1962); H. L. Strauss, T. J. Katz, and G. K. Fraenkel. J. Amer. Chem. Soc. **85**, 2360 (1963).
4. H. P. Fritz and H. Keller. Z. Naturforsch, **16b**, 231 (1961); P. G. Farrell and S. F. Mason. Z. Naturforsch. **16b**, 848 (1961).
5. H. C. Longuet-Higgins. *In* Theoretical organic chemistry. Papers presented to the Kekule Symposium organized by The Chemical Society, London, 1958. Butterworths Scientific Publications, London. 1959. pp. 9 ff; D. P. Craig. *In* Reference 2a. Chapter 1; R. Breslow, J. Brown, and J. J. Gajewski. J. Amer. Chem. Soc. **89**, 4383 (1967).
6. Cf. D. Bryce-Smith and W. A. Perkins. J. Chem. Soc. 1339 (1962).
7. L. Eberson, K. Nyberg, M. Finkelstein, R. C. Petersen, S. D. Ross, and J. J. Uebel. J. Org. Chem. **32**, 16 (1967).
8. (*a*) E. J. Smutny, M. C. Caserio, and J. D. Roberts. J. Amer. Chem. Soc. **82**, 1793 (1960). (*b*) Reference 2c. Chapter 7.
9. G. L. Buchanan and D. R. Lockhart. J. Chem. Soc. 3586 (1959); Reference 2b. Chapter 6.
10. (*a*) D. J. Bertelli and T. G. Andrews, Jr. Tetrahedron Lett. 4467 (1967); J. Amer. Chem. Soc. **91**, 5280 (1969). (*b*) D. J. Bertelli, T. G. Andrews, Jr., and P. O. Crews. J. Amer. Chem. Soc. **91**, 5286 (1969).
11. Reference 2b. Chapter 5.
12. M. Brookhart, M. Ogliaruso, and S. Winstein. J. Amer. Chem. Soc. **89**, 1965 (1967).
13. S. Wawzonek. J. Amer. Chem. Soc. **62**, 745 (1940).
14. P. Yates and E. Lewars. Chem. Comm. 622 (1967); E. Lewars, J. K. Stowell, S. Wawzonek,

Can. J. Chem. Downloaded from www.nrcresearchpress.com by 210.87.254.42 on 09/05/12
For personal use only.

and P. YATES. Chem. Ind. 344 (1968). P. YATES and E. LEWARS. Can. J. Chem. This issue.
15. M. P. CAVA and K. W. RATTS. J. Org. Chem. **27**, 752 (1962).
16. D. MCINTYRE, G. R. PROCTOR, and L. REES. J. Chem. Soc. (C), 985 (1966).
17. V. I. BENDALL and J. F. NEUMER. Abstracts of papers presented at the 153rd National Meeting of the American Chemical Society, Miami Beach, Florida, April, 1967. O88.
18. A. C. COPE and S. W. FENTON. J. Amer. Chem. Soc. **73**, 1668 (1951).
19. Cf. W. THALER. J. Amer. Chem. Soc. **85**, 2607 (1963).
20. Cf. D. N. JONES and M. A. SAEED. J. Chem. Soc. 4657 (1963).
21. E. CIDRANESCU, A. BACUR, M. BANCIU, and C. D. NENITZESCU. Rev. Roumaine Chim. **10**, 141 (1965); Chem. Abstr. **63**, 11456 (1965).
22. A. C. COPE and R. D. SMITH. J. Amer. Chem. Soc. **77**, 4596 (1955).
23. N. J. LEONARD, A. J. KRESGE, and M. OKI. J. Amer. Chem. Soc. **77**, 5078 (1955).
24. Cf. (*a*) W. G. DAUBEN and W. N. EPSTEIN. J. Org. Chem. **24**, 1595 (1959); (*b*) W. H. T. DAVISON. J. Chem. Soc. 2456 (1951).
25. G. HERZBERG. Molecular spectra and molecular structure. II. Infrared and Raman spectra of polyatomic molecules. D. van Nostrand Co., Inc., Princeton, New Jersey, 1945. p. 198.
26. R. N. JONES and C. SANDORFY. *In* Chemical applications of spectroscopy. *Edited by* W. West. Interscience Publishers, Inc., New York, 1956. p. 481.
27. Cf. P. D. BARTLETT and M. STILES. J. Amer. Chem. Soc. **77**, 2806 (1955).
28. F. SONDHEIMER. *In* Aromaticity. Special Publication No. 21, The Chemical Society, London, 1967. p. 75.
29. Cf. W. B. SMITH and B. A. SHOULDERS. J. Amer. Chem. Soc. **86**, 3118 (1964).
30. A. A. BOTHNER-BY. Advan. Magn. Resonance, **1**, 195 (1965).
31. V. I. BENDALL. Ph.D. Thesis, Brown University, Providence, Rhode Island, 1964.
32. R. STEWART, M. R. GRANGER, R. B. MOODY, and L. J. MUENSTER. Can. J. Chem. **41**, 1065 (1963).
33. Cf. R. F. CHILDS and S. WINSTEIN. J. Amer. Chem. Soc. **89**, 6348 (1967).
34. M. STILES and A. J. LIBBY, JR. J. Org. Chem. **22**, 1243 (1957).

Can. J. Chem. Downloaded from www.nrcresearchpress.com by 210.87.254.42 on 09/05/12
For personal use only.

Can. J. Chem. Downloaded from www.nrcresearchpress.com by 210.87.254.42 on 09/05/12
For personal use only.

Cyclooctatetraenoquinones. II. The synthesis and transformations of compounds related to dibenzo[*a*,*e*]cyclooctene-5,6,11(12*H*)-trione

PETER YATES AND ERROL G. LEWARS
Lash Miller Chemical Laboratories, University of Toronto, Toronto 5, Ontario

Received September 11, 1969

Bromination of 11-acetoxydibenzo[*a*,*e*]cycloocten-5(6*H*)-one (**6**) gave the 6-bromo derivative (**8**), which on further bromination gave a hydrogen bromide adduct (**12** or **13**) of 6,6,12-tribromodibenzo-[*a*,*e*]cyclooctene-5,11(6*H*,12*H*)-dione (**14**). Treatment of this adduct with aqueous-ethanolic ammonia followed by sublimation gave 11-oxoindeno[1,2-*c*]isocoumarin (**4**), not dibenzo[*a*,*e*]cyclooctene-5,6,11(12*H*)-trione (**3**) as earlier suggested. The conversion of **12** or **13** to **4** has been shown to involve the formation of 3-bromo-2-(*o*-carboethoxyphenyl)indone (**17**), which gave **4** and ethyl bromide on being heated at 180°. Oxidation of dibenzo[*a*,*e*]cyclooctene-5,11(6*H*,12*H*)-dione with selenium dioxide gave a bimolecular product **25** considered to be derived by loss of carbon monoxide from the dimer of dibenzo-[*b*,*f*]pentalene-5,10-dione (**27**), a selenium-containing product, **28**, and the hydrate **29** of **3**.

Canadian Journal of Chemistry, **48**, 796 (1970)

1,2-Cyclooctatetraenoquinone (**1**) and its 1,4-isomer (**2**) are of interest because of their possible aromaticity (1). The first reference in the chemical literature to a potential cyclooctatetraenoquinone derivative appeared in 1940 when the preparation of a compound provisionally assigned structure **3** was reported (2). This would be converted by enolization to a hydroxydibenzo derivative of **1**. We report here on a reinvestigation of the structure of the supposed trione **3**, which has led to the assignment to it of the revised structure (**4**),[1] and on experiments directed towards the synthesis of compound **3**.

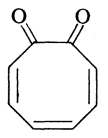

1

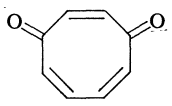

2

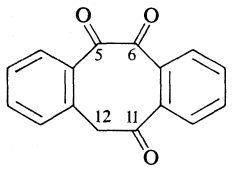

3

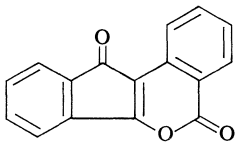

4

The product earlier considered to be **3** was obtained (2) by a series of reactions starting from dibenzo[*a*,*e*]cyclooctene-5,11(6*H*,12*H*)-dione[2] (**5**).

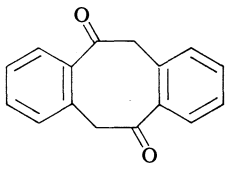

5

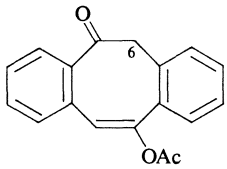

6

This dione was originally prepared from diphenylsuccinonitrile, but is obtained more conveniently from 5,6,11,12-tetrahydrodibenzo[*a*,*e*]cyclooctene (1). Treatment of **5** with acetic anhydride and potassium acetate gave the enol acetate **6** as previously described (2). This product showed bands in its infrared (i.r.) spectrum at 5.66 (enol ester C=O stretch), 5.96 (conjugated ketone C=O stretch), and 7.33 μ (medium; acetate C—H bend) in good accord with the structural assignment **6**. Its proton magnetic resonance (p.m.r.) spectrum in deuteriochloroform showed signals at δ 2.17 (3H) and 6.82 (1H), assignable to the acetyl methyl and vinyl protons, respectively, and multiplets at δ 7.0–7.6 (7H) and 8.1–8.3 (1H), assignable to the aromatic protons; in addition there were two 1-proton multiplets at δ 3.9–4.3 and 4.3–4.9, which must be assigned to the methylene protons at C-6 if structure **6** is correct. This pattern could be accounted for in terms of this structure if at the temperature of the probe (27°) the two tub conformations **7***a* and *b* were undergoing interconversion at a rate slow on the p.m.r. time scale. That this is indeed the case was shown by recording the p.m.r. spectrum in carbon disulfide at 27 and 0°. At the former temperature the spectrum resembled that in deuteriochloro-

[1]Preliminary accounts of this work have appeared previously (3, 4); Wawzonek and Stowell (5) have also made this structural revision.

[2]See footnotes 4 and 6 in reference 1.

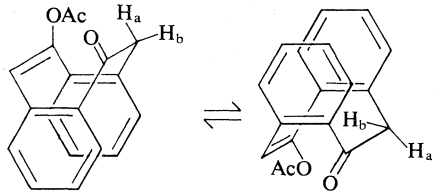

7a *7b*

form, but at the latter temperature the methylene protons gave rise to a simple AB system with δ 3.80 and 4.63 and J_{gem} = 12.5 Hz. Thus when the temperature is lowered the 8-membered ring becomes conformationally "frozen" and the individual signals for H_a and H_b in *7a* or *b* can be observed (6). In dimethyl sulfoxide at 27°, the protons in question give rise to an envelope at δ 4.0–4.6, but at 40° this becomes a broad singlet at δ 4.30 (half-height width = 5.5 Hz); clearly the interconversion of *7a* and *b* at the higher temperature has become rapid on the p.m.r. time scale.

Treatment of **6** with bromine in acetic acid gave the compound that was previously considered to be **8**; this structure was preferred to **9** because of the apparent unreactivity of the bromo compound when treated with potassium acetate in boiling acetic acid (2). While its i.r. spectrum [λ_{max} 5.64, 5.90, and 7.31 μ (m)] did not provide an unambiguous basis for choice between structures **8** and **9**, the p.m.r. spectrum of the bromo compound in deuteriochloroform [δ 2.23 (s, 3H), 7.00 (s, 2H), 7.2–7.6 (m, 6H), 7.7–8.0 (m, 1H), and 8.3–8.5 (m, 1H)] definitively excluded structure **8** since it showed no signal corresponding to the C-6 methylene protons. However, the latter spectrum

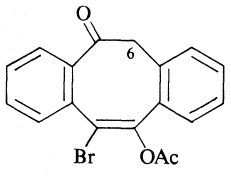

8

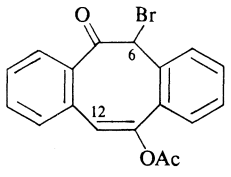

9

could only be reconciled with structure **9** by assuming that the signals of the protons at C-6 and C-12 were accidentally superimposed. That this was indeed the case was revealed by spectra taken in trifluoroacetic acid or dimethyl sulfoxide, which showed two 1-proton singlets in place of the 2-proton signal; the apparent singlet could also be resolved in deuteriochloroform at 100 MHz, when the separation of the component signals was ca. 1 Hz.

Also in accord with the assignment of structure **9** was the observation that brief treatment of the bromo compound with zinc in boiling acetic acid returned **6** in virtually quantitative yield. With respect to the reactivity of the bromo compound with potassium acetate (*vide supra*), we have found that reaction in boiling acetonitrile or acetic acid, although slow, does occur with the formation of a compound whose i.r. spectrum included a carbonyl-stretching band at 5.80 μ; this product was not obtained pure. Some analogy for the bromination of **6** to give **8**

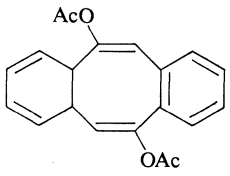

10

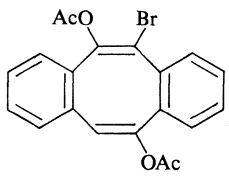

11

appeared to be provided by the claim that treatment of the diacetate **10** with bromine gave the bromo compound **11**. However, in our hands the product from this reaction was the bromo ketone **9**, which by coincidence has a closely similar carbon and hydrogen (but not bromine) content to that of **11**.

Further bromination of **9** in chloroform gave a polybromo product that was not purified or characterized in the earlier work, but was treated with boiling aqueous–ethanolic ammonia followed by sublimation to give the compound considered to be **3** (2). In the present case the polybromo compound was purified and assigned the formula $C_{16}H_{10}Br_4O_2$. Its i.r. spectrum (Nujol) showed a weak hydroxyl-stretching band at 2.95 μ, but no band in the carbonyl-stretching region. Its p.m.r. spectrum showed a 1-proton singlet at δ 4.71, assignable to a hydroxyl proton since it was absent after brief treatment with D_2O, and a 1-proton singlet at δ 5.66, together with 6- and 2-proton multiplets in the aromatic proton region. The polybromo compound is therefore assigned either structure **12** or **13**. These structures are very closely related for both are hydrogen bromide adducts of the tribromo dione **14**. The lability that would be expected of a compound of this type was displayed in several ways. The polybromo compound melted with gas evolution; on attempted purification by thin-layer

Can. J. Chem. Downloaded from www.nrcresearchpress.com by 210.87.254.42 on 09/05/12
For personal use only.

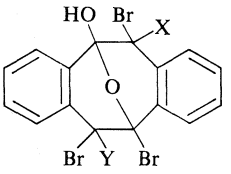

12 X = Br; Y = H
13 X = H; Y = Br

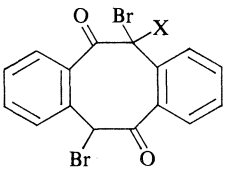

14 X = Br
15 X = H

chromatography (t.l.c.) it decomposed to give at least 5 products, all showing carbonyl absorption in their i.r. spectra; although its i.r. spectrum in Nujol or ethanol-free chloroform lacked carbonyl absorption, a band at 5.80 μ immediately developed in the spectrum of a solution in chloroform containing ethanol. The formation of **12** or **13** from **9** can be interpreted as occurring via attack of bromine on the enol acetate function to give the dibromo dione **15** (cf. the conversion of **10** to **9**), followed by bromination at a position adjacent to a carbonyl group to give the tribromo dione **14**; alternatively, bromination at the position adjacent to the carbonyl group of **9** may precede attack at the enol acetate function. The bromination next to the carbonyl group provides the hydrogen bromide that converts **14** to **12** or **13** by transannular addition.

When the polybromo compound was treated briefly with boiling aqueous-ethanolic ammonia and the resulting crude product was sublimed at ca. 200°, the compound previously assigned structure **3** was obtained as orange needles, m.p. 254–255° [lit. (2) m.p. 254–256°]. Its i.r. spectrum [λ_{max} (CCl_4) 5.69, 5.80 (m), 5.84, and 6.13 μ] and p.m.r. spectrum [δ ($CDCl_3$) 7.3–7.9 (m, 6H) and 8.2–8.5 (m, 2H)] clearly showed that it could not be **3**. Indeed the latter spectrum indicated that its formula was $C_{16}H_8O_3$ rather than $C_{16}H_{10}O_3$, and this was confirmed by the observation of a molecular ion peak with *m/e* 248 in its mass spectrum. The spectral data and mechanistic considerations suggested that it was 11-oxoindeno-[1,2-*c*]isocoumarin (**4**). This was proved by direct comparison with an authentic sample of **4** prepared by the method of Pailer *et al.* (7) by condensation of phthalide and phthaldehydic acid to give 2-(*o*-carboxyphenyl)-indan-1,3-dione (**16**) followed by dehydration, eq. [1].

[1] 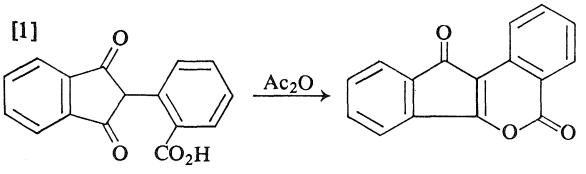

16 **4**

The next goal was the elucidation of the course of this interesting transformation. Thin-layer chromatography established that the indeno-isocoumarin **4** was not present in the crude product formed on treatment of the polybromo compound with aqueous-ethanolic ammonia, and thus **4** must be formed during the sublimation. This crude product was similarly shown to contain neither the acid **16** nor its ethyl ester. Column chromatography of the crude product on silica readily effected the separation of an intensely yellow oil, which was the least polar component of the crude product and represented ca. 25% of its weight. This gave **4** in high yield on being heated at 180° (20 mm). High resolution mass spectrometry established the composition of the yellow compound as $C_{18}H_{13}BrO_3$; its p.m.r. spectrum showed signals at δ (CCl_4) 1.12 (t, J = 7.0 Hz, 3H) and 4.14 (q, J = 7.0 Hz, 2H) indicating the presence of a $-CO_2CH_2CH_3$ grouping, and multiplets at δ 7.0–7.7 (7H) and 7.9–8.16 (1H) attributable to aromatic protons. These data and the fact that the yellow compound is the precursor of **4** led to the assignment to it of structure **17**. Its i.r. spectrum [λ_{max} (CCl_4) 5.84 μ] and ultraviolet (u.v.) spectrum [λ_{max} (C_6H_{14}) 235 (log ε 4.6), 242 (log ε 4.6), 252 (infl., log ε 4.4), 328 (log ε 2.8), and 392 mμ (log ε 3.2)] were in full accord with this structural assignment (8) Its conversion to **4** may be envisaged as occurring via the intermediacy of either **18** or **19** (see Scheme 1). Loss of bromide ion to give **20** or **21** followed by nucleophilic attack of bromide ion on the ethyl group would then give **4** and ethyl bromide. Alternatively, in the case of **18**, a concerted 4-center reaction could lead to the direct elimination of ethyl bromide; in the case of **19**, however, the analogous 6-center concerted elimination is sterically inhibited. It seems reasonable to postulate that such polar reactions could occur in the reaction melt. Analogous formation of lactones by elimination of alkyl bromides has been observed previously (9). In the case at hand the formation of ethyl bromide in the conversion of **17** to **4** was established by trapping it in dichloromethane and identifying it by p.m.r. and mass spectrometry.

The formation of **17** by the action of aqueous–

Can. J. Chem. Downloaded from www.nrcresearchpress.com by 210.87.254.42 on 09/05/12
For personal use only.

Can. J. Chem. Downloaded from www.nrcresearchpress.com by 210.87.254.42 on 09/05/12
For personal use only.

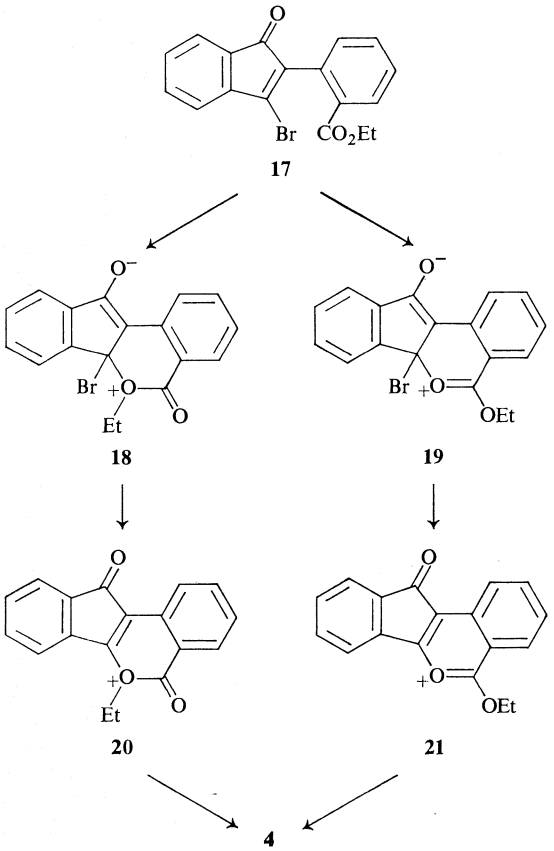

SCHEME 1

ethanolic ammonia on the polybromo compound **12** or **13** can be interpreted as involving initial reversion to the tribromo dione **14** by loss of the elements of hydrogen bromide in the basic medium, followed by ethanolysis to give **22** (see Scheme 2). Cyclization of this to either **23** or **24** followed by elimination of hydrogen bromide would then give **17**.

Having shown that the compound hitherto considered to be the trione **3** was in fact **4**, we investigated an alternative route for the synthesis of **3**, viz., the oxidation of the dione **5** with selenium dioxide. The reaction was carried out in boiling aqueous dioxane, conditions under which cyclooctane-1,2-dione is formed from cyclooctanone in 65% yield (10). The progress of the reaction was followed by vapor-phase chromatography (v.p.c.), and the mixture was worked up after $3\frac{1}{2}$ days when little starting material remained. Three products were obtained: red, yellow, and colorless. The red compound was indicated to have the formula $C_{31}H_{16}O_3$ by mass spectrometry, and its p.m.r. spectrum [δ ($CDCl_3$) 7.1–8.3 (m, 13H) and 8.3–8.8 (m, 3H)] suggested that all of its protons were aromatic and that 3 of them were in the *ortho* relationship to carbonyl groups. On this basis it was concluded that the red product was compound **25**, which had been obtained previously by Brand and Stephan (11) from the dione **26** by oxidation with selenium

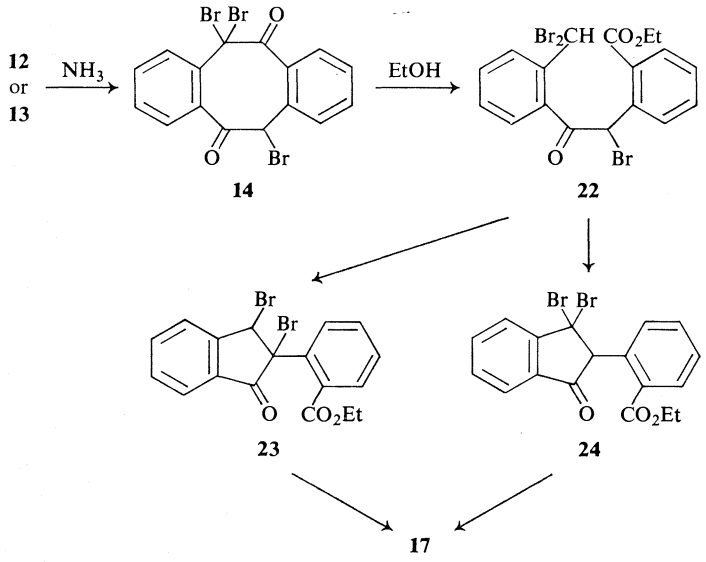

SCHEME 2

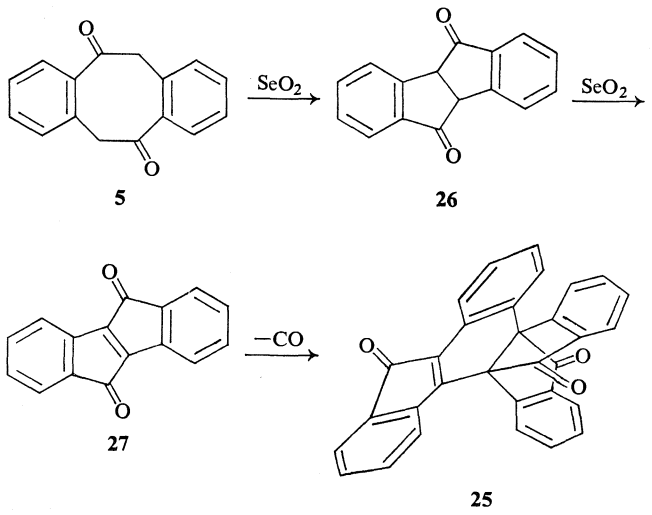

SCHEME 3

dioxide. This conclusion was confirmed by direct comparison with a sample of **25** prepared from **26**, which was itself obtained from α,β-diphenylsuccinic acid (12). The conversion of **5** to **25** can be considered as involving initial oxidation to **26**, followed by further oxidation to **27** and Diels–Alder dimerization (13) of this intermediate with subsequent loss of carbon monoxide (see Scheme 3) as proposed previously (11). Compound **25** was obtained in 4% yield from **5**.

The yellow compound formed on treatment of **5** with selenium dioxide was shown by mass spectrometry and elemental analysis to have the formula $C_{16}H_{10}O_2Se$. Its i.r. spectrum showed a band at 5.92 μ, and its p.m.r. spectrum showed signals at δ ($CDCl_3$) 4.50 (s, 2H), 7.24–7.52 (m, 6H), and 7.84–8.15 (m, 2H). On this basis it is assigned structure **28**. It was obtained in 20% yield.

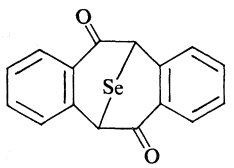

28

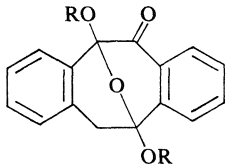

29 R = H
30 R = $COCH_3$

The major product (70%) was a colorless solid shown by its i.r. spectrum [λ_{max} ($CHCl_3$) 2.95 (ms) and 5.90 μ] to be a hydroxy ketone. Its p.m.r. spectrum (CF_3CO_2H) showed an AB system at δ 3.35 and 3.78 (J = 16 Hz, 2H) and aromatic proton signals at 6.9–8.05 (m, 8H). These spectra suggested structure **29**, and high resolution mass spectrometry established that the formula of the product corresponded to this structure, although the elemental analytical data could only be reconciled with it by the assumption that it was a hydrate $C_{16}H_{12}O_4 \cdot 1/4\ H_2O$.[3] Acetylation with acetic anhydride and sulfuric acid gave a diacetate, whose i.r. [λ_{max} (CCl_4) 5.65 and 5.84 μ] and p.m.r. spectra [δ ($CDCl_3$) 2.13 (s, 3H), 2.25 (s, 3H), 3.17 and 3.87 (AB system, J = 16 Hz, 2H), 6.9–7.65 (m, 7H), and 7.85–8.1 (m, 1H)] were in good accord with its formulation as **30**. The spectra of the diol and its diacetate could conceivably also be interpretable in terms of structures without bridging of the 8-membered ring, such as **31** and **32**, if they are assumed to be conformationally frozen at room temperature, as in the case of **6** at 0° (*vide supra*). However, the

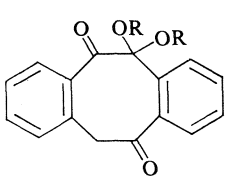

31 R = H
32 R = $COCH_3$

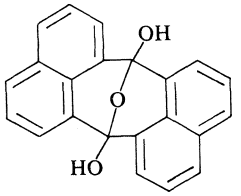

33

[3]The tendency of compounds of this type to exist as hydrates is high (14).

Can. J. Chem. Downloaded from www.nrcresearchpress.com by 210.87.254.42 on 09/05/12
For personal use only.

Can. J. Chem. Downloaded from www.nrcresearchpress.com by 210.87.254.42 on 09/05/12
For personal use only.

positions of the methylene proton signals in the p.m.r. spectra of the 2 compounds and the occurrence in the p.m.r. spectrum of the acetate of only a 1-proton signal attributable to a proton in the *ortho* relationship to a carbonyl group favor structures **29** and **30**. The former finds analogy in compound **33** which is obtained by hydration of the corresponding dione (15).

Compound **29** is a hydrate of the desired trione **3** (as is **31**), and attempts were made to dehydrate it. Like **33** it was unaffected by treatment with *p*-toluenesulfonic acid in boiling benzene with distillation of the solvent to remove any water formed as its azeotrope with benzene. A solution of the compound and dicyclohexylcarbodiimide showed no change after standing for several months. The compound melted at 198–199° without decomposition and sublimed unchanged at ca. 150° (10^{-2} mm), behavior that again paralleled the properties of **33** (15). However, on being heated at 300° (20 mm) the melt evolved gas, and a new product sublimed. The i.r. spectrum of the crude product showed that it was again a hydroxy ketone [λ_{max} ($CHCl_3$) 2.9 (wm) and 5.86 μ]; its p.m.r. spectrum showed a broad 1-proton signal at δ 2.9 that can be assigned to a hydroxyl proton since its position was concentration-dependent, a 1-proton singlet at δ 4.25, and an 8-proton aromatic multiplet at δ 7.2–8.2. These data suggest the assignment to this product, which was not further characterized, of structure **34**, whose formation can be rationalized as involving an intramolecular aldol condensation of the elusive trione **3**, eq. [2].

[2] 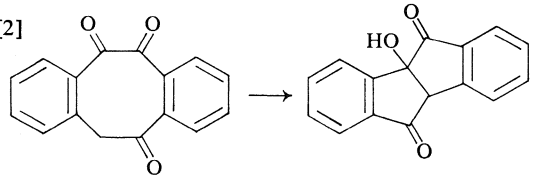

3 34

Experimental

Melting points were determined in capillary tubes with a Thomas–Hoover "Uni-Melt" apparatus and are uncorrected.

Infrared spectra were recorded in carbon tetrachloride solutions, unless otherwise stated, and were calibrated with the 3.51, 6.24, and 9.72 μ bands of polystyrene film. Proton magnetic resonance spectra were recorded in deuteriochloroform solutions, unless otherwise stated. The band positions are reported in parts per million downfield from tetramethylsilane as internal reference (δ scale).

Analytical t.l.c. was carried out with thin layers of silica gel (Merck) on microscope slides. Preparative t.l.c. was carried out with 1.0 mm thick layers of silica gel (Merck) on 20 × 20 cm square glass plates. Unless otherwise stated, thin-layer chromatograms were developed with dichloromethane, analytical chromatograms were made visible with iodine vapor, and preparative chromatograms by the quenching of a u.v. phosphor added to the silica gel.

Solutions in organic solvents were dried over anhydrous magnesium sulfate and stripped of solvent with a rotary evaporator in conjunction with a water aspirator. The term "aqueous workup" used here means that the solution in question was poured into about 3 times its volume of water and extracted 3 times with dichloromethane, and the dichloromethane solution was washed 3 times with water, dried, and stripped of solvent.

11-Acetoxydibenzo[a,e]cycloocten-5(6H)-one (6)

Compound **6** was prepared by treating dibenzo[*a,e*]cyclooctene-5,11-(6*H*,12*H*)-dione (**5**) (1) with acetic anhydride and potassium acetate, as described by Wawzonek (2). Several recrystallizations from 95% ethanol gave colorless rhomboidal platelets, m.p. 137–138° [lit. (2) m.p. 138–139°]; λ_{max} 5.66, 5.96, 7.33 (ms), and 8.35 μ; δ 2.17 (s, 3H), 3.9–4.3 (m, 1H), 4.3–4.9 (m, 1H), 6.82 (s, 1H), 7.0–7.6 (m, 7H), and 8.1–8.3 (m, 1H). At 27° in carbon disulfide, the nuclear magnetic resonance (n.m.r.) spectrum was similar to that in deuteriochloroform, but at 0°, the two 1-proton envelopes in the δ 3.9–4.9 region became an AB signal system, δ 3.80 and 4.63, J = 12.5 Hz. In dimethyl sulfoxide at 27°, the protons in question gave rise to an envelope at δ 4.0–4.6; at 40° this had become a broad singlet at δ 4.30 (half-height width = 5.5 Hz).

11-Acetoxy-6-bromodibenzo[a,e]cycloocten-5(6H)-one (9)

Compound **9** was obtained when the enol acetate **6** was treated with bromine in acetic acid as described by Wawzonek (2). Recrystallization from benzene gave colorless prisms, m.p. 229–229.5° (without gas evolution) [lit. (2) m.p. 219–223° with gas evolution]; λ_{max} 5.64, 5.90, 7.31 (m) and 8.36 μ; δ 2.23 (s, 3H), 7.00 (s, 2H), 7.2–7.6 (m, 6H), 7.7–8.0 (m, 1H), and 8.3–8.5 (m, 1H); δ (CF_3CO_2H) 2.47 (s, 3H), 7.02 (s, 1H), 7.20 (s, 1H), 7.3–7.75 (m, 6H), 7.75–8.05 (m, 1H), and 8.3–8.6 (m, 1H); the p.m.r. spectrum in DMSO-d_6 showed 1-proton singlets at δ 7.00 and 7.27.

Anal. Calcd. for $C_{18}H_{13}BrO_3$: C, 60.50; H, 3.65; Br, 22.38. Found: C, 60.59; H, 3.80; Br, 22.39.

Reduction of 9 with Zinc and Acetic Acid. Formation of 6

In a 5 ml round-bottomed flask were placed compound **9** (10.5 mg, 0.029 mmole), zinc dust (3.6 mg, 0.055 mmole), and acetic acid (2 ml). The mixture was boiled under reflux for 0.5 h, then a further 3 mg of zinc dust was added, and the mixture was boiled under reflux for another 5 min, allowed to cool, filtered, and subjected to aqueous workup. The product was the enol acetate **6** (8 mg, 100%); the i.r. spectrum of this "crude" product was identical with that of authentic **6**, and t.l.c. showed only one spot, corresponding to **6**. Recrystallization from

Can. J. Chem. Downloaded from www.nrcresearchpress.com by 210.87.254.42 on 09/05/12
For personal use only.

95% ethanol gave colorless platelets, m.p. 139–139.5°, undepressed on admixture with authentic **6**.

*Treatment of **9** with Potassium Acetate*

A mixture of **9** (126 mg, 0.353 mmole) and potassium acetate (107 mg, 1.09 mmoles) in acetonitrile (5 ml) was boiled under reflux for 3 h; much of the potassium acetate failed to dissolve. The mixture was poured into water, and the solid that precipitated was collected by filtration. The light orange solid weighed 74 mg, after being dried over phosphorus pentoxide. Its i.r. spectrum was similar to that of the starting material, but there was an additional band at 5.80 μ (m). Recrystallization from benzene–hexane gave canary-yellow prisms, m.p. 225–229.5°, identified as starting material (**9**) by mixture m.p. and i.r. spectral comparison; the yellow color of the recovered **9** is attributed to a small amount of impurity. The material which gave rise to the 5.80 μ band presumably remained in the mother liquor from recrystallization of the recovered **9**, and was not investigated.

When **9** was heated at reflux for 4 h with potassium acetate in acetic acid, aqueous workup gave a sticky orange solid, the i.r. spectrum of which was very similar to that of the solid obtained by treating **9** with potassium acetate in boiling acetonitrile (*vide supra*).

*Treatment of **9** with Dimethyl Sulfoxide and Collidine*

A solution of **9** (4 mg, 0.011 mmole) and collidine (2.5 mg, 0.021 mmole) in dimethyl sulfoxide (0.5 ml) was heated at 130° for 6 h. Aqueous workup gave a yellow oil (2.5 mg), the i.r. spectrum of which was similar to that of the material obtained by treating **9** with potassium acetate (*vide supra*).

*Treatment of **9** with Silver Nitrate*

A solution of **9** (10 mg, 0.028 mmole) and silver nitrate (6.8 mg, 0.040 mmole) in acetonitrile (4 ml) was boiled under reflux in the dark for 18 h under nitrogen. Aqueous workup gave a bright yellow smear (7 mg); λ_{max} 5.66 (m) and 5.80 μ.

When the reaction mixture was stirred in the dark at 23° for 24 h instead of being boiled under reflux for 18 h, aqueous workup gave a solid, m.p. 225–228°, the i.r. spectrum of which was virtually identical to that of **9** (69% recovery).

*5,11-Diacetoxydibenzo[a,e]cyclooctene (**10**)*

Compound **10** was prepared by heating the dione **5** in acetic anhydride containing a little sulfuric acid, as described by Wawzonek (2). Aqueous workup gave a yellow oil that was recrystallized from 95% ethanol to give colorless rosettes, m.p. 149–150° [lit. (2) m.p. 150–151°]; λ_{max} 5.66, 7.34 (m), and 8.31 μ; δ 2.12 (s, 6H), 6.78 (s, 2H), 7.1–7.4 (m with spike at δ 7.23, 8H).

*Treatment of **10** with Bromine. Formation of **9***

A solution of bromine (58 mg, 0.36 mmole) in acetic acid (0.4 ml) was added to a solution of **10** (45 mg, 0.14 mmole) in acetic acid (1.5 ml) in a Pyrex tube. The tube was sealed and left at 23° for 7 h, during which time crystals were deposited. The tube was opened and the orange supernatant solution was removed. The colorless prisms were washed with benzene, giving **9** (30 mg, 60%), m.p. 122–128.5°; its i.r. spectrum was identical with that of authentic **9**. Recrystallization from benzene gave colorless cubes, m.p. 230–231.5°, undepressed on admixture with authentic **9**, m.p. 229–229.5°; mixed t.l.c. with authentic **9** gave a single spot.

The original supernatant solution was stripped of solvent to give a colorless solid (22.5 mg), the i.r. spectrum of which indicated it to be **9**, contaminated with material giving rise to a band at 5.79 (m) μ.

*Treatment of **9** with Bromine. Formation of **12** or **13***

Bromine (0.8 ml, 14.6 mmoles) was added to a solution of **9** (400 mg, 1.12 mmoles) in chloroform (16 ml) in a Pyrex tube. The tube was sealed and left at 23° for 48 h, during which time no change could be discerned. The tube was opened and the solution was stripped of solvent to give a yellow solid (689 mg), m.p. 172–179° with gas evolution [lit. (2) m.p. 173–178° with gas evolution]. Recrystallization from hexane–chloroform (ethanol-free) gave microprisms, m.p. 199–200° with gas evolution; λ_{max} (Nujol) 2.95 (w) μ; δ 4.71 (s, 1H, absent after treatment with D_2O), 5.66 (s, 1H), 7.2–7.7 (m, 6H), and 7.7–8.2 (m, 2H). The i.r. spectrum in ethanol-free chloroform was similar to that in Nujol, but in chloroform containing 0.75% of ethanol included a weak band at 5.80 μ.

Anal. Calcd. for $C_{16}H_{10}Br_4O_2$: C, 34.70; H, 1.82; Br, 57.72. Found: C, 34.55; H, 1.79; Br, 58.43.

The crude tetrabromo compound was obtained from **9** in essentially quantitative yield, and recrystallization gave material in ca. 55% yield that melted sharply with gas evolution. Recrystallization gave material with m.p. varying from 199–200° to 205–206.5°; sometimes the m.p. was slightly lowered by further recrystallization. This behavior may be due to dimorphism; when the m.p. was taken with a microscope-hot-stage unit, a change in crystalline form appeared to occur at ca. 180°. When the tetrabromo compound was subjected to preparative t.l.c., decomposition occurred to give at least 5 compounds, all showing carbonyl absorption in their i.r. spectra; no tetrabromo compound was recovered. The tetrabromo compound did not dissolve appreciably in aqueous ammonia, but when it was shaken with this reagent the aqueous ammonia slowly became yellow. On adding aqueous ammonia to a suspension of the compound in 95% ethanol, the tetrabromo compound readily dissolved to give a light yellow solution which became bright yellow during about 2 min.

*Treatment of the Tetrabromo Compound **12** or **13** with Aqueous-ethanolic Ammonia Followed by Sublimation. Formation of 11-Oxoindeno[1,2-c]isocoumarin (**4**)*

A mixture of crude tetrabromo compound **12** or **13** (736 mg), 95% ethanol (17 ml), and concentrated aqueous ammonia (5 ml) was boiled under reflux for 10 min. Aqueous workup gave a yellowish solid (337 mg); λ_{max} 3.1 (br, wm), 5.82, and 5.90 (sh, s) μ. This crude solid was sublimed at 180° (20 mm) to give **4** (84 mg, 26%), m.p. 150–200°. Recrystallization from ethyl acetate gave orange needles, m.p. 254–255° [lit. (2) m.p. 254–256°]; λ_{max} 5.69, 5.80 (m), 5.84, and 6.13 (m) μ; δ 7.3–7.9 (m, 6H) and 8.2–8.5 (m, 2H).

Mol. Wt. Calcd. for $C_{16}H_8O_3$: 248. Found: *m/e* 248.

The use of recrystallized tetrabromo compound, m.p. 199–200°, gave **4** in 52% yield.

An authentic sample of **4** was prepared from phthalide

Can. J. Chem. Downloaded from www.nrcresearchpress.com by 210.87.253.12 on 05/05/12
For personal use only.

and phthalaldehydic acid via the acid **16** by the method of Pailer *et al.* (7); m.p. 255.5–256.5° [lit. (7) m.p. 257°]. A mixture of this with the compound obtained from the tetrabromo compound had m.p. 255–256°; the i.r. spectra and t.l.c. behavior of the 2 samples were identical.

*Treatment of the Tetrabromo Compound **12** or **13** with Aqueous-ethanolic Ammonia. Formation of 3-Bromo-2-(o-carboethoxyphenyl)indone (**17**)*

The recrystallized tetrabromo compound **12** or **13**, m.p. 199–200°, (920 mg) was treated with aqueous-ethanolic ammonia (*vide supra*) to give a crude solid (440 mg), which was chromatographed on silica gel (28 g, 19 × 1.8 cm). The column was eluted with benzene, and the eluate corresponding to the most mobile colored band was collected. This eluate gave **17** as an intensely yellow oil (116 mg, 26%); λ_{max} 5.84 μ; λ (C_6H_{12}) 235 (log ε 4.6), 242 (log ε 4.6), 252 (infl., log ε 4.4), 328 (log ε 2.8), and 392 mμ (log ε 3.2); δ (CCl_4) 1.12 (t, J = 7.0 Hz, 3H), 4.14 (q, J = 7.0 Hz, 2H), 7.0–7.7 (m, 7H), and 7.9–8.16 (m, 1H).

Calcd. for $C_{18}H_{13}{}^{79}BrO_3$: 356.0048. Found: *m/e* 356.0021.

The rest of the reaction mixture consisted of red, polar, solid material (eluted with 1–10% methanol in dichloromethane) with i.r. absorption at 2.9, 5.9, 6.1, and 6.3 μ; it did not give **4** on heating, and was not investigated further.

It was shown by t.l.c. that the acid **16** was not present in the original reaction mixture; p.m.r. spectroscopy showed that the ethyl ester of **16**, 2-(*o*-carboethoxyphenyl)-indan-1,3-dione, (*vide infra*) was absent; t.l.c. and i.r. spectroscopy demonstrated the absence of **4**.

2-(o-Carboethoxyphenyl)indan-1,3-dione

The acid **16** (750 mg, 2.82 mmoles) was added to methanol (30 ml), and the suspension was stirred while a distilled solution of diazoethane (ca. 200 mg, ca. 3.6 mmoles) in ether (150 ml) (16) was added rapidly. The mixture was stirred for a further 5 min, treated with acetic acid (0.2 ml), and stripped of solvent. The residue was crystallized from benzene–hexane to give the ester as a yellow solid (205 mg, 25%), m.p. 156–165°. Recrystallization from dichloromethane–hexane gave very pale yellow needles, m.p. 160.5–164°; λ_{max} 5.71 (wm) and 5.84 μ; δ 1.15 (t, J = 7.0 Hz, 3H), 4.03 (q, J = 7.0 Hz, 2H), 4.77 (s, 1H), and 7.2–8.2 (m, 8H).

Anal. Calcd. for $C_{18}H_{14}O_4$ (mol. wt. 294.0891): C, 73.46; H, 4.80. Found (*m/e* 294.0920): C, 73.64; H, 4.66.

*Pyrolysis of **17**. Formation of **4** and Ethyl Bromide*

When compound **17** (11 mg) was heated at 180° (20 mm) in a Pyrex tube, a bright orange compound rapidly sublimed onto the cool, upper part of the tube. This compound (6.9 mg, 90%) was shown to be **4** by i.r. spectral comparison with an authentic sample.

Pyrolysis of **17** (70 mg) was also carried out at 180° in a closed system evacuated at the water aspirator. The gas evolved was collected directly in a p.m.r. tube containing dichloromethane cooled in liquid nitrogen, while **4** sublimed onto the cooler parts of the pyrolysis tube. The p.m.r. tube, with its contents frozen, was sealed and detached from the rest of the apparatus. The presence of ethyl bromide in the dichloromethane was shown by p.m.r. and mass spectrometry, the spectra being compared with those of authentic solutions of ethyl bromide in dichloromethane. The p.m.r. spectrum indicated that ca. 2 mg (10%) of ethyl bromide was dissolved in the dichloromethane.

*Oxidation of **5** with Selenium Dioxide. Formation of Compounds **25**, **28**, and **29***

A mixture of **5** (1.20 g, 5.1 mmoles), selenium dioxide (B.D.H.; 0.74 g, 6.7 mmoles), dioxane (Fisher Certified; freshly refluxed and distilled over sodium; 24 ml), and water (2 ml) was boiled under reflux for 84 h, at the end of which time v.p.c. indicated that very little starting material was present. Aqueous workup gave a bright orange–red solid, which was chromatographed on a column of silica gel (119 g, 29 × 3 cm). Elution with benzene and with benzene containing 1% dichloromethane gave compound **25** (51 mg, 4%); recrystallization from dichloromethane gave red prisms, m.p. 289–289.5°; λ_{max} 5.82 μ; δ 7.1–8.3 (m, 13H) and 8.3–8.8 (m, 3H).

Mol. Wt. Calcd. for $C_{31}H_{16}O_3$: 436. Found: *m/e* 436.

An authentic sample of **25** was prepared by heating the dione **26** (12) with selenium dioxide in acetic acid as previously described (11). Recrystallization from acetic acid gave red prisms, m.p. 288–289° [lit. (11) m.p. 284°]. A mixture of this with the red compound obtained from **5** had m.p. 287.5–289.5°; the i.r. spectra of the two samples were identical.

Elution with benzene containing 2% dichloromethane and with dichloromethane gave compound **28**, as yellow platelets (82 mg, 4%); recrystallization from dichloromethane–hexane gave yellow rhomboidal platelets, m.p. 235–236°; λ_{max} 5.97 μ; δ 4.50 (s, 2H), 7.24–7.52 (m, 6H), and 7.84–8.15 (m, 2H).

Anal. Calcd. for $C_{16}H_{10}O_2Se$ (mol. wt. 314): C, 61.37; H, 3.22. Found (*m/e* 314): C, 61.56; H, 3.30.

Elution with dichloromethane containing 2% methanol gave **29** as a white solid (954 mg, 70%); recrystallization from dichloromethane–hexane gave small, colorless prisms, m.p. 195.5–198°; λ_{max} (Nujol) 3.06 (m) and 5.94 μ; λ_{max} ($CHCl_3$) 2.95 (ms) and 5.89 μ; δ (CF_3CO_2H) 3.38 (A part of AB signal system, J = 16 Hz, 1H), 3.75 (B part of AB system, J = 16 Hz, 1H), and 6.95–8.1 (m, 8H); the solubility of **29** in deuteriochloroform was too low for the signal due to the hydroxyl protons to be discerned, but signals were seen at δ 3.17 and 3.67 (AB system, J = 16 Hz), and 6.9–7.8 (m).

Anal. Calcd. for $C_{16}H_{12}O_4 \cdot 1/4\ H_2O$: C, 70.44; H, 4.62. Found: C, 70.30, 70.08; H, 4.37, 4.34.

Mol. Wt. Calcd. for $C_{16}H_{12}O_4$: 268.0736. Found: *m/e* 268.0734.

*Acetylation of **29**. Formation of the Diacetate **30***

Compound **29** (5 mg) was dissolved in acetic anhydride (1 ml), and concentrated sulfuric acid (1 drop) was added. The mixture was left at 23° in a stoppered flask for 24 h. Aqueous workup gave a white powder (5 mg), m.p. 197–202°; λ_{max} 5.65, 5.84, 7.34, 7.80, and 8.33 μ; δ 2.13 (s, 3H), 2.25 (s, 3H), 3.17 (A part of AB system, J = 16 Hz, 1H), 3.87 (B part of AB system, J = 16 Hz, 1H), 6.9–7.65 (m, 7H), and 7.85–8.1 (m, 1H).

*Attempted Dehydration of **29**. Formation of **34***

Compound **29** melted without decomposition, and

sublimed without decomposition at 150° (10^{-2} mm) as demonstrated by i.r. spectroscopy. When heated at 300° (20 mm) in a Pyrex tube by insertion of the lower part of the tube into a preheated electric furnace, it evolved gas and gave a product that distilled onto the cooler, upper part of the tube. The crude pyrolysate was a pale yellow oil; λ_{max} 2.9 (br, m) and 5.86 μ; δ 2.9 (br s, 1H, position concentration-dependent), 4.25 (s, 1H), and 7.2–8.1 (m, 8H). The i.r. and n.m.r. spectra of the pyrolysate resembled those of **26** (12); λ_{max} 5.86 μ; δ 4.40 (s, 2H), and 7.3–8.1 (m, 8H). A solution of **29** (5 mg) and *p*-toluenesulfonic acid (1 mg) in benzene (30 ml) was boiled under reflux for 72 h under a drying tube in a flask fitted with a Soxhlet extractor containing calcium carbide. The colorless reaction solution was evaporated in a stream of dry nitrogen. The i.r. spectrum of the residue indicated that it was a mixture of **29** and *p*-toluenesulfonic acid.

Compound **29** (2 mg, 0.007 mmole) and dicyclohexylcarbodiimide (2 mg, 0.01 mmole) were dissolved in dichloromethane (0.5 ml) in a Pyrex tube; the tube was sealed, and the mixture was allowed to stand at 23°. After 2 months no change in appearance was noted; in particular, there was no sign of the very insoluble dicyclohexylurea.

We thank the National Research Council of Canada for generous support of this work. One of us (E. G. L.) gratefully acknowledges the awards of an Alcan Jamaica Independence Overseas Scholarship, a Shell Canada Fellowship, a Special Open University of Toronto Fellowship, and an NRCC Scholarship.

1. P. YATES, E. G. LEWARS, and P. H. MCCABE. Can. J. Chem. This issue.
2. S. WAWZONEK. J. Amer. Chem. Soc. **62**, 745 (1940).
3. P. YATES and E. G. LEWARS. Chem. Commun. 622 (1967).
4. E. G. LEWARS, J. K. STOWELL, S. WAWZONEK, and P. YATES. Chem. Ind. 344 (1968).
5. S. WAWZONEK and J. K. STOWELL. J. Org. Chem. **33**, 896 (1968).
6. Cf. E. L. ELIEL, N. L. ALLINGER, S. J. ANGYAL, and G. A. MORRISON. Conformational analysis. Interscience Publishers, Inc., New York. 1955. p. 153.
7. M. PAILER, H. WÖRTHER, and A. MELLER. Monatsh. **92**, 1037 (1961).
8. Cf. F. YA. FREIMANS and G. YA. VANAG. J. Gen. Chem. USSR, **30**, 3328 (1960); **34**, 448 (1964).
9. Cf. L. J. HAYNES and J. R. PLIMMER. Quart. Rev. **14**, 292 (1960).
10. G. WITTIG and A. KREBS. Ber. **94**, 3260 (1951).
11. K. BRAND and H. W. STEPHAN. Ber. **72**, 2168 (1939).
12. A. C. COPE and S. W. FENTON. J. Amer. Chem. Soc. **73**, 1668 (1951).
13. Cf. E. N. GARBISCH and P. F. SPRECHER. J. Amer. Chem. Soc. **88**, 3433, 3434 (1966).
14. Cf. P. YATES, S. N. EĞE, G. BÜCHI, and D. KNUTSEN. Can. J. Chem. **45**, 2927 (1967).
15. W. C. AGOSTA. J. Amer. Chem. Soc. **89**, 3505 (1967).
16. P. YATES, D. G. FARNUM, and D. W. WILEY. Tetrahedron, **18**, 881 (1962).

Can. J. Chem. Downloaded from www.nrcresearchpress.com by 210.87.254.42 on 09/05/12
For personal use only.

Electron spin resonance studies of oriented NO_2 and NF_2 in inert matrices at low temperatures

C. A. McDowell, H. Nakajima,[1] and P. Raghunathan
Department of Chemistry, University of British Columbia, Vancouver 8, British Columbia
Received October 14, 1969

Preferentially oriented NO_2 and NF_2 in inert matrices have been studied in some detail by electron spin resonance methods at 4.2 °K. Methods are discussed which may optimize the degree of preferential orientation of the paramagnetic species in appropriate matrices. The results demonstrate that while neon is the best host matrix for orienting NO_2, argon is to be preferred for NF_2. The *g*-values and hyperfine splitting data have been accurately determined and are compared with earlier values. Motional processes are suggested to explain the spectra obtained for NF_2 in an argon matrix in the temperature range 4–30 °K.

Canadian Journal of Chemistry, **48**, 805 (1970)

Can. J. Chem. Downloaded from www.nrcresearchpress.com by 210.87.254.42 on 09/05/12
For personal use only.

Introduction

Some recent low-temperature electron spin resonance (e.s.r.) studies of paramagnetic molecules in inert-gas matrices have shown that the spectra and their dependence on the orientation of the magnetic field are characteristic of highly oriented species (1, 2). The particular species which has been frequently investigated by the e.s.r. method is the NO_2 molecule, and its preferential orientation in a neon matrix has been cursorily indicated some time ago (1). The exact experimental conditions causing this "preferential orientation", however, are far from being well-established, and this paper reports a more detailed study of how an inert-gas matrix and appropriate physical conditions together may influence the nature and extent of orientation of a paramagnetic species. Analysis of the e.s.r. spectra of a σ-radical (NO_2), and a π-radical (NF_2), isolated in appropriate inert-gas matrices are also presented, together with a study of their motional effects which depend on temperature. Computer-simulated spectra were generated to compare the experimental data with theory. Several refinements have been made of an earlier experimental arrangement which led to well-resolved and well-oriented spectra of matrix-isolated paramagnetic molecules.

Experimental

An X-band superheterodyne spectrometer was employed for the detection of the e.s.r. and the microwave power-level was kept about 30 dB below the 200 mW klystron output. The signal at the detector was phase-detected at 400 Hz and displayed on a recorder. For the measurement of the magnetic field strength, a proton magnetometer was used and the proton-probe was placed as close as possible to the cavity. To estimate the *g*-values, the microwave frequency was measured using a Hewlett–Packard (5255A) frequency convertor and the frequency counter. The errors in the measurements were within ± 0.0002 for *g*-values, and ± 0.25 G for the hyperfine splittings.

The low-temperature apparatus was essentially similar in design to the ones previously described in the literature (2, 3), but with certain important modifications. First, a thin copper target, ground flat, was used in place of the sapphire rod generally employed inside the TE_{102} microwave cavity. The "Q" of the cavity was negligibly affected by this change. The target, which was rotatable about an axis perpendicular to the magnetic field, was conduction-cooled by direct contact with a liquid helium cryostat. The use of copper as target material (4) not only led to the rapid establishment and continued maintenance of a low surface-temperature of the target, but also conveniently eliminated several unwanted signals often observed with sapphire. Secondly, the overall cryogenics of the system were improved by mounting the cavity in such a way that it was in good contact with the bottom of the helium cryostat at all times. A very sizable gradient was thus ensured between the initial temperature of the radical–matrix mixture and the final temperature at the time of deposition. While the temperature of the cavity was thus kept not warmer than about 25 °K, the copper target itself was maintained at the temperature of liquid helium by direct thermal contact with the bottom of the helium dewar. This arrangement helped to improve the degree of orientation of molecules directly impinging on the cold target-face. A schematic set-up of the cryostat is shown in Fig. 1.

Research grade matrix and paramagnetic gases were premixed and equilibrated at room temperature for several hours before being sprayed onto the cold surface by means of a thin-walled quartz nozzle located very close to it. To achieve enhanced sample orientation, it was necessary to use a uniformly controlled rate of sample spray. In a typical experiment, well-resolved and intense

[1]Permanent address: Department of Physics, Faculty of Science, Hokkaido University, Sapporo, Hokkaido, Japan.

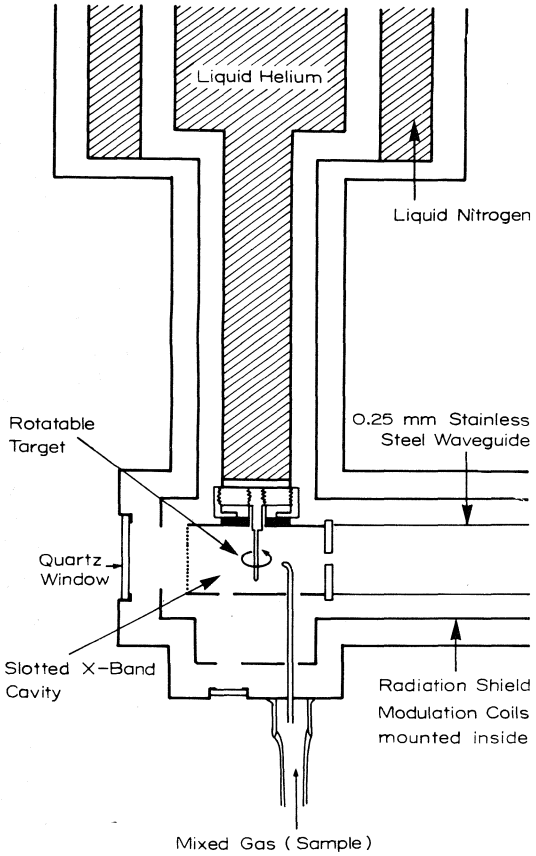

FIG. 1. Cross section of the low temperature apparatus (for deposition of mixed gas) and the microwave cavity.

spectra were recorded after using a spray rate of 2×10^{18} molecules/min of mixed gas and a spraying time of about 20 min.

Results and Discussion

NO_2 in a Neon Matrix

The e.s.r. spectra of NO_2 in neon matrix were obtained as described above. In Fig. 2 are shown typical experimental spectra recorded as a function of θ, the angle between the plane of sample deposition and the external magnetic field (for example, θ = 90° when the plane of deposition is held normal to the direction of the external field). These spectra have several features different from the ones reported earlier for this species in neon (1), argon (5), and dinitrogen tetroxide (6) matrices. The turning points of the spectrum corresponding to the *a*, *b*, and *c* components of the **g**-tensor for the $m_I = 0$ transition are here clearly resolved. We use the subscripts *a* and *b* to refer to the axes in the plane of the NO_2 molecule and, in particular, *b* is the molecular symmetry axis; *c* is the component perpendicular to the molecular plane. Previous studies (1, 6) have confirmed the assignment we have adopted for the **g**- and **A**-components in Fig. 2. A clue to the degree of preferential orientation of the species is afforded by the fact that the intensities of the hyperfine lines of the spectrum in Fig. 2 definitely vary with θ.

It is of interest to examine whether the above-mentioned "degree of orientation" is influenced by the matrix-to-radical ratios, and to investigate this point we studied the spectra obtained with

FIG. 2. The e.s.r. spectra of NO_2/neon (~1/2500) at 4.2 °K, recorded as a function of θ (defined in the text). Microwave frequency = 9356.3 MHz; magnetic field center = 3337.22 G; field modulation amplitude = 0.5 G. (All spectra in this work are presented as first derivatives of the absorption.)

Can. J. Chem. Downloaded from www.nrcresearchpress.com by 210.87.254.42 on 09/05/12
For personal use only.

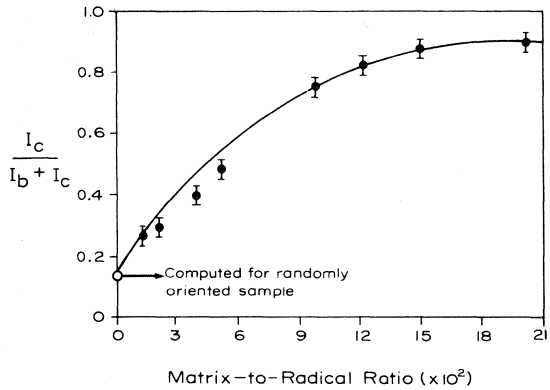

FIG. 3. The "orientation parameter", $I_c/(I_b + I_c)$, as a function of the concentration of NO_2 radicals in neon at $\theta = 90°$.

M/R ratios ranging from 100 to over 2000. To obtain an estimate of the dependence of orientation on concentration, the ratio of peak heights of the high-field ($m_I = -1$) components, $I_c/(I_b + I_c)$, was chosen for the perpendicular configuration of the target. The spectra obtained for this position of the target possessed sharply-defined *a*, *b*, and *c* components; and the *c* component of the hyperfine pattern can be used to indicate the degree of orientation of the molecular planes parallel to the target; i.e. the condensing surface. The results obtained by keeping a rigidly-controlled rate of deposition of the matrix–radical mixture (2×10^{18} molecules/min) are shown in Fig. 3. It can be seen from this figure that it is most satisfactory to choose matrix-to-radical ratios of over 1000 for obtaining a well-oriented specimen.

The degree of orientation of the species in its matrix relative to the target surface can be analyzed by means of line-shape simulation computing techniques. In Fig. 4, the computed spectrum for randomly oriented NO_2 is presented; this was obtained by choosing a Gaussian line-shape function with a line width of 1.5 G and taking the principal values of **g**- and **A**-tensors to be the ones shown later in Table 1. The spectrum in Fig. 4 was plotted using a Fortran IV program which solved the e.s.r. spin Hamiltonian, as in eq. [1]

$$[1] \quad \mathcal{H} = g_c\beta H_z S_z + g_b\beta H_y S_y + g_a\beta H_x S_x + A_c I_z S_z + A_b I_y S_y + A_a I_x S_x$$

to second order in hyperfine interaction (7);

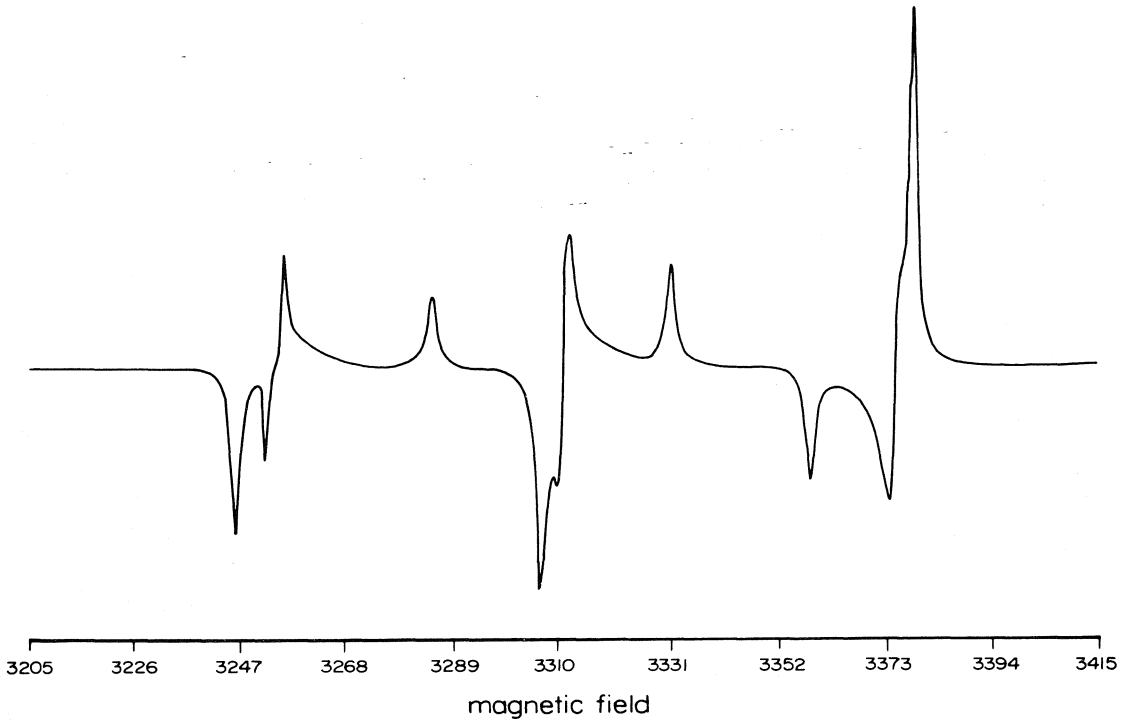

FIG. 4. Computer simulated e.s.r. spectrum of randomly oriented NO_2, using the values of *g* and *A* reported in this work. A Gaussian line-width of 1.5 G has been assumed.

Can. J. Chem. Downloaded from www.nrcresearchpress.com by 210.87.254.42 on 09/05/12
For personal use only.

Can. J. Chem. Downloaded from www.nrcresearchpress.com by 210.87.254.42 on 09/05/12
For personal use only.

TABLE 1

Data on g and A values for NO_2 in different matrices

	Principal g values			Principal A values (G)			Isotropic values		
Matrix	g_a	g_b	g_c	A_a	A_b	A_c	g	A (G)	Reference
Argon	1.9920	2.0033		44.6	59.6				
	± 0.0005	± 0.0005	—	± 1.0	± 1.0	—	—	—	5
	($g_\parallel$)	($g_\perp$)		($A_\parallel$)	($A_\perp$)				
Neon	1.9920	2.0030		45.80	61.70	51.70	2.0004		1
N_2O_4	1.9913	2.0015	2.0062	2.0054	|48.15|	|67.25|	|50.35|		|55.25|
	± 0.0004	± 0.0004	± 0.0004	$\pm$ 0.15	± 0.0004	± 0.15	± 0.15	1.9994	± 0.08 6
Neon	1.9919	2.0026	2.0054	45.90	63.05	50.90			
	± 0.0002	± 0.0002	± 0.0002	± 0.25	± 0.25	± 0.25	1.9999	—	This work
Argon	1.9914	2.0024	2.0051	45.40	63.10	50.60			53.10*
	± 0.0002	± 0.0002	± 0.0002	± 0.25	± 0.25	± 0.25	1.9997	± 0.1	This work
NO_2(gas)	1.991015	2.001990	2.006178	45.23	66.02	45.60	1.9997 (3)	52.28	9

*The relative signs of the hyperfine interaction tensors for nitrogen and fluorine were of course not determinable in our experiment, but have been arrived at from theoretical considerations (11) of the corresponding isotropic components.

Can. J. Chem. Downloaded from www.nrcresearchpress.com by 210.87.254.42 on 09/05/12
For personal use only.

the subscripts in this equation represent the principal-axis coordinate system of the **g**- and **A**-tensors. The applied field was taken along the *c*-axis. The overall agreement between the computed spectrum in Fig. 4 and the experimental one for $\theta = 45°$ (see Fig. 1*b*) is good. However, the lines due to the *c* component of the hyperfine interaction are stronger in the experimental spectrum. This can be interpreted to mean that while the in-plane (*a*, *b*) molecular axes are distributed fairly randomly in the trapping sites in the matrix, the out-of-plane (*c*) component is frozen in with a distribution *far from random.*

This type of distribution, which in fact measures the inclination of the molecular planes of the radical away from the surface of deposition, was first observed by Kasai *et al.* (2) for the case of $Cu(NO_3)_2$ molecules isolated in a neon matrix. The trial-and-error line-shape computation employed by these workers led to quite a reasonable approximation of the extent of orientation of the Cu^{2+} molecular species parallel to the cold target surface.

An independent means of assessing the nature of the distribution in our experiment has been sought by using the following method: the parameter $I_i/(I_i + I_o)$ was measured at each m_I region of the spectrum for several values of θ ranging from 0 to 90°; here I_i is the intensity of the in-plane component lines and I_o that of the out-of-plane component line. An exponentially decreasing plot of this "distribution parameter" against θ, going from a maximum to a minimum, would indicate a substantial degree of orientation. From our experimental data the distribution shown in Fig. 5 was obtained and is seen to lie between $e^{-\theta}$ and $e^{-2\theta}$.

Several trial polynomials in θ having the form suggested by the above analysis were used to weight the in-plane and out-of-plane components before performing the numerical integration (8) to obtain the computed spectrum. The computer subroutines that handled these calculations, written in Fortran IV, were essentially similar to the ones used by Kasai *et al.* (2). The derivatives of the absorption spectrum were plotted for the two extreme cases, $\theta = 90°$ and $\theta = 0°$. These are shown in Figs. 6*a* and *b*, respectively, which are seen to simulate the corresponding experimental spectra of Fig. 2 remarkably well. It is concluded, then, that a large majority of the molecular planes of NO_2 molecules are oriented

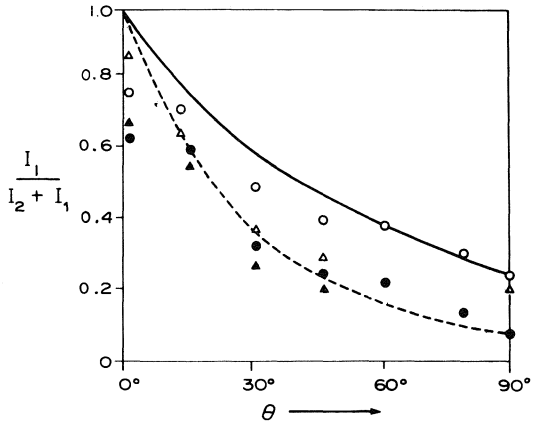

FIG. 5. Relative intensities of the in-plane and out-of-plane hyperfine components as a function of θ (NO_2/neon ~1/2500). ○, $I_b/I_b + I_c$) for $m_I = 0$; ●, $I_a/(I_a + I_c)$ for $m_I = 0$; ▲, $I_a/(I_a + I_c)$ for $m_I = +1$; △, $I_b/(I_b + I_c)$ for $m_I = +1$.

parallel to the surface of deposition. The experimental technique provides much useful information if the **g**- and **A**-tensors have an orthorhombic or axial symmetry, considering that the external magnetic field has explored only the *a*–*c* plane.

The principal values of the **g**- and **A**-tensors consistent with the best fit to the experimental spectra are listed in Table 1, along with a set of other comparable results for NO_2. The average width of the component lines of our spectra, assuming a Gaussian line-shape, was found to be 1.0 G. This is consistent with the best resolution obtained so far for NO_2 trapped in polycrystalline matrices.

NF_2 in Neon and Argon Matrices

A spectrum of NF_2 randomly oriented in neon at 4.2 °K has been investigated by Farmer *et al.* (3) and by Kasai and Whipple (10). Following these workers, the axes of the **g**- and **A**-tensors are labeled as shown in Fig. 7. The main features of the oriented spectrum are that it consists of a triplet of triplets, and that a small but clearly resolved anisotropy of the **g**-tensor is revealed in the $m_I(N) = 0$, $m_I(2F) = 0$ central peak. In the present study, the overall pattern is the same as described above, but the central region of the spectra, shown in Fig. 8, has led to the following significant advances over earlier efforts: (*a*) The region corresponding to the $m_I(2F) = 0$ transition (± 60 G from the center) has been fully resolved, revealing a fairly

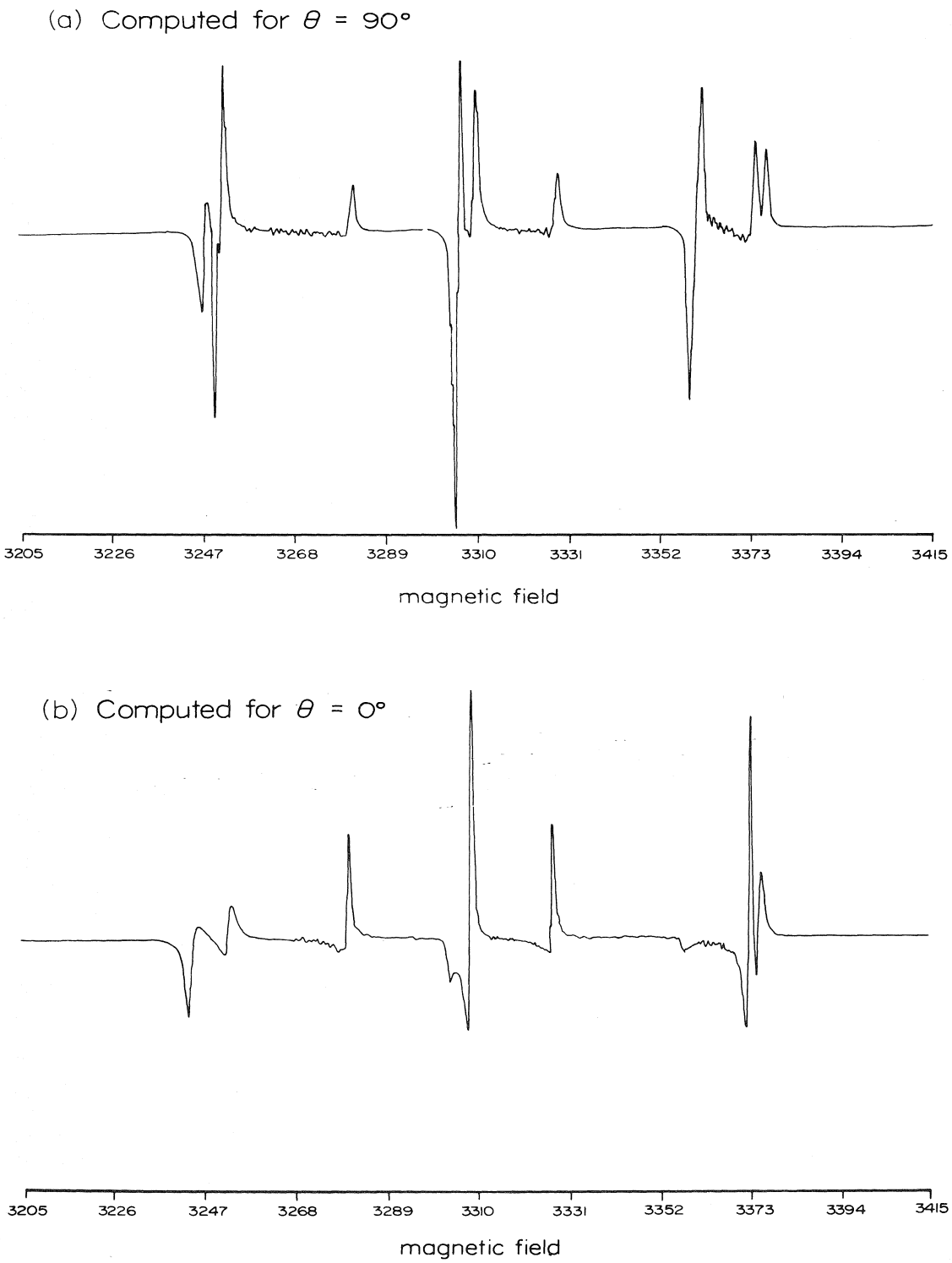

FIG. 6. Computer simulated e.s.r. spectra of preferentially oriented NO_2: (*a*) $\theta = 90°$, (*b*) $\theta = 0°$. The in-plane components of **g** and **A** are randomly distributed in the *a*–*b* plane, while the out-of-plane component is heavily weighted around the magnetic field axis.

Can. J. Chem. Downloaded from www.nrcresearchpress.com by 210.87.254.42 on 09/05/12
For personal use only.

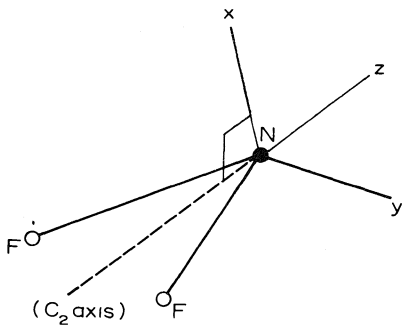

FIG. 7. Definition of the principal axes of **g** and **A** for the NF_2 radical.

complex structure due to the smaller hyperfine constants of nitrogen and fluorine; the points of inflexion of the strong central line can be precisely located, and these, therefore, have led to values of the **g**-tensor components accurate to ± 0.0002. (*b*) Argon has been found preferable to neon as matrix material in that it leads to a well-defined orientation effect.

A set of equal-intensity triplets due to the $m_I(2F) = \pm 1$ transition are observed on the sides of the strong center-structure on the low- and high-field sides. The rise and fall of these outer triplets with respect to θ (these triplets have been left out of Fig. 8 and subsequent figures) coincided with those of *x*-component lines in the $m_I(2F) = 0$ transition. The NF_2 radical is known to be "π-type", and the unpaired electron occupies an orbital of b_1 symmetry (3). Therefore, the component of the hyperfine tensor causing the largest splitting will be directed outward from the molecular plane, which becomes the *x*-component in our notation. Thus the outermost triplets may be assigned conclusively to the $m_I(2F) = \pm 1$ region of A_x.

The *g*- and *A*-values measured for NF_2/argon and NF_2/neon are listed in Table 2. These values are seen to be essentially the same for the two matrices. However, the angular dependence of the spectra was markedly different in the two matrices. This difference is illustrated in Fig. 8*a* (neon) and Fig. 8*b* (argon). In the argon matrix, only the *x*-component becomes progressively more prominent as the surface of deposition is rotated, and reaches a maximum intensity for the perpendicular configuration ($\theta = 90°$). It may be concluded therefore that in the argon matrix the molecular plane of NF_2 is oriented parallel to the surface of deposition. This orientation effect has not been so clearly observed in neon in our experiments. This lack of orientation may be due to the "softness" of the neon matrix.

From the measurements reported in Table 2, values of 16.10 and 76.2 G are calculated for the anisotropic (dipolar) part of the hyperfine interaction of the unpaired electron with the nitrogen and fluorine nuclei, respectively. These values are in complete agreement with the ones reported earlier (10). In using their data to estimate the p orbital contribution of nitrogen to the molecular orbital of NF_2, Kasai and Whipple (10) have employed the spectroscopic values of Barnes and Smith (12) for the $<1/r^3>_{2p}$ of nitrogen. This leads to a slight overestimate of the spin density on nitrogen. We, however, prefer to use a value (11, 13) of 3.10 a.u. for $<1/r^3>_{2p}$ for nitrogen and calculate the dipolar part in the hyperfine interaction as

$$(2/5)\,(\mu_I\beta_I/I)\,<1/r^3>_{2p} = 17.05 \text{ G}$$

the symbols on the left hand side of the above equation having their usual meaning. On comparing this quantity with the corresponding experimental estimate of 16.10 G, we obtain a value of 0.98 for the spin density on the nitrogen nucleus.

Temperature Dependence of the NF_2/Argon Spectrum

It has been noted earlier that the central peak of the NF_2/argon spectrum exhibits structure due to the anisotropy of the **g**-tensor. Certain kinds of motion, with frequencies of the order of 5 to 10 MHz, i.e. typically of the order of the difference between two anisotropic *g*-values (in frequency units), would tend to average out the structure of the center of the spectrum (3, 14). The temperature dependence of the central peak was examined in the temperature range 4–30 °K, and the results are illustrated in Fig. 9. First, a line appeared between the *z*- and *y*-components and grew larger, while a corresponding peak was not seen between the *z*- and *x*-components. Next, the distinction between the *y*- and *z*-components disappeared, but the *x*-component was still present. Finally, even the *x*-component disappeared above 30 °K and molecular tumbling was now presumably fast enough to bring about a narrowing of the central peak. The whole spectrum became an isotropic triplet set of triplets.

The above changes in the spectrum may be explained as follows: the first noticeable motion

Can. J. Chem. Downloaded from www.nrcresearchpress.com by 210.87.254.42 on 09/05/12
For personal use only.

Can. J. Chem. Downloaded from www.nrcresearchpress.com by 210.87.254.42 on 09/05/12
For personal use only.

TABLE 2

Data on the g and A values of NF_2 in inert gas matrices

Matrix	Principal g values			Principal A values (G)						Isotropic g value	Isotropic A value (G)		Reference
				Nitrogen			Fluorine						
	g_x	g_y	g_z	A_x	A_y	A_z	A_x	A_y	A_z		Nitrogen	Fluorine	
Argon	2.0022 ±0.0004	2.0051 ±0.0004	2.0066 ±0.0004	—	—	—	—	—	—	2.0053	17 ±2.0	60 ±2.0	3
Krypton	—	—	—	—	—	—	—	—	—	2.0053	17 ±2.0	60 ±2.0	3
Neon	2.0011 ±0.0005	2.0079 ±0.0005	2.0042 ±0.0005	49 ±0.5	0 ±1.0	0 ±1.0	212 ±2.0	−16.9 ±1.0	−16.9 ±1.0	2.0044	16 ±1.0	59 ±1.0	10
Neon	2.0019 ±0.0002	2.0086 ±0.0002	2.0050 ±0.0002	49.2 ±0.25	1.0 ±0.25	1.0 ±0.25	212.8 ±0.25	−16.6 ±0.25	−16.6 ±0.25	2.0052	—	—	This work*
Argon	2.0022 ±0.0002	2.0085 ±0.0002	2.0051 ±0.0002	49.3 ±0.25	1.0 ±0.25	1.0 ±0.25	212.0 ±0.25	−16.5 ±0.25	−16.5 ±0.25	2.0053	17.1±0.25	60.2±0.25	This work
Krypton	,,	,,	,,	49.5 ±0.25	,,	,,	,,	,,	,,	,,	17.3±0.3	60.6±0.3	This work

*See footnote of Table 1.

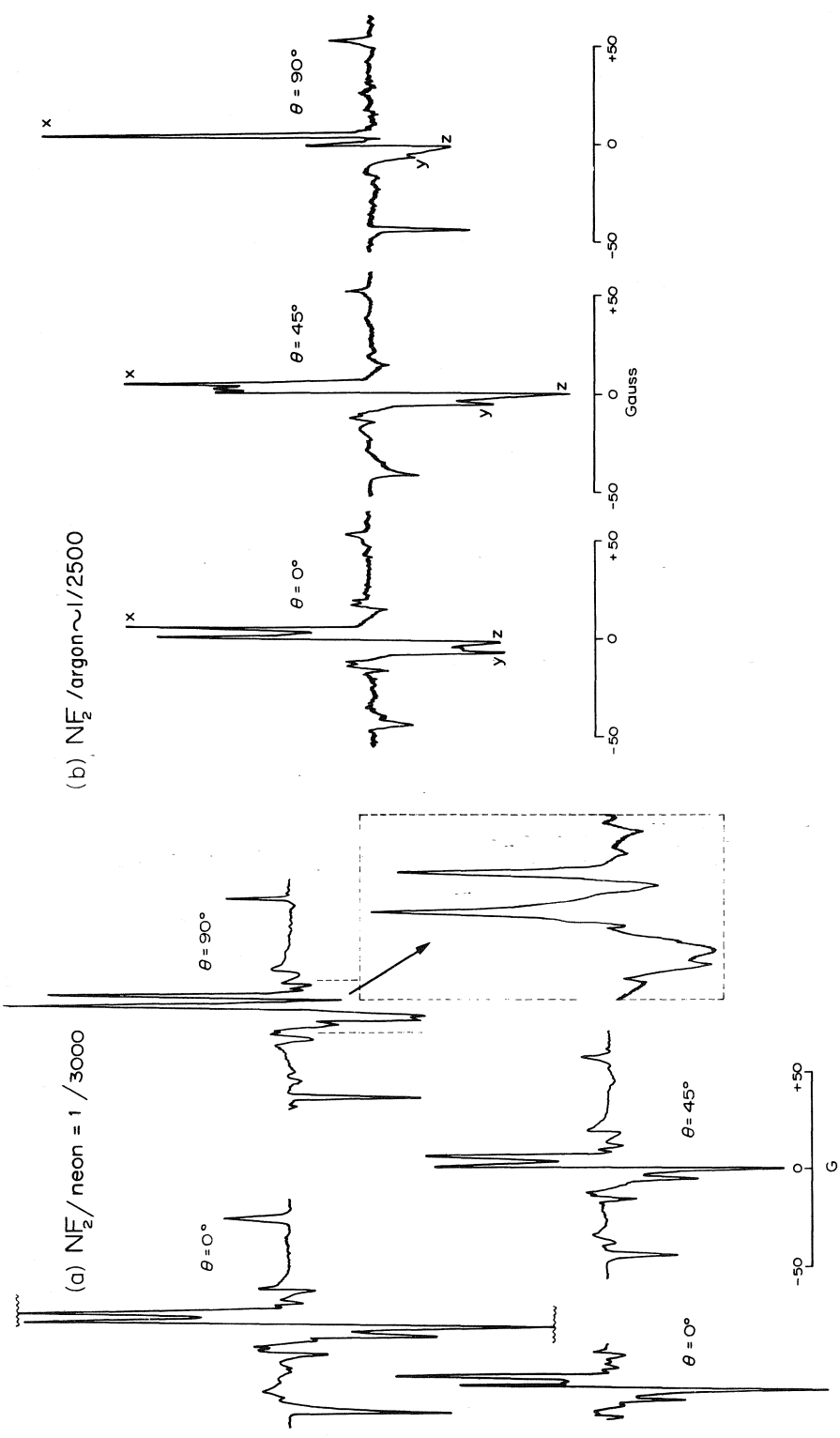

FIG. 8. The central region of the e.s.r. spectra of NF_2 at 4.2 °K, recorded in neon (*a*) and argon (*b*) matrices as a function of θ. The insets in (*a*) show expanded scans of the central peak, using a lower signal amplitude.

Can. J. Chem. Downloaded from www.nrcresearchpress.com by 210.87.254.42 on 09/05/12
For personal use only.

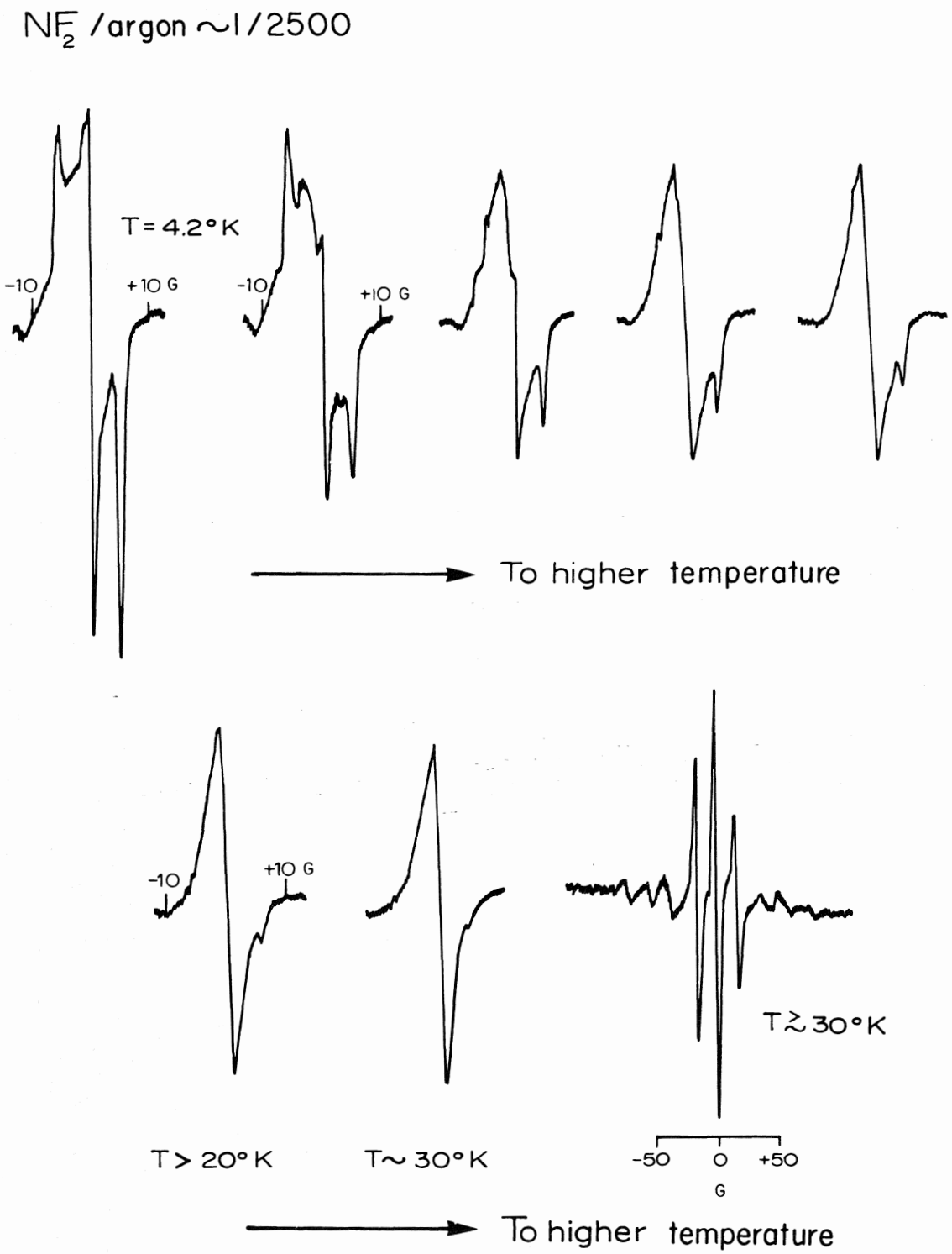

FIG. 9. The temperature dependence of the central peak of NF_2/argon (~1/2500); the spectra were recorded for $\theta = 0°$.

Can. J. Chem. Downloaded from www.nrcresearchpress.com by 210.87.254.42 on 09/05/12
For personal use only.

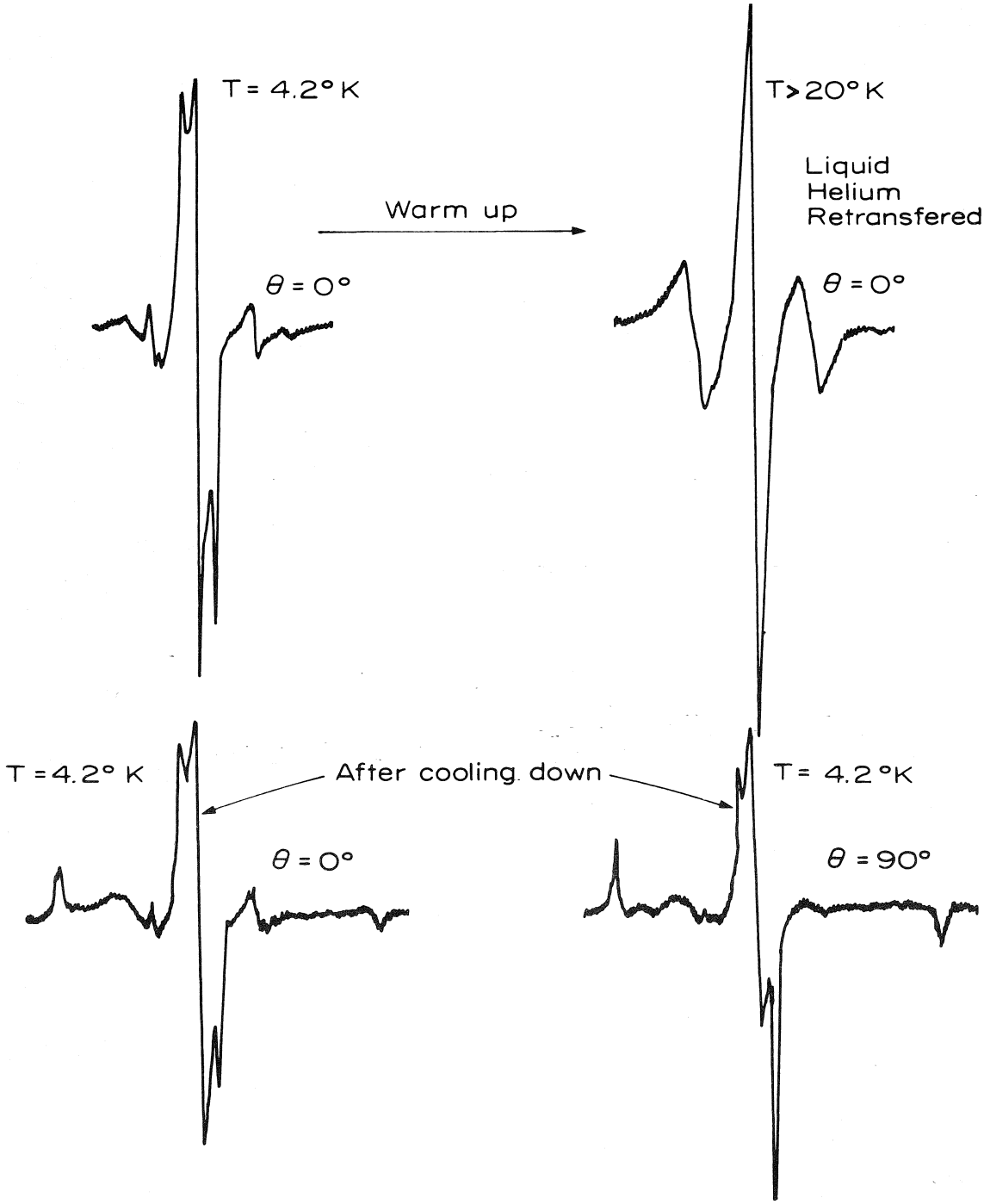

FIG. 10. The central peak of the e.s.r. spectrum of NF_2/argon obtained when the sample was warmed up and cooled down again to 4.2 °K.

Can. J. Chem. Downloaded from www.nrcresearchpress.com by 210.87.254.42 on 09/05/12
For personal use only.

Can. J. Chem. Downloaded from www.nrcresearchpress.com by 210.87.254.42 on 09/05/12
For personal use only.

is a rotation about the molecular x-axis (3). Then some other mode of rotation sets in, such as a rotation about the y-axis (C_2 symmetry axis). Finally, at a still higher temperature, the NF_2 radical rotates almost isotropically around more than two axes about a fixed center of gravity. This leads to the isotropic g-value of 2.0053 recorded in Table 2.

It is of interest to note that the above-mentioned situation arises while the matrix is still oriented. To examine this matter in more detail, the deposit was warmed to a temperature below the sublimation point of the matrix in vacuum when the aforementioned isotropic lines just began to appear and the temperature was cooled down to 4.2 °K by a slow transfer of liquid helium to the experimental cryostat. The helium transfer at this stage of the experiment presented the following difficulty: the reading of the ionization gauge attached to the main evacuation port of the dewar system, which usually stood at 1×10^{-7} mm Hg, temporarily went up to 6×10^{-4} mm during this transfer before settling down again to the original value, thus indicating some loss of the sample deposit. As a consequence, there was a slight decrease in the overall intensity of the spectrum recorded after this cooling down process. A typical result of this operation is recorded in Fig. 10.

The remarkable feature of these spectra is that the orientation of radicals is still seen in these samples after the cooling down process has been completed. This leads to the conclusion that, prior to cooling, isotropic rotations were going on in the matrix which was previously preferentially oriented. It is known (15) that vapor-deposited argon at 4.2 °K tends to have its (111) plane oriented parallel to the surface of deposition, and it is conceivable that this dictates the general pattern of alignment of the radical species. However, in a more detailed interpretation of the orientation process one includes the following considerations.

The chief driving force in the mechanism of crystal growth with preferred orientations usually arises from the surface energies of the crystallographic planes. The experimental data pertaining to this subject have been extensively reviewed by Bauer (16). If the condensing gas is streamed at a low angle of incidence to the target surface, as was done in our experiment, an "anisotropic" molecular supply results. Consequently, the growth form of the crystal would deviate somewhat from the normal isometric form. Thus the formation of columnar crystals or platelets, for instance, could be visualized. The crystal planes of such structures would possess larger surface energies than their corresponding "equilibrium" forms and it is probable that this excess energy induces eventual ordering in the structure.

Alternatively, the mechanism of oriented growth could involve the electrical double layer at the metal target surface, which polarizes the condensing matrix gas (17, 18). This proposal has been made by Shereshefsky and Mazumder (18) to explain the orientation observed in the condensation of krypton and methane monolayers on highly homogeneous metal surfaces. It is likely that such a mechanism is operative in the present experiment, at least for the first few layers of the sample deposit. As the molecular population on the surface increases, the induced dipoles

FIG. 11. The central region of the e.s.r. spectrum of NF_2/nitrogen (~1/2000); obtained at 4.2 °K and $\theta = 90°$.

would of course counteract the field at the metallic surface.

NF_2 in Matrices other than Neon and Argon

The NF_2 radicals trapped in krypton and nitrogen matrices were also studied at 4.2 °K. Since the van der Waals radii of krypton and argon are not much different (r_v = 1.91 Å for argon, 2.01 Å for krypton), it is not surprising that orientation was also observed in the krypton matrix. Every spectroscopic parameter was almost identical for the spectra obtained with krypton and argon, but the radicals appeared to be oriented to a somewhat lesser degree in krypton.

On the other hand, the spectrum obtained in nitrogen matrix had much broader lines and did not show any orientation effect. The central region of this spectrum is shown in Fig. 11. The poor resolution and the width of the lines may be ascribed to radical motion which promotes the spin–rotational relaxation of the species. The outer triplets due to the $m_I(2F) = \pm 1$ transitions were hardly observable in this matrix.

We wish to thank the National Research Council of Canada for generous grants in supporting this research work. We are also much indebted to Professor J. B. Farmer for many most helpful discussions and assistance.

1. P. H. KASAI, W. WELTNER, JR., and E. B. WHIPPLE. J. Chem. Phys. **42**, 1120 (1965).
2. P. H. KASAI, E. B. WHIPPLE, and W. WELTNER, JR. J. Chem. Phys. **44**, 2581 (1966).
3. J. B. FARMER, M. C. L. GERRY, and C. A. MCDOWELL. Mol. Phys. **8**, 253 (1964).
4. J. P. GOLDSBOROUGH and T. R. KOEHLER. Phys. Rev. **133**, A135 (1964).
5. F. J. ADRIAN. J. Chem. Phys. **36**, 1692 (1962).
6. T. J. SCHAAFSMA, G. A. V.D. VELDE, and J. KOMMANDEUR. Mol. Phys. **14**, 501 (1968).
7. R. E. D. MCCLUNG. Can. J. Phys. **46**, 2271 (1968).
8. C. P. POOLE, JR. Electron spin resonance. Interscience Publishers, Inc., New York. 1967. pp. 825–835.
9. G. R. BIRD, J. C. BAIRD, A. W. JACHE, J. A. HODGSON, R. F. CURL, A. C. KUNKLE, J. W. BRANSFORD, J. RASTRUP-ANDERSEN, and J. ROSENTHAL. J. Chem. Phys. **40**, 3378 (1964).
10. P. H. KASAI and E. B. WHIPPLE. Mol. Phys. **9**, 497 (1965).
11. A. J. FREEMAN and R. E. WATSON. *In* Magnetism, Vol. IIA. *Edited by* G. T. Rado and H. Suhl. Academic Press, Inc., New York. 1965. p. 248.
12. R. G. BARNES and W. V. SMITH. Phys. Rev. **93**, 95 (1954).
13. J. R. MORTON. Chem. Rev. **64**, 456 (1964).
14. J. MARUANI, C. A. MCDOWELL, H. NAKAJIMA, and P. RAGHUNATHAN. Mol. Phys. **14**, 349 (1968).
15. H. S. PEISER. *In* Formation and trapping of free radicals. *Edited by* A. Bass and H. P. Broida. Academic Press, Inc., New York. 1960. p. 319.
16. E. BAUER. *In* Single crystal films. *Edited by* M. H. Francombe and H. Sato. The Pergamon Press, Ltd., London. 1964. p. 43.
17. J. C. P. MIGNOLET. Discuss. Faraday Soc. **8**, 104 (1950).
18. J. L. SHERESHEFSKY and B. R. MAZUMDER. J. Phys. Chem. **63**, 1630 (1959).

Can. J. Chem. Downloaded from www.nrcresearchpress.com by 210.87.254.42 on 09/05/12
For personal use only.

Can. J. Chem. Downloaded from www.nrcresearchpress.com by 210.87.254.40 on 09/05/12
For personal use only.

Synthesis, resolution, and absolute configuration of 1-phenyl-1-methyl-1-silacyclohexanone-2[1,2]

A. G. BROOK, H. W. KUCERA,[3] AND D. M. MACRAE[4]
Department of Chemistry, University of Toronto, Toronto 181, Ontario

Received September 24, 1969

The synthesis and resolution of 1-phenyl-1-methyl-1-silacyclohexanone-2 by oxidative hydroboration of the related silacyclohexene to the silacyclohexanol, resolution of this via the strychnine salt of the phthalate half-ester, and subsequent oxidation of the silacyclohexanol to the silacyclohexanone is described. The carbon analog 1-phenyl-1-methylcyclohexanone-2 was also synthesized in optically active form. The (+)-enantiomers of the two ketones had similar optical rotatory dispersion curves, presenting convincing evidence for the identity of their configurations, and the carbon compound could be degraded without affecting the asymmetric center to (−)-(*R*)-2-phenyl-2-methylhexandioic acid, thereby establishing the absolute configurations of both compounds.

Canadian Journal of Chemistry, **48**, 818 (1970)

As part of our continuing interest in the chemistry of acylsilanes (1) we have resolved and determined the absolute configuration of 1-phenyl-1-methyl-1-silacyclohexanone-2 (**1**). At the time that this research was initiated only two cyclic systems containing an asymmetric silicon center in the ring were known. These were **2** (2), and **3** (3). In these latter systems, the resolving agent,

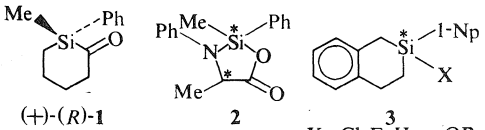

an optically active amino acid for **2**, and *l*-menthol for **3** were bonded directly to the asymmetric silicon center through reactive Si—O and Si—N bonds. These methods did not appear to be suitable for the resolution of cyclic acylsilanes; however, certain developments discussed below suggested that a resolution might be effected through the carbinol precursor to the ketone **1**, 1-phenyl-1-methyl-1-silacyclohexanol-2 (**8**).

It has been shown previously that hydroboration of cyclic silylalkenes such as 1,1-diphenylsilacyclohexene-2 (**4**) results in the formation of the α-silylcarbinol, **5**, as the only isolated product (see Scheme 1) (4). The carbinol can then be oxidized in reasonable yield using the DMSO/

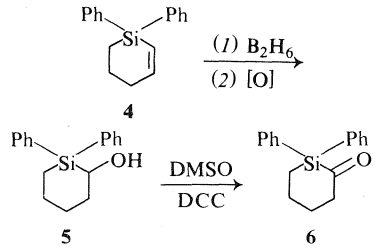

SCHEME 1

dicyclohexylcarbodiimide (DCC) reagent to the corresponding acylsilane **6**.

Upon investigating such a synthetic route to the ketone, **1**, it was found that treatment of racemic 1-phenyl-1-methyl-1-silacyclohexene-2 (**7**) with excess diborane resulted after oxidative workup in the carbinol **8**, whose gas–liquid phase chromatography (g.l.p.c.) analysis showed that it consisted of the two possible diastereomeric carbinols in the proportions of about 95:5 (Scheme 2).

That the diastereomeric carbinols had indeed

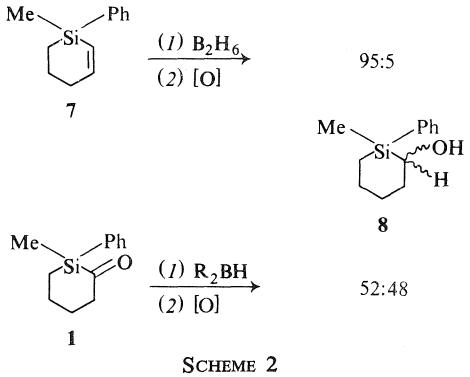

SCHEME 2

[1]Taken in part from the M.Sc. thesis of H. W. Kucera, University of Toronto, 1968.
[2]Part of this material was presented at the Second International Symposium on Organosilicon Chemistry, Bordeaux, France, July, 1968, Abstracts Page 26.
[3]Holder of an NRCC Bursary, 1966–1967.
[4]Holder of a Dow Corning Silicones Fellowship, 1968–1969.

Can. J. Chem. Downloaded from www.nrcresearchpress.com by 210.87.254.40 on 09/05/12
For personal use only.

been separated on the column was shown by reducing the racemic acylsilane **1**, with diisopinocamphenylborane (R_2BH) (5). A g.l.p.c. analysis of the crude reduction product indicated that approximately equal amounts of the diastereomeric carbinols had been produced.

Thus, although the reaction of R_2BH with the ketone exhibits low stereoselectivity, the reaction of B_2H_6 with the alkene **7**, is highly stereoselective. This remarkable fact makes it possible to introduce a second reactive asymmetric center into the molecule, whose configuration is directly related to the configuration at the silicon center. We are attempting to establish the configuration at the carbinol center of the predominant diastereomer.

It seemed feasible to resolve this system through its new asymmetric carbinol center, and a successful resolution was achieved through the phthalic acid-ester of the α-silylcarbinol **8**. This material could be crystallized to diastereomeric purity since the carbinol isolated from the hydrolysis of the crystalline acid-ester showed only one peak by g.l.p.c. analysis, corresponding to the more abundant diastereomer.

On preparing the strychnine salt of the acid-ester in chloroform–acetone, the less soluble diastereomer precipitated and could be recrystallized readily to a constant melting point and rotation. Reisolation of the carbinol ($[\alpha]_D^{25}$ $-73.5°$) and oxidation with DMSO using the method reported by Brook and Pierce (4) gave the optically pure ketone, $[\alpha]_D^{24}$ $-160°$. Isolation of the carbinol from the more soluble strychnine salt followed by oxidation gave (+)-**1** of lower optical purity, $[\alpha]_D^{24}$ $+73.5°$. The optical rotatory dispersion (o.r.d.) spectrum of (+)-**1** showed a positive Cotton effect with a maximum at 400 mμ[5] as shown in Fig. 1.

A considerable amount of effort was expended in trying to devise a workable scheme whereby the absolute configuration of **1** could be determined by degradative reactions. However, the stereochemistry to be expected in displacement reactions at silicon in a new cyclic silicon system is uncertain, since the rules found to apply to Sommer's acyclic 1-naphthylphenylmethylsilyl system (6) are not always applicable to Corriu's cyclic 2-(1-naphthylsila)-1,2,3,4-tetrahydronaphthalene system (**3**) (3, 7). Therefore, chemical degradation to compounds of known absolute configuration was considered to be a hazardous and unreliable approach.

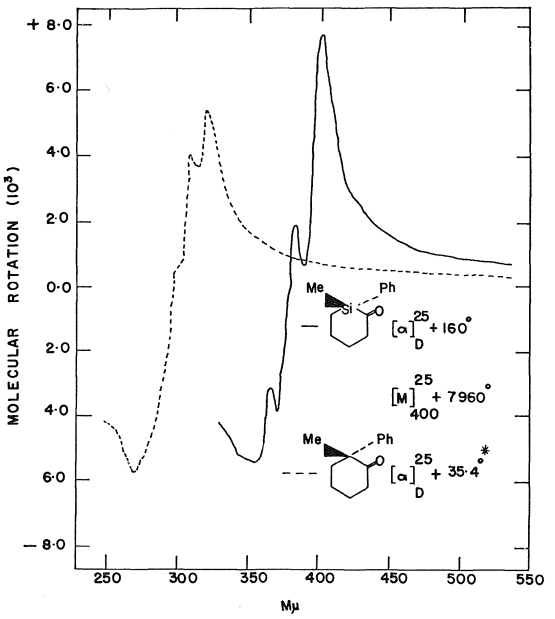

FIG. 1. Optical rotatory dispersion curves obtained in cyclohexane for the analogous carbon and silicon cyclohexanones. *The amplitude of the curve for the carbon ketone is not on an absolute scale since the optical purity of this material is unknown.

The possibility of relating the configurations of the silicon ketone, **1** and its carbon analog **9**, was considered. The relation of the configuration at the silicon and carbon centers could be based upon the reasonable assumption that analogous silicon and carbon compounds with similar o.r.d. curves and Cotton effects of the same sign have the same absolute configuration, as was proposed and confirmed in earlier studies (8).

The resolution of 1-phenyl-1-methylcyclohexanone-2 (**9**) (9), has not been previously reported. Thus, a method for resolving this ketone had to be found. The method used for the analogous silicon ketone was not considered practical, since hydroboration of the alkene **10** would be expected to give rise to a mixture of products bearing the carbinol function at the 2 and 3 positions (10).

Instead it was decided to reduce selectively one enantiomer of the ketone **9** (Scheme 3), using 1/2 mole-equivalent of optically active diisopinocamphenylborane (R_2BH) (5). Selective reduction

[5]The interpretation of the o.r.d. spectra in these systems is currently under study in these laboratories.

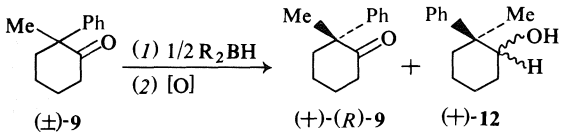

SCHEME 3

was carried out at 0 °C in diglyme to yield after separation of the carbinol, **12**, residual ketone **9**, $[\alpha]_D^{25}$ +35.4°. The optical purity of this ketone has not been determined; however, this is not important for the work that follows.

The recent work of Cram and Hoffman (11) in which they report the absolute configuration of (−)-(*R*)-2-phenyl-2-methylhexandioic acid **14**, greatly simplified the approach to the determination of the absolute configuration of **9**. The degradation used was as follows (Scheme 4):

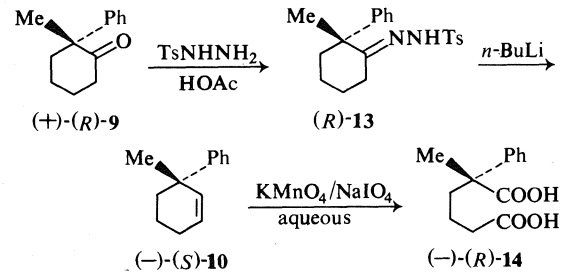

SCHEME 4

The ketone, (+)-**9**, was converted to its tosylhydrazone, **13**, in absolute ethanol in the presence of a few drops of glacial acetic acid and this in turn was converted directly to the alkene (−)-**10** by treatment with 2 mole-equivalents of *n*-butyllithium in ether (12). The alkene was then oxidized with sodium periodate in the presence of a catalytic amount of potassium permanganate (13) to the diacid (−)-**14**. The spectral characteristics and mixed melting point with authentic material prepared by an alternate route (14) confirmed the identity of this compound.

Since (+)-**9** gave rise to (−)-**14** via a series of reactions not involving the asymmetric center, it is possible to assign the absolute configuration of (+)-**9** as *R*, as shown.

Furthermore, since (+)-(*R*)-**9** has a positive Cotton effect, it is reasonable to assign the same absolute configuration to the cyclic acylsilane (+)-(*R*)-**1** as shown since it also exhibits a positive Cotton effect having a similar character.

This work represents the first assignment of absolute configuration to a cyclic organosilicon compound, asymmetric at silicon. Furthermore, it prepares the way for the assignment of absolute configurations to a number of other compounds. For example, treatment of (+)-(*R*)-**1** with diazomethane (15) (Scheme 5), gives rise to (−)-(*S*)-1-phenyl-1-methyl-1-silacycloheptanone-3 (**15**) as the major product whose configuration must be as shown since this reaction has been demonstrated to proceed with retention of configuration at silicon (16). Minor amounts of material presumed to be **16** on the basis of nuclear magnetic resonance (n.m.r.) data were detected.

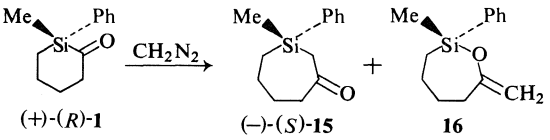

SCHEME 5

Hopefully, it will be possible to relate the stereochemistry of this system to other systems such as Corriu's naphthylsilatetralene compounds (3) whose absolute configurations have not yet been established.

Experimental

General

Nuclear magnetic resonance spectra were run on either a Varian A-60 or A-56/60 instrument using carbon tetrachloride or deuterochloroform as specified. Infrared (i.r.) spectra were obtained on a Perkin–Elmer model 237-B grating i.r. spectrophotometer in carbon tetrachloride or as a liquid film as specified. Ultraviolet (u.v.) spectra were obtained on a Perkin–Elmer model 350 spectrophotometer in the solvent specified.

Optical rotations were obtained on a Galileo manual polarimeter at the Sodium D line using a 1 dm cell. Optical rotatory dispersion spectra were obtained on a Jasco Model ORD/UV-5 spectrophotometer.

Boiling points and melting points are uncorrected.

Preparation of 1-Phenyl-1-methyl-1-silacyclohexene-2 (7)

To 34.0 g (0.204 mole) of 1,1-dichloro-1-silacyclohexene-2 (17) in 125 ml anhydrous ether were added 145 ml (0.213 mole) of phenyllithium solution, over a period of 30 min. The mixture was left at ambient temperature for 22 h and then the clear solution was decanted off leaving a precipitate of lithium chloride. The ether was removed on a rotary evaporator and the residue was distilled under vacuum. Three fractions were isolated. The first consisted of 6.7 g (20%) of unreacted 1,1-dichloro-1-silacyclohexene-2, the third of 4.5 g (9%) of 1,1-diphenyl-1-silacyclohexene-2.

The central fraction consisted of 24.1 g (57%) of 1-chloro-1-phenyl-1-silacyclohexene-2, b.p. 120–125° (4.5 mm). This was not characterized but methylated directly with methylmagnesium bromide.

Can. J. Chem. Downloaded from www.nrcresearchpress.com by 210.87.254.40 on 09/05/12
For personal use only.

Can. J. Chem. Downloaded from www.nrcresearchpress.com by 210.87.254.40 on 09/05/12
For personal use only.

To a solution of 19.4 g (0.093 mole) of 1-chloro-1-phenyl-1-silacyclohexene-2 in 100 ml anhydrous tetrahydrofuran (THF) was added 0.21 mole of methylmagnesium bromide solution (1.5 *M* in ether). Most of the diethyl ether was distilled off and the residual THF solution was refluxed overnight. The mixture was acidified with 10% HCl solution and extracted 3 times with diethyl ether. The combined ether extracts were washed with dilute sodium bicarbonate solution and were dried over anhydrous magnesium sulfate. Removal of the ether on a rotary evaporator followed by distillation of the high boiling residue gave 16.1 g (93%) of the desired alkene, b.p. 80–84° (0.8 mm); i.r. (film) λ_{max} 6.29 (C=C), 7.0, 9.0 (SiPh), 8.0 (SiMe) μ; n.m.r. (CCl_4) δ 7.2–7.6 (Ar, complex, 5), 6.9 (olefinic, doublet (J = 14 c.p.s.) of triplets (J = 4 c.p.s.), 1), 5.8 (olefinic, d, J = 14 c.p.s., 1), 1.7–2.4 (aliph, m, 4) 0.7–1.1 (aliph, m, 2), 0.35 (SiMe, s, 3) p.p.m.

Anal. Calcd. for $C_{12}H_{16}Si$: C, 76.52; H, 8.57. Found: C, 76.35; H, 8.38.

Preparation of 1-Phenyl-1-methyl-1-silacyclohexanol-2 (8)

To a solution of 16.5 g (0.088 mole) of 1-phenyl-1-methyl-1-silacyclohexene-2 in 40 ml of anhydrous THF cooled with an ice bath were added 100 ml of diborane solution (1.0 *M* in THF) over 30 min. After the addition was complete, the mixture was left at 0° for an additional 4 h and then the solvents were removed on a rotary evaporator. The residual oil was *carefully* acidified with 5% HCl solution and was extracted 3 times with ether. Removal of the ether from the combined extracts on a rotary evaporator left a viscous oil which was dissolved in 175 ml of THF. This solution was cooled on an ice bath and a solution of 2.5 g of sodium hydroxide (0.063 mole) in 45 ml water was added, followed by 35 ml of 30% hydrogen peroxide solution. The mixture was left at room temperature for 18 h and then was acidified with 10% HCl solution. The organic products were isolated by 3 ether extractions. After drying the combined extracts over anhydrous magnesium sulfate, the ether was removed on a rotary evaporator and the residue was distilled. The desired carbinol, 15.0 g (84%) was isolated as a constant boiling fraction, b.p. 117° (0.4 mm); i.r. (film) λ_{max} 2.8–3.1 (OH), 7.0, 9.0 (SiPh), 8.0 (SiMe) μ; n.m.r. (CCl_4) δ 7.2–7.6 (Ar, m, 5), 3.35–3.7 (C*H*OH, m, 1), 0.5–2.0 (aliph, m, 8), 0.25 (SiMe, s, 3) p.p.m.

Anal. Calcd. for $C_{12}H_{18}SiO$: C, 69.84; H, 8.79. Found: C, 69.49; H, 8.88.

An n.m.r. spectrum in DMSO showed a doublet at δ 4.2 p.p.m. J_{AB} = 4.5 c.p.s., which disappeared on the addition of D_2O. This is consistent with the secondary carbinol function.

The g.l.p.c. analysis of this carbinol using a 10 ft, 10% neopentylglycol sebacate column at 225 °C indicated a 95:5 ratio of the two possible diastereomeric carbinols.

Resolution of 1-Phenyl-1-methyl-1-silacyclohexanone-2 (1)

(a) Preparation of the Phthalic Acid-ester of 1-Phenyl-1-methyl-1-silacyclohexanol-2

A solution containing 68 g (0.33 mole) of 1-phenyl-1-methyl-1-silacyclohexanol-2, 49 g (0.33 mole) of phthalic anhydride, and 50 ml of pyridine in 300 ml of dry benzene was refluxed for 3 h. The solvent was then removed on a rotary evaporator and the residue was extracted with dilute sodium bicarbonate solution. The aqueous phase was washed with ether to remove any non-acidic organic residues. Acidification of the aqueous phase with 10% HCl precipitated the acid-ester as an oil which was extracted with chloroform. The chloroform solution was then dried over anhydrous sodium sulfate and the solvent was removed on a rotary evaporator. The residual oil was taken up in approximately 300 ml of carbon tetrachloride and 700 ml of petroleum ether (b.p. 60–70°) were added. On cooling to 5° the acid-ester crystallized in hemispherical clusters, over a period of 4 days.

The crude crystals were filtered and recrystallized 3 times from the same mixed solvent system (2:3, CCl_4: petroleum ether (60–70 °C)) to yield 68 g (57%) of pure acid-ester, m.p. 116–118 °C.

Anal. Calcd. for $C_{20}H_{22}O_4Si$: C, 67.76; H, 6.26. Found: C, 67.55; H, 6.15.

(b) Resolution of the Phthalic Acid-Ester of 1-Phenyl-1-methyl-1-silacyclohexanol-2

To 15 g (0.042 mole) of the acid-ester in 400 ml of acetone at reflux, were added 14 g (0.042 mole) of strychnine partially dissolved in 50 ml chloroform. This mixture was left at reflux for 10 min and then cooled to 5 °C. The less soluble diastereomer crystallized from the solution overnight, yielding 10.9 g (38%) of colorless crystals, m.p. 225–230 °C (decomposition).

The strychnine salt was recrystallized to constant melting point and optical rotation using the following procedure. The salt was dissolved in excess chloroform (50 ml $CHCl_3$ for every 10 g of salt) and the solution was then concentrated to approximately half its volume on a rotary evaporator. To this solution at reflux was added hot acetone (150 ml acetone per 10 g of salt). Crystallization commenced almost immediately and after approximately 1 h the solution was filtered and the crystals were washed with acetone. Table 1 summarizes the relevant recrystallization data.

TABLE 1

Resolution of silacyclohexanol acid phthalate

Recrystallization no.	Yield (g)	$[\alpha]_D^{23}$(°)	Melting point (°C)
1	8.3	−61	225–230
2	5.5	−58	228–230
3	4.8	−59	230–231
4	4.2	−59	229–230

(c) Reisolation of the Acid-Ester

To a suspension of 4.0 g (0.0057 mole) of the strychnine salt of the acid-ester ($[\alpha]_D^{25}$ −59°) in 50 ml of ether were added 50 ml of 10% HCl and the mixture was stirred vigorously for 15 min. To this were added 100 ml water and the suspension was filtered to remove the precipitated strychnine hydrochloride. This precipitate was then washed well with ether and the ether phase was isolated and was extracted with dilute sodium bicarbonate solution. Acidification of the bicarbonate phase with 10% HCl precipitated the acid-ester as an oil which was

Can. J. Chem. Downloaded from www.nrcresearchpress.com by 210.87.254.40 on 09/05/12
For personal use only.

isolated by ether extraction in the normal fashion. The residue, on removing the ether on a rotary evaporator, was crystallized from 20 ml of *n*-hexane and sufficient carbon tetrachloride such that the acid-ester did not oil out on cooling to −20 °C. After a few weeks at this temperature the acid-ester had precipitated to yield 1.5 g (75%) of the crystalline acid-ester, $[\alpha]_D^{24}$ + 150° ($CHCl_3$), m.p. 84–86 °C. A second recrystallization did not alter the optical rotation although the melting point range was changed to 85–86 °C. An i.r. spectrum of this material in carbon tetrachloride was identical to that of the racemic acid-ester.

(d) Hydrolysis of the Acid-ester

To 17 g (0.048 mole) of the resolved acid-ester (from the strychnine salt having $[\alpha]_D^{24}$ −59°, m.p. 230–231 °C) in 30 ml THF were added 100 ml of 1.5 *N* sodium hydroxide solution. The mixture was then heated on a steam bath for 15 min and then was extracted with ether. The aqueous phase was again heated on a steam bath for an additional 15 min and then was extracted with ether. This cycle was repeated 2 more times. In the last cycle the aqueous phase was heated for 1 h on the steam bath. The carbinol was isolated from the ether extracts in the normal manner. Distillation of the residue gave 7.4 g (75%) of the desired optically active carbinol, b.p. 85–95 °C (0.2 mm). This material solidified on standing to a waxy solid m.p. 32.5–33°, $[\alpha]_D^{22}$ −73.5°. The n.m.r. and i.r. spectra of this material were identical to those of an authentic sample of racemic carbinol.

*(e) The Oxidation of 1-Phenyl-1-methyl-1-silacyclohexanol-2 (**8**)*

To a solution of 7.43 g (0.0361 mole) of the resolved 1-phenyl-1-methyl-1-silacyclohexanol-2 and 12.4 g (0.062 mole) of dicyclohexylcarbodiimide in a solvent mixture of 30 ml anhydrous ether and 100 ml dry DMSO (distilled from calcium hydride) were added slowly 7.0 g (0.036 mole) of pyridinium trifluoroacetate in 50 ml dry DMSO. This mixture was left overnight, under nitrogen, at room temperature. It was then filtered to remove the precipitated dicyclohexylurea and the precipitate was washed well with ether. The filtrate was extracted with 100 ml of water and the aqueous phase in turn was re-extracted with ether. The combined ether phases were then washed well with water to remove any DMSO and then were dried over anhydrous magnesium sulfate. Removal of the ether on a rotary evaporator left a residue which was distilled on a spinning band column to yield 4.20 g (57%) of the desired ketone, b.p. 85° (0.02 mm) n_D^{21} 1.5448, $[\alpha]_D^{24}$ −160° (*c*, 2.15, cyclohexane); i.r. (film) λ_{max} 6.08 (C=O) μ; n.m.r. (CCl_4) δ 7.4 (Ar, m, 5) 2.4 ($COCH_2$, t, (J = 6 c.p.s.), 2), 1.0–2.0 (aliph, m, 6), 0.4 (SiMe, s, 3) p.p.m.; u.v. λ_{max} (ε) (cyclohexane) 336 (157), 361 (217), 390 (204) mμ.

Anal. Calcd. for $C_{12}H_{16}OSi$: C, 70.53; H, 7.89. Found: C, 70.54; H, 7.84.

*1-Phenyl-1-methylcyclohexanone-2 (**9**)*

The ketone, **9**, was prepared according to the literature procedure (9). However, g.l.p.c. analysis of the product indicated presence of a small amount of material tentatively identified as 1-methyl-3-phenylcyclohexanone-2. This could be removed by chromatography on neutral alumina with carbon tetrachloride, or by preparative g.l.p.c. on 20% SE-30 on Chromosorb W. Boiling point 98° (1.5 mm) n_D^{25} = 1.5327; i.r. (carbon tetrachloride) λ_{max} 5.84 (C=O) μ; n.m.r. (CCl_4) δ 7.0–7.5 (Ar, m, 5), 2.7, 2.25, 1.8 (aliph, 3m, 8), 1.2 (CMe, s, 3).

*Selective Asymmetric Reduction of 1-Phenyl-1-methylcyclohexanone-2 (**9**)*

To a solution of 7.9 g (0.0584 mole) of α-pinene, $[\alpha]_D^{25}$ +40.8° (neat), in 75 ml of dry diglyme were added 21.9 ml of a 1.0 *M* solution of sodium borohydride in diglyme (0.0219 mole). While cooling in an ice bath, 4.15 g (0.0292 mole) of boron trifluoride etherate were added dropwise with stirring. Following the above addition, the mixture was stirred overnight at 0 °C. A thick white precipitate formed in the mixture to which 10.0 g (0.053 mole) of (rac)-1-phenyl-1-methylcyclohexanone-2 (**9**) were added all at once in 20 ml of dry diglyme. The reaction mixture was stirred at 0 °C until all of the precipitate had disappeared (approximately 20 h). Stirring at room temperature was continued overnight and the reaction was worked-up by pouring the clear solution into 30 ml of 30% NaOH. Exactly 30 ml of 30% H_2O_2 solution were added dropwise over 15 min and the mixture was stirred for 1 h. The reaction mixture was extracted with diethyl ether, washed with water, and the ether layer dried over anhydrous magnesium sulfate.

The solvent was removed and the mixture was distilled under vacuum. Following removal of residual diglyme and isopinocamphenol, the product was distilled over a range of 94–115 °C (0.9 mm). Three fractions were collected, the first 2 of which consisted of approximately equal amounts of ketone and carbinol. The third consisted of a small amount of almost pure carbinol. The ketone was separated from the carbinol by column chromatography on neutral alumina (Woelm) using 2:1 benzene–chloroform. Analysis by g.l.p.c. (3/8 in. × 20 ft, 20% SE-30 on Chromosorb W) showed the presence of pure ketone whose spectral data were identical to those of the racemic material. The ketone was isolated in 50% yield after distillation, b.p. 98° (1.5 mm), $[\alpha]_D^{25}$ +35.4° (*c*, 9.32 cyclohexane). An o.r.d. spectrum showed a positive Cotton effect with the first maximum at 321 mμ in cyclohexane.[5] Further elution of the alumina column with chloroform yielded the carbinol (+)-**12**, b.p. 116–118° (1.0 mm), n_D^{20} = 1.5467; $[\alpha]_D^{25}$ +4.45° (*c*, 9.41, cyclohexane).

Anal. Calcd. for $C_{13}H_{18}O$: C, 82.06; H, 9.59. Found: C, 82.07; H, 9.41.

*Conversion of (+)-(R)-**9** to (−)-(S)-1-Phenyl-1-methylcyclohexene-2 ((−)-(S)-**10**)*

Treatment of 1.48 g (0.0078 mole) of the ketone (+)-(*R*)-1-phenyl-1-methylcyclohexanone-2 with 1.5 g (0.0080 mole) of tosylhydrazine in absolute ethanol in the presence of a few drops of glacial acetic acid yielded after work-up a white crystalline tosylhydrazone, **13**, that was not purified further. The tosylhydrazone was treated with slightly more than 2 mole-equivalents of *n*-butyllithium in ether at room temperature. The mixture was extracted with ether and water, the ether layer was dried over anhydrous magnesium sulfate, and the solvent was removed by rotary evaporator. The yellow oil was introduced onto a basic alumina column and eluted with pentane. Removal of the pentane and distillation of the

oil yielded 0.6 g (45%) of (−)-(*S*)-3-phenyl-3-methylcyclohexene **10**, b.p. 71° (2.5 mm), n_D^{25} 1.5349; $[\alpha]_D^{25}$ −16.6°; (*c*, 9.37, cyclohexane); n.m.r. (CCl_4) δ 1.35 (CMe, s, 3) 5.5–6.0 (vinyl, m, 2), 7.0–7.3 (Ar, m, 5), 1.3–2.2 (aliph, m, 6) p.p.m., i.r. (carbon tetrachloride) λ_{max} 6.05 (weak) (C=C) μ.

Anal. Calcd. for $C_{13}H_{10}$: C, 90.60; H, 9.40. Found: C, 90.61; H, 9.42.

*Oxidation of alkene (−)-(S)-**10** to (−)-(R)-2-Phenyl-2-methylhexandioic Acid ((−)-(R)-**14**)*

To 50 ml of an aqueous solution containing 4.0 g (0.019 mole) of sodium periodate, 0.25 g potassium permanganate, and 5.0 g potassium carbonate were added, 0.5 g (0.0029 mole) of (−)-(*R*)-**10**. The mixture was stirred vigorously for 48 h at room temperature. The mixture was extracted with diethyl ether to remove any unreacted alkene and then the aqueous layer was acidified. The aqueous layer was extracted a second time with diethylether and the ether layer was dried over anhydrous magnesium sulfate. The solvents were removed and the gummy material after pumping under vacuum at 100 °C for 15 h had $[\alpha]_D^{25}$ −7.90° (*c*, 6.98, ethanol). A small amount of racemic material crystallized from benzene–petroleum ether (b.p. 60–70°) m.p. 75–78°. When this was heated under vacuum to 80° the melt resolidified m.p. 113–114°, mixed m.p. 113–115° with authentic material (14). Crystals were obtained from the residue dissolved in carbon tetrachloride, m.p. 111–119 °C; $[\alpha]_D^{25}$ −10.3° (*c*, 4.53, ethanol); lit. (11) m.p. 126.3–127.5°, $[\alpha]_{546}^{25}$ −25.65° for optically pure material. The i.r. and n.m.r. spectra confirmed identity of this compound.

*Preparation of (−)-(S)-1-Phenyl-1-methyl-1-silacycloheptanone-3 ((−)-(S)-**15**)*

The acylsilane (+)-(*R*)-1-phenyl-1-methyl-1-silacyclohexanone-2, $[\alpha]_D^{25}$ +73.5°, (containing 73% of one enantiomer) was treated with diazomethane according to the published method (15).

Examination of the n.m.r. spectrum of the crude reaction product revealed 2 singlets δ 3.81 and 4.05 p.p.m. These were assigned to the cyclic siloxyalkene **16**, whose yield, while not isolated, was estimated at 5–10% by integration. Distillation of the oil yielded 76% of (−)-(*S*)-1-phenyl-1-methyl-1-silacycloheptanone-3, $[\alpha]_D^{25}$ −47.2° (*c*, 3.18, cyclohexane), b.p. 105–106° (0.1 mm); n.m.r. (neat with external TMS standard) δ −0.05 (SiMe, s, 3), 2.02, 2.37 ($SiCH_2CO$, 2d, J = 10 c.p.s., 2), 1.98, 1.30, 0.55 (aliph, 3m, 8), 7.0 (Ar, m, 5) p.p.m.; i.r. (film) λ_{max} 5.93 (C=O) μ; u.v. λ_{max} (ε) (cyclohexane), 248 (358), 253 (418), 259 (470), 263 (425), 266 (480), 271 (342), 296 (100), 305 (65) mμ; o.r.d. (cyclohexane) negative Cotton effect, first maximum 308 mμ.

Anal. Calcd. for $C_{13}H_{18}SiO$: C, 71.50; H, 8.31. Found: C, 71.25; H, 8.17.

1. A. G. Brook. Adv. Organometal. Chem. **7**, 95 (1968).
2. J. F. Klebe and H. Finkbeiner. J. Amer. Chem. Soc. **88**, 4740 (1966).
3. R. J. P. Corriu and J. P. Masse. Chem. Commun. 1287 (1967).
4. A. G. Brook and J. B. Pierce. J. Org. Chem. **30**, 2566 (1965).
5. H. C. Brown and D. B. Bigley. J. Amer. Chem. Soc. **83**, 3166 (1961).
6. L. H. Sommer. Stereochemistry, mechanism, and silicon. McGraw-Hill Inc., New York, 1965. p. 114.
7. R. J. P. Corriu and J. P. Masse. Tetrahedron Lett. 5797 (1968).
8. A. G. Brook. J. Amer. Chem. Soc. **85**, 3051 (1963).
9. M. S. Newman and M. D. Farbman. J. Amer. Chem. Soc. **66**, 1550 (1944).
10. H. C. Brown. Hydroboration. W. A. Benjamin Inc., New York, 1962. p. 205.
11. T. D. Hoffman and D. J. Cram. J. Amer. Chem. Soc. **91**, 1000 (1969).
12. R. H. Shapiro and M. J. Heath. J. Amer. Chem. Soc. **89**, 5735 (1967).
13. J. Meinwald and P. G. Gassman. J. Amer. Chem. Soc. **82**, 2857 (1960).
14. M. S. Newman and R. D. Closson. J. Amer. Chem. Soc. **66**, 1553 (1944).
15. A. G. Brook, W. W. Limburg, D. M. MacRae, and S. A. Fieldhouse. J. Amer. Chem. Soc. **89**, 704 (1967).
16. A. G. Brook, W. W. Limburg, and D. M. MacRae. J. Amer. Chem. Soc. **89**, 5493 (1967).
17. R. Benkeser and R. F. Cunico. J. Organometal. Chem. **4**, 284 (1965).

Can. J. Chem. Downloaded from www.nrcresearchpress.com by 210.87.254.40 on 09/05/12
For personal use only.

Can. J. Chem. Downloaded from www.nrcresearchpress.com by 210.87.254.105 on 09/05/12
For personal use only.

Internal rotation in the methyl esters of dimethylcarbamic acid and thio derivatives

ALBERTA E. LEMIRE AND JAMES C. THOMPSON
Lash Miller Chemical Laboratories, University of Toronto, Toronto, Ontario

Received August 22, 1969

The kinetic parameters for hindered rotation about the C—N bond have been determined by total nuclear magnetic resonance line shape analysis for the methyl esters of *N,N*-dimethyldithiocarbamic acid, and *N,N*-dimethylmonothiocarbamic acid. A qualitative picture of the effect of substituents on the potential barrier in carbamate and thiocarbamate esters is presented.

Canadian Journal of Chemistry, **48**, 824 (1970)

High resolution nuclear magnetic resonance (n.m.r.) studies have led to the discovery of hindered rotation about the C—N bond in various molecules (1, 2). Pauling (3) postulated that delocalization of the lone pair of electrons on nitrogen leads to a polar carbon–nitrogen double bond (*b*).

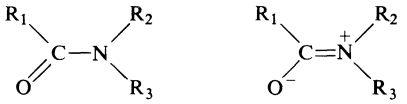

a *b*

In the past, various attempts have been made to determine the kinetic parameters for hindered rotation by n.m.r. There has, however, been considerable controversy about the results obtained.

Arrhenius activation parameters obtained from one parameter approximations (i.e. peak separation, etc.) of the exchange equations derived from the Bloch equations have proved to be unreliable. An excellent review on the errors involved in these approximations has recently been published by Allerhand *et al.* (4).

It is now believed that the only reliable methods to determine exchange rates are by using total n.m.r. line shape fitting methods or the spin echo technique. The spin echo method has, however, been reported to yield activation energies which are approximately 10–15% too low (5).

Unfortunately, only a few molecules have been studied by these latter methods. Neuman *et al.* have studied *N,N*-dimethylcarbamoyl chloride, *N,N*-dimethylthiocarbamoyl chloride, and *N,N*-dimethylacetamide-d_3 by total line shape analysis (2, 6). Inglefield *et al.* have studied *N,N*-dimethylcarbamoyl chloride by the spin echo method and *N,N*-dimethylformamide by spin echo and total line shape analysis (5). Rabinovitz and Pines have studied *N,N*-dimethylformamide by total line shape analysis (7). It should be noted that the values obtained by the latter two sets of workers for *N,N*-dimethylformamide are in excellent agreement [i.e. $E_a = 20.8 \pm 0.6$ kcal/mole (5) and $E_a = 20.5 \pm 0.2$ kcal/mole (7)]. This is in sharp contrast to the situation existing in the earlier literature where values for the activation energy ranged from 7–24 kcal/mole (5).

Since total line shape analysis appears to be the only method to yield results which are reliable enough to allow one to make meaningful comparisons between molecules, it seems advisable to extend the range of compounds studied by this method. A consideration of some interest is the effect of varying the substituents X and Y in compounds of the form $Me_2NC(Y)X$ upon the potential barrier to rotation. For means of comparison with some continuing work[1] on some trimethylsilyl carbamates, we decided first to study the related methyl esters of carbamic and thiocarbamic acids.

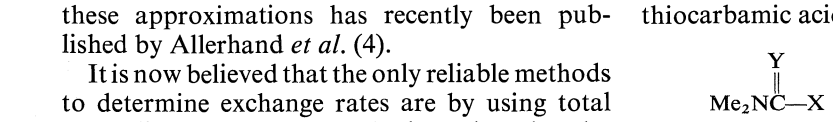

Of these compounds, only the methyl ester of *N,N*-dimethyldithiocarbamic acid has been studied by total line shape analysis (8).

Some qualitative information is, however, available on the other methyl esters of the series. Drago has reported that the $-NMe_2$ peak is a single resonance for $MeOC(O)NMe_2$ and $MeSC(O)NMe_2$ at -46 °C for 25% solutions in methylene chloride and toluene (9). However, Lustig *et al.* have reported hindered rotation

[1]Lemire and Thompson. To be published.

about the C—N bond in $Me_2NC(O)OMe$ in $CHCl_3$ solutions below −25 °C (10).

The compound $MeOC(S)NMe_2$ has not been studied by total line shape methods prior to this study. It has been studied using the intensity ratio method by Sandström (11).[2] We observed a splitting of the —NMe_2 peak at room temperature and above, both in the neat liquid and in a variety of solvents.

Experimental

(A) Variable Temperature Spectra

The n.m.r. spectra were obtained from a Varian A56-60D n.m.r. spectrometer. At each temperature, curvature, homogeneity and resolution adjustments were made in an attempt to obtain an optimum constant homogeneity. Several spectra were run in each direction at each temperature. Temperature was measured using the methanol and ethylene glycol standards supplied by Varian; temperature readings were made before and after each spectrum was recorded.

The charts supplied by Varian have been shown to be somewhat unreliable. Hence the temperatures were calculated by means of the equations reported by Van Geet (12).[2] Temperatures are believed to be accurate to ± 0.60 °C. The 500 c.p.s. sweep width was calibrated using the separation between the TMS and chloroform signals. Because of the slight temperature dependence of this separation, slightly different values were used for the high temperature and low temperature regions. The 50 c.p.s. sweep width was calibrated using the separation between the —SMe and —NMe_2 peaks of $MeSC(O)NMe_2$. The separation was measured by the side band technique. To take into account the temperature dependence of this separation, several measurements of the separation were made at each temperature studied and a least squares plot of separation vs. temperature was constructed. To avoid distortion due to saturation, spectra were run at a low field strength. Values for T_2 for each spectrum were obtained from an internal cyclohexane standard or from the —XMe peak.

The solutions were prepared using large volumes from which small samples were drawn out and sealed *in vacuo* in thick walled n.m.r. tubes. Samples were degassed by the freeze–thaw method.

The choice of solvent is important in these studies. Whittaker and Siegal have described the rather extensive effects of solvent on the internal rotation about the C– N bond in amides (13, 14). Neuman and Jonas (6) and Rabinovitz and Pines (7) have reported dimerization of amides in CCl_4 solutions.

In this study, saturated hydrocarbon solvents were used to minimize solvent–solute interactions (15). It has however, been pointed out that minimizing solvent–solute interactions may tend to favor solute–solute interactions.[3] Dilute solutions were used in hope of minimizing solute–solute interactions.

(B) Calculations of Theoretical Spectra and Activation Parameters

A Fortran IV program was written to compute the theoretical proton absorption line shape for an uncoupled 2-site exchange using the method of Gutowsky and Holm (1). The input consists of experimental intensities at about 25–50 frequency points as well as initial guesses for τ and the non-exchanging chemical shift $\delta\omega\infty$. The theoretical plots were normalized to the experimental spectra. T_2 was obtained separately for each spectrum as described previously. The non-exchanging chemical shift, $\delta\omega\infty$, was varied to give the best spectral fit.

The final value of τ was that which gave the best fit (in a least squares sense) between theoretical and experimental intensities; the calculated and experimental intensities may be compared either visually or analytically.

If protons are exchanging between sites A and B, then the average lifetime of protons at each site is

$$\tau_A = 1/k_A = \tau/p_B$$
$$\tau_B = 1/k_B = \tau/p_A$$
$$\tau = \tau_A\tau_B/(\tau_A + \tau_B)$$

For an equally populated 2-site system $\tau_A = \tau_B = 2\tau$. Thus the lifetime is 2τ and the rate constant is $1/2\tau$. From the Arrhenius equation, one may derive the activation energy and log A from a plot of log $(1/2\tau)$ vs. $1/T$ (16).

$$[1] \qquad \log(1/2\tau) = \log A - E_a/2.30RT$$

The limits of 95% confidence in E_a and log A may be found by means of the formula given in (17). However, the values obtained using this statistical procedure seemed rather unrealistically low (i.e. less than 0.2% deviation for E_a for neat $Me_2NC(S)OMe$). Several authors have pointed out that statistical deviations do not reflect the true error situation and that systematic errors may be very serious for the line shape method (4, 18). Hence the error limits shown for the activation parameters were estimated from the error of all the values involved in the calculations.

(C) Materials

$Me_2NC(S)OMe$

This compound was prepared by the method of Nambury (19) from a 30% aqueous solution of dimethylamine and MeOC(S)SK. A 69% yield of a colorless liquid boiling at 188–190 °C was obtained (lit. b.p. 190–191 °C). We found that on distillation at this temperature, the compound partially rearranged to the *S*-methyl ester. Hence the compound was purified by repeated distillations at reduced pressure.

$Me_2NC(S)SMe$

This compound was prepared by the method of Holloway and Gitlitz (8) from the sodium salt of *N,N*-dimethyldithiocarbamic acid and methyl iodide. The compound was purified by recrystallization from pentane. A 76% yield of white crystals melting at 45–46 °C (lit. 45–47 °C) was obtained.

$Me_2NC(O)OMe$

This compound was prepared by the method of Middaugh *et al.* (9) from dimethylamine and methyl chloroformate. Identified on basis of n.m.r. (Table 1).

[2]We are grateful to the referees for pointing out to us the results in references 11, 12.

[3]Dr. W. F. Reynolds. Private communication.

Can. J. Chem. Downloaded from www.nrcresearchpress.com by 210.87.254.105 on 09/05/12
For personal use only.

$Me_2NC(O)SMe$

This compound was prepared from $Me_2NC(O)SH \cdot HNMe_2$ and methyl iodide by procedure *C* of Tilles (20) using hexane as a solvent. Identified on the basis of n.m.r.

TABLE 1

Proton magnetic resonance spectra

Compound	Chemical shift* δ in p.p.m.	Reference
[a]$MeSC(O)NMe_2$[b]	a 2.26 (lit. 2.28) b 2.97 (lit. 3.00)	9
[a]$MeOC(O)NMe_2$[b]	a 3.60 (lit. 3.60) b 2.87 (lit. 2.87)	9
[a]$MeOC(S)NMe_2$[b]	a 3.94 b 3.34 3.11	This work
[a]$MeSC(S)NMe_2$[b]	a 2.58 b 3.44	This work

*All compounds were run as 10% solution in CCl_4.

Results

(A) $Me_2NC(O)OMe$

Drago (9) has reported no splitting of the $-NMe_2$ peak at room temperature for the pure liquid and for 10% solutions in benzene, CCl_4, and CCl_4–benzene (50% by volume), and at −46 °C for 25% solutions in methylene chloride and toluene. Lustig *et al.*, on the other hand have found that there is a splitting of the peak into a doublet below −25 °C for solutions in $CHCl_3$ and that the maximum splitting observed is dependent upon concentration (10). We have found no splitting of the $-NMe_2$ signal at the ambient temperature of the probe for the neat liquid and for dilute solutions in *n*-hexane. We did, however, observe the splitting reported by Lustig *et al.* in chloroform solution at low temperatures.

The results in chloroform solutions may well be due to a hydrogen bonding interaction of the sort shown below:

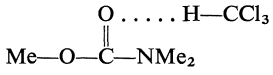

This would be expected to increase delocalization of the lone pair of electrons on nitrogen into the carbon–nitrogen bond, increasing its double bond character and hence increasing the barrier to rotation.

On the other hand, we found no splitting of the $-NMe_2$ peak in *n*-hexane as low as −58 °C although there appeared to be some broadening.

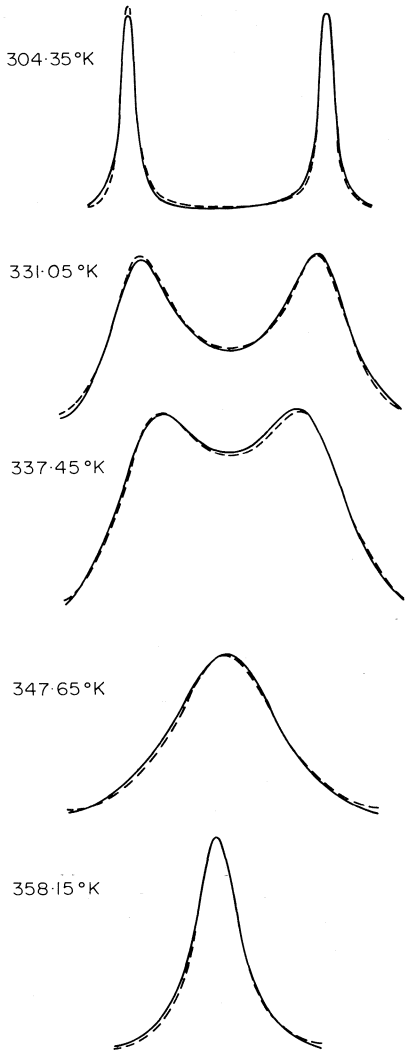

FIG. 1. Experimental (---) and theoretical (—) spectra for neat $Me_2NC(S)OMe$.

(B) $Me_2NC(O)SMe$

There is no splitting of the $-NMe_2$ signal at room temperature in the neat liquid nor in solutions in CCl_4 or benzene. Middaugh *et al.* (9) also report no splitting at −46 °C for 25% solutions in methylene chloride and toluene. We found no splitting at −20 °C for a dilute solution in $Me_2NC(S)OMe$.

No splitting was observed in the neat liquid at −10.5 °C. A splitting of 1.2 c.p.s. was observed in a dilute solution in chloroform at −32.4 °C. More detailed work is continuing on chloroform solutions.

Can. J. Chem. Downloaded from www.nrcresearchpress.com by 210.87.254.105 on 09/05/12
For personal use only.

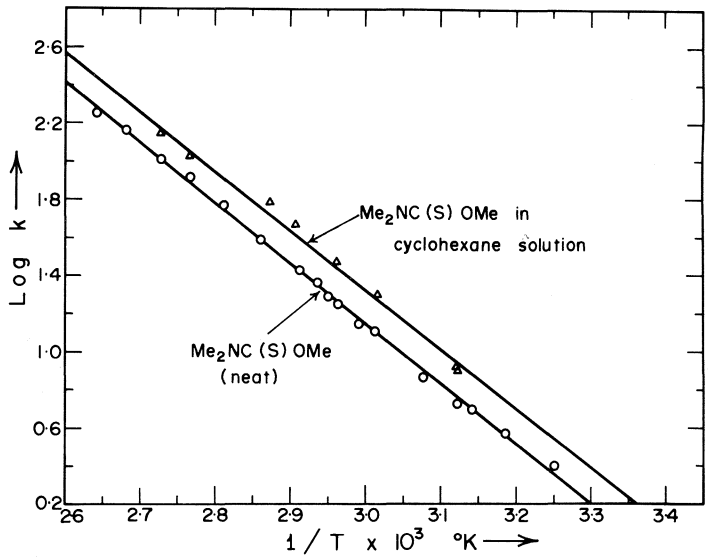

FIG. 2. Arrhenius plots for the process of internal rotation in $Me_2NC(S)OMe$ neat (O) and a 1.5 mole % solution in cyclohexane (Δ).

(C) $Me_2NC(S)OMe$

The *O*-methyl ester of *N*,*N*-dimethylmonothiocarbamic acid was studied both as a neat liquid and as a 1.5 mole % solution in cyclohexane. The $-NMe_2$ resonance of this compound is split into a doublet at room temperature.

Exchange rates were determined by comparing experimental and theoretical spectra as explained earlier. A comparison between theoretical and experimental spectra is shown in Fig. 1.

A least means square plot yielded the following activation parameters. For the neat liquid, $E_a = 14.5 \pm 0.4$ kcal/mole, $\log A = 10.7 \pm 0.3$, $\Delta H^{\ddagger}_{298.2} = 13.9$ kcal/mole, $\Delta G^{\ddagger}_{298.2} = 17.4$ kcal/mole, $\Delta S^{\ddagger} = -11.7$ e.u.

For the 1.5 mole % solution in cyclohexane, the activation parameters were $E_a = 14.2 \pm 0.5$ kcal/mole, $\log A = 10.6 \pm 0.3$, $\Delta H^{\ddagger}_{298.2} = 13.6$ kcal/mole, $\Delta G^{\ddagger}_{298.2} = 17.1$ kcal/mole, $\Delta S^{\ddagger} = -11.7$ e.u.

The Arrhenius plots are shown in Fig. 2.

The results obtained by Sandström (11) for the neat liquid were $E_a = 16.4 \pm 0.2$ kcal/mole, $\log A = 12.0 \pm 0.2$.

Such differences in results obtained by the intensity ratio method and the total line shape method are not unexpected as shown by a comparison between the activation energies obtained by Rogers and Woodbrey (21) by the intensity ratio for *N*,*N*-dimethylformamide and *N*,*N*-dimethylacetamide and those obtained later by total line shape methods (Table 2).

TABLE 2

Comparison of E_a values obtained by two methods

Compound	Method	
	Intensity ratio	Total line shape
DMF	18.3 kcal/mole	20.5 kcal/mole
DMA	10.6 kcal/mole	19.6 kcal/mole

(D) $Me_2NC(S)SMe$

The *S*-methyl ester of *N*,*N*-dimethyldithiocarbamic acid was studied in dilute solution in *n*-hexane. The following activation parameters were obtained $E_a = 13.0 \pm 0.6$ kcal/mole, $\log A = 11.6 \pm 0.5$, $\Delta H^{\ddagger}_{298.2} = +12.5$ kcal/mole, $\Delta G^{\ddagger}_{298.2} = 14.7$ kcal/mole, $\Delta S^{\ddagger} = -7.4$ e.u.

This compound has previously been studied by Holloway and Gitlitz (8) who reported the activation parameters $E_a = 10.3 \pm 0.3$ kcal/mole, $\log A = 9.62 \pm 0.18$, $\Delta G^{\ddagger}_{298.2} = 14.7$ kcal/mole.

They report a peak separation of 10 c.p.s. for the $-NMe_2$ doublet at the lowest temperature investigated, 248.0 °K. We found a peak separation of 10.4 c.p.s. at 261.4 °K. Below this temperature, crystals began to come out. It did not seem feasible to decrease the concentration further, as there was already considerable noise

Can. J. Chem. Downloaded from www.nrcresearchpress.com by 210.87.254.105 on 09/05/12
For personal use only.

TABLE 3
Activation parameters

Compound	Solvent	E_a in kcal/mole	log A	$\Delta G^{\ddagger}_{298.2}$ kcal/mole	$\Delta H^{\ddagger}_{298.2}$ kcal/mole	$\Delta S^{\ddagger}$ e.u.	References
$Me_2NC(S)OMe$	Neat	14.5 ± 0.4	10.7 ± 0.3	17.4	13.9	−11.7	This work
	1.5 mole % in cyclohexane	14.2 ± 0.5	10.6 ± 0.3	17.1	13.6	−11.7	"
$Me_2NC(S)SMe$	*n*-Hexane	13.0 ± 0.6	11.6 ± 0.5	14.7	12.5	−7.4	This work
	n-Hexane	10.3 ± 0.3	9.6 ± 0.18	14.7			8
$Me_2NC(O)CD_3$	Neat	19.6 ± 0.3	13.8 ± 0.2	18.2	19.0	+2.7	6
	9.5% in DMSO-d_6	20.6 ± 0.3	14.3 ± 0.3	18.6	20.0	+4.7	6
$Me_2NC(O)Cl$	Neat	16.9 ± 0.5	12.9 ± 0.4	16.8			2
	Neat	14.0 ± 0.7				−10	5
	10.4 mole % in CCl_4	17.7 ± 0.9	13.8 ± 0.7	16.3			2
$Me_2NC(S)Cl$	CCl_4	19.5	13.2	19			2
$Me_2NC(O)H$	Neat	20.5 ± 0.2			20.2 ± 0.2	−1.7	7
	Neat	20.8 ± 0.6				0 ± 1	5

and smooth lines had to be drawn through the n.m.r. curves adding an additional source of error.

The coalescence temperature of this compound appears to be quite sensitive to solvent. J. M. Potter has found that while the coalescence temperature is 2–3 °C in CS_2 and CCl_4, it is greater than 19.5 °C in $CHCl_3$ and above room temperature in acetonitrile.[4]

Discussion

The activation parameters obtained by the total line shape method in this study and for some related amide compounds are summarized in Table 3.

The qualitative results observed in this set of compounds, at first, seem rather inexplicable. Why, for instance, should $Me_2NC(S)OMe$ exhibit hindered rotation about the C—N bond while $Me_2NC(O)SMe$ does not? The differences can, however, be partially rationalized if one divides the compounds studied into two groups; one analogous to substituted thioamides

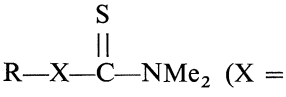

R—X—C—NMe_2 (X = S, O); and the other

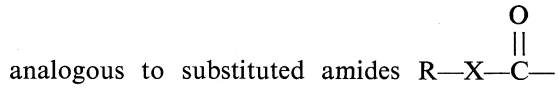

analogous to substituted amides R—X—C—NMe_2 (X = S, O).

Middaugh *et al.* (9) and Rogers and Woodbrey (21) have explained the results for the amide-like compounds by invoking a "cross conjugation" of the R—X— group with the amide system; this π-interaction could weaken the C—N π-bonding enough to make the barrier too small to be observed by n.m.r. methods. Thus for an —OR or —SR substituent the loss in C—N π-bonding energy in the transition state is partially compensated for by an increase in the C—X (X = O, S) π-bonding. Hence barriers to rotation would be lower than in amides where there is no possibility of π-bonding in the transition state.

Considering the results obtained in this study, we might also now extend this picture to the thioamide-like derivatives.

In general, it appears that activation energies are higher than those for amides. Since the polar form $X^-—C{=}N^+$ where X is oxygen or sulfur probably determines the value of E_a, the contribution of this form appears to be higher in thioamides than in amides in spite of the higher electronegativity of oxygen relative to sulfur. This conclusion has been supported by several workers (22–25). Mautner and Kumler (26) have postulated that this may be due to the ability of the

[4]E. A. V. Ebsworth and J. M. Potter. Private communication.

Can. J. Chem. Downloaded from www.nrcresearchpress.com by 210.87.254.105 on 09/05/12
For personal use only.

Can. J. Chem. Downloaded from www.nrcresearchpress.com by 210.87.254.105 on 09/05/12
For personal use only.

3d orbitals on sulfur to accept electrons and stabilize the polar form.

Hence one would expect the barriers to rotation in the compounds $Me_2NC(S)XMe$ (X = O, S) to be higher than those in $MeXC(O)NMe_2$ (X = O, S) as we have indeed, found. The fact that the barrier in $Me_2NC(S)SMe$ is lower than that in $Me_2NC(S)OMe$ might perhaps suggest that the —SMe group is better able to participate in π-bonding in the transition state than the —OMe group, thus stabilizing the transition state and leading to a lower barrier.

Moreover, the activation energies for the compounds $Me_2NC(S)OMe$ and $Me_2NC(S)SMe$ are lower than those obtained for *N,N*-dimethylformamide and *N,N*-dimethylacetamide by previous workers. This is what is predicted in the light of the π-bonding capabilities of the former compounds.

The values for the log *A* factor obtained in this study seem rather low compared to those obtained for amides. It has been suggested that entropies of activation for amides should be small for this type of internal rotation and that log *A* should be approximately equal to 13 (i.e. $\Delta S^{\ddagger} = 0$). As Neuman and Young point out, "this value of a frequency factor for a unimolecular process has enjoyed somewhat magical status which is undeserved for reactions in condensed phases due to probable differences in solvation of ground and transition states" (23). Since low frequency factors indicate a loss in entropy in proceeding to the transition state, it is difficult to rationalize them for internal rotation in amides where the ground state should be more polar than the transition state. It has hence been suggested that frequency factors higher than 10^{13} should not be unexpected. On the other hand, for esters such as those studied in this work, where there appears to be π-bonding in both ground and transition state, it is difficult to say exactly what the entropy of activation should be.

Moreover, the error range in $\Delta S^{\ddagger}$ is usually quite large, for the activation parameters E_a and $\Delta S^{\ddagger}$ are sensitive to any systematic errors.

Before any meaningful discussion is possible regarding activation parameters (on anything but qualitative terms), measurements should be made on many more related compounds using as many techniques (i.e. n.m.r., spin echo) as possible.

Allerhand *et al.* (4) have suggested that a more reliable parameter is the free energy of activation $\Delta G^{\ddagger}$. It appears to be less sensitive to systematic errors; for the values for this parameter have been relatively consistent for different groups of workers. The $\Delta G^{\ddagger}_{298.2}$ values obtained in this study are also listed in Table 3. Here again the values obtained are smaller than those for amides.

The authors thank the National Research Council of Canada and the Ontario Department of University Affairs for financial assistance and Dr. W. F. Reynolds for many helpful discussions. One of us (A.E.L.) gratefully acknowledges the financial support provided by a Province of Ontario Graduate Fellowship award.

1. H. S. Gutowsky and C. H. Holm. J. Chem. Phys. **25**, 1228 (1956).
2. R. C. Neuman, Jr., D. N. Roark, and V. Jonas. J. Amer. Chem. Soc. **89**, 3412 (1967).
3. L. Pauling. The nature of the chemical bond. 2nd edition. Cornell University Press, Ithaca, New York, 1948. p. 207.
4. A. Allerhand, H. S. Gutowsky, J. Jonas, and R. A. Meinzer. J. Amer. Chem. Soc. **44**, 3185 (1966).
5. P. R. Inglefield, E. Krakower, L. W. Reeves, and R. Stewart. Mol. Phys. **15**, 65 (1968).
6. R. C. Neuman, Jr. and V. Jonas. J. Amer. Chem. Soc. **90**, 1970 (1968).
7. M. Rabinovitz and A. Pines. J. Amer. Chem. Soc. **91**, 1585 (1969).
8. C. E. Holloway and M. H. Gitlitz. Can. J. Chem. **45**, 2659 (1967).
9. R. L. Middaugh, R. S. Drago, and R. J. Niedzielski. J. Amer. Chem. Soc. **86**, 388 (1964).
10. E. Lustig, W. R. Benson, and N. Duy. J. Org. Chem. **32**, 851 (1967).
11. J. Sandström. J. Phys. Chem. **71**, 2318 (1967).
12. A. L. Van Geet. Anal. Chem. **40**, 2227 (1968).
13. A. G. Whittaker and S. Siegal. J. Chem. Phys. **42**, 3320 (1965).
14. A. G. Whittaker and S. Siegal. J. Chem. Phys. **43**, 1575 (1965).
15. A. D. Buckingham, R. Scheafer, and W. G. Schneider. J. Chem. Phys. **32**, 1227 (1960).
16. K. J. Laidler. Reaction kinetics. Vol. 1. The Pergamon Press, Ltd., London, 1963. p. 85.
17. P. D. Lark, B. R. Craven, and R. C. Bosworth. The handling of chemical data. The Pergamon Press, London, 1968. p. 148.
18. A. Mannschreck, A. Mettheus, and G. Rissmann. J. Mol. Spectry. **23**, 15 (1967).
19. C. N. V. Nambury. J. Vikram Univ. 2, No. 1, 101 (1958).
20. H. Tilles. J. Amer. Chem. Soc. **81**, 714 (1959).
21. M. T. Rogers and J. C. Woodbrey. J. Phys. Chem. **66**, 540 (1962).
22. A. Loewenstein, A. Melera, P. Rigny, and W. Walter. J. Phys. Chem. **68**, 1597 (1964).
23. R. C. Neuman, Jr. and L. Brewster Young. J. Phys. Chem. **69**, 2570 (1965).
24. M. J. Janssen. Rec. Trav. Pays Bas, **82**, 1936 (1963).
25. C. M. Lee and W. D. Kumler. J. Org. Chem. **27**, 2052 (1962).
26. H. G. Mautner and W. D. Kumler. J. Amer. Chem. Soc. **78**, 98 (1956).

Can. J. Chem. Downloaded from www.nrcresearchpress.com by 210.87.254.40 on 09/05/12
For personal use only.

Synthesis of DL-chalcose from acrolein dimer

R. M. SRIVASTAVA[1] AND R. K. BROWN
Department of Chemistry, University of Alberta, Edmonton, Alberta

Received August 29, 1969

1,6:2,3-Dianhydro-4-deoxy-β-DL-*ribo*-hexopyranose (**1**), a product obtained from acrolein dimer (3,4-dihydro-2*H*-pyran-2-carboxaldehyde), has been converted to 1,6-anhydro-4-deoxy-3-*O*-methyl-β-DL-*xylo*-hexopyranose (**2**) by reaction with acidic methanol or sodium methoxide in methanol. The structure and conformation of **2** have been confirmed by nuclear magnetic resonance spectroscopy. The reaction of **2** with methanol in the presence of Amberlite IR-120 (H^+) gave a 2:1 mixture of the α and β isomers of methyl 4-deoxy-3-*O*-methyl-DL-*xylo*-hexopyranoside (**3**) from which the individual α and β isomers of the di-*p*-nitrobenzoates could be obtained as crystalline solids.

Conversion of **3** to the corresponding di-*O*-*p*-toluenesulfonates **4**, followed by selective reduction of these diesters with $LiAlH_4$ gave a mixture of the α and β isomers of methyl 4,6-dideoxy-3-*O*-methyl-2-*O*-*p*-toluenesulfonyl-DL-*xylo*-hexopyranoside (**5**). Reaction of **5** with sodium methoxide in methanol gave a 2:1 mixture of the α and β isomers of methyl 4,6-dideoxy-3-*O*-methyl-DL-*xylo*-hexopyranoside (**6**) (methyl DL-chalcoside) from which only the α isomer could be separated in pure form by column chromatography or gas–liquid chromatography. The α isomer, **6**-α, upon acid-catalyzed hydrolysis in aqueous dioxane, gave a mixture of the α and β isomers of 4,6-dideoxy-3-*O*-methyl-DL-*xylo*-hexopyranose (DL-chalcose) which gave the same nuclear magnetic resonance spectrum in D_2O as did authentic D-chalcose. Yields are good to excellent in the various steps from **1** on.

Canadian Journal of Chemistry, **48**, 830 (1970)

From the acid degradation and the methanolysis of the antibiotic chalcomycin there have been obtained the crystalline compounds chalcose and methyl chalcoside (1). Determination of the structure (1) and stereochemistry (2) of these substances revealed that crystalline chalcose is 4,6-dideoxy-3-*O*-methyl-α-D-*xylo*-hexopyranose while the methyl chalcoside possessed the structure methyl 4,6-dideoxy-3-*O*-methyl-β-D-*xylo*-hexopyranoside. The hexose lankavose, obtained from the acid hydrolysis of the antibiotic lankamycin has been found to be identical with chalcose (3). Additional support for the structural assignment was provided by the conversion of desosamine (3,4,6-trideoxy-3-dimethylamino-D-*xylo*-hexopyranose) to chalcose (4, 5) and final proof was obtained by the synthesis of chalcose from methyl 4,6-*O*-benzylidene-3-*O*-methyl-2-*O*-tosyl-α-D-*gluco*-pyranoside (6) and from 4-deoxy-D-*xylo*-hexopyranose (7). A recent report (8) describes a facile synthesis of chalcose from 1,2:5,6-*di*-*O*-isopropylidene-3-*O*-methyl-α-D-glucofuranose.

We now wish to report the preparation of DL-chalcose from acrolein dimer. To our knowledge this has not yet been described.[2]

[1]Postdoctoral Fellow.

[2]When the present work was completed, a report appeared describing the preparation of an analogous compound, ethyl 3,4,6-trideoxy-3-dimethylamino-β-DL-*xylo*-hexopyranoside from 2-methyl-3,4-dihydro-2*H*-pyran (9) and benzyl 3,4-dideoxy-3-amino-β-DL-*threo*-pentopyranoside from 2-ethoxy-5,6-dihydro-2*H*-pyran (10).

Results and Discussion

The key substance required for the synthesis of DL-chalcose was 1,6:2,3-dianhydro-4-deoxy-β-DL-*ribo*-hexopyranose (**1**) (Scheme 1). This compound had been prepared previously in this laboratory (11) from acrolein dimer (3,4-dihydro-2*H*-pyran-2-carboxaldehyde). The present route to **1** followed that described (11) but with the following observations and modifications. (*a*) Reduction of the acrolein dimer by aluminum isopropoxide also provides the alcohol 2-hydroxymethyl-3,4-dihydro-2*H*-pyran (**1** in ref. 11) in 60–65% yield, but a contaminant, the isopropyl ester of 2-carboxy-3,4-dihydro-2*H*-pyran which was formed as a byproduct of this reduction to the extent of 10–15%, was difficult to remove, hence the sodium borohydride reduction previously employed (11) was still preferred. (*b*) Bromination of 6,8-dioxabicyclo[3.2.1]octane (**2** in ref. 11) gave a mixture of *endo*- and *exo*-[3] 4-bromo-6,8-dioxabicyclo[3.2.1]octane (**3** in ref. 11) (12), contrary to the previous suggestion (11) that only one isomer is formed. (*c*) In the dehydrohalogenation, only *trans*-4-bromo-6,8-dioxabicyclo[3.2.1]octane dehydrohalogenated readily to form the olefin 6,8-dioxabicyclo[3.2.1]oct-3-ene (**4** in ref. 11). Care was necessary in the dehydrohalogenation to avoid high temperatures and prolonged reaction time since this olefin is now

[3]The *endo* and *exo* terminology is used to signify *cis* and *trans* position of the bromine atom with respect to the 1,5-anhydro ring.

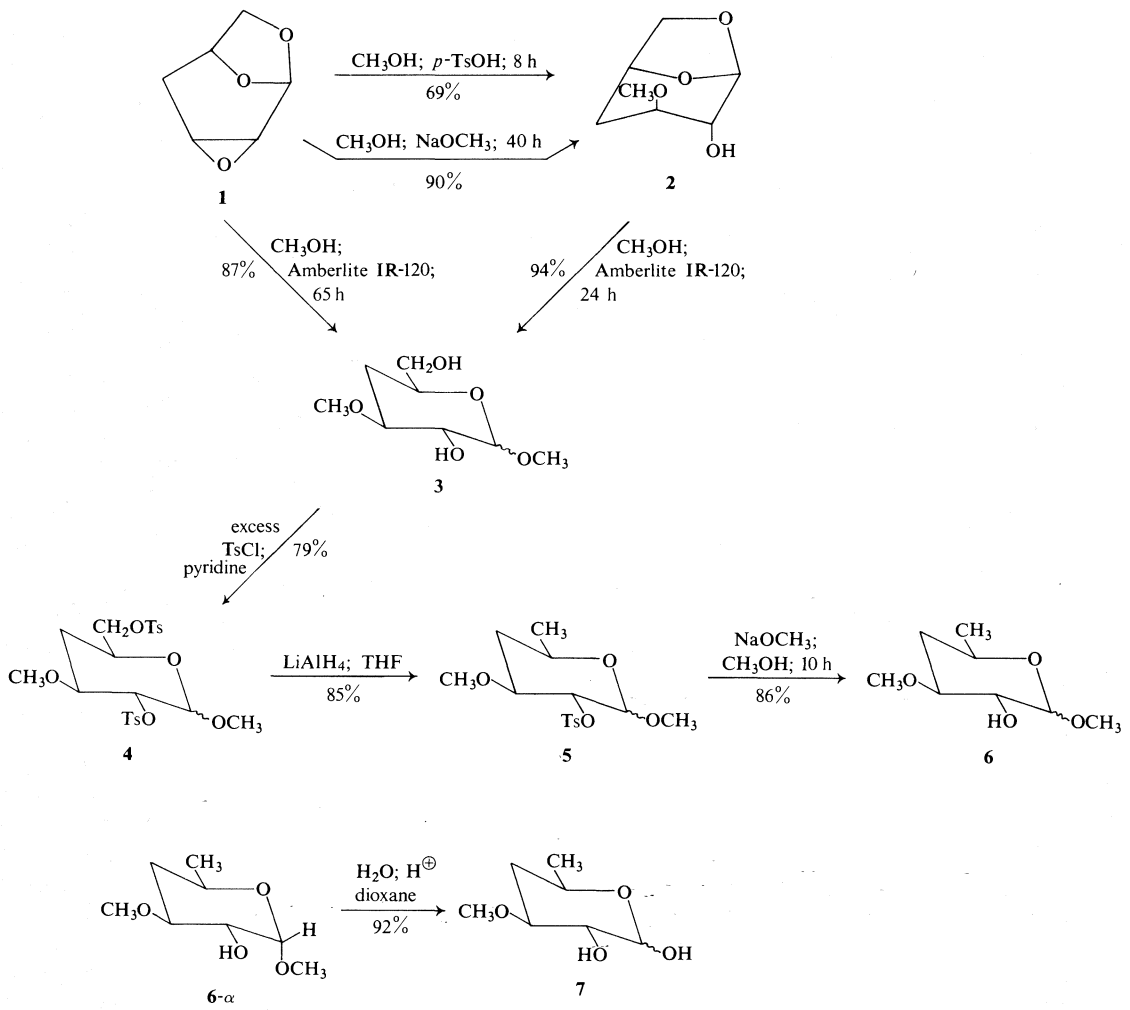

THF = tetrahydrofuran; Ts = p-$CH_3C_6H_4So_2^-$

SCHEME 1

known to isomerize to 6,8-dioxabicyclo[3.2.1]-oct-2-ene under vigorous base catalyzed dehydrohalogenation conditions (12). The use of sodium hydride and a small amount of dry ethanol in 1,2-dimethoxyethane facilitated the dehydrohalogenation and avoided isomerization (12). (*d*) The time required to produce the epoxide **1** by the reaction of *m*-chloroperoxybenzoic acid with 6,8-dioxabicyclo[3.2.1]oct-3-ene could be reduced from 10 days (11) to less than 24 h by using methylene chloride rather than dry ether as solvent.

Along with product **1** there was obtained an impurity in ~ 5% yield (as shown by gas–liquid chromatography (g.l.c.) and the nuclear magnetic resonance (n.m.r.) spectrum) considered previously (11) to be the isomer 1,6:2,3-dianhydro-4-deoxy-β-DL-*lyxo*-hexopyranose (**6** in ref. 11). This is now supported by the fact that the n.m.r. spectrum of authentic material now prepared in this laboratory (13) shows the identical anomeric proton signal (doublet, $J \sim 3$ Hz, at τ 4.32). This impurity could be largely removed (residue < 2%) by repeated crystallization of **1** from ether, using a dry ice – acetone bath. The n.m.r. spectrum of purified **1** is devoid of signals of the contaminating *lyxo* isomer. The remaining trace of this contaminant gave no problem in the subsequent reaction of **1**.

Heating **1** for 8 h, in refluxing methanol in the

Can. J. Chem. Downloaded from www.nrcresearchpress.com by 210.87.254.40 on 09/05/12
For personal use only.

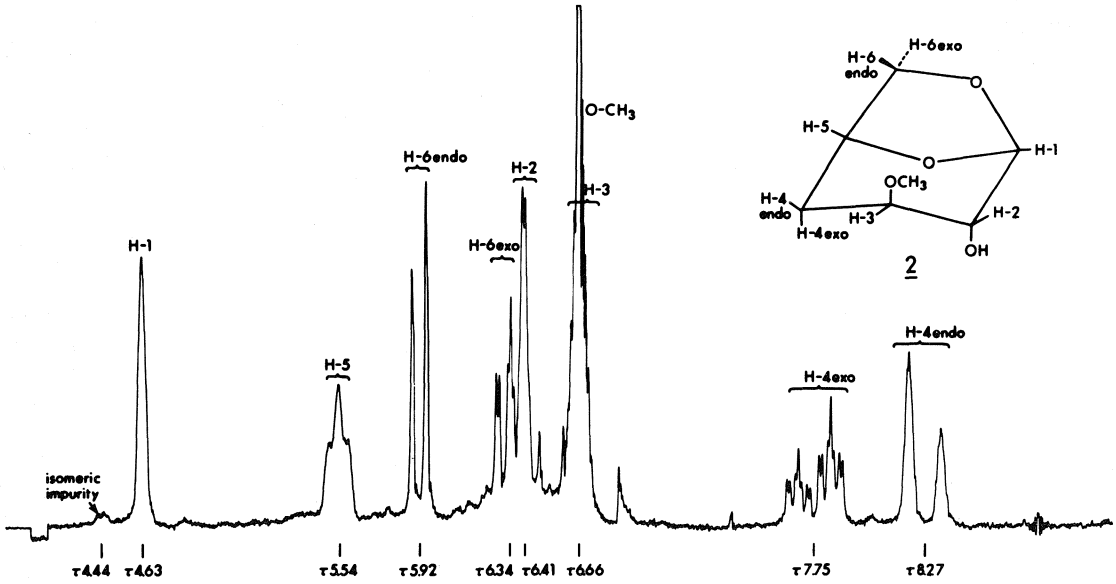

FIG. 1. 100 MHz n.m.r. spectrum of 1,6-anhydro-4-deoxy-3-*O*-methyl-β-DL-*xylo*-hexopyranose (**2**). Contains a very small amount of isomeric impurity (signal at τ 4.44). In $CDCl_3$ with tetramethylsilane as reference.

presence of a catalytic amount of *p*-toluenesulfonic acid monohydrate gave a mixture of 1,6-anhydro-4-deoxy-3-*O*-methyl-β-DL-*xylo*-hexopyranose, **2** (69%), and unreacted **1** (Scheme 1). Longer reaction times resulted in some opening of the 1,6-anhydro ring as well. The unreacted **1** could be removed readily by chromatography on an alumina column, and provided **2** as a viscous liquid whose elemental analysis was that required by structure **2**. The same compound, **2**, was obtained in 90% yield when **1** was heated for 40 h in refluxing dry methanol containing an excess of sodium methoxide. In both of these preparations of **2** from **1** a very small amount of impurity, possibly the *arabino* isomer, was evident from the small signal that is perceived at τ 4.44 in the n.m.r. spectrum of **2** (Fig. 1). The *p*-nitrobenzoate of **2**, a crystalline material obtained in 78% yield, gave the elemental analysis required.

It is clearly seen that the reaction of the epoxide group in the 1,6:2,3-dianhydro compound **1** with methanol in the presence of acid or with sodium methoxide in methanol, can give only two products, the *xylo* structure **2** and/or its *arabino* isomer. Judging from previous work (11) in which the reaction of aqueous potassium hydroxide with **1** had produced 1,6-anhydro-4-deoxy-β-DL-*xylo*-hexopyranose (**7** in ref. 11), apparently exclusively, and from the observation that such α,β epoxy acetals do prefer to break the C—O bond of the epoxy function which is more remote from the anomeric carbon (14), it is expected that the product obtained in the present case is compound **2**. The n.m.r. spectrum of compound **2**, shown in Fig. 1, as well as that of the *p*-nitrobenzoate of **2** provides evidence that the compound has in fact the structure and conformation indicated in **2**. This was further confirmed by spin decoupling experiments.

When heated for 24 h in refluxing methanol containing Amberlite IR-120 (H^+), compound **2** was converted in 94% yield to **3**, a syrupy mixture of the α and β isomers of methyl 4-deoxy-3-*O*-methyl-DL-*xylo*-hexopyranoside. Treatment of the dianhydro compound **1** under the same conditions, but for 65 h, gave **3** in 87% yield. All attempts to separate the α and β isomers or their silyl derivatives (15) failed. Both α and β isomers of **3** are strongly absorbed in the columns and do not come off. Of the several g.l.c. columns tried, only one (10% Carbowax 6000 on Gas–Chrom W, acid-washed) showed two overlapping peaks for the silyl derivatives in the approximate ratio of 2:1. The 60 MHz spectrum of **3** in $CDCl_3$ showed two anomeric proton signals at τ 5.20 (doublet, $J \simeq 2.5$ Hz) and 5.82 (doublet, $J \simeq 7.0$ Hz) also in the approximate ratio of 2:1. These

Can. J. Chem. Downloaded from www.nrcresearchpress.com by 210.87.254.40 on 09/05/12
For personal use only.

Can. J. Chem. Downloaded from www.nrcresearchpress.com by 210.87.254.40 on 09/05/12
For personal use only.

clearly are the anomeric proton signals for the α and β isomers respectively.

The mixture of α and β isomers **3** was converted to the respective di-*p*-nitrobenzoates (**3**-α and **3**-β) from which both the α and β isomers were separated by chromatography as pure crystalline solids.

Treatment of the isomeric mixture, **3**, with excess *p*-toluenesulfonyl chloride in pyridine gave a good yield of the di-*p*-toluenesulfonate **4** as a semisolid mass which could not be crystallized. Attempts to convert **3** to the mono-*p*-toluenesulfonate gave a mixture from which a crystalline di-*p*-toluenesulfonate could be obtained in ~ 8% yield. The n.m.r. spectrum of this product possessed only one anomeric proton signal (at τ 5.25), a doublet, $J \simeq 3.5$ Hz, which clearly shows that this must be the α isomer.

Selective lithium aluminum hydride reduction of the di-*p*-toluenesulfonate, **4**, gave 85% of crude methyl 4,6-dideoxy-3-*O*-methyl-2-*O*-*p*-toluenesulfonyl-α,β-DL-*xylo*-hexopyranoside (**5**) which in turn could be saponified to methyl 4,6-dideoxy-3-*O*-methyl-α,β-DL-*xylo*-hexopyranoside (**6**) in 86% (crude) yield. The n.m.r. spectrum showed this to be composed of the α and β isomers in the ratio of 2:1 respectively, but also contaminated with a very small amount of unreacted **5**. The unreacted **5** could be separated from **6**-α,β by passage through a column of alumina.

The α isomer was separated by chromatography on an alumina column or by preparative g.l.c. Reinjection gave only one peak of the same retention time as observed previously. Both the elemental analysis and the n.m.r. spectrum agreed with the structure as the α isomer of **6**. The "β isomer" was isolated similarly, but upon reinjection showed the same two, well separated peaks corresponding to the α and β isomers. The n.m.r. spectrum of this "β isomer" isolated by g.l.c. also showed two anomeric proton signals corresponding to the α and β isomers. It is thus obvious that isomerization of the β isomer, but not the α isomer, had occurred during some phase of the g.l.c. analysis.

The 100 MHz spectrum of the α isomer of **6** and the signal assignments made by the use of double irradiation are in complete agreement with the chair conformation of the α isomer of compound **6**.

When the pure α isomer of **6** was heated for 4 h at 100° in a mixture of dioxane and 1.5% aqueous sulfuric acid, a viscous liquid was obtained which, when twice distilled in a sublimation apparatus, provided a colorless semisolid material in 92% yield which gave the elemental analysis required for compound **7**, 4,6-dideoxy-3-*O*-methyl-α,β-DL-*xylo*-hexopyranose (α,β-DL-chalcose).

The 100 MHz n.m.r. spectrum of **7** in $CDCl_3$ agreed with the structure, showing the two anomeric proton signals of the α and β isomers at τ 4.76 (doublet, $J \simeq 3$ Hz) and τ 5.50 (doublet, $J \simeq 7.5$ Hz) in the approximate area ratio of 1:1. The 60 MHz spectrum in D_2O 1 h after the solution had been made, showed the α and β isomers to be present in the ratio 1.0:1.5 respectively. Five hours later, the same solution showed this ratio to be α:β ≃ 1:2 thus indicating that mutarotation had occurred. No further change was observed over an additional 16 h.

Final evidence that **7** is indeed chalcose was obtained by comparison of the 60 MHz spectrum in D_2O with the 60 MHz spectrum (in D_2O) of authentic α-D-chalcose.[4]

Experimental

All boiling points and melting points are uncorrected. The boiling points of the liquids isolated in small quantities, were determined in a two-bulb micro boiling point apparatus under vacuum, with the lower bulb immersed in the heating bath which was heated very slowly. When the liquid began to distill, the temperature of the bath was taken as the "boiling point".

The g.l.c. analyses were carried out with an F and M apparatus (Model 700) or an Aerograph Autoprep Model A-700, using primarily a column (12′ × 1/8″) packed with 20% butanediol succinate (BDS) on Gas–Chrom P (60–80 mesh). Helium was the carrier gas.

Elemental analyses were made by Mrs. Darlene Mahlow of this Department or by Dr. C. Daessle, Organic Microanalyses, 5757 Decelles Ave., Montreal.

The 60 MHz n.m.r. spectra were made by Mr. Robert Swindlehurst of this Department, using a Varian A-60 instrument. The 100 MHz n.m.r. spectra and the spin decoupling experiments were done by Mr. Glen Bigham of this Department, using a Varian HR-100 MHz instrument. Unless otherwise stated, deuteriochloroform was the solvent for n.m.r. analyses, with tetramethylsilane as reference. All the *J* values were estimated by measuring the spacings on the spectra and are therefore approximate values.

Infrared (i.r.) spectra were obtained with a Perkin–Elmer Model 337 Grating Infracord. The expanded

[4]We are deeply indebted to Dr. Woo of the Research Division of Parke, Davis and Company, Detroit 32, Michigan, U.S.A. for copies of the spectra of D-chalcose.

Can. J. Chem. Downloaded from www.nrcresearchpress.com by 210.87.254.40 on 09/05/12
For personal use only.

spectra were taken by Mr. Robert Swindlehurst using a Perkin–Elmer Model 421 Grating spectrometer.

Thin-layer chromatography (t.l.c.) was carried out on microscope slides using aluminum oxide G (E. Merck and Co.) as adsorbent. Detection of spots on the t.l.c. was made by exposure to iodine vapor. Solvents were removed under vacuum in a rotary evaporator unless otherwise stated.

2-Hydroxymethyl-3,4-dihydro-2H-pyran

The compound was prepared by the method of Sweet and Brown (11) in 81–86% yield; b.p., 94–95° at 35 mm; $\eta_D^{23.5}$, 1.4770 (lit. b.p., 102° at 45 mm; η_D^{25}, 1.4772 (11). The g.l.c., using a BDS column at 160° and a carrier gas flow rate of 40 ml/min, showed two components in the ratio of 1.0:14.3 in order of appearance. The minor component had the same retention time as did 6,8-dioxabicyclo[3.2.1]octane. Since the n.m.r. spectrum of 2-hydroxymethyl-3,4-dihydro-2*H*-pyran before g.l.c. showed only a trace of an anomeric proton signal corresponding to that of the bicyclooctane, passage of the hydroxymethyl compound through the g.l.c. column must have caused some ring closure to the bicyclo compound.

4-Bromo-6,8-dioxabicyclo[3.2.1]octane

Bromination of 83.3 g (0.73 mole) of 6,8-dioxabicyclo-[3.2.1]octane (**2**) (11) in 1.5 l of dry carbon tetrachloride, containing 300 g (2.83 mole) of dry sodium carbonate was carried out essentially according to published direction (11) by addition of 116 g (0.72 mole) of bromine in 250 ml of carbon tetrachloride over a period of 2.5 h. A liquid was obtained (92.4 g, 66%) boiling at 75° at 1.7 mm; η_D^{26}, 1.5195 (lit. b.p., 90° at 4.5 mm; η_D^{27}, 1.5176 (11)). The g.l.c. on a BDS column at 180° showed two closely overlapping peaks in the ratio of 1.0:0.8 (*endo*:*exo*).

In another run, to 66.4 g (0.58 mole) of 6,8-dioxabicyclo[3.2.1]octane in 1200 ml of carbon tetrachloride containing 130 g (1.23 mole) of dry sodium carbonate, was added a solution of 100 g (0.63 mole) of bromine in 200 ml of carbon tetrachloride over a 2.5 h period. The oil which was obtained was fractionally distilled. The three fractions boiled at (*i*) 64–65° at 0.7–0.8 mm (33.6 g), (*ii*) 65–66° at 0.7 mm (10.25 g) and (*iii*) 65–66° at 0.7 mm (13.0 g) with a combined yield of 51%. The g.l.c. of each fraction showed the two overlapping peaks in the *endo*:*exo* area ratio respectively of (*i*) 1.0:3.4, (*ii*) 1.0:6.4, (*iii*) 1.0:9.5; η_D^{25} for the third fraction, 1.5202.

6,8-Dioxabicyclo[3.2.1]oct-3-ene

The following modification of the published directions (11) avoided isomerization of the product 6,8-dioxabicyclo[3.2.1]oct-3-ene to the oct-2-ene.

To a quantity (40 g, 0.207 mole) of the isomeric bromides **3** (in this case *endo*:*exo* $\simeq$ 0.7:1.0 by g.l.c.) stirred well in 300 ml of dry 1,2-dimethoxyethane (DME) was added a total of 5.1 g (0.21 mole) of sodium hydride in 1 g lots. The addition of the first gram of hydride was followed by 1 ml of dry ethanol. Then two 1 g quantities of hydride were added in succession, followed again by 1 ml of dry ethanol. The remainder of the hydride was then added in 1 g lots. The mixture was stirred for 1 h at room temperature, then under reflux for 1.5 h. Removal of 270 ml of solvent at atmospheric pressure by fractional distillation left a liquid which deposited a solid (NaBr) when cooled and diluted with 200 ml of ether. The solid was separated and the filtrate fractionally distilled to give 10.45 g of the bicyclo[3.2.1]oct-3-ene boiling at 83–84° at 51.5 mm; η_D^{22}, 1.4795 (lit. b.p., 54° at 9 mm; η_D^{25}, 1.4772). The residual liquid was subjected to careful fractional distillation with a spinning band column and afforded an additional 1.4 g of the oct-3-ene (total yield 51%) and 10.1 g of unreacted bromide which proved to be the *endo* isomer when compared with authentic material (12).

The i.r. spectrum of the 6,8-dioxabicyclo[3.2.1]oct-3-ene showed a weak band at 1638 cm^{-1} (C=C).

The n.m.r. spectrum was identical to that found for authentic bicycloolefin (12) and differed from that reported (11) for the oct-3-ene by omission of the signals specific for 6,8-dioxabicyclo[3.2.1]oct-2-ene.

*1,6:2,3-Dianhydro-4-deoxy-*β*-*DL*-ribo-hexopyranose (**1**)*

A solution of 4.7 g (0.042 mole) of 6,8-dioxabicyclo-[3.2.1]oct-3-ene in 65 ml of dry methylene chloride and 10.35 g (0.06 mole) of *m*-chloroperoxybenzoic acid, protected from moisture, was stirred magnetically for 22.5 h and at the same time, kept at room temperature by means of a water bath. A precipitate of *m*-chlorobenzoic acid appeared. The reaction mixture was then poured into 50 ml of water and the organic layer separated. The aqueous layer was extracted with methylene chloride (3 × 50 ml) and the combined methylene chloride solutions washed with 10% aqueous sodium carbonate (5 × 20 ml), then with water (4 × 20 ml), and finally dried ($MgSO_4$). Removal of the solvent left 5.4 g of crude **1**. This was combined with material, (9.5 g), obtained from a second run (10.2 g of the oct-3-ene) in which the time of epoxidation was 17.5 h. Distillation of the combined crude material (14.9 g) gave 10.3 g of material boiling at 61–62° at 0.5 mm. Extraction of the aqueous washings with methylene chloride for 2 days afforded an additional 1 g of the epoxide. Total yield 67%.

The g.l.c. (BDS column at 160°) indicated the presence of a contaminant (< 5%). Several crystallizations from ether cooled by a dry ice – acetone bath reduced the contaminant to < 2%.

*1,6-Anhydro-4-deoxy-3-O-methyl-*β*-*DL*-xylo-hexopyranose (**2**)*

(a) By Acid Catalysis

A solution of the epoxide **1** (isomeric contaminant < 2%) (4.5 g, 0.035 mole) in 50 ml of anhydrous methanol containing 50 mg of *p*-toluenesulfonic acid monohydrate, was refluxed for 8.5 h and then cooled. Sodium methoxide was added to destroy the acid (p*H* ~ 9). The methanol was removed and the residue diluted with 100 ml of methylene chloride. The organic solution was washed with saturated aqueous sodium carbonate (2 × 10 ml), then with water (5 × 10 ml), and dried (Na_2SO_4). The solid was removed by filtration and the solution freed from solvent to provide 1.5 g of viscous liquid whose n.m.r. spectrum showed the presence of only two compounds, **2** and **1** in the approximate ratio 1.6:1.0. A further quantity (3.0 g) of viscous liquid was obtained when the combined aqueous layer, left after methylene chloride extraction, plus the aqueous sodium carbonate and water

Can. J. Chem. Downloaded from www.nrcresearchpress.com by 210.87.254.40 on 09/05/12
For personal use only.

washings, were extracted with methylene chloride in a liquid–liquid extractor for 24 h. This material was **2** contaminated with a trace of **1** according to t.l.c. (solvent, 1% methanol in benzene).

The above 3.0 g of material were subjected to chromatography on a 0.5 in. column of 20 g of neutral alumina. Elution by 100 ml of benzene gave 1.6 g of viscous liquid. A further 100 ml quantity of benzene gave an additional 1.35 g of this liquid. The former fraction was contaminated with a trace of epoxide **1** while the latter was pure **2** according to their t.l.c. and n.m.r. spectra.

The second fraction (1.35 g) was distilled in a 2-bulb apparatus to give a colorless liquid boiling at 89° at 0.3 mm. Total yield of **2** was 69%. For analysis, the material was freed from traces of water by azeotropic distillation with benzene.

Anal. Calcd. for $C_7H_{12}O_4$: C, 52.49; H, 7.55. Found: C, 52.36; H, 7.36.

The 100 MHz n.m.r. spectrum of this material is shown in Fig. 1 and agrees with the structure **2**.

(b) By Reaction with Sodium Methoxide

A solution of epoxide **1** (1 g, 0.0078 mole) and 1.0 g (0.018 mole) of sodium methoxide in 25 ml of dry methanol was refluxed for 40 h. Removal of the methanol gave crude **2** contaminated with sodium methoxide. This residue was diluted with 50 ml of water and extracted with methylene chloride (5 × 25 ml). The extract was washed with water (4 × 10 ml) and dried (Na_2SO_4). Removal of the solvent gave 50 mg of crude liquid which t.l.c. indicated to be composed of two substances believed to be the epoxide **1** and the product **2**. This was not considered further.

The aqueous layer left after methylene chloride extraction, and the water washings above were combined and cautiously treated with concentrated hydrochloric acid until the p*H* of the solution reached 9. The resulting solution was continuously extracted with methylene chloride for 3 days. The methylene chloride extract was dried (Na_2SO_4) and freed from solvent to provide 1.13 g (90%) of colorless liquid.

The n.m.r. spectrum of this crude liquid was identical to the n.m.r. spectrum of **2** isolated from the acid-catalyzed reaction of **1** with methanol. The presence of a very small signal at τ 4.50 in the anomeric proton region indicated the presence of an impurity, ~ 3%, possibly the 1,6-anhydro-4-deoxy-2-*O*-methyl-β-DL-*arabino*-hexopyranose. This liquid boiled at 93° at 0.4 mm.

A solution of compound **2** (400 mg, 0.0025 mole) and 0.5 g (0.0027 mole) of *p*-nitrobenzoyl chloride in 5 ml of dry pyridine was heated under reflux for ~ 10 min. The cooled solution produced a solid when poured onto ice. The bulk of the pyridine could be removed by washing the solid with water. A solution of the solid in 100 ml of ether was washed with 5% aqueous sodium carbonate (4 × 10 ml), with water (5 × 5 ml), dried (Na_2SO_4), and filtered. The drying agent was extracted with 20 ml of chloroform. The combined ether and chloroform solutions were freed from solvents and gave 0.8 g of crude material. Three crystallizations from 95% ethanol gave 0.6 g (78%) of pure *1,6-anhydro-4-deoxy-3-O-methyl*-β-DL-*xylo*-*hexopyranose*-*p*-*nitrobenzoate* (**2**-α), m.p., 124–125°.

Anal. Calcd. for $C_{14}H_{15}O_7N$: C, 54.37; H, 4.89; N, 4.53. Found: C, 54.23; H, 4.92; N, 4.70.

The i.r. spectrum in carbon tetrachloride showed a strong band at 1727 cm^{-1} (ester carbonyl).

The 100 MHz n.m.r. spectrum is consistent with the structure **2**-α.

Methyl 4-Deoxy-3-O-methyl-α,β-DL-xylo-hexopyranoside (3)

(a) From 2

A solution of 1.6 g (0.01 mole) of **2** in 50 ml of anhydrous methanol containing 2 ml of Amberlite IR-120 (H^+) was heated under reflux for 12 h. The solution was cooled, freed from the resin by filtration, and then from solvent under reduced pressure. The n.m.r. spectrum of the crude material showed, from the anomeric proton signals, that the product was contaminated by ~ 35% of unreacted **2**. Accordingly, the crude material was subjected to an additional 12 h treatment with 50 ml of refluxing methanol containing 3 ml of the Amberlite resin. The oil, obtained as described above, was dried in a vacuum desiccator and gave 1.8 g (94%) of **3** as a syrup.

Anal. Calcd. for $C_8H_{16}O_5$: C, 49.98; H, 8.39. Found: C, 49.90; H, 8.56.

The 60 MHz n.m.r. spectrum showed two anomeric proton signals, one at τ 5.20 (doublet, $J \simeq 2.5$ Hz) and the other at τ 5.81 (doublet, $J \simeq 7.0$ Hz) in the approximate area ratio of 2:1. These were due respectively to the α and β isomers of *methyl 4-deoxy-3-O-methyl*-DL-*xylo-hexopyranoside* (**3**).

(b) From 1

A solution of 5 g (0.039 mole) of **1** in 75 ml of anhydrous methanol containing 10 ml of Amberlite IR-120 (H^+) was heated under reflux for 65 h. The mixture was then worked up as described in (*a*) above and gave 6.5 g (87%) of **3**. Here again the ratio of α:β was about 2:1 as determined by the n.m.r. spectrum. When the reaction was interrupted after 26 h of reflux, the n.m.r. spectrum of the crude oil obtained showed the presence of a significant quantity of **2** (shown by the characteristic anomeric proton signal of **2**, see Fig. 1) thus indicating that the epoxide ring is broken first.

Di-p-nitrobenzoate of 3

A solution of 0.4 g (0.0021 mole) of **3** (a 2:1 mixture of α and β isomers) and 0.8 g (0.0043 mole) of *p*-nitrobenzoyl chloride in 5 ml of dry pyridine was heated under reflux for 5 min. The cooled material was poured onto 50 g of crushed ice. The resulting semisolid was washed several times with water to remove excess pyridine. A chloroform (100 ml) solution of this semisolid was washed first with 5% aqueous sodium bicarbonate (4 × 10 ml), then with water (4 × 5 ml), and dried (Na_2SO_4). Filtration and solvent removal afforded 0.95 g of crude brown solid. A t.l.c. of this material (solvent, 1:3 benzene–chloroform) showed two spots with R_f values of 0.38 and 0.54.

The brown solid was subjected to chromatography on a column (i.d. 0.5″) of 15 g of alumina (BDH) using benzene–hexane as eluent in the proportions first 1:1 then 3:1. The solid obtained was thrice crystallized from methylene chloride – hexane, giving 205 mg of crystalline material melting at 163.5–165.5°. The total yield of the isolated di-*p*-nitrobenzoate of **3** was 20%. The solid (m.p.,

Can. J. Chem. Downloaded from www.nrcresearchpress.com by 210.87.254.40 on 09/05/12
For personal use only.

163.5–165.5°) was dried at 80° for 10 h under vacuum and analyzed.

Anal. Calcd. for $C_{22}H_{22}O_{11}N_2$: C, 53.88; H, 4.52; N, 5.71. Found: C, 53.64; H, 4.63; N, 5.49.

The 100 MHz n.m.r. spectrum is in complete agreement with the structure as *methyl 4-deoxy-3-O-methyl-2,6-di-O-p-nitrobenzoyl-α-*DL*-xylo-hexopyranoside* (**3**-α).

A final elution of the alumina column with benzene gave 70 mg of material showing only one spot on the t.l.c. This material, when crystallized once from methylene chloride – hexane gave a reddish material whose n.m.r. spectrum clearly showed it to be impure. After treatment with charcoal in methylene chloride and two further crystallizations from methylene chloride – hexane, a colorless crystalline material was obtained (22 mg) melting at 155–158°. For analysis this was dried for 4 h at 80° under vacuum.

Anal. Calcd. for $C_{22}H_{22}O_{11}N_2$: C, 53.88; H, 4.52; N, 5.71. Found: C, 53.71; H, 4.62; N, 5.52.

The 100 MHz n.m.r. spectrum was in complete agreement with the structure as *methyl 4-deoxy-3-O-methyl-2,6-di-O-p-nitrobenzoyl-β-*DL*-xylo-hexopyranoside* (**3**-β).

*Methyl 4-Deoxy-3-O-methyl-2,6-di-O-p-toluenesulfonyl-α,β-*DL*-xylo-hexopyranoside (**4**)*

To an ice-cold solution of 1.5 g (0.0078 mole) of **3** in 4.5 ml of dry pyridine was added a cold solution of 4.5 g (0.024 mole) of *p*-toluenesulfonyl chloride in 6 ml of dry pyridine. The mixture was kept at 0° for 4 h, in a refrigerator for 1 day, and then stirred for 2 days at 30°. It was then poured onto crushed ice whereupon the ester separated as a thick viscous liquid. This was washed with water and dissolved in chloroform. The chloroform solution was washed with 5% aqueous sodium bicarbonate solution (5 × 10 ml), then with water (3 × 10 ml), and dried (Na_2SO_4). The filtered solution was freed from solvent, giving 3.1 g (79%) of crude material which could not be crystallized. An analytical sample was obtained by shaking a solution of 50 mg of this crude material in methylene chloride with some activated charcoal. The charcoal was separated by filtration and washed with methylene chloride (5 ml). The combined methylene chloride solutions were freed from solvent and the residue was dried under vacuum (oil pump) at room temperature and gave 43 mg of material.

Anal. Calcd. for $C_{22}H_{28}O_9S_2$: C, 52.78; H, 5.64. Found: C, 52.62; H, 5.94.

*Attempted Selective Monotosylation. Methyl 4-Deoxy-3-O-methyl-2,6-di-O-p-toluenesulfonyl-α-*DL*-xylo-hexopyranoside (**4**-α)*

To a stirred cold solution (ice–salt bath) of 1 g (0.0052 mole) of **3** in 5 ml of dry pyridine was added dropwise a solution of 1.08 g (0.00524 mole) of *p*-toluenesulfonyl chloride in 8 ml of dry pyridine over a period of 0.5 h. The stirred mixture was then kept cold for 4 h with a salt–ice bath, then stirred at room temperature overnight. The bulk of the pyridine was removed at room temperature by fractional distillation under vacuum and the residue was dissolved in 75 ml of benzene. This was washed with 10% aqueous sodium bicarbonate (5 × 10 ml), water (5 × 10 ml), and dried (Na_2SO_4). Removal of the solid and then the solvent gave 1.45 g of material.

This was subjected to chromatography on 35 g of alumina (BDH) (column i.d. 2 cm). Elution with 450 ml of benzene gave nine 50 ml fractions which were combined to give 250 mg of viscous liquid showing only one spot on t.l.c. (R_f = 0.68; solvent, $CHCl_3$). The viscous liquid was dissolved in a minimum quantity of methylene chloride, and ether was added to faint turbidity. Crystallization occurred. Two more such crystallizations gave 200 mg (7.7%) of colorless needles, m.p. 125–126°.

Anal. Calcd. for $C_{22}H_{28}O_9S_2$: C, 52.78; H, 5.64; S, 12.81. Found: C, 52.75, 52.40; H, 5.97, 5.67; S, 12.15, 12.30.

The i.r. spectrum in chloroform showed no absorption for OH.

The n.m.r. spectrum was in complete agreement with the structure as **4**-α (see Discussion).

Further elution of the alumina column with 100 ml of benzene gave 25 mg of a mixture (t.l.c.) of two substances one of which was **4**-α. This was not considered further. Elution of the column with chloroform and then with 5% methanol in chloroform gave 0.83 g of syrup. Although this showed one spot on the t.l.c. it could not be induced to crystallize. The i.r. spectrum indicated the presence of free hydroxyl by a broad band at 3540 cm^{-1} and it is believed that this material is the mono ester *methyl 4-deoxy-3-O-methyl-6-O-p-toluenesulfonyl-α,β (?)-*DL*-xylo-hexopyranoside* although the elemental analysis was not satisfactory.

The 60 MHz n.m.r. spectrum indicated that this was a mixture of α and β isomers. It showed a doublet at τ 5.29 ($J \simeq 2.8$ Hz) due to the anomeric proton of the α isomer. The signal for the anomeric proton of the β isomer was masked by the other proton signals and could not be defined.

*$LiAlH_4$ Reduction of **4**. Methyl 4,6-Dideoxy-3-O-methyl-2-O-p-toluenesulfonyl-α-*DL*-xylo-hexopyranoside (**5**-α)*

A solution of 2.7 g (0.0054 mole) of **4** in 20 ml of dry tetrahydrofuran was added dropwise over a period of 20 min to a solution of 0.61 g (0.016 mole) of $LiAlH_4$ in 20 ml of dry tetrahydrofuran. The solution was then heated under reflux for 30 h. Removal of ~ 25 ml of solvent by fractional distillation at atmospheric pressure left a residue which was cooled and treated with 25 ml of water containing 14.0 g of sodium potassium tartrate. The mixture was then extracted with ether (8 × 25 ml), and the combined ether extract washed with water (5 × 10 ml), dried (Na_2SO_4), and filtered. Removal of the solvent gave 1.6 g (90%) of crude yellow oil, **5**.

This oil was subjected to chromatography on a column (i.d. ~0.5″) of 20 g of alumina (BDH) and 50 ml fractions were collected. Elution with hexane provided 4 fractions (470 mg, 26.4%) of oil which showed a single spot on t.l.c. (benzene:chloroform, 3:1). This was crystallized by solution in a minimum quantity of ether to which cyclohexane was carefully added to faint turbidity. Yield, 430 mg (24.2%) of crystals melting at 56–57°.

For analysis, the sample was dried for 24 h under vacuum (oil pump) at room temperature.

Anal. Calcd. for $C_{15}H_{22}O_6S$: C, 54.54; H, 6.70; S, 9.71. Found: C, 54.80; H, 6.88; S, 9.47.

The 60 MHz n.m.r. spectrum was completely consistent with the structure as **5**-α.

Further fractions (5 and 6) obtained by elution of the column above with benzene gave respectively 220 mg and 30 mg of viscous oil which could not be induced to crystallize. The 60 MHz n.m.r. spectrum of fraction 5 (220 mg) indicated that it was largely **5**-α. The t.l.c.

showed two spots. The second component could be the β isomer.

Methyl α,β-DL-Chalcoside (Methyl 4,6-dideoxy-3-O-methyl-α,β-DL-xylo-hexopyranoside) (6)

A solution of 5.5 g (0.011 mole) of **4** in 50 ml of dry tetrahydrofuran was added dropwise over a period of 0.5 h to a magnetically stirred solution of 1.25 g (0.033 mole) of $LiAlH_4$ in 35 ml of dry tetrahydrofuran. The solution was then heated under reflux for 6 h. Most of the solvent (~ 70 ml) was then removed by fractional distillation under reduced pressure. The cooled residue was treated with 50 ml of water containing 28 g of sodium potassium tartrate, followed by 50 ml of water. This was continuously extracted with ether for 24 h. The ether extract was dried (Na_2SO_4) and freed from solvent to provide 3.1 g (85.4%) of crude **5**.

To 3.05 g (0.0092 mole) of this crude **5** dissolved in 10 ml of dry methanol were added 7.5 g (0.139 mole) of sodium methoxide in 65 ml of methanol and the mixture heated under reflux for 10 h. The solvent was removed and the residue was diluted with 75 ml of water. The aqueous solution was brought to p*H* 9 by dropwise addition of dilute hydrochloric acid. The methylene chloride extract (7 × 25 ml) of this aqueous solution was washed with water (3 × 10 ml) and dried (Na_2SO_4). Solvent removal afforded 1.4 g (86%) of crude **6**.

The 60 MHz n.m.r. spectrum of this crude material (**6**), indicated the presence of two anomeric proton signals, at τ 5.29 (doublet, $J \simeq 2.8$ Hz) and at τ 5.90 (doublet, $J \simeq 8$ Hz) due to the α and β isomers in the respective area ratio of ~ 2:1. A small amount of unreacted **5** was evident in the n.m.r. spectrum as shown by the signals in the region τ 2.0–3.0 characteristic of aromatic protons.

The 1.4 g of crude **6** was subjected to chromatography on a column (i.d. ~ 0.5″) of 15 g of alumina (BDH). Fractions of 100 ml were collected. The first fraction obtained with hexane gave 1 g of oil which was largely **6** contaminated with **5**. Fractions 2 and 3 obtained with hexane and 4 and 5 obtained with chloroform gave in total 250 mg of material free of **5** and apparently a mixture of the α and β isomers of **6**.

Fractions 2–5 were combined and separated by g.l.c. on a column (1/4″ × 6′) of 10% Carbowax on Gas Chrom W (acid washed) at 155° with a carrier gas flow rate of 60 ml/min. Two peaks appeared with retention times of 9 1/4 and 12 3/4 min.

Reinjection of the material with retention time 9 1/4 min gave the same single peak. It was an oil, b.p., 65–67° at 0.08 mm; $\eta_D^{27.5}$, 1.4492.

Anal. Calcd. for $C_8H_{16}O_4$: C, 54.54; H, 9.15. Found: C, 54.28; H, 9.21.

The i.r. spectrum showed a broad band at 3450 cm^{-1} (OH).

The 100 MHz n.m.r. spectrum is consistent with the structure as *methyl 4,6-dideoxy-3-O-methyl-α-DL-xylo-hexopyranoside (methyl α-DL-chalcoside)* (**6**-α). The material of retention time 12 3/4 min, when reinjected gave two peaks (retention time 9 1/4 min and 12 3/4 min) in the area ratio ~ 2:1 (α and β isomers) respectively; b.p. of this mixture 66–67° at 0.2 mm (2-bulb method).

The impure fraction 1 above (1 g) was subjected to careful chromatography on 40 g of alumina (BDH). Elution with hexane, 3:1 hexane–benzene, 1:1 hexane–benzene, 1:3 hexane–benzene and 9:1 benzene–chloroform removed **5** and other impurities. Further elution with 3:1 benzene–chloroform gave six 50 ml fractions from which 350 mg of pure (**6**-α) was obtained. Nine more 50 ml fractions (1:1 benzene–chloroform, then chloroform) gave in each case mixtures of the α and β isomers of **6** (total weight, 305 mg).

4,6-Dideoxy-3-O-methyl-α,β-DL-xylo-hexopyranose (α,β-DL-Chalcose) (7)

Methyl α-DL-chalcoside (**6**-α) 200 mg, 0.0011 mole) in 2 ml of *p*-dioxane containing 5 ml of 1.5% aqueous sulfuric acid was heated for 4 h on a water bath at ~ 100°. The solution was cooled and neutralized with barium carbonate and then filtered. The solvent was removed and the residue dried in a desiccator overnight under vacuum. The viscous material, dissolved in methylene chloride, was dried (Na_2SO_4), filtered, and freed from solvent. The crude material (190 mg) was distilled in a small sublimation apparatus at 65° (oil bath temperature) at 0.3 mm and gave 170 mg (92%) of colorless thick viscous material.

Anal. Calcd. for $C_7H_{14}O_4$: C, 51.84; H, 8.70. Found: C, 51.99; H, 8.80.

The 60 MHz n.m.r. spectrum in D_2O is identical with the 60 MHz n.m.r. spectrum (in D_2O) of authentic α,β-D-chalcose kindly provided by Dr. Woo (2).

The authors wish to thank the National Research Council of Canada for financial assistance for a portion of this work.

We wish to thank Dr. Woo of the Parke, Davis Company for the copy of the 60 MHz n.m.r. spectrum of D-chalcose in D_2O.

1. P. W. K. Woo, H. W. Dion, and Q. R. Bartz. J. Amer. Chem. Soc. **83**, 3352 (1961).
2. P. W. K. Woo, H. W. Dion, and L. F. Johnson. J. Amer. Chem. Soc. **84**, 1066 (1962).
3. W. Keller-Schierlein and G. Roncari. Helv. Chim. Acta, **45**, 138 (1962).
4. A. B. Foster, M. Stacey, J. M. Webber, and J. H. Westwood. Proc. Chem. Soc. 279 (1963).
5. A. B. Foster, M. Stacey, J. M. Webber, and J. H. Westwood. J. Chem. Soc. 2318 (1965).
6. N. K. Kochetkov and A. I. Usov. Tetrahedron Lett. 519 (1963).
7. S. McNally and W. G. Overend. Chem. Ind. (London), 2021 (1964).
8. B. T. Lawton, D. J. Ward, W. A. Szarek, and J. K. N. Jones. Can. J. Chem. **47**, 2899 (1969).
9. V. B. Mochalin, Y. N. Porshnev, and G I. Samokhvalov. Zhur. Obshch. Khim. **39**, 701 (1969). Index chemicus, **34** issue 296 115 606 (1969).
10. V. B. Mochalin, Y. N. Porshnev, and G. I. Samokhvalov. Zhur. Obshch. Khim. **39**, 681 (1969). Index chemicus **34**, issue 296 115 605 (1969). cf. also V. B. Mochalin, Y. N. Porshnev, and G. I. Samokhvalov. J. Gen. Chem. U.S.S.R. **38**, 82 (1968) (Engl. Ed.).
11. F. Sweet and R. K. Brown. Can. J. Chem. **46**, 2289 (1968).
12. C. S. Williams and R. K. Brown. Unpublished results.
13. J. E. Roff and R. K. Brown. Unpublished results.
14. F. Sweet and R. K. Brown. Can. J. Chem. **46**, 707 (1968).
15. C. C. Sweeley, R. Bentley, M. Makita, and W. W. Wells. J. Amer. Chem. Soc. **85**, 2497 (1963).

Can. J. Chem. Downloaded from www.nrcresearchpress.com by 210.87.254.40 on 09/05/12
For personal use only.

Can. J. Chem. Downloaded from www.nrcresearchpress.com by 210.87.254.40 on 09/05/12
For personal use only.

Vibrational spectra of some isonitrile complexes of cobalt(I) and (II)

P. M. BOORMAN, P. J. CRAIG, AND T. W. SWADDLE
Department of Chemistry, The University of Calgary, Calgary 44, Alberta

Received October 9, 1969

The Raman and low-frequency infrared spectra of the trigonal-bipyramidal complexes $Co(RNC)_5ClO_4$ (R = Me, Et, Ph) have been recorded and assigned. It is found that δ(CoCN) modes occur at higher frequencies than ν(Co—CN) modes. Although Raman spectra of the blue and yellow forms of $Co(PhNC)_5(ClO_4)_2$ could not be obtained, the low-frequency infrared spectra are consistent with the C_{4v} structure previously suggested (1). The dimeric complexes $Co_2(RNC)_{10}(ClO_4)_4$ (R = Me, Et) have been studied, and tentative assignments of the Raman and infrared spectra made on the basis of D_{4d} symmetry. Spectra of the complexes $Co_2(RNC)_{10}I(ClO_4)_3$ (R = Me, Et) strongly support the previously suggested structural formulation (2) $[(MeNC)_5Co—I—Co(MeNC)_5](ClO_4)_3$, and furthermore indicate that the Co—I—Co skeleton is linear.

Canadian Journal of Chemistry, **48**, 838 (1970)

Introduction

Although the vibrational spectra of metal carbonyls have been extensively studied (ref. 3, p. 121), there have been relatively few reports of the spectra of the isoelectronic isonitrile complexes. Previous spectroscopic investigations of isonitrile complexes of Co(I) and Co(II) have been mainly concerned with the ν(CN) region of the infrared spectrum (1, 4). We now report the results of our studies of the complexes $Co(RNC)_5ClO_4$ (R = Me, Et, Ph), $Co_2(RNC)_{10}(ClO_4)_4$ (R = Me, Et), $Co(PhNC)_5(ClO_4)_2$, and $Co_2(RNC)_{10}I(ClO_4)_3$ (R = Me, Et). Low-frequency infrared, and in most cases Raman, spectra have been obtained. This is therefore the first complete vibrational spectroscopic investigation of such complexes to be reported. The object of our studies was to examine and assign the spectra of the relatively simple D_{3h} and C_{4v} complexes, to extend the study to the more complicated D_{4d} complexes, and then to apply this knowledge to the compounds $Co_2(RNC)_{10}I(ClO_4)_3$, whose structures were not absolutely known. In as many cases as possible, solution spectra and the comparison of methyl and ethyl isonitrile complex spectra were utilized to avoid any ambiguities introduced by solid-state effects.

Experimental

Preparation of the Complexes

The complexes $[Co_2(CH_3NC)_{10}](ClO_4)_4$ (2), $[Co(CH_3NC)_5]ClO_4$ (2), $[Co(PhNC)_5(H_2O)](ClO_4)\cdot\frac{1}{2}H_2O$ (5), $Co(PhNC)_5(ClO_4)_2$ (1), $Co(PhNC)_5ClO_4$ (2), and $[Co_2(CH_3NC)_{10}I](ClO_4)_3$ (2) were prepared by published methods and found to be analytically pure. The new complexes $[Co_2(C_2H_5NC)_{10}](ClO_4)_4$, $[Co(C_2H_5NC)_5]ClO_4$, and $[Co_2(C_2H_5NC)_{10}I](ClO_4)_3$ were prepared by exactly the same methods as their methyl isonitrile analogues (2). Analytical data, yields, and melting points are presented in Table 1.

Infrared Spectra

Infrared spectra were measured as Nujol mulls between CsI plates, on a Perkin–Elmer Model 621 spectrophotometer, in the region 4000–200 cm^{-1}. For the range 350–33 cm^{-1}, a Beckman IR-11 spectrophotometer was used, with polyethylene cell windows. Where possible, the spectra of the compounds were also measured in methylene chloride in the ν(CN) region. Good agreement with the solid spectra was usually obtained, indicating the absence of solid state effects.

Raman Spectra

Raman spectra of the solids were obtained with a Cary 81 spectrometer using helium–neon laser excitation. The coaxial mode of sampling was employed, and in cases where sample decomposition tended to occur a glycerol film was applied to the sample surface for protection. In the case of the phenyl derivatives, this procedure was to no avail, as decomposition was sudden and violent. Hence no Raman data were obtained for

TABLE 1
Analytical data for EtNC complexes

Complex	Found (%)			Calculated (%)			Yield (%)	Melting point (°C)
	C	H	N	C	H	N		
$Co(C_2H_5NC)_5ClO_4$	32.9	5.0	13.2	33.8	4.7	13.1	45	Decomposes below m.p.
$Co_2(C_2H_5NC)_{10}(ClO_4)_4$	41.8	6.1	15.9	41.5	5.8	16.1	56	163–5*
$[Co_2I(C_2H_5NC)_{10}](ClO_4)_3$	32.4	4.7	12.7	32.9	4.6	12.8	62	155

*With decomposition.

TABLE 2
Vibrational frequencies of $Co(RNC)_5ClO_4$ (D_{3h})

Vibrational frequency, cm^{-1}*						
$Co(CH_3NC)_5ClO_4$		$Co(C_2H_5NC)_5ClO_4$		$Co(C_6H_5NC)_5ClO_4$		
Infrared	Raman	Infrared	Raman	Infrared	Assignment	
		2251 m				
	2238 s		2216 s		A_1'	
		2203 m		2185 shw		
2198 s		2169 vs		2137 shs	A_2''	ν(CN)
	2178 m		2159 vs		A_1'	
2139 vs	2142 m	2130 vs	2129 s	2108 vs	E'	
	600 m		590 m		E''	
522 vs		535 vs		562 vs	A_2''	δ(CoCNR)
510 vs	510 shw	521 shs	526 shw	529 shm	E'	
487 shs	485 vvs	480 shw†	478 m†	486 s	E'	
412 w			400 w	438 vw	A_2''	
386 w	388 m	344 w	347 m	285 vw	E'	
344 w						ν(Co—CNR)
324 m	325 m		320 m			
	285 vs	264 vw	258 vs	240 vvw	A_1'	
	225 m		200 s			
203 s		170 w		170 vw		
140 w						
	106 shs		105 shs			δ(CCoC) and others
88 w		88 w				
		56 vw				
38 w		44 w				

*s = strong, v = very, m = medium, w = weak, sh = shoulder.
†Coincident with a C_2H_5NC vibration.

these complexes. Attempts to obtain solution spectra were also unsuccessful in all cases, regardless of the solvent (e.g. methylene chloride, acetone, chloroform) used. Although no decomposition of the samples occurred, the laser beam was rapidly absorbed by the solution, preventing more than one or two passes through the rectangular cell.

Results and Discussion

The compounds investigated fall into two distinct classes: the five-coordinate cobalt(I) complexes and the various types of cobalt(II) compounds.

Data presented in the Tables which follow have been compiled so as to exclude bands due to the vibrations of the perchlorate anions, or the alkyl or aryl group of the isonitrile. We have also excluded any Raman bands which were shown to be artefacts.

Pentacoordinate Cobalt(I) Complexes, $[Co(RNC)_5]ClO_4$ (R = Me, Et, Ph)

The structure of $[Co(MeNC)_5]ClO_4$ has been determined by X-ray crystallography (6) and shown to be approximately trigonal-bipyramidal, with some slight crystallographic distortions of the $Co(MeNC)_5^+$ framework. It might be predicted that with the sterically bulkier ethyl and phenyl groups, these distortions would be enhanced, and that the spectroscopic selection rules would become increasingly likely to break down. The selection rules for the D_{3h} point group predict three Raman-active and two infrared-active ν(CoC) and ν(CN) modes, one of which (E') should be common to both spectra. In the case of the isoelectronic molecule $Fe(CO)_5$, the E' mode occurs as the lowest frequency carbonyl stretching vibration, and we find for $[Co(MeNC)_5]ClO_4$ that the lowest-frequency ν(CN) mode ($\sim 2140\ cm^{-1}$) is coincident in the Raman and infrared spectra (Table 2). We therefore assign this band to the E' mode. The higher-frequency Raman bands are assigned to A_1' stretching vibrations, whilst the infrared band at $2198\ cm^{-1}$ is assigned to the A_2'' mode. Hence these spectra are in excellent agreement with the predictions based on the known trigonal-bipyramidal structure.

The Raman spectrum of the compound $[Co(EtNC)_5]ClO_4$ is very similar in this region,

Can. J. Chem. Downloaded from www.nrcresearchpress.com by 210.87.254.40 on 09/05/12
For personal use only.

Can. J. Chem. Downloaded from www.nrcresearchpress.com by 210.87.254.40 on 09/05/12
For personal use only.

although the bands occur at $\sim 20\ cm^{-1}$ to lower energy. The infrared spectrum contains two extra weak bands, suggesting a possible distortion from true D_{3h} symmetry. The infrared spectrum of the phenyl isonitrile analogue is similar, again showing two strong bands, plus an extra weak shoulder. It resembles the solution spectrum reported by Pratt and Silverman (1), rather than their solid-phase spectrum. An examination of the frequencies of the two strong infrared bands for the three compounds studied indicates that they follow the order MeNC > EtNC > PhNC. This trend suggests that there is an increasing degree of metal–carbon π-bonding from the methyl to ethyl to phenyl isonitrile complexes.

In the lower-frequency region of the infrared spectra (Table 2), two distinct series of bands occur; a more intense series centered around $500\ cm^{-1}$, and a weaker set near $300–400\ cm^{-1}$. Again we draw an analogy with carbonyl complexes, in which the δ(MCO) modes give rise to more intense bands of higher frequency than those caused by metal–carbon stretching vibrations (7). Indeed, for many stereochemical situations this also appears to be true for cyano-complexes (ref. 3, p. 119). An assignment of ν(NC) and δ(MCN) modes made on this basis for the isonitrile complexes is consistent with their trigonal-bipyramidal structures, whereas the reverse assignments would be incompatible with the selection rules for the D_{3h} point group. We would therefore assign bands in the $500\ cm^{-1}$ region to δ(MCN) modes, and those around $300–400\ cm^{-1}$ to cobalt–carbon stretches. This is also consistent with the assignment of the spectrum of $Ni(CO)_3MeNC$ made by Bigorgne (8).

The selection rules for D_{3h} symmetry allow four Raman-active and three infrared-active δ(CoCN) modes, with two coincidences (E'). For the methyl and ethyl isonitrile complexes, we observe three infrared bands in the $500\ cm^{-1}$ region, two of which have Raman equivalents. For $Co(PhNC)_5(ClO_4)_2$, again three infrared bands are observed. For the methyl and ethyl isonitrile complexes, an additional Raman band occurs at $\sim 600\ cm^{-1}$; which by comparison with the spectra of $Fe(CO)_5$ (ref. 3, p. 121) we assign as an E'' mode, while the exclusively infrared-active vibration (for example at 522 cm^{-1} for $Co(MeNC)_5ClO_4$) is assigned to the A_2'' mode. Thus our assignments are completely consistent with δ(CoCN) occurring at higher energy than ν(Co—C) for these complexes.

The vibrations in the $300–400\ cm^{-1}$ region are weak in the infrared and harder to assign. As for ν(CN), four ν(CoC) modes are expected, of which three are Raman-active, two infrared-active, with one coincidence. Coincident peaks occur at $386\ cm^{-1}$ (MeNC complex) and 344 cm^{-1} (EtNC), and are assigned as E' modes, while the other infrared bands at higher energy (one per compound) are readily assigned to the A_2'' asymmetric stretching vibration of the axial cobalt–carbon bonds. This is the highest-frequency infrared stretching vibration, again analogous to the spectrum of the isoelectronic iron pentacarbonyl. Although two Raman-active A_1' vibrations are predicted, only one peak is observed which could be assigned to these modes.

Bands at lower frequencies have not been specifically assigned, but presumably most are associated with δ(CCoC) modes.

Cobalt(II) Complexes, $Co(PhNC)_5(ClO_4)_2$

The simplest complexes of cobalt(II) have been shown to be formed with phenyl isonitrile. Two forms of $Co(PhNC)_5(ClO_4)_2$ have been identified by Pratt and Silverman (1). These are an anhydrous yellow form, which it was concluded has a square-pyramidal structure, and a blue hydrate, in which the sixth coordination position of the octahedron is occupied by a water molecule. For the C_{4v} point group, to which both the above cations appear to belong, three infrared-active ν(CN) and ν(CoC) modes and four δ(CoCN) modes should occur.

The infrared spectra (Table 3) are very similar indeed. Three ν(CN) bands occur, which by comparison with assignments made for analogous carbonyl complexes (9, 10) are assigned to the E ($\sim 2210\ cm^{-1}$), the A_1 (mainly axial CN stretching at $\sim 2187\ cm^{-1}$), and the A_1 (mainly radial CN stretching mode at $\sim 2233\ cm^{-1}$) modes, respectively. At lower frequencies, the bands observed are tentatively assigned to the various types of vibration by comparison of band positions and intensities with those of the D_{3h} species outlined above. In the case of these phenyl isonitrile complexes we were unable to obtain Raman spectra (see Experimental Section). We could not unambiguously identify a $\nu(Co—OH_2)$ band in the spectrum of the blue complex, but the remarkable general similarity of the spectra of

TABLE 3

Infrared vibrational frequencies for the blue and the yellow forms of $Co(C_6H_5NC)_5(ClO_4)_2$

Frequency, cm^{-1}*			
Blue form†	Yellow form‡	Assignment	
2236 shw	2233 shw	A_1(equatorial)	ν(CN)
2209 vs	2211 vs	E	
2184 s	2187 s	A_1(axial)	
548 s	550 s		δ(CoCN)
521 w	521 w		
510 w	513 w		
428 vw	427 vw		ν(Co—CN)
	328 vw		
300 vw	303 vw		
263 vw	267 vw		
230 vw			
183 vw	180 vw		δ(CCoC) and others
	168 vw sh		
110 w	121 vw		

*s = strong, v = very, w = weak, sh = shoulder.
†$[Co(C_6H_5NC)_5(H_2O)][ClO_4]_2.\frac{1}{2}H_2O$.
‡$Co(C_6H_5NC)_5(ClO_4)_2$.

these two complexes would certainly support the suggestion (1) that both the blue and yellow forms have the same C_{4v} symmetry.

$[Co_2(RNC)_{10}](ClO_4)_4$ (R = Me, Et)

It has been shown by X-ray crystallography (11) that the structure of $Co_2(MeNC)_{10}(ClO_4)_4$ contains the $[Co_2(MeNC)_{10}]^{4+}$ cation, which possesses approximately D_{4d} symmetry. For this system, group theory would predict four Raman-active and three infrared-active vibrations, for the ν(CoC) and ν(CN) modes. None of these would be coincident. Alternatively, for somewhat similar systems, such as $(CO)_5Mn—Hg—Mn(CO)_5$, it is sometimes possible to interpret the spectra on the basis of local C_{4v} symmetry (7). Under these circumstances, the same number of Raman and infrared bands should be observed as for D_{4d}, but there would now be three coincidences. For both the complexes investigated, we find that a treatment based on the D_{4d} point group is more appropriate. A recent publication (12), which appeared after completion of our experimental work, reports the Raman and infrared spectra of the compound $Co_2(MeNC)_{10}(ClO_4)_4$. In some respects, our spectra (Table 4) do not agree with these, particularly in the ν(CN) region, but for this region our data agree quite closely with the infrared spectrum reported by Pratt (1). For both the methyl and ethyl isonitrile complexes, whose spectra are so similar as to indicate that the compounds are isostructural, we find three infrared bands in the ν(CN) region. The pattern of intensities resembles those reported by various workers (13–15) for similar carbonyl complexes. Thus, the most intense peak (2264 cm^{-1} for the MeNC complex) is assigned to the E' mode, the higher-frequency shoulder (2285 cm^{-1}) to the B_2 vibration involving mainly the radial isonitrile ligands, and the lower frequency shoulder to a B_2 mode involving mostly the axial isonitrile groups. Flitcroft and co-workers (13) found that for $Mn_2(CO)_{10}$ the higher-frequency shoulder was more intense than predicted for such a system (ref. 3, p. 119 and ref. 9). We notice the same effect here, so that some mixing of the two B_2 vibrations may be occurring. The infrared spectrum of the ethyl isonitrile complex also exhibits the same features.

The Raman spectra of both $Co_2(MeNC)_{10}(ClO_4)_4$ and $Co_2(EtNC)_{10}(ClO_4)_4$ contain only two very strong bands in the ν(CN) region, rather than the predicted four. For the analogous $Re_2(CO)_{10}$ molecule, it was found that the E_3 mode was very weak and at lower frequency than the infrared bands (14, 15), so we do not assign either of our bands to this mode. The Raman band which is higher than any of the infrared absorption bands we assign to an A_1 vibration involving radial groups, in accordance with the

Can. J. Chem. Downloaded from www.nrcresearchpress.com by 210.87.254.40 on 09/05/12
For personal use only.

TABLE 4
Vibrational frequencies of $Co_2(RNC)_{10}(ClO_4)_4$ (D_{4d})

Frequency, cm^{-1}*					
$Co_2(CH_3NC)_{10}(ClO_4)_4$		$Co_2(C_2H_5NC)_{10}(ClO_4)_4$ (D_{4d})			
Infrared	Raman	Infrared	Raman		Assignment
	2291 vs		2283 vs	A_1	ν(CN)
2285 sh		2269 shs		B_2	
	2269 vs		2255 vs	E_2 or A_1	
2264 vs		2250 vs		E_1	
2236 shm		2220 shs		B_2	
522 vs	522 m	528 vs	534 m		δ(CoCN)
512 vs		505 shm			
	490 m	488 shm†	489 m†		
464 w					
391 w	389 m	375 w	375 w		ν(Co—CN)
	349 m		335 w		
323 w	325 s				
	186 s		192 s		ν(Co—Co)
230 sh		266 w	261 w		δ(CCoC) and others
222 m		204 vw			
171 vw		142 vw			
114 m	110 shvs	90 m	109 s		
64 vw		56 vw			

*s = strong, v = very, m = medium, w = weak, sh = shoulder.
†Coincident with a C_2H_5NC vibration.

assignment for $Re_2(CO)_{10}$ (14, 15). The other Raman peak is assigned to the E_2 and/or A_1 vibration. Since two separate, strong bands occur for $Re_2(CO)_{10}$ it seems likely that in the present cases the two vibrations are accidentally degenerate.

In the lower regions of the spectra, fewer Raman and infrared peaks are observed than are predicted by group theory. In the infrared spectra, two distinct areas of absorption occur which we assign to δ(CoCN) and ν(CoC) modes, respectively, but no attempt has been made to individually assign the peaks.

For both the methyl and ethyl isonitrile complexes, it should be possible to identify a Raman peak associated with the cobalt–cobalt stretching vibration. Strong Raman bands occur at 186 and 192 cm^{-1}, respectively, and also at $\sim$ 110 cm^{-1} in both spectra. On the grounds of intensity alone, both these bands might be considered as candidates for such an assignment. However, the 110 cm^{-1} bands have infrared counterparts and also occur in the spectra of some complexes without metal–metal bonds. We therefore conclude that the 192 and 186 cm^{-1} peaks should be assigned as Co—Co stretching vibrations for ethyl and methyl isonitrile complexes, respectively. This assignment agrees with that made by Griffith and Wickham (12), who placed ν(Co—Co) at 190 cm^{-1} for $Co_2(MeNC)_{10}(ClO_4)_4$.

$[Co_2(RNC)_{10}I](ClO_4)_3$ (R = Me, Et)

The complex $Co_2(MeNC)_{10}I(ClO_4)_3$ was first reported by Sacco and Freni (2). On the basis of analytical and conductivity data it was formulated as μ-iododecakis(methylisocyano)cobalt(II) perchlorate, $[(MeNC)_5Co—I—Co(MeNC)_5](ClO_4)_3$. We have measured the vibrational spectra of this complex and its ethyl isonitrile analogue, and have confirmed the presence of cobalt–iodine bonding. Furthermore, our data suggest that the Co—I—Co skeleton is linear rather than bent.

Of the two possible iodine-bridged structures, the bent one leads to C_{2v} symmetry, while for a linear system the point group would be D_{4d} (or possibly D_{4h}). The group theoretical predictions for the former system would lead to eight infrared-active ν(CN) and ν(CoC) modes, while for D_{4d} symmetry a much simpler spectrum would result, with only three ν(CoC) or ν(CN) bands.

Can. J. Chem. Downloaded from www.nrcresearchpress.com by 210.87.254.40 on 09/05/12
For personal use only.

TABLE 5
Vibrational frequencies of $[Co_2(RNC)_{10}I][ClO_4]_3$

Frequency, cm^{-1}*					
$[Co_2(MeNC)_{10}I](ClO_4)_3$		$[Co_2(EtNC)_{10}I](ClO_4)_3$			
Infrared	Raman	Infrared	Raman		Assignment
	2266 s		2249 m	A_1	ν(CN)
2254 shs		2240 shs		B_2	
2234 vs		2219 vs		E_1	
	2231 m			E_2	
2226 shvs		2207 shvs		B_2	
	2221 s		2208 m	A_1	
	534 w				δ(CoCN)
517 vs		532 s			
496 vs		521 shm			
	491 m				
471 shw		483 shw†			
			476 w		
422 w		422 w			ν(Co—CN)
411 w		410 w			
	411 w				
375 w		356 w			
	367 m				
353 w		344 w			
	345 w				
	245 vvs		222 vvs		ν(Co—I—Co) symmetric
220 shm		270 wbr			δ(CCoC) and others
215 m		180 wbr			
150 shw	160 shs		145 shs		
126 w		117 w			
108 vw	80 shs	96 w	110 shs		
36 vw		59 vw			

*s = strong, v = very, m = medium, w = weak, sh = shoulder, br = broad.
†Coincident with C_2H_5NC vibration.

Studies on systems of this type have been made by other workers. In spite of a complex infrared spectrum, Ruff (16) suggested that the $[M_2(CO)_{10}I]^-$ ion (M = Cr, Mo, W) has a linear M—I—M bridge, ascribing the extra bands to impurities. However, in a more recent publication (17), reference was made to an X-ray crystal structure of $[Cr_2(CO)_{10}I]^-$ in which the Cr—I—Cr bond angle was found to be 118°. Lindner and Behrens (18) studied $Cr_2(CO)_{10}I$ and found only three ν(CO) bands in the infrared spectrum, and suggested that a linear Cr—I—Cr bridge was present. Furthermore, the infrared spectrum of the complex $Cl_2Sn[Co(CO)_4]_2$ presents a complex ν(CO) region (19), whereas the linear $Hg[Co(CO)_4]_2$ only displays three fundamental ν(CO) absorption bands (20); so the symmetry of the metal skeleton does have a large effect on the ν(CO) region of the spectrum.

We have applied similar criteria to examining the ν(CN) region of the spectra of the isonitrile complexes. The infrared spectra (Table 5) of both complexes are very simple, having one strong absorption band due to ν(CN), with a shoulder on either side. This is in accordance with the predictions of group theory for the D_{4d} point group. The Raman spectra are also simple, with three bands occurring in the case of the MeNC complex, and only two for the EtNC analogue. In the former case, two of the Raman bands are very close in energy to infrared bands, while in the latter case one of the two Raman bands is almost coincident with an infrared band. The assignments (Table 5) are made on the same basis as those made for the metal–metal bonded complexes, assuming D_{4d} symmetry.

Infrared and Raman spectra in the δ(MCN) and ν(CoC) regions were similar to those of $Co_2(RNC)_{10}(ClO_4)_4$ (Table 4). The notable feature of the Raman spectra of each complex is an intense peak, at 245 and 222 cm^{-1} for methyl and ethyl derivatives, respectively. No infrared

Can. J. Chem. Downloaded from www.nrcresearchpress.com by 210.87.254.40 on 09/05/12
For personal use only.

bands occurred at these frequencies. It is therefore reasonable to assign these bands to symmetric ν(CoICo) vibrations. For a linear Co—I—Co skeleton, group theory predicts (21) that the symmetric stretch will be Raman-active, while an asymmetric stretching vibration normally occurs at higher frequency, exclusively in the infrared spectrum. For a bent system, both the symmetric and asymmetric stretching frequencies should exhibit Raman and infrared activity. No second Raman peak is observed, which again is consistent with a linear Co—I—Co bond system. By comparison with the spectra of $Co_2(RNC)_{10}(ClO_4)_4$, we find no infrared band we can unequivocally assign to the asymmetric ν(Co—I—Co) mode, perhaps because of a coincidence with a skeletal vibration. It has been noted that metal–iodine stretches are sometimes weak in the infrared (see, for example, ref. 22).

The combined evidence of the isonitrile (CN) stretching frequencies and the Co—I stretching vibrations are strongly indicative of a linear bridging iodide ion. However, in view of the C_{2v} structure of $[(CO)_5CrICr(CO)_5]^-$ quoted above it would be interesting to determine the structure by an X-ray study.

We acknowledge the financial support of the National Research Council of Canada, particularly in providing funds for the purchase of the Cary 81 laser Raman spectrometer. We thank Dr. J. M. Bertie and his colleagues at the University of Alberta for the use of a Beckman IR-11 spectrometer, and we are grateful to Mrs. S. Swaddle for carrying out all microanalyses.

1. J. M. Pratt and P. R. Silverman. J. Chem. Soc. A, 1286 (1967).
2. A. Sacco and M. Freni. Gazz. Chim. Ital. **89**, 1800 (1959).
3. D. M. Adams. Metal–ligand and related vibrations. Edward Arnold and Co., London. 1967.
4. F. A. Cotton and R. V. Parish. J. Chem. Soc. 1440 (1960).
5. A. Sacco. Gazz. Chim. Ital. **84**, 370 (1954).
6. F. A. Cotton, T. G. Dunne, and J. S. Wood. Inorg. Chem. **4**, 318 (1965).
7. D. M. Adams and A. Squire. J. Chem. Soc. A, 2817 (1968).
8. M. Bigorgne. J. Organometal. Chem. **1**, 101 (1963).
9. L. E. Orgel. Inorg. Chem. **1**, 25 (1962).
10. M. A. El-Sayed and H. D. Kaesz. J. Mol. Spectrosc. **9**, 310 (1962).
11. F. A. Cotton, T. G. Dunne and J. S. Wood. Inorg. Chem. **3**, 1495 (1964).
12. W. P. Griffith and A. J. Wickham. J. Chem. Soc. A, 834 (1969).
13. N. Flitcroft, D. K. Huggins and H. D. Kaesz. Inorg. Chem. **3**, 1123 (1964).
14. I. J. Hymans, D. Jones and E. R. Lippincott. J. Chem. Soc. A, 1987 (1967).
15. J. Lewis, A. R. Manning, J. R. Miller, M. J. Ware, and F. Nyman. Nature, **207**, 142 (1965).
16. J. K. Ruff. Inorg. Chem. **7**, 1821 (1968).
17. J. K. Ruff and R. B. King. Inorg. Chem. **7**, 180 (1969).
18. E. Lindner and H. Behrens. Spectrochim. Acta, **23A**, 3025 (1967).
19. D. J. Patmore and W. A. G. Graham. Inorg. Chem. **5**, 1405 (1966).
20. G. Bor and L. Marko. Spectrochim. Acta, **16**, 1105 (1960).
21. K. Nakamoto. Infrared spectra of inorganic and coordination compounds. John Wiley and Sons, Inc., New York. 1963. p. 76.
22. J. M. Jenkins and J. G. Verkade. Inorg. Chem. **6**, 2250 (1967).

Can. J. Chem. Downloaded from www.nrcresearchpress.com by 210.87.254.40 on 09/05/12
For personal use only.

Can. J. Chem. Downloaded from www.nrcresearchpress.com by 210.87.254.40 on 09/05/12
For personal use only.

A new route to 5- and 6-membered ring sultones

T. Durst and K.-C. Tin
Department of Chemistry, University of Ottawa, Ottawa 2, Ontario

Received October 3, 1969

Reaction of 1,2- or 1,3-alkanedisulfonate esters with one equivalent of *n*-butyllithium in tetrahydrofuran at −78 to 10° affords 5- and 6-membered ring sultones. Similar treatment of alkanesulfonate esters of 1,2-halohydrins gives 5-membered ring sultones. 1,2-Diols and 1,2-halohydrins of known stereochemistry were converted into 5-membered ring sultones in which the stereochemistry at 2 of the 3 ring carbon atoms is uniquely defined. Extension of these reactions to the formation of 7- and 8-membered ring sultones was not successful and products derived from an initial intermolecular reaction were obtained.

Canadian Journal of Chemistry, **48**, 845 (1970)

Introduction

The synthesis of sultones is generally carried out either by cyclization of the appropriate halo- or hydroxyalkanesulfonic acid (1) or by sulfonation of olefins with dioxane – sulfur trioxide (1,2). Both of these methods are rather limited; the former suffers from a lack of ready preparation of all but the most simple of the required precursors, while the latter is generally useful only in the synthesis of 3,3-dialkyl-3-hydroxypropanesulfonic acid sultones.

The recent reports of the preparation of α-sulfonate ester carbanions (3–5) have prompted us to investigate their use in the synthesis of sultones according to eq. [1]. Such cyclizations appeared to have considerable potential for the production of a variety of sultones because of the ready availability of the potential precursors i.e. diols or halohydrins.

Discussion of Results

Initial experiments were carried out on 1,2-ethylene dimethanesulfonate (**1**) and 1,3-propylene dimethanesulfonate (**2**). Treatment of either **1** or **2** in tetrahydrofuran at −78° with one equivalent of *n*-butyllithium followed by warming to 0° for 30 min yielded the sultones **3** and **4** in 68[1] and 88% yield respectively. The cyclization of the corresponding ethane- and phenylmethanesulfonate esters was carried out similarly except that longer reaction times were required. The crude products from these reactions were generally contaminated with up to 20% of starting materials even when the reaction time was 2 days. The yields of the purified monosubstituted sultones ranged from 47–74% (Table 1). Analytical and spectroscopic properties were in agreement with the assigned structures and are recorded in the Experimental section.

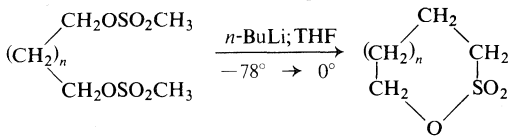

1 $n = 0$ — **3** $n = 0$ (68%)
2 $n = 1$ — **4** $n = 1$ (88%)

Dimethanesulfonate esters of unsymmetrical diols, e.g. 1,2-propane- or 1,3-butanediol, cyclized as expected, with displacement occurring preferentially at the least substituted carbon. Thus the dimesylates **5** and **6** afforded the sultones **7** and **8** in 81 and 75% yield respectively. Nuclear magnetic resonance (n.m.r.) inspection of the total crudes indicated the absence of significant amounts of the isomeric sultones **9** and **10**. Equilibration of the two isomeric lithio derivatives **11***a* and **11***b* is expected to be facile (6) thereby allowing the preferential production of

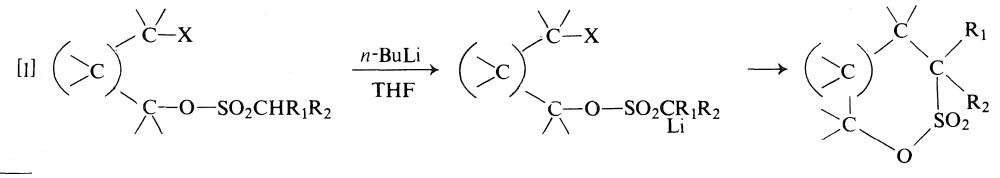

[1]The lower yield of **3** was probably due to its ease of hydrolysis. It was found that only about 70% of a sample of **3** could be recovered when put through the workup conditions (5).

TABLE 1

Formation of 5- and 6-membered ring sultones

Precursor	Sultone	Yield (%)
1,2-Ethylene dimethanesulfonate	Propane-1,3-sultone	68
1,3-Propylene dimethanesulfonate	Butane-1,4-sultone	88
1,2-Ethylene diphenylmethanesulfonate	3-Hydroxy-1-phenylpropanesulfonic acid 1,3-sultone	47
1,3-Propylene diphenylmethanesulfonate	4-Hydroxy-1-phenylbutanesulfonic acid 1,4-sultone	51
1,3-Propylene diethanesulfonate	4-Hydroxy-1-methylbutanesulfonic acid 1,4-sultone	74
1,2-Propylene dimethanesulfonate	3-Hydroxy-3-methylpropanesulfonic acid 1,3-sultone	81
1,3-Butylene dimethanesulfonate	4-Hydroxy-4-methylbutanesulfonic acid 1,4-sultone	75
β-Chloroethyl methanesulfonate	Propane-1,3-sultone	19
β-Chloroethyl phenylmethanesulfonate	3-Hydroxy-1-phenylpropanesulfonic acid 1,3-sultone	30*
trans-2-Bromocyclohexyl methanesulfonate	**15**	33,39†
trans-2-Bromocyclooctyl methanesulfonate	**17**	36,64†
cis-1,2-Cyclooctenyl dimethanesulfonate	**19**	17,48†

*Yield determined by n.m.r.
†Yield based on consumed starting material.

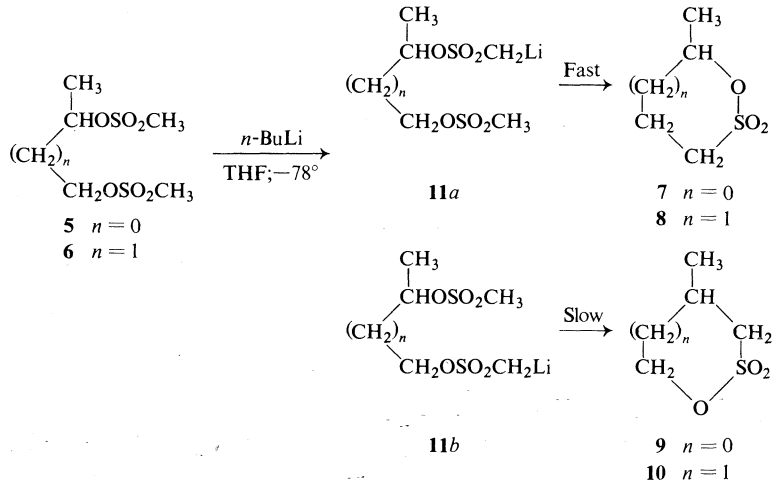

SCHEME 1

the isomer resulting from the faster cyclization (Scheme 1). Although the experimental data is to date very limited it seems reasonable to expect high selectivity in the cyclization of mono-lithio derivatives of other unsymmetrically substituted 1,2- and 1,3-disulfonate esters.

Alkanesulfonate esters of 1,2-halohydrins have also been used for the synthesis of 5-membered ring sultones. The yields of cyclized product from these compounds were considerably lower than those obtained from the disulfonate esters (Table 1); in general they roughly parallel the ease of displacement of the leaving group ($^-OSO_2R > Br^- > Cl^-$). For instance, β-chloroethyl phenylmethanesulfonate (**12**) gave the sultone **13** in 30% yield, while the mesylate of *trans*-2-bromocyclohexanol (**14**) afforded a 33% yield of the *cis*-bicyclic sultone (**15**). The structural assignment of **15** rests on its mode of synthesis, analytical and spectroscopic data. The infrared (i.r.) spectrum showed strong bands at 1340, 1150, 908, and 810 cm^{-1}; n.m.r. absorption occurred at δ = 4.8–5.0 (*m*, 1H, *H*—C—O), an 8-line multiplet from δ = 3.0–3.8 (2H) due to CH—CH_2SO_2— with J_{gem} = 13 c.p.s. and J_{vic} 7.0 and 3.0 c.p.s., and multiplets at δ = 2.5–2.9 (1H) and 1.2–2.4 (8H).

The attractiveness of the above route is the ready availability of 1,2-halohydrins and 1,2-

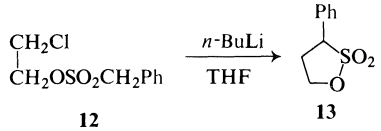

Can. J. Chem. Downloaded from www.nrcresearchpress.com by 210.87.254.40 on 09/05/12
For personal use only.

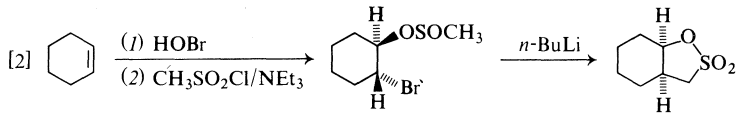

14 **15**

diols of known stereochemistry which in turn can lead to sultones having at least part of their stereochemistry uniquely defined e.g. as in eq. [2].

To illustrate the above claim we have synthesized from *cis*-cycloöctene both the *cis*- and *trans*-fused bicyclic sultones **17** and **19**; the final step being the cyclization of the *trans*-2-bromocyclooctyl methanesulfonate (**16**) and *cis*-1,2-cyclooctylene dimesylate (**18**) respectively (Scheme 2). The i.r. and n.m.r. spectra are in agreement with the gross structure of both **17** and **19**. The stereochemical assignment is however based solely on the mode of synthesis and could in these particular cases not be verified by the spectroscopic methods.

The success achieved in the formation of 5- and 6-membered ring sultones could not be duplicated for the 7-membered ring species. Cyclization reactions were attempted with a number of sulfonate esters among them **20** and **21**. The crude reaction mixture from the attempted cyclization of the mesylate of 4-chlorobutanol (**20**) was separated by preparative t.l.c. In addition to significant amounts of starting material, 34% of a colorless oil was obtained which was identified by spectroscopic methods (i.r. peaks at 1330 (s), 1155 (s), and 920 (s) cm^{-1}; n.m.r. absorption δ = 4.2–4.6(m, 2H), 3.4–3.9 (m, 3H), and 1.5–2.4 (12H)) and by independent synthesis as 4-chlorobutyl cyclopentanesulfonate (**22**). The alternate synthesis of **22** and its probable mode of formation from **20** are shown in Scheme 3. The products from the other cyclization attempts were similarly separated. Spectroscopic data in each case indicated that the product was analogous to **22**, i.e. an ester of a cyclopentanesulfonic acid e.g. **23**. The products were not further characterized. A single attempt to obtain an 8-membered ring sultone from **24** was unsuccessful and the starting material was recovered.

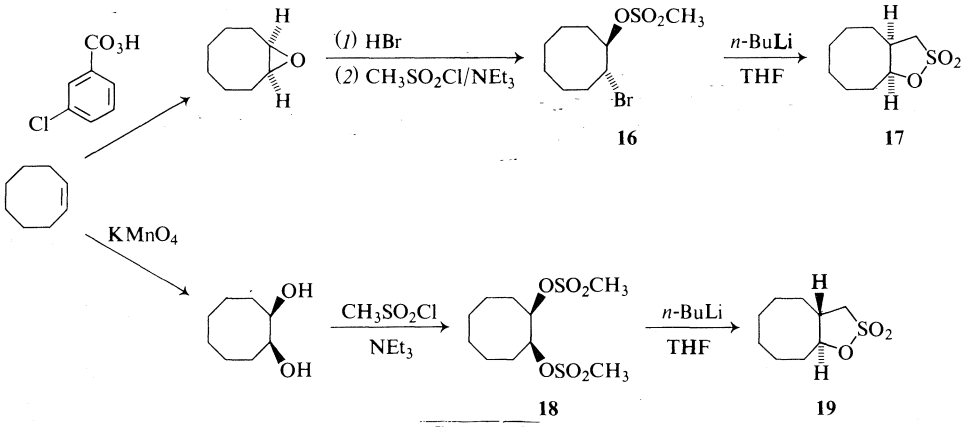

16 **17** **18** **19**

SCHEME 2

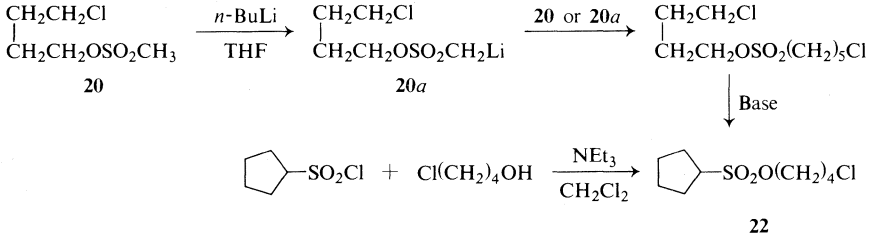

20 **20*a*** **22**

SCHEME 3

Can. J. Chem. Downloaded from www.nrcresearchpress.com by 210.87.254.40 on 09/05/12
For personal use only.

Can. J. Chem. Downloaded from www.nrcresearchpress.com by 210.87.254.40 on 09/05/12
For personal use only.

TABLE 2

Preparation of alkanesulfonate esters

Ester	Yield (%)	Melting point or boiling point/mm (°C)	Analysis (Found) (%)	Spectroscopic properties	
				n.m.r. (δ)	i.r. (cm^{-1})
1,2-Ethylene diphenylmethanesulfonate	74	141	C, 51.79 H, 4.09	4.23 (s, 2H), 4.40 (s, 2H) 7.40 (s, 5H)	1352 (s), 1160 (s) 905 (s)
1,3-Propylene diethanesulfonate	53	dec.*	C, 32.28 H, 6.17	1.34 (t, 6H), 2.12 (quint., 2H) 3.08 (quart., 4H), 4.28 (t, 4H)	1340 (vs), 1158 (s) 920 (s)
1,3-Propylene diphenylmethanesulfonate	55	109–110	C, 53.08 H, 5.32	1.90 (quint., 2H), 4.05 (s, 2H) 4.32 (s, 2H), 7.37 (s, 5H)	1350 (vs), 1160 (s) 922 (s)
trans-2-Bromocyclohexyl methanesulfonate	50	59	C, 32.71 H, 5.04 S, 12.33 Br, 31.24	1.1–2.7 (m, 8H), 3.10 (s, 3H) 3.9–4.3 (m, 1H), 4.4–4.8 (m, 1H)	1350 (vs), 1160 (s) 960 (s), 940 (m), 895 (s), 867 (s) 817 (s)
trans-2-Bromocyclooctyl methanesulfonate	96†	dec.*		1.2–2.4 (m, 12H), 3.10 (s, 3H) 4.1–4.5 (m, 1H), 4.6–5.1 (m, 1H)	1342 (s), 1160 (s) 908 (s)
cis-1,2-Cyclooctylene dimethanesulfonate	75	69–70	C, 39.76 H, 6.73 S, 20.85	1.2–2.4 (m, 12H), 3.10 (s, 6H) 4.9–5.2 (m, 2H)	1350 (s), 1160 (s) 890 (s)
4-Chlorobutyl methanesulfonate	74	100–103/1.5	C, 32.29 H, 5.96	1.8–2.1 (m, 4H) 3.02 (s, 3H), 3.5–3.7 (m, 2H) 4.2–4.4 (m, 2H)	1340 (vs), 1165 (s) 930 (vs)

*Substance decomposed on attempted distillation at 0.2 mm.
†Crude yield, estimated purity by n.m.r. > 90%.

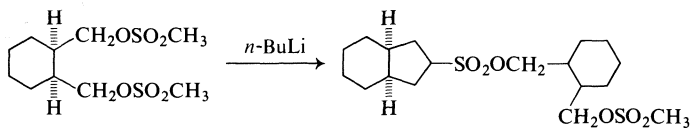

21 23

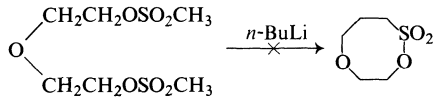

24

Experimental

Melting points were determined with a Thomas Hoover apparatus and are not corrected; boiling points are also not corrected. Infrared spectra were recorded on a Beckmann IR8 or Beckmann IR20 i.r. spectrophotometers and n.m.r. spectra were obtained on Varian Associates model HA-100 or T-60 spectrophotometers.

Preparation of the Sulfonate Esters

In general the diol was dissolved in dry methylene chloride containing 2.2 equivalents of alkanesulfonyl chloride. The solution was cooled in an acetone – dry ice bath and treated with dropwise addition of 2.2 equivalents of triethylamine in methylene chloride. After the addition of the triethylamine was complete the reaction mixture was allowed to warm to room temperature and poured into water. The methylene chloride layer was separated, dried over magnesium sulfate, and the solvent evaporated. The products were purified either by recrystallization, column chromatography, or distillation under reduced pressure. The yields refer to purified products. The monosulfonate esters of the halohydrins were similarly prepared except that for each equivalent of halohydrin only 1.1 equivalents of sulfonyl chloride and triethylamine were employed.

The following esters have been described in the literature: 1,2-ethylene dimethanesulfonate (7), 1,2-propylene dimethanesulfonate (8), 1,3-propylene dimethanesulfonate (7), 1,3-butylene dimethanesulfonate (9), β-chloroethyl methanesulfonate (10), β-chloroethyl phenylmethanesulfonate (10), and the dimethanesulfonate **22** (11). The physical and spectroscopic properties of the other sulfonate esters are reported in Table 2.

Formation of the Lithio Derivatives of the Sulfonate Ester and Subsequent Cyclization. General Procedure

To a tetrahydrofuran solution of disulfonate ester or β-halosulfonate ester at −78° under nitrogen atmosphere was added via syringe 1.05–1.10 equivalent of *n*-butyllithium (Foote Mineral Co., 1.6 *M* in hexane). The reaction mixture was allowed to warm to −20, 0°, or room temperature for the times specified. It was then poured into water and extracted with methylene chloride. The organic extracts were dried over magnesium sulfate and the solvent evaporated. The crude products were usually purified by preparative thin-layer chromatography (t.l.c.); yields refer to purified materials.

1,3-Propane Sultone

(a) From 1,2-Dimethanesulfonate

1,2-Ethylene dimethanesulfonate (1.00 g, 4.6 mmoles) was dissolved in 30 ml of tetrahydrofuran at −78° and then treated with 3.0 ml (4.8 moles) of *n*-butyllithium. The reaction mixture was warmed to −20° for 30 min during which time a colorless precipitate was formed. Workup gave 380 mg (68%) of 1,3-propane sultone, identified by comparison of t.l.c. behavior and i.r. spectrum with authentic commercial material.[2]

(b) From β-Chloroethyl Methanesulfonate

To a solution of 1.28 g (6.6 mmoles) of the ester in 50 ml of tetrahydrofuran at −78° were added dropwise 7.2 mmoles of *n*-butyllithium. The reaction mixture was stored for 2 days. The crude product (316 mg) was separated by preparative t.l.c. and yielded 155 mg (19%) of 1,3-propane sultone.

1,4-Butane Sultone

To a solution of 780 mg (3.36 mmoles) of 1,3-propylene dimethanesulfonate in 30 ml of tetrahydrofuran at −78° were added 2.2 ml (3.5 mmoles) *n*-butyllithium. Workup of the reaction mixture after it had been stored at −20° for 30 min gave 400 mg (88%) of 1,4-butane sultone whose i.r. was identical with that of authentic material.[2]

*3-Hydroxy-1-phenylpropanesulfonic Acid 1,3-Sultone (**13**)*

(a) From 1,2-Ethylene Diphenylmethanesulfonate

1,2-Ethylene diphenylmethanesulfonate (255 mg, 0.69 mmole) was dissolved in 10 ml of tetrahydrofuran at −78° and treated with 0.70 mmole of *n*-butyllithium. The reaction mixture was stored at 0° for 3 days. Workup gave 129 mg of crude material whose n.m.r. spectrum indicated approximately 85% product and 15% starting material; n.m.r. yield approximately 80%. Purification by preparative t.l.c. gave 64 mg (47%) of sultone m.p. 93.5–96° (methylene chloride – pentane). The i.r. spectrum ($CHCl_3$) showed strong bands at 1350, 1160, and 990 cm^{-1}; n.m.r. peaks occurred at δ = 2.6–3.1 (m, 2H), 4.2–4.7 (m, 3H), and 7.40 (s, 5H).

Anal. Calcd. for $C_9H_{10}O_3S$: C, 54.54; H, 5.09; S, 16.15. Found: C, 54.15; H, 5.16; S, 16.19.

[2]Supplied by the Aldrich Chemical Co. Ltd., Milwaukee, Wis.

Can. J. Chem. Downloaded from www.nrcresearchpress.com by 210.87.254.40 on 09/05/12
For personal use only.

Can. J. Chem. Downloaded from www.nrcresearchpress.com by 210.87.254.40 on 09/05/12
For personal use only.

(b) From β-Chloroethyl Phenylmethanesulfonate

Sulfonate ester (1.50 g, 6.4 mmoles) was converted into its lithio salt in the usual manner at −78°. The reaction mixture was stored at 5° for 3 h. An n.m.r. spectrum of the crude product (674 mg) indicated a 30% yield of the sultone **13**.

3-Hydroxy-3-methylpropanesulfonic Acid 1,3-Sultone

1,2-Propylene dimethanesulfonate (1.57 g, 6.8 mmoles) was dissolved in 40 ml tetrahydrofuran at −78° and reacted with 7.5 mmoles *n*-butyllithium. The reaction mixture was kept at 10° for 12 h during which time a colorless precipitate was formed. Workup, followed by flash distillation of the crude product, gave 0.75 g (81%) of sultone **7**. The n.m.r. spectrum was in agreement with that given by Ohline *et al.* (12).

4-Hydroxy-1-phenylbutanesulfonic Acid 1,4-Sultone

A solution of 2.01 g (5.2 mmoles) of 1,3-propylene diphenylmethanesulfonate in 30 ml of tetrahydrofuran at −78° was treated with 5.5 mmoles of *n*-butyllithium, and then stored at room temperature overnight. Workup gave 1.22 g of crude product from which 0.56 g (51%) of pure sultone, m.p. 157–158.5°, was obtained after two recrystallizations from methylene chloride – pentane. Spectroscopic properties were as follows: i.r. ($CHCl_3$), 1350 (vs), 1162 (s), 1010 (s) and 925 (s) cm^{-1}; n.m.r. peaks ($CDCl_3$), δ = 1.8–2.8 (m, 4H), 4.22 (d of d, J = 4 and 12 c.p.s., 1H), 4.3–4.8 (m, 2H) and 7.3–7.6 (m, 5H).

Anal. Calcd. for $C_{10}H_{12}O_3S$: C, 56.60; H, 5.70; S, 15.08. Found: C, 56.53; H, 5.72; S, 15.24.

4-Hydroxy-1-methylbutanesulfonic Acid 1,4-Sultone

To a solution of 1.74 g (6.7 mmoles) of 1,3-propylene diethanesulfonate in 40 ml of tetrahydrofuran at −78° were added dropwise 7.5 mmoles of *n*-butyllithium. The reaction mixture was stored at 10° for 2 h. Distillation of the crude product gave 0.74 g (74%) of sultone (11).

4-Hydroxy-4-methylbutanesulfonic Acid 1,4-Sultone

n-Butyllithium (6.7 mmoles) was added to a solution of 1.55 g (6.3 mmoles) of 1,3-butylene dimethanesulfonate in 35 ml of tetrahydrofuran at −78°. The reaction mixture was stored at −20° for 2 h (colorless precipitate) then at 5° for a further 12 h. Distillation of the crude product gave 0.71 g (75%) of sultone **10**, n_D^{20} = 1.460, lit. (13) n_D^{25} = 1.4586.

*Sultone **15***

A solution of 1.03 g (4.0 mmoles) of *trans*-2-bromocyclohexyl methanesulfonate in 35 ml tetrahydrofuran was treated with 4.8 mmoles of *n*-butyllithium and then stored at 5° for 2 days. Workup gave 0.672 g of crude material from which was obtained by preparative t.l.c. 0.232 g (33%, 39% based on recovered starting material) of sultone **15**, m.p. 54–55° (methylene chloride – pentane).

Anal. Calcd. for $C_7H_{12}O_3S$: C, 47.72; H, 6.87; S, 18.16. Found: C, 47.73; H, 6.93; S, 18.01.

*cis-Sultone **17***

n-Butyllithium (4.7 mmoles) was added dropwise to a solution of 1.13 g (3.9 mmoles) of *trans*-2-bromocyclooctyl methanesulfonate in 30 ml of tetrahydrofuran which had been cooled to −78°. The reaction mixture was kept at 10° for 18 h. Workup gave 830 mg of crude product as a yellowish oil whose n.m.r. spectrum indicated a 1:1 mixture of starting material and sultone **17**. The sultone was isolated by preparative t.l.c. (3:2 pentane–ether). The yield was 294 mg (36%, 64% based on recovered starting material). Recrystallization from methylene chloride – pentane gave colorless flakes m.p. 56.5–57.5°. The n.m.r. spectrum ($CDCl_3$) showed multiplets from δ = 1.2–2.3 (12H), 2.8–3.6 (3H) and 4.8–5.0 (1H); i.r. peaks ($CHCl_3$), 1340 (vs), 1155 (s), and 910 (s) cm^{-1}.

Anal. Calcd. for $C_9H_{16}O_3S$: C, 52.93; H, 7.90; S, 15.67. Found: C, 53.08; H, 7.89; S, 15.54.

*trans-Sultone **19***

To a solution of 2.80 g (9.0 mmoles) of *cis*-dimesylate **18** in 50 ml of tetrahydrofuran at −78° were added dropwise 9.9 mmoles of *n*-butyllithium. The reaction mixture was kept at 10° overnight. Workup gave 2.30 g of crude product whose n.m.r. spectrum indicated a 3:1 mixture of starting material and product. Separation by preparative t.l.c. (3:2 pentane–ether) gave 304 mg (17%, 48% based on consumed starting material) of the *trans*-sultone **19** as colorless needles m.p. 56–57° (mixed m.p. with the *cis*-sultone **17**, 35–50°). The n.m.r. spectrum ($CDCl_3$) showed multiplets at δ = 1.2–2.4 (12H), 2.6–3.7 (3H), and 4.5–4.8 (1H); i.r. peaks ($CHCl_3$), 1340 (vs), 1155 (s), 905 (m), 880 (m), 848 (m) cm^{-1}.

Anal. Calcd. for $C_9H_{16}O_3S$: C, 52.93; H, 7.93; S, 15.67. Found: C, 52.79; H, 7.90; S, 15.53.

Reaction of 4-Chlorobutyl Methanesulfonate with n-Butyllithium

n-Butyllithium (7 ml, 11.2 mmoles) was added dropwise to a solution of 2.01 g (10.7 mmoles) of 4-chlorobutyl methanesulfonate in 50 ml of tetrahydrofuran at −78°. The reaction mixture was stored at room temperature for 2 days. The crude product (1.04 g) was purified by preparative t.l.c. and gave 475 mg (34%) of the ester **22** whose n.m.r. and i.r. spectra were identical to those obtained by reacting cyclopentanesulfonyl chloride with 4-chlorobutanol in methylene chloride in the presence of triethylamine (see below).

Reaction of Cyclopentanesulfonyl Chloride with 4-Chlorobutanol

Cyclopentanesulfonyl chloride (14) (5.35 g, 32 mmoles) and 3.8 g (35 mmoles) of 4-chlorobutanol were dissolved in 45 ml of methylene chloride at −78° and treated with dropwise addition of 3.5 g (35 mmoles) of triethylamine. The reaction mixture was warmed to room temperature and worked up in the usual manner. Two distillations of the crude product gave a slightly yellowish oil 4.25 g (57%), b.p. 145–150/0.75 mm.

Anal. Calcd. for $C_9H_{17}ClO_3S$: C, 44.91; H, 7.12; O, 19.92; S, 13.28. Found: C, 44.96; H, 6.91; O, 20.18; S, 13.49.

*Diester **23***

To a solution of 2.04 g (6.7 mmoles) of dimethanesulfonate **21** in 40 ml of tetrahydrofuran at −78° were added dropwise 7.3 mmoles of *n*-butyllithium. Workup gave 1.47 g of crude product from which 0.50 g of starting material was obtained by recrystallization. The remainder was purified by preparative t.l.c. and yielded 311 mg (23%) of the diester **23**. The i.r. and n.m.r. spectra were in agreement with the proposed structural assignment.

The compound tended to decompose and was not analyzed.

Financial support by the National Research Council of Canada is gratefully acknowledged. The authors would also like to thank A. Benderly, A. Gauthier, and K. Stevens for the preparation of some of the known sulfonate esters.

1. D. S. Breslow and H. Skolnik. *In* The chemistry of heterocyclic compounds. Vol. 21. Part I. *Edited by* A. Weissberger. Interscience Publishers Inc., New York, 1966. pp. 79–87; Vol. 21. Part II. pp. 774–780.
2. F. G. Bordwell, R. D. Chapman, and C. E. Osborne. J. Amer. Chem. Soc. **81**, 2002 (1959).
3. E. J. Corey and T. Durst. J. Amer. Chem. Soc. **88**, 5656 (1966); **90**, 5548 (1968).
4. W. E. Truce and D. J. Vrencur. Can. J. Chem. **47**, 860 (1969).
5. T. Durst and J. du Manoir. Can. J. Chem. **47**, 1230 (1969).
6. D. J. Cram. Fundamentals of carbanion chemistry. J. Wiley and Sons Inc., New York, 1965. Chapter II.
7. G. M. Timms. Br. Pat. 700 677; C. A. **49**, 1773 (1955).
8. J. H. Chapman and L. N. Owen. J. Chem. Soc. 579 (1950).
9. A. G. Koslova and L. B. Leont'eva. Zhur. Obshchei Khim. **30**, 3541 (1960); C. A. **55**, 20944 (1961).
10. W. J. C. Ross and W. Davis. J. Chem. Soc. 2420 (1957).
11. G. A. Haggis and L. N. Owen. J. Chem. Soc. 389 (1953).
12. R. W. Ohline, A. L. Allred, and F. G. Bordwell. J. Amer. Chem. Soc. **86**, 4641 (1964).
13. W. E. Truce and F. D. Hoerger. J. Amer. Chem. Soc. **76**, 5357 (1964).
14. C. Ziegler and J. M. Sprague. J. Org. Chem. **16**, 621 (1951).

Can. J. Chem. Downloaded from www.nrcresearchpress.com by 210.87.254.40 on 09/05/12
For personal use only.

Can. J. Chem. Downloaded from www.nrcresearchpress.com by 210.87.254.5 on 09/05/12
For personal use only.

Microwave spectrum of paraldehyde

R. KEWLEY
Department of Chemistry, Queen's University, Kingston, Ontario

Received August 6, 1969

The microwave spectrum of paraldehyde has been investigated in the range 14 to 26 GHz using commercial reagent grade samples. The spectrum of the symmetric rotor triequatorial methyl conformer was found, giving the value $B_0 = 1822.41 \pm 0.05$ MHz. The effects of low energy molecular vibrations are prominent in the spectrum.

Canadian Journal of Chemistry, **48**, 852 (1970)

Recently studies have been made in this laboratory of the microwave spectra of the heteroalicyclic compounds tetrahydropyran (1) and morpholine (2). Work in this area has now been extended by the present investigation in which the rotational spectrum of paraldehyde (2,4,6-trimethyl s-trioxane) has been observed in the 14 to 26 GHz region.

Four possible chair form conformational models of the molecule may be constructed:

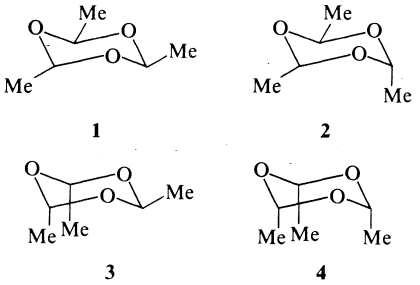

Because of the repulsion between the axial methyl group, conformers **3** and **4** would not be expected to be energetically favorable and in fact are not known to exist. In an electron diffraction study using a sample of boiling point 124.0 ± 0.2 °C, Carpenter and Brockway (3) established the chair form structure of the ring but were unable to distinguish between structures **1** and **2**, although the presence of structures **3** and **4** was ruled out. In a nuclear magnetic resonance (n.m.r.) investigation Diehl and Freeman (4), using a B.D.H. reagent grade paraldehyde sample, found the spectrum of the triequatorial methyl conformer **1** and showed that any other conformer, if present, must be at a concentration of less than 2 mole %.

Using the paraldehyde filtrate from the commercial production of metaldehyde, Craven *et al.* were able to effect a separation of two forms of paraldehyde by gas chromatography and also record their infrared (i.r.) spectra (5). These investigators concluded that the two forms isolated corresponded to structures **1** and **2** above and also determined their boiling points and refractive indices η_D^{20} to be respectively 124 °C, 1.4048 and 125 °C, 1.4082. In a later n.m.r. study of the products of radiolysis of polyacetaldehyde, also separated by gas chromatography, Jungnickel and Reilly (6) were able to obtain the spectra of both conformers **1** and **2**.

In the present investigation commercially available samples were used. The frequency measurements and 18–26 GHz sweep were done using a Fisher Scientific Company reagent grade sample for which the refractive index was measured as $\eta_D^{20} = 1.4044 \pm 0.0002$. The 14–18 GHz sweep was carried out with a reagent grade Anachemia Chemical Company sample of measured refractive index $\eta_D^{20} = 1.4054 \pm 0.0002$. The 20–22 GHz region was also swept using this sample as a check.

Preliminary calculations of expected rotational constants were carried out for structures **1** and **2** using the structural parameters C—C = 1.533, C—O = 1.410, and C—H = 1.108 Å with all bond angles assumed to be tetrahedral. The predicted constants for the symmetric rotor form, conformer **1**, were $B = 1805.1$ and $C = 962.8$ MHz. Conformer **2** is highly asymmetric with calculated constants $A = 2181.3$, $B = 1655.4$, and $C = 1119.8$ MHz and $K = 0.0092$. The calculated spectrum of this form is one with both *a* and *c*

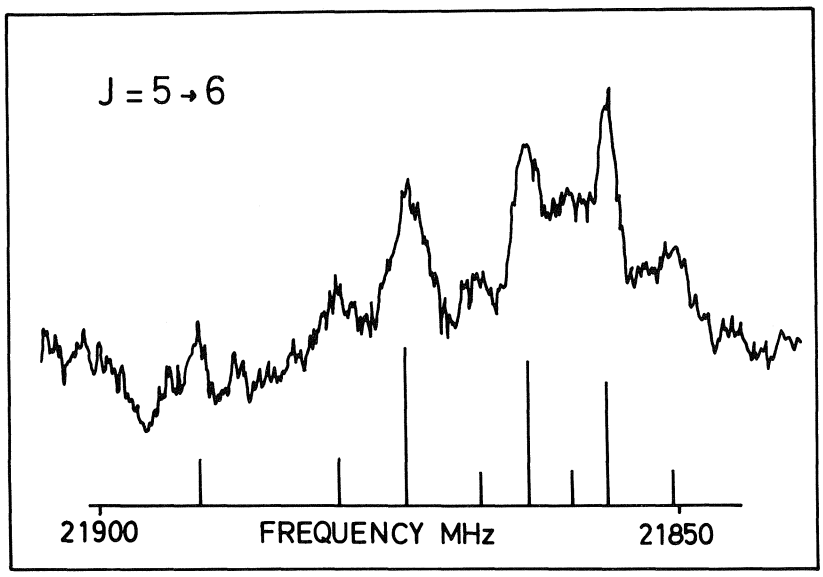

FIG. 1. Recorder trace of the $J = 5 \rightarrow 6$ transition of paraldehyde, triequatorial methyl conformer. Stark field is 164 V/cm and the pressure is 175 μ. The trace was taken at room temperature (22 °C).

type transitions distributed fairly evenly throughout the entire region studied.

The observed spectrum showed the expected absorption lines due to conformer **1** together with nearby vibrational satellite peaks. A number of other peaks were also noticed which could not be matched with the calculated pattern for conformer **2** since large gaps occurred between 14 and 18 GHz and also 24 and 26 GHz in which regions many *a* and *c* type R-branch transitions were calculated to fall. Some of these peaks, particularly a group of lines situated near 21.0 GHz, were found with both samples, being more intense with the Fisher sample. These peaks are thought to be due to an unidentified impurity and not conformer **2**. A number of related molecules such as acetaldehyde, formic acid, acetic acid, and methyl formate were considered as possible impurities but none of these has a spectrum of the form observed.

The line frequencies in $J = 4 \rightarrow 5$, $5 \rightarrow 6$, and $6 \rightarrow 7$ transitions of the triequatorial methyl conformer were measured and are given in Table 1. In calculating the B values, effects of centrifugal distortion were ignored. The pattern for a particular rotational transition consists of a number of broad lines which are not well resolved, see Fig. 1. The lines are much more closely spaced than those in the spectrum of the related molecule s-trioxane (7) because of the greater mass of the paraldehyde molecule. Some of the weaker lines in the pattern could only be measured with difficulty which necessitated working at relatively large pressures. In addition to the ground vibrational state rotational transition it is expected that peaks will be present due to excitation of low frequency vibrations involving ring deformation and methyl torsion. The latter should give rise to strong satellite peaks corresponding to degenerate (ν_e) and symmetric (ν_a) torsional modes. In paraldehyde the methyl group would experience an environment similar to that in the CH_3CF_2H molecule in which the barrier to rotation about the C—C bond is 1110 cm^{-1} (8). For this reason it is anticipated that in paraldehyde only small oscillations of the methyl

TABLE 1
Rotational transition frequencies (in MHz) of paraldehyde, triequatorial methyl conformer

$J = 4 \rightarrow 5$	$J = 5 \rightarrow 6$	$J = 6 \rightarrow 7$	B (MHz)
	21850.6	25491.5	1820.85
18216.3	21859.6	25503.0	1821.63
	21864.9	25508.9	1822.07
18224.0	21868.9	25514.2	1822.41
	21873.6	25519.5	1822.81
18232.0	21879.0	25525.7	1823.24
	21883.5	25530.2	1823.60
	21894.7	25543.8	1824.55

Can. J. Chem. Downloaded from www.nrcresearchpress.com by 210.87.254.5 on 09/05/12
For personal use only.

Can. J. Chem. Downloaded from www.nrcresearchpress.com by 210.87.254.5 on 09/05/12
For personal use only.

FIG. 2. Recorder traces of the $J = 6 \rightarrow 7$ transition, in each case with a Stark field of 164 V/cm; *upper*: at room temperature (26 °C) and a pressure of 145 μ; *lower*: at -13 ± 5 °C and at the vapor pressure of paraldehyde (approximately 15 μ)

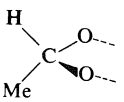

paraldehyde

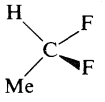

1,1-difluoroethane

hydrogens will occur. No information appears to be available concerning the far i.r. spectrum of paraldehyde. However, in the Raman spectrum, displacements of 258, 274, 371, 424, 470, 525, and 575 cm^{-1} have been recorded (9), which are typical for ring deformation modes. It is possible that there are other vibrational frequencies lower than 258 cm^{-1}. The degenerate torsional vibration (ν_e) would most probably be Raman and i.r. inactive. Because of the fairly large number of low lying vibrational states of the molecule and because of the incomplete state of the vibrational data, it has not been possible to carry out detailed analysis of the observed vibrational satellites. At room temperature the intensities of absorption peaks on recorder traces of the $J = 4 \rightarrow 5, 5 \rightarrow 6$, and $6 \rightarrow 7$ transitions suggest that for the ground vibrational state of the molecule the B_0 value might be 1821.63, 1822.41, or 1823.24 MHz. The first excited state of a degenerate vibration of frequency 145 cm^{-1} would give rise to a satellite peak having intensity equal to that of the ground state peak at 22 °C. This indicates that two of the three large peaks in each transition are due to methyl torsion. A study of the $J = 6 \rightarrow 7$ transition carried out at a lower temperature showed that the peak at 25 514.2 MHz is most likely the ground state on account of its increase in intensity relative to the other nearby peaks, see Fig. 2. It is therefore likely that $B_v = 1823.24$ and $B_v = 1821.63$ MHz correspond to $v = 1$ for the ν_a and ν_e torsional satellites respectively. The remaining lines in the pattern are to be attributed to the low frequency deformation modes of the ring. The weakest line in each of the $J = 5 \rightarrow 6$ and $6 \rightarrow 7$ transitions is about 1/5 of the ground state at room temperature indicating a vibrational frequency in the range 300–500 cm^{-1}, allowing for the possibility of double degeneracy.

Experimental

The spectrum was recorded and measured using a 100 KHz Stark modulation spectrometer which has been described previously (1, 2). Frequency measurements using a Micronow model 101D frequency standard are accurate to ±0.1 MHz. All the frequency measurements in Table 1 were made at room temperature (22 °C) and at pressures in the range 50 to 100 μ. Refractive index measurements were made at 20 °C using a Bausch and Lomb Abbe-3L refractometer calibrated against a standard test piece of refractive index 1.5125 with 1-bromonaphthalene as the contact liquid.

The work was supported by operating grants provided by the National Research Council of Canada and the Department of University Affairs, Ontario.

1. V. M. Rao and R. Kewley. Can. J. Chem. **47**, 1289 (1969).
2. J. J. Sloan and R. Kewley. Can. J. Chem. **47**, 3453 (1969).
3. D. C. Carpenter and L. O. Brockway. J. Amer. Chem. Soc. **58**, 1270 (1936).
4. P. Diehl and R. Freeman. Mol. Phys. **4**, 39 (1961).
5. E. C. Craven, H. Jewitt, and W. R. Ward. J. Appl. Chem. **12**, 526 (1962).
6. J. L. Jungnickel and C. A. Reilly. J. Mol. Spect. **16**, 135 (1965).
7. T. Oka, K. Tsuchiya, S. Iwata, and Y. Morino. Bull. Chem. Soc. Jap. **37**, 4 (1964).
8. D. R. Herschbach. J. Chem. Phys. **25**, 358 (1956).
9. R. W. Wood. J. Chem. Phys. **5**, 287 (1937).

Solvent effects in the Cope rearrangement

Donald C. Wigfield and Steve Feiner
Department of Chemistry, Carleton University, Ottawa 1, Ontario

Received October 7, 1969

Mechanistic ambiguity in the kinetic results of certain Cope rearrangements has been resolved. It is concluded from rate studies in solvents of widely differing polarity that there is negligible contribution of an ionic mechanism, even in rearrangements of substrates structurally best suited to this mechanism.

Canadian Journal of Chemistry, **48**, 855 (1970)

It has long been generally accepted that the Cope rearrangement of 1,5-hexadienes proceeds by a concerted mechanism through a transition state in which the 3,4 bond is being ruptured while the 1,6 bond is being formed (1), as shown in Fig. 1.

Can. J. Chem. Downloaded from www.nrcresearchpress.com by 210.87.254.5 on 09/05/12
For personal use only.

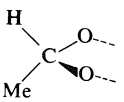
paraldehyde

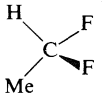
1,1-difluoroethane

hydrogens will occur. No information appears to be available concerning the far i.r. spectrum of paraldehyde. However, in the Raman spectrum, displacements of 258, 274, 371, 424, 470, 525, and 575 cm^{-1} have been recorded (9), which are typical for ring deformation modes. It is possible that there are other vibrational frequencies lower than 258 cm^{-1}. The degenerate torsional vibration (ν_e) would most probably be Raman and i.r. inactive. Because of the fairly large number of low lying vibrational states of the molecule and because of the incomplete state of the vibrational data, it has not been possible to carry out detailed analysis of the observed vibrational satellites. At room temperature the intensities of absorption peaks on recorder traces of the $J = 4 \rightarrow 5, 5 \rightarrow 6$, and $6 \rightarrow 7$ transitions suggest that for the ground vibrational state of the molecule the B_0 value might be 1821.63, 1822.41, or 1823.24 MHz. The first excited state of a degenerate vibration of frequency 145 cm^{-1} would give rise to a satellite peak having intensity equal to that of the ground state peak at 22 °C. This indicates that two of the three large peaks in each transition are due to methyl torsion. A study of the $J = 6 \rightarrow 7$ transition carried out at a lower temperature showed that the peak at 25 514.2 MHz is most likely the ground state on account of its increase in intensity relative to the other nearby peaks, see Fig. 2. It is therefore likely that $B_v = 1823.24$ and $B_v = 1821.63$ MHz correspond to $v = 1$ for the ν_a and ν_e torsional satellites respectively. The remaining lines in the pattern are to be attributed to the low frequency deformation modes of the ring. The weakest line in each of the $J = 5 \rightarrow 6$ and $6 \rightarrow 7$ transitions is about 1/5 of the ground state at room temperature indicating a vibrational frequency in the range 300–500 cm^{-1}, allowing for the possibility of double degeneracy.

Experimental

The spectrum was recorded and measured using a 100 KHz Stark modulation spectrometer which has been described previously (1, 2). Frequency measurements using a Micronow model 101D frequency standard are accurate to ±0.1 MHz. All the frequency measurements in Table 1 were made at room temperature (22 °C) and at pressures in the range 50 to 100 μ. Refractive index measurements were made at 20 °C using a Bausch and Lomb Abbe-3L refractometer calibrated against a standard test piece of refractive index 1.5125 with 1-bromonaphthalene as the contact liquid.

The work was supported by operating grants provided by the National Research Council of Canada and the Department of University Affairs, Ontario.

1. V. M. Rao and R. Kewley. Can. J. Chem. **47**, 1289 (1969).
2. J. J. Sloan and R. Kewley. Can. J. Chem. **47**, 3453 (1969).
3. D. C. Carpenter and L. O. Brockway. J. Amer. Chem. Soc. **58**, 1270 (1936).
4. P. Diehl and R. Freeman. Mol. Phys. **4**, 39 (1961).
5. E. C. Craven, H. Jewitt, and W. R. Ward. J. Appl. Chem. **12**, 526 (1962).
6. J. L. Jungnickel and C. A. Reilly. J. Mol. Spect. **16**, 135 (1965).
7. T. Oka, K. Tsuchiya, S. Iwata, and Y. Morino. Bull. Chem. Soc. Jap. **37**, 4 (1964).
8. D. R. Herschbach. J. Chem. Phys. **25**, 358 (1956).
9. R. W. Wood. J. Chem. Phys. **5**, 287 (1937).

Solvent effects in the Cope rearrangement

Donald C. Wigfield and Steve Feiner
Department of Chemistry, Carleton University, Ottawa 1, Ontario

Received October 7, 1969

Mechanistic ambiguity in the kinetic results of certain Cope rearrangements has been resolved. It is concluded from rate studies in solvents of widely differing polarity that there is negligible contribution of an ionic mechanism, even in rearrangements of substrates structurally best suited to this mechanism.

Canadian Journal of Chemistry, **48**, 855 (1970)

It has long been generally accepted that the Cope rearrangement of 1,5-hexadienes proceeds by a concerted mechanism through a transition state in which the 3,4 bond is being ruptured while the 1,6 bond is being formed (1), as shown in Fig. 1.

Can. J. Chem. Downloaded from www.nrcresearchpress.com by 210.87.254.105 on 09/05/12
For personal use only.

FIG. 1. Concerted mechanism for the Cope rearrangement.

Evidence supporting this type of mechanism includes the facts that the reaction proceeds with first order kinetics (2), that the reaction is intramolecular, no exchange of groups being observed (3), and that *both* substituted allyl groups become inverted in the process (3). The activation parameters, $\Delta H^{\ddagger}$ 26–28 kcal mole^{-1}, $\Delta S^{\ddagger}$ -11 to -14 e.u., have also been quoted in favor of this mechanism (4, 5).

Not all Cope rearrangements, however, behave with these characteristics and, in particular, pyrolysis of 3,4-diphenyl-1,5-hexadiene (**1**) yields a mixture of 1,6-diphenyl-1,5-hexadiene (**2**) and 1,4-diphenyl-1,5-hexadiene (**3**) (6), a result which is clearly inconsistent with a concerted mechanism. Koch suggested that this result indicated the intermediacy of two phenylvinylmethyl radicals, formed by cleavage of the 3,4 bond prior to construction of the 1,6 link (Fig. 2).

More recently, the existence of such a mechanism has been confirmed by Hammond and DeBoer (7) by observation of similar results in conjugation with near zero entropies of activation, thus establishing the *duality of mechanism* in the Cope rearrangement.[1]

These results suggest the intriguing possibility of the existence of the *third* type of mechanism, that involving heterolytic cleavage of the 3,4 bond to give an ion pair which on recombination would yield the product. Clearly, the only type of compounds that would be expected to exhibit this mechanism would be those able to accommodate charge development, particularly the negative charge of the potential carbanion. In order to probe this possibility, we have prepared and isomerized 2-allyl-2-(1-ethyl-1-propenyl)-malononitrile (**4***a*). Compounds of this type may conveniently be synthesized by the 2-step procedure of Cope *et al.* (2), illustrated in Fig. 3. Diethyl ketone is condensed with the appropriate active methylene compound and the resulting adducts (**6**) are reacted with allyl bromide to generate the 1,5-hexadiene system.

The ionic mechanism of isomerization, as shown in Fig. 4, for compound **4***a* seems attractive and not unreasonable since it involves as intermediates the highly stabilized malononitrile anion and allyl cation. Furthermore, recent results on the mechanism of the pyrolysis of pyrazolines have shown that while pyrazolines of the type **7** decompose in a concerted fashion to form olefins, those with an additional nitrile group at C-3, such as **8** show considerable ionic character in their decomposition, presumably due to initial (at least partial) heterolytic cleavage of the 2–3 bond.[2]

Interestingly, much of the initial mechanistic work on the Cope rearrangement, by Cope and his co-workers (1–3) was done on compounds similar to dienes **4***a–c*, in the sense that they possessed electron-withdrawing groups at position 3 of the hexadiene system, probably owing to the greater ease of synthesis of this type of system. A critical examination of the mechanistic evidence certainly confirms it to be consistent in all aspects with a concerted process; it does not, however, rule out the possibility of an ion pair intermediate, provided that the ion pair is sufficiently "tight" or short-lived to prevent exchange or inversion of the allyl groups. The concerted mechanism was favored on the basis of the negative entropy of activation, caused by loss of rotational freedom in the transition state (4); nevertheless, it is now well recognized that development of charge also gives rise to negative entropies of activation (8), owing to electrostriction of solvent around the ions produced, and consequently this type of evidence does not constitute a distinction between the two mechanisms. More recently, similar ambiguities have arisen from the negative values of the volume of activa-

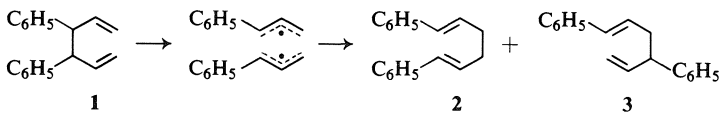

1 2 3

FIG. 2. Biradical mechanism for the Cope rearrangement.

[1]In these rearrangements steric restrictions prevent the normal mechanism.

[2]See reference 12. We are very grateful to Dr. D. E. McGreer for communicating his results to us prior to publication.

Can. J. Chem. Downloaded from www.nrcresearchpress.com by 210.87.254.105 on 09/05/12
For personal use only.

TABLE 1
Spectral properties of compound **5**, and rates* of conversion of compound **4***a* to compound **5**, in various solvents

Solvent	λ_{max} (mμ)	ε	$k \times 10^5$ (s^{-1})	$t_{\frac{1}{2}} \times 10^{-4}$ (s)
Cyclohexane	240	10 200	0.42	16.5
1,4-Dioxane	246	9 300	4.7	1.47
Ethanol	243	10 500	4.9	1.41
1:1 Ethanol–water	243	10 600	7.0	0.99

*All rates measured at 79° with a hexadiene concentration of 2.5×10^{-4} *M*.

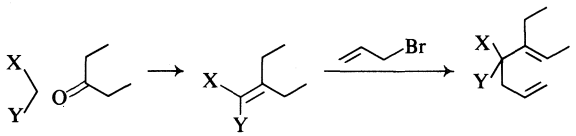

6 **4**

a X = Y = CN
b X = CN, Y = CO_2Et
c X = Y = CO_2Et

FIG. 3. Synthetic scheme to 1,5-hexadienes.

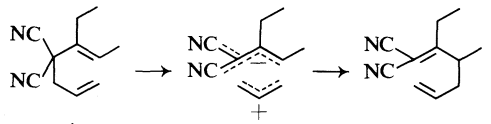

4*a* **5**

FIG. 4. Ionic mechanism for the Cope rearrangement.

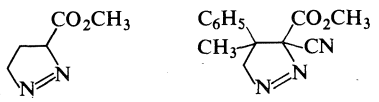

7 **8**

tion obtained on Cope rearrangement of compound **4***b* (9). One highly interesting piece of information regarding the isomerization of compounds of the type **4**, lies in the fact that the presence of the electron-withdrawing groups on the 1,5-hexadiene greatly increase the rate of isomerization, the magnitude of the increase depending on the strength of the electron-withdrawing substituents (2). This is certainly demanded by the ionic mechanism, although it does not exclude the concerted mechanism (1).

In order to provide definite distinction between the ionic and concerted mechanisms, we have measured the rates of isomerization as a function of solvent polarity. This appears never to have been performed on 1,5-hexadienes with electron-withdrawing groups at the 3 position, presumably because the original method of measuring the kinetics (change in refractive index) did not lend itself to a study of solution kinetics. Following the reaction by the appearance of the α,β-unsaturated dinitrile absorption band at about 240 mμ (depending on the solvent) proved to be a convenient method of measurement for these studies.

The results obtained are shown in Table 1. They show that even for compound **4***a*, with the two nitrile groups to heavily stabilize a potential carbanion, the rate of isomerization changes only by a factor of 17 with the drastic change in solvent from cyclohexane to ethanol–water. This small rate increase corresponds to a difference in free energy of activation of $\Delta\Delta G^{\ddagger} = 2.0$ kcal $mole^{-1}$. On this basis we feel that the possibility of the reaction proceeding by way of ions, or indeed, of any significant charge development in the transition state must be rejected. We conclude that the negative value of the entropy of activation (4, 5) is indeed due to a cyclic transition state and not due to charge development. Furthermore, since compound **4***a* was deliberately chosen as structurally best suited to exhibit an ionic mechanism, it seems highly unlikely that the Cope rearrangement of any other compounds so far investigated would proceed by this mechanism. Very recently (10), secondary deuterium isotope effects for the isomerization of compound **4***a* have been reported, and it would now appear valid to interpret these interesting values in terms of a purely concerted mechanism.

Experimental

Infrared (i.r.) spectra were obtained on a Perkin–Elmer Model 237 spectrophotometer and ultraviolet (u.v.) spectra on a Perkin–Elmer Model 202 spectrophotometer. Proton magnetic resonance (p.m.r.) spectra were measured as neat liquids, with tetramethylsilane as the internal standard, on a Jeolco C-60 instrument.

*2-(1-Ethylpropylidene)malononitrile (**6**, X = Y = CN)*

Malononitrile was condensed with 3-pentanone under the conditions of Cope and Hoyle (11) to give the title

Can. J. Chem. Downloaded from www.nrcresearchpress.com by 210.87.254.105 on 09/05/12
For personal use only.

compound, b.p. 120–123° (23 mm), n_D^{25} 1.4692, ν_{max}(film) 2240 cm^{-1} (strong), λ_{max}(EtOH) 237 mμ (ε 10 200), p.m.r. δ 1.17 (6H, triplet, J = 7.6 c.p.s., CH_3) and 2.60 p.p.m. (4H, quartet, J = 7.6 c.p.s., CH_2), (lit. (11) b.p. 121–122° (20 mm), n_D^{22} 1.4694).

2-Allyl-2-(1-ethyl-1-propenyl)malononitrile (4a)

Allyl bromide was reacted with the sodium anion of compound **6** (X = Y = CN), as described by Cope *et al.* (2), to yield the 1,5-diene, n_D^{18} 1.4641, ν_{max}(film) 2250 cm^{-1} (weak), λ_{max}(EtOH) 246 mμ (ε 1360), p.m.r. δ 1.05 (3H, triplet, J = 7.5 c.p.s., CH_3), 1.62 (3H, doublet, J = 7.0 c.p.s., allylic CH_3), 1.9–2.8 (4H, multiplet, allylic CH_2) and 5.0–6.1 p.p.m. (4H, multiplet, olefinic protons), (lit. (2) n_D^{25} 1.4639).

2-(1-Ethyl-2-methyl-4-pentenylidene)malononitrile (5)

Compound **4** (X = Y = CN) was heated as a neat liquid for 4 h at 150° (2). The rearranged product was purified by distillation, b.p. 121–123° (26 mm), n_D^{18} 1.4845, ν_{max}(film) 2230 cm^{-1} (strong), λ_{max}(EtOH) 243 mμ (ε 10 500), p.m.r. δ 1.17 (3H, doublet, J = 7.0 c.p.s., CH—CH_3), 1.20 (3H, triplet, J = 7.5 c.p.s., CH_2—CH_3), 2.1–3.3 (5H, multiplet, allylic protons) and 4.8–6.0 p.p.m. (3H, multiplet, olefinic protons), (lit. (2) b.p. 148–149° (25 mm), n_D^{25} 1.4839).

Kinetic Measurements

Solvents

All solvents used were of spectroscopic grade and were freshly redistilled before use.

Procedure

Isomerizations of the hexadiene were performed by heating an approximately 2.5 × 10^{-4} M solution (accurately prepared) in a constant temperature (79°) bath. Aliquots were taken at appropriate time intervals (30 or 60 min.), immediately cooled in ice, and the absorbance value of the solution measured on a Gilford Model 240 spectrophotometer. The wavelength at which absorbance values were measured was that of maximum absorbance of compound **4***a* in the particular solvent of interest. These wavelengths are recorded in Table 1. Readings were taken for 2 half-life periods. The final (infinity) absorbance value was determined either by allowing the reaction to proceed for 6 half-life periods or by calculation from the initial concentration of the solution. Data were treated in the normal first-order manner (2), and each rate constant was measured at least in duplicate to ensure reproducibility. The mean values of the rate constants are recorded in Table 1.

The generous support of the National Research Council of Canada is gratefully acknowledged.

1. S. J. Rhoads. Molecular rearrangements. P. de Mayo, *editor*. Interscience Publishers Inc., New York, 1963. pp. 684–696.
2. A. C. Cope, K. E. Hoyle, and D. Heyl. J. Amer. Chem. Soc. **63**, 1843 (1941).
3. A. C. Cope, C. M. Hofmann, and E. M. Hardy. J. Amer. Chem. Soc. **63**, 1852 (1941).
4. E. G. Foster, A. C. Cope, and F. Daniels. J. Amer. Chem. Soc. **69**, 1893 (1947).
5. G. R. Aldridge and G. W. Murphy. J. Amer. Chem. Soc. **73**, 1158 (1951).
6. H. P. Koch. J. Chem. Soc. 1111 (1948).
7. G. S. Hammond and C. D. DeBoer. J. Amer. Chem. Soc. **86**, 899 (1964).
8. R. Stewart. The investigation of organic reactions. Prentice–Hall, Inc., Englewood Cliffs, N. J. 1966. pp. 74–76.
9. C. Walling and M. Naiman. J. Amer. Chem. Soc. **84**, 2628 (1962).
10. K. Humski, T. Strelkov, S. Borcic, and D. E. Sunko. Chem. Commun. 693 (1969).
11. A. C. Cope and K. E. Hoyle. J. Amer. Chem. Soc. **63**, 734 (1941).
12. D. E. McGreer and Y. Y. Wigfield. Can. J. Chem. **47**, 3965 (1969); D. E. McGreer and I. M. Masters. Can. J. Chem. **47**, 3975 (1969).

Friedel–Crafts alkylation of benzene with 1,1-d_2-1-chloropropane

C. C. Lee and D. J. Woodcock

Department of Chemistry and Chemical Engineering, University of Saskatchewan, Saskatoon, Saskatchewan

Received September 18, 1969

The $AlCl_3$ catalyzed reaction of 1,1-d_2-1-chloropropane with benzene was carried out in excess benzene at about 5° or in 1,2,4-trichlorobenzene as solvent at 0°. The products, *n*-propylbenzene and isopropylbenzene, were examined by nuclear magnetic resonance and mass spectrometry. The results indicated only very minor amounts of isotope position scrambling in the propyl side chain, suggesting no major involvement of protonated cyclopropane intermediates in the reaction. The mass spectral data, however, demonstrated that the products are quite labile in the reaction medium, with extensive intermolecular hydride and deuteride transfers taking place.

Canadian Journal of Chemistry, **48**, 858 (1970)

Deno and coworkers (1) have recently reported that when cyclopropane was introduced into deuterated benzene (c-C_6D_6) in the presence of $AlCl_3$ moistened with D_2O, both of the resulting *n*-propyl- and isopropylbenzenes contained one deuterium atom which was statistically

Can. J. Chem. Downloaded from www.nrcresearchpress.com by 210.87.254.105 on 09/05/12
For personal use only.

compound, b.p. 120–123° (23 mm), n_D^{25} 1.4692, ν_{max}(film) 2240 cm^{-1} (strong), λ_{max}(EtOH) 237 mμ (ε 10 200), p.m.r. δ 1.17 (6H, triplet, J = 7.6 c.p.s., CH_3) and 2.60 p.p.m. (4H, quartet, J = 7.6 c.p.s., CH_2), (lit. (11) b.p. 121–122° (20 mm), n_D^{22} 1.4694).

2-Allyl-2-(1-ethyl-1-propenyl)malononitrile (4a)

Allyl bromide was reacted with the sodium anion of compound **6** (X = Y = CN), as described by Cope *et al.* (2), to yield the 1,5-diene, n_D^{18} 1.4641, ν_{max}(film) 2250 cm^{-1} (weak), λ_{max}(EtOH) 246 mμ (ε 1360), p.m.r. δ 1.05 (3H, triplet, J = 7.5 c.p.s., CH_3), 1.62 (3H, doublet, J = 7.0 c.p.s., allylic CH_3), 1.9–2.8 (4H, multiplet, allylic CH_2) and 5.0–6.1 p.p.m. (4H, multiplet, olefinic protons), (lit. (2) n_D^{25} 1.4639).

2-(1-Ethyl-2-methyl-4-pentenylidene)malononitrile (5)

Compound **4** (X = Y = CN) was heated as a neat liquid for 4 h at 150° (2). The rearranged product was purified by distillation, b.p. 121–123° (26 mm), n_D^{18} 1.4845, ν_{max}(film) 2230 cm^{-1} (strong), λ_{max}(EtOH) 243 mμ (ε 10 500), p.m.r. δ 1.17 (3H, doublet, J = 7.0 c.p.s., CH—CH_3), 1.20 (3H, triplet, J = 7.5 c.p.s., CH_2—CH_3), 2.1–3.3 (5H, multiplet, allylic protons) and 4.8–6.0 p.p.m. (3H, multiplet, olefinic protons), (lit. (2) b.p. 148–149° (25 mm), n_D^{25} 1.4839).

Kinetic Measurements

Solvents

All solvents used were of spectroscopic grade and were freshly redistilled before use.

Procedure

Isomerizations of the hexadiene were performed by heating an approximately 2.5 × 10^{-4} M solution (accurately prepared) in a constant temperature (79°) bath. Aliquots were taken at appropriate time intervals (30 or 60 min.), immediately cooled in ice, and the absorbance value of the solution measured on a Gilford Model 240 spectrophotometer. The wavelength at which absorbance values were measured was that of maximum absorbance of compound **4***a* in the particular solvent of interest. These wavelengths are recorded in Table 1. Readings were taken for 2 half-life periods. The final (infinity) absorbance value was determined either by allowing the reaction to proceed for 6 half-life periods or by calculation from the initial concentration of the solution. Data were treated in the normal first-order manner (2), and each rate constant was measured at least in duplicate to ensure reproducibility. The mean values of the rate constants are recorded in Table 1.

The generous support of the National Research Council of Canada is gratefully acknowledged.

1. S. J. Rhoads. Molecular rearrangements. P. de Mayo, *editor*. Interscience Publishers Inc., New York, 1963. pp. 684–696.
2. A. C. Cope, K. E. Hoyle, and D. Heyl. J. Amer. Chem. Soc. **63**, 1843 (1941).
3. A. C. Cope, C. M. Hofmann, and E. M. Hardy. J. Amer. Chem. Soc. **63**, 1852 (1941).
4. E. G. Foster, A. C. Cope, and F. Daniels. J. Amer. Chem. Soc. **69**, 1893 (1947).
5. G. R. Aldridge and G. W. Murphy. J. Amer. Chem. Soc. **73**, 1158 (1951).
6. H. P. Koch. J. Chem. Soc. 1111 (1948).
7. G. S. Hammond and C. D. DeBoer. J. Amer. Chem. Soc. **86**, 899 (1964).
8. R. Stewart. The investigation of organic reactions. Prentice–Hall, Inc., Englewood Cliffs, N. J. 1966. pp. 74–76.
9. C. Walling and M. Naiman. J. Amer. Chem. Soc. **84**, 2628 (1962).
10. K. Humski, T. Strelkov, S. Borcic, and D. E. Sunko. Chem. Commun. 693 (1969).
11. A. C. Cope and K. E. Hoyle. J. Amer. Chem. Soc. **63**, 734 (1941).
12. D. E. McGreer and Y. Y. Wigfield. Can. J. Chem. **47**, 3965 (1969); D. E. McGreer and I. M. Masters. Can. J. Chem. **47**, 3975 (1969).

Friedel–Crafts alkylation of benzene with 1,1-d_2-1-chloropropane

C. C. Lee and D. J. Woodcock

Department of Chemistry and Chemical Engineering, University of Saskatchewan, Saskatoon, Saskatchewan

Received September 18, 1969

The $AlCl_3$ catalyzed reaction of 1,1-d_2-1-chloropropane with benzene was carried out in excess benzene at about 5° or in 1,2,4-trichlorobenzene as solvent at 0°. The products, *n*-propylbenzene and isopropylbenzene, were examined by nuclear magnetic resonance and mass spectrometry. The results indicated only very minor amounts of isotope position scrambling in the propyl side chain, suggesting no major involvement of protonated cyclopropane intermediates in the reaction. The mass spectral data, however, demonstrated that the products are quite labile in the reaction medium, with extensive intermolecular hydride and deuteride transfers taking place.

Canadian Journal of Chemistry, **48**, 858 (1970)

Deno and coworkers (1) have recently reported that when cyclopropane was introduced into deuterated benzene (c-C_6D_6) in the presence of $AlCl_3$ moistened with D_2O, both of the resulting *n*-propyl- and isopropylbenzenes contained one deuterium atom which was statistically

Can. J. Chem. Downloaded from www.nrcresearchpress.com by 210.87.254.42 on 09/05/12
For personal use only.

TABLE 1

The number of deuterium atoms at the various positions of the side chain of *n*-propylbenzene or isopropylbenzene as determined by n.m.r.

Experiment	Solvent	Reaction time (min)	*n*-Propylbenzene			Isopropylbenzene	
			C_α	C_β	C_γ	C_α	$2C_\beta$
1	Excess PhH	1.5	2	0	0	0	2
2	Excess PhH	45	2	0	0	0	2
3	Excess PhH	240	1.8	0	0	0.1	2
4	Excess PhH	240	1.8	0	0	0.2	2
5	1,2,4-Cl_3Ph	45	1.4	0	0	0.1	1.6
6	1,2,4-Cl_3Ph	45	1.4	0	0	0.1	1.5

distributed in the *n*-propyl or isopropyl side chain, while the phenyl group remained free of hydrogen. These findings were interpreted as resulting from the formation of protonated (or deuteronated) cyclopropane, *c*-$C_3H_6D^+$, which isomerized to scramble the deuterium before alkylating the benzene, each alkylation ejecting a D^+ which in turn reacted with new *c*-C_3H_6 to give *c*-$C_3H_6D^+$. In the present work, the Friedel–Crafts alkylation of benzene with 1,1-d_2-1-chloropropane (**1**-d_2) was investigated with the object of finding out if protonated cyclopropane intermediates would play any part in the reaction.

The Friedel–Crafts reaction between benzene and **1**-d_2 was carried out in the presence of $AlCl_3$ at about 5° for 1.5, 45, or 240 min in excess benzene, or for 45 min at 0° in 1,2,4-trichlorobenzene as solvent. The *n*-propyl- and isopropylbenzenes (**2** and **3**) obtained were purified by preparative vapor-phase chromatography (v.p.c.) and then analyzed by nuclear magnetic resonance (n.m.r.) and by mass spectrometry. Using the phenyl absorptions in the n.m.r. spectra as an internal standard of 5 protons, the H contents and, by difference, the number of D atoms at the various positions of the *n*-propyl and isopropyl side chains were determined. The results are given in Table 1. From the mass spectra, the isotopic compositions were calculated, using the appropriate peak heights after correcting for natural isotopic abundance (2), for the molecular M^+ and the $(M—C_2H_5)^+$ ions from **2**, and for the molecular M^+ and the $(M—CH_3)^+$ ions from **3**. The data are summarized in Table 2.

From Tables 1 and 2, it can be seen that no measurable isotope position rearrangement in the side chain of **2** could be detected by n.m.r., while the mass spectral data suggested the possibility that rearrangement of the D-label from C_α to C_β and C_γ in **2** might have occurred to the extent of only about 0.1 D atom or about 5% of the total of 2 D atoms. These results indicated that protonated cyclopropane intermediates did not intervene in the major pathways involved in the Friedel–Crafts alkylation of benzene with **1**.

Both n.m.r. and mass spectral analyses gave results in fairly good agreement regarding the total deuterium contents in **2** and **3**. In experiments 3 and 4, there was apparently some loss of deuterium in **2** and some gain of deuterium in **3**, while in experiments 5 and 6, loss of deuterium was observed in both **2** and **3**. These findings strongly suggest the intermolecular transfer of hydride and deuteride ions.

It is also of interest to note from the mass spectral data (Table 2) that extensive changes in isotopic composition were observed in the products obtained under different experimental conditions. For the reactions carried out with excess benzene as solvent (experiments 1–4) the amount of **2** formed with only one deuterium atom in the molecule apparently increased with longer reaction time. When the reaction was effected in 1,2,4-trichlorobenzene for 45 min (experiments 5–6), significant amounts of d_0 species also appeared. Similarly, variations in the amounts of d_0, d_1, d_2, and d_3 species were found in **3**.

The present results may be rationalized on the basis of conclusions previously arrived at by Brown and coworkers (3, 4) regarding Friedel–Crafts alkylations and by Roberts and coworkers (5–7) regarding disproportionations of alkylbenzenes. Brown and coworkers have proposed that Friedel–Crafts alkylations with primary halides,

Can. J. Chem. Downloaded from www.nrcresearchpress.com by 210.87.254.42 on 09/05/12
For personal use only.

Can. J. Chem. Downloaded from www.nrcresearchpress.com by 210.87.254.42 on 09/05/12
For personal use only.

TABLE 2

Data from the mass spectra of *n*-propylbenzene and isopropylbenzene

	n-Propylbenzene (2)								Isopropylbenzene (3)									
	M^+				$(M—C_2H_5)^+$					M^+					$(M—CH_3)^+$					
	Composition (%)			Total D	Composition (%)			Total D	D atoms at	Composition (%)				Total D	Composition (%)				Total D	D atoms at
Experiment	d_0	d_1	d_2	atoms*	d_0	d_1	d_2	atoms†	$C_{\beta\gamma}$‡	d_0	d_1	d_2	d_3	atoms§	d_0	d_1	d_2	d_3	atoms‖	C_α¶
1	0	5	95	1.95	3	8	89	1.86	0.09	0	8	91	1	1.85	50	2	48	0	1.00	0.15
2	0	8	92	1.92	3	7	90	1.87	0.05	0	7	90	3	1.96	48	4	47	1	1.01	0.06
3	0	19	81	1.82	6	21	74	1.70	0.12	0	6	81	13	2.08	45	8	41	6	1.09	0.10
4	0	20	81	1.80	5	23	72	1.67	0.13	0	4	85	11	2.07	42	10	41	7	1.13	0.19
5	20	14	66	1.46	25	18	57	1.32	0.14	20	6	68	6	1.60	56	6	35	3	0.85	0.10
6	23	4	74	1.51	28	8	65	1.37	0.14	23	5	71	0	1.48	61	3	36	0	0.74	0.00

*Corresponds to the number of D atoms at C_α, C_β, and C_γ of *n*-propylbenzene.
†Corresponds to the number of D atoms at C_α of *n*-propylbenzene.
‡Difference between * and †.
§Corresponds to the number of D atoms at $C_\alpha + 2C_\beta$ of isopropylbenzene.
‖Corresponds to the number of D atoms at $C_\alpha + C_\beta$ of isopropylbenzene.
¶Calculated from § and ‖.

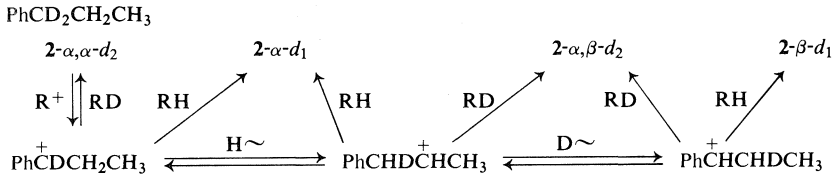

SCHEME 1

such as **1**, took place by a direct displacement mechanism. The formation of **3** in the reaction of **1** with benzene was suggested as the result of a concurrent isomerization of the *n*- to isopropyl halide prior to the rapid alkylation. In the present work, more **3** was formed when 1,2,4-trichlorobenzene instead of excess benzene was used as solvent (see Experimental). Presumably, the rate of alkylation of the benzene was decreased by the presence of the inert solvent, thus giving more opportunity for **1** to isomerize prior to the alkylation. Subsequent changes in the initial alkylation products, by processes such as disproportionation and transalkylation, would account for the variations in isotopic compositions as given in Table 2.

Roberts and coworkers (5, 6) have found that in the $AlCl_3$ catalyzed disproportionation of ^{14}C-labeled **2** (carried out under more drastic conditions than those used in the present work, typically at 80–100° for 6.5 h), scrambling of the ^{14}C-label between C_α and C_β took place without involving C_γ. From extensive studies with **2** and with other alkylbenzenes and from the isolation of diphenylalkanes in these reactions, Roberts and coworkers (7) postulated a mechanistic scheme which could correlate dealkylations, fragmentations, rearrangements, and disporportionations in alkylbenzenes. The scheme involved hydride transfers via carbonium ions, but with the formation of primary carbonium ions specifically avoided, phenyl and methyl shifts, and formation of diphenylalkanes as intermediates and by-products. Under the relatively mild conditions of the present experiments, extensive isotopic scrambling between C_α and C_β was not observed. To account for the small amount (about 5%) of isotope position rearrangements of the D-label in the side chain and the formation of d_1 species in **2** (experiments 1–4, Table 2), it is sufficient to suggest a modified version of Roberts' mechanism, depicted in Scheme 1, involving hydride and deuteride shifts and intermolecular hydride and deuteride transfers via carbonium ions derived from the initially formed alkylation product, *n*-propylbenzene-α,α-d_2 (**2**-α,α-d_2). When the reaction was carried out in 1,2,4-trichlorobenzene as solvent (experiments 5 and 6), a longer lifetime for the carbonium ions would allow several cycles of hydride or deuteride transfers to occur, converting, for example, **2**-d_1 to **2**-d_0 as indicated by the experimental results. The isopropylbenzene (**3**) in the reaction mixture could, of course, be involved in some of the processes in Scheme 1, for example, by taking part in hydride or deuteride transfers through the formation of the dimethylphenylmethyl cation. Abstraction of a deuteride ion by this carbonium ion would result in the formation of **3**-d_3 with a gain of deuterium at C_α. On the other hand, a carbonium ion derived from such processes as fragmentation or dealkylation would not have the skeletal structure of **2** or **3**. Transfer of deuteride ions to such carbonium ions would result in a net loss of deuterium from **2** and **3** as observed, for example, in experiments 5 and 6.

The above discussions thus have adequately explained the observed results as recorded in Tables 1 and 2. It should be pointed out, in conclusion, that although the Friedel–Crafts alkylation of benzene with **1** gave the expected products, **2** and **3**, and that there was only a very minor amount, if any, of isotope position scrambling in the propyl side chain of **2**, the present mass spectral data have demonstrated the lability of the alkylation products in the Friedel–Crafts reaction medium. Extensive intermolecular and possibly some intramolecular hydride (and deuteride) migrations could take place even when the reaction was carried out at 0°.

Experimental

*1,1-d_2-1-Chloropropane (**1**-d_2)*

1,1-d_2-1-Propanol was obtained from the reduction of propionaldehyde with lithium aluminum deuteride. The alcohol was converted to the tosylate and then to the chloride by reaction with $CaCl_2$ in ethylene glycol as described

Can. J. Chem. Downloaded from www.nrcresearchpress.com by 210.87.254.42 on 09/05/12
For personal use only.

previously in the analogous preparation of 1-*t*-1-chloropropane (8).

Reaction of **1**-d_2 *with Excess Benzene (Experiments 1–4)*

To a suspension of 1.0 g (7.5 mmoles) of $AlCl_3$ in 23 ml of dry benzene, cooled to near its freezing point (about 5°), was added rapidly a solution of 1.0 g (12 mmoles) of **1**-d_2 in 2 ml of cold, dry benzene. The reaction mixture was stirred at about 5° for the desired length of time (1.5, 45, or 240 min) before being quenched with ice–water. The benzene layer was separated, washed with water and with $NaHCO_3$ solution and then dried over anhydrous $MgSO_4$. Most of the benzene was fractionated off, and the products, *n*-propylbenzene (**2**) and isopropylbenzene (**3**), were isolated from the residue by preparative v.p.c., using a Pye chromatograph with a 36 ft × 3/8 in. glass column packed with 20% Carbowax 20M on Chromosorb P. The ratio of products, **3**:**2**, was about 55:45 and the total yields were 0.7–0.8 g (about 50%) regardless of the length of reaction time.

Reaction of **1**-d_2 *with Benzene in 1,2,4-Trichlorobenzene (Experiments 5 and 6)*

To a suspension of 4.0 g (30 mmoles) of $AlCl_3$ in 12.0 g (154 mmoles) of dry benzene and 40 g of 1,2,4-trichlorobenzene, cooled to 0° in an ice bath, was added rapidly a solution of 4.0 g (50 mmoles) of **1**-d_2 in 20 g of trichlorobenzene, also cooled to 0°. The reaction mixture was stirred at 0° for 45 min and then quenched in ice–water. The organic layer was washed with water and with $NaHCO_3$ solution and dried over anhydrous $MgSO_4$. The crude products were isolated by fractional distillation, the fraction boiling between 81–170° being collected. Pure **2** and **3** were then separated by preparative v.p.c. as described above. The total yield was about 2.0 g (33%) and the product ratio, **3**:**2**, was about 85:15.

Nuclear Magnetic Resonance and Mass Spectra

The n.m.r. and mass spectra of pure **2** and **3** obtained from the above experiments were taken with the HA 100 and MS 12 spectrometers.

The financial assistance given by the National Research Council of Canada is gratefully acknowledged.

1. N. C. Deno, D. La Vietes, J. Mockus, and P. Scholl. J. Amer. Chem. Soc. **90**, 6457 (1968).
2. J. H. Beynon. Mass spectrometry. Elsevier Publishing Co., New York, N.Y. 1960. Appendix I.
3. H. Jungh, C. R. Smoot, and H. C. Brown. J. Amer. Chem. Soc. **78**, 2185 (1956).
4. C. R. Smoot and H. C. Brown. J. Amer. Chem. Soc. **78**, 6249 (1956).
5. R. M. Roberts and S. G. Brandenberger. J. Amer. Chem. Soc. **79**, 5484 (1957).
6. R. M. Roberts and J. E. Douglass. J. Org. Chem. **28**, 1225 (1963).
7. R. M. Roberts, A. A. Khalaf, and R. N. Greene. J. Amer. Chem. Soc. **86**, 2846 (1964).
8. C. C. Lee, B.-S. Hahn, K.-M. Wan, and D. J. Woodcock. J. Org. Chem. **34**, 3210 (1969).

Nucleotide syntheses using O^2,2′-anhydrouridine

K. K. Ogilvie and D. Iwacha[1]

Department of Chemistry, University of Manitoba, Winnipeg, Manitoba

Received October 2, 1969

The synthesis of a nucleotide derivative (**3**) which can lead directly to O^2,2′-anhydro- and arabino-analogues of 1-β-D-ribofuranosyluracil nucleotides is described.

Canadian Journal of Chemistry, **48**, 862 (1970)

Arabinonucleotides have recently received a great deal of attention. Wechter (1) has studied the biological properties of nucleotides containing the antiviral nucleoside arabinocytidine. Smrt and Sorm (2) have found that trinucleotides containing arabinouridine or arabinocytidine in the third position do not stimulate the binding of transfer RNA to ribosomes. Lunzmann and Schramm (3) have reported studies on the biologically active arabinoadenosine and nucleotides containing arabinouridine. Very recently Nagyvary (4) has described the synthesis of arabinocytidine 3′-phosphate from O^2,2′-anhydrocytidine 3′-phosphate. We wish to report the synthesis of nucleotides containing anhydrouridine as convenient precursors to arabinouridine nucleotides. Work is in progress to adapt the procedure to nucleosides derived from all common purines and pyrimidines.

The chemistry is illustrated by the synthesis of the anhydronucleotide derivative (**3**), indicated in Scheme 1. In this case 1.0 g (2.0 mmole) of 5′-*O*-monomethoxytritylanhydrouridine (**1**) was phosphorylated (5) with pyridinium β-cyanoethyl phosphate (8.0 mmole) using dicyclohexylcarbodiimide (32.0 mmole) in pyridine. The product **2**

[1]NRCC Scholarship Recipient, 1968–present.

Can. J. Chem. Downloaded from www.nrcresearchpress.com by 210.87.254.42 on 09/05/12
For personal use only.

previously in the analogous preparation of 1-*t*-1-chloropropane (8).

Reaction of **1**-d_2 *with Excess Benzene (Experiments 1–4)*

To a suspension of 1.0 g (7.5 mmoles) of $AlCl_3$ in 23 ml of dry benzene, cooled to near its freezing point (about 5°), was added rapidly a solution of 1.0 g (12 mmoles) of **1**-d_2 in 2 ml of cold, dry benzene. The reaction mixture was stirred at about 5° for the desired length of time (1.5, 45, or 240 min) before being quenched with ice–water. The benzene layer was separated, washed with water and with $NaHCO_3$ solution and then dried over anhydrous $MgSO_4$. Most of the benzene was fractionated off, and the products, *n*-propylbenzene (**2**) and isopropylbenzene (**3**), were isolated from the residue by preparative v.p.c., using a Pye chromatograph with a 36 ft × 3/8 in. glass column packed with 20% Carbowax 20M on Chromosorb P. The ratio of products, **3**:**2**, was about 55:45 and the total yields were 0.7–0.8 g (about 50%) regardless of the length of reaction time.

Reaction of **1**-d_2 *with Benzene in 1,2,4-Trichlorobenzene (Experiments 5 and 6)*

To a suspension of 4.0 g (30 mmoles) of $AlCl_3$ in 12.0 g (154 mmoles) of dry benzene and 40 g of 1,2,4-trichlorobenzene, cooled to 0° in an ice bath, was added rapidly a solution of 4.0 g (50 mmoles) of **1**-d_2 in 20 g of trichlorobenzene, also cooled to 0°. The reaction mixture was stirred at 0° for 45 min and then quenched in ice–water. The organic layer was washed with water and with $NaHCO_3$ solution and dried over anhydrous $MgSO_4$. The crude products were isolated by fractional distillation, the fraction boiling between 81–170° being collected. Pure **2** and **3** were then separated by preparative v.p.c. as described above. The total yield was about 2.0 g (33%) and the product ratio, **3**:**2**, was about 85:15.

Nuclear Magnetic Resonance and Mass Spectra

The n.m.r. and mass spectra of pure **2** and **3** obtained from the above experiments were taken with the HA 100 and MS 12 spectrometers.

The financial assistance given by the National Research Council of Canada is gratefully acknowledged.

1. N. C. Deno, D. La Vietes, J. Mockus, and P. Scholl. J. Amer. Chem. Soc. **90**, 6457 (1968).
2. J. H. Beynon. Mass spectrometry. Elsevier Publishing Co., New York, N.Y. 1960. Appendix I.
3. H. Jungh, C. R. Smoot, and H. C. Brown. J. Amer. Chem. Soc. **78**, 2185 (1956).
4. C. R. Smoot and H. C. Brown. J. Amer. Chem. Soc. **78**, 6249 (1956).
5. R. M. Roberts and S. G. Brandenberger. J. Amer. Chem. Soc. **79**, 5484 (1957).
6. R. M. Roberts and J. E. Douglass. J. Org. Chem. **28**, 1225 (1963).
7. R. M. Roberts, A. A. Khalaf, and R. N. Greene. J. Amer. Chem. Soc. **86**, 2846 (1964).
8. C. C. Lee, B.-S. Hahn, K.-M. Wan, and D. J. Woodcock. J. Org. Chem. **34**, 3210 (1969).

Nucleotide syntheses using O^2,2′-anhydrouridine

K. K. Ogilvie and D. Iwacha[1]
Department of Chemistry, University of Manitoba, Winnipeg, Manitoba

Received October 2, 1969

The synthesis of a nucleotide derivative (**3**) which can lead directly to O^2,2′-anhydro- and arabino-analogues of 1-β-D-ribofuranosyluracil nucleotides is described.

Canadian Journal of Chemistry, **48**, 862 (1970)

Arabinonucleotides have recently received a great deal of attention. Wechter (1) has studied the biological properties of nucleotides containing the antiviral nucleoside arabinocytidine. Smrt and Sorm (2) have found that trinucleotides containing arabinouridine or arabinocytidine in the third position do not stimulate the binding of transfer RNA to ribosomes. Lunzmann and Schramm (3) have reported studies on the biologically active arabinoadenosine and nucleotides containing arabinouridine. Very recently Nagyvary (4) has described the synthesis of arabinocytidine 3′-phosphate from O^2,2′-anhydrocytidine 3′-phosphate. We wish to report the synthesis of nucleotides containing anhydrouridine as convenient precursors to arabinouridine nucleotides. Work is in progress to adapt the procedure to nucleosides derived from all common purines and pyrimidines.

The chemistry is illustrated by the synthesis of the anhydronucleotide derivative (**3**), indicated in Scheme 1. In this case 1.0 g (2.0 mmole) of 5′-*O*-monomethoxytritylanhydrouridine (**1**) was phosphorylated (5) with pyridinium β-cyanoethyl phosphate (8.0 mmole) using dicyclohexylcarbodiimide (32.0 mmole) in pyridine. The product **2**

[1]NRCC Scholarship Recipient, 1968–present.

Can. J. Chem. Downloaded from www.nrcresearchpress.com by 210.87.254.105 on 09/05/12
For personal use only.

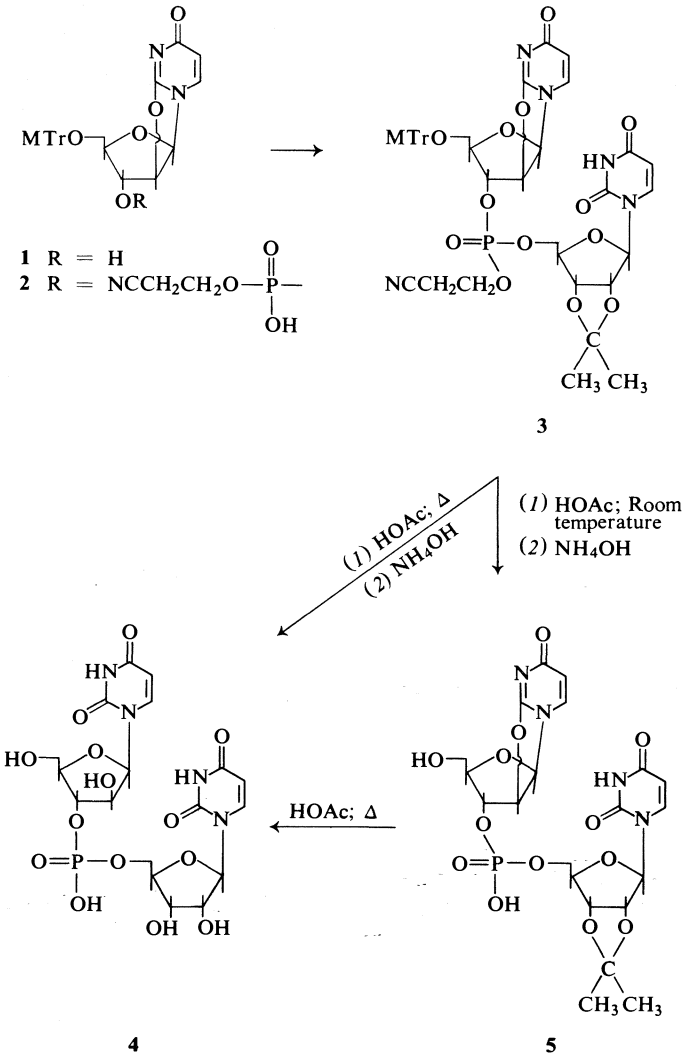

SCHEME 1

was extracted into chloroform, transferred to 5 ml of pyridine, and stirred with 1.2 g (4.0 mmole) of triisopropylbenzenesulfonyl chloride and 0.9 g (3.2 mmole) of isopropylidineuridine for 24 h (6). Water (5 ml) was added to the solution and the product was extracted into chloroform (75 ml). The chloroform solution was concentrated and on addition of ether a gummy residue was obtained which was dissolved in tetrahydrofuran and applied to silica gel thick layer plates (20 × 20 cm). The plates were developed first in ethyl acetate and then in tetrahydrofuran. The product (R_f 0.23, tetrahydrofuran) was eluted with tetrahydrofuran which was concentrated and on addition of hexane yielded 480 mg of **3**, m.p. 150–155 °C (softens at 135 °C). The ultraviolet (u.v.) spectrum in ethanol showed λ_{max} 232 (ε 25 500) and sh 250 mμ (ε 18 500) and λ_{min} 226 mμ (ε 25 000). Treatment of **3** with refluxing 80% acetic acid (2 h) followed by brief treatment with ammonium hydroxide afforded arabinouridylyl-(3′–5′)-uridine (araUpU **4**); u.v. spectrum in water showed λ_{max} 260 mμ and λ_{min} 232 mμ. Assay of **4** with snake venom phosphodiesterase yielded arabinouridine (araU) and uridine 5′-phosphate (1.1:1) while spleen enzyme yielded

Can. J. Chem. Downloaded from www.nrcresearchpress.com by 210.87.254.105 on 09/05/12
For personal use only.

arabinouridine 3′-phosphate and uridine (1.1:1).

Compound **3** also proved useful in yielding a new nucleotide, 0^2,2′-anhydrouridylyl-(3′–5′)-isopropylidineuridine (**5**). Treatment of **3** with 80% acetic acid at room temperature (1 1/2 h) followed by brief exposure to ammonium hydroxide afforded **5** (u.v. spectrum in water: λ_{max} 255 mμ, and λ_{min} 236 mμ). Compound **5** was readily converted to araUpU (**4**) on treatment with 80% acetic acid (steam bath, 2 h).

Attempts to convert **5** to uridylyl-(3′–5′)-isopropylidineuridine using sodium benzoate and benzoic acid in refluxing dimethylformamide (7) have not been successful. Instead, equal amounts of uridine 2′,3′-phosphate and 2′,3′-*O*-isopropylidineuridine are produced. Results similar to these have been obtained with **3**. This reaction is under investigation along with the use of phosphate protecting groups (on **3**) other than cyanoethyl in an effort to convert anhydroribonucleotides into ribonucleotides.

Financial assistance from the National Research Council of Canada and the faculty of Graduate Studies of the University of Manitoba is gratefully acknowledged.

1. W. J. WECHTER, A. J. MIKULSKI, and M. LASKOWSKI. Biochem. Biophys. Res. Commun. **30**, 318 (1968); W. J. WECHTER. J. Med. Chem. **10**, 762 (1967).
2. J. SMRT and F. SORM. Biochem. Biophys. Acta, **138**, 210 (1967); Coll. Czech. Chem. Commun. **32**, 3169 (1967).
3. C. LUNZMANN and C. SCHRAMM. Biochem. Biophys. Acta, **169**, 263 (1968); C. SCHRAMM and I. ULMER-SCHURNBRAND. Biochem. Biophys. Acta, **145**, 7 (1967).
4. J. NAGYVARY. J. Amer. Chem. Soc. **91**, 5409 (1969).
5. G. M. TENER. J. Amer. Chem. Soc. **83**, 159 (1961).
6. R. L. LETSINGER and K. K. OGILVIE. J. Amer. Chem. Soc. **91**, 3550 (1969).
7. J. J. FOX and N. C. MILLER. J. Org. Chem. **28**, 936 (1963).

Can. J. Chem. Downloaded from www.nrcresearchpress.com by 210.87.254.105 on 09/05/12
For personal use only.

Can. J. Chem. Downloaded from www.nrcresearchpress.com by 210.87.254.5 on 09/05/12
For personal use only.

Polar effects at solid/liquid interfaces

A. C. LOWE AND A. C. RIDDIFORD
Department of Chemistry, University of Victoria, Victoria, British Columbia

Received November 25, 1969

Studies of the advancing contact angle of water upon several alkylchlorosilaned glass surfaces at 22 °C lead to the view that, at zero or very low interfacial velocities, the free energy per unit area of the solid/liquid interface is governed by both dispersive and polar forces. At higher velocities, the polar forces may be neglected.

Canadian Journal of Chemistry, **48**, 865 (1970)

We have measured the advancing contact angle, θ_A, at 22 °C, as a function of the linear velocity, $\dot{r}$, with which a water/saturated air interface is caused to move over five different surfaces, prepared by adsorbing dialkyl- and trialkylchlorosilanes on to clean glass plates from the vapor phase using an established technique (1, 2). In Table 1, $\theta_{A,min}$ denotes the constant value of θ_A found when $\dot{r} \leqslant \dot{r}_{min}$, a first critical velocity ranging from 0.5–2.5 mm min^{-1} according to the particular surface studied. Above $\dot{r}_{min}$, θ_A increases until beyond a second critical velocity, $\dot{r}_{max}$, ranging from 3.0–6.0 mm min^{-1}, it again becomes independent of $\dot{r}$. These latter values are denoted by $\theta_{A,max}$ in Table 1. The results for the dimethylsilaned surface are in close agreement with those found for a surface prepared by adsorption from solution (1, 2).

Expressing the difference cos $\theta_{A,min}$ − cos $\theta_{A,max}$ by $\Delta \cos \theta_A$, then, from Young's equation, $\gamma_{LV}\Delta \cos \theta_A$ is clearly a measure of $\Delta\gamma_{SL}$, the increase in the free energy per unit area of the solid/liquid interface, where γ_{LV} is the surface tension of water at 22 °C and is assumed to be independent of $\dot{r}$ (3). This increase in γ_{SL}, and hence in θ_A, has been discussed (1, 2) in the light of Hansen and Miotto's theory (4), that when $\dot{r} < \dot{r}_{min}$, there is ample time for water molecules in the freshly generated solid/liquid interface to relax to their equilibrium orientations, i.e., $\theta_{A,min}$ can be identified with the particular static contact angle appropriate to the unpenetrated surface. When $\dot{r} > \dot{r}_{min}$, however, there is insufficient time for this orientation to be completed at a given point on the surface before the three-phase line of contact has moved beyond the (short) range of influence of this point. The degree of disorientation, with consequent increase in γ_{SL} and in θ_A, reaches a maximum when $\dot{r} \geqslant \dot{r}_{max}$, and the water molecules at the solid surface immediately behind the three-phase line of contact may then be regarded as being randomly oriented. No clear account has been given, however, of the forces acting across the solid/liquid interface for the regions $\dot{r} \leqslant \dot{r}_{min}$ and $\dot{r} \geqslant \dot{r}_{max}$.

The view that $\theta_{A,min}$, or the static contact angle for the unpenetrated surface, is governed by purely dispersive forces (5, 6) is difficult to reconcile with the present results. Apart from minor

TABLE 1
Dynamic contact angles

Silane	$\theta_{A,min}$ (deg)	$\theta_{A,max}$ (deg)	$\gamma_{LV}\Delta \cos \theta_A$ (erg cm^{-2})	A (erg Å)
$(CH_3)_3SiCl$	80	90	12.5	1.4×10^{-14}
$(C_2H_5)_3SiCl$	78.5	80	1.85	
$(CH_3)_2SiCl_2$	105	115	11.8	1.1×10^{-14}
$(C_2H_5)_2SiCl_2$	101.5	105	4.3	
$(CH_2)_5SiCl_2$	90	92	2.5	

variations in the nature and packing density of the outermost alkyl groups, there is an important difference between the surfaces under consideration and that of a bulk solid hydrocarbon. Whether the chlorosilanes are adsorbed on to the glass substrate as monolayers or, as is possible in the case of the dialkylsilanes, as polysiloxane multilayers (7), the extent to which the surface may be treated as non-polar depends upon the extent to which the alkyl substituent groups shield the water molecules from the underlying, and extremely polar, Si—O bonds (μ = 2.6 D). The decrease in $\gamma_{LV}\Delta \cos \theta_A$ in passing from methyl- to ethylsilaned surfaces strongly suggests that it is necessary to consider electrostatic interactions in addition to those arising from dispersion forces. Viewed in this light, $\theta_{A,min}$ is governed by both types of interaction, the orientation of the water molecules being caused by the electrostatic forces. In passing from $\dot{r}_{min}$ to $\dot{r}_{max}$, this electrostatically induced orientation is progressively destroyed until, when $\theta_A = \theta_{A,max}$, only dispersion forces need be considered.

To test this hypothesis, we have made the following simplifying assumptions: that the number of Si—O bonds, and the number of water molecules, do not vary from surface to surface; that the distance of closest approach of water molecules is the same for each surface; and that the alkyl chains behave as uniform dielectrics. On these assumptions, there would be maximum electrostatic interaction between the water molecules and an induced (positive) surface charge on the outermost hydrogen atoms when $0 \leqslant \dot{r} \leqslant \dot{r}_{min}$, this latter charge decreasing linearly with d^{-3}, where d is the distance between the outermost hydrogen atoms and the nearest underlying silicon atom. It then follows that $\gamma_{LV}\Delta \cos \theta_A$ should also vary linearly with d^{-3}.

Figure 1 shows that the predicted linear relationship holds for the dialkyl surfaces and, although only two points are available for the trialkyl surfaces, the slopes, A, of the two lines are closely similar.

This interpretation, if accepted, provides a direct experimental means for assessing dipolar contributions to the free energy of a number of solid/liquid interfaces, and suggests that, for such interfaces, dynamic studies are essential before static observations can properly be interpreted. Fuller details will be reported in due course.

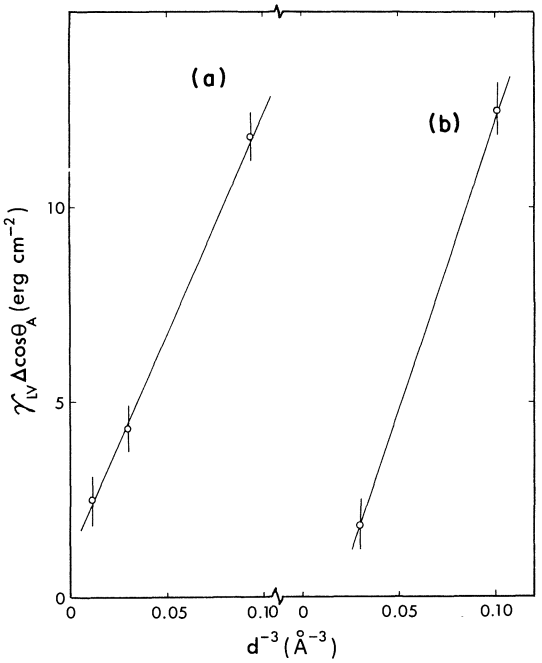

FIG. 1. Plot of $\gamma_{LV}\Delta \cos \theta_A$ vs. d^{-3}: (*a*) for dialkyl surfaces, (*b*) for trialkyl surfaces.

Acknowledgment of financial support for this work is made to the Iraq Petroleum Co., Ltd. and to the National Research Council of Canada.

1. G. E. P. ELLIOTT and A. C. RIDDIFORD. Nature, **195**, 795 (1962).
2. G. E. P. ELLIOTT and A. C. RIDDIFORD. J. Colloid. Sci. **23**, 389 (1967).
3. A. F. VANDEGRIFT. J. Colloid. Sci. **23**, 43 (1967).
4. R. S. HANSEN and M. MIOTTO. J. Amer. Chem. Soc. **79**, 1765 (1957).
5. M. C. PHILLIPS and A. C. RIDDIFORD. J. Colloid. Sci. **22**, 149 (1966).
6. F. M. FOWKES. Advan. Chem. Ser. **43**, 99 (1964).
7. R. L. BASS. Chem. Ind. London. 912 (1959).

Can. J. Chem. Downloaded from www.nrcresearchpress.com by 210.87.254.5 on 09/05/12
For personal use only.

Isolation of indole (β-carboline), pyridine, and indole–pyridine alkaloids from *Nauclea diderrichii*

STEWART MCLEAN AND D. G. MURRAY
Department of Chemistry, University of Toronto, Toronto, Ontario

Received December 5, 1969

The bark of *N. diderrichii* has afforded alkaloids of novel structure and of biogenetic significance. Pyridines, β-carbolines, and more complex alkaloids that contain both of these units or modifications of them have been identified among the bases isolated.

Canadian Journal of Chemistry, **48**, 867 (1970)

Can. J. Chem. Downloaded from www.nrcresearchpress.com by 210.87.254.5 on 09/05/12
For personal use only.

The genus *Nauclea* (*Sarcocephalus*) of the *Rubiaceae* appears to have attracted relatively little phytochemical interest in the past (1). We have now isolated a considerable number of bases, each in low yield, from the bark of Nigerian *N. diderrichii*. The alkaloids were separated by thin-layer chromatography (t.l.c.), their molecular formulae were determined mass spectrometrically, and as many spectroscopic characteristics were recorded as the amounts of material obtained would allow. Structures deduced on the basis of these data were in most cases confirmed by synthesis, but in some of the more complex cases structural assignments are still incomplete. We have identified pyridines, β-carbolines, and alkaloids that incorporate both an indole component, apparently tryptamine-derived, and a pyridine component that may be of terpenoid origin. Although the first reports of the coexistence of both pyridine and "C_{19}-indole" alkaloids in a single plant have appeared recently (2), the indole–pyridine alkaloids we describe appear to constitute a new structural class. This structural novelty and the potential biogenetic significance of the isolation of all 3 classes of alkaloids from a single plant lead us to give a preliminary account of our results.

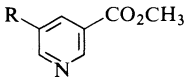

1

a R = $CH_3\dot{C}HOH$
b R = $CH_3\dot{C}HOMe$
c R = $CH_3\dot{C}HNH_2$
d R = $CH_2{=}\dot{C}H$
e R = $CH_3\dot{C}{=}O$
f R = —COCl

(i) Simple Pyridines

Four 5-substituted derivatives of methyl nicotinate (**1***a–d*) were obtained, and each was synthesized from nicotinic acid through the ketone **1***e*, m.p. 90–92°, by standard methods. The natural materials **1***a–c* were optically active and all, including **1***d*, were obtained as oils, as were the racemic synthetic products; identity was therefore demonstrated by comparison of spectroscopic and t.l.c. characteristics.

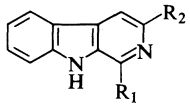

2

a $R_1 = CH_3$; $R_2 = H$
b $R_1 = CO_2Me$; $R_2 = H$
c $R_1 = CH_3$; $R_2 = CO_2Me$
d $R_1 = CONH_2$; $R_2 = H$

(ii) Simple β*-Carbolines*

Three β-carbolines (**2***a–c*), which have been described previously (3), were obtained. Harman (**2***a*) is readily available and comparison samples of **2***b* and **2***c* were synthesized by established procedures (4). From one extraction, which employed ammonia, **2***d* was isolated; this was also obtained by the reaction of synthetic **2***b* with ammonia, and is therefore probably an artifact.

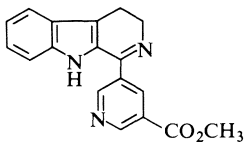

3

(iii) Indole–pyridine Alkaloids

Three of the bases isolated have been placed with some confidence in this group: $C_{18}H_{15}N_3O_2$,

Can. J. Chem. Downloaded from www.nrcresearchpress.com by 210.87.254.5 on 09/05/12
For personal use only.

m.p. 84–90°, $C_{19}H_{19}N_3O_2$, m.p. 102–124°, and $C_{21}H_{21}N_3O_3$, m.p. 108–114°. Structure **3**, assigned to the first alkaloid, has been confirmed by its synthesis from tryptamine and **1***f* under Bischler–Napieralski conditions (5). Present data, which include λ_{max}(MeOH) 224 (ε 40 700), 276 (ε 9500), 290 mμ (sh, ε 7900), λ_{max}($CHCl_3$) 5.80 μ, a methyl singlet at τ 6.14, and signals from 4 indole protons near τ 2.7 and 3 pyridine protons at τ 1.03 (d, $J \sim 2$ Hz), 1.48 (d, $J \sim 2$ Hz), and 1.89 (3 lines, splitting ~ 2 Hz) in the nuclear magnetic resonance spectrum, indicate that the second is a tetracyclic secondary amine (acylable) and contains a simple indole unit and an isolated 5-substituted methyl nicotinate unit. The third appears, on the basis of data of a similar nature, to be a pentacyclic tertiary amine and to contain a simple indole unit and a disubstituted (probably 4,5-) methyl nicotinate unit.

(iv) Other Alkaloids

At least 6 other bases are present in the extract, including $C_{18}H_{17}N_3O_2$, m.p. 229–232° and $C_{21}H_{26}N_2O_4$, m.p. 209–211°; the former probably belongs in group (*iii*), but it appears structurally more complex than those already assigned to that group. All extractions afforded a considerable amount of a component which had the characteristics of a high molecular weight polyhydroxy base.

The composition of the total extract was variable and appeared to depend on factors such as the age of the tree from which the bark was obtained. The question of whether pyridines are true alkaloids or artifacts produced by reaction of a precursor with ammonia during isolation has been raised previously (6). Our earlier procedures did employ ammonia in the extraction and chromatography steps, but, in a control isolation which carefully avoided ammonia at every stage, we obtained the same pyridine as in the former procedure; unfortunately, none of the more complex alkaloids was isolated by either procedure on this occasion.

We thank Professor D. M. James, University of Ibadan, and her collaborators for collecting and identifying the plant material. Operating and Scholarship support from the National Research Council of Canada and a Province of Ontario Graduate Fellowship are gratefully acknowledged.

1. E. Fujita, T. Fujita, and T. Suzuki. Chem. Pharm. Bull. **15**, 1682 (1967); L. A. Silva, L. N. Prista, and A. C. Alves. Garcia de Orta, **11**, 89 (1963); F. E. King and L. Jurd. J. Chem. Soc. 1192 (1953).
2. A. B. Ray and A. Chatterjee. Tetrahedron Lett. 2763 (1968); H. R. Arthur, S. R. Johns, J. A. Lamberton, and S. N. Loo. Aust. J. Chem. **20**, 2505 (1967).
3. H. Achenbach and K. Biemann. J. Amer. Chem. Soc. **87**, 4177 (1965); L. D. Antonaccio and H. Budzikiewicz. Monatsh. Chem. **93**, 962 (1962).
4. H. R. Snyder, H. G. Walker, and F. X. Werber. J. Amer. Chem. Soc. **71**, 527 (1949); H. R. Snyder, C. H. Hansch, L. Katz, S. M. Parmerter, and E. C. Spaeth. J. Amer. Chem. Soc. **70**, 219 (1948).
5. A. Szakolcai. Unpublished results from this laboratory.
6. N. K. Hart, S. R. Johns, and J. A. Lamberton. Aust. J. Chem. **21**, 1321 (1968). W. A. Ayer and T. E. Habgood. The alkaloids. Vol. XI. *Edited by* R. H. F. Manske. Academic Press, New York, 1968. Chap. 12.

Reaction of trialkylboranes with diazoacetaldehyde. A new synthesis of aldehydes

John Hooz and Geoffrey F. Morrison
Department of Chemistry, University of Alberta, Edmonton, Alberta

Received December 12, 1969

A new aldehyde synthesis has been developed, based on the reaction of organoboranes with diazoacetaldehyde.

Canadian Journal of Chemistry, **48**, 868 (1970)

Previous publications have described syntheses of ketones (1), nitriles (2), esters (2), and diketones (3), in which olefins, via their organoborane derivatives, have been simultaneously functionalized and homologated. We have expanded this versatile method to include a new, mild aldehyde synthesis which permits a 2-carbon-atom extension (ethanalation) of olefins by the reaction of

Can. J. Chem. Downloaded from www.nrcresearchpress.com by 210.87.254.5 on 09/05/12
For personal use only.

m.p. 84–90°, $C_{19}H_{19}N_3O_2$, m.p. 102–124°, and $C_{21}H_{21}N_3O_3$, m.p. 108–114°. Structure **3**, assigned to the first alkaloid, has been confirmed by its synthesis from tryptamine and **1***f* under Bischler–Napieralski conditions (5). Present data, which include λ_{max}(MeOH) 224 (ε 40 700), 276 (ε 9500), 290 mμ (sh, ε 7900), λ_{max}($CHCl_3$) 5.80 μ, a methyl singlet at τ 6.14, and signals from 4 indole protons near τ 2.7 and 3 pyridine protons at τ 1.03 (d, $J \sim 2$ Hz), 1.48 (d, $J \sim 2$ Hz), and 1.89 (3 lines, splitting ~ 2 Hz) in the nuclear magnetic resonance spectrum, indicate that the second is a tetracyclic secondary amine (acylable) and contains a simple indole unit and an isolated 5-substituted methyl nicotinate unit. The third appears, on the basis of data of a similar nature, to be a pentacyclic tertiary amine and to contain a simple indole unit and a disubstituted (probably 4,5-) methyl nicotinate unit.

(iv) Other Alkaloids

At least 6 other bases are present in the extract, including $C_{18}H_{17}N_3O_2$, m.p. 229–232° and $C_{21}H_{26}N_2O_4$, m.p. 209–211°; the former probably belongs in group (*iii*), but it appears structurally more complex than those already assigned to that group. All extractions afforded a considerable amount of a component which had the characteristics of a high molecular weight polyhydroxy base.

The composition of the total extract was variable and appeared to depend on factors such as the age of the tree from which the bark was obtained. The question of whether pyridines are true alkaloids or artifacts produced by reaction of a precursor with ammonia during isolation has been raised previously (6). Our earlier procedures did employ ammonia in the extraction and chromatography steps, but, in a control isolation which carefully avoided ammonia at every stage, we obtained the same pyridine as in the former procedure; unfortunately, none of the more complex alkaloids was isolated by either procedure on this occasion.

We thank Professor D. M. James, University of Ibadan, and her collaborators for collecting and identifying the plant material. Operating and Scholarship support from the National Research Council of Canada and a Province of Ontario Graduate Fellowship are gratefully acknowledged.

1. E. Fujita, T. Fujita, and T. Suzuki. Chem. Pharm. Bull. **15**, 1682 (1967); L. A. Silva, L. N. Prista, and A. C. Alves. Garcia de Orta, **11**, 89 (1963); F. E. King and L. Jurd. J. Chem. Soc. 1192 (1953).
2. A. B. Ray and A. Chatterjee. Tetrahedron Lett. 2763 (1968); H. R. Arthur, S. R. Johns, J. A. Lamberton, and S. N. Loo. Aust. J. Chem. **20**, 2505 (1967).
3. H. Achenbach and K. Biemann. J. Amer. Chem. Soc. **87**, 4177 (1965); L. D. Antonaccio and H. Budzikiewicz. Monatsh. Chem. **93**, 962 (1962).
4. H. R. Snyder, H. G. Walker, and F. X. Werber. J. Amer. Chem. Soc. **71**, 527 (1949); H. R. Snyder, C. H. Hansch, L. Katz, S. M. Parmerter, and E. C. Spaeth. J. Amer. Chem. Soc. **70**, 219 (1948).
5. A. Szakolcai. Unpublished results from this laboratory.
6. N. K. Hart, S. R. Johns, and J. A. Lamberton. Aust. J. Chem. **21**, 1321 (1968). W. A. Ayer and T. E. Habgood. The alkaloids. Vol. XI. *Edited by* R. H. F. Manske. Academic Press, New York, 1968. Chap. 12.

Reaction of trialkylboranes with diazoacetaldehyde. A new synthesis of aldehydes

John Hooz and Geoffrey F. Morrison
Department of Chemistry, University of Alberta, Edmonton, Alberta

Received December 12, 1969

A new aldehyde synthesis has been developed, based on the reaction of organoboranes with diazoacetaldehyde.

Canadian Journal of Chemistry, **48**, 868 (1970)

Previous publications have described syntheses of ketones (1), nitriles (2), esters (2), and diketones (3), in which olefins, via their organoborane derivatives, have been simultaneously functionalized and homologated. We have expanded this versatile method to include a new, mild aldehyde synthesis which permits a 2-carbon-atom extension (ethanalation) of olefins by the reaction of

trialkylboranes with diazoacetaldehyde (eq. [1]).

$$[1] \qquad R_3B + N_2CHCHO \xrightarrow[H_2O]{-N_2} RCH_2CHO$$

This process conveniently augments the repertory of organoborane-based aldehyde syntheses, which to date have been limited to 1- (4) and 3-carbon-atom (5) chain-lengthening reactions.

Some typical examples are summarized in Table 1. The reactions of organoboranes derived from 1-alkenes as well as cyclopentene proceed in good yield (77–98%); yields are lower, however, for sterically-hindered trialkylboranes. Triarylboranes also react successfully, as exemplified by the conversion of triphenylborane to phenylacetaldehyde (76%).

Although the hydroboration of monosubstituted terminal olefins produces approximately 94% primary and 6% secondary alkyl groups (6), the product from reaction of the trialkylborane derived from 1-butene was hexanal; no evidence (gas–liquid phase chromatography (g.l.p.c.)) for the formation of 3-methylpentanal was observed. Since a similar migrational preference of primary over secondary alkyl groups has also been noted in the organoborane-diazoacetic ester reaction (2), these developments permit the synthesis of functional derivatives free of isomeric contaminants. By way of contrast, the 3-carbon aldehyde homologation, involving reaction of trialkylboranes with acrolein (5), gives products derived from preferential migration of the secondary alkyl groups in the organoborane.[1]

Functional diazo substrates react with organoboranes to produce intermediates which undergo hydrolysis with extreme ease (2). The g.l.p.c. analysis of a crude tributylborane–diazoacetaldehyde reaction mixture after complete consumption of diazo compound, but prior to the addition of water, revealed the presence of some hexanal. The infrared (i.r.) spectrum exhibited absorption at 1730 (aldehyde carbonyl) and 1670 cm^{-1} (enol ether ?); the latter disappeared at the expense of the former after addition of water. This observation is highly reminiscent of the formation of enol borinates (5) from the 1,4-addition of trialkylboranes to acrolein, and implies a similar intermediate.[2]

TABLE 1

Conversions of olefins into aldehydes by the reaction of the corresponding trialkylboranes with diazoacetaldehyde in the presence of water

Olefin*	Product	Yield† (%)
Ethylene‡	Butanal	88
1-Butene	Hexanal	77
Cyclopentene	Cyclopentylacetaldehyde	98
Isobutylene	4-Methylpentanal	67
2-Butene	3-Methylpentanal	33

*Each olefin was converted to the corresponding trialkylborane following the procedure of ref. 6.

†By g.l.p.c. analysis. Yield based on diazoacetaldehyde. The molar ratio of diazoacetaldehyde:trialkylborane:water was 1:1.5:10, although we have not determined that these excesses are necessary. A 1:1 molar ratio of organoborane to diazo compound gives somewhat lower yields.

‡Triethylborane was obtained from Alfa Inorganics, Inc.

Rather than conduct the hydrolysis in a separate stage, however, we have observed that higher yields of aldehydes and an experimentally more convenient procedure is achieved by adding water to a solution of organoborane in THF prior to the addition of diazo compound. This permits the rapid, in situ hydrolysis of the functional boron intermediate.

The straightforward experimental procedure is illustrated for the preparation of cyclopentylacetaldehyde.[3] To a mixture of tricyclopentylborane (47 mmole) in 23 ml THF and 1.8 ml (100 mmole) of water, was added (60 min) 8.4 mmole of diazoacetaldehyde[4] in 10 ml THF at

[1]A limitation of the R_3B-diazo reaction at present, a difficulty also encountered in the propanalation process, is that but one alkyl moiety is utilized. Although B-alkyl-9-borabicyclo[3.3.1]nonane (B-R-9-BBN) derivatives have recently been very effectively employed to circumvent this difficulty in the carbonylation reaction and the alkylation of α-halocarbanions (7), diazo substrates react with B-R-9-BBN derivatives with preferential B-cyclooctyl bond migration (8, 9).

However, B-R-9-BBN derivatives fail to react with acrolein.

[2]Also, trialkylboranes react with diazo ketones and esters in the presence of deuterium oxide to furnish α-deuterio ketones and esters with incorporation of one deuterium atom in high yield and isotopic purity (10). The interesting consequences of these developments, suggestive of a mechanistic convergence of the R_3B-diazo and R_3B-carbonyl systems, warrant further detailed elaboration, although at present our primary concerns have been focused on the novel synthetic aspects of the R_3B-diazo reaction.

[3]Organoboranes derived from 1-alkenes react at 0–10°, boranes from 1,1-disubstituted olefins at 40°, whereas those derived from 1,2-disubstituted olefins require a brief reflux period before nitrogen evolution ceases.

[4]Prepared according to the method of Z. Arnold (11) from β-(*N*-methylanilino)-acrolein and *p*-toluenesulfonyl azide. *Caution*! Although we experienced no difficulties in numerous reactions of this material, adequate safety precautions should be observed in its preparation and isolation. Arnold reports that diazoacetaldehyde detonates very violently when overheated.

We have also synthesized this material in a convenient manner by reacting formic acetic anhydride with excess diazomethane. (Unpublished results of G. F. Morrison.) Org. Prep. Proc. Int., 3, 227 (1971).

Can. J. Chem. Downloaded from www.nrcresearchpress.com by 210.87.254.5 on 09/05/12
For personal use only.

25°. Nitrogen evolution was quantitative after an additional stirring period of 60 min at 25°; g.l.p.c. analysis indicated a 98% yield of product.[5] In a duplicate experiment (98% yield), the crude mixture was first processed with aqueous sodium borohydride, then alkaline hydrogen peroxide. The isolated yield of 2-cyclopentylethanol was 72%.

We wish to thank the National Research Council of Canada for financial support, and the University of Alberta for the award of a Bursary (G.F.M.).

[5]Lower yields were obtained by attempting to distill the sensitive product directly from the crude reaction mixture. Other workers (5) have also observed that direct distillation of aldehydes from residual boron-containing materials leads to product loss. Consequently, we have employed g.l.p.c. to determine yields and isolate pure samples in the preliminary study of this new process.

1. J. Hooz and S. Linke. J. Amer. Chem. Soc. **90**, 5936 (1968).
2. J. Hooz and S. Linke. J. Amer. Chem. Soc. **90**, 6891 (1968).
3. J. Hooz and D. M. Gunn. Chem. Commun. 139 (1969).
4. H. C. Brown, R. A. Coleman, and M. W. Rathke. J. Amer. Chem. Soc. **90**, 499 (1968).
5. H. C. Brown, M. M. Rogić, M. W. Rathke, and G. W. Kabalka. J. Amer. Chem. Soc. **89**, 5709 (1967).
6. (*a*) H. C. Brown. Hydroboration. W. A. Benjamin, Inc., New York, N.Y., 1962; (*b*) G. Zweifel and H. C. Brown. Org. React. **13**, 1 (1963).
7. H. C. Brown, E. F. Knights, and R. A. Coleman. J. Amer. Chem. Soc. **91**, 2144 (1969); H. C. Brown, M. M. Rogić, H. Nambu, and M. W. Rathke. J. Amer. Chem. Soc. **91**, 2147 (1969).
8. H. C. Brown and M. M. Rogić. J. Amer. Chem. Soc. **91**, 2146 (1969).
9. J. Hooz and D. M. Gunn. Tetrahedron Lett. 3455 (1969).
10. J. Hooz and D. M. Gunn. J. Amer. Chem. Soc. **91**, 6195 (1969).
11. Z. Arnold. Chem. Commun. 299 (1967).

Mechanism of silicon hydride addition to hydridocarbonyltris(triphenylphosphine)iridium(I)

J. F. Harrod and C. A. Smith
Chemistry Department, McGill University, Montreal, Quebec

Received December 9, 1969

Canadian Journal of Chemistry, **48**, 870 (1970)

The discovery of the oxidative addition of simple covalent molecules to transition metal complexes has led to major advances in the field of homogeneous catalysis (1, 2). Our interest has been directed towards the reactions of silicon hydrides (3–5) in the hope that a detailed understanding of their oxidative addition reactions would help to solve one of the outstanding problems in homogeneous catalysis, namely, the activation of saturated hydrocarbons.

We have previously reported (5) reaction [1], which was shown to result in *cis* addition of the silicon hydride.

[1] 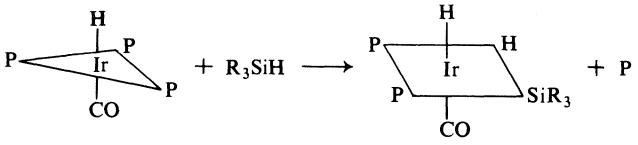

1 2

The only definitive reaction mechanism that has thus far been demonstrated for oxidative addition to a five-coordinate d^8 complex is that shown in reactions [2] and [3], according to Collman and Roper (1)

[2] 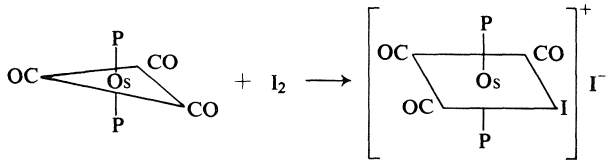

3 4

Can. J. Chem. Downloaded from www.nrcresearchpress.com by 210.87.254.5 on 09/05/12
For personal use only.

25°. Nitrogen evolution was quantitative after an additional stirring period of 60 min at 25°; g.l.p.c. analysis indicated a 98% yield of product.[5] In a duplicate experiment (98% yield), the crude mixture was first processed with aqueous sodium borohydride, then alkaline hydrogen peroxide. The isolated yield of 2-cyclopentylethanol was 72%.

We wish to thank the National Research Council of Canada for financial support, and the University of Alberta for the award of a Bursary (G.F.M.).

[5]Lower yields were obtained by attempting to distill the sensitive product directly from the crude reaction mixture. Other workers (5) have also observed that direct distillation of aldehydes from residual boron-containing materials leads to product loss. Consequently, we have employed g.l.p.c. to determine yields and isolate pure samples in the preliminary study of this new process.

1. J. Hooz and S. Linke. J. Amer. Chem. Soc. **90**, 5936 (1968).
2. J. Hooz and S. Linke. J. Amer. Chem. Soc. **90**, 6891 (1968).
3. J. Hooz and D. M. Gunn. Chem. Commun. 139 (1969).
4. H. C. Brown, R. A. Coleman, and M. W. Rathke. J. Amer. Chem. Soc. **90**, 499 (1968).
5. H. C. Brown, M. M. Rogić, M. W. Rathke, and G. W. Kabalka. J. Amer. Chem. Soc. **89**, 5709 (1967).
6. (*a*) H. C. Brown. Hydroboration. W. A. Benjamin, Inc., New York, N.Y., 1962; (*b*) G. Zweifel and H. C. Brown. Org. React. **13**, 1 (1963).
7. H. C. Brown, E. F. Knights, and R. A. Coleman. J. Amer. Chem. Soc. **91**, 2144 (1969); H. C. Brown, M. M. Rogić, H. Nambu, and M. W. Rathke. J. Amer. Chem. Soc. **91**, 2147 (1969).
8. H. C. Brown and M. M. Rogić. J. Amer. Chem. Soc. **91**, 2146 (1969).
9. J. Hooz and D. M. Gunn. Tetrahedron Lett. 3455 (1969).
10. J. Hooz and D. M. Gunn. J. Amer. Chem. Soc. **91**, 6195 (1969).
11. Z. Arnold. Chem. Commun. 299 (1967).

Mechanism of silicon hydride addition to hydridocarbonyltris(triphenylphosphine)iridium(I)

J. F. Harrod and C. A. Smith
Chemistry Department, McGill University, Montreal, Quebec

Received December 9, 1969

Canadian Journal of Chemistry, **48**, 870 (1970)

The discovery of the oxidative addition of simple covalent molecules to transition metal complexes has led to major advances in the field of homogeneous catalysis (1, 2). Our interest has been directed towards the reactions of silicon hydrides (3–5) in the hope that a detailed understanding of their oxidative addition reactions would help to solve one of the outstanding problems in homogeneous catalysis, namely, the activation of saturated hydrocarbons.

We have previously reported (5) reaction [1], which was shown to result in *cis* addition of the silicon hydride.

[1] 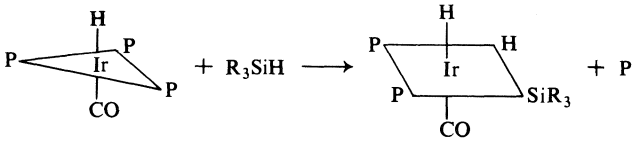

1 2

The only definitive reaction mechanism that has thus far been demonstrated for oxidative addition to a five-coordinate d^8 complex is that shown in reactions [2] and [3], according to Collman and Roper (1)

[2] 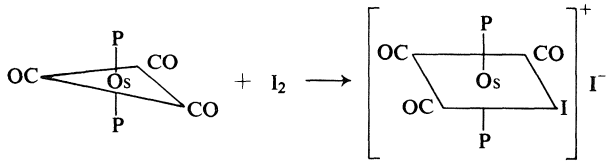

3 4

Can. J. Chem. Downloaded from www.nrcresearchpress.com by 210.87.254.40 on 09/05/12
For personal use only.

[3] 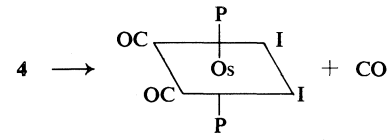

5

Although a sequence of reactions analogous to [2] and [3] for reaction [1] would result in the correct stereochemistry, the requirement of either an uncoordinated silyl- or hydride-ion is most unattractive.

A second possible mechanism involves a bimolecular reaction between **1** and silicon hydride, with phosphine leaving from a seven-coordinate transition state. Such a mechanism has been proposed, without experimental support, for the activation of hydrogen by **1** (6).

We have now confirmed that reaction [1] proceeds by a third mechanism, predissociation of **1** followed by addition of silicon hydride to a four-coordinate intermediate. Thus

[4] 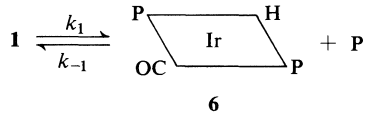

6

[5] $$\mathbf{6} + R_3SiH \xrightarrow{k_2} \mathbf{2}$$

Under pseudo-zero order conditions with respect to [P] and [R_3SiH], the rate of disappearance of **1** obeyed the rate law

[6] $$-\frac{d[Ir^I]}{dt} = k_a[Ir^I]$$

Analysis of reactions [4] and [5] yield the relationship

[7] $$k_a = \frac{k_1k_2[R_3SiH]}{k_{-1}[P] + k_2[R_3SiH]}$$

Plots of $1/k_a$ vs. [P] and $1/[R_3SiH]$ for triethoxysilane are shown in Fig. 1. The linearity of these plots confirms the predissociative mechanism and the intercepts and slopes of such plots yielded values of k_1 and k_{-1}/k_2. At 20 °C these values were 2.8×10^{-2} s^{-1} and 56, respectively, for triethoxysilane and 2.9×10^{-2} s^{-1} and 15 for triphenylsilane.

The activation parameters for k_1 in the case of triethoxysilane were $\Delta H_1\dagger = 23$ Kcals and $\Delta S_1\dagger = 15$ e.u. The value of k_{-1}/k_2 was, within experimental error, independent of temperature, indicating that the greater reactivity of Ph_3P relative to $(C_2H_5O)_3SiH$ was almost entirely attributable to a $\Delta S\dagger$ that was more favorable by about 8 e.u. The greater reactivity of Ph_3SiH relative to $(C_2H_5O)_3SiH$ is in line with previous results, where the rates of reaction of a series of silicon hydrides were found to increase as ethoxy groups were replaced by methyl groups (4).

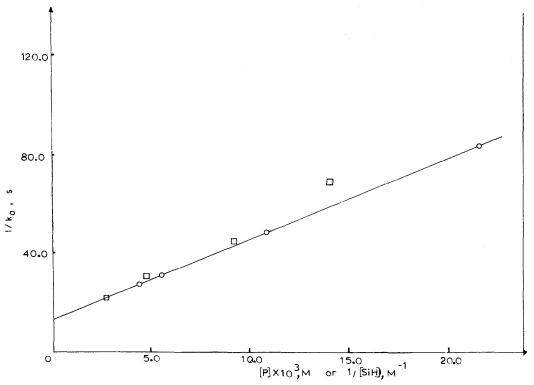

FIG. 1. Dependence of the rate of addition of $(C_2H_5O)_3SiH$ to $P_3(CO)HIr$ on [P] (□) and [SiH] (○), at 27.6 °C. [Ir] = 1.4×10^{-4} *M*. (□) [SiH] = 1.86×10^{-1} *M*, (○) [P] = 4.65×10^{-3} *M*.

It is clear that the kinetic study of reaction [1], and others using similar five-coordinate d^8 complexes, in addition to providing data on the energetics and mechanism of oxidative addition, can also provide data on the dissociation of the starting complex. Quantitative data on the unimolecular dissociation of five-coordinate d^8 complexes is almost nonexistent (7).

We are presently pursuing these studies in the direction of (*i*) varying the phosphine in **1**, (*ii*) varying the silane, and (*iii*) examining other d^8 complexes.

1. J. P. COLLMAN and W. R. ROPER. Advan. Organometal. Chem. **7**, 53 (1968).
2. L. VASKA. Accounts Chem. Res. **1**, 335 (1968).
3. A. J. CHALK and J. F. HARROD. J. Amer. Chem. Soc. **87**, 16 (1965).
4. J. F. HARROD and C. A. SMITH. J. Amer. Chem. Soc. In press.
5. J. F. HARROD, D. F. R. GILSON and R. CHARLES. Can. J. Chem. **47**, 2205 (1969).
6. L. VASKA. Inorg. Nucl. Chem. Lett. **1**, 89 (1965).
7. F. BASOLO and R. PEARSON. Mechanisms of inorganic reactions. John Wiley and Sons Inc., New York. 1968. Chap. 7.

Can. J. Chem. Downloaded from www.nrcresearchpress.com by 210.87.254.40 on 09/05/12
For personal use only.

Can. J. Chem. Downloaded from www.nrcresearchpress.com by 210.87.254.105 on 09/05/12
For personal use only.

Canadian Journal of Chemistry

Published by THE NATIONAL RESEARCH COUNCIL OF CANADA

VOLUME 48 MARCH 15, 1970 NUMBER 6

Absolute rate constants for hydrocarbon autoxidation. XVIII. Oxidation of some acyclic ethers[1]

J. A. HOWARD AND K. U. INGOLD

Division of Chemistry, National Research Council of Canada, Ottawa, Canada

Received November 5, 1969

Propagation and termination rate constants have been measured for autoxidation of benzyl phenyl ether, benzyl *t*-butyl ether, isopropyl ether, and benzyl ether. In the case of isopropyl ether and benzyl ether, estimates have been made of inter- and intramolecular propagation rate constants. Reactivities of acyclic ethers towards the *t*-butylperoxy radical have been determined. Rate constants for autoxidation of cyclic and acylic ethers have been summarized and compared.

Canadian Journal of Chemistry, **48**, 873 (1970)

Introduction

The previous publication in this series (1) reported absolute propagation and termination rate constants for the autoxidation of some cyclic ethers. Acyclic ethers also react with molecular oxygen to give α-hydroperoxides. For example, isopropyl ether gives a mixture of a mono- and a dihydroperoxide (2). This is because the α-alkoxyalkylperoxy radical can abstract a hydrogen atom by an intramolecular as well as by an intermolecular reaction.[2] At oxygen pressures above about 100 mm Hg, the oxidation of acyclic ethers can be represented by the following free-radical chain reaction

Initiation

Production of free radicals

Propagation

[1] $E^{\cdot} + O_2 \longrightarrow EOO^{\cdot}$

[2] $EOO^{\cdot} + EH \xrightarrow{k_2} EOOH + E^{\cdot}$

[3] 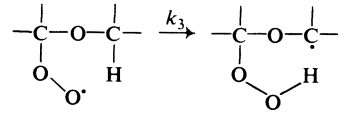

(EOO·) (D·)

[4] $D^{\cdot} + O_2 \longrightarrow DOO^{\cdot}$

[5] $DOO^{\cdot} + EH \xrightarrow{k_5} DOOH + E^{\cdot}$

[6] $EOO^{\cdot} + EOO^{\cdot} \xrightarrow{2k_6}$

[7] $EOO^{\cdot} + DOO^{\cdot} \xrightarrow{2k_7}$ } Non-radical products

[8] $DOO^{\cdot} + DOO^{\cdot} \xrightarrow{2k_8}$

where $E^{\cdot}$ represents an α-alkoxyalkyl radical; $EOO^{\cdot}$, an α-alkoxyalkylperoxy radical; EOOH, a monohydroperoxide; $D^{\cdot}$, an α′-hydroperoxy-α-alkoxyalkyl radical; $DOO^{\cdot}$, an α′-hydroperoxy-α-alkoxyalkylperoxy radical; and DOOH, a dihydroperoxide. The overall rate of oxidation, R_S, at long chain lengths can be represented in the usual way, i.e.

[I] $$R_S = k_p[ROO^{\cdot}][EH]$$

or

[II] $$R_S = k_p[EH]\, R_i^{1/2}/(2k_t)^{1/2}$$

where k_p is an overall propagation rate constant made up of contributions from k_2, k_3, and k_5, and $2k_t$ is an overall termination rate constant made up of contributions from $2k_6$, $2k_7$, and

[1]NRCC No. 11 145.

[2]Intramolecular reactions have also been observed for alkylperoxy radicals (3) and alkenylperoxy radicals (4).

$2k_8$. The radical concentration, [ROO·], is defined by $(R_i/2k_t)^{1/2}$, where R_i is the rate of chain initiation. The rate of oxidation is also given by

$$[III] \quad R_S = (k_2[EOO^·] + k_5[DOO^·])[EH] + k_3[EOO^·]$$

or

$$[IV] \quad R_S = (k_2[EOO^·] + 2k_5[DOO^·])[EH]$$

since $k_3[EOO^·] = k_5[DOO^·][EH]$. Equation [IV] can be solved explicitly to yield the rather complex kinetic expression

$$[V] \quad R_S = \frac{(k_2k_5[EH] + 2k_3k_5)[EH]R_i^{1/2}}{(2k_5^2k_6[EH]^2 + 4k_3k_5k_7[EH] + 2k_3^2k_8)^{1/2}}$$

If it is assumed that $k_6 = k_7 = k_8 = k_t$, then $[ROO^·] = [EOO^·] + [DOO^·]$ and hence

$$k_p[ROO^·] = k_p([EOO^·] + [DOO^·]) = k_2[EOO^·] + 2k_5[DOO^·]$$

Making the further reasonable assumption that $k_2 = k_5$, we obtain

$$[VI] \quad k_2k_p[EH] + k_3k_p = k_2^2[EH] + 2k_2k_3$$

The overall propagation rate constant, k_p, can be calculated from the oxidation rate, and the value of $2k_t$ found by the rotating sector technique. The rate-constant ratio k_2/k_3 can be determined from concentrations of monohydroperoxide and of dihydroperoxide from the relation

$$[VII] \quad \frac{[EOOH]}{[DOOH]} = \frac{k_2[EH]}{k_3}$$

Some acyclic ethers, e.g., benzyl phenyl ether, cannot undergo an intramolecular propagation reaction and reactions [3], [4], [5], [7], and [8] do not apply. The measured propagation rate constant, k_p, is then equivalent to k_2 and the measured termination rate constant, $2k_t$, is equivalent to $2k_6$.

It is well known that α-alkoxyalkyl radicals can undergo β-scission. This reaction is particularly facile when the resulting alkyl radical is stabilized by resonance (5, 6). For example, the α-benzyloxybenzyl radical, formed by oxidation of benzyl ether with *t*-butoxy radicals at 110 °C, gives benzaldehyde and a benzyl radical (5)

$$[9] \quad PhCH_2OCHPh \rightarrow PhCH_2^· + PhCHO$$

The possibility that β-scission occurs during autoxidation of acyclic ethers has to be considered, since it will introduce even more radicals into the oxidation chain.

The present paper reports overall absolute propagation and termination rate constants for the oxidation of some acyclic ethers. Where possible, rate constants for the individual propagation steps have been estimated.

Experimental

Materials

n-Butyl, *t*-butyl isopropyl, benzyl, isopropyl, and α-methylbenzyl ethers, chlorobenzene, and carbon tetrachloride were commercial products purified by distillation. α-Methylbenzyl ether was also prepared from α-methylbenzyl alcohol (7). Benzyl *t*-butyl ether was prepared by the reaction of potassium *t*-butoxide with benzyl chloride (8). Benzyl phenyl ether was prepared from benzyl bromide and potassium phenoxide (8). The preparation and purification of the hydroperoxides used in this work has been described previously (1).

Product Analysis

Total hydroperoxide concentrations were determined by iodometric titration. Relative concentrations of mono- and dihydroperoxides were determined after reduction of the total hydroperoxide with a slight excess of triphenylphosphine. For example, the monohydroperoxide from benzyl ether gives benzaldehyde and benzyl alcohol

$$PhCH_2OCH(OOH)Ph \rightarrow [PhCH_2OCH(OH)Ph] \rightarrow PhCHO + PhCH_2OH$$

while the dihydroperoxide gives benzaldehyde and water

$$PhCH(OOH)OCH(OOH)Ph \rightarrow [PhCH(OH)OCH(OH)Ph] \rightarrow 2PhCHO + H_2O$$

Concentrations of products after reduction were determined by gas–liquid chromatography (g.l.c.) and infrared analyses. Infrared analysis was also used to measure the yields of carbonyl compounds formed before reduction of the oxidized ethers.

Kinetic Procedure

Methods used to measure rates of oxidation, rates of chain initiation, and absolute rate constants have been described previously (1). Whenever necessary, termination rate constants have been corrected for a kinetically first-order contribution. All rate constants presented in this paper were measured at 30 °C.

Can. J. Chem. Downloaded from www.nrcresearchpress.com by 210.87.254.105 on 09/05/12
For personal use only.

Can. J. Chem. Downloaded from www.nrcresearchpress.com by 210.87.254.105 on 09/05/12
For personal use only.

Results and Discussion

Isopropyl ether, benzyl ether, and benzyl *t*-butyl ether oxidize to give ether hydroperoxides in almost 100% yield at 30 °C and at oxygen partial pressures between 80 mm and 740 mm Hg (Table 1). This means that β-scission of α-alkoxyalkyl radicals (E˙) (reaction [9]) is not important at this temperature.[3]

Isopropyl acetate is a major non-hydroperoxidic product formed by oxidation of isopropyl ether. From our knowledge of hydrocarbon oxidations (9) it seems probable that the acetate results from β-scission of alkoxy radicals formed by non-terminating reactions of 2-isopropoxy-2-propylperoxy radicals

[10] $$EOO^{\cdot} + EOO^{\cdot} \rightleftharpoons EO_4E \longrightarrow \underbrace{\boxed{EO^{\cdot}\,O_2\,{}^{\cdot}OE}}_{\text{cage}} \begin{cases} \nearrow EO_2E + O_2 \\ \searrow EO^{\cdot} + O_2 + EO^{\cdot} \end{cases}$$

[11] $$\underset{(EO^{\cdot})}{CH_3-\overset{CH_3}{\underset{H}{C}}-O-\overset{CH_3}{\underset{CH_3}{C}}O^{\cdot}} \longrightarrow CH_3-\overset{CH_3}{\underset{H}{C}}-O-\underset{CH_3}{C}{=}O + CH_3^{\cdot}$$

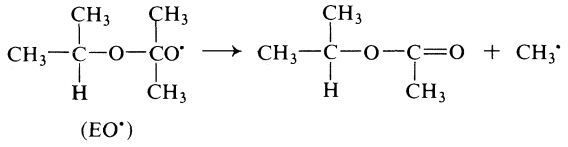

Methyl radicals formed in reaction [11] will add oxygen to give methylperoxy radicals, which will enter into chain propagation and termination. The termination rate constant for the oxidation of isopropyl ether will therefore contain contributions from reactions [12] and [13]

$$\left.\begin{array}{ll} [12] & CH_3OO^{\cdot} + EOO^{\cdot} \rightarrow \\ [13] & CH_3OO^{\cdot} + DOO^{\cdot} \rightarrow \end{array}\right\} \text{Non-radical products}$$

The small amount of benzaldehyde produced by oxidation of benzyl ether at 30° may be formed by β-scission of α-benzyloxybenzyl radicals or may be formed in the termination reaction

[14] $$2PhCH_2O\underset{OO^{\cdot}}{C}(H)Ph \rightarrow PhCH_2O\underset{O}{C}Ph + PhCHO + PhCH_2OH$$

Rate constants for oxidation of *n*-butyl, *t*-butyl isopropyl, α-methylbenzyl, benzyl phenyl, benzyl *t*-butyl, isopropyl, and benzyl ethers are given in Table 2. Low chain lengths for oxidation of *n*-butyl ether and *t*-butyl isopropyl ether prevented measurement of their absolute rate constants. A propagation rate constant for *n*-butyl ether was calculated from $k_p/(2k_t)^{\frac{1}{2}}$, using a termination rate constant for α-ethoxyethylperoxy radicals (i.e., the monoperoxy radical from ethyl ether). This rate constant was obtained by oxidation of benzyl ether in the presence of α-ethoxyethyl hydroperoxide (see later). A value of $k_p/(2k_t)^{\frac{1}{2}}$ for α-methylbenzyl ether was estimated from eq. [I], but absolute rate constants could not be calculated because of the presence of a large and irreproducible first-order termination reaction.

The termination rate constant for isopropyl ether is lower than for the two secondary ethers but is higher than is usually found for tertiary peroxy radicals from hydrocarbons (9, 10) and cyclic ethers (1), for which $2k_t$ is normally in the range 10^3–10^5 M^{-1} s^{-1}. This may well be due to the involvement of methylperoxy radicals in termination (reactions [10] and [11]). The termination rate constant for benzyl *t*-butyl ether is in the range normally found for alkyl or aralkyl α-substituted toluenes, e.g., ethylbenzene and bibenzyl (10). The termination rate constant for benzyl ether is about 8 times larger, which makes it similar to that for toluene (10). The difference between the two benzyl ethers suggests that termination may be quite sensitive to steric factors.

The propagation rate constant for oxidation of benzyl ether or isopropyl ether is expected to vary with the ether concentration. At low ether concentrations, k_p will equal $2k_5$ and at high ether concentrations, k_p should approach k_2. Since k_5 is probably about equal to k_2, the maximum change which can be expected in k_p is about two. Within the experimental accuracy, there was no variation in k_p for benzyl ether in the concentration range 1.2 to 5.3 *M*.

[3] β-Scission does play an important role at higher temperatures. For example, the autoxidation of benzyl ether at 65 °C gives almost 100% benzaldehyde, based on the oxygen absorbed, at an oxygen pressure of 200 mm Hg, while at 740 mm Hg, the yield of benzaldehyde is about 50%.

Can. J. Chem. Downloaded from www.nrcresearchpress.com by 210.87.254.105 on 09/05/12
For personal use only.

TABLE 1

Primary reaction products formed from oxidation of some acyclic ethers at 30 °C

Ether	Concentration, M	Chain length	Oxygen pressure mm Hg	Oxygen absorbed $\times 10^2$ M	Titratable hydroperoxide $\times 10^2$ M	[EOOH] $\times 10^2$ M	[DOOH] $\times 10^2$ M	Benzaldehyde $\times 10^2$ M	Isopropyl acetate $\times 10^2$ M
Isopropyl	7.1	35	150	3.7	4.0	2.2	0.9	—	0.37
Isopropyl	7.1	21	550	2.2	2.2	1.4	0.4	—	0.2
Benzyl-*t*-butyl	5.6	190	740	11*	9.5	9.5	—	—	—
Benzyl	0.6	10	600	2.1	2.7	0.22	1.1	—	—
	1.2	15	81	1.0	1.1	—	—	0.05	—
	1.2	20	650	2.0	2.0	—	—	0.12	—
	2.6	40	600	9.8	10	2.7	2.85	—	—
	5.3	50	740	20	21	9.0	5.5	0.02	—

*The carbonyl yield was approximately 0.2% based on the oxygen absorbed.

TABLE 2

Rate constants for oxidation of some acyclic ethers at 30 °C

Ether	Concentration, M	$R_i \times 10^7$ $M\ s^{-1}$	$R_s \times 10^6$ $M\ s^{-1}$	$k_p/(2k_t)^{\frac{1}{2}} \times 10^3$ $M^{-\frac{1}{2}}\ s^{-\frac{1}{2}}$	k_p $M^{-1}\ s^{-1}$	$2k_t \times 10^{-7}$ $M\ s^{-1}$
n-Butyl	5.9	1.8	0.25	~0.1	~1.2	14*
t-Butyl isopropyl	6.5	2.2	0.44	~0.1	—	—
α-Methyl benzyl	5.26	0.11	0.16	0.3	—	—
Benzyl phenyl	4.5	0.5	0.28	0.3	1.5	2.4
Benzyl *t*-butyl	1.13	0.54	0.57	2.2	13.2	3.6
	5.63	0.09	1.7	3.2	—	—
	5.63	0.48	3.36	2.7	9.3	1.2
	5.63	0.65	3.3	2.6	8.6	1.1
	5.63	2.1	7.0	3.0	14.7	2.4
Isopropyl	7.1	0.048	0.17	3.4	—	—
	7.1	0.17	0.35	3.7	0.44	0.14
	7.1	0.31	0.46	3.7	0.35	0.09
	7.1	0.5	0.6	3.7	0.47	0.16
	7.1	0.78	0.74	3.7	0.30	0.065
Benzyl	1.2	0.67	2.5	8.0	80	17
	1.2	2.0	4.6	8.5	85	10
	2.65	6.1	13.5	7.1	83	16
	5.3	2.2	14.6	5.8	66	13
	5.3	4.9	24.6	6.7	98	21
	5.3	8.3	30.3	6.4	85.5	17.5

*Assumed to be equal to $2k_t$ for α-ethoxyethylperoxy radicals.

In the presence of sufficient quantities of added hydroperoxide, free-radical oxidations can be propagated and terminated by the peroxy radicals derived from the hydroperoxide (1). Intramolecular propagation reactions which occur with acyclic ethers, such as benzyl ether or isopropyl ether, are eliminated. Thus, the oxidation of 0.42 M benzyl ether in the presence of 2.0 M *t*-butyl hydroperoxide gave only monohydroperoxide, while the same concentration of benzyl ether in the absence of *t*-butyl hydroperoxide gave 87% of dihydroperoxide. The measured propagation rate constants represent the intermolecular reaction between a peroxy radical derived from the hydroperoxide and the ether. Rate constants for oxidation of *t*-butyl isopropyl, *n*-butyl, α-methylbenzyl, isopropyl, benzyl phenyl, benzyl *t*-butyl, and benzyl ethers in the presence of *t*-butyl hydroperoxide or cumene hydroperoxide are given in Table 3. Rates of oxidation of benzyl ether and isopropyl ether were constant above about 1 M *t*-butyl hydroperoxide, and the average value of the termination rate constant for *t*-butylperoxy radicals was $1.2 \times 10^3\ M^{-1}\ s^{-1}$. This value is in good agreement with the value found in tetrahydrofuran (1) and with the value obtained by electron spin resonance (e.s.r.) spectroscopic measurement of the steady-state *t*-butylperoxy radical concentration at a known rate of initiation (9). The k_p values in the presence of *t*-butylhydroperoxide given in Table 3 were calculated using this termination rate constant.

Rate constants for oxidation of benzyl ether in the absence or presence of tetralin hydroperoxide or two secondary ether hydroperoxides are given in Table 4. Termination rate constants measured under these conditions are in good agreement with the values found in cyclic ethers (1).

We have previously concluded (1, 11, 12) that secondary peroxy radicals are more reactive in hydrogen atom abstraction than tertiary peroxy radicals. This conclusion receives further support from the data in Tables 2, 3, and 4. For example, benzyl *t*-butyl ether and benzyl ether are 10–20 times more reactive towards secondary peroxy radicals than towards *t*-butylperoxy radicals.

α-Methylbenzyl ether is unexpectedly resistant to oxidation. Towards *t*-butylperoxy radicals, the propagation rate constant for this ether is only about 1/15 of the value for benzyl ether and benzyl *t*-butyl ether. This is unusual in autoxidations, because steric effects normally do not

Can. J. Chem. Downloaded from www.nrcresearchpress.com by 210.87.254.105 on 09/05/12
For personal use only.

TABLE 3

Rate constants for the oxidation of some acyclic ethers in the presence of *t*-butyl hydroperoxide or cumene hydroperoxide at 30 °C

Ether	Concentration, M	Hydroperoxide	Concentration, M	$R_i \times 10^7$ $M\ s^{-1}$	Chain length	$k_p/(2k_t)^{\frac{1}{2}} \times 10^3$ $M^{-\frac{1}{2}}\ s^{-\frac{1}{2}}$	k_p* $M^{-1}\ s^{-1}$
t-Butyl isopropyl	5.7	*t*-Butyl	1.25	2.2	7	0.6	0.02
n-Butyl	4.7	*t*-Butyl	2.0	0.094	95	1.9	0.064
α-Methyl benzyl	4.2	*t*-Butyl	2.0	1.17	33	2.7	0.09
	4.2	*t*-Butyl	2.0	0.08	112	2.4	0.08
Isopropyl	6.2	*t*-Butyl	1.24	0.043	280	3.2	0.11
	5.7	*t*-Butyl	2.0	2.2	40	3.3	0.11
	4.4	*t*-Butyl	3.72	0.043	302	3.45	0.12
Benzyl phenyl	0.4	*t*-Butyl	1.7	0.24	15	5.6	0.2
Benzyl *t*-butyl	1.13	Cumyl	0.26	0.3	50	18	1.4
	1.13	Cumyl	0.53	0.44	45	19	1.5
	1.13	*t*-Butyl	2.0	0.22	246	32	1.1
Benzyl	0.4	*t*-Butyl	0.85	5.1	18	37.5	1.3
	0.4	*t*-Butyl	1.7	8.0	19	36.5	1.3
	0.42	*t*-Butyl	2.0	0.22	109	39	1.35
	0.42	*t*-Butyl	4.0	0.22	101	36	1.25

*k_p in this table is the rate constant for attack of a *t*-butylperoxy (or cumylperoxy) radical on the ether. The value of $2k_t$ was taken to be $1.2 \times 10^3\ M^{-1}\ s^{-1}$ for *t*-butylperoxy and $6 \times 10^3\ M^{-1}\ s^{-1}$ for cumylperoxy radicals.

TABLE 4

Rate constants for oxidation of benzyl ether in the presence of some secondary hydroperoxides at 30 °C

Hydroperoxide	Concentration, M	$R_i \times 10^7$ $M\ s^{-1}$	Chain length	$k_p/(2k_t)^{\frac{1}{2}} \times 10^3$ $M^{-\frac{1}{2}}\ s^{-\frac{1}{2}}$	k_p $M^{-1}\ s^{-1}$	$2k_t \times 10^{-7}$ $M^{-1}\ s^{-1}$
None	—	—	—	7.1	83	16
α-Ethoxyethyl	0.21	2.9	7.0	3.1	35	13
α-Ethoxyethyl	0.28	3.0	6.5	3.0	37	15
α-Tetrahydropyranyl	0.13	2.5	14	5.9	31	2.8
α-Tetrahydropyranyl	0.25	2.35	13	5.3	20.5	1.5
Tetralyl	0.09	3.0	9	4.0	20	2.5
Tetralyl	0.18	3.5	7	4.0	18	2.0

outweigh the polar and radical stabilizing effects of alkyl substitution at the reaction center. That is, although decreases in the propagation rate constant on going from a secondary substrate to a structurally related tertiary substrate are common when the attacking peroxy radical is derived from the substrate (10), they are unusual when substrates are attacked by the same peroxy radicals (11). We have previously observed only one example of this phenomena, viz., *sec*-amylbenzene is less reactive per hydrogen towards cumylperoxy radicals ($k_p = 0.07\ M^{-1}\ s^{-1}$) than ethylbenzene ($k_p/H = 0.11\ M^{-1}\ s^{-1}$) (11). Sensitivity of k_p to steric factors is also indicated by the fact that, towards the *t*-butylperoxy radical, the value of k_p/H for *t*-butyl isopropyl ether is less than half as large as that for isopropyl ether.

We have shown previously that secondary ether peroxy radicals have about the same reactivity as secondary hydrocarbon peroxy radicals in hydrogen atom abstraction (1). Since added hydroperoxides eliminate intramolecular reactions, it is reasonable to assume that the intermolecular propagation rate constant, k_2, for oxidation of benzyl ether is approximately 30 $M^{-1}\ s^{-1}$, an average of the propagation rate constants in Table 4. (This corresponds to $k_p/H = 7.5\ M^{-1}\ s^{-1}$, in good agreement with the value of $5.8\ M^{-1}\ s^{-1}$ for benzyl *t*-butyl ether.) It also seems reasonable to assume that k_2 for isopropyl ether will be approximately equal to the rate constant for attack on this ether by *t*-butylperoxy radicals, i.e., $0.11\ M^{-1}\ s^{-1}$. These values of k_2 have been combined with ratios of k_2/k_3 for isopropyl ether and benzyl ether to

Can. J. Chem. Downloaded from www.nrcresearchpress.com by 210.87.254.105 on 09/05/12
For personal use only.

TABLE 5

Propagation rate constants for oxidation of isopropyl ether and benzyl ether at 30 °C

Ether	Concentration, M	k_2/k_3 M^{-1}	k_p $M^{-1}s^{-1}$	k_2* $M^{-1}s^{-1}$	k_3* s^{-1}	k_2† $M^{-1}s^{-1}$	k_3† s^{-1}
Isopropyl	7.1	0.48	0.4	0.11	0.23	0.33	0.68
Benzyl	1.2	0.35	83	30	86	49	140
Benzyl	5.3	0.35	83	30	86	61.5	176

*Calculated assuming that $k_2 = k_p$ for reaction of the ether with an alkylperoxy radical (see text).
†Calculated from eq. [VI].

TABLE 6

Collected rate constants for oxidation of ethers at 30 °C

Ether	$k_p/(2k_t)^{\frac{1}{2}} \times 10^3$ $M^{-\frac{1}{2}}s^{-\frac{1}{2}}$	k_2/H* $M^{-1}s^{-1}$	$2k_t \times 10^{-7}$ $M^{-1}s^{-1}$	k_p/H for Bu^{t}OO· $M^{-1}s^{-1}$
1,4-Dioxan	0.07	0.12	5	—
n-Butyl	0.1	0.3	14	0.016
Isopropyl *t*-butyl	0.1	0.02	0.0043	0.02
Tetrahydropyran	0.12	0.14	2.1	0.006
α-Methylbenzyl	0.3	—	—	0.042
Benzyl phenyl	0.3	0.75	2.4	0.10
Tetrahydrofuran	0.78	1.1	3.1	0.085
Benzyl *t*-butyl	2.75	5.75	2.1	0.55
Isopropyl	3.7	0.055†	0.1	0.055
Benzyl	7.1	7.5†	16	0.325
2,5-Dimethyltetrahydrofuran	22.5	2.4	0.0046	0.4
Phthalan	42.5	108	10.5	—

*Equivalent to k_p/H for the cyclic ethers and acyclic ethers which do not undergo intramolecular propagation.
†Estimated intermolecular rate constant for the monoperoxy radical (see text).

obtain k_3 (Table 5). The ratios k_2/k_3 were calculated from data in Table 1 using eq. [VII]. The two ratios are quite similar, even though the absolute magnitudes of k_2 and k_3 for the ethers are so different. It would be interesting to know whether k_2/k_3 is about the same for all acyclic ethers and whether it varies significantly with temperature.

The rate constants k_2 and k_3 can also be calculated from eq. [VI][4]. The values obtained by this method for two benzyl ether concentrations do not agree because there was no measurable difference in k_p at the two concentrations. The values of k_2 and k_3 for benzyl ether and for isopropyl ether differ somewhat from the values estimated from propagation rate constant measurements on systems containing the ethers and appropriate hydroperoxides. Although the disagreement may be within the limits of experimental accuracy, it is also quite probable that one or more of the assumptions involved in either method of separating k_2 and k_3 is at fault.

Rate constants for the oxidation of cyclic and acyclic ethers are summarized in Table 6. Intermolecular propagation rate constants (k_2) per α-hydrogen are given for those acyclic ethers which undergo intramolecular propagation reactions, so that they can be more easily compared with the cyclic ethers and the acyclic ethers which do not undergo intramolecular propagation reactions. Rate constants per α-hydrogen for abstraction from ethers by *t*-butylperoxy radicals have also been included in Table 6.

Absolute rate constants for neat *t*-butyl isopropyl ether have been estimated from data for the oxidation in the presence of *t*-butyl hydroperoxide by assuming that the crossed and uncrossed propagation rate constants are equal. That is, it has been assumed that rate constants for hydrogen abstraction by the *t*-butylperoxy radical and the peroxy radical derived from *t*-butyl isopropyl ether are the same. The termination rate constant for neat ether is then obtained from the value of $k_p/(2k_t)^{\frac{1}{2}}$. Using this assumption, it would appear that the value of $2k_t$ for *t*-butyl isopropyl ether is about 20 times lower than for isopropyl ether. This difference

[4]We are indebted to a referee for pointing out this method of calculating k_2 and k_3.

Can. J. Chem. Downloaded from www.nrcresearchpress.com by 210.87.254.105 on 09/05/12
For personal use only.

Can. J. Chem. Downloaded from www.nrcresearchpress.com by 210.87.254.105 on 09/05/12
For personal use only.

in $2k_t$ for the two isopropyl ethers is in the same direction as the difference in $2k_t$ between benzyl *t*-butyl ether and benzyl ether.

Five- and six-membered cyclic hydrocarbons which have a π-electron system as part of the ring have about the same reactivity towards peroxy radicals (11). However, the 5-membered cyclic ether tetrahydrofuran is about 10 times more reactive towards peroxy radicals than the 6-membered cyclic ethers tetrahydropyran and 1,4-dioxan. We previously concluded that this difference in reactivity was due to steric repulsion between the α and β hydrogens being released to a greater extent by abstraction from the 5-membered ring than from the less strained 6-membered ring (1). It is, however, difficult to see why such an effect should show up in ethers and not in hydrocarbons. The present work implies that ethers are quite sensitive to steric effects both in propagation and termination and this may explain the difference between cyclic hydrocarbons and cyclic ethers.

Tetrahydrofuran and 2,5-dimethyltetrahydrofuran are both less reactive towards *t*-butylperoxy radicals than towards their own peroxy radicals. For tetrahydrofuran, this is due to the usual difference in reactivity between tertiary and secondary peroxy radicals. However, this explanation cannot apply to 2,5-dimethyltetrahydrofuran. Oxidation of this ether may be quite complicated, since thin-layer chromatography revealed the presence of more than one hydroperoxide. Though 2-hydroperoxy-2,5-dimethyltetrahydrofuran is the major product, there is a small amount of a slower-running hydroperoxide which can be readily removed from the principal hydroperoxidic product by extraction with water. This second hydroperoxide is not H_2O_2 but might possibly be 2,5 - dihydroperoxy - 2,5-dimethyltetrahydrofuran formed by an intramolecular propagation reaction.[5] This implies that the measured rate constants for the neat ether may contain contributions from more than just the intermolecular propagation reaction.

Russell and Williamson (8) reported that benzyl phenyl ether reduced the rate of oxidation of benzyl ether at 60° much more than would be expected of an inert diluent. For example, 0.4 *M* benzyl ether and 0.2 *M* benzyl phenyl ether oxidized at 1/4 the rate of 0.5 *M* benzyl ether. From this, they concluded that benzyl phenyl ether must have a higher termination rate constant than benzyl ether. When benzyl ether was oxidized in the presence of benzyl phenyl ether at 30°, we did not observe nearly as large a reduction in rate. However, the rate was slightly lower than would be expected from an inert diluent. This was also true of mixtures of benzyl *t*-butyl ether and benzyl phenyl ether. The cause of the small deviation from linearity is apparently not due to a difference in termination rate constants (see Table 6) and at present we have no obvious explanation of this phenomenon.

A comparison of the propagation rate constants in Table 6 with our previous data for hydrocarbons (10) indicates that an alkoxy group is less activating than a phenyl ring or a double bond. For example, isopropyl ether gives $k_p/H = 0.055\ M^{-1}\ s^{-1}$, cumene gives $k_p/H = 0.18\ M^{-1}\ s^{-1}$, and 2,5-dimethylhexene-3 gives $k_p/H = 0.8\ M^{-1}\ s^{-1}$. Peroxy radicals derived from ethers also appear to have about the same reactivity towards hydrogen atom abstraction as structurally related peroxy radicals from hydrocarbons.

[5]Aqueous extraction of oxidized isopropyl ether removes the slower-running dihydroperoxide.

1. J. A. Howard and K. U. Ingold. Can. J. Chem. **47**, 3809 (1969).
2. K. I. Ivanov, V. K. Savinova, and E. G. Mikhailova. J. Gen. Chem. USSR Engl. Transl. **16**, 1003, (1946); **16**, 1015 (1946).
3. F. F. Rust. J. Amer. Chem. Soc. **79**, 4000 (1957).
4. J. L. Bollard and P. ten Have. Trans. Faraday Soc. **45**, 93 (1949).
5. R. L. Huang and S. S. Si-Hoe. *In* Vistas in free-radical chemistry. *Edited by* W. A. Waters. The Pergamon Press, Inc., New York. 1959. p. 242.
6. R. E. Lovins, L. J. Andrews, and R. M. Keefer. J. Org. Chem. **30**, 4150 (1965).
7. J. Kenyon and H. Phillips. J. Chem. Soc. 1676 (1930).
8. G. A. Russell and R. C. Williamson, Jr. J. Amer. Chem. Soc. **86**, 2357 (1964).
9. J. A. Howard, K. Adamic, and K. U. Ingold. Can. J. Chem. **47**, 3793 (1969) and references cited therein.
10. J. A. Howard and K. U. Ingold. Can. J. Chem. **45**, 793 (1967).
11. J. A. Howard, K. U. Ingold, and M. Symonds. Can. J. Chem. **46**, 1017 (1968).
12. J. A. Howard, W. J. Schwalm, and K. U. Ingold. Advan. Chem. Ser. **75**, 6 (1968).

Crystallographic studies of cobalt arsenates. I. Crystal structure of $Co_3(AsO_4)_2$

N. KRISHNAMACHARI AND C. CALVO

Department of Chemistry and Institute for Materials Research, McMaster University, Hamilton, Ontario

Received June 19, 1969

$Co_3(AsO_4)_2$, an analogue of the mineral xanthiosite, crystallizes in the monoclinic space group $P2_1/c$ with $Z = 4$. The unit cell parameters are $a = 5.830(4)$ Å, $b = 9.675(2)$ Å, and $c = 10.34(2)$ Å with $\beta = 93.42(5)°$. The intensity of 2261 independent reflections were estimated either from integrated precession photographs or by direct measurement using a scintillation counter. The final value of the reliability index is 0.072 for a full matrix least-square refinement where all the atoms have anisotropic thermal parameters. The three independent cations are surrounded octahedrally by oxygen atoms with mean Co—O bond lengths of 2.12 Å and a range from 1.99 to 2.29 Å. One of the arsenate ions, AsO_4^{4-}, is a nearly regular tetrahedron with a mean As—O bond length of 1.70 Å; while the second, with an angular irregularity primarily introduced by one oxygen atom, shows a mean As—O bond length of 1.69 Å. This structure consists of nearly hexagonally close packed layers of oxygen atoms normal to the *b* axis repeating every four layers.

Canadian Journal of Chemistry, **48**, 881 (1970)

Can. J. Chem. Downloaded from www.nrcresearchpress.com by 210.87.254.40 on 09/05/12
For personal use only.

Introduction

The crystallography of anhydrous arsenates has, until recently, been relatively unexplored. Although early work indicated that a number of arsenates and phosphates are isostructural, this relationship may not be true often enough to be useful. For example, although $Mn_3(PO_4)_2$ and $Mn_3(AsO_4)_2$ (1) can be crystallized with the graftonite structure, $Co_3(PO_4)_2$ crystallizes in the "γ" $Zn_3(PO_4)_2$ structure (2) which is substantially different than the structure of $Co_3(AsO_4)_2$.

Taylor and Heyding (3) used powder X-ray diffractometry to study the various compounds obtained upon reacting CoO with As_2O_5 in various molar ratios. In particular, they reported that $3CoO.As_2O_5$ crystallized in the orthorhombic system. Davis, Hey, and Kingsbury (4) have shown that the mineral analogue of the nickel orthoarsenate, previously reported to have the same structure as $3CoO.As_2O_5$ (3), is in fact monoclinic with cell parameters and symmetry similar to those reported here. A second composition $6MO.As_2O_5$, M = Ni or Co, was also reported to be orthorhombic by Taylor and Heyding (3). However, Davis *et al.* (4) have shown the nickel analogue, as the mineral aerugite, to be monoclinic. Here we show, in passing, that although the cobalt analogue can be assigned to a monoclinic cell of the same size and symmetry as aerugite, the true symmetry is rhombohedral.

Recently determined arsenate structures with divalent metal cations have shown As—O bond lengths lying between 1.65 and 1.71 Å in $Cu_3(AsO_4)_2$ (5) and 1.63 and 1.72 Å in stranskiite (6). The coordination numbers of the cations are 5 in the former compound and 5 and 4 in the latter compound. In stranskiite there are two additional oxygen atoms lying 3.2 Å away, suggesting an enormous Jahn–Teller distortion of the "octahedral" environment about the Cu^{2+} ion or, more probably, virtually no bond at all. In $Co_3(AsO_4)_2$, where a more nearly isotropic octahedral environment is expected, a nearly close packed arrangement is found consistent with an average tetrahedral As—O bond length of about 1.7 Å and a mean metal–oxygen atom bond length of about 2.0 Å.

Experimental

Single crystals were grown from hydrated $Co_3(AsO_4)_2$ obtained from Alpha Inorganic Inc. A sample was heated in a platinum crucible until it had melted and then cooled slowly across the melting temperature. The product obtained showed two distinct crystalline forms. One gave a monoclinic pattern with unit cell parameters substantially the same as reported by Davis *et al.* (4) for the mineral xanthiosite whose composition was nearly that of $Ni_3(AsO_4)_2$. The second crystal gave the pattern of a *C*-centered monoclinic crystal and lattice parameters nearly those reported by these same authors for aerugite. The fact that Davis *et al.* (4) pointed out that the $a:b$ ratio is nearly equal to $\sqrt{3}$ suggested that our crystal could be rhombohedral. This suspicion has been confirmed by taking precession photographs with the hexagonal *c* axis parallel to the X-ray beam. The study of the structure of the Co analogue of aerugite is presently in hand.

Accurate parameters were determined from the measurement of films calibrated with TiO_2 reflections whose lattice parameters were taken to be $a = 4.5929$ Å and $c = 2.9591$ Å (7). The parameters obtained after least-squares refinement are: $a = 5.830(4)$ Å, $b =$

Can. J. Chem. Downloaded from www.nrcresearchpress.com by 210.87.254.40 on 09/05/12
For personal use only.

9.675(2) Å, c = 10.34(2) Å, and β = 93.42(5)°. There are four molecules per unit cell. The extinction $h0l$, l = odd, and $0k0$, k = odd, leads uniquely to space group $P2_1/c$. The density was not determined since a suitable sample of reliable purity was not available.

Reflections of the type hkn with n = 0, 1, 2, 3 and hml, m = 0, 1, 2, 3, 4 were measured, using MoKα radiation, from integrated precession photographs. Reflections of the type rkl with r = 0, 1, 2, 3, 4 were measured with a manually oriented scintillation counter mounted on a Supper Weissenberg camera. An ω scan on the Weissenberg camera was used and the background measured near the Bragg reflection. The values obtained were corrected, where necessary, for the effects of saturation of the counter. All the data were corrected for the Lorentz polarization and absorption effects. Since the crystals used had dimensions 0.1 × 0.1 × 0.2 mm^3, neglect of absorption would lead to an average variation in intensity of the order of 20%.

Trial y and z coordinates for the Co^{2+} and As^{5+} ions were determined from solving the Patterson function using $0kl$ data. Structure factor calculations using these positions resulted in a reliability index, $R = \Sigma(|F_o| - |F_c|)/\Sigma|F_o|$, of 0.35. The x coordinates were determined from three-dimensional Patterson functions computed at intervals of 5/60 along the a axis. Once the positions of the Co^{2+} and As^{5+} ions had been confirmed, oxygen atom positions were sought at about 1.7 Å from the As^{5+} ions and such as to be shared by at least two Co^{2+} ions. These criteria together with that of a psuedo-tetrahedral environment of oxygen atoms about the As^{5+} ions allowed the positioning of all the oxygen atoms.

The refinement was completed using weights chosen equal to 0.136 for $F_o < 50$, $(0.33\,F_o - 8.0)^{-1}$ for $50 < F_o < 90$, and $(351.65 - 8.30\,F_o + 0.052\,F_o^2)^{-1}$ for $F_o > 90$. These functions, with small discontinuities at the boundaries, were determined by least squares after examining a plot of $|F_o - F_c|$ vs. F_o. A reasonable fit with one weighting expression R would require a higher order polynominal in F_o. Atomic scattering factors were taken from Thomas and Umeda (8) and corrected, where appropriate, for dispersion.

Each layer of data was scaled independently and scale constants of multiply observed reflections assigned randomly to one of the groups from which they emanated. The value of R was reduced to 0.10 when individual isotropic thermal parameters were assigned to each atom. The value of

$$R_2 = \left[\frac{\sum W(|F_0| - |F_c|)^2}{\sum WF_0^2}\right]^{1/2}$$

was 0.12 at this stage. When anisotropic thermal parameters were refined, R_1 became 0.072 and R_2 fell to a value of 0.082.

The refinement was terminated when the calculated change in the parameters was less than 1/3 of the estimated standard deviation. The final atomic positional parameters are shown in Table 1 and the observed and calculated structure factors are shown in Table 2.

Since other members of this series of cobalt arsenates (9) showed nonstoichiometric composition, an attempt was made to refine a model where the site occupancy was varied. The occupancy of the Co sites changed by about 3/4 of the estimated standard deviation, while that of As by about 1.5 times its estimated standard deviation. These changes were regarded as insignificant.

Description of the Structure

The structure consists of nearly hexagonally close packed layers of oxygen atoms parallel to [010] with the cobalt ions distributed in octahedral holes and the arsenic ions in tetrahedral holes. Figure 1 shows a view normal to these layers. This structure is related to that of olivine, basically Mg_2SiO_4, where the magnesium ions are in the octahedral interstices and the Si in the tetrahedral ones (10). Olivine, illustrated in Fig. 2, is orthorhombic with a repeat of two pseudo-hexagonally close packed layers. In $Co_3(AsO_4)_2$, the repeat is four oxygen atom layers.

The first and third layer possess a center of symmetry while the second and fourth layers, related to each other by inversion, are generated by the glide plane. The Co ions, lying in the interstices of successive layers, are related either by centers of symmetry or by c glides. In contrast to $Co_3(AsO_4)_2$, in the olivine structure one of the cations lies on a center of symmetry and thus the closest packed oxygen atom layers are related by this symmetry operation. In addition, the layer itself has a mirror plane perpendicular to it, upon which all the atoms lie, save one oxygen atom per formula unit.

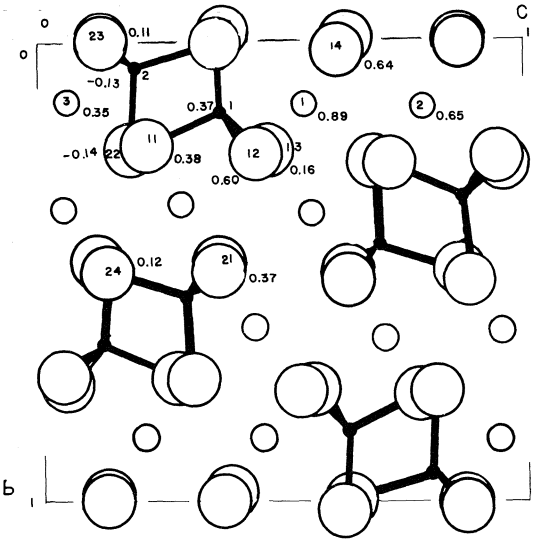

FIG. 1. The structure of $Co_3(AsO_4)_2$ is shown projected onto the bc face. The smallest circles represent As ions; the next larger, Co ions; and the largest, oxygen ions. The approximate fractional X coordinates of the cations are shown.

Can. J. Chem. Downloaded from www.nrcresearchpress.com by 210.87.254.40 on 09/05/12
For personal use only.

TABLE 1

Atomic positional and thermal parameters* for $Co_3(AsO_4)_2$

	Coordinates			Thermal parameters ($\times 10^4$) Å^2					
Atom	x	y	z	U_{11}	U_{22}	U_{33}	U_{12}	U_{13}	U_{23}
Co(1)	−0.1129(2)	0.1352(1)	−0.4670(1)	147(7)	119(5)	133(5)	−6(4)	14(4)	−3(4)
Co(2)	−0.3502(2)	0.1401(1)	−0.2163(1)	160(7)	110(4)	127(5)	12(4)	13(4)	−3(4)
Co(3)	0.3547(2)	0.1235(1)	0.0586(1)	153(7)	117(5)	122(5)	13(4)	9(4)	8(4)
As(1)	0.3675(2)	0.1549(1)	0.3809(1)	93(5)	82(3)	93(3)	−11(3)	10(3)	−10(3)
As(2)	−0.1283(2)	0.0523(1)	0.2032(1)	84(5)	81(3)	85(3)	−4(3)	−4(3)	1(2)
O(11)	0.3835(12)	0.2217(7)	0.2312(6)	125(32)	106(23)	116(23)	16(21)	−4(21)	18(19)
O(12)	0.6035(14)	0.2389(8)	0.4534(6)	150(32)	161(27)	119(24)	−15(25)	3(22)	−7(22)
O(13)	0.1582(13)	0.2283(7)	0.4636(6)	163(34)	126(24)	117(24)	−47(23)	8(22)	−51(20)
O(14)	−0.3638(12)	0.0177(7)	0.6204(7)	94(31)	96(22)	169(27)	−46(21)	9(22)	−33(21)
O(21)	0.3723(12)	0.4867(7)	0.3777(6)	135(32)	137(23)	56(21)	1(23)	−5(19)	27(19)
O(22)	−0.1365(12)	0.2255(6)	0.1909(6)	131(31)	60(20)	133(24)	19(20)	14(21)	3(17)
O(23)	0.1083(12)	−0.0104(8)	0.1325(7)	93(31)	148(26)	186(28)	46(24)	39(23)	42(23)
O(24)	0.1212(13)	0.5061(7)	0.1391(6)	216(36)	123(24)	61(21)	34(24)	−11(21)	−21(18)

*Estimated standard deviations in parentheses.

Can. J. Chem. Downloaded from www.nrcresearchpress.com by 210.87.254.40 on 09/05/12
For personal use only.

TABLE 2

Observed and calculated structure factors for $Co_3(AsO_4)_*$

Part A. Observable reflections

K	L	Fo	Fc	K	L	Fo	Fc	K	L	Fo	Fc	K	L	Fo	Fc	K	L	Fo	Fc	K	L	Fo	Fc	K	L	Fo	Fc
K	L		H = 0	17	8	34	-23	10	-7	33	-35	1	-7	33	-34	9	-14	39	-41	2	-15	43	47	10	7	9	11	8	-3	82	-80
				18	9	29	-24	10	-6	20	-24	1	-6	36	37	9	-12	29	-30	2	-14	23	-32	10	8	24	-24	8	-2	73	-71
				18	11	23	32	10	-5	20	-21	1	-5	36	38	9	-11	22	-21	2	-13	43	45	10	10	42	44	8	-1	22	21
0	2	21	-18	19	5	36	43	10	-3	46	50	1	-4	147	152	9	-10	54	-56	2	-12	14	15	10	11	38	-37	8	1	22	-22
0	4	11	13					10	-2	63	55	1	-3	167	166	9	-8	13	12	2	-10	26	-26	10	12	59	-60	9	1	36	40
0	6	34	-34	K	L		H = 1	10	-1	49	49	1	-2	65	63	9	-5	35	36	2	-9	82	81	11	-16	18	25	9	2	62	60
0	8	22	-21					10	1	65	-61	1	-1	24	26	9	-4	82	79	2	-8	18	16	11	-13	26	26	10	-2	55	-54
0	10	25	30	0	-18	61	-54	10	2	57	-54	1	0	27	27	9	-3	58	-56	2	-7	42	40	11	-9	22	21	10	-1	41	-43
0	12	173	-177	0	-16	43	-40	10	3	49	52	1	1	31	31	9	-2	25	26	2	-6	25	-29	11	-7	74	-75	10	0	14	12
0	14	9	13	0	-12	102	-97	10	7	29	35	1	2	76	79	9	-1	44	47	2	-5	55	49	11	-6	29	27	10	2	28	32
0	16	10	11	0	-10	38	-39	10	8	39	40	1	5	29	-25	9	0	28	29	2	-4	22	21	11	-5	27	31	10	3	30	29
1	2	30	33	0	-8	68	-69	10	9	23	28	1	6	28	30	9	1	47	44	2	-3	116	110	11	-4	52	-49	12	-3	80	76
1	3	92	-100	0	-6	151	155	10	10	27	-31	1	7	14	-14	9	2	37	36	2	-2	56	52	11	-3	55	-52	11	-2	21	-22
1	4	35	-37	0	-4	104	108	10	12	13	-20	1	8	80	-81	9	5	29	-30	2	-1	85	84	11	-2	42	42	11	1	19	-18
1	5	112	111	0	-2	92	-86	11	-11	18	-20	1	9	95	-96	9	6	33	33	2	0	26	-23	11	-1	28	-29	11	2	30	-33
1	6	110	-122	0	0	49	-46	11	-9	50	-51	1	10	46	48	9	7	58	-59	2	1	25	28	11	2	34	38				
1	7	151	-165	0	2	83	81	11	-8	72	69	1	11	28	-23	9	8	35	-38	2	2	36	38	11	3	55	-58	K	L		H = 6
1	8	37	-38	0	4	52	53	11	-2	52	49	1	12	16	18	9	9	36	39	2	3	16	13	11	4	26	27				
1	10	58	59	0	6	52	52	11	1	39	40	1	13	16	21	9	10	43	46	2	4	17	13	11	5	62	65	0	-8	19	-23
1	13	14	19	0	8	40	-37	2	-19	30	28	9	11	28	-27	2	5	30	-28	11	6	11	-15	0	-6	154	161
1	15	59	54	0	10	76	75	11	3	80	79	2	-17	15	14	10	-14	24	-22	2	6	15	-12	11	7	51	-53	0	-4	19	-20
1	16	9	-16	0	12	101	99	11	8	28	34	2	-14	14	-14	10	-13	15	13	2	7	36	-36	11	8	11	15	0	-2	21	-21
2	-12	18	-18	0	14	43	41	11	9	19	21	2	-12	25	26	10	-12	24	23	2	8	17	14	11	9	12	11	0	0	62	59
2	-8	14	-10	0	18	64	-65	11	10	20	23	2	-11	10	10	10	-10	31	31	2	10	28	-29	11	10	24	24	0	2	27	-27
2	0	24	22	1	-13	26	-32	11	11	22	-27	2	-10	27	-27	10	-8	50	-49	2	12	20	20	12	-16	12	-11	0	4	19	21
2	1	74	-71	1	-12	23	26	12	-5	20	-21	2	-9	141	136	10	-7	34	33	2	13	26	-29	12	-15	19	-26	0	6	198	-194
2	2	65	-73	1	-11	21	26	12	-4	20	-23	2	-8	49	37	10	-6	21	24	2	15	40	-42	12	-14	17	21	1	-11	21	19
2	3	95	-115	1	-10	100	97	12	-2	21	-16	2	-7	15	-12	10	-5	47	45	3	-16	19	-25	12	-13	13	-17	1	-10	40	-40
2	4	47	-70	1	-9	109	104	12	-1	37	41	2	-6	57	-53	10	-4	22	26	3	-14	20	27	12	-11	30	34	1	-9	54	-52
2	5	50	52	1	-8	58	-56	12	2	21	22	2	-5	13	12	10	-2	52	55	3	-13	86	88	12	-9	23	-24	1	-7	47	49
2	6	24	28	1	-7	14	-16	12	4	26	29	2	-4	21	22	10	-1	56	60	3	-12	11	-10	12	-8	44	-47	1	-5	25	26
2	7	48	49	1	-6	84	83	12	6	29	-37	2	-3	88	84	10	0	13	-12	3	-10	15	16	12	-7	9	-13	1	-4	40	41
2	9	44	44	1	-5	58	57	12	7	35	44	2	-2	68	64	10	1	25	-29	3	-9	44	-43	12	-6	9	-10	1	-2	35	35
2	10	36	36	1	-4	63	63	12	8	19	-23	2	-1	66	64	10	2	44	-44	3	-8	13	-15	12	-5	34	-33	1	-1	112	107
2	11	46	44	1	2	145	-171	12	9	79	-81	2	0	61	-61	10	3	43	-47	3	-7	65	-64	12	-4	52	53	1	0	96	-92
2	14	32	34	1	3	174	-213	12	10	20	-22	2	2	66	69	10	4	48	48	3	-6	87	-82	12	-3	25	24	1	1	64	-60
2	15	65	61	1	4	131	139	13	-6	49	-51	2	3	221	-243	10	5	35	-37	3	-4	29	-28	12	-2	17	-18	1	3	31	27
2	17	32	-28	1	5	68	-65	13	0	44	-45	2	4	35	-34	10	7	30	-29	3	-3	15	12	12	-1	34	36	1	5	26	32
3	-10	14	-11	1	6	19	24	13	2	24	-25	2	5	24	-22	10	8	40	-41	3	-2	57	55	12	0	42	41	1	7	21	-25
3	-5	44	-42	1	7	21	21	13	6	19	25	2	6	96	84	10	10	20	-22	3	-1	100	-104	12	1	34	-37	1	8	21	-16
3	1	93	99	1	8	26	-26	13	7	35	37	2	8	24	-27	10	11	48	46	3	1	27	-29	12	4	61	60	1	9	34	33
3	2	61	-65	1	10	35	-35	15	5	30	-30	2	10	25	-27	10	12	15	-15	3	2	20	22	12	5	29	30	1	10	31	29
3	3	4	-7	1	11	33	37					2	11	34	37	11	-15	18	21	3	3	30	28	12	7	33	32	2	-13	22	-24
3	4	17	-21	1	12	44	-44	K	L		H = 2	2	12	26	27	11	-14	41	-42	3	4	40	40	12	8	60	-60	2	-12	18	19
3	6	112	-131	1	13	21	-20					2	13	18	-18	11	-13	25	-24	3	5	48	49	13	-13	22	-25	2	-11	28	-28
3	7	85	90	2	-15	62	66	0	-12	36	38	2	15	70	79	11	-12	15	-9	3	6	95	94	13	-12	12	15	2	-9	60	60
3	8	44	-45	2	-14	25	29	0	-8	25	27	3	-19	30	-21	11	-11	31	31	3	7	42	-44	13	-7	12	-7	2	-8	36	-35
3	9	48	47	2	-13	27	-29	0	-6	*262	-388	3	-17	34	33	11	-10	25	27	3	8	30	30	13	-6	33	35	2	-7	69	67
3	10	7	11	2	-12	25	-29	0	0	61	-50	3	-16	27	-36	11	-9	25	-25	3	9	37	-38	13	-5	33	-33	2	-6	18	17
3	13	90	-89	2	-10	17	18	0	2	41	43	3	-12	50	-49	11	-8	14	17	3	13	49	51	13	-3	24	-18	2	-4	20	-22
3	14	40	37	2	-9	44	48	0	4	25	-21	3	-11	24	-25	11	-7	11	15	3	14	29	-29	13	-2	38	38	2	-3	64	62
4	0	16	-14	2	-8	46	46	0	6	*265	400	3	-10	31	-27	11	-5	32	-31	4	-15	34	-40	13	-1	47	49	2	-1	28	-30
4	0	109	-123	2	-7	19	-21	1	-13	79	77	3	-8	33	31	11	-4	30	-28	4	-13	21	21	13	1	34	35	2	1	33	33
4	1	97	-96	2	-6	67	-65	1	-12	34	-38	3	-7	90	95	11	-2	67	-70	4	-12	9	-9	13	2	26	-29	2	3	56	-56
4	2	83	-84	2	-4	57	57	1	-11	34	-36	3	-6	27	-26	11	-1	73	-70	4	-11	12	-12	13	3	19	-18	2	4	35	34
4	3	108	118	2	-3	*253	-370	1	-10	20	15	3	-5	145	-150	11	-1	23	-24	4	-10	9	-7	13	6	35	-37	2	5	41	-40
4	4	52	-55	2	-2	67	-70	1	-9	84	81	3	-4	125	123	11	1	20	-23	4	-9	35	36	13	7	12	11	2	6	21	-23
4	5	54	-58	2	-1	23	-23	1	-7	46	44	3	-3	77	-67	11	2	53	-52	4	-8	20	18	13	8	18	-16	2	7	26	27
4	6	48	52	2	0	99	100	1	-6	* 17	-1	3	-2	72	72	11	4	40	-39	4	-7	54	-53	13	11	26	-22	2	8	21	21
4	7	82	-81	2	1	52	-56	1	-5	24	-26	3	-1	96	-137	11	5	19	19	4	-6	65	-65	14	-9	39	-39	2	9	24	23
4	8	21	21	2	*	66	-68	1	-4	74	-71	3	0	52	53	11	7	11	13	4	-5	48	-45	14	-8	26	-26	3	-13	14	13
4	9	86	86	2	4	43	-44	1	-3	40	36	3	1	54	54	11	8	53	53	4	-4	30	29	14	-1	24	24	3	-12	20	20
4	10	17	17	2	5	71	71	1	-2	70	-63	3	2	17	-16	11	9	48	48	4	-3	103	96	14	3	21	22	3	-11	21	19
4	11	23	-23	2	6	56	55	1	-1	169	-213	3	3	24	-23	11	10	19	-21	4	-2	50	50	14	4	10	11	3	-10	17	-20
4	12	46	47	2	7	13	-8	1	0	148	178	3	5	80	-77	11	11	28	27	4	-1	35	34	14	7	20	-22	3	-8	32	33
4	13	26	27	2	8	56	-55	1	1	151	176	3	6	59	57	11	14	16	16	4	0	104	92	14	9	26	31	3	-7	96	94
4	14	42	-42	2	9	184	135	1	2	48	47	3	7	109	116	12	-14	13	-14	4	1	26	25	15	-8	30	-32	3	-5	43	-43
4	15	33	-30	2	10	20	22	1	3	49	-44	3	8	43	-44	12	-10	32	33	4	2	70	69	15	-7	24	23	3	-2	14	-15
4	16	33	28	2	12	31	-32	1	4	39	-40	3	9	37	39	12	-9	64	-68	4	3	54	-58	15	-5	20	21	3	-1	51	-53

Can. J. Chem. Downloaded from www.nrcresearchpress.com by 210.87.254.40 on 09/05/12
For personal use only.

TABLE 2 (Continued)

K	L	Fo	Fc	K	L	Fo	Fc	K	L	Fo	Fc	K	L	Fo	Fc	K	L	Fo	Fc	K	L	Fo	Fc	K	L	Fo	Fc	K	L	Fo	Fc
5	1	43	-43	2	14	18	12	1	5	17	-14	3	10	76	79	12	-8	33	34	4	4	20	17	15	-3	20	19	3	0	78	-74
5	2	97	-94	3	-13	61	57	1	9	74	-70	3	11	72	76	12	-7	39	40	4	5	37	37	15	-2	42	47	3	2	20	-20
5	4	179	219	3	-11	97	-31	1	10	23	-26	3	13	34	-34	12	-6	45	47	4	7	70	71	15	0	12	15	3	3	23	26
5	5	21	19	3	-10	100	96	1	11	58	53	4	-20	14	-15	12	-5	23	24	4	8	30	-32	15	2	44	-47	3	4	21	-23
5	7	35	37	3	-9	36	-38	1	12	50	-45	4	-18	26	-21	12	-4	23	-26	4	9	63	-64	15	3	20	22	3	5	45	-45
5	8	147	164	3	-8	34	-31	1	13	88	-78	4	-17	38	-37	12	-1	21	-17	4	10	21	-21	15	4	21	23	3	7	29	-29
5	9	7	14	3	-7	101	-101	1	14	42	-34	4	-16	30	-30	12	0	16	14	4	11	24	24	15	8	13	15	3	8	23	24
5	10	66	-63	3	-6	76	75	2	-13	33	32	4	-15	25	23	12	1	30	-30	4	12	56	-56	15	9	13	-13	3	9	15	15
5	12	28	-24	3	-5	53	56	2	-12	25	-27	4	-14	28	-28	12	3	57	100	4	15	26	27	15	10	23	-23	3	11	15	14
5	14	38	38	3	-2	63	-54	2	-11	40	44	4	-13	15	16	12	5	20	-22	5	-15	18	17	16	-11	23	24	3	12	45	43
5	15	23	-23	3	-1	114	-118	2	-10	17	17	4	-12	65	64	12	6	12	-10	5	-14	25	28	16	-6	27	30	3	13	24	-20
5	16	27	-26	3	0	67	68	2	-9	103	-105	4	-11	46	-44	12	7	14	-18	5	-13	11	13	16	-5	28	26	4	-11	11	9
6	0	101	108	3	1	190	230	2	-8	54	54	4	-10	34	33	12	10	24	25	5	-12	11	-11	16	-4	25	-24	4	-9	54	-54
6	1	105	-104	3	2	112	-112	2	-7	85	-85	4	-8	72	76	12	12	30	-30	5	-10	64	-62	16	-3	22	-20	4	-8	20	-20
6	3	147	149	3	3	90	89	2	-6	18	-20	4	-7	31	-29	12	13	31	30	5	-9	8	-9	16	-1	36	40	4	-7	20	22
6	4	90	-96	3	4	139	142	2	-4	48	49	4	-6	11	11	12	15	41	-42	5	-8	131	125	16	1	38	-39	4	-6	23	-22
6	5	61	-59	3	5	168	177	2	-3	31	-30	4	-5	92	92	13	-17	23	-23	5	-7	45	-41	16	2	10	-13	4	-5	11	-10
6	6	6	-11	3	6	25	-25	2	-2	49	46	4	-4	68	56	13	-16	29	27	5	-6	11	12	16	4	28	-29	4	-4	32	-34
6	7	74	-80	3	7	82	-83	2	-1	47	47	4	-3	20	-16	13	-12	37	34	5	-5	51	-45	16	7	30	-29	4	-3	28	31
6	8	90	93	3	8	29	31	2	1	56	-59	4	-2	76	73	13	-11	25	28	5	-4	121	104	16	8	36	37	4	-2	11	8
6	11	82	-84	3	9	12	-8	2	2	43	-47	4	-1	71	66	13	-7	32	-33	5	-3	19	-15	16	10	14	10	4	-1	36	37
6	12	40	-42	3	11	39	41	2	3	55	61	4	0	136	-141	13	-6	25	25	5	-2	47	43	17	-8	14	-17	4	0	41	-41
6	15	58	-52	3	12	62	-56	2	4	54	-54	4	1	71	67	13	-5	30	29	5	-1	12	10	17	-7	12	11	4	1	54	-54
6	16	10	11	3	13	44	-41	2	5	25	27	4	3	15	15	13	-4	65	-66	5	0	24	-15	17	-6	25	20	4	2	26	26
6	17	10	12	4	-14	56	49	2	6	25	25	4	4	29	-29	13	-2	27	28	5	1	26	31	17	-4	40	-39	4	3	71	71
6	18	10	14	4	-13	18	-18	2	7	57	-56	4	5	45	44	13	0	35	-35	5	2	99	98	17	-3	19	19	4	4	37	36
6	19	43	35	4	-12	12	13	2	8	43	-45	4	6	60	53	13	1	47	-50	5	4	169	-168	17	-1	27	-27	4	5	27	-27
6	20	33	-28	4	-11	70	65	2	9	83	-80	4	7	56	-55	13	4	12	16	5	5	18	15	17	1	18	-19	4	6	68	68
7	1	56	-56	4	-10	58	57	2	10	17	-14	4	8	20	-19	13	5	52	53	5	6	24	-24	17	4	41	36	4	7	17	17
7	2	39	40	4	-9	24	-24	2	11	33	33	4	9	14	-14	13	6	49	-50	5	8	102	-103	17	8	30	26	4	8	38	36
7	3	38	39	4	-8	49	46	2	12	19	22	4	10	54	-53	13	8	29	33	5	9	8	-7	18	-7	12	-14	4	9	29	-29
7	4	77	84	4	-7	57	-52	3	-13	40	-40	4	11	47	49	13	10	44	-40	5	10	31	32	18	-4	15	14	5	-2	132	-128
7	6	47	-47	4	-6	123	-123	3	-12	59	-54	4	12	19	22	13	11	15	-18	5	11	11	-14	18	1	24	-26	5	-1	29	-32
7	7	49	-53	4	-5	62	66	3	-8	64	-61	4	13	17	-21	14	-13	15	-14	5	12	27	30	19	-8	21	18	5	0	18	17
7	8	34	36	4	-3	21	20	3	-7	118	-129	4	14	29	-37	14	-12	29	-25	5	14	36	-41	19	-5	34	-36	5	1	22	-29
7	9	39	-38	4	-2	79	-80	3	-3	46	45	5	-20	13	13	14	-11	24	25	5	16	33	36	K	L	H = 5		5	2	75	76
7	10	8	8	4	-1	60	59	3	-2	110	-95	5	-18	16	13	14	-9	24	-22	6	-15	36	-41	0	-10	26	33	6	-2	80	-76
7	11	8	-8	4	0	90	94	3	-1	113	113	5	-17	13	-7	14	-6	15	-12	6	-14	12	16	0	-8	49	45	6	-1	26	23
7	13	67	63	4	1	109	-110	3	0	138	163	5	-16	12	9	14	-5	52	-53	6	-12	25	23	0	-6	96	-95	6	0	18	15
7	18	31	29	4	2	55	-57	3	1	74	-72	5	-14	30	31	14	-4	24	-23	6	-11	67	-66	0	-4	87	-85	6	1	52	-54
8	0	114	126	4	4	83	-82	3	2	84	98	5	-13	14	12	14	-2	39	-39	6	-9	8	-12	0	-2	62	62	6	2	44	46
8	2	94	94	4	6	69	66	3	3	39	-40	5	-12	17	-19	14	-1	46	43	6	-8	87	-82	0	0	29	-33	7	-2	28	-28
8	3	31	-32	4	7	37	-40	3	4	28	27	5	-11	20	17	14	0	14	18	6	-7	61	-56	0	2	43	-44	7	-1	21	23
8	4	7	8	4	8	65	-67	3	5	43	43	5	-10	122	113	14	2	14	-21	6	-6	23	21	0	4	19	-24	7	0	30	-32
8	5	70	72	4	10	17	-13	3	7	81	83	5	-8	9	-10	14	3	44	46	6	-5	66	-60	0	6	36	38	7	2	48	49
8	6	29	-28	4	11	35	-34	3	8	53	-52	5	-6	72	-64	14	4	14	18	6	-4	62	53	0	10	58	-52	8	-1	23	-30
8	7	50	51	4	12	68	-63	3	10	15	-16	5	-5	32	-28	14	6	12	-14	6	-3	143	-133	1	-12	22	-26	8	0	15	15
8	10	68	-69	4	13	22	21	3	11	15	-9	5	-4	55	-48	14	7	41	41	6	-2	24	-24	1	-10	70	-65	8	1	33	40
8	11	31	-22	5	-16	82	80	3	12	62	-61	5	-3	42	-31	14	8	28	23	6	-1	48	46	1	-9	68	-67	9	-2	41	40
8	12	27	-26	5	-12	39	-41	3	13	43	43	5	-1	56	-59	14	10	29	23	6	0	75	-70	1	-7	37	36	9	-1	23	-26
8	14	10	-10	5	-10	46	-47	4	-13	47	-45	5	0	67	61	14	11	33	-38	6	1	88	86	1	-6	40	-44	9	1	62	58
8	15	24	24	5	-8	21	-26	4	-12	55	-54	5	1	43	-45	15	-12	26	23	6	2	11	-8	1	-5	37	-39	9	2	24	-26
9	1	32	32	5	-7	60	-57	4	-11	17	-19	5	2	75	-74	15	-11	15	-14	6	3	68	-63	1	-4	86	-85	10	-1	18	17
9	2	15	20	5	-6	41	43	4	-10	12	17	5	3	21	16	15	-10	31	-27	6	4	83	78	1	-2	20	-18	10	2	29	31
9	4	59	-64	5	-5	44	-43	4	-9	76	78	5	4	76	-74	15	-7	13	12	6	5	20	13	1	0	20	14	11	2	33	-34
9	5	89	-92	5	-4	120	-134	4	-8	28	28	5	5	32	29	15	-6	13	14	6	7	60	63	1	1	21	21	K	L		H = 7
9	6	53	-64	5	-2	50	49	4	-7	37	-36	5	6	45	43	15	-5	25	25	6	8	61	-58	1	2	110	112	0	-6	83	80
9	7	33	32	5	-1	36	35	4	-6	84	80	5	7	56	53	15	-4	15	-18	6	9	51	-51	1	3	113	122	0	-4	36	36
9	8	60	-62	5	0	78	77	4	-3	100	86	5	9	26	21	15	-1	30	29	6	11	57	54	1	4	47	-45	0	-2	20	22
9	10	37	35	5	1	87	83	4	-2	41	39	5	10	39	-46	15	0	16	-22	6	12	40	41	1	5	21	23	0	0	54	-51
9	11	14	-15	5	2	23	28	4	-1	85	-79	5	11	11	15	15	1	26	26	6	15	38	37	1	8	41	41	0	2	61	-62
9	12	9	-9	5	3	40	46	4	0	33	31	5	12	32	-35	15	2	37	37	7	-13	68	-68	1	11	22	-20	0	4	54	48
9	17	66	54	5	4	62	-60	4	1	94	92	6	-17	40	-40	15	4	31	32	7	-11	15	15	2	-13	27	31	1	-7	20	16
10	0	131	-142	5	5	49	46	4	2	61	-67	6	-16	38	36	15	5	20	-21	7	-9	48	45	2	-12	19	22	1	-6	27	-27
10	1	26	25	5	7	17	17	4	3	103	-113	6	-15	41	42	15	7	32	-30	7	-8	19	15	2	-11	19	20	1	-4	72	-71
10	2	43	42	5	10	112	105	4	7	35	-35	6	-12	58	-58	16	-13	24	18	7	-7	39	36	2	-9	49	-45	1	-3	75	-75
10	3	6	-15	5	11	25	-25	4	8	41	-40	6	-11	24	-24	16	-10	15	-14	7	-6	53	-46	2	-8	33	-30	1	0	[illegible]	[illegible]
10	4	20	-24	5	13	37	-29	4	9	63	62	6	-10	18	17	16	-8	26	-26	7	-5	33	29	2	-7	16	14	1	1	22	[illegible]
10	5	23	-26	6	-13	43	-43	4	10	16	-17	6	-9	28	-30	16	-7	20	21	7	-4	70	67	2	-6	37	37	1	2	63	-63
10	8	8	9	6	-11	36	38	4	11	19	-19	6	-7	84	-80	16	-6	30	-28	7	-3	24	-20	2	-4	41	-41	1	4	21	16
10	9	21	22	6	-10	75	-69	4	12	37	38	6	-6	17	15	16	-5	15	-15	7	-2	38	-38	2	-3	172	-172	1	[illegible]	57	53
10	10	55	-53	6	-9	67	-64	4	13	57	-53	6	-5	30	27	16	-4	24	25	7	-1	88	82	2	-2	31	30	2	-1	21	[illegible]
10	11	60	57	6	-8	37	-37	5	-2	242	253	6	-4	71	-73	16	-2	30	31	7	1	16	13								
10	12	78	72	6	-6	92	82	5	-1	31	31	6	-3	64	-56	16	0	12	-18	7	2	7	-13								

Can. J. Chem. Downloaded from www.nrcresearchpress.com by 210.87.254.40 on 09/05/12
For personal use only.

TABLE 2 (Concluded)

K	L	Fo	Fc	K	L	Fo	Fc	K	L	Fo	Fc	K	L	Fo	Fc	K	L	Fo	Fc	K	L	Fo	Fc	K	L	Fo	Fc	K	L	Fo	Fc
11	1	9	10	6	-9	75	79	5	0	38	-36	6	-2	70	-70	16	8	24	-24	7	3	41	-40	2	-1	18	-14	2	-9	49	-49
11	2	56	-55	6	-8	25	-29	5	1	17	14	6	0	89	96	16	10	20	-19	7	4	65	-61	2	0	56	-56	2	-8	14	-17
11	3	75	76	6	-7	135	-129	5	2	133	-213	6	1	102	97	17	-9	31	-31	7	5	27	-21	2	2	20	22	2	-7	17	16
11	4	51	-49	6	-1	132	-129	6	-3	62	60	6	2	14	-16	17	-2	32	34	7	6	30	31	2	3	40	40	2	-6	30	27
11	5	61	-62	6	0	83	-82	6	-2	139	139	6	3	102	107	17	-1	33	-30	7	7	27	25	2	4	38	36	2	-5	14	20
11	6	17	19	6	2	80	80	6	-1	76	-76	6	4	21	16	17	1	35	33	7	8	41	-41	2	5	49	-51	2	-4	25	-26
11	7	86	85	6	3	17	-21	6	1	92	89	6	5	82	80	17	3	38	-38	7	9	22	23	2	6	37	-36	2	-3	24	-23
11	8	21	-24	6	4	103	100	6	2	99	-106	6	6	40	-41	17	4	26	26	7	10	19	-18	2	8	37	39	2	-2	29	31
11	9	21	-21	6	5	19	16	6	3	113	-117	6	8	32	34	18	-9	15	-18	7	12	11	15	2	9	145	-138	2	2	30	-33
11	10	21	9	6	7	93	-94	7	-3	62	-62	6	9	34	-32	18	-8	27	31	7	13	34	-36	2	10	18	-12	2	3	125	123
11	11	10	-21	6	9	65	-67	7	-2	65	62	6	10	66	65	18	-7	26	23	7	16	26	27	3	-13	46	-44	2	4	17	16
11	12	27	19	6	10	22	-21	7	-1	43	-44	6	11	21	20	18	-6	29	29	8	-11	29	-31	3	-11	60	58	2	5	16	18
11	13	49	-42	6	11	31	-34	7	0	47	46	6	12	25	-30	18	-5	24	23	8	-10	53	51	3	-10	64	-61	2	6	35	-36
11	14	35	28	6	12	52	49	7	1	19	16	6	13	37	-42	18	-4	25	-24	8	-9	26	25	3	-9	22	21	2	7	18	-12
11	15	10	9	7	-13	41	-38	7	2	75	-75	7	-17	28	-31	18	-3	15	-17	8	-8	22	-20	3	-8	14	13	3	-12	23	26
11	17	10	9	7	-11	85	80	7	3	42	44	7	-16	52	54	18	-2	32	33	8	-7	34	31	3	-7	22	23	3	-11	18	16
12	0	55	-59	7	-10	85	-79	8	-1	73	66	7	-11	33	33	18	-1	35	-30	8	-6	32	31	3	-6	50	-48	3	-10	22	23
12	1	38	38	7	-7	92	89	8	1	81	-76	7	-8	16	-9	18	0	16	-16	8	-5	58	53	3	-5	22	-21	3	-8	15	-14
12	2	18	20	7	-6	83	76	9	-2	80	-80	7	-7	65	-66	18	1	15	-21	8	-3	42	-39	3	-4	21	-22	3	-7	55	-55
12	3	72	-73	7	-5	26	32	9	-1	64	54	7	-6	26	-24	19	-5	23	-22	8	-2	52	-57	3	-3	31	-35	3	-6	15	14
12	4	43	-42	7	-4	163	-168	9	0	69	68	7	-5	133	125	19	-4	23	23	8	0	74	-73	3	-2	92	89	3	-5	67	66
12	5	31	-28	7	1	57	-55	9	1	82	-71	7	-3	35	31	19	-3	31	-34	8	1	24	23	3	-1	34	-31	3	-4	62	-61
12	6	71	69	7	2	57	-55	9	2	69	71	7	-2	84	85	19	-2	15	-18	8	2	79	-81	3	1	124	-125	3	-3	30	30
12	7	9	-12	7	3	34	-37	9	3	42	44	7	-1	101	103	19	-1	20	-18	8	3	44	-42	3	2	79	79	3	-2	23	-24
12	8	33	29	7	5	132	-132	10	-1	38	-32	7	0	0	10	19	2	35	30	8	4	46	-45	3	3	55	-52	3	-1	28	31
12	12	10	15	7	6	21	-22	10	1	22	24	7	1	39	-38	20	-1	20	18	8	5	44	-42	3	4	66	-64	3	0	23	-26
12	13	10	-11	7	7	51	50	10	2	28	-33	7	2	23	22					8	10	54	54	3	5	82	-82	3	1	15	-15
12	15	35	-29	7	8	22	-22	11	-1	105	98	7	3	36	-35	K	L		H = 4	8	11	11	16	3	6	14	13	3	4	25	24
12	17	17	16	7	9	25	32	11	0	13	-17	7	4	18	19					8	12	36	30	3	7	30	32	3	5	50	53
13	1	57	-56	7	11	42	-42	11	1	80	-78	7	5	68	65	0	-12	102	111	9	-12	16	-16	3	8	15	14	3	6	28	-24
13	2	38	42	7	13	49	45	11	2	34	37	7	6	20	20	0	-10	32	-32	9	-10	34	34	3	9	15	-12	3	7	68	-65
13	4	9	17	8	-11	26	-30	12	-2	89	83	7	7	105	-110	0	-8	18	-15	9	-8	40	-40	3	10	15	-12	3	8	37	35
13	5	31	30	8	-10	33	-37	12	-1	34	-35	7	8	48	-45	0	-8	18	-15	9	-7	18	-19	3	11	41	-41	3	9	28	-27
13	6	43	41	8	-9	94	92	12	1	43	44	7	9	17	-14	0	-6	70	68	9	-6	44	-44	3	12	39	37	4	1	33	-36
13	11	10	17	8	-8	24	21	12	2	88	-84	7	10	15	12	0	-4	22	-21	9	-5	87	84	4	13	49	45	4	10	35	-36
13	12	10	10	8	-3	145	132					7	11	64	-66	0	-2	36	37	9	-5	87	84	4	-12	35	-35	4	11	37	-34
13	13	35	36	8	-2	99	97	K	L		H = 3	7	13	25	25	0	C	*255	-391	9	-4	25	-23	4	-11	55	-56	4	-8	39	42
13	14	33	-27	8	-1	36	-36					8	-18	15	10	0	6	29	-26	9	-1	26	-28	4	-10	39	-40	4	-7	15	17
14	0	67	65	8	0	81	-80	0	-22	21	13	8	-17	15	17	0	8	35	35	9	0	19	15	4	-9	21	21	4	-6	36	-36
14	1	9	9	8	4	21	28	0	-20	21	-28	8	-16	26	28	0	10	20	-20	9	1	21	-19	4	-8	43	-43	4	-5	54	-55
14	6	49	-44	8	5	21	-22	0	-18	52	64	8	-15	15	-17	0	12	144	149	9	2	28	-31	4	-7	28	29	4	-4	27	-28
14	11	10	-12	8	8	88	87	0	-16	21	23	8	-12	54	-54	1	-16	29	-36	9	3	18	-18	4	-6	86	83	4	-3	15	13
14	12	35	-27	8	9	88	87	0	-14	45	43	8	-9	71	71	1	-15	42	-45	9	4	54	59	4	-5	60	-60	4	-2	44	-43
14	13	31	-24	8	10	20	-20	0	-12	88	-90	8	-8	80	-81	1	-14	16	-16	9	5	61	59	4	-4	39	40	4	-1	27	-31
15	1	9	11	8	12	63	56	0	-10	76	-74	8	-7	31	-28	1	-11	15	10	9	6	50	48	4	-2	60	61	4	0	76	78
15	2	63	59	9	-11	20	16	0	-8	46	47	8	-5	34	-34	1	-10	46	49	9	7	36	-39	4	-1	32	33	4	1	45	-48
15	3	26	-27	9	-10	64	62	0	-6	115	-105	8	-4	21	-21	1	-8	34	-34	9	8	46	44	4	1	73	74	4	2	19	20
15	6	10	15	9	-9	50	-49	0	-4	56	-54	8	-3	26	22	1	-7	120	121	9	10	11	-16	4	2	22	21	4	4	25	23
15	7	24	-23	9	-8	20	-17	0	-2	62	-61	8	-2	21	-20	1	-6	90	-87	9	11	25	25	4	4	59	59	4	5	22	-23
15	8	31	-29	9	-7	80	77	0	0	89	91	8	-1	26	26	1	-5	69	-64	10	-12	51	-53	4	5	40	-46	4	7	36	36
15	9	10	16	9	-1	34	-36	0	2	72	78	8	0	79	85	1	-4	12	8	10	-11	48	48	4	6	75	-76	5	-2	21	-22
15	10	27	26	9	0	27	31	0	4	89	-87	8	1	30	32	1	-3	80	73	10	-10	41	42	4	7	36	38	5	-1	21	19
15	11	10	-11	9	1	90	-82	0	6	88	-82	8	2	67	-66	1	-1	53	51	10	-9	36	37	4	8	17	18	5	0	28	-31
15	14	44	-39	9	2	73	-67	0	8	48	47	8	3	107	-113	1	1	35	-39	10	-8	8	11	4	11	23	21	5	2	52	56
16	0	10	12	9	3	91	94	0	10	26	27	8	4	56	57	1	2	38	-41	10	-7	9	-12	5	-2	20	-15	6	-2	29	32
16	1	64	63	9	4	73	71	0	12	44	47	8	5	25	20	1	3	43	45	10	-6	17	-17	5	0	65	-63	6	-1	20	-17
16	4	31	32	9	5	66	-65	1	-19	15	15	8	6	56	-54	1	4	58	57	10	-4	37	34	5	1	38	-41	6	0	56	-60
16	5	32	27	9	7	20	-25	1	-18	15	-14	8	10	32	34	1	5	109	-111	10	-3	22	-23	6	-1	84	80	7	-2	68	-63
16	7	24	26	9	10	39	-36	1	-16	32	-35	8	11	15	-17	1	6	97	96	10	-2	22	-26	6	0	19	11	7	-1	24	-27
16	8	49	-42	9	11	23	24	1	-15	32	-36	8	13	24	-24	1	7	56	58	10	0	103	107	6	2	46	-48	7	0	22	19
16	11	44	36	9	12	36	-34	1	-13	42	43	8	14	46	50	1	8	43	44	10	1	40	-42	7	-2	21	12	7	2	21	24
16	13	27	-21	9	13	57	44	1	-12	44	-46	8	15	47	46	1	10	24	-29	10	2	34	-34	7	-1	65	-65	10	-2	24	-27
17	1	32	29	10	-13	36	36	1	-11	31	-36	9	-16	19	-24	1	11	33	-40	10	3	8	-11	7	0	27	28				
17	4	57	-49	10	-8	49	49	1	-10	66	-67	9	-15	33	36	2	-17	20	-23	10	6	11	11	7	1	122	117				

* Photocopies of Table 2, Part B (unobserved reflections) may be obtained free of charge, upon request, from the Depository of Unpublished Data, National Science Library, National Research Council of Canada, Ottawa, Canada.

+ Unreliable reflections are marked with an asterisk.

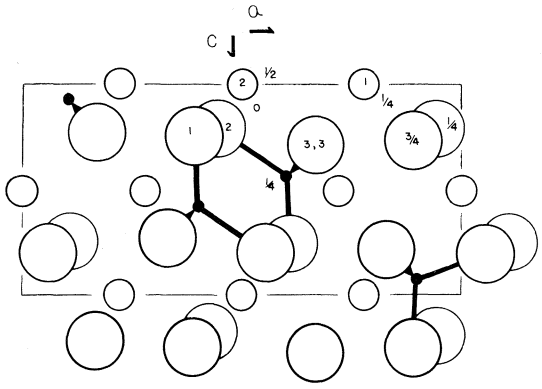

FIG. 2. The olivine structure is shown projected down the *b* axis. The closest packed direction is along *c*. The small filled circles represent the ions in tetrahedral sites; the next larger circles, those in octahedral sites. There are two cations superimposed on the site labelled 1/4, 3/4, and those symmetry related to it. The oxygen ions are represented by large circles with two oxygens superimposed in projection where there are doubled circles.

The arsenate ion has nearly tetrahedral symmetry although the deviations are significant. The average AsO bond lengths are 1.69 Å for As(1) and 1.70 Å for As(2). The two longest AsO bonds involve those oxygen atoms, O(12) and O(21), bonded to more than two Co^{2+} ions. The O—As—O bond angles about As(2) all lie within 2° of their mean value of 109.3°, whereas the analogous angles about As(1) range from 98 to 119°. The geometries of the anions are summarized in Table 3. This latter distortion is entirely due to a displacement of O(21) by about 0.3 Å from the ideal value. The arsenate ions are arranged such that their pseudo mirror planes parallel each other and the [100] plane. These tetrahedra form a nonbonded chain generated by a pseudo 2_1 axis parallel to a^*. The oxygen atoms coplanar with the As ions at about the same *y* value nearly superimpose in projection (see Fig. 1); thus the *a* axis length (5.830 Å) is governed by the sum of two oxygen atom van der Waals contact distances.

The CoO_6 octahedra deviate significantly from regularity. The average Co—O bond lengths are nearly identical, being 2.11, 2.12, and 2.13 Å for cobalt 1, 2, and 3, respectively. The range of CoO distances is 1.991 to 2.181 Å for Co(1), 2.042 to 2.292 Å for Co(2), and 2.021 to 2.287 Å for Co(3). The longer Co—O bond distances involve those oxygen atoms, O(21) and O(12), bonded to three Co ions in addition to an As ion. The mutual arrangement of these octahedra is shown in Fig. 3.

Discussion

The structures of $Mg_3(VO_4)_2$ (11) and $Co_3(AsO_4)_2$ are similar in that both are based upon closest packed layers of oxygen atoms, with all the divalent metal ions in octahedral sites and the pentavalent ions in tetrahedral sites. The major difference in these structures lies in the fact that $Mg_3(VO_4)_2$ (11), and therefore its analogues $Ni_3(VO_4)_2$ (12), $Zn_3(VO_4)_2$, and $Co_3(VO_4)_2$ (13), show cubic closest packed layers stacked normal to $[01\bar{1}]$.

The structure of sarcopside, $(Fe, Mn, Mg)_3(PO_4)_2$ (14), has been reported to be olivine-like, although the space group symmetry is in fact $P2_1/a$. The stacking is parallel to *b*, which is equal to 1/2 of the *b* axis in $Co_3(AsO_4)_2$, and the 10.48-Å axis is in the glide direction. One can anticipate that one of the cations lies at the center of symmetry in order to satisfy the stoichiometry of the crystal. In order for a transformation to occur between these phases, the ABAC stacking in $Co_3(AsO_4)_2$ has to

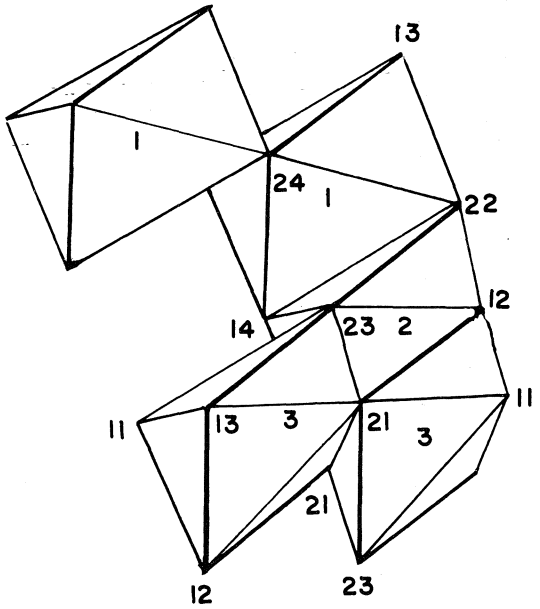

FIG. 3. The mutual arrangement of the three CoO_6 octahedra are shown schematically. The cobalts, labelled as in Table 2, lie at the center of each octahedron. The oxygen atoms are numbered as in Table 2.

Can. J. Chem. Downloaded from www.nrcresearchpress.com by 210.87.254.40 on 09/05/12
For personal use only.

Can. J. Chem. Downloaded from www.nrcresearchpress.com by 210.87.254.40 on 09/05/12
For personal use only.

TABLE 3

Bonding geometry in $Co_3(AsO_4)_2$*

Atoms	Bond length† (Å)	Atoms	Bond angle† (deg)	Atoms	Bond angle† (deg)
As(1)—O(11)	1.685(6)	O(11)—As(1)—O(12)	97.5(3)	O(12)—As(1)—O(13)	99.2(3)
—O(12)	1.722(7)	—O(13)	112.6(3)	—O($\bar{1}$4)	119.0(3)
—O(13)	1.688(7)	—O($\bar{1}$4)	112.6(3)	O(13)—As(1)—O($\bar{1}$4)	114.6(3)
—O($\bar{1}$4)	1.670(7)				
As(2)—O($\bar{2}$1′)	1.728(7)	O($\bar{2}$1′)—As(2)—O(22)	108.1(3)	O(22)—As(2)—O(23)	109.9(3)
O(22)	1.681(6)	—O(23)	108.9(3)	O($\bar{2}$4′)	109.6(3)
O(23)	1.710(7)	—O($\bar{2}$4′)	110.0(3)	O(23)—As(2)—O($\bar{2}$4′)	110.2(3)
O($\bar{2}$4′)	1.689(6)				

Atoms	Bond length† (Å)	Atoms	Bond length† (Å)	Atoms	Bond length† (Å)
Co(1)—O(12′)	2.072(7)	Co(2)—O(11′)	2.096(7)	Co(3)—O(11)	2.021(6)
—O(13)	1.991(7)	O(12′)	2.138(7)	—O(12′)	2.287(8)
—O(14)	2.099(7)	—O($\bar{2}$1′)	2.292(7)	—O(13′)	2.048(7)
—O(22)	2.128(6)	—O(22′)	2.075(7)	—O(21′)	2.161(6)
—O($\bar{2}$4′)	2.173(7)	—O(14)	2.061(7)	—O($\bar{2}$1′)	2.143(7)
—O(24′)	2.181(7)	—O($\bar{2}$3)	2.042(7)	—O(23)	2.111(8)

Atoms	Bond angle† (deg)	Atoms	Bond angle† (deg)	Atoms	Bond angle† (deg)
O(12′)—Co(1)—O($\bar{2}$4′)	88.5(3)	O($\bar{2}$1)—Co(2)—O(11′)	85.4(3)	O(21′)—Co(3)—O(13′)	89.1(3)
—O(22)	85.0(3)	—O(12′)	79.4(3)	—O(12′)	79.0(3)
—O(24′)	165.4(3)	—O(22′)	171.8(3)	—O(11)	172.4(3)
—O(13)	105.8(3)	—O(14)	92.7(3)	—O(23)	94.6(3)
—O(14)	82.6(3)	—O($\bar{2}$3)	88.8(3)	—O($\bar{2}$1′)	83.6(3)

Atoms	Bond angle† (deg)	Atoms	Bond angle† (deg)	Atoms	Bond angle† (deg)
O($\bar{2}$4′)—Co(1)—O(22)	173.4(3)	O(11′)—Co(2)—O(12′)	74.4(3)	O(13′)—Co(3)—O(12′)	73.4(3)
—O(24′)	92.0(3)	—O(22′)	86.4(3)	—O(11)	96.3(3)
—O(13)	86.8(3)	—O(14)	99.4(3)	—O(23)	103.3(3)
—O(14)	93.4(3)	—O($\bar{2}$3)	169.8(3)	—O($\bar{2}$1′)	164.4(3)
O(22)—Co(1)—O(24′)	94.5(3)	O(12′)—Co(2)—O(22′)	98.5(3)	O(12′)—Co(3)—O(11)	97.3(3)
—O(13)	94.5(3)	—O(14)	170.2(3)	—O(23)	172.7(3)
—O(14)	86.2(3)	—O($\bar{2}$3)	96.3(3)	—O($\bar{2}$1′)	91.6(3)
O(24′)—Co(1)—O(13)	88.8(3)	O(22′)—Co(2)—O(14)	88.6(3)	O(11)—Co(3)—O(23)	89.5(3)
—O(14)	82.8(3)	—O($\bar{2}$3)	99.4(3)	—O($\bar{2}$1′)	89.9(3)
O(13)—Co(1)—O(14)	171.6(3)	O(14)—Co(2)—O($\bar{2}$3)	89.2(3)	O($\bar{2}$1′)—Co(3)—O(23)	91.1(3)

*Atom $\bar{n}$ is obtained from n by an inversion through the origin and n' by the c glide operation changing x, y, z to $x, 1/2 - y, 1/2 + z$.
†Estimated standard deviations in parentheses.

change to the ABAB stacking in sarcopside.[1] Small displacement could then occur giving rise to a center of symmetry at cation site 2.

A further indication that this layer stacking is the appropriate feature to emphasize is the fact that the structures of both $Co_6As_3O_{16}$ and $Co_8As_2O_{16}$ (9) basically have the olivine-like structures. In addition, Davis *et al.* have pointed out that the unit cell dimensions of aerugite are strongly suggestive of layer arrangement. In this sense, the arsenates of the same cations seem to differ substantially from the analogous phosphates, where regular packing of oxygen atom layers rarely occurs. This no doubt is related to the fact that the oxygen–oxygen distances about an As ion are comparable to those about a Co ion and thus close packed structures should occur even more commonly among the vanadates, since the tetrahedral V—O bond length is somewhat larger than the As—O bond length in arsenates.

[1]These letters designate an entire oxygen atom layer and indicate the set of interstices occupied by the oxygen atom. Because of the packing of the cations in $Co_3(AsO_4)_2$, the layers distort and the two A layers in the unit cell are not crystallographically equivalent, of course.

This work was supported by a grant from the National Research Council of Canada.

1. N. KRISHNAMACHARI. Ph.D. Thesis, McMaster University, Hamilton, Ontario. 1970.
2. C. CALVO. J. Chem. Phys. Solids, **24**, 141 (1963).
3. J. B. TAYLOR and R. D. HEYDING. Can. J. Chem. **36**, 597 (1958).
4. R. J. DAVIS, M. H. HEY, and A. W. G. KINGSBURY. Mineral. Mag. **35**, 72 (1965).
5. S. J. POULSEN and C. CALVO. Can. J. Chem. **46**, 917 (1968).
6. C. CALVO and K. Y. LEUNG. Z. Krist. To be published.
7. D. T. CROMER and K. HERRINGTON. J. Amer. Chem. Soc. **77**, 4708 (1955).
8. L. H. THOMAS and K. UMEDA. J. Chem. Phys. **26**, 293 (1957).
9. N. KRISHNAMACHARI and C. CALVO. Can. J. Chem. To be published.
10. N. V. BELOV, E. N. BELOVA, N. H. ANDRIANOVA, and P. F. SMIRNOVA. Dokl. Akad. Nauk. SSSR, **81** 399 (1951).
11. A. DURIF. Anal. Chem. **31**, 1741 (1959).
12. A. DURIF and E. F. BERTAUT. J. Phys. Radium, **20**, 54S (1959).
13. C. BRISI. Ric. Sci. **30**, 1339 (1960).
14. M. E. MROSE and D. E. APPLEMAN. American Crystallographic Association, Annual Meeting, Program and Abstracts, University of Colorado, Boulder, Colorado. 1961.

Can. J. Chem. Downloaded from www.nrcresearchpress.com by 210.87.254.40 on 09/05/12
For personal use only.

Can. J. Chem. Downloaded from www.nrcresearchpress.com by 210.87.254.5 on 09/05/12
For personal use only.

Refinement of the structure of $Mg_2As_2O_7$

C. CALVO AND K. NEELAKANTAN[1]

Department of Chemistry and Institute for Materials Research, McMaster University, Hamilton, Ontario

Received September 10, 1969

The crystal structure of $Mg_2As_2O_7$ has been refined by full matrix least squares procedures using 587 observed reflections. The structure of $Mg_2As_2O_7$ is of the thortveitite type, as reported by Łukaszewicz, with space group $C2/m$ and unit cell dimensions $a = 6.567(2)$ Å, $b = 8.524(4)$ Å, $c = 4.739(1)$ Å, $\beta = 103.8(1)°$, and $Z = 2$. The As—O—As group in the anion appears to be linear but the central oxygen atom undergoes considerable disorder in the plane perpendicular to this group. The AsO bond distances uncorrected for thermal motion are 1.67 Å for the As—O(—As) bond and 1.66 and 1.65 Å for the terminal As—O bonds. The final R value obtained is 0.088.

Canadian Journal of Chemistry, **48**, 890 (1970)

Introduction

Łukaszewicz (1) has determined that $Mg_2As_2O_7$ structurally is a member of the thortveitite, $(Sc,Y)_2Si_2O_7$, series. His analysis, based upon data from two projections, led to an average As—O bond length of 1.7 Å. In detail, however, the As—O(—As) bond length at 1.71 Å was considerably smaller than one of the terminal As—O bonds. The As—O_{II} bond length, which lies in the mirror plane of the anion, was reported to be 1.78 Å. A number of reasonably accurate arsenate structure (2–5) have been determined recently and they indicate a mean As—O bond length, when tetrahedrally coordinated, near 1.70 Å, in agreement with the results of Lukaszewicz for $Mg_2As_2O_7$. The variation from the mean in this structure determination is, however, at variance with the trend predicted by Cruickshank (6) upon condensation in phosphate systems. His expectations, based upon $p\pi$–$d\pi$ bonding, have been extensively confirmed experimentally in phosphate systems (7, 8). Further, in virtually all the analogues of the thortveitite structure studied to date, the central oxygen atom showed enhanced disorder and those refinements allowing for anisotropic thermal motion indicated that the disorder was in the plane perpendicular to the Y–Y vector of the anion Y_2O_7. Therefore, in order to examine in detail the analogy with the pyrophosphates, divanadates, and disilicates, a more detailed refinement of $Mg_2As_2O_7$ was needed.

Experiments

Crystals of $Mg_2As_2O_7$ were grown in a manner analogous to that reported by Łukaszewicz except for the fact that $MgHAsO_4$ was doped with 0.1% Mn^{2+} before decomposing and that a Vycor container was employed. The crystals were doped with Mn^{2+} in quest of samples large enough for concurrent electron paramagnetic resonance studies. Unfortunately, crystals suitable for such a study were not obtained.

Three crystals of dimensions of the order of 0.15 × 0.15 × 0.10 mm³ with the c axis along one of the longer directions, were selected for study. Accurate lattice parameters were determined from a Debye–Scherrer diagram by least square refinement using 44 lines. The lattice parameters obtained are: $a = 6.567(2)$ Å, $b = 8.524(4)$ Å, $c = 4.739(1)$ Å, and $\beta = 103.8(1)°$ using Mo $K\alpha_1$ radiation with wavelength 0.70930 Å. Thus the calculated density of 4.004 g/cm³ for $Z = 2$ agrees with the experimental value of 3.982 g/cm³ reported by Łukaszewicz. The extinctions are all reflections with $h + k$ odd. This is consistent with space group $C2$, Cm, and $C2/m$. The latter has been chosen primarily because all other members of this series have been shown to be of this symmetry (9–12).

Weissenberg photographs containing data of the $n = 0$, 1, 2, 3, 4 layers of [001] zone and the first three layers of the [121] zone were recorded. The 0th and the first two upper layers of the [010] zone together with the [100] zone were taken with a precession camera. All data were collected using Mo $K\alpha$ radiation and the intensities were visually estimated using calibrated strips and corrected for Lorentz and polarization effects. No absorption corrections were made and thus a systematic error of the order of 5% may have been introduced since the average value of μr is 0.9. A total of 769 independent reflections were recorded and 587 reflections had intensities strong enough to be observed.

The refinement was started with the coordinates reported by Łukaszewicz (1). Mg^{2+}, As^{5+}, and O^- scattering curves were taken from the International tables for X-ray crystallography (13) and corrected for dispersion. A full matrix least squares program written by Stephens for use on the IBM 7040 was employed. After the positional parameters had ceased to show significant shifts the thermal parameters were also allowed to vary. Finally, for the last cycles, the atoms were assigned anisotropic thermal parameters whose components were varied together with all the variable positional parameters.

Weights, w, were chosen so that $w(\Delta F)^2$, $\Delta F =$

[1]Present Address: Department of Chemistry, University of Toronto, Toronto 181, Ontario.

TABLE 1
Atomic parameters of $Mg_2As_2O_7$*

Atom	Positional Symmetry at nuclei	Coordinate x	y	z
Mg	2	0	0.3119(5) [0.303]	1/2
As	m	0.2285(2) [0.230]	0	0.9031(3) [0.892]
O_I	$2/m$	0	0	0
O_{II}	m	0.4002(11) [0.406]	0	0.2214(20) [0.239]
O_{III}	1	0.2313(11) [0.230]	0.1646(8) [0.165]	0.7163(17) [0.708]

Atom	Thermal† ($\times 10^4$) Å^2 U_{11}*	U_{22}	U_{33}	U_{12}	U_{13}	U_{23}
Mg	102(16)	16(16)	153(26)		−1(8)	
As	260(36)	50(4)	23(7)		6(2)	
O_I	105(92)	2066(24)	818(255)		79(60)	
O_{II}	52(24)	16(28)	110(46)		7(12)	
O_{III}	200(29)	101(29)	174(42)	10(11)	−9(13)	−30(11)

*Values obtained by Łukaszewicz in brackets and estimated standard deviations in parentheses.
†The values of U_{ij} have been computed from $\beta_{ij} = 2\pi^2 b_i b\, U_{ij}$ where the β_{ij}'s appear as a thermal effect through $\exp[-(\beta_{11}h^2 + 2\beta_{12}hk + \ldots)]$ in the structure factor expression and b_i are the reciprocal lattice vectors. The estimated standard deviations are calculated from the inverse matrix arising in the least-squares refinement.

$F_c - F_o$, the difference between the calculated and observed structure factor, was independent of the magnitude of the observed structure factor, F. The weighting function determined by least squares methods was

$$w = [2.5 + 0.38F + 0.03F^2]^{-1}$$

Individual scale constants were assigned to each layer of data and multiply-observed reflections were assigned randomly to one of the data sets from which they arose. The final value of the reliability index including all the data is 0.088, while the value of R_2

$$R_2 = \left\{ \frac{\Sigma\, \omega(|F| - |F_c|^2)}{\Sigma\, \omega|F|^2} \right\}^{1/2}$$

is 0.107. Unobserved reflections were assigned zero weight if the minimum possible observable value exceeded the calculated value of the structure factors. The final atomic coordinates are found in Table 1 while the observed and calculated structure factors are compared in Table 2.[2]

Description of the Structure

The structure of $Mg_2As_2O_7$ is based upon sheets composed of double layers of oxygen atoms extended in the *ab* plane. The cations are octahedrally coordinated to these oxygen atoms and form edge-shared octahedra arranged in the hexagonal pattern depicted in Fig. 1. The As—O—As part of the anion lies above the empty octahedral site and causes an elongation of the ***a*** axis beyond that to be expected for an ideal packing of MgO_6 octahedra. Adjacent sheets pack such that the As ion on one side of the anion shares one oxygen atom with the first

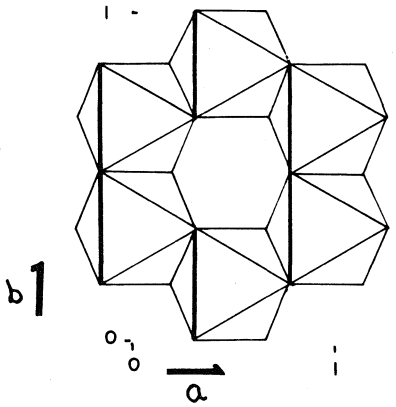

FIG. 1. An idealized view of the packing of a sheet of edge-sharing cation octahedra. The oxygen atoms lie at corners while the cations lie at the center of the octahedra.

[2]Table 2 has been placed in the National Depository for Unpublished Data. Photocopies may be obtained free of charge, upon request, from the Depository of Unpublished Data, National Research Council of Canada, Ottawa, Canada.

Can. J. Chem. Downloaded from www.nrcresearchpress.com by 210.87.254.5 on 09/05/12
For personal use only.

TABLE 3
Bond distances and angles in $Mg_2As_2O_7$*

Atoms	Bond length (Å)	Atoms	Bond angle (deg)
As_2O_7 group			
As—O_I	1.671(1)†	O_I—As—O_{II}	102.1(3)
		—O_{III}	105.8(3)
As—O_{II}	1.653(5)	O_{II}—As—O_{III}	113.2(3)
		O_{III}—As—$O_{III'}$	115.2(3)
As—O_{III}	1.661(7)		
O_I—O_{II}	2.587(7)		
—O_{III}	2.657(8)		
O_{II}—O_{III}	2.751(8)		
O_{III}—$O_{III'}$	2.806(8)		
MgO_6 group			
Mg—O_{II}	2.080(8)	O_{II}—Mg—O_{III}	150.9(3)
O_{III}	2.046(7)	—$O_{III'}$	78.7(3)
$O_{III'}$	2.252(8)	—O_{II}	79.2(3)
		—$O_{III'}$	93.1(3)
		O_{III}—Mg—$O_{III'}$	169.8(3)
		—$O_{III''}$	113.3(3)

*Estimated standard deviations in parentheses.
†The estimated standard deviation on this bond length is artifically small since As in on a special position.

sheet of cation octahedra and two oxygen atoms with the next adjacent sheet as shown in Fig. 2. The remaining half of the anion is generated by the apparent center of symmetry at the bridging atom. The anion has an apparent C_{2h} symmetry and the cations lie on two-fold axes.

The MgO_6 groups adjacent along the ***b*** axis share a pair of O_{II} atoms with a cation oxygen atom bond length of 2.080(8) Å. This group shows a positive axial distortion, that is an elongation, along the ***a*** axis as indicated by the MgO_{III} bond length of 2.252(8) Å. The remaining unique Mg—O bonds are 2.046(7) Å in length to a pair of oxygen atoms rotated about 20° about the two-fold axis from the positions required for a perfect

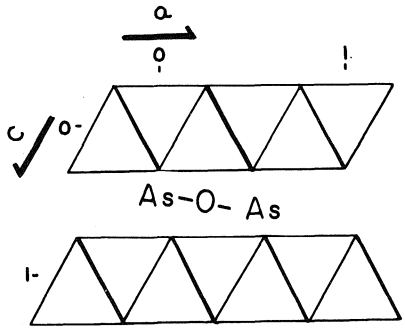

FIG. 2. A view of the packing of adjacent sheets down the ***b*** axis. Two layers are separated by the As—O—As part of the anion while the remaining oxygen atoms are at the corners of the octahedra.

octahedron. The bond lengths and angles are listed in Table 3.

The anion consists of corner-shared tetrahedra with the bridging oxygen atom, O_I, lying 1.671Å from the As ion. The As oxygen atom bond lying in the mirror plane, involving O_{II}, shows a length of 1.653(5) Å and the remaining unique As—O bond is 1.661(7) Å in length. Since the average estimated standard deviation is 0.006 Å these lengths cannot be regarded as significantly different as they stand. However, the large vibration of O_I, primarily in the plane perpendicular to the As—As vector, suggests a thermal correction of about 0.04 Å could be applied. In common with previous determinations of structures of thortveitite analogues (7, 14–16), the terminal O—As—O angles are larger than that expected for a perfect tetrahedron, whereas the O—As—O angles which include the bridging oxygen atom are smaller. That is, it appears that the As ion is displaced from the center of its tetrahedron towards the terminal oxygen atom.

Discussion

The structure of no other diarsenate has been reported although a powder pattern together with a suggested indexing have been proposed for $Ni_2As_2O_7$ and $Co_2As_2O_7$ (17). This indexing is wrong, however, since single crystal work has shown $Co_2As_2O_7$ to have a triclinic structure

Can. J. Chem. Downloaded from www.nrcresearchpress.com by 210.87.254.5 on 09/05/12
For personal use only.

probably closely related to the structure reported here (18). In addition, Weissenberg and precession photographs of $Zn_2As_2O_7$ and $Cd_2As_2O_7$ taken in this laboratory indicate that both their structures are closely related and probably almost identical to that reported here. Unfortunately, only twinned crystals of the former compound could be obtained.

The large disorder at the central oxygen atom suggests that the structure might be described as having a positionally disordered anion. A model allowing for static disorder in the structure of $\beta Cu_2P_2O_7$ (7) was found to give a reasonable interpretation of the data. If the anion were bent but positionally disordered so that randomly in half the cells O_I were displaced along the positive ***b*** axis and the remainder along the negative ***b*** axis from the center of symmetry, the apparent amplitude of vibration along ***b***, $\sqrt{U_{22}}$, should be large and the amplitude of vibration along ***a***, $\sqrt{U_{11}}$, should be small with the amplitude of vibration along ***c***, $\sqrt{U_{33}}$, normal for this atom. The large value of U_{33}, although smaller than U_{22}, suggests some disorder in the *bc* plane and the structure permits this oxygen atom to be displaced along ***a*** vector at 60° to the ***b*** axis. Here the steric repulsion of the neighboring oxygen atoms would be minimal. The difference between this model and one showing rotational disorder with potential wells every 60° becomes marginal, and it would be hard to distinguish between them with data of the present quality. However, a refinement of a model with a bent but disordered anion with the oxygen atom displaced only along the $\pm$***b*** direction did not yield a significantly better agreement than is reported here. We thus can regard the matter of the nature of the disorder in $Mg_2As_2O_7$ as an open question.

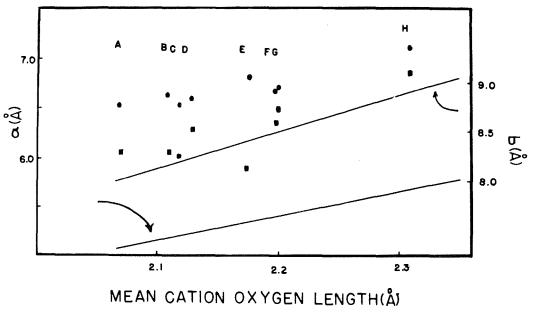

FIG. 3. The lengths of the ***a*** and ***b*** axes are plotted vs. the mean cation–oxygen atom length in a variety of systems showing the thortveitite structure. The letters A through H represent $\beta Mg_2P_2O_7$, $\beta Zn_2P_2O_7$, $\beta Ni_2P_2O_7$, $Mg_2As_2O_7$, $\beta Cu_2P_2O_7$, $Mn_2P_2O_7$, $Mn_2V_2O_7$, and $Cd_2V_2O_7$ in that order.

Let us regard the ideal thortveitite structure as consisting of perfect octahedra with Mg—O bond lengths of 2.13 Å arranged as in Fig. 1, and with a three-fold axis through the center of the layer. The predicted lengths of the ***a*** and ***b*** axes are 5.22 and 8.23 Å and are calculated from the relations

$$a = \sqrt{6}\,(\text{M—O})$$

and

$$b = \sqrt{2}(1 + \sqrt{3})(\text{M—O})$$

where M—O is the metal–oxygen atom bond length. The actual average bond lengths were used to compare the predicted ***a*** and ***b*** axes with the experimental ones as shown in Fig. 3. The

TABLE 4

Comparison of the parameters of the thortveitite series of compounds with the ideal structure

Compound	y_m	$x_{O_{II}}$	$x_{O_{III}}$	$y_{O_{III}}$
Ideal structure	0.3175	0.3660	0.1725	0.1825
$Mg_2As_2O_7$	0.3119	0.4002	0.2313	0.1646
$Mn_2V_2O_7$*	0.3114	0.409	0.232	0.160
$Cd_2V_2O_7$†	0.3052	0.3881	0.2378	0.1566
$\beta Ni_2P_2O_7$‡	0.310	0.387	0.220	0.151
$\beta Cu_2P_2O_7$§	0.3122	0.3759	0.2035	0.1533
$Mn_2P_2O_7$‖	0.3106	0.3765	0.2183	0.1488
$\beta Zn_2P_2O_7$¶	0.3092	0.3781	0.2262	0.1559
$\beta Mg_2P_2O_7$**	0.3124	0.3997	0.2217	0.1549

*Reference 20.
†Reference 16.
‡Reference 21.
§Reference 7.
‖Our unpublished results, details available from authors.
¶Reference 14.
**Reference 15.

Can. J. Chem. Downloaded from www.nrcresearchpress.com by 210.87.254.5 on 09/05/12
For personal use only.

predicted value of the ***a*** axis is invariably about 25% too small while the experimental ***b*** axis is within about 5% of the predicted value. Proceeding along the same lines the predicted values of the y_M and $y_{O_{III}}$ parameters are 0.3175 and 0.1825, respectively, and lie quite near the experimental values. In contrast, the $x_{O_{II}}$ and $x_{O_{III}}$ values are all substantially larger than the predicted values of 0.3360 and 0.1725, respectively. These effects are attributed to an expansion of this structure along the ***a*** axis in order to accommodate the bridging oxygen atom. A further indication of this effect is that the layer spacing perpendicular to the octahedral sheets is smaller than the value of 4.8 Å expected for closest packing of spheres of oxygen atom. In the disilicates of Ho, Y, and Er (19), the disilicate ions pack with the Si—O—Si at an angle of 30° to the ***b*** axis and 120° to each other rather than collinear as is the case in $Mg_2As_2O_7$. The resultant space group is $P2_1/a$ with the a the order of 5.55 Å and b the order of 10.8 Å. In this case the ***a*** axes length is that predicted while the ***b*** axis is predicted to be 8.75 Å in length.

This research has been supported by a grant from the National Research Council of Canada.

1. K. Łukaszewicz. Bull. Acad. Polon. Sci. Ser. Sci. Chim. **11**, (7), 361 (1963).
2. S. J. Poulsen and C. Calvo. Can. J. Chem. **46**, 917 (1968).
3. C. Calvo and K. Y. Leung. To be published. (1969).
4. N. Krishnamachari and C. Calvo. Can. J. Chem. This issue.
5. K. H. Jost. Acta Cryst. **21**, 808 (1966).
6. D. W. J. Cruickshank. J. Chem. Soc. 5486 (1961).
7. B. E. Robertson and C. Calvo. Can. J. Chem. **46**, 605 (1968).
8. D. W. J. Cruickshank. Acta Cryst. **17**, 672 (1964).
9. J. G. Chambers, W. R. Datars, and C. Calvo. J. Chem. Phys. **41**, 806 (1964).
10. J. S. Leung, W. R. Datars, and C. Calvo. J. Chem. Phys. **46**, 798 (1967).
11. C. V. Stager. Can. J. Phys. **46**, 807 (1968).
12. W. R. Datars and C. Calvo. J. Chem. Phys. **47**, 3224 (1967).
13. International tables for X-ray crystallography, Vol. III. Kynoch Press, Birmingham. 1962.
14. C. Calvo. Can. J. Chem. **43**, 1147 (1965).
15. C. Calvo. Can. J. Chem. **43**, 1139 (1965).
16. P. K. L. Au and C. Calvo. Can. J. Chem. **45**, 2297 (1967).
17. J. B. Taylor and R. D. Heyding. Can. J. Chem. **36**, 597 (1958).
18. J. Ozog, N. Krishnamachari, and C. Calvo. Can. J. Chem. **48**, 388 (1970).
19. Yu. I. Smolin and Yu. F. Shepelev. Izv. Akad. Nauk. SSR. Neorg. Mater. **4**, 1133 (1968).
20. E. Dorm and B. Marinder. Acta Chem. Scand. **21**, 590 (1967).
21. A. Pietraszko and K. Łukaszewicz. Bull. Acad. Polon. Sci. Ser. Sci. Chem. **16**, 183 (1968).

Can. J. Chem. Downloaded from www.nrcresearchpress.com by 210.87.254.5 on 09/05/12
For personal use only.

A fluorine magnetic resonance study of the solid addition compounds $SF_4 . AsF_5$ and $IF_7 . AsF_5$

M. R. BARR[1] AND B. A. DUNELL

Department of Chemistry, The University of British Columbia, Vancouver 8, British Columbia

Received September 2, 1969

A broad-line fluorine magnetic resonance study of the solid addition compounds $SF_4 . AsF_5$ and $IF_7 . AsF_5$ shows that each has two types of chemically distinct fluorine in the ratios of 1:2 and 1:1, respectively. The fine structure and the second moments of the spectra are consistent with the ionic formulations $SF_3^+AsF_6^-$ and $IF_6^+AsF_6^-$. Bond lengths in the iodine compound are discussed in relation to the observed second moment at liquid-nitrogen temperature and the calculated rigid-lattice second moment based on the detailed sodium-chloride-type crystal structure of Beaton. The chemical shifts of the fluorines in the three ionic species are measured relative to trifluoracetic acid and to HF. Reorientations of the ions in the solid state are discussed on the basis of the change in second moment with temperature for each compound. A very rough estimate of the anisotropy of chemical shift in $IF_6^+AsF_6^-$ is made from the slope of the second moment vs. field-squared line at liquid-nitrogen temperature.

Canadian Journal of Chemistry, **48**, 895 (1970)

Can. J. Chem. Downloaded from www.nrcresearchpress.com by 210.87.254.5 on 09/05/12
For personal use only.

The adducts of AsF_5 with SF_4 and IF_7 are relatively new compounds. In 1956, Bartlett and Robinson (1) reported that SF_4 coordinated with AsF_5 in the ratio of one mole of each to form a new compound, a white solid. In the following year they observed that a displacement reaction involving this adduct provided a convenient method of purifying SF_4 (2). In 1958, Seel and Detmer reported both $SF_4 . AsF_5$ and $IF_7 . AsF_5$ (3), and in a subsequent paper (4) they discussed the compounds more fully and suggested an ionic formulation for them. Bartlett and Robinson (5) also were led to suggest that an ionic formulation might be appropriate for a number of coordination compounds formed by the tetrafluorides of the sulfur subgroup. The existence of the ion AsF_6^- in solutions of addition complexes and in the solid state has also been discussed (6–12). Beaton (13), as well as Christe and Sawodny (14), have concluded from X-ray and infrared studies that the adduct $IF_7 . AsF_5$ is an ionic salt, $IF_6^+AsF_6^-$.

Experimental

The addition compounds used in this study were prepared by Beaton from analytical reagent-grade As_2O_3, or arsenic metal, and cylinder fluorine, which gave AsF_5; from purified cylinder IF_5 (Matheson Company) and cylinder fluorine, which gave IF_7; and from cylinder SF_4. Purity of the reagents IF_7, SF_4, and AsF_5 was checked by their infrared spectra and by the X-ray diffraction pattern of the solid formed by the reaction of AsF_5 with ONF.

[1]Present address: Royal Roads Military College, Victoria, British Columbia.

The fluorine magnetic resonance spectra were recorded on two Varian 4250-type broad-line spectrometers and on a Varian HA100 high-resolution spectrometer. One of the broad-line spectrometers was a DP60 with a Varian 12 in. electromagnet and fixed-frequency radio-frequency (r.f.) units at 56.4 and 40 MHz. The other broad-line spectrometer employed a Varian 6 in. electromagnet, a 30 MHz V-4310A fixed frequency r.f. unit, and a 2–16 MHz V-4210A variable frequency r.f. unit. On the HA100 instrument, the 2000 Hz side bands of the integrator/decoupler were used to provide sweep modulation. Since the resonance lines of the solids were very much wider than 2000 Hz, the resulting spectra were the familiar derivative signals customarily observed in broad-line work. Since the normal method of calibrating the modulation amplitude of a lock-in detector by recording the derivative of a liquid line could not be used on the high-resolution spectrometer, a minor problem was encountered in determining the amplitude of the modulation. However, when a liquid signal is scanned, the integrator/decoupler may be adjusted to give zero amplitude for the center band. At that point there is then a known modulation index from which the modulation amplitude may be determined (15). Since this required adjustment of the coarse amplitude control in the interior of the instrument, it was difficult to reproduce this exact value for each series of runs without recording a tedious series of signals on a strip recorder each time. However, it was always simple to ensure that the amplitude was below the point of known amplitude which in itself was safe (about 1.2 G peak-to-peak) and that modulation broadening was absent. A more serious problem was encountered in obtaining a pure absorption derivative of the resonance signal. Balancing and phasing were quite critical and laborious. Operation on wide-line diode detection with the introduction of absorption leakage was quicker and surer than phase detection. It also produced a better signal-to-noise ratio. Standard operating procedures were employed on the two broad-line spectrometers. For the compound $SF_4 . AsF_5$, useful spectra were obtainable at 94.1 MHz and 77 °K with

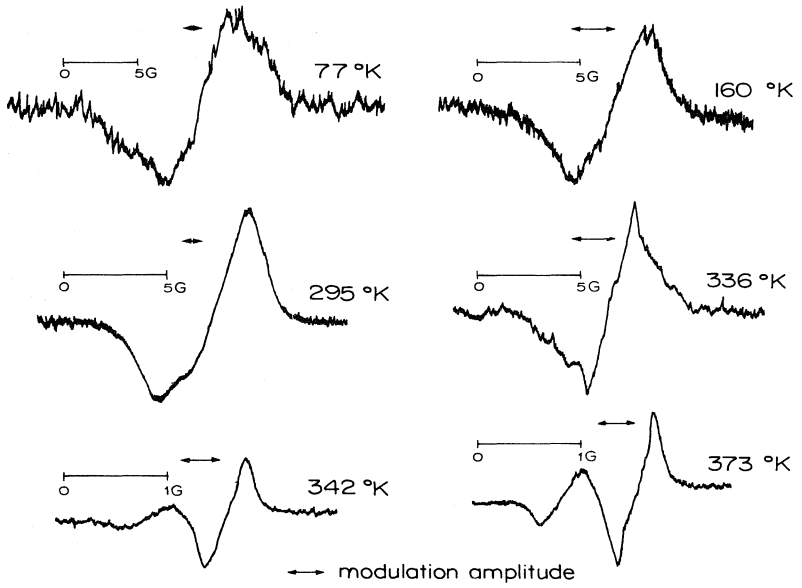

FIG. 1. Dependence of derivative line shape on temperature at 30 MHz for $SF_3^+AsF_6^-$.

the aid of a specially constructed Dewar vessel. For $IF_7.AsF_5$, the 94.1 MHz spectra at 77 °K were not useable because the very small sample required a high r.f. field, which produced saturation effects, and a lower H_1 field gave a very bad signal-to-noise ratio.

The temperature dependence of the nuclear magnetic resonance (n.m.r.) spectra was studied over the range 77–370 °K at 30 MHz.[2] Spectra were also run at 94.1, 56.4, 40, and 30 MHz at room temperature and at 77 °K for both compounds. For low-temperature runs at 30 MHz, the temperature was controlled by cooled tank-nitrogen passed through a flow system. A Dry Ice – acetone bath can be used to cool the gas to achieve temperatures above 220 °K; below that a liquid-nitrogen bath is required. Temperature control was approximately ±5° near 100 °K and ±1° above 150 °K. At 94.1 MHz, the standard Varian V-4341 variable-temperature system was used. Its temperature range is stated to be −60 to +200 °C, but it was found that −100 °C could be reached. Maximum temperature variation for the Varian system is ±1° within the specified range, and calibration is about ±3°.

The samples were polycrystalline, and their spectra were independent of their orientation in the external magnetic field. Preliminary spectra were run at each frequency to check the r.f. level for saturation, the field H_1 being varied over the range from about 0.05 to 45 mG. When an r.f. region was found where line widths remained constant as the power was lowered, forward and reverse scans were run to check that line shape was the same for both directions. When an apparently satisfactory r.f. level was thus established, it was further reduced to ascertain that no additional line shape changes occurred. H_1 values of about 0.5 to 1.0 mG were generally found to be safe. A sweep modulation of only about 0.5 G peak-to-peak was used in taking at least one or two spectra to ensure that detail in the line structure was not lost. Depending on packing factor, signal-to-noise ratio varied from about 4:1 in some unfavorable cases to 20:1 under good conditions; all at 77 °K.

The chemical shifts of the compounds, with respect to CF_3COOH, were obtained at 77 °K at all the external fields used. The chemical shift of the CF_3COOH reference sample was +76.2 p.p.m. relative to Freon 11. Two side bands were imposed on the fluorine resonance signal of the reference sample with an audio-oscillator. The external magnetic field was scanned through one of the side bands and, while scanning proceeded, the reference was replaced by the sample, the probe rebalanced if necessary, and the spectrum recorded. The sample was then replaced by the reference and the other side band recorded. The position of the reference resonance was taken as the midpoint between the two side bands.

A minimum of four spectra were recorded at each temperature in the temperature dependence runs. In the external-field dependence runs, ten or more referenced spectra were recorded at each frequency at 77 °K. In addition, a number of non-referenced spectra were run at each frequency at 77 °K.

Results and Discussion

$SF_4.AsF_5$

Experimental Line Shape, Second Moment, and Chemical Shift

Figure 1 shows the dependence of the derivative line shape on temperature at 30 MHz; and Fig. 2,

[2]For $IF_7.AsF_5$, the highest temperature at which detailed studies were made was 295 °K. In a preliminary observation, however, Mr. C. R. Eaton in this laboratory had found that the line width and shape for $IF_7.AsF_5$ were essentially unchanging between 250 and 375 °K.

Can. J. Chem. Downloaded from www.nrcresearchpress.com by 210.87.254.5 on 09/05/12
For personal use only.

Can. J. Chem. Downloaded from www.nrcresearchpress.com by 210.87.254.5 on 09/05/12
For personal use only.

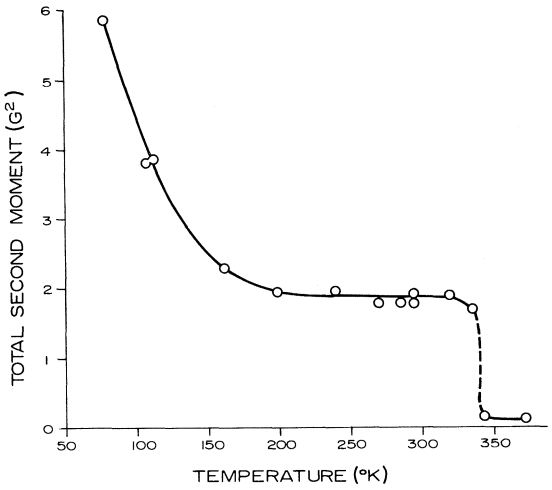

FIG. 2. Temperature dependence of second moment at 30 MHz for $SF_3^+AsF_6^-$.

the change in average second moment with temperature at 30 MHz. The second moment at 77 °K does not appear to correspond to a rigid-lattice value. From a value of 5.9 ± 0.3 G^2 at 77 °K, it drops in a progressively less steep curve to 1.85 ± 0.1 G^2 near 200 °K, remains constant at this value until 336 °K, and then drops sharply to a value of about 0.1 G^2 by 342 °K; beyond which it remains constant to 373 °K, the highest temperature investigated. At and above 342 °K there is an almost complete resolution of the spectrum into two components shifted by 97.5 ± 5 p.p.m. from one another.

The dependence of the derivative line shape on the external field is shown in Fig. 3 for 300 °K. It was found that the corresponding integrated absorption spectra at 94.1 MHz could be resolved into two symmetrical peaks, the smaller peak lying to lower external field. The resolution gave a ratio of areas of components of 1, at low field, to 2.2, at high field, and a shift of 105 ± 10 p.p.m. between the components; in good agreement with the observation at 342 °K and 30 MHz. The relative areas of the components indicate that twice as many fluorine atoms are resonating at high field as at low field, a condition consistent with a formulation $SF_3^+AsF_6^-$ for the addition compound, with the AsF_6^- fluorines being more diamagnetically shielded than the SF_3^+ fluorines. The shift, in G, of the centroid of the spectrum of the addition compound (the point about which the first moment was zero) with respect to the position of a trifluoroacetic acid signal is plotted against the external field in Fig. 4. The slope of the straight line through the points showed a chemical shift of -40 ± 15 p.p.m. for the centroid relative to CF_3COOH. One may combine this with the approximate shift of 100 ± 10 p.p.m. between components and the shift of -117 p.p.m. of CF_3COOH relative to HF (16) to obtain a shift of -120 ± 20 for the AsF_6^- component and a shift of -220 ± 20 for the SF_3^+ component relative to HF. This is in excellent agreement with the value of Christe *et al.* (17) of -126.6 p.p.m. for the chemical shift of

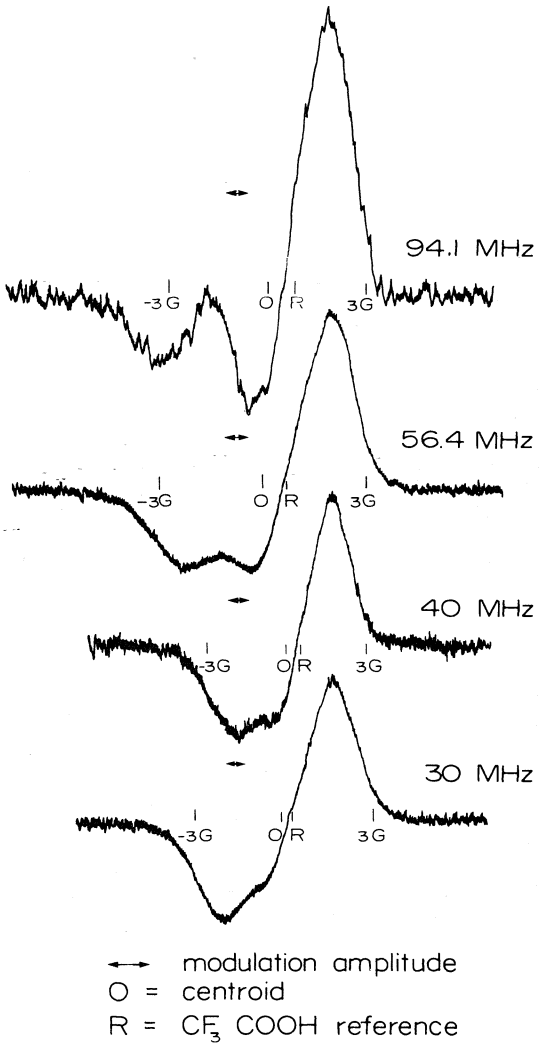

FIG. 3. Dependence of derivative line shape on external field at 300 °K for $SF_3^+AsF_6^-$.

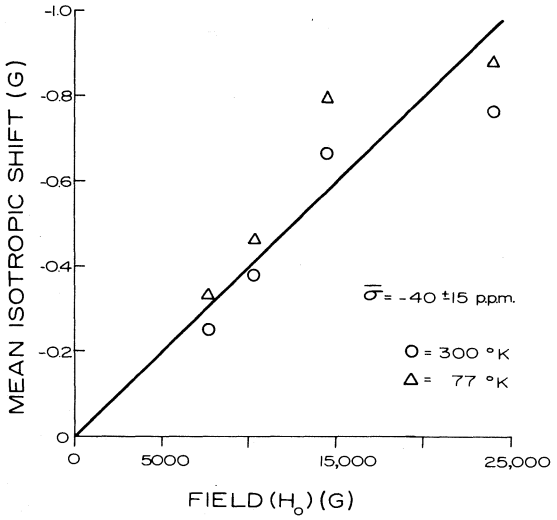

FIG. 4. Chemical shift at 77 and 300 °K of the centroid of the $SF_3^+AsF_6^-$ spectrum relative to CF_3-COOH as a function of external field.

AsF_6^- in HF solution, relative to HF. For the 77 °K spectrum, the resolution was less straightforward, and, although a ratio of areas of 1, at low field, to 1.9, at high field, was obtained for the resolved components, their separation was found to be 185 ± 20 p.p.m. Further support for a shift of nearly 100 p.p.m. between the two ionic groups comes from the slope of the straight line obtained from a plot of second moment of the total spectrum against the square of the external field, shown in Fig. 5 for the two temperatures 77 and 300 °K. If one can assume whatever anisotropy of chemical shift that may exist is averaged out by molecular motion, the second moment is given by

$$S = S_D' + (2H_0^2/9)(\bar{\sigma}_{AsF_6^-} - \bar{\sigma}_{SF_3^+})^2$$

where $\bar{\sigma}$ represents an isotropic chemical shift equal to Tr $\boldsymbol{\sigma}/3$ and S_D' is the zero-field, non-rigid-lattice dipolar second moment. At 300 °K there is no evidence of asymmetry in the resolved components of the spectra, and the small second moments of the components, which will be discussed next, indicate an amount of motion which should average out the effects of anisotropy of chemical shift. In that case, the slope of the 300 °K line in Fig. 5 should be $2(\sigma_{AsF_6^-} - \sigma_{SF_3^+})^2/9$, and one finds that the shift between components is 87 ± 10 p.p.m. The slope of the 77 °K line is only slightly greater, and indicates that $\Delta\bar{\sigma}$ is at most 110 ± 10 p.p.m. (for $\sigma_{\parallel} - \sigma_{\perp} = 0$).

Lattice Motions

To discuss adequately lattice motions from the evidence of second moments, one should have a close estimate of the rigid-lattice second moment. This is certainly not available from the experimental value at 77 °K, and no detailed X-ray diffraction study of the compound has been published. One can, however, make a first-order approximation to the rigid-lattice second moment from the following reasonable guess for the atom positions in the unit cell. Since As—F and Sb—F bond lengths are approximately equal (18), the unit cell for $SF_3^+AsF_6^-$ was assumed to be the same as that of $SF_3^+SbF_6^-$ determined by Bartlett and Robinson at 291 °K (5); namely, a simple cubic structure with $a = 5.625 \pm 0.002$ Å and $Z = 1$. The orientation of the AsF_6^- octahedra at the corners of the cube was chosen by trial and error so that models which used 1.77 Å for the As—F bond length and Pauling's van der Waals radius of 1.35 Å for fluorine (19) would fit into the assumed unit cell. The SF_3^+ group was placed with the triangle defined by the three fluorines centered on (1/2,1/2,1/2) and parallel to the *ab* plane of the cell. The sulfur atom was located on an axis perpendicular to this plane and passing through (1/2,1/2,1/2). Following Bartlett and Robinson (5), it was assumed that the ion has a tetrahedral configuration because of the electron lone-pair on the sulfur, and the S—F bond length was taken to be 1.56 Å (18). Unit cell coordinates for the nine fluorines were generated on the basis of this model of the ionic structure $SF_3^+AsF_6^-$ and a rigid-lattice second moment calculated using a computer program for contributions from pairs

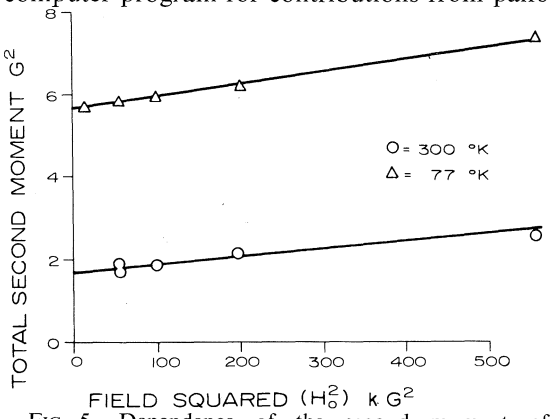

FIG. 5. Dependence of the second moment of $SF_3^+AsF_6^-$ on the square of the external field for 77 and 300 °K.

Can. J. Chem. Downloaded from www.nrcresearchpress.com by 210.87.254.5 on 09/05/12
For personal use only.

TABLE 1

Calculated rigid-lattice contributions to the second moment of $SF_3^+AsF_6^-$*

Group		Second moment, G^2 F—F	F—As	Total
$SF_3^+AsF_6^-$,	total†	8.90	0.52	9.42
$SF_3^+AsF_6^-$,	intra	4.72	0.51	5.23
AsF_6^-,	total (to 6 Å)	5.96	0.51	6.47
AsF_6^-,	intra	3.62	0.50	4.12
SF_3^+,	total (to 6 Å)	2.63	0.01	2.64
SF_3^+,	intra	0.77	0.00	0.77

*Every contribution in the table is based on a 9 fluorine unit ($SF_3^+AsF_6^-$), even in the case of the AsF_6^- and the SF_3^+ group contributions, which therefore add directly to give the total second moment of the system.

†Includes integral contribution over 6 Å of 0.31 G^2 to F—F.

of nuclei closer than 6 Å apart, integrating the contribution from pairs separated by more than 6 Å on the assumption that density of nuclei is effectively uniform outside a sphere of 6 Å radius. Contributions from dipolar interactions between fluorine and arsenic were not neglected, but fluorine-to-^{33}S interactions were ignored. The various calculated contributions to the rigid-lattice second moment are listed in Table 1. The rigid-lattice value of 9.4 G^2 calculated from this model is not unreasonable, but may be a little high. The count of internuclear distances, which the computer program so conveniently provides, shows that the SF_3^+ group is somewhat crowded in this assumed model. It has four intergroup contacts below 2.7 Å (double the fluorine van der Waals radius). Two of these are not too severe, being 2.5 and 2.6 Å, but the remaining two are 2.2 Å. This crowding would be reduced if one assumed a F—S—F bond angle rather smaller than 109° 28′, and this would be in accord with greater repulsion between lone pairs and bond pairs than between two bond pairs (20). It would also agree with the ease of rotational reorientation that we attribute to the SF_3^+ group in this substance. Since the intragroup F—F distance of 2.5 Å in SF_3^+ in the assumed model would be diminished by the suggested modification and the four close contacts with AsF_6^- fluorines relieved, the second moment would not change greatly. A tilting of the threefold axis of the SF_3^+ group would also modify contacts with surrounding AsF_6^- groups and therefore alter the second moment. These details were not examined. If $SF_3^+AsF_6^-$ had, like $IF_6^+AsF_6^-$, a NaCl-type structure, the second moment would not likely be greatly different from that estimated here. Only the inter-ion contributions would be expected to be different. In $IF_6^+AsF_6^-$, which has a NaCl-type structure, the ratio of the intra-ion F—F contribution to the second moment to the total F—F contribution to the second moment is 4.75/9.13. If the same ratio were to apply to $SF_3^+AsF_6^-$ with a NaCl structure, the intra-ion F—F contribution of 4.39 G^2 would imply a total F—F second moment contribution of 8.43 G^2 and a total second moment of 8.95 G^2, compared with the estimated value of 9.42 G^2 for the CsCl-type structure. An estimate of 9.0 ± 0.5 G^2 is probably reasonable for $SF_3^+AsF_6^-$.

The observed second moment of 5.9 G^2 at 30 MHz and 77 °K, which includes a contribution of the order of 0.1 G^2 from an isotropic chemical shift of 100 p.p.m., shows, by comparison with the rigid-lattice value of some 9.0 G^2, that there is significant rotational oscillation or reorientation at frequencies of at least 10^4 or 10^5 s^{-1} by groups in the lattice at liquid-nitrogen temperature. Although the 30 MHz spectra are not readily resolved into components corresponding to the cation and anion resonances, there is some evidence that the cation component of the spectrum is somewhat broader than the anion component and its second moment reduced from the rigid-lattice value to a smaller extent. Correspondingly, one may suggest that the almost-spherical AsF_6^- ions can orient about more than one axis, though not freely at 77 °K, whereas the SF_3^+ ion may be restricted to oscillation or hindered reorientation about its threefold axis at 77 °K. By 220 °K, the total second moment of the 30 MHz spectrum has fallen to about 1.9 G^2 and remains at this value to 336 °K. Removal of about 0.1 G^2 for the effect of chemical shift at 30 MHz leaves 1.8 G^2 as the second moment. If the AsF_6^- ion rotated freely about a fourfold axis, the intra-ion contribution to the second moment would be 0.74 G^2; and if the SF_3^+ ion rotated freely about its threefold axis, the intra-ion contribution to the second moment would be 0.2 G^2. The remaining intergroup contribution (4.1 to 4.5 G^2 for the supposed rigid lattice) might be reduced by a factor of 1/2 to 1/4 if rotation took place about one axis only (21), giving a contribution of 1.1 to 2.3 G^2. This would give a total second moment of 2.0 to 3.2 G^2. Again there is some evidence

Can. J. Chem. Downloaded from www.nrcresearchpress.com by 210.87.254.5 on 09/05/12
For personal use only.

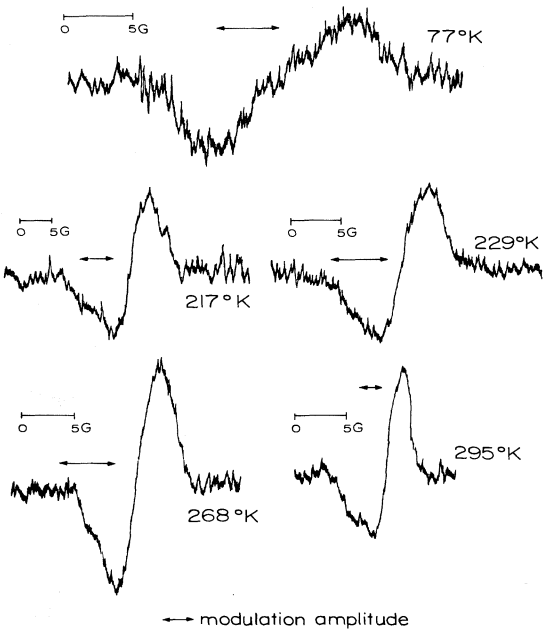

FIG. 6. Dependence of derivative line shape on temperature at 30 MHz for $IF_6^+AsF_6^-$.

suggesting that line narrowing and second moment decrease is greater for the AsF_6^- component of the spectrum than for the SF_3^+ component. An acceptable interpretation of the observed second moment might then be that the AsF_6^- group is rotating freely about more than one axis, while the SF_3^+ group may still be constrained to rotate only about its threefold axis between 220 and 336 °K.

The transition between 336 and 342 °K is so abrupt that it probably corresponds to a phase change. The second moment of little more than 0.1 G^2 at 30 MHz indicates very extensive motion in the solid, including diffusion of ions. Although the sample had a somewhat plastic appearance at 373 °K, it remained solid and showed no indication of melting even when held at that temperature for several hours.

$IF_7.AsF_5$

Experimental Line Shape, Second Moment, and Chemical Shift

Figure 6 shows the variation of the derivative line shape with temperature at 30 MHz for $IF_7.AsF_5$, and Fig. 7 shows the change in second moment with temperature at 30 MHz. The second moment is constant at 11.6 ± 0.6 G^2 from 77 to about 205 °K. This value probably corresponds to a rigid-lattice condition. Between 205 and 235 °K, the second moment drops to 2.1 ± 0.2 G^2 and remains constant thereafter up to 295 °K.

The nature of derivative line-shape dependence on external field at 295 °K is illustrated in Fig. 8. The 94.1 MHz spectrum can be resolved into two quite symmetrical components, the ratio of whose areas is 1.1 to 1, and which are shifted 153 ± 10 p.p.m. with respect to one another. Another evaluation of the shift between components comes from the slope of the plot of second moment against external-field-squared at 295 °K, shown in Fig. 9. If at 295 °K the anisotropy of chemical shift is averaged out by molecular motion, as the symmetry of the resolved components and the low second moment of 2.1 G^2 at 30 MHz suggest, the second moment can be expressed by

$$S = S_D' + H_0^2(\bar{\sigma}_{IF_6^+} - \bar{\sigma}_{AsF_6^-})^2/4$$

where S_D' is the zero-field, non-rigid-lattice dipolar second moment and $\bar{\sigma}$ represents an isotropic chemical shift. The slope of the 295 °K line in Fig. 9 indicates a value of 135 ± 8 p.p.m. for $\Delta\bar{\sigma}$ on the reasonable assumption that anisotropy of chemical shift has been averaged to zero. The shift between the two components of the spectrum will be taken as 143 ± 15 p.p.m.

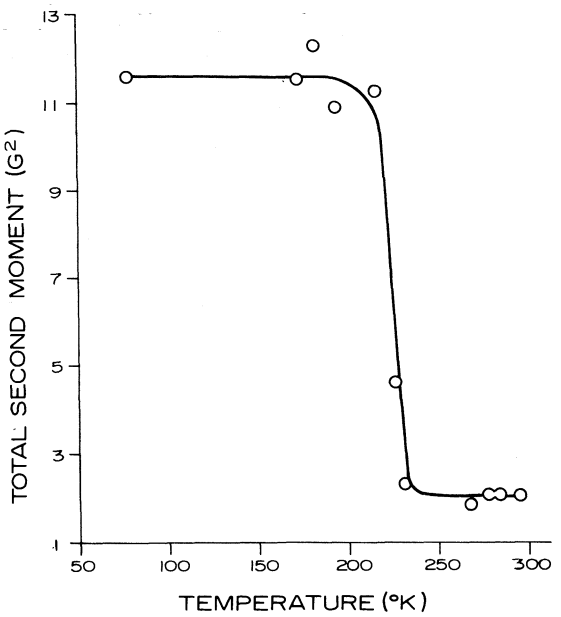

FIG. 7. Temperature dependence of second moment at 30 MHz for $IF_6^+AsF_6^-$.

Can. J. Chem. Downloaded from www.nrcresearchpress.com by 210.87.254.5 on 09/05/12
For personal use only.

Can. J. Chem. Downloaded from www.nrcresearchpress.com by 210.87.254.5 on 09/05/12
For personal use only.

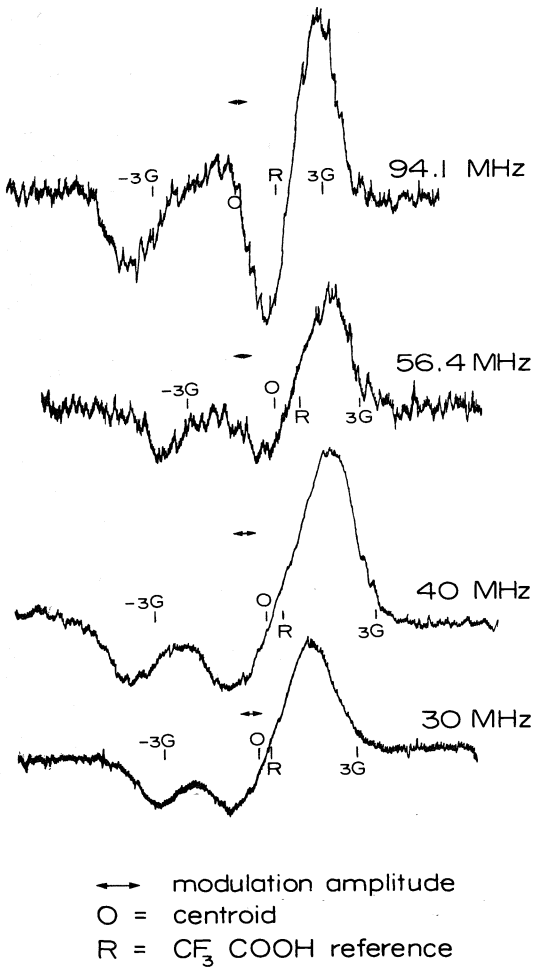

FIG. 8. Dependence of derivative line shape on external field at 295 °K for $IF_6^+AsF_6^-$.

The components are equidistant to either side of the centroid of the total spectrum, and the shift of this centroid with respect to CF_3COOH at various external fields is shown in Fig. 10 for both 295 and 77 °K to be -54 ± 9 p.p.m. This gives a shift relative to HF of -99 ± 16 p.p.m. for the high field component and -243 ± 16 p.p.m. for the low field component. The 1.1-to-1 ratio of areas corresponds most closely to the ionic formulation $IF_6^+AsF_6^-$ for the addition compound, and the chemical shift for the high field component corresponds reasonably well to that for AsF_6^- in $SF_3^+AsF_6^-$, viz., -120 ± 20 p.p.m.

Although it may be most clearly seen from integral absorption spectra, it can be deduced

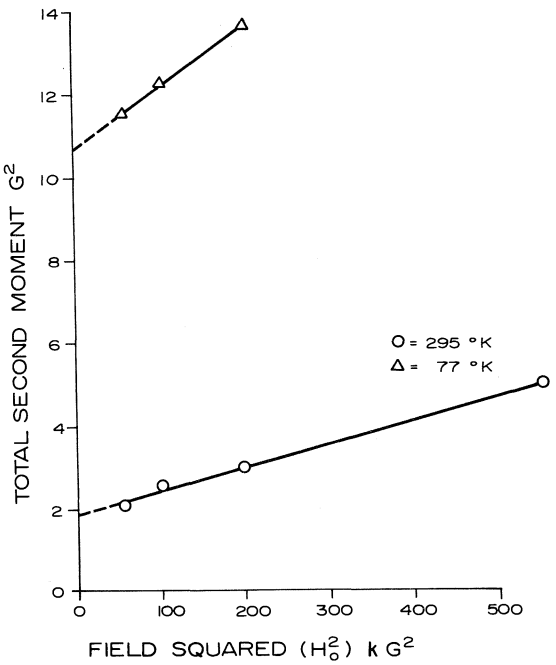

FIG. 9. Dependence of the second moment of IF_6^+-AsF_6^- on the square of the external field for 77 and 295 °K.

from inspection of the derivative spectra that at 77 °K the n.m.r. absorption line tails to high field, whereas at room temperature it tails to low field. One concludes that anisotropy of chemical shift becomes important at low temperature, where molecular motion is no longer effective in averaging out its effect, and causes the observed reversal of the asymmetry of the spectrum. This view is supported by the considerable increase in slope of the second moment vs. H_0^2 plot as one

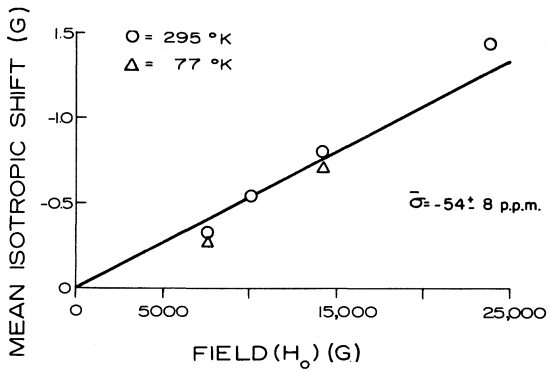

FIG. 10. Chemical shift at 77 and 295 °K of the centroid of the $IF_6^+AsF_6^-$ spectrum relative to CF_3-COOH as a function of external field.

goes from 295 to 77 °K. If the rigid-lattice second moment can be given by

$$S = S_D + 4H_0^2(\overline{\sigma_{\parallel} - \sigma_{\perp}})^2/45 + H_0^2(\bar{\sigma}_{AsF_6^-} - \bar{\sigma}_{IF_6^+})^2/4$$

where S_D is the rigid-lattice, zero-field dipolar second moment and $\overline{\sigma_{\parallel} - \sigma_{\perp}}$ is an average value of the chemical shift anisotropy for the two ions; if one assumes an isotropic shift of 143 p.p.m. between the two groups, the average anisotropy is calculated to be 333 ± 20 p.p.m. Since the low temperature spectrum tails to high field and the broadening function for anisotropy of chemical shift is (22)

$$f(h) = (2\sqrt{3}a)^{-1}(1 + h/a)^{-1/2} \qquad -a \leqslant h \leqslant 2a$$

where

$$a = H_0(\sigma_{\parallel} - \sigma_{\perp})/3$$

and h represents the increment to the average external field required to bring a particular nucleus into resonance at given frequency, one concludes that the average $\sigma_{\parallel} - \sigma_{\perp}$ for the two ions must be positive.

Theoretical Second Moment

The crystal structure of $IF_6^+AsF_6^-$ at room temperature has been determined by Beaton (13) from X-ray diffraction powder photographs. The unit cell is cubic, space group $Pa3$, a_0 = 9.4935 ± 0.0005 Å (see also ref. 14). From the atomic parameters (Table 2), coordinates for all atoms may be obtained and the following bond lengths calculated: As—F, 1.67 Å; and I—F, 1.75 Å. Since the X-ray results were not corrected for thermal motion, the bond lengths may be somewhat short. Noting the result of Copeland *et al.* (23), in which they found an As—F bond length of 1.65 Å uncorrected for thermal motion and 1.78 Å corrected for thermal motion, Beaton suggests that the bond lengths obtained from his powder photographs might be increased by 0.1 Å or more. We have arbitrarily increased all the bond lengths by 0.1 Å and calculated another set of atomic coordinates for the fluorines. Both sets of coordinates have then been used to obtain a rigid-lattice second moment for the substance. Using the coordinates uncorrected for thermal motion we obtain a second moment of 12.56 G^2; and using the thermally corrected coordinates, a second moment of 10.50 G^2. Details of the several contributions to this value are given in Table 3. The zero-field second moment of 10.7 G^2 at 77 °K is thought to represent a rigid-lattice value, decreased only by zero-point vibrational motion. Since the theoretical second moment is based on a crystal structure obtained at room temperature, the calculated rigid-lattice second moment will be too small because thermal contraction of the lattice as it goes from 295 to 77 °K has been ignored. It seems highly probable, therefore, that a thermal correction of about 0.1 Å or slightly less in the bond lengths is required.

TABLE 2

Atomic parameters of $IF_6^+AsF_6^-$

Atom	Coordinate		
	x	y	z
As (4*a*)	0	0	0
I (4*b*)	½	½	½
F (24*d*)	0.0980	0.1377	−0.0489
F (24*d*)	0.6001	0.6431	0.4411

TABLE 3

Calculated rigid-lattice contributions to the second moment of $IF_6^+AsF_6^-$*

Group		Second moment, G^2			
		F—F	F—As	F—I	Total
$IF_6^+AsF_6^-$	total†	9.13	0.39	0.98	10.50
AsF_6^-,	total (to 6 Å)	4.71	0.38	0.04	5.13
AsF_6^-,	intra	2.71	0.38	0	3.09
IF_6^+,	total (to 6 Å)	4.07	0.01	0.93	5.01
IF_6^+,	intra	2.04	0	0.93	2.97

*Every contribution in this table is based on a 12 fluorine unit ($IF_6^+AsF_6^-$), even in the case of the IF_6^+ and AsF_6^- group contributions, which therefore add directly to give the total second moment of the system. The contributions are calculated from the crystal structure of Beaton (13), but assuming As—F = 1.77 Å and I—F = 1.85 Å.

†Includes integral contribution over 6 Å of 0.35 G^2 to F—F and 0.1 to F—I.

Can. J. Chem. Downloaded from www.nrcresearchpress.com by 210.87.254.5 on 09/05/12
For personal use only.

Ionic Reorientations

The observed second moment above the transition near 200 °K is 2.1 G^2. If each ion were a symmetrical octahedron and rotated freely about one of its fourfold axes, the intragroup contribution to the second moment would be 1.30 G^2. If the intergroup rigid-lattice contribution of 4.4 G^2 is reduced by a factor of 1/2 to 1/4 (21) under this condition, the total expected second moment, including 0.3 G^2 for the 143 p.p.m. separation between components, would be 2.7 to 3.8 G^2 at 30 MHz. It seems probable, then, that the ionic groups rotate about more than one axis. Random reorientation about the symmetry axes of the octahedron would, however, reduce the second moment to a value only a little larger than 1 G^2 (24). As in the case of $SF_3^+AsF_6^-$, no satisfactory resolution of the 30 MHz spectrum into components, one for each ion, was obtained. There was some indication, however, that the line width and second moment of the AsF_6^- component were smaller than those of the IF_6^+ component. This suggests more extensive motion for the AsF_6^- groups than for the IF_6^+ groups.

The authors gratefully acknowledge the financial support of a grant-in-aid from the National Research Council of Canada and a grant from the Committee on Research of the University of British Columbia. We are most indebted to Dr. S. P. Beaton for preparing the compounds and to Professor Neil Bartlett for valuable discussions. Our thanks are also due to Dr. T. J. R. Cyr for advice on computer programming.

1. N. Bartlett and P. L. Robinson. Chem. Ind. London, 1351 (1956).
2. N. Bartlett and P. L. Robinson. Proc. Chem. Soc. 230 (1957).
3. F. Seel and O. Detmer. Angew. Chem. **70**, 163, (1958); **70**, 470 (1958).
4. F. Seel and O. Detmer. Z. Anorg. Allg. Chem. **301**, 113 (1959).
5. N. Bartlett and P. L. Robinson. J. Chem. Soc. 3417 (1961).
6. L. Kolditz and W. Schaeffer. Z. Chem. **1**, 124 (1961).
7. L. Kolditz and W. Schaeffer. Z. Anorg. Allg. Chem. **315**, 35 (1962).
8. L. Kolditz and E. Roesel. Z. Anorg. Allg. Chem. **341**, 88 (1965).
9. K. O. Christe and A. E. Pavlath. Z. Anorg. Allg. Chem. **335**, 210 (1965).
10. L. Kolditz and W. Rehak. Z. Anorg. Allg. Chem. **342**, 32 (1966).
11. F. N. Trebbe and E. L. Muetterties. Inorg. Chem. **6**, 129 (1967).
12. A. R. Young, II, and D. Moy. Inorg. Chem. **6**, 178 (1967).
13. S. P. Beaton. Ph.D. Thesis, the University of British Columbia, Vancouver, British Columbia. 1966.
14. K. O. Christe and W. Sawodny. Inorg. Chem. **6**, 1783 (1967).
15. W. I. Orr (*Editor*). The radio handbook. 16th ed. Editors and Engineers, Ltd., New Augusta, Indiana. 1962. p. 316.
16. J. A. Pople, W. G. Schneider, and H. J. Bernstein. High resolution nuclear magnetic resonance. McGraw-Hill Book Co., Inc., New York. 1959.
17. K. O. Christe, J. P. Guertin, A. E. Pavlath, and W. Sawodny. Inorg. Chem. **6**, 533 (1967).
18. Interatomic distances. Spec. Publ. No. 11, Chem. Soc. London. 1958; Suppl. Spec. Publ. No. 18, 1965.
19. L. Pauling. The nature of the chemical bond. 3rd ed. Cornell University Press, Ithaca, New York. 1960. p. 260.
20. R. J. Gillespie and R. S. Nyholm. Quart. Rev. London, **11**, 339 (1957).
21. G. W. Smith. J. Chem. Phys. **42**, 4229 (1965).
22. E. R. Andrew and D. P. Tunstall. Proc. Phys. Soc. London, **81**, 986 (1963).
23. R. F. Copeland, S. H. Connor, and E. A. Meyers. J. Phys. Chem. **70**, 1288 (1966).
24. G. R. Miller and H. S. Gutowsky. J. Chem. Phys. **39**, 1983 (1963).

Can. J. Chem. Downloaded from www.nrcresearchpress.com by 210.87.254.5 on 09/05/12
For personal use only.

Can. J. Chem. Downloaded from www.nrcresearchpress.com by 210.87.254.42 on 09/05/12
For personal use only.

Properties relating to critical phenomena in the acetic anhydride – acetone – carbon disulfide system

A. N. Campbell and E. M. Kartzmark
Department of Chemistry, University of Manitoba, Winnipeg, Manitoba

Received September 5, 1969

The following physical properties of the acetic anhydride – acetone – carbon disulfide system have been investigated: congruent compositions, excess volumes, dielectric constants. For the system acetone – carbon disulfide, the excess volumes and the molar polarizations are much greater than those required by the mixture rule. From this we deduced that this system is very non-ideal and might, at a suitable temperature, form two layers; two liquid layers did indeed form at −73 °C, the upper critical solution temperature occurring somewhere between this temperature and 0 °C. We offer it as a general rule that, if the deviation from additivity of molar polarization is large and positive, two layers will form at a sufficiently low temperature, provided that solid phases do not intervene. This deduction becomes almost a certainty if large positive deviations from additivity of molar volume and large positive heats of mixing are also present.

Canadian Journal of Chemistry, **48**, 904 (1970)

On previous occasions (1, 2), we studied congruent compositions, heats of mixing, and dielectric constants of the binary system acetic anhydride – carbon disulfide. We have now conducted isothermal studies of the same system in the presence of acetone. The properties we have studied are congruent compositions, partial molar excess volumes, dielectric constants, and viscosity. From our results we deduced that the system acetone – carbon disulfide should form a partially miscible liquid pair and we have found this to be so at −73 °C.

Experimental

Purity of Materials

Acetic anhydride, acetone, and carbon disulfide were purchased as "certified reagents", but they were further purified by methods given in Purification of Laboratory Chemicals (3); the densities and refractive indices were in exact agreement with literature values.

Methods

All the experimental methods have been described previously, as follows: congruent concentrations (1), partial molar excess volumes and viscosity (4), and dielectric constants (2). Congruent solutions were analyzed from density and refractive index measurements.

Results

Congruent concentrations (in mole %), at 0 and 25 °C, are expressed graphically in Fig. 1, and at −73 °C in Fig. 2. The critical compositions (in mole %) at 25 and 0.0 °C are, respectively: acetone, 3.0 and 13.9; carbon disulfide, 68.0 and 62.7; acetic anhydride, 29.0 and 23.5. There is obviously no critical composition at −73 °C, since the miscibility gaps in the two binary systems acetic anhydride – carbon disulfide and carbon disulfide – acetone run into one another.

The changes of volume on mixing (molar excess volumes) can be represented by the equation of Redlich and Kister (5), viz.

$$[1]\quad V^{E} = X_1X_2[A + B(X_1 - X_2) + C(X_1 - X_2)^2 + D(X_1 - X_2)^3]$$

where X_1 and X_2 are the mole fractions of the two components. The values of the constants A, B, C, and D are given for each system in Table 1. To determine the constants, we used the computer program of Myers and Scott (6). This program has the advantage that it states how many constants are justifiable by a given set of data. Our measurements were made at 25 °C and the constants apply to this temperature. For the purpose of studying properties in the neighborhood of the critical state, a pseudobinary system, represented by a straight line on the triangular diagram, drawn parallel to the tielines at 25 °C and touching the consolute curve tangentially at the plait point was investigated. It represents a state of affairs for which all concentrations are homogeneous but, in the critical region, only just so. Solutions **A** and **B** were made up to the following compositions: Solution **A**, 6.46 mole % acetone, 93.54 mole % acetic anhydride; solution **B**, 1.39 mole % acetone, 98.61 mole % carbon disulfide. The excess properties used in the calculation are total, that is, they include the changes of property associated with the

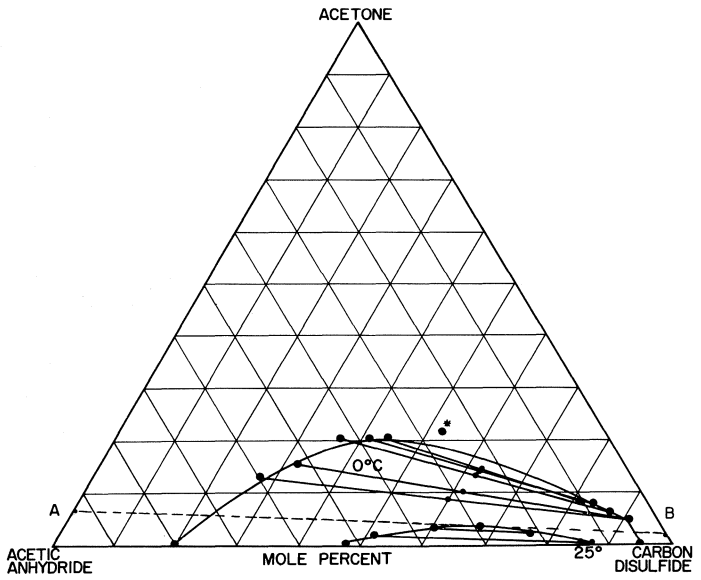

FIG. 1. Congruent compositions at 25 and 0 °C. (*, homogeneous at 0 °C).

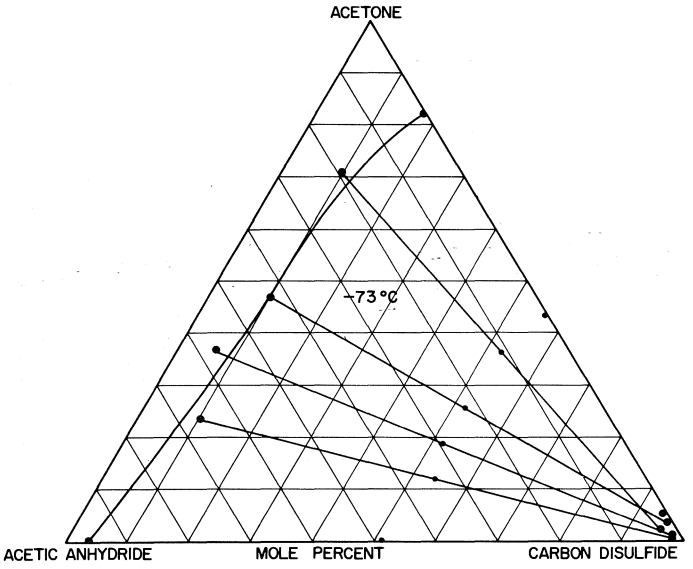

FIG. 2. Congruent compositions at −73 °C.

formation of solutions **A** and **B**, respectively. Calculated and experimental values of excess volumes are represented graphically in Figs. 3 and 4.

Knowing the constants for all four systems listed in Table 1, it was possible to calculate the partial molar excess volumes, using the second set of equations of Redlich and Kister (5), viz.

$$[2]\quad \bar{V}_1^{E} = (1 - X_1)^2[A + B(4X_1 - 1) + C(2X_1 - 1)(6X_1 - 1) + D(2X_1 - 1)^2(8X_1 - 1)]$$

and

$$[3]\quad \bar{V}_2^{E} = X_1^2[A + B(4X_1 - 3) + C(2X_1 - 1)(6X_1 - 5) + D(2X_1 - 1)^2(8X_1 - 7)]$$

Can. J. Chem. Downloaded from www.nrcresearchpress.com by 210.87.254.42 on 09/05/12
For personal use only.

TABLE 1
Values of constants for eq. [1]

System	Constant			
	A	*B*	*C*	*D*
Carbon disulfide – acetone	4.053	−0.835	0.081	—
Acetic anhydride – carbon disulfide	4.726	4.290	−10.376	7.257
Acetic anhydride – acetone	−0.784	−0.166	−0.546	0.440
Pseudo-binary	4.893	0.559	1.236	—

always using only as many constants as the experiments justify. The results are expressed graphically in Figs. 5 and 6. In order to use the above expressions for the ternary system acetone – acetic anhydride – carbon disulfide, it was necessary to recalculate compositions as if acetone was not present.

Figure 7 represents the molar polarizations of the mixtures. The so-called "permanent polarization" is obtained by subtracting the molar refraction (distortion polarization) from the molar polarization. We determined these molar refractions and found them always to be additive, within the experimental error. The viscosities are represented in Figs. 8 and 9.

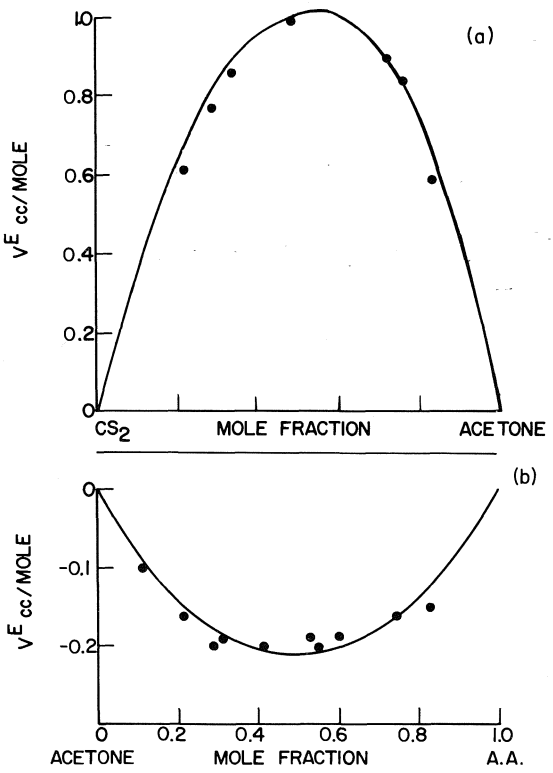

FIG. 3. Excess volumes in cm^3 per mole: (*a*) carbon disulfide – acetone, (*b*) acetone – acetic anhydride. The solid curve is calculated from the constants given in the text.

Discussion

The excess volumes of the system acetone – acetic anhydride are small and negative; those of the other systems, including the system acetone – carbon disulfide, are large and positive, amounting to a maximum value of $+1.25$ cm^3 for the acetone – carbon disulfide system. The same is true of the partial molar excess volumes (Figs. 5 and 6), amounting to values of $+6$ or $+7$ cm^3 for acetone – carbon disulfide, at infinite dilution. This led us to conclude that while the system acetone – acetic anhydride is an almost ideal solution, the system acetone – carbon disulfide and, of course, the system acetic anhydride – carbon disulfide, which shows a miscibility gap at 25 °C, are very non-ideal. The molar polarization figures lead to the same conclusion. The molar polarizations of acetone – acetic anhydride are practically additive, but those of acetone – carbon disulfide show a strong positive deviation, amounting to $+11.84$ cm^3 for a solution containing 56.30 mole % carbon disulfide. We had previously concluded (2) that strong positive deviation from additivity in molar polarization was an indication of a tendency towards formation of a miscibility gap. Therefore, despite the fact that partial miscibility of solutions containing acetone is almost unknown, we felt that such a gap might exist in the system acetone – carbon disulfide, and we therefore investigated the equilibrium conditions at 0 and at −73 °C (Figs. 1 and 2). At 0 °C, the field of partial miscibility is greatly increased for the ternary system and at −73 °C it has spread completely over to the acetone – carbon disulfide side. The system acetone – carbon disulfide shows a very

Can. J. Chem. Downloaded from www.nrcresearchpress.com by 210.87.254.42 on 09/05/12
For personal use only.

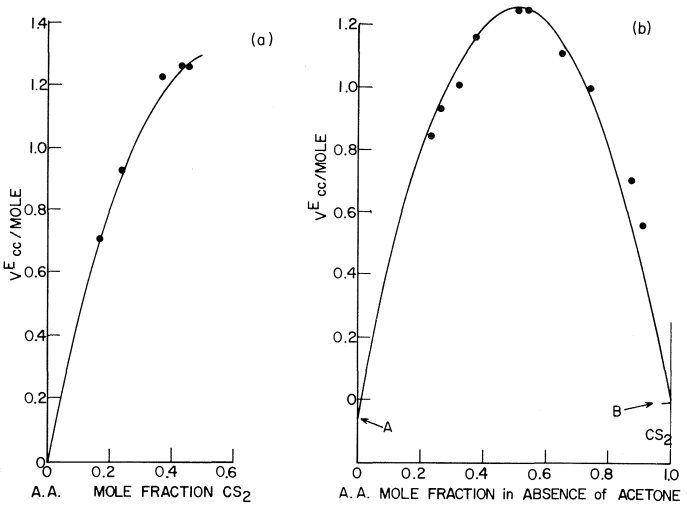

FIG. 4. Excess volumes in cm^3 per mole: (*a*) acetic anhydride – carbon disulfide, (*b*) pseudo-binary. The solid curve is calculated from the constants given in the text.

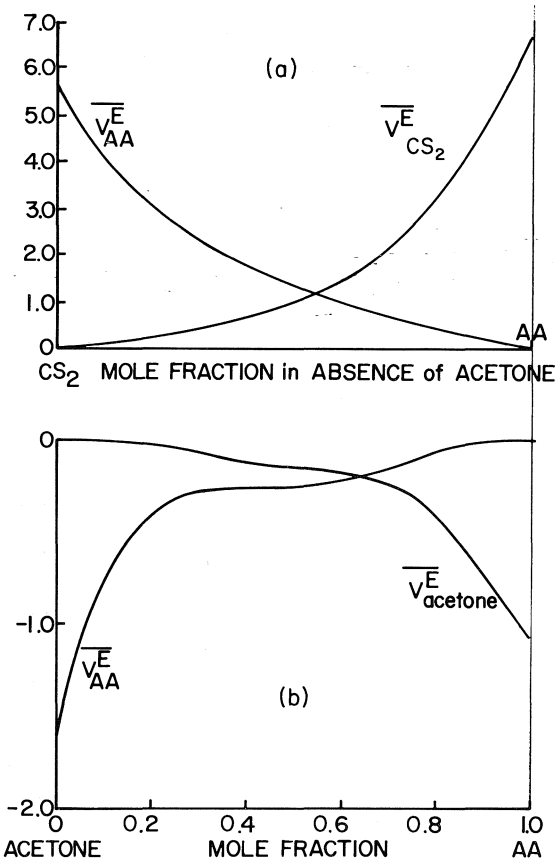

FIG. 5. Partial molar excess volumes, in cm^3 per mole: (*a*) pseudo-binary, (*b*) acetone – acetic anhydride.

Can. J. Chem. Downloaded from www.nrcresearchpress.com by 210.87.254.42 on 09/05/12
For personal use only.

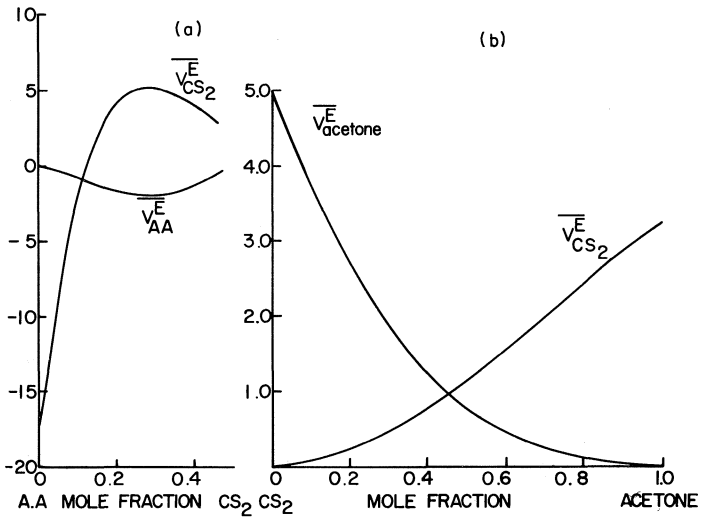

FIG. 6. Partial molar excess volumes: (*a*) acetic anhydride – carbon disulfide, (*b*) carbon disulfide – acetone.

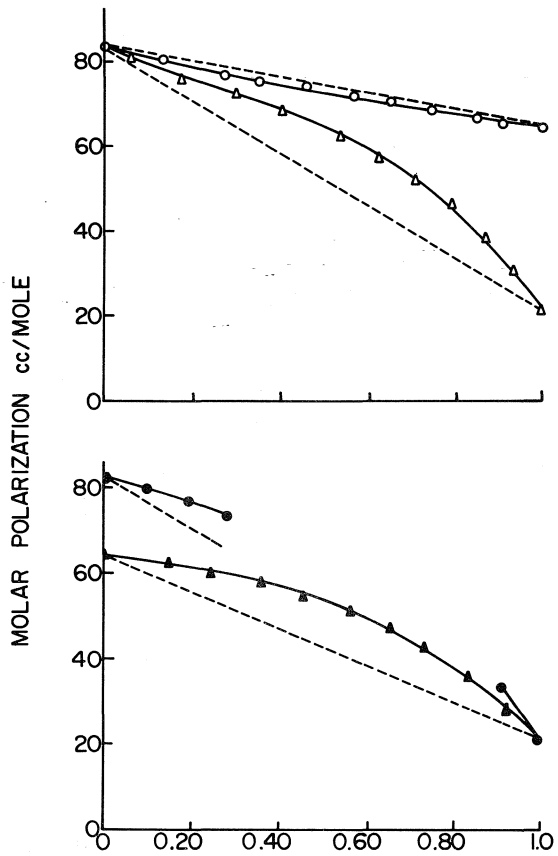

FIG. 7. Molar polarizations in cm^3 per mole. ○, acetone – acetic anhydride (mole fraction acetone); △, pseudo-binary (mole fraction CS_2 in absence of acetone); ●, acetic anhydride – carbon disulfide (mole fraction CS_2); ▲, acetone – carbon disulfide (mole fraction CS_2).

Can. J. Chem. Downloaded from www.nrcresearchpress.com by 210.87.254.42 on 09/05/12
For personal use only.

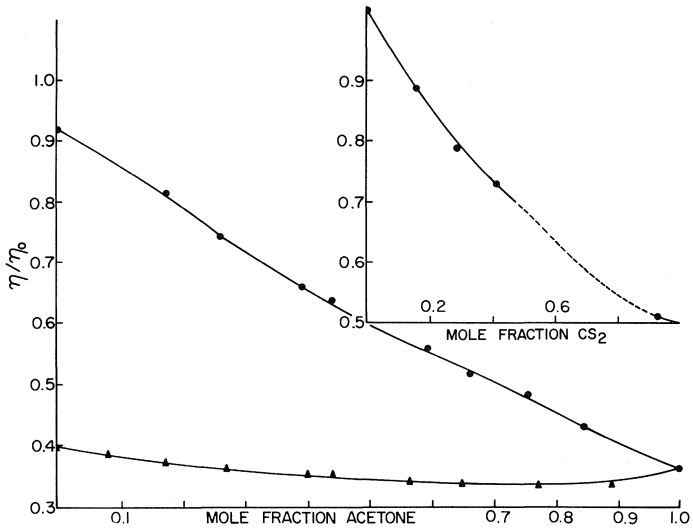

FIG. 8. Relative viscosity. Acetic anhydride – acetone, ●; carbon disulfide – acetone, ▲; inset, acetic anhydride – carbon disulfide.

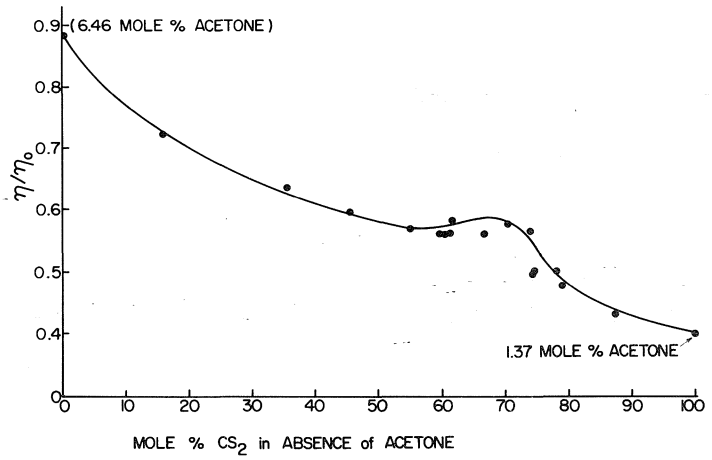

FIG. 9. Relative viscosity in pseudo-binary system.

large miscibility gap at −73 °C. We consider ourselves justified in suggesting that if the deviation from additivity in the molar polarization is large and positive, two layers will form at a sufficiently low temperature; provided, of course, that solid phases do not intervene. This deduction will receive support if there are large positive deviations from additivity of molar volume and large positive heats of mixing.

In all cases, the viscosity is less than required by additivity, most markedly so in the less-ideal system. The pseudo-binary system shows the phenomenon of anomalous viscosity, common to all systems which are in the neighborhood of the critical state.

We are at present completing work on the thermal properties of the above systems and the results bear out the above conclusions.

1. A. N. CAMPBELL and E. M. KARTZMARK. Can. J. Chem. **45**, 2433 (1967).
2. A. N. CAMPBELL and E. M. KARTZMARK. Can. J. Chem. **47**, 619 (1969).
3. D. D. PERRIN, W. L. F. ARMAREGO, and D. R. PERRIN. Purification of laboratory chemicals. The Pergamon Press, Ltd., New York. 1966. pp. 56, 57, and 104.
4. A. N. CAMPBELL, E. M. KARTZMARK, S. C. ANAND, Y. CHENG, H. P. DZIKOWSKY, and S. M. SKRYNYK. Can. J. Chem. **46**, 2399 (1968).
5. O. REDLICH and A. T. KISTER. Ind. Eng. Chem. **40**, 345 (1948).
6. D. B. MYERS and R. L. SCOTT. Ind. Eng. Chem. **55**, 431 (1963).

Can. J. Chem. Downloaded from www.nrcresearchpress.com by 210.87.254.42 on 09/05/12
For personal use only.

Can. J. Chem. Downloaded from www.nrcresearchpress.com by 210.87.254.6 on 09/05/12
For personal use only.

Volumes of activation for the aquation of $Co(NH_3)_5Cl^{2+}$ and $Cr(NH_3)_5NCS^{2+}$ complex ions in solution

D. L. Gay and Robert Nalepa[1]
Department of Chemistry, Xavier College, Sydney, Nova Scotia

Received August 29, 1969

The volumes of activation for the aquation of $Co(NH_3)_5Cl^{2+}$ and $Cr(NH_3)_5NCS^{2+}$ in aqueous acidic solution (0.1 *M* $HClO_4$) have been measured and found to be -7.5 ± 1 and -8.6 ± 1 ml/mole, respectively. These values are more consistent with an S_N1 than an S_N2 pathway for the aquation of both of these complexes.

Canadian Journal of Chemistry, **48**, 910 (1970)

Introduction

At present, there is some doubt about the exact role of solvent water in the aquation reaction [1]

[1] $M(NH_3)_5X^{2+} + H_2O \rightarrow M(NH_3)_5OH_2^{3+} + X^-$

where M = Co(III), Cr(III), etc. and $X^- = Cl^-$, Br^-, I^-, NCS^-, etc. Some authors suggest that solvation of the leaving anion is the dominating factor in this reaction (1). Others have been divided on whether or not solvent water acts as a nucleophile in forming the transition state (2–4).

Volumes of activation have been used to determine reaction mechanisms (5, 6), and several authors, using them, have demonstrated the participation of solvent water in forming the transition state of both organic (6–8) and inorganic (9–11) reactions.

This study is concerned with the measurement of the volume of activation of reaction [1], with the hope of discovering the role played by the solvent water in forming the transition state of this reaction.

Experimental

Preparation of Compounds

Aquopentamminechromium(III) nitrate ammonium nitrate was prepared as described in ref. 12. The crude product was converted into the perchlorate salt by the addition of 60% perchloric acid to a saturated solution of the nitrate. The product was recrystallized twice from aqueous perchloric acid, washed with water, alcohol, and ether, and dried over phosphorous pentoxide.

Anal. Calcd. for $[Cr(NH_3)_5OH_2](ClO_4)_3$: NH_3, 24.05; equiv. wt., 151.2. Found: NH_3, 24.0; equiv. wt., 151.2.

Thiocyanatopentamminechromium(III) perchlorate was prepared from the aquopentammine salt, by the method used for the analogous cobalt(III) complex (13).

Anal. Calcd. for $[Cr(NH_3)_5NCS](ClO_4)_2$: NH_3, 21.6; Cr, 13.2; equiv. wt., 197.1. Found: NH_3, 21.5; Cr, 13.2; equiv. wt., 197.2

[1]Summer student.

Chloropentamminecobalt(III) chloride was prepared by the air oxidation of an ammoniacal solution of cobaltous nitrate and ammonium chloride. This was converted to the perchlorate salt by precipitation with 60% perchloric acid. The complex was checked for purity by spectral analysis. Maxima were found at 532 and 362 mμ with molar extinction coefficients of 50.8 and 45.8, respectively; these were in good agreement with published values (14, 15).

Reaction Kinetics

(*a*) *Atmospheric Pressure*

Solutions of the complex ion in 0.1 *M* $HClO_4$, were made up in 100-ml volumetric flasks. These were placed in a constant-temperature bath whose temperature was controlled to $\pm 0.2°$ and left to equilibrate for 30 min. The rate of aquation was followed by withdrawing aliquots of the reaction mixture at definite time intervals, cooling them in ice-cold water and analyzing the solution spectrophotometrically for complex ion.

(*b*) *High Pressure*

The high-pressure apparatus is shown schematically in Fig. 1. In the pressurization process, valve *2* is closed and valve *1* is open. The pressure in A, an Aminco micro series vessel, is developed by pumping paraffin oil by means of a hand operated pump, Blackhawk P-228, P. Fine adjustments to the pressure can then be made by closing valves *1* and *3*, and operating the screw injector, B. When the desired pressure is obtained, valves *2* and *1* are closed and remain closed for the duration of the run. The pressure is measured by the Bourdon gauge, G. Pressure regulation did not present any problems, and was easily controlled to ± 5 atm.

The reaction vessel was a 5-ml hypodermic syringe sealed at one end and with a portion of the barrel sawed off. This was filled with the reaction solution, and placed inside the pressure vessel. The pressure vessel was filled with oil, assembled, and immersed in an oil bath thermostated at the desired temperature. The pressure was then brought to the desired value as quicly as possible. The times taken to assemble (5 min) and to pressurize (3 min) the system were recorded and kept the same for every run. The system was then left for 30 min, after which the pressure was released. The syringe was removed, wiped clean of oil, and cooled in ice-cold water. The reaction solution was analyzed for complex ion spectrophotometrically. This reading was taken as that for time zero.

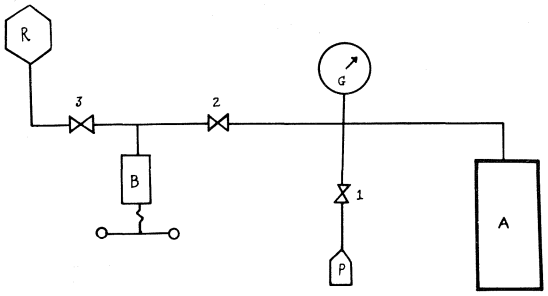

FIG. 1. Schematic representation of the high-pressure system: R, oil reservoir; B, screw injector; G, Bourdon gauge; P, pressure pump; A, pressure vessel; *1*, *2*, and *3* are valves.

Other samples were put into the pressure vessel and left for times of 1, 1½, 2 h. Four points were taken for each run and three runs were performed at each pressure.

Results and Discussion

In all experiments, the rate of disappearance of complex ion obeyed the first-order rate law [2]

$$[2] \qquad k_1 t = 2.303 \log_{10} (C_0/C),$$

where C_0 and C are the concentrations of the complex ion at times zero and t, respectively. First-order rate constants, k_1, accurate to ±3%, were obtained for the aquation of $Co(NH_3)_5Cl^{2+}$ and $Cr(NH_3)_5NCS^{2+}$ at 59.8 and 79.8 °C, respectively, in the pressure range 1 to 1360 atm (Table 1).

The activation volumes, ΔV, were determined graphically from plots of $\log_{10} (k_P/k_1)_T$ against pressure, Fig. 2, according to the expression [3]

$$[3] \qquad d \log_{10} k_P/dP = -(\Delta V/2.303\ RT)$$

where k_P and k_1 are the first-order rate constants at pressure P and atmospheric pressure, respectively. The activation volume for the aquation of $Co(NH_3)_5Cl^{2+}$ is −7.5 ml/mole and that for $Cr(NH_3)_5NCS^{2+}$ is −8.6 ml/mole. These values are accurate to ±1 ml/mole. The following discussion of these activation volumes will be largely in terms of the S_N1 and S_N2 mechanisms.

TABLE 1

Rate constants for the aquation of $Co(NH_3)_5Cl^{2+}$ and $Cr(NH_3)_5NCS^{2+}$ in 0.1 *M* $HClO_4$ solution

	Rate constant, $10^5 k_1$, s^{-1}	
Pressure, atm	$Co(NH_3)_5Cl^{2+}$ at 59.8 °C	$Cr(NH_3)_5NCS^{2+}$ at 79.8 °C
1	8.607	5.977
340	9.623	6.751
681	10.44	
1020		7.910
1361	12.63	9.125

In any discussion of the activation volumes of ionic reactions such as [1], three factors are important. These factors are the intrinsic volumes of the ions, the electrostriction of the solvent, and the compressibilities of the ions (16). The data necessary for the calculation of activation volumes, such as the compressibility of the ions, is grossly lacking. Therefore, no attempt will be made to estimate the activation volumes in this manner. Rather, an estimate will be obtained from the volume changes of a series of related reactions.

If the aquation reaction [4] goes via an S_N1

$$[4] \quad Co(NH_3)_5Cl^{2+} + OH_2 \rightarrow Co(NH_3)_5{}^{+3} + Cl^- + OH_2$$

pathway (4), the activation volume is expected to be in the range −6.8 to −9.2 ml/mole. This value is obtained from the sum of the volume changes in reactions [5] and [6]

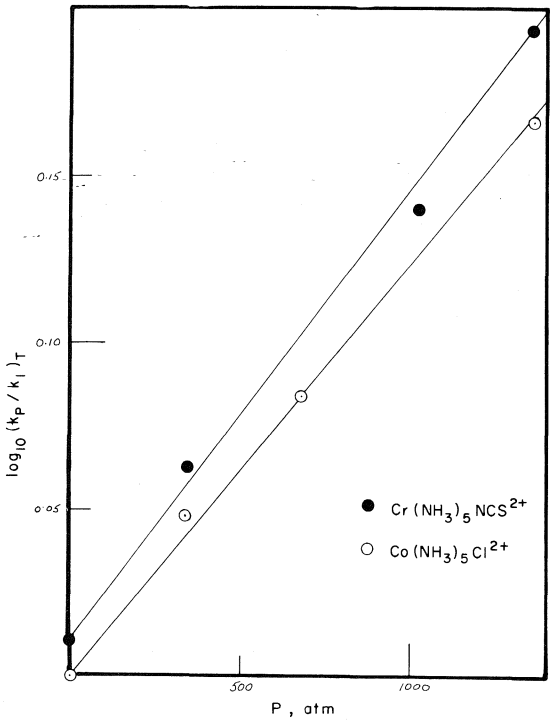

FIG. 2. Graphs of $\log_{10} (k_P/k_1)$ vs. P, where k_P and k_1 are the rate constants at pressure P and 1 atm, respectively, $A = 0.00$ for $Co(NH_3)_5Cl^{2+}$ and 0.01 for $Cr(NH_3)_5NCS^{2+}$.

Can. J. Chem. Downloaded from www.nrcresearchpress.com by 210.87.254.6 on 09/05/12
For personal use only.

[5] $Co(NH_3)_5Cl^{2+} + OH_2 \rightarrow Co(NH_3)_5OH_2^{3+} + Cl^-$

[6] $Co(NH_3)_5OH_3^{3+} \rightarrow Co(NH_3)_5^{3+} + OH_2$

The overall volume change for reaction [5] is -10.4 ml/mole (17) and that for reaction [6] is $+1$ to $+3.6$ ml/mole (11). Reaction [6] is the rate determining step for the S_N1 water exchange reaction of $Co(NH_3)_5OH_2^{3+}$.

However, if the aquation proceeds via an S_N2 pathway, reaction [7]

[7] $Co(NH_3)_5Cl^{2+} + OH_2 \rightarrow H_2O—Co(NH_3)_5Cl^{2+}$

then the activation volume is expected to be in the range -1 to -3.6 ml/mole (11); that is, the difference in volume between a water molecule bound in the first coordination sphere and a water molecule in bulk solvent. This estimate may be more positive due to decreased electrostriction on forming a transition state of decreased charge density.

On the basis of the above arguments, it seems that the measured activation volume of -7.5 ml/mole is more in agreement with an S_N1 than an S_N2 pathway. However, an intermediate mechanism cannot be ruled out entirely.

If the mechanism of aquation of $Cr(NH_3)_5NCS^{2+}$ is S_N2, then the activation volume is expected to be in the range -1 to -3.6 ml/mole and can be more positive. The measured activation volume of -8.6 ml/mole is not in agreement with this. The authors, therefore, prefer to think of this reaction as proceeding via a pathway which is not pure S_N2 and more likely is S_N1 in nature.

The authors wish to thank the National Research Council of Canada and St. Francis Xavier University for support of this work.

1. D. L. Gay and G. C. Lalor. J. Chem. Soc. A, 1179 (1966).
2. A. Haim and H. Taube. Inorg. Chem. **2**, 1199 (1963).
3. R. G. Pearson and J. W. Moore. Inorg. Chem. **3**, 1334 (1964).
4. C. H. Langford. Inorg. Chem. **4**, 265 (1965).
5. S. D. Hamann. *In* High pressure physics and chemistry. Vol. 2. *Edited by* R. S. Bradley. Academic Press, Inc., New York. 1963. Ch. 8.
6. E. Whalley. Advan. Phys. Org. Chem. **2**, 93 (1964).
7. J. Koskikallio and E. Whalley. Trans. Faraday Soc. **55**, 815 (1959).
8. B. T. Baliga and E. Whalley. Can. J. Chem. **42**, 1019 (1964).
9. H. E. Brower, L. Hathaway, and K. R. Brower. Inorg. Chem. **5**, 1899 (1966).
10. J. P. Caldin and J. Halpern. Inorg. Chem. **4**, 1086 (1965).
11. H. R. Hunt and H. Taube. J. Amer. Chem. Soc. **80**, 2643 (1958).
12. F. Basolo and R. Murmann. *In* Inorganic synthesis IV. *Edited by* J. Bailar. McGraw–Hill Book Co., Inc., New York. 1953. p. 171.
13. Gmelins Handbuch der anorganischen Chemie. **8**, No. 58, 181 (1930).
14. C. H. Langford and W. R. Muir. J. Phys. Chem. **71**, 2602 (1967).
15. H. Taube. J. Amer. Chem. Soc. **82**, 524 (1960).
16. E. Whalley. J. Chem. Phys. **38**, 1400 (1963).
17. T. G. Spiro, A. Revesz, and J. Lee. J. Amer. Chem. Soc. **90**, 4000 (1968).

Can. J. Chem. Downloaded from www.nrcresearchpress.com by 210.87.254.6 on 09/05/12
For personal use only.

Can. J. Chem. Downloaded from www.nrcresearchpress.com by 210.87.254.40 on 09/05/12
For personal use only.

Thermal decomposition of cyclopentene

G. I. MACKAY AND R. E. MARCH
Department of Chemistry, Trent University, Peterborough, Ontario

Received June 23, 1969

The thermal decomposition of cyclopentene, which had previously been shown to proceed by a gas-phase homogeneous process, has been found to be accelerated in the presence of glass wool fibers. The roles of products in the lowering of the overall rate in the later stages of decomposition have been investigated.

Canadian Journal of Chemistry, **48**, 913 (1970)

Introduction

The homogeneous thermal decomposition of cyclopentene has been studied (1) in a flow system where it was observed that at 850 °C, with a pressure of 10 Torr and a contact time sufficient to produce about 20% decomposition, 0.96 mole of hydrogen and 0.93 mole of cyclopentadiene are formed from each mole of cyclopentene decomposed. Only small amounts of other hydrocarbons were found. In an experiment carried out in a static system at 552 °C, it was reported (2) that 80% of the products of less than 5 carbon atoms consist of hydrogen.

It would appear in the light of later work that the extent of decomposition in this experiment was not limited to the initial reactant. Vanas and Walters (3) in their experiments in a static system, over a temperature range 483–548 °C at pressures from 38 to 249 Torr, observed that the main reaction was the dehydrogenation of cyclopentene to cyclopentadiene and hydrogen

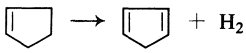

During the early portion of the decomposition it appeared that the pressure increase was a satisfactory indication of the amount of dehydrogenation. Measurements of $t_{1/4}$ (the time for 25% pressure increase) at different initial pressures showed that the reaction was first order. However, the value of the rate constant obtained from pressure measurements decreased in the later stages of the decomposition. It was found that addition of propylene to the system had no appreciable effect on the kinetics of the reaction; this implied that a chain mechanism was not involved in the reaction. A 28-fold increase in the surface-to-volume ratio did not cause any significant change in the overall pressure–time curve. Tanji *et al.* (4) studied the decomposition at low pressures (12–30 Torr) in the temperature range 416–532 °C. Propylene and ethylene were detected as minor products of decomposition. Knecht (5) reported that at the quarter time of the pyrolysis of cyclopentene these minor substances, relative to the main dehydrogenation products, amounted to about 5–6% of the reaction. Neither Tanji nor Knecht reported any experiments in which the surface-to-volume ratio was changed.

The work presented here was concerned with the decrease in the rate constant as the reaction proceeded and a re-examination of any surface effects on the reaction.

Experimental

The cyclopentene used was obtained from the Aldrich Scientific Company. The mass spectrum of a sample which had been cooled to liquid nitrogen temperature and thoroughly outgassed several times and then distilled to a further trap and outgassed once more was taken using an MS-12 mass spectrometer. No extraneous materials were detected.

The cyclopentadiene was prepared by cracking, in a 32-cm fractionating column, dicyclopentadiene obtained from Fisher Scientific Co. The monomer was kept at liquid nitrogen temperature until used. It was thoroughly outgassed and underwent trap-to-trap distillation immediately prior to use.

The reaction vessel was a wire-wound Pyrex cylinder with a volume of 692.5 cm^3, with a thermocouple well at one end. The vessel was connected directly to the manometer in such a way as to keep the "dead space" volume to a minimum. The temperature was measured by an iron–constantan thermocouple located in the well near the center of the reaction vessel. The thermocouple was attached to a Leeds and Northrup (No. 7645) potentiometer, was standardized against a standard Weston cell, and calibrated against the melting point of aluminum. It is estimated that the accuracy of the temperature measurements should be within ±1 °C.

The packed reaction vessel contained 60 g of Pyrex glass wool and had a minimum surface-to-volume ratio of about 30 times that of the unpacked vessel. In order to obtain consistent results it was necessary to flush the

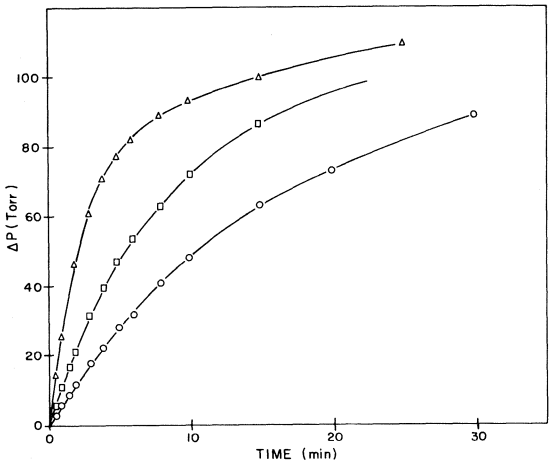

FIG. 1. The rate of change of pressure with time at 530 °C: □, cyclopentene in unpacked vessel, P_0 = 177.5 Torr; △, cyclopentene in packed vessel (60 g Pyrex wool), P_0 = 174.0 Torr; ○, cyclopentene plus cyclopentadiene in unpacked vessel at equal initial pressures of 173.0 Torr.

reaction vessel with cyclopentene at an elevated temperature whenever the vessel had come into contact with air. The pressure measurements were made with a mercury manometer which had to be heated several times in order to remove compounds of low volatility which may have been products of the decomposition. It was found that in air and at room temperature cyclopentene reacts with mercury to form a brown amorphous solid. A similar substance was observed in the manometer and also tended to block the mercury diffusion pump at intervals.

The analysis of the products was done with an MS-12 mass spectrometer. The sample tube, containing products and undecomposed reactant, was removed from the system subsequent to the filling operation and placed in liquid nitrogen until the mass spectrum was about to be taken. Spectra consisted mainly of molecular ions.

Results and Discussion

The pressure–time curves in Fig. 1 show the initial rates of increase of pressure with time obtained in the decomposition of cyclopentene. The results of a number of experiments are shown in Table 1; those results obtained with cyclopentene alone in an unpacked vessel compare favorably with values obtained by other workers, as shown in Table 2. First-order plots of ln $(2P_0 - P)$ vs. t were found to be linear for all cases (that is, cyclopentene with and without cyclopentadiene, packed and unpacked vessel) up to 30% conversion. This indicated that first-order kinetics were observed in all cases.

The data obtained with a packed vessel indicated that an accelerated reaction was occurring. These data were reproducible once the reaction vessel and glass wool had been conditioned by flushing with cyclopentene for 2 h at a temperature of about 500 °C. Comparison of the rates for the unpacked and packed vessel indicated an increase in rate for the packed vessel of almost 6-fold at 488 and 2-fold at 530 °C. This observation differs from that of Vanas and Walters in that they found no significant difference in the rate of reaction for a packed vessel with a 28-fold increase in surface-to-volume ratio, where they used thin-walled Pyrex tubes.

The acceleration effect is well manifested at relatively low temperatures. It can be seen from Table 1 that the value of $t_{1/4}$ at 487 °C was approaching 40 min for the unpacked vessel, while the value at 488 °C for the packed vessel was reduced to approximately 7 min. No appreciable reaction was found in the unpacked vessel at 470 °C; however, at the same temperature of 470 °C in the packed vessel, appreciable reaction occurred, as is shown by the value of $t_{1/4}$ of approximately 20 min. This may indicate that the calculated value of the surface area of the glass wool is too low in these experiments by perhaps as much as 10 to 100 times.

TABLE 1
Rate of decomposition of cyclopentene at different temperatures and pressures

Temperature (°C)	P_0 (cyclopentene) (Torr)	$t_{25\%}$ (min)	$k \times 10$ (min^{-1})
470	166.3*,†	20.5	0.200
482	167.6*,†	12.6	0.311
487	158.5†	39.0	0.078
487	195.0†	38.2	0.110
488	166.0*	6.80	0.670
502	174.0*	4.8	0.800
508	153.5†	10.8	0.392
510	200.5	9.3	0.480
513	139.0	7.6	0.556
513	94.2†,‡	17.5	0.229
523	169.0*,§	4.3	1.06
525	160.8*,§	2.8	1.81
528	164.3	5.75	0.767
528	172.3‡	10.4	0.410
530	177.5	4.3	0.933
530	173.0‡	9.0	0.450
530	174.0*	1.9	1.96
542	175.5	3.0	1.21
542	151.0	2.7	1.18
545	160.5	2.0	2.12
545	137.0‡	4.0	1.33
550	191.6*	0.90	5.14
558	170.5	1.8	3.14

*Packed vessel (60 g Pyrex wool).
†Induction period observed.
‡Equal pressure of cyclopentadiene added.
§Mass spectrum taken of product mixture.

Can. J. Chem. Downloaded from www.nrcresearchpress.com by 210.87.254.40 on 09/05/12
For personal use only.

TABLE 2

Comparison of kinetic results for the first-order thermal decomposition of cyclopentene

Source	Pressure range (Torr)	Activation energy (kcal/mole)	Pre-exponential factor ($s^{-1} \times 10^{-12}$)
Vanas and Walters (3)	110–120	58.8	11
Tanji *et al.* (4)	12–30	59.9	22
Knecht (5)	4–34	57.7	6.3
This work	94–200	61	6.0

Can. J. Chem. Downloaded from www.nrcresearchpress.com by 210.87.254.40 on 09/05/12
For personal use only.

The calculated value of the surface area was based on treatment of the fibers as rod-like and did not take into account the heterogeneous nature of the glass surface. However, fair agreement with the calculated value of the surface area was obtained with the nitrogen absorption technique. It would thus appear that if the accelerated reaction is not due to a change in surface-to-volume ratio then the nature of the surface may differ between tubing and glass wool.

It should be pointed out here that the decomposition of cyclopentene is suggested in a well-known text (6) as a suitable experiment for senior undergraduates. Students are directed away from experiments in which the surface-to-volume ratio is changed as "[this] system . . . should be free from serious wall effects." The possibility of wall effects now deserves a close re-examination.

When the reaction has proceeded for a time the rate is observed to decrease. This would seem to indicate that the products are beginning to affect the rate. In an effort to determine the influence of cyclopentadiene on the reaction, the initial rates of the reaction of cyclopentene with and without an equal concentration of cyclopentadiene were measured.

Comparison of pairs of runs carried out at 528, 530, and 545 °C in Table 1 shows that the initial rate of reaction is decreased by almost a factor of two on the addition of cyclopentadiene.

The influence of hydrogen may be estimated from a comparison of the initial rate constant for an equimolar mixture of cyclopentene and cyclopentadiene with the rate constant at $t_{1/2}$ obtained from runs with cyclopentene alone.

In Table 3 are shown the results of four pairs of runs with which this comparison may be made. It is seen that the initial rate constant for the decomposition of cyclopentene in the presence of an equal concentration of cyclopentadiene is virtually identical with the rate constant obtained at 50% conversion of cyclopentene (i.e. equal concentrations of cyclopentene, cyclopentadiene, and hydrogen, neglecting minor products). It appears that hydrogen has negligible effect on the reaction, which is in agreement with the findings of Knecht (5).

TABLE 3

Comparison of initial rate constants for reaction of cyclopentene–cyclopentadiene 1:1 mixtures with rate constants at $t_{50\%}$ for reaction of cyclopentene

	$k \times 10$ (min^{-1})	
Temperature (°C)	Cyclopentene, rate constant at $t_{50\%}$	1:1 Cyclopentene–cyclopentadiene, initial rate constant
513	0.180	0.229
528	0.400	0.410
530	0.452	0.450
545	1.31	1.33

In an attempt to explain the decelerating effect of cyclopentadiene on the reaction, the tendency of cyclopentadiene (and cyclopentene) to form dimers was considered. While no direct evidence is yet available, the observed effect can be predicted by a simple mechanism which incorporates a metastable molecule ($C_{10}H_{14}$) formed by the condensation of cyclopentadiene with cyclopentene.

In Table 4 are given the ratios of the final pressure P_f to the initial pressure P_0 for several runs. All values of pressure given in this table are corrected for the "dead space" in the reaction system outside the furnace. The values of P_f/P_0 compare favorably with those of Vanas and Walters except for the run with the vessel packed

TABLE 4

Ratio of final pressure (P_f) to initial pressure (P_0), reaction of cyclopentene

Temperature (°C)	P_0 (Torr)	P_f/P_0
523	168*	1.99
530	170	1.87
558	163	1.89

*Packed vessel (60 g Pyrex wool).

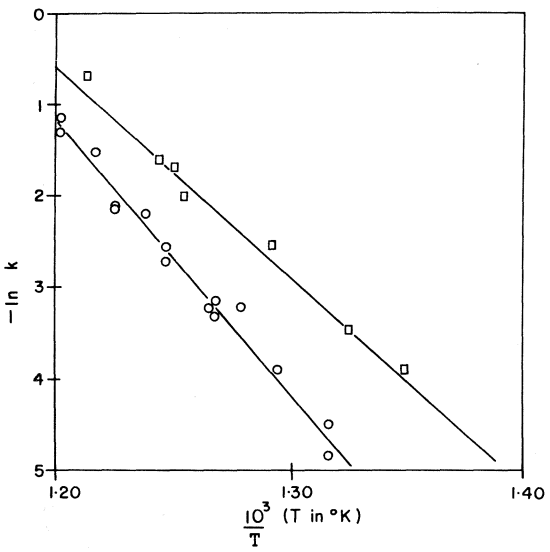

FIG. 2. Arrhenius plots for cyclopentene: ○, unpacked vessel; □, packed vessel (60 g Pyrex wool).

with 60 g of Pyrex wool, for which a value of 1.99 was obtained at 523 °C.

The mass spectra of the product mixtures from several experiments were taken, including two from this packed vessel. These mass spectra indicated that cyclopentadiene and hydrogen were the main products. However, more detailed analyses are required now, particularly for runs with the packed vessel and those in which cyclopentadiene was added. This work is to be pursued.

In Fig. 2 are shown Arrhenius plots for data obtained with the packed and unpacked reaction vessels. Careful consideration of the data for the unpacked vessel indicated that a value of the activation energy of 62 kcal/mole could be realized from experiments in which the initial pressure was varied from 140–170 Torr; whereas for those experiments in which the initial pressure was in excess of 170 Torr, a lower value of 55 kcal/mole could be obtained. A combination of all the data obtained with the unpacked vessel yielded an activation energy of 61 kcal/mole and a frequency factor of 6.0×10^{12} s^{-1}. A comparison of these values with those found by other workers is shown in Table 2. Data obtained with the packed vessel, in which the marked surface effect was noted, yielded an activation energy of 45 kcal/mole and a frequency factor of 6.7×10^{9} s^{-1}.

At low temperatures, an apparent lag in the pressure–time curve, or induction period, was observed at the start of each run and was reproducible within the limits of experimental error. For the cyclopentene plus cyclopentadiene system, the lag was evident only at 513 °C (the lowest temperatures at which this system was investigated); for cyclopentene alone in the unpacked vessel, the lag was evident in each run carried out at a temperature of 508 °C and below; for cyclopentene in the packed vessel, the lag was evident at a temperature of 482 °C and below.

An explanation for this lag is not readily available. It may be due to consumption of inhibiting impurities but once the induction period was complete the reaction proceeded as expected and rate data obtained from cyclopentene alone are in agreement with those of other workers.

Summary

The decomposition of cyclopentene has been investigated in a static system in the region 470 to 558 °C, at pressures from 94 to 201 Torr. Cyclopentadiene and hydrogen have been identified as the major products. Pressure measurements indicate that a slight induction period is present and that the initial reaction is first order. The overall rate constant can be expressed as $k = 6.0 \times 10^{12}\, e^{-61\,000/RT}\, s^{-1}$. Measurements in which an equal concentration of cyclopentadiene was added indicate that this is the main factor influencing the lowering of the overall rate as the reaction proceeds.

Experiments with the vessel packed with glass wool indicate that an accelerated reaction occurs which has been shown to be a first-order reaction initially. The first-order rate constant of this reaction can be expressed as $k = 6.7 \times 10^{9}\, e^{-45\,000/RT}$ s^{-1}.

The financial support of the National Research Council of Canada and the Department of University Affairs of the Province of Ontario is gratefully acknowledged.

The authors are grateful to the referee for helpful comments.

1. F. O. RICE and M. T. MURPHY. J. Amer. Chem. Soc. **64**, 896 (1942).
2. K. KUCHLER. Z. Phys. Chem. Frankfurt **B53**, 307 (1943).
3. D. W. VANAS and W. D. WALTERS. J. Amer. Chem. Soc. **70**, 4035 (1948).
4. H. TANJI, M. UCHIYAMA, A. AMANO, and H. TOKUHISA. Kogyo Kagaku Zasshi, **70**, 307 (1967).
5. D. A. KNECHT. Diss. Abstr. **B29**, 1627 (1968).
6. D. P. SHOEMAKER and C. W. GARLAND. Experiments in physical chemistry. 2nd ed. McGraw-Hill Book Co., Inc., New York. 1967. p. 232, Experiment 28.

Can. J. Chem. Downloaded from www.nrcresearchpress.com by 210.87.254.40 on 09/05/12
For personal use only.

Can. J. Chem. Downloaded from www.nrcresearchpress.com by 210.87.254.105 on 09/05/12
For personal use only.

Proton magnetic resonance studies of ionic solvation in ion-exchange resins. Part I. Sulfonated cation-exchange resins

T. E. GOUGH, H. D. SHARMA[1], AND N. SUBRAMANIAN
Department of Chemistry, University of Waterloo, Waterloo, Ontario

Received September 29, 1969

The proton magnetic resonance spectra of cation-exchange resins of crosslinkage X1 to X16 in the H^+, Li^+, Na^+, K^+, Rb^+, Cs^+, and NH_4^+ forms have been recorded and the values of the molal chemical shift, $\delta_{M^+}{}^0$, are found to be -0.321, -0.005, 0.041, 0.031, 0.028, 0.015, and 0.00 (assumed) p.p.m./mole, respectively, for the cations. These values are very nearly equal to those observed in corresponding aqueous solutions, indicating that ion–solvent interactions are similar in both the resin matrix and the aqueous solution. The temperature dependence of the chemical shift shows the same trend. The effective hydration numbers calculated from the temperature dependence are 2.0 (4.81 *m*) for the H^+ form, 4.8 (3.25 *m*) and 3.6 (5.26 *m*) for the Na^+ form, 4.4 (3.9 *m*) for the K^+ form, and 2.4 (6.18 *m*) for the Cs^+ form. The ions in the resin phase behave as solutions of strong electrolyte, which is consistent with the polyelectrolyte gel model for the ion-exchange resin.

Canadian Journal of Chemistry, **48**, 917 (1970)

Introduction

Nuclear magnetic resonance (n.m.r.) has been extensively applied to the study of ionic solvation and three reviews (1–3) serve to indicate the extent and scope of present interest in the field. The n.m.r. studies fall into four categories: measurements of (*i*) relaxation times, (*ii*) peak areas, (*iii*) dependence of chemical shift upon solute concentration, and (*iv*) dependence of chemical shift upon temperature. A frequent goal of the studies has been the measurement of solvation number; under suitable, though unfortunately uncommon, conditions, solvent exchange may be slowed down sufficiently to allow the observation of cationic solvation shells, leading to a direct determination of the primary solvation number of the cation (4). In contrast, solvation numbers determined by observation of chemical shifts in electrolyte solutions have a less obvious significance, since both cationic and anionic effects contribute to the chemical shift. Malinowski and co-workers (5–7) have performed a series of such experiments, observing the proton chemical shift of aqueous electrolyte solutions at several temperatures and obtaining an "effective" solvation number.

It is of interest to perform similar experiments on ion-exchange resin in as quantitative a manner as possible, so that insight may be gained as to the environments of the ionic species within the resin.

Experimental

All salts used were of analytical grade, of 99+% purity. Deionized, doubly distilled water was used in the preparation of all solutions. Ion-exchange resins were procured from Bio-Rad Laboratories, Richmond, California as Dowex AG 50W in the H^+ form. They were converted to the desired ionic form by standard column procedures. The water content of the resin was determined by the Karl Fischer titration (8). The capacities of resins in the H^+ form, X1 to X16, were determined by a titration method (9). A weighed amount of air-dried resin was contacted with a large excess of 2*M* NaCl solution for a sufficiently long time and the mixture titrated against standard alkali. The capacities were calculated in meq/g of dry resin, and agreed with the specifications stated by the suppliers. The capacities of resins X1 to X16 in their other ionic forms were calculated from the corresponding values for the H^+ form (10). The proton magnetic resonance measurements were made with a Varian A-60 spectrometer, in conjunction with a Varian V-6040 temperature controller. Sample temperatures were calibrated by measurement of the chemical shifts of the hydroxylic protons of methanol and ethylene glycol and are believed to be accurate to ± 1 °C. Freshly prepared samples of resin beads of different sizes ranging from 20–50 to 200–400 mesh were suspended in doubly distilled, deionized water in 5-mm precision cells supplied by Wilmad Glass Co. Both the spectral and water-content measurements were made at least three times. Where overlap was considerable, the peaks in the n.m.r. spectra were resolved by the use of a hybrid analog–digital computer routine developed by the Computing Center, University of Waterloo (11).

Results

The n.m.r. spectrum of a suspension of ion-exchange resin beads in a solvent usually shows distinct signals of solvent protons inside and outside the resin beads (12–14). Identification of the proton resonance signals can be easily made, since the "internal" solvent peak is invariably sharper than the "external" solvent peak (12). In some cases, where the two peaks are close to each other, only a broad, unsymmetrical band

[1]To whom all correspondence should be addressed.

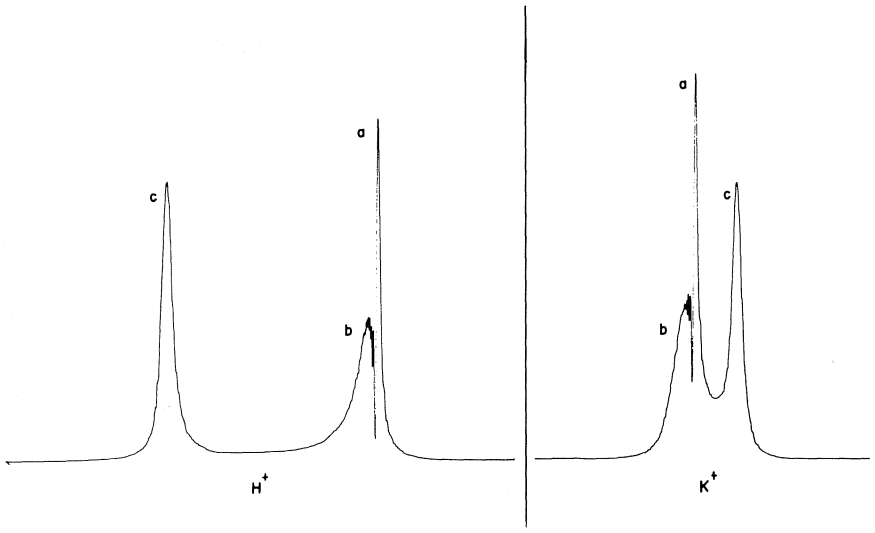

FIG. 1. Nuclear magnetic resonance spectra of suspensions of the H^+ form and K^+ form of Dowex AG 50W (X8) (200–400 mesh) in water (resin beads not allowed to settle): (*a*) "bulk" water, (*b*) "external" water, and (*c*) "internal" water peaks.

results. When water is the solvent, the n.m.r. spectrum consists of two bands: the broader "external water" line and the sharper "internal water" line, provided that the resin beads are allowed to settle down in the n.m.r. tube. When the spectra are taken without allowing the resin particles to settle down (the n.m.r. tube is well-shaken prior to insertion in the probe), a third sharp signal appears as a shoulder to the "external water" proton signal. This third resonance is evidently that of bulk water remote from the surface of the beads, which is excluded as the resin settles. Therefore, the "external water" must be located at the surface of the resin, and is not able, within the n.m.r. time-scale, to exchange with the bulk region. A typical spectrum showing all three resonances is given in Fig. 1. The resonance peaks show a slight skewness, presumably indicating exchange between the "external water" and "internal water" at the surface of the beads only. The "internal" solution is not affected by the exchange at the surface.

The molalities and the chemical shifts for the ion-exchange resins of varying crosslinkages and in different ionic forms are given in Table 1. The shift, $\Delta\nu$, in c.p.s. represents the chemical shift of the "internal water" signal with respect to the "external water" signal, i.e., ($\nu_{ext.\ H_2O} - \nu_{int.\ H_2O}$). A negative value of $\Delta\nu$ means that the internal water peak is downfield with respect to the external water peak. Values of δ_{soln}, defined as $\Delta\nu/60$ (p.p.m.), are plotted against the molalities of the ionic species in Fig. 2.

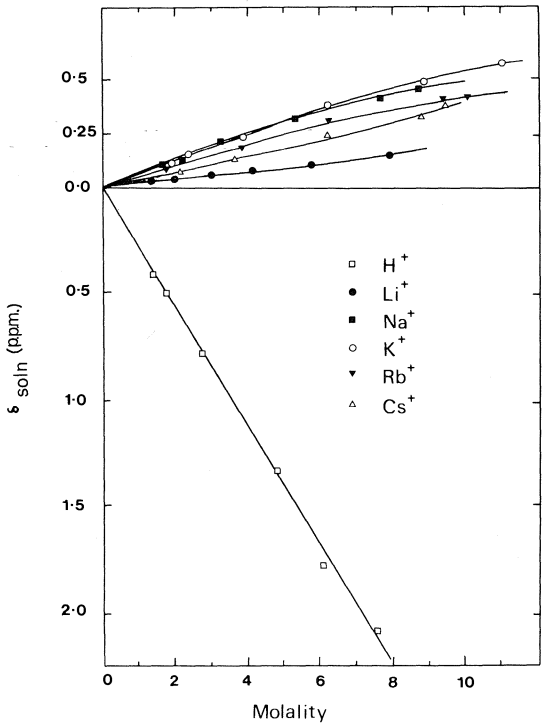

FIG. 2. Chemical shift as a function of concentration of ion inside the ion-exchange resin at 25 °C.

Can. J. Chem. Downloaded from www.nrcresearchpress.com by 210.87.254.105 on 09/05/12
For personal use only.

TABLE 1

Concentration dependence of proton resonance of water at 25 °C, for ion-exchange resins of various crosslinkages and ionic forms

Ionic form	Parameter	Resin crosslinkage X1	X2	X4	X8	X12	X16
H^+	Molality	1.39	1.76	2.79	4.81	6.10	7.57
	Δν*	−25.0	−31.2	−47.5	−80.0	−107.2	−125.5
Li^+	Molality	1.39	2.01	2.94	5.12	6.74	7.94
	Δν	1.6	2.0	2.5	4.1	5.8	8.4
Na^+	Molality	1.59	2.26	3.25	5.26	7.64	8.74
	Δν	6.5	7.6	12.1	18.8	24.0	27.7
K^+	Molality	1.90	2.38	3.90	6.17	8.89	11.06
	Δν	6.8	7.8	13.3	22.5	29.0	34.2
Rb^+	Molality	1.76	2.23	3.88	6.29	9.46	10.15
	Δν	5.3	7.0	11.0	18.5	23.5	25.5
Cs^+	Molality	—	2.19	3.66	6.18	8.82	9.45
	Δν	—	4.7	7.4	14.1	19.4	23.4
NH_4^+	Molality	—	2.01	3.30	5.70	—	—
	Δν	—	2.7	5.0	9.5	—	—

*Δν in c.p.s.

Malinowski *et al.* (5) have shown that the proton shift of water, measured with respect to gaseous ethane, varies with temperature according to the equation

$$[1] \quad \delta_{H_2O}{}^{ethane} = 0.00956\,t - 4.38 \quad \text{p.p.m.}$$

where t is the temperature in °C. Creekmore and Reilley (15) have recently obtained a value of 0.00958 p.p.m./°C for the slope from independent measurements. For the case of ion-exchange resin in water, the observed value at any temperature is equal to $\nu_{ext.\ H_2O} - \nu_{int.\ H_2O}$. Hence, $\nu_{int.\ H_2O}{}^{ethane}$ can be evaluated at a given temperature, if $\nu_{ext.\ H_2O}{}^{ethane}$ is known at that particular temperature. $\nu_{ext.\ H_2O}{}^{ethane}$ at different temperatures was obtained from eq. [1] and was used to calculate the corresponding $\delta_{soln}{}^{ethane}$ values. $\delta_{soln}{}^{ethane}$ values over the temperature range 16–60 °C for the H^+, Na^+, K^+, and Cs^+ forms of the resin are given in Table 2. The effect of temperature beyond 60 °C cannot be studied conveniently, at least in the present cases (except for H^+), since at higher temperatures overlap of the peaks becomes considerable. A plot of $\delta_{soln}{}^{ethane}$ (p.p.m.) vs. t (°C) is shown in Fig. 3. The slopes of the lines, $d\delta_{soln}{}^{ethane}/dt$, were calculated by the method of least squares using an IBM 360/75 computer and are included in Table 2.

Discussion

Accuracy of Data

The main source of error in the estimation of ion molality inside the resin comes from water content determination. We find that the Karl Fischer technique is capable of yielding values of the water content (percent, w/w) in sulfonic-acid-type resins within a maximum error of ±2% (8). The upper limit of error in capacity determination is ±0.05 meq/g. The error due to the exchange of water on the surface of the resin beads is negligible, since it does not affect the molality of cations inside the beads. The overall error in the value of molalities reported here can be considered to be not more than ±3%.

The n.m.r. shifts were found to be reproducible within 1 c.p.s. All the shifts recorded are the results of at least three separate measurements. The bands obtained with samples of ion-exchange resins suspended in water are relatively broader than those encountered in homogeneous aqueous solutions (12). The ν values, therefore, can only be estimated to a precision of ±1 c.p.s. The fluctuation of temperature inside the probe was within ±1 °C, as was shown by careful calibration of temperature using samples of methanol and ethylene glycol. Since δ_{soln} is a function of both concentration and temperature, the effect of temperature on δ_{soln} cannot be studied if the molality of the ion inside the resin (in other words, the water content) varies considerably over the range of temperature studied. We determined the water content of the H^+ form of resin X12 (where the internal and external water peaks are well separated) from 15 to

Can. J. Chem. Downloaded from www.nrcresearchpress.com by 210.87.254.105 on 09/05/12
For personal use only.

TABLE 2

Temperature dependence of proton resonance of water, for H^+, Na^+, K^+, and Cs^+ forms of ion-exchange resins*

Ionic form	Crosslinkage	Ion concentration m	Temperature °C	δ_{soln} p.p.m.	δ_{soln}^{ethane} p.p.m.	$d\delta_{soln}^{ethane}/dt$ p.p.m./°C
H^+	X8	4.81	16	−1.32	−5.54	0.00761
			25	−1.34	−5.48	
			35	−1.35	−5.39	
			40	−1.37	−5.36	
			50	−1.39	−5.28	
			60	−1.41	−5.21	
Na^+	X4	3.25	16	0.22	−4.01	0.00690
			25	0.20	−3.94	
			35	0.17	−3.87	
			40	0.15	−3.84	
			50	0.13	−3.76	
			60	0.09	−3.71	
Na^+	X8	5.26	16	0.34	−3.89	0.00635
			25	0.31	−3.83	
			35	0.28	−3.76	
			40	0.25	−3.74	
			50	0.22	−3.67	
			60	0.19	−3.61	
K^+	X4	3.90	16	0.23	−4.00	0.00662
			25	0.22	−3.92	
			35	0.19	−3.85	
			40	0.17	−3.82	
			50	0.14	−3.75	
			60	0.09	−3.71	
Cs^+	X8	6.18	16	0.25	−3.98	0.00699
			25	0.24	−3.90	
			35	0.20	−3.84	
			40	0.18	−3.81	
			50	—	—	
			60	—	—	

*$\delta_{soln} = \delta_{ext.\ H_2O} - \delta_{int.\ H_2O}$; δ_{soln}^{ethane} values were computed from the $\delta_{pure\ H_2O}^{ethane}$ values reported in ref. 5.

75 °C by a method suggested by de Villiers and Parrish (14). The change in percent (w/w) water content over this temperature range was found to be no more than 3%, which is within the limits of experimental error in the determination of molalities.

Size 200–400 mesh beads were used throughout, except in the case of X1 resins, where only 50–100 mesh could be obtained. It was found that the δ_{soln} value was not affected to any significant extent by change in the size of resin particles, provided the molality of the cation is the same. The n.m.r. spectra of resins in the H^+ (X8 and X12), Na^+ (X8), and K^+ (X8) forms with sizes ranging from 20–50 mesh to 200–400 mesh show that δ_{soln} is independent of the bead size in all three cases.

Concentration Dependence

Hindman (16) studied the dependence of the chemical shift of water protons on the concentration of alkali-metal salts in aqueous solution. He assumed an empirical relationship between δ, the chemical shift of the solution with respect to pure water, and m, the molality

$$[2] \qquad \delta = \delta_{salt}^{0}(m) + B(m)^2$$

where δ_{salt}^{0} is the value of δ/m at infinite dilution and B is a constant characteristic of the electrolyte. He further assumed that, for a uni–uni electrolyte

$$[3] \qquad \delta_{salt}^{0} = \delta_{M^+}^{0} + \delta_{X^-}^{0}$$

where $\delta_{M^+}^{0}$ and $\delta_{X^-}^{0}$ are the infinite dilution shift values for the cation and anion, respectively. By determining the δ_{salt}^{0} values for the ammonium salts and by assuming $\delta_{NH_4^+}^{0} = 0$, he obtained a set of $\delta_{X^-}^{0}$ values for anions. $\delta_{M^+}^{0}$ values for alkali-metal ions were then obtained by subtracting $\delta_{X^-}^{0}$ from δ_{salt}^{0}. In the present work, the $\delta_{M^+}^{0}$ values have similarly been

Can. J. Chem. Downloaded from www.nrcresearchpress.com by 210.87.254.105 on 09/05/12
For personal use only.

Can. J. Chem. Downloaded from www.nrcresearchpress.com by 210.87.254.105 on 09/05/12
For personal use only.

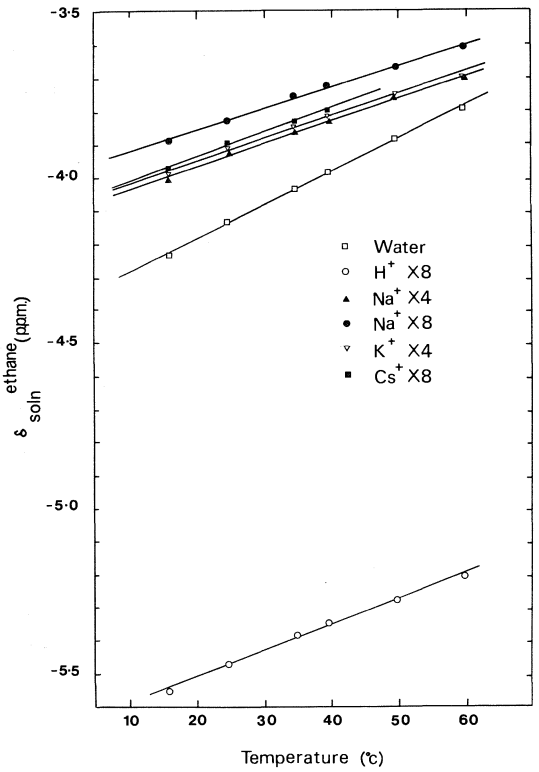

FIG. 3. Chemical shift of "internal" water as a function of temperature (pure water line is from ref. 5).

obtained by assuming $\delta_{x^-}{}^0 = 0.021$ p.p.m. for the fixed anionic group in the resin and by assuming $\delta_{NH_4^+}{}^0 = 0$ in the resin. These values are listed in Table 3. The experimental values of δ_{soln}, when plotted as a function of ionic concentration in the resin matrix (Fig. 2), show that the δ_{soln} value extrapolates to 0 for $m = 0$; the external and internal water thus have the same chemical shift.

Since δ_{soln} is zero when the "electrolyte" concentration is zero, and since it is not a function of bead size, it is satisfactory to interpret δ_{soln} directly as the shift of the water resonance produced by the ionic interactions with solvent within the bead and to omit susceptibility corrections. We attribute the shift between external and bulk water to susceptibility effects ($(\chi_{H_2O} - \chi_{resin}) \approx 0.03$ p.p.m.) and its value is dependent on the ionic form of the resin, as discussed by Gordon (12).

It can be seen from Fig. 2 that δ_{soln} vs. molality curves resemble the corresponding ones in aqueous solutions (16). The $\delta_{M^+}{}^0$ values for alkali-metal ions in the resin matrix differ by $\sim|0.013|$ p.p.m. from the respective ones in aqueous solutions. It appears that the chemical shifts are lower by this magnitude regardless of the sign. We offer no explanation for this behavior except to point out that the pore liquid inside the resin matrix is under pressure and is dispersed in an organic matrix, and the anionic groups are not mobile in the matrix. Nevertheless, it would appear from these observations that the cations act as salt solutions of strong electrolytes.

The deviation from linearity of the lines in Fig. 2 at high concentrations of ions (X12 and X16) parallels similar observations in homogeneous aqueous solutions (16–19). Except for H^+, where linearity exists almost up to 7 m, δ_{soln} for all the alkali-metal ions is not directly proportional to molality over the entire concentration range. The chemical shift values therefore

TABLE 3

Comparison of molal chemical shifts for cations in ion-exchange resin and in aqueous solution at 25 °C

	Molal shift (p.p.m.)			
Cation	Ion-exchange $\delta_{salt}{}^0$	Aqueous solution $\delta_{M^+}{}^0$ Hindman, ref. 16	Ion-exchange $\delta_{M^+}{}^0$	$\delta_{ion\text{-}ex.} - \delta_{aq.soln}$
H^+	−0.300	−0.344	−0.321	0.023
Li^+	0.017	−0.016	−0.005	0.011
Na^+	0.062	0.050	0.041	−0.009
K^+	0.052	0.047	0.031	−0.016
Rb^+	0.049	0.037	0.028	−0.009
Cs^+	0.036	0.027	0.015	−0.012
NH_4^+	0.021	0.0 (assumed)	0.0 (assumed)	

Can. J. Chem. Downloaded from www.nrcresearchpress.com by 210.87.254.105 on 09/05/12
For personal use only.

cannot be used to characterize the resin unambiguously in all ionic forms, contrary to a suggestion by de Villiers and Parrish (14).

Temperature Dependence

With a view to obtaining further evidence regarding the nature of the "electrolyte" inside the ion-exchange resin, the effect of temperature on the chemical shift of the "internal" water proton was studied in some typical cases. The experimental data were analyzed according to the method proposed by Malinowski *et al.* (5–7). The values of $d\delta_{soln}/dt$ listed in Table 2 compare very well with those reported for aqueous solutions of alkali-metal chlorides of approximately the same concentration (15).

To follow Malinowski's method for the determination of hydration numbers (5), it is necessary to obtain values of $d\delta/dt$, where t is the temperature in °C. As stated earlier, Malinowski *et al.* (5) and Creekmore and Reilley (15) have found a linear relationship of δ_{bulk} with temperature.

We may relate ν_{int} to ν_{bulk} as follows

$$\Delta\nu = \nu_{ext} - \nu_{int}$$
$$\nu_{int} = -\Delta\nu + \nu_{ext}$$
$$\nu_{int} = -\Delta\nu + \nu_{bulk} + S$$

where S is a susceptibility correction. Differentiating with respect to temperature

$$\frac{d\nu_{int}}{dt} = -\frac{d\Delta\nu}{dt} + \frac{d\nu_{bulk}}{dt} + \frac{dS}{dt}$$

Measured values of $d\delta/dt$ are approximately 0.002 p.p.m./°C. The value of dS/dt will be controlled by the difference in the temperature coefficients of the susceptibilities of the beads and of bulk water. The diamagnetic susceptibility of water changes by 0.0002 p.p.m./°C and this may be taken as an upper limit for dS/dt. Hence, within the accuracy of the present experiments, we neglect dS/dt, and therefore

$$\frac{d\nu_{int}}{dt} = \frac{d\nu_{bulk}}{dt} - \frac{d\Delta\nu}{dt}$$

The value of $d\delta_{soln}{}^{ethane}/dt$ for an electrolyte in the resin might be expected to yield hydration numbers of the resinates directly. The expression (ref. 7)

$$[4] \quad h = \frac{55.55}{m} \times \left[1 - \left(\frac{m + 111.02}{111.02}\right)\left(\frac{d\delta_{soln}{}^{ethane}/dt}{d\delta_{H_2O}{}^{ethane}/dt}\right)\right]$$

is used to calculate the hydration number of H^+, while for the alkali-metal ions, h is computed by

$$[5] \quad h = \frac{55.55}{m} \times \left[\frac{d\delta_{H_2O}{}^{ethane}/dt - d\delta_{soln}{}^{ethane}/dt}{d\delta_{H_2O}{}^{ethane}/dt}\right]$$

The values of h, along with the relevant concentration values, are compared with those obtained in homogeneous aqueous solutions in Table 4. The hydration number decreases with increase in concentration of electrolyte, similar to the observations for NaCl solutions by Malinowski *et al.* (5). When the ionic concentrations are comparable to the aqueous solution concentrations, similar values for h result. The value of h for H^+ in the ion-exchange resin is 2.0, which is lower than the value of 3.4 ± 0.4 for the same ion in aqueous HCl (7). The small size of H^+ and its greater tendency to form ion pairs might be responsible for the low hydration number in the resin. Creekmore and Reilley obtained even lower values of the hydration number for the sodium salt of *p*-toluene sulfonic acid (15); it would appear that resin acts as a stronger acid. The hydration numbers obtained by the ion-exchange method (20) are in general lower than those obtained by the n.m.r. resin or aqueous solution methods (Table 4).

It would appear that the concentration dependence of the chemical shift of water protons due to ions in both ion-exchange resins and homogeneous solutions show similar trends. The hydration numbers of alkali-metal ions in cation-exchange resin as calculated from the temperature dependence are also in agreement with those obtained for the corresponding aqueous solutions. These observations are consistent with the polyelectrolyte gel model of the ion-exchange resin (20). This medium offers an advantage in studying ion–solvent interactions at fairly high concentrations of ions, which are difficult to attain in homogeneous solutions due to solubility limitations.

The authors are grateful to the National Research Council of Canada for providing financial support for this work and for a Post-Graduate Scholarship to one of us (N.S.). We are also indebted to Dr. R. C. Vasishth, Research Director, Reichhold Chemicals (Canada) Ltd., Weston, Ont. for making available to us the use of the Varian A-60 spectrometer.

TABLE 4

Comparison of hydration numbers of cations

	Nuclear magnetic resonance method					
	Ion-exchange resin		Aqueous solution			
Ion	Ion concentration (m)	h	Chloride concentration (m)	h	Reference	Ion-exchange (ref. 20) h
H^+	4.81	2.0	0.00 to 4.77	3.4	7	3.9
Na^+	3.25	4.8	3.08	4.6	15	1.5
			3.00	4.7	5	
	5.26	3.6	5.00	3.9	15	
K^+	3.90	4.4	2.99	4.6	15	0.6
Cs^+	6.18	2.4	3.02	3.9	15	0.0

1. J. F. HINTON and E. S. AMIS. Chem. Rev. **67**, 367 (1967).
2. J. BURGESS and M. C. R. SYMONS. Quart. Rev. London, **22**, 276 (1968).
3. C. DEVERELL. Progr. NMR Spectrosc. **4**, 235 (1969).
4. J. A. JACKSON, J. F. LEMONS, and H. TAUBE. J. Chem. Phys. **32**, 553 (1960).
5. E. R. MALINOWSKI, P. S. KNAPP, and B. FEUER. J. Chem. Phys. **45**, 4274 (1966).
6. E. R. MALINOWSKI and P. S. KNAPP. J. Chem. Phys. **48**, 4989 (1968).
7. P. S. KNAPP, R. O. WAITE, and E. R. MALINOWSKI. J. Chem. Phys. **49**, 5459 (1968).
8. H. D. SHARMA and N. SUBRAMANIAN. Anal. Chem. **41**, 2063 (1969).
9. F. HELFFERICH. Ion exchange. McGraw-Hill Book Co., Inc., New York. 1962. p. 91.
10. H. P. GREGOR, J. A. BERGMAN, F. GUTOFF, R. D. BRADLEY, D. E BALDWIN, and C. G. OVERBERGER. J. Colloid Sci. **6**, 20 (1951). R. G. FESSLER and H. A. STROBEL. J. Phys. Chem. **67**, 2562 (1963).
11. A. WEERHEIM. Private communication.
12. J. E. GORDON. J. Phys. Chem. **66**, 1150 (1962).
13. R. H. DINIUS, M. T. EMERSON, and G. R. CHOPPIN. J. Phys. Chem. **67**, 1178 (1963).
14. J. P. DE VILLIERS and J. R. PARRISH. J. Polym. Sci. Part A, **2**, 1331 (1964).
15. R. W. CREEKMORE and C. N. REILLEY. J. Phys. Chem. **73**, 1563 (1969).
16. J. C. HINDMAN. J. Chem. Phys. **36**, 1000 (1962).
17. J. N. SHOOLERY and B. J. ALDER. J. Chem. Phys. **23**, 805 (1955).
18. B. P. FABRICAND and S. GOLDBERG. J. Chem. Phys. **34**, 1624 (1961).
19. S. GOTO and T. ISEMURA. Bull. Chem. Soc. Jap. **37**, 1693 (1964).
20. E. GLUECKAUF and G. P. KITT. Proc. Roy. Soc. London, Ser. A, **228**, 322 (1955).

Can. J. Chem. Downloaded from www.nrcresearchpress.com by 210.87.254.105 on 09/05/12
For personal use only.

Can. J. Chem. Downloaded from www.nrcresearchpress.com by 210.87.254.42 on 09/05/12
For personal use only.

The Hg 6($^3P_1$) photosensitized decomposition of methyl vinyl ether

R. V. Morris and S. V. Filseth
Department of Chemistry, Harvey Mudd College, Claremont, Calif. 91711

Received August 11, 1969

The mercury 6($^3P_1$) photosensitized decomposition of methyl vinyl ether has been studied in the vapor phase in a static system at 55 °C between 0.2 and 10.0 Torr. The principal products are propanal and ethane. It is concluded that the primary process involves the direct production of methyl and vinoxy radicals with no more than 3% participation of a competing step producing ethylene. Neither carbon–hydrogen bond breaking nor the production of primary excited molecules is observed.

Canadian Journal of Chemistry, **48**, 924 (1970)

Introduction

Recent studies of the mercury 6($^3P_1$) photosensitized decomposition of dimethyl ether (1, 2) and of methyl ethyl ether (3) have demonstrated that the only primary decomposition process in the simple ethers above 1 Torr is rupture of a carbon–hydrogen bond. The overall decomposition mechanisms seem to differ little from those of corresponding hydrocarbons, with the exception that the ether quenching cross-sections are considerably larger.

A very different behavior has been observed in the only reported study of an unsaturated aliphatic ether. The sensitized and direct decomposition of ethyl vinyl ether (4) has been observed to produce ethyl and vinoxy radicals in at least 75% of the primary processes, while ethylene and acetaldehyde are formed directly in the remainder. In this work, the possibility was raised that an excited state subject to collisional deactivation might participate in the direct photodecomposition.

A comparison of the primary processes in the sensitized decomposition of saturated and unsaturated analogs of an aliphatic ether should be particularly interesting in view of the possibility of competition between the carbon–hydrogen bond breaking step established for saturated hydrocarbons and ethers and an excited-molecule mechanism characteristic of unsaturated hydrocarbons. The simplest such pair is methyl vinyl and methyl ethyl ethers. A comparison of relevant quenching cross-sections measured on the chemical basis by the competitive nitrous oxide technique is given in Table 1. The present work was begun to quantitatively assess the importance of competing primary steps in methyl vinyl ether. Of particular interest was the possibility that ethylene might be formed from an excited intermediate subject to collisional deactivation as suggested by earlier work (3) on methyl ethyl ether.

Experimental

Matheson methyl vinyl ether was purified by preparative gas chromatography and by successive trap-to-trap distillation, and stored at room temperature behind a metal valve. Its purity was determined to be 99.5%, with acetaldehyde and dimethyl ether the principal impurities.

Irradiations were carried out in a static system and products were analyzed by combined gas chromatography and mass spectrometry. The light intensities employed in these studies averaged 5×10^{14} quanta $cm^{-2}\,s^{-1}$ of 2537 Å radiation reaching the interior of the vessel. Details of the apparatus and procedure have been described previously (3). There is no appreciable direct absorption by the ether at wavelengths longer than about 2300 Å.

Results and Discussion

The principal products in the sensitized decomposition of methyl vinyl ether between 0.2 and 10.0 Torr at 55 °C are propanal and ethane. In addition, smaller amounts of ethanal, ethylene, carbon monoxide, propane, methane, and *n*-butanal are observed together with polymer. No hydrogen is observed and analysis for formaldehyde was not attempted.

On the basis of previous work on saturated (1–3) and unsaturated (4, 5) ethers, several

TABLE 1

Chemical quenching cross-sections for Hg 6($^3P_1$), at 328 °K

Molecule	σ_Q^2 (Å^2)	Reference
CH_3OCH_3	3.3	2*
$CH_3OCH_2CH_3$	10.3	3†
$CH_3OCH{=}CH_2$	31.5	This work†

*Relative to $\sigma_{n-C_4H_{10}}^2 = 3.6$ Å^2, 298 °K.
†Relative to $\sigma_{N_2O}^2 = 18.0$ Å^2, 328 °K.

TABLE 2
Product quantum yields for varying irradiation time of 0.82 Torr methyl vinyl ether

Product	Quantum yield for irradiation time (s)			
	60	120	240	960
Propanal	0.159	0.147	0.135	0.132
Ethane	0.065	0.063	0.063	0.059
Ethanal	0.032	0.012	0.017	0.021
Ethylene	0.016	0.009	0.010	0.014
Carbon monoxide	0.008	0.006	0.012	0.027
Propane, methane, *n*-butanal	0.005	0.005	0.005	0.009

primary processes may be considered for the methyl vinyl ether decomposition. A carbon–hydrogen bond breaking step, as

[1] $Hg\ 6(^3P_1) + CH_3OCH{=}CH_2 \rightarrow CH_2OCH{=}CH_2 + H + Hg\ 6(^1S_0)$

may be eliminated by the failure to observe anticipated final products such as ethyl vinyl ether or methyl isopropyl ether. Similarly, the absence of propylene and dimethyl ether in the product distribution excludes a primary carbon–oxygen bond breaking step, as

[2] $Hg\ 6(^3P_1) + CH_3OCH{=}CH_2 \rightarrow CH_3O + CH{=}CH_2 + Hg\ 6(^1S_0)$

The composition of the product distribution and its behavior under conditions of varying intensity and varying pressure and irradiation time as described below suggests that the principal primary process can be written as

[3] $Hg\ 6(^3P_1) + CH_3OCH{=}CH_2 \rightarrow CH_3 + CH_2{=}CHO + Hg\ 6(^1S_0)$

An analogous primary process has been proposed in the sensitized decomposition of anisole (5). The vinoxy radical formed in reaction [3] is a resonance-stabilized tautomer of the formyl methyl radical, CH_2CHO.

The major stable products result from combination of these primary radicals. The results of measurements of product quantum yields as a function of period of irradiation are recorded in Table 2. Propanal, ethane, ethanal, and ethylene appear to be primary products, whereas the others result at least in part from secondary decomposition of primary products. Propanal seems clearly to result from the combination of methyl and formyl methyl radicals. Similarly, *n*-butanal has been observed as the major product in the sensitized decomposition of ethyl vinyl ether (6). Disproportionation to methane and presumably ketene occurs with less than 4% probability.

Recombination of the vinoxy tautomer with the methyl radical could regenerate the substrate ether and thereby go undetected or result in the formation of propanal as indicated above. The reaction of two vinoxy radicals could lead to ethanal and ketene through disproportionation, as

[4] $2CH_2CHO \rightarrow CH_3CHO + CH_2CO$

for which a reasonable six-membered ring intermediate can be written. No ketene was detected in this work, but it would not be expected to survive attempts to separate it chromatographically (7). In addition, polymerization is a likely alternate fate of the radical.

As the irradiation period is extended, the quantum yield of propanal decreases. This fact, together with the near-equality of the methane, propane, and *n*-butanal yields, suggests the following pattern of secondary reactions

[5] $Hg\ 6(^3P_1) + CH_3CH_2CHO \rightarrow CH_3CH_2 + CHO + Hg\ 6(^1S_0)$

[6] $CH_3CH_2 + CH_2CHO \rightarrow n\text{-}C_3H_7CHO$

[7] $CH_3CH_2 + CH_3 \rightarrow C_3H_8$

[8] $CHO + CH_3 \rightarrow CO + CH_4$

[9] $CH_2CHO + CHO \rightarrow CO + CH_3CHO$

Near-equal yields of methane, propane, and *n*-butanal would be expected on the basis of this reaction sequence, as is observed, and reaction [5] is expected to be the dominant primary process in the sensitized decomposition of propanal on the basis of previous work on ethanal (8).

The overall mechanism, including reactions [3]–[9] and propanal production through recombination of methyl and formyl methyl

Can. J. Chem. Downloaded from www.nrcresearchpress.com by 210.87.254.42 on 09/05/12
For personal use only.

TABLE 3

Product yield of irradiation of methyl vinyl ether at varying pressures and intensities

	Product yield* (nmole)					
Product	Exp. 1	Exp. 2	Exp. 3	Exp. 4	Exp. 5	Exp. 6
Propanal	38.4	13.8	30.0	41.4	44.4	—
Ethane	26.3	26.0	19.2	25.8	31.8	33.6
Ethanal	7.8	26.8	6.0	10.8	—	—
Ethylene	2.8	1.7	2.4	2.4	2.4	2.4
Propane	0.6	0.6	1.2	1.2	1.2	1.2
Methane	1.1	2.5	1.2	1.2	1.2	1.2
n-Butanal	0.6	0.1	0.6	0.6	0.6	—

*Experimental conditions for Exps. 1 to 6 are: ether pressure = 0.82, 0.82, 0.21, 0.92, 4.30, 10.00 Torr; intensity I_0 = 1.00, 0.01, 1.00, 1.00, 1.00, 1.00; and irradiation time = 100, 10 000, 60, 60, 60, 60 s, respectively.

radicals, is the basis for a quantitative mass balance at low intensity, as seen from the data in Table 3, for which the yield of methyl-radical containing products equals that of vinoxy tautomer products. The mass balance is incomplete at higher intensity, with methyl-radical products in the excess. This may reflect the disappearance of the vinoxy tautomer with the formation of polymer which was observed at high intensity.

By analogy with the results of studies of ethyl vinyl ether (4), and as suggested by a previous study of methyl ethyl ether (3), a primary process to produce ethylene might be expected. Ethylene is formed in fact as a primary product, but this appears to be a very minor process accounting for no more than 3% of the ether decomposition.

The effect on product yields of the variation of substrate pressure as recorded in Table 3 provides no evidence for the presence of an excited intermediate capable of collisional deactivation. Within the limitation of this diagnostic test, it is concluded that the production of such a precursor is not an important feature of the mechanism at pressures above 0.2 Torr.

The authors thank the Pomona College Chemistry Department for the use of its mass spectrometer. This research was supported in part by grants from the Petroleum Research Fund of the American Chemical Society and from Harvey Mudd College.

1. L. F. Loucks and K. J. Laidler. Can. J. Chem. **45**, 2763 (1967).
2. R. Payette, M. Bertrand, and Y. Rousseau. Can. J. Chem. **46**, 2693 (1968).
3. S. V. Filseth. J. Phys. Chem. **73**, 793 (1969).
4. E. Murad. J. Amer. Chem. Soc. **83**, 1327 (1961).
5. J. B. Homer, I. P. Fisher, and F. P. Lossing. Abstracts Sixth Informal Photochemistry Conference, University of California, Davis, June 1964.
6. R. V. Morris and S. V. Filseth. Unpublished results.
7. H. E. Avery and R. J. Cvetanović. J. Chem. Phys. **48**, 380 (1968).
8. F. P. Lossing. Can. J. Chem. **35**, 305 (1957).

Can. J. Chem. Downloaded from www.nrcresearchpress.com by 210.87.254.42 on 09/05/12
For personal use only.

Supersonic molecular beam intensities

RODNEY L. LEROY[1]
Department of Chemistry, University of Colorado, Boulder, Colorado 80302

AND

THOMAS R. GOVERS[2] AND JACQUES M. DECKERS
Lash Miller Chemical Laboratories, University of Toronto, Toronto 181, Ontario

Received August 25, 1969

This paper attempts to obtain agreement between theoretical and experimental supersonic molecular beam intensities. Measurements of absolute beam intensities are presented, corrected for the effect of background scattering in the expansion chamber. It is found that these intensities are considerably lower than those predicted by existing theories. This is true even when losses due to imperfect skimming are negligible. A new mechanism is therefore proposed which postulates a considerable attenuation of the beam due to "self-scattering" collisions upstream of the skimmer and downstream of the onset of translational freezing. Using this mechanism it is possible to reasonably reproduce the experimental intensities.

Canadian Journal of Chemistry, **48**, 927 (1970)

Can. J. Chem. Downloaded from www.nrcresearchpress.com by 210.87.254.5 on 09/05/12
For personal use only.

Introduction

Numerous attempts have been made to predict the intensities of molecular beams which are formed by skimming-off the core of an expanding free jet (1–7). All of these efforts have yielded theoretical beam intensities which are several times larger than most of the experimental intensities which have been reported.[3] In an attempt to understand the low experimental intensities, several "non-ideal" effects have been postulated: skimmer interference with the flow (9–13), self-scattering collisions among beam molecules downstream of the skimmer (14, 15), and attenuation due to scattering on background gas which penetrates the jet in the expansion chamber (10, 12, 13, 16, 17).

We report here some careful measurements of absolute beam intensities, made using a range of nozzle–skimmer separations and five sets of source conditions. In each case intensities were recorded at a number of values of the background pressure (p_b) in the expansion chamber. The intensity which would be observed in the absence of background scattering in this region could thus be deduced by logarithmic extrapolation of these measurements to $p_b = 0$ (13). In every case it was found that the intensities obtained in this way were still considerably lower than those predicted by any of the ideal beam equations. This was true even at large nozzle–skimmer separations, where effects due to skimmer interference and self-scattering downstream of the skimmer almost certainly have a negligible effect on the observed intensities.

We discuss a new mechanism which, we believe, resolves the discrepancy between theory and experiment. The effect is a consequence of the translational freeze phenomenon which was described, e.g., by Anderson and Fenn (5). In particular we argue that collisions among beam particles downstream of the onset of translational freezing may result in the effective removal of the collision partners from the beam. Taking this effect into account, we are able to predict intensities in satisfactory agreement with experiment. Only beams of monatomic gases are considered, so as to avoid the complications introduced by rotational and vibrational freezing in the expanding jet.

Experimental

The apparatus has been described previously (13, 18). No collimating orifice was used between the skimmer and the detector. The geometric parameters of the beam defining elements were: geometric nozzle exit diameter (D), 0.0266 cm; skimmer throat diameter, 0.033 cm; skimmer–detector distance, 99.6 cm; solid angle subtended by detector, 1.43×10^{-5} steradians.

[1]Present address: Department of Chemistry, Yale University, New Haven, Connecticut 06520.

[2]Present address: FOM Institute, Kruislaan 407, Amsterdam, The Netherlands.

[3]A notable exception is the agreement between theory and experiment reported recently by Bossel, Hurlbut, and Sherman (8). These authors utilized an unusually high pumping capacity in the expansion chamber in order to produce free jets which could be "skimmed" in the region of isentropic flow, with a minimum of non-ideal effects.

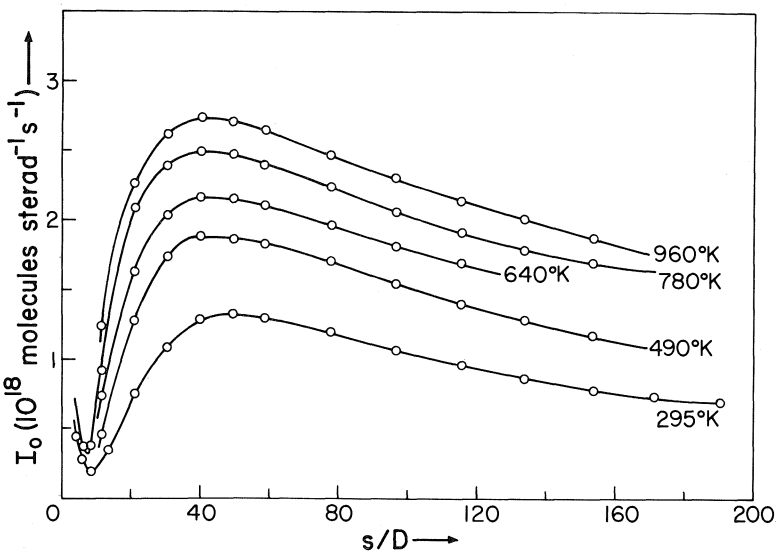

FIG. 1. Centerline beam intensities, obtained by extrapolation to $p_b = 0$. The flow through the nozzle is 2.7×10^{19} particles/s. Dimensions of the beam defining elements are given in text.

An absolute calibration of the ionization gauge detector was obtained using known effusive flows from a small orifice. The calibration procedure has been described in detail by Govers (18). Argon was used throughout. For all experiments reported, the flow through the nozzle was held constant at 2.7×10^{19} particles/s. Source temperatures (T_0) were determined using the constant flow technique described by Govers, LeRoy, and Deckers (13). The nozzle discharge coefficient was ~ 0.83, and was roughly independent of the source temperature (13).

Centerline beam intensities were measured as a function of nozzle–skimmer separation (s), at five values of T_0 ranging from 295 to 960 °K. At each value of s, the background pressure in the expansion chamber was varied between 4.4×10^{-4} and 2.5×10^{-3} Torr, so that the beam intensity in the absence of background scattering (I_0) could be determined by logarithmic extrapolation to $p_b = 0$ (13). The resulting intensities are plotted in Fig. 1. The error resulting from the extrapolation procedure is estimated to be $\pm 4\%$ or less. Intensities here and throughout this paper are expressed per unit of solid angle, where solid angles are measured from the center of the skimmer opening.

"Ideal" Molecular Beam Intensities

Molecular beam intensities can be readily calculated, if skimmer interference and other non-ideal effects are ignored. For a centerline detector far downstream of a skimmer, the "ideal" intensity may be approximated by (6, 19)

$$[1] \qquad I_0 \simeq n v_b s^2 (1 - e^{-S_\perp^2 \alpha_s^2})$$

Here n is the number density of beam particles at the skimmer orifice, v_b is the average velocity of beam particles in the radial direction, s is the nozzle–skimmer separation, $S_\perp \equiv v_b/c_\perp$ is the perpendicular speed ratio at the skimmer, and $\alpha_s \equiv \arctan(r_s/s)$ is one-half the angle which the skimmer opening subtends at the nozzle throat. $c_\perp$ is a reference velocity, defined by $c_\perp \equiv (2kT_\perp/m)^{1/2}$, where m is the mass of a beam particle, k is the Boltzmann constant, and $T_\perp$ is the perpendicular temperature (the "temperature" of a two-dimensional Boltzmann distribution function which describes the local speed distribution in the plane perpendicular to the radial direction). r_s is the skimmer radius.

We have compared eq. [1] with a more exact expression which can take account of any anisotropy of the local speed distribution at the skimmer (19). This comparison shows that when the local speed distribution at the skimmer is isotropic, eq. [1] is a good approximation provided only that $S^2 = S_\perp^2 \gg 3/2$. In the other limit, where the flow is isentropic to a distance $x = x_q$ from the nozzle throat,[4] and is free molecular thereafter ($T_\perp/T_q = x_q^2/s^2$), the corresponding requirements are $r_s \ll x_q$ and $S_q \gg 3/2$. Most realistic cases fall between these two extremes. For the conditions of the experiments

[4]The symbol x is used to denote the distance from a point of interest in the expansion to the nozzle throat. The subscript q identifies isentropic flow parameters at $x = x_q$.

Can. J. Chem. Downloaded from www.nrcresearchpress.com by 210.87.254.5 on 09/05/12
For personal use only.

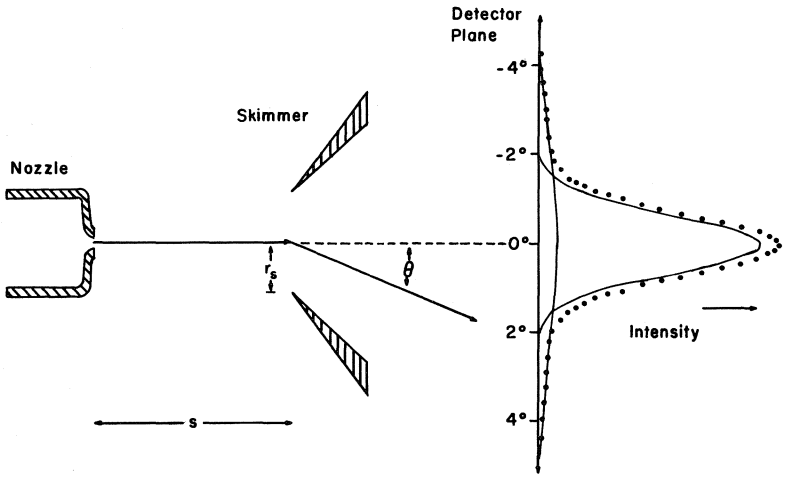

FIG. 2. Origin of the self-scattering losses. The broad intensity profile corresponds to $T_\perp = 2.1$ °K, and represents beam molecules which suffer collisions downstream of the onset of translational freezing. The sharper profile ($T_\perp = 0.19$ °K) represents an equal number of beam particles which do not suffer such collisions. The dotted curve is the sum of these two contributions.

reported in this paper, eq. [1] always approximates the exact ideal beam intensity within 10%.

In evaluating eq. [1] below, the expansion is assumed to be isentropic to $x = x_q$, where the local Mach number is $M = M_q$. For $s > x_q$ it is assumed that

$$n = n_q(x_q/s)^2$$

$$v_b = M_q[(5/3)kT_q/m]^{1/2}$$

and that the parallel temperature $T_\parallel$ (the "temperature" which describes the local distribution of molecular speeds in the radial direction) is a constant, equal to T_q. Ashkenas and Sherman's fitting formula (20) for the centerline Mach number in a free jet is used to relate x ($\leqslant x_q$) and M, and the "terminal" Mach number M_q (and thus x_q, T_q, and n_q) is calculated from Anderson and Fenn's empirical relation for argon expansions (5).

Beam Attenuation due to "Self-Scattering" Upstream of the Skimmer

Solutions of the Boltzmann equation for the source flow problem suggest that the perpendicular temperature[5] in a free jet should approach a dependence on the inverse of the distance from the source (21, 22). On the other hand, experimental determinations of $T_\perp$ (23–25) show a dependence on the nozzle–skimmer separation which is intermediate between the collision-dominated form ($T_\perp = T_\parallel \propto s^{-4/3}$) and the form expected in the free molecular limit ($T_\perp \propto s^{-2}$). This apparent discrepancy was clarified by Edwards and Cheng's analysis (26) of their asymptotic solution. They found that this *does* predict $T_\perp' \propto x^{-2}$, provided that only the portion of the distribution function near the centerline in velocity space is used in evaluating $T_\perp'$.[6] The overall $T_\perp' \propto x^{-1}$ dependence is due to the effect of collisions downstream of the onset of translational freezing. Because a large anisotropy develops in the local velocity distribution, such collisions impart relatively large transverse velocities to the particles involved. They can thus effectively remove both collision partners from a beam which is formed by sampling the core of the jet. When these "self-scattering" losses are accounted for, centerline beam intensities may be predicted from equations such as [1] using an s dependence of $T_\perp$ which varies from $T_\perp \propto s^{-4/3}$ in the collision dominated region of the expansion to $T_\perp \propto s^{-2}$ at large distances from the source (27).

The origin of the self-scattering attenuation is illustrated schematically in Fig. 2. This figure shows intensity profiles measured by a detector

[5]Evaluated by fitting an ellipsoidal function to the entire theoretical speed distribution (21).

[6]Primed quantities are evaluated in the expansion at a distance x from the source.

Can. J. Chem. Downloaded from www.nrcresearchpress.com by 210.87.254.5 on 09/05/12
For personal use only.

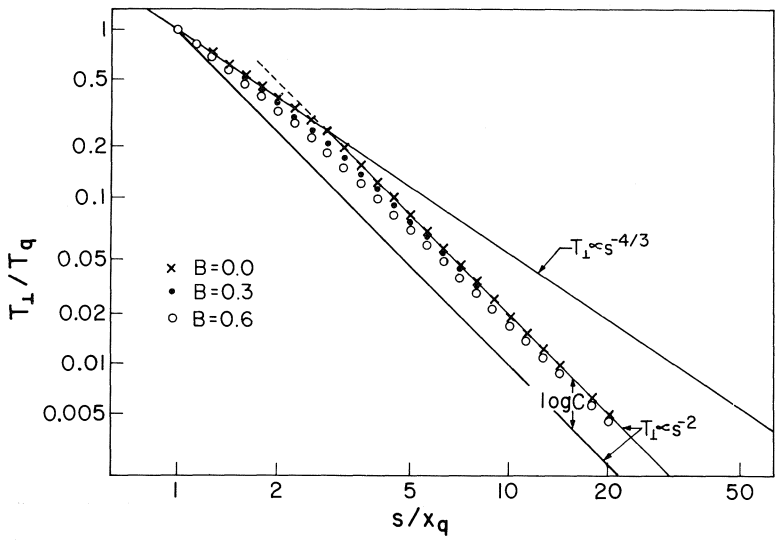

FIG. 3. Typical variations of the perpendicular temperature with nozzle–skimmer separation. The points are calculated from eq. [2] for three values of the parameter B; C is set equal to 2.

which is moved across the beam, perpendicular to the centerline. The broad curve ($T_\perp = 2.1$ °K) represents those particles which have suffered collisions downstream of the onset of translational freezing, while the sharper curve ($T_\perp = 0.19$ °K) represents those particles which have not. The dotted profile is derived from the sum of these two contributions. The particular perpendicular temperature used is taken from Fig. 3 of ref. 27 and it corresponds to a nozzle–skimmer separation of 40 nozzle diameters. The perpendicular temperature of particles which have collided is arbitrarily set at one-half the value of $T_\parallel$ taken from ref. 27 at $s/D = 40$. In constructing Fig. 2, it was assumed that one-half of the particles passing the skimmer had suffered collisions downstream of the onset of translational freezing.

Self-scattering collisions upstream of the skimmer do not affect the total flux through the skimmer. However, the profiles of Fig. 2 show clearly that particles which have suffered such collisions make only a small contribution to the beam intensity measured by a centerline detector. This contribution decreases as the nozzle–skimmer separation is increased.

We use an analytical expression to describe the variation from $T_\perp \propto s^{-4/3}$ to $T_\perp \propto s^{-2}$, a hyperbola on a log–log plot of $T_\perp/T_q$ vs. s/x_q. This hyperbola has asymptotes of slope $-4/3$ and -2 (cf. Fig. 3), and it is constructed so that $T_\perp = T_q$ at $s = x_q$:

$$[2]\quad \log\left(\frac{T_\perp}{T_q}\right) = -\frac{5}{3}\log\left(\frac{s}{x_q}\right) + \frac{1+B^2}{2}\log C - \frac{1}{3}\left\{\left[\log\left(\frac{s}{x_q}\right) - 1.5(1-B^2)\log C\right]^2 + 9B^2[\log C]^2\right\}^{1/2}$$

The function has two parameters: C is the number of times $T_\perp$ in the limit $s \to \infty$ is larger than the value it would have if the flow became suddenly free molecular at $x = s_q$; and $B\,(0 \leqslant B \leqslant 1)$ is a measure of how rapidly the transition from $T_\perp \propto s^{-4/3}$ to $T_\perp \propto s^{-2}$ takes place.[7] When B

[7]Specifically B is the ratio of two differences on the log–log plot: the difference between $\log(T_\perp/T_q)$ and the asymptotic line of slope $-4/3$ at $s/x_q = 1$, and the same difference at $s/x_q = x_0/x_q$, where $x_0 = x_q C^{1.5(1-B^2)}$ is the abscissa of the origin of the hyperbola.

Can. J. Chem. Downloaded from www.nrcresearchpress.com by 210.87.254.5 on 09/05/12
For personal use only.

Can. J. Chem. Downloaded from www.nrcresearchpress.com by 210.87.254.5 on 09/05/12
For personal use only.

is small the transition is sharp, while for large B it is quite gradual (Fig. 3).

In order to estimate the extent of beam attenuation due to self-scattering upstream of the skimmer, we make three approximations. (*a*) At a distance x_q from the nozzle, $T_{\|}'$ freezes at the value of the local temperature calculated for an isentropic expansion, T_q. (*b*) Self-scattering losses are limited to the interval between $x = c_s x_q$ and s, where $c_s \geqslant 1$. In other words, when $x \geqslant c_s x_q$, $T_{\perp}'$ and $T_{\|}'$ are assumed to have diverged sufficiently that any collision will result in removal of both collision partners from the final beam. Downstream of the skimmer, the sharp decrease in density[8] quenches further self-scattering losses. (*c*) The collision frequency in the interval $c_s x_q \leqslant x \leqslant s$ is governed by a one-dimensional Maxwellian speed distribution corresponding to a temperature T_q.

With these approximations, the collision probability per unit length is given by

$$[3] \qquad \xi(x) = \frac{n'}{v_b}\frac{m}{2kT_q}\int_{-\infty}^{\infty}\int_{-\infty}^{\infty}(\sigma(v_r))^2 v_r \exp\left(\frac{-m(v_1^2 + v_2^2)}{2kT_q}\right) dv_1\, dv_2$$

where $n' = n_q(x_q/x)^2$ is the number density at x, $\sigma(v_r)$ is the collision diameter of the beam particles, and $v_r \equiv |v_1 - v_2|$ is the relative speed of particles 1 and 2. To approximate $\sigma(v_r)$ we assume a "classical" dependence on v_r (28).

$$[4] \qquad \sigma(v_r) = \sigma_0\left(\frac{16kT_{rt}}{\pi m}\right)^{1/6} v_r^{-1/3}$$

σ_0 is the collision diameter for particles which collide with a relative velocity equal to its average value in a room temperature ($T_{rt} = 298$ °K) gas. Integration of eq. [3] now yields

$$[5] \qquad \xi(x) = 4.1 \times 10^{-7}\frac{n_q s_q^2 \sigma_0^2}{x^2 v_b}\left(\frac{T_q}{m^3}\right)^{1/6} \equiv \beta/x^2$$

where T_q is in degrees Kelvin and all other quantities are in c.g.s. units.

According to our assumptions, the probability that a beam particle will not suffer a collision between $c_s x_q$ and s is equal to the ratio of the beam intensities in the presence (I) and absence (I_0) of self-scattering. This probability is now readily derived (29) to be

$$[6] \qquad I/I_0 = \exp\left[-\beta\left(\frac{1}{c_s x_q} - \frac{1}{s}\right)\right]$$

The ratio I/I_0 is plotted in Fig. 4 for several values of the parameters σ_0 and c_s. The source conditions correspond closely to the high and low temperature results reported in Fig. 1. n_q, x_q, T_q, and v_b were evaluated as described in the preceding section. Note that an increase in source temperature decreases the amount of self-scattering at large nozzle–skimmer separations.

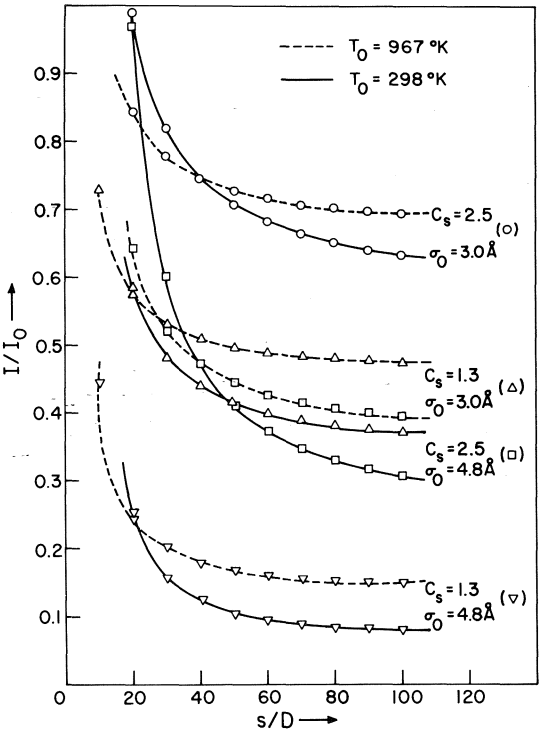

FIG. 4. Some typical variations of the self-scattering attenuation with nozzle–skimmer separation.

We should emphasize that the estimation of collision frequencies at low local temperatures such as are encountered in the free jet ($T_{\|} \simeq 10$ °K for $T = 295$ °K) is a risky matter. This is especially true for beam gases, including argon,

[8]See, for example, the derivation in ref. 15 of the collision free density downstream of a skimmer.

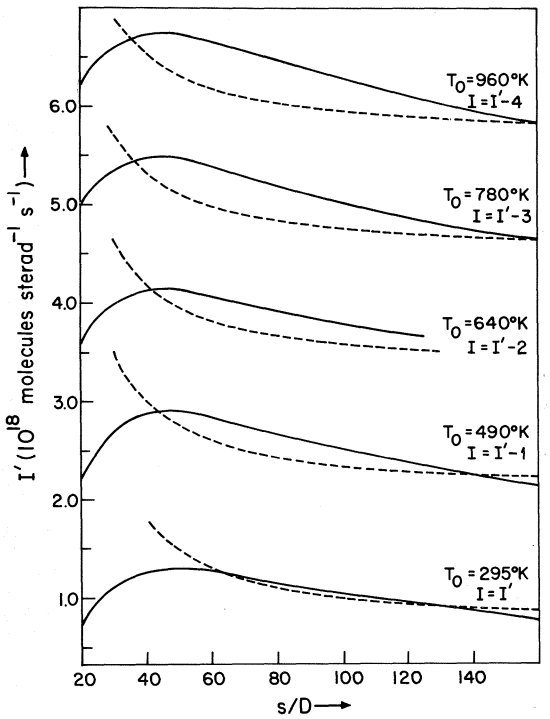

FIG. 5. Comparison of theoretical and experimental centerline intensities. The solid curves are transferred directly from Fig. 1, while the broken curves are calculated from eq. [7] using the parameters $\sigma_0 = 5.5$ Å, $c_s = 2.0$, $B = 0.4$, and $C = 1.5$.

which become "supercooled" at these temperatures. Thus eq. [6] must be viewed as a rough approximation to the self-scattering attenuation.

Predictions of Supersonic Beam Intensities Using the Self-Scattering Model: Comparison with Experiment

When the core of a monatomic free jet is sampled downstream of the onset of translational freezing eqs. [1] and [6] may be combined to predict the centerline intensity of the resulting beam

$$[7]\quad I = nv_b s^2(1 - e^{-S_\perp^2 \alpha_s^2}) \times \exp\left[-\beta\left(\frac{1}{c_s x_q} - \frac{1}{s}\right)\right]$$

$S_\perp$ is calculated using $T_\perp$ from eq. [2].

We have used eq. [7] to predict the beam intensities corresponding to the experimental conditions of Fig. 1. Figure 5 illustrates the results obtained using $B = 0.4$ and $C = 1.5$ to evaluate $S_\perp$, and $\sigma_0 = 5.5$ Å and $c_s = 2.0$ to estimate the self-scattering attenuation. However, this choice of parameters is certainly not unique as, for example, comparable agreement was obtained using $\sigma_0 = 4.7$ Å and $c_s = 1.5$. "Quitting" parameters were again calculated from Anderson and Fenn's empirical relation (5), as explained above. To determine x_q, we used the "effective nozzle diameter" (13, 20) corresponding to the experimental discharge coefficient.

Discussion

Equation [7] predicts absolute intensities which are in qualitative agreement with experimental measurements, and it also predicts qualitatively the variation of intensity with source temperature which is observed (cf. Fig. 5). This is true at nozzle–skimmer distances which are large enough that the effect of skimmer interference with the flow is negligible ($s/D \gtrsim 60$ in Fig. 5). At very large nozzle–skimmer separations, the predicted variation of beam intensity with source temperature is found to be in excellent agreement with experiment.

The agreement at intermediate nozzle–skimmer separations and elevated source temperatures is less satisfactory. The predicted intensities fall more and more rapidly with respect to the experimental results as the source temperature is increased. We shall not attempt to rationalize these discrepancies in detail. However, we will examine how the idealizations of the model and the possible dependence of the parameters on source conditions might affect the agreement.

The two parameters, σ_0 and c_s, of the self-scattering model are obviously related, since the limiting attenuation at large nozzle–skimmer separations is

$$I_\infty/I_0 = e^{-\beta/c_s x_q}$$

where β is proportional to σ_0^2. Thus for given source conditions an infinite number of combinations of σ_0 and c_s can lead to the same attenuation at large nozzle–skimmer separations. However, larger values of c_s will tend to shift the theoretical curves of Fig. 5 to the right, and thus bring them into closer agreement with experiment. On the other hand the predicted variation of intensity with source temperature becomes somewhat weaker as c_s is increased.

It is possible that both the parameters B and C depend on the source conditions. The curves of Fig. 5 were recalculated for $B = 0.2$ and 0.6. The effect of increasing B, and hence of making the transition from $T_\perp \propto s^{-4/3}$ to $T_\perp \propto s^{-2}$ more gradual (see Fig. 3), is to increase the predicted intensities at intermediate s/D. How-

Can. J. Chem. Downloaded from www.nrcresearchpress.com by 210.87.254.5 on 09/05/12
For personal use only.

Can. J. Chem. Downloaded from www.nrcresearchpress.com by 210.87.254.5 on 09/05/12
For personal use only.

ever this effect is very small, and has a negligible effect on the agreement obtained. A variation of C could be more significant, but it is difficult to estimate what effect this would have.

Perhaps the most important cause of the discrepancies between the theoretical and experimental curves of Fig. 3 is the assumption of a sudden onset of losses due to self-scattering collisions. In fact the onset of such losses will be quite gradual, starting upstream of $x = c_s x_q$. If proper account were taken of this effect, the self-scattering curves of Fig. 4, and thus the intensity curves of Fig. 5, would fall off more gradually with increasing nozzle–skimmer separation. Some error may also be introduced by our assumption that the flow becomes suddenly free molecular at the skimmer orifice, but this should be small. Certainly the intensities measured using very large nozzle–skimmer separations (cf. Fig. 5) have not been measurably affected by "self-scattering" downstream of the skimmer (14, 15).

The four parameters σ_0, c_s, B, and C are closely related, and in principle they can all be derived from a careful analysis of the appropriate solution of the Boltzmann equation (21, 22). In fact the self-scattering mechanism which we invoke is an artifact, since it is likely that the intensity losses which it predicts would be accounted for if the complete theoretical distribution function at the skimmer were used in predicting beam intensities. However, the self-scattering model is valuable, since with a "reasonable" choice of parameters it can reasonably approximate the experimental intensities. Furthermore, it offers a clear physical interpretation of the discrepancies between theory and experiment which have previously been unexplained.

We gratefully acknowledge stimulating discussions about the self-scattering mechanism with Professors G. Scoles, J. B. Anderson, and R. P. Andres. This work was made possible by the support of the National Research Council of Canada and of the U.S. Atomic Energy Commission (Contract AT(30–1) 1957). Two of us (T.R.G. and R.L.L.) are also indebted to the National Research Council of Canada for scholarship awards.

1. A. KANTROWITZ and J. GREY. Rev. Sci. Instr. **22**, 328 (1951).
2. H. M. PARKER, A. R. KUHLTHAU, R. ZAPATA, and J. E. SCOTT. *In* Rarefied gas dynamics. *Edited by* F. M. Devienne. The Pergamon Press, Inc., New York, 1960. p. 69.
3. J. B. ANDERSON, R. P. ANDRES, and J. B. FENN. *In* Advances in atomic and molecular physics. *Edited by* D. R. Bates and I. Estermann. Academic Press, Inc., New York. 1965. p. 345.
4. J. B. FRENCH. AGARDograph 112, NATO. April, 1966.
5. J. B. ANDERSON and J. B. FENN. Phys. Fluids, **8**, 780 (1965).
6. O. F. HAGENA and H. S. MORTON, JR. *In* Rarefied gas dynamics. Vol. 2. *Edited by* C. L. Brundin. Academic Press, Inc., New York. 1967. p. 1369.
7. E. L. KNUTH, N. M. KULUVA, and J. P. CALLINAN. Entropie, **18**, 38 (1967).
8. U. BOSSEL, F. C. HURLBUT, and F. S. SHERMAN. *In* Rarefied gas dynamics. Vol. 2. *Edited by* L. Trilling and H. Y. Wachman. Academic Press, Inc., New York, 1969, p. 945. U. BOSSEL. Aeronautical Sciences Division Report No. AS-68-6. University of California, Berkeley. August, 1968.
9. J. B. FENN and J. M. DECKERS. *In* Rarefied gas dynamics. Vol. 1. *Edited by* J. A. Laurmann. Academic Press, Inc., New York. 1963. p. 497.
10. K. BIER and O. HAGENA. *In* Rarefied gas dynamics. Vol. 2. *Edited by* J. H. DeLeeuw. Academic Press, Inc., New York. 1966. p. 260.
11. J. B. FRENCH and G. E. MCMICHAEL. *In* Rarefied gas dynamics. Vol. 2. *Edited by* C. L. Brundin. Academic Press, Inc., New York. 1967. p. 1385.
12. R. F. BROWN and J. H. HEALD, JR. *In* Rarefied gas dynamics. Vol. 2. *Edited by* C. L. Brundin. Academic Press, Inc., New York. 1967. p. 1407.
13. T. R. GOVERS, R. L. LEROY, and J. M. DECKERS. *In* Rarefied gas dynamics. Vol. 2. *Edited by* L. Trilling and H. Y. Wachman. Academic Press, Inc., New York. 1969. p. 985.
14. J. P. VALLEAU and J. M. DECKERS. Can. J. Chem. **42**, 225 (1964).
15. J. P. VALLEAU and J. M. DECKERS. Can. J. Chem. **43**, 6 (1965).
16. J. B. FENN and J. B. ANDERSON. *In* Rarefied gas dynamics. Vol. 2. *Edited by* J. H. DeLeeuw. Academic Press, Inc., New York. 1966. p. 311.
17. R. L. LEROY, T. R. GOVERS, and J. M. DECKERS. Can. J. Chem. **47**, 2305 (1969).
18. T. R. GOVERS. Ph.D. Thesis, University of Toronto, Toronto, Ontario. 1969.
19. R. L. LEROY and T. R. GOVERS. Can. J. Chem. In press.
20. H. ASHKENAS and F. S. SHERMAN. *In* Rarefied gas dynamics. Vol. 2. *Edited by* J. H. DeLeeuw. Academic Press, Inc., New York. 1966. p. 84.
21. B. B. HAMEL and D. R. WILLIS. Phys. Fluids, **9**, 829 (1966).
22. R. H. EDWARDS and H. K. CHENG. A.I.A.A. Journal, **4**, 558 (1966).
23. N. ABAUF, J. B. ANDERSON, R. P. ANDRES, J. B. FENN, and D. R. MILLER. *In* Rarefied gas dynamics. Vol. 2. *Edited by* C. L. Brundin. Academic Press, Inc., New York. 1967. p. 1317.
24. S. S. FISHER. University of California Department of Engineering Report No. 67–5, Los Angeles. March 1967. S. S. FISHER and E. L. KNUTH. A.I.A.A. Journal, **7**, 1174 (1969).
25. G. SCOLES and F. TORELLO. Meccanica, **3**, 20 (1968). C. GAZZOLA, G. SCOLES, and F. TORELLO. *In* Rarefied gas dynamics. Vol. 2. *Edited by* L. Trilling and H. Y. Wachman. Academic Press, Inc., New York. 1969. p. 977.
26. R. H. EDWARDS and H. K. CHENG. *In* Rarefied gas dynamics. Vol. 2. *Edited by* C. L. Brundin. Academic Press, Inc., New York. 1967. p. 819.
27. R. L. LEROY and J. M. DECKERS. Can. J. Chem. **47**, 2161 (1969)
28. F. VON BUSCH. Z. Phys. **193**, 412 (1966).
29. R. D. PRESENT. Kinetic theory of gases. McGraw-Hill Book Co., Ltd., New York. 1958. pp. 27–30.

Long-range spin–spin coupling in *N*-methyl 2-carbomethoxy-4,6-dinitroaniline[1]

J. A. McCubbin and R. Y. Moir
Department of Chemistry, Queen's University, Kingston, Ontario

AND

G. A. Neville
Research Laboratories, Food and Drug Directorate, Department of National Health and Welfare, Ottawa, Ontario

Received September 11, 1969

Long-range coupling ($^5J \simeq 0.5$ Hz) between the amino proton and the C-5 ring proton of *N*-methyl 2-carbomethoxy-4,6-dinitroaniline (**1**) was established unequivocally by comparison of the proton magnetic resonance spectra of the 3-*d* and 5-*d* analogs of **1** together with the *N*-deutero derivatives of the above compounds. Deuterium decoupling experiments indicated that *meta*-deuterium coupling was of the order of band resolution (< 0.2 Hz). Elucidation of the source of long-range coupling with the amino proton enabled the chemical shifts of the aromatic protons to be assigned. The relative magnitude of these chemical shifts is discussed in terms of the shielding effects operative in the predominant conformer in which the amino hydrogen is intramolecularly hydrogen bonded to the oxygen of the ester carbonyl group.

Canadian Journal of Chemistry, **48**, 934 (1970)

Can. J. Chem. Downloaded from www.nrcresearchpress.com by 210.87.254.42 on 09/05/12
For personal use only.

Introduction

When the present system involving long-range coupling between the anilino proton and a ring *meta*-proton was first reported, relatively few examples of long-range H^1–H^1 spin–spin coupling in aromatic systems had been documented (1). Now, however, much of the previously published but widely scattered data for long-range coupling between aromatic ring and α-protons and for coupling across hetero atoms in aromatic systems has been compiled by Brügel (2), and very recently Sternhell (3) has reviewed various classes of spin–spin coupling which have appeared in the literature since his earlier review of the subject (1).

Kowalewski and Kowalewski (4) first reported several long-range couplings across 5 bonds involving the aldehydic proton ($J_{OCH\text{-}5} \sim 0.50$–0.90 Hz) in some di-substituted benzaldehydes. Karabatsos and Vane (5) extended this work by studying some 65 substituted benzaldehydes from which they concluded that the coupling followed a *trans–trans* coplanar path (the so-called M or W path). Earlier, Meinwald and Lewis (6) had proposed that long-range interactions may involve the direct overlap between the small orbitals of carbon atoms in a zigzag configuration, and the similarity between their theoretical model and some extended zigzag configurations present in unsaturated structures exhibiting long-range coupling had been noted by Banwell and Sheppard (7). Shortly afterward, the Kowalewski team demonstrated the existence of an additional weaker coupling between the *trans–trans* aldehydic and *ortho* protons ($J_{OCH\text{-}4} \sim 0.15$–0.25 Hz) in various di-substituted benzaldehydes (8) and also found multiple long-range spin–spin coupling between the formyl and ring protons of various salicylaldehydes where $J_{OCH\text{-}3}$, $J_{OCH\text{-}4}$, and $J_{OCH\text{-}6}$ were all of the order of 0.10 Hz (9). More examples of long-range couplings involving the aldehydic proton and ring protons in substituted benzaldehydes may be found in Brügel's compilation (2).

Toluene and its derivatives also provide an instructive system for the study of various coupling effects. In a definitive and elegant study in which the nuclear magnetic resonance (n.m.r.) spectrum of toluene was completely analyzed in terms of chemical shifts and coupling constants, Williamson *et al.* (10) have shown that the aromatic protons form a very strongly coupled spin system which is completely modified by the extra splittings due to the long-range couplings with the methyl protons. The long-range coupling constants of toluene, interestingly, were found to be almost identical (maximum deviation of 0.1 Hz) to those found by Kotowycz and Schaefer (11) in 2-bromo-5-chlorotoluene. Schaefer *et al.* (12) have demonstrated that the C—H bond of the dichloro methyl group of α,α-2,6-tetrachlorotoluene at −40 °C lies in the

[1]Taken in part from the M.Sc. Thesis (Queen's University) of J. A. McCubbin, and reported in part at the 48th Annual Chemical Institute of Canada Conference, Montreal, Quebec, June 1, 1965.

Can. J. Chem. Downloaded from www.nrcresearchpress.com by 210.87.254.42 on 09/05/12
For personal use only.

plane of the ring and that the C—H proton is involved in a stereospecific 5-bond coupling with a ring proton in the *meta* position.

Until the relatively recent conformational study of polynitroanilines by Weil *et al.* (13), no long-range couplings involving anilino protons had been reported for substituted anilines. In the above work, the authors reported J_{NH,H_5} as 0.3 and 0.7 Hz for 2,4-dinitroaniline and *N*-methyl 2,4-dinitroaniline respectively. To the best of our knowledge no further long-range couplings involving anilino protons have been reported for substituted anilines. Coupling of the anilino proton with those on adjacent carbon atoms (J = 5–6 Hz) has been reported for nitro-substituted *N*-methylanilines (14, 15) and *N*-ethylanilines (15), alkylaminoanthraquinones (16), 2-methylaminopyridine (17), and for several polyfluorinated *N*-methylanilines (18). Since the disappearance of the *N*-alkyl multiplet, being dependent on the rate of proton exchange, should reflect the basicity of the aniline, a series of anilines might be found having pK_a values such that at some point in the series a change in coupling to non-coupling might be observed in the proton magnetic resonance (p.m.r.) spectra. Such a sequence has been found by Rae (19) for deuterochloroform solutions of substituted *N*-methylanilines where no coupling of the H—C—N—H system was observed for those anilines with pK_a > 3.5 at 25 °C owing to the rapidity of proton exchange in solution. *N*-Methyl 2-carbomethoxy-4,6-dinitroaniline (**1**) shows both H—C—N—H coupling and a long-range coupling across the hetero atom involving the anilino proton. It is the purpose of this paper to provide an unequivocal proof that it is the C-5 ring proton that couples with the anilino proton of **1**.

Results and Discussion

Spectral Features and Long-Range Coupling

Four absorption regions are found in the p.m.r. spectrum of *N*-methyl 2-carbomethoxy-4,6-dinitroaniline in chloroform-*d* solution. The doublet centered at 2.90 p.p.m. (J_{HNCH_3} = 5.6 Hz) is assigned to the protons of the *N*-methyl group, and this chemical shift and coupling constant are consistent with the following values reported for the corresponding proton absorption in *N*-methyl 2,4,6-trinitroaniline; 2.98 p.p.m. (J = 5.9 Hz) ($CDCl_3$) (19), 3.04 p.p.m. (J = 5.6 Hz) (nitrobenzene) (15), and 2.95[2] p.p.m. (J = 5.6 Hz) (CH_2Cl_2) (14). Since the *N*-methyl protons of *N*-methyl 2-carbomethoxy-4,6-dinitroaniline couple with the amino proton and give J as high as 5.6 Hz, this aniline would fall into the third group of Rae's classification of anilines (19), as based on their basicities, and presumably it would have a pK_a of less than 1.3.

In addition to a singlet at 3.97 p.p.m. which is in the accepted region for methyl protons of a carbomethoxy group attached to a benzene ring, a very broad absorption is seen at 9.4 p.p.m. (approximately 30 Hz wide) which is attributed to the amino proton. From infrared (i.r.) spectroscopic studies of **1**[3] in chloroform and carbon tetrachloride solutions it is known that the amino proton of the major portion of the solute is hydrogen bonded to the oxygen of the ester carbonyl group ($\nu_{C=O}$ = 1697; ν_{N-H} = 3279 cm^{-1}). A minor portion of the solute resides in the other conformation in which the amino proton is hydrogen bonded to an oxygen of the *ortho* nitro group ($\nu_{C=O}$ = 1722; ν_{N-H} = 3316 and 3248 cm^{-1}, shoulders on the medium intensity 3279 cm^{-1} band). Since hydrogen bonding is known to deshield the proton nucleus (20), the low-field frequency observed for the amino proton is expected and is consistent with the value of 9.2 p.p.m. (nitrobenzene) obtained for the amino proton[4] of *N*-methyl 2,4,6-trinitroaniline (15).

The p.m.r. spectral region of main interest (Fig. 1) concerns the two doublets (J_m = 2.6 Hz) centered at 8.75 and 8.90 p.p.m. arising from the 2 aromatic protons *meta* to each other. A range of 1 to 3 Hz has been quoted by Pople *et al.* (21) for *meta* coupling. Comparison with the *N*-deuterated compound (Fig. 2) shows that the upfield doublet of the ABX pattern (Fig. 1) is broadened relative to the down-field doublet, and distinct long-range coupling is seen in Fig. 1

[2]Heidberg *et al.* (14) reported their chemical shifts relative to the CH_2Cl_2 peak. The above frequency has been recalculated on the basis of the CH_2Cl_2 peak being at 5.30 p.p.m. from TMS.

[3]The extensive i.r. study of this compound and of its *N*-, 3-*d*, and 5-*d* deuterated analogs in both the solid and solution state will be reported later.

[4]Heidberg *et al.* (14) reported that the amino peaks of various nitrated *N*-methylanilines used in their study were broad and barely detectable. Rae (19) did not report the amino proton frequencies of his nitrated *N*-methylanilines, but Lamm (15) used spin decoupling to record the amino proton frequencies from the same series of nitrated *N*-methylanilines.

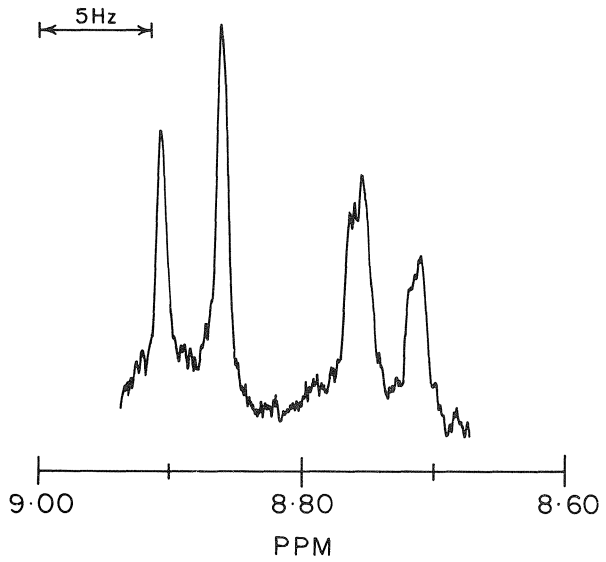

FIG. 1. The p.m.r. spectrum of the aromatic region of *N*-methyl 2-carbomethoxy-4,6-dinitroaniline in $CDCl_3$.

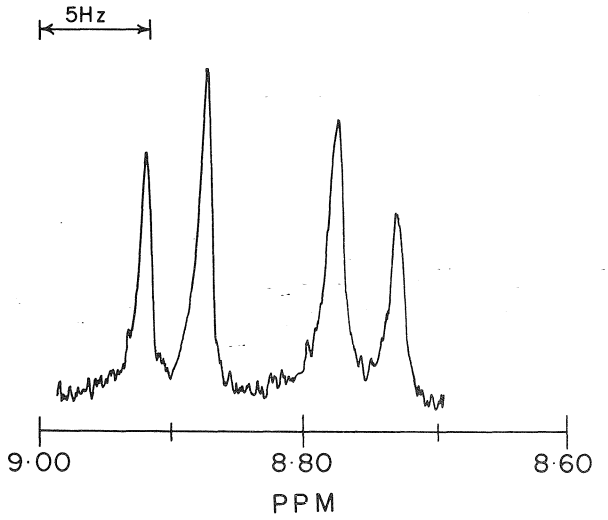

FIG. 2. The p.m.r. spectrum of the aromatic region of *N*-deutero-*N*-methyl 2-carbomethoxy-4,6-dinitroaniline in $CDCl_3$.

which disappears upon *N*-deuteration. The complete collapse of ABX pattern to an AB pattern rules out the possibility of two conformers[5] causing this splitting and indicates a long-range coupling (^5J) between the amino protons and one of the ring protons. By comparison, it is interesting that Heidberg *et al.* (14) found the 3- and 5-phenyl protons of *N*-methyl 2,4,6-trinitroaniline and of *N*-methyl 2,6-dinitroaniline to become nonequivalent at low temperatures (down to $-60\,^{\circ}C$). No mention is made of any evidence for long-range coupling by the amino proton, and the illustrated aromatic portions of the low temperature spectra were limited to the *N*-deutero picryl derivative (14).

To discover which of the two protons is interacting, it was possible to partially deuterate the

[5]Although i.r. spectroscopy provided evidence for the existence of 2 intramolecularly hydrogen bonded conformers in solution, p.m.r. spectra taken near ambient temperature showed only (as was to be expected) lines each of which was the average of the corresponding lines of the pure conformers. The coupling constants and shifts so observed of course correspond to averages weighted in favor of the dominant, more strongly bonded (amino-to-carbonyl) conformer.

Can. J. Chem. Downloaded from www.nrcresearchpress.com by 210.87.254.42 on 09/05/12
For personal use only.

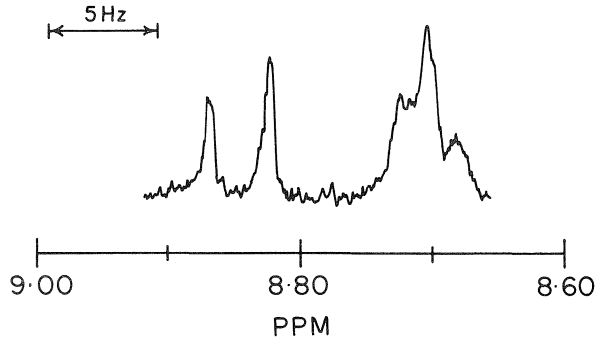

FIG. 3. The p.m.r. spectrum of the aromatic region of partially deuterated *N*-methyl 2-carbomethoxy-4,6-dinitroaniline-3-*d* in $CDCl_3$.

ring at the 3 position. The p.m.r. spectrum of the partially deuterated 3-*d* derivative (Fig. 3) shows decreased area of the down-field doublet relative to the up-field doublet. This change indicated that the fine coupling seen in the up-field doublet must arise from interaction of the amino proton with the C-5 proton. In order to further verify that only the C-5 proton couples with the amino protons, both the 3-*d* and 5-*d* derivatives were prepared in high purity. With the 3-*d* derivative (Fig. 4), the singlet given by the proton at C-5 was broad (band width at half height = 1.3 Hz) due mainly to interaction with the amino proton. With the 5-*d* derivative (Fig. 5), a sharp singlet (band width at half height = 0.9 Hz) was obtained for the proton at C-3 indicative of non-interaction with the amino proton. Although *meta*-deuterium coupling is expected to be less than 0.2 Hz, deuterium decoupling experiments were performed on each deuterium derivative in an attempt to further simplify the aromatic bands. No change occurred in either the H_3 or H_5 aromatic band with deuterium decoupling except for slight broadening due to the decoupling experiment itself. Sharper aromatic singlets were obtained without the decoupler indicating that the magnitude of the deuterium coupling in these compounds is of the order of resolution of the equipment.

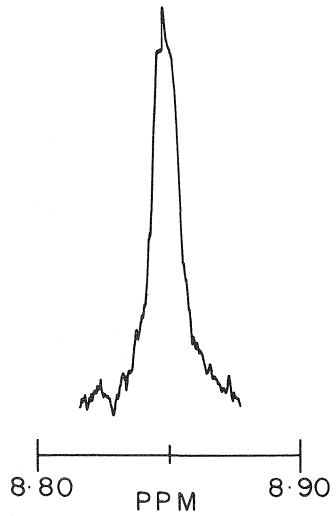

FIG. 4. The p.m.r. spectrum of the aromatic region of completely deuterated *N*-methyl 2-carbomethoxy-4,6-dinitroaniline-3-*d*.

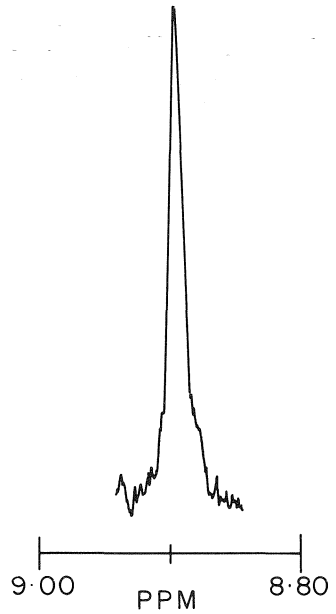

FIG. 5. The p.m.r. spectrum of the aromatic region of completely deuterated *N*-methyl 2-carbomethoxy-4,6-dinitroaniline-5-*d*.

Can. J. Chem. Downloaded from www.nrcresearchpress.com by 210.87.254.42 on 09/05/12
For personal use only.

TABLE 1

Chemical shifts (δ)* for selected aromatic protons from the 4′-carbomethoxy-2′-nitro-(**4**) and 2′,4′-dinitro-(**5**) derivatives of anisole (R = CH_3) and of 7-metameconine (R = $C_{10}H_9O_4$)†

R	Proton	δ **4**	δ **5**	Δδ
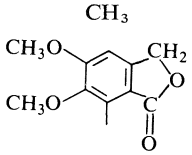	H_e	8.48	8.72	0.24
	H_f	8.22	8.47	0.25
	H_e	8.68	8.89	0.21
	H_f	8.08	8.28	0.20

*In $CDCl_3$ solution, expressed in p.p.m. of band centers downfield from tetramethylsilane internal reference.

† 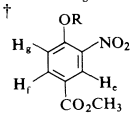

4

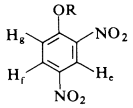

5

The long-range coupling between the amino and C-5 proton of *N*-methyl 2-carbomethoxy-4,6-dinitroaniline therefore follows the conventional *trans–trans* route and presumably the path is also coplanar since maximum coupling occurs when the substituent group is coplanar with the ring (4). This finding is also in agreement with the i.r. results which show the methylamino group to be coplanar with the ring. In this conformation the π electron system is conjugated with the amino group and favorable for the mechanism of coupling proposed by Gutowsky and Porte (22) for aromatic systems. The interaction between the π electrons with the lone pair of electrons of the amino nitrogen could affect the electrons of the N—H bond resulting in perturbation of the field around the amino proton nucleus.

Conformational Influence on Aromatic Proton Frequencies

Before the 3-*d* and 5-*d* analogs of *N*-methyl 2-carbomethoxy-4,6-dinitroaniline (**1**) were synthesized and the aromatic seat of long-range coupling with the amino protons was established unequivocally, we were inclined to regard the high-field doublet of the aromatic pattern at 8.74 p.p.m. (Fig. 1) as arising from the H_3 proton. Although such an assignment would have constituted an exception to the W-rule, it seemed likely that the more shielded aromatic proton ought to be located between the nitro and carbomethoxy groups. From the data in Table 1, derived from conformational studies by p.m.r. spectroscopy of substituted diphenyl ethers and their corresponding anisoles having planar nitro and carbomethoxy groups (23), it was noted that a nitro group exhibits a deshielding effect of 0.20–0.25 p.p.m. greater than a carbomethoxy group depending on the nature of the remaining aryl moiety. When this chemical shift difference is subtracted from 8.98 p.p.m. (14, 25) for the 3,5-protons of *N*-methyl 2,4,6-trinitroaniline (**2**) by way of an estimate of the effect of replacing a coplanar nitro group of **2** with the coplanar carbomethoxy group of **1**, the values obtained are very near the smaller chemical shift of 8.74 p.p.m. for **1**. Moreover, while the fine multiplicity for the C-5 proton, which disappears upon *N*-deuteration, of *N*-methyl 2-carbomethoxy-4-nitroaniline (**3**) (Fig. 6) constitutes its own indicator of the source of long-range coupling in this compound, neither the chemical shifts of 8.82 and 8.18 p.p.m. for the C-3 and C-5 protons respectively of **3** provide any immediate help in assigning the chemical shifts convincingly to the aromatic protons of **1**. Heidberg *et al.* (14) reported that the introduction of one planar nitro group reduced the shielding of its *ortho* protons approximately 50 Hz. Tori and Kuriyama (24) have shown that the nitro group exhibits shielding and deshielding volumes similar to those of a carbonyl group. Rae (25), using the magnetic susceptibilities determined by Yamaguchi (26) for the nitro group, showed that anisotropic deshielding by the nitro group

Can. J. Chem. Downloaded from www.nrcresearchpress.com by 210.87.254.42 on 09/05/12
For personal use only.

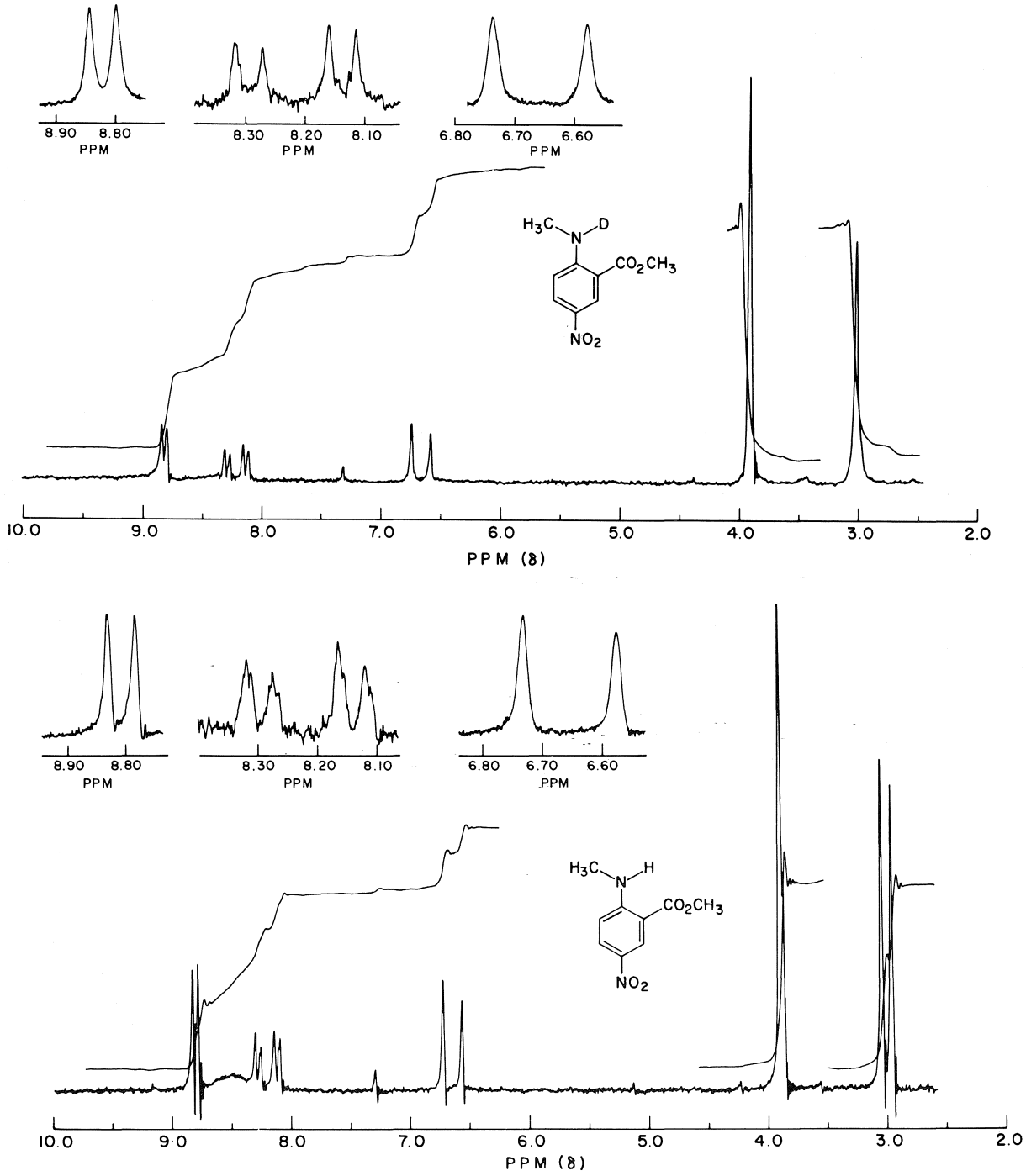

FIG. 6. The p.m.r. spectrum of *N*-methyl 2-carbomethoxy-4-nitroaniline and of its *N*-deutero analog in $CDCl_3$.

Can. J. Chem. Downloaded from www.nrcresearchpress.com by 210.87.254.42 on 09/05/12
For personal use only.

might be suspected to decrease by some 40 Hz as the angle of rotation approached 90°. In retrospect, therefore, it is seen that introduction of a nitro group at C-6 in **3** to obtain **1** deshields the C-5 proton by approximately 30 Hz indicating that the *ortho*-nitro group is only partially rotated from the plane of the ring by steric interaction from the *N*-methyl substituent.

Experimental

Apparatus

The p.m.r. spectra were recorded on a Varian A-60 spectrometer in chloroform-*d* solution using tetramethylsilane (TMS) as an internal reference. All chemical shifts are reported in p.p.m. down-field from TMS. Since all the compounds examined are sparingly soluble in chloroform, all p.m.r. spectra were obtained from saturated solutions at ambient probe temperature of 40 ± 2°.

Deuterium decoupling experiments were performed using a Varian DA-60 n.m.r. spectrometer equipped with an external locking system for field stabilization. Double irradiation experiments were carried out using an n.m.r. Specialties SD-60 spin decoupler operating at 9.2 MHz.

Infrared spectra were recorded on a Perkin–Elmer Model 21 spectrometer. All undesignated melting points were taken on a Kofler hot stage with microscope attachment and are reported uncorrected. The melting determinations designated precision (prec.) were obtained with Anschutz immersion thermometers using an electrically heated precision melting apparatus (27) containing Dow Corning 550 fluid. Thin-walled capillary tubes drawn from thoroughly cleaned and dry pyrex tubing were employed for these determinations.

Synthesis

Methyl 2-Chloro-3,5-dinitrobenzoate, Methyl 2-Chloro-3,5-dinitrobenzoate-4-d, and Methyl 2-Chloro-3,5-dinitrobenzoate-6-d

The method of chlorodehydroxylation is similar to that used by Borrows *et al.* (28) for the replacement of a hydroxyl group by chlorine in dinitrophenols.

Methyl 3,5-dinitrosalicylate (30 g, m.p. 132–134°, prepared from methyl salicylate) was suspended in freshly opened phosphorus oxychloride (89 ml). While the mixture was vigorously stirred and maintained at 10–15° by an ice-bath, *N,N*-dimethylaniline (34 ml, 2.22 moles) was slowly added dropwise to the suspension over a period of 30–35 min. The solid slowly dissolved during the addition, and when approximately 75% of the dimethylaniline had been added, the reaction mixture developed a dark orange–brown color. On completion of the addition, the mixture was stirred in the ice-bath for 1 h after which it was allowed to warm up to room temperature. The mixture was poured with stirring onto crushed ice (1 l) and immediately a dark green solid formed. After having been crushed and washed well with water, the damp solid was recrystallized from methanol using decolorizing charcoal to obtain solid (dry, 19.6 g, 60% yield) melting 89–90°. Two more recrystallizations from methanol gave the analytical sample melting at 90.3–91.0° (prec.). The p.m.r. spectrum showed a singlet for the ester methyl protons (4.05) and an AB quartet with line frequencies at 8.85, 8.88, 8.97, and 9.02 (J_m = 7.1 Hz) for the aromatic protons.

Anal. Calcd. for $C_8H_5N_2O_6Cl$: C, 36.87; H, 1.93; N, 10.75. Found: C, 36.97, 37.16; H, 2.21, 2.24; N, 10.81, 10.72.

The small quantities of methyl 3,5-dinitrosalicylate-4-*d* and methyl 3,5-dinitrosalicylate-6-*d*, reported elsewhere (29), were treated with phosphorus oxychloride in the same way except that the reactions were conducted in a flask and hand agitated. The crude, brown 4-*d* and 6-*d* chloro compounds were used without further purification in the next reaction step.

N-Methyl 2-Carbomethoxy-4,6-dinitroaniline, N-Methyl 2-Carbomethoxy-4,6-dinitroaniline-3-d, and N-Methyl 2-Carbomethoxy-4,6-dinitroaniline-5-d

Methyl 2-chloro-3,5-dinitrobenzoate (10.0 g, m.p. 90–92°) was dissolved in benzene (150 ml). Excess methylamine gas (generated from a saturated aqueous solution of methylamine hydrochloride (10.0 g) dropped on sodium hydroxide pellets (20 g)) was passed through the benzene solution producing some yellow solid. On completion of the reaction, the mixture was heated to the boiling point and filtered hot to remove the methylamine hydrochloride by-product. After boiling the filtrate to reduce its volume by ½, a solid cake of crystals formed on standing at room temperature. The solid was washed free with diethyl ether and collected to obtain the crude product (9.3 g, 95% yield) melting at 132.5–135.5°. Two recrystallizations from methanol gave the analytical sample melting at 133.2–134.2° (prec.).

Anal. Calcd. for $C_9H_9N_3O_6$: C, 42.36; H, 3.56; N, 16.47. Found: C, 42.46, 42.39; H, 3.72, 3.70; N, 16.66, 16.50.

The entire quantity of methyl 2-chloro-3,5-dinitrobenzoate-4-*d*, as described earlier, was reacted and purified essentially as above. The yellow crystals (0.184 g, 21% overall yield from methyl 4-iodosalicylate (29)) after 1 recrystallization melted at 133.2–134.2° (prec.) and a mixture with authentic undeuterated material melted at 132.8–133.8° (prec.). The p.m.r. spectrum showed only 1 singlet (7.25) in the aromatic region.

Similarly, the entire quantity of methyl 2-chloro-3,5-dinitrobenzoate-6-*d*, described earlier, was reacted with methylamine gas in benzene and crystallized from methanol. The yellow crystals (0.178 g, 3.2% overall yield from methyl 2-chloro-6-nitrobenzoate (29)) after 1 recrystallization melted at 133.2–134.2° (prec.). A mixture with the authentic undeuterated compound melted at 133.4–134.2° (prec.). The p.m.r. spectrum revealed only 1 singlet (7.05) in the aromatic region.

Methyl 2-Chloro-5-nitrobenzoate

2-Chloro-5-nitrobenzoic acid (10.0 g, Eastman) was heated under reflux with anhydrous methanol (225 ml) and concentrated sulfuric acid for 24 h. Crystals formed on pouring the methanolic solution into excess water. The solid was collected, washed, and dried to give 9.9 g, of product melting at 70.0–71.0°; lit. value 73° (30).

Methyl 2-Carbomethoxy-4-nitroaniline

Methyl 2-chloro-5-nitrobenzoate (3.00 g, m.p. 70.0–71.0°) was dissolved in benzene (30 ml) and treated with excess methylamine gas (generated from methylamine hydrochloride (3.8 g, Eastman) and sodium hydroxide

Can. J. Chem. Downloaded from www.nrcresearchpress.com by 210.87.254.42 on 09/05/12
For personal use only.

pellets (18 g)). On completion of the reaction, the mixture was heated to boiling and filtered hot to remove the methylamine hydrochloride by-product. By reducing the volume of the filtrate successively by boiling, a total of 1.44 g (49%) of crude product was obtained by crystallization. Two recrystallizations of the crude solid from benzene with decolorizing charcoal followed by a single recrystallization from benzene alone gave the analytical sample melting at 148.0–148.6° (prec.). The p.m.r. spectrum (Fig. 6) showed a doublet for the *N*-methyl protons (2.97, 3.07; $J_{HNCH_3} = 5.1$ Hz), a singlet for the ester methyl protons (5.58), a doublet for H_3 (8.80, 8.85; $J_{3,5} = 2.8$ Hz), a quartet for H_5 (8.12, 8.15, 8.27, 8.32; $J_{3,5} = 2.8$, $J_{5,6} = 9.4$ Hz), a doublet for H_6 (6.28, 6.73; $J_{5,6} = 9.4$ Hz), and a moderately broad band at 8.52 for the amino proton.

Anal. Calcd. for $C_9H_{10}N_2O_4$: C, 51.42; H, 4.80; N, 13.33. Found: C, 51.54, 51.53; H, 4.90, 4.89; N, 13.29, 13.31.

Preparation of N-Deuterated Isomers

Each nitro-aniline was dissolved in acetic acid-d_1 and the flask was connected to a vacuum line. Each mixture was allowed to stand overnight before being warmed to 60° under a pumping vacuum to remove the acetic acid-d_1. The product was handled in a dry box (N_2 and P_2O_5). The absence of any N—H stretching bands in the i.r. spectra indicated that *N*-deuteration was complete.

We are grateful to Dr. Robert R. Fraser, University of Ottawa, for the ring deuterium decoupling experiments.

1. S. STERNHELL. Rev. Pure and Appl. Chem. **14**, 15 (1964).
2. W. BRÜGEL. Nuclear magnetic resonance spectra and chemical structure. Academic Press, Inc., New York, 1967. Vol. 1. pp. 15–25.
3. S. STERNHELL. Quart. Rev. **23**, 236 (1969).
4. D. G. DE KOWALEWSKI and V. J. KOWALEWSKI. J. Chem. Phys. **37**, 1009 (1962).
5. G. J. KARABATSOS and F. M. VANE. J. Amer. Chem. Soc. **85**, 3886 (1963).
6. J. MEINWALD and A. LEWIS. J. Amer. Chem. Soc. **83**, 2769 (1961).
7. C. N. BANWELL and N. SHEPPARD. Discuss. Faraday Soc. **34**, 115 (1962).
8. D. G. DE KOWALEWSKI and V. J. KOWALEWSKI. Mol. Phys. **9**, 331 (1965).
9. D. G. DE KOWALEWSKI and V. J. KOWALEWSKI. Mol. Phys. **9**, 319 (1965).
10. M. P. WILLIAMSON, R. J. KOSTELNIK, and S. M. CASTELLANO. J. Chem. Phys. **49**, 2218 (1968).
11. G. KOTOWYCZ and T. SCHAEFER. Can. J. Chem. **44**, 2743 (1966).
12. T. SCHAEFER, R. SCHWENK, C. J. MACDONALD, and W. F. REYNOLDS. Can. J. Chem. **46**, 2187 (1968).
13. J. A. WEIL, A. BLUM, A. H. HEISS, and J. K. KINNAIRD. J. Chem. Phys. **46**, 3136 (1967).
14. J. HEIDBERG, J. A. WEIL, G. A. JANUSONIS, and J. K. ANDERSON. J. Chem. Phys. **41**, 1033 (1964).
15. B. LAMM. Acta Chem. Scand. **19**, 2316 (1965).
16. S. M. BLOOM and R. F. HUTTON. Tetrahedron Lett. 1993 (1963).
17. M. FREIFELDER, R. W. MALTOON, and Y. H. NG. J. Org. Chem. **29**, 3730 (1965).
18. J. BURDON. Tetrahedron, **21**, 1101 (1965).
19. I. D. RAE. Aust. J. Chem. **19**, 409 (1966).
20. B. G. SOMMERS and H. S. GUTOWSKY. J. Amer. Chem. Soc. **85**, 3065 (1963).
21. J. A. POPLE, W. G. SCHNEIDER, and H. J. BERNSTEIN. High-resolution nuclear magnetic resonance. McGraw-Hill Company, Inc., New York, 1959.
22. H. S. GUTOWSKY and A. L. PORTE. J. Chem. Phys. **35**, 839 (1961).
23. W. D. CHANDLER, W. MACFARLANE SMITH, and R. Y. MOIR. Can. J. Chem. **42**, 2549 (1964).
24. K. TORRI and K. KURIYAMA. Tetrahedron Lett. 3939 (1964).
25. I. D. RAE. Aust. J. Chem. **18**, 1807 (1965).
26. I. YAMAGUCHI. Mol. Phys. **6**, 105 (1963).
27. E. B. HERSHBERG. Ind. Eng. Chem. (Anal. Ed.) **8**, 312 (1936).
28. E. T. BORROWS, J. C. CLAYTON, B. A. HEMS, and A. G. LONG. J. Chem. Soc. S190 (1949).
29. J. A. MCCUBBIN, R. Y. MOIR., and G. A. Neville. Can. J. Chem. This issue.
30. P. J. MONTAGNE. Rec. Trav. Chim. **19**, 57 (1900).

Can. J. Chem. Downloaded from www.nrcresearchpress.com by 210.87.254.42 on 09/05/12
For personal use only.

Synthesis of the deutero-specific 4-*d* and 6-*d* methyl 3,5-dinitrosalicylates

J. A. McCubbin and R. Y. Moir
Department of Chemistry, Queen's University, Kingston, Ontario
AND
G. A. Neville
Research Laboratories, Food and Drug Directorate, Department of National Health and Welfare, Ottawa, Ontario
Received September 11, 1969

The synthesis is described of several specifically labelled deuterium derivatives of salicylic acid needed for the study of long-range coupling and in infrared studies of aromatic conformation.
Canadian Journal of Chemistry, **48**, 942 (1970)

Can. J. Chem. Downloaded from www.nrcresearchpress.com by 210.87.254.5 on 09/05/12
For personal use only.

Introduction

In a paper devoted to a proton magnetic resonance (p.m.r.) study of molecular overcrowding in *N*-alkyl-*o*-nitroanilines, Rae (1) has noted the particular attention that has been given the study of nitroanilines and the wealth of information about conjugation in aromatic systems, hydrogen bonding, association by charge transfer, and molecular overcrowding. Heidberg *et al.* (2) have also studied the conformation and internal rotation of several nitro aromatic amines in solution by p.m.r. spectroscopy. Weil *et al.* (3) recently reported an extensive study of spectra and conformation in nitroanilines and nitroacetanilides and, in particular, observed a long-range coupling between amino hydrogen and a *meta* proton. When the latter work was published, an extensive series of *N*-alkylated 2-carbomethoxy-4,6-dinitroanilines and related compounds had been prepared and examined by p.m.r. spectroscopy in our laboratory. In the context of this work a novel, long-range coupling (^5J) was observed to involve the amino proton and one of the aromatic protons of the *N*-alkyl-2-carbomethoxy-4,6-dinitroaniline system (4). It is the purpose of this communication to report the extensive chemical transformations performed in order to obtain the appropriately deuterium labelled phenolic precursors to *N*-methyl-2-carbomethoxy-4,6-dinitroaniline-3-*d* and *N*-methyl-2-carbomethoxy-4,6-dinitroaniline-5-*d* by which the aromatic seat of this long-range coupling was elucidated.

Synthesis and Proof of Structure

Synthesis of 2-Carbomethoxy-4,6-dinitrophenol-3-d

The sequence of reactions that finally proved successful is shown in Fig. 1. Although the initial oxidation required surprisingly close control, the main interest and difficulty occurred in the third step, the reduction of the nitro group.

In our original plan for the sequence from this step onward (Fig. 2), the nitro group was to be replaced with deuterium, and the chloro group was to survive the synthesis. Repeated attempts to reduce the nitro group with ferrous sulfate and ammonia, or with sodium sulfide, all failed, and when the reduction was attempted with hydrogen and palladium, some of the chlorine was found to be replaced at the same time. Graceful acceptance of the reversed roles for nitro and chlorine still left us two problems. We could not proceed by replacing amine with chlorine (Fig. 3), since the resulting ester could not be dinitrated. We therefore chose the route via methyl salicylate (Fig. 1), whose nitration is easy. Even so, when the reduction of the nitro group (Step 3, Fig. 1) with palladium-on-charcoal was carried out in ethanol, the chlorine was replaced, not by deuterium, but by hydrogen. In dioxane solution, equal amounts of the two isotopes were introduced at position 3. Obviously the exchange between deuterium gas and acidic hydrogen was fast compared to the rate of dehalogenation. However, complete deuteration at position 3, without any disturbance of other aryl hydrogen, was achieved when the reduction took place in dioxane whose very small water content had been swamped by the addition of deuterium oxide, and, at the same time, when the deuterium gas had been dried over a molecular sieve. The further refinement of boiling the catalyst with deuterium oxide prior to the reaction proved both unnecessary and harmful.[1]

[1]Dioxane solutions of D_2O had been used earlier to prepare the *N*-deutero-*N*-alkyl 2-carbomethoxy-4,6-dinitroanilines.

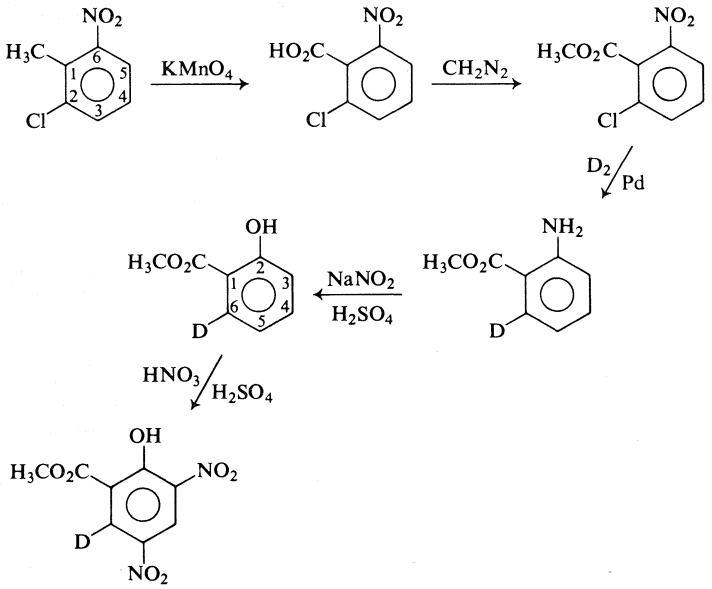

FIG. 1. Sequence of reactions leading to 2-carbomethoxy-4,6-dinitrophenol-3-*d*.

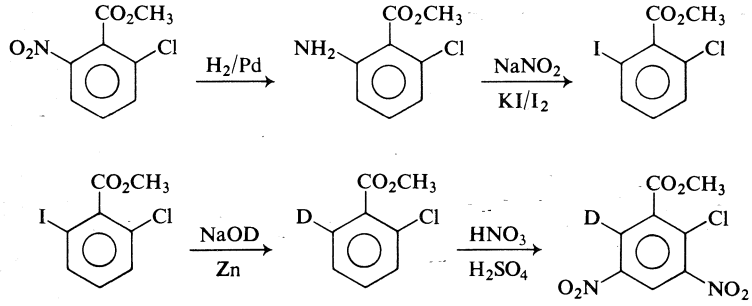

FIG. 2. The proposed reaction sequence to produce methyl 2-chloro-3,5-dinitrobenzoate-6-*d* by reduction with hydrogen.

Completion of the synthesis by conversion of hydroxyl to chlorine is described in the companion paper (4).

Synthesis of 2-Carbomethoxy-4,6-dinitrophenol-5-d

The sequence of reactions by which 2-carbomethoxy-4,6-dinitrophenol-5-*d* was prepared is shown in Fig. 4.

Good yields in the esterification of 4-aminosalicylic acid were obtained only if very close control was maintained over the periods of heating and of standing. Furthermore, if too much solvent was removed at the end of the reaction, crystallization would not occur, while

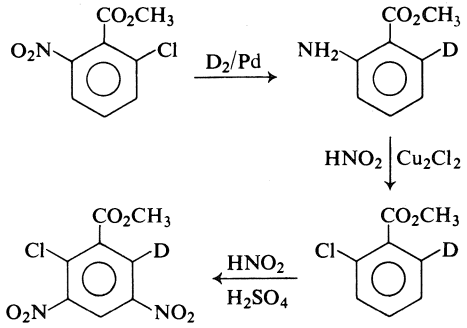

FIG. 3. The proposed reaction sequence to produce methyl 2-chloro-3,5-dinitrobenzoate-6-*d* by reduction with deuterium.

Can. J. Chem. Downloaded from www.nrcresearchpress.com by 210.87.254.5 on 09/05/12
For personal use only.

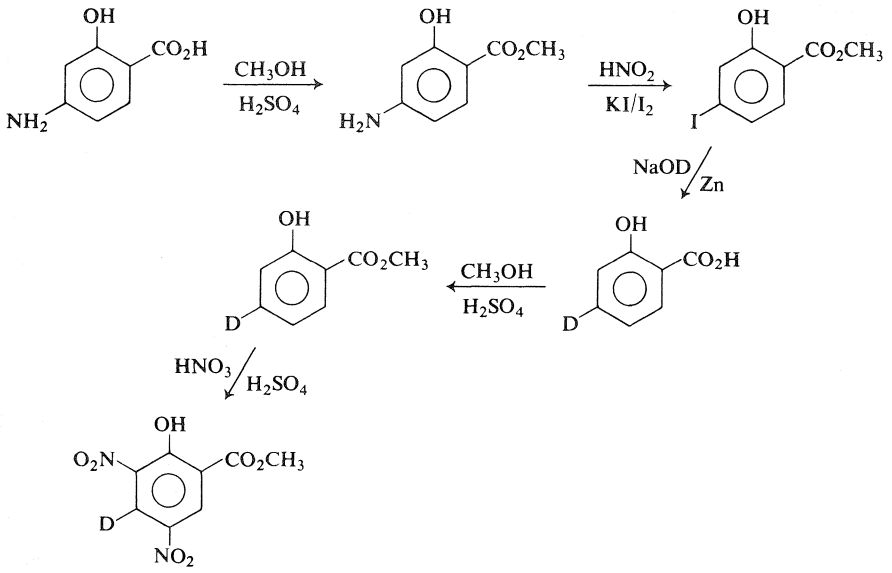

FIG. 4. The reaction sequence to produce 2-carbomethoxy-4,6-dinitrophenol-5-*d*.

if not enough was removed the subsequent yields were very low. After recrystallization from benzene, the methyl 4-aminosalicylate was characterized by a melting point (5).

The diazotization of 4-aminosalicylic acid was found to be unsuccessful unless the acid was esterified. This was probably due to either the solubility of the final product and the consequent difficult separation, or to different electronic effects of the carboxyl and carbonyl groups. The simultaneous extraction with chloroform was found to be the most effective way to remove the product, methyl 4-iodosalicylate, from the reaction mixture starting from the ester. The product was characterized by its p.m.r. spectrum and eventually and with difficulty, by analysis for carbon and hydrogen (see Experimental), as well as by its derivatives.

The reaction of methyl 4-iodosalicylate with sodium hydroxide-d_1 and zinc was found to be a very effective way of placing a deuterium in the 4 position on the ring. However, as reduction and ester hydrolysis occurred together, the product was salicylic acid-4-*d*. This was then easily esterified with methanol to give methyl salicylate-4-*d* which was characterized by p.m.r. spectroscopy. The subsequent reactions were then identical to the first sequence and the final product *N*-methyl 2-carbomethoxy-4,6-dinitroaniline was identified by melting point and by p.m.r. spectroscopy.

Experimental

Apparatus

All undesignated melting points were taken on a Kofler hot stage with microscope attachment and are reported uncorrected. The melting points designated precision (prec.) were obtained with Anschutz immersion thermometers using an electrically heated melting apparatus (6) containing a Dow Corning 550 fluid. Thin-walled capillary tubes drawn from thoroughly cleaned and dry pyrex tubing were employed for these determinations.

Infrared i.r. spectra were recorded on a Perkin–Elmer Model 21 spectrometer. Spectra were recorded from potassium bromide discs (2 mg sample in 250 mg KBr) and in saturated chloroform solutions (1–8%). All i.r. frequencies are reported in cm^{-1}.

The p.m.r. spectra were obtained in saturated $CDCl_3$ solutions at ambient probe temperature of 40 ± 2° from a Varian A-60A spectrometer. Tetramethylsilane (TMS) was used as internal reference, and all chemical shifts are reported in p.p.m. downfield from TMS.

Syntheses

2-Chloro-6-nitrobenzoic Acid and Methyl Ester

The method employed by S. K. Guha *et al.* (7) had to be modified. Sodium bicarbonate (10 g), 2-chloro-6-nitrotoluene (10 g, steam distilled, m.p. 27–28°) and water (1000 ml) were heated to reflux temperature. Potassium permanganate (30 g) was added in small amounts over a

Can. J. Chem. Downloaded from www.nrcresearchpress.com by 210.87.254.5 on 09/05/12
For personal use only.

Can. J. Chem. Downloaded from www.nrcresearchpress.com by 210.87.254.5 on 09/05/12
For personal use only.

period of 1 h. This mixture was heated under reflux[2] for 9 h when more potassium permanganate (10 g) was added. Heating was continued for another 4 h. Product was recovered in the usual way as white needles (5.0 g, 43%), m.p. 160–165°. Guha *et al.* (7) reported m.p. 161°. The procedure had to be repeated 30 times to obtain enough product. No success was experienced with chromic acid as the oxidant.

The methyl ester was obtained by reaction with diazomethane (8), as monoclinic crystals (from petroleum ether), m.p. 94–96°, yield 75%. Goldstein and Pretiner (9) reported m.p. 94–95°.

Methyl Anthranilate-6-d

Methyl 2-chloro-6-nitrobenzoate (1.0 g, m.p. 94–96°, prepared from 2-chloro-6-nitrobenzoic acid) was dissolved in dioxane (10 ml, spectrograde) and deuterium oxide (1.5 ml, 99.7% isotopic purity, Merck, Sharp and Dohme). Palladium-on-charcoal (0.78 g, 10%, Englehard) was added to the solution and deuterium gas (760 mm pressure, dried with molecular sieve type 4 A, Matheson) was passed into the flask. The 50 ml round bottom flask was shaken in an oil bath at 70°. The reaction mixture absorbed 545 ml of deuterium in 4½ h. After the catalyst had been removed and washed with water (20 ml) the combined filtrate was made alkaline with sodium bicarbonate solution (50 ml, 2%) which caused a white inorganic solid to form. The mixture was extracted 5 times with ether (25 ml each time) and the ethereal extracts were dried over anhydrous magnesium sulfate. The solvent was removed on the rotary evaporator under vacuum and a yellowish oil was left. This was distilled under vacuum (0.05 mm, 80°). The i.r. spectra showed 2 peaks, 3370 and 3480 cm^{-1} (characteristic of primary amines). The p.m.r. spectrum had a singlet at 3.8 which is characteristic of a carbomethoxy absorption. Some of the product of a similar but undeuterated reaction was heated under reflux in a sodium hydroxide solution (10 ml, 40%) for 20 min. This was neutralized with concentrated hydrochloric acid and extracted 5 times with ether (25 ml each time). The solvent was removed leaving a white solid (m.p. 149–151°). A mixture with authentic anthranilic acid (m.p. 152–154°, Eastman) melted between 151 and 153°.

The entire product was used in the following step as were all products in the subsequent reactions in the sequence and overall yield will be given at the end of the series.

This reaction was only done once under conditions described above. However a number of attempts were made to reduce the nitro group of this compound as mentioned earlier. Firstly, ferrous sulfate and ammonia were tried and then sodium sulfide was used. Repeated variations with these reagents failed.

Hydrogen, with a palladium catalyst, was found to remove the chlorine as well as reduce the nitro-group so deuterium gas was used. This was only found successful when dry deuterium and dioxane with deuterium oxide were used.

[2]Two condensers, one with hot and one with cold water, were used to prevent the toluene from solidifying in the condenser.

Methyl Salicylate-6-d

Concentrated sulfuric acid (10 ml) and water (8 ml) were used to wash all the methyl anthranilate-6-*d* (from the above experiment) into the reaction flask. This solution was cooled to 0° in an ice–salt bath and aqueous sodium nitrite solution (15 ml, 3%) was added over a period of 20 min while the solution was being stirred. This was left in the ice–salt bath for 3 hours after which it was removed and urea was added until the reaction mixture did not give the reaction with starch iodide paper. Steam was passed into the flask and the milky distillate was collected in a receiver immersed in an ice bath, during 45 min. Methyl salicylate was recovered from the distillate in the usual way, and then redistilled (0.05 mm pressure, bath temperature 50°) to give an oil which was nitrated directly.

Methyl 4-Aminosalicylate

Methyl 4-aminosalicylate was prepared by the method of Balica (5). 4-Aminosalicylic acid (10 g, m.p. 143–144°) was dissolved in methanol (275 ml) with gentle heating. The solution was then cooled to room temperature and concentrated sulfuric acid (17 ml) was added slowly. A fluffy white precipitate formed when the first few ml were added. This solid quickly dissolved when more acid was added. The solution was then heated under reflux for 17 h and allowed to stand at room temperature for 5 h.

All but 75 ml of solution was distilled off and upon cooling the residue formed large pink crystals. Water (200 ml) was added and the mixture was stirred. The resulting suspension was neutralized to alkacid test paper with sodium bicarbonate solution (10%). The product was dried over sodium hydroxide under vacuum yielding 9.1 g (83%) of light brown crystals. The melting point of 120–123° was improved to 123–125° after 1 recrystallization from stock benzene. Balica (5) reported 119–120° and Tsatsas and Sandris (10) reported 118°.

Methyl 4-Iodosalicylate

Water (50 ml) and concentrated hydrochloric acid (13 ml) were cooled to a temperature of 2° in an ice salt bath. Methyl 4-aminosalicylate (1 g, m.p. 120–123°), prepared as above, was added slowly along with an aqueous sodium nitrite solution (10 ml, 13%) to the stirred reaction mixture. This addition took 30 min and the solution was stirred in the ice–salt bath for 45 min longer.

The flask was removed from the bath and urea was added until the solution gave a negative reaction to starch iodide test paper. Chloroform (40 ml) was added directly to the reaction flask. A solution of potassium iodide (2.0 g) and iodine (1.0 g) in water (21 ml) was added to the vigorously stirred mixture over a period of 20 min. The purple chloroform layer was separated, and the remaining aqueous phase was extracted 4 times with chloroform (20 ml each time). The chloroform extracts were stirred rapidly with an aqueous sodium bisulfite solution (40 ml, 10%) and sulfur dioxide was passed in until the dark purple solution gradually turned to a dark yellow color and finally became light yellow. This yellow chloroform solution was washed 4 times with water (20 ml each time) and dried for 2 h over magnesium sulfate. The solvent was then removed on the rotary evaporator under vacuum leaving the yellow product to crystallize. These crude crystals (1.2 g, 74.1%) melted between 63 and 67°.

Can. J. Chem. Downloaded from www.nrcresearchpress.com by 210.87.254.5 on 09/05/12
For personal use only.

Purification was accomplished by sublimation at reduced pressure (0.05 mm., 60°) and the white solid melted between 69.8 and 70.4° (prec.).

This procedure was repeated 12 times with only minor changes in the method. It was found that the destruction of nitrous acid by urea in the substitution was essential for reasonable yield. The simultaneous extraction with chloroform also improved the yield substantially. There has been no report of this compound in the literature.

Analyses of the compound are reported in Table 1 (in the order received) to call attention to difficulties recently experienced in the analyses of aromatic halogen compounds in several independent series made in this laboratory.

The samples for the first 2 analyses were recrystallized from methanol. The remaining 4 samples were first sublimed under vacuum and then recrystallized from methanol.

TABLE 1
Analyses of methyl 4-iodosalicylate*

Analysis†	% C	% H	% I
1	35.53	2.74	46.73
2	35.28	2.61	46.99
3	35.37	2.76	46.80
4	34.62	2.27	42.79
5	35.27	2.84	46.85
6	35.24	2.91	46.74
Calcd.	34.62	2.52	45.65

*The p.m.r. spectrum showed a large singlet (3.90) which is characteristic of a methyl ester peak. There was also a complex multiplet from 7.27 to 7.52.
†Analyses by Alfred Bernhardt (Mulheim), except for row 4, Daessle (Montreal).

Salicylic Acid and Salicylic Acid-4-d

These compounds were prepared by the procedure used by Safe (11) for the removal of aromatic halogen. Methyl 4-iodosalicylate (1 g, m.p. 63–67°), prepared as above, and zinc dust (1.5 g) were suspended in a solution of sodium hydroxide (8.0 ml, 40%) and water (8 ml). This mixture was heated under reflux for $2\frac{1}{2}$ h after which time the solid was removed by filtration and the solution was neutralized to alkacid test paper with hydrochloric acid. The neutral solution and fine white precipitate were extracted 4 times with ether (25 ml each time) and combined extracts were dried over anhydrous magnesium sulfate. The solvent was removed on a rotary evaporator under vacuum, leaving a white solid. This procedure was repeated twice for the undeuterated material and then in another run sodium hydroxide-d_1 (8.0 ml, 40%, Merck, Sharp and Dohme) and deuterium oxide (8.0 ml, 99.7%, isotopic purity Merck, Sharp and Dohme) were substituted for the sodium hydroxide in water in reaction with methyl 4-iodosalicylate (1 g) and zinc dust (1.5 g). The resulting salicylic acid-4-*d* was characterized by the p.m.r. spectrum of its dinitro-ester. The entire deuterated product from this reaction was used in the following esterification reaction. The same is true for all subsequent reactions; consequently, a yield is reported only for the final product.

Methyl Salicylate and Methyl Salicylate-4-d

The method used by Fisher (12) in preparing the undeuterated methyl salicylate from methanol and salicylic acid was used to prepare methyl salicylate-4-*d*. The white solid from the nondeuterium reaction of the iodo-compound was washed directly into a flask with methanol (20 ml) and concentrated sulfuric acid (0.5 ml). This solution was heated under reflux for 14 h and allowed to stand at room temperature for 4 h. The methanol was distilled off through a fractionating column.[3] The residue (5 ml) was neutralized to alkacid with a sodium bicarbonate solution (10%). This neutral mixture was extracted 5 times with chloroform (20 ml each time) and the combined extracts were dried over anhydrous magnesium sulfate. Removal of the solvent was done on the rotary evaporator under vacuum and the brown oil left was distilled under reduced pressure (0.05 mm, 60°) yielding a clear colorless oil which had the characteristic odor of methyl salicylate. The p.m.r. spectrum of the distilled product was found to be identical to that of authentic methyl salicylate.

The entire deuterated product from the above reduction was esterified in exactly the same way as the undeuterated compound. The deuterated product was a clear colorless oil that had the characteristic odor of methyl salicylate and was characterized by its dinitro-derivative.

Methyl salicylate-6-*d* and methyl salicylate-4-*d* were made by 2 different methods but the subsequent reactions leading to the 2 final products are identical.

Methyl 3,5-Dinitrosalicylate, Methyl 3,5-Dinitrosalicylate-4-d, and Methyl 3,5-Dinitrosalicylate-6-d

Methyl salicylate was nitrated by a method similar to that used by Cavill (13). Since the overall yield and completeness of nitration of the product is sensitive to the strength of the fuming acid and reaction conditions used,[4] the refined procedure developed for the nitration of the 4- and 6-*d* analogs is reported.

Fuming nitric acid (3.0 ml, sp. gr. 1.5) and concentrated sulfuric acid (1.7 ml) were cooled in an ice–salt bath to −2°. Methyl salicylate (0.55 g, Eastman) was mixed with an equal volume of glacial acetic acid. This mixture was added slowly to the well agitated cold mineral acids, and the temperature was kept below 6°. The flask was removed from the cooling bath, and the contents were stirred at room temperature for 1 h. The dark orange solution was poured over ice (25 g) and lemon yellow crystals separated immediately. The collected, dry, crude product (0.93 g, 87%, m.p. 126–132°) melted 132-134° after a single recrystallization from methanol. No depression of m.p. was observed on admixture with authentic methyl 3,5-dinitrosalicylate.

The small quantities of methyl salicylate-4-*d* and methyl salicylate-6-*d* were nitrated and purified in exactly the same way. No depression of m.p. was observed on admixture of either deutero analog with the non-deuterated methyl 3,5-dinitrosalicylate. The p.m.r. spectrum of

[3]The fractionating column was 16 cm long, 2 cm in diameter, and filled with glass Fenske helices. When an efficient column was not used the characteristic odor of methyl salicylate could be detected in the distillate indicating only trace amounts of the ester.

[4]For example, weak fuming nitric acid or higher reaction temperatures lead to considerable formation of the mono-nitroisomers.

methyl 3,5-dinitrosalicylate-4-*d* showed a single aromatic peak (6.63) whereas the non-deuterated material showed 2 aromatic singlets (6.72 and 6.78). The methyl 3,5-dinitrosalicylate-6-*d* was characterized by conversion to *N*-methyl 2-carbomethoxy-4,6-dinitroaniline-3-*d* (4).

1. I. D. RAE. Aust. J. Chem. **18**, 1807 (1965).
2. J. HEIDBERG, J. A. WEIL, G. A. JANUSONIS, and J. K. ANDERSON. J. Chem. Phys. **41**, 1033 (1964).
3. J. A. WEIL, A. BLUM, A. H. HEISS, and J. K. KINNAIRD. J. Chem. Phys. **46**, 3132 (1967).
4. J. A. McCUBBIN, R. Y. MOIR, and G. A. NEVILLE, Can. J. Chem. This issue.
5. GH. BALICA. Rev. Chim. **11**, 171 (1960).
6. E. B. HERSHBERG. Ind. Eng. Chem. (Anal. Ed.) **8**, 312 (1936).
7. S. K. GUHA, J. N. CHATEREA, and A. K. SINA. J. Indian Chem. Soc. **32**, 780 (1955).
8. TH. J. DE BOER. Rec. Trav. Chim. **73**, 229 (1954).
9. H. GOLDSTEIN and G. PRETINER. Helv. Chim. Acta, **27**, 612 (1944).
10. G. TSATSAS and C. SANDRIS. Prakt. Akad. Athenon. **35**, 372 (1960).
11. S. SAFE. Ph.D. Thesis, Queen's University, Kingston, Ontario (1963).
12. H. L. FISHER. Laboratory manual of organic chemistry. 4th Ed. J. Wiley & Sons, Inc., New York (1938).
13. G. W. K. CAVILL. J. Soc. Chem. Ind. **64**, 212 (1945).

Can. J. Chem. Downloaded from www.nrcresearchpress.com by 210.87.254.5 on 09/05/12
For personal use only.

Can. J. Chem. Downloaded from www.nrcresearchpress.com by 210.87.254.105 on 09/05/12
For personal use only.

Total synthesis of spirobenzylisoquinoline alkaloids: (±)-ochotensimine

STEWART MCLEAN, MEI-SIE LIN, AND JOHN WHELAN
Department of Chemistry, University of Toronto, Toronto, Ontario

Received October 27, 1969

A synthesis of ochotensimine that can be modified to lead to related spirobenzylisoquinoline alkaloids is described.

Canadian Journal of Chemistry, **48**, 948 (1970)

In 1940 Manske (1) reported the isolation of the alkaloids ochotensine and ochotensimine from the fumariaceous plant *Corydalis ochotensis* Turcz. A few years ago the structures **1***a* and **1***b*, respectively, were assigned to these alkaloids on the basis of chemical, spectroscopic, and X-ray crystallographic evidence (2). Ochotensine and ochotensimine were of considerable interest since they appeared to belong to a new structural class of alkaloids in which the basic benzylisoquinoline framework had been modified to incorporate a spiro union. Several further fumariaceous alkaloids have very recently been assigned structures incorporating the same type of skeleton (3).

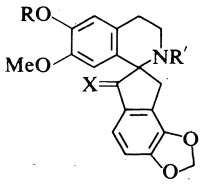

1

a R = H; R′ = Me; X = CH_2
b R = Me; R′ = Me; X = CH_2
c R = H; R′ = H; X = O
d R = Me; R′ = Me; X = O

In 1968 we communicated a preliminary report of the total synthesis of (±)-ochotensimine (4); since then Irie *et al.* (5) have reported a synthesis that closely parallels our own and there have been several reports of syntheses of analogs by related routes (5, 6). Very recently Shamma (7) has reported a very interesting synthesis of the spiro skeleton by a completely different route that may be related to the biosynthesis of this class of alkaloids. We now report the details of our own synthesis, some steps of which we have improved since our preliminary communication (4).

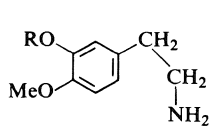

2

a R = Me
b R = H

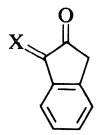

3

a X = H_2
b X = O

The Pictet–Spengler reaction (8) has found extensive use for the synthesis of tetrahydroisoquinolines, but in almost all of the vast amount of work on the reaction the carbonyl component has been an aldehyde. The literature does, however, contain a few isolated references to the use of the reaction with pyruvic acid derivatives (9) and, in one case, with cyclic ketones (10). Both classes of ketones offered potential routes to the spiro skeleton and this led us to investigate first the applicability of the method with model cyclic ketones.

We were pleased to find conditions, utilizing hot 85% phosphoric acid, under which homoveratrylamine (**2***a*) reacted with 2-indanone (**3***a*) to form the tetracylic product **4***a* which incorporated the required skeleton. 1,2-Indanedione (**3***b*) then appeared to be ideal as the next model carbonyl component: it can be anticipated that of the two carbonyl groups present, the one at position 2 should be the more reactive in the cyclization reaction, and the second carbonyl should be retained in the product (**4***b*) at the precise position where an exocyclic methylene must eventually be introduced. When the reaction was carried out, the yield of **4***b* was, in fact, higher than that of **4***a* in the earlier case and no trace of the isomer resulting from reaction at position 1 was isolated.

Treatment of **4***b* with formic acid and formaldehyde converted it to its *N*-methyl derivative **4***c* by the Eschweiler–Clarke reaction. A

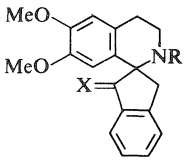

4

a R = H; X = H_2
b R = H; X = O
c R = Me; X = O
d R = Me; X = CH_2

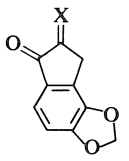

5

a X = O
b X = H_2
c X = NOH
d X = H,OAc

standard Wittig reaction employing methylenetriphenylphosphorane transformed **4***c* to **4***d*, which has all the structural features of ochotensimine except the methylenedioxy substituent. The spectroscopic characteristics of these compounds were in accord with the structural assignments made; in particular, the nuclear magnetic resonance (n.m.r.) spectrum of **4***d* was remarkably similar to that of ochotensimine except that it exhibited signals for two further aromatic protons in place of those of the methylenedioxy protons in the alkaloid.

The synthesis of the model compound **4***d* indicated that it should be possible to use the same route to ochotensimine if **5***a*, the appropriate methylenedioxy derivative of **3***b*, could be obtained as the starting material for the sequence. This task required the use of a surprisingly large number of synthetic steps. Many substituted methylenedioxybenzenes are readily available as starting materials, but all of the common examples are derivatives of piperonal and it seemed inevitable that synthetic elaboration of these would lead to undesired isomers of **5***a*. It was therefore necessary to use a sequence incorporating the methylenation of a suitably substituted catechol, a reaction that frequently presents technical difficulties.

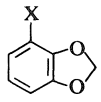

6

a X = COOH
b X = CH_2OH
c X = CHO
d X = CH=CHCOOH
e X = CH_2CH_2COOH

Perkin and Trikojus (11) have described a convenient preparation of the methylenedioxybenzoic acid **6***a* from 2,3-dihydroxybenzoic acid

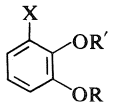

7

a X = CHO; R = Me; R′ = H
b X = CHO; R = Me; R′ = Me
c X = COOH; R = Me; R′ = Me
d X = COOH; R = H; R′ = H
e X = CHO; R = H; R′ = H

(**7***d*), which is now commercially available. We have been able to repeat this and obtain **6***a* in yields of 52% for this step. They converted **6***a* to the methylenedioxycinnamic acid **6***d* by a sequence which we have modified, with a considerable improvement in convenience and yield, by the use of reagents not available to them: **6***a* was reduced with lithium aluminum hydride to the alcohol **6***b*, which was oxidized to the aldehyde **6***c* by chromium trioxide in pyridine (12). Perkin's original preparation of 2,3-dihydroxybenzoic acid (**7***d*) started with *o*-vanillin (**7***a*), which is still a very convenient starting material. However, it was unfortunately necessary to methylate **7***a* to protect the phenolic group, oxidize the aldehyde group of the *o*-veratraldehyde (**7***b*) obtained, and then remove both methyl groups from the product **7***c* in order to obtain **7***d*; furthermore the oxidation level required at **6***c*, an aldehyde, is the same as in **7***a* but it was necessary, in order to introduce the methylenedioxy group, to go through the lengthy series of oxidations and reductions described. We have now been able to devise a method for converting *o*-vanillin (**7***a*) to **6***c* in two steps and in excellent yield. The demethylation of *o*-vanillin to 2,3-dihydroxybenzaldehyde (**7***e*) by hydrobromic acid can be accomplished on a large scale by the method of Pauly *et al.* (13); yields of up to 60% were obtained. The product can then be converted directly to **6***c* in 64% yield by the method that Tomita and Aoyagi have recently described (14), where methylenation is carried out by methylene iodide in dimethylformamide in the presence of cupric oxide and potassium carbonate. The aldehyde (**6***c*) produced by this method was of a very good quality and could be converted by condensation with malonic acid under Perkin's conditions (11) to the methylenedioxycinnamic acid **6***d* in 96% yield; the yield was considerably lower if less pure starting material was used. The conversion

Can. J. Chem. Downloaded from www.nrcresearchpress.com by 210.87.254.105 on 09/05/12
For personal use only.

Can. J. Chem. Downloaded from www.nrcresearchpress.com by 210.87.254.105 on 09/05/12
For personal use only.

of **6***d* to **6***e* was effected in 92% yield by reduction with sodium amalgam.

The conversion of **6***e* to the indanone **5***b* was accomplished by a Friedel–Crafts cyclization, a reaction which has received a considerable amount of study in a wide variety of contexts. The conclusions that can be drawn from these studies are, in summary, that the optimum conditions for cyclization are remarkably dependent on the precise constitution of the substrate, and yields are liable to fall rapidly if the reaction conditions are allowed to diverge from the optimum. The cyclization of **6***e* was typical. In our original method **6***e* was heated with phosphorus pentoxide and converted to **5***b* in a yield of 25%; this result is comparable with that of Irie *et al.* (5) and, like them we observed the formation of a by-product with infrared (i.r.) absorption at 5.67 μ. We now find that **6***e* can be converted via its acid chloride to **5***b* in 76% yield, the cyclization being effected by treatment of the acid chloride with aluminum chloride in methylene chloride at −10°; the temperature used was extremely critical since at a few degrees below the optimum the rate of the reaction fell rapidly, while raising the temperature caused an appreciable increase in the formation of the by-product at the expense of **5***b*.

In the model series 1,2-indanedione (**3***b*) was conveniently prepared by nitrosation of 1-indanone and hydrolysis of the product with hydrochloric acid in the presence of formaldehyde (15). The methylenedioxyindanone **5***b* was readily converted to the oximino ketone **5***c* by *n*-butyl nitrite as in the model series, but we were unable to obtain useful amounts of **5***a* by acid-catalyzed hydrolysis of **5***c*; our conditions were either too gentle and **5***c* was recovered, or too vigorous and extensive degradation resulted. Although Irie and his co-workers (5) have now reported that they have found conditions under which this hydrolysis can be carried out, the very marked difference in behavior of **5***c* and the analogous compound in the model series gives evidence that the reactions at the 2 position of an indanone can be markedly influenced by the presence or absence of a methylenedioxy group on the aromatic ring, an observation that is unexpected, unexplained, and an ill omen for the next stage of the synthesis. We did, in fact, succeed in converting **5***c* to **5***a* by Eistert's method (16) which required the methylation of **5***c* with diazomethane and acid-catalyzed hydrolysis of the product, but in our most convenient synthesis of **5***a*, **5***b* was acetoxylated with lead tetraacetate (17) and the product, **5***d*, was hydrolyzed to the corresponding hydroxyketone and then oxidized to **5***a* by the Jones reagent; when this sequence was carried out rapidly and with care to avoid the degradation of the somewhat unstable intermediates, yields of 70% were achieved.

With **5***a* available we turned our attention to completing the synthesis of ochotensimine (**1***b*) by the route established in the synthesis of the model compound **4***d*. However, as the results of the attempted acid-catalyzed hydrolysis of **5***c* had led us to fear, the Pictet–Spengler reaction of **5***a* with homoveratrylamine (**2***a*) under the conditions used in the model series led to no recognizable product. Since one potential source of difficulty was the methylenedioxy group which may not have survived the strongly acid conditions, we sought less vigorous conditions for the reaction. It soon became apparent that a more reactive phenylethylamine was required, so we turned to the phenolic compound **2***b* and found that this reacted with **5***a* in the presence of dilute hydrochloric acid and that excellent yields of the spiro compound **1***c* could be obtained by careful control of the concentration of acid and temperature. The product (**1***c*) was *O*-methylated with diazomethane and *N*-methylated by the Eschweiler–Clarke reaction as in the model series, the product, **1***d*, being obtained in excellent yield. The final step to (±)-ochotensimine (**1***b*), the Wittig reaction, was also carried out under the same conditions as in the model series. The product was non-crystalline, as is natural ochotensimine, and the identity of the two materials in every respect but optical activity was established by i.r., ultraviolet (u.v.), and n.m.r. spectroscopy as well as by their mass spectrometric fragmentation patterns and their behavior in thin-layer chromatography (t.l.c.). Intermediate **1***c* has also been converted to (±)-ochotensine (**1***a*) by Irie *et al.* (5) and by Beckett and Kelly (6).

We have carried out a number of unsuccessful attempts to resolve our synthetic products; the resolving agents *d*-10-camphorsulfonic acid, the 2′-chloro, 2′-bromo, and 2′-nitro derivatives of (2*R*,3*R*)- and (2*S*,3*S*)-tartranilic acid (18) were used with **1***b*, **1***c*, and **1***d*, the toluenesulfonate

esters of D- and L-leucine were used with **1***b*, and the di-*p*-toluoyl derivatives of D- and L-tartaric acids (19) were used with **1***c* and **1***d*.

Experimental

Melting points were determined on a Thomas–Kofler micro hot stage. Spectrometers used were: Beckman IR 8 for i.r. spectra, Bausch and Lomb Spectronic 505 and Unicam SP. 800 for u.v. spectra, and Varian A-60 and HA-100 for n.m.r. spectra. Unless otherwise indicated, i.r. spectra were obtained with chloroform solutions, u.v. spectra with methanol solutions, and n.m.r. spectra with chloroform-*d* solutions.

*6,7-Dimethoxy-1,2,3,4-tetrahydroisoquinoline-1-spiro-2′-indane (**4a**)*

Homoveratrylamine (**2***a*) (5.4 g; 30 mmoles), 2-indanone (**3***a*) (20) (4.2 g; 32 mmoles), and 11 ml 85% phosphoric acid were heated together at 80–90° under nitrogen for 21 h. The dark suspension that resulted was poured into 60 ml water, extracted with chloroform, made basic with sodium hydroxide, and then extracted with ether. The ether afforded a residue (1.4 g) which failed to crystallize from common solvents. Treatment with acetic anhydride and a little pyridine at room temperature overnight converted the residue to the crystalline *N*-acetyl derivative of **4***a* (1.3 g; 4 mmoles), which had, after recrystallization from methanol, m.p. 152–153°.

Anal. Calcd. for $C_{21}H_{23}NO_3$: C, 74.75; H, 6.87; N, 4.15. Found: C, 74.80; H, 6.91; N, 4.22.

The i.r.: λ_{max} 6.11 μ; u.v.: λ_{max} 232 (inflect. ε 8300), 266 (ε 2600), 272 (ε 3900), 278 (ε 3400), 282 (ε 3400), and 288 mμ (inflect.); n.m.r. (τ; A-60): 2.85 (4H; s), 3.42 (1H; s), 3.57 (1H; s), 6.19 (3H; s), 6.58 (3H; s), 7.81 (3H; s), 5.92, 6.86 (2H each; apparently AB quartet, *J* 16 Hz), 6.31, 7.17 (2H each; apparently components of A_2B_2 multiplet).

*6,7-Dimethoxy-2-methyl-1,2,3,4-tetrahydroisoquinoline-1-spiro-2′-indanone-1′ (**4c**)*

Homoveratrylamine (**2***a*) (1.6 g; 9 mmoles), 1,2-indanedione (**3***b*) (15) (1.4 g; 9.5 mmoles), and 10 ml 85% phosphoric acid were subjected to the treatment just described. The product, **4***b*, (0.83 g) (5.84 μ peak in i.r.), which failed to crystallize, was acetylated as in the previous case. The *N*-acetyl derivative was crystalline, m.p. 177–179°, but appeared to be hygroscopic and gave unreproducible microanalytical results ("best values" are quoted).

Anal. Calcd. for $C_{21}H_{21}NO_4$: C, 71.79, H, 6.02; N, 3.99. Found: C, 72.02; H, 6.34; N, 3.94.

The i.r. λ_{max} 5.80, 6.10 μ; u.v.: λ_{max} 239 (ε 18 300) and 286 mμ (ε 6100); n.m.r. (τ; A-60): 2.10–2.71 (4H; complex); 3.33 (1H; s), 3.84 (1H; s), 6.17 (3H; s), 6.60 (3H; s), 6.00–7.18 (6H; complex), 7.82 (3H; s).

A mixture of **4***b* (6.2 g; 20 mmoles), 7 ml 85% formic acid, and 5 ml 40% formaldehyde was heated on a steam-bath for 10 h and then evaporated under reduced pressure to a syrup. The syrup was diluted with 30 ml water, made basic with 1 *N* sodium hydroxide, and thoroughly extracted with chloroform. The chloroform extract afforded **4***c* as a brown solid (6.4 g; 20 mmoles) which, after chromatography on alumina (Brockmann activity I) with ether elution and recrystallization from methanol–ether, was obtained as yellow crystals, m.p. 136–138°.

Anal. Calcd. for $C_{20}H_{21}NO_3$: C, 74.28; H, 6.55; N, 4.33. Found: C, 74.11; H, 6.57; N, 4.34.

The i.r.: λ_{max} 5.85 μ; u.v. λ_{max} 246 (ε 15 600), 287 (ε 5400), and 301 mμ (inflect.); n.m.r. (τ; A-60): 2.10–2.68 (4H; complex), 3.37 (1H; s), 3.92 (1H; s), 6.18 (3H; s), 6.50 (3H; s), 6.53–7.20 (6H; complex), 7.70 (3H; s). Methiodide, m.p. 145–148°.

Anal. Calcd. for $C_{21}H_{24}NO_3I$: C, 54.19; H, 5.16; N, 3.01. Found: C, 54.17; H, 5.66; N, 3.04.

*Des(methylenedioxy)ochotensimine (**4d**)*

Methyltriphenylphosphonium bromide (2.15 g; 6 mmoles) and 4.2 ml of 14.9% butyl lithium (6 mmoles) were stirred together under nitrogen at room temperature for 2 h. A solution of **4***c* (646 mg; 2.0 mmoles) in 30 ml tetrahydrofuran was added, and the reaction mixture was refluxed 9 h, and then poured into 100 ml water. Extraction with chloroform afforded a product (1.54 g) which was chromatographed on 45 g neutral alumina (Brockmann activity I) with elution first with benzene – petroleum ether and then benzene. The benzene fractions afforded **4***d* as a noncrystalline residue (285 mg; 0.89 mmoles): i.r. λ_{max} 6.22 (m)μ; u.v. λ_{max} 227 (ε 37 700), 281 (ε 6300), 289 (ε 6100), and 300 mμ (ε 4000); n.m.r. (τ; A-60): 2.10–2.76 (4H; complex), 3.41 (1H; s), 3.65 (1H; s), 4.19 (1H; s), 4.95 (1H; s), 6.15 (3H; s), 6.40 (3H; s), 6.68 (2H; AB quartet, *J*, 18 Hz, internal chemical shift 27 Hz), 7.04–7.42 (4H; complex), 7.88 (3H; s). Treatment of **4***d* with methyl iodide in acetone–ether converted it to its methiodide which was obtained crystalline, m.p. 130–134°, after recrystallization from acetone–ether.

Anal. Calcd. for $C_{22}H_{26}NO_2I$: C, 56.92; H, 5.61; N, 3.02. Found: C, 56.77; H, 5.92; N, 2.95.

*2,3-Methylenedioxybenzaldehyde (**6c**)*

Method A

o-Vanillin (**7***a*) was converted into 2,3-dihydroxybenzaldehyde (**7***e*) in 60% yield by the method of Pauly *et al.* (13). A mixture of **7***e* (10.0 g; 72.5 mmoles), methylene iodide (31.4 g; 117 mmoles), potassium carbonate (30.0 g; 218 mmoles), cupric oxide (1.0 g) and 85 ml dimethylformamide was heated to 100–110° under nitrogen and vigorously stirred for 3½ h (14). The reaction mixture was cooled, diluted with 1400 ml ice-water, and thoroughly extracted with ether. The ether extract, after it had been washed successively with 3% hydrochloric acid, 10% aqueous potassium carbonate, and water, yielded crystalline **6***c* (7.0 g; 47 mmoles), m.p. 32–34° (lit. (11) 34°).

Method B

2,3-Methylenedioxybenzoic acid (**6***a*) (19.8 g; 119 mmoles), prepared from 2,3-dihydroxybenzoic acid (11), in 600 ml tetrahydrofuran was added dropwise to a suspension of lithium aluminum hydride (4.75 g; 125 mmoles) in 600 ml ether under nitrogen. The reaction mixture was refluxed 4 days, cooled, treated with ice, and made acid with 10% sulfuric acid. The aqueous layer was thoroughly extracted with ether, and the combined ether extracts yielded a brown oil (18.9 g) from which **6***b*, (16.3 g; 108 mmoles) m.p. 34–35° (lit. (21) 34–35°) was obtained as tan needles.

Can. J. Chem. Downloaded from www.nrcresearchpress.com by 210.87.254.105 on 09/05/12
For personal use only.

Can. J. Chem. Downloaded from www.nrcresearchpress.com by 210.87.254.105 on 09/05/12
For personal use only.

A solution of **6***b* (12.4 g; 81.5 mmoles) in 50 ml pyridine was added in one portion to a chilled, well-stirred suspension of chromium trioxide (24.4 g; 244 mmoles) in 600 ml pyridine. The suspension, which immediately turned greenish brown, was stirred for 20 min and then allowed to stand at room temperature 22 h. The solution was diluted with 250 ml ether and the precipitate removed by filtration. The filtrate was diluted with 600 ml water and thoroughly extracted with ether and the combined ether extracts, after they had been washed successively with 10% hydrochloric acid, 4% aqueous sodium carbonate, and water, yielded yellowish crystals of **6***c* (7.95 g; 53 mmoles), m.p. 32–34°.

2,3-Methylenedioxydihydrocinnamic Acid (6e)

The aldehyde **6***c* was converted in 96% yield by Perkin's method (11) into 2,3-methylenedioxycinnamic acid (**6***d*), m.p. 190–194°; recrystallization from methanol gave material m.p. 194–196°; i.r.: λ_{max} 3–4, 5.92, 6.12 μ; u.v.: λ_{max} 230 (ε 20 600), 275 (ε 20 300), and 335 mμ (ε 4240); n.m.r.: (τ; A-60; acetone-d_6): 2.15–2.78 (3H; complex), 2.85 (2H; AB quartet, *J*, 16 Hz, internal chemical shift 59 Hz), 3.86 (2H; s).

Freshly prepared 2% sodium amalgam (88 g; 77 mmoles Na) was added to a well-stirred solution of **6***d* (7.68 g; 40.0 mmoles) in 18 ml 2.5 *N* sodium hydroxide over 1 h. The mixture was filtered and the filtrate was acidified with dilute hydrochloric acid. The acid **6***e* (7.11 g; 37 mmoles), m.p. 80–82°, was precipitated.

Anal. Calcd. for $C_{10}H_{10}O_4$: C, 61.85; H, 5.19. Found: C, 61.65; H, 5.01.

The i.r.: λ_{max} 3–4, 5.84 μ; u.v.: λ_{max} 233 (ε 2900) and 282 mμ (ε 2700); n.m.r. (τ; A-60): 3.30 (3H; m), 4.09 (2H; s), 6.99–7.45 (4H; complex).

4,5-Methylenedioxy-1-indanone (5b)

Method A

A solution of **6***e* (2.0 g; 10.3 mmoles) in 4 ml purified thionyl chloride was stirred with the exclusion of moisture for 2 h at room temperature. The excess thionyl chloride was evaporated under reduced pressure and the amber oil which resulted was dissolved in 5 ml dry methylene chloride and added dropwise over 7 min to a vigorously stirred suspension of finely powdered aluminum chloride (1.8 g; 13.7 mmoles) in 125 ml methylene chloride at −10°. The reaction was stopped by the addition of 30 ml 10% hydrochloric acid, and the aqueous layer was separated and extracted with further methylene chloride; the combined organic layers were washed successively with water, 2% sodium hydroxide, and water. The organic extract afforded a white solid which was recrystallized from acetone–ether and **5***b* (1.3 g; 7.6 mmoles), m.p. 165–168°, was obtained.

Method B

Phosphorus pentoxide (6 g) was added in small portions with shaking to a boiling solution of **6***e* (1.1 g; 5.6 mmoles) in 30 ml benzene. After the mixture had been refluxed with occasional agitation for 5 h, it was poured on to 100 g crushed ice and successively extracted with ether and ethyl acetate. The combined extracts, after they had been washed with saturated aqueous sodium bicarbonate and water, afforded a residue (0.66 g) which consisted of **5***b* and an impurity which showed i.r. absorption at 5.67 μ. Pure **5***b* (effective yield ~25%) m.p. 165–168°, was obtained by repeated recrystallization of the residue from acetone–ether.

Anal. Calcd. for $C_{10}H_8O_3$: C, 68.18; H, 4.58. Found: C, 68.38; H, 4.39.

The i.r.: λ_{max} 5.88, 6.12 μ; u.v.: λ_{max} 235 (ε 24 800), 286 (ε 7300), and 305 mμ (inflect., ε 5500); n.m.r. (τ; A-60): 2.87 (2H; AB quartet, *J*, 8 Hz, internal chemical shift 31 Hz), 3.92 (2H; s), 6.84–7.46 (4H; complex).

4,5-Methylenedioxy-1,2-indanedione (5a)

Method A

A solution of **5***b* (0.35 g; 2.0 mmoles) in 25 ml glacial acetic acid containing 7 ml of acetic anhydride was heated to 78° with stirring and red lead oxide (Pb_3O_4; 2.75 g; 4.0 mmoles) was added in portions over 1 h (care was taken that each portion of lead oxide had completely reacted before the next was added). The solution was kept at 78° for a further $3\frac{3}{4}$ h and 10 ml methanol were then added and the stirring was continued for a further 15 min. The solution was cooled to room temperature and added to 225 ml of cold water. The aqueous solution was thoroughly extracted with methylene chloride, and the extract was filtered through Celite and washed with water until the wash water was neutral. The extract afforded a yellow solid from which the acetoxyindanone **5***d* (0.3 g; 1.35 mmoles), m.p. 129–131° was isolated by recrystallization from hexane – carbon tetrachloride.

Anal. Calcd. for $C_{12}H_{10}O_5$: C, 61.54; H, 4.30. Found: C, 61.77; H, 4.51.

The i.r.: λ_{max} 5.75, 5.82 μ; u.v. λ_{max} 238 (ε 22 500) 294 (ε 7400), and 309 mμ (inflect.): n.m.r. (τ; HA-100) 2.85 (2H; AB quartet, *J*, 8.0 Hz, internal chemical shift 54 Hz), 3.91 (2H; narrow multiplet), 4.60, 6.40, 7.10 (1H each; AMX pattern, J_{AM} 5Hz, J_{AX} 9 Hz, J_{MX} 18 Hz), 7.84 (3H; s).

A solution of **5***d* (95 mg; 0.405 mmoles) in 35 ml methanol was kept at 0° under nitrogen and a solution of 1.2 ml of 2% aqueous sodium hydroxide in 15 ml methanol was added dropwise over about 15 min. The solution was poured into 100 ml of ice-water and immediately acidified with 10% hydrochloric acid. The solution was thoroughly extracted with methylene chloride, and, after the extract had been washed with water, it yielded an unstable yellow solid (75 mg) [Mol. Wt. Calcd. for $C_{10}H_8O_4$: 192.0422. Found (mass spectrometry): 192.0423] which was immediately dissolved in 5 ml acetone at 10° and the Jones reagent (22) was added until an orange–brown color persisted (~0.25 ml reagent was required). The solution was diluted with 40 ml water and thoroughly extracted with methylene chloride. The extract afforded **5***a* (73 mg; 0.385 mmoles) m.p. 158–168° (value strongly dependent on rate of heating; material appeared to decompose near its m.p.).

Anal. Calcd. for $C_{10}H_6O_4$: C, 63.16; H, 3.18. Found: C, 63.33; H, 3.27.

The i.r.: λ_{max} 5.66, 5.82 μ; u.v.: λ_{max} 239 (ε 20 500), 294 (ε 7400), and 311 mμ (ε 6600); material too insoluble for useful n.m.r. spectrum.

Method B

To an ice-cooled, well-stirred solution of **5***b* (3.02 g; 17.1 mmoles) in 300 ml methanol were added *n*-butyl nitrite (2.1 g; 20.3 mmoles) and 2 ml concentrated hydrochloric acid. The mixture was stirred 1 h and then left

Can. J. Chem. Downloaded from www.nrcresearchpress.com by 210.87.254.105 on 09/05/12
For personal use only.

at room temperature 20 h. The precipitate of **5***c* (2.95 g; 14.4 mmoles), m.p. 257–260°, which formed was recrystallized from acetone–tetrahydrofuran and obtained as crystals m.p. 258–260°.

Anal. Calcd. for $C_{10}H_7NO_4$: C, 58.54; H, 3.44; N, 6.83. Found: C, 58.67; H, 3.60; N, 6.70.

The i.r.: λ_{max}(KBr) 5.89, 6.17 μ; u.v.: λ_{max} 253 (ε 10 900), 313 (inflect.), and 340 mμ (ε 4800); n.m.r. (τ; A-60; DMSO-d_6): −2.79 (1H; s), 2.78 (2H; AB quartet, *J*, 8 Hz, internal chemical shift 21 Hz), 3.77 (2H; s), 6.38 (2H; s).

A suspension of **5***c* (112 mg; 0.54 mmole) in 100 ml tetrahydrofuran containing a few drops of methanol was stirred for 21 h with 25 ml ethereal diazomethane (~ 8.3 mmoles). The residue (120 mg), m.p. 185–186°, recovered after evaporation of the solvent, was recrystallized from acetone–ether and obtained as yellow crystals, m.p. 188–189°, showing i.r. absorption at 5.92 and 6.38 μ. Hydrolysis of this material (55 mg) in 9% hydrochloric acid at room temperature for 7 days converted it to a product (43 mg), m.p. 150–173°, which consisted largely of **5***a*, but which could be purified by recrystallization from acetone–ether only with difficulty and with poor recovery of material.

*6,7-Dimethoxy-2-methyl-1,2,3,4-tetrahydroisoquinoline-1-spiro-2′-(4′,-5′-methylenedioxy-1′-indanone) (**1***d*)*

A suspension of finely powdered **5***a* (380 mg; 2.0 mmoles) and β-(3-hydroxy-4-methoxyphenyl)ethylamine hydrochloride (**2***b*) (500 mg; 2.0 mmoles) in 15 ml 2.5% hydrochloric acid was stirred vigorously at 49–52° for 4 days. Unchanged **5***a* (237 mg; 1.25 mmoles) was recovered by extraction of the reaction mixture with methylene chloride. The reaction mixture was then made slightly basic with saturated aqueous sodium bicarbonate and re-extracted with methylene chloride. The extract afforded an amber oil (310 mg) which was purified by preparative layer chromatography on silica gel G. Crystalline **1***c* (230 mg; 0.68 mmoles), m.p. 104–107°, was then obtained from acetone. This material corresponds to that obtained by Kelly and Beckett (6) and we thank Professor Kelly for a sample of his material for direct comparison with ours; the material obtained by Irie *et al.* (5) is apparently a different crystalline modification. The material we obtained gave erratic analytical results, probably because of tenacious retention of variable amounts of solvent.

Spectroscopic results: i.r.: λ_{max} 2.83, 5.85 μ; u.v.: λ_{max} 237 (ε 27 600), 292 (ε 11 800), and 310 mμ (inflect., ε 8000); n.m.r. (τ; CD_3OD: HA-100): 2.79 (2H; AB quartet, *J*, 8.0 Hz, internal chemical shift 46 Hz), 3.45 (1H; s), 3.88 (3H; probably 2 superimposed singlets), 6.45 (3H; s), remainder of spectrum confused by partially exchanged solvent, etc.

Treatment of **1***c* (251 mg) in 2 ml methanol with an excess of diazomethane in ether converted it quantitatively to its methyl ether which, after purification by t.l.c. (9:1 methylene chloride – methanol on silica gel G) and recrystallization from acetone–hexane, afforded crystals m.p. 179–181°.

Anal. Calcd. for $C_{20}H_{19}NO_5$: C, 67.98; H, 5.42; N, 3.96. Found: C, 67.85; H, 5.49; N, 4.13.

The i.r.: λ_{max} 5.85 μ; u.v.: λ_{max} 237 (ε 37 600), 292 (ε 11 800), and 310 mμ (inflect., ε 10 500); n.m.r. (τ; HA-100): 2.78 (2H; AB quartet, *J*, 8.0 Hz, internal chemical shift 59 Hz), 3.41 (1H; s), 3.84 (1H; s), 3.90 (2H; AB quartet, $J \sim 1.5$ Hz; internal chemical shift ~ 3.5 Hz), 6.18 (3H; s), 6.40 (3H; s), 6.2–7.3 (6H; complex), 7.86 (1H; s; removed by D_2O).

A mixture of the methyl ether (180 mg; 0.53 mmole), 5 ml 91% formic acid and 0.2 ml 40% formaldehyde was heated on a steam-bath for 9½ h. The solution, when cool, was poured into 50 ml water, made basic with saturated aqueous sodium bicarbonate, and thoroughly extracted with methylene chloride. The extract afforded **1***d* (155 mg; 0.44 mmole), m.p. 162–165°, after recrystallization from acetone–hexane.

Anal. Calcd. for $C_{21}H_{21}NO_5$: C, 68.65; H, 5.76; N, 3.81. Found: C, 68.88; H, 5.69; N, 3.70.

The i.r.: λ_{max} 5.86 μ; u.v.: λ_{max} 237 (ε 32 000), 292 (ε 12 600), and 310 mμ (inflect., ε 9600); n.m.r. (τ; HA-100): 2.80 (2H; AB quartet, *J*, 8.0 Hz, internal chemical shift 58 Hz), 3.41 (1H; s), 3.88 (3H; probably 1H singlet superimposed on very narrow 2H multiplet), 6.19 (3H; s), 6.44 (3H; s), 6.60 (2H; AB quartet; *J*, 18 Hz; internal chemical shift 23 Hz), 6.8–7.3 (4H; m), 7.71 (3H; s).

*(±)-Ochotensimine (**1***b*)*

Methyltriphenylphosphonium bromide (152 mg; 0.42 mmoles) and *n*-butyl lithium (0.37 mmoles) in 1.6 ml hexane were stirred together under nitrogen at room temperature for 2 h. A solution of **1***d* (45 mg; 0.125 mmoles) in 4 ml tetrahydrofuran was added and the reaction mixture was refluxed 7.5 h, and, when cool, poured into 60 ml water. Extraction with methylene chloride afforded a material which was purified by t.l.c. (11:1 ether–methanol on silica gel G). The product (26.5 mg; 0.073 mmoles) was a pale yellow oil which showed the same behavior on t.l.c. (6 systems) as natural ochotensimine and the n.m.r., i.r., u.v., and mass spectra of the synthetic and natural materials were identical in all significant characteristics.

We thank the National Research Council of Canada for financial support of this work and for a Graduate Fellowship (J.W.); a Province of Ontario Department of University Affairs Graduate Fellowship (M.-S.L.) is also gratefully acknowledged.

1. R. H. F. MANSKE. Can. J. Res. **18** B, 75 (1940).
2. S. McLEAN and M.–S. LIN. Tetrahedron Lett. 3819 (1964). S. McLEAN, M.–S. LIN, and R. H. F. MANSKE. Can. J. Chem. **44**, 2449 (1966). S. McLEAN, M.–S. LIN, A. C. MACDONALD, and J. TROTTER. Tetrahedron Lett. 185 (1966). A. C. MACDONALD and J. TROTTER. J. Chem. Soc. (B) 929 (1966).
3. J. K. SAUNDERS, R. A. BELL, C.–Y. CHEN, D. B. MacLEAN, and R. H. F. MANSKE. Can. J. Chem. **46**, 2873, 2876 (1968).
4. S. McLEAN, M.–S. LIN, and J. WHELAN. Tetrahedron Lett. 2425 (1968).
5. H. IRIE, T. KISHIMOTO, and S. UYEO. J. Chem. Soc. (C) 3051 (1968).
6. B. A. BECKETT and R. B. KELLY. J. Heterocycl. Chem. **5**, 685 (1968). R. B. KELLY and B. A. BECKETT. Can. J. Chem. **47**, 2501 (1969).
7. M. SHAMMA and C. D. JONES. J. Amer. Chem. Soc. **91**, 4009 (1969).

8. W. M. WHALEY and T. R. GOVINDACHARI. Org. React. **6**, 151 (1951).
9. G. HAHN and K. STIEHL. Ber. **69**, 2627 (1936). G. R. CLEMO and G. A. SWAN. J. Chem. Soc. 487 (1949).
10. J. GARDENT. Ann. Chim. (Paris), **10**, 413 (1955).
11. W. H. PERKIN, jun., and V. M. TRIKOJUS. J. Chem. Soc. 2925 (1926).
12. J. R. HOLUM. J. Org. Chem. **26**, 4814 (1961).
13. H. PAULY, K SCHÜBEL, and K. LOCKEMANN. Ann. **383**, 288 (1911).
14. M. TOMITA and Y. AOYAGI. Chem. Pharm. Bull. (Japan), **16**, 523 (1968).
15. H. O. HOUSE, W. F. GANNON, R. S. RO, and D. J. WLUKA. J. Amer. Chem. Soc. **82**, 1463 (1960).
16. B. EISTERT, R. MÜLLER, H. SELZER, and E.-A. HACKMANN. Chem. Ber. **97**, 2469 (1964).
17. P. D. GARDNER. J. Amer. Chem. Soc. **78**, 3421 (1956).
18. T. A. MONTZKA, T. L. PINDELL, and J. D. MATISKELLA. J. Org. Chem. **33**, 3993 (1968).
19. R. B. WOODWARD, F. E. BADER, H. BICKEL, A. J. FREY, and R. W. KIERSTEAD. Tetrahedron **2**, 1 (1958).
20. W. E. ROSEN, L. DORFMAN, and M. P. LINFIELD. J. Org. Chem. **29**, 1723 (1964).
21. T. S. STEVENS. J. Chem. Soc. 725 (1935).
22. C. DJERASSI, R. R. ENGLE, and A. BOWERS. J. Org. Chem. **21**, 1547 (1957).

Can. J. Chem. Downloaded from www.nrcresearchpress.com by 210.87.254.105 on 09/05/12
For personal use only.

Can. J. Chem. Downloaded from www.nrcresearchpress.com by 210.87.254.40 on 09/05/12
For personal use only.

Free radicals by mass spectrometry. XLII. Ionization potentials and ionic heats of formation for C_1—C_4 alkyl radicals[1]

F. P. Lossing and G. P. Semeluk[2]
Division of Chemistry, National Research Council of Canada, Ottawa, Canada

Received November 10, 1969

Ionization potentials for C_1—C_4 alkyl free radicals have been re-measured by electron impact, using an energy-resolved electron beam from a double-hemispherical electrostatic monochromator. From these values and kinetic data for heats of formation of the radicals, ionic heats of formation for C_1—C_4 alkyl ions have been calculated. New values for the four isomeric butyl ions are given. The ionization efficiency curves for the simpler radicals show linear sections corresponding to excitation of vibrational levels; for larger radicals these segments are not resolved and only a smooth upward curvature is seen. In disagreement with earlier results, no evidence for formation of low-lying excited states of the ions could be found, either for parent or fragment ions.

Canadian Journal of Chemistry, **48**, 955 (1970)

Introduction

Earlier data on the ionization potentials (IP) of alkyl free radicals obtained with conventional mass spectrometric ion sources has been shown, by retarding potential difference (RPD) electron impact (1, 2) and photon impact (PI) (3, 4, 5), to be generally too high by 0.1 to 0.6 V. The reason for this over-estimate is that the probability of ionization to the zeroth vibrational level of the ion may for some species be quite small, becoming rapidly larger for vibrational levels a few tenths of a volt higher, corresponding to allowed vertical transitions in the Franck–Condon sense. Using electrons with a relatively wide (0.6–1.0 V) spread, the energy resolution at the onset of ionization is low, and the customary data treatment yields apparent ionization onsets corresponding approximately to the part of the ionization efficiency curve where the steep rise begins. This energy excess can be as little as < 0.1 V (CH_3 radical (5)) or as much as 1.0 V (CF_3 radical (6)) depending on the threshold ionization probabilities.

The RPD electron impact experiments (1, 2) have given greatly improved threshold measurements for alkyl radicals as a result of the increased resolution and sensitivity. These data suggest further, however, that ionization efficiency curves exhibit considerable structure in the first volt or two above the threshold. This structure, generally appearing to consist of straight line sections separated by upward breaks in slope common to both direct ionization of the radical and to formation of the radical ion in fragmentation processes, has been interpreted (7, 8) as corresponding to formation of various excited states of the radical ion. The reality of this structure, or more precisely the form which this structure has been thought to exhibit, has been questioned (5, 9), since corresponding features are not observed in photoionization efficiency curves. Indeed, the questions of whether photon and electron impact data should show only corresponding features, for both direct ionization and autoionization, and whether electron impact ionization is in fact governed by the Franck–Condon principle, have been the subject of some discussion (10–12).

In view of the current interest in such questions it was thought that further electron impact measurements on free radicals, using an energy-resolved electron beam, would be of value. Improved IP data and threshold ionization efficiency curves for C_1—C_4 alkyl radicals, obtained using a double-hemispherical energy selector for electrons combined with a quadrupole mass spectrometer, are presented here. From these IP's, and preferred values for heats of formation of the neutral radicals (13), heats of formation for the alkyl ions have been recalculated.

Experimental

The design and arrangement of the electron energy selector, ionization chamber, ion extractor, and quadrupole mass filter have been described (14). To reduce contamination of critical surfaces the vacuum chamber

[1]Issued as NRCC No. 11132.
[2]Visiting scientist. Present address: Department of Chemistry, University of New Brunswick, Fredericton, N.B.

TABLE 1
Ionization potentials of C_1—C_4 alkyl free radicals

Radical	This work	RPD (ref.)	PI (ref.)	Other (ref.)
CH_3	9.84 ± 0.03	9.80 (1), 9.87 (2)	9.82 (4), 9.82 (5)	9.843 (19)
C_2H_5	8.38 ± 0.05	8.25 (1), 8.34 (2)	< 8.4 (4), (8.45 ± 0.2) (9)	—
n-C_3H_7	8.10 ± 0.05	8.15 (1), 8.13 (2)	< 8.1 (4), (7.2 ± 0.2) (18)	—
s-C_3H_7	7.55 ± 0.05	7.52 (1), 7.57 (2)	< 7.5 (4)	—
n-C_4H_9	8.01 ± 0.05	8.01 (2)	—	—
iso-C_4H_9	8.01 ± 0.05	—	—	—
s-C_4H_9	7.41 ± 0.05	—	—	—
t-C_4H_9	6.93 ± 0.05	—	—	(6.90 indirect (26))

containing the energy selector is separately pumped, and communicates with the ionization chamber only through an electron beam defining aperture 0.64 mm in diameter. By appropriate design of the ionization chamber and good collimation of the electron beam, spurious effects resulting from wall bombardment by electrons have been minimized. Performance characteristics for some simple molecules (15) and PH_2 radicals (16) have been reported recently.

The alkyl free radicals R were produced in reasonable yields by pyrolysis of the appropriate alkyl nitrite esters RCH_2ONO at low pressures in a fused-silica capillary furnace (17). For CH_3 radicals a slightly better yield was obtained from the pyrolysis of di-*t*-butyl peroxide.

Samples of *n*-pentane and neo-pentane used for the dissociative ionization measurements were NBS standard samples. The methyl iodide was an Eastman Organic Chemicals sample, further purified by distillation.

Results and Discussion

The threshold energies, obtained from extrapolation of linear or nearly-linear initial portions of the ionization efficiency curves for the C_1—C_4 alkyl radicals, are given in Table 1. Extrapolation of the approximately linear portion of a curve for an added krypton standard was used to calibrate the energy scale. For comparison are given also other recent values by RPD electron impact, and photoionization and spectroscopic data where available. For CH_3 radicals, as shown in Fig. 1, a linear extrapolation of the first segment of the curve to give an adiabatic IP is clearly justified. For the C_2H_5 and larger radicals, as shown in Figs. 2–7, an initial linear segment, if present, was not clearly resolved. In these cases the ionization threshold obtained by extrapolation of the first "segment" should properly be regarded as an upper limit to the adiabatic IP (4). Nevertheless, even in the most unfavorable cases the onset can be clearly distinguished within ±0.05 V.

Within the limits cited, the present data and the RPD and photoionization data are in excellent agreement. The only possible disagreement is for *n*-C_3H_7 radical. The present value agrees well with the observed threshold for direct photoionization (4). However a value of 7.2 V has been derived from appearance potentials (AP) of fragment ions (18). By comparison with C_2H_5 radical this seems improbably low, and it is likely that this value corresponds to formation of the *s*-$C_3H_7^+$ ion by rearrangement.

No evidence for the occurrence of autoionization processes could be found. Within experimental error the curves in Figs. 1–7 appear to be free from discontinuities except for structures attributable to vibrational excitation. On the grounds that bonding in the radicals is generally weaker than in normal molecules, it is reasonable to suppose that for excited states of the radicals predissociation may predominate over autoionization.

Further details of the ionization efficiency curves are discussed under separate headings below.

CH_3 Radical and Fragment Ion

The ionization curve for CH_3 radical shown in Fig. 1 was obtained from radicals produced in the pyrolysis of di-*t*-butyl peroxide. Curves obtained using ethyl nitrite as a source of CH_3 were essentially the same. All curves showed two linear sections, with a distinct break about 0.36 V above the onset. Extrapolation of the linear portions of the Kr^+ and CH_3^+ curves gave 9.84 V as the threshold for ionization of CH_3 radical. The curved foot at the onset for both gases is consistent with an electron energy width at half maximum of about 0.07 V. The uncertainty in the scale calibration and the extrapolation probably does not exceed ± 0.03 V, and the agreement with values from PI (4, 5) spectroscopy (19) and RPD electron impact (1, 2) is excellent.

The first differential of the CH_3^+ curve, which should have approximately the same shape as the

Can. J. Chem. Downloaded from www.nrcresearchpress.com by 210.87.254.40 on 09/05/12
For personal use only.

Can. J. Chem. Downloaded from www.nrcresearchpress.com by 210.87.254.40 on 09/05/12
For personal use only.

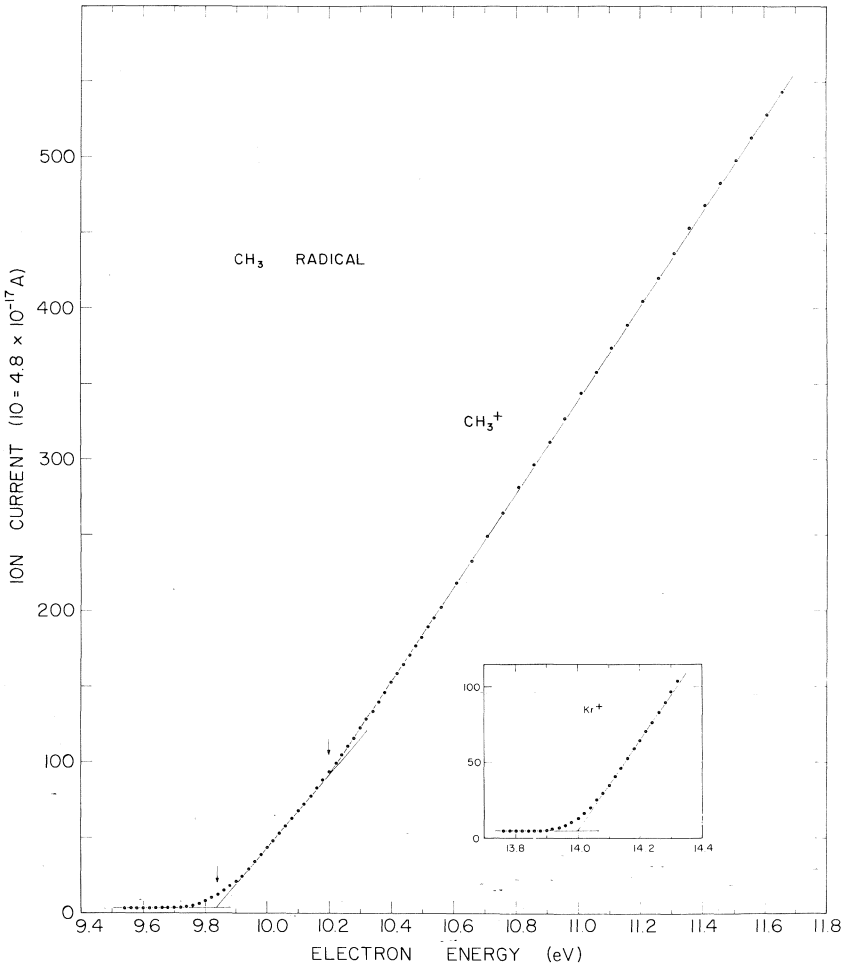

FIG. 1. Ionization efficiency curve for methyl radical produced by pyrolysis of di-*t*-butyl peroxide.

photoionization efficiency curve (20), is shown in Fig. 8. When allowance is made for the larger energy spread, this differential curve is in fact quite similar to Fig. 2 given by Chupka and Lifschitz (5). The step at about 10.2 V is clearly visible in both curves. This feature appears to correspond to excitation of a vibrational level of CH_3^+ ion, most probably the symmetric stretch mode. From Fig. 8, the ratio of step heights would give a Franck–Condon factor of 0.23 for this transition, relative to 1.00 for the $0 \rightarrow 0$ transition. From the photoionization data (5) the ratio is closer to 0.14. In view of the combined uncertainties this difference is likely not significant. The probability for excitation of higher vibrational levels appears to be vanishingly small for both photon and electron impact.

Aside from the break at about 10.2 V, the ionization efficiency plot for CH_3 radical appears to be a straight line for at least 1.8 V above the threshold. No sign of the breaks at 10.7 V and 11.4 V observed in the earlier RPD measurements (1) could be found. To investigate this point further, the AP curves for the formation of CH_3^+ fragment ion from CH_4 and CH_3I were obtained. The curves, given in Figs. 9 and 10 respectively, show only a smooth increase in CH_3^+ ion yield with increasing electron energy, without indication of the breaks reported earlier for these processes (7). For both these curves the observed thresholds are in good agreement with AP's calculated for reactions as shown in eqs. [1] and [2]. Heats of formation employed in these calculations are those for 298°K given in Kerr's comprehensive review article (13). The reason for the difference between these results and the

Can. J. Chem. Downloaded from www.nrcresearchpress.com by 210.87.254.40 on 09/05/12
For personal use only.

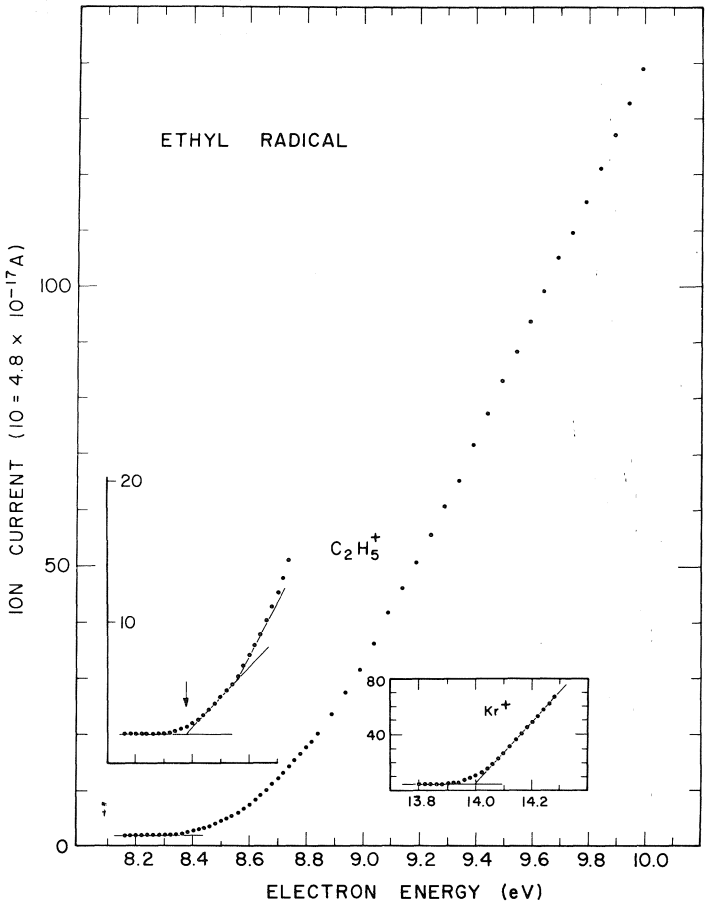

FIG. 2. Ionization efficiency curve for ethyl radical produced by pyrolysis of *n*-propyl nitrite.

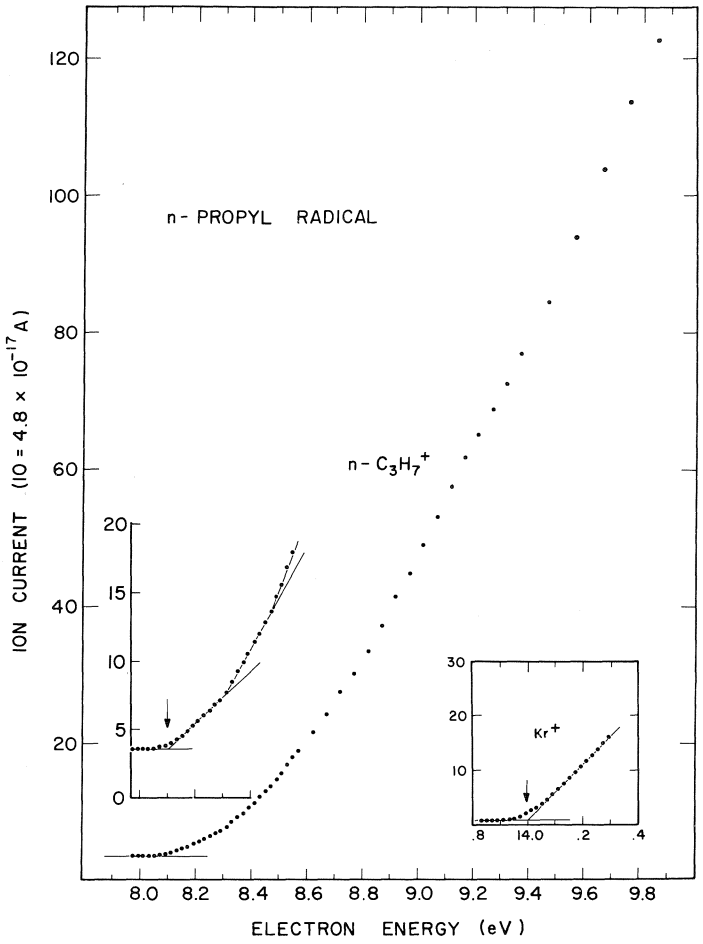

FIG. 3. Ionization efficiency curve for *n*-propyl radical produced by pyrolysis of *n*-butyl nitrite.

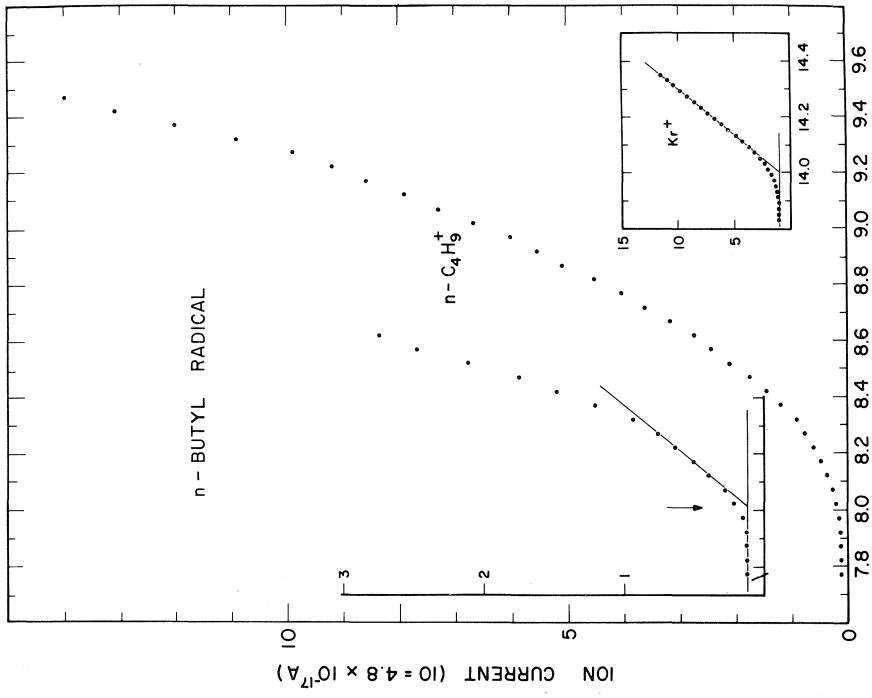

FIG. 5. Ionization efficiency curve for *n*-butyl radical produced by pyrolysis of *n*-pentyl nitrite.

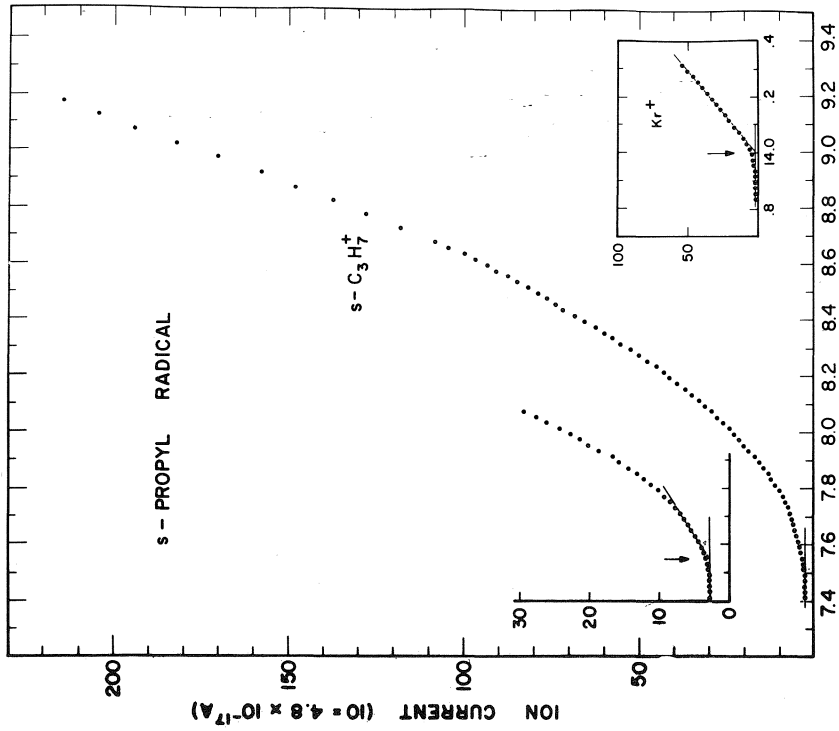

FIG. 4. Ionization efficiency curve for *s*-propyl radical produced by pyrolysis of nitrite ester of 2-methyl-1-propanol.

Can. J. Chem. Downloaded from www.nrcresearchpress.com by 210.87.254.40 on 09/05/12
For personal use only.

Can. J. Chem. Downloaded from www.nrcresearchpress.com by 210.87.254.40 on 09/05/12
For personal use only.

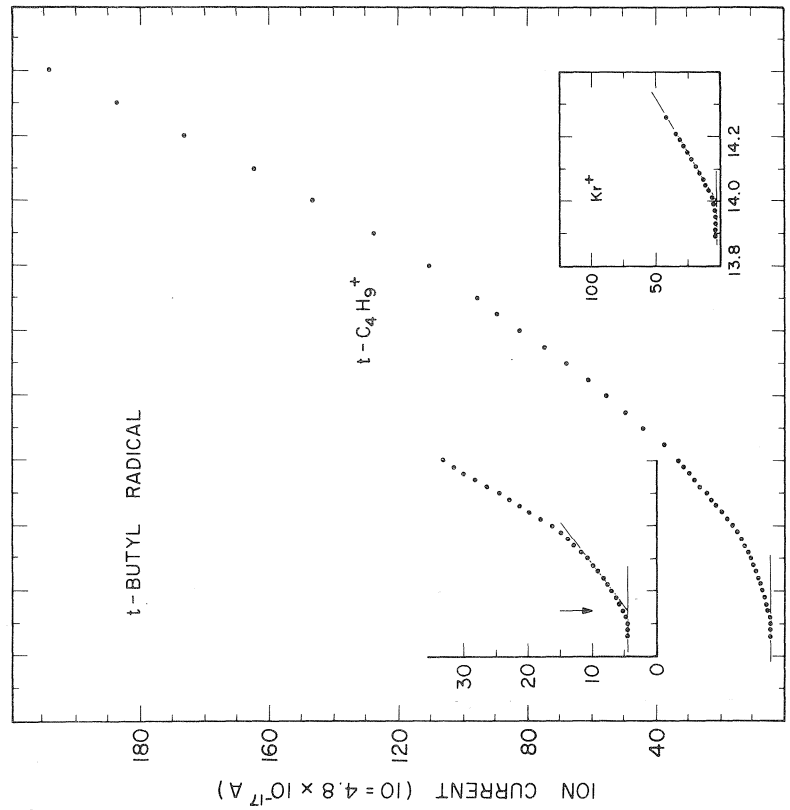

FIG. 7. Ionization efficiency curve for *t*-butyl radical produced by pyrolysis of the nitrite ester of neo-pentyl alcohol.

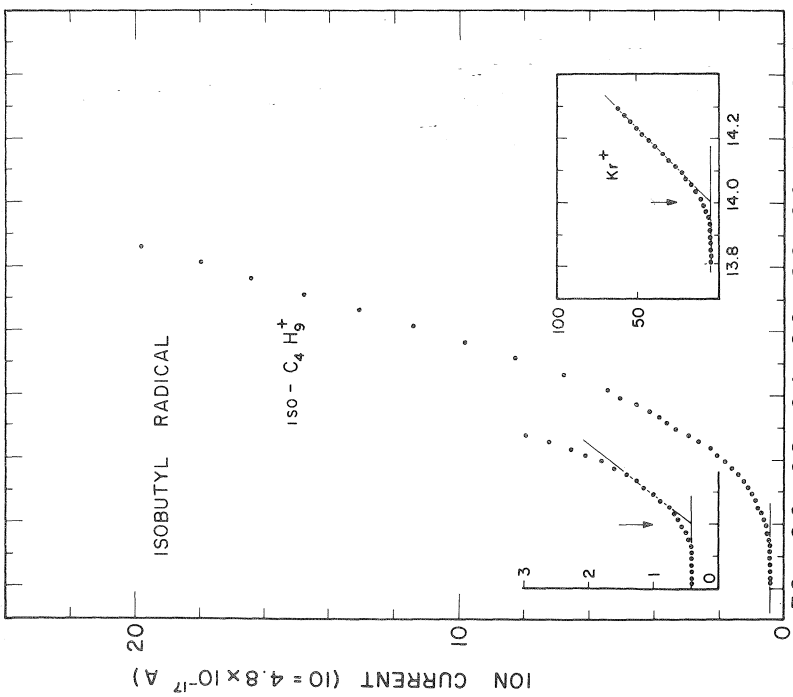

FIG. 6. Ionization efficiency curve for iso-butyl radical produced by pyrolysis of the nitrite ester of isoamyl alcohol.

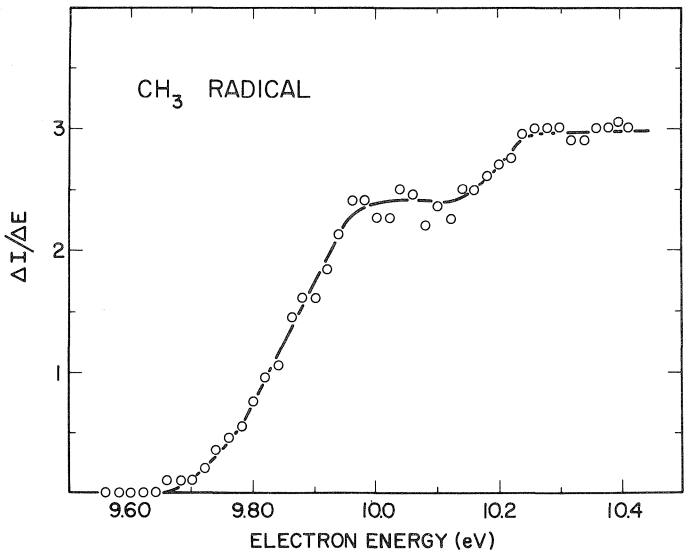

FIG. 8. Plot of first differential of ionization efficiency curve for CH_3 radical. The experimental points at 0.02 V intervals from Fig. 1 were used without smoothing.

[1] $CH_4 + e \rightarrow CH_3^+ + H + 2e$
AP_{obs} 14.30 V, AP_{calcd} 14.35 V

[2] $CH_3I + e \rightarrow CH_3^+ + I(^2P_{3/2}) + 2e$
AP_{obs} 12.22 V, AP_{calcd} 12.28 V

RPD results with respect to the presence of distinct segments and breaks for formation of CH_3^+ ion as a parent ion and a fragment ion is not understood. If confirmed, the present data would suggest that there are no easily accessible low-lying electronic states of CH_3^+ (8) within 1.8 V above the ground state.[3] The absence of structure in the available PI curves for formation of CH_3^+ fragment from CH_4 (21, 22) tends to support this result.

It is of interest to note that in Fig. 10 no significant change in slope occurs at the threshold energy for formation of the neutral I-atom fragment in its $^2P_{1/2}$ state (eq. [3]).

[3] $CH_3I + e \rightarrow CH_3^+ + I(^2P_{1/2}) + 2e$
AP_{calcd} 13.2 V

Recent findings have indicated a 1.127-power law or even higher power laws for threshold ionization of H-atom (23), helium (24, 25), and argon (25). In this respect, the close correspondence of the ionization cross-section behavior of CH_3 radical to a first-power law found here is interesting. In our instrument also the shape of the threshold curve for helium is non-linear and corresponds closely to that reported by these authors. The difference in threshold law between ionization of CH_3 and of H-atom and the rare gases may therefore be real, and not merely an instrumental effect.

Ethyl and Propyl Radicals

The ionization efficiency curves for ethyl and *n*-propyl radicals, shown in Figs. 2 and 3, appear to have two short nearly linear sections near the onset, above which no further structure appears. The curve for *s*-propyl radical (Fig. 4) is more strongly curved and may have one short linear segment at the onset, although rather poorly defined. The curves for ethyl and *n*-propyl become nearly linear about 0.8 V above the onset. The corresponding point for the *s*-propyl curve is not reached until about 1.2 V above the onset.

Butyl Radicals

The curves for *n*-, iso-, and *t*-butyl radicals, shown in Figs. 5, 6, and 7 respectively, were of the same general shape as the curve for *s*-propyl. An initial linear portion, if present, was too short to be resolved. In the absence of a linear portion, the "extrapolation" shown in the figures is an estimate based mainly on a comparison of the

[3]Using RPD electron impact, Bünau and Potzinger (30) have also reported structure in the AP curves for CH_3^+ from CH_4 and CH_3I, which they attributed to low-lying excited levels of CH_3^+.

Can. J. Chem. Downloaded from www.nrcresearchpress.com by 210.87.254.40 on 09/05/12
For personal use only.

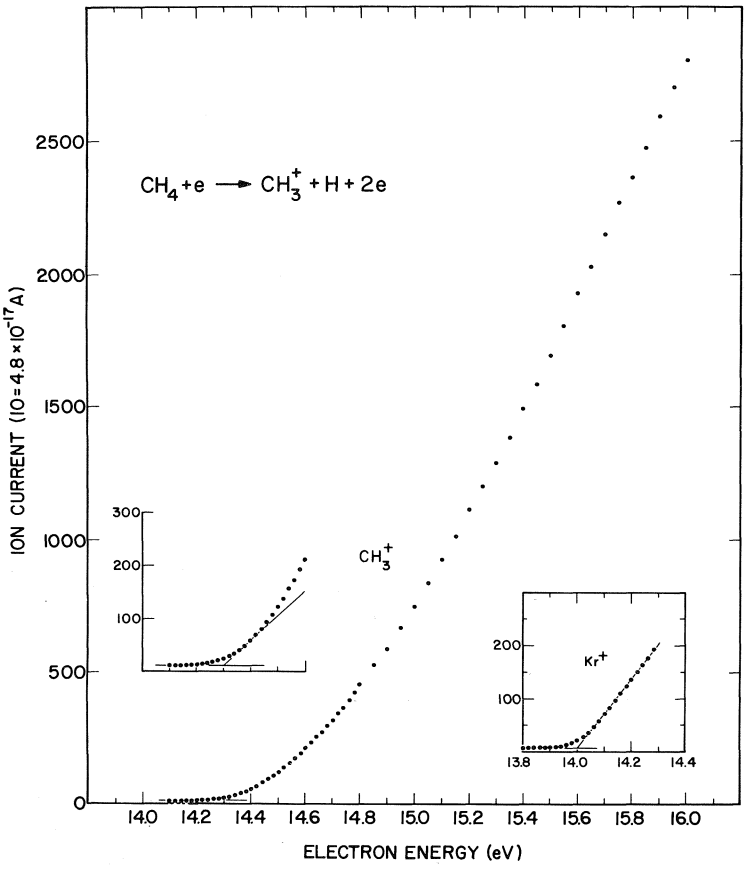

FIG. 9. Appearance potential curve for formation of CH_3^+ fragment from methane.

shape of the curved foot resulting from the electron energy spread with that for the krypton standard. An alternative method, estimation of the onset energies by comparing the positions of the first detectable upward break in ion current for the unknown and standard gas, gave the same set of values within ± 0.03 V. Both these methods for estimating the onset energies are less accurate than a linear extrapolation, since they depend on the relative threshold ionization probabilities and concentrations of krypton and the radical. A curve for *s*-butyl radical is not shown, since it was indistinguishable in shape from that for iso-butyl.

As seen from Table 1, existing data for the IP's of butyl radicals, aside from the earlier low-resolution values (17), are quite limited. The present value for *n*-C_4H_9 agrees well with the RPD value (2). It is interesting to note that the discrepancy between the earlier "direct" value for IP (*t*-butyl), 7.42 V (17) and the "indirect" value of Stevenson, 6.90 V (26), is resolved in favor of the latter.

Heats of Formation of Alkyl Ions

It seems probable from Kerr's review (13) that heats of formation of C_1—C_4 alkyl radicals at 298 °K have now been established from kinetic data to an accuracy of ± 2 kcal/mole or better. Combining these with the IP's from Table 1, which are probably accurate to about ±1 kcal/mole, we can obtain ionic heats of formation as given in Table 2. These differ only slightly from those given in a recent compilation by Franklin *et al.* (27) except for the $C_4H_9^+$ ions, which were calculated from the earlier direct IP's, and for which the current values are 10–15 kcal/mole lower.

A comparison of the values in Table 2 with heats of formation calculated from AP's for

Can. J. Chem. Downloaded from www.nrcresearchpress.com by 210.87.254.40 on 09/05/12
For personal use only.

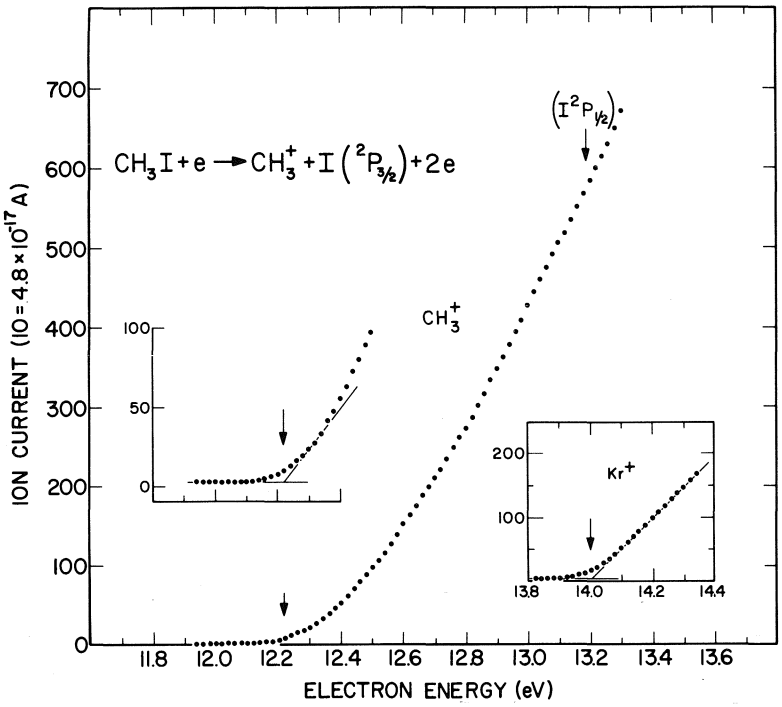

FIG. 10. Appearance potential curve for CH_3^+ fragment from methyl iodide. The upper arrow indicates the energy required for formation of the neutral I-atom in the $^2P_{1/2}$ state.

TABLE 2

Heats of formation of alkyl radicals and ions (kcal/mole 298 °K)

Radical	$\Delta H_f(R)$*	Ionization potential†	$\Delta H_f(R^+)$
CH_3	34.0	226.9	261
C_2H_5	25.7	193.3	219
n-C_3H_7	21.0	186.8	208
s-C_3H_7	17.6	174.1	192
n-C_4H_9	16.0	184.7	201
iso-C_4H_9	14.0	184.7	199
s-C_4H_9	12.4	170.9	183
t-C_4H_9	6.8	159.8	167

*Ref. 13.
†Table 1.

fragment ions, given in ref. 27, is of interest with respect to ionic rearrangement reactions. For example, the AP's for $C_3H_7^+$ from n- and iso-butanes and pentanes give $\Delta H_f(C_3H_7^+)$ in the range 189–196 kcal/mole, clearly too low to correspond to a primary $C_3H_7^+$, for which ΔH_f is 208 kcal/mole. The necessary isomerization is evidently rapid and requires little activation energy. The new values for $\Delta H_f(C_4H_9^+)$ ions allow a similar deduction to be drawn from corresponding data for butyl fragment ions. The photoionization AP's for CH_3 loss from n- and iso-pentane (3) give $\Delta H_f(C_4H_9^+) = 183.6$ and 182.2 kcal/mole respectively, both of which evidently correspond to s-$C_4H_9^+$ ($\Delta H_f = 183$ kcal/mole, Table 2). The heats of formation for $C_4H_9^+$ ions from photon impact (3) on n-hexane (185 kcal/mole) and n-heptane (186 kcal/mole) show that these are also evidently not primary $C_4H_9^+$ ions ($\Delta H_f = 201$ kcal/mole, Table 2). The only case reported in ref. 27 in which an n-$C_4H_9^+$ ion may be formed as a threshold fragment is in the dissociative ionization of n-C_4H_9ONO, from which a value of $\Delta H_f(C_4H_9^+) = 201$ kcal/mole has been derived (28).

For comparison with the PI result, the AP curve for $C_4H_9^+$ from n-pentane was investigated with the present apparatus. The curve is shown in Fig. 11. The threshold energy, 10.98 ± 0.05 V, is in good agreement with the PI threshold of 10.96 V (3). A second break at 11.10 V reported by these authors was not observed. Calculated AP's for the isomeric $C_4H_9^+$ ions, using the heats of formation in Table 2, $\Delta H_f(CH_3) = 34.0$ kcal/mole (13), and standard heats of formation for the pentanes (29), are indicated in Fig. 11. It can be

Can. J. Chem. Downloaded from www.nrcresearchpress.com by 210.87.254.40 on 09/05/12
For personal use only.

Can. J. Chem. Downloaded from www.nrcresearchpress.com by 210.87.254.40 on 09/05/12
For personal use only.

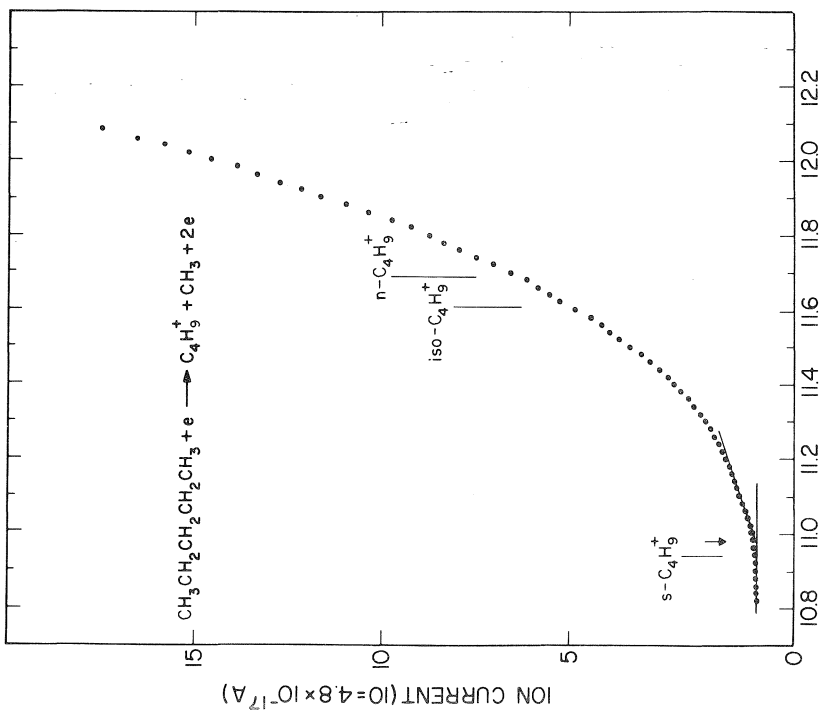

FIG. 11. Appearance potential curve for formation of $C_4H_9^+$ fragment from *n*-pentane. Energies corresponding to formation of *s*-$C_4H_9^+$, iso-$C_4H_9^+$ and *n*-$C_4H_9^+$ (Table 2) are indicated on the curve.

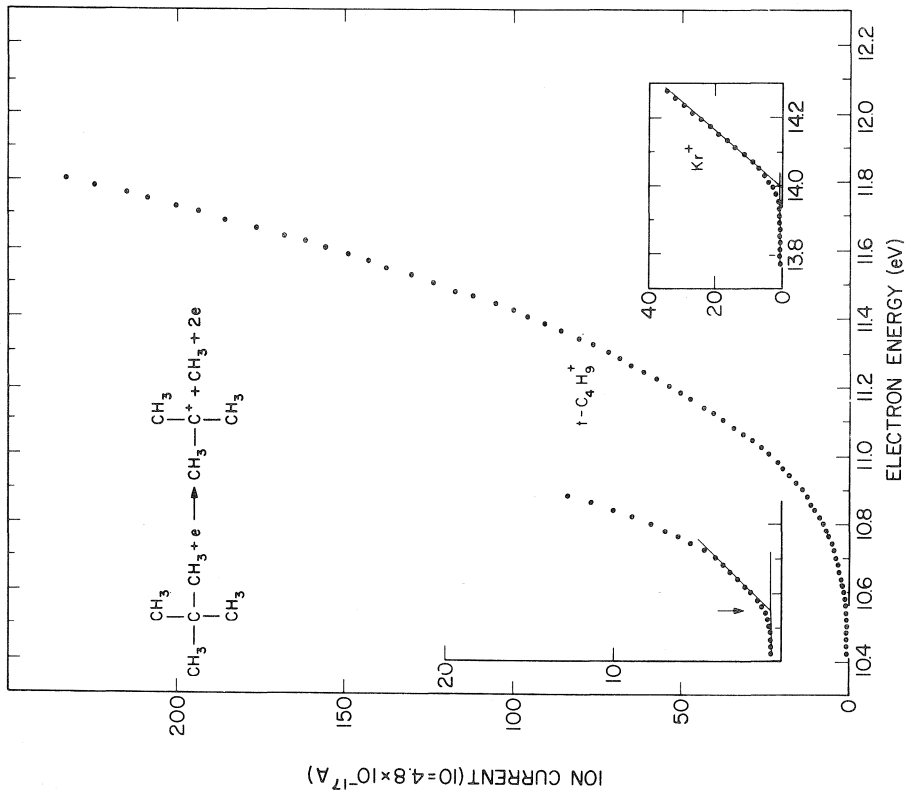

FIG. 12. Appearance potential curve for $C_4H_9^+$ fragment from neo-pentane.

seen that the threshold agrees closely with the formation of s-$C_4H_9^+$ with less than 1 kcal/mole excess energy available to bring about isomerization. As the rising ion yield curve crosses the energy threshold for primary $C_4H_9^+$ ion formation, no perceptible change in the rate of increase in the ion yield can be detected. It would appear that the "conductivity" of this second reaction channel, that of direct bond scission, is negligibly small compared to that of the channel involving decomposition by way of rearrangement from a primary to a secondary ion. In view of this evident ease of isomerization it is surprising that the AP for $C_4H_9^+$ from iso-pentane, as mentioned above, corresponds to an s-$C_4H_9^+$ ion and not a t-$C_4H_9^+$ ion, which could be formed by a rearrangement analogous to that forming s-$C_4H_9^+$ from n-pentane. It would seem that the rupture of one of the secondary C—CH_3 bonds in iso-pentane ion must be so fast that the preliminary manoeuvres necessary to t-$C_4H_9^+$ ion formation are precluded.

In Fig. 12 is shown the ion efficiency curve for formation of $C_4H_9^+$ fragment from neo-pentane. The observed AP, 10.56 V, agrees well with the 10.55 V obtained by photoionization (3). This gives $\Delta H_f(C_4H_9^+) = 170$ kcal/mole, which can only be a t-butyl ion ($\Delta H_f = 167$ kcal/mole, Table 2).

1. C. E. Melton and W. H. Hamill. J. Chem. Phys. **41**, 3464 (1964).
2. J. M. Williams and W. H. Hamill. J. Chem. Phys. **49**, 4467 (1968).
3. B. Steiner, C. F. Giese, and M. G. Inghram. J. Chem. Phys. **34**, 189 (1961).
4. F. A. Elder, C. F. Giese, B. Steiner, and M. G. Inghram. J. Chem. Phys. **36**, 3292 (1962).
5. W. A. Chupka and C. Lifschitz. J. Chem. Phys. **48**, 1109 (1968).
6. C. Lifschitz and W. A. Chupka. J. Chem. Phys. **47**, 3439 (1967).
7. S. Tsuda, C. E. Melton, and W. H. Hamill. J. Chem. Phys. **41**, 689 (1964).
8. C. E. Melton and H. W. Joy. J. Chem. Phys. **42**, 1986 (1965).
9. W. A. Chupka and J. Berkowitz. J. Chem. Phys. **47**, 2921 (1967).
10. D. P. Stevenson. J. Amer. Chem. Soc. **82**, 5961 (1960).
11. J. W. McGowan, M. A. Fineman, E. M. Clarke, and H. P. Hanson. Phys. Rev. **167**, 52 (1968).
12. C. E. Brion. Chem. Phys. Lett. **3**, 9 (1969).
13. J. A. Kerr. Chem. Rev. **66**, 465 (1966).
14. K. Maeda, G. P. Semeluk, and F. P. Lossing. Intern. J. Mass Spectry. Ion Phys. **1**, 395 (1968).
15. F. P. Lossing and G. P. Semeluk. Intern. J. Mass Spectry. Ion Phys. **2**, 408 (1969).
16. T. McAllister and F. P. Lossing. J. Phys. Chem. **73**, 2996 (1969).
17. F. P. Lossing and J. B. de Sousa. J. Amer. Chem. Soc. **81**, 281 (1959).
18. E. Murad and M. G. Inghram. J. Chem. Phys. **40**, 3263 (1964).
19. G. Herzberg and J. Shoosmith. Can. J. Phys. **34**, 523 (1956).
20. F. H. Dorman, J. D. Morrison, and A. J. C. Nicholson. J. Chem. Phys. **32**, 378 (1960).
21. W. A. Chupka. J. Chem. Phys. **48**, 2337 (1968).
22. V. H. Dibeler, M. Krauss, R. M. Reese, and F. N. Harlee. J. Chem. Phys. **42**, 3791 (1965).
23. J. W. McGowan and E. M. Clarke. Phys. Rev. **167**, 43 (1968).
24. C. E. Brion and G. E. Thomas. Phys. Rev. Lett. **20**, 241 (1968).
25. P. Marchand, C. Paquet, and P. Marmet. Phys. Rev. **180**, 123 (1969).
26. D. P. Stevenson. Disc. Faraday Soc. **10**, 35 (1951).
27. J. L. Franklin, J. G. Dillard, H. M. Rosenstock, J. T. Herron, and K. Draxl. Ionization potentials, appearance potentials, and heats of formation of gaseous positive ions. National Bureau of Standards, Washington. June 1969.
28. S. Tsuda and W. H. Hamill. Adv. Mass Spectrometry **3**, 249 (1966).
29. F. D. Rossini *et al.* Selected values of physical and thermodynamic properties of hydrocarbons and related compounds. Carnegie Press, Pittsburgh, 1953.
30. G. von Bünau and P. Potzinger. Bunsenges. Phys. Chem. **73**, 472 (1969).

Can. J. Chem. Downloaded from www.nrcresearchpress.com by 210.87.254.40 on 09/05/12
For personal use only.

Can. J. Chem. Downloaded from www.nrcresearchpress.com by 210.87.254.6 on 09/05/12
For personal use only.

Lead tetraacetate oxidation of hindered alicyclic ketoximes

G. JUST AND K. DAHL[1]
Department of Chemistry, McGill University, Montreal, Quebec
Received September 29, 1969

Lead tetraacetate oxidation of 2,2,6,6-tetramethylcyclohexanone oxime and structurally related ketoximes caused C—C bond fission to yield acetyl hydroxamates. Severely hindered ketoximes gave nitrile oxides as intermediates which were trapped by 1,3-dipolar cycloaddition reaction.

Canadian Journal of Chemistry, **48**, 966 (1970)

In our preliminary communication, we reported about a facile oxidative cleavage reaction of 2,2,6,6-tetramethylcyclohexanone oxime (**1**) and structurally related ketoximes with lead tetraacetate (1). A mechanism was proposed involving the intermediacy of nitrile oxides. We now wish to report about the spectroscopic detection and trapping of these intermediates.

Lead tetraacetate oxidation of sterically hindered cyclohexanone oximes in acetic acid gave mainly acetyl hydroxamates. Equation [1][2] shows two plausible mechanisms to account for the reaction products, and Table 1 gives a summary of the results.

Low temperature oxidation of ketoxime **1** in the presence of excess methyl acrylate produced the adducts **2**, **3***a*, and **3***b*, thus providing evidence for mechanism *a* (2). Isolation of the adducts was effected by thin-layer chromatography (t.l.c.). The nuclear magnetic resonance (n.m.r.) spectra of **2**, **3***a*, and **3***b* are diagnostic. The isopropylidene groups adjacent to the isoxazoline and acetate group in **2** appear as two singlets at 1.20 (6H) and 1.37 p.p.m. (6H), respectively. A singlet at 1.92 p.p.m. (3H) was assigned to the acetate group. The methylene protons appear as a complex multiplet from 1.2 to 2 p.p.m. Two almost superimposed doublets centered at 3.13 p.p.m. (2H) were assigned to the methylene group in the isoxazoline ring. The other ring proton gives rise to a set of two doublets centered at 4.85 p.p.m. (1H) showing coupling constants of 8.0 and 9.1 Hz. A singlet at 3.75 p.p.m. (3H) was assigned to the carbomethoxy group. The olefinic components **3***a* and **3***b* could not be separated by t.l.c. and the mixture was analyzed. Spectral data arising from the isoxazoline and saturated hydrocarbon portion of **3***a* and **3***b* are almost identical to those of compound **2**. The vinylic protons of **3***a* appear as a poorly resolved triplet centered at 4.64 p.p.m. (J_{gem} = 0.8 Hz) while the olefinic proton of **3***b* appears as a partly resolved triplet centered at 5.05 p.p.m. (J_{vic} = 6.0 Hz). Integration of the two

TABLE 1
Oxidative cleavage of ketoximes

Ketoxime	Solvent	% Cleavage*
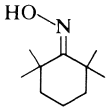	CH_3COOH	90
	CF_3COOH	>90 (30)†
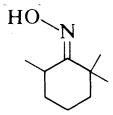	CH_3COOH	<10
	CF_3COOH	54†
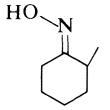	CH_3COOH	Not detected
	CF_3COOH	30
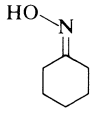	CH_3COOH	Not detected
	CF_3COOH	Not detected
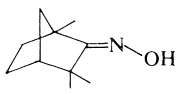	CH_3COOH	>90
	CH_2Cl_2	>90
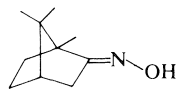	CH_3COOH	70

*Estimate based on spectral analysis (i.r., n.m.r.).
†Analytically pure material.

[1]To whom inquiries should be directed. Present address, Raychem Corporation, 300 Constitution Drive, Menlo Park, California 94025.
[2]Analogous considerations apply to camphor and fenchone oxime.

[1]

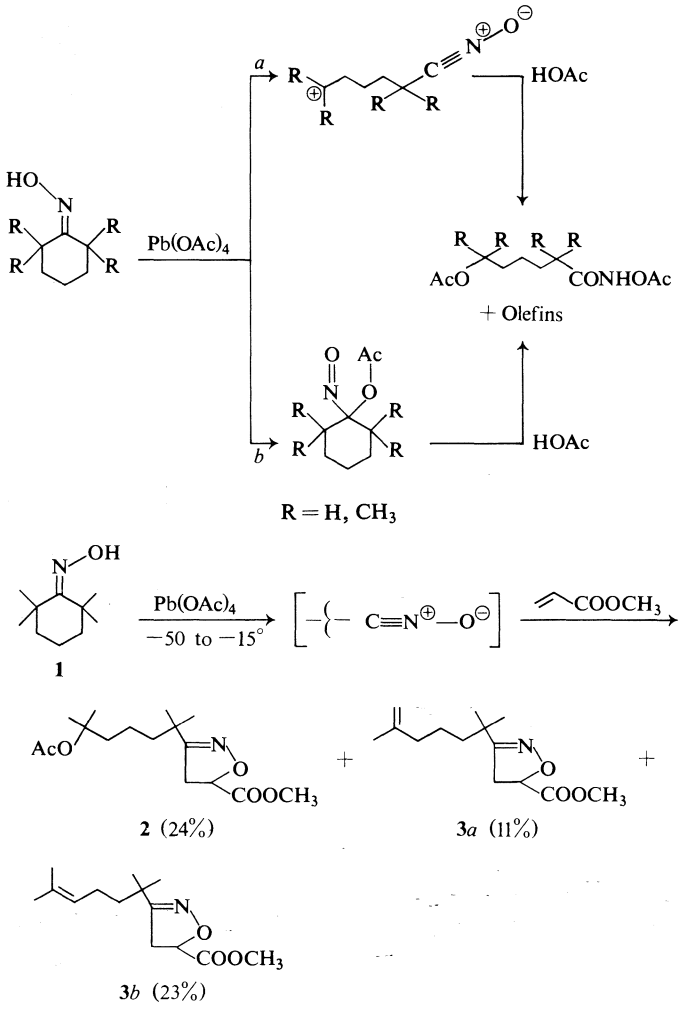

MECHANISM *a*

signals indicated for **3***a* and **3***b* a ratio of 1:2. Two slightly broadened singlets at 1.58 and 1.66 p.p.m. were assigned to the methyl groups which are attached to the double bond of **3***a* and **3***b*.

Interception of the nitrile oxide was also achieved with vinyl acetate. However, the instability of the resulting isoxazolinyl acetates permitted only spectral characterization (3). While reaction in methylene chloride caused very little cleavage, the extent of cleavage increased with acetic acid concentration. When a mixture of acetic acid and methylene chloride was used, and work-up was conducted below 0°, the resulting product mixture contained a substantial amount of material which showed a strong infrared (i.r.) band at 2280 cm^{-1}. This band is indicative of nitrile oxides.

Interception of a nitrile oxide and its i.r. spectroscopic detection was also realized in the oxidation of fenchone oxime. No such intermediate, however, was detected for camphor oxime although ring cleavage did occur to give mainly acetyl hydroxamates. Oxidation of camphor oxime was accompanied by formation of a deep blue color which was stable below 0°, but faded at room temperature. The rate of fading was accelerated by addition of acetic acid. This observation suggests the intermediacy of a geminal nitroso-acetate of the type found in the oxidation of unhindered aliphatic ketoximes (4), and would satisfy reaction path *b* (eq. [1]). A possible mechanism for the rearrangement of the nitroso-acetate to give acetyl hydroxamates is shown in eq. [2].

Can. J. Chem. Downloaded from www.nrcresearchpress.com by 210.87.254.6 on 09/05/12
For personal use only.

[2] 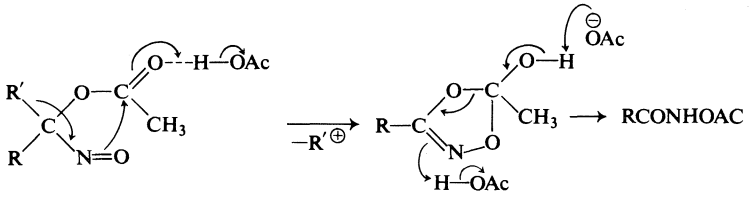

Common to all lead tetraacetate oxidations of the ketoximes investigated was the occurrence of a green color which appeared at about $-70°$ and was accompanied by formation of a heavy white precipitate which was assumed to be lead diacetate. This color faded irreversibly when raising the temperature above $-30°$. Electron spin resonance measurements (5) have shown that iminoxyl radicals are formed in the lead tetraacetate oxidation of oximes, and it is conceivable that these radicals are intermediates in the oxidative cleavage reaction. This mechanistic assumption could also explain the oxidation products obtained from aromatic ketoximes (*6a–d*). A discussion of these results was published in a previous paper (*6d*).

Experimental

Melting points were measured in a capillary tube in a sulfuric acid bath and are corrected. Analyses were performed by Beller Mikroanalytisches Laboratorium, Göttingen, and Bernhard Mikroanalytisches Laboratorium, Mühlheim, Germany. The n.m.r. spectra were recorded on a Varian A-60 spectrometer with tetramethylsilane serving as internal standard. The i.r. spectra were recorded on Perkin–Elmer Infracord, 337, and 521 spectrometers. Ultraviolet (u.v.) spectra were recorded with a Beckmann DK spectrometer.

Lead Tetraacetate

The lead tetraacetate (Matheson, Coleman, and Bell) contained 4–7% acetic acid and was used as such for all oxidations.

Ketoximes

2,2,6,6-Tetramethylcyclohexanone oxime (m.p. 151.5°) was prepared from 2-methylcyclohexanone by exhaustive methylation (7), followed by oximation (8). All other ketoximes were prepared from commercially available ketones using standard procedures (9).

*Oxidation of 2,2,6,6-Tetramethylcyclohexanone Oxime (**1**) in Acetic Acid*

Lead tetraacetate (6.036 g, 13.6 mmoles) was added with stirring to a solution of **1** (2.000 g, 11.8 mmoles) in acetic acid (10 ml). After 5 min, acetic acid was removed by distillation (20°/0.1 mm), affording a pale green oil and lead diacetate which was suspended in a mixture of chloroform and ether (1:2) and filtered. The filtrate was washed with cold saturated sodium bicarbonate solution, dried ($MgSO_4$), and freed of solvent (40°/20 mm) to give 3.39 g of a pale green oil. Titration with 0.1 *N* sodium hydroxide solution indicated 90 ± 5% of acetyl 6-acetoxy-2,2,6-trimethylheptanohydroxamate (**4**): the n.m.r. ($CDCl_3$) δ 1.20 [s, 6H, $(CH_3)_2CCO$], 1.36 [s, 6H, $(CH_3)_2COAc$], 1.90 (s, 3H, *Ac*OC), 2.17 (s, 3H, *Ac*ON), and 9.5 (s, 1H, NH, exchangeable) p.p.m.; i.r. (CCl_4) 3350 (NH), 1790 (*N*-acetate C=O), 1740 (ester C=O) and 1720 (hydroxamate C=O) cm^{-1}. The material gave a negative ferric chloride test.[3]

*Hydrolysis of Hydroxamate **4***

A methanolic solution of 341 mg of **4** was neutralized at room temperature with 2 *N* aqueous potassium carbonate solution. After stirring for 24 h, solvent was removed (20°/0.2 mm) and the residue was dissolved in water (10 ml) and ether (50 ml), then acidified with a drop of dilute acetic acid. The aqueous phase was separated and extracted with ether. The combined ether extracts were dried ($MgSO_4$) and freed of solvent (30°/20 mm) to produce 320 mg of crystalline material. Recrystallization from hexane gave 245 mg (1.0 mmoles, 84%) of 6-acetoxy-2,2,6-trimethylheptanohydroxamic acid: m.p. 74–75°; n.m.r. ($CDCl_3$) δ 1.18 [s, 6H, $(CH_3)_2CCO$], 1.41 [s, 6H, $(CH_3)_2COAc$], 1.98 (s, 3H, *Ac*O), and 9.0 (s,[4] 2H, *NHOH*, exchangeable) p.p.m.; i.r. (CCl_4) 3450 and 3290 (*NHOH*), 1730 (ester C=O), and 1660 (hydroxamic acid C=O), cm^{-1}.

Anal. Calcd. for $C_{12}H_{23}NO_4$: C, 58.75; H, 9.45; N, 5.71. Found: C, 59.07; H, 9.46; N, 6.22.

*Oxidation of Ketoxime **1** in Trifluoroacetic Acid*

Lead tetraacetate (21.0 g, 47.4 mmoles) was dissolved in 210 ml of trifluoroacetic acid and stirred for 1 h. This reagent was added to a solution of 7.20 g (42.5 mmoles) of **1** in 35 ml of trifluoroacetic acid. The reaction mixture was stirred at room temperature for 0.5 h, then diluted with cold water followed by extraction with ether. The combined extracts were washed with saturated sodium bicarbonate solution and water, then dried ($MgSO_4$), and freed of solvent (40°/20 mm) to give 9.39 g of crystalline material. Repeated recrystallization from hexane afforded 3.82 g (12.8 mmoles, 30%) of 6-trifluoroacetoxy-2,2,6-trimethylheptanohydroxamic acid (**5**): m.p. 81.5–82°; n.m.r. ($CDCl_3$) δ 1.18 [s, 6H, $(CH_3)_2CCO$], 1.53 [s, 6H, $(CH_3)_2COCOCF_3$], and 9.0 (s, 2H, *NHOH*, exchangeable) p.p.m.; i.r. (CCl_4) 3450 and 3250 (NHOH),

[3]All subsequently described hydroxamic acids gave a positive ferric chloride test.

[4]The 2-proton peak was resolved in $(CD_3)_2SO$ solution into 2 signals: 8.43 (s, 1H, *NH*) and 10.23 (s, 1H, *NOH*) p.p.m.; analogous resolution was achieved for other hydroxamic acids given.

Can. J. Chem. Downloaded from www.nrcresearchpress.com by 210.87.254.6 on 09/05/12
For personal use only.

Can. J. Chem. Downloaded from www.nrcresearchpress.com by 210.87.254.6 on 09/05/12
For personal use only.

1780 (ester C=O), and 1660 (hydroxamic acid C=O) cm^{-1}; u.v. max (95% C_2H_5OH) 211 mμ (ε 1550).

Anal. Calcd. for $C_{12}H_{20}F_3NO_4$ (299.29): C, 48.17; H, 6.74; F, 18.90; N, 4.68. Found ((mass spectrum) 299): C, 48.57; H, 6.71; F, 19.25; N, 4.80.

Hydrolysis of Hydroxamic Acid **5**

A solution of 36.0 mg (0.1204 mmoles) of **5** in water (2 ml) was boiled for 10 min, then cooled to room temperature and saturated with ammonium sulfate. Ether extraction afforded 23.0 mg (0.1134 mmoles, 94%) of 6-hydroxy-2,2,6-trimethylheptanohydroxamic acid: m.p. 112–113°; n.m.r. ($CDCl_3$) δ 1.20 [s, 12H, $(CH_3)_2$-COH, and $(CH_3)_2CCO$], 6.3[5] (s, 3H, *OH* and *NHOH*, exchangeable) p.p.m.; i.r. ($CHCl_3$) 3605 (OH), 3455 and 3300 (NHOH), and 1655 (hydroxamic acid C=O) cm^{-1}; u.v. max (95% C_2H_5OH) 212 mμ (ε 1520).

Anal. Calcd. for $C_{10}H_{21}NO_3$: C, 59.08; H, 10.40; N, 6.89. Found: C, 59.60; H, 10.51; N, 6.77.

Oxidation of 2,2,6-Trimethylcyclohexanone Oxime (6)

Lead tetraacetate (670 mg, 1.52 mmoles) was dissolved in 10 ml of trifluoroacetic acid, stirred for 1 h, and then added to a solution of 180 mg (1.16 mmoles) of ketoxime **6** in 2 ml of trifluoroacetic acid. The reaction was completed within a few seconds at room temperature. Trifluoroacetic acid was removed by distillation (20°/0.5 mm), and to the oily distillation residue was added cold saturated sodium bicarbonate solution, followed by ether extraction. The combined ether extract gave 247 mg of a colorless oil. Crystallization from pentane afforded 180 mg (0.631 mmoles, 54%) of 2,6-dimethyl-6-trifluoroacetoxyheptanohydroxamic acid: m.p. 79.5–80.5°; n.m.r. ($CDCl_3$) δ 1.14 (d, 3H, J = 6.7 Hz, $HCCH_3$), 1.54 [s, 6H, $(CH_3)_2COCOCF_3$], and 8.5 (s, 2H, *NHOH*) p.p.m.; i.r. (CCl_4) 3430 and 3210 (NHOH), 1790 (ester C=O), and 1660 (hydroxamic acid C=O) cm^{-1}.

Anal. Calcd. for $C_{11}H_{18}F_3NO_4$: C, 46.30; H, 6.36; N, 4.96. Found: C, 46.52; H, 6.27; N, 4.92.

Nitrile Oxide Interception in the Oxidation of Ketoxime **1**

A mixture of 1.00 g (5.90 mmoles) of ketoxime **1**, 15 ml of methyl acrylate, 15 ml of methylene chloride, and 6 ml of acetic acid was cooled to −50° and a cold (−50°) solution of 3.08 g (6.9 mmoles) of lead tetraacetate in 20 ml of methylene chloride and 1 ml of acetic acid was slowly added with stirring. The reaction mixture was kept at −50° for 1.5 h, then the temperature was raised to −15° within 0.5 h. The solution was re-cooled to −50° and 20 ml of cold triethylamine was added dropwise with stirring. The temperature was raised to 25° and 100 ml of ether was added, followed by extraction with water. The organic phase was dried ($MgSO_4$) and freed of volatile material (30°/20 mm and 85°/0.005 mm) to yield 1.405 g of a yellow oil. Separation by t.l.c. [SiO_2, hexane/ether (30%) as solvent] gave 2 oily fractions. These were rechromatographed on precleaned (methanol) plates, affording 445 mg (1.42 mmoles, 24%) of isoxazoline **2** and 500 mg (1.98 mmoles, 34%) of isoxazolines **3***a* and **3***b*. Compound **2** did not crystallize; distillation at 140–145° (bath)/0.0005 mm caused partial decomposition to give **3***a* and **3***b*. Isoxazoline **2** was, therefore, analyzed as such: n_D^{20} 1.4632; i.r. (neat) 1730 (ester C=O) cm^{-1}.

Anal. Calcd. for $C_{16}H_{27}NO_5$: C, 61.32; H, 8.68; N, 4.47. Found: C, 61.15; H, 8.72; N, 4.65.

Compounds **3***a* and **3***b* were distilled at 110–115° (bath)/0.0005 mm to give a colorless oil: n_D^{20} 1.4752; i.r. (neat) 1740 (ester C=O), 1650 and 1615 (C=C) cm^{-1}.

Anal. Calcd. for $C_{14}H_{23}NO_3$: C, 66.37; H, 9.15; N, 5.53. Found: C, 66.15; H, 9.23; N, 5.65.

This work was supported by the National Research Council of Canada. One of us (K.D.) gratefully acknowledges the award of fellowships from the Canadian Industries Ltd. (1964–1965) and the National Research Council of Canada (1965–1966). We thank Prof. R. Huisgen, University of Munich, for having made available space and equipment to conduct the trapping experiments.

1. G. Just and K. Dahl. Tetrahedron Lett. No. 21, 2441 (1966).
2. R. Huisgen. Angew. Chem. **75**, 604 and 633 (1963).
3. G. Just and K. Dahl. Tetrahedron, **24**, 5251 (1968).
4. H. Kropf and R. Lambeck. Ann. Chem. **700**, 1 and 18 (1966) and references cited therein.
5. B. C. Gilbert and R. O. C. Norman. J. Chem. Soc. B, 123 (1968).
6. (*a*) Y. Yukawa, M. Sakai, and S. Suzuki. Bull. Chem. Soc. Japan, **39**, 2266 (1966); (*b*) O. L. Chapman, D. C. Heckert, J. W. Reasoner, and S. P. Thackaberry. J. Amer. Chem. Soc. **88**, 5550 (1966); (*c*) S. P. Thackaberry. Ph.D. Thesis. Iowa State University, Ames, Iowa, 1968; (*d*) M. M. Frojmovic and G. Just. Can. J. Chem. **46**, 3719 (1968). See also S. Kaufmann, L. Tökés, J. W. Murphy, and P. Crabbé. J. Org. Chem. **34**, 1618 (1969).
7. F. Bohlmann and K. Kieslich. Ber. **87**, 1363 (1954).
8. R. Cornubert. Bull. Soc. Chim. France, 541 (1927).
9. E. Hauser. *In* Methoden der organischen Chemie (Houben–Weyl) Vol. 2. E. Müller, *editor*, G. Thieme Verlag, Stuttgart (1953). p. 446.

[5]In $(CD_3)_2SO$ the *tert* OH appeared as 1-H singlet at 3.95 p.p.m.

Non-Chugaev products from the pyrolysis of *S*-*p*-bromophenacyl xanthates of primary alcohols[1]

R. E. GILMAN,[2] J. D. HENION, S. SHAKSHOOKI, J. I. H. PATTERSON, M. J. BOGDANOWICZ, R. J. GRIFFITH, D. E. HARRINGTON, R. K. CRANDALL, AND K. T. FINLEY

Department of Chemistry, Rochester Institute of Technology, One Lomb Memorial Drive, Rochester, New York, 14623

Received July 21, 1969

The study of the pyrolysis of *S*-*p*-bromophenacyl xanthates of 1-hexanol, cyclohexanemethanol, and 2-phenylethanol are reported. The complex reaction mixtures were found to be composed of carbonyl sulfide, carbon disulfide, the corresponding alkenes, alkyl bromides, and starting alcohols, and 4′-bromoacetophenone. The formation of the non-Chugaev products in significant amounts indicates that these pyrolyses are quite different from the *cis*-elimination that is characteristic of *S*-methyl xanthates. The occurrence of the alkyl bromides is particularly significant. Possible mechanisms for the formation of all of these products are discussed.

Canadian Journal of Chemistry, 48, 970 (1970)

Can. J. Chem. Downloaded from www.nrcresearchpress.com by 210.87.254.5 on 09/05/12
For personal use only.

The pyrolysis of xanthate esters, the Chugaev reaction, has been extensively studied from a mechanistic point of view, especially for *S*-methyl xanthates derived from secondary alcohols (1, 2). The usual products are the alkene, carbonyl sulfide, and methanethiol.

We have found that the pyrolysis of xanthates of primary alcohols that contain the *S*-*p*-bromophenacyl group rather than the *S*-methyl group proceeds in a dramatically different manner to give a complex mixture of products, most of which are not formed in the normal Chugaev reaction.

The compounds used in this study, the *S*-*p*-bromophenacyl xanthates of 1-hexanol, cyclohexanemethanol, and 2-phenylethanol, were prepared by standard methods (3, 4). The pyrolysis of these xanthates in a semi-micro distillation apparatus at 240° for 90 min gave the products shown in Table 1. The components of the complex pyrolysis mixtures were separated by preparative-scale gas chromatography. Structural assignments were made on the basis of comparisons of infrared (i.r.) spectra with those of authentic compounds. The alkene, the normal Chugaev product, was obtained in low yields in all cases, but the mercaptan, 4′-bromo-2-mercaptoacetophenone, was not observed. This compound was synthesized by a modification of the method of Kretov *et al.* (5) and found to decompose rapidly under our pyrolysis conditions to yield 4′-bromoacetophenone as the only significant product. This route undoubtedly accounts for some of the 4′-bromoacetophenone that is found in the pyrolysis of each of the xanthates. The large amount of 1-methylcyclohexene formed in the pyrolysis of the xanthate of cyclohexanemethanol can be attributed to a rearrangement of the methylenecyclohexane. Toluene was present only in the pyrolysate of the xanthate of cyclohexanemethanol. This is possibly explained as a dehydrogenation product of the cycloalkenes formed in this reaction.

The remaining pyrolysis products are quite different from those expected from the normal Chugaev reaction. The formation of these non-Chugaev products; alkyl bromide, 4′-bromoacetophenone, starting alcohol, and in one case hydrocarbon; in substantial amounts suggests that either the Chugaev products (alkene and mercaptan) react to form intermediates that subsequently decompose or that the pyrolysis proceeds to a large extent by a different mechanism. The most probable intermediates that might be formed are the corresponding alkyl-*p*-bromophenacyl sulfides since alkenes and mercaptans are known to yield sulfides under relatively mild conditions (6). To determine whether or not the non-Chugaev products were formed from a sulfide intermediate, the preparation and pyrolysis of *n*-hexyl-*p*-bromophenacyl sulfide was investigated. The sulfide was prepared from *n*-hexyl mercaptan and 2,4′-dibromoacetophenone by standard methods (7). Pyrolysis of this sulfide under conditions comparable to those for xanthate pyrolysis gave *n*-hexyl mercaptan and 4′-bromoacetophenone as the only major distillable products. Since no significant amount of alkyl mercaptan was found in any of the xanthate

[1]Part of this work was presented at the 156th National Meeting of the American Chemical Society, Atlantic City, New Jersey, September, 1968.

[2]To whom inquiries should be directed.

Can. J. Chem. Downloaded from www.nrcresearchpress.com by 210.87.254.5 on 09/05/12
For personal use only.

TABLE 1

Pyrolysis products of alkyl *S*-*p*-bromophenacyl xanthates

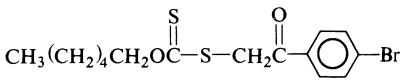 **1***b*	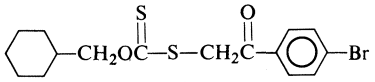 **1***a*	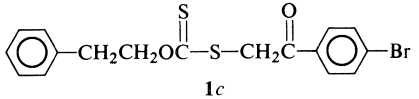 **1***c*
Products (yield)*	Products (yield)*	Products (yield)*
COS†	COS†	COS†
CS_2	CS_2	CS_2
$CH_3(CH_2)_3CH{=}CH_2$ (29 ± 4%)	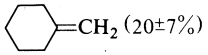 (20±7%)	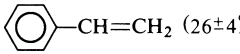 (26±4%)
$CH_3(CH_2)_2CH{=}CHCH_3$ (~1%)‡	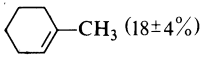 (18±4%)	
	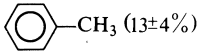 (13±4%)	
$CH_3(CH_2)_4CH_2Br$ (24 ± 8%)	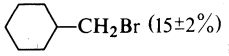 (15±2%)	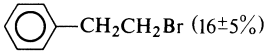 (16±5%)
$CH_3(CH_2)_4CH_2OH$ (35 ± 8%)	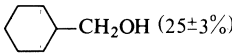 (25±3%)	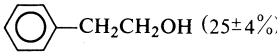 (25±4%)
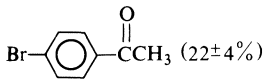 (22±4%)	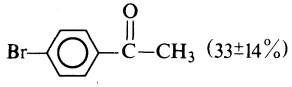 (33±14%)	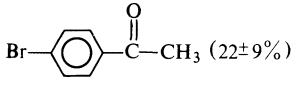 (22±9%)
—	—	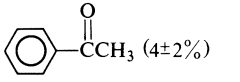 (4±2%)
—	—	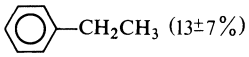 (13±7%)

*Yields are reported as percentages of theoretical yields and are averages of results from 4 pyrolyses.
†Carbonyl sulfide was identified by comparison of the i.r. spectrum of the gaseous products with an authentic sample of COS.
‡The amount of rearranged alkene was estimated by collection of the hexene peak and reinjection into a 12 ft × 1/8 in. column of 30% $AgNO_3$–diethyleneglycol on Chromosorb W, 80–100 mesh.

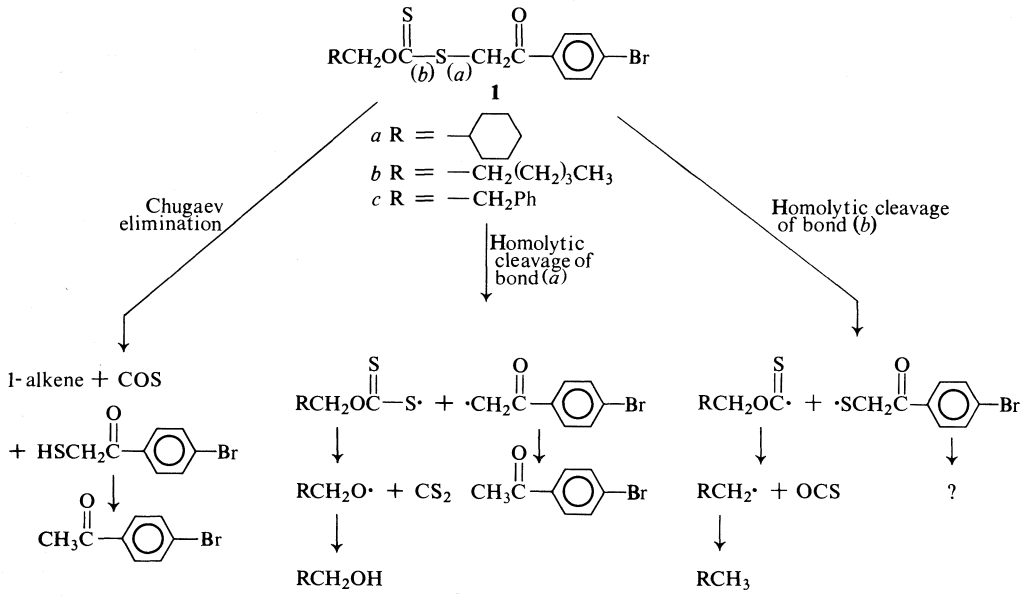

SCHEME 1

pyrolysates, we conclude that these alkyl-*p*-bromophenacyl sulfides are not important intermediates in this pyrolysis.

The formation of the respective alkyl bromides (1-bromohexane, bromomethylcyclohexane, and 1-bromo-2-phenylethane) is particularly significant since aryl halides are generally unreactive. Two experiments were conducted in order to demonstrate that the bromine originated from the *para* position of the starting xanthate rather than from possible impurities. First, the pyrolysis of an analytically pure sample of cyclohexylmethyl *S*-*p*-bromophenacyl xanthate gave results identical to those shown in Table 1. Secondly, the pyrolysis of cyclohexylmethyl *S*-*p*-chlorophenacyl xanthate gave no bromomethylcyclohexane and only a trace of chloromethylcyclohexane.

The most significant difference between the pyrolyses of the 3 xanthates studied is the presence of ethylbenzene in the pyrolysate of the xanthate of 2-phenylethanol. The corresponding hydrocarbons were not formed in detectable amounts in the other 2 cases.

We suggest that the competitive pathways indicated in Scheme 1 represent a plausible, although highly tentative, explanation for all of the products except the bromides and acetophenone. The alkyl bromides could be formed from the reaction of hydrogen bromide or bromine atoms, formed in the decomposition of the aryl part of the xanthate, with either the alkene or the alcohol. Gas chromatographic comparison of the pyrolysates with authentic samples of the isomeric bromides (2-bromohexane, 1-bromo-1-phenylethane, and 1-bromo-1-methylcyclohexane) indicated that these bromides were not present in the product mixture. This is consistent with either a direct reaction of HBr with the primary alcohol or a free radical addition of HBr to the 1-alkene. Acetophenone has been identified as a minor product in only one of these cases, but its formation lends support to a free radical mechanism for the cleavage of the aromatic carbon–bromine bond. Since considerable tar is formed in all of these pyrolyses, the identification of the specific compound that may be decomposing to hydrogen bromide was not attempted.

Experimental

Melting points were taken on a Fisher–Johns Melting Point Apparatus and are corrected. Boiling points are uncorrected. The i.r. spectra were recorded on either a Perkin–Elmer Model 137 or Model 257 recording spectrophotometer. The nuclear magnetic resonance (n.m.r.) spectra were recorded on a Hitachi Model R-20 n.m.r. spectrometer and chemical shift data are given in p.p.m. downfield (δ) from tetramethylsilane as an internal standard (multiplicity: s, singlet; d, doublet; t, triplet; m, multiplet). Elemental analyses were performed by Micro-Tech Laboratories, Skokie, Illinois and Baron Consulting Company, Orange, Connecticut.

Can. J. Chem. Downloaded from www.nrcresearchpress.com by 210.87.254.5 on 09/05/12
For personal use only.

Can. J. Chem. Downloaded from www.nrcresearchpress.com by 210.87.254.5 on 09/05/12
For personal use only.

*Cyclohexylmethyl S-p-Bromophenacyl Xanthate (**1a**)*

Cyclohexanemethanol (57 g, 0.5 mole) was added dropwise (15 min) to a suspension of sodium hydride (26.4 g, 0.6 mole of 56% oil dispersion) in 50 ml of anhydrous ether. The mixture was stirred for 75 min and then carbon disulfide (76 g, 1.0 mole) was added with stirring and cooling over a period of 30 min. Additional portions of ether (200 ml total) were added as needed to keep the suspension fluid. Stirring was continued for 30 min and then the solid product (115 g) was collected by filtration and purified in 10 g portions. The crude sodium salt (10 g) was dissolved in reagent acetone (25 ml) and filtered to remove impurities. Dilution of the filtrate with anhydrous ether (500 ml) and refrigeration overnight resulted in the formation of 5.8 g of crystalline sodium xanthate. Concentration of the filtrate to 50 ml followed by the addition of 200 ml of anhydrous ether gave an additional 1.6 g. The total yield of 7.4 g represents an 80% conversion. This salt was used for the preparation of cyclohexylmethyl *S-p*-bromophenacyl xanthate by the method of Berger and Uldall (3) without characterization or further purification.

A solution of sodium xanthate (4.0 g, 0.02 mole) in 50 ml of reagent acetone was added to a solution of 2,4′-dibromoacetophenone (5.5 g, 0.02 mole) in 10 ml of reagent acetone. After 5 min, 200 ml of ice was added and the solid xanthate was collected and recrystallized from 95% ethanol to give 6.4 g (80%) of **1***a*: m.p. 88–89°; ν_{max} (nujol) 2860, 1662, 1560, 1440, 1365, 1300, 1275, 1220, 1186, 1055, 984, 822, 810, 757 cm^{-1}; n.m.r. ($CDCl_3$), δ 0.9–1.9 [11H, m], 4.3 [2H, d, J = 6 Hz, CH_2O], 4.6 [2H, s, CH_2S], 7.5, 7.6, 7.8, 7.9 [4H, m, phenyl protons].

Anal. Calcd. for $C_{16}H_{19}BrO_2S_2$: C, 49.50; H, 4.90; Br, 20.60; S, 16.50. Found: C, 49.77; H, 4.89; Br, 20.42; S, 16.38.

*n-Hexyl S-p-Bromophenacyl Xanthate (**1b**)*

1-Hexanol was converted to the crystalline sodium xanthate in 78% yield by the procedure described for the sodium xanthate of cyclohexanemethanol. Reaction with 2,4′-dibromoacetophenone according to the procedure of Berger and Uldall (3) gave **1***b* in 85% yield: m.p. 60–61° (lit. (3) m.p. 60–61°); ν_{max} (nujol) 2820, 1660, 1565, 1440, 1355, 1335, 1060, 1040, 980, 825, 810, 770, 723 cm^{-1}; n.m.r. ($CDCl_3$), δ 0.9–1.9 [11H, m], 4.5 [t, J = 6 Hz, CH_2O], 4.6 [s, SCH_2], 7.5, 7.6, 7.8, 7.9 [4H, m, phenyl protons].

*2-Phenylethyl S-p-Bromophenacyl Xanthate (**1c**)*

2-Phenylethanol was converted to the crystalline sodium xanthate in 75% yield by the procedure described for the sodium xanthate of cyclohexanemethanol. Reaction with 2,4′-dibromoacetophenone according to the procedure of Berger and Uldall (3) gave **1***c* in 82% yield: m.p. 76–77° (lit. (3) m.p. 76°); ν_{max} (nujol) 2980, 2900, 1675, 1565, 1480, 1470, 1440, 1380, 1210, 1175, 1060, 982, 810, 770, 750, 695 cm^{-1}; n.m.r. ($CDCl_3$), δ 3.0 [2H, t, J = 7 Hz, CH_2O], 4.5 [s, CH_2S], 4.7 [t, J = 7 Hz, $PhCH_2$], 7.2 [5H, s, phenyl protons], 7.5, 7.6, 7.7, 7.8 [4H, m, phenyl protons].

*Pyrolysis of Cyclohexylmethyl S-p-Bromophenacyl Xanthate (**1a**)*

All pyrolyses were carried out in a 25 ml distilling flask to which had been attached a 90° connecting tube that was in turn connected through a ☒ 14/20 joint to the receiving flask.

Xanthate **1***a* (3.0 g, 7.7 mmole) was placed in the pyrolysis flask and the entire apparatus was flushed with a slow stream of dry nitrogen for 30 min. The pyrolysis vessel was then immersed in a bath of silicone oil that had been preheated to 240°. The temperature was maintained at 240° for 90 min and the volatile products were collected by cooling the receiving flask in a Dry Ice bath. The weight of tarry residue was 0.8 g. The distillate was allowed to warm up to room temperature. The gas that was evolved at this point was found by i.r. spectroscopy to be mainly COS and CS_2. The remaining distillate (1.7 g) was then analyzed by gas chromatography. The components of the complex mixture were separated by preparative scale gas–liquid partition chromatography (g.l.p.c.) on a Varian 1520B gas chromatograph using 10 ft × 3/8 in. columns of 15% Carbowax 20M on Chromosorb W, 30–60 mesh. Comparison of the i.r. spectra of these collected compounds with those of authentic samples showed the mixture to consist of the components shown in Table 1. Quantitative gas chromatographic results were then obtained by use of the area normalization method (8).

*Pyrolysis of n-Hexyl S-p-Bromophenacyl Xanthate (**1b**)*

Compound **1***b* (3.0 g) was pyrolyzed under conditions identical to those used for **1***a*. Gas chromatographic analysis of the pyrolysate indicated the presence of the components shown in Table 1.

*Pyrolysis of 2-Phenylethyl S-p-Bromophenacyl Xanthate (**1c**)*

Compound **1***c* (3.0 g) was pyrolyzed under conditions identical to those used for **1***a*. Gas chromatographic analysis of the pyrolysate indicated the presence of the components shown in Table 1.

4′-Bromo-2-mercaptoacetophenone

A solution of sodium thiosulfate pentahydrate (35.5 g, 0.14 mole) in 50 ml of water was added with stirring over a period of 15 min to a refluxing solution of 2,4′-dibromoacetophenone (36.1 g, 0.13 mole) in 95% ethanol. The reaction mixture was heated at reflux temperature for an additional 75 min, then cooled in an ice bath. Ether (300 ml) was added and the solid product was collected by suction filtration, washed with ether, and dried in a vacuum oven over anhydrous calcium chloride. The crystalline solid (36 g, 83%) was used without further purification.

Sodium p-bromophenacyl thiosulfate (36 g, 0.13 mole) was heated with stirring at reflux temperature with 200 ml of 6 *N* HCl and 300 ml of reagent chloroform for 1 h under a nitrogen atmosphere. The chloroform layer was separated, washed with water (100 ml), dried ($MgSO_4$), and concentrated at reduced pressure. The white solid residue (22.2 g, 89%) was dissolved in chloroform and the solution was then mixed with 375 ml of ligroin. The mixture was filtered to remove precipitated disulfide and the filtrate was concentrated to dryness under reduced pressure. Recrystallization of the solid residue from cyclohexane gave 14.3 g (58%) of white needles: m.p. 87–91°; ν_{max} (melt) 3090, 2960, 2930, 2580, 1680, 1590, 1570, 1485, 1395, 1315, 1300, 1205, 1180, 1070, 1005, 810 cm^{-1}; n.m.r. ($CDCl_3$), δ 2.1 [1H, t, J = 8 Hz, SH], 3.9 [2H, d, J = 8 Hz, $COCH_2S$], 7.5, 7.7, 7.8, 7.9 [4H, m, phenyl protons].

Can. J. Chem. Downloaded from www.nrcresearchpress.com by 210.87.254.5 on 09/05/12
For personal use only.

Anal. Calcd. for C_8H_7BrOS: C, 41.58; H, 3.05; Br, 34.58; S, 13.87. Found: C, 41.77; H, 3.07; Br, 34.33; S, 13.67.

Pyrolysis of 4′-Bromo-2-mercaptoacetophenone

Solid (3.0 g) was pyrolyzed in the same apparatus and under the same conditions as were described above for the xanthates. The distillate (0.5 g) was analyzed by g.l.p.c. and found to consist of 4′-bromoacetophenone (~94%) and one unidentified minor component (~6%). The remaining distillate was dissolved in ether, dried ($CaCl_2$), and treated with Norit. Slow evaporation of the ether solution yielded colorless crystals of 4′-bromoacetophenone.

n-Hexyl-p-Bromophenacyl Sulfide

n-Hexylmercaptan (14.2 g, 0.13 mole) was added with stirring to a cold solution of sodium hydroxide (5.0 g, 0.13 mole) in 50 ml of 50% aqueous ethanol (7). 2,4′-Dibromoacetophenone (35.0 g, 0.13 mole) was added in one portion and the reaction mixture was refluxed for 1 h, cooled, diluted with 2 volumes of water, and finally extracted with 3 100 ml portions of ether. The combined ether extracts were dried (Na_2SO_4) and evaporated to dryness. Recrystallization of the residue from pentane gave 26 g (66%) of white crystals: m.p. 32–33°; ν_{max} (nujol) 2965, 2940, 2860, 1682, 1590, 1570, 1488, 1465, 1420, 1400, 1380, 1308, 1280, 1180, 1075, 1012, 845, 772, 754 cm^{-1}; n.m.r. ($CDCl_3$), δ 0.8 [3H, t, J = 5 Hz, $—CH_3$], 1.0–1.7 [8H, m], 2.5 [2H, t, J = 7 Hz, $SCH_2—$], 3.6 [2H, s, $COCH_2S$], 7.4, 7.5, 7.7, 7.8 [4H, m, phenyl protons].

Anal. Calcd. for $C_{14}H_{19}BrOS$: C, 53.40; H, 6.04; Br, 25.40; S, 10.17. Found: C, 53.13; H, 6.09; Br, 25.23; S, 10.08.

Pyrolysis of n-Hexyl-p-Bromophenacyl Sulfide

The sulfide (4.6 g) was pyrolyzed under conditions identical to those described for xanthate **1***a*. The distillate (0.11 g) was analyzed by gas chromatography (10 ft × 1/8 in. Carbowax 20M on Chromosorb W, 80–100 mesh). Comparison with authentic samples showed the mixture to consist of 1-hexanethiol (50%) and 4′-bromoacetophenone (35%) along with small amounts of unidentified components.

Cyclohexylmethyl S-p-Chlorophenacyl Xanthate

A solution of cyclohexylmethyl *S*-sodium xanthate (15.8 g, 0.07 mole) in reagent acetone (180 ml) and water (18 ml) was added to a solution of 2-bromo-4′-chloroacetophenone (16.5 g, 0.07 mole) in reagent acetone. The solution was stirred for 15 min at 5° and then diluted with 500 ml of ice water. Filtration followed by vacuum drying gave 21.1 g of white solid. Recrystallization from 95% ethanol gave 18.1 g (75%) of white crystals: m.p. 80–81°; ν_{max} (melt) 3090, 2920, 2850, 1680, 1590, 1570, 1490, 1450, 1400, 1285, 1230, 1090, 1065, 990, 830, 820, 780 cm^{-1}; n.m.r. ($CDCl_3$), δ 0.9–1.9 [11H, m], 4.3 [2H, d, J = 6 Hz, CH_2O], 4.6 [2H, s, CH_2S], 7.3, 7.4, 7.8, 8.0 [4H, m, phenyl protons].

Anal. Calcd. for $C_{16}H_{19}ClO_2S_2$: C, 56.10; H, 5.58; Cl, 10.35; S, 18.71. Found: C, 56.00; H, 5.65; Cl, 10.26; S, 18.52.

Pyrolysis of Cyclohexylmethyl S-p-Chlorophenacyl Xanthate

This xanthate (6.0 g, 0.018 mole) was pyrolyzed under conditions identical to those described previously for xanthate **1***a*. The distillate (3.5 g) was analyzed by gas chromatography (10 ft × 1/8 in., 15% Carbowax 20M on Chromosorb W, 80–100 mesh). Comparison with authentic samples showed the mixture to consist of methylenecyclohexane (6%), 1-methylcyclohexene (2%), toluene (1%), chloromethylcyclohexane (< 1%), cyclohexanemethanol (27%), 4′-chloroacetophenone (66%).[3] Comparison of the pyrolysate with an authentic sample of bromomethylcyclohexane indicated that the latter was not present.

We gratefully acknowledge financial support from the Undergraduate Research Participation Program of the National Science Foundation (Grants GY 2889 and GY 4610) and the donors of the Petroleum Research Fund (Grant 2849-B), administered by the American Chemical Society.

J. D. H. and S. S. wish to acknowledge financial support from the E. I. DuPont de Nemours Company and the U.S. Office of Education, Department of Health, Education, and Welfare, respectively.

We wish to thank Dr. Earl Krakower of this Department for assistance in securing and interpreting the n.m.r. spectra.

1. C. H. DePuy and R. W. King. Chem. Rev. **60**, 431 (1960).
2. H. R. Nace. Org. React. **12**, 57 (1962).
3. J. Berger and I. Uldall. Acta Chem. Scand. **18**, 1353 (1964).
4. J. D. Roberts and C. W. Sauer. J. Amer. Chem. Soc. **71**, 3925 (1949).
5. A. E. Kretov, A. N. Panchenko, and A. Konovalchik. J. Gen. Chem. (U.S.S.R.), **1**, 390 (1931); Chem. Abstr. **26**, 2442 (1932).
6. W. A. Pryor. Mechanism of sulfur reactions. McGraw–Hill Book Co., Inc., New York, 1962. p. 71.
7. E. E. Reid. Organic chemistry of bivalent sulfur. Vol. II. Chemical Publishing Co., New York, 1960. p. 24.
8. S. Dal Nogard and R. S. Juvet, Jr. Gas–liquid chromatography. John Wiley and Sons, New York, 1962. p. 255.

[3]Percentages were estimated from peak areas.

Can. J. Chem. Downloaded from www.nrcresearchpress.com by 210.87.254.40 on 09/05/12
For personal use only.

Tetrahydropyranyl protecting group. II.[1] 3-Bromo-2-(tetrahydropyran-2-yloxy)-propene, a masked acetonyl bromide

D. E. Horning, G. Kavadias, and J. M. Muchowski[2]
Bristol Laboratories of Canada, Candiac, Quebec
Received November 3, 1969

It is shown that the sodium hydride (in dimethyl formamide) induced elimination of hydrogen bromide from 1,3-dibromo-2-(tetrahydropyran-2-yloxy)propane (**3**) can be considered to result in the in situ formation of 3-bromo-2-(tetrahydropyran-2-yloxy)propene (**4**). When generated in this manner, **4** was shown to function as a masked acetonyl bromide of considerable utility. Under similar conditions, 1,3-dibromo-2-methoxypropane was assumed to produce 3-bromo-2-methoxypropene, which also was shown to be a useful masked acetonyl bromide.

The pyrolytic elimination of methanol from bromoacetone dimethyl ketal was shown to produce a 1:1 mixture of the two possible isomeric enol ethers, rather than pure 3-bromo-2-methoxypropene as stated in the literature (2).

Canadian Journal of Chemistry, **48**, 975 (1970)

The introduction of an acetonyl moiety into a molecule possessing an activated methylene position is usually effected directly with acetonyl bromide (3) or acetonyl chloride (4). Alternatively, 2-step processes, involving alkylation with propargyl bromide followed by mercuric salt catalyzed hydration of the terminal acetylenic function (5), or, alkylation with 2,3-dichloropropene and subsequent hydrolysis of the vinylic chloride with concentrated sulfuric acid (6,7), are often used when the direct method is unsatisfactory. The great reactivity of bromo- and chloroacetone towards nucleophilic species reduces their usefulness as sources of the acetonyl group (e.g. a solution of the sodium salt of ethyl malonate in ethanol evidently gave only ethoxyacetone, see (4)), and the vigorous conditions necessary for the hydrolysis of the vinylic chloride often promote secondary reactions, such as cyclization and dehydration (see (7), for example), which limit the utility of the dichloropropene method. In contrast, the sequential introduction and hydration of a propargyl group at an activated methylene position is not subject to the above drawbacks, and consequently, this method is more widely applicable than the others.

In connection with various synthetic objectives, we required a masked acetonyl halide which retained the desirable characteristics of both 2,3-dichloropropene and the propargylic halides, and, in addition, had a proclivity to undergo substitution at the terminal carbon atom (C-3) subsequent to insertion at an activated (methylene) position. These requirements were likely to be met by a molecule which incorporated the functionalities of an allylic halide and an enol ether as in **1**. Hydrolysis of the alkylation product **2** obtained therefrom (eq. [1]), would unmask the acetonyl group, or electrophilic substitution of **2** could, at least in principle (8), result in the formation of an ω-substituted acetonyl moiety.

The tetrahydropyranyl ether **3** (eq. [2]), was chosen as a potential precursor of **1** (R = tetrahydropyran-2-yl) because of its ease of synthesis from commercially available, inexpensive starting materials. A solution of the dibromide **3** in anhydrous dimethyl formamide (DMF) containing an excess of sodium hydride was stable

[1]

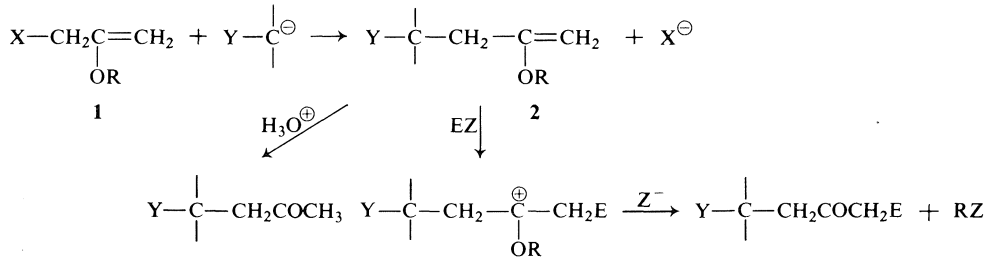

---

[1]For Part I, see ref. 1.
[2]To whom enquiries concerning this paper should be addressed.

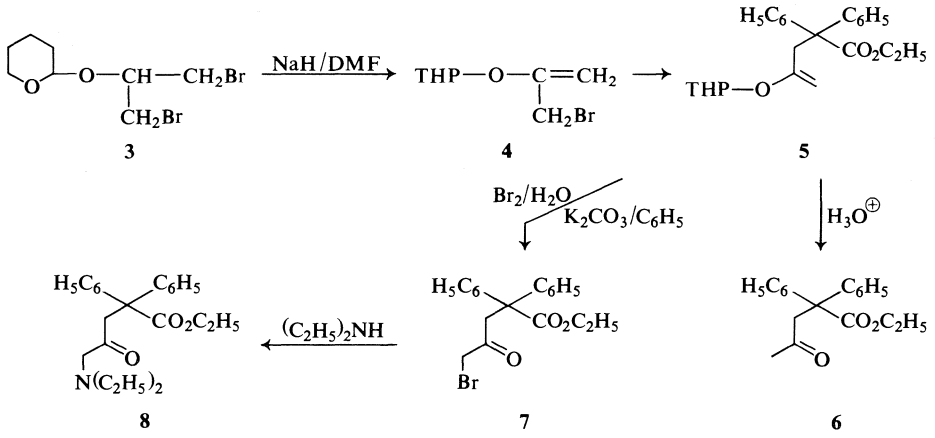

at 0°, but on warming to 10–20° a brisk evolution of hydrogen occurred.[3,4] Addition of ethyl diphenylacetate to the reaction mixture, which was assumed to contain **4** (THP = tetrahydropyran-2-yl), caused a further gas evolution, and after aqueous workup, the enol ether **5** was obtained. Acid catalyzed hydrolysis of **5** gave ethyl-2,2-diphenyllevulinate (**6**). Various reaction conditions for the preparation of **6** were studied (see Table 1, trials *a*, *b*, and *c*), and it was found that a 1.5:1 molar ratio of the dibromide to ethyl diphenylacetate (trial *b*) consistently gave satisfactory yields of **6**. Under similar conditions (see Table 4 in Experimental), fair to good yields of other compounds containing an acetonyl group could be prepared (see Table 3).[5] For example, 2,2-diphenyl-4-oxovaleronitrile was obtained in 73% yield as compared to a 55% overall yield recently reported (5) for the 2-step propargyl group process (vide supra). In addition, alkylation of the pyrrolidine enamine of cyclohexanone and subsequent hydrolysis gave 2-acetonyl cyclohexanone in 24% yield. This was somewhat lower (40%) than was obtained from the direct alkylation of this enamine with acetonyl bromide (10), but the latter procedure invariably gave a product which was contaminated with ca. 15 mole % of 2 - methyl - 4,5,6,7 - tetrahydrobenzofuran (see Experimental).

Under carefully controlled conditions, it was possible to utilize the intermediate enol ethers for the preparation of compounds containing an ω-substituted acetonyl moiety. For example, the synthesis of the basic keto ester **8** (eq. [2]) was accomplished by the bromination of the tetrahydropyranyl enol ether **5**, under conditions which probably generated hypobromous acid, followed by treatment of the α-bromoketone **7** thus produced with diethylamine. Compound **8** was prepared in 49% overall yield from ethyl diphenylacetate, which is remarkably high when the complex nature of the functionality present in **8** is considered.[5]

Although 3 - bromo - 2 - (tetrahydropyran - 2-yloxy)propene (**4**) served notably well as a masked acetonyl group, several instances were envisioned where a 3-bromo-2-alkoxy propene (**9**) would be

[3]The elimination of the elements of hydrogen bromide from β-halogeno ethers with powdered potassium hydroxide is well known (9).

[4]Aqueous workup of the reaction at this stage gave a benzene soluble oily mixture which readily decolorized bromine in carbon tetrachloride, rapidly gave a precipitate of silver bromide with aqueous alcoholic silver nitrate, and which had a medium intensity i.r. absorption at 1634 cm^{-1}. This mixture was judged to contain 60–70% of compound **4** (THP = tetrahydropyran-2-yl) by comparison of the intensity of the n.m.r. signal for the allylic methylene group (singlet at δ 3.88) or the C-2 proton of the tetrahydropyranyl moiety (singlet with fine structure at δ 4.78) with that (singlet with fine structure at δ 1.68) ascribed to the protons on C_3–C_5 of the tetrahydropyran ring. The resonance(s) for the olefinic protons were obscured by the absorptions due to the contaminant(s).

[5]A referee has commented that the main advantage of the 2-alkoxyallyl bromides described herein over bromoacetone, lies in the facile preparation of substituted acetonyl compounds such as **8** from the former. The powerful lachrymatory properties of bromoacetone as well as its poor bench stability (bromoacetone stored at 0° in brown bottles becomes dark colored after 2–3 months and must be redistilled before use; cf., **3** in Experimental) makes **3** (hence **4**) attractive as a source of the acetonyl group. The generality of this approach to acetonyl substituted compounds would, however, be greatly increased if a simple ex situ synthesis of pure 3-bromo-2-methoxypropene, or a derivative thereof, could be devised.

Can. J. Chem. Downloaded from www.nrcresearchpress.com by 210.87.254.40 on 09/05/12
For personal use only.

TABLE 1

Determination of the optimum conditions for the preparation of **6**

Trial	Alkylating agent: Compound	Mode of addition*	mmoles†	Reaction time (h)	Yield‡ of **6** (%)	Number of runs
a	**3**	N	10	17	31–57	4
b	**3**§	I	15	13–15	66–69	2
c	**4**‖	N	12¶	22	44	1
d	**11****	I	15	16	73	1
e	**9***a*††	N	10–15‡‡	17	50–59	2
f	**9***b*	N	15‡‡	18	59	1

*N = Normal, i.e. alkylating agent added to sodium salt of ester and excess sodium hydride. I = Inverse; ester added to alkylating agent and sodium hydride.
†Ten mmoles of the ester were used throughout.
‡Yield of pure product.
§Assumed to involve the in situ generation of **4**.
‖Generated ex situ; see footnote 4 in text.
¶Based on the assumption that the mixture described in footnote 4 in text was pure **4**.
Assumed to involve the in situ generation of **9*a*.
††Prepared according to (2).
‡‡These quantities were adjusted for the presence of the isomeric 1-bromo-2-alkoxypropene.

synthetically more versatile.[6] We were surprised to discover that one such compound, 3-bromo-2-methoxypropene (**9***a*), was reported (2) to be the sole thermolysis product of bromoacetone dimethyl ketal. Repetition of this reaction gave a

[3] $CH_3-C(OR)_2-CH_2Br \longrightarrow$

R = CH_3, C_2H_5

$CH_2=C(OR)-CH_2Br$ + $CH_3-C(OR)=CHBr$

9 **10**

a R = CH_3 *a* R = CH_3

b R = C_2H_5 *b* R = C_2H_5

product in about 40% yield, which was shown by nuclear magnetic resonance (n.m.r.) spectroscopy to contain only 43% of the desired alkoxyallyl bromide **9***a* admixed with 50% of 1-bromo-2-methoxypropene (**10***a*) and 7% bromoacetone (eq. [3]). A similar reaction with the diethyl ketal gave a mixture which was significantly richer in the required component **9***b* (75–77% **9***b*, 19–25% **10***b*, and 0–4% bromoacetone). It is probable that the thermolysis products of the other bromoacetone dialkyl ketals studied by Bruce and Ban (2) were also mixtures. The mixtures containing **9***a* and **9***b* were tested as sources of the acetonyl group,[7] however, as judged from the yields of **6** (see Table 1, trials *e* and *f*), they did not have any significant advantages over **4**. Consequently, a method, analogous to that which had been used for the synthesis of **4** from **3**, was then applied to the in situ generation of **9***a* free of **10***a*. Dehydrohalogenation of 2-methoxy-1,3-dibromopropane [prepared by the aluminum chloride catalyzed diazomethane methylation (12) of 1,3-dibromo-2-propanol][8] was effected by briefly heating a DMF solution of this compound with sodium hydride at 60° (eq. [4]). The resulting solution, which presumably contained **9***a*, also was a useful source of the acetonyl group. For example, ethyl-2,2-diphenyllevulinate (**6**) and 2-acetonyl cyclohexanone were prepared therefrom in 73 (see trial *d*, Table 1) and 19% yields, respectively. The utilization of **9***a* for the synthesis of compounds containing a 3-substituted acetonyl moiety has not yet been examined.

[6]For example, reaction of the tetrahydropyranyl enol ether **5** with an aryl diazonium salt would be expected to produce a mixture of 2 hydrazones, *a* and *b*, whereas the corresponding alkoxy compound would give only *a* (11).

5 $\xrightarrow{ArNHNH_2}$ H_5C_6, C_6H_5, $CO_2C_2H_5$, O, NHHAr (*a*) + HO, O, H, NNHAr (*b*)

[7]Bruce and Ban (2) utilized these mixtures to prepare a series of 5-substituted-5-(2-alkoxyallyl)barbituric acids, and also to alkylate diethyl allylmalonate, but curiously, none of these compounds were converted to their acetonyl derivatives.

[8]This compound is not readily prepared directly from allyl bromide (see (13)).

Can. J. Chem. Downloaded from www.nrcresearchpress.com by 210.87.254.40 on 09/05/12
For personal use only.

[4] $BrCH_2\underset{OH}{\underset{|}{C}}HCH_2Br + CH_2N_2 \xrightarrow{AlCl_3} BrCH_2\underset{OCH_3}{\underset{|}{C}}H-CHBr \xrightarrow[60^\circ]{NaH/DMF} CH_2=\underset{OCH_3}{\underset{|}{C}}CH_2Br$

11 **9a**

[5] $THP-O-\underset{CH_2Br}{\underset{|}{CH}}-CH_2CH_2Br \longrightarrow THP-O-\underset{CH_2}{\underset{||}{C}}-CH_2CH_2Br \longrightarrow \longrightarrow$ 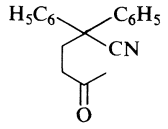

12 **13**

Finally, it was of interest to determine the feasibility of extending the principles discussed above to the introduction of groups other than the acetonyl moiety. Therefore, the tetrahydropyranyl ether **12** was subjected to the elimination conditions described above. Addition of diphenylacetonitrile to this solution gave, after the usual workup, the δ-ketonitrile **13** in 36% yield (eq. [5]) (isolated as the crystalline semicarbazone; see Table 3). A somewhat purer product was obtained (37%) when the dibromide **11** was added to the sodium salt of diphenylacetonitrile and an excess of sodium hydride (as in trial *a*, Table 1).

A number of other synthetic applications of the principles described herein will be submitted for publication in the near future.

Experimental

The melting points were determined in a Gallenkamp melting point apparatus and are not corrected. The infrared (i.r.) spectra were recorded with a Perkin–Elmer 237-B grating spectrophotometer and a Unicam SP-200G i.r. spectrophotometer. The n.m.r. spectra were recorded at 60 Mc.p.s. on a Varian A-60A spectrometer and are expressed in p.p.m. (δ) from internal tetramethylsilane.

1,3-Dibromo-2-(tetrahydropyran-2-yloxy)propane (3)

1,3-Dibromo-2-propanol (217.9 g, 1 mole) containing 12 drops of 48% hydrobromic acid was cooled to 0° with stirring, and 132 g (1.5 moles) of dihydropyran were added dropwise at a rate such that the reaction temperature did not exceed 10°. After 1 h at 0° and 17 h at room temperature, 100 ml of dichloromethane and 10 g of potassium carbonate were added, and the mixture was stirred for 1/2 h. The solids were removed by filtration, the filtrate was concentrated *in vacuo*, and the residual oil was fractionally distilled under high vacuum from 40 g of potassium carbonate. A forerun, b.p. 68–83°/0.06–0.10 mm, was discarded, and the fraction with b.p. 76–83°/0.002–0.005 mm (232.7 g, 77.1%) was collected. A portion of the product was redistilled, and a center cut, b.p. 76°/0.002 mm, was analyzed.

Anal. Calcd. for $C_8H_{14}Br_2O_2$: Br, 52.93. Found: Br, 53.20.

1,3-Dibromo-2-(tetrahydropyran-2-yloxy)propane can be stored at 0° for at least 6 months with no observable loss in its ability to serve as a source of the acetonyl group.

The n.m.r. and i.r. spectra of this and the other halogeno compounds prepared in this work are collected in Table 2.

1,4-Dibromo-2-(tetrahydropyran-2-yloxy)butane (12)

This tetrahydropyranyl ether was prepared in 43% yield from 1,4-dibromo-2-butanol (15) in the manner described above. It had b.p. 92–93°/0.002 mm and was used without further characterization.

1,3-Dibromo-2-methoxypropane (11)

Commercial 1,3-dibromo-2-propanol was strongly acidic to litmus paper, and consequently, a dichloromethane solution of the alcohol was stirred with a paste of sodium carbonate and water until neutrality was achieved. After removal of the solvent, the alcohol was distilled *in vacuo*, and the fraction, b.p. 83–85°/12 mm was collected.

A solution of 1,3-dibromo-2-propanol (23.5 g, 107 mmoles) in 150 ml of dry ether containing 800 mg of anhydrous aluminum chloride, was cooled to 0° with stirring. An ethereal solution of diazomethane (prepared from 41.2 g of nitrosomethylurea) was added dropwise over a 1 h period, then stirring at 0° was continued until gas evolution had become slow (4.5 h). A few drops of acetic acid were added and the mixture was filtered through Celite. The filtrate was washed successively with 10% hydrochloric acid and water, dried over sodium sulfate, and evaporated *in vacuo*. The residual oil, which contained some starting material, was taken up in dichloroethane and this solution was placed on a dry packed column of 400 g of Fluka neutral alumina (activity II). The product was eluted with dichloroethane and was contained in the first 150 ml of the eluate. The solvent was evaporated and the residue was distilled *in vacuo* to give 17.89 g (73%) of a colorless oil, b.p. 72–73°/11 mm [lit. (12), b.p. 83°/13 mm].

3-Bromo-2-methoxypropene (9a) and 1-Bromo-2-methoxypropene (10a)

Bromoacetone dimethyl ketal was thermally cracked by fractionation in a Nester–Faust spinning band column, according to the method described by Bruce and Ban (2). A fraction, b.p. 60.5–61.5°/70 mm [lit. (2), b.p. 65–67°/60–62 mm] was obtained in 41% yield. It was shown by n.m.r. spectroscopy to consist of a mixture of 50% 1-bromo-2-methoxypropene, 43% 3-bromo-2-methoxypropene, and 7% bromoacetone.

Can. J. Chem. Downloaded from www.nrcresearchpress.com by 210.87.254.40 on 09/05/12
For personal use only.

TABLE 2

Spectral properties of some bromo compounds

Compound (No.)		Infrared (cm^{-1})*	Nuclear magnetic resonance (δ)†,‡
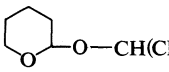	(**3**)	1131, 1034, 981	1.65(bs,6H), 3.28–4.47(m,7H), 4.67 (bs,1H)§
$CH_3O—CH(CH_2Br)_2$	(**11**)	1101,1081	3.50(s,3H), 3.58(s,4H), 3.85(quin.,1H)
$CH_3O—C(=CH_2)—CH_2Br$	(**9***a*)	1663(m),1634, 1308,1212,1169, 1138,1066,862,824	3.65(s,3H), 3.92(s,2H), 4.15(d,1H; J_{AB} = 2.6), 4.35(d,1H; J_{AB} = 2.6)
$CH_3O—C(CH_3)=CHBr$	(**10***a*)		2.00(s,3H), 3.58(s,3H), 5.20(s,1H)
$CH_3CH_2O—C(=CH_2)—CH_2Br$	(**9***b*)	1664(m),1631,1306 1206,1190,1139 1070,854(m),816	1.35(t,3H; J = 7.2), 3.87(q,2H; J = 7.2), 3.92(s,2H), 4.16(d,1H; J_{AB} = 2.5), 4.35(d,1H; J_{AB} = 2.5)
$CH_3CH_2OC(CH_3)=CHBr$	(**10***b*)		1.20(t,3H; J = 7.0), 2.02(s,3H), 3.57(q,2H; J = 7.0), 5.23(s,1H)

*Infrared spectra measured as neat liquids.
†Recorded in deuteriochloroform with internal tetramethylsilane unless specified otherwise. J values given in c.p.s.
‡bs = Broad singlet, d = doublet, m = multiplet, q = quartet, quin. = quintet, s = singlet, and t = triplet.
§Measured in carbon tetrachloride.

*3-Bromo-2-ethoxypropene (**9b**) and 1-Bromo-2-ethoxypropene (**10b**)*

Bromoacetone diethyl ketal was thermally cracked as above to give an oil, b.p. 53–55°/26 mm, in about 50% yield. This fraction was shown by n.m.r. spectroscopy to be a mixture of 75–77% 3-bromo-2-ethoxypropene, 19–25% 1-bromo-2-ethoxypropene, and 0–4% bromoacetone. This mixture was not further characterized.

Conditions for the Alkylation Reaction

The preparation of ethyl-2,2-diphenyllevulinate (**6**) exemplifies a typical procedure; modifications are described below as well as in Tables 1 and 4.

A 100 ml, 3-necked flask was flame dried and then charged with 1200 mg (27.5 mmoles) of a 55% dispersion of sodium hydride in mineral oil, while a flow of purified dry nitrogen was maintained through the apparatus. The sodium hydride was freed of the carrier by washing with several portions of hexane, and then it was layered with 30 ml of dry DMF and cooled with stirring to 0°. A solution of 4.53 g (15 mmoles) of 1,3-dibromo-2-(tetrahydropyran-2-yloxy)propane in 5 ml of dry DMF was added all at once, and the apparatus was removed from the cooling bath. At 10° hydrogen evolution commenced and thereafter the reaction temperature rose steadily, but was not allowed to exceed 25°. When the evolution of gas had become slow (ca. 45 min), the mixture was cooled to 0°, and 2.40 g (10 mmoles) of crystalline ethyl diphenylacetate were added all at once. The cooling bath was removed, and the reaction temperature was maintained at 20–25° until gas evolution had become slow. The reaction mixture was stirred at room temperature for 13–15 h under a slight positive pressure of nitrogen. The solution was then poured into a large volume of cold water containing a little sodium chloride, and the product was extracted into benzene. The extract was washed well with water, dried over sodium sulfate, and the solvent was removed *in vacuo* at 40° leaving a quantitative yield of the crystalline tetrahydropyranyl ether **5**. It had i.r. (neat) absorptions at 1733 and 1636 cm^{-1}. Since it was not readily recrystallized and because it partially decomposed (to **6** and presumably dihydropyran) on sublimation at 80°/0.001 mm, it was used without further purification. The crude enol ether was dissolved in 90 ml of methanol and 10 ml of 10% hydrochloric acid, and the solution was heated at reflux temperature for ca. 10 min. The resultant was concentrated to a volume of about 10 ml *in vacuo*, the mixture was diluted with a large amount of water and the product was extracted into benzene. The extract was washed well with water, dried over sodium sulfate, and then evaporated *in vacuo*. The residue was crystallized from methanol to give 1.752 g of a crystalline solid, m.p. 110–112°. Workup of the mother liquor in the usual manner gave an additional 0.187 g of the product m.p. 109–111°. The spectral data for this compound are given in Table 3.

Modifications

(*i*) The rate of dehydrohalogenation of 1,3-dibromo-2-methoxypropane was slower than that of the tetrahydropyranyl ether **3**. As a consequence, the DMF solution containing **11** and excess sodium hydride was thrice heated to 60° and then allowed to cool spontaneously to room temperature. The solution of **9***a* thus obtained was then used as above.

(*ii*) The alkylation of the pyrrolidine enamine of cyclohexanone was carried out under the usual conditions except that a 1:1 molar ratio of the alkylating

Can. J. Chem. Downloaded from www.nrcresearchpress.com by 210.87.254.40 on 09/05/12
For personal use only.

Can. J. Chem. Downloaded from www.nrcresearchpress.com by 210.87.254.40 on 09/05/12
For personal use only.

TABLE 3

Yields and properties of some ketonic compounds

Compound	Yield (%)*	Calcd. C	Calcd. H	Found C	Found H	Melting point (°C) or boiling point (°C/mm)	Other means of characterization	
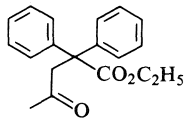	66–69	77.00	6.80	76.93	6.75	110–112†	n.m.r. (δ)‡	1.13(t,3H;J = 7.0),2.00(s,3H) 3.58(s,2H),4.13(q,2H;J = 7.0) 7.20(s,10H)
							i.r.(cm^{-1})§	1731
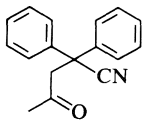	73	81.90	6.06	81.62	6.02	103–105‖	n.m.r.	2.10(s,3H),3.52(s,2H),7.28 (s,10H)
							i.r.	2247(w),1729
							lit. (5)	m.p. 105–107°
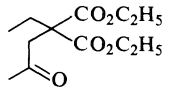	55	59.00	8.25	58.73	8.44	145–150/9¶	n.m.r.	0.87(t,3H;J = 7.5),1.25(t,3H; J = 7.2),2.10(q,2H;J = 7.5), 2.18(s,3H),3.02(s,2H),4.27 (q,2H;J = 7.2)
							i.r.	1757(sh), 1731[neat]
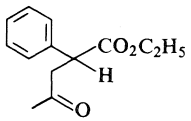	42	—	—	—	—	95–100/0.04	i.r.	1734,1725[neat]
						36.5–39**	lit. (14)	m.p.41–42. Saponification of the ester gave an acid m.p. 126–127°, [lit.(14)m.p.127°]††
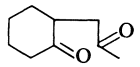	24	—	—	—	—	95/1.0¶	Identical to an authentic specimen prepared according to ref. 10.	
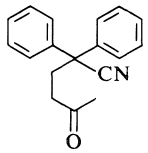	36–37‡‡	71.22	6.29	71.35	6.33	171–173	n.m.r.	1.83(s,3H),2.53(m,4H),5.98 (s,2H),7.42(m,10H),8.80(s,1H)
							i.r.	3520,3468,3400,3378,3208 1697,1569

*Yields of pure products.
†After crystallization from methanol and sublimation at 85°/0.001 mm.
‡See † and ‡ in Table 2.
§Measured in chloroform unless specified otherwise.
‖After crystallization from 2-propanol and sublimation at 90°/0.001 mm.
¶Evaporative distillation; air bath temperature.
**After crystallization from petroleum ether b.p. 60–90°.
††After crystallization from ether.
‡‡Yield, analysis, m.p., and spectral data are those of the semicarbazone.

TABLE 4
Conditions for the preparation of some ketonic compounds

Compound	Moles dibromide*/mole active methylene compound	Reaction temperature (°C)	Time (h)
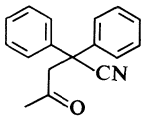	1.5	25	2
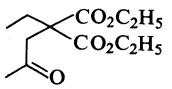	1.5	25	19
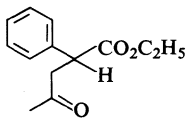	1	50	17
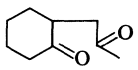	1	25	15
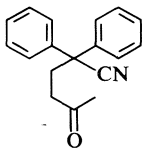	1.5	25	15

*Dibromide **3** was used for the first 4 compounds and dibromide **12** for the last compound.

agent to the enamine was used (see Table 4). When the reaction was completed the solution was poured into a large excess of water and then left at room temperature for 1 h. The product was then isolated in the usual way by extraction with benzene. Removal of the solvent gave the crude keto enol ether (4.90 g from a 20 mmole reaction using **4** prepared in situ) which was taken up in 200 ml of dichloromethane. The solution was stirred vigorously at room temperature with 35 ml of 10% hydrochloric acid and 185 ml of water. After 1 h, the organic phase was separated, washed well with water, and dried over sodium sulfate. The solvent was removed *in vacuo* leaving an oil which was distilled *in vacuo*. The material thus obtained, b.p. 70–110°/0.7 mm (2.72 g) was shown to be a 2 component mixture by thin-layer chromatography (t.l.c.) on alumina (benzene). This mixture was taken up in benzene and placed on a column of 100 g of Fluka neutral alumina (activity II; packed in benzene). The chromatogram was developed with benzene (250 ml) and then chloroform (350 ml). The impurity was contained in the benzene eluate, the product in the chloroform eluate. After removal of the solvent *in vacuo*, the residual oil was evaporatively distilled at 95°/1 mm [lit. (10), b.p. 91–93°/1.1 mm], to give 745 mg of a colorless liquid (see Table 3) with an i.r. (neat) absorption at 1713 cm^{-1}. When prepared by the method of Baumgarten *et al.* (10), 2-acetonylcyclohexanone was contaminated with ca. 15 mole % of 2-methyl-5,6,7,8-tetrahydrobenzofuran (determined by integration of the absorption for the olefinic proton at δ 5.82). The i.r. spectrum of 2-acetonylcyclohexanone obtained in this way had a weak band at 1627 cm^{-1}, but was otherwise identical to the specimens prepared by our procedures.

(*iii*) For the preparation of 2,2-diphenyl-5-oxocapronitrile (**13**), the best procedure was to add the dibromide **12** to the sodium salt of diphenylacetonitrile and excess sodium hydride. When the reaction was completed, the crude product was taken up in methanol and treated with an excess of aqueous–methanolic semicarbazine. The product, m.p. 168–171°, crystallized from solution and was collected by filtration. After two crystallizations from aqueous alcohol (3:4) the melting point was raised to 171–173° (see Table 3).

*Ethyl-2,2-diphenyl-5-diethylaminolevulinate (**8**)*

To a vigorously stirred cooled (5°) mixture of potassium carbonate (415 mg, 3 mmoles) and 55 μl of water (55 mg, 3.05 mmoles) in 25 ml of benzene containing 1.14 g (3 mmoles) of the tetrahydropyranyl ether **5**, was added a solution of 528 mg (0.17 ml, 3.3 mmoles) of bromine in 5 ml of benzene at a rate such that the reaction temperature did not exceed 10°. When the addition was completed,

Can. J. Chem. Downloaded from www.nrcresearchpress.com by 210.87.254.40 on 09/05/12
For personal use only.

the cooling bath was removed, and the mixture was stirred vigorously for 20 min. At the end of this time, the mixture was again cooled to 5°, and 438 mg (0.63 ml, 6 mmoles) of diethylamine were added all at once. The cooling bath was removed, and after stirring for 2 h at room temperature, a few mls of sodium carbonate solution (200 g/l) and 50 ml of water were added. The organic phase was separated and combined with a benzene extract of the aqueous phase. The benzene phase was extracted alternately with 10% hydrochloric acid (4 × 30 ml) and water (4 × 30 ml). The aqueous acidic extract was made basic with sodium carbonate solution (200 g/l), and the liberated base was extracted into dichloromethane. The extract was dried over sodium sulfate, and the solvent was removed *in vacuo* leaving 0.64 g of a yellow oil which was converted to its hydrobromide salt in ether. The crude salt was taken up in about 50 ml of hot 2-propanol, and this solution was made up to ca. 250 ml with ether. A beautifully crystalline solid, m.p. 195–197° was obtained in 48.6% yield (0.653 g). The n.m.r. spectrum (free base in $CDCl_3$) had resonances at δ 0.93 (t, 6H; J = 7.1), 1.17 (t, 3H; J = 7.1), 2.48 (q, 4H; J = 7.1), 3.00 (s, 2H); 3.73(s, 2H), 4.18(q, 2H; J = 7.1), and 7.23 (m, 10H). The i.r. spectrum (Nujol mull) of the salt had a strong absorption at 1734 cm^{-1}.

For analysis, the above material was thrice crystallized from 2-propanol. The melting point was thus raised to 198–200°.

Anal. Calcd. for $C_{23}H_{29}NO_3 \cdot HBr$: C, 61.60; H, 6.74; N, 3.12. Found: C, 61.71; H, 6.69; N, 3.39.

1. D. E. Horning and J. M. Muchowski. Can. J. Chem. **46**, 2617 (1968).
2. W. F. Bruce and M. Ban. U.S. Patent No. 2 786 057 (1957); Chem. Abstr. **51**, 18015 (1957).
3. H. Gault and T. Salomon. C. R. **174**, 754 (1922).
4. A. W. Dox and B. Houston. J. Amer. Chem. Soc. **46**, 252 (1924).
5. J. F. Cavalla, R. Simpson, and A. C. White. British Patent No. 1 124 682 (1968); Chem. Abstr. **70**, 28671*p* (1969).
6. P. T. Lansbury and E. J. Nienhouse. J. Amer. Chem. Soc. **88**, 4290 (1966).
7. E. J. Nienhouse, R. M. Irwin, and G. R. Finni. J. Amer. Chem. Soc. **89**, 4557 (1967).
8. F. Effenberger. Angew. Chem. Int. Ed. Engl. **8**, 295 (1969).
9. W. M. Lauer and M. A. Spielman. J. Amer. Chem. Soc. **53**, 1533 (1931).
10. H. E. Baumgarten, P. L. Creger, and C. E. Villars. J. Amer. Chem. Soc. **80**, 6609 (1958).
11. M. Seefelder and H. Eilingsfeld. Angew. Chem. Int. Ed. Engl. **2**, 484 (1963).
12. E. Mueller, R. Meischkeil, and M. Bauer. Ann. **677**, 55 (1964).
13. L. Sattler, M. Altamura, and S. Prener. J. Amer. Chem. Soc. **57**, 333 (1935).
14. Huan. Bull. Soc. Chim. **5**, 1341 (1938).
15. C. D. Lunsford, J. W. Ward, A. J. Pallotta, T. W. Tusing, E. K. Rose, and R. S. Murphey. J. Med. Pharm. Chem. **1**, 73 (1959).

Can. J. Chem. Downloaded from www.nrcresearchpress.com by 210.87.254.40 on 09/05/12
For personal use only.

Titanium tetrachloride promoted conversion of carboxylic acids to carboxamides

JAMES D. WILSON AND HAROLD WEINGARTEN
Monsanto Co., Central Research Department, St. Louis, Mo. 63166

Received October 16, 1969

In the presence of approximately stoichiometric amounts of $TiCl_4$, carboxylic acids and amines react at room temperature and atmospheric pressure to form carboxamides in good yields. The mono- and diformyl derivatives of 1,2-dimethylhydrazine exhibit unusual nuclear magnetic resonance spectra which are briefly discussed.

Canadian Journal of Chemistry, **48**, 983 (1970)

Can. J. Chem. Downloaded from www.nrcresearchpress.com by 210.87.254.5 on 09/05/12
For personal use only.

A classic method for the preparation of *N*-substituted carboxamides involves the pyrolytic dehydration of the appropriate substituted-ammonium carboxylate salts. We have found that it is possible to effect virtually the same reaction under very mild conditions of temperature by allowing an acid or its salt to react with the mixed Ti^{IV} amide/amine/chloride complexes formed (1) by the interaction of $TiCl_4$ and aliphatic amines. These reagents have previously been shown to convert ketones to enamines (2) and/or ketimines (3).

In a typical reaction formic acid was dissolved in a solution of ethylamine in tetrahydrofuran, the ethylamine being in excess of that required by the stoichiometry of eq. [1]. To the

[1] $$2\,HCOOH + 6\,C_2H_5NH_2 + TiCl_4 = 2\,HCONHCH_2CH_3 + 4\,C_2H_5NH_3Cl + TiO_2$$

resulting suspension, cooled to $-70°$[1] under a nitrogen atmosphere, titanium tetrachloride was added in small portions, neat, until a small excess over the stoichiometric quantity was present. The resulting dark brown mixture was allowed to warm to 25° and remain at that temperature for about 8 h, during which time the color faded. From the filtrate of this mixture *N*-ethylformamide was isolated in 82% yield by distillation. This general procedure was used to prepare the amides listed in Table 1, the main variations from it being the length of time allowed for the reaction to go to completion.[2]

[1]Mixing the reagents at this temperature is convenient because the high heat of reaction of $TiCl_4$ with bases is thus rapidly dissipated.

[2]Working at elevated temperatures does not increase the yield, since heating these reaction mixtures above 50° for extended periods or above 90° causes the reduction of Ti^{IV}, giving species which are ineffective as condensing agents. Presumably the amines are oxidized in this redox reaction (1, 4) which is signalled by the formation of dark tars during the reaction and by a blue precipitate after hydrolysis.

From Table 1 it can be inferred that this method can be used to prepare virtually any *N*-alkyl or *N,N*-dialkyl carboxamide; examples representing all the common variations are listed there. However, the reaction fails when aromatic amines are employed with hindered acids; no *N*-methylpivalanilide could be detected from the reaction of pivalic acid with *N*-methylaniline under these conditions. Thus the method is useful in effecting the condensation of all but the most hindered acids with the most weakly basic amines.

Under certain conditions, some amides can be further aminated, amidinium ions and/or endiamines being formed. A full account of these findings is in preparation.

Although the mechanism of the reaction has not been studied it seems likely that the rate-determining step in the reaction involves transfer of an amide ligand from Ti to C in an intermediate Ti^{IV} complex (or family of such species) containing both carboxylate and amide ligands. If this is the case then the reaction should be slowed by factors which sterically impede the ligand transfer, exactly what is observed.

The reaction of formic acid with 1,2-dimethylhydrazine (generated in situ from the dihydrochloride plus triethylamine) gave a mixture of 1-formyl-1,2-dimethylhydrazine (**1**, 24% yield) and 1,2-diformyl-1,2-dimethylhydrazine (5) (**2**, 14%), the first of which has not previously been prepared. These two formamides exhibit interestingly complex nuclear magnetic resonance (n.m.r.) spectra (described below) which imply that rotation about the nitrogen–carbonyl–carbon bond is hindered, as is common in other amides (6). The spectrum of **2** is especially interesting in that at room temperature there appears to be "slow" interconversion among three rotamers, two of which are present in equal concentration,

TABLE 1

Some amides prepared by $TiCl_4$-promoted condensations

Amide formed	Reaction conditions		
	Time	Solvent	Yield (%)*
N-Ethylformamide	8 h	THF	82
N,*N*-Diethylbenzamide	20 h†, ‡	Hexane	76
N-Pivaloylpyrrolidine	7 days‡	THF	31
N,*N*′-Bis(tetramethylene) malonamide	2 days	THF	66
Tetramethyloxamide	3 days	$(CH_3)_2NH$	73
N,*N*,*N*′,*N*′-Tetramethyl-1,4-cyclohexanedicarboxamide	5 days	THF	67

*No special effort was made to maximize the yield.
†Run at 60°. The starting material was sodium benzoate.
‡Some Ti^{III} formed.

the third of which is present in considerably smaller amount. If rotation about the nitrogen–nitrogen bond is fast, three rotamers are expected (Fig. 1), two of which, (*a*) and (*c*), possess a center of symmetry and should thus exhibit single "formyl" and "methyl" resonances. The other (*b*) is not symmetrical, and may exhibit two formyl and two methyl resonances. Four formyl and four methyl resonances are observed, in the approximate relative areas 2:1:1:0.16, which implies that rotamer *b* and either *a* or *c* dominate the mixture and the other of *a* or *c* is the minor constituent. Such behavior is not normally expected for such a symmetrical compound; however, it can be rationalized by hypothesizing an interaction between the carbonyl groups to give an oxadiazolinium-type structure (see Fig. 1).[3,4] Such ring closure is possible for rotamers *a* and *b* but not for *c*, and thus interaction could stabilize those two at the expense of the third.

Experimental

The chemicals and solvents employed in this work were obtained from Fisher Scientific or Aldrich Chemical Company. Tetrahydrofuran and amines were distilled from CaH_2 before use. Infrared (i.r.) spectra were obtained as neat liquid films or KBr discs using a Beckman IR-4 spectrophotometer; n.m.r. spectra were obtained on a Varian A-60, with $CDCl_3$ or CD_3CN

[3]We thank Dr. J. J. Bloomfield for suggesting this mechanism.

[4]1,2-Diacylhydrazines are readily converted to oxadiazoles (7).

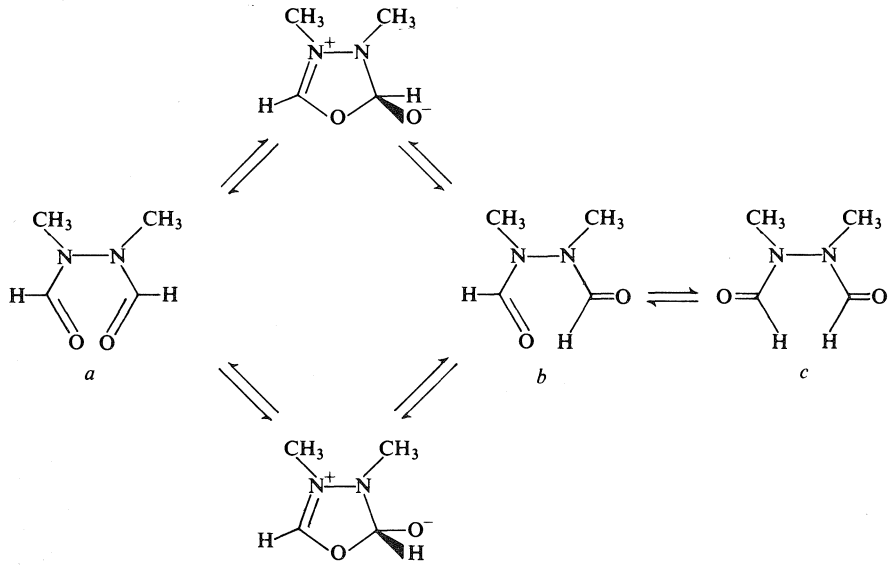

FIG. 1. Rotamers of 1,2-dimethyl-1,2-diformylhydrazine.

Can. J. Chem. Downloaded from www.nrcresearchpress.com by 210.87.254.5 on 09/05/12
For personal use only.

Can. J. Chem. Downloaded from www.nrcresearchpress.com by 210.87.254.5 on 09/05/12
For personal use only.

solvent and tetramethylsilane internal standard. Mass spectra were obtained on a CEC-103 mass spectrometer.

N,N′-Bis(tetramethylene)malonamide

In a 200 ml 3-neck round-bottom flask equipped with mechanical stirrer, N_2-inlet, and dropping funnel were placed malonic acid (2.08 g, 0.02 mole) and pyrrolidine (10 ml, >0.12 mole); tetrahydrofuran (THF: 100 ml) was added, giving a suspension of the pyrrolidinium malonate. This was cooled to −70° under N_2, with stirring, and $TiCl_4$ (2.2 ml, 0.02 mole) was introduced in small portions from the dropping funnel, the reaction mixture turning dark brown in the process. After addition of $TiCl_4$ was complete the cooling bath was removed and the reaction allowed to warm to ambient temperature, at which temperature it was allowed to remain for 48 h. During this time the color faded to light yellow. A small amount of water (~2 ml) was added to destroy any complex Ti species remaining, then the mixture was filtered. The precipitate was washed with THF and twice with CCl_4; the filtrate and washings were combined and flash-evaporated to give crude *N,N′*-bis(tetramethylene)-malonamide (2.77 g, 66%). Part of the amide was sublimed (90° at 0.02 Torr) and then recrystallized from CCl_4 to give colorless crystals, m.p. 109–110°.

Anal. Calcd. for $C_{11}H_{18}O_2N_2$: C, 62.83; H, 8.62; N, 13.33. Found (210 (mass spectroscopy)): C, 62.66; H, 8.65; N, 13.35.

The n.m.r. spectrum consisted of a complex multiplet centered at τ 6.4 (8H), a singlet at τ 6.7 (2H), and a complex multiplet centered at τ 8.1 (8H). The i.r. spectrum contained a band at 1650 cm^{-1} characteristic of tertiary amides (8), as well as strong bands at 2900, 2730, 1450, and 1420 cm^{-1}.

N-Pivaloylpyrrolidine

Using exactly the same procedure, pivalic acid (5.1 g, 0.05 mole) was allowed to react with pyrrolidine and $TiCl_4$ for 7 days at 25°. Some reduction of Ti^{IV} to Ti^{III} was observed. *N*-Pivaloylpyrrolidine was obtained as colorless needles (2.40 g, 31%), m.p. 56–59°. It exhibited an n.m.r. spectrum consisting of a complex multiplet centered at τ 6.5 (4H) and τ 8.2 (4H) and a singlet at τ 8.8 (9H) assigned to the α- and β-protons of the pyrrolidine ring and the *t*-butyl group, respectively.

Anal. Calcd. for $C_9H_{17}NO$: C, 69.62; H, 11.06; N, 9.02. Found (155 (mass spectroscopy)): C, 69.41; H, 11.03; N, 8.78.

N-Ethylformamide

In the procedure described generally in the text, 3.7 g formic acid (0.08 mole) was allowed to react with 4.5 ml $TiCl_4$ (0.04 mole) and excess ethylamine. *N*-Ethylformamide (5.05 g, 87%) was isolated by distillation of the THF solution obtained by filtration of the reaction mixture, b.p. 94–96/12 Torr (ca. 200°/760 Torr), lit. 197–199° (9). It exhibited an n.m.r. spectrum consisting of a singlet at τ 2.0 (1H), a quintet at 6.7 (2H) and a triplet at 8.9 (3H). Molecular weight (mass spectroscopy) 73; the cracking pattern is consistent with this structure.

N,N-Diethylbenzamide

By a similar procedure, in hexane solvent, *N,N*-diethylbenzamide (5.35 g, 76%) was obtained from 5.76 g (0.04 mole) sodium benzoate, 2.2 ml $TiCl_4$ (0.02 mole), and excess diethylamine as a liquid, b.p. 75°/1 Torr (lit. 175°/135 Torr, 280–282°/760 Torr) (10). Structure confirmed by its mass spectrum: M^+ required, 177; found, 177; the cracking pattern is in accord with this structure.

N,N,N′,N′-Tetramethyl-1,4-cyclohexanedicarboxamide

By a similar procedure, in THF, *N,N,N′,N′*-tetramethyl-1,4-cyclohexanedicarboxamide (11.4 g, 67%) was obtained, from 13.8 g (0.083 mole) $TiCl_4$ and 40 ml (6 mole) dimethylamine, by recrystallization from THF as colorless crystals, m.p. (corr.) 201–203°, lit., 201° (11). The n.m.r. spectrum consisted of a broad doublet centered at τ 7.0 (12H), a very broad resonance at τ 7.4 (2H), and an unresolved complex multiplet at τ 8.3 (8H).

Tetramethyloxamide

Titanium tetrachloride (4.5 ml, ca. 0.04 mole) was placed in a Pyrex citrate bottle, under nitrogen, *carefully* cooled to −70° in a dry ice–acetone bath, and attached through a rubber stopper to an evacuated manifold. The bottle and manifold were evacuated to about 100 Torr, then pumping was discontinued and about 50 ml dimethylamine allowed to distil into the citrate bottle. When the operation was complete, the bottle was stoppered and allowed to warm slowly toward room temperature, during which time the $TiCl_4$ melted and reacted vigorously with the dimethylamine. When this reaction had subsided the vessel was cooled to about −20° and oxalic acid (3.60 g, 0.04 mole) was added. The bottle was again capped and heated in a water bath at 40° for 3 days. The bottle was then cooled to 0°, opened, and 50 ml THF added, plus a few drops of water. The resulting mixture was filtered and from the filtrate the product was isolated by evaporation of solvent. Recrystallization from THF gave 4.20 g (73%) of tetramethyloxamide, m.p. 79–80° (12), which exhibited a single resonance in the n.m.r. ($CDCl_3$ solution) at 7.1 τ identical with that of an authentic sample.

Formylation of 1,2-Dimethylhydrazine

In the manner described above 13.3 g (0.1 mole) 1,2-dimethylhydrazine dihydrochloride and 9.2 g (0.2 mole) formic acid were allowed to react with 12 ml (0.11 mole) $TiCl_4$ in the presence of excess triethylamine for 7 days at 25° in THF solvent. The liquid obtained by evaporation of the solvent from the filtrate of this reaction mixture was distilled under vacuum, boiling 70–110°/8 Torr. Analysis of this mixture by gas–liquid chromatography (g.l.c.) (SE-52 on Diatoport-5, initial temperature 85°, programmed rise 2°/min) showed the presence of 2 major components which were identified by mass spectrometry as 1-formyl-1,2-dimethylhydrazine (**1**, M^+ = 88 and fragments M—CH_3, M—CO, M—CHO, and M—NCH_3) and 1,2-diformyl-1,2-dimethylhydrazine (**2**, M^+ = 116 and fragments M—CO, M—CHO, and M/2). Samples of the 2 compounds, not analytically pure, were obtained by preparative g.l.c. (KOH/Carbowax, 50° initial, 5.9°/min rise to 200°), the yields quoted (above) were determined from the g.l.c. results. Compound **1** exhibits an n.m.r. spectrum (38°, $CDCl_3$ solvent, TMS internal standard) consisting of singlets at τ 1.6 (3H), 1.9 (1H), 5.8 (4H, broad), 6.90 (3H), 6.95 (9H), 7.35 (9H), and 7.40 (3H) which becomes at 100° singlets at 1.9, 6.0, 6.9, and 7.4 (area 1:1:3:3); and i.r. bands at

3500 and 1690 cm^{-1}. Compound **2** exhibits an n.m.r. spectrum (38°, $CDCl_3$ TMS) consisting of 4 resonances near τ 1.9 (relative areas 2:1:0.16:1) and 4 resonances between τ 6.7 and τ 6.9 (areas 1:0.16:2:1) which becomes at 100° 2 singlets at τ 1.8 (1H) and 6.9 (3H); its i.r. spectrum includes a band at 1700 cm^{-1} but none near 3500 cm^{-1}.

1. R. T. COWDELL and G. W. A. FOWLES. J. Chem. Soc. 2522 (1960).
2. W. A. WHITE and H. WEINGARTEN. J. Org. Chem. **32**, 213 (1967).
3. H. WEINGARTEN, J. P. CHUPP, and W. A. WHITE. J. Org. Chem. **32**, 3246, (1967).
4. W. R. TROST. Can. J. Chem. **30**, 835 (1952); M. ANTLER and A. W. LAUBENGAYER. J. Amer. Chem. Soc. **77**, 5250 (1955).
5. J. THIELE. Ber. **42**, 2575 (1909).
6. W. D. PHILLIPS. J. Chem. Phys. **23**, 1363 (1955).
7. L. C. BEHR. *In* Five- and six-membered compounds with nitrogen and oxygen. R. H. Wiley, *editor*, Interscience Publishers, New York, N.Y., 1962.
8. L. J. BELLAMY. Infra-red spectra of complex molecules. 2nd Ed., John Wiley and Sons, Inc., New York, N.Y., 1954. p. 203 *et seq.*
9. R. C. WEAST. *Editor*. Handbook of chemistry and physics, 47th ed. The Chemical Rubber Publishing Co., Cleveland, Ohio, 1966. p. C-327.
10. F. HALLMAN. Ber. **9**, 846 (1877); L. H. ULICH and R. ADAMS. J. Amer. Chem. Soc. **43**, 660 (1921).
11. F. H. MCMILLAN, K. A. KUN, C. B. MCMILLAN, and J. A. KING. J. Amer. Chem. Soc. **78**, 4077 (1956).
12. A. D. N. FRANCHIMONT and H. A. ROUFFAER. Rec. Trav. Chim. **13**, 331 (1895).

Can. J. Chem. Downloaded from www.nrcresearchpress.com by 210.87.254.5 on 09/05/12
For personal use only.

Can. J. Chem. Downloaded from www.nrcresearchpress.com by 210.87.254.42 on 09/05/12
For personal use only.

Triplet state of orotic acid and orotic acid methyl ester in solution[1,2]

R. W. YIP AND W. D. RIDDELL[3]
Division of Chemistry, National Research Council of Canada, Ottawa, Canada

AND

A. G. SZABO
Division of Biology, National Research Council of Canada, Ottawa, Canada

Received October 14, 1969

Flash photolysis of orotic acid and orotic acid methyl ester in aqueous solution was studied. The transients were identified as triplet excited states on the basis of their lifetimes, sensitization, quenching, and self-quenching experiments. The rate constants for self-quenching and for decay of the triplet were measured and discussed in terms of dimerization and competing unimolecular and pseudo-unimolecular processes. A triplet energy of 60 kcal mole^{-1} was deduced for both orotic acid and orotic acid methyl ester from triplet energy transfer measurements.

Canadian Journal of Chemistry, **48**, 987 (1970)

The photochemistry of pyrimidines (1) is interesting both biologically and chemically. In the first instance ultraviolet (u.v.) irradiation of microorganisms (2) causes mutagenic and lethal effects and is a powerful probe to investigate repair mechanisms operating in the cell (3). Photodimerization of the pyrimidines is one of the reactions which contributes to these effects. Chemically, the mechanisms of photodimerization of pyrimidines bear directly on the general and important problem of the nature of the photochemically induced cycloaddition process of unsaturated carbonyl compounds. Specific questions yet to be answered concern the particular spin state in a given solvent and state of aggregation (4), the extent of self-quenching caused by dimer formation, and the rate constant for reaction by triplet excited states. On a slightly more subtle level, questions regarding the intervention of complex formation preceding dimer formation have lately been raised (5, 6).

Sztumpf and Shugar (7) have shown that orotic acid (**1***a*) and orotic acid methyl ester (**1***b*) (methyl orotate) dimerize in aqueous solution, and that the rate of dimerization is reduced by oxygen, confirming the earlier observations of Beukers and Berends (8) on the oxygen effect. From a quantitative analysis of the oxygen quenching (assuming a quenching rate constant, k_q, of oxygen as $10^{10}\ M^{-1}\ s^{-1}$) Sztumpf–Kulikowska *et al.* (9) inferred a lifetime of 2 μs for the reactive state, almost certainly the triplet. We therefore felt that there was a good probability of directly observing the triplet state of orotic acid and of methyl orotate. Subsequently, we have learned that Boag and Godfrey (10) had observed a short-lived transient prior to our investigation. In this paper we have identified the triplet state of orotic acid in aqueous solution by sensitization, quenching, and self-quenching experiments. We have measured the rate constants for dimerization and for decay of the triplet (in the absence of dimerization) and for triplet energy transfer in aqueous solution. The experimental rate constants for energy transfer are important in themselves in connection with the theory of triplet energy transfer and especially if reasonable values of triplet lifetimes are to be obtained by Stern–Volmer type quenching experiments. Most experiments were carried out with the methyl ester to avoid the complication of dissociation of the acid to its anion since we have no information on the pK of the triplet excited state. During the course of our investigation, Herbert *et al.* (11) reported the observation of the triplet state of orotic acid in water at pH 5 by flash photolysis and measured the rate constants for reactions under this condition.

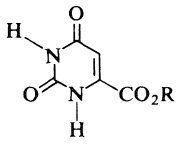

1

a R = H
b R = CH_3

[1]Issued as NRCC No. 11124.
[2]Presented in part at the Northeast Photobiology Group, Cornell University, Ithaca, New York, on May 10, 1969.
[3]NRCC Postdoctoral Fellow, 1968–1969.

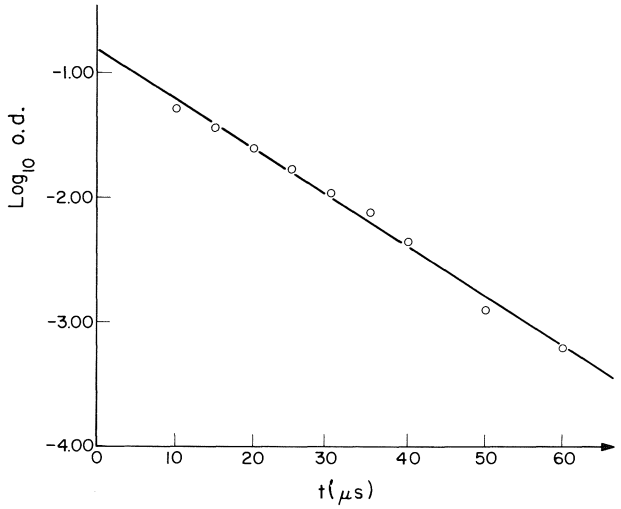

FIG 1. Plot of $\log_{10}$ o.d. vs. time (μs); [methyl orotate] = 4×10^{-5} *M*; monitoring wavelength, 340 mμ; data obtained from Fig. 2.

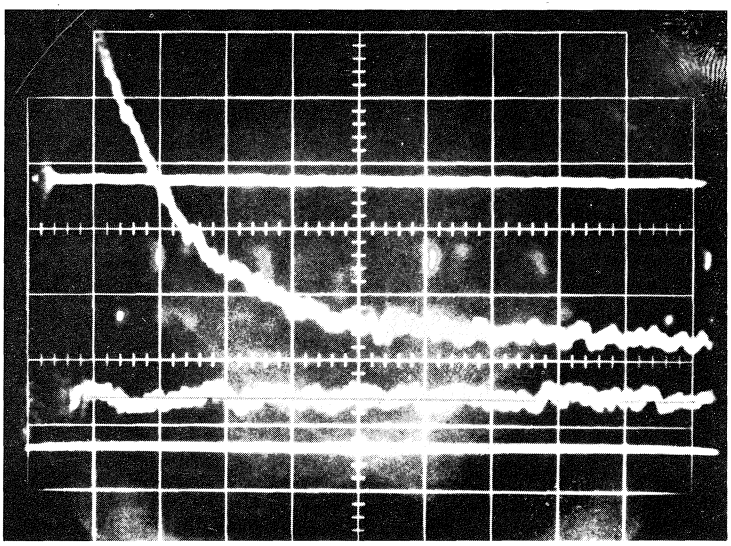

FIG. 2. Typical oscilloscope trace of transient observed on flashing aqueous solutions of methyl orotate or orotic acid; [methyl orotate] = 4×10^{-5} *M*; monitoring wavelength, 340 mμ; timebase, 10 μs/cm; transient voltage, 0.05 V/cm; photoflash energy, 67 J.

Results

Flash excitation of either orotic acid or its methyl ester in aqueous solution at p*H* 5 produced a transient which decayed by first order kinetics (eq. [1]) (Fig. 1). A typical trace is shown

$$[1] \qquad 2.303 \log (\text{o.d.}) = k_{obs}t + \text{constant}$$

in Fig. 2. Flash excitation of aqueous solutions of orotic acid and HCl (p*H* 0.6) (or to a lesser extent with H_2SO_4, p*H* 0.7), produced a long-lived transient in addition to the principal first order transient. The long-lived transient could not be detected when the photoflash was filtered with 1 cm of neat acetic acid. Flash excitation of an HCl (p*H* 0.6) solution alone without filter gave a strong long-lived transient. Therefore the long-lived transient observed with orotic acid at p*H* 0.6 most probably originates from photolysis of the HCl. The transient observed on photolysis of either orotic acid or its methyl ester was assigned as the triplet state of these pyrimidines on

Can. J. Chem. Downloaded from www.nrcresearchpress.com by 210.87.254.42 on 09/05/12
For personal use only.

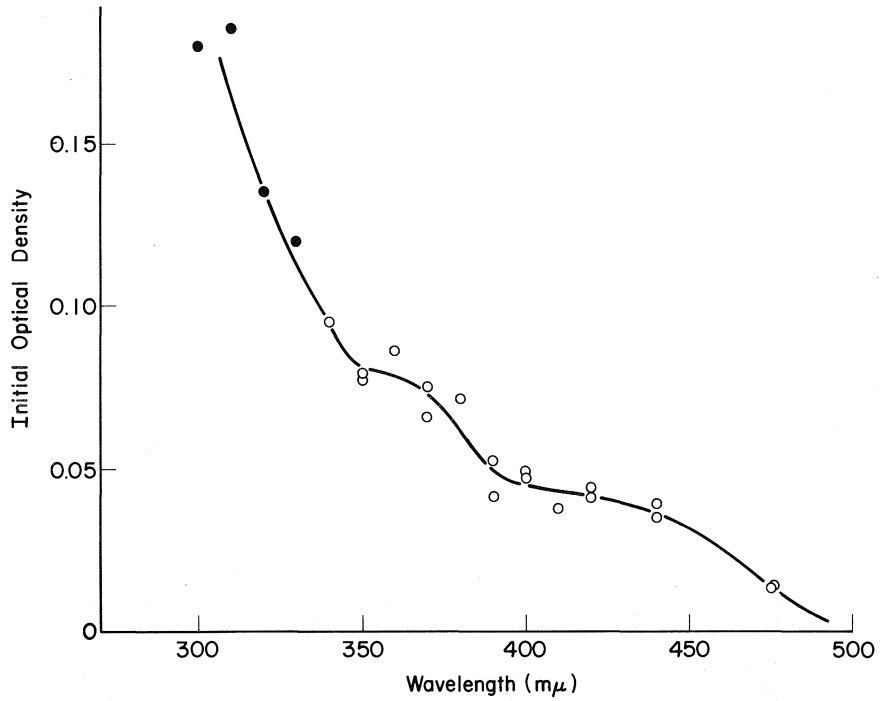

FIG. 3. Absorption spectrum of triplet orotic acid in aqueous solution, pH 5; ○ [orotic acid] = 2×10^{-5} M (half bandwidth, 11 mμ); ● [orotic acid] = 0.5×10^{-5} M (half bandwidth, 20 mμ); effective pathlength 16 cm; photoflash filtered through 2 mm Vycor glass; photoflash energy, 108 J.

the basis of the following experiments and observations.

Transient Absorption Spectra

The absorption spectra of the transients from flash excitation of orotic acid and methyl orotate in water at pH 5 are shown in Figs. 3 and 4. Both are very broad, extending from about 475 mμ, no clear maxima being evident in the region scanned. To obtain reliable data from wavelengths below 320 mμ, it was necessary to work with very dilute solutions. Because of ground state absorption, it was not possible to scan much below 300 mμ. Our results on the spectrum of the transient from orotic acid are not in agreement with a maximum at 320 mμ as reported by Herbert *et al.* (11).

Acetone Sensitization

Acetone was chosen as a sensitizer on the basis of its triplet energy (12), solubility, and ground state absorption. In addition, there is little overlap of the absorption spectrum of triplet acetone (13) with that of the acceptor transient. Moreover the lifetime of triplet acetone in aqueous solution, 18 μs, (13) is sufficiently long to permit efficient transfer to methyl orotate at low ester concentrations. At orotate concentrations of greater than 1–2 $\times 10^{-4}$ M, the transient lifetime lies beyond the time resolution of the instrument because of self-quenching.

Flash excitation, through a 2 mm Pyrex filter, of an aqueous solution of 0.05 M acetone and 2×10^{-5} M methyl orotate gave a strong signal at 340 mμ (Fig. 5*a*) which decayed by first order kinetics with a lifetime of 19 μs. Note the slow rise time (compared with the direct photolysis shown in Fig. 2) of the sensitized transient which is expected for an acceptor triplet (14). While the greater part of the transient absorption was due to sensitization, a small part of the absorption was the result of direct excitation of the methyl ester, as was revealed in a separate control experiment. In this experiment, 2×10^{-5} M methyl orotate alone was flashed under identical conditions (Fig. 5*b*). Finally, to demonstrate that the acetone triplet absorption does not interfere, a solution containing 0.05 M acetone alone was flashed under the same conditions and as can be seen in Fig. 5*c* gave no measurable transient at 340 mμ.

Can. J. Chem. Downloaded from www.nrcresearchpress.com by 210.87.254.42 on 09/05/12
For personal use only.

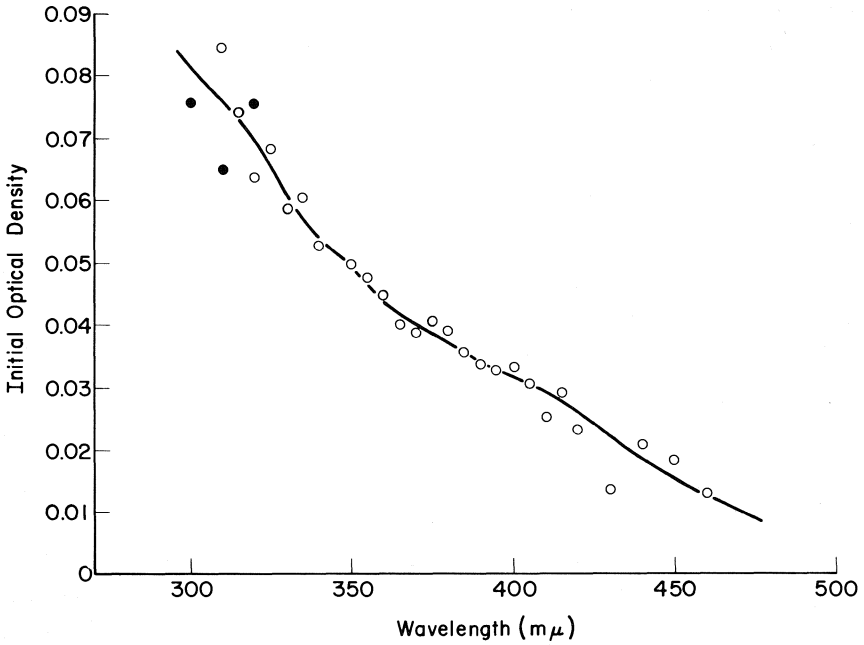

FIG. 4. Absorption spectrum of triplet methyl orotate in aqueous solution, pH 5; ○ [methyl orotate = 2×10^{-5} M (half bandwidth, 11 mμ); ● [methyl orotate] = 0.25×10^{-5} M (half bandwidth, 20 mμ); effective pathlength, 20 cm; photoflash energy, 92 J.

Quenching of Sensitizer Triplets by Methyl Orotate in Aqueous Solution

The rates of decay of sensitizer triplets (T) under certain conditions can be represented by eq. [2],

$$[2] \qquad \frac{d[T]}{dt} = k_o + k_q [Q],$$

where [Q] is the concentration of added quencher and k_0 is a composite pseudo first order rate constant. In the present work, low sensitizer concentrations ($1 \times 10^{-5} - 3.7 \times 10^{-5}$ M) and low flash energies ($\sim$ 100 J) were used to reduce the likelihood of complex formation and self-quenching by the sensitizer, and triplet–triplet annihilation which would introduce a term which is second order in triplet-concentration. In all samples except one, excellent first order rate plots were obtained. The exception was the case of naphthalene with no added methyl orotate. Here, long triplet lifetime and lack of competitive quenching from the presence of added quencher resulted in considerable deviation from first order decay due to triplet–triplet annihilation. However, first order kinetics was easily restored in this case by adding a Corex filter to reduce the flash intensity and hence the triplet concentration.

The results of these quenching experiments, recorded in Table 1, show a clear correlation between k_q and the triplet energy of the sensitizer.

Quenching of Methyl Orotate Transient in Aqueous Solution

The lifetime of the transient observed on flash excitation of methyl orotate in water was reduced by the addition of 2,4-hexadien-1-ol and dimethyl fumarate (E_T 59.5 and $\sim$ 60 kcal mole^{-1} respectively (15, 16)). By varying the concentration of the quenchers, rate constants of $2.88 \pm 0.15 \times 10^9$, and 2.3×10^9 M^{-1} s^{-1} were obtained for quenching by hexadienol and by fumarate respectively. The extent of consumption of ground state methyl orotate in the presence and absence of hexadienol is shown in Fig. 6. Clearly, the rate of decomposition of methyl orotate is markedly reduced in the presence of hexadienol. Hexadienol quenching of the transient from orotic acid in water was also carried out and a k_q of $2.93 \pm 0.12 \times 10^9$ M^{-1} s^{-1} was obtained (Fig. 7). It was not possible to obtain a rate constant for hexadienol quenching of the transient from orotic acid in water at pH 0.6 because

Can. J. Chem. Downloaded from www.nrcresearchpress.com by 210.87.254.42 on 09/05/12
For personal use only.

Can. J. Chem. Downloaded from www.nrcresearchpress.com by 210.87.254.42 on 09/05/12
For personal use only.

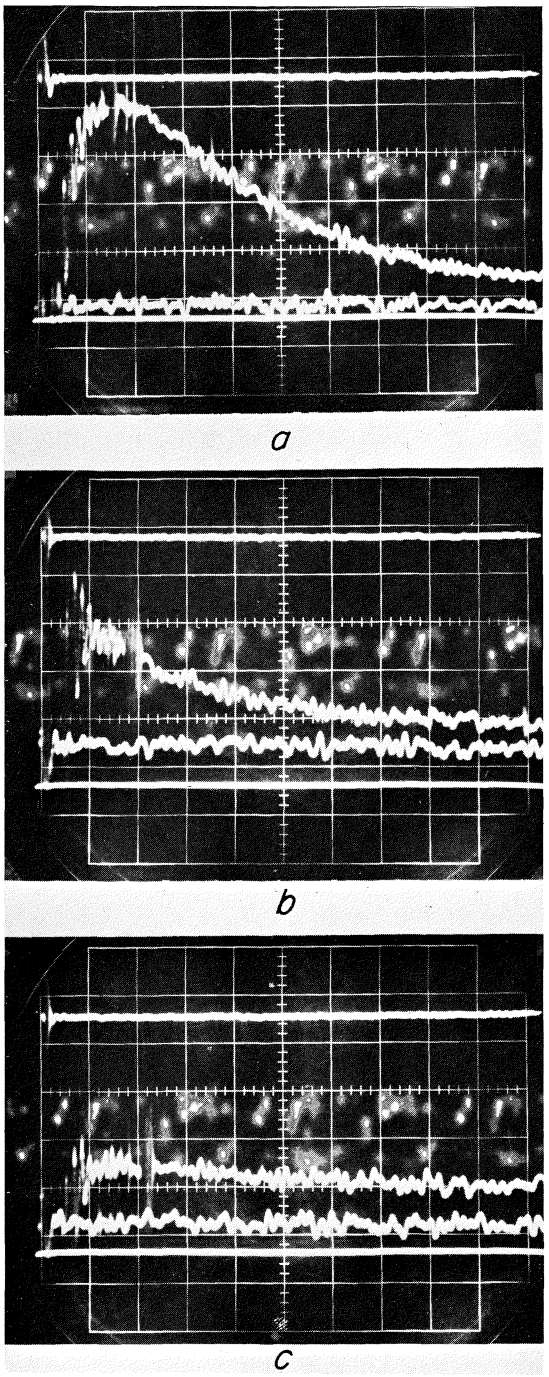

FIG. 5. Oscilloscope traces showing acetone sensitized formation of triplet methyl orotate in aqueous solution. Conditions for all 3 traces are identical. Monitoring wavelength, 340 mμ, optical half bandwidth, 45 mμ; photoflash filtered through 2 mm Pyrex glass; timebase, 10 μs/cm; in each trace the lowest line is the baseline; uppermost line is the initial transmission, 0.1 V/cm; transient voltage, 0.01 V/cm. *a*, (upper trace) [acetone] = 0.05 *M*, [methyl orotate] = 2×10^{-5} *M*; *b*, (middle trace) [methyl orotate] = 2×10^{-5} *M* (acetone absent); *c*, (lower trace) [acetone] = 0.05 *M* (methyl orotate absent).

of the rapid dehydration of hexadienol to hexatriene under these conditions.

For comparison of the above-mentioned quenching rate constants with those of triplet energy transfer in aqueous solution, the rate constants for quenching of triplet excited 2-acetonaphthone (E_T 59.3 kcal mole^{-1} (17, 18)) and 1-acetonaphthone (E_T 58 kcal mole^{-1}, (19)) by hexadienol in aqueous solution were also measured. The hexadienol quenching results are summarized in Table 2.

Rate Constants for Photodimerization of Orotic Acid and Methyl Orotate in Aqueous Solutions

The observed pseudo first order rate constant k_{obs} for decay of the transient in the presence of orotic acid (OA) (or its methyl ester) can be written as eq. [3], where k_0 is the rate constant at

$$[3] \qquad k_{obs} = k_0 + k_{dim}[OA]$$

infinite dilution of orotic acid. Values of k_{dim} were obtained from the gradients of plots of k_{obs} against [OA] (Figs. 8, 9) and are recorded together with values of k_0 in Table 3. The results show that these values of k_{dim} for orotic acid at p*H* 0.6 and methyl orotate at p*H* 5 (both neutral species in the ground state), are very similar (1.91×10^9 and 2.20×10^9 M^{-1} s^{-1}, respectively) and are significantly higher than that for orotic acid at p*H* 5 (1.13×10^9 M^{-1} s^{-1}) where the acid is fully dissociated in the ground state. In absolute terms, these rate constants are exceedingly large and are almost diffusion-controlled.

Discussion

Identification of the Transient

A transient lifetime of 78 μs observed for flash excitation of orotic acid at p*H* 5 is considerably longer than, but of the correct order of magnitude expected for, the lifetime of the triplet inferred on the basis of the oxygen quenching measurements of Sztumpf–Kulikowska *et al.* (9) and of the experimentally measured k_q for oxygen quenching of the transient (11). First order decay kinetics are interpretable in terms of a triplet excited state rather than a radical intermediate. Quenching by

TABLE 1

Rate constants for quenching of sensitizer triplets by methyl orotate in aqueous solution*

Sensitizer (concentration M)	E_T (kcal mole^{-1})	Analysis wavelength (mμ)	τ_0† (μs)	$k_q \times 10^{-9}$ (M^{-1} s^{-1})
Xanthen-9-one§ (1.14×10^{-5})	74	600	37.7	2.78 ± 0.24
Naphthalene¶ (1.72×10^{-5})	60.9	415	246	2.35 ± 0.16
				(2.22 ± 0.07)‡,¶
2-Acetonaphthone‖ (1×10^{-5})	59.3	430	244	0.71 ± 0.09
1-Acetonaphthone‖ (1×10^{-5})	56.4	500	277	0.82 ± 0.04
9-Fluorenone (3.7×10^{-5})	53.3	430	110	0.026 ± 0.01

*pH 5.
†Lifetime of unquenched sensitizer.
‡Rate constant for quenching of naphthalene triplet by orotic acid in aqueous solution at pH 5. Naphthalene concentration 2.7×10^{-5} M.
§Soft glass as filter.
‖Pyrex as filter.
¶Corex as filter.

ground state orotic acid (or methyl orotate) referred to here as self-quenching implicates the transient in the photodimerization process and the exceedingly high self-quenching rate constants of 10^9 M^{-1} s^{-1} (see Table 3) demonstrate that the transient is an extremely reactive species as might be expected of an excited state molecule.

The assignment of the triplet state to the observed transient is further supported by the hexadienol and dimethyl fumarate quenching results. The quenching rate constants, which appear to represent a limiting value for triplet energy transfer characteristic of the solvent, are essentially identical with those obtained for the quenching of triplet 1-acetonaphthone and 2-acetonaphthone by hexadienol and for the quenching of triplet xanthenone by methyl orotate. As well, substantial quenching by a

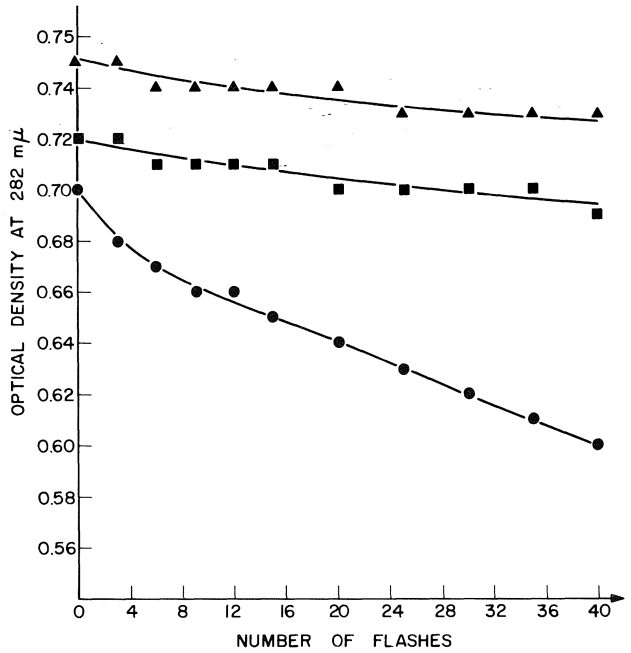

FIG. 6. Plot of decrease in optical density at 282 mμ with successive flashes of aqueous solutions of [methyl orotate] = 1×10^{-5} M and varying [hexadienol]; ● [hexadienol] = 0; ■ [hexadienol] = 3×10^{-5} M; ▲ [hexadienol] = 1×10^{-4} M. (The variation in optical density at 0 flash results from minor variations in [methyl orotate] and minor absorption from the added hexadienol.)

Can. J. Chem. Downloaded from www.nrcresearchpress.com by 210.87.254.42 on 09/05/12
For personal use only.

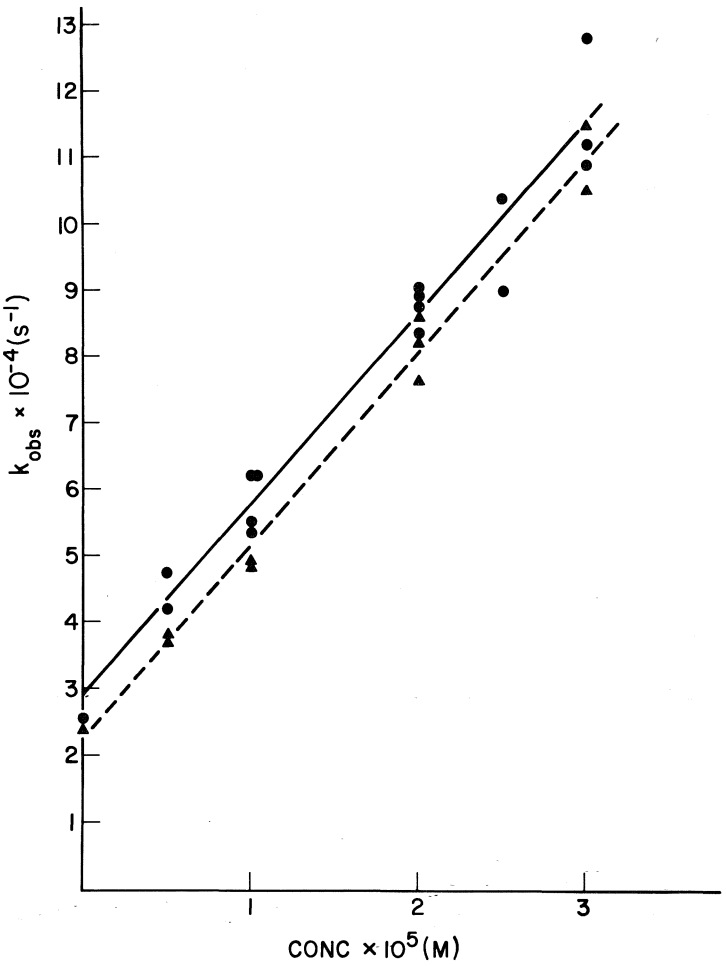

FIG. 7. Plot of k_{obs} vs. [hexadienol] for quenching studies of methyl orotate and orotic acid, pH 5, triplets; ● [methyl orotate] = 1×10^{-5} M; ▲ [orotic acid] = 1×10^{-5} M.

chemical reaction between triplet methyl orotate and hexadienol is eliminated by the negligible rate of decrease of ground state methyl orotate in the presence of hexadienol (see Fig. 6).

TABLE 2
Quenching of pyrimidine transients and sensitizer triplets by 2,4-hexadien-1-ol*

Sensitizer†	E_T (kcal mole^{-1})	$k_q \times 10^{-9}$ (M^{-1} s^{-1})
Orotic acid	—	2.93 ± 0.12
Methyl orotate	—	2.88 ± 0.15
		(2.3 ± 0.2)‡
2-Acetonaphthone	59.3	2.69 ± 0.08
1-Acetonaphthone	56.4	2.41 ± 0.08

*In aqueous solution at pH 5.
†Concentration of sensitizer 1×10^{-5} M.
‡Rate constant for quenching of methyl orotate transient by dimethyl fumarate in aqueous solution at pH 5.

The results of the acetone sensitization confirm the triplet assignment. The control experiments show that the transient observed on sensitization arises mainly from excitation of acetone but is not triplet acetone. The lifetime of the sensitized species is, within experimental error, identical with the lifetime of the transient observed from directly excited methyl orotate. Since singlet energy transfer is unlikely due to the low concentration of methyl orotate used (2×10^{-5} M), the sensitized species is triplet methyl orotate formed by triplet energy transfer. The slow risetime of the sensitized species is consistent with this view.

Can. J. Chem. Downloaded from www.nrcresearchpress.com by 210.87.254.42 on 09/05/12
For personal use only.

Can. J. Chem. Downloaded from www.nrcresearchpress.com by 210.87.254.42 on 09/05/12
For personal use only.

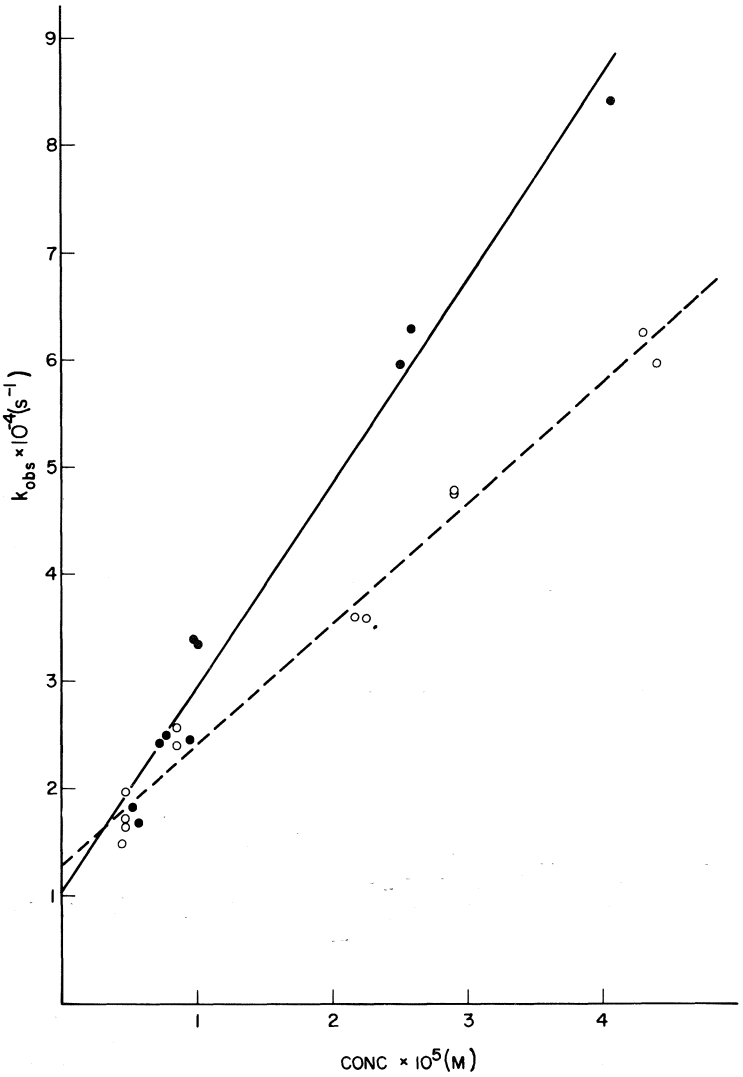

FIG. 8. Plot of k_{obs} vs. [orotic acid]; ● p*H* 0.6; ○ p*H* 5.

Triplet Energy Transfer in Solution and Triplet Energy of Methyl Orotate and Orotic Acid

The measured rate constants for methyl orotate quenching of triplet xanthenone (E_T 74 kcal mole^{-1}) and naphthalene (E_T 61 kcal mole^{-1}) shown in Table 1 are $\sim 2.5 \times 10^9$ M^{-1} s^{-1} and this suggests that in both cases, triplet energy transfer is exothermic. It appears to be the general case, at least for non-viscous solvents, that the experimental value of k_q is lower than the value calculated by the Debye equation (7×10^9 M^{-1} s^{-1} for water at 23 °C) by a factor of at least 3 (20). With sensitizers having triplet energies of 59 kcal mole^{-1} or less, quenching by methyl orotate becomes substantially less efficient. On the basis of these quenching results, we infer that the energy of the lowest triplet state of methyl orotate is close to 60 kcal mole^{-1}. Since orotic acid at p*H* 5 (which exists in the anion form in the ground state) quenches naphthalene triplet with a rate constant of 2.22×10^9 M^{-1} s^{-1}, almost identical with that of the ester, therefore the triplet energy of orotic acid is most probably the same as the ester. The triplet energies thus deduced for the neutral species and for the anion, are in

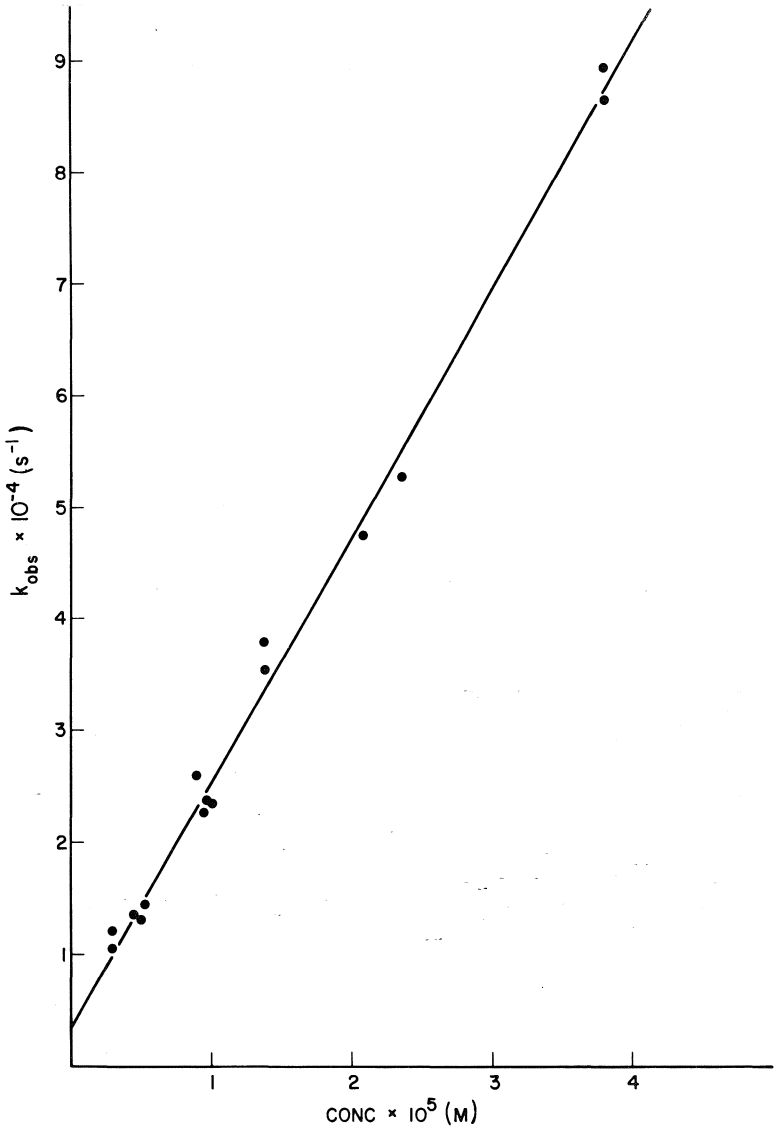

FIG. 9. Plot of k_{obs} vs. [methyl orotate].

agreement with the value obtained by Haug and Douzou (21) for orotic acid from phosphorescence measurements (see Table 4).

Hexadienol quenching of triplet methyl orotate and orotic acid at pH 5 is surprisingly efficient ($k_q \sim 3 \times 10^9\ M^{-1}\ s^{-1}$). This value taken together with the quenching rates of triplet 2-acetonaphthone (E_T 59.3 kcal mole^{-1}) and 1-acetonaphthone (E_T 56.4 kcal mole^{-1}) by hexadienol indicates that the reported E_T of 2,4-hexadienol of 59.6 kcal mole^{-1} (15) should be revised to a lower value. It should be kept in mind however, that the optical triplet energies of dienes are known with less certainty than are those of aromatic molecules. Chemical quenching is unlikely to account for the large k_q because of the effectiveness with which hexadienol suppresses the consumption of methyl orotate (Fig. 6). This implies that if products are formed between methyl orotate and hexadienol, the quantum yield of formation is low. The rate constants for quenching of triplet orotic acid at pH 1.1 and 5

Can. J. Chem. Downloaded from www.nrcresearchpress.com by 210.87.254.42 on 09/05/12
For personal use only.

TABLE 3

Rate constants for photodimerization* of orotic acid and methyl orotate in aqueous solution

Compound	pH	% Dissociated in the ground state	$k_0 \times 10^{-4}$ (s^{-1})	τ_0 (μs)	$k_{dim} \times 10^{-9}$ ($M^{-1}\ s^{-1}$)
Orotic acid	5	100	1.27 ± 0.11	78 ± 6	1.13 ± 0.05
Orotic acid	0.6	6	1.03 ± 0.19	97 ± 18	1.91 ± 0.1
Methyl orotate	5	—	0.35 ± 0.09	287 ± 72	2.20 ± 0.05

*Vycor as filter.

TABLE 4

Triplet energy of orotic acid and methyl orotate

Compound	Solvent	E_T (kcal $mole^{-1}$)	Method	Reference
Orotic acid	Propylene glycol/H_2O 1:1 (v/v)	69.8	Phosphorescence*	23
Orotic acid	Propylene glycol/H_2O 1:1 (v/v) (in HCl)	60.9	Phosphorescence*	23
Orotic acid	Ethanol	60.9	Phosphorescence*	22
Orotic acid	DMF/EtOH/ether‡ 1:1:1.7 (v/v)	60.9	Phosphorescence*	21
Orotic acid	H_2O§	~60	Energy transfer†	This work
Methyl orotate	H_2O§	~60	Energy transfer†	This work

*77 °K.
†300 °K.
‡pH 12 ref. (24).
§pH 5.

by oxygen reported by Whillans and Johns (25) are considerably lower than our values for hexadienol. These workers also found a different k_q for the neutral form as compared with the anion. In the case of oxygen quenching of triplet fluorescein in aqueous solution, Kasche and Lindqvist (26) obtained a k_q of $1.2 \times 10^9\ M^{-1}\ s^{-1}$ for both the monoanion and the neutral molecule. It is interesting that the quenching rate of 1-acetonaphthone triplet by methyl orotate is slightly greater than that of 2-acetonaphthone (0.82×10^9 cf. $0.71 \times 10^9\ M^{-1}\ s^{-1}$). In view of the inefficiency of endothermic energy transfer in this case other processes may compete more effectively, such as chemical reaction.

Lifetime and Reactivity of the Triplet State

The lifetime of triplet orotic acid determined in this work by flash photolysis (97 μs at pH 0.6, Table 3) is considerably longer than the value obtained by Sztumpf–Kulikowska *et al.* (9) from their oxygen quenching study of the rates of disappearance of orotic acid in aqueous solution. If we recalculate their results using the k_q determined by Whillans and Johns (25) instead of $10^{10}\ M^{-1}\ s^{-1}$ used by Sztumpf–Kulikowska and co-workers (9), a lifetime of 5 μs can be inferred from the oxygen quenching studies. The discrepancy between the recalculated lifetime and the directly measured lifetime would seem large but is perhaps not unexpected. All triplet lifetimes indirectly inferred from triplet quenching studies depend on a reaction of the triplet excited state and it therefore requires a relatively long extrapolation to obtain the lifetime in the absence of reaction. On the other hand, lifetimes obtained by flash photolysis are more accurate in the absence of reaction when the lifetime is longest and the extrapolation to infinite dilution least.

The rate constant k_0 for decay of triplet orotic acid or methyl orotate in the absence of self-quenching does not reflect any impurity quenching. We can represent the composite rate constant k_0 by eq. [4], where the term $k_q(Q)$ rep-

$$[4] \qquad k_0 = k_q(Q) + k_{chem} + k_i$$

resents impurity quenching of the triplet, k_{chem} represents a unimolecular reaction of the triplet, and k_i, the intrinsic rate of decay of the triplet. If $k_q(Q)$ were to dominate, we would expect identical decay times for triplet orotic acid and methyl orotate in water, contrary to the results shown in Table 3. In addition, if k_i were independent of phase, the phosphorescence results of Haug and Douzou (21) would suggest that k_i

Can. J. Chem. Downloaded from www.nrcresearchpress.com by 210.87.254.42 on 09/05/12
For personal use only.

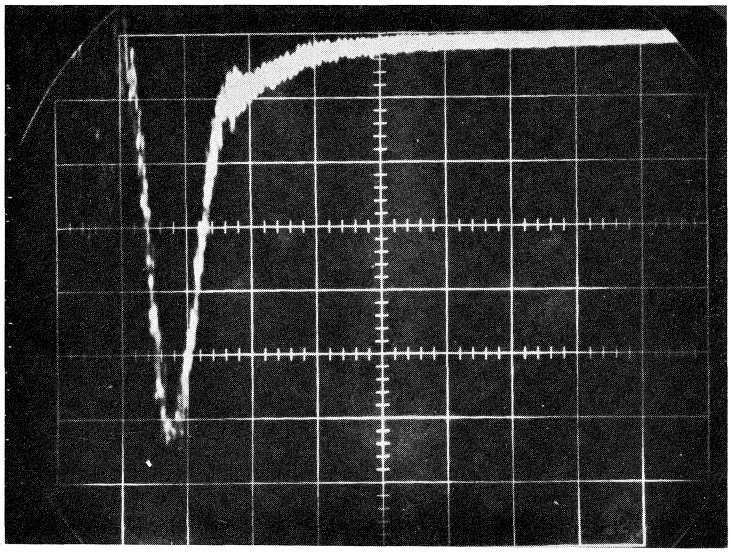

FIG. 10. Oscilloscope trace of photoflash pulse; monitoring wavelength, 350 mμ; timebase, 1 μs/cm; voltage, 0.5 V/cm.

might be small compared to k_0. We might therefore speculate that k_0 is in fact a reflection of unimolecular reaction(s) of the triplet state, for instance, decarboxylation or ring cleavage.

At present we have no evidence to suggest that the self-quenching rate constant k_{dim} does not represent the rate constant for dimerization. The value of k_{dim} for triplet orotic acid at p*H* 5 is approximately a factor of 2 smaller than either the values for orotic acid at p*H* 0.6, or methyl orotate at p*H* 5. The smaller value would seem reasonable if triplet orotic acid exists in the anion form at p*H* 5. Since ground state orotic acid is fully dissociated at p*H* 5, the rate constant for reaction between two like charged species would be expected to be slower than for reaction between neutral species.[4] Wagner has reported rate constants for dimerization of uracil and thymine obtained from quenching studies and found a smaller value for thymine as compared to uracil. He attributed the differences to steric effects. Comparison of his values with ours shown in Table 3 would suggest that such steric effects are not important and that the electronic distribution of the molecule is the more important factor controlling reactivity (6).

[4]The Debye treatment for diffusion rates predicts a factor of 0.45 or 0.60 for spheres of 5 or 7.5 Å, respectively, of similar unit charge as compared with 2 uncharged species (20*b*).

Experimental

Apparatus

The flash apparatus was identical with the 5 μs dual beam flash photoelectric apparatus already described (27), except for the discharge circuit and lamps. Instead of series connections of the lamps, each of the 2 lamps was operated from 2 separate capacitor-spark gap circuits which are triggered synchronously. Each circuit used a 0.3 μF 25 kV capacitor. The lamps had a cross-sectional area of 3.74 mm^2 and an arc length of 100 mm and were filled with 4 cm argon and 1 cm hydrogen. A light pulse width of 0.9, 1.1, and 2.3 μs at 1/2, 1/3, and 1/10 of its peak value respectively was obtained (Fig. 10). The absorption cells were all quartz in construction, 22 mm o.d. and 100 mm path length. For degassing they were connected to a Pyrex vessel by means of a graded seal.

Instruments

Gas–liquid chromatography (g.l.c.) was carried out using a Hewlett–Packard 5754 gas chromatograph with a flame ionization detector. Infrared (i.r.) spectra were determined on a Perkin–Elmer 257 i.r. spectrophotometer. Ultraviolet (u.v.) spectra were measured on a Cary 15, dual beam u.v. spectrophotometer. Nuclear magnetic resonance (n.m.r.) spectra were recorded on a Varian A-100 spectrometer, using tetramethylsilane as an internal standard. Melting points are uncorrected and were measured on a Fisher–Johns melting point apparatus. Low p*H* values were determined spectrophotometrically using *p*-nitroaniline according to the method outlined by Albert and Serjeant (28), otherwise p*H* was measured using a Radiometer p*H* meter.

Procedure

Prior to being filled with the sample solution the photolysis cell and degassing chamber were pumped continuously under high vacuum. During the pumping,

Can. J. Chem. Downloaded from www.nrcresearchpress.com by 210.87.254.42 on 09/05/12
For personal use only.

Can. J. Chem. Downloaded from www.nrcresearchpress.com by 210.87.254.42 on 09/05/12
For personal use only.

the apparatus was briefly flamed. Solutions were degassed under vacuum through several freeze–pump–thaw–shake cycles and the cell sealed off with a flame. No noticeable difference in lifetime was found using an oil diffusion pump as compared with a mercury diffusion pump.

The concentration of orotic acid or methyl orotate was monitored before and between flashes by u.v. absorption measurement of the 10 cm path photolysis cell using a Bausch and Lomb single beam double grating spectrophotometer.

Hexadienol solutions were degassed immediately upon preparation to prevent oxidation to the aldehyde. Neat hexadienol keeps well but very dilute solutions were easily oxidized. Dilute aqueous solutions of hexadienol dehydrate rapidly to the triene at pH 0.6.

The transient trace was shifted from the baseline to facilitate measurement. Sufficiently long sweep times were used to allow unambiguous definition of the baseline from the transient trace alone. Any variation in the shape of the baseline was used to correct the transient trace. In general, data were taken out to at least 2 half-lives of the transient. For each sample, at least 5 traces were taken and the results averaged. Data taken from the Polaroid photographs, or from their enlargements, were processed using an IBM 360/50 computer from which best value rate constants were obtained. The decay kinetics were plotted on an X–Y recorder linked to the output of the computer.

Materials

Orotic acid was obtained from Sigma Chemical Co. and was recrystallized from water and dried in a desiccator prior to use. Its pK_a was determined spectrophotometrically to be 1.7 (29).

Methyl orotate was prepared according to the method of Fox *et al.* (30) and was recrystallized from water and dried prior to use, m.p. 248–249° (lit. (30) m.p. 243–245°, (31) m.p. 248–250°); ν_{max} ($CHCl_3$), 3380, 1730, 1705, 1600 cm^{-1}; λ_{max} (H_2O) (log ε), 284 (3.89) mμ; δ (DMSO-d_6) 3.86 (3H, s), 6.04 (1H, d, J = 2 c.p.s.), 11.09 (1H, br), 11.36 (1H, br) p.p.m.

The sensitizers xanthen-9-one, 2-acetonaphthone, 1-acetonaphthone, and fluoren-9-one were obtained from J. T. Baker Chemical Co., and were used without further purification. Naphthalene was zone refined by Koch Light Laboratories. The 2,4-hexadienol was obtained from Aldrich Chemical Co., and distilled prior to use, b.p. (22 mm) 83–84°. The g.l.c. on C-20M, 6 ft, 100°, indicated it was largely a single isomer (90%). Dimethyl fumarate was prepared according to the method of Fischer Spiers (32) and purified by distillation, m.p. 102°. The g.l.c. on C-20M, 6 ft, 80°, indicated it to be free of dimethyl maleate and no impurity with concentration greater than 0.5% could be detected.

NOTE ADDED IN PROOF: We have identified and measured the kinetics of the triplet state of thymine in acetonitrile solutions and found that k_{dim} was $5.3 \times 10^8\ M^{-1}\ s^{-1}$ and the lifetime was 14 μs (Can. J. Chem. In press).

One of us (W.D.R.) wishes to thank the National Research Council of Canada for the award of a post-doctoral fellowship (1968–1969). We are grateful to Mr. Peter Tolg for his excellent technical assistance, and to Mr. R. Lauzon for assistance in the data processing. We are indebted to Mr. P. Clay for the development of the computer program.

1. (*a*) J. G. BURR. *In* Advances in photochemistry. Vol. 6. *Edited by* W. A. Noyes, Jr., G. S. Hammond, and J. N. Pitts. Interscience Publishers, Inc., New York. 1968. p. 193. (*b*) A. D. MCLAREN and D. SHUGAR. Photochemistry of proteins and nucleic acids. Pergamon Press, Inc., New York. 1964.
2. J. K. SETLOW. *In* Comprehensive biochemistry. Vol. 27; Photobiology, ionizing radiations. *Edited by* M. Florkin and E. H. Stotz. Elsevier Publishing Co., Amsterdam. 1967. p. 157.
3. B. S. STRAUSS. *In* Current topics in microbiology and immunology. Vol. 44. Springer-Verlag, Berlin. 1968. p. 1.
4. R. LISEWSKI and K. L. WIERZCHOWSKI. Chem. Commun. 348 (1969).
5. R. O. LOUTFY, P. DE MAYO, and M. F. TCHIR. J. Amer. Chem. Soc. **91**, 3986 (1969).
6. P. J. WAGNER and D. J. BUCHECK. J. Amer. Chem. Soc. **90**, 6530 (1968).
7. E. SZTUMPF and D. SHUGAR. Photochem. Photobiol. **4**, 719 (1965).
8. (*a*) R. BEUKERS and W. BERENDS. Biochim. Biophys. Acta, **38**, 573 (1960). (*b*) B. BEUKERS, J. IJLSTRA, and W. BERENDS. Rec. Trav. Chim. **78**, 879 (1959).
9. E. SZTUMPF-KULIKOWSKA, D. SHUGAR, and J. W. BOAG. Photochem. Photobiol. **6**, 41 (1967).
10. J. W. BOAG and T. GODFREY. Private communication, August, 1968.
11. M. A. HERBERT, J. W. HUNT, and H. E. JOHNS. Biochem. Biophys. Res. Commun. **33**, 643 (1968).
12. R. F. BORKMAN and D. R. KEARNS. J. Chem. Phys. **44**, 945 (1966).
13. G. PORTER and R. W. YIP. Unpublished observations.
14. S. ARAI and L. M. DORFMAN. J. Phys. Chem. **69**, 2239 (1965).
15. R. E. KELLOGG and W. T. SIMPSON. J. Amer. Chem. Soc. **87**, 4230 (1965).
16. G. S. HAMMOND, J. SALTIEL, A. A. LAMOLA, N. J. TURRO, J. S. BRADSHAW, D. O. COWAN, R. C. COUNSELL, V. VOGT, and C. DALTON. J. Amer. Chem. Soc. **86**, 3197 (1964).
17. J. G. CALVERT and J. N. PITTS, JR. Photochemistry. John Wiley and Sons, Inc., New York. 1967. p. 298.
18. W. G. HERKSTROETER, A. A. LAMOLA, and G. S. HAMMOND. J. Amer. Chem. Soc. **86**, 4537 (1964).
19. G. N. LEWIS and M. KASHA. J. Amer. Chem. Soc. **66**, 2100 (1944).
20. (*a*) P. J. DEBYE. Trans. Electrochem. Soc. **82**, 265 (1942). (*b*) E. F. CALDIN. Fast reactions in solution. Blackwell Scientific Publications, Oxford. 1964. p. 12.
21. A. HAUG and P. DOUZOU. Z. Naturforsch. **20***b*, 509 (1965).
22. M. CHARLIER and C. HÉLÈNE. Photochem. Photobiol. **6**, 501 (1967).
23. M. CHARLIER, C. HÉLÈNE, and M. DOURLANT. J. Chim. Phys. **66**, 700 (1969).
24. R. G. SHULMAN and R. O. RAHN. J. Chem. Phys. **45**, 2940 (1966).
25. D. W. WHILLANS, and H. E. JOHNS. Photochem. Photobiol. **9**, 323 (1969).

26. V. KASCHE and L. LINDQVIST. J. Phys. Chem. **68**, 817 (1964).
27. R. W. YIP. Rev. Sci. Instr. **40**, 1035 (1969).
28. A. ALBERT and E. P. SERJEANT. Ionization constants of acids and bases. Methuen and Co. Ltd., London. 1962. p. 78.
29. D. SHUGAR and J. J. FOX. Biochim. Biophys. Acta, **9**, 199 (1952).
30. J. J. FOX, N. YUNG, and I. WEMPEN. Biochim. Biophys. Acta, **23**, 295 (1957).
31. G. BISCARO and E. BELLONI. Ann. Soc. Chim. Milano, **18** II, 71 (1905).
32. A. I. VOGEL. Elementary practical organic chemistry. Longmans, Green and Co., Ltd. London. 1958. p. 310.

Can. J. Chem. Downloaded from www.nrcresearchpress.com by 210.87.254.42 on 09/05/12
For personal use only.

Can. J. Chem. Downloaded from www.nrcresearchpress.com by 210.87.254.42 on 09/05/12
For personal use only.

NOTES

Emission from benzene excited by pulse radiolysis

A. R. HORROCKS[1]

Department of Chemistry, University of British Columbia, Vancouver 8, British Columbia

Received October 20, 1969

The emission spectra from deaerated benzene solutions of varying concentration, excited by 3 ns duration electron pulses at dose rates of 10^{13} rads/s are described. These compare favorably with the photoexcited spectra for similar benzene systems. The effects of chloroform and oxygen on the emission from liquid benzene are reported.

Canadian Journal of Chemistry, **48**, 1000 (1970)

Benzene excited by ultraviolet light emits the well characterized excimer and monomer fluorescence when it is in concentrated solution or its liquid state (1, 2). Recent work (3, 4) concerning the irradiation of benzene by 100 keV electrons suggested that only excimer emission was observed from the liquid state at dose rates of 10^7 rads/s. Both monomer and excimer bands were reported to appear when the sample was irradiated by 100 keV X-rays at a dose rate of 100 rads/s. This difference in emission spectral profiles was attributed to a dose rate effect where the monomer emission is assumed to be quenched preferentially by species generated only at high dose rates.

This note reports the emission spectra of various benzene systems excited by a field-emission Febetron 600 keV, 3 ns electron pulser at a high dose rate of the order of 10^{13} rads/s. All samples were contained in a vacuum-tight aluminum cell fitted with a stainless steel electron window of 3 mm diameter and 0.001 in. thickness. The cell was constructed so that the irradiated sample could be replaced by fresh sample from a reservoir under vacuum after every pulse. This ensured that any radiolysis products which might quench the luminescence were removed before each successive pulse of an experimental run. Light emitted by the irradiated benzene was viewed at right angles to the electron beam axis by a silica rod of 4 mm diameter fitted into the cell such that its collecting face was 1.5 mm from this axis. In this way an attempt was made to minimize the intensity of unwanted Cerenkov emission as well as reducing self-absorption of emission by the benzene samples.

The silica rod light guide transmitted the emission to the entry slit of a Jarrell-Ash 82–420 grating monochromator whose exit slit was coupled to an IP28 phototube. The signal from the latter was displayed on a Tektronix 454 oscilloscope. All electronic components were shielded from both electrical and X-ray interference and great care was taken to match all impedances in the detector circuit. The time resolution of the detector system was approximately 2 ns.

All samples studied were degassed to 10^{-3} mm Hg by the normal freeze–pump–thaw technique, unless otherwise stated. On pulsing electrons into the cell containing a nonluminescent liquid, no emission was observed to arise from the silica light guide itself over the wavelength range 260–400 mμ. The oscilloscope trace of sample emission decay following a pulse showed a sizeable Cerenkov emission component having a lifetime equal to that of the electron pulse to be present. To eliminate this from interfering with measurements of the longer lived benzene emission, the decay curves were analyzed 20 ns after the commencement of each pulse. From the first order decay constants found, the benzene emission intensity extrapolated to the electron pulse maximum (i.e. zero time) was calculated for each trace. To allow for any apparatus geometrical changes occurring between experiments, these intensity values were recorded relative to the arbitrary standard of the Cerenkov intensity at 380 mμ. At this wavelength benzene emission intensity is negligible. Each intensity point at any wavelength in the results below is

[1]Present address: Research Department, ICI Fibres Ltd., Pontypool, Mon., England.

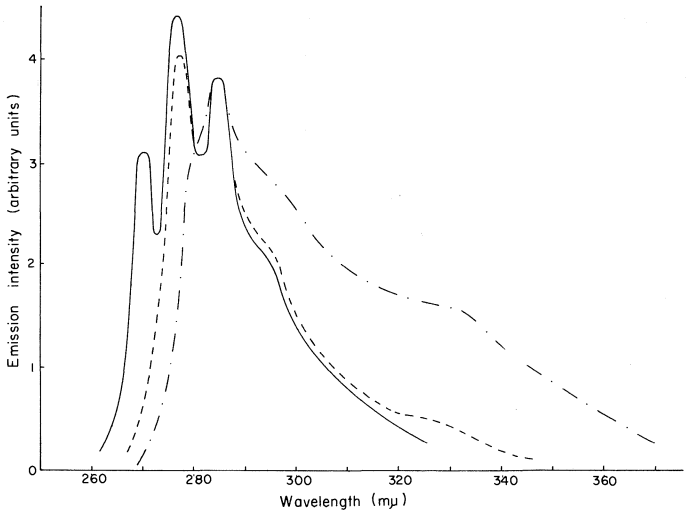

FIG. 1. The emission spectra of various benzene systems normalized at the 285 mμ maximum and uncorrected for detector wavelength sensitivity; (*i*) – · – ·, 11.1 *M* benzene; (*ii*) - - - - -, 1.11 *M* benzene in cyclohexane; (*iii*) ——, 1.1×10^{-2} *M* benzene in cyclohexane.

the average of at least two pulses; the root-mean-square deviation of measured intensity at any one wavelength over a series of 20 pulses was about ±5%.

The results for various benzene samples are shown in Fig. 1; the spectra are uncorrected for detector wavelength sensitivity. The emission spectra for benzene at 11.1, 1.11, and 1.1×10^{-2} *M* in Fig. 1 resemble those for the same systems reported by Birks for photoexcitation (2). Self absorption of the shorter wavelength region of the monomer fluorescence band caused some distortion in the more concentrated benzene systems, but this does not detract from the general inference that emission from benzene is independent of the mode of excitation. The lifetimes of liquid benzene monomer emission at 285 mμ and excimer emission at 320 mμ are shown in Table 1. These are in good agreement with those reported by Cooper and Thomas (5) for benzene emission below 350 mμ excited by pulse radiolysis. The wavelength independence of τ is in agreement with the postulate that monomer and excimer are in dynamic equilibrium with each other in liquid benzene (6). The lifetimes of monomer emissions from the two benzene solutions in cyclohexane are much longer than for liquid benzene or for photoexcited benzene solutions in hexane (1).

The effects of atmospheric oxygen and added chloroform are shown in Table 1 on both the emission intensity immediately after the pulse and the lifetime for liquid benzene. Oxygen is seen to decrease the lifetime of both monomer and excimer by equal amounts but does not noticeably scavenge the precursors of the singlet

TABLE 1

Lifetimes and intensities of emission spectra from the various benzene systems

	Monomer, 285 mμ		Excimer, 320 mμ	
Benzene Concentration	τ (ns)	*I*	τ (ns)	*I*
11.1 *M* (liquid) deaerated	28.8	3.75	26.0	1.70
11.1 *M* aerated	15.3	3.00	15.5	1.90
11.1 *M* deaerated + 0.3 *M* $CHCl_3$	25.2	1.88	25.6	0.93
1.1 *M* in deaerated cyclohexane	40.2			
1.1×10^{-2} *M* in deaerated cyclohexane	41.5			

Can. J. Chem. Downloaded from www.nrcresearchpress.com by 210.87.254.42 on 09/05/12
For personal use only.

excited states. Chloroform, however, assumed to be a scavenger of electrons (7, 8), reduces both monomer and excimer emission by equal amounts whilst only slightly decreasing their respective lifetimes. These results suggest that both the monomer and excimer arise from common precursors. It seems most likely that the latter generate either monomer or excimer species followed by rapid equilibration.

The intense Cerenkov emission monitored during this work suggests that, since such emission has maximum intensity in the direction of the irradiating particle beam, the benzene luminescence yield is appreciably less than that for Cerenkov emission over the spectral region 260–360 mμ. It is likely, therefore, that some benzene emission will arise from absorption of Cerenkov photons; the chloroform scavenging experiment shows that this is not a major contribution, however.

The author is indebted to Dr. D. C. Walker for advice during this work carried out at the University of British Columbia and to the National Research Council of Canada for financial support.

1. T. V. Ivanova, G. A. Mokeeva, and B. Ya. Sveshnikov. Opt. Spectrosc. **12**, 325 (1962).
2. J. B. Birks, C. L. Braga, and M. D. Lumb. Proc. Roy. Soc. London, Ser. A, **283**, 83 (1965).
3. J. G. Carter, L. G. Christophorou, and M-E. M. Abu-Zeid. J. Chem. Phys. **47**, 3879 (1967).
4. L. G. Christophorou, M-E. M. Abu-Zeid, and J. G. Carter. J. Chem. Phys. **49**, 3775 (1968).
5. R. Cooper and J. K. Thomas. J. Chem. Phys. **48**, 5097 (1968).
6. J. B. Birks. Chem. Phys. Lett. **1**, 625 (1968).
7. W. Van Dusen, Jr. and W. H. Hamill. J. Amer. Chem. Soc. **84**, 3648 (1962).
8. E. P. Bertin and W. H. Hamill. J. Amer. Chem. Soc. **86**, 1301 (1964).

Signs of methyl–methyl proton spin–spin coupling constants in xylene derivatives (interbenzylic coupling)

C. J. Macdonald[1] and W. F. Reynolds
Department of Chemistry, University of Toronto, Toronto 181, Ontario

Received October 23, 1969

The signs of the intermethyl proton spin–spin coupling constants in ortho, meta, and para xylene derivatives (interbenzylic coupling) have been determined by double resonance techniques. $J_{CH_3,CH_3}{}^{o}$, $J_{CH_3,CH_3}{}^{m}$, and $J_{CH_3,CH_3}{}^{p}$ are positive, negative, and positive, respectively, in agreement with the predictions of theories based on σ–π interactions. The magnitudes of the coupling constants are discussed in terms of the values predicted by these theories.

Canadian Journal of Chemistry, **48**, 1002 (1970)

Introduction

The signs of the long range α-side-chain proton – ring proton (benzylic) coupling constants in toluene and substituted toluenes, $J_{H,CHXY}{}^{o}$, $J_{H,CHXY}{}^{m}$, and $J_{H,CHXY}{}^{p}$ are known to be negative, positive, and negative, respectively (1–4). A substantial measure of agreement between theory (5–7) and experiment (1–4, 8–11) has led to the conclusion that the signs and magnitudes of the ortho and para benzylic coupling constants are primarily determined by π-electron contributions, transmitted to the benzylic proton by σ–π exchange polarization. For the meta coupling constant, although agreement between theory and experiment is reasonable for an unsubstituted methyl group (1–7), experimental results indicate substantial σ-electron contributions, at least in situations where a benzylic proton is constrained to lie in the nodal plane of the π-electron system (8, 12, 13).

These theories further predict that substitution of a second benzylic group for the ring proton should invert the signs of the corresponding α-side-chain proton – α′-side-chain proton (interbenzylic[2]) coupling constants in xylenes, i.e. $J_{CHXY,CHX'Y'}{}^{o}$, $J_{CHXY,CHX'Y'}{}^{m}$, and $J_{CHXY,CHX'Y'}{}^{p}$ should be positive, negative, and positive, respectively (5–7).

In this note, we describe the determination of the signs of $J_{CH_3,CH_3}{}^{o}$, $J_{CH_3,CH_3}{}^{m}$, and $J_{CH_3,CH_3}{}^{p}$ in

[1]Postdoctoral Fellow, 1968–1969.

[2]Name suggested by M. Neeman (14).

Can. J. Chem. Downloaded from www.nrcresearchpress.com by 210.87.254.42 on 09/05/12
For personal use only.

excited states. Chloroform, however, assumed to be a scavenger of electrons (7, 8), reduces both monomer and excimer emission by equal amounts whilst only slightly decreasing their respective lifetimes. These results suggest that both the monomer and excimer arise from common precursors. It seems most likely that the latter generate either monomer or excimer species followed by rapid equilibration.

The intense Cerenkov emission monitored during this work suggests that, since such emission has maximum intensity in the direction of the irradiating particle beam, the benzene luminescence yield is appreciably less than that for Cerenkov emission over the spectral region 260–360 mμ. It is likely, therefore, that some benzene emission will arise from absorption of Cerenkov photons; the chloroform scavenging experiment shows that this is not a major contribution, however.

The author is indebted to Dr. D. C. Walker for advice during this work carried out at the University of British Columbia and to the National Research Council of Canada for financial support.

1. T. V. Ivanova, G. A. Mokeeva, and B. Ya. Sveshnikov. Opt. Spectrosc. **12**, 325 (1962).
2. J. B. Birks, C. L. Braga, and M. D. Lumb. Proc. Roy. Soc. London, Ser. A, **283**, 83 (1965).
3. J. G. Carter, L. G. Christophorou, and M-E. M. Abu-Zeid. J. Chem. Phys. **47**, 3879 (1967).
4. L. G. Christophorou, M-E. M. Abu-Zeid, and J. G. Carter. J. Chem. Phys. **49**, 3775 (1968).
5. R. Cooper and J. K. Thomas. J. Chem. Phys. **48**, 5097 (1968).
6. J. B. Birks. Chem. Phys. Lett. **1**, 625 (1968).
7. W. Van Dusen, Jr. and W. H. Hamill. J. Amer. Chem. Soc. **84**, 3648 (1962).
8. E. P. Bertin and W. H. Hamill. J. Amer. Chem. Soc. **86**, 1301 (1964).

Signs of methyl–methyl proton spin–spin coupling constants in xylene derivatives (interbenzylic coupling)

C. J. Macdonald[1] and W. F. Reynolds
Department of Chemistry, University of Toronto, Toronto 181, Ontario

Received October 23, 1969

The signs of the intermethyl proton spin–spin coupling constants in ortho, meta, and para xylene derivatives (interbenzylic coupling) have been determined by double resonance techniques. $J_{CH_3,CH_3}{}^{o}$, $J_{CH,CH_3}{}^{m}$, and $J_{CH_3,CH_3}{}^{p}$ are positive, negative, and positive, respectively, in agreement with the predictions of theories based on σ–π interactions. The magnitudes of the coupling constants are discussed in terms of the values predicted by these theories.

Canadian Journal of Chemistry, **48**, 1002 (1970)

Introduction

The signs of the long range α-side-chain proton – ring proton (benzylic) coupling constants in toluene and substituted toluenes, $J_{H,CHXY}{}^{o}$, $J_{H,CHXY}{}^{m}$, and $J_{H,CHXY}{}^{p}$ are known to be negative, positive, and negative, respectively (1–4). A substantial measure of agreement between theory (5–7) and experiment (1–4, 8–11) has led to the conclusion that the signs and magnitudes of the ortho and para benzylic coupling constants are primarily determined by π-electron contributions, transmitted to the benzylic proton by σ–π exchange polarization. For the meta coupling constant, although agreement between theory and experiment is reasonable for an unsubstituted methyl group (1–7), experimental results indicate substantial σ-electron contributions, at least in situations where a benzylic proton is constrained to lie in the nodal plane of the π-electron system (8, 12, 13).

These theories further predict that substitution of a second benzylic group for the ring proton should invert the signs of the corresponding α-side-chain proton – α′-side-chain proton (interbenzylic[2]) coupling constants in xylenes, i.e. $J_{CHXY,CHX'Y'}{}^{o}$, $J_{CHXY,CHX'Y'}{}^{m}$, and $J_{CHXY,CHX'Y'}{}^{p}$ should be positive, negative, and positive, respectively (5–7).

In this note, we describe the determination of the signs of $J_{CH_3,CH_3}{}^{o}$, $J_{CH_3,CH_3}{}^{m}$, and $J_{CH_3,CH_3}{}^{p}$ in

[1]Postdoctoral Fellow, 1968–1969.

[2]Name suggested by M. Neeman (14).

Can. J. Chem. Downloaded from www.nrcresearchpress.com by 210.87.254.6 on 09/05/12
For personal use only.

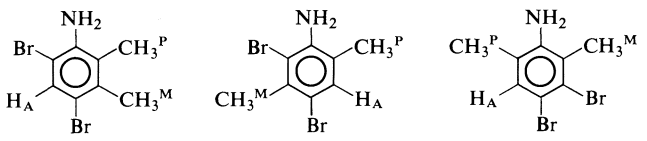

FIG. 1. Structural formulae of **1**, 4,6-dibromo-2,3-dimethylaniline; **2**, 4,6-dibromo-2,5-dimethylaniline; **3**, 3,4-dibromo-2,6-dimethylaniline. The protons of interest are labelled in a conventional way according to their magnetic resonance spectra at 100 MHz.

ortho, meta, and para xylene derivatives relative to the known signs of benzylic coupling constants.

Experimental

Preparation of Compounds

4,6-Dibromo-2,3-dimethylaniline (**1**) was prepared by the bromination of 2,3-dimethylaniline (Eastman Organic Chemicals) in acetic acid. Recrystallization from petroleum ether (30–60°) afforded the dibromide as white needles, m.p. 54–55 °C (reported m.p., 56 °C (15)).

4,6-Dibromo-2,5-dimethylaniline (**2**) was obtained similarly from 2,5-dimethylaniline (Eastman) as white needles, m.p. 63–64 °C (reported m.p., 65 °C (15)).

3,4-Dibromo-2,6-dimethylaniline (**3**) was synthesized in two steps from 2,6-dimethylaniline (Eastman). Bromination in acetic acid afforded 4-bromo-2,6-dimethylaniline, which was then meta brominated in concentrated sulfuric acid containing one equivalent of silver ion after the method of Gorvin (16). Preferential recrystallization from petroleum ether (30–60°) gave the dibromide **3**, substantially (95%) free from both unreacted starting material and the 3,4,5-tribromide also found in the reaction product. A recrystallized sample was obtained as white needles, m.p. 50 °C (reported m.p. 51 °C (15)).

Nuclear Magnetic Resonance Experiments

Compounds **1**, **2**, and **3**, prepared as 3-, 3-, and 6-mole % solutions (respectively) in carbon disulfide containing about 3 mole % of tetramethylsilane, were degassed by the freeze–pump–thaw technique and sealed. The sample of **3** used contained about 5% of 4-bromo-2,6-dimethylaniline whose nuclear magnetic resonance (n.m.r.) peaks did not overlap those of **3**.

Proton resonance spectra were obtained on a Varian HA-100 n.m.r. spectrometer, operating in the frequency sweep mode, locked to the TMS, and at sweep rates of 0.01 or 0.02 Hz/s. Peak positions, calculated from at least 5 sweeps calibrated at <5 Hz intervals, were obtained with a reproducibility of $\leqslant 0.03$ Hz. Half-line widths were 0.15–0.20 Hz. Double resonance spectra were obtained in the usual manner (17, 18) using a Hewlett–Packard 4204A oscillator.

Results

Structural formulae of the compounds are shown in Fig. 1, with appropriate labelling of the protons. Final parameters obtained are collected in Table 1.

TABLE 1

Nuclear magnetic resonance parameters derived for carbon disulfide solutions of **1**, 4,6-dibromo-2,3-dimethylaniline; **2**, 4,6-dibromo-2,5-dimethylaniline; and **3**, 3,4-dibromo-2,6-dimethylaniline*

	Compound		
Parameter	**1**	**2**	**3**
δ_A†	7.3447±0.0005	7.0490±0.0005	7.0004±0.0005
δ_M	2.2683±0.0005	2.4407±0.0005	2.2208±0.0008
δ_P	2.1111±0.0005	2.1029±0.0005	1.9868±0.0008
J_{AM}	+0.36± 0.03	+0.38 ±0.03	−0.57 ±0.03
J_{AP}	−0.61± 0.03	−0.76 ±0.03	−0.77 ±0.03
J_{MP}	+0.40± 0.03	+0.62 ±0.03	−0.19 ±0.04

	Compound		
Computer output‡	**1**	**2**	**3**
No. of experimental peaks fitted	27	26	26
Worst fit of any peak (in Hz)	0.045	0.042	0.034
Average fit for all peaks (in Hz)	±0.014	±0.012	±0.008
Computed probable errors	0.0021–0.0032	0.0015–0.0020	0.0014–0.0025
Sums of squares of residuals (energy level fitting)	0.0068	0.0086	0.0024

*Chemical shifts in p.p.m. to low field of TMS; coupling constants in Hz.
†Protons identified as in Fig. 1.
‡From the output of a TWOSUM iterative fitting.

Can. J. Chem. Downloaded from www.nrcresearchpress.com by 210.87.254.6 on 09/05/12
For personal use only.

Can. J. Chem. Downloaded from www.nrcresearchpress.com by 210.87.254.6 on 09/05/12
For personal use only.

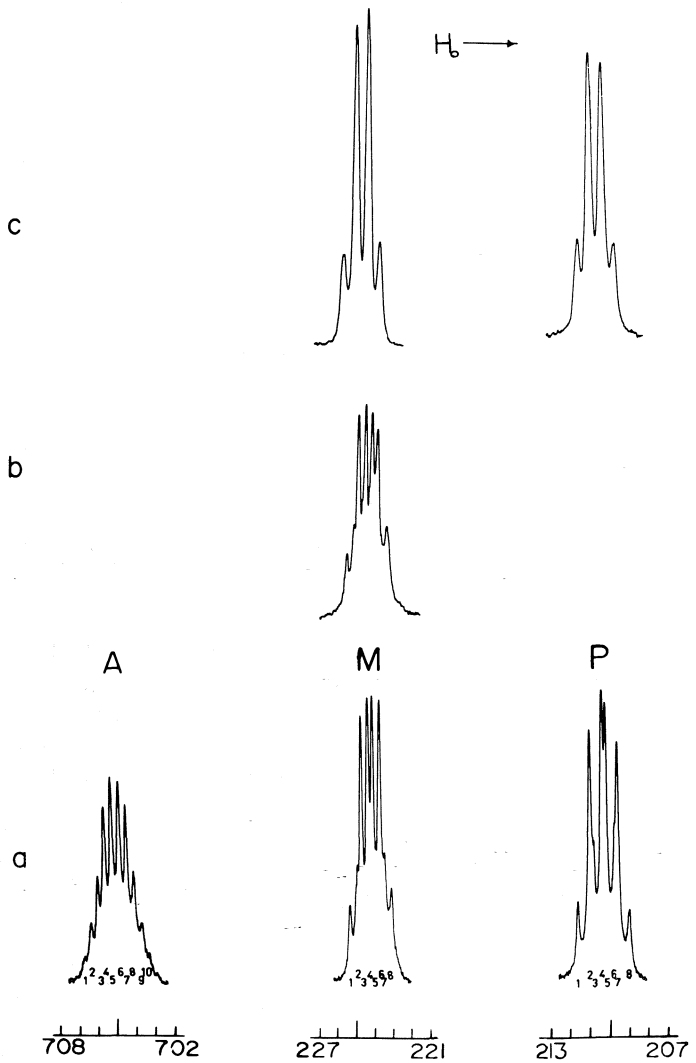

FIG. 2. Magnetic resonance spectra of **2**, 4,6-dibromo-2,5-dimethylaniline, in carbon disulfide at 100 MHz. The scale is in Hz to low field of internal TMS. (*a*) The single resonance spectrum, with the experimental peaks which can be distinguished numbered from low to high field. The amino proton spectrum is not reproduced; (*b*) the spectrum of the protons M when weak decoupling irradiation is centered on the quartet of peaks A_1–A_4; (*c*) the spectrum of the methyl groups with the ring proton decoupled.

The analysis methods used are illustrated with reference to 4,6-dibromo-2,5-dimethylaniline (**2**), whose AM_3P_3 spectrum (Fig. 2*a*) shows J_{H,CH_3} magnitudes of approximately 0.4 and 0.8 Hz. Since $J_{H,CH_3}{}^m$ and $J_{H,CH_3}{}^o$ have magnitudes of about 0.4 and 0.7 Hz, respectively (1–4, 12, 13), the protons must be assigned as in Fig. 1. Decoupling of the A protons (Fig. 2*c*) clearly shows the coupling of about 0.6 Hz magnitude between the methyl groups.

The double-irradiation experiments which establish the relative sign of J_{MP} in **2** may be understood by reference to the schematic single-resonance spectrum (Fig. 3), in which 12 of the A-proton resonances are seen to overlap in pairs, giving the observed 10 peaks. Methyl groups are considered as composite nuclei, and spin states of protons coupled to a nucleus involved in a given transition are labelled with plus and minus signs (spin states of the methyl group are 3+, +, −,

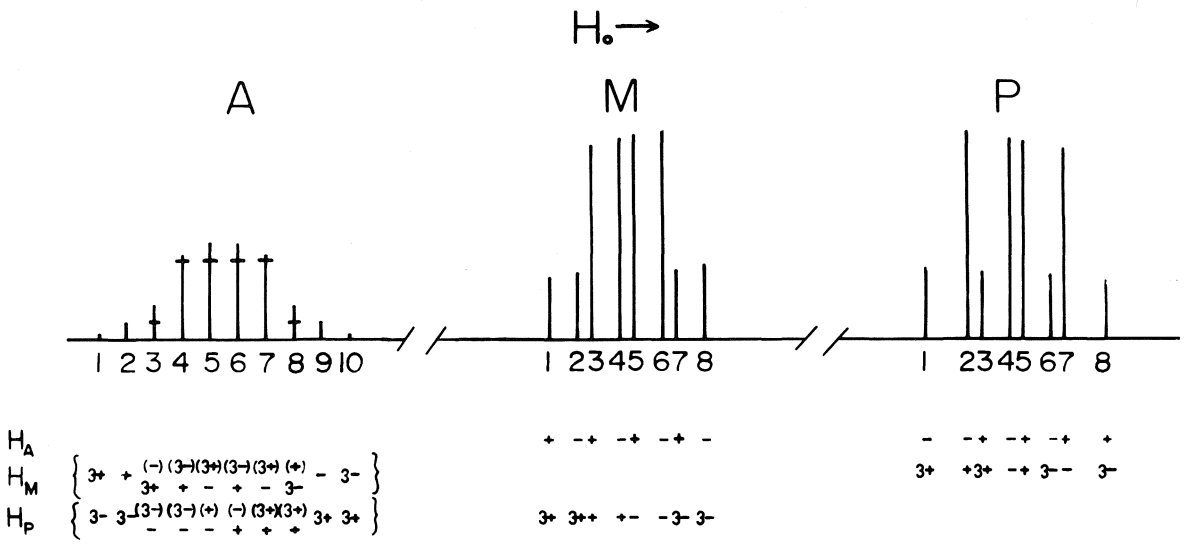

FIG. 3. Stick diagram of the proton resonance of **2**, 4,6-dibromo-2,5-dimethylaniline. Spin states of the coupled nuclei are labelled as discussed in the text (see Results). Spin states in brackets refer to the upper transition of the stick diagram in cases involving coincident transitions.

and 3−), with the convention that a plus sign below a low-field peak indicates a positive coupling to the nucleus in question. $J_{H,CH_3}{}^o$ and $J_{H,CH_3}{}^m$ are known to be negative and positive, respectively (1–3), and if J_{MP} in **2** is assumed to be positive, the spin assignment of Fig. 3 follows. Peaks A_1–A_4 involve substantially transitions in which the P protons are all in the same spin state (3−). Weak decoupling irradiation centered in the middle of peaks A_1–A_4 causes coalescence of transitions M_7 and M_8 (Fig. 2*b*),[3] showing that the signs of J_{AP} and J_{MP} in **2** are opposite. Since $J_{AP} \equiv J_{H,CH_3}{}^o$ is negative in sign, $J_{MP} \equiv J_{CH_3,CH_3}{}^p$ must be positive in sign. Confirmation of all the relative signs was obtained by several further double-resonance (both tickling and decoupling) experiments.

These sign assignments and the experimental peak positions, when analyzed by the TWOSUM program (19), led to the parameters shown in Table 1, which also records the results of similar experiments performed on compounds **2** and **3**. The small magnitude of $J_{CH_3,CH_3}{}^m$ leads to rather greater uncertainties in some of the derived parameters of **3** compared to **1** and **2**.

[3]Because peaks A_3 and A_4 also contain transitions other than those with the P protons in the 3− spin state, other slight changes occur. However, these do not obscure the essential point of the experiment: peaks M_7 and M_8, but not M_1 and M_2, are affected.

Discussion

The signs found for $J_{CH_3,CH_3}{}^o$, $J_{CH_3,CH_3}{}^m$, and $J_{CH_3,CH_3}{}^p$ (positive, negative, and positive, respectively) are those predicted for the π-electron contribution (5–7). However, the magnitudes found in this work and in previous investigations (20–24) are at variance (Table 2) with some of the values predicted by Barfield and Chakrabarti (7), and the values given by the modified McConnell relationship

$$[1] \qquad J_{CH_3,CH_3} \propto Q_{CCH}Q_{CCH}$$

if it is assumed that the constant of proportionality is identical to that for the corresponding benzylic coupling constant relationship

$$[2] \qquad J_{H,CH_3} \propto Q_{CH}Q_{CCH}$$

and Q_{CH}, Q_{CCH}, $J_{H,CH_3}{}^o$, $J_{H,CH_3}{}^m$, and $J_{H,CH_3}{}^p$ have the values −23 G, +25 G, −0.7 Hz, +0.4 Hz, and −0.6 Hz, respectively (4).

The magnitudes found for $J_{CH_3,CH_3}{}^p$ are those predicted for the π-electron contribution (within experimental uncertainty), confirming previous suggestions that the σ-electron contribution to $J_{H,CH_3}{}^p$ is negligible (4, 8, 12). It may be reasonably assumed that σ-electron contributions to $J_{CH_3,CH_3}{}^p$ are also negligible. However, the magnitudes observed for $J_{CH_3,CH_3}{}^m$ and $J_{CH_3,CH_3}{}^o$ appear to suggest contributions from other than the π-electron system. In view of the essentially sub-

Can. J. Chem. Downloaded from www.nrcresearchpress.com by 210.87.254.6 on 09/05/12
For personal use only.

TABLE 2

Comparison of calculated π-electron contributions to interbenzylic coupling in xylenes with available experimental data

Compound	J_{CH_3,CH_3}^{o}	J_{CH_3,CH_3}^{m}	J_{CH_3,CH_3}^{p}	Reference
McConnell prediction, xylenes	+0.76*	−0.43	+0.65	
Barfield prediction, xylenes	+0.74	−0.60	+0.63	7
Compounds **1–3**	+0.40	−0.19	+0.62	†
Mesitylene		|<0.35|		20
3,4-Dibromo-2,6-dimethylphenol		|0.21|		21
2,4,6-Trimethylbenzaldehyde		|0.25|		4
6-Bromo-2,4-dimethyl-5-nitroaniline		|0.23|		22
2-Carbomethoxy-5,6-dimethylbenzofuran	|0.37|			23
7,12-Dimethylbenz[*a*]anthracene			|0.55|‡	24

*In Hz.
†This work.
‡Value deduced from line-width narrowing on decoupling one methyl group from the other.

stituent-independent (< 25% variation) values found for J_{H,CH_3} in a large number of molecules (1–4), discrepancies between the observed and predicted values of J_{CH_3,CH_3} are not expected to be principally due to substituent effects. Consideration of the factors involved leads to several interesting, if rather tentative, conclusions.

Barfield and Chakrabarti have suggested (7) that the magnitude of the π-electron contribution to J_{CH_3,CH_3}^{m} calculated by his valence-bond method is too large because of errors inherent in that method (over-correlation of electrons in the same subset of an alternant system). Both experimental (8, 12, 13) and theoretical (25) considerations suggest the existence of substantial σ-electron contributions to J_{H,CH_3}^{m}. Comparing the value of $|J_{CH_3,CH_3}^{m}|$ found in 2,4,6-trimethylbenzaldehyde with the observed range of $|J_{H,CH_3}^{m}|$ in toluenes in the light of the methyl group replacement technique for assessing π-electron contributions to J values (26), it has been concluded (4) that σ-electron contributions to J_{H,CH_3}^{m} amount to approximately one-third of the observed magnitude. The values of J_{CH_3,CH_3}^{m} in Table 2 indicate that this is probably a lower limit to the σ-electron contribution to J_{H,CH_3}^{m}. In the absence of other information, it is inappropriate to discuss the importance of σ-electron contributions to J_{CH_3,CH_3}^{m}, although it may be noted that they cannot be discounted on theoretical grounds.

On the basis of the methyl group replacement technique (26), the decrease of 0.2 to 0.4 Hz between $|J_{H,CH_3}^{o}|$ and $|J_{CH_3,CH_3}^{o}|$ suggests a substantial σ-electron contribution (one-third to one-half) to the magnitude of J_{H,CH_3}^{o}, contrary to previous conclusions (4, 27). The symmetry of the methyl groups negates any possible explanations for the low value of J_{CH_3,CH_3}^{o} (such as reduced Q_{CCH} values) based on the known existence (28) of preferred conformers in ortho xylenes, and arguments based on steric crowding in **1** appear inappropriate in view of the similarity of the J_{CH_3,CH_3}^{o} value in 2-carbomethoxy-5,6-dimethylbenzofuran (23). Some small measure of support for the existence of significant σ-contributions to J_{H,CH_3}^{o} can perhaps be gleaned from the observation of approximately equal $|J_{H,CH}^{o}|$ and $|J_{H,CH}^{m}|$ values in several dihydrocinnamic acid derivatives, in which the benzylic methine proton is held approximately in the plane of the π-electrons (12). In addition, *cisoid* $^4J_{H,CHXY}$ values in cyclic 2,3-disubstituted butanes **4** (R = O, $(CH_3)_2$) (29) and epoxides **5** (R = H, halogen) (30, 31), which are in the range −0.1 to −0.4 Hz, cannot be due to π-electrons. All these factors point to the possibility of significant

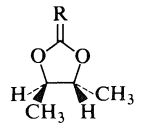

4

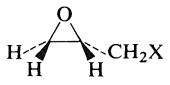

5

contributions to J_{H,CH_3}^{o}, independent of the π-electron system. Alternatively, the small magnitude of J_{CH_3,CH_3}^{o} may be due to the relative importance of "direct" or "through space" contributions, which are expected to be negative in sign, and most important in the vicinity of eclipsed conformations (32). Experiments designed to test the validity of σ-bond contributions to J_{H,CH_3}^{o} are currently being pursued in this laboratory.

Can. J. Chem. Downloaded from www.nrcresearchpress.com by 210.87.254.6 on 09/05/12
For personal use only.

We are grateful to the author for a listing of TWOSUM, to Dr. M. Barfield for a preprint of his review article, and to the National Research Council of Canada for financial support.

1. G. KOTOWYCZ and T. SCHAEFER. Can. J. Chem. **44**, 2743 (1966).
2. D. GAGNAIRE and TRINH-HUU-ICH. Bull. Chem. Soc. France, 3763 (1966).
3. M. P. WILLIAMSON, R. KOSTELNIK, and S. M. CASTELLANO. J. Chem. Phys. **49**, 2218 (1968).
4. T. SCHAEFER, S. S. DANYLUK, and C. L. BELL. Can. J. Chem. **47**, 1507 (1969) and references therein.
5. H. M. MCCONNELL. J. Chem. Phys. **30**, 126 (1959).
6. H. M. MCCONNELL. Mol. Spectrosc. **1**, 11 (1957).
7. M. BARFIELD and B. CHAKRABARTI. J. Amer. Chem. Soc. **91**, 4346 (1969).
8. T. SCHAEFER, R. SCHWENK, C. J. MACDONALD, and W. F. REYNOLDS. Can. J. Chem. **46**, 3132 (1967).
9. D. T. WITIAK, D. B. PATEL, and Y. LIN. J. Amer. Chem. Soc. **89**, 1908 (1967).
10. W. C. RIPKA and D. E. APPLEQUIST. J. Amer. Chem. Soc. **89**, 4035 (1967).
11. D. J. BLEARS, S. S. DANYLUK, and T. SCHAEFER. Can. J. Chem. **46**, 654 (1968).
12. G. P. NEWSOROFF and S. STERNHELL. Aust. J. Chem. **21**, 747 (1968).
13. T. SCHAEFER, C. M. WONG, and K. C. TAM. Can. J. Chem. **47**, 3688 (1969).
14. M. BARFIELD and B. CHAKRABARTI. Chem. Rev. In press.
15. F. M. JAEGER and J. J. BLANKSMA. Rec. Trav. Chim. **25**, 352 (1906).
16. J. H. GORVIN. J. Chem. Soc. 1237 (1953).
17. R. FREEMAN and W. A. ANDERSON. J. Chem. Phys. **37**, 3053 (1962).
18. J. D. BALDESCHWIELER and E. W. RANDALL. Chem. Rev. **63**, 81 (1963).
19. G. R. DE MARE and J. S. MARTIN. J. Amer. Chem. Soc. **88**, 5033 (1966).
20. J. V. ACRIVOS. Mol. Phys. **5**, 1 (1962).
21. W. G. B. HUYSMANS, J. G. WESTRA, W. J. MIJS, H. A. GAUR, J. VRIEND, and J. SMIDT. Tetrahedron Lett. 4345 (1968).
22. C. J. MACDONALD and W. F. REYNOLDS. Unpublished results.
23. A. D. COHEN and K. A. MCLAUCHLAN. Mol. Phys. **9**, 49 (1965).
24. K. D. BARTLE, D. W. JONES, and R. S. MATTHEWS. Tetrahedron, **25**, 2701 (1969).
25. H. FRISCHLEDER and G. BÄR. Mol. Phys. **11**, 359 (1966).
26. R. HOFFMAN. Ark. Kem. **17**, 1 (1961).
27. S. STERNHELL. Quart. Rev. London, **23**, 236 (1969).
28. W. R. WOOLFENDEN and D. M. GRANT. J. Amer. Chem. Soc. **88**, 1496 (1966).
29. F. A. L. ANET. J. Amer. Chem. Soc. **84**, 747 (1962).
30. D. D. ELLEMAN, S. L. MANATT, and C. D. PEARCE. J. Chem. Phys. **42**, 650 (1965).
31. C. J. MACDONALD and W. F. REYNOLDS. To be published.
32. M. BARFIELD. J. Chem. Phys. **41**, 3825 (1964).

Composition and stability of some bivalent transition metal complexes of 3,5-dinitrosalicylic acid

S. S. DUBE AND S. S. DHINDSA
Department of Chemistry, Government College, Kota (Rajasthan), India

Received June 2, 1969

The interaction of Zn^{2+}, Mn^{2+}, Hg^{2+}, and Cd^{2+} ions with 3,5-dinitrosalicylic acid was investigated by potentiometric titrations in aqueous 0.1 *M* KNO_3 medium. In all cases the formation of 1:1 complex was indicated. The stability constants in the p*H* ranges 4.5–8.0, 4.5–8.0, 5.0–8.0, and 5.5–8.0 were determined by applying the Calvin and Melchior's extension of Bjerrum's method and the log *K* values were found to be 3.70, 2.95, 3.20, and 2.85, respectively. A comparative study of the complexes of 3,5-dinitrosalicylic acid with other bivalent metal ions has also been incorporated. The stability constants of the transition metal complexes obey the order Cu > Ni > Co > Zn > Mn, in agreement with Irving and William's rule.

Canadian Journal of Chemistry, **48**, 1007 (1970)

Introduction

3,5-Dinitrosalicylic acid (3,5-DNS) falls in an important group of organic compounds, hydroxy carboxylic acids, and provides two possible coordination sites, viz., —COOH and —OH groups. A survey of literature revealed that the complexation tendency of this ligand has not yet been explored, and hence in previous communications the authors had reported the investigations on the complex formation between 3,5-DNS and Ni^{2+} (1), Co^{2+} (1), Mg^{2+} (2), Cu^{2+} (3), Pb^{2+} (3), and Be^{2+} (4). In view of the interesting results obtained, it was considered worthwhile to extend studies on the interaction of 3,5-DNS with bivalent transition metal ions, viz., Zn^{2+}, Mn^{2+}, Hg^{2+}, and Cd^{2+}. The attention has been focussed mainly on the composition and stabilities of the complexes and also on the determination of free energy changes accompanying the reactions.

Can. J. Chem. Downloaded from www.nrcresearchpress.com by 210.87.254.6 on 09/05/12
For personal use only.

We are grateful to the author for a listing of TWOSUM, to Dr. M. Barfield for a preprint of his review article, and to the National Research Council of Canada for financial support.

1. G. KOTOWYCZ and T. SCHAEFER. Can. J. Chem. **44**, 2743 (1966).
2. D. GAGNAIRE and TRINH-HUU-ICH. Bull. Chem. Soc. France, 3763 (1966).
3. M. P. WILLIAMSON, R. KOSTELNIK, and S. M. CASTELLANO. J. Chem. Phys. **49**, 2218 (1968).
4. T. SCHAEFER, S. S. DANYLUK, and C. L. BELL. Can. J. Chem. **47**, 1507 (1969) and references therein.
5. H. M. MCCONNELL. J. Chem. Phys. **30**, 126 (1959).
6. H. M. MCCONNELL. Mol. Spectrosc. **1**, 11 (1957).
7. M. BARFIELD and B. CHAKRABARTI. J. Amer. Chem. Soc. **91**, 4346 (1969).
8. T. SCHAEFER, R. SCHWENK, C. J. MACDONALD, and W. F. REYNOLDS. Can. J. Chem. **46**, 3132 (1967).
9. D. T. WITIAK, D. B. PATEL, and Y. LIN. J. Amer. Chem. Soc. **89**, 1908 (1967).
10. W. C. RIPKA and D. E. APPLEQUIST. J. Amer. Chem. Soc. **89**, 4035 (1967).
11. D. J. BLEARS, S. S. DANYLUK, and T. SCHAEFER. Can. J. Chem. **46**, 654 (1968).
12. G. P. NEWSOROFF and S. STERNHELL. Aust. J. Chem. **21**, 747 (1968).
13. T. SCHAEFER, C. M. WONG, and K. C. TAM. Can. J. Chem. **47**, 3688 (1969).
14. M. BARFIELD and B. CHAKRABARTI. Chem. Rev. In press.
15. F. M. JAEGER and J. J. BLANKSMA. Rec. Trav. Chim. **25**, 352 (1906).
16. J. H. GORVIN. J. Chem. Soc. 1237 (1953).
17. R. FREEMAN and W. A. ANDERSON. J. Chem. Phys. **37**, 3053 (1962).
18. J. D. BALDESCHWIELER and E. W. RANDALL. Chem. Rev. **63**, 81 (1963).
19. G. R. DE MARE and J. S. MARTIN. J. Amer. Chem. Soc. **88**, 5033 (1966).
20. J. V. ACRIVOS. Mol. Phys. **5**, 1 (1962).
21. W. G. B. HUYSMANS, J. G. WESTRA, W. J. MIJS, H. A. GAUR, J. VRIEND, and J. SMIDT. Tetrahedron Lett. 4345 (1968).
22. C. J. MACDONALD and W. F. REYNOLDS. Unpublished results.
23. A. D. COHEN and K. A. MCLAUCHLAN. Mol. Phys. **9**, 49 (1965).
24. K. D. BARTLE, D. W. JONES, and R. S. MATTHEWS. Tetrahedron, **25**, 2701 (1969).
25. H. FRISCHLEDER and G. BÄR. Mol. Phys. **11**, 359 (1966).
26. R. HOFFMAN. Ark. Kem. **17**, 1 (1961).
27. S. STERNHELL. Quart. Rev. London, **23**, 236 (1969).
28. W. R. WOOLFENDEN and D. M. GRANT. J. Amer. Chem. Soc. **88**, 1496 (1966).
29. F. A. L. ANET. J. Amer. Chem. Soc. **84**, 747 (1962).
30. D. D. ELLEMAN, S. L. MANATT, and C. D. PEARCE. J. Chem. Phys. **42**, 650 (1965).
31. C. J. MACDONALD and W. F. REYNOLDS. To be published.
32. M. BARFIELD. J. Chem. Phys. **41**, 3825 (1964).

Composition and stability of some bivalent transition metal complexes of 3,5-dinitrosalicylic acid

S. S. DUBE AND S. S. DHINDSA
Department of Chemistry, Government College, Kota (Rajasthan), India

Received June 2, 1969

The interaction of Zn^{2+}, Mn^{2+}, Hg^{2+}, and Cd^{2+} ions with 3,5-dinitrosalicylic acid was investigated by potentiometric titrations in aqueous 0.1 *M* KNO_3 medium. In all cases the formation of 1:1 complex was indicated. The stability constants in the p*H* ranges 4.5–8.0, 4.5–8.0, 5.0–8.0, and 5.5–8.0 were determined by applying the Calvin and Melchior's extension of Bjerrum's method and the log *K* values were found to be 3.70, 2.95, 3.20, and 2.85, respectively. A comparative study of the complexes of 3,5-dinitrosalicylic acid with other bivalent metal ions has also been incorporated. The stability constants of the transition metal complexes obey the order Cu > Ni > Co > Zn > Mn, in agreement with Irving and William's rule.

Canadian Journal of Chemistry, **48**, 1007 (1970)

Introduction

3,5-Dinitrosalicylic acid (3,5-DNS) falls in an important group of organic compounds, hydroxy carboxylic acids, and provides two possible coordination sites, viz., —COOH and —OH groups. A survey of literature revealed that the complexation tendency of this ligand has not yet been explored, and hence in previous communications the authors had reported the investigations on the complex formation between 3,5-DNS and Ni^{2+} (1), Co^{2+} (1), Mg^{2+} (2), Cu^{2+} (3), Pb^{2+} (3), and Be^{2+} (4). In view of the interesting results obtained, it was considered worthwhile to extend studies on the interaction of 3,5-DNS with bivalent transition metal ions, viz., Zn^{2+}, Mn^{2+}, Hg^{2+}, and Cd^{2+}. The attention has been focussed mainly on the composition and stabilities of the complexes and also on the determination of free energy changes accompanying the reactions.

Can. J. Chem. Downloaded from www.nrcresearchpress.com by 210.87.254.5 on 09/05/12
For personal use only.

Can. J. Chem. Downloaded from www.nrcresearchpress.com by 210.87.254.5 on 09/05/12
For personal use only.

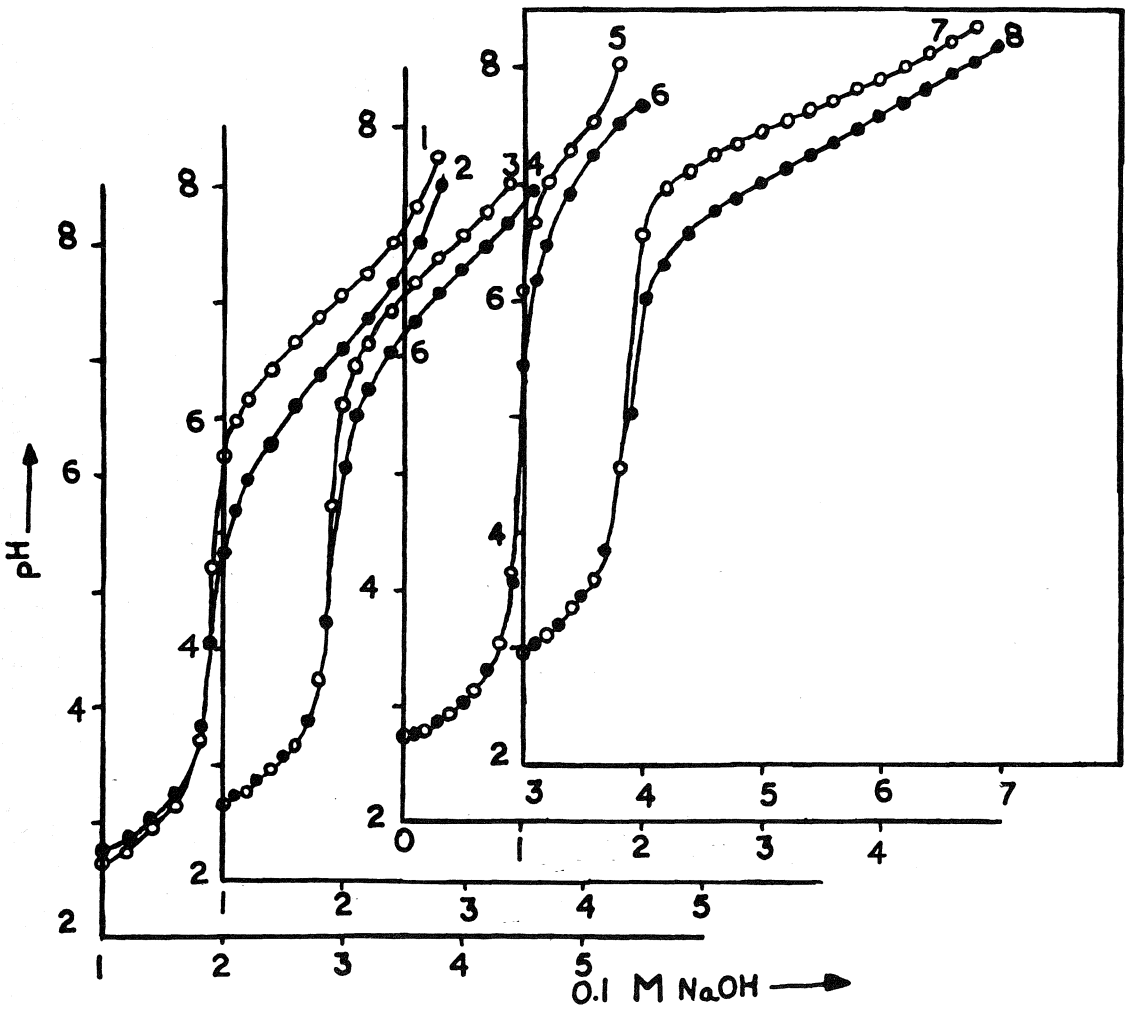

FIG. 1. Potentiometric titrations of 3,5-DNS in the absence and presence of metal ions with 0.1 *M* NaOH: curves *1* and *3*, 1×10^{-2} *M* 3,5-DNS; curve *2*, 1×10^{-2} *M* 3,5-DNS + 2.5×10^{-3} *M* $ZnSO_4$; curve *4*, 1×10^{-2} *M* 3,5-DNS + 2.5×10^{-3} *M* $MnCl_2$; curve *5*, 5×10^{-3} *M* 3,5-DNS; curve *6*, 5×10^{-3} *M* 3,5-DNS + 1×10^{-3} *M* $HgCl_2$; curve *7*, 2×10^{-2} *M* 3,5-DNS; curve *8*, 2×10^{-2} *M* 3,5-DNS + 5×10^{-3} *M* $CdSO_4$.

Experimental

Anal-R (British Drug Houses) reagents zinc sulfate, manganese chloride, mercuric chloride, and cadmium sulfate were used and their solutions were prepared in doubly distilled water. Reidel's (Germany) 3,5-dinitrosalicylic acid was used.

A Cambridge (bench type) p*H* meter using glass and calomel electrodes was used for p*H* measurements. The p*H* meter was calibrated with aqueous buffers (p*H* 4.0 and 9.18) before and after titration.

The experimental procedure consisted in performing a series of p*H* titrations of 3,5-DNS with standard NaOH, in the absence and presence of metal ions at various metal-to-ligand ratios, viz., 1:1, 1:2, and 1:3, in aqueous 0.1 *M* KNO_3 medium at 35 °C.

Calculations

The stability constants were calculated from potentiometric titration data employing the Calvin and Melchior's (5) extension of Bjerrum's (6) method. The evaluation of $\bar{n}$ values was made from Fig. 1. The horizontal distances between the curves *1* and *2*, *3* and *4*, *5* and *6*, and *7* and *8* measure quite accurately the additional base consumed or the total number of A^{2-} complexed.

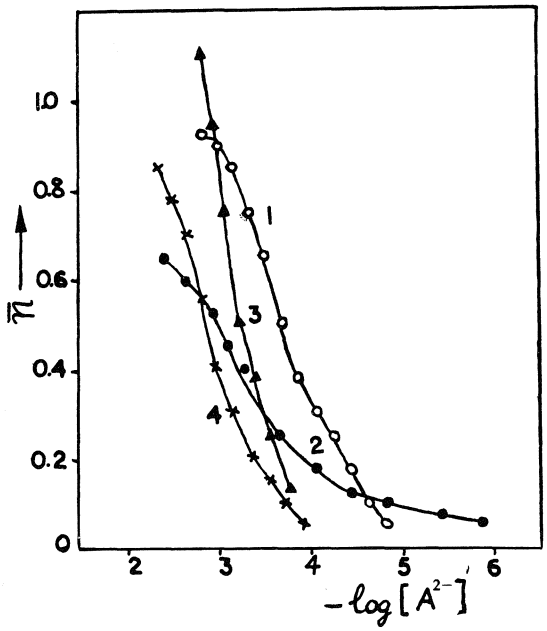

FIG. 2. Plot of $\bar{n}$ against $-\log [A^{2-}]$; curve *1*, for Zn complex; curve *2*, for Mn complex; curve *3*, for Hg complex; curve *4*, for Cd complex.

This number divided by total $[M^{2+}]$ is $\bar{n}$. At any p*H*, $[A^{2-}]$ was calculated as

$$[1] \quad [A^{2-}] = \frac{[H_2A]_{total} - [MA]}{[H^+]^2/K_{a_1}K_{a_2} + [H^+]/K_{a_2} + 1}$$

Where K_{a_1} and K_{a_2} are the first and second dissociation constants of the acid (7). Plots of $\bar{n}$ vs. $-\log [A^{2-}]$ for Zn^{2+}, Mn^{2+}, Hg^{2+}, and Cd^{2+} complexes are shown in Fig. 2. The values of log *K* were read directly from the graph at $\bar{n} = 0.5$, and were found to be 3.70, 2.95, 3.20, and 2.85 for Zn^{2+}, Mn^{2+}, Hg^{2+}, and Cd^{2+} complexes, respectively.

The values of overall changes in free energy (ΔF) of complex formation were evaluated at 35 °C from the expression $\Delta F = -RT \ln K$, where *R* is the gas constant and *T* the absolute temperature.

Results and Discussion

Titrations of 1:1 mixtures of ligand and metal with standard alkali indicate that the affinity of Zn^{2+}, Mn^{2+}, Hg^{2+}, and Cd^{2+} for the ligand is not great enough to compete with the relatively high concentration of hydrogen ions, and consequently zinc, manganese, mercury, and cadmium complexes are not formed below p*H* values 4.5, 4.5, 5.0, and 5.5, respectively. Above these p*H* values the affinity of ligand for metal increases, as a result of which an appreciable decrease in the corresponding p*H* values (as compared with the free ligand titration curve) is observed. The inflections at $m = 2$, where *m* denotes the moles of NaOH per mole of ligand, observed in the titration curves of 1:1 mixtures of metal ions and ligand vs. standard alkali, indicate the formation of 1:1 metal–ligand complexes as follows

[2] 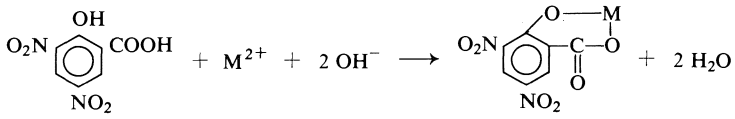

where M = Zn or Mn. On further addition of NaOH, second inflections at $m = 4$ are observed, and precipitates of $Zn(OH)_2$ (gelatinous white) and $Mn(OH)_2$ (brownish) are obtained. This shows the complete decomposition of the complex as below

[3] 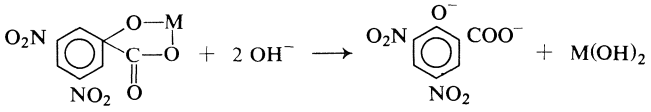

An inflection at $m = 3.5$, in the titration curve of the 1:1 mixture of ligand and Hg^{2+} ions vs. standard alkali, indicates the formation of 1:1 metal–ligand complex as in eq. [2] with M = Hg, followed by its disproportionation into HgO and hydroxo complex

Can. J. Chem. Downloaded from www.nrcresearchpress.com by 210.87.254.5 on 09/05/12
For personal use only.

TABLE 1
Stability constants of some bivalent metal complexes of 3,5-DNS

Serial number	Complex	pH range	log K_1	log K_2	$-\Delta F$ (kcal/mole)
1	Cu–3,5-DNS	2.5–4	7.0	—	9.96
2	Ni–3,5-DNS	4–9	4.80	—	6.81
3	Co–3,5-DNS	4–10	3.88	—	5.50
4	Be–3,5-DNS	2.7–9	7.13	5.29	17.34
5	Zn–3,5-DNS	4.5–8	3.70	—	5.25
6	Hg–3,5-DNS	5–8	3.20	—	4.55
7	Mn–3,5-DNS	4.5–8	2.95	—	4.18
8	Cd–3,5-DNS	5.5–8	2.85	—	4.04
9	Mg–3,5-DNS	6–9	2.65	—	3.75

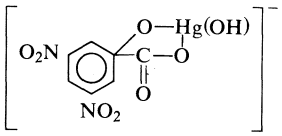

Gelatinous grey precipitate begins to appear above pH 8.0. The validity of the above course of reaction was further confirmed by gravimetric estimation of Hg in HgO and hydroxo complex. It was observed that 50% of Hg was present in HgO and the remaining 50% in hydroxo complex. This is in fair agreement with the above view.

An inflection at $m = 3$, in the titration curve of the 1:1 mixture of ligand and Cd^{2+} ions vs. standard alkali, indicates the formation of 1:1 metal–ligand complex as in eq. [2] with M = Cd, followed by its disproportionation into basic salt of cadmium

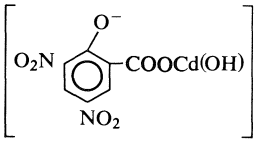

The precipitate begins to appear above pH 8.0.

When 2:1 mixtures of ligand and metal ions were titrated against standard alkali, the shift in inflections corresponds to the neutralization of excess ligand (1 mole).

Table 1 shows the stability constants of the complexes of some bivalent metal ions with 3,5-DNS at 35 °C. The stability of the transition metal ion complexes with 3,5-DNS are in the order Cu > Ni > Co > Zn > Mn, which is in agreement with the Irving and William's rule (8).

The correlation of log K values with atomic numbers of transition metal ions is shown in Fig. 3.

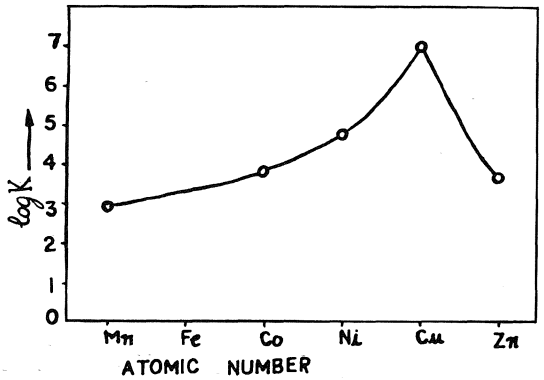

FIG. 3. Correlation of log K with atomic numbers of transition metal ions.

The authors wish to express their thanks to Dr. C. S. Bhatnagar and Dr. M. L. Mittal for valuable suggestions, and to University Grants Commission, New Delhi for the award of a research scholarship to one of them (S. S. Dhindsa).

1. S. S. DUBE and S. S. DHINDSA. Indian J. Chem. **7**, 823 (1969).
2. S. S. DUBE and S. S. DHINDSA. Z. Naturforsch. In press.
3. S. S. DUBE and S. S. DHINDSA. J. Indian Chem. Soc. **46**, 838 (1969).
4. S. S. DUBE and S. S. DHINDSA. Z. Naturforsch. **24b**, 967 (1969).
5. M. CALVIN and N. C. MELCHIOR. J. Amer. Chem. Soc. **70**, 3270 (1948).
6. J. BJERRUM. Metal amine formation in aqueous solutions. P. Haase and Co. Copenhagen. 1941.
7. S. S. DUBE and S. S. DHINDSA. Curr. Sci. **37**, 642 (1968).
8. H. IRVING and R. WILLIAM. Nature, **162**, 746 (1948).

Can. J. Chem. Downloaded from www.nrcresearchpress.com by 210.87.254.5 on 09/05/12
For personal use only.

Dehydration of alcohols derived from 1-*t*-butyl-3-dimethylaminopropan-1-one; a novel cleavage reaction involving 2,6-dichlorobenzylmagnesium bromide

A. F. CASY AND R. R. ISON
Faculty of Pharmacy and Pharmaceutical Sciences, University of Alberta, Edmonton, Alberta

Received October 20, 1969

The acid-catalyzed dehydration of 1-*t*-butyl-3-dimethylamino-1-phenylpropan-1-ol gives *cis*(*t*-Bu/H)1-*t*-butyl-3-dimethylamino-1-phenylprop-1-ene exclusively. Dehydration of the product of reaction between 1-*t*-butyl-3-dimethylaminopropan-1-one and 2,6-dichlorobenzylmagnesium bromide gives *cis* and *trans* 2-*t*-butyl-1-2,6-dichlorophenyl-4-dimethylaminobut-2-ene plus the *cis* aminopropene of the first reaction. The formation of the aminopropene, together with that of its precursor tertiary alcohol, represents a novel cleavage reaction of 2,6-dichlorobenzylmagnesium bromide. The configurations of the aminoalkenes were established from proton magnetic resonance spectroscopic data, the *cis*(*t*-Bu/H)but-2-ene providing a further example of a magnetically non-equivalent *t*-butyl group.

Canadian Journal of Chemistry, **48**, 1011 (1970)

Can. J. Chem. Downloaded from www.nrcresearchpress.com by 210.87.254.40 on 09/05/12
For personal use only.

During the course of a study of structure-activity relationships among aminobutenes with antihistaminic properties (1), the acid-catalyzed dehydration of some tertiary alcohols derived from 1-*t*-butyl-3-dimethylaminopropan-1-one (**1**) was investigated. Reaction between this Mannich base and lithium phenyl gave a mixture of the

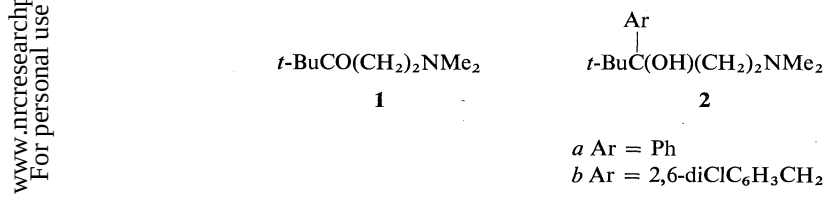

tertiary alcohol **2***a* and unchanged **1** which could not be resolved. The alcohol **2***a* was isolated as a hydrochloride, however, from the product of treating unpurified material from the reaction with an acetic–hydrochloric acid mixture (reflux, 4 h), together with a 1-*t*-butyl-3-dimethylamino-1-phenylprop-1-ene. The dehydration procedure allows the equilibration of isomers (2), hence the product obtained represents the more stable form (the proton magnetic resonance (p.m.r.) spectrum of the total base displayed a single vinylic signal so only one isomer appears to be produced). This is probably the *cis* *t*-Bu/H propene **3** since Catalin models reveal that interactions between adjacent substituents are undoubtedly of a higher order in the corresponding *trans* isomer (*cis* *t*-Bu/CH_2NMe_2). This assignment is supported by the near-coincidence of the aminopropene's vinylic chemical shift with that of the model **4**, of known configuration (3).

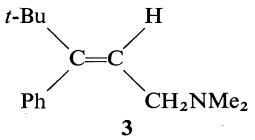

3

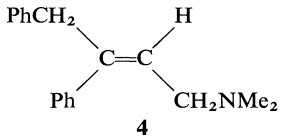

4

The mixture resulting from reaction between the Mannich base **1** and 2,6-dichlorobenzylmagnesium bromide was dehydrated in the same manner, and the product fractionally crystallized after acidification with hydrogen chloride or hydrogen bromide. Three aminoalkenes were isolated, yields being low because the precursor contained a substantial amount of non-alcoholic impurity (chiefly **1**). Two were the isomeric

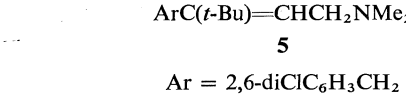

aminobut-2-enes **5** derived from the tertiary alcohol **2***b*, the anticipated product of the Grignard reaction (the configurations of **5** are discussed below). The third, however, was the aminopropene **3**; this unexpected result was corroborated by subsequent isolation of its precursor tertiary alcohol **2***a* from the total product of the Grignard reaction. Reaction between 2,6-dichlorobenzylmagnesium bromide and **1** must therefore involve some loss of aryl halogens and methylene group from the substituted benzyl fragment (the purity of the halide used to prepare the Grignard reagent was confirmed from integral data of its p.m.r. spectrum and by gas–liquid chromatography (g.l.c.)). This loss may be linked with the highly hindered nature of the 2 components of

TABLE 1

The p.m.r. characteristics* of the aminopropene **3** and the aminobutenes **5**

Alkene (*t*-Bu/H configuration)	Vinylic†	CH_2Ar	CH_2N	NMe_2§	*t*-Bu‖
cis **3** HCl	4.05	—	6.72‡	7.33	8.88
cis **5** HCl	4.55	6.90‖	6.30¶	7.28	8.82 (6 protons) 8.12** (3 protons)
trans **5** HBr	4.18	6.13**	6.90††	7.43	8.77

*Chemical shifts in τ from TMS, coupling constants in Hz; solvent $CDCl_3$.
†Triplet (J = 7.5).
‡Center of doublet of doublets (J = 5 and 7.5).
§Doublet (J = 6, $\overset{+}{N}HMe_2$).
‖Singlet.
¶Center of broad band.
**Broad singlet.
††Deformed triplet.

the reaction, since the less crowded Mannich base **6**, with the same Grignard reagent, gave a 40% yield of the expected tertiary alcohol **7**, no abnormal products being detected. There are few references to the use of 2,6-dichlorobenzyl halides in Grignard reactions (4), and the degradative phenomenon noted here appears to be novel; the mechanism involved is obscure.

$PhCO(CH_2)_2NMe_2$ **6**

$ArPhC(OH)(CH_2)_2NMe_2$ **7**

Ar = 2,6-di$ClC_6H_3CH_2$

The aminobutene **5** isolated as a hydrochloride was assigned a *cis*, and that isolated as a hydrobromide a *trans* *t*-Bu/H configuration on the grounds of differences in the chemical shifts of their vinylic, benzylic methylene, and *t*-butyl signals, as previously described for the related compounds **5** (Ar = $PhCH_2$ and 2-ClC_6H_4-CH_2) (5). The *t*-butyl signals differed in a striking manner, that of *trans* **5** being a sharp 9-proton singlet while the *cis* signal was a sharp 6- plus a broad 3-proton singlet. Signal appearance in the last case is attributed to magnetic non-equivalence of the *t*-butyl group (5), now a well documented phenomenon (6).

The *t*-butylaminoalkene **3** and its reduction product, 1-*t*-butyl-3-dimethylamino-1-phenylpropane, failed to antagonize histamine-induced contractions of the guinea-pig ileum. We thank Drs. R. T. Brittain and R. G. W. Spickett for these data.

Experimental

The p.m.r. spectra were recorded on a Varian A-60D spectrometer using $CDCl_3$ or DMSO-d_6 as solvent and TMS as reference standard. The p.m.r. characteristics of the aminobutenes **3** and **5** are given in Table 1.

1-t-Butyl-1-phenyl-3-dimethylaminopropan-1-ol, its Propene and Propane Analogs

A mixture of the Mannich base **1** (5) (17.1 g) and lithium phenyl prepared from bromobenzene (17.1 g), lithium (1.65 g) and ether (100 ml) was treated under reflux for 1 h, and then decomposed with NH_4Cl–ice. The organic layer was dried ($CaCl_2$) and evaporated to give a mixture of **1** and the *t*-alcohol **2***a* (i.r. evidence); fractional crystallization of the hydrochloride, m.p. 170–175°, obtained from this base failed to separate the components. A similar product resulted after **1** and lithium phenyl had been heated in toluene at the reflux temperature for 18 h.

The mixture (6 g) was heated under reflux with acetic acid (40 ml) and concentrated hydrochloric acid (20 ml) for 4 h, the base recovered as usual (7), (its p.m.r. spectrum in $CDCl_3$ displayed a single vinylic signal at 4.33 τ) acidified with ethanolic hydrogen chloride and fractionally crystallized. Products isolated were: the *cis* (*t*-Bu/H) prop-1-ene **3** hydrochloride (0.45 g), m.p. 250°.

Anal. Calcd. for $C_{15}H_{24}ClN$: C, 71.0; H, 9.5; N, 5.5. Found: C, 70.8; H, 9.5; N, 5.8.

The *t*-alcohol **2***a* hydrochloride (0.6 g), m.p. 185–187°.

Anal. Calcd. for $C_{15}H_{26}ClNO$: C, 66.3; H, 9.6; N, 5.15. Found: C, 66.45; H, 9.7; N, 4.95.

A mixture of **3** hydrochloride (0.38 g), 10% palladized charcoal (0.3 g), and ethanol (100 ml) was stirred with hydrogen at atmospheric pressure until gas absorption ceased (5 h required). The product was filtered through kieselguhr, the filtrate evaporated and the residue recrystallized to give 1-*t*-butyl-3-dimethylamino-1-phenylpropane hydrochloride (0.3 g), m.p. 201–202° from acetone.

Anal. Calcd. for $C_{15}H_{25}ClN$: C, 70.5; H, 10.2. Found: C, 70.2; H, 10.0.

Reaction of the Mannich Base 1 with 2,6-Dichlorobenzylmagnesium Bromide and Dehydration of the Product

The Mannich base **1** (15 g) in ether was added to a Grignard reagent prepared from 2,6-dichlorobenzyl bromide (p.m.r. integral ratio Ar—H:CH_2; 3.0:2.0) (45.8 g), magnesium (4.9 g) and ether (250 ml), and the mixture heated under reflux for 2.5 h, then decomposed with NH_4Cl–ice. The base, recovered as usual, formed a

Can. J. Chem. Downloaded from www.nrcresearchpress.com by 210.87.254.40 on 09/05/12
For personal use only.

hydrochloride (14.1 g), m.p. 150–160° (a butanol–**1** mixture) which was fractionally crystallized from ethanol–ether to give similar mixtures together with a pure crop of **2***a* hydrochloride (0.8 g), m.p. and mixed m.p. 185–187° (i.r. and p.m.r. spectra identical with those of authentic sample).

Anal. Calcd. for $C_{15}H_{26}ClNO$: C, 66.3; H, 9.6. Found: C, 66.55; H, 9.6.

The total base (10 g) was dehydrated in a mixture of acetic acid and hydrochloric acids as before and the following products isolated:

The *cis* prop-1-ene **3** hydrochloride, (0.58 g), m.p. and mixed m.p. 242–243° (i.r. and p.m.r. spectra identical with those of authentic sample).

The *cis* (*t*-Bu/H) but-2-ene **5** hydrochloride, (0.39 g), m.p. 208–210°.

Anal. Calcd. for $C_{16}H_{24}Cl_3N$: C, 57.1; H, 7.2; N, 4.2. Found: C, 57.4; H, 7.4; N, 4.1.

The *trans* (*t*-Bu/H) but-2-ene **5** hydrobromide, (0.25 g), m.p. 223°.

Anal. Calcd. for $C_{16}H_{24}BrCl_2N$: C, 50.4; H, 6.35; N, 3.7. Found: C, 50.7; H, 6.5; N, 3.5.

The Mannich base **1** hydrochloride (1.11 g) was also recovered.

The purity of the sample of 2,6-dichlorobenzyl bromide m.p. 55°, identical with reported value (8), used in this experiment was checked by its g.l.c. behavior in an F and M Scientific 700 laboratory chromatograph (hydrogen flame ionization detector, 6 ft 1% silicon gum rubber, diameter 1/8 in. column with OV-17, 80–100 mesh DMCS stationary phase). It gave rise to a single peak of retention time 20.5 min at 120°. Under the same conditions, the retention time of bromobenzene (a probable contaminant which could lead to **2***a* and **3**) was 1.2 min, while a 50:50 mixture of the 2 halides displayed peaks corresponding with those of the pure materials.

1-(2,6-Dichlorophenyl)-4-dimethylamino-2-phenylbutan-2-ol

The Mannich base **6** (9) (16 g) was treated with a Grignard reagent prepared from 2,6-dichlorobenzyl bromide (35.9 g) and magnesium (4.9 g) as before. The base product after acidification with ethanolic hydrogen chloride yielded hydrochlorides of **6** (0.6 g) and *t*-butanol **7** (11.2 g), m.p. 234–235°.

Anal. Calcd. for $C_{18}H_{22}Cl_3NO$: C, 57.7; H, 5.9. Found: C, 57.6; H, 5.65.

Its p.m.r. spectrum in DMSO-d_6 (10% w/v) displayed a characteristic 8-proton aryl signal at 2.65 τ and a 2-proton methylene signal at 6.61 τ (both broad singlets). The hydroxyl signal was at 4.70 τ (broad singlet, which collapsed after the addition of a drop of D_2O).

The authors thank the Medical Research Council of Canada for financial support.

1. A. F. Casy and A. P. Parulkar. Can. J. Chem. **47**, 423 (1969).
2. A. F. Casy, A. H. Beckett, and M. A. Iorio. Tetrahedron, **23**, 1405 (1967).
3. A. F. Casy and P. Pocha. Tetrahedron, **23**, 633 (1967).
4. M. S. Kharasch and O. Reinmuth. Grignard reactions of non-metallic substances. Prentice-Hall, Englewood Cliffs, 1954.
5. A. F. Casy and R. R. Ison. Tetrahedron, **25**, 641 (1969).
6. F. A. Anet and M. St. Jacques. J. Amer. Chem. Soc. **88**, 2586 (1966); F. A. Anet, M. St. Jacques, and G. N. Chnurny. J. Amer. Chem. Soc. **90**, 5243 (1968); J. P. N. Brewer, H. Heaney, and B. A. Marples. Chem. Commun. 27 (1967); A. Rieker, N. Zeller, and H. Kessler. J. Amer. Chem. Soc. **90**, 6566 (1968); W. E. Heyd and C. A. Cupas. J. Amer. Chem. Soc. **91**, 1559 (1969).
7. A. F. Casy, J. L. Myers, and P. Pocha. Tetrahedron, **22**, 1001 (1966).
8. F. Krohnke, K. Ellegast, and E. Bertran. Ann. **600**, 176 (1956).
9. A. Pohland and H. R. Sullivan. J. Amer. Chem. Soc. **75**, 4458 (1953).

Acid-catalyzed rearrangement of 3-carene-2,5-dione (3,7,7-trimethylbicyclo[4.1.0]hept-3-ene-2,5-dione)

I. W. J. Still[1] and G. W. Nathan
Department of Chemistry, University of Toronto, Toronto 181, Ontario

Received October 14, 1969

The reaction of 3-carene-2,5-dione (**2**) with acetic anhydride – concentrated sulfuric acid at 25° has been shown to lead exclusively to the formation of 2-methyl-6-isopropenylhydroquinone diacetate (**3***b*).

Canadian Journal of Chemistry, **48**, 1013 (1970)

The recently published findings of Bellamy and Whitham (1) on the reductive and mineral acid catalyzed rearrangements of 3-methylcar-4-en-2-one (**1**) led us to examine the effect of acid on 3-carene-2,5-dione (**2**). In the case of compound **1** it was found that preferential acid-catalyzed cleavage of the C_1—C_7 bond occurred, with exclusive formation of *p*-menthane derivatives. In the case of 3-carene-2,5-dione the presence of a second carbonyl group might be expected to lead,

[1]Author to whom enquiries should be addressed.

Can. J. Chem. Downloaded from www.nrcresearchpress.com by 210.87.254.40 on 09/05/12
For personal use only.

hydrochloride (14.1 g), m.p. 150–160° (a butanol–**1** mixture) which was fractionally crystallized from ethanol–ether to give similar mixtures together with a pure crop of **2***a* hydrochloride (0.8 g), m.p. and mixed m.p. 185–187° (i.r. and p.m.r. spectra identical with those of authentic sample).

Anal. Calcd. for $C_{15}H_{26}ClNO$: C, 66.3; H, 9.6. Found: C, 66.55; H, 9.6.

The total base (10 g) was dehydrated in a mixture of acetic acid and hydrochloric acids as before and the following products isolated:

The *cis* prop-1-ene **3** hydrochloride, (0.58 g), m.p. and mixed m.p. 242–243° (i.r. and p.m.r. spectra identical with those of authentic sample).

The *cis* (*t*-Bu/H) but-2-ene **5** hydrochloride, (0.39 g), m.p. 208–210°.

Anal. Calcd. for $C_{16}H_{24}Cl_3N$: C, 57.1; H, 7.2; N, 4.2. Found: C, 57.4; H, 7.4; N, 4.1.

The *trans* (*t*-Bu/H) but-2-ene **5** hydrobromide, (0.25 g), m.p. 223°.

Anal. Calcd. for $C_{16}H_{24}BrCl_2N$: C, 50.4; H, 6.35; N, 3.7. Found: C, 50.7; H, 6.5; N, 3.5.

The Mannich base **1** hydrochloride (1.11 g) was also recovered.

The purity of the sample of 2,6-dichlorobenzyl bromide m.p. 55°, identical with reported value (8), used in this experiment was checked by its g.l.c. behavior in an F and M Scientific 700 laboratory chromatograph (hydrogen flame ionization detector, 6 ft 1% silicon gum rubber, diameter 1/8 in. column with OV-17, 80–100 mesh DMCS stationary phase). It gave rise to a single peak of retention time 20.5 min at 120°. Under the same conditions, the retention time of bromobenzene (a probable contaminant which could lead to **2***a* and **3**) was 1.2 min, while a 50:50 mixture of the 2 halides displayed peaks corresponding with those of the pure materials.

1-(2,6-Dichlorophenyl)-4-dimethylamino-2-phenylbutan-2-ol

The Mannich base **6** (9) (16 g) was treated with a Grignard reagent prepared from 2,6-dichlorobenzyl bromide (35.9 g) and magnesium (4.9 g) as before. The base product after acidification with ethanolic hydrogen chloride yielded hydrochlorides of **6** (0.6 g) and *t*-butanol **7** (11.2 g), m.p. 234–235°.

Anal. Calcd. for $C_{18}H_{22}Cl_3NO$: C, 57.7; H, 5.9. Found: C, 57.6; H, 5.65.

Its p.m.r. spectrum in DMSO-d_6 (10% w/v) displayed a characteristic 8-proton aryl signal at 2.65 τ and a 2-proton methylene signal at 6.61 τ (both broad singlets). The hydroxyl signal was at 4.70 τ (broad singlet, which collapsed after the addition of a drop of D_2O).

The authors thank the Medical Research Council of Canada for financial support.

1. A. F. Casy and A. P. Parulkar. Can. J. Chem. **47**, 423 (1969).
2. A. F. Casy, A. H. Beckett, and M. A. Iorio. Tetrahedron, **23**, 1405 (1967).
3. A. F. Casy and P. Pocha. Tetrahedron, **23**, 633 (1967).
4. M. S. Kharasch and O. Reinmuth. Grignard reactions of non-metallic substances. Prentice-Hall, Englewood Cliffs, 1954.
5. A. F. Casy and R. R. Ison. Tetrahedron, **25**, 641 (1969).
6. F. A. Anet and M. St. Jacques. J. Amer. Chem. Soc. **88**, 2586 (1966); F. A. Anet, M. St. Jacques, and G. N. Chnurny. J. Amer. Chem. Soc. **90**, 5243 (1968); J. P. N. Brewer, H. Heaney, and B. A. Marples. Chem. Commun. 27 (1967); A. Rieker, N. Zeller, and H. Kessler. J. Amer. Chem. Soc. **90**, 6566 (1968); W. E. Heyd and C. A. Cupas. J. Amer. Chem. Soc. **91**, 1559 (1969).
7. A. F. Casy, J. L. Myers, and P. Pocha. Tetrahedron, **22**, 1001 (1966).
8. F. Krohnke, K. Ellegast, and E. Bertran. Ann. **600**, 176 (1956).
9. A. Pohland and H. R. Sullivan. J. Amer. Chem. Soc. **75**, 4458 (1953).

Acid-catalyzed rearrangement of 3-carene-2,5-dione (3,7,7-trimethylbicyclo[4.1.0]hept-3-ene-2,5-dione)

I. W. J. Still[1] and G. W. Nathan
Department of Chemistry, University of Toronto, Toronto 181, Ontario

Received October 14, 1969

The reaction of 3-carene-2,5-dione (**2**) with acetic anhydride – concentrated sulfuric acid at 25° has been shown to lead exclusively to the formation of 2-methyl-6-isopropenylhydroquinone diacetate (**3***b*).

Canadian Journal of Chemistry, **48**, 1013 (1970)

The recently published findings of Bellamy and Whitham (1) on the reductive and mineral acid catalyzed rearrangements of 3-methylcar-4-en-2-one (**1**) led us to examine the effect of acid on 3-carene-2,5-dione (**2**). In the case of compound **1** it was found that preferential acid-catalyzed cleavage of the C_1—C_7 bond occurred, with exclusive formation of *p*-menthane derivatives. In the case of 3-carene-2,5-dione the presence of a second carbonyl group might be expected to lead,

[1]Author to whom enquiries should be addressed.

Can. J. Chem. Downloaded from www.nrcresearchpress.com by 210.87.254.40 on 09/05/12
For personal use only.

Can. J. Chem. Downloaded from www.nrcresearchpress.com by 210.87.254.40 on 09/05/12
For personal use only.

via protonation of a carbonyl group in acidic media, either to C_6—C_7 or C_1—C_7 cleavage and production of a tertiary carbonium ion, or as a less likely alternative, to C_1—C_6 cleavage and formation of a secondary carbonium ion. Loss of a proton from one of the methyl groups at C-7 and enolization of the remaining carbonyl group would lead in the first two instances to the aromatic derivatives **3***a* or **4***a* respectively, while C_1—C_6 cleavage would have the additional disadvantage energetically of leading to non-benzenoid products. We have used the same reaction conditions as Bellamy and Whitham (concentrated sulfuric acid in acetic anhydride), as it was felt that the diacetates (**3***b* or **4***b*) would be less labile than the parent hydroquinones (**3***a* or **4***a*).

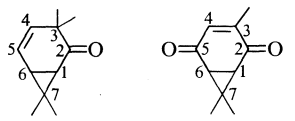

1 **2**

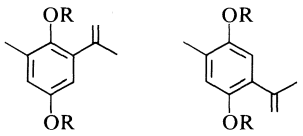

3 **4**

a R = H *a* R = H
b R = Ac *b* R = Ac

Treatment of **2** under these conditions led to the formation of a single liquid product (68% after distillation), the homogeneity of which was established by thin-layer chromatography (t.l.c.) and gas–liquid chromatography (g.l.c.). The product showed no hydroxylic absorption in the infrared (i.r.) and a single carbonyl band at 1764 cm^{-1}. In addition, there were bands present characteristic of a benzenoid ring, a phenolic (or enolic) acetate and the grouping $\diagdown C{=}CH_2$. The ultraviolet (u.v.) spectrum combined the main absorption bands observed for α-methylstyrene and hydroquinone diacetate. Elemental analysis and mass spectral data were in accord with the formula $C_{14}H_{16}O_4$, as was the nuclear magnetic resonance (n.m.r.) spectrum (see Experimental). This spectroscopic evidence could be accommodated by either **3***b* or **4***b*.

A decision between the two possibilities was made possible by catalytic hydrogenation of the rearrangement product over palladium which resulted in the uptake of 1.14 moles of hydrogen. The reduced acetate which resulted (75% after distillation) was shown by t.l.c. to be a single compound, the purity of which was not less than 97% by g.l.c. analysis. The acetate revealed i.r. bands at 1767, 1215, and 1174 cm^{-1} and aromatic region bands similar to those in the precursor, but the band at 910 cm^{-1} due to the $\diagdown C{=}CH_2$ grouping had disappeared. This liquid acetate was clearly different from the previously described solid thymoquinol diacetate **6**, an authentic sample of which was prepared from thymoquinone by reductive acetylation (2, 3). Table 1 compares the i.r., u.v., and n.m.r. spectra of **5** and **6**. As would be expected for two such positional isomers, the differences between the respective u.v. and i.r. spectra are extremely small, and are only slightly more marked in the case of the n.m.r. data. Furthermore, since **3***b* and **4***b* are the only aromatic structures which are mechanistically likely for the rearrangement product itself, it follows that our reduced acetate is actually **5** and the rearrangement product must therefore be 2-methyl-6-isopropenylhydroquinone diacetate (**3***b*).

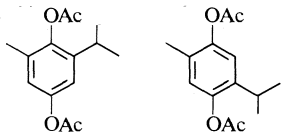

5 **6**

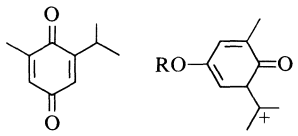

7 **8**

Several attempts have been made to convert **5** into the corresponding quinone **7** by mild hydrolysis followed by oxidation. Although in one instance i.r. evidence suggested the presence of a quinone in the crude oxidation product, we were unable to isolate **7** in pure form. Examination of the literature has revealed that 2,6-dialkyl *p*-quinones are relatively rare, the 2,6-diethyl derivative (4) being the closest analogue of **7** that we could find.

TABLE 1
Spectral comparison of diacetates **5** and **6**

Compound	Spectrum (solvent)		
	Nuclear magnetic resonance (pyridine-d_5) δ, p.p.m.	Infrared (CCl_4) cm^{-1}	Ultraviolet (MeOH) nm
5	1.10 (6H, d, J = 6.8 Hz) 2.05 (3H, s) 2.16 (3H, s) 2.24 (3H, s) 3.01 (1H, sept, J = 6.8 Hz) 6.93 (2H, m)	1767 1215 1174	216 (ε, 10800) 274 (ε, 2400)
6	1.11 (6H, d, J = 6.5 Hz) 2.06 (3H, s) 2.23 (3H, s) 2.26 (3H, s) 3.05 (1H, sept, J = 6.5 Hz) 7.11 (2H, m)	1767 1215 1160	215 (ε, 7800) 274* (ε, 950)

*Fine structure of slightly lower intensity at 265–270 nm.

The selective formation of 2-methyl-6-isopropenylhydroquinone diacetate rather than the 2,5-isomer **4** may be attributed to steric and electronic factors. If the electrophile R^+ leading to the presumed intermediate carbonium ion **8** is the acetylium ion rather than a proton, then attack at the C_5-carbonyl would be preferred on steric grounds. The same result might reasonably be predicted on the basis that electron release from the C_3-methyl group should selectively enhance the basicity of the C_5-carbonyl group. Loss of a proton from one of the C_7-methyl groups in **8**, enolization, and acetylation then lead to **3***b*.

Experimental

Infrared spectra were recorded neat or in CCl_4 on a Perkin–Elmer Model 237B grating spectrophotometer and the u.v. spectra in methanol on a Unicam SP800 recording spectrophotometer. The n.m.r. spectra were obtained on a Varian HA-100 instrument with tetramethylsilane as internal standard. Mass spectra were measured on an AEI MS-902 spectrometer and elemental analyses were carried out in the laboratory of A. B. Gygli, Toronto. The g.l.c. analyses were carried out on a 10 ft × 3/4 in., 10% SE-30 column, using the Aerograph Autoprep A-700 instrument. All melting points and boiling points are uncorrected.

*3-Carene-2,5-dione (**2**)*

This compound was prepared by deoximation of 3-carene-2,5-dione-5-oxime (5) using the sodium nitrite – acetic acid procedure (6), and purified by sublimation.

*2-Methyl-6-isopropenylhydroquinone Diacetate (**3b**)*

Concentrated sulfuric acid (1.25 g, 0.012 mole) in acetic anhydride (36 ml) was added slowly with vigorous stirring to a solution of 3-carene-2,5-dione **2** (4.0 g, 0.025 mole) in acetic anhydride (120 ml). The mixture was stirred for 1 h at 25° before adding to water (800 ml) and shaking to hydrolyze excess acetic anhydride. Solid sodium carbonate was then added until the solution was slightly alkaline. The aqueous solution was extracted thoroughly with ether and the combined ether extracts filtered through a cone of anhydrous sodium sulfate before final drying ($MgSO_4$). Evaporation afforded a thick yellow oil (83%), which on distillation gave a viscous light yellow liquid (4.1 g, 68%), b.p. 136°/0.8 mm, n_D^{25} 1.5086. This liquid showed only a single spot on t.l.c. in several solvent systems and was at least 95% pure by g.l.c. analysis. The u.v. spectrum showed λ_{max}(MeOH) 273 (ε, 818), 234 (ε, 7920) and 216 nm (ε, 10 300). The i.r. spectrum (neat) showed bands at 1764 (C=O), 1642 (C=C), 1597, 1473, and 1435 (benzenoid), 1209 and 1170 (C—O), and 910 cm^{-1} (>C=CH_2). The n.m.r. spectrum (CCl_4) had signals at δ 1.98 (3H, s), 2.08 (6H, s), 2.10 (3H, s), 4.99 (1H, m), 5.12 (1H, m) and 6.84 (2H, m) p.p.m. The mass spectrum revealed a molecular ion at *m/e* 248 in agreement with the formula $C_{14}H_{16}O_4$.

Anal. Calcd. for $C_{14}H_{16}O_4$: C, 67.70; H, 6.51. Found: C, 67.51; H, 6.70.

*2-Methyl-6-isopropylhydroquinone Diacetate (**5**)*

2-Methyl-6-isopropenylhydroquinone diacetate (**3***b*) (1.6 g, 0.0065 mole) was hydrogenated in ethanol over 10% Pd/C (45 mg). Hydrogen uptake was complete after 3.5 h. Filtration and concentration of the reaction mixture gave on distillation a viscous, pale yellow liquid (1.20 g, 75%), b.p. 115°/0.3 mm, n_D^{25} 1.4937. The essential homogeneity and purity (> 97%) of the reduced acetate was again revealed by t.l.c. and g.l.c. The u.v. spectrum showed λ_{max}(MeOH) 216 (ε, 10 800) and 274 nm (ε, 2400). The i.r. spectrum (CCl_4) showed bands at 1767 (C=O), 1215 and 1174 cm^{-1} (C—O). The n.m.r. spectrum (pyridine-d_5) had signals at δ 1.10 (6H, d, J = 6.8 Hz), 2.05 (3H, s), 2.16 (3H, s), 2.24 (3H, s), 3.01 (1H, sept, J = 6.8 Hz) and 6.93 (2H, m) p.p.m. The mass spectral data showed the expected molecular ion at *m/e* 250.

Can. J. Chem. Downloaded from www.nrcresearchpress.com by 210.87.254.40 on 09/05/12
For personal use only.

Anal. Calcd. for $C_{14}H_{18}O_4$: C, 67.26; H, 7.28. Found: C, 67.44; H, 7.39.

Thymoquinol Diacetate (6)

This compound was obtained by reductive acetylation of thymoquinone (2) in an acetic anhydride – zinc dust – hydrochloric acid mixture by a modification of a standard procedure (3). The product was obtained as a white solid (79% yield) m.p. 70–71° (lit. (7) m.p. 73–75°) from petroleum ether (b.p. 60–70°).

Financial support of this work by the National Research Council of Canada is gratefully acknowledged. We wish to acknowledge also the valuable experimental contributions of Mr. R. W. Mulligan.

1. A. J. Bellamy and G. H. Whitham. Tetrahedron **24**, 247 (1968).
2. E. Kremers, N. Wakeman, and R. M. Hixon. Organic syntheses. Coll. Vol. I, 2nd Ed., John Wiley and Sons, Inc., New York, 1941. pp. 511–513.
3. L. F. Fieser. Organic experiments. 2nd Ed., Raytheon Education Co., Lexington, Massachusetts, 1968. pp. 221–222.
4. E. C. S. Jones and J. Kenner. J. Chem. Soc. 1842 (1931).
5. E. J. Corey and H. J. Burke. J. Amer. Chem. Soc. **78**, 174 (1956).
6. G. L. Buchanan, R. A. Raphael, and I. W. J. Still. J. Chem. Soc. 4372 (1963).
7. Dictionary of organic compounds. 4th Ed., Vol. 3. Eyre and Spottiswoode, London, 1965. p. 1958.

Wavelength dependency of the relative proportions of singlet/triplet methylenes from the photolysis of diazomethane[1]

G. W. Taylor[2] and J. W. Simons

Chemistry Department, New Mexico State University, Las Cruces, New Mexico 88001

Received August 21, 1969

Results of a high pressure study of the photolysis of diazomethane/*cis*-butene-2/ethylene mixtures at 4358 and 3660 Å under various conditions are reported. These results indicate that the proportion of ground triplet state methylene radicals, produced in the primary photolysis of diazomethane, is independent of photolysis wavelength.

Canadian Journal of Chemistry, **48**, 1016 (1970)

The separate reactivities of singlet and triplet electronic state methylene radicals toward C—H bonds and C=C bonds have been extensively investigated (1–12). The presence of both electronic states of methylene in the photolysis of ketene and diazomethane has been established (1–15). It has been found that the ratio of triplet to singlet methylenes varies significantly with wavelength in the photolysis of ketene (7, 8). A study of the wavelength dependence of the relative amounts of triplet and singlet methylenes from the photolysis of diazomethane/*cis*-2-butene/ethylene mixtures at high total pressures is presented here.

The experimental and analytical procedures used have been reported (16). The limited vapor pressure of *cis*-2-butene made it necessary to add ethylene in order to increase total pressures above $\sim$ 100 cm. Photolyses were carried out in 4 different sized reactors; 2 of relatively small volume (4.3 and 5.9 cc) and 2 of larger volume (15.0 and 19.6 cc). Identical pressure runs were made at each of the photolysis wavelengths of 4358 and 3660 Å for each reactor employed. In order to test the effect of varying the diazomethane (DM) concentration relative to the total pressure (P_t), several sets of experiments were performed with $DM/P_t \sim 1/10$ and $\sim 1/30$. In addition, a series of packed vessel experiments were performed in 5.8 and 26.7 cc glass wool-packed reactors with $DM/P_t \sim 1/10$ and $\sim 1/30$, respectively. Dark reactions in the 5.9 cc reactor at high total pressure with added ethylene gave none of the C_5-products of interest.

The pertinent reaction scheme and kinetic parameters for singlet methylene radicals have been reported (16). Plots of the ratio of *trans*- to *cis*-1,2-dimethylcyclopropane (TDMC/CDMC) vs. pressure are presented in Figs. 1 and 2. The data in Fig. 1 were taken from photolysis runs in which $DM/P_t \sim 1/10$ while Fig. 2 presents data taken from photolysis runs with $DM/P_t \sim 1/30$. The lower solid curves in Figs. 1 and 2 represent the predicted behavior of TDMC/CDMC vs. pressure if only singlet methylenes were present;

[1]This work was supported by National Science Foundation under Grant No. GP-6124.
[2]National Defence Education Act Predoctoral Fellow.

Can. J. Chem. Downloaded from www.nrcresearchpress.com by 210.87.254.40 on 09/05/12
For personal use only.

Anal. Calcd. for $C_{14}H_{18}O_4$: C, 67.26; H, 7.28. Found: C, 67.44; H, 7.39.

Thymoquinol Diacetate (6)

This compound was obtained by reductive acetylation of thymoquinone (2) in an acetic anhydride – zinc dust – hydrochloric acid mixture by a modification of a standard procedure (3). The product was obtained as a white solid (79% yield) m.p. 70–71° (lit. (7) m.p. 73–75°) from petroleum ether (b.p. 60–70°).

Financial support of this work by the National Research Council of Canada is gratefully acknowledged. We wish to acknowledge also the valuable experimental contributions of Mr. R. W. Mulligan.

1. A. J. Bellamy and G. H. Whitham. Tetrahedron **24**, 247 (1968).
2. E. Kremers, N. Wakeman, and R. M. Hixon. Organic syntheses. Coll. Vol. I, 2nd Ed., John Wiley and Sons, Inc., New York, 1941. pp. 511–513.
3. L. F. Fieser. Organic experiments. 2nd Ed., Raytheon Education Co., Lexington, Massachusetts, 1968. pp. 221–222.
4. E. C. S. Jones and J. Kenner. J. Chem. Soc. 1842 (1931).
5. E. J. Corey and H. J. Burke. J. Amer. Chem. Soc. **78**, 174 (1956).
6. G. L. Buchanan, R. A. Raphael, and I. W. J. Still. J. Chem. Soc. 4372 (1963).
7. Dictionary of organic compounds. 4th Ed., Vol. 3. Eyre and Spottiswoode, London, 1965. p. 1958.

Wavelength dependency of the relative proportions of singlet/triplet methylenes from the photolysis of diazomethane[1]

G. W. Taylor[2] and J. W. Simons

Chemistry Department, New Mexico State University, Las Cruces, New Mexico 88001

Received August 21, 1969

Results of a high pressure study of the photolysis of diazomethane/*cis*-butene-2/ethylene mixtures at 4358 and 3660 Å under various conditions are reported. These results indicate that the proportion of ground triplet state methylene radicals, produced in the primary photolysis of diazomethane, is independent of photolysis wavelength.

Canadian Journal of Chemistry, **48**, 1016 (1970)

The separate reactivities of singlet and triplet electronic state methylene radicals toward C—H bonds and C=C bonds have been extensively investigated (1–12). The presence of both electronic states of methylene in the photolysis of ketene and diazomethane has been established (1–15). It has been found that the ratio of triplet to singlet methylenes varies significantly with wavelength in the photolysis of ketene (7, 8). A study of the wavelength dependence of the relative amounts of triplet and singlet methylenes from the photolysis of diazomethane/*cis*-2-butene/ethylene mixtures at high total pressures is presented here.

The experimental and analytical procedures used have been reported (16). The limited vapor pressure of *cis*-2-butene made it necessary to add ethylene in order to increase total pressures above $\sim$ 100 cm. Photolyses were carried out in 4 different sized reactors; 2 of relatively small volume (4.3 and 5.9 cc) and 2 of larger volume (15.0 and 19.6 cc). Identical pressure runs were made at each of the photolysis wavelengths of 4358 and 3660 Å for each reactor employed. In order to test the effect of varying the diazomethane (DM) concentration relative to the total pressure (P_t), several sets of experiments were performed with $DM/P_t \sim 1/10$ and $\sim 1/30$. In addition, a series of packed vessel experiments were performed in 5.8 and 26.7 cc glass wool-packed reactors with $DM/P_t \sim 1/10$ and $\sim 1/30$, respectively. Dark reactions in the 5.9 cc reactor at high total pressure with added ethylene gave none of the C_5-products of interest.

The pertinent reaction scheme and kinetic parameters for singlet methylene radicals have been reported (16). Plots of the ratio of *trans*- to *cis*-1,2-dimethylcyclopropane (TDMC/CDMC) vs. pressure are presented in Figs. 1 and 2. The data in Fig. 1 were taken from photolysis runs in which $DM/P_t \sim 1/10$ while Fig. 2 presents data taken from photolysis runs with $DM/P_t \sim 1/30$. The lower solid curves in Figs. 1 and 2 represent the predicted behavior of TDMC/CDMC vs. pressure if only singlet methylenes were present;

[1]This work was supported by National Science Foundation under Grant No. GP-6124.
[2]National Defence Education Act Predoctoral Fellow.

Can. J. Chem. Downloaded from www.nrcresearchpress.com by 210.87.254.40 on 09/05/12
For personal use only.

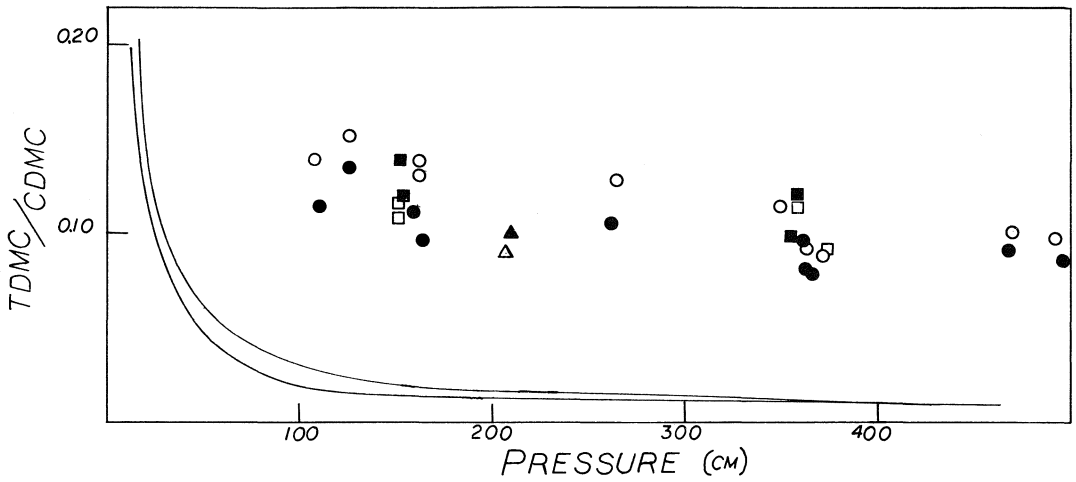

FIG. 1. Open and closed circles are data taken from runs in the 4.3 and 5.9 cc reactors at 3660 and 4358 Å, respectively. Open and closed squares represent data from the 15.0 and 19.6 cc reactor runs at 3660 and 4358 Å, respectively. The open and closed triangles are packed vessel experiments in a 5.8 cc reactor at 3660 and 4358 Å, respectively. All data points were taken with $DM/P_t \sim 1/10$.

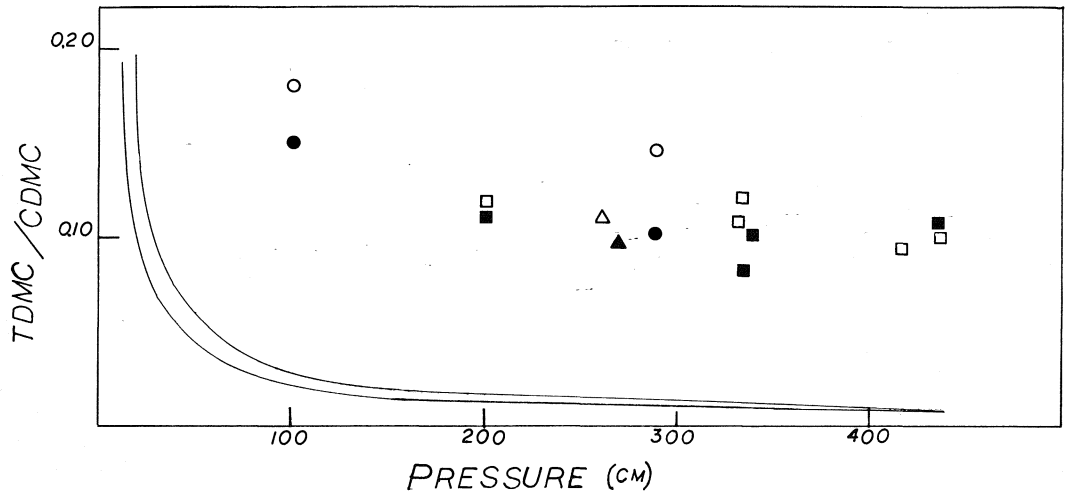

FIG. 2. Open and closed circles represent data taken from photolysis runs in the 15.0 cc reactor at 3660 and 4358 Å, respectively. The open and closed squares are 3660 and 4358 Å data, respectively, from 19.6 cc reactor experiments. Open and closed triangles are packed vessel experiments done in a 26.7 cc reactor at 3660 and 4358 Å, respectively. All photolysis experiments represented in this figure were performed with $DM/P_t \sim 1/30$.

i.e., extrapolated from lower pressure experiments (< 20 cm Hg) in the presence of oxygen. The discrepancy between these curves and the experimental points obtained in the absence of oxygen indicate the presence and effect of triplet methylene radicals in this system. In all cases the data decrease with increasing pressure to a high pressure value of 0.10 ± 0.01. In few cases do the TDMC/CDMC ratios differ by more than 10% between the 2 photolysis wavelengths at the same total pressure.

At the pressures of this study any significant difference in the TDMC/CDMC values at the 2 wavelengths probably are due to differences in the percent triplet methylene at the 2 photolysis wavelengths.

Can. J. Chem. Downloaded from www.nrcresearchpress.com by 210.87.254.40 on 09/05/12
For personal use only.

Can. J. Chem. Downloaded from www.nrcresearchpress.com by 210.87.254.40 on 09/05/12
For personal use only.

It is seen from Fig. 1 that in each pair of experiments at 3660 and 4358 Å the 3660 Å point always plots slightly above the 4358 Å point for the 4.3 and 5.9 cc volumes. When similar runs were made in the 15.0 and 19.6 cc vessels, these points were observed to invert; i.e., the 4358 Å point plotted slightly above the 3660 Å point. This effect suggested the possibility of a surface reaction and, accordingly, packed vessel experiments were done. No important surface effect was observed from the packed vessel experiments as seen in Figs. 1 and 2.

It was thought that an additional factor which might affect the observed results would be the DM/P_t ratio. Therefore, this ratio was reduced by a factor of 3 for the runs presented in Fig. 2. It is obvious that no large effect is observed. The data still decrease to a value of 0.10 at the highest pressure and only a small difference exists between data at the 2 wavelengths. The experiments done in the 5.9 cc reactor with $DM/P_t \sim 1/30$ seem to exhibit a larger wavelength effect. However, product yields for these runs were quite low and the experimental uncertainties were thus enhanced.

The slight decrease in the TDMC/CDMC ratios with increasing pressure above 100 cm Hg observed in all cases is probably due to the slightly larger selectivity of ethylene compared to *cis*-2-butene for triplet state methylene radical double bond addition compared to their selectivities for singlet methylene radical double bond addition (18). As mentioned earlier, pressures were increased above 100 cm by addition of ethylene to the reaction mixtures. The apparent insensitivity of the TDMC/CDMC ratio to the factors investigated over a wide range of pressures at both photolysis wavelengths leads us to the conclusion that the percent triplet methylene is constant and demonstrates little, if any, dependence on the photolysis energy. This conclusion supports the findings of Herzog and Carr (10).

A mechanism for ketene photolysis that seems to account qualitatively for the wavelength dependency of the proportion of triplet methylene radicals has been proposed (17). This mechanism suggests that the wavelength dependency arises essentially from a large energy difference between the singlet and triplet excited electronic states of ketene. Assuming a similar mechanism was operative in the photolysis of diazomethane, one might postulate that the lack of wavelength dependency for this system was indicative of a small energy difference between excited singlet and triplet diazomethanes.

An earlier mechanism postulated by Rabinovitch *et al.* (5) suggested that triplet methylenes arise from an intersystem crossing involving singlet and triplet states of ketene and diazomethane. A similar mechanism could explain qualitatively the invariance of triplet methylene with photolysis wavelength in this system. If it were supposed that the singlet and triplet excited electronic states of diazomethane were both repulsive, non-bonding or weakly bonding states having a narrow energy separation and a low lying intersystem crossing point on the potential energy surfaces then the lack of wavelength dependency would be explained. This latter proposal may seem more acceptable since the only evidence for pressure quenching of the singlet or triplet electronically excited states of diazomethane have been liquid experiments by Ring and Rabinovitch indicating quenching of triplet states (19).

1. J. W. Simons and B. S. Rabinovitch. J. Phys. Chem. **68**, 1322 (1964).
2. F. H. Dorer and B. S. Rabinovitch. J. Phys. Chem. **68**, 1952 (1964).
3. S. Ho, I. Unger, and W. A. Noyes, Jr. J. Amer. Chem. Soc. **87**, 2297 (1965).
4. H. M. Frey. Chem. Commun. 260 (1965).
5. B. S. Rabinovitch, K. W. Watkins, and D. F. Ring. J. Amer. Chem. Soc. **87**, 1960 (1965).
6. R. F. W. Bader and J. I. Generosa. Can. J. Chem. **43**, 1631 (1965).
7. R. W. Carr, Jr., and G. B. Kistiakowsky. J. Phys. Chem. **70**, 118 (1966).
8. R. W. Carr, Jr. J. Phys. Chem. **70**, 1970 (1966).
9. M. L. Halberstadt and J. R. McNesby. J. Amer. Chem. Soc. **89**, 3417 (1967).
10. B. M. Herzog and R. W. Carr, Jr. J. Phys. Chem. **71**, 2688 (1967).
11. D. F. Ring and B. S. Rabinovitch. J. Phys. Chem. **72**, 191 (1968).
12. J. W. Simons, C. J. Mazac, and G. W. Taylor. J. Phys. Chem. **72**, 749 (1968).
13. W. Kirmse. Carbene chemistry. Academic Press, Inc., New York, N.Y., 1964. And references therein.
14. W. B. Demore and S. W. Benson. Advances in photochemistry. Vol. 2. Interscience Publishers, New York, N.Y., 1964. p. 219.
15. H. M. Frey. Progress in reaction kinetics. Vol. 2. McMillan Co., New York, N.Y., 1964. p. 131.
16. J. W. Simons and G. W. Taylor. J. Phys. Chem. **70**, 952 (1966).
17. A. N. Strachan and D. E. Thornton. J. Phys. Chem. **70**, 952 (1966).
18. S. Krzyzanowski and R. J. Cvetanovic. Can. J. Chem. **45**, 665 (1967).
19. D. F. Ring and B. S. Rabinovitch. Int. J. Chem. Kin. **1**, 11 (1969).

Electron transference in homolytic aromatic substitution reactions

DENNIS D. DAVIS AND FAUZIA Y. AHMED
Department of Chemistry, New Mexico State University, Las Cruces, New Mexico 88001

Received August 6, 1969

The selectivity of methyl radicals in the homolytic substitution reaction on naphthalene was studied as a function of solvent. The selectivity decreases as the solvent dielectric increases. A possible explanation of these effects based upon a charge-transfer contribution to the transition state leading to σ-complex formation is offered.

Canadian Journal of Chemistry, **48**, 1019 (1970)

Can. J. Chem. Downloaded from www.nrcresearchpress.com by 210.87.254.5 on 09/05/12
For personal use only.

Dipolar effects in homolytic alkylation reactions of aromatic compounds have been suggested as an explanation of the directive effects in the cyclohexylation of substituted benzenes (1) and of the reactivities of substituted benzenes toward the trifluoromethyl radical (2). In order to further elucidate the nature of possible polar effects in homolytic aromatic substitution reactions, we have studied the methylation of naphthalene in a series of solvents.

Experimental

Solvents were reagent grade materials distilled prior to use. Naphthalene (Baker) was recrystallized from benzene.

"Lucidol", a solution of acetyl peroxide in dimethyl phthalate, and "Lupersol 7", *t*-butyl peracetate in benzene, products of the Lucidol Organic Peroxides Co., were used as supplied.

In a typical experiment, naphthalene (12.5 mmoles), solvent (200 mmoles), previously flushed with nitrogen or argon, and peroxide (2.5 mmoles) were maintained at 80° in an oil bath under a nitrogen or argon atmosphere for at least 4 half-lives of the peroxide. The reaction mixture was then analyzed directly by vapor-phase chromatography (v.p.c.) utilizing a 5′ × 1/8″ SE-30 column in an Aerograph flame ionization gas chromatograph, model 600-C. 1- and 2-Methylnaphthalenes were identified and the detector response calibrated by comparison with authentic samples supplied by the Columbia Organic Chemicals Co. and the Aldrich Chemical Co. respectively.

Results

Methyl radicals were generated by the thermal decomposition of acetyl peroxide or *t*-butyl peracetate in a dilute (5%) solution of naphthalene in the solvent under consideration. The ratio of the substitution products, 1-methylnaphthalene and 2-methylnaphthalene (1-/2-), was determined by v.p.c., Table 1. The 1-/2- ratio is independent, within experimental error, of the relative concentrations of radical precursor and naphthalene. Control experiments also show that neither isomer is selectively destroyed under the reaction conditions.

For the series of aromatic solvents, benzene, chlorobenzene, *o*-dichlorobenzene, and pyridine, the 1-/2- ratio decreases as the dielectric constant of the solvent increases. The remaining non-aromatic solvents follow a parallel pattern, however there appears to be no inclusive correlation with any of the common physical or empirical solvent parameters.

TABLE 1
Solvent effects on the 1-/2- ratio, 80°C

Solvent	Ratio*	Dielectric constant, 25°†
Benzene	7.0 ± 0.2	2.3
Chlorobenzene	6.2 ± 0.1‡	5.6
o-Dichlorobenzene	5.8 ± 0.2	9.9
Pyridine	4.0 ± 0.2	12.3
Acetic acid	9.0 ± 0.1	6.2
N,*N*-Dimethylformamide	5.2 ± 0.2	37

*Errors are standard deviation of the mean.
†Reference 14.
‡A value of 6.3 is obtained by extrapolation of data given in ref. 3.

The phenylation of naphthalene (4) exhibits a smaller solvent effect than that observed for methylation, the 1-/2- ratios for phenylation in pyridine, DMF, and benzene being 2.5, 3.1, and 3.8 respectively. These results are parallel to those for methylation.

Discussion

The concept of one-electron nucleophilicity or electrophilicity of alkyl radicals implies some degree of charge transfer in the transition state leading to the σ-complex in the substitution reaction.

$$ArH + R\cdot \rightarrow [ArH^{\delta+} \cdots R^{\delta-}]\ddagger \rightarrow \sigma\text{-complex}$$

Can. J. Chem. Downloaded from www.nrcresearchpress.com by 210.87.254.5 on 09/05/12
For personal use only.

A model for this type of resonance contribution based on Huckel MO theory and Mulliken's approach for charge transfer complexes (5) of aromatic compounds predicts that the reactivity of the aromatic substrate should be a function of the ionization potential of the donor, or the energy of the highest occupied molecular orbital (HOMO) (6). The reactivities of the acceptor alkyl radicals would be proportional to their electron affinities. Additionally, a stabilizing effect on the transition state should be noted in polar solvents.

The reactivities of aromatic molecules toward trifluoromethyl radicals are linearly related to their ionization potentials (2). Methyl (7), ethyl (8), and trichloromethyl (9) affinities of polycyclic aromatics can be correlated to the energies of the HOMO. Radical affinities, however, are also correlated by a number of other reactivity indices (7). The order of the electron affinities of alkyl radicals (10), $CF_3 > CCl_3 > CH_3 \approx C_2H_5$, is in the same order as their reactivities in homolytic aromatic substitution reactions.

The decrease in selectivity in the methylation of naphthalene as the solvent dielectric increases can be explained by an increased stabilization of the charge-separated resonance form of the transition state. As Hammond's postulate (11) would predict, stabilization of the transition state by polar solvents lowers the activation energy for the process and causes the transition state to occur earlier along the reaction path resulting in a decrease in selectivity. In solvents of similar size and type the stabilization of charge-transfer complexes is directly related to the static dielectric constant (12). The effect noted in acetic acid and DMF may well be due to a drastic change in the structure of the solvent sheath surrounding the transition state induced by the change in solvent type.

We have assumed that the electron transfer is from the aromatic substrate to the alkyl radical. Consideration of the energies involved in ionization (13) and electron gain (10) and the relationship between radical reactivities and electron affinities is best explained if alkyl radicals are acting as electron acceptors in the homolytic substitution reaction.

The methylation of naphthalene was chosen for study because of the presumed small dipolar character of methyl radicals and the high ionization potential of naphthalene, a system with a predicted minimum charge-transfer character. The solvent effect is readily discernible and it is to be expected that such effects would be even more important for other polycyclic aromatic compounds. In view of these results, the common assumption that solvent effects are unimportant in homolytic alkylation reactions of polycyclic aromatics is invalid.

Acknowledgment is made to the donors of The Petroleum Research Fund, administered by the American Chemical Society, for partial support of this research.

1. J. R. Shelton and C. W. Uzelmier. J. Amer. Chem. Soc. **88**, 5222 (1966).
2. I. M. Whittemore and M. Swarc. J. Amer. Chem. Soc. **84**, 3799 (1962).
3. J. A. Kent and R. O. C. Norman. J. Chem. Soc. 1724 (1959).
4. R. Huisgen and R. Grashey. Leibigs Ann. **607**, 46 (1957).
5. R. S. Mulliken. J. Amer. Chem. Soc. **72**, 600 (1950); J. Amer. Chem. Soc. **74**, 8110 (1952); J. Phys. Chem. **56**, 801 (1952).
6. R. S. Mulliken. Phys. Rev. **74**, 736 (1948).
7. M. Swarc and J. H. Binks. *In* Theoretical organic chemistry. Special Publication No. 12, The Chemical Society, Butterworths Scientific Publications, London, 1959. p. 262.
8. J. Smid and M. Swarc. J. Amer. Chem. Soc. **78**, 3322 (1956).
9. E. C. Kooyman and E. Farenhorst. Trans. Faraday Soc. **49**, 58 (1953).
10. H. O. Pritchard. Chem. Rev. **52**, 529 (1953); R. K. Curran. J. Chem. Phys. **34**, 2007 (1961).
11. G. S. Hammond. J. Amer. Chem. Soc. **77**, 334 (1955).
12. N. Matage, T. Okada, and N. Yamamoto. Bull. Chem. Soc. Japan, **39**, 2562 (1966).
13. D. W. Turner. *In* Advances in physical organic chemistry. Vol. 4, Academic Press, New York, 1966. p. 65.
14. E. M. Kosower. An introduction to physical organic chemistry. John Wiley and Sons, New York, 1968. p. 269.

Neutral terpenes from the bark of Sitka spruce [*Picea sitchensis* (Bong.) Carr.][1]

I. H. ROGERS AND L. R. ROZON
Department of Fisheries & Forestry, Canadian Forestry Service, Forest Products Laboratory, Vancouver, British Columbia

Received August 28, 1969

Four of the minor components of the neutral triterpene fraction of Sitka spruce bark have been isolated and characterized as 3β,21α-dihydroxy-Δ^{14}-serratene (**1**) (serratenediol), 3α,21β-dimethoxy-Δ^{14}-serratene (**2**), 3α-methoxy-21-keto-Δ^{14}-serratene (**3**), and 3β-hydroxy-21-keto-Δ^{14}-serratene (**4**). 13-Epimanool was characterized as its 3,5-dinitrobenzoate derivative.

Canadian Journal of Chemistry, **48**, 1021 (1970)

Can. J. Chem. Downloaded from www.nrcresearchpress.com by 210.87.254.40 on 09/05/12
For personal use only.

Previous work (1, 2) on the neutral triterpene fraction of the bark of Sitka spruce has resulted in the isolation and structural identification of 5 compounds which are the most plentiful in the extract. These compounds are related to serratenediol **1** in which ring C is 7-membered (3–5). Compounds of this type have also been isolated from the bark of various species of pine (genus *Pinus*) (6), from a Japanese club moss (*Lycopodium* sp.) (3), and from the rhizome of a fern (*Polypodium* sp.) (7). We report now on the separation and characterization of 4 of the minor components of the triterpene fraction and a diterpene alcohol in the bark of Sitka spruce.

Isolation

The recovery of the crude triterpene fraction from the cork layer of the bark and its preliminary separation on an alumina column was described earlier (2). This yielded crude fractions containing a ketol (compound D) and a diol (compound H). Elution of a similar column with petroleum ether yielded a triterpene dimethyl ether while use of petroleum ether – benzene (7:3) yielded a mixed fraction. Rechromatography of this fraction on another alumina column yielded a mixture of 2 methoxy ketones not previously isolated. Acetylation of the most polar fraction of the original crude extract and separation by column chromatography yielded, amongst other components, the diacetate derivative of an unknown triterpene and the diacetates of serratenediol and 21-episerratenediol.

3β,21α-Dihydroxy-Δ^{14}-serratene (1)

The serratenediol diacetate from the column chromatographic separation was contaminated with 21-episerratenediol diacetate from which it was separated by fractional crystallization from ethanol. The pure acetate had m.p. 325–328 °C (21-episerratenediol diacetate m.p. 214 °C) and had the empirical formula $C_{34}H_{54}O_4$, as determined by high resolution mass spectrometry. The presence of acetate functional groups was apparent from the infrared (i.r.) spectrum (1725 and 1242 cm^{-1}) and a trisubstituted double bond was also indicated (1640 and 795 cm^{-1}). The mass spectrum of this compound indicated a molecular ion at *m/e* 526 and satellite ions at M-60, M-75, M-120, and M-135 corresponding to loss of 2 acetate groups and 1 methyl group. After deacetylation the reaction product was purified by column chromatography and had thin-layer chromatography (t.l.c.) properties identical with an authentic sample of serratenediol and with compound H isolated directly from the original crude triterpene extract (2).

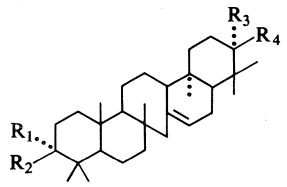

1 $R_2 = R_3 = OH$; $R_1 = R_4 = H$
2 $R_1 = R_4 = OCH_3$; $R_2 = R_3 = H$
3 $R_1 = OCH_3$; $R_2 = H$; $R_3, R_4 = O$
4 $R_2 = OH$; $R_1 = H$; $R_3, R_4 = O$

Compound H, m.p. 256–270°, was not obtained in a pure state. The spectral evidence indicated the presence of hydroxyl functions and a trisubstituted double bond. This was confirmed in the mass spectrum which had molecular ion satellites corresponding to the loss of 2 hydroxyls and 1 methyl group. Moreover the cleavage fragments observed at *m/e* 302 (ion X, $R_1 = OH$, 6.6%), 207 (ion Y, $R_1 = OH$, 22.6%), and 220 (ion Z, $R_2 = OH$, 16%) were in agreement with this compound having the Δ^{14}-serratene skeleton

[1]Preliminary communication, see ref. 12.

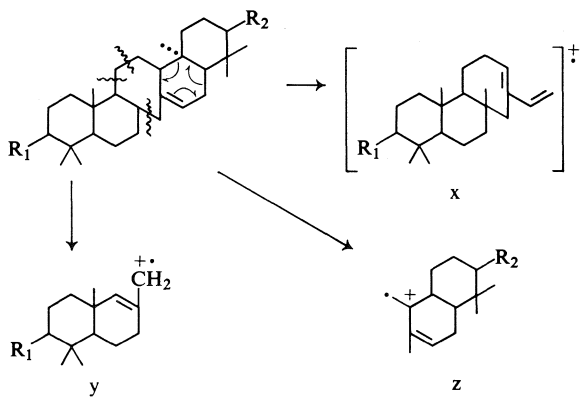

SCHEME 1

(9). The characterization of the diol was completed by a gas–liquid chromatography (g.l.c.) investigation of its trimethylsilyl (TMS) ether which showed behavior identical with that of an authentic standard of the serratenediol derivative.

3α,21β-Dimethoxy-Δ^{14}-serratene (2)

This compound was present in very low yield and was purified by high-vacuum sublimation. High-resolution mass spectrometry indicated the empirical formula $C_{32}H_{54}O_2$. The i.r. and nuclear magnetic resonance (n.m.r.) spectral evidence indicated the presence of a trisubstituted double bond and 2 methoxyl groups of secondary type. The mass spectral fragmentation of this substance was that expected of a compound with a Δ^{14}-serratene skeleton as discussed earlier (9). Thus, besides the expected molecular ion satellites at M-15, M-32, M-47, M-64, and M-79 there were present important ionic fragments at *m/e* 316 (ion X, $R_1 = OCH_3$, 22%), 221 (ion Y, $R_1 = OCH_3$, 75%), and 234 (ion Z, $R_2 = OCH_3$, 41%) (see Scheme 1).

Comparison with the methyl ether derivatives of the previously characterized compounds A and B (2) showed that compound B methyl ether is identical in all respects with the unknown derivative, to which we therefore assign the structure 3α,21β-dimethoxy-Δ^{14}-serratene (**2**).

3α-Methoxy-21 Keto-Δ^{14}-serratene (3)

This compound was isolated by preparative t.l.c. The empirical formula was determined as before to be $C_{31}H_{50}O_2$ and the i.r. and n.m.r. spectra indicated the presence of a trisubstituted double bond, a secondary methoxyl group, and a carbonyl function. The mass spectral fragmentation showed the expected satellite ions at M-15, M-32, and M-47 and also prominent ions at *m/e* 221 (ion Y, $R_1 = OCH_3$, 77%) and 218 (ion Z, $R_2 = O$, 60%) of the Δ^{14}-serratene type. The absence of an ion of type X in this case is explained by the presence of the ketone group in the molecule, which we have observed to quench the retro Diels–Alder cleavage giving rise to ion X (9).

Comparison with the known compound B ketone (2) by t.l.c., mixed m.p. and quantitative i.r. spectra, established that these compounds are identical and we therefore assign the structure as 3α-methoxy-21 keto-Δ^{14}-serratene (**3**).

3β-Hydroxy-21 Keto-Δ^{14}-serratene (4)

This material, compound D, was separated from a minor contaminant by preparative t.l.c. The physical properties as determined on a somewhat impure sample were listed previously (2), but it was not possible at that time to define the structure.

The i.r. and n.m.r. spectral evidence again showed the presence of the hydroxyl function and a trisubstituted double bond. However, this compound also possesses a carbonyl group in a 6 or larger membered ring (1707 cm^{-1}). The ketonic function gives rise to a negative Cotton effect (α 26.2) typical of a C-21 keto group in a Δ^{14}-serratene system (4). Further evidence for the presence of such a skeleton was again forthcoming from a study of the mass spectral fragmentation pattern where ions of types Y (*m/e* 207, $R_1 = OH$, 100%) and Z (*m/e* 218, $R_2 = O$, 84%) were observed. Apparently, therefore, this com-

Can. J. Chem. Downloaded from www.nrcresearchpress.com by 210.87.254.40 on 09/05/12
For personal use only.

Can. J. Chem. Downloaded from www.nrcresearchpress.com by 210.87.254.40 on 09/05/12
For personal use only.

pound is a ketol with a C-21 keto function and a hydroxyl group of unknown configuration.

Acetylation yielded a derivative, with the empirical formula $C_{32}H_{50}O_3$. Confirmation that this was a keto-acetate was obtained from the i.r. spectrum which showed the expected acetate and ketonic absorption bands. The n.m.r. spectrum contained the usual olefinic proton multiplet, a sharp 3-proton singlet at τ 8.00 arising from the acetate function and a 1-proton multiplet centered at τ 5.55 due to the secondary hydrogen geminal to the acetate group. The width of this signal (18 Hz) suggested that the acetate group is equatorial.

Reduction of the keto-acetate with $LiAlH_4$ allowed us to isolate a mixture of 2 triterpene diols whose t.l.c. behavior ($CHCl_3$; R_f 0.32 and 0.42 ratio about 10 to 1) was identical with standard samples of the compounds serratenediol and 21-episerratenediol respectively. This evidence was reinforced by g.l.c. analysis of the TMS ether derivatives which indicated the reduction product to be mainly serratenediol with a trace of 21-episerratenediol. This is as expected in that reductions of ketones with complex metal hydrides tend to favor the formation of equatorial over axial hydroxyl groups in the absence of any large steric effects (10). We therefore assign the structure 3β-hydroxy-21 keto-Δ^{14}-serratene **4** to this compound which is identical with a compound previously reported from pine bark (6).

13-Epimanool

By a combination of column chromatography on the neutral fraction of the petroleum ether bark extract followed by high vacuum distillation, a pale yellow liquid diterpene alcohol was isolated. The spectral properties of this compound together with the physical constants of its 3,5-dinitrobenzoate derivative identified it as 13-epimanool, as discussed by Rowe and Scroggins (11).

Experimental

Column chromatography was performed on neutral Woelm aluminum oxide, either as supplied (activity I) or after deactivation by the addition of 6% by weight of water (activity III). Preparative scale t.l.c. plates were prepared from silica gel G (E. Merck) and the activated plates were sprayed with a 2% alcoholic solution of Rhodamine 6G, (8) then reactivated for 1 h at 130 °C. The solvent systems used in development of the plates were either chloroform or benzene – ethyl acetate (4:1 v/v).

The n.m.r. spectra were determined in deuteriochloroform using a Varian HA 100 spectrometer. Signal positions are quoted in terms of the Tiers τ scale relative to tetramethylsilane as internal standard. Mass spectra were recorded using an Atlas CH4 or an AEI MS9 double-focusing mass spectrometer with high resolution measurements being obtained with the latter instrument. Samples for i.r. spectra were prepared as KBr disks and were recorded on a Perkin-Elmer 521 spectrophotometer. Melting points were measured on a Mettler FP1 automatic apparatus and are uncorrected. The g.l.c. analyses were performed on a Varian Aerograph Model 204-1.

Isolation and Purification

The preparation of the crude triterpene fraction and its preliminary separation on an alumina (III) column was described earlier (2). Thus 2.014 g crude extract yielded 30 mg impure compound D (**4**) and 20 mg impure compound H (serratenediol **1**). A similar separation performed on 21.939 g crude extract yielded 74 mg of a dimethyl ether **2** and 7.375 g of a mixture of methoxy ketones and methoxy alcohols. Further chromatography of the latter on an alumina (I) column eluted with benzene–ether yielded a total of 1.527 g of a partially resolved mixture of 2 methoxy ketones. This could be separated by preparative t.l.c. with about 60% recovery of the material applied. In this fashion we obtained 261 mg of the less polar compound (**3**) and 458 mg of the other which was reserved for future work.

The most polar fraction of the original 21.939 mg of triterpene extract was recovered by stripping the alumina III with ether and methanol (yield 890 mg). This was acetylated with acetic anhydride – pyridine and the crude acetate extract (960 mg) separated on alumina III. Elution with petroleum ether – benzene (7:3) yielded a mixture (210 mg) of 2 triterpene diacetates which was separated by fractional crystallization from ethanol into 2 components, m.p. 221 °C and 325–328 °C corresponding to 21-episerratenediol diacetate and serratenediol diacetate respectively. Elution of the column with petroleum ether – benzene (1:1) yielded 61 mg of the diacetate of an unknown triterpene containing a methoxyl group and this was reserved for future work.

The neutral mother liquor fraction (27.7 g) obtained from the petroleum ether extract of the bark after removal of the crystalline triterpenes was chromatographed on alumina III. Elution with petroleum ether yielded a fraction containing the known triterpene methoxy alcohols B and C (2) together with an unknown diterpene alcohol. Crops of crystals of the triterpenes were removed from petroleum ether solution and the residue (5.459 g) was distilled (220 °C at 0.2 mm Hg) to give the pure diterpene alcohol (**5**) as a pale yellow oil (1.930 g).

*3β, 21α-Dihydroxy-Δ^{14}-serratene (Serratenediol) (**1**)*

The physical and chemical properties of an impure sample, m.p. 256–270 °C, were listed in a previous publication (2) where it was referred to as compound H; ν_{max}: 3400–3300 (OH), 1387 and 1365 (geminal dimethyl), and 795 (trisubstituted double bond). The n.m.r.: 4.72 (multiplet, 1H, olefinic), 6.79 and 6.90 (overlapping triplets, J = 5.0 Hz, 2H, H—C—OH), 8.78 and 9.06–9.35 (CH_3).

Mass spectrum (MS9): fragments at *m/e* 427 (M-15),

424 (M-18), 409 (M-33), 406 (M-36), and 391 (M-51); 302 (ion X), 220 (ion Z), 207 (ion Y), other prominent fragments at 187, 147, and 135.

Anal. Calcd. for $C_{30}H_{50}O_2$ (molecular weight 442.381): C, 81.45; H, 11.31; O, 7.24. Found (442.380): C, 80.66; H, 12.03; O, 7.50.

The diacetate, m.p. 325–328 °C was isolated in a separate experiment; ν_{max}: 1725 and 1242 (OAc), 1640 and 795 (trisubstituted double bond). Mass spectrum (CH4): fragments at *m/e* 466 (M-60), 451 (M-75), 406 (M-120), and 391 (M-135). Mol. Wt. Calcd. for $C_{34}H_{54}O_4$ 526.402. Found: 526.402.

The diacetate (15 mg) was reduced with excess $LiAlH_4$ in refluxing dry tetrahydrofuran (THF) for 3 h and the excess reducing agent destroyed by the addition of moist solvent. The product was filtered, taken up in $CHCl_3$, dried, and evaporated. Elution from a small alumina III column yielded the corresponding diol (10 mg) with t.l.c. properties in ethyl acetate – benzene corresponding to an authentic sample of serratenediol contaminated with a trace of 21-episerratenediol, R_f 0.30, serratenediol 0.30, and 21-episerratenediol 0.42.

The identity of compound H was confirmed by g.l.c. analysis of the TMS ether derivative using a 6 ft × 1/8 in. stainless steel column packed with 1.5% SE 30 silicone gum rubber on gas Chrom Q (100–200 mesh). In a linear temperature programmed run from 200–300 °C, at 4 °C/min temperature gradient, serratenediol was eluted at 297 °C and 21-episerratenediol at 286°. Compound H showed 2 fractions emerging at 286° and 296° in the ratio 3 parts to 100.

3α,21β-Dimethoxy-Δ¹⁴-serratene (2)

This compound was purified by high vacuum sublimation, m.p. 254–256 °C; ν_{max}: 1090 (OCH_3), 1640 and 795 (trisubstituted double bond). The n.m.r.: 4.63 (multiplet, 1H, olefinic H), 6.72 (singlet, 6H, 2 OCH_3), 7.16 and 7.22 (overlapping triplets, J = 2.5 Hz, 2H, $CH_3O-\underset{|}{C}-H$), and 9.09–9.32 (17.5H, CH_3). Mass spectrum (CH4): fragments observed at *m/e* 455 (M-15), 438 (M-32), 423 (M-47), 406 (M-64), and 391 (M-79); other prominent fragments at *m/e* 316 (ion X), 221 (ion Y), 234 (ion Z), 284, 269, 189, 149, and 135. Mol. Wt. Calcd. for $C_{32}H_{54}O_2$: 470.412. Found: 470.415.

This compound was compared with the known compound B methyl ether (2) on a t.l.c. plate; $CHCl_3$ (R_f 0.88, compound B methyl ether 0.88); benzene–ether (10:1) (R_f 0.80, compound B methyl ether 0.80). Quantitative comparison of the i.r. spectra as KBr disks showed the compounds are identical and the mass spectra and n.m.r. spectra were also identical.

3α-Methoxy-21 Keto-Δ¹⁴-serratene (3)

After high vacuum sublimation this compound had m.p. 240–242 °C; $[\alpha]_D^{20}$ − 70.6°; ν_{max} 1707 (carbonyl), 1090 (OCH_3), 1640 and 795 (trisubstituted double bond). The n.m.r. 4.63 (multiplet, 1H, olefinic), 6.67 (singlet, 3H, OCH_3), 7.20 (triplet, J 2.5 Hz, 1H, $H-\underset{|}{C}-OCH_3$), and 8.90–9.16 (22.8H, CH_3). Mass spectrum (CH4): fragments at *m/e* 439 (M-15), 422 (M-32), 407 (M-47); other prominent fragments at *m/e* 221 (ion Y), 218 (ion Z), 284, 203, 190, 189, 149, and 135. Mol. Wt. Calcd. for $C_{31}H_{50}O_2$: 454.381. Found: 454.380.

This substance was compared with the known B ketone (2). The substances showed identical behavior when developed with $CHCl_3$ (R_f 0.38) and with benzene–ether (10:1) (R_f 0.61); compound B ketone, m.p. 238–239.5 °C, mixed m.p. 239–242 °C. The compounds are identical on the basis of quantitative i.r. spectral comparison and consideration of optical rotation, n.m.r., and mass spectral data.

3β-Hydroxy-21 Keto-Δ¹⁴-serratene (4)

The physical and chemical properties of an impure sample of this substance were listed in a previous publication (2) where it was referred to as compound D. White crystals from ethanol, m.p. 245–247 °C; optical rotatory dispersion (o.r.d.) (*c*, 0.02, CH_3OH), 21 °C: $[\phi]_{700}$ −231°, $[\phi]_{589}$ −231°, $[\phi]_{314}$ −2168°, $[\phi]_{276}$ +461°, $[\phi]_{240}$ −2906°; molecular amplitude −26.2; ν_{max}: 3500 (OH), 1707 (carbonyl), 1387 and 1370 (geminal dimethyl), and 797 (trisubstituted double bond). The n.m.r.: 4.65 (multiplet, 1H, olefinic), 6.84 (multiplet, 1H, $H-\underset{|}{C}-OH$), 8.94–9.25 (22.6H, CH_3). Mass spectrum (CH4): fragments observed at *m/e* 425 (M-15), 422 (M-18), and 407 (M-33); 218 (ion Z), 207 (ion Y); other prominent fragments at 189, 177, 149, 147, 138, and 135. Mol. Wt. Calcd. for $C_{30}H_{48}O_2$: 440.365. Found: 440.369.

A sample of the compound was acetylated in pyridine – acetic anhydride at room temperature. After standing for 2 days the crude acetate was recovered in the usual fashion and purified on a short alumina column (yield 15 mg). White platelets from acetone, m.p. 325–327 °C; ν_{max} $CHCl_3$: 1720 and 1255 (OAc) and 1702 (carbonyl). The n.m.r.: 4.55 (multiplet, 1H, olefinic), 5.50 (multiplet, 1H, $H-\underset{|}{C}-OAc$, 1/2 height width 18 Hz), 7.92 (singlet, 3H, OAc), 8.90–9.14 (CH_3). Mass spectrum (MS9): fragments observed at *m/e* 467 (M-15), 422 (M-60), and 407 (M-75); 218 (ion Z); other prominent fragments at 249, 203, 190, 189, 147, and 135. Mol. Wt. Calcd. for $C_{32}H_{50}O_3$: 482.375. Found: 482.376.

The acetate was reduced with excess $LiAlH_4$ in refluxing THF for 3 h. Workup in the usual fashion yielded a product shown by t.l.c. in ethyl acetate – benzene (1:4) to be free of starting material and to have properties similar to an authentic standard of serratenediol; R_f serratenediol 0.30, 21-episerratenediol 0.42, reaction product 2 spots R_f 0.32 and 0.42 in ratio about 10 to 1. The g.l.c. analysis of the TMS ether derivatives under the conditions previously described showed serratenediol eluted at 295 °C, 21-episerratenediol at 288 °C, and the reaction product gave two peaks at 286 and 296 °C in the ratio 1 to 30.

13-Epimanool (5)

Pale yellow oil, $[\alpha]_D^{22}$ (*c*, 1.0, $CHCl_3$) + 40.9°; λ_{max} (*n*-heptane): 228, shoulder 276 (ε 190 and 60); ν_{max} (liquid film): 3300 (OH), 3065 (vinyl or terminal methylene), 1635 (non-conjugated double bond), 1410, 990, and 915 (vinyl), 878 (terminal methylene), and 1383 and 1365 (geminal dimethyl). The n.m.r.: ABX system from vinyl group

Can. J. Chem. Downloaded from www.nrcresearchpress.com by 210.87.254.40 on 09/05/12
For personal use only.

4.15 (1H, quartet, J_{trans} = 17.5 Hz, J_{cis} = 10.5 Hz, H_a in system 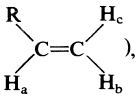), 4.88 (1H, quartet J_{trans} = 17.5 Hz, J_{gem} = 1.5 Hz, H_c), 5.05 (1H, quartet, J_{cis} = 10.5 Hz, J_{gem} = 1.5 Hz, H_b), 5.26 and 5.55 (2H, pair of wide multiplets, exocyclic methylene), 8.57 (singlet, OH, moved to 8.65 when temperature raised from 30 to 50°), 8.79 (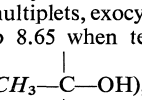), and 9.17–9.36 (CH_3). Mass spectrum (MS9): highest observed fragment at *m/e* 272, major fragments at 257, 204, 189, 161, 137, and 135.

Anal. Calcd. for $C_{20}H_{34}O$: C, 82.69; H, 11.80; O, 5.51. Found: C, 82.20; H, 12.19; O, 5.62.

The mass spectrum did not reveal a molecular ion peak. However, high resolution mass measurement on the *m/e* 272 peak gave the value 272.251. Mol. Wt. Calcd. for $C_{20}H_{32}$: 272.250. This peak therefore corresponds to $M^+ - H_2O$.

The alcohol (227 mg) was reacted with freshly prepared and recrystallized 3,5-dinitrobenzoyl chloride (227 mg) in dry pyridine (3 ml) for 2 days. The pyridine was removed by distillation *in vacuo* and the product recrystallized twice from CH_2Cl_2—MeOH. Needles, m.p. 119–120 °C; $[\alpha]_D^{22}$ (*c*, 1.0, $CHCl_3$) + 36.6°. The n.m.r.: 0.80 (1H, triplet, J = 2.0 Hz, aromatic C_4), 0.88 and 0.90 (2H, singlets, aromatic C_2 and C_6), 3.89 (1H, quartet, J_{trans} = 18 Hz, J_{cis} = 10 Hz, H_a in system 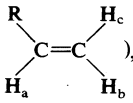), 4.74 and 4.76 (2H, overlapping multiplets, H_c and H_b), 5.15 and 5.49 (2H, multiplets, exocyclic methylene), 8.27 (3H, singlet,), and 9.12–9.32 (CH_3).

Anal. Calcd. for $C_{27}H_{36}N_2O_6$: C, 66.92; H, 7.49; N, 5.78. Found: C, 66.99; H, 7.60; N, 5.67.

Compounds **1**, **4**, and **5** were first isolated in the course of doctoral thesis work in the Chemistry Department, University of British Columbia.

1. J. P. KUTNEY and I. H. ROGERS. Tetrahedron Lett. 761 (1968).
2. J. P. KUTNEY, I. H. ROGERS, and J. W. ROWE. Tetrahedron. **25**, 3731 (1969).
3. Y. INUBUSHI, T. SANO, and Y. TSUDA. Tetrahedron Lett. 1303 (1964).
4. Y. TSUDA, T. SANO, K. KAWAGUCHI, and Y. INUBUSHI. Tetrahedron Lett. 1279 (1964).
5. Y. INUBUSHI, Y. TSUDA, T. SANO, T. KONITA, S. SUZUKI, H. AGETA, and Y. OTAKE. Chem. Pharm. Bull. Japan, **15**, 1153 (1967).
6. J. W. ROWE and C. L. BOWER. Tetrahedron Lett. 2745 (1965).
7. G. BERTI, F. BOTTARI, A. MARSILI, I. MORELLI, and A. MANDELBAUM. Chem. Commun. 50, (1967).
8. J. AVIGAN, D. S. GOODMAN, and D. STEINBERG. J. Lipid Res. **4**, 100 (1963).
9. J. P. KUTNEY, G. EIGENDORF, and I. H. ROGERS. Tetrahedron. **25**, 3753 (1969).
10. O. H. WHEELER and J. L. MATEOS. Can. J. Chem. **36**, 1431 (1958).
11. J. W. ROWE and J. H. SCROGGINS. J. Org. Chem. **29**, 1554 (1964).
12. I. H. ROGERS and L. R. ROZON. Bi-Monthly Res. Notes **25** (1), 2 (1969).

Notes 25 (1), 2 (1969).

Protonated cyclopropanes. IV.[1] Trifluoroacetolysis of 1-^{14}C-1-propyl tosylate

C. C. LEE AND W. KAO-YING CHWANG

Department of Chemistry and Chemical Engineering, University of Saskatchewan, Saskatoon, Saskatchewan

Received October 9, 1969

The trifluoroacetolysis of 1-^{14}C-1-propyl tosylate was carried out either with or without the presence of an equivalent of sodium trifluoroacetate. Both 1-propyl and 2-propyl trifluoroacetates were obtained, the latter being the major product if the sodium salt was not present. Isotope position rearrangements from C-1 to C-2 and C-3 were observed in the 1-propyl trifluoroacetate to the extent of about 2 and 17%, respectively, for the reactions effected with and without sodium trifluoroacetate. The rearranged ^{14}C-label was about equally distributed at C-2 and C-3. It is proposed that these rearrangements may be explained on the assumption that part of the overall reaction proceeds through equilibrating protonated cyclopropane intermediates.

Canadian Journal of Chemistry, **48**, 1025 (1970)

As a part of a general scrutiny of reactions with the 1-propyl system that might involve protonated cyclopropane intermediates (1–5), a study was made on the solvolysis of 1-^{14}C-1-propyl tosylate (**1**-OTs-1-^{14}C) in trifluoroacetic acid. The use of trifluoroacetic acid is of interest since it is an even more "limiting" solvent than the commonly used formic acid because of its higher ionizing power and/or more poorly nucleophilic character (6).

[1]For paper III, see ref. 4.

Can. J. Chem. Downloaded from www.nrcresearchpress.com by 210.87.254.40 on 09/05/12
For personal use only.

4.15 (1H, quartet, J_{trans} = 17.5 Hz, J_{cis} = 10.5 Hz, H_a in system 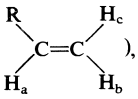), 4.88 (1H, quartet J_{trans} = 17.5 Hz, J_{gem} = 1.5 Hz, H_c), 5.05 (1H, quartet, J_{cis} = 10.5 Hz, J_{gem} = 1.5 Hz, H_b), 5.26 and 5.55 (2H, pair of wide multiplets, exocyclic methylene), 8.57 (singlet, OH, moved to 8.65 when temperature raised from 30 to 50°), 8.79 (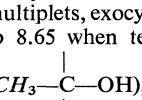), and 9.17–9.36 (CH_3). Mass spectrum (MS9): highest observed fragment at *m/e* 272, major fragments at 257, 204, 189, 161, 137, and 135.

Anal. Calcd. for $C_{20}H_{34}O$: C, 82.69; H, 11.80; O, 5.51. Found: C, 82.20; H, 12.19; O, 5.62.

The mass spectrum did not reveal a molecular ion peak. However, high resolution mass measurement on the *m/e* 272 peak gave the value 272.251. Mol. Wt. Calcd. for $C_{20}H_{32}$: 272.250. This peak therefore corresponds to $M^+ - H_2O$.

The alcohol (227 mg) was reacted with freshly prepared and recrystallized 3,5-dinitrobenzoyl chloride (227 mg) in dry pyridine (3 ml) for 2 days. The pyridine was removed by distillation *in vacuo* and the product recrystallized twice from CH_2Cl_2—MeOH. Needles, m.p. 119–120 °C; $[\alpha]_D^{22}$ (*c*, 1.0, $CHCl_3$) + 36.6°. The n.m.r.: 0.80 (1H, triplet, J = 2.0 Hz, aromatic C_4), 0.88 and 0.90 (2H, singlets, aromatic C_2 and C_6), 3.89 (1H, quartet, J_{trans} = 18 Hz, J_{cis} = 10 Hz, H_a in system 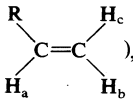), 4.74 and 4.76 (2H, overlapping multiplets, H_c and H_b), 5.15 and 5.49 (2H, multiplets, exocyclic methylene), 8.27 (3H, singlet,), and 9.12–9.32 (CH_3).

Anal. Calcd. for $C_{27}H_{36}N_2O_6$: C, 66.92; H, 7.49; N, 5.78. Found: C, 66.99; H, 7.60; N, 5.67.

Compounds **1**, **4**, and **5** were first isolated in the course of doctoral thesis work in the Chemistry Department, University of British Columbia.

1. J. P. KUTNEY and I. H. ROGERS. Tetrahedron Lett. 761 (1968).
2. J. P. KUTNEY, I. H. ROGERS, and J. W. ROWE. Tetrahedron. **25**, 3731 (1969).
3. Y. INUBUSHI, T. SANO, and Y. TSUDA. Tetrahedron Lett. 1303 (1964).
4. Y. TSUDA, T. SANO, K. KAWAGUCHI, and Y. INUBUSHI. Tetrahedron Lett. 1279 (1964).
5. Y. INUBUSHI, Y. TSUDA, T. SANO, T. KONITA, S. SUZUKI, H. AGETA, and Y. OTAKE. Chem. Pharm. Bull. Japan, **15**, 1153 (1967).
6. J. W. ROWE and C. L. BOWER. Tetrahedron Lett. 2745 (1965).
7. G. BERTI, F. BOTTARI, A. MARSILI, I. MORELLI, and A. MANDELBAUM. Chem. Commun. 50, (1967).
8. J. AVIGAN, D. S. GOODMAN, and D. STEINBERG. J. Lipid Res. **4**, 100 (1963).
9. J. P. KUTNEY, G. EIGENDORF, and I. H. ROGERS. Tetrahedron. **25**, 3753 (1969).
10. O. H. WHEELER and J. L. MATEOS. Can. J. Chem. **36**, 1431 (1958).
11. J. W. ROWE and J. H. SCROGGINS. J. Org. Chem. **29**, 1554 (1964).
12. I. H. ROGERS and L. R. ROZON. Bi-Monthly Res. Notes **25** (1), 2 (1969).

Notes 25 (1), 2 (1969).

Protonated cyclopropanes. IV.[1] Trifluoroacetolysis of 1-^{14}C-1-propyl tosylate

C. C. LEE AND W. KAO-YING CHWANG

Department of Chemistry and Chemical Engineering, University of Saskatchewan, Saskatoon, Saskatchewan

Received October 9, 1969

The trifluoroacetolysis of 1-^{14}C-1-propyl tosylate was carried out either with or without the presence of an equivalent of sodium trifluoroacetate. Both 1-propyl and 2-propyl trifluoroacetates were obtained, the latter being the major product if the sodium salt was not present. Isotope position rearrangements from C-1 to C-2 and C-3 were observed in the 1-propyl trifluoroacetate to the extent of about 2 and 17%, respectively, for the reactions effected with and without sodium trifluoroacetate. The rearranged ^{14}C-label was about equally distributed at C-2 and C-3. It is proposed that these rearrangements may be explained on the assumption that part of the overall reaction proceeds through equilibrating protonated cyclopropane intermediates.

Canadian Journal of Chemistry, **48**, 1025 (1970)

As a part of a general scrutiny of reactions with the 1-propyl system that might involve protonated cyclopropane intermediates (1–5), a study was made on the solvolysis of 1-^{14}C-1-propyl tosylate (**1**-OTs-1-^{14}C) in trifluoroacetic acid. The use of trifluoroacetic acid is of interest since it is an even more "limiting" solvent than the commonly used formic acid because of its higher ionizing power and/or more poorly nucleophilic character (6).

[1]For paper III, see ref. 4.

Can. J. Chem. Downloaded from www.nrcresearchpress.com by 210.87.254.6 on 09/05/12
For personal use only.

TABLE 1

Yields of 1-propyl trifluoroacetate (**1**-TFA) and 2-propyl trifluoroacetate (**2**-TFA) from trifluoroacetolyses of 1-propyl tosylate (**1**-OTs) with or without added sodium trifluoroacetate (NaTFA)*

Reaction time (days)	3		4		5		6	
	With NaTFA	No NaTFA	With NaTFA	No NaTFA	With NaTFA	No NaTFA	With NaTFA	No NaTFA
Unreacted **1**-OTs (g)	2.55	3.37	1.94	1.71	1.26	0.51	0.81	0.00
1-TFA (g)	1.77	0.54	1.62	0.47	1.79	0.37	1.65	0.24
2-TFA (g)	1.28	3.00	1.12	3.50	1.27	2.94	1.20	1.78

*Each experiment was carried out at reflux temperature using 8.00 g of 1-OTs, with or without an equivalent of NaTFA, in 35 ml of F_3CCOOH; the product mixture was analyzed by n.m.r. (see Experimental).

The trifluoroacetolysis of **1**-OTs-1-^{14}C, either with or without the presence of an equivalent of sodium trifluoroacetate, was carried out by refluxing the reaction mixture for 5 days. Both 1-propyl trifluoroacetate (**1**-TFA-^{14}C) and 2-propyl trifluoroacetate (**2**-TFA-^{14}C) were obtained. The reaction time of 5 days was chosen because results from preliminary trials with inactive materials, given in Table 1, suggested that this length of refluxing gave reasonably good yields of **1**-TFA relative to the yields of **2**-TFA and unreacted **1**-OTs. It should also be noted from Table 1 that when the solvolysis was effected without any sodium trifluoroacetate, the dominant product was **2**-TFA. However, when sodium trifluoroacetate was present in the reaction mixture, more **1**-TFA was formed. The mixture of **1**-TFA-^{14}C and **2**-TFA-^{14}C obtained from each solvolysis run was hydrolyzed to give the alcohols, **1**-OH-^{14}C and **2**-OH-^{14}C, which were subsequently separated by preparative vapor phase chromatography (v.p.c.) (1). The active 1-propanol (**1**-OH-^{14}C) so obtained was degraded by conversion to propionic acid, to acetic acid, to methylamine, as described previously (1) to give the ^{14}C- distribution in the 1-propyl group; the results are summarized in Table 2.

From Table 2, it is seen that there was much less isotopic scrambling in the **1**-TFA-^{14}C when the trifluoroacetolysis of **1**-OTs-1-^{14}C was carried out with added sodium trifluoroacetate. Moreover, the rearranged isotopic label was about equally distributed between C-2 and C-3. When the reaction was effected in the presence of trifluoroacetate ions from the added salt, apparently there was a larger S_N2 component which gave rise to unrearranged **1**-TFA. This conclusion would be compatible with the product distribution given in Table 1, which showed that the presence of sodium trifluoroacetate led to the formation of more **1**-TFA. When the trifluoroacetolysis was effected without added salt, the S_N1 component, which could give rise to **2**-TFA and to isotopically rearranged **1**-TFA, would be the dominant process.

The finding of about equal amounts of rearranged ^{14}C-label at C-2 and C-3 in the **1**-TFA-^{14}C product from the present work is similar to the results observed in the nitrous acid deamination of 1-^{14}C-1-propylamine (1, 5), although the extents of rearrangement were different for the different reactions. As was concluded in the earlier work (1–5), the rearrangement of the label in the 1-propyl system from C-1 to both C-2 and C-3 could be best accommodated by the intervention of equilibrating protonated cyclopropane intermediates. Thus the 1-propyl cation generated in the trifluoroacetolysis of **1**-OTs-1-^{14}C could rearrange to the 2-propyl cation and to equilibrating protonated cyclopropanes, the latter giving rise to **1**-TFA with equal amounts of ^{14}C-label at each of the 3 carbon positions.

The equal distribution of the rearranged label at C-2 and C-3 does not permit a differentiation between face-protonated cyclopropane (**3**), equilibrating corner-protonated cyclopropanes (methyl-bridged ions) (***4a*** $\rightleftarrows$ ***4b***), and equilibrating edge-protonated cyclopropanes (***5a*** $\rightleftarrows$ ***5b***) (7) (Scheme 1). There is, however, general agreement that face-protonated **3** is not the stable structure (8–10) and that probably, the edge-protonated intermediates may be preferred over the corner-protonated species (1, 8–11). Collins has pointed out (7 and private communications) that starting from **1**-X-1-^{14}C, after all intermediates have reached equilibrium, equal amounts of **1**-Y-2-^{14}C and **1**-Y-3-^{14}C would be obtained from either ***4a*** $\rightleftarrows$ ***4b*** or ***5a*** $\rightleftarrows$ ***5b***. On the

Can. J. Chem. Downloaded from www.nrcresearchpress.com by 210.87.254.6 on 09/05/12
For personal use only.

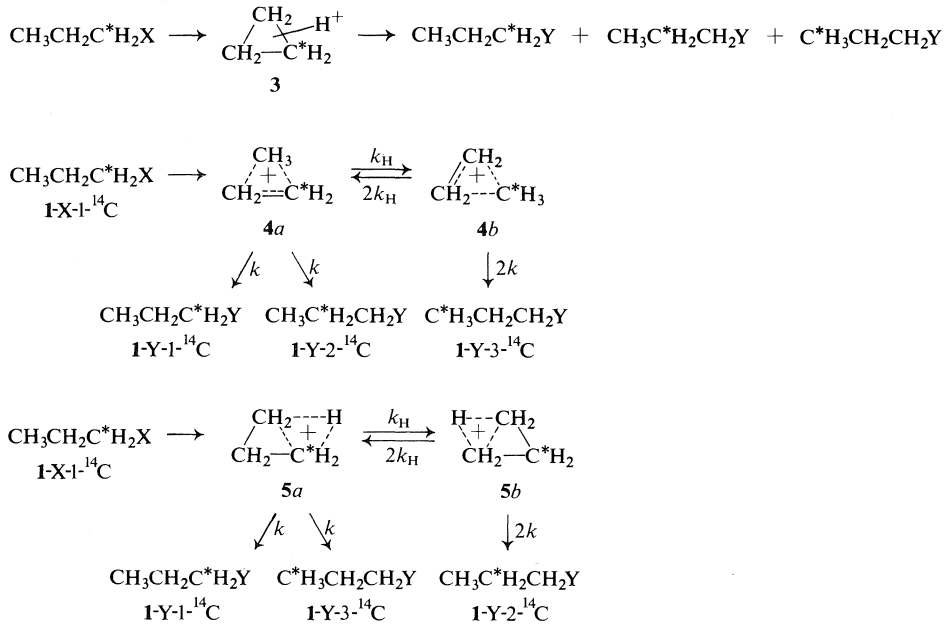

SCHEME 1

other hand, if products were formed before equilibrium has been established, from processes involving corner-protonation (**4***a* ⇄ **4***b*), **1**-Y-3-^{14}C can never be greater than **1**-Y-2-^{14}C, while from processes involving edge-protonation (**5***a* ⇄ **5***b*), **1**-Y-3-^{14}C can be greater than **1**-Y-2-^{14}C. One of the original objectives of the present work was to find out if the trifluoroacetolysis of **1**-OTs-1-^{14}C would give a **1**-TFA-^{14}C product with more ^{14}C-label at C-3 than C-2, thus providing experimental evidence for edge-protonation. Since the results indicated about equal amounts of ^{14}C-label at C-2 and C-3, in the trifluoroacetolysis of **1**-OTs-1-^{14}C, the equilibrating protonated cyclopropane intermediates must have reached equilibrium before formation of the product, **1**-TFA-^{14}C.

ADDENDUM

When the present note was being prepared for publication, a communication by Reich *et al.* (13) on the trifluoroacetolysis of certain primary alkyl tosylates has appeared. Among the compounds studied was **1**-OTs labelled with deuterium in various positions. The products obtained (at 100 or 125°) ranged from 10.3–16.3% **1**-TFA and 83.7–89.7% **2**-TFA. These product distributions can be regarded as in substantial agreement with those observed in the present work; for example, it can be seen from Table 1 that when the trifluoroacetolysis mixture was refluxed (about 73°) for 6 days without the presence of sodium trifluoroacetate, the product ratio was 12% **1**-TFA and 88% **2**-TFA. Reich *et al.* also reported that the nuclear magnetic resonance (n.m.r.) examination of the **1**-TFA derived from D-labelled **1**-OTs, such as **1**-OTs-1,1-d_2, showed essentially no isotopic scrambling (less than 2%), and this is distinctly at variance with the present results. The determination of isotope position rearrangements by ^{14}C-tracers would be more sensitive than the n.m.r. technique. The isotope position rearrangement of about 1% from C-1 to each of C-2 and C-3, observed in the trifluoroacetolysis of **1**-OTs-1-^{14}C with added sodium trifluoroacetate, would have been missed by the n.m.r. method. On the other hand, the total of about 17% rearrangement from C-1 to C-2 and C-3, found in the trifluoroacetolysis of **1**-OTs-1-^{14}C without the presence of sodium trifluoroacetate, should be readily detectable by n.m.r. and D-labelling. The absence of isotope position rearrangements reported by

Can. J. Chem. Downloaded from www.nrcresearchpress.com by 210.87.254.6 on 09/05/12
For personal use only.

Can. J. Chem. Downloaded from www.nrcresearchpress.com by 210.87.254.6 on 09/05/12
For personal use only.

TABLE 2

Activity distributions in the x-^{14}C-1-propyl trifluoroacetate (**1**-TFA-^{14}C) from trifluoroacetolysis of 1-^{14}C-1-propyl tosylate (**1**-OTs-1-^{14}C) with or without added sodium trifluoroacetate (NaTFA)

Compound assayed	Specific activity (c.p.m./mmole)*				% ^{14}C at C-2,3				% ^{14}C at C-3			
	With NaTFA		No NaTFA		With NaTFA		No NaTFA		With NaTFA		No NaTFA	
	Run 1	Run 2	Run 1	Run 2	Run 1	Run 2	Run 1	Run 2	Run 1	Run 2	Run 1	Run 2
C_2H_5COOH†	106 500	106 800	30 700	118 000	—	—	—	—	—	—	—	—
CH_3COOH†	2 040	2 220	5 400	18 900	1.9	2.1	17.6	16.0	—	—	—	—
CH_3NH_2‡	950	1 000	2 590	9 710	—	—	—	—	0.9	0.9	8.4	8.2

*Measured by a liquid scintillation counter.
†Assayed as the *p*-bromophenacyl ester.
‡Assayed as *N*-methyl-*p*-toluenesulfonamide.

Reich *et al.* apparently applies to trifluoroacetolysis without added salt, and this discrepancy, therefore, remains to be resolved.[2]

Experimental

The Solvolysis Reaction

A solution of 8.00 g (0.037 mole) of 1-^{14}C-1-propyl tosylate (**1**-OTs-1-^{14}C) (2) in 35 ml of trifluoroacetic acid, with or without 5.10 g (0.037 mole) of sodium trifluoroacetate, was heated under reflux in an oil-bath for 5 days, the top of the reflux condenser being protected by a drying tube. The resulting solution was poured into a separatory funnel containing about 200 ml of ice and water. The organic layer (about 4.0 g) was separated, washed with a small amount of water, and then distilled, the fraction boiling between 65 and 90° being collected. (The b.p. of 1-propyl and 2-propyl trifluoroacetates (**1**-TFA and **2**-TFA) (12) are 82.5 and 73.5°, respectively.)

The above crude product was hydrolyzed by heating under reflux for 3 h with 50 ml of 10% NaOH solution. To the hydrolyzate, about 1.0 g of ordinary 1-propanol (**1**-OH) was added as carrier, and the material was then continuously extracted with ether for 24 h. After drying over anhydrous $MgSO_4$, the ether was fractionated off. From the residue, the **1**-OH-^{14}C was separated from the **2**-OH-^{14}C by preparative v.p.c. as previously described (1). More **1**-OH carrier was added, if necessary, to give a total of about 3.0 g of x-^{14}C-1-propanol before it was used for the subsequent degradation.

Product Analysis Studies

The trifluoroacetolysis, using 8.00 g of ordinary **1**-OTs, with or without an equivalent of sodium trifluoroacetate, in 35 ml of trifluoroacetic acid, was carried out as described above, the reaction time being 3, 4, 5, or 6 days. The organic material recovered from the reaction mixture was not distilled, and after weighing, it was analyzed directly by n.m.r. using an HA-100 spectrometer. Comparison with the n.m.r. spectra of authentic samples showed the presence of **1**-TFA, **2**-TFA and unreacted **1**-OTs. Based on the integration of the absorptions centered at τ 4.85, 5.74, and 6.07, respectively, for the one C-2 proton of **2**-TFA, the two C-1 protons of **1**-TFA, and the two C-1 protons of unreacted **1**-OTs, the relative molar composition of the product mixture was estimated. Knowing the mole fractions and molecular weights of the three components and the total weight of the mixture, the weights of each component can be calculated. The results are summarized in Table 1.

As a test of the stability of **1**-TFA and **2**-TFA in the trifluoroacetolysis medium, an authentic sample of each of these compounds was refluxed in trifluoroacetic acid for 5 days. The n.m.r. analysis of the recovered material showed no isomerization of **1**-TFA to **2**-TFA or vice versa.

Degradations

Each sample of **1**-OH-^{14}C derived from the solvolysis runs was degraded by conversion to propionic acid, to acetic acid, and then to methylamine as described previously by Lee and Kruger (1). The degradation products were converted to the appropriate solid derivatives which were rigorously purified before being used for the determination of their radioactivity (1).

The financial support given by the National Research Council of Canada is gratefully acknowledged.

1. C. C. Lee and J. E. Kruger. Tetrahedron **23**, 2539 (1967).
2. C. C. Lee and J. E. Kruger. Can. J. Chem. **44**, 2343 (1966).
3. C. C. Lee and L. Gruber. J. Amer. Chem. Soc. **90**, 3775 (1968).
4. C. C. Lee, W. K-Y. Chwang, and K.-M. Wan. J. Amer. Chem. Soc. **90**, 3778 (1968).
5. C. C. Lee and K.-M. Wan. J. Amer. Chem. Soc. **91**, 6416 (1969).
6. J. E. Nordlander and W. G. Deadman. J. Amer. Chem. Soc. **90**, 1590 (1968).
7. C. J. Collins. Chem. Rev. **69**, 543 (1969).
8. R. Hoffmann. J. Chem. Phys. **40**, 2480 (1964).
9. J. D. Petke and J. L. Whitten. J. Amer. Chem. Soc. **90**, 3338 (1968).
10. C. C. Lee. *In* Progress in physical organic chemistry. Vol. 7. A. Streitivieser, Jr. and R. W. Taft, *editors*. Interscience publishers, New York. 1969. In press.
11. R. L. Baird and A. A. Aboderin. J. Amer. Chem. Soc. **86**, 252 (1964).
12. T. R. Norton. J. Amer. Chem. Soc. **72**, 3523 (1950).
13. I. L. Reich, A. Diaz, and S. Winstein. J. Amer. Chem. Soc. **91**, 5635 (1969).

[2]In a private communication from Dr. Diaz, it was pointed out that the n.m.r. assays were carried out on the reaction mixture itself, which would contain unreacted **1**-OTs-d_2 and **2**-TFA-d_2 besides the **1**-TFA-d_2. Thus the amount of C-1 H-absorption for the **1**-TFA-d_2 product would be difficult to measure with great accuracy. The conclusion drawn was that the extent of isotopic scrambling from C-1 to C-2 and C-3 was low, perhaps no more than 10% and this conclusion may be regarded as indicating no substantial disagreement between the results obtained with D- or ^{14}C-labeling. It was also pointed out that in the present work, the concentration of **1**-OTs-1-^{14}C in the reaction solution was relatively high and there could be the possibility that the HOTs liberated during the solvolysis might cause more extensive isotopic scrambling.

Can. J. Chem. Downloaded from www.nrcresearchpress.com by 210.87.254.6 on 09/05/12
For personal use only.

Diels–Alder reaction between cyclopentadiene and 3-*O*-acetyl-5,6-dideoxy-1,2-*O*-isopropylidene-6-nitro-α-D-*xylo*-hex-5-enose

W. A. SZAREK AND J. S. JEWELL
Department of Chemistry, Queen's University, Kingston, Ontario

Received September 19, 1969

A Diels–Alder reaction between cyclopentadiene and 3-*O*-acetyl-5,6-dideoxy-1,2-*O*-isopropylidene-6-nitro-α-D-*xylo*-hex-5-enose (**3**) gave a crystalline adduct, whose structure has been established to be that of 5-*endo*-nitro-6-*exo*-(3′-*O*-acetyl-1′,2′-*O*-isopropylidene-α-D-*xylo*-tetrofuranos-4′-yl)-2-norbornene (**4**) by nuclear magnetic resonance spectroscopy.

Une réaction de Diels–Alder entre le cyclopentadiène et le 3-*O*-acétyl-5,6-didésoxy-1,2-*O*-isopropylidène-6-nitro-α-D-*xylo*-hex-5-ènose (**3**) conduit à un composé cristallin, dont la structure a été démontrée par spectroscopie de résonance magnétique nucléaire: il s'agit de le 5-*endo*-nitro-6-*exo*-(3′-*O*-acétyl-1′,2′-*O*-isopropylidène-α-D-*xylo*-tétrofuranos-4′-yl)-2-norbornène (**4**).

Canadian Journal of Chemistry, **48**, 1030 (1970)

Can. J. Chem. Downloaded from www.nrcresearchpress.com by 210.87.254.5 on 09/05/12
For personal use only.

Although there exists considerable literature on the Diels–Alder reaction in general organic chemistry, examples in the carbohydrate field are rare. Recently Inch and Rich (1) reported the facile dimerization of (2*R*,3*R*)-5-benzoyl-2,3-dihydro-2,3-*O*-isopropylidenefuran-2,3-diol (**1**) by a Diels–Alder reaction in which the conjugated α,β-unsaturated carbonyl compound functions both as a diene and as a dienophile. At about the same time Baer and Kienzle (2) reported that the dehydroacetylation of methyl 2,4,6-tri-*O*-acetyl-3-deoxy-3-nitro-β-D-glucopyranoside and of its D-*manno* and D-*galacto* isomers gave, as a reaction intermediate, a derivative (**2**) of 2*H*-pyran which dimerized spontaneously in a Diels–Alder reaction to a tricyclic product. We describe now a Diels–Alder reaction between cyclopentadiene and the carbohydrate nitroolefin 3-*O*-acetyl-5,6-dideoxy-1,2-*O*-isopropylidene-6-nitro-α-D-*xylo*-hex-5-enose (**3**) (3, 4).

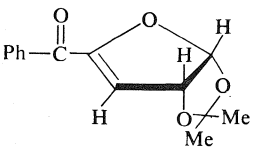

1

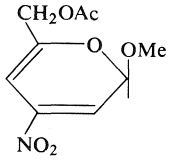

2

Compound **3** was prepared in the present work by the addition of nitryl iodide (NO_2I) to 3-*O*-acetyl-5,6-dideoxy-1,2-*O*-isopropylidene-α-D-*xylo*-hex-5-enose, followed by dehydrohalogenation of the resultant iodo-*C*-nitro adduct (4). The configuration of the double bond in **3** has been determined (4) to be *trans* by nuclear magnetic resonance (n.m.r.) spectroscopy. In nitroethylene the vicinal proton coupling constants J_{trans} and J_{cis} have been estimated (5) to be 13.4 and 4.9 Hz, respectively. The observed coupling constant for the vinyl protons in the spectrum of **3** is approximately 14 Hz which indicates that the nitroolefin has the *trans* stereochemistry.

Diels–Alder reactions between cyclopentadiene and nitroolefins have been reported previously (6). Structures can be assigned to the diastereomeric adducts from their n.m.r. spectra (5, 7). Thus Noland *et al.* (5) have determined that in the addition to cyclopentadiene of nitroethylene and some *trans* nitroolefins (1-nitropropene, 1-nitro-1-butene, and various 2-aryl-1-nitroethylenes) there was a predominance of the *endo*-nitro *trans* stereoisomer; *endo*/*exo* ratios from 3:1 to 9:1 were observed.

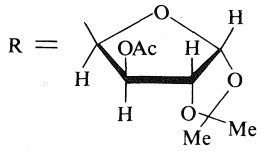

Treatment of compound **3** with refluxing cyclopentadiene gave a crystalline adduct in 26% yield and a syrupy residue. The structure of 5-*endo*-nitro-6-*exo*-(3′-*O*-acetyl-1′,2′-*O*-isopropylidene-α-D-*xylo*-tetrofuranos-4′-yl)-2-norbornene (**4**) has been assigned to the crystalline compound on the basis of its n.m.r. spectrum (Fig. 1). The signal assignments were made with the aid of spin decoupling, and by comparison with published (5) n.m.r. data for 5-nitro-6-

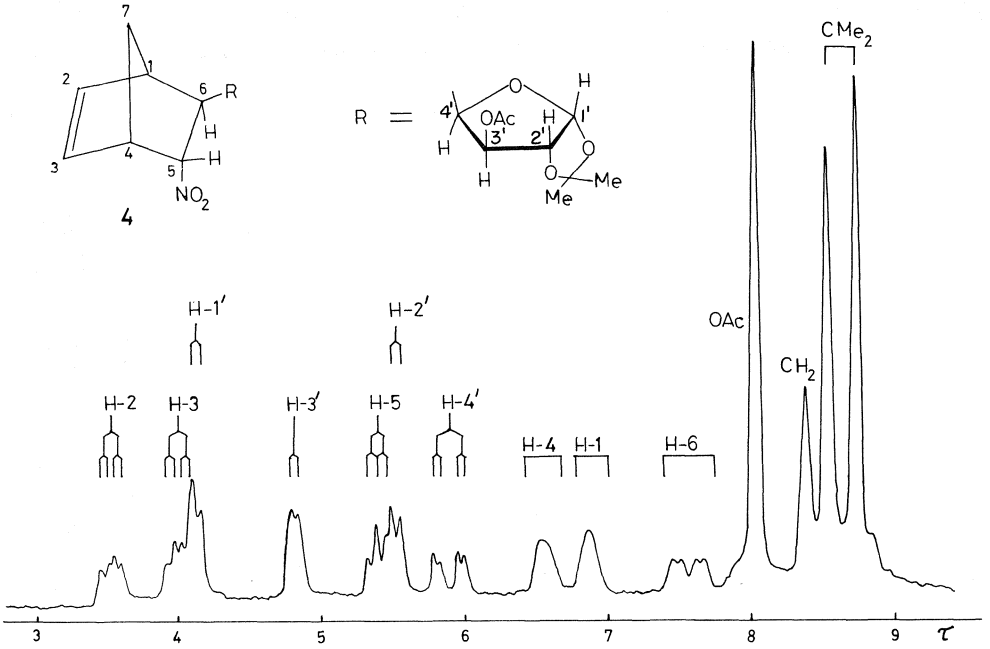

FIG. 1. The 60 MHz nuclear magnetic resonance spectrum of 5-*endo*-nitro-6-*exo*-(3′-*O*-acetyl-1′,2′-*O*-isopropylidene-α-D-*xylo*-tetrofuranos-4′-yl)-2-norbornene (**4**) in chloroform-*d*.

substituted-2-norbornenes. The absorption for the vinyl protons is centered at τ 3.74, and appears as two 4-line multiplets because of coupling of the vinyl and bridgehead (H-1 and H-4) protons. The downfield multiplet, centered at τ 3.50, has been attributed to H-2 (see below) with $J_{2,3}$ = 5.0 and $J_{2,1}$ = 2.2 Hz; the H-3 multiplet is centered at τ 3.97, and $J_{3,4}$ = 2.6 Hz. The 2 broad peaks at τ 6.41–6.61 and 6.78–6.98 have been assigned to the 2 bridgehead protons H-4 and H-1, respectively; it is assumed that the electron-withdrawing inductive and field effects of the 5-nitro group would cause the signal for H-4 to occur further downfield than that for the more remote H-1 (5). Irradiation of H-4 caused the quartet centered at τ 3.97 to collapse to a doublet with a splitting of 5.0 Hz, and the triplet at τ 5.39 to collapse to a doublet with a splitting of 4.0 Hz. The former result shows that the signal at τ 3.97 is that of H-3, and $J_{3,2}$ = 5.0 Hz. The triplet can be assigned to the 5-*exo* proton with $J_{5,4} = J_{5,6}$ = 4.0 Hz. Noland *et al.* (5) have reported that the 5-*exo* protons in their 5-*endo*-nitro-6-*exo*-substituted-2-norbornenes occurred in the region τ 4.97–5.57, and all appeared as triplets as a result of the fortuitous equivalence of the coupling constants (4–5 Hz) for the 4,5-*exo* and 5-*exo*, 6-*endo* interactions. The 5-*endo* protons in the 5-*exo*-nitro stereoisomers, however, occurred upfield in the region τ 5.43–6.21, and usually appeared as quartets owing to non-equivalence of the coupling constants for the 5-*endo*, 6-*exo* (4–5 Hz) and long range 5-*endo*, 7-*syn* (2 Hz) interactions. Irradiation of H-1 caused the quartet centered at τ 3.50 to collapse to a doublet with a splitting of 5.0 Hz, a result

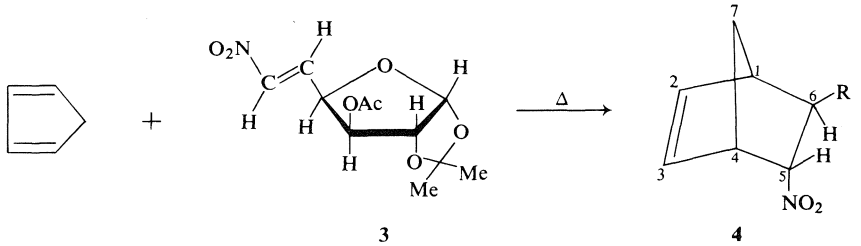

3 4

Can. J. Chem. Downloaded from www.nrcresearchpress.com by 210.87.254.5 on 09/05/12
For personal use only.

which corroborates the assignment of this signal to H-2. The multiplet centered at τ 7.50 has been assigned to the 6-*endo* proton with $J_{6,4'} = 10.0$ Hz, since irradiation at τ 5.88 (H-4′) caused the multiplet to appear as a broad band, in addition to causing the doublet at τ 4.78 to collapse to a singlet, whereas irradiation at τ 7.50 caused the quartet at τ 5.88 to appear as a broad band, and also simplified the H-5 triplet at τ 5.39 to a doublet with a splitting of 4.0 Hz ($J_{5,4}$). The value of τ 7.50 for the 6-*endo* proton is in agreement with values reported by Noland *et al.* (5) in their 5-*endo*-nitro-6-*exo*-substituted-2-norbornenes (τ 6.45–7.93). The doublet at τ 4.78 can be assigned to H-3′ with $J_{3',4'} = 3.0$ Hz; irradiation at τ 4.78 caused the H-4′ quartet at τ 5.88 to collapse to a doublet with a splitting of 10.0 Hz ($J_{4',6}$). The two doublets at τ 4.11 and τ 5.50 have been assigned to H-1′ and H-2′, respectively, with $J_{1',2'} = 3.8$ Hz; irradiation at τ 4.11 caused the doublet at τ 5.50 to collapse to a singlet. Finally, the remaining peaks at τ 7.98, 8.33, 8.48, and 8.66 have been assigned to the acetyl group, the methylene bridge at C-7, and the isopropylidene–methyl protons, in that order. The values obtained for the coupling constants for the ring proton interactions of the tetrofuranose moiety are in agreement with those reported (8) previously for 1,2-*O*-isopropylidene-α-D-*xylo*-hexofuranose derivatives, and indicate that the carbohydrate ring adopts the $\mathbf{T}_2^3$ conformation.

The n.m.r. spectrum of the syrupy residue indicated that it was a mixture which contained a small amount of compound **4**. A resolution of the mixture by thin-layer chromatography (t.l.c.) was not possible, since the other component(s) migrated in a variety of solvents at almost the same rate as **4**.

Experimental

Melting points were determined on a Fisher–Johns apparatus and are uncorrected. Optical rotations were measured with a Perkin–Elmer model 141 automatic polarimeter at 27 ± 2°. Infrared (i.r.) spectra were measured on a Beckman-IR5A spectrophotometer. Nuclear magnetic resonance spectra were determined on a Varian T-60 spectrometer in chloroform-*d* and tetramethylsilane as internal standard; signal assignments were made on a first-order basis with the aid of spin decoupling, and coupling constants were measured at 250 Hz sweep widths. The t.l.c. was performed with Silica Gel G as the adsorbent, and 4:1 (v/v) petroleum ether (b.p. 60–80°) – ethyl acetate as the developing solvent. The developed plates were air dried, sprayed with 5% ethanolic sulfuric acid and heated at about 150°.

Reaction of 3-O-Acetyl-5,6-dideoxy-1,2-O-isopropylidene-6-nitro-α-D-xylo-hex-5-enose (3) with Cyclopentadiene

A solution of compound **3** (100 mg) in freshly prepared (9) cyclopentadiene was heated for 3 h at reflux temperature. The solution was concentrated then under reduced pressure to 1/2 of its original volume, and left overnight at room temperature. Long needles were formed, which were removed by filtration and dried under reduced pressure; the filtrate was concentrated to dryness to yield a yellow syrup. Recrystallization of the needles from 1:1 ethyl acetate – petroleum ether gave the pure adduct **4** (33 mg, 26%), m.p. 185–186°, $[\alpha]_D$ +61 ± 3° (*c*, 0.5 in chloroform); R_F 0.29 (t.l.c.); λ_{max} (Nujol) 5.72 (OAc), 6.1 (C=C), 6.42, 6.50 (C—NO_2) 7.25 μm (CMe_2). The n.m.r. spectrum of **4** is shown in Fig. 1.

Anal. Calcd. for $C_{16}H_{21}O_7N$: C, 56.6; H, 6.2; N, 4.1. Found: C, 56.6; H, 6.3; N, 4.0.

The authors thank Professor J. K. N. Jones for his interest and encouragement, and the National Research Council of Canada and the Department of University Affairs in the Province of Ontario for financial support of this research.

1. T. D. Inch and P. Rich. Carbohyd. Res. **6**, 244 (1968).
2. H. H. Baer and F. Kienzle. J. Org. Chem. **33**, 1823 (1968).
3. H. H. Baer and W. Rank. Can. J. Chem. **43**, 3330 (1965).
4. W. A. Szarek, D. G. Lance, and R. L. Beach. Chem. Commun. 356 (1968); Carbohyd. Res. To be published.
5. W. E. Noland, B. A. Langager, J. W. Manthey, A. G. Zacchei, D. L. Petrak, and G. L. Eian. Can. J. Chem. **45**, 2969 (1967).
6. Ref. 5, and references therein.
7. R. R. Fraser. Can. J. Chem. **40**, 78 (1962).
8. R. J. Abraham, L. D. Hall, L. Hough, and K. A. McLauchlan. J. Chem. Soc. 3699 (1962).
9. L. F. Fieser. Organic experiments. 2nd ed. Raytheon Education Co., Lexington, Massachusetts. 1968. p. 86.

Can. J. Chem. Downloaded from www.nrcresearchpress.com by 210.87.254.5 on 09/05/12
For personal use only.

1033-1153

Canadian Journal of Chemistry

Published by THE NATIONAL RESEARCH COUNCIL OF CANADA

VOLUME 48 APRIL 1, 1970 NUMBER 7

Nuclear magnetic resonance spectra of the epihalohydrins. I. Signs of long-range spin–spin coupling constants in epichlorohydrin[1]

C. J. MACDONALD[2,3] AND T. SCHAEFER

Chemistry Department, University of Manitoba, Winnipeg, Manitoba

Received October 17, 1969

The complete analysis of the proton magnetic resonance spectrum of epichlorohydrin as 10 mole % solutions in benzene and in acetonitrile is reported. Extensive tickling experiments demonstrate that the *cisoid* coupling constants over four bonds are negative, while the corresponding *transoid* coupling constants are positive. Detailed results for the benzene solution, in which the non-equivalent protons of the $-CH_2Cl$ moiety have almost identical chemical shifts, show that although all the resonances may be unequivocally identified and measured to a high order of precision (± 0.03 Hz), an iterative computer fit (LAOCOON-3) has a larger uncertainty for the derived parameters than indicated by the "probable errors" furnished by the computer program. Analysis of the acetonitrile solution, however, furnishes a less ambiguous result. In addition, it is noted that use of relative apparent intensities of resonance peaks can lead to the wrong sign of those coupling constants whose magnitudes are near zero.

Canadian Journal of Chemistry, **48**, 1033 (1970)

Introduction

The nuclear magnetic resonance (n.m.r.) spectra of the epihalohydrins, **1**, have been investigated by several workers (1–5). Only in the case of the parent propylene oxide (X = H) have the signs of the long-range proton–proton coupling constants been unequivocally determined.[4] In propylene oxide, $^4J_{CH_3,H_A}$ is negative, while $^4J_{CH_3,H_B}$ is positive (6). When X = halogen in **1**, H_D and H_E are magnetically non-equivalent (7). Previous analysis of the n.m.r. spectra of epichlorohydrin (1, 3) and epifluorohydrin (4), which utilized iterative computer methods in matching observed and calculated peak positions together with visual comparisons of calculated and observed peak intensities, have variously suggested that (*a*) all four ^4J are positive (4); (*b*) all four ^4J are negative (3); (*c*) one ^4J involving H_B is positive, the other three ^4J are negative (1).

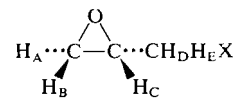

1

A re-investigation of the n.m.r. spectra of the 3-substituted propylene oxides therefore appeared to be warranted. This paper reports the method of analysis used to determine unequivocally the signs of the long-range coupling constants. Its application to the proton magnetic resonance spectrum of epichlorohydrin is illustrated. Because of the ambiguities present in the analysis of a benzene solution of epichlorohydrin, an acetonitrile solution was also analyzed. A second paper by one of us (C.J.M.) will present the results and discussion for all the epihalohydrins (8).

Experimental

Reagent-grade epichlorohydrin from Eastman was prepared as a degassed 10 mole % solution in benzene containing some tetramethylsilane (TMS). A similar 10 mole % solution in acetonitrile was also prepared. Proton resonance spectra were recorded in the frequency sweep mode (sweep rate 0.01–0.02 Hz/s) on a Varian

[1]Presented, in part, at the 51st Annual C.I.C. Conference, Vancouver, British Columbia, June 2–7, 1968.

[2]Postdoctorate Fellow 1967–1968.

[3]Present address: Department of Chemistry, University of Toronto, Toronto 181, Ontario.

[4]A recent sign determination for epifluorohydrin, using the results of "tickling" experiments, is of dubious value because of the wrong signs reported for $^3J_{CD}$, $^3J_{CE}$, and $^2J_{DE}$ (5). These authors find $^4J_{AD}$, $^4J_{AE}$, $^4J_{BE} < 0$, and $|^4J_{BD}| < 0.1$.

Can. J. Chem. Downloaded from www.nrcresearchpress.com by 210.87.254.5 on 09/05/12
For personal use only.

Can. J. Chem. Downloaded from www.nrcresearchpress.com by 210.87.254.5 on 09/05/12
For personal use only.

4802118

TABLE 1

Chemical shifts and proton–proton coupling constants for epichlorohydrin*

Parameter	This work		Reference 1 (Neat)	Reference 2 (Neat)	Reference 3 (Neat)
	Benzene†	Acetonitrile			
ν_A	-2.0093 ± 0.0005‡	-2.6448 ± 0.0003‡	-2.650 ± 0.003	-2.620 ± 0.003	-2.622 ± 0.005
ν_B	-2.2180 ± 0.0005	-2.8222 ± 0.0003	-2.840	-2.820	-2.805
ν_C	-2.6740 ± 0.0005	-3.1882 ± 0.0003	-3.200	-3.190	-3.155
ν_D	-2.9643 ± 0.005	-3.7478 ± 0.0003	-3.740	—	-3.698
ν_E	-2.9618 ± 0.005	-3.4612 ± 0.0003	-3.470	—	-3.453
J_{AB}	5.04 ± 0.03	4.91 ± 0.02	5.0 ± 0.2	5.2 ± 0.3	4.8 ± 0.15
J_{AC}	2.39 ± 0.03	2.45 ± 0.02	2.4	2.2	2.3
J_{AD}	-0.27 ± 0.14	-0.26 ± 0.02	-0.1	—	-0.1
J_{AE}	-0.35 ± 0.13	-0.30 ± 0.02	-0.2	—	-0.2
J_{BC}	3.85 ± 0.03	3.99 ± 0.02	4.0	3.8	3.9
J_{BD}	0.06 ± 0.19	0.03 ± 0.02	-0.1	—	-0.1
J_{BE}	0.56 ± 0.20	0.39 ± 0.02	0.6	—	-0.4
J_{CD}	4.75 ± 0.35	3.89 ± 0.02	4.0	—	3.9§
J_{CE}	6.00 ± 0.36	6.78 ± 0.02	6.6	—	6.4§
J_{DE}	-11.63 ± 0.05	-11.84 ± 0.02	-11.7	—	-11.5§

*Chemical shifts, ν, in p.p.m. from "internal" TMS. Values from ref. 3 are adjusted to allow for the cyclohexane reference used. Proton–proton coupling constants J in Hz.

†Solution A^1, deemed to be the most correct solution.

‡Error estimates in this work obtained as noted in the text.

§Signs patently in error are corrected in this Table.

TABLE 2

Approximate magnitudes of chemical shifts and coupling constants from n.m.r. spectrum on a first-order basis*

Chemical shift		Coupling constant		Coupling constant	
Parameter	Value	Parameter	Value	Parameter	Value
ν_A	−121	$^2J_{AB}$	5.0	$^4J_{BD}$, $^4J_{BE}$	0.4, 0.6
ν_B	−133	$^3J_{AC}$	2.4		
ν_C	−161	$^4J_{AD}$, $^4J_{AC}$	0.2, 0.3	$^3J_{CD}$	4.2 (5.2)
ν_D	−178			$^3J_{CE}$	6.0 (5.5)
ν_E	−178	$^3J_{BC}$	3.8	$^2J_{DE}$	11.6

*All units in Hz; all values for solution *A*; those values for solution *B* which differ from solution *A* are in parentheses.

DA60-I spectrometer locked on the TMS signal. Peak positions relative to TMS were determined by interpolation, with a standard deviation of not more than 0.03 Hz. Double-resonance experiments were performed according to standard procedures (9, 10). Resolved peaks had widths at half height of 0.12 Hz or better.

Results

The final shift and coupling constant parameters are given in Table 1.

1. Initial Analysis of the Benzene Solution Spectrum

The ABCDE proton resonance spectrum of epichlorohydrin in benzene is shown in Fig. 1. Several weak transitions were discernible at higher radiofrequency power levels. Resonance peaks from H_A, H_B, and H_C in **1** were readily assigned as shown on the basis of previous findings that $^2J_{gem} \sim 5$ Hz and $^3J_{cis} > {}^3J_{trans}$ in epoxide rings (6, 11, 12). Peaks arising from H_D and H_E were less easily differentiated because of the small chemical shift between these two protons.

Consideration of the spectrum on a first-order basis led to the *approximate* chemical shifts, ν (in Hz relative to TMS), and two possible coupling constants, J, in Hz (magnitudes ± 0.2 Hz) shown in Table 2.

From previous work (6), all the three-bond and two-bond coupling constants are positive, except for $^2J_{DE}$. Spectra incorporating this information were computed on an IBM systems 360/65 computer using the LAOCOON-3 program (13). Setting $|\nu_D - \nu_E| = 1$ Hz facilitated the elucidation of the spin assignments in the energy levels generated by the program. Owing to the complexity of the spectrum, a self-consistent assignment of the observed peak positions to particular transitions proved difficult. This task was simplified by utilization of the transition diagram (14) in conjunction with the results of extensive double-resonance ("tickling") experiments.

2. Double Irradiation and Relative Signs of J_{HH} in Benzene Solution

The irradiation experiments are described by the notation (15) in which, for example, $A\{C_{16}\}$ indicates observation of A transitions during weak irradiation of transition C_{16}. As is well known, such weak irradiations or "tickling" experiments indicate which observed transitions have common energy levels (9). Because different sign alternatives for the coupling constants correspond to different energy-level arrangements of the spin system, the relative signs may also be obtained by these experiments. The parameters in epichlorohydrin are such that it is most advantageous to irradiate C transitions. Proton C undergoes three-bond, positive couplings only. Therefore the spin states of the other protons for both solutions *A* and *B* are easily assigned for the outer H_C peaks (C_1, C_2, C_{15}, C_{16}) as in Table 3. By convention, a minus sign under the low-field peak indicates a positive coupling from H_C to the proton in question.

TABLE 3

Spin states of protons

	Spin state in peak			
Proton	C_1	C_2	C_{15}	C_{16}
H_A	−	+	−	+
H_B	−	−	+	+
H_C				
H_D	−	−	+	+
H_E	−	−	+	+

Can. J. Chem. Downloaded from www.nrcresearchpress.com by 210.87.254.5 on 09/05/12
For personal use only.

Can. J. Chem. Downloaded from www.nrcresearchpress.com by 210.87.254.5 on 09/05/12
For personal use only.

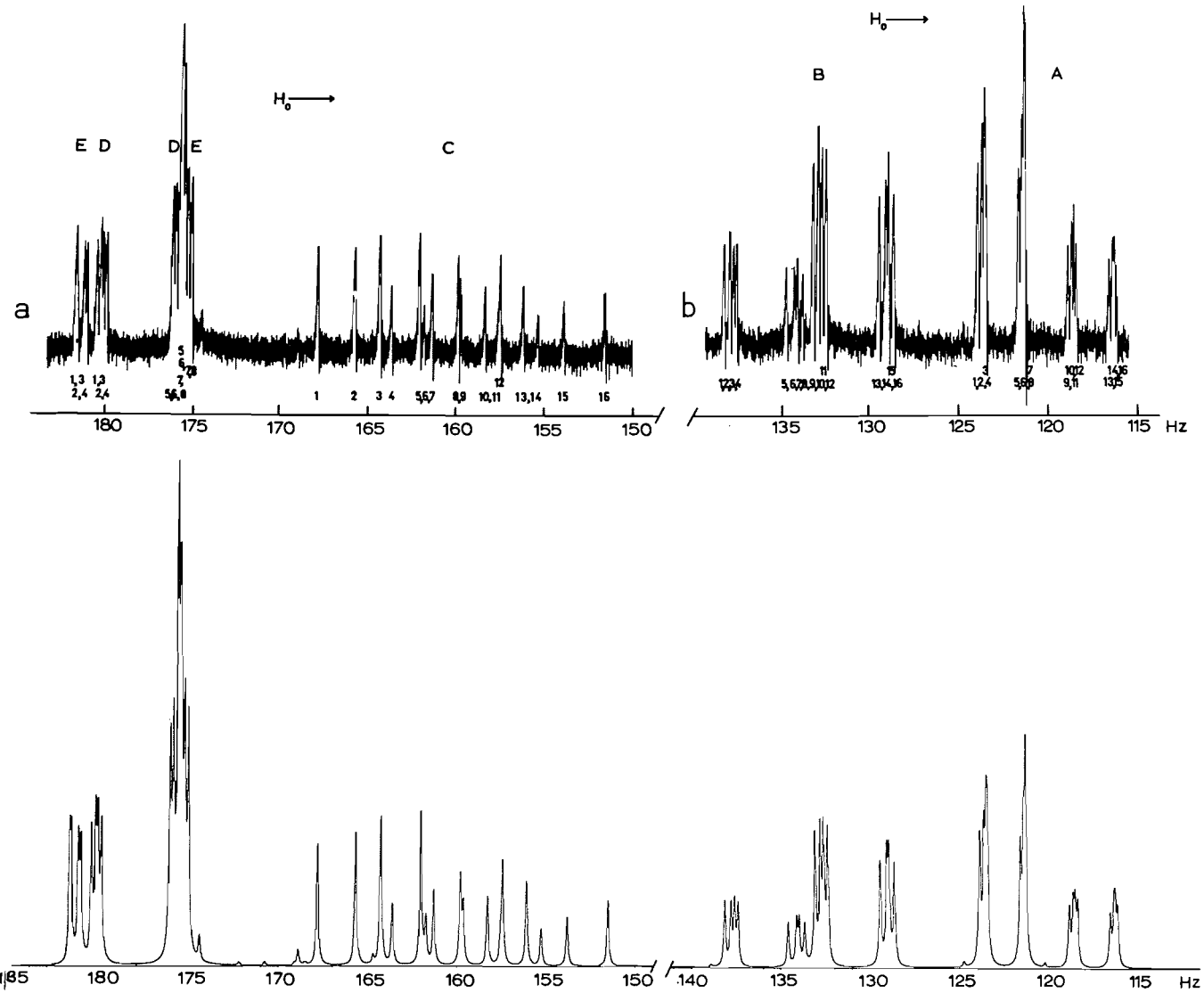

FIG. 1. Epichlorohydrin in benzene: the single-resonance spectrum. The upper trace records the experimental spectrum, the lower trace is the Calcomp trace compiled using the parameters in Table 1, assuming Lorentzian peak shapes with half-line widths of 0.12 Hz. Experimental trace (*b*) was obtained using higher spectrometer "gain" than that used for trace (*a*).

Can. J. Chem. Downloaded from www.nrcresearchpress.com by 210.87.254.5 on 09/05/12
For personal use only.

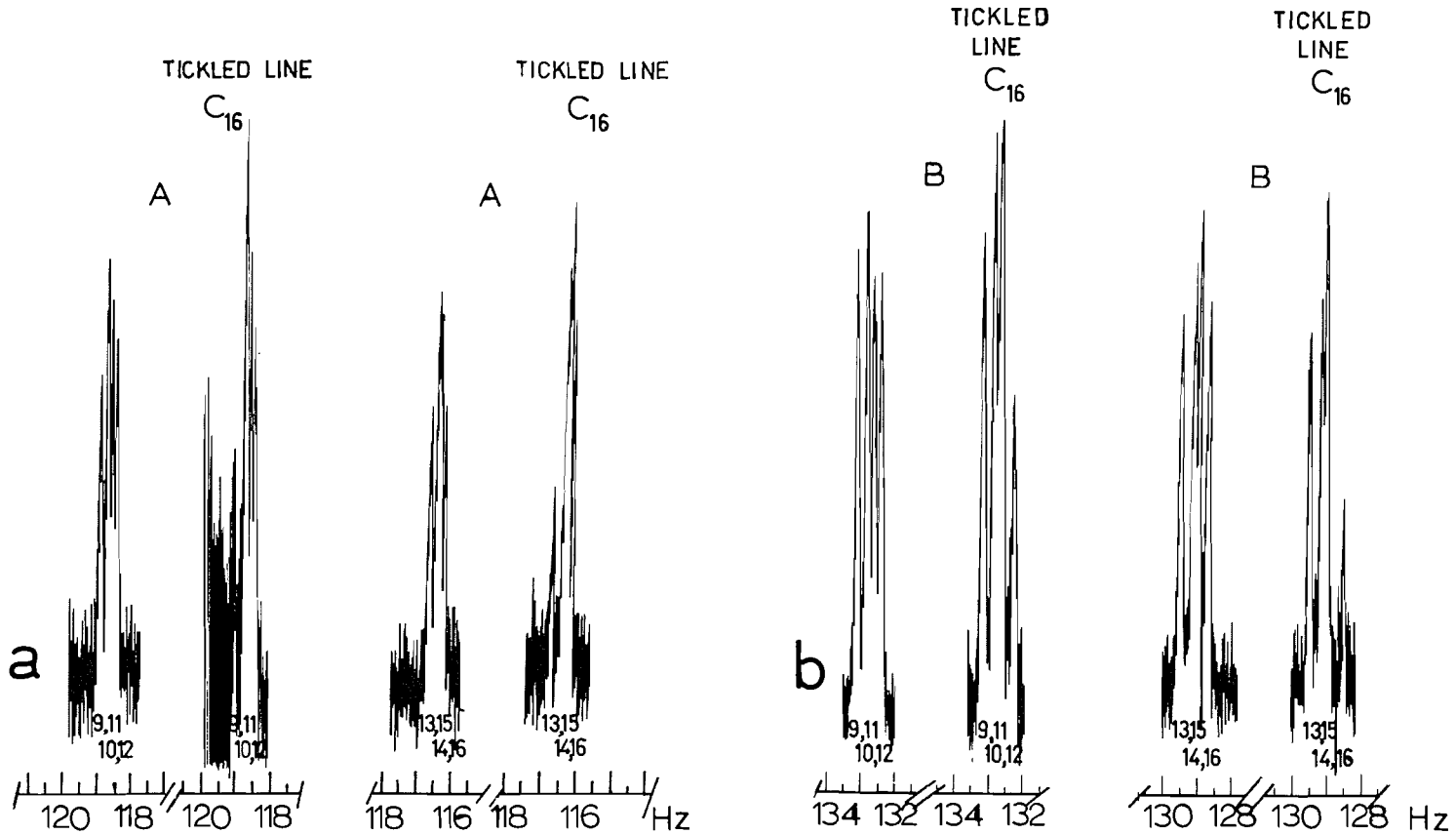

FIG. 2. Epichlorohydrin in benzene: the double-resonance experiments. In (*a*) the partial single (left-hand side) and double (right-hand side) resonance spectra show the effect on A resonances caused by tickling C_{16} (experiment A{C_{16}}). Ringing in the double-resonance trace (caused by coincidence of the sweep frequency with a spurious weak signal from the double-resonance oscillator) does not obscure the pertinent features of the experiment. (*b*) Traces showing the effect of the experiment B{C_{16}}. Only those portions of the A and B resonances affected by the double resonance are shown.

Can. J. Chem. Downloaded from www.nrcresearchpress.com by 210.87.254.5 on 09/05/12
For personal use only.

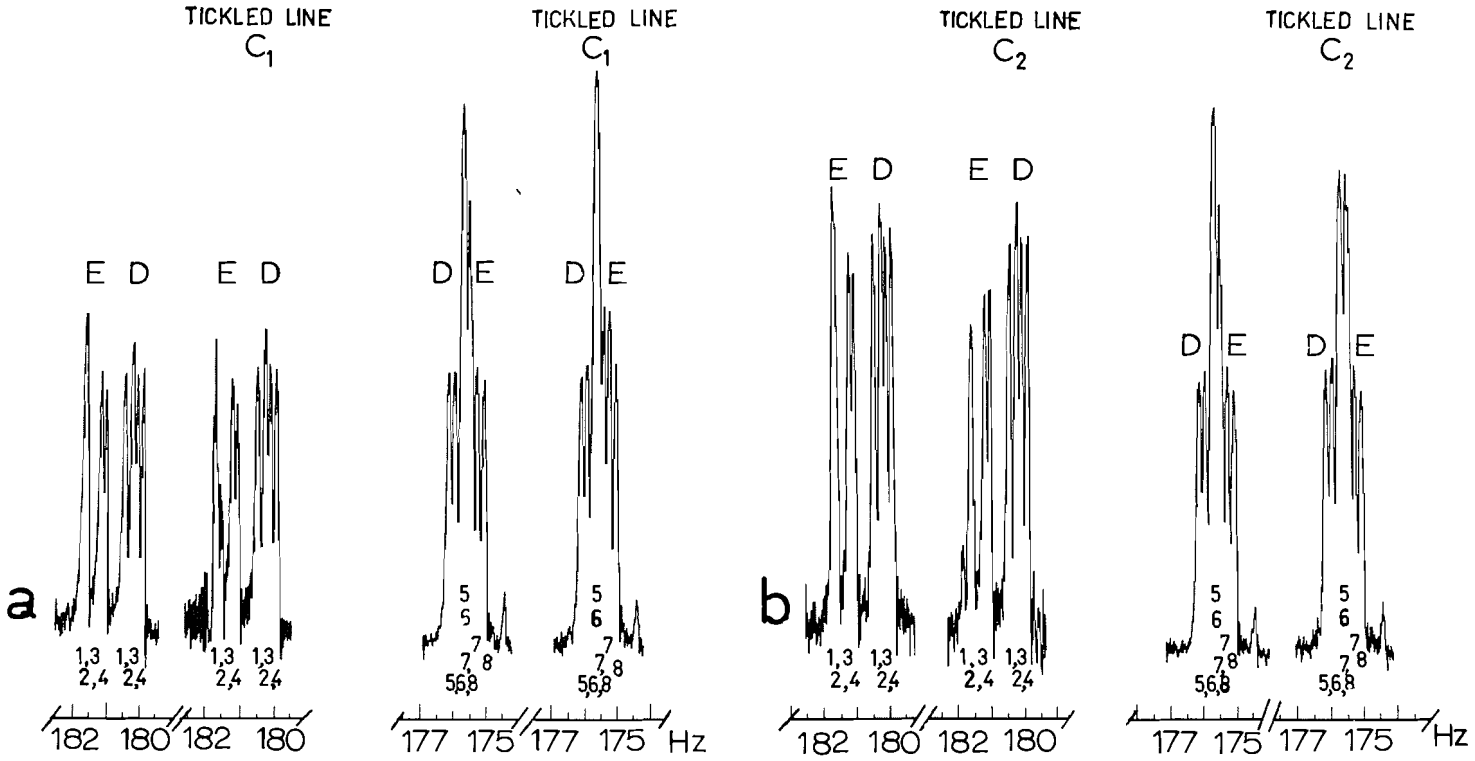

FIG. 3. Epichlorohydrin in benzene: the double-resonance experiments. Partial single- and double-resonance spectra (as in Fig. 2) for the experiment DE{C_1} (*a*) and for the experiment DE{C_2} (*b*).

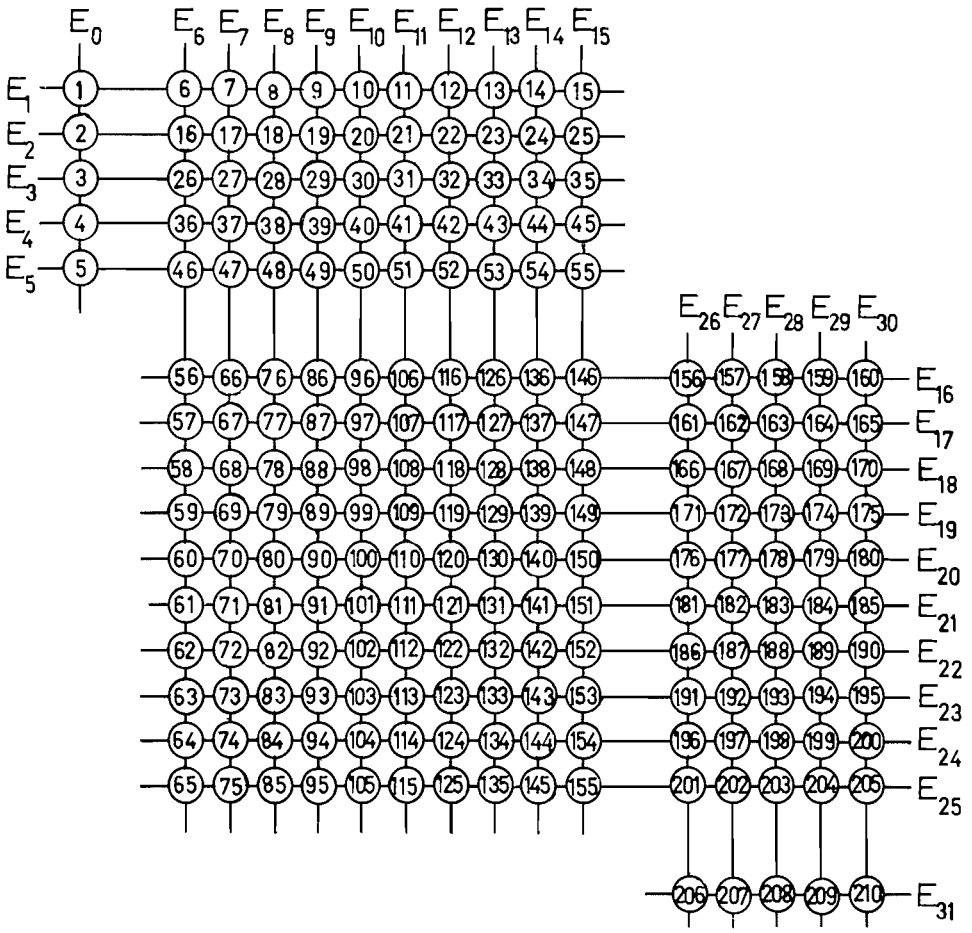

FIG. 4. Transition diagram for a 5-spin system. Energy level and transition numbering corresponds to that used in the LAOCOON-3 program. In the benzene solution, 74 of these transitions could be identified and were used in the final iterative computer fitting. A total of 81 transitions were used for the acetonitrile solution.

(a) $A\{C_n\}$ Experiments

In the experiment $A\{C_{16}\}$, peaks A_9 and A_{13} are perturbed (Fig. 2*a*). In first order, the theory (9) then shows that $J_{AB}/J_{BC} > 0$, J_{AD}/J_{CD} and $J_{AE}/J_{CE} < 0$. On the assumption that the three-bond couplings are positive, it follows that $J_{AB} > 0$, $J_{AD} < 0$, and $J_{AE} < 0$. Of course, the present single-resonance spectrum is not first order, but the subsequent iterative fit confirmed the first-order assignment. Other $A\{C_n\}$ experiments reinforced these conclusions and also delineated further connected transitions.

(b) $B\{C_n\}$ Experiments

In the $B\{C_{16}\}$ experiment, those peaks having H_B, H_D, and H_E in positive spin states and H_C in either spin state are perturbed. Figure 2*b* shows splitting of peaks B_{12} and B_{16}, suggesting that *all* couplings to H_B have the same sign and are therefore positive. Confirmation was obtained by further $B\{C_n\}$ and $C\{B_n\}$ experiments, and also by the iterative computer fit.

(c) $DE\{C_n\}$ Experiments

In benzene solution, H_D and H_E have almost identical chemical shifts. In Fig. 1*a*, the peak assignment incorporates the results of the complete analysis (very weak transitions are not numbered). Figure 3*a* shows that in the experiment $DE\{C_1\}$, E_2 and E_6 are perturbed, while in Fig. 3*b*, the experiment $DE\{C_2\}$ is seen to cause splitting of E_1 and E_5. While assignment of these peaks as E rather than D is expected from the iterative fit where $\nu_D > \nu_E$ and the fact

Can. J. Chem. Downloaded from www.nrcresearchpress.com by 210.87.254.5 on 09/05/12
For personal use only.

Can. J. Chem. Downloaded from www.nrcresearchpress.com by 210.87.254.5 on 09/05/12
For personal use only.

that $^2J_{DE}$ is negative for an sp^3-hydridized, aliphatic CH_2 group, it is interesting to note that the peak assignments remain unchanged for $(\nu_E - \nu_D) = \pm 2$ Hz; a result not, of course, in accord with first-order expectations.

In other experiments (not shown), $\{C_{15}\}$ perturbed D_4 and D_8, whereas $\{C_{16}\}$ perturbed D_2 and D_7. These results again suggest that $^4J_{AD}$, $^4J_{AE} < 0$ and $^4J_{BD}$, $^4J_{BE} > 0$.

3. *Iterative Computer Fitting of the Benzene Solution Spectrum*

The tickling experiments clearly show the spin assignments of many observed peaks. These assignments, together with the transition diagram appropriate to a 5-spin system (Fig. 4), lead to the unequivocal identification of every resolved transition by means of the LAOCOON-3 program (13). Further information was available from several of the double-resonance experiments. For example, the experiments $DE\{C_1\}$ and $DE\{C_2\}$ show that $E_1 - E_2 = 0.06 \pm 0.02$ Hz (Figs. 3*a*, 3*b*). In addition, the experimental precision is sufficient to allow decomposition of composite peaks using repeated spacing rules (16) and peak widths. The iterative procedure from *both* approximate solutions *A* and *B* (using 74 assigned peaks) then converges rapidly on the solution A^1 (Table 1), with a "total root-mean-square (r.m.s.) error" (13) of 0.011 Hz, and the *worst* fit of any resolved or interpolated peak $\leqslant 0.03$ Hz. However, it was noted that the "probable errors" (13) in the derived parameters given by the computer fell into two ranges, $\leqslant 0.003$ Hz and $\leqslant 0.03$ Hz (i.e., some parameters were better determined than others), raising some doubt as to the validity of the results.

Attempts to gauge the accuracy of the iterative result by changing several of the experimental frequencies within the uncertainty limits of their measurement (± 0.03 Hz) led to a range of solutions without the "probable errors" indicated in the computer results. For all these apparent solutions, the total r.m.s. error is $\leqslant 0.020$ Hz, the "probable errors" for each parameter are computed to be $\leqslant 0.06$ Hz,[5] and the *worst* fit of any resolved or interpolated peak $\leqslant 0.05$ Hz, whereas the derived parameters were in the ranges

$\nu_A = -120.560 \pm 0.002$	$J_{AB} = 5.036 \pm 0.001$	$J_{BD} = 0.13 \pm 0.12$
$\nu_B = -133.086 \pm 0.002$	$J_{AC} = 2.387 \pm 0.002$	$J_{BE} = 0.49 \pm 0.11$
$\nu_C = -160.438 \pm 0.009$	$J_{AD} = -0.23 \pm 0.10$	$J_{CD} = 4.92 \pm 0.18$
$\nu_D = -178.02 \pm 0.15$	$J_{AE} = -0.39 \pm 0.09$	$J_{CE} = 5.83 \pm 0.19$
$\nu_E = -177.57 \pm 0.15$	$J_{BC} = 3.848 \pm 0.002$	$J_{DE} = -11.600 \pm 0.020$

where ν and J are both in Hz.

Insofar as the numbered peaks in Fig. 1 serve as a measure of peak intensity, all the "solutions" gave equally valid fits, since intensity variations between them are $<1\%$ for any given peak. The only difference between these "solutions" lies in the intensities of the several weak peaks in the CDE portion of the spectrum, as indicated in Table 4 for solution A^1 and one of the other solutions. Comparison of all the "solutions" with the experimental spectrum intensities strongly indicates solution A^1 as the most correct solution. Experimental and computed spectra based on A^1 may be compared in Fig. 1.

Although the signs of the coupling constants appear to be reliably given by the tickling experiments and the iterative fitting results, doubts as to the reliability of the parameter magnitudes remain, however. For example, if the reliability of any of the better determined parameters (e.g. ν_A, ν_B, J_{AB}, etc.) is taken to be ~ 0.03 Hz (i.e., five times the indicated "probable error"), then a similar multiplication factor leads to the value $\sim \pm 0.2$ Hz as the reliability

[5]It should be noted that, whereas the "probable errors" in those parameters which are invariant in these solutions are $\leqslant 0.006$ Hz, the varying parameters have "probable errors" of 0.02–0.06 Hz. In addition, the "error vector and standard error" table (13) shows that, while the "standard error" in each invariant parameter is $\leqslant 0.006$ Hz, the corresponding "standard error" for variable parameters could be as great as 0.10 Hz (for some of the coupling constants) and 0.17 Hz (for ν_D). It is significant that the *sums* of the varying parameters (e.g. $\nu_D + \nu_E$, $J_{AD} + J_{AE}$) remain constant in these solutions, and that varying parameter values occur when small differences in these parameters (e.g. $\nu_D - \nu_E$, $J_{AD} - J_{AE}$, etc.) are important in the zero-order Hamiltonian for the system. Thus, whereas the sums of these parameters appear to be well determined, the differences are not so well defined.

TABLE 4
Comparison of experimental and calculated peak intensities

Solution A^1		Experimental		One "apparent solution"	
Frequency (Hz)	Intensity	Frequency (Hz)	Relative intensity*	Frequency (Hz)	Intensity
164.12	0.029	~164.0	vw, sh	164.12	0.024
164.72	0.089	164.74	3	164.71	0.081
164.75	0.011			—	<0.02
168.50	0.023	~168.5	vw	—	<0.02
168.59	0.019	~168.6	vw	—	<0.02
168.94	0.178	168.95	5	168.94	0.125
169.14	0.027	169.11	vw, sh	—	<0.02
170.80	0.046	170.81	2	170.80	0.030
172.24	0.037	172.23	1	172.23	0.024
174.46	0.290	174.45	10	174.46	0.227

*vw = very weak, sh = shoulder.

in the less well determined parameters. This factor is of the order of the coupling constants J_{AD}, J_{AE}, J_{BD}, and J_{BE}.

4. Analysis of the Acetonitrile Solution Spectrum

The ambiguities present in the parameter extraction for the benzene solution spectrum of epichlorohydrin are probably related to the near equivalence of ν_D and ν_E, together with the near equality of coupling constants between these protons and any other given proton. In acetonitrile solution, $(\nu_D - \nu_E) \sim 16$ Hz, a value which allows ready differentiation of resonances due to protons D and E.

Initial first-order analysis indicated the proton assignment shown in Fig. 5*a*, and the approximate solution (magnitudes only, in Hz)

$$\nu_A = -159 \qquad J_{AB} = 4.9 \qquad \left.\begin{matrix} J_{BD} \\ J_{BE} \end{matrix}\right\} = 0.1, 0.5$$
$$\nu_B = -169 \qquad J_{AC} = 2.4$$
$$\nu_C = -191 \qquad \left.\begin{matrix} J_{AD} \\ J_{AE} \end{matrix}\right\} = 0.2, 0.35 \qquad J_{CD} = 3.7$$
$$\nu_D = -224 \qquad J_{CE} = 6.2$$
$$\nu_E = -208 \qquad J_{BC} = 3.7 \qquad J_{DE} = 11.5$$

In the tickling experiments, ABDE$\{C_{15}\}$ perturbed A_9, A_{13}, B_3, B_8, D_4, D_8, E_3, and E_8 (Fig. 6*a*, *b*), while the experiment ABDE$\{C_{16}\}$ showed perturbation to peaks A_9, A_{13}, B_{11}, B_{16}, D_3, D_7, E_1, and E_6 (Fig. 6*a*, *c*). If J_{AB}, J_{AC}, J_{BC}, J_{CD}, and J_{CE} are accepted as positive, and J_{DE} as negative, in sign, these results are then consistent with $J_{AD}, J_{AE} < 0$ and $J_{BD}, J_{BE} > 0$ (but note that the indicated spin assignments are not first order). The connected transitions indicated by these experiments, together with the transition diagram (Fig. 4) and repeated spacing rules, then lead to the identification and assignment of all the peaks in Fig. 5*a*. Starting from the approximate solution above, this assignment leads to only one solution; variation of peak positions within the uncertainty limits in their measurement (±0.03 Hz) failing to alter the derived parameters by more than 0.02 Hz. In the final iterative fit, the composite peaks were decomposed as in the previous example. The total indicated r.m.s. error is 0.010 Hz, the probable error for *all* parameters 0.002–0.004 Hz, "standard errors" of each parameter 0.002–0.005 Hz, and the *worst* fit of any resolved or interpolated peak (a total of 81 fitted) is 0.021 Hz. This solution is shown in Table 1, and the computed and experimental spectra may be compared in Fig. 5*a*, *b*.

Discussion

(a) The Analysis Procedure

The extensive analysis of the benzene solution of epichlorohydrin demonstrates the caution

Can. J. Chem. Downloaded from www.nrcresearchpress.com by 210.87.254.5 on 09/05/12
For personal use only.

Can. J. Chem. Downloaded from www.nrcresearchpress.com by 210.87.254.5 on 09/05/12
For personal use only.

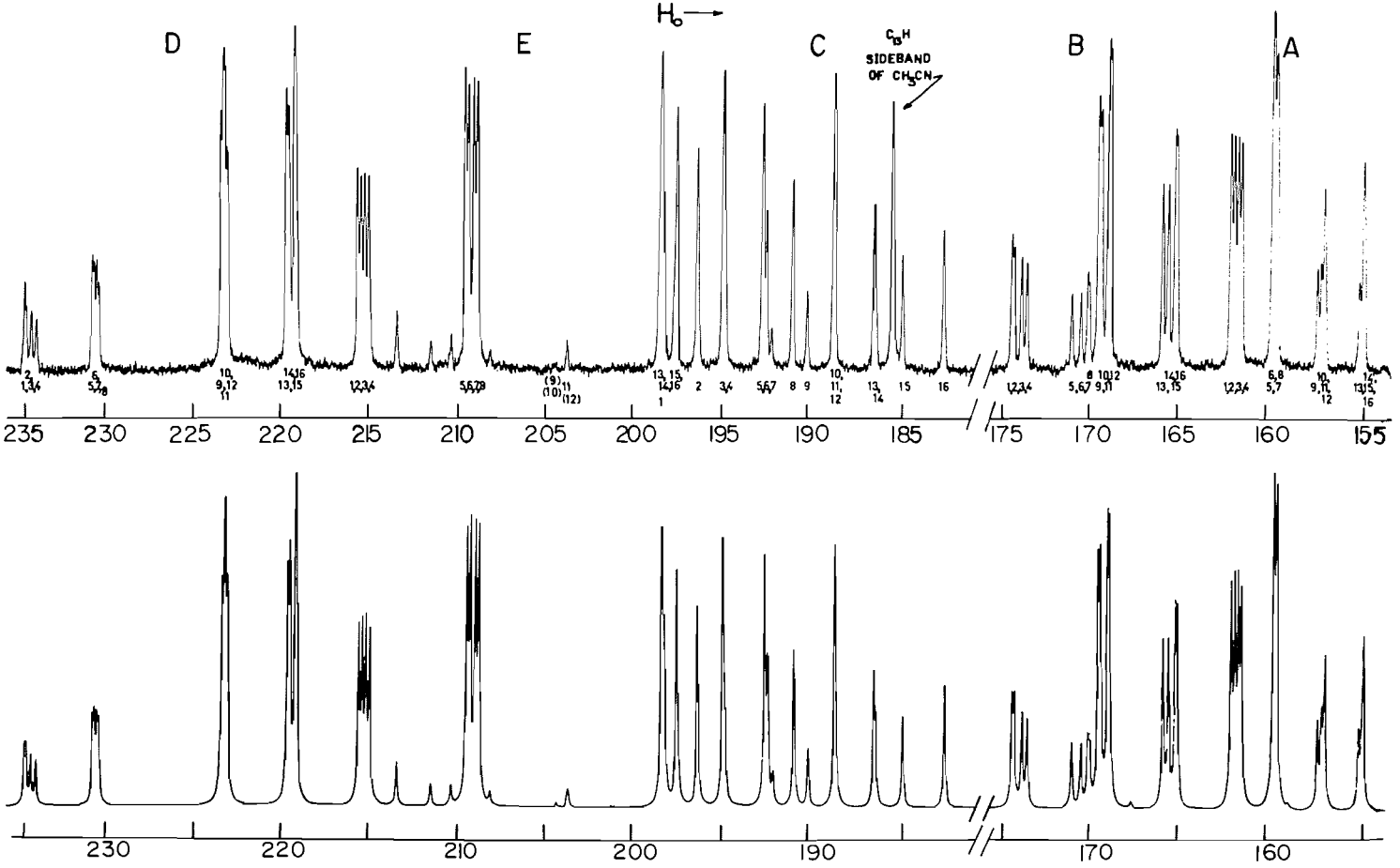

FIG. 5. Epichlorohydrin in acetonitrile: the single-resonance spectrum. Below the experimental trace is the Calcomp trace obtained using the parameters in Table 1, assuming Lorentzian peak shapes with half-line widths of 0.12 Hz.

Can. J. Chem. Downloaded from www.nrcresearchpress.com by 210.87.254.5 on 09/05/12
For personal use only.

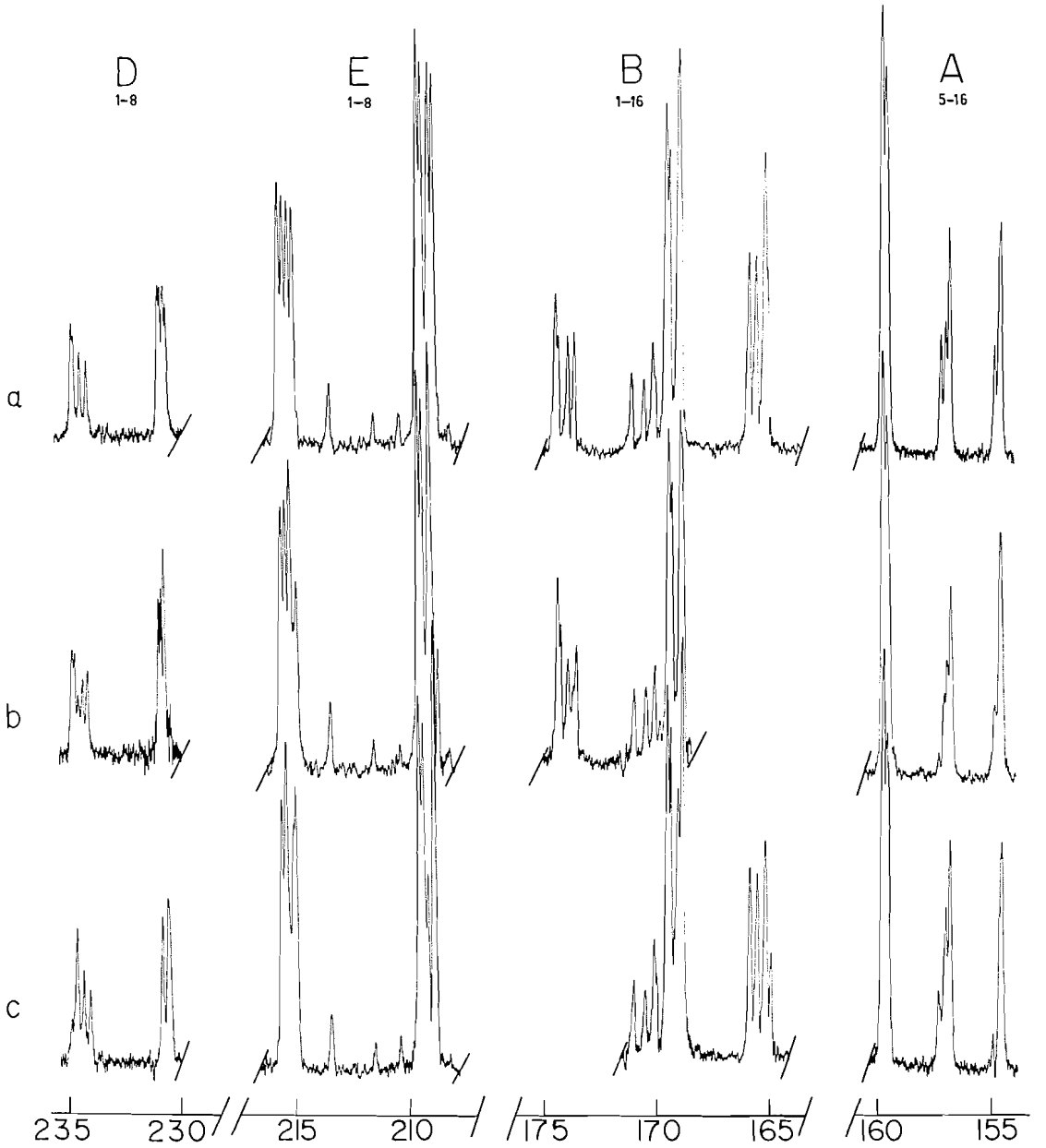

FIG. 6. Epichlorohydrin in acetonitrile: the double-resonance experiments. (*a*) Partial single-resonance trace of the indicated peaks, (*b*) partial trace showing the results of experiment ABDE{C_{15}}, (*c*) partial trace for the experiment ABDE{C_{16}}.

which must be used during the interpretation and computer fitting of complex n.m.r. spectra. Although it has been conjectured that tracing the energy-level diagram by weak double irradiations should furnish a unique solution for complex spectra (6), the present results indicate that accurate peak positions and delineation of connected transitions notwithstanding, ambiguities in parameter extractions can exist in complex spectra, at least in cases involving near-degeneracy. Although the parameter signs appear to be well established by this method, the large

Can. J. Chem. Downloaded from www.nrcresearchpress.com by 210.87.254.5 on 09/05/12
For personal use only.

variations in several parameters possible within the constraints of excellent r.m.s. error fitting suggest a measure of caution in accepting the results as definitive.

No such ambiguity is found for the acetonitrile spectrum, and the changes in the derived parameters are found to be consistent with those expected (assuming solution A^1 to be correct) on going from benzene to a more polar solvent, and with the data available for other epihalohydrins (8). This further evidence suggests that solution A^1 is the most correct, and probably unique, solution for the benzene sample, the other "solutions" being artifacts occasioned by the relatively large uncertainties in the measurement of several small peak separations crucial to the analysis.[6]

Two points of particular relevance to the use of purely iterative computer fitting of spectra are underlined by this study. First, the spin labelling of several transitions in both samples are not those expected on a first-order basis, even though $(\nu_X - \nu_Y)/J_{XY} \gg 10$. For example, in both samples, although $(\nu_A - \nu_D)/J_{AD} \sim 200$ and $(\nu_A - \nu_E)/J_{AE} \sim 150$, the true labels of H_D and H_E for several A transitions are interchanged from those expected in first order. While this may not be surprising in the benzene sample, where $(\nu_D - \nu_E)/J_{DE} \ll 1$, it is more surprising in the acetonitrile solution, where $(\nu_D - \nu_E)/J_{DE} \sim 1$. Without the benefit of spin tickling to positively identify the peaks, many of these label "switches" would not be detected in the closely spaced peaks. Secondly, very slight "reference phase" changes in the radiofrequency unit of the spectrometer were found to lead to a reversal of the apparent intensities of closely spaced peaks without, however, causing a detectable change in the symmetry of the peaks at their base line. The import of both these factors on purely iterative fitting of peak positions coupled with visual intensity comparisons is very clear. Perhaps it explains the discrepancies between the present and previous results on epichlorohydrin.

[6]The existence of more than one solution to ABX and ABC spectra is well known (16, 17), and has led to a cautioning against the automatic acceptance of the uniqueness of solutions given by iterative computer fits (18). Although techniques are available that allow investigation of all possible solutions to ABX and ABC spectra (19), these cannot be extended to systems with more than 3 non-equivalent protons, and therefore it is not possible to exclude other solutions for this case with any certainty.

It is perhaps pertinent here to argue against the frequent practice of quoting as "error estimates" the data generated by iterative computer fits to n.m.r. spectra. In the usual experiment, spectra are calibrated at <5 Hz intervals and peak positions obtained by interpolation.[7] Typically, such a method furnishes errors of 0.02–0.04 Hz for an exact AB or ABX analysis where it is easy to compute the effect of errors in position measurements. However, the "probable error" or "error vector" computed by the LAOCOON programs for these same, or more complex (as here), spectra, can be as low as 0.002–0.004 Hz. Thus, this measure is not so much a real error estimate as a measure of the accuracy with which the computer can fit the observed (averaged) peak positions. Perhaps a more real error estimate would be obtained by varying a significant number of peak positions within the error limits in their measurement, iterating again, and comparing results. This method has been used in estimating the probable errors for the present work, as shown in Table 1.

(b) The Coupling Constants

The tickling experiments clearly demonstrate that in both benzene and acetonitrile solutions $^4J_{AD}$ and $^4J_{AE} < 0$, while $^4J_{BD}$ and $^4J_{BE} > 0$, a result consistent with $^4J_{H_A,CH_3} < 0$ and $^4J_{H_B,CH_3} > 0$ in propylene oxide (6). There exists considerable interest in the stereochemical significance of the signs and magnitudes of $^4J_{HH}$ (20–23). Barfield has derived formulations for ^4J as a function of the two dihedral angles involved in simple acyclic fragments (20), and Barfield and Chakrabarti have pointed out problems in separating conformational and substituent effects in substituted fragments (24). The bonding scheme is not simple in epichlorohydrin. At any rate, these formulations do not lead to agreement between the experimental $^4J_{HH}$ values and reasonable conformations (25) for epichlorohydrin. A fuller discussion for all epihalohydrins will be given in a second paper (8). Vicinal coupling constants (26) will also be considered.

NOTE ADDED IN PROOF: Since completing this manuscript, a recent paper co-authored by one of the authors of the LAOCOON-3 program

[7]A more accurate if tedious method would use continuous sweep and lock frequency monitoring at a very slow, $\leqslant 0.01$ Hz/s, sweep rate.

has touched on one of the points raised in the present paper (27). In assessing the confidence limits to be placed on the LAOCOON-3 derived parameters for α,α,α-trifluorotoluene, these workers decline to use the computer-generated "probable errors" (noted to be all < 0.010 Hz), but rather use as a criterion the reproducibility of the results. It may be noted that this latter method gives an uncertainty of 0.02–0.03 Hz. It is explicitly stated in this paper that "calculated probable errors furnish only a measure of the precision of the experimental determinations but not necessarily their accuracy. The latter can be estimated in fact only by comparison of the results of repeated independent measurements".

It therefore appears that it is not the intention of the authors of the LAOCOON-3 program to use the computer-generated "probable errors" as a measure of the *accuracy* of derived parameters. However, inspection of almost any paper using LAOCOON-3 will show that this is in fact the way that the "probable error" table is interpreted in almost every instance.

The present paper reaches much the same conclusion as that quoted above, and perhaps goes further in stating that the "probable error" is a measure of the precision of fitting (not experimental determination). Further, the results quoted clearly show the dangers of accepting these "probable errors" as such. We feel that our comments on this topic, and the experimental results which led to them, are therefore apt, and worthy of discussion.

We are grateful to the National Research Council of Canada and the Manitoba Graduate Research Fund for financial assistance. Mr. R. Wasylishen kindly prepared the trace of the theoretical spectra on a Calcomp plotter. We are indebted to Drs. S. Castellano and A. A. Bothner-By for a listing of LAOCOON-3 and to Dr. Barfield for a preprint of his review. The helpful comments of a referee concerning the significance of the "error vector and standard error" table given by the LAOCOON-3 computer program is gratefully acknowledged.

1. C. A. Reilly and J. D. Swalen. J. Chem. Phys. **35**, 1522 (1961); see also footnote 9 in J. Chem. Phys. **37**, 3012 (1962).
2. E. Lippert and H. Prigge. Ber. Bunsenges. Phys. Chem. **67**, 415 (1963).
3. G. Aruldhas and V. Nayar. Indian J. Appl. Phys. **4**, 361 (1966).
4. W. A. Thomas. J. Chem. Soc. B, 1187 (1968).
5. P. Granger and D. Canet. C. R. **268C**, 1661 (1969).
6. D. D. Elleman, S. L. Manatt, and C. D. Pearce. J. Chem. Phys. **42**, 650 (1965).
7. J. S. Waugh and F. A. Cotton. J. Phys. Chem. **65**, 562 (1961).
8. C. J. Macdonald and W. F. Reynolds. Can. J. Chem. This issue.
9. R. Freeman and W. A. Anderson. J. Chem. Phys. **37**, 2053 (1962).
10. J. D. Baldeschwieler and E. W. Randall. Chem. Rev. **63**, 81 (1963).
11. C. A. Reilly and J. D. Swalen. J. Chem. Phys. **32**, 1378 (1960); **34**, 980 (1961).
12. G. Allen, D. J. Blears, and K. H. Webb. J. Chem. Soc. 810 (1965).
13. S. Castellano and A. A. Bothner-By. LAOCOON-3. Mellon Institute Publication, Pittsburgh. 1967.
14. S. Castellano and A. A. Bothner-By. J. Chem. Phys. **47**, 5443 (1967).
15. J. D. Baldeschwieler and E. W. Randall. Discuss. Faraday Soc. **34**, 156 (1962).
16. M. T. Emerson and S. M. Cohen. J. Mol. Spectrosc. **20**, 159 (1966).
17. R. Yamamoto and S. Fujiwara. Bull. Chem. Soc. Jap. **39**, 333 (1966).
18. S. Castellano and J. S. Waugh. J. Chem. Phys. **34**, 295 (1961).
19. J. W. Emsley, J. Feeney, and L. H. Sutcliffe. High resolution NMR spectroscopy. Vol. 1. The Pergamon Press, Ltd., New York. 1965. p. 374.
20. M. Barfield. J. Chem. Phys. **41**, 3825 (1964); **47**, 3831 (1967); **48**, 4463 (1968).
21. S. Sternhell. Rev. Pure Appl. Chem. **14**, 15 (1964).
22. V. F. Bystrov and A. U. Stepanyants. J. Mol. Spectrosc. **21**, 241 (1966).
23. K. G. R. Pachler and W. G. E. Underwood. Tetrahedron, **23**, 1817 (1967).
24. M. Barfield and B. Chakrabarti. Chem. Rev. To be published.
25. M. Igarashi. Bull. Chem. Soc. Jap. **28**, 58 (1955).
26. M. Karplus. J. Chem. Phys. **30**, 11 (1959).
27. R. J. Kostelnik, M. P. Williamson, D. E. Wisnosky, and S. M. Castellano. Can. J. Chem. **47**, 3313 (1969).

Can. J. Chem. Downloaded from www.nrcresearchpress.com by 210.87.254.5 on 09/05/12
For personal use only.

Can. J. Chem. Downloaded from www.nrcresearchpress.com by 210.87.254.6 on 09/05/12
For personal use only.

Nuclear magnetic resonance spectra of the epihalohydrins. II. Spectral analyses and structural correlations for all the epihalohydrins[1]

C. J. MACDONALD[2,3]
Department of Chemistry, University of Manitoba, Winnipeg, Manitoba

AND

W. F. REYNOLDS
Department of Chemistry, University of Toronto, Toronto 181, Ontario

Received October 17, 1969

Complete analyses of the proton magnetic resonance spectra of propylene oxide, epifluorohydrin, epibromohydrin, and epiiodohydrin shows that in all cases the *cisoid* coupling constants over four bonds are negative, and the *transoid* coupling constants positive. Dipole moments, together with the vicinal coupling constants of the $CH—CH_2X$ moiety, are used to establish the probable conformations for all the epihalohydrins. Conformational factors appear to obscure any possible relationship between substituent electronegativity and long-range coupling constants.

Canadian Journal of Chemistry, **48**, 1046 (1970)

Introduction

Although the epihalohydrins, **1** (X = F, Cl, Br, I), have been investigated previously by nuclear magnetic resonance (n.m.r.) spectroscopy (1–5), the published data are incomplete, especially with regard to the signs and magnitudes of the long-range proton–proton coupling constants ($^4J_{HH}$). A recent unequivocal sign determination for epichlorohydrin by one of us (6) has buttressed the conclusion that care is required in the spectral analysis of this series of compounds (7).

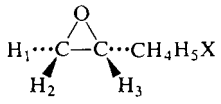

1

In this paper, the extension of the study to the complete series of epihalohydrins is described. Additional structural information was sought from dipole moment determinations. The investigation had three principal objectives: (*a*) to obtain complete and reliable spectral parameters, including relative signs of the coupling constants; (*b*) to correlate these parameters and the dipole moment data with molecular conformations; and (*c*) to monitor variations in the $^4J_{HH}$ with substituent and conformation.

[1]Presented, in part, at the 51st Annual C.I.C. Conference, Vancouver, British Columbia, June, 1968.
[2]Postdoctorate Fellow, 1967–1968.
[3]Present address: Department of Chemistry, University of Toronto, Toronto 181, Ontario.

Experimental

Compounds

Propylene oxide (**1**, X = H), epifluorohydrin, epichlorohydrin, epibromohydrin, benzene, and tetramethylsilane (TMS) were commercially available. Epiiodohydrin, synthesized from epichlorohydrin and potassium iodide in dry acetone (2), had b.p. 59–60 °C/16 mm, n_D^{25} 1.5493 (lit. (2) b.p. 63 °C/20 mm). The iodo compound, which decomposed if distilled at atmospheric pressure and discolored readily on standing in light without observable change in its n.m.r. spectrum, was stored in the dark over copper wire.

Nuclear Magnetic Resonance Spectra and Analyses

Vapor phase chromatography (v.p.c.) and n.m.r. spectra showed all the compounds to be 99% pure, or better. 10 mole % solutions in Analar benzene containing 2–3 mole % of TMS were degassed by the freeze–pump–thaw technique and sealed.

Proton magnetic single- and double-("tickled") resonance spectra were obtained and calibrated as described previously (6), using a Varian DA60-I spectrometer operating in the frequency sweep mode. Peak positions were obtained with standard deviations of not more than 0.03 Hz, and half-line widths for resolved lines were $\leqslant 0.12$ Hz. The probe temperature was 30 ± 1 °C, as shown by the standard Varian methanol sample and calibration chart.

Analysis involved mapping the energy-level diagram by extensive selective spin-tickling experiments and iterative computer fitting (6) using either the LAOCOON-3 (8) or TWOSUM (9) computer programs. Identical results were obtained by either program, but in some cases the TWOSUM program was preferred since it furnished energy levels explicitly and thus allowed more ready identification of the observed transitions. Epibromohydrin and epiiodohydrin were solved as ABCDE spectra, the proton spectrum of epifluorohydrin as the ABCDE part of an ABCDEX spectrum, and propylene oxide as an $ABCD_3$ spectrum. No attempt was made to

Can. J. Chem. Downloaded from www.nrcresearchpress.com by 210.87.254.6 on 09/05/12
For personal use only.

repeat the previous sign determination on propylene oxide (7). In assessing the uncertainty values of the derived parameters, a significant number ($\sim 1/3$) of the experimental peak positions were varied within the confidence limits in their measurement (± 0.03 Hz), and the iterative solutions repeated. This method is considered (6) to give rather larger, but somewhat more realistic confidence limits than the "probable errors" furnished by the computer programs.

Experimental Determinations of Dipole Moments

Distilled propylene oxide, epichlorohydrin, and epibromohydrin were free of detectable impurities (< 0.2% by v.p.c.). The principal impurity ($\sim 1\%$) in epifluorohydrin appeared to be 1,4-dioxane from its n.m.r. and v.p.c. response (4); a pure sample was prepared by preparative v.p.c. After repeated distillations, epiiodohydrin contained 0.5–1% of epichlorohydrin as the only detectable impurity. Preparative v.p.c. was abandoned because of sample decomposition. These compounds were stored over Linde molecular sieve (type 4A). Reagent-grade (thiophene-free) benzene was partially frozen, the liquid portion ($\sim 1/5$) discarded, and the thawed benzene dried by repeated shaking over molecular sieve. Physical constants of the compounds used are collected in Table 1.

TABLE 1

Physical constants of compounds used in dipole moment measurements

Compound	Boiling point (°C)	$n_D^{25.1}$
Propylene oxide	35	1.3648
Epifluorohydrin	84–85	1.3686
Epichlorohydrin	117–117.5	1.4363
Epibromohydrin	135–136	1.4804
Epiiodohydrin	59–60/16 mm	1.5493
Benzene	—	1.4980

Standard methods (10, 11) were used to determine the dipole moments of the epihalohydrins and propylene oxide in benzene solution. Dielectric constants of dilute benzene solutions were determined on a previously calibrated (12) Wissenschaftliche Technische Werkstatten (WTW) DMOl Dipolmeter, using a 30 ml cell thermostated at 25.15 ± 0.01 °C by water rapidly circulated from a large water bath. Specific volumes of solutions at this temperature were found using a calibrated, stoppered pycnometer of approximately 13 ml volume which had a graduated capillary stem. Experimental data are summarized in Table 2.

TABLE 2

Raw data for dipole moment determinations. Weight fraction, W, dielectric constant, E, and specific volume, V, of benzene solutions at 25.15 °C

Compound	$W \times 10^4$	E	V
Propylene oxide			
	0	2.2734	1.14486
	7.3735	2.2781	1.14494
	15.0645	2.2833	1.14500
	20.5237	2.2870	1.14505
	30.6661	2.2931	1.14515
	37.6425	2.2977	1.14518
Epifluorohydrin			
	0	2.2730	1.14487
	0	2.2731	1.14486
	3.2588	2.2760	1.14484
	5.7315	2.2785	1.14481
	5.8218	2.2789	1.14480
Epichlorohydrin			
	0	2.2733	1.14486
	7.3805	2.2778	1.14473
	19.9130	2.2854	1.14441
	27.0774	2.2898	1.14422
	37.0794	2.2956	1.14396
Epibromohydrin			
	0	2.2734	1.14486
	9.2482	2.2768	1.14441
	20.3156	2.2811	1.14385
	28.6859	2.2842	1.14342
	40.9089	2.2887	1.14284
Epiiodohydrin			
	0	2.2738	1.14485
	7.9944	2.2758	1.14435
	17.5878	2.2779	1.14374
	25.1511	2.2797	1.14308
	42.2428	2.2838	1.14205

Total molar polarizations (P_T) were calculated from the experimental data (least-squares treatment) using the Halverstadt and Kumler modification (13) of the Hedestrand equation (14). Molar electron polarizations (P_E)

TABLE 3

Structural and bond dipole data used to compute expected dipole moments in the epihalohydrins

Structural factors				Bond dipoles	
Parameter	Value	Parameter	Value	Parameter	Value
C—C_{ring}	1.471 Å	C—C_{side}	1.513 Å	μ (propylene oxide)	1.90 D
C—O	1.436 Å	C—H_{side}	1.09 Å	μ_{C-F}	1.51 D
C—H_{ring}	1.082 Å	C—F	1.379 Å	μ_{C-Cl}	1.56 D
∠H_2CC	158° 6′	C—Cl	1.767 Å	μ_{C-Br}	1.48 D
∠HCH	116° 15′	C—Br	1.935 Å	μ_{C-I}	1.29 D
∠C—C—C	120° 57′	C—I	2.207 Å	μ_{H-C}	0.3 D
∠CC⊥*	33° 47′	∠XCH_{side}	109° 30′		

*Angle between C—CH_2X bond and perpendicular to the ring through the ring carbon atom.

Can. J. Chem. Downloaded from www.nrcresearchpress.com by 210.87.254.6 on 09/05/12
For personal use only.

TABLE 4

Chemical shifts and coupling constants for propylene oxide and epihalohydrins in benzene

Parameter*	Value, X = H	F	Cl	Br	I
δ_1	2.001±0.0005	2.060±0.0005	2.009±0.0005	1.994±0.0005	1.966±0.0005
δ_2	2.326±0.0005	2.223±0.0005	2.218±0.0005	2.273±0.0005	2.325±0.0005
δ_3	2.577±0.0005	2.703±0.0005	2.674±0.0005	2.719±0.0005	2.696±0.0005
δ_4	0.975±0.0005	3.758±0.0005	2.962±0.0005	2.824±0.0005	2.664±0.0005
δ_5		4.083±0.0005	2.964±0.0005	2.744±0.0005	2.490±0.0005
δ_X		—	—	—	—
J_{12}	5.33 ±0.03	5.11 ±0.03	5.04 ±0.03	5.05 ±0.03	5.08 ±0.03
J_{13}	2.53 ±0.03	2.54 ±0.03	2.39 ±0.03	2.37 ±0.03	2.36 ±0.03
J_{14}	−0.38 ±0.03	−0.23 ±0.03	−0.35 ±0.13	−0.32 ±0.03	−0.36 ±0.03
J_{15}		−0.31 ±0.03	−0.27 ±0.14	−0.26 ±0.03	−0.23 ±0.03
J_{1X}		−1.44 ±0.03	—	—	—
J_{23}	3.83 ±0.03	4.21 ±0.03	3.85 ±0.03	3.82 ±0.03	3.80 ±0.03
J_{24}	0.51 ±0.03	0.17 ±0.03	0.56 ±0.20	0.67 ±0.03	0.81 ±0.03
J_{25}		0.09 ±0.03	0.06 ±0.19	0.01 ±0.02	0.02 ±0.02
J_{2X}		3.74 ±0.03	—	—	—
J_{34}	5.15 ±0.03	6.03 ±0.03	6.00 ±0.36	6.18 ±0.03	5.94 ±0.03
J_{35}		2.52 ±0.03	4.75 ±0.35	5.44 ±0.03	6.46 ±0.03
J_{3X}		11.87 ±0.03	—	—	—
J_{45}	Insensitive to	−10.66 ±0.03	−11.63 ±0.05	−10.58 ±0.03	−10.13 ±0.03
J_{4X}	this parameter	47.34 ±0.03	—	—	—
J_{5X}		47.87 ±0.03	—	—	—
Total r.m.s. error, Hz	0.012	0.011	0.011	0.009	0.011
No. of assigned peaks	80	160	74	70	88
Worst fit of any peak, Hz	0.029	0.025	0.034	0.024	0.024

*δ in p.p.m. to low field of internal TMS, J in Hz.

Can. J. Chem. Downloaded from www.nrcresearchpress.com by 210.87.254.6 on 09/05/12
For personal use only.

were estimated using Vogel bond-refraction values (15). At least in the case of propylene oxide (P_E^{Vogel} = 15.92, P_E^{expt} = 15.67, 16.21 (16, 17)), this approximation may be shown to lead to no significant error. Molar atom polarizations (P_A) were assigned at the reasonable value of (0.1 × P_E), following the usual practice (10).

Dipole moments were then calculated from the Debye equation (18).

Vector Model Computation of Dipole Moments

Assuming that the skeleton of propylene oxide, established by microwave spectroscopy (19), held for all the epihalohydrins, and further assuming reasonable values for the carbon–halogen bond lengths (20), dipole moments expected for a bond vector model were computed as a function of the dihedral angle ϕ (Fig. 1). Bond dipoles and other data used in the computation are collected in Table 3.

Results

The final n.m.r. parameters are collected in Table 4. Experimental dipole moments are listed in Table 5, while the computed dipole moments are summarized graphically in Fig. 1.

Discussion

1. Experimental Dipole Moments

The dipole moment of propylene oxide found in this study is in good agreement (Table 5) with previously reported values (16, 17, 21). The decreasing preponderance of polar conformers with increasing size of halogen is obvious from the trend in the series.

2. Comparison with Previous n.m.r. Results

Taking cognizance of the effects of benzene upon chemical shifts, the n.m.r. parameters derived for propylene oxide in benzene compare very favorably with those previously determined for a neat sample (7). Recently, two analyses of the n.m.r. spectra of epifluorohydrin have been reported (4, 5). Although the magnitudes of the coupling constants agree with those obtained in this study (see Table 6), several signs are at variance. Two points can be made in favor of the signs reported here. First, although Granger and Canet (5) utilized, at least in part, the results of spin-tickling experiments in their analysis, the signs of the vicinal coupling constants J_{34} and J_{35} and the geminal coupling constants J_{45} (respectively reported as negative, negative, and positive) are obviously in error. Since sign determinations by double resonance are relative, this may account for some of the further disagreements in signs for the $^4J_{HH}$. Secondly, Thomas (4) relied upon visual intensity comparisons together with the "goodness" of the computer fit to establish the signs of $^4J_{HF}$ and $^4J_{HH}$. However, we found that equally "good" computer fits, as indicated by root-mean-square errors of $\leqslant$ 0.02 Hz, worst peak fitting of $\leqslant$ 0.05

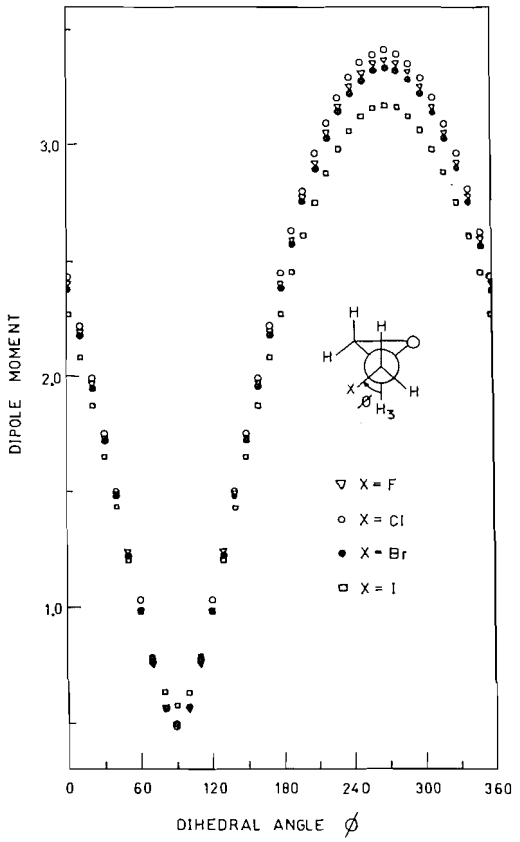

FIG. 1. Dipole moments calculated for the epihalohydrins as a function of the dihedral angle ϕ, using a bond vector model. ϕ = 0 corresponds to the eclipsing of C—X and C—H_3.

TABLE 5

Experimentally determined dipole moments of propylene oxide and epihalohydrins

Compound	Dipole moment, D
Propylene oxide	1.90*
Epifluorohydrin	2.66
Epichlorohydrin	2.29
Epibromohydrin	2.19
Epiiodohydrin	1.93

*Reported values, 1.90–1.98 D (16, 17, 21).

Can. J. Chem. Downloaded from www.nrcresearchpress.com by 210.87.254.6 on 09/05/12
For personal use only.

TABLE 6

Comparison of n.m.r. parameters derived for epifluorohydrin with previously reported values*

Parameter	Value		
	This work (Benzene)	Reference 4 (CCl_4)	Reference 5 (Neat)
δ_1	2.060	2.5571	2.573
δ_2	2.223	2.7577	2.776
δ_3	2.703	3.1430	3.196
δ_4	3.758	4.2066	4.148
δ_5	4.083	4.5660	4.681
J_{12}	5.11	5.14	4.84
J_{13}	2.54	2.55	2.68
J_{14}	−0.23	0.25	−0.38
J_{15}	−0.31	0.25	−0.21
J_{1X}	−1.44	−1.32	1.40
J_{23}	4.21	4.20	4.16
J_{24}	0.17	0.15	|<0.1|
J_{25}	0.09	0.15	−0.11
J_{2X}	3.74	3.60	4.31
J_{34}	6.03	5.83	−6.41
J_{35}	2.52	2.73	−2.09
J_{3X}	11.87	11.74	12.06
J_{45}	−10.66	−10.57	10.75
J_{4X}	47.34	47.18	47.20
J_{5X}	47.87	47.84	47.71

*δ in p.p.m. to low field of internal TMS, J in Hz.

Hz, and visual comparisons of observed and calculated peak intensities, were obtained for the solution with $^4J_{14}, {}^4J_{15} > 0 > {}^4J_{24}, {}^4J_{25}$, as for the solution with $^4J_{24}, {}^4J_{25} > 0 > {}^4J_{14}, {}^4J_{15}$. Furthermore, it was noted that slight changes of the "reference phase" of the radiofrequency unit of the spectrometer caused apparent reversal of peak intensities of several closely spaced lines of comparable intensity without noticeably affecting the symmetry of the peaks at the base line. This further failure to obtain a unique solution using iterative computer fitting coupled with visual intensity comparisons reinforces previous observations (6, 7) about the dangers of this method of relative sign determination, at least in cases involving small coupling constants.

3. *Assignment of Protons 4 and 5*

There are two possible relative assignments for protons 4 and 5

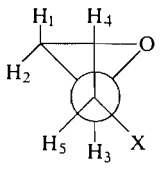

2*a*

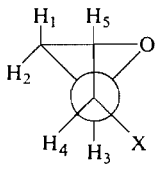

2*b*

In the case of epifluorohydrin, Thomas favored assignment **2***a* on the basis of the magnitudes and solvent dependences of J_{34} and J_{35}. Our results support this assignment. Assignment of protons H_4 and H_5 as shown in Table 4 leads to two smooth (intersecting) curves when chemical shifts are plotted vs. electronegativity of X (X = halogen). No regularity is found for alternate assignments. This assignment is also compatible with the dipole moment data (see below).

4. *Stereochemistry about the CH—CH_2X Bond*

Assuming that the propylene oxide skeleton remains basically unchanged in all of the epihalohydrins, then the only remaining source of geometrical uncertainty in this series resides in the stereochemistry about the CH—CH_2X bond. Little information about this point exists in the literature. On the basis of electron diffraction spectroscopy results, it has been concluded that epichlorohydrin (22*a*) and epibromohydrin (22*b*) exist as conformer **3***a* in the gas phase. On the other hand, n.m.r. results have been interpreted as showing that **3***b* is the major conformer in epifluorohydrin in solution (4) and **3***d* the major conformer in 2,3-epoxypropanol (23). Semiempirical calculations based on Lennard-Jones "6–12" potentials, after the method of Scott and Scheraga (24), show that potential minima correspond to conformers **3***b*–**3***d* with some distortion of conformer **3***d* in the case of the larger halogens, due to severe non-bonded repulsions between halogen and proton H_1 (25). There is no potential minimum corresponding to conformer **3***a*.

Certain general conclusions concerning

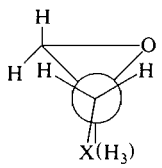

3*a*

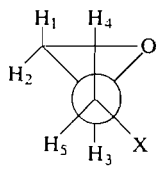

3*b*

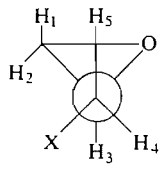

3*c*

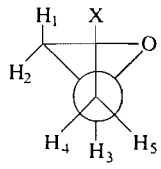

3*d*

Can. J. Chem. Downloaded from www.nrcresearchpress.com by 210.87.254.6 on 09/05/12
For personal use only.

changes in stereochemistry with substituent can be drawn from our dipole moment and vicinal coupling constant data.

In the series **1** (X = F, Cl, Br, I), the decrease in dipole moment with increasing substituent size can only be explained in terms of a corresponding increase in the fractional population of conformer **3***c*, since this conformer has a small dipole moment, while conformers **3***b* and **3***d* have large and relatively similar dipole moments. It is not possible to further discriminate between **3***b* and **3***d* on the basis of dipole moments because of this similarity. The observed dipole moments also show that epifluorohydrin, because of its large moment, can contain only a very small proportion of conformer **3***c*. On the other hand, the value in epiiodohydrin suggests that this compound contains close to 50% of conformer **3***c*.

Corroboratory information can be obtained from the magnitudes of the vicinal coupling constants J_{34} and J_{35}. The dihedral angle dependence of vicinal coupling constants (26) is well known. For the series X = F, Cl, Br, and I, J_{35} increases while J_{34} remains nearly constant. This result can only be rationalized by assuming that the fractional population of conformer **3***c* increases at the expense of **3***d*, since during this process J_{35} is increasingly converted from a *gauche* to a *trans* coupling constant, whereas J_{34} retains its *gauche* character. The nearly constant value of J_{34} in the series also appears to preclude any large change in population of conformer **3***b* at the expense of **3***c* or **3***d*, because J_{34} is a *trans* coupling constant in conformer **3***b* and *gauche* in the other two. However, there is probably a small decrease in the fractional population of **3***b* with increasing substituent size. It is well established that increasing substituent electronegativity results in a decrease in rotationally-averaged vicinal coupling constants (27, 28). More recent work suggests that this effect is due primarily to a decrease in the *gauche* coupling constants in those cases where at least one of the *gauche* protons is *trans* to the electronegative group (29, 30). Other *gauche* and *trans* coupling constants are relatively little affected by substituent electronegativity. Consequently, replacement of conformer **3***d* by **3***c* would be expected to lead to a slight increase in J_{34}, since proton H_3 is *trans* to the halogen in conformer **3***d* while neither proton H_3 or H_4 is *trans* to an electronegative group in **3***c*. Since J_{34} does not in fact change, it is possible that a small increase in conformer **3***c* at the expense of **3***b* does occur in the series. One process would tend to increase J_{34}, the other to decrease it. It should be noted that the intermediate value for all the J_{34} implies that all of the compounds must contain appreciable fractions of **3***b*.

In the foregoing discussion, we have preferred to emphasize the qualitative or discriminatory aspects of the Karplus relationship because of the uncertain quantitative effects of substituent electronegativity and orientation on explicit calculations in this series. It may be noted that calculations based on the reasonable values (30) $J_{trans} = 11$ Hz, $J_{gauche}{}^{g} = 3$ Hz (no electronegative substituent *trans* to either proton), $J_{gauche}{}^{t} = 1.5$ Hz (an electronegative substituent *trans* to at least one proton) give fractional populations consistent with the arguments developed above, and furnish good agreement between computed and experimental dipole moments.[4]

In summary, we believe that the dipole moment and vicinal coupling constant data can best be explained by assuming that conformer **3***b* is a major conformer for all the compounds, that **3***d* is a second major conformer in epifluorohydrin, and that as X increases in size, the population of **3***c* increases, while **3***d* and possibly **3***b* decrease, so that in epiiodohydrin **3***c* is the second major conformer. These conclusions are consistent with all the data and most of the conclusions made by Thomas in the case of epifluorohydrin (4), the only disagreement being the fact that Thomas concluded that **3***d* was the least populated conformer. The discrepancy between the reported gas-phase conformations of epichlorohydrin and epibromohydrin, and the conformers found in this study for solutions of these compounds may be more apparent than real. The electron diffraction spectra on which the gas-phase structures are based have extremely broad peaks. This broadness could be due to rapid interconversion of two conformers. If these conformers were **3***b* and **3***c*, as indicated in the present study, the observed result would approximate the "observed" conformer **3***a*.

A final comment may be made as to the solvent chosen for this study. Although benzene is

[4]Assignment of protons H_4 and H_5 as in **2***b* leads to marked disagreement between observed dipole moments and those computed from the observed coupling constants.

known to cause anomalies in n.m.r. chemical shifts (31) and to stabilize polar conformers to a greater degree than expected from its dielectric constant (32), it was nevertheless used in this study for two principal reasons. First, it is the preferred solvent for dipole moment determinations. Secondly, its n.m.r. absorption is well removed from that of the solutes, and it furnishes sharp and generally well-separated solute resonance peaks.

5. Long-Range Coupling Constants

The conformational dependence of four-bond proton–proton coupling constants in aliphatic systems is well established (33). Recently, substituent electronegativity dependence has also been demonstrated in the compounds $(CH_3)_2$-CXY, where increasing electronegativity of X or Y causes increasing magnitudes for the rotationally averaged $^4J_{HH}$ (34). Barfield has commented on the difficulties involved in separating dihedral angle and substituent electronegativity effects in systems containing variable conformer ratios (33), and failure of the Barfield formulation to accurately predict $^4J_{HH}$ values in epichlorohydrin has been noted (6).

Reference to Table 4 shows that the magnitudes of the *cisoid* coupling constants, $^4J_{14}$ and $^4J_{15}$, remain approximately constant with decreasing electronegativity of X, so that their average also remains constant. In the positive *transoid* couplings, J_{25} is nearly zero for all substituents and J_{24} decreases with increasing substituent electronegativity, so that their average also decreases. The trends in the averaged $^4J_{HH}$ therefore cannot be explained in terms of the electronegativity effect noted in the compounds $(CH_3)_2CXY$.

However, at least part of the trends in the individual $^4J_{HH}$ may be rationalized in terms of the changes in the average orientations in the series. Both theoretical considerations (33) and previous experimental results (7, 35) are in agreement with the *cisoid* coupling constants being negative, and variations in conformer populations between **3***c* and **3***d* as a function of substituent are not expected to appreciably change the *cisoid* couplings, as observed. *Transoid* coupling constants are expected to be positive, and increase in the relative population of conformer **3***c* at the expense of **3***d* is expected to decrease J_{25} (not observed) and increase J_{24} (observed). On the basis of the available evidence, it is not clear why J_{25} does not decrease as expected.

It therefore appears that while substituent electronegativity effects are obscured by conformational factors in this series, conformational factors cannot account for all the observed trends.

We are grateful to the National Research Council of Canada and the Manitoba Graduate Research Fund for financial assistance. One of us (C.J.M.) is grateful for the help and encouragement of Professor T. Schaefer, University of Manitoba, in whose laboratory the n.m.r. spectra were determined and analyzed. We are indebted to Drs. S. Castellano and A. A. Bothner-By, and J. S. Martin, for listings of LAOCOON-3 and TWOSUM, respectively, and to Professor K. Yates, University of Toronto, for permission to use the WTW Dipolmeter.

1. C. A. Reilly and J. D. Swalen. J. Chem. Phys. **35**, 1522 (1961); see also footnote 9 in J. Chem. Phys. **37**, 3012 (1962).
2. E. Lippert and H. Prigge. Ber. Bunsenges. Phys. Chem. **67**, 415 (1963).
3. G. Aruldhas and V. Nayar. Indian J. Appl. Phys. **4**, 361 (1966).
4. W. A. Thomas. J. Chem. Soc. B, 1187 (1968).
5. P. Granger and D. Canet. C. R. **268C**, 1661 (1969).
6. C. J. Macdonald and T. Schaefer. Can. J. Chem. This issue.
7. D. D. Elleman, S. L. Manatt, and C. D. Pearce. J. Chem. Phys. **42**, 650 (1965).
8. S. Castellano and A. A. Bothner-By. LAOCOON-3. Mellon Institute Publication, Pittsburgh. 1967.
9. J. S. Martin. Private communication.
10. J. W. Smith. Electric dipole moments. Butterworth's, London. 1955. Chaps. 3, 9.
11. C. P. Smyth. Dielectric behaviour and structure. McGraw-Hill Book Co. Inc., New York. 1955. pp. 16–50.
12. B. Scott. Ph.D. Thesis. University of Toronto, Toronto. 1967.
13. I. F. Halverstadt and W. D. Kumler. J. Amer. Chem. Soc. **64**, 2988 (1942).
14. G. Hedestrand. Z. Phys. Chem. **B2**, 428 (1929).
15. A. I. Vogel. A textbook of organic chemistry. 3rd. ed. Longmans, Green and Co., Ltd., London. 1961. p. 1035.
16. M. T. Rogers. J. Amer. Chem. Soc. **69**, 2544 (1947).
17. C. W. N. Cumper and A. I. Vogel. J. Chem. Soc. 3521 (1959).
18. P. Debye. Phys. Z. **13**, 97 (1912).
19. J. D. Swalen and D. R. Herschbach. J. Chem. Phys. **27**, 100 (1957).
20. L. E. Sutton. (*Editor*) Tables of interatomic distances and configuration in molecules and ions. Chem. Soc. Spec. Publ. No. 11. Chemical Society, London. 1958; Chem. Soc. Spec. Publ. No. 18. Chemical Society, London. 1965.
21. J. S. Allen and H. Hibbert. J. Amer. Chem. Soc. **56**, 1398 (1934).
22. (*a*) M. Igarashi. Bull. Chem. Soc. Jap. **28**, 58 (1955); (*b*) **34**, 365 (1961).

Can. J. Chem. Downloaded from www.nrcresearchpress.com by 210.87.254.6 on 09/05/12
For personal use only.

23. J.-L. PIERRE, R. PERRAUD, P. CHAUTEMPS, and P. ARNAUD. Bull. Soc. Chim. France, 1325 (1969).
24. R. A. SCOTT and H. A. SCHERAGA. J. Chem. Phys. **42**, 2209 (1965); **45**, 2091 (1966).
25. C. J. MACDONALD, W. F. REYNOLDS, and D. J. WOOD. Unpublished results.
26. M. KARPLUS. J. Chem. Phys. **30**, 11 (1959).
27. N. SHEPPARD and R. M. LYNDEN-BELL. Proc. Roy. Soc. London, Ser. A, **269**, 385 (1962).
28. R. J. ABRAHAM and K. G. R. PACHLER. Mol. Phys. **7**, 165 (1964).
29. R. J. ABRAHAM, L. CAVALLI, and K. G. R. PACHLER. Mol. Phys. **11**, 471 (1966).
30. G. M. WHITESIDES, J. P. SEVENAIR, and R. W. GOETZ. J. Amer. Chem. Soc. **89**, 1135 (1967).
31. J. W. EMSLEY, J. FEENEY, and L. H. SUTCLIFFE. High resolution nuclear magnetic resonance spectroscopy. Vol. 1. The Pergamon Press, Ltd., Oxford. 1965. p. 258.
32. K. CHITOKU and K. HIGASI. Bull. Chem. Soc. Jap. **40**, 773 (1967).
33. M. BARFIELD and B. CHAKRABARTI. Chem. Rev. In press.
34. D. J. SARDELLA. J. Mol. Spectrosc. **31**, 70 (1969).
35. K. G. R. PACHLER and W. G. E. UNDERWOOD. Tetrahedron, **23**, 1817 (1967) and references therein.

Can. J. Chem. Downloaded from www.nrcresearchpress.com by 210.87.254.6 on 09/05/12
For personal use only.

Can. J. Chem. Downloaded from www.nrcresearchpress.com by 210.87.254.5 on 09/05/12
For personal use only.

Kinetics of aquation of the fluoropentaamminecobalt(III) ion

T. W. SWADDLE AND W. E. JONES
Department of Chemistry, The University of Calgary, Calgary 44, Alberta

Received October 27, 1969

The kinetics of the hydrogen-ion-independent pathway for the replacement of fluoride in aqueous $(NH_3)_5CoF^{2+}$ by H_2O have been reinvestigated using a specific fluoride-ion electrode, with due regard for the concomitant autocatalytic loss of the ammine ligands. In perchlorate media of ionic strength 0.1 *M*, the first-order rate coefficient is 1.22×10^{-6} s^{-1} at 45°, and the kinetics are represented by $\Delta H^* = 24.4$ kcal mole^{-1} and $\Delta S^* = -9$ cal deg^{-1} mole^{-1} over the range 35–75° at least. The relationship of these data to those for the aquation of other species of the type ML_5X^{n+} is discussed.

Canadian Journal of Chemistry, **48**, 1054 (1970)

Introduction

The purpose of this study was primarily to re-evaluate the enthalpy ΔH^* and entropy ΔS^* of activation for the acid-independent aquation of the fluoropentaamminecobalt(III) ion, since the previously reported values of Chan (1) seemed to us to be strikingly anomalous. To this end, it was necessary to find an improved analytical technique for the estimation of aqueous fluoride ion, and to consider whether aquation of the supposedly "inert" ammine ligands (2, 3) is a serious complicating factor in the study of the replacement of less-labile ligands X, such as fluoride, in $Co^{III}(NH_3)_5X^{n+}$.

Activation parameters for the acid-independent pathways of some aquations of the type

[1] $$ML_5X^{2+} + H_2O \rightarrow ML_5OH_2^{3+} + X^-$$

have been critically re-evaluated (where necessary) from data in the existing literature, and are collected in Table 1. It will be seen at once that the values of ΔH^* and ΔS^* obtained from the data of Chan (1) for the aquation of $Co(NH_3)_5F^{2+}$ are quite different from those of the Cr(III) complexes, despite an overall similarity in the values of these parameters for other corresponding compounds of the series $Co(NH_3)_5X^{2+}$, $Cr(NH_3)_5X^{2+}$, and $Cr(H_2O)_5X^{2+}$. It is probably wrong to expect a *close* correlation between the data for these series, since it appears that the cobalt(III) ammines react by an extreme dissociative interchange ("I_d") mechanism (12, 13) whereas associative activation by the incoming water-ligand is evidently of comparable importance to dissociative activation by the departing X^- (an "I_a" mechanism) in the reactions of the $Cr(H_2O)_5X^{2+}$ series (14–16). Nevertheless, the influence of the departing ligand X^- on the kinetic parameters does seem to follow a roughly similar pattern in these three series of reactions, with the apparent exception of $Co(NH_3)_5F^{2+}$ (and $Co(NH_3)_5I^{2+}$ (5), in which instance redox phenomena complicate the kinetic measurements).

It has been claimed (7, 8, 17) that ΔH^* and ΔS^*

TABLE 1

Activation parameters* for the acid-independent replacement of X^- by H_2O in ML_5X^{2+}

	ΔH^*, kcal mole^{-1}			ΔS^*, cal deg^{-1} mole^{-1}		
X	$Co(NH_3)_5X^{2+}$	$Cr(H_2O)_5X^{2+}$	$Cr(NH_3)_5X^{2+}$	$Co(NH_3)_5X^{2+}$	$Cr(H_2O)_5X^{2+}$	$Cr(NH_3)_5X^{2+}$
F	(19.6)†	28.7	24.6	(−25)†	−3.9	−6.4
F	24.4‡			−8.9‡		
Cl	23.3	24.3	21.7	−6.8	−7.1	−8.7
Br	23.2	23.8	21.8	−3.8	−3.5	−3.6
I	(19)†	23.0	21.6	(−16)†	−0.2	0.3
NO_3	24.3	21.6	18.6	1.9	−5.1	−11.1
NCS	30.1	27.5	24.6§	−0.8	−3.5	−8.3§
N_3	33.2	32.4	—	13.1	16.2	—

*Activation parameters taken from refs. 4 through 10, or recalculated by a least-squares method from rate data given therein.
†Disputed value; see text.
‡This work.
§This figure, from Gay and Lalor (4), differs from that of Duffy and Earley (11).

Can. J. Chem. Downloaded from www.nrcresearchpress.com by 210.87.254.5 on 09/05/12
For personal use only.

are abnormally large (in the absolute sense) for both $Cr(H_2O)_5F^{2+}$ and $Cr(NH_3)_5F^{2+}$; certainly, the logical sequence $F \ll Cl < Br < I$ (or vice versa) is not followed. This phenomenon probably originates in a lower degree of solvation of the fluoro group, as compared with other leaving groups, in the transition state; this has been attributed to a greater degree of associative activation by the incoming water molecule (8), or alternatively to the separation of the basic fluoro-ligand as an entity approximating to HF rather than F^- (7, 17). The true mechanism probably involves features of *both* models, but we shall retain the latter view as a working hypothesis, since it focuses attention on the Brønsted basicity of the departing ligand; unusually positive ΔS^* values seem to be associated with acid-independent aquation pathways involving other basic ligands, notably azide (7, 18, 19). Noting that $(H_2O)_5CrN_3^{2+}$ (18) and $(NH_3)_5CoN_3^{2+}$ (19, 20) show closely similar behavior in this respect (Table 1), it might be anticipated that the true value of ΔH^* lies between 24 and 29 kcal $mole^{-1}$ and ΔS^* between -10 and 0 cal deg^{-1} $mole^{-1}$ for $Co(NH_3)_5F^{2+}$, and accordingly it was decided to redetermine these parameters using a wider temperature range and modern analytical methods.

Experimental

Materials

Reagents were purified in the usual ways (6). Polyethylene laboratory ware was used for the kinetic experiments and the long-term storage of fluorine-containing solutions. Fluoropentaamminecobalt(III) nitrate was made by the standard method (21) and reprecipitated as the perchlorate salt using $LiClO_4$ solution at 0°. The product was analyzed for NH_3 by a Kjeldahl-type method, and for fluoride using a specific fluoride-ion electrode (see below).

Anal. Calcd. for $CoN_5O_8H_{15}FCl_2$: NH_3, 23.53; F, 5.25. Found: NH_3, 23.5; F, 5.2.

Baker-analyzed sodium fluoride (100.0% NaF) was used as a primary standard for fluoride ion, and lanthanum nitrate solutions were made from La_2O_3 (Matheson, Coleman and Bell) as directed by Lingane (22).

Kinetic Measurements

For kinetic runs without p*H* control, a weighed sample of fluoropentaamminecobalt(III) perchlorate was dissolved quickly at "zero time" in a thermally pre-equilibrated 0.1 *M* $LiClO_4$ solution contained in a polyethylene bottle in a thermostat bath. The complex concentration was 5×10^{-3} *M* in all cases. Samples (30 ml) were withdrawn at appropriate intervals over the first 8% of fluoride aquation, and stored at 0° until required for analysis, at which time they were brought quickly to 25° and aliquots (25.0 ml) were transferred to a thermostatted (25°) polyethylene beaker and slowly stirred magnetically. The p*H* (as measured with a glass electrode) was adjusted to 5.9 or slightly less with dilute $HClO_4$, and then millivolt readings were taken using a specific fluoride-ion electrode (Orion Research Inc., Model 94-09) in conjunction with a Beckman Research Model p*H* meter and Beckman No. 40459 fluoride-resistant frit junction calomel reference electrode, after titers of 0.00, 1.00, 2.00, 3.00, 4.00, 7.00, and 10.00 ml of a standard 0.005 *M* NaF solution (0.1 *M* in $LiClO_4$) had been added.

The original concentrations of fluoride were calculated from these electromotive force values (e.m.f.) by Gran's method, as described by Liberti and Mascini (23), using a linear least-squares program with a Hewlett–Packard 9100A calculator. The correlation coefficient for the seven points on the Gran plot was generally better than 0.9999.

In some experiments, the hydrogen-ion concentration was varied 30-fold (p*H* 5.8 to 4.3) by adding a small amount of perchloric acid. In experiments requiring buffer solutions, these were made up by adding the appropriate quantity of organic base to 0.1 *M* $HClO_4$, thus maintaining ionic strength 0.1 *M* in all cases.

Results

Use of Fluoride–Ion Electrode

The direct use of the e.m.f. of a fluoride-ion electrode (24) as an index of fluoride-ion concentration (as referred to a calibrating NaF solution) was found to be inadequate for the present purpose because of the logarithmic nature of the relationship between activity and e.m.f., and so the electrode was used instead as an end-point detector for a titrimetric method. We developed Lingane's lanthanum nitrate titration method (22) in much the same way as did Liberti and Mascini (23) independently, and their recommendations (23) were ultimately adopted and found to give better than $\pm 2\%$ accuracy in $[F^-]$ at 10^{-5} *M* and better than $\pm 1\%$ at 10^{-3} *M*. This represents a marked improvement over the thorium nitrate/sodium alizarinsulfonate method used by Chan (1); standard deviations in the latter technique can amount to $\pm 10\%$ even for conveniently high (0.02 *M*) fluoride concentrations (25).

Kinetic Experiments

Preliminary experiments at 45–75° showed that $Co(NH_3)_5F^{2+}$ solutions lose ammonia and deposit hydrated cobalt oxides before a substantial portion of the fluoride aquation is completed. Chan (1) reports that his first-order plots were linear up to 40–50% aquation of fluoride,

Can. J. Chem. Downloaded from www.nrcresearchpress.com by 210.87.254.5 on 09/05/12
For personal use only.

and that the reaction went to 85–90% completion. However, in a run at 45° using Chan's conditions (for which the half-life of bound fluoride is about 10 days, on the basis of Chan's data), we observed that hydrated cobalt oxides were deposited after only 6 days, and that the p*H* rose concomitantly from 6.08 to 6.60 because of ammonia release.

On the assumption that the observed decomposition was that of the aquation product, $Co(NH_3)_5OH_2^{3+}$, the spectrum of a centrifuged solution of $[Co(NH_3)_5OH_2](ClO_4)_3$ was followed as a function of time. A small decrease in the 498 mμ maximum had occurred after 2.5 days, after which time this absorption decreased rapidly; after 5 days, the p*H* had risen from 5.7 to 8.0. Thus, the loss of ammine ligands is autocatalytic, as suggested by Lamb and Marden (2). Presumably, release of NH_3 causes a rise in p*H* which in turn causes further rapid base hydrolysis of the aquo-ammine species, until finally hydrated cobalt oxides precipitate.

In order to obtain meaningful kinetic data, two alternative methods were tried: (*a*) the p*H* of the solutions was controlled with cationic buffers (26) so as to suppress the autocatalysis of NH_3 loss (addition of strong acid was not attempted, since the aquation of $Co(NH_3)_5F^{2+}$ is strongly acid-catalyzed (1)); and (*b*) the reaction kinetics were followed over the first few percent of fluoride release only, i.e., before a significant amount of NH_3 could accumulate.

Kinetics in Buffered Solutions

The buffering approach seemed promising, since an unbuffered solution of $Co(NH_3)_5F^{2+}$ deposited hydrous cobalt oxide within 0.5 h at 75° while a similar one buffered to p*H* 5 remained clear for at least 24 h. Possible complications due to ion-pairing were avoided by use of amine salt buffers such as pyridine/pyridinium (26). However, a strong shoulder at 340 mμ was seen to develop in the spectrum of $Co(NH_3)_5OH_2^{3+}$ in aqueous pyridine/pyridinium perchlorate buffer (p*H* 4.6, $I = 0.1$ *M*, 75.0°) with a half-period of roughly 3 h, and the same absorption appeared in an equimolar $Co(NH_3)_5F^{2+}$ solution under the same conditions once aquation had progressed sufficiently; the spectrum of the buffer solution alone was shown to be invariant under these conditions. Thus, a slow reaction of some kind was occurring between $Co(NH_3)_5OH_2^{3+}$ and pyridine, but the product was *not* simply $Co(NH_3)_5(C_5H_5N)^{3+}$, since this species is known (27) to have a stronger absorption maximum (ε 63.8) at 474 mμ than that at 340 mμ (ε 54), yet no such 474 mμ band was observed in our experiments. Generally similar results were obtained with aniline/anilinium buffer, and even with the very weakly nucleophilic quinaldine/quinaldinium perchlorate (28).

In the face of evidence for an interaction between $Co(NH_3)_5OH_2^{3+}$ and the buffer, one cannot strictly interpret the fluoride concentration data for buffered solutions in terms of the aquation reaction reaching the equilibrium

[2] $(NH_3)_5CoOH_2^{3+} + F^- \rightleftarrows (NH_3)_5CoF^{2+} + H_2O$

and indeed the fit of the data to the appropriate integrated rate equation

$$[3] \quad k_{aq}t = \frac{x_e}{(2a - x_e)} \ln \frac{ax_e + x_t(a - x_e)}{a(x_e - x_t)}$$

where a is the concentration of fluoro-complex at zero time and x_t and x_e are the concentrations of F^- at time t and at equilibrium, respectively, was not very satisfactory. However, the values of the aquation rate coefficient, k_{aq}, so obtained were close to those obtained by following only the first 8% of reaction either with buffer or without (see below), so the actual aquation process is not directly affected by the presence of buffer. The equilibrium quotient for the reaction [2] (i.e., the "stability constant" of $Co(NH_3)_5F^{2+}$) in pyridine/pyridinium perchlorate buffer of $I = 0.1$ *M* and p*H* 4.5 was determined by direct equilibrium measurements and from eq. [3] as 170 ± 30 M^{-1} in the range 45–75°; in view of the apparent interaction of $Co(NH_3)_5OH_2^{3+}$ with the buffer, this value represents a lower limit.

Kinetics in Unbuffered Solutions

In view of the uncertainties described in the preceding section, the definitive kinetic studies were done by following the first 8% only of the fluoride aquation reaction, without p*H* control; beyond this extent of reaction, ammonia aquation became significant, the p*H* rising from an initial value of about 5.5 to as high as 6.9 after 10% fluoride release. The free fluoride concentrations measured over this period gave good first-order kinetics with respect to $[Co(NH_3)_5F^{2+}]$; at least two independent measurements of k_{aq} were made at each temperature, and the agreement was invariably to within 3%. These results are summarized in Table 2.

TABLE 2

First-order rate coefficients, k_{aq}, for the acid-independent aquation pathway of $Co(NH_3)_5F^{2+}$ in aqueous $LiClO_4$, ionic strength 0.12 M, initial pH 5.3

Temperature, °C	$10^7 k_{aq}$, s^{-1}	
	This work	Reference
25.0	0.87*	0.87
35.0	3.30	2.44
45.0	12.2	7.50
55.0	44.5	
65.0	127	
75.0	365	

*Extrapolated from the higher temperatures.

In some experiments at 55 and 65°, the hydrogen-ion concentration was varied 30-fold (pH 5.8 to 4.3), but there was no significant effect on k_{aq}; thus, neither base- nor acid-catalyzed hydrolysis is significant in our experiments, and k_{aq} corresponds to the acid-independent aquation pathway alone.

The data of Table 2 give a good linear plot of $\ln(k_{aq}/T)$ vs. $(1/T)$, and a non-linear least-squares computer program gave $\Delta H^* = 24.4 \pm 0.3$ kcal $mole^{-1}$ and $\Delta S^* = -8.9 \pm 1.0$ cal deg^{-1} $mole^{-1}$; the same program gave $\Delta H^* = 19.6 \pm 0.9$ kcal $mole^{-1}$ and $\Delta S^* = -25 \pm 3$ cal deg^{-1} $mole^{-1}$ from Chan's data (1).

Discussion

We consider that our kinetic data (Table 2) and revised activation parameters, $\Delta H^* = 24.4$ kcal $mole^{-1}$ and $\Delta S^* = -9$ cal deg^{-1} $mole^{-1}$, for the acid-independent aquation of $Co(NH_3)_5F^{2+}$ supersede those of Chan (1), because (*a*) the Liberti–Mascini method for fluoride estimation is superior to the Th(IV)/sodium alizarinsulfonate titration, (*b*) the need to remove unreacted $Co(NH_3)_5F^{2+}$ by ion-exchange before titration is obviated, (*c*) attention has been paid to interference from the auto-catalytic loss of the ammine ligands, and (*d*) our experiments extend over a wider temperature range (40° as against 20°). Care has also been taken to maintain constant ionic strength, though this is only of minor importance (6). It is gratifying, however, to note that Chan's rate coefficient agrees well with our extrapolated value at 25° (Table 2).

The equilibrium quotient Q for reaction [2] cannot be determined with any certainty from our measurements, and we have been unable to devise an accurate method for the direct measurement of the rate coefficient for anation of $Co(NH_3)_5OH_2^{3+}$ by F^-. Nevertheless, it appears that Q is not less than 100 M^{-1} at 25° and I = 0.1 M, even if the reaction [2] is strongly endothermic, so that the value $20 \leqslant Q \leqslant 30$ M^{-1} which can be obtained from Chan's data (1) is probably incorrect. Thus, $Co(NH_3)_5F^{2+}$ may not fit the Langford linear free-energy relationship (L.f.e.r.) (12) as well as was formerly believed, though the deviation would not be great.

The aquation of fluoropentaamminecobalt(III) ion, then, is kinetically closely analogous to those of the other fluoro- and azido-complexes of Table 1, and the mechanistic models advanced (7, 8, 17, 18, 20) to accommodate the data on the latter compounds will apply to $Co(NH_3)_5F^{2+}$ too. A rather rough fit in the L.f.e.r. is almost to be expected, since the cancellation of excess ΔH^* and ΔS^* components, arising from differences in the extent of solvation of the transition states in the series $Co(NH_3)_5X^{2+}$, need not be exact (29).

With the emergence of a fairly general pattern in the activation parameters for aquation of $Co(NH_3)_5X^{2+}$, $Cr(NH_3)_5X^{2+}$, and $Cr(H_2O)_5X^{2+}$, it seems that appropriate activation parameters for $Co(NH_3)_5I^{2+}$ would be $\Delta H^* \sim 24$ kcal $mole^{-1}$ and $\Delta S^* \sim -1$ cal deg^{-1} $mole^{-1}$, so that $k_{aq} \sim 9.5 \times 10^{-6}$ s^{-1} at 25°. Yalman's experimental value (5) of $k_{aq} = 8.3 \times 10^{-6}$ s^{-1} is in agreement with this prediction, but the experimental values of ΔH^* and ΔS^* seem to be inordinately low. Our attempts to extend Yalman's work were frustrated by redox decomposition of the iodo-complex, and the question is likely to remain unresolved for this reason.

Finally, using the data of Table 1, values of $\Delta H^* \sim 33$ kcal $mole^{-1}$ and $\Delta S^* \sim 15$ cal deg^{-1} $mole^{-1}$ can be predicted for the acid-independent aquation of $Cr(NH_3)_5N_3^{2+}$.

We thank the International Nickel Company, Ltd., for a Fellowship (to W. E. Jones), the National Research Council of Canada for further financial support, and Dr. T. P. Jones for making his detailed experimental data on the $Cr(NH_3)_5X^{2+}$ series available to us.

1. S. C. Chan. J. Chem. Soc. 2375 (1964).
2. A. B. Lamb and J. W. Marden. J. Amer. Chem. Soc. **33**, 1873 (1911).
3. F. Basolo, J. G. Bergmann, and R. G. Pearson. J. Phys. Chem. **56**, 22 (1952).

Can. J. Chem. Downloaded from www.nrcresearchpress.com by 210.87.254.5 on 09/05/12
For personal use only.

4. D. L. GAY and G. C. LALOR. J. Chem. Soc. A, 1179 (1966).
5. R. G. YALMAN. Inorg. Chem. **1**, 16 (1962).
6. W. E. JONES, R. B. JORDAN, and T. W. SWADDLE. Inorg. Chem. **8**, 2504 (1969).
7. T. W. SWADDLE. J. Amer. Chem. Soc. **89**, 4338 (1967).
8. T. P. JONES and J. K. PHILLIPS. J. Chem. Soc. A, 674 (1968).
9. M. A. LEVINE, T. P. JONES, W. E. HARRIS, and W. J. WALLACE. J. Amer. Chem. Soc. **83**, 2453 (1961).
10. T. P. JONES. Private communication.
11. N. V. DUFFY and J. E. EARLEY. J. Amer. Chem. Soc. **89**, 272 (1967).
12. C. H. LANGFORD and H. B. GRAY. Ligand substitution processes. W. A. Benjamin, Inc., New York. 1966.
13. W. E. JONES and T. W. SWADDLE. Chem. Commun. 998 (1969).
14. T. W. SWADDLE and G. GUASTALLA. Inorg. Chem. **7**, 1915 (1968).
15. J. H. ESPENSON. Inorg. Chem. **8**, 1554 (1969).
16. J. BURGESS. Ann. Rept. Progr. Chem. **65A**, 400 (1968).
17. T. W. SWADDLE and E. L. KING. Inorg. Chem. **4**, 532 (1965).
18. T. W. SWADDLE and E. L. KING. Inorg. Chem. **3**, 234 (1964).
19. G. C. LALOR and E. A. MOELWYN-HUGHES. J. Chem. Soc. 1560 (1963).
20. T. W. SWADDLE and G. GUASTALLA. Inorg. Chem. **8**, 1604 (1969).
21. F. BASOLO and R. K. MURMANN. Inorg. Syn. **4**, 171 (1953).
22. J. J. LINGANE. Anal. Chem. **39**, 881 (1967).
23. A. LIBERTI and M. MASCINI. Anal. Chem. **41**, 676 (1969).
24. M. S. FRANT and J. W. ROSS, JR. Science, **154**,1553 (1966).
25. C. A. HORTON. Treatise on analytical chemistry. Pt. II, Vol. 7. *Edited by* J. M. Kolthoff and P. J. Elving. Interscience Publishers Inc., New York. 1961. p. 207.
26. T. P. JONES, W. E. HARRIS, and W. J. WALLACE. Can. J. Chem. **39**, 2371 (1961).
27. F. NORDMEYER and H. TAUBE. J. Amer. Chem. Soc. **90**, 1162 (1968).
28. J. G. PRITCHARD and F. A. LONG. J. Amer. Chem. Soc. **79**, 2365 (1957).
29. M. E. BALDWIN, S. C. CHAN, and M. L. TOBE. J. Chem. Soc. 4637 (1961).

Can. J. Chem. Downloaded from www.nrcresearchpress.com by 210.87.254.5 on 09/05/12
For personal use only.

Free-radical and molecular processes in the pyrolysis of ethylbenzene

W. D. CLARK[1] AND S. J. PRICE
Department of Chemistry, University of Windsor, Windsor, Ontario
Received August 12, 1969

From 910 to 1089 °K, at pressures of 20 to 36 mm, the pyrolysis of ethylbenzene in a toluene carrier flow system occurs primarily by three reactions

[1] $C_6H_5CH_2CH_3 \rightarrow C_6H_5CH_2 + CH_3$

[11] $C_6H_5CH_2CH_3 \rightarrow C_6H_6 + C_2H_4$

[12] $C_6H_5CH_2CH_3 \rightarrow C_6H_5C_2H_3 + H_2$

The Arrhenius equation for the reaction [1], $\log k_1\ (s^{-1}) = 14.7 - (70\,100/2.3RT)$, is in agreement with a previous aniline carrier study and with thermochemical calculations. Reaction [11] is surface dependent and yields widely scattered results. For experiments in a conditioned quartz vessel, $\log k_{11}\ (s^{-1}) = 9.06 - (51\,700/2.3RT)$. Values of k_1 and k_{12} are unaffected by the nature of the surface and by changes in the surface-to-volume ratio. The rate constants for reaction [12] are somewhat scattered, but yield the approximate equation $\log k_{12}\ (s^{-1}) = 12.7 - (64\,000/2.3RT)$. E_1 should possibly be increased by about 1 kcal to allow for the effect of reaction [−1], the recombination of methyl and benzyl species.

Canadian Journal of Chemistry, 48, 1059 (1970)

Can. J. Chem. Downloaded from www.nrcresearchpress.com by 210.87.254.6 on 09/05/12
For personal use only.

Introduction

The pyrolysis of ethylbenzene has previously been investigated by the toluene carrier technique (1), by aniline carrier studies (2), and more recently by a toluene carrier procedure using a stirred flow reactor (3). Szwarc (1) assumed the decomposition into methyl and benzyl could be followed by measuring the methane produced. He reported $\log k\ (s^{-1}) = 13.0 - (63\,200/2.3RT)$. Esteban *et al.* (2) also based their calculations on the rate of methane formation. Using primarily an aniline carrier technique, with some toluene carrier runs interspersed, they obtained $\log k\ (s^{-1}) = 14.6 - (70\,100/2.3RT)$. These higher Arrhenius parameters are supported by studies of the recombination of methyl and benzyl which, together with thermo-chemical data, lead to $\log k\ (s^{-1}) = 14.9 - (70\,500/2.3RT)$ (4).

Crowne *et al.* (3) have shown that Szwarc's activation energy may be low because no allowance was made for the recombination of methyl and benzyl. Making no correction, they obtain $\log k\ (s^{-1}) = 13.1 - (62\,200/2.3RT)$. Applying a correction based on the rate constant for the recombination process (4), they obtain $\log k\ (s^{-1}) = 14.7 - (69\,200/2.3RT)$. Although the activation energy obtained by Crowne *et al.* (3) is close to that obtained by the aniline carrier method, the rate constants from the stirred reactor work are approximately a factor of two greater. In the present work, the range of decomposition has been extended and concurrent modes of decomposition have been investigated.

Experimental

Materials

(*a*) The toluene used was prepared from sulfonic acid, Eastman Organic X325. It was dried by refluxing over sodium ribbon under vacuum and then degassed by bulb-to-bulb distillation.

(*b*) The ethylbenzene used was supplied by Eastman Organic Chemicals. It was fractionally distilled and degassed before use.

The above materials were analyzed on a 0.02 in. i.d. × 150 ft poly(propylene glycol) Golay column using a Perkin–Elmer Model 800 gas chromatograph with flame ionization detector. The major impurities were never greater than 1 part in 5000 of the liquid being analyzed.

Apparatus and Procedure

The experiments were carried out using a system similar to that used in previous work (5). The gaseous products were analyzed using a Perkin–Elmer Model 154 gas chromatograph equipped with a 1/4 in. 6 ft silica gel column. The column was maintained at 80 °C, and a helium flow rate of 20 cm^3 per min was used. A nitrogen carrier was used when hydrogen analysis was desired.

The liquid products which condensed along with the toluene in an acetone – Dry Ice trap were analyzed using the Perkin–Elmer Model 800 gas chromatograph equipped with 150 ft × 0.02 in. i.d. Golay column coated with poly(propylene glycol) (isothermal operation at 60 °C; inlet pressure of N_2 carrier, 7 lb).

[1]NRCC Studentship holder. Present address: Chemistry Department, Brandeis University, Waltham, Massachusetts.

Can. J. Chem. Downloaded from www.nrcresearchpress.com by 210.87.254.6 on 09/05/12
For personal use only.

TABLE 1

Pyrolysis of ethylbenzene

P (cm)	Temperature (°K)	Time* (min)	Toluene (g)	Ethylbenzene (mole × 10^4)	Products from ethylbenzene† (mole × 10^4)				t_c (s)	log k_1
					Methane	Styrene	Ethylene	Hydrogen		
2.23	1089	3,9,3	6.52	9.70	6.77	—	0.246		0.484	0.392‡,§
2.11	1089	3,12,3	8.44	16.10	9.45	3.95	0.370		0.424	0.318‡,§
2.90	1084	3,9,3	10.17	9.67	6.36	1.72	0.168		0.674	0.200
2.39	1081	3,13,3	9.47	11.1	6.93	3.09	1.11	4.37	0.649	0.177§
2.36	1062	3,18,3	12.29	6.25	4.46	0.845	0.376		0.742	0.225
2.27	1048	3,18,3	12.67	16.4	4.47	1.07	0.394		0.421	−0.122‡,§
2.19	1043	3,18,3	10.42	15.6	6.93	2.22	0.188		0.827	−0.148
3.49	1034	3,9,3	13.50	20.4	4.93	1.55	0.188		0.385	−0.144‡
2.33	1034	3,15,10	15.04	10.3	2.89	0.618	0.236		0.430	−0.120‡,§
2.32	1032	3,15,3	11.19	10.3	2.96	0.588	0.244		0.432	−0.106‡,§
2.32	1025	3,18,3	12.22	9.41	3.31	0.623	0.061		0.761	−0.245
1.97	1015	3,18,3	10.77	14.5	3.65	1.05	0.086		0.741	−0.410
2.26	1008	3,18,3	10.40	10.4	1.98	0.439	0.106		0.681	−0.510‡
2.24	1008	3,18,3	10.19	12.3	2.30	0.558	0.093		0.688	−0.522‡
2.07	998	3,18,3	11.48	11.8	1.92	0.690	0.046		0.743	−0.621
2.35	995	3,18,15	15.82	11.6	2.35	0.525	0.955		0.920	−0.609§
2.29	995	3,18,10	15.68	12.6	2.13	0.414	0.964		0.778	−0.625§
2.33	995	3,18,3	12.27	16.4	2.09	0.341	0.905		0.784	−0.615§
2.30	977	3,18,3	10.71	7.93	0.614	0.118	0.031		0.693	−0.935‡
2.24	967	3,18,3	12.68	12.6	0.374		0.250		0.451	−1.176‡,§
2.26	966	3,18,10	16.59	14.4	0.409		0.262		0.449	−1.193‡,§
3.60	966	3,12,3	17.06	8.64	0.450		0.013		0.673	−1.099
2.24	966	3,18,3	12.43	11.2	0.693		0.018		0.765	−1.078
2.23	956	3,18,3	12.27	13.9	0.440	0.125	0.615	0.200	0.667	−1.318§
2.32	951	3,18,3	11.58	11.5	0.468		0.014		0.864	−1.317
2.36	951	3,18,3	12.46	12.0	0.453		0.016		0.817	−1.327
2.24	943	3,18,3	12.38	16.5	0.356	0.093	0.398	0.146	0.673	−1.490§
2.31	943	3,18,3	12.86	11.2	0.111		0.074		0.470	−1.671‡,§
2.22	927	3,18,3	12.30	16.4	0.182			0.086	0.684	−1.785§
2.24	926	3,18,3	12.37	15.6	0.239		0.642	0.095	0.686	−1.648§
2.30	911	3,18,3	11.78	13.1	0.090		0.079		0.881	−2.111§
2.28	910	3,18,3	12.48	11.8	0.035		0.007		0.495	−2.218‡
2.56	910	3,18,15	12.19	12.0	0.135		0.144		1.423	−2.100§

*Prerun, ethylbenzene flow, postrun.
†Corrected for decomposition of toluene.
‡Runs in reaction vessel packed with small quartz tubes; surface-to-volume ratio a factor of 10 greater than in unpacked vessel.
§Unconditioned reaction vessel.

Can. J. Chem. Downloaded from www.nrcresearchpress.com by 210.87.254.6 on 09/05/12
For personal use only.

Results and Discussion

The experimental results are given in Table 1. They may be discussed in terms of the following mechanism

[1] $C_6H_5C_2H_5 \rightarrow C_6H_5CH_2 + CH_3$

[2] $C_6H_5CH_3 \rightarrow C_6H_5CH_2 + H$

[3] $CH_3 + C_6H_5CH_3 \rightarrow CH_4 + C_6H_5CH_2$

[4] $H + C_6H_5CH_3 \rightarrow H_2 + C_6H_5CH_2$

[5] $H + C_6H_5CH_3 \rightarrow C_6H_6 + CH_3$

[6] $CH_3 + C_6H_5C_2H_5 \rightarrow CH_4 + C_6H_5C_2H_4$

[7] $H + C_6H_5C_2H_5 \rightarrow H_2 + C_6H_5C_2H_4$

[8] $H + C_6H_5C_2H_5 \rightarrow C_6H_6 + C_2H_5$

[9] $C_6H_5C_2H_4 \rightarrow C_6H_5C_2H_3 + H$

[10] $C_2H_5 \rightarrow C_2H_4 + H$

[11] $C_6H_5C_2H_5 \rightarrow C_6H_6 + C_2H_4$

[12] $C_6H_5C_2H_5 \rightarrow C_6H_5C_2H_3 + H_2$

All of these reactions undoubtedly occur to some extent. However, the failure to observe any effect of wide variation in the toluene-to-ethylbenzene ratio on the rate of decomposition indicates that reactions [6]–[10] are of minor importance.

Since no detectable ethane was observed, it has been assumed in this work, as in previous studies of this pyrolysis, that k_1 may be calculated from the rate of formation of methane (corrected for the contribution of reaction [5] using data from earlier work in this laboratory (6)). Rate constants calculated on this basis, making no allowance for concurrent decomposition by reactions [11] and [12], are shown in Fig. 1. The first-order rate constants are independent of concentration, surface-to-volume ratio, and total pressure (over the rather narrow range 1.97–3.49 cm).

No particular significance is attached to the fact that the packed-vessel runs at low conversion fall below the curve. The correction for the decomposition of toluene is quite small in most runs. However, in the packed vessel at 966 °K it was estimated that 20% of the methane was from toluene, while at 943 and 910 °K, a figure of 35–40% was used. These estimates are based on rate constants for the essentially heterogeneous decomposition of toluene in an untreated, packed, quartz vessel (6). Since the packing used in the present work had been conditioned, the estimated corrections are probably too large.

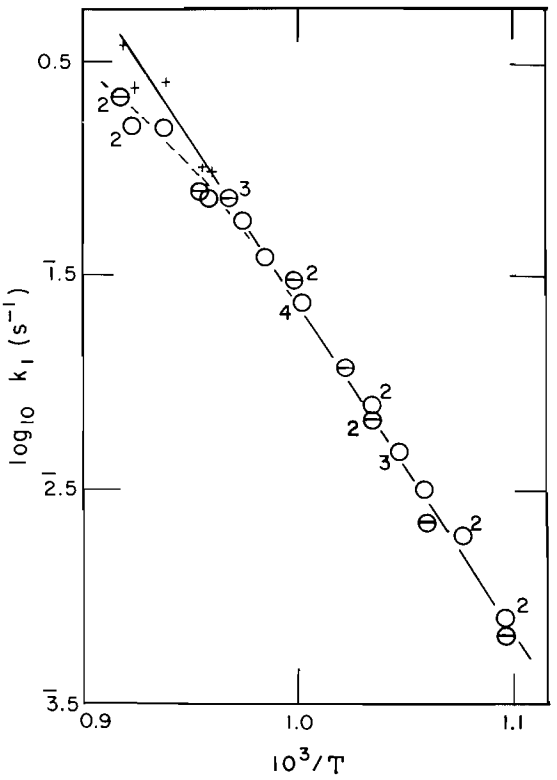

FIG. 1. Arrhenius plot of k_1. The numbers beside the points are the number of runs averaged to obtain the points; the open circles (unpacked vessel) and divided circles (packed vessel) represent values of k_1 calculated from the rate of formation of CH_4 (corrected for toluene decomposition), assuming no concurrent modes of decomposition; +, values of k_1 estimated by using extrapolated values of k_{11} and k_{12} to determine k_1 from the parallel reaction scheme. Below 1043 °K the two methods of calculating k_1 give virtually identical results.

Values of k_1 have also been calculated based on the parallel reaction scheme involving reactions [1], [11], and [12]. The only significant differences from the values of k_1 calculated from the yield of CH_4 occur when the percent decomposition is above about 35%. As may be seen from Fig. 1, allowance for reactions [11] and [12] leads to an approximately linear Arrhenius plot over the entire range of decomposition. The least-mean-squares line shown in Fig. 1 may be represented by $\log k_1\,(s^{-1}) = 14.7 - (70\,100/2.3RT)$.

No allowance has been made for reaction [−1], the recombination of methyl and benzyl. Using reactions [−1] and [3] and assuming

Can. J. Chem. Downloaded from www.nrcresearchpress.com by 210.87.254.6 on 09/05/12
For personal use only.

reactions [2] and [4]–[6] are negligible gives

$$\frac{\text{moles } C_6H_5C_2H_5 \text{ from reaction } [-1]}{\text{moles } CH_4} = \frac{k_{-1}[C_6H_5CH_2]}{k_3[C_6H_5CH_3]}$$

An upper limit may be set on the average benzyl concentration by using basically the same type of calculation previously employed in evaluating k_{-1} (4), but assuming that no benzyl radicals are removed in the reaction zone. Then

$$[C_6H_5CH_2] = \frac{1}{2}\frac{2(\text{moles } CH_4)}{V}\frac{t_c}{t}$$

where V = volume of the reaction zone, t_c = residence time, and t = total time of the run.

Calculations based on these expressions indicate a negligible correction for reaction [−1] at the lowest temperatures used in the present work. The magnitude of the correction gradually increases until in an experiment at 1025 °K (approximately 35% decomposition) about 15% of the ethylbenzene undergoing decomposition would be expected to be regenerated.

Considering the extent of recombination calculated in this way over the range of experimental conditions used leads to the conclusion that the present value of E_1 should be increased by 2–3 kcal. Similar calculations on the toluene carrier runs done in conjunction with the aniline carrier studies (2) give an estimated correction of 1–2 kcal, while Szwarc's value should apparently be increased by 3–4 kcal.

However, a number of factors have been omitted which tend to make the calculated corrections too large. These involve minor corrections, such as allowance for ring abstraction from toluene and allowance for reaction [6], but these are considered negligible. Of more importance are the increasing nonuniformity of radical concentrations as the percent decomposition increases, and the omission of a negative term in the numerator of the expression for $[C_6H_5CH_2]$ to allow for benzyl removed by the combination process. Also, no allowance has been made for that fraction of the recombination product which undergoes subsequent redissociation. Another major correction is required because recent work from this laboratory on the recombination of methyl radicals (8) indicates that our published values for $\log k_{-1}$ are too high by about 0.15 log units. The exact correction that should be made to E_1 is uncertain. Plausible figures might be about 0.5 kcal for the aniline carrier studies, 1 kcal for the present work, and about 2 kcal for Szwarc's work.

As shown in Fig. 2, the present results for reaction [1] are in excellent agreement with the aniline carrier results (2). Szwarc's data at low decomposition agree well with both the aniline carrier work and the present results, but fall below these more recent studies as the extent of decomposition increases. Crowne *et al.* (3), using a stirred flow reactor, obtained results, previously quoted in the introduction, which indicated that the low activation energy obtained by Szwarc was due to failure to allow for reaction [−1]. As may be seen from the discussion in the previous paragraph, failure to allow for this reaction could explain a difference of 1–2 kcal mole^{-1} between the results of Szwarc and those of later plug-flow work, but certainly cannot account for the observed difference of approximately 7 kcal mole^{-1}.

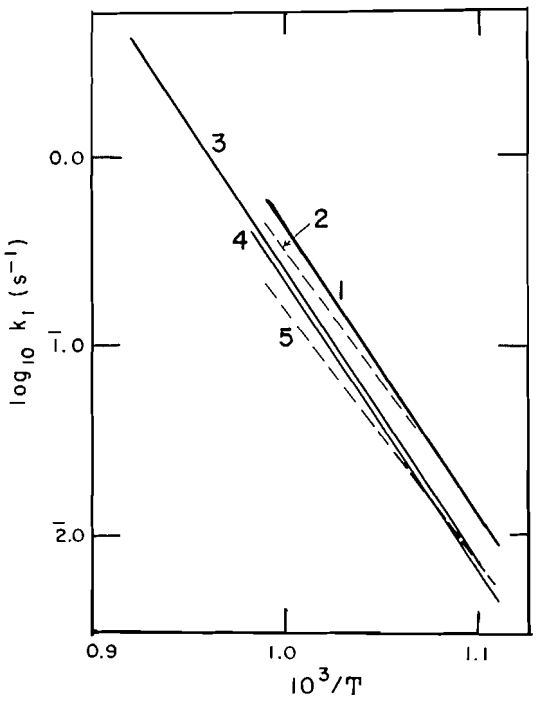

FIG. 2. Comparison of Arrhenius plots for k_1. (*1*) Crowne *et al.* (3), allowance made for recombination of methyl and benzyl; (*2*) Crowne *et al.*, no allowance made for recombination; (*3*) present work; (*4*) Esteban *et al.* (2); (*5*) Szwarc (1).

Can. J. Chem. Downloaded from www.nrcresearchpress.com by 210.87.254.6 on 09/05/12
For personal use only.

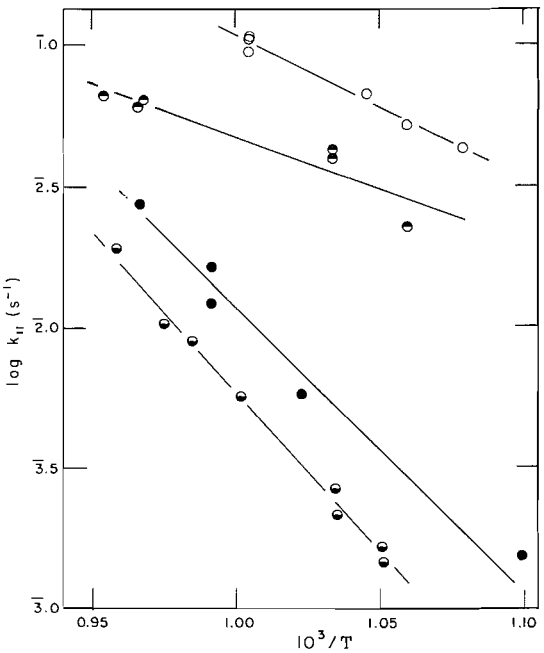

FIG. 3. Arrhenius plot of k_{11}. ○, unconditioned vessel; ◓, unconditioned vessel packed with conditioned packing; ●, conditioned vessel packed with conditioned packing; ◒, conditioned vessel. Surface-to-volume ratio in packed vessel approximately ten times that in unpacked vessel.

It is also apparent from Fig. 2 that although the stirred reactor work yields a value of E_1 close to that obtained in the aniline carrier work and in the present study, the rate constants obtained are considerably higher. Crowne *et al.* (3) did not correct for the decomposition of toluene, but this should account for only a small part of the observed difference. These workers state that their value of log A_1 (s^{-1}) may be high by as much as 0.5 (a decrease of 0.25–0.30 would give good agreement with other work) but their reasons for this statement are not clear.

The present work did use contact times in most runs that are short enough to potentially lead to low rate constants due to failure to achieve thermal equilibrium in a small fraction of the residence time (7). However, limited results from the present work indicate no appreciable effect as t_c is lowered from 1.4 to 0.88 s at 910 °K or from 0.92 to 0.78 s at 995 °K. Esteban *et al.* used residence times in most runs that are well within the recommendations of Mulcahy and Pethard (7). The agreement of the present results with these aniline and toluene carrier studies is further indication that it is unlikely that significant thermal equilibrium problems exist in the present investigation.

It should be possible to calculate values of k_{11} from the rate of formation of either benzene or ethylene. The apparent yield of benzene was in most cases considerably higher than that of ethylene. However, the procedure used in the gas chromatographic analysis of the liquids was primarily designed to give good styrene analysis and the accuracy of the benzene results is open to considerable question. Values of k_{11} have therefore been calculated from the ethylene yield. As may be seen from Fig. 3, these rate constants are very sensitive to the nature of the surface.

In an untreated quartz vessel, log k_{11} (s^{-1}) = $4.0 - (22\,900/2.3RT)$; while in a vessel rinsed with nitric acid prior to use, log k_{11} (s^{-1}) = $9.06 - (51\,700/2.3RT)$. The packed vessel runs were carried out using a vessel packed with small quartz tubes which had been nitric acid treated (surface-to-volume ratio approximately ten times that in unpacked vessel). The results with the packed treated vessel indicate that even in the acid rinsed vessel, k_{11} still contains a significant heterogeneous component. The runs with the

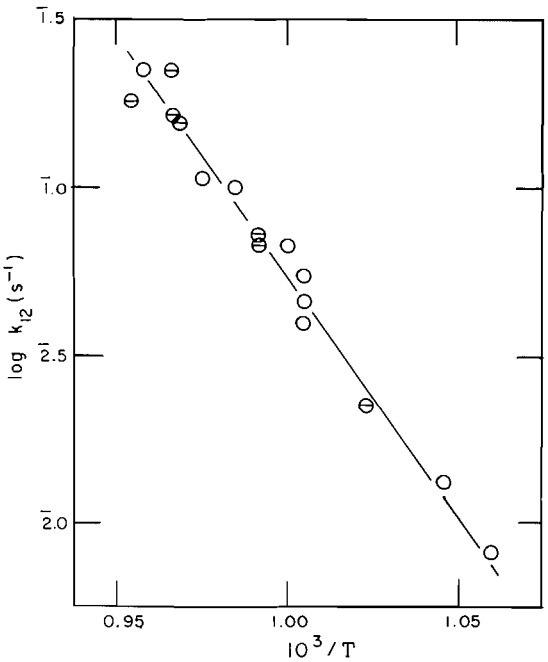

FIG. 4. Arrhenius plot of k_{12}. ⊖, runs in packed reaction vessel. Nitric acid treatment of the quartz reaction vessel had no effect on k_{12}.

conditioned packing, but unconditioned vessel, show the interference by the packing with diffusion to the active walls.

Values of k_{12} based on styrene have been used to construct the Arrhenius plot shown in Fig. 4. The curve shown may be represented by $\log k_{12}\,(s^{-1}) = 12.7 - (64\,000/2.3RT)$. It should be noted that to be consistent with the proposed mechanism, reactions [11] and [12] have been treated as first-order processes. Although the results using a variety of ethylbenzene concentrations seem to fit the appropriate curves in Figs. 3 and 4 and therefore support the assumption of first-order behavior, the surface dependence of k_{11} and the scatter in k_{12} preclude any reliable estimate of the order of these reactions.

It should also be possible to calculate k_{12} from the quantity of hydrogen formed. Only five hydrogen analyses were done, since the rate of hydrogen formation, corrected for the contribution from toluene pyrolysis, is in excellent agreement with the results obtained in the aniline carrier studies (2). As may be seen from Table 1, the corrected hydrogen yield is consistently greater than the yield of styrene. This may be due to other hydrogen-producing reactions, such as the pyrolysis of a portion of the benzene produced. It is also possible that limited polymerization of the styrene occurs, although no evidence for this could be found. In either case, A_{12} is about two orders of magnitude less than A_1. This is consistent with the more rigid activated complex expected in the molecular decomposition.

This work has been supported by a grant from the National Research Council of Canada.

1. M. SZWARC. J. Chem. Phys. **17**, 431 (1949).
2. G. L. ESTEBAN, J. A. KERR, and A. F. TROTMAN-DICKENSON. J. Chem. Soc. 3873 (1963).
3. C. W. P. CROWNE, V. J. GRIGULIS, and J. J. THROSSELL. Trans. Faraday Soc. **65**, 1051 (1969).
4. R. J. KOMINAR, M. G. JACKO, and S. J. PRICE. Can. J. Chem. **45**, 757 (1967).
5. M. KRECH and S. J. PRICE. Can. J. Chem. **41**, 224 (1963).
6. S. J. PRICE. Can. J. Chem. **40**, 1310 (1962).
7. M. F. R. MULCAHY and M. R. PETHARD. Aust. J. Chem. **16**, 527 (1961).
8. A. N. DUNLOP, R. J. KOMINAR, and S. J. PRICE. To be published.

Can. J. Chem. Downloaded from www.nrcresearchpress.com by 210.87.254.6 on 09/05/12
For personal use only.

The effect of the cation on the ^2E_g $[Cr(CN)_6]^{3-}$ and $^3T_{1g}$ $[Co(CN)_6]^{3-}$ emissions: a study of $Ag_3[Cr_xCo_{1-x}(CN)_6]$

ALEXANDER D. KIRK[1] AND HANS L. SCHLÄFER
Institut für physikalische Chemie der Universität Frankfurt/Main, Germany

AND

ANDREAS LUDI
Institut für anorganische, analytische und physikalische Chemie der Universität Bern, Switzerland

Received October 9, 1969

The luminescence behavior of the compounds $Ag_3[Cr_xCo_{1-x}(CN)_6]$ has been found to differ in several respects from that of the related compounds $K_3[Cr_xCo_{1-x}(CN)_6]$. In the silver compounds at room temperature, the Co(III) $^3T_{1g}$ emission is too weak to be seen; the Cr(III) ^2E_g emission appears to be quenched to a greater extent, and is displaced about 1.5 kK to higher energy. At 77 °K, where the Co(III) $^3T_{1g}$ emission can be seen, it is found to be displaced about 0.5 kK to higher energy. These effects, and also the shifts of the $[Cr(CN)_6]^{3-}$ and $[Co(CN)_6]^{3-}$ absorption bands in the reflectance spectra of the compounds, are discussed on the basis of interaction of the Ag^+ ion with the $[Cr(CN)_6]^{3-}$ and $[Co(CN)_6]^{3-}$ ions. Furthermore, the variation of Cr ^2E_g emission intensity with mole percent Cr has its maximum at a lower Cr concentration in the silver salts, indicative of more extended interaction between Cr^{3+} ions than in the potassium salts.

Canadian Journal of Chemistry, 48, 1065 (1970)

Can. J. Chem. Downloaded from www.nrcresearchpress.com by 210.87.254.105 on 09/05/12
For personal use only.

Introduction

In a previous paper (1), we described a qualitative and quantitative study of the luminescence, both from Cr(III) and Co(III), of the system $K_3[Cr_xCo_{1-x}(CN)_6]$, where x ranged from 0.0001 to 1.0. In contrast to the more usual single-crystal technique, this work made use of a technique of intensity and spectral studies on tablets formed by pressing powdered starting materials prepared by precipitation. For some types of work, this method offers advantages, amongst which is the ability to obtain precise relative luminescence intensity data for compounds that cannot easily be prepared in large crystalline form.

This paper describes such an investigation. The luminescence of the series of compounds $Ag_3[Cr_xCo_{1-x}(CN)_6]$ has been found to differ from that of the corresponding potassium salts, and comparison of the systems suggests some conclusions about the interaction of the Ag^+ ion with the ion $[Cr(CN)_6]^{3-}$.

Experimental

Preparation of $Ag_3[Cr_xCo_{1-x}(CN)_6]$

Aqueous solutions of $K_3[Cr(CN)_6]$ and $K_3[Co(CN)_6]$ were mixed in the proportions appropriate to the mole % Cr desired in the final product. To these solutions, an equivalent amount of 0.1 *M* $AgNO_3$ was then added, with stirring. The resulting precipitate was filtered, washed with water, and dried in vacuo.

The starting materials, $K_3[Cr(CN)_6]$ and $K_3[Co(CN)_6]$, were prepared by standard methods (2), recrystallized three times from aqueous solution, and checked by analysis for Cr, Co, K, C, and N.

X-Ray Measurements

Powder photographs of these materials were taken using a focussing camera of the Guinier – de Wolff type. Fe Kα radiation was used.

Luminescence Measurements

The technique used to prepare tablets from the starting materials, to measure their luminescence spectra and relative integrated emission intensities, and to record the reflectance spectra of the tablets were as described in detail previously (1), the sole change being that tablets of these silver compounds were made at an applied force of 1.5 (metric) tons (dial gauge reading on MATRA press, corresponding to a sample pressure of about 1.1 tons cm^{-2}). The luminescence spectrometer used was that described in ref. 3.

Light Sources used for Excitation

For the wavelengths 579, 550, 474, 434, and 404 mμ, an Osram 100 W mercury lamp was used together with a 10 cm water filter, a blue optical filter (B.G. 23 Jenaer Glaswerk Schott, Mainz), and an appropriate interference filter (Schott). For the wavelengths 365 and 313 mμ, a Bausch and Lomb 33 8602 UV grating monochromator was used in conjunction with an Osram 200 W mercury lamp and the 10 cm water filter.

Results

Crystallographic Studies

Examination of the different samples by X-ray powder techniques showed that they all had the

[1]Address: University of Victoria, Victoria, British Columbia. On leave of absence during the 1968–1969 academic year.

Can. J. Chem. Downloaded from www.nrcresearchpress.com by 210.87.254.105 on 09/05/12
For personal use only.

same hexagonal unit cell as $Ag_3[Co(CN)_6]$, of which the crystal structure has recently been determined (4). The powder patterns of the Cr-doped compounds, as well as of $Ag_3[Cr(CN)_6]$, showed somewhat broader reflections than $Ag_3[Co(CN)_6]$, but there was no large change in the lattice spacings as one steadily replaced the cobalt by chromium

$Ag_3[Co(CN)_6]$ $a = 7.03$ Å $c = 7.13$ Å

$Ag_3[Cr(CN)_6]$ $a = 7.12$ Å $c = 7.48$ Å

It was demonstrated also that the pressing of tablets had no influence on the X-ray pattern.

Luminescence Properties

A preliminary survey of the room-temperature luminescence properties of the $Ag_3[Cr_xCo_{1-x}(CN)_6]$ system showed that Cr ^2E_g luminescence could be seen, although the Co $^3T_{1g}$ luminescence also found in the potassium compounds was absent. We should also like to report here that a parallel study of the systems $K_3[Cr_xFe_{1-x}(CN)_6]$ and of $Ag_3[Cr_xFe_{1-x}(CN)_6]$ revealed no Cr emission either at room temperature or at 130 °K, due probably to inner filtering by the $[Fe(CN)_6]^{3-}$ ion at low percentages of Cr and to Cr/Cr quenching processes at high concentrations of Cr (1).

Test of Procedure

To check that the procedure of tablet formation caused no dramatic changes in the luminescence properties of the substances, the Cr emission spectrum of a tablet of the 5% Cr compound was compared with the spectrum of the original powder, both at room temperature and at 77 °K. The spectra of the two forms were not resolved into very sharp lines even at 77 °K, so the test can not be regarded as extremely sensitive. However, no significant differences could be seen either in band position, resolution, or relative band intensity (Fig. 2*d*). Whether changes occur in the total emission intensity is clearly impossible to say, but in view of the spectral identity it seems unlikely.

A comparison of the reflectance spectrum of the 5% compound as a tablet and as a powder similarly showed no differences in the positions of the band maxima and the band widths, although the usual differences in band intensities were to be seen. In all cases, and particularly for the pure Co compound, however, care had to be taken to press the tablets at relatively low pressures (1.1 tons cm^{-2}) or the material flowed, resulting in a tablet of relatively glassy appearance and with a reflectance spectrum in which the absorption bands were broadened. With the exception of the compound $Ag_3[Co(CN)_6]$, no luminescence work was done with such tablets.

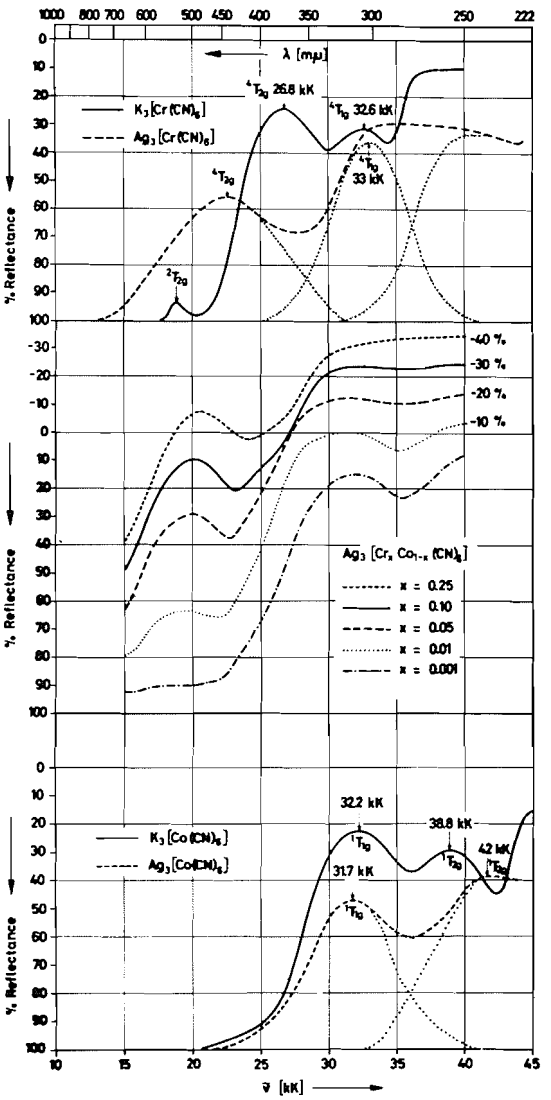

FIG. 1. Reflectance spectra of $Ag_3[Cr_xCo_{1-x}(CN)_6]$, $K_3[Cr(CN)_6]$, and $K_3[Co(CN)_6]$ obtained on the tablets used in the luminescence work, except for $Ag_3[Cr(CN)_6]$ and $Ag_3[Co(CN)_6]$, where the spectra shown are of MgO-diluted powders. As indicated on the right-hand side, the mixed-crystal spectra have been progressively displaced by 10% increments for clarity.

Can. J. Chem. Downloaded from www.nrcresearchpress.com by 210.87.254.105 on 09/05/12
For personal use only.

Reflectance Spectra

The reflectance spectra of tablets of the doped compounds are shown in Fig. 1, which also shows the reflectance spectra of pure $K_3[Cr(CN)_6]$ and $K_3[Co(CN)_6]$. In the silver compounds, the $[Cr(CN)_6]^{3-}$ $^4T_{2g} \leftarrow {}^4A_{2g}$ absorption band is displaced a significant amount to the red, appearing at about 500 mμ. No such large shift of the $^1T_{1g} \leftarrow {}^1A_{1g}$ $[Co(CN)_6]^{3-}$ absorption band is revealed by comparison of the silver and potassium salts of $[Co(CN)_6]^{3-}$, but the $^1T_{2g} \leftarrow {}^1A_{1g}$ absorption is moved significantly to the ultraviolet.

Chromium Emission Spectrum

The spectrum of the Cr emission at room temperature and 77 °K is reproduced in Fig. 2*a* and 2*d* and was the same for all percentages of Cr up to 10% (Fig. 2*a*). No emission could be seen from the pure compound $Ag_3[Cr(CN)_6]$, presumably due to the effectiveness of Cr/Cr quenching processes in this substance. The spectrum resembles that of the potassium salts (Fig. 2*b*) or the ion $[Cr(CN)_6]^{3-}$ in solution (5) and we do not doubt that it is the emission $^2E_g \rightarrow {}^4A_{2g}$. However, the most intense band occurs at 13.49 kK, compared with 12.05 kK for the potassium salts, being thus shifted ca. 1.5 kK to higher energy in the silver compounds. No such pronounced shift was seen in the ^2E_g emission of $Pb_3[Cr(CN)_6]_2$ (Fig. 2*c*), which was examined to see if this was a general effect of class B cations.

$^3T_{1g}$ Emission of Co(III)

At room temperature, $Ag_3[Co(CN)_6]$ did not emit, but on cooling to 77 °K, the $^3T_{1g}$ emission was seen; broad, as in the potassium compound, and with the band maximum at 14.3 kK. The $^3T_{1g}$ emission spectra at 77 °K of the Ag^+ and K^+ compounds are compared in Fig. 2*e*, and a shift of about 0.5 kK to higher energy is to be seen for the Ag compound.

Emission Intensity Concentration Dependence

Figure 3 shows a plot of the variation of Cr ^2E_g emission intensity with mole fraction of Cr

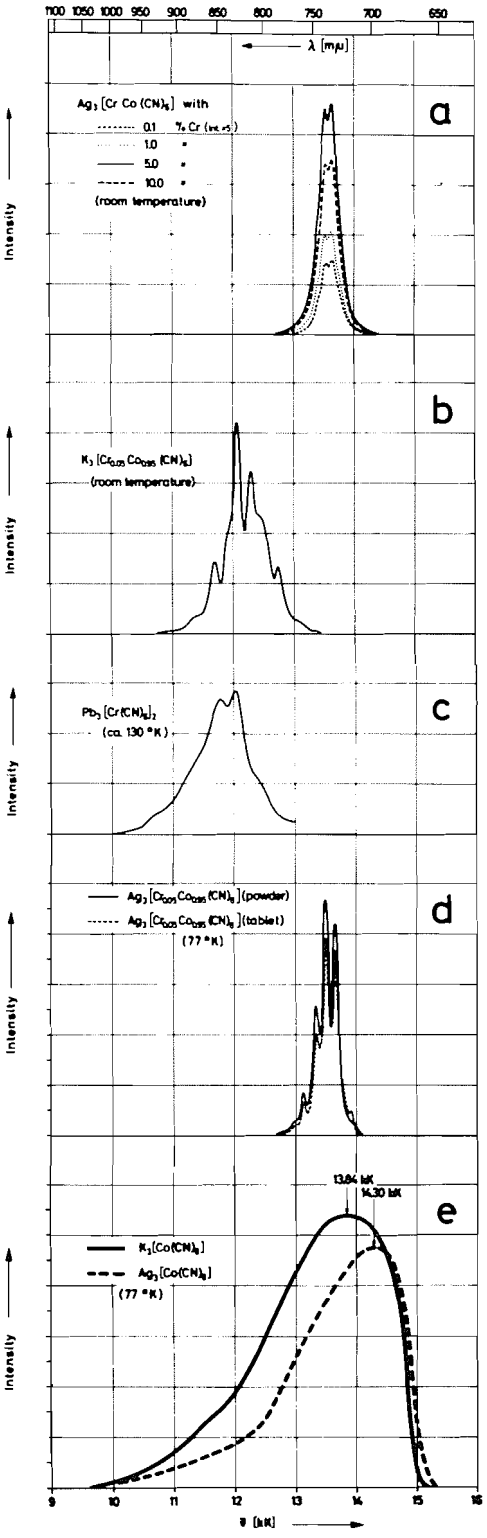

FIG. 2. Emission spectra: (*a*) $Ag_3[Cr_xCo_{1-x}(CN)_6]$ at room temperature; the spectrum is independent of Cr concentration up to at least 10% Cr; (*b*) $K_3[Cr_{0.05}Co_{0.95}(CN)_6]$ at room temperature; (*c*) $Pb_3[Cr(CN)_6]_2$ at ca. 130 °K; (*d*) $Ag_3[Cr_{0.05}Co_{0.95}(CN)_6]$ at 77 °K, as tablet and as powder; (*e*) $K_3[Co(CN)_6]$ and $Ag_3[Co(CN)_6]$ at 77 °K.

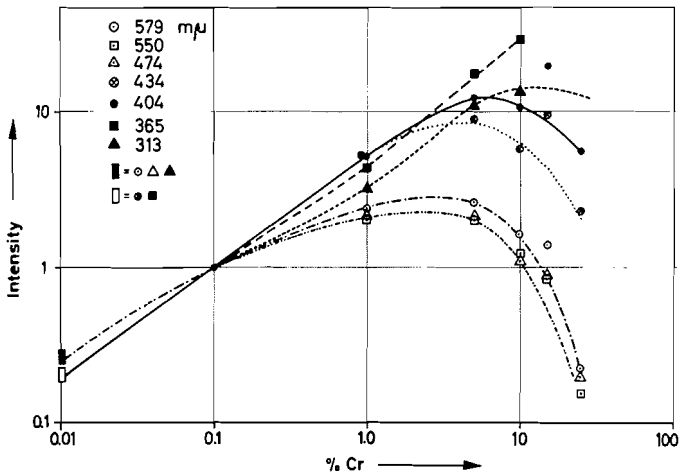

FIG. 3. log (relative integrated Cr ^2E_g emission intensity) vs. log (Cr concentration (mole fraction)) for various excitation wavelengths. Conditions: room temperature; monochromator slit 2 mm, centered at 13.65 kK (band width 13.3 to 14.0 kK).

The term relative integrated emission intensity is used here to indicate that the emission intensities for various concentrations of Cr were measured relatively, but over the total spectral range of the emission (integrated) (1). The concentration dependence curves for different excitation wavelengths have been made comparable by assigning the relative integrated emission intensity for the 0.1% tablet as 1.0, independent of wavelength, and normalizing the remaining concentration data on this basis.

using several different wavelengths of excitation. At those wavelengths where the absorption process is predominantly into $[Cr(CN)_6]^{3-}$ (579, 550, and 474 mμ, Fig. 1) then the same behavior is obtained, independent of exciting wavelength. This curve, after correction of the data for sample reflectivity (see caption to Fig. 3), shows an increase of emission intensity with Cr concentration to a maximum at about 2 to 4% Cr, followed by an increasingly rapid loss of intensity for greater Cr concentrations. This behavior is qualitatively the same as that previously found for the corresponding potassium system (1), but the differences found in slope and in the position of the intensity maximum are significant.

Comparison of K and Ag Salt Emission Intensities

A comparison of the total Cr emission intensity for the 1.0% Cr silver and potassium compounds yielded the value 7.4 for the ratio (K salt Cr emission intensity)/(Ag salt Cr emission intensity), after allowance for the sample reflectivities and the difference in the average photomultiplier sensitivity over the respective emission regions.

Discussion

An obvious difference between the systems $K_3[Cr_xCo_{1-x}(CN)_6]$ and $Ag_3[Cr_xCo_{1-x}(CN)_6]$ is their totally different crystal structure, despite the similarity in ionic radius of K^+ and Ag^+; and it emphasizes the importance of the d^{10} configuration of Ag^+ in influencing its solid-state interactions. The consequent preference of Ag^+ for linear two-fold coordination is undoubtedly an important factor in determining the approximately linear arrangement (...NC M CN Ag NC...) (M = Co^{3+}, Cr^{3+}) seen in the lattice of the silver compounds. The following discussion shows that the singularities that occur in the absorption spectrum and in the luminescence behavior of the silver salts also derive from the specific solid-sate interactions of the ions Ag^+ and $[Cr(CN)_6]^{3-}$.

Band Shifts in Absorption and Emission Spectra

Our observed spectroscopic information is summarized and compared with the potassium-salt data in Table 1. (Band positions have been rounded to two significant figures where uncertain.)

Since the reflectance spectra of both $Ag_3[Cr(CN)_6]$ and $Ag_3[Co(CN)_6]$ resemble the spectra of the respective "isolated" complex ions, the effects of the Ag^+ ion are relatively secondary and there is no requirement to interpret the spectra in a drastically different way; e.g., on a band model,

Can. J. Chem. Downloaded from www.nrcresearchpress.com by 210.87.254.105 on 09/05/12
For personal use only.

Can. J. Chem. Downloaded from www.nrcresearchpress.com by 210.87.254.105 on 09/05/12
For personal use only.

a charge transfer basis, or pair spectra. Thus, we assume that the usual ligand field model is applicable.

Starting from the strong-field limit, allowing for interelectronic repulsion and neglecting the small effects of configuration interaction, one obtains expressions for the energy levels of d^3 and d^6 systems which lead to the following transition energies (6).

$$\begin{aligned} &Cr^{3+} \\ &\Delta E(^4T_{2g} \leftarrow {}^4A_{2g}) = \Delta \\ &\Delta E(^4T_{1g} \leftarrow {}^4A_{2g}) = \Delta + 12B \\ &\Delta E(^2E_g \leftarrow {}^4A_{2g}) = 9B + 3C \\ &Co^{3+} \\ &\Delta E(^1T_{1g} \leftarrow {}^1A_{1g}) = \Delta - C \\ &\Delta E(^1T_{2g} \leftarrow {}^1A_{1g}) = \Delta + 16B - C \\ &\Delta E(^3T_{1g} \leftarrow {}^1A_{1g}) = \Delta - 3C \end{aligned} \qquad [1]$$

From the experimental transition energies shown in Table 1, one then obtains values of the ligand field strength parameter, Δ, and the Racah parameters, B and C, for $K_3[Cr(CN)_6]$, $Ag_3[Cr(CN)_6]$, $K_3[Co(CN)_6]$, and $Ag_3[Co(CN)_6]$, Table 2. The experimental uncertainties in the wavelengths of the band maxima, and the uncertainties in assumed Stokes shifts used to calculate the absorption maxima from emission maxima, (see footnotes to Table 1) result in some uncertainty in the values of Δ, B, and C obtained. Nevertheless, the trend is clearly the same for both complex ions: Δ and C decrease, and B increases, and on this basis all the spectral shifts observed are consistently explained. The simultaneous decrease in C and increase in B requires a decrease of the ratio C/B on forming the Ag^+ complexes.

TABLE 1

Transition energies for Ag and K salts of $[Cr(CN)_6]^{3-}$ and $[Co(CN)_6]^{3-}$

	ΔE (kK)		
Transition	Ag salt	K salt	Lit. value for complex ion in solution (6)
$[Cr(CN)_6]^{3-}$			
$^4T_{2g} \leftarrow {}^4A_{2g}$	22.5	26.8	26.7
$^4T_{1g} \leftarrow {}^4A_{2g}$	33	32.6	32.6
$^2E_g \leftarrow {}^4A_{2g}$	14.0*	12.7*	13.1 (5)
$[Co(CN)_6]^{3-}$			
$^1T_{1g} \leftarrow {}^1A_{1g}$	31.7	32.3	32.4
$^1T_{2g} \leftarrow {}^1A_{1g}$	42	38.8	39
$^3T_{1g} \leftarrow {}^1A_{1g}$	29†	28.5‡	—

*Our experimental data give the band maximum in emission. In order to obtain results comparable to the quartet–quartet absorption band maxima, we have taken the band maxima of the K^+ and Ag^+ emission spectra and added 0.7 kK to obtain estimates of the position of the maxima in absorption for the solid. This figure of 0.7 kK is twice the difference between the maximum in emission and the 0–0 band of the K salt identified by Forster (7). (We assume a mirror relationship of absorption and emission spectra.)

†Calculated from the emission maximum assuming the same Stokes shift as for $K_3[Co(CN)_6]$.

‡Calculated value, using $\Delta = 33.45$ kK, $B_{35} = 0.410$ kK and $C = 4B$(6).

On a ligand field basis, the parameter Δ may be considered approximately to be made up of four parts: a purely electrostatic ($\Delta_{Coul.}$), a ligand σ-bonding ($\Delta\sigma$), a metal-to-ligand π-bonding ($\Delta\pi(M \rightarrow L)$), and a ligand-to-metal π-bonding ($\Delta\pi(L \rightarrow M)$) contribution. While there is no basis for true additivity of these terms, we may for the present qualitative discussion write

$$\Delta = \Delta_{Coul.} + \Delta\sigma + \Delta\pi(M \rightarrow L) + \Delta\pi(L \rightarrow M)$$

where the last term would be expected to be negative, the others positive. It is certain that the first two terms are most significant in determining the value of Δ.

TABLE 2

Ligand field strength parameter, Δ, and Racah parameters, B and C, for $K_3[Cr(CN)_6]$, $Ag_3[Cr(CN)_6]$, $K_3[Co(CN)_6]$ and $Ag_3[Co(CN)_6]$*

Compound	Δ (kK)	B (kK)	C (kK)	C/B	B_{35} (kK)† Calcd.	B_{35} (kK)† Lit.	B_{55} (kK)† Calcd.
$K_3[Cr(CN)_6]$	26.8	0.48_3‡	2.78‡	5.7	0.48_3§	0.49	0.60§
$Ag_3[Cr(CN)_6]$	22.5	0.87_5‡	2.04‡	2.1	0.87_5§	—	0.67§
Cr^{3+} (free ion)	—	—	—	—	0.91_4 (6)	—	—
$K_3[Co(CN)_6]$	34.1	0.41_2	1.85	(4.0)‖	(0.41_2)‖	0.410	—
$Ag_3[Co(CN)_6]$	33.1	0.64_5	1.35	2.1	0.64_5	—	—
Co^{3+} (free ion)	—	—	—	—	1.10 (6)	—	—

*All calculated values are based on the transition energies of Table 1.

†All the values quoted are uncorrected for any effects of configuration interactions.

‡B and C were calculated solving eq. [1], assuming that B was the same for interelectronic repulsion in the t_{2g}^3 and $t_{2g}^2 e_g^1$ configurations.

§Calculated taking $\Delta E(^2E_g \leftarrow {}^4A_{2g}) = 21B_{55}$ (i.e. $C_{55} = 4B_{55}$) and $\Delta E(^4T_{1g} \leftarrow {}^4T_{2g}) = 12B_{35}$.

‖We assumed $C = 4B$ and $B = 0.410$ kK in calculating the energy of the $^3T_{1g}$ state in $K_3[Co(CN)_6]$. See footnotes to Table 1.

Can. J. Chem. Downloaded from www.nrcresearchpress.com by 210.87.254.105 on 09/05/12
For personal use only.

In explaining how interactions in the silver salts could alter Δ, it is unreasonable to expect large differences in the coulombic effect of Ag^+ and K^+ on the $[Cr(CN)_6]^{3-}$ ion in view of their similarity of size and identity of charge. However, unlike K^+, Ag^+ will σ bond to species such as N, and one may expect Cr—C≡N—Ag σ bonding to occur in the silver salt. Such σ bonding would reduce the σ-electron density available for Cr/C σ bonding and reduce the magnitude of the Δσ term. The same effect will also increase B, as the central-ion d electrons will be less delocalized on the ligands (this is later discussed in more detail.)

Changes in π-bonding effects may also change B and decrease Δ. The t_{2g} orbitals of the metal ion are π bonded to the ligands and yield orbitals of the correct symmetry also to π bond with the d_{xz} and d_{yz} orbitals of the silver ion. The configuration of the C—N—Ag bond is not too far from linear (157°) (4); therefore, d electrons of Ag^+ are able to interact with the t_{2g} electrons of the Cr^{3+} and Co^{3+}. This would also increase B and decrease Δ, through a decrease in the negative term $\Delta\pi(L \rightarrow M)$.

Thus, one may consistently rationalize the observed spectral shifts, both in emission and absorption, in terms of bonding between the Ag^+ ion and the N of the Cr/Co cyanide ligands.

It is interesting to press this treatment somewhat further. For Cr, the starting equations [1] are not strictly accurate because they fail to recognize that in an octahedral complex, the radial functions for $t_{2g}(\gamma_5)$ electrons and $e_g(\gamma_3)$ electrons are expected to be different. Thus, one should recognize the existence of three differing interelectronic repulsion parameters, B_{33}, B_{35}, and B_{55}. Since the ^2E_g and $^4A_{2g}$ states of Cr both arise from the strong-field configuration t_{2g}^3, we should write

$$[2] \qquad \Delta E(^2E_g \leftarrow {}^4A_{2g}) = 9B_{55} + 3C_{55}$$

Similarly, since the two $^4T_{2g}$ and $^4T_{1g}$ states arise from $t_{2g}^2 e_g^1$, we may write

$$[3] \qquad \Delta E(^4T_{2g} \leftarrow {}^4A_{2g}) = \Delta$$

$$[4] \qquad \Delta E(^4T_{1g} \leftarrow {}^4A_{2g}) = \Delta + 12B_{35}$$

If $C = 4B$, we may calculate B_{55} from

$$[5] \qquad \Delta E(^2E_g \leftarrow {}^4A_{2g}) = 21B_{55}$$

The difference between the transition energies of the two quartet → quartet bands is clearly $12B_{35}$. In this way, we obtain the values of B_{35} and B_{55} shown in Table 2. The value of B_{35} $(=B)$ for cobalt is also given.

Observe that formation of the Ag salts causes a small, significant increase in B_{55} for $[Cr(CN)_6]_6^{3-}$ and a very large increase in B_{35} for both ions; in the case of Cr, raising the value almost up to the value for the free ion ($B(Cr^{3+})$ = 914 cm^{-1}, $B(Co^{3+})$ = 1 100 cm^{-1}). The usual explanation for the lowering of metal-ion B values on formation of octahedral complexes is that delocalization of electron density onto the ligands through the σ-antibonding nature of the e_g orbitals very much reduces interelectronic repulsion between electrons occupying them. Therefore, β_{33} and β_{35} are generally much below 1.0, with β_{55} somewhat larger. The reduction of the extent of σ bonding between Cr^{3+} and CN^- postulated by us to explain the decrease in Δ in the silver salt, however, implies inhibition of the e_g electron delocalization and consequently an increase in B_{35} and, to a lesser extent, in B_{55} over the K salt values. These effects appear to be much smaller for $Ag_3[Co(CN)_6]$ than for $Ag_3[Cr(CN)_6]$.

Concentration Dependence of the Chromium Emission Intensity

In our previous work (1) on the system $K_3[Cr_xCo_{1-x}(CN)_6]$, a satisfactory theoretical treatment of the intensity dependence was possible. However, it was necessary to show first that energy transfer from Co to Cr was not an important process, and then to assume that the ratio of the solution extinction coefficients could be applied to the solid systems for the purpose of calculating the proportion of the absorbed radiation going into the Cr. For these silver salts, such an approach is clearly invalid, since their reflectance spectra are so completely different from the solution spectra of the individual ions. Thus, in the absence of any way of calculating the extent to which the light is absorbed by each component of the solids, and of determining whether energy transfer occurs in the system, the highest hope we can fulfill with the data is a semiquantitative clarification.

Reference to Fig. 3 shows that the form of the intensity/mole-fraction-Cr plot is strongly dependent on the exciting wavelength. Comparison between Figs. 1 and 3 shows further that as one

goes to those wavelengths at which Co absorption becomes more predominant (404, 365, 313 mμ), the maximum tends to move to higher Cr mole-fraction. This is to be expected as a result of Co inner filtering, but the picture is clearly more complicated, because in the high Co absorption region the slope of the log (intensity)/log (Cr mole-fraction) plot is not 1.0 as it should be on the basis of our simple theory. It may be that this is caused by Co/Cr energy transfer effects under these conditions, but we have no method of proceeding further with the data in this region.

The best that can be done is with the data at 574, 550, and 474 mμ, where the Co absorption coefficient is clearly much smaller than that for Cr and the same curve for the intensity dependence is obtained independent of wavelength.

In our previous work (1), theoretical expressions for the intensity of Cr emission as a function of the Cr mole-fraction were derived on the following assumptions.

(1) The raw luminescence intensity data could be corrected for the effects of sample reflectivity by dividing by the fraction of the light actually absorbed by the tablet, f_{abs}

$$[6] \qquad f_{abs} = (100 - R)/100$$

where R is the percent diffuse reflectance of the tablet. (This correction has been made to the data plotted in Figs. 3 and 4.)

(2) Energy transfer from Co to Cr was not a significant mechanism for Cr emission. Cr emission therefore only arose from that fraction of the absorbed light actually absorbed by Cr

$$[7] \qquad (f_{abs})_{Cr} = \varepsilon_{Cr}X_{Cr}/(\varepsilon_{Cr}X_{Cr} + \varepsilon_{Cr}X_{Co})$$

where X is the mole fraction and the ε quantities were taken to be the molar decadic solution extinction coefficients on the assumption that their ratio would still give the ratio of Cr/Co absorption in the solid state.

(3) Excited Cr states would be quenched only if they had a second Cr ion as one of a set of Z neighbor ions. Otherwise, they were expected to emit with a constant quantum yield, ϕ_{phos}, at a given temperature, independent of the mole fraction of Cr. A simple statistical treatment then showed that the fraction of the total Cr absorption that goes to such single emitting ions was given by

$$[8] \qquad (f_{abs})_{Cr\ singles} = (1 - X_{Cr})^Z$$

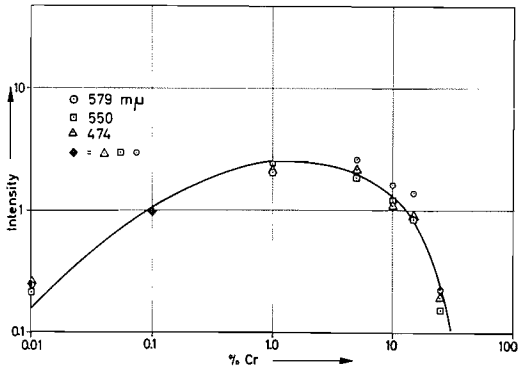

FIG. 4. log/log comparison of eq. [9] (for $\varepsilon_{Cr}/\varepsilon_{Co} = 500$ and $Z = 9$) with the 579, 550, and 474 mμ data of Fig. 3. The solid line is calculated from eq. [9].

Combination of these expressions and cognizance of the relative nature of all the intensity data gives for the reflectivity-corrected emission intensities

$$[9] \qquad \frac{(I_{lum})_{Cr} \times 100}{100 - R} = C_\lambda I_0 \phi_{phos} \left\{1 + \frac{\varepsilon_{Co}X_{Co}}{\varepsilon_{Cr}X_{Cr}}\right\}^{-1} (1 - X_{Cr})^Z$$

where I_0 is the absolute incident intensity (never measured), and the constant C_λ allows for the limited aperture of the apparatus, the change of I_0 with wavelength, etc. Figure 3 is a log/log plot of the left-hand side of eq. [9] vs. X_{Cr}.

Assumption *2*, on which eq. [9] was obtained, does not apply in the case of these silver salts, particularly at those wavelengths where the Co absorption is large relative to Cr (404, 434, 365, and 313 mμ.) For the remaining data at 579, 550, and 474 mμ, a semiquantitative fit of the data may be obtained from eq. [9] by choosing an appropriate value of $\varepsilon_{Cr}/\varepsilon_{Co}$ and Z. By trial and error, the best fit was obtained for $Z = 9$ and $\varepsilon_{Cr}/\varepsilon_{Co} = 500$, and this curve is compared with the experimental data in Fig. 4.

The fit is mediocre, particularly when one considers that these are log/log plots, but the choice of parameters is reasonable. The value of $\varepsilon_{Cr}/\varepsilon_{Co}$ is consistent with the reflectance spectra of the pure $Ag_3[Cr(CN)_6]$ and $Ag_3[Co(CN)_6]$ compounds (Fig. 1) and the choice of $Z = 9$ is rational.

Thus for those wavelengths of irradiation for which absorption by $[Cr(CN)_6]^{3-}$ predominates, the mechanism of luminescence and quenching is

Can. J. Chem. Downloaded from www.nrcresearchpress.com by 210.87.254.105 on 09/05/12
For personal use only.

likely to be the same as that found previously for the potassium compounds (1). The somewhat larger number, ca. 9 as opposed to 6, of effective quencher neighbors necessary to account for the concentration dependence of emission intensity is evidence for longer-range interactions, perhaps through the intermediacy of Ag^+.

An approximate absolute comparison was made of the ratio of the Cr luminescence intensity for the 1% tablets of the K and Ag salts. The value obtained for the optimum wavelength, 404 mμ, for this experiment was 7.4 for K salt Cr emission/Ag salt Cr emission. At first, it was thought that the ratio of Cr/Co absorption in the two tablets would be the same and that correction for the reflectivity would then yield the ratio of the absolute Cr quantum yields. Our analysis of the reflectance spectra shows this initial assumption to be quite untrue. The band shifts in the reflectance spectra suggest, however, that at 404 mμ the quantity $(f_{abs})_{Cr}$ is likely to be smaller for the Ag salts than the K salts. Thus, we conclude that this value of 7.4 is a lower limit for the ratio of absolute Cr/Co quantum yields. At 1% Cr, the ^2E_g state is therefore produced with a lower intersystem crossing yield or quenched to a significantly greater extent in the silver salts.

Although these complexities have hindered the precise quantitative study of these $Ag_3[Cr_xCo_{(1-x)}(CN)_6]$ salts, the work has still yielded useful information. Both the absorption spectra and emission spectrum show changes on formation of the silver salts and these are explainable in terms of interaction of Ag^+ with the N end of the cyanide ligand. As further evidence of such interaction, one finds that the concentration dependence of the Cr emission intensity implies more extended interaction of Cr ions in the lattice.

The authors wish to acknowledge the financial support of the Deutsche Forschungsgemeinschaft, the Schweizerischen Nationalfonds, and the Alexander von Humboldt-Stiftung (stipendium, A.D.K.). We are particularly grateful to W. Schroeder for preparation of the diagrams.

1. A. D. KIRK, A. LUDI, and H. L. SCHLÄFER. Ber. Bunsenges. Phys. Chem. **73**, 669 (1969).
2. W. C. FERNELIUS (*Editor*). Inorganic syntheses. Vol. II. McGraw-Hill Book Co., Inc. 1964. pp. 203, 225.
3. H. L. SCHLÄFER, H. GAUSMANN, and H. WITZKE. Z. Phys. Chem. Frankfurt, **56**, 55 (1967).
4. A. LUDI and H. U. GÜDEL. Helv. Chim. Acta, **51**, 1762 (1968).
5. H. L. SCHLÄFER, H. GAUSMANN, H. R. WASGESTIAN, and H. U. ZANDER. Z. Phys. Chem. **51**, 274 (1966).
6. C. K. JORGENSEN. Advan. Chem. Phys. **5**, 33 (1963).
7. R. A. CONDRATE and L. S. FORSTER. J. Chem. Phys. **48**, 1514 (1968).

Can. J. Chem. Downloaded from www.nrcresearchpress.com by 210.87.254.105 on 09/05/12
For personal use only.

Magnetic interactions in the Mn(II)/cyanide system

E. ROTLEVI AND D. R. EATON
Department of Chemistry, McMaster University, Hamilton, Ontario
Received October 20, 1969

A well-resolved electron spin resonance spectrum has been observed from frozen aqueous, methanol/water mixtures, and acetonitrile/water mixtures of potassium manganocyanide. Hyperfine splitting from at least two manganese atoms is present. The sharpness of the lines indicates that a rate process capable of averaging the anisotropic dipole–dipole interactions is operative. These results are discussed in terms of the known chemical and magnetic properties of Mn(II)/cyanide systems. It is suggested that an exchange process involving low-spin and high-spin manganese ions in the same molecule occurs.

Canadian Journal of Chemistry, 48, 1073 (1970)

Can. J. Chem. Downloaded from www.nrcresearchpress.com by 210.87.254.40 on 09/05/12
For personal use only.

Introduction

Potassium manganocyanide is a well-characterized material. It is one of the few manganese compounds known which contain Mn(II) in its low-spin form. The complex has a magnetic moment of 2.18 B.M. (1), agreeing well with the value expected for one unpaired electron. The electron spin resonance (e.s.r.) spectrum of a magnetically dilute single crystal containing $K_4Mn(CN)_6.3H_2O$ in the isomorphous diamagnetic ferrocyanide has been examined by Baker, Bleaney, and Bowers (2). Owing to the short relaxation time, they were unable to observe hyperfine structure at temperatures higher than 12 °K and at this temperature they report lines of approximately 13 G half-width. They found substantial anisotropy in both the g values ($g_x = 2.624$, $g_y = 2.182$, and $g_z = 0.63$) and the hyperfine coupling constant ($A_x = 84.5$, $A_y = 46.5$, $A_z = 104 \times 10^{-4}$ cm^{-1}). As a consequence of these findings, one would not expect to be able to observe an e.s.r. spectrum from a polycrystalline sample containing $K_4Mn(CN)_6$ at liquid-nitrogen temperature.

In aqueous solution, $K_4Mn(CN)_6$ is subject to dissociation. Chadwick and Sharpe (3) state that it is soluble without decomposition in solutions of potassium cyanide of at least 1.5 *M* concentration. In the absence of excess cyanide ion, a product of stoichiometry $KMn(CN)_3$ is precipitated. The same product can be obtained by reaction of $MnCl_2$ with a limited amount of potassium cyanide. There is some parallel here to the chemistry of the Co(II)/cyanide system, in which the stable species is $Co(CN)_5^{3-}$ rather than $Co(CN)_6^{4-}$. The structure of $KMn(CN)_3$ is unknown, but it has been suggested (3) that it might well be more correctly formulated as $K_2Mn[Mn(CN)_6]$, analogous to the known compound $K_2Fe[Fe(CN)_6]$. The reported magnetic moment of 4.22 B.M. (4) is consistent with this formulation, since it is intermediate between the value expected for low-spin Mn(II) (one unpaired electron) and that for high-spin Mn(II) (five unpaired electrons). The structure of Prussian blue, $K_2Fe[Fe(CN)_6]$, has been investigated by Robin (5). The essential structural feature is a lattice of iron ions, each octahedrally surrounded by cyanide groups so that both the carbon and the nitrogen of each cyanide moiety is bonded to a metal ion. Thus half the metal ions are bonded to the carbon of cyanide groups and half to the nitrogen. It has been shown by Shriver, Shriver, and Anderson (6) that when bonded through nitrogen, CN^- is a relatively weak-field ligand. In its normal carbon bonded orientation it is of course a strong-field ligand. The expectation that $K_2Mn[Mn(CN)_6]$, assuming it has a Prussian-blue structure, will have half of the manganese ions low-spin and half high-spin is therefore a reasonable one. This situation should be distinguished from that obtaining in many Prussian-blue structures which contain equal numbers of metal ions in two different *oxidation* states (7). In the present paper, we wish to report e.s.r. spectra which appear to be associated with interaction between two manganese ions in different spin states present in the same molecule. This type of situation does not appear to have been considered previously.

Results

The e.s.r. spectrum obtained from a frozen aqueous solution of potassium manganocyanide at liquid-nitrogen temperature is shown in Fig. 1. Very similar spectra, but with slightly better resolution, are obtained from frozen methanol/

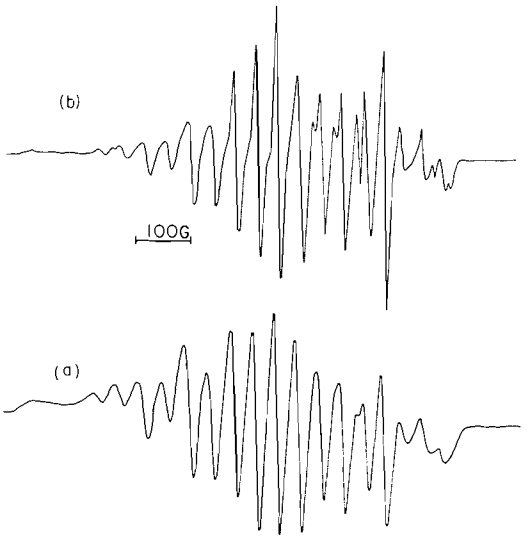

FIG. 1. (*a*) Electron spin resonance spectrum of solution of $K_4Mn(CN)_6$ in ice at 77 °K. (*b*) Electron spin resonance spectrum in frozen aqueous/methanol solution, 77 °K. The field increases from right to left in all spectra.

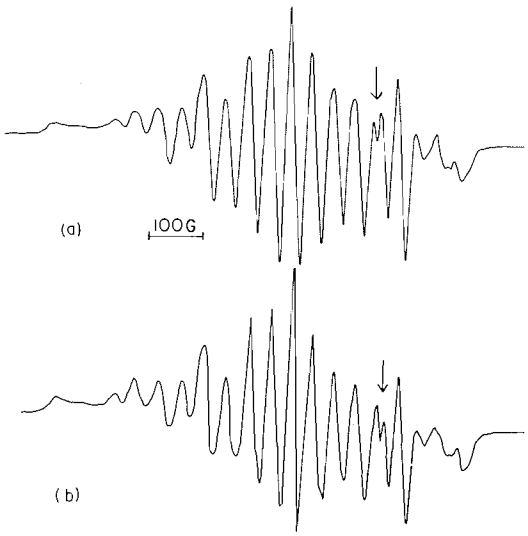

FIG. 2. (*a*) Electron spin resonance spectrum of freshly prepared solution of $K_4Mn(CN)_6$ in frozen D_2O at 77 °K. (*b*) Same sample after standing three days at Dry-Ice/acetone temperature. The change in the spectrum is marked by the arrow.

water or acetonitrile/water mixtures. Such a spectrum is also shown in Fig. 1. Some small, but significant, changes in the relative intensities of the lines can be observed in some of the spectra and these are illustrated in Fig. 2. These differences suffice to demonstrate that more than one paramagnetic chemical species is involved. The lines are slightly broader at high concentrations but no other concentration effect is observed. If the samples are allowed to warm from liquid-nitrogen temperature, the spectra diminish in intensity and eventually disappear. The disappearance is complete at temperatures well below the melting point of the matrix. The spectrum can also be suppressed almost completely by adding an excess of potassium cyanide.

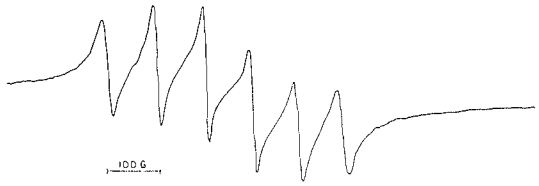

FIG. 3. Electron spin resonance spectrum of "$KMn(CN)_3$" in liquid ammonia.

Qualitatively, the spectra of Fig. 1 contain at least eleven or twelve sharp lines together with some broader absorptions in the wings. The center of the spectrum is located at $g = 1.98$. The spacing of the major lines is close to 40 G. This is about half of the usual 75–95 G isotropic splitting found in Mn(II) compounds (8). The widths of the central lines are around 10 G. It should also be noted that these lines show a true derivative line shape rather than the half derivative characteristic of powder e.s.r. spectra. A frozen aqueous solution of Mn(II) ions shows no resolvable hyperfine structure under comparable instrumental conditions. It must be concluded that a mechanism is operative which averages out the anisotropic dipole–dipole interactions which usually broaden the e.s.r. spectra of polycrystalline mixtures. Solid samples of the compound "$KMn(CN)_3$" prepared by the methods described in the literature show no resolvable e.s.r. spectrum. This material is slightly soluble in liquid ammonia and gives a six-line spectrum with a hyperfine splitting of 89 G, as illustrated in Fig. 3. As anticipated, only the high-spin Mn(II) ions are contributing to the spectrum.

Discussion

Initially, it is apparent that the spectra of Fig. 1 are not produced from the starting material $K_4Mn(CN)_6$. From the results of Baker, Bleaney, and Bowers (2), spectra are not expected to be observed from this compound under the experi-

Can. J. Chem. Downloaded from www.nrcresearchpress.com by 210.87.254.40 on 09/05/12
For personal use only.

Can. J. Chem. Downloaded from www.nrcresearchpress.com by 210.87.254.40 on 09/05/12
For personal use only.

mental conditions used; there are too many lines in the observed spectrum and the measured parameters do not agree with those reported. In addition to these spectroscopic arguments, there is the chemical argument that the spectrum is suppressed by the addition of KCN, which should increase the concentration of $Mn(CN)_6^{4-}$ ions.

The proposition that the spectrum arises from the decomposition product "$KMn(CN)_3$" is also unattractive. By direct experiment, this latter material does not exhibit the observed spectrum in the solid phase. In liquid-ammonia solution the observed spectrum is that of solvated Mn^{2+} ions. Neither does it seem feasible to explain the nature of the spectrum on a model based on an *extended* Prussian-blue type lattice such as has been proposed for $KMn(CN)_3$. We are therefore led to the conclusion that an intermediate (or intermediates) in the decomposition process gives rise to the spectra. In this context, it is interesting to note that precipitation of $KMn(CN)_3$ is not apparent until several minutes after preparing solutions of $K_4Mn(CN)_6$, and that freezing of the freshly prepared, clear solutions produces the observed spectrum.

It is reasonable to suppose that the initial step in the decomposition of $Mn(CN)_6^{4-}$ is loss of a cyanide group and that this could be followed by formation of a cyanide bridge, i.e.

$$Mn(CN)_6^{4-} \rightarrow Mn(CN)_5^{3-} + CN^-$$

$$Mn(CN)_5^{3-} + Mn(CN)_6^{4-} \rightarrow [(CN)_5Mn{-}C{\equiv}N{-}Mn(CN)_5]^{7-}$$

Continued loss of cyanide groups and formation of bridges leads to the Prussian-blue structure. The analogous loss of a cyanide in the Co(II) system has already been pointed out, and the formation of a cyanide bridge in the reaction of $Co(CN)_5^{3-}$ and $Co(NH_5)_5CN^{2+}$ has been demonstrated by Halpern and Nakamura (9). These authors showed that oxidation of the cobalt(II) cyanide proceeds by an inner-sphere mechanism and that the resulting N-bonded cyanide complex rearranges to the thermodynamically more stable C-bonded complex with a characteristic half-life of around 1.6 s.

We would like to propose that the e.s.r. spectra reported in the present paper arise from relatively low molecular weight species containing the —Mn—C≡N—Mn grouping. It is further postulated that in such a grouping, one manganese atom will be high-spin and one low-spin. In bridged complexes of this nature, hyperfine coupling from both metal atoms may be observed, as has been demonstrated for a variety of copper complexes (10, 11). Further, as was first shown by Slichter (12), it is expected that the magnitude of the hyperfine coupling will only be half as great as that found in the monomeric species, providing there is interaction between the two paramagnetic centers. Thus, for the above grouping, an eleven-line spectrum with relative intensities 1:2:3:4:5:6:5:4:3:2:1 and hyperfine coupling half of the usual manganese value is expected. These predictions are in qualitative agreement with the observed spectra, although they do not account for all the lines present. The doubling of some of the lines with variable relative intensity illustrated in Figs. 1 and 2 can be readily ascribed to slightly different environments for different pairs of manganese atoms. Thus it is possible that in some cases, one or more cyanide groups might be replaced by solvent molecules on the high-spin manganese. The presence of trimers, tetramers, and higher polymers could serve to account for some of the additional broader lines observed in the wings of the spectrum. The observed g value is also consistent with this interpretation, since it is intermediate between the values expected for high-spin and low-spin Mn(II).

It should be noted that there is considerable precedent in the literature for cyanide bridges in structures other than Prussian blue. Perhaps the closest example to the present case is the compound

$$Ba_3[(NC)_5FeCNCo(CN)_5]16H_2O$$

discussed by Dows, Haim, and Wilmarth (13). Other papers have discussed cyanide bridges using X-ray (14) and infrared (15) methods of examination. Haim and Wilmarth (16) have reported several compounds involving cyanide bridges formed from cobalt pentacyanide, and Taube and Myers (17) have shown that reduction of ferricyanide by Cr(II) occurs via a bridging CN and that the bridge persists in the product. There is also analogy between the e.s.r. spectra reported here and those observed for certain peroxy-bridged cobalt complexes. Thus Bayston, Looney, and Winfield (18) obtained a fifteen-line spectrum (corresponding to coupling with two cobalt ions with nuclear spin 7/2) from $[(CN)_5Co{-}O{-}O{-}Co(CN)_5]^{5-}$. In this case, the effect is attributed

Can. J. Chem. Downloaded from www.nrcresearchpress.com by 210.87.254.40 on 09/05/12
For personal use only.

to electron exchange between Co(III) and Co(IV). Ebsworth and Weil (19) obtained similar results with $[(NH_3)_5Co—O—O—Co(NH_3)_5]^{5+}$.

However, the mere presence of the —Mn—C≡N—Mn grouping is not sufficient to account for the observed e.s.r. spectrum. The extremely narrow lines observed indicate that some mechanism is present which effectively averages out the magnetic dipole–dipole interactions. Rotation of radicals such as $CH_3\cdot$ in solid matrices can produce this effect and allow resolution of the hyperfine splitting. It is difficult to envisage free rotation of dimeric manganese cyanides in ice at liquid-nitrogen temperature. We wish to suggest that the averaging is produced by rapid exchange between manganese ions in low-spin and high-spin states. Such a time-dependent phenomenon could result in averaging of the dipole–dipole interactions. Spin equilibria have previously been reported in Ni(II) systems (20), Fe(II) systems (21, 22), and Fe(III) systems (23). It seems probable that changes in the spin state will usually be accompanied by relatively large changes in the bond lengths or geometry of the complex. Thus, in a crystal they usually cannot occur without disruption of the crystal (22). In the Prussian-blue structures, it appears that both the oxidation state and spin state of each metal atom are fixed (7). One would expect a great deal more flexibility in the relatively low molecular weight oligomers considered here, and hence easier spin exchange. Thus, one possible specific mechanism could be rotation of the bridging cyanide, i.e.

$$—Mn—C\equiv N—Mn \rightleftharpoons Mn—N\equiv C—Mn$$

which could result in exchange of the high-spin and low-spin manganese ions with consequent narrowing of the e.s.r. lines. However, other mechanisms can also be envisaged. Thus, a manganese ion surrounded by six carbon-bonded cyanides clearly has a low-spin ground state, whereas an ion surrounded by six nitrogen-bonded cyanides has a high-spin ground state. For intermediate situations, e.g., three C-bonded and three N-bonded ligands, the two states may be close in energy and rather modest changes in bond distances might suffice to convert one to the other. The present data does not suffice to establish a specific mechanism.

In summary, the e.s.r. spectra reported in the present paper clearly show hyperfine interactions with at least two manganese atoms, and are thought to arise from species intermediate between the initial $K_4Mn(CN)_6$ molecule and the final insoluble polymeric decomposition product $KMn(CN)_3$. In proceeding from $K_4Mn(CN)_6$ to $KMn(CN)_3$, it is necessary to convert half of the manganese ions from a low-spin state to a high-spin state. The abnormally sharp lines observed in the present e.s.r. spectra suggest that the intermediate is such as to allow rapid interconversion between spin-paired and spin-free states, although the present data is insufficient to provide positive proof of this hypothesis. If correct, such an interconversion suggests facile ligand rearrangements in the intermediate. Such a conclusion is perhaps not surprising in view of the fact that Prussian-blue structures are apparently completely ordered with respect to the cyanide groups; and if such a structure is to be formed by polymerization of manganocyanide ions, some reorganization of the cyanide ligands is inevitable.

Experimental

Samples of potassium manganocyanide were purchased from Alfa Inorganic Co. Electron spin resonance spectra were obtained using a JEOLCO spectrometer Model JES 3BS equipped with a cylindrical cavity.

We are indebted to the National Research Council of Canada for financial support of this research.

1. B. N. Figgis. Trans. Faraday Soc. **57**, 204 (1961).
2. J. M. Baker, B. Bleaney, and K. D. Bowers. Proc. Phys. Soc. London, B, **69**, 1205 (1956).
3. B. M. Chadwick and A. G. Sharpe. Advan. Inorg. Radiochem. **8**, 83 (1966).
4. N. Goldenberg. Trans. Faraday Soc. **36**, 847 (1940).
5. M. B. Robin. Inorg. Chem. **1**, 337 (1962).
6. D. F. Shriver, S. A. Shriver, and S. E. Anderson. Inorg. Chem. **4**, 725 (1965).
7. M. B. Robin and P. Day. Advan. Inorg. Radiochem. **10**, 247 (1967).
8. S. I. Chan, B. M. Fung, and H. Lutje. J. Chem. Phys. **47**, 2121 (1967).
9. J. Halpern and S. Nakamura. J. Amer. Chem. Soc. **87**, 3002 (1965).
10. G. F. Kokoska, M. Linzer, and G. Gordon. Inorg. Chem. **7**, 1730 (1968).
11. G. F. Kokoska, H. C. Allen, and G. Gordon. J. Chem. Phys. **42**, 3693 (1965); **46**, 3020 (1967).
12. C. P. Slichter. Phys. Rev. **99**, 479 (1955).
13. D. A. Dows, A. Haim, and W. K. Wilmarth. J. Inorg. Nucl. Chem. **21**, 33 (1961).
14. R. Nast and W. Pfab. Naturwiss. **39**, 300 (1952).
15. M. F. A. El-Sayed and R. K. Sheline. J. Amer. Chem. Soc. **78**, 702 (1956).
16. A. Haim and W. K. Wilmarth. J. Amer. Chem. Soc. **83**, 509 (1961).
17. H. Taube and H. Myers. J. Amer. Chem. Soc. **76**, 2103 (1954).

18. J. H. BAYSTON, F. D. LOONEY, and M. E. WINFIELD. Instrum. J. Chem. **16**, 557 (1963).
19. E. A. V. EBSWORTH and J. A. WEIL. J. Phys. Chem. **63**, 1890 (1959).
20. D. R. EATON, W. D. PHILLIPS, and D. J. CALDWELL. J. Amer. Chem. Soc. **85**, 397 (1963).
21. J. P. JESSON, S. TROFIMENKO, and D. R. EATON. J. Amer. Chem. Soc. **89**, 3158 (1967).
22. J. P. JESSON, J. F. WEIHER, and S. TROFIMENKO. J. Chem. Phys. **48**, 2058 (1968).
23. E. KONIG and K. MADYA. Inorg. Chem. **6**, 48 (1967).

Can. J. Chem. Downloaded from www.nrcresearchpress.com by 210.87.254.40 on 09/05/12
For personal use only.

Radiolysis of ethane. I. Liquid phase at 195 °K with added cyclopentene

P. T. HOLLAND AND J. A. STONE
Chemistry Department, Queen's University, Kingston, Ontario
Received October 29, 1969

The radiolysis of liquid ethane at 195 °K gives as major products H_2, C_2H_4, and n-C_4H_{10}. Minor products are CH_4 and C_3H_8. The initial yields of H_2 and C_2H_4 can only be determined indirectly due to the high rate of H-atom addition to product ethylene. c-C_5H_8 in low concentration effectively scavenges H atoms and hence protects C_2H_4. The derived initial yields are: $G(H_2) = 5.97$, $G(C_2H_4) = 2.96$, $G(CH_4) = 0.44$, and $G(C_3H_8) = 0.55$. The yields of scavengeable H atoms and $\cdot C_2H_5$ radicals are 2.29 and 5.81, respectively. The problem of direct measurement of initial $G(H_2)$ values for saturated hydrocarbons at low temperatures is discussed.

Canadian Journal of Chemistry, 48, 1078 (1970)

Introduction

The radiation chemistry of liquid ethane has received scant study in comparison with that of higher hydrocarbons. Ethane does possess the advantage that, with only one C—C bond, the products at low dose are few in number and their analysis is comparatively easy. We have studied the radiolysis of ethane in the liquid phase at 195 °K and in the fluid phase above the critical temperature (305 °K) to examine the effect of temperature on the radiolysis. This paper reports some of our results obtained at 195 °K.

Gillis (1) irradiated liquid ethane at 195 °K and observed product yields which were linear with dose over the range 2–10 $\times$ 10^{19} eV/ml. He argued that the absence of curvature in the yield–dose plots demonstrates an absence of observable competition between abstraction and addition to product olefin in the fate of radiolytic H atoms. He concluded that in the dose range studied, all H atoms are removed by ethylene, even when its concentration is as low as 3 $\times$ 10^{-4} M. Improved analytical techniques have allowed us to measure product concentrations obtained at doses down to 3 $\times$ 10^{18} eV/g. We find a region of non-linearity in the yield curves of H_2 and C_2H_4, in confirmation of Gillis' prediction of the role played by H atoms in ethane radiolysis. The protective effect of another olefin, cyclopentene, has been used to obtain $G(H\cdot) = 2.29$ and $G(\cdot C_2H_5) = 5.81$. The former value is in excellent agreement with that recently reported by Bakale and Gillis (2) who used ethylene-d_4 to protect ethylene. We find further confirmation of $G(H\cdot)$ from HD formation in the liquid ethane/D_2S system.

Experimental

Phillips Research Grade Ethane (> 99.99% pure, but containing ~ 100 p.p.m. ethylene) was condensed at 77 °K onto 5A molecular sieve which had been heated under vacuum at 300–400 °C overnight. After several partial thawings and freezings to distribute the ethane more evenly throughout the sieve, the tube was immersed in a solid CO_2 - acetone bath at 195 °K and left for ½ h. The ethane was then slowly distilled off under vacuum, the first small amount and the last third being rejected. Several trap-to-trap distillations with continuous pumping were carried out to remove traces of methane and air. Gas chromatography revealed the purified material contained less than 0.1 p.p.m. ethylene and 1 p.p.m. methane.

J. T. Baker cyclopentene contained 0.22 volume % cyclopentane as major impurity and was used as received. D_2S (Stohler Isotopes, > 98% D) was also used as received.

Samples were irradiated in thoroughly baked and degassed Pyrex tubes having long, narrow, easily breakable necks. One g of ethane was condensed under vacuum in each flask. The appropriate amounts of cyclopentene (measured by micropipette) and D_2S (measured by PVT) were degassed and introduced into the sample tubes which were then sealed off. The sample tubes were immersed in a solid CO_2-acetone bath at 195 °K and irradiated in a Gammacell 220 (Atomic Energy of Canada, Limited). The dose rate, measured by Fricke dosimetry, was 6.3 $\times$ 10^{19} eV/g ethane h.

After irradiation, the sample tubes were broken under vacuum and the contents were transferred to a 1 l flask. Hydrogen and part of the methane were removed at 77 °K, measured volumetrically, and analyzed by mass spectrometry (using an A.E.I. MS10 instrument). When D_2S was present, the methane was a mixture of CH_4, CH_3D, and CH_2D_2. Cracking patterns and relative sensitivities for these were obtained from A.P.I. tables. The 1 l flask was allowed to warm to room temperature and an aliquot of its contents was injected into a gas chromatograph by means of a gas sampling valve. Ethylene and the remainder of the methane was determined using a ¼ in., 12 ft Porapak N column at 60 °C. Propane and butane were determined by temperature programing a ¼ in., 6 ft activated alumina column from 60 to 180 °C. Mixtures of

Can. J. Chem. Downloaded from www.nrcresearchpress.com by 210.87.254.6 on 09/05/12
For personal use only.

Can. J. Chem. Downloaded from www.nrcresearchpress.com by 210.87.254.6 on 09/05/12
For personal use only.

ethylene, methane, propane, and butane in ethane, with compositions closely resembling those obtained by radiolysis, were prepared for use as chromatographic standards.

Results

The major products from the radiolysis of pure liquid ethane which were studied in detail are hydrogen, methane, ethylene, propane, and *n*-butane. Acetylene was a minor product ($G < 0.1$) and apart from the initial determination of its presence and approximate yield no further measurements were made. Another product was detected with a yield less than that of acetylene. From its chromatographic retention time, it was thought to be a butene. Again no further measurements were carried out.

The effect of total dose in the range 0.3–6 $\times$ 10^{19} eV/g on the yields of hydrogen and ethylene is shown in Fig. 1. Results were obtained up to 9.5 $\times$ 10^{19} eV/g, but the shorter dose range is presented in Fig. 1 to emphasize our observation of the marked change in slope of the yield curves at low dose which was forecast by Gillis (1). The upper broken line on the H_2 curve represents an extrapolation of the curve at higher dose and gives $G(H_2) = 3.68$ at high dose, which is in good agreement with the value of 3.78 reported by Bakale and Gillis (2) and the value of 3.75 $\pm$ 0.15 obtained by Stone, Quirt, and Miller (3). The initial yields of H_2 and C_2H_4 derived as described later in this paper are represented by the broken lines at low dose.

Figure 2 shows the effect of total dose on the remaining major products. The methane and propane yields are, within experimental error,

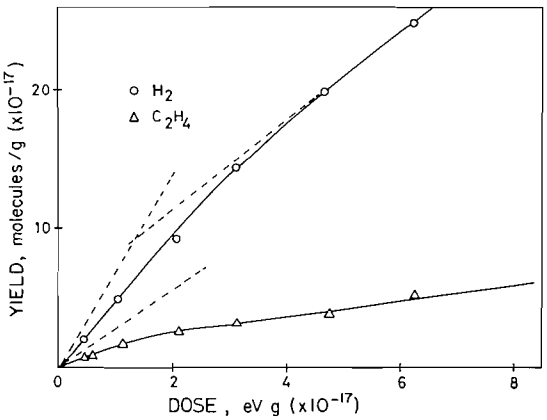

FIG. 1. H_2 and C_2H_4 yields from irradiated liquid ethane at 195 °K.

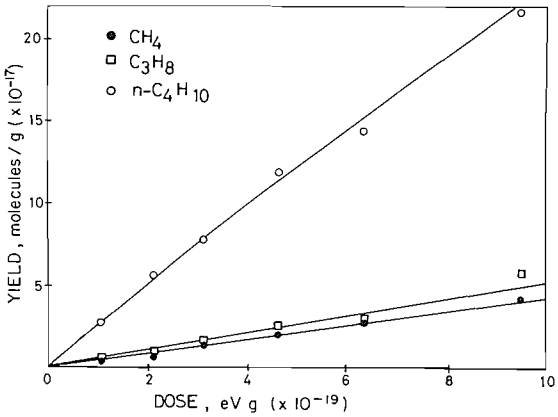

FIG. 2. CH_4, C_3H_8, and n-C_4H_{10} yields from liquid ethane at 195 °K.

linear with dose, the G values being 0.44 and 0.55, respectively. The *n*-butane yield plot shows a slight curvature and gives $G = 2.61$ at low dose and 2.25 at the highest dose.

At 5 $\times$ 10^{19} eV/g, the C:H ratio for the products is 1:3.05. It is improbable that any major product remains undetected.

The effect of up to 1.7 mole % of cyclopentene on $G(H_2)$, $G(C_2H_4)$, and $G(C_4H_{10})$ is shown in Fig. 3. These yields are independent of dose in the range 1–5 $\times$ 10^{19} eV/g. The yield of cyclopentane is also shown. The correction required for the cyclopentane impurity in the cyclopentene makes the accuracy of these points, particularly at the higher cyclopentene concentrations, rather low. $G(C_3H_8)$ is reduced by $\sim$ 0.2 units by cyclopentene, but $G(CH_4)$ remains unchanged.

The yields of H_2, HD, and D_2 from solutions of D_2S in liquid ethane are shown in Fig. 4. The G values are based on energy absorbed by the ethane alone. A correction has been applied to the D_2 yield to account for direct radiolysis of D_2S.

Discussion

The effect of total dose and of added cyclopentene on product yields will be discussed entirely in terms of the reactions of free radicals. These may, of course, have ionic precursors but we find no evidence for ionic reactions playing a major role in the phenomena under discussion.

The major transient species observed by electron paramagnetic resonance in irradiated liquid ethane is the ethyl radical (4). Small concentrations of methyl and vinyl radicals are also present.

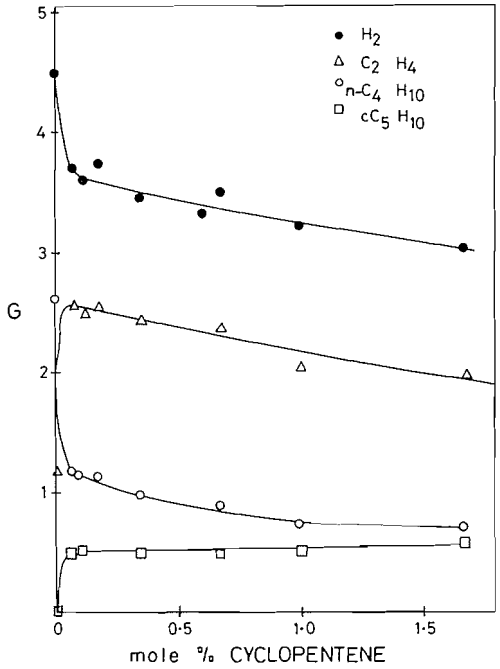

FIG. 3. The effect of cyclopentene on $G(H_2)$, $G(C_2H_4)$, and $G(n\text{-}C_4H_{10})$ for liquid ethane at 195 °K. (Dose = 2×10^{19} eV/g ethane.)

Although H atoms are not observed, this does not signify their absence from the system; rather it is most probable that their lifetime is too short for a detectable concentration to be present. We therefore formulate our mechanism for radical reactions in pure liquid ethane in terms of H·, $\cdot CH_3$, and $\cdot C_2H_5$ as follows

[1] $\quad H\cdot + C_2H_6 \rightarrow H_2 + \cdot C_2H_5$

[2] $\quad H\cdot + C_2H_4 \rightarrow \cdot C_2H_5$

[3a] $\quad 2\cdot C_2H_5 \rightarrow n\text{-}C_4H_{10}$

[3b] $\quad \rightarrow C_2H_4 + C_2H_6$

[4a] $\quad \cdot CH_3 + \cdot C_2H_5 \rightarrow CH_4 + C_2H_4$

[4b] $\quad \rightarrow C_3H_8$

The decreases in $G(H_2)$ and $G(C_2H_4)$ with increasing dose are explicable in terms of competition between reactions [1] and [2]. When the ethylene concentration is very low, i.e., at very low dose, reaction [1] should predominate over reaction [2]. Information on this competition at 195 °K is not available. Recourse must be made to extrapolation of data obtained at much higher temperature in the gas phase. Even here, very little information on the temperature dependence of the competition is available. Yang (5) has studied the gas-phase radiolysis of propane containing small concentrations of ethylene and propylene and has interpreted his results in terms of H-atom addition to olefin competing with abstraction of H from propane. Although this picture may be a little too simple by neglect of the probable occurrence of ion–molecule reactions, the results, when extrapolated to 298 °K, are in agreement with the isothermal ones reported by Cvetanovič and co-workers (6, 7) for

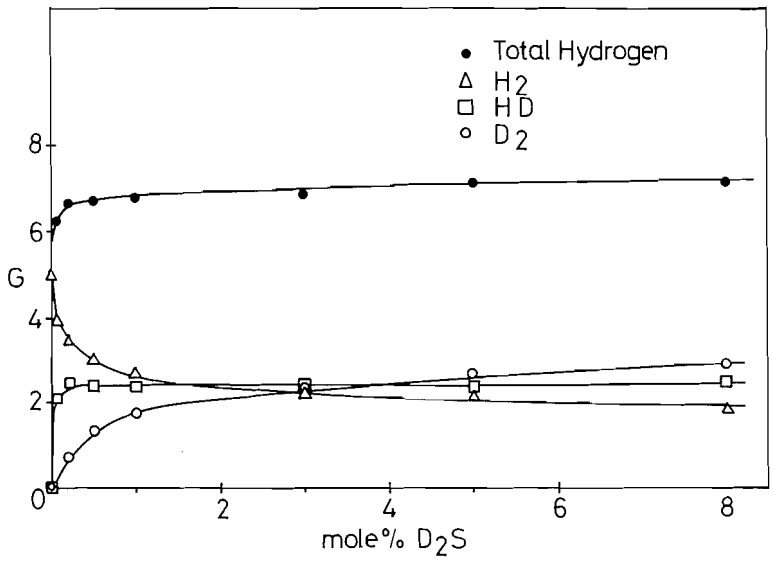

FIG. 4. H_2, HD, and D_2 yields from liquid ethane at 195 °K containing D_2S. (Dose = 2×10^{19} eV/g ethane.)

Can. J. Chem. Downloaded from www.nrcresearchpress.com by 210.87.254.6 on 09/05/12
For personal use only.

Can. J. Chem. Downloaded from www.nrcresearchpress.com by 210.87.254.6 on 09/05/12
For personal use only.

photochemically generated H atoms. If Yang's temperature coefficients are used, and assuming no changes in either the pre-exponential factors or the differences in activation energies, then, as an approximation at 195 °K we expect $k_{abstraction}/k_{addition}$ to fall in the range 10^{-4}–10^{-7}. We shall later show that our results are consistent with such an assumption, i.e., H-atom addition to olefin will predominate over H-atom abstraction from paraffin when the olefin concentration exceeds $\sim 10^{-4}$ *M*.

In the above reaction scheme, the only results of increasing dose, i.e., increasing ethylene concentration, are decreases in $G(H_2)$ and $G(C_2H_4)$. As reaction [2] supercedes reaction [1], there is no change in the total number of ethyl radicals which react via reactions [3] and [4]. There is a small decrease in $G(C_4H_{10})$, but no change in $G(CH_4)$ or $G(C_3H_8)$. The change in $G(C_4H_{10})$ is small and continuous over the whole dose range, unlike the more abrupt changes observed for ethylene and hydrogen. We therefore feel justified in ascribing the major cause of the changes in slope of the curves in Fig. 1 to H-atom scavenging by product ethylene. This is confirmed by the results obtained when cyclopentene is added. The extra reactions to be considered are

[5] $c\text{-}C_5H_8 + H\cdot \rightarrow c\text{-}C_5H_9\cdot$

[6*a*] $c\text{-}C_5H_9\cdot + \cdot C_2H_5 \rightarrow c\text{-}C_5H_9C_2H_5$

[6*b*] $\rightarrow c\text{-}C_5H_8 + C_2H_6$

[6*c*] $\rightarrow c\text{-}C_5H_{10} + C_2H_4$

[7*a*] $2c\text{-}C_5H_9\cdot \rightarrow c\text{-}C_5H_8 + c\text{-}C_5H_{10}$

[7*b*] $\rightarrow (c\text{-}C_5H_9)_2$

Only cyclopentane of the new products was detected and quantitatively determined. Dicyclopentyl and regenerated cyclopentene were not searched for.

$G(H_2)$ is reduced to 3.6 by the addition of less than 0.1 mole % ($\sim 10^{-2}$ *M*) cyclopentene. This value is essentially that (3.68) obtained from pure liquid ethane at high dose. Increasing olefin concentration leads to a further, very gradual decrease in $G(H_2)$. Accompanying the rapid decrease in $G(H_2)$ is an immediate increase in $G(C_2H_4)$ to a maximum value of 2.50 and a decrease in $G(C_4H_{10})$ to 1.15. Both product yields then decrease slowly with increasing cyclopentene concentration. *G*(cyclopentane) assumes a value of 0.5 ± 0.1 at the lowest cyclopentene concentration and, within experimental error, this value remains unchanged when the olefin concentration is increased by a factor of thirty. The abrupt changes in yields in the presence of a small amount of cyclopentene are readily interpreted as protection of product ethylene by cyclopentene, which scavenges all freely diffusing hydrogen atoms, i.e., reaction [5] effectively supercedes reactions [1] and [2]. Reactions involving hot hydrogen atoms or thermalized hydrogen atoms reacting in cages and spurs will not be affected at these low olefin concentrations.

The following equations describe the product balance in the formation of ethylene and butane. (In order to simplify the presentation we ignore, for the present, the disappearance of $\cdot C_2H_5$ radicals by reaction [4]. A correction is later applied for this omission.) A measured or partial yield of a final product is designated *G*, while the yield of a transient species is designated *g*. G_M represents that portion of a product yield which is not affected by radical scavengers, i.e., that part formed by nonradical processes together with that from radical reactions occurring in spurs which are not altered by the low concentration of the scavengers we employ.

(*a*) In pure ethane at high dose when all H atoms are scavenged by product ethylene

$$[\mathrm{I}]\quad G(C_2H_4) = 0.67 = G_M(C_2H_4) + \frac{k_{3b}}{k_{3a}}\{G(C_4H_{10}) - G_M(C_4H_{10})\} - g(H\cdot)$$

$$[\mathrm{II}]\quad G(C_4H_{10}) = 2.45 = \tfrac{1}{2}\left(\frac{k_{3a}}{k_{3a}+k_{3b}}\right) \times \{g(\cdot C_2H_5) + g(H\cdot)\} + G_M(C_4H_{10})$$

$G(C_2H_4) = 0.67$ is obtained from the slope of the $G(C_2H_4)$ line at high dose (Fig. 1). As noted earlier, the mechanism proposed in reactions [1]–[4] should lead to no change in $G(C_4H_{10})$ with increasing dose; experimentally a small change is noticed. Since we do not know the cause of this, we take the value for $G(C_4H_{10})$ as 2.45, which is an average of the value over the dose range shown in Fig. 2. The value is essentially that obtained at a dose of 5×10^{19} eV/g when H-atom scavenging is complete. A value of $G_M(C_4H_{10}) = 0.51$ is obtained when D_2S is used as a radical scavenger (8). Bakale and Gillis (2) find k_{3b}/k_{3a} to be 0.41 ± 0.06 from their measurements of the yields of

Can. J. Chem. Downloaded from www.nrcresearchpress.com by 210.87.254.6 on 09/05/12
For personal use only.

labelled products obtained by radiolysis of C_2D_4 in C_2H_6 at 195 °K. They note that this ratio is far larger than that observed in the gas phase; however, it is consistent with the move to higher values which has been observed (9) in the liquid phase.

(*b*) In the presence of cyclopentene when all the H atoms are scavenged by this solute

$$[III]\quad G(C_2H_4) = 2.60 = G_M(C_2H_4) + \frac{k_{3b}}{k_{3a}} \times \{G(C_4H_{10}) - G_M(C_4H_{10})\} + 0.13g(\cdot C_2H_5)_6$$

$$[IV]\quad G(C_4H_{10}) = 1.20 = \tfrac{1}{2}\left(\frac{k_{3a}}{k_{3a} + k_{3b}}\right) \times \{g(\cdot C_2H_5) - g(\cdot C_2H_5)_6\} + G_M(C_4H_{10})$$

The values of 2.60 and 1.20 for $G(C_2H_4)$ and $G(C_4H_{10})$, respectively, are obtained by a linear extrapolation of the gently sloping portions of the yield curves to 0 mole % cyclopentene. Since simple H-atom scavenging should not be responsible for the decreasing C_2H_4 yields above 0.2 mole % cyclopentene, other reactions must be assuming importance as the olefin concentration increases. The extrapolations should minimize any complications caused by these reactions.

$g(\cdot C_2H_5)_6$ is the yield of ethyl radicals which react with cyclopentyl radicals in reaction [6]. The factor 0.13 in eq. [III] is Holroyd's estimate of the fraction of the total number of encounters between ethyl and cyclopentyl radicals which lead to ethylene production (10).

Equations [I]–[IV] were solved to obtain the remaining four unknowns. The results are $g(H\cdot) = 2.29 \pm 0.2$, $g(\cdot C_2H_5) = 3.18 \pm 0.4$, $G_M(C_2H_4) = 2.16 \pm 0.1$, and $g(\cdot C_2H_5)_6 = 1.23 \pm 0.5$. The error estimates represent the expected variation arising from the errors in measured product G values, which are thought to be accurate to 0.1 units. Inclusion of the estimated error limits of ± 0.06 in the ratio $k_{\text{disproportionation}}/k_{\text{combination}}$ for ethyl radicals (2) would approximately double the stated limits.

The value for $g(H\cdot)$ is supported by the HD yield in the C_2H_6/D_2S system (Fig. 4). G(HD), which measures $g(H\cdot)$ (11), attains a maximum value of 2.4 at very low D_2S concentrations when ion scavenging, whose magnitude is indicated by the D_2 yield, plays only a small part. HD is formed in reaction [7], which competes effectively with reactions [1] and [2].

$$[7]\qquad H\cdot + D_2S \rightarrow HD + DS\cdot$$

At very low dose, when all H atoms react by abstraction, the initial yield of hydrogen, ethyl radicals, and ethylene are as follows

$$G(H_2) = G_M(H_2) + g(H\cdot) = 5.97$$

$$G(\cdot C_2H_5) = g(\cdot C_2H_5) + g(H\cdot) + g(\cdot C_2H_5)_4$$

where $g(\cdot C_2H_5)_4$ is the yield of $\cdot C_2H_5$ which reacts with $\cdot CH_3$ as in reactions [4*a*] and [4*b*]; it can be estimated from experiments with D_2S as scavenger. D_2S (10^{-2} *M*) reduces $G(C_3H_8)$ by 0.3 units, after which further addition has a negligible effect. For methyl and ethyl radicals, $k_{\text{disproportionation}}/k_{\text{combination}} = 0.14$ (2), making $G(\cdot C_2H_5)_4 = 0.34$. Therefore, $G(\cdot C_2H_5) = 5.81$.

$$G(C_2H_4) = G_M(C_2H_4) + \left(\frac{k_{3b}}{k_{3a} + k_{3b}}\right)\frac{g(\cdot C_2H_5)}{2} = 2.96$$

Table 1 summarizes our results and compares them with those of Bakale and Gillis (2). It is gratifying to see that the agreement is very good.

TABLE 1

Product yields in the radiolysis of liquid ethane at 195 °K

Measured yields	This work	Bakale and Gillis (2)
$G_M(H_2)$	3.68±0.05	3.78
$G(CH_4)$	0.44±0.05	0.39
$G(C_3H_8)$	0.55±0.05	0.52
$G(n\text{-}C_4H_{10})$	2.6 ±0.1	2.45
$G_M(C_2H_4)$	0.67±0.05	~0.74
Derived values	**This work**	**Bakale and Gillis (2)**
$g(H\cdot)$	2.3 ±0.2	2.3±0.2
$g(\cdot C_2H_5)$	5.81±0.6	—
$G(H_2)$*	5.97±0.25	6.08
$G(C_2H_4)$*	2.96±0.25	—

*Calculated for infinitely small dose.

Bakale and Gillis derive a competition equation which describes the dose dependence of ethylene concentration in terms of the ratio k_2/k_1 and of the initial G values (G^0) for ethylene and hydrogen atom. Taking $G(H\cdot) = 2.3$, a best fit to the experimental curve for C_2H_4 production is obtained with $k_2/k_1 = 5 \pm 3 \times 10^5$ and $G^0(C_2H_4) = 2.8 \pm 0.2$. Using our derived values

Can. J. Chem. Downloaded from www.nrcresearchpress.com by 210.87.254.6 on 09/05/12
For personal use only.

of $G(H\cdot) = 2.29$ and $G^0(C_2H_4) = 2.96$, we obtain a best fit to our ethylene results (Fig. 1) with $k_2/k_1 = 10 \pm 2 \times 10^5$. The agreement between the two ratios is excellent, considering the low concentrations of ethylene which have to be measured at the lowest doses. With $k_2/k_1 = 10 \pm 2 \times 10^5$, and assuming equal pre-exponential factors, we obtain an activation energy difference of 5.4 ± 0.2 kcal mole^{-1}. Yang (5) obtained $\Delta E_a = 4.4$ kcal mole^{-1} for the competition of $H + C_2H_4$ and $H + C_3H_8$. Taking E_a for $H + C_2H_6$ as 9.9 kcal mole^{-1} and for $H + C_3H_8$ as 8.4 kcal mole^{-1} (12), then Yang's (5) results yield $\Delta E_a = 5.9$ kcal mole^{-1} for the difference in activation energy between $H + C_2H_4$ and $H + C_2H_6$. Gas-phase rate-constant ratios for H-atom reactions appear to be equally applicable to the liquid phase.

Our results emphasize the difficulty in experimentally determining initial product yields in studies of the radiolysis of saturated hydrocarbons. These yields are only obtainable if they are measurable at a dose sufficiently low that significant H-atom scavenging by product olefin is eliminated. At 298 °K, when $k_2/k_1 \sim 2$–4×10^4, we require doses no higher than $\sim 1 \times 10^{19}$ eV/ml. At 195 °K, the dose will have to be about 100 times less. At the moment, product yield measurements at such doses are impracticable and therefore numerical analyses such as ours must be resorted to to obtain initial yields.

It is of interest to note that the initial hydrogen yield for ethane (5.97) at 195 °K is practically the same as we obtain at 313 °K (5.7) for ethane at a density of 0.45 g/ml. (8). The latter is an experimental value obtained by extrapolation to zero dose and may therefore be slightly low. There is therefore little, if any, change in $G(H_2)$ from liquid ethane over a temperature range of more than 100 °K, and it may be that many of the reported temperature coefficients of $G(H_2)$ for hydrocarbons (13, 14) simply reflect the increasing difficulty of experimentally obtaining true initial yields as temperature decreases.

Bakale and Gillis (2) discuss the possibility of ion–molecule reactions occurring at the higher C_2D_4 concentrations. They suggest that charge transfer from $C_2H_6^+$ to C_2D_4 can explain the concentration dependence of both the decreasing H_2 yield and the relatively small yields of HD and D_2. Such a reaction should lead to a decrease in the C_2H_4 yield, since its production via neutralization of $C_2H_6^+$ should be inhibited. Confirmation of this decrease is hampered by the difficulty in determining C_2H_4 in the presence of large amounts of C_2D_4. We have no such difficulty with C_2H_4 in the presence of c-C_5H_8, and Fig. 3 shows that as the concentration of the latter increases, $G(C_2H_4)$ decreases. The most abundant initial ion must surely be $C_2H_6^+$. Possible exothermic reactions of this ion with cyclopentene which might lead to a reduction in $G(C_2H_4)$ are charge transfer, proton transfer, and H_2 transfer. We cannot distinguish between these, although the apparent constancy of $G(c\text{-}C_5H_{10})$ with increasing c-C_5H_8 would appear to rule out the occurrence of H_2 transfer. We are, however, surprised at the precision of our measurements of the c-C_5H_{10} concentration (Fig. 3), since a large correction is applied for the presence of this compound in the c-C_5H_8 used. We therefore hesitate to rule out the occurrence of this reaction.

The authors thank the National Research Council of Canada, the Province of Ontario, and Atomic Energy of Canada, Ltd., Commercial Products, for financial support. The authors thank Dr. H. A. Gillis for allowing them access to the manuscript of ref. 2 prior to publication.

1. H. A. Gillis. J. Phys. Chem. **67**, 1399 (1963).
2. G. Bakale and H. A. Gillis. J. Phys. Chem. **73**, 2178 (1969).
3. J. A. Stone, A. R. Quirt, and O. A. Miller. Can. J. Chem. **44**, 1175 (1966).
4. R. W. Fessenden and R. H. Schuler. J. Chem. Phys. **39**, 2147 (1963).
5. K. Yang. J. Amer. Chem. Soc. **84**, 719 (1962).
6. R. K. Jennings and R. J. Cvetanovič. J. Chem. Phys. **35**, 1233 (1961).
7. G. R. Woolley and R. J. Cvetanovič. J. Chem. Phys. **50**, 4697 (1969).
8. P. T. Holland and J. A. Stone. Unpublished results.
9. P. S. Dixon, A. P. Stefani, and M. Szwarc. J. Amer. Chem. Soc. **85**, 2551 (1963).
10. R. A. Holroyd. J. Phys. Chem. **66**, 730 (1962).
11. Von G. Meissner and A. Henglein. Ber. Bunsenges. Phys. Chem. **69**, 264 (1965).
12. B. A. Thrush. Progr. React. Kinet. **3**, 89 (1965).
13. T. J. Hardwick. J. Phys. Chem. **66**, 117 (1962).
14. H. Widmer and T. Gaumann. Helv. Chim. Acta, **46**, 944 (1964).
15. A. A. Scala, S. G. Lias, and P. Ausloos. J. Amer. Chem. Soc. **88**, 5701 (1966).

Can. J. Chem. Downloaded from www.nrcresearchpress.com by 210.87.254.42 on 09/05/12
For personal use only.

Platinum–acetylene or –ethylene complexes with bridging or chelating ethylenediamine derivatives[1]

T. Theophanides and P. C. Kong
Department of Chemistry, University of Montreal, Montreal 250, Quebec

Received September 24, 1969

The reaction intermediates of $K[Pt(ac)X_3]$ with ethylenediamine and its N-substituted derivatives have been studied in water and organic solvents. The general reaction is

$$K[Pt(ac)X_3] \xrightarrow[-KX]{+en} Pt(ac)(en)X_2 \longrightarrow [Pt(ac)(en)X]X$$

1 2 3

where ac = $(CH_3)_2C(Y)C{\equiv}CC(Y)(CH_3)_2$, en = ethylenediamine, Y = OH, OCH_3, and X = Cl, Br. The five-coordinate intermediates **2** are isolated and characterized from conductivity data, molecular weight determinations, and infrared, nuclear magnetic resonance (n.m.r.), and ultraviolet (u.v.)–visible absorption spectra. The stability of complexes **2** (see equation above) in terms of alkyl substitution of the NH_2 groups is approximately

$$enMe_4 > enMe_2Et_2 > enH_2Me_2 > en$$

where $enMe_4 = (CH_3)_2N(CH_2)_2N(CH_3)_2$, $enMe_2Et_2 = CH_3C_2H_5N(CH_2)_2NC_2H_5CH_3$, $enH_2Me_2 = CH_3HN(CH_2)_2NHCH_3$, $enEt_4 = (C_2H_5)_2N(CH_2)_2N(C_2H_5)_2$. In contrast to these reactions, the Zeise salt, $K[PtC_2H_4Cl_3]$, reacts with ethylenediamines and gives only stable, bridged compounds of the formula $(PtC_2H_4Cl_2)_2(en)$. Bridged compounds, $(Pt(ac)Cl_2)_2(en)$, are also obtained with $K[Pt(ac)Cl_3]$, but only in the presence of a large excess of KCl in the reaction solutions.

Canadian Journal of Chemistry, **48**, 1084 (1970)

Introduction

The tetramethylbutynendioltrichloro platinum(II), $K[Pt(ac)Cl_3]$, was first prepared by Bukhovets (1), and its molecular structure was discussed later by Chatt *et al.* (2) and Allen and Theophanides (3).

Recently, the *trans*-$[Pt(Bu^tC{\equiv}CBu^t)Cl_2(p\text{-toludine})]$ has been studied by X-ray diffraction (4) and it was confirmed that the acetylenic ligand is perpendicular to the plane of the molecule. Due to the high *trans* effect of the acetylenic bond, the *trans* chlorine in $K[Pt(ac)Cl_3]$ is strongly labilized and easily replaced by nucleophilic ligands such as amines. As a result of this high *trans* labilization, many zero-charged complexes have been made by direct substitutions (2, 3, 5). In a previous study, the reactions of Bukhovet's salt with ethylenediamines have been reported and a series of cationic complexes have been isolated (6).

In the reactions of $K[Pt(ac)Cl_3]$ in organic solvents, the yellow solutions change immediately to an intense red color on addition of ethylenediamine and subsequently the color disappears to form the white product, [Pt(ac)(en)Cl]Cl.

The intermediate products $Pt(ac)(en)X_2$ have been isolated and characterized. We report here, in detail, the preparation and chemical reactions of these complexes, which are five-coordinated if (ac) is considered as a monodentate ligand (4).

Bridged ethylenediamine complexes of the general formula $(Pt(ac)Cl_2)_2(en)$ are also isolated and described. These complexes were prepared from water solution in the presence of excess KCl, and are similar to the ethylene analogs, $(PtC_2H_4Cl_2)_2(en)$ (7).

Results and Discussion

The overall reactions of Bukhovet's salt with ethylenediamines are shown in Scheme 1. Various N-alkyl derivatives of ethylenediamine have been used to investigate the effect of alkyl groups on the stability and type of product obtained.

When a solution of ethylenediamine in an organic solvent is added dropwise to a solution of $K[Pt(ac)X_3]$ (see Scheme 1) or to a solution of *trans*-$[Pt(ac)(py)X_2]$, also in organic solvent, a red spot first is observed around the drop. The lifetime of the red spot depends greatly on the

[1]This paper was presented in part at the 52nd C.I.C. Conference, May 25–28, 1969, Montreal, Quebec.

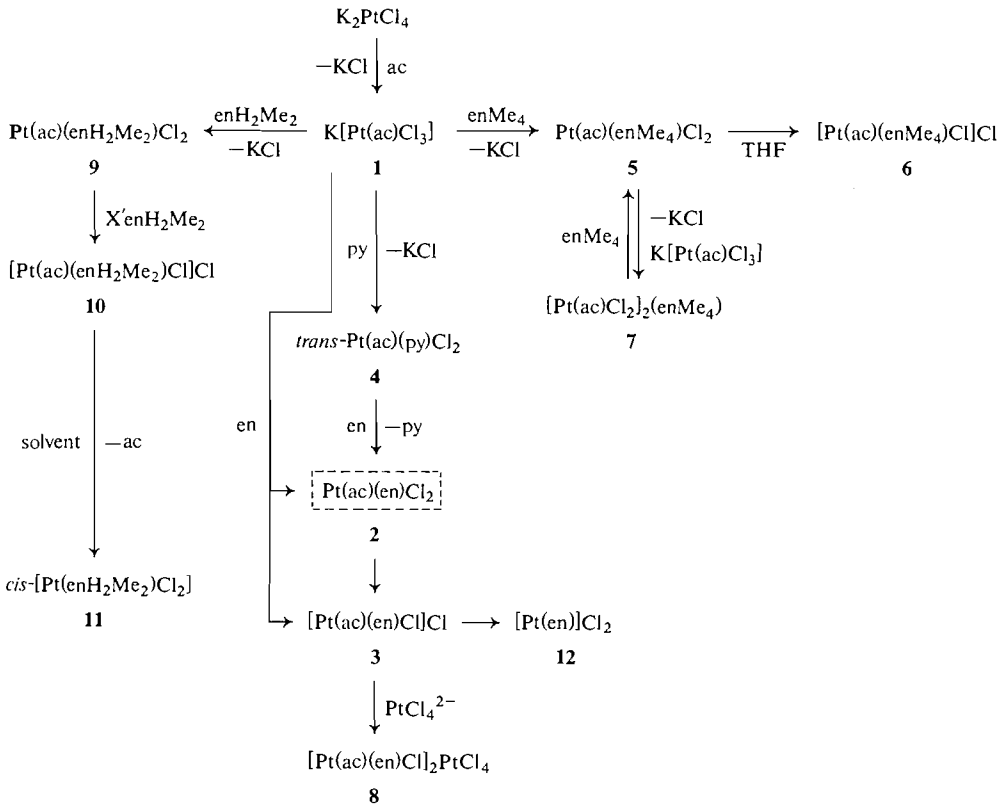

SCHEME 1

bulkiness of the N-alkyl groups. In the case of ethylenediamine itself, the initially red solution changes quickly and a white precipitate **3** is obtained. When N-tetramethyl-substituted ethylenediamine ($enMe_4$) is used, the red solution persists longer and red complexes can be isolated having the formula $Pt(ac)(enMe_4)X_2$. These five-coordinate complexes rearrange in solution to the cationic complexes $[Pt(ac)(enMe_4)X]X$ (6) in about 2 h (see Fig. 3).

The five-coordinate complexes seem to be intermediates in all these reactions (8). Compound **5** (see Scheme 1) in the presence of $K[Pt(ac)X_3]$ gives the bridged complex **7** which reverts to five-coordinate **5** in the presence of excess $enMe_4$. A five-coordinate intermediate has also been isolated with $enMe_2Et_2$, which with excess $K[Pt(ac)X_3]$ reacts further and forms the bridged analogue $(Pt(ac)X_2)_2(enMe_2Et_2)$. This, however, does not give the reverse reaction with excess $enMe_2Et_2$, as in the case of complex **7**.

The five-coordinate intermediates are also obtained with enH_2Me_2, but they are very unstable at room temperature and quickly rearrange into cationic complexes **10** which lose acetylene and give the yellow, stable precipitates **11** (see Scheme 1). Several attempts to prepare the complex $Pt(ac)Cl_2(enEt_4)$ were unsuccessful.

The physical properties, analytical data, and infrared characteristic group frequencies of the five-coordinate compounds with chelating ethylenediamine derivatives are given in Tables 1 and 2. Similar data for the compounds with bridging ethylenediamines are given in Table 3. Plots of conductivity vs. time for the five-coordinate complexes in methanol, in the absence or presence of methyl iodide, are shown in Figs. 1–3. The conductivity measurements indicate that there is a dissociation of the five-coordinate complex into cationic species and that the methyl iodide does not alter the measurements. This indicates that the tetramethylethylenediamine is coordinated from both ends (9, 10). The steady increase in conductance due to

Can. J. Chem. Downloaded from www.nrcresearchpress.com by 210.87.254.42 on 09/05/12
For personal use only.

Can. J. Chem. Downloaded from www.nrcresearchpress.com by 210.87.254.42 on 09/05/12
For personal use only.

TABLE 1

Analytical data and properties of the five-coordinate complexes

Compound	Melting point (°C)	Molecular weight		Analysis, %									
				C		H		N		X		Pt	
		Found	Calcd.	Found	Calcd.	Found	Calcd.	Found	Calcd.	Found	Calcd.	Found	Calcd.
$Pt(ac)(enMe_4)Cl_2$	87	495	524	32.10	31.31	5.73	5.41	5.34	5.13			36.96	37.25
$Pt(ac)(enMe_4)Br_2$	82	—	—	28.32	27.90	5.12	4.97	4.41	4.64	26.56	26.50	32.30	32.37
$Pt(ac)(enMe_2Et_2)Cl_2$	83	520	552	34.11	34.78	6.05	6.18	5.24	5.07			35.13	35.33
$Pt(ac)(dipy)Cl_2$	82	—	—	38.56	38.31	4.07	3.93	4.86	4.96			34.70	34.57

TABLE 2

Infrared characteristic frequencies of the five-coordinate complexes*

Compound	Frequency, cm^{-1}				
				ν_{Pt-X}	
	ν_{OH}	ν_{NH}	$\nu_{C\equiv C}$	X = Cl	X = Br
$Pt(ac)(enMe_4)Cl_2$	3450sh 3417s		1918w 1896m	326s	
$Pt(ac)(enMe_4)Br_2$	3430s		1916w 1888m		257vs
$Pt(ac)(enMe_2Et_2)Cl_2$	3502s		1919w 1865m	310s	
$Pt(ac)(enH_2Me_2)Cl_2$	3470s	3270vs	1878w 1865m	335s	
$Pt(ac')(enMe_4)Cl_2$	3500s		1918w 1892m	325s	
$Pt(ac)(dipy)Cl_2$	3505s		1817w 1892m	330s	

*s = strong, m = medium, w = weak, sh = shoulder, v = very; ac′ = $(CH_3)_2C(OCH_3)C{\equiv}CC(OCH_3)(CH_3)_2$.

quaternization of the $-N(CH_3)_2$ groups is not taking place; cf. Figs. 1 and 2. Figure 2 shows the rate of conversion of $Pt(ac)(enMe_4)Cl_2$ into the cationic compound $[Pt(ac)(enMe_4)Cl]Cl$.

The ultraviolet–visible spectra of the five-coordinate complexes differ significantly from

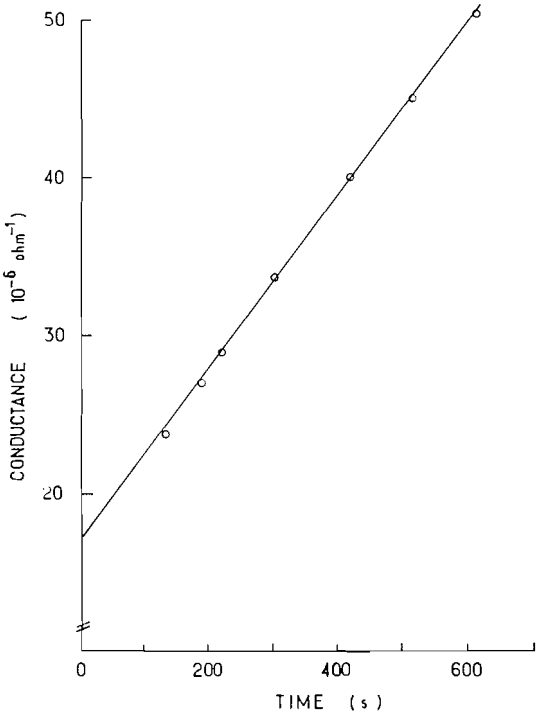

FIG. 1. Conductivity changes of N,N,N′,N′-tetramethylethylenediamine in methanol (1 mmole) with added CH_3I (2%), at 25 °C.

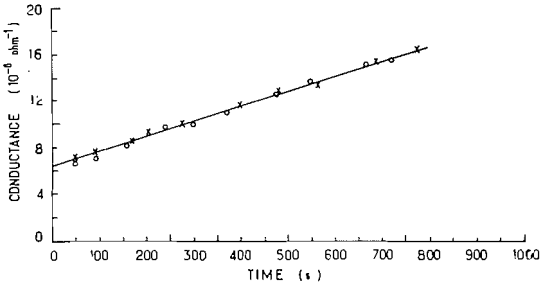

FIG. 2. Conductivity changes of the five-coordinate complex $Pt(ac)(enMe_4)Cl_2$ in methanol (1 mmole) as a function of time at 25 °C: ○, with CH_3I (2%); ×, no CH_3I was added.

those of the square-planar complexes of platinum(II). The low-frequency band at 3000 Å (ε = 1900) and the weak one at 3700 Å (ε = 280) do indicate a five-coordinate complex and suggest a local ligand geometry of trigonal-bypyramidal (11). In general, the colors, band intensities, and positions of these complexes are quite different from those of the square-planar complexes, e.g., K_2PtCl_4, $K[Pt(ac)Cl_3]$, and $[Pt(ac)(enMe_4)Cl]Cl$.

Nuclear magnetic resonance spectra of the complex $Pt(ac)(enMe_4)Cl_2$ in chloroform show a single $-CH_3$ signal shifted downfield by about 0.6 p.p.m. from its uncomplexed, free $(CH_3)_2NCH_2CH_2N(CH_3)_2$ position, indicating that both nitrogens are coordinated.

The infrared spectra of five-coordinate complexes show a strong band in the region 1900–1800 cm^{-1}, which is assigned to the triple-bond

Can. J. Chem. Downloaded from www.nrcresearchpress.com by 210.87.254.42 on 09/05/12
For personal use only.

Can. J. Chem. Downloaded from www.nrcresearchpress.com by 210.87.254.42 on 09/05/12
For personal use only.

TABLE 3

Analytical data and properties of the bridged complexes*

Compound	Color	Melting point (°C)	Calculated, %					Found, %				
			C	H	N	X	Pt	C	H	N	X	Pt
$(PtC_2H_4Cl_2)_2(en)$	Light yellow	163	11.11	2.47	4.32	21.98	60.19	10.90	2.64	4.84	21.90	60.00
$(PtC_2H_4Cl_2)_2(enH_2Me_2)$	Yellow	134	13.35	2.96	4.14		57.60	13.68	2.98	4.45		57.88
$(PtC_2H_4Cl_2)_2(enMe_4)$	Yellow	115	17.05	3.41	3.98		55.40	17.19	3.73	4.33		54.25
$(Pt(ac)Cl_2)_2(en)$	Yellow	155	24.50	4.15	3.23	16.40	45.00	23.97	4.00	3.59	16.66	44.95
$(Pt(ac)Cl_2)_2(enH_2Me_2)$	Bright yellow	122	26.55	4.42	3.10		43.14	27.32	4.77	3.88		41.38
$(Pt(ac)Cl_2)_2(enMe_4)$	Yellow	124	28.33	4.72	3.00		41.85	28.63	4.94	2.94		42.16
$(PtC_2H_4Br_2)_2(en)$	Orange yellow	153	8.73	1.94	3.39	38.70	47.22	9.52	2.56	3.46	39.00	47.02

*Analyses were done by Schwarzkopf Microanalytical Laboratory, 56–19, 37th Avenue, Woodside, New York 11377.

TABLE 4

Infrared characteristic group frequencies of the dinuclear bridged complexes

Compound	Frequency, cm^{-1}*			
	ν_{OH}	ν_{NH}	$\nu_{C\equiv C}$	ν_{Pt-X}
$(Pt(ac)Cl_2)_2(en)$	3454s	3260sh	2040vw	337s
	3426	3216s		
		3140s		
$(Pt(ac)Cl_2)_2(enH_2Me_2)$	3287vsbr	3171s	2034vw	334s
$(Pt(ac)Cl_2)_2(enMe_4)$	3506sh		2040vw	338s
	3440s			324sh
$(Pt(ac)Cl_2)_2(enMe_2Et_2)$	3508s		2020vw	338vs
$(Pt(ac')Cl_2)_2(enMe_4)$	3515s		2036vw	340vs

*s = strong, w = weak, sh = shoulder, v = very, br = broad.

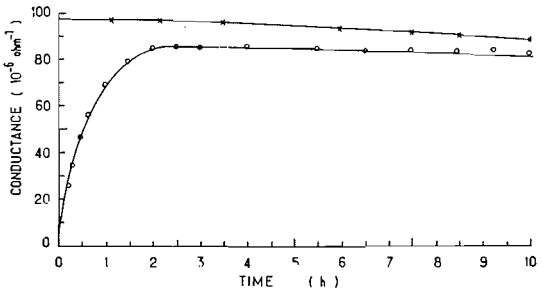

FIG. 3. Conductivity changes of the cationic complex [Pt(ac)(enMe$_4$)Cl] Cl (○) and the five-coordinate complex Pt(ac)(enMe$_4$)Cl$_2$ (×) in methanol (1 mmole) at 25 °C.

stretching frequency $\nu_{C\equiv C}$, lowered on complexation by 300–400 cm^{-1} (see Table 2). These frequencies are lower by 150–200 cm^{-1} than the frequencies of absorption of the $\nu_{C\equiv C}$ in square-planar complexes (2, 3, 6) and the bridging ethylenediamine dinuclear complexes (see Table 4). The intensities of $\nu_{C\equiv C}$ absorption bands in five-coordinate complexes are also greatly enhanced with respect to those of the square-planar or bridging complexes, where this absorption is very weak (see Fig. 4).

The further lowering of the triple-bond absorptions in the five-coordinate complexes, and the strong intensity of the band, as compared to the square-planar and bridging complexes, reveal a stronger involvement of the triple bond with the platinum metal in π bonding, due to a more negative pentacoordinate platinum atom. The high intensity of the band is no doubt due to an asymmetrical disposition of the acetylenic ligand with respect to platinum. The acetylenic bond, from kinetic substitution (12) considerations, should be in the trigonal plane. A deviation from this position towards the axial direction could lead to a rapid decrease in π back-donation due to poor overlap of the orbitals in question.

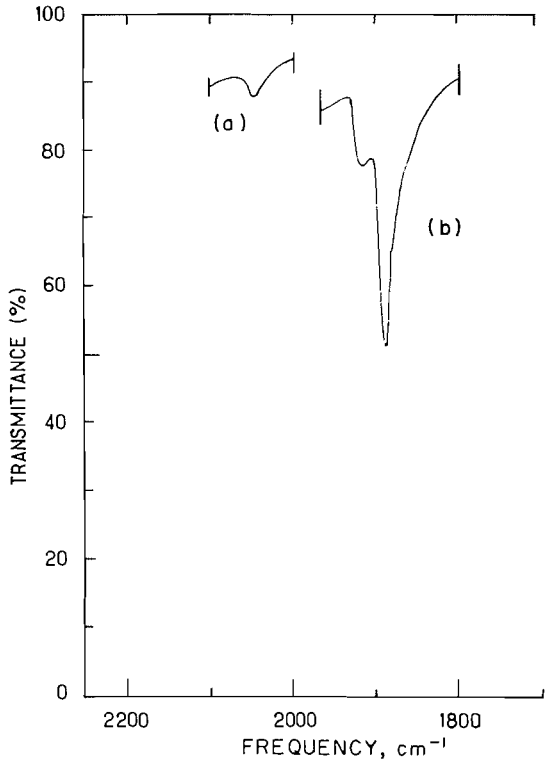

FIG. 4. Comparison of the positions and intensities of the $\nu_{C\equiv C}$ absorption of (*a*) the bridged complex $(Pt(ac)Cl_2)_2enMe_4$ and (*b*) the five-coordinate complex Pt(ac)(enMe$_4$)Cl$_2$.

The OH groups absorb in the region 3450–3500 cm^{-1} in solid samples. The experimental fact that the acetylenic glycol is recovered on decomposition in all these complexes excludes any Pt–O bonding.

Can. J. Chem. Downloaded from www.nrcresearchpress.com by 210.87.254.42 on 09/05/12
For personal use only.

Can. J. Chem. Downloaded from www.nrcresearchpress.com by 210.87.254.42 on 09/05/12
For personal use only.

The Pt—N stretchings are completely masked by the strong C—C≡C—C skeletal modes and could not be assigned. The Pt—Cl stretching frequency gives one sharp band in the 330-cm^{-1} region, which also indicates that the two chlorines are equivalent along the axial positions of the trigonal bypyramid.

The isolation and identification of five-coordinate complexes as intermediates in these platinum complexes is strong evidence of the bimolecular substitution mechanism in the square-planar complexes (12). In the first step of the reaction, one end of ethylenediamine rapidly replaces the highly labilized *trans* chlorine, followed by a fast chelation of the ethylenediamine molecule to form a five-coordinate intermediate (8); this subsequently undergoes a bond rupture of Pt—Cl, giving the cationic complex **3** (see Scheme 2), which loses the acetylenic ligand. The chloride ion then enters the inner coordination sphere by directly replacing the acetylenic ligand, or by means of a solvolytic mechanism, or both (8)

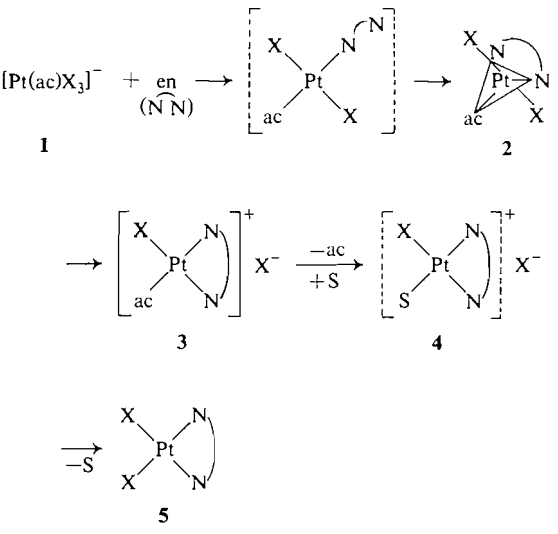

SCHEME 2

where N⌒N = ethylenediamine derivative, S = solvent, X = Cl, Br.

This mechanism is similar to that proposed by Uguagliati *et al.* (13), except for the intermediate pentacoordinate complex **2**.

The reaction of Zeise's salt with ethylenediamine and its N-derivatives, however, does not give stable five-coordinate intermediates and the cationic analogs of the acetylenic complexes (6). The reaction of $PtC_2H_4Cl_2(py)$ with ethylenediamine in tetrahydrofuran gives a white precipitate immediately (no red spot is observed at all here) which is the cationic salt $[PtC_2H_4(en)Cl]Cl$. Unfortunately, this compound does not analyze well, as it is very unstable and changes rapidly into the non-ionic, yellow compound *cis*-$PtCl_2(en)$. The same result is obtained with N-alkyl derivatives of ethylenediamine. The Zeise's-salt-in-water solution reacts rapidly with ethylenediamine (7, 14) or its derivatives (15) and gives the bridged complexes.

Complete infrared assignments for the dinuclear bridging ethylenediamine complexes, $(PtAX_2)_2B$, where A = CO, C_2H_4, or C_2D_4 and B = ethylenediamine or its N-alkyl derivatives, are published (15). Analytical data and physical properties of the bridged complexes $(PtAX_2)_2B$, where A = ac or C_2H_4, are given in Table 3 and infrared characteristic group frequencies in Table 4.

No chelation of ethylenediamine takes place when the Zeise's salt or the carbonyl analog (16) is used, and bridging complexes are always formed. When N-tetramethylethylenediamine is used, a yellow ionic precipitate is formed, of the formula

$$[Me_2\overset{+}{H}N(CH_2)_2\overset{+}{N}HMe_2][PtC_2H_4Cl_3]_2$$

which is easily identified by its infrared spectrum.

The following reactions take place

$$2K[PtC_2H_4Cl_3] + enMe_4 + 2H_2O \rightarrow [enH_2Me_4][PtC_2H_4Cl_3]_2 + 2KOH$$

$$enMe_4 + 2H_2O \rightarrow [enH_2Me_4]^{2+} + 2OH^-$$

The platinum atom in the Zeise's salt apparently is not positive enough to attract and form two coordinate bonds with the two nitrogens of the $enMe_4$ molecule.

The stabilization and isolation of five-coordinate complexes with the acetylenic ligands may also be due to the interaction of the oxygen atoms of the hydroxyl or methoxyl groups with platinum (3). Five-coordinate complexes were obtained only with the ligands $(CH_3)_2C(OH)C{\equiv}CC(OH)(CH_3)_2$ and $(CH_3)_2C(OCH_3)C{\equiv}CC(OCH_3)(CH_3)_2$, but not with $(CH_3)_3CC{\equiv}CC(CH_3)_3$.

The apparent stabilities of the complexes for the above two ligands which gave five-coordinate

Can. J. Chem. Downloaded from www.nrcresearchpress.com by 210.87.254.42 on 09/05/12
For personal use only.

intermediates in terms of N-alkyl ethylenediamine substitution are found to be in the order

$$enMe_4 > enMe_2Et_2 > enH_2Me_2 > en$$

From this order, it is seen that an inductive effect is needed on the nitrogens in order to have a stable complex. The steric effect, however, also plays a great role in the formation of these complexes. The two nitrogen atoms apparently cannot effectively approach the platinum atom when two bulky ethyl groups are on them, and no reaction was observed with this ligand.

Experimental

Preparation of the Five-coordinate Complexes

1. Pt(ac)(enMe$_4$)Cl$_2$

An ice-cold aqueous solution (2 ml) of 0.5 g K[Pt(ac)Cl$_3$] was added to 2 ml of ice-cold 50% aqueous solution of N,N,N′,N′,-tetramethylethylenediamine with continuous stirring. The deep-orange precipitate was crystallized by persistent rubbing against the walls of the beaker. This was left in an ice-bath for about 15 min and then filtered, washed with cold water, and dried in vacuo in the presence of P_2O_5.

2. Pt(ac)(enMe$_4$)Br$_2$

An ice-cold water solution (5 ml) of K[Pt(ac)Br$_3$] (~0.5 g) was added slowly to an ice-cold 50% solution of N,N,N′,N′-tetramethylethylenediamine (2 ml). A deep-red precipitate appeared immediately. This was left in contact with an ice bath for 15 min, and agitated frequently. The precipitate was filtered, washed with cold water, and dried in vacuo over P_2O_5.

3. Pt(ac)(enMe$_2$Et$_2$)Cl$_2$

An ice-cold water solution of K[Pt(ac)Cl$_3$] (0.5 g) was slowly added to 2 ml of an ice-cold 50% solution of N,N′-dimethyl-N,N′-diethylethylenediamine. By stirring continuously and slightly scrubbing the walls of the beaker, after a few minutes a deep orange–red precipitate appeared. This was left in an ice-bath for about 15 min and then filtered, washed with cold water, and dried in vacuo in the presence of P_2O_5.

4. Pt(ac′)(enMe$_4$)Cl$_2$, where ac′ = (CH$_3$)$_2$C(OCH$_3$)C≡CC(OCH$_3$)(CH$_3$)$_2$

An ice-cold solution (2 ml) of 0.5 g K[Pt(ac′)Cl$_3$] (3) was added to 2 ml of an ice-cold solution of N,N,N′,N′-tetramethylethylenediamine. A deep orange–red precipitate appeared immediately. This was left in contact with an ice-bath for 15 min and agitated frequently. The precipitate was then filtered, washed with cold water, and dried in vacuo over P_2O_5. M.p. 90 °C.

5. Pt(ac)(enH$_2$Me$_2$)Cl$_2$

An ice-cold 50% aqueous solution of N,N′-dimethylethylenediamine was added dropwise to a solution (3 ml) of 0.5 g K[Pt(ac)Cl$_3$]. At first a yellow precipitate appeared, then by continuing the dropwise addition of N,N′-dimethylethylenediamine solution and agitating frequently, the precipitate became deep red. The precipitate was then filtered and washed with cold water. This complex is very unstable at room temperature and an elemental analysis could not be made.

Preparation of the Bridged Dinuclear Complexes

1. (Pt(ac)Cl$_2$)$_2$(en)

(*a*) One g of K[Pt(ac)Cl$_3$] was dissolved in 2 ml of ice-cold water and excess potassium chloride (1 g) was added. An 8 ml ice-cold aqueous solution (saturated with KCl) containing 0.06 g of ethylenediamine was then added dropwise. A yellow precipitate was formed immediately and continued to precipitate until the solution became slightly yellow. More water was then added to dissolve all the potassium chloride and the precipitate was filtered off and washed with cold water, dried in a desiccator over calcium chloride, and recrystallized from THF–ether (1:4).

(*b*) An ice-cold aqueous solution (5 ml) of 0.48 g of K[Pt(ac)Cl$_3$] and 0.06 g of ethylenediamine dihydrochloride was made. To this a dilute solution (~0.1 N) of sodium bicarbonate was slowly added dropwise with agitation until a yellow precipitate was formed and the solution became slightly yellow. The solution was then treated as in *1a*.

2. (Pt(ac)Cl$_2$)$_2$(enH$_2$Me$_2$)

The complex was prepared as in *1a* or *1b*, but the reaction was carried out at room temperature.

3. (Pt(ac)Cl$_2$)$_2$(enMe$_4$)

(*a*) A mixture of 0.968 g (2 mmole) of K[Pt(ac)Cl$_3$], 0.188 g (1 mmole) of N,N,N′,N′-tetramethylethylenediamine dihydrochloride, and 0.168 g (2 mmole) of sodium bicarbonate was ground into a fine powder. The mixture was then cooled in an ice-bath and a few drops of water added to make a paste. This was kept in an ice-bath for about 30 min. The yellow precipitate formed was then washed with water, filtered, and dried at 66 °C under vacuum, over P_2O_5.

(*b*) The five-coordinate complex, Pt(ac)(enMe$_4$)Cl$_2$, prepared from 0.5 g of K[Pt(ac)Cl$_3$], was added to an ice-cold aqueous solution (3 ml) containing 0.5 g of K[Pt(ac)Cl$_3$], and agitated for 30 min. The deep-red suspension changed into a yellow suspension, which was filtered off and treated as in *a*.

4. (PtC$_2$H$_4$Cl$_2$)$_2$(en)

This complex was prepared as in *1b* (see also refs. 7 and 14).

5. (PtC$_2$H$_4$Cl$_2$)$_2$(enH$_2$Me$_2$)

The complex was prepared as in *1b*.

6. (PtC$_2$H$_4$Br$_2$)$_2$(en)

This complex was prepared by addition of aqueous ethylenediamine (20%) to a 5-ml solution of K[PtC$_2$H$_4$Br$_3$] (0.5 g). When the supernatant solution became slightly yellow, the precipitate was filtered, washed with cold water, and dried in vacuo over P_2O_5.

7. (PtC$_2$H$_4$Cl$_2$)$_2$(enMe$_4$)

Ethylene gas was passed through a suspension of (Pt(ac)Cl$_2$)$_2$(enMe$_4$) (0.2 g) in 100 ml of ether. After 30 min acetylene in the complex was displaced by ethylene, and the resulting ethylene complex was filtered off (the free acetylene was washed out with ether). The product was dried over P_2O_5 under vacuum. This is one of the rare examples in which ethylene displaces acetylene in a complex.

Infrared spectra were obtained in Nujol mulls or KCl and KBr pellets in the region 4000–200 cm^{-1}, with a Perkin–Elmer Model 621 spectrophotometer. Ultraviolet–visible spectra were obtained at room temperature in methanol or in KBr disks with a Cary 14 spectrophotometer. Nuclear magnetic resonance spectra were obtained with a Varian A-60 spectrometer using tetramethylsilane (TMS) as the internal reference. Conductance measurements were done with 1-mmole solutions of the complexes; a type COM 2C No. 29477 Radiometer, Bach–Simpson, Ltd. and a type E365B Conductoscope, Metrohm, Ltd. being used.

We wish to thank the National Research Council of Canada for financial assistance.

1. S. V. BUKHOVETS. Izv. Sekt. Platiny i Drug. Blagorod. Metal. Inst. Obshch. Neorg. Khim. Akad. Nauk. USSR, **29**, 55 (1955).
2. J. CHATT, R. G. GUY, L. A. DUNCANSON, and D. T. THOMSON. J. Chem. Soc. 5170 (1963).
3. A. D. ALLEN and T. THEOPHANIDES. Can. J. Chem. **44**, 2703 (1966).
4. G. R. DAVIES, W. HEWVERTSON, R. H. B. MAIS, and P. G. OWSTON. Chem. Commun. 423 (1967).
5. S. V. BUKHOVETS and K. A. MOLODOVA. Zh. Neorg. Khim. **2**, 776 (1957).
6. P. C. KONG and T. THEOPHANIDES. Can. J. Chem. **45**, 3193 (1967).
7. A. D. GELMAN and E. A. MEILAKH. C. R. Acad. Sci. USSR, **51**, (3), 207 (1946).
8. J. HUBERT and T. THEOPHANIDES. Inorg. Chim. Acta, **3**, 391 (1969).
9. G. DYER, M. O. WORKMAN, and D. W. MEEK. Inorg. Chem. **6**, 1404 (1967).
10. R. C. TAYLOR, R. DOBSON, and R. A. KOLODNY. Inorg. Chem. **7**, 1886 (1968).
11. M. J. NORGETT, J. H. M. THORNLEY, and L. M. VENANZI. J. Chem. Soc. A, 540 (1967).
12. C. H. LANGFORD and H. B. GRAY. Ligand substitution processes. W. A. Benjamin, Inc., New York. 1965. Chap. 2.
13. P. UGUAGLIATI, UMBERTO BELLUCO, UGO CROATTO, and ROSARIO PIETROPAOLO. J. Amer. Chem. Soc. **89**, 1336 (1967).
14. D. B. POWELL and N. SHEPPARD. J. Chem. Soc. 3089 (1959).
15. P. C. KONG and T. THEOPHANIDES. Can. J. Spectrosc. **14**, 105 (1969).
16. P. C. KONG and T. THEOPHANIDES. To be published.

Can. J. Chem. Downloaded from www.nrcresearchpress.com by 210.87.254.42 on 09/05/12
For personal use only.

Preparation and some reactions of thiomethyl derivatives of aluminum

J. M. LALANCETTE, Y. BEAUREGARD, AND M. BHEREUR
Département de Chimie, Faculté des Sciences, Université de Sherbrooke, Sherbrooke, Québec

Received September 29, 1969

The preparation of $(CH_3S)_2AlCH_3$ and $(CH_3S)_3Al$ from trimethylaluminum and methanethiol is reported. The reaction of CO_2, COS, and CS_2 with $(CH_3S)_2AlCH_3$ yields $(CH_3S)_3C—C(CH_3S)_3$ and thiocarbonates respectively, besides dimethyl disulfide. With the same disubstituted aluminum derivative, phenylacetylene reacted to give $C_5H_5C(SCH_3)CH_2$. A study with deuterated phenylacetylene has permitted us to establish the mechanism of this reaction.

Canadian Journal of Chemistry, **48**, 1093 (1970)

Can. J. Chem. Downloaded from www.nrcresearchpress.com by 210.87.254.42 on 09/05/12
For personal use only.

The reactions of boron derivatives incorporating sulfur and other chalcogens (B_2S_3, $(RS)_3B$, $NaBH_2S_3$, $NaBH_2Te_3$) with various organic substrates have led to new reactions of great synthetic interest (1–4). We have extended this study to the lower elements of group IIIA in order to ascertain the chemistry of similar compounds with the main organic functions. This paper reports some aspects of the reactivity observed with derivatives of aluminum of general formula $(CH_3S)_X\ Al(CH_3)_Y$ where $X + Y = 3$.

Preparation

The literature mentions two preparative techniques concerning the formation of thiomethyl derivatives of aluminum. The first method from Davidson and Brown (5) calls for the direct action of methanethiol on trimethylaluminum. From these authors, this reaction leads to the formation of two compounds: $(CH_3)_2AlSCH_3$ (as a dimer) and the adduct, $(CH_3)_2S \rightarrow Al(CH_3)_3$. Although the mixing of these two reagents can be done on a small scale, using vacuum line techniques we have found that such a procedure cannot be used on a preparative scale since it is extremely hazardous. The second reference is a patent reporting the formation of compounds of formulae $(RS)Al(CH_3)_2$, $(RS_2)AlCH_3$, and $(RS)_3Al$ when 1 mole of trimethylaluminum is treated with 1, 2, or 3 moles of the appropriate mercaptan respectively, in a hydrocarbon solvent (6). We have reproduced this experiment, following exactly the procedure described by the patent and we have never found the compound corresponding to the complete substitution of thiomethyl groups for the 3 methyl groups, even in the presence of a very large excess of methanethiol and prolonged reaction time. What was obtained, in the presence of petroleum ether as diluent, was the compound in which 2 methyl groups were substituted: the methyl bis(methylthio)aluminum designated in this text as the disubstituted compound. If ethyl ether was used as diluent, instead of a hydrocarbon solvent as specified by the patent, then a quantitative yield of the tris(methylthio)aluminum was obtained, the trisubstituted compound. Both compounds appeared as white solids decomposing around 150 °C without a sharp melting point and completely insoluble in the usual solvents with which they do not react. Their composition was established by elementary analysis for aluminum and when indicated, by determination of the volume of methane evolved upon hydrolysis. The determination of aluminum (titrimetric and gravimetric) proved to be difficult because of the tendency of these compounds to retain solvent and excess methanethiol. But when the samples were thoroughly dried under high vacuum and when *extreme* precautions were taken to exclude water from the system, then both methods gave results in very good agreement with the proposed formulation: $(CH_3S)_2AlCH_3$ and $(CH_3S)_3Al$ respectively. In the case of the disubstituted derivative, the sole methyl group on the aluminum was determined as methane by hydrolysis, absorption of the mercaptan over silver nitrate and measurement of CH_4 over saturated potassium hydroxide. This measurement was also in accordance with the proposed formulation. The degree of polymerization of the di- and trisubstituted compounds has not been established since molecular weight measurements could not be performed for lack of solubility. These polymers must be relatively strongly bonded since upon heating there is no sublimation or distillation, decomposition occurring around 150 °C as indicated before.

Reaction with Some Gaseous Species

Upon attempts to study the chemistry of

[1] 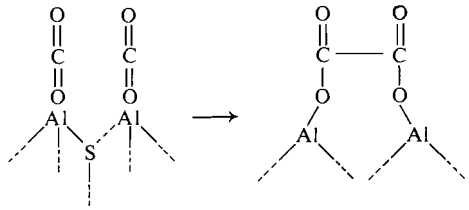 $+ SCH_3 \longrightarrow (CH_3S)_3C{-}C(SCH_3)_3 + CH_3SSCH_3$

[2] $$C_6H_5\overset{\beta}{C}{\equiv}\overset{\alpha}{C}H + (CH_3S)_2AlCH_3 \xrightarrow[2)H_2O]{1)\ \Delta} C_6H_5C(SCH_3){=}CH_2 + Al(OH)_3 + CH_3SH + CH_4$$

[3] $$C_6H_5C(SCH_3){=}CH_2 \xrightarrow[EtOH]{H^{\oplus}} \left[C_6H_5C(OH){=}CH_2\right] \longrightarrow C_6H_5{-}\overset{\overset{O}{\|}}{C}{-}CH_3$$

thiomethyl derivatives of aluminum it was noted that many common gases and solvents were reacting with these derivatives. It was first necessary to ascertain the nature of these reactions. The first gas tried was carbon dioxide. When the disubstituted derivative was treated with a stream of CO_2 at 55–57°, hexathiomethyl ethane $(CH_3S)_3C{-}C(CH_3S)_3$ and dimethyl disulfide $(CH_3S)_2$ were recovered. Those 2 compounds were identified by elementary analysis, infrared (i.r.), nuclear magnetic resonance (n.m.r.), and mass spectrometry. This reaction is heterogeneous and the very nature of the products formed suggests a radical mechanism. The formation of the ethane derivative could be understood as a radical condensation proceeding in a similar fashion as the pinacol reaction (eq. [1]). A dimerization of the CH_3S radical appearing in the course of the reaction would then explain the formation of dimethyl disulfide.

In the case of carbon disulfide, 3 products were obtained from the reaction with the disubstituted aluminum derivative: dimethyl disulfide, methyl dithiocarbonate $(CH_3S)_2C{=}O$, and methyl trithiocarbonate $(CH_3S)_2C{=}S$. Those substances were identified by the usual measurements (n.m.r., i.r., and mass spectrometry) and by comparison with synthetic samples.[1] With carbon oxisulfide COS, only dimethyl disulfide and methyl trithiocarbonate were observed. The absence of dimerization with carbon disulfide and carbon oxisulfide suggested a mechanism different from the one observed for CO_2, although, probably still radicalar in nature because of the presence of dimethyl disulfide in large amounts in the reaction products. No reactions were observed, below 100 °C, with carbon monoxide, ammonia, or hydrocyanic acid.

Reactions with Alkynes

The reaction of the disubstituted aluminum derivative with phenyl acetylene gave 1-thiomethyl - 1 - phenylethene $C_6H_5(CH_3S)C{=}CH_2$ with a yield of the order of 50%, even in the presence of a large excess of the disubstituted aluminum derivative (eq. [2]). The structure of the aromatic olefin was established through the usual measurements and the position of the $S{-}CH_3$ groups was confirmed by hydrolysis of the SCH_3 group, leading exclusively to acetophenone (eq. [3]).

In relation with the mechanism of this reaction, the first point examined was the source of the hydrogen appearing on the α-carbon of the alkyne. Three sources are possible, a priori: from the methyl group on aluminum, from water in the course of the hydrolysis, or from a second molecule of phenylacetylene. From n.m.r. measurements, the presence of the methylene group in the reaction mixture can be established before hydrolysis. The reaction was repeated using d_1-phenylacetylene. Under these conditions, even with hydrolysis by H_2O, an olefin fully deuterated in the α position was obtained, indicating that

[1]The presence of the methyl dithiocarbonate is explained by the easy oxidation of methyl trithiocarbonate, the reaction in that case being done in the presence of air.

Can. J. Chem. Downloaded from www.nrcresearchpress.com by 210.87.254.42 on 09/05/12
For personal use only.

[4] $$2C_6H_5C{\equiv}CD + (CH_3S)_2AlCH_3 \xrightarrow[2)\ H_2O]{1)\ \Delta} C_6H_5C(SCH_3){=}CD_2 + C_6H_5C{\equiv}CH + \text{other products.}$$

hydrogen must come from a second molecule of starting alkyne and neither water nor methyl group on aluminum (eq. [4]).

If the reaction mixture obtained with non-deuterated phenylacetylene is hydrolyzed with heavy water, the olefin does not contain deuterium but the unreacted alkyne then incorporates deuterium. Under the experimental conditions used for the hydrolysis we have shown that less than 5% of the phenylacetylene exchanged with heavy water. Consequently, the formation of deuterated phenylacetylene in the course of the hydrolysis by D_2O of the reaction mixture cannot be a mere exchange reaction. The 50% yield of olefin and the presence of deuterated phenylacetylene in the reaction products can be explained by the following mechanism (eq. [5]).

A similar reaction was tried with 1-phenyl-1-butyne, -1-hexyne, and 3,3-dimethyl-1-butyne but the starting material was recovered in all cases unaffected by the treatment. Consequently, it appears that both a terminal triple bond and activation by the aromatic group, as in phenylacetylene, are required to promote the reaction.

Experimental

Infrared measurements were made on a Perkin–Elmer spectrometer, model 257, in carbon tetrachloride solutions. The n.m.r. measurements were performed with a Varian A-60 instrument, using tetramethylsilane as internal reference. Mass spectrometric determinations were made with a Hitachi Perkin–Elmer machine, model RMV-6D. Melting points are not corrected; elementary analysis are from Schwarzkopf Microanalytical Laboratory, New York. Vapor-phase chromatography (v.p.c.) measurements were made with a Microteck G-2000-R instrument.

1. Preparation of Thiomethyl Derivatives of Aluminum

1.1 Preparation of Methyl Bis(methylthio)aluminum

The reaction was performed in a 5 l flask bearing a pressure equilibrated adding funnel of 1 l capacity, a condenser operating at −70° with Dry Ice and a system for introduction of trimethylaluminum. The whole system was flushed with nitrogen and dried by flame warming. After cooling, 2 l of dry pentane were introduced in the flask and 250 g of trimethylaluminum (K & K Chemicals) added in 1 portion to the diluent. Extreme caution must be exercised in the course of this experiment since trimethylaluminum inflames spontaneously in air and explodes violently upon contact with water. Methanethiol was then added to the solution of trimethylaluminum. The mercaptan (1 kg, large excess) was diluted (50/50 in volume) with pentane and was added over a period of 1 h, the reaction mixture being stirred magnetically and kept at a temperature of 6–12° with an acetone/Dry Ice bath during the addition. After 2 h, the precipitation of a white solid began and the system was allowed to reach room temperature over a 24 h period. Pentane was then evaporated and the white solid lumps (433 g) broken

[5]

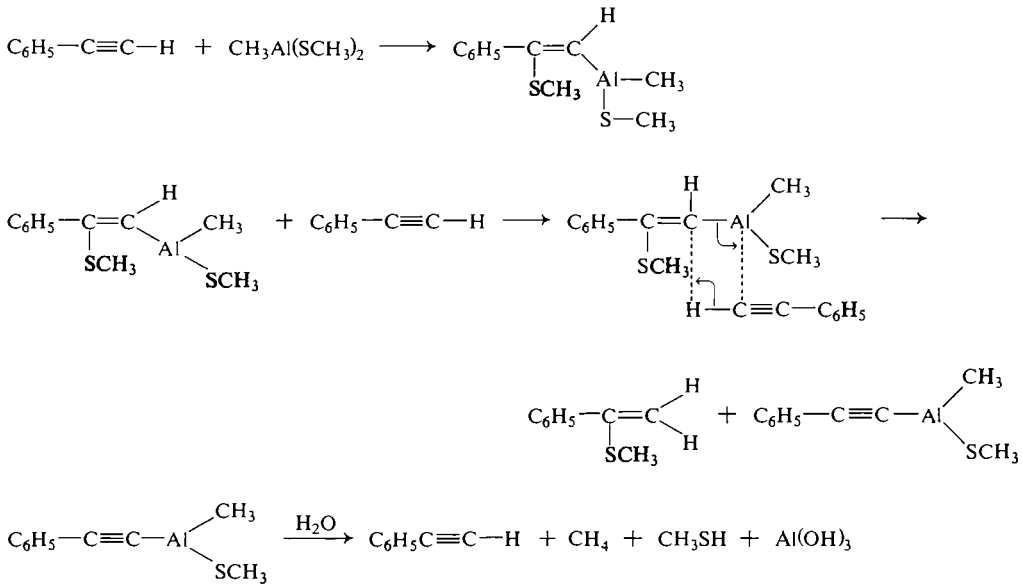

Can. J. Chem. Downloaded from www.nrcresearchpress.com by 210.87.254.42 on 09/05/12
For personal use only.

Can. J. Chem. Downloaded from www.nrcresearchpress.com by 210.87.254.42 on 09/05/12
For personal use only.

under nitrogen atmosphere, was methyl bis(methylthio)-aluminum. This material decomposed without a sharp melting point around 150°. It was insoluble in all common solvents, such as benzene, pentane, ether and gave reactions with solvents bearing carbonyl groups. The analysis for aluminum was not easily performed. First, the last traces of pentane and excess mercaptan proved very difficult to remove, except under high vacuum for 24 h. Secondly, the slightest hydrolysis, the compound is extremely hygroscopic, produced aluminum oxide that could not be dissolved. So, the whole manipulation of the sample, even after weighing had to be carried out under nitrogen atmosphere. When these precautions were used, it was then possible to obtain reproducible results in accordance with the formulation proposed above. Two different methods for the evaluation of the aluminum were used.

The first method was gravimetric, using hydroxyquinoline as complexing agent (7). In a typical experiment, a 0.152 g sample was dissolved in 20 ml of concentrated sulfuric acid. This solution was then diluted to 250 ml and an aliquot of 25 ml analyzed for aluminum gave 20.6% Al. Calculated for Al in $(CH_3S)_2AlCH_3$: 19.8%.

The second method was titrimetric (8). The sample (0.134 g) was dissolved in concentrated sulfuric acid (20 ml) and diluted to 250 ml. A 20 ml aliquot was then adjusted at p*H* 3.0 with NaOH 0.1 *N*. The curve of the variation of p*H* when titrating this solution with 0.05 *N* NaOH, against volume of NaOH was traced and the difference between the 2 p*H* plateau was related to the aluminum content of the solution. Found for Al: 20.1%.

A third analysis was performed by hydrolysis of $(CH_3S)_2AlCH_3$, measuring the methane evolved. The methanethiol and methane formed upon hydrolysis were carried by a stream of CO_2. The mercaptan was absorbed by silver nitrate scrubbers and methane measured over a concentrated solution of potassium hydroxide, in a similar fashion as the Dumas determination of nitrogen. Volume of CH_4 calculated for 0.100 g of $(CH_3S)_2AlCH_3$: 16.4 ml. Found: 16.5 ml.

1.2 Preparation of Tris(methylthio)aluminum

Using a similar technique as described in 1.1, except that ethyl ether instead of pentane was used as solvent, the tris-methylthio derivative was obtained. It is a white solid, insoluble in common solvents and decomposing around 150°. Calculated for $(CH_3S)_3Al$: Al 16.0%. Found (gravimetric) 16.1%; (titrimetric) 16.3%.

2. Reaction with Carbon Dioxide

A 5 g sample of the disubstituted derivative was treated by a slow stream of CO_2 at 80° for 1 h. In the course of this reaction, the white solid aluminum derivative was slowly transformed in a viscous yellow liquid. After cooling, the reaction mixture was taken up with 150 ml of ether and hydrolyzed with 10 ml of water. The ether fraction was filtrated, dried over magnesium sulfate, and the solvent distilled. The residual material (2.50 g of a yellow oil) was fractionated by v.p.c. The first fraction (20%) was identified as dimethyl disulfide by comparison of i.r. and n.m.r. with an authentic sample. The crude reaction mixture, by chromatography over aluminum oxide (Woehm, activity I in petroleum ether) gave 2.0 g of a white solid, m.p. 55–57°: hexathiomethylethane.

The following measurements on $(CH_3S)_3CC(SCH_3)_3$ proved its structure: n.m.r. singlet at 2.15 δ; mass spectrum: *m/e* 153 ($(CH_3S)_3C$), 91 (CH_3S—C=S), 76 (CS_2), 47 (CH_3S).

Anal. Calcd. for $C_8H_{18}S_2$: C, 31.37; H, 6.22; S, 62.41. Found: C, 32.81; H, 6.42; S, 60.89.

The discrepancies between calculated and found values are explained by the very high percentage of sulfur in the compound, rending difficult the elementary analysis.

3. Reaction with Carbon Disulfide

In a 250 ml flask, a 10 g sample of the disubstituted compound was treated by 20 g of CS_2 in 100 ml of dry pentane. The reaction mixture was stirred at room temperature for 25 h. The reaction products were extracted with ethyl ether after hydrolysis. Filtration, drying of the solvent, and evaporation gave 6.3 g of a yellow oil. By v.p.c. analysis, the crude product contained 3 substances, dimethyl disulfide (42%), methyldithio carbonate $(CH_3S)_2C$=O (36%), and methyl trithiocarbonate $(CH_3S)_2C$=S (22%). Dimethyl disulfide was identified as above. By chromatography over aluminum oxide (Woehm, activity I in petroleum ether) methyl dithiocarbonate and methyl trithiocarbonate were separated. The structure of these 2 thiocarbonates was established by comparing i.r., n.m.r., and mass spectrometry measurements on the reaction products with those on synthetic samples. Methyl dithiocarbonate was prepared by the action of methanethiol on phosgene (9). The n.m.r.: singlet at 2.41 δ; i.r.: bands at 1660 (strong), 1430 (medium), 1380 (medium), 1250 (strong), 1055 cm^{-1} (strong); mass spectrometry: *m/e* 122 ($(CH_3S)_2C$=O), 94 (CH_3SSCH_3), 75 (CH_3SCO), 48 (CH_3SH), 15 (CH_3). Methyl trithiocarbonate was obtained by the reaction of methanethiol on thiophosgene (10). The n.m.r.: singlet at 2.61 δ; i.r.: bands at 1440 (strong), 1425 (medium), 1100 (very strong), 1080 (strong), 985 (medium), 970 cm^{-1} (medium); mass spectrometry: *m/e* 138 ($(CH_3S)_2C$=S), 91 (CH_3S—C=S), 76 (CS_2), 48 (CH_3SH), 15 (CH_3).

4. Reaction with Carbon Oxysulfide

A 2.0 g sample of the disubstituted derivative was treated by a slow stream of COS at 160° for 48 h. After extracting the reaction mixture with ether, 0.50 g of a yellow oil was obtained. From v.p.c. analysis, this oil was a mixture of dimethyl disulfide (20%) and methyltrithiocarbonate (80%). These products were separated by chromatography over alumina, as indicated above and physical measurements (n.m.r., i.r., and mass spectrometry) confirmed their identity.

5. Reactions with CO, NH_3, HCN

A 2.0 g sample of the disubstituted derivative was treated by a slow stream of CO at 25° and subsequently at 100°. No reaction was observed. A similar behavior was noted with ammonia and anhydrous hydrocyanic acid.

6. Reaction with Alkynes

6.1 Reaction with Phenylacetylene

In a 250 ml flask, a suspension of 10 g of the disubstituted derivative in 150 ml of petroleum ether was refluxed for 48 h with 10 g of phenylacetylene. After hydrolysis by 10 ml of water at 0 °C, the solution was filtered, dried and the solvent evaporated. This way,

5.4 g of a liquid, b.p. 116–120°/12 mm, was obtained. It was identified as 1-thiomethyl 1-phenyl ethene. Infrared bands at 1590 (medium), 1575 (medium), 1495 (strong), 1450 (medium), 1230 (medium), 1070 (medium), 1030 (medium), 850 cm^{-1} (strong); n.m.r.: singlet at 2.21 (3H), singlet at 4.91 (1H), singlet at 5.36 (1H), multiplet around 7.3 δ (5H); mass spectrometry: *m/e* 150 (molecular ion), 149 ($C_6H_5C_3H_4S$), 135 ($C_6H_5C_2H_2S$), 103 ($C_6H_5C_2H_2$), 91 ($C_6H_5CH_2$), 77 (C_6H_5).

6.2 Preparation of Phenylacetylene-d_1

In a 500 ml flask 12 g of $NaNH_2$ in the presence of 250 ml of anhydrous ethyl ether were treated with 20 g of phenylacetylene. After a 2 h reflux, the reaction mixture was hydrolyzed with D_2O. The usual operations gave a phenylacetylene 85% d_1. To increase this percentage, the partially deuterated compound was kept in contact with CaO in the presence of D_2O for 25 h. The usual operations gave $C_6H_5C{\equiv}CD$, 96% d_1. The i.r.: bands at 2595 (very strong), 1480 (very strong), 1445 cm^{-1} (very strong); n.m.r.: multiplet at 7.41 δ; mass spectrometry *m/e*: 103 (C_6H_5—$C{\equiv}CD$), 77 (C_6H_5).

6.3 Reaction of Phenylacetylene-d_1

Starting with $C_6H_5C{\equiv}CD$ and using a procedure similar as in 6.1, the reaction gave $C_6H_5(CH_3S)C{=}CD_2$ exclusively, the hydrolysis being done with ordinary water. The i.r.: bands at 1670 (strong), 1590 (medium), 1575 (medium), 1490 (medium), 1480 (strong), 1440 (strong), 1260 (strong), 980 (medium), 780 (strong), 750 cm^{-1} (very strong); n.m.r.: singlet at 2.21 (3H), multiplet at 7.3 δ (5H); mass spectrometry *m/e*: 152 (molecular ion), 105 ($C_6H_5C_2D_2$), 77(C_6H_5).

When the hydrolysis of the crude reaction mixture obtained in 6.1 was done with D_2O, $C_6H_5(CCH_3)C{=}CH_2$ was the sole product of the reaction, by its i.r., n.m.r., and mass spectra. But the unreacted phenylacetylene was then incorporating more than 95% of d_1. In order to establish that the phenylacetylene-d_1 was not produced by an exchange reaction, ordinary phenylacetylene, D_2O, and the disubstituted derivative were placed simultaneously in ethyl ether and refluxed for 1 h, in conditions similar to those used in the course of the hydrolysis. Then, only 5% of deuterium was introduced by the phenylacetylene, as indicated by i.r. and n.m.r.

6.4 Reaction with Other Alkynes

Attempted reactions with 1-phenyl-1-butyne, -1-hexyne, and 3,3-dimethyl-1-butyne according to the procedure as in 6.1 led to the quantitative recovery of the starting alkynes.

We thank the National Research Council of Canada and the Defence Research Board of Canada (grant 9530-30) for financial assistance.

1. J. Brault and J. M. Lalancette. Can. J. Chem. **42**, 2903 (1964).
2. J. M. Lalancette and A. Lachance. Can. J. Chem. **47**, 859 (1969).
3. J. M. Lalancette and A. Freche. Can. J. Chem. **47**, 739 (1969).
4. J. M. Lalancette and M. Arnac. Can. J. Chem. **47**, 3695 (1969).
5. N. Davidson and H. C. Brown. J. Amer. Chem. Soc. **64**, 320 (1942).
6. K. Kctosaka *et al.* U.S. Patent 3 082 234 (1963).
7. A. Claassen and L. Bastings. Anal. **92**, 614 (1967).
8. G. Charlot. Les méthodes de la chimie analytique. Masson et Cie, Paris, 1966, p. 299.
9. H. Pelster and E. Muhlbauer. Holland Patent 1 181 205 (1964).
10. H. C. Godt and R. E. Wann. J. Org. Chem. **26**, 4047 (1961).

Can. J. Chem. Downloaded from www.nrcresearchpress.com by 210.87.254.42 on 09/05/12
For personal use only.

Can. J. Chem. Downloaded from www.nrcresearchpress.com by 210.87.254.105 on 09/05/12
For personal use only.

Nuclear magnetic resonance studies. XX.[1] Structures and ^1H nuclear magnetic resonance parameters of the bromination products of some substituted bicyclo[2.2.2]octenes

M. GORDON, GURUDATA,[2] AND J. B. STOTHERS
Department of Chemistry, University of Western Ontario, London, Ontario

Received October 27, 1969

The stereochemical course of the reaction of some 7,8-dicarboxylate derivatives of 1,3,5,5-tetramethylbicyclo[2.2.2]oct-2-ene with bromine has been established. The proton magnetic resonance parameters of these products are discussed.

Canadian Journal of Chemistry, **48**, 1098 (1970)

Introduction

In a recent investigation of the proton magnetic resonance (p.m.r.) parameters of bicyclo-[2.2.2]octenes (1) a number of 7,8-disubstituted derivatives of 1,3,5,5-tetramethylbicyclo[2.2.2]-oct-2-ene (**1**) were synthesized. As confirmation

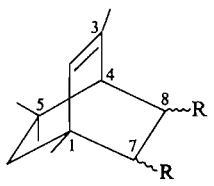

1

of the assignments for the C-7, -8 carboxyl substituents, the bromination of these unsaturated materials was examined since bromolactones are expected to form in those cases in which a carboxyl function is in an *endo* orientation with respect to the olefinic bond. It has been found that the stereochemical course of the bromination reaction depends on the orientation of these substituents and these results for 4 bicyclic olefins, **2**–**5**, are summarized in Scheme 1. We wish to describe these experiments in the present paper and to compare the proton nuclear magnetic resonance (n.m.r.) parameters with those in the less strained bicyclo[2.2.2]octane systems.

Experimental

Infrared (i.r.) spectra were obtained with either a Beckman IR 5A or a Beckman IR 10 spectrophotometer. The n.m.r. parameters were determined from spectra obtained with a Varian HA 100 spectrometer. Comparisons of these spectra with those calculated using the LAOCOON III program[3] permitted complete analyses of the spectra for most compounds; the signs of the coupling constants are positive unless otherwise indicated. In a few cases a complete set of parameters could not be obtained because of overlapping multiplets. The precision of the data is judged to be within 0.01 p.p.m. for the shieldings and 0.1 Hz for the coupling constants. Elemental analyses were performed by A. Bernhardt, Mulheim, Germany.

Preparation of **6**

(a) Bromination of Anhydride **2**

Adduct **2** (1.0 g) was dissolved in a warm solution of potassium hydroxide (1.5 g) in water (25 ml) and bromine was added until a pale yellow color persisted. After acidifying, a crystalline precipitate formed which was separated and crystallized from methanol, m.p. 214–215°. This material gave a positive test for bromine. Treatment with ethereal diazomethane in the usual fashion yielded the crystalline bromolactone ester **6**. Recrystallization from either petroleum ether or ether gave **6**, m.p. 152–153°, ν ($CHCl_3$) 1785, 1735 cm^{-1}.

Anal. Calcd. for $C_{15}H_{21}O_4Br$: C, 52.18; H, 6.13; Br, 23.15. Found: C, 52.04; H, 6.18; Br, 22.98.

(b) Bromination of cis-Diester **3**

Treatment of **3** (0.82 g), dissolved in acetic acid, with a solution of bromine in acetic acid until the color persisted afforded, after work-up, **6** (0.98 g) having physical constants identical to those noted above.

Debromination of **6**

A solution of **6** (275 mg) in glacial acetic acid (10 ml) was refluxed with 200 mg of zinc dust for 15 min. A crystalline solid separated out on cooling and the rest was isolated by chloroform extraction to yield a total of 210 mg of crude product. After recrystallization from a petroleum ether – benzene mixture, the product was

[1]Part XIX see ref. (7).

[2]Petroleum Research Fund Predoctoral Fellow, 1964–1965; Ontario Graduate Fellowship 1966–1967. Present address, Department of Chemistry, Sir George Williams University, Montreal, Canada.

[3]We wish to thank Prof. A. A. Bothner-By and Dr. S. Castellano for kindly providing a listing of their LAOCOON III program and Dr. John Wasson for his assistance in adjusting the program to fit on the U.W.O. 7040 computer.

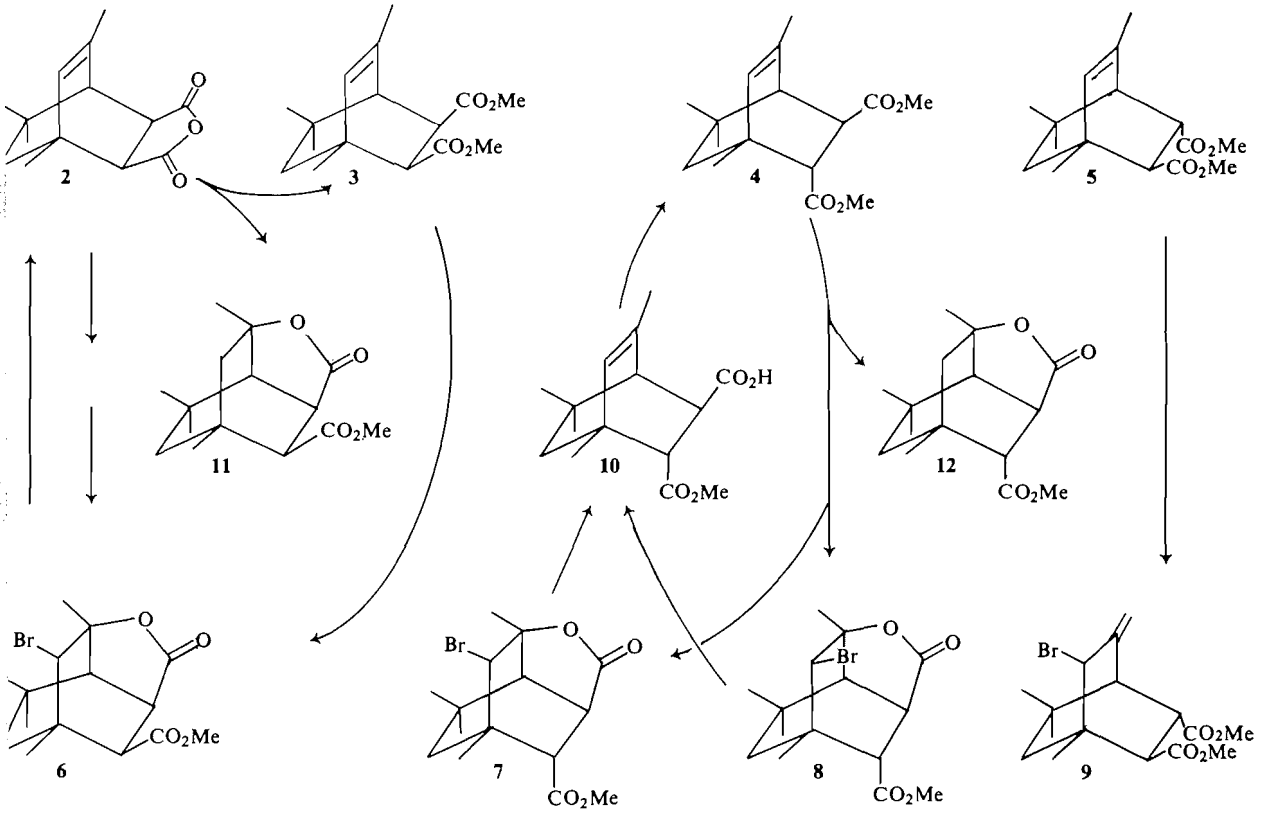

SCHEME 1

shown to be identical to the *cis-endo* anhydride **2** (1) by mixed melting point (99.0–100.0 °C) and its i.r. and n.m.r. spectra.

Bromination of trans-Diester 4

(a) Isolation of 8

To a solution of 7.3 g of **4** in ca. 50 ml of glacial acetic acid was added a 5% (v/v) solution of bromine in glacial acetic acid dropwise with continuous stirring. When a pale orange color persisted, the addition was stopped and the reaction mixture allowed to stand for ca. 1 h.

After dilution with water, the product was extracted with chloroform. After the usual work-up, the residue was cooled and a small amount of anhydrous ether added; immediate crystallization of part of the product occurred.

From a total crude yield of 8.8 g, 3.5 g of crystalline material was obtained. Recrystallization from diethyl ether gave **8**, m.p. 176–177°; ν ($CHCl_3$) 1786, 1739 cm^{-1}.

Anal. Calcd. for $C_{15}H_{21}O_4Br$: C, 52.18; H, 6.13; Br, 23.15. Found: C, 52.02; H, 6.04; Br, 23.08.

(b) Isolation of 7 and 12

The mother liquors were chromatographed on a column made from silicic acid (Fisher) which had been heated at 135 °C for 5 days. Several fractions were eluted with ether–benzene (1:9) to yield a total of 2.85 g of crude material. These were grouped on the basis of their p.m.r. spectra.

Group 1 (1.2 g) comprised several components which were inseparable while the second group (1.23 g) yielded crystalline **7** (from ether), m.p. 128° (decomposition); ν ($CHCl_3$) 1775, 1730 cm^{-1}.

Anal. Calcd. for $C_{15}H_{21}O_4Br$: C, 52.18; H, 6.13; Br, 23.15. Found: C, 52.05; H, 6.18; Br, 23.34.

A third group yielded 195 mg of a white crystalline solid (from ether) which was shown to be **12** (1).

Preparation of 12 from 4

Compound **4** (1 g) was dissolved in a few ml of glacial acetic acid and 100 ml of 5% sulfuric acid added; a small amount of methanol was added to redissolve the solid which separated out. The mixture was warmed overnight on a steam bath. On cooling, starting material was recovered unchanged.

The recovered material was dissolved in 50 ml of glacial acetic acid and refluxed for about 1 h. The solvent was removed on a rotary evaporator and the residue dissolved in ether. After washing with 10% aqueous sodium carbonate followed by water, the neutral ether solution was dried over anhydrous magnesium sulfate.

Removal of drying agent and solvent yielded 0.7 g of a white crystalline material. Recrystallization from petroleum ether (35–60°) gave a product, melting at

Can. J. Chem. Downloaded from www.nrcresearchpress.com by 210.87.254.105 on 09/05/12
For personal use only.

Can. J. Chem. Downloaded from www.nrcresearchpress.com by 210.87.254.105 on 09/05/12
For personal use only.

100.5–101.0°, whose i.r. spectrum and p.m.r. spectra were identical with those of **12** (1).

Debromination of 7 and 8

Bromolactone **8** (500 mg) was dissolved in 10 ml of methanol and 5 ml of glacial acetic acid was added followed by 200 mg of zinc dust. The mixture was refluxed for 2 h. After cooling, the zinc was removed by filtration, the filtrate diluted with water and extracted with several portions of chloroform. The work-up gave a syrupy liquid (350 mg) which crystallized on standing. Compound **10** melts at 148–149°; ν ($CHCl_3$) 1720, 1700 cm^{-1} and broad OH absorption.

Anal. Calcd. for $C_{15}H_{22}O_4$: C, 67.64; H, 8.33. Found: C, 67.72; H, 8.59.

The above procedure with **7** gave identical results.

Methylation of Compound 10

A solution of 100 mg of the half ester, **10**, in anhydrous ether was cooled in an ice-bath and a slight excess of an ethereal solution of diazomethane added dropwise. Removal of excess diazomethane and evaporation of solvent gave a quantitative yield of **4**, the identity of the 2 compounds being established by mixed melting point, i.r., and p.m.r. spectroscopy.

Bromination of trans-Diester 5

The bromination was carried out in the manner described for the bromolactonization of **4**. Reaction of 135 mg of 7-*endo*-8-*exo*-diester gave 136 mg of crude product (melting range 115–120 °C). After 2 recrystallizations from anhydrous ether, compound **9** melted at 127.5–129.5°, ν ($CHCl_3$) 1730, 1620, 900 cm^{-1}.

Anal. Calcd. for $C_{16}H_{23}O_4Br$: C, 53.49; H, 6.45; Br, 22.24. Found: C, 53.88; H, 6.33; Br, 22.20.

Ozonolysis of 9

The ozonolysis was carried out at −70 °C on 28 mg of the compound in ethyl acetate. Work-up with a formic acid – hydrogen peroxide (3:1) mixture gave 25 mg of crude product which was crystallized from chloroform. Its proton spectrum showed no peaks corresponding to CH_3—C=O, —COOH, or —CHO while its i.r. spectrum showed absorption at 1725 cm^{-1}. This ketone gave a 2,4-dinitrophenylhydrazone, melting at 121–122°.

Results and Discussion

The chemical and physical evidence necessary for the structural assignments of the bromination products **6–9** are described before a more detailed consideration of the proton parameters is presented. Some of the latter are mentioned briefly as a part of the structural elucidation and amplified in the final section.

Treatment of the *endo*-adduct **2** in dilute base with bromine proceeds smoothly and virtually quantitatively to give a single crystalline product which is readily methylated to yield a crystalline bromolactone ester **6**. The same compound is formed directly, and in comparable yield, by treatment of *cis*-diester **3** with bromine in acetic acid. The presence of the γ-lactone function is shown by its i.r. absorption at 1783 cm^{-1} in addition to that of the carbomethoxyl at 1735 cm^{-1}. Since all methyl groups give rise to singlet signals in the proton spectrum the point of attachment of the lactone must be C-3. The bromine atom is assigned the *anti*[4] orientation since no long-range coupling is resolved in the absorption of the C-7 proton. That the C-2 proton is long-range coupled (J = 2.2 Hz) to the *exo* proton on C-6 was established by a decoupling experiment in which the splitting of the C-2 proton signal was eliminated by irradiation in the C-6 methylene region. Since the same bromolactone is produced in very high yield from anhydride **2** and diester **3**, in basic and acidic media, respectively, there is little likelihood of epimerization at C-7. Proof that skeletal rearrangement does not accompany bromination is given by the regeneration of **2** from **6** by treatment with zinc dust. The formation of **6**, therefore, proceeds in the expected manner.

In contrast to the bromination of **3**, *trans*-diester **4** gives 3 major products upon treatment with bromine in acetic acid, 2 of which, **7** and **8**, contain bromine and both have a γ-lactone ring as shown by their i.r. absorptions at 1775 and 1786 cm^{-1}, respectively. The point of attachment again must be C-3 since the methyl signals are singlets for each. The bicyclo[2.2.2]octene skeleton has not rearranged since both compounds are readily converted back to the starting material by reaction with zinc dust to give **10**, a half ester, which may be methylated with diazomethane to **4**. Thus, the orientation of the carboxyl functions is not affected by this reaction sequence. Further confirmation of the *exo*-carbomethoxyl grouping at C-7 is provided by the C-7 proton pattern. This signal is an apparent "triplet" and was shown by spin-decoupling to be long-range coupled to both the *endo*-C-6 and C-8 protons. The orientation of the bromine atom in **7** and **8** is assigned on the basis of n.m.r. evidence. For **7**, the C-2 proton absorption is similar to that in **6** having a long-range coupling to the *exo*-C-6 proton and the C-3 methyl signal appears at the same position in **6** and **7**, δ 1.79,

[4]For convenience, we distinguish the orientation of the bromine atom on C-2 by the terms *syn* and *anti* with respect to the C-7,8 bond and the orientation of substituents on the C-5,6 and C-7,8 bonds as *exo* or *endo* relative to the C-2,3 bond, by analogy with the bicyclooctenes.

Can. J. Chem. Downloaded from www.nrcresearchpress.com by 210.87.254.105 on 09/05/12
For personal use only.

indicating that the C-2 bromine is *anti*. In the spectrum of **8**, however, the C-2 proton appears as a singlet with no resolved long-range coupling constant, the C-3 methyl group appears at higher field, 1.61 p.p.m., while the C-7 proton is deshielded by 0.17 p.p.m. relative to that in **7**. On this basis, the C-2 bromine is assigned the *syn* orientation. An interesting feature of the bromination of **4** is that **8** is the predominant product (ca. 50%) and it has the *cis*-arrangement for the bromine and lactone groups. The simplest view is that *cis*-addition occurs preferentially, although other routes may be envisaged. An indication that addition proceeds on the less-hindered side of the double bond in **4** is the fact that catalytic hydrogenation yields the corresponding saturated diester, i.e. that in which the C-3 methyl is *anti* (1).

The third product isolated also contains a γ-lactone ring, ν ($CHCl_3$) 1770 cm^{-1}, and an ester (1735 cm^{-1}) but no bromine. Again the lactone involves the C-3 position since the methyl signals are singlets. Structure **12** was assigned to this compound since it can be generated from **4** by treatment with acid, as reported previously (1).

A third variation in the course of the bromination reaction of this series was found for *trans*-diester **5**. A single crystalline product **9** was isolated in good yield (ca. 70%). The presence of an olefinic bond is indicated by i.r. and proton spectra in $CDCl_3$ solution. The latter also shows that 2 carbomethoxyl functions are present (δ 3.67 and 3.70) as well as 3 methyl groups on quaternary carbons (δ 0.85, 0.95, 1.12). The *trans* disposition of the carbomethoxyl groups is retained since the vicinal coupling of the C-7 and C-8 protons at 3.01 and 2.90 p.p.m. respectively is 7.9 Hz; the latter is coupled, $J = 1.8$ Hz, to the bridgehead proton at δ 2.90. Two olefinic protons δ 4.07, are readily attributed to an *exo*-methylene group at C-3, accounting for the "loss" of one methyl signal. The C-2 proton appears at 5.85 p.p.m. The C-5 protons absorb at 0.96 and 1.32 p.p.m. ($J_{AB} = -12.7$ Hz) with the former long-range coupled to the bridgehead proton, $J = 3.6$ Hz. Comparison with the computed spectrum for the 6-spin system including the methine protons and the C-6 methylene group showed each line to be within 0.2 Hz of the observed position. The mass spectrum[5] of **9** exhibits 2 almost equally intense peaks at *m/e* 358 and 360 consistent with the molecular formula $C_{16}H_{23}O_4Br$. The formation of an allylic bromide from **5** appears to be a reasonable consequence of the fact that the carbomethoxyl group on C-8 is *exo*. Thus, the intermediate carbonium ion resulting from attack of Br^+ at C-2 on the less-hindered side, preferentially loses a proton before any available nucleophile reacts at C-3. Skeletal rearrangement of the system to a bicyclo[3.2.1]-octane derivative is ruled out by the fact that there are only 3 methyl signals.

Ozonolysis of **9** afforded a single crystalline product whose proton spectrum contained no signals attributable to acetyl, carboxyl, or formyl protons. Its i.r. spectrum showed carbonyl absorption at 1725 cm^{-1} and a 2,4-dinitrophenylhydrazone derivative formed readily. Structure **9** is consistent with each of these observations. A similar result has been reported recently (2) for the bromination of *exo-cis*-3,6-endoxo-4-methyl-Δ^4-tetrahydrophthalic anhydride (**13**); the *exo*-methylene derivative **14** was obtained in 91% yield.

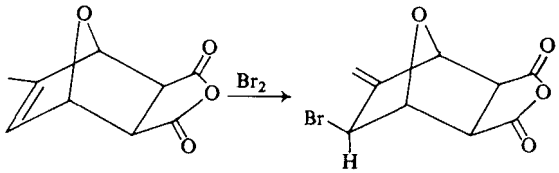

13 **14**

The data extracted from the spectra of compounds **6–8** are collected in Tables 1 and 2. These were obtained in chloroform solution in all cases although a few were examined in carbon tetrachloride or benzene as well. The parameters of the corresponding lactones lacking bromine are included for comparison although these have been discussed previously (1). The complete analysis of **12** has been carried out in the interim and these results are listed.

As noted earlier, the shifts of the C-3 methyl protons indicate the orientation of the vicinal bromine. In the *cis* configuration the bromine deshields these methyl protons by 0.2 p.p.m. ($CDCl_3$), but by only 0.05 p.p.m. in the *trans* by comparison with the results for **11** and **12**; similar comparisons show that the C-1 methyl absorption is shifted downfield by ca. 0.1 p.p.m. by the C-2 bromine. Undoubtedly the shieldings

[5]The mass spectrometry was performed by Prof. D. R. Bidinosti to whom we are indebted.

Can. J. Chem. Downloaded from www.nrcresearchpress.com by 210.87.254.105 on 09/05/12
For personal use only.

TABLE 1

Proton shifts in some substituted bicyclo[2.2.2]octyl γ-lactones (p.p.m. from TMS, 5 mole % solutions)

		Proton positions											
		C-2			C-6		C-7		C-8				
Compound	Solvent	*syn*	*anti*	C-4	*exo*	*endo*	*exo*	*endo*	*exo*	C-1 Me	C-3 Me	C-5 Me	OMe
6	$CDCl_3$	5.01	—	2.14	1.11	2.00	2.99	—	2.94	1.06	1.77	1.10, 1.22	3.68
	C_6H_6	5.22	—	1.44	0.58	1.70	2.68	—	2.59	0.96	1.56	0.58, 0.85	3.41
7	$CDCl_3$	4.12	—	2.02	1.55	1.66	—	2.55	3.02	1.13	1.79	1.23, 1.23	3.75
	CCl_4	4.15	—	1.98	1.54	1.62	—	2.49	2.87	1.12	1.75	1.22, 1.22	3.74
8	$CDCl_3$	—	3.98	2.13	1.91	1.24	—	2.72	3.08	1.08	1.61	1.15, 1.21	3.72
	C_6H_6	—	3.49	1.46	1.69	0.71		2.79	2.98	0.95	1.25	0.62, 0.94	3.24
11	$CDCl_3$	*	*	2.07	*	*	2.64	—	2.92	0.93	1.57	1.01, 1.08	3.67
12	$CDCl_3$	1.79	1.54	1.97	1.52	1.03	—	2.40	3.05	1.01	1.56	1.09, 1.18	3.69

*Complex multiplets obscured by methyl absorption.

TABLE 2

^1H–^1H Coupling constants of some substituted bicyclo[2.2.2]octyl γ-lactones (Hz)

Compound	Geminal J	Vicinal*			Long-range*			
		$J_{4,8}$	$J_{7,8\ exo}$	$J_{7,8\ endo}$	$J_{2,6\ exo}$	$J_{2,7\ exo}$	$J_{6,7}$	$J_{2,4}$
6	− 14.2 (C-6)	3.3	9.8	—	2.2	<0.2	—	2.0
7	†	4.2	—	2.3	~1	<0.5	1.4	—
8	− 14.5 (C-6)	4.1	—	2.3	—	<0.1	2.1	—
11	− 15.0 (C-2)	4.4	9.8	—	1.6	1.5	—	—
12	− 13.6 (C-6) − 14.8 (C-2)	4.3	—	2.2	2.8	—	2.1	0.8

*Subscripts indicate location of coupled protons.
†Obscured by methyl absorption.

of other protons are affected by the presence of the bromine atom but quantitative comparisons can be made for only a few. For the C-7 *endo*-proton in **7** and **8** a shift of − 0.17 p.p.m. is found for the *anti* → *syn* change in orientation at C-2, for which a shift of + 0.42 p.p.m. is observed for the C-6 *endo* proton. These deshielding effects of the bromine atom on closely neighboring protons may be due to a dispersion effect (3) although the magnetic anisotropy of the C—Br bond can also contribute. Some evidence that the latter factor may be appreciable is given by the upfield shift of 0.36 p.p.m. found for the 6-*exo* proton in **7** relative to that in **8**. The assignments of the C-6 methylene protons in **6** and **8** is straightforward since only one exhibits resolvable long-range coupling in each case and for 4-bond couplings via σ-networks it is well-known that the interaction through a "W" pathway is the largest (4). In **7**, however, both methylene protons are long-range coupled and, furthermore, absorb so closely that their pattern is an ill-defined multiplet. Spin-decoupling experiments were employed for the assignments listed in Table 1.

Another rather large shift difference is observed for the C-2 and *exo* C-6 protons in **6** vs. **7**. A change in orientation of the 7-carbomethoxyl group from *endo* to *exo* moves the former signal upfield by 0.9 p.p.m. while the latter is shifted downfield 0.44 p.p.m. Presumably this is primarily a result of the relative orientation of these protons with respect to the carbonyl bond; this contribution has been discussed in detail for closely related systems (1). The rest of the shielding data exhibit trends closely analogous to those described previously for the bicyclo[2.2.2]octenes **2**–**5** and their saturated derivatives (1).

The coupling constants for these lactones (Table 2) are similar to those found for the starting materials. The geminal couplings are comparable to those reported for a variety of bicyclo[2.2.2]octane systems (1, 5) and indicate little strain in the system. The vicinal interactions, however, show some interesting deviations from the values found in similar systems lacking the lactone grouping. The $J_{4,8}$ values for **7**, **8**, **11**, and **12** are larger by ca. 2 Hz than the corresponding couplings in **3** and **4** while $J_{7,8}$ for **7**, **8**, and **12** are smaller (ca. 3.5 Hz) than $J_{7,8}$ in **4**. These trends are consistent with the expected change in geometry caused by the formation of the γ-lactone between C-3 and C-8. Closure of this ring tends to twist the *exo*-C_8—H bond relative to the *endo*-C_7—H and C_4—H bonds such that the dihedral angles, φ, are reduced. In **4**, these φ values will be very close to 120 and 60°, respectively, as in I, whereas in **7**, **8**, and **12** these angles are ca. 110 and 50°, (see II), as estimated from models. Thus it is expected that $J_{7,8}$ will decrease while $J_{4,8}$ increases on the basis of the well-known dependence of vicinal couplings on φ (6). The strain introduced by formation of the lactone ring may also affect the vicinal couplings so it would be unwise to estimate the dihedral angles from the n.m.r. results. Another indication that the lactone ring does indeed twist the bicyclic skeleton in these systems is the fact that the vicinal coupling $J_{7,8}$, of **6** and **11** is 9.8 Hz or 1.2 Hz less than the corresponding value for **3** (1). The long-range couplings are as expected for 4-bond interactions through σ-bonds (3) with values > 1 Hz for those following a "W" path.

It is interesting that the orientation of the bromine atom apparently exerts some influence

Can. J. Chem. Downloaded from www.nrcresearchpress.com by 210.87.254.105 on 09/05/12
For personal use only.

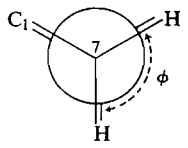

Ia

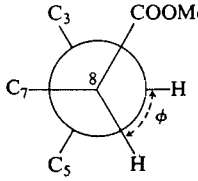

Ib

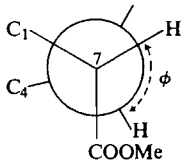

IIa

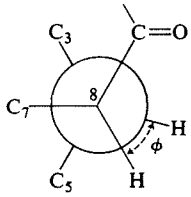

IIb

on these long-range couplings. For example, $J_{6,7}$ (*endo–endo*) changes from 1.4 to 2.1 Hz as the bromine atom moves from the *anti* to the *syn* position. This presumably could be due to slight variations in geometry. A comparable difference, 1.6 to 2.2 Hz, is found for $J_{2,6}$ upon introduction of the bromine (cf. **11** vs. **6**) which could be due to both steric and electronic perturbations.

In summary it can be seen that the proton spectra of the series **6–9** provide a reasonably straightforward means of elucidation of their structure and stereochemistry with the data giving some insight into the factors affecting the proton parameters.

We are grateful for the financial support of the National Research Council of Canada and the Petroleum Research Fund, administered by the American Chemical Society. We wish to thank Mrs. Mary Warren for some preliminary experiments.

1. GURUDATA and J. B. STOTHERS. Can. J. Chem. **47**, 3515 (1969).
2. J. MANTECÓN, L. CORTÉS, E. PAYO, and C. PIEMONTI. J. Org. Chem. **33**, 1235 (1968).
3. T. YONEMOTO. Can. J. Chem. **44**, 223 (1966).
4. S. STERNHELL. Rev. Pure Appl. Chem. **14**, 15 (1964).
5. K. TORI, Y. TAKANO, and K. KITAHONOKI. Ber. **97**, 2798 (1964).
6. M. KARPLUS. J. Amer. Chem. Soc. **85**, 2870 (1963).
7. P. W. RABIDEAU, R. G. HARVEY, and J. B. STOTHERS. Chem. Commun. 1005 (1969).

Can. J. Chem. Downloaded from www.nrcresearchpress.com by 210.87.254.105 on 09/05/12
For personal use only.

Can. J. Chem. Downloaded from www.nrcresearchpress.com by 210.87.254.6 on 09/05/12
For personal use only.

Ozonolysis of podocarpic acid

R. A. Bell and M. B. Gravestock
Department of Chemistry, McMaster University, Hamilton, Ontario

Received October 17, 1969

Low temperature ozonolysis of methyl podocarpate in methanol – methylene chloride results in the formation in high yield of 8β-hydroperoxy-8α-hydroxy-(13 → 17)-pentanorlabd-9(11)-en-12,19-dioic acid 19-methyl ester 8 → 12-lactone **4**. Ozonolysis followed by hydrogen peroxide work-up gives the lactone-acid **14***a*, whilst ozonolysis followed by reduction with sodium borohydride gives keto-acid **3***a* and lactones **16** and **17** derived from peroxide **4** together with δ-lactone **19** possessing all 18 carbon atoms of methyl podocarpate. The lactone **16** is shown to possess an 8β-configuration by application of the nuclear Overhauser effect.

Canadian Journal of Chemistry, **48**, 1105 (1970)

The partial ozonolysis of phenols has been of little use in synthetic organic chemistry. Phenol itself is completely degraded by ozone into one- and two-carbon fragments (1). The aromatic ring is more resistant to attack by ozone than a simple olefin[1] but, once the aromaticity has been destroyed by the first mole of ozone, the residual diene is rapidly cleaved (3). Polycyclic aromatic phenols likewise suffer sequential destruction of the hydroxyl containing ring upon exposure to ozone. 2-Naphthol is typical and on limited ozonolysis in non-hydroxylic solvents (4) gives a mixture of *O*-carboxycinnamic acid, phthalaldehydic acid, and phthalic acid, whilst ozonolysis in the participating solvent methanol (5) results in the formation of 4-methoxy-2,3-benzodioxan-1-ol (**1**). To our knowledge, the only ring opening of a substituted benzene ring by a single mole of ozone which is of preparative value, is the example recorded by Woodward *et al.* (6) in their synthesis of strychnine. Here a *meta* substituted catechol dimethyl ether was cleaved to a diene-diacid in good yield. The diene was apparently resistant to further attack by ozone because of the steric interactions resulting from the bulky *meta* substituent.

In connection with the synthesis of (13 → 17)-pentanorlabdane derivatives for the construction of a variety of bicyclic diterpenes (7), we considered that ozonolysis of the phenolic diterpene, podocarpic acid[2] **2***a*, might lead to useful synthetic intermediates since the 11-position of **2** is known (8) to be very hindered to electrophilic attack. We here report an examination of the ozonolysis of podocarpic acid and conditions for a high-yield, 2-step synthesis of the valuable keto-acid **3***a*, previously obtainable only by a 6-step sequence (9) from podocarpic acid.

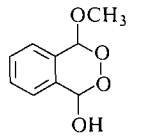

1

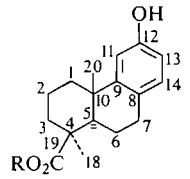

2
a R=H
b R=CH$_3$

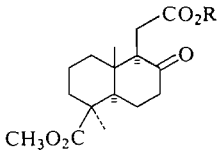

3
a R=H
b R=CH$_3$

Discussion and Results

Preliminary ozonolyses at moderate temperatures in hydroxylic or non-hydroxylic solvents showed that **2***a* or *b* were degraded to a multitude of products. However, slow ozonolysis at low temperatures in hydroxylic solvents was found to give relatively few products and the definitive experiments were therefore conducted at −78° using either methanol – methylene chloride or methanol–trichlorofluoromethane solvent mixtures. The ozonolysis reaction mixtures were

[1]See for example the ozonolysis of isoeugenol to give vanillin (2).

[2]The nomenclature used here is that proposed by the IUPAC Committee on Diterpene Nomenclature, July, 1968.

worked up in 3 ways: (*i*) direct isolation; (*ii*) oxidation with basic hydrogen peroxide; and (*iii*) reduction with sodium borohydride. The experiments carried out are conveniently discussed under these categories.

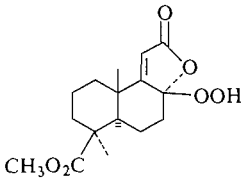

4

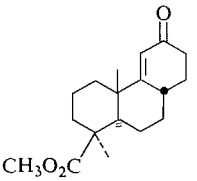

5

Direct Isolation

Careful removal of all solvents and volatile materials from the crude ozonolysis products of **2***b* resulted in the isolation of a crystalline material. The proton magnetic resonance (p.m.r.) spectrum showed the material to be 85–90% pure and a single crystallization gave the pure compound which has been assigned the lactone-hydroperoxide structure **4**. This structure is an unusual product to obtain from the ozonolysis of a substituted phenol since, on the basis of precedent (5), a more likely product would be a 2,3-dioxolan derivative analogous to **1**. However, the structure of **4** rests firmly on both spectral and chemical evidence. Thus in its infrared (i.r.) spectrum, **4** showed typical absorptions for an hydroxyl group at 3500 and 3250 cm^{-1}, and a strained, 5-membered unsaturated lactone at 1765 and 1640 cm^{-1}. There was also present a weak absorption at 870 cm^{-1} which is considered (10) to be characteristic of the O—O bond stretching of a peroxide. The ultraviolet (u.v.) spectrum, which showed $\lambda_{max}(CH_3OH)$ 218 mμ (ε 11 000), was also in agreement with the presence of an unsaturated lactone. The trisubstituted nature of the conjugated double bond was shown by the presence of only one, very sharp ($W_{h/2}$ = 0.5 Hz) singlet at 5.79 p.p.m. in the p.m.r. spectrum of **4**. The appearance of the hydroperoxide proton signal at 9.08 p.p.m. is consistent with the chemical shift of other hydroperoxides (11).

Additional evidence for the presence of the 9(11)-olefin could be inferred from the chemical shift of the C-20 methyl group. As has been noted previously, the central methyl group of terpenes and steroids is a sensitive probe of the functional groups and geometry of the A, B, and C rings (12). Thus the absorption of the C-20 methyl group of **4** at 1.13 p.p.m. showed the geometrical and deshielding influences of a 9(11)-double bond and a 12 → 8-lactone, and may be compared to the observed resonances of the C-20 methyl groups of the 9(11)-unsaturated compounds **5** and **16** which occur at 0.94 and 0.99 p.p.m. respectively. These latter absorptions are considerably deshielded from their saturated counterparts which occur at 0.68 and 0.77 p.p.m. respectively (9). The slight deshielding of the C-20 methyl of **4** by 0.19 and 0.14 p.p.m. in comparison with **5** and **16** is consistent with a β stereochemistry of the C-8 hydroperoxide. An axial hydroperoxide can be expected to deshield a 3-axial methyl group to the same extent as an axial hydroxyl group[3] and hydroxyl-methyl 1,3-diaxial interactions normally result in the methyl group being deshielded by 0.18 to 0.25 p.p.m. (12*b*, *c*, 13).

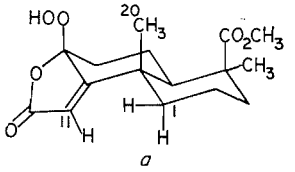

a

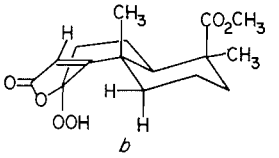

b

FIG. 1. Conformation (*a*) of 8β-hydroperoxide and (*b*) of 8α-hydroperoxide.

Additional evidence for the stereochemistry of the lactone-hydroperoxide derives from the absence of a nuclear Overhauser effect (n.O.e.) (14) between the C-11 vinylic proton and the C-20 methyl group. The two possible configurations for the C-8 hydroperoxide are depicted in Fig. 1. In the β-hydroperoxide (*a*), the planarity of the lactone ring constrains ring B to an almost classical chair conformation and the internuclear distance between the C-20 carbon atom and the C-11 proton is 3.88 Å. The α-hydroperoxide (*b*) on the other hand can only exist with ring B in a

[3]This statement is supported in the sequel by the observation that the resonance of the C-20 methyl group of **6** is indistinguishable from that of **4**.

Can. J. Chem. Downloaded from www.nrcresearchpress.com by 210.87.254.6 on 09/05/12
For personal use only.

Can. J. Chem. Downloaded from www.nrcresearchpress.com by 210.87.254.6 on 09/05/12
For personal use only.

twist conformation[4] and this places the C-20 carbon and the C-11 proton 3.16 Å apart. Since in **4** there was no observable n.O.e. between the C-20 methyl and the C-11 proton, their distance apart can be assessed as 3.6 Å or greater (16) and this separation clearly invalidates stereochemistry (*b*) but is satisfied by (*a*).

The structure of **4** was finally and unequivocally established on chemical grounds. Thus, the iodide test for a peroxide was positive and 1 mole-equivalent of iodine was released in less than 2 min (17). This indicates the presence of a hydroperoxide rather than a peroxide as the latter liberates iodine at a relatively slow rate.[5] The peroxide bond of **4** could also be selectively reduced by aqueous methanolic sodium sulfite to give a 98% yield of the unsaturated lactone-hemiketal **6**. Finally, palladium catalyzed hydrogenation of **4** or **6** at atmospheric pressure resulted in the formation in over 90% yield of the known (9,19) keto-acid **3***a*. Production of this compound is conclusive evidence for the carbon skeleton present in the lactone-hydroperoxide.

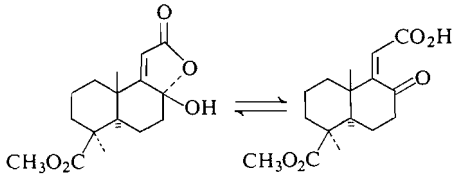

6 7

A minor, but interesting point of comparison between the saturated keto-acid **3***a* and the unsaturated keto-acid **7** is the observation that **7** in non-polar solvents existed entirely in the lactone-hemiketal form **6** whereas **3***a* existed solely in the keto-acid form. The stereochemistry of **6** is assigned on the basis of the similarity between its i.r. and p.m.r. spectra and those of hydroperoxide **4**. The factors causing this change in equilibrium between the 2 keto-acids are most reasonably a combination of bond angle changes (20) introduced by the 9(11)-double bond and steric interactions between the C-11 H and hydrogens at C-1 (21). In **3***a*, rotation about the 9,11-bond can enable the side chain to adopt suitable conformations which minimize the C-1, C-11 hydrogen interactions. However, keto-acid **7** has no such possibilities open to it and inspection of a molecular model places the C-11 H only 1.9 Å away from the C-1 equatorial H and 2.3 Å from the axial H (sum of the van der Waals radii of 2 H's 2.4 Å). This interaction with the C-1 equatorial H is removed in the lactone-hemiketal form where the C-11 H is midway between the C-1 axial and equatorial H's and at distances of 2.3 and 2.5 Å respectively.

Although there is precedent for electrophilic attack at the 13-position (8,22) and the 8-position (13) of methyl podocarpate, we consider that on the basis of previous work, ozone will attack initially *ortho* to the phenolic OH (13-position). A mechanism for the formation of the lactone-hydroperoxide **4** following this pathway is shown in Scheme 1. The initial molozonide **8** should cleave with breakage of the 11,12-bond preferentially towards the 12-position[6] because of the inductive effect of the hydroxyl group (24) and attack of the Criegee zwitterion (25) by methanol

[4]The possibility of the lactone-hydroperoxide possessing structure (*b*) cannot be immediately dismissed on the grounds of its probable instability since the ketone (**i**) with an sp^2-hybridized carbon at C-9 has been shown to preferentially exist in a twist conformation (15).

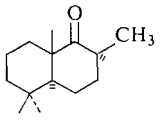

i

[5]Compare also the lead tetraacetate test to differentiate peroxides and hydroperoxides (18).

[6]The alternative mode of cleavage of molozonide **8** may also possibly occur. The hydroperoxide (**iv**) on treatment with water would be unstable (23) and decompose to hydroperoxide **4**. Although this process is quite reasonable, it is felt that it represents a minor pathway since there were no observable extra vinylic absorptions (other than the C-11 H of **4**) in the p.m.r. spectrum of crude **4** isolated by direct evaporation of the methanol – methylene chloride solvent. (We thank a referee for pointing out this alternative reaction pathway.)

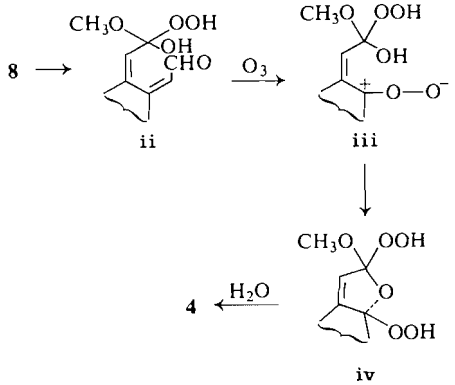

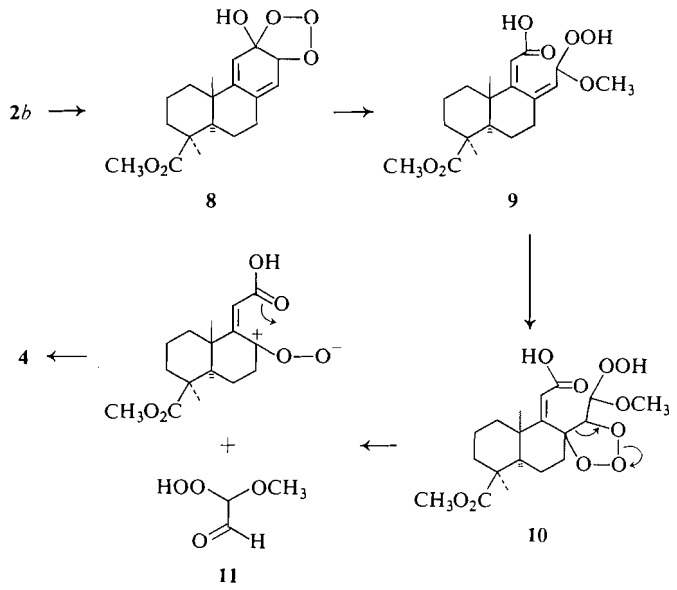

SCHEME 1

solvent will lead to the acid-hydroperoxide **9**. Of the 2 remaining double bonds in **9** the 8(14)-double bond is relatively unencumbered and attack by a further molecule of ozone leads to the molozonide **10** which in turn can undergo breakage of the 8(14)-bond in either a concerted fashion, or in a sequential manner via the Criegee zwitterion and subsequent cyclization of the lactone ring to give **4**. As only the 8β-hydroperoxide was observed in the reaction mixture, the latter possibility is considered correct. Ozone attack of the 8(14)-double bond should preferentially occur from the α-face of **9**. Concerted reaction should therefore lead to a predominance of the α-hydroperoxide, but sequential reaction would give the Criegee zwitterion a finite lifetime and enable the carboxyl group to attack from the most favorable side, namely the α-face and give the β-hydroperoxide. The lack of reactivity of the 9(11)-double bond under the reaction conditions must be attributed to steric shielding by the C-20 methyl group and the hydrogens at C-1. This double bond was certainly attacked by ozone at higher temperatures (0°) as was evidenced by loss of the C-11 H in the p.m.r. spectra of products from exploratory reactions.

The fate of the 2 carbon unit **11** which is cleaved from methyl podocarpate was not investigated in this study. However, on the basis of the work by Johnson and Bailey (26) the glyoxal derivative which is ejected during the fragmentation of the molozonide **10** most likely undergoes a 1,2-shift during warm-up to room temperature to give the intermediate **12** (Scheme 2) and finally, after proton transfer, a molecule of methyl formate and formic acid.

Oxidative Treatment

When the ozonolysis reaction mixture was treated directly with hot aqueous H_2O_2–NaOH, the lactone-acid **14***a* was isolated. This compound was characterized as its methyl ester **14***b* and the structure follows from its i.r. spectrum which showed absorption for an ester at 1720 cm^{-1} and a δ-lactone at 1730 cm^{-1}, and its p.m.r. spectrum which showed the C-11 proton as a single, sharp signal at 6.22 p.p.m. and the 2 protons at C-7 as a multiplet at 4.20 p.p.m. In addition the u.v.

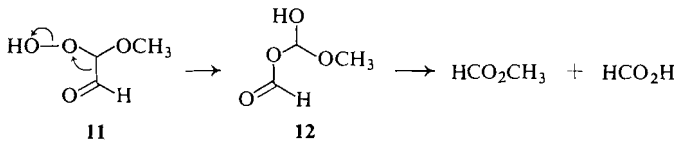

SCHEME 2

Can. J. Chem. Downloaded from www.nrcresearchpress.com by 210.87.254.6 on 09/05/12
For personal use only.

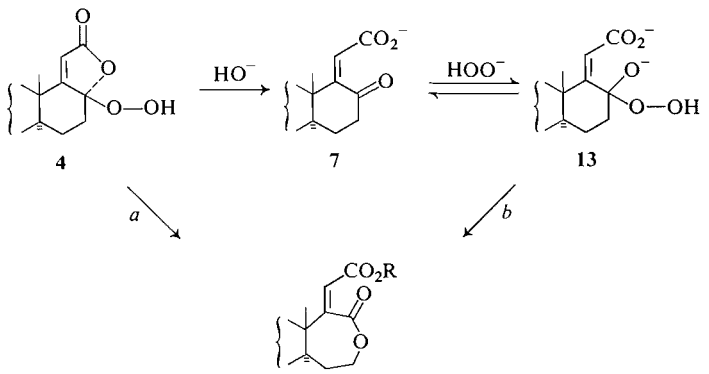

SCHEME 3

spectrum of **14***b* showed maxima at 214 mμ (ε 10 400) and 280 mμ (ε 190).

The origin of **14***a* is readily rationalized on the assumption that it is a rearrangement product of the hydroperoxide **4**. This was confirmed by subjecting pure **4** to H_2O_2–NaOH treatment when **14***a* was obtained in 90% yield. A simple mechanism for the formation of **14***a* can be depicted (Scheme 3 path *a*) as a 1,2-shift (26) of the 7,8-bond of **4** followed by hydroxide ion attack at C-8 and then proton loss and ring opening of the γ-lactone to give the lactone-acid. The presence of hydrogen peroxide appears unnecessary in this mechanism, but reactions conducted in its absence led to a high yield of the decalone **15** and smaller quantities of unidentified acidic materials. Presumably aqueous base alone results in attack at the γ-lactone carbonyl of **4** to give **7** and hydroperoxide anion. Further base attack at C-11 of **7** followed by a reverse aldol then gives **15**. This mechanism was further substantiated when base treatment of the pure hemiketal **6** likewise gave **15** in good yields. The rearrangement mechanism of **4** is therefore more likely to follow path *b* with the initial formation of keto-acid **7**. Attack of **7** by hydroperoxide anion then leads to **13** which subsequently undergoes rearrangement to **14***a*.

Reductive Treatment

The major products formed by sodium borohydride reduction of the ozonolysis reaction mixture are shown in Scheme 4. Their origin is reasonably rationalized on the basis of the hydroperoxide **4** being the sole precursor. The relative proportions of each component varied with the temperature at which the reducing agent was added. Thus very low temperatures (−78°) gave the unsaturated lactone **16** in yields as high as 85%, whereas higher temperatures (refluxing ethanol) gave largely **3***a* and the known (19) saturated lactone **17**. Small quantities of the diol **18** resulting from more extensive reduction were also present.

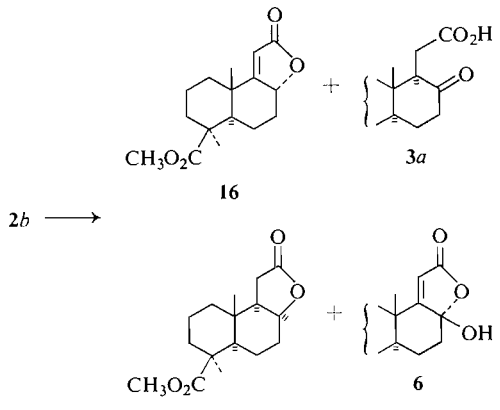

SCHEME 4

The structure of the unsaturated lactone **16** follows from the presence of a single olefinic absorption at 6.20 p.p.m. and a single proton adjacent to the lactone oxygen as an octet ($J_{7a,8}$ = 11.5, $J_{7e,8}$ = 7.5, $J_{8,11}$ = 1.5 Hz) at 4.86 p.p.m. in its p.m.r. spectrum and a band characteristic of a γ-lactone at 1755 cm^{-1} in its

Can. J. Chem. Downloaded from www.nrcresearchpress.com by 210.87.254.6 on 09/05/12
For personal use only.

Can. J. Chem. Downloaded from www.nrcresearchpress.com by 210.87.254.6 on 09/05/12
For personal use only.

i.r. spectrum. The 8β-configuration assigned to **16** is based on the coupling constants of the C-8 H. The long range allylic coupling with C-11 H ($J_{8,11}$ = 1.5 Hz) is more consistent with a β-orientation of C-8 since the dihedral angle between the C-8 H bond and the C-11 H bond is closer to 90° for a β-orientation than an α-orientation (27). More definitively, there is an 18% n.O.e. at the C-8 H when the C-20 CH_3 is saturated and therefore the C-8 H must be on the same side of the molecule as the C-20 CH_3; that is possess a β-orientation.

The formation of keto-acid ***3a*** in yields as high as 35% by reduction in hot ethanol can be ascribed to a 1,4-addition of borohydride (28) to the neutral lactone-hemiketal **6**. The keto-acid was presumably preserved in the reaction medium as the carboxylate anion whilst the excess borohydride was destroyed by solvent. The lactone **17** on the other hand, could either originate by reduction of ***3a*** or by 1,4-reduction of **16**.

A minor component was obtained from reductions of the crude ozonolysis product over the temperature range −55 to 0° in yields varying from 10–30% which, from its high resolution mass spectrum, had molecular formula $C_{18}H_{26}O_5$. The proposed structure **19** for this compound is compatible with the recorded spectroscopic data. Thus **19** showed in its p.m.r. spectrum the vinylic C-11 proton at 6.1 p.p.m., the C-17 proton as a triplet (J = 5.5 Hz) at 4.68 p.p.m. and the hydroxymethylene protons as a doublet (J = 5.5 Hz) at 3.82 p.p.m. The coupling of the C-17 proton and the hydroxymethylene protons was conclusively established by double resonance experiments. The i.r. spectrum of **19** showed an hydroxyl absorption at 3610 and 3500 cm^{-1} and the C-19 ester and (12 → 17)-lactone as an intense band at 1730 cm^{-1}, and the u.v. spectrum showed a maximum at 214 mμ (ε 10 000) characteristic of a 9,11-unsaturated lactone system (cf. the maximum of γ-lactone **16**). The high resolution mass spectrum was also consistent with the proposed structure (Scheme 5) and the molecular ion (intensity temperature dependent) showed an M-18 peak which corresponded with the ion **20**, $C_{18}H_{24}O_4$ indicating the loss of a molecule of water. The ion **20** in turn gave rise to an M-46 peak (base peak) which corresponded to the ion **21**, $C_{17}H_{24}O_3$. The stable, aromatic ion **21** results from the loss of a hydrogen atom and carbon monoxide from **20** and is a reasonable fragmentation for a cyclic lactone (29).

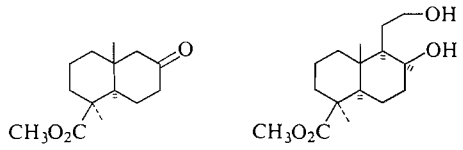

15 **18**

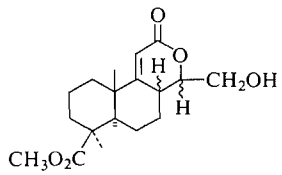

19

A rationale for the formation of the hydroxylactone **19** is not readily apparent and, in view of the lack of significant precursors to it from either the reductive, oxidative, or direct isolation experiments, a detailed mechanistic scheme is unwarranted at this point. The value of **19** in bicyclic diterpenoid syntheses is evident and it is reasonable that its yield can be increased by the use of solvents other than those used in this study.

Summary

The ozonolysis of methyl podocarpate ***2b*** in methanol – methylene chloride at −78° with a slight excess of ozone and direct isolation at room temperature results in the formation of the hydroperoxide **4** in high yield. The structure and stereochemistry of **4** are deduced from its spectroscopic properties and its conversion on catalytic hydrogenation into the known keto-acid ***3a***. Direct oxidation of the methyl podocarpate

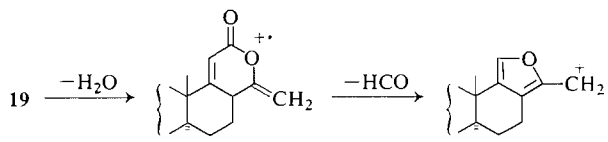

20 **21**

SCHEME 5

Can. J. Chem. Downloaded from www.nrcresearchpress.com by 210.87.254.6 on 09/05/12
For personal use only.

ozonolysis product gives the acid-lactone **14** in 90% yield whilst direct reductive work up with sodium borohydride affords largely a mixture of intermediate reduction products of **4** together with a smaller quantity of a compound possessing all 18 carbon atoms of methyl podocarpate and assigned the hydroxy-lactone structure **19**.

Experimental

Melting points were determined on a Kofler micro hot-stage apparatus and are uncorrected. Spectra were recorded in the following solvents and instruments: i.r. ($CHCl_3$) Perkin–Elmer 337; u.v. (MeOH) Carey 14; p.m.r. ($CDCl_3$) Varian Associates A-60 and HA-100, tetramethylsilane as internal standard; mass spectra, Hitachi Perkin–Elmer RMU-6A (at 80 eV) and C.E.C. 21-110. Carbon, hydrogen, and oxygen microanalyses were performed by Spang Microanalytical Laboratories, Ann Arbor, Michigan, U.S.A. In the experimental descriptions to follow the organic substrates were isolated via extraction with the appropriate solvent (2 ×) followed by washing of the combined solvent layer with water, saturated brine, and finally drying with anhydrous Na_2SO_4. The solvents were removed by evaporation at reduced pressure on a Buchi Rotavapor.

The ozonolysis experiments were conducted at −78° (Dry Ice – acetone bath) using dry air in a Welsbach model T408 ozonizer operating at 7–8 p.s.i. gas pressure, 80 V primary potential, and a flow rate of 0.5 s.l.p.m. These instrument settings gave an ozone concentration of 2 mg O_3/l gas. Excess ozone was always removed from the reaction vessel by passing through a stream of dry nitrogen for 20–30 min before further manipulation of the product.

8β-Hydroperoxy-8α-hydroxy-(13 → 17)-pentanorlabd-9(11)-en-12,19-dioic Acid 19-Methyl Ester 8α → 12-Lactone (4)

Methyl podocarpate **2***b*, (m.p. 208–210°), 10.0 g (34.8 mmole) was dissolved by warming in 100 ml methylene chloride and 100 ml methanol (both dried over molecular sieves) in a 250 ml gas absorption vessel fitted with a fritted-glass bubbler and, after cooling to −78°, treated with ozone for 6 h. A slight excess of ozone was present at this point and after its removal the solution was transferred to a flask with the aid of methanol and the solvent removed *in vacuo* at 30–40° to give the crude hydroperoxide **4** as a colorless solid. The solid was unstable in this state and was dissolved in 200 ml of chloroform and washed with 500 ml water, 200 ml brine, filtered through anhydrous Na_2SO_4, and evaporated *in vacuo* at 40° to give 10.75 g (100%) of **4** as a colorless solid of 80–90% purity by p.m.r. analysis. Recrystallization from 50 ml of chloroform and 100 ml of hexane added at the boiling point gave 7.30 g (68%) of **4**, m.p. 183–187° (d). One further crystallization from the same solvent gave the analytical sample as colorless prisms, m.p. 185–187° (d); i.r. ν_{max}, 3500, 3250 (—OOH), 1765 (γ-lactone), 1725 (ester), 1640 (C=C), 870 cm^{-1} (O—O); u.v. λ_{max} 218 mμ (ε 11 000); p.m.r. δ, 1.135 (s, 3H, C-20 CH_3), 1.22 (s, 3H, C-18 CH_3), 3.72 (s, 3H, C-19 $COOCH_3$), 5.79 (s, 1H, vinylic H), 9.08 p.p.m. (s, 1H, $W_{h/2}$ = 2.0 Hz, OOH).

Anal. Calcd. for $C_{16}H_{22}O_6$: C, 61.92; H, 7.15; O, 30.93. Found: C, 61.86; H, 7.14; O, 30.86.

In runs where trichlorofluoromethane (Freon 11) was substituted for methylene chloride similar yields of **4** were obtained although there were problems arising from decreased methyl podocarpate solubility.

Iodometric determination of peroxidic oxygen was carried out by the procedure of Wagner *et al.* (17). One mole of **4** released 0.98 ± 2 mole of active oxygen. The reaction was quantitative within a period of 2 min.

8-Dihydroxy-(13 → 17)-pentanorlabd-9(11)-en-12,19-dioic Acid 19-Methyl Ester 8α → 12-Lactone (6)

To a solution of 0.50 g of hydroperoxide **4** (m.p. 183–187°) in 50 ml of 95% ethanol was added 0.5 g sodium sulfite in 20 ml water and the mixture stirred at room temperature for 2 h. Dilution with 500 ml of water and isolation via benzene gave 465 mg (98%) of crystalline lactone hemi-ketal **6** which p.m.r. analyses showed to be > 95% pure. Recrystallization from 1:1 chloroform–hexane gave **6** as colorless plates, m.p. 198–201° (d); i.r. ν_{max} 3570, 3350 (—OH), 1760, (γ-lactone), 1725 (ester), 1640 cm^{-1} (C=C); u.v. λ_{max} 220 (ε 11 200), 280 mμ (sh) (ε 19); p.m.r. δ, 1.125 (s, 3H, C-20 CH_3), 1.22 (s, 3H, C-18 CH_3), 3.71 (s, 3H, C-19 $COOCH_3$), 4.1–4.9 (s, 1H, $W_{h/2}$ = 5 Hz, —OH), 5.63 p.p.m. (s, 1H, vinylic H).

Anal. Calcd. for $C_{16}H_{22}O_5$: C, 65.29; H, 7.53; O, 27.15. Found: C, 65.38; H, 7.47; O, 27.15.

8-Oxo-(13 → 17)-pentanorlabdan-12,19-dioic Acid 19-Methyl Ester (3a)

The hydroperoxide **4** (m.p. 183–187°), 7.3 g was added in 75 ml 95% ethanol to a pressure bottle containing a suspension of 0.7 g 5% palladium–charcoal catalyst in 75 ml ethanol which had been prehydrogenated for 15 min. The mixture was shaken under 3 atm of hydrogen overnight. The reaction mixture was filtered through "Celite" with thorough washing of the filter pad and evaporated *in vacuo* to give 6.8 g (98%) of keto-acid **3***a* as colorless crystals (95% pure by p.m.r. analysis). Recrystallization from 1:2 ethyl acetate – hexane gave **3***a* as colorless needles, m.p. 171–172° (lit. (9), 171–172°).

Hydrogenation of lactone-hemiketal **6** with 5% palladium–charcoal also gave an almost quantitative yield of **3***a*.

7-Hydroxy-(13 → 17)-pentanor-7,8-secolabd-9(11)-en-8,12,19-trioic Acid 12,19-Dimethyl Ester 7 → 8-Lactone (14b)

A solution of 10.0 g (36 mmole) methyl podocarpate in 100 ml of 1:1 methanol – methylene chloride was ozonized for 2.25 h. The reaction mixture was allowed to warm to room temperature and treated with 50 ml 30% H_2O_2 and 100 ml NaOH and the whole heated at reflux for 30 min. The cooled solution was acidified with 2 *N* H_2SO_4 and the organic material isolated via benzene to give 10.45 g of an oil. The p.m.r. spectrum of this showed the presence of ca. 70% **14***a*. The crude acid was methylated in ether with diazomethane and the ester chromatographed on 200 g Florisil. Elution with 5% ethyl acetate – benzene gave 4.46 g impure **14***b* as an oil and elution with 20% ethyl acetate – benzene gave 4.61 g

Can. J. Chem. Downloaded from www.nrcresearchpress.com by 210.87.254.6 on 09/05/12
For personal use only.

pure **14***b*. Crystallization from 1:10 ethyl acetate – hexane gave **14***b* as colorless prisms, m.p. 95–96°; i.r. ν_{max} 3040 (C=C—*H*), 1742 (lactone), 1730 (C-19 ester), 1720 (C-12 ester), 1640 cm^{-1} (C=C); u.v. λ_{max} 214 (ε 10 400), 280 mμ (sh) (ε 190); p.m.r. (100 MHz) δ, 0.97 (s, 3H, C-20 CH_3), 1.20 (s, 3H, C-18 CH_3), 3.65 and 3.70 (s, 3H each, C-12 and C-19 $COOCH_3$), 4.14 (m, 2H, CH_2—O, unresolved at 30°, 3-line m at 40°, 4-line m at 50°, 6-line m at 70°), 5.85 p.p.m. (s, 1H, vinylic H).

Anal. Calcd. for $C_{17}H_{24}O_6$: C, 62.95; H, 7.46; O, 29.60. Found: C, 63.09; H, 7.28; O, 29.39.

In another experiment 0.50 g of pure hydroperoxide **4** in 25 ml methanol was treated with 10 ml 30% H_2O_2 and 25 ml of 10% NaOH for 30 min at reflux. Work-up gave 0.50 g (95%) of the acid-lactone **14***a* as colorless crystals. The p.m.r. analysis showed this to be > 95% pure.

*1β-Carbomethoxy-1α,10β-dimethyldecal-6-one (**15**)*

To a solution of 0.200 g of hydroperoxide **4** (m.p. 183–187°) in 10 ml of ethanol was added 10 ml of 1 *N* NaOH and the whole heated at the steam bath under nitrogen for 4 h. The cooled reaction mixture was diluted with 200 ml water and the organic material isolated via benzene to give 106 mg (70%) of **15** as a colorless oil almost analytically pure. Crystallization from hexane at − 20° gave 60 mg of **15** as colorless plates, m.p. 62–63° (softens 54°); i.r. ν_{max} 1720 (ester), 1705 (ketone), 1460, 1240, 1160, 1150, 1095, 985 cm^{-1}; u.v. λ_{max} 290 (ε ca. 50); p.m.r. δ, 0.715 (s, 3H, C-10 CH_3), 1.23 (s, 3H, C-4 CH_3), 3.55 p.p.m. (s, 3H, $COOCH_3$); mass spectrum *m/e*, 238 (M^+), 223 (M-15), 179 (M-59); mol. wt. 238.

Anal. Calcd. for $C_{14}H_{22}O_3$: C, 70.55; H, 9.31. Found: C, 70.61; H, 9.46.

The base soluble fraction from the above reaction was acidified and isolation via benzene gave 42 mg of colorless oil. The p.m.r. analysis showed it to be a mixture of 45% lactone-hemiketal **6**, 25% of an unknown compound (C-20 CH_3 at 1.03 p.p.m.), and 30% of an unknown acid (C-20 CH_3 at 0.85 p.p.m.).

Similar treatment of the pure **6** in aqueous ethanolic base at reflux for 6 h gave a 60% yield of **15** and 30% of the unknown acid.

Borohydride Reductions

*8α-Hydroxy-(13 → 17)-pentanorlabd-9(11)-en-12,19-dioic Acid 19-Methyl Ester 8α → 12-Lactone (**16**)*

A solution of 2.00 g (6.9 mmole) of methyl podocarpate **2***b* in 40 ml of 1:1 methanol – methylene chloride was cooled to −78° and ozonized air passed through for 55 min (slight excess of ozone). The cold solution was then treated with 1.5 g $NaBH_4$ in 20 ml of 50% aqueous ethanol and allowed to warm to room temperature with stirring. After further stirring at room temperautre for 30 min the reaction mixture was poured into 200 ml water and the products isolated via benzene–ether (1:3) extraction to give 1.70 g (90%) of the unsaturated lactone **16** as colorless crystals (ca. 90% pure by p.m.r. analysis). Crystallization of **16** from 1:3 ethyl acetate – hexane gave colorless slabs, m.p. 144–145°; i.r. ν_{max} 1750 (γ-lactone), 1720 (ester), 1635 cm^{-1} (C=C); u.v. λ_{max} 218 (ε 18 000), 280 mμ (ε 40); p.m.r. (100 MHz) δ, 0.99 (s, 3H, C-20 CH_3), 1.22 (s, 3H, C-18 CH_3), 3.66 (s, 3H, $COOCH_3$), 4.86 (2 quartets, 1H, $J_{7\alpha,8}$ = 11.5 Hz, $J_{7e,8}$ = 7.5 Hz, $J_{8,11}$ = 1.5 Hz, C-8 βH), 5.53 p.p.m. (q, 1H, $J_{8,11}$ = 1.5 Hz, $J_{7e,11}$ = 0.6 Hz, vinylic H); mass spectrum *m/e* 278 (M^+), 263 (M-15), 248 (M-30), 234 (M-45), 219 (M-59); mol. wt. 278.

Anal. Calcd. for $C_{16}H_{22}O_4$: C, 69.04; H, 7.97. Found: C, 68.88; H, 8.22.

The aqueous residues from the above experiment were acidified with 2 *N* H_2SO_4 and extracted with benzene. Isolation gave 0.25 g (11%) of an oil which from its p.m.r. spectrum was largely the δ-lactone-alcohol **19** (see below).

*17-Hydroxymethylene-17-hydroxy-(13 → 16)-tetranorlabd-9(11)-en-12,19-dioic Acid 19-Methyl Ester 12 → 17-Lactone (**19**)*

In an identical manner to the above preparation, a solution of 1.00 g (3.45 mmole) methyl podocarpate **2***b* in 20 ml of 1:1 methanol – methylene chloride was treated with ozonized air for 28 min. The solution was allowed to warm to −50 to −20° and then a solution of 1.05 g $NaBH_4$ in 10 ml 50% aqueous ethanol added. The stirred solution was allowed to warm to room temperature, held there for 30 min and finally warmed at the steam bath for 30 min. After solvent had been removed *in vacuo* the product was acidified with 5% NaH_2PO_4 and isolated via benzene to give 0.80 g of a light yellow oil. The p.m.r. spectrum of this showed it to be largely keto-acid **3***a* together with δ-lactone-alcohol **19**. The mixture was esterified with diazomethane and chromatographed on Florisil. Elution with 5% ethyl acetate – benzene gave 400 mg of keto-ester **3***b* and elution with 15% ethyl acetate – benzene gave 300 mg (26%) of **19**. Crystallization of **19** from 1:9 ethyl acetate – hexane gave colorless micro-crystals, m.p. 119–120°; i.r. ν_{max} 3590, 3410 (—OH), 1730 (δ-lactone, ester), 1570, 1470, 1238, 1068, 1036 cm^{-1}; u.v. λ_{max} 227 (ε 8300), 280 mμ (ε 40); p.m.r. (100 MHz) δ, 0.92 (s, 3H, C-20 CH_3), 1.23 (s, 3H, C-18 CH_3), 3.64 (s, 3H, $COOCH_3$), 3.82 (d, 2H, J = 5.5 Hz, C-21 CH_2O), 3.5–5.5 (variable), (broad s, 1H, OH), 4.68 (t, 1H, J = 5.5 Hz, C-17 H), 6.07 p.p.m. (s, 1H, vinylic H); mass spectrum (80 eV) *m/e* 322 (M^+, calcd. for $C_{18}H_{26}O_5$: 322.1793; found: 322.1780), 304 (M-H_2O, calcd. for $C_{18}H_{24}O_4$: 304.1679; found: 304.1674), 291 (M-CH_3O, calcd. for $C_{17}H_{23}O_4$: 291.1607; found: 291.1596), 275 (M-H_2O-HCO, calcd. for $C_{17}H_{23}O_3$: 275.1647; found: 275.1660), 263 (M-$COOCH_3$, calcd. for 263.1647; found: 263.1621).

Anal. Calcd. for $C_{18}H_{26}O_5$: C, 67.06; H, 8.13. Found: C, 67.10; H, 8.31.

*8β-Hydroxy-(13 → 17)-pentanorlabdan-12,19-dioic Acid 19-Methyl Ester 8 → 12-Lactone (**16**)*

The solution from the ozonolysis of 1.00 g (3.45 mmole) of methyl podocarpate **2***b* (see above) was allowed to warm to room temperature and treated with a solution of 1.5 g $NaBH_4$ in 20 ml 50% aqueous ethanol. The reaction mixture was stirred at room temperature for 30 min and then heated at reflux for 1 h. The cooled reaction mixture was diluted with water, extracted with benzene, and the aqueous layer then acidified with 2 *N* H_2SO_4 and further extracted with benzene. Isolation gave 540 mg neutral fraction which from its p.m.r. spectrum consisted of **16**, **17**, and **18** in the ratio of 2:2:1 respectively. Chromatography on Florisil and elution with benzene gave 190 mg **16** and elution with 5% ethyl

acetate – benzene gave 200 mg **17** as a colorless oil which crystallized on standing. Crystallization from 1:9 ethyl acetate – hexane gave **17**, m.p. 160–161° (lit. (19), 163–164°); i.r. 1775 (lactone), 1725 cm^{-1} (ester); p.m.r. δ, 0.77 (s, 3H, C-20 CH_3), 1.23 (s, 3H, C-18 CH_3), 2.5 (m, 2H, C-11 CH_2), 3.66 (s, 3H, $COOCH_3$), 4.5 p.p.m. (m, 1H, C-8 H); mass spectrum *m/e*, 280 (M^+), 262 (M-18), 248 (M-32), 234 (M-46), 221 (M-59); mol. wt. 280.

Elution of the above column with 10% ethyl acetate – benzene gave 110 mg of *8,12-dihydroxy-(13 → 17)-pentanorlabdan-19-oic acid 19-methyl ester* **18** as a colorless oil. Crystallization from 1:4 ethyl acetate – hexane gave **18** as colorless needles, m.p. 112–113°; i.r. ν_{max} 3615, 3420, 1725 (ester), 1155, 1035, 1000 cm^{-1}; p.m.r. δ, 0.83 (s, 3H, C-20 CH_3), 1.18 (s, 3H, C-18 CH_3), 3.65 (s, 3H, $COOCH_3$), 3.75 (m, 2H, C-12 CH_2O), 4.03 (m, 1H, C-8 H), 1.75–4.75 p.p.m. (concentration dependent, s, 2H, $W_{h/2}$ = 5 Hz, OHs).

Anal. Calcd. for $C_{16}H_{28}O_4$: C, 67.57; H, 9.93. Found: C, 67.35; H, 10.25.

We wish to thank the National Research Council of Canada for financial support of this work and for a Fellowship to Mr. M. B. Gravestock. We thank Mr. J. K. Saunders for the nuclear Overhauser effect experiments.

1. E. Bernatek and C. Frengen. Acta Chem. Scand. **15**, 471 (1961).
2. E. Briner and S. Fliszar. Helv. Chim. Acta, **42**, 1310 (1959).
3. See for example: (*a*) P. S. Bailey. Chem. Rev. **58**, 985 (1958), and references therein. (*b*) J. P. Wibaut and F. L. J. Scixma. Rec. Trav. Chim. **71**, 761 (1952). (*c*) E. Bernatek, J. Moskeland, and K. Valen. Acta Chem. Scand. **15**, 1454 (1961).
4. E. Bernatek and C. Frengen. Acta Chem. Scand. **16**, 2421 (1962).
5. P. S. Bailey, S. S. Bath, F. Dobinson, F. J. Garcia-Sharp, and C. D. Johnson. J. Org. Chem. **29**, 697 (1964).
6. R. B. Woodward, M. P. Cava, W. D. Ollis, A. Hunger, H. U. Daeniker, and K. Schenker. J. Amer. Chem. Soc. **76**, 4749 (1954).
7. A. Ogiso and S. W. Pelletier. Chem. Commun. 94 (1967); S. W. Pelletier, L. B. Hawley, Jr., and K. W. Gopinath. Chem. Commun. 96 (1967); S. W. Pelletier, K. N. Iyer, C. W. J. Chang, and A. Ogiso. Tetrahedron Lett. 3819 (1968).
8. B. R. Davis and W. B. Watkins. Aust. J. Chem. **21**, 2769 (1968).
9. R. A. Bell and M. B. Gravestock. Can. J. Chem. **47**, 3661 (1969).
10. R. T. Conley. Infrared spectroscopy. Allyn and Bacon, Inc. Boston. 1966. p. 131.
11. W. P. Keaveney, M. G. Berger, and J. P. Pappas. J. Org. Chem. **32**, 1537 (1967).
12. (*a*) N. S. Bhacca and D. H. Williams. Applications of NMR spectroscopy in organic chemistry. Holden-Day. San Francisco. 1964. Chapter II. (*b*) R. F. Zürcher. Helv. Chim. Acta, **46**, 2054 (1963). (*c*) A. I. Cohen and S. Rock, Jr. Steroids, 243 (1964). (*d*) J. W. ApSimon, W. G. Craig, P. V. Demarco, D. W. Mathieson, and W. B. Whalley. Tetrahedron, **23**, 2375 (1967).
13. G. F. Burkinshaw and B. R. Davis. Tetrahedron, **23**, 4147 (1967).
14. F. A. L. Anet and A. R. J. Bourn. J. Amer. Chem. Soc. **87**, 5250 (1965); P. A. Hart and J. P. Davis. J. Amer. Chem. Soc. **91**, 512 (1969) and references therein.
15. M. Adinolfi, G. Laonigro, and L. Mangoni. Gazz. Chim. Ital. **98**, 107 (1968).
16. R. A. Bell and J. K. Saunders. This issue.
17. C. D. Wagner, R. H. Smith, and E. D. Peters. Anal. Chem. **19**, 976 (1947). V. R. Kakatner and N. Jelling. J. Amer. Chem. Soc. **63**, 1432 (1941).
18. N. A. Milas, P. Davis, and J. T. Nolan, Jr. J. Amer. Chem. Soc. 77, 2536 (1955); R. M. Carman and D. E. Cowley. Tetrahedron Lett. 2723 (1968).
19. V. P. Arya, H. Erdtman, and T. Kubota. Tetrahedron, **16**, 255 (1961).
20. E. L. Eliel, N. L. Allinger, S. J. Angyl, and G. A. Morrison. Conformational analysis. John Wiley and Sons, Inc. New York, N.Y. 1965. p. 345.
21. W. Nagata, T. Terasawa, and K. Tori. J. Amer. Chem. Soc. **86**, 3746 (1964).
22. R. A. Raphael and R. Hodges. J. Chem. Soc. 52 (1960).
23. J. Renard and S. Fliszar. Can. J. Chem. **47**, 3333 (1969).
24. S. Fliszar and M. Granger. J. Amer. Chem. Soc. **91**, 3330 (1969).
25. R. Criegee and G. Wenner. Ann. **564**, 9 (1949). R. Criegee. Ann. **583**, 1 (1953). R. Criegee. Rec. Chem. Progr. **18**, 111 (1957).
26. C. D. Johnson and P. S. Bailey. J. Org. Chem. **29**, 703 (1964).
27. S. Sternhell. Quart. Rev. **23**, 236 (1969) and references therein.
28. H. C. Brown and H. M. Hess. J. Org. Chem. **34**, 2206 (1969).
29. H. Budzikiewicz, C. Djerassi, and D. H. Williams. Mass spectrometry of organic compounds. Holden-Day, Inc., San Francisco, Calif. 1967. p. 205.

Can. J. Chem. Downloaded from www.nrcresearchpress.com by 210.87.254.6 on 09/05/12
For personal use only.

Can. J. Chem. Downloaded from www.nrcresearchpress.com by 210.87.254.5 on 09/05/12
For personal use only.

Correlation of the intramolecular nuclear Overhauser effect with internuclear distance

R. A. Bell and J. K. Saunders
Department of Chemistry, McMaster University, Hamilton, Ontario

Received September 3, 1969

A linear relationship between the intramolecular nuclear Overheauser effect (n.O.e.) and the sixth power of the internuclear distance for protons in reasonably compact organic molecules in deuteriochloroform solution is derived. Examples of H—H and CH_3—H interactions from this work and the literature have been used to demonstrate the validity of this relationship. It is shown that application of the observed n.O.e. between two protons or between a proton and a methyl group can be used to determine internuclear distances in unknown structures.

Canadian Journal of Chemistry, 48, 1114 (1970)

Since the first demonstration of the nuclear Overhauser effect (n.O.e.) in proton systems by Kaiser (1), and by Anet and Bourn (2), the phenomenon has been used with striking success in a wide variety of structural and conformational (3) problems in organic chemistry. It is the intention of this paper to show that careful measurement of intramolecular n.O.e.'s leads not only to qualitative structural information but also to quantitative information on internuclear distances. Only proton systems have been studied and the molecules chosen possess unequivocal and fairly rigid structures. Although the theory advanced is based on simple principles and uses first order results, the internuclear distance information obtainable from n.O.e. measurements is remarkably accurate.

Qualitatively, the n.O.e. experienced by a specific proton arises from changes in the proton's longitudinal relaxation time T_1. The factors which contribute to the observed T_1 of a proton include intermolecular effects such as external dipoles, fluctuating magnetic fields, paramagnetic species etc., and intramolecular effects such as anisotropic bonds, time dependent scalar spin–spin interactions, and neighboring dipoles. The total T_1 can be computed from the reciprocal relationship (4) in eq. [1], where T_α,

$$[1] \qquad \frac{1}{T_1} = \frac{1}{T_\alpha} + \frac{1}{T_\beta} + \frac{1}{T_\gamma} + \ldots .$$

T_β, etc., are measures of the contribution of each specific type of relaxation mechanism open to the proton. In many examples of organic molecules which are not undergoing chemical exchange, the dominant intramolecular contributor to T_1 appears to be the dipole–dipole interaction between a given proton and its nearest neighbors (4, 5).

Quantitatively, the n.O.e. can be treated by considering the Bloch phenomenological equations as derived by Solomon (6) and Abragam (7). For 2 weakly coupled and mutually interacting protons A and B, any perturbation of the system results in a return to equilibrium given by eqs. [2] and [3], where M_z^A is the instantaneous

$$[2] \qquad \frac{dM_z^A}{dt} = -\frac{1}{T_{AA}}(M_z^A - M_0^A) - \frac{1}{T_{BA}}(M_z^B - M_0^B)$$

$$[3] \qquad \frac{dM_z^B}{dt} = -\frac{1}{T_{BB}}(M_z^B - M_0^B) - \frac{1}{T_{AB}}(M_z^A - M_0^A)$$

magnetization of proton A, M_0^A is the equilibrium magnetization, T_{AA} is the total of the intermolecular and the intramolecular contributions to the longitudinal relaxation time of proton A, and T_{BA} is the specific contribution to the longitudinal relaxation time of A arising from the interaction of A with B. The terms involving the B proton are similarly defined. If we saturate the resonance signal of A, eq. [2] is no longer valid, and $M_z^A = 0$; and further, when the system has regained equilibrium, $dM_z^B/dt = 0$ and eq. [3] becomes, on rearranging, eq. [4]. That is, the observed area of the B resonance signal will *increase* by the

$$[4] \qquad M_z^B = M_0^B + M_0^A \frac{T_{BB}}{T_{AB}}$$

Can. J. Chem. Downloaded from www.nrcresearchpress.com by 210.87.254.5 on 09/05/12
For personal use only.

fraction M_0^A. T_{BB}/T_{AB} and a knowledge of the relative values of T_{BB} and T_{AB} can lead to an assessment of the area increase to be expected for the B signal.[1] In the general case of 2 interacting nuclear dipoles of spins I and S, the ratio of the relaxation times in the limit of extreme narrowing is given by (9) eq. [5]. For protons the maximum

$$[5] \qquad \frac{T_{II}}{T_{IS}} = \frac{I(I+1)}{2S(S+1)}$$

value of the ratio T_{BB}/T_{AB} is 1/2 and the maximum area increase expected for the proton B signal is 50%. The theoretical assessment of T_{BB} and T_{AB} can be carried out by expressing the time constants in terms of transition probabilities (6, 8) which in turn can be expressed in terms of distances and simple forces (9). Thus, provided the A–B dipolar interaction is the dominant intramolecular relaxation mechanism and that the solute molecules are spherical and the forces exerted on the molecule are spherically symmetric, the time constant T_{AB} can be evaluated as (9) shown in eq. [6], where r_{AB} is the internuclear separation

$$[6] \qquad \frac{1}{T_{AB}} = \frac{3}{10}\hbar^2\gamma_H{}^4 \frac{1}{r_{AB}{}^6}\left[\frac{2\tau_r}{1+(\omega_A+\omega_B)^2\tau_r{}^2} - \frac{1}{3}\frac{\tau_r}{1+(\omega_A-\omega_B)^2\tau_r{}^2}\right]$$

of protons A and B, τ_r is the isotropic molecular rotational correlation time, ω_A and ω_B are the resonance frequencies of A and B,[2] and the other symbols have their usual significance. In the limit of extreme narrowing, that is when $\omega_A{}^2\,\tau_r{}^2$ and $\omega_B{}^2\,\tau_r{}^2 \ll 1$, a situation which is valid for dilute solution in non-viscous solvents, eq. [6] reduces to eq. [7].

$$[7] \qquad \frac{1}{T_{AB}} = \tfrac{1}{2}\hbar^2\gamma_H{}^4 \frac{1}{r_{AB}{}^6}\tau_r$$

The time constant T_{BB} can be written as a sum of an intramolecular and an intermolecular contribution, eq. [8]. The first term in this expression is given by (9) eq. [9], and if the A–B dipolar interaction is the sole interaction present, then $r = r_{AB}$ and in the limit of extreme narrowing eq. [9] becomes eq. [10]. In the general situation

$$[8] \qquad \frac{1}{T_{BB}} = \left(\frac{1}{T_1{}^{BB}}\right)_{intra} + \left(\frac{1}{T_1{}^{BB}}\right)_{inter}$$

$$[9] \qquad \left(\frac{1}{T_1{}^{BB}}\right)_{intra} = \frac{3}{10}\hbar^2\gamma_H{}^4 \frac{1}{r^6}\left[\frac{1}{3}\frac{\tau_r}{1+(\omega_B-\omega_A)^2\tau_r{}^2} + \frac{\tau_r}{1+\omega_B{}^2\tau_r{}^2} + \frac{2\tau_r}{1+(\omega_A+\omega_B)^2\tau_r{}^2}\right]$$

$$[10] \qquad \left(\frac{1}{T_1{}^{BB}}\right)_{intra} = \hbar^2\gamma_H{}^4 \frac{1}{r_{AB}{}^6}\tau_r$$

where more than one proton relaxes B, the contributions to $(1/T_1{}^{BB})_{intra}$ can be approximated by adding additional like terms to eq. [10] where r adopts values corresponding to the various internuclear distances. This approximation neglects cross relaxation terms which is considered (9) a valid approximation for solutes in dilute solution.

The intermolecular term in eq. [8] is more complex and, since we are concerned with a solute in dilute solution, we must take into account the relaxation effects of the solvent. A general expression for such a situation (10), in the limit of extreme narrowing is eq. [11], where $\sum_S$

$$[11] \qquad \left(\frac{1}{T_1{}^{BB}}\right)_{inter} = \frac{6}{5}\hbar^2\gamma_H{}^4 \frac{\tau_t}{r_B{}^6} + \frac{2}{5}\hbar^2\gamma_H{}^2\tau_t \sum_S \gamma_S{}^2 S(S+1) \sum_b^\infty \frac{1}{r^6}$$

represents the sum over all possible solvent nuclei of spin S, r_B is the distance between proton B and other solute protons, r is the distance between proton B and all other solvent nuclei, b is the radius of closest approach, and τ_t is the isotropic translational correlation time. The first term in this expression can be neglected for dilute solutions as the distance r_B which refers to distances between solute molecules will be large. In addition the summation $\sum_b^\infty 1/r^6$ can be well approximated by $1/b^6$, since solvent molecules beyond those at the distance of closest approach, the first solvation sphere of proton B, will contribute very little to the summation

[1] A signal decay technique can be readily used to determine T_{BB} and T_{BA} (8).

[2] This formulation is true if A and B have different chemical shifts where for a given field strength H_0, $|\omega_A - \omega_B| \gg \frac{1}{T_2{}^A}, \frac{1}{T_2{}^B}$ (9).

Can. J. Chem. Downloaded from www.nrcresearchpress.com by 210.87.254.5 on 09/05/12
For personal use only.

because of the sixth power relationship. Hence eq. [11] can be expressed as eq. [12]. Substituting

$$[12]\quad \left(\frac{1}{T_1^{BB}}\right)_{inter} = \frac{2}{5}\hbar^2\gamma_H{}^2\tau_t\sum_S \gamma_S{}^2 S(S+1)\frac{1}{b^6}$$

eqs. [10] and [12] into eq. [8] gives eq. [13].

$$[13]\quad \frac{1}{T_{BB}} = \hbar^2\gamma_H{}^4\tau_r\frac{1}{r_{AB}{}^6} + \frac{2}{5}\hbar^2\gamma_H{}^2\tau_t\sum_S \gamma_S{}^2 S(S+1)\frac{1}{b^6}$$

We can now write the ratio T_{AB}/T_{BB} from eqs. [9] and [13] as eq. [14]. Inspection of the terms

$$[14]\quad \frac{(1/T_{BB})}{(1/T_{AB})} = \frac{\hbar^2\gamma_H{}^4\tau_r\frac{1}{r_{AB}{}^6} + \frac{2}{5}\hbar^2\gamma_H{}^2\tau_t\sum_S \gamma_S{}^2 S(S+1)\frac{1}{b^6}}{\frac{1}{2}\hbar^2\gamma_H{}^4\tau_r\frac{1}{r_{AB}{}^6}} = 2 + \left[\frac{4}{5}\frac{1}{\gamma_H{}^2}\frac{\tau_t}{\tau_r}\sum_S \gamma_S{}^2 S(S+1)\frac{1}{b^6}\right] r_{AB}{}^6$$

in brackets shows that for a given solvent, and temperature all the terms are constant with the exception of $1/b^6$ and the ratio τ_t/τ_r which should be solute dependent. However, if we note that in the examples studied below all the protons are on the periphery of the solute molecule and the deuteriochloroform solvent molecules will be able to approach these protons to within approximately the same distance. That is, we can reasonably assume that the distance of closest approach of the deuteriochloroform to the protons of different solutes will be approximately constant. The correlation times τ_t and τ_r both refer to isotropic motion and when this is true, the ratio τ_t/τ_r is constant (7). However, very few organic molecules possess a spherically symmetric framework and the molecular reorientation rate should be considered independently along orthogonal axes. Hertz (9) has treated the case of an ellipsoidal molecule and has shown that, provided the molecule is not of the long chain type, the ratio of the reorientation times along the 2 ellipse axes is close to unity. In all the examples studied below we are concerned with the relaxation of a proton on a fairly rigid and compact molecular system and hence the assumption of representing the molecular motion as isotropic would appear a valid approximation. This assumption receives some justification from the work of Zeidler (11) where the ratio of τ_t/τ_r for benzene, pyridine, and cyclohexane was found to be approximately constant. Hence, to first order the ratio of τ_t/τ_r for different solutes of reasonably compact structure may be taken as constant and therefore the whole expression in brackets in eq. [14] may be taken as approximately constant for different solutes. Thus rewriting eq. [4] as eq. [15] and

$$[15]\quad \frac{M_z{}^B - M_0{}^B}{M_0{}^A} = \text{n.O.e.} = \frac{T_{BB}}{T_{AB}}$$

substituting in eq. [14] gives eq. [16] where A is a

$$[16]\quad \frac{1}{\text{n.O.e.}} = 2 + Ar_{AB}{}^6$$

constant. This relationship is however a combination of two separate equations which take into account the 50% maximum present in the dependence of an n.O.e. on the internuclear distance. When r_{AB} assumes small values, less than some value $r^0{}_{AB}$ say, which must be experimentally determined, the n.O.e. approaches the limiting value of 1/2 and eq. [16] becomes simply eq. [16*a*]. When r_{AB} has values greater

$$[16a]\quad \frac{1}{\text{n.O.e.}} = 2$$

than this distance $r^0{}_{AB}$, then eq. [16] must be represented as eq. [16*b*].

$$[16b]\quad \frac{1}{\text{n.O.e.}} = Ar_{AB}{}^6$$

To test the validity of this equation and to assess its application to structural problems, we have chosen a set of compounds where single proton–proton interactions can be examined, and where interactions between a proton and CH_3-protons can be studied. To avoid problems arising from bond angle distortion compounds with H—H distances of the order of the sum of the van der Waals' radii of hydrogen (2.2–2.4 Å) and greater have been selected.

TABLE 1

Observed n.O.e. and internuclear distance for H–H interaction

No.	Structure	Proton irradiated	Proton observed	n.O.e. (%)	Internuclear distance (Å)
1	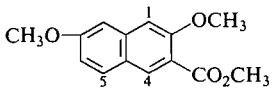	C_5-H	C_4-H	25	2.44
2*	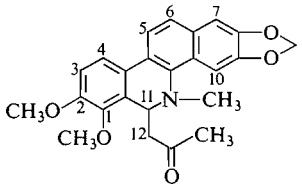	C_6-H	C_7-H	27	2.44
3†	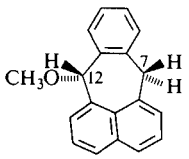	C_7-H (ax.)	C_{12}-H	28	2.40
4	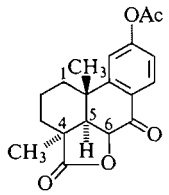	C_5-H	C_6-H	22	2.50
5‡	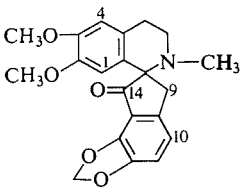	C_9-H	C_{10}-H	10	2.88
6	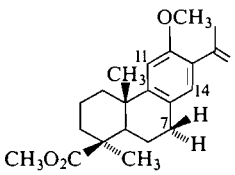	C_7-H (eq.) C_7-H (ax.)	C_{14}-H C_{14}-H	18 12	2.58 2.79
7	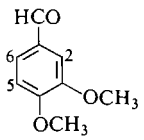	C_5-H	C_6-H	29	2.42

*(3*i*).
†(12).
‡(3*a*).

Can. J. Chem. Downloaded from www.nrcresearchpress.com by 210.87.254.5 on 09/05/12
For personal use only.

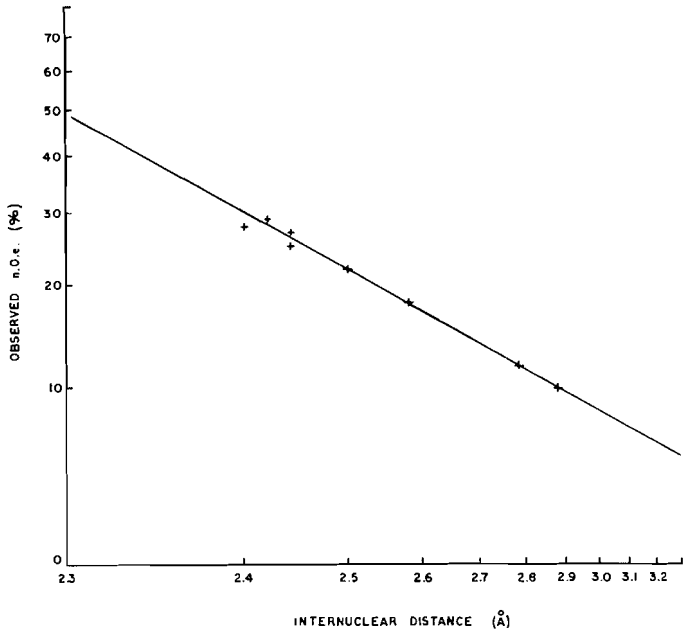

FIG. 1. Plot of observed n.O.e. against internuclear distance for H—H interaction (logarithmic axes).

Results and Discussion

The n.O.e. results obtained when irradiating and observing single protons are shown in Table 1 together with the internuclear distance as measured from Dreiding models. From these data a plot of n.O.e. against internuclear distance (logarithmic axes) has been constructed (Fig. 1). The plot shows a straight line of slope -6 as predicted by eq. [16*b*]. Considering the errors possible, $\pm 1\%$ in observed n.O.e. and ± 0.04 Å for the distance, the points all fall well within the bounds of experimental error. The slope of the line is further evidence for the dominance of the dipole–dipole relaxation mechanism within an all proton system and for moderately dilute solutions the intramolecular interactions greatly predominate over intermolecular effects (12). The excellent linearity of the experimental points indicates that the gross approximations of taking τ_1/τ_r and $1/b^6$ as constant for different solutes are either remarkably good approximations or alternatively, that there is perhaps a compensation of the 2 effects. Clearly, from an experimental viewpoint, even though the solute molecular size and solvent properties (4, 13) are important factors in the absolute measurements of T_1, in the measurement of n.O.e.'s they appear to play a very minor role.

Table 2 shows the results obtained for the CH_3—H interactions, these being represented by a plot in Fig. 2. The slope of the straight line obtained is again -6. The internuclear distance measured in this instance is that between the single proton and the point defined by the intersection of the 3-fold rotation axis of the CH_3 group and the plane through the 3 protons of the CH_3 group. This vector was taken since the rotational motion of the CH_3 group will be very fast compared to the relaxation rate of the single proton and the net effect at the single proton must

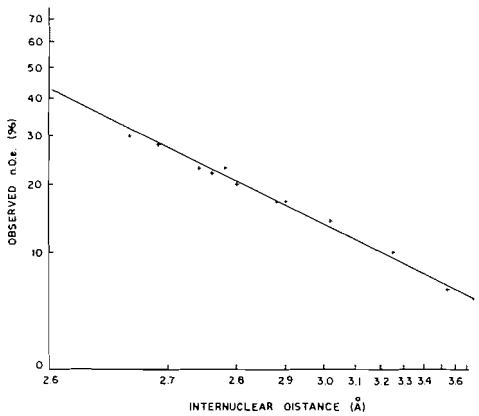

FIG. 2. Plot of observed n.O.e. against internuclear distance for CH_3—H interaction (logarithmic axes).

Can. J. Chem. Downloaded from www.nrcresearchpress.com by 210.87.254.5 on 09/05/12
For personal use only.

TABLE 2

Observed n.O.e. and internuclear distance for CH_3–H interaction

No.	Structure	Proton irradiated	Proton observed	n.O.e. (%)	Internuclear distance (Å)
8	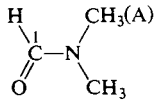	$CH_3(A)$	C_1-H	28	2.69
2	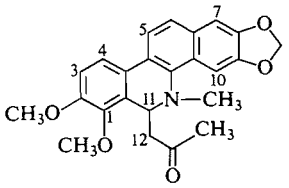	N-CH_3	C_{10}-H	30	2.66
		N-CH_3	C_{11}-H	23	2.78
9*	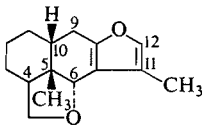	C_{11}-CH_3	C_{12}-H	17	2.88
		C_{11}-CH_3	C_6-H	6	3.56
		C_5-CH_3	C_6-H	23	2.74
10†	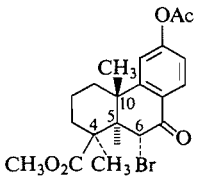	C_4-CH_3	C_6-H	22	2.76
		C_{10}-CH_3	C_6-H	10	3.25
4	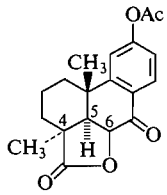	C_4-CH_3	C_5-H	20	2.80
		C_4-CH_3	C_6-H	14	3.02
11‡	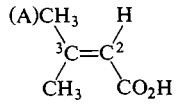	$CH_3(A)$	C_2-H	17	2.90

*(3*f*).
†(3*b*).
‡(2).

be averaged over this motion. In the most rigorous sense the length and direction of the internuclear vector should be defined as averaged over the specific conformations available to the CH_3 group and this may well place the end of the vector at some point off the methyl-3-fold axis. However, the errors inherent in locating the most likely methyl conformations makes attempts at more rigorous measurements unattractive and it is felt that the vector used here is adequate for the accuracy of the current n.O.e. data. ApSimon *et al.* (14) in a study of methyl group chemical shift changes arising from neighboring anisotropic bonds have measured distances to the CH_3

Can. J. Chem. Downloaded from www.nrcresearchpress.com by 210.87.254.5 on 09/05/12
For personal use only.

TABLE 3

Nuclear Overhauser effects for protons with more than one relaxation pathway

No.	Structure	Proton irradiated	Proton observed	n.O.e. (%)	Internuclear distance (Å)
7	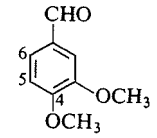	C_4-OCH_3	C_5-H	25	—
12	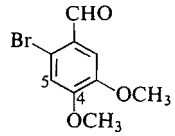	C_4-OCH_3	C_5-H	40	—
13*	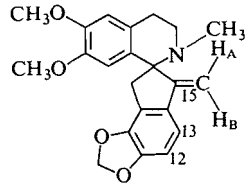	C_{15}-H_A	C_{15}-H_B	40	1.82
		C_{13}-H	C_{15}-H_B	8	2.40
		C_{15}-H_B	C_{13}-H	24	2.40
		C_{12}-H	C_{13}-H		2.42

*(15).

group in a similar manner and found the method to be quite satisfactory.

As in the case of H—H interactions, the deviations of individual CH_3—H interaction points from the straight line of Fig. 2 are remarkably small and carry similar implications about the assumptions made in deriving eq. [16] as were noted above. The constant, A, of eq. [16] has values for the H—H and CH_3—H interactions of 1.8×10^{-2} and 0.98×10^{-2} respectively. The slightly lower value of A for the CH_3—H interaction may perhaps be a result of the CH_3 group decreasing the solvent effect on the single proton by virtue of its size; that is causing an increase in the effective value of b. However, detailed interpretation of the specific value of A is considered to be unwarranted at this point in the absence of more extensive data on additional compounds and solvent systems. The most significant empirical implication of the data in Figs. 1 and 2 is that it is possible by observing n.O.e.'s in an unkown structure, to deduce with reasonable accuracy the internuclear distance between individual protons and between protons and methyl groups. This knowledge should aid greatly in structure determination problems and also in conformational problems.

Extrapolation of the plots of Figs. 1 and 2 back to n.O.e.'s of the order of 5% shows that measurable H—H and CH_3—H interactions should be present at distances of 3.4 Å and 3.7 Å respectively. However, this situation is valid only if a proton is relaxed solely by another proton or by a single methyl group. In most practical cases a proton will be relaxed by more than one proton or group of protons and then it may not be possible to observe n.O.e.'s at such large distances as deduced from the plots. In quantitative terms, if we have a proton A relaxed intramolecularly by protons B, C, ... then neglecting any cross terms, we have, from eq. [1], eq. [17] which by

$$[17] \qquad \frac{1}{T_1^{A}} = \frac{1}{T_1^{AB}} + \frac{1}{T_1^{AC}} + \ldots .$$

application of eq. [16] gives eq. [18] with a maximum n.O.e. (A) = 50%.

$$[18] \quad \text{n.O.e. (A)} = \text{n.O.e. (AB)} + \text{n.O.e. (AC)} + \ldots .$$

Thus an observed n.O.e. can be less than indicated by Figs. 1 and 2 because of efficient relaxation by more than one proton. In Table 3 this effect is illustrated by replacing the C-6

Can. J. Chem. Downloaded from www.nrcresearchpress.com by 210.87.254.5 on 09/05/12
For personal use only.

Can. J. Chem. Downloaded from www.nrcresearchpress.com by 210.87.254.5 on 09/05/12
For personal use only.

proton of **7** by the much less efficient relaxing bromine atom (compound **12**) and comparing the difference in observed n.O.e. between the C_4—OMe and the C_5—H. In compound **12** the n.O.e. is 40% whereas in **7**, with the proton at C_6, the observed n.O.e. is reduced to 25%. Another example of this effect is noted for the alkaloid ochotensimine (15) (Table 3). The internuclear distance between C_{15}—H_A and H_B is 1.82 Å with an observed n.O.e. at H_B of 40% which is less than the 50% expected from the graph. Irradiation of C_{13}—H results in an 8% area enhancement in C_{15}—H_B. In this situation with 2 nuclei very close to the proton H_B, it is no longer possible to uniquely deduce each of the 2 internuclear distances. However, it is possible to deduce a value for the ratio of the 2 internuclear distances from the n.O.e. data. Thus, if the distance of H_B from C_{15}—H_A is taken as r_1 and the distance of H_B from C_{13}—H is taken as r_2 then the ratio $1/r_1^6 : 1/r_2^6$ has a value of 5.2:1 and this compares favorably with the ratio of 5:1 observed for the 2 n.O.e.'s at H_B. The validity of this procedure will be dealt with in a subsequent publication.

In the general case of multiple relaxation by unlike spins then, it is only possible to directly obtain internuclear distances from the plots of Figs. 1 and 2 when the protons are beyond the sum of their van der Waals' radii and each of the n.O.e.'s is fairly small. In other cases where the protons closely approach one another only ratios of the internuclear distances are obtainable.[3]

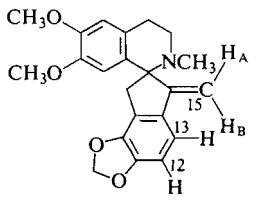

13

[3]In many cases additional outside information may be available which would lead to an assessment of individual internuclear distances. For example in the case of ochotensimine **13** above, the distance between geminal protons is a well-established quantity and its knowledge leads directly to an estimate of the C_{15}—H_B to C_{13}—H distance.

A technique which can be very useful in determining whether a particular proton is interacting with more than one other proton, is based on the non-equivalence of T_{BA} with T_{AB} (eqs. [2] and [3]). A typical example of this is found in ochotensimine **13**, where irradiation of C_{13}—H causes an 8% n.O.e. at C_{15}—H_B but reversal of the process causes a 24% n.O.e. at C_{13}—H when C_{15}—H_B is irradiated. This difference arises because both H_B and C_{13}—H have additional and different protons contributing to their relaxations.

It is important to note that in order to obtain *reliable* n.O.e. data which may be applied to internuclear distance determinations, special care must be paid to sample preparation. There should be no traces of paramagnetic materials present; solid particles should be removed by filtration (fine sintered glass) and dissolved oxygen removed by at least 5 freeze–thaw cycles on a good high vacuum line. Care must also be taken during the double resonance experiment that the combined H_1 and H_2 r.f. fields do not cause saturation of the observed spectral lines and that the H_2 field is precisely positioned.

Summary

A linear relationship between the reciprocal of an n.O.e. between 2 protons and the sixth power of the internuclear distance has been constructed for compounds in dilute solution. Using a number of examples from this work and the literature, it has been shown that measurement of the n.O.e. between 2 protons or between a proton and a methyl group can be used to predict with reasonable accuracy the internuclear distance. With the methyl group the distance is measured from the center of the circle formed by rotation of the 3 methyl protons. When more than one proton or group of non-equivalent protons relax a single proton, it is generally not possible to uniquely determine each internuclear distance but only their ratios.

Experimental

All compounds used were of analytical purity and were obtained from the following sources (references are given to structure proof where pertinent): 2,7-dimethoxy-3-carbomethoxynapthalene (**1**), P. K. Oommen (16*a*); 11-acetonyl-dehydrocheleryther ine (**2**), D. B. MacLean (3*i*); 12-acetoxy-6β-hydroxy-7-oxopodocarp-8,11,13-triene-19-oic acid (6 → 19)-lactone (**4**), E. N. C. Osakwe (17*a*); fumariline (**5**), D. B. MacLean (3*a*); methyl 14-isopropylidene-12-methoxypodocarp-8,11,13-triene-19-oate (**6**),

P. K. Oommen (16*a*, 18); veratraldehyde (7), Eastman Kodak Ltd.; methyl 12 - acetoxy - 6α - bromo - 7 -oxo-podocarp-8,11,13-triene-19-oate (**10**), E. N. C. Osakwe (17*a*, 19); 6-bromoveratraldehyde (**12**), C.-Y. Chen (20); ochotensimine (**13**), S. McLean (21).

All spectra were recorded on a Varian Associates HA-100 spectrometer using frequency sweep mode. The second r.f. field was obtained by using a Hewlett Packard model 201 C audio generator. The strength of the r.f. field was measured on the oscilloscope incorporated in the instrument, calibration in units of mG being obtained as described by Baldeschweiler (22) using a degassed $CHCl_3$ in CCl_4 solution.

The spectra of all compounds were run as filtered (fine sintered glass) and carefully degassed $CDCl_3$ solutions, the concentration varying between 5 and 10%. A small amount of TMS was added as an internal lock.

The Overhauser effects were measured as area increases using the electronic integrator of the instrument. All area measurements were recorded with the second r.f. field on. The spectra were run with the oscillator at a position well away from any proton absorption to check that no saturation was occuring. The oscillator frequency was then placed at the required frequency to saturate the proton in question and the area recorded. The frequency and the strength of H_2 were then optimized to give a maximum area increase. Finally H_2 was moved to a frequency greater than 30 Hz from any proton absorption to give a standard area. The area at each frequency was measured at least 10 times and after each area had been recorded, the system was allowed to return to equilibrium by waiting for a period of time, varying from 30 s to 5 min depending on the proton being observed. The possibility of the position of H_2 affecting the integral was checked and it was found that providing H_2 was greater than 25 Hz away from H_1 its position had no effect on the recorded standard area.

It is felt that the above method is the most accurate available as results reproducible to ± 1% have been obtained by changing samples, instrument probes and operators. Some workers (3*j*) have measured intensities directly but this method can be slightly suspect particularly if small coupling occurs between the 2 protons in question.

The internuclear distance measurements were made with the aid of Dreiding molecular models (23) and are the average of several measurements on models assembled from different units. The CH_3—H distances were measured following the method of ApSimon *et al.* (24).

We thank the individuals named above for their generous gifts of samples and Professor J. W. ApSimon for his gift of a CH_3—H measurement device. We thank the National Research Council of Canada for financial support of this work and for a Fellowship to J. K. Saunders. We wish to acknowledge the helpful criticism of the referees.

1. R. Kaiser. J. Chem. Phys. **42**, 1838 (1965).
2. F. A. L. Anet and A. J. R. Bourn. J. Amer. Chem. Soc. **87**, 5250 (1965).
3. (*a*) J. K. Saunders, R. A. Bell, C.-Y. Chen, D. B. MacLean, and R. H. F. Manske. Can. J. Chem. **46**, 2876 (1968). (*b*) R. A. Bell and E. N. C. Osakwe. Chem. Commun. 1093 (1968). (*c*) K. Tori, M. Ohtsuru, I. Horibe, and K. Takeda. Chem. Commun. 943 (1968). (*d*) D. J. Aberhart, K. H. Overton, and S. Hunek. Chem. Commun. 162 (1969). (*e*) T. Tomimatsu, H. Hashimoto, T. Shingu, and K. Tori. Chem. Commun. 168 (1969). (*f*) Y. Ishizaki, Y. Tanahashi, T. Takahashi, and K. Tori. Chem. Commun. 551 (1969). (*g*) G. R. Newkome and N. S. Bhacca. Chem. Commun. 385 (1969). (*h*) E. L. Eliel and F. Nader. J. Amer. Chem. Soc. **91**, 536 (1969). (*i*) D. B. MacLean, D. E. F. Gracey, J. K. Saunders, R. Rodrigo, and R. H. F. Manske. Can. J. Chem. **47**, 1951 (1969). (*j*) P. A. Hart and J. P. Davis. J. Amer. Chem. Soc. **91**, 512 (1969) and references cited therein.
4. N. Bloembergen, E. M. Purcell, and R. V. Pound. Phys. Rev. **73**, 679 (1948).
5. I. Solomon and N. Bloembergen. J. Chem. Phys. **25**, 261 (1956); R. Kaiser. J. Chem. Phys. **42**, 1838 (1965).
6. I. Solomon. Phys. Rev. **99**, 559 (1955).
7. A. Abragam. The principles of nuclear magnetism. Oxford University Press, New York, 1961. Chapter VIII.
8. R. A. Hoffman and S. Forsén. J. Chem. Phys. **45**, 2049 (1966).
9. H. G. Hertz. Progr. Magn. Resonance, **3**, 159 (1967); see also reference (7).
10. H. S. Gutowsky and D. E. Woessner. Phys. Rev. **104**, 843 (1956); see also J. G. Powles. Ber. Bunsenges. Phys. Chem. **67**, 328 (1963).
11. M. D. Zeidler. Ber. Bunsenges. Phys. Chem. **69**, 659 (1963).
12. J. C. Colson, P. T. Lansbury, and F. D. Saeva. J. Amer. Chem. Soc. **89**, 4987 (1967).
13. F. A. Bovey. J. Chem. Phys. **32**, 1877 (1963).
14. J. W. ApSimon, W. G. Craig, P. V. Demarco, D. W. Mathieson, L. Saunders, and W. B. Whalley. Tetrahedron, **23**, 2357 (1967); see also A. D. Cross and I. T. Harrison. J. Amer. Chem. Soc. **85**, 3223 (1963).
15. R. A. Bell and J. K. Saunders. Can. J. Chem. **46**, 3421 (1968).
16. (*a*) P. K. Oommen. Ph.D. Thesis. McMaster University, Hamilton, Ontario, 1968. (*b*) S. V. Sunthanker and H. Gilman. J. Org. Chem. **16**, 8 (1951).
17. (*a*) E. N. C. Osakwe. Ph.D. Thesis. McMaster University, Hamilton, Ontario, 1969. (*b*) E. Wenkert, P. Beak, R. W. J. Carney, J. W. Chamberlain, P. B. R. Johnston, C. D. Roth, and A. Tahara. Can. J. Chem. **41**, 1924 (1963).
18. W. R. Campbell and D. Todd. J. Amer. Chem. Soc. **62**, 1287 (1940).
19. R. C. Cambie, C. R. Clark, D. R. Crump, and T. N. Waters. Chem. Commun. 183 (1968).
20. C.-Y. Chen. Private communication.
21. S. McLean, M.-S. Lin, and R. H. F. Manske. Can. J. Chem. **44**, 2449 (1966); S. McLean, M.-S. Lin, A. C. MacDonald, and J. Trotter. Tetrahedron Lett. 3819 (1964).
22. J. D. Baldeschweiler. J. Chem. Phys. **40**, 459 (1964).
23. A. Dreiding. Helv. Chim. Acta, **42**, 1339 (1959).
24. J. W. ApSimon, W. G. Craig, A. Demayo, and A. A. Raffler. Can. J. Chem. **46**, 809 (1968).

Can. J. Chem. Downloaded from www.nrcresearchpress.com by 210.87.254.5 on 09/05/12
For personal use only.

Structure of a galactomannan from seed of *Crotalaria mucronata*

A. M. UNRAU AND Y. M. CHOY
Department of Chemistry, Simon Fraser University, Burnaby 2, British Columbia
Received August 21, 1968[1]

A galactomannan, purified by repeated complexation with copper acetate, was shown to be composed of D-mannose and D-galactose in a molar ratio of 3:1. Methylation of the polysaccharide followed by hydrolysis gave 2,3,4,6-tetra-*O*-methyl-D-mannose, 2,3,4,6-tetra-*O*-methyl-D-galactose, 2,3,6-tri-*O*-methyl-D-mannose, 2,4,6-tri-*O*-methyl-D-mannose, 3,4,6-tri-*O*-methyl-D-mannose (from 1→ 2-linkages), and 2,3-di-*O*-methyl-D-mannose (molar ratio 1:23:28:11:4:26). Periodate degradation further indicated that the galactose units occupied single unit branch points linked (1 → 6). One in every 6 mannose units was resistant to periodate attack further suggesting the presence of (1 → 3)-linkages. An approximately equimolar occurrence of 2-*O*-β-D-mannopyranosyl-D-erythritol and *O*-β-D-mannopyranosyl-(1 → 3)-2-*O*-β-D-mannopyranosyl-D-erythritol indicated a significant frequency of isolated and consecutive (1 → 3)-linkages. In conjunction with results from methylation experiments a relatively simple structure may be assigned.

Canadian Journal of Chemistry, 48, 1123 (1970)

Discussion

A rather large number of gums of varying composition and varying degrees of structural complexity have been isolated from seed of legumes. Ordinarily, the neutral gums mostly found in the endosperm are less complex structurally (composed of D-mannose and D-galactose in varying ratios) than the acid polysaccharides which are more characteristically associated with seed coats and usually contain more than just 2 building units.

Extraction of broken seed of *Crotalaria mucronata* with hot water resulted in a highly viscous solution upon cooling. Usual alcohol precipitation resulted in a characteristic grey, stringy precipitate. The polysaccharide was purified by repeated complexation with copper acetate (1, 2) ($[\alpha]_D^{22}$ 6–10° in 0.1 *N* NaOH). This low value suggests that the glycosidic linkages in the main chain have the β-anomeric configuration as has been found for numerous similar galactomannans (3). Since the galactomannan was unaffected by prolonged treatment with emulsin, p*H* 7.0, 22 °C, it would appear that the galactose units are attached by α-linkages.[2] Ultracentrifugation showed a single peak and from the sedimentation rate, an approximate molecular weight of 50 000 was obtained. Hydrolysis of the polysaccharide gave D-mannose and D-galactose in a molar ratio of 3:1. The galactose content is higher than that found in some of the more commonly known galactomannans such as guar gum (16% galactose), Carob bean (14–27% galactose), and Kentucky coffee bean (20% galactose), although some galactomannans are known which have up to 50% galactose (4).

Hydrolysis of the fully methylated gum gave the following partially methylated sugars: 2,3,4,6-tetra-*O*-methyl-D-galactose, 2,3,4,6-tetra-*O*-methyl-D-mannose, 2,4,6-tri-*O*-methyl-D-mannose, 2,3,6-tri-*O*-methyl-D-mannose, 3,4,6-tri-*O*-methyl-D-mannose, and 2,3-di-*O*-methyl-D-mannose, molar ratio 23:1:11:28:4:26 (from vapor phase chromatography (v.p.c.)). The presence of the above sugars is in agreement with the periodate oxidation results, namely, approximately 1 of every 6 mannose units is linked (1 → 3) and the occurrence of a small number of (1 → 2)-linkages is also indicated. All of the galactose units occupy terminal, non-reducing "branch point" positions since the ratio of tetra-*O*-methyl-galactose to di-*O*-methylmannose is essentially 1:1 (the slightly lower tetra-*O*-methyl-D-galactose quantity, Table 1, is probably due to inadvertent loss during evaporation). The absence of 2,4-di-*O*-methyl-D-mannose indicated that no (1 → 3)-linked mannose units were associated with branching at C-6. The approximate size of the repeating unit based on the amount of tetra-*O*-methylmannose found was 80. Since from ultracentrifugation

[1]Revision received September 26, 1969.
[2]Ample evidence is cited in the literature regarding the specificity of the enzyme(s) found in almond emulsin. Emulsin displays the combined ability found for the separate enzymes β-glucosidase, β-galactosidase, β-D-fucosidase (see for example ref. 18).

Can. J. Chem. Downloaded from www.nrcresearchpress.com by 210.87.254.42 on 09/05/12
For personal use only.

TABLE 1

Vapor phase chromatography of TMS derivatives of partially methylated sugars

TMS derivative	Retention time (min)	Molar ratio
2,3,4,6-M*	16.5	1
2,3,4,6-Gal†	15.3 (α-anomer) 18.9 (β-anomer)	23
2,4,6-M	12.2	11
3,4,6-M	10.6	4
2,3,6-M	13.5	28
2,3-M	8.5	26

*2,3,4,6-M = 2,3,4,6-tetra-*O*-methyl-D-mannose.
†2,3,4,6-G = 2,3,4,6-tetra-*O*-methyl-D-galactose.

an approximate molecular weight of 50 000 may be deduced, approximately 4 repeating units constitute 1 macromolecule.

Treatment of the polysaccharide with periodate (4–5 °C) resulted in periodate consumption of slightly less than 1 mole per hexose unit. Reduction of the polyaldehyde with borohydride followed by mild acid hydrolysis (Smith degradation) gave glycerol, erythritol (no threitol), and 2 non-reducing components with slower paper chromatographic mobilities than galactose. Analysis of the hydrolysis mixture for intact hexose by the phenol – sulfuric acid method (5) indicated that 18–20% had survived periodate attack. No oligomeric fragments were found at the starting boundaries of the paper chromatograms. The relatively large amount of glycerol formed may be attributed to terminal, non-reducing mannose and galactose units, mostly the latter since galactose residues are ordinarily not linked (1 → 4) or (1 → 6) along the main chain. Furthermore, threitol, which was not present, would arise from galactose units consecutively linked (1 → 4). The relatively major quantity of erythritol produced shows that the main chain of the polysaccharide is composed of mannopyranose units predominantly joined by β-(1 → 4)-glycosidic linkages. The above findings indicate that the galactose units are present as single unit branch points primarily linked (1 → 6) to approximately every third mannose unit of the main chain. The presence of the 2 non-reducing oligosaccharide fractions indicated that a smaller proportion of other than (1 → 4)- and (1 → 4)-(1 → 6)-linkages existed. Hydrolysis of component **1**, $R_{Man} = 0.61$, gave mannose and erythritol in a molar ratio of 1:1. This finding indicates that a minor proportion of mannose units were linked (1 → 3) and these were flanked by (1 → 4)-linked units, e.g., D-Manp*1,4*βD-Manp*1,3*βD-Manp*1,4*β. Oligosaccharide II, $R_{Man} = 0.33$, the molar ratio of I and II being approximately 1:1, when hydrolyzed, gave mannose and erythritol in a ratio of 2:1 indicating a minor proportion of mannose units consecutively linked (1 → 3), e.g., D-Manp*1,4*βD-Manp*1,3*βD-Manp*1,3*βD-Manp*1,4*β. A further Smith type periodate degradation of II gave a non-reducing component (shown by hydrolysis to consist of mannose and glycerol, molar ratio 1:1), glycerol, and formaldehyde. Formaldehyde would be expected from C-4 of the erythritol moiety of II, whereas glycerol would arise from the terminal, non-reducing mannose unit joined (1 → 3) to the subsequent "internal" hexose unit. The internal (1 → 3)-linked mannose unit would be immune to periodate attack.

From the methylation and periodate oxidation experiments, a reasonably simple structure for the particular galactomannan may be assigned with relative certainty, particularly since the polysaccharide was immune to action of emulsin and the identity of the methylated sugars was definitely established directly or through degradation. The structure shown in Chart 1 is consistent with the experimental results obtained. The low incidence of (1 → 2)-linkages in the main mannose chain (4 in 70) is, due to complexity of representation, not included in the above structural notation. It is not intended that the structural notation given necessarily implies a regularized sequence since a more random sequence can also fit the results.

Experimental

All evaporations were carried out under reduced pressure. Melting points quoted are uncorrected. Solvent systems used in qualitative identification of sugars as well as in quantitative separations were: (A) ethyl acetate:acetic acid:water (8:2:2); (B) ethyl acetate: pyridine:water (8:2:1); (C) butanone:water azeotrope; (D) butanol:ethanol:water (upper phase) (4:1:5); (E) benzene:ethanol:water (85:15:1). Chromatographic spray reagents used were F, *p*-anisidine-trichloroacetic acid (6) and G, Tollens solution (7).

Isolation of Galactomannan

Broken seed was slurried in boiling water for 3 to 4 h after which the solids were removed by centrifugation. The cooled, viscous solution was slowly poured with vigorous stirring into 4 volumes of alcohol whereupon a light grey, stringy precipitate formed. The solid material was removed by filtration, washed with acetone, and dried in a dessicator.

Purification of Galactomannan with Copper Acetate

To a portion (2 g) of polysaccharide in 0.5 *N* NaOH

Can. J. Chem. Downloaded from www.nrcresearchpress.com by 210.87.254.42 on 09/05/12
For personal use only.

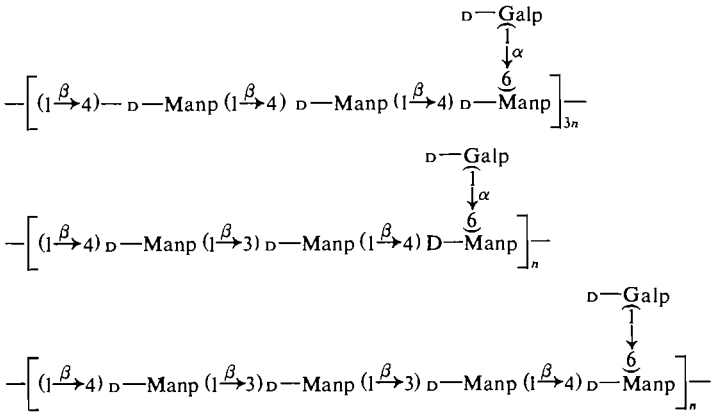

CHART 1

(400 ml) was added with stirring 5% copper acetate (w/v) (75 ml). A gelatinous precipitate resulted which was removed by centrifugation. Addition of a further volume (75 ml) of copper acetate solution resulted in further precipitation of a copper complex which was not further investigated at this time. The gelatinous complex was suspended in alcohol and acidified with hydrochloric acid and after maceration in a Waring blendor, the light grey precipitate was removed by centrifugation and washed free of acid with alcohol. Complexation with Cu^{2+} was repeated twice more as described and resulting in no observable change in sugar ratio (see succeeding section), yield 1.2 g, $[\alpha]_D^{22}$ 6–10° in 0.1 *N* NaOH (*c*, 0.3).

Ultracentrifugation

Solutions of galactomannan (0.5 to 1% concentration) in alkali (1 to 5 *N* NaOH) were centrifuged for 2 h, rotor speed 60 000 r.p.m., exposure intervals, 16 min. A sedimentation pattern (0.8% galactomannan in 5 *N* NaOH) is shown in Fig. 1.

Hydrolysis of Polysaccharide

(a) With 1 N Sulfuric Acid

A small portion (250 mg) of the polysaccharide was refluxed (6 h) in mineral acid followed by neutralization ($BaCO_3$) and paper (Whatman No. 1) chromatography of the syrupy residue after evaporation of the filtrate. Mannose and galactose were identified as the only sugar components using solvents A and B, spray reagent E. Oxidation of a small portion (100 mg) of mixture with nitric acid gave mucic acid, m.p. 219 °C. Separation (Whatman 3MM) of a further portion (100 mg) of mixture using solvent B gave D-mannose, 60 mg, further characterized as the phenylhydrazone, m.p. 199 °C $[\alpha]_D^{22}$ 33° in pyridine (*c*, 0.9) and D-galactose, 28 mg, $[\alpha]_D^{22}$ 80° in water, (*c*, 0.8). The molar ratio of the 2 sugars was further confirmed by elution of each sugar from a single chromatogram followed by analysis employing the phenol–sulfuric acid method (5), and by v.p.c. of the mixture of trimethylsilyl derivatives (8) using a 5′ × 1/4″ stainless steel column packed with 20% SE 30 on HMDS treated chromosorb W. A mannose–galactose ratio of 3:1 was obtained in all cases.

(b) Hydrolysis with Emulsin

To a sterile solution (15 ml), p*H* 7.0, of galactomannan (25 mg) was added emulsin (10 mg). The solution was incubated at 25 °C for 3 days. No observable change in the reducing power (3,5-dinitrosalicylic acid reagent) was found. The solution was evaporated and the residue was shown, by paper chromatography solvents A and B, reagents F and G, to contain no detectable galactose (or mannose) and no evidence of smaller oligomers.

Methylation Analysis

A portion (2.0 g) of the galactomannan was initially treated with 30% NaOH and dimethylsulfate followed by extended treatment with silver oxide and methyl iodide. A fully methylated polymer (1.5 g) (no OH-absorption evident in the infrared (i.r.) spectrum) was dissolved in cold 75% H_2SO_4, 5 ml, (9) the mixture was held at room temperature for 1 h after which the solution was diluted with ice-water to approximately 2 *N* and boiled for 7 h. The syrupy mixture (1.2 g) which was obtained after neutralization ($BaCO_3$) and evaporation of the filtrate was analyzed by paper chromatography using solvents C, D, and E. The molar ratio of the partially methylated sugars was determined by the phenol–H_2SO_4 procedure and by v.p.c. of TMS derivatives (20% neopentylglycol-succinate on Gas Chromatograph 900, 3/16″ by 12′ column, 180 °C, flame ionization detector) (10). As is the case for unsubstituted hexoses and pentoses where the difference in molar sensitivity to the phenol–H_2SO_4 reagent may be significant (e.g., glucose vs. galactose) (5) a similar variability exists when analyzing a mixture of partially methylated sugars (*O*-methyl glucoses and galactoses). The appropriate corrections were made in the usual standardization involving plots of absorbance vs. molar concentration. It has been shown that the molar response for isomeric tri-*O*- and di-*O*-methyl hexoses in v.p.c. analysis of the TMS derivatives varies (11), consequently the detector response was firstly correlated with the phenol–H_2SO_4 results and where authentic synthetic samples were available, the detector (thermal conductivity and hydrogen flame) response was calibrated. Comparison with published results (11) where similar although not identical v.p.c. conditions had been employed

Can. J. Chem. Downloaded from www.nrcresearchpress.com by 210.87.254.42 on 09/05/12
For personal use only.

Can. J. Chem. Downloaded from www.nrcresearchpress.com by 210.87.254.42 on 09/05/12
For personal use only.

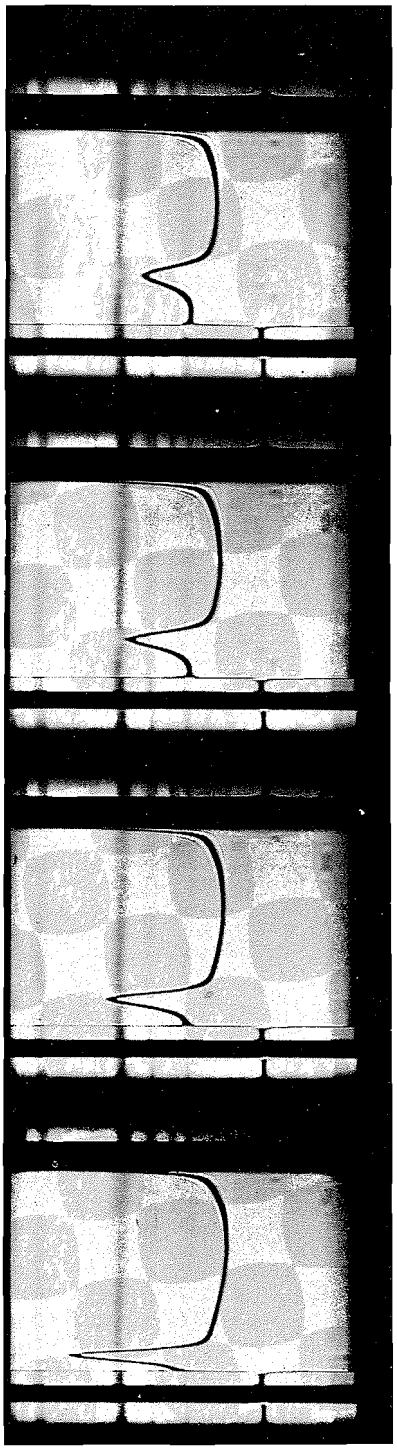

FIG. 1. Sedimentation pattern of *Crotalaria* galactomannan (0.8% galactomannan in 5 *N* NaOH, rotor speed 60 000 r.p.m., time: 2 h, 16 min exposure intervals).

Can. J. Chem. Downloaded from www.nrcresearchpress.com by 210.87.254.42 on 09/05/12
For personal use only.

indicated similar results. The mixture of partially methylated sugars was separated using Whatman 3MM paper, solvent C, and the individual sugars characterized.

Component 1 was identified as follows: Authentic 2,3,4,6-tetra-*O*-methyl-D-mannose was prepared by methylation of methyl-α-D-mannopyranoside with NaH in dimethylsulfoxide (12) followed by hydrolysis (1.0 *N* H_2SO_4, 6 h) to generate the free tetra-*O*-methyl sugar. Component 1 and the synthetic tetra-*O*-methyl sugar showed identical R_f (solvent C) 0.79 and R_g (solvent E) 0.96 and retention time of TMS derivatives 16.5 min.

Component 2, 38 mg, $[\alpha]_D^{22}$ 118° in water (*c*, 0.4), gave upon treatment with aniline in dry ethanol containing a trace of glacial acetic acid 2,3,4,6-tetra-*O*-methyl-*N*-phenyl-D-galactosylamine, m.p. 190–191 °C, $[\alpha]_D^{22}$ 40° in acetone (*c*, 0.5) (13). Further confirmation of identity was established by synthesis, as described for component 1. Component 2 and authentic 2,3,4,6-tetra-*O*-methyl-D-galactose showed identical R_f (solvent C) 0.69 and R_g (solvent E) 0.88 and retention time of TMS derivatives, 15.3 min α, 18.9 min β.

Component 3, 18 mg, $[\alpha]_D^{22}$ ca. 15° in water (*c*, 0.3), was treated with aniline as above to give 2,4,6-tri-*O*-methyl-*N*-phenyl-D-mannosylamine, m.p. 133–135 °C, $[\alpha]_D^{22}$ −8° in methanol (*c*, 0.4) (14). The identity of component 3 was further established by the following series of reactions. A small portion (about 10 mg) was subjected to sodium borohydride reduction (24 h, room temperature) followed by treatment with methanol–HCl to remove borate. The product was treated with periodic acid (0.5 *M*) for 16 h (room temperature). The solution (25 ml) was treated with barium chloride to remove iodate and periodate and after evaporation, the residue was hydrolyzed (100 °C) with 35% hydrobromic acid for 30 min to effect demethylation. Mannitol was identified by comparative (*i*) paper chromatography, (*ii*) v.p.c., and (*iii*) physical constants of the hexaacetates.

Component 4, a portion (51 mg), $[\alpha]_D^{22}$ −9° in water (*c*, 0.9), was dissolved in dry pyridine, a 10% molar excess *p*-nitrobenzyl chloride was added followed by heating to 65 °C for 30 min. The mixture was cooled, saturated solution of $NaHCO_3$ added, followed by extraction of the suspension with chloroform. After recrystallization from methanol, the solid was identified as the 1,4-di-*p*-nitrobenzoyl-2,3,6-tri-*O*-methyl-D-mannose and had m.p. 187–189 °C, $[\alpha]_D^{22}$ + 33° in $CHCl_3$ (*c*, 1.0) (15). Component 4 was further analyzed as follows. Thin-layer chromatography (t.l.c.) on silica gel, using solvent C, showed 3 components with R_g values of 0.78, 0.76, and 0.68. In solvent E, 3 components were also evident with R_g of 0.52, 0.50 and 0.45 thus indicating three tri-*O*-methyl sugars. The v.p.c. analysis of TMS derivatives (conditions described previously) showed the presence by comparison with authentic compounds, of 2,4,6-tri-*O*-methyl mannose, 12.2 (minor proportion), 3,4,6-tri-*O*-methyl mannose, 10.6 (minor proportion), and 2,3 6-tri-*O*-methyl mannose, 13.5 min (major proportion). A portion (100 mg) of component 4 was subjected to the following series of reactions: (*i*) reduction with borohydride, (*ii*) oxidation with periodic acid, (*iii*) reduction with borohydride, (*iv*) demethylation with 35% hydrobromic acid, (*v*) deionization, and (*vi*) identification by paper and gas chromatography of degradation products. Ethylene glycol and erythritol were identified and would arise from 2,3,6-tri-*O*-methyl mannose. Arabinitol was identified by comparison with authentic D-arabinitol obtained via the above series of reactions carried out on 3,4,6-tri-*O*-methyl-D-mannose prepared by a published procedure (16). The retention time of the TMS derivatives of authentic D-arabinitol and that obtained from component 4 was identical (3.4 min, 170 °C, otherwise conditions as described previously), m.p. of pentaacetates 75–77 °C. D-Arabinitol would arise from 3,4,6-tri-*O*-methyl-D-mannose (the same pentitol would arise from 2,3,4-tri-*O*-methyl-D-mannose; however, the absence of this sugar was established previously from v.p.c. results, see Table 2). Mannitol was identified by comparison with authentic compound, the TMS derivatives of both having retention times of 4.4 min, (170 °C, otherwise conditions as described previously). Mannitol would be derived from 2,4,6-tri-*O*-methyl-D-mannose via the above series of reactions.

TABLE 2

Paper chromatographic separation of partially methylated sugars

Component	Butanone–H_2O azeotrope R_f	Butanol–EtOH–H_2O R_g*	Proposed compound†	Molar ratio†
1	0.79	0.96	2,3,4,6-M	1
2	0.69	0.88	2,3,4,6-Gal	20
3	0.56	0.82	2,4,6-M	10
4	0.50	0.81	2,3,6- and 3,4,6-M	25
5	0.21	0.57	2,3-M	26

*Mobility with reference to 2,3,4,6-tetra-*O*-methyl-D-glucose.
†From chromatographic results in butanone–H_2O azeotrope.

Component 5, 51 mg, $[\alpha]_D^{22}$ 15° in water (*c*, 1.0) gave upon treatment with *p*-nitrobenzoyl chloride, as above, 1,4,6-tri-*p*-nitrobenzoyl-2,3-di-*O*-methyl-D-mannose, m.p. 192–194 °C, $[\alpha]_D^{22}$ +65° in $CHCl_3$ (*c*, 1.0) (4). The v.p.c. analysis of the TMS derivative revealed the presence of one compound which had the identical retention time of authentic TMS 2,3-di-*O*-methyl-D-mannose.

Smith Periodate Degradation

To a portion (500 mg) of galactomannan dissolved in water (200 ml) was added 0.5 *M* periodic acid (10 ml) and the solution stored at 5 °C. Periodate consumption reached 0.95 moles per hexose unit in 2 days with little change thereafter. To the polyaldehyde was added $NaBH_4$ (500 mg) and the solution stored at room temperature for 16 h. Analysis of the solution of polyalcohol with phenol–H_2SO_4 indicated intact hexose to the extent of 18–20% (in terms of mannose) of the original polysaccharide. The solution was passed through a cation exchange column (Amberlite IR 120), the acidic solution evaporated and borate removed by repeated evaporation with methanol. The residue was dissolved in 0.5 *N* hydrochloric acid (50 ml), stored at room (21–22 °C) temperature for 8 h, followed by inorganic ion removal with cation and anion exchange resins. Paper chromatography, solvents A and B, indicated the presence of glycerol and

erythritol, molar ratio 1:2 as determined by the periodate – chromotropic acid method (17) and 2 non-reducing components, $R_{Man} = 0.61$ (Component I) and $R_{Man} = 0.33$ (Component II). The compounds were separated by paper chromatography (solvent B, Whatman 3 MM paper) and characterized as follows:

Glycerol (approximately 30 mg) was dissolved in dry pyridine, 10% molar excess *p*-nitrobenzoyl chloride added, and the mixture heated to 75 °C for 30 min. After cooling to room temperature, an excess saturated $NaHCO_3$ solution was added and the insoluble precipitate collected and washed with water. The tri-*p*-nitrobenzoate, after recrystallization from alcohol had m.p. and mixed m.p. 191 °C.

Erythritol (approximately 60 mg) was treated in the same manner as glycerol. The tetra-*p*-nitrobenzoate had m.p. and mixed m.p. 250 °C.

Component I (approximately 5 mg) was hydrolyzed in 1 *N* H_2SO_4 (10 ml) (100 °C, 6 h) and the hydrolysate shown by paper chromatography, using solvents A and B and spray reagent G, to contain mannose and erythritol in a 1:1 molar ratio (mannose, by phenol–H_2SO_4; erythritol, by chromotropic acid).

Component II (approximately 8 mg) a portion (4 mg) was hydrolyzed as I above and the hydrolysate shown to contain mannose and erythritol in a 2:1 molar ratio. The remaining portion of II was degraded with periodate (Smith degradation) whereupon 1 molar proportion of formaldehyde was produced (analyzed before borohydride reduction) and glycerol and a non-reducing component (III) with slightly faster mobility than I were formed upon mild acid hydrolysis. Complete hydrolysis of III, as described for I gave mannose and glycerol in a 1:1 molar ratio.

The authors gratefully acknowledge financial support from the National Research Council of Canada.

1. A. J. Erskine and J. K. N. Jones. Can. J. Chem. **34**, 821 (1956).
2. D. G. Easterby and J. K. N. Jones. Nature **165**, 614 (1950).
3. C. Leschziner and A. S. Cerezo. Carbohyd. Res. **11**, 113 (1969).
4. F. Smith and R. Montgomery. *In* Chemistry of plant gums and mucilages. ACS Monograph no. 141, Reinhold Publishing Corp., 1959.
5. N. Dubois, J. K. Hamilton, K. A. Gilles, P. A. Rebers, and F. Smith. Anal. Chem. **28**, 350 (1956).
6. L. Hough, J. K. N. Jones, and W. H. Wadman. J. Chem. Soc. 1702 (1950).
7. S. M. Partridge. Nature, **158**, 270 (1946).
8. C. C. Sweeley, R. Bentley, M. Makita, and W. W. Wells. J. Amer. Chem. Soc. **85**, 2497 (1963).
9. I. Croon, G. Herrstrom, G. Kull, and B. Lindberg. Acta Chem. Scand. **14**, 1338 (1960).
10. P. A. J. Gorin and J. F. T. Spencer. Can. J. Chem. **46**, 2299 (1968).
11. S. S. Bhattacharjee and P. A. J. Gorin. Can. J. Chem. **47**, 1207 (1969).
12. S-I. Hakomori. J. Biochem. (Japan), **55**, 205 (1964).
13. L. Hough and J. K. N. Jones. J. Chem. Soc. 1199 (1950).
14. W. N. Haworth, R. L. Heath, and S. Peat. J. Chem. Soc. 833 (1941).
15. P. A. Rebers and F. Smith. J. Amer. Chem. Soc. **76**, 6097 (1954).
16. G. O. Aspinall, C. S. Hudson, and M. L. Wolfrom (*Editors*). Advances in carbohydrate chemistry. Vol. 8. Academic Press Inc., New York, 1953. p. 217.
17. M. Lambert and A. C. Neisch. Can. J. Res. **28B**, 83 (1950).
18. J. Cankie, A. L. Gelman, and G. A. Levoy. Biochem. J. **103**, 609 (1967).

Can. J. Chem. Downloaded from www.nrcresearchpress.com by 210.87.254.42 on 09/05/12
For personal use only.

Can. J. Chem. Downloaded from www.nrcresearchpress.com by 210.87.254.40 on 09/05/12
For personal use only.

Infrared spectra and structure of methane – noble gas mixed crystals: the influence of temperature and methane concentration on the ν_3 vibration band of methane[1]

A. Chamberland, R. Belzile, and A. Cabana[2]
Département de chimie, Université de Sherbrooke, Sherbrooke, Québec

Received October 22, 1969

The infrared spectra of CH_4, at low concentrations in the noble gases, were obtained at temperatures ranging from 4 °K up to the respective boiling points of argon, krypton, or xenon. It is concluded from this study that methane occupies substitutional cavities in these lattices. Furthermore, it is established that the potential hindering the rotation of the molecules perturbs the higher rotational levels to a greater extent than the low lying levels.

In a second series of experiments, the methane concentration was varied from 0.06 to 55% for krypton; narrower ranges were used for argon and xenon. The experimental results clearly demonstrate that the influence of the CH_4 concentration is different for the three systems and that the fine structure does not result from molecular aggregation.

The spectrum of 0.06% CD_4 in solid krypton shows fine structure which confirms the rotational origin of the four components observed for CH_4. The CD_4 spectra previously published were complicated with additional lines that probably arose from the nonhomogeneity of the samples.

Les spectres infrarouges du CH_4 en faibles concentrations dans les gaz nobles furent enregistrés à des températures allant de 4 °K jusqu'aux points d'ébullition de l'argon, du krypton ou du xénon. Cette étude nous a permis de conclure que le méthane occupe des cavités substitutionnelles dans ces réseaux. On a de plus constaté que le potentiel s'opposant à la rotation des molécules se manifeste à un plus haut degré sur les niveaux de rotation élevés que sur les premiers niveaux.

La concentration de méthane fut ensuite variée de 0.06 à 55% pour le krypton; des domaines moins étendus furent utilisés pour l'argon ou le xénon. Les résultats expérimentaux obtenus démontrent clairement que l'effet de la concentration en CH_4 est différent pour les trois systèmes et que la structure fine n'est pas causée par l'agglomération des molécules.

Le spectre du CD_4 en solution à 0.06% dans le krypton montre une structure fine qui confirme la nature rotationnelle des quatre composantes observées pour le CH_4. Les spectres de CD_4 publiés antérieurement étaient compliqués par des raies additionnelles probablement attribuables à l'inhomogénéité des échantillons.

Canadian Journal of Chemistry, 48, 1129 (1970)

Introduction

Since the first report of molecular rotation of HCl in solid argon (1), the problem of the fine structure observed on the vibrational bands of small molecules isolated in noble gas crystals has been of considerable interest. The present work is an extension of the research on the infrared absorption spectra of CH_4 or CD_4 trapped in inert gas matrices (2) and in liquid solutions with the noble gases (3). The spectral features observed on the ν_3 and ν_4 bands were previously ascribed to the quantized molecular rotation. The Raman spectrum of a mixed crystal, grown from a melt, was also found to be consistent with the concept of rotation, although the resolution achieved was insufficient to permit a detailed analysis (4). The time dependence of the intensities of the spectral features of CH_4 in crystalline argon has been taken as evidence of equilibration between the three possible spin species of CH_4 (5). These experimental studies have aroused interest in theoretical investigations on the nature of rotation in these solids, particularly for tetrahedral molecules trapped in octahedral cavities (6). All these studies are based on the assumption that the host molecules replace noble gas atoms in undistorted face-centered cubic (f.c.c.) lattices. Although it is known that, at least in the low concentration range, CH_4 forms solid solutions with krypton (7) or argon (8), it appeared desirable to obtain additional data which could yield information on the nature of the sites occupied and on the distribution of the molecules over the available cavities.

Two different sets of experiments seemed appropriate to the solution of the problem. In the first series, the effect of the temperature on the fine structure of the ν_3 band was investigated in the range extending from 4 °K up to the boiling points of the noble gases used. In the second, the

[1]Work supported, in part, by the Defence Research Board of Canada (Grant No. 9511–67).
[2]To whom all correspondence should be addressed.

Can. J. Chem. Downloaded from www.nrcresearchpress.com by 210.87.254.40 on 09/05/12
For personal use only.

influence of the solute concentration of the ν_3 band was studied. The concentration was varied from 0.06 up to 55% in the case of the CH_4–krypton system; fewer solutions and narrower ranges were investigated for the argon and xenon systems. The present study should bring support to the interpretation of the nature of the fine structure presented by Cabana *et al.* (2) and thus to the reported spin equilibration discussed by Frayer and Ewing (5).

Experimental

All the spectra were taken with a Perkin–Elmer Model 125 prism–grating spectrometer; under the experimental conditions prevailing, the actual resolving power varied from 0.5 to 1.5 cm^{-1}, depending upon the spectral regions and the optical quality of our samples. The factory calibration was checked during each run by recording appropriate gas-phase spectra and comparing with the values given in the Tables of Wavenumbers (9). The frequencies quoted later are accurate to ± 0.3 cm^{-1} for sharp peaks which are relatively free of overlapping. A conventional cryostat equipped with a variable pressure gas exchanger was used to obtain any selected temperature in the range 4 to 170 °K with liquid helium or nitrogen as the coolant. The control thus achieved was relatively rough but it could be improved by introducing small electrical heaters around the filling tube and the sample cell. The heater around the filling tube was found particularly useful to prevent clogging if the tube inadvertently touched the nitrogen shield; it also created a temperature gradient through the cell diameter and prevented the formation of bubbles in the middle of our samples. The temperature was measured with a copper–constantan thermocouple and a carbon resistor, both embedded in the cell body; the accuracy is better than $\pm 1°$ above 50 °K, but considerably worse at the lowest temperatures, where it can be of the order of $\pm 5°$.

The gaseous mixtures were prepared in a Pyrex system previously pumped down to pressures lower than 1×10^{-5} mm Hg and outgassed. Research-grade methane and noble gases (Matheson of Canada, Ltd.) were used. The samples were prepared by condensing the mixture to the liquid phase in the experimental cell and, whenever necessary, cooling through the freezing point. Various cooling rates were tried without any noticeable difference in the observed spectra. The samples were often kept for rather long periods of time at temperatures close to their melting points; spectra recorded at different intervals were found identical. The crystals, which were perfectly transparent at 77 °K, had a tendency to crack upon further cooling.

The thickness of the sample cell was of the order of a few microns for high methane concentrations and 2 mm for the low concentrations; the small spacings were determined approximately by counting the interference fringes (10). The window material was either sapphire or Irtran-2 and the seals were achieved with 0.010 in. diameter indium wire squeezed between the windows and the cell body, which was copper. The design was such that the coolant surrounded the sample, thus providing lower temperatures. In addition, KBr windows were placed in the beam holes of the nitrogen shield and narrow-band-pass filters were used on the outside window; these two additional precautions helped in obtaining lower sample temperatures.

Results

The spectra of the 0.06% CH_4–argon mixed crystal, 0.1% CH_4–krypton crystal, and 0.06% CH_4–xenon crystal are shown in Fig. 1; the frequencies are collected in Table 1. The temperatures at which the spectra were recorded are indicated on each tracing. The bottom spectrum of each set is that of the liquid solution. Only the ν_3 vibration region was scanned. The low-temperature spectra of the three systems exhibit similar patterns, contrary to those reported previously (2). As the temperature is raised, the four lines gradually blend together and finally they form a continuous band more typical of the liquid state or of disordered crystals. It is observed that the intensities of the various components do not vary the same way as the temperature is raised. In particular, this effect gives rise to a shift of the band at temperatures, T, approaching 40 or 50 °K. At higher temperatures, the shifts are smooth up to the melting points, where discontinuities occur: a sudden high-frequency displacement for the xenon system, a slight low shift for krypton, and a larger downward shift for argon.

The spectra of CH_4 at various concentrations in argon are given in Fig. 2; in krypton, Fig. 3; and in xenon, Fig. 4; the temperature during the runs was kept as close as possible to that of liquid helium. The frequencies at maximum intensity are collected in Table 2. In argon, the CH_4 concentration ranged from 0.06 to 35%; in krypton, concentrations up to 55% were used; while in xenon only two solutions were prepared: 0.06 and 20% CH_4. It is readily seen that the influence of the solute concentration was very different for the three systems. Figure 5 summarizes the effect of the concentration on three lines of the ν_3 vibration band of methane in krypton. The low-temperature spectrum ($T < 10$ °K) of 0.06% CD_4 in solid krypton is shown in Figs. 6 and 7.

Discussion

A. The Influence of Temperature on the ν_3 Absorption Band

The spectra recorded at low temperatures have

Can. J. Chem. Downloaded from www.nrcresearchpress.com by 210.87.254.40 on 09/05/12
For personal use only.

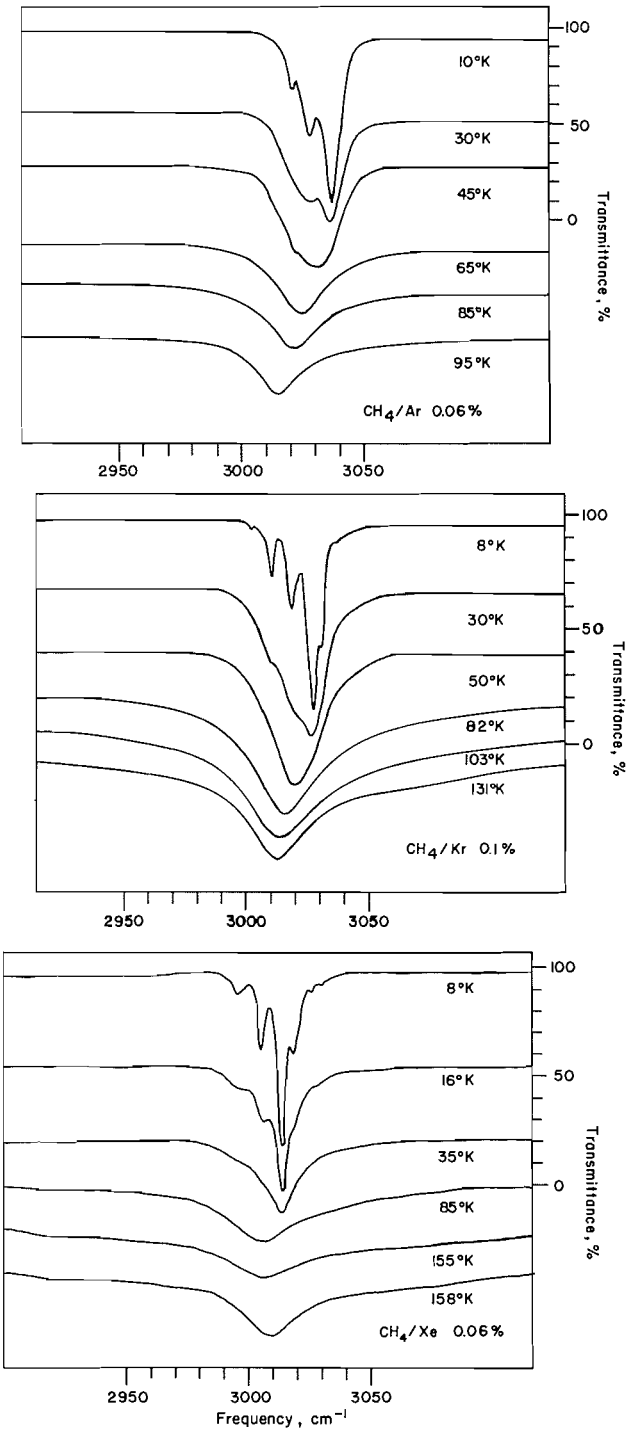

FIG. 1. (*Upper*) Infrared spectra of 0.06% CH_4 in crystalline argon at various temperatures; at 95 °K, the solution is liquid. (*Middle*) Infrared spectra of 0.1% CH_4 in crystalline krypton at various temperatures; at 131 °K, the solution is liquid. (*Lower*) Infrared spectra of 0.06% CH_4 in crystalline xenon at various temperatures; at 158 °K, the solution is liquid.

Can. J. Chem. Downloaded from www.nrcresearchpress.com by 210.87.254.40 on 09/05/12
For personal use only.

TABLE 1

Frequencies of the components of the ν_3 vibration band of methane*

Matrix	Temperature (°K)	Frequency, cm^{-1} P(1)	Q	R(0)	R(1)
Xe	8	2995.6	3005.3	3013.3	3018.3
Xe	16	2996	3005.9	3013.2	3019
Xe	35			3012.9	
Xe	85		3004.8		
Xe	155		3004.9		
Xe	158†		3007.4		
Kr	8	3010.1	3018.3	3026.5	3030.0
Kr	30			3026.1	
Kr	50		3017.0		
Kr	82		3016.0		
Kr	103		3014.1		
Kr	131†		3011.7		
Ar	10	3021.6	3028.6	3037.4	‡
Ar	30		3028.4	3036.5	
Ar	45			3033.0	
Ar	65		3025.5		
Ar	85		3022.3		
Ar	95†		3015.1		

*CH_4 concentration was 0.06% for the argon and xenon systems and 0.10% for the krypton system.
†Liquid state.
‡Shoulder.

TABLE 2

Frequencies of the components of the ν_3 vibration band of methane; temperature lower than 10 °K

% concentration	System	Frequency, cm^{-1} P(1)	Q		R(0)	R(1)
0.06	CH_4–Xe	2995.6	3005.3		3013.3	3018.3
20	CH_4–Xe	2997	3005.3		3013.4	†
0.06	CH_4–Kr	3010.1	3018.3		3026.5	3030.0
0.1	CH_4–Kr	3009.8	3017.7		3026.1	3029.6
5.0	CH_4–Kr	3009.4	3018.4		3024.7	†
10	CH_4–Kr	3009.4	3017.3		3024.7	†
13	CH_4–Kr	3009.2	3016.4		3022.9	†
15	CH_4–Kr	3009.6	3016.0		3021.1	†
18	CH_4–Kr	3009.1	3015.3		3020.6	†
24	CH_4–Kr	3008.9	3015.2		3020.6	†
35	CH_4–Kr	3009.4	3014.7		3019.5	†
55	CH_4–Kr*	3008	3013		3016	
0.06	CH_4–Ar	3021.6	3028.6		3037.4	†
3.0	CH_4–Ar			3026		
6.0	CH_4–Ar			3026		
20	CH_4–Ar			3017		
35	CH_4–Ar			3016		

*Three lines are observed; their nature is uncertain.
†Shoulder.

Can. J. Chem. Downloaded from www.nrcresearchpress.com by 210.87.254.40 on 09/05/12
For personal use only.

shown the time dependence ascribed by Frayer and Ewing (5) to spin equilibration. Our results agree with this; thus no further discussion regarding this particularity will be carried out here.

Three aspects of these experimental results inevitably draw attention: (*a*) The observation of opposite shifts for the ν_3 vibration of CH_4 in xenon and in argon upon melting of the mixed crystals. (*b*) The different behavior of the intensities for the various components as the temperature is increased. (*c*) The rapid broadening of the individual lines with increasing temperature. These observations will now be discussed in terms of the nature of the fine structure of the unsymmetrical stretching vibration band of methane and of the kinds of sites occupied by the molecules.

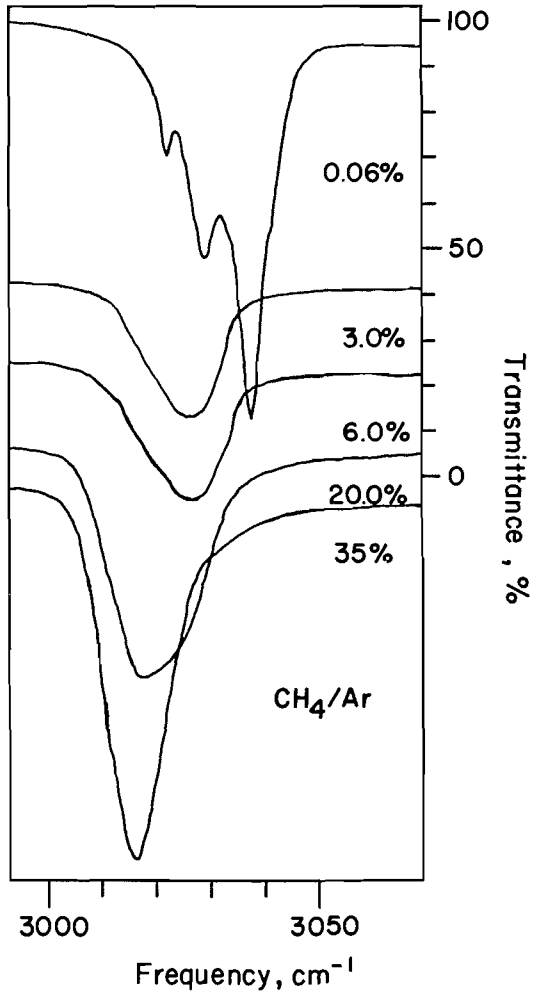

FIG. 2. Infrared spectra of CH_4 in solid argon at 8 °K. The concentrations, ranging from 0.06 to 35% CH_4, are indicated on each spectrum.

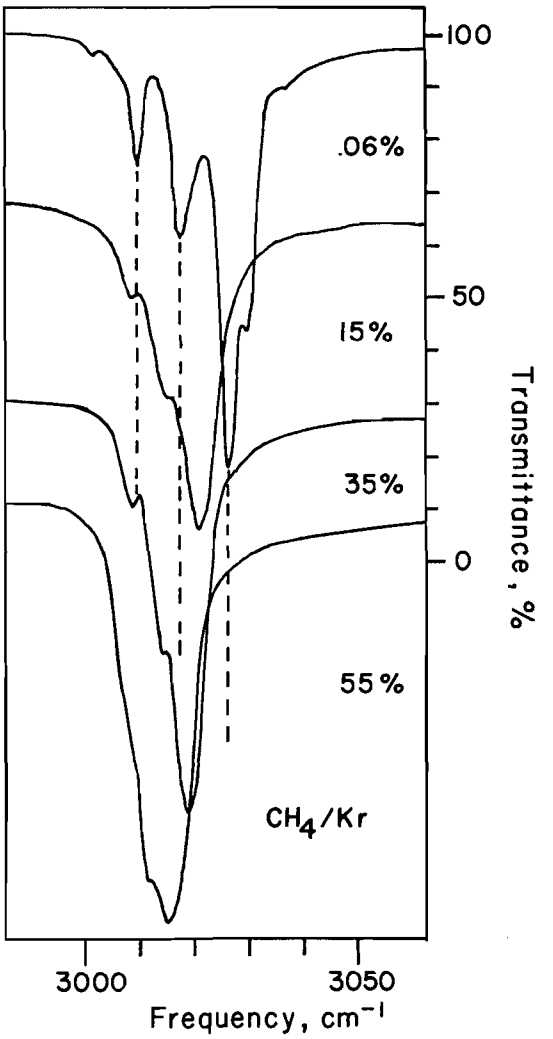

FIG. 3. Infrared spectra of CH_4 in solid krypton at 8 °K. The concentrations, ranging from 0.06 to 55% CH_4, are indicated on each spectrum.

The low-frequency displacements of the ν_3 vibration band of CH_4 dissolved in liquid argon (-3 cm^{-1}), krypton (-7 cm^{-1}), and xenon (-11 cm^{-1}) indicate that the predominant interaction between the molecules and the atoms is attractive. Upon solidification of these solutions, shifts of $+7.2$, 2.3, and -2.5 cm^{-1} are measured for the band in argon, krypton, and xenon, respectively. Thus, upon formation of the

Can. J. Chem. Downloaded from www.nrcresearchpress.com by 210.87.254.40 on 09/05/12
For personal use only.

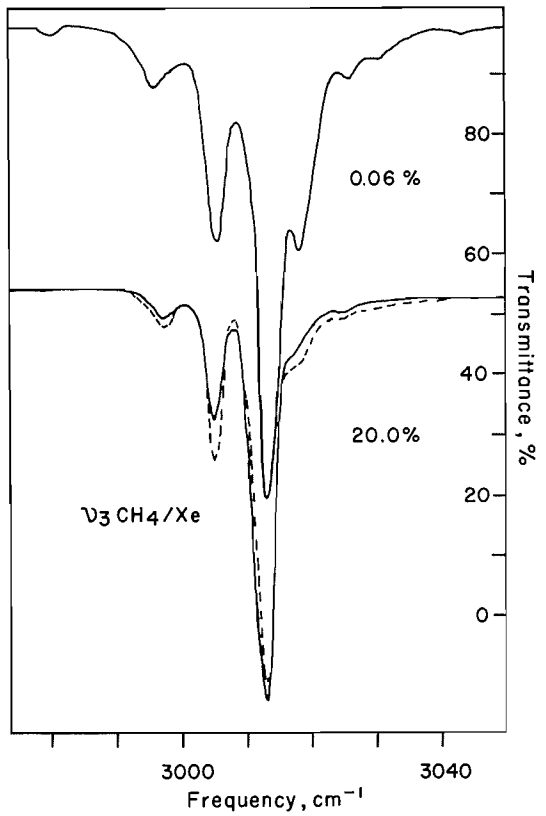

FIG. 4. Infrared spectra of 0.06 and 20% CH_4 in solid xenon at 8 °K.

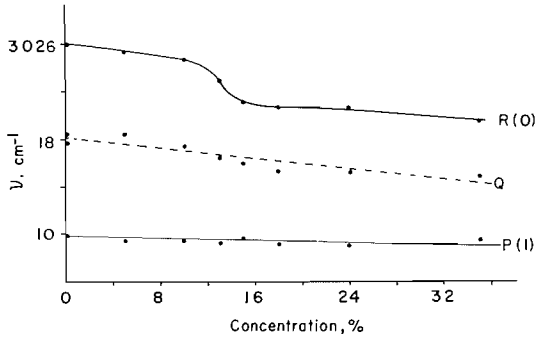

FIG. 5. Frequencies of the R(0), Q, and P(1) lines of methane in crystalline krypton as a function of the methane concentration, at 8 °K.

lattice, the repulsive forces acting on the molecule augment in argon and in krypton, but diminish in xenon. *This is precisely what is predicted for these mixed crystals if a molecule occupies a substitutional cavity created by the displacement of a noble gas atom.* The diameters of the holes formed by withdrawing an atom from a lattice site are 3.8 Å for argon, 4.0 Å for krypton, and 4.4 Å for xenon (11), as compared to 4.1 Å, the diameter of the stationary CH_4 molecule. Thus, while the molecule inherits a larger cavity as xenon crystallizes, it is squeezed into smaller cavities in krypton and even more so in argon. Additional support for this arrangement of the molecules in the crystals is provided by the frequency shifts of the stretching vibration, which occur upon contraction of the lattice as the temperature is lowered: $+6\ cm^{-1}$ for 75° lowering of temperature in argon, $+4\ cm^{-1}$ for 100° in krypton, and no shift in xenon over 120°.

The relative intensity of the four lines observed in the ν_3 vibration band at low temperature is altered as the temperature is raised (see Fig. 1). At the lowest temperature, the line labelled R(0) is the strongest component; gradually the line labelled Q, on the low-frequency side of R(0), gains intensity and finally around 50 °K it becomes the predominant feature. After the fine structure is lost, some information may still be gained from the spectra by studying the band

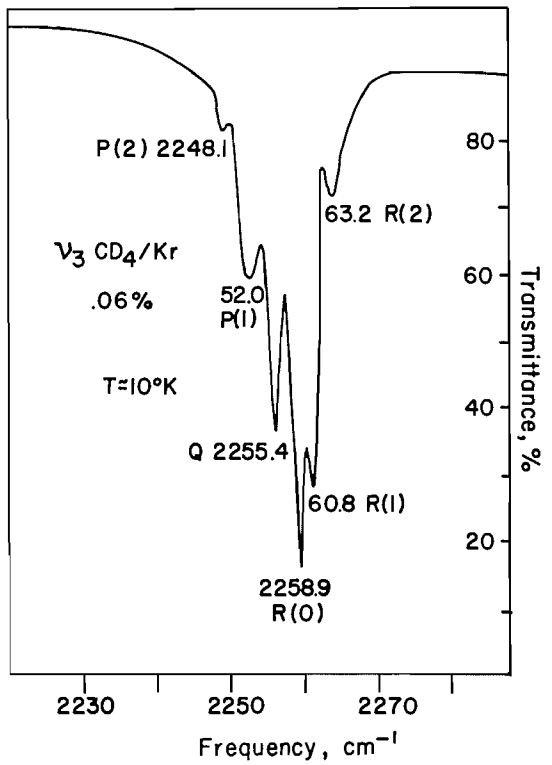

FIG. 6. The ν_3 vibration band of 0.06% CD_4 in crystalline krypton, at 8 °K.

TABLE 3

Intensities of the vibration–rotation transitions of freely rotating methane molecules

	Intensity					
	With spin equilibration			Without spin equilibration		
	4.4 °K	8.8 °K	17.6 °K	17.6 °K	40.0 °K	75 °K
R(8)						0.1
R(7)						0.5
R(6)					0.1	2.0
R(5)					0.5	3.1
R(4)			0.1		3.8	8.4
R(3)			1.8	1.7	11.1	13.0
R(2)		3.0	13.3	11.6	12.6	8.4
R(1)	13.2	33.0	30.6	29.8	10.7	5.3
R(0)	77.0	36.0	14.3	29.9	15.3	6.5
Q	7.7	21.0	27.4	23.4	28.0	31.1
P(1)	2.6	7.0	6.1	4.6	2.1	1.1
P(2)		1.0	5.6	3.0	5.4	3.6
P(3)			1.0	1.0	6.2	7.2
P(4)			0.1	0.3	2.7	5.3
P(5)					0.4	3.1
P(6)					0.1	1.5
P(7)						0.4
P(8)						0.1

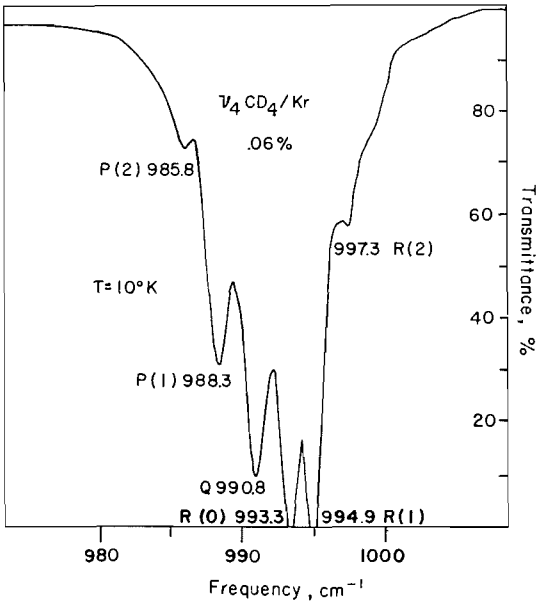

FIG. 7. The ν_4 vibration band of 0.06% CD_4 in crystalline krypton, at 8 °K.

shape. At the higher temperatures, the bands are unsymmetrical, the high-frequency side being wider and more intense. Such an observation is consistent with the concept of rotation, since the R branch is always more intense than the P branch (see Table 3). There is, however, a difficulty: the band center grows too rapidly in comparison with the wings. There does not seem to be an easy answer to this problem, but several factors may contribute to this phenomenon if a barrier opposing rotation exists in these solids as indicated from earlier studies (2, 5). For example, theoretical calculations for a tetrahedral molecule undergoing rotation in an octahedral field indicate that the splitting of the rotational levels increases with increasing J and that some sublevels converge to the $J = 0$ state (6). Also of importance is the fact that, as the temperature is raised, the vibrational amplitude of the lattice increases, possibly modifying the interactions between the atoms and the molecules. *Thus we can summarize by stating that the molecules trapped in crystals of the noble gases undergo some type of quantized rotational motion; the departure from free rotation is certainly much more evident at the higher temperatures, indicating that the levels having high J numbers are more perturbed than those with low J.* Agreement between experimental and theoretical (6) data is only qualitative.

B. The Influence of the CH_4 Concentration

Argon, krypton, xenon, and CH_4 all crystallize in the f.c.c. lattice, although it has been shown that the close-packed hexagonal structure can be

Can. J. Chem. Downloaded from www.nrcresearchpress.com by 210.87.254.40 on 09/05/12
For personal use only.

Can. J. Chem. Downloaded from www.nrcresearchpress.com by 210.87.254.40 on 09/05/12
For personal use only.

obtained as a metastable phase for pure argon, or as a stable phase, near the melting point, in certain argon-based solid solutions (12). For the methane–argon system, it was recently shown that the crystal structure is f.c.c. (8). At least for the mixed crystals with low CH_4 concentrations discussed in the previous section, it can be considered established that the structure is f.c.c. and that the molecules occupy substitutional cavities. We wish now to find out what happens to the f.c.c. lattice when the concentration of methane is increased and if possible find out something about the distribution of the molecules within the mixed crystal. The three systems under investigation have shown widely different behavior with respect to the concentration, as shown in Figs. 2 to 5, although their spectra at low concentration have revealed identical structures.

In the argon–methane system, the ν_3 vibration band of CH_4 clearly demonstrates that at concentrations of CH_4 as low as 3%, the solid has modified its structure; the lines resolved at 0.06% have collapsed. The band shape and the frequency at maximum intensity coincide with those of an amorphous solid of very low solute concentration, easily obtained with the spray technique by slow deposition at very low temperature without annealing. At 20% CH_4, and even more so at 35%, the band narrows and the frequency at maximum intensity moves close to that of pure solid CH_4. It seems that microcrystals of pure CH_4 are being formed and that a two-phase system is obtained; this deduction is consistent with the results obtained from X-ray diffraction studies (8).

The methane–krypton system shows a more intricate behavior. As the CH_4 concentration is increased in the range 0.06 to 10%, no modification of the spectrum was observed except for a small low-frequency shift (see Fig. 5). This shift arises from lattice expansion resulting from the introduction of slightly larger species in the matrix. In the range 10–14% CH_4, the line labelled R(0) undergoes a very rapid displacement, while the three other lines are simply subjected to the low-frequency shift just discussed; it may seem that the Q line is subjected to a larger shift than R(1) or P(1), but closer examination reveals that this effect results from an increased overlapping of that line with the very strong R(0) component. In the range from 14 to 35% (and very likely up to 50%), all lines are again shifted slowly to lower frequencies as the lattice expands. An additional experiment with a crystal containing 55% CH_4 has yielded a spectrum showing major modifications.

We now have to justify why the R(0) line was influenced differently from the others. The answer to this question lies in the fact that this line and only this line (since the 0–0 transition is forbidden) originates from nonrotating molecules in the ground vibrational state. It seems reasonable to believe that these nonrotating molecules will interact with the surroundings differently from those in the $J = 1$ or higher states. In other words, these molecules may orient themselves in the direction of maximum interaction. Thus, a modification of the structure of the mixed crystal may very well manifest itself differently on R(0) than on R(1), Q(1), or P(1).

For a random distribution of the molecules over the lattice sites, major modifications of the ν_3 vibration band are expected in the low concentration range. This is contrary to our findings. It has already been shown that while very few molecules are located on adjacent sites at a concentration of 0.06% CH_4, 25% of them are paired at 5% CH_4 (13). Molecules on adjacent sites would certainly have a different spectrum than those truly isolated. *We are led to conclude that the distribution is not random and we have to find an array consistent with the observed spectral changes.* It need not surprise us to find that the molecules are distributed in an ordered manner in these crystals since intuitively it appears to be an arrangement that minimizes the strain energy. Let us consider what happens when molecules enter the krypton crystal: the molecule, larger than the available substitutional cavities, will displace the surrounding atoms, creating strain in a given region of the crystal. If another molecule is introduced in the immediate vicinity of the first one, the strain introduced is expected to be larger than that created by the first molecule, since the crystal was already distorted in that region. On the contrary, if the molecule migrates to an undistorted portion of the solid, it will create a repetition of the first phenomenon. It seems that the lowering of the repulsive forces obtained by this regular distribution is high enough to compensate for the loss in entropy.

Something may be learned about the "organized distribution" of the molecules over the lattice sites from a discussion of the observed

Can. J. Chem. Downloaded from www.nrcresearchpress.com by 210.87.254.40 on 09/05/12
For personal use only.

irregular displacements of the CH_4 R(0) line in the krypton crystal. Several arrays of the molecules could produce the spectral changes found at a 12.5% CH_4 concentration, but if the structure of the mixed crystal remains f.c.c. at these concentrations, the molecules have to occupy fourth nearest neighbor sites separated by a distance $2\sqrt{2}a_0$ (where a_0 is the length of the cube edge of the primitive cell). After 12.5% of the sites are filled, the spectrum is expected to be very sensitive to the introduction of more CH_4, since each additional molecule creates six next-nearest neighbors which interact with each other. Such a model, although very attractive, has to be abandoned for the higher concentrations, since it predicts additional spectral changes at 25% CH_4 and it fails to account for those observed at 50%. Amongst the structures consistent with a change at a concentration of 50% CH_4, the most appealing ones seem to be the sodium chloride and cesium chloride lattices, where the anions are the molecules and the cations the atoms or vice versa. In the sodium chloride lattice, the anions occupy a set of f.c.c. sites and the cations another set. The structure of the "mixed crystal" is simple cubic. The most usual way to look at it is to consider the chloride ions on a f.c.c. lattice and the sodium ions in its octahedral cavities. In the methane–krypton system, since both species have about the same diameter, the noble-gas lattice has to be expanded in order to accommodate the molecules or a structural transformation occurs and the structure becomes simple cubic or body-centered cubic. In both cases, there are no pairs formed at concentrations as high as 50%, but in the first case at exactly 50% CH_4 the molecules are surrounded by six atoms, while they are surrounded by eight in the second. These suggestions may be regarded as highly speculative; nevertheless the observed spectral changes taking place upon increasing the methane concentration require structural modifications. X-Ray diffraction studies of the CH_4–Kr system seem most desirable and promise to be more informative than those on the CH_4–Ar (8) or CH_4–Xe mixed crystals.

The CH_4–Xe system was not as thoroughly investigated as the other two; nevertheless, the results obtained are interesting. The spectrum of the 0.06% CH_4 solution was identical to that of the 20%, except for a slight broadening of the lines which seems at least partly responsible for the loss of the R(1) feature. It is therefore believed that no major changes of structure occurred within that range of methane concentration. However, this spectrum is possibly less sensitive to structural modifications because the molecules fit loosely into the substitutional cavities.

C. The "Additional Lines" Observed for Microcrystals Formed by the Spray Technique

In an earlier paper (2), "additional lines" were reported to be found in the ν_3 vibration band of methane dispersed in argon and krypton crystals. In argon, a line was found at 3033 cm^{-1} and a band with some structure appeared on the low-frequency side of the main components; in the krypton crystal, only one "additional line" was seen, at 3022 cm^{-1}. None of these was ever detected when the crystals were grown slowly from the liquid, but instead the four-line pattern always showed up exclusively.

We wish to discuss the origin of the additional features, starting with the prominent band of the argon system that develops (2) during the annealing process and which was believed to be caused by diffusion inside the matrix. In view of the results reported in this paper, it becomes clear that this interpretation is erroneous. Since this band is never found with closed cells, it appears to result from preferential sublimation of the most volatile component (argon) from the surface of the film when the temperature is raised to the temperatures of annealing. Thus we conclude that this band results from microcrystals at the surface of the film.

The nature of the 3022 cm^{-1} line found in krypton and the 3033 cm^{-1} line found in argon is certainly different from that of the prominent band. These two lines are likely to have the same origin. Their intensities and positions are not exactly reproducible from run to run (ref. 14 and unpublished data from this laboratory). We have shown, in a previous section, that only the line labelled R(0) was highly sensitive to the methane concentration (see Fig. 5). Few experiments were carried out with the argon system, but a large number with the krypton system; the position of the additional lines was always in the range of the R(0) frequencies found with various CH_4 concentrations. Since the spectrum of the xenon system has been shown to be insensitive to methane concentration in the range 0.06–20%, it should not show the additional line when the

Can. J. Chem. Downloaded from www.nrcresearchpress.com by 210.87.254.40 on 09/05/12
For personal use only.

crystals are prepared from a spray. This is precisely what is observed. It is thus concluded that the microcrystals obtained with the spray technique are inhomogeneous, some portions having high concentrations of molecules while others will have low concentrations.

D. The Vibration–Rotation Band of CD_4 in the CD_4–Krypton System

The crystals grown from liquid solutions yielded reproducible spectra of higher quality than those resulting from films prepared from a spray. ν_3 and ν_4 now show identical features (Figs. 6 and 7), labelled from high to low frequencies, R(2), R(1), R(0), Q, P(1), and P(2). The measured intensities of the seven lines agree rather well with those calculated for a free rotator assuming complete spin equilibration and a temperature close to 5 °K. The discrepancies probably result from incomplete equilibration. These spectra confirm the rotational nature of the fine structure proposed earlier. For this reason, it may be interesting to compare the frequency spacings observed in the matrix to those between the rotational levels of CD_4 in the gas phase.

The gas-phase spacing for ν_3 of CD_4 is about $2B(1 - \xi_3) = 4.5\,cm^{-1}$, while that for ν_4 is $2B(1 - \xi_4) = 3.5\,cm^{-1}$ (15). The measured values for ν_3 of CD_4 in solid krypton are: R(2) − R(1) = 2.4 cm^{-1}, R(1) − R(0) = 1.9 cm^{-1}, R(0) − Q = 3.5 cm^{-1}, Q − P(1) = 3.4 cm^{-1}, and P(1) − P(2) = 3.9 cm^{-1}. In ν_4, R(2) − R(1) = 2.4 cm^{-1}, R(1) − R(0) = 1.6 cm^{-1}, R(0) − Q = 2.5 cm^{-1}, Q − P(1) = 2.5 cm^{-1}, and P(1) − P(2) = 2.5 cm^{-1}. Hence it is clear that the matrix does decrease the separations between successive rotational levels. However, it seems appropriate to correct for the effects of the Coriolis coupling in order to compare directly the gas-phase spacings to those observed in the matrix for the ν_3 and ν_4 vibration–rotation bands. This correction will be carried out in the usual manner (16) with the approximation used previously (5). The following combination differences, written in a form appropriate for the gas phase are needed

$$R(2) - Q(2) = F_1^{(-)}(3) - F_1^{(0)}(2)$$

$$R(1) - Q(2) = F_1^{(-)}(2) - F_1^{(0)}(2) + F_0(2) - F_0(1)$$

$$R(0) - Q(1) = F_1^{(-)}(1) - F_1^{(0)}(1) + F_0(1) - F_0(0)$$

$$Q(2) - P(2) = F_1^{(0)}(2) - F_1^{(+)}(1)$$

$$Q(1) - P(1) = F_1^{(0)}(1) - F_1^{(+)}(0)$$

From these combination differences, appropriate corrections to the observed spacings in the matrix can be made and thus one obtains the energy-level differences for CD_4 in the matrix, free from Coriolis interaction. Table 4 summarizes the results. It can be seen that the energy-level differences as determined from either ν_3 or ν_4 are roughly equal for both vibrational states. The crystal field reduces all the spacings and it seems to be more important for the excited vibrational state than for the ground state.

TABLE 4

Rotational energy-level differences for CD_4, corrected for Coriolis coupling

	Energy-level difference, cm^{-1}		
	Gas phase	Matrix	
$F_v(J+1) - F_v(J)$	ν_3 and ν_4	ν_3	ν_4
$F_1(3) - F_1(2)$	$6B = 15.9$	10.3	11.8
$F_1(2) - F_1(1)$	$4B = 10.6$	7.1	7.7
$F_1(1) - F_1(0)$	$2B = 5.3$	4.3	4.3
$F_0(2) - F_0(1)$	$4B = 10.6$	9.0	8.0
$F_0(1) - F_0(0)$	$2B = 5.3$	4.2	4.3

Conclusions

The methane molecules occupy substitutional cavities in any of the solid noble gases when the concentration of methane is low enough; the limit of solute concentration is different for the three noble gases used. The temperature-dependence study shows that the motion of the molecules is more complex than free rotation and that the high rotational levels $J \geqslant 2$ are more highly perturbed than the two lowest ones. The aggregation of the molecules as a possible cause of the fine structure has to be definitively ruled out. The influence of the methane concentration on the structures of the three systems is different; this is likely the result of the strain energy, which is highly different in the three different mixed crystals. X-Ray diffraction studies of the methane–krypton system are needed; more information about intermolecular forces should be obtained from this system than from the

methane–argon or methane–xenon mixed crystals. As regards the thin films deposited on a cold plate suspended in vacuum, it has been shown that their composition or structure, or both, are not uniform over the entire sample. Raman spectra of solutions with low CH_4 concentrations will be reinvestigated. Using the high-power lasers now available, it should be possible to obtain spectra of much higher quality than those reported previously (4). Because of the different selection rules, such spectra would certainly be very useful to the solution of the problems discussed in this paper.

Generous financial assistance from the National Research Council of Canada is acknowledged. We are grateful to Professor G. E. Ewing for helpful discussions and to Professor S. Kimel for sending us preprints of his papers.

1. L. J. SCHOEN, D. E. MANN, C. KNOBLER, and D. WHITE. J. Chem. Phys. **37**, 1146 (1962).
2. A. CABANA, G. B. SAVITSKY, and D. F. HORNIG. J. Chem. Phys. **39**, 2942 (1963).
3. A. CABANA, R. BARDOUX, and A. CHAMBERLAND. Can. J. Chem. **47**, 2915 (1969).
4. A. CABANA, A. ANDERSON, and R. SAVOIE. J. Chem. Phys. **42**, 1122 (1965).
5. F. H. FRAYER and G. E. EWING. J. Chem. Phys. **46**, 1994 (1967); **48**, 781 (1968).
6. H. F. KING and D. F. HORNIG. J. Chem. Phys. **44**, 4520 (1966). H. FRIEDMANN, A. SHALOM, and S. KIMEL. J. Chem. Phys. In press.
7. J. G. ASTON. Phys. Chem. Solids, **18**, 62 (1961).
8. S. C. GREER and L. MEYER. J. Chem. Phys. **50**, 4299 (1969).
9. Tables of wavenumbers. Butterworths, Inc., Washington, D.C. 1961.
10. J. L. HOLLENBERG and D. A. DOWS. J. Chem. Phys. **34**, 1061 (1961).
11. E. R. DOBBS and G. O. JONES. Rep. Progr. Phys. **20**, 560 (1957).
12. C. S. BARRETT, L. MEYER, and J. WASSERMAN. J. Chem. Phys. **44**, 998 (1966).
13. R. E. BEHRINGER. J. Chem. Phys. **29**, 537 (1958).
14. H. P. HOPKINS, R. F. CURL, and K. S. PITZER. J. Chem. Phys. **49**, 2959 (1968).
15. J. HERRANZ, J. MORCILLO, and A. GÓMEZ. J. Mol. Spectrosc. **19**, 226 (1966).
16. G. HERZBERG. Infrared and Raman spectra. D. van Nostrand Co., Inc., Princeton, N. J. 1945. pp. 446 *ff*.

Can. J. Chem. Downloaded from www.nrcresearchpress.com by 210.87.254.40 on 09/05/12
For personal use only.

Thermal decomposition of methyl azide[1]

M. S. O'DELL, JR.[2] AND B. DEB. DARWENT
The Martin Maloney Chemistry Laboratory, The Catholic University of America, Washington, D.C. 20017
Received October 14, 1969

The thermal decomposition of gaseous methyl azide has been investigated at conversions of less than 1% at 155, 170, and 200 °C. The reaction has been shown to be homogeneous and unimolecular, the first-order rate constant being $k_{uni} = 2.85 \times 10^{14} \exp -(40\,500/RT)$. The decomposition results in the formation of $CH_3N(X^3\Sigma^-)$ and $N_2(X^1\Sigma_g^+)$. The $CH_3N(X^3\Sigma^-)$ do not react with CH_3N_3 to produce N_2, but do form a polymer of composition similar to hexamethylene tetramine and also react with olefins. The major products are N_2 and polymer; small amounts of H_2 and CH_4, but no C_2H_6, are formed.

Canadian Journal of Chemistry, 48, 1140 (1970)

Can. J. Chem. Downloaded from www.nrcresearchpress.com by 210.87.254.105 on 09/05/12
For personal use only.

Introduction

The early investigations (1, 2) of the thermal decomposition of methyl azide showed the reaction to be homogeneous and of the first order. However, those investigations were conducted at rather high conversions (20–60%), and the complexity of the products (N_2, NH_3, C_2H_6, C_2H_4) was such that secondary reactions may have been important. It is therefore not clear whether the process is truly unimolecular or that short chains were not present. A subsequent investigation (3) was more concerned with the possibility of stabilizing the methyl imino radical (CH_3N) than with the details of the decomposition.

A recent investigation (4) of the photochemical decomposition showed that a short chain, carried by CH_3N, was present and led to a quantum yield of two or slightly higher.

The thermal decomposition of methyl azide has been re-investigated at low conversion and the effects of olefins, as free-radical scavengers, and of the surface studied. These experiments have shed light on the details of the thermal decomposition and the nature of the CH_3N radicals.

Experimental

A. Apparatus

The apparatus was an all-glass, conventionally designed gas kinetic system. Special precautions were taken to exclude mercury from that portion of the system in which the azide was to be handled, since contamination by mercury could lead to the formation of an easily detonated product (5).

The reaction vessel was a Pyrex bulb of 397-ml capacity with a surface-to-volume ratio of 0.68 cm^{-1}; the temperature was maintained constant, to within 0.2 °C, by a temperature controller. These sections of the apparatus were evacuated by a three-stage oil diffusion pump backed by a rotary pump, and were capable of maintaining a vacuum of at least 10^{-5} mm Hg.

The analytical section was the only portion of the apparatus that contained mercury. It consisted of a Toepler pump – gas buret, a McLeod gauge, and a mercury manometer. A two-stage mercury diffusion pump backed by a separate rotary pump was used to evacuate this section. The analytical section connected through a trap and a stopcock to the low vacuum side of a single-stage oil diffusion pump, the high vacuum side of which connected to the reaction section of the mercury-free system. The stopcock was opened only after the trap had been immersed in liquid nitrogen (or CO_2–acetone mixture) and the diffusion pump turned on.

A Bourdon-type Pyrex spiral gauge, having a sensitivity of ±0.1 mm Hg and capable of withstanding ±1.0 atm differentials, was used as a null instrument in measuring the pressure of gases. A CEC Model 21 620-A mass spectrometer, a Perkin–Elmer infracord spectrometer, and a gas chromatograph were used for analysis and identification of products.

B. Materials

The methyl azide was prepared by the methylation of a slightly alkaline solution of sodium azide in a manner very similar to the original procedure of Dimroth and Wislicenus (6) and its modifications (3). It was found that yields were greatly facilitated if the azide was distilled from the alkaline medium in an open system protected from the moisture of the atmosphere by a short tube containing anhydrous calcium chloride. The fraction distilling from a Vigreaux column at 20–21 °C was transferred to the purification section of the vacuum system, and further purified by trap-to-trap distillation. The middle third fraction distilling from a −78 °C bath was retained. The methyl azide was analyzed by both mass spectrometry and gas chromatography before use. Occasionally further distillation from −78 °C bath was necessary to remove

[1]This research was supported by the U.S. Army Engineer Research and Development Laboratories, Corps of Engineers, Fort Belvoir, Virginia under Contract No. DA-44-009-AMC-516 (T) with the Catholic University of America.

[2]Abstracted from a Dissertation submitted by M. S. O'Dell, Jr., to the Graduate School of Arts and Sciences in partial fulfillment of the requirements for the Ph.D. degree of the Catholic University of America.

Can. J. Chem. Downloaded from www.nrcresearchpress.com by 210.87.254.105 on 09/05/12
For personal use only.

an impurity which appeared as a mass 44 peak. It was found that each of eight different preparations gave rates of production of nitrogen that were identical within 2% under the same conditions. As a precautionary measure, only a small portion of a given preparation was stored on the vacuum system in a blackened bulb, while the remainder was stored in a separate flask at −78 °C, away from the system and shielded from light.

The carbon dioxide, ethylene, and propylene were Matheson research grade specimens and, after purification by trap-to-trap distillation and mass spectral analysis, were used without further treatment.

C. Technique and Analysis

The required pressure of azide was transferred to a precisely known and variable volume and then a portion was admitted to the reaction vessel. The amount of azide admitted was calculated from the change in pressure in the known volume. A similar technique was used for mixtures of azide and other gases and, in those experiments, analysis of the mixture before and after expansion showed that there had not been any detectable alteration in the composition of the mixture due, for example, to different diffusion rates of the components.

At the end of the decomposition, the reaction vessel was opened to two traps in series, cooled in liquid nitrogen, and then to a small oil diffusion pump and the Toepler pump – gas buret. The traps were then isolated from the reaction vessel and their contents thawed and frozen until all the uncondensable gas had been removed.

Synthetic mixtures containing nitrogen, hydrogen, and methane were prepared for calibration of the mass spectrometer. The ratios of the sensitivities of mass numbers 2:28 and 16:28 were calculated from the observed peak heights of the standard mixtures. The uncondensable fractions were analyzed by the mass spectrometer, and the peak heights of mass numbers 2, 16, and 28 corrected for their leak rates. With these measurements and the ratios of the sensitivities obtained from the standard mixtures, the ratios of hydrogen/nitrogen and methane/nitrogen in the products were calculated.

The condensable fractions were warmed to −155 °C, and the distillate collected at liquid-nitrogen temperature. The container was transferred to the gas chromatograph for analysis on a 3-ft silica gel column at 70 °C for the presence of any C_2 fraction in the products. The residue from the −155 °C fractionation was then warmed to room temperature and the distillate collected at liquid-nitrogen temperature. The sample was analyzed on a 3-ft Silicone (Dow-Corning 203) – Chromosorb W column at 25 °C. This column had previously been found satisfactory for the separation of all the expected products in the room temperature fraction from the decomposition of methyl azide.

After several decompositions, a solid product was found in the trap nearest the reaction vessel. That trap was sealed off under vacuum and the product analyzed for carbon and hydrogen.

The remaining procedure for the foreign gas mixtures was the same as in the case of the azide alone, except that with the azide–ethylene mixtures it was necessary to remove traces of ethylene from the uncondensable fraction before final measurement in the gas buret. This was accomplished by admitting the gases to a small U-shaped trap immersed in liquid nitrogen and expanding back into the buret. With this procedure, no peak due to the presence of ethylene was observed in the spectra of the uncondensable fractions.

Results

A. Products

The uncondensable gases were found to consist mainly of nitrogen, with small amounts of hydrogen and methane. The hydrogen ranged from 6% of the nitrogen at the lowest pressure, to less than 1% at the highest pressure studied. Methane was less than 2% of the nitrogen and this ratio remained essentially constant over the entire pressure range.

Neither ethane nor ethylene was found in the −155 °C distillate. Either would have been detected if it had been present to the extent of 5% of the nitrogen. The residue of the −155° fractionation yielded only a trace of a component identifiable as HCN by its retention time on the Silicone – Chromosorb W column, and then only after collecting the products from several low-pressure runs. Neither HN_3 nor NH_3 was detected chromatographically in the −155° residue. While the column used was efficient in separating HN_3 and CH_3N_3 in mixtures of proportions of 1:9 HN_3/CH_3N_3 in the presence of a very large excess of CH_3N_3, as was the case in these experiments, tailing of the CH_3N_3 obscured the HN_3 peak. Hence HN_3 may have been produced in this reaction.

Two white solid products were formed. One was found deposited on the walls of the trap into which the decomposition mixture was first expanded. It appeared to be of low vapor pressure, and remained on the walls after being pumped on at room temperature for several hours. It was not sublimed by a boiling water bath, but did decompose when warmed by a soft flame. The products of that decomposition were nitrogen, hydrogen, and methane in poorly reproducible ratios. The trap was sealed off under vacuum and the material subjected to elemental analysis. Assuming the material to consist solely of carbon, hydrogen, and nitrogen, the analysis was 53.06% carbon, 8.97% hydrogen, and, by difference, 37.97% nitrogen. Since the amount of product obtainable for analysis was small (only 0.63 mg) the error in the analysis may be as high as 5%. This sample was the accumulated product from a large number of runs. Further attempts to obtain stoichiometric results were abandoned when it

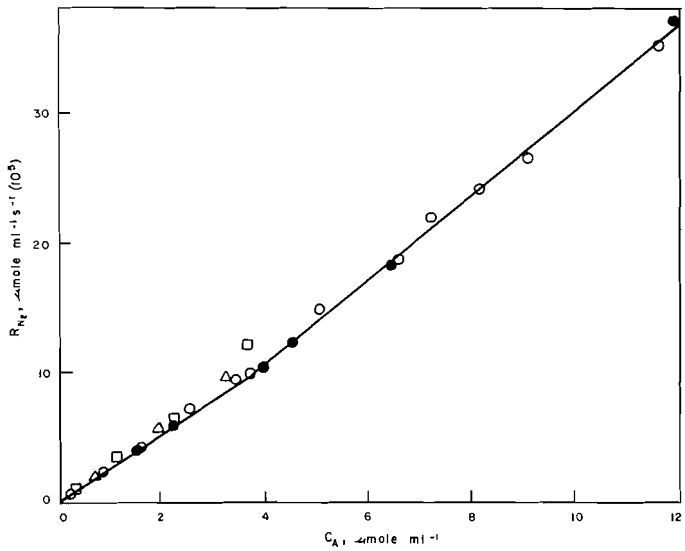

FIG. 1. The effects of concentration of azide, ○; increased surface, ●; propene, △; and ethylene, □, on the rate of formation of N_2 at 200 °C. $[C_3H_6]/[CH_3N_3] = 1.0$; $[C_2H_4]/[CH_3N_3] = 0.10$.

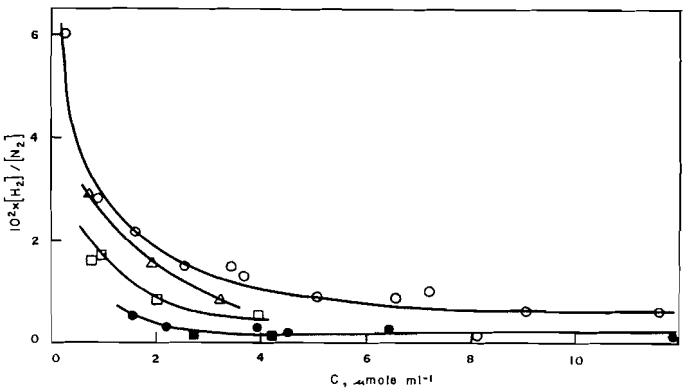

FIG. 2. The effects of concentration of azide, ○; increased surface, ●; propene, △; and ethylene, □, on the rate of formation of H_2 at 200 °C. [Olefin]/[azide] = 1.0.

was observed that a portion of the polymer remained in the dead space of the reaction vessel.

The other solid material was deposited on the walls throughout the sections of the apparatus to which the products of the decomposition were exposed. It was also deposited on the walls of the gas buret and so was more volatile than the solid found on the walls of the first trap. The analysis of this substance was not feasible.

B. Rates

The effect of time on the rates of formation of N_2, CH_4, and H_2 was investigated at 22 mm of azide and at 200 °C. The rate of formation of N_2 was independent of time up to 20 min (4% conversion) and the ratios H_2/N_2 and CH_4/N_2 were also independent of time; the values of these ratios were $2.3 \pm 0.2 \times 10^{-2}$ and $1.5 \pm 0.2 \times 10^{-2}$, respectively.

The effects of concentration of azide (C), surface-to-volume ratio (S/V), and free-radical scavengers (C_2H_4, C_3H_6) were investigated at small conversion (<1%) at 200 °C. The results of these experiments are presented in Figs. 1 and 2. From Fig. 1, it is evident that the rate of formation of N_2 (R_{N_2}) is approximately directly proportional to C at large C and deviates from linearity at low C as expected for a unimolecular

Can. J. Chem. Downloaded from www.nrcresearchpress.com by 210.87.254.105 on 09/05/12
For personal use only.

TABLE 1

Effect of concentration and surface/volume ratio on the rate of the thermal decomposition of CH_3N_3 at 200 °C

Concentration (μmole ml^{-1})	Decomposition (%)	Rate (N_2) (μmole ml^{-1} $s^{-1} \times 10^6$)	$[H_2]/[N_2]$ ($\times 10^2$)	$[CH_4]/[N_2]$ ($\times 10^2$)	k_{unf} ($s^{-1} \times 10^5$)
0.24	0.69	5.5	6.0	1.8	2.28
0.88	0.77	22.6	2.8	1.5	2.57
1.54*	—	40.7	0.5	1.1	2.64
1.60	0.77	43.0	2.2	1.5	2.69
2.20*	—	59.4	0.3	1.1	2.70
2.52	0.81	73.4	1.5	1.9	2.89
3.40	0.84	95.6	1.5	1.5	2.81
3.68	0.82	100.0	1.3	1.7	2.74
3.91*	—	105.5	0.3	1.3	2.70
4.50*	—	124	0.2	1.3	2.75
5.03	0.89	149.5	0.9	1.5	2.96
6.45*	—	185	0.3	1.6	2.87
6.58	0.88	188.5	0.9	1.1	2.86
7.20	0.92	221.5	1.0	1.2	3.07
8.11	0.90	243.5	0.1	1.5	3.01
4.05	0.88	266	0.6	1.2	2.94
11.60	0.92	354	0.6	1.1	3.05
11.90*	—	375	0.1	1.2	3.15

*Packed reaction vessel; $S/V = 12.7$.

reaction in the "fallen-off" region; the rate is also independent of S/V, of the addition of C_3H_6 equal to C, and of small amounts of C_2H_4. The addition of larger amounts of C_2H_4 increased R_{N_2} significantly. From these data we may conclude that the reaction is homogeneous and that chains are unimportant. One noticeable effect of the addition of C_2H_4 was that the formation of polymer was suppressed. The fact that the polymer was not formed suggests that some other product, e.g., N-methyl ethylene imine, should have been produced. We were unable to detect such compounds, possibly due to the formation of the quaternary ammonium azide by reaction with the excess azide present.

Although R_{N_2} was unaffected by S/V or scavengers, the ratio H_2/N_2 was drastically influenced by these changes (Fig. 2). Thus H_2/N_2 was decreased significantly by increasing C and S/V and by the addition of olefins. Although these data are not of the highest precision, it is evident that C_2H_4 is more effective than C_3H_6 and that the surface plays an important role in the formation of H_2.

The ratio CH_4/N_2 appeared to be completely unaffected by C or S/V, but it was reduced by the addition of olefins.

These experiments were restricted to conversions of less than 1%, so that C remained essentially constant and the rates were quite accurately the initial values. Accordingly, the order of the reaction could be determined by plotting log R_{N_2} against log C. Those plots (Fig. 3) are quite accurately linear and lead to reaction orders of 1.08, 1.10, and 1.06 at 200, 170, and 155 °C, respectively, and suggest that the reaction is of first order at all temperatures investigated. The values on which these plots were based are given in Tables 1 and 2.

The limiting values for k_∞, the defined first-order rate constant for the formation of N_2, were determined by the method suggested by Johnston (7) in which k was plotted as a function of $1/C$. These plots (Fig. 4) were satisfactorily linear at high C and gave values of 3.47×10^{-7}, 1.67×10^{-6}, and 3.21×10^{-5} s^{-1} for k_∞ at 155, 170, and 200 °C, respectively. The Arrhenius plot of these values (Fig. 5) was also linear and leads to $k_\infty = 2.85 \times 10^{14} \exp -(40\,800/RT)$.

Although the reaction was not investigated over a very wide range of pressures (only between 7 and 350 mm) the solution of Kassel's integral suggests that 11 ± 1 oscillators were effective. This number did not change with temperature.

Discussion

The results of this investigation show that the thermal decomposition of methyl azide is quite

Can. J. Chem. Downloaded from www.nrcresearchpress.com by 210.87.254.105 on 09/05/12
For personal use only.

Can. J. Chem. Downloaded from www.nrcresearchpress.com by 210.87.254.105 on 09/05/12
For personal use only.

TABLE 2

Effect of concentration on the rate of the thermal decomposition of CH_3N_3 at 155 °C and 170 °C

Concentration (μmole ml^{-1})	Decomposition (%)	Rate (N_2) (μmole ml^{-1} s^{-1} × 10^6)	$[H_2]/[N_2]$ (× 10^2)	$[CH_4]/[N_2]$ (× 10^2)	k_{unl} (s^{-1} × 10^6)
(a) 155 °C					
0.81	0.19	0.212	2.4	1.4	0.222
0.91	0.23	0.279	2.2	1.4	0.307
1.68	0.22	0.503	1.6	1.1	0.300
2.18	0.23	0.641	1.9	1.6	0.301
2.52	0.22	0.783	1.8	1.3	0.315
3.63	0.23	1.165	1.0	1.6	0.321
4.81	0.37	1.59	0.8	1.7	0.331
5.09	0.24	1.675	1.0	1.6	0.329
6.12	0.28	1.98	0.6	1.3	0.324
8.61	0.37	2.92	0.5	1.8	0.339
9.01	0.37	3.06	0.5	1.0	0.339
(b) 170 °C					
0.96	0.48	1.29	2.2	1.3	1.35
1.13	0.45	1.47	2.2	1.3	1.30
2.82	0.54	4.19	1.2	1.2	1.49
3.61	0.58	5.50	1.3	1.3	1.53
5.56	0.56	8.75	0.6	1.2	1.58
6.54	0.58	10.6	0.6	1.2	1.60
9.00	0.58	14.6	0.6	1.3	1.62

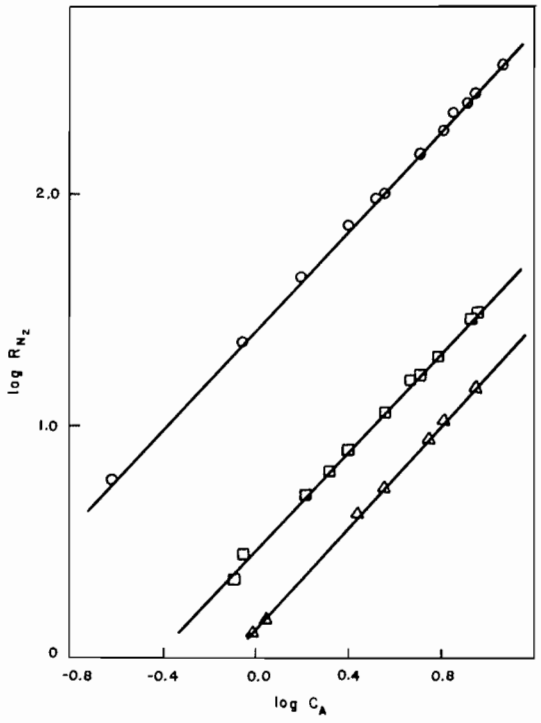

FIG. 3. Determination of the order of the reaction. ○, 200 °C, $k \times 10^6$; △, 170 °C, $k \times 10^6$; □, 155 °C, $k \times 10^7$.

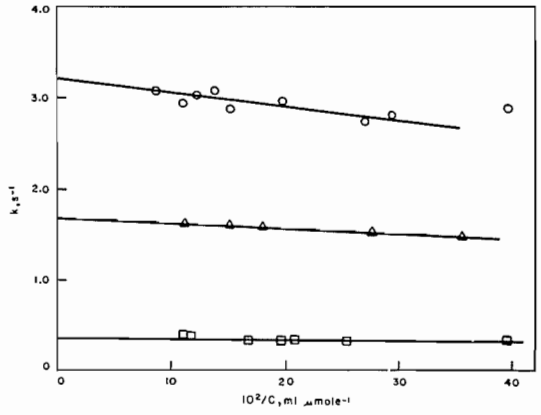

FIG. 4. Determination of k_∞. ○, 200 °C; △, 170 °C; □, 155 °C. k's multiplied by 10^5 (200 °C), 10^6 (170 °C), 10^7 (155 °C).

accurately of the first order, homogeneous, and free from chains. The small yield of CH_4 and the complete absence of C_2H_6 suggest that CH_3 is not formed to any significant extent. Accordingly, the most important initial step in the thermal decomposition is certainly

[1] $$CH_3N_3 \rightarrow CH_3N + N_2$$

The observation that olefins do not reduce the rate of formation of N_2 but do inhibit the forma-

Can. J. Chem. Downloaded from www.nrcresearchpress.com by 210.87.254.105 on 09/05/12
For personal use only.

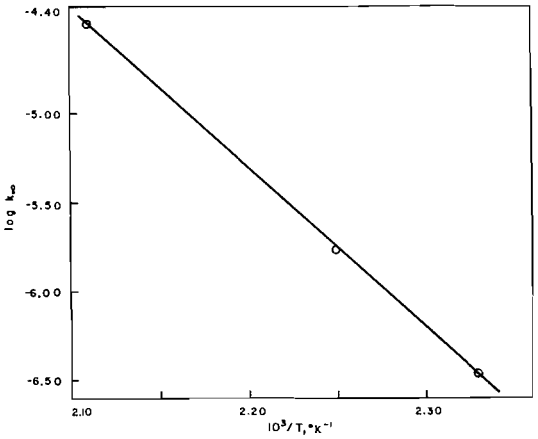

FIG. 5. Arrhenius plot of k_∞ vs. $1/T$.

tion of the polymer suggests strongly that CH_3N do not react with CH_3N_3 to produce N_2, as they do in the photochemical decomposition of methyl azide (4), but combine with each other

$$[2] \qquad 2CH_3N \rightarrow (CH_3N)_2$$

with subsequent formation of the polymer, or react with added olefins, possibly by addition to the double bond. This is consistent with the ability of olefins to inhibit the formation of the polymer.

The most probable source of H_2 is the decomposition of CH_3N

$$[3] \qquad CH_3N \rightarrow H_2 + HCN$$

and this is supported by the fact that HCN was identified in the products, though in very small amounts. The application of the usual steady-state assumption to the above three reactions leads to

$$d[CH_3N]/dt = 0 = k_1C - k_2[CH_3N]^2 - k_3[CH_3N]$$

Even though the estimation of the polymer is not possible, the material balance requires that the rate of disappearance of CH_3N to form the polymer be about equal to the rate of formation of N_2, since the only other detectable products (H_2, CH_4) were much less than N_2. Accordingly, reaction [3] will be much slower than reaction [2], so that $[CH_3N] \approx (k_1C/k_2)^{1/2}$ or

$$[4] \qquad R_{H_2}/R_{N_2} = (k_3/k_2^{1/2})R_{N_2}^{-1/2}$$

The ratio $[H_2]/[N_2]$ is shown as a function of $R_{N_2}^{-1/2}$ in Fig. 6 and eq. [4] is shown to be obeyed, with more or less precision, at all three temperatures.

Since an increase in S/V decreases the value of $[H_2]/[N_2]$, it is evident that, if reactions [2] and [3] adequately explain the formation of polymer and H_2, the combination of the radicals [2] must occur, at least partially, on the walls, but at a rate that is second order in $[CH_3N]$ in the gas. One explanation of this requirement is that the surface be sparsely covered and that the combination occur between two adsorbed radicals. Polymerization may then proceed, not through the repeated addition of CH_3N to $(CH_3N)_2$(ads), but by repeated combinations of $(CH_3N)_2$(ads).

The fact that no C_2H_6 could be detected analytically requires the CH_4 to be formed directly as such and not by reactions of CH_3 with, e.g., CH_3N_3. The reaction

$$CH_3 + CH_3N_3 \rightarrow CH_4 + CH_2N_3$$

is expected to be slow, especially at the lower temperatures and pressures, so that some detectable C_2H_6 should have been formed under those conditions. Furthermore, the ratio $[CH_4]/[N_2]$ is independent of T, C, and S/V, so that the CH_4

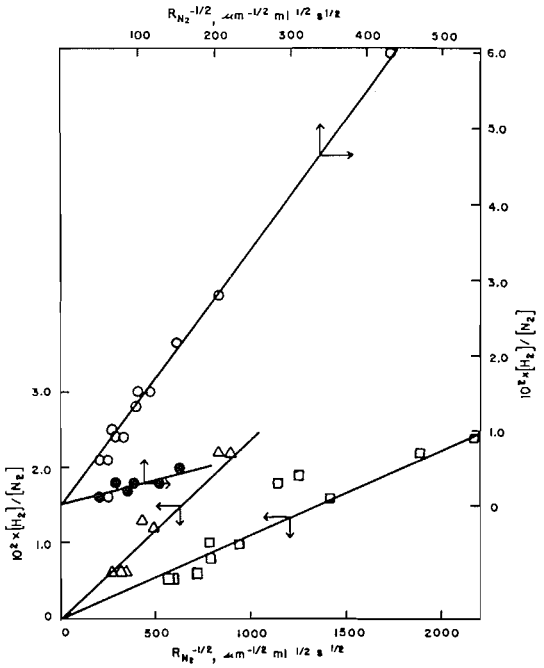

FIG. 6. The effect of concentration (R_{N_2}) on the ratio $[H_2][/N_2]$: ○, 200 °C; △, 170 °C; □, 155 °C. Filled circles: data from packed vessel at 200 °C.

TABLE 3

Composition of the polymers formed by the thermal and photochemical decomposition of CH_3N_3

Analysis for	CH_3N	Hexamethylene-tetramine	Photochemical (ref. 4)	Thermal	
				Rice and Grelecki (ref. 3)	Present investigation
%C	41.4	51.4	41.4	51.4	53.1±2.6
%H	10.3	8.7	10.3	8.7	9.0±0.45
%N	48.3	40.0	48.2	40.0	38.0±1.9

must have been formed by a reaction of the same type and order as the principal means of disappearance of CH_3N. This requires CH_4 to be formed by

$$[4] \qquad 2CH_3N \xrightarrow{\text{(wall)}} CH_4 + CH_2N_2$$

where CH_2N_2 may be diazomethane or diazirine or some absorbed species. This substance would have been formed in small amounts, approximately equivalent to CH_4, or 1.5% of the N_2, and could easily have escaped detection.

The elemental analysis (Table 3) shows that the polymer has the approximate composition $(CH_2)_6N_4$ or a higher polymer of similar composition. It is similar to that reported by Rice and Grelecki (3) but is obviously very different from the photochemically produced polymer.

Some information concerning the details of the decomposition process [1] and the nature of the CH_3N may be obtained from the present data. Since there is no information about the bond dissociation energy of CH_3N—N_2 and the triplet–singlet separations of CH_3N, we assume that they are not very different from those in HN_3. Adopting the values given by Okabe (8) for HN_3 and assuming they are about the same for CH_3N_3, we have

$$[1a] \qquad CH_3N_3 \rightarrow CH_3N(X^3\Sigma^-) + N_2(X^1\Sigma_g^+) \qquad \Delta H = 9.5 \text{ kcal mole}^{-1}$$

$$[1b] \qquad CH_3N_3 \rightarrow CH_3N(a^1\Delta) + N_2(X^1\Sigma_g^+) \qquad \Delta H = 46.5 \text{ kcal mole}^{-1}$$

$$[1c] \qquad CH_3N_3 \rightarrow CH_3N(b^1\Sigma^+) + N_2(X^1\Sigma_g^+) \qquad \Delta H = 71.0 \text{ kcal mole}^{-1}$$

The value of E (40.5 kcal mole^{-1}) found in the present experiments rules out the possibility of reaction [1c] but, in view of the uncertainty in transposing the values for HN_3 to CH_3N_3, we cannot eliminate reaction [1b] on the basis of energy, since ΔH for that process may well be as low as 40 kcal mole^{-1}. However, even such a low value of ΔH would require the reverse reaction to have little or no activation energy, so that the reaction may exhibit some of the characteristics of a first-order reaction opposed by a second-order reaction. A mechanism based on reactions [1], [−1], and [2], assuming a steady state in $[CH_3N]$ and also that $k_2[CH_3N]^2 \gg k_{-1}[CH_3N][N_2]$, leads to

$$R_{N_2} = k_1[CH_3N_3] - k_{-1}(k_1/k_2)^{1/2}[CH_3N_3]^{1/2}[N_2]$$

If the rate of reaction [−1] were at all comparable to that of reaction [1], the reaction should depart from first-order behavior at high conversion. The earlier work (2) did not show any detectable departure from first-order kinetics up to 60% conversion. This suggests that reaction [−1] is unimportant and, if a rapid reaction [−1] is a necessary consequence to reaction [1b], that the initial decomposition is by reaction [1a], even though the process is spectroscopically forbidden.

A more compelling reason for preferring reaction [1a] to [1b] is obtained by contrasting the reactivities of CH_3N produced thermally and photochemically (4). The photochemical radicals react readily with both CH_3N_3 and C_2H_4, and the addition of quite small concentrations of C_2H_4 decreased the quantum yield of N_2 by a factor of two. The thermal CH_3N also react with olefins, since the polymerization is inhibited by C_2H_4, but do not react with CH_3N_3 to produce N_2, since the rate of N_2 is unaffected by small amounts of olefins. The selection rules are much more stringent for the photochemical than for the thermal process and much more energy (85–112 kcal mole^{-1}) was available in the former. Accordingly, the photochemical CH_3N were very probably ($a^1\Delta$) or ($b^1\Sigma^+$), and we conclude that the

Can. J. Chem. Downloaded from www.nrcresearchpress.com by 210.87.254.105 on 09/05/12
For personal use only.

unreactive thermal radicals were in the ($X^3\Sigma^-$) ground state.

The magnitude of the frequency factor (ca. 3×10^{14} s^{-1}) appears, at first sight, to be inconsistent with a forbidden process. However, frequency factors in the range 10^{15}–10^{17} s^{-1} have been reported for many unimolecular decompositions, so that the frequency factor is not inconsistent with a value in the range 10^{15}–10^{17} s^{-1}, coupled with a transmission coefficient in the range 10^{-1}–10^{-3}, as would be expected in a system of light atoms that reacts contrary to the selection rules. This suggests that the singlet surface of CH_3N_3, which connects with $CH_3N(a^1\Delta)$ and $N_2(X^1\Sigma_g^+)$, is intersected by a triplet, probably repulsive, surface at about 40.5 kcal above the zero-point energy of the ground state.

1. H. C. RAMSPERGER. J. Amer. Chem. Soc. **51**, 2134 (1929).
2. J. A. LEERMAKERS. J. Amer. Chem. Soc. **55**, 3098 (1933).
3. F. O. RICE and C. T. GRELECKI. J. Phys. Chem. **61**, 830 (1957).
4. C. L. CURRIE and B. DEB. DARWENT. Can. J. Chem. **41**, 1552 (1963).
5. C. L. CURRIE and B. DEB. DARWENT. Can. J. Chem. **41**, 1048 (1963).
6. O. DIMROTH and W. WISLICENUS. Chem. Ber. **38**, 1573 (1905).
7. H. S. JOHNSTON. J. Chem. Phys. **20**, 1103 (1952).
8. H. OKABE. J. Chem. Phys. **49**, 2726 (1968).

Can. J. Chem. Downloaded from www.nrcresearchpress.com by 210.87.254.105 on 09/05/12
For personal use only.

Can. J. Chem. Downloaded from www.nrcresearchpress.com by 210.87.254.105 on 09/05/12
For personal use only.

Oxidation of ascorbic acid by osmium(VIII)

U. S. MEHROTRA AND S. P. MUSHRAN
Department of Chemistry, University of Allahabad, Allahabad, India

Received May 29, 1969

Reduction of osmium(VIII) by ascorbic acid has been studied in the presence of hydrochloric acid. The reaction is found to be directly proportional to the concentration of ascorbic acid and osmium(VIII) and to the reciprocal of the hydrogen ion concentration. In the proposed mechanism, the reacting species have been shown to be perperosmic acid and ascorbate ion; this was supported by the negligible effect of the ionic strength. Influence of temperature was studied in the range 25–40 °C, and the energy and entropy of activation were calculated as 14.1 ± 0.2 kcal mole^{-1} and −8.6 ± 0.1 e.u., respectively. Osmium(IV) was found to be a product of the reaction.

Canadian Journal of Chemistry, 48, 1148 (1970)

Introduction

Osmium tetroxide has been extensively used as an oxidizing agent as well as a catalyst. Like all platinum metals, osmium(VIII) has been found to catalyze many organic and inorganic oxidation processes. Solymosi and Csik (1) have described osmium tetroxide as a general catalyst for all oxidations involving hexacyano-ferrate(III) as the oxidant. Its catalytic role has been explained through the intermediate formation of osmium-(VI) (2).

Criegee (3) studied the oxidation by osmium-(VIII) of some organic compounds in alkaline media and showed that the oxidant was reduced to osmium(VI). Cook and Schoental (4) investigated the oxidation of anthracene by osmium tetroxide and found a brown ester complex formed in a slow process, as the product. Osmium(VIII) has been found to oxidize several pyrimidine nucleosides at different rates but no kinetic conclusion could be drawn from this investigation (5).

Osmium tetroxide dissolves in an alkaline medium, giving a red-brown solution which becomes colorless in the presence of mineral acid due to the formation of perperosmic acid (6) (H_2OsO_5). In the present investigation, the kinetics of the reduction of octavalent osmium by ascorbic acid in an acidic medium has been reported.

Experimental

An aqueous solution of osmium tetroxide was prepared by dissolving a Johnson–Mathey sample of the reagent in 5×10^{-5} *M* sodium hydroxide solution; it was standardized iodometrically using a starch indicator. An aqueous solution of ascorbic acid was prepared fresh from a G.R., S. Merck sample of the reagent; it was titrated against a standard iodine solution using a starch indicator. All other reagents were of analytical grade. Doubly distilled water from a glass still was employed. Reaction vessels were of Jena glass and were coated outside with Japan black to exclude all photochemical effects.

Requisite amounts of osmium tetroxide and hydrochloric acid were kept in a water thermostat; ascorbic acid was pipetted in to start the reaction. Perperosmic acid was reduced to hexachlorosmate ion ($OsCl_6^{2-}$), which develops a yellow color at a definite interval of time in the reaction mixture (7). Aliquots were withdrawn from the reaction mixture; the kinetics was followed by colorimetrically estimating the amount of osmium(IV) formed, using a Klett–Summerson Photoelectric Colorimeter with blue filter No. 42 (transmission 400–450 mμ).

Results

It is reported that osmium(VIII) reacts with ascorbic acid to give dehydroascorbic acid and osmium(IV) (8), and that the yellow color developed during the reduction is due to quadrivalent osmium. Thus the reaction may be represented by the following stoichiometric equation

$$2C_6H_8O_6 + Os(VIII) = 2C_6H_6O_6 + Os(IV) + 4H^+$$

The reduction of Os(VIII) by ascorbic acid was studied at 30 °C with various concentrations of the oxidant, ranging from 2.43×10^{-5} to 7.29×10^{-5} *M* with [ascorbic acid] = 8×10^{-4} *M* and [HCl] = 0.8 *M*. This threefold change in [Os(VIII)] had no effect on the apparent first-order rate constants with respect to perperosmic acid. The average value of this constant was $(9.60 \pm 0.02) \times 10^{-4}$ s^{-1}. The order of the reaction with respect to ascorbic acid was obtained from experiments done at 30 °C with [Os(VIII)] = 3.64×10^{-5} *M* and [HCl] = 0.8 *M*. First-order plots of log $(a/(a - x))$ vs. time were linear for experiments with [ascorbic

Can. J. Chem. Downloaded from www.nrcresearchpress.com by 210.87.254.105 on 09/05/12
For personal use only.

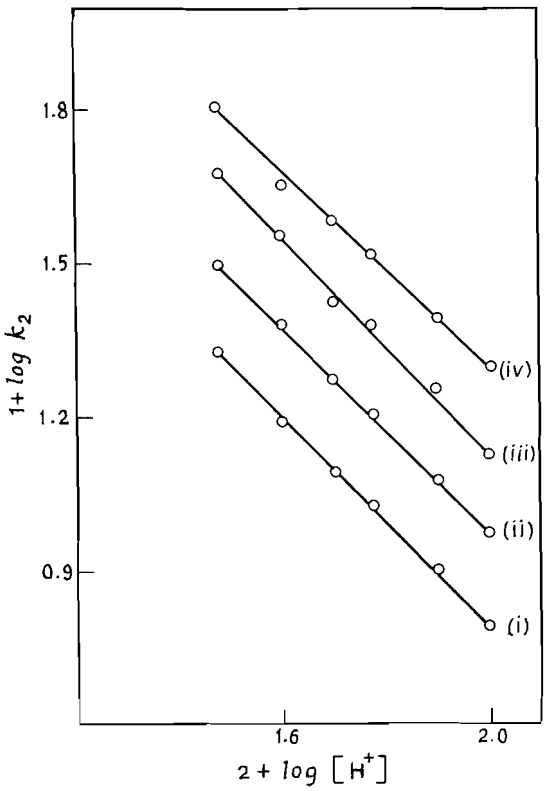

FIG. 1. Plot of log k_2 vs. log [H^+] at (*i*) 25, (*ii*) 30, (*iii*) 35, and (*iv*) 40 °C. [ascorbic acid] = 8×10^{-4} *M*, [Os(VIII)] = 4.86×10^{-5} *M*, $k_2 = k_1$/[ascorbic acid].

acid] = 4.0, 8.0, 12.0, 16.0, and 20.0×10^{-4} *M*; the second-order rate constants, calculated from the slopes of these plots and the concentrations of ascorbic acid, were 1.15, 1.20, 1.13, 1.14, and 1.16 l mole^{-1} s^{-1}, respectively. These two sets of data show that the rate is first order in both [Os(VIII)] and [ascorbic acid].

It was observed that the rate depended strongly on the concentration of hydrochloric acid. A plot of log k vs. log [H^+], where k is the second-order rate constant, is linear (Fig. 1), with a negative slope of unity at all temperatures studied. Thus the rate of the reaction is proportional to the reciprocal of the hydrogen ion concentration.

Variation of ionic strength was accomplished by addition of various amounts of potassium chloride in experiments done at 30 °C with [Os(VIII)] = 4.86×10^{-5} *M*, [ascorbic acid] = 8×10^{-4} *M*, and [HCl] = 0.8 *M*. For [KCl] = 0.02, 0.04, 0.06, 0.08, 0.10, and 0.12 *M*, the apparent first-order rate constants with respect to [Os(VIII)] were 9.60, 9.60, 9.83, 10.0, and 10.1×10^{-4} s^{-1}, respectively. Clearly the sixfold increase in the ionic strength was insignificant.

Measurements were made at 25, 30, 35, and 40 °C. A linear plot of log k vs. $1/T$ was obtained which led to a frequency factor of $(13.0 \pm 0.3) \times 10^{10}$ l mole^{-1} s^{-1}, $E_{act} = 14.1 \pm 0.2$ kcal mole^{-1}, and thus, to $\Delta S^{\dagger} = -8.6 \pm 0.1$ cal deg^{-1} mole^{-1}.

Discussion

Perperosmic acid is known to be a very weak acid (dissociation constant = 8×10^{-13} mole l^{-1} for the first hydrogen) (6) and so reacts as an unionized molecule rather than in the ionized state. From studies of the reduction of osmium(VIII) by hydrobromic acid, Krishman and Crowell (9) suggested that the reacting species in the rate determining step are perperosmic acid, hydrogen ion, and bromide ion. Thus the following scheme may be proposed to account for the reduction of osmium(VIII)

[1] $$AH_2 \underset{k_{-1}}{\overset{k_1}{\rightleftharpoons}} AH^- + H^+$$

This is the reversible ionization of ascorbic acid (AH_2) which is followed by the rate determining step [2]

[2] $$H_2OsO_5 + AH^- \xrightarrow{k_2} A + H_2OsO_4 + OH^-$$

The formation of ascorbate ion (AH^-) has been supported by Khan and Martell (10). The hexavalent osmium formed reacts with another ascorbate ion in the fast step [3] to give the end product dehydroascorbic acid (A)

[3] $$H_2OsO_4 + AH^- \xrightarrow{k_3} A + H_2OsO_3 + OH^-$$

[4] $$H_2OsO_3 + 6HCl \longrightarrow OsCl_6^{2-} + 3H_2O + 2H^+$$

Applying the steady-state condition to [H_2OsO_4] and [AH^-] and assuming $k_{-1}[H^+] \gg k_2[H_2OsO_5]$, the rate of disappearance of perperosmic acid may be represented as

$$[5] \quad -\frac{d}{dt}[H_2OsO_5] = Kk_2\frac{[H_2OsO_5][AH_2]}{[H^+]}$$

where $k_1/k_{-1} = K$.

Equation [5] correctly predicts the observed

dependence of the rate of the reduction of perosmic acid on the concentration of osmium-(VIII), ascorbic acid, and the reciprocal of the concentration of hydrogen ion.

In the proposed mechanism, the rate determining step involves an interaction between a charged ion and an uncharged molecule, and thus should correspond to a negative entropy change and a negligible salt effect. This is also in complete accordance with the experimental data.

The authors thank the Council of Scientific and Industrial Research, New Delhi, India for a Senior Research Fellowship to U.S.M.

1. F. SOLYMOSI and J. CSIK. Chem. Anal. **49**, 12 (1960).
2. U. S. MEHROTRA and S. P. MUSHRAN. J. Indian Chem. Soc. **45**, 526 (1968).
3. R. CRIEGEE. Ann. Chem. **522**, 75 (1936).
4. J. F. W. COOK and R. SCHOENTAL. Nature, **161**, 237 (1948).
5. K. BURTON and T. W. RILEY. Biochem. J. **98**, 70 (1966).
6. D. M. YOST and R. J. WHITE. J. Amer. Chem. Soc. **50**, 81 (1928).
7. W. P. GRIFFITH. Quart. Rev. London, **19**, 224 (1965).
8. W. WAWRZYCHEK. Z. Anal. Chem. **148**, 191 (1961).
9. H. D. KRISHMAN and CROWELL. J. Amer. Chem. Soc. **59**, 20 (1937).
10. M. M. T. KHAN and A. E. MARTELL. J. Amer. Chem. Soc. **89**, 4176 (1967).

Can. J. Chem. Downloaded from www.nrcresearchpress.com by 210.87.254.105 on 09/05/12
For personal use only.

Can. J. Chem. Downloaded from www.nrcresearchpress.com by 210.87.254.40 on 09/05/12
For personal use only.

A refinement of the crystal structures of K_2ReCl_6, K_2ReBr_6, and K_2PtBr_6

H. D. GRUNDY AND I. D. BROWN
Institute for Materials Research, McMaster University, Hamilton, Ontario

Received September 3, 1969

The crystal structures of K_2ReCl_6, K_2ReBr_6, and K_2PtBr_6 have been refined using data collected on a single-crystal X-ray diffractometer to give weighted agreement indices ranging from 0.026 to 0.054 for 75 to 90 nonequivalent reflections. The following bond lengths were obtained: Re—Cl = 235 pm,[1] Re—Br = 248 pm, Pt—Br = 246 pm, K—Cl = 348 pm, and K—Br = 367 and 364 pm in the Re and Pt compounds, respectively. The differences in the root-mean-square angles of libration of the MX_6^{2-} ions in these and a number of isomorphous crystals are discussed.

Canadian Journal of Chemistry, 48, 1151 (1970)

Introduction

Since the determination of the cubic structure of K_2PtCl_6 by Ewing and Pauling (1) in 1928, a large number of compounds of the generic formula R_2MX_6 have been found to possess the same structure. Because of the simplicity of this structure, it has been customary to characterize these compounds by X-ray powder diffraction which yields a value for the unit cell length, a_0, and in some cases the value of the parameter, x, giving the position of the halogen atom in the unit cell. With single-crystal X-ray diffraction methods, it is also possible to measure values for the four independent anisotropic temperature factors, as well as to obtain much more accurate values of x. Recently a number of such determinations have been reported (2–5).

Experimental

Crystals of the K_2PtCl_6 type belong to space group $Fm3m$ (O_h^5) with R in 8(*c*), M in 4(*a*), and X in 24(*e*) with x about 0.25. Regular octahedral crystals of K_2ReCl_6, K_2ReBr_6, and K_2PtBr_6 having a maximum radius such that the spherical absorption term μR was less than 1.0 were selected. About 300 independent measurements of the intensities of 75 to 90 independent reflections from each crystal were made using a θ–2θ scan on a General Electric automatic X-ray diffractometer with molybdenum radiation. After the application of spherical crystal absorption corrections, the intensities of equivalent reflections were averaged. An analysis of the standard deviations observed between such equivalent reflections indicated that the correct standard error to apply to any given intensity measurement was either one-tenth of the observed intensity or the standard error calculated from the counting statistics, whichever was the larger. This standard error was used in weighting the intensities during a least-squares refinement of the scale factor, x, β_{11}(M), β_{11}(X), β_{22}(X), and β_{11}(K). Unobserved reflections for which $F_{min} > F_{calcd}$ and reflections obviously suffering from extinction were given zero weight in the final rounds of refinement. The results are summarized in Table 1. The errors quoted are those derived from random errors and do not take into account possible systematic errors. The structure factors are given in Table 2. The unit cell lengths, a_0, were not measured in this study since accurate values of these have already been published.

Discussion

The values of x for K_2ReCl_6 and K_2ReBr_6 agree with the values given in earlier powder diffraction studies by Aminoff (6) and Templeton and Dauben (7), respectively, although Templeton and Dauben's measurement of the lattice parameter (1044.5 $\pm$ 0.5 pm) is in considerable disagreement with most other measurements (8–10), none of which differ significantly from 1038.5 pm. No value for x has previously been determined for K_2PtBr_6.

An examination of Table 1 shows that for all three compounds, the component of thermal vibration of the halogen atom parallel to the metal–halogen bond is similar to that of the metal atom, but the component perpendicular to the bond is much larger. Similar results have been found in other crystals of this type. If one assumes that these results can be interpreted as arising from a rigid-body libration of the MX_6^{2-} ion, it is possible to calculate the root-mean-square amplitude of libration ($\theta_{r.m.s.}$) of the ion and to correct the M—X bond lengths for this effect (11). Table 3 summarizes these values for a number of crystals.

In such an analysis of temperature effects, a variety of assumptions have to be made. The neglect of the internal modes of vibration of the

[1] 1 pm is equal to 1×10^{-2} Å.

TABLE 1

Crystallographic data for K_2ReCl_6, K_2ReBr_6, and K_2PtBr_6*

Parameter	Value		
	K_2ReCl_6	K_2ReBr_6	K_2PtBr_6
a_0, pm	984.0±0.1 (15)	1038.5±0.2 (8, 9, 10)	1029.3±1 (16)
x	0.2391±0.0003	0.2391±0.0004	0.2393±0.0003
β_{11} (Re,Pt)	0.0036±0.0001	0.0034±0.0002	0.0025±0.0001
β_{11} (Cl,Br)	0.0042±0.0003	0.0043±0.0005	0.0034±0.0002
β_{22} (Cl,Br)	0.0108±0.0001	0.0126±0.0002	0.0108±0.0001
β_{11} (K)	0.0090±0.0002	0.0083±0.0008	0.0080±0.0005
R_1 (unweighted)	0.025	0.071	0.041
R_2 (weighted)	0.026	0.054	0.042
Bond lengths in pm			
(Re,Pt)—(Cl,Br)	235.3±0.4	248.3±0.5	246.3±0.3
K—(Cl,Br)	347.9±0.1	367.2±0.1	364.0±0.1
Root-mean-square thermal displacements in pm			
Re,Pt	13.3±0.3	13.4±0.4	11.6±0.2
Cl,Br (along bond)	14.4±0.3	15.0±0.7	13.5±0.2
Cl,Br (perpendicular to bond)	23.0±0.1	25.8±0.2	24.0±0.1
K	21.0±0.4	20.9±0.9	20.7±0.7

*No allowance has been made for possible systematic errors in the standard errors quoted.

MX_6^{2-} ion will have the effect of increasing the calculated value of $\theta_{r.m.s.}$, but probably not by more than the standard error. The corrected values of the bond length will also tend to be too short by an amount which could be as large as 1 pm. The uncertainty in the values of the corrected bond lengths cannot, therefore, be less than this amount. It is also well known that the root-mean-square thermal displacements of an atom calculated from X-ray data are particularly susceptible to systematic error caused by such effects as the neglect of absorption and extinction or the use of peak height rather than integrated intensity measurements of the X-ray reflections. However, such errors will tend to increase or decrease the apparent mean square displacements of all the atoms in the crystal by the same amount, and since the estimates of the angle of libration and bond length corrections depend only on the differences between two such values, such systematic errors will be minimal in the present case.

In an earlier paper (12), one of us (I.D.B.) pointed out that crystals of the K_2PtCl_6 type were liable to distort if the value of the radius ratio, defined as the size of the alkali metal atom in terms of the space available to it in the crystal, was less than unity. Crystals with radius ratios lying between 0.89 and 0.98 are found to be undistorted at room temperature but have distorted structures at lower temperatures. Crystals

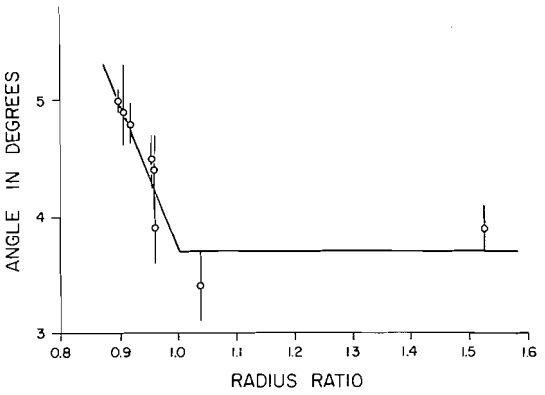

FIG. 1. The r.m.s. libration angle of the MX_6^{2-} ions at room temperature plotted as a function of radius ratio.

with a radius ratio less than 0.89 are distorted at room temperature. This distortion arises from a co-operative twisting of the MX_6^{2-} ions by an amount between 7 and 9° about one of the axes of the MX_6 octahedron. Since the librations of the MX_6^{2-} ion in the cubic crystals are rotational oscillations about these same axes, it is not surprising to find that the measured values of $\theta_{r.m.s.}$ at room temperature also vary with the radius ratio. Figure 1 shows that for radius ratios greater than 1.0, root-mean-square libration angles of about $3\frac{1}{2}$° are found. With a decrease in radius ratio, the libration angle increases to a value of about 5°, beyond which point

Can. J. Chem. Downloaded from www.nrcresearchpress.com by 210.87.254.40 on 09/05/12
For personal use only.

Can. J. Chem. Downloaded from www.nrcresearchpress.com by 210.87.254.40 on 09/05/12
For personal use only.

TABLE 2

Observed and calculated structure factors and standard errors used in the least squares refinement*

K_2ReCl_6

H	K	L	FØBS	FCALC	SIGMA	H	K	L	FØBS	FCALC	SIGMA	H	K	L	FØBS	FCALC	SIGMA	H	K	L	FØBS	FCALC	SIGMA
2	0	0	262.13	260.49	9.28	9	1	1	163.38	159.87	4.72	8	8	2	100.95	99.39	3.14	5	5	5	178.42	172.54	8.92
6	0	0	182.38	170.00	5.27	3	3	1	195.45	196.14	5.65	10	8	2	80.68	79.95	2.47	7	5	5	125.56	121.31	3.63
8	0	0	306.05	299.62	8.84	5	3	1	210.05	203.86	4.30	10	10	2U	34.17	35.57	4.33	9	5	5	117.81	120.33	3.40
10	0	0	102.63	101.98	3.47	7	3	1	131.89	128.45	2.69	3	3	3	171.01	164.47	8.56	7	7	5	85.89	88.72	3.15
2	2	0	253.54	266.45	3.66	9	3	1	146.27	143.55	2.99	5	3	3	182.22	176.11	5.27	9	7	5	91.99	91.31	2.38
4	2	0	219.28	212.88	4.49	5	5	1	206.16	201.42	5.96	7	3	3	116.24	113.60	3.36	9	9	5	86.07	85.32	3.72
6	2	0	193.60	183.24	3.95	7	5	1	134.24	134.29	2.75	9	3	3	130.42	129.41	3.77	6	6	6U	22.53	26.31	12.38
8	2	0	154.68	148.37	3.15	9	5	1	140.44	138.68	2.87	5	5	3	187.20	176.99	5.40	8	6	6	100.26	98.17	3.17
10	2	0	112.22	110.02	2.51	7	7	1	94.63	93.94	2.91	7	5	3	122.03	120.12	2.49	10	6	6U	35.07	35.23	4.02
4	4	0X	416.62	442.42	12.04	9	7	1	103.16	102.38	2.28	9	5	3	126.29	125.87	2.58	8	8	6	82.20	79.94	3.55
6	4	0	158.90	153.16	3.57	9	9	1	98.43	98.23	3.40	7	7	3	86.42	85.28	2.99	10	8	6	68.03	66.59	2.83
8	4	0	254.98	254.48	5.21	2	2	2	145.60	-138.80	7.26	9	7	3	93.36	93.87	2.31	10	10	6U	35.01	34.30	5.28
10	4	0	94.27	94.28	2.16	4	2	2	228.54	226.19	6.61	9	9	3	90.48	90.64	3.59	7	7	7	73.32	67.57	6.45
6	6	0	141.20	149.16	4.08	6	2	2U	40.53	-23.96	3.13	4	4	4	360.92	357.92	18.05	9	7	7	74.62	71.37	3.62
8	6	0	116.58	114.76	2.38	8	2	2	162.79	156.71	4.70	6	4	4	146.49	138.71	4.23	9	9	7	72.97	67.89	3.88
10	6	0	91.85	90.24	2.29	10	2	2U	31.36	25.49	3.54	8	4	4	219.66	218.98	6.36	8	8	8	104.73	100.75	6.65
8	8	0	167.98	166.37	4.86	4	4	2	191.36	185.15	5.52	10	4	4	87.61	86.98	3.24	10	8	8	56.28	54.24	4.82
10	8	0	75.31	74.36	2.76	6	4	2	167.99	163.98	3.44	6	6	4	131.03	127.07	3.78	10	10	8	49.28	47.13	5.26
10	10	0	64.54	63.14	4.45	6	4	2	132.76	133.61	2.97	8	6	4	105.00	104.67	2.18	9	9	9	63.31	61.34	8.11
1	1	1X	294.17	302.83	14.70	10	4	2	103.40	101.39	2.18	10	6	4	82.67	83.62	2.39	10	10	10U	31.00	29.46	12.33
3	1	1	235.48	239.58	6.81	6	6	2U	29.30	11.91	3.39	8	8	4	150.10	145.82	4.34						
5	1	1	251.54	239.40	7.26	8	6	2	121.77	122.15	2.49	10	8	4	70.02	68.64	2.63						
7	1	1	154.06	146.25	4.45	10	6	2U	34.42	32.70	2.61	10	10	4	62.18	58.80	4.85						

K_2ReBr_6

H	K	L	FØBS	FCALC	SIGMA	H	K	L	FØBS	FCALC	SIGMA	H	K	L	FØBS	FCALC	SIGMA	H	K	L	FØBS	FCALC	SIGMA
2	0	0X	337.96	390.39	6.54	3	3	1	162.73	164.28	3.73	3	3	3	102.04	113.99	5.60	9	5	5	137.89	153.41	6.54
4	0	0X	698.52	901.45	21.47	5	3	1	230.32	229.32	2.80	5	3	3	183.27	179.97	4.67	7	7	5	77.21	78.15	7.47
8	0	0	451.77	461.51	26.14	7	3	1	100.08	92.35	4.67	7	3	3	74.87	71.03	4.67	9	7	5	90.75	104.52	8.40
10	0	0	113.34	105.05	12.14	9	3	1	184.67	178.18	7.47	9	3	3	162.54	153.52	7.47	9	9	5	91.96	104.75	12.14
2	2	0	142.75	143.47	3.73	5	5	1	257.49	256.28	4.67	5	5	3	219.86	211.90	4.67	6	6	6	77.68	-47.58	13.07
4	2	0	303.70	315.78	5.60	7	5	1	132.85	131.38	3.73	7	5	3	110.54	109.29	3.73	8	6	6	84.96	93.49	13.07
6	2	0	114.83	106.25	6.54	9	5	1	184.01	179.12	7.47	9	5	3	147.51	156.67	5.60	10	6	6	33.42	8.72	14.00
8	2	0	221.54	211.29	10.27	2	2	2X	403.50	-478.98	11.20	9	7	3	99.90	102.55	13.07	8	8	6	87.67	96.62	13.07
10	2	0	79.64	75.39	6.54	4	2	2	149.19	152.87	3.73	4	4	4X	532.71	558.33	14.94	10	8	6	59.94	65.97	12.14
4	4	0X	625.42	695.49	14.00	6	2	2	226.68	-226.63	8.40	6	4	4	191.48	178.79	6.54	10	10	6	44.72	25.71	9.34
6	4	0	212.21	198.95	7.47	8	2	2	146.76	146.77	8.40	8	4	4	321.53	320.74	10.27	7	7	7	43.32	50.68	11.20
8	4	0	391.55	382.91	16.80	10	2	2	75.62	-51.79	7.47	10	4	4	83.56	92.85	8.40	9	7	7	63.02	75.01	18.67
10	4	0	108.30	99.08	8.40	4	4	2	266.73	271.01	4.67	6	6	4	88.97	94.21	9.34	9	9	7	108.48	78.28	23.34
10	6	0	70.95	69.81	18.67	6	4	2	113.34	113.90	3.73	8	6	4	116.31	131.37	10.27	8	8	8	110.16	128.81	14.94
1	1	1X	302.58	332.50	8.40	8	4	2	156.80	186.03	8.40	10	6	4	68.53	70.91	11.20	10	8	8	47.61	59.80	8.40
3	1	1	226.40	233.31	4.67	10	4	2	76.37	78.92	6.54	8	8	4	159.93	198.11	15.87	10	10	8	54.80	48.89	28.01
5	1	1	279.52	290.23	5.60	8	6	2	110.44	114.35	11.20	10	8	4	69.27	75.19	11.20	9	9	9	75.06	72.64	26.14
7	1	1	128.37	119.53	6.54	10	6	2	61.43	-13.19	11.20	5	5	5	231.25	223.36	8.40	10	10	10	77.77	27.79	12.14
9	1	1	216.22	207.82	8.40	10	8	2	60.78	76.95	12.14	7	5	5	142.19	129.60	5.60						

K_2PtBr_6

H	K	L	FØBS	FCALC	SIGMA	H	K	L	FØBS	FCALC	SIGMA	H	K	L	FØBS	FCALC	SIGMA	H	K	L	FØBS	FCALC	SIGMA
2	0	0	383.20	404.41	22.14	10	4	2	88.78	91.97	8.47	0	6	6	79.76	101.12	18.13	1	7	9	209.44	206.10	8.36
4	0	0X	783.23	929.11	45.26	1	3	3	187.21	180.07	10.85	2	6	6	131.96	-117.88	9.11	1	7	9	141.41	136.93	9.22
6	0	0	243.64	248.92	14.11	3	3	3	116.88	129.31	20.73	4	6	6	56.51	106.43	10.20	3	7	9	122.42	122.46	8.47
8	0	0	482.18	505.00	27.89	5	3	3	197.84	197.15	11.39	6	6	6U	68.59	-52.29	31.47	5	7	9	127.52	127.36	8.03
10	0	0	124.59	132.54	13.24	7	3	3	79.33	84.07	9.52	8	6	6	100.93	107.51	11.07	1	9	9	156.06	150.49	11.28
6	2	0	124.15	118.83	5.96	9	3	3	170.16	174.45	10.85	10	6	6U	63.82	11.31	15.85	3	9	9	146.62	136.81	12.05
8	2	0	231.38	236.80	10.31	9	5	3	188.95	181.95	8.47	7	1	7	95.72	80.18	12.15	5	9	9	132.40	132.52	12.48
10	2	0	88.12	87.92	7.92	0	2	4	347.07	335.97	14.22	1	5	7	150.85	150.39	8.13	7	9	9	106.68	101.15	12.92
10	6	0	78.25	82.63	8.13	0	4	4	694.56	732.51	40.16	3	5	7	127.09	126.58	6.83	9	9	9	84.76	97.68	30.50
1	1	1	322.53	347.57	32.24	2	4	4	299.31	294.25	17.26	3	7	7	69.46	67.89	10.75	10	0	10	82.70	70.64	19.43
3	1	1	252.22	248.77	14.54	4	4	4X	537.10	600.18	53.72	5	7	7	95.50	93.79	10.64	0	4	10	125.56	125.52	7.38
5	1	1	312.77	307.96	18.13	6	4	4	200.44	206.07	11.62	7	7	7U	59.48	61.46	29.73	2	6	10U	49.16	-14.02	15.09
7	1	1	134.90	136.85	8.47	8	4	4	346.09	365.27	19.97	9	7	7	93.98	93.40	12.15	10	6	10U	63.27	33.66	38.75
9	1	1	226.17	231.68	13.02	10	4	4	115.15	118.46	10.85	0	4	8	413.70	427.30	16.93	0	8	10	106.68	105.25	9.11
7	3	1	107.66	107.61	6.73	10	6	4	81.83	84.03	8.90	0	6	8	171.03	173.52	8.13	2	8	10	95.61	91.81	9.44
9	3	1	201.75	200.70	9.00	1	5	5	263.07	246.24	10.75	2	6	8	120.47	126.68	7.92	4	8	10	93.00	98.71	10.20
0	2	2	164.22	158.49	9.77	1	5	5	280.22	278.52	16.17	4	6	8	156.39	158.31	7.38	6	8	10	84.00	81.13	9.00
2	2	2X	428.35	-473.62	16.17	3	5	5	230.83	233.20	13.35	6	8	8	269.58	273.68	13.45	2	10	10U	57.84	25.00	28.11
4	2	2	166.26	162.51	9.55	5	5	5	235.28	249.63	23.55	2	8	8	163.44	157.21	10.53	4	10	10	94.63	69.83	13.68
6	2	2	239.19	-231.46	13.79	7	5	5	153.67	150.75	9.66	4	8	8	240.71	238.52	13.89	8	10	10	77.49	64.05	14.54
8	2	2	146.29	156.27	9.44	9	5	5	168.11	182.16	11.18	6	8	8	132.73	122.26	11.39	10	10	10U	65.99	38.60	43.20
10	2	2L	73.69	-55.83	10.53	0	4	6	231.60	226.27	10.31	8	8	8	160.18	163.45	22.90						
8	4	2	210.87	212.76	9.44	2	4	6	126.32	124.83	5.96	10	8	8	94.20	81.49	12.81						

*Unobserved reflections are marked U and reflections suspected of suffering from extinction are marked X.

TABLE 3

Bond lengths and r.m.s. libration angles found in R_2MX_6 compounds at room temperature

Crystal	Metal–halogen bond (pm)		r.m.s. angle of libration (deg)	Radius ratio	Reference
	Uncorrected	Corrected			
$(NH_4)_2SiF_6$	168.8±0.3	169.6	3.9±0.2	1.53	4
Cs_2TeBr_6	269.5±0.4	270.7	3.4±0.3	1.04	2
K_2TeCl_6	235.0±1.0	236.1	3.9±0.3	0.96	5
K_2ReCl_6	235.3±0.4	236.8	4.5±0.2	0.96	*
$(NH_4)_2TeCl_6$	252.8±0.7	254.3	4.4±0.3	0.96	3
K_2PtBr_6	246.4±0.3	248.1	4.8±0.2	0.92	*
K_2ReBr_6	248.3±0.5	250.2	4.9±0.3	0.91	*
$(NH_4)_2TeBr_6$	268.1±0.2	270.1	5.0±0.1	0.90	2

*This work.

distorted structures are found. The distorted structure would then appear to be related to an instability in the librational modes of the cubic crystal.

Recent nuclear quadrupole resonance studies of K_2PtCl_6 (13) and K_2PdCl_6 (14), both of which have radius ratios close to unity, have revealed a low-frequency lattice vibration which has been identified with this librational mode. Taking the root-mean-square libration angle as equal to $(kT/I\omega^2)^{1/2}$ and substituting the values of the effective moment of inertia ($I = 2.1 \times 10^{-44}$ kg m^2) and frequency (ω = 33 and 42 cm^{-1}, respectively) measured by Armstrong and his co-workers (13, 14), it is found that $\theta_{r.m.s.}$ in these crystals at room temperature should be 4.0 and 3.2°, respectively, values which are in encouraging agreement with the values expected from Fig. 1.

We wish to thank the National Research Council of Canada for operating grants.

1. F. J. Ewing and L. Pauling. Z. Krist. **68**, 223 (1928).
2. A. K. Das and I. D. Brown. Can. J. Chem. **44**, 939 (1966).
3. A. C. Hazell. Acta Chem. Scand. **20**, 165 (1966).
4. E. O. Schlemper, W. C. Hamilton, and J. J. Rust. J. Chem. Phys. **44**, 2499 (1966).
5. M. Elder, J. E. Fergusson, G. J. Gainsford, J. H. Hickford, and B. R. Penfold. J. Chem. Soc. A, 1423 (1967).
6. B. Aminoff. Z. Krist. **94**, 246 (1936).
7. D. H. Templeton and C. H. Dauben. J. Amer. Chem. Soc. **73**, 4492 (1951).
8. H. Mueller. Z. Anorg. Allg. Chem. **321**, 124 (1963).
9. K. Schwochau. Z. Naturforsch. **19a**, 1237 (1964).
10. R. Ikeda, A. Sasane, D. Nakamura, and M. Kubo. J. Phys. Chem. **70**, 2926 (1966).
11. W. R. Busing and H. A. Levy. Acta Cryst. **17**, 142 (1964).
12. I. D. Brown. Can. J. Chem. **42**, 2758 (1964).
13. K. R. Jeffrey and R. L. Armstrong. Phys. Rev. **174**, 359 (1968).
14. R. L. Armstrong. Private communication.
15. H. E. Swanson, M. C. Morris, R. P. Stinchfield, and E. H. Evans. Natl. Bur. Stand. Monograph 25. Washington, D.C. 1963. Section 2, p. 28.
16. H. E. Swanson, N. T. Gilfrich, M. I. Cook, R. Stinchfield, and P. C. Parks. Natl. Bur. Stand. Circ. 539. Vol. 8. Washington, D.C. 1959. p. 40.

Can. J. Chem. Downloaded from www.nrcresearchpress.com by 210.87.254.40 on 09/05/12
For personal use only.

Can. J. Chem. Downloaded from www.nrcresearchpress.com by 210.87.254.5 on 09/05/12
For personal use only.

Studies of specifically fluorinated carbohydrates. Part VI.[1] Some pentofuranosyl fluorides

L. D. HALL AND P. R. STEINER[2]
Department of Chemistry, The University of British Columbia, Vancouver 8, B.C.

AND

C. PEDERSEN
Department of Chemistry, The Technical University of Denmark, Lyngby, Denmark

Received September 11, 1969

Detailed analyses of the ^1H and ^{19}F nuclear magnetic resonance spectra of seven pentofuranosyl fluoride derivatives are reported. With the help of ^1H-{^{19}F} heteronuclear decoupling experiments, some unexpectedly large ^4J couplings have been detected between F and H-4; when these substituents are *trans* the coupling is 5.5–7.9 Hz while the *cis* relationship gives couplings of 1.0–1.8 Hz. The ^4J couplings between F and H-3 are smaller when these groups are *trans* (< 0.7 Hz) than when they are *cis* oriented (1.7–2.4 Hz). These, and the other coupling constants are discussed in terms of the favored conformations of these derivatives. The ring conformations of the anomeric tri-*O*-benzoyl-D-ribofuranosyl fluorides differ from each other.

Canadian Journal of Chemistry, 48, 1155 (1970)

Introduction

It has become apparent that the determination of furanose conformations (and configurations) by nuclear magnetic resonance (n.m.r.) spectroscopy is often a difficult task. Yet, the important role of the ribofuranose system in many biochemical processes, provides a compelling reason to persevere with such conformational studies since n.m.r. spectroscopy still constitutes the only method generally applicable to the liquid phase. In the previous paper of this series (1) we described studies of some "model" fluorinated furanose systems, which had been chosen in anticipation that they might have a reasonable degree of conformational "rigidity" (meaning that they have a limited number of degrees of conformational freedom). We now describe attempts to use both ^1H and ^{19}F n.m.r. spectroscopy to study the conformations of furanosyl fluoride derivatives derived from D-ribose, D-arabinose, and D-xylose. The recent isolation (2) from natural sources of a nucleoside of 4-deoxy-4-fluoro-D-ribofuranose provided an additional impetus to our interest in fluorinated furanoses.

Before discussing the problem at hand we feel it necessary to point out some of the general limitations inherent in all conformational studies of furanose sugars and, indeed, of other 5-membered ring systems. Although these comments apply regardless of the absolute accuracy of the method being used, we shall center our discussion on the n.m.r. method.

It has been calculated (3, 4) that for cyclopentane, the barrier for conformational inversion is in the range 3–4 kcal/mole. *If it is valid to draw an analogy between the properties of a cyclopentane ring and those of a furanose ring*,[3] this low barrier implies that at any temperature experimentally available at this time, conformational inversion will be fast on the n.m.r. time scale. It follows that conformational studies of furanose derivatives by n.m.r. methods are automatically limited to the determination of conformations which are to a greater, or lesser, extent time-averaged.

It is convenient to confine discussion solely to those furanose conformations having a (nominal) symmetry relationship with the "C_s" and "C_2" conformations of cyclopentane (3), that is the "envelope" (V) and "twist" (T) conformations (5). These are related by the pseudorotational scheme[4] (hereafter, *Cyclops*) shown in Fig. 1. For

[1]For Part V see ref. 1.
[2]Recipient of an NRCC Scholarship, 1968–1969.

[3]It is clear that an analogous comparison between the 6-membered cyclohexane and pyranose rings is valid, since they both have approximately the same barrier for chair:chair interconversion. Interestingly the increased substitution on a pyranose ring does not appear to significantly increase the barrier.

[4]Strictly each of the symbols should include an indication of the absolute configuration of the sugar being described, e.g. $^2T_1$-(D). Since we are only concerned here with sugars in the D-series we shall consistently omit the D suffix.

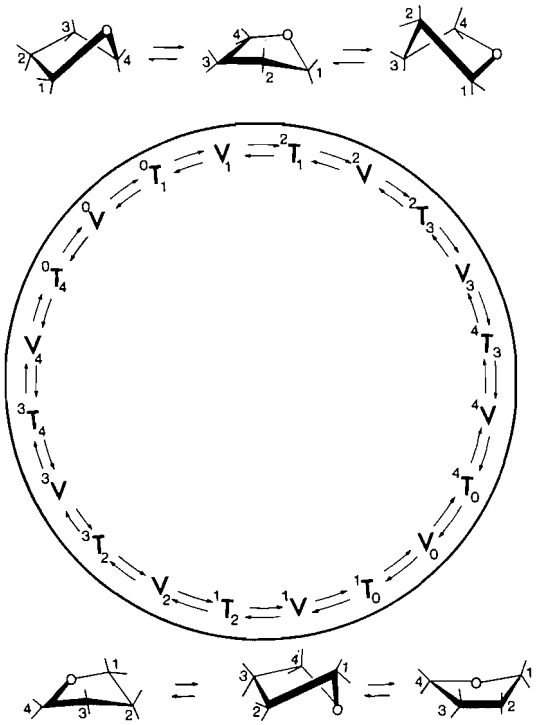

FIG. 1. CYCLe Of PSeudorotation (*Cyclops*) for furanose sugars. The symbols T and V designate the Twist and enVelope conformations respectively.

Numerical superscripts indicate the atom displaced above the reference plane defined by the remaining ring atoms while subscripts indicate an atom which is below the plane. Restricted sections of the overall cycle are represented at the top and bottom of the figure.

most substituted furanose sugars a combination of steric and dipolar interactions will significantly populate only a limited segment of *Cyclops* and the various conformations within that segment will freely interconvert. In this situation it is questionable whether it is possible to interpret any n.m.r. parameters in terms of a unique conformation; this would only be appropriate if one particular conformation were to be *exclusively* populated, as is likely for certain fused-ring systems. Instead, discussions should generally be limited to a definition of which particular section of *Cyclops* is populated.

The only situation not covered by the above treatment occurs, for example, when steric considerations populate one particular segment of *Cyclops* while dipolar (or other) considerations significantly populate some remote segment. Clearly in this situation the time-averaged conformation determined by n.m.r. spectroscopy will bear no direct relation with those conformations which are actually populated. It is quite unlikely that this circumstance will arise for any fully esterified furanose system; however, it is likely to be important when hydrogen bonding and similar interactions can operate, as in nucleoside systems.

We shall also be concerned in this study with developing a more rigorous formalism for evaluating furanose conformations on the basis of the somewhat uncertain accuracy of dihedral angles derived from *vicinal* couplings. It is necessary to make the following basic assumptions:

(*i*) All the ring carbons have precise "tetrahedral" symmetry, meaning that all 4 angles at every carbon are equal to 109°28′. Clearly, any deviations from this idealized state will mean that dihedral angles between *vicinal* C—H bonds will no longer equal those between the corresponding C—C bonds which actually define the ring geometry. Hendrickson's calculations (4) on the cyclopentane system indicate that the internal ring angle lies in the range 100–106°.

(*ii*) As in the development of *Cyclops*, only envelope and twist conformations are considered; in other words, our conformational evaluation is concerned with determining which of 20 possible conformers are favored. In view of the limited accuracy of the n.m.r. method (vide infra) it does not seem sensible to consider any of the conformations between the envelope and twist forms. Thus, this assumption does not seriously prejudice or limit any discussions.

(*iii*) "Maximal" puckering of the ring always occurs. This implies that an envelope conformation will resemble one end of a cyclohexane, chair conformation. Having based a conformational assignment on this "maximal" basis it is a simple matter to consider the effect of a decrease in the extent of puckering.

(*iv*) Coupling constants associated with C-1, C-2 will be somewhat smaller than those associated with other pairs of *vicinal* carbons. No numerical allowance will be made for this effect, rather a general tolerance will be applied (vide infra).

Discussion

The syntheses of the derivatives used in this study followed conventional procedures, and have been described previously (6). The n.m.r. spectra provided further proof of the structures.

Can. J. Chem. Downloaded from www.nrcresearchpress.com by 210.87.254.5 on 09/05/12
For personal use only.

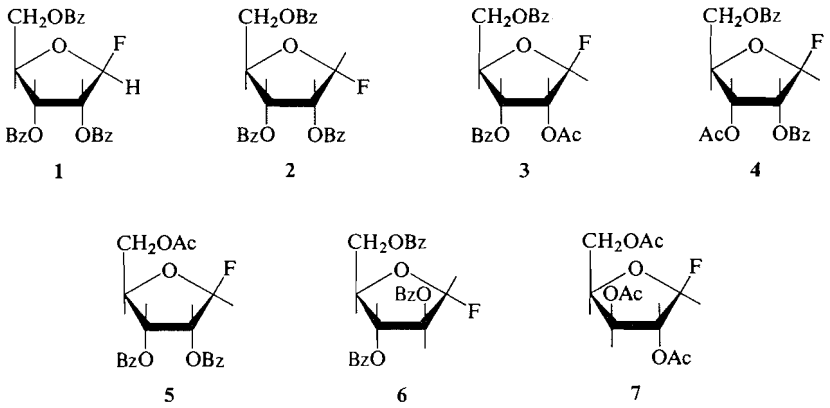

Much of the pertinent information in the series of compounds (**1**–**7**) studied comes from the anomeric pair of tri-*O*-benzoyl-D-ribofuranosyl fluorides **1** and **2**. Hence we shall discuss their n.m.r. spectra and conformations in some detail.

The normal ^{1}H n.m.r. spectrum of the β-anomer (**1**) is shown in Fig. 2*A*, together with the "fluorine-decoupled" spectrum (Fig. 2*B*). The general assignment of the H-1, H-4, and H-5 resonances was initially straightforward. The observation that $J_{1,2} < 0.5$ Hz immediately confirmed the β-configuration. The H-2 and H-3 resonances are closely coupled, with shifts at τ 4.04 and 3.98 respectively. The identity of the H-3 resonance was secured by observing the complex region centered about τ 4.1 while simultaneously irradiating both the ^{19}F and H-4 resonances (7); the H-3 resonance collapsed to the anticipated doublet. The appearance of the H-2, H-3 resonances in the ^{19}F decoupled spectrum (Fig. 2*B*)

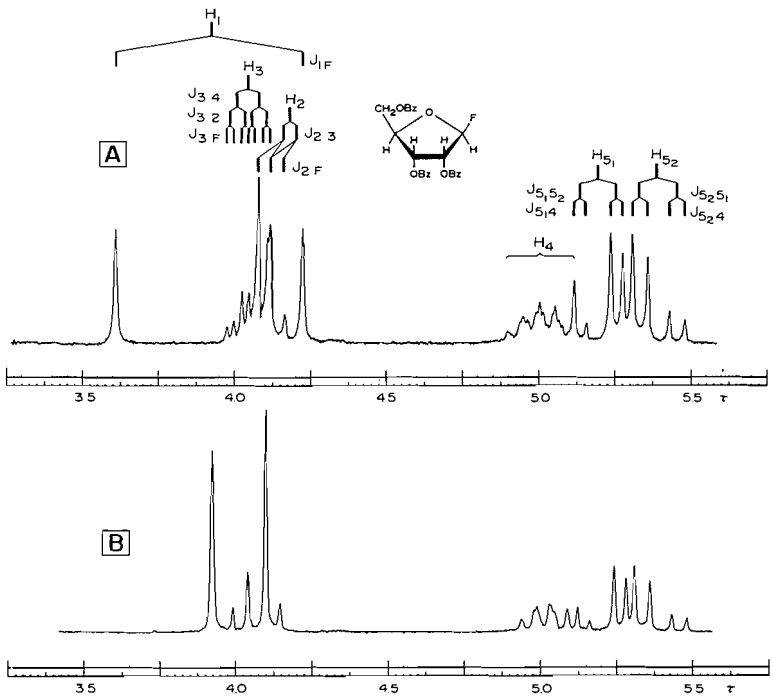

FIG. 2. Partial ^{1}H n.m.r. spectra (100 MHz) of 2,3,5-tri-*O*-benzoyl-β-D-ribofuranosyl fluoride (**1**) in acetone-d_6 solution. (*A*), normal spectrum. (*B*), spectrum obtained with simultaneous irradiation at the ^{19}F frequency (94.083, 045 MHz).

Can. J. Chem. Downloaded from www.nrcresearchpress.com by 210.87.254.5 on 09/05/12
For personal use only.

Can. J. Chem. Downloaded from www.nrcresearchpress.com by 210.87.254.5 on 09/05/12
For personal use only.

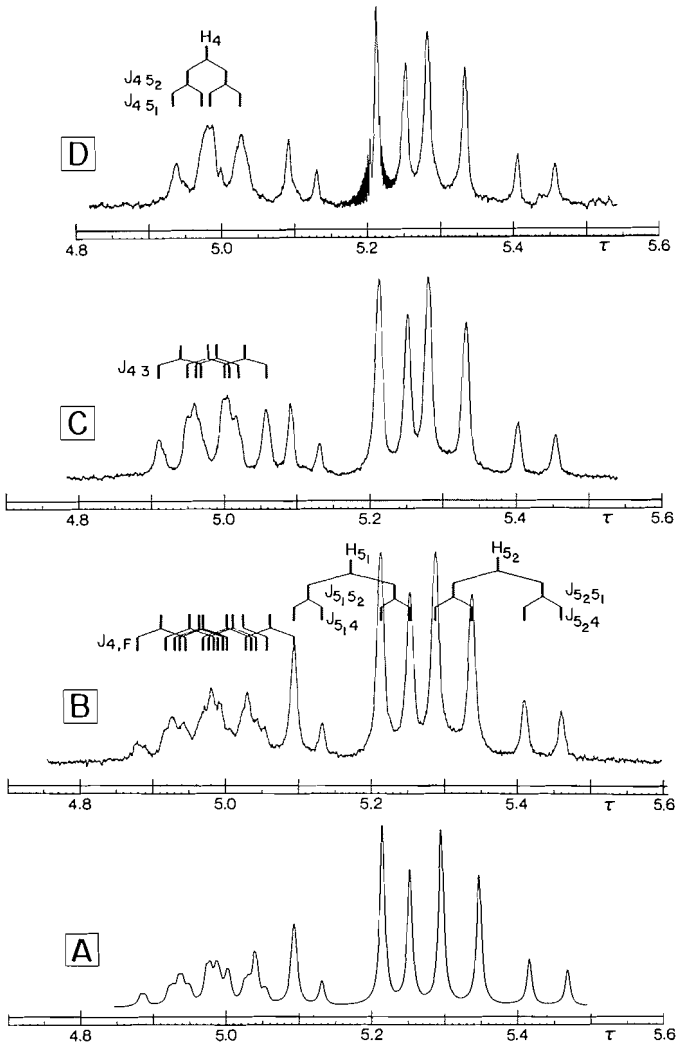

FIG. 3. ^{1}H n.m.r. spectra (100 MHz) of the H-4 and H-5 resonances of **1** in acetone-d_6 solution. (*A*), Computer simulated spectrum using LAØCØØN III with the SMASH plot-routine. (*B*), Normal spectrum. (*C*), ^{19}F decoupled spectrum. (*D*), As for (*C*) but with irradiation of the H-3 resonance. The transition at τ 5.2 is partially obscured by an audio-beat-signal. The first-order assignments are based on the coupling constants in Table 1.

deserves comment at this time, since the multiplet located about τ 4.2 does not accord with expectations based on the first-order assignment given above Fig. 2*A*; indeed this multiplet cannot now be assigned on a first-order basis. We attribute this behavior to a decrease in the relative chemical shift separation between the H-2 and H-3 resonances: this decrease in shift is induced by the temperature increase which attends the application of the high power-output (5 W) of the heteronuclear decoupler. These small, temperature-induced shifts are a common occurrence but are only a hazard when strongly coupled systems are being studied.[5] The complications in the present case could be precisely simulated with a computer. Further support for the original assignment follows analysis of the spectrum of the configurationally identical compound **3**. In this case the H-2 and H-3 resonances are separated by ca. 20

[5]Subsequent to this assignment, Mr. Robert Malcolm of this laboratory suggested that the H-2, H-3 resonances of compound **1** should be regarded as a special case (8) of a "deceptively-simple" (9) ABX-system. This attractive alternative does not, however, have to be invoked.

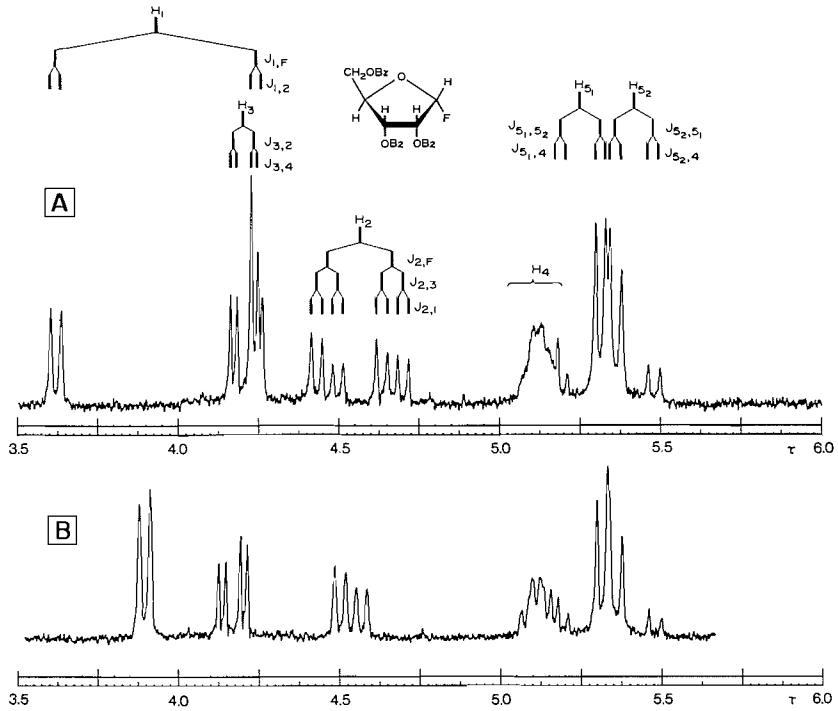

FIG. 4. Partial ^{1}H n.m.r. spectra (100 MHz) of 2,3,5-tri-*O*-benzoyl-α-D-ribofuranosyl fluoride (**2**) in chloroform-*d* solution. (*A*), Normal spectrum. (*B*), Spectrum with irradiation of the fluorine (94.099, 115 MHz). The first-order assignment is indicated. Note the temperature induced changes in chemical shifts which accompany spin-decoupling.

Hz and hence not subject to any ambiguity; straightforward analysis gives the same coupling constants (see Table 1) as previously obtained for **1**.

Aside from the complications associated with the H-2, H-3 resonances of **1**, the most interesting resonance of this spectrum is that of H-4; this is shown in greater detail in Fig. 3. The H-5 resonances also shown, constitute the AB-part of an ABM-system and require no further comment. The H-4 resonance is clearly coupled to a number of other nuclei, which accounts for its "poor resolution" (Fig. 3*B*). Application of a powerful radiofrequency field to the ^{19}F resonance caused the band-width at half-height of the H-4 resonance to decrease by 6.6 Hz (Fig. 3*C*). Further simplification of this resonance occurs when the H-3 resonance is also strongly irradiated (Fig. 3*D*). Now the H-4 resonance clearly has the form anticipated for the M-part of an ABM-system.[6]

[6]The additional broadening of the H-4 transitions is likely due to the presence of unresolved long-range couplings from H-1 and H-2, together with the effects of incomplete ^{1}H–^{1}H decoupling.

The observation of this large long-range coupling between F-1 and H-4 was a surprise to us, even though the ^{19}F spectrum itself has indicated that one proton or other had a coupling of this magnitude. Nevertheless, its detection enabled us to complete successfully a computer-based simulation of the "normal" proton magnetic resonance (p.m.r.) spectrum of **1**; part of the simulated spectrum is shown in Fig. 3*A*.

The general assignment of the p.m.r. spectrum of tri-*O*-benzoyl-α-D-ribofuranosyl fluoride (**2**), shown in Fig. 4, was very straightforward and does not require special comment. The temperature induced changes in chemical shifts attending the use of the strong ^{19}F decoupling field are obvious. The value of $J_{1,2}$ (3.2 Hz) indicated this to be the α-anomer.

In view of the large ^4J, F-1 to H-4 coupling observed previously for **1**, the H-4 resonance of this spectrum was examined carefully; this is illustrated in Fig. 5. It was soon apparent that in this instance $J_{F,4}$ was much smaller (1.0 Hz) than before. The computer simulation (LAΦCΦΦN III with SMASH plot routine) of the spectrum

Can. J. Chem. Downloaded from www.nrcresearchpress.com by 210.87.254.5 on 09/05/12
For personal use only.

TABLE 1

First-order coupling constants for furanosyl fluorides (Hz)

Compound*		H_1F	H_1H_2	H_2F	H_2H_3	H_3F	H_3H_4	H_4F	$H_4H_{5_1}$	$H_4H_{5_2}$	$H_{5_1}H_{5_2}$
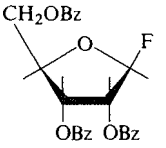 1	(*a*)	61.5	< 0.5	4.8	4.8	2.2	5.8	6.6	3.9	5.2	−12.2
	(*c*)	61.2	< 0.5	4.9	4.9	2.2	6.2	7.3	3.9	5.2	−11.9
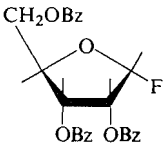 2	(*a*)	64.4	3.2	20.6	6.9	≃ 0	2.3	1.0	3.1	3.5	−12.1
	(*c*)	63.6	3.5	20.6	6.9	≃ 0	2.5	1.8	3.2	3.8	−12.3
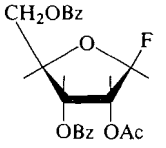 3	(*a*)	60.9	< 0.5	4.7	4.7	2.4	6.9	6.7	3.5	4.6	−11.9
	(*c*)	61.4	< 0.5	4.8	4.7	1.9	6.7	6.8	3.8	5.6	−12.5
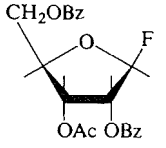 4	(*a*)	61.6	< 0.5	4.5	5.0	1.7	5.0	7.9	4.5	5.4	−12.4
	(*c*)	61.1	—	—	—	—	—	—	—	—	—
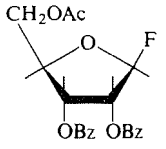 5	(*a*)	61.3	< 0.5	4.9	4.9	2.1	4.9	7.2	3.6	5.3	−12.1
	(*c*)	61.4	< 0.5	—	—	—	—	—	3.8	5.3	−12.2
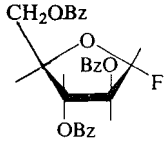 6	(*a*)	58.4	0.9	6.4	< 0.5	< 0.7	4.4	1.5	3.3	5.8	−12.1
	(*c*)	58.1	< 0.5	6.1	1.0	0.5	3.5	1.0	3.0	6.5	−12.1
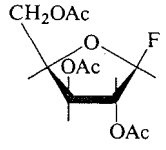 7	(*a*)	—	—	—	—	—	—	—	—	—	—
	(*c*)	60.5	1.0	5.2	< 0.5	< 0.5	5.5	5.2	5.3	7.1	−11.4

*The compounds above are measured in (*a*) acetone-d_6 and (*c*) chloroform-*d* solutions.

Can. J. Chem. Downloaded from www.nrcresearchpress.com by 210.87.254.5 on 09/05/12
For personal use only.

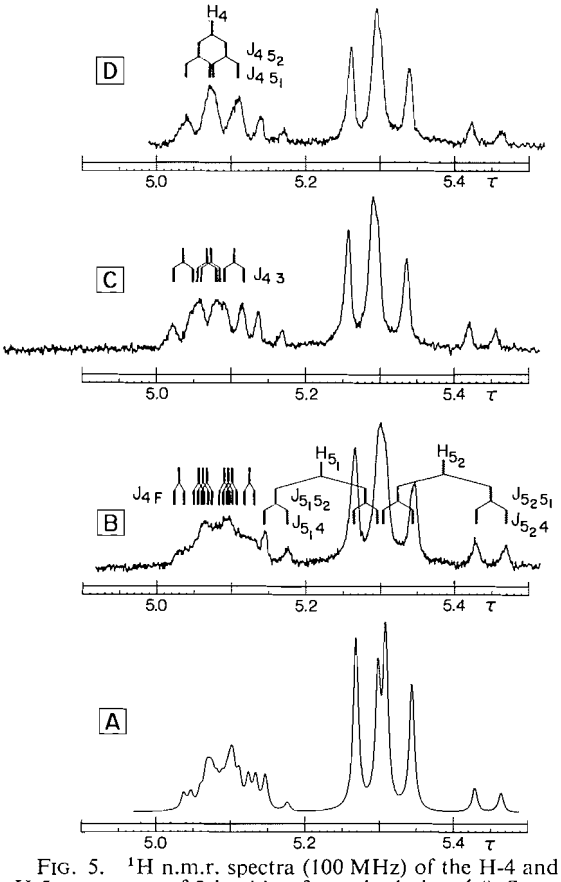

FIG. 5. ^{1}H n.m.r. spectra (100 MHz) of the H-4 and H-5 resonances of **2** in chloroform-*d* solution. (*A*), Spectrum simulated by computer (see text). (*B*), Normal spectrum. (*C*), Fluorine-decoupled spectrum. (*D*), As for (*C*), but with simultaneous irradiation of H-3. The first-order assignments are based on the couplings listed in Table 1, and the room-temperature chemical shifts.

was based on the ambient temperature chemical shifts listed in Table 2, whereas the "normal" spectrum in Fig. 5*B* was of a sample which had previously been subjected to a period of ^{19}F decoupling.

It was indeed fortunate that of the two anomers, **1** and **2**, the one giving the most complex ^{1}H n.m.r. spectrum was also the one where configurationally related compounds were available for comparison purposes. Analyses of the spectra of these derivatives (**3**, **4**, and **5**) confirmed the validity of parameters derived for **1** and, in particular, the magnitude of the ^4J, F-1 to H-4 coupling (vide infra).

It is convenient at this juncture to complete a comparison of derivatives **1** and **2**. The anomeric configuration of these derivatives was assigned originally on the basis of the values of $J_{1,2}$; the near 90° dihedral angle required to give a near zero value for $J_{1,2}$ can only be obtained when H-1 and H-2 are *trans*. Apparently the magnitudes of $J_{F,2}$ and of $J_{F,4}$ provide an equally unambiguous distinction for these anomers. Although there is only a small shift separation between the H-1 resonances of **1** and **2**, the ^{19}F shift difference is 17 p.p.m., with that of the α-anomer being to higher field.

Inspection of the *vicinal* ^{1}H–^{1}H couplings of these two derivatives indicates quite clearly that they have different ring conformations. The values of $J_{2,3}$ differ by ca. 30% while those of $J_{3,4}$ differ by 60%; the latter difference is particularly significant. We shall derive first the conformation(s) favored by **1**, using the limiting formalism outlined earlier. Table 3 shows the estimated dihedral angles (Dreiding models) possible for all 20 of the possible "symmetric" conformations of the furanose ring. Included also are the *vicinal* coupling constants together with a very conservative estimate of the corresponding dihedral angles. Because it is so difficult to choose which conformation is in fact favored, we start by discounting those conformations obviously at variance with one or more of the experimentally determined dihedral angles.

Consider first the small value of $J_{1,2}$, which corresponds to a dihedral separation of 80–100°; all of those conformations requiring a dihedral angle ($\phi_{1,2}$) beyond this range are discounted. This immediately limits the allowed conformations to the sector of the *Cyclops* between $^4T_0$ and $^3T_4$, inclusive; if $J_{1,2}$ were precisely zero the V_0 or ^3V conformations would be indicated. If the value of $J_{3,4}$ is considered, only those conformations between the $^1T_2$ and $^0T_1$ symmetries are relevant. It is encouraging to observe that these two evaluations of "acceptable" segments of *Cyclops* have a single overlap, located in the region ^1V, $^1T_2$, V_2. The overlap is not perfect, since the "best" fit for $J_{2,3}$ does not coincide with that for $J_{1,2}$; however, the effect of the second oxygen substituent attached to C-1 should increase the value of $\phi_{1,2}$ corresponding to a value of $J_{1,2}$ ca. 0.5 Hz.

A similar process of conformational assignment can be applied to the α-anomer (**2**) which leads to the conclusion that either of two segments of *Cyclops* are populated, namely V_3, $^4T_3$ or ^1V, $^1T_2$. We reject the latter assignment on symmetry

Can. J. Chem. Downloaded from www.nrcresearchpress.com by 210.87.254.5 on 09/05/12
For personal use only.

TABLE 2

First-order chemical shifts (τ and ϕ values) for furanosyl fluorides

Compound*		F	H_1	H_2	H_3	H_4	H_{5_1}	H_{5_2}	OBz	OAc
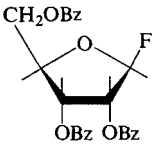 1	(*a*)	115.9	3.82	4.04	3.98	4.89	5.11	5.31	1.9–2.8	—
	(*c*)	116.1	4.04	4.54	4.43	5.10	5.26	5.43	1.9–2.8	—
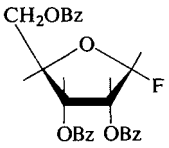 2	(*a*)	133.3	3.70	4.49	4.14	5.07	5.24	5.39	1.9–2.8	—
	(*c*)	133.6	3.86	4.53	4.16	5.10	5.23	5.41	1.9–2.8	—
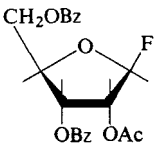 3	(*a*)	115.8	4.20	4.45	4.26	5.21	5.32	5.49	1.9–2.7	7.85
	(*c*)	116.0	4.21	4.24	4.38	5.23	5.29	5.48	1.9–2.7	7.95
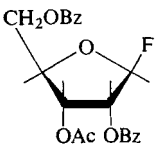 4	(*a*)	115.5	4.05	4.30	4.38	5.26	5.32	5.58	1.9–2.7	6.98
	(*c*)	115.7	—	—	—	—	—	—	—	—
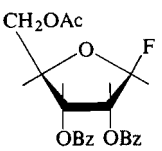 5	(*a*)	115.7	3.96	4.19	4.25	5.18	5.39	5.75	2.0–2.8	7.95
	(*c*)	—	4.09	—	—	5.32	5.38	5.75	2.0–2.8	7.90
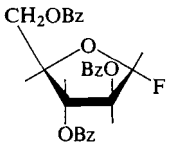 6	(*a*)	123.8	3.83	4.26	4.25	5.05	5.12	5.27	1.9–2.8	—
	(*c*)	124.7	4.01	4.35	4.43	5.15	5.20	5.31	1.8–2.8	—
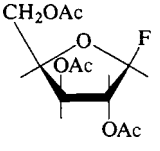 7	(*a*)	—	—	—	—	—	—	—	—	—
	(*c*)	113.2	4.37	4.82	4.66	5.30	5.71	5.80	—	7.95 7.98

*The compounds above are measured in (*a*) acetone-d_6 and (*c*) chloroform-*d* solutions.

Can. J. Chem. Downloaded from www.nrcresearchpress.com by 210.87.254.5 on 09/05/12
For personal use only.

Can. J. Chem. Downloaded from www.nrcresearchpress.com by 210.87.254.5 on 09/05/12
For personal use only.

TABLE 3

Data for the evaluation of the favored conformations[a] of compound **1**

Table 3*a*

J	Observed couplings (Hz)	Dihedral angle ranges°
H_1H_2	<0.5	80–100
H_2F	4.8	30–50; 140–150
H_2H_3	4.8	30–50; 130–150
H_3H_4	6.0	20–40; 140–160

Table 3*b*

Conformation	Dihedral angle (degrees) H_1H_2	H_2F	H_2H_3	H_3H_4	Evaluation
V_1	170*	50	30	120	X
$^2T_1$	180*	60	50	100	X
^2V	170*	50	50	90*	X
$^2T_3$	170*	50	60	90*	X
V_3	150*	30	50	70	X
$^4T_3$	140*	20	50	60	X
^4V	120	0*	30	70	X
$^4T_0$	100	20	20	50	X
V_0	90	30	0*	90*	X
$^1T_0$	70	50	20	100*	X
^1V	70	50	30	120	
$^1T_2$	60	60	50	140	
V_2	70	50	50	150	
$^3T_2$	70	50	60	170*	X
^3V	90	30	50	170*	X
$^3T_4$	100	20	50	180*	X
V_4	120	0*	30	170*	X
$^0T_4$	140*	20	20	170*	X
^0V	150*	30	0	150	X
$^0T_1$	170*	50	30	150	X

[a]A cross (X) in the "evaluation" column indicates that this conformer has been eliminated. An asterisk indicates the parameters having the maximum deviation for that particular conformation.

grounds since it seems highly improbable that **1** and **2** could have identical conformations and yet have different values of $J_{3,4}$ (5.8 and 2.3 Hz respectively). Nevertheless the "$\cos^2 \phi$" function in the Karplus relationship does make this possible in principle.

If these deductions are correct, then **1** and **2** have ring conformations approximating to those depicted in **A** and **B**. Although it is not easy to define which positions have "axial" and which have "equatorial" character, it does seem that in both **A** and **B** the fluorine substituent occupies a "pseudo-axial" orientation.

Application of a similar set of evaluations to the D-*arabino* and D-*xylo* derivatives **6** and **7**, respectively, leads to the conformational assignments listed in Table 4. Direct application of the formalism outlined earlier led to an ambiguous assignment for **6**; the former may be the correct assignment because it brings the $J_{F,2}$ value into line with those found for derivatives **1**, **7**, which also have a *cis* relationship between F-1 and H-2.

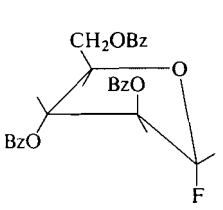

C

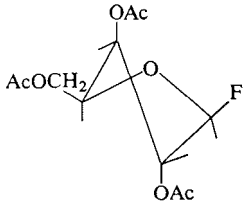

D

TABLE 4

The favored conformations of pentofuranosyl fluoride derivatives, based on considerations of their *vicinal* ^1H–^1H and ^{19}F–^1H coupling constants

Derivative	Favored conformers
1, 3, 4	^1V, $^1T_2$, V_2
2	V_3, $^4T_3$
5	$^1T_2$, V_2, $^3T_2$
6	V_1, V_3, $^4T_3$
7	V_2, $^3T_2$, ^3V

Inspection of the conformation of **6** and **7**, depicted in **C** and **D**, shows again an apparent preference of the fluorine substituent for a "pseudo-axial" disposition. In view of the uncertainty of the methods used for evaluating these conformations, it would be most unwise to attempt to make a dogmatic statement on this point. However, such a preference already has a well documented precedent (10) in the pentopyranose system, where even the tri-*O*-acetyl-β-D-xylopyranosyl fluoride (**E**) favors the $^1C_4$ conformation.

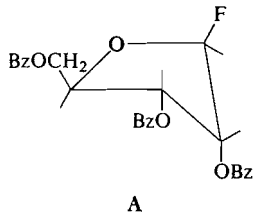

A

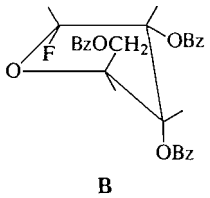

B

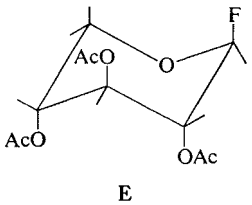

E

TABLE 5

Conformations of pentofuranose per-esters based on the *vicinal* ^1H–^1H couplings of Stevens and Fletcher (11)

Compound tetraester	Conformation		
	Stevens and Fletcher (11)	This study	Bishop and Cooper (12)
β-D-Ribofuranose	$^3T_2$	V_2, $^3T_2$, ^3V	^3V
α-D-Ribofuranose	$^2T_1$, ^2V	^2V, $^2T_3$, V_3	^2V
α-D-Arabinofuranose	$^0T_1$	$^2T_3$, V_3, $^4T_3$	$^2T_3$, $^3T_2$
β-D-Xylofuranose	$^3T_2$, ^3V	V_2, $^3T_2$, ^3V	$^2T_3$, V_3

During the course of this work, Stevens and Fletcher (11) reported a study of a series of pentofuranose derivatives, and made the conformational assignments listed in Table 5. It was of interest for us to re-evaluate their parameters using our formalism and this led us to the assignments also listed in Table 5. There is a satisfactory agreement between these two sets of evaluations except for the α-D-arabinofuranose system. We have also included in Table 5 the conformational assignments of Bishop and Cooper (12); there is a major disagreement in the assignment for the β-D-xylofuranose system.

The conformations deduced by us for each pentofuranosyl peracetate and the corresponding pentofuranosyl fluoride, appear to be the same or nearly so. This is an interesting result, since even if our formalism for evaluating furanose conformations is incorrect, the identity of the two sets of conformations will remain. It is appropriate to note at this juncture that the consensus of all n.m.r. and X-ray (13, 14) studies of furanose conformations to date is that either C-2 or C-3 (or both) are the out-of-plane atoms. This implies that the oxygen substituent contributes a lower interaction energy than a carbon atom, when it is required to be an in-plane atom.

We shall now discuss the long-range (^4J) ^{19}F–^1H couplings detected for these furanosyl fluoride derivatives. The configurational significance of these couplings is immediately obvious. When the F-1 and H-4 substituents have a *trans* relationship, as in the β-*ribo* and β-*xylo* derivatives **1**, **3**, **4**, **5**, and **7**, the ^4J coupling is large (5.5–7.9 Hz); a *cis* relationship, as in the α-*ribo* and α-*arabino* system, **2** and **6**, gives a much smaller coupling (1.0–1.8 Hz). For the F-1, H-3 couplings the reverse situation pertains since the *cis* relationship (as in **1**) gives a larger coupling (1.7–2.4 Hz) than does the *trans* relationship (**2**, **6**, **7**) where the coupling is 0.7 Hz. It is questionable whether it is worthwhile discussing these couplings further until the signs of these couplings are known, which requires specifically deuterated derivatives not available at this time. It is interesting to note however, that the apparent specificity of the $^4J_{F,3}$ couplings parallels that already established for pyranose derivatives (15).

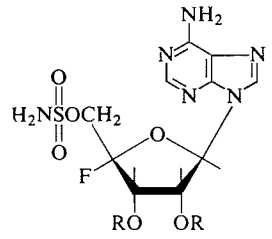

8

After we had completed this work, Webb informed us (2) of his group's investigation of nucleodin **8** which is the first example of a naturally occurring nucleoside containing fluorine.

The relevant coupling constants published for this derivative are listed in Table 6, together with those of derivative **2**, which is configurationally related. The close agreement between the appropriate pairs of couplings $J_{1,2}$, $J_{3,4}$; $J_{2,3}$, $J_{2,3}$;

TABLE 6

Coupling constants (Hz) for nucleodin (**8**)* and **2**

Nucleodin†	**2**‡
$J_{1,2}$ = 2.2	$J_{3,4}$ = 2.3
$J_{2,3}$ = 6.5	$J_{2,3}$ = 6.9
$J_{F,3}$ = 18.0	$J_{F,2}$ = 20.6

*Data from ref. 2.
†In pyridine-d_5 solution.
‡In chloroform-*d* solution.

Can. J. Chem. Downloaded from www.nrcresearchpress.com by 210.87.254.5 on 09/05/12
For personal use only.

$J_{F,3}$, $J_{F,2}$, and the absence of detectable splittings between F-4, H-1 and between F-4, H-2, provides additional support for the claimed structure and further suggests that the furanose ring of **8** favors conformers in the vicinity of the ^3V conformation.

The observation that for **8** the two 5′,F coupling constants are approximately equal, and relatively small (9.6 and 12.6 Hz), indicated that the *favored* rotamer about the C_4', C_5' bond is that shown in **F**. Interestingly, this positions the sulphonamide group over the furanose ring.

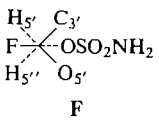

F

While the formalism for evaluating furanose conformations, which is described in this paper has the advantage of enabling *vicinal* coupling constants to be used in a very conservative fashion, it is not without some disadvantages of its own. Most notable of these is the presupposition of a maximal-puckering model for the furanose ring. In practice the furanose ring will be less puckered than the maximal model would imply. It is simple to allow for this effect. All *cis* couplings increase as the furanose ring becomes less puckered. The situation for *trans* couplings is more complex. For protons which are *trans* and "equatorial", the coupling constants increase as the ring becomes less puckered while coupling constants which are related to *trans* "diaxial" protons will decrease as the ring flattens.

It is interesting to note that generally, this formalism indicates that only one segment of the pseudorotational cycle is significantly populated, which seems a sensible conclusion. That we have evaluated other workers' *vicinal* ^1H–^1H couplings in terms of conformers somewhat different from those previously postulated (11) indicates that our current appreciation of the problems associated with furanose conformations is still not final. We plan to invoke computer techniques in an attempt to improve the unsatisfactory situation which now pertains to the n.m.r. approach.

It is obvious that some further experiments should be performed in order to determine the significance of the dipolar interactions associated with the anomeric center of furanose derivatives.

Experimental

The general methods used, followed those of earlier studies (1). Most of the furanosyl fluoride derivatives were available from other studies (6).

2,3,5-Tri-O-acetyl-β-D-xylofuranosyl Fluoride (7)

A sample of **7** was prepared by the reaction of D-xylofuranose tetraacetate (500 mg) with anhydrous HF (1 ml) and diethyl ether (100 ml) in a polyethylene flask surrounded by an acetone – Dry Ice bath. The reaction mixture was swirled several times and then allowed to warm to room temperature (20 min). The mixture was poured into a beaker containing a saturated sodium hydrogen carbonate solution (100 ml) and diethyl ether (100 ml). Upon neutralization of excess hydrogen fluoride, the ether layer was separated, dried over Na_2SO_4, and evaporated at reduced pressure to give a crude syrup **7**. Most impurities were removed by column chromatography (Silicar CC7) using 25% ethyl acetate/75% petroleum ether. The final product was an almost colorless syrup which ran as a single spot on thin-layer chromatography plates. The p.m.r. spectrum showed that while the product was substantially pure some minor impurities were present which gave resonance at ca. τ 8. Since these did not interfere with the n.m.r. analysis, no attempts were made to further purify this product.

It is a pleasure for L. D. H. to thank the National Research Council of Canada for their generous financial support of this work, especially for an Equipment Grant (E 1338) which made available the heteronuclear decoupler.

1. L. D. HALL and P. R. STEINER. Can. J. Chem. **48**, 451 (1970).
2. J. S. WEBB. Private Communication, January 6, 1969; G. O. MORTON, J. E. LANCHASTER, G. E. VAN LEAR, W. FULMOR, and W. E. MEYER. J. Amer. Chem. Soc. **91**, 1535 (1969).
3. J. E. KILPATRICK, K. S. PITZER, and R. S. SPITZER. J. Amer. Chem. Soc. **69**, 2483 (1947); K. S. PITZER and W. E. DONATH. J. Amer. Chem. Soc. **81**, 3213 (1959).
4. J. D. HENDRICKSON. J. Amer. Chem. Soc. **83**, 4537 (1961).
5. L. D. HALL. Chem. Ind. (London), 950 (1963).
6. N. GREGERSEN and C. PEDERSEN. Acta Chem. Scand. **22**, 1307 (1968).
7. R. BURTON and L. D. HALL. Can. J. Chem. **48**, 59 (1970).
8. R. B. MALCOLM. M.Sc. Thesis, University of British Columbia, Vancouver, B.C., 1969.
9. R. J. ABRAHAM and H. J. BERNSTEIN. Can. J. Chem. **39**, 216 (1961).
10. L. D. HALL and J. F. MANVILLE. Can. J. Chem. **47**, 20 (1969).
11. J. D. STEVENS and H. G. FLETCHER. J. Org. Chem. **33**, 1799 (1968).
12. C. T. BISHOP and F. D. COOPER. Can. J. Chem. **41**, 2743 (1963).
13. G. A. JEFFREY and R. D. ROSENSTEIN. Advan. Carbohyd. Chem. **19**, 7 (1964).
14. M. SUNDARALINGAM. J. Amer. Chem. Soc. **87**, 599 (1965).
15. A. B. FOSTER, R. HEMS, L. D. HALL, and J. F. MANVILLE. Chem. Commun. 158 (1968).

Can. J. Chem. Downloaded from www.nrcresearchpress.com by 210.87.254.5 on 09/05/12
For personal use only.

Can. J. Chem. Downloaded from www.nrcresearchpress.com by 210.87.254.5 on 09/05/12
For personal use only.

Circular dichroism of some copper(II) diamide complexes

M. PARRIS AND A. E. HODGES
Chemistry Department, Carleton University, Ottawa, Canada

Received October 27, 1969

The absorption spectra and circular dichroism spectra of some Cu(II) N,N′-diglycylethylenediamine analogues are interpreted in terms of a square-planar structure of the biuret type.

Canadian Journal of Chemistry, **48**, 1166 (1970)

We wish to report the preparation of some dissymmetric diamides of formula $H_2N{\cdot}CHR{\cdot}CO{\cdot}NH{\cdot}CHR'{\cdot}CHR''{\cdot}NH{\cdot}CO{\cdot}CHR{\cdot}NH_2$, together with the circular dichroism of their Cu(II) complexes. These ligands are bis(glycyl)- or -(alanyl) amides of ethylenediamine (en), 1,2-propanadiamine (pn), 2,3-butanediamine (bn), or 1,2-cyclohexanediamine (chxn): **1**, gly_2(*R*)pn; **2**, gly_2(*SS*)bn; **3**, gly_2(*SS*)chxn; **4**, (*S*)ala_2en; **5**, (*S*)ala_2(*SS*)chxn; **6**, (*S*)ala_2(*RR*)-chxn; **7**, (*S*)ala_2(*RS*)chxn; **8**, (*S*)ala_2(*RS*)bn. Our interest in these is concerned with their complete reduction to the corresponding 1,4,7,10-tetra-azadecanes, that is, to substituted triethylene-tetramines which are stereospecific tetradentate ligands, as has already been shown for **1**–**4** (1, 2). Such ligands are potentially useful in the study of stereoselectivity in certain metal-catalyzed reactions (3 and references therein). The circular dichroism (c.d.) spectra of the 1:1 amide–Cu(II) complexes (of the biuret type) are in themselves of interest in connection with octant or double-octant rules (4), however.

These 1:1 amide–Cu(II) complexes belong strictly to the point groups C_1 (**1**, **7**, **8**) and C_2(**2**–**6**). However, so far as the donor-atoms' symmetry is concerned, they may all be considered as approximating to the group D_{4h}, for the tetragonal distortion usual for a Cu(II) complex will be heightened by the ligand geometry. Taking the *z* axis as the out-of-plane direction, we expect three transitions: $^2B_{1g} \leftarrow {}^2A_{1g}$ (or $d_{x^2-y^2} \leftarrow d_{z^2}$), low in energy; $^2B_{1g} \leftarrow {}^2B_{2g}$ (or $d_{x^2-y^2} \leftarrow d_{xy}$), and $^2B_{1g} \leftarrow {}^2E_g$ (or $d_{x^2-y^2} \leftarrow d_{yz}, d_{xz}$), both higher in energy.

Each transition is electric-dipole forbidden and only the two high-energy transitions are magnetic-dipole allowed. Coupling with the three u normal vibrations in D_{4h}(a_{2u}, b_{2u}, and e_u) gives rise to only two transitions which can be simultaneously and collinearly electric- and magnetic-dipole-allowed: the degenerate $d_{x2-y2} \leftarrow d_{xz}, d_{yz}$ transitions. The species arising from vibronic coupling are indicated in Table 1. E_g and E_u (D_{4h}) correlate with $B(C_2)$, and so for these two transitions only will the rotational strength be non-zero. Only the $d_{x2-y2} \leftarrow d_{xz}, d_{yz}$ absorption is expected to show strong optical activity. On the other hand, all transition moments are strictly electric- and magnetic-dipole-allowed in the group C_2. If the complex becomes sufficiently distorted by conformational preference in the chelate rings, then all three absorption bands will show optical activity in this model.

TABLE 1
Species arising from vibronic coupling of the ^2D terms in D_{4h}

Transition	Vibrational mode	Representation	Polarization	Rotation
$d_{x^2-y^2} \leftarrow d_{z^2}$	—	B_{1g}	—	—
	a_{2u}	B_{2u}	—	—
	b_{2u}	A_{2u}	z	—
	e_u	E_u	x,y	—
$d_{x^2-y^2} \leftarrow d_{xy}$	—	A_{2g}	—	R_z
	a_{2u}	A_{1u}	—	—
	b_{2u}	B_{1u}	—	—
	e_u	E_u	x,y	—
$d_{x^2-y^2} \leftarrow d_{xz}, d_{yz}$	—	E_g	—	R_x,R_y
	a_{2u}	E_u	x,y	—
	b_{2u}	E_u	x,y	—
	e_u	A_{1u}	—	—
		A_{2u}	z	—
		B_{1u}	—	—
		B_{2u}	—	—

The absorption and c.d. spectra of the Cu(II) – amide-complex solutions using ligands **2**, **5**–**8** are shown in Fig. 1. The spectra of the **1**, **3**, and **4**

Can. J. Chem. Downloaded from www.nrcresearchpress.com by 210.87.254.5 on 09/05/12
For personal use only.

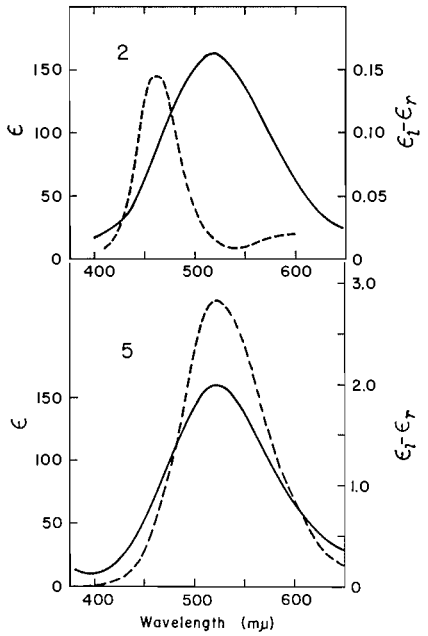

FIG. 1*a*. Absorption spectra (—) and associated circular dichroism (---) for copper(II) complexes of bis(glycyl)-*SS*-butanediamine (**2**) and bis(*S*-alanyl)-*RR*-cyclohexanediamine (**5**).

complexes have been previously published (5). It will be seen that the spectra fall into two groups: those (**3**–**8**) in which optical activity is apparent over the whole of the visible absorption spectrum, and those (**1** and **2**) in which circular dichroism appears mainly in the highest-energy component. The chirality of the complexes of **3**, **5**, and **6** is determined by the cyclohexanediamine ring, conformation λ for *RR*. It appears that the alanine likewise confers a strong preference for a dissymmetric structure to the **4** complex. By analogy with the cyclohexanediamine derivatives, this must involve a δ conformation for the bridging ethylenediamine ring in the case of *S*-alanine; that is, the methyl groups are axial if the C—N—C—O system is to be planar. These complexes are highly distorted from D_{4h}, whereas the remaining two (**1** and **2**) may be supposed to be much less so. It has been pointed out (6) that the methyl groups in **1** and **2** may be axial, as in **4**, giving a λ conformation for bridging *R*-propanediamine or *RR*-butanediamine. However, comparison with the c.d. spectra of the cyclohexanediamine derivatives shows that the opposite is more likely, for the c.d. of **1** and **2** at ca. 530 mμ is, if anything, negative.

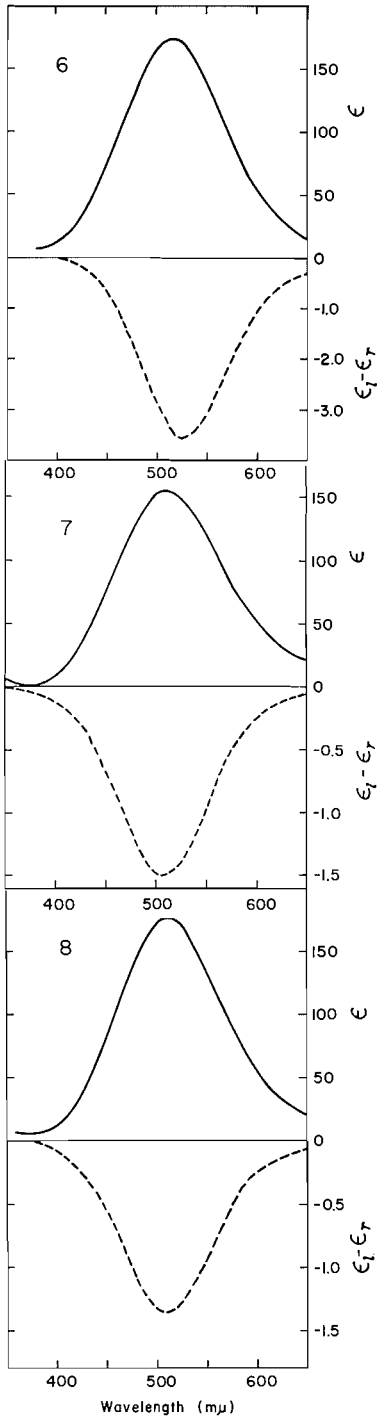

FIG. 1*b*. Absorption spectra (—) and associated circular dichroism (---) for Cu(II) complexes of bis(*S*-alanyl)-*SS*-cyclohexanediamine (**6**), bis(*S*-alanyl)-*RS*-cyclohexanediamine (**7**), and bis-(*S*-alanyl)-*RS*-butanediamine (**8**).

Can. J. Chem. Downloaded from www.nrcresearchpress.com by 210.87.254.5 on 09/05/12
For personal use only.

Finally, the lack of any specific abnormality associated with the C_1 symmetry of **1** is evidenced by the fact that the **7** and **8** complexes show a "normal" circular dichroism.

Experimental

Bis(glycyl)-R-propanediamine (1)

The preparation procedure was adapted from that of Sheehan and Frank (7). (−)Propanediamine dihydrochloride (22.9 g), $|\alpha|_D$, +3.8 (5%, aqueous) was slurried with magnesium oxide (40 g) in water (400 ml). The temperature was maintained at 5–10 °C during the slow (1 h) addition of phthaloylglycyl chloride (60.5 g) dissolved in *p*-dioxane (400 ml). The insoluble product was extracted into and crystallized from warm glacial acetic acid. The m.p. was higher than 300 °C.

The bis(phthaloylglycyl)propanediamine (12.6 g) was refluxed for 2 h with hydrazine hydrate (3.5 g) in absolute ethanol (250 ml), and the solvent removed under vacuum. Concentrated HCl (50 ml) was added, the mixture warmed to 45 °C for 5 min, rapidly cooled, the phthalazine-1,4-dione filtered off, and the filtrate evaporated to dryness under vacuum over KOH. The hydrochloride was converted to the free base by ion exchange (Dowex 1, OH form) and recovered from its aqueous solution by repeated evaporation with absolute ethanol. After recrystallization from *n*-butanol, the m.p. was 84–87 °C; $|\alpha|_D$, −13.7 (16%, aqueous).

Anal. Calcd. for $C_7H_{16}N_4O_2$: C, 44.7; H, 8.51; N, 29.8. Found: C, 44.3; H, 8.44; N, 29.6.

Bis(glycyl)-SS-butanediamine (2)

The same procedure was followed as for the propanediamine compound, using (+)butanediamine dihydrochloride (7.7g), $|\alpha|_D$, −6.5 (7.5%, aqueous), MgO (9 g), H_2O (100 ml), phthaloylglycyl chloride (18.3 g), *p*-dioxane (100 ml).

The bis(phthaloylglycyl)butanediamine (1.4 g) was refluxed with hydrazine hydrate (0.28 g) in absolute ethanol (50 ml). M.p., 176 °C; $|\alpha|_D$, −4.91 (1.6%, aqueous).

Anal. Calcd. for $C_8H_{18}N_4O_2$: C, 47.5; H, 8.91; N, 27.7. Found: C, 47.0; H, 8.89; N, 27.6.

Bis(glycyl)-RR-cyclohexanediamine (3)

The same procedure was followed as for the propanediamine and butanediamine compounds, using (−)*trans*-cyclohexanediamine dihydrochloride (4.05 g), $|\alpha|_D$, −15 (15%, aqueous), MgO (10 g), H_2O (150 ml), phthaloylglycyl chloride (16 g), *p*-dioxane (100 ml). The bis(phthaloylglycyl)cyclohexanediamine (2.5 g) was refluxed with hydrazine hydrate (0.6 g) in absolute ethanol (40 ml). After recrystallization from *n*-butyl ether, the m.p. was 174 °C; $|\alpha|_D$, +97.5 (4%, aqueous).

Anal. Calcd. for $C_{10}H_{20}N_4O_2$: C, 52.6; H, 8.77; N, 24.6. Found: C, 52.6; H, 8.74; N, 24.6.

Bis(S-alanyl)ethylenediamine (4)

The procedure was adapted from that of Erlanger and Brand (8). N-Benzyloxycarbonyl L-α-alanine hydrazide was prepared from L-α-alanine (Nutritional Biochemicals Corp., $|\alpha|_D$, +14.25 (2*M*, 2*N* HCl)). The carbobenzyloxyalanine hydrazide (40 g) was dissolved in glacial acetic acid (200 ml) and hydrochloric acid (800 ml, 0.6 *M*) added. Sodium nitrite (14.4 g) as a saturated aqueous solution was slowly added, the temperature being kept at −5 °C. The azide was extracted into cold ether (600 ml), washed with water (200 ml), sodium bicarbonate solution (400 ml, 3%), and water (200 ml). The cold solution was dried over sodium sulfate for 15 min and ethylenediamine (10 g) in an ether:benzene mixture (20:80 v/v) was slowly added to it (30 min). The insoluble product was recrystallized from methanol. M.p., 185–188 °C.

Anal. Calcd. for $C_{24}H_{26}N_4O_6$: C, 61.5; H, 6.4; N, 11.9. Found: C, 61.6; H, 6.8; N, 12.4.

The bis(carbobenzyloxyalanyl)ethylenediamine (5 g) was dissolved in methanol (200 ml) and hydrogenolyzed (6 h, room temperature, atmospheric pressure) using Palladium-black catalyst (1 g). The methanol was removed under vacuum and the residue recrystallized from THF. M.p., 140 °C; $|\alpha|_D$, +14.8 (4%, methanol).

Anal. Calcd. for $C_8H_{18}N_4O_2$: C, 47.5; H, 8.9; N, 27.7. Found: C, 47.0; H, 8.94; N, 26.9.

Bis(S-alanyl)-RR-cyclohexanediamine (5)

The procedure was adapted from that of Sheehan and Hess (9). (−)Transcyclohexanediamine, (dihydrochloride, $|\alpha|_D$, −16.0 (3.8%, aqueous)), (9.5 g), dissolved in methylene chloride (20 ml), was added to a cooled (−5°) solution of phthaloyl-L-alanine (37.0 g) in methylene chloride (100 ml). A solution of N,N′-dicyclohexylcarbodimide (35.2 g) in methylene chloride (25 ml) was slowly added (30 min) with continued cooling and the mixture stirred for 4 h. The N,N′-dicyclohexylurea (40 g) was removed by filtration and the filtrate evaporated to dryness. The residue was recrystallized from ethanol:water (75:25 v/v). Yield, 29.9 g; m.p., 232–233 °C; $|\alpha|_D$, +51 (0.5%, ethanol).

The bis(phthaloylalanyl)cyclohexanediamine (28.4 g) was refluxed for 4 h with hydrazine hydrate (6.0 g) in absolute ethanol (500 ml), and the solvent removed under vacuum. HCl (100 ml, 0.2 *M*) was added, the mixture warmed to 60 °C for 10 min, then cooled to 0 °C, and the phthalazine-1,4-dione (17.8 g) filtered off. After evaporation of the filtrate to dryness, the residue was recrystallized from ethanol:water (75:25 v/v). Yield, 16.5 g.

The hydrochloride was converted to the free base in the same manner as **1** and recrystallized from absolute ethanol. M.p., 189–190 °C; $|\alpha|_D$, +93 (1%, aqueous).

Anal. Calcd. for $C_{12}H_{24}N_4O_2$: C, 56.2; H, 9.44; N, 21.9. Found: C, 56.2; H, 9.36; N, 21.8.

Bis(S-alanyl)-SS-cyclohexanediamine (6)

The same procedure was followed as for the *RR*-cyclohexanediamine compound, using (+) *trans*-cyclohexanediamine (7.3 g) (dihydrochloride, $|\alpha|_D$, +16.0, 3%, aqueous), phthaloyl-L-alanine (28 g), N,N′-dicyclohexylcarbodiimide (27 g) in methylene chloride (750 ml total volume).

After removal of N,N′-dicyclohexylurea (26 g) and evaporation, the residue was recrystallized from ethanol. Yield, 26 g; m.p., 274–275 °C; $|\alpha|_D$, +11.7 (0.8%, $CHCl_3$).

The hydrazinolysis was carried out upon the bis(phthaloylalanyl)cyclohexanediamine (24.7 g) using hydrazine hydrate (5.25 g) in absolute ethanol (500 ml) as

before. Yield, 14.2 g. The hydrochloride was converted to the free base in the same manner as **1**, then recrystallized from absolute ethanol. M.p., 195–196 °C; $|\alpha|_D$, −78 (0.5%, aqueous).

Anal. Calcd. for $C_{12}H_{24}N_4O_2$: C, 56.2; H, 9.44; N, 21.9. Found: C, 56.3; H, 9.39; N, 21.7.

Bis(S-alanyl)-RS-cyclohexanediamine (7)

The same procedure was followed as for **5** and **6**, using *cis*-cyclohexanediamine (6.6 g), phthaloyl-L-alanine (25 g), N,N′-dicyclohexylcarbodiimide (24 g) in methylene chloride (250 ml total volume).

After removal of N,N′-dicyclohexylurea (22.5 g) and evaporation, the residue was recrystallized from ethanol. Yield, 24 g; m.p., 159–160 °C; $|\alpha|_D$, −2.6 (0.5%, $CHCl_3$).

The hydrazinolysis was carried out upon the bis-(phthaloylalanyl)cyclohexanediamine (235 g) using hydrazine hydrate (4.6 g) in absolute ethanol (500 ml) as before. Yield, 11.7 g. The free base was obtained from the hydrochloride by ion exchange as before, and crystallized, with difficulty. M.p., 123–124 °C; $|\alpha|_D$, +10.1 (0.7%, aqueous).

Anal. Calcd. for $C_{12}H_{24}N_4O_2$: C, 56.2; H, 9.44; N, 21.9. Found: C, 56.1; H, 9.47; N, 21.8.

Bis(S-alanyl)-RS-butanediamine (8)

The same procedure was followed as for **5**–**7**. The yield of bis(phthaloyl)butanediamine was 23 g; m.p., 223–234 °C; $|\alpha|_D$, −11.5 (1.6%, aqueous). The yield of free base was 6.5 g; m.p., 174–175 °C; $|\alpha|_D$, +13 (1%, aqueous).

Anal. Calcd. for $C_{10}H_{22}N_4O_2$: C, 52.1; H, 9.63; N, 24.3. Found: C, 50.9; H, 9.5; N, 23.7.

Cupric bis(amide) complexes

Aqueous solutions were prepared 10^{-3} *M* in cupric sulfate and 10^{-2} *M* in ligand, and the p*H* adjusted with NaOH to lie between 10.0 and 10.5. At this p*H*, the absorption at 510–520 mμ had attained its maximum value and the solutions were used immediately to record their c.d. spectra.

Upon standing at room temperature for several hours, the red colors gave place to blue, presumably due to the amides' hydrolysis. This was not further investigated.

Circular dichroism spectra were recorded using a Durrum-Jasco ORD/UV/CD/5 with a cell length of 10 mm at a temperature of 28 ± 1 °C, the instrument being standardized by means of camphorsulphonic acid, m.p. +193 °C, Δε (292 mμ) 2.3. Absorption spectra were recorded using a Cary Model 14 spectrophotometer, a cell length of 10 mm, and a temperature of 25 ± 0.1 °C.

We would like to express our gratitude to Badische Anilin u. Soda Fabrik AG for a generous supply of cyclohexanediamine, to Dr. P. Morand of The University of Ottawa for provision of c.d. facilities, and to the Ontario Department of University Affairs for financial assistance.

1. R. G. Asperger and C. F. Liu. Inorg. Chem. **4**, 1395 (1965).
2. M. Goto, M. Saburi, and S. Yoshikawa. Inorg. Chem. **8**, 35 (1969).
3. D. A. Buckingham, C. M. Foster, and A. M. Sargeson. J. Amer. Chem. Soc. **90**, 6032 (1968).
4. R. B. Martin, J. M. Tsangaris, and J. W. Chang. J. Amer. Chem. Soc. **90**, 821 (1968).
5. M. Parris and E. A. Hodges. J. Amer. Chem. Soc. **90**, 1909 (1968).
6. R. S. Downing and F. L. Urbach. J. Amer. Chem. Soc. **90**, 5344 (1968).
7. J. C. Sheehan and V. S. Frank. J. Amer. Chem. Soc. **71**, 1856 (1949).
8. B. F. Erlanger and E. Brand. J. Amer. Chem. Soc. **73**, 3508 (1951).
9. J. C. Sheehan and G. P. Hess. J. Amer. Chem. Soc. **77**, 1067 (1955).

Spectrophotometric determination of the hydrolysis constant of bromine at 25 °C

Judith M. Pink (Mrs.)

Department of Chemistry, St. Francis Xavier University, Antigonish, Nova Scotia

Received October 21, 1969

A spectrophotometric determination of the equilibrium constant for the hydrolysis of bromine in water is described.

Canadian Journal of Chemistry, **48**, 1169 (1970)

While carrying out a quantitative analysis of some kinetic results of oxidations in bromine water, it was found that no reliable value of K_h, the hydrolysis constant of bromine water, was available.

$$[1] \qquad K_h = \frac{[HOBr][H^+][Br^-]}{[Br_2]}$$

K_h was determined by Liebhafsky (1) to be 5.8×10^{-9} at 25 °C. This value, however, was questioned later. Eigen and Kustin (2), using a temperature jump relaxation technique, found the value to be 6.9×10^{-9} at 20°. Deno and Potter (3) used Eigen's value at 20° and Liebhafsky's temperature correction to calculate K_h at 25° to be 9×10^{-9}. In a later publication,

Can. J. Chem. Downloaded from www.nrcresearchpress.com by 210.87.254.5 on 09/05/12
For personal use only.

before. Yield, 14.2 g. The hydrochloride was converted to the free base in the same manner as **1**, then recrystallized from absolute ethanol. M.p., 195–196 °C; $|\alpha|_D$, −78 (0.5%, aqueous).

Anal. Calcd. for $C_{12}H_{24}N_4O_2$: C, 56.2; H, 9.44; N, 21.9. Found: C, 56.3; H, 9.39; N, 21.7.

Bis(S-alanyl)-RS-cyclohexanediamine (7)

The same procedure was followed as for **5** and **6**, using *cis*-cyclohexanediamine (6.6 g), phthaloyl-L-alanine (25 g), N,N′-dicyclohexylcarbodiimide (24 g) in methylene chloride (250 ml total volume).

After removal of N,N′-dicyclohexylurea (22.5 g) and evaporation, the residue was recrystallized from ethanol. Yield, 24 g; m.p., 159–160 °C; $|\alpha|_D$, −2.6 (0.5%, $CHCl_3$).

The hydrazinolysis was carried out upon the bis-(phthaloylalanyl)cyclohexanediamine (235 g) using hydrazine hydrate (4.6 g) in absolute ethanol (500 ml) as before. Yield, 11.7 g. The free base was obtained from the hydrochloride by ion exchange as before, and crystallized, with difficulty. M.p., 123–124 °C; $|\alpha|_D$, +10.1 (0.7%, aqueous).

Anal. Calcd. for $C_{12}H_{24}N_4O_2$: C, 56.2; H, 9.44; N, 21.9. Found: C, 56.1; H, 9.47; N, 21.8.

Bis(S-alanyl)-RS-butanediamine (8)

The same procedure was followed as for **5**–**7**. The yield of bis(phthaloyl)butanediamine was 23 g; m.p., 223–234 °C; $|\alpha|_D$, −11.5 (1.6%, aqueous). The yield of free base was 6.5 g; m.p., 174–175 °C; $|\alpha|_D$, +13 (1%, aqueous).

Anal. Calcd. for $C_{10}H_{22}N_4O_2$: C, 52.1; H, 9.63; N, 24.3. Found: C, 50.9; H, 9.5; N, 23.7.

Cupric bis(amide) complexes

Aqueous solutions were prepared 10^{-3} *M* in cupric sulfate and 10^{-2} *M* in ligand, and the p*H* adjusted with NaOH to lie between 10.0 and 10.5. At this p*H*, the absorption at 510–520 mμ had attained its maximum value and the solutions were used immediately to record their c.d. spectra.

Upon standing at room temperature for several hours, the red colors gave place to blue, presumably due to the amides' hydrolysis. This was not further investigated.

Circular dichroism spectra were recorded using a Durrum-Jasco ORD/UV/CD/5 with a cell length of 10 mm at a temperature of 28 ± 1 °C, the instrument being standardized by means of camphorsulphonic acid, m.p. +193 °C, Δε (292 mμ) 2.3. Absorption spectra were recorded using a Cary Model 14 spectrophotometer, a cell length of 10 mm, and a temperature of 25 ± 0.1 °C.

We would like to express our gratitude to Badische Anilin u. Soda Fabrik AG for a generous supply of cyclohexanediamine, to Dr. P. Morand of The University of Ottawa for provision of c.d. facilities, and to the Ontario Department of University Affairs for financial assistance.

1. R. G. Asperger and C. F. Liu. Inorg. Chem. **4**, 1395 (1965).
2. M. Goto, M. Saburi, and S. Yoshikawa. Inorg. Chem. **8**, 35 (1969).
3. D. A. Buckingham, C. M. Foster, and A. M. Sargeson. J. Amer. Chem. Soc. **90**, 6032 (1968).
4. R. B. Martin, J. M. Tsangaris, and J. W. Chang. J. Amer. Chem. Soc. **90**, 821 (1968).
5. M. Parris and E. A. Hodges. J. Amer. Chem. Soc. **90**, 1909 (1968).
6. R. S. Downing and F. L. Urbach. J. Amer. Chem. Soc. **90**, 5344 (1968).
7. J. C. Sheehan and V. S. Frank. J. Amer. Chem. Soc. **71**, 1856 (1949).
8. B. F. Erlanger and E. Brand. J. Amer. Chem. Soc. **73**, 3508 (1951).
9. J. C. Sheehan and G. P. Hess. J. Amer. Chem. Soc. **77**, 1067 (1955).

Spectrophotometric determination of the hydrolysis constant of bromine at 25 °C

Judith M. Pink (Mrs.)

Department of Chemistry, St. Francis Xavier University, Antigonish, Nova Scotia

Received October 21, 1969

A spectrophotometric determination of the equilibrium constant for the hydrolysis of bromine in water is described.

Canadian Journal of Chemistry, **48**, 1169 (1970)

While carrying out a quantitative analysis of some kinetic results of oxidations in bromine water, it was found that no reliable value of K_h, the hydrolysis constant of bromine water, was available.

$$[1] \qquad K_h = \frac{[HOBr][H^+][Br^-]}{[Br_2]}$$

K_h was determined by Liebhafsky (1) to be 5.8×10^{-9} at 25 °C. This value, however, was questioned later. Eigen and Kustin (2), using a temperature jump relaxation technique, found the value to be 6.9×10^{-9} at 20°. Deno and Potter (3) used Eigen's value at 20° and Liebhafsky's temperature correction to calculate K_h at 25° to be 9×10^{-9}. In a later publication,

Can. J. Chem. Downloaded from www.nrcresearchpress.com by 210.87.254.6 on 09/05/12
For personal use only.

Can. J. Chem. Downloaded from www.nrcresearchpress.com by 210.87.254.6 on 09/05/12
For personal use only.

Deno and Fruit (4) revised this to 6.7×10^{-9}, though the earlier computation appears to be correct. Since the value of K_h is a prerequisite for any quantitative study in the bromine water system, its determination at 25° was undertaken by the present author.

The equilibrium constant, K_3, for tribromide formation is known to be (5)

$$[2] \quad K_3 = \frac{[Br_3^-]}{[Br_2][Br^-]} = 16.85 \pm 0.09$$

and therefore K_h can be evaluated spectrophotometrically if the extinction coefficients for Br_2, Br_3^-, HOBr, and OBr^- are known.

A new determination of the spectra of HOBr and of OBr^- gave essentially the same results as obtained by previous workers (6, 7). However, no reliable set of extinction coefficients had been found for Br_2 in water for the same wavelength region. Earlier workers (8, 9) ignored both the hydrolysis reaction and tribromide formation. Since the tribromide absorption is high, even small amounts present may cause significant errors. The extinction coefficients of Br_2 and Br_3^- determined by the author are listed in Table 1.

TABLE 1

Extinction coefficients of Br_2 and of Br_3^- between 390 and 250 mμ

Wavelength (mμ)	$\varepsilon_{Br_2} \times 10^{-2}$	$\varepsilon_{Br_3} \times 10^{-2}$
390	1.73	3.09
380	1.63	4.88
370	1.42	7.65
360	1.11	9.37
350	0.78	11.20
340	0.50	15.48
330	0.30	23.60
320	0.20	41.7
310	0.17	64.6
300	0.24	98.7
290	0.40	155.9
280	0.69	257.9
270	1.03	346.2
260	1.21	337.4
250	1.31	193.8

In the spectrophotometric determination of the concentrations of the various species in eq. [1] for bromine water solutions containing varying amounts of bromide, any contribution from OBr^- was neglected, since the solutions analyzed had a p*H* between 3 and 5. The concentration terms listed in Table 2 are the average values of eight sets of simultaneous equations solved for each run. The values of K_h were calculated from eq. [1] using these concentrations and the $[H^+]$ computed from the p*H* reading of each solution.

The values of K_h determined are expected to be more reliable at low bromide concentration than at high values because of the strong absorption of Br_3^- relative to all the other species at all wavelengths studied. This is clearly confirmed by the greater deviations shown by runs 1 and 3 (Table 2). On the basis of the other three runs, the average value of K_h is 9.6×10^{-9}. This is in agreement with Deno and Potter's calculation (3) and also with the value 8.8×10^{-9} recently estimated from kinetic considerations by Perlmutter–Hayman and Weissman (10). This latter value was found in solutions of fairly high ionic strength.

Experimental

British Drug Houses AnalaR-grade reagents were used and the water was doubly distilled. p*H* measurements were made with a Radiometer TTT1 titrator in conjunction with a type PHA630T Scale Expander. The ultraviolet spectra were recorded on a Cary Model 14 spectrophotometer.

Bromine–water solutions were freshly made up by dissolving bromine either in distilled water or in a bromide solution of known concentration and equilibrating the resulting solutions at 25°. Samples were withdrawn for measuring their p*H* and determining their oxidizing power iodometrically. Ultraviolet spectra of the remaining solutions were run against water or bromide solutions as references.

Determination of the Tribromide Extinction Coefficient

Solutions, all 2.75×10^{-2} *M* in $HClO_4$ (in order to suppress hydrolysis) and containing varying amounts of known bromide, were prepared. The total oxidant concentration, determined iodometrically, is given by

$$[Ox] = [Br_2] + [Br_3^-]$$

This equation, in conjunction with eq. [2], was used to determine the equilibrium concentrations of Br_2 and of Br_3^-. The extinction coefficients were calculated by comparing pairs of spectra at a chosen wavelength, assuming that the only absorbing species were Br_2 and Br_3^- and that Beer's law was obeyed.

Determination of the Concentrations of the Various Species in Bromine Water

The simultaneous concentrations of the different species were determined at several wavelengths using pairs of the set of equations

$$\varepsilon_{Br_2}^{\lambda}[Br_2] + \varepsilon_{Br_3}^{\lambda}[Br_3^-] + \varepsilon_{HOBr}^{\lambda}[HOBr] = [O.D.]^{\lambda}$$

together with

$$[Br_2] + [Br_3^-] + [HOBr] = [Ox]$$

where $\varepsilon_{Br_2}^{\lambda}$ designates the extinction coefficient of Br_2 and

TABLE 2

Calculated hydrolysis constant for bromine water at 25 °C

Run No.	$[H^+]$ $\times 10^5$, (M)	[Ox] $\times 10^3$, (M)	$[Br_2]$ $\times 10^3$, (M)	$[Br^-]$ $\times 10^4$, (M)	[HOBr] $\times 10^3$, (M)	K_h $\times 10^9$, (M^2)
1	1.12	0.442	0.304	24.17	0.126	11.2
2	2.74	5.520	3.469	5.938	2.016	9.46
3	3.98	0.396	0.347	20.84	0.037	8.95
4	15.1	3.441	2.255	2.053	1.182	9.55
5	16.2	3.486	2.250	1.199	1.144	9.90

$[O.D.]^{\lambda}$ is the absorbance of the bromine solution, both at wavelength λ.

The computations were carried out on an IBM 1620 computer.

The author thanks the National Research Council of Canada and the St. Francis Xavier University Council for Research for grants, Miss K. Crouse for carrying out some of the measurements, and one of the referees for pointing out a serious typographical error.

1. H. A. Liebhafsky. J. Amer. Chem. Soc. **61**, 3513 (1939).
2. M. Eigen and K. Kustin. J. Amer. Chem. Soc. **84**, 1355 (1962).
3. N. C. Deno and N. H. Potter. J. Amer. Chem. Soc. **89**, 3550 (1967).
4. N. C. Deno and R. E. Fruit, Jr. J. Amer. Chem. Soc. **90**, 3502 (1968).
5. D. B. Scaife and H. J. V. Tyrrel. J. Amer. Chem. Soc. **80**, 386 (1958).
6. L. Farkas and F. S. Klein. J. Chem. Phys. **16**, 886 (1948).
7. M. Anbar and I. Dostrovsky. J. Chem. Soc. 1106 (1954).
8. C. L. Child and O. J. Walker. Trans. Faraday Soc. **34**, 1506 (1938).
9. R. G. Aickin, N. S. Bayliss and A. L. G. Rees. Proc. Royal Soc. London, Ser. A, **169**, 234 (1938).
10. B. Perlmutter-Hayman and Y. Weissman. J. Amer. Chem. Soc. **91**, 668 (1969).

Electron impact-induced rearrangements of substituted 1-phenylpropynes[1,2,3]

S. Safe and W. D. Jamieson

Atlantic Regional Laboratory, National Research Council of Canada, Halifax, Nova Scotia

AND

W. R. Pilgrim and Saul Wolfe

Department of Chemistry, Queen's University, Kingston, Ontario

Received August 20, 1969

The primary ion mass spectra of the C_9H_8 isomers indene and 1-phenylpropyne were remarkably similar. Examination of ion and metastable peak intensities and their energy spectrum indicate that their common M-1 ($C_9H_7^+$) fragment ion has the same structure. The mass spectra of several substituted phenylpropynes were also similar to that of the parent hydrocarbon below mass *m/e* 115 but showed no substituent or kinetic effect. The mass spectra of 1-phenylpropyne-d_3 clearly shows H/D randomization in the molecular ion and linear ion structures are proposed.

Canadian Journal of Chemistry, **48**, 1171 (1970)

The electron impact induced fragmentations and rearrangements of acetylenic compounds tend to give fragment ions which are typically derived from aromatic systems (1–4). The acyclic alcohol (**1**) and its C_7H_8O isomer, benzyl alcohol, give similar primary ion mass spectra with identical metastable peaks. Moreover, both α-*d*-benzyl alcohol and α-*d*-all-*trans*-hepta-2,4-dien-6-yn-1-ol show almost 100% H/D randomization in the $C_7H_7^+$ ion (3). Aplin and Safe (2) also showed that the mass spectra and metastable peaks of the C-10 polyacetylene (**2**) and indene (**3**) were similar.

[1]NRCC No. 11133
[2]Part I in the series "Aspects of acetylene chemistry".
[3]Part V in the series "Mass spectra of aromatic and acetylenic compounds".

Can. J. Chem. Downloaded from www.nrcresearchpress.com by 210.87.254.6 on 09/05/12
For personal use only.

TABLE 2

Calculated hydrolysis constant for bromine water at 25 °C

Run No.	$[H^+]$ $\times 10^5$, (M)	[Ox] $\times 10^3$, (M)	$[Br_2]$ $\times 10^3$, (M)	$[Br^-]$ $\times 10^4$, (M)	[HOBr] $\times 10^3$, (M)	K_h $\times 10^9$, (M^2)
1	1.12	0.442	0.304	24.17	0.126	11.2
2	2.74	5.520	3.469	5.938	2.016	9.46
3	3.98	0.396	0.347	20.84	0.037	8.95
4	15.1	3.441	2.255	2.053	1.182	9.55
5	16.2	3.486	2.250	1.199	1.144	9.90

$[O.D.]^{\lambda}$ is the absorbance of the bromine solution, both at wavelength λ.

The computations were carried out on an IBM 1620 computer.

The author thanks the National Research Council of Canada and the St. Francis Xavier University Council for Research for grants, Miss K. Crouse for carrying out some of the measurements, and one of the referees for pointing out a serious typographical error.

1. H. A. Liebhafsky. J. Amer. Chem. Soc. **61**, 3513 (1939).
2. M. Eigen and K. Kustin. J. Amer. Chem. Soc. **84**, 1355 (1962).
3. N. C. Deno and N. H. Potter. J. Amer. Chem. Soc. **89**, 3550 (1967).
4. N. C. Deno and R. E. Fruit, Jr. J. Amer. Chem. Soc. **90**, 3502 (1968).
5. D. B. Scaife and H. J. V. Tyrrel. J. Amer. Chem. Soc. **80**, 386 (1958).
6. L. Farkas and F. S. Klein. J. Chem. Phys. **16**, 886 (1948).
7. M. Anbar and I. Dostrovsky. J. Chem. Soc. 1106 (1954).
8. C. L. Child and O. J. Walker. Trans. Faraday Soc. **34**, 1506 (1938).
9. R. G. Aickin, N. S. Bayliss and A. L. G. Rees. Proc. Royal Soc. London, Ser. A, **169**, 234 (1938).
10. B. Perlmutter-Hayman and Y. Weissman. J. Amer. Chem. Soc. **91**, 668 (1969).

Electron impact-induced rearrangements of substituted 1-phenylpropynes[1,2,3]

S. Safe and W. D. Jamieson

Atlantic Regional Laboratory, National Research Council of Canada, Halifax, Nova Scotia

AND

W. R. Pilgrim and Saul Wolfe

Department of Chemistry, Queen's University, Kingston, Ontario

Received August 20, 1969

The primary ion mass spectra of the C_9H_8 isomers indene and 1-phenylpropyne were remarkably similar. Examination of ion and metastable peak intensities and their energy spectrum indicate that their common M-1 ($C_9H_7^+$) fragment ion has the same structure. The mass spectra of several substituted phenylpropynes were also similar to that of the parent hydrocarbon below mass *m/e* 115 but showed no substituent or kinetic effect. The mass spectra of 1-phenylpropyne-d_3 clearly shows H/D randomization in the molecular ion and linear ion structures are proposed.

Canadian Journal of Chemistry, **48**, 1171 (1970)

The electron impact induced fragmentations and rearrangements of acetylenic compounds tend to give fragment ions which are typically derived from aromatic systems (1–4). The acyclic alcohol (**1**) and its C_7H_8O isomer, benzyl alcohol, give similar primary ion mass spectra with identical metastable peaks. Moreover, both α-*d*-benzyl alcohol and α-*d*-all-*trans*-hepta-2,4-dien-6-yn-1-ol show almost 100% H/D randomization in the $C_7H_7^+$ ion (3). Aplin and Safe (2) also showed that the mass spectra and metastable peaks of the C-10 polyacetylene (**2**) and indene (**3**) were similar.

[1]NRCC No. 11133
[2]Part I in the series "Aspects of acetylene chemistry".
[3]Part V in the series "Mass spectra of aromatic and acetylenic compounds".

Can. J. Chem. Downloaded from www.nrcresearchpress.com by 210.87.254.5 on 09/05/12
For personal use only.

TABLE 1

Compound	$[C_9H_7^+$ *m/e* 115]/$[C_9H_8^+$ *m/e* 116] 70 eV	15 eV	[68.9]*/$[C_7H_5^+$ *m/e* 89] 70 eV†
Indene (**3**)	1.2	0.75	.02
1-Phenylpropyne (**4**, X = H)	0.8	0.78	.02

*Metastable peak for *m/e* 115 $-C_2H_2$ *m/e* 89 fragmentation.
†Metastable ions are too weak at 15 eV.

$HC{\equiv}C\cdot CH{=}CH\cdot CH{=}CH\cdot CH_2OH$

(**1**)

$CH_3\cdot CH{=}CH\cdot(C{\equiv}C)_2\cdot CH{=}CH\cdot CH_2R$

(**2**, R = OH, OAc)

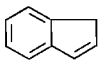

(**3**)

In the present study the mass spectral fragmentations of indene (**3**) and 1-phenylpropyne (**4**, X = H) and substituted 1-phenylpropynes were studied in order to investigate the fragment ion structures and particularly the ubiquitous $C_9H_7^+$ (*b*, *m/e* 115) ion.

The similar primary ion mass spectra of the two C_9H_8 isomeric hydrocarbons (**3** and **4**, X = H) are shown (Fig. 1). The molecular ion (*a*, *m/e*, 116) for (**4**, X = H) decomposes to give a strong M-1 ion at *m/e* 115 (*b*, $C_9H_7^+$) which in turn loses C_2H_2 to give the $C_7H_5^+$ ion (*c*). Both of these fragmentations are accompanied by strong metastable ions at *m/e* 112 and 68.9 respectively. The $C_7H_5^+$ ion (*c*) also expels acetylene to give the $C_5H_3^+$ ion (*d*) and a weak metastable peak at *m/e* 44.6. The fragmentation pathway described by **4** (X = H) (eq. [1]) is identical to that previously reported for indene (**3**) (2). Table 1 shows a comparison of the *b*/*a* values obtained for both **3** and **4** (X = H) as well as their respective ratio of [metastable ion at *m/e* 68.9]/[(*c*)] for the fragmentation $b \rightarrow c$. These data indicate that at least a fraction of the decomposing *b* ions for both hydrocarbons have the same structure and energy (5).

The energy spectrum of the ion beam (6) impinging on the beam monitor electrode was recorded by scanning the ion accelerating voltage at constant electrostatic voltage. The energy spectrum yields the relative concentrations of ions produced by "metastable" processes in the ion beam following acceleration of the ion beam and prior to its impinging on the beam monitor electrode. The energy spectrum for both **3** and **4** (X = H) showed a major species in the ion beam having 77% of the accelerating energy. This species has the energy expected for the product of the reaction $b \rightarrow c$. Moreover the ratio of [daughter ion species, *m/e* 89]/[total ion current] was 1.35 ($\pm$1%) $\times$ 10^{-3} for both **3** and **4** (X = H). Therefore, it is likely that in the mass spectra of **3** and **4** (X = X) the $C_9H_7^+$ ion (*b*) is both formed and decomposed by identical processes.

In order to further probe the breakdown of 1-phenylpropyne (**4**, X = H) a series of substituted analogs were prepared so that the presence (or absence) of a substituent or kinetic effect could be ascertained (7). The values obtained for $[M^+]/[M^+{-}X]$ (X = Cl, Br, CH_3, NO_2) are similar

[1]

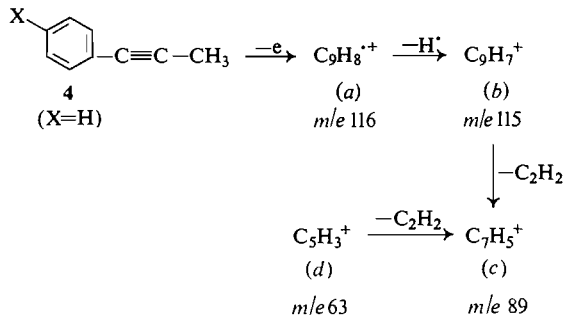

Can. J. Chem. Downloaded from www.nrcresearchpress.com by 210.87.254.5 on 09/05/12
For personal use only.

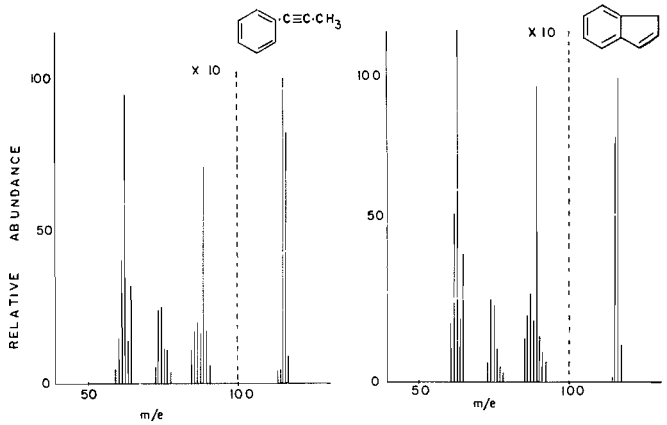

FIG. 1. A comparison of mass spectral fragmentation patterns.

for all substituents (i.e., 0.70, 0.80, 0.90, 0.70 respectively). The result indicates rapid loss of the substituent to give ion *b* which then fragments as already described for **3** and **4** (X = H). The methoxyl derivative **4** (X = OMe) gives an anomalous result which is typical for strongly electron-donating groups (8) and the fragmentation proceeds as shown (eq. [2]) (9). The fluoro group in **4** (X = F) acts as a heavy atom label (10) in which the ions *a*, *b*, *c*, and *d* are replaced by their corresponding fluoro analogs ($C_9H_7F^+$, $C_9H_6F^+$, $C_7H_4F^+$, and $C_5H_2F^+$ respectively). To a lesser extent, however, the fragmentation also proceeds as already described for the other substituted 1-phenylpropynes (**4**, X = Br, Cl, CH_3, NO_2). The complexity of the spectrum of the fluoro derivative does not readily permit a quantitative estimate of the H/F randomization.

The mass spectrum of the deuterated compound (**5**) provides further insight into the nature and mechanism of the formation of the $C_9H_7^+$ ion (*b*). The results (eq. [3]) clearly show that the molecular ion *e* loses both hydrogen and deuterium with the ratio of *f* $(M^+-H)/g$ (M^+-D) being 5:3. This is precisely the atomic H/D ratio in **5** indicating 100% H/D scrambling in the molecular ion *e* prior to fragmentation. The mass spectra of several other aromatic compounds [i.e., benzene (11), nitrosobenzene (12), halogenobenzene (5), pyridine (13), and benzonitrile (14)] also shows H/D randomization in the molecular ion.

It has been suggested (15) that the H/D scrambling occurs via valence bond isomerism in which no C—H bond cleavage occurs (typical of photochemical processes). This mechanism clearly cannot be operative with 1-phenylpropyne (**4**, X = H) and indene (**3**) since the H/D scrambling in the molecular ion necessitates C—H (*d*) bond rupture prior to the formation of the $C_9H_7^+$ ion (*b*). A more likely structure for *a* and *b* is a linear ion formed by rupture of the benzene ring followed by rapid hydrogen randomization via processes analogous to prototropic rearrangement. It is also conceivable that the linear ion might reversibly recyclize. The existence of the linear $C_6H_5^+$ ion has previously

[2] $$\mathbf{4}\ (X{=}OMe) \longrightarrow C_{10}H_{10}O^{\cdot+} \xrightarrow{-CH_3} C_9H_7O^+ \xrightarrow{-CO} C_8H_7^+ \xrightarrow{-C_2H_2} C_6H_5^+$$

[3] $$\text{(5)}\ -C{\equiv}C{\cdot}CD_3 \xrightarrow{-e} C_9H_5D_3^{\cdot+}\ (e)\ m/e\ 119 \xrightarrow{-H^{\cdot}} C_9H_4D_3^+\ (f)\ m/e\ 118 \qquad C_9H_4D_3^{\cdot+} \xrightarrow{-D^{\cdot}} C_9H_5D_2^+\ (g)\ m/e\ 117$$

Can. J. Chem. Downloaded from www.nrcresearchpress.com by 210.87.254.5 on 09/05/12
For personal use only.

been shown to result from the electron-impact fragmentation of benzene (16) and these non-cyclic ions may conceivably play a more important role in the mass spectra of aromatic and acetylenic compounds.

Experimental

Mass spectra were obtained on a Consolidated Electrodynamics Corporation 21-110B mass spectrometer operating at 70 eV and using electrical detection. Samples were introduced by a direct introduction technique using a low temperature probe (18) at -50 to $-30°$ to avoid thermal reactions in the inlet system.

All of the compounds were of analytical purity and, except for the *p*-nitro were prepared from the corresponding acetophenone by reaction successively with phosphorus pentachloride, 3 moles of lithium amide, and an excess of methyl iodide (17). In the case of **9**, trideuteromethyl iodide was employed in the final step. The *p*-nitro compound was prepared, most conveniently, from the reaction of *p*-nitroiodobenzene with propynyl copper (17).

The work at Queen's University was supported by a grant from the National Research Council of Canada and by the award of a Studentship to W. R. Pilgrim. The authors wish to thank Mr. D. Embree for his assistance in recording the mass spectra.

1. S. MEYERSON, J. P. MCCOLLUM, and P. N. RYLANDER. J. Amer. Chem. Soc. **83**, 1401 (1961).
2. R. T. APLIN and S. SAFE. Chem. Commun. 140 (1967).
3. R. T. APLIN and S. SAFE. Can. J. Chem. **47**, 1599 (1969).
4. F. BOHLMANN, C. ZDERO, H. BETHKE, and D. SCHUMANN. Chem. Ber. **101**, 1553 (1968).
5. D. H. WILLIAMS, S. W. TAM, and R. G. COOKS. J. Amer. Chem. Soc. **90**, 2150 (1968) and references cited herein.
6. J. H. BEYNON, J. W. AMY, and W. E. BARTINGER. Chem. Commun. 723 (1969).
7. M. M. BURSEY. Org. Mass Spec. **1**, 31 (1968) and references cited herein.
8. (*a*) M. M. BURSEY and F. W. MCLAFFERTY. J. Amer. Chem. Soc. **88**, 4484 (1966); (*b*) J. M. S. TAIT, T. W. SHANNON, and A. G. HARRISON. J. Amer. Chem. Soc. **84**, 4 (1962).
9. H. BUDZIKIEWICZ, C. DJERASSI, and D. H. WILLIAMS. *In* Interpretation of mass spectra of organic compounds. Holden-Day Inc., San Francisco. 1964. p. 190.
10. M. M. BURSEY, R. D. RIEKE, T. A. ELWOOD, and L. R. DUSOLD. J. Amer. Chem. Soc. **90**, 1557 (1968).
11. K. JENNING. Z. Naturforsch, **229**, 454 (1967).
12. I. R. KING and G. W. KIRBY. J. Chem. Soc. C, 1334 (1966).
13. D. H. WILLIAMS and J. RONAYNE. Chem. Commun. 1129 (1967).
14. R. G. COOKS, R. S. WARD, and D. H. WILLIAMS. Chem. Commun. 850 (1967).
15. R. G. COOKS, I. HOWE, S. W. TAM, and D. H. WILLIAMS. J. Amer. Chem. Soc. **90**, 4064 (1968).
16. J. MOMIGNY, L. BRAKIER, and L. D'OR. Bull. Cl. Sci. Roy. Belges, **48**, 1002 (1962).
17. S. WOLFE and W. R. PILGRIM. In preparation.
18. W. D. JAMIESON and F. MASON. In preparation.

Erratum: Kinetics of the pyrolysis of propylene. Part I

M. SIMON AND M. H. BACK
Chemistry Department, University of Ottawa, Ottawa, Canada

Received February 17, 1970

(Ref.: Can. J. Chem. **48**, 317 (1970))

Canadian Journal of Chemistry, **48**, 1174 (1970)

The ordinates of Figs. 1, 3, and 4 should be multiplied by 10^9, and that of Fig. 2 should be multiplied by 10^8.

Can. J. Chem. Downloaded from www.nrcresearchpress.com by 210.87.254.5 on 09/05/12
For personal use only.

Can. J. Chem. Downloaded from www.nrcresearchpress.com by 210.87.254.40 on 09/05/12
For personal use only.

Canadian Journal of Chemistry

Published by THE NATIONAL RESEARCH COUNCIL OF CANADA

VOLUME 48 APRIL 15, 1970 NUMBER 8

Influence of inert gases on the catalytic oxidation of SO_2

A. A. YERAMIAN,[1] P. L. SILVESTON, AND R. R. HUDGINS

Department of Chemical Engineering, University of Waterloo, Waterloo, Ontario

Received[2] August 16, 1968

A study was made of the influence of diluent gases on the reaction rate and activation energy of the oxidation of sulfur dioxide over vanadium pentoxide catalyst, an effect noted by Baron, Manning, and Johnstone in 1952. Results confirmed the occurrence of the effect in a still lower temperature range (350–470 °C). Using non-adsorbing gases, helium and argon, the effect was demonstrated to be free from chemisorption of the diluents.

Data on activation energy vs. molecular weight of the gas phase, using helium and argon, were in qualitative agreement with predictions based on a momentum-exchange model of Baron *et al.* However, comparison of rates obtained with argon (monatomic) and nitrogen (diatomic) as diluents, combined with independent study of the rate controlling steps, casts doubt on the adequacy of the explanation offered by Baron *et al.*

Canadian Journal of Chemistry, 48, 1175 (1970)

Introduction

Baron, Manning, and Johnstone (1) reported that the rates and activation energies for the oxidation of sulfur dioxide over vanadium pentoxide depended upon the gas used to dilute the reactants. This curious discovery has not been mentioned further in the literature. Baron *et al.* postulated that the desorption of SO_3 must be one of the rate controlling steps and explained the effect through a momentum-exchange model in which the rates and the overall activation energy depended upon the average molecular weight of the gas phase. Helium, nitrogen, and carbon dioxide were used as diluents, and the activation energies observed with these gases were found to be in qualitative agreement with theory.

The object of this study was to dissociate the Baron observations from both the complex reactor model previously utilized and the possible chemisorption of nitrogen and carbon dioxide by employing the non-adsorbing gases helium and argon. In addition, an attempt was made to establish the rate controlling step by the modelling approach of Yang–Hougen–Watson (2, 3) to assist the interpretation of the inert gas effect. It was a further object of this study to obtain data free from transport effects, a pitfall which many of the previous investigators of SO_2 oxidation have taken insufficient pains to avoid.

The literature offers a variety of mechanistic and rate control proposals for SO_2 oxidation over vanadium oxide catalysts. The reaction over sodium promoted vanadium oxide was judged to be controlled by a surface reaction between adsorbed SO_2 and gas-phase oxygen by Calderbank (4), but others (5–7), using a potassium promoted catalyst, found the rate to be controlled by a surface reaction between chemisorbed O and SO_2. Kubota *et al.* (8) found that over pure V_2O_5, below 450 °C, O_2 adsorption controls, although this model is not satisfactory for data taken at low SO_3 pressure (9). Mathur and Thodos (10), using a commercial potassium promoted catalyst, inferred a change of control from surface reaction at 372 °C to desorption of SO_3 at 400 °C. Their conclusions have been criticized on several counts (11, 12). Peveney (13) measured the activity of several catalysts for SO_2 oxidation, including V_2O_5 promoted with BaO, and found a direct relation between catalyst activity and the rate of desorption of SO_3. Mars and van Krevelen (14), and later Boreskov *et al.* (15), concluded that

[1]Present address: Facultad de Ciencias Exactax, Universidad Nacional de La Plata, La Plata, Argentina.

[2]Revision received August 20, 1969.

Can. J. Chem. Downloaded from www.nrcresearchpress.com by 210.87.254.40 on 09/05/12
For personal use only.

oxygen uptake by the catalyst was the controlling step. Mars and Maessen (16) suggested that the strong inhibition of the reaction rate by SO_3 was related to the equilibrium $SO_2 + V_2O_5 \rightleftarrows SO_3 + V_2O_4$. A molten phase has been reported as low as 400 °C (17) and attributed to an eutectic formed by vanadium pentoxide and the promoter (18). The melting point is sensitive to the composition of the catalyst and the presence of SO_2 and SO_3 dissolved in the molten phase. These findings indicate an interaction between the gas phase and the catalyst resulting in a change of catalyst composition and activity. They also cast doubt on the validity of much of the previous work, in which variation of gas composition was used to obtain kinetic models and postulate the rate controlling step.

Recent papers (19–21) indicate that the masking of the kinetics by mass transfer must be considered even for millimeter-sized catalyst particles in the higher temperature ranges. Calderbank's study (4) reported a sharp increase in site density when a very fine catalyst powder was used in place of the 10–14 mesh catalyst employed for most of his work. This result suggests pore diffusion interference.

The existence of a long induction period for the catalyst, particularly in the lower temperature ranges, has been found by different workers (9, 12, 22) and may have confounded the interpretation of previous kinetic studies (12).

Experimental

In our experiments, the problem of interaction of catalyst and gas phases was minimized by maintaining a constant SO_2/O_2 mole ratio and by keeping the conversion low and relatively constant through adjusting the amount of catalyst. Also, the temperature range was chosen to avoid a molten catalyst phase at low partial pressures of SO_2.

As an independent investigation of the rate controlling step, four reaction models of the Langmuir–Hinshelwood type (2, 3) were considered. Rate controlling steps were taken as (*i*) adsorption of O_2, (*ii*) adsorption of SO_2, (*iii*) desorption of SO_3, (*iv*) surface reaction between adsorbed SO_2 and adsorbed oxygen. In all models, oxygen was assumed to dissociate upon adsorption. Models were compared for their goodness of fit to the data, as described in *Modelling Studies* below.

Apparatus

A detailed description of the apparatus is available elsewhere (23). Oxygen and diluent gases were passed through separate silica gel dryers and rotameters and mixed with SO_2 in a manifold. All SO_2-carrying lines were heated to prevent condensation. The absolute pressure was measured behind the manifold. Adequate mixing of the feed gases was insured by using a manifold of twice the diameter of the feed lines and by allowing 350 tube-diameters in a preheater of 1/4 in. stainless steel tubing before the catalyst bed. The gas mixtures passed downward through the catalyst bed containing either 0.18 or 9.31 g of catalyst in a 1/4 in. diameter stainless steel tube. Thermocouples clad in stainless steel were located immediately before and after the bed. The entire preheater and reactor were immersed in a Cole-Parmer fluidized sand bath. Temperatures between ends of the catalyst sample varied by not more than 1 °C during runs. Thus, the reaction took place isothermally. Reacted gas passed from the reactor via a heated tube to a sampling train.

Materials

Nitrogen (prepurified grade), oxygen (commercial grade), anhydrous sulfur dioxide, and high purity argon and helium were obtained from Matheson Co. Oxygen and the diluents were dried over silica gel, but no gases were refined further. The promoted V_2O_5 ("Aero") catalyst was obtained from Cyanamid of Canada, who supplied its typical analysis: $V_2O_5 = 9.1\%$, $K_2O = 10.1\%$ (both by weight), bulk density = 0.7 g/cm^3, and specific surface = < 1 m^2/g. The catalyst support was diatomaceous silica, and catalyst was received in the form of 1/8 in. × 1/8 in. cylindrical pellets. These were crushed and sieved and the 20/30 mesh fraction, U.S. Sieve Size (averaging 0.7 mm diameter), was used for the rate measurements.

Analysis

Analysis was accomplished by collecting a gas sample and titrating. The procedure was developed after testing various methods reported in the literature (23). The sampling train consisted of two bulbs containing a measured quantity of isopropanol cooled in a Dry-Ice – acetone bath to −72 °C. Product gases passed through the sample train for a measured period, whereupon the bulbs were removed and analyzed. It was estimated that less than 2% of the effluent SO_3 escaped from the train with this system. A known quantity of deionized water was added to the contents of the collecting flasks while still cold and the solution was allowed to warm to room temperature. SO_2 was partially purged using a stream of N_2. Water served to keep the SO_3 in the system during purging, which was done to reduce the error in chemical analysis by lowering the SO_2/SO_3 ratio. Total acidity of a sample was determined by microburet titration. The SO_2 content in another sample of purged solution was determined by titrating with iodine solution. The difference between the titers of NaOH and I_2, corrected for a blank, was used to calculate the conversion to SO_3. The method was checked for accuracy and found to be $\pm 2\%$ of the known value. Precision of a measurement was also $\pm 2\%$.

Procedure

In most runs, mass velocities were about 230 g/cm^2 h, and conversions ranged from 0.1 to 2%. Thus, the reactor was differential with respect to conversion of SO_2 and oxygen, permitting rates to be calculated directly from conversions. Mole fractions of SO_2 averaged 0.168 and O_2 averaged 0.252, but varied between 0.16 to 0.17 and 0.245 to 0.27, respectively. The remainder was diluent gas. Total pressures in the system were varied from 0.6 to 6.2

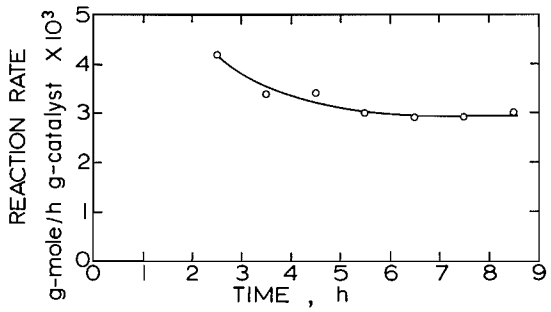

FIG. 1. Catalyst stabilization in a typical run. Conditions: temperature, 422 °C; total pressure, 1.03 atm; flow rate, 1.20 mole/h; weight of catalyst, 0.314 g. Mole fractions: $O_2 = 0.25$, $SO_2 = 0.17$, $N_2 = 0.58$.

atm to obtain the pressure dependence of the rate of reaction. Runs to find the temperature dependence were performed at about atmospheric pressure. During a run, operating conditions were maintained constant and, after two successive rate measurements which agreed to within the apparent standard deviation were obtained an hour apart, a stabilized condition of the catalyst was assumed. It usually required 6 h to obtain steady conditions (although at temperatures below 400 °C and with helium as a diluent, stabilization periods of up to 12 h were required). Similar behavior has been observed by Kubota (9) and Boreskov (22). Figure 1 shows a sequence of rate measurements made in a run at 442 °C, 1.03 atm pressure, with mole fractions of SO_2, oxygen, and nitrogen of 0.17, 0.25, and 0.58, respectively. The flow rate was 1.20 g-mole/h over 0.314 g catalyst.

The standard deviation of replicate measurements of the reaction rate was about 10%.

In addition to the stabilization problem already noted, an induction period of 30 to 40 h of on-stream time was required to stabilize fresh catalyst. Thereafter, there was no apparent change in the stable catalyst activity with further use.

Initially, considerable conversion was obtained from the metal surface in the empty reactor. After one week, however, the activity of this surface had fallen to a negligible level.

Results and Discussion

Transport Effects

The absence of an internal diffusion contribution for the pressure used to study the inert-gas effect was verified experimentally by measuring rates at 442 °C, 1 atm, with catalyst particles of 0.7 (20/30 mesh) and 0.3 mm (40/60 mesh) diameter. As shown in Table 1, there was no significant difference in the rates observed, despite a two-fold difference in size. This result could be anticipated from the low value of the specific surface (less than 1 m^2/g). However, for this condition, the Weisz–Hicks criterion (24)

TABLE 1

Reaction rate for varying mean particle diameter*

Mean particle diameter (mm)	Reaction rate (g-mole/h g catalyst × 10^2)
0.3	0.53
0.3	0.57
0.7	0.56
0.7	0.60
0.7	0.64

*442 °C, 1 atm, 1.20 g-mole/h total flow, mole fractions as in Fig. 3, 0.184 g catalyst.

$$\frac{\bar{r}\rho R_0^2 \exp(\gamma\beta/(1+\beta))}{C_s D_{eff}} \leqslant 1$$

($\bar{r}$ = measured reaction rate, ρ = bulk density of a single catalyst pellet, R_0 = pellet radius, C_s = concentration of gaseous reactant at pellet surface, ε = porosity within a pellet, ΔH = exothermicity of the reaction, K = thermal conductivity of pellet, T_s = temperature at pellet surface, $\gamma = \Delta H/RT_s$, R = gas constant) may be used to indicate the absence of concentration and temperature gradients within the catalyst. Substitution in the criterion gave 0.1. The only value which had to be assumed was the effective diffusivity, D_{eff}. This was calculated from the relation $D_{eff} = D_{Bulk\ SO_2}\,\varepsilon/\tau$ assuming a tortuosity, τ, of 2. This relation is believed to be a good approximation for a macro-pore system which the low specific surface suggests for our catalyst. The thermicity factor

$$\beta = D_{eff}\, C_s\, \Delta H/(\kappa T_s)$$

was found to be about 0.02. This low value indicates that the catalyst pellets are isothermal (24).

Estimates were also made of the concentration difference between the gas phase and the catalyst surface using actual rate data to see whether the mass transport to or from the catalyst was rate limiting. A mass transfer correlation of Sen Gupta and Thodos (25) was employed, using a conservative value of the exponent of the Reynolds number, as recommended by Boudart and Chambers (26). These calculations, employing measured rates of reaction, indicated no appreciable concentration or thermal gradients at the solid–fluid interface.

Inert-Gas Effect

An Arrhenius plot, Fig. 2, shows that the inert-gas effect is observed approximately 80 °

Can. J. Chem. Downloaded from www.nrcresearchpress.com by 210.87.254.40 on 09/05/12
For personal use only.

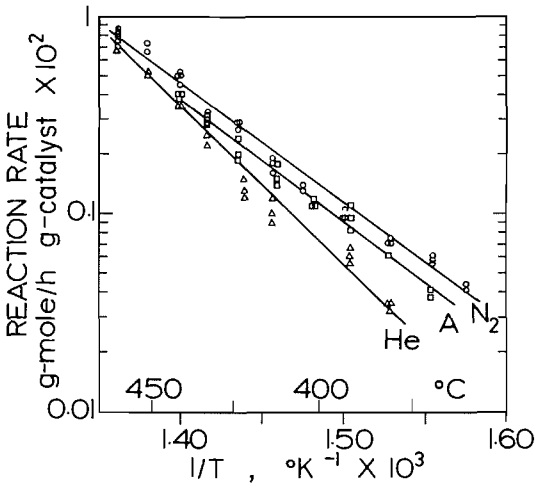

FIG. 2. Arrhenius plots for SO_2 oxidation using different diluents. Total pressure = 1.03 atm. Mole fractions: O_2 = 0.25, SO_2 = 0.17, diluent gas = 0.58. Diluent gas: ○, nitrogen; □, argon; △, helium.

below the range studied by Baron *et al.* (1). Rates appear to converge towards similar values at about 470 °C, but to diverge at about 90° higher. Figure 2 shows considerable scatter, but only in the high temperature region beyond about 430 °C is the scatter becoming clearly of the same order of magnitude as the difference in the effects. At lower temperatures, there is a difference of 100% between the rates with He and with A, while the scatter in some cases is 25 to 30%.

Experimental proof that the inert-gas effect is not due to diffusional control of reaction may be seen in that an increase in molecular weight of the gas phase increases the reaction rate. This result is opposite to what would be expected of a diffusion controlled process.

The possibility of a change in the activation energy between low and high temperature regions is suggested by both the helium and the nitrogen data of Fig. 2. The break appears to be located near 420 °C, which is close to the observation of Mars and Maessen (16). However, there are insufficient data to establish a definite slope change. Therefore, the least-squares values of the activation energy using the three diluent gases were obtained and are compared with those of Baron *et al.* in Table 2. Rather large differences are noted between the activation energies obtained in the two studies. However, different catalysts were used and the temperature ranges overlap only partially so that there may be different rate controlling steps for the two studies. With the exception of Baron's value for the CO_2 diluent, both sets of activation energies are within the ranges usually found for oxidation over V_2O_5 (16).

The crucial observation is the difference in activation energies using helium and argon, two non-adsorbing gases. It is clear that the inert-gas effect may be explained without recourse to arguments involving competition for sites, or lateral interactions arising from chemisorption of the diluent gas. Baron *et al.* appear to have been wholly justified in looking elsewhere for an explanation of the diluent gas effect.

Baron *et al.* (1) proposed the following model, postulating that the reaction was controlled by desorption of the product gas, where desorption occurs strictly as a result of momentum exchange from impinging gas molecules. Assuming spherical gas and adsorbate molecules, the rate, r, is given by

$$[1] \quad r = d^2 N p P \left(\frac{2\pi}{m_B R T}\right)^{1/2} \theta_A \times \exp\left[-\frac{(1+\alpha)^2}{4\alpha}\frac{E_d}{RT}\right]$$

for

$$\left(\frac{(1+\alpha)^2}{4\alpha}\frac{E_d}{RT}\right)^{1/2} > 3$$

where A refers to the molecule being desorbed from the surface through a collision with gas-phase molecule B, d is the sum of the molecular radii of A and B, $\alpha = m_A/m_B$, m = molecular mass, p = pressure, P = steric factor, R = gas constant, T = temperature in °K, θ_A = surface concentration of A, N = Avogadro's number, E_d = energy of desorption of A. Only when $\alpha = 1$ will the measured activation energy be

TABLE 2

Comparison of activation energies for inert-gas diluents

	Activation energy, kcal/mole	
Diluent	370–462 °C (This study)	450–550 °C (Reference 1)
Helium	35.7 ± 2.4	21.5
Nitrogen	28.6 ± 1.4	15.8
Argon	28.5 ± 2.0	—
Carbon dioxide	—	9.5

Can. J. Chem. Downloaded from www.nrcresearchpress.com by 210.87.254.40 on 09/05/12
For personal use only.

TABLE 3
Predicted and observed activation energies

Diluent gas X	M	M_{av}	α	E_{He}/E_X Predicted Eq. [1]	E_{He}/E_X Predicted Eq. [2]	E_{He}/E_X Observed, showing 95% confidence interval
He	4.00	20.0	4.00	1	1	
N_2	28.0	34.4	2.32	1.31	1.12	1.25 ± 0.14
A	39.9	41.0	1.95	1.40	1.14	1.25 ± 0.16

equal to the actual energy necessary to desorb a molecule from the catalyst surface.

Reasoning from Bodenstein's interpretation (27) of the mechanism, Baron *et al.* developed an alternative model which assumed that the catalytic oxidation of SO_2 was controlled by surface diffusion of the adsorbed SO_2 to reaction sites. Collision of impinging gas molecules with adsorbed SO_3 then freed the sites for further reaction. This view led to the following modification of eq. [1]

$$[2] \quad r = \frac{k''}{M_{av}^{1/6}} \theta_{SO_2}^{2/3} \times \exp\left(-\left[\frac{2}{3} + \frac{(1+\alpha)^2}{12\alpha}\right]\frac{E_d}{RT}\right)$$

where k'' = a temperature-dependent constant, M_{av} = average molecular weight of the gas phase, E_d = activation energy for desorption which is assumed equal to the activation energy of surface diffusion, and θ_{SO_2} = fraction of surface sites occupied by adsorbed SO_2.

Both eqs. [1] and [2] predict that the activation energy decreases if nitrogen or argon are substituted for helium. Our experiments verify this, as may be seen in Fig. 2 or Table 2. However, as shown in Table 3, the experimental ratios of E_{He}/E_{N_2} and E_{He}/E_A with 95% confidence intervals include the values predicted from both eqs. [1] and [2]. Thus, no discrimination between theories is possible from these results.

Table 2 also shows that the activation energies obtained using argon and nitrogen were almost identical, although eq. [1] predicts that the activation energy using the nitrogen diluent should have been about 7% greater. The scatter in the Arrhenius plots results in an E ratio ($E_{N_2}/E_A = 1.00 \pm 0.12$) whose confidence limits are larger than this difference.

Equation [1] suggests that increasing the molecular weight of the impinging spherical gas molecule should increase the reaction rate. This may be because d varies only slightly from one pair of molecules to another, P remains constant for spherical molecules, and the exponential term for values of the physical parameters expected in this reaction increases more rapidly with m_B than the term $m_B^{-1/2}$ decreases. This behavior was observed by Baron *et al.* (1). However, Fig. 2 shows that the reaction rate decreases when argon ($M = 39.9$) is substituted for nitrogen ($M = 28.0$). It may be, however, that this discrepancy occurs because nitrogen, being diatomic, transfers rotational and vibrational energy in addition to translational energy on colliding with an adsorbed species. Since the momentum-transfer model was derived for colliding spheres, it is likely that helium and argon are closer to the assumed model than is nitrogen. The rotational and vibrational energy contributions of the reactants, SO_2 and O_2, would also be expected to cause some departure from the simple model.

The interpretation of the activation energies reported above requires some comment. The values of E given in Table 2 are obtained from the slopes of Fig. 2. This procedure implies a power-law model of the form

$$[3] \quad r = k_0[\exp(-E/RT)]p_{SO_2}^{m}p_{O_2}^{n}p_{SO_3}^{q}$$

for the catalytic oxidation. Several variants of this general power-law model have been employed in the literature to correlate measurements over V_2O_5 catalysts (28, 29, 4). Some recent researchers (5, 1) however, have favored models of the Langmuir–Hinshelwood type such as that shown in Table 4.

Calculating E in the manner noted above can only be done if the following conditions are

Can. J. Chem. Downloaded from www.nrcresearchpress.com by 210.87.254.40 on 09/05/12
For personal use only.

Can. J. Chem. Downloaded from www.nrcresearchpress.com by 210.87.254.40 on 09/05/12
For personal use only.

TABLE 4

Results of fitting kinetic models to data of Fig. 3*

(*a*) Description of models

Model number	Controlling stage	Equation
I	Oxygen adsorption	$r = \dfrac{k_I p_{O_2}}{\left(1 + \dfrac{K_{O_2}^{1/2} p_{SO_3}}{K_p p_{SO_2}} + K_{SO_2} p_{SO_2} + K_{SO_3} p_{SO_3}\right)^2}$
II	SO_2 adsorption	$r = \dfrac{k_{II} p_{SO_2}}{1 + K_{O_2}^{1/2} p_{O_2}^{1/2} + \dfrac{K_{SO_2} p_{SO_3}}{K_p p_{O_2}^{1/2}} + K_{SO_3} p_{SO_3}}$
III	SO_3 desorption	$r = \dfrac{k_{III} p_{SO_2} p_{O_2}^{1/2}}{1 + K_{O_2}^{1/2} p_{O_2}^{1/2} + K_{SO_2} p_{SO_2} + K_p K_{SO_3} p_{SO_3} p_{O_2}^{1/2}}$
IV	Surface reaction	$r = \dfrac{k_{IV} p_{SO_2} p_{O_2}^{1/2}}{(1 + K_{SO_2} p_{SO_2} + K_{O_2}^{1/2} p_{O_2}^{1/2} + K_{SO_3} p_{SO_3})^2}$

(*b*) Values of parameters

Model	$k_i \times 10^2$	K_{O_2}	K_{SO_2}	K_{SO_3}	RSS $\times 10^5$
I	2.29	0.750	0.144	1.99×10^{-6}	2.05
II	4.86	0.512	1.31	0.266	5.43
III	7.84	0.500	6.34×10^{-5}	1.16×10^{-3}	1.637
IV	8.27	1.44×10^{-4}	0.981	5.94×10^{-3}	1.633

*Units of the rate constants are: k_I, k_{II}: g-mole atm^{-1} h^{-1} g-catalyst^{-1}; k_{III}, k_{IV}: g-mole atm$^{-3/2}$ h^{-1} g-catalyst^{-1}. K_p is the equilibrium constant in terms of partial pressures for the reaction

$$SO_2 + \tfrac{1}{2}O_2 \rightleftharpoons SO_3$$

At 442 °C, K_p was taken as 179 atm$^{-1/2}$.

closely approximated: (*i*) the partial pressures p_{O_2} and p_{SO_2} are constant, (*ii*) either P_{SO_3} is constant or the reaction rate is insensitive to p_{SO_3}, (*iii*) the temperature dependence of any of the adsorption coefficients in the denominator of models such as those in Table 4 does not confound the estimation of E under the reaction conditions used. Condition *i* is satisfied in that a constant ratio of O_2 and SO_2 was used at about 1 atm, and the conversions of SO_2 and O_2 were differential. Condition *ii* was satisfied in that there appeared to be no sensitivity of the reaction rate to p_{SO_3}, as the following results indicate. Four runs, plotted in Fig. 3, were carried out at 1 atm and with identical flows of reagents, using two different weights of catalyst. Conversions were, respectively, 0.41, 0.45, 0.78, and 0.80%, while the corresponding rates were 4.5, 5.0, 5.0, and 5.2 mg-mole/h g-catalyst. While conversion (and thus p_{SO_3}) almost doubled between the first and second pairs of runs, the rates did not differ significantly. Thus, the exponent q in eq. [3] may be assumed to equal zero. In addition, from

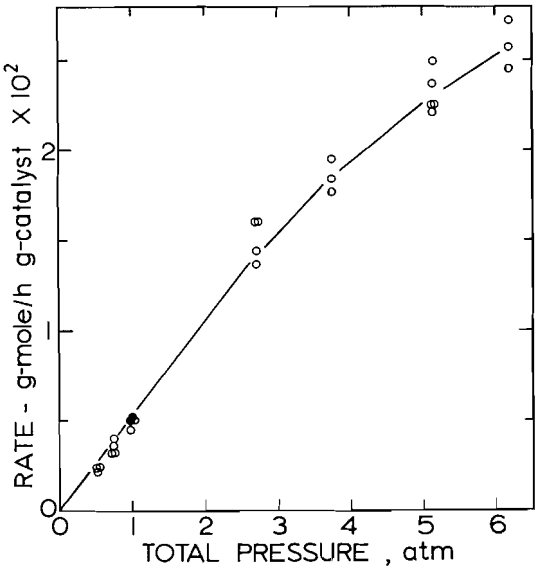

FIG. 3. Reaction rate vs. total pressure. Temperature = 442 °C; mole fraction: O_2 = 0.25, SO_2 = 0.17, N_2 = 0.58; flow rate, 0.70 to 2.40 mole/h; weight of catalyst, 0.184 g (two runs with 0.314 g are shown as ●).

Can. J. Chem. Downloaded from www.nrcresearchpress.com by 210.87.254.40 on 09/05/12
For personal use only.

Table 4 it can be seen that the adsorption equilibrium constant K_{SO_3} at 442 °C was negligibly small in all models considered in this study. Using this result, it is now possible to determine whether condition *iii* was satisfied.

Calderbank (4) measured adsorption equilibrium constants and heats of adsorption for SO_2 and O_2. If we assume that these values can be used with the models of Table 4, an estimate of the change in the denominator for the experimental conditions used in this study may be made. As the temperature increases from 370 to 442 °C, the denominator decreases by about 50% in the worst case (Model IV), while the rate increases twenty-fold. This calculation suggests that the slopes of Fig. 2 give a satisfactory approximation of the value of the activation energy.

Modelling Studies

With the object of examining the model postulated for the diluent gas effect by Baron *et al.* in eq. [1], data were taken on the effect of pressure on the oxidation rate, as shown in Fig. 3, to identify the rate controlling step by means of model fitting (2, 3). The four models usually proposed for SO_2 oxidation are shown in Table 4. These models were tested against the experimental data by means of a non-linear least-squares technique using a direct search of the sum-of-squares surface. To eliminate bias in selection, the best model was found by the use of likelihood ratios. This method, formalized by Barnard *et al.* (30, 31), makes use of the sums-of-squares of the residuals (that is, goodness-of-fit measurements) for each model, and results in the test

$$\frac{L_i}{L_j} = \left(\frac{\mathrm{RSS}_j}{\mathrm{RSS}_i}\right)^{N/2}$$

where L_i is the likelihood function of Model i, where the error is normally distributed by a variance σ_i^2 whose value is unknown. L_i is a function of σ_i^2; RSS_i, the residual sum of squares calculated from the data and the predicted response for Model i; and N, the number of observations. The likelihood ratio, L_i/L_j, or odds ratio, is a measure of the evidence for Model i as compared with Model j and may be considered the odds that Model i is the correct model rather than j. Results are given in Table 5.

It can be seen from Table 5 that Model II may be rejected on the basis of an extremely small probability, while Model I appears to be somewhat less probable than Models III and IV. The standard deviations of Models I, III, and IV are approximately the error in the measured rate; thus, these models provide a satisfactory fit of the rate data at 442 °C. The values of the adsorption constants (Table 4) obtained by fitting do not agree with those obtained by Calderbank (4) in static measurements ($K_{O_2} = 9.35\ \mathrm{atm}^{-1}$ and $K_{SO_2} = 7.1\ \mathrm{atm}^{-1}$).

TABLE 5

Likelihood ratios for Langmuir–Hinshelwood kinetic models*

	L_i/L_j, i =			
j	I	II	III	IV
I	1	3.3×10^{-4}	19	19
II	3×10^{5}	1	6×10^{6}	6×10^{6}
III	0.053	1.7×10^{-5}	1	1.0
IV	0.052	1.7×10^{-5}	1.0	1

*See Table 4.

Our modelling studies consequently were not adequate to verify the rate controlling step assumed by Baron *et al.* in their explanation of the inert-gas effect.

Conclusion

Our experiments verify the previous observation of an inert-gas effect associated with molecular weight on the rate and activation energy of the oxidation of SO_2 over a V_2O_5 catalyst. Measurements reported extend the range of conditions over which this curious effect is observed. They also eliminate chemisorption of the inert gas and mass and heat transfer as grounds for the observation. However, our attempts to verify the explanation for the effect proposed by Baron *et al.* were unsuccessful and this remains an open question.

The authors wish to acknowledge financial assistance provided for this study by the National Research Council of Canada. Catalyst was provided by Cyanamid of Canada, Ltd.

The likelihood-ratio analysis was kindly directed by Professor P. M. Reilly and carried out by Messrs. S. Hawkins and W. G. Rhodey.

1. T. Baron, W. R. Manning, and H. F. Johnstone. Chem. Eng. Progr. **48**, 125 (1952).
2. K. H. Yang and O. A. Hougen. Chem. Eng. Progr. **46**, 146 (1950).
3. O. A. Hougen and K. M. Watson. Chemical process principles, part 3, kinetics and catalysis. John Wiley and Sons, Inc., London. 1947.

4. P. L. CALDERBANK. J. Appl. Chem. London, **2**, 482 (1952).
5. M. GOLDMAN, L. N. CANJAR, and R. B. BECKMAN. J. Appl. Chem. London, **7**, 274 (1957).
6. G. K. BORESKOV. Zh. Fiz. Khim. **19**, 535 (1945).
7. B. DAVIDSON and G. THODOS. Amer. Inst. Chem. Eng. J. **10**, 568 (1964).
8. H. KUBOTA, M. ISHIZAVA, and M. SHINDO. Ryusan, **12**, 243 (1959).
9. H. KUBOTA. Private communication.
10. G. MATHUR and G. THODOS. Chem. Eng. Sci. **21**, 1191 (1966).
11. M. BOUDART. Chem. Eng. Sci. **22**, 1387 (1967).
12. A. A. YERAMIAN, R. R. HUDGINS, and P. L. SILVESTON. Chem. Eng. Sci. **23**, 952 (1968).
13. N. I. PEVENEY. Zh. Fiz. Khim. **14**, 981 (1940).
14. P. MARS and D. W. VAN KREVELEN. Chem. Eng. Sci. **3**, 41 (1954), Spec. Suppl.
15. G. K. BORESKOV, R. A. BUYANOV, and A. A. IVANOV. Kinet. i Katal. **8**, 153 (1967).
16. P. MARS and J. G. H. MAESSEN. Proc. Intern. Congr. Catal. 3rd, Amsterdam, 266 (1964).
17. R. KIYOURA. Kagaku Tokyo, **10**, 126 (1940); Chem. Abstr. **34**, 7169 (1940).
18. F. A. TOPSOE and A. NIELSEN. Trans. Dan. Acad. Technol. Sci. **1**, 3 (1948).
19. S. WEYCHERT and A. URBANEK. Intern. Congr. Catal. 4th, Moscow. 1968. Symp. III, paper No. 22.
20. A. A. IVANOV, G. K. BORESKOV, B. S. BESKOV. Intern. Congr. Catal. 4th, Moscow. 1968. Symp. III, paper No. 21.
21. B. KADLEC, A. REGNER, J. VOSOLSOBE, V. POUR. Intern. Congr. Catal. 4th, Moscow. 1968. Symp. III, paper No. 20.
22. G. K. BORESKOV. Private communication.
23. A. A. YERAMIAN. M.A.Sc. Thesis. University of Waterloo, Waterloo, Ontario. 1968.
24. P. B. WEISZ and J. S. HICKS. Chem. Eng. Sci. **17**, 265 (1962).
25. A. SEN GUPTA and G. THODOS. Amer. Inst. Chem. Eng. J. **9**, 751 (1963).
26. M. BOUDART and R. CHAMBERS. J. Catal. **6**, 141 (1966).
27. M. BODENSTEIN. Z. Phys. Chem. Frankfurt, **B2**, 345 (1929).
28. G. K. BORESKOV and T. I. SOKOLOVA. J. Chem. Ind. U.S.S.R. **14**, 1241 (1937).
29. E. L. KRISCHEVSKAYA. Zh. Fiz. Khim. **21**, 287 (1947).
30. G. A. BARNARD. J. Roy. Statist. Soc. **B11**, 116 (1949).
31. G. A. BARNARD, G. M. JENKINS, and C. B. WINSTEN. J. Roy. Statist. Soc. A**125**, part 3, 321 (1962).

Can. J. Chem. Downloaded from www.nrcresearchpress.com by 210.87.254.40 on 09/05/12
For personal use only.

Can. J. Chem. Downloaded from www.nrcresearchpress.com by 210.87.254.105 on 09/05/12
For personal use only.

Crystalline-field effects on the infrared and Raman spectra of powdered alkali-metal, silver, and thallous nitrates

M. H. Brooker and D. E. Irish
Department of Chemistry, University of Waterloo, Waterloo, Ontario

Received August 7, 1969

Infrared and Raman spectra have been recorded for room-temperature-phase, powdered samples of $LiNO_3$, $NaNO_3$, KNO_3, $RbNO_3$, $CsNO_3$, $AgNO_3$, and $TlNO_3$. For the trigonal systems, the nitrate pairs $LiNO_3$, $NaNO_3$ and $RbNO_3$, $CsNO_3$ give almost identical spectra. For the orthorhombic systems, $AgNO_3$ and $TlNO_3$ give similar spectra, whereas that of KNO_3 is significantly different. Site and correlation field perturbations are considerably more pronounced in the antisymmetric stretching region (ν_3 ca. 1400 cm^{-1}) than in the antisymmetric bending region (ν_4 ca. 700 cm^{-1}). Although lifting of the degeneracy of E' modes was frequently observed, the reported split of the $\nu_4(E')$ mode (ca. 716 cm^{-1}) of the aragonite form of KNO_3 could not be confirmed. Multiple internal reflectance techniques have been employed to observe the extremely intense $\nu_3(E')$ infrared fundamental ca. 1400 cm^{-1}.

Canadian Journal of Chemistry, 48, 1183 (1970)

Introduction

It has long been established that selection rules for solids do not conform to the free-ion approximation but are related to the crystallographic space group. Bhagavantam and Venkatarayudu (1) first developed methods to deduce selection rules in molecular crystals by considering the simplest unit cell as a super molecule on which a vibrational analysis could be performed. Halford's (2*a*) site symmetry analysis has proven useful, although it is not an exact treatment.[1] Later, Hornig (3) and Winston and Halford (4) developed a factor group analysis which extended the site symmetry treatment to include molecular coupling; results analogous to those developed by Bhagavantam and Venkatarayudu were obtained. The latter treatment often predicts theoretically distinguishable frequencies which are indistinguishable in practice, and the site symmetry approximation adequately accounts for observations.

For complete spectral analysis, one should examine a single crystal with polarized light along each of the crystallographic axes. However, considerable information can be obtained from the spectrum of a solid powder, since the observed spectrum is an average, the result of all orientations.

Schroeder *et al.* (5) have recorded infrared spectra of single-crystal ionic nitrates at low temperature but did not report splitting of degenerate modes. Three independent infrared studies of single crystals of aragonite KNO_3 (6–8) give contradictory evidence concerning crystal splittings of $\nu_4(E')$. Newman and Halford (9) have described and interpreted infrared spectra of oriented single crystals of NH_4NO_3 and $TlNO_3$. Shultin and Karpov (10) have made a similar study with $CsNO_3$. Infrared studies of powdered ionic nitrates in organic mulling agents or KBr pellets have also been reported (11, 12) but no multiplet structure was observed. These infrared methods are undesirable for ionic nitrates, since mulling agents obscure important spectral regions, while KBr disks are prone to ion exchange. All of the above authors have been unable to obtain valid spectra for the intensely infrared-active ν_3 fundamental ca. 1400 cm^{-1}.

Early Raman spectra of solid nitrates (13, 14) failed to show any multiplet structure, but several authors (8, 15–18) have since observed splitting of ν_3 in the aragonite form of KNO_3. Recently, James and Leong (8) have reported extensive multiplet structure in the infrared and Raman spectra of single crystals of Group I nitrates.

In this laboratory we have observed the infrared and Raman spectra of powdered alkali-metal, silver, and thallous nitrate salts. Multiple internal reflectance (m.i.r.) techniques were useful for obtaining infrared spectra in the intense ν_3 region ca. 1400 cm^{-1}. Raman spectra were recorded on a Cary 81 Raman spectrophotometer employing a conical sample cell similar to that described by Busey and Keller (19). This type of cell gives excellent spectra of solid powders with

[1]Also pertinent are the corrections of L. Couture (2*b*) and Halford's reply in ref. 4.

Can. J. Chem. Downloaded from www.nrcresearchpress.com by 210.87.254.105 on 09/05/12
For personal use only.

signal-to-noise ratio and background superior to the pellet or tube methods described by Ferraro (20). The resulting infrared and Raman spectra show multiplet structure for both ν_3 and ν_4 frequencies of Rb, Cs, Ag, and Tl nitrates. For KNO_3, splitting of ν_3 is observed, whereas for Li and Na nitrates no multiplet structure is detectable. For $LiNO_3$ and $NaNO_3$, the frequencies are best assigned on the basis of a factor group analysis, whereas for the other nitrates site group approximations are adequate.

Recently, spectra obtained from molten salts (21–25) and concentrated aqueous solutions (26, 27) have been interpreted in terms of local order or a perturbed lattice that exists for sufficient time to be observed spectroscopically. Vibrational analysis has been performed (24) on these quasi-lattice units. The present work on solid nitrates provides an indication of the magnitude of spectral changes expected in molten salts and concentrated solutions.

Experimental

The chemicals used were $LiNO_3$, Fisher certified reagent; $NaNO_3$, KNO_3, and $TlNO_3$, B.D.H. analar reagent grade; $RbNO_3$, Alfa Inorganics; $CsNO_3$, K and K Laboratories 99.9%; $AgNO_3$, Johnson Matthey and Mallory Ltd. The salts were recrystallized from aqueous solution after filtering the solution through fine sintered glass. Except for $AgNO_3$, the powdered samples were dried at 110 °C for at least 12 h and loaded into the sampling devices in a drybox. $AgNO_3$ was dried over P_2O_5. Only for $LiNO_3$ is the drying procedure critical.

Most Raman spectra were obtained from powdered samples in a thermostated (25 °C) conical cell sealed from the atmosphere, and recorded on a Cary 81 spectrophotometer. Both 4358 Å and 4046 Å mercury lines were used as excitation. No filter solution was used with the 4046 Å line but the 4358 Å line was isolated by removing ultraviolet radiation with either a Kodak Wratten 2A gelatin filter or 10 *M* aqueous KNO_2, while mercury lines in the visible region were removed with an ethyl-violet – *o*-nitrotoluene – isopropanol solution. Lines from the mercury lamp at 148 cm^{-1} and 172 cm^{-1} from 4358 Å occurred in most spectra. A slit width of 4 cm^{-1} or less was used for all Raman spectra. Spectra for Rb, Cs, and $AgNO_3$ in the 1400 cm^{-1} region were also recorded with a Spex Double Monochrometer, Model 1400, after excitation with a Spectra-Physics Model 140 argon-ion laser.

Infrared spectra were obtained from powdered solids pressed against the surface of a KRS-5 or AgBr prism cut with a face angle of 60°, placed in the Wilks Model 9 m.i.r. attachment. $AgNO_3$ could not be used with KRS-5 since a reaction occurs. There is no evidence of any exchange phenomena with any of the other nitrates. Infrared transmission spectra of the powders in the 700–1100 cm^{-1} region were also obtained after pressing (1000 p.s.i.) the powder into a thin disk or mechanically depositing the powder on a AgBr plate. No evidence of the Christiansen filter effect was observed (9). Single crystals of KNO_3 and $CsNO_3$ were grown from aqueous solutions of the salts. After polishing to about 0.5 mm thickness, the spectra were recorded with the *z* axis parallel to the slit entrance. Spectra were recorded on a Beckman IR-9 infrared (i.r.) spectrophotometer, using the double-beam mode with the reference beam attenuated. Transmission spectra for the thin films and single crystals were recorded at "standard" program slits (~1.5 cm^{-1} at 700 cm^{-1}) and a scan speed of 1.6 cm^{-1}/min. The m.i.r. spectra were recorded at "3 times the standard" program slits and a scan speed of 8 cm^{-1}/min. The infrared spectra were recorded at the temperature of the infrared beam, ca. 40 °C. The sample compartment of the spectrophotometer was purged with dry air and desiccated with P_2O_5. The extreme weakness of the water vapor bands, ca. 1600 cm^{-1}, attested to the dryness of the sample compartment.

Williamson *et al.* (24) make use of the very intense bands ca. 700 cm^{-1} of carbon tetrachloride and benzene as a criterion for confidence in attenuated total reflectance (a.t.r.) spectra. The extinction coefficient, $n\kappa$, for carbon tetrachloride has maxima at 762 and 786 cm^{-1}, with the latter intensity the greater. The $n\kappa$ curve for benzene has a symmetric maximum at 675 cm^{-1} (28). The refractive index of most nitrates studied is similar to that of benzene and carbon tetrachloride, i.e. 1.5, but the $n\kappa$ maxima for nitrates are less than for benzene and carbon tetrachloride (24). If no distortion occurs in the observed spectra of benzene and carbon tetrachloride, then no distortion should be expected in the spectra of ionic nitrates under the same conditions. In our spectra of carbon tetrachloride and benzene using a small surface area centrally located on the AgBr and KRS-5 m.i.r. plates, no noticeable distortion or frequency shifts occurred.

Although gratifying, these results seemed contradictory to both Devlin and co-workers (24) and Crawford and co-workers (28), who obtained distorted spectra for carbon tetrachloride and benzene using a single-pass a.t.r. KRS-5 70° prism. To investigate the discrepancy, we recorded spectra for these organic compounds with a single reflection at 62° angle of incidence to a KRS-5 a.t.r. prism on a Beckman a.t.r. unit. The recorded spectra now showed both frequency shifts and reversal of relative intensities for the carbon tetrachloride doublet. It appears that single-reflection a.t.r. spectra are subject to more distortion than multiple-reflection spectra. In single-reflection spectra, the dispersion of the incident light may result in some components striking the surface with less than the prescribed angle of incidence. In m.i.r., compensation for the dispersion occurs on reflection, decreasing the possibility of distortion.

Confidence in our m.i.r. data is enhanced by the excellent agreement between the m.i.r. and transmission frequencies and intensities. Slight line distortion is present in the $TlNO_3$ m.i.r. spectrum due to the higher refractive index of $TlNO_3$, 1.7.

All recorded frequencies are expected to be accurate to ± 1 cm^{-1}, with the exception of the broad bands in the ν_3 region, which may only be accurate to ± 5 cm^{-1}. The

Can. J. Chem. Downloaded from www.nrcresearchpress.com by 210.87.254.105 on 09/05/12
For personal use only.

Beckman IR-9 i.r. spectrophotometer was calibrated with polystyrene or atmospheric water vapor and carbon dioxide. The Cary 81 spectrophotometer was calibrated with carbon tetrachloride and benzene. Raman intensities relative to the ν_1 symmetric stretch were obtained from band areas with a standard polar planimeter. Infrared intensities relative to the ν_2 mode were obtained from peak heights. No attempts were made to measure the intensity of the ν_3 infrared region, due to the band-width as well as baseline complications created by the order-break discontinuity at 1200 cm^{-1}.

Results

Infrared and Raman frequency and intensity data for the powdered alkali-metal, silver, and thallous nitrates are contained in Tables 1–4. Included are the far-infrared results of Ferraro and Walker (29), James and Leong (8), and Nakagawa and Walter (30). Photographs of m.i.r. spectra are shown in Fig. 1. Photographs of portions of infrared transmission spectra for the powders pressed into a disk are presented in Fig. 2, while the photographs of the ν_4 region from spectra of KNO_3 and $CsNO_3$ single crystals are presented in Fig. 3. Photographs of portions of Raman traces are shown in Figs. 4 and 5.

The unperturbed nitrate ion, D_{3h} symmetry, would generate the following spectrum: $\nu_1(A_1')$, Raman active, ca. 1050 cm^{-1}; $\nu_2(A_2'')$ infrared active, ca. 825 cm^{-1}; $\nu_3(E')$ and $\nu_4(E')$, both Raman and infrared active, ca. 1380 cm^{-1} and 720 cm^{-1}, respectively. In all of our Raman spectra, the ν_1 frequency appears as a single, sharp band with frequency that is cation dependent. Although forbidden in the infrared spectrum, ν_1 can be seen as a single infrared band for KNO_3, $RbNO_3$, $CsNO_3$, $AgNO_3$, and $TlNO_3$, with frequency, within experimental error, equal to the Raman value. In all the Raman spectra and in the infrared spectra of KNO_3, $RbNO_3$, and $CsNO_3$, a weak band was observed at (ν_1 − 20) cm^{-1} which is due to the naturally abundant isotopic species $^{14}N^{16}O_2{}^{18}O^-$ (31).

In the infrared spectrum, ν_2 appears as a single, sharp band with frequency that is cation dependent. A small band at (ν_2 − 20) cm^{-1} was present in all spectra and assigned to the naturally abundant isotopic species $^{15}N^{16}O_3{}^-$ (31, 32). Both site and factor group analysis predict that ν_2 should become Raman active for K, Rb, Cs, Ag, and Tl nitrates; consequently this region was studied exhaustively. Only for solid $AgNO_3$ and $TlNO_3$ did the ν_2 mode become Raman active (Fig. 4).

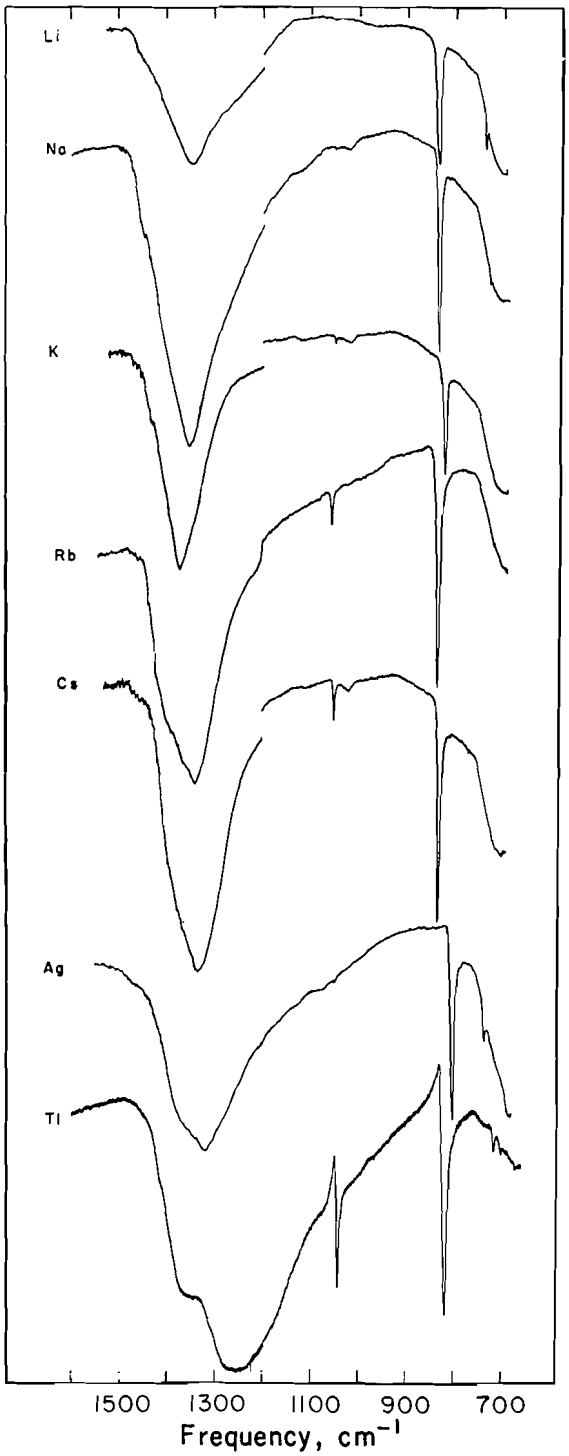

FIG. 1. Photographs of m.i.r. infrared spectra obtained for powdered polycrystalline $LiNO_3$, $NaNO_3$, KNO_3, $RbNO_3$, $CsNO_3$, $AgNO_3$, and $TlNO_3$.

Can. J. Chem. Downloaded from www.nrcresearchpress.com by 210.87.254.105 on 09/05/12
For personal use only.

TABLE 1

Vibrational analysis of crystalline $LiNO_3$, $NaNO_3$; calcite type, space group D_{3d}^6, 2 molecules per unit cell*

Internal modes of NO_3^-			ν observed (cm^{-1})			
Free-ion approximation, point group D_{3h} ν in cm^{-1}	Site group D_3	Factor group D_{3d}	$LiNO_3$		$NaNO_3$	
			Raman	Infrared	Raman	Infrared
ν_3(1380) E' (R,I)	E (R,I)	E_g (R)	1384 (0.25)	—	1386 (0.25)	—
		E_u (I)	—	1345 (vs)	—	1350 (vs)
ν_1(1050) A_1' (R)	A_1 (R)	A_{1g} (R)	1071 (1.0)	—	1068 (1.0)	—
		A_{1u} (ia)	—	—	—	—
ν_2(825) A_2'' (I)	A_2 (I)	A_{2g} (ia)	—	—	—	—
		A_{2u} (I)	—	838 (1.0)	—	836 (1.0)
ν_4(720) E' (R,I)	E (R,I)	E_g (R)	735 (0.085)	—	726 (0.083)	—
		E_u (I)	—	738 (0.25)	—	726 (0.02)
Lattice modes			ν observed (cm^{-1})			
Point group D_{3h}	Site group D_3	Factor group D_{3d}	$LiNO_3$		$NaNO_3$	
			Raman	Infrared	Raman	Infrared
Inferred from nitrate site†						
		Rotatory				
A_2' (ia)	A_2 (I)	A_{2g} (ia)	—	—	—	—
		A_{2u} (I)	—	96 (w)‡	—	89 (m, sp)‡
E'' (R)	E (R,I)	E_g (R)	238 (0.78)	—	186 (1.0)	—
		E_u (I)	—	166 (m, sp)‡	—	145‡
		Translatory				
A_2'' (I)	A_2 (I)	A_{2g} (ia)	—	—	—	—
		A_{2u} (I)	—	321 (s)‡	—	217 (s)‡
E' (R,I)	E (R,I)	E_g (R)	128 (0.05)	—	100 (0.28)	—
		E_u (I)	—	152 (w, sh)‡	—	173 (s, sp)‡

Can. J. Chem. Downloaded from www.nrcresearchpress.com by 210.87.254.105 on 09/05/12
For personal use only.

TABLE 1 (*Concluded*)

Lattice modes			
Site group S_6	Factor group D_{3d}	ν observed (cm^{-1})	
		$LiNO_3$, i.r.	$NaNO_3$, i.r.
Inferred from cation site†			
	Translatory		
A_u (I)	A_{1u} (ia)	—	—
	A_{2u} (I)	Acoustic	Acoustic
E_u (I)	E_u (I)	277 (sh)‡	217 (s)‡
	E_u (I)	Acoustic	Acoustic

*R = Raman active, I = i.r. active, ia = inactive, v = very, s = strong, m = medium, w = weak, sh = shoulder, sp = sharp, br = broad. Raman intensities relative to ν_1 and infrared absorbances relative to ν_2 are given in parentheses after the frequency.

†Assignments are inferred from consideration of the particular ion and its symmetry group. Strictly, all atoms may be involved in the motion. Where the species symbols for nitrate and cation translatory modes are the same (e.g. E_u), both ions are involved in the motion.

‡Obtained from refs. 8, 29, and 30.

Can. J. Chem. Downloaded from www.nrcresearchpress.com by 210.87.254.105 on 09/05/12
For personal use only.

Splitting of $\nu_3(E')$ is observable for K, Rb, Cs, Ag, and Tl nitrates in both infrared and Raman spectra, whereas Li and Na nitrates have only one band in this region (Figs. 1, 5). Infrared and Raman spectra (Figs. 2–4) show that ν_4 is clearly one band for Li, Na, and K nitrates, but two for Rb, Cs, Ag, and Tl nitrates. The intensity of ν_4 for Ag and Tl nitrates shows a marked increase in both infrared and Raman spectra compared to the alkali-metal nitrates. A close similarity exists in the features of the infrared and Raman spectra for the pairs of salts $LiNO_3$, $NaNO_3$ and $RbNO_3$, $CsNO_3$.

Discussion

$LiNO_3$, $NaNO_3$

Both crystals have the calcite structure (33–35), space group D_{3d}^6-$R\bar{3}c$, with two molecules per unit cell. The center-of-mass of the nitrate ion is on a D_3 site, while the cation is on a C_{3i} site. Factor group analysis (1, 5, 36) indicates that there should be 6 active normal internal modes, viz. 3 Raman and 3 non-coincident infrared lines, as well as 7 active external modes, viz. 2 Raman and 5 non-coincident infrared lines. The observed frequencies conform to the factor group analysis (Table 1). Without the benefit of conclusions

TABLE 2

Vibrational analysis of crystalline KNO_3; aragonite type, space group D_{2h}^{16}, 4 molecules per unit cell*

Internal modes of NO_3^-				
Free-ion approximation, point group D_{3h} ν in cm^{-1}	Site group $C_s(yz)$	Factor group D_{2h}	ν observed (cm^{-1}) Raman	Infrared
ν_3(1380) E' (R,I)	A' (R,I)	A_g (R), B_{3g} (R)	1361 (0.11)	—
		B_{1u} (I), B_{2u} (I)	—	1375 (s)
	A'' (R,I)	A_u (ia), B_{3u} (I)	—	—
			—	1340 (sh)
		B_{1g} (R), B_{2g} (R)	1345 (0.09)	—
ν_1(1050) A_1' (R)	A' (R,I)	A_g (R), B_{3g} (R)	1051 (1.0)	—
		B_{1u} (I), B_{2u} (I)	—	1051 (0.07)
ν_2(825) A_2'' (I)	A' (R,I)	A_g (R), B_{3g} (R)	—	—
			—	—
		B_{2u} (I), B_{1u} (I)		828 (1.0)
ν_4(720) E' (R,I)	A' (R,I)	A_g (R), B_{3g} (R)	717 (0.085)	—
		B_{2u} (I), B_{1u} (I)	—	717 (0.001)
	A'' (R,I)	A_u (ia), B_{3u} (I)		
		B_{1g} (R), B_{2g} (R)	717	—

TABLE 2 (*Concluded*)

Lattice modes			ν observed (cm^{-1})	
Point group D_{3h}	Site group $C_s(yz)$	Factor group D_{2h}	Raman	Infrared
Inferred from nitrate site†				
	Rotatory			
A_2' (ia)	A'' (R,I)	B_{1g} (R) B_{2g} (R)	126 (0.04)	
		A_u (ia) B_{3u} (I)		130 (sh)‡
E'' (R)	A' (R,I)	B_{1u} (I) B_{2u} (I)		—
		A_g (R) B_{3g} (R)	85 (1.1)	
	A'' (R,I)	B_{1g} (R) B_{2g} (R)		
		A_u (ia) B_{3u} (I)		—
	Translatory			
A_2'' (I)	A' (R,I)	A_g (R) B_{3g} (R)	—	
		B_{1u} (I) B_{2u} (I)		152 (s)‡
E' (R,I)	A' (R,I)	B_{1u} (I) B_{2u} (I)		—
		A_g (R) B_{3g} (R)	52 (0.30)	
	A'' (R,I)	B_{1g} (R) B_{2g} (R)		
		A_u (ia) B_{3u} (I)		—
Inferred from cation site†				
	Translatory			
	$2A'$ (R,I)	$2(A_g$ (R) B_{3g} (R))		
		$2(B_{1u}$ (I) B_{2u} (I))		
	A'' (R,I)	B_{1g} (R) B_{2g} (R)		
		A_u (ia) B_{3u} (I)		

*R = Raman active, I = i.r. active, ia = inactive, s = strong, sh = shoulder. Raman intensities relative to ν_1 and infrared intensities relative to ν_2 are given in parentheses after the frequency.

†Assignments are inferred from consideration of the particular ion and its symmetry group. Strictly all atoms may be involved in the motion. Where the species symbols for nitrate and cation translatory modes are the same (e.g. A_g) both ions are involved in the motion. One each of B_{1u}, B_{2u}, and B_{3u} are assigned to acoustic modes.

‡Obtained from refs. 8 and 29.

TABLE 3

Observed infrared and Raman frequencies for $RbNO_3$ and $CsNO_3$*

ν $RbNO_3$ (cm^{-1})		ν $CsNO_3$ (cm^{-1})	
Raman	Infrared	Raman	Infrared
62 (0.25)		55 (0.02)	60 (sh)†
108 (1.0)		114 (1.9)	~110 (sp)†
130 (0.30)			~300 (br)†
707 (0.04)	705 (0.002)	705 (0.025)	707 (0.001)
722 (0.05)	722 (0.01)	717 (0.060)	717 (0.006)
	836 (1.0)		833 (1.0)
1057 (1.0)	1057 (1.0)	1051 (1.0)	1051 (0.18)
1352 (0.15)	1340 (s)	1347 (0.09)	1330 (s)
1405 (0.15)	1395 (sh)	1395 (0.21)	1390 (sh)
1442 (0.03)		1420 (0.03)	

*sh = shoulder, sp = sharp, br = broad, s = strong. Raman intensities relative to ν_1 and infrared intensities relative to ν_2 are given in parentheses.

†Estimated from ref. 52.

Can. J. Chem. Downloaded from www.nrcresearchpress.com by 210.87.254.105 on 09/05/12
For personal use only.

TABLE 4

$AgNO_3$, $TlNO_3$

Observed infrared and Raman frequencies for $AgNO_3$ and $TlNO_3$*

ν $AgNO_3$ (cm^{-1})		ν $TlNO_3$ (cm^{-1})	
Raman	Infrared	Raman	Infrared
		39 (0.03)	
44 (0.2)		49 (0.02)	
	80 (w)†		
96 (0.3)		95 (0.01)	
	103 (w)†		
	125 (sh)†		
138 (0.85)		109 (0.75)	
	170 (s)†		
195 (0.15)		144 (0.15)	
713 (0.013)	713 (0.01)	699 (0.006)	699 (0.06)
733 (0.019)	733 (0.15)	713 (0.048)	713 (0.09)
809 (0.003)	802 (1.0)	819 (0.002)	819 (1.0)
1046 (1.0)	1046 (0.01)	1042 (1.0)	1042 (0.5)
			1255 (vs)
		1292 (0.025)	
1326 (0.03)	1316 (s)		
1350 (0.12)	1360 (sh)		1350 (sh)
		1382 (0.12)	
		1395 (0.10)	
		1405 (0.02)	

*w = weak, sh = shoulder, s = strong, v = very. Intensities relative to ν_1 (Raman) and ν_2 (i.r.) are given in parentheses.
†Obtained from refs. 8, and 29.

from vibrational analysis, the rotatory modes would be expected to lie at higher frequencies and be more intense than the translatory modes. The calculations of Nakagawa and Walter (30), however, suggest otherwise and their assignments are used. For $LiNO_3$, Ferraro and Walker (29) and James and Leong (8) report a line at 152 cm^{-1}. This frequency is assigned to an E_u mode, as it is more compatible with the 128 cm^{-1} E_g mode than the 321 cm^{-1} proposed by Nakagawa and Walters. Two distinct frequencies for the infrared external A_{2u} and E_u modes of $NaNO_3$ have not been observed. Ferraro (private communication) reports that the 217 cm^{-1} infrared line splits with application of pressure into a line which remains at 217 cm^{-1} and a line which moves toward ~260 cm^{-1}. Thus, the A_{2u} and E_u rotatory modes may be accidentally degenerate. Rousseau *et al.* (37), by careful isotopic studies, have assigned the Raman bands at 186 and 100 cm^{-1} of $NaNO_3$ to the rotatory and translatory E_g modes, respectively, of the nitrate ion. Miller *et al.* (38) have also confirmed assignment of the Raman bands at 237 and 124 cm^{-1} of $LiNO_3$ to E_g modes, from depolarization studies.

An almost total lack of coincidence between the infrared and Raman spectra is consistent with the presence of a center of symmetry. The symmetric stretch ν_1 remains only Raman active, while ν_2 remains only infrared active. The difference between the two components of ν_3 is about 30 cm^{-1}, whereas the components of ν_4 are almost coincident. This fact indicates that ν_3 is more sensitive to intermolecular coupling. Raman frequencies of Li and Na nitrates are in excellent agreement with the literature (14, 17, 22, 38). Multiple internal reflectance frequencies are considered to be accurate and reproducible to ± 5 cm^{-1}, which is an improvement on previously published data. Ketelaar *et al.* (39) have also reported ν_3 at 1353 cm^{-1} in the infrared reflectance spectrum of $NaNO_3$.

KNO_3

At room temperature, KNO_3 has the aragonite crystal structure (35, 40, 41), space group D_{2h}^{16}-*Pnma*, with 4 molecules per unit cell. Both the NO_3^- ions and the K^+ ions are on C_s sites. Factor group analysis (5–7) requires 30 Raman-active vibrations (12 internal NO_3^- modes and 18 lattice modes) and 21 non-coincident infrared-active vibrations (10 internal NO_3^- modes and 11 lattice vibrations). From Table 2, it is clear

Can. J. Chem. Downloaded from www.nrcresearchpress.com by 210.87.254.105 on 09/05/12
For personal use only.

Can. J. Chem. Downloaded from www.nrcresearchpress.com by 210.87.254.105 on 09/05/12
For personal use only.

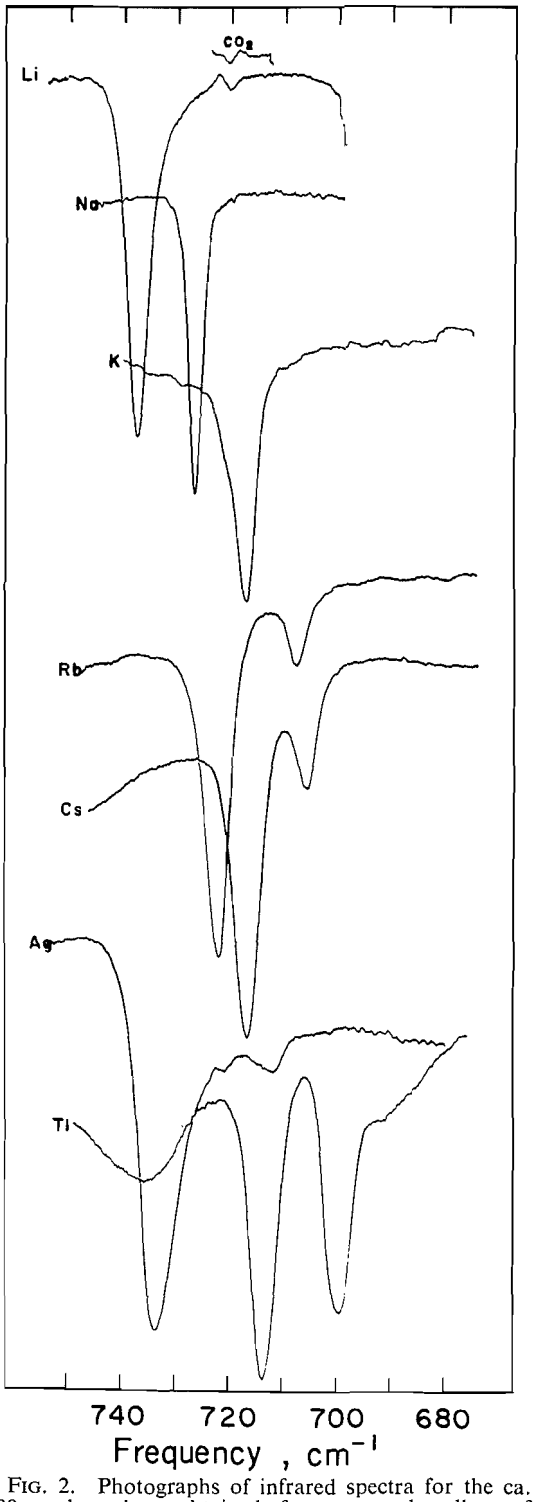

FIG. 2. Photographs of infrared spectra for the ca. 700 cm^{-1} region, obtained from pressed pellets of $LiNO_3$, $NaNO_3$, KNO_3, $RbNO_3$, $CsNO_3$, $AgNO_3$, and $TlNO_3$. The atmospheric CO_2 band at 721 cm^{-1} was recorded under identical spectral conditions.

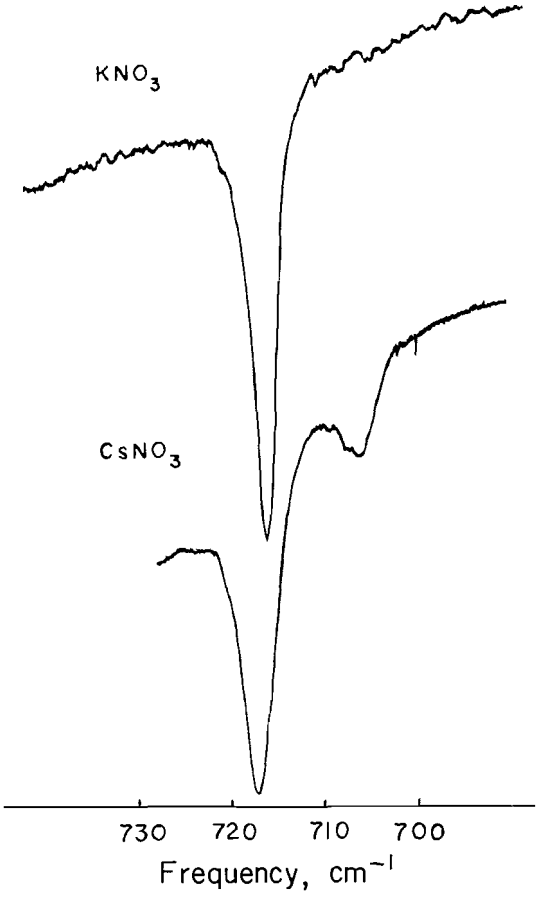

FIG. 3. Photographs of infrared spectra for the ca. 700 cm^{-1} region, obtained from single crystals of KNO_3 and $CsNO_3$.

that data are not sufficient to warrant a factor group analysis. Recent polarization studies on a single crystal of KNO_3 (7) show that for ν_1 and ν_4, the correlation field splittings are of the order of 1 cm^{-1} and are not detectable in this work.

Site symmetry approximations predict 6 active internal NO_3^- vibrations coincident in the infrared and Raman spectrum, as well as 9 coincident infrared- and Raman-active lattice modes. Although the agreement is better than with factor group analysis, the site group analysis is still not suitable. The ν_2 mode is not observed in the Raman as predicted and splitting of the degenerate ν_4 mode is not observed. However, Raman polarization studies (15, 16, 18) of single crystals of KNO_3 indicate that ν_4 is split into two accidentally coincident components.

Khanna *et al.* (6) reported splitting of ν_4 into 3 components at 715, 719, and 729 cm^{-1} for the

Can. J. Chem. Downloaded from www.nrcresearchpress.com by 210.87.254.105 on 09/05/12
For personal use only.

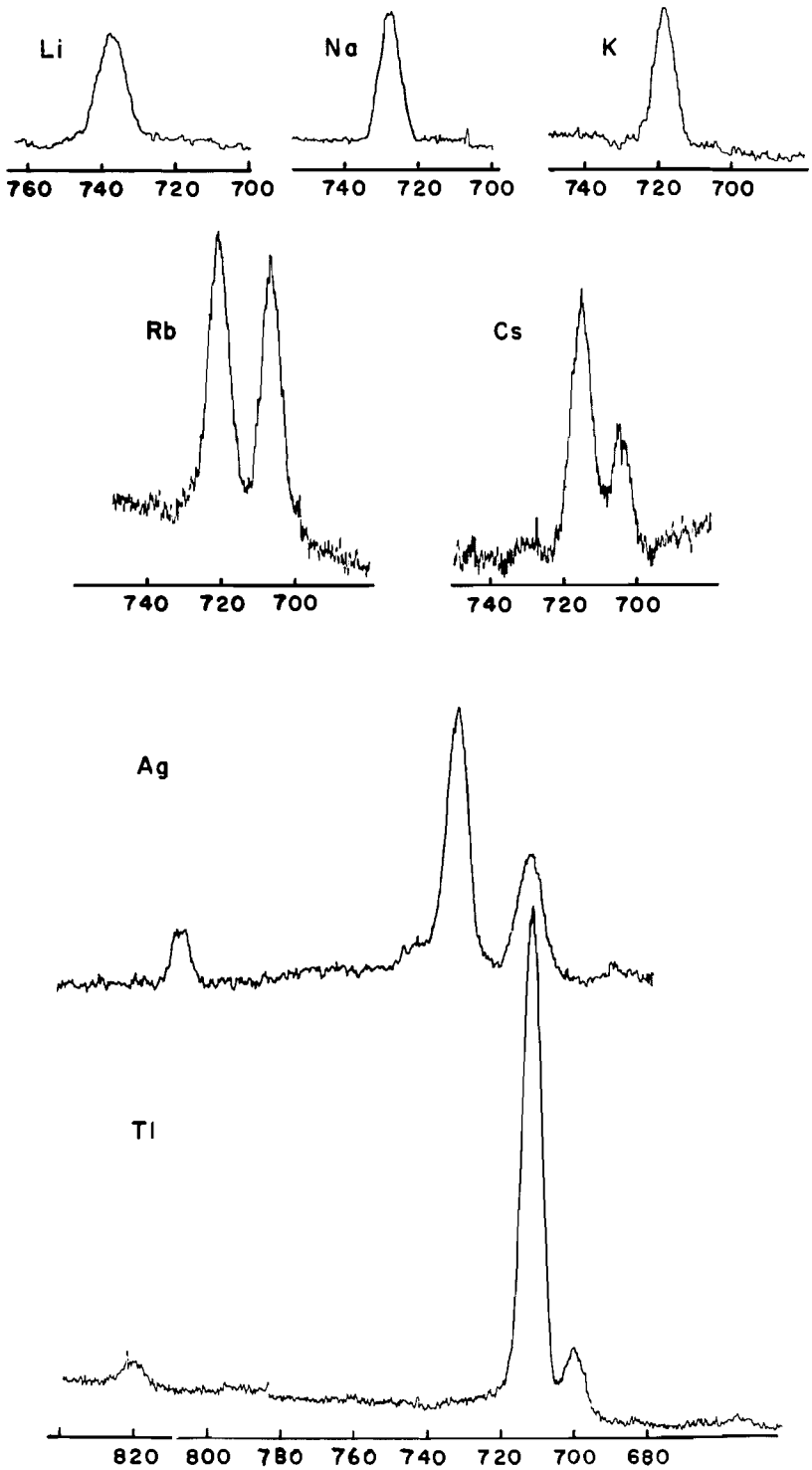

FIG. 4. Photographs of portions of Raman spectra (700 cm^{-1} region) obtained from powdered polycrystalline $LiNO_3$, $NaNO_3$, KNO_3, $RbNO_3$, $CsNO_3$, $AgNO_3$, and $TlNO_3$.

Can. J. Chem. Downloaded from www.nrcresearchpress.com by 210.87.254.105 on 09/05/12
For personal use only.

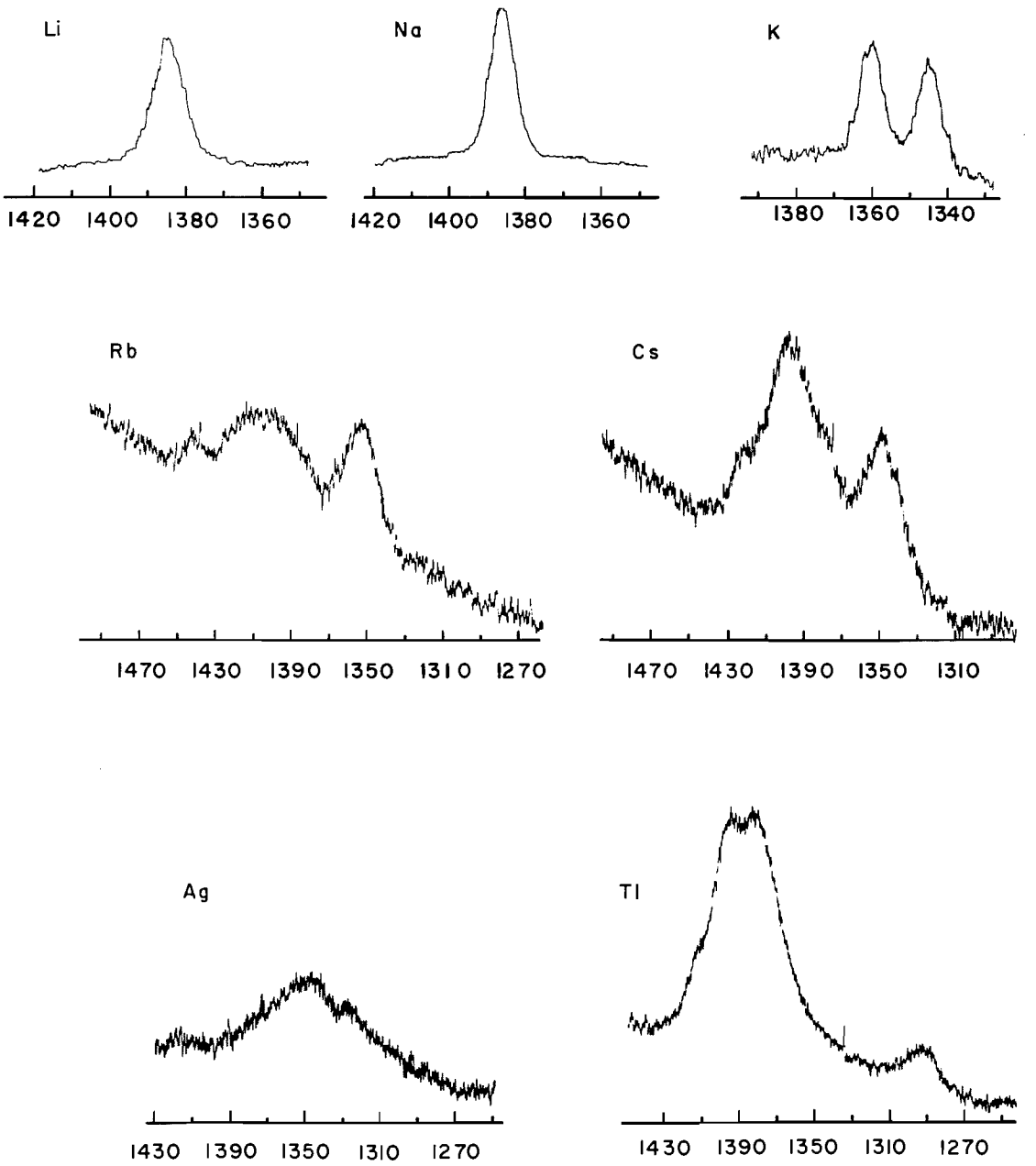

FIG. 5. Photographs of portions of Raman spectra (1300 cm^{-1} region) obtained from powdered polycrystalline $LiNO_3$, $NaNO_3$, KNO_3, $RbNO_3$, $CsNO_3$, $AgNO_3$, and $TlNO_3$.

room-temperature phase of a single crystal of KNO_3. The bands were assigned to B_{1u}, B_{2u}, and B_{3u} species predicted by factor group analysis. James and Leong (8) reported components at 700 and 713 cm^{-1}. We were unable to verify these observations. The spectral region obtained from a single crystal of KNO_3 is shown in Fig. 3. The crystal orientation and spectrophotometer conditions are as reported by Khanna *et al.* (6), except that dry nitrogen was used to purge the infrared machine. Clearly, only one symmetric band centered at 716 cm^{-1} is apparent. If the

Can. J. Chem. Downloaded from www.nrcresearchpress.com by 210.87.254.105 on 09/05/12
For personal use only.

nitrogen purge was not used then, under the high-resolution conditions necessary to obtain the spectrum of KNO_3, an intense, well-resolved spectrum of the P, Q, and R branches of ν_2 for carbon dioxide was observed (ca. 700 cm^{-1}) even on double beam operation, due to a slight difference in path length. An unusually strong line of carbon dioxide is observable at 720 cm^{-1} (42). We propose that the band observed by Khanna *et al.* (6) at 719 cm^{-1} was, in fact, the carbon dioxide band. We can offer no explanation for their report of the weakest component at 729 cm^{-1} or the convergence of the three components on heating. The band observed by James and Leong at 700 cm^{-1} may be due to the naturally abundant $N^{16}O_2{}^{18}O^-$ ion. Our observation of only one infrared component at 716 cm^{-1} for the $\nu_4(E')$ mode of KNO_3 is consistent with the single-crystal, polarized infrared study of Karpov and Shulton (7). They observed two components at 715.2 and 714.5 cm^{-1}. It is also consistent with the single band observed in the Raman spectrum at 716 cm^{-1}.

$RbNO_3$, $CsNO_3$

Early structural investigations of the room-temperature phases of $RbNO_3$ (33, 43) and $CsNO_3$ (44, 45) could not determine the nitrate positions, although they appeared to indicate isomorphous crystals, space group C_{3v}^2-$P31m$, with 9 molecules per unit cell. However, recent work indicates much lower symmetry. Shultin and Karpov (10) conclude from optical activity of single crystals that $CsNO_3$ must crystallize in the space group C_3^1-$P3$. Two sites, C_1 and C_3, are possible for the nitrate ion, but the same authors have used polarized infrared studies to show the site is C_1. A general site is consistent with the splitting of ν_3 and ν_4 and the appearance of ν_1 in the infrared spectrum of $CsNO_3$ (Table 3). Brown and McLaren (46) show from systematic absences in X-ray patterns that $RbNO_3$ crystallizes in either D_3^3-$P3_112$ or D_3^5-$P3_212$, with 9 molecules per unit cell. Possible sites for either space group are C_2 or C_1. Either site will provide explanation of the observed splittings of ν_3 and ν_4, as well as the appearance of ν_1 in the infrared (Table 3). We tend to favor the general site, on the basis of almost identical infrared and Raman spectra for $RbNO_3$ and $CsNO_3$ (Figs. 1, 2, 4, 5). The magnitude of the split in ν_4 for $RbNO_3$ and $CsNO_3$ is similar to that observed for NH_4NO_3(V) (9), which has since been shown to have nitrate ions on general sites (47).

A factor group analysis is not practical for these crystals, due to the large number of molecules per unit cell and the extremely low site symmetry. If one of the three Raman bands in the ν_3 region is assigned to an overtone, a site group analysis is acceptable.

The coincidence of the infrared and Raman frequencies is consistent with the lack of a center of symmetry in the crystals. Once again, ν_2 fails to become Raman active even though other perturbations in the spectra are rather large.

James and Leong (8) have proposed a two-site description for these crystals. The two sites suggested are C_s and C_{3v} (on the basis of C_{3v}^2 space group); the former twice as plentiful as the latter. As well as being in disagreement with the more recent structure determinations (10, 46) described above, two bands necessary for the two-site description, ca. 810 and 1033 cm^{-1}, can more plausibly be assigned to isotopic species (31).

$AgNO_3$, $TlNO_3$

Niggli (48) reported D_2^{2-4}-$P222_1$, -$P2_12_12$, -$P2_12_12_1$ as possible space groups for $AgNO_3$, whereas Lindley and Woodward (49) give the space group as D_{2h}^{15}-$Pcba$, the difference being the presence of a center of symmetry reported by the latter authors. If the space group is D_{2h}^{15}, the nitrate ions are on general sites; for D_2^{2-4}, the possible sites are general or groups of non-equivalent C_2 sites. The results of either would be consistent with our observations (Figs. 1, 2, 4, 5 and Table 4). A factor group analysis would require lack of coincidence between the infrared and Raman spectra for a D_{2h}^{15} space group, but not for D_2^{2-4}. From Table 4 it can be seen that considerable coincidence exists. This coincidence does not rule out the possibility of a center of symmetry in $AgNO_3$, since similar coincidence was observed for KNO_3, which has a center of symmetry.

The occurrence of ν_2 in the Raman spectrum (Fig. 4) is noteworthy. In view of the magnitude of other crystallographic perturbations, the ν_1 infrared frequency is surprisingly feeble (Fig. 1).

A structural study of thallous nitrate phase III has been performed by Kennedy and Patterson (50). Again, some uncertainty exists concerning the correct space group. Two equally acceptable

Can. J. Chem. Downloaded from www.nrcresearchpress.com by 210.87.254.105 on 09/05/12
For personal use only.

structures are possible, each with 8 molecules per unit cell: D_{2h}^{16}-*Pnma*, with nitrate ions on two sets of perpendicular C_s planes; C_{2v}^{9}-*Pbn*2_1, with nitrate ions on general sites. Again, the data (Table 4) are consistent with either possible site, and the presence of a center of symmetry cannot be ascertained. Like $AgNO_3$, the ν_2 mode ca. 820 cm^{-1} appears in the Raman spectrum (Fig. 4). There are, however, major differences in the ν_3 region for the two crystals (Fig. 5). The band at 1292 cm^{-1} may indicate substantial covalency or strong polarization in the $TlNO_3$ crystals. For $AgNO_3$ and $TlNO_3$, marked increases in the relative intensities of the ν_4 region are apparent in both the infrared and Raman spectra.

Crystals vs. Melts and Solutions

Although the long-range order characteristic of the ionic lattice does not exist in the molten salt or the concentrated electrolyte solution, there is considerable evidence for the persistence of short-range order. Low-frequency bands, ca. 200–400 cm^{-1}, in the infrared spectra of molten alkali metal nitrates have been assigned to lattice-like modes (51). Wegdam *et al.* (52) observed very little change in the far-infrared lattice modes of $NaNO_3$ and $CsNO_3$ on fusion of these salts. The authors conclude that "the liquid nitrates possess a phonon spectrum that is rather similar to the phonon spectrum of solid nitrates." Thus, at temperatures just above the melting point, order prevails.

Although density of molten alkali metal nitrates decreases by about 30% on fusion, it has been shown that the metal–oxygen distances are not likely to increase, but may even decrease. X-Ray data (34, 35) for the $NaNO_3$ crystal give a Na—O distance of 2.4 Å, whereas X-ray distribution curves for molten $NaNO_3$ (53) suggest distances of 2.3 Å. For fluids, some sort of ion cluster separated by holes is indicated. The frequency of the symmetric stretching mode, $\nu_1(A_1')$, always decreases on fusion. However, the decrease is irregular: $LiNO_3$, 4 cm^{-1}; $NaNO_3$, 15 cm^{-1}; KNO_3, 4 cm^{-1}; $RbNO_3$, 11 cm^{-1}; $CsNO_3$, 9 cm^{-1}; $AgNO_3$, 11 cm^{-1}; $TlNO_3$, 6 cm^{-1} (our crystal frequencies, compared with melt frequencies in refs. 22 and 25). The melt frequencies correlate with polarizing power of the cations (22, 25, 54). Insensitivity of ν_1 to temperature changes (22) is contrary to expectation if the change of frequency is related to change in free

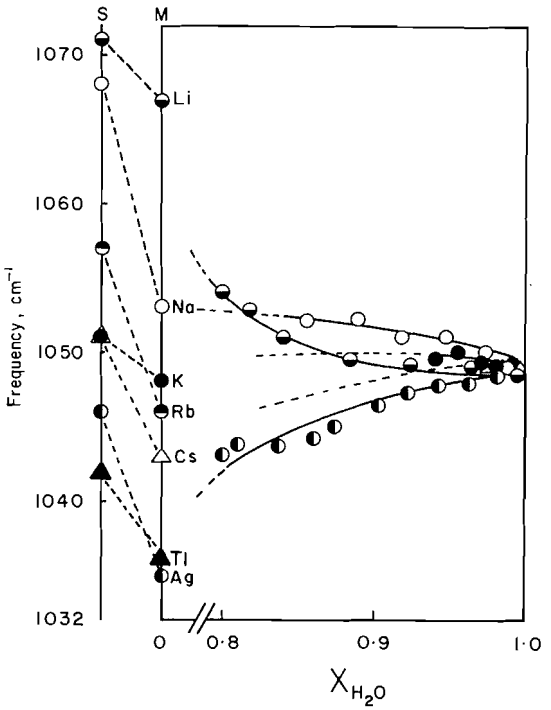

FIG. 6. The $\nu_1(A_1')$ nitrate frequency for the solids (s), molten salts (M), and aqueous solutions (plotted vs. X_{H_2O}, the mole fraction water) of Li, ◒; Na, ○; K, ●; Rb, ◓; Cs, △; Ag, ◐; and $TlNO_3$, ▲.

volume (17, 54). The decrease on melting is consistent with a lower force constant, possibly resulting from the shorter cation–anion distances in the melts. Knowledge of these distances is not available and thus further speculation is premature. On addition of water, the frequency continues to drop for the Li and Na salts, but increases for all the others and approaches the value 1049 cm^{-1} in the limit of dilute solution (Fig. 6) (55). This value is characteristic of the aquated nitrate ion.

For $AgNO_3$ and $TlNO_3$, the infrared and Raman spectra of the powders are very similar to those reported for the molten salts (23, 25, 56). In this laboratory, the weak ν_2 band, ca. 820 cm^{-1}, has also been observed in the Raman spectrum of concentrated aqueous solutions of $AgNO_3$ (27). The splittings of ν_3 for $LiNO_3$, $NaNO_3$, and KNO_3 melts reported by Williamson *et al.* (24) are of similar magnitude to some observed for solid nitrates, although the spectra of solid $LiNO_3$ and $NaNO_3$ show no splitting in this region. The same authors reported two

components for ν_2 in the infrared spectra of molten $LiNO_3$ and $NaNO_3$. We observe only one component for the crystalline nitrates.

Conclusions

Vibrational spectral changes due to crystal field perturbations of the nitrate ion are reported. Accurate infrared frequencies for the intense ν_3 region have been obtained using m.i.r. techniques. Factor group analysis seems appropriate only for the calcite-type crystals, $LiNO_3$ and $NaNO_3$. In the other crystals, the magnitude of the correlation field coupling is small and site group approximations allow at least partial interpretation. Because of the small correlation field effects our data are insufficient to resolve the problem of whether or not $AgNO_3$ has a center of symmetry. The magnitude of the splitting of the degenerate ν_4 antisymmetric bend, ca. 720 cm^{-1}, is similar for $RbNO_3$, $CsNO_3$, $AgNO_3$, $TlNO_3$, and NH_4NO_3(V). A strong possibility exists that the NO_3^- ion resides on a general site in all of these crystals.

This work was supported by grants from the National Research Council of Canada. The authors are indebted to A. Anderson of the University of Waterloo, Department of Physics for the use of the laser Raman instrument, as well as his helpful comments. The technical assistance of Mr. G. Hill of the Chemistry Department Glass Shop is gratefully acknowledged.

1. S. Bhagavantam and T. Venkatarayudu. Proc. Indian Acad. Sci. Sect. A, 9, 224 (1939); S. Bhagavantam. Proc. Indian Acad. Sci. **13**A, 543 (1941).
2. (*a*) R. S. Halford. J. Chem. Phys. **14**, 8 (1946). (*b*) L. Couture. J. Chem. Phys. **15**, 153 (1947).
3. D. F. Hornig. J. Chem. Phys. **16**, 1063 (1948).
4. H. Winston and R. S. Halford. J. Chem. Phys. **17**, 607 (1949).
5. R. A. Schroeder, C. E. Weir, and E. R. Lippincott. J. Res. Nat. Bur. Stand. A, **66**, 407 (1962).
6. R. K. Khanna, J. Lingscheid, and J. C. Decius. Spectrochim. Acta, **20**, 1109 (1964).
7. S. V. Karpov and A. A. Shultin. J. Phys. Chem. Solids, **29**, 475 (1968).
8. D. W. James and W. H. Leong. J. Chem. Phys. **49**, 5089 (1968).
9. R. Newman and R. S. Halford. J. Chem. Phys. **18**, 1276 (1950); **18**, 1291 (1950).
10. A. A. Shultin and S. V. Karpov. Soviet Phys. Cryst. Engl. Transl. **13**, 601 (1969).
11. K. Buijs and C. J. H. Schutte. Spectrochim. Acta, **18**, 307 (1962).
12. F. Vratney. Appl. Spectrosc. **13**, 59 (1959).
13. P. Krishnamurti. Indian J. Phys. **5**, 1 (1930).
14. H. Nisi. Proc. Physico-Math. Soc. Jap. **15**, 114 (1933); Chem. Abstr. **27**, 5248.
15. T. M. K. Nedungadi. Proc. Indian Acad. Sci. Sect. A, **14**, 242 (1941).
16. L. Couture. C. R. **220**, 656 (1945).
17. W. Bues. Z. Phys. Chem. Frankfurt, **10**, 1 (1957).
18. M. Balkanski, M. K. Teng, and M. Nusimovici. Phys. Rev. **176**, 1089 (1968).
19. R. H. Busey and O. L. Keller, Jr. J. Chem. Phys. **41**, 215 (1964).
20. J. R. Ferraro. *In* Raman spectroscopy theory and practice. *Edited by* H. A. Szymanski. Plenum Press, New York. 1967. Chap. 2, p. 62.
21. G. J. Janz and S. C. Wait, Jr. *In* Raman spectroscopy theory and practice. *Edited by* H. A. Szymanski. Plenum Press, New York. 1967. Chap. 5, p. 151.
22. G. J. Janz and D. W. James. J. Chem. Phys. **35**, 739 (1961).
23. J. P. Devlin, K. Williamson, and G. Austin. J. Chem. Phys. **44**, 2203 (1966).
24. K. Williamson, P. Li, and J. P. Devlin. J. Chem. Phys. **48**, 3891 (1968).
25. G. J. Janz, T. R. Kozlowski, and S. C. Wait. J. Chem. Phys. **39**, 1809 (1963).
26. D. E. Irish and A. R. Davis. Can. J. Chem. **46**, 943 (1968).
27. D. E. Irish and T. G. Chang. Unpublished results.
28. A. C. Gilby, J. Burr, Jr., W. Krueger, and B. Crawford, Jr. J. Phys. Chem. **70**, 1525 (1966).
29. J. R. Ferraro and A. Walker. J. Chem. Phys. **42**, 1273 (1965).
30. I. Nakagawa and J. L. Walter. J. Chem. Phys. **51**, 1389 (1969).
31. M. H. Brooker and D. E. Irish. Can. J. Chem. This issue.
32. J. C. Decius. J. Chem. Phys. **22**, 1941 (1954); **23**, 1290 (1955).
33. W. H. Zachariasen. Skr. Norske Vidensk. Akad. Oslo I: Mat. Naturvidensk. Kl. (1928); C.A. **23**, 1791.
34. R. W. G. Wyckoff. Phys. Rev. **16**, 149 (1920).
35. R. W. G. Wyckoff. Crystal structures. Vol. 2. Interscience Publishers, Inc., New York. 1963. Chap. 7, pp. 359–374.
36. R. Loudon. Advan. Phys. **13**, 423 (1964).
37. D. L. Rousseau, R. E. Miller, and G. E. Leroi. J. Chem. Phys. **48**, 3409 (1968).
38. R. E. Miller, R. R. Getty, K. L. Treuil, and G. E. Leroi. J. Chem. Phys., **51**, 1385 (1969).
39. J. A. A. Ketelaar, C. Haas, and J. Fahrenfort. Physica, **20**, 1259 (1954).
40. W. L. Bragg. Proc. Roy. Soc. London Ser. A, **105**, 16 (1924).
41. D. A. Edwards. Z. Krist. **80**, 154 (1931).
42. P. E. Martin and E. F. Barker. Phys. Rev. **41**, 291 (1932).
43. L. Pauling and J. Sherman. Z. Krist. **84**, 213 (1933).
44. L. Waldbauer and D. C. McCann. J. Chem. Phys. **2**, 615 (1934).
45. C. Findbak and O. Hassel. J. Chem. Phys. **5**, 460 (1937).
46. R. N. Brown and A. C. McLaren. Acta Cryst. **15**, 974 (1962).
47. J. L. Amorós, F. Arrese, and M. Canut. Z. Krist. **117**, 92 (1962).
48. A. Niggli. Z. Krist. **111**, 269 (1959).
49. P. F. Lindley and P. Woodward. J. Chem. Soc. A, 123 (1966).
50. S. W. Kennedy and J. H. Patterson. Z. Krist. **116**, 143 (1961).
51. J. K. Wilmshurst and S. Senderoff. J. Chem. Phys. **35**, 1078 (1961).

Can. J. Chem. Downloaded from www.nrcresearchpress.com by 210.87.254.105 on 09/05/12
For personal use only.

52. G. H. WEGDAM, R. BONN, and J. VAN DER ELSKEN. Chem. Phys. Lett. **2**, 182 (1968).
53. K. FURUKAWA. Discuss. Faraday Soc. **32**, 53 (1961).
54. D. W. JAMES. *In* Molten salt chemistry. *Edited by* M. Blander. John Wiley and Sons, New York. 1964. p. 524.
55. D. E. IRISH. *In* Ionic interactions: dilute solutions to molten salts. *Edited by* S. Petrucci. Academic Press. In press.
56. G. E. WALRAFEN and D. E. IRISH. J. Chem. Phys. **40**, 911 (1964).

Can. J. Chem. Downloaded from www.nrcresearchpress.com by 210.87.254.105 on 09/05/12
For personal use only.

Can. J. Chem. Downloaded from www.nrcresearchpress.com by 210.87.254.105 on 09/05/12
For personal use only.

Vibrational frequency assignments of isotopically different forms of nitrate ion in ionic nitrate crystals

M. H. Brooker and D. E. Irish
Department of Chemistry, University of Waterloo, Waterloo, Ontario

Received August 7, 1969

Infrared and Raman spectra of powdered ionic nitrates contain low intensity vibrational bands which are assigned to isotopically different species. Bands at $\sim(\nu_1 - 20)$ and $\sim(\nu_4 - 13)$ cm^{-1} are assigned to the $^{14}N^{16}O_2{}^{18}O^-$ ion whereas the band at $\sim(\nu_2 - 20)$ cm^{-1} is assigned to the $^{15}N^{16}O_3{}^-$ ion. Failure of the ratio of band intensities to agree with predicted isotopic ratios is discussed.

Canadian Journal of Chemistry, 48, 1198 (1970)

Introduction

In the course of current studies of the infrared and Raman spectra of powdered ionic nitrates (1, 2) we have detected several low intensity vibrational bands on the low frequency side of ν_1 (A_1'), ν_2 (A_2''), and ν_4 (E'). The occurrence of bands at these frequencies has been observed by other authors but explanations of their origin differ. James and Leong (3) have assigned bands in the ν_1 and ν_2 regions to either site symmetry perturbation of the nitrate ion or an extraneous band due to reflection at the surface of the crystal. Schroeder, Weir, and Lippincott (4) assign series of weak bands observable at liquid nitrogen temperatures to combinations involving fundamental and librational modes. Decius (5), Newman and Halford (6), Karpov and Shultin (7) have assigned bands[1] at $\sim(\nu_2 - 20)$ cm^{-1} to the species $^{15}N^{16}O_3{}^-$. Our interpretation is in agreement with the latter. We also assign bands at $\sim(\nu_1 - 20)$ cm^{-1} in the infrared and Raman spectra and $\sim(\nu_4 - 13)$ cm^{-1} in the infrared spectra to the isotopic species $^{14}N^{16}O_2{}^{18}O^-$. The assignments are in excellent agreement with the vibrational frequencies observed and calculated by Kato and Rolfe (9) for isotopically enriched $NO_3{}^-$ ions in KBr crystals.

Experimental

Nitrates used were all reagent grade. Infrared spectra of powders were recorded with a Beckman IR-9 spectrophotometer. The finely divided powders were either mechanically deposited on an AgBr plate or pressed (1000 p.s.i.) into an extremely thin pure disc. Raman spectra were recorded for powders contained in a conical cell similar to that used by Busey and Keller (8) on a Cary 81 Raman spectrophotometer. Raman intensities were determined from band areas. Infrared relative absorbance measurements were obtained from peak heights although some spectra were recorded on the absorbance scale and the relative absorbance ratio determined by areas. The two methods were in good agreement. Because of the problem of comparing two bands of such unequal magnitude the observed ratios are estimated to have uncertainties of 0.001 for the Raman and 0.005 for the infrared.

[1]The abbreviation $\sim(\nu_2 - 20)$ etc. is used to signify the frequency of a line about 20 cm^{-1} lower than the intense ν_2 line of the most abundant isotopic form of $NO_3{}^-$. This nomenclature is convenient because the positions of the lines ν_1, ν_2, and ν_4 differ for different salts but the isotopic shift is almost constant. The differences between the two observed frequencies are not expected to be given exactly by relations such as $\sim(\nu_2 - 20)$ because of differences in the host lattices. See Results and Discussion section.

Results and Discussion

The observed infrared and Raman frequencies for the ν_1, ν_2, and ν_4 regions for a collection of ionic metal nitrates are given in Tables 1 to 3. The frequencies are expected to be accurate to ± 1 cm^{-1}. Typical spectra are shown in Figs. 1–3. The ν_3 region of nitrate is too broad at room temperature to allow resolution of bands from naturally occurring isotopic species.

From the Table of Natural Isotopes (10) it follows that $^{15}N^{16}O_3{}^-$, $^{14}N^{16}O_2{}^{18}O^-$, and $^{14}N^{16}O_2{}^{17}O^-$ are the most naturally abundant isotopically substituted nitrate ions. The ratios of $^{15}N^{16}O_3{}^-$, $^{14}N^{16}O_2{}^{18}O^-$, and $^{14}N^{16}O_2{}^{17}O^-$ to $^{14}N^{16}O_3{}^-$ are 0.00366, 0.00613, and 0.0011, respectively. Other isotopically different ions are present to less than 0.001%. No contributions from $^{14}N^{16}O_2{}^{17}O^-$ have been observed in the spectra reported here. Both $^{14}N^{16}O_3{}^-$ and $^{15}N^{16}O_3{}^-$ belong to the point group D_{3h} and consequently the 6 normal modes of vibration are ν_1 (A_1'), ν_2 (A_2''), ν_3 (E'), and ν_4 (E'). The $^{14}N^{16}O_2{}^{18}O^-$ ion belongs to the point group C_{2v} and the 6 normal modes are now A_1, B_1, and 2 ($A_1 + B_2$) which may be considered as derived

Can. J. Chem. Downloaded from www.nrcresearchpress.com by 210.87.254.105 on 09/05/12
For personal use only.

TABLE 1

Vibrational frequencies of ν_1 of nitrate

	Raman			Infrared		
	Frequency (cm^{-1})		Intensity ratio $I_{N^{16}O_2{}^{18}O^-}/I_{N^{16}O_3^-}$	Frequency (cm^{-1})*		Absorbance ratio $A_{N^{16}O_2{}^{18}O^-}/A_{N^{16}O_3^-}$
Nitrate	$N^{16}O_3^-$	$N^{16}O_2{}^{18}O^-$		$N^{16}O_3^-$	$N^{16}O_2{}^{18}O^-$	
Li	1071	1050	0.0053	—	—	—
Na	1068	1049	0.0051	—	—	—
K	1050	1030	0.0050	1051	1032	0.02
Rb	1057	1037	0.0052	1057	1037	0.05
Cs	1051	1030	0.0050	1051	1031	0.05
Ag	1046	1026	0.0040	1046 (vw)	—	—
Tl	1043	1023	0.0042	1042	—	—
Sr	1056	1036	0.0048	1055 (vw)	—	—
Ba	1048	1027	0.0050	1047 (vw)	—	—
Pb	1045	1025	0.0042	1045 (vw)	—	—

*vw = very weak.

from the fundamental modes of the $^{14}N^{16}O_3^-$ ion.

Substitution with ^{15}N should affect the frequency of the out-of-plane deformation ν_2 much more than the symmetric stretch ν_1 or the antisymmetric bend ν_4. Decius (5) has shown that an observed shift of 21.7 cm^{-1} for the infrared active ν_2 mode on substitution with ^{15}N in $NaNO_3$ is in excellent agreement with the Teller–Redlich product rule. Kato and Rolfe (9), employing a general harmonic force field, calculate a change of 22 cm^{-1} for ν_2 but only 1 cm^{-1} for each of ν_1 and ν_4 on ^{15}N substitution.

Conversely, substitution of the nitrate ion with ^{18}O should affect the symmetric stretch and antisymmetric bend more than the out-of-plane deformation. Kato and Rolfe (9) calculate a 19.5 cm^{-1} frequency change for ν_1 but only a 3.6 cm^{-1} shift of ν_2 for $^{14}N^{16}O_2{}^{18}O^-$. Both frequency differences are in qualitative agreement with the Teller–Redlich product rule if one assumes that the $^{14}N^{16}O_2{}^{18}O^-$ gives one third of the shift of the completely substituted $^{14}N^{18}O_3^-$ species. The asymmetric bend should split into A_1 and B_2 components in $^{14}N^{16}O_2{}^{18}O^-$. Kato and Rolfe predict that these will be 10.9 and 15.9 cm^{-1}, respectively, from the ν_4 (E') mode of the non-substituted species. If in fact the A_1 and B_2 components are not fully resolved one may expect to find the band for $N^{16}O_2{}^{18}O^-$ at $\sim (\nu_4 - 13)$ cm^{-1}.

From Tables 1 to 3 it can be seen that in all cases the agreement between our data and the proposed calculated frequency differences for bands generated from the various isotopically different nitrate ions is excellent. One should expect small differences between the designations $\sim (\nu_1 - 20)$ etc. and the difference between the frequency of the line of $^{14}N^{16}O_3^-$ and the line of the isotopically different form. The intense lines of the former arise from nitrate ions

TABLE 2

Infrared vibrational frequencies of ν_2 of nitrate

	Frequency (cm^{-1})		Absorbance ratio $A_{^{15}NO_3^-}/A_{^{14}NO_3^-}$
Nitrate	$^{14}NO_3^-$	$^{15}NO_3^-$	
Li	838	818	0.04
Na	836	815	0.035
K	828	812	0.020
Rb	836	816	0.015
Cs	834	814	0.020
Ag	802	784	0.050
Tl	819	800	0.020
Sr	814	796	0.045
Ba	817	797	0.025
Pb	807	787	0.020

TABLE 3

Infrared vibrational frequencies of ν_4 of nitrate

	Frequency (cm^{-1})		Absorbance ratio
Nitrate	$N^{16}O_3^-$	$N^{16}O_2{}^{18}O^-$	
Sr	738	727	0.02
Ba	731	716	0.02
		721	0.02
Pb	725	713	0.02

Can. J. Chem. Downloaded from www.nrcresearchpress.com by 210.87.254.105 on 09/05/12
For personal use only.

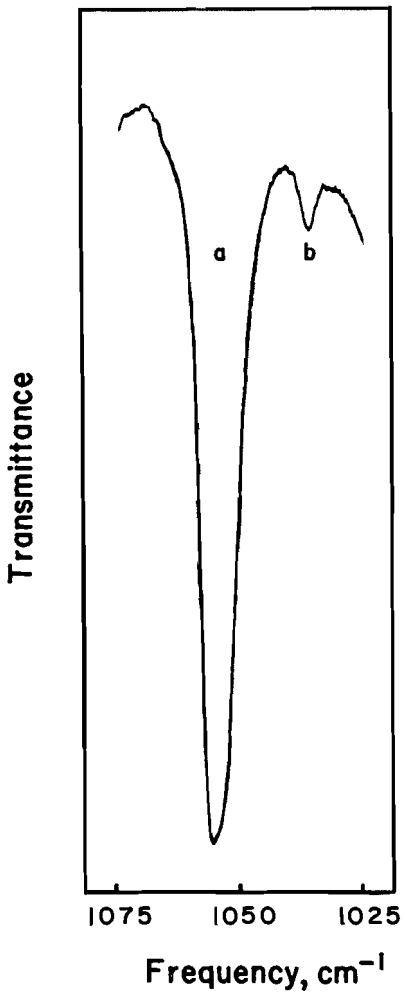

FIG. 1. A portion of infrared spectrum of $RbNO_3$, (*a*) ν_1, $^{14}N^{16}O_3^-$; (*b*) $(\nu_1 - 20)$ cm^{-1}, $^{14}N^{16}O_2{}^{18}O^-$.

"coupled" throughout the lattice. These frequencies are affected by both the site and the correlation field effect; the magnitude of the perturbation will be different for different lattice types. The dilute species ($^{15}NO_3^-$ etc.) to a good approximation occupy the same sites but are partially "decoupled" and hence the correlation field effects are not operative to the same extent. The fact that, within a few wavenumbers, the designations $(\nu_1 - 20)$ etc. satisfy the data indicates that the correlation field effects are either constant and/or small in these crystals. Previously it has been observed that coupling manifests itself most for $LiNO_3$ and is undetectable for powdered nitrates containing heavy cations (1).

Generally the ratios of band intensities are not in good agreement with the predicted ratios of the naturally occurring isotopic forms. In the infrared spectra the bands from $^{15}N^{16}O_3^-$ and $^{14}N^{16}O_2{}^{18}O^-$ are more intense than predicted, indicating a substantial increase in the dipole moment change. Khanna *et al.* (11) have reported a decidedly greater intensity in the ^{15}N region than in the ^{14}N region for the ν_2 mode of nitrate ion in a 50% mixture of $K^{15}NO_3$ and $K^{14}NO_3$ at room temperature. Their system differs from ours in that all nitrate ions in their 1:1 mixture were coupled.

The infrared spectrum of $Pb(NO_3)_2$ shown in Fig. 2 does not show a band at 831 cm^{-1} as reported by Newman and Halford (6). The presence of this band had caused these authors to doubt their assignment of bands at $\sim (\nu_2 - 20)$

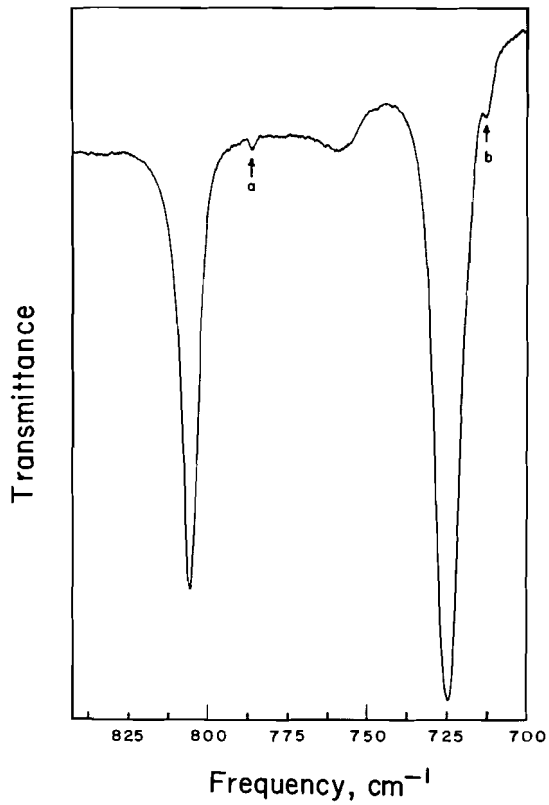

FIG. 2. A portion of infrared spectrum of $Pb(NO_3)_2$, (*a*) $(\nu_2 - 20)$ cm^{-1}, $^{15}N^{16}O_3^-$; (*b*) $\sim(\nu_4 - 13)$ cm^{-1}; $^{14}N^{16}O_2{}^{18}O^-$.

Can. J. Chem. Downloaded from www.nrcresearchpress.com by 210.87.254.105 on 09/05/12
For personal use only.

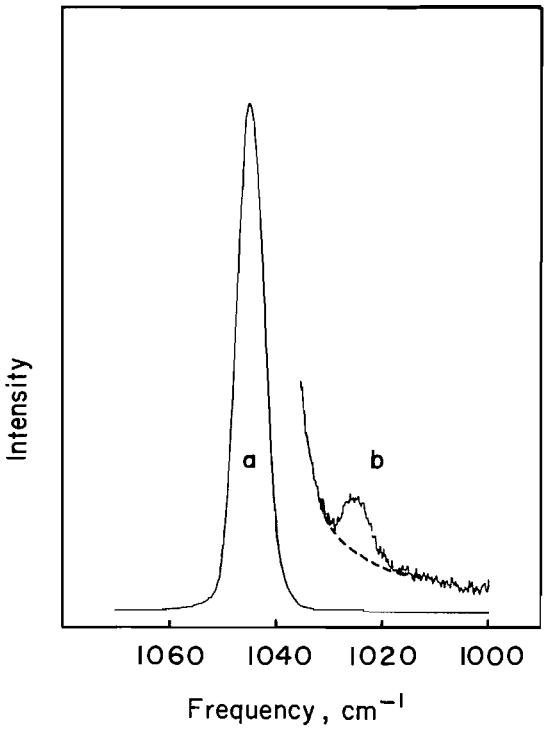

FIG. 3. Portions of Raman spectra of $AgNO_3$, (*a*) ν_1, $^{14}N^{16}O_3^-$ (sensitivity 5); (*b*) $\sim(\nu_1 - 20)$ cm^{-1}, $^{14}N^{16}O_2{}^{18}O^-$ (sensitivity 100).

cm^{-1} to $^{15}NO_3^-$ as they had done for other nitrates. It is possible that an alkali metal impurity or ion exchange with the plate was responsible for the occurrence of this extraneous absorption band.

The band due to $N^{16}O_2{}^{18}O^-$ at $\sim(\nu_1 - 20)$ cm^{-1} is expected in the infrared spectrum since it is allowed under C_{2v} selection rules. The ν_1 fundamental for $^{14}N^{16}O_3^-$ is not infrared allowed under D_{3h} selection rules and its appearance is usually attributed to perturbation by the environment. The crystals for which ν_1 ($^{14}N^{16}O_3^-$) is weak or absent in the infrared also do not show the isotopic analogue. In the Raman spectra the $\sim(\nu_1 - 20)$ cm^{-1} band occurs for all of the nitrates studied. The spectrum obtained for $AgNO_3$ in the 1050 cm^{-1} region is shown in Fig. 3. The observed intensity ratios listed in Table 1 are less than predicted from isotopic abundances and probably reflect the loss of symmetry that accompanies the ^{18}O substitution.

In the infrared ν_4 nitrate region (ca. 720 cm^{-1}) a band attributed to $N^{16}O_2{}^{18}O^-$ is observable as a shoulder on the $N^{16}O_3^-$ peak for $Ba(NO_3)_2$, $Sr(NO_3)_2$, and $Pb(NO_3)_2$ (Fig. 2). This band is probably only seen for these compounds because the ν_4 ($N^{16}O_3^-$) band is single, sharp, and extremely intense. In most other nitrates the band is much weaker and often split by lattice forces. The $\sim(\nu_4 - 13)$ cm^{-1} band was beyond the detectability limit of our Cary 81 Raman spectrophotometer.

The assignment of bands at $\sim(\nu_1 - 20)$ cm^{-1} and $\sim(\nu_4 - 13)$ cm^{-1} to the species $^{14}N^{16}O_2{}^{18}O^-$ and the band at $\sim(\nu_2 - 20)$ cm^{-1} to the species $^{15}N^{16}O_3^-$ in naturally occurring metal nitrates provides a realistic and consistent analysis of the vibrational spectra of solid metal nitrates. From this study it can be seen that considerable fundamental information relating to band intensities, dipole moments, and polarizabilities can be obtained for the nitrate ion by comparing intensities of isotopically-enriched species.

This work was supported by a grant from the National Research Council of Canada. A National Research Council Postgraduate Fellowship to M.H.B. is also gratefully acknowledged.

1. M. H. BROOKER and D. E. IRISH. Can. J. Chem. This issue.
2. M. H. BROOKER, D. E. IRISH, and G. E. BOYD. To be published.
3. D. W. JAMES and W. H. LEONG. J. Chem. Phys. **49**, 5089 (1968).
4. R. A. SCHROEDER, C. E. WEIR, and E. R. LIPPINCOTT. J. Res. Nat. Bur. Stand. **66A**, 407 (1962).
5. J. C. DECIUS. J. Chem. Phys. **22**, 1941 (1954).
6. R. NEWMAN and R. S. HALFORD. J. Chem. Phys. **18**, 1276 (1950); **18**, 1291 (1950).
7. S. V. KARPOV and A. A. SHULTIN. J. Phys. Chem. Solids, **29**, 475 (1968).
8. R. H. BUSEY and O. L. KELLER, JR. J. Chem. Phys. **41**, 215 (1964).
9. R. KATO and J. ROLFE. J. Chem. Phys. **47**, 1901 (1967).
10. J. M. HOLLANDER, I. PERLMAN, and G. T. SEABORG. Table of isotopes, Rev. Mod. Phys. **25**, 469 (1953).
11. R. K. KHANNA, J. LINGSCHEID, and J. C. DECIUS, Spectrochim. Acta, **20**, 1109 (1964).

Raman, infrared, and proton magnetic resonance investigation of solutions of zinc nitrate in anhydrous methanol

S. A. AL-BALDAWI, M. H. BROOKER,[1] T. E. GOUGH,[2] AND D. E. IRISH
Department of Chemistry, University of Waterloo, Waterloo, Ontario

Received November 10, 1969

Raman, infrared, and proton magnetic resonance spectra of solutions of zinc nitrate in anhydrous methanol are reported. It is concluded that above −30 °C the zinc and nitrate ions can form contact ion-pairs, but that below −30 °C association is limited to the formation of solvent-separated ion-pairs. The apparent solvation number of zinc, as determined by area measurements on the proton magnetic resonance spectra, decreases with increasing solute concentration, and an interpretation of this effect is given.

Canadian Journal of Chemistry, **48**, 1202 (1970)

Can. J. Chem. Downloaded from www.nrcresearchpress.com by 210.87.254.105 on 09/05/12
For personal use only.

Introduction

The determination of primary cationic solvation numbers through observation of the nuclear magnetic resonance (n.m.r.) spectra of solvent molecules bound to cations is now an accepted technique. The majority of reported solvation numbers are, within experimental error, equal to 6 (1–6), although lower values have been reported (7–10), and assumed to reflect the replacement of solvent molecules by anions in the first coordination shell of the cation (9, 10).

For example, for solutions of zinc perchlorate in methanol (10) at 0.2 *M* concentration, the measured solvation number was close to 6, but as the concentration was increased the solvation number decreased until at 1.5 *M*, values close to 4 were obtained. Furthermore, as the concentration increased, the resonance of the hydroxylic protons in the solvation shell of zinc shifted to higher fields, an effect compatible with the postulated contact between the zinc and perchlorate ions.

Such association was chemically somewhat unexpected, but there seems to be no obvious microscopic experiment with which to test these conclusions, particularly since the Raman spectra of several perchlorates in solution show no evidence of perturbation by cations (11). However, the nitrate ion has been shown to be an excellent spectroscopic probe with which to investigate ionic interactions. An unperturbed nitrate ion with D_{3h} symmetry generates four vibrational frequencies: ν_1, 1050 cm^{-1} (Raman); ν_2, 825 cm^{-1} (infrared); ν_3, 1380 cm^{-1} (infrared, Raman); and ν_4, 720 cm^{-1} (infrared, Raman). From studies of metal nitrates in aqueous solution, it has been proposed (12, 13) that the appearance of a band close to 740 cm^{-1} is diagnostic of contact ion-pairing. Confirmatory evidence for such complexing of the nitrate ion usually exists in the form of new bands at slightly lower frequencies than the ν_1 and ν_2 free nitrate bands, and the appearance of at least two maxima in the ν_3 region, usually separated by more than 150 cm^{-1} and resolvable into at least four lines (13–15).

Accordingly, we have examined solutions of zinc nitrate in methanol, studying the infrared and Raman spectra of the nitrate anion and the proton resonance spectrum of the methanol.

Experimental

Anhydrous zinc nitrate was prepared by the reaction, at room temperature, between a block of zinc metal and nitrogen tetroxide (16). The reaction was performed in a cylindrical vessel with two side arms, one carrying a standard n.m.r. tube, and the other stopcocks for evacuating the vessel and for admitting nitrogen tetroxide. A drying tube containing phosphorus pentoxide was used to protect the contents of the vessel from atmospheric moisture and to vent evolved gases. When the dissolution of the zinc was complete, excess nitrogen tetroxide was pumped off under low vacuum, and the vessel was then connected to a high-vacuum line. The last traces of nitrogen tetroxide were removed by heating at 100 °C under a high vacuum to form a white solid, stuck to the side of the vessel, which dissolved readily in anhydrous methanol with the evolution of heat. Thorough removal of nitrogen tetroxide is important, since its presence colors the solutions, interfering with the Raman measurements, and also impairs the resolution of the n.m.r. spectra.

Anhydrous methanol was prepared as described previously (10) and distilled in vacuo onto the anhydrous zinc nitrate. A portion of the resulting solution was poured into the n.m.r. tube and sealed off, while the remainder of the solution was analyzed to determine the concentration of zinc (17).

[1]Present address: Department of Chemistry, University of Tennessee, Knoxville, Tennessee.
[2]To whom all correspondence should be addressed.

Can. J. Chem. Downloaded from www.nrcresearchpress.com by 210.87.254.105 on 09/05/12
For personal use only.

Recording of the n.m.r. spectra, calibration of chemical shifts, measurement of temperatures, and the determination of solvation numbers were performed as previously described (10).

Infrared spectra were recorded on a Beckman IR-9 spectrophotometer operated at three times the "standard" slit program provided by the manufacturer. Transmission spectra were obtained using a thermostated cell ("R.I.I.C." cell), equipped with silver bromide windows and a 0.025 mm teflon gasket, supplied by Research and Industrial Instrument Company. No reference cell was used, but some attenuation of the reference beam was obtained by placing a sheet of silver bromide in it. A Haake constant-temperature circulator was used to obtain temperatures above 15 °C; temperatures below 15 °C were obtained by passing a regulated stream of cold nitrogen gas through the outer jacket of the R.I.I.C. cell. Temperatures so obtained were determined with a copper–constantan thermocouple attached directly to the silver bromide windows. Frosting was prevented by purging the IR-9 instrument with dry nitrogen.

For all infrared studies, the n.m.r. samples were opened in a drybox and the solution quickly drawn into the infrared cell and resealed. After each spectrum was recorded, the cell was flushed several times with dry methanol and finally with dry nitrogen. At the time of filling the infrared cells, a portion of the solution was withdrawn and analyzed for water by the Karl Fischer method. The highest water concentration found was 0.02 *M*, and the majority of samples contained considerably less than this value. The complete infrared spectrum of 1.5 *M* zinc nitrate in methanol was recorded using a Wilks Model 9 multiple internal reflectance attachment equipped with a silver bromide prism.

The relative molar absorbance for uncomplexed nitrate was determined by recording spectra of a series of solutions of lithium nitrate (anhydrous Fisher certified reagent dried for 1 week at 110 °C) in methanol under the same conditions as the solutions of zinc nitrate.

The Raman spectrum of a saturated solution (~1.3 *M*) of zinc nitrate in methanol was recorded using a Cary 81 Raman spectrophotometer and the 4358 Å mercury exciting line. Extraneous mercury lines were filtered with a 10 *M* potassium nitrite solution, or with an ethyl-violet – *o*-nitrotoluene solution; a slit width of 10 cm^{-1} was used. A freshly prepared solution of zinc nitrate in anydrous methanol was filtered in vacuo through a fine sintered disk into a Raman cell by applying a slight pressure of dry nitrogen. The filled Raman cell was sealed, and removed from the vacuum line. The degrees of depolarization of the Raman lines were estimated from spectra obtained with incident light polarized by concentric cylinders of polaroid film having their polarizing axes either perpendicular or parallel to the axis of the Raman cell.

Results

Proton magnetic resonance spectra of solutions of zinc nitrate in methanol were recorded for solute concentrations up to 1.0 *M* at sample temperatures between −90 and +30 °C. The results were, qualitatively, very similar to those previously presented for solutions of zinc perchlorate in methanol (10), and so only those results of interest to the following discussion are presented in detail.

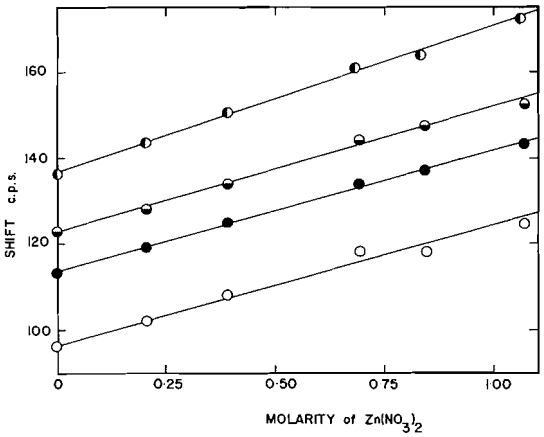

FIG. 1. The dependence of the chemical shift of hydroxylic protons upon solute molarity for solutions of zinc nitrate in anhydrous methanol. Shifts are in c.p.s. downfield from the methyl proton resonance. Sample temperatures: ○, 20; ●, −6; ◒, −26; ◐, −58 °C.

The addition of zinc nitrate to methanol causes a downfield shift of the resonance of the hydroxylic protons, linear with concentration (see Fig. 1). Below −60 °C the hydroxyl resonance experiences asymmetric broadening and below −75 °C it splits, as expected, into two separate absorptions, assigned conventionally as "bound" and "bulk" methanol. The chemical shift, with reference to the methyl resonance, of the bound hydroxylic protons is plotted as a function of concentration in Fig. 2, where for the purposes of discussion the corresponding results for solutions of zinc perchlorate in methanol (10) are also plotted. Both sets of measurements were recorded at a sample temperature of −82 °C. Unlike the resonance of bulk methanol (not shown), the resonance of bound methanol moves to higher fields as concentration increases. This shift to higher fields is much greater per mole of zinc perchlorate than per mole of zinc nitrate.

From measurements of the relative areas of the two hydroxyl proton resonances and of the concentration of zinc nitrate, estimates were made of the average number of methanol molecules bound to each zinc ion (see Fig. 3). Measurements were made of the densities, at −78 °C, of methanol and of methanolic solutions of zinc

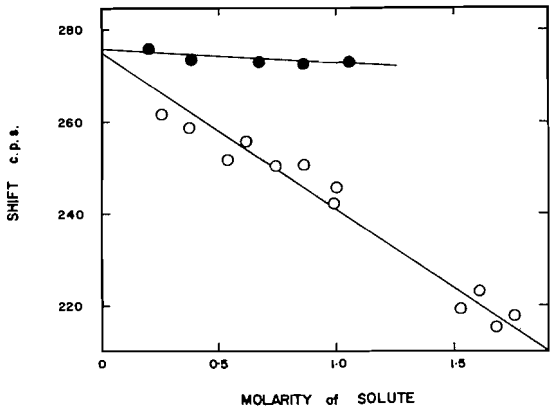

FIG. 2. The dependence of the chemical shift of cationically bound hydroxylic protons upon solute molarity for solutions of ○, zinc perchlorate; and ●, zinc nitrate in anhydrous methanol. Shifts are in c.p.s. downfield from the methyl proton resonance. Sample temperature −82 °C.

nitrate in order to determine whether variations in sample density with concentration are responsible for the observed trend in solvation numbers; such was not the case.

The infrared and Raman frequencies, assignments, and polarizations are reported in Table 1. The most noteworthy features in the infrared spectra are the doublet in the 800 cm^{-1} region (Fig. 4) and a new band at 754 cm^{-1}. The relative

TABLE 1

Infrared and Raman frequencies for solutions of zinc nitrate in anhydrous methanol

Frequency*, cm^{-1}		
Infrared	Raman†	Assignment
	380 vw (p?)	Zn—$OHCH_3$
	715 m (dp)	ν_4 free NO_3^-
754 w	753 m (dp)	bound NO_3^-
817 m		bound NO_3^-
828 m		ν_2 free NO_3^-
‡	1044 vs (p)	ν_1 free NO_3^-
1310 m	1310 w (p)	bound NO_3^-
‡	‡	ν_3 free NO_3^-
1500 sh?	‡	bound NO_3^-

*w = weak, m = medium, s = strong, sh = shoulder, v = very.
†p = polarized, dp = depolarized.
‡Region obscured by solvent.

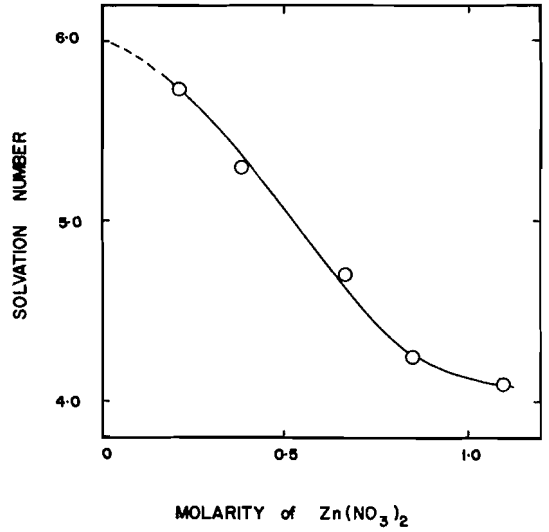

FIG. 3. The dependence of the measured solvation number of zinc upon solute molarity for solutions of zinc nitrate in anhydrous methanol. Sample temperature −82 °C.

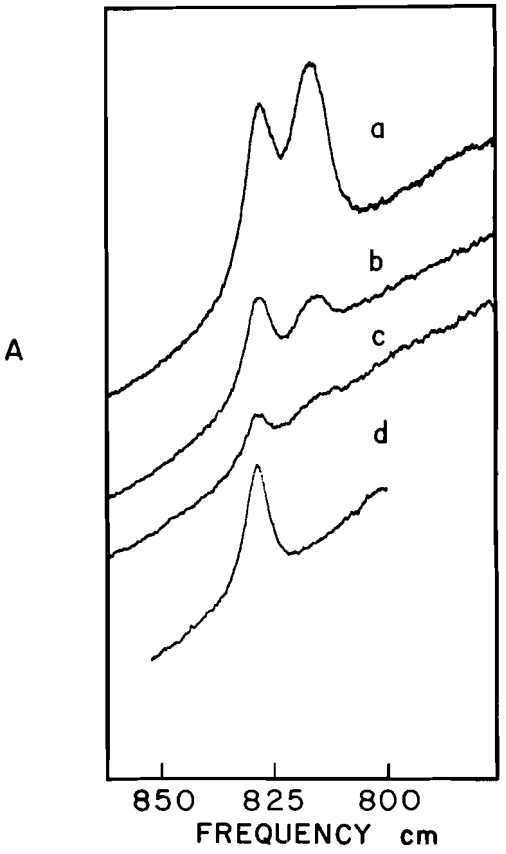

FIG. 4. Infrared spectra, in the 800 cm^{-1} region, for solutions in methanol of (*a*) 1.82 *M* zinc nitrate, (*b*) 0.76 *M* zinc nitrate, (*c*) 0.32 *M* zinc nitrate, (*d*) 1.0 *M* lithium nitrate.

Can. J. Chem. Downloaded from www.nrcresearchpress.com by 210.87.254.105 on 09/05/12
For personal use only.

Can. J. Chem. Downloaded from www.nrcresearchpress.com by 210.87.254.105 on 09/05/12
For personal use only.

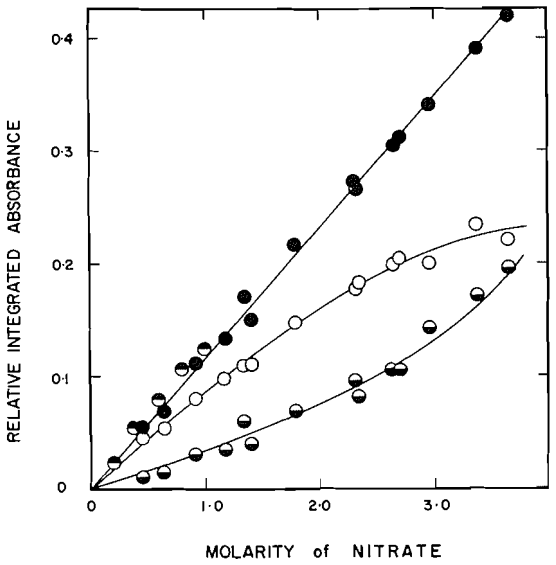

FIG. 5. Relative integrated absorbances plotted as functions of solute molarity for ◒, 817 cm^{-1} band of zinc nitrate; ○, 828 cm^{-1} band of zinc nitrate; ●, sum of the 817 and 828 cm^{-1} bands of zinc nitrate; and ◓, the 828 cm^{-1} band of lithium nitrate. Solvent, anhydrous methanol; sample temperature, 25 °C.

integrated absorbances of the 817 and 828 cm^{-1} bands were obtained through area measurements using a standard polar planimeter; the area of the 828 cm^{-1} band was determined on the assumption that the band is symmetric about its absorption maximum, while the area of the 817 cm^{-1} band was obtained by subtracting the area of the 828 cm^{-1} band from the total area. The sum of the relative integrated absorbances of the bands at 817 and 828 cm^{-1} is proportional to nitrate concentration, and, within experimental error, is equal to the relative integrated absorbance of the 828 cm^{-1} band of lithium nitrate in methanol. Plots of relative integrated absorbances of the 817 and 828 cm^{-1} bands, and of their sum as a function of nitrate concentration, are given in Fig. 5.

The band at 754 cm^{-1} observed for a 1.5 *M* solution decreased in intensity and shifted to lower frequencies on dilution. Figure 6 shows the Raman spectrum near 700 cm^{-1} of a saturated solution of zinc nitrate in methanol; both of these bands were found to be depolarized. However, Raman bands at 1044 and 1310 cm^{-1} were found to be polarized. A strong band due to methanol prevents detection of an expected nitrate Raman band near 1500 cm^{-1}, while an infrared- and Raman-active band of methanol at 1020 cm^{-1} partly obscures the Raman band at 1044 cm^{-1} and precludes detection of any infrared absorption by nitrate in this region. The 1200 to 1500 cm^{-1} region is partially obscured by methanol bands in the infrared and Raman spectra. The infrared and Raman bands due to methanol in the solution of zinc nitrate were identical to those of pure methanol at 25 °C, and agreed well with the reported literature values (18).

The infrared spectra were strongly temperature dependent (Fig. 7). A decrease in temperature causes a decrease in the relative absorbance of the band at 817 cm^{-1} compared to that for the band at 828 cm^{-1}. At −30 °C, only the 828 cm^{-1} band was observable; the band at 754 cm^{-1} behaved as did the 817 cm^{-1} band, becoming weaker as the temperature was decreased, and disappearing at −30 °C.

Discussion

We accept, as the starting point for our discussion, the postulate (12, 13) that the appearance of a band ca. 740 cm^{-1} in the infrared and Raman spectra of the nitrate ion is diagnostic of contact between nitrate and, in the present case, zinc

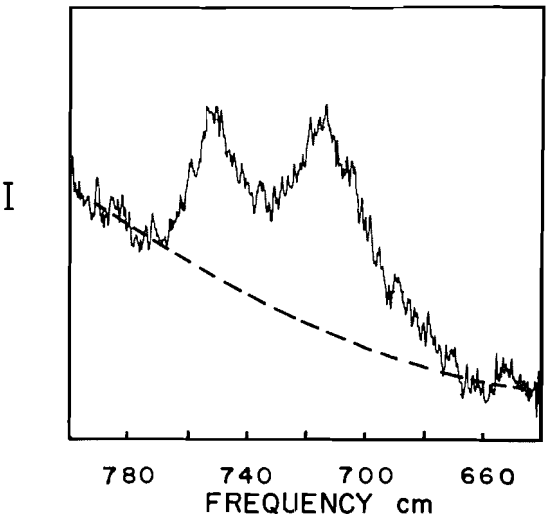

FIG. 6. The Raman spectrum in the 700 cm^{-1} region, of a saturated solution of zinc nitrate in methanol. Sample temperature 40 °C.

Can. J. Chem. Downloaded from www.nrcresearchpress.com by 210.87.254.105 on 09/05/12
For personal use only.

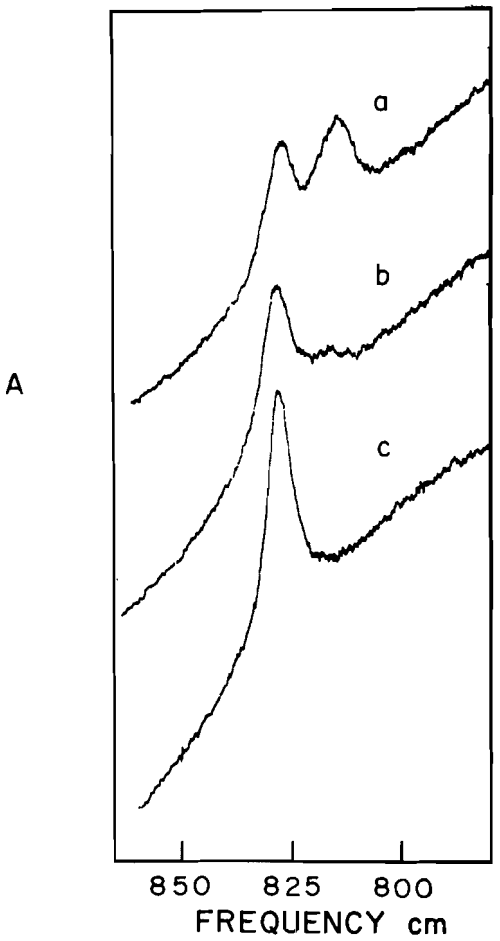

FIG. 7. Infrared spectra, in the 800 cm^{-1} region, of a 1.2 *M* solution of zinc nitrate in anhydrous methanol. Sample temperature: (*a*) 38, (*b*) −10, (*c*) −30 °C.

ions. Therefore, the observation of a band at 754 cm^{-1} at temperatures above −30 °C indicates the formation of contact ion-pairs of zinc nitrate in anhydrous methanol. Below −30 °C, however, this species is not present in detectable amounts. Polarization of the Raman band at 1310 cm^{-1} is evidence for monodentate bonding via oxygen of nitrate to zinc within the ion pair (19). For nitrate complexes having some covalence within their metal–oxygen interactions, Raman spectra exhibit a band ca. 270 cm^{-1} attributed to the metal–oxygen stretching frequency (12, 14, 20–22). Such a zinc–oxygen stretch was not observed for the present system, indicating that the bonding between the zinc and nitrate ions is largely electrostatic, as has already been reported for solutions of zinc nitrate in acetonitrile (23). The weak band observed at 380 cm^{-1} is probably due to a zinc–oxygen stretch between zinc and methanol, since it is close to the 390 cm^{-1} band reported for the aquo-zinc ion (24).

Although the 754 cm^{-1} absorption is a satisfactory qualitative indication of the presence of contact ion-pairs, its low intensity makes it unsatisfactory for quantitative studies. However, since the 754 and 817 cm^{-1} bands have parallel dependences upon concentration and temperature, it is possible to use the more intense 817 cm^{-1} absorption, assigned as the out-of-plane mode of associated nitrate, as the basis of a quantitative study. Since the sum of the areas of the 817 and the 828 cm^{-1} bands for a solution of zinc nitrate equals the area, for the same nitrate concentration, of the 828 cm^{-1} band of lithium nitrate, which we take to be fully dissociated, all three absorptions must have the same relative molar absorbance, which may be obtained from the slope of the straight-line plot in Fig. 5. Using the superscripts b and f to denote bound and free, respectively, *C* to denote concentration, and assuming that the predominant associated species is $ZnNO_3^+$, a plot of $C_{NO_3^-}{}^b$ vs. $(C_{Zn^{2+}}{}^f . C_{NO_3^-}{}^f)$ should be a straight line, of slope equal to the association constant K_1, passing through the origin. This plot is shown in Fig. 8, from which K_1 at 25 °C = 3.00 ± 0.04 l $mole^{-1}$. A similar calculation assuming that the predominant associated species is $Zn(NO_3)_2$ gave a non-linear plot that did not pass through the origin. However, evidence for the stepwise formation of $Zn(NO_3)_2$ was found, especially at higher temperatures; for instance, at 60 °C, when the concentration exceeded 1.2 *M*, the average number of nitrates bound per zinc ion, $C_{NO_3^-}{}^b/C_{Zn^{2+}}$, exceeded 1.0. Assuming both associated species to be present, treatment of the data as suggested by Rossotti and Rossotti (25), gave, at 25 °C, $K_1 \sim 2.6$ and $K_2 \sim 0.05$ l $mole^{-1}$.

The temperature dependence of the equilibrium is illustrated in Fig. 7 for a 1.2 *M* $Zn(NO_3)_2$ solution. Below −30 °C no infrared evidence was found for the formation of contact ion-pairs. From the temperature dependence of K_1, neglecting K_2, ΔH^0 for the association was found to be approximately 3 kcal/mole.

Knowledge of the extent of association of zinc nitrate under various conditions facilitates discussion of the n.m.r. data. Comparing the

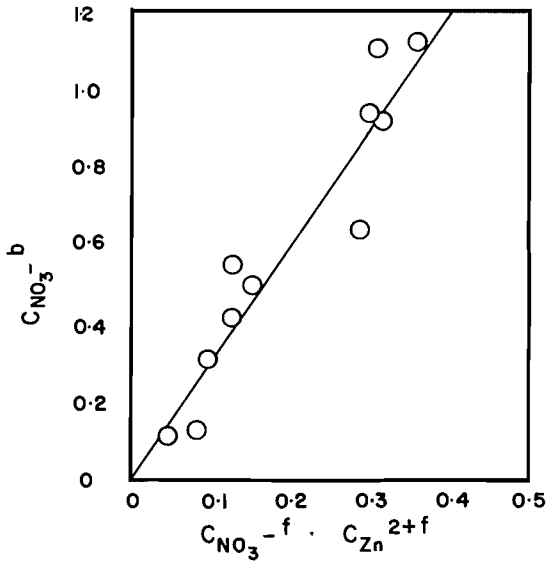

FIG. 8. Plot used to determine the association constant, K_1, of zinc nitrate in methanol at 25 °C. For significance of axes labels see text.

infrared and n.m.r. results obtained at room temperature, it is evident that a linear relationship between the hydroxylic proton resonance frequency and the concentration of electrolyte is not a reliable criterion for the absence of ionic association.

The results of the experiments to determine the solvation number of zinc in solutions of zinc nitrate are analogous to those obtained for solutions of zinc perchlorate (10). However, in the light of the present Raman and infrared evidence, the interpretation of these concentration-dependent solvation numbers requires modification. It is obviously incorrect to invoke the presence, at −80 °C, of contact ion-pairs in these systems. Nevertheless, because the hydroxyl resonance frequency of the cationically bound methanol depends upon the anion, and upon concentration (Fig. 2), the zinc ion must be forming solvent-separated ion pairs with the nitrate and perchlorate anions. The perchlorate ion of the solvent-separated species produces larger upfield shifts of the resonance of bound methanol than does the nitrate ion. (cf. total molar shifts for perchlorate and nitrate in water (26)).

At −80 °C, even though exchange between solvent and the primary solvation shells of cations is slow, exchange between solvent and the solvation shells of anions is rapid. Furthermore, exchange between sites within a cationic solvation shell is slow, as is shown by the observation of more than one "bound" resonance for cobalt (3) and magnesium (1) salts in aqueous methanol. Therefore, when solvent-separated ion pairs are formed, it is necessary to distinguish between three sites for solvent molecules: (*i*) bound between the cation and anion, (*ii*) bound at the remaining sites within the cation's solvation shell, (*iii*) bulk, where this last category includes any anionic solvation shells as well as solvent remote from any ion. At −80 °C, exchange between (*i*) and (*ii*), and between (*ii*) and (*iii*), is slow. The rate of exchange between (*i*) and (*iii*) is of importance to the determination of solvation numbers via area measurements. Should the exchange be slow, both (*i*) and (*ii*) will be counted as within the solvation shell, and the formation of solvent-separated ion pairs will have no effect on the measured solvation number. However, should the exchange between (*i*) and (*iii*) be rapid, then resonance (*i*) will not be counted as within the solvation shell. Therefore, if the anion of a solvent-separated ion pair promotes rapid exchange between bulk solvent and that portion of the cationic solvation shell adjacent to the anion, the measured solvation numbers will decrease from the true value, even though the anion is not displacing solvent from the solvation shell of the cation.

This work was supported by grants from the National Research Council of Canada, by the Government of Ontario in the form of an Ontario Graduate Fellowship to M.H.B., and by the Gulbenkian Foundation in the form of a scholarship to S.A.Al-B.

1. J. H. SWINEHART and H. TAUBE. J. Chem. Phys. **37**, 1579 (1962).
2. S. NAKAMURA and S. MEIBOOM. J. Amer. Chem. Soc. **89**, 1765 (1967).
3. Z. LUZ and S. MEIBOOM. J. Chem. Phys. **40**, 1058 (1964); **40**, 1066 (1964); **40**, 2682 (1964).
4. A. FRATIELLO and D. P. MILLER. Mol. Phys. **11**, 37 (1966).
5. A. FRATIELLO and D. P. MILLER. Mol. Phys. **12**, 111 (1967).
6. A. FRATIELLO, R. E. LEE, V. M. NISHIDA, and R. E. SCHUSTER. J. Chem. Phys. **47**, 4951 (1967).
7. T. J. SWIFT and H. H. LO. J. Amer. Chem. Soc. **89**, 3988 (1967).
8. R. N. BUTLER and M. C. R. SYMONS. Trans. Faraday Soc. **65**, 945 (1969).
9. A. FRATIELLO, V. M. NISHIDA, R. E. LEE, and R. E. SCHUSTER. J. Chem. Phys. **50**, 3624 (1969).
10. S. A. AL-BALDAWI and T. E. GOUGH. Can. J. Chem. **47**, 1417 (1969).

Can. J. Chem. Downloaded from www.nrcresearchpress.com by 210.87.254.105 on 09/05/12
For personal use only.

11. R. E. HESTER and R. A. PLANE. Inorg. Chem. **3**, 769 (1964).
12. D. E. IRISH, A. R. DAVIS, and R. A. PLANE. J. Chem. Phys. **50**, 2262 (1969).
13. D. E. IRISH, G. CHANG, and D. L. NELSON. Inorg. Chem. **9**, 425 (1970).
14. A. R. DAVIS and D. E. IRISH. Inorg. Chem. **7**, 1699 (1968).
15. A. R. DAVIS and R. A. PLANE. Inorg. Chem. **7**, 2565 (1968).
16. C. C. ADDISON and N. LOGAN. Preparative inorganic reactions. Vol. 1. *Edited by* W. L. Jolly. Interscience Publishers, Inc., New York. 1964. p. 141.
17. A. I. VOGEL. Textbook of quantitative inorganic analysis. John Wiley and Sons, Inc., New York, 1967. p. 433.
18. G. HERZBERG. Infrared and Raman spectra of polyatomic molecules. D. Van Nostrand Co. (Canada), Ltd., Toronto. 1964. p. 335.
19. H. BRINTZINGER and R. E. HESTER. Inorg. Chem. **5**, 980 (1966).
20. R. E. HESTER, R. A. PLANE, and G. E. WALRAFEN. J. Chem. Phys. **38**, 249 (1963).
21. A. R. DAVIS. Ph.D. thesis, University of Waterloo, Waterloo, Ontario. 1967.
22. R. P. OERTEL and R. A. PLANE. Inorg. Chem. **7**, 1192 (1968).
23. C. C. ADDISON, D. W. AMOS, and D. SUTTON. J. Chem. Soc. A, 2285 (1968).
24. D. E. IRISH, B. MCCARROLL, and T. F. YOUNG. J. Chem. Phys. **39**, 3436 (1963).
25. F. J. C. ROSSOTTI and H. ROSSOTTI. The determination of stability constants. McGraw-Hill Book Co., Inc., New York. 1961. p. 91.
26. J. N. SHOOLERY and B. J. ALDER. J. Chem. Phys. **23**, 805 (1955).

Can. J. Chem. Downloaded from www.nrcresearchpress.com by 210.87.254.105 on 09/05/12
For personal use only.

Can. J. Chem. Downloaded from www.nrcresearchpress.com by 210.87.254.40 on 09/05/12
For personal use only.

Reaction of CF_3 radicals with methylchlorosilanes

T. N. Bell and U. F. Zucker[1]
Department of Chemistry, Simon Fraser University, Burnaby 2, British Columbia

Received November 14, 1969

Arrhenius parameters have been measured for H abstraction from the alkylchlorosilanes CH_3SiCl_3, $(CH_3)_2SiCl_2$, and $(CH_3)_3SiCl$, and also for $(CH_3)_4Si$

$$k = 10^{11.3}\,e^{-9350/RT} \quad CH_3SiCl_3$$
$$k = 10^{11.8}\,e^{-9230/RT} \quad (CH_3)_2SiCl_2$$
$$k = 10^{12.3}\,e^{-9130/RT} \quad (CH_3)_3SiCl$$
$$k = 10^{11.9}\,e^{-7290/RT} \quad (CH_3)_4Si$$

where k is in ml mole^{-1} s^{-1}. Halogen abstraction does not occur with these compounds nor with $SiCl_4$. CF_2CH_2 is formed from the hot molecule produced when the silylmethyl radical combines with CF_3

$$CF_3 + CH_2SiX_3 \rightarrow CF_3CH_2SiX_3^* \xrightarrow{M} CF_3CH_2SiX_3$$
$$CF_3CH_2SiX_3^* \rightarrow CF_2CH_2 + FSiX_3$$

Canadian Journal of Chemistry, 48, 1209 (1970)

Introduction

This work is a continuation of previous studies concerning the interaction of free radicals with volatile inorganic compounds. In the particular case of silicon compounds, a few such studies have been made (1–9). Introduction of a silicon atom profoundly modifies the molecule as compared with carbon analogues, probably through such factors as electronegativity, size, and dπ–pπ bonding involving empty Si d orbitals. These studies were undertaken to obtain further information on the parameters affecting the reactivity of molecules towards free-radical attack.

Experimental

Materials

(*a*) Hexafluoroacetone (Allied Chemical) was repeatedly fractionated through traps at −96, −135, and −196 °C. The fraction collecting at −135° was thoroughly degassed at that temperature and stored in a blackened bulb.

(*b*) Methylchlorosilanes (Penninsular Chemical Research) were each distilled using a spinning-band column. Large head and tail fractions were rejected. A procedure of fractionation and degassing on the line then followed. $SiCl_4$ was similarly treated.

Apparatus and Procedure

This was as described previously (6).

Results

Trifluoromethyl radicals were produced (10) from the photolysis of hexafluoroacetone (HFA)

[1] $$HFA \xrightarrow{h\nu} 2CF_3 + CO$$

In the presence of the alkyl chlorosilanes the volatile products of reaction consisted of CO, C_2F_6, CF_3H, and CF_2CH_2. No methane or CF_3Cl was detected. Previous work (6) on the reaction of CF_3 radicals with the methylfluorosilanes gave the same products which were established as arising from radical reactions.

Hydrogen Abstraction

Reactions [2] and [3] are proposed to account for the formation of CF_3H and C_2F_6

[2] $$CF_3 + CH_3Si{\lessgtr} \rightarrow CF_3H + CH_2Si{\lessgtr}$$

[3] $$CF_3 + CF_3 \rightarrow C_2F_6$$

Assuming that the reaction between CF_3 and $CH_2Si{\lessgtr}$ leads to insignificant amounts of CF_3H, we have, from reactions [2] and [3]

[4] $$R_{CF_3H}/R_{C_2F_6}{}^{1/2} = k_2\,[\text{silane}]/k_3{}^{1/2}$$

A test of this equation is seen in Fig. 1, where $R_{CF_3H}/R_{C_2F_6}{}^{1/2}$ is plotted against [silane], for a fixed HFA pressure of 20 mm at a temperature of 200 °C.

A determination of $k_2/k_3{}^{1/2}$ was made for each of the silanes at various temperatures by the application of eq. [4] to the experimental results. The results are tabulated in Table 1. Variation of

[1]Present address: DuPont of Canada, Ltd., Central Research Laboratory, Maitland, Ontario.

Can. J. Chem. Downloaded from www.nrcresearchpress.com by 210.87.254.40 on 09/05/12
For personal use only.

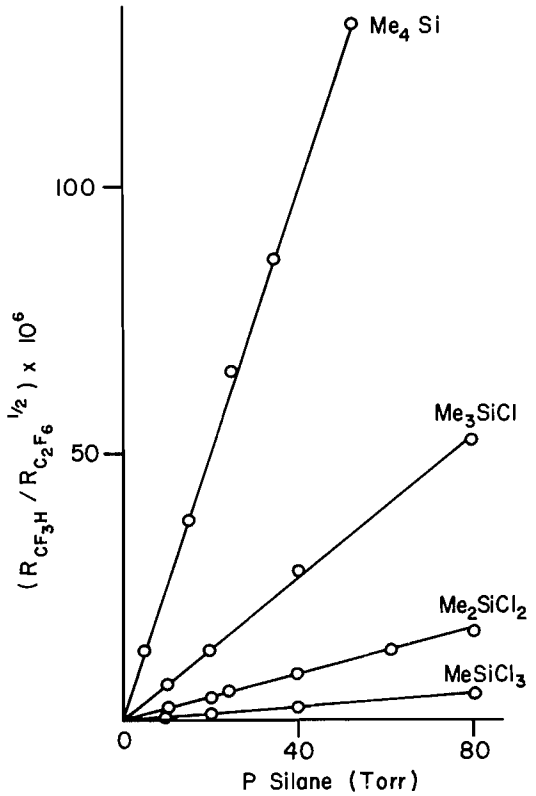

FIG. 1. Variation of $R_{CF_3H}/R_{C_2F_6}{}^{1/2}$ with p_{silane}. Temperature, 200 °C (Me_4Si, ref. 6).

the HFA pressure had no effect on $k_2/k_3{}^{1/2}$. Decomposition of the silane was kept to <2%.

An Arrhenius plot of the results is shown in Fig. 2. Using Ayscough's (11) value for $k_3 = 2.3 \times 10^{13}$ cm^3 mole^{-1} s^{-1}, a least-squares evaluation of the Arrhenius parameters yields the results given in Table 2. Included in Table 2 are the values obtained for k_2 by Cheng and Szwarc (5) at one temperature, 180 °C, and calculated from our results at that temperature. Reasonable agreement is seen. The Arrhenius parameters for H abstraction by CF_3 from the methylfluorosilanes and tetramethylsilane (6) are also included.

Chlorine Abstraction

No evidence was obtained for CF_3Cl formation with the methylchlorosilanes, nor has previous work shown this to occur (3, 5, 7). There is a possibility that the competitive H abstraction process completely precludes chlorine abstraction. In an attempt to measure the Arrhenius parameters for this process, HFA was photolyzed in the presence of $SiCl_4$ at temperatures up to 350 °C. No CF_3Cl could be detected.

We conclude that reaction [5] is unimportant under our experimental conditions

[5] $$CF_3 + ClSi\begin{matrix}\diagup\\ \diagdown\end{matrix} \rightarrow CF_3Cl + Si\begin{matrix}\diagup\\ \diagdown\end{matrix}$$

CF_2CH_2 Formation

All the methylchlorosilanes gave this product, as was also found (12) with the methylfluorosilanes and $(Me)_4Si$. Two sources were apparent: (*a*) from a dark reaction observed only after periods of photolysis, and (*b*) from a much faster process during the photolysis of the HFA–silane systems.

By analogy with our previous conclusions (12) on the methylfluorosilane system, we suggest the second source is from a radical combination process, reaction [6], leading to a hot molecule which may stabilize, reaction [7*a*], or decompose, reaction [7*b*]

[6] $$CF_3 + CH_2SiX_3 \rightarrow CF_3CH_2SiX_3^*$$

[7*a*] $$CF_3CH_2SiX_3^* \xrightarrow{M} CF_3CH_2SiX_3$$

[7*b*] $$\hookrightarrow CF_2CH_2 + FSiX_3$$

where X = Cl and/or Me.

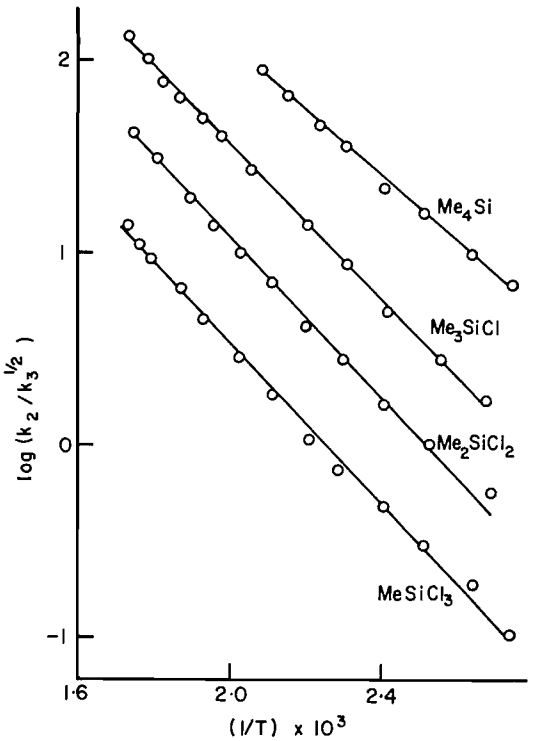

FIG. 2. Arrhenius plot, $\log k_2/k_3{}^{1/2}$ *vs.* $1/T$ (Me_4Si, ref. 6).

Can. J. Chem. Downloaded from www.nrcresearchpress.com by 210.87.254.40 on 09/05/12
For personal use only.

TABLE 1

Hydrogen abstraction from methyl chlorosilanes by CF_3

Temperature (°C)	P silane (Torr)	$R_{C_2F_6} \times 10^{10}$ (mole ml^{-1} s^{-1})	$R_{CF_3H} \times 10^{10}$ (mole ml^{-1} s^{-1})	$k_2/k_3^{1/2}$ (ml$^{1/2}$ mole$^{-1/2}$ s$^{-1/2}$)
		Substrate CH_3SiCl_3		
90.5	78.1	2.523	0.050	0.12
105.6	75.0	2.863	0.078	0.182
125.3	65.6	2.833	0.111	0.297
143.5	70.7	2.731	0.186	0.469
163.5	73.8	2.553	0.287	0.719
179.3	42.3	0.841	0.141	1.07
198.5	40.5	0.708	0.205	1.77
219.5	33.6	1.974	0.449	2.80
245.0	36.9	1.788	0.760	4.54
261.6	35.7	1.610	1.002	6.52
282.4	34.5	1.406	1.292	9.31
291.8	34.0	1.238	1.406	11.0
301.6	33.4	0.227	0.702	13.0
		Substrate $(CH_3)_2SiCl_2$		
98.6	30.6	2.121	0.086	0.57
122.1	28.8	2.201	0.143	0.99
141.8	24.9	1.781	0.177	1.57
161.6	32.8	2.134	0.447	2.75
181.4	25.0	1.777	0.474	4.19
200.8	61.1	1.174	1.454	6.48
200.8	79.8	1.048	1.756	6.33
200.8	24.0	1.583	0.699	6.84
219.5	23.1	1.348	0.899	9.9
237.1	22.4	1.149	1.121	13.8
253.2	21.6	0.949	1.362	19.1
279.3	20.6	0.655	1.722	30.4
298.3	19.9	0.471	1.970	42.6
		Substrate $(CH_3)_3SiCl$		
100.0	25.4	1.005	0.149	1.73
117.5	24.2	1.070	0.238	2.80
140.1	22.9	0.956	0.380	5.0
159.8	21.8	0.800	0.573	8.66
179.3	21.9	2.609	1.670	13.9
179.3	20.9	0.656	0.770	13.4
212.3	19.5	0.565	1.343	27.1
231.9	18.7	0.386	1.541	39.1
245.0	18.2	0.320	1.727	49.4
261.6	17.7	0.252	1.960	64.9
273.3	17.3	0.200	2.154	81.9
288.6	16.9	0.155	2.366	105.1
301.6	16.5	0.114	2.533	134.4

TABLE 2

Arrhenius parameters for H abstraction from methyl-, methylchloro-, and methylfluorosilanes by CF_3

Substrate	log A	E (kcal/mole)	$k_2 \times 10^{-8}$ (180 °C) (ml mole^{-1} s^{-1}*)	$k_2 \times 10^{-8}$ (180 °C) (ml mole^{-1} s^{-1}*)
CH_3SiCl_3	11.31±0.13	9.35±0.21	0.06	0.07 (5)
$(CH_3)_2SiCl_2$	11.79±0.10	9.23±0.18	0.2	0.44 (5)
$(CH_3)_3SiCl$	12.25±0.06	9.13±0.09	0.7	1.4 (5)
CH_3SiF_3	11.98±0.04	11.71±0.09	0.02 (6)	
$(CH_3)_2SiF_2$	12.27±0.06	10.53±0.12	0.2 (6)	
$(CH_3)_3SiF$	12.43±0.05	9.48±0.09	0.8 (6)	
$(CH_3)_4Si$	11.91±0.09	7.29±0.14	2.6 (6)	3.5 (5)
$(CH_3)_4Si$	11.90±0.05	7.23±0.09	2.7 (8)	

*Reference numbers in parentheses.

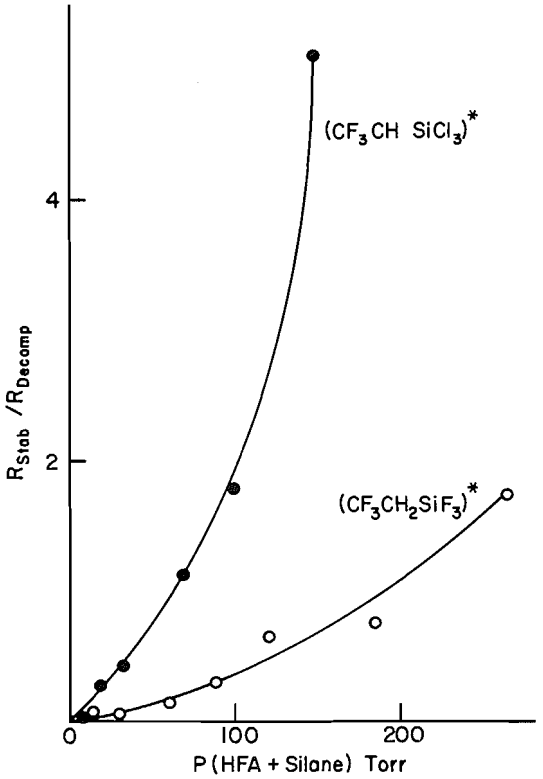

FIG. 3. Variation of R_{stab}/R_{decomp} with total pressure. Temperature, 200 °C. ● $(CF_3CH_2SiCl_3)^*$, ○ $(CF_3CH_2SiF_3)^*$.

The dark production of CF_2CH_2 is considered to arise from pyrolysis of the product formed in reaction [7*a*]

[8] $$CF_3CH_2SiX_3 \rightarrow CF_2CH_2 + FSiX_3$$

This β-fluorosilane pyrolysis reaction is well established (13, 14). From reactions [7*a*] and [7*b*]

[9] $$R_{stab}/R_{decomp} = k_{7a}[M]/k_{7b}$$

A series of experiments were carried out to determine the ratio R_{stab}/R_{decomp} for the system HFA + CH_3SiCl_3 as a function of pressure, for equal amounts of each reactant at 200 °C. R_{decomp} was determined from the CF_2CH_2 formed during photolysis (the correction for the pyrolysis reaction [8] is negligible for the photolysis times of 2 min). R_{stab} was measured in a separate experiment by pyrolyzing, at 300 °C, the $CF_3CH_2SiCl_3$ formed during photolysis, and determining the resulting CF_2CH_2. The results are plotted in Fig. 3; included here for comparison are the corresponding results for the HFA + CH_3SiF_3 system (12).

Discussion

In their earlier work, Kerr, Slater, and Young (1, 2) discussed silane reactivity in terms of abnormally high A factors. However, in view of more recent results, they (7, 8) conclude that normal A factors prevail. These conclusions are confirmed in the present work. The observed increase in A factor with decreasing chlorine substitution leads to changes in the rate constant such that $k_{\rightarrow SiCl} \sim 3k_{\rightarrow SiCl_2} \sim 10k_{\rightarrow SiCl_3}$. The same trend is apparent in H abstraction by CF_3 radicals from the fluorosilanes (6) and the chloromethanes (15), also in the tabulated data of the reactions of methyl radicals with the halomethanes (16, 17). It should be pointed out that the A factor for tetramethylsilane does not fit into this pattern, which result parallels the position of methane in abstraction from this and the halomethanes. When normalized per methyl group or per hydrogen atom, the effect of variations in the A factor on the rate of reaction is considerably reduced.

The activation energy differences between the chlorosilanes are slight, and have little effect on the silane reactivity. This is in marked contrast to our observations on hydrogen abstraction from the fluorosilanes (Table 2). In the latter case the variations in activation energy were linked to changes in electron density on the hydrogen atom, the lowest activation energy being associated with the H having the highest electron density. This polar effect involving attack by the electrophilic CF_3 radical would be expected to occur with the methyl chlorosilanes, where the inductive effect of the Cl atoms should decrease the H electron density with increasing chlorine substitution.

We suggest that the inductive effect is offset to some extent by $d\pi \leftarrow p\pi$ bonding which is expected to be more important with chlorine than with fluorine, when the orbitals involved are considered. Gowenlock and Thomas (18) have suggested that this back-coordination reaches a maximum when three chlorine atoms are attached to silicon. On this basis, the effective inductive effect may well be approximately the same for mono-, di-, and tri-chloro substitution, leading to a similar electron density on the hydrogen atom, and thus a constant polar effect.

The constancy of the observed activation energies would furthermore imply that the C—H bond strength is the same in the three chlorosilanes. This view is supported by the constancy

Can. J. Chem. Downloaded from www.nrcresearchpress.com by 210.87.254.40 on 09/05/12
For personal use only.

Can. J. Chem. Downloaded from www.nrcresearchpress.com by 210.87.254.40 on 09/05/12
For personal use only.

of the activation energies observed (2) for methyl attack on the methylchlorosilanes, where polar effects would be expected to be minimal.

The activation energy difference $E_{\text{chlorosilane}} - E_{\text{Si(Me)}_4}$ for CF_3 attack is approximately 2 kcal, while the corresponding difference for CH_3 attack is ~1 kcal (2, 4, 8); presumably the latter is due to changes in the silane C—H bond energy term.

We suggest that the greater difference in the CF_3 case is a result of this bond energy difference plus a polar effect, which should favor a lowering of the activation energy for compounds whose H atoms have greater electron density. In the case under discussion, the inductive effect of chlorine should decrease the electron density on the H atom, compared to the hydrogen atoms in $Si(Me)_4$.

These results confirm the observation by Cheng and Szwarc (5) that increased chlorine substitution leads to a decrease in reactivity of the silanes, and that this correlates with the proton chemical shift.

In support of the suggestion that $d\pi \leftarrow p\pi$ bonding is important is the observation that chlorine abstraction is not observed with the chlorosilanes nor with $SiCl_4$. Such interactions would result in a strong Si—Cl bond; this has been estimated (19, 20) at between 82 and 120 kcal. The absence of Cl abstraction at 350 °C would suggest an endothermic process for reaction [5], and supports the upper estimate for $D_{\text{Si-Cl}}$.

The formation of CF_2—CH_2 in all cases involving the methylchlorosilanes and the methylfluorosilanes (6) points to the hot molecule rearrangement–elimination reaction being general (12)

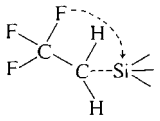

In Fig. 3, the results for $(CF_3CH_2SiCl_3)^*$ are compared to those for $(CF_3CH_2SiF_3)^*$. In both cases the plots of $R_{\text{stab}}/R_{\text{decomp}}$ are curved, which is suggestive of a multistage deactivation process (21, 22). This is to be expected if our estimate (12) for the excess energy above the activation energy is correct ($(CF_3CH_2SiF_3)^*$ excess estimated 45 kcal). This may well be less for $(CF_3CH_2SiCl_3)^*$, where our pyrolysis measurements indicate a greater half-life for $CF_3CH_2SiCl_3$, compared with $CF_3CH_2SiF_3$. Indeed, if the fluorine transfer process involves interaction of the β fluorine atom with the silicon d orbitals, we would expect that significant amounts of back-bonding (proposed above) would make this transfer a more difficult process.

This effect would alter the ratio $R_{\text{stab}}/R_{\text{decomp}}$ in favor of the chlorosilane over the fluorosilane for a given pressure. That this is the case is shown in Fig. 3. A similar effect would of course occur if the effective number of oscillators is greater in the case of chlorosilanes as against fluorosilanes.

We thank the National Research Council of Canada for financial support and Mr. R. McDaniel for computer assistance.

1. J. A. KERR, D. H. SLATER, and J. C. YOUNG. J. Chem. Soc. A, 104 (1966).
2. J. A. KERR, D. H. SLATER, and J. C. YOUNG. J. Chem. Soc. A, 134 (1967).
3. T. N. BELL and B. B. JOHNSON. Aust. J. Chem. **20**, 1545 (1967).
4. A. U. CHAUDHRY and B. G. GOWENLOCK. J. Organometal. Chem. **16**, 221 (1969).
5. W. J. CHENG and M. SZWARC. J. Phys. Chem. **72**, 494 (1968).
6. T. N. BELL and U. F. ZUCKER. J. Phys. Chem. In press.
7. J. A. KERR, A. STEPHENS, and J. C. YOUNG. Int. J. Chem. Kinet. **1**, 371 (1969).
8. J. A. KERR, A. STEPHENS, and J. C. YOUNG. Int. J. Chem. Kinet. **1**, 339 (1969).
9. E. R. MORRIS and J. C. J. THYNNE. J. Organometal. Chem. **17**, 3 (1969).
10. P. B. AYSCOUGH and E. W. R. STEACIE. Proc. Roy. Soc. London, Ser. A, **476**, 234 (1956).
11. P. B. AYSCOUGH. J. Chem. Phys. **24**, 944 (1956).
12. T. N. BELL and U. F. ZUCKER. Can. J. Chem. **47**, 1701 (1969).
13. R. N. HASZELDINE, P. J. ROBINSON, and R. F. SIMMONS. J. Chem. Soc. 1890 (1964).
14. G. FISHWICK, R. N. HASZELDINE, C. PARKINSON, P. J. ROBINSON, and R. F. SIMMONS. Chem. Commun. 383 (1965).
15. W. G. ALCOCK and E. WHITTLE. Trans. Faraday Soc. **62**, 134 (1966).
16. G. Porter (*Editor*) Progress reaction kinetics. Vol. 3. Pergamon Press. 1965. pp. 50, 104, 106.
17. S. W. BENSON. Foundations of chemical kinetics. McGraw-Hill Book Co., Inc. 1960. p. 296.
18. B. G. GOWENLOCK and K. E. THOMAS. J. Chem. Soc. London, 5068 (1965).
19. G. G. HESS, F. W. LAMPE, and L. H. SOMMER. J. Amer. Chem. Soc. **86**, 3174 (1964); **87**, 5327 (1965).
20. J. A. CONNOR, G. FINNEY, G. J. LEIGH, R. N. HASZELDINE, P. J. ROBINSON, R. D. SEDGWICK, and R. F. SIMMONS. Chem. Commun. 178 (1966).
21. G. O. PRITCHARD and R. L. THOMMASON. J. Phys. Chem. **71**, 1674 (1967).
22. J. T. BRYANT and G. O. PRITCHARD. J. Phys. Chem. **71**, 3439 (1967).

Can. J. Chem. Downloaded from www.nrcresearchpress.com by 210.87.254.40 on 09/05/12
For personal use only.

Viscosity of associated liquids

R. C. MAKHIJA AND R. A. STAIRS[1]
Department of Chemistry, Trent University, Peterborough, Ontario

Received November 13, 1969

Viscosity data for ammonia, methylamine, and 1,2-diaminopropane have been obtained in the temperature ranges −65 to −35, −65 to −10, and −35 to +50 °C, respectively, using an Ubbelohde viscometer. The results were compared with existing data, and all the data were fitted to the Fulcher (Tammann–Hesse) equation by the method of least squares. The significance of the values of T_0 in this equation for these and other associated liquids was considered.

Les valeurs de viscosité pour l'ammoniac liquide, la méthylamine et le 1,2-diaminopropane ont été obtenues dans les intervalles de température suivants: −65 à −35, −65 à −10 et −35 à +50 °C, respectivement, utilisant un viscosimètre Ubbelohde. Les résultats ont été comparés aux valeurs existantes, et les constantes de l'équation Fulcher (Tammann–Hesse) ont été trouvées par la méthode des moindres carrés. La signification des valeurs de T_0 dans cette équation a été considérée pour ces liquides contenant des liaisons hydrogène et d'autres composés similaires.

Canadian Journal of Chemistry, 48, 1214 (1970)

In the search for a simple equation to express the dependence of the viscosity, η, of liquids on absolute temperature, T, over an extended range, the equation apparently first proposed by Fulcher (1)

$$[1] \qquad \log \eta = A + B/(T - T_0)$$

and used by Tammann and Hesse (2), Prasad (3), Gutmann and Simmons (4, 5), and recently by Miller (6), has been somewhat neglected. Part of this neglect may be due to the fact that it is not simply explicable in terms of an "activation energy for flow."

Gutmann and Simmons showed that eq. [1] is obtained if the activation energy, E_0, varies with temperature as $E_0/(a + b/T)$, where a and b are constants. This, however, is an unsatisfying form, hard to relate to molecular or thermodynamic concepts. They also succeeded in deriving the equation from what they described as a quantum form of the Maxwell–Boltzmann distribution law, attributing the deviation of the viscosity from the Andrade equation (7)

$$[2] \qquad \eta = A' \, e^{E/RT}$$

where A' is a constant and R is the gas constant, to other causes than inconstancy of E. It must be admitted that the theoretical justification for eq. [1] is uncertain, but it does fit the data for diverse liquids well, and is not too difficult to apply. Gutmann and Simmons have derived normal equations for least-squares fitting of eq. [1] to data, but we prefer eqs. [3] for this purpose, as they throw less undue weight on the higher-temperature points.

$$[3a] \quad nA + T_0 \sum(y/T) + D \sum(1/T) - \sum y = 0$$

$$[3b] \quad A \sum(y/T) + T_0 \sum(y^2/T^2) + D \sum(y/T^2) - \sum(y^2/T) = 0$$

$$[3c] \quad A \sum(1/T) + T_0 \sum(y/T^2) + D \sum(1/T^2) - \sum(y/T) = 0$$

where $y = \log \eta$, T = absolute temperature, $D = B - AT_0$, and A, B, and T_0 are the constants in eq. [1].

Using a computer, we have fitted the Fulcher equation to data for the viscosity of several oxygen- and nitrogen-containing associated liquids. The results are listed in Table 3. Data for the alcohols, glycol, and glycerol were obtained from various literature sources (8–10). Data for ammonia in the literature were included with our own, and our own data were used for methylamine and 1,2-diaminopropane.

Experimental

The viscosities of liquid ammonia, methylamine, and 1,2-diaminopropane were measured by capillary flow, using Ubbelohde (suspended-level) viscometers, adapted for use in a closed system as shown in Fig. 1. The design permits introduction of sample without admission of air, by distillation or through the side-arm, and makes it unnecessary to know the volume of the liquid; the working volume being that between the upper meniscus (moving

[1]Temporary address until August 1, 1970: c/o Department of Chemistry, University of California, Berkeley, Calif. 94720.

Can. J. Chem. Downloaded from www.nrcresearchpress.com by 210.87.254.40 on 09/05/12
For personal use only.

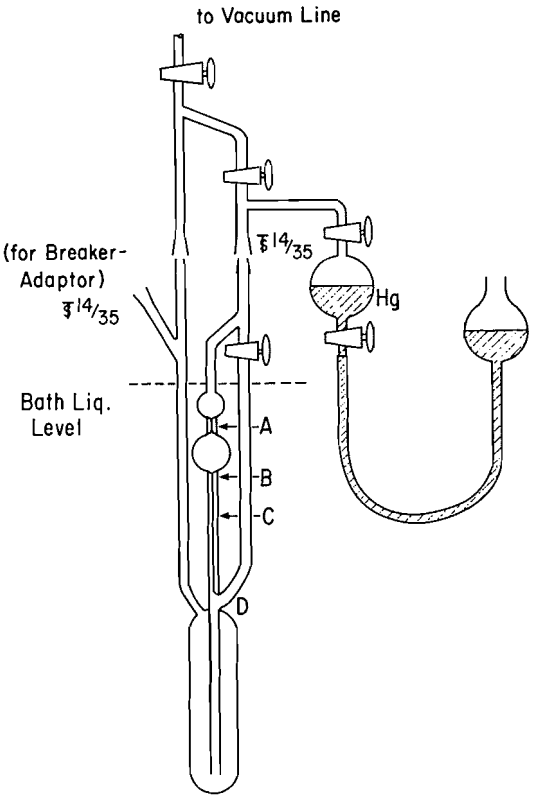

FIG. 1. Viscometer for use with air-sensitive liquids and solutions.

between the marks at *A* and *B*) and the bottom of the capillary at *D*. The viscometers were calibrated against water in the temperature range 0–50 °C, using data for the viscosity and density of water from the Handbook of Chemistry and Physics (10).

Ammonia (Matheson) was distilled from the cylinder onto sodium in the vacuum line. After allowing a portion to escape, together with any hydrogen formed, a further portion was subjected to two bulb-to-bulb fractionations, and finally distilled into the viscometer. Methylamine was similarly treated, except that lithium replaced sodium, and 24 h were allowed for reaction with water or any other reducible impurities.

1,2-diaminopropane (various sources, including B.D.H., Ana Chimia, and BASF) was purified by refluxing overnight with potassium hydroxide, followed by distillation under nitrogen over sodium wire. It was again distilled and a middle fraction of boiling range 117.5–118.5 °C was retained. This distilled product was finally distilled under vacuum into a number of break-seal vials, which were then sealed off from the line where indicated in Fig. 2*a*. The contents of a vial were transferred to the viscometer without access of air or entry of broken glass by means of the adaptor with fritted disk, illustrated in Fig. 2*b*.

The gas used to move the liquids in the viscometer was hydrogen (Matheson, electrolytic) purified by passage over a "Deoxo" catalytic purifier and phosphorus pentoxide.

Temperature control above 0 °C was achieved by a water-bath thermostat of conventional design, and temperatures in this range were measured by a mercury-in-glass thermometer, graduated to 1/10 degree, and corrected at ice point. Temperature control at lower temperatures was achieved by a thermostat of special design. Methanol contained in a large Dewar vessel was circulated through a copper coil, immersed in Dry Ice – acetone in another vessel, by a centrifugal pump which was controlled by a YSI thermistor controller. By this means, the temperature could be controlled within 0.1 degree at any point down to about −70 °C.

In the present work, time was measured manually, using an electrical stop watch.

The method employed yields the kinematic viscosity $\nu = \eta/\rho$, where η is viscosity and ρ the density of the liquid. The required densities for ammonia were taken from Johnson and Martens (11, 12), and for methylamine from Felsing and Thomas (13). Densities for 1,2-diaminopropane not being available, they were measured by means of a dilatometer fitted with a ground joint for attachment to the vacuum line and a stopcock. It was filled by distillation under vacuum with the diamine, purified as described. With the stopcock closed, it was removed from the line, weighed, and the position of the meniscus in the "Trubore" neck observed with a cathetometer at different temperatures. It was calibrated using distilled water.

The observed times were related to viscosity through the equation

$$\nu = \eta/\rho = At - B/t$$

where A and B are constants which we did not attempt to calculate absolutely, but obtained, by calibration with water and *n*-butanol at a number of temperatures, from the intercept and slope of a plot of ν/t vs. $1/t^2$. The values for the various viscometers used are listed in Table 1.

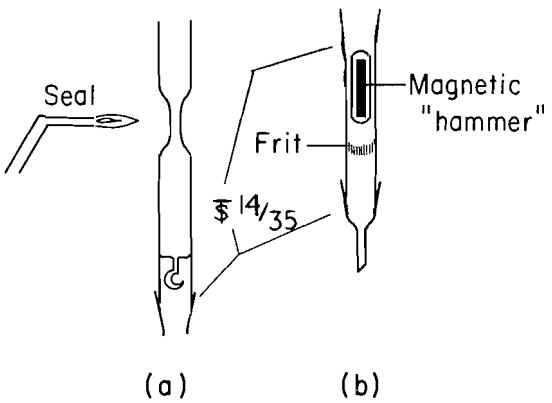

FIG. 2. (*a*) Break-seal vial. (*b*) Breaker-adaptor.

TABLE 1
Calibration of viscometers

Viscometer	Used with	$A \times 10^3$	B/A
I	Ammonia	1.288	(negligible)
II	Ammonia	3.128	4.77
III	Methylamine	5.768	2.69
IV	1,2-Diaminopropane	1.160	(negligible)

Because of the disparity between the temperatures of calibration and measurement, the effect of thermal expansion of the Pyrex glass of the viscometers was calculated, and found to be negligible.

Results and Discussion

The values of the viscosity of ammonia obtained in this work, together with some earlier measurements made using the same method by Stairs (unpublished), and our results for viscosity of methylamine and viscosity and density of 1,2-diaminopropane are collected in Table 2. The results for ammonia agree within 0.33% with those in the Handbook of Chemistry and Physics (10), and support, by a short extrapolation, the value 0.2543 cP at −33.5 °C found by Elsey (14). Fitzgerald's value at this temperature appears to be nearly 5% high (15). A large graph of log η vs. reciprocal temperature, on which all the available data were plotted, made it apparent that the data of Pinevich (16) are inconsistent with the others, being too high at his higher temperatures (30, 60 °C) by as much as 25%. The data of Carmichael and Sage (17) tend towards low values at higher temperatures (70, 100 °C), but this seems to be a real effect, due to the increasing specific volume of ammonia under its own vapor pressure at these temperatures. These two sets of data were accordingly excluded from those used to fit the Fulcher equation, which was not expected to be valid under conditions of grossly-varying specific volume.

The only available data for methylamine were those of Fitzgerald (15), who gives η as 0.2364 cP at 0 °C, and of Berns *et al.* (18), who give values differing from that of Fitzgerald at 0 °C by 16%. Our measurements agree with Fitzgerald at the highest temperature and with Berns *et al.* at the

TABLE 2
(*a*) Viscosity of ammonia and methylamine at various temperatures

Ammonia				Methylamine	
t (°C)	η (cP)	t (°C)	η (cP)	t (°C)	η (cP)
−65.0	0.4314	−41.8	0.290	−70	0.802
−60.0	0.3906	−40.6	0.2826	−65	0.681
−55.0	0.3562	−40.1	0.2817	−60	0.604
−53.2	0.347	−40.0	0.2823	−55	0.540
−50.4	0.331	−39.8	0.2794	−50	0.484
−50.0	0.3285	−39.5	0.280	−45	0.443
−47.8	0.319	−38.0	0.2714	−40	0.404
−45.1	0.305	−37.2	0.271	−35	0.374
−45.0	0.3002	−36.7	0.269	−30	0.348
−42.2	0.290	−35.0	0.2632	−25	0.323
				−20	0.301
				−15	0.280
				−10	0.266

(*b*) Viscosity and density of 1,2-diaminopropane at various temperatures

t (°C)	η (cP)	ρ (g/ml)	t (°C)	η (cP)	ρ (g/ml)
−35	16.47	0.9140	10	2.206	0.8690
−30	13.20	0.9087	15	1.925	0.8639
−25	9.372	0.9030	20	1.709	0.8580
−20	6.965	0.8987	25	1.570	0.8540
−15	5.322	0.8935	30	1.395	0.8487
−10	4.354	0.8880	35	1.227	0.8440
−5	3.610	0.8834	40	1.173	0.8397
0	3.032	0.8787	45	1.045	0.8351
+5	2.704	0.8737	50	0.940	0.8303

Can. J. Chem. Downloaded from www.nrcresearchpress.com by 210.87.254.40 on 09/05/12
For personal use only.

Can. J. Chem. Downloaded from www.nrcresearchpress.com by 210.87.254.40 on 09/05/12
For personal use only.

lowest. There seemed no way of choosing between them, so we used our results only to fit the Fulcher equation. The only data for 1,2-diaminopropane were estimates found in industrial bulletins (19, 20), with which our measurements appear to agree. We again fitted the equation to our data alone.

TABLE 3

Viscosity of methylamine by Berns *et al.* (18)

t (°C)	η (cP)
0	0.2742
−22.8	0.3532
−63.3	0.6704
−78.3	0.9120

On examining the Fulcher equation constants in Table 4 for trends of possible significance, we noted that the quantity T_0 (written as $-C$ by some authors) is largest for those liquids in which very extensive hydrogen bonding is possible, leading to possible formation of chains or networks. This is apparent in the sequence of water and the normal alcohols, where, as the hindrance to polymerization through hydrogen bonding due to the bulk of the alkyl group increases, T_0 tends rapidly to small values. In the sequence of compounds $H(CHOH)_nH$, however, the value of T_0 tends to maintain the value (about −120 to −140) characteristic of water. At these temperatures, the quantity RT is about 1/10 of the energy of dissociation of a hydrogen bond between two oxygens (about 3 kcal/mole), and it appears that the liquids at these and lower temperatures are, in effect, brittle glasses. (The glass transition temperature, where it can be observed, seems to occur a few degrees above T_0. See, for example, refs. 2 and 21.)

The tendency towards extensive polymerization is less apparent in ammonia, the value of T_0 being less than half that of water, but in the diamine, the two hydrogen-bonding groups restore the tendency to polymerize. That methylamine shows a larger value of T_0 than does methanol is puzzling, but the range of the measurements is not great and the extrapolation is long, so the value of T_0 for methylamine may be in error.

The significance of the other constants remains obscure. There is a tendency for B to increase with increasing molecular weight, but its significance as proportional to an activation energy, which would be in keeping with this observation, is obscure, as was remarked above. The significance of A, which in the Andrade equation can be interpreted as a "jump frequency factor", is also obscure.

TABLE 4

Fit of viscosity of associated liquids to the Fulcher equation $\log \eta = A + B/(T - T_0)$

Liquid	Constants in eq. [1] A	B	T_0	Percent error of fit*	Range (°C)
Ammonia	−1.7520	218.76	50.701	0.76	−69 to +40
Methylamine	−1.3634	126.389	102.886	0.32	−70 to −10
1,2-Diaminopropane	−1.0755	165.754	166.751	1.10	−35 to +50
Methanol	−1.6807	354.876	48.585	2.05	−98.3 to +50
Water	−1.5668	230.298	146.797	0.51	−10 to +160
Ethanol	−2.4401	774.414	−15.249	2.66	−98.11 to +70
Glycerin	−2.8834	997.586	128.481	4.50	−42 to +30
Ethylene glycol	−1.5923	438.064	141.617	0.18	+20 to +100
n-Propanol	−2.4907	725.903	37.474	1.10	0 to +70
n-Butanol	−3.0037	1033.306	−4.3828	0.80	−50.9 to +100

*Defined as

$$100\left\{\frac{\Sigma\left(\frac{\eta_{calcd}-\eta}{\eta}\right)^2}{n-3}\right\}^{\frac{1}{2}}$$

The authors wish to thank DuPont of Canada, Limited, for the gift of a quantity of 1,2-diaminopropane.

1. G. S. FULCHER. J. Amer. Ceram. Soc. **8**, 339 (1925).
2. G. TAMMANN and W. HESSE. Z. Anorg. Allg. Chem. **156**, 245 (1926).
3. B. PRASAD. Phil. Mag. **16**, 263 (1933).
4. F. GUTMANN and L. M. SIMMONS. Aust. J. Sci. **13**, 109 (1951).
5. F. GUTMANN and L. M. SIMMONS. J. Appl. Phys. **23**, 977 (1952).
6. A. A. MILLER. Science, **163**, 1325 (1969).
7. E. N. DA C. ANDRADE. Nature, 125 (1930).
8. International critical tables. Vols. 5 and 7. McGraw-Hill Book Co., Inc. 1930.

9. J. TIMMERMANS. Physico-chemical constants of pure organic compounds. Elsevier Publ. Co., Inc., Amsterdam. 1950.
10. C. D. HODGMAN (*Editor*). Handbook of chemistry and physics. The Chemical Rubber Co., Cleveland, Ohio. 1964.
11. W. L. JOLLY and C. J. HALLADA. *In* Non-aqueous solvent systems. *Edited by* T. C. Waddington. Academic Press, Inc., New York. 1965. p. 4.
12. W. C. JOHNSON and R. I. MARTENS. J. Amer. Chem. Soc. **58**, 15 (1936).
13. W. A. FELSING and A. R. THOMAS. Ind. Eng. Chem. **21**, 1269 (1929).
14. H. M. ELSEY. J. Amer. Chem. Soc. **42**, 2454 (1920).
15. F. F. FITZGERALD. J. Phys. Chem. **16**, 621 (1912).
16. G. PINEVICH. Kholod. Tekh. **20**, 30 (1948); Chem. Abstr. **43**, 8813*e*.
17. L. T. CARMICHAEL and B. H. SAGE. Ind. Eng. Chem. **44**, 2728 (1952).
18. D. S. BERNS, E. C. EVERS, and P. W. FRANK, JR. J. Amer. Chem. Soc. **82**, 310 (1960).
19. Propylenediamine. Union Carbide Chemicals, Product bulletin F-40669A, April, 1966.
20. 1,2-Propylenediamine. Badishe Anilin and Sodafabrik A.G. (BASF), Ludwigshafen/Rhein. Provisional leaflet.
21. I. YANNAS. Science, **160**, 298 (1968).

Can. J. Chem. Downloaded from www.nrcresearchpress.com by 210.87.254.40 on 09/05/12
For personal use only.

Can. J. Chem. Downloaded from www.nrcresearchpress.com by 210.87.254.42 on 09/05/12
For personal use only.

Synthesis of polymer intermediates containing the bicyclo[3.2.2]nonane ring

LUDEK TAIMR[1] AND JAMES G. SMITH
Department of Chemistry, University of Waterloo, Waterloo, Ontario

Received October 8, 1969

The preparation of 1,5-biscarbethoxybicyclo[3.2.2]nonane and 1,5-bis(hydroxymethyl)bicyclo[3.2.2]-nonane is described. The procedure generally followed that reported for the analogous bicyclo[2.2.2]-octanes. However, certain differences in chemical behavior were observed and are reported.

The alkylation of the sodium salt of diethyl succinylsuccinate produced the expected 1,5-biscarb-ethoxybicyclo[3.2.2]nonane-6,8-dione along with a by-product which was shown to be 1,5-biscarbethoxy-bicyclo[4.2.1]nonane-7,9-dione. It was also shown that this compound arose by isomerization of the bicyclo[3.2.2]nonane analogue after the alkylation occurred.

Conversion of these compounds to thioketals with 1,3-propanedithiol was also examined in detail. The reaction between 1,3-propanedithiol and 1,5-biscarbethoxybicyclo[3.2.2]nonane-6,8-dione generated an equilibrating system of 4 compounds. Three of these are shown to be the monothioketal, the bisthioketal, and a mixed thioketal–vinylthioether.

Canadian Journal of Chemistry, 48, 1219 (1970)

For the purposes of continuing our study (1, 2) into the relationship between the structure of condensation polymers and their physical properties, it became necessary to prepare bifunctional bridgehead derivatives of bicyclo[2.2.2]octane and bicyclo[3.2.2]nonane. While syntheses for the former compounds had been documented (3, 4), syntheses for the latter compounds were incomplete (4, 5). It seemed logical, however, that the synthetic sequence employed for the bicyclo[2.2.2]octane system (3) would be equally applicable to the bicyclo[3.2.2]nonane system (see Scheme 1). While broadly speaking this was true, certain interesting differences have been observed and these are described here.

[1]Dr. L. Taimr is a visiting scientist from the Institute of Macromolecular Chemistry of the Czechoslovak Academy of Sciences, Prague, Czechoslovakia.

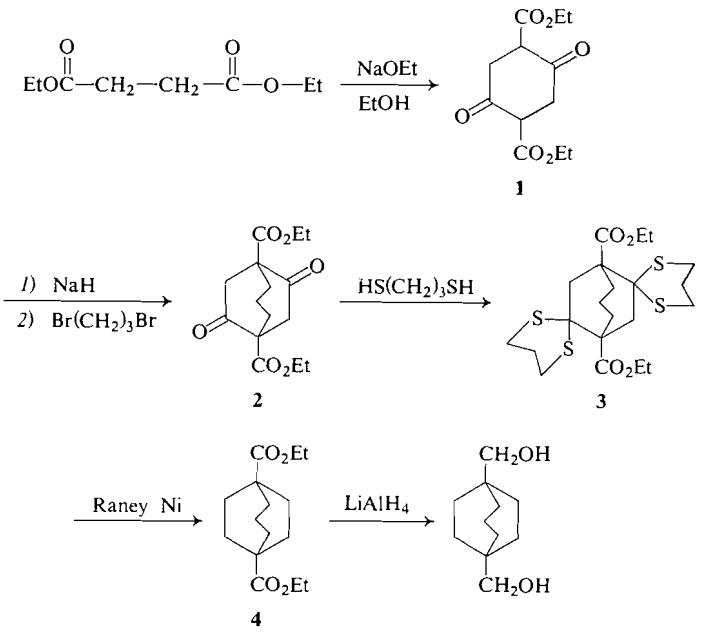

SCHEME 1

Can. J. Chem. Downloaded from www.nrcresearchpress.com by 210.87.254.42 on 09/05/12
For personal use only.

Alkylation of the sodium salt of diethyl succinylsuccinate (**1**) with 1,3-dibromopropane using the procedure of Wood and Woo (5) produced an acceptable yield of the expected product 1,5-biscarbethoxybicyclo[3.2.2]nonane-6,8-dione (**2**). From the filtrates a small yield of a second product crystallized which proved to have the same analysis as the main product **2** but a different melting point. The possibility that this second product was a different crystalline modification was eliminated by a mixture melting point and by the fact that the main product **2** and the by-product each gave a different thioketal with either 1,2-ethanedithiol or 1,3-propanedithiol.

Isolation of this by-product was not accomplished with equal facility in every preparation. However, its presence was demonstrated in every preparation either by its isolation through fractional crystallization or by the infrared (i.r.) spectrum of the mixture remaining after the majority of the main product was removed by crystallization.

The close relationship of the structures of the main product **2** and the by-product was evident from their spectral properties. The i.r. spectra of these 2 compounds were very similar in overall appearance but differed in the position of several bands in the fingerprint region. In addition, both the nuclear magnetic resonance (n.m.r.) and mass spectra were very similar. Concerning this last observation, ring isomers have been reported (6) to have similar fragmentation patterns.

Efforts to remove the carbonyl groups from the by-product by thioketal formation and desulfurization were frustrated. Only a monothioketal could be prepared with either ethane- or propanedithiol. This behavior undoubtedly indicates a steric hindrance of one of the carbonyl groups (9).

Ring-opening reactions based on a reversed Claisen condensation were next examined.

The chief product of the reaction with potassium hydroxide was a tricarboxylic acid which decarboxylated above 100° to a dicarboxylic acid. Both these compounds had been described by Guha (4) as arising from the main product **2** itself. This was confirmed; both the main product **2** and the by-product gave the same tricarboxylic acid and the same dicarboxylic acid after decarboxylation. Identity was established by m.p., mixture m.p., and i.r. spectra. Such a behavior was explained by assigning structure **5**, 1,5-biscarbethoxybicyclo[4.2.1]nonane-7,9-dione, to the by-product and the above reactions are shown in Scheme 2. The structure **5** also satisfied the requirement that one of the carbonyl groups be more sterically hindered than the other.

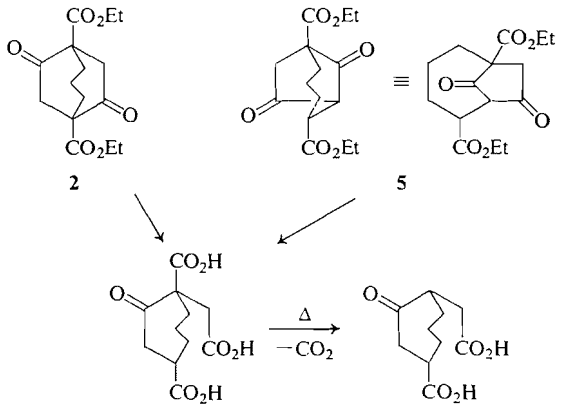

SCHEME 2

The formation of compound **5** must occur by isomerization of the main product **2** after alkylation. This isomerization can be pictured as occurring through carbanionic intermediates formed under the influence of the base also present in the reaction.

In order to test this mechanism, the main product **2** was treated with sodium acetate in refluxing ethanol and isomerization of the bicyclo[3.2.2]nonane system to the bicyclo[4.2.1]-nonane structure of the by-product **5** did occur. The presence of **5** in the isomerized product was evident from the i.r. spectrum of the crude

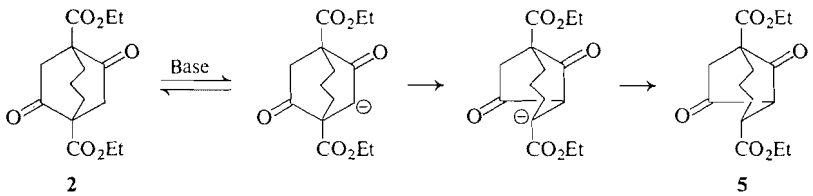

Can. J. Chem. Downloaded from www.nrcresearchpress.com by 210.87.254.42 on 09/05/12
For personal use only.

crystallized reaction mixture. A comparison of this i.r. spectrum with the spectra of mixtures of **2** and **5** showed that this material contained only these 2 compounds in the ratio of 2:1. By fractional crystallization **5** was isolated to further confirm its presence. In addition to **2** and **5**, the isomerized product contained a non-crystallizable oil.

This same oil was the only product (other than starting material) isolated in an attempt to isomerize **5** to **2**. The i.r. spectrum of this oil resembled that of **2** and **5** but had its own characteristic features. Since compound **5** is capable of stereoisomerism, it is possible that this oil contains an isomer of **5**. Irrespective of this, its formation from both **2** and **5** suggested that the isomerization of the bicyclo[3.2.2]nonane ring system proceeded through **5** to other, as yet unidentified, products.

Thioketal formation with 1,2-ethanedithiol was quite straightforward. The only difference between the reaction of the bicyclo[2.2.2]octane and bicyclo[3.2.2]nonane compounds was the considerably slower rate of reaction of the latter. However, when 1,3-propanedithiol was used, thioketal formation from the bicyclo[3.2.2] compound was much more complex than from the bicyclo[2.2.2] analogue.

The reaction product from 1,5-biscarbethoxybicyclo[3.2.2]nonane-6,8-dione and excess 1,3-propanedithiol using toluenesulfonic acid as a catalyst contained 4 compounds, all well resolved on thin-layer or paper chromatography. Of these products, only 2 were major. One of these proved to be crystalline and readily isolable. Its properties established that it was the expected bisthioketal **3** (Scheme 1).

The remaining 3 were isolated by column chromatography but proved to be non-crystallizable at the time. A repetition of this reaction using the 1,5-biscarbomethoxybicyclo[3.2.2]-nonane-6,8-dione gave the analogous mixture of 4 products. These were separated chromatographically and one of the minor products was obtained crystalline. This was identified as the monothioketal on the basis of its analysis, n.m.r., and i.r. spectra. The corresponding monothioketal of **2** (the diethyl ester) crystallized slowly on storage.

The second minor product was not closely investigated. From the molecular weight of the dimethyl ester it would appear to be a dimer resulting possibly through intermolecular thioketal formation.

The second major product, both as diethyl or dimethyl ester, resisted all attempts to crystallize it. Its analysis, after purification by column chromatography, showed it to be isomeric with the crystalline bisthioketal, **3**. Either of these 2 isomeric bisthioketals on treating with excess 1,3-propanedithiol and catalyst produced a mixture of both compounds; in the absence of the dithiol, a mixture of all 4 products was produced.

The n.m.r. spectrum of the liquid bisthioketal showed one feature which clearly distinguished it from **3**, the solid bisthioketal; a singlet at 6.2 indicative of a vinylic proton. In addition, the presence of a mercapto group, while not visible in the i.r. spectrum, could be demonstrated by the reaction of the liquid bisthioketal with sodium and by the preparation of a nitrophthalate and a 3,5-dinitrobenzoate derivative (both liquids).

Desulfurization of the bisthioketal, **3**, the solid bisthioketal, produced 1,5-biscarbethoxybicyclo-[3.2.2]nonane (**4**). The liquid bisthioketal on desulfurization produced the same product and consequently the carbon skeleton of both bisthioketals must be the same.

Two possibilities exist for the structure of the liquid bisthioketal, either **6** or **7**. Structure **7** may appear strange at first glance but molecular models of it using either Dreiding or Stuart–Briegleb models can be built with no difficulty. It also offers the advantage of explaining why complex mixtures of thioketals are not obtained with 1,2-ethanedithiol.

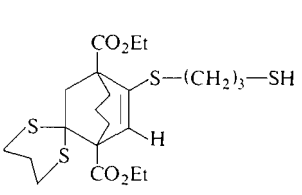

6

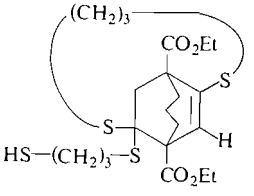

7

It thus appears that thioketal formation from 1,3-propanedithiol and 1,5-biscarbethoxybicyclo-[3.2.2]nonane-6,8-dione is not a simple reaction. Four products are formed and these exist as a complex equilibrating system. The 2 main products are the bisthioketal and a mixed thioketal–vinylthioether.

The desulfurization of the 1,2-ethanedithiol thioketal of 1,5-biscarbethoxybicyclo[3.2.2]-nonane-6,8-dione was effected with Raney nickel. The reduction of the 1,5-biscarbethoxybicyclo-[3.2.2]nonane so obtained with lithium aluminum hydride to 1,5-bishydroxymethylbicyclo[3.2.2]-nonane was uneventful.

Experimental

The melting points are uncorrected and were determined in an open capillary using a Mel-temp melting point apparatus. The n.m.r. spectra were recorded on a Varian T-60 spectrometer using a 10–15% solution of the compound in chloroform-*d*. Chemical shifts are in p.p.m. downfield from the internal standard, tetramethylsilane. The i.r. spectra were recorded on a Beckmann IR-10 spectrophotometer using thin films or solutions in chloroform. Column chromatography was performed with 70–325 mesh silica gel supplied by E. Merck.

Precoated silica gel sheets (Eastman Chromagram) were used for all thin-layer chromatography (t.l.c.) results reported. Ketoesters and thioketals were developed by benzene containing 4% of ethyl ether and the spots were detected by iodine vapor. A mixture of benzene (90 ml) methanol (16 ml) and glacial acetic acid (8 ml) was used for developing derivatives containing carboxylic groups (7). The developed silica gel sheets were dried 15 min at room temperature *in vacuo* to remove the acetic acid and the spots were detected by spraying with bromcresol green.

1,5-Biscarbethoxybicyclo[3.2.2]nonane-6,8-dione (2)

Diethyl succinylsuccinate (128 g, 0.5 mole, prepared according to (5), m.p. 129–130 °C) was added in small portions to the mixture of sodium hydride (1.11 mole, 53.3 g of a 50% dispersion in mineral oil) and 700 ml of dry monoglyme. The mixture was refluxed 3.5 h until no more hydrogen was formed. Approximately 500 ml of monoglyme was removed by distillation (the temperature of oil bath was kept below 140 °C). Then 625 ml of 1,3-dibromopropane was added and the slurry was refluxed 22 h. The mixture was filtered and the filtrate was distilled *in vacuo*. The residue was diluted with 75 ml of ethanol and allowed to crystallize. This product was isolated by filtration and washed with a small amount of ethanol and petroleum ether. After recrystallization from ethanol, 52.5 g (35.4%) of pure **2**, m.p. 134 °C (lit. (4) m.p. 132°, lit. (5) m.p. 130–132.5°) were obtained.

The i.r. spectrum of **2** (in $CHCl_3$) showed 2 carbonyl bands at 1720 and 1740 cm^{-1}. In the 950–1200 region 3 characteristic bands of medium intensity were observed at 1040, 1100, and 1130 cm^{-1}.

The n.m.r. spectrum of **2** showed a triplet centered at 1.25 (CH_3, J = 7 c.p.s., 6.0 H), a quartet at 4.22 (ethyl CH_2, 3.9 H) and a complex assemblage of peaks from 1.6–4.0 (10.2 H). A double doublet was visible in this last group centered at 2.7 and 3.4 (J = 19 c.p.s., 4.4 H) which was assigned to the non-equivalent —CH_2—CO— protons.

The ethanol filtrate from this main product on standing overnight deposited a small amount of a second material. This by-product after recrystallization from ethanol afforded 3.6 g (2.4% yield) of a compound m.p. 97–98 °C. The mixture m.p. of both products was 85–92°.

Anal. Calcd. for $C_{15}H_{20}O_6$ (mol. wt. 296): C, 60.80; H, 6.80. Found (301): C, 61.04; H, 6.77.

The i.r. spectrum of the by-product (in $CHCl_3$) showed only one broad carbonyl absorption band at 1720–1740 cm^{-1}, a strong band at 1270 cm^{-1}, and 3 characteristic absorptions of medium intensity at 1020, 1090, and 1115 cm^{-1}.

The n.m.r. and mass spectra of the by-product were very similar to those of the main product **2**.

1,5-Biscarbomethoxybicyclo[3.2.2]nonane-6,8-dione

1,5-Biscarbethoxybicyclo[3.2.2]nonane-6,8-dione (10 g) was hydrolyzed by refluxing with 125 ml of 6 *N* hydrochloric acid for 8 h (3). After cooling, the diacid was isolated by filtration (6.36 g, m.p. 239–241 °C with decomposition). The diacid (5.4 g, 0.0225 mole) was refluxed 18 h with 30 ml of thionyl chloride and 40 ml of dioxane. After removing the dioxane and excess thionyl chloride by distillation, the crude molten chloride was poured into 50 ml of methyl alcohol. After 10 min refluxing, the excess of methanol was distilled off and the residue crystallized by treating with petroleum ether. After washing with petroleum ether, a small amount of methanol, 2 *N* sodium hydroxide solution, and water and recrystallization from ethanol, 2.5 g of solid was obtained, m.p. 129 °C.

The n.m.r. spectrum showed the methyl groups as a singlet at 3.75 (5.8 H). A double doublet due to the —CH_2—CO— groups was centered at 2.72 and 3.38 (J = 18 c.p.s., 4.6 H) and the remaining trimethylene bridge protons generated a complex spectrum between 1.6 and 2.5.

Cleavage of Ketoesters to 2-Carboxymethylcyclo-heptanone-2,6-dicarboxylic Acid

A 1 g sample of 1,5-biscarbethoxybicyclo[3.2.2]nonane-6,8-dione (**2**) or 1,5-biscarbethoxybicyclo[4.2.1]nonane-7,9-dione (**5**) was dissolved in a solution of potassium hydroxide (1.5 g) in 99% ethanol (15 ml) and the mixture was refluxed and stirred for 30 min. The precipitated potassium salt was isolated by filtration, dissolved in a small amount of water, and acidified with hydrochloric acid. The mixture was dried *in vacuo* and the residue extracted with 99% ethanol (20 ml, 5 min refluxing). The oil (0.66 g) obtained after evaporating the ethanol was mixed with a small amount of ether and allowed to crystallize. Recrystallization of this isolated product from an acetone – petroleum ether mixture gave 0.16 g of solid from **2**, 0.27 g of solid from **5**, (m.p.: at about 150 °C decarboxylation took place; m.p. of decarboxylated product was 176–178 °C).

The identity of the product from the 2 sources was established by the behavior of the 2 materials, and a mixture, on melting and by an identical behavior on t.l.c. The i.r. spectra (Nujol mull) of the 2 products were identical over the range 4000–400 cm^{-1} (AgCl windows); this included even the minor absorption bands which were recorded with thick samples.

Anal. Calcd. for $C_{11}H_{14}O_7$: C, 51.16; H, 5.46. Found: C, 50.56; H, 5.43.

Can. J. Chem. Downloaded from www.nrcresearchpress.com by 210.87.254.42 on 09/05/12
For personal use only.

Can. J. Chem. Downloaded from www.nrcresearchpress.com by 210.87.254.42 on 09/05/12
For personal use only.

Decarboxylation of 2-Carboxymethylcycloheptanone-2,6-dicarboxylic Acid

The acid (3.59 g) was decarboxylated by heating from 140 °C to 185 °C within 20 min. The molten material solidified on cooling to room temperature and this solid (2.94 g, calculated 2.98 g assuming loss of 1 mole of carbon dioxide) was fractionally crystallized from acetone – petroleum ether mixture and 2 compounds of m.p. 180–181° and 200–204° were isolated. The latter compound was obtained in only small quantities and in experiments performed on a 1 g scale could not be isolated. The compound of m.p. 180–181° was obtained on decarboxylation of the tricarboxylic acid from either **2** or **5**. Identity was established through i.r. spectra and mixture m.p. The i.r. spectra of the 180° dicarboxylic acid (Nujol mull) showed a broad asymmetric carbonyl band at 1700 cm^{-1} and a broad band of medium strength at 950 cm^{-1} due to the H-bonded dimer of the acid. The spectrum of the 200–204° acid was quite similar to that of the 180° compound.

For the compound m.p. 180°:

Anal. Calcd. for $C_{10}H_{14}O_5$ (mol. wt. 214): C, 56.07; H, 6.59. Found (248): C, 56.23; H, 6.36.

For the compound m.p. 200–204°:

Found (mol. wt. 242): C, 53.20; H, 6.88.

Guha (4) reported the formation of 3 compounds m.p. 163°, 181°, and 199–200°.

Isomerization of Ketoesters

(*a*) 1,5-Biscarbethoxybicyclo[3.2.2]nonane-6,8-dione (**2**) (1 g) and fused sodium acetate (0.2 g) were dissolved in absolute ethanol (25 ml) and the solution was refluxed 21 h. Ethanol was distilled off and the residue was mixed with water (50 ml) and allowed to crystallize. The crude product (a mixture of solid and colorless oil, 0.82 g) was isolated by filtration. Crystallization from ethanol gave solid (0.4 g, m.p. 87–115 °C) which was shown by i.r. spectroscopy to be a mixture of the starting ketoester **2** and 1,5-biscarbethoxybicyclo[4.2.1]nonane-7,9-dione (**5**). A mixture of **2** and **5** in the ratio of 2:1 gave an i.r. spectrum identical to that of this crystalline material. The presence of the bicyclo[4.2.1]nonane derivative, **5**, in this crystalline mixture was further confirmed by fractional crystallization from ethanol whereby 0.06 g of **5** was obtained and shown to be identical (i.r. spectrum, mixture m.p.) to an authentic sample.

(*b*) 1,5-Biscarbethoxybicyclo[4.2.1]nonane-7,9-dione (**5**) (1 g) was treated with sodium acetate in the same way. Crystallization of the crude product (0.8 g) from ethanol gave pure starting material (0.45 g). From the filtrate a colorless oil (0.3 g) was obtained after evaporation of ethanol. The i.r. spectroscopy suggested that the oil consisted predominantly of some material similar in structure to both **2** and **5** but identical with neither.

Preparation of Thioketals

Method (a)

The ketoester (1 mole, 296 g) was dissolved in 600 ml of chloroform, 1,2-ethanedithiol or 1,3-propanedithiol (4 mole), and boronfluoride ethyl ether (625 ml, approximately 5 mole) were added at 10 °C, and the mixture was allowed to stand at room temperature for 18 h. The mixture was diluted with diethyl ether and shaken twice with water, 3 times with 2 *N* sodium hydroxide solution, again twice with water, and dried over anhydrous magnesium sulfate. Ocassionally, solid material crystallized during extraction; a small amount of chloroform was added to dissolve it. After removing the solvent by distillation *in vacuo*, the crude product was obtained.

Method (b)

The ketoester (1 mole, 296 g), 1,2-ethanedithiol or 1,3-propanedithiol (4 mole), and *p*-toluenesulfonic acid (100 g) were dissolved in 5000 ml of benzene by heating, and the mixture was refluxed 24 h. The evolved water was removed continuously by the benzene azeotrope. The product was isolated as described in method (*a*).

Bisthioketal of 1,2-Ethanedithiol and 1,5-Biscarbethoxybicyclo[3.2.2]nonane-6,8-dione

The crude product prepared from 0.1 mole of ketoester **2** and 1,2-ethanedithiol using method (*a*) was recrystallized from ethanol to give 38.6 g (86%) of solid, which was isolated in 2 crystalline modifications, m.p. 104 and 115 °C respectively.

Anal. Calcd. for $C_{19}H_{28}O_4S_4$ (mol. wt. 448.7): C, 50.86; H, 6.29; S, 28.58. Found (464): C, 50.75; H, 6.23; S, 28.25.

Using the method (*b*), the same product was obtained in 76% yield.

The i.r. spectrum showed a carbonyl band at 1710 cm^{-1} and bands at 1250 and 1035 cm^{-1} due to the ester group. The n.m.r. spectrum showed the ethyl group as a triplet centered at 1.27 (CH_3, J = 7 c.p.s., 6.1 H) and a quartet at 4.05 (CH_2, 4.1 H). The —SCH_2—CH_2—S— produced a singlet at 3.27 and the isolated CH_2—, a double doublet at 2.80 and 3.40 (J = 16 c.p.s.). The protons of the trimethylene bridge appeared in a complex band from 1.6 to 2.6.

Thioketals of 1,5-Biscarbethoxybicyclo[4.2.1]nonane-7,9-dione (5)

The thioketal was prepared from 0.01 mole of **5** and 1,2-ethanedithiol using method (*a*). After recrystallization from ethanol, 3.1 g (83% yield) of product was obtained, m.p. 125–126°.

Anal. Calcd. for $C_{17}H_{24}O_5S_2$ (mol. wt. 372.5): C, 54.82; H, 6.49; S, 17.22. Found (382): C, 54.59; H, 6.47; S, 17.35.

Method (*b*) afforded the same product in 81% yield. The i.r. spectrum showed 2 overlapping carbonyl bands at 1710 and 1730 cm^{-1} and bands due to the ester groups at 1030, 1270, and/or 1250 cm^{-1}. The n.m.r. spectrum showed the ethyl groups as a triplet at 1.33 (CH_3, J = 7 c.p.s., 6.0 H) and a quartet at 4.30 (CH_2, 3.9 H). The ethanedithiol moiety appeared as a singlet at 3.40 (4.6 H) and the remaining protons as a complex spectrum between 3.4 and 1.6.

The related thioketal from 1,3-propanedithiol prepared by method (*a*) in 56% yield had a m.p. 124.5–125.5° and depressed the melting point of the 1,2-ethanedithiol derivative.

Anal. Calcd. for $C_{18}H_{26}O_5S_2$: C, 55.95; H, 6.78; S, 16.59. Found: C, 56.65; H, 6.96; S, 16.62.

The i.r. spectrum was very similar to that of the 1,2-ethanedithiol derivative and showed two overlapping carbonyl bands at 1710 and 1730 cm^{-1} as well as bands due to the ester groups at 1030 and 1270 cm^{-1}. The n.m.r. spectrum showed the ethyl groups as a triplet at 1.30

Can. J. Chem. Downloaded from www.nrcresearchpress.com by 210.87.254.42 on 09/05/12
For personal use only.

(CH_3, J = 7 c.p.s., 5.9 H) and a quartet at 4.17 (CH_2, 3.9 H). The remaining protons produced a complex spectrum in which a pair of overlapping triplets at 2.90 (4.0 H, —S—CH_2) could be distinguished.

Reaction of 1,5-Biscarbethoxybicyclo[3.2.2]nonane-6,8-dione (2) with 1,3-Propanedithiol

Using method (*a*), only non-crystallizable gums were formed. Using method (*b*), 46.5 g of oil was obtained from 0.1 mole of starting ketoester. According to t.l.c., the oil consisted of 2 main products (A, B) and 2 minor products (C, D). Silica gel column chromatography using benzene containing 4% of ethyl ether as solvent was carried out. From fractions containing mainly B (18.9 g) a crystalline bisthioketal was obtained. Recrystallization from ethanol gave 7.3 g of pure substance, m.p. 146–147 °C. After a sample of solid B was available it was more convenient to seed the crude oil diluted with a small amount of ethanol and to separate the crystallized solid before column chromatography of the filtrate.

Anal. Calcd. for $C_{21}H_{32}O_4S_4$ (mol. wt. 476.8): C, 52.91; H, 6.77; S, 26.90. Found (500): C, 53.24; H, 6.89; S, 26.71.

The i.r. spectrum (CCl_4 solution) showed a carbonyl band at 1725 cm^{-1}, a band at 1040 cm^{-1} attributed to the ester group and 2 prominent bands at 1210 and 1270 cm^{-1}. The n.m.r. spectrum showed the ethyl group as a triplet at 1.37 (CH_3, J = 7 c.p.s., 6.0 H) and a quartet at 4.18 (CH_2, 3.9 H). Of the remaining protons only half the double doublet due to the isolated methylene groups of the bicyclo ring system could be distinguished, at 3.63 (J = 16 c.p.s., 2.5 H). This crystalline bisthioketal has structure **3**.

From fractions containing mainly A (24.8 g), those fractions which were chromatographically pure A (8.5 g) were combined and dried several hours at 100 °C *in vacuo* (0.2 mm Hg):

Anal. Found (mol. wt. 482): C, 52.88; H, 6.70; S, 26.98.

The i.r. spectrum (CCl_4 solution) resembled that of the solid derivative B; a carbonyl band at 1735 cm^{-1}, an ester band at 1060 cm^{-1} and 2 bands at 1220 and 1620 cm^{-1}. The n.m.r. spectrum showed 2 different ethyl groups as 2 triplets centered at 1.33 and 1.37 (CH_3, J = 7 c.p.s., 6.3 H) and 2 quartets at 4.17 and 4.20 (CH_2, 4.0 H). The vinylic proton appeared as a singlet at 6.23 (1.0 H) and again the isolated methylene group of the bicyclo ring generated a double doublet of which one doublet only was clearly visible centered at 3.40 (J = 16 c.p.s., 1.3 H) (note the decrease in the area of this signal compared with that of the solid derivative B). The remaining protons generated a complex spectrum between 1.6 and 3.2. No change was apparent in the spectrum after shaking the sample with deuterium oxide.

Fractions containing the third product C were combined and the solvent removed. The residue was an oil which finally crystallized after storing for 3 months, m.p. 72–74°.

Anal. Calcd. for $C_{18}H_{26}O_5S_2$: C, 55.93; H, 6.78; S, 16.95. Found: C, 55.41; H, 6.93; S, 17.48.

The i.r. and n.m.r. spectra of this material were compatible with the compound being a monothioketal of **2**.

Reaction of 1,5-Biscarbomethoxybicyclo[3.2.2]nonane-6,8-dione with 1,3-Propanedithiol

The reaction was carried out using 2 g of 1,5-biscarbomethoxybicyclo[3.2.2]nonane - 6,8 - dione and method (*a*). The oily product (2.15 g) contained (t.l.c.) 2 main products (A′, B′) and 2 minor products (C′, D′) analogous to those in the reaction mixture from the biscarbethoxy derivate (using method (*b*)). The products were separated chromatographically in the manner already described. The product A′ did not crystallize (0.8 g). From fractions containing the product B′, 0.46 g of solid was obtained after recrystallization from ethanol, m.p. 164–165 °C.

Anal. Calcd. for $C_{19}H_{28}O_4S_4$ (mol. wt. 448.7): C, 50.86; H, 6.29; S, 28.58. Found (452): C, 50.86; H, 6.27; S, 28.29.

From fractions containing the by-product C′ (0.2 g), 0.1 g of solid was obtained after recrystallization from ethanol, m.p. 168–169 °C.

Anal. Calcd. for $C_{16}H_{22}O_5S_2$: C, 53.61; H, 6.19; S, 17.89. Found: C, 53.42; H, 6.52; S, 18.07.

The product D′ did not crystallize (0.2 g). Found: S, 21.40; mol. wt. 1198. The product D′ was not further investigated.

The n.m.r. spectra of a somewhat impure sample of A′ (in CCl_4) showed the vinylic proton as a singlet at 6.04 (0.7 H) and the methyl groups as a singlet at 3.65 (5.4 H). The remaining protons generated a complex spectrum between 1.1 and 3.2. A spectrum of the solid bisthioketal compound B′ was equally complex. The only identifiable feature being a strong singlet at 3.70 (6.3 H) due to the methyl groups. The remaining protons generating a complex set of bands in the 1.5–3.5 region. Compound C′, the mono thioketal, produced an equally complex spectrum with the methyl peak at the same position and a complex band in the region 1.6–3.5.

Acid Isomerization of Thioketals

The products A, B, and C (oil, chromatographically purified on a silica gel column) obtained from the reaction of 1,5 - biscarbethoxybicyclo[3.2.2]nonane - 6,8 - dione with 1,3-propanedithiol were investigated in the following manner:

(*a*) 0.2 g of the product was dissolved in 1 ml of chloroform, 0.5 ml of 1,3-propanedithiol, and 0.3 ml of boron fluoride ethyl ether were added and the mixture was allowed to stand at room temperature 24 h. The solution was then diluted with ether, shaken with sodium hydroxide solution, and analyzed with the help of t.l.c.

Mixtures of A and B approximately in the ratio of 1:1 were obtained from each of the 3 products.

(*b*) This same procedure was repeated with omission of the 1,3-propanedithiol. Each of the 2 compounds A or B produced a similar mixture of A, B, D, and a small amount of C. On the other hand, product C did not change.

Desulfurization of the Thioketals

The thioketal (0.03 mole) was added to a mixture of 200 g of Raney nickel slurry in 200 ml of ethyl alcohol. The mixture was stirred and refluxed for 48 h. After cooling, the catalyst was removed by filtration and the solvent by distillation. The residue was distilled under vacuum, to give 1,5-biscarbethoxybicyclo[3.2.2]nonane b.p. 96–98° at 0.05 mm, colorless liquid weighing 7.3 g (90% yield).

Anal. Calcd. for $C_{15}H_{24}O_4$: C, 67.13; H, 9.01. Found: C, 67.18; H, 8.88.

By a comparison of the i.r. spectra, identical products

Can. J. Chem. Downloaded from www.nrcresearchpress.com by 210.87.254.42 on 09/05/12
For personal use only.

were obtained on desulfurizing the 1,2-ethanedithiol and both the solid (product B) and the liquid (product A) 1,3-propanedithiol thioketals of 1,5-biscarbethoxybicyclo-[3.2.2]nonane-6,8-dione.

The i.r. spectrum (CCl_4 solution) showed a carbonyl band at 1730 cm^{-1} and bands due to the ester groups at 1050, 1200, and 1260 cm^{-1}. The n.m.r. spectrum showed the ethyl groups as a triplet at 1.20 (CH_3, J = 7 c.p.s., 6.5 H) and a quartet at 4.03 (CH_2, 3.8 H). The remaining protons appeared as 2 closely spaced singlets at 1.78 and 1.83 approximately equivalent to 4 H and 10 H respectively.

3,5-Dinitrobenzoyl Thioester of 1,3-Propanedithiol Thioketal, Product A

A solution of 0.2 g of 3,5-dinitrobenzoyl chloride in 2 ml of benzene was added to a solution of 0.4 g of 1,3-propanedithiol thioketal A in 1 ml of benzene and 1 ml of pyridine. The mixture was allowed to stand at room temperature 30 min then refluxed 30 min. After diluting the reaction mixture with ether, it was washed with water, 5% sulfuric acid, water, sodium bicarbonate solution, and water and then dried over magnesium sulfate. The solvent was evaporated and the product crystallized from ether at −60° and dried at 110° under vacuum. The yellow, glassy product contained only traces of starting material as was demonstrated by t.l.c. (chloroform: petroleum ether (1:1) as developing solvent). The i.r. spectrum (CCl_4 solution) showed aromatic CH at 3110 and 690 cm^{-1}. The presence of the nitro groups was indicated by bands at 1550, 1350, and 730 cm^{-1}. An ester carbonyl band was visible at 1730 cm^{-1} and a thiol-ester carbonyl band at 1675 cm^{-1}. The n.m.r. spectrum showed the aromatic protons in a band 8.9–9.3 (3.2 H), the vinylic proton a singlet at 6.2 (1.1 H), the remaining protons (30 H) appeared in a complex pattern stretching from 1.0–4.6. Only the ethyl of the carbethoxy groups could be distinguished, the CH_3 (7.3 H) appearing as a triplet centered at 1.33 (J = 7 c.p.s.), the CH_2 (3.6 H) appearing as a double quartet centered approximately at 4.15.

A second attempt at obtaining a solid derivative was made using 3-nitrophthalic anhydride (8). The product was again non-crystalline although t.l.c. clearly demonstrated that a derivative free of starting material had been obtained.

Interaction of the 1,3-Propanedithiol Ketal A with Sodium

In a test tube, freshly cut sodium (about 0.05 g) was covered with dry monoglyme (2 ml). When 0.1 g of the dry thioketal A was added, hydrogen gas was evolved in clearly observable amounts.

A similar experiment carried out with the solid 1,3-propanedithiol thioketal B produced only a few bubbles of hydrogen.

1,5-Bis(hydroxymethyl)bicyclo[3.2.2]nonane

A solution of 1,5-biscarbethoxybicyclo[3.2.2]nonane (5.4 g, 0.02 mole) in dry tetrahydrofuran (50 ml) was added dropwise to a mixture of lithium aluminum hydride (2 g) and tetrahydrofuran (50 ml) with stirring and refluxing. The mixture was then refluxed a further 20 h. Tetrahydrofuran was removed by distillation. Wet ether followed by water was added to destroy the excess of lithium aluminum hydride. The mixture was then acidified with dilute sulfuric acid and the product extracted with ether. After drying over magnesium sulfate, removing the ether, and crystallization of the residue from benzene, a solid (2.8 g, 76% yield) was obtained. Recrystallization from benzene gave an analytical sample, m.p. 102–103°.

Anal. Calcd. for $C_{11}H_{20}O_2$: C, 71.69; H, 10.94. Found: C, 71.48; H, 10.74.

The i.r. spectrum of the diol showed hydroxyl bands at 3640 and 3460 cm^{-1}. The n.m.r. spectrum showed a rather broad singlet at 1.47 (14.6 H) for the bicyclo ring protons, a singlet at 1.70 (1.6 H) for the hydroxyl groups, and a singlet at 3.17 (3.7 H) for the —CH_2·O groups.

The authors are indebted to the Defence Research Board of Canada for their financial support of this research. We also thank Mr. H. M. H. Ghonima for his assistance in some of the experimental work.

1. C. J. Kibler, A. Bell, and J. G. Smith. J. Polym. Sci. (A) **2**, 2115 (1964).
2. A. Bell, J. G. Smith, and C. J. Kibler. J. Polym. Sci. (A) **3**, 19 (1965).
3. J. D. Roberts, W. T. Moreland, Jr., and W. Fraser. J. Amer. Chem. Soc. **75**, 637 (1953).
4. P. C. Guha. Ber. **72B**, 1359 (1939).
5. G. Wood and E. P. Woo. Can. J. Chem. **46**, 3713 (1968).
6. D. S. Weinberg and C. Djerassi. J. Org. Chem. **31**, 115 (1966).
7. H. J. Petrowitz and G. Pastuska. J. Chromatogr. **7**, 128 (1962).
8. E. Wertheim. J. Amer. Chem. Soc. **51**, 3661 (1939).
9. W. Reusch. Deoxygenation of carbonyl compounds. *Edited by* R. L. Augustine. M. Dekker, Inc. New York, 1968. p. 195. Reduction.

Can. J. Chem. Downloaded from www.nrcresearchpress.com by 210.87.254.42 on 09/05/12
For personal use only.

Sur la réduction par $LiAlH_4$ de quelques dérivés du méthylène-3 camphre[1]

JEAN-CLAUDE RICHER ET YVON PÉPIN[2]
Département de Chimie, Université de Montréal, B.P. 6128, Montréal, P.Q.

Reçu le 4 novembre, 1969

L'action de $LiAlH_4$ sur le chlorométhylène-3 camphre, le pipéridinométhylène-3 camphre, les éthylidène-3 camphres *cis* et *trans*, et le furfurylidène-3 camphre a été examinée. La nature des produits de ces réactions a été établie. Les quantités relatives d'addition 1:2 vs. 1:4 de l'hydrure sur ces dérivés sont déterminées; les résultats obtenus sont discutés en fonction de l'isomérie des substituants sur la double liaison et du caractère électroaffinitaire ou électrorépulsif des substituants.

Canadian Journal of Chemistry, 48, 1226 (1970)

Introduction

Il a été établi antérieurement (1, 2) que la réduction des méthylène-3 camphres substitués (**1**) par les hydrures complexes peut conduire à des quantités variables d'addition 1:2 et 1:4 des hydrures sur le groupement carbonyle conjugué. Afin d'évaluer d'une manière plus précise la nature des facteurs pouvant influencer le cours de ces réactions, il s'avérait intéressant d'examiner l'effet de divers substituants X; les résultats de cette étude font l'objet de la présente communication.

Partie expérimentale

Les points de fusion sont déterminés sur un "Hot Stage Apparatus" de la compagnie Reichert (Autriche) et ne sont pas corrigés. Les indices de réfraction sont mesurés sur un réfractomètre du type Abbé de la compagnie Karl Zeiss. Les indices de rotation ont été mesurés à l'aide d'un polarimètre Bellingham et Stanley, modèle A; une moyenne de 10 lectures est effectuée pour chaque mesure et à moins d'indication contraire le benzène est utilisé comme solvant. Les poids moléculaires sont déterminés au moyen d'un osmomètre à pression de vapeur de la compagnie Hewlett-Packard, modèle 301 A.[3] Les spectres infrarouges (i.r.) sont pris sur un spectrophotomètre Beckman, modèle IR-8 à double faisceau, entre 2 plaques de NaCl; à moins d'indication contraire, les spectres des solides sont pris comme émulsion dans le Nujol alors que ceux des liquides sont pris à l'état pur. Les spectres ultra-violets (u.v.) sont pris sur un spectrophotomètre Bausch et Lomb, modèle 505, en solution dans l'éthanol 95%. Les spectres de résonance magnétique nucléaire (r.m.n.) sont mesurés pour des solutions dans le CCl_4 à l'aide d'un appareil Jeol, modèle C-60-H; les déplacements chimiques (δ) sont exprimés en p.p.m. et se réfèrent au TMS utilisé comme référence interne. Les spectres de masse sont déterminés sur un spectromètre Hitachi, modèle RMU-6D à 70 éV. Les chromatographies en phase gazeuse (c.p.g.) sont effectuées à l'aide d'un appareil Microtek à ionisation à flamme; les colonnes utilisées sont: (*a*) 10% SE-52 sur Chromosorb W, 10′ × 1/4″, 145 °C, N_2/70 ml/min; (*b*) 15% Polyester succinate de Craig sur Chromosorb P, 10′ × 1/4″, 190 °C, N_2/70 ml/min; (*c*) 15% de diglycérol sur Chromosorb W, 10′ × 1/4″, 100 °C, N_2/40 ml/min; (*d*) 10% de SE-30 sur Chromport XXX, 12′ × 1/4″, 200 °C, N_2/60 ml/min.

1 Sur la réduction du chlorométhylène-3 camphre (1b)

1.1 Produits de référence

Le méthylène-3 camphre (**1***f*), les méthyl-3 camphres (**4***f*) sous forme de mélange d'isomères, les méthylène-3 bornéols (**2***f* et **3***f*), et les méthyl-3 bornéols (**5***f*) sont disponibles d'une étude précédente (2).

1.1.1 Chlorométhylène-3 camphre (1b)

Préparé par action du chlorure de thionyle sur l'hydroxyméthylène-3 camphre (**1***a*), ce dérivé se présente sous forme de liquide de p.é.: 101–102 °C/7 mm Hg (litt. (3) 113 °C/12.5 mm Hg); n_D^{22} 1.5066; $[\alpha]_D^{25}$ + 175.7° (litt. (3) + 180.28°); r.m.n.: proton vinylique à 7.07 p.p.m. sous forme de doublet J = 0.5 c.p.s.; i.r.: bandes à 1735 (C=O) et à 1642 cm^{-1} (C=C); u.v.: λ_{max} à 243 nm, ε: 11 500; spectre de masse: ions parents à *m/e* de 198 et 200 d'intensités relatives 100:32.

1.1.2 Chlorométhylène-3 bornéols (2b et 3b)

La réduction de 3 g de la cétone **1***b* par 20 g d'isopropylate d'aluminium dans 150 ml d'alcool isopropylique en éliminant l'acétone au fur et à mesure de sa formation conduit, après extractions à la manière habituelle, à 2.8 g (94% du rendement théorique) de produits qui contiendraient, d'après la c.p.g. à l'aide de la colonne de polyester de Craig ou par intégration dans le spectre r.m.n. des protons carbinoliques, 30% de l'alcool *endo* (**3***b*) et 70% de l'alcool *exo* (**2***b*); le chlorométhylène-3 isobornéol (**2***b*) obtenu à l'état pur présente les caractéristiques suivantes: p.f.: 39–41 °C; $[\alpha]_D^{28}$: + 122.9° (*c*, 1.36 g/100 ml); i.r.: bandes à 3630, 3500, 1656, et 1070 cm^{-1}; r.m.n.: C*H*OH à 3.82 p.p.m. (doublet, J = 1.5 c.p.s.) et proton vinylique à 6.03 p.p.m. (quadruplet, J = 0.8 et 1.6 c.p.s.); spectre de masse: ions parents à *m/e* de 200 et 202 d'intensités relatives de 100:34.

1.1.3 Chlorométhyl-3 camphres (4b)

Un mélange formé de 5 ml de pyridine, 5 ml de chlorure

---

[1]Les résultats rapportés dans cette communication sont extraits de la thèse présentée par M. Yvon Pépin en vue de l'obtention du grade de Ph.D. (Faculté des Sciences, Université de Montréal, juin 1968).

[2]Adresse actuelle: Département de Chimie, Université du Québec (constituante de Montréal).

[3]Les auteurs remercient le Dr. Fliszar et ses collaborateurs pour ces mesures.

Can. J. Chem. Downloaded from www.nrcresearchpress.com by 210.87.254.42 on 09/05/12
For personal use only.

de sulfuryle et de 5 g d'hydroxyméthyl-3 camphres (**4***a*) disponibles d'une étude précédente (2) est chauffé au bain-marie pendant une demi-heure et fourni, après extractions à la manière habituelle et purification par distillation, 2 g (36% du rendement théorique) de chlorométhyl-3 camphres (**4***b*) de p.f.: 46–49 °C (litt. (4) 53–54 °C); $[\alpha]_D^{24}$: +103.8° (*c*, 1.99 g/100 ml); i.r.: bande à 1740 cm^{-1}; r.m.n.: pics à 2.25, 2.78, 3.41, et 3.85 p.p.m.; spectre de masse: ions parents à *m/e* de 200 et 202 d'intensités relatives de 100:33.9.

*1.2 Réductions du chlorométhylène-3 camphre (**1***b*) par $LiAlH_4$*

A 0.9 g (23.6 mmoles) de $LiAlH_4$ dans 100 ml d'éther anhydre, 1 g (5.04 mmoles) du dérivé chloré **1***b* dissous dans 40 ml d'éther anhydre est ajouté à la température de la pièce puis porté à reflux durant 2 h. Après décomposition de l'excès d'hydrure et des complexes intermédiaires à l'aide de 10 ml d'une solution aqueuse de NaOH 10%, l'extraction des produits par de l'éther à la manière habituelle conduit à 1.01 g (100% du rendement théorique) de produits. L'analyse par c.p.g. a permis d'établir: 1° à l'aide de la colonne de SE-52 que le mélange est constitué: (*a*) de 2.4% de méthyl-3 camphres (**4***f*) et de méthylène-3 bornéols (**2***f* et **3***f*), (*b*) de 1.6% d'un produit inconnu, et (*c*) de 96% de chlorométhylène-3 bornéols (**2***b* et **3***b*) correspondant à plus de 96% d'addition 1:2 sur le système conjugué original; 2° à l'aide de la colonne de polyester de Craig que les chlorométhylène-3 bornéols sont présents dans le rapport 90% *exo* (**2***b*)/10% *endo* (**3***b*).

*2 Sur la réduction du pipéridinométhylène-3 camphre (**1***c*)*

2.1 Synthèse des produits de référence

*2.1.1 Pipéridinométhylène-3 camphre (**1***c*)*

Une solution de 15 g (80 mmoles) d'hydroxyméthylène-3 camphre (**1***a*) et 10 ml de pipéridine (102 mmoles) dans 150 ml de benzène anhydre est chauffé à reflux dans un ballon surmonté d'une trappe à eau. Lorsque la quantité théorique d'eau est receuillie, le benzène est évaporé et les produits (20 g, 97% du rendement théorique) sont extraits à la manière habituelle; après recristallisations dans l'éther de pétrole, le dérivé **1***c* se présente sous forme de solide blanc: p.f.: 64–66 °C (litt. (5) 60–61 °C); $[\alpha]_D^{23}$: + 457° (*c*, 2.35 g/100 ml); i.r.: bandes à 1685, 1590, et 955 cm^{-1}; u.v.: λ_{max}: 320 nm et ε: 25 100; r.m.n.: proton vinylique à 6.70 p.p.m. (singulet); spectre de masse: pic parent à *m/e* de 247.

*2.1.2 Pipéridinométhyl-3 camphres (**4***c*)*

*(a) Par hydrogénation catalytique de **1***c*.* Une suspension de 9 mg de PtO_2 dans 2.5 ml d'éthanol contenant 0.085 ml d'acide chlorhydrique concentré et 180 mg de la cétone **1***c* est agitée en présence d'hydrogène pendant 1 h à pression et température normales. Lorsque l'absorbtion cesse, les produits (166 mg, 91% du rendement théorique) sont extraits à la manière habituelle; après recristallisation dans l'éther de pétrole, les cétones **4***c* se présentent sous forme de solide de p.f.: 53–56 °C (litt. (6): 38–40 °C); $[\alpha]_D^{25}$: + 57.5° (*c*, 2.12 g/100 ml); i.r.: bandes de Bohlmann entre 2690 et 2800 cm^{-1} et carbonyle à 1740 cm^{-1}; spectre de masse: ion parent à *m/e* de 249.

*(b) Par oxydation chromique des pipéridinométhyl-3 bornéols (**5***c*).* L'oxydation de 3.1 g (12.3 mmoles) des alcools **5***c* (obtenus par réduction, voir section 2.1.3) par 3 g d'anhydride chromique dans 30 ml de pyridine conduit avec un rendement de 66% à un produit ayant les mêmes caractéristiques que celui décrit plus haut.

*2.1.3 Pipéridinométhyl-3 bornéols (**5***c*)*

Le mélange des produits basiques (5.9 g, 23.6 mmoles) obtenu lors de la réduction du pipéridinométhylène-3 camphre par $LiAlH_4$ (voir section 2.2.1) est traité par 2 g (52 mmoles) de cet hydrure dans l'éther. Le mélange réactionnel livre, après hydrolyse à la manière habituelle, 5.6 g (95% du rendement théorique) des alcools **5***c* qui se présentent sous forme de liquide de p.é.: 116–117 °C/0.35 mm Hg; i.r.: bandes hydroxyles faibles à 3685 et 3635 cm^{-1}, bande hydroxyle forte à 3400 cm^{-1} et bandes de Bohlmann entre 2800 et 2700 cm^{-1}; r.m.n.: C*H*OH à 3.68 et 3.83 p.p.m.; spectre de masse: pic parent à *m/e* de 251.

*2.2 Réductions du pipéridinométhylène-3 camphre (**1***c*)*

2.2.1 Réduction par $LiAlH_4$ dans l'éther

(a) Avec décomposition des intermédiaires par de l'eau. A une suspension de 600 mg (15.8 mmoles) de $LiAlH_4$ dans 30 ml d'éther anhydre sous atmosphère d'azote, 1 g (4.05 mmoles) de la cétone **1***c* en solution dans 10 ml d'éther anhydre est ajouté goutte à goutte puis le tout est chauffé à reflux pendant 2 h. Après refroidissement du mélange réactionnel dans un bain de glace, les complexes intermédiaires sont décomposés par addition de 10 ml d'eau puis 10 ml d'une solution aqueuse de NaOH à 10% et les produits extraits à l'éther; cette phase éthérée est lavée par 3 × 30 ml d'une solution aqueuse d'acide chlorhydrique à 20%. La fraction neutre livre 256 mg (38% de rendement basé sur l'obtention de méthyl-3 camphre **4***f*) de produits alors que les extraits acides fournissent, après alcalinisation et extraction à l'éther, 646 mg (64% du rendement théorique) de produits basiques. La c.p.g. des produits neutres à l'aide de la colonne de polyester de Craig indique la présence de méthylène-3 camphre (**1***f*): 15%, de méthyl-3 camphres (**4***f*): 40%, de méthylène-3 bornéols (**2***f* et **3***f*): 15% et de méthyl-3 bornéols (**5***f*): 30%. La chromatographie sur gel de silice des produits basiques permet d'établir, en isolant les produits, que les pipéridinométhyl-3 camphres (**4***c*) forment 52% du total pour 48% des pipéridinométhyl-3 bornéols. Tous les produits, neutres et basiques, proviennent d'une addition 1:4 de l'hydrure sur le système conjugué initial.

(b) Avec décomposition des intermédiaires par l'acétate d'éthyle suivie de base. La réduction de **1***c* utilisant un protocole expérimental semblable à celui décrit dans le paragraphe précédent, à l'exception du fait que les complexes intermédiaires sont décomposés en premier lieu par addition d'acétate d'éthyle, conduit à 19% de produits neutres composés à plus de 95% de méthylène-3 camphre (**1***f*) et à 81% de produits basiques ne contenant que le pipéridinométhyl-3 camphre (**4***c*).

2.2.2 Réduction par $LiAlH_4$ dans le diglyme

La réduction de 1 g (4.05 mmoles) de cétone **1***c* est effectuée à l'aide de 600 mg (15.8 mmoles) de $LiAlH_4$ chauffé à 100 °C pendant 24 h dans 50 ml de diglyme. L'extraction des produits, en utilisant la technique décrite dans la section 2.2.1 (*b*), conduit à 96% de

Can. J. Chem. Downloaded from www.nrcresearchpress.com by 210.87.254.42 on 09/05/12
For personal use only.

produits neutres [formés de 89% de méthyl-3 camphre (**4***f*) et de 11% de méthylène-3 bornéols (**2***f* et **3***f*)] et 4% de produits basiques composés essentiellement de cétone **4***c*.

*3 Sur la réduction des éthylidène-3 camphres cis (**1***g*) et trans (**1***d*)*

3.1 Synthèse des produits de référence

*3.1.1 Synthèse des éthylidène-3 camphres cis (**1***g*) et trans (**1***d*)*

La condensation de 38 g de chlorométhylène-3 camphre (**1***c*) et de 27.4 g d'acétoacétate d'éthyle en suivant les indications de Rupe et Burckhard (7) fournit 26.3 g (55% du rendement théorique) des esters **1***h* et **1***i* qui sont hydrolysés à l'aide de 100 ml d'acide chlorhydrique concentré pour conduire à 19 g (72% du rendement théorique) d'un mélange des acides correspondants **1***j* et **1***k*; la recristallisation de ces acides dans de l'éther de pétrole/benzène permet d'isoler un des isomères: p.f.: 105–107 °C (litt. (7) 106 °C); $[\alpha]_D^{25}$: + 135° (*c*, 1.37 g/100 ml); i.r.: bande large à 2900 cm^{-1} et bandes à 1730, 1695, et 1675 cm^{-1}; u.v.: λ_{max}: 239 nm, ε: 9800; r.m.n.: pics à 0.78, 0.92, et 0.97 p.p.m. (3 singulets dus aux méthyles), 2.71 p.p.m. (H_4, doublet, J = 3.5 c.p.s.), 3.17 p.p.m. (CH_2—CO—, doublet, J = 7 c.p.s.), 6.37 p.p.m. (proton vinylique, triplet, J = 7 c.p.s.) et 11.3 p.p.m. (proton acide, singulet); spectre de masse: pic parent à *m/e* de 222. La décarboxylation, par chauffage à 160 °C sous un vide partiel de 13 mm Hg, de 16.3 g (73 mmoles) de l'acide **1***k* conduit à 12.5 g (92% du rendement théorique) d'un produit qui serait formé, d'après la c.p.g. à l'aide de la colonne de diglycérol, de 54% de **1***g*, 39% de **1***d*, et 7% de vinyl-3 camphre (**4***l*). Le chauffage de ce mélange permet de transformer le vinyl-3 camphre en éthylidène-3 camphres (**1***d* et **1***g*); dans ces conditions, une partie de l'isomère *cis* **1***g* se transforme en isomère *trans* **1***d* et la composition du produit isomérisé serait de 50% de **1***d* et 50% de **1***g*. La chromatographie de ce mélange sur gel de silice utilisant le CCl_4 comme éluant permet d'isoler chacun des isomères.

(*a*) L'éthylidène-3 camphre *trans* (**1***d*) se présente sous forme de solide de p.f.: 27–28 °C (litt. (3) 28–29 °C); $[\alpha]_D^{24}$: + 172.2° (*c*, 1.95 g/100 ml) [litt. (3): + 178.58]; i.r.: bandes à 1730, 1665, et 935 cm^{-1}; u.v.: λ_{max}: 240 nm, ε: 9600; r.m.n.: pics à 0.76, 0.91, et 0.97 p.p.m. (singulets dus aux méthyles), 1.75 p.p.m. (CH—CH_3, doublet, J = 7 c.p.s.) 2.78 p.p.m. (H_4, doublet, J = 3.5 c.p.s.) et 6.34 p.p.m. (proton vinylique, quadruplet, J = 7 c.p.s.); spectre de masse: pic parent à *m/e* de 178.

(*b*) L'éthylidène-3 camphre *cis* (**1***g*) présente les caractéristiques suivantes: p.é.: 81 °C/5 mm Hg; n_D^{24}: 1.4905; $[\alpha]_D^{25}$: + 175.7° (*c*, 1.81g/100 ml) [litt. (7): p.é.: 101–102 °C/10 mm Hg; $[\alpha]_D$: + 203.4°]; i.r.: bandes à 1725, 1660, et 935 cm^{-1}; u.v.: λ_{max}: 241 nm, ε: 9100; r.m.n.: bandes à 0.80, 0.89, et 0.92 p.p.m. (singulets dus aux méthyles), 2.05 p.p.m. (CH—CH_3, doublet, J = 7 c.p.s.), 2.44 p.p.m. (H_4, doublet, J = 4 c.p.s.) et 5.74 p.p.m. (proton vinylique, quadruplet, J = 7 c.p.s.); spectre de masse: pic parent à *m/e* de 178.

L'équilibration de ces cétones conjuguées par chauffage dans de la potasse alcoolique conduit à des mélanges contenant 89% de l'isomère *trans* (**1***d*) et 11% de l'isomère *cis* (**1***g*).

*3.1.2 Ethyl-3 camphres (**4***d*)*

L'hydrogénation catalytique de 5 g d'un mélange d'éthylidène-3 camphres (**1***d* et **1***g*) en présence de 3 g de nickel de Raney et 30 ml d'éthanol conduit à 4.3 g (86% du rendement théorique) des éthyl-3 camphres (**4***d*) de p.é.: 111 °C/16 mm Hg (litt. (8): 108 °C/14 mm Hg) et $[\alpha]_D^{26}$: + 47° (litt. (8): + 44°).

3.1.3 Les éthylidène-3 bornéols

*(a) Les éthylidène-3 bornéols trans (**2***d* et **3***d*).* La réduction de 0.5 g (2.8 mmoles) de cétone **1***d* par 5 g d'isopropylate d'aluminium conduit à 0.47 g (95% du rendement théorique) des alcools désirés qui, d'après la c.p.g. sur la colonne de diglycérol, comporteraient 53% de l'alcool *exo* (**2***d*) et 47% de l'alcool *endo* (**3***d*).

*(b) Les éthylidène-3 bornéols cis (**2***g* et **3***g*).* La réduction de 130 mg (0.73 mmole) de cétone **1***g* par 1.3 g d'isopropylate d'aluminium conduit à 110 mg (82% du rendement théorique) d'un produit qui serait formé, d'après la c.p.g. sur la colonne de diglycérol, de 15% de cétone qui n'a pas réagie, 63% de l'alcool *exo* (**2***g*) et 22% de l'alcool *endo* (**3***g*).

3.1.4 Réduction des éthyl-3 camphres.

La réduction de 1 g des cétones **4***d* par 500 mg de $LiAlH_4$ dans 50 ml d'éther anhydre à température de la pièce pendant 1 h conduit à 937 mg (94% du rendement théorique) d'un mélange qui comprendrait, d'après la c.p.g. sur la colonne de diglycérol, les 4 éthyl-3 bornéols (**5***d*) dans la proportion 70:21:7:2 (temps de rétention croissants).

*3.2 Réductions des éthylidène-3 camphres **1***d* et **1***g*

*3.2.1 Réduction de l'éthylidène-3 camphre trans (**1***d*)*

La réduction de 200 mg (1.12 mmole) de cétone **1***d* par 170 mg de $LiAlH_4$ dans 5 ml d'éther anhydre conduit à 195 mg (97% du rendement théorique) d'un produit qui serait composé, d'après la c.p.g. sur la colonne de diglycérol, de 40% d'éthyl-3 camphres (**4***d*), 2% d'éthyl-3 bornéols (**5***d*), 52% d'éthylidène-3 isobornéol *trans* (**2***d*) et 6% d'éthylidène-3 bornéol *trans* (**3***d*) soit 58% d'addition 1:2 sur le système conjugué initial.

*3.2.2 Réduction de l'éthylidène-3 camphre cis (**1***g*)*

Le produit de la réduction effectuée de la manière décrite dans le paragraphe précédent serait formé de 4% d'éthyl-3 camphres (**4***d*), 1% d'éthyl-3 bornéols (**5***d*), 78% d'éthylidène-3 isobornéol *cis* (**2***g*), et 17% d'éthylidène-3 bornéol *cis* (**3***g*) soit 95% d'addition 1:2 sur le système conjugué initial.

*4 Réduction du furfurylidène-3 camphre (**1***e*)*

4.1 Synthèse des produits de référence

*4.1.1 Furfurylidène-3 camphre (**1***e*)*

Préparé avec un rendement de 50% à partir du furfural et du camphre sodé et en suivant les indications de Wolff (9), ce dérivé se présente sous forme de solide de p.f.: 50–52 °C (litt. (9): 64 °C); $[\alpha]_D^{29}$: + 326.4° (*c*, 3.65 g/100 ml de toluène) [litt. (9): + 339°]; i.r.: bandes à 1710 et 1635 cm^{-1}; u.v.: maxima à 208, 243, et 324 nm (ε respectifs de 3600, 1400, et 25 400); r.m.n.: pics à 0.77 (un méthyle), 0.96 (2 méthyles), 3.32 (H_4, doublet, J = 3.5 c.p.s.), 6.92 (proton vinylique, singulet) et 6.41, 6.58, et 6.72 p.p.m. (protons du noyau furanne); spectre de masse: pic parent à *m/e* de 230.

Can. J. Chem. Downloaded from www.nrcresearchpress.com by 210.87.254.42 on 09/05/12
For personal use only.

4.1.2 Furfurylidène-3 bornéols (2e et 3e)

La réduction de 2 g (8.7 mmoles) de la cétone **1***e* par 20 g (100 mmoles) d'isopropylate d'aluminium dans 150 ml d'alcool isopropylique conduit à 2 g d'alcools **2***e* et **3***e* qui, par chromatographie sur une colonne de gel de silice utilisant le benzène comme éluant, peuvent être isoler à l'état pur. Le furfurylidène-3 bornéol (**3***e*) se présente sous forme de solide de p.f.: 92–93 °C; $[\alpha]_D^{27}$: + 352° (*c*, 1.79 g/100 ml); i.r.: bandes à 3615, 3370, et 1056 cm^{-1}; u.v.: maxima à 267, 274, et 286 nm (ε respectifs de 15 500, 18 000, et 13 700); r.m.n.: pics à 0.80, 0.88, et 0.91 p.p.m. (singulets dus aux méthyles), 2.92 p.p.m. (H_4, doublet, J = 3.5 c.p.s.), 4.17 p.p.m. (C*H*OH, singulet), 6.20 p.p.m. (proton vinylique, singulet) et à 6.03, 6.20, et 7.25 p.p.m. (protons du noyau furanne); spectre de masse: pic parent à *m/e* de 232. Le furfurylidène-3 isobornéol (**2***e*) présente les caractéristiques suivantes: p.f.: 61–62 °C; $[\alpha]_D^{24}$: + 280.3° (*c*, 1.74 g/100 ml); i.r.: bandes à 3630, 3485, et 1066 cm^{-1}; u.v.: maxima à 266, 273.5, et 284.5 nm (ε respectifs à 20 300, 24 200, et 16 800); r.m.n.: pics à 0.85, 0.92, et 0.95 p.p.m. (singulets dus aux groupes méthyles), 3.03 p.p.m. (H_4, doublet, J = 3.5 c.p.s.), 3.84 p.p.m. (C*H*OH, singulet), 6.25 p.p.m. (proton vinylique, singulet) et à 6.07, 6.25 et 7.27 p.p.m. (protons du noyau furanne); spectre de masse: pic parent à *m/e* de 232.

4.1.3 Furfurylméthyl-3 camphres (4e)

La réduction de 2 g de cétone **1***e* par 28 g d'amalgame de sodium en suivant les indications de Wolff (9) conduit à 2 g (99% du rendement théorique) de la cétone **4***e* de p.é.: 93–96 °C/0.3 mm Hg; n_D^{22}: 1.5053; $[\alpha]_D^{24}$: + 88° (litt. (9): + 108.6° dans le toluène); i.r.: bande à 1739 cm^{-1}.

4.2 Réduction du furfurylidène-3 camphre (1e) par $LiAlH_4$

La réduction de 1 g de la cétone **1***e* par 0.6 g de $LiAlH_4$ dans 40 ml d'éther conduit à 1.01 g (100% de rendement) d'un produit qui, d'après la c.p.g. sur la colonne de SE-30, serait composé uniquement des alcools insaturés **2***e* et **3***e*; par comparaison dans le spectre r.m.n. des intégrations des pics correspondants aux protons carbinoliques (3.84 et 4.17 p.p.m.) il est possible d'indiquer que l'isomère *endo* **3***e* forme 7 à 8% du total pour 92 à 93% de l'alcool *exo* **2***e*. L'oxydation de ces produits par le CrO_3 dans la pyridine ne fournit que la cétone insaturée **1***e*.

Résultats et discussion

Les résultats obtenus au cours du présent travail tant au point de vue des pourcentages d'addition 1:4 de l'hydrure sur le système conjugué des méthylène-3 camphres substitués (**1**) qu'au point de vue de la stéréochimie de l'addition 1:2 de l'hydrure sur le groupement carbonyle peuvent être résumés dans le tableau 1; pour fins de comparaison, les résultats obtenus au cours de travaux précédents y sont inclus. De ces résultats, il ressort qu'alors que les groupes électroaffinitaires comme le furanne, le chlore ou le *N*-méthylanilino inhibent presque complètement

TABLEAU 1

Réductions par $LiAlH_4$ de méthylène-3 camphres substitués

Méthylène-3 camphres	% Addition 1:4	% Addition *endo*
X = Furanne	pas observé	92
X = Chlore	3	90
X = *N*-Méthylanilino*	5	
X = Méthyle (*cis*)	7	83
X = Thiobutyle†	23	
X = Méthyle (*trans*)	42	90
X = Hydrogène†	62	
X = Butoxyle*	90	
X = Pipéridino	100	

*Voir référence 1.
†Voir référence 2.

les additions 1:4 sur le système conjugué du méthylène-3 camphre, les groupes susceptibles de fournir facilement des électrons à ce système, comme le butoxy et le pipéridino, ont un effet contraire et la réduction de ces dérivés fournit presqu'exclusivement des produits provenant d'une addition 1:4 de l'hydrure sur le système conjugué initial. Ces résultats pourraient être rationalisés en faisant l'hypothèse que les groupes électrorépulsifs favorisent un déplacement des électrons de la double liaison du groupement méthylène vers le cycle et le groupement carbonyle laissant ainsi sur le carbone exocyclique une charge positive susceptible de réaction avec un hydrure; les groupes électroaffinitaires ayant comme effet d'accumuler une charge négative sur le carbone méthylénique exocyclique rendraient cette réaction avec un hydrure moins facile.

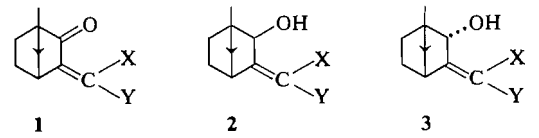

1 **2** **3**

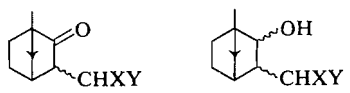

4 **5**

a X = H; Y = OH
b X = H; Y = Cl
c X = H; Y = pipéridino
d X = H; Y = CH_3
e X = H; Y = 2-furyle
f X = H; Y = H
g X = CH_3; Y = H
h X = H; Y = CH_2COOEt
i X = CH_2COOEt; Y = H
j X = H; Y = CH_2COOH
k X = CH_2COOH; Y = H
l X = Y = CH_2

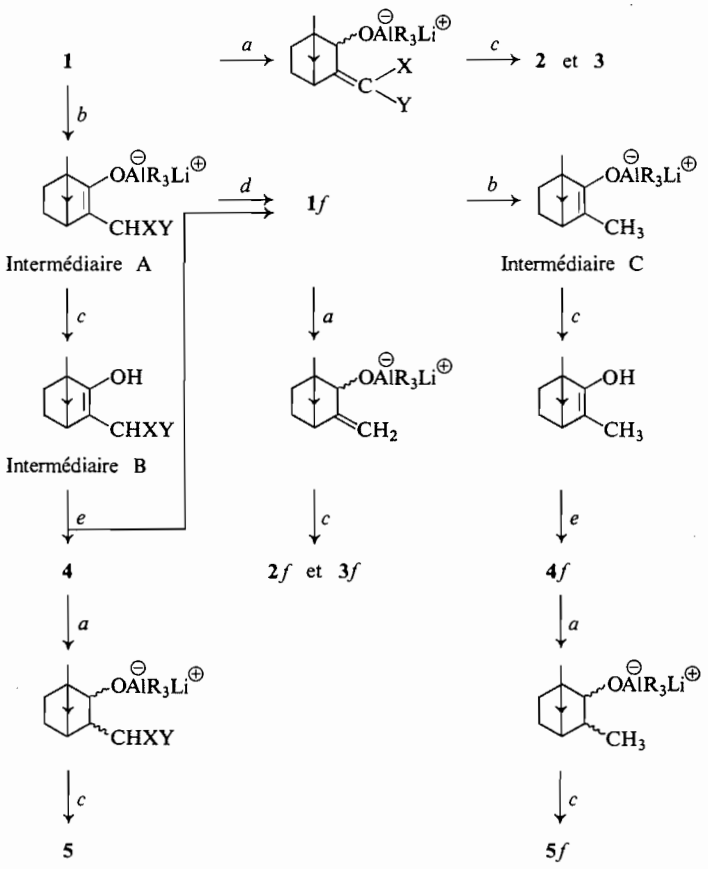

SCHEME 1

(*a*) Addition 1:2 d'hydrure sur un carbonyle; (*b*) addition 1:4 d'hydrure sur un système conjugué; (*c*) hydrolyse; (*d*) élimination, si X ou Y s'y prêtent, de $Li^+AlR_3X^-$; (*e*) réaction de cétonisation.

Les résultats obtenus lors de la réduction des éthylidène-3 camphres *cis* (**1***g*) et *trans* (**1***d*) permettent de mettre en évidence l'influence stérique que peuvent provoquer les substituants qui se trouvent orienter entre les groupements carbonyle et méthylène; cette influence permet d'étayer l'hypothèse selon laquelle la réduction de cétones conjuguées formant un système cisoïde s'effectue par l'intermédiaire d'un mécanisme cyclique à 6 centres.

D'une manière générale, la nature des produits formés au cours de ces réactions de réduction peut être expliquée aisément à l'aide du schéma réactionnel 1. Des particularités ont toutefois pu être mises en évidence lors de la réduction du pipéridinométhylène-3 camphre (**1***c*) par $LiAlH_4$. Si cette réduction est effectuée dans l'éther à température de la pièce et suivie d'une décomposition des complexes intermédiaires par de l'acétate d'éthyle puis de la soude, elle conduit essentiellement à un mélange formé de 82% de pipéridinométhyl-3 camphres (**4***c*) et de 19% de méthylène-3 camphre (**1***f*). Puisque le méthylène-3 camphre en présence d'hydrure en excès serait réduit, on peut donc affirmer que cette cétone non saturée s'est formée au cours de l'isolement des produits; considérant toutefois que dans les conditions d'extraction la cétone basique **4***c* ne se décompose pas en cétone non-saturée **1***f*, on doit donc en conclure que cette dernière se produirait au moment même de l'hydrolyse et l'on doit envisager que l'énol intermédiaire B pourrait, au moment de la cétonisation, soit suivre cette dernière voie ou perdre une molécule de pipéridine

Can. J. Chem. Downloaded from www.nrcresearchpress.com by 210.87.254.42 on 09/05/12
For personal use only.

Can. J. Chem. Downloaded from www.nrcresearchpress.com by 210.87.254.42 on 09/05/12
For personal use only.

par un mécanisme favorisé par une proximité possible des éléments à éliminer. Les résultats obtenus lors de la réduction de **1***c* par $LiAlH_4$ dans l'éther à température de la pièce suivie d'une hydrolyse des complexes intermédiaires peuvent être rationalisés en acceptant comme hypothèse: (*a*) que la vitesse d'hydrolyse de ces intermédiaires et de leur transformation en produits cétoniques est au moins aussi grande que la vitesse d'hydrolyse des hydrures en excès dans le milieu; (*b*) que les hydrures résiduels réagissent normalement avec les produits cétoniques qui se forment. Tous les résultats obtenus pour la réduction de **1***c* avec $LiAlH_4$ dans l'éther indiquent donc: (*a*) que cette réaction se produit presqu' exclusivement par une addition 1:4 de l'hydrure sur le système conjugué initial qui conduit à l'intermédiaire A et (*b*) que la diversité des produits obtenus reflète le cours des réactions que peut suivre l'intermédiaire B, son produit d'hydrolyse. Les résultats obtenus lors de la réduction de **1***c* par $LiAlH_4$ dans le diglyme à 100 °C tout en indiquant que l'attaque initiale sur le système conjugué se produit essentiellement en 1:4 suggèrent que la réaction d'élimination de $Li^+AlR_3(C_5H_{10}N)$ qui n'intervient pas à la température de la pièce se produirait à 100 °C et donnerait ainsi naissance au méthylène-3 camphre (**1***f*) qui par réduction subséquente conduirait à tous les produits observés.

Il a donc été établi maintenant que la nature de l'agent réducteur (2, 10), le caractère électroaffinitaire ou électrorépulsif du groupement X porté par le groupe méthylène (pour fins de comparaison, voir la référence 11) et l'effet stérique des substituants à proximité du centre réactionnel (travail actuel et référence 11) peuvent influencer sur les quantités relatives d'addition 1:2 vs. 1:4 d'hydrure auxquelles peut donner lieu la réduction de méthylène-3 camphres substitués. Les résultats obtenus au cours du présent travail ont aussi permis de mettre en évidence le fait que dans des composés contenant le groupe —O—AlR_3, ou un des R = H, l'hydrolyse du lien O—Al est au moins aussi rapide que l'hydrolyse du lien Al—H.

Les auteurs remercient vivement le Conseil National de Recherches du Canada et la Compagnie Shawinigan Chemicals du Canada pour l'aide financière apportée sous forme d'octrois de recherches et de bourses d'étude. L'un de nous (J.-C.R.) tient à exprimer sa gratitude au Dr. Pierre Maroni et à Mlle Marthe Benoit de la Faculté des Sciences de Toulouse pour l'accueil et l'aide apportés au cours de la préparation de ce manuscrit.

1. J.-C. RICHER et R. CLARKE. Tetrahedron Lett. 935 (1964).
2. J.-C. RICHER et C. LAMARRE. Can. J. Chem. **45**, 1581 (1967).
3. H. RUPE et M. ISELIN. Chem. Ber. **49**, 25 (1916).
4. H. RUPE, A. AKERMAN, et H. TAKAGI. Helv. Chim. Acta, **1**, 452 (1918).
5. H. RUPE, M. SEIBERTH, et W. KUSSMAUL. Helv. Chim. Acta, **3**, 50 (1920).
6. P. SHENONE et G. MINARDI. Farm. (Pavia), Ed. Sci. **17**, 291 (1962); C. A. **58**, 4601 (1963).
7. H. RUPE et E. BURCKHARD. Chem. Ber. **49**, 2547 (1916).
8. A. HALLER et J. LOUVRIER. Ann. Chim. [9], **9**, 189 (1918).
9. N. WOLFF. Ann. Chim. [9], **20**, 87 (1923).
10. H. C. BROWN et H. M. HESS. J. Org. Chem. **34**, 2206 (1969).
11. K. IQBAL et W. R. JACKSON. J. Chem. Soc. (C), 616 (1968).

Radiation-induced oxidation of 2-propanol by hydrogen peroxide in aqueous solutions[1]

C. E. BURCHILL AND I. S. GINNS
Department of Chemistry, University of Manitoba, Winnipeg 19, Manitoba

Received December 15, 1969

The radiation-induced oxidation of 2-propanol by hydrogen peroxide in neutral deaerated aqueous solution has been investigated. 2-Propanol is oxidized to acetone, and hydrogen peroxide reduced in stoichiometrically equivalent high yields. The yields are independent of hydrogen peroxide concentration in the range 5×10^{-2} to 10^{-3} *M* and linearly dependent on alcohol concentration in the range 0.13 to 1.05 *M*. The reaction yields increased with decreasing dose rate.

The results are explained by a chain mechanism in which initiation occurs via H-atom abstraction from 2-propanol to form either $(CH_3)_2\dot{C}OH$ (**1**) or $CH_3\,CHOH\,\dot{C}H_2$ (**2**). **1** reacts with H_2O_2 in a chain propagating reaction

$$\mathbf{1} + H_2O_2 \rightarrow \text{acetone} + H_2O + OH$$

2 may abstract the α hydrogen from the parent alcohol

$$\mathbf{2} + \text{2-propanol} \rightarrow \text{2-propanol} + \mathbf{1}$$

or undergo bimolecular termination. A lower limit of 53 ± 10 l mole^{-1} s^{-1} is estimated for the rate constant for this radical conversion reaction.

Canadian Journal of Chemistry, **48**, 1232 (1970)

Introduction

The peroxidation of 2-propanol has been studied using a variety of radical initiation techniques. Merz and Waters (1) have studied the chain oxidation of 2-propanol using Fenton's reagent. The photolysis of hydrogen peroxide in aqueous solutions of 2-propanol has been investigated (2, 3). The reaction of H_2O_2 has been studied in solution in pure 2-propanol using both photochemical (4) and thermal (5) initiation. The disappearance of hydrogen peroxide by a chain process during the γ irradiation of aqueous solutions of 2-propanol has been described by Allan and Beck (6).

Mechanisms have been proposed for these oxidations and for the similar radiation-induced oxidation of ethanol by hydrogen peroxide in aqueous solution (7). During a preliminary study of the radiation-induced reaction of 2-propanol and hydrogen peroxide, we observed features of the dependence of the yields on solute concentrations which were inconsistent with the accepted mechanism. We now present the results of an extensive study of this reaction and a revised mechanism to explain them.

Experimental

2-Propanol (Fisher Certified Reagent) and hydrogen peroxide (30% unstabilized Fisher Certified Reagent) were used as received. Water was redistilled from alkaline $KMnO_4$ solution and acidic $K_2Cr_2O_7$ solution. Analytical reagents were of reagent grade and used without further treatment.

Solutions were prepared using freshly distilled water, irradiated, and analyzed on the same day. Ten-ml aliquots of the solutions were placed in 25 ml Pyrex bulbs fitted with demountable vacuum-seated stopcocks. Before irradiation the samples were degassed under vacuum by successive freeze–pump–thaw cycles.

Most samples were irradiated at room temperature in a ^{60}Co Gammacell 220 source (Atomic Energy of Canada, Ltd.) at an average dose rate of 1.70×10^{19} eV l^{-1} s^{-1}. Lead shields supplied with the Gammacell were used to provide attenuation to a nominal 10%. For studies at lower dose rates, an Eldorado Model A ^{60}Co source at the Manitoba Cancer Treatment and Research Foundation was used. Dose rates were estimated using the Fricke dosimeter and assuming $G(Fe^{3+}) = 15.6$. For all solutions it was assumed that the absorbed dose was proportional to the electron density, and the dose rates estimated for the solutions were adjusted for variations in electron density with solution composition.

Acetone was determined spectrophotometrically using the salicylaldehyde method of Berntsson (8). Hydrogen peroxide was determined by the iodide method (9).

Results

The reduction of hydrogen peroxide during irradiation in the presence of a constant (0.52 *M*) concentration of 2-propanol is shown in Fig. 1. The figure is a composite of the results from a series of experiments with different initial concentrations of hydrogen peroxide. It is clear that the rate of hydrogen peroxide reduction is independent of its concentration in the range 5×10^{-2} to 10^{-3} *M* H_2O_2. $G(-H_2O_2)$ is found

[1]This work was supported in part by the Defence Research Board of Canada, Grant No. 9530-78, and in part by Atomic Energy of Canada, Limited, Commercial Products Division.

TABLE 1

G(acetone) and $G(-H_2O_2)$ from water–2-propanol solutions*

2-Propanol (mole l^{-1})	G(acetone)	$G(-H_2O_2)$
0.13	36.1	38.1
0.26	39.9	
0.52	51.8	51.8
0.78	58.1	
1.05	70.1	70.8
2.09	77.4	
3.66	103.3	
5.23	95.7	
9.15	53.1	
Pure 2-propanol	16.3	

*Constant initial $[H_2O_2] = 0.01$ M, dose rate = 1.70×10^{19} eV l^{-1} s^{-1}.

from the slope of this graph and is 51.8 ± 2.0 for this concentration of 2-propanol. Additional $G(-H_2O_2)$ values for various concentrations of 2-propanol are given in Table 1.

Acetone formation yields for a constant initial concentration of 0.01 M H_2O_2 and various concentrations of 2-propanol are also shown in Table 1. The stoichiometric equivalence of the

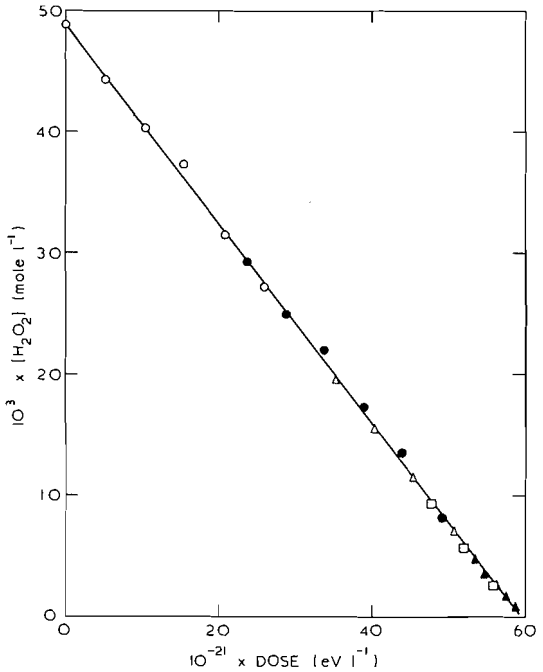

FIG. 1. Radiation-induced reduction of H_2O_2 in deaerated aqueous 2-propanol (0.52 M) solutions. Dose rate = 1.70×10^{19} eV l^{-1} s^{-1}. Initial $[H_2O_2]$: ○, 0.05; ●, 0.03; △, 0.02; □, 0.01; ▲, 5×10^{-3} M.

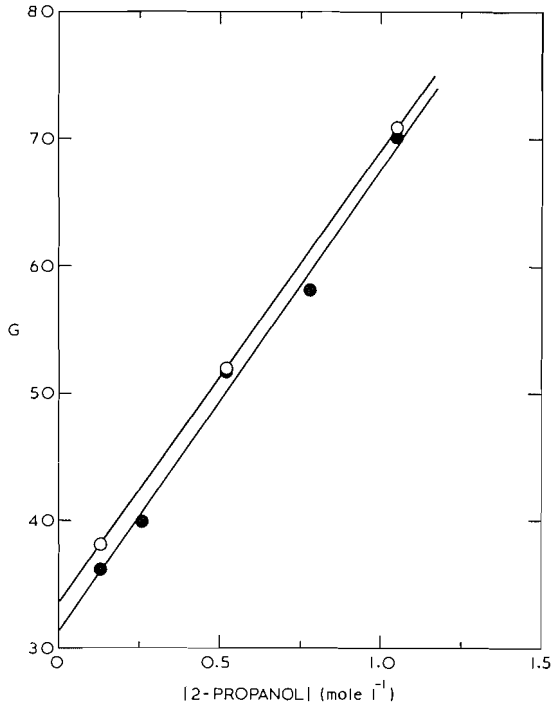

FIG. 2. Variation of yields with 2-propanol concentration. Initial $[H_2O_2] = 0.01$ M, dose rate = 1.70×10^{19} eV l^{-1} s^{-1}. ○, $G(-H_2O_2)$; ●, G(acetone).

acetone formation and peroxide reduction yields is evident for those systems in which both quantities were measured. This equivalence is also illustrated in Fig. 2, which further demonstrates that both yields increase linearly with increasing alcohol concentration in the range 0.13 to 1.05 M 2-propanol. Extrapolation of both yields as shown in Fig. 2 leads to the result G^0 (H_2O_2) = 33.4 ± 1.0 and G^0 (acetone) = 31.2 ± 1.0 at zero 2-propanol concentration.

As the 2-propanol concentration is increased beyond 1.05 M, the initial yield of acetone continues to increase but it is no longer a linear function of alcohol concentration. G(acetone) reaches a maximum of ~ 100 at a concentration of 2-propanol ~ 3.7 M and then decreases to 16 ± 1 in pure 2-propanol. Initial yields of acetone formation are shown as a function of mole fraction 2-propanol in Fig. 3.

The effect of varying dose-rate on the oxidation of 2-propanol by hydrogen peroxide is shown in Fig. 4 for solutions 0.01 M in H_2O_2 and 0.52 M in 2-propanol. An increase in G(acetone) with decreasing dose rate is clearly demonstrated.

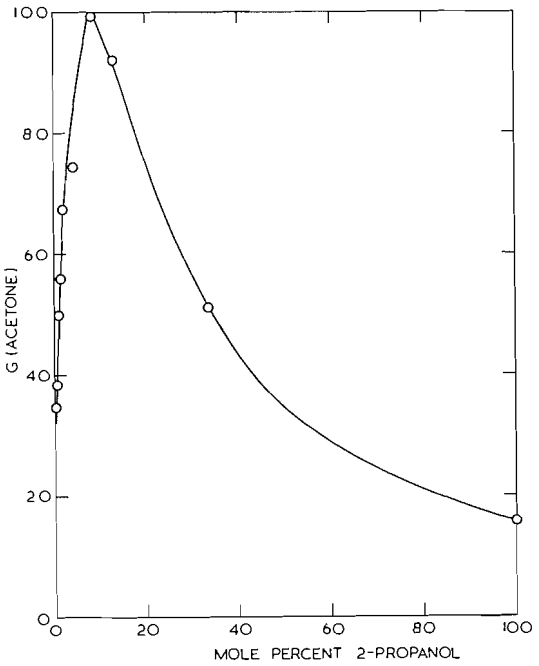

FIG. 3. Initial acetone formation yields as a function of mole percent 2-propanol. Initial $[H_2O_2] = 0.01$ *M*, dose rate = 1.70×10^{19} eV l^{-1} s^{-1}.

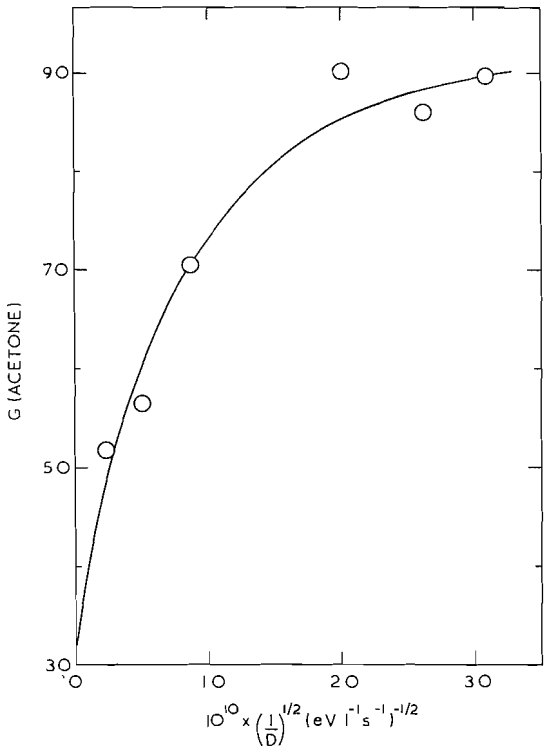

FIG. 4. Variation of *G*(acetone) with dose rate. [2-Propanol] = 0.52, initial $[H_2O_2] = 0.01$ *M*.

Table 2 contains data demonstrating the effect of varying dose-rate for other concentrations of 2-propanol.

At concentrations of $H_2O_2 < 10^{-3}$ *M*, the rate of peroxide reduction in the presence of 0.52 *M* 2-propanol is dependent on the concentration of H_2O_2, as is demonstrated in Fig. 5. The figure is again a composite of the results obtained from experiments with different initial concentrations of H_2O_2. The peroxide concentration approaches a steady-state value of $\sim 3 \times 10^{-6}$ *M*. *G*(acetone) at the steady-state concentration of H_2O_2 is 0.97 $\pm$ 0.05.

TABLE 2

Dose-rate effect on *G*(acetone) from water–2-propanol solutions*

2-Propanol (mole l^{-1})	*G*(acetone) Unattenuated dose rate	*G*(acetone) Dose rate attenuated to 26%
0.52	51.8	56.5
5.23	95.7	138.3
9.15	53.1	73.7
Pure 2-propanol	16.3	22.0

*Initial $[H_2O_2] = 0.01$ *M*, unattenuated dose rate = 1.70×10^{19} eV l^{-1} s^{-1}.

Discussion

0–1.0 M 2-Propanol/5 × 10⁻²–10⁻³ M H_2O_2

In this concentration region, the significant features of the results are that the yields of acetone formation and hydrogen peroxide reduction are essentially equal, linearly dependent upon the alcohol concentration, and independent of the peroxide concentration. The linear plot of *G* vs. 2-propanol concentration extrapolates to a significant chain value at zero alcohol concentration and the radiation–chemical yields show an inverse dependence upon dose rate.

In this range of solute concentrations, we may assume without serious error that the γ radiation interacts primarily with the solvent water to form the species e_{aq}^-, H, OH, H_3O^+, H_2O_2, H_2. The hydrated electron will react rapidly with the solute hydrogen peroxide

[1] $$e_{aq}^- + H_2O_2 \rightarrow \cdot OH + OH^-$$

Since

$$k_{OH+(CH_3)_2CHOH} > k_{OH+H_2O_2}$$

$$k_{H+(CH_3)_2CHOH} \simeq k_{H+H_2O_2} \quad (10)$$

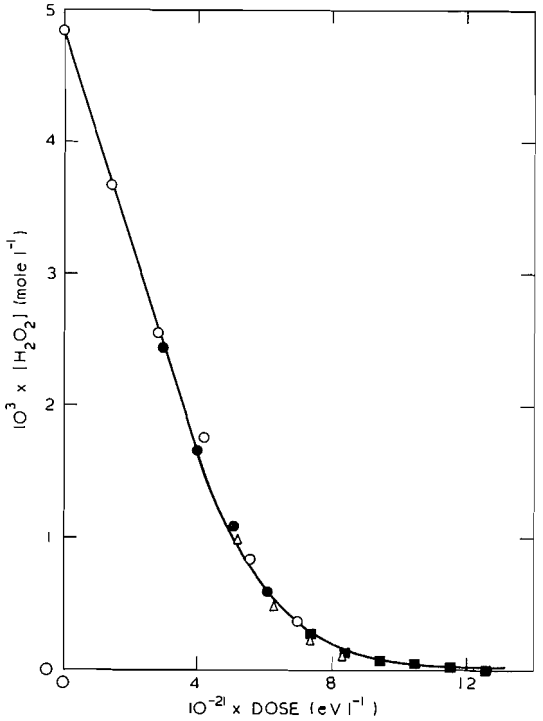

FIG. 5. Reduction of H_2O_2 at low concentrations. [2-Propanol] = 0.52 *M*, dose rate = 1.70×10^{19} eV l^{-1} s^{-1}. Initial $[H_2O_2]$: ○, 5×10^{-3}; ●, 2.5×10^{-3}; △, 10^{-3}; ■, 3×10^{-4}*M*.

and

$$[\text{2-propanol}] \gg [H_2O_2]$$

all H and OH will react with 2-propanol. Previous authors (1–5) have assumed reactions proceed entirely by abstraction of an H atom from the α position of the alcohol.

[2] $H + (CH_3)_2CHOH \rightarrow H_2 + \mathbf{1}$

[3] $OH + (CH_3)_2CHOH \rightarrow H_2O + \mathbf{1}$

where **1** represents the radical $(CH_3)_2\dot{C}OH$. The chain reaction has been attributed to the propagating reaction [4] with termination of the

[4] $\mathbf{1} + H_2O_2 \rightarrow (CH_3)_2CO + H_2O + OH$

chain by bimolecular reaction of **1**

[5] $\mathbf{1} + \mathbf{1} \rightarrow (CH_3)_2CO + (CH_3)_2CHOH$

This simple reaction scheme, however, may be shown to predict a first-order dependence of the reaction rate on the concentration of H_2O_2 and no dependence on alcohol concentration, whereas we have observed that the reaction rate under irradiation is independent of peroxide concentration and linearly dependent upon the alcohol concentration. We propose the following modification of the reaction scheme to explain the observed results

$$H_2O \rightsquigarrow e_{aq}^-, H, OH, H_3O^+, H_2O_2, H_2$$

[1] $e_{aq}^- + H_2O_2 \rightarrow OH^- + OH$

[2] $H + (CH_3)_2CHOH \rightarrow H_2 + (CH_3)_2\dot{C}OH$
$(CH_3)_2\dot{C}OH = \mathbf{1}$

[7] $H + (CH_3)_2CHOH \rightarrow H_2 + CH_3CHOH\dot{C}H_2$
$CH_3CHOH\dot{C}H_2 = \mathbf{2}$

[3] $OH + (CH_3)_2CHOH \rightarrow H_2O + \mathbf{1}$

[8] $OH + (CH_3)_2CHOH \rightarrow H_2O + \mathbf{2}$

[4] $\mathbf{1} + H_2O_2 \rightarrow (CH_3)_2CO + H_2O + OH$

[9] $\mathbf{2} + (CH_3)_2CHOH \rightarrow (CH_3)_2CHOH + \mathbf{1}$

[10] $\mathbf{2} + \mathbf{2} \rightarrow$ 2,5-hexanediol or
$(CH_3)_2CO + (CH_3)_2CHOH$

The novel features of this proposal are the inclusion of abstraction reactions from the methyl groups of the alcohol, reactions [7], [8], and the radical conversion reaction [9].

The rate constants for reactions [3] and [7] have been assessed (10), and it is clear from their values that the abstraction from the α position is not entirely specific and that reaction [7] must be considered in addition to reaction [3]. No rate data are available for the abstraction of α and β hydrogens from simple alcohols by OH radicals, although it might be argued that if abstraction by H atoms is not entirely specific to the α position, that by OH radicals would be even less specific by virtue of its greater exothermicity. Allan and Beck (6) have suggested that the OH radical may not react specifically at the α position of 2-propanol. More convincing evidence for the lack of specificity is provided by the observation of electron spin resonance (e.s.r.) spectra attributed to both radicals **1** and **2** in the photoinitiated reaction of H_2O_2 with 2-propanol (11). These radicals, whose formation was attributed to OH radical abstraction of H atoms from the alcohol, were present in concentrations within the same order of magnitude, and the spectrum attributed to radical **2** became increasingly prominent as the system was diluted with water. We therefore contend that the abstraction of H atoms from the β position of the alcohol cannot be neglected in any mechanistic description of these free-radical reactions.

FOR ERRATA SEE
v.4.8.#18,1970 P. 2948

The radical conversion reaction [9] was suggested, in part, by the form of the experimental results. The linear dependence of the radiolytic yields on alcohol concentration suggests that the chain length is determined by the competition between a radical terminating reaction and the reaction of that radical with the alcohol. In view of the high rate of its reaction with the alcohol (10) and the large concentration of the alcohol, it is unlikely that the steady-state concentration of OH is sufficient for it to play any role in chain termination. Chain termination involving radical **1** would be in competition with the propagating reaction [4] and would lead to some dependence of chain length on H_2O_2 concentration. There remains the possibility of reaction [9] as the rate-controlling propagation step in competition with reaction [10] as the terminating step. While this reaction appears to predict the appropriate kinetic form of the results, this is not sufficient to conclude that the reaction occurs. Examination of the literature, however, has brought to light considerable evidence that such a reaction may occur.

Thomas (12) has observed the reaction of methyl radicals with 2-propanol, presumably by abstraction of the α hydrogen of the alcohol. Radical **2**, being an alkyl radical, may well undergo a similar reaction, although in view of the greater degree of ordering required in the formation of a transition rate, the rate constant might well be less than the value $3.4 \times 10^3\ M^{-1}\ s^{-1}$ observed for the methyl radical. Livingston and Zeldes (11, 13) observed the e.s.r. spectrum of radical **2** during the photolysis of H_2O_2 in 2-propanol–water mixtures, but its intensity was reduced in mixtures of high alcohol concentration and the spectrum was not observed in pure 2-propanol. This may be argued as evidence for the occurrence of reaction [9]. With increasing alcohol concentration, the rate of reaction [9] would increase with a consequent decrease in the steady-state concentration of radical **2**. It was also noted (11) that as the solution (75% 2-propanol, 25% H_2O) was cooled from 30 to −5 °C the spectrum of **2** was enhanced. This observation is also consistent with the occurrence of a reaction such as [9], a relatively slow reaction, with a significant energy of activation. With a decrease in temperature, the rate of the reaction would be reduced and the steady-state concentration of **2** increased. Norman and West (14) have recently suggested reaction [9] to explain the variation in intensity of e.s.r. spectra with changing substrate concentration in the metal-ion catalyzed reaction of organic compounds with hydrogen peroxide.

The presence of 2,5-hexanediol as a reaction product was demonstrated qualitatively by vapor-phase chromatography, using flame-ionization detection and a 6 ft column (2% Carbowax 20 M on 60/80 chromosorb W).

Returning then to the proposed mechanism, we may derive an expression for the radiation–chemical yields in the system using the normal steady-state approximations

$$[11] \qquad G(-H_2O_2) = \left[G_{e_{aq}^-} - G_{H_2O_2} + G_H \left\{ \frac{k_2 (k_3 + k_8)}{k_8 (k_2 + k_7)} \right\} + \frac{k_3}{k_8} (G_{e_{aq}^-} + G_{OH}) \right] + \left(1 + \frac{k_3}{k_8} \right) k_9 \left(\frac{G_{e_{aq}^-} + G_H + G_{OH}}{2k_{10}D} \right)^{\frac{1}{2}} [\text{2-propanol}]$$

(D is the dose rate in units of 6.02×10^{25} eV l^{-1} s^{-1}). G(acetone) differs only marginally from $G(-H_2O_2)$, depending upon the exact stoichiometry of the terminating reaction, [10].

Note that this mechanism predicts a linear dependence of the yields on 2-propanol concentration, no dependence on H_2O_2 concentration, and a non-zero intercept at zero alcohol concentration corresponding to the first portion of the yield equation (in square brackets). This conforms precisely to the experimental results as represented in Figs. 1 and 2.

Equating the $G(-H_2O_2)$ intercept from Fig. 2 (33.4 ± 1.0) to the portion of eq. [11] in square brackets, we may estimate a value of k_3/k_8 using accepted values for the primary yields in irradiated water (15) and the literature values for k_2, k_7, and $(k_3 + k_8)$ (10). The ratio of k_3/k_8 so calculated is 6.2. Assuming the value of $k_3 + k_8$ to be 1.4×10^9 l mole^{-1} s^{-1} gives

$$k_3 = 1.2 \times 10^9 \quad \text{l mole}^{-1}\,\text{s}^{-1}$$

$$k_8 = 2 \times 10^8 \quad \text{l mole}^{-1}\,\text{s}^{-1}$$

The second part of eq. [11], as previously noted, predicts a linear dependence of radiation-chemical yields on 2-propanol concentration, and the coefficient of [2-propanol] corresponds to the slope of the line in Fig. 2. However, this coefficient includes a dose-rate dependent term which predicts an inverse square-root dependence on the dose rate and extrapolation to the zero-alcohol intercept at high dose rates. As seen from Fig. 4, the yield is not the predicted linear function of $(1/D)^{\frac{1}{2}}$, although the yield decreases with increasing dose rate and the curve can, without difficulty, be extrapolated to the zero-alcohol intercept. The fact that there is a significant dose-rate effect confirms that there is a bimolecular termination, but the curvature of Fig. 4 indicates that there is, in addition, an apparent first-order termination which becomes increasingly important at low dose rates. If it is assumed that at the highest dose rate used (1.75×10^{19} eV $\text{l}^{-1}\,\text{s}^{-1}$), termination is primarily by the bimolecular process [10], then it is possible to estimate a lower limit for the rate constant of the conversion reaction [9]. Using $k_3/k_8 = 6.2$, assuming that the bimolecular termination reaction has a rate constant $2k_{10} = 2.0 \times 10^9$ l $\text{mole}^{-1}\,\text{s}^{-1}$ and using Buxton's (15) values for the primary radical yields, k_9 can be calculated from the slope of $G(-H_2O_2)$ vs. [2-propanol] (Fig. 2). The lower limit of k_9 so estimated is 53 ± 10 l $\text{mole}^{-1}\,\text{s}^{-1}$. This estimate is nearly two orders of magnitude less than the observed rate constant for the corresponding methyl-radical reaction (12), but this, in view of the highly ordered transition state required for such a reaction, may not be unreasonable.

In the low dose-rate studies, a reduction in the yield of acetone was observed on increasing the concentration of hydrogen peroxide, suggesting that a reaction such as [12] may be the competing "first-order" terminating reaction.

[12] $CH_3CHOH\dot{C}H_2 + H_2O_2 \rightarrow (CH_3)_2CHOH + HO_2$

High Propanol Concentration /0.01 M H_2O_2

As the concentration of 2-propanol is increased to values greater than 1.0 *M*, the yield of acetone increases less rapidly, reaching a maximum in the region of 3.7 *M*. This levelling-off in the yield of acetone could be attributed to the increasing rate of reaction [9] with increasing alcohol concentration. If reaction [9] becomes sufficiently rapid, it may no longer be exclusively rate controlling and the chain length would be determined in part by competition between reactions [4] and [6]

[4] $\mathbf{1} + H_2O_2 \rightarrow (CH_3)_2CO + H_2O + OH$

[6] $\mathbf{1} + \mathbf{1} \rightarrow (CH_3)_2CO + (CH_3)_2CHOH$

This would result in a transition to a situation in which the reaction becomes independent of alcohol concentration and first-order in hydrogen peroxide. In fact, in this region, the yield–dose curve for hydrogen peroxide reduction becomes non-linear, although at none of the higher alcohol concentrations is it completely first order.

At alcohol concentrations in excess of 4.0 *M*, the chain yield of acetone decreases to a limiting value of 16 ± 1 in pure 2-propanol. There are at least two possible explanations for this decrease. The argument presented above suggests that, with increasing alcohol concentration, the yield should increase to a maximum limiting value and then remain constant. This assumes, however, that the primary yields of free-radical intermediates remain unchanged, which is highly improbable as the system is changed from pure water as solvent to pure 2-propanol. A decrease in the primary yields with increasing alcohol concentrations could account for the decreasing yield. However in a study of the photo-induced reaction, Barrett *et al.* (3) found an almost identical change in the quantum yield for hydrogen peroxide reduction, although the primary quantum yield of peroxide homolysis is said to remain constant in this concentration range. The decreasing yield was attributed by Barrett *et al.* to reaction of the product OH radicals with alcohol molecules in the "primary photochemical cage". The parallel between the radiation-chemical results reported here and the photochemical results makes this explanation unlikely, since the radiation chemical "spur" is not analogous to the photochemical "cage". We suggest that with increasing alcohol concentration, and consequent increase in the rate of reaction [9], reaction [4] becomes the principle rate-controlling propagation step and that the rate constant for [4] decreases with increasing alcohol concentration as a result of the decrease in dielectric constant.

[4] 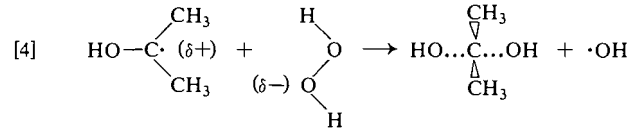

The reaction of the polar radical **1** with the polar molecule H_2O_2 would involve the formation of a polar transition state and would be expected to decrease in rate with decreasing dielectric constant (16).

At high 2-propanol concentrations, there is a significant dose-rate effect on the yields of acetone (Table 2). This dose-rate effect approaches, but never equals, a simple inverse square-root dependence, suggesting that even in pure 2-propanol termination by reaction [10] may still be significant.

Sherman (17) has reported the formation of methane and acetic acid in chain yields in addition to acetone in the radiation-induced oxidation of alkaline 2-propanol by nitrous oxide. The formation of methane and acetic acid was accounted for by the stoichiometric reaction

[13] $(CH_3)_2CHOH + N_2O \rightarrow CH_3CO_2H + N_2 + CH_4$

We detected no significant formation of methane in the oxidation of neutral 2-propanol by hydrogen peroxide, thus ruling out a reaction with H_2O_2 analogous to reaction [13].

Aqueous 2-Propanol/$< 10^{-3}$ M Hydrogen Peroxide

At a constant concentration of 2-propanol (0.52 *M*), the rate of reduction of hydrogen peroxide becomes dependent on its concentration (Fig. 3) and becomes essentially first-order in H_2O_2 below 10^{-4} *M*. We take this to indicate that the rate of reaction [4] has become sufficiently slow to become rate determining at these low peroxide concentrations.

When the concentration of H_2O_2 reaches its steady-state value, the requirement of oxidation–reduction balance in the system predicts that

[14] $G(\text{net oxidation}) = G(\text{net reduction})$

[15] $G(\text{acetone}) = G(H_2) = G_{H_2} + G_H$

This latter value is expected to be of the order of 1.0 (15), in good agreement with the experimental value of $G(\text{acetone}) = 0.97 \pm 0.05$.

The magnitude of the steady-state concentration of H_2O_2 could be used to determine the relative rates of terminating and propagating reactions, but we found this quantity to be rather irreproducible, varying from one experiment to another by as much as a factor of two.

Summary

The abstraction of hydrogen atoms from 2-propanol by OH radicals is suggested to be less specific as to the site of reaction than previously believed. The ratio of the rates of abstraction at the α and β position is

$$k_\alpha/k_\beta = 6.2$$

It is proposed that the radical formed by abstraction of a β hydrogen, $CH_3CHOH\dot{C}H_2$, can react with 2-propanol to abstract the α hydrogen, forming the α radical $(CH_3)_2\dot{C}OH$. A lower limit for the rate constant for this reaction is estimated as 53 ± 10 l mole^{-1} s^{-1}.

The authors gratefully acknowledge the cooperation of the Manitoba Cancer Treatment and Research Foundation and, particularly, the assistance of Dr. D. V. Cormack in performing the low dose-rate irradiations.

1. J. H. Merz and W. A. Waters. Discuss. Faraday Soc. **2**, 179 (1947).
2. J. H. Baxendale and J. A. Wilson. Trans. Faraday Soc. **53**, 344 (1957).
3. J. Barrett, A. L. Mansell, and R. J. M. Ratcliff. Chem. Commun. 48 (1968).
4. S. Paszyc and W. Augustyniak. Photochem. Photobiol. **8**, 235 (1968).
5. A. Burghardt, Z. Kulicki, and T. Mazonski. Chem. Stosow. Ser. A, **10**, 253 (1966).
6. J. T. Allan and C. M. Beck. J. Amer. Chem. Soc. **86**, 1483 (1964).
7. W. A. Seddon and A. O. Allen. J. Phys. Chem. **71**, 1914 (1967).
8. S. Berntsson. Anal. Chem. **28**, 1337 (1956).
9. A. O. Allen, C. J. Hochanadel, J. A. Ghormley, and J. W. Davis. J. Phys. Chem. **56**, 697 (1952).
10. M. Anbar and P. Neta. Int. J. Appl. Radiat. Isotop. **18**, 493 (1967).
11. R. Livingston and H. Zeldes. J. Amer. Chem. Soc. **88**, 4333 (1966).
12. J. K. Thomas. J. Phys. Chem. **71**, 1919 (1967).
13. R. Livingston and H. Zeldes. J. Chem. Phys. **44**, 1245 (1966).
14. R. O. C. Norman and P. R. West. J. Chem. Soc. B, 389 (1969).
15. G. V. Buxton. Radiat. Res. Rev. **1**, 209 (1968).
16. K. J. Laidler. Chemical kinetics. 2nd ed. McGraw–Hill Book Co., Inc., New York. 1965. p. 228.
17. W. V. Sherman. J. Phys. Chem. **71**, 1695 (1967).

Polyatomic cations of selenium. III. Compounds of the Se_8^{2+} cation

R. J. GILLESPIE AND P. K. UMMAT
Department of Chemistry, McMaster University, Hamilton, Ontario
Received November 19, 1969

The preparation and characterization of the compounds $Se_8(Sb_2F_{11})_2$ and $Se_8(AsF_6)_2$ are described. Both compounds are shown to contain the Se_8^{2+} cation.

Canadian Journal of Chemistry, 48, 1239 (1970)

Can. J. Chem. Downloaded from www.nrcresearchpress.com by 210.87.254.6 on 09/05/12
For personal use only.

In Part I of this series (1) it was shown that selenium dissolves in 100% sulfuric acid, oleum, or fluorosulfuric acid to give green solutions which, with time or the addition of a suitable oxidizing agent, become yellow. From studies of the conductivities, freezing points, absorption spectra, and magnetic susceptibilities of these solutions, it was concluded that the green solutions contain the species Se_8^{2+} and the yellow solutions contain the species Se_4^{2+}. In Part II (2) we described the preparation and characterization of some compounds of Se_4^{2+}. In this paper we describe the preparation of the compounds $Se_8(Sb_2F_{11})_2$ and $Se_8(AsF_6)_2$, and we show that they contain the Se_8^{2+} cation and the anions $Sb_2F_{11}^-$ and AsF_6^-, respectively.

Results and Discussion

In the preparation of the yellow compound $Se_4(Sb_2F_{11})_2$ by direct reaction of selenium and antimony pentafluoride (2), it was noted that the first product was a green material which on prolonged heating at 100–140 °C changed to the final yellow product. By carrying out the reaction between powdered selenium and antimony pentafluoride dissolved in liquid SO_2 at −23 °C for several days, a green solid was obtained on pumping off the SO_2. This solid was extracted several times with sulfur dioxide, leaving a white residue which was shown to be antimony trifluoride. A microcrystalline green solid was obtained from the sulfur dioxide solution which had an analysis consistent with the formulation $Se_8(Sb_2F_{11})_2$. The overall equation for the reaction may be written as follows

$$8Se + 5SbF_5 \rightarrow Se_8(Sb_2F_{11})_2 + SbF_3$$

It was also found that selenium could be conveniently oxidized to the green species by means of a solution of arsenic pentafluoride in anhydrous HF. This reaction was carried out at 0 °C over a period of a few days. Arsenic trifluoride was identified as a volatile product of the reaction. After removal of the solvent from the dark green solution, a semicrystalline green material was obtained in an amount corresponding to quantitative conversion of the selenium to the compound $Se_8(AsF_6)_2$, and this composition was confirmed by analysis. Thus the overall reaction may be formulated as follows

$$8Se + 3AsF_5 \rightarrow Se_8(AsF_6)_2 + AsF_3$$

Both compounds darken rapidly on exposure to moist air and instantly decompose to red selenium when added to water. They dissolve readily in 100% sulfuric acid, oleum, and fluorosulfuric acid to produce green solutions. On heating in a sealed tube, $Se_8(AsF_6)_2$ melted at 178–182 °C to form a green liquid and on further heating, black selenium was deposited. The other compound, $Se_8(Sb_2F_{11})_2$, gave a yellow melt over the range 180–190 °C and finally black selenium was deposited at approximately 200 °C. Presumably the $Sb_2F_{11}^-$ anion further oxidizes the Se_8^{2+} cation to the yellow Se_4^{2+} cation on heating.

The absorption spectra of solutions of both compounds in fluorosulfuric acid were identical with the spectrum reported for Se_8^{2+} in Part I (1) with absorption maxima at 295, 470, and 685 nm and an extinction coefficient for the 295 nm peak of 980 mole(Se)$^{-1}$ l cm^{-1}, which is in reasonable agreement with the value of 930 mole(Se)$^{-1}$ l cm^{-1} reported previously, showing that both compounds dissolve to give a quantitative yield of Se_8^{2+}.

The infrared spectrum of $Se_8(Sb_2F_{11})_2$ was essentially identical with that of $CsSb_2F_{11}$ over the range 450–1800 cm^{-1} and, in particular, contained a broad band at 650–770 cm^{-1} assigned to Sb—F stretching modes, and a weaker band at 476 cm^{-1} which appears to be characteristic of $Sb_2F_{11}^-$. This band has been observed previously at 523 cm^{-1} in $VO_2^+Sb_2F_{11}^-$ (3), at 485 cm^{-1}

Can. J. Chem. Downloaded from www.nrcresearchpress.com by 210.87.254.6 on 09/05/12
For personal use only.

in $Se_4^{2+}(Sb_2F_{11}^-)_2$ (4), and at 479 cm^{-1} in $Cs^+Sb_2F_{11}^-$ (5). The infrared spectrum of $Se_8(AsF_6)_2$ had a strong absorption at 700 cm^{-1}. Cesium hexafluoroarsenate has a similar strong absorption at 699 cm^{-1} (6).

The ^{19}F nuclear magnetic resonance (n.m.r.) spectrum in SO_2 at -90 °C consisted of a multiplet at 92 p.p.m., a doublet of doublets at 111 p.p.m., and a quintet at 133 p.p.m. from external $CFCl_3$. These chemical shifts agree well with those observed previously (7) for the $Sb_2F_{11}^-$ ion (**1**): multiplet F_a 89–91 p.p.m., doublet of doublets, F_b 109–111 p.p.m., and quintet F_c, 131–135 p.p.m. The coupling constants $J_{ab} = 60$ and $J_{bc} = 102$ Hz are in good agreement with the values of $J_{ab} = 59$ Hz and $J_{bc} = 102$ Hz obtained previously in SO_2 solution (7). In addition, a weak doublet was observed at 100 p.p.m. which is attributed to the complex $SbF_5 \cdot SO_2$ which arises from a small amount of solvolysis of $Sb_2F_{11}^-$. The ^{19}F spectrum of a solution of $Se_8(Sb_2F_{11})_2$ in fluorosulfuric acid had a broad peak F_d at 166 p.p.m. which may be assigned to SbF_6^-, a doublet F_e at 156 p.p.m., and a quintet F_f at 184 p.p.m. with a coupling constant of 100 Hz which may be assigned to the $SbF_5(SO_3F)^-$ anion (**11**) (8). The doublet arises from the four equivalent fluorines F_e and the quintet from F_f. The relative areas of signals from F_d and F_e were 5.9/4.0, in good agreement with the expected ratio of 6.0/4.0 for the formation of equal amounts of SbF_6^- and $SbF_5(SO_3F)^-$ according to the equation

$$Sb_2F_{11}^- + SO_3F^- \rightarrow SbF_6^- + SbF_5(SO_3F)^-$$

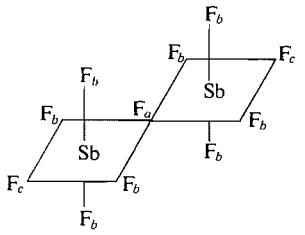

I

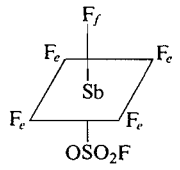

II

A weak spectrum due to $Sb_2F_{11}^-$ was also observed, indicating that solvolysis of the anion was incomplete.

The ^{19}F n.m.r. spectrum of a solution of $Se_8(AsF_6)_2$ in fluorosulfuric acid had only one broad signal at $\delta_{CCl_3F} = 61.6$ p.p.m., in addition to that from the solvent. A solution of $Bu_4N^+AsF_6^-$ in fluorosulfuric acid gave a signal at $\delta_{CCl_3F} = 63$ p.p.m., in addition to the solvent peak. The spectra remained essentially unchanged on cooling the solution to -80 °C.

It is clear that the two compounds have the ionic structures $Se_8^{2+}(Sb_2F_{11}^-)_2$ and $Se_8^{2+}(AsF_6^-)_2$. The structure of the Se_8^{2+} cation is of great interest and low-frequency laser Raman studies and X-ray crystallographic investigations are in progress.

NOTE ADDED IN PROOF: A preliminary report of an X-ray crystallographic study of the structure of Se_8^{2+} has appeared since this paper was submitted for publication (11).

Experimental

Preparation of $Se_8(Sb_2F_{11})_2$

In a typical experiment, antimony pentafluoride (0.015 mole) was added to powdered selenium (0.025 mole) in SO_2 at -63 °C; the mixture was allowed to warm up to -23 °C and stirred for three days. A very dark green solution containing some dark solid was obtained which gave a green solid on pumping off the sulfur dioxide. The solid was extracted with approximately 30 ml of sulfur dioxide four times until the remaining solid residue was white. This white solid was identified as antimony trifluoride, which is insoluble in liquid sulfur dioxide. The Raman spectrum was identical with that of an authentic sample and the oxidation state of antimony was confirmed by the Rhodamine-B test. The sulfur dioxide extract was evaporated under vacuum and a dark green microcrystalline solid was obtained.

Anal. Calcd. for $Se_8(Sb_2F_{11})_2$: Se, 41.40; Sb, 31.60; F, 27.30. Found: Se, 40.4; Sb, 30.5; F, 28.7.

Preparation of $Se_8(AsF_6)_2$

In a typical experiment, arsenic pentafluoride (0.0095 mole) was condensed onto powdered selenium (0.025 mole) in anhydrous hydrogen fluoride at -78 °C and the mixture was allowed to warm up to 0 °C over a period of 3 days. A volatile product was condensed out in an adjoining trap. This was identified as arsenic trifluoride by means of the infrared spectrum of the vapor. On removal of the solvent under vacuum, a semicrystalline dark green solid product was obtained, the weight of which corresponded to quantitative formation of $Se_8(AsF_6)_2$ (0.0032 mole).

Anal. Calcd. for $Se_8(AsF_6)_2$: Se, 62.57; AsF_6, 37.43. Found: Se, 63.1; AsF_6, 37.0.

Materials

Commercially available pure selenium was dried in a vacuum desiccator over P_2O_5. Antimony pentafluoride was obtained from Ozark-Mahoning Company and distilled twice in glass apparatus immediately before use. Arsenic pentafluoride was obtained from the Ozark-Mahoning Co. Its purity was checked by gas-phase infrared spectroscopy. Hydrogen fluoride (99.9%) was obtained from the Matheson Co. and was distilled directly from the cylinder.

Absorption Spectra

These spectra were obtained on a Cary Model 14 spectrometer using 1 cm quartz cells and quartz inserts to give path length down to 0.005 cm.

Infrared Spectra

The infrared spectra of both compounds were obtained on the powder between silver chloride plates using a Perkin–Elmer Model 337 spectrophotometer.

Nuclear Magnetic Resonance

^{19}F n.m.r. spectra were obtained at 56.4 Hz using a Varian DP-60 spectrometer.

Analysis

The compound $Se_8(Sb_2F_{11})_2$ was analyzed by Alfred Bernhardt (5251 Elbach über Engelskirchen, Fritz-Pregl-Strasse, 14–16, West Germany).

Selenium. Weighed quantities of each compound were decomposed with water and dissolved in the minimum volume of warm nitric acid. The dilute solution was warmed with an excess of hydrazine sulfate for 1 h, and the resulting grey selenium was filtered, dried, and weighed.

AsF_6^-. The method of Dess *et al.* (9, 10) was used to determine AsF_6^-, in which AsF_6^- was precipitated as tetraphenylarsonium hexafluoroarsenate from an acid solution and weighed as such after drying at 110 °C.

1. J. Barr, R. J. Gillespie, R. Kapoor, and K. C. Malhotra. Can. J. Chem. **46**, 149 (1968).
2. J. Barr, D. B. Crump, R. J. Gillespie, R. Kapoor, and P. K. Ummat. Can. J. Chem. **46**, 22 (1968).
3. J. Weidlein and K. Dehnicke. Z. Anorg. Allg. Chem. **348**, 278 (1966).
4. R. J. Gillespie and G. Pez. Inorg. Chem. **8**, 1229 (1969).
5. P. A. W. Dean and R. J. Gillespie. Unpublished results.
6. C. M. Begun and A. C. Rutenberg. Inorg. Chem. **6**, 2212 (1967).
7. P. A. W. Dean, J. Bacon, and R. J. Gillespie. Can. J. Chem. **47**, 1655 (1969).
8. R. C. Thompson, J. Barr, R. J. Gillespie, J. B. Milne, and R. A. Rothenbury. Inorg. Chem. **4**, 1641 (1965).
9. H. M. Dess, R. W. Parry, and G. L. Vidall. J. Amer. Chem. Soc. **78**, 5734 (1956).
10. H. H. Willard and H. Diehl. Advanced quantitative analysis. D. Van Nostrand Company Ltd., London.
11. R. K. McMullan. D. J. Prince, and J. D. Corbelt. Chem. Commun. 1438 (1969).

Can. J. Chem. Downloaded from www.nrcresearchpress.com by 210.87.254.6 on 09/05/12
For personal use only.

Can. J. Chem. Downloaded from www.nrcresearchpress.com by 210.87.254.6 on 09/05/12
For personal use only.

Anodic oxidation of copper in alkaline solution

M. J. DIGNAM AND D. B. GIBBS[1]
Department of Chemistry, University of Toronto, Toronto 181, Ontario

Received September 10, 1969

The anodic formation of Cu_2O on electropolished polycrystalline copper has been examined galvanostatically in a borate buffer solution over a range of current densities and temperatures. A model for film formation based on rapid formation of oxide nuclei followed by their lateral growth has been developed and shown to be in quantitative agreement with the data. According to this model, an oxygen-containing adsorbed intermediate, formed in an electrochemical step, reacts with metal at the peripheries of oxide patches to form more oxide. Both one- and two-dimensional lateral growth mechanisms were considered, the former being found to represent the data appreciably better. Assuming the initial electrochemical step to be $H_2O \xrightarrow{k_f} (OH)_s + H_{aq}^+ + e$, where $(OH)_s$ represents the adsorbed intermediate, the first-order rate constant, k_f, calculated at the equilibrium electrode potential, is given by $k_f = 10^{13.3} \exp(-19\,400/RT)\ s^{-1}$.

Canadian Journal of Chemistry, **48**, 1242 (1970)

Introduction

Since the early work of Muller (1) and others, potential steps on the galvanostatic charging curves for copper anodes in alkaline solution have been identified mainly with the formation of Cu_2O, CuO, and $Cu(OH)_2$. Higher oxides, such as Cu_2O_3, have also been claimed.

It is generally agreed (2–8) that the lowest oxide, Cu_2O, first forms on a clean copper anode, probably according to the overall reaction

$$2Cu + 2OH^- \rightleftharpoons Cu_2O + H_2O + 2e$$

However, this process has not been investigated in any detail. Considerably greater attention has been given in the literature to the formation of CuO and $Cu(OH)_2$ (2–9), either or both of which may be associated with potential plateaus following that for Cu_2O, and which probably result from oxidation of Cu_2O.

In spite of much introductory work on the behavior of the copper electrode, it remains true that little more than a qualitative understanding of the anodic processes on copper in alkaline solution exists at present. Quantitative experimental conditions and methods of surface preparation which have been used by different workers make correlation of the various results difficult. However, it is clear that a study of the copper anode must begin with a good understanding of the initial oxidation process, namely the formation of Cu_2O. It is with this subject that the present paper is principally concerned.

In this work, electropolished polycrystalline copper specimens of ultra-high purity were anodically oxidized at constant current in a borate buffer solution. Experiments were carried out in a carefully purified nitrogen atmosphere, with a pre-electrolysis procedure being used to reduce the concentrations of dissolved oxygen and other impurities to very low levels. The cell was designed to permit the transfer of each copper electrode from a hydrogen reduction furnace into the electrolyte without exposing it to air.

Experimental

Instrumentation

An instrument for control of current or potential (three-electrode system) was constructed from Philbrick operational amplifiers. It functioned as a galvanostat for the experimental runs to be described, and as a potentiostat during pre-electrolysis. The potential of the working electrode was monitored with either a recording potentiometer or a Tektronix oscilloscope and camera. An additional operational amplifier, connected as a limited-frequency differentiator, was used to follow the time derivative of the electrode potential.

Materials

Experiments were carried out under an atmosphere of nitrogen purified by passage first through Fieser's solution (10), then through a five-ft column packed with finely dispersed copper on Kieselguhr (11) and heated to 220 °C (after Nagayama and Cohen (12)). Before entering the cell, the nitrogen passed through a bubbler containing the experimental electrolyte solution.

The 0.05 *M* borax solution was prepared by dissolving AR sodium tetraborate decahydrate in doubly-distilled water. Following transfer to the cell, purified nitrogen was bubbled through the solution for several h, followed by pre-electrolysis while passing nitrogen over the solution and stirring with a magnetic stirring bar.

The pre-electrolysis, using an auxiliary Pt electrode, was carried out at a potential just above that of the

[1]Present address: Division of Chemistry, National Research Council of Canada, Ottawa, Canada.

Can. J. Chem. Downloaded from www.nrcresearchpress.com by 210.87.254.6 on 09/05/12
For personal use only.

reversible hydrogen electrode, until the current density dropped to 0.25 μA/cm².

The test electrodes were punched from 99.999+ % copper sheet obtained from American Smelting and Refining Company. They were in the form of sheets 1.0 × 0.25 × 0.050 in., with handles 1.5 in. long, and were suspended vertically in the cell so that the geometric area exposed to the solution was 4.0 cm². After a thorough degreasing in acetone or benzene, followed by a 10 s etch in 1:1 nitric acid, they were annealed in flowing hydrogen at 350 °C for 4 h, then electropolished in a phosphoric acid bath (13) to a very bright, smooth finish.

Cell Design

The cell was of conventional design and was provided with an outer jacket for temperature control. The counter electrode was a piece of copper foil shaped as a cylinder with elliptic cross section, and surrounding the working electrode. It was given a preliminary oxidation to ensure saturation of the solution with copper. The Hg/HgO reference electrode (14) was housed within the cell, in a compartment which terminated in a Luggin capillary. It was checked for accuracy against a hydrogen electrode and for stability, periodically, against a saturated calomel electrode.

The cell was fitted with an air-tight lid into which was sealed an overhead vertical furnace. The working electrode, mounted on a polished stainless steel rod which emerged from the top of the furnace through a Teflon-plug seal, could be given a final reduction in hydrogen, and then after cooling be lowered directly into the electrolyte solution out of contact with air. Cathodic reduction immediately following immersion of the electrode into the electrolyte gave no indication of any film material reducible above the reversible hydrogen potential (15).

In order to maintain a low concentration of dissolved oxygen, pre-electrolysis with stirring was continued at all times except during experiments. All runs were done in unstirred solution.

The entire apparatus was enclosed in a box painted flat black inside to eliminate any possible photoelectric or photochemical effects.

Results

Rest Potential

Upon immersion in the electrolyte, the test electrode assumed an initial open-circuit potential of −0.50 to −0.55 V vs. the Hg/HgO reference electrode, but attained a steady value close to −0.40 V within less than a minute. Some twenty determinations of this rest potential were carried out. It was found that the same potential was reached from above or below; i.e., by a freshly-immersed electrode, or by open-circuit decay of an electrode on which some Cu_2O had been anodically formed, or by a fresh electrode which was first polarized cathodically to approximately the reversible hydrogen electrode potential and then left to decay on open circuit. The mean value was −0.400 ± 0.010 V vs. Hg/HgO. In the following sections, the anode potential will often be given with respect to this potential, and referred to as the overpotential for Cu_2O formation.

Oxidation and Reduction Curves

We first examine the complete anodic charging curve, extending from the initial rest potential up to the steady oxygen evolution potential. Such a curve, obtained at a current density of 6.7 μA/cm², is shown in Fig. 1. The initial potential arrest, terminating at L, is believed to correspond solely to Cu_2O formation. Beyond point L, a second potential arrest of about one-half the length of the first (possibly CuO formation) is followed by a long, steady rise before levelling off, due to oxygen evolution, at about +0.76 V vs. Hg/HgO. Just prior to reaching this value, the potential fluctuates erratically.

We now turn to a more detailed study of the initial portion of this curve, which will be referred to as the "Cu_2O formation" region. A series of charging curves for this region were recorded at various current densities covering a range of two decades. The results for runs at 25 °C will be described first.

The characteristic inflection point at L, Fig. 1, was taken as indicating the onset of a new electrode process, most probably CuO formation. Provided oxidation was carried well beyond point L, its position could usually be determined graphically. In order to measure the current efficiency for oxidation up to point L, however, an alternative method was used which allowed the current direction to be reversed, and cathodic reduction carried out, as soon as this point was reached. The method involved monitoring the time derivative of the anode potential. Since the derivative

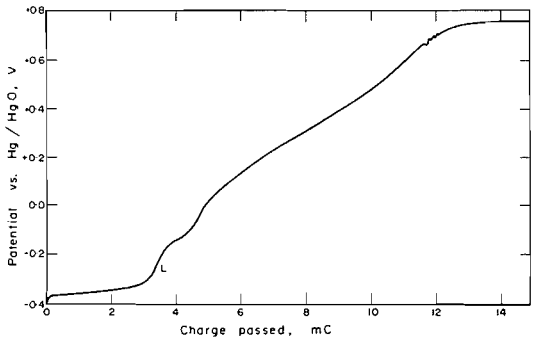

FIG. 1. Anodic polarization curve for copper, extending from the Cu/Cu_2O rest potential up to the oxygen evolution region. (Temperature 25 °C, current density 6.7 μA/cm².)

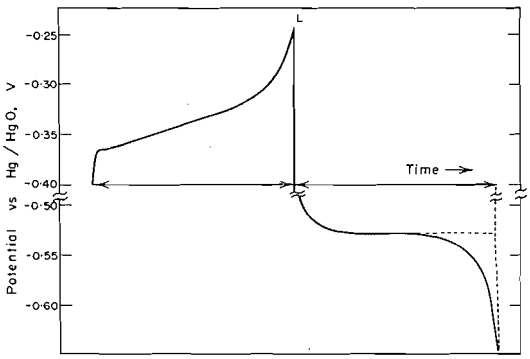

FIG. 2. Oxidation and reduction curves for Cu_2O. (Temperature 25 °C, current density 10.1 μA/ cm², oxidation and reduction periods are each 90 s.)

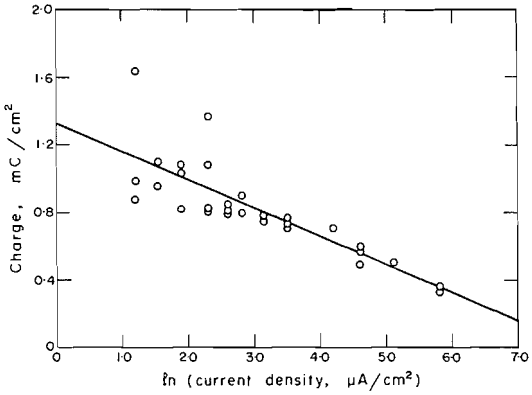

FIG. 4. Dependence of the limiting oxidation charge for Cu_2O formation on current density. (Temperature 25 °C.)

passed through a sharp maximum at L, cathodic reduction could be started as soon as it was evident that the maximum had been passed.

A potential–time curve obtained in this manner is depicted in Fig. 2. The oxidation section consists of an initial rapid rise of potential with a small, rounded peak, followed by a long, more or less linear, region in which the potential increases gradually. Finally, a more rapid increase toward the inflection point L occurs. The reduction curve consists of only one plateau followed by a rapid drop to hydrogen evolution. All reductions were carried out at a current density of 10.1 μA/cm². The reduction plateau was not always horizontal, particularly for films formed at high current densities, where there was instead a linear region of negative slope.

Effect of Current Density

The effect of current density on the shape of the oxidation curve is seen in Fig. 3. The amount of charge q_L consumed during oxidation from zero

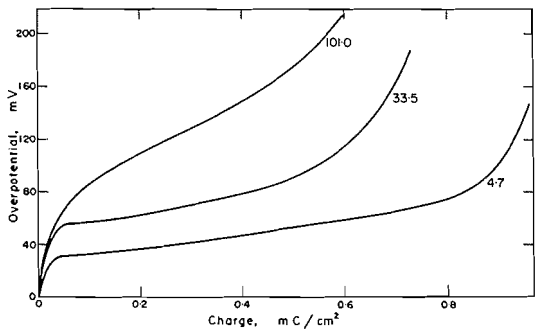

FIG. 3. Polarization curves for Cu_2O formation. (Temperature 25 °C; current densities of 4.7, 33.5, and 101 μA/cm².)

time up to point L is depicted as a function of current density in Fig. 4. A plot of q_L vs. ln (current density) appears to be approximately linear, and a least-squares straight line has been drawn through the points. It is clear that the reproducibility is poorer at the low current densities.

The current efficiencies for Cu_2O formation, measured from curves of the type shown in Fig. 2, were always 100 ± 2%, even at the lowest current density. Hence, the mean limiting film thickness X_L can be estimated from either the oxidation charge or the reduction charge, assuming a roughness factor of unity, and using the bulk density of Cu_2O, 6.0 g/cm³ (16). The thicknesses, X_L, calculated in this manner range from about 5 to 15 Å. No correction of X_L for double-layer capacitance was made. Assuming the ionic double-layer capacitance to be of the order of 20 to 40 μF/cm², the fraction of q_L used in double-layer charging will be small, even at the highest current density. For example, with $q_L \simeq 0.4$ mC/cm² and a potential range of ~200 mV, the double-layer charge amounts to only 1 to 2% of q_L.

Inflection Point, L

As stated earlier, the marked increase of potential in the vicinity of point L was taken to indicate the onset of a new electrode reaction. This interpretation is supported by the fact that whenever oxidation was carried past point L, an additional cathodic reduction plateau appeared at about −0.27 V vs. Hg/HgO, the associated charge for which depended on the amount of charge passed

Can. J. Chem. Downloaded from www.nrcresearchpress.com by 210.87.254.6 on 09/05/12
For personal use only.

Can. J. Chem. Downloaded from www.nrcresearchpress.com by 210.87.254.6 on 09/05/12
For personal use only.

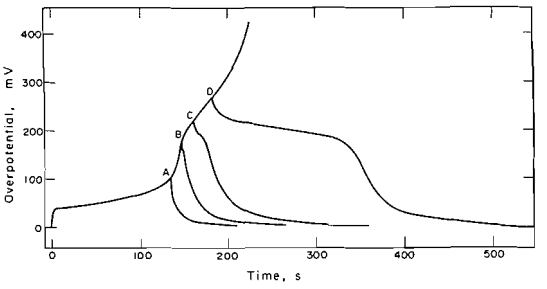

FIG. 5. Open-circuit potential decay curves starting at various points along the anodic polarization curve. (Temperature 25 °C, polarizing current density 6.7 μA/cm².)

beyond point L during oxidation. Further support comes from open-circuit potential decay experiments. Figure 5 shows an anodic polarization curve recorded at 6.7 μA/cm² up to an overpotential of 400 mV, along with decay curves recorded at four different starting overpotentials. The inflection point L occurs at an overpotential of about 145 mV. Curve *A*, which originates below this point, drops rapidly and approaches the zero overpotential line in a straightforward manner. However, curve *B*, which begins above the inflection point, displays a subtle kink near the beginning, a hint of the additional plateau which is shown with increasing prominence in curves *C* and *D*. The onset of the kink was observed to begin at an overpotential coinciding within experimental uncertainty to the position of the inflection point.

Effect of Temperature

Two series of experiments similar to those described for 25 °C were carried out at temperatures of 14 and 36 °C, respectively. The overpotentials

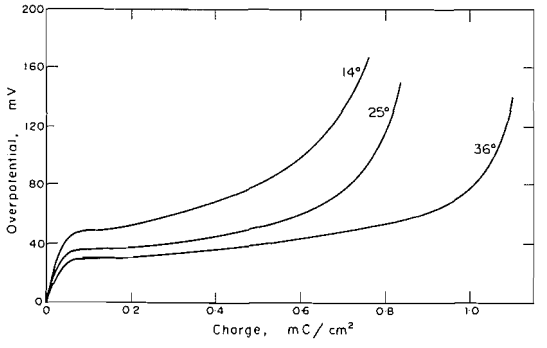

FIG. 6. Dependence of the polarization curve for Cu_2O formation on temperature. (Temperatures of 36, 25, and 14 °C; current density 6.7 μA/cm².)

were determined with respect to the Cu/Cu_2O rest potential at the experimental temperature. In Fig. 6 are shown three curves recorded at the same current density, one at each temperature. Two trends with increasing temperature are apparent: the overpotential for oxidation decreases, and the amount of charge q_L increases. This behavior is observed at all current densities.

Discussion

One of the features of the anodic charging curves which must be accounted for by any proposed mechanism for Cu_2O formation, is the existence of a limiting film thickness. Thus, any viable mechanism must account for the rapid increase of overpotential in the vicinity of point L followed by the onset of a new anodic process. A number of possible explanations were considered, including rate control by (*1*) a diffusion process within a film assumed to be uniformly distributed over the surface, (*2*) electron tunnelling, and (*3*) diffusion of a reactant in solution. None of these approaches gave results consistent with the data. The proposed model, which was found to be in excellent agreement with the data, is described in the following sections.

Nucleation; Two-Dimensional Growth

We suppose that upon application of current, patches of oxide nucleate rapidly at energetically favorable sites on the metal surface, and that these nuclei subsequently grow laterally and eventually coalesce to cover the surface. It is clear that for such a mechanism the measured film thickness X must be interpreted as a mean value.

One mechanism which will give rise to this type of growth follows. The forward electrochemical step is assumed to involve the discharge of an hydroxyl ion at the bare metal surface to form a mobile surface species $(OH)_s$

$$[I'] \qquad OH_{aq}^- \xrightarrow{k_f'} (OH)_s + e$$

This adsorbed intermediate can either undergo an electrochemical reaction which is the reverse of (I′)

$$[II] \qquad (OH)_s + e \xrightarrow{k_r} OH_{aq}^-$$

or it can move about the surface, periodically encountering the growing oxide patches. Successful encounters lead to formation of metal oxide at the peripheries of the patches. For example

Can. J. Chem. Downloaded from www.nrcresearchpress.com by 210.87.254.6 on 09/05/12
For personal use only.

[III] $(OH)_s + M \xrightarrow{k_s} M—OH$

followed by a fast reaction such as

[IV] $M—OH + (OH)_s \rightarrow MO + H_2O$

where MO represents the oxide product. It is to be noted that this mechanism leads to lateral growth of the oxide patches, but not to an increase in their thickness. The oxide patches will therefore maintain essentially a constant thickness, X_o, during their growth. Possible variations in the details of this mechanism will be discussed later.

A proper treatment of this model must take account of impingement of growing oxide patches on one another. For this purpose, an adaptation (17) of an approach by Avrami (18) will be used. His result gives the fraction of the surface actually covered with oxide (X/X_o in the present case) as

$$[1] \qquad -\ln (1 - X/X_o) = N\pi r^2$$

where we have assumed for simplicity that the patches (concentration N per unit area) are circular cylinders of radius r.

The radial growth rate of the centers will be proportional to the number of oxygen atoms incorporated into the peripheries of the growing crystallites per unit time per unit peripheral length, which from reactions [III] and [IV] is given by $k_s[(OH)_s]$. We can therefore write

$$[2] \qquad dr/dt = k_s[(OH)_s]\Omega/X_o$$

where Ω is the volume of the oxide per oxygen atom. The current density i corresponding to film formation is clearly given by

$$[3] \qquad i = (2e/\Omega)(dX/dt)$$

in which e is the charge on the proton. The factor 2 is introduced since reaction [I′] must occur twice for each oxygen atom incorporated. Differentiating eq. [1] with respect to t leads to the result

$$[4] \qquad dX/dt = 2\pi Nr(X_o - X)\, dr/dt$$

Eliminating dX/dt, dr/dt, and r from eqs. [1], [2], [3], and [4] gives

$$[5] \qquad i = 4e(N\pi)^{1/2}k_s(1 - X/X_o) \times [-\ln (1 - X/X_o)]^{1/2}[(OH)_s]$$

Now the rate of consumption of (OH_s) per unit area of bare metal on the electrode via reaction [III] is given by

$$[6] \qquad -(d[(OH)_s]/dt)_{III} = i/e(1 - X/X_o)$$

The expression for the net rate of consumption of $(OH)_s$ via reactions [I′], [II], and [III] can then be written (denoting by $[OH_{aq}^-]_p$ the concentration of hydroxyl ion in the pre-electrode layer) as

$$[7] \qquad -d[(OH)_s]/dt = -k_f'[OH_{aq}^-]_p \exp(\beta e\eta/kT) + k_r[(OH)_s] \exp(-[1 - \beta]e\eta/kT) + i/e(1 - X/X_o)$$

Here we have made use of the usual equation relating current density and overpotential, η, for an activation-controlled anodic process.

Applying the steady-state approximation, i.e., setting $d[(OH)_s]/dt \simeq 0$, and eliminating $[(OH)_s]$ between eqs. [5] and [7] gives

$$[8] \qquad i = i_2 y(1 - X/X_o) \exp(e\eta/kT)/\{1 + a_2 y \cdot \exp[(1 - \beta)e\eta/kT]\}$$

where

$$i_2 = 4e(k_f'k_s/k_r)(N\pi)^{1/2}[OH_{aq}^-]_p$$

$$a_2 = 4(N\pi)^{1/2}(k_s/k_r)$$

and

$$y = [-\ln (1 - X/X_o)]^{1/2}$$

Rearranging eq. [8], we obtain

$$[9] \qquad \eta = (kT/e)\{\ln (i/i_2) + \ln (y^{-1} + a_2 \exp[(1 - \beta)e\eta/kT]) - \ln (1 - X/X_o)\}$$

The first term is independent of thickness, while the second term varies with thickness in a complicated manner, both y and η being functions of X. This term will be important when X is small, but the third term will clearly be the most important one as X approaches X_o.

Nucleation; One-Dimensional Growth

In the foregoing treatment, nucleation of oxide may be supposed to take place primarily at point heterogeneities on the metal surface. There is no reason, however, why growth of nuclei need be two-dimensional, and indeed one-dimensional growth, such as broadening of ribbon-like nuclei which have formed along linear heterogeneities (steps and/or grain boundaries) seems not unlikely. An equation for such a case can be derived in a manner similar to eq. [9]. In place of eq. [1] we write

$$[10] \qquad -\ln (1 - X/X_o) = 2Wr$$

in which W is the total length of nuclei per unit

Can. J. Chem. Downloaded from www.nrcresearchpress.com by 210.87.254.6 on 09/05/12
For personal use only.

area, X_o their thickness, and r the half-width of the growing nuclei in the direction in which growth occurs. Equations [2] and [3] are unchanged, but eq. [4] becomes

$$[11] \qquad dX/dt = 2W(X_o - X)\, dr/dt$$

This leads to the relation

$$[12] \qquad i = 4Wek_s[(OH)_s](1 - X/X_o)$$

and we eventually obtain, analogous to eq. [9]

$$[13] \qquad \eta = (kT/e)\{\ln(i/i_1) + \ln(1 + a_1 \exp[(1 - \beta)e\eta/kT]) - \ln(1 - X/X_o)\}$$

with

$$i_1 = 4We(k_f' k_s/k_r)[OH_{aq}^-]_p$$

and

$$a_1 = 4W(k_s/k_r)$$

This result is similar to eq. [9], differing only in the form of the second term.

Test of Models

An attempt was made to distinguish between the two types of growth by testing which equation best described the experimental results. The overpotential–thickness data for all runs were fitted to eqs. [9] and [13] by a non-linear least-squares method. The parameter β was set equal to 0.5, alternate values failing to give consistent improvement. The procedure amounted to choosing values of the three variables ($\ln(i/i_2)$, a_2, and X_o; or $\ln(i/i_1)$, a_1, and X_o) which minimized the variance in η. (Since η appears on both sides of the equations, an iterative method was used.)

The standard deviations in η for the two equations are tabulated for runs at 25 °C in Table 1. Comparison shows that in nearly all cases, eq. [13] gave a better fit to the data than did eq. [9]; in some cases the improvement is substantial. Similar results were found at 36 and 14 °C.

Applying Snedecor's F-test at the 99% confidence level to the total variance in η on combining all the runs at a given temperature led to the result that the improved fit of eq. [13] over eq. [9] is statistically significant for the data at 25 °C, but not for that at 14 or 36 °C. The data at 36 °C passes the test at the 95% confidence level, while that at 14 °C passes it at the 90% confidence level. To test the mechanisms further, we define C_1 and C_2 as follows

$$[14] \qquad C_j = i_j/a_j \qquad j = 1, 2$$

TABLE 1
Standard deviations in η for polarization data at 25 °C fitted in turn to eqs. [9] and [13]

Formation current density (μA/cm²)	Standard deviation in η (mV)	
	Equation [9]	Equation [13]
3.35	10.4	4.39
	3.93	1.54
	5.59	2.02
4.69	7.70	5.59
	5.16	3.69
6.70	5.45	4.38
	5.70	3.58
	4.59	1.53
10.1	4.88	3.25
	5.11	3.76
	2.37	1.12
	5.30	3.23
13.4	4.13	2.99
	1.99	2.58
	7.43	3.64
16.8	2.92	1.87
	1.74	1.79
23.4	3.45	2.91
	3.26	1.92
33.5	4.96	4.71
	2.16	2.32
	3.38	3.59
67.0	8.18	7.86
	8.54	8.19
101	5.31	4.75
	8.03	7.37
	7.58	7.25
168	4.43	4.09
335	11.7	11.4
	6.16	6.00

The important property of the C_j is that they are independent of the density of nuclei, a number which one would expect to vary considerably from specimen to specimen. The C_j should therefore display considerably less scatter than either the i_j or a_j, as indeed was found to be the case. Making use of the relationship

$$[15] \qquad \ln(i/C_j) = \ln(i/i_j) + \ln a_j$$

the left-hand side of eq. [15] could be calculated for each run once the parameters $\ln(i/i_j)$ and a_j had been found by the least-squares fitting procedure. It follows that if either of the two mechanisms is valid, a plot of the corresponding $\ln(i/C_j)$ vs. $\ln i$ must be linear with unit slope.

The graphs of $\ln(i/C_j)$ are shown for the runs at 25 °C in Fig. 7. The straight lines are least-squares lines of slope unity. The agreement is

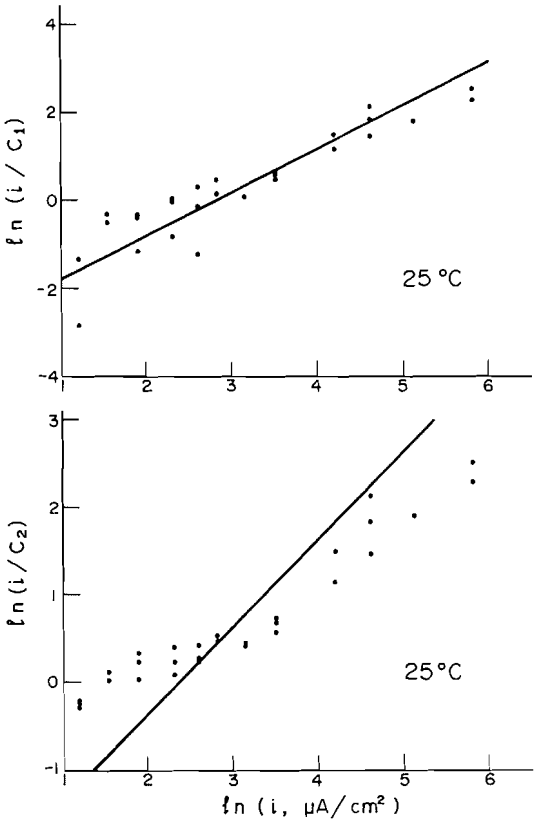

FIG. 7. Plots of (ln i/C_1) and (ln i/C_2) vs. ln i at 25 °C. (In both cases the slopes have been set equal to unity and the intercepts determined by least-squares.)

clearly better for the one-dimensional growth mechanism, a result found to hold also for the corresponding plots at the other temperatures.

Of course, the growth of nuclei need not be restricted to either one- or two-dimensions, but might instead be some combination of the two. The one-dimensional model, however, gives a consistently better fit, and one which is within experimental scatter. The remainder of the discussion will therefore be concerned solely with this type of growth.

Figure 8 illustrates how well eq. [13] is able to account for the form of the polarization curves. The agreement is excellent at low and medium current densities and quite good at the highest current densities.

Calculation of k_f and its Temperature Dependence

From the expression for C_1

$$[16] \qquad C_1 = k_f' e[OH_{aq}^-]_p$$

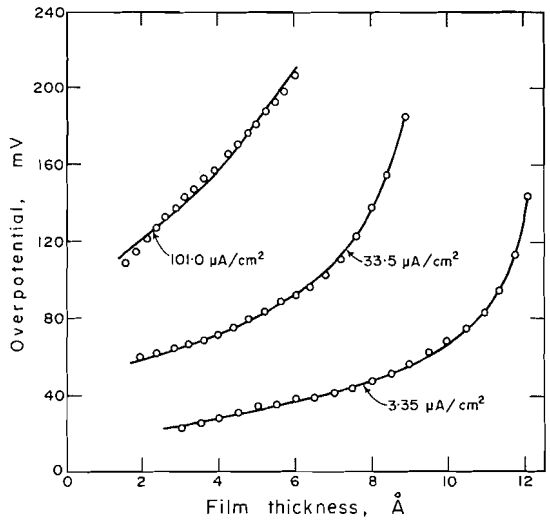

FIG. 8. Comparison of experimental and calculated (eq. [13]) polarization curves using the least-squares parameters. The data are represented by open circles. (Temperature 25 °C.)

it is apparent that a plot of ln C_1 vs. $1/T$ will yield the Arrhenius activation energy for k_f', provided that the temperature dependence of $[OH_{aq}^-]_p$ may be neglected. If in place of the reaction step [I'], we write

$$[I] \qquad H_2O \xrightarrow{k_f} (OH)_s + H_{aq}^+ + e$$

leaving the other steps unchanged, C_1 will be given by

$$[17] \qquad C_1 = k_f e[H_2O]_p$$

where $[H_2O]_p$ is the surface concentration of water molecules in the pre-electrode layer. That the source of oxygen might be H_2O rather than OH^- seems not unlikely for the present system. In either event, however, the activation energy (corresponding to k_f' or k_f) can be determined from the temperature dependence of C_1. The value of ln C_1 at 25 °C is obtained directly from the intercept of Fig. 7, upper graph. Values for ln C_1 at 14 and 36 °C were obtained from similar plots for data at these temperatures, the three values being plotted against $1/T$ in Fig. 9. The points are collinear within experimental error, the vertical bars representing 95% confidence limits. The slope yields an activation energy of 19.4 kcal/mole.

In order to calculate the pre-exponential factor for k_f' or k_f, clearly we must choose between eqs. [16] and [17] (i.e., between reactions [I'] and [I])

Can. J. Chem. Downloaded from www.nrcresearchpress.com by 210.87.254.6 on 09/05/12
For personal use only.

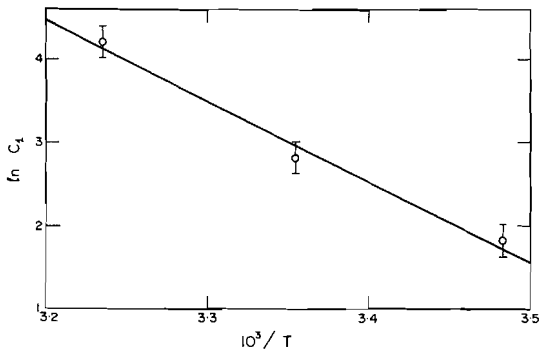

FIG. 9. Arrhenius plot of C_1 (Temperature in ° K). The vertical bars represent 95% confidence limits on C_1.

and obtain an estimate of the relevant concentration term. This is difficult to do in the case of eq. [16], since the relevant adsorption isotherm is not known. In the case of eq. [17], however, we may assume that the concentration of water in the pre-electrode layer will be essentially that for bulk water, $[H_2O]$, so that $[H_2O]_p \simeq [H_2O]^{2/3} = 1.04 \times 10^{15}$ molecules/cm^2. This leads to

[18] $\quad k_f = 10^{13.3} \exp(-19\,400/RT) \quad s^{-1}$

which corresponds to an eminently reasonable value for the pre-exponential factor (i.e., a value of the order of kT/h).

It should be noted that on replacing reaction [I'] with [I], the electrochemical step [II] is no longer the reverse of the forward electrochemical step. Equation [13] will apply to this case, therefore, only if β has essentially the same value for each of steps [I] and [II], a condition, nevertheless, likely to be satisfied within experimental accuracy since $\beta \simeq 0.5$.

TABLE 2

Least-squares parameters for the polarization data at 25 °C fitted to the one-dimensional growth equation, [13]*

Formation current density, μA/cm^2	ln i_1 (i_1 in μA/cm^2)	a_1 (dimensionless)	X_0 (Å)
3.35	0.265 —	−0.057 —	20.4 (0.06)
	0.719 (0.052)	0.159 (0.032)	12.4 (0.02)
	0.415 (0.070)	0.026 (0.018)	11.0 (0.03)
4.69	1.043 (0.062)	0.366 (0.041)	14.3 (0.12)
	1.016 (0.051)	0.424 (0.024)	12.5 (0.08)
6.70	0.967 (0.088)	0.265 (0.019)	14.6 (0.14)
	1.118 (0.051)	0.321 (0.017)	13.3 (0.06)
	0.955 (0.037)	0.117 (0.027)	10.4 (0.02)
10.1	1.420 (0.092)	0.389 (0.032)	14.3 (0.10)
	1.424 (0.060)	0.356 (0.019)	18.0 (0.11)
	1.968 (0.098)	0.721 (0.067)	10.5 (0.01)
	1.394 (0.109)	0.176 (0.088)	10.5 (0.06)
13.4	1.971 (0.354)	0.464 (0.073)	10.5 (0.12)
	2.293 (0.089)	0.993 (0.114)	10.3 (0.02)
	1.225 (0.084)	0.074 (0.013)	10.8 (0.04)
16.8	2.006 (0.103)	0.512 (0.148)	11.9 (0.04)
	2.499 (0.108)	1.132 (0.140)	10.4 (0.02)
23.4	2.267 (0.284)	0.421 (0.086)	10.0 (0.04)
	2.284 (0.089)	0.443 (0.148)	9.6 (0.03)
33.5	3.115 (0.118)	1.086 (0.154)	9.8 (0.02)
	2.860 (0.085)	0.976 (0.175)	9.4 (0.03)
	3.092 (0.133)	1.195 (0.179)	9.1 (0.02)
67.0	3.907 (0.276)	2.328 (0.749)	9.2 (0.07)
	3.785 (0.384)	2.910 (1.146)	9.1 (0.06)
101	4.163 (0.263)	2.773 (0.731)	7.6 (0.04)
	4.125 (0.414)	3.828 (1.501)	8.0 (0.06)
	4.046 (0.791)	4.779 (3.422)	6.9 (0.08)
168	4.637 (0.451)	4.122 (1.810)	7.2 (0.06)
335	5.308 (1.122)	6.001 (6.422)	5.1 (0.10)
	5.181 (1.395)	6.615 (7.500)	4.9 (0.09)

*The numbers in parentheses are standard deviations.

Can. J. Chem. Downloaded from www.nrcresearchpress.com by 210.87.254.6 on 09/05/12
For personal use only.

Can. J. Chem. Downloaded from www.nrcresearchpress.com by 210.87.254.6 on 09/05/12
For personal use only.

Other changes in the details of the reaction mechanism may be made without bringing about any changes in the form of eq. [13]. For example, there are only mild restrictions on the nature of the surface intermediate and the solution species from which it is formed. Again, the fast reaction, [IV], may assume one of several forms. An alternative to the one already suggested might be

$$[IV'] \quad M{-}OH + OH_{aq}^- \rightarrow MO + H_2O + e$$

in which case the expression for a_1 becomes

$$[19] \qquad a_1 = 2W(k_s/k_r)$$

Current Dependence of i_1, a_1, and X_0

The least-squares parameters obtained on fitting the runs at 25 °C to eq. [13] (one-dimensional growth) are given in Table 2. In addition to the random scatter, a systematic variation of the parameters with the formation current density is evident, a result also found at 14 and 36 °C, as well as for the two-dimensional growth model. No systematic variation of i_1/a_1 exists, however, as evidenced by the lack of any systematic deviation between the points and line of Fig. 7 (upper graph). This result is most easily accounted for by assuming that W, the total length of oxide nuclei on the surface, increases with increasing formation current density, a result rather to be expected. That X_0, the thickness of the growing nuclei, should decrease with increasing formation current density is likewise not unexpected, since a more rapid lateral growth rate for the nuclei will provide a shorter time for the maximum thickness to be achieved. On the basis of this explanation, a variation of X_0 during a single galvanostatic run would also be expected, thus requiring a modification of eq. [13]. As X_0 varies only slowly with i, however, its variation during a single run can be neglected to a first approximation.

Concluding Remarks

The model has been shown to give an excellent quantitative account of the experimental data as well as providing an explanation for the extremely thin Cu_2O films found. The slightly poorer agreement found for charging curves obtained at high current densities (Fig. 8) is probably due to the following: (*1*) no attempt has been made to allow for double-layer charging, (*2*) a steady-state approximation has been made which will break down at sufficiently high current densities, and (*3*) the kinetics of formation of the nuclei have not been considered.

The initial segments of the charging curves were not analyzed, since this would require detailed knowledge of the nucleation and double-layer charging processes. Furthermore, the steady-state approximation relating to the concentration of $(OH)_s$ could no longer be made.

This work was supported by the National Research Council of Canada. One of us (D. B. Gibbs) also wishes to acknowledge financial aid in the form of a Province of Ontario Graduate Fellowship and a National Research Council of Canada Studentship.

1. E. MULLER. Z. Elektrochem. **13**, 133 (1907).
2. W. FEITKNECHT and H. W. LENEL. Helv. Chim. Acta, **27**, 775 (1944).
3. A. HICKLING and D. TAYLOR. Trans. Faraday Soc. **44**, 262 (1948).
4. A. R. TOURKY and S. E. S. EL WAKKAD. J. Chem. Soc. 740 (1948); 749 (1948); S. E. S. EL WAKKAD. J. Chem. Soc. 3563 (1950).
5. S. E. S. EL WAKKAD and S. H. EMARA. J. Chem. Soc. 3508 (1953).
6. J. S. HALLIDAY. Trans. Faraday Soc. **50**, 171 (1954).
7. R. W. OHSE. Z. Phys. Chem. Frankfurt, **21**, 406 (1959).
8. A. M. SHAMS EL DIN and F. M. ABD EL WAHAB. Electrochim. Acta, **9**, 113 (1964).
9. F. BOUILLON, J. PIRON, and J. STEVENS. Bull. Soc. Chim. Belg. **67**, 643 (1958).
10. L. F. FIESER. J. Amer. Chem. Soc. **46**, 2639 (1924).
11. R.-R. MEYER and G. RONGE. Angew. Chem. **52**, 637 (1939).
12. M. NAGAYAMA and M. COHEN. J. Electrochem. Soc. **109**, 781 (1962).
13. R. W. POWERS. Electrochem. Technol. **2**, 274 (1964).
14. B. D. CAHAN, J. B. OCKERMAN, R. F. AMLIE, and P. RUELSCHI. J. Electrochem. Soc. **107**, 725 (1960).
15. F. BOUILLON, M. OFFERGELD-JARDINIER, J. PIRON, J. STEVENS, and G. VAN DER SCHRICK. Bull. Soc. Chim. Belg. **68**, 153 (1959).
16. C. D. HODGMAN (*Editor*). Handbook of chemistry and physics. 50th ed. The Chemical Rubber Company, Cleveland, Ohio. 1969–1970.
17. M. J. DIGNAM and W. R. FAWCETT. J. Electrochem. Soc. **113**, 663 (1966).
18. M. AVRAMI. J. Chem. Phys. **7**, 1103 (1939); **8**, 212 (1940); **9**, 177 (1941).

Can. J. Chem. Downloaded from www.nrcresearchpress.com by 210.87.254.40 on 09/05/12
For personal use only.

Complexes of stannic chloride and alkyl phenols and the influence of these complexes and of free phenol on the cationic polymerization of isobutene

R. F. BAUER, R. T. LAFLAIR, AND K. E. RUSSELL
Department of Chemistry, Queen's University, Kingston, Ontario

Received August 5, 1969

The polymerization of isobutene in ethyl chloride solution at −78.5 °C has been studied using stannic chloride as catalyst and alkyl substituted phenols as cocatalysts. In preliminary experiments, the nature and extent of the complexing between phenols and stannic chloride was examined and it was shown that σ-complexing occurs between the oxygen of the phenol and the stannic chloride. Equilibrium constants were determined over the temperature range 30 to −50 °C and were used, together with hydrogen bonding data, to estimate the concentrations of complex and free phenol in the polymerization mixtures at −78.5 °C. The active initiator in the polymerization is probably the σ-complex but the free phenol acts as a chain terminating agent. This explains the ability of the cocatalyst to decrease the rate of polymerization under some experimental conditions. For isobutene concentrations up to 3 *M* and at constant dielectric constant the rate of polymerization and the molecular weight are proportional to the monomer concentration. A mechanism is proposed to account for the main features of the experimental results.

Canadian Journal of Chemistry, 48, 1251 (1970)

Introduction

The low temperature polymerization of isobutene to give a high molecular weight polymer can be effected by the addition of a variety of Lewis acids including aluminum chloride (1), boron trifluoride (2), titanium tetrachloride (2), and stannic chloride (3). Boron trifluoride, titanium tetrachloride, and stannic chloride do not initiate polymerization by themselves but require a so-called cocatalyst to be present. The rate of polymerization varies with the nature of the catalyst and cocatalyst; the reaction is extremely rapid at low temperatures with boron trifluoride and water (4) but lower rates have been obtained with e.g. stannic chloride and water (3). The general field of cationic polymerization has been the subject of major reviews by Plesch (5), Pepper (6), and Kennedy and Langer (7) and these include critical summaries of recent work on isobutene polymerization.

The influence of cocatalysts on the rates of other Lewis acid catalyzed reactions has also been studied, including the polymerization of α-methyl styrene (8) and the isomerization of 2-butene (9). It is generally agreed that initiation of polymerization occurs by transfer of a proton from the complex acid to the monomer to give a carbonium ion or ion pair. The exact nature of the complex acid is frequently not known but it is usually assumed to be a 1:1 or 1:2 complex of catalyst and cocatalyst. Direct studies of complexing at room temperature show that, in some cases, at least 2 complexes coexist in solution. For example, Clayton and Eastham have studied the complexing between boron trifluoride and water in ethylene chloride solution (9) and have determined the equilibrium constant for the reaction between boron trifluoride and its dihydrate to give the monohydrate at 25 °C. They show that the kinetics of isomerization of 2-butene may require the assumption that a third complex $2BF_3:H_2O$ is the most active catalyst.

In the present study we have chosen to use stannic chloride as catalyst because it gives rise to relatively low rates of polymerization of isobutene at low temperatures. In previous work with water as cocatalyst (10) it was found that the kinetics of polymerization at −78.5 °C in the solvent ethyl chloride could best be interpreted by assuming that the initiator is a 1:1 complex of stannic chloride and water, effectively all the water present being converted to this lowest hydrate if the stannic chloride concentration is sufficiently high. Very little evidence existed for 5-coordinate tin at that time although Ulich *et al.* (11) had suggested in 1932 that 1:1 complexes of stannic chloride and ketones or ethers exist in equilibrium with 1:2 complexes. More recent studies (12) have shown that 1:1 complexes frequently occur in solutions of oxygen- and nitrogen-containing donors and that the equbilirium constant for 1:1 complex formation is generally greater than the equilibrium constant for 1:2 complex formation from donor and 1:1 complex. The concentration of 1:2 complex is usually low if the donor is weak or if complex

Can. J. Chem. Downloaded from www.nrcresearchpress.com by 210.87.254.40 on 09/05/12
For personal use only.

formation is subject to considerable steric hindrance. It has been suggested that higher complexes of stannic chloride and acetic acid e.g. $SnCl_4 \cdot 3CH_3COOH$, exist in solution at room temperature (13). Results for this system are however difficult to interpret and it is unlikely that significant concentrations of higher complexes exist in solutions of stannic chloride and the cocatalysts employed in the present work.

It was known from earlier studies that although phenol is a more active cocatalyst than water, it gives measurable rates of polymerization at −78.5 °C. It was anticipated that the extent of complexing with stannic chloride could be controlled by use of ortho substituents in the phenol and that the effect of both catalyst complex and free phenol on the rate and degree of polymerization could be studied. The solubilities of phenols and their complexes with stannic chloride in ethyl chloride – isobutene mixtures are appreciable so that all reaction mixtures should be homogeneous.

Phenol interacts with stannic chloride via the oxygen atom to form a σ-complex and via π-electrons of the aromatic ring to form a π-complex; it also undergoes hydrogen bonding. In the present work the formation of σ-complexes and hydrogen-bonded phenol dimers has been investigated by means of nuclear magnetic resonance (n.m.r.); the formation of π-complexes has been studied using ultraviolet (u.v.) measurements. The concentrations of catalyst complex and free cocatalyst in the polymerization mixtures were then calculated using the results of the preliminary equilibrium studies. Rates and degrees of polymerization have been determined for a wide range of initial experimental conditions and a simple mechanism is proposed which accounts for the main features of the results.

Experimental

Materials

Isobutene (99.6%, Phillips Petroleum Co.) and ethyl chloride (Ohio Chemical Co.) were subjected to 8–10 bulb-to-bulb distillations from −78.5 to −196 °C on the vacuum line and stored at −78.5 °C. Isobutane (Matheson instrument grade) was dried over molecular sieves and distilled 4 times on the vacuum line. Stannic chloride was given 3 bulb-to-bulb distillations on the vacuum line before use in spectroscopic studies. For kinetic work, distillation was continued until a mixture of isobutene, ethyl chloride, and stannic chloride showed no observable polymerization over a period of 1 h.

The 2,3,4,6-tetramethylphenol was recrystallized from an ethanol–water mixture. Other phenols were used as received from the Aldrich Chemical Co. Phenol-*d* was prepared by dissolving phenol in methanol-*d* and evaporating the methanol under reduced pressure; the process was repeated. Reagent grade benzene, toluene, mesitylene, and methylene chloride were degassed on the vacuum line and stirred with Drierite for several hours. Diisobutylene (Eastman Kodak) was used as solvent in the determination of intrinsic viscosities of polymer solutions.

Procedure

(i) Spectroscopic Studies

Spectra in the near u.v. of solutions of stannic chloride and aromatic hydrocarbon or phenol in methylene chloride were obtained at room temperature using a DK-1 spectrophotometer. Solvent and hydrocarbon or phenol were placed in a closed optical cell of 1 cm path length in an atmosphere of dry nitrogen and stannic chloride was added from a micrometer burette. The mixture was stirred with a motor-driven stirrer. Spectra at low temperatures were determined using a Unicam SP-800 spectrophotometer. The cylindrical cell of 5.52 cm path length was similar in design to one used by Caldin and Trickett (14) for low temperature optical measurements. The cell was maintained at low temperatures by a surrounding bath of methanol which was cooled by Dry Ice and controlled to ±0.1 °C by a thermistor unit.

The n.m.r. spectra of solutions of stannic chloride and phenols were determined using a Varian A-60 spectrometer equipped with a V-6040 variable temperature controller. Solutions were made up in an atmosphere of dry nitrogen and used immediately since the spectra changed over a period of a few days. The solvent was normally chloroform-*d* but in some experiments at very low temperatures a mixture of chloroform-*d* and methylene chloride-d_2 was used. The temperature of the probe was estimated from the separation of the methyl and hydroxyl proton peaks in pure methanol. Tetramethylsilane was used as internal reference.

(ii) Polymerization Technique

Polymerization mixtures were made up using a vacuum technique similar to that employed in earlier work (10). The reaction tubes were evacuated at about 300 °C and filled with dry nitrogen. A known amount of phenol was introduced by weighing or by micrometer burette and the tube evacuated while the phenol was cooled by liquid nitrogen. In some experiments with phenol and phenol-*d*, the reaction tube was evacuated and the phenol introduced by freezing down a known pressure from a bulb on the vacuum line. Stannic chloride and ethyl chloride were added and the mixture warmed until mixing occurred. The mixture was again frozen, isobutene was added, and the tube was sealed.

For rate measurements at −78.5 °C the reaction vessel consisted of a precision capillary tube with bulbs at each end. The frozen reagents in the larger bulb were warmed sufficiently to allow mixing to occur on shaking and the tube was then inverted and immersed in a Dry Ice – acetone mixture which had been prepared 3 h earlier in a strip-silvered Dewar flask. The level of the meniscus was determined using a cathetometer; it was found that non-reacting mixtures reached a constant level after about 70 s using this procedure. Rates of polymerization were determined from initial rates of change of height of meniscus knowing that 100% reaction gave rise to a

Can. J. Chem. Downloaded from www.nrcresearchpress.com by 210.87.254.40 on 09/05/12
For personal use only.

movement of 6.9 ± 0.5 cm. The densities of isobutene and ethyl chloride at −78.5 °C are 0.708 g/ml (15) and 1.027 g/ml (16) respectively. Initial rates of polymerization determined dilatometrically and by polymer precipitation agreed within the general reproducibility which was about ±8%.

For molecular weight measurements and for rate studies at temperatures other than −78.5 °C, the reaction vessel consisted of a simple tube of internal diameter 10 mm. The frozen reactants in the sealed tube were warmed sufficiently to allow mixing to occur on shaking and the tube immersed in a Dry Ice – acetone mixture or placed in a thermostat whose temperature was controlled to ±0.2 °C. The polymerization was allowed to proceed for a measured length of time, the conversion being usually of the order of 15%, and the tube was then immersed in liquid nitrogen. Ethanol at −78.5 °C was stirred with the reaction mixture and the precipitated polymer was washed with ethanol, dried in a vacuum oven, and weighed.

(iii) Molecular Weight Studies

Molecular weight determinations were generally made by means of viscometry. Relative viscosities in diisobutylene at 20.0 °C were determined using an Ubbelohde viscometer with a solvent flow time of 151.4 s. The average molecular weight $\bar{M}$ was determined from the relationship (17) shown in eq. [1]. This equation was

$$[1] \qquad \log \bar{M} = 5.376 + 1.56 \log (\ln \eta_r/c)$$

developed using fractionated polymers of narrow molecular weight range and the derived value of $\bar{M}$ will only be close to the number average molecular weight, $\bar{M}_n$, if the polymer samples have a comparable molecular weight distribution.

Gel permeation chromatography was used to obtain the molecular weight distribution and to afford a second estimate of average molecular weight. The Waters Associates instrument with a resolution of 998 plates/ft was calibrated using standard polystyrene and polypropylene glycol samples. The instrument was operated at 60 °C with a toluene flow rate of 1 ml/min and the polymer solution consisted of 0.005–0.01 g polyisobutene dissolved in 1 ml toluene. Molecular weights were calculated both by the Q factor method with $Q = 21.7/\text{Å}$ and by the "universal" calibration technique of Grubisic *et al.* (18). Number average and weight average molecular weights were derived from the experimental data and viscosity average molecular weights were calculated using an α value of 0.64 (α is the exponent in the intrinsic viscosity – molecular weight relationship).

Number average molecular weights for some of the polymer samples were determined using a Hewlett Packard Model 501 Membrane Osmometer with toluene as solvent. For low molecular weight samples (< 15 000) it was necessary to extrapolate the osmotic pressures to zero time to correct for a slight leakage of solute through the membrane.

Results

Complexes of Stannic Chloride and Phenols

The n.m.r. spectrum of a solution of an alkyl substituted phenol in chloroform-*d* is affected only slightly by the addition of stannic chloride at room temperature. With 2,6-dimethylphenol (0.52 M), for example, the addition of stannic chloride (0.21 M) gives rise to a change in δ for the OH proton from 4.57 to 4.67 p.p.m. At lower temperatures, stannic chloride causes a much larger change in the position of the OH proton resonance. At −46 °C the value of δ for a 2,6-dimethylphenol solution (0.56 M) is 4.92 p.p.m. but this changes to 5.40 p.p.m. on the addition of stannic chloride (0.21 M). No significant change in δ is observed when stannic chloride is added to solutions of 2-*t*-butylphenol, 2-*t*-butyl-6-methylphenol, and 2,6-di-*t*-butyl-4-methylphenol. Each of these phenols possesses a *t*-butyl group in one of the positions ortho to the OH group and it appears that this large group strongly hinders the ability of the oxygen to enter into complex formation. It is concluded that complexing between the oxygen of the phenol and stannic chloride to give a σ-complex is responsible for the increase in n.m.r. shift.

In order to use proton shifts to estimate the amounts of σ-complex present in solution, it is necessary to know equilibrium constants for dimerization of the phenols, ArOH, in chloroform.

$$[2] \qquad 2\text{ArOH} \rightleftharpoons [\text{ArOH}]$$

The equilibrium constants were determined from n.m.r. data for phenol solutions in the temperature range 30 to −50 °C. The results were interpreted by means of eq. [3], where δ_M, δ_D

$$[3] \qquad \delta_{obs} = \frac{[P_M]}{[P_T]}\delta_M + \frac{[P_T] - [P_M]}{[P_T]}\delta_D$$

are the OH proton shifts for monomeric and dimeric phenol respectively and $[P_M]$, $[P_T]$ are the concentrations of phenol monomer and of total phenol in the solution. The assumption that hydrogen bonding leads only to dimers is probably correct for all the ortho-substituted phenols but there is some evidence (19) that trimer is present in solutions of phenol itself. The equilibrium constant for reaction [2], K_H, is given by eq. [4]. δ_M is obtained by extrapolating a plot of

$$[4] \qquad K_H = \frac{(\delta_M - \delta_{obs})(\delta_M - \delta_D)}{2(\delta_{obs} - \delta_D)^2[P_T]}$$

δ_{obs} vs. $[P_T]$ to zero concentration. Various values of δ_D are then assumed and values of K_H and δ_D are chosen to fit the range of experimental data.

Can. J. Chem. Downloaded from www.nrcresearchpress.com by 210.87.254.40 on 09/05/12
For personal use only.

TABLE 1

Association constants, K_H, at −40 °C and ΔH values for hydrogen bonding of phenols in chloroform

Phenol	K_H (l/mole)	ΔH (kcal/mole)
Phenol	3.2 ± 1.1	−4.2 ± 0.5*
2-*sec*-Butylphenol	0.99 ± 0.4	−4.6 ± 1.0
2,6-Dimethylphenol	0.32 ± 0.05	−2.2 ± 0.5
2,6-Diisopropyl-phenol	0.28 ± 0.17	−5.6 ± 1.0
2,3,4,6-Tetra-methylphenol	0.65 ± 0.27	−2.2 ± 0.5

*Quoted uncertainty takes into account uncertainty in individual values of K_H and in slope of least squares line.

TABLE 2

Equilibrium constants, K_X, at −40 °C and ΔH values for σ-complex formation between stannic chloride and phenols

Phenol	K_X (l/mole)	ΔH (kcal/mole)
Phenol	2.5 ± 0.8	−7.5 ± 1.0
2-*sec*-Butylphenol	2.0 ± 0.5	−5.9 ± 1.0
2,6-Dimethylphenol	0.45 ± 0.1	−3.6 ± 1.0
2,6-Diisopropyl-phenol	0.20 ± 0.07	0 ± 1.0
2,3,4,6-Tetra-methylphenol	2.7 ± 1.1	−5.0 ± 1.5

The equilibrium constants at −40 °C and the values of ΔH for the dimerization are recorded in Table 1.

The n.m.r. results for mixtures of stannic chloride and phenols are interpreted on the assumption that the only species present in solution are the 1:1 σ-complex of stannic chloride, X, the hydrogen bonded dimer of the phenol, and the free monomeric phenol. If the rate of exchange between these species is sufficiently rapid, the observed chemical shift for the OH proton, δ_{obs}, is given by eq. [5] where $[P_D]$ is the concentration

$$[5] \quad \delta_{obs} = \frac{[X]}{[P_T]}\delta_X + \frac{[P_M]}{[P_T]}\delta_M + \frac{2[P_D]}{[P_T]}\delta_D$$

of the phenol dimer; δ_M, δ_D are known from hydrogen bonding studies. δ_X was determined in the case of the 2,3,4,6-tetramethylphenol σ-complex by cooling solutions of 2,3,4,6-tetramethylphenol and stannic chloride in a chloroform-*d*-methylene chloride-d_2 mixture to −90 °C. Under these conditions an absorbance with a maximum shift of δ = 10.83 p.p.m. is observed in addition to absorptions associated with uncomplexed phenol. The integrated area of the low field absorption is close to that expected for the σ-complex. The value of 10.83 p.p.m. was assumed for δ_X for all σ-complexes formed between stannic chloride and phenols. Values of [X] were derived using eq. [5]. Equilibrium constants K_X for the reaction

$$[6] \quad ArOH + SnCl_4 \rightleftharpoons \begin{matrix} Ar \\ \diagdown \\ O \rightarrow SnCl_4 \\ \diagup \\ H \end{matrix}$$

were determined over the temperature range 30 to −45 °C. Table 2 gives K_X at −40 °C and ΔH for the complex formation. These values have been used to estimate the concentrations of complex and phenol monomer and dimer in solution at various temperatures; the results for a mixture of 2,3,4,6-tetramethylphenol (0.027 *M*) and stannic chloride (0.185 *M*) are shown graphically in Fig. 1. With 2-*sec*-butylphenol, 2,6-dimethylphenol, 2,6-diisopropylphenol, and 2,3,4,6-tetramethylphenol it is thought that the absolute concentrations of the various species at −78.5 °C are known to better than ±20%. The assumptions that (*i*) phenol itself hydrogen bonds to give only dimer and (*ii*) complexes with stannic chloride to give only the 1:1 σ-complex are probably not correct and the errors may be larger in this instance.

An attempt has been made to estimate the effect of solvent on extents of complexing of stannic chloride and phenols. The n.m.r. spectra were

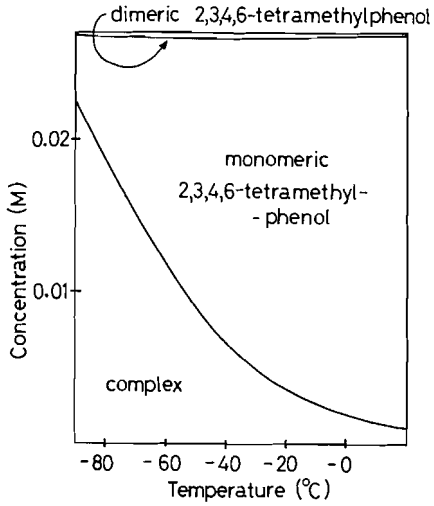

FIG. 1. Concentrations of monomeric and dimeric 2,3,4,6-tetramethylphenol and of σ-complex in chloroform solution as a function of temperature. Initial stannic chloride concentration, 0.185 *M*; initial 2,3,4,6-tetramethylphenol concentration, 0.027 *M*.

Can. J. Chem. Downloaded from www.nrcresearchpress.com by 210.87.254.40 on 09/05/12
For personal use only.

obtained of ethyl chloride solutions of 2-*sec*-butylphenol (0.75 *M*) and 2,3,4,6-tetramethylphenol (0.59 *M*) with and without stannic chloride (0.2 *M*) in the temperature range 0 to −50 °C. 2-*sec*-Butylphenol hydrogen bonds to itself and σ-complexes with stannic chloride to a lesser extent in ethyl chloride solution than in chloroform solution. 2,3,4,6-Tetramethylphenol forms hydrogen bonded dimers and σ-complexes with stannic chloride to about the same extent in the two solvents. Most of the polymerization experiments however were performed with a 3.2 *M* solution of isobutene in ethyl chloride. The n.m.r. studies of tetramethylethylene–chloroform solutions of 2,3,4,6-tetramethylphenol and stannic chloride suggest that the extent of σ-complexing may be slightly lower in polymerization mixtures than in ethyl chloride solution. The actual concentrations of σ-complexes in polymerization mixtures are thus probably overestimated when the assumption is made that they are the same as in chloroform solution; the true concentrations are probably between 75 and 95% of the estimated values.

In u.v. studies of solutions of stannic chloride (0.02–0.12 *M*) and phenols (0.02–0.1 *M*) in the solvent methylene chloride, it is found that the absorbance at 355 mμ increases linearly with stannic chloride concentration at 25 °C for all the phenols studied. The absorbance is of the same order as that observed for alkyl benzenes such as toluene and mesitylene (13) and increases as the number of alkyl substituents is increased. The absorbance in the near u.v. of solutions of alkyl benzenes and stannic chloride has been ascribed to the formation of weak π-complexes and it is probable that a similar explanation applies to phenol – stannic chloride solutions. As the temperature is lowered, the extent of complex formation slowly increases whether the donor is an aromatic hydrocarbon or a phenol. At −50 °C for a given stannic chloride concentration, the absorbance falls off slightly as the concentration of 2,6-dimethylphenol is increased but this is probably due mainly to the incidence of σ-complex formation rather than to an appreciable proportion of the stannic chloride being converted to π-complex. In general the extent of π-complexing between phenol and stannic chloride appears to be small and its effect on the concentrations of σ-complex and free phenol has been neglected in this work.

Polymerization Rates

In the absence of a cocatalyst, stannic chloride does not initiate the polymerization of a solution of isobutene (3.2 *M*) in ethyl chloride at −78.5 °C. Addition of small amounts of phenol, 2-*sec*-butylphenol, 2,6-dimethylphenol, 2,6-diisopropylphenol, or 2,3,4,6-tetramethylphenol results in rapid polymerization with half lives of the order of 1/4 h. Reactions proceed to completion and the conversion of monomer to polymer follows an approximately first order curve when the polymer is soluble in the reaction medium. Addition of the more hindered phenols, 2-*t*-butylphenol, 2-*t*-butyl-6-methylphenol, and 2,6-di-*t*-butyl-4-methylphenol, does not lead to polymerization and these phenols are therefore not considered to be cocatalysts in this reaction.

The cocatalytic action of the unsubstituted phenol has been investigated over a wide concentration range (0.001–0.070 *M*) and it is found that the rate of polymerization first increases with phenol concentration, reaches a maximum, and then decreases as more cocatalyst is added (Fig. 2). In the low concentration range (0.001–0.01 *M*) replacement of the phenolic hydrogen atom by deuterium decreases the overall rate of polymerization by a factor of 2.5 ± 0.5. Some of the results of the effect of phenol and stannic chloride concentration on the rate are given in Table 3. In the range of concentrations of 2,6-dimethylphenol and 2,3,4,6-tetramethylphenol convenient for dilatometric study (0.004–0.02 *M*) the rate increases with increasing amount of cocatalyst. With 2-*sec*-butylphenol and 2,6-diisopropylphenol however it was convenient to use a concentration range of 0.03–0.14 *M* and, under these conditions, the rate *decreases* with increasing cocatalyst concentration. The rate of polymerization rises when the stannic chloride concentration is increased (Table 3).

The effect of monomer concentration on the polymerization rate at −78.5 °C when the concentrations of stannic chloride and the cocatalyst 2-*sec*-butylphenol are maintained at 0.185 and 0.071 *M* respectively is shown in Fig. 3. The rate of polymerization reaches a maximum value of about 0.0025 mole/l s when the monomer concentration is 2.3 *M* and decreases to about 1/10 of this value when the monomer concentration is 7 *M*. If however the dielectric constant of the medium is maintained constant by addition of isobutane, the overall rate of polymerization is

Can. J. Chem. Downloaded from www.nrcresearchpress.com by 210.87.254.40 on 09/05/12
For personal use only.

TABLE 3

The effect of phenol and stannic chloride concentration on the rate of polymerization at −78.5 °C*

Phenol	Phenol concentration (mole/l)	Stannic chloride concentration (mole/l)	Polymerization rate × 10^4 (mole/l s)
Phenol	0.0010	0.160	2.3
	0.0033	0.160	6.6
	0.013	0.160	18.3
	0.020	0.185	22.6
	0.038	0.185	11.6
	0.071	0.185	7.9
	0.071	0.092	5.3
2-*sec*-Butylphenol	0.036	0.185	15.9
	0.071	0.185	10.6
	0.142	0.185	4.8
	0.249	0.185	5.9
	0.178	0.008	0.36
	0.178	0.039	2.3
	0.178	0.092	4.0
2,6-Dimethylphenol	0.009	0.185	4.5
	0.012	0.185	4.0
	0.019	0.185	6.1
	0.018	0.370	12.9
2,6-Diisopropylphenol	0.063	0.185	1.20
	0.156	0.185	0.63
	0.312	0.185	0.52
	0.470	0.185	0.62
2,3,4,6-Tetramethylphenol	0.004	0.185	13.9
	0.013	0.185	19.8
	0.024	0.185	30.2
	0.024	0.185	29.7

*3.2 *M* Isobutene in ethyl chloride.

found to be proportional to the monomer concentration for concentrations up to 3.2 *M* (Fig. 3). The results emphasize that the medium may exert a considerable effect on the rate of the cationic polymerization of isobutene.

Molecular Weight Studies

The polymer isolated with phenol, 2-*sec*-butylphenol and 2,6-diisopropylphenol as cocatalysts generally has an average molecular weight in the range 6000 to 60 000 under the conditions of these experiments (Table 4). Analysis by gel permeation chromatography shows that the molecular weight distributions of polymer samples are relatively narrow, values of $\overline{M}_w/\overline{M}_n$ being normally between 1.3 and 1.6. When 2,6-dimethylphenol and 2,3,4,6-tetramethylphenol are used as cocatalysts at low concentrations, the molecular weights determined by the viscosity method vary from 80 000 to 300 000 and the values of $\overline{M}_w/\overline{M}_n$ range as high as 2.8. Most of the polymer samples obtained in

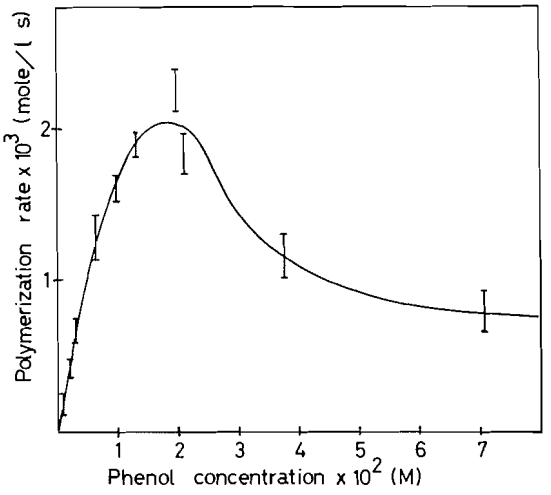

FIG. 2. Dependence of rate of polymerization at −78.5 °C on the concentration of added phenol. Initial stannic chloride concentration, 0.185 *M*; isobutene concentration, 3.2 *M*.

this investigation are of narrow distribution and the viscosity method gives a fair estimate of the required $\overline{M}_n$ value; this has been confirmed experimentally in the cases where comparative measurements have been made with the membrane osmometer. For the samples of high molecular weight however, the quoted values are significantly higher than values of $\overline{M}_n$.

The results in Table 4 show that the molecular weight decreases with increasing 2-*sec*-butylphenol concentration when the stannic chloride concentration is 0.185 *M* and the initial isobutene concentration is 3.2 *M*. Increasing the stannic chloride concentration at constant cocatalyst concentration causes a small increase in molecular weight. Similar effects are observed when phenol, 2,6-dimethylphenol, 2,6-diisopropylphenol, and 2,3,4,6-tetramethylphenol are used as cocatalysts (Table 4).

The influence of isobutene concentration on the polymer molecular weight was determined with a stannic chloride concentration of 0.185 *M*

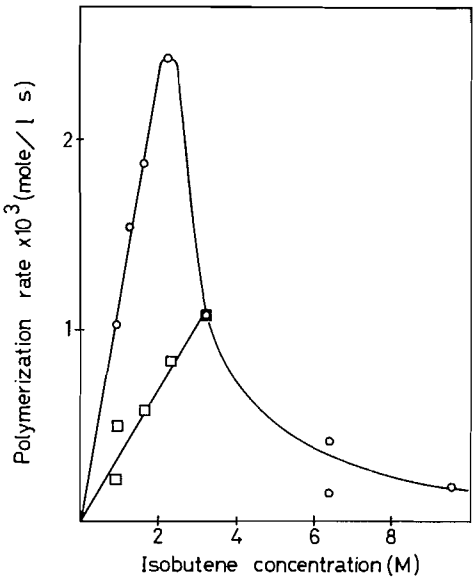

FIG. 3. Dependence of rate of polymerization on monomer concentration; ○, dielectric constant decreases with increasing [M]; □, constant dielectric constant.

TABLE 4

The effect of phenol and stannic chloride concentration on the molecular weight at −78.5 °C*

Phenol	Phenol concentration (mole/l)	Stannic chloride concentration (mole/l)	Molecular weight
Phenol	0.021	0.185	60 000
	0.037	0.185	47 000
	0.062	0.185	18 600
	0.071	0.185	12 900
	0.071	0.039	7 900
	0.071	0.092	10 000
2-*sec*-Butylphenol	0.075	0.185	26 000
	0.178	0.185	14 200
	0.258	0.185	11 400
	0.427	0.185	6 300
	0.178	0.037	9 800
	0.178	0.092	10 800
2,6-Dimethylphenol	0.010	0.185	215 000
	0.018	0.185	151 000
	0.037	0.185	79 000
	0.018	0.007	105 000
	0.018	0.092	126 000
2,6-Diisopropylphenol	0.063	0.185	19 500
	0.312	0.185	6 500
	0.156	0.008	17 200
	0.156	0.092	10 600
2,3,4,6-Tetramethylphenol	0.013	0.185	363 000
	0.024	0.185	265 000
	0.030	0.185	174 000
	0.044	0.185	116 000
	0.030	0.007	117 000
	0.030	0.390	279 000

*3.2 *M* Isobutene in ethyl chloride.

Can. J. Chem. Downloaded from www.nrcresearchpress.com by 210.87.254.40 on 09/05/12
For personal use only.

TABLE 5
Dependence of molecular weight on conversion*

Phenol	Stannic chloride concentration (mole/l)	Conversion (%)	Molecular weight
Phenol	0.037	17	51 000
	0.037	21	47 000
	0.037	33	37 000
2,6-Dimethylphenol	0.185	3.6	173 000
	0.185	8.1	136 000
	0.185	15.1	149 000
2,3,4,6-Tetramethylphenol	0.185	14.5	347 000
	0.185	35	258 000
	0.185	54.5	364 000

*3.2 *M* Isobutene in ethyl chloride; approximate phenol concentration 0.02 *M*.

and a 2-*sec*-butylphenol concentration of 0.071 *M*. The molecular weight is proportional to the monomer concentration for [M] < 3 *M* but it reaches a maximum at 4 *M* isobutene and falls sharply beyond about 8 *M* isobutene (Fig. 4). If the dielectric constant of the medium is maintained effectively constant through the addition of isobutane, the molecular weight results for isobutene concentrations up to 3.2 *M* are the same within experimental error as those observed when isobutane is not added to the system.

The molecular weight does not vary greatly with extent of reaction for conversions up to 50%. The results of some experiments are given in Table 5.

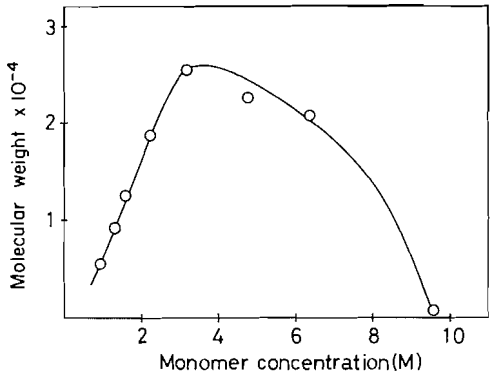

FIG. 4. Dependence of molecular weight on monomer concentration. Initial stannic chloride concentration, 0.185 *M*; 2-*sec*-butylphenol concentration, 0.071 *M*.

Discussion

Phenol, 2-*sec*-butylphenol, 2,6-dimethylphenol, 2,6-diisopropylphenol, and 2,3,4,6-tetramethylphenol act as cocatalysts in the stannic chloride-catalyzed polymerization of isobutene in ethyl chloride solution at −78.5 °C. The hindered phenols, 2-*t*-butylphenol, 2-*t*-butyl-6-methylphenol, and 2,6-di-*t*-butyl-4-methylphenol show no cocatalytic behavior. All of these phenols form π-complexes with stannic chloride as judged by the development of an absorbance in the near u.v. but only the unhindered phenols are able to form σ-complexes with the oxygen atom as donor center. It is thus likely that π-complexes of phenols and stannic chloride are not polymerization initiators and that σ-complexing is necessary before an active initiator is developed. The n.m.r. experiments at −90 °C give a δ value of the OH proton of 10.83 p.p.m. for the 2,3,4,6-tetramethylphenol – stannic chloride complex; this compares with a value of 12.42 p.p.m. for the $BF_3 \cdot H_2O$ complex dissolved in acetone (20). The value for the monomeric 2,3,4,6-tetramethylphenol is 4.42 p.p.m. and the large change is presumably associated with a considerable increase of acidic character when the phenol forms a σ-complex with stannic chloride.

The rate of polymerization of isobutene at −78.5 °C with low concentrations of phenol is reduced by a factor of 2.5 ± 0.5 when the phenol is deuterated. The rate constant for propagation is probably not affected by deuteration of the cocatalyst and if one of the rate constants for termination is reduced there should be an increase in overall rate of polymerization. The observed isotope effect can therefore be interpreted as strong evidence that the initiation reaction involves proton transfer from the catalyst–cocatalyst complex to a monomer molecule. Water cocatalysis probably leads to a similar initiation process, for the overall rate of polymerization is reduced by a

Can. J. Chem. Downloaded from www.nrcresearchpress.com by 210.87.254.40 on 09/05/12
For personal use only.

Can. J. Chem. Downloaded from www.nrcresearchpress.com by 210.87.254.40 on 09/05/12
For personal use only.

factor of 1.7 ± 0.3 when water is replaced by heavy water (23). The molecular weight of the polymer is simultaneously increased by a factor of 2 so that the isotope effect on the initiation rate is probably greater than 1.7. An isotope effect was observed in the polymerization of α-methylstyrene initiated by stannic chloride – water mixtures at 55 °C (8) and was taken as evidence that the initiation step in this reaction also involves proton transfer.

The kinetic studies give further information concerning the initiation process. The overall order of reaction with respect to monomer is 1.0 ± 0.2 when isobutane is added to ensure that the dielectric constant does not vary significantly. This order may be slightly less than the true order because replacement of isobutane by isobutene may affect the extent of σ-complexing of stannic chloride and phenol. If the overall reaction is first order with respect to monomer and the polymer molecular weight is proportional to monomer concentration, the rate of initiation is independent of monomer concentration. Two mechanisms (eqs. [7*a*,*b*]) can be considered (7, 21). It is somewhat more plausible to consider transfer of a proton from the strongly acid complex of stannic chloride and phenol to a π-complexed monomer molecule. The alternative reaction [7*b*] is not excluded with phenols as cocatalysts but it seems the less likely alternative with water as cocatalyst at −78.5 °C. The ion pairs formed in the initiation reaction may be partly dissociated into free ions; conductivity studies of polymerizing mixtures indicate that the concentrations of such free ions must be very low.

[7*a*] $SnCl_4 \cdot ArOH \cdot CH_2{=}C(CH_3)_2 \rightarrow (CH_3)_3C^+ \cdot O\bar{A}r \cdot SnCl_4$

[7*b*] $SnCl_4 \cdot CH_2{=}C(CH_3)_2 + ArOH \rightarrow (CH_3)_3C^+ \cdot O\bar{A}r \cdot SnCl_4$

The rate and molecular weight results can be discussed in terms of the propagation reaction [8] and the termination reactions [9] and [10]. It is recognized that reaction [9] can also give rise to $-CH{=}C(CH_3)_2$ end groups and possibly C—[OAr] groups. The square brackets around the OAr in the C—[OAr] end groups indicate that the OAr group may be attached to the polymer chain through the oxygen or through a carbon–carbon bond to the aromatic ring.

The number of polymer molecules produced is usually only a small fraction of the number of molecules of catalyst–cocatalyst σ-complex or of cocatalyst present in the reaction system. The molecular weight of the polymer produced does not increase with time (Table 5). It thus seems likely that a steady state concentration of carbonium ion pairs is attained. The above kinetic scheme leads to the following expression for R_p, the overall rate of polymerization,

$$[11] \qquad R_p = \frac{k_p k_i [X][M]}{k_{t_1} + k_{t_2}[P_M]}$$

where k_i, k_p, k_{t_1}, and k_{t_2} are the rate constants for reactions [7*a*], [8], [9], and [10]. Experimentally it is observed that the rate of polymerization is proportional to the monomer concentration for $[M] < 3\ M$ when [X], $[P_M]$, and the dielectric constant of the medium are essentially constant. The kinetic results are thus consistent with a rate of initiation which is independent of monomer concentration. Further information is however required before the detailed nature of reaction [7] can be established.

Equation [11] may be written as eq. [12]. The

[8] 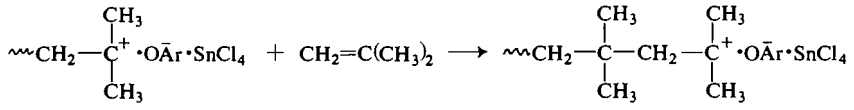

[9] 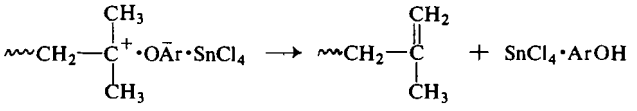

[10] 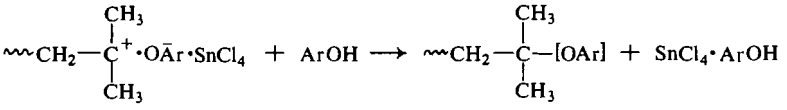

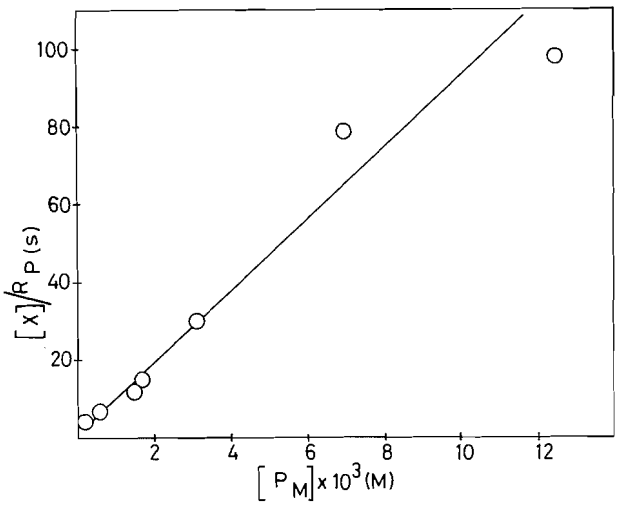

FIG. 5. Plot of $[X]/R_p$ vs. concentration of free monomeric phenol, $[P_M]$. Initial isobutene concentration, 3.2 *M*.

$$[12] \qquad \frac{[X]}{R_p} = \frac{k_{t_2}[P_M]}{k_p k_i[M]} + \frac{k_{t_1}}{k_p k_i[M]}$$

mechanism therefore requires that plots of $[X]/R_p$ vs. $[P_M]$ should be linear if the initial monomer concentration is constant. Approximately linear plots are obtained for all the phenols studied over a wide range of catalyst and cocatalyst concentrations; Fig. 5 shows the plot for phenol as cocatalyst. This is taken as strong support for the mechanism and in particular for the importance of a termination step involving attack of the growing polymer chain on the free phenol. Under some conditions, increase of cocatalyst concentration may cause $[P_M]$ to increase much more rapidly than [X] and in this way give rise to the decrease in rate with added phenol which is observed with 2-*sec*-butylphenol, 2,6-diisopropylphenol, and phenol at high concentrations. Values of $k_{t_2}/k_p k_i$, derived from the slopes of $[X]/R_p$ vs. $[P_M]$ plots, are given in Table 6. These results apply to the polymerization of 3.2 *M* in ethyl chloride at -78.5 °C and over ranges of catalyst and cocatalyst concentrations typified by the values in Table 3.

The mechanism predicts that the number average degree of polymerization, *DP*, varies with isobutene and phenol concentrations according to eq. [13]. The *DP* is found experimentally

$$[13] \qquad \frac{1}{DP} = \frac{1}{k_p[M]}(k_{t_1} + k_{t_2}[P_M])$$

to be proportional to the monomer concentration under conditions when $[P_M]$ and [X] are essentially constant provided that [M] does not exceed 3 *M* (Fig. 4). At higher isobutene concentrations the molecular weight reaches a maximum and eventually decreases with [M]. This result has been observed with certain other initiators and has been interpreted by Plesch (22) in terms of chain-breaking impurities in the system. If impurities are the cause of the rapid drop in molecular weight at high [M], their concentration must increase very rapidly with monomer concentration. The intercept of the plot of $1/DP$ vs. $1/[M]$ is close to zero if only monomer concentrations up to 3 *M* are considered (Fig. 6). This implies that the transfer reaction between growing polymer cation and isobutene proceeds at a negligible rate at -78.5 °C.

TABLE 6

Values of $k_{t_2}/k_i k_p$ and k_{t_2}/k_p for the stannic chloride-catalyzed polymerization of isobutene in ethyl chloride at -78.5 °C

Cocatalyst	$k_{t_2}/k_i k_p$ (s)	k_{t_2}/k_p
Phenol	28 000 ± 5 000	0.45 ± 0.15*
2-*sec*-Butylphenol	9 600 ± 3 000	0.22 ± 0.06
2,6-Dimethylphenol	730 ± 300	0.05 ± 0.02*
2,6-Diisopropylphenol	2 200 ± 500	0.19 ± 0.05
2,3,4,6-Tetramethylphenol	2 000 ± 500	0.04 ± 0.01*

*Estimated errors based on least squares lines. Absolute errors probably greater (see text).

Can. J. Chem. Downloaded from www.nrcresearchpress.com by 210.87.254.40 on 09/05/12
For personal use only.

Can. J. Chem. Downloaded from www.nrcresearchpress.com by 210.87.254.40 on 09/05/12
For personal use only.

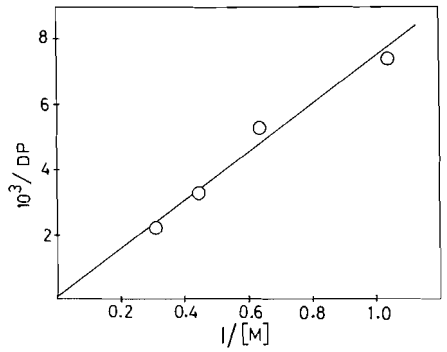

FIG. 6. Plot of $1/DP$ vs. $1/[M]$. Initial stannic chloride concentration, 0.185 *M*; 2-*sec*-butylphenol concentration 0.071 *M*.

For reactions in which the initial monomer concentration is the same, plots of $1/DP$ vs. $[P_M]$ give fairly good straight lines over the range of phenol and stannic chloride concentrations studied. Figure 7 is the plot for the cocatalyst 2-*sec*-butylphenol. Linear plots are not obtained when $1/DP$ is plotted against [X] (Fig. 8) showing that attack on the σ-complex is not the major chain-breaking process. The results are therefore consistent with the assumption that the main mode of termination at the relatively high free phenol concentrations of the present work involves attack by the growing polymer chain on the free monomeric phenol; a simultaneous attack on the free phenol dimer is not however excluded. Values of k_{t_2}/k_p derived from the plots of $1/DP$ vs. $[P_M]$ are given in Table 6. Errors in the values of *DP* used in these plots may be particularly large with 2,6-dimethylphenol and 2,3,4,6-tetramethylphenol as cocatalysts because of the use of the viscosity method in estimating the average molecular weight, and values of k_{t_2}/k_p for these phenols must be regarded as approximate. Combination of the results of rate and molecular weight measurements leads to rough estimates of k_i, assuming that initiation proceeds by way of reaction [7*a*]. These rate constants are of the order of 10^{-5} s^{-1}.

The kinetic and molecular weight results do not distinguish between propagation by free ions and by ion pairs. A change in dielectric constant which greatly affects the rate of polymerization has practically no effect on the molecular weight. The lack of dependence of molecular weight on dielectric constant implies that the propagation rate and overall termination rate are affected to about the same extent. The higher rate of polymerization in a medium of slightly higher dielectric constant must then be due to a higher rate of initiation of polymerization. The dielectric constant of the medium can affect concentrations of both ion pairs and free ions and the part they play in the initiation process remains unclear.

The concentrations of free phenol and σ-complex in the polymerization mixtures are not accurately known because of the uncertainty in K_X and of the simplifying assumptions concerning the nature of the σ-complex and the hydrogen bonded polymers of phenols. Nevertheless the simple mechanism presented here explains the

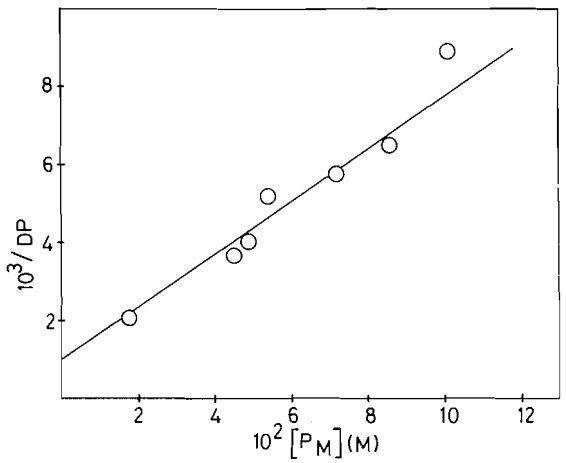

FIG. 7. Plot of $1/DP$ vs. concentration of free monomeric 2-*sec*-butylphenol, $[P_M]$. Initial isobutene concentration, 3.2 *M*.

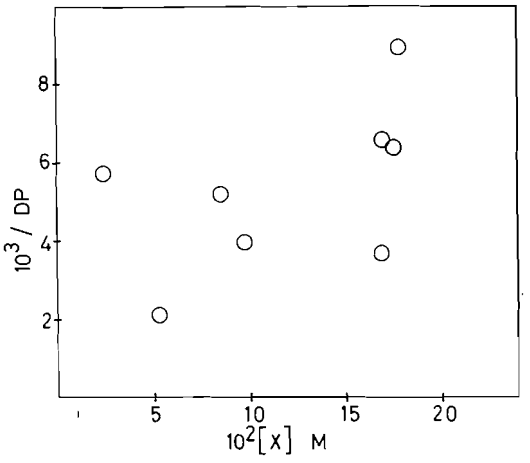

FIG. 8. Plot of $1/DP$ vs. concentration of σ-complex of 2-*sec*-butylphenol and stannic chloride. Initial isobutene concentration, 3.2 *M*.

main features of the kinetic and molecular weight data. It predicts that a fraction of the polymer contains end groups derived from the cocatalyst. The fraction of end groups derived from the phenol has been estimated for the cocatalysts 2-*sec*-butylphenol and 2,6-diisopropylphenol from u.v. absorption spectra of polyisobutene samples in chloroform solution. It is found that a high proportion of the polyisobutene molecules contain aromatic end groups when the concentration of free cocatalyst is of the order of 0.1 *M*. The mechanism also predicts the shapes of the plots of polymerization rate vs. phenol concentration for high concentrations of the cocatalysts 2,6-dimethylphenol and 2,3,4,6-tetramethylphenol. These predictions will be examined in future work.

The authors are grateful to the Polymer Corporation Ltd., and the National Research Council of Canada for financial support of this work. They thank Dr. G. Wilson, Polymer Corporation Ltd. for helpful discussion and Dr. C. C. Hsu, Queen's University, for considerable assistance with the gel permeation chromatography studies. They gratefully acknowledge the technical assistance of Mr. R. W. Horsey, Queen's University in some of this work.

1. R. M. THOMAS, W. J. SPARKS, P. K. FROLICH, M. OTTO, and M. MUELLER-CUNRADI. J. Amer. Chem. Soc. **62**, 276 (1940).
2. A. G. EVANS, D. HOLDEN, P. H. PLESCH, M. POLANYI, H. A. SKINNER, and M. A. WEINBERGER. Nature, **157**, 102 (1946).
3. R. G. W. NORRISH and K. E. RUSSELL. Nature, **160**, 543 (1947).
4. A. G. EVANS and G. W. MEADOWS. Trans. Faraday Soc. **46**, 327 (1950).
5. P. H. PLESCH. The chemistry of cationic polymerization. The MacMillan Company, New York, 1963; P. H. PLESCH. *In* Progress in high polymers. Vol. 2. *Edited by* J. C. Robb and F. W. Peaker. Heywood Books, London, 1968.
6. D. C. PEPPER. *In* Friedel-Crafts and related reactions. Vol. 2. *Edited by* G. A. Olah. Interscience Publishers Inc., New York, 1964.
7. J. P. KENNEDY and A. W. LANGER. Fortschr. Hochpolym.-Forsch. **3**, 508 (1964).
8. F. S. DAINTON and R. H. TOMLINSON. J. Chem. Soc. **151**, (1953).
9. J. M. CLAYTON and A. M. EASTHAM. J. Amer. Chem. Soc. **79**, 5368 (1957).
10. R. G. W. NORRISH and K. E. RUSSELL. Trans. Faraday Soc. **48**, 91 (1952).
11. H. ULICH, E. HERTEL, and W. NESPITAL. Z. Phys. Chem. B, **17**, 21 (1932).
12. T. L. BROWN and M. KUBOTA. J. Amer. Chem. Soc. **83**, 331 (1961); J. LAANE and T. L. BROWN. Inorg. Chem. **3**, 148 (1964); D. P. N. SATCHELL and J. C. WARDELL. Proc. Chem. Soc. 86 (1963); J. J. MYHER and K. E. RUSSELL. Can. J. Chem. **42**, 1555 (1964).
13. D. P. N. SATCHELL. J. Chem. Soc. 4388 (1960).
14. E. F. CALDIN and J. C. TRICKETT. Trans. Faraday Soc. **49**, 772 (1953).
15. R. R. DREISBACH. Physical properties of chemical compounds II. No. 22. Advances in chemistry series. Amer. Chem. Soc. 1959.
16. T. MCMULLEN, E. D. CROZIER, and R. L. MCINTOSH. Can. J. Chem. **46**, 2945 (1968).
17. W. R. KRIGBAUM and P. J. FLORY. J. Amer. Chem. Soc. **75**, 1775 (1953).
18. Z. GRUBISIC, P. REMPP, and H. BENOIT. Polym. Lett. **5**, 753 (1967).
19. N. D. COGGESHALL and E. L. SAIER. J. Amer. Chem. Soc. **73**, 5414 (1951).
20. R. J. GILLESPIE and J. S. HARTMAN. Can. J. Chem. **45**, 859 (1967).
21. B. ELLIOTT, A. G. EVANS, and E. D. OWEN. J. Chem. Soc. 689 (1962).
22. P. H. PLESCH. J. Chem. Soc. 104 (1964).
23. R. T. LAFLAIR. M.Sc. Thesis. Queen's University, Kingston, Ontario. 1962.

Can. J. Chem. Downloaded from www.nrcresearchpress.com by 210.87.254.40 on 09/05/12
For personal use only.

Can. J. Chem. Downloaded from www.nrcresearchpress.com by 210.87.254.6 on 09/05/12
For personal use only.

Hydrogen bonding and long-range proton coupling constants in some ortho disubstituted aniline derivatives. Intramolecular proton exchange and degree of nonplanarity of the amino group

R. WASYLISHEN AND T. SCHAEFER
Chemistry Department, University of Manitoba, Winnipeg, Manitoba

Received October 22, 1969

Long-range spin–spin coupling constants over five bonds between the two amino protons and the ring protons are reported for some ortho disubstituted aniline derivatives in cyclohexane and benzene-d_6 solutions. Equal coupling of both amino protons to the meta protons in unsymmetrically ortho disubstituted aniline derivatives indicates the occurrence of intramolecular exchange of the amino protons. The absence of any observable coupling over six bonds to the para proton places an upper limit on the degree of nonplanarity of the amino group in the 2,6-dibromo- and 2,6-dichloroanilines. A relatively basic compound like 2,4,6-trimethylaniline does not display long-range couplings of the amino protons, very likely because intermolecular proton exchange occurs.

Canadian Journal of Chemistry, 48, 1263 (1970)

Introduction

Indirect spin–spin coupling constants of protons in a substituent to ring protons in toluene (1), benzaldehyde (2), and their derivatives (3–9) are well known. The coupling to a ring proton in the para position over six bonds, ^6J, is apparently dominated by a σ–π mechanism and its magnitude is therefore at a maximum when the C—H bond in the side-chain lies perpendicular to the plane of the benzene ring (10, 11). The coupling over five bonds to the meta proton, ^5J, appears to have contributions from both σ and σ–π mechanisms (9, 12). It is largest when the two C—H bonds are arranged as in **1** (X = C, N, or O) and is smallest in **2** (8, 9, 12–14). Neither ^6J nor ^5J are markedly

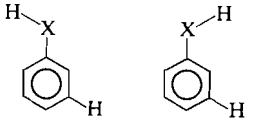

1 **2**

sensitive to the electronic nature of other ring substituents (1, 3, 7, 9) but may be influenced by the steric effects of the substituents on conformational preferences.

Phenolic protons couple to ring protons in the meta position (13, 15, 16), particularly when an intramolecular hydrogen bond determines a planar conformation **1**. The hydrogen-bond prevents rapid intermolecular exchange of the phenolic protons (16). Such exchange renders the coupling unobservable in a slow-passage single resonance experiment.

Similarly, $^5J_m^{H,NH} = 0.7$ Hz in *N*-methyl-2,4-dinitroaniline (17), where hydrogen bonding between the amino proton and the 2-nitro group results in a conformation **1** for the N—H and relevant C—H bond. No coupling is observed to the other meta proton (H_5). The presence of the N—H···O bond in ortho nitro aniline derivatives can be inferred from the low shielding of the amino proton (17–21), the infrared (i.r.) stretching frequencies (22–28), and the coplanarity of the nitro group as determined by X-ray measurements in the solid state (29).

Spin–spin coupling between ring protons and both protons in the unsubstituted amino group has not been previously reported. We here report the observation of such couplings in a number of ortho disubstituted aniline derivatives. The occurrence of intramolecular exchange of the amino protons is inferred from the experimental data and a limit is placed on the degree of nonplanarity of the amino group involved in intramolecular hydrogen bonds.

Experimental

The aniline derivatives were obtained from Aldrich Chemical Company and were used without further purification. The presence of small amounts of impurities is of no importance as long as they do not lead to intermolecular exchange of the amino protons. Such exchange would render the long-range couplings unobservable. However, it is clear from the results that intermolecular

TABLE 1

Amino and ring proton chemical shifts and spin–spin coupling constants in some ortho disubstituted anilines

Compound	Solvent (concentration)‡	Chemical shift*			Coupling constants†	
		Amino	$H_{3,5}$	H_4	$J_m^{H,NH}$	Others
2,6-DiCl	C_6H_{12} (3)	4.32	7.035	6.452	0.33 ± 0.02	$J_o^{H,H} = 8.10$
	C_6D_6 (3)	3.87	6.851	6.126	0.34	$J_o^{H,H} = 8.08$
2,6-DiBr	C_6H_{12} (3)	4.42	7.233	6.318	0.36	$J_o^{H,H} = 8.02$
	C_6D_6 (3)	4.02	7.039	5.990	0.34	$J_o^{H,H} = 7.98$
2,4,6-TriCl	C_6H_{12} (3)	4.28	7.078	—	0.36	
	C_6D_6 (3)	3.72	6.859	—	0.35	
2,4-DiBr-3,6-diCl	C_6H_{12} (1.5)	§	7.403	—	0.32	
	C_6D_6 (1.5)	3.86	7.048	—	0.33	
2-Br-4,6-diNO_2	C_6H_{12} (insoluble)	—	—	—	—	
	C_6D_6 (< 1)	5.93	7.871 (H_3) 8.540 (H_5)		0.40	$J_m^{H,H} = 2.63$
2,4,6-TriCH_3	C_6H_{12} (3)	3.13	6.599	—	—	
	C_6D_6 (3)	2.82	6.712	—	—	

*Ring proton chemical shifts are precise to at least 0.003 p.p.m. while amino proton shifts are precise to 0.01–0.02 p.p.m.; to low field of internal TMS.
†Coupling constants in Hz between ring protons are precise to at least 0.05 Hz while $J^{H,NH}$ are precise to 0.02 Hz.
‡Concentration of aniline derivative in mole %.
§Unobserved.

exchange was absent in all but the solutions of 2,4,6-trimethylaniline.[1]

The anilines were normally prepared as 3 mole % solutions in cyclohexane or in benzene-d_6 if their solubility allowed. Tetramethylsilane (TMS) served as an internal reference and locking signal in the measurement of the proton magnetic resonance (p.m.r.) spectra of the degassed solutions at 30 °C on a DA60I Varian spectrometer operated in the frequency sweep mode. Peak positions were calibrated by reading sweep and manual oscillator frequencies at intervals of a few Hz.

Results

In Table 1 the proton chemical shifts relative to internal TMS and the observed proton–proton coupling constants are given. Complex spectra were analyzed as ABX_2 or AB_2X_2, *not* $ABXX^1$ or AB_2XX^1, cases. Line widths at half-height of the amino proton peaks varied between 13 and 25 Hz at 60 MHz (^{14}N quadrupole relaxation effects).

The chemical shifts in benzene solution, although accurately measured, are sensitive to the concentration of the internal reference. At low concentrations of TMS the shifts depend linearly on TMS concentration. Our measurements show that the shifts in Table 1 lie within 0.3 to 0.5 Hz (at 60 MHz) of the shifts extrapolated to zero concentration of TMS. For our present purposes these deviations are of no interest.[2]

In the cyclohexane solutions the concentrations of TMS are not at all critical.

In Fig. 1, the ring proton spectrum of an 11.8 mole % solution (near saturation) of 2,6-dibromoaniline in benzene-d_6 demonstrates the resolution attainable with a degassed solution of an aniline derivative. Note the absence of observable coupling of amino protons to proton 4. The linewidth at half-height of the antisymmetric transition of proton 4 in this spectrum is less than or equal to 0.17 Hz.

The sign of $^5J_m^{H,NH}$ in Table 1 is unknown. The analogous couplings in toluene, benzaldehyde, and phenol derivatives (3, 8, 13, 32) are positive. It is highly likely that $^5J_m^{H,NH}$ is also positive.

Discussion

The ring proton chemical shifts and the coupling constants between ring protons in

[1]Some authors (17, 30) have performed extensive purifications of solvents and amines but have not always observed long-range couplings. The solvents themselves may compete with the ortho substituents in forming hydrogen bonds with the amino group. Of course, that is the reason for using benzene-d_6 and cyclohexane as solvents in the present study. In previous work in this laboratory we have carefully purified aniline but have never succeeded in observing long-range coupling of its amino protons.

[2]However, in the studies of solvent shifts induced by aromatic solvents (ASIS) the internal concentrations of TMS are seldom reported (31). For an ASIS of 1 p.p.m., relatively small differences in TMS concentrations could easily lead to differences of 0.03 p.p.m. in the ASIS values reported by different workers.

Can. J. Chem. Downloaded from www.nrcresearchpress.com by 210.87.254.6 on 09/05/12
For personal use only.

Can. J. Chem. Downloaded from www.nrcresearchpress.com by 210.87.254.6 on 09/05/12
For personal use only.

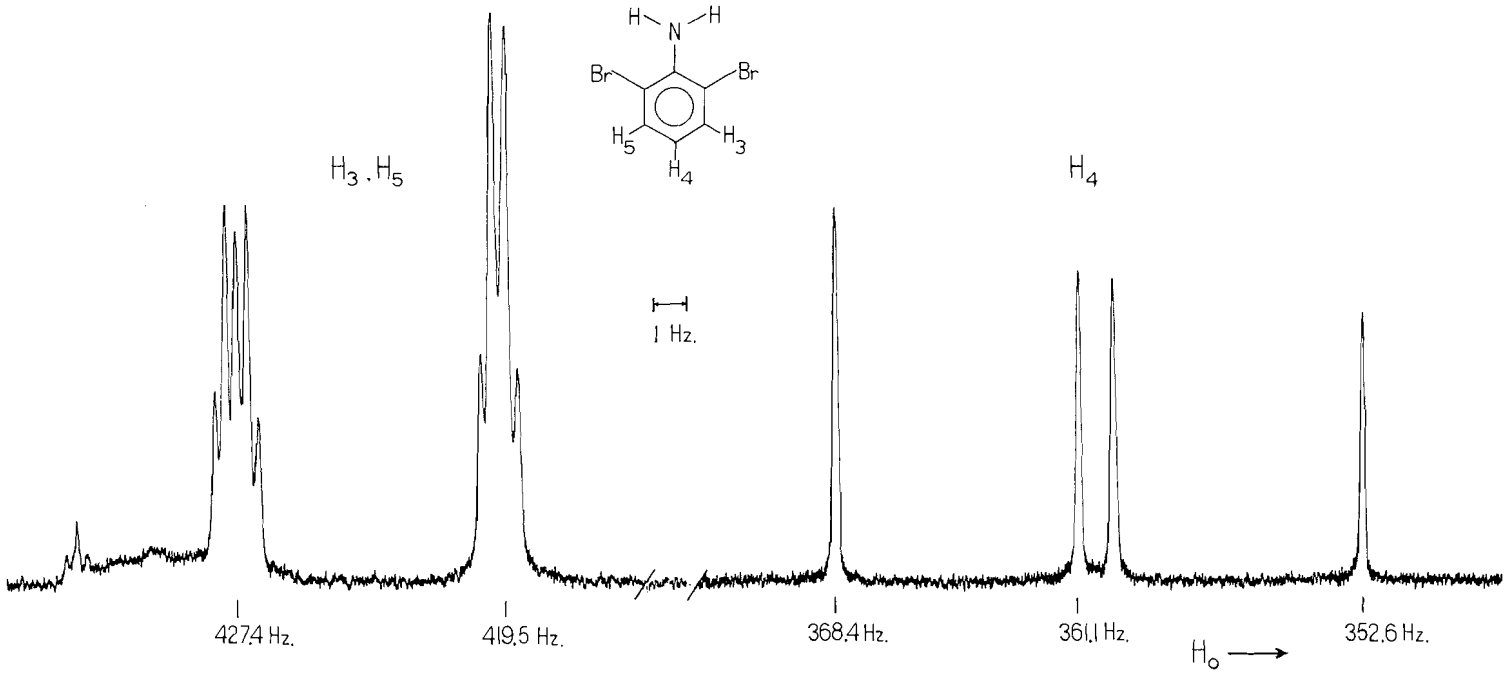

FIG. 1. The ring proton magnetic resonance spectrum at 30 °C of an 11.8 mole% solution of 2,6-dibromoaniline in benzene-d_6 taken at 60 MHz. The scale is in Hz to low-field of internal TMS. Long-range coupling of H_3 and H_5 to the amino protons is clearly resolved. The triplet of low intensity at lowest field arises from the ring protons of 2,4,6-tribromoaniline. The broad resonance just to high field of the small triplet is due to residual, incompletely deuterated solvent molecules.

Can. J. Chem. Downloaded from www.nrcresearchpress.com by 210.87.254.6 on 09/05/12
For personal use only.

Table 1 are of interest in studies of substituent effects and solvent effects on these parameters and will eventually be fully discussed in connection with similar data on many benzene derivatives.

1. $^5J_m^{H,NH}$ *and Intramolecular Hydrogen Bonding*

The absence of an observable long-range coupling in 2,4,6-trimethylaniline[3] implies the occurrence of intermolecular proton exchange. This implication is in agreement with the work of Rae (20), who shows that in substituted *N*-methylanilines the coupling between the amino proton and the methyl protons becomes unobservable due to rapid intermolecular proton exchange when $pK_a > 3.5$ for the aniline derivative. The pK_a of 2,4,6-trimethylaniline is greater than 3.5 (33). On the other hand, the other compounds in Table 1 are clearly much less basic than the trimethylaniline. The observation of $^5J_m^{H,NH}$ and the implied lack of appreciable proton exchange in the other compounds, is probably related to the small fraction of amine molecules existing as the conjugate acid under the present solvent conditions.

Consequently, the observation of $^5J_m^{H,NH}$ in Table 1 does not prove the existence of intramolecular hydrogen bonding. However, the relatively large deshielding of the amino protons caused by ortho halogen or nitro substituents in Table 1 (the amino proton shift of aniline in cyclohexane is 3.35 p.p.m. from TMS (34)) is best interpreted (34) in terms of the formation of nonlinear N—H···X bonds when X = Cl, Br, or NO_2. The N—H stretching frequencies in ortho substituted anilines have been variously interpreted (22, 24–28) but have also been used as evidence in favor of intramolecular hydrogen bonds when X = Cl, Br, or NO_2 (22).

2. Intramolecular Exchange of the Amino Protons

An increase in the concentration of 2,6-dibromoaniline to 11.8 mole% in benzene-d_6 and an increase in temperature to 60 °C produced no broadening of the ring proton peaks. Hence the mean lifetime before intermolecular exchange must be greater than 1 s even under these conditions.[4]

[3]Decoupling of the 4-methyl protons leads to a septet for the ring protons, the peaks of which have widths at half-height of 0.25 Hz.

[4]Long-range coupling of the amino protons was not observed in a recent study (35) of this compound as a 20 weight% solution in carbon tetrachloride.

The observation of *equal* coupling of both amino protons to *any* meta proton in Table 1 indicates an *intramolecular* exchange of the two amino protons. This conclusion is reached as follows. As discussed in the introduction, $^5J_m^{H,NH}$ is stereospecific and in conformation **1** is equal to 0.7 Hz but is near 0 Hz in **2**. If **1** and **2** were interconverting at a rate greater than about 0.7 s^{-1} and were equally populated, the observed coupling to both meta protons would be $(0.7 + 0.0)/2 = 0.35$ Hz (spin state of amino proton conserved during interconversion). In Table 1 the observed couplings are all near 0.35 Hz.

However, in the presence of two, identical ortho substituents, an apparently equal coupling of the amino protons to both meta protons does not necessarily imply intramolecular exchange of the amino protons. For example, for 2,4,6-trichloroaniline the proton spectrum corresponds to the case AA^1XX^1 in the absence of intramolecular exchange. The four-bond coupling between the meta protons in the ring must be 2.0 ± 0.2 Hz, as follows from known additivity schemes for the effect of substituents on *J* (36) and from $J_m^{H,H} = 2.1 \pm 0.2$ Hz in 1,3,5-trichlorobenzene (37). Hence, set $J_{AA^1} = 2.1$, $J_{AX} = J_{A^1X^1} = 0.7$, and $J_{AX^1} = J_{A^1X} = 0$ Hz. Direct calculation (38) then shows that for $^2J^{H,NH} \equiv J_{XX^1} = 0$ Hz, the A region consists of a 1:2:1 triplet with a spacing of 0.35 Hz. However, if $J_{XX^1} = \pm 2$ Hz, the A region consists of a 3:2:3 triplet with a spacing of 0.35 Hz. When $J_{XX^1} = \pm 3 \mp 1$ or $\pm 1 \mp 1$ Hz, the A resonance is more complex.

In ammonia, $|^2J^{H,H}| \approx 10$ Hz (39). In the aniline derivative, the hybridization state of the nitrogen atom probably lies between sp^2 and sp^3 (see below) in which case the coupling may well be lower than 10 Hz in magnitude (compare $^2J^{H,H} = -12.5$ Hz in methane (40) and $^2J^{H,H} = 2.5$ Hz in ethylene (41)). In the absence of intramolecular exchange, the observed 1:2:1 triplet with a spacing of 0.35 Hz in 2,4,6-trichloroaniline would therefore exclude $^2J^{H,NH}$ values lying between the limits of $\pm 3 \mp 1$ and $\pm 1 \mp 1$ Hz. Therefore the observed triplet can arise either from certain reasonable values of $^2J^{H,NH}$ or from intramolecular exchange which occurs with a rate constant, $k > 0.7\ \pi/\sqrt{2}\ s^{-1}$.

If the two ortho substituents are not identical, absence of intramolecular exchange entails different chemical shifts of the two amino protons (compare 2,6-dichloro- and 2,6-dibromoaniline

Can. J. Chem. Downloaded from www.nrcresearchpress.com by 210.87.254.6 on 09/05/12
For personal use only.

in Table 1). For instance, in 2,4-dibromo-3,6-dichloroaniline a shift difference of 0.1 p.p.m. between the amino protons would, in the absence of exchange, give rise to a resolvable quartet in the ring proton spectrum instead of the observed triplet (this conclusion assumes an ABX spectrum with $J_{AB} \leq 14, J_{AX} = 0.7, J_{BX} = 0.0$ Hz). Hence intramolecular exchange very probably occurs in this compound (the amino proton resonance is too broad to yield information on amino proton shift difference).

In 2-bromo-4,6-dinitroaniline an equal coupling of 0.40 ± 0.02 Hz to the two ring protons is again observed. An amino proton placed ortho to a nitro group has a shift of about 8 p.p.m. (18–21). The shift of an amino proton situated ortho to a bromine substituent is about 4 p.p.m. in benzene-d_6 (Table 1). Rapid intramolecular exchange, with a mean lifetime prior to exchange of about 10^{-3} s then causes an observed proton shift of about 6 p.p.m. in a 2-bromo-6-nitroaniline derivative. The observed shift in our compound is 5.9 p.p.m. Consequently, both the long-range coupling magnitude[5] and the observed shift are consistent with an intramolecular exchange of the amino protons in 2-bromo-4,6-dinitroaniline in benzene-d_6 solution. Rapid intermolecular exchange would average the amino proton shifts but would also lead to apparently zero long-range coupling constants. Hence intramolecular exchange is a necessary and sufficient condition for the observation of an averaged amino proton shift together with an averaged, non-zero long-range coupling of the amino and meta protons. The present data set an upper limit on the lifetime before exchange of amino protons. There is no reason to believe that intramolecular exchange does not also occur in the other hydrogen bonded anilines in Table 1.

The intramolecular exchange may simply occur by rotation about the C—NH_2 bond. The N—H bond itself may be disrupted during the exchange (although this seems unlikely) without a loss in long-range coupling; as long as it breaks and reforms in a time short compared to the lifetime of the spin state of the proton.

[5]In *N*-*n*-butyl-2,4-dinitroaniline in benzene-d_6 solution we have observed $^5J_m^{H_5,NH} = 0.78 \pm 0.02$ Hz, suggesting that nitro groups increase the magnitude of $^5J_m^{H,NH}$ over that observed for halogen substituents. The observed, averaged $^5J_m^{H,NH} = 0.40 \pm 0.02$ Hz, in 2-bromo-4,6-dinitroaniline is consistent with this suggestion.

3. Planarity of the Amino Group

In the gas phase the angle between the bisector of the HNH angle (114°) and the extension of the C—N bond of aniline is 39° (42). Consequently the angle between the ring plane and the plane defined by the nuclei in the C—N—H bond is 20°. When the amino protons are involved in intramolecular bonds this angle may decrease. Infrared data (22) suggests an HNH angle of 115° in 2,4,6-tribromoaniline and 2,4,6-trichloroaniline but an angle of 120° in 2,6-dinitroaniline. Coplanarity of the amino group and the aromatic ring is therefore indicated in the latter compound.

The following arguments place a plausible upper limit on the degree of nonplanarity of the amino group in 2,6-dibromoaniline and 2,6-dichloroaniline. From the linewidth of the transition between the antisymmetric spin states in these compounds we conclude that $^6J_p^{H,NH} < 0.07$ Hz.

J_p^{H,CH_3} in toluene (1) and $J_p^{H,CHO}$ in benzaldehyde (9) derivatives are evidently proportional to $\cos^2\theta$ (π electron mechanism) where θ is the angle between the H—C—C_1 plane and the pπ orbital on the C_1 carbon atom of the aromatic ring. Furthermore, as many as four halogen substituents do not significantly affect J_p^{H,CH_3} (43). Turning to $^5J_m^{H,NH}$ in Table 1, their magnitude of 0.35 ± 0.04 Hz compares with 0.37 ± 0.02 Hz in benzaldehyde (2) and a number of its halogen and nitro derivatives (9), and with 0.36 Hz in toluene (1) and some of its derivatives (3, 4, 12, 43). In all these cases, $^5J_m^{H,XH}$ is evidently largely independent of the state of hybridization of X or of the substituents in the ring.

$J_p^{H,CHO} = -0.03$ Hz in benzaldehyde (2), a planar molecule (44). Furthermore, $J_p^{H,CHCl_2} \approx 0$ Hz in $\alpha,\alpha,2,6$-tetrachlorotoluene at -40 °C when the C—H bond of the dichloromethyl group lies in the plane of the ring (14). On the plausible assumption that $J_p^{H,XH}$ magnitudes depend primarily on geometry we write

$$\cos^2\theta = (J(\pi/2) - J)/(J(\pi/2) - J(O))$$

where $J(\pi/2)$ and $J(O)$ are the respective J values for coplanar and orthogonal conformations of the amino group relative to the plane of the aromatic ring. The methyl group in toluene rotates freely (45) and hence $\langle\cos^2\theta\rangle = 1/2$. But $J_p^{H,CH_3} = -0.62$ Hz in toluene (1) and therefore $J_p^{H,CH_3} = -1.2$ Hz for $\theta = 0$.

Can. J. Chem. Downloaded from www.nrcresearchpress.com by 210.87.254.6 on 09/05/12
For personal use only.

Assuming the same value of $J_p^{H,NH}$ for $\theta = 0$, the observed value of $J_p^{H,NH} < 0.07$ Hz yields $\theta > 76°$. In agreement with the i.r. (22) and Kerr constant (46) data, the present result suggests that hydrogen bonding to halogen substituents tends to decrease the degree of nonplanarity of the aniline molecule found in the gas phase. Unfortunately, the present method is insensitive in the region $70° < \theta < 90°$ but note that for $\theta = 70°$ (as in gaseous aniline) the above treatment would yield $J_p^{H,NH} = 0.14$ Hz, easily measurable on our spectrometer.[6]

The pK_a of aniline itself is so high that intermolecular proton exchange occurs at a rate sufficient to obscure long-range coupling of the amino protons, which has not been observed (47). The observation of $^6J_p^{H,NH}$ probably requires an *N*-alkyl-2,6-diXaniline derivative in which X is not a proton acceptor. If X and the alkyl group are bulky enough then the N—H bond may well be situated in a nonplanar, time-averaged conformation. We have yet to succeed in the synthesis of such a compound in which no intermolecular proton exchange occurs.

We are grateful to the National Research Council of Canada for financial support and thank a referee for helpful comments.

1. M. P. Williamson, R. J. Kostelnik, and S. M. Castellano. J. Chem. Phys. **49**, 2218 (1968).
2. R. J. Kostelnik, M. P. Williamson, D. E. Wisnosky, and S. M. Castellano. Can. J. Chem. **47**, 3313 (1969).
3. G. Kotowycz and T. Schaefer. Can. J. Chem. **44**, 2743 (1966).
4. D. Gagnaire and Trinh-Huu-Ich. Bull. Chem. Soc. (France), 3763 (1966).
5. D. J. Blears, S. S. Danyluk, and T. Schaefer. J. Chem. Phys. **47**, 5037 (1967).
6. G. P. Newsoroff and S. Sternhell. Aust. J. Chem. **21**, 747 (1968).
7. D. T. Witiak, D. B. Patel, and Y. Lin. J. Amer. Chem. Soc. **89**, 1908 (1967).
8. D. G. De Kowalewski and S. Castellano. Mol. Phys. **16**, 567 (1969).
9. C. L. Bell, S. S. Danyluk, and T. Schaefer. Can. J. Chem. **47**, 3529 (1969).
10. H. M. McConnell. J. Chem. Phys. **30**, 126 (1959); M. Barfield and B. Chakrabarti. J. Amer. Chem. Soc. **91**, 4346 (1969).
11. M. J. S. Dewar and R. C. Fahey. J. Amer. Chem. Soc. **85**, 2704 (1963).
12. T. Schaefer, C. Wong, and C. K. Tam. Can. J. Chem. **47**, 3688 (1969).
13. S. Forsén and R. A. Hoffman. J. Mol. Spectrosc. **20**, 168 (1966).
14. T. Schaefer, R. Schwenk, C. J. MacDonald, and W. F. Reynolds. Can. J. Chem. **46**, 2187 (1968).
15. R. Freeman. Mol. Phys. **6**, 535 (1963).
16. T. Schaefer and G. Kotowycz. Can. J. Chem. **46**, 2865 (1968).
17. J. A. Weil, A. Blum, A. H. Heiss, and J. K. Kinnaird. J. Chem. Phys. **46**, 3132 (1967).
18. B. M. Lynch, B. C. Macdonald, and J. G. K. Webb. Tetrahedron, **24**, 3595 (1968).
19. R. F. C. Brown, L. Radom, S. Sternhell, and I. D. Rae. Can. J. Chem. **46**, 2577 (1968).
20. I. D. Rae. Aust. J. Chem. **19**, 409 (1966).
21. B. Lamm. Acta Chem. Scand. **19**, 2316 (1965).
22. P. J. Krueger. Can. J. Chem. **40**, 2300 (1962); **41**, 363 (1963).
23. K. B. Wetsel, W. E. Robertson, and M. W. Krell. Anal. Chem. **30**, 1598 (1958).
24. A. G. Moritz. Spectrochim. Acta, **20**, 1642 (1964).
25. A. N. Hambley and B. V. O'Grady. Aust. J. Chem. **15**, 627 (1962).
26. L. K. Dyall and J. E. Kemp. Spectrochim. Acta, **22**, 467 (1966).
27. L. K. Kyall. Aust. J. Chem. **20**, 93 (1967).
28. L. K. Dyall. Spectrochim. Acta, **25A**, 1423 (1969) and references therein.
29. J. R. Holden and C. Dickinson. J. Phys. Chem. **73**, 1199 (1969).
30. J. Heidberg, J. A. Weil, G. A. Janusonis, and J. K. Anderson. J. Chem. Phys. **41**, 1033 (1964).
31. P. Laszlo. *In* Progress in nuclear magnetic resonance spectroscopy. Volume 3. *Edited by* J. W. Emsley, J. Feeney, and L. H. Sutcliffe. Pergamon Press, London. 1968.
32. S. Forsén, T. Alm, B. Gestblom, S. Rodmar, and R. A. Hoffman. J. Mol. Spectrosc. **17**, 13 (1965).
33. H. C. Brown, D. H. McDaniel, and O. Hoefliger. *In* Determination of organic structures by physical methods. *Edited by* E. A. Braude and F. C. Nachod. Academic Press, New York. 1955.
34. T. Yonemoto, W. F. Reynolds, H. M. Hutton, and T. Schaefer. Can. J. Chem. **43**, 2668 (1965).
35. A. Kumar and B. D. Nageswaro Rao. Mol. Phys. **15**, 377 (1968).
36. T. Schaefer, G. Kotowycz, H. M. Hutton, and J. W. S. Lee. Can. J. Chem. **46**, 2531 (1968).
37. H. M. Hutton, W. F. Reynolds, and T. Schaefer. Can. J. Chem. **40**, 1758 (1962).
38. P. L. Corio. Structure of high resolution n.m.r. spectra. Academic Press, New York. 1966.
39. R. A. Bernheim and H. Batiz-Hernandez. J. Chem. Phys. **40**, 3446 (1964).
40. R. A. Bernheim and B. J. Lavery. J. Chem. Phys. **42**, 1464 (1965).
41. R. M. Lynden Bell and N. Sheppard. Proc. Roy. Soc. **269A**, 385 (1962).
42. D. G. Lister and J. K. Tyler. Chem. Commun. 152 (1966).
43. H. Rottendorf and S. Sternhell. Aust. J. Chem. **17**, 1315 (1964).
44. S. Forsén and P. N. Skancke. *In* Selected topics in structure chemistry. *Edited by* P. Andersen, O. Bastiansen, and S. Furberg. Universitetsforlaget, Oslo. 1967.
45. H. Rudolph, H. Dreizler, A. Joeschke, and P. Wendling. Z. Naturf. **22a**, 940 (1967).
46. R. J. W. LeFèvre, R. Radom, and G. L. D. Ritchie. J. Chem. Soc. B, 913 (1969).
47. S. Castellano, C. Sun, and R. Kostelnik. Tetrahedron Lett. 5205 (1967).

[6]We feel that a coupling of 0.05 Hz would have been detectable in our very careful line width comparisons (we have achieved line widths of 0.07 Hz), leading to $\theta > 78°$. However, the more conservative estimate above is probably more reliable.

Can. J. Chem. Downloaded from www.nrcresearchpress.com by 210.87.254.6 on 09/05/12
For personal use only.

Hydrogen abstraction from toluene by methyl radicals and the pressure dependence of the recombination of methyl radicals

A. N. DUNLOP,[1] R. J. KOMINAR,[2] AND S. J. W. PRICE
Department of Chemistry, University of Windsor, Windsor, Ontario
Received August 28, 1969

Using dimethylzinc, dimethylmercury, and trimethylbismuth as sources of methyl radicals, values of $k_1/k_2^{1/2}$

[1] $$CH_3 + C_6H_5CH_3 \rightarrow CH_4 + C_7H_7$$

[2] $$2CH_3 + M \rightarrow C_2H_6 + M$$

have been calculated from 338 to 610 °C over the pressure range 4.5–204 mm. M is predominantly toluene. The observed pressure dependence of reaction [2] is in agreement with that found when M = benzene, but is somewhat greater, and the fall-off occurs at higher pressures, than for ethane dissociation. However, reasonable agreement is obtained if it is assumed that the efficiency of toluene as a third body in reaction [2] is about 1/10th that of ethane.

Extrapolation to infinite pressure, where it is assumed that $E_2 = 0$ and $A_2 = 10^{13.34}$ cm^3 mole^{-1} s^{-1}, gives $E_1 = 8.0 \pm 0.3$ kcal mole^{-1} and $A_1 = 10^{11.07}$ cm^3 mole^{-1} s^{-1}.

Canadian Journal of Chemistry, **48**, 1269 (1970)

Introduction

Previous investigations of the abstraction of hydrogen from toluene by methyl radicals have given activation energies from 7.3–9.5 kcal mole^{-1} over the temperature range 100–300 °C (1–5). Previous discrepancies are discussed and the values reported are considered as a possible example of the temperature dependence of Arrhenius parameters.

The pressure dependence of the recombination of methyl radicals and of the dissociation of ethane have been the subject of many investigations. Eleven of these have been discussed in a review article (6). A further study by Trenwith (7) is included in results of the ethane dissociation discussed by Lin and Laidler in a theoretical paper (8). Using the classical Kassel theory, Loucks (9) found a value of s between 8 and 9 best fitted his data for methyl-radical recombination (200–300 °C). Grotewold *et al.* (10) suggest that the observed pressure dependence of methyl radical recombination indicates a semirigid activated complex and that, as a result, the commonly accepted A factor for this reaction at infinite pressure, $10^{13.34}$ cm^3 mole^{-1} s^{-1}, is at least an order of magnitude too large. These conclusions are not confirmed by other investigations and seem unfounded. In particular, the results of Hole and Mulcahy (11) and the discussions of Lin and Laidler (8) indicate a rather loose complex.

Experimental

Materials

(*a*) Dimethylmercury was prepared by adding methyl magnesium iodide to an ether slurry of mercuric chloride (12).

(*b*) Dimethylzinc was prepared by refluxing excess zinc metal with dimethylmercury under a nitrogen atmosphere. After refluxing for 12 h, the fraction boiling at 41 °C at 712 mm was removed. The reflux was allowed to continue for an additional 4 h, at which time the fraction boiling at 42 °C at 722 mm was collected. The alkyl was degassed and stored under its own vapor pressure at −78 °C. The dimethylzinc had a vapor pressure of 122 mm at 0 °C, which is in agreement with the literature (13).

(*c*) Trimethylbismuth was prepared by adding anhydrous bismuth trichloride to methyl magnesium iodide (14). The addition was carried out under a nitrogen atmosphere over a period of 3 h. The mixture was refluxed for an additional 3 h. The excess Grignard was hydrolyzed by pouring the solution over an ice–water mixture containing ammonium chloride. The ether layer was separated, washed three times with distilled water, and dried over sodium sulfate. The ether fraction was removed at reduced pressure and the remaining solution fractionally distilled under a nitrogen atmosphere. The fraction boiling at 52 to 53.5 °C at 120 mm was collected and stored under its own vapor pressure at −78 °C. Small fractions were discarded until the vapor pressure agreed with the literature value of 104 mm at 0 °C (15).

(*d*) Toluene from sulfonic acid (Eastman Organic X325) was prepared for use by refluxing over sodium under vacuum for 24 h and then degassing twice by bulb-to-bulb distillation.

[1]Present address: Department of Applied Chemistry, University of Toronto, Toronto, Ontario.
[2]Present address: Department of Chemistry, Waterloo Lutheran University, Waterloo, Ontario.

Can. J. Chem. Downloaded from www.nrcresearchpress.com by 210.87.254.6 on 09/05/12
For personal use only.

Apparatus and Procedure

The experiments were carried out using the same plug-flow system previously used in studying the decomposition of dimethylmercury in a benzene carrier (12). The gaseous products which passed a trap at −120 °C were analyzed using a Perkin–Elmer Model 154 gas chromatograph equipped with a 1/4 in. × 6 ft silica gel column. The column was maintained at 80 °C and a helium flow rate of 20 cm^3/min was used.

The liquid products which condensed along with the toluene in an acetone – Dry Ice trap were analyzed using a Perkin–Elmer Model 800 gas chromatograph equipped with a 150 ft × 0.02 in. (inside diameter) Golay column coated with poly(propylene glycol) (isothermal operation at 50 °C; inlet pressure of N_2 carrier, 7 lb).

Results and Discussion

The reactions of methyl radicals generated by the thermal decomposition of metal alkyls in the presence of a large excess of toluene may be represented by the following scheme

[1] $$CH_3 + C_6H_5CH_3 \rightarrow CH_4 + C_7H_7$$

[2] $$2CH_3 + M \rightarrow C_2H_6 + M$$

At the temperatures used in the present work, 338–610 °C, the C_7H_7 formed in reaction [1] is predominantly $C_6H_5CH_2$. The work of Cher *et al.* (5) shows that E_1 and $E_{\text{side chain}}$ should be virtually identical, while A_1 should be about $10^{0.04}$ greater than $A_{\text{side chain}}$. Therefore, although the Arrhenius parameters obtained in the present work refer to the overall abstraction process, they should not differ significantly from those associated with abstraction from the side chain of toluene.

The experimental results are given in Table 1, and Arrhenius plots at various fixed pressures are shown in Fig. 1. The observed pressure effect is assumed to arise solely from the third-body requirements of reaction [2]. The infinite-pressure curve was obtained by extrapolation based primarily on the curves for the four highest pressures, using the procedure suggested by Oref and Rabinovitch (16).

The pressure dependence agrees with that observed when M = benzene (17). If it is assumed that the efficiency of benzene and toluene as third bodies in reaction [2] is only about 1/10th that of ethane, then the present results agree very well with those of Trenwith (7), but show a somewhat stronger pressure dependence than suggested by Lin and Laidler (8).

The Arrhenius curves of $k_1/k_2^{1/2}$ at infinite pressure and 4.5 mm may be represented, respectively, by

TABLE 1

Variation of $k_1/k_2^{1/2}$ with temperature and pressure

Radical source	Total pressure mm	Temperature °K	$k_1/k_2^{1/2}$	Number of runs averaged*
$Zn(CH_3)_2$	200	857	308	
	200	847	236	
	101	840	259	3
	48	883	385	
	48	869	400	
	48	842	372	
$Hg(CH_3)_2$	204	777	160	2
	204	744	122	
	204	733	121	2
	204	714	97	2
	106	744	132	
	106	733	141	2
	106	714	99	2
	86	731	128	2
	72	715	116	4
	51	781	219	2
	51	769	189	2
	51	756	179	
	46	714	125	
	28	798	335	
	27	794	321	
	26	798	322	
	21	799	365	
	16	798	381	
	14	714	157	
	12	799	443	
	9.6	799	444	
	8.2	714	181	
	7.0	798	473	
	5.7	798	501	
	4.5	847	950	4
	4.5	840	846	4
	4.5	829	752	3
	4.5	813	656	7
	4.5	800	570	4
	4.5	787	516	6
	4.5	772	424	2
$Bi(CH_3)_3$	204	649	54	
	204	629	51	
	106	630	51	2
	106	611	36	2
	86	628	50	4
	51	631	49	
	51	626	48	
	51	622	48	
	24	693	114	
	24	683	113	2
	24	672	88	2
	4.5	703	184	2
	4.5	694	168	
	4.5	685	158	2
	4.5	676	148	8
	4.5	659	105	2

*Number of runs averaged to obtain the given value of $k_1/k_2^{1/2}$. Variation in individual runs $< \pm 10\%$ in the value of $k_1/k_2^{1/2}$.

$$(k_1/k_2^{1/2})_\infty = 2.5 \times 10^4 \exp(-8000 \pm 300/RT) \quad \text{mole}^{-1/2}\,(\text{cm}^3)^{1/2}\,\text{s}^{-1/2}$$

and

$$(k_1/k_2^{1/2})_{4.5} = 1 \times 10^6 \exp(-11\,900 \pm 300/RT) \quad \text{mole}^{-1/2}\,(\text{cm}^3)^{1/2}\,\text{s}^{-1/2}$$

If E_1 is independent of pressure, then E_2 at 4.5 mm is -7.8 kcal mole^{-1}. This is consistent with the results of Hole and Mulcahy (11) who estimate that in the third-order region $E_2 = -13$ kcal mole^{-1}.

In Fig. 2, the present results are compared with previous studies of reaction [1]. The work of Trotman-Dickenson and Steacie (1) agrees quite well with that of Mulcahy *et al.* (4) and of Cher *et al.* (5), but has been omitted because of the uncertainty in correction for isotopic impurity. The latter two studies give $E_1 = 9.2$ and 9.5 kcal mole^{-1}, respectively. Over their concurrent temperature range, these two studies can be adequately represented by a single curve, the solid portion for curve *2* in Fig. 2. This may be somewhat fortuitous since the results of Mulcahy *et al.* may be in a pressure dependent region and should probably be decreased by about 0.1 log units, putting them more in line with those of Burkley and Rebbert (3) (curve *3*, Fig. 2).

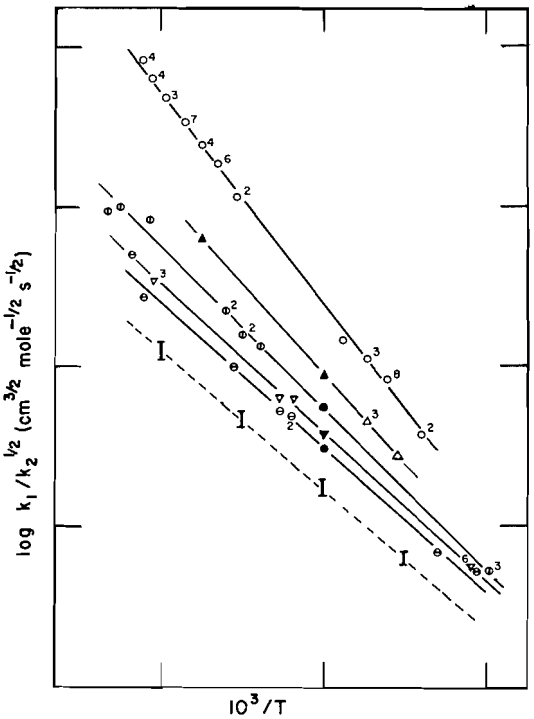

FIG. 1. Arrhenius plot of $k_1/k_2^{1/2}$ at various pressures. Numbers beside the points indicate number of runs averaged to obtain the point. Full points are from curves of $k_1/k_2^{1/2}$ vs. pressure and are usually coincident with experimental points. Pressure: ○, 4.5; △, 24; ◑, 50; ▽, 106; ⊖, 204 mm; I = infinite pressure; length of bar indicates estimated uncertainty in the extrapolated value.

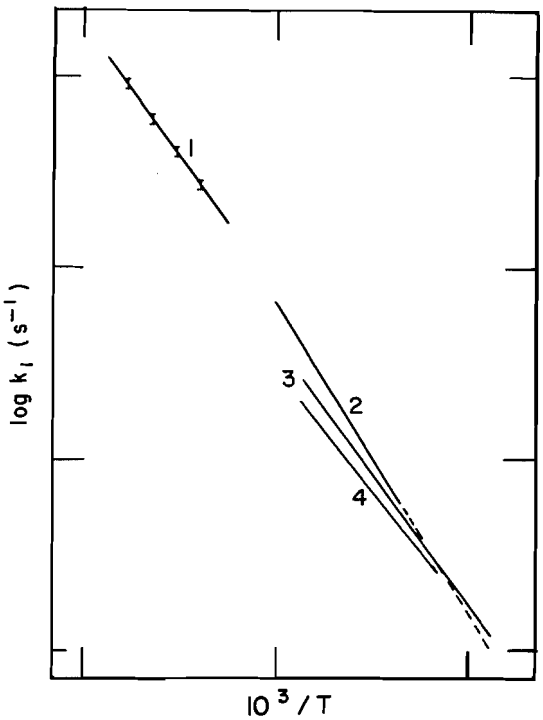

FIG. 2. Arrhenius plots of abstraction of hydrogen from toluene by methyl radicals. All values based on $k_2 = 10^{13.34}$ mole^{-1} cm^3 s^{-1}. *1*, this work, bars indicate estimated uncertainty; *2*, composite of results of Cher, Hollingsworth, and Sicilio (5) and of Mulcahy, Williams, and Wilmshurst (4); dashed curve indicates the additional temperature range covered by Cher *et al* (5); *3*, Burkley and Rebbert (3); *4*, Rebbert and Steacie (2).

The present results are basically in agreement with previous investigations, although the activation energy obtained is 1.2–1.5 kcal below the most recent results at lower temperatures (4, 5). At least part of this difference may be real. Marshall and Purnell (18) predict a *minimum* temperature dependence of $T^{-1/2}$ for the activation energy of the abstraction reaction. This leads to an expected minimum difference of 0.3 kcal, compared to the experimental difference of 1.4 ± 0.6 kcal. Whether the actual temperature dependence could explain the complete difference is uncertain.

The calculations of Marshall and Purnell also indicate that the *A* factor for reaction [2] at infinite pressure should decrease by at least 0.15

Can. J. Chem. Downloaded from www.nrcresearchpress.com by 210.87.254.6 on 09/05/12
For personal use only.

log units from room temperature to 475 °K and then should show little variation from this temperature up to at least 900 °K. It is possible, therefore, that all the curves shown in Fig. 2 should be lowered by at least 0.08 log units. This effect would also explain at least a significant part of the curvature in the Arrhenius plot of $k_1/k_2^{1/2}$ observed by Cher *et al.* (5) below approximately 425 °K.

This work has been supported by a grant from the National Research Council of Canada.

1. A. F. TROTMAN-DICKENSON and E. W. R. STEACIE. J. Chem. Phys. **19**, 329 (1951).
2. R. E. REBBERT and E. W. R. STEACIE. J. Chem. Phys. **21**, 1723 (1953).
3. I. B. BURKLEY and R. E. REBBERT. J. Phys. Chem. **67**, 168 (1963).
4. M. F. R. MULCAHY, D. J. WILLIAMS, and J. R. WILMSHURST. Aust. J. Chem. **17**, 1329 (1964).
5. M. CHER, C. S. HOLLINGSWORTH, and F. SICILIO. J. Phys. Chem. **70**, 877 (1966).
6. K. J. LAIDLER and D. J. MCKENNEY. *In* The chemistry of the ether linkage. *Edited by* S. Patai. Interscience Publishers, Inc., London. 1967. p. 193.
7. A. B. TRENWITH. Trans. Faraday Soc. **62**, 1538 (1966).
8. M. C. LIN and K. J. LAIDLER. Trans. Faraday Soc. **64**, 79 (1968).
9. L. F. LOUCKS. Can. J. Chem. **45**, 2775 (1967).
10. J. G. GROTEWOLD, E. A. LISSI, and M. G. NEUMANN. J. Chem. Soc. A, 375 (1968).
11. K. J. HOLE and M. F. R. MULCAHY. J. Phys. Chem. **73**, 177 (1969).
12. M. KRECH and S. J. PRICE. Can. J. Chem. **41**, 224 (1963).
13. L. H. LONG and J. CATTANACH. J. Inorg. Nucl. Chem. **20**, 341 (1961).
14. L. H. LONG and J. F. SACKMAN. Trans. Faraday Soc. **50**, 1177 (1954).
15. C. H. BAMFORD, D. L. LEVI, and D. M. NEWITT. J. Chem. Soc. 468 (1946).
16. I. OREF and B. S. RABINOVITCH. J. Phys. Chem. **72**, 4488 (1968).
17. M. KRECH and S. J. W. PRICE. Can. J. Chem. **45**, 157 (1967).
18. R. M. MARSHALL and J. H. PURNELL. J. Chem. Soc. A, 2301 (1968).

Can. J. Chem. Downloaded from www.nrcresearchpress.com by 210.87.254.6 on 09/05/12
For personal use only.

Can. J. Chem. Downloaded from www.nrcresearchpress.com by 210.87.254.105 on 09/05/12
For personal use only.

Radiolysis of ethyl iodide – chloromethane mixtures

R. M. LEBLANC AND M. A. WEST[1]
Davy Faraday Research Laboratory, Royal Institution, London, W.1.

R. J. WOODS
Department of Chemistry and Chemical Engineering, University of Saskatchewan, Saskatoon, Saskatchewan

AND

J. A. HERMAN
Département de chimie, Université Laval, Québec 10, Québec

Received November 7, 1969

Mixtures of ethyl iodide with chloroform, carbon tetrachloride, and dichloromethane have been irradiated with ^{60}Co γ-radiation. Reduced yields of iodine, hydrogen iodide, and hydrogen chloride from ethyl iodide – chloroform and ethyl iodide – dichloromethane mixtures and of chlorinated ethanes from ethyl iodide – chloroform are attributed to radical scavenging by iodine and dissociative electron capture by the chlorinated methane.

Electron capture by carbon tetrachloride followed by ion–molecule reactions between ethyl iodide cations and ethyl iodide, or neutralization of these cations by chlorine anions, explains iodine yields observed at low ethyl iodide concentrations in carbon tetrachloride greater than those expected on the basis of partition of absorbed energy. In this mixture, neutralization of an ethyl iodide cation by a chlorine anion gives rise to an enhanced hydrogen chloride yield.

Canadian Journal of Chemistry, 48, 1273 (1970)

Introduction

Initial experiments to study the radiation-induced rearrangement of 2-phenylethyl iodide in solution in chloroform and carbon tetrachloride indicated that solutions in the two solvents behaved quite differently (1), although the physical properties of the solvents are similar. The role of these solvents in the radiolysis of a simpler iodide, ethyl iodide, was examined. In the solid phase, radiolysis of mixtures of ethyl iodide and carbon tetrachloride indicated that the iodine was produced by a sensitization mechanism (2), and it was decided to examine the results with the same system in the liquid phase. The radiolysis of liquid ethyl iodide (3–5), chloroform (6, 7), and carbon tetrachloride (7, 8) separately has been studied quite extensively, and binary mixtures of chloroform and carbon tetrachloride (8) and ethyl iodide with hydrocarbons (e.g. ref. 9) have been irradiated.

In the present experiments, the yield of a major product from each component of the mixture irradiated was estimated and then plotted as a function of the composition of the mixture. The products determined were I_2 and HI from C_2H_5I; HCl from $CHCl_3$, CCl_4, and CH_2Cl_2; C_2Cl_6 from $CHCl_3$ and CCl_4; and a mixture of other chlorinated products from $CHCl_3$ (the main components of the mixture are believed to be 1,1,2,2-tetrachloroethane and pentachloroethane).

[1]To whom all correspondence should be addressed.

Experimental

The purification of ethyl iodide and carbon tetrachloride has already been described (2). Chloroform (Fisher Certified Reagent) and dichloromethane (B.D.H.) were stirred successively with concentrated sulfuric acid, distilled water (×2), sodium bicarbonate solution, and distilled water (×2); then dried over anhydrous calcium chloride, and fractionated using either a preparative gas chromatograph (Wilkins Autoprep) or a column of 40 theoretical plates. Middle fractions were collected and stored over phosphorus pentoxide in the dark until needed.

Trichloroiodomethane was prepared by the method of Dehn (10). The colorless product (b.p. 140–142 °C/760 mm) darkened rapidly and quantitative analysis was not feasible. Gas chromatography of the liquid using a flame ionization detector gave a major peak, assumed to be CCl_3I, and a minor peak having the same retention time as C_2Cl_6.

Samples of about 3 ml, prepared by weighing the components, were irradiated in Pyrex tubes. Air was removed by repeating cycles of freezing, pumping (to about 5 Torr), and thawing or by trap-to-trap distillation. Irradiations were carried out at room temperature (20–30 °C) in ^{60}Co "Gammacell 220" irradiators (A.E.C.L.) at doses ranging from 2×10^{19} to 5×10^{19} eV g^{-1} and a dose rate of $\sim 3 \times 10^{17}$ eV min^{-1}.

Yields are reported relative to $G = 15.6$ for the Fricke dosimeter, but corrections were made for the low-energy

components in the cylindrical ^{60}Co irradiator, which cause a significant increase in the energy absorbed by the iodine atoms (11).

Chemical analysis of HCl and HI by spectrophotometry has already been described (2). Iodine was determined spectrophotometrically. Standard solutions of I_2 in mixtures of the halogenated methanes were prepared to determine the wavelength of maximum absorption and the extinction coefficient of I_2 in the solvent mixture used.

The chlorinated ethanes were determined by gas chromatography using a Wilkins 204 chromatograph equipped with a flame ionization detector. Product peaks were identified by peak reinforcement using authentic samples of the substituted hydrocarbon. 1,1,2,2-Tetrachloroethane and pentachloroethane (Aldrich) had the same retention time, and the peak due to these compounds is referred to as "$Cl_4 + Cl_5$ product" and assumed to have the molecular weight of C_2HCl_5.

Results

Irradiation of pure C_2H_5I, $CHCl_3$, CCl_4, and CH_2Cl_2 gave yields of major products consistent with yields reported by other workers (3–7).

Yields of I_2 from degassed mixtures of C_2H_5I–$CHCl_3$, C_2H_5I–CCl_4, and C_2H_5I–CH_2Cl_2 are plotted in Fig. 1 against the electron fraction of ethyl iodide in the mixture. Figure 2 illustrates the effect of mixture composition upon the yields of chlorinated ethanes from $CHCl_3$ and CCl_4. Figures 3 and 4 show the yield of HCl and HI, respectively, from the three mixtures. Most points represent the average of several determinations and the broken line represents the yield expected if the components of the mixture had no effect upon each other and if absorbed energy is partitioned between the components of the mixture in proportion to their electron fractions.

The yield of I_2 and HI from C_2H_5I is rapidly reduced by added $CHCl_3$ or CH_2Cl_2, and almost no I_2 is released if the mixture contains an

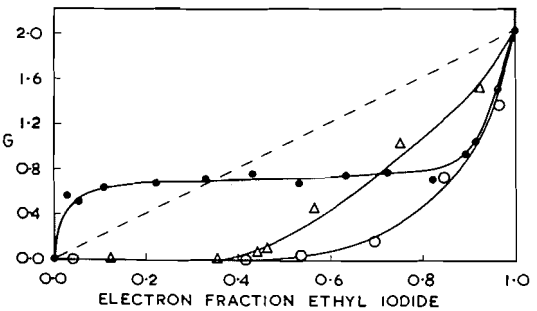

FIG. 1. Yield of I_2 from C_2H_5I–$CHCl_3$ mixtures (○), C_2H_5I–CCl_4 mixtures (●), and C_2H_5I–CH_2Cl_2 mixtures (△) as a function of electron fraction ethyl iodide.

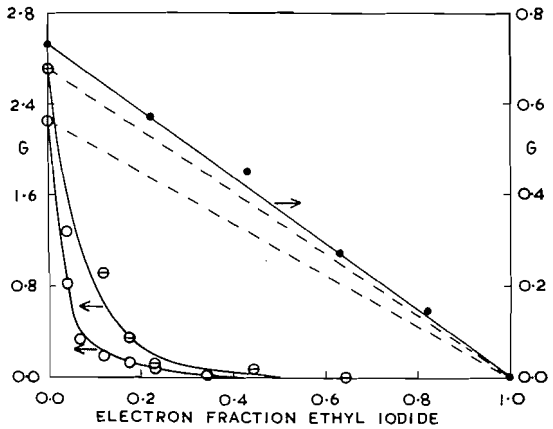

FIG. 2. Yield of C_2Cl_6 (○) and "$Cl_4 + Cl_5$ product" (⊖) from C_2H_5I–$CHCl_3$ mixtures and yield of C_2Cl_6 (●) from C_2H_5I–CCl_4 mixtures as a function of electron fraction ethyl iodide.

electron fraction less than about 0.55 C_2H_5I. Similarly, added C_2H_5I rapidly reduces the yield of chlorinated ethanes and HCl from $CHCl_3$ and the yield of HCl from CH_2Cl_2.

Addition of CCl_4 to C_2H_5I reduces the yield of I_2, but only to a limiting value of $G(I_2) \approx 0.7$, which is maintained until the proportion of C_2H_5I in the mixture falls below an electron fraction of ~ 0.1. Carbon tetrachloride reduces the yield of HI from C_2H_5I more efficiently than $CHCl_3$ or CH_2Cl_2. Addition of C_2H_5I to CCl_4 has apparently no effect upon the yield of C_2Cl_6. Addition of small amounts of C_2H_5I to CCl_4 produces an initial large HCl yield ($G(HCl) \approx$

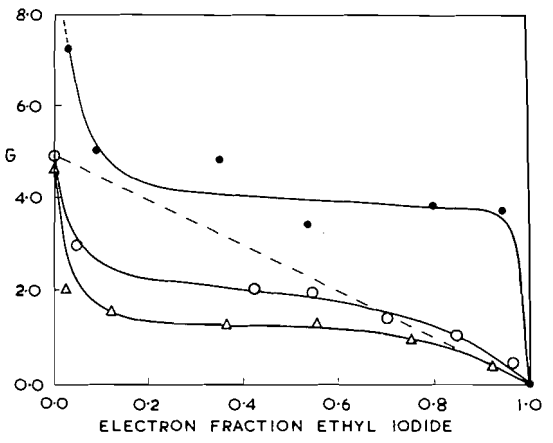

FIG. 3. Yield of HCl from C_2H_5I–$CHCl_3$ mixtures (○), C_2H_5I–CCl_4 mixtures (●), and C_2H_5I–CH_2Cl_2 mixtures (△) as a function of electron fraction ethyl iodide.

Can. J. Chem. Downloaded from www.nrcresearchpress.com by 210.87.254.105 on 09/05/12
For personal use only.

Can. J. Chem. Downloaded from www.nrcresearchpress.com by 210.87.254.105 on 09/05/12
For personal use only.

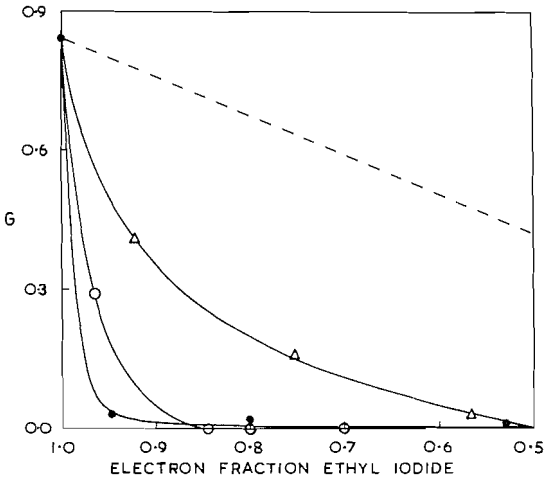

FIG. 4. Yield of HI from C_2H_5I–$CHCl_3$ mixtures (○), C_2H_5I–CCl_4 mixtures (●), and C_2H_5I–CH_2Cl_2 mixtures (△) as a function of electron fraction ethyl iodide.

8.5) which then falls, as more C_2H_5I is added, in a manner similar to the reduction in $G(I_2)$ upon addition of CCl_4 to C_2H_5I.

Figure 5 shows the dependence of I_2 production on dose for various mixtures of C_2H_5I and CCl_4,

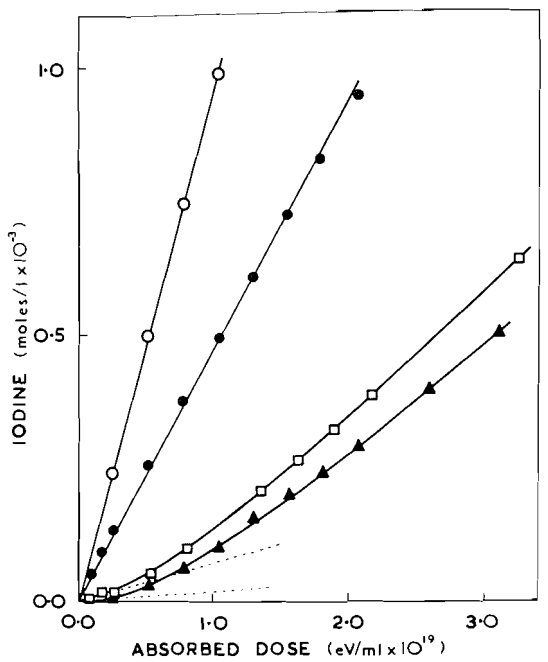

FIG. 5. Formation of molecular I_2 in C_2H_5I–CCl_4 mixtures as a function of absorbed dose. ○, pure C_2H_5I; ●, 95 e% C_2H_5I; □, 62 e% C_2H_5I; ▲, 9 e% C_2H_5I.

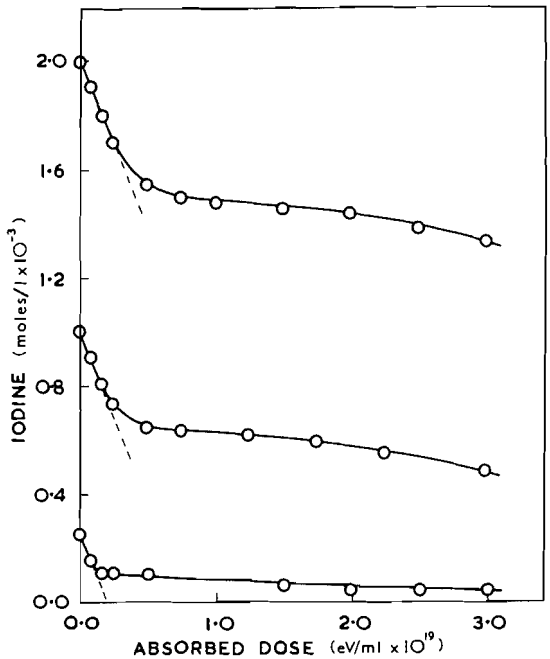

FIG. 6. Disappearance of molecular I_2 in I_2–CCl_4 mixtures as a function of absorbed dose.

and Fig. 6 shows the consumption of I_2 in irradiated mixtures of I_2 in CCl_4 as a function of dose.

Discussion

Four primary processes occur in mixtures of C_2H_5I with a chloromethane, RX, represented in this work by $CHCl_3$, CCl_4, and CH_2Cl_2

[1*a*] $C_2H_5I \rightsquigarrow C_2H_5I^+ + e^-$

[1*b*] $\rightsquigarrow C_2H_5I^*$

[2*a*] $RX \rightsquigarrow RX^+ + e^-$

[2*b*] $\rightsquigarrow RX^*$

Further reaction of these ions and excited molecules occurs by capture of thermalyzed electrons, charge transfer, ion–molecule reactions, and decomposition of the neutral excited molecules. These processes have already been described in detail (2) and are mentioned briefly below.

Electron capture processes of organic halides are described by the following reactions

[3*a*] $C_2H_5I + e^- \rightarrow C_2H_5 + I^-$

[3*b*] $\rightarrow C_2H_5I^-$

[4*a*] $RX + e^- \rightarrow R + X^-$

[4*b*] $\rightarrow RX^-$

Can. J. Chem. Downloaded from www.nrcresearchpress.com by 210.87.254.105 on 09/05/12
For personal use only.

Positive charge transfer processes (eq. [5]) are possible since the ionization potential of RX is higher than that of ethyl iodide (12)

[5] $RX^+ + C_2H_5I \rightarrow RX + C_2H_5I^+$

Ion–molecule reactions involving the cation of ethyl iodide are possible, and one of the transient absorption bands observed in the pulse radiolysis of alkyl iodides has been attributed to either R_2I^+ or $(RI)_2^+$ (13), e.g.

[6*a*] $C_2H_5I^+ + C_2H_5I \rightarrow (C_2H_5I)_2^+$

[6*b*] $\rightarrow (C_2H_5)_2I^+ + I$

The decomposition of $C_2H_5I^*$ and RX^* can be represented by the following scheme

[7*a*] $C_2H_5I^* \rightarrow (C_2H_5 + I)$

[7*b*] $\rightarrow (C_2H_4 + HI)$

[8] $RX^* \rightarrow (R + X) \rightarrow R + X$

The products of these reactions may react together or with the solvent, either in the spurs in which they are formed or after escaping from the spurs. The formation of HI in the radiolysis of pure liquid C_2H_5I is explained by the following, in-spur, disproportionation reaction

[7*c*] $(C_2H_5 + I) \rightarrow C_2H_4 + HI$

while iodine molecules arise from dimerization of iodine atoms both in the spurs and after spur expansion (5).

Charge neutralization and radical recombination processes are described below and correlated with the stable products observed.

Some attempt has been made with the mixed halide systems studied in this work to correlate "non-linear" effects with the electron attachment coefficients of the mixture constituents. In the solid phase, the calculated dissociative capture cross sections give a ratio $\sigma_{CCl_4}/\sigma_{C_2H_5I}$ of 16 (2), a value similar to the coefficients determined in the gas phase (14). It is reasonable to assume that in the liquid phase this ratio should be of the same order of magnitude as in the solid phase. In the gas phase, the electron attachment coefficient for CCl_4 is 9.0; C_2H_5I, 0.5; $CHCl_3$, 0.6; and CH_2Cl_2, 5×10^{-3} (14), indicating that electron attachment by C_2H_5I is likely to be important in the radiolysis of C_2H_5I–CH_2Cl_2 mixtures and, conversely, that electron attachment by CCl_4 will be important in the radiolysis of C_2H_5I–CCl_4 mixtures. (Although the electron attachment coefficients for I_2 and HI are significant (15), electron capture by these compounds can be neglected at the low concentrations present in our systems.)

Chloroform and ethyl iodide have almost the same electron attachment coefficient, and the radiolytic behavior of a mixture of these two halides has thus been used as a model for comparison with the mixture C_2H_5I–CCl_4 (and to a lesser extent, the mixture C_2H_5I–CH_2Cl_2).

Radical Reactions at High Chloroform Concentrations

Radicals escaping from the spurs in irradiated pure $CHCl_3$ will be mainly Cl and $CHCl_2$ (which may also be produced by electron attachment) and they will react in the following manner (6, 7)

[9] $Cl + CHCl_3 \rightarrow HCl + CCl_3$

[10] $CHCl_2 + CHCl_3 \rightarrow CH_2Cl_2 + CCl_3$

[11] $CHCl_2 + CCl_3 \rightarrow C_2HCl_5$

[12*a*] $2\,CCl_3 \rightarrow C_2Cl_6$

[12*b*] $2\,CHCl_2 \rightarrow C_2H_2Cl_4$

In the presence of ethyl iodide, free radicals from $CHCl_3$ may react with I_2. These reactions include

[13] $Cl + I_2 \rightarrow ICl + I$

[14] $CHCl_2 + I_2 \rightarrow CHCl_2I + I$

[15] $CCl_3 + I_2 \rightarrow CCl_3I + I$

and would lead to a reduction in both iodine and chlorinated ethane yields compared with the yields expected on the basis of the partition of absorbed energy.

At high $CHCl_3$ concentrations ($\leqslant 0.2$ electron fraction C_2H_5I), reactions [13]–[15] would be expected to reduce the yield of C_2Cl_6 formed by secondary radicals (CCl_3) more rapidly than the yield of "Cl_4 + Cl_5 product" formed by primary radicals ($CHCl_2$), as is observed (Fig. 2). A rough estimate (9) of molecular product yields based on free-radical mechanisms indicates that this mechanism is consistent with the observed absence of I_2 at low C_2H_5I concentrations and of chlorinated ethanes at high concentrations of C_2H_5I. Since $G(I)$ is about 10.2 for pure C_2H_5I (16) and G(radical) is 11–12 for pure $CHCl_3$ (7), the net I_2 production would be expected to fall to zero for solutions where the electron fraction of C_2H_5I was less than 0.75.

At the higher concentrations of $CHCl_3$, the reaction of primary radicals from $CHCl_3$ with

Can. J. Chem. Downloaded from www.nrcresearchpress.com by 210.87.254.105 on 09/05/12
For personal use only.

C_2H_5I might be expected to reduce yields of the higher chlorinated compounds by reactions [16] and [17]

[16] $$Cl + C_2H_5I \rightarrow HCl + C_2H_4 \cdot I$$

[17] $$CHCl_2 + C_2H_5I \rightarrow CH_2Cl_2 + C_2H_4 \cdot I$$

If this were the case, small amounts of C_2H_5I would not change G(HCl), since reaction [16] would replace reaction [9] without effect upon the hydrogen chloride yield. The decrease in G(HCl) observed when C_2H_5I is added to $CHCl_3$ shows that these two reactions can be neglected. Since $G(Cl) \approx G(CHCl_2) = 5.6$ (7), the higher chlorinated products derived from $CHCl_2$ radicals cannot be reduced by reaction [17].

In the C_2H_5I–CH_2Cl_2 mixtures, no I_2 is observed at high concentrations of the chloro compound. A similar mechanism involving radical scavenging by iodine atoms explains this result.

Enhanced Iodine Yields at High Carbon Tetrachloride Concentrations

The absence of I_2 from mixtures of $CHCl_3$ and CH_2Cl_2 with small amounts of C_2H_5I contrasts with the enhanced iodine yield observed from C_2H_5I–CCl_4 mixtures (Fig. 1). Trichloroiodomethane, the expected radical scavenging product (eq. [15]), was not detected in irradiated C_2H_5I–CCl_4 mixtures. A peak tentatively assigned to this compound, or possibly dichloroiodomethane (b.p. of CCl_3I is 142 °C and that of $CHCl_2I$ is 132 °C (17)), was observed when irradiated mixtures of $CHCl_3$ and C_2H_5I were analyzed by gas chromatography. This observation suggests that the reduction in iodine yield due to radical scavenging by iodine might be offset in part by subsequent reaction of the rather unstable CCl_3I and ClI in C_2H_5I–CCl_4 mixtures (eq. [18])

[18] $$Cl + CCl_3I \text{ (or ClI)} \rightarrow I + CCl_4 \text{ (or } Cl_2)$$

Bimolecular reaction of CCl_3I to produce I_2 and C_2Cl_6 is unlikely at the low radiolytic conversions used in this work.

The iodine production vs. dose plot (Fig. 5) for C_2H_5I–CCl_4 mixtures gives some insight into the importance of reaction [18]. At low C_2H_5I concentrations, plots of I_2 concentration vs. dose consist of two parts: a non-linear region at doses less than 0.5×10^{19} eV/ml followed by a steeper linear region up to doses of 4×10^{19} eV/ml. Between 0.1 and 0.8 electron fraction C_2H_5I in CCl_4, $G(I_2)$ increases from 0.3 to 0.7 as the absorbed dose is increased from 0.5×10^{19} to 10^{19} eV/ml. The induction period is also present in plots of the disappearance of I_2 from I_2–CCl_4 mixtures upon irradiation (Fig. 6). The initial rapid loss of I_2 is presumably due to radical scavenging. G(radicals) from CCl_4 calculated from initial slopes in Fig. 6 is 17 and agrees with values found by Bouby *et al.* (18) and Chapiro (19) of 18.3 and 19 ± 1, respectively. On the other hand, graphs of I_2 concentration vs. dose were perfectly linear for all mixtures studied (at an equivalent dose) of C_2H_5I–$CHCl_3$ and C_2H_5I–CH_2Cl_2. There seems to be good evidence, therefore, that reaction [18] explains the change of slope observed and consequently explains why CCl_3I could not be detected by gas chromatography at doses of $\sim 5 \times 10^{19}$ eV/ml in C_2H_5I–CCl_4 mixtures.

The enhanced I_2 yields at low concentrations of C_2H_5I in CCl_4 cannot be accounted for on the basis of radical reactions [13]–[15], and are possibly due to energy transfer from ionized (eq. [5]) or excited (eq. [19]) CCl_4 molecules to C_2H_5I

[19] $$RX^* + C_2H_5I \rightarrow RX + C_2H_5I^*$$

and subsequent reaction of the "activated" C_2H_5I molecules to eventually give I_2. However, these reactions (eqs. [5] and [19]) can also occur with $CHCl_3$ and CH_2Cl_2, which do not yield iodine when mixed with low concentrations of C_2H_5I and irradiated. If G(radical) for these three chlorinated compounds is about the same, some other mechanism must be involved in the CCl_4 system.

An alternative explanation for the I_2 production in CCl_4 mixtures at low concentrations of C_2H_5I is as follows: ejected electrons, reaction [2*a*], are removed by dissociative electron attachment by CCl_4 with the formation of Cl^-. Since the positively charged molecule RX^+ can migrate (20) (eq. [20]), C_2H_5I having a low ionization potential would be expected to trap the charge (eq. [5]) and subsequently take part in ion–molecule (eq. [6]) and neutralization (eq. [21]) reactions

[20] $$RX^+ + RX \rightarrow RX + RX^+$$

[21] $$C_2H_5I^+ + Cl^- \rightarrow HCl + C_2H_4 + I$$

Either reaction would result in a net yield of molecular I_2. Although a similar process could

Can. J. Chem. Downloaded from www.nrcresearchpress.com by 210.87.254.105 on 09/05/12
For personal use only.

occur with the other two chlorinated compounds, their lower electron affinities would reduce its importance. In addition, CCl_3 radicals produced from CCl_4 by electron attachment are much less reactive towards I_2 than the primary radicals derived from $CHCl_3$ and CH_2Cl_2.

Hydrogen Chloride Formation at High Concentrations of Chloromethanes

Extrapolation of G(HCl) from CCl_4 to zero electron fraction C_2H_5I (Fig. 3) gives a value of ~8.5. The high HCl yield at low C_2H_5I concentrations cannot be explained by reaction [16], but may arise through electron attachment (eqs. [4*a*], [21]).

Figure 3 suggests a "plateau" value for G(HCl) from reaction [21] of ~4 and the g-value for eq. [16] will be given by $g(Cl) = g(HCl) = 8.5 - 4 = 4.5$. This figure agrees with $G(Cl)_{CCl_4}$ of 4.6 (21) and 3.5 ± 0.35 (22).

Increasing the electron fraction of C_2H_5I in CCl_4 from 0.01 to 0.1 causes a decrease in G(HCl) (Fig. 3). This result can be explained by the fact that the yield of chlorine atoms decreases as C_2H_5I is added, due to energy transfer processes (eqs. [5] and [19]).

In the C_2H_5I–$CHCl_3$ and C_2H_5I–CH_2Cl_2 mixtures, electron capture processes involving the chlorinated compounds are less important and the initial G(HCl) lower. In this, a decrease in G(HCl) due to energy transfer processes to the C_2H_5I (eqs. [5], [19]) is expected as the proportion of C_2H_5I is increased; this would not reduce G(HCl) to zero since HCl is also produced by reaction [21]. The importance of this reaction is governed by the relative electron affinities $CCl_4 > CHCl_3 > CH_2Cl_2$, in agreement with the trend $G(HCl)_{CCl_4} > G(HCl)_{CHCl_3} > G(HCl)_{CH_2Cl_2}$ seen in Fig. 3.

Reduced Iodine and Hydrogen Iodide Yields at Low Concentrations of Chloromethanes

With all three chlorinated compounds, their addition in small quantities to C_2H_5I results in a decrease in the yield of both I_2 and HI and the appearance of HCl. At high concentrations of C_2H_5I (0.8–1.0 electron fraction C_2H_5I), the energy is absorbed mainly by C_2H_5I and energy and charge transfer from the chloromethane to C_2H_5I will be slight. However, there will be competition for thermalized electrons, the importance of capture decreasing in the series $CCl_4 > C_2H_5I \approx CHCl_3 > CH_2Cl_2$. The decrease in $G(I_2)$ with added chloromethane is observed to be in the same order as that of the importance of electron capture, suggesting that competition for thermalized electrons is the process responsible for the disappearance of molecular iodine. This explanation for the decrease in $G(I_2)$ is also consistent with the observed decrease in G(HI).

Yield of Hexachloromethane in Carbon Tetrachloride Mixtures

The yield of C_2Cl_6 from CCl_4 appears largely unaffected by the factors which govern the yield of I_2 from these mixtures (Fig. 2). One explanation is that C_2Cl_6 is formed only in spur reactions where radical scavenging by iodine is unlikely.

Alternatively, the observed linear yield may be the result of competition between two reaction schemes which involve an ion–molecule reaction and a positive charge transfer process, respectively. At high CCl_4 concentrations, dissociative electron capture (eq. [4]) will give rise to an enhanced CCl_3 yield. At these concentrations, $C_2H_5I^+$ ions (arising from positive charge transfer from CCl_4^+) cannot take a significant part (23) in the ion–molecule reaction (eq. [6]) but disappear by a charge transfer process which effectively removes CCl_3 radicals (eq. [23]), since the CCl_3^+ ion produced will not give rise directly to C_2Cl_6 (the relative ionization potentials of C_2H_5I and CCl_3 are consistent with reaction [23]).

$$[23] \qquad C_2H_5I^+ + CCl_3 \rightarrow CCl_3^+ + C_2H_5I$$

As the concentration of C_2H_5I is increased, reaction [23] will be reduced in importance because of the diminished yield of CCl_3 radicals (from consideration of energy absorption) and the gradual disappearance of $C_2H_5I^+$ ions by reaction [6].

The financial support of the National Research Council of Canada is gratefully acknowledged. We thank Dr. A. J. Swallow for helpful comments on the manuscript.

1. M. A. West and C. C. Lee. Personal communication.
2. R. M. Leblanc, F. C. Thyrion, and J. A. Herman. Can. J. Chem. **46**, 1625 (1968).
3. R. H. Schuler and R. C. Petry. J. Amer. Chem Soc. **78**, 3954 (1956).
4. H. A. Gillis, R. R. Williams, and W. H. Hamill. J. Amer. Chem. Soc. **83**, 17 (1961).
5. R. N. Schindler. Radiochim. Acta, **2**, 69 (1963).
6. M. Ottolenghi and G. Stein. Radiat. Res. **14**, 281 (1961).

7. H. R. WERNER and R. F. FIRESTONE. J. Phys. Chem. **69**, 840 (1965).
8. T. H. CHEN, K. Y. WANG, and F. J. JOHNSTON. J. Phys. Chem. **64**, 1023 (1960).
9. T. S. CROFT and R. J. HANRAHAN. J. Phys. Chem. **66**, 2188 (1962).
10. W. M. DEHN. J. Amer. Chem. Soc. **31**, 1220 (1909).
11. W. BERNSTEIN and R. H. SCHULER. Nucleonics, **13**, 110 (1955).
12. Bond energies, ionization potentials and electron affinities. *Translated by* W. C. Price from the Russian. Edward Arnold, Ltd., London. 1966.
13. C. CAPELLOS and A. J. SWALLOW. J. Phys. Chem. **73**, 1077 (1969).
14. T. G. LEE. J. Phys. Chem. **67**, 360 (1963).
15. J. P. GUARINO, M. R. RONAYNE, and W. H. HAMILL. Radiat. Res. **17**, 329 (1962).
16. R. H. SCHULER and W. H. HAMILL. J. Amer. Chem. Soc. **74**, 6171 (1952).
17. R. C. WEAST (*Editor*). Handbook of chemistry and physics. The Chemical Rubber Co., Cleveland, Ohio. 1967.
18. L. BOUBY, A. CHAPIRO, M. MAGAT, E. MIGIRDICYAN, A. PREVOT-BERNAS, L. REINISCH, and J. SEBBAN. Proc. Int. Conf. Peaceful Uses At. Energy, Geneva, 1955, **7**, 612 (1955).
19. A. CHAPIRO. J. Phys. Chem. **63**, 801 (1959).
20. T. SHIDA and W. H. HAMILL. J. Chem. Phys. **44**, 2369 (1966).
21. J. DURUP. J. Chim. Phys. **56**, 873 (1959).
22. J. W. SCHULTE. J. Amer. Chem. Soc. **79**, 4643 (1957).
23. J. P. MITTAL and W. H. HAMILL. J. Amer. Chem. Soc. **89**, 5749 (1967).

Can. J. Chem. Downloaded from www.nrcresearchpress.com by 210.87.254.105 on 09/05/12
For personal use only.

Can. J. Chem. Downloaded from www.nrcresearchpress.com by 210.87.254.6 on 09/05/12
For personal use only.

Synthesis of an analog of ochrobirine

R. H. F. MANSKE AND QUAZI A. AHMED
Department of Chemistry, University of Waterloo, Waterloo, Ontario

Received November 18, 1969

An analog of ochrobirine in which one of the methylenedioxy groups is absent has been synthesized.

Canadian Journal of Chemistry 48, 1280 (1970)

In recent years several papers have appeared on the synthesis of ochotensine (1, 2) (**1**), ochotensimine (1, 3) (**2**), and their related analogs (1, 3, 4). These alkaloids have various substituents on the aromatic rings such as hydroxy, methoxy, or methylenedioxy besides an exocyclic methylene or hydroxy (5) or carbonyl (5) group in the 5-membered ring. Recently Manske *et al.* (6) have reported the isolation and structure elucidation of ochrobirine (**3**) which possesses the spiro-structure with two hydroxy groups at C-9 and C-14 of the 5-membered ring.

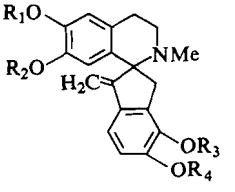

1 R_1=H,R_2=Me,R_3 + R_4=CH_2
2 R_1=R_2=Me,R_3 + R_4=CH_2

We are interested in the total synthesis of **3** which is the first example of an alkaloid possessing a spiro-structure in the naturally occurring benzylisoquinoline alkaloids having two hydroxy groups in the 5-membered ring. Moreover, its synthesis would add further confirmation to the structure given. Before proceeding with the synthesis of ochrobirine (**3**), we prepared a model compound **8**, which the present communication describes.

Homopiperonylamine (**4**) was treated with

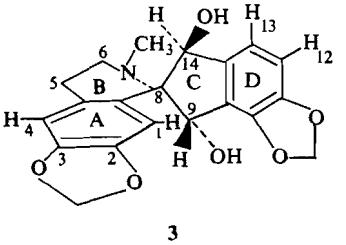

3

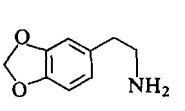

4

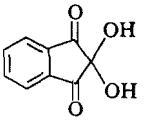

5

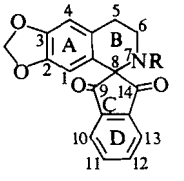

6 R=H
7 R=Me

ninhydrin (**5**) in absolute ethanol at 0° for 25 min. The reaction mixture was then cooled to about −78° (Dry Ice – acetone) and dry hydrogen chloride gas bubbled over the surface of the mixture until a clear solution was obtained. Workup of the reaction mixture afforded the crystalline hydrochloride of **6** in 86% yield. The hydrochloride, on treatment with ammonium hydroxide, gave the free amine **6**[1] in 93% yield as yellow crystalline flakes, m.p. 164–165°. The infrared (i.r.), nuclear magnetic resonance (n.m.r.) spectra, the analytical data of the amine **6**, and all the succeeding compounds were consistent with the assigned structures (see Experimental). The free amine was converted to the

[1]After we independently obtained the desired Pictet–Spangler condensation product **6** by reacting homopiperonylamine with ninhydrin, we became aware of a similar condensation made by treating ninhydrin with 3-hydroxy-4-methoxyphenethylamine to give 3-hydroxy-2-methoxyochotensinan-8,13-dione (**a**) in low yield (16.5%).

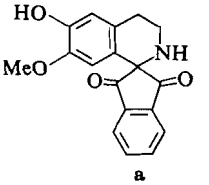

a

Can. J. Chem. Downloaded from www.nrcresearchpress.com by 210.87.254.6 on 09/05/12
For personal use only.

N-methylamine **8** by refluxing with an aqueous mixture of formic acid and formaldehyde for 5 min. The sodium borohydride reduction of the *N*-methylamine **7** in tetrahydrofuran–methanol for 24 h gave an oil. Chromatography of this product over neutral alumina afforded a dihydroxy-*N*-methylamine in 75% yield. The n.m.r. spectrum revealed it to be a mixture of **8** and **9** in the ratio 1:2. Several attempts to separate **9** from **8** on thin-layer chromatography over silica or alumina using different solvent systems were unsuccessful because of identical R_f values of the compounds. The mixture shows a singlet of area 3 at 2.60 δ assigned to the $N—CH_3$ group while a complex of area 4 at 2.70–3.45 δ is attributed to the protons at C-5 and C-6. A sharp singlet of area 1 at 4.74 δ is assigned to the proton geminal to the hydroxyl group at C-9 (6) and two broad singlets of area 0.33 and 0.66 at 5.28 and 5.47 δ are due to the protons geminal to the hydroxyl group at C-14 of **8** and C-14 of **9** (6). A singlet of area 2 at 5.74 δ corresponds to the methylenedioxy group. The two singlets of area 1 at 5.84 and 6.55 δ are assigned to the aromatic protons at C-1 and C-4 respectively; the other aromatic protons in ring D appear as a singlet of area 4 at 7.33 δ. The synthesis of ochrobirine is in progress in our laboratories and will be the subject of a future communication.

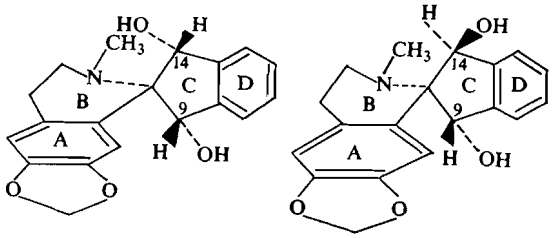

8 **9**

Experimental

All melting points were taken on a Thomas Hoover apparatus and are uncorrected. Infrared spectra were determined on a Perkin–Elmer model 237B recording spectrophotometer in chloroform solution unless otherwise noted. Ultraviolet (u.v.) spectra were observed in 95% ethanol on a Cary model 14 spectrophotometer. The n.m.r. spectra were determined in deuteriochloroform containing tetramethylsilane as internal reference with a Varian A-60 spectrometer.

Materials

3,4-Methylenedioxy-β-nitrostyrene was prepared employing the method of Gensler and Samour (8). Its reduction to homopiperonylamine (**4**) was carried out according to the procedure of Erne and Ramirez (9).

Attempted Condensation

(*1*) The procedure of Beckett and Kelly (4) was followed. A mixture of the hydrochloride of **4** (0.20 g, 0.99 mmole) and ninhydrin (0.177 g, 0.9 mmole) in 10 ml of ethanol and 3 ml of concentrated hydrochloric acid was heated to reflux over a period of 15 min, then allowed to reflux for 40 min. The reddish solution on cooling deposited colorless needles of the hydrochloride of **4** in almost quantitative yield (0.18 g); identified by m.p., mixed m.p., and i.r. spectrum.

(*2*) A solution of the amine **4** (0.148 g, 0.89 mmole) in 5 ml of absolute ethanol was added to a stirred solution of ninhydrin (0.158 g, 0.89 mmole) in 5 ml of absolute ethanol in presence of 5% hydrochloric acid and the mixture was kept at 50–60° for 1 h. Work-up of the reaction mixture gave hydrochloride of **4** (0.13 g); identified by m.p. and i.r. spectrum.

(*3*) A solution of ninhydrin (2.75 g, 15.4 mmole) in 50 ml of absolute ethanol was placed in a 500-ml three-necked flask equipped with a mechanical stirrer, pressure equalized dropping funnel, and condenser provided with a calcium chloride guard-tube. The flask was cooled to 0° in an ice-water bath and a solution of the amine **4** (2.55 g, 15.4 mmole) in 25 ml of absolute ethanol was added over a period of 2 min from the dropping funnel under a nitrogen atmosphere. A white precipitate separated within 3 min and 50 ml more of absolute ethanol were added to facilitate the stirring of the mixture. After vigorously stirring the mixture for 25 min, the ice-water bath was replaced by a Dry Ice – acetone bath. The contents of the flask were stirred for an additional 5 min after which dry hydrogen chloride gas was bubbled over the surface of the mixture until all the precipitate had dissolved giving a clear slightly dark red solution. The Dry Ice bath was then removed and the solution slowly heated to 80–85° on a water bath and kept at this temperature for about 7 min with stirring. Most of the solvent was removed in a Buchi rotary evaporator under reduced pressure and the solution allowed to cool when crystals separated. The crystals were filtered and recrystallized from ethanol to yield 5.3 g (86%) of the hydrochloride of **6** as light yellow needles, m.p. 221–223° (sintering at 219°); i.r. λ_{max}(Nujol) 2733–2393 (ammonium bands), 1753, and 1718 cm^{-1} (carbonyl groups); u.v. 226.5, 252.5 (sh), and 293.8 mμ (log ε 4.72, 4.22 and 3.71).

Anal. Calcd. for $C_{18}H_{14}NO_4Cl$: C, 62.90; H, 4.10; N, 4.07. Found: C, 62.81; H, 4.01; N, 3.91.

The hydrochloride (3.0 g) was placed in 50 ml of chloroform and the suspension cooled in an ice–water bath. A solution of 50 ml of ammonium hydroxide (5%) was added with stirring and the organic layer separated. The alkaline aqueous solution was extracted once more with 25 ml of chloroform. The combined organic extracts were washed with water, dried over anhydrous sodium sulfate, and the solvent was removed in a rotary evaporator under reduced pressure. Crystallization of the residue from a methylene chloride – methanol mixture afforded 2.5 g (93%) of free base **6** as shiny yellow flakes: m.p. 164–165°; i.r. λ_{max}(KBr) 3288 (NH), 1748, and 1718 cm^{-1} (carbonyl groups); u.v. 227, 252.5 (sh), and

293.7 mμ (log ε 4.62, 4.05, and 3.65); n.m.r. δ 1.95 (1H, s, NH), 2.78 (2H, t, $J = 6$ Hz, NCH_2), 3.44 (2H, t, $J = 6$, benzylic CH_2), 5.80 (2H, s, methylenedioxy), 5.96 (1H, s, H at C_1), 6.66 (1H, s, H at C_4), and 7.77–8.23 (4H, complex, H at C-10, 11, 12, 13). The NH proton at 1.95 p.p.m. exchanged with D_2O.

Anal. Calcd. for $C_{18}H_{13}NO_4$: C, 70.35; H, 4.26; N, 4.56. Found: C, 70.69; H, 4.55; N, 4.31.

Preparation of N-Methylamine 7

A solution of amine **6** (0.20 g, 0.65 mmole) in 2 ml each of 90% formic acid and 40% formaldehyde was refluxed with stirring for 5 min. The solution was then cooled and diluted with 5 ml of water and basified with concentrated ammonium hydroxide solution. The mixture was extracted twice with 25-ml portions of methylene chloride. The organic layers were combined, washed with water, dried over anhydrous sodium sulfate, and evaporated to dryness under reduced pressure. The product was twice crystallized from a mixture of methylene chloride and methanol to afford 0.085 g (40%) of **7** as yellow-orange needles, m.p. 174–175°; i.r. λ_{max}(KBr) 1738 and 1708 cm^{-1} (carbonyl groups); no absorption due to N–H around 3200–3400 cm^{-1} was observed; u.v. 228.6, 252.5 (sh), and 293.7 mμ (log ε 4.64, 4.07, and 3.59); n.m.r. δ 2.36 (3H, s, NCH_3), 3.0 (2H, t, $J = 6$ Hz, NCH_2), 3.36 (2H, t, $J = 6$ Hz, benzylic, $—CH_2$), 5.80 (2H, s, methylenedioxy), 5.90 (1H, s, H at C_1), 6.70 (1H, s, H at C_4), and 7.76–8.29 (4H, complex, H at C-10, 11, 12, 13).

Anal. Calcd. for $C_{19}H_{15}NO_4$: C, 71.02; H, 4.71; N, 4.36. Found: C, 71.17; H, 4.79; N, 4.46.

Reduction of N-Methylamine 7 by Sodium Borohydride

Sodium borohydride (0.15 g) was slowly added to a stirred solution of *N*-methylamine 7 (0.20 g, 0.62 mmole) in 10 ml of tetrahydrofuran and 10 ml of methanol over a period of 10 min. The color of the solution soon started to fade and after about 1 h, an additional amount of sodium borohydride (0.05 g) was added to the reaction mixture. After 24 h, the colorless solution was cooled in an ice-water bath and acidified with acetic acid. Removal of most of the solvent in a rotary evaporator under reduced pressure left a semi-solid residue which was basified with concentrated ammonium hydroxide solution. The precipitates were extracted into two 25 ml portions of chloroform and the combined organic extracts washed with water, dried over anhydrous sodium sulfate, and the solvent was removed under reduced pressure. The oily product was dissolved in 5 ml of ethyl acetate and passed through a 1.4 × 2 cm column of neutral alumina (100–200 mesh, Bio-Rad Laboratories). The column was eluted with 25 ml of ethyl acetate. This fraction on concentration followed by addition of ether deposited 0.15 g (75%) of a mixture of **8** and **9**, m.p. 207–213°. Recrystallization from a mixture of methylene chloride and ether yielded minute white crystals; m.p. 209–214°; i.r. 3565 (s) and 3265 cm^{-1} (m, b); no carbonyl absorption was observed; u.v. 202.5, 238.7, and 292.5 mμ (log ε 4.56, 3.44 and 3.54).

Anal. Calcd. for $C_{19}H_{19}NO_4$: C, 70.14; H, 5.89; N, 4.30. Found: C, 70.08; H, 5.97; N, 4.27.

This research was supported in part by grants from the National Research Council of Canada.

1. H. IRIE, T. KISHIMOTO, and S. UYEO. J. Chem. Soc. 3051 (1968).
2. R. B. KELLY and B. A. BECKETT. Can. J. Chem. **47**, 2501 (1969).
3. S. MCLEAN, M.-S. LIN, and J. WHELAN. Tetrahedron Lett. 185 (1966).
4. B. A. BECKETT and R. B. KELLY. J. Heterocycl. Chem. **5**, 685 (1968).
5. J. K. SAUNDERS, R. A. BELL, C.-Y. CHEN, D. B. MACLEAN, D. E. F. GRACEY, and J. K. SAUNDERS. Can. J. Chem. **47**, 3589 (1969).
6. R. H. F. MANSKE, R. G. A. RODRIGO, D. B. MACLEAN, D. E. F. GRACEY, and J. K. SAUNDERS. Can. J. Chem. **47**, 3589 (1969).
7. T. KAMETANI, S. TAKANO, and S. HIBINO. Yakugaku Zasshi. **88**, 1123 (1968).
8. W. J. GENSLER and C. M. SAMOUR. J. Amer. Chem. Soc. **73**, 5555 (1951).
9. M. ERNE and F. RAMIREZ. Helv. Chim. Acta, **33**, 912 (1950).

Can. J. Chem. Downloaded from www.nrcresearchpress.com by 210.87.254.6 on 09/05/12
For personal use only.

Lemon-peel pectin. II. Isolation of homogeneous pectins and examination of some associated polysaccharides

G. O. Aspinall and I. W. Cottrell
Department of Chemistry, Trent University, Peterborough, Ontario, Canada
Received November 7, 1969

Two electrophoretically homogeneous pectins have been isolated from dried lemon-peel under conditions of minimum degradation by extraction with cold water and with disodium ethylenediaminetetraacetate. Some properties of polysaccharides which occur in association with the pectins are reported.

Canadian Journal of Chemistry, **48**, 1283 (1970)

Can. J. Chem. Downloaded from www.nrcresearchpress.com by 210.87.254.6 on 09/05/12
For personal use only.

Previous studies on dried lemon-peel (1) have shown that extraction under the mildest possible conditions, namely with water at room temperature, furnishes pectin A which, after chromatography on diethylaminoethyl-Sephadex, may be obtained in chemically homogeneous form as pectin C. This pectin was shown to contain 75% of galacturonic acid residues, of which approximately 80% were esterified. Neutral sugars, including galactose, arabinose, rhamnose, xylose, and fucose, were present as constituents, and characterization of oligosaccharides formed on depolymerization provided direct evidence for the structural role of rhamnose and xylose residues in the acidic polysaccharide. The water-extracted pectin, however, accounts for only about a third of the total pectin in the peel, and we now report the extraction of a second homogeneous pectin, under non-degradative conditions, together with an examination of certain structural features of polysaccharides which occur in association with pectin C.

Dried lemon-peel was extracted with water at room temperature, as described previously (1), to give pectin A together with a polysaccharide fraction from which polysaccharide F was isolated. Pectin A gave a single peak on electrophoresis in pyridine – acetic acid buffer (Fig. 1), but two minor peaks were detected in addition to the main peak in borate buffer (Fig. 2). Fractionation of pectin A by chromatography on diethylaminoethyl-Sephadex furnished electrophoretically homogeneous pectin C (Fig. 3), and small amounts of polysaccharide fractions D and E. Partial acid hydrolysis of pectin C afforded inter alia acidic oligosaccharides with the chromatographic mobilities of 2-*O*-(α-D-galactopyranosyluronic acid)-L-rhamnose, 4-*O*-(β-D-glucopyranosyluronic acid)-L-fucose, and 6-*O*-(β-D-glucopyranosyluronic acid) - D - galactose, thus providing further evidence that these oligosaccharides were genuine fragments from the pectin and did not arise solely from associated polysaccharides.

Samples of water-extracted lemon-peel were further extracted at 90° with (*i*) water acidified to p*H* 2.1, (*ii*) disodium ethylenediaminetetraacetate/sodium lauryl sulfate at p*H* 5,[1] and (*iii*) sodium hexametaphosphate at p*H* 4.2 to give pectins G, H, and J (see Table 1). Pectins G and H were essentially identical in composition, but in each case electrophoresis showed that the major component was contaminated with a component of the same mobility as pectin C. Control experiments showing that treatment of pectin A under extraction conditions (*i*) and (*ii*) caused no change in electrophoretic mobility indicated that the two components in pectins G and H are not artifacts arising from the extraction procedures. Pectin J, however, had a much higher electrophoretic mobility and the much lower methoxyl content suggested that the extraction conditions had caused partial saponification. Treatment of pectins with alkaline reagents (3) and even with hot phosphate buffer at p*H* 6.8 (4) causes not only de-esterification but also base-catalyzed β-elimination resulting in rupture of glycosidic linkages and in the formation of unsaturated uronic acid residues. A control experiment showed that pectin A when treated with sodium hexametaphosphate at p*H* 4.2 underwent de-esterification

[1]The assumed role of EDTA in the extraction of pectins is to complex divalent metal ions such as calcium, and complexing is normally most effective at ca. p*H* 7. Nevertheless, the isolated yields of pectins are not markedly lowered when extractions are conducted at p*H* 4.5–5 (2) when the chelating efficiency of EDTA is very low. Our extractions were carried out at p*H* 5 in order to avoid inadvertent base-catalyzed degradation.

Can. J. Chem. Downloaded from www.nrcresearchpress.com by 210.87.254.6 on 09/05/12
For personal use only.

TABLE 1

Isolation of lemon-peel pectin fractions

Pectin	Method of isolation	Galacturonic acid (%)	OMe (%)	$[\alpha]_D°$	Electrophoretic mobility ($\mu \times 10^5$)*	
					Borate buffer	Pyridine – acetic acid buffer
A	(1) Extraction of peel with H_2O at room temperature	75	10.5	+206	(4.1) (6.3) 11.2	5.4
C	Chromatography of pectin A	75	10.1	+212	11.3	
G	(2) Residual peel from (1) extracted with H_2O at p*H* 2.1 at 90°	80	10.3	+220		(5.4) 5.9
H	(3) Residual peel from (1) extracted with EDTA/sodium lauryl sulfate at 90°	83	10.3	+212		(5.8) 6.3
J	(4) Residual peel from (1) extracted with sodium hexametaphosphate at 90°	82	2.2	+237		12.5
K	(5) Residual peel from (1) extracted with water at 50°	83	9.1	+210	12.0	(5.4) 6.2
L	(6) Residual peel from (1) and (5) extracted with EDTA at p*H* 5.0 at 90°	84	8.8	+214	12.0	6.3

*Figures in parentheses indicate mobilities of minor components.

Can. J. Chem. Downloaded from www.nrcresearchpress.com by 210.87.254.6 on 09/05/12
For personal use only.

FIG. 1. Electrophoretic pattern of pectin A. Buffer: pyridine (1%, v/v) – acetic acid (0.4%, v/v), 220 V, 13 mA, 95 min.

FIG. 3. Electrophoretic pattern of pectin C. Buffer: 0.05 *M* sodium tetraborate, 150 V, 13 mA, 155 min.

and that the formation of unsaturated uronic acid residues could be detected by light absorption at 235 mμ. However, no apparent de-esterification as judged by the absence of change in electrophoretic mobility was detected when pectin A was heated with sodium hexametaphosphate buffer at p*H* 3.7.

The following procedure was adopted for the large scale isolation under conditions of minimum degradation of a second homogeneous pectin. Water-extracted lemon-peel was treated with water at 50° to give pectin K, which was shown by electrophoresis to contain components with the mobilities of pectins C and L (Fig. 4). Subsequent extraction of the peel with disodium ethylenediaminetetraacetate at p*H* 5 gave homogeneous pectin L with the same electrophoretic mobility as the major components of pectins G and H (Fig. 5). Analysis of pectin L showed that it had a higher galacturonic acid content (84%) and a lower methoxyl content (8.8%) than those (75 and 10.1%) of pectin C. When both pectins C and L were chromatographed on diethylaminoethylcellulose using stepwise elution (5), in each case more than one polysaccharide fraction was obtained (Fig. 6). In the light of subsequent experiments on the fractionation of the derived pectic acids (6) and of the electrophoretic homogeneity of the pectins we consider that these fractionations probably indicate variations in degree of esterification within each preparation.

In the following paper it is shown that the pectic acids formed on saponification of pectins C and L contain slightly different average proportions of galacturonic acid residues, but that analyses of the sub-fractions derived from these preparations indicate overlap in galacturonic acid content of molecules within each spectrum of molecular species. The differences between the parent pectins are therefore compounded of differences in galacturonic acid content and in methoxyl content as a measure of the degree of esterification. The combined differences, when expressed in these terms, do not seem large, but when expressed as percentages of *non-esterified* galacturonic acid residues, 25 and 41% in pectins C and L respectively, the differences between the two pectins appear to be more substantial. These latter differences are indicated in the relatively low degree of overlap in elution pattern when the two pectins were chromatographed on diethylaminoethylcellulose (Fig. 6). Inasmuch as the physical properties of pectins (7) may be markedly influenced by both esterification of galacturonic acid residues and interruptions in the structural regularity of the linear galacturonan portion of the molecule by neutral sugar residues inserted in the main chain, e.g.

FIG. 2. Electrophoretic pattern of pectin A. Buffer: 0.05 *M* sodium tetraborate, 150 V, 13 mA, 174 min.

FIG. 4. Electrophoretic pattern of pectin K. Buffer: pyridine (1%, v/v) – acetic acid (0.4%, v/v), 220 V, 13 mA, 105 min.

FIG. 5. Electrophoretic pattern of pectin L. Buffer: pyridine (1%, v/v) – acetic acid (0.4%, v/v), 220 V, 13 mA, 108 min.

rhamnose, and attached in side-chains, e.g. arabinose, galactose, and xylose, the observed differences in composition between pectins C and L probably account for the differences in ease of extraction and may reflect differences in biological function in the plant.

During the extraction and fractionation of lemon-peel pectin C three polysaccharide fractions containing high proportions of neutral sugars were isolated. Although pectins are especially susceptible to inadvertent degradation involving, for example, hydrolysis of acid-labile arabinofuranosidic linkages or base-catalyzed β-elimination from methyl galacturonate residues, the mildest possible conditions were used throughout and we regard these polysaccharides as genuine components of the peel. Since only small quantities of these fractions were obtained, information on structure was limited to that obtained from small-scale experiments using chromatographic procedures for identification.

Fractionation by chromatography on diethylaminoethyl-Sephadex of the mother liquors from the precipitation of pectin A furnished an arabinan. This arabinan had a high negative specific rotation ($[\alpha]_D$ −140°) typical of other arabinans associated with pectins, e.g. that from mustard seeds (8), and the highly branched nature of the polysaccharide was established by the detection of 2,3,5-tri-, 2,3-di-, and 2-*O*-methylarabinose as cleavage products from the methylated derivatives.

Previous studies (1) have shown that fractionation of lemon-peel pectin A by chromatography on diethylaminoethyl-Sephadex gives two minor polysaccharide fractions D and E, both containing galactose and arabinose as major constituents, but with different proportions of galacturonic acid residues. When this separation was repeated we found that polysaccharide D was obtained as an arabinogalactan devoid of galacturonic acid residues. Chromatographic identifications showed that the main cleavage products from the methylated polysaccharide included 2,3,5-tri- and 2,3-di-*O*-methylarabinose, and 2,3,6-tri-*O*-methylgalactose. Minor cleavage products included 2-*O*-methylarabinose and 2,6-di-*O*-methylgalactose, but these results do not permit a distinction to be made between polysaccharide D as an arabinogalactan and as a mixture of polysaccharides, e.g. an arabinan and a galactan.

Electrophoresis showed that polysaccharide fraction E was heterogeneous, but insufficient quantities were available for further separation. However, evidence for the nature of the neutral sugar constituents was obtained by the detection inter alia of 2,3,5-tri- and 2,3-di-*O*-methylarabinose, and 2,3,4,6-tetra-, 2,3,4-, 2,3,6-, and 2,4,6-tri-, and 2,4-di-*O*-methylgalactose as cleavage products from the methylated derivative, and by

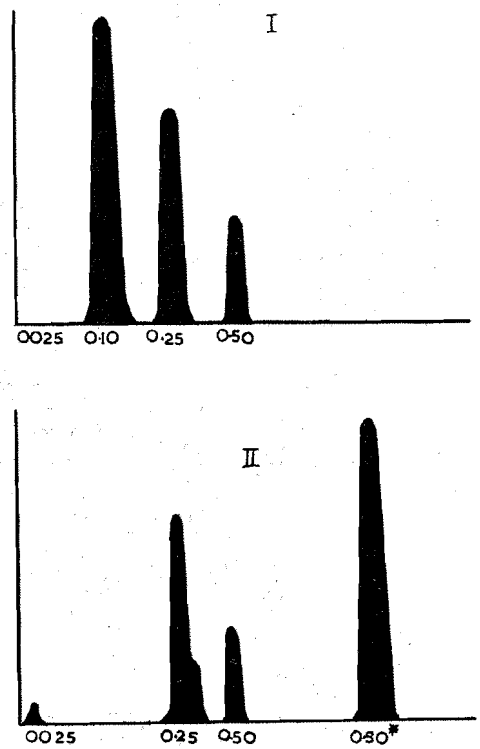

FIG. 6. Chromatographic elution patterns of (I) pectin C and (II) pectin L from diethylaminoethylcellulose using 0.025 *M*, 0.10 *M*, 0.25 *M*, and 0.50 *M* phosphate buffer at p*H* 6, and (*) 0.50 *M* sodium hydroxide.

Can. J. Chem. Downloaded from www.nrcresearchpress.com by 210.87.254.6 on 09/05/12
For personal use only.

Can. J. Chem. Downloaded from www.nrcresearchpress.com by 210.87.254.6 on 09/05/12
For personal use only.

the chromatographic identification of 3-*O*-, 4-*O*-, and 6-*O*-galactopyranosylgalactose as products of partial acid hydrolysis. The presence of branched arabinogalactans in which galactose residues are joined by 1 → 3 and 1 → 6 in addition to the 1 → 4 linkages commonly associated with pectic substances may be inferred. Small quantities of branched arabinogalactans have also been encountered in association with pectins from alfalfa (9) and suspension cultured sycamore cells (10).

Experimental

Analyses

Galacturonic acid contents were determined by (*i*) a modified carbazole – sulfuric acid procedure (11), (*ii*) potentiometric titration with 0.1 *N* sodium hydroxide, and (*iii*) decarboxylation (12). Electrophoresis of polysaccharide solutions (1%) was performed in either 0.05 *M* sodium tetraborate buffer at p*H* 9.25 or pyridine (1%, v/v) – acetic acid (0.4%, v/v) buffer at p*H* 5.5, using a Tiselius type, Spinco Model H apparatus with Schlieren optics, and currents of 13 mA were maintained. Polysaccharide samples were hydrolyzed in *N* sulfuric acid in sealed tubes at 100° for 12 h. Paper chromatography was carried out in the following solvent systems (v/v): (*A*) ethyl acetate – pyridine – water (10:4:3): (*B*) ethyl acetate – acetic acid – formic acid – water (18:3:1:4); (*C*) ethyl acetate – acetic acid – formic acid – water (18:8:3:9); and (*D*) butanone – water – ammonia (200:17:1). Gas–liquid partition chromatography was carried out on columns of (*a*) dichlorodimethylsilane treated Celite coated with 5% by weight of neopentylglycol adipate polyester at 165°, (*b*) Chromosorb W coated with 10% by weight of Carbowax 20M at 190°, and (*c*) dichlorodimethylsilane treated Celite coated with 5% by weight of silicone gum XE-60 at 125 and 150°. Unless otherwise stated, optical rotations were observed for aqueous solutions at ca. 18°.

Isolation of Pectin C and Polysaccharide Fractions D, E, and F

Powdered lemon-peel (700 g) was extracted with water at room temperature to give pectin A (56 g) as described previously (1). Electrophoresis of pectin A in borate buffer showed the presence of a major and two minor polysaccharide components (see Table 1). The supernatant solutions from the precipitations of pectin A with acetone were combined and concentrated. During the concentration polysaccharide fraction 2 (1 g) separated as a fine precipitate and was removed by centrifugation. Hydrolysis of the fraction gave glucose as the main product with traces of galacturonic acid, galactose, arabinose, xylose, and rhamnose. The above concentrated solution was poured into acetone (25 volumes), the resulting sticky precipitate was dissolved in water, and the solution was extracted with chloroform in a liquid/liquid extractor for 48 h to remove coloring matter and saponins, and then freeze-dried to give polysaccharide fraction 3 (10 g), $[\alpha]_D$ +10° (*c*, 0.24). Hydrolysis of fraction 3 gave arabinose as the major product with smaller amounts of galacturonic acid, galactose, glucose, xylose, and rhamnose.

Polysaccharide fraction 3 contained 25% of carbohydrate [estimated as arabinose by the phenol – sulfuric acid method (13)]. Aqueous 7% cupric acetate (100 ml) was added slowly with stirring to the polysaccharide fraction (10 g) in water (100 ml) and the further addition of ethanol (3 volumes) gave a precipitate which was removed by centrifugation. The supernatant liquid was concentrated to remove ethanol, dialyzed to remove copper salts, and freeze-dried to give fraction 3A (0.62 g), $[\alpha]_D$ −9° (*c*, 1.2) [Found: uronic acid residues (*i*), 19%]. Hydrolysis of fraction 3A gave arabinose as the main neutral sugar. The copper precipitate was dispersed in water containing 1% of hydrochloric acid and polysaccharide was precipitated by the addition of ethanol (3 volumes). This procedure was repeated four times, and the resulting precipitate was redissolved in water, precipitated with ethanol, and freeze-dried to give polysaccharide fraction 3B (0.88 g), $[\alpha]_D$ +181° (*c*, 1.42) [Found: uronic acid residues (*i*), 76%]. The supernatant liquid from the above precipitations was dialyzed and freeze-dried to give polysaccharide fraction 3C (0.50 g), $[\alpha]_D$ +83° (*c*, 0.86) [Found: uronic acid residues (*i*), 46%]. Hydrolysis of fractions 3B and 3C gave arabinose as the major neutral sugar, but the fractions were not examined further. Polysaccharide fraction 3A (600 mg) was adsorbed on a column (8 g) of diethylaminoethyl-Sephadex A-50 (formate form). The column was eluted with water (500 ml), the eluate was concentrated and poured into ethanol (10 volumes), and the precipitate was dissolved in water and freeze-dried to give polysaccharide F (322 mg), $[\alpha]_D$ −140° (*c*, 0.50), which gave only arabinose on hydrolysis.

Pectin A (12 g) was fractionated by chromatography on diethylaminoethyl-Sephadex A-50 (formate form) as described previously (1) and in a typical separation furnished polysaccharide fraction D (0.44 g), $[\alpha]_D$ +10° (*c*, 0.74) [Found: uronic acid residues, nil], polysaccharide E (0.275 g), $[\alpha]_D$ +71° (*c*, 0.36) [Found: uronic acid residues, 25; OMe, 4.7%], and pectin C (7.522 g). Chromatography of pectin C on diethylaminoethyl-cellulose (5) (Fig. 6) showed that neutral polysaccharide was absent. Electrophoresis of pectin C in borate buffer gave a single peak (Fig. 3).

Pectin C (500 mg) was hydrolyzed with *N* sulfuric acid on a boiling-water bath for 5.5 h. Insoluble degraded polysaccharide was removed by centrifugation and hydrolysis gave only galacturonic acid. The supernatant liquid was neutralized with barium carbonate, and the solution was filtered, treated with Amberlite resin IR-120 (H), concentrated, and adsorbed on a column (5 g) of diethylaminoethyl-Sephadex A-25 (formate form). The column was eluted successively with water, 0.05 *N* formic acid, a gradient of 0.05–0.4 *N* formic acid, and 0.5 *N* formic acid. Fractions were collected, concentrated, and examined by chromatography in solvents *B* and *C*. Acidic sugars with the mobilities of galacturonic acid, 2-*O*-(galactopyranosyluronic acid)rhamnose, 4-*O*-(glucopyranosyluronic acid)fucose, 6-*O*-(glucopyranosyluronic acid)galactose, galacturonobiose and galacturonotriose (1) were detected.

Polysaccharide D

Polysaccharide D (200 mg) was methylated with methyl iodide and sodium hydride in dimethylsulfoxide as

Can. J. Chem. Downloaded from www.nrcresearchpress.com by 210.87.254.6 on 09/05/12
For personal use only.

described by Sandford and Conrad (14), and furnished methylated arabinogalactan (82 mg), $[\alpha]_D$ −65° (*c*, 0.31 $CHCl_3$) [Found: OMe, 40.1%]. A sample of the methylated polysaccharide was methanolyzed and gas–liquid chromatography (g.l.c.) on columns *a* and *b* showed the presence of components with the retention times of methyl glycosides of 2,3,5-tri- (+++) and 2,3-di-*O*-methylarabinose (++), and 2,3,4,6-tetra- (+), 2,3,6-tri- (+++), and 2,6-di-*O*-methylgalactose (+). A sample of the mixture of methyl glycosides was hydrolyzed with *N* sulfuric acid and, in addition to the above-mentioned sugars, small amounts of arabinose and 2-*O*-methylarabinose were detected by paper chromatography in solvent *D*.

Polysaccharide E

Electrophoresis of polysaccharide E in pyridine – acetic acid buffer gave a single broad peak (μ, 3.2 × 10^{-5} cm^2 V^{-1} s^{-1}), but examination in borate buffer showed two peaks (μ, 5.7 and 10.3 × 10^5 cm^2 V^{-1} s^{-1}). After saponification (7) electrophoresis of the polysaccharide in borate buffer showed three peaks (μ, 2.7, 4.2, and 10.2 × 10^{-5} cm^2 V^{-1} s^{-1}). A sample of the polysaccharide (50 mg) was partially hydrolyzed in 0.5 *N* sulfuric acid (12 ml) on a boiling-water bath for 6 h and paper chromatography of the hydrolysate in solvents *A* and *B* showed the presence of oligosaccharides with the mobilities of 3-*O*-, 4-*O*-, and 6-*O*-β-D-galactopyranosyl-D-galactose.

Polysaccharide fraction E (500 mg) was methylated with methyl iodide and sodium hydride in dimethylsulfoxide (14) and furnished methylated arabinogalactan E′ (292 mg), $[\alpha]_D$ −95° (*c*, 0.48 $CHCl_3$) [Found: OMe, 40.2%]. A sample of the methylated polysaccharide was methanolyzed and g.l.c. of the methanolysate on columns *a* and *c* showed the presence of components with the retention times of methyl glycosides of 2,3,5-tri- (+++), and 2,3- (++) and 2,5-di-*O*-methylarabinose (+), 2,3,4,6-tetra- (+), 2,3,4- (++), 2,3,6- (++), and 2,4,6-tri- (+), and 2,4-di-*O*-methylgalactose (++). A sample of the mixture of methyl glycosides was hydrolyzed and, in addition to the above-mentioned sugars, small amounts of arabinose and 2-*O*-methylarabinose were detected by paper chromatography in solvent *D*.

Polysaccharide F

Polysaccharide F (160 mg) was methylated with methyl iodide and sodium hydride in dimethylsulfoxide (14) to give methylated arabinan (144 mg), $[\alpha]_D$ −153° (*c*, 1.44 $CHCl_3$) [Found: OMe, 37.9%]. A sample of the methylated polysaccharide was methanolyzed and g.l.c. of the methanolysate on columns *a* and *b* showed the presence of components with the retention times of methyl glycosides of 2,3,5-tri- and 2,3-di-*O*-methylarabinose in approximately equal proportions. Although no methyl glycosides of 2-*O*-methylarabinose were detected, paper chromatography of the hydrolysate from the methylated arabinan showed the presence of 2,3,5-tri-, 2,3-di-, and 2-*O*-methylarabinose in approximately equal proportions with traces of arabinose and 3-*O*-methylarabinose.

Further Extraction of Water-extracted Lemon-peel

Dried lemon-peel (500 g) was extracted four times with water at room temperature and gave pectin A (49 g). The residual peel was divided into three portions. The first portion was extracted with water acidified to p*H* 2.1 with hydrochloric acid at 90° for 3 h. Peel was removed by centrifugation and acetone (1.5 volumes) was added to the supernatant liquid. The resulting gelatinous precipitate was removed at the centrifuge, washed several times with acetone–water (7:3), dissolved in water, and freeze-dried to give pectin G (23 g). The second portion of the peel was extracted with aqueous 2% disodium ethylenediaminetetraacetate containing 0.2 *M* sodium lauryl sulfate (p*H* 4) at 90° for 3 h. The peel was removed at the centrifuge, and the supernatant liquid was dialyzed to remove EDTA and freeze-dried. The resulting solid was stirred in butanone–water (9:1) to dissolve sodium lauryl sulfate, and the residue was dissolved in water, precipitated by the addition of acetone (1.5 volumes), redissolved in water, and freeze-dried to give pectin H (21 g). The third portion of peel was extracted with aqueous 1% sodium hexametaphosphate (p*H* 4.2) at 90° for 3 h. The supernatant liquid was dialyzed for several days to remove inorganic salts and concentrated, acetone (1.5 volumes) was added, and the resulting precipitate was dissolved in water and freeze-dried to give pectin J (26 g). Chemical and physical properties of pectins G, H, and J are given in Table 1. Hydrolysis of the three pectin samples gave galacturonic acid (+++), arabinose (++), galactose (++), xylose (+), and rhamnose (+).

Treatment of Pectin A under Conditions of Further Extraction

Samples (ca. 1 g) of pectin A were heated for periods of 40 min in solutions similar to those for the above three extractions. Recovery of the polysaccharide samples gave respectively pectins G′, H′, and J′ which were examined by electrophoresis in pyridine – acetic acid buffer (μ, 5.2, 5.4, and 8.3 × 10^{-5} cm^2 V^{-1} s^{-1}). The decreased methoxyl content [Found: OMe, 5.2%] of pectin J′ also indicated that de-esterification had taken place. The u.v. spectrum of pectin J′ showed significant absorption at 235 mμ indicative of unsaturated uronic acid residues (4) which absorption was absent in pectin A. When a sample of pectin A was heated with a solution of sodium hexametaphosphate in which the p*H* was adjusted to 3.7 the recovered polysaccharide showed no change in electrophoretic mobility (2).

Isolation of Pectin L

Lemon-peel (500 g), which had been exhaustively extracted with cold water, was stirred twice with water (8 000 ml) at 50° for 4 h. The peel was removed by centrifugation and acetone (1.5 volumes) was added to the combined supernatant liquids to give pectin K (12.5 g). Electrophoresis of pectin K in pyridine – acetic acid buffer gave two peaks (μ, 5.4 and 6.2 × 10^{-5} cm^2 V^{-1} s^{-1}) (Fig. 4). The water-extracted peel was extracted twice by stirring with aqueous 2% disodium ethylenediaminetetraacetate (p*H* 5) at 80° for 4 h. The combined aqueous extracts were poured into acetone (1.5 volumes), the precipitate was dissolved in water, and the solution was dialyzed for several days and freeze-dried to give pectin L (62 g). Chemical and physical properties of pectins K and L are given in Table 1. Hydrolysis of pectin L gave galacturonic acid (+++), arabinose (++), galactose (+), and rhamnose (+). A sample of

pectin L was chromatographed on diethylaminoethylcellulose (5) (Fig. 6). Electrophoresis in pyridine – acetic acid buffer gave a single peak (Fig. 5).

The authors wish to acknowledge financial support from the National Research Council of Canada and, during the early stages of the investigation, from Unilever Research Limited. Thanks are also expressed to Dr. C. T. Greenwood and Dr. C. T. Bishop for the provision of facilities for electrophoresis, and to Dr. J. W. T. Craig for assistance in some of the early experiments.

1. G. O. ASPINALL, J. W. T. CRAIG, and J. L. WHYTE. Carbohyd. Res. **7**, 442 (1968).
2. R. W. STODDART, A. J. BARRETT, and D. H. NORTHCOTE. Biochem. J. **102**, 194 (1967).
3. P. ALBERSHEIM, H. NEUKOM, and H. DEUEL. Arch. Biochem. Biophys. **90**, 46 (1960).
4. B. VOLLMERT. Makromol. Chem. **5**, 110 (1950).
5. H. NEUKOM, H. DEUEL, W. J. HERI, and W. KUNDIG. Helv. Chim. Acta, **43**, 64 (1960).
6. G. O. ASPINALL, I. W. COTTRELL, J. A. MOLLOY, and M. UDDIN. Can. J. Chem. This issue.
7. D. A. REES. Advan. Carbohyd. Chem. **24**, in press (1969).
8. E. L. HIRST, D. A. REES, and N. G. RICHARDSON. Biochem. J. **95**, 453 (1965); D. A. REES and N. G. RICHARDSON. Biochem. **5**, 3099 (1966).
9. G. O. ASPINALL and J. A. MOLLOY. J. Chem. Soc. (*C*), 2994 (1968).
10. G. O. ASPINALL, J. A. MOLLOY, and J. W. T. CRAIG. Can. J. Biochem. **47**, 1063 (1969).
11. T. BITTER and H. M. MUIR. Anal. Biochem. **4**, 330 (1962).
12. D. M. W. ANDERSON. Talanta, **2**, 73 (1959).
13. M. DUBOIS, K. A. GILLES, J. K. HAMILTON, P. A. REBERS, and F. SMITH. Anal. Chem. **28**, 350 (1956).
14. P. A. SANDFORD and H. E. CONRAD. Biochem. **5**, 1508 (1966).

Can. J. Chem. Downloaded from www.nrcresearchpress.com by 210.87.254.6 on 09/05/12
For personal use only.

Can. J. Chem. Downloaded from www.nrcresearchpress.com by 210.87.254.40 on 09/05/12
For personal use only.

Lemon-peel pectin. III. Fractionation of pectic acids from lemon-peel and lucerne

G. O. Aspinall and I. W. Cottrell
Department of Chemistry, Trent University, Peterborough, Ontario, Canada

and

J. A. Molloy and M. Uddin
Department of Chemistry, University of Edinburgh, Scotland

Received November 7, 1969

The pectic acids formed on saponification of lemon-peel pectins C and L have been fractionated by graded precipitation with sodium acetate. The results of analytical and electrophoretic studies on the pectic acid fractions have been interpreted as being typical of those of the fractionation of chemically homogeneous polydisperse systems. Similar fractionations of lucerne polysaccharides have indicated the presence of a single component in pectic acid A and of two components in pectic acid B. The nature of polysaccharide heterogeneity in pectic acid preparations is discussed.

Canadian Journal of Chemistry, **48**, 1290 (1970)

Previous investigations (1, 2) have shown that two homogeneous pectins may be isolated from dried lemon-peel. The two pectins show slight differences in uronic acid content and in degrees of esterification and it has been suggested that the higher proportion of non-esterified galacturonic acid residues in pectin L than in pectin C accounts for the differences in ease of extraction from the peel (2). In order to compare the two polysaccharides and to assess the homogeneity of each in respects other than the degree of esterification of galacturonic acid residues, the pectins have been saponified under the mildest possible conditions (3) to give acid-insoluble pectic acids C and L. Similar pectic acids have been prepared from pectins A and B isolated from lucerne (alfalfa) by extraction with disodium ethylenediaminetetraacetate (4) and with water alone (5).

As indicated by the compositions of the parent lemon-peel pectins, analysis showed that pectic acid L contained a higher proportion of galacturonic acid and a correspondingly lower proportion of neutral sugar residues than pectic acid C (see Table 1). Bhattacharjee and Timell (6) have isolated from Amabilis fir bark a polysaccharide preparation which may be separated into a galacturonan and a pectic acid with galacturonic acid as the dominant sugar but with neutral sugars as integral constituents. Zitko and Bishop (7) have similarly interpreted the results of fractionations of various pectic acids by graded precipitation with sodium acetate as indicating the presence of two such polysaccharides in other pectins. Lemon-peel pectic acids C and L were therefore fractionated in the same way in order to see if the differences in composition of the two pectic acids could be accounted for by the presence in each of two polysaccharides, but in different proportions. Similar fractionations have been performed on the lucerne pectic acids.

Lemon-peel pectic acid C was electrophoretically homogeneous in both borate and pyridine – acetic acid buffers. Graded precipitation with sodium acetate gave four polysaccharide fractions and a fifth fraction was obtained by precipitation with ethanol. Table 1 shows some of the properties of these fractions and those from pectic acid L, and Figs. 1–8 show some typical electrophoretic patterns. Pectic acid fractions C 1–5 contained varying proportions of galacturonic acid residues, but all gave neutral sugars on hydrolysis. Pectic acid C 1 with the highest galacturonic acid content (94%) gave on partial hydrolysis acidic oligosaccharides with neutral sugar constituents which were more fully characterized previously from the less rigorously fractionated pectin A (1). Despite differences in composition the pectic acid fractions all gave a single peak of the same mobility on electrophoresis in pyridine – acetic acid buffer (Fig. 1). Similarly all (see Fig. 2) except fraction C 3 (Fig. 3) gave single electrophoretic peaks in borate buffer. This fraction represented ca. 40% of pectic acid C, but for reasons discussed below we consider the detection of two peaks, which were not detected in the unfractionated pectic acid, to be due to causes other than polysaccharide heterogeneity.

Pectic acid C 3 was treated again under the

TABLE 1
Fractionation of lemon-peel pectic acids

Pectic acid fraction	Precipitant (*M*)	Galacturonic acid (%)	$[\alpha]_D^\circ$	Electrophoretic mobility ($\mu \times 10^5$)* in Pyridine – acetic acid buffer	Electrophoretic mobility ($\mu \times 10^5$)* in Borate buffer	% of Parent pectic acid
C		84	+242	13.9	11.8	
C 1	sodium acetate (0.12)	94	+288	14.6	n.d.	5
C 2	sodium acetate (0.14)	88	+265	15.1	10.8	24
C 3	sodium acetate (0.14)	85	+257	15.9	(11.6) 12.3	40
C 4	sodium acetate (0.22)	82	+240	14.9	10.8	12
C 5	ethanol	68	+186	15.3	11.0	8
L		87	+251	14.5	10.9	
L 1*a*	sodium acetate (0.10)	93	+285	n.d.	11.1	5
L 1*b*	sodium acetate (0.12)	89	+278	14.2	11.1	67
L 2	sodium acetate (0.14)	84	+257	14.6	11.1	3
L 3	sodium acetate (0.18)	76	+224	12.3 14.1	9.7 10.6	16

*Figures in parentheses indicate mobilities of minor components.

conditions used for pectin saponification. Although the polysaccharide was recovered in only 50% yield re-examination of the pectic acid by electrophoresis in borate buffer showed a single peak. Selective recovery of one component may have occurred, but we consider it more likely that some unexplained 'aging' phenomenon had been observed. Pectic acid C 3 had been stored as a freeze-dried solid for 3 months before examination in borate buffer. Pectic acid L 1*b* (see Table 1) gave a single peak when a freshly prepared sample was examined by electrophoresis in borate buffer, but on re-examination after 3 months, the sample showed two peaks similar to those observed for pectic acid C 3. No similar multiplicity of peaks was observed on electrophoresis of these pectic acids in pyridine – acetic acid buffer.

Pectic acid L also gave single peaks on electrophoresis in both buffers. Graded precipitation with sodium acetate gave three polysaccharide fractions. The first fraction was sub-fractionated, but fraction L 1*a* with the highest galacturonic acid content (93%) still contained the characteristic neutral sugar constituents. Fraction L 3 gave a second peak on electrophoresis in both buffers (Figs. 4 and 5) indicating the presence of a minor component amounting to approximately 5% of the whole which had not been detected in pectic acid L.

Aside from showing that pectic acid L contains a second minor polysaccharide component, the results from these fractionation experiments point to the presence of single homogeneous polysaccharide components in lemon-peel pectic acids C and L. No evidence was obtained for the presence in either pectic acid preparation of a galacturonan devoid of neutral sugar residues. We consider that the results point to the sub-fractionation of polydisperse systems in which each contains a continuous spectrum of closely-related molecular species. Pectic acids C and L contained slightly different average proportions of galacturonic acid residues, but the analyses of the sub-fractions derived from these preparations indicate a substantial degree of overlap in galacturonic acid content of molecules within each

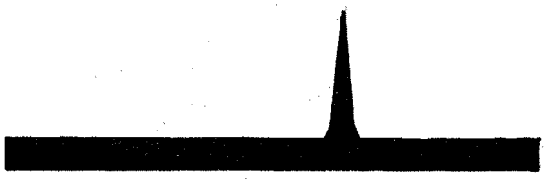

FIG. 1. Electrophoretic pattern of lemon-peel pectic acid C. Buffer: pyridine (1%, v/v) – acetic acid (0.4%, v/v), 220 V, 13 mA, 50 min.

FIG. 2. Electrophoretic pattern of lemon-peel pectic acid C 4. Buffer: 0.05 *M* sodium tetraborate, 150 V, 13 mA, 161 min.

Can. J. Chem. Downloaded from www.nrcresearchpress.com by 210.87.254.40 on 09/05/12
For personal use only.

Can. J. Chem. Downloaded from www.nrcresearchpress.com by 210.87.254.40 on 09/05/12
For personal use only.

FIG. 3. Electrophoretic pattern of lemon-peel pectic acid C 3. Buffer: 0.05 *M* sodium tetraborate, 150 V, 13 mA, 138 min.

FIG. 6. Electrophoretic pattern of lucerne pectic acid B. Buffer: 0.05 *M* sodium tetraborate, 150 V, 13 mA, 141 min.

spectrum of molecular species. Since the parent pectins were distinct polysaccharides with a relatively low degree of overlap when chromatographed on diethylaminoethylcellulose (2) it is probable that the differences between the pectins are due more to differences in degree of esterification than to sugar composition.

Previous studies (4, 5) on the pectic substances from lucerne (alfalfa) have shown that the main pectin component may be extracted with ammonium oxalate or disodium ethylenediaminetetraacetate. This pectin (A), which contains 73% of galacturonic acid residues and has a low degree of esterification (5), is similar to lemon-peel pectin C in having integral neutral sugar constituents. Extraction of lucerne with water alone yields, in addition, small amounts of pectin B which were separated from associated polysaccharides and protein. Pectins A and B were saponified to give the corresponding pectic acids which were sub-fractionated by graded precipitation with sodium acetate to give fractions whose properties are recorded in Table 2.

Pectic acid A gave single symmetrical peaks on electrophoresis in both pyridine – acetic acid and borate buffers. Since pectic acid A contained ca. 81% of galacturonic acid units and previous studies had shown neutral sugars to be integral constituents, it appeared improbable that a galacturonan was present in admixture with a second acidic polysaccharide carrying neutral constituents. Pectic acid fractions A 1 to A 5 had progressively lower proportions (92 to 78%) of galacturonic acid units, all gave neutral sugars on hydrolysis, but electrophoresis in pyridine – acetic acid buffer indicated the presence of single

FIG. 4. Electrophoretic pattern of lemon-peel pectic acid L 3. Buffer: 0.05 *M* sodium tetraborate, 150 V, 13 mA, 122 min.

FIG. 7. Electrophoretic pattern of lucerne pectic acid B 3. Buffer: 0.05 *M* sodium tetraborate, 150 V, 13 mA, 90 min.

FIG. 5. Electrophoretic pattern of lemon-peel pectic acid L 3. Buffer: pyridine (1%, v/v) – acetic acid (0.4%, v/v), 220 V, 13 mA, 68 min.

FIG. 8. Electrophoretic pattern of lucerne pectic acid B 5. Buffer: 0.05 *M* sodium tetraborate, 150 V, 13 mA, 90 min.

TABLE 2
Fractionation of lucerne pectic acids

Pectic acid fraction	Precipitant (*M*)	Galacturonic acid (%)	$[\alpha]_D°$	Electrophoretic mobility ($\mu \times 10^5$)* in Pyridine – acetic acid buffer	Electrophoretic mobility ($\mu \times 10^5$)* in Borate buffer	% of Parent pectic acid
A		81	+239	14.7	12.2	
A 1	sodium acetate (0.12)	92	+268	15.1	(11.0) 11.9	6
A 2	sodium acetate (0.14)	87	+255	14.5	(11.3) 12.0	14
A 3	sodium acetate (0.18)	84	+248	14.9	11.6	9
A 4	sodium acetate (0.22)	83	+244	14.7	12.3	17
A 5	ethanol	78	+236	14.6	(9.5) 11.6	35
B		81	+227	n.d.	(10.5) 11.1	
B 1	sodium acetate (0.12)	94	+267	14.2	11.7	23
B 2	sodium acetate (0.14)	90	+254	n.d.	n.d.	3
B 3	sodium acetate (0.16)	87	+237	n.d.	12.2	13
B 4	sodium acetate (0.18)	83	+230	n.d.	n.d.	1
B 5	ethanol	61	+170	11.9 14.2	10.7 11.6	28

*Figures in parentheses indicate mobilities of minor components.

components of essentially the same mobility in each fraction. The results of electrophoresis in borate buffer were somewhat less simple, but indicated the presence of the same polysaccharide as the sole component of fractions A 3 and A 4, and as the dominant component of fractions A 1, A 2, and A 5. Electrophoresis of pectic acids A 1 and A 2 showed the presence of a shoulder on the trailing side of the main peak. Since these polysaccharide fractions contained higher proportions of uronic acid residues than pectic acids A 3 and A 4 which were electrophoretically homogeneous, we consider it more likely that these shoulders represent artifacts of the type observed in lemon-peel pectic acid C 3 rather than genuine polysaccharide contaminants. In contrast, pectic acid A 5, which was of markedly lower uronic acid content, showed a second component of significantly lower mobility. This second component, however, probably amounted to less than 5% of the total pectic acid preparation.

The presence of two polysaccharide components in lucerne pectic acid B was shown by electrophoresis of the original preparation (Fig. 6). Graded precipitation of the pectic acid afforded three main fractions. The two main fractions (B 1 and B 3) of higher uronic acid content were electrophoretically homogeneous (see Fig. 7) and therefore consisted of a single polysaccharide essentially similar to that in pectic acid A. The second polysaccharide component was concentrated in the third main fraction (B 5) (see Fig. 8) which was of substantially lower acid content. Although pectic acid B 5 was not obtained in sufficient quantity to permit the isolation of the second component, the mode of isolation of the parent pectin and the electrophoretic mobility of the second polysaccharide indicate that it must be acidic. We conclude therefore that pectic acid B consists of two acidic polysaccharides both of which contain neutral sugars but in markedly different proportions.

Our results from the fractionations of pectic acids are in general agreement with those of Zitko and Bishop (7) in that pectic acids of higher galacturonic acid content are preferentially precipitated by sodium acetate. Although no details are supplied of the extraction procedure which was used for the isolation of their sample of citrus pectin from mixed oranges and lemons, fractionation of the derived pectic acid (7) gave surprisingly similar results to those reported in this paper. Two main fractions, amounting to 89% of the total, were electrophoretically homogeneous and contained neutral sugar residues. In this instance we find no compelling reason to support their conclusion that the unfractionated pectic acid consisted of a mixture of two distinct molecular species, one a galacturonan and the other a 'pectic acid' which contained all the neutral sugar residues. On the contrary, we regard those fractionations of pectic acids, such as those of Zitko and Bishop's citrus and apple pectic acids, our citrus pectic acids, and lucerne pectic acid A, which give electrophoretically homogeneous subfractions of differing acid content, as typical of polydisperse systems rather than indicative of chemical heterogeneity.

Can. J. Chem. Downloaded from www.nrcresearchpress.com by 210.87.254.40 on 09/05/12
For personal use only.

Can. J. Chem. Downloaded from www.nrcresearchpress.com by 210.87.254.40 on 09/05/12
For personal use only.

Gibbons (8) has suggested the term *polydisperse* to describe natural polymer preparations in which the variations of all measurable parameters, e.g. relative proportions of neutral and acid units, and degrees of branching, are continuous or *unimodal*. Provided the variation is not great, a sample may be termed homogeneous. The molecules in such a preparation are not identical but constitute statistically a single population. On the other hand, if the variation of any parameter is *bi-* or *poly-modal*, i.e. discontinuous, the preparation is heterogeneous. Inasmuch as two electrophoretically separable components are observable in our unfractionated lucerne pectic acid B, and in the less readily precipitable fractions from lucerne pectic acid A, lemon-peel pectic acid L, and Zitko and Bishop's citrus and apple pectic acids, we consider that it is probable that both polysaccharides contain neutral sugars, but in markedly different proportions. While molecules within each polysaccharide species may be expected to show relatively small but continuous variations in the proportions of neutral and acid sugar residues, the variations in these proportions between polysaccharide species would be discontinuous.

The presently available evidence suggests that pure galacturonans devoid of neutral sugar residues are of infrequent natural occurrence. The pectic acid from sunflower heads (7, 9) is in our opinion the only example of such a galacturonan, which, to date, has been fully authenticated. The galacturonan isolated by Bhattacharjee and Timell (6) from Amabilis fir bark *may* provide a second example. This pectin, however, was extracted from bark which had been treated previously with hot potassium acetate (6). In the light of Barrett and Northcote's observations that homogeneous apple pectin may be degraded on heating with phosphate buffer at p*H* 6.8 to give two structurally dissimilar degraded polysaccharides, one of them a galacturonan (10), the occurrence of a native undegraded galacturonan in Amabilis fir bark remains open to doubt.

Experimental

The general experimental procedures were as described in Part II (2). Lemon-peel pectins C and L were isolated as described in Part II (2). Since previous investigations (4, 5) had shown no discernible differences between corresponding polysaccharide fractions isolated from lucerne leaves and stems, lucerne pectin A was isolated as ammonium pectinate after extraction of the whole plant with disodium ethylenediaminetetraacetate (4). Water-extracted lucerne leaf polysaccharide fractions 5–9 and stem polysaccharide fractions 5–8 (5) were combined as lucerne pectin B.

Saponification of Lemon-peel Pectin C and Fractionation of Pectic Acid C

Sodium hydroxide (1 *N*) was added dropwise with stirring to pectin C (20 g) in water (2000 ml) at 0° until p*H* 12 was reached. The solution was kept at 0° for 2 h while the p*H* was maintained at 12. Aqueous 18% hydrochloric acid was added dropwise with stirring to the clear solution. When precipitation of polysaccharide was complete the pectic acid gel was squeezed through a linen cloth and washed successively with ethanol–water (3:2, containing 5 ml of concentrated hydrochloric acid per l), ethanol–water (3:2), ethanol, and ether. The polysaccharide was dispersed in water and freeze-dried to give pectic acid C (15.3 g) (see Table 1). The supernatant liquid was poured into ethanol (5 volumes), and the precipitate was removed by centrifugation, washed with ethanol–water (3:2), dissolved in water, and freeze-dried to give acid-soluble polysaccharide (0.4 g), $[\alpha]_D$ + 100° (*c*, 0.31) [Found: uronic acid residues (method *i*), 36%], which gave galactose and arabinose as the main neutral sugars with traces of xylose and rhamnose.

Pectic acid C (14 g) was dissolved by dispersion in water (1400 ml) followed by the addition of *N* sodium hydroxide to give a solution of p*H* 6.5. Sodium acetate (2 *M*, 90 ml) was added with vigorous stirring and the solution was kept at 0° for 18 h. The resulting precipitate was removed by centrifugation and washed with 0.12 *M* sodium acetate. The sodium pectate was dissolved in water and precipitated as pectic acid by the addition of acidified ethanol (1 volume; containing 4% of acetic acid). The precipitate was removed by centrifugation, washed free of acetic acid with ethanol–water (1:1), dispersed in water, and freeze-dried to give pectic acid C 1 (0.7 g). Pectic acid fractions C 2 (3.3 g), C 3 (5.6 g), and C 4 (1.7 g) were isolated in a similar manner after precipitation of the sodium pectates by the further addition of 2 *M* sodium acetate (10, 20, and 20 ml) to the supernatant liquids from the previous precipitations. Addition of more sodium acetate gave no further precipitates and pectic acid fraction C 5 (1.2 g) was isolated after addition of ethanol (1 volume) to the final aqueous solution. The pectic acid fractions were analyzed for galacturonic acid content (methods *i* and/or *ii*), the specific rotations of the sodium salts were determined, and the electrophoretic mobilities were determined (for summary of results see Table 1). Hydrolysis of all pectic acid fractions gave galacturonic acid as the main component together with small amounts of galactose, arabinose, rhamnose, and xylose.

Further Electrophoretic Examination of Pectic Acid Fractions

Electrophoresis of pectic acid C 3 in borate buffer (Table 1) showed two peaks, whereas only one peak was shown by pectic acid fractions C 2 and C 4 in the same buffer. Both peaks were observed when mixtures of fractions C 2 + C 3, and C 3 + C 4 were examined by electrophoresis in borate buffer. The electrophoretic patterns showed that the faster-moving component of fraction C 3 corresponded to the single components of both

fractions C 2 and C 4. The parent pectic acid was 'reconstituted' by admixture of the fractions and electrophoresis showed the presence of the slower-moving component from fraction C 3 which had not been observed in the original pectic acid C. Since electrophoresis in borate buffer was carried out 3 months after electrophoresis in pyridine – acetic acid buffer, an 'aging' phenomenon was suspected, but reexamination of fraction C 3 in the latter buffer again showed a single symmetrical peak. A sample of pectic acid C 3 was re-saponified as described previously and electrophoretic examination of the regenerated pectic acid (recovered in 50% yield) in borate buffer then showed a single peak corresponding to the peaks given by fractions C 2 and C 4.

Partial Acid Hydrolysis of Pectic Acid C 1

Pectic acid C 1 (500 mg) was hydrolyzed with *N* sulfuric acid on a boiling-water bath for 5.5 h. Acidic sugars were fractionated as described previously [for pectin C (2)] by chromatography on diethylaminoethyl-Sephadex A-25 (formate form). Sugars with the mobilities of galacturonic acid, 2-*O*-(galactopyranosyluronic acid)rhamnose, 4-*O*-(glucopyranosyluronic acid)fucose, 6-*O*-(glucopyranosyluronic acid)galactose, galacturonobiose, and galacturonotriose were detected by paper chromatography.

Lemon-peel Pectic Acid L

Saponification of pectin L (20 g), as described above, afforded pectic acid L (18.5 g) and acid-soluble polysaccharide (0.4 g), $[\alpha]_D$ +36° (*c*, 0.48) [Found: uronic acid residues (*i*), 28%]. Pectic acid L was fractionated by graded precipitation with sodium acetate as described for pectic acid C to give pectic acid fractions L 1 (13.2 g), L 2 (0.5 g), and L 3 (2.75 g) which were precipitated respectively with 0.12, 0.14, and 0.18 *M* sodium acetate. Fraction L 1, which had $[\alpha]_D$ +279° (*c*, 0.30; as sodium salt) [Found: uronic acid residues (*i*), 90%], was refractionated to give fractions L 1*a* (0.8 g) and L 1*b* (12 g) which were precipitated with 0.10 and 0.12 *M* sodium acetate. Hydrolysis of all pectic acid fractions gave galacturonic acid as the main component together with small amounts of arabinose, galactose, and rhamnose. Analyses for uronic acid content, specific rotations of the sodium salts, and electrophoretic mobilities of freshly prepared pectic acids are shown in Table 1. Reexamination by electrophoresis in borate buffer of a sample of pectic acid L 1*b*, which had been stored as a freeze-dried solid for 3 months, showed two peaks in addition to the single peak observed in the freshly prepared sample.

Lucerne Pectic Acid A

Saponification of pectin A (10 g) furnished pectic acid A (8.3 g). Pectic acid A (8 g) was fractionated to give pectic acid fractions A 1 (0.45 g), A 2 (1.1 g), A 3 (0.7 g), A 4 (1.38 g), and A 5 (2.3 g), which were precipitated respectively with 0.12, 0.14, 0.18, and 0.22 *M* sodium acetate, and with ethanol. All fractions gave on hydrolysis galacturonic acid as the main component, together with small amounts of galactose, arabinose, rhamnose, and xylose. Analyses and physical constants are shown in Table 2.

Lucerne Pectic Acid B

Pectin B (3.4 g) was dissolved in water (400 ml) and insoluble material (0.23 g, largely protein) was removed by centrifugation. Saponification of the soluble pectin furnished pectic acid B (2.4 g) and acid-soluble polysaccharide (0.14 g), $[\alpha]_D$ +86° (*c*, 0.4) [Found: uronic acid residues (*i*), 38%]. Fractionation of pectic acid B (2 g) gave pectic acid fractions B 1 (0.45 g), B 2 (0.05 g), B 3 (0.25 g), B 4 (1.016 g), and B 5 (0.55 g), which were precipitated respectively with 0.12, 0.14, 0.16, and 0.18 *M* sodium acetate, and with ethanol. All fractions gave on hydrolysis galacturonic acid as the main component, together with small amounts of galactose, arabinose, rhamnose, and xylose. Analyses and physical constants are shown in Table 2.

The authors wish to acknowledge financial support from the National Research Council of Canada and, during the early stages of the investigation, from Unilever Research Limited and the United States Department of Agriculture. Thanks are also expressed to Dr. C. T. Greenwood and Dr. C. T. Bishop for the provision of facilities for electrophoresis.

1. G. O. Aspinall, J. W. T. Craig, and J. L. Whyte. Carbohyd. Res. **7**, 442 (1968).
2. G. O. Aspinall and I. W. Cottrell. Can. J. Chem. This issue.
3. C. Hatanaka and J. Ozawa. Nippon Nogei Kagaku Kaishi, **40**, 421 (1966); C.A. **66**, 91876 (1966).
4. G. O. Aspinall, B. Gestetner, J. A. Molloy, and M. Uddin. J. Chem. Soc. *C*, 2554 (1968).
5. G. O. Aspinall and J. A. Molloy. J. Chem. Soc. *C*, 2994 (1968).
6. S. S. Bhattacharjee and T. E. Timell. Can. J. Chem. **43**, 758 (1965).
7. V. Zitko and C. T. Bishop. Can. J. Chem. **43**, 3206 (1965).
8. R. A. Gibbons. Nature, **200**, 665 (1963).
9. V. Zitko and C. T. Bishop. Can. J. Chem. **44**, 1275 (1966).
10. A. J. Barrett and D. H. Northcote. Biochem. J. **94**, 617 (1965).

Can. J. Chem. Downloaded from www.nrcresearchpress.com by 210.87.254.40 on 09/05/12
For personal use only.

Can. J. Chem. Downloaded from www.nrcresearchpress.com by 210.87.254.6 on 09/05/12
For personal use only.

Solvation differences in the hydrolysis of certain alicyclic bromides[1]

H. S. GOLINKIN,[2] D. M. PARBHOO,[3] AND R. E. ROBERTSON[4]
Division of Chemistry, National Research Council of Canada, Ottawa, Canada

Received November 3, 1969

A detailed study of the hydrolysis in water of the *cis* and *trans* cyclopentyl and cyclohexyl bromohydrins reveals significant differences in the apparent heat capacity of activation ($\Delta C_p^{\ddagger}$). The *cis* isomers have values of $\Delta C_p^{\ddagger} \simeq 68 \pm 6$ cal deg^{-1} mole^{-1}; the same value as found for cyclopentyl bromide, but more negative by 10 cal deg^{-1} mole^{-1} than that found for the hydrolysis of cyclohexyl bromide. By contrast, the corresponding value for *trans* isomers was about -45 cal deg^{-1} mole^{-1}. The differences in $\Delta C_p^{\ddagger}$ can be explained in terms of different mechanisms. Secondary β-deuterium isotope effects of 2.28 for the *cis*-2-bromocyclopentanol-1-*d* and 2.45 for *cis*-2-bromocyclohexanol-1-*d* confirm hydrogen participation in these cases. The corresponding ketones were the only products detected.

Canadian Journal of Chemistry, **48**, 1296 (1970)

Introduction

In a recent paper, Blandamer and co-workers (1) reported a study of the effect of substituting —OH, —OMe, and —SMe on the mechanism of hydrolysis of alkyl halides in water and on the accompanying solvent reorganization. Particular attention was given to the latter as indicated by the temperature coefficient of $\Delta H^{\ddagger}$ ($\Delta C_p^{\ddagger}$). In one sense, the present paper represents an extension of this earlier study of the alicyclic systems, but the more rigid structure of the cyclic compounds, cyclopentyl and cyclohexyl bromohydrin, and the new and different mechanistic alternatives available to *cis* and *trans* conformers introduce factors in the activation process which were not present, or were present but to a limited degree, in the corresponding straight-chain compounds.

For the *trans* chloro conformers, Mousseron and co-workers (2, 3) propose a mechanism

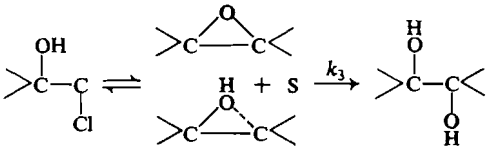

where S is solvent, while that for the *cis* conformers involved hydrogen participation, hydrogen transfer, and the loss of a proton from the hydroxyl group

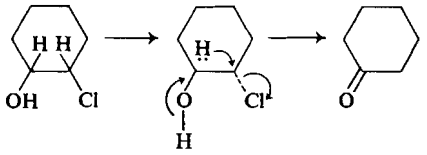

We accepted their findings as a general framework of reference. Hence our problem, aside from those attending the kinetic study, was to attempt to account for the determined values of $\Delta C_p^{\ddagger}$ in terms of our working hypotheses.

Experimental

trans-2-Bromocyclopentanol

The compound was prepared according to the general method used by Winstein and Buckles (4) by the addition of N-bromosuccinimide to cyclopentene; b.p. 41–48 °C at 1 mm.

Anal. Calcd. for C_5H_9OBr: C, 36.39; H, 5.50; Br, 48.42. Found: C, 36.02; H, 5.73.

cis-2-Bromocyclopentanol

Bromopentanone was prepared by the addition of bromine in chloroform to cyclopentanone (5). The crude mixture of bromopentanones in ethereal solution was added dropwise to a slight excess of $LiAlH_4$ in ether cooled with Dry-Ice – MeOH mixture. The product was recovered by the usual method to give a product, b.p. 40–44 °C at 1 mm. This material did not give a linear first-order plot on hydrolysis, hence the 18 g of product was added to 50 ml water at 90 °C with stirring for 10 min; 2.9 g of the bromopentanone was recovered and passed through Al_2O_3 (Fisher for Adsorption); this material showed acceptable kinetic purity; b.p. 49–51 °C at 7 mm.

trans-2-Bromocyclohexanol

This was a very pure sample supplied by Dr. R. A. A. B. Bannard of the National Defence Research Laboratories.

cis-2-Bromocyclohexanol

The same method was followed as for the C-5 compound. The product was stirred for 1½ h with 750 ml of 0.1% Na_2CO_3 to destroy the *trans* isomer.

---

[1]NRCC No. 11 176.
[2]Postdoctorate Fellow, 1966-1968.
[3]Postdoctorate Fellow, 1967-1969.
[4]Present address: Department of Chemistry, The University of Calgary, Calgary, Alberta.

TABLE 1

Empirical constants for the rate–temperature relation defined by eq. [1]

Compound	$-A$	$-B$	C	$n_{T_1}^{T_2*}$
Cyclopentyl bromide	9 722.079	32.273_8	110.6865	47_{50}^{75}
cis-Bromocyclopentanol	10 455.0154	33.5433	112.3863	40_{50}^{86}
trans-Bromocyclopentanol	8 774.5361	22.0975	77.9905	37_{50}^{90}
Cyclohexyl bromide	9 723.659	28.696_0	98.02657	$41_{27.5}^{70}$
cis-Bromocyclohexanol	11 489.689	34.3886	114.8969	38_{54}^{78}
trans-Bromocyclohexanol	8 951.000	19.879	72.0511	63_{60}^{100}

*n gives the number of replicate runs at a given temperature. T_2 and T_1 indicate the upper and lower limits of the experimental temperature range.

Anal. Calcd. for $C_6H_{11}OBr$: C, 40.24; H, 6.19; Br, 44.63. Found: C, 40.42; H, 6.13; Br, 44.68.

cis-2-Bromocyclopentanol-1-d and cis-2-Bromocyclohexanol-1-d

The same method was used as for the protium compounds, with the exception that $LiAlD_4$ was used in the reduction of the ketone and the excess was destroyed with D_2O.

Anal. Calcd. for C_5H_8ODBr: C, 36.17; H, 4.86; Br, 48.12. Found: C, 36.02; H, 4.8; Br, 48.3; D, 0.95 mole/mole.

Anal. Calcd. for $C_6H_{10}ODBr$: C, 40.00; H, 5.59; Br, 44.36. Found: C, 40.20; H, 5.4; Br, 44.0; D, 0.91 mole/mole.

Kinetic Procedure

In all cases, satisfactory conformance of the hydrolysis rates to first-order linearity was regarded as the test for acceptable purity of the compounds used for kinetic studies. Rate determinations, temperature control and measurement, and calculations were the same as used previously in this laboratory (6, 7). The reaction solutions were made up in distilled water by dispersing about 2 μml of the solute on Kieselguhr and adding the latter to 50 ml distilled water containing 0.001 *M* KBr as backing electrolyte. After shaking, this reaction mixture was forced into the reaction cells through a suitable filter.

Product Analysis

The fact that the *trans*-glycol results from the hydrolysis of the *trans*-halohydrins had been established by Mousseron and co-workers (2) for hydrolysis in 50/50 dioxane–water. This was accepted as the course of reaction here, where reaction conditions favoring the *trans*-glycol were more favorable. Since Mousseron proposed a mechanism involving hydrogen participation for the *cis* compound, product analysis under our conditions was considered significant. Fifty μml of the *cis*-2-Br-pentanol and of the *cis*-2-Br-hexanol were dissolved in 2 ml water. The mixture was stirred at 65 °C for 12 half-lives and then extracted 10 times with 1 ml of methylene chloride. The extract was analyzed by gas–liquid chromatography, using an 8.5 ft × 1/4 in. (i.d.) column of 40% duodecylphthalate on Chromosorb W at 120 °C, flow rate 100 ml min^{-1}. Control experiments indicated 95–100% ketone product. This result is in agreement with the results reported by Mousseron for the solvolysis of the corresponding chloride in 50/50 dioxane–water (2).

Rate Data

The rate data obtained for this series showed a temperature dependence which, consistent with past experience, could be fitted to an equation of the form

$$[1] \qquad \log k = A/T + B \log T + C$$

using the transformations previously described (7). The corresponding constants determined by the least-mean-squares method are given in Table 1. The smoothed rates calculated from these temperature–rate relationships agreed in all cases with the determined values within experimental reproducibility.[5]

By making the usual assumptions with respect to the differentiability of log k with respect to T, and accepting as valid the formalism of transition-state theory and the further assumption that $d\Delta C_p^*/dT = 0$, the quasi-thermodynamic parameters characterizing the hydrolysis of these compounds can be derived. These are given in Table 2. We do not intend to imply that $d\Delta C_p^*/dT$ actually is negligible (e.g. see ref. 8), but rather, for the purpose of this paper, we choose to regard it so. In any case, if $d\Delta C_p^*/dT \neq 0$, the value of ΔC_p^* at the mid temperature range will be the same as if we assumed $d\Delta C_p^*/dT = 0$. From Table 2, it will be readily apparent how the calculated errors in the derived terms increase for temperature removed from the midpoint of the experimental range.

Discussion

With the exception of *cis*-2-Br-cyclohexanol, we find the qualitative effect of a *cis* and *trans* —OH substituent for hydrolysis of the bromide in water gives rise to the same pattern of rates as was reported earlier by Mousseron and co-workers (2) for solvolytic displacement of the corresponding —Cl in the poorer ionizing medium 50/50 dioxane–water. Quantitative differences exist, as will be apparent from a comparison

[5]The experimental rates have been placed in the Depository of Unpublished Data. Photocopies may be obtained free of charge, upon request, from: Depository of Unpublished Data, National Science Library, National Research Council of Canada, Ottawa, Canada.

Can. J. Chem. Downloaded from www.nrcresearchpress.com by 210.87.254.6 on 09/05/12
For personal use only.

Can. J. Chem. Downloaded from www.nrcresearchpress.com by 210.87.254.6 on 09/05/12
For personal use only.

TABLE 2

Quasi-thermodynamic parameters for the hydrolysis of a series of cyclic halides

	Compound	Temperature (°C)	$\Delta G^{\ddagger}$ (cal mole^{-1})	$\Delta H^{\ddagger}$ (cal mole^{-1})	$\Delta S^{\ddagger}$ (cal deg^{-1} mole^{-1})	$-\Delta C_p^{\ddagger}$ (cal deg^{-1} mole^{-1})	10^6k, 50 °C (s^{-1})
1	Cyclopentyl bromide	35	23 299 ± 0.4	23 498 ± 11	0.84 ± 0.04	68 ± 1	1269
		50	23 251 ± 0.8	22 475 ± 28	−2.40 ± 0.09		
2	*cis*-2-Bromocyclopentanol	50	25 104 ± 1.3	25 670 ± 42	1.75 ± 0.18	69 ± 3	70.84
		70	25 111 ± 0.9	24 297 ± 19	−2.37 ± 0.05		
3	*trans*-2-Bromocyclopentanol	50	25 791 ± 1	25 319 ± 44	−1.4 ± 0.13	46 ± 2	24.34
		70	25 848 ± 0.7	24 399 ± 13	−4.22 ± 0.04		
4	Cyclohexyl bromide	50	24 991 ± 0.4	25 422 ± 8	1.33 ± 0.02	59 ± 1	84
		70	25 000 ± 0.8	24 245 ± 28	−2.2 ± 0.08		
5	*cis*-2-Bromocyclohexanol	50	25 807 ± 2.6	26 405 ± 121	1.85 ± 0.4	70 ± 7	23.83
		70	25 812 ± 0.8	25 000 ± 31	−2.37 ± 0.09		
6	*trans*-2-Bromocyclohexanol	50	27 148 ± 4	27 549 ± 84	1.24 ± 0.34	42 ± 3	2.93
		70	27 149 ± 0.8	26 304 ± 16	−1.25 ± 0.09		

Can. J. Chem. Downloaded from www.nrcresearchpress.com by 210.87.254.6 on 09/05/12
For personal use only.

TABLE 3
Comparison of rates of hydrolysis of a series of alicyclic halides (X)

Compound RX	Relative rate, X = Cl (50/50 dioxane/water, 100 °C)	Relative rate, X = Br (Water, 50 °C)
Cyclohexyl X	100	100
-*trans* —OH	58	3
-*cis* —OH	133	28
Cyclopentyl X	100	100
-*trans* —OH	9	2
-*cis* —OH	32	6

of the relative effectiveness of the —OH substitutions, in Table 3.

The substitution of —OH on a carbon adjacent to a center from which a halogen is to be displaced introduces both steric and inductive considerations, the latter resulting in a rate reduction of about 10^{-2} (9). For *trans* substitution, the rate reduction for the hydrolysis of cyclohexyl bromide is about the same (1/30) as was found for 2-bromoethanol (1), suggesting that, while the presence of the —OH might forestall rearside nucleophilic attack of water, leading to the *cis* glycol, anchimeric assistance as such was small. Under the somewhat poorer ionizing conditions used by Mousseron (2, 3) the importance of neighboring-group effects became accentuated and the retarding inductive effect of the *trans* —OH was largely cancelled out in the cyclohexyl case, but to a much lesser degree in the cyclopentyl series. In the latter, anchimeric assistance is much less important in the activation process. In neither example was there evidence of strong internal nucleophilic interaction as was found in the acetolysis for *trans*-acetoxy (10) or the *trans* chloro, bromo, and iodo tosylates (11). The question of anchimeric effects on relative rates has been discussed repeatedly in the past (9, 12). In this respect, the present work merely provides further quantitative data for a particular system, supplementing earlier work by Winstein and his co-workers. In one respect there is a difference which may be unique for hydrolysis in aqueous systems. Thus, in the acetolysis of cyclohexyl *p*-Br-benzenesulfonate, it is normal to expect β-substituents to reduce the rate, the effect being greater for the *cis* than for the *trans* if there is any possibility of participation. Thus, $k_H = 1$; k_{trans}(-2-OAc) = 0.30; k_{cis}(-2-OAc) = 4.5×10^{-4} (11). For acetolysis of the *cis*- and *trans*-$OSO_2C_6H_4Br$, where participation is unlikely, k_s/k_H ($k_s = k$ substituted) is about 7×10^{-5} in both cases (10). A very different relationship is apparent in Table 3. Mousseron and co-workers attribute the enhanced rates for the *cis*-OH substituted compounds to hydrogen participation, analogous to that found by Winstein and Takahashi (12) for the solvolysis of 3-methyl-2-butyl tosylate in acetic acid.

It is not unexpected that this alternative mechanism gives evidence of enhanced anchimeric effects for displacement from cyclohexyl compared to cyclopentyl. The cyclopentyl system is more readily activated, hence will be less affected by supplementary assistance. This differential behavior will be more apparent in the poorer ionizing solvent, where greater charge separation is required at the transition state.

In both series, the corresponding ketones were the only products reported by Mousseron (2, 3) for the hydrolysis of the *cis*-OH chloro compounds. We have shown by gas–liquid chromatography that the same ketones are the only products obtained for the hydrolysis of the corresponding bromides in water.

To confirm the postulate of β-hydrogen participation advanced by Mousseron, we synthesized the corresponding deuterated compounds and found the rate constant at 67.5 °C to be 2.44×10^{-4} s^{-1}, leading to a value of $k_H/k_D = 2.28$, for the cyclopentyl compounds. The corresponding rate for the *cis*-cyclohexyl bromohydrin was $k_{67.5} = 8.06 \times 10^{-5}$ s^{-1}, resulting

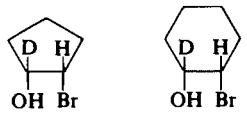

in a value of $k_H/k_D = 2.45$. The first ratio represents about the same degree of hydrogen participation as was found by Winstein and Takahashi (12) for the solvolysis of 3-methyl-2-butyl tosylate in acetic acid, and as found by Inomoto and co-workers (13) for the hydrolysis of the corresponding mesylate in water. It is worth noting that acceleration of the rate of hydrolysis by an electron-withdrawing substituent appears to be a property of the cyclic series (contrast the rate reduction of 1/30 for 2-bromoethanol (1)) and of —OH compared to such substituents as AcO^-, Br^-, Cl^-, and $OSO_2C_6H_5Br$ (9); hydrogen

Can. J. Chem. Downloaded from www.nrcresearchpress.com by 210.87.254.6 on 09/05/12
For personal use only.

participation does not seem to be brought about by any of the latter. Further contrast is provided by the fact that in the acetolysis of 3-Me-2-butyl tosylate and in the hydrolysis of the corresponding mesylate, hydrogen participation seems to be brought about by the electron-releasing 3-methyl group. When displacement occurs at a secondary carbon atom, judging from the rate ratio of hydrolysis, k(*n*-propyl)/k(isobutyl) = 1.5 (for the iodide (14)), no similar enhancement is induced for displacement from a primary carbon. This rate data does not exclude the above possibility but rather indicates that S_N2 nucleophilic displacement is the preferred mode of reaction. The elaboration of these differences is postponed until data from allied systems and for hydrolysis in D_2O are available.

The relation of the observed $\Delta C_p^{\ddagger}$ values to the probable contributions from solvent reorganization and to the above indications of mechanistic change seem relatively straightforward.

The more negative value of $\Delta C_p^{\ddagger}$ normally found for those molecules which react by a so-called ionizing mechanism (S_N1), compared to the value of this coefficient found for those compounds reacting by an S_N2 mechanism, is attributed to the requirement for a more extensive disruption of the solvent about the forming cation at the first transition state (15). There we may assume that the exothermic solvation of the anion has proceeded to some indeterminate degree from the well-known sensitivity of such reactions to the ionizing properties of the solvent medium (16). As a working hypothesis, we assume that the level of charge on the quasi-cation at the transition state for the S_N1 reaction will be such that

$$\text{water–water interaction} = \text{water–anion interaction}$$

Accordingly, where charge is distributed over a large ion (e.g. *t*-butyl, cyclobutonium) extensive solvent disruption would be expected at the transition state and reflected in larger negative values of $\Delta C_p^{\ddagger}$ and more positive values of $\Delta S^{\ddagger}$ (6).[6] While we feel relatively confident with respect to the first inference, the second is less certain, and it is just on this point that the Albery and Robinson deduction (15), as extended and developed by Scott (17), may very well contribute in an important way to our understanding of the apparent values of the derived quasi-thermodynamic parameters. Where charge development on the cation is more localized, we anticipate that the transition state will be reached at a lower net charge separation; in a series of solvents of differing ionizing power, such compounds will show a lesser dependency on the ionizing properties of the solvent. It follows that for solvolysis in water, the contribution to the observed $\Delta C_p^{\ddagger}$ values arising from solvent reorganization will be less negative than for cations which are larger and hence have the effect of charge development more dispersed (20). An examination of the $\Delta C_p^{\ddagger}$ values derived from the temperature dependence of the rates of hydrolysis for the compounds reported in this study show that cyclopentyl bromide, *cis*-bromocyclopentanol, and -cyclohexanol have $\Delta C_p^{\ddagger}$ values about -68 cal deg^{-1} mole^{-1}. Cyclohexyl bromide has a somewhat more positive value (-59 cal deg^{-1} mole^{-1}), about the same as found for the hydrolysis of 2-bromopropane (18).

To understand the mechanistic significance of these indications of similarity with respect to the extent of solvent reorganization in the activation process, it is necessary to examine briefly the implications of β-deuterium substitution on the same rates of hydrolysis. We have already noted that in the case of the *cis*-cyclopentyl and -cyclohexyl halohydrins, a relatively large secondary deuterium isotope effect was determined in such reactions. The overall secondary deuterium isotope effect for the hydrolysis of cyclopentyl 2,2,4,4-d_4 bromide was 1.60 (19). This compares with a value of 1.56 for the hydrolysis of isopropylmethanesulfonate-d_6 and 1.34 for the corresponding bromide (17). Saunders and Finley (21) reported a value of 2.34 for the acetolysis of cyclohexyl 2,2,6,6-d_4 tosylate under conditions where a higher degree of charge separation may be assumed at the transition state. Shiner and Jewett (22) provide proof of hydrogen participation in the solvolysis of the *cis*-4-*t*-butylcyclohexyl brosylate. In their view, "Since this participation is from a secondary hydrogen to an adjacent secondary solvolytic center, it is difficult to conceive of any driving force for it except the formation of a stabilized, bridged, nonclassical intermediate carbonium ion". They calculate that the secondary deuterium isotope effect associated

[6]The assumption that the contribution from this source can be regarded as zero (15) is noted but is not considered here.

Can. J. Chem. Downloaded from www.nrcresearchpress.com by 210.87.254.6 on 09/05/12
For personal use only.

with this bridging hydrogen is $k_H/k_D = 2.2$, comparable to the values determined for the *cis*-halohydrins, but higher than were observed for the more mobile cyclohexyl or cyclopentyl compounds. No similar analysis of secondary deuterium isotope effects has been made for the unsubstituted cyclohexyl or cyclopentyl compounds under our reaction conditions. What the present work shows is that the solvent reorganization as indicated by $\Delta C_p^{\ddagger}$ is about the same for the unsubstituted and for the *cis*-OH compounds, and quite different from the corresponding value found for the *trans*-OH compounds.

The large degree of hydrogen participation accompanying hydrolysis of the *cis*-OH compounds effectively predicates an S_N1 mechanism. In water, we assume that the transition state corresponds to that point where a combination of thermal activation and internal factors (in the present case, H-participation), coupled with some degree of interaction between the solvent and the quasi-anion, results in a critical charge density on the quasi-cation. Localization of the charge near the seat of reaction can result in less solvent reorganization than for a dispersed charge. This is the hypothesis proposed to account for the difference in the value of $\Delta C_p^{\ddagger}$ for cyclobutyl chloride ($\Delta C_p^{\ddagger} = -103$) and cyclopentyl bromide ($\Delta C_p^{\ddagger} = -68$). Supplementary evidence will be required to extend this argument to account for the value of $\Delta C_p^{\ddagger} = -59$ found for the hydrolysis of cyclohexyl bromide. An alternative would be that the more positive value for the latter is evidence of "mixed kinetics". Our conclusion is that the values of $\Delta C_p^{\ddagger}$ for compounds **1**, **2**, **4**, **5** (Table 2) are all characteristic of an S_N1 displacement of Br from a secondary carbon.

The $\Delta C_p^{\ddagger}$ values calculated for the *trans*-cyclohexyl and -cyclopentyl compounds are about the same, and much less negative than values found for the four related compounds noted above. Conformation probably excludes the —OH from having much effect on the water structure about the bromide in the unactivated molecule and so modifying water structure in that area (1). While it seems unlikely that any strong anchimeric interaction is established at the rear of the C-1, it seems highly probable that sufficient interaction occurs between the —OH group and the empty orbital at the rear of C-1 in the activated molecule to exclude either nucleophilic attack or reduce the possibility of hydrogen participation from a β-H. A reasonable alternative, consistent with the fact that the *trans*-bromohydrin leads to the *trans*-glycol, would be nucleophilic displacement of —OH from C_2 to C_1 by water. The $\Delta C_p^{\ddagger}$ then would correspond to that characteristic of an S_N2 displacement reaction, as is found ($\Delta C_p^{\ddagger} = -43$ cal deg^{-1} mole^{-1}). Mousseron and co-workers have proposed that an equilibrium is set up involving the formation of the *cis*-epoxide which reacts to give the *trans*-glycol (3). The double-labelling experiments required to distinguish between these two mechanisms have not yet been done. If the hypothesis advanced by Mousseron proves correct, then the observed value of $\Delta C_p^{\ddagger}$ (which is just about what would be expected for the hydrolysis of a bromide by an S_N2 mechanism) must be regarded as an interesting coincidence.

1. M. J. Blandamer, H. S. Golinkin, and R. E. Robertson. J. Amer. Chem. Soc. **91**, 2678 (1969).
2. H. Bodot, J. J. Jullien, and M. Mousseron. Bull. Soc. Chim. France, 1101 (1958).
3. H. Bodot, J. J. Jullien, and M. Mousseron. Bull. Soc. Chim. France, 1110 (1958).
4. S. Winstein and R. E. Buckles. J. Amer. Chem. Soc. **64**, 2780 (1942).
5. J. V. Machinsbain and A. S. Podberegina. J. Gen. Chem. U.S.S.R. **28**, 1550 (1958).
6. R. E. Robertson. Progr. Phys. Org. Chem. **4**, 213 (1967).
7. R. E. Robertson and S. E. Sugamori. J. Amer. Chem. Soc. **91**, 7524 (1969).
8. L. Treindle, R. E. Robertson, B. Rossall, and S. E. Sugamori. Can. J. Chem. **47**, 4199 (1969).
9. S. Winstein and E. Grunwald. J. Amer. Chem. Soc. **70**, 828 (1948).
10. S. Winstein, E. Grunwald, and L. L. Ingraham. J. Amer. Chem. Soc. **70**, 821 (1948).
11. S. Winstein, R. E. Buckles, and C. Hanson. J. Amer. Chem. Soc. **70**, 816 (1948).
12. S. Winstein and I. Takahashi. Tetrahedron Lett. **2**, 316 (1958).
13. Y. Inomoto, R. E. Robertson, and G. Sarkis. Can. J. Chem. **47**, 4599 (1969).
14. R. E. Robertson and S. E. Sugamori. Unpublished results.
15. W. J. Albery and B. H. Robinson. Trans. Faraday Soc. **65**, 980 (1969).
16. E. D. Hughes. Trans. Faraday Soc. **37**, 603 (1941).
17. J. M. W. Scott. Private communication.
18. R. L. Heppolette and R. E. Robertson. Can. J. Chem. **44**, 677 (1966).
19. R. E. Robertson and S. E. Sugamori. Unpublished results.
20. K. T. Leffek, R. E. Robertson, and S. E. Sugamori. Can. J. Chem. **39**, 1981 (1961).
21. W. H. Saunders and K. T. Finley. J. Amer. Chem. Soc. **87**, 1384 (1965).
22. V. J. Shiner and V. G. Jewett. J. Amer. Chem. Soc. **87**, 1382 (1965).

Can. J. Chem. Downloaded from www.nrcresearchpress.com by 210.87.254.105 on 09/05/12
For personal use only.

Reactions of nitro sugars. XVII. Koenigs–Knorr syntheses[1]

HANS H. BAER, WERNER RANK, AND FRANK KIENZLE
Department of Chemistry, University of Ottawa, Ottawa 2, Canada

Received November 6, 1969

Starting from methyl 3-deoxy-3-nitro-β-D-glucopyranoside (**1**), the free sugar 3-deoxy-3-nitro-α-D-glucopyranose (**2**), its tetraacetate (**3**), and 2,4,6-tri-*O*-acetyl-3-deoxy-3-nitro-α-D-glucopyranosyl bromide (**4**) were prepared. Another sequence of reactions commencing with **1** gave the 6-*O*-trityl (**6**), the 2,4-di-*O*-acetyl-6-*O*-trityl (**7**), the 2,4,6-tri-*O*-acetyl (**8**), and the 2,6-di-*O*-acetyl (**10**) derivatives of **1**, whereas the 2,4-di-*O*-acetyl derivative (**9**) could not be isolated in pure form because of acetyl group migration. Reaction of the bromide **4** with water, methanol, and benzyl alcohol, respectively, led to 2,4,6-tri-*O*-acetyl-3-deoxy-3-nitro-β-D-glucopyranose (**5**) and the corresponding methyl and benzyl β-D-glycosides (**8** and **11**). Condensation of **4** with 1,2,3,4-tetra-*O*-acetyl-β-D-glucopyranose (**12**), and condensation of tetra-*O*-acetyl-α-D-glucopyranosyl bromide (**14**) with the trityl compound **6**, furnished derivatives of gentiobiose having a deoxynitro function at C-3′ (**13**) and C-3 (**15**), respectively.

Canadian Journal of Chemistry, **48**, 1302 (1970)

The synthesis of nitro sugar derivatives and their use as versatile intermediates for preparative purposes has been much investigated in recent years (1, 2). Interest in this class of compounds will doubtless receive further stimulation by the first discovery (3) of a nitro sugar, evernitrose, in nature. Although various aspects of the special reactivity conferred upon sugars by the activating and directing effects of a nitro substituent have already been studied and reviewed (2), certain common reactions widely employed in general carbohydrate chemistry have seldom or not at all been performed with nitro sugars in particular. This applies to the Koenigs–Knorr reaction, one of the most useful methods for the synthesis of glycosides and disaccharides (4). It was felt that an investigation in this area was warranted, with a view to expanding the potential utility of nitro sugars. We report here on the preparation of suitable reactants for, and on the performance of, some Koenigs–Knorr syntheses involving 3-deoxy-3-nitro-D-glucose.

3-Deoxy-3-nitro-α-D-glucose and Some Derivatives

The hitherto unknown reducing sugar 3-deoxy-3-nitro-D-glucose (**2**) was obtained by acid hydrolysis of its methyl β-glycopyranoside (**1**). Although this hydrolysis required more vigorous conditions (6 *N* HCl at 100°) than are ordinarily needed for the cleavage of glycosides, it afforded **2** in high yield and in crystalline form (as the downward-mutarotating α-anomer). In order to verify that no unexpected structural or configurational change had occurred in the reaction, **2** was hydrogenated catalytically, and the crystalline product isolated after *N*-acetylation proved to be identical with the known 3-acetamido-3-deoxy-β-D-glucose.

Boron trifluoride-catalyzed acetylation (5) of **2** gave 1,2,4,6-tetra-*O*-acetyl-3-deoxy-3-nitro-α-D-glucopyranose (**3**). Alternatively, **3** was produced by sulfuric acid-catalyzed acetylation, with concomitant acetolysis, of the glycoside **1**. Treatment of the tetraacetate **3** with hydrogen bromide in glacial acetic acid furnished a 77% yield of 2,4,6-tri-*O*-acetyl-3-deoxy-3-nitro-α-D-glucopyranosyl bromide (**4**), the key compound for the Koenigs–Knorr reactions planned.[2] Debromination of **4** with silver carbonate in aqueous acetone gave crystalline 2,4,6-tri-*O*-acetyl-3-deoxy-3-nitro-β-D-glucopyranose (**5**).

Next, a partially protected nitro sugar having a free hydroxyl group at C-6 was desired as a component for the synthesis of a disaccharide. The glycoside **1** was therefore selectively tritylated on its primary hydroxyl group. The 6-*O*-trityl derivative (**6**), which was obtained without serious difficulties, was to be acetylated and, subsequently, detritylated to give, in turn, methyl 2,4-di-*O*-acetyl-3-deoxy-3-nitro-6-*O*-trityl-β-D-glucopyranoside (**7**) and methyl 2,4-di-*O*-acetyl-3-deoxy-3-nitro-β-D-glucopyranoside (**9**).

[1]For part XVI in this series see ref. 19.

[2]This glycosyl bromide appeared to be quite stable as it could be stored in a desiccator for several weeks without showing signs of decomposition. One attempt was made to prepare it directly from the free sugar **2** by the method of Bárczai-Martos and Körösy (6), but this was unsuccessful, and the tetraacetate **3** was the only product isolated.

Can. J. Chem. Downloaded from www.nrcresearchpress.com by 210.87.254.105 on 09/05/12
For personal use only.

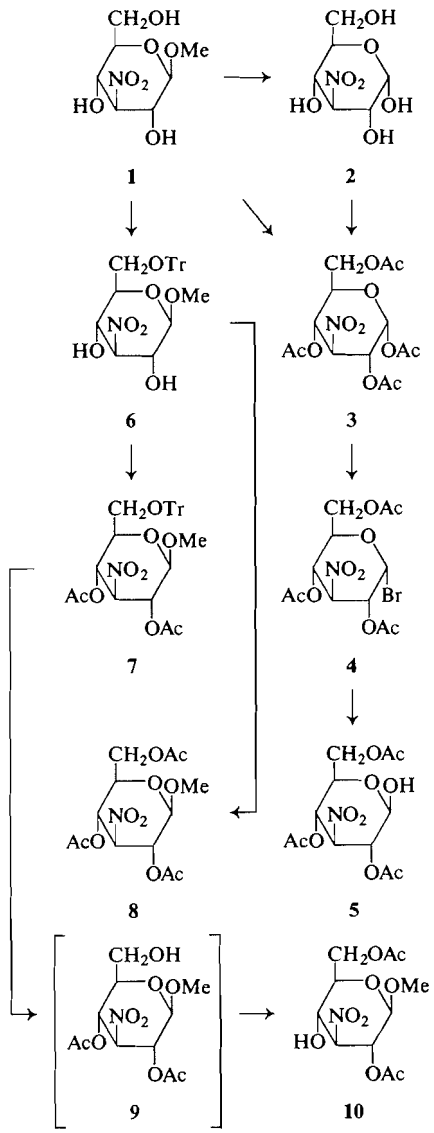

However, acetylation of **6** with acetic anhydride in ether–pyridine at +5°, or with acetic anhydride and sodium acetate at +25°, afforded **7** in moderate yields only and always accompanied by large proportions of an unidentified, yellow by-product. The latter exhibited a strong ultraviolet (u.v.) absorption band at λ_{max} 360 mμ, lacked carbonyl frequencies in the infrared (i.r.), and appeared to possess a nitro group situated on an unsaturated system (ν_{max} 1525 cm^{-1}). It is recalled that in the pyridine-catalyzed acetylation (5) of **1** a similar, yellow by-product arose; the latter was revealed (7) to be an isochromene derivative whose formation was due to a complicated sequence of reactions initiated by an extremely facile dehydroacetylation of the acetylated nitro glycoside. The inference may be drawn that the yellow compound now encountered resulted from an analogous aromatization.

When the trityl ether **6** was acetylated with acetic anhydride containing a catalytic amount of boron trifluoride,[3] the trityl group was split off and the known methyl 2,4,6-tri-*O*-acetyl-3-deoxy-3-nitro-β-D-glucopyranoside (**8**) was produced instead of **7**. A satisfactory way of preparing **7** was eventually found when **6** was treated with acetyl chloride in the presence of triethylamine.

The detritylation of **7** was readily effected by ethereal hydrogen chloride. However, spectral evidence indicated that the crude product obtained, which presumably was the 2,4-diacetate **9**, underwent a structural change during recrystallization. Thus, the *O*-acetyl proton resonances (in $CDCl_3$ solution) were observed at τ 7.92 and 7.97 *before*, but at τ 7.84 and 7.93 *afterwards*, and in the i.r. spectrum the carbonyl stretching absorption changed from a single peak (1730 cm^{-1}) to a double peak (1730, 1750 cm^{-1}). The recrystallized product was methyl 2,6-di-*O*-acetyl-3-deoxy-3-nitro-β-D-glucopyranoside (**10**), resulting from acetyl migration in **9**. Acetyl migrations have long been known to occur in partially acetylated sugars (9), but the great ease of reaction observed in the present case seems noteworthy. The assignment of the 2,6-diacetate structure (**10**) was based on the analysis of ring proton signals in the 100 MHz nuclear magnetic resonance (n.m.r.) spectrum (in $CDCl_3$) of **10**, aided by a comparison of the spectra of the precursors **6** and **7**. In the non-acetylated trityl ether (**6**), the ring proton signal appearing at lowest field (τ 5.50) was a symmetrical triplet (1H) assignable to H-3 ($J_{2,3} = J_{3,4} = 10$ Hz), and the signal following upfield (τ 5.78) was a doublet (1H) due to the anomeric proton ($J_{1,2} = 8$ Hz). In the acetylated trityl ether (**7**), the corresponding 1-proton signals were shifted slightly downfield, to τ 5.30 (H-3; $J_{2,3} = J_{3,4} = 10$ Hz) and τ 5.56 (H-1; $J_{1,2} = 8$ Hz), respectively, and at even lower field there appeared a quartet centered at τ 4.52 and superimposed by a triplet

[3]Glycoside, benzylidene acetal, and ordinary ether linkages had been found (5, 8) to remain unaffected by this reagent.

Can. J. Chem. Downloaded from www.nrcresearchpress.com by 210.87.254.105 on 09/05/12
For personal use only.

at τ 4.50. These two signals (combined intensity, 2H) were attributable to H-2 and H-4, respectively ($J_{1,2}$ = 8 Hz, $J_{2,3}$ = 10 Hz; $J_{3,4} = J_{4,5}$ = 10 Hz). Compound **10** also exhibited a symmetrical triplet (1H) for H-3 at τ 5.32 ($J_{2,3} = J_{3,4}$ = 10 Hz) and a doublet (1H) for H-1 at 5.55 ($J_{1,2}$ = 8 Hz), but farther downfield there was only a single, 1-proton signal (τ 4.65), which indicated that only one of the positions 2 and 4 carried an acetoxyl group. The signal was a quartet assignable to H-2 ($J_{1,2}$ = 8 Hz, $J_{2,3}$ = 10 Hz).

Koenigs–Knorr Reactions

The Koenigs–Knorr reaction of 2,3,4,6-tetra-*O*-acetyl-α-D-glucopyranosyl halides is well-known to proceed with inversion of the anomeric configuration (4). When the "acetobromo" sugar **4** was condensed with methanol in the presence of silver carbonate, the known methyl β-D-glycoside **8** was obtained, and this provided chemical proof for the structure and configuration of **4**. By reaction with benzyl alcohol we also prepared the corresponding benzyl β-D-glycoside **11**, in a yield of 65%. The synthesis of **11** was undertaken in view of its potential usefulness for work requiring a subsequent hydrogenolytic rather than hydrolytic glycoside cleavage.

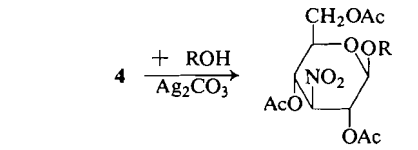

8 R = Me
11 R = CH_2Ph

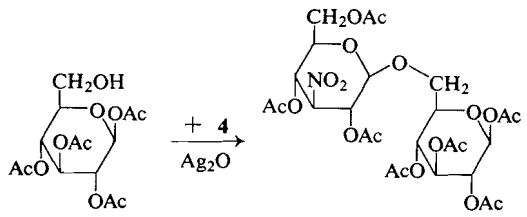

12 **13**

Condensation of **4** with 1,2,3,4-tetra-*O*-acetyl-β-D-glucopyranose (**12**) furnished in 25% yield a 3′-deoxy-3′-nitro derivative of gentiobiose, namely, 6-*O*-(3-deoxy-3-nitro-β-D-glucopyranosyl)-β-D-glucopyranose heptaacetate (**13**). We had planned to synthesize in similar fashion a gentiobiose derivative having a nitro group in the other monosaccharide unit, by condensing tetra-*O*-acetyl-α-D-glucopyranosyl bromide (**14**) with the nitro glycoside 2,4-diacetate **9**. This project had to be postponed when **9** could not be isolated in pure form because of its spontaneous isomerization to **10**. However, an alternate approach to such a disaccharide was successful. It consisted of condensation of the bromide **14** with the trityl ether **6** in nitromethane solution in the presence of silver perchlorate, according to Bredereck and associates (10). We thus obtained in 14% yield a partially acetylated methyl β-glycoside of 3-deoxy-3-nitro-gentiobiose, namely, methyl 6-*O*-(2,3,4,6-tetra-*O*-acetyl-β-D-glucopyranosyl)-3-deoxy-3-nitro-β-D-glucopyranoside (**15**).

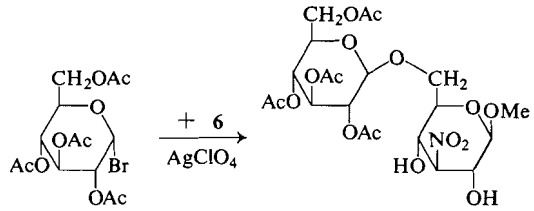

14 **15**

The specific rotations of the new disaccharides **13** and **15** in chloroform solution, $[\alpha]_D$ − 7.8° and −25.6°, respectively, confirm the β-configuration of the 1 → 6 linkages, the corresponding values calculated on the basis of Hudson's rules of isorotation being $[\alpha]_D$ −7.5° for **13** and −18.5° for **15** (see Experimental).

Only a few disaccharides that contain nitro sugars had previously been synthesized. The first one was a sucrose-type compound obtained by nitromethane cyclization (11), and two anomeric methyl glycosides of a 1 → 2 linked disaccharide related to sophorose as well as several 2 → 2 linked methyl glycosides (bisglycosidyl ethers and bisglycosidylamines) have been obtained more recently by way of nucleophilic addition reactions (8, 12).

Experimental

Melting points were taken in capillaries in an electric aluminum block apparatus. Infrared spectra were obtained from Nujol mulls with a Beckman IR-8 instrument, and significant data are reported as ν_{max} values (in cm^{-1}). Nuclear magnetic resonance spectra were taken in chloroform-*d* solution, with internal tetramethylsilane standard, on a Varian HA 100 Spectrometer. Optical rotations were determined at about 25° by use of a Perkin–Elmer 141 automatic polarimeter. Thin-layer chromatography (t.l.c.) was performed on silica gel G

Can. J. Chem. Downloaded from www.nrcresearchpress.com by 210.87.254.105 on 09/05/12
For personal use only.

plates with 2:3 (v/v) ethyl acetate – petroleum ether (b.p. 30–60°), unless otherwise indicated.

3-Deoxy-3-nitro-α-D-glucopyranose (2)

A solution of the nitro glycoside **1** (13, 14) (300 mg) in half-concentrated hydrochloric acid (50 ml) was heated on a steam bath for 1 h. The solution was then evaporated, and the residue was coevaporated several times with water and thereafter recrystallized from ethyl acetate – ether, to give **2** (223 mg, 80.5%). The melting point (169–172°, decomp.) was raised to 176–177° (decomp.) by one recrystallization from acetone–chloroform and then remained constant. $[\alpha]_D$ +99.6° (6 min) → +73.9° (130 min, constant) (*c*, 1.3 in water); ν_{max} (cm^{-1}) 3530, 3340 (OH), 1545 (NO_2), 1140, 1090, and 1050–1010 (four bands).

Anal. Calcd. for $C_6H_{11}NO_7$ (209.2): C, 34.40; H, 5.32; N, 6.70. Found: C, 34.22; H, 5.45; N, 6.60.

When hydrolyses of **1** were attempted with *N* hydrochloric acid or *N* sulfuric acid, the starting material was recovered.

Hydrogenation of 2

A solution of **2** (700 mg) in 0.1 *N* hydrochloric acid (40 ml) was hydrogenated with platinum catalyst (200 mg of PtO_2, prehydrogenated). The uptake of hydrogen (230 ml, ca. 3 molar equiv) was complete after 5 h. Evaporation of the filtered solution yielded a colorless syrup that crystallized upon coevaporation with ethanol. The slightly hygroscopic crystals of *3-amino-3-deoxy-D-glucose hydrochloride* exhibited in paper chromatography[4] one main spot (R_{GN} 1.1) and two very minor contaminants (R_{GN} 0.6 and 2.4). The hydrochloride was *N*-acetylated (14) to give crystalline *3-acetamido-3-deoxy-β-D-glucose*, m.p. 201–203° (decomp.), in a yield of 72% (based on **2**). The i.r. spectrum of the *N*-acetyl derivative was identical with that of an authentic sample (14), and a mixture melting point was 200–202° (decomp.).

1,2,4,6-Tetra-O-acetyl-3-deoxy-3-nitro-α-D-glucopyranose (3)

(a) By Acetylation of 2

The nitro sugar **2** (700 mg) was acetylated (5) with acetic anhydride (14 ml) and boron trifluoride etherate (5 drops). After completion of the reaction (30 min at room temperature), the mixture was evaporated with the addition of several small portions of toluene, and the remaining syrup was crystallized from ethyl acetate – petroleum ether to give **3** (953 mg, 75.6%): m.p. 112–113°; $[\alpha]_D$ +95.5° (*c*, 0.7 in 1,2-dichloroethane); ν_{max} (cm^{-1}) 1770, 1745 (ester C=O), 1558 (NO_2), 1240 and 1215 (all strong), 1035 (broad), 1138, 1100, 952, 896 and 656 (medium).

Nuclear magnetic resonance data: τ 3.58, doublet (H-1) with $J_{1,2}$ = 3.5 Hz; τ 4.45, triplet (H-4) with $J_{3,4}$ = $J_{4,5}$ = 9.8 Hz; τ 4.48, quartet (H-2) with $J_{1,2}$ = 3.5 Hz and $J_{2,3}$ = 10.5 Hz; τ 5.02, triplet (H-3), *J* ca. 10 Hz; τ 5.6–6.0, overlapping multiplets (H-5, H-6,6′); τ 7.82, 7.91, 7.93, 7.99, singlets (acetyl).

Anal. Calcd. for $C_{14}H_{19}NO_{11}$ (377.3): C, 44.56; H, 5.08; N, 3.71. Found: C, 44.80; H, 5.25; N, 3.83.

[4]By the descending technique in ethyl acetate – pyridine – water – acetic acid (5:5:3:1, v/v) according to Fischer and Dörfel (15); R_{GN} = mobility relative to 2-amino-2-deoxy-D-glucose hydrochloride.

(b) By Acetolysis of 1

Sulfuric acid (0.2 ml) was added to a solution of the glycoside **1** (200 mg) in glacial acetic acid (3 ml) and acetic anhydride (3 ml). The mixture was allowed to stand at room temperature. The t.l.c. revealed that, after 3 h, **1** was completely replaced by a product travelling slightly faster than **3**, and that, after 5 days, this product was in turn replaced by **3**.[5] The mixture was then diluted with chloroform, the sulfuric acid was removed by shaking the solution with Dowex-1 X8 (CO_3^{2-} form) anion exchange resin, and the filtrate therefrom was evaporated with several consecutive additions of toluene. The residue was recrystallized from ethyl acetate–petroleum ether to give **3** (226 mg, 67%), m.p. 111–112°, which was identified with **3** from (*a*) by i.r. spectra and a mixture melting point.

2,4,6-Tri-O-acetyl-3-deoxy-3-nitro-α-D-glucopyranosyl Bromide (4)

The tetraacetate **3** (3.90 g) was dissolved in glacial acetic acid (80 ml) that had been saturated at 0° with hydrogen bromide. The reaction mixture was kept at room temperature for 2.5 h. After removal of part of the hydrogen bromide by aeration with a stream of nitrogen, the solution was poured into ice water (1 l). After brisk stirring for 10 min the white precipitate was isolated, washed with cold water, and dried *in vacuo* (24 h at 0.1 mm) over potassium hydroxide. The yield was 3.80 g (92.5%) of **4** showing $[\alpha]_D$ +190.0° (*c*, 0.95 in chloroform) and m.p. 118–119° (unchanged after storage for 3 weeks over KOH). The compound had ν_{max} 1740 (ester C=O), 1565 (NO_2), 1245, 1222, and 1045 (strong), 1115 and 898 (medium), 1160, 1085, 940, 863, and 679 cm^{-1} (moderate or weak).

Nuclear magnetic resonance data: τ 3.30, doublet (H-1) with $J_{1,2}$ = 4 Hz; τ 4.42, triplet (H-4) with $J_{3,4}$ = $J_{4,5}$ = 10 Hz; τ 4.70, quartet (H-2) with $J_{1,2}$ = 4 Hz and $J_{2,3}$ = 10 Hz; τ 5.0–5.9, multiplets (H-3, H-5, H-6,6′); τ 7.90, singlet corresponding to 9 protons (3 acetyl groups).

Anal. Calcd. for $C_{12}H_{16}BrNO_9$ (398.2): Br, 20.07. Found: Br, 20.08.

When the preparation of **4** was attempted by treatment of the free sugar **2** (1.70 g) with acetic anhydride and perchloric acid followed by addition of red phosphorus and bromine, as described (6) for the preparation of **14**, the crude product isolated (1.95 g) contained only 2.7% of bromine. It showed m.p. 105–107° and $[\alpha]_D$ +93.5° (*c*, 0.8 in 1,2-dichloroethane). After recrystallization from ether-pentane it melted at 112° and was free from bromine, and its i.r. and n.m.r. spectra revealed it to be the tetraacetate **3**.

2,4,6-Tri-O-acetyl-3-deoxy-3-nitro-β-D-glucopyranose (5)

The bromide **4** (410 mg) was dissolved in acetone (15 ml), water (10 ml) and silver carbonate (700 mg) were added, and the mixture was stirred for 90 min at room temperature. Upon filtration, partial evaporation, and cooling (1 h at 5°), the solution yielded a white precipitate

[5]Presumably the intermediary product was the glycoside triacetate **8**. This assumption received support when, in a separate experiment, the mixture was worked up after 3 h and found to contain methoxyl (n.m.r. singlet at τ 6.55).

(251 mg), m.p. 165°. Recrystallization from chloroform – petroleum ether gave fine needles with an unchanged melting point. $[\alpha]_D$ +9.6° (5 min) → +14.0° (1 h) → +47.0° (24 h) → +65.5° (72 h) → +70.5° (96 h, constant) (*c*, 1 in methanol); ν_{max} 3525 (OH), 1745 (ester C=O), 1568 (NO_2), 1242, 1220, 1155, 1065, 885 cm^{-1}.

Anal. Calcd. for $C_{12}H_{17}NO_{10}$ (335.3): C, 42.99; H, 5.11; N, 4.19. Found: C, 43.03; H, 5.09; N, 4.03.

Methyl 3-Deoxy-3-nitro-6-O-trityl-β-D-glucopyranoside (6)

Trityl chloride (2.40 g, freshly recrystallized from benzene containing a small amount of acetyl chloride) was added to a solution of the glycoside **1** (1.60 g) in pyridine (15 ml, dried over calcium hydride). After standing for 24 h at room temperature, the reaction mixture was poured into vigorously stirred ice-water to give a white precipitate that became crystalline within 30 min. The dried material was extracted with petroleum ether by repeated, careful trituration, and recrystallized from ethanol to give **6** (2.40 g), m.p. 99–102°. The product was shown by t.l.c. to contain a small amount of triphenylcarbinol. The latter was difficult to remove by recrystallization. An analytical sample was purified by preparative t.l.c. using silica gel HF 254 (E. Merck A.G., Darmstadt). Zone extraction with chloroform furnished pure **6** which was recrystallized once from ethanol–water before analysis. For preparative purposes, the crude material was purified by passage through a column (2.5 cm x 50 cm) of silica gel (70–325 mesh), with the t.l.c. solvent mixture serving as eluant. The fast-moving triphenylcarbinol was thus removed easily, and 2.26 g (65%) of pure **6** was obtained.

When the analytical sample, m.p. 106–107° and $[\alpha]_D$ −39.9° (*c*, 1 in chloroform), was dried *in vacuo* at 25° it retained 1.5 moles of water of crystallization.

Anal. Calcd. for $C_{26}H_{27}NO_7 \cdot 1.5\ H_2O$ (492.5): C, 63.73; H, 5.89; N, 2.51. Found: C, 63.40; H, 5.94; N, 2.81.

The sesquihydrate showed ν_{max} 3300 (OH, broad), 1565 and 1550 (NO_2), and it had a detailed fingerprint spectrum with strong peaks at 1100, 1050, 765, 755, 720, and 705 cm^{-1} (in Nujol). A spectrum in chloroform exhibited a single peak (1560 cm^{-1}) for NO_2. Drying of the sample at 64° caused a loss in weight corresponding to 1.3 moles of water. The i.r. spectrum in Nujol then showed a single, sharp nitro band also (1560 cm^{-1}), but considerable band broadening occurred in the fingerprint region.

Nuclear magnetic resonance data: τ 2.5–2.8, multiplet (trityl); τ 5.50, triplet (H-3) with $J_{2,3} = J_{3,4} = 10$ Hz); τ 5.78, doublet (H-1) with $J_{1,2} = 8$ Hz; τ 6.08, quartet (presumably H-2) with splittings of 8 and 10 Hz; τ 6.25–6.75, multiplets for the remaining ring protons, and singlet (τ 6.47) for OCH_3. There were broad signals in the τ 7 region (OH) which disappeared on deuterium exchange.

Methyl 2,4-Di-O-acetyl-3-deoxy-3-nitro-6-O-trityl-β-D-glucopyranoside (7)

Acetyl chloride (0.93 ml) was added with stirring and cooling (0°) to a solution of triethylamine (1.5 ml) in dry ether (30 ml). To this mixture was added a chilled solution of **6** (500 mg) in ether (5 ml). After continued stirring for 40 min the white precipitate was dissolved by addition of water (25 ml). Subsequent evaporation of the ether caused **7** to separate from the mixture as a solid which was filtered off, washed thoroughly with cold water, and dried. Recrystallized from ethanol, **7** (372 mg, 67%) melted at 165–166° and showed $[\alpha]_D$ +9.0° (*c*, 1.0 in chloroform); ν_{max} 1750 (C=O), 1555 (NO_2), 790–690 cm^{-1} (6 bands, trityl).

Nuclear magnetic resonance data: τ 2.45–2.75, multiplet (trityl); τ 4.50, triplet (H-4) with $J_{3,4} = J_{4,5} = 10$ Hz; τ 4.52, quartet (H-2) with $J_{1,2} = 8$ Hz and $J_{2,3} = 10$ Hz; τ 5.30, triplet (H-3) with $J_{2,3} = J_{3,4} = 10$ Hz; τ 5.56, doublet (H-1) with $J_{1,2} = 8$ Hz); τ 6.42, singlet (OCH_3) superimposed on multiplet (H-5); 6.75, multiplet (H-6,6′); τ 7.94, 8.25, singlets (acetyl).

Anal. Calcd. for $C_{30}H_{31}NO_9$ (549.6): C, 65.60; H, 5.69; N, 2.55. Found: C, 65.51; H, 5.60; N, 2.64.

The Yellow By-Product

A solution of **6** (200 mg), acetic anhydride (0.8 ml), and pyridine (2 ml) in ether (10 ml) was stored overnight at 5°. The mixture was extracted twice with 3 ml of water, then with dilute acetic acid until the aqueous phase showed acidic reaction, and finally, twice more with water. The ether phase was dried (Na_2SO_4) and evaporated to give a syrup that crystallized in part from ethanol. A crop of **7** (47 mg, 19.5%) melting at 162–164° was isolated. The t.l.c. of the mother liquor indicated the presence, besides additional **7**, of a large proportion of a faster-moving product, a part of which could be isolated by concentration of the ethanolic solution. (In one experiment, only this product and no **7** was obtained.) It formed yellow crystals, m.p. 183–185°, λ_{max} 360 mμ (in methanol). The i.r. spectrum lacked carbonyl absorption but showed a nitro band (1525 cm^{-1}) as well as bands attributable to unsaturation and to the trityl group (1650, 1600, 750, and 700 cm^{-1}). Treatment of **6** with acetic anhydride and anhydrous sodium acetate (24 h at 25°) also gave mixtures of **7** and the yellow by-product as revealed by i.r. spectra and t.l.c.

Methyl 2,4,6-Tri-O-acetyl-3-deoxy-3-nitro-β-D-glucopyranoside (8)

(a) From the Bromide 4

A solution of the bromide **4** (85 mg) in methanol (10 ml) was stirred for 2 h with silver carbonate. The filtered solution was evaporated to give a crystalline residue that was at once recrystallized from aqueous ethanol. The colorless prisms so obtained (38 mg) melted at 152–153°. Comparison of i.r. spectra, and an undepressed mixture melting point with an authentic sample, proved the product to be the known (5) glycoside **8**.

(b) From the Trityl Ether 6

An ice-cooled mixture of **6** (200 mg), acetic anhydride (3 ml), and boron trifluoride etherate (2 drops) was stirred for 15 min and then poured into ice water. The solid precipitate was washed with water and recrystallized from ethanol to give **8** (117 mg, 78%), m.p. 153–154°.

Methyl 2,6-Di-O-acetyl-3-deoxy-3-nitro-β-D-glucopyranoside (10)

The compound **7** (100 mg) was dissolved in anhydrous ether (10 ml) saturated with hydrogen chloride. After 30 min the solvent was evaporated, and two portions of ethanol were subsequently evaporated from the residue.

Can. J. Chem. Downloaded from www.nrcresearchpress.com by 210.87.254.105 on 09/05/12
For personal use only.

Can. J. Chem. Downloaded from www.nrcresearchpress.com by 210.87.254.105 on 09/05/12
For personal use only.

The residue was then dissolved in ether, and addition of petroleum ether (b.p. 60–80°) produced an off-white solid (48 mg). The i.r. spectrum of this crude material showed a single, sharp carbonyl band (1730 cm^{-1}) and two bands in the hydroxyl region (3500 and 3250 cm^{-1}), and the n.m.r. spectrum exhibited *O*-acetyl signals at τ 7.92 and 7.97. The compound was presumed to be the *2,4-diacetate* **9**.

Recrystallization of **9** from water gave crystals (40.5 mg, 72%) of the *2,6-diacetate* **10**; m.p. 107–108°, $[\alpha]_D$ −45° (*c*, 1.0 in chloroform), ν_{max} 3400 (single OH peak), 1750 and 1730 (two C=O bands), 1560 cm^{-1} (NO_2).

Anal. Calcd. for $C_{11}H_{17}NO_9$ (307.3): C, 43.00; H, 5.58; N, 4.56. Found: C, 43.24; H, 5.54; N, 4.42.

Nuclear magnetic resonance data: τ 4.65, quartet (H-2) with $J_{1,2}$ = 8 Hz and $J_{2,3}$ = 10 Hz; τ 5.32, triplet (H-3) with $J_{2,3}$ = $J_{3,4}$ = 10 Hz; τ 5.55, doublet (H-1) with $J_{1,2}$ = 8 Hz; τ 6.48, singlet (OCH_3); τ 7.84, 7.93, singlets (two *O*-acetyl groups). The remaining protons gave signals in the region τ 5.35–6.0 and near τ 6.4; assignments could not be made although the integration of the spectrum was correct.

*Benzyl 2,4,6-Tri-O-acetyl-3-deoxy-3-nitro-β-D-glucopyranoside (**11**)*

A mixture of dried, redistilled nitromethane (5 ml), benzyl alcohol (100 mg), Drierite (0.5 g), and freshly prepared (16) silver carbonate (0.3 g) was stirred, in the dark, for 30 min. The bromide **4** (200 mg) was then added, and stirring was continued overnight. The mixture was filtered through a layer of Celite, and the filtrate was evaporated to yield a crystalline residue. Recrystallization from ethanol containing a small proportion of water gave **11** (139 mg, 65%) as white needles, m.p. 104–105° $[\alpha]_D$ −53.6° (*c*, 1.0 in chloroform), ν_{max} 1755, 1735 (C=O), 1555 (NO_2), 760, 705 cm^{-1} (aryl).

Anal. Calcd. for $C_{19}H_{23}NO_{10}$ (425.4): C, 53.65; H, 5.44, N, 3.29. Found: C, 53.71; H, 5.24; N, 3.39.

*1,2,3,4-Tetra-O-acetyl-6-O-(2,4,6-tri-O-acetyl-3-deoxy-3-nitro-β-D-glucopyranosyl)-β-D-glucopyranose (**13**)*

A solution of the tetraacetate **12** (17) (162 mg) in dry, ethanol-free chloroform (4 ml) was stirred for 1 h together with silver oxide (120 mg) and Drierite (0.5 g). Then a few small crystals of iodine and a solution of the bromide **4** (165 mg) in chloroform (4 ml) were added, and stirring was continued, in the dark, for 18 h. The t.l.c. revealed that **4** had been completely consumed by that time, and that two slow-moving products had been formed. Filtration of the mixture was aided by the addition of Celite, and evaporation of the filtrate resulted in a foamy residue which crystallized partially on trituration with ethanol. The crystals (70 mg, 25%) were collected, washed with ethanol, and dried; m.p. 203–205° (203–204° upon recrystallization from ethanol), $[\alpha]_D$ −7.8° (*c*, 0.96 in chloroform), ν_{max} 1750 (C=O), 1560 cm^{-1} (NO_2).

Anal. Calcd. for $C_{26}H_{35}NO_{19}$ (665.6): C, 46.90; H, 5.30; N, 2.10. Found: C, 47.01; H, 5.39; N, 2.06.

*Methyl 6-O-(2,3,4,6-Tetra-O-acetyl-β-D-glucopyranosyl)-3-deoxy-3-nitro-β-D-glucopyranoside (**15**)*

A suspension of silver perchlorate (103.6 mg) and Drierite (0.5 g) in nitromethane (10 ml) was stirred for 15 min, after which the trityl compound **6** (275 mg) was added and the mixture was cooled to 0°. A solution of the bromide **14** (6) (207.5 mg) in nitromethane was then added, which produced a voluminous precipitate. The reaction mixture was vigorously stirred for 5 min and then filtered. The filter residue was washed with nitromethane and the filtrate was extracted once with cold sodium hydrogen carbonate solution and twice with water. Triphenyl carbinol crystallized during these washing procedures and was removed. The washed nitromethane solution was diluted with chloroform (15 ml), dried (Na_2SO_4), and evaporated to give a crystalline residue that was dissolved in ethanol. Addition of some water furnished another crop of triphenyl carbinol, m.p. 161–162°. The aqueous–alcoholic mother liquor was brought to dryness, and crystallization of the residue from ethyl acetate – ether finally gave **15** (45 mg, 14%) as white crystals, m.p. 184–186°, $[\alpha]_D$ −25.6° (*c*, 0.9 in chloroform), ν_{max} 3470 (OH), 1753, 1725 (C=O), 1555 cm^{-1} (NO_2).

Anal. Calcd. for $C_{21}H_{32}NO_{16}$ (554.5): C, 45.50; H, 5.83; N, 2.53. Found: C, 45.60, H, 5.93; N, 2.53.

Calculation of Optical Rotations

The molecular rotations calculated for **13** and **15** are

$$M_{13} = M_A - M_B + M_C = -5002°,$$

$$M_{15} = M_A - M_D + M_E = -10252°$$

where, M_A = −3394° (molecular rotation of β-gentiobiose octaacetate, from mol. wt. 678.8 and $[\alpha]_D$ −5.0°, ref. 17); M_B = −6775° (molecular rotation of methyl β-D-glucopyranoside tetraacetate, from mol. wt. 362.3 and $[\alpha]_D$ −18.7°, ref. 18); M_C = −8383° (molecular rotation of **8**, from mol. wt. 349.3 and $[\alpha]_D$ −24°, ref. 5); M_D = +4180° (molecular rotation of **12**, from mol. wt. 348.3 and $[\alpha]_D$ +12°, ref. 17); and M_E = −2678° (molecular rotation of **1**, from mol. wt. 223.2 and $[\alpha]_D$ −12°, ref. 13).

The specific rotations following from M_{13} and M_{15} are −7.5° (found, −7.8°) and −18.5° (found, −25.6°) for **13** and **15**, respectively. All $[\alpha]_D$ values used refer to chloroform solutions, with the exception of that of **1**, which refers to an aqueous solution and may therefore be a factor causing the slight discrepancy in the values calculated and found for **15**.

The authors are grateful to the National Research Council of Canada for the support of their work. F. Kienzle thanks the Ogilvie Flour Mills Co. for a post-graduate fellowship.

1. J. C. SOWDEN. Advan. Carbohyd. Chem. **6**, 291 (1951).
2. H. H. BAER. Advan. Carbohyd. Chem. **24**, 67 (1969).
3. A. K. GANGULY, O. Z. SARRE, and H. REIMANN. J. Amer. Chem. Soc. **90**, 7129 (1968).
4. W. KOENIGS and E. KNORR. Ber. **34**, 957 (1901). W. L. EVANS, D. D. REYNOLDS, and E. A. TALLEY. Advan. Carbohyd. Chem. **6**, 27 (1951). L. J. HAYNES and F. H. NEWTH. Advan. Carbohyd. Chem. **10**, 207 (1955).
5. H. H. BAER, F. KIENZLE, and F. RAJABALEE. Can. J. Chem. **46**, 80 (1968).
6. M. BÁRCZAI-MARTOS and F. KÖRÖSY. Nature **165**, 369 (1950). See also R. U. LEMIEUX. *In* Methods in

carbohydrate chemistry. Vol. II. Academic Press Inc., New York 1963. p. 221.
7. H. H. BAER and F. KIENZLE. J. Org. Chem. **33**, 1823 (1968).
8. H. H. BAER and F. KIENZLE. Can. J. Chem. **47**, 2819 (1969).
9. B. HELFERICH and A. KLEIN. Ann. **450**, 219 (1926). B. HELFERICH and A. KLEIN. Ann. **455**, 173 (1927). B. HELFERICH and H. BREDERECK. Ber. **64**, 2411 (1931).
10. H. BREDERECK, A. WAGNER, G. FABER, H. OTT, and J. RAUTHER. Ber. **92**, 1135 (1959).
11. H. H. BAER and A. AHAMMAD. Can. J. Chem. **44**, 2893 (1966).
12. H. H. BAER and F. RAJABALEE. Can. J. Chem. **47**, 4086 (1969).
13. H. H. BAER. Ber. **93**, 2865 (1960).
14. H. H. BAER. J. Amer. Chem. Soc. **83**, 1882 (1961).
15. F. G. FISCHER and H. DÖRFEL. Z. Physiol. Chem. **301**, 224 (1955).
16. C. M. MCCLOSKEY and G. H. COLEMAN. Org. Syntheses. Coll. Vol. **3**, 434 (1955).
17. E. A. TALLEY. *In* Methods in carbohydrate chemistry. Vol. II. Academic Press Inc., New York. 1963. p. 337.
18. J. STANĚK, M. ČERNÝ, J. KOCOUREK, and J. PACÁK. The Monosaccharides. Academic Press, Inc., New York. 1963. p. 276.
19. H. H. BAER and F. RAJABALEE. Carbohyd. Res. **12** (241) 1970.

Can. J. Chem. Downloaded from www.nrcresearchpress.com by 210.87.254.105 on 09/05/12
For personal use only.

Can. J. Chem. Downloaded from www.nrcresearchpress.com by 210.87.254.40 on 09/05/12
For personal use only.

Etude cinétique de la réduction des ozonides de styrènes substitués dans le noyau par la triphénylphosphine[1]

J. Carles et S. Fliszár
Département de Chimie, Université de Montréal, Montréal, Québec

Reçu le 20 octobre 1969

Les vitesses de réduction k[ozonide][triphénylphosphine] ont été étudiées, dans le chloroforme, pour une série d'ozonides de styrènes substitués dans le noyau. Les constantes k de deuxième ordre satisfont l'équation de Hammett, avec $\rho = 0.72$, ce qui confirme le caractère nucléophile de l'attaque de la triphénylphosphine sur les ozonides. La formation d'un oxyphosphorane cyclique intermédiaire instable semble constituer l'étape cinétique déterminante en raison de l'effet de solvant pratiquement nul sur k.

The rates of reduction k[ozonide][triphenylphosphine] have been studied, in chloroform solution, for ozonides of ring-substituted styrenes. The second order rate constants k fit the Hammett equation with $\rho = 0.72$, thus confirming that the reduction proceeds via a nucleophilic attack of the triphenylphosphine on the ozonide ring. The absence of any significant kinetic solvent effect indicates that the rate determining step is in the formation of an unstable six-membered ring oxyphosphorane intermediate.

Canadian Journal of Chemistry, **48**, 1309 (1970)

L'étude de la réduction des ozonides par la triphénylphosphine, effectuée par Lorenz et Parks (1) dans le cas de quelques ozonides aliphatiques, a montré que cette réduction est quantitative et qu'elle se prête à des fins analytiques en vue de la détermination de quantités inconnues d'ozonide (2). De plus, la nature de l'ozonide soumis à la réduction peut être déterminée par l'identification des composés carbonylés engendrés lors de cette réaction. Par analogie avec la réaction de la triphénylphosphine avec les sulfures (3), il a été supposé que l'attaque de la triphénylphosphine se produit selon un processus nucléophile sur l'un des oxygènes peroxydiques du cycle ozonique (1).

Une récente étude (4) de la réduction, par la triphénylphosphine, des ozonides du styrène, stilbène, β-méthylstyrène, et du triphényléthylène, marqués à l'aide d'oxygène-18 dans la position éther, a montré que l'attaque a lieu très sélectivement sur les atomes d'oxygène en position peroxydique. Les effets stériques semblent jouer un rôle important lors de la distribution des points d'attaque (O-1 ou O-2), ce qui est montré par l'abstraction très sélective de l'atome d'oxygène O-2 lors de la réduction de l'ozonide du triphényléthylène ($R_1 = R_2 = R_3 = Ph$) (schéma 1).

En ce qui a trait à la distribution des positions d'attaque (O-1 ou O-2), les effets électroniques dus aux substituants semblent jouer un rôle moins prononcé que les facteurs stériques. Ainsi, par exemple, lors de la réduction de l'ozonide du styrène, environ 55% de l'attaque a lieu sur l'atome d'oxygène O-1; dans le cas de l'ozonide du β-méthylstyrène, sous l'influence combinée des groupements phényle (attracteur d'électrons) et méthyle (donneur d'électrons), l'attaque en O-1 est favorisée, mais ne s'élève qu'à 60% environ (4). Ces résultats indiquent que des groupements attracteurs d'électrons, rattachés à un atome de carbone du cycle ozonique, favorisent l'attaque par la triphénylphosphine sur l'oxygène peroxydique adjacent à cet atome de carbone,

[1]Extrait du mémoire de Doctorat de M. J. C.

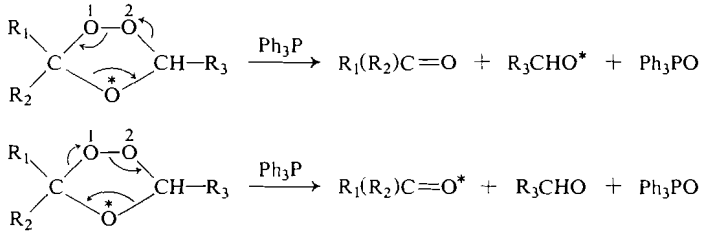

Schéma 1

TABLEAU 1

Spectres de résonance magnétique nucléaire des ozonides **1**–**6***

R	τ_{H_α}	$\tau_{H_{\alpha'}}$	τ_{H_β}	$\tau_{aromatique}$	J_{ortho}†,‡	τ_{CH_3}§	$\bar{\nu}_{C-O-C}$‖
p-CH_3O	4.62	4.75	4.10	H(2) H(6) 2.57 H(3) H(5) 3.12	9.0	6.18	1069
p-CH_3	4.80	4.90	4.17	H(2) H(6) 2.75 H(3) H(5) 2.75	0	6.70	1067
H	4.89	4.94	4.19	H(2) H(6) 2.78 H(3) H(5) 2.78	0	—	1064
p-Cl	4.80	4.85	4.16	H(2) H(6) 2.72 H(3) H(5) 2.72	0	—	1068
m-Cl	4.77	4.82	4.12	H(2) H(6) 2.73 H(3) H(5) 2.73	0	—	1066
p-NO_2	4.67	4.70	3.90	H(2) H(6) 2.36 H(3) H(5) 1.76	8.0	—	1073

*Les valeurs de τ sont données en p.p.m., avec le TMS comme référence, dans le CCl_4.
†Les constantes de couplage sont exprimées en c.p.s.
‡Seules les constantes de couplage ortho peuvent être déterminées.
§Protons du CH_3 du substituant.
‖Fréquence i.r., en cm^{-1}.

tandis que des groupements donneurs d'électrons agissent en sens contraire.

Le but du présent travail est de préciser, au moyen d'études cinétiques, les effets électroniques dus aux substituants ainsi que la nature de la réaction entre ozonides aromatiques et la triphénylphosphine, en solution dans du chloroforme.

Ozonides utilisés

Les ozonides de styrènes substitués dans le noyau suivants ont été utilisés.

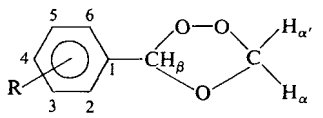

1 R = *p*-CH_3O **4** R = *p*-Cl
2 R = *p*-CH_3 **5** R = *m*-Cl
3 R = H **6** R = *p*-NO_2

Les caractéristiques des spectres de résonance magnétique nucléaire (r.m.n.) et de spectroscopie infrarouge (i.r.) des composés **1** à **6** sont résumées dans le tableau 1.

L'examen de ce tableau indique qu'il ne se produit, en r.m.n., aucun couplage à travers le cycle ozonique, puisque les protons H_α, $H_{\alpha'}$, et H_β apparaissent tous sous forme de singulet. Ce fait se retrouve également dans les ozonides aliphatiques (5), ainsi que dans les ozonides du *p*-méthoxy-cinnamate de méthyle (6). On observe aussi que les protons méthylèniques H_α et $H_{\alpha'}$ apparaissent comme deux singulets séparés, ce qui est en bon accord avec les observations de Murray et Williams (7). La constante de couplage géminé est nulle, fait que l'on retrouve dans de nombreux hétérocycles oxygénés. La position (*cis* ou *trans*) de H_α (ou de $H_{\alpha'}$) par rapport au cycle aromatique n'a pu être précisée à partir des présentes données expérimentales.

En ce qui concerne les protons aromatiques, on observe pour les ozonides ayant des groupements moyennement donneurs ou attracteurs d'électrons (R = *p*-CH_3, H, *p*-Cl, *m*-Cl) que les influences du cycle ozonique et du substituant du noyau aromatique se compensent. Dès lors, un seul signal peut être observé pour les protons aromatiques. Par contre, dans le cas de l'ozonide du *p*-méthoxystyrène, porteur d'un groupement fortement donneur d'électrons, on observe un blindage des protons H-3 et H-5 qui donnent un signal à un champ supérieur à celui des protons H-2 et H-6. Dans le cas de l'ozonide du *p*-nitrostyrène, porteur d'un groupement fortement attracteur d'électrons, l'effet de déblindage dû au groupement NO_2 est très net pour les protons H-3 et H-5 qui donnent un signal à un champ plus faible que les protons H-2 et H-6. Les constantes de couplage observées correspondent bien à un couplage ortho.

En spectroscopie i.r. on reconnaît, pour chacun des ozonides étudiés, la bande d'absorption caractéristique, vers 1060–1070 cm^{-1}, due à la vibration du groupement C—O—C. Le substituant R n'affecte que faiblement la fréquence d'absorption de cette bande.

Can. J. Chem. Downloaded from www.nrcresearchpress.com by 210.87.254.40 on 09/05/12
For personal use only.

Can. J. Chem. Downloaded from www.nrcresearchpress.com by 210.87.254.40 on 09/05/12
For personal use only.

Etude cinétique de la réduction

La réduction des ozonides par la triphénylphosphine a été étudiée à température contrôlée, en solution dans le chloroforme, par l'observation de la formation, au cours de la réaction, de l'aldéhyde aromatique. Cette formation d'aldéhyde a été suivie en spectroscopie i.r. par l'évolution de la bande d'absorption due à la vibration de son groupement carbonyle.

La stoechiométrie de la réaction a été vérifiée par des analyses des mélanges réactionnels. Après un temps de réaction de 48 h, à 25 °C, la réduction de l'ozonide du styrène (0.1 *M*) par la triphénylphosphine (0.1 *M*) est pratiquement quantitative (> 99% de réaction), d'après les analyses d'aldéhyde benzoïque et d'oxyde de triphénylphosphine formés. L'aldéhyde formique, qui est également un produit de cette réaction, n'a pas pu être dosé, en raison de sa grande volatilité. Il a été vérifié, dans le cas de l'ozonide du styrène, que la réduction d'une mole d'ozonide conduit à la formation d'une mole d'aldéhyde aromatique et d'une mole d'oxyde de triphénylphosphine. Dans 4 expériences indépendantes, 0.997, 0.998, 0.996, et 0.998 mmole de Ph_3PO et, respectivement, 0.998, 0.996, 0.998, et 0.995 mmole de PhCHO ont été formés lors de la réduction de 1.0 mmole d'ozonide de styrène par 1.0 mmole de Ph_3P, dans 10 ml de $CHCl_3$, à 25°, après 48 h de réaction.

En admettant, par conséquent, que la réaction est du deuxième ordre, soit du premier ordre par rapport à chacun des réactifs, la formation d'aldéhyde aromatique (ArCHO) est décrite par l'équation [1].

$$[1] \quad d[ArCHO]/dt = k[\text{ozonide}][Ph_3P]$$

Dans toutes les expériences, des concentrations initiales égales en ozonide et en triphénylphosphine ont été utilisées. Si a désigne ces concentrations initiales et x la concentration en aldéhyde aromatique formé au temps $t = t$, il s'ensuit, d'après la stoechiométrie de la réaction, que

$$[2] \quad dx/dt = k(a - x)^2$$

et

$$[3] \quad x/a\,(a - x) = kt$$

En admettant la loi de Lambert–Beer, la densité optique D de l'aldéhyde aromatique engendré est

$$[4] \quad D = \varepsilon x l$$

avec ε = coéfficient d'extinction moléculaire de l'aldéhyde et l = longueur de la cellule. Lorsque l'ozonide est quantitativement réduit, donc pour $x = a$, la densité optique de l'aldéhyde aromatique est

$$[5] \quad D_\infty = \varepsilon a l$$

En divisant, l'une par l'autre, les expressions [4] et [5] il résulte

$$[6] \quad x = aD/D_\infty$$

et, en remplaçant cette dernière expression pour x dans l'équation [3],

$$[7] \quad kt = D/a(D_\infty - D)$$

Par un réarrangement de l'équation [7], on obtient l'équation [8] qui permet une analyse facile des mesures expérimentales des densités optiques en vue du calcul de la constante de vitesse k.

$$[8] \quad 1/D = 1/D_\infty + (1/aD_\infty k)(1/t)$$

Les mesures de densités optiques (D) de l'aldéhyde au cours de la réaction permettent de tracer la courbe $1/D$ en fonction de $1/t$. On vérifie ainsi que la réaction est bien du deuxième ordre, ainsi que postule l'équation [2], par l'obtention d'une droite satisfaisant l'équation [8]. La pente de cette droite permet le calcul de la valeur de la constante de vitesse k. L'ordonnée à l'origine ($1/t \to 0$) permet le calcul de D_∞. La valeur de D_∞ calculée à partir de données cinétiques peut être ainsi facilement contrôlée par des mesures directes de D_∞ obtenues soit par sa détermination après un temps de réaction suffisamment long, soit par la comparaison avec une solution d'aldéhyde de concentration $x = a$ (fig. 1).

La constante de vitesse de réaction k peut être également calculée directement à partir de l'équation [8], en y insérant les valeurs de D observées aux temps t. L'exemple donné par le tableau 2, qui se rapporte à la réduction de l'ozonide du styrène à 15 °C, illustre bien la constance de k jusqu'à un fort degré d'avancement de la réaction.

Les équations cinétiques utilisées ont également été vérifiées, dans le cas de la réduction de l'ozonide du styrène, par des mesures des temps de demi-réaction $t_{1/2}$ observés pour des solutions de différentes concentrations initiales (a) en

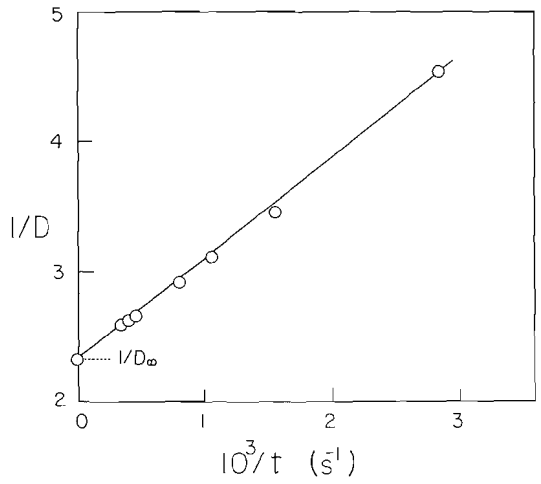

FIG. 1. Application de l'équation [8] à l'étude de la cinétique de réduction de l'ozonide du styrène à 15 °C.

ozonide et en triphénylphosphine. Les résultats rapportés au tableau 3 montrent bien la constance des valeurs de k ainsi calculées ($k = 1/at_{1/2}$).

Lors de chaque étude cinétique, la constante de vitesse a été déterminée au moins 5 fois, par des expériences indépendantes. Les résultats retenus à partir des déterminations indépendantes de k sont exprimés avec une limite de confiance de 95%.

Résultats et discussion

Les constantes de vitesse de réduction, à 25 °C, des ozonides de styrènes substitués dans le noyau sont indiquées dans le tableau 4. La dépendance de k en fonction de la température a été étudiée pour la réduction des ozonides du styrène et du *p*-méthoxystyrène (tableau 5, fig. 2). Ainsi que l'indique la fig. 2, la loi d'Arrhenius est bien

TABLEAU 2

Réduction de l'ozonide du styrène à 15 °C; $a = 0.1$ M

t (s)	10^2 D	10^2 k (1 mole^{-1} s^{-1})
0	0	—
355	22	2.95
638	29	3.24
949	32	3.06
1265	34	2.98
2130	37.5	3.20
2480	38.0	3.06
2870	38.5	2.98
∞	43.0	—
		moy. 3.06±0.15

TABLEAU 3

Réduction de l'ozonide du styrène par la triphénylphosphine à 25 °C

a (M)*	$t_{1/2}$ (s)	k (1 mole^{-1} s^{-1})
0.05	302	6.62 10^{-2}
0.10	152	6.57
0.15	101	6.60
0.20	75	6.66

*a = concentration initiale en ozonide.
= concentration initiale en triphénylphosphine.

suivie et conduit à des énergies d'activation de 12.7 kcal/mole pour la réduction de l'ozonide du styrène et de 10.4 dans le cas de l'ozonide du *p*-méthoxystyrène.

L'examen des résultats du tableau 4 permet l'étude de l'influence des substituants R du noyau aromatique sur les constantes de vitesse k. Il résulte, notamment, que l'équation de Hammett

$$[9] \qquad \log (k/k_0) = \rho\sigma$$

est bien vérifiée, ainsi que l'illustre la fig. 3.

La pente positive de la droite de Hammett ($\rho = 0.72$) indique que les ozonides possédant un substituant R attracteur d'électrons dans le noyau aromatique se réduisent plus rapidement que les ozonides comprenant un groupement donneur d'électrons. Ce résultat confirme donc les observations précédentes (1, 4) qui indiquent que l'attaque de la triphénylphosphine se fait selon un processus nucléophile.

Les expériences cinétiques rapportées ne permettent cependant pas de préciser la position

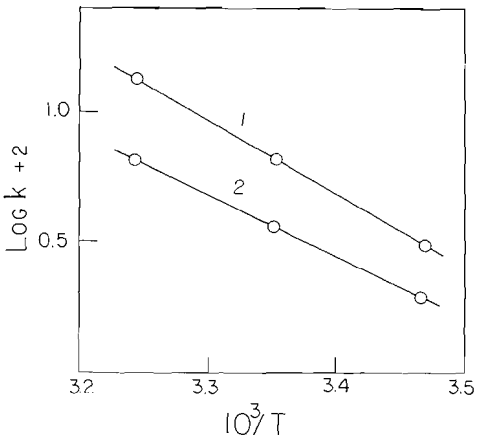

FIG. 2. Application de la loi d'Arrhenius : log k vs. $1/T$, pour les ozonides du styrène (*1*) et du *p*-méthoxystyrène (*2*).

Can. J. Chem. Downloaded from www.nrcresearchpress.com by 210.87.254.40 on 09/05/12
For personal use only.

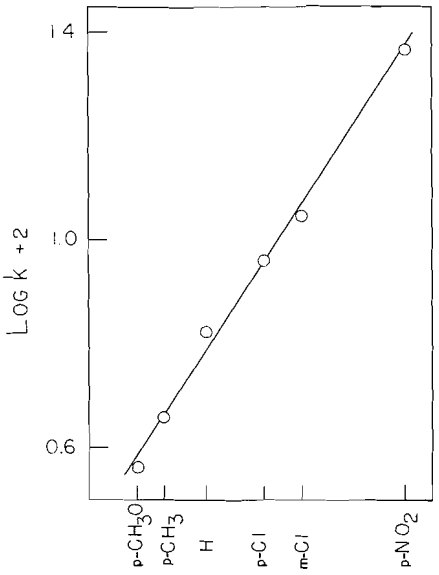

FIG. 3. Application de l'équation de Hammett : log k vs. σ de Hammett (25 °C).

d'attaque (O-1 ou O-2) sur la molécule d'ozonide. Il convient, à cet égard, de considérer les possibilités suivantes:

(*i*) L'attaque de la triphénylphosphine pourrait s'effectuer par un processus unique, par une étape où les deux atomes d'oxygène peroxydique sont simultanément mis en jeu, cette étape contrôlant la cinétique (schéma 2). Le processus impliqué pourrait alors correspondre à la formation d'un

TABLEAU 4

Constantes de vitesse de réduction des ozonides de styrènes substitués dans le noyau, à 25 ± 0.1 °C, dans le chloroforme

Substituant	$10^2 k$ (l mole^{-1} s^{-1})
p-CH_3O	3.66 ± 0.29
p-CH_3	4.55 ± 0.18
H	6.64 ± 0.17
p-Cl	9.10 ± 0.45
m-Cl	11.10 ± 0.51
p-NO_2	23.15 ± 0.75

TABLEAU 5

Constantes de vitesse de réduction des ozonides du styrène (k_H) et du *p*-méthoxystyrène (k_{CH_3O}) à diverses températures, dans le chloroforme

Température (°C)	$10^2 k_H$ (l mole^{-1} s^{-1})	$10^2 k_{CH_3O}$ (l mole^{-1} s^{-1})
15 ± 0.1	3.28 ± 0.24	1.96 ± 0.06
25 ± 0.1	6.64 ± 0.17	3.66 ± 0.29
35 ± 0.1	13.26 ± 0.88	6.46 ± 0.23

produit d'addition intermédiaire instable, semblable à l'oxyphosphorane suggéré par Adam *et al.* (8) pour la réduction de β-peroxylactones par des nucléophiles de phosphore trivalent. La formation d'oxyphosphoranes lors de la réaction de phosphites trisubstitués avec les peroxydes a également été mise en évidence par Denney et Jones (9).

L'intermédiaire se décomposerait ensuite très rapidement selon les 2 voies possibles : la voie *1*, conduisant à l'incorporation de l'oxygène du pont éther dans l'aldéhyde aromatique, et la voie *2*, où cet oxygène se retrouverait dans le formaldéhyde.

Un tel mécanisme serait en accord avec les équations cinétiques [1], [2], et [8], donc avec les résultats expérimentaux, et ne sont pas contredits par l'observation d'une droite de Hammett, d'après l'équation [9]. Il est à noter que certains oxyphosphoranes, ne présentant pas de pont éther, sont relativement stables (10). Des études cristallographiques aux rayons X ont montré que les angles des liaisons O—P—O et P—O—C peuvent subir de grandes distorsions et que les interactions de non-liaison peuvent déterminer des stabilités et des modes de rupture différents pour des oxyphosphoranes présentant de forts encombrements stériques (11). Un tel argument pourrait être invoqué ici pour expliquer les effets stériques marqués, mentionnés précédemment (4), qui interviennent lors de la distribution des sites d'attaque (O-1 ou O-2).

(*ii*) La réduction des ozonides peut avoir lieu par deux mécanismes parallèles (schéma 3), l'un

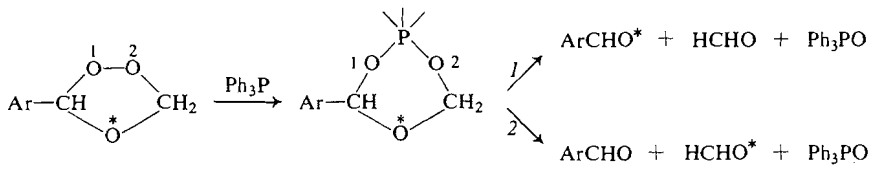

SCHÉMA 2

Can. J. Chem. Downloaded from www.nrcresearchpress.com by 210.87.254.40 on 09/05/12
For personal use only.

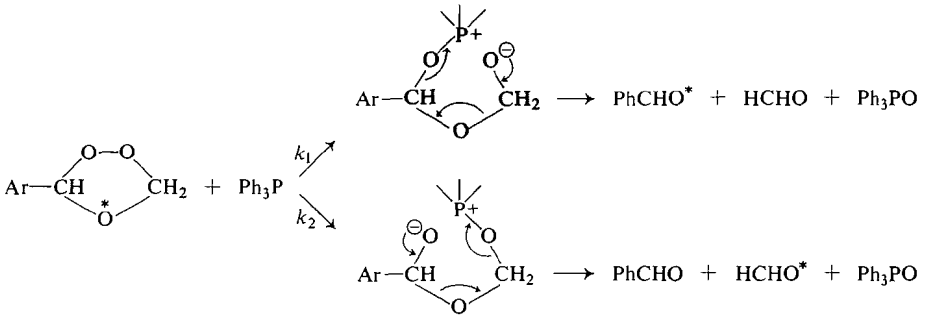

SCHÉMA 3

d'entre eux s'effectuant par une attaque sur l'oxygène O-1 (avec une vitesse v_1 et une constante de vitesse k_1) et l'autre ayant lieu par une attaque sur l'oxygène O-2 (avec une vitesse v_2 et une constante k_2).

Dans cette hypothèse, la vitesse de réaction observée expérimentalement deviendrait

$$[10] \quad v = v_1 + v_2 = (k_1 + k_2)[\text{ozonide}][\text{Ph}_3\text{P}]$$

En appliquant à k_1 et k_2 l'équation de Hammett [9], les expressions suivantes sont obtenues :

$$[11] \quad \log (k_1/k_{1,0}) = \rho_1\sigma$$
$$\log (k_2/k_{2,0}) = \rho_2\sigma$$

qui, à l'aide des équations [1] et [10], conduisent à l'équation [12].

$$[12] \quad k = k_1 + k_2 = k_{1,0}\, 10^{\rho_1\sigma} + k_{2,0}\, 10^{\rho_2\sigma}$$

Cette dernière équation peut être réarrangée comme suit :

$$[13] \quad \log (k/k_{1,0}) = \rho_1\sigma + \log[1 + (k_{2,0}/k_{1,0})10^{(\rho_2-\rho_1)\sigma}]$$

Il paraîtrait, à première vue, que les processus (*i*) et (*ii*) devraient pouvoir être distingués l'un de l'autre du fait que, dans l'hypothèse de l'applicabilité de la relation de Hammett à cette réaction, le processus (*i*) demande une relation linéaire entre k et σ (éq. [9]), tandis que (*ii*) implique une relation non linéaire entre k et σ (éq. [13]).

L'examen de l'équation [13] montre, cependant, que les mécanismes (*i*) et (*ii*) ne sauraient être distingués par un tel critère. On connait, en effet, d'après les expériences effectuées avec l'ozonide du styrène marqué par O-18 (4), qu'environ 55% de l'oxygène O-1 et, par conséquent, 45% de l'oxygène O-2, se retrouvent dans l'oxyde de triphénylphosphine. Dès lors, $k_{2,0}/k_{1,0} \simeq 0.45\,k/0.55\,k \simeq 0.82$. Il paraît raisonable de supposer que les effets électroniques dus à R sont plus prononcés sur l'atome d'oxygène O-1, adjacent au carbone porteur du groupement aromatique, que sur O-2 et que, dès lors, $\rho_1 > \rho_2$. Par ailleurs l'influence relativement faible des facteurs électroniques sur la distribution des sites d'attaque (4) indique que ρ_1 et ρ_2 devraient être assez semblables. Or, en insérant dans l'équation [13] $k_{2,0}/k_{1,0} = 0.82$ et $\rho_2 - \rho_1 = -0.5$, on vérifie facilement que le terme logarithmique, figurant dans [13] à côté de $\rho_1\sigma$, est quasi linéairement relié à σ. Même en admettant cette différence relativement importante entre ρ_1 et ρ_2, la courbure est, en effet, trop faible pour être significative lorsqu'elle est comparée aux erreurs expérimentales entachant les valeurs de k qui sont utilisées pour l'étude de $k = k(\sigma)$. Pour des différences moindres entre ρ_1 et ρ_2, la courbure s'atténue encore et, à la limite $\rho_1 = \rho_2$, le terme logarithmique devient constant. En conclusion, la relation linéaire entre les constantes de vitesse k et les constantes de Hammett σ, telle qu'elle a été observée expérimentalement, ne saurait être invoquée pour favoriser le mécanisme (*i*) par rapport à (*ii*).

Par contre, la comparaison des étapes cinétiques supposées pour les mécanismes (*i*) et (*ii*) indique que l'intermédiaire intervenant dans le mécanisme (*ii*) possède un caractère nettement plus polaire que celui postulé pour le mécanisme (*i*). Dès lors, l'étude de l'effet du solvant sur les constantes de vitesse peut permettre la distinction entre les deux mécanismes. Les résultats rapportés au tableau 6 indiquent que les constantes de vitesse de réaction dépendent très peu des solvants utilisés. En conclusion, ce faible effet de

Can. J. Chem. Downloaded from www.nrcresearchpress.com by 210.87.254.40 on 09/05/12
For personal use only.

TABLEAU 6

Constantes de vitesse de réduction de l'ozonide du styrène, à 25 ± 0.1 °C, dans différents solvants

Solvant	Constante diélectrique (25°)	$10^2 k$ (l mole^{-1} s^{-1})
CCl_4	2.228	5.04 ± 0.19
$CHCl_3$	4.718	6.64 ± 0.17
CH_2ClCH_2Cl	10.36	6.14 ± 0.16
CH_3OH	32.63	6.28 ± 0.16

solvant semble nettement favoriser le mécanisme (*i*).

Partie expérimentale

Préparation des ozonides

L'ozonide du styrène a été préparé d'après la méthode exposée précédemment (12). Quant aux ozonides des styrènes comportant un substituant dans le noyau aromatique, leurs analyses élémentaires et propriétés physiques sont résumées dans le tableau 7. Les microanalyses ont été effectuées, par le Dr. C. Daesslé (Organic Microanalyses, Montréal).

Ozonide du p-méthoxystyrène

Cinq millimoles (670 mg) de *p*-méthoxystyrène, en solution dans 25 ml de pentane, ont été ozonés à la température de la pièce avec 90% de la quantité théorique d'ozone. Après évaporation du solvant par un courant d'azote sec, l'ozonide est isolé par chromatographie sur colonne en utilisant 300 g de silica gel Baker. L'oléfine non consommée et les aldéhydes formés sont élués avec du tétrachlorure de carbone. L'ozonide est élué avec un mélange de benzène–hexane (55/45). La fraction contenant l'ozonide est évaporée à sec, permettant ainsi de receuillir un solide blanc. La recristallisation dans le méthanol s'avère difficile. Après recristallisation dans l'éther éthylique, on obtient 25 mg d'ozonide (rendement : 10%).

Ozonide du p-méthylstyrène

Dix millimoles (1.18 g) de *p*-méthylstyrène, en solution dans 25 ml de CCl_4, sont ozonées à 0 °C avec 80% de la quantité théorique d'ozone. Après évaporation du solvant sous un courant d'azote sec, l'ozonide est isolé par chromatographie sur colonne en utilisant 300 g de silica gel Baker. L'ozonide est élué avec un mélange 50/50 de benzène–hexane. Après purification par une nouvelle chromatographie, on a obtenu 245 mg d'ozonide (rendement : 15%). Lors d'une expérience similaire, dans laquelle le tétrachlorure de carbone a été remplacé par le pentane, on a obtenu 288 mg d'ozonide purifié.

Ozonide du p-chlorostyrène

Dix millimoles (1.385 g), en solution dans 25 ml de CCl_4, ont été ozonées à la température de la pièce avec 80% de la quantité théorique d'ozone. L'ozonide a été isolé et purifié dans les conditions employées pour l'ozonide du *p*-méthylstyrène (rendement : 180 mg). Le produit se présente sous forme d'un liquide visqueux.

Ozonide du m-chlorostyrène

Cet ozonide a été préparé comme son isomère para. Il a été obtenu un rendement de 201 mg d'ozonide purifié à partir de 10 mmole d'oléfine (11%).

Ozonide du p-nitrostyrène

Une solution de 2.08 mmole (300 mg) de *p*-nitrostyrène dans 25 ml de CCl_4 a été ozonée à 25° avec 80–90% de la quantité théorique d'ozone. Après évaporation de la majeure partie du solvant par un courant d'azote sec, l'ozonide est isolé par chromatographie sur colonne en utilisant 500 g de silica gel Baker. L'oléfine n'ayant pas réagi avec l'ozone est éluée avec le CCl_4 et l'ozonide est élué au moyen d'un mélange 1:1 de benzène–hexane. La fraction contenant l'ozonide est évaporée à sec. Le solide blanc ainsi obtenu est recristallisé 3 fois dans le méthanol. Il a ainsi été obtenu un rendement de 33 mg d'ozonide (17%), de couleur blanche.

Mesures cinétiques

Les solutions d'ozonide (0.2 *M*) et de triphénylphosphine (0.2 *M*), dans le chloroforme, ont été préparées par pesée. Pour chaque étude cinétique, des volumes égaux des deux solutions ont été mélangés, après équilibration de la température. Le mélange (0.1 *M* en chacun des réactifs) est maintenu dans un thermostat à ±0.1 °C. Aux intervalles de temps appropriés, des prélevements sont analysés rapidement en spectroscopie i.r., au moyen d'un appareillage Perkin–Elmer 621. Les densités optiques ont été mesurées aux fréquences correspondantes aux vibrations de valence C—O dues aux aldéhydes aromatiques engendrés par la réaction, entre 1704 et 1717 cm^{-1}. Les courbes de calibration pour les aldéhydes et l'oxyde de triphénylphosphine ont été établies de manière similaire.

TABLEAU 7

Analyses et propriétés physiques (indices de réfraction n_D^{25} et points de fusion) des ozonides de styrènes substitués dans le noyau aromatique

R	Calculé (%)				Trouvé (%)				n_D^{25}	Point de fusion
	C	H	N	Cl	C	H	N	Cl		
p-CH_3	65.05	6.07	—	—	65.19	5.99	—	—	1.4508	—
p-NO_2	48.73	3.58	7.10	—	48.69	3.75	6.97	—	—	78
p-CH_3O	59.34	5.49	—	—	59.42	5.34	—	—	—	64
m-Cl	51.52	3.78	—	19.01	51.92	4.03	—	19.30	1.5468	—
p-Cl	51.52	3.78	—	19.01	51.29	3.63	—	18.82	1.5389	—

Can. J. Chem. Downloaded from www.nrcresearchpress.com by 210.87.254.40 on 09/05/12
For personal use only.

Nous tenons à remercier le Conseil National de Recherches du Canada pour une subvention qui a permise ces recherches.

1. O. LORENZ et C. R. PARKS. J. Org. Chem. **30**, 1976 (1965).
2. O. LORENZ. Anal. Chem. **37**, 101 (1965).
3. P. D. BARTLETT et G. MEGUERIAN. J. Amer. Chem. Soc. **78**, 3710 (1956).
4. J. CARLES et S. FLISZÁR. Can. J. Chem. **47**, 1113 (1969).
5. R. W. MURRAY, R. D. YOUSSEFYEH, et P. R. STORY. J. Amer. Chem. Soc. **88**, 3143 (1966).
6. P. KOLSAKER. Acta Chem. Scand. **19**, 223 (1965).
7. R. W. MURRAY et G. J. WILLIAMS. J. Org. Chem. **34**, 1891 (1969).
8. W. ADAM, R. J. RAMÍREZ, et SHIH-CHUAN TSAI. J. Amer. Chem. Soc. **91**, 1254 (1969).
9. D. B. DENNEY et D. H. JONES. J. Amer. Chem. Soc. **91**, 5821 (1969).
10. F. RAMÍREZ et N. B. DESAI. J. Amer. Chem. Soc. **82**, 2652 (1960); **85**, 3252 (1963). F. RAMÍREZ, N. RAMANATHAN, et N. B. DESAI. J. Amer. Chem. Soc. **85**, 3465 (1963). F. RAMÍREZ, A. V. PATWARDHAN, N. B. DESAI, N. RAMANATHAN, et C. V. GRECO. J. Amer. Chem. Soc. **85**, 3056 (1963). F. RAMÍREZ. *Dans* Organophosphorus compounds. International Symposium, Heidelberg, 1964, IUPAC, Butterworth and Co., Ltd., London, 1964. p. 337–369.
11. F. RAMÍREZ. Accounts Chem. Res. **1**, 168 (1968). W. C. HAMILTON, S. J. LAPLACA, F. RAMÍREZ, et C. P. SMITH. J. Amer. Chem. Soc. **89**, 2268 (1967). R. D. SPRATLEY, W. C. HAMILTON, et J. LADELL. J. Amer. Chem. Soc. **89**, 2272 (1967). F. RAMÍREZ, M. NAGABHUSHANAM, et C. P. SMITH. Tetrahedron, **24**, 1785 (1968).
12. J. CASTONGUAY, M. BERTRAND, J. CARLES, S. FLISZÁR, et Y. ROUSSEAU. Can. J. Chem. **47**, 919 (1969).

Can. J. Chem. Downloaded from www.nrcresearchpress.com by 210.87.254.40 on 09/05/12
For personal use only.

Electron spin resonance spectra of nitric oxide adsorbed on zeolites[1,2]

C. L. GARDNER AND M. A. WEINBERGER[3]
Defence Research Establishment Ottawa, Ottawa 4, Canada

Received[4] June 9, 1969

Electron spin resonance (e.s.r.) spectra of NO adsorbed on the 4 zeolites Linde 4A, 5A, 13X, and hydrogen mordenite were measured at 77 °K. No e.s.r. signal was observed for NO on silica gel. By use of expressions for the line shapes of polycrystalline samples, assuming axially symmetric **g**-tensors, and taking into account also isotropic coupling, values of $\mathbf{g}_{\parallel}$, $\mathbf{g}_{\perp}$, and line width were derived by an iterative procedure. From these, the crystal field splitting, Δ, of the $2p\pi$ levels, which become non-degenerate on adsorption, were calculated. By relating Δ to the interaction of the non-axial components of the quadrupole moment with the corresponding electric field gradients, the non-axial component of the latter is estimated for the surface fields of the zeolites.

Canadian Journal of Chemistry, **48**, 1317 (1970)

Can. J. Chem. Downloaded from www.nrcresearchpress.com by 210.87.254.6 on 09/05/12
For personal use only.

Introduction

Experimental evidence has indicated intense electrostatic fields at the surface of both ionic and covalent insulator materials. Sheppard and Yates (1), for example, have estimated the electrostatic field at a porous glass surface by measuring the infrared intensity of adsorbed H_2. Their results showed a field of 7×10^6 V/cm. The structure of zeolites is known to consist of an open, negatively charged network with cations on the surface of this open network structure. Extremely intense electrostatic fields exist in the cavities due to the poor shielding of the cations. For instance, Monod *et al.* (2) estimate this field, from the heat of adsorption of helium, to be 1.6×10^8 V/cm in faujasite. Calculations of Dempsey (3, 4) also indicate fields of this order of magnitude.

The influence of electrostatic fields of this order of magnitude on the mechanism of catalytic reactions has been shown by the calculations of Hoijtink (5, 6). He has shown that the difference in structure of the products obtained by homogeneous reduction and catalytic hydrogenation of aromatic hydrocarbons can be explained in terms of the influence of the electric field of the electrical double layer at the catalyst–solution interface on the electronic structure of the intermediately formed dinegative ions.

The electron spin resonance (e.s.r.) spectrum of NO is known in the gas phase (7). Early attempts (8) to detect NO trapped in rare-gas matrices were unsuccessful. The reason for this failure was believed to be due to partial quenching of the orbital momentum. Partial quenching of the orbital angular momentum of NO adsorbed on silica gel has been indicated by magnetic susceptibility measurements (9, 10). Electron spin resonance spectra have been reported (11, 12) of what has been assigned as NO trapped in a crystal in a $^2\Sigma$ state. Recently, Lunsford (14) has reported the spectrum of NO adsorbed on MgO, ZnO, and several zeolites in a $^2\Pi$ state in which the orbital momentum has been substantially quenched by the surface fields. The results we report for NO on zeolites are in essential agreement with those of Lunsford.

The purpose of the present work has been to identify those parameters characteristic of the surface field that can be determined from this type of experiment, and to study quantitatively how these vary from one material to another. The zeolite systems were chosen as these materials are well characterized structurally as compared to many catalyst systems.

Experimental

In these experiments, samples of the zeolites (Linde 4A, 5A, 13X, and hydrogen mordenite)[5] as well as silica gel (Fisher) were degassed for about 15 h at 300 °C and a pressure less than 10^{-4} mm. Nitric oxide (Matheson research grade) was allowed to adsorb onto the sample at 10 cm pressure. The sample tube was then sealed and the e.s.r. measurements made at 77 °K. The e.s.r. spectra

[1]D.R.E.O. No. 609.
[2]Presented in part at the 3rd Catalysis Symposium, Hamilton, Ontario, 1967.
[3]Present address: Defence Research Analysis Establishment, Ottawa 4, Canada.
[4]Revision received November 4, 1969.

[5]We are indebted to Dr. G. R. Findlay of Norton Company for providing us with a sample of hydrogen mordenite, to Dr. J. R. Morton for samples of Linde 4A and 5A molecular sieves, and to Union Carbide Corporation for a sample of Linde 13X molecular sieve.

Can. J. Chem. Downloaded from www.nrcresearchpress.com by 210.87.254.6 on 09/05/12
For personal use only.

TABLE 1

Line width and g-tensor values for NO adsorbed on zeolites*

Zeolite	$g_\perp$	$g_\parallel$	Line width (G)
Faujasite	1.970	1.786	71.6
Mordenite	1.967	1.773	65.8
Linde 5A	1.990	1.859	44.5

*Isotropic hyperfine interaction: 17.0 G in all cases.

did not change from the initial recording to one made several weeks later. During the cooling process, the faujasite (Linde 13X) and mordenite samples became brown and purple, respectively.

Electron spin resonance spectra were recorded for NO adsorbed on all four zeolites investigated. No e.s.r. spectrum was observed for NO on silica gel. The e.s.r. spectra were obtained with a Varian spectrometer (V4500). They were digitized with a Gerber scaler, and each was then fitted[6] with a calculated curve based on a Lorentzian lineshape and an axially symmetric g-tensor. The theoretical expression used was that of Searl *et al.* (29) for polycrystalline samples, which is applicable if the anisotropies are small. The expression was modified to include the ^{14}N isotropic hyperfine interaction, for which a value of 17 G was assumed (13). Important anisotropic interactions are undoubtedly present (14), but the corresponding hyperfine lines were either not resolved in the spectra or were very rudimentary (Fig. 1*b*). Instead of attempting to guess the magnitude of these interactions, the problem was circumvented by including the effect of the interactions in an empirical linewidth. Since the disposition of the underlying hyperfine lines is symmetrical, the *g*-value assignments should not be affected. An iteration procedure (15) was applied to deduce the optimal values for the linewidth and g-tensor in each case, the calculations being programmed for a CDC 3200 computer. For faujasite, the more accurate, but much more complicated, treatment of Ibers and Swalen (16) was also used. Although this yielded the same parameters as the simpler procedure, the fit to the experimental "points" was better. A comparison of the calculated curves with curves calculated using the data in Tables 1 and 2 and assuming the anisotropic hyperfine tensor for NO given by Ohigashki and Kurita (13) showed that they were almost identical. This validates the use of empirical linewidths. Figures 1*a*–1*c* show comparisons of the digitized e.s.r. spectra (points) with the calculated curves, and Table 1 gives the derived parameters. The fit of the calculated curves to the experimental curve is not too good in most cases. It seems likely, however, that the variation is in part caused by the inclusion in the linewidth of the effects of anisotropic hyperfine interactions, which in addition make the linewidths quite large. Lunsford (14) has given a number of other causes for line broadening in the e.s.r. spectrum of NO adsorbed on NaY zeolites.

[6]No fit was made for the e.s.r. spectrum of NO on Linde 4A, as this spectrum, shown in Fig. 1*d*, is complicated and not understood completely.

Discussion

(a) g-Values

Nitric oxide in its ground state is a regular $^2\Pi$ state. The splitting (17) between the $^2\Pi_{1/2}$ and the low lying $^2\Pi_{3/2}$ state is 121 cm^{-1}. The *g*-values of a $^2\Pi$ state in an electrostatic field depend on the relative magnitudes of λ, the spin–orbit coupling constant, and Δ and E, parameters which define the crystal field splitting of the $2p\sigma^*$ and $2p\pi$ orbitals (Fig. 2).

Känzig *et al.* (18–20) have derived equations for the principal *g*-values of a $^2\Pi$ state, such as O_2^-, which has a $^2\Pi_{3/2}$ ground state. Their equations, modified because of the change of sign of λ, become for NO

$$[1]\quad g_{xx} = \frac{g_e\Delta}{\sqrt{\lambda^2+\Delta^2}} - \frac{\lambda}{E}\left\{\frac{\Delta}{\sqrt{\lambda^2+\Delta^2}} - \frac{\lambda}{\sqrt{\lambda^2+\Delta^2}} - 1\right\}$$

$$[2]\quad g_{yy} = \frac{g_e\Delta}{\sqrt{\lambda^2+\Delta^2}} - \frac{\lambda}{E}\left\{\frac{\Delta}{\sqrt{\lambda^2+\Delta^2}} + \frac{\lambda}{\sqrt{\lambda^2+\Delta^2}} + 1\right\}$$

$$[3]\quad g_{zz} = g_e - \frac{2l\lambda}{\sqrt{\lambda^2+\Delta^2}}$$

where g_e = free-electron *g*-value, l = effective

TABLE 2

Calculated values of parameters

Zeolite	$\Delta \times 10^{-3}$ (cm^{-1})	$E \times 10^{-4}$ (cm^{-1})	$g_{xx} - g_{yy}$	$\left(\frac{\partial^2 V}{\partial x^2} - \frac{\partial^2 V}{\partial y^2}\right)_0 \times 10^{-16}$ ($V\ cm^{-2}$)
Faujasite	1.11	1.2	0.022 (38 G)	−0.46
Mordenite	1.05	1.1	0.024 (41 G)	−0.42
Linde 5A	1.69	3.7	0.007 (12 G)	−0.70

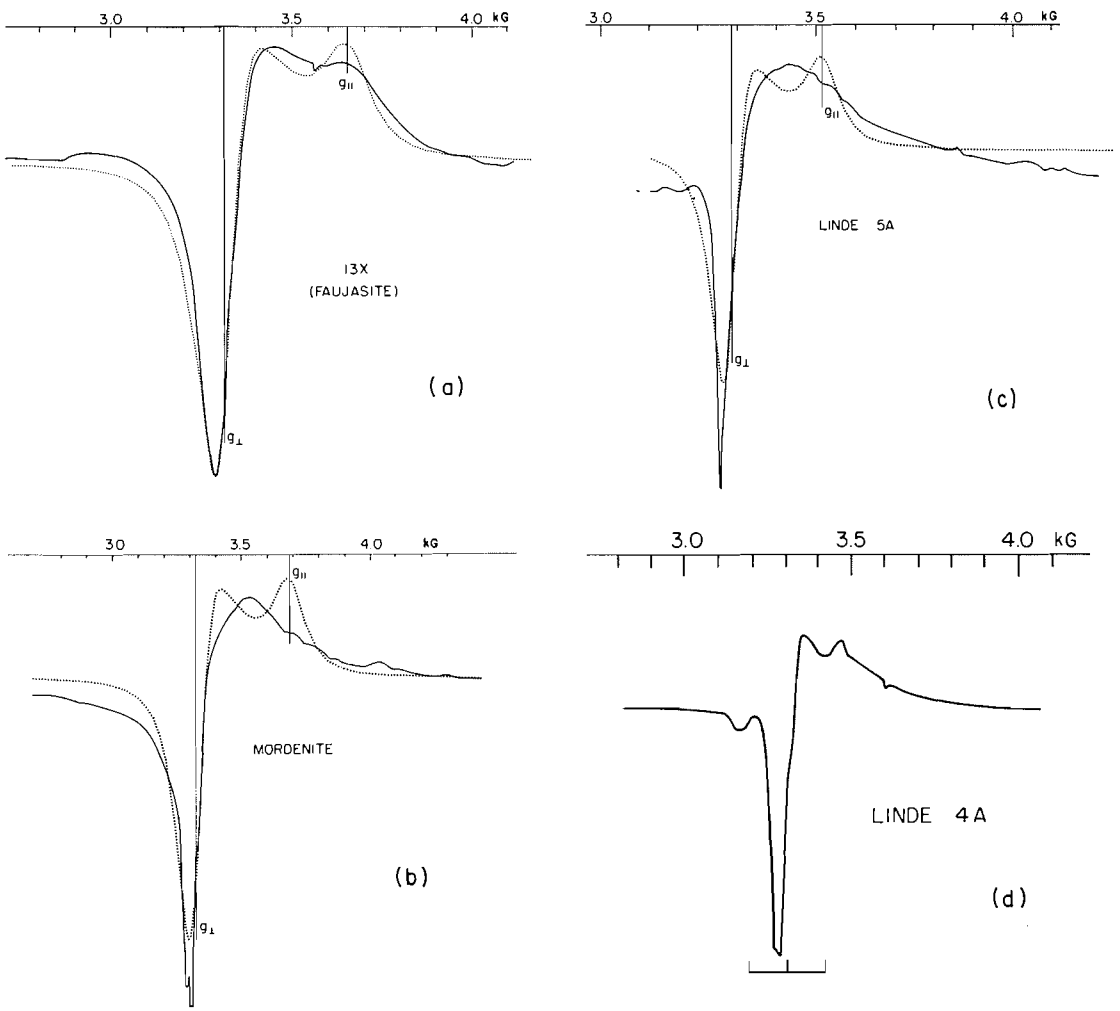

FIG. 1. Calculated (line) and digitized experimental (points) e.s.r. spectra of NO adsorbed on (*a*) faujasite, (*b*) mordenite, (*c*) Linde 5A, (*d*) Linde 4A zeolite.

g-factor for the orbital contribution ($l = 1$ for the free molecule but may change on adsorption).

The determination of the parameters Δ, E, and l from our experimental data is ambiguous, as we have only two experimentally determined *g*-values. The work of Känzig *et al.* (18–20) and Vanotti and Morton (21) indicates, however, that the value of l may be expected to be close to unity, and we assume this value here. The apparent axial symmetry must be the result of λ/E being small, but the theory indicates that some deviation from axial symmetry should exist. The polycrystalline spectrum of a species with an anisotropic **g**-tensor is well known (22). In this case, an infinite singularity occurs (assuming a δ-function line shape) at g_{yy}, and we conclude that the experimentally determined *g*-values are g_{yy} and g_{zz}. We are unable to determine g_{xx}, because of the small deviation from axial symmetry. The values of Δ and E derived using the experimental *g*-values and eqs. [1]–[3] are given in Table 2. Also included in this table are the calculated values of $g_{xx} - g_{yy}$. In all cases, this is seen to be less than the linewidth, giving support to the procedure used. The values of Δ for the zeolites are only about one-half the value of Lunsford for MgO. This is not surprising, since the values of Δ for O_2^- on Na–Y zeolite and MgO (14) are similarly related.

It is interesting to note that the calculations

Can. J. Chem. Downloaded from www.nrcresearchpress.com by 210.87.254.6 on 09/05/12
For personal use only.

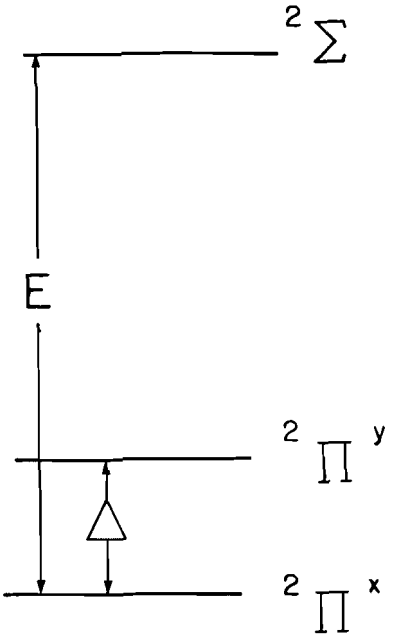

FIG. 2. Energy levels of NO when adsorbed on surface.

indicate that, on adsorption, the $^2\Sigma$ state is shifted much closer in energy to the $^2\Pi$ state. In the free molecule, this separation (17) is 4.4×10^4 cm^{-1}. In the case of faujasite and mordenite, the predicted position of the $^2\Sigma$ state should give a transition in the red or near infrared. Experimentally, at 77 °K these samples were purple and brown, respectively, in reasonable agreement with the prediction.

(b) The Surface Field

In this section we wish to see what information can be obtained about the surface from the magnitude of the splittings Δ and E.

We define orbital energies ε_i^0 which are eigenvalues of the free-molecule Hamiltonian H_0 with eigenfunctions ψ_i^0. In the presence of the surface field, the energies, to first order, are given by

$$[4] \qquad \varepsilon_i = \varepsilon_i^0 + \langle \psi_i^0 | \mathscr{H}' | \psi_i^0 \rangle$$

where $\mathscr{H}'$ is the Hamiltonian representing the perturbation due to the surface environment.

Classically, the energy W corresponding to this Hamiltonian can be considered as arising from the interaction of the charge distribution due to the surface, $\rho_s(r)$, with the molecular charge density, $\rho_{NO}(R)$. Hence (23)

$$W = \iint \frac{\rho_s(r)\rho_{NO}(R)\, dr\, dR}{|r - R|}$$

where r and R are taken to have origin at the molecular center of mass.

Expansion of $1/|r - R|$, in terms of the usual normalized spherical harmonics, enables separation of the terms relating to surface (lower case) and molecule (capitals). Thus

$$\frac{1}{|r - R|} = \sum_{l=0}^{\infty} \sum_{m=-l}^{l} \frac{4\pi}{2l+1} \frac{R^l}{r^l + 1} \times Y_l^m(\theta_s, \phi_s) Y_l^{-m}(\Theta, \Phi)$$

$$[5] \quad W = \int \sum_{l,m} \sqrt{\frac{4\pi}{2l+1}} \frac{\rho_s(r)}{r^l + 1} Y_l^m(\theta_s, \phi_s)\, dr \times \int \sum_{l,m} \sqrt{\frac{4\pi}{2l+1}}\, \rho(R) R^l Y_l^{-m}(\Theta, \Phi)\, dR$$

Instead of the continuous charge distribution $\rho_s(r)$, we assume for the surface a discrete set of charged particles, e_i. For the molecule, $\rho(R)$ will be described by the wave functions ψ_i. The Hamiltonian operator equivalent to eq. [5] may then be written as

$$\mathscr{H}' = \sum_{l,m} \left\{ \left[\sqrt{\frac{4\pi}{2l+1}} \sum_i e_i r_i^{-(l+1)} Y_l^m(\theta_s^i, \phi_s^i) \right] \times \left[-e \sqrt{\frac{4\pi}{2l+1}} R^l Y_l^{-m}(\Theta, \Phi) \right] \right\}$$

Substitution in eq. [4] yields

$$[6] \qquad \varepsilon_i = \varepsilon_i^0 + \sum_{l,m} A_l^m B_l^{-m}$$

where

$$A_l^m = \sqrt{\frac{4\pi}{2l+1}} \sum_i e_i r_i^{-(l+1)} Y_l^m(\theta_s^i, \phi_s^i)$$

$$B_l^{-m} = -e \sqrt{\frac{4\pi}{2l+1}} \langle \psi_i^0 | R^l Y_l^{-m}(\Theta, \Phi) | \psi_i^0 \rangle$$

Assuming rhombic symmetry, the first terms in the expansion of eq. [6] are

$$[7.1] \quad \varepsilon_i = \varepsilon_i^0 + A_1^0 B_1^0 + A_2^0 B_2^0 + (A_2^{-2} B_2^2 + A_2^2 B_2^{-2}) + \cdots$$

The spherical harmonics necessary to evaluate these terms are (24)

$$Y_1^0(\theta, \phi) = \sqrt{\frac{3}{4\pi}} \cos\theta$$

Can. J. Chem. Downloaded from www.nrcresearchpress.com by 210.87.254.6 on 09/05/12
For personal use only.

$$Y_2^0(\theta, \phi) = \sqrt{\frac{5}{4\pi}} \cdot \tfrac{1}{2}(3\cos^2\theta - 1)$$

$$Y_2^{\pm 2}(\theta, \phi) = \frac{1}{4}\sqrt{\frac{15}{2\pi}} \sin^2\theta\, e^{\pm 2i\phi}$$

Noting that $V = \sum_i e_i r_i^{-1}$ is the potential of the charged particles responsible for the surface field, we can interpret the terms in the expansion [7.1] as follows

$$[7.2] \quad A_1^0 B_1^0 = -\sum_i e_i r_i^{-2} \cos\theta_s{}^i \times (e\langle\psi_i^0|R\cos\Theta|\psi_i^0\rangle) = \left(\frac{\partial V}{\partial z}\right)_0 e\langle Z\rangle$$

This term represents the interaction of the surface field with the dipole $\mu_{NO} = e\langle Z\rangle$ of the NO molecule.

$$[7.3] \quad A_2^0 B_2^0 = -\sum_i e_i r_i^{-3} \cdot \tfrac{1}{2}(3\cos^2\theta_s{}^i - 1) \times (e\langle\psi_i^0|R^2 \cdot \tfrac{1}{2}(3\cos^2\Theta - 1)|\psi_i^0\rangle) = -\frac{e}{2}\left(\frac{\partial^2 V}{\partial z^2}\right)_0 \left\langle\frac{3Z^2 - R^2}{2}\right\rangle$$

This term gives the interaction of the axial component of the quadrupole moment

$$Q_{zz} = \langle(3Z^2 - R^2)/2\rangle$$

with the axial component of the field gradient. Finally

$$[7.4] \quad A_2^{-2} B_2^2 + A_2^2 B_2^{-2} = -\frac{3}{4}\sum_i e_i r_i^{-3} \times \sin^2\theta^i \cos 2\phi^i (e\langle\psi_i^0|R^2 \sin^2\Theta \cos 2\Phi|\psi_i^0\rangle) = -\frac{e}{2}\left(\frac{\partial^2 V}{\partial x^2} - \frac{\partial^2 V}{\partial y^2}\right)_0 \cdot \left\langle\frac{X^2 - Y^2}{2}\right\rangle$$

gives the interaction of the non-axial component of the field gradient with the non-axial component of the quadrupole moment

$$Q_{xx} - Q_{yy} = \langle(X^2 - Y^2)/2\rangle$$

Experimentally (25), NO has a dipole moment of 0.158 D. Monod *et al.* (2) have estimated the electric field in the interior of faujasite to be about 1.6×10^8 V/cm. It is very likely that the interaction of this dipole with the field will orient the molecule in the field direction, the energy of the interaction being $\sim 400\ \text{cm}^{-1}$ for a field of this strength. Interaction with the axial component of the quadrupole moment and polarizability terms will also contribute to this alignment. In the discussion that follows, we therefore assume that the molecular axis and field direction coincide.

Moffitt (26) has discussed the contributions of the σ and π electrons to the total dipole moment of CO ($\mu = \mu_\sigma + \mu_\pi$). He finds that the σ dipole moment is of opposite sign but almost equal in magnitude to the π dipole moment. This explains the observed small dipole moment (0.118 D) of CO. Moffitt suggests that a similar explanation holds for NO, where the dipole moment is also relatively small.

If we consider the effect of the electric field term [7–2] on the orbital energies of NO, it is clear that the interaction with the field will not remove the degeneracy of the π levels (i.e. the π_x and π_y orbitals have the same dipole moment).

The axial component of the quadrupole moment will be the same for the π_x and π_y orbitals, and hence the term [7–3] will not remove the degeneracy of the π levels. The non-axial component, $Q_{xx} - Q_{yy} = \tfrac{1}{2}\langle X^2 - Y^2\rangle$, on the other hand, will shift the π_x and π_y orbitals by an equal amount but with opposite sign, and hence the degeneracy is removed. The energy separation caused by this interaction is given by

$$[8] \quad \Delta = -e\left\langle\frac{X^2 - Y^2}{2}\right\rangle\left(\frac{\partial^2 V}{\partial x^2} - \frac{\partial^2 V}{\partial y^2}\right)_0$$

To estimate the quadrupole moment of a π_x orbital we make the crude approximation that the p_x orbitals may be replaced by a point model, where a half unit charge is placed at an average distance $d_i/2$ from the nucleus. The values of d_i for nitrogen and oxygen, d_N and d_O, were obtained from the approximation used by Parr (27). He approximated the p orbital by two tangential uniform spheres of diameter $d_i = 4.597\, Z_p^{-1} \times 10^{-8}$ cm, where Z_p is the effective nuclear charge as defined by Slater's rules (28). We place the half unit charge at the center of these spheres.

Using this method the following values for Q_{zz} and $Q_{xx} - Q_{yy}$ are evaluated

$$Q_{zz} = \left\langle\frac{3Z^2 - R^2}{2}\right\rangle = 0.36 \times 10^{-16} \text{ cm}^2$$

$$Q_{xx} - Q_{yy} = \left\langle\frac{X^2 - Y^2}{2}\right\rangle = 0.30 \times 10^{-16} \text{ cm}^2$$

Can. J. Chem. Downloaded from www.nrcresearchpress.com by 210.87.254.6 on 09/05/12
For personal use only.

where the values

$$d_N = 1.18 \text{ Å}$$
$$d_O = 1.02 \text{ Å}$$
$$r_e = \text{NO bond distance} = 1.15 \text{ Å}$$

have been used. The values given for Q_{zz} and $Q_{xx} - Q_{yy}$ cannot be expected to be accurate, but may at least provide a rough estimate. Using these values and eq. [8], an estimate can be made of the non-axial component of the field gradient. These results are included in Table 2.

The only contributions we have considered so far are the first-order contributions to the electrostatic interaction between the molecule and the surface. While they will not be discussed in detail, it is perhaps worthwhile to make a few comments about the second-order contributions. It appears that, since the polarizability tensor will be axially symmetric, the interaction of the electric field with the induced dipole moment will not remove the degeneracy of the π levels. It is not clear to us, however, what the effect of dispersion forces might be.

A discussion of the terms contributing to Δ is simplified to a large extent by symmetry restrictions. The same is not true, however, when discussing E, and in this case any sort of quantitative discussion is difficult. The Σ–Π separation will in fact be affected by the first-order electric field – dipole and axial field gradient – quadrupole interactions, as well as the second-order electric-field-induced dipole contribution. It seems likely that all these terms may be roughly of the same order of magnitude.

The authors are indebted to Dr. E. J. Casey and Dr. R. A. McIvor for valuable advice and encouragement.

We are grateful to Dr. P. Raghunathan for calculating the spectra based on the anisotropic $\mathbf{g}$ and hyperfine tensors for us.

1. N. Sheppard and D. Yates. Proc. Roy. Soc. London, Ser. A, **238**, 69 (1956).
2. P. Monod, J. A. Cowen, and W. N. Hardy. J. Phys. Chem. Solids, **27**, 727 (1966).
3. J. A. Rabo, C. L. Angell, P. H. Kasai, and V. Schomaker. Discuss. Faraday Soc. **41**, 328 (1966).
4. P. E. Pickert, J. A. Rabo, E. Dempsey, and V. Schomaker. Proc. 3rd Int. Congr. Catal. Amsterdam, 1965. p. 714.
5. G. J. Hoijtink. Rec. Trav. Chim. **76**, 869, 885 (1957).
6. G. J. Hoijtink. Proc. Symp. Heterogeneous Catal. Amsterdam, 1959. p. 90.
7. R. Beringer and J. G. Castle. Phys. Rev. **78**, 581 (1950).
8. C. K. Jen, S. N. Foner, E. L. Cochran, and V. A. Bowers. Phys. Rev. **112**, 1169 (1958).
9. A. Solbakken and L. H. Reyerson. J. Phys. Chem. **63**, 1622 (1959).
10. A. Solbakken. Acta Chem. Scand. **21**, 1123 (1967).
11. C. Jaccard. Phys. Rev. **124**, 60 (1961).
12. D. Mergerian and S. A. Marshall. Phys. Rev. **127**, 2015 (1962).
13. H. Ohigashi and Y. Kurita. J. Phys. Soc. Jap. **24**, 654 (1968).
14. J. Lunsford. J. Chem. Phys. **46**, 4347 (1967); J. Phys. Chem. **72**, 2141 (1968); **72**, 4163 (1968).
15. W. C. Davidon. Argonne Nat. Lab. Rep. ANL 5990 (1959).
16. J. A. Ibers and J. D. Swalen. Phys. Rev. **127**, 1914 (1962).
17. G. Herzberg. Spectra of diatomic molecules. D. van Nostrand Co., Inc., New York. 1950.
18. W. Känzig and M. H. Cohen. Phys. Rev. Lett. **3**, 509 (1959).
19. H. R. Zeller, R. T. Shuey, and W. Känzig. J. Phys. **28**, C4-81 (1967).
20. H. R. Zeller and W. Känzig. Helv. Phys. Acta, **40**, 845 (1967).
21. L. E. Vannotti and J. R. Morton. Phys. Rev. **161**, 282 (1967).
22. F. K. Kneubühl. J. Chem. Phys. **33**, 1074 (1960).
23. A. Abragam. The principles of nuclear magnetism. Oxford Univ. Press, London. 1967. pp. 159–164. A similar discussion.
24. A. D. Edmonds. Angular momentum in quantum mechanics. Princeton Univ. Press, Princeton, N.J. 1957.
25. D. E. and A. P. Stogryn. Mol. Phys. **11**, 371 (1966).
26. W. Moffitt. Proc. Roy. Soc. London, Ser. A, **196**, 524 (1949).
27. R. G. Parr. J. Chem. Phys. **20**, 1499 (1952).
28. J. C. Slater. Phys. Rev. **36**, 57 (1930).
29. J. W. Searl, R. C. Smith, and S. J. Wyard. Proc. Phys. Soc. London, **74**, 491 (1959).

Can. J. Chem. Downloaded from www.nrcresearchpress.com by 210.87.254.6 on 09/05/12
For personal use only.

Pyrochlores. VI. Preparative chemistry of sodium and silver antimonates and related compounds[1]

DAVID J. STEWART AND OSVALD KNOP
Department of Chemistry, Dalhousie University, Halifax, Nova Scotia
Received December 11, 1969

A number of pyrochlore-structure antimonates MSb_yO_z (M = Na, Ag, K) have been prepared by dry-firing methods. Each M forms a series of compounds which adopt the pyrochlore structure up to a maximum ratio of M:Sb; the ratio depends on M. Antimony in these compounds is usually present simultaneously in trivalent and pentavalent states.

The preparation of the above antimonates by wet methods was also examined. The products obtained were found to depend on the p*H* of the solution. In acid solution a polyantimonate ion exists which on addition of M salts leads to compounds of formula MSb_3O_z, while in alkaline solution the $Sb(OH)_6^-$ ion exists and $MSb(OH)_6$ antimonates are obtained.

A previous literature claim that $NaSbO_3$ occurs with the pyrochlore structure has been disproved. It has been shown that $NaSb_yO_z$ pyrochlore phases exist only for Na:Sb less than 1:1.5.

The preparation of antimonates in the presence of Cl^- and from hydrated reactants was carried out. It was concluded that neither Cl^- nor OH^- or H_2O play a significant part in causing an antimonate of Na, Ag, or K to adopt the pyrochlore structure.

Canadian Journal of Chemistry, **48**, 1323 (1970)

Can. J. Chem. Downloaded from www.nrcresearchpress.com by 210.87.254.6 on 09/05/12
For personal use only.

Introduction

The work reported in this paper began as an extension of previous work (1–5) which examined in detail complex oxides having the pyrochlore structure and containing various combinations of trivalent and tetravalent cations (3–4 pyrochlores). It was hoped to complete this survey of oxide pyrochlores by investigating the analogous 2–5 and 1–5 pyrochlores. However, the preparation of some of these compounds introduced several complications that had not been anticipated. Also, it was found that the existence field of the 1–5 pyrochlores is considerably more extensive than was previously thought. Because of these factors, only 1–5 pyrochlores[2] are discussed in this paper; the 2–5 pyrochlores will be dealt with in a subsequent publication.

The only compounds previously reported to be 1–5 pyrochlores, other than the poorly defined hydrated antimonates described below, are the antimonates $AgSbO_3$ (6–8, 27) and $NaSbO_3$ (6, 7). However, while silver antimonate has always been found to have a pyrochlore structure, regardless of the method of preparation, $NaSbO_3$ has been obtained with the pyrochlore structure only by treating "antimonic acid", in solution or as a suspension, with excess of a sodium salt (6, 7).[3] All other methods gave a product having the *ilmenite* structure (6–10). In view of the known ability of Cl^-, F^-, and OH^- to stabilize the pyrochlore structure,[4] the question arises: does the wet method yield sodium antimonate of the pyrochlore type because introduction of Cl^- (from the $SbCl_5$ used in the preparation of the "antimonic acid" or from NaCl) or H_2O into the antimonate causes stabilization of the pyrochlore structure?

The method which yields the pyrochlore antimonate is also distinguished from the others in that it is the only one involving antimonic acid as an intermediate. Therefore, even if the pyrochlore structure is not stabilized by Cl^- or H_2O, a further question may be asked: is it some property of antimonic acid in solution that causes the antimonate to adopt the pyrochlore structure?

It was the aim of this investigation to answer these questions, and also to find whether other 1–5 pyrochlore-type oxides could be prepared.

The hydrated sodium antimonate, stated to exist with the pyrochlore structure (6–9),[5] can be obtained only in a poorly crystalline state

[1]For Part V, see ref. 5.

[2]Since detailed structure determinations have not as yet been made for all compounds whose preparations are reported in this paper, the term "pyrochlore" is used to denote any compound that gave an X-ray powder pattern consistent with the space group and dimensions of the classical pyrochlore structure.

[3]This product was called β_2-$NaSbO_3$ by Schrewelius (6, 7). It gives a sharp X-ray powder pattern of the pyrochlore type.

[4]The mineral pyrochlore contains F^- and OH^-, and the fluoride ion, for example, has been shown to stabilize the pyrochlore structure in calcium antimonate even when present in only small concentrations (11, 12).

[5]This is the β_1-$NaSbO_3$ of Schrewelius (6, 7). It gives a diffuse X-ray powder pattern of the pyrochlore type.

Can. J. Chem. Downloaded from www.nrcresearchpress.com by 210.87.254.6 on 09/05/12
For personal use only.

as an intermediate during the dehydration of $NaSb(OH)_6$. Prolonged heating of the latter compound at 200–400 °C in air is necessary to produce the pyrochlore X-ray pattern, and on heating above 400 °C the ilmenite pattern develops. Montmory *et al.* (9) consider the pyrochlore to have the formula $Na_2Sb_2O_5(OH)_2$, but it has been suggested that the representation $Na_2Sb_2O_6(H_2O)$ is more likely (8).

Schrewelius (6) has reported the preparation of a potassium antimonate which gave an X-ray powder pattern containing a number of weak and diffuse lines that correspond to a pyrochlore pattern. He prepared it by repeated evaporation and rehydration of a saturated solution of $KSb(OH)_6$, followed by prolonged heating at 110 °C. Again, it is likely that water or OH^- participate in the structure.

Experimental

The following methods have been used in the past to prepare metal antimonates: (*a*) firing of a mixture of an antimony oxide and a metal salt (6–8, 13); (*b*) precipitation of the metal antimonate from a solution of "$KSb(OH)_6$" by adding the appropriate metal salt (6–8, 14, 15); (*c*) oxidation of an alkaline solution of Sb_2S_3 using H_2O_2, followed by addition of an alkali hydroxide (16); (*d*) precipitation of the metal antimonate by adding the appropriate metal salt to colloidal "antimonic acid" (6, 7, 17); (*e*) oxidation of Sb_2O_3 in alkaline solution using $KMnO_4$ (18) or H_2O_2 (17); (*f*) firing antimony metal with saltpeter and leaching the product with water (15).

Of these methods, only (*d*) has been found to yield an antimonate with the pyrochlore structure (6, 7). This is an indirect method since the "antimonic acid" must first be prepared. The term "antimonic acid" is used loosely to denote both the antimonate ion in solution and the solid that precipitates when the concentration of the sparingly soluble antimonate ion is increased. The precipitated material has also been referred to as a "hydrated antimonic oxide", which is probably a more correct description. The term is used in its looser meaning here. Antimonic acid can be prepared by acidification of "$KSb(OH)_6$" solutions, hydrolysis of $SbCl_5$, or oxidation of Sb_2S_3 with fuming nitric acid followed by hydration with water. According to refs. 19 and 20, the best way of obtaining the acid free of electrolytes (which adsorb strongly on the solid) is to drop $SbCl_5$ into iced water. This method was used primarily in this work, but acidification of "$KSb(OH)_6$" solution was also used because it did not involve Cl^-.

Materials

For the wet preparations, either $SbCl_5$ (Baker and Adamson Reagent) or "$KSb(OH)_6$" (B.D.H. AnalaR Reagent) was used. The former was checked by titration with $KMnO_4$ for Sb(III) content, which was found to be negligible. However, the commercial "$KSb(OH)_6$" was found to be better represented as $KSbO_3.n\ H_2O$, where n was always less than the value of three necessary to give a formula of $KSb(OH)_6$; the AnalaR Reagent material analyzed to $KSbO_3.(2.77\ H_2O)$. Each batch was therefore checked by thermogravimetric analysis (t.g.a.) and titration with standard $AgNO_3$ solution before use.

In the dry preparations, Sb_2O_3 (Fisher Certified Reagent) was always used because analysis of the available commercial "antimony pentoxide" chemicals showed one (Baker Analyzed Reagent) to be amorphous, with an approximate formula of $Sb_2O_{4.4}$, and another (Fisher Certified Reagent) to have an X-ray powder pattern of the Sb_2O_4 type and an oxygen content close to this formula. Where an antimony(V) oxide was required for a preparation, it was obtained by hydrolysis of a weighed amount of $SbCl_5$.

Other materials used in this investigation were: Baker Analyzed Reagent Na_2CO_3, $AgNO_3$, and $Na_2C_2O_4$; B.D.H. AnalaR Reagent KNO_3; B.D.H. Reagent Ag_2CO_3 and Bi_2O_3; Baker and Adamson Reagent Li_2CO_3; Koch–Light $RbNO_3$ (3 *N*); and CIBA optical-grade reagent Ta_2O_5 (> 3 *N*).

Preparation of Antimonates: Wet Methods

(*i*) $SbCl_5$ was added to crushed ice giving a white semicolloidal precipitate of antimonic acid. This precipitate could be filtered only with difficulty because of the fine particle size and had to be passed a number of times through the porous porcelain filtering crucible before a clear filtrate could be obtained. The precipitate was washed with cold water until the washings showed no trace of Cl^- when tested with $AgNO_3$. After drying at room temperature, the antimonic acid was shaken with distilled water to form a suspension, to which the appropriate metal ion was added. Boiling this mixture for some hours produced a crystalline precipitate of the metal antimonate.

(*ii*) $SbCl_5$ was hydrolyzed as above and the appropriate metal ion added directly to the semicolloidal solution, which was then boiled until a crystalline product resulted. This method avoided the tedious separation of the antimonic acid precipitate required in (*i*), but meant that precipitation of the metal antimonate occurred in strongly acid solution containing Cl^-.

(*iii*) Antimonic acid was prepared from $KSb(OH)_6$ solution by precipitation with acid and treated according to (*i*).

(*iv*) Antimonic acid obtained from $KSb(OH)_6$ as in (*iii*) was reacted directly with metal ions as in (*ii*).

(*v*) The appropriate metal ion was added directly to a solution of $KSb(OH)_6$ and the precipitate filtered as described in (*i*).

The antimonates obtained by methods (*i*)–(*v*) were finally dried to constant weight either at room temperature or at 500–700 °C. In each case, the temperature necessary to achieve an anhydrous product without causing decomposition was previously determined by t.g.a. using a small amount of the sample dried at room temperature.

Preparation of Antimonates: Dry Methods

Either Sb_2O_3 or antimonic acid of known Sb content was mixed with the appropriate weight of a metal carbonate, oxalate, nitrate, or acetate. The reagent powders were then ground and mixed in an agate mortar

Can. J. Chem. Downloaded from www.nrcresearchpress.com by 210.87.254.6 on 09/05/12
For personal use only.

TABLE 1

Dry preparation of antimonates

Preparation No.	Reactants	Heat treatment*	Product†		$a_0(P)$, Å‡
			Type	Composition	
91	$Na_2CO_3 + 5Sb_2O_3$	410/35, 550/19, 830/21, 1000/17	*P*	$NaSb^{III}_{3.75}Sb^{V}_{1.25}O_{9.25}$	10.290
99	$Na_2ox + 3Sb_2O_3$	415/21, 750/16, 850/17, 840/26, 880/67	*P*	$NaSb^{III}_{1.12}Sb^{V}_{1.88}O_{6.88}$	10.291
33	$Na_2ox + 3Sb_2O_3$	680/17, 1010/23	*P*	$NaSb^{III}_{1.09}Sb^{V}_{1.91}O_{6.91}$	10.291
77	$2Na_2CO_3 + 5Sb_2O_3$	245/31, 510/22, 750/45, 940/22	*P*	$NaSb^{III}_{0.70}Sb^{V}_{1.80}O_{6.05}$	10.291
76	$Na_2CO_3 + 2Sb_2O_3$	245/31, 510/22, 750/45, 940/22	*P*	$NaSb^{III}_{0.50}Sb^{V}_{1.50}O_{5.00}$	10.289
86	$2Na_2CO_3 + 3Sb_2O_3$	460/22, 640/22, 990/17, 900/19	*P* + *I*	$(NaSb^{III}_{0.34}Sb^{V}_{1.16}O_{3.91})$§	10.281
34	$Na_2ox + Sb_2O_3$	760/19, 1035/66	*I*	$NaSb_{1.00}O_{2.95}$	
49	$NaSb(OH)_6$	1070/8	*I*	$NaSb_{1.00}O_{2.99}$	
89	Na_2CO_3 + antimonic acid	460/22, 640/22	*I*	$NaSb_{1.00}Sb_{3.00}$	
112	$2KNO_3 + 5Sb_2O_3$	345/19, 690/16, 850/15, 880/18	*P*	$KSb^{III}_{1.43}Sb^{V}_{3.57}O_{11.57}$	10.312
62	$KSb(OH)_6 + Sb_2O_3$	675/17, 825/22, 1010/70, 1050/47	*P*	$KSb^{III}_{2.54}Sb^{V}_{0.46}O_{5.54}$	10.343
93	$KNO_3 + Sb_2O_3$	450/22, 1000/18, 1000/21, 1140/7	Complex		
63	$2KNO_3 + Sb_2O_3$	450/23, 760/27, 900/18, 1050/44	*I* + ?	$(KSb_{1.00}O_{3.0})$§	
60	$KSb(OH)_6$	945/17	*I* + ?	$(KSb_{1.00}O_{3.0})$§	
59*c*	$2AgNO_3 + 3Sb_2O_3$	400/12, 645/18, 825/23	*P*	$AgSb^{III}_{0.81}Sb^{V}_{2.19}O_{7.19}$	10.296
59*d*	59*c*	1010/70	*P*	Uncertain	10.278
110	$AgNO_3 + Sb_2O_3$	345/19, 690/16, 850/15, 880/18	*P*	$AgSb^{III}_{0.36}Sb^{V}_{1.64}O_{5.14}$	10.290
111	$4AgNO_3 + 3Sb_2O_3$	345/19, 690/16, 850/15, 880/18	*P*	$AgSb^{III}_{0.30}Sb^{V}_{1.20}O_{3.95}$	10.280
64	$2AgNO_3 + Sb_2O_3$	425/19, 870/21, 925/23	*P*	$AgSb^{III}_{0.12}Sb^{V}_{0.88}O_{2.88}$	10.249
51	$AgSb(OH)_6$	780/48	*P*	$AgSb_{1.00}O_{3.0}$	10.249‖
88	$2AgNO_3 + Sb_2O_3$	350/½, 460/22, 640/22, 780/21, 900/19, 935/17	*P* + Ag	$(Ag_{1.50}SbO_{2.53})$§	10.249

*410/35 stands for 410 °C for 35 h.

†*P*, pyrochlore; *I*, ilmenite. The empirical formulae have been normalized to 1 M (M = Na, K, Ag). Errors in the formulae arise mainly from impurity of reactants and handling losses during firing. These factors probably cause errors of up to ±0.2% in the overall weight of product obtained. For example, the composition of preparation No. 91 would be $Na_{1.00\pm0.02}Sb^{III}_{3.75\pm0.08}Sb^{V}_{1.25\pm0.03}O_{9.25\pm0.18}$, and similar error margins are to be applied to the other compositions.

‡The uncertainty in the $a_0(P)$ values is ±0.001 Å.

§Overall composition of product.

‖The same value (±0.002 Å) was obtained by Sleight (27) for all his preparations, while Schrewelius (6, 7) reported a value of 10.25 Å (converted from kX).

TABLE 2
Comparison of analytical methods

Compound	Wt. % oxygen		
	Wt. measurement	Vacuum fusion	Theory
$NaSb_3O_7$	22.3	22.2±0.3	22.4
$AgSbO_3$	17.3	17.1±0.3	17.3

and placed in a sintered alumina or zirconia crucible for firing in an electric muffle furnace in air. Table 1 summarizes the various heat treatments. A preliminary firing at about 400 °C was found necessary, particularly for mixtures of Sb_2O_3 and Na carbonate or oxalate, to avoid fusion of the mixture. After each firing the sample was checked for weight change, reground, weighed again, and returned to the furnace for further firing, until reaction appeared to have ceased.

Chemical Analysis

Wet Preparations

Antimony present in the sample was taken to be that added either as $SbCl_5$ or as $KSb(OH)_6$. A check for dissolved Sb (using KI and back titration with $Na_2S_2O_3$ after oxidation with H_2O_2) showed no significant amounts were present in the filtrates. The Ag or Na content of each antimonate was determined as the difference between the weight added and that remaining in the filtrate. A flame-spectrophotometric method was used to determine the Na content of filtrates, while Ag was analyzed for by a standard gravimetric method (AgCl).

Dry Preparations

All attempts to dissolve the antimonates were unsuccessful, so that standard analytical methods could not be used. It was therefore necessary to calculate the composition of each product from the weights of reactants used. The oxygen content could be calculated from the difference between the mass of the product and the calculated weight of metal atoms. From the amount of oxygen present, the relative proportions of Sb(III) and Sb(V) in the antimonate were then calculated. As a check on the accuracy of this procedure, two of the preparations were analyzed for oxygen by vacuum fusion. The results obtained were in excellent agreement with those from the weight measurements (Table 2).

Instrumental Analysis

Details of the t.g.a., X-ray diffraction, and infrared techniques are given in refs. 1 and 3. Analysis of sodium was made on a Cary Model 511 spectrophotometer using the Na emission line at 5889.965 Å. A graph of emission peak height vs. concentration was prepared using a set of standard Na solutions, and the concentrations of samples were estimated by measuring the emission intensities and interpolating on the graph.

Results and Discussion

Sodium Antimonates: Wet Preparations

Table 3 summarizes the compositions of these products. In all experiments in which Na^+ was added to acidic solutions of antimonate ion, the anhydrous product obtained after drying at 600 °C for 24 h contained an Na:Sb ratio of close to 1:3, except where insufficient Na was added to realize this ratio. These products gave X-ray powder patterns of the pyrochlore type.

Addition of Na^+ to solutions of pH > 8 always gave a precipitate of $NaSb(OH)_6$.[6] On firing this material to about 400 °C, the ilmenite-type $NaSbO_3$ resulted, confirming that it contained an Na:Sb ratio of 1:1. No matter what pH was tried, a precipitate of the ilmenite phase could not be obtained directly.

The results of the wet preparations indicate that different ions exist in antimonate solutions, depending on the pH. In acid solution a polymeric species of formula $Sb_{3x}O_zH_u^{x-}$ appears to exist, which on addition of metal ions, yields salts of formula $M_x^{I}Sb_{3x}O_zH_u$.[7] On drying, compounds of formula MSb_3O_z are formed with an M:Sb ratio of 1:3. Investigations by various authors of the formula of the polymeric species have produced results that are not in good agreement with each other. Souchay and Peschanski (21) propose the formula $HSb_5O_{17}^{2-}$, while Ricca *et al.* (22) suggest $HSb_6O_{17}^{3-}$. If these ions were present in acid solution, the products upon addition of metal ions should contain M:Sb ratios of 3:5 or 2:3, respectively, which we did not obtain. However, the ionic weight of 960 measured by Jander and Joachim (23), who suggest a hexaantimonate, is close to that of, e.g., $Sb_6O_{14}^{2-}$ (ionic weight 955), and this would lead to a compound of Na:Sb = 1:3, in agreement with our results.

There is good agreement amongst various authors (21, 23–25) that, as was observed in this investigation, the ion present in solutions of high pH is $Sb(OH)_6^-$. The addition of metal ions to

[6]As described for "$KSb(OH)_6$", this formula can only apply if sufficient water is present in the material. The product obtained after several days at room temperature had an empirical formula close to $NaSb(OH)_6$ (= $NaSbO_3.3H_2O$), but in general a better representation would be $NaSbO_3.n\,H_2O$, where n is often less than 3. Material with $n < 3$ still showed only X-ray lines of $NaSb(OH)_6$. Since the $NaSb(OH)_6$ structure cannot be retained for less than 3 molecules of water per $NaSbO_3$ unit, it appears that a mixture of $NaSb(OH)_6$ and an amorphous component of formula $NaSbO_3.(3-x)H_2O$ must be formed.

[7]The hydrogen included in this formulation is not intended to represent an acidic hydrogen, but rather hydrogen present as covalent OH or H_2O. The hydrogen in the formulae of refs. 21 and 22 is, however, considered acidic.

Can. J. Chem. Downloaded from www.nrcresearchpress.com by 210.87.254.6 on 09/05/12
For personal use only.

TABLE 3
Pyrochlore antimonates prepared by wet methods*

Method	Reactants	Product No.	Sb (M)	Na or Ag (M)	Product composition	$a_0(P)$ (Å)
Sodium antimonates						
i	$SbCl_5 + H_2O + NaCl$	1	0.147	0.907	$Na_{1.0}Sb_3O_{6.8}$	10.288
		2	0.105	0.126	$Na_{1.0}Sb_3O_{6.8}$	
		3	0.088	0.907	$Na_{0.9}Sb_3O_{6.9}$	
		4	0.079	0.126	$Na_{0.9}Sb_3O_{7.0}$	
ii	$SbCl_5 + H_2O + NaCl$	5	0.135	0.171	$Na_{0.8}Sb_3O_{6.5}$	10.291
		6	0.133	0.017	$Na_{0.4}Sb_3O_{6.5}$†	
		7	0.133	0.007	$Na_{0.2}Sb_3O_{5.8}$†	
		8	0.131	0.171	$Na_{1.1}Sb_3O_{6.4}$	
		9	0.132	0.069	$Na_{0.9}Sb_3O_{6.9}$	
		10	0.084	0.862	$Na_{1.0}Sb_3O_{6.5}$	
ii	$SbCl_5 + H_2O + NaOH$	11	0.121	0.541	$Na_{1.0}Sb_3O_{7.0}$	
		12	0.109	0.134	$Na_{1.0}Sb_3O_{6.7}$	
iii	$KSb(OH)_6 + H^+ + NaCl$	13	0.154	0.171	$Na_{1.0}Sb_3O_{8.1}$‡	10.286
		14	0.152	0.069	$Na_{1.0}Sb_3O_{8.1}$‡	
		15	0.148	0.776	$Na_{1.0}Sb_3O_{8.2}$‡	
iii	$KSb(OH)_6 + H^+ + NaNO_3$	16	0.141	0.536	$Na_{1.0}Sb_3O_{8.2}$‡	
iv	$KSb(OH)_6 + H^+ + NaCl$	17	0.144	0.171	$Na_{1.0}Sb_3O_{7.9}$‡	
		18	0.127	0.776	$Na_{1.0}Sb_3O_{8.1}$‡	
iv	$KSb(OH)_6 + H^+ + NaNO_3$	19	0.151	0.536	$Na_{0.9}Sb_3O_{8.1}$‡	
		20	0.140	0.536	$Na_{1.0}Sb_3O_{8.1}$‡	
v	$KSb(OH)_6 + NaCl$	21	0.155	0.171	$Na_{1.0}SbO_{3.0}$	(Ilmenite)
		22	0.160	0.069	$Na_{1.0}SbO_{2.9}$	(Ilmenite)
Silver antimonates						
iv	$KSb(OH)_6 + H^+ + AgNO_3$	23	0.150	0.171	$Ag_{1.0}Sb_3O_{7.3}$	10.269
		24	0.155	0.989	$Ag_{1.0}Sb_3O_{6.9}$	
		25	0.098	0.070	$Ag_{1.0}Sb_3O_{7.1}$	
v	$KSb(OH)_6 + AgNO_3$	26	0.143	0.171	$Ag_{1.0}SbO_{3.0}$	
		27	0.140	0.989	$Ag_{1.0}SbO_{3.0}$	

*The compositions were determined after firing the reaction products to constant weight at 500–700 °C. They are expressed relative to 3 Sb or 1 Sb. The uncertainties in the empirical formulae are estimated to be ± 0.1 for Na, ± 0.05 for Sb, ± 0.5 for oxygen in the sodium antimonates; ± 0.02 for Ag, ± 0.05 for Sb, and ± 0.35 for oxygen in the silver antimonates. The uncertainties arise partly from the analysis errors and partly from errors caused in separating the fine precipitates of products from solution. The larger errors in the oxygen figures arise because oxygen was determined by difference to 100%. Thus the errors in the metal figures are compounded in the oxygen value and magnified because of the small atomic weight of oxygen compared to those of the metal atoms. For each compound, the error in the oxygen figure is therefore dependent on the other two errors. The uncertainty in the $a_0(P)$ values is ± 0.001 Å.
†Insufficient sodium was added to realize a Na:Sb ratio of 1:3.
‡The oxygen figures are erroneously high owing to contamination by potassium impurity.

alkaline solutions therefore yields compounds with Na:Sb ratios of unity.

The interconversion of the $Sb_{3x}O_zH_u^{x-}$ and $Sb(OH)_6^-$ ions with changing pH could be verified by (*a*) titration of a suspension of $NaSb(OH)_6$ with acid, and (*b*) titration of a suspension of $NaSb_3O_7$ with NaOH. These titrations were followed with a pH meter. Whilst the polymerization of the $Sb(OH)_6^-$ ion occurred rapidly, even in cold solution, the depolymerization of the $Sb_{3x}O_zH_u^{x-}$ ion was very slow, even at 100 °C. The powder pattern of the precipitate obtained after titration (*b*) contained lines of the pyrochlore antimonate as well as those of $NaSb(OH)_6$, even though the solution had been boiled for more than 10 h.

Antimonic acid prepared from $KSb(OH)_6$ apparently adsorbed potassium ions from solution. Thus, addition of NaCl yielded a sodium antimonate that spectrographic analysis showed to contain as much as 1% K for a Na content of 3%. The presence of potassium in products 13–20 (Table 3) is reflected in an erroneously high figure for oxygen content. This arises because after determination of the Na and Sb contents of the preparations, the remaining weight was taken to be entirely oxygen and no potassium was allowed for.

Other Antimonates: Wet Preparations

Because K antimonates are appreciably soluble, no attempt was made to prepare them by wet methods. However, the products obtained on adding an Ag salt to an antimonate solution were analogous in composition to those obtained on addition of Na^+ (see Table 3).

Dry Preparations

Table 1 summarizes the dry preparations of

Can. J. Chem. Downloaded from www.nrcresearchpress.com by 210.87.254.6 on 09/05/12
For personal use only.

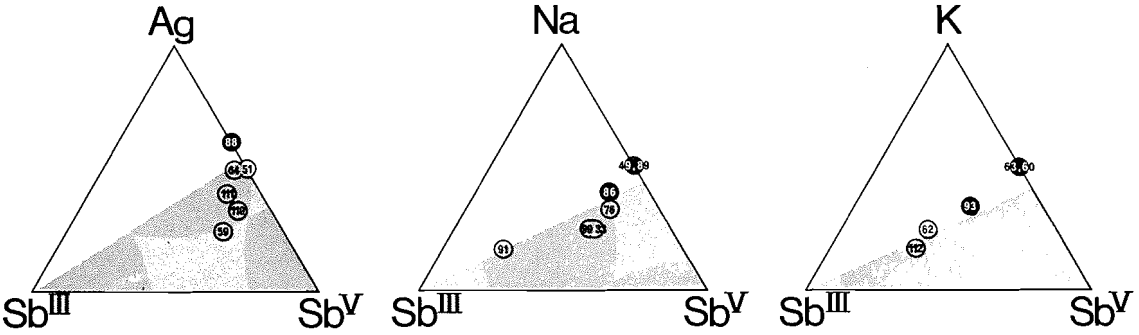

FIG. 1. Products of preparation of MSb_yO_z antimonates by dry methods (Table 1). Open circles: a homogeneous pyrochlore phase $M^{I}Sb^{III}_{t}Sb^{V}_{y-t}O_z$ ($z = 0.5 + 2.5\,y - t$) is the sole product; full circles, other results. The estimated existence fields of the homogeneous pyrochlore phases are shaded grey. The phase and structural relationships along the line Sb^{III}–Sb^{V} are not considered here.

metal antimonates. For each of the systems Ag–Sb–O, Na–Sb–O, and K–Sb–O, a range of M:Sb ratios gave compounds with the pyrochlore structure. The ranges of composition that yielded pyrochlore phases were different for each system, as shown in Fig. 1. In all the systems, the M:Sb ratio of 1:3 was included in the pyrochlore field, but otherwise no special compositional stability was attributable to phases having this ratio. It must therefore be concluded that the pyrochlore products of the wet methods form with an M:Sb ratio of 1:3 entirely because of the structure of the antimonate ion in acid solution, and not from any special stability that distinguishes this ratio. In confirmation of this conclusion, when the precipitated antimonic acid is removed from solution before being reacted dry with excess Na_2CO_3 (see No. 89, Table 1), an ilmenite-type $NaSbO_3$ is obtained rather than the pyrochlore $NaSb_3O_z$ which was obtained in solution. That a pyrochlore-type product is always obtained when an Ag salt is added to an antimonate solution, irrespective of the pH, is clearly because the Ag:Sb ratio of 1:1, as well as that of 1:3, is included in the pyrochlore existence field.

Since in this work controlled atmospheres were not used, it was not possible to control the Sb(III):Sb(V) ratio in the products, although, at a given temperature, a particular ratio could usually be maintained. The Sb(III):Sb(V) ratios for the various antimonates in Table 1 are therefore merely the ratios that resulted for the firing schedules quoted, and not necessarily equilibrium values. The reduction of Sb(V) to Sb(III) did not appear to have any significant effect on the stability of the pyrochlore structure since for the same M:Sb ratio products could be prepared with different Sb(III):Sb(V) ratios.

As shown in Fig. 1, the magnitudes of the composition ranges for which the metal antimonates exist with the pyrochlore structure follow an order Ag > Na > K. Since the stability of the pyrochlore structure has been shown, for the 3–4 pyrochlores at least, to depend on the relative and absolute sizes of the cations involved (*cf.*, for example, refs. 3–5), it might be expected that the above order would be K > Ag > Na, i.e. the same as the sequence of ionic radii.[8] It thus appears that the different electronic structure of Ag, compared to K and Na, must be important in causing silver antimonate to adopt a pyrochlore-type structure. Perhaps Ag enters into a different bonding arrangement than Na and K, such as bonding via d orbitals, that would not be possible with these latter ions. However, it is also possible that some of the structural features of the Ag antimonates, such as cation distribution and site occupancy, differ from those of the Na and K compounds. A detailed investigation of the crystal structures of the antimonates is therefore necessary before justifiable conclusions can be drawn. Work with this aim is in progress.

Table 4 summarizes a number of attempts to prepare mixed-metal antimonates. These preparations were tried to investigate the effect of ionic size of the metal combined with Sb and, where Bi was substituted for Sb, the effect of trivalent ions in place of pentavalent ions. However, none of

[8]The Shannon and Prewitt (26) ionic radii for six-coordination are 1.38 Å for K^+, 1.15 Å for Ag^+, and 1.02 Å for Na^+.

Can. J. Chem. Downloaded from www.nrcresearchpress.com by 210.87.254.6 on 09/05/12
For personal use only.

TABLE 4

Preparation of mixed antimonates and related phases*

Preparation No.	Reactants	Heat treatment	Product	
			Type	Overall composition
78	$Li_2CO_3 + 3Sb_2O_3$	550/25, 930/21, 1000/21	Not *P*	$LiSb_3O_{8.0}$
73	$2RbNO_3 + 3Sb_2O_3$	415/21, 830/32, 970/23, 1000/17	*P* + ?	$RbSb^{III}_{0.56}Sb^{V}_{2.44}O_{7.44}$
97	$Na_2CO_3 + 2AgNO_3 + 2Sb_2O_3$	425/48, 680/23, 850/18	*P* + *I*	$NaAgSb^{III}_{0.52}Sb^{V}_{1.48}O_{5.48}$
87	$Na_2CO_3 + 2KNO_3 + 2Sb_2O_3$	460/22, 640/22, 990/17, 900/19, 935/17, 1120/27, 1000/22	*P* + *I*	$NaKSb^{III}_{0.50}Sb^{V}_{1.50}O_{5.50}$
98	$KNO_3 + AgNO_3 + Sb_2O_3$	680/23, 850/18, 920/18	*P* + ?	$KAgSb^{III}_{0.50}Sb^{V}_{1.50}O_{5.50}$
92	$Na_2CO_3 + Bi_2O_3 + 2Sb_2O_3$	450/22, 650/70, 740/21, 1000/27, 1000/22, 1030/23, 1090/½	*P* + ?	$NaBiSb^{III}_{0.64}Sb^{V}_{1.36}O_{6.36}$
90	$Ag_2CO_3 + Ta_2O_5$	415/23, 615/23, 680/21, 990/17, 900/19, 1015/22	†	$AgTaO_{2.87}$
96	$Ag_2CO_3 + 2KNO_3 + 2Ta_2O_5$	450/18, 550/25, 930/21, 1000/21, 1140/7	Not *P*	$AgKTa_2O_{5.83}$

*See footnotes to Table 1.
†Cubic perovskite (cf. refs. 28 and 29).

the preparations yielded single-phase pyrochlore products.

Effect of Anion Substitution

The pyrochlore antimonates obtained by wet methods in which Cl^- was present during precipitation did not show any enhanced stability, either structural or thermal, in comparison with products obtained free of chloride. Also, infrared and t.g.a. methods showed that the pyrochlore structure was stable without any detectable water or OH^- being present. Furthermore, an attempt to introduce OH^- or H_2O into the antimonate by reacting antimonic acid (hydrated antimony pentoxide) with Na_2CO_3 (No. 89, Table 1) resulted in the ilmenite-type $NaSbO_3$ and not a pyrochlore antimonate.

The hydrated Na antimonate ("β_1-$NaSbO_3$") described by Schrewelius (6, 7), Montmory *et al.* (9), and Brisse (8) does not seem to be a compound of fixed water content, since the weak X-ray lines of the pyrochlore phase persist throughout successive firings, even though a weight loss can be observed on each occasion. Rather than attempting to ascribe a definite formula of $Na_2Sb_2O_5(OH)_2$ or $Na_2Sb_2O_6(H_2O)$, it appears that the compound should be regarded as a reaction intermediate of formula $NaSbO_3 . xH_2O$, where x decreases with increasing heating time and temperature. Because the rate of transformation from $NaSb(OH)_6$ to $NaSbO_3$ is very slow at temperatures around 350 °C, the pyrochlore-like intermediate structure appears to have a finite existence. If a pyrochlore of definite formula *does* exist, then the thermal decomposition product of $NaSb(OH)_6$, which gives a pyrochlore-type X-ray powder pattern, must be a mixture containing, besides the pyrochlore of definite formula, an amorphous component of indeterminate composition. The proportion of the latter increases with temperature, and at constant temperature very slowly with time, thus accounting for the loss in weight. Presumably this amorphous component is the precursor of the ilmenite $NaSbO_3$.

A recent investigation by Sleight (27) of the role of Cl^-, F^-, and OH^- in the $AgSbO_3$ structure led him to conclude that these ions are not important, in agreement with the results of this work.

It must therefore be concluded that only the M:Sb ratio is of importance in determining whether or not a pyrochlore structure is adopted in a given M–Sb–O system.

General Observations

Although wet method *i* is the same as that by which Schrewelius (6, 7) claimed to have prepared $NaSbO_3$ with the pyrochlore structure ("β_2-$NaSbO_3$"), the product we obtained always contained an Na:Sb ratio of 1:3. Furthermore, the dry preparations confirmed that whilst $NaSb_3O_z$ has the pyrochlore structure, the ilmenite structure is obtained for a Na:Sb ratio of unity. Also, Schrewelius described how firing the pyrochlore antimonate (β_2) to 1000 °C caused it to convert

Can. J. Chem. Downloaded from www.nrcresearchpress.com by 210.87.254.6 on 09/05/12
For personal use only.

Can. J. Chem. Downloaded from www.nrcresearchpress.com by 210.87.254.6 on 09/05/12
For personal use only.

partially to the ilmenite structure, but not entirely, even on prolonged heating. This is consistent with an antimonate containing a high proportion of Sb, since a disproportionation could occur, for example

$$2NaSb_3O_7 \rightarrow NaSbO_3 + NaSb_5O_{11}$$

Schrewelius's observation cannot, however, be explained if the pyrochlore had the formula $NaSbO_3$, unless a loss of Na by volatilization had occurred at 1000 °C. To the contrary, our experiments showed that high temperatures caused a loss of Sb oxide rather than Na. Prolonged firing of a pyrochlore antimonate at 1300 °C eventually caused complete conversion to the ilmenite structure, and crystals of Sb_2O_3 and Sb_2O_4 could be collected from the cooler parts of the furnace tube. The conclusion then is that Schrewelius was mistaken in assigning the formula $NaSbO_3$ to the pyrochlore antimonate ("β_2-$NaSbO_3$") he prepared, and that no pyrochlore of this formula exists.

An implication of the composition–structure fields of Fig. 1 is that compounds of formula $M^{I}_{x}Sb^{III}_{t}Sb^{V}_{y-t}O_z$ ($z = 0.5x + 2.5y - t$) adopt the pyrochlore structure even when x is very small. Pyrochlore-type potassium antimonates with as little as 1 wt. % K have already been reported by Schrewelius, and similar compounds were prepared in this investigation. Further discussion of this aspect is reserved for a subsequent publication.

The variation of the lattice parameter a_0 with composition of the antimonates obtained by dry methods is shown in Fig. 2. Because of the increasing reduction of Sb(V) and accompanying loss of oxygen that occurs as the proportion of Sb(III) increases, a simple linear relationship between a_0 and composition would not be expected. However, despite the effect of the Sb(III):Sb(V) ratio, there is, in general, an increase in a_0 of MSb_yO_z (M = Na, Ag, K) antimonates with increasing ionic size of M (for the same M:Sb ratio) as would be expected.

The $a_0(P)$ values of the single-phase sodium antimonate products obtained by dry methods do not vary significantly with change in Na:Sb ratio. Nor is there any large variation between a_0's of wet preparations. The slight variation that does occur is probably due to differences in annealing of different samples.

In contrast to the Na antimonates, a change in Ag:Sb ratio caused a marked variation in a_0 of the Ag antimonate unit cell (Fig. 2). This is illustrated by preparation 59*d* (Table 1), obtained from 59*c* ($AgSb_3O_{7.19}$) by firing a further 70 h at 1010 °C. The loss of Sb caused by this treatment resulted in a decrease in a_0 from 10.296 Å (59*c*) to 10.278 Å (59*d*). Wet preparations of silver antimonates also resulted in products of differing a_0 values, sensitive to variation in Ag:Sb ratio. An unexpected result was the a_0 of the wet-prepared $AgSb_3O_z$, which was 10.269 Å rather than 10.296 Å as was found for the antimonate prepared by the dry method. We cannot at present offer any explanation for this discrepancy.

The curves drawn in Fig. 2 would be expected to extrapolate to Sb_2O_5 (or Sb_2O_z) when the ratio of M:Sb becomes zero. However, literature values for the a_0 of Sb_2O_5 and other antimony oxides with the pyrochlore structure vary considerably, from 10.305 Å (30) to 10.281 Å (31), 10.26 Å (32), and 10.23–10.27 Å (33).[9] It is almost certain that this variation is due to differences in preparation of the various samples and probably also to the presence of impurities (metal ions) in the preparations. In addition, the proportion of Sb(III) in these "Sb_2O_5" and "Sb_3O_6OH" samples is unknown. At present, therefore, attempts at extrapolation are impractical.

Conclusions

(*1*) Contrary to a previous report by Schrewelius (6, 7), $NaSbO_3$ can be prepared only with the ilmenite structure. Dry methods (Nos. 34 and 89, Table 1) yield $NaSbO_3$ directly, as does thermal decomposition of $NaSb(OH)_6$ when carried to complete removal of water (No. 49, Table 1; Nos. 21 and 22, Table 3; *cf.* also refs. 6–10). X-Ray powder photographs of the ilmenite phase are well defined, with sharp lines.

(*2*) Wet conversion of "antimonic acid" (methods *i–iv*) does not yield a pyrochlore with the formula $NaSbO_3$. Instead, pyrochlore products of approximately 1:3 sodium-to-antimony ratio are obtained, which on drying in air give X-ray powder patterns of the pyrochlore type, with well defined lines. Heating these products above 500 °C results in anhydrous products which give very sharp X-ray patterns of the pyrochlore type.

(*3*) The pyrochlore structure of the antimonates does not appear to be stabilized by the substitution of Cl^- or OH^- for oxygen.

[9]The last three values have been converted from kX.

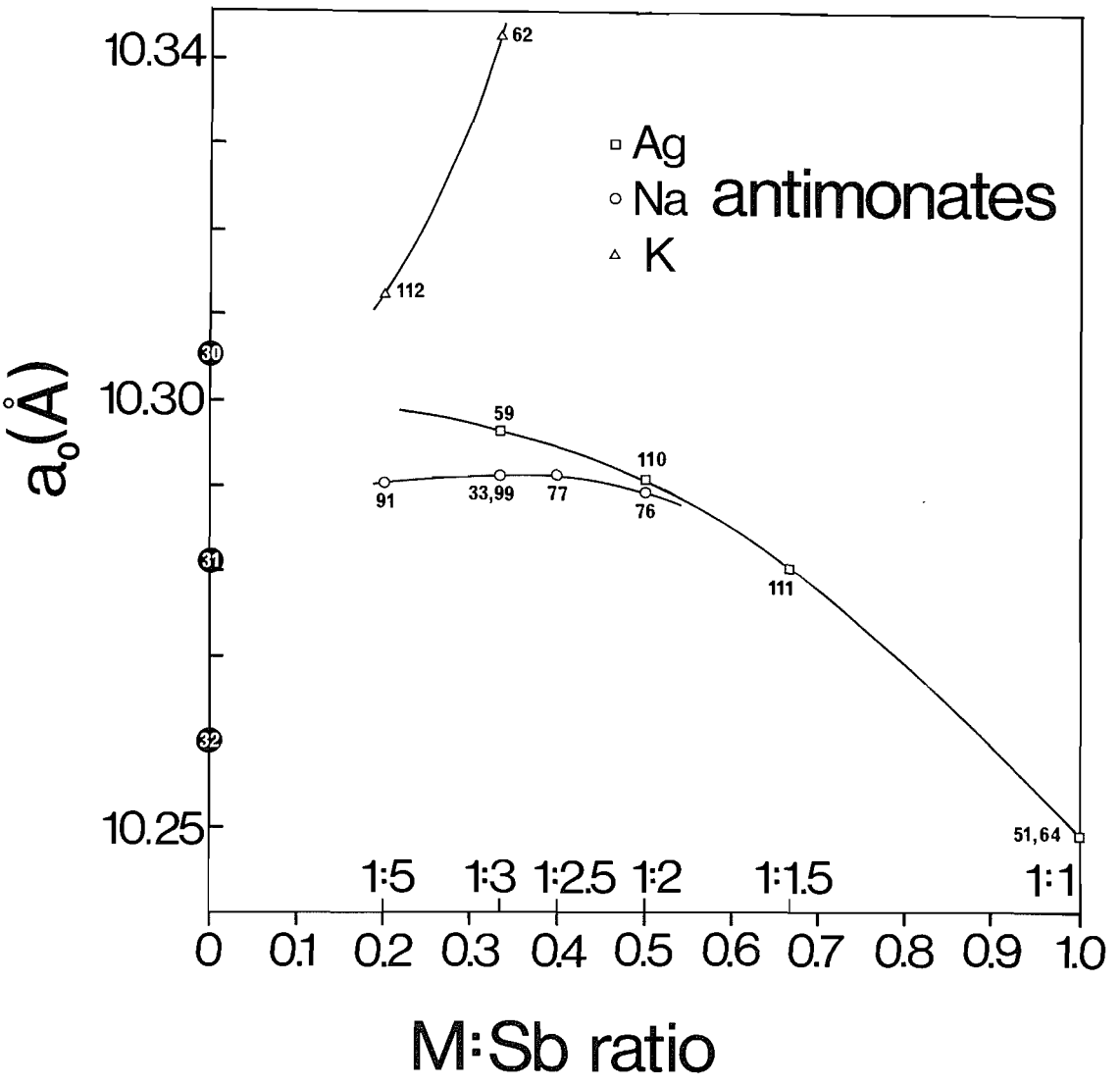

FIG. 2. Variation of a_0 with the M:Sb atomic ratio for homogeneous pyrochlore antimonates $M^{I}Sb^{III}_{t}Sb^{V}_{y-t}O_z$ ($z = 0.5 + 2.5\,y - t$) (Table 1). Full circles: literature values (reference number inside circle) of the lattice parameter of the pyrochlore phase(s) of limiting composition (M:Sb $\rightarrow$ 0; see text).

(*4*) Sodium, potassium, and silver do not form pyrochlore-type antimonates with a unique formula. Instead, $M_xSb_yO_z$ systems (M = Ag, Na, K) exist, where the M:Sb ratio has a definite maximum for each M. The maximum ratio for Ag antimonates is 1:1, while for Na it is approximately 1:1.5, and for K it is closer to 1:2. The antimony is usually present in both valence states, and the limiting ratios M:Sb depend on the ratio of Sb(III) to Sb(V). The minima in the composition fields are bordered by compounds of such small M contents that their formulae are close to Sb_2O_z; the departure of z from the value of five depends on the amount of Sb(III) present.

(*5*) Silver antimonates are anomalous in comparison with the sodium and potassium compounds. Apparently, either the cation distributions (or site occupancies, or both) in the Ag antimonates are different from those in the two alkali antimonates, or else the bonding of the Ag atom in the pyrochlore structure differs from that of Na and K.

Can. J. Chem. Downloaded from www.nrcresearchpress.com by 210.87.254.6 on 09/05/12
For personal use only.

(*6*) Incomplete thermal decomposition of $NaSb(OH)_6$ leads to an intermediate hydrated compound of uncertain formula which gives a weak pyrochlore X-ray powder pattern. The pyrochlore structure persists only as long as water is present.

(*7*) From the formulae of the antimonates obtained by wet conversion of "antimonic acid" it appears that the antimonate ion in acid solution is a polymeric species with a formula $Sb_{3x}O_zH_u^{x-}$. In alkaline solution, the ion present is $Sb(OH)_6^-$. Thus, addition of M^+ ions to an acid solution of antimonate yields products of formula $M_xSb_{3x}O_zH_u$, while addition of M^+ to an alkaline solution produces $MSb(OH)_6$ compounds.

(*8*) Preparation of antimonates from acid solutions in which potassium is present can lead to products containing considerable potassium impurity. This is apparently a consequence of the marked ability of antimonic acid to adsorb metal ions (see refs. 19 and 20).

The present work is a continuation and extension of a preliminary study of pyrochlore antimonates initiated in this laboratory by Dr F. Brisse (8).

We are indebted to Dr C. R. Masson and Mr J. Uher for oxygen analyses by vacuum fusion, and to Dr P. J. Wangersky for the use of a flame spectrophotometer.

Financial support of this investigation by the National Research Council of Canada and by the Geological Survey of Canada through grants in aid of research is hereby acknowledged.

1. O. KNOP, F. BRISSE, L. CASTELLIZ, and SUTARNO. Can. J. Chem. **43**, 2812 (1965).
2. F. BRISSE and O. KNOP. Can. J. Chem. **45**, 609 (1967).
3. F. BRISSE and O. KNOP. Can. J. Chem. **46**, 859 (1968).
4. O. KNOP, F. BRISSE, R. E. MEADS, and J. BAINBRIDGE. Can. J. Chem. **46**, 3829 (1968).
5. O. KNOP, F. BRISSE, and L. CASTELLIZ. Can. J. Chem. **47**, 971 (1969).
6. N. SCHREWELIUS. Doctoral thesis, University of Stockholm, Stockholm, Sweden. 1943.
7. N. SCHREWELIUS. Z. Anorg. Allg. Chem. **238**, 241 (1938).
8. F. BRISSE. Ph.D. thesis. Dalhousie University, Halifax, Nova Scotia. 1967.
9. M.-C. MONTMORY, A. DURIF-VARAMBON, and X. PARÉ. Bull. Soc. Fr. Mineral. Cristallogr. **86**, 434 (1963).
10. W. W. COFFEEN. J. Amer. Ceram. Soc. **39**, 154 (1956).
11. M. A. AIA, R. W. MOONEY, and C. W. W. HOFFMAN. J. Electrochem. Soc. **110**, 1048 (1963).
12. K. H. BUTLER, M. J. BERGIN, and V. M. B. HANNAFORD. J. Electrochem. Soc. **97**, 117 (1950).
13. P. SPIEGELBERG. Ark. Kemi, Mineral Geol. **14A**, No. 5 (1940).
14. G. VON KNORRE and P. OLSCHEWSKY. Ber. Deut. Chem. Ges. **18**, 2353 (1885).
15. F. BEILSTEIN and O. VON BLAESE. Ber. Deut. Chem. Ges. **22**, 530 (1889).
16. G. JANDER and L. BRANDT. Z. Anorg. Allg. Chem. **147**, 5 (1925).
17. G. JANDER and W. BRÜLL. Z. Anorg. Allg. Chem. **158**, 321 (1926).
18. A. REYNOSO. C.R. **32**, 644 (1851).
19. E. BUCHHOLTZ. Doctoral thesis, Dresden. 1927 (quoted in ref. 6).
20. A. LOTTERMOSER. Z. Elektrochem. **33**, 514 (1927).
21. P. SOUCHAY and D. PESCHANSKI. Bull. Soc. Chim. France, **46**, 439 (1948).
22. B. RICCA, G. D'AMORE, and A. BELLOMO. Ann. Chim. Rome, **46**, 491 (1956).
23. G. JANDER and H. JOACHIM. Z. Anorg. Allg. Chem. **315**, 241 (1962).
24. B. RICCA and G. D'AMORE. Ann. Chim. Rome, **46**, 483 (1956).
25. H. BRINTZINGER. Z. Anorg. Allg. Chem. **256**, 98 (1948).
26. R. D. SHANNON and C. T. PREWITT. Acta Crystallogr. **B25**, 925 (1969).
27. A. W. SLEIGHT. Mater. Res. Bull. **4**, 377 (1969).
28. M. H. FRANCOMBE and B. LEWIS. Acta Cryst. **11**, 175 (1958).
29. H. BRUSSET, J. J. P. MARTIN, and G. IANSON. Bull. Soc. Chim. France, 1323 (1968).
30. H. E. SWANSON, M. I. COOK, E. H. EVANS, and J. H. DE GROOT. Nat. Bur. Stand. Circ. 539. Vol. 10, Washington, D.C. 1960. p. 10.
31. K. DIHLSTRÖM and A. WESTGREN. Z. Anorg. Allg. Chem. **235**, 153 (1937).
32. U. DEHLINGER. Z. Kristallogr. **66**, 108 (1927).
33. G. NATTA and M. BACCAREDDA. Gazz. Chim. Ital. **66**, 308 (1936).

Can. J. Chem. Downloaded from www.nrcresearchpress.com by 210.87.254.6 on 09/05/12
For personal use only.

Can. J. Chem. Downloaded from www.nrcresearchpress.com by 210.87.254.40 on 09/05/12
For personal use only.

NOTES

Photosensitization by Cd $^3P_1$ atoms. I. Decomposition of acetone

B. L. KALRA AND A. R. KNIGHT

Department of Chemistry and Chemical Engineering, University of Saskatchewan, Saskatoon, Saskatchewan

Received November 20, 1969

The photodecomposition of acetone vapor at 255 °C sensitized by Cd $^3P_1$ atoms has been investigated. On irradiation of the Cd–acetone system at 3261 Å, both direct and sensitized reaction occur. CO and CH_4 are the only significant volatile products, and their yield is decreased by addition of SF_6 as inert quenching gas. The required participation of triplet acetone molecules in the sensitized reaction and the virtual identity of the direct and sensitized decompositions provide additional evidence for the importance of this excited species in direct photolysis.

Canadian Journal of Chemistry, 48, 1333 (1970)

Introduction

To initiate a series of investigations of the reactions of Cd $^3P_1$ atoms, we have examined briefly the sensitized decomposition of acetone vapor. The purpose of the study was to establish that the experimental approach to be used in the series is appropriate and to obtain data on this previously uninvestigated aspect of acetone photochemistry.

Two previous studies of acetone are particularly relevant to the present work. Lossing and co-workers (1, 2) determined that the primary process in Hg $^3P_1$ sensitization is the same as in direct photolysis. Shaw and Toby (3) recently re-examined the effect on the direct photolysis of temperature between 121 and 298 °C over a pressure range of 0.1 to 220 Torr.

Experimental

A conventional vacuum system was employed. The reaction cell was a Pyrex cylinder, 11.5 cm in length and 3.5 cm o.d. with a side-arm containing Cd metal. The cell and side arm were enclosed in separate furnaces with independent temperature control. In sensitization experiments the side arm was maintained at 245 ± 2 °C while the temperature of the cell was set 10 °C higher to prevent cadmium vapor deposition on the cell windows. The light source was a Phillips 93107E Cd-spectral lamp. A Corning 0160 filter, together with the Pyrex cell window, excluded wavelengths less than ca. 3000 Å.

Baker reagent acetone was employed after degassing and trap-to-trap distillation at reduced pressure. SF_6 (Matheson) was degassed at −196 °C before use. The cadmium metal was Alpha Inorganics, Inc., 99.999% purity.

Reaction products were routinely measured in a gas buret and analyzed by gas chromatography. The substrate and possible products condensable at −196 °C were analyzed using a carbowax 20 M column.

At each acetone pressure, experiments were performed initially with the cadmium-containing side-arm at room temperature to determine the extent of direct photolysis. Subsequently, the arm was heated and the product yields for the combined and direct decompositions measured. Reaction cell temperature was the same in both cases. Because of the relative concentrations and extinction coefficients of Cd and CH_3COCH_3 at 3261 Å, direct absorption by the substrate is significant. A higher operating temperature would have increased the proportion of the sensitized reaction but made less meaningful comparisons with results obtained over the normally investigated temperature range in direct photolysis. The contribution of the sensitized decomposition here, however, is sufficient to detect any appreciable changes in product distribution attributable to sensitization.

Results and Discussion

The only significant volatile products from both the direct and sensitized decomposition are carbon monoxide and methane. Trace amounts of ethane could be detected only in the sensitized reaction. CO and CH_4 rates for the direct and combined decompositions are shown in Fig. 1. As the acetone pressure is increased, the fraction of incident radiation being absorbed by Cd atoms, and hence that leading to photosensitization, decreases. At 20 Torr the latter accounts for about 64% of methane production and about 22% at 160 Torr.

The rate of formation of these two products due to the sensitized decomposition can be determined by difference from the curves of Fig. 1. Both products show an increase in rate to a more or less constant value at about 70 Torr acetone. The rise in rates would correspond to increasing quenching of Cd $^3P_1$ atoms.

Table 1 presents the rate data obtained in the

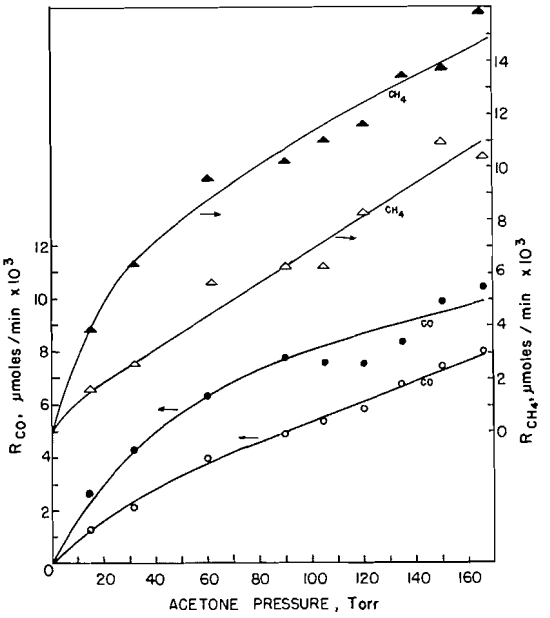

FIG. 1. Rate of production of CO and CH_4 for the direct photolysis at 3261 Å (open symbols) and the combined direct and Cd $^3P_1$ sensitized photolysis (filled symbols) of acetone at 255 °C as a function of substrate pressure. Exposure time was 120 min.

presence of SF_6, expected to act as a quencher of excited species, in the sensitized reaction. Both direct and combined photolyses were carried out and the rates shown in the table calculated. This addend decreases product yields, and at high concentrations prevents completely the sensitized mode. For the direct photolysis there is also a decline, but the effect is less pronounced.

The primary process in the cadmium sensitized decomposition of acetone must involve the formation of triplet acetone, which subsequently would be expected to yield CH_3 and CH_3CO radicals as in direct photolysis. The average value observed for R_{CH_4}/R_{CO}, 1.82, in the sensitized case, indicates that unimolecular decomposition accounts for at least 90% of the acetyl radicals. The decomposition of triplet acetone under these conditions thus effectively produces CO and two CH_3 radicals directly. CH_4 presumably arises via H-atom abstraction from the substrate.[1]

TABLE 1

Rate of CO and CH_4 production in the Cd-sensitized decomposition of acetone in the presence of SF_6*

$P(SF_6)$, Torr	R_{CH_4}†	R_{CO}†
0	4.30	2.50
4.5	2.28	0.73
10	2.34	1.61
22	2.00	1.39
51	1.65	0.85
410	Trace	Trace

*Acetone pressure, 52 Torr; exposure time, 120 min.
†(μmoles/min) × 10^3.

The effect of SF_6 may be due to competitive quenching of Cd $^3P_1$ atoms, deactivation of triplet acetone molecules, or both. Since rates decline in both direct and sensitized systems, it would appear that triplet acetone deactivation makes at least some contribution to the sensitized reaction.

Further investigations of this system will require data on quenching cross sections for acetone and possible addends, and the development of a suitable actinometer. A variety of fundamental investigations on Cd-sensitized reactions will be necessary to obtain data of that type. To this end, studies with some hydrocarbon substrates are currently underway in this laboratory.

The authors gratefully acknowledge the financial assistance of the National Research Council of Canada in this work.

1. J. B. FARMER, F. P. LOSSING, D. G. H. MARSDEN, and E. W. R. STEACIE. J. Chem. Phys. **23**, 1169 (1955).
2. F. P. LOSSING. Can. J. Chem. **35**, 305 (1957).
3. H. SHAW and S. TOBY. J. Phys. Chem. **72**, 2337 (1968).

[1]The CH_2COCH_3 radicals formed in this process could give rise to several nonvolatile products. In view of the small amount of these products (of the order of 1 μmole total, even at high pressures) and the probability of their being adsorbed in the vacuum system, it is not surprising that they were not detected here by thermal conductivity gas chromatography.

Can. J. Chem. Downloaded from www.nrcresearchpress.com by 210.87.254.40 on 09/05/12
For personal use only.

Reaction of azide ion with 9-[2,3-anhydro-5-*O*-(*p*-tolylsulfonyl)-β-D-lyxofuranosyl]adenine[1]

MICHEL HUBERT-HABART AND LEON GOODMAN
Life Sciences Research, Stanford Research Institute, Menlo Park, California 94025

Received[2] April 17, 1969

The reaction of 9-[2,3-anhydro-5-*O*-(*p*-tolylsulfonyl)-β-D-lyxofuranosyl]adenine (7) with sodium azide afforded 9-(2,5-anhydro-3-azido-3-deoxy-β-D-arabinofuranosyl)adenine (**11**) rather than the anticipated 5′-azido-2′,3′-anhydrolyxoside (**8**). Treatment of the azide **11** with sodium benzyl mercaptide resulted in formation of the Schiff base **15** via the 3′-amino-2′,5′-anhydroarabinoside (**12**). Compound **12** was also formed directly by hydrogenation of the azide **11**.

Canadian Journal of Chemistry, **48**, 1335 (1970)

Can. J. Chem. Downloaded from www.nrcresearchpress.com by 210.87.254.42 on 09/05/12
For personal use only.

The opening with nucleophilic reagents, of epoxide rings in the sugar moieties of nucleosides has provided important biochemicals or precursors of them. For example, ring openings, with ammonia, of 2-methylmercapto-6-dimethylamino-9-(2,3-anhydro-β-D-lyxofuranosyl)purine was a key step in one of the syntheses of the antibiotic puromycin (1). Further, the action of sodium benzoate in *N*,*N*-dimethylformamide on 9-(2,3-anhydro-β-D-lyxofuranosyl)adenine (**1**) provided the first synthesis (2) of 9-(β-D-arabinofuranosyl)adenine (**2**), a compound with antitumor (3) and antiviral (4) activity. The epoxide **1** could also be opened smoothly with sodium azide in aqueous 2-methoxyethanol at 80° to give mainly the 3-azidoarabinoside **3** with a small yield of the 2-azidoxyloside **5**.[3] Reaction of **1** with sodium benzyl mercaptide in refluxing methanol furnished excellent yields of the ring-opened products **4** and **6** in a ratio of about 5:1 (5). Based on the results with **1** we reasoned that similar opening of the epoxide ring of the 5′-amino analog **9** of **1** would provide a group of interesting nucleosides. This note describes the unexpected results of our efforts toward this goal.

The tosylation of **1** was straightforward and gave a good yield of the anhydronucleoside **7**. In comparison to most 5′-sulfonate esters of the 9-(β-pentofuranosyl)adenines which form 3,5′-cyclonucleosides readily (6), compound **7** was very stable. On being heated at 95° in dimethylformamide for 24 h there was evidence for cyclization but 37% of the starting material was recovered. When the temperature was raised to 105°, all of the epoxide (**7**) was converted to the 3,5′-cyclonucleoside, a hygroscopic solid with the typical (6) ultraviolet (u.v.) absorption at 272 mμ (p*H* 1 and 7). Reaction of **7** with sodium azide gave good yields of a compound which we assumed to be the azidoepoxide **8** and which could be smoothly converted to an amino compound, presumed to be the aminoepoxide **9**, by catalytic hydrogenation. All attempts to open the expected epoxide ring of the aminonucleoside gave negative results. Both sodium benzoate and sodium azide in dimethylformamide at 135–140° gave back starting material. Similar employment of sodium benzyl mercaptide resulted in recovery of most of the starting material accompanied by a small amount of a Schiff base. Nucleophilic attack on the compound assumed to be **8** was also studied and again sodium benzoate and sodium azide under vigorous conditions failed to effect reaction. Sodium benzyl mercaptide with the azido compound gave the Schiff base mentioned above which could also be formed by reaction of the aminonucleoside with benzaldehyde and which was best characterized as a dimethylaminomethylene derivative (7). When sodium ethyl mercaptide was allowed to react with the azidonucleoside, reduction again occurred to give the aminonucleoside.

The anomalous behavior to nucleophiles of the aminonucleoside and the azidonucleoside made their formulation as 2′,3′-anhydronucleosides

[1]This investigation was partly supported by the Cancer Chemotherapy National Service Center, National Cancer Institute, National Institutes of Health, Public Health Service, Contract No. PH-43-64-500. M. H-H, from I.N.S.E.R.M., Paris, France, was the holder of an Eleanor Roosevelt International Cancer Fellowship awarded by the International Union Against Cancer.
[2]Revision received December 9, 1969.
[3]A. P. Martinez and W. W. Lee. Unpublished work.

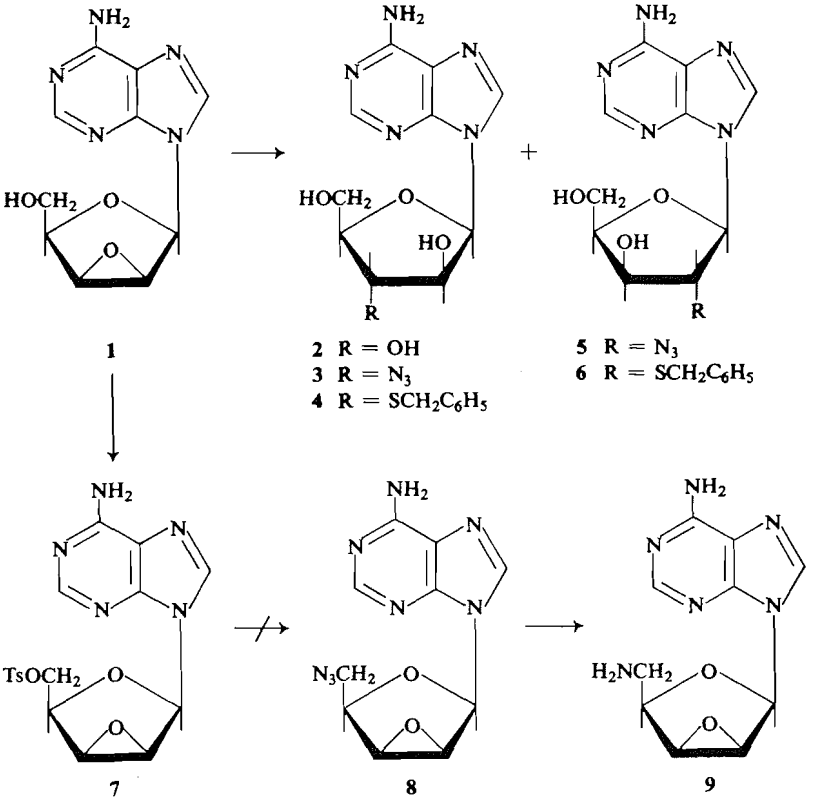

suspect.[4] Isomeric 2′,5′-anhydronucleoside structures would provide a logical explanation for the observed chemistry and such structures would result if azide attack on **7** took place preferentially at C-3′ rather than at C-5′, with intramolecular displacement of the 5′-tosylate by the initially formed anionoid oxygen of the intermediate **10** following. The reduced accessibility of C-5′ to S_N2 displacement correlates with the stability of **7** towards 3,5′-cyclonucleoside formation. The azidonucleoside then would be **11**, the aminonucleoside **12**, the Schiff base **15**, and its dimethylaminomethylene derivative **14**.

That this latter reaction course is the correct one was demonstrated spectrally and chemically. An authentic 2′,5′-anhydroarabinoside was prepared by conversion of 9-(β-D-arabinofuranosyl)-adenine **2** to its 5′-tosylate **13** which, by treatment with methanolic sodium methoxide, gave a good yield of the 2′,5′-anhydro sugar **16**.[5] The nuclear magnetic resonance (n.m.r.) spectra of **16** showed patterns for the sugar protons that were reproduced in the spectra of **11** and **12** when consideration was given to the changes in chemical shift of the proton at C-3′ in the three compounds and which were markedly different from the sugar proton pattern in the 2′,3′-epoxide **1**. In particular the 5′-protons of **1** appeared as a triplet at τ 6.37 while those of **11**, **12**, and **14** appeared as pairs of doublets centered at τ 5.75–5.94. When the 3′-azido derivative **3**[2] was treated analogously, tosylation gave the 5′-tosylate **18**, accompanied by a substantial amount of the ditosylate **19**. Reaction of **18** with sodium hydride in dimethylformamide afforded in very low yield, **11**, shown to be identical to the product from **7** by thin-layer

[4]Our initial assumptions were that the reaction product from **7** was the 2′,3′-anhydronucleoside **8** which was then converted to the aminonucleoside **9**; we were unable to explain the lack of reactivity of these compounds to nucleophiles. Drs. B. A. Otter, K. A. Watanabe, and J. J. Fox of the Sloan-Kettering Institute for Cancer Research suggested the alternative (and correct) 2′,5′-anhydronucleoside formulation and the mechanistic rationalization (**10**) for such a result. We wish to express our appreciation to Drs. Otter, Watanabe, and Fox for resolving our dilemma.

[5]The preparation of **13** and its conversion to **16** were first carried out by Dr. E. J. Reist in connection with another problem. We are grateful to Dr. Reist for the detailed directions for these conversions.

Can. J. Chem. Downloaded from www.nrcresearchpress.com by 210.87.254.42 on 09/05/12
For personal use only.

Can. J. Chem. Downloaded from www.nrcresearchpress.com by 210.87.254.42 on 09/05/12
For personal use only.

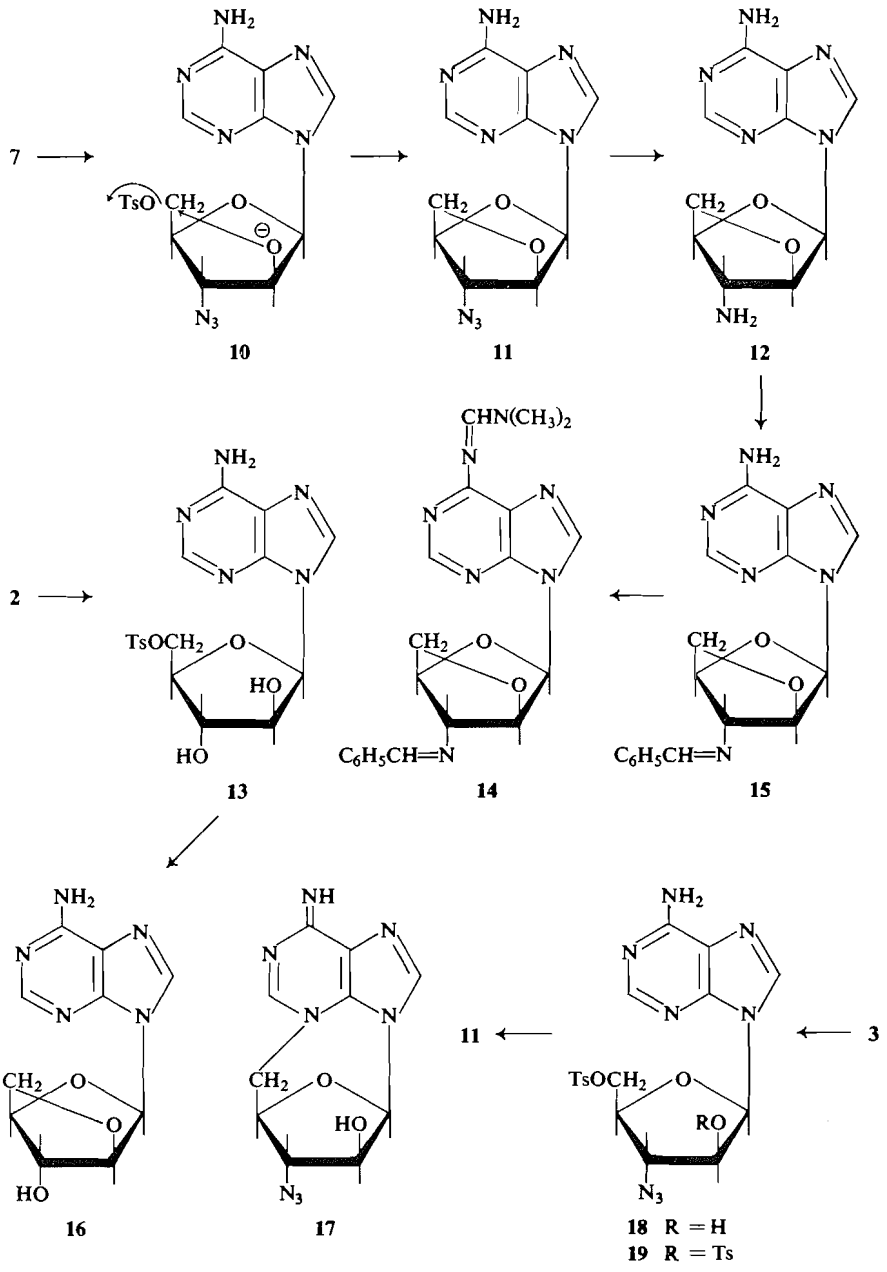

chromatographic (t.l.c.) comparison. Reaction of **3** with methanesulfonyl chloride in pyridine gave the cyclonucleoside **17**, characterized by its p*H* 7 u.v. maximum at 271 mμ, as the only isolable product. The 5′-tosylate **18** was so easily converted to cyclonucleoside **17** (as its tosylate salt) that the n.m.r. spectrum in dimethylsulfoxide solution showed initially a mixture of **18** and **17** tosylate which quite rapidly became the spectrum of **17** tosylate. This instability to cyclonucleoside formation may be responsible for the low yield of **11** from **18**.

A plausible rationalization for the formation of the Schiff base **15** from the reaction of **11** and

Can. J. Chem. Downloaded from www.nrcresearchpress.com by 210.87.254.42 on 09/05/12
For personal use only.

sodium benzyl mercaptide would seem to be reduction to **12** by the mercaptide followed by reaction with thiobenzaldehyde to give **15**. The conversion of sodium benzyl mercaptide to thiobenzaldehyde is analogous to the formation of benzaldehyde from sodium benzyloxide (8).

Experimental

Melting points, taken on the Fisher–Johns apparatus are uncorrected. Thin-layer chromatograms were run (detection by u.v. light) on silica gel HF (solvents *a*, *b*, and *c*) and paper chromatograms on Whatman No. 1 paper (solvents *d* and *e* with adenine as a reference) and the spots detected with u.v. light. The solvent systems were: *a*, chloroform–methanol (9:1); *b*, ethyl acetate – methanol (9:1); *c*, ethyl acetate – methanol (7:3); *d*, 1-butanol – acetic acid – water (4:1:1); *e*, 5% aqueous sodium dihydrogen phosphate. All evaporations were done *in vacuo*, either with a water aspirator or a vacuum pump, keeping the bath temperature below 50°.

9-(2,3-Anhydro-5-O-(p-tolylsulfonyl)-β-D-lyxofuranosyl)-adenine (7)

A mixture, protected from moisture, of 0.499 g (2 mmoles) of 9-(2,3-anhydro-β-D-lyxofuranosyl)adenine (**1**), 1.52 g (8 mmoles) of *p*-toluenesulfonyl chloride, and 200 ml of dry pyridine was stirred at room temperature for 24 h, then was treated with a small piece of ice. The pyridine was evaporated and water was added to the residue. The insoluble material was filtered and crystallized from 175 ml of 95% ethanol to give 0.614 g (68%) of white solid, m.p. 187–189°, $[\alpha]_D^{19}$ + 3.0 (0.73% in dimethylformamide), chromatographically homogeneous in solvents *a* and *b* with R_f 0.22 and 0.41, respectively.

Anal. Calcd. for $C_{17}H_{17}N_5O_5S \cdot 2\frac{1}{2}\ H_2O$: C, 45.53; H, 4.94; N, 15.62; S, 7.15. Found: C, 45.51; H, 4.70; N, 15.87; S, 7.05.

9-(2,5-Anhydro-3-azido-3-deoxy-β-D-arabinofuranosyl)-adenine (11)

(a) From the Tosylate 7

A stirred mixture of 1.12 g (2.5 mmoles) of the tosylate **7**, 0.32 g (5.0 mmoles) of sodium azide and 250 ml of dry *N,N*-dimethylformamide was maintained at 50–60° for 24 h. The solvent was evaporated. The residue was thoroughly triturated with three 50-ml portions of boiling chloroform, then the combined extracts were evaporated and the remaining solid was slurried with 10 ml of acetone and filtered to give 0.545 g (78%) of a colorless solid that was suitable for further reactions and was homogeneous in solvents *a* and *c* with R_f 0.47 and 0.78, respectively. It showed the typical azide infrared (i.r.) absorption at 4.7 μ. A small quantity of the azide was crystallized from methanol to give colorless crystals, m.p. 204–206°, $[\alpha]_D^{20}$ + 23.7° (0.92% in water). The 100 MHz n.m.r. spectrum in deuterated dimethylsulfoxide with tetramethylsilane showed singlet resonances at τ 1.69 and 1.87 (H_2 and H_8), 2.76 (broad, NH_2), 3.63 (H_1') and 5.20 (H_2'). Proton H_4' and H_3' appeared as quartets centered at 5.36 and 5.26, respectively, and H_5' as a pair of doublets centered at 5.83.

Anal. Calcd. for $C_{10}H_{10}N_8O_2 \cdot 1/4\ H_2O$: C, 43.09; H, 3.80; N, 40.20. Found: C, 43.21; H, 3.59; N, 40. 50.

(b) From the Tosylate 18

A suspension of 0.123 g of the tosyl nucleoside **18** in 5 ml of dry dimethylformamide was stirred, with exclusion of moisture, at 0° and 14 mg of a suspension of sodium hydride (58%) in mineral oil was added. The now red solution was stirred at 0° for 21 h, then poured into 20 ml of ice-water giving a solution. The solution was neutralized with glacial acetic acid and was allowed to evaporate spontaneously to dryness. The residue was triturated with 5 ml of water which left about 5 mg of solid which was filtered. The t.l.c. of this residue in solvents *a* and *c* showed it to move identically with **11**. The i.r. spectrum of this solid run in Nujol, showed absorption bands that agreed with all the major bands in the spectrum of crystalline **11**, but, because of the amorphous nature of the residue, this comparison does not provide a proof of identity. There was insufficient solid for recrystallization.

9-(3-Amino-2,5-anhydro-3-deoxy-β-D-arabinofuranosyl)-adenine (12)

(a) By Hydrogenation

A suspension of 0.548 g (2.0 mmoles) of the azide **11** and 0.030 g of palladium black in 200 ml of water was stirred at room temperature under one atmosphere of hydrogen for 24 h. The mixture was filtered through Celite and the filtrate was evaporated to dryness giving 0.377 g (76%) of a colorless solid whose i.r. spectrum showed the loss of the 4.7 μ absorption. The material was chromatographically homogeneous in solvents *c* and *e* with R_f 0.21 and R_{Ad} 0.75, respectively. The analytical sample was obtained by two crystallizations from absolute ethanol, m.p. 256–258°, $[\alpha]_D^{20}$ + 61.5° (0.85% in water). The 100 MHz n.m.r. spectrum in deuterated dimethylsulfoxide with tetramethylsilane as internal standard showed singlet resonances at τ 1.72 and 1.88 (H_2 and H_8), 2.79 (broad, exchangeable, purine NH_2), 3.42 (H_1'), 5.63 (H_2') and 7.89 (broad, exchangeable, sugar NH_2). Proton H_4' appeared as a multiplet at 5.81, H_3' as a doublet at 6.30, and H_5' as a pair of doublets centered at 5.94.

Anal. Calcd. for $C_{10}H_{12}N_6O_2$: C, 48.39; H, 4.88; N, 33.86. Found: C, 48.18; H, 4.90; N, 33.70.

(b) From Attempted Epoxide Opening with Sodium Ethyl Mercaptide

A mixture of 0.441 g (7.1 mmoles) of ethanethiol, 0.324 g (6.0 mmoles) of sodium methoxide, 0.200 g (0.71 mmole) of the azide **11** and 200 ml of methanol was heated at reflux, under nitrogen for 24 h. The solution was evaporated and the residue was partitioned between 20 ml each of water and ether. The aqueous layer was evaporated and the residue was extracted with five 10-ml portions of boiling chloroform. Evaporation of the chloroform extracts left 0.099 g (56%) of solid which was identical with the 3′-aminonucleoside **12**, described above.

9-(2,5-Anhydro-3-benzylidenimino-3-deoxy-β-D-arabinofuranosyl)adenine (15)

(a) From the Aminonucleoside 12

A mixture of 0.100 g (0.40 mmole) of the 3′-aminonucleoside **12**, 0.048 g (0.45 mmole of benzaldehyde) and 100 ml of dry *N,N*-dimethylformamide was stirred at

Can. J. Chem. Downloaded from www.nrcresearchpress.com by 210.87.254.42 on 09/05/12
For personal use only.

100–110° for 24 h, under nitrogen. The solvent was evaporated and the residue stirred in water, filtered, and washed with ethanol to give 0.115 g (85%) of a colorless solid, chromatographically homogeneous in solvent *a* with R_f 0.47. Recrystallization from *N,N*-dimethylformamide gave the analytical sample, m.p. > 295°.

Anal. Calcd. for $C_{17}H_{16}N_6O_2$: C, 60.71; H, 4.80; N, 24.90. Found: C, 59.93; H, 5.04; N, 25.08.

(b) From Attempted Ring-opening of the 3′-Azidonucleoside ***11*** *or of the 3′-Aminonucleoside* ***12***

A solution of 0.164 g (3.0 mmoles) of sodium methoxide and 0.446 g (3.6 mmoles) of α-toluenethiol in 5 ml of methanol was stirred for a few minutes, then evaporated to dryness. The residue was dissolved with 15 ml of dry *N,N*-dimethylformamide, 0.092 g (0.33 mmole) of the 3′-azidonucleoside **11** was added and the mixture heated at 100°, under nitrogen, for 4½ h. The solvent was evaporated, water (200 ml) and ether (250 ml) were added, and the crystalline material (0.066 g, 59%) was collected. It was identical in all respects with the Schiff base prepared above. When the 5′-aminonucleoside **12** was treated similarly with sodium benzyl mercaptide for 21 h, 10% of the Schiff base **15** was isolated. Chromatographic examination of the residues showed them to consist mainly of the starting material **12** accompanied by a small amount of an unknown, u.v.-absorbing material that moved faster than **9** in solvent *c*.

*N-6-(Dimethylaminomethylene)-9-(2,5-anhydro-3-benzylidenimino-3-deoxy-*β-D-*arabinofuranosyl)-adenine (****14****)*

To a suspension of 0.050 g (0.15 mmole) of the Schiff base **15** in 10 ml of dry *N,N*-dimethylformamide was added 0.5 ml (large excess) of the dimethyl acetal of *N,N*-dimethylformamide. After it had been stirred at room temperature for 2 h, protected from moisture, the mixture became homogeneous and was kept at room temperature for 15 h. The solvent was evaporated and the residue stirred with dry ether. The crystalline solid, 0.047 g (80%) was collected and dried, m.p. 186–189°. The 100 MHz n.m.r. spectrum obtained in chloroform-*d* with tetramethylsilane as the internal standard showed singlet resonances at τ 1.02 (N=CH—N<), 1.47 (C_6H_5CH=N), 1.42 and 1.60 (H_2 and H_8), 3.06 (H_1'), 6.74 and 6.82 [$N(CH_3)_2$] with phenyl protons as multiplets at τ 2.1–2.3 and 2.45–2.65, H_2' and H_3' at 5.32–5.37, and H_4' as a doublet at 5.63 with H_5' as a partially-obscured quartet centered at 5.78.

Anal. Calcd. for $C_{20}H_{21}N_7O_2$: C, 61.36; H, 5.41; N, 25.05. Found: C, 60.88; H, 5.60; N, 24.93.

*9-[5-O-(p-Tolylsulfonyl)-*β-D-*arabinofuranosyl]-adenine (****13****)*

A stirred suspension of 0.50 g (1.87 mmoles) of arabinofuranosyladenine **2** in 15 ml of pyridine was chilled to 0°, then 0.75 g (3.95 mmoles) of *p*-toluenesulfonyl chloride was added and the mixture was stirred at 0–5° for 18 h with all the solid slowly dissolving. A few drops of water were added to the yellow solution at 0° and, after 1 h, the solution was poured onto 50 ml of ice and water giving a white precipitate which was filtered, washed with water, then chloroform to give 0.44 g (56% yield) of **13** which softened at 145–148° and liquefied with decomposition at 220°.

*9-(2,5-Anhydro-*β-D-*arabinofuranosyl)adenine (****16****)*

The tosylate **13** (0.25 g) was suspended in 5 ml of absolute ethanol. Excess sodium methoxide (0.1 g) was added and the mixture was stirred at room temperature for 1 h to dissolve all the solids. The mixture was refrigerated for 18 h, then neutralized with glacial acetic acid and evaporated *in vacuo*. Water was added to the residue to give 0.14 g of a white solid which was recrystallized from water to give crystals which darkened near 220° and liquefied with decomposition at 300°. The 100 MHz n.m.r. spectrum in deuterated dimethylsulfoxide with tetramethylsilane as internal standard showed singlet resonances at τ 1.72 and 1.90 (H_2 and H_8), 2.80 (broad, NH_2), 3.50 (H_1') and 5.60 (H_2'). Proton H_3' appeared as a triplet at 5.46, H_4' as a multiplet centered at 5.77, H_5' as a pair of doublets centered at 5.91 and the hydroxyl proton as a doublet at 3.98. When **16** was converted to the 3′-*O*-acetate with acetic anhydride – pyridine, the resulting solid showed singlet resonances at 3.56 (H_1') and 5.25 (H_2') with a doublet at 4.64 (H_3'), a multiplet at 5.35 (H_4') and a pair of doublets centered at 5.79 (H_5') in addition to the purine, amino and acetyl methyl protons.

Anal. Calcd. for $C_{10}H_{11}N_5O_3 \cdot 1/4\ H_2O$: C, 47.5; H, 4.56; N, 27.6. Found: C, 47.7; H, 4.57; N, 27.8.

For comparison the n.m.r. spectrum of **1** in deuterated dimethylsulfoxide showed singlet resonances at τ 1.82 and 1.87 (H_2 and H_8), 2.68 (broad, exchangeable, NH_2) and 3.76 (H_1'). The OH proton was an exchangeable triplet centered at 5.02, protons H_2', H_3' and H_4' were found under two groups of signals centered at 5.72 and 5.87 while H_5' was a triplet, collapsed to a doublet after exchange, centered at 6.37.

*9-[3-Azido-3-deoxy-5-O-(p-tolylsulfonyl)-*β-D-*arabinofuranosyl]adenine (****18****) and 9-[3-Azido-3-deoxy-2,5-di-O-(p-tolylsulfonyl)-*β-D-*arabinofuranosyl]adenine (****19****)*

A stirred suspension of 0.75 g (2.57 mmoles) of the azide **3** in 20 ml of dry pyridine was chilled to 0° and 1.28 g (6.70 mmoles) of *p*-toluenesulfonyl chloride was added. (When 1.5 moles of tosylchloride/mole **3** were employed, the rate of solution of **3** was much slower and the reaction product contained much unchanged **3**.) The suspension was stirred at 0–5° for 43 h with exclusion of moisture, by which time all the solid had dissolved. The dark solution was processed as in the preparation of **13** giving 0.83 g of tan solid which was a mixture of **18** and **19**. This solid was stirred for 1 h at 0° with 40 ml of acetonitrile and the suspension was filtered leaving 0.30 g (26%) of **18** as a yellow, crystalline solid, m.p. 230–232°, dec.

Anal. Calcd. for $C_{17}H_{18}N_8O_5S$: C, 45.7; H, 4.06; N, 25.1. Found: C, 45.6; H, 3.92; N, 25.2.

The acetonitrile filtrate from **18** was evaporated *in vacuo* to give a brown residue that was crystallized from isopropyl alcohol then recrystallized from the same solvent to give a solid that melted indistinctly in the range 140–150°.

Anal. Calcd. for $C_{24}H_{24}N_8O_7S_2$: C, 48.0; H, 4.03; N, 18.7. Found: C, 47.7; H, 4.07; N, 18.6.

The authors wish to acknowledge the preparation of the necessary amounts of the epoxide **1** by Mr. O. P. Crews and his group and of the azide **3** by Mr. A. P. Martinez. They also acknowledge the help of Dr. Terry Barrett, Mrs. Lynn Stietzel, and Mr. K. J. Ryan in obtaining and in interpreting the n.m.r. spectra.

1. B. R. BAKER and R. E. SCHAUB. J. Amer. Chem. Soc. **77**, 5900 (1955).
2. W. W. LEE, A. BENITEZ, L. GOODMAN, and B. R. BAKER. J. Amer. Chem. Soc. **82**, 2648 (1960).
3. G. A. LEPAGE and I. G. JUNGA. Cancer Res. **23**, 739 (1963).
4. F. A. MILLER, G. J. DIXON, J. EHRLICH, F. M. SCHABEL, JR., and I. W. MCCLEAN, JR. Abstracts of Eighth Interscience Conference on Antimicrobiol. Agents and Chemotherapy, Oct. 21–23, 1968, New York, page 54.
5. A. P. MARTINEZ, W. W. LEE, and L. GOODMAN. J. Org. Chem. **31**, 3263 (1966).
6. V. M. CLARK, A. R. TODD, and J. ZUSSMAN. J. Chem. Soc. 2952 (1951).
7. J. ZEMLICKA and A. HOLY. Collect. Czech. Chem. Commun. **32**, 3159 (1967).
8. Y. SPRINZAK. J. Amer. Chem. Soc. **78**, 466 (1956) and prior references.

Partition coefficients and ultraviolet absorption maxima for the cinnamoyl derivatives of some long-chain and large-ring amines

D. J. CURRIE AND H. L. HOLMES
Chemistry Section, Defence Research Establishment Suffield, Ralston, Alberta

Received October 10, 1969

Partition coefficients of the title compounds in the system cyclohexane–water do not increase steadily with increasing chain length or ring size but level off to a limiting value. Reasons are advanced to account for this observation. Absorption maxima, on the other hand, are not influenced by the size of the ring or the length of the chain but are dependent only upon the degree of substitution on the amide nitrogen atom.

Canadian Journal of Chemistry, 48, 1340 (1970)

In developing π values for atoms and groups (1) it was found that the π-value concept breaks down for 1,4-naphthoquinones with a long alkyl chain, as present in vitamin K_1. This anomaly prompted the examination of the partition coefficients of a series, **1**, of *trans*-cinnamoyl derivatives of some long-chain and large-ring amines, prepared by the method of Papa *et al.* (2), to determine the effect of these hydrophobic groups upon partition coefficient.

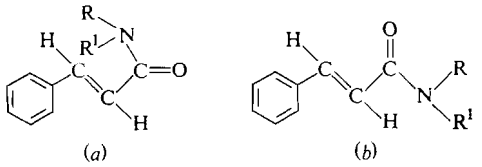

(*a*) (*b*)

R = H, R^1 = alkyl, or
R = R^1 = alkyl or
R—R^1 = polymethylene

1

Logarithms of the partition coefficients, log *K*, in cyclohexane–water were determined by methods previously described (1, 3, 4), and these values are listed in Table 1, along with those calculated from eq. [1].

[1] $\log K = \Sigma\pi + \Sigma\pi$ interaction $- 1.30$

The terms π and π interaction of eq. [1], as recorded in refs. 1, 3, and 4, are, respectively, substituent- and interaction-constants for the component groups in the molecule. Since this paper deals only with the change in log *K* with the introduction of *n*-CH_2 groups into the R group or groups in the carboxyamide group, for this purpose it is sufficient to say that $\pi_H = 0$ and $\pi_{CH_3} = 0.65$ log units.

log *K* values for the N-alkyl (**1**, R = H, R^1 = alkyl)- and symmetrical N,N-dialkyl (**1**, R = R^1 = alkyl)-derivatives of cinnamamide increased steadily as the total number of carbon atoms in R and R^1 increased from 1–8, when a plateau was reached. In general, log *K* values for the cinnamoyl derivatives of primary cycloalkylamines and of secondary polymethyleneimines **1** (R—R^1 = *n*-CH_2) were approximately the same as those for the cinnamoyl derivatives of acyclic amines containing one less carbon atom, **1** (R = alkyl, R^1 = H) or **1** (R = R^1 = alkyl). The plateau in the log *K* values probably stems from intramolecular solvation of the carboxyamide group by the coiled alkyl group or groups or the puckered cycloalkyl or polymethylene groups.

Can. J. Chem. Downloaded from www.nrcresearchpress.com by 210.87.254.42 on 09/05/12
For personal use only.

The authors wish to acknowledge the preparation of the necessary amounts of the epoxide **1** by Mr. O. P. Crews and his group and of the azide **3** by Mr. A. P. Martinez. They also acknowledge the help of Dr. Terry Barrett, Mrs. Lynn Stietzel, and Mr. K. J. Ryan in obtaining and in interpreting the n.m.r. spectra.

1. B. R. BAKER and R. E. SCHAUB. J. Amer. Chem. Soc. **77**, 5900 (1955).
2. W. W. LEE, A. BENITEZ, L. GOODMAN, and B. R. BAKER. J. Amer. Chem. Soc. **82**, 2648 (1960).
3. G. A. LEPAGE and I. G. JUNGA. Cancer Res. **23**, 739 (1963).
4. F. A. MILLER, G. J. DIXON, J. EHRLICH, F. M. SCHABEL, JR., and I. W. MCCLEAN, JR. Abstracts of Eighth Interscience Conference on Antimicrobiol. Agents and Chemotherapy, Oct. 21–23, 1968, New York, page 54.
5. A. P. MARTINEZ, W. W. LEE, and L. GOODMAN. J. Org. Chem. **31**, 3263 (1966).
6. V. M. CLARK, A. R. TODD, and J. ZUSSMAN. J. Chem. Soc. 2952 (1951).
7. J. ZEMLICKA and A. HOLY. Collect. Czech. Chem. Commun. **32**, 3159 (1967).
8. Y. SPRINZAK. J. Amer. Chem. Soc. **78**, 466 (1956) and prior references.

Partition coefficients and ultraviolet absorption maxima for the cinnamoyl derivatives of some long-chain and large-ring amines

D. J. CURRIE AND H. L. HOLMES
Chemistry Section, Defence Research Establishment Suffield, Ralston, Alberta

Received October 10, 1969

Partition coefficients of the title compounds in the system cyclohexane–water do not increase steadily with increasing chain length or ring size but level off to a limiting value. Reasons are advanced to account for this observation. Absorption maxima, on the other hand, are not influenced by the size of the ring or the length of the chain but are dependent only upon the degree of substitution on the amide nitrogen atom.

Canadian Journal of Chemistry, 48, 1340 (1970)

In developing π values for atoms and groups (1) it was found that the π-value concept breaks down for 1,4-naphthoquinones with a long alkyl chain, as present in vitamin K_1. This anomaly prompted the examination of the partition coefficients of a series, **1**, of *trans*-cinnamoyl derivatives of some long-chain and large-ring amines, prepared by the method of Papa *et al.* (2), to determine the effect of these hydrophobic groups upon partition coefficient.

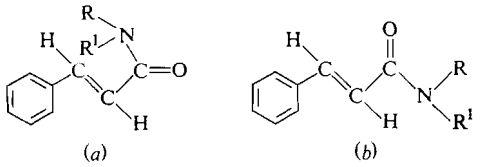

(*a*) (*b*)

R = H, R^1 = alkyl, or
R = R^1 = alkyl or
R—R^1 = polymethylene

1

Logarithms of the partition coefficients, log *K*, in cyclohexane–water were determined by methods previously described (1, 3, 4), and these values are listed in Table 1, along with those calculated from eq. [1].

[1] $\log K = \Sigma\pi + \Sigma\pi$ interaction $- 1.30$

The terms π and π interaction of eq. [1], as recorded in refs. 1, 3, and 4, are, respectively, substituent- and interaction-constants for the component groups in the molecule. Since this paper deals only with the change in log *K* with the introduction of *n*-CH_2 groups into the R group or groups in the carboxyamide group, for this purpose it is sufficient to say that $\pi_H = 0$ and $\pi_{CH_3} = 0.65$ log units.

log *K* values for the N-alkyl (**1**, R = H, R^1 = alkyl)- and symmetrical N,N-dialkyl (**1**, R = R^1 = alkyl)-derivatives of cinnamamide increased steadily as the total number of carbon atoms in R and R^1 increased from 1–8, when a plateau was reached. In general, log *K* values for the cinnamoyl derivatives of primary cycloalkylamines and of secondary polymethyleneimines **1** (R—R^1 = *n*-CH_2) were approximately the same as those for the cinnamoyl derivatives of acyclic amines containing one less carbon atom, **1** (R = alkyl, R^1 = H) or **1** (R = R^1 = alkyl). The plateau in the log *K* values probably stems from intramolecular solvation of the carboxyamide group by the coiled alkyl group or groups or the puckered cycloalkyl or polymethylene groups.

Can. J. Chem. Downloaded from www.nrcresearchpress.com by 210.87.254.42 on 09/05/12
For personal use only.

TABLE 1

Melting points, analytical figures, and partition coefficients for some cinnamoyl derivatives of some long-chain and large-ring amines

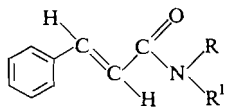

R	R^1	Melting point* (°C)	Percent N		log partition coefficient	
			Calcd.	Found	log K	$\Sigma\pi - 1.30$
cyclo-C_3H_5	H	117.0–117.6	7.48	7.65	−0.62	−0.60
cyclo-C_5H_9	H	145.0–145.6	6.50	6.56	+0.82	+0.70
cyclo-C_6H_{11}	H	179.2–180.2	Prepared previously (4)		1.39	1.35
cyclo-C_7H_{13}	H	192.2–192.8	5.75	5.80	2.04	2.00
cyclo-C_8H_{15}	H	186.0–186.5	5.44	5.34	2.48	2.65
cyclo-$C_{12}H_{23}$	H	176.0–176.8	4.47	4.40	4.14	3.30
—$(CH_2)_5$—		118.5–119.5†	Prepared previously (4)		1.44	1.35
—$(CH_2)_6$—		121.8–122.4†	6.18	6.12	1.97	2.00
—$(CH_2)_7$—		99.2– 99.8†	5.75	5.82	2.46	2.65
—$(CH_2)_8$—		69.5– 70.2†	5.44	5.41	3.11	3.30
cyclo-C_5H_9	*cyclo*-C_5H_9	134.4–135.4†	4.94	5.05	3.50	3.95
cyclo-C_6H_{11}	*cyclo*-C_6H_{11}	117.0–117.5	4.49	4.56	>4.40	3.95
$CH_3(CH_2)_6$	H	58.8– 59.8†	5.71	5.79	2.72	2.65
$CH_3(CH_2)_7$	H	76.4– 77.4†	5.40	5.43	3.21	3.30
$CH_3(CH_2)_8$	H	72.8– 73.8†	5.12	5.19	3.17	3.30
$CH_3(CH_2)_9$	H	57.0– 58.0†	4.87	5.01	~3.46	3.30
$CH_3(CH_2)_{11}$	H	73.0– 74.0† (6)	—	—	3.45	3.30
n-C_6H_{13}	*n*-C_6H_{13}	176–179/0.05 mm	4.44	4.63‡	—	—

*Unless stated otherwise, the compounds were crystallized from ethanol.
†Crystallized from benzene–hexane mixture.
‡Anal. Calcd. for $C_{21}H_{33}ON$: C, 79.95; H, 10.54. Found: C, 80.22; H, 10.23.

In order to mathematically describe the limiting value of log K as a function of the number of carbon atoms in the chain or ring, a discontinuous function must be employed such as Heavysides' unit step function, $U(t - a)$ (5). In this connection, $U(t - a)$ is defined as 1 for $t > a$ and 0 for $t \leqslant a$. Therefore, the values of π_R for compounds with $R = C_nH_{2n+1}$, $R^1 = H$ are given by eq. [2]

$$[2] \quad \pi_R = 0.65n - U(n - 8)[0.65(n - 8)]$$

Similarly, the π values for the substituents in symmetrically substituted amides, **1** ($R = R^1 =$ alkyl), $\pi_R + \pi_{R^1}$, are given by eq. [3]

$$[3] \quad \pi_R + \pi_{R^1} = 0.65(n + n^1) - U(n + n^1 - 8)[0.65(n + n^1 - 8)]$$

Finally, the π values for substituents in cinnamamides containing cycloalkyl groups, **1** (R = cycloalkyl, $R^1 = H$), or polymethylene groups, **1** (R, $R^1 = n$-CH_2), π_{RR^1} are given by eq. [4].

$$[4] \quad \pi_{RR^1} = 0.65(n - 1) - U(n - 9) \times [0.65(n - 9)]$$

The relative constancy (7×10^{-3} to 7×10^{-4} M) of the solubility in cyclohexane of **1** compounds (Table 2) where $R^1 = H$ and R varies from CH_3 to *n*-C_8H_{17} requires that changes in the partition coefficients with increase in the number of carbon atoms in the substituent chain must be due, primarily, to variation in their solubilities in water. Accordingly, calculations of the water solubilities (Table 2) of the above series of compounds gave values from 1×10^{-2} to $\sim 2 \times 10^{-6}$ M. These solubility relationships were just reversed for cinnamamides derived from secondary amines containing two identical alkyl groups.

The number of carbon atoms in the chain or ring of N-monosubstituted cinnamamides do not materially alter the ultraviolet absorption spectra from that of cinnamamide, **1** ($R = R^1 = H$), when recorded in ethanolic solution.[1] For example, $\lambda_{max}^{C_2H_5OH}$ (mμ) and (ε) for cinnamamide are ~298 (—),[2] 272 (21 000), 222 (15 600), 216.2

[1]The concentration ranged from 5×10^{-4} to 1×10^{-3} M.

[2]Evaluation of this figure was rendered difficult by virtue of the peak being a shoulder on another peak.

Can. J. Chem. Downloaded from www.nrcresearchpress.com by 210.87.254.42 on 09/05/12
For personal use only.

TABLE 2

Solubilities of some cinnamoyl derivatives of some long-chain and large-ring amines in cyclohexane and water

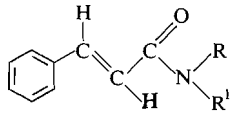

R	R^1	Solubility, mole per l in Cyclohexane	Water
CH_3	H	6.99×10^{-4}	1.31×10^{-2}
CH_3CH_2	H	1.66×10^{-3}	6.39×10^{-3}
$CH_3(CH_2)_2$	H	2.36×10^{-3}	2.30×10^{-3}
$CH_3(CH_2)_3$	H	4.48×10^{-3}	9.70×10^{-4}
$CH_3(CH_2)_4$	H	1.99×10^{-3}	8.20×10^{-5}
$CH_3(CH_2)_6$	H	3.98×10^{-3}	7.60×10^{-6}
$CH_3(CH_2)_7$	H	2.26×10^{-3}	1.39×10^{-6}
$CH_3(CH_2)_8$	H	3.29×10^{-3}	2.22×10^{-6}
$CH_3(CH_2)_9$	H	7.30×10^{-3}	2.53×10^{-6}
$CH_3(CH_2)_{11}$	H	5.91×10^{-3}	2.10×10^{-6}
CH_3	CH_3	1.88×10^{-2}	1.67×10^{-2}
CH_3CH_2	CH_3CH_2	1.43×10^{-1}	7.45×10^{-3}
$CH_3(CH_2)_2$	$CH_3(CH_2)_2$	1.16×10^{0}	2.89×10^{-3}
cyclo-C_3H_5	H	7.58×10^{-4}	3.15×10^{-3}
cyclo-C_5H_9	H	1.48×10^{-3}	2.28×10^{-4}
cyclo-C_6H_{11}	H	9.90×10^{-4}	4.04×10^{-5}
cyclo-C_7H_{13}	H	3.91×10^{-4}	3.57×10^{-6}
cyclo-C_8H_{15}	H	8.03×10^{-4}	2.66×10^{-6}
cyclo-$C_{12}H_{23}$	H	5.40×10^{-4}	3.91×10^{-8}
cyclo-C_5H_9	*cyclo*-C_5H_9	2.48×10^{-3}	7.75×10^{-7}
cyclo-C_6H_{11}	*cyclo*-C_6H_{11}	1.42×10^{-1}	$<5.68\times10^{-6}$
	$-(CH_2)_5-$	2.64×10^{-2}	9.6×10^{-4}
	$-(CH_2)_6-$	2.29×10^{-2}	2.46×10^{-4}
	$-(CH_2)_7-$	7.40×10^{-2}	2.56×10^{-4}
	$-(CH_2)_8-$	3.17×10^{-1}	2.46×10^{-4}

(18 000), ~210 (—), 204.6 (14 800), while those for the N-monocycloalkyl derivatives of **1** (R = H, $R^1 = C_nH_{2n-1}$) are ~300 (—), 274 (24 500), 223.8 (14 600), 217.7 (17 000), 212.2 (14 300), 206 (14 900), and those for the N-monoalkyl derivatives of **1** (R = C_nH_{2n+1}, R^1 = H) are ~298 (—), 273 (24 400), 222.7 (15 000), 216.5 (17 900), ~212 (—), 205 (15 600). Unless the conjugated system in cinnamamide is skewed, then the above results suggest that the planarity of the —CH=CH—C=O group in these series is maintained despite changes in the size of R. The absorption spectra of the N,N-disubstituted cinnamamides, on the other hand, differ markedly from those above, but again are constant within the series. The $\lambda_{max}^{C_2H_5OH}$ and (ε) for these compounds are 281–282 (22 000), 225 (12 500), 219.4 (45 400), ~214 (—), 206.5–208.8 (13 800). This difference in the spectra of the N-monosubstituted cinnamamides and of the N,N-disubstituted cinnamamides may stem from interference between the R and/or R^1 group with the benzylic hydrogen atom. To relieve steric strain in the N,N-disubstituted cinnamamides, the molecule may assume the conformation **1***b* rather than the **1***a* of cinnamamide.

If the above is true, then the variation in the water solubility of the N-monosubstituted cinnamamides must be ascribed to the rotation of the —NHR group about the C—N bond of the carboxyamide bond to a position less favorable for hydration than the planar structure shown in

Can. J. Chem. Downloaded from www.nrcresearchpress.com by 210.87.254.42 on 09/05/12
For personal use only.

2*a*.[3] Conformation **1***b* for the N,N-disubstituted cinnamamides is free from the above restriction

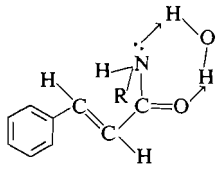

2a

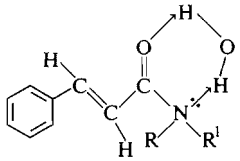

2b

and so hydration of **2***b* will occur independently of the size of R and R^1, while increase in R and R^1 will favor solubility in cyclohexane.

[3]This rotation of the —NHR group about the *C*—N bond of the carboxyamide bond should manifest itself in other properties. Rotation about the C—N bond would damp the contribution of the polar form of **3** to amide resonance and lead to lower melting points and increased solubility in cyclohexane.

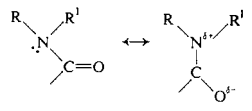

3

It is interesting then to find a linear relationship between the solubilities of these compounds in cyclohexane and their melting points. They fit in equations of the form $y = mx + b$, where $y = \log [\mathbf{1}]_{\text{cyclohexane}}$, x = melting point in °C. For N-alkylcinnamamides and N,N-dialkylcinnamamides, $m = -0.0172, -0.0344$; $b = -1.16$, $+1.68$, respectively. The slope of the line for the disubstituted amides is greater than that for the monosubstituted analogs by a factor of 2 and this is in accord with expectation that two alkyl groups on the amide nitrogen atom are more effective than one in altering the conformation (i.e. **1***a* or **1***b*) or the rotation about the C—N bond.

Similar linear relationships obtain for **1** compounds where R = cycloalkyl, R^1 = H and for compounds where R—R^1 are polymethylene groups. The slopes of these lines are, respectively, ~ -0.0063 and -0.0217. Fusion of the alkyl group with itself in **1** compounds (R = alkyl, R^1 = H) to give N-cycloalkylcinnamamides, or fusion of the two alkyl groups in **1** (R = R^1 = alkyl) to give N,N-polymethylenecinnamamides restricts the spatial gyrations of these atoms. Since this probably reduces the interference between the nitrogen substituents and the benzylic hydrogen atom, it would in part account for the decrease in the slopes of the melting point – solubility lines, relative to the unfused analogues. It follows that the corresponding steric effects would be greater in the N,N-dicycloalkylcinnamamides, **1**(R = R^1 = cycloalkyl), than in the N-cycloalkylcinnamamides, **1** (R = cycloalkyl, R^1 = H). In accord with this, a slope greater for the former than for the latter is found.

Determination of the partition coefficients by Mr. C. E. Lough and of the analytical figures for the new compounds by Mr. R. P. Hicken is gratefully acknowledged.

1. D. J. Currie, C. E. Lough, R. F. Silver, and H. L. Holmes. Can. J. Chem. **44**, 1035 (1966).
2. D. Papa, E. Schwenk, F. Villani, and E. Klingsberg. J. Amer. Chem. Soc. **72**, 3885 (1950).
3. C. E. Lough, R. F. Silver, and F. K. McClusky. Can. J. Chem. **46**, 1943 (1968).
4. A. D. Delaney, D. J. Currie, and H. L. Holmes. Can. J. Chem. **47**, 3273 (1969).
5. H. S. Carslaw and J. C. Jaeger. Operational methods in applied mathematics. 2nd ed. Oxford University Press, London. 1953. p. 7.
6. B. A. Hunter. Iowa State Coll. J. Sci. **15**, 223 (1941); C.A. **36**, 4474 (1942).

Signs of long-range amino proton – ring proton coupling constants in *N*-ethyl-4-chloro-2-nitroaniline

T. Schaefer and R. Wasylishen
Chemistry Department, University of Manitoba, Winnipeg, Manitoba

Received December 11, 1969

In *N*-ethyl-4-chloro-2-nitroaniline there exists a measurable indirect spin–spin coupling constant of $\pm 0.39 \pm 0.03$ Hz between the methylene protons and ring proton 6. The amino proton is coupled to ring protons 5 and 6 and also to the methylene protons. Consequently, although the amino proton resonance is broad due to incompletely relaxed coupling to ^{14}N, normal multiple resonance experiments show that $^5J_m^{H,NH} = 0.67 \pm 0.03$ Hz and $^4J_o^{H,NH} = -0.35 \pm 0.03$ Hz.

Canadian Journal of Chemistry, **48**, 1343 (1970)

1) Spectrum Analysis and Sign Determinations

The signs of the indirect, spin–spin coupling constants between ring protons and methyl protons in toluene and its derivatives (1–3), aldehydic protons in benzaldehyde and its derivatives (4–7), and hydroxyl protons in phenol

Can. J. Chem. Downloaded from www.nrcresearchpress.com by 210.87.254.42 on 09/05/12
For personal use only.

2*a*.[3] Conformation **1***b* for the N,N-disubstituted cinnamamides is free from the above restriction

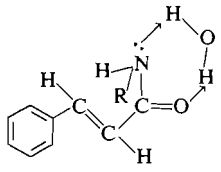

2a

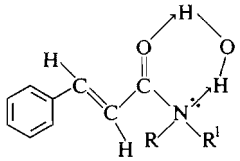

2b

and so hydration of **2***b* will occur independently of the size of R and R^1, while increase in R and R^1 will favor solubility in cyclohexane.

[3]This rotation of the —NHR group about the *C*—N bond of the carboxyamide bond should manifest itself in other properties. Rotation about the C—N bond would damp the contribution of the polar form of **3** to amide resonance and lead to lower melting points and increased solubility in cyclohexane.

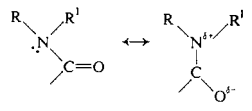

3

It is interesting then to find a linear relationship between the solubilities of these compounds in cyclohexane and their melting points. They fit in equations of the form $y = mx + b$, where $y = \log [\mathbf{1}]_{\text{cyclohexane}}$, x = melting point in °C. For N-alkylcinnamamides and N,N-dialkylcinnamamides, $m = -0.0172, -0.0344$; $b = -1.16$, $+1.68$, respectively. The slope of the line for the disubstituted amides is greater than that for the monosubstituted analogs by a factor of 2 and this is in accord with expectation that two alkyl groups on the amide nitrogen atom are more effective than one in altering the conformation (i.e. **1***a* or **1***b*) or the rotation about the C—N bond.

Similar linear relationships obtain for **1** compounds where R = cycloalkyl, R^1 = H and for compounds where R—R^1 are polymethylene groups. The slopes of these lines are, respectively, ~ -0.0063 and -0.0217. Fusion of the alkyl group with itself in **1** compounds (R = alkyl, R^1 = H) to give N-cycloalkylcinnamamides, or fusion of the two alkyl groups in **1** (R = R^1 = alkyl) to give N,N-polymethylenecinnamamides restricts the spatial gyrations of these atoms. Since this probably reduces the interference between the nitrogen substituents and the benzylic hydrogen atom, it would in part account for the decrease in the slopes of the melting point – solubility lines, relative to the unfused analogues. It follows that the corresponding steric effects would be greater in the N,N-dicycloalkylcinnamamides, **1**(R = R^1 = cycloalkyl), than in the N-cycloalkylcinnamamides, **1** (R = cycloalkyl, R^1 = H). In accord with this, a slope greater for the former than for the latter is found.

Determination of the partition coefficients by Mr. C. E. Lough and of the analytical figures for the new compounds by Mr. R. P. Hicken is gratefully acknowledged.

1. D. J. Currie, C. E. Lough, R. F. Silver, and H. L. Holmes. Can. J. Chem. **44**, 1035 (1966).
2. D. Papa, E. Schwenk, F. Villani, and E. Klingsberg. J. Amer. Chem. Soc. **72**, 3885 (1950).
3. C. E. Lough, R. F. Silver, and F. K. McClusky. Can. J. Chem. **46**, 1943 (1968).
4. A. D. Delaney, D. J. Currie, and H. L. Holmes. Can. J. Chem. **47**, 3273 (1969).
5. H. S. Carslaw and J. C. Jaeger. Operational methods in applied mathematics. 2nd ed. Oxford University Press, London. 1953. p. 7.
6. B. A. Hunter. Iowa State Coll. J. Sci. **15**, 223 (1941); C.A. **36**, 4474 (1942).

Signs of long-range amino proton – ring proton coupling constants in *N*-ethyl-4-chloro-2-nitroaniline

T. Schaefer and R. Wasylishen
Chemistry Department, University of Manitoba, Winnipeg, Manitoba

Received December 11, 1969

In *N*-ethyl-4-chloro-2-nitroaniline there exists a measurable indirect spin–spin coupling constant of $\pm 0.39 \pm 0.03$ Hz between the methylene protons and ring proton 6. The amino proton is coupled to ring protons 5 and 6 and also to the methylene protons. Consequently, although the amino proton resonance is broad due to incompletely relaxed coupling to ^{14}N, normal multiple resonance experiments show that $^5J_m^{H,NH} = 0.67 \pm 0.03$ Hz and $^4J_o^{H,NH} = -0.35 \pm 0.03$ Hz.

Canadian Journal of Chemistry, **48**, 1343 (1970)

1) Spectrum Analysis and Sign Determinations

The signs of the indirect, spin–spin coupling constants between ring protons and methyl protons in toluene and its derivatives (1–3), aldehydic protons in benzaldehyde and its derivatives (4–7), and hydroxyl protons in phenol

Can. J. Chem. Downloaded from www.nrcresearchpress.com by 210.87.254.6 on 09/05/12
For personal use only.

Can. J. Chem. Downloaded from www.nrcresearchpress.com by 210.87.254.6 on 09/05/12
For personal use only.

derivatives (8), are known. These couplings, when observable, are negative over four or six bonds and are positive over five bonds. The six-bond couplings are apparently dominated by a σ–π mechanism (2, 6, 9–12), which also contributes to the coupling over four or five bonds (11, 12), but for these a σ mechanism is probably also important (12–15).

Coupling over five bonds, $J_m^{H,NH}$, between amino protons and ring protons in the meta position has been observed in a number of aniline derivatives (16, 17). The observation of the coupling evidently depends on the presence of proton accepting substituents which form intramolecular hydrogen bonds, N—H...X, and thereby hinder intermolecular exchange of the amino protons. The amino proton resonance is normally broad and featureless (width at half-height $\approx$ 10–20 Hz). Consequently, even fairly sophisticated multiple resonance experiments (8), when confined to the proton spectrum, cannot be used to determine the sign of $J_m^{H,NH}$.

When *N*-ethyl-4-chloro-2-nitroaniline (**1**) is studied as a 3.8 mole % solution in benzene-d_6, its proton magnetic resonance (p.m.r.) spectrum

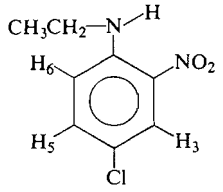

1

at 30 °C displays coupling between H_6 and the amino proton, $^4J_o^{H,NH}$, between H_6 and the methylene protons, $^5J^{H,CH_2}$, and between H_5 and the amino protons, $^5J_m^{H,NH}$. It follows that normal, multiple, homonuclear resonance experiments (18, 19) can be employed to determine the signs of $^5J_m^{H,NH}$ and $^4J_o^{H,NH}$ even though the spin-lattice relaxation time of ^{14}N is such that the amino proton resonance cannot be directly used in these experiments.

Weak irradiation with a second radiofrequency field of selected transitions of H_6 and observation of the relevant H_5 transitions (18) showed that $J_m^{H,NH}/J_o^{H,NH} < 0$. Decoupling of H_3 with simultaneous weak irradiation of the appropriate transitions of the methylene protons while observing the resonance of H_6 proved that $J_o^{H,NH}/^3J^{NH,CH_2} < 0$.

TABLE 1

Refined spectral parameters

Chemical shifts (p.p.m.)	Coupling constants (Hz)
$\nu_{CH_3} = -0.756 \pm 0.008$	$^3J^{CH_2,CH_3} = 7.15 \pm 0.07$
$\nu_{CH_2} = -2.506 \pm 0.008$	$^3J^{CH_2,NH} = 5.20 \pm 0.08$
$\nu_{NH} = -7.53 \pm 0.03$	$^3J^{H_5,H_6} = 9.14 \pm 0.04$
$\nu_3 = -8.058 \pm 0.003$	$^4J^{H_3,H_5} = 2.59 \pm 0.04$
$\nu_5 = -6.887 \pm 0.003$	$^4J^{H_6,NH} = -0.35 \pm 0.03$
$\nu_6 = -6.021 \pm 0.006$	$^5J^{H_3,H_6} = 0.38 \pm 0.06$
	$\lvert^5J^{H_6,CH_2}\rvert = 0.39 \pm 0.04$
	$^5J^{H_5,NH} = 0.67 \pm 0.03$
	$^5J^{H_3,NH} < \pm 0.1$

Vicinal proton coupling constants involving the fragments H—C—C—H (20), H—C—O—H (21), H—C—S—H (22), and H—C—P—H (23) are known to be positive. There is no reason to believe that such is not the case for the fragment H—C—N—H. Furthermore, the couplings in the

fragments H—C—N—H and H—C—N—H in *N*-methylformamide are positive (24–26). Therefore we set $J_o^{H,NH} < 0$. The coupling between the ring protons were of the same sign and are positive.

Other decoupling experiments simplified the H_6 multiplets sufficiently well to determine the spacings caused by the long-range couplings from H_6. At 60 MHz the proton resonance spectrum is nearly first-order. Refinement of the first-order parameters by means of LAOCN3 (27) yielded the chemical shifts relative to internal tetramethylsilane and the proton–proton coupling constants (quoted errors about eight times larger than probable errors) (Table 1).

2) Long-range Coupling Constants

The signs of the coupling constants between the amino and ring protons in the ortho and meta position are the same as the corresponding couplings in toluene (1–3), phenol (8), and benzaldehyde (4–7) derivatives. The five-bond coupling, $^5J^{H,NH}$, displays the stereospecificity expected from the zig–zag rule (8, 28) and its magnitude lies in the range 0.4–0.8 Hz observed for couplings of this type. The coupling over four bonds, $^4J^{H,NH} = -0.35 \pm 0.03$ Hz is the first to be observed in aniline derivatives. Its sign is the same but its magnitude is greater than the analogous coupling in a series of para substituted benzaldehydes (13). In the latter the magnitude of $^4J^{H,CHO}$ depends on the double bond character of the C—CHO bond (13). A similar situation

may prevail for **1** because **2** will clearly contribute both to the strength of the intramolecular hydrogen bond and to the double bond character of the C_1—NH bond. On the other hand, steric

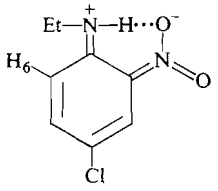

2

hindrance between the ethyl group and C—H_6 or between N—H and the NO_2 group (29) may introduce some nonplanarity of the N—H bond. Then the σ–π mechanism could contribute to $^4J^{H,NH}$. Such a coupling mechanism would also contribute to $J_p^{H,NH}$ and compounds of the requisite structure are being synthesized.

The five-bond coupling between the methylene protons and H_6 is unknown in sign but its magnitude is reminiscent of the *negative* coupling between ring protons and the protons in the methoxy group in anisole derivatives (8, 30–32). In the latter, $^5J^{H,OCH_3}$ has a relatively large magnitude when a bulky substituent forces the methyl group in OCH_3 to lie near the ortho proton. The internal hydrogen bond in **1** clearly forces a similar, close approach of the methylene protons and H_6 (the presence of an intramolecular hydrogen bond is unequivocally demonstrated by the chemical shift of the amino proton and by the stereospecific couplings of the latter). We have observed a coupling between H_6 and methylene protons in *N*-*n*-butyl-2,4-dinitroaniline, so that its presence in **1** is not unique.

Experimental

N-Ethyl-4-chloro-2-nitroaniline from Aldrich Chemical Company was prepared as a 3.8 mole % solution in benzene-d_6. The sample was degassed by the freeze–pump–thaw technique and p.m.r. spectra were recorded on a DA-60-I spectrometer in the frequency sweep mode. Tetramethylsilane served as an internal reference and as a locking signal. Peak positions were calibrated by reading oscillator frequencies at 5 Hz intervals and averaging over a number of spectra. Multiple resonance experiments were carried out in the normal way (18, 19).

The resonance peaks from the ethyl protons were distinctly broad compared to the ring proton peaks. Increasing the temperature to 65 °C did not change the linewidth of these peaks nor did the long-range coupling from the amino proton change in an observable way. Decoupling of the amino proton also had no effect on the linewidth of the ethyl proton peaks. It is likely that the breadth is caused by incompletely relaxed coupling to ^{14}N.

We are grateful to the National Research Council of Canada for financial assistance.

1. M. P. Williamson, R. J. Kostelnik, and S. M. Castellano. J. Chem. Phys. **49**, 2218 (1968).
2. D. J. Blears, S. S. Danyluk, and T. Schaefer. J. Chem. Phys. **47**, 5037 (1967).
3. T. Schaefer, C. M. Wong, and K. C. Tam. Can. J. Chem. **47**, 3688 (1969).
4. R. J. Kostelnik, M. P. Williamson, D. E. Wisnosky, and S. M. Castellano. Can. J. Chem. **47**, 3313 (1969).
5. D. G. DeKowalewski and V. J. Kowalewski. Mol. Phys. **9**, 331 (1965).
6. C. L. Bell, S. S. Danyluk, and T. Schaefer. Can. J. Chem. **47**, 3529 (1969).
7. S. Forsén, T. Alm, B. Gestblom, S. Rodmar, and R. A. Hoffman. J. Mol. Spectrosc. **17**, 13 (1965).
8. S. Forsén and R. A. Hoffman. J. Mol. Spectrosc. **20**, 168 (1966).
9. H. M. McConnell. J. Chem. Phys. **30**, 126 (1959).
10. M. Barfield and B. Chakrabarti. J. Amer. Chem. Soc. **91**, 4346 (1969).
11. M. Barfield and J. J. Reed. J. Chem. Phys. **51**, 3039 (1969).
12. C. J. Macdonald and W. F. Reynolds. Can. J. Chem. **48**, 1002 (1970).
13. S. S. Danyluk, C. L. Bell, and T. Schaefer. Can. J. Chem. **47**, 4005 (1969).
14. H. Frischleder and G. Bär. Mol. Phys. **11**, 359 (1966).
15. M. Barfield and M. Karplus. J. Amer. Chem. Soc. **91**, 1 (1969).
16. J. A. Weil, A. Blum, A. H. Heiss, and J. K. Kinnaird. J. Chem. Phys. **46**, 3132 (1967).
17. R. Wasylishen and T. Schaefer. Can. J. Chem. This issue.
18. R. Freeman and W. A. Anderson. J. Chem. Phys. **37**, 2053 (1962).
19. R. Kaiser. J. Chem. Phys. **39**, 2435 (1963).
20. D. N. Silverman and B. P. Dailey. J. Chem. Phys. **51**, 655 (1969).
21. F. Hruska, T. Schaefer, and C. A. Reilly. Can. J. Chem. **42**, 697 (1964).
22. V. F. Bystrov and O. P. Yablonsky. J. Mol. Spectrosc. **26**, 213 (1968).
23. W. McFarlane and J. A. Nash. Chem. Commun. 127 (1969).
24. A. J. R. Bourn and E. W. Randall. Mol. Phys. **8**, 568 (1964).
25. R. J. Chuck, D. G. Gillies, and E. W. Randall. Mol. Phys. **16**, 121 (1969).
26. W. McFarlane and R. R. Dean. J. Chem. Soc. A, 1535 (1968).
27. S. Castellano and A. A. Bothner-By. J. Chem. Phys. **41**, 3863 (1964).
28. C. N. Banwell and N. Sheppard. Discuss. Faraday Soc. **34**, 115 (1962).
29. L. K. Dyall. Spectrochim. Acta, **25A**, 1727 (1969).
30. S. Forsén. J. Phys. Chem. **67**, 1740 (1963).
31. H. Angad Gaur, J. Vriend, and W. G. B. Huysmans. Tetrahedron Lett. 1999 (1969).
32. R. W. Crecely, K. W. McCracken, and J. H. Goldstein. Tetrahedron, **25A**, 877 (1969).

Can. J. Chem. Downloaded from www.nrcresearchpress.com by 210.87.254.6 on 09/05/12
For personal use only.

Can. J. Chem. Downloaded from www.nrcresearchpress.com by 210.87.254.105 on 09/05/12
For personal use only.

Orientation in nitration and sulfonation of 2,5-dimethylbenzoic acid[1]

ALLAN N. FUJIWARA AND EDWARD M. ACTON
Life Sciences Research, Stanford Research Institute, Menlo Park, California 94025

Received November 7, 1969

Nitration of 2,5-dimethylbenzoic acid was only 29% at the *meta*[2] position vs. 41% at the *ortho*, in contrast to sulfonation which was 85% *meta* vs. 15% *para*. Identity of the products (and of their derived amino esters and phenolic esters) was determined from the nuclear magnetic resonance spectra and confirmed by chemical means.

Canadian Journal of Chemistry, 48, 1346 (1970)

In some synthetic studies related to alkaloids, we required the *meta*-substitution[2] products from the nitration and sulfonation of 2,5-dimethylbenzoic acid (**3**). When carried out, these reactions showed striking differences in orientation effects, illustrative of the complex interplay of electronic and steric influences in reactions of a poly-substituted benzene. Nitration of **3** with fuming nitric acid occurred mainly in the *ortho*[2] position, despite the considerable steric hindrance, to form a mixture of *meta*- and *ortho*-nitro acids, **1** and **2** (in 29 and 41% yields, respectively). In contrast, sulfonation of **3** with oleum afforded mostly the *meta* sulfonate (about 85%, isolated as the sodium salt **4**) accompanied by about 15% of the *para* isomer **5**. This sulfonation was previously reported (1) to form only the *meta* product **4**, but inspection of the n.m.r. spectrum readily disclosed the presence of the *para* isomer.[3] In the nitration of **3**, the ratio of isomers closely resembled that reported (2*a*) for nitration of 2,5-dimethylacetophenone. Other, similarly substituted benzenes have also given predominantly *o*-nitration (2*b*).

The *m*-nitro acid **1** was separated from the mixture of **1** and **2** by crystallization. The *o*-nitro acid **2** was then purified after treatment with methanolic hydrogen chloride, which selectively esterified **1** and left the hindered *ortho* isomer unchanged. This *o*-nitro acid **2** could be esterified successfully only with diazomethane or with methanol – sulfuric acid (3). The sulfonation product (mixture of **4** and **5**) was subjected to alkali fusion (1), and the nuclear magnetic resonance (n.m.r.) spectra showed that the *meta* to *para* ratio of phenolic acids **6** and **7** was essentially the same as the ratio of sodium sulfonates **4** and **5**. Separation of isomers was possible only after esterification of **6** and **7**, when the predominant *meta* methyl ester **11** could be purified by fractional crystallization; a small sample of the *para* ester **12** was obtained from the mother liquors.

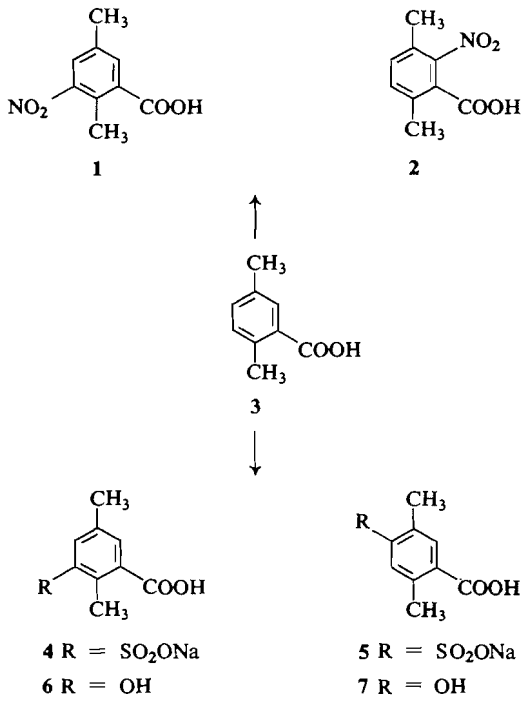

[1]This work was carried out under the auspices of the Cancer Chemotherapy National Service Center, National Cancer Institute, National Institutes of Health, Public Health Service, Contract No. PH-43-64-500. The opinions expressed in this paper are those of the authors and not necessarily those of the Cancer Chemotherapy National Service Center.

[2]The terms *ortho*, *meta*, and *para* refer to the carboxyl as point of reference.

[3]Though no *ortho* sulfonation was detected, a referee has pointed out the likelihood that the *ortho* position may be the site of kinetically governed reaction, but that, since sulfonation is a reversible reaction, the more thermodynamically stable *meta* and *para* products were obtained under conditions used.

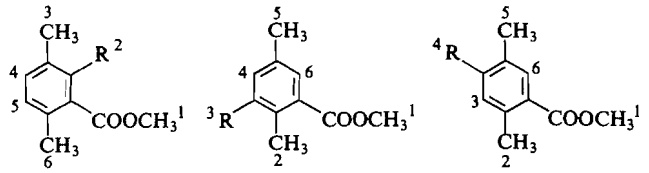

8 R = NH_2 **9** R = NH_2 **10** R = NH_2
11 R = OH **12** R = OH

The compounds could be readily identified from the n.m.r. spectra by observing splitting patterns of the 2 aryl protons in each isomer. Characteristic coupling constants (4) were $J_{para} < 1$ Hz, $J_{meta} = 2$–3 Hz, and $J_{ortho} = 7.5$ Hz, determined respectively from sharp singlets, broad singlets partially resolved, and an AB quartet. Spectra of the nitration products were best studied after esterification and reduction of **1** and **2** to form the amino esters **8** and **9**, because (*a*) the distinctly different *para* isomer **10**, methyl 4-amino-2,5-dimethylbenzoate, was then available (5) for comparison, and (*b*) in the *o*-nitro compounds (**2** and its methyl ester) the aryl protons had identical resonances so that the resultant 2-proton singlets gave no information as to the orientation. The *p*-hydroxy ester **12** exhibited proton chemical shifts nearly identical to those for the corresponding protons in the *p*-amino ester **10**. Chemical shifts of the aryl protons were generally as predicted from summation of known shielding effects (6) of the various substituents. Although no attempt was made in the present work to study spectra at high dilutions or with rigorously calibrated instrumentation, the additive shielding parameters developed by several workers (6) could usually be applied to the assigned structures.

For instance, the large differences in shielding of the aryl protons for the *p*-amino ester **10** ($\delta_{H-3} - \delta_{H-6} = 1.27$ p.p.m.) and the *p*-hydroxy ester **12** ($\delta_{H-3} - \delta_{H-6} = 1.14$ p.p.m.) were predictable. Relative to benzene (δ 7.32) as standard (or to *p*-xylene, δ 7.05), the C_3-protons in **10** and **12** (δ 6.43 and 6.58) were shifted upfield by the adjacent 4-NH_2 and 4-OH (shielding) but were little affected by the *meta*-oriented $COOCH_3$ (deshielding); the $COOCH_3$ shifted the adjacent 6-H's downfield (δ 7.70 and 7.72), with little effect on the 6-H's from the *meta*-oriented OH or NH_2. In contrast, the *m*-amino and *m*-hydroxy esters **9** and **11** showed little difference in the aryl protons ($\delta_{H-4} - \delta_{H-6} = 0.45$ and 0.38 p.p.m., respectively). Upfield shift of the 4-H's (δ 6.55 and 6.85) by the adjacent NH_2 and OH was still observed, though somewhat lessened perhaps by the $COOCH_3$ now *para* to these 4-H's. Surprisingly, the 6-H's (δ 7.00 and 7.23) in **9** and **11** were little affected by the 1-$COOCH_3$ (deshielding expected) or were perhaps at the same time shielded by a strong *para* effect of the 3-NH_2 or 3-OH. A strong shielding effect by *p*-NH_2 seemed to be evident in the *o*-amino ester **8**, where 1 proton (apparently H-5, *para* to the 2-NH_2) was as far upfield (δ 6.47) as the proton in **10** (δ 6.43) that was *ortho* to the NH_2. The other proton in **8** (H-4, δ 6.98) seemed to be as much affected by the *m*-NH_2 (shielding) as by the *p*-$COOCH_3$.

Similar substituent effects were seen on resonances of the aryl methyl groups, i.e., the shielding tendency of an adjacent amino group, the deshielding tendency of an adjacent methoxycarbonyl. This was clearly observed with the *p*-amino ester **10**. The 5-CH_3 (δ 2.12) was shielded relative to the CH_3's in *p*-xylene (δ 2.30) by the adjacent 4-NH_2, and the 2-CH_3 (δ 2.52) was deshielded by the 1-$COOCH_3$. In the *ortho* isomer **8**, the 3-CH_3 (δ 2.12) was shielded by the adjacent 2-NH_2, but the 6-CH_3 was only slightly deshielded by the adjacent $COOCH_3$, perhaps a reflection of steric restriction on the $COOCH_3$ at this crowded position, interfering with its free rotation or its planarity with the ring.[4] In the *m*-amino isomer **9**, the NH_2 and $COOCH_3$ groups are *ortho* to the 2-CH_3 and are *meta* to the 5-CH_3; the opposing effects were nearly cancelled out, and the methyl resonances were nearly coincident (δ 2.26 and 2.20).

[4]Some further chemical evidence of steric crowding in the *ortho* series was the difficulty of *N*-acetylating the anthranilic acid obtained on reduction of **2**. Only a low yield of *N*-acetyl product was obtained with refluxing acetic anhydride overnight, though yields in the analogous *meta* and *para* series were quantitative after a few hours. We are indebted to Mr. Nasser Sadri for this observation.

Can. J. Chem. Downloaded from www.nrcresearchpress.com by 210.87.254.105 on 09/05/12
For personal use only.

Can. J. Chem. Downloaded from www.nrcresearchpress.com by 210.87.254.105 on 09/05/12
For personal use only.

Experimental

Melting points were determined on a Fisher–Johns micro hot stage and are uncorrected. The n.m.r. spectra were determined with a Varian A-60A spectrometer on 25–30% (w/v) solutions in chloroform-*d* (4% internal tetramethylsilane as standard, $\delta = 0$), and, with external tetramethylsilane, in dimethylsulfoxide-d_6 (DMSO) and in D_2O. Signals were observed as singlets (s) or doublets (d). Accuracy was ± 0.07 p.p.m. for chemical shifts, ± 0.2 Hz for coupling constants. Signals exchangeable with D_2O are not recorded.

Paper chromatography was done by the descending technique on Whatman No. 1 paper, in 1-butanol – ethanol – 15 *M* ammonium hydroxide – water (4:1:1:4), spots detected under ultraviolet (u.v.) light.

2,5-Dimethyl-3-nitrobenzoic Acid (1)

To 150 ml of red fuming nitric acid (*d* 1.50) at 5° were added, with stirring, 25.0 g (0.167 mole) of 2,5-dimethylbenzoic acid (Eastman) in portions, over 35 min, while the temperature was maintained at 5–10°. The solution was allowed to stand another 60 min at 10° and was poured onto 1.5 kg of ice with stirring. The white precipitate was collected on a filter and washed with water (in a typical experiment, the dried weight amounted to a 75% yield). Paper chromatography showed 2 isomers were present, R_f 0.51 (**2**) and R_f 0.59 (**1**). The damp solid was recrystallized from 225 ml of hot ethanol by adding 375 ml of water; after 15 h at room temperature, 7.5 g of the *meta* isomer **1** was collected, m.p. 130–160°. Recrystallization from 150 ml of benzene then afforded 6.4 g (20%), m.p. 178–181° with a crystal transition at 165–175° (lit. (*2a*) m.p. 168–170°), chromatographically homogeneous with R_f 0.59; n.m.r. (DMSO-d_6) δ 7.86 broad s (H-4, estimated $J_{4,6}$ ca. 2 Hz), 7.62 broad s (H-6, estimated $J_{4,6}$ ca. 2 Hz), 2.57 s and 2.39 (aryl CH_3's). The yield was consistently 20%, even on 10 times the scale. An analytical sample melted at 180–181.5° with crystal transition at 163–175°.

Anal. Calcd. for $C_9H_9NO_4$: C, 55.4; H, 4.65; N, 7.18. Found: C, 55.8; H, 4.64; N, 7.00.

3,6-Dimethyl-2-nitrobenzoic Acid (2)

The combined mother liquors from **1** were evaporated to yield a mixture of the isomers (ca. 50% based on **3**; estimated 41% **2** and 9% **1**, from n.m.r.). A 15 g sample of the solid mixture was refluxed with 175 ml of saturated anhydrous methanolic hydrogen chloride overnight. The solution was concentrated to a residual solid, which was suspended in 150 ml of dichloromethane and extracted with 2 100-ml portions of 5% aqueous sodium hydroxide. Acidification of the combined extracts to p*H* 2 with 12 *M* hydrochloric acid afforded 10.1 g (34% based on **3**) of precipitated 2-nitro acid **2**, m.p. 143–145°. An analytical sample, previously obtained (16% yield) by recrystallization of the crude mixture of acids from benzene–methanol, then methanol–water, melted at 141–143°; n.m.r. (DMSO-d_6) δ 7.23 s (H-4 and H-5), 2.27 s and 2.18 s (aryl CH_3's).

Anal. Calcd. for $C_9H_9NO_4$: C, 55.4; H, 4.65; N, 7.18. Found: C, 55.6; H, 4.72; N, 7.27.

The extracted dichloromethane solution contained 3.8 g of a syrupy mixture of the *m*-nitro and *o*-nitro esters, in a ratio of 2:1 as estimated from the n.m.r. spectrum.

Methyl 3,6-Dimethyl-2-nitrobenzoate

This compound was obtained (*a*) in quantitative yield by esterification of the acid **2** in tetrahydrofuran with diazomethane in ether (7), and (*b*) in 47% yield with 100% sulfuric acid and methanol (3). The syrup crystallized on standing, m.p. 36–40°; n.m.r. ($CDCl_3$) δ 7.24 s (H-4 and H-5), 3.82 s ($COOCH_3$), 2.39 s and 2.35 s (aryl CH_3's).

Anal. Calcd. for $C_{10}H_{11}NO_4$: C, 57.4; H, 5.30; N, 6.70. Found: C, 57.6; H, 5.19; N, 6.71.

Methyl 3,6-Dimethyl-2-aminobenzoate (8)

This compound was obtained by hydrogenation with platinum oxide in methanol, as a syrup in quantitative yield; n.m.r. ($CDCl_3$) δ 6.98 d (H-4, $J_{4,5} = 7.5$ Hz), 6.47 d (H-5, $J_{4,5} = 7.5$ Hz), 3.88 s ($COOCH_3$), 2.40 s and 2.10 s (aryl CH_3's).

Anal. Calcd. for $C_{10}H_{13}NO_2$: C, 67.0; H, 7.31; N, 7.82. Fonud: C, 66.7; H, 7.20; N, 7.97.

Methyl 2,5-Dimethyl-3-nitrobenzoate

This compound was obtained from **1** by esterification with refluxing anhydrous methanolic hydrogen chloride and was recrystallized from methanol (5 ml/g), m.p. 57–58° (81%); n.m.r. ($CDCl_3$), 7.78 broad s (H-4, estimated $J_{4,6}$ ca. 2 Hz), 7.63 broad s (H-6, estimated $J_{4,6}$ ca. 2 Hz), 3.91 s ($COOCH_3$), 2.54 s and 2.39 s (aryl CH_3's).

Anal. Calcd. for $C_{10}H_{14}NO_4$: C, 57.4; H, 5.30; N, 6.70. Found: C, 57.4; H, 5.30; N, 6.58.

Methyl 2,5-Dimethyl-3-aminobenzoate (9)

This compound was obtained by hydrogenation of the nitro ester with platinum oxide in methanol, as a syrup in quantitative yield; n.m.r. ($CDCl_3$) δ 7.00 broad s (H-6, estimated $J_{4,6}$ ca. 2 Hz), 6.55 broad s (H-4, estimated $J_{4,6}$ ca. 2 Hz), 3.81 s ($COOCH_3$), 2.26 s and 2.20 s (aryl CH_3's).

Anal. Calcd. for $C_{10}H_{13}NO_2$: C, 67.0; H, 7.31; N, 7.82. Found: C, 66.7; H, 7.36; N, 7.75.

Sulfonation of 2,5-Dimethylbenzoic Acid (3)

This acid, when prepared as described by Charlesworth and Levene (1), yielded quantitatively the mixture of sodium sulfonates **4** and **5**; n.m.r. (D_2O) δ 7.85 broad s (H-4 of **4**, estimated $J_{4,6}$ ca. 2 Hz), 7.53 broad s (H-6 of **4**, estimated $J_{4,6}$ ca. 2 Hz), 2.63 s and 2.31 s (aryl CH_3's of **4**); contamination with ca. 17% of the *para*-substituted isomer **5** was indicated by singlets at δ 7.72 and 7.76 (H-3 and H-6) and at 2.52 and 2.43 (aryl CH_3's).

Potassium Hydroxide Fusion (1)

Fusion of the mixture of **4** and **5** at 210° for 1.5 h afforded the mixture of hydroxy acids **6** and **7**, isolated by acidification with concentrated hydrochloric acid and reprecipitated from a bicarbonate solution. The yield was 61%, m.p. 162–164° (lit. (1) 163–165°); n.m.r. (DMSO) δ 6.95 broad s (H-6 of **6**, estimated $J_{4,6}$ ca. 2 c.p.s.), 6.71 broad s (H-4 of **6**, estimated $J_{4,6}$ ca. 2 c.p.s.), 2.22 s and 2.08 s (aryl CH_3's of **6**); singlets at 7.59 (H-6) and 6.57 (H-3), and at 2.37 and 2.01 (aryl CH_3's) indicated the presence of 12% of the 4-hydroxy isomer **7**.

*Methyl 2,5-Dimethyl-3-hydroxybenzoate (**11**)*

This benzoate was obtained from the mixture of **6** and **7** with refluxing anhydrous methanolic hydrogen chloride after 2 h; the residual oil crystallized on standing and was washed with water (97% yield), m.p. 61–74°. Most of the 4-hydroxy isomer **12** (ca. 15% estimated by n.m.r.) was removed by recrystallization from benzene – petroleum ether (1:1, 15 ml/g), then from carbon tetrachloride (4 ml/g), to yield 58% of **11** (96% purity), m.p. 77.5–79.5°. Further fractional recrystallization from benzene afforded an analytical sample (free of **12**), m.p. 79–79.5°; n.m.r. ($CDCl_3$) δ 7.22 broad s (H-6, $J_{4,6}$ estimated 2 Hz), 6.78 broad s (H-4, $J_{4,6}$ estimated 2 Hz), 3.91 s ($COOCH_3$), 2.41 s and 2.23 s (aryl CH_3's).

Anal. Calcd. for $C_{10}H_{12}O_3$: C, 66.6; H, 6.71. Found: C, 66.6; H, 6.66.

*Methyl 2,5-Dimethyl-4-hydroxybenzoate (**12**)*

This compound was obtained from the mother liquors of **11** as light white needles, along with the dense prisms of **11**, and was separated and recrystallized from benzene – petroleum ether (1:1), m.p. 116–117°; n.m.r. ($CDCl_3$) δ 7.72 s (H-6), 6.58 s (H-3), 3.80 s ($COOCH_3$), 2.49 s and 2.19 s (aryl CH_3's). The sample was identical to an authentic sample, m.p. 116–117°, obtained by diazotization of 2,5-dimethyl-4-aminobenzoic acid (5), hydrolysis of the diazonium salt, and esterification of the resultant **7**.

Anal. Calcd. for $C_{10}H_{12}O_3$: C, 66.6; H, 6.71. Found: C, 66.6; H, 6.69.

The authors are indebted to Dr. Joseph I. DeGraw for initial studies of the nitration, to Dr. Carol Mosher for preparation of compound **9**, to Mr. Osborne Crews and Mr. R. B. Bicknell for large scale nitrations and sulfonations, and to Dr. Leon Goodman for helpful suggestions.

1. E. H. Charlesworth and L. Levene. Can. J. Chem. **41**, 1071 (1963).
2. (*a*) C. A. Howe and A. Howe. J. Chem. Soc. 6064 (1963); (*b*) C. A. Howe, A. Howe, C. R. Hamel, H. W. Gibson, and R. R. Flynn. J. Chem. Soc. 795 (1965); C. D. Johnson and M. J. Northcott. J. Org. Chem. **32**, 2029 (1967).
3. M. S. Newman. J. Amer. Chem. Soc. **63**, 2431 (1941).
4. R. M. Silverstein and G. C. Bassler. Spectrometric identification of organic compounds. 2nd ed., John Wiley and Sons, New York, 1967. p. 145.
5. A. N. Fujiwara, E. M. Acton, and L. Goodman. J. Heterocycl. Chem. **5**, 853 (1968).
6. Reviewed by J. W. Emsley, J. Feeney, and L. H. Sutcliffe. High resolution nuclear magnetic resonance spectroscopy. Vol. 2, Pergamon Press, New York, 1966. pp. 749–767.
7. Org. Syn., coll. Vol. II, p. 166, note 3.

Can. J. Chem. Downloaded from www.nrcresearchpress.com by 210.87.254.105 on 09/05/12
For personal use only.

Can. J. Chem. Downloaded from www.nrcresearchpress.com by 210.87.254.42 on 09/05/12
For personal use only.

Canadian Journal of Chemistry

Published by THE NATIONAL RESEARCH COUNCIL OF CANADA

VOLUME 48 MAY 1, 1970 NUMBER 9

Effect of the structure of phosphylating agents on their reaction with ethanolamine, an ambident nucleophile[1-3]

R. GREENHALGH,[4] R. M. HEGGIE, AND M. A. WEINBERGER[5]

Defence Research Establishment Ottawa, Defence Research Board, Ottawa, Canada

Received November 3, 1969

The reactions of a series of phosphylating agents (RR′P(O)X) with ethanolamine have been examined, and relative yields of the products from the nucleophilic amino and hydroxyl moieties determined. In general the amount of *O*-phosphylation increased as R and R′ were changed from dimethylamino through alkoxy to methyl and as the leaving group (X) was changed from OP(O)RR′ to CN. The only exceptions occurred when R was dimethylamino and X was Cl. When X was F, only *O*-phosphylation was observed. Thus, a wide range of essentially continuously varying selectivities was found.

The results are discussed in terms of the amount of charge transfer involved in the formation of the transition state which is assumed to be determined by the electrophile. When the charge transfer is small, the contributions to the activation energy of such factors as solvation and ionization potential of the nucleophile are most important, resulting in *N*-phosphylation. As the amount of charge transfer increases, the energy of bond formation becomes the dominant factor and *O*-phosphylation is preferred.

Canadian Journal of Chemistry, 48, 1351 (1970)

Introduction

In an earlier study (1) it was shown that, when reacted with ethanolamine in chloroform solution, phosphofluoridates give exclusively *O*-phosphylation whereas phosphochloridates give mainly *N*-phosphylation. This study has now been extended to examine the reactions of ethanolamine with a wider variety of phosphylating agents (RR′P(O)X). The compounds studied included phosphorodiamides (R = R′ = Me_2N), phosphoramidates (R = Me_2N, R′ = EtO), phosphates (R = R′ = Pr^iO), phosphonates (R = Pr^iO, R′ = Me), and phosphinic compounds (R = R′ = Me) in which the leaving group (X) was changed from F to Cl, CN, and OP(O)RR′.

[1]D.R.E.O. Report No. 613.

[2]Presented at the 52nd meeting of the Chemical Institute of Canada, Montreal, Quebec, May, 1969.

[3]The term phosphylation is used in this paper to cover phosphorylation, phosphonylation, and phosphinylation.

[4]Present address: Analytical Chemistry Research Service, Canada Department of Agriculture, Central Experimental Farm, Ottawa 3, Canada.

[5]Present address: Defence Research Analysis Establishment, Ottawa 4, Canada.

Results

The percentages and ^{31}P chemical shifts of the various components of the reaction mixtures are shown in Table 1.

In most reactions examined the products were also isolated and, in Table 2, the percentage yields as determined by ^{31}P nuclear magnetic resonance (n.m.r.) analysis and isolation are compared.

The ^{31}P n.m.r. method of product analysis has certain deficiencies. For reactions which do not go to completion, its lack of sensitivity has to be considered when no other products are reported. In addition ^{31}P n.m.r. does not differentiate between an *O*,*N*-diphosphylated product and mixtures of the *O*- and *N*-phosphylated compounds. Isolation of the products by chromatography did, however, distinguish between these possibilities. The only occasion when any diphosphylated compound was isolated was from the reaction of ethanolamine with dimethylphosphinic chloride. However, because of the losses involved in isolation of the products, the yields as determined by n.m.r. are considered to be more accurate and these will be used in discussing the results of this study.

Can. J. Chem. Downloaded from www.nrcresearchpress.com by 210.87.254.42 on 09/05/12
For personal use only.

TABLE 1

Reaction conditions and products from the reaction of ethanolamine with phosphylating agents

Phosphylating agent ($RR'P(O)X$)			Chemical shift (p.p.m.)	^{31}P Chemical shifts (p.p.m.) and % material at end of reaction				Reaction conditions	
R	R′	X		*N*-Phosphyl derivative	*O*-Phosphyl derivative	RR′P(O)OH	Other products	Time (h)	Temperature†
Me_2N	Me_2N	Cl	−29.7	−23.6 (22%)	−19.0 (3.5%)			24	R.T.
EtO	Me_2N	Cl	−16.9	−18.8 (84%)	−11.1 (11%)		−30.9 (2%), −7.2 (3%)	28	R.T.
EtO	Me_2N	OP(O)RR′	0	−18.6 (4%)			+12.7 (1%)	24	Reflux
EtO	Me_2N	F	−5.2*		−11.9 (13%)			120	R.T.
Pr^iO	Pr^iO	OP(O)RR′	+15	−7.9 (44%)	+2.0 (3%)	+2.0 (50%)	+9.6 (3%)	72	R.T.
Pr^iO	Pr^iO	CN	+24.2	−8.1 (22%)	+2.5 (78%)			56	R.T.
Pr^iO	CH_3	OP(O)RR′	−20.5	−32.5 (43%)	−29.9 (4%)	−19.8 (53%)		72	R.T.
Pr^iO	CH_3	CN	−10.5		−29.6 (95%)	−19.8 (5%)		48	R.T.
CH_3	CH_3	Cl	−62.0	−41.1 (61%)	−55.7 (15%)	−33.3 (21%)		2	R.T.
CH_3	CH_3	OP(O)RR′	−51.5	−39.0 (22%)	−54.4 (19%)	−33.9 (59%)		24	R.T.

*Doublet.
†R.T. stands for room temperature.

TABLE 2

Comparison of product analysis by ^{31}P n.m.r. and isolation

Phosphylating agent (RR′P(O)X)			% Yield of product			
			Nuclear magnetic resonance analysis		Isolation	
R	R′	X	N—P	O—P	N—P	O—P
EtO	Me_2N	Cl	84	11	71	10
Pr^iO	Pr^iO	OP(O)RR′	88	7	72	—
Pr^iO	Pr^iO	CN	22	78	10	68
Pr^iO	Me	OP(O)RR′	86	8	74	—
Pr^iO	Me	CN	—	95	—	69
Me	Me	Cl	61	15	42	—
Me	Me	OP(O)RR′	44	38	—	18

TABLE 3

Chemical shifts and coupling constants ($CDCl_3$) for the methylenic protons in the *N*- and *O*-phosphyl derivatives of ethanolamine

Product RR′P(O)X		X = $NHCH_2CH_2OH$				X = $OCH_2CH_2NH_2$			
		τ (p.p.m.)		*J* (Hz)		τ (p.p.m.)		*J* (Hz)	
R	R′	P—NCH_2	CH_2O	CH_2CH_2	$PNCH_2$	P—OCH_2	CH_2N	CH_2CH_2	$POCH_2$
Pr^iO	Me_2N	6.98	6.36	4.9	10.2	6.04	7.08	5.75	7.7
Pr^iO	Pr^iO	6.96	6.36	4.75	9.7	5.98	7.06	5.30	7.1
Pr^iO	Me	6.98	6.34	4.75	9.3	6.00	7.08	5.42	7.0
Me	Me	6.90	6.36	4.85	10.4	6.01	7.06	5.35	7.5

The reaction products were identified by comparison of the ^{31}P chemical shifts with those of known products (1) and this identification was confirmed, in most cases, by isolation. In the phosphinyl series, where no authentic products were available, characterization was by proton n.m.r. only. The reliability of this method of identification is demonstrated in Table 3 which shows that, irrespective of the substituents on phosphorus, the chemical shifts and coupling constants of the methylenic protons are quite characteristic and different for the *N*- and *O*-phosphylated compounds.

It was found that the phosphinyl group undergoes a facile N → O migration on heating, as shown by ^{31}P n.m.r. spectra of *N*-2-hydroxyethyl-*P*,*P*-dimethylphosphinamide before distillation, −41.4 p.p.m. (P—N, 100%); after distillation, −54 p.p.m. (P—O, 58%), −41 p.p.m. (P—N, 22%), and −34 p.p.m. (20%). To ensure that migration had not occurred during the reaction with ethanolamine, a blank run was performed. Over a 6 h period no change was observed in the ^{31}P spectrum of *N*-(2-hydroxyethyl)-*P*,*P*-dimethylphosphinamide in chloroform containing triethylamine. It was thus concluded that no migration took place under the reaction conditions employed. This had already been demonstrated for phosphoryl and phosphonyl derivatives of ethanolamine (1).

The fact that the hydroxyl and amino moieties of ethanolamine function as two separate entities is shown by the products of the reaction of diisopropyl phosphorocyanidate with an equimolar mixture of *n*-propylamine and *n*-propyl alcohol in chloroform in the presence of triethylamine as acid acceptor. The percentage yields of each product (76% P—O and 24% P—N) were almost identical to those obtained with ethanolamine.

Discussion

Various hypotheses (e.g. 2, 3) have been put forward to explain the change in selectivity towards two nucleophiles as the structure of the electrophile is changed. The results of the present study will be discussed in terms of the semi-empirical treatment of Hudson (3). When there is no charge transfer involved in the transition

Can. J. Chem. Downloaded from www.nrcresearchpress.com by 210.87.254.42 on 09/05/12
For personal use only.

TABLE 4

Variation in selectivity with phosphylating agent (RR′P(O)X)

R	R′	Sum of Hammett σ values of R and R′	Selectivity $\left(\ln \frac{\text{yield P—N}}{\text{yield P—O}}\right)$ X = Cl	OP(O)RR′	CN	F
Me_2N	Me_2N	−1.2	1.8	—	—	—
Me_2N	EtO	−0.85	2.04	—	1.15	< −4
Pr^iO	Pr^iO	−0.57	3.13	2.68	−1.27	< −4
Pr^iO	Me	−0.46	2.35	2.37	< −4	< −4
Me	Me	−0.34	1.39	0.02	—	—
P—X Bond Energy (kcal) (21)			80	96	80.5*	120

*Value for P—CH_3.

state (S_N1 reaction), no selectivity is to be expected if statistical and entropy factors are the same for both nucleophiles. For small charge transfer the more easily polarized nucleophile is preferred. However, as the charge transfer is increased the energy required from the bond formed becomes more important and a faster reaction is observed with the less easily polarized nucleophile, which forms the stronger nucleophile to electrophile bond. In this treatment it is assumed that the amount of charge transfer is determined almost exclusively by the electrophile and that the changes from nucleophile to nucleophile are small. This is presented schematically in Fig. 1, where the charge transfer is shown as a function of the natural logarithm of the ratio of the rate constant for the more easily polarized nucleophile (N_1) to that for the more difficultly polarizable one (N_2).

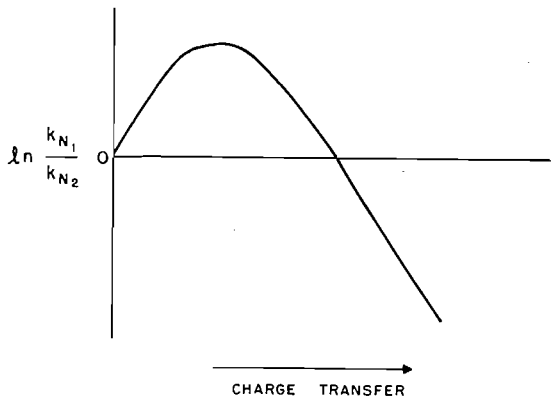

FIG. 1. Variation in selectivity with charge transfer in the transition state (3).

Assuming that the mechanisms of the reaction of the amino and hydroxyl functions of ethanolamine with any one phosphylating agent are similar, the product ratio can be used to represent the velocity constant ratio. This still remains true if the mechanism changes between phosphylating agents, providing that both the amino and hydroxyl moieties are similarly affected. Dostrovsky and Halmann (4) deduced that diisopropyl phosphorochloridate reacts by the same mechanism with amines and alcohols. In Table 4 the natural logarithms of the product ratios obtained in this and the previous study (1) are given for comparison with Fig. 1.

Considering first the effect of changes in R and R′, for a constant leaving group, it can be seen (most clearly from the results with the cyanidates and pyro compounds) that the preference for the less polarizable nucleophile (hydroxyl) increases as the substituents are changed from dimethylamino through alkoxy to methyl. The effect of these substituents on the character of the phosphorus atom will depend on the sum of their inductive and mesomeric effects. For the inductive effect alone the positive nature of the phosphorus will increase in the order C < N < O. Interactions of the π electrons of the substituent with the d orbitals of the phosphorus to give p_π–d_π bonding results in the phosphorus becoming more positive in the order N < O < C. Since this latter effect is important in pentavalent phosphorus compounds (5), an increase in the positive nature of the phosphorus atom would be expected as we descend the table. The same order of increase in the positive nature of the phosphorus would be predicted from the Hammett σ values (6) for the substituents. These values are also shown in Table 4. This increase in the positive character of the phosphorus would be expected to lead to greater charge transfer in the transition state and, as observed, a preference for the less polarizable nucleophile. In addition, the rate of

Can. J. Chem. Downloaded from www.nrcresearchpress.com by 210.87.254.42 on 09/05/12
For personal use only.

Can. J. Chem. Downloaded from www.nrcresearchpress.com by 210.87.254.42 on 09/05/12
For personal use only.

reaction with nucleophiles should increase as we descend Table 4 and this has been observed (7). Attempts to correlate the charge on phosphorus with ground state phenomena, such as ^{31}P chemical shifts, P—F coupling constants and the infrared absorption of the P → O bond were not successful.

When the leaving group (X) is varied, increased *O*-phosphylation is observed in the order Cl < OP(O)RR′ < CN < F. In considering these results the energy of the bond broken during the reaction must be taken into account. In an earlier paper (1), the exclusive *O*-phosphylation obtained with phosphofluoridates was explained by assuming that, because of the strength of the P—F bond, a significant part of the driving force for the reaction is derived from the energy of the bond formed. This results in a need for high charge transfer in the transition state. It should be noted that the effect of p_π–d_π overlap between the leaving group and phosphorus is included in the strength of the bond broken. However, although the relative energies of the bonds broken can explain the increased selectivity for the hydroxyl moiety in going from chlorides to pyro compounds and fluorides, the high preference for phosphylation of oxygen shown by cyanidates cannot be explained on this basis. The position of the cyanidates in Table 4 may be explained by the high electron-withdrawing power of the cyano group resulting in a highly positive phosphorus atom. The value of Taft σ^* which is a measure of the electron-withdrawing power is +1.3 for CN as compared to +1.05 for F and +1.01 for Cl (8).

An examination of all the results in Table 4 which were obtained with a series of closely analogous compounds shows that they cover a large part of the selectivity curve in Fig. 1. The chloro compounds span the portion of the curve where maximum selectivity for the more polarizable amino function is observed. The pyro compounds studied fall in the range from maximum selectivity for the amino function to the point where the rates of phosphylation of the two nucleophiles are virtually identical. The cyanidates show reversal of selectivity and the fluoridates demonstrate, within experimental error, complete *O*-phosphylation. A similar wide range of essentially continuously varying selectivities or charge transfers cannot be observed with closely analogous carbon compounds. Here the selectivity variation is restricted to the narrow ranges characteristic of the charge transfer allowed to a carbon in sp^3 or sp^2 hybridization. The sp^3 transition state for substitution at a carbonyl function is akin to an addition intermediate and involves strong binding. Nucleophilic attack at a saturated carbon center results in only weak bonding and a low charge transfer. Some studies of the relative rates of reaction of different nucleophiles at an aromatic center suggest that these reactions may involve an intermediate degree of charge transfer (3*a*). Thus, although in carbon chemistry the whole range of charge transfer can be spanned, it is by no means as continuous a variation as observed with phosphorus. The transition state for the reactions examined in this study is sp^3d, and the stability of compounds with this hybridization state in phosphorus chemistry is highly dependent on the nature of the substituents. Stable compounds of this type are known but only with highly electronegative substituents (9). It is, therefore, not surprising that a wide range of selectivities and charge transfers is observed in nucleophilic substitution at a pentavalent phosphorus center.

In phosphorus chemistry S_N1 reactions are few, since they require a substituent on phosphorus with very high electron density (e.g. a negatively charged group) to stabilize the required metaphosphate intermediate (10). Hall (11) suggested that *N*,*N*,*N*′,*N*′-tetramethylphosphonic chloride hydrolyzed by an S_N1 mechanism. The selectivity value of 1.8 obtained for this compound in the present study suggests a low charge transfer but does not indicate a pure S_N1 reaction.

The Brönsted coefficient (z) is directly related to charge transfer under specific reaction conditions (3). Our results would therefore suggest that the Brönsted coefficient would decrease in the order

fluorides > cyanides > pyro compounds > chlorides

Green *et al.* (12) quoted a value of 0.82 for the reaction of hydroxamic acids with isopropyl methylphosphonofluoridate. Although hydroxamic acids are α-nucleophiles (13), the high Brönsted coefficient does confirm that a high degree of charge transfer is associated with nucleophilic attack on phosphofluoridates. Brönsted coefficients for ethyl *N*,*N*-dimethylphosphoramidocyanidate (0.55) and tetraethyl pyrophosphate (0.7) are lower (12), and it is concluded that selectivity reversal for the nucleophilic moieties of ethanolamine occurs in the range of $z = 0.5$ to 0.7. However, the present data suggest that,

Can. J. Chem. Downloaded from www.nrcresearchpress.com by 210.87.254.42 on 09/05/12
For personal use only.

under our experimental conditions at least, the Brönsted coefficient for cyanides will be higher than that for the corresponding pyro compounds. No Brönsted coefficients have been reported for chlorides but a low value has been measured in these laboratories.[6]

To summarize, it has been shown that, by changing the substitution on phosphorus, the amount of charge transfer in the transition state can be varied predictably with consequent changes in the selectivity for phosphylation of the amino and hydroxyl moieties of ethanolamine. Because of the comparative stability of the sp^3d transition state of phosphorus a wide range of selectivities/charge transfers are observed. A similar wide range cannot be observed with closely analogous carbon compounds. Our results lead us to believe that, for any one series, the values for the Brönsted coefficient will be in the order F > CN > OP(O)RR′ > Cl.

Experimental

Ethanolamine

This compound was distilled before use, b.p. 171–172°.

Triethylamine

This was distilled from KOH prior to use, b.p. 89–90°.

Phosphorus Compounds

The chloro compounds were prepared by standard methods: ethyl *N,N*-dimethylphosphoramidochloridate, b.p. 51°/0.01 mm, lit. 73°/4 mm (14); diisopropyl phosphorochloridate, b.p. 84°/10 mm, lit. 93°/15 mm (15); isopropyl methylphosphonochloridate, b.p. 81°/15 mm, lit. 83°/22 mm (16); and dimethylphosphinic chloride, m.p. 67–69°, lit. 68–72° (17); tetramethylphosphodiamidic chloride, b.p. 106–109°/10 mm, lit. 110°/10 mm (18).

Using these chloro compounds, the pyro analogs were prepared by the method of Toy (19), and the fluoro by the procedure of Goldwhite and Saunders (20) with ammonium fluoride substituted for sodium fluoride. The cyano analogs were prepared by the reaction of cyanogen bromide with tervalent phosphorus esters (14). The purity of each compound was established by ^{31}P, ^{1}H n.m.r. and infrared spectra.

Nuclear magnetic resonance spectra were determined on a Varian 4300B/HA60IL spectrometer operating at 60 MHz for protons and 24.288 MHz for phosphorus. All the phosphorus spectra were referenced to 85% H_3PO_4 and determined in a non-spinning 15 mm tube. For proton spectra the internal lock signal was provided by tetramethyl silane. Infrared spectra were obtained using a Perkin–Elmer 421 spectrophotometer.

Reaction of Phosphylating Agents with Ethanolamine

With the exception of the dimethylphosphinic compounds, the phosphylating agents were reacted with ethanolamine according to the procedure previously reported (1). Equimolar amounts (0.025 *M*) of agent and ethanolamine were reacted in the presence of a slight excess of triethylamine in chloroform as solvent. The alcohol was removed from the chloroform prior to use by passing it through a column of silica gel. During the addition of agent to ethanolamine, the temperature was maintained at 10–15°, after which the conditions were as recorded in Table 1. A ^{31}P n.m.r. spectrum was obtained on the crude product remaining after removal of the triethylamine salt and solvent. The relative amounts of phosphorus in different environments was determined by peak area measurements (square count).

Reaction of Dimethylphosphinic Chloride with Ethanolamine

Dimethylphosphinic chloride (5.6 g) was weighed in a dry box and dissolved in chloroform (35 ml). This solution was added with stirring to ethanolamine (3 g) and triethylamine (15 ml) in chloroform (30 ml), in a nitrogen atmosphere. The reaction temperature was kept below 10° during the addition, and then allowed to rise to room temperature. After 2 h the solvent was removed by a stream of dry nitrogen, and the resulting mixture of oil and crystals filtered. A ^{31}P n.m.r. spectrum of the crude oil showed the presence of three major products: −55.7 p.p.m. (15%), −41.1 p.p.m. (61%), −33.3 p.p.m. (21%), but no starting material (−62.0 p.p.m.).

An aliquot (4.6 g) of the crude product was chromatographed on alumina (Woelm, basic III). An oil (882 mg) was eluted with chloroform–ether (2:1), and distilled at 125–130°/0.05 mm. The ^{31}P n.m.r. spectrum of this oil showed 2 peaks: −56.8 p.p.m. (53%) and −42.5 p.p.m. (47%), which suggested it was a mixture of *O,N-bis*-dimethylphosphinyl ethanolamine and a small amount of 2-aminoethyl dimethylphosphinate.

The second fraction was also an oil (2.07 g), which was eluted with methanol–chloroform (1:1). This material in chloroform showed a single peak at −43.1 p.p.m. (^{31}P n.m.r.). Proton n.m.r. ($CDCl_3$): PCH_3, doublet (τ = 8.49, J_{PH} = 13.9 Hz); NCH_2, multiplet, (τ = 6.90, J_{P-NCH_2} = 10.4 Hz); OCH_2, triplet (τ = 6.36, $J_{CH_2CH_2}$ = 4.85 Hz). Infrared (film): 3370 and 3250 cm^{-1}, OH and NH; 1304 cm^{-1}, P—CH_3; 1180 cm^{-1}, P → O; 1110, 1020, and 945 cm^{-1}, P—C and P—N. This compound was assigned the structure *N*-2-hydroxyethyl-*P,P*-dimethylphosphinamidate on the basis of its spectral characteristics.

Attempts to distil this oil at 120–130°/0.05 mm resulted in decomposition as illustrated by the ^{31}P n.m.r. spectrum before distillation, −41.1 p.p.m. (100%); and after, −54 p.p.m. (58%), −40 p.p.m. (22%), and −34.5 p.p.m. (20%).

Reaction of Tetramethylphosphinic Anhydride with Ethanolamine

Tetramethylphosphinic anhydride (8.5 g) in chloroform (25 ml) was added to a solution of ethanolamine (3 g) and triethylamine (15 ml) in chloroform (35 ml). The reaction was carried out in a dry nitrogen environment at room temperature for 24 h. Removal of the solvent gave a clear oil, the ^{31}P n.m.r. spectrum of which showed three peaks: −54.4 p.p.m. (19%), −39 p.p.m. (22%), and −33.9 p.p.m. (59%). The absence of a peak at −51.5 p.p.m. indicated that all the starting material had reacted.

[6]R. Greenhalgh and M. A. Weinberger. Unpublished results.

Chromatography of the crude product on alumina (Woelm, basic III) did not result in the separation of pure compounds. Three fractions eluted with chloroform, whose ^{31}P n.m.r. spectra showed the presence of a compound at -56.2 p.p.m. ($CHCl_3$) in amounts greater than 80%, were combined and distilled. The bulk of the material which distilled at 80–85°/0.05 mm was an oil, whose ^{31}P n.m.r. spectrum showed a single peak at -56.1 p.p.m. ($CHCl_3$). Proton n.m.r. ($CHCl_3$): PCH_3, doublet ($\tau = 8.48, J_{P-CH_3} = 14.1$ Hz); NCH_2, triplet ($\tau = 7.06, J_{CH_2-CH_2} = 5.35$ Hz); OCH_2, double triplet ($\tau =: 6.01, J_{CH_2CH_2} = 5.35, J_{P-OCH_2} = 7.5$ Hz). Infrared (film) 3440 and 3360 cm^{-1}, NH_2; 1302 cm^{-1}, P—CH_3; 1205 cm^{-1}, P→O; 1010, 940, and 870 cm^{-1}, P—C and P—N.

Anal. Calcd. for $C_4H_{12}NO_2P + H_2O$: C, 31.00; H, 9.02; N, 9.02. Found: C, 31.35; H, 8.71; N, 9.28.

The elemental analysis and spectral characteristics of this compound are consistent with it being 2-aminoethyl dimethylphosphinate. The original product, therefore, consisted of 19% P—O, 22% P—N, and 59% acid.

The authors wish to thank Miss P. M. Lutley for n.m.r. spectra and product analyses and Mr. Y. Marois for the infrared spectra. Mr. N. Gibson assisted with some of the synthetic and kinetic experiments.

1. R. GREENHALGH and M. A. WEINBERGER. Can. J. Chem. **45**, 495 (1967).
2. J. O. EDWARDS and R. G. PEARSON. J. Amer. Chem. Soc. **84**, 16 (1962).
3. (*a*) R. F. HUDSON. Chim. **16**, 173 (1962). (*b*) R. F. HUDSON. Structure and mechanisms in organophosphorus chemistry. Academic Press Inc., London. 1965.
4. I. DOSTROVSKY and M. HALMANN. J. Chem. Soc. 516 (1953).
5. E. W. CRUNDEN and R. F. HUDSON. J. Chem. Soc. 3591 (1962).
6. H. H. JAFFE. Chem. Rev. **53**, 191 (1953).
7. J. R. COX, JR. and O. B. RAMSAY. Chem. Rev. **64**, 617 (1964).
8. R. W. TAFT, JR. J. Chem. Phys. **26**, 93 (1957).
9. R. F. HUDSON and M. GREEN. Angew. Chem. Int. Ed. **2**, 11 (1963).
10. F. H. WESTHEIMER. Special Publication No. 8. The Chemical Society, London. 1957. p. 180.
11. H. K. HALL. J. Org. Chem. **21**, 248 (1956).
12. A. L. GREEN, B. SAVILLE, G. L. SAINSBURY, and M. STANSFIELD. J. Chem. Soc. 1583 (1958).
13. J. EPSTEIN, P. L. CANNON, H. O. MICHEL, B. E. HACKLEY, and W. A. MOSHER. J. Amer. Chem. Soc. **89**, 2937 (1967).
14. G. SCHRADER. Die Entwicklung neuer Insektizide auf Grundlage organischer Fluor und Phosphor-Verbindungen. 2. Erweiterte Auflage. Verlag Chemie, GMBH., Weinheim/Bergstr, 1952.
15. R. A. MCIVOR, G. D. MCCARTHY, and G. A. GRANT. Can. J. Chem. **34**, 1819 (1956).
16. Z. PELCHOWICZ. J. Chem. Soc. 238 (1961).
17. M. J. HARWOOD and K. A. POLLART. US Pat. 3 104 259 (1963).
18. H. TOLKMITH. J. Amer. Chem. Soc. **75**, 5270 (1953).
19. A. D. F. TOY. J. Amer. Chem. Soc. **70**, 3882 (1948).
20. H. GOLDWHITE and B. C. SAUNDERS. J. Chem. Soc. 2040 (1955).
21. (*a*) S. P. HARTLEY, W. S. HOLMES, J. K. JAQUES, M. F. MOLE, and J. C. MCCOUBREY. Quart. Rev. **17**, 216 (1963). (*b*) E. NEALE, L. T. D. WILLIAMS, and V. T. MOORE. J. Chem. Soc. 422 (1956).

Can. J. Chem. Downloaded from www.nrcresearchpress.com by 210.87.254.42 on 09/05/12
For personal use only.

Can. J. Chem. Downloaded from www.nrcresearchpress.com by 210.87.254.40 on 09/05/12
For personal use only.

Mechanism of the reaction of sarin with methanol in the presence of amines[1]

M. A. WEINBERGER,[2] R. GREENHALGH,[3] AND P. M. LUTLEY (MISS)[4]
Defence Research Establishment Ottawa, Defence Research Board, Ottawa, Canada

Received November 3, 1969

In pyridine or 2-methyl-2-propanol solution, the kinetics of the reaction of sarin with methanol in the presence of amines to produce the ester, methyl isopropyl methylphosphonate, is shown to be of first order with respect to each of the three components. By varying the amine it was deduced that the amine acts as a general base catalyst but the catalysis is subject to large steric effects.

Canadian Journal of Chemistry, **48**, 1358 (1970)

Introduction

It has previously been shown (1) that alcohol–amine mixtures react with sarin (isopropyl methylphosphonofluoridate) to form esters, in contrast to the production of amides when the chloridate is used as the phosphylating agent. The presence of amine is, however, apparently required for ester formation to proceed. This reaction has now been examined in further detail by kinetic methods.

Experimental

Sarin is extremely toxic and quite volatile. It is normally handled only in a highly efficient fume-hood with the operator showing no exposed skin and wearing a gas mask.

(a) Method

The course of the reaction was followed by determining, at various times, the nuclear magnetic resonance (n.m.r.) spectra (Varian HA60IL spectrometer operating in HR mode) of the reaction mixtures in the regions characteristic of OMe and PMe protons. The development of the ester POMe doublet vs. the disappearance of the methanol OMe singlet served as an index of reaction progress, as did, independently, the appearance of the ester PMe doublet compared with the disappearance of the sarin PMe quartet. This double determination of the extent of reaction was not possible with those amines whose proton spectra obscured the PMe region. Integrated spectra and, in some cases, peak heights were used to determine the relative concentrations of the reagents.

The choice of solvent was limited by the requirements of non-reactivity and a non-interfering n.m.r. spectrum. The effect of varying the amine was examined in 2-methyl-2-propanol, in which all components remained in solution, but in which the PMe peaks appeared on the shoulder of the large solvent peak. 2-Methyl-2-propanol did not react with sarin in the time allotted to the experiments. Attempts to use deuterated 2-methyl-2-propanol led to irreproducible results, as the commercially available samples appeared to contain a non-removable component which interfered with the reaction. The system on which the detailed kinetic evaluations were made consisted of sarin-d_6 [$(CD_3)_2CHOP(O)(CH_3)F$], methanol, with ethylene diamine as the amine and pyridine as the solvent. Use of sarin-d_6 ensured a clear view of the PMe protons, and all the required n.m.r. peaks were well separated from one another. However, the amine salt precipitated during the reaction. Pyridine, even at the high concentration in which it is present as the solvent, is ineffective as a base for the sarin–methanol reaction and can be considered inert.

The reactions were studied in n.m.r. tubes at 29 °C. To determine reaction order, runs were made with the reagents in equimolar proportions at three concentrations (0.37, 0.48, and 0.68 *M*). The relative proportions of the reagents were also varied (sarin, 0.74; MeOH, 0.37; $(CH_2NH_2)_2$, 0.37 *M*). These high concentrations were required because of the lack of sensitivity of the n.m.r. method. The ratio of the total integrated OMe to PMe peaks was averaged over the run and used to correct the nominal methanol concentration.

The preparation of the reaction mixtures was complicated by the precautions which had to be taken because of the toxicity of sarin and to protect the reagents from moisture. The operations were carried out in a glove box (dry nitrogen atmosphere) inside a fume-hood. Quantities of reagents (30–60 μl) were measured by micropipet into a mixing vessel, before transfer to a 5 mm n.m.r. tube which was closed with a tightly fitting neoprene cap.

(b) Materials

Sarin-d_6

This was prepared by the reaction of 2-propanol-d_6 [$(CD_3)_2CHOH$] (Merck, Sharp and Dohme of Canada Ltd.) with a mixture of methylphosphonic dichloride and methylphosphonic difluoride (2). The product, b.p. 42 °C/0.9 mm, was characterized by its ^1H and ^{31}P n.m.r. and infrared spectra.

Methanol

This was stored over molecular sieve (Linde type 3A) and distilled from calcium hydride; b.p. 65 °C.

Pyridine

This was stored over KOH and fractionated; b.p. 115 °C.

---

[1]D.R.E.O. Report No. 614.

[2]Present address: Defence Research Analysis Establishment, Ottawa 4, Canada.

[3]Present address: Analytical Chemistry Research Service, Department of Agriculture, Central Experimental Farm, Ottawa, Canada.

[4]Present address: Dalhousie University, Halifax, Nova Scotia.

TABLE 1
Kinetics of the sarin–methanol–ethylene diamine reaction

c_0 (M)	Relative concentrations Sarin:MeOH:en	Kinetic equation	$10^4 k''' c_0^2$ (s^{-1})	$10^4 k'''$ ($M^{-2}\ s^{-1}$)
0.38	1:1.00:1	[1]	2.0	13.8
0.48	1:1.16:1	[1]	2.7	11.5
0.48	1:0.90:1	[1]	4.2	18.0
0.67	1:0.96:1	[1]	6.3	14.1
0.68	1:0.92:1	[1]	6.5	14.0
0.37	2:0.98:1	[2]	2.6	19.5
0.37	1:1.97:1	[2]	2.6	19.5

2-Methyl-2-propanol

This was distilled from calcium hydride; b.p. 81–82 °C, m.p. 24–25 °C.

Amines

Ethylene diamine, triethylamine, diethylamine, piperidine, and collidine were stored over KOH and distilled prior to use. 1,4-Diazabicyclo[2.2.2]octane and quinuclidine[5] were purified by recrystallization.

(c) Base Strengths in 2-Methyl-2-propanol

The base (0.5 M) in 2-methyl-2-propanol saturated with KCl was half neutralized with a solution of trifluoroacetic acid in KCl-saturated 2-methyl-2-propanol. From the potential difference, E, measured between calomel and glass electrodes immersed in the solution (Metrohm pH meter), the relative base strengths of quinuclidine and 1,4-diazabicyclo[2.2.2]octane with respect to triethylamine were calculated by $\Delta pK = (F/2.303\ RT)\Delta E$.

Results

The product of the reaction was shown to be methyl isopropyl methylphosphonate by comparison of its n.m.r. and infrared spectra with those of an authentic sample. There was no n.m.r. evidence for the formation of isopropyl *P*-methylphosphonamidates or isopropyl methylphosphonic acid. However, it must be borne in mind that n.m.r. is not a very sensitive method for detecting impurities.

In the runs with ethylene diamine (en) its hydrofluoride precipitated from the pyridine solution and this degraded the quality of the n.m.r. spectra. If the salt is only involved in the reaction mechanism as a final product, the kinetics will not be affected. The ratio of the integrated peaks due to OMe to those from PMe protons was constant to ±3–4% during each run. This ratio was used to correct the nominal methanol concentration which, because of the method of addition and the volatility of methanol, was most likely to be in error. The extents of reaction at a given time, as measured by the relative distribution of OMe and PMe among reagents and products were almost identical, except in the runs at lowest concentration (0.37–0.38 M), where the methanol disappearance lagged somewhat behind the sarin consumption.

The results obtained in pyridine solution were analyzed by applying the relevant relation for third-order kinetics. In the case of equimolar concentration (c_0) of two reagents, with the third reagent concentration slightly different at $c_0 + \delta c$, the simple third-order expression

$$\frac{1}{2}\left\{\left(\frac{c_0}{c}\right)^2 - 1\right\} = k''' c_0^2 t$$

is modified by a correction term to give

$$[1] \qquad \frac{1}{2}\left\{\left(\frac{c_0}{c}\right)^2 - 1\right\} - \frac{\delta c}{3c_0}\left\{\left(\frac{c_0}{c}\right)^3 - 1\right\} = k''' c_0^2 t$$

where k''' is the third-order rate constant and c is the concentration at time t.

When the proportion of reactants is 2:1:1, the relation is

$$[2] \qquad \ln\left(\frac{2}{1 + c_0/c}\right) + \frac{c_0}{c} - 1 = k''' c_0^2 t$$

where c_0 and c are the concentrations of the reactants present in smaller quantity. No concentration corrections were applied in this case. Typical plots against time of the left-hand side of eq. [1], evaluated for three concentrations of equimolar reaction mixtures, are shown in Fig. 1. Values of $k''' c_0^2$ derived from the slopes of these plots and those of eq. [2] are shown in Table 1. A plot with least-square constraint of $k''' c_0^2$ vs.

[5]The authors thank Dr. D. H. Rosenblatt, Edgewood Arsenal, Maryland for donating this amine.

Can. J. Chem. Downloaded from www.nrcresearchpress.com by 210.87.254.40 on 09/05/12
For personal use only.

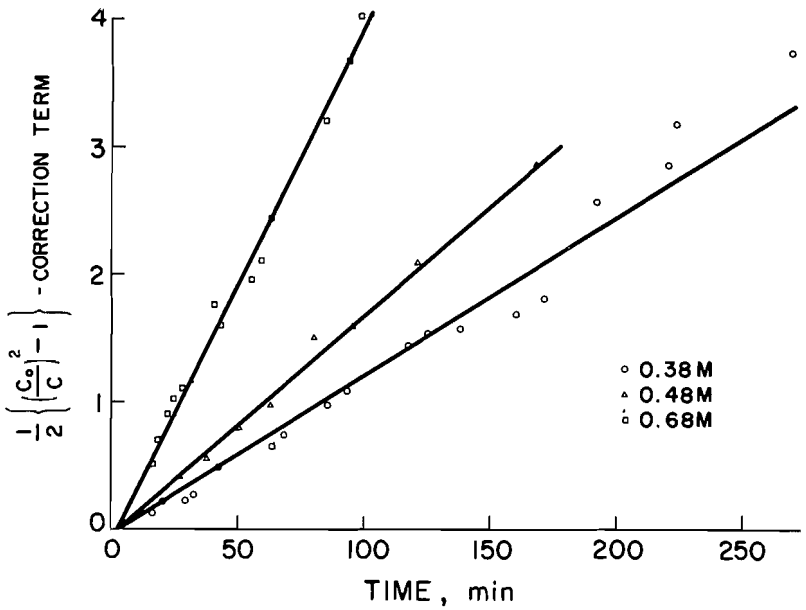

FIG. 1. Plots to 65–70% reaction of left-hand side of eq. [1] vs. time.

c_0^2 yielded a line through the origin of slope $k''' = 1.45 \pm 0.08 \times 10^{-3}\ M^{-2}\ s^{-1}$.

Third-order rate constants for the reactions with various amines in 2-methyl-2-propanol solution are shown in Table 2, which is arranged according to increasing base strength in water. Reaction mixtures were usually 1:1:1 in reagents, each at a concentration 0.45–0.5 M. The pK_a values of the bases in water and the differential pK_a values with respect to triethylamine in 2-methyl-2-propanol are also shown.

Discussion

In considering these results, it should be remembered that n.m.r. is not capable of giving, in the present experiments, highly accurate kinetic measurements. The results are, however, adequate to establish that the reaction kinetics are overall third order. A second-order expression does not fit the data as well as the third-order expression used and, furthermore, the values of $k''c_0$ which can be deduced from the second-order (c_0/c vs. t) plots do not lie on a line through the origin when graphed against c_0. It should also be remembered that no reaction occurs when either methanol or amine is missing from the reaction medium.

The following three mechanisms were considered in order to explain the function of the amine. Only the third was found to be consistent with all the kinetic and other reaction data.

(*a*) Specific catalysis or nucleophilic attack by amine

$$\text{sarin} + \text{amine} \rightarrow [\text{—P—N—}]$$

$$[\text{—P—N—}] + \text{MeOH} \rightarrow \text{ester} + \text{amine.HF}$$

This mechanism is unlikely, because when amidates rather than esters are produced by a suitable change of the leaving group (e.g. from F to Cl), they are found to be stable. For example, when ethanolamine is reacted with the chloro analogue of sarin, a high yield of the *N*-phosphylated product is isolated in contrast to the reaction of ethanolamine with sarin which results in *O*-phosphylation (1). It has also been shown that diethylamine hydrofluoride neither reacts with sarin nor catalyzes the conversion of *N*-phosphylated ethanolamine to *O*-phosphylated ethanolamine. Furthermore, a tertiary amine would lead to a positive nitrogen in a phosphonamidate intermediate, yet the rate constant with quinuclidine is not too different from that with diethylamine.

(*b*) The amine reacts with methanol in a fast equilibrium reaction to produce the true nucleophile, methoxide ion, probably present in an ion pair, the attack of methoxide ion on sarin being

Can. J. Chem. Downloaded from www.nrcresearchpress.com by 210.87.254.40 on 09/05/12
For personal use only.

TABLE 2

Rate constants of the sarin–methanol–amine reaction in 2-methyl-2-propanol

Amine	pK_a (aq)	pK_a (*t*-BuOH)	$10^4 k'''$ (M^{-2} s^{-1})
Collidine	7.6		0.0017
1,4-Diazabicyclo[2.2.2]octane	8.9	−0.85	0.76
Quinuclidine	10.7	+0.4	3.8 ±0.2
Triethylamine	10.8	ref	0.73±0.02
Diethylamine	11.0		5.8 ±0.7
Piperidine	11.2		10.7 ±0.5

the rate-determining step

$$\text{amine} + \text{MeOH} \overset{K}{\rightleftharpoons} \text{MeO}^- + \text{amine.H}^+$$

$$\text{MeO}^- + \text{sarin} \overset{k}{\rightarrow} \text{ester} + \text{F}^-$$

At first sight, it would appear that this mechanism could be immediately eliminated on kinetic grounds for, on the assumption that $K \ll 1$, it does not lead to third-order kinetics but, for equal initial reactant concentrations, to $1/2[(c_0/c)-1]^2 = kKc_0t$. This expression does not fit the data. However, since it was found that ethylene diamine hydrofluoride is sparingly soluble in and precipitates from pyridine solution, third-order kinetics may still result as long as supersaturation does not occur ($k''' = kK/\sqrt{K_s}$, where $K_s = [\text{amine.H}^+][\text{F}^-]$).

This mechanism can, however, be ruled out on other grounds. Firstly, the reaction also shows third-order kinetics in 2-methyl-2-propanol, where the salt stays in solution. Secondly, the effect of the base on the rate of the reaction should be controlled by its strength, since it is involved only in a non-rate-determining proton transfer equilibrium. However, a comparison (Table 2) of the results with triethylamine with those with quinuclidine suggests that factors other than base strength are involved. There is a fivefold increase in velocity constant with quinuclidine over triethylamine although the pK_a values for the two amines are virtually identical in aqueous solution and differ by a factor of only 2.5 in 2-methyl-2-propanol solution. The amino group of quinuclidine is not sterically hindered. It is well known that triethylamine exhibits considerable steric hindrance as compared to diethylamine (see, for example, Lemieux and Lineback (3)). It would appear, therefore, that the reaction mechanism must be one which involves steric hindrance in the function of the amine.

(*c*) The amine acts as a general base catalyst by facilitating the removal of the hydroxyl proton in the transition state of the reaction between sarin and methanol. All the facts given above are consistent with this mechanism. A similar mechanism has been suggested by Dudek and Westheimer (4) for the propanolysis of tetrabenzyl pyrophosphate in the presence of lutidine or collidine and by Hudson and Greenhalgh (5) for the catalysis by butylamine of the hydrolysis of diisopropyl phosphorofluoridate. General base catalysis subject to steric effects is perhaps not a universally accepted phenomenon, but it has been used by Covitz and Westheimer (6) to explain the hydrolysis of ethylene methyl phosphate. The third-order rate constant reflects interaction of the base with a large organic transition state complex at the moment when a proton is transferred from one to the other. It is reasonable to suppose that this interaction is subject to different steric conditions from those which affect the ionization constant of the base. When steric conditions are similar, as in quinuclidine and 1,4-diazabicyclo[2.2.2]octane, it can be seen from Table 2 that the rate constants follow the basicities with an indicated Brönsted coefficient of 0.5 to 0.6.

The authors are grateful to Dr. R. M. Heggie for valuable advice and encouragement.

1. R. Greenhalgh and M. A. Weinberger. Can. J. Chem. **45**, 495 (1967).
2. B. M. Zeffert, P. B. Coulter, and H. Tannenbaum. J. Amer. Chem. Soc. **82**, 3842 (1960).
3. R. U. Lemieux and D. R. Lineback. Can. J. Chem. **43**, 94 (1968).
4. G. O. Dudek and F. H. Westheimer. J. Amer. Chem. Soc. **81**, 2641 (1959).
5. R. F. Hudson and R. Greenhalgh. J. Chem. Soc. B, **325** (1969).
6. F. Covitz and F. H. Westheimer. J. Amer. Chem. Soc. **85**, 1773 (1963).

Can. J. Chem. Downloaded from www.nrcresearchpress.com by 210.87.254.40 on 09/05/12
For personal use only.

Can. J. Chem. Downloaded from www.nrcresearchpress.com by 210.87.254.5 on 09/05/12
For personal use only.

Mass spectral studies of metal chelates. V. Mass spectra and appearance potentials of some fluorine-substituted acetylacetonates[1,2]

C. REICHERT,[3] G. M. BANCROFT,[4] AND J. B. WESTMORE
Department of Chemistry, University of Manitoba, Winnipeg, Manitoba

Received July 10, 1969

The mass spectra of the hexafluoroacetylacetonates (hfacac) and trifluoroacetylacetonates (tfacac) of Al(III), Cr(III), Fe(III), Fe(II), Cu(II), and Zn(II) are reported. The main features of the spectra are discussed. Compared with the spectra of the acetylacetonates (acac), substitution of CF_3 for CH_3 in these complexes leads to more extensive fragmentation of the molecular ions. For example, ions corresponding to loss of $\cdot CF_3$ radicals are more abundant than those corresponding to loss of $\cdot CH_3$ radicals. The appearance potentials (a.p.'s) of the molecular ions and, where possible, of fragment ions formed from the molecular ion by loss of $\cdot CF_3$, $\cdot CH_3$, or ligand radicals are reported. The a.p.'s of the molecular ions are more sensitive to the nature of the ligand than to the metal. Thus, for the metal chelates studied here the a.p.'s of the molecular ions from ML_2 and ML_3 (L stands for ligand) were 9.95 ± 0.25 V for L = hfacac, 9.05 ± 0.35 V for L = tfacac, and 8.3 ± 0.35 V for L = acac. The energy required to dissociate a $\cdot CF_3$ or $\cdot CH_3$ radical from the molecular ion is sensitive to the nature and valency of the metal M, being low (relatively) for Al(III) and Fe(III), and high (relatively) for Cr(III) (inferred) and Fe(II). This variation is discussed in terms of the effect of substituent, and of interaction of metal d orbitals with the ligands.

Canadian Journal of Chemistry, 48, 1362 (1970)

Introduction

Although the metal acetylacetonates have long been studied, there still remains much to be understood about the bonding in these molecules. There is general agreement that, in those complexes in which coordination to the metal occurs through the oxygen atoms, the chelate ring is planar and the π electrons are partially delocalized over the chelate ring (2). Other conclusions are less certain. Substantial progress has been made in the interpretation of their electronic spectra. Although Barnum (3) has obtained good agreement between calculated and observed energies for spectral transitions of a number of octahedral acetylacetonates, there is still considerable disagreement over the band assignments.

Recent mass spectral studies of metal β-diketonates have been useful in elucidating the bonding in these compounds (4–9). However, differences in appearance potential values, although they should be easier to assess than changes in absorption spectra (4), were not in agreement with those expected on the basis of Barnum's simple molecular orbital calculations and assuming Koopmans' theorem (10) to hold. Yet the results have been consistent with the loss of an electron from an orbital localized mainly on the ligand, and the changes in appearance potentials for a number of substituted acetylacetonates (5) could be correlated with the bonding properties of the various substituents to a ring which has aromatic character.

In this paper, we report mass spectra of a number of bis and tris chelates formed from hexafluoroacetylacetone ($CF_3COCH_2COCF_3$) and trifluoroacetylacetone ($CF_3COCH_2COCH_3$). Also recorded are the appearance potentials of the molecular ions and other selected ions. These results are again consistent with the loss of an electron from a molecular orbital localized mainly on the ligand. The large variation in C—CF_3 and C—CH_3 bond dissociation energies (from the molecular ion) from compound to compound is discussed in terms of relative stabilization of the molecular and fragment ions.

Experimental

All the metal chelates, with the exception of $Fe(tfacac)_2$, were prepared using the aqueous solution synthesis described by Fernelius and Bryant (11). Iron(II) trifluoroacetylacetonate was prepared using a modification of the method of Buckingham *et al.* (12). Trifluoroacetylacetone was added to a solution of $FeSO_4$ in deoxygenated water containing a few drops of H_2SO_4 and a few drops of hydrazine to reduce any iron(III) impurities present. The precipitate was filtered off and washed with a large volume of deoxygenated water. It was dried in vacuo. All compounds were purified by fractional sublimation at reduced pressure.

[1]See ref. 1 for Part IV.
[2]Presented, in part, at the 51st Conference and Exhibition, Chemical Institute of Canada, Vancouver, May, 1968.
[3]Present address: Mass Spectrometry Center, University of Kentucky, Lexington, Kentucky.
[4]Present address: University Chemical Laboratory, Lensfield Road, Cambridge, England.

TABLE 1

Relative intensities of metal-containing ions in the mass spectra of the tris-complexes of fluorinated acetylacetonates, at an electron energy of 50 V and an ionization chamber temperature of 150 °C*

Ion or *e/m*	Relative intensity of daughter ion from					
	$Al(hfacac)_3$	$Cr(hfacac)_3$	$Fe(hfacac)_3$‡	$Al(tfacac)_3$	$Cr(tfacac)_3$	$Fe(tfacac)_3$
L_3M^+ (*a*)	5	20	18	3	24	10
$(L_3M—F)^+$ (*b*)	1[a]	4	2	—	2	—
$(L_3M—CF_3)^+$ (*c*)	6[ab]	6[ab]	7	—	—	0.5
L_2M^+ (*d*)	100[ac]	100[ac]	100	100[a]	100	100
$(L_2M—F)^+$	5	—	—	—	—	—
$(L_2M—CH_3)^+$	—	—	—	—	—	3
$(L_2M—CF_2)^+$ (*e*)	17[d]	21[d]	37[d]	9[d]	8	27[d]
$(L_2M—CF_3)^+$ (*f*)	3	3[bc]	21	1.5	21[e]	20
$(L_2M—2CF_2)^+$ (*g*)	1	—	—	7	—	0.5
$(LMOCCH)^+$	—	—	—	—	—	3
$(L_2M—CF_3—CF_2)^+$	1	—	—	—	—	4
LMF^+ (*h*)	—	70[d]†	8	12	40	5
LM^+ (*i*)	—	64[f]	7[ef]	3[e]	30[e]	20
$(LMF—CF_2)^+$ (*j*)	10	23[h]†	6	39[gh]	25[h]	—
$(LM—CF_2)^+$ (*k*)	11	35[i]	57[i]	—	40	80[i]
$(LM—CF_3)^+$	—	38	—	—	3	—
207	—	w	—	—	—	—
189	—	w	—	—	—	—
169	m	m	m	—	—	—
154	—	—	w	—	—	—
139	w	—	w	—	w	w
119	m[j]	m[j]	m[k]	—	—	—
115	—	—	—	—	—	m
91	m	w	vw	—	—	—
87	—	—	—	—	—	m
85	—	—	—	w	w	m
75	m	m	m	—	—	—
71	m	m	—	—	—	—
69	s	s	s	m	w	m
67	—	—	—	m	w	m
43	—	—	—	s	s	s

*Identified metastable transitions are indicated by superscripts which relate the daughter ion to its precursor as labelled in column 1. (The relative intensities of the ions in the lower part of the table, which do not contain a metal atom, are indicated qualitatively by s = strong, m = medium, w = weak.)

†Incorrectly reported in ref. 5.

‡Temperature = 80 °C.

The mass spectra were obtained on a Hitachi Perkin–Elmer RMU-6D single focussing mass spectrometer. The samples were introduced via the heated inlet system (150 °C). The masses of the high-mass ions were verified by the simultaneous introduction into the ion source of perfluorokerosene, which gives ions of known mass, at small mass intervals, to masses beyond 1000. Appearance potentials were determined, as described previously (4), by the semi-logarithmic method (13) using xenon as a standard.

Results and Discussion

Mass Spectra

The relative intensities of all metal-containing ions (except for very minor peaks, i.e. less than 1% relative intensity) in the mass spectra of the tri- and hexa-fluoroacetylacetonates of Al(III), Cr(III), Fe(III), Fe(II), Cu(II), and Zn(II) are given in Tables 1 and 2. Also present in the spectra were ligand fragments, and only the most important of these are reported in the tables. They were of variable intensity and possibly could arise from ionization and fragmentation of the metal chelate or a thermal decomposition product, although, except for the Fe(III) chelates, evidence of thermal decomposition was minimal. In some cases, however, the presence of a metastable peak confirmed that these non-metal-containing ions did arise from metal-containing precursor. These cases will be discussed later.

It is first appropriate to point out some general features of the spectra. Compared with the spectra of the acetylacetonates (4, 6), it is apparent that substitution of CF_3 for CH_3 in these complexes leads to a more extensive fragmentation of the molecule under electron impact. There is a

Can. J. Chem. Downloaded from www.nrcresearchpress.com by 210.87.254.5 on 09/05/12
For personal use only.

TABLE 2

Relative intensities of metal-containing ions in the mass spectra of the bis-complexes of fluorinated acetylacetonates, at an electron energy of 50 V and an ionization chamber temperature of 150 °C*

Ion or *e/m*	Relative intensity of daughter ion from					
	$Fe(hfacac)_2$	$Cu(hfacac)_2$	$Zn(hfacac)_2$	$Fe(tfacac)_2$	$Cu(tfacac)_2$	$Zn(tfacac)_2$
$(L_2M)^+$ (*a*)	83	9	9	100	5	44
$(L_2M—F)^+$ (*b*)	4	—	—	—	—	—
$(L_2M—CH_3)^+$ (*c*)	—	—	—	6	1	21
$(L_2M—CF_2)^+$ (*d*)	30[a]	—	—	28[a]	—	—
$(L_2M—CH_2CO)^+$	—	—	—	—	8	—
$(L_2M—CFO)^+$	—	—	—	—	8[a]	—
$(L_2M—CF_3)^+$ (*e*)	44[ab]	24[ab]	27[a]	31[d]	11	100[a]
$(LMOCCH_2)^+$ (*f*)	—	—	—	4	—	40[e]
$(L_2M—138)^+$† (*g*)	—	23[e]	2.5	—	27[e]	—
$(LMF)^+$	8	—	—	6	—	—
$(LM)^+$ (*h*)	13[e]	1.5	19[e]	23	8	54[cf]
$(LM—CH_3)^+$	—	—	—	—	10	—
$((L—CF_3)MOCCH)^+$?	—	—	—	—	—	9
$(LM—CF_2)^+$ (*i*)	100[h]	—	100[h]	71		67[h]
$(LM—CF_3)^+$ (*j*)	—	100[h]	12	—	100[g]	9
$(MCOCH_2)^+$	—	—	—	—	59[J]	—
$(MCOCH)^+$	—	11	6	—	18	12
$(LMF—CF_2)^+$	9	—	—	—	—	—
M^+	—	82[J]	46	—	44	28
169	m	—	vw	—	—	—
154	—	—	—	w	—	—
153	—	—	—	—	w[g]	—
139	m	m	w	w	—	w
119	m[J]	w	m	w	—	w
97	—	—	—	w	m	—
91	w	m	m	w	m	m
85	—	—	—	m	m	m
75	m	w	m	w	—	—
69	s	s	s	s	w	s
67	—	—	—	m	—	m
43	—	—	—	s	m	s

*Identified metastable transitions are indicated by superscripts which relate the daughter ion to its precursor as labelled in column 1. (The relative intensities of the ions in the lower part of the table, which do not contain a metal atom, are indicated qualitatively by s = strong, m = medium, w = weak.)

†See text for interpretation of this ion.

decrease in relative intensity (compared with the total ion current) of the molecular ion, and a consequent increase in the number and intensity of the fragment ion peaks in the spectra of the fluorinated species. The greater fragmentation of the fluorinated chelates can be attributed to (*a*) the relative instability of the molecular ion due, for example, to weak C—CF_3 bonds in the molecular ion, (*b*) the relative stability of fragment ions in which rearrangement allows formation of strong metal–fluorine bonds, and (*c*) the destabilization of a C—CH_3 or C—CF_3 bond owing to the increase of positive charge on the carbon atom via the electron withdrawing power of the CF_3 substituents. Evidence to support (*a*) is given by the appearance potential measurements to be discussed in this paper, and to support (*b*) is given later in this section. Evidence in favor of (*c*) has already been discussed (5). It is noteworthy that observation (*c*) is consistent with the relative stabilities of benzylic bonds meta or para to another functional group in the mass spectra of benzene derivatives and in which correlations with Hammett sigma constants have been made (14). Thus, in analogous compounds of the same metal, the peak corresponding to loss of a $\cdot CF_3$ radical is always considerably more intense than the corresponding peak due to loss of a $\cdot CH_3$ radical. Indeed, the latter peaks are very small or undetectable in the spectra of most of the trifluoroacetylacetonates presented here. This suggests that, in the molecular ion, the C—CF_3 bond is weaker than the C—CH_3 bond. This is confirmed in the cases of $Zn(tfacac)_2$ and H(tfacac), in which the appearance potentials of both $(P—CF_3)^+$ and $(P—CH_3)^+$ could be measured

Can. J. Chem. Downloaded from www.nrcresearchpress.com by 210.87.254.5 on 09/05/12
For personal use only.

TABLE 3

Appearance potentials of selected ions in the mass spectra of fluorinated acetylacetonates*

Compound	Appearance potential, V							
	P^+	$(P—CF_3)^+$	$(P—CH_3)^+$	$(P—L)^+$	$\Delta(CF_3)$	$\Delta(CH_3)$	$\Delta(L)$	P^+(lit.)
$Al(hfacac)_3$	9.80	10.7	—	11.2	0.9	—	1.4	10.30†
$Cr(hfacac)_3$	10.13±0.05	—	—	14.3	—	—	4.2	9.97†
$Fe(hfacac)_3$	10.2	11.1	—	10.2§	0.9	—	0§	10.34†
$Fe(hfacac)_2$	9.7	13.2±0.2	—	—	3.5	—	—	—
$Cu(hfacac)_2$	9.86±0.05	11.6	—	—	1.7	—	—	—
$Zn(hfacac)_2$	10.07±0.05	11.35	—	15.3±0.2	1.3	—	5.2	—
H(hfacac)	10.55±0.05	11.2	—	—	0.6	—	—	10.68†
$Al(tfacac)_3$	9.05	—	—	10.2	—	—	1.15	—
$Cr(tfacac)_3$	9.09±0.05	—	—	11.9	—	—	2.8	—
$Fe(tfacac)_3$	9.10±0.05	—	—	9.2§	—	—	0.1§	9.38†
$Fe(tfacac)_2$	8.75	12.6	—	14.5	3.85	—	5.75	—
$Cu(tfacac)_2$	9.05	11.5	—	13.1	2.45	—	4.05	—
$Zn(tfacac)_2$	9.40	11.3	11.7	14.6	1.9	2.3	5.2	—
H(tfacac)	9.8	10.6±0.2	11.7	—	0.8	1.9	—	9.96†
$Al(acac)_3$	7.95±0.05	—	—	9.1±0.2	—	—	1.15	8.27†
$Cr(acac)_3$	8.10±0.05	—	—	11.3	—	—	3.2	7.87†
$Fe(acac)_3$	8.45±0.05	—	—	9.4	—	—	0.95	8.64†
$Fe(acac)_2$	8.1 ±0.05	—	11.7	13.9	—	3.6	5.8	—
$Cu(acac)_2$	8.31±0.05	—	10.9	13.1±0.2	—	2.6	4.8	—
$Zn(acac)_2$	8.62±0.05	—	10.9	14.1±0.2	—	2.3	5.5	—
H(acac)	9.2	—	10.7	—	—	1.5	—	8.87‡

*P = parent molecular ion. Ionization chamber temperature = ~150 °C. Experimental error = ±0.1 V unless otherwise stated. Error in Δ values = ±0.2 V in most cases.
†See ref. 7.
‡Photoionization value, see ref. 36.
§May be low because of the possibility of thermal decomposition to the bischelate in the ion source.

(Table 3) and a direct comparison of the bond dissociation energies in the same molecular ion can be made assuming that the excess energies due to kinetic and excitation effects are the same.

The general features of the mass spectra can be interpreted in terms of the relative stabilities of odd- or even-electron ions, and the tendency of the metal to undergo valency change (4–6). Thus, if, as we propose (5), an electron is removed from the π-system of a chelate ring, the elimination of neutral odd-electron species (·F, $\cdot CF_3$, $\cdot CH_3$, ·acac, ·tfacac, ·hfacac) will produce a relatively stable, even-electron fragment ion. Further elimination of odd-electron neutral species from this fragment ion will not occur readily unless a valency change (reduction) of the metal occurs, and consequently these reactions occur most readily for the Fe(III) and Cu(II) chelates, and least readily for the Al(III) chelates, consistent with the familiar facile reduction of Fe(III) to Fe(II) and Cu(II) to Cu(I) in the general chemistry of these metals. Even-electron ions tend to lose even-electron neutral species (CF_2, CH_2CO, L—F), and no valency change of the metal is required in these reactions.

There are many metastable peaks which aid in the interpretation of the mass spectra. These are recorded in Tables 1 and 2. Of notable interest are the peaks due to the following metastable transitions in which a neutral, metal-containing species is eliminated

$$(FM(hfacac)—CF_2)^+ \rightarrow MF_3 + CF_2COCHCO^+ \quad \text{for M = Al, Cr}$$

$$(Fe(hfacac)—CF_2)^+ \rightarrow FeF_2 + CF_2COCHCO^+$$

$$(Al(hfacac)_2—CF_2)^+ \rightarrow (Al(hfacac)_2—CF_2—CF_3) + CF_3^+$$

$$((tfacac)Cu \cdot CH_3)^+ \rightarrow CuCH_3 + tfacac^+$$

There are a number of noteworthy transitions, involving loss of CF_2 or (L—F), in the spectra. The corresponding loss of CH_2 was not observed in the spectra of the acetylacetonates (4, 6). In many cases, a one step process is indicated by the presence of a metastable peak for the transition. A mechanism for the elimination of CF_2 has been proposed previously (5) and involves the rearrangement of a fluorine atom to the metal. The elimination of L—F would also involve rearrangement of a fluorine atom to the metal. That metal–fluorine bonds are indeed formed is confirmed by

Can. J. Chem. Downloaded from www.nrcresearchpress.com by 210.87.254.5 on 09/05/12
For personal use only.

Can. J. Chem. Downloaded from www.nrcresearchpress.com by 210.87.254.5 on 09/05/12
For personal use only.

the observations of Clobes *et al.* (15), who observed metastable peaks for the elimination of neutral metal fluorides from fragment ions in the mass spectra of hexafluoroacetylacetonates of Cr(III), Fe(III), and Co(III), and also by our own observations given above. Additionally, King (16) has reported elimination of neutral FeF_2 in the mass spectra of some transition-metal fluorocarbon complexes.

The formation of metal–fluorine bonds is thus well documented. Since a strong carbon–fluorine bond must be broken in the reaction, the process should be favored when the metal–fluorine bond energy is high. From recent data, the mean bond energies, in kcal/mole, in the following compounds are computed: AlF_3, 140 (17); CrF_3, 119 ± 4 (18); CrF_2, 113.5 ± 2 (19); FeF_3, 110 ± 6 (18); FeF_2, 115 ± 5 (20); CoF_2, 111.5 (21); CuF_2, 90 (21); ZnF_2, 92 (21); CF_4, 117.5 ± 1 (22). Thus, for Al, Cr, Fe, and Co the metal–fluorine bonds are almost as strong as, or stronger than, the carbon–fluorine bond. For Cu and Zn the metal–fluorine bonds are 25–30 kcal/mole weaker than the carbon–fluorine bond. No evidence for Cu—F bond formation is observed in the mass spectra of the copper chelates, but elimination of CF_2 is apparently a very favorable process in the zinc chelate fragmentations. It is apparent that, if the metal–fluorine bond is not too weak, the odd- or even-electron character of the ion, and the ability of the metal to change valency, are of prime importance.

Since CF_2 is an even-electron species, it would preferentially be eliminated from even-electron ions rather than from odd-electron ions. Elimination of CF_2 has not been observed from the molecular ions of any of the trischelates (i.e. $(L_3M—CF_2)^+$ ion peaks have not been detected), either because the L_3M^+ ions are odd-electron species or because the concerted mechanism proposed (5) may be sterically hindered. $(L_2M—CF_2)^+$ ion peaks are observed for all the trischelates and also for $Fe(hfacac)_2$ and $Fe(tfacac)_2$. For these latter two compounds the L_2M^+ ion is an odd-electron species unless metal-to-ligand electron transfer occurs, i.e. oxidation of the metal occurs. It is just in the case of Fe(II) that oxidation of the metal should occur most readily. $(LM—CF_2)^+$ ion peaks are observed in most of the spectra but are absent from the spectra of the Cu(II) chelates. Elimination of CF_2 seems to occur more readily in fragmentation of the hexafluorochelates than the trifluorochelates, possibly because of the greater statistical probability of occurrence (twice as many CF_3 groups).

The elimination of CF_2 has also been observed in organometallic compounds (23, 24) and organic compounds (25, 26). In organic compounds, the elimination of CF_2 has been attributed to the comparative stability of CF_2, although, until recently, reliable thermochemical data were not available. The latest data (22) give the average bond energy in CF_2 as 124 ± 3 kcal/mole, indicating a slight strengthening of the carbon–fluorine bonds with respect to CF_4, so that the energy gain, from this contribution alone, on elimination of CF_2 from an ion is quite small.

In the spectra of $Cu(hfacac)_2$, $Zn(hfacac)_2$, and $Cu(tfacac)_2$ are fragment ions labelled as $(L_2M—138)^+$. These could be due to loss of $2 \cdot CF_3$ radicals from the molecular ion or of loss of $CF_3COCHCO$ (or $\cdot CF_3 + COCHCO$). By using ligands deuterated at the central carbon atom, it was established that for $Cu(hfacac)_2$ this ion corresponded to loss of $2 \cdot CF_3$ radicals from the parent ion. At the same time, the assignment of the base peak in this spectrum to $(Cu(hfacac)—CF_3)^+$ rather than to $(Cu(hfacac)_2—4CF_3)^+$ was confirmed. For $Cu(tfacac)_2$, both processes occur with equal probability (within the accuracy of the determination). Owing to the broadness of the metastable peak, it was not possible to determine whether, in the spectrum of the deuterated compound, the daughter ion of the metastable transition was $(L_2M—138)^+$ or $(L_2M—139)^+$. In the formation of the $(Cu(tfacac)_2—2CF_3)^+$ ion, the CF_3 substituents are lost from different chelate rings, a reaction which can rarely be confirmed. The $(Cu(tfacac)_2—CF_3COCHCO)^+$ ion corresponds to $((tfacac)Cu \cdot CH_3)^+$, and migration of a methyl group to copper is indicated. Further support for the methyl migration is given by the observation of a metastable peak given above for a transition in which neutral $CuCH_3$ is eliminated.

The identity of the $(Zn(hfacac)_2—138)^+$ ion was not established, since it is a minor peak.

The simplicity of the negative-ion mass spectra supports the foregoing rationalizations. For example, at 70 eV, the only negative ions with relative intensity greater than 0.5% of the base peak in the mass spectrum of $Cu(tfacac)_2$ were CuL_2^- (100%), L^- (69%), and $(L—CH_3)^-$ (2%). Under these conditions CF_3^- and CH_3^-

Can. J. Chem. Downloaded from www.nrcresearchpress.com by 210.87.254.5 on 09/05/12
For personal use only.

were not detected. Thus, although $\cdot CF_3$ likely has a high electron affinity, it seems that the reaction

$$P + e \rightarrow (P—CF_3)^+ + CF_3^- + e$$

is not important in these spectra, and that the CF_3 substituent is preferentially eliminated from the molecular ions as a radical rather than as a negative ion.

Appearance Potentials

(a) Molecular Ions

The appearance potentials of the molecular ions depend much more upon the nature of the ligand than upon the nature of the metal. Thus, for all the bis- and tris-hexafluoroacetylacetonates listed here (Table 3), the appearance potentials lie within the range 9.95 ± 0.25 V; for the bis- and tris-trifluoroacetylacetonates, within the range 9.05 ± 0.35 V; and for the bis- and trisacetylacetonates, within the range 8.3 ± 0.35 V. Thus, replacement of a CH_3 substituent by a CF_3 substituent increases the appearance potential by 0.6 to 1.1 V. It should also be noted that the values for the complexes always lie appreciably below those of the parent ligand, HL. These generalizations are thus consistent with our previous observations, and support the suggestion that the electron removed on ionization of the molecule comes from an orbital which has mainly ligand character, i.e. a π orbital localized mainly on the ligand (4, 5). In addition, for some copper β-diketonates, recent data (9, 27) also show the dominating effect of the ligand upon the appearance potential values.

The appearance potentials of some of the complexes studied here have been reported by Schildcrout, Pearson, and Stafford (7) (see Table 3). In most cases, the agreement between the two sets of results is within ± 0.3 V, even though they used a different method (vanishing current method) for their determinations. They also infer that ionization of the complexes involves an orbital concentrated on the ligand and suggest either that Koopmans' theorem (10) is not valid for these complexes, or that possibly inversion of the e_g and the π orbitals occurs upon ionization.

Recently, another simple Hückel treatment has been applied to the metal(III) trisacetylacetonates (28). These authors claim that some aspects of Barnum's original treatment (3) are incorrect, but also fail to reproduce even qualitatively the trends in the electron impact appearance potentials, and suggest that the approximations inherent in the Hückel approach and the apparent non-applicability of Koopmans' theorem do not allow a more quantitative description of the trends in the appearance potentials.

(b) Fragment Ions

In some of the chelates studied here it was possible to measure the energy required to dissociate a $\cdot CF_3$ or $\cdot CH_3$ radical from the molecular ion. (The dissociation of a neutral radical rather than a negative ion is assumed because of the non-detectability of CF_3^- or CH_3^- in the negative-ion mass spectrum. The difference in energy between the dissociation of a radical or a negative ion is a constant amount, namely, the electron affinity of the radical, and will not alter any trends as the metal atom is varied.) These energies, for the following reactions, vary widely from compound to compound

$$ML_3^+ \rightarrow (ML_3—CF_3)^+ + \cdot CF_3 \qquad \text{for L = hfacac or tfacac}$$

$$ML_3^+ \rightarrow (ML_3—CH_3)^+ + \cdot CH_3 \qquad \text{for L = tfacac or acac}$$

The energy of dissociation of $\cdot CF_3$ or $\cdot CH_3$ from the molecular ion is represented as $\Delta(CF_3)$ or $\Delta(CH_3)$ in Table 3. The values are obtained from

$$\Delta(CF_3) = \text{a.p.}[(ML_3—CF_3)^+] - \text{a.p.}[ML_3^+]$$

and

$$\Delta(CH_3) = \text{a.p.}[(ML_3—CH_3)^+] - \text{a.p.}[ML_3^+]$$

for a given compound. It is assumed that the excess energy associated with the ionization processes is small, or, for comparison purposes, at least constant from compound to compound. In principle, contributions to $\Delta(CF_3)$ and $\Delta(CH_3)$ can be divided into σ and π bond energy terms (29), but the situation is actually more complicated than this. For example, in the molecule RR′, when the R—R′ bond is breaking, adjustments of the other bonds (lengths and angles) in the product radicals may occur. This contribution has been called the "reorganizational energy". To minimize this difficulty, the assumption is made that the σ bond energy term in D(R—R′) is identical to that in an analogous system which involves no π conjugation, and the difference between the D values for the two systems is associated mainly with the π energies as the bond is broken. The π contribution to D(R—R′) is

Can. J. Chem. Downloaded from www.nrcresearchpress.com by 210.87.254.5 on 09/05/12
For personal use only.

often appreciable when compared with typical σ bond energies and can be positive or negative depending upon whether the greater π energy (stabilization) is associated with RR′ or the product radicals.

For molecules in which the π contributions are expected to be small, the bond dissociation energies, in kcal/mole, available (30) are: $D(CF_3—CF_3) = 86$, $D(CH_3—CH_3) = 88$, $D(CF_3—H) = 106$, $D(CH_3—H) = 104$. These values suggest that the σ contribution to $D(C_{sp^3}—C_{sp^3})$ is about 85–90 kcal/mole for H or F substituents. The σ contribution to $D(C_{sp^2}—C_{sp^3})$ is expected to be about 5 kcal/mole higher (31), and hence the energy required to dissociate a $\cdot CH_3$ or $\cdot CF_3$ radical from the chelate ring in the neutral metal chelates under study here should be about 90–95 kcal/mole (about 4 eV/molecule), since, again, the π contribution should be small; i.e. an unoccupied, low-energy π orbital in which to place the unpaired electron is not available. We expect that the σ contribution to the energy required to dissociate a $\cdot CH_3$ or $\cdot CF_3$ radical from the molecular ions also has a value of about 4 eV/molecule, since we have assumed that the positive charge is delocalized over the chelate ring. However, it is not essential to our argument to assume this value, since similar values of the σ contribution to $\Delta(CH_3)$ and $\Delta(CF_3)$ would be expected for the molecular ions of all metals, and the large variations in these quantities can safely be attributed to differences in π contributions. The values of $\Delta(CH_3)$ and $\Delta(CF_3)$ are always lower than 4 eV/molecule, usually much lower. This indicates that the molecular ions are less π-stabilized than the fragment ions. The smaller the value of $\Delta(CF_3)$ or $\Delta(CH_3)$, the smaller is the relative π stabilization of the molecular ion.

An explanation for the variations in $\Delta(CF_3)$ or $\Delta(CH_3)$ must be sought in the structures and bonding of the molecular and fragment ions. Upon ionization of the molecule, an electron is removed from the π system of one of the chelate rings to give **1**. Homolytic dissociation of α_1 from the ring will leave an unpaired electron on the ring carbon atom, as in **2**, which may then transfer to the vacancy in the partially delocalized, bonding molecular orbital on the chelate ring to give **3**. This should give considerable π stabilization to **3** with respect to **1**. Furthermore, little structural or geometrical rearrangement should accompany this process. This stabilization

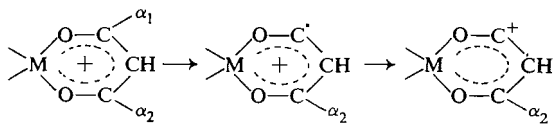

1 **2** **3**

will lead to small values of $\Delta(CF_3)$ and $\Delta(CH_3)$, i.e. values appreciably lower than 4 eV. The metal should have little effect on the π stabilization of **3**, and we assume that the large variations in $\Delta(CF_3)$ observed are due to different π stabilizations of the molecular ion. The smallest values of $\Delta(CF_3)$ are observed with Al(III), Fe(III), and Zn(II), and the largest value with Fe(II). For the Cr(III) chelates, no values could be obtained due to the low relative intensities of the $(L_3M—CF_3)^+$ and $(L_3M—CH_3)^+$ peaks. This probably means that the energy required to dissociate a $\cdot CF_3$ or $\cdot CH_3$ group from the molecular ion is high, i.e. $\Delta(CF_3)$ and $\Delta(CH_3)$ are large, indicating a large π stabilization of the molecular ion.

We propose that the stabilization of the molecular ion by the metals is accomplished by expansion of the metal d orbitals into the positively charged chelate ring, thus further delocalizing the positive charge. The amount of stabilization will clearly depend upon the symmetry of the molecular ion. For the nearly octahedral trischelates, the metal orbitals allowed by symmetry to interact with the ligand π orbitals are the metal t_{2g} orbitals. Thus, for Al(III) (d^0) the chelate molecular ion cannot be stabilized by this type of interaction and consequently the reaction **1** → **3** occurs readily (low $\Delta(CF_3)$). For Cr(III), (t_{2g}^3) stabilization of the chelate molecular ion by metal d orbital expansion can occur, which should make reaction **1** → **3** more difficult (high $\Delta(CF_3)$ and $\Delta(CH_3)$). For Fe(III), ($t_{2g}^3\ e_g^2$) expansion of the t_{2g} orbitals should occur, but little stabilization of the molecular ions is apparent. Possibly this is an effect due to the antibonding e_g electrons, since the e_g orbitals are expected to contract when the t_{2g} orbitals expand. It is perhaps worth noting that metal d orbital expansion should parallel the ease of oxidation of the trivalent metals. In the first transition series, the stability of the +4 oxidation state decreases in the sequence Ti through Co. Thus, Fe(IV) is less stable than Cr(IV), consistent with the relative stabilization of the molecular ions of their chelates.

The structures of the bischelates have been dis-

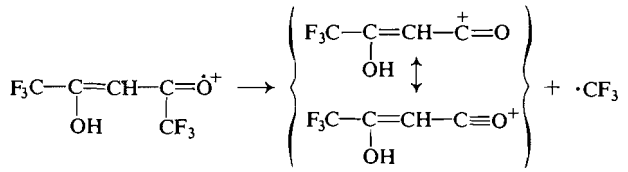

4 5

cussed in a review (2). The structures of the Fe(II) and Zn(II) complexes have not been determined in the gas phase, but are said to be tetrahedral (2). $Cu(acac)_2$ is planar in the gas phase (32). For the Fe(II) chelates, the high values of $\Delta(CF_3)$ suggest stabilization of the molecular ion, **1**, presumably by metal d orbital expansion. This is in agreement with the wellknown ready conversion of Fe(II) to Fe(III). Oxidation of Zn(II) and Cu(II) occurs much less readily and, in agreement with this, much lower values of $\Delta(CF_3)$ and $\Delta(CH_3)$ are observed. As might be expected, it seems that metal d orbital expansion is slightly easier for Cu(II) than for Zn(II).

Although the data are rather limited, it appears that when the electronegative CF_3 group remains attached to the chelate ring in the fragment ion, greater stabilization of the fragment ion results than when the CH_3 group remains. For example, $\Delta(CF_3)$ is 1.7 V for $Cu(hfacac)_2$ and 2.45 V for $Cu(tfacac)_2$; it is 1.3 V for $Zn(hfacac)_2$ and 1.9 V for $Zn(tfacac)_2$; $\Delta(CH_3)$ is 2.3 V for both $Zn(tfacac)_2$ and $Zn(acac)_2$. It seems that electronegative groups on the ring enhance transfer of the unpaired electron from the ring carbon of **2** to the π system. This observation is consistent with arguments given previously (5) in the interpretation of the mass spectra of substituted chromium acetylacetonates, and also earlier in this paper.

Substantial stabilization energies are involved in the dissociation of $\cdot CH_3$ or $\cdot CF_3$ from the HL^+ species. This reaction is well known (33) and is illustrated for $H(hfacac)^+$.

It is more difficult to assess the significance of the $\Delta(L)$ values. Apart from electronic reorganization, there may be, and probably are in many cases, structural rearrangements, and, for small metal atoms, steric relaxations to consider. Furthermore, since L^- ions are present in the negative-ion mass spectrum of $Cu(tfacac)_2$, it is possible that some $(P—L)^+$ ions are formed by ion-pair production in addition to loss of ligand radicals from the molecular ion. For the compounds studied here, $\Delta(L)$ is significantly larger for the bischelates than for the trischelates.

In principle (see ref. 1), the values of $D(FeL_2—L)$ can be obtained from

$$D(FeL_2—L) = \text{a.p.}(FeL_2^+ \text{ from } FeL_3) - \text{a.p.}(FeL_2^+ \text{ from } FeL_2)$$

assuming that a ligand radical is eliminated from FeL_3^+. The values obtained from Table 3 are 0.5, 0.45, and 1.3 eV for L = hfacac, tfacac, and acac, respectively. No significance is attached to these values, since (*a*) negative-ion formation may accompany formation of FeL_2^+, (*b*) it is likely that the a.p. of FeL_2^+ from FeL_3 is too low, since some decomposition of Fe(III) β-diketonates to Fe(II) chelates in the ion source has been observed (4, 7).

It would have been of interest to obtain the a.p.'s of CF_3^+, CH_3^+, and L^+ from the various chelates. Unfortunately, for CF_3^+, the ionization efficiency curves showed extreme tailing and had several inflexions, suggesting that several ionization processes were involved. A similar problem would be encountered for CH_3^+. The intensities of the L^+ ion currents were too low for a.p. measurements and here, again, the L^+ ion may not arise from a single process.

(c) Structures of the Ions

There has been much debate over the "charge localization" concept in mass spectra, and many ion decomposition reactions have been rationalized in terms of this concept (33). Shannon and co-workers proposed ion decomposition reactions for metal acetylacetonates (6) and other chelates (34) based on charge localization, as we ourselves have also done (4). We now believe that the energetic data presented here invalidate the structures proposed for some of the ions. For example, the $(P—CH_3)^+$ ions were assigned (6) the resonance stabilized structure, **6**. Formation of ions such as this from the proposed molecular ion (**1**) would require breaking of a metal–oxygen bond, disruption of the π system, and possibly

Can. J. Chem. Downloaded from www.nrcresearchpress.com by 210.87.254.5 on 09/05/12
For personal use only.

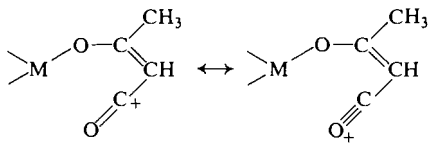

6

considerable rearrangement of the ion, as well as breaking of the C—CH_3 bond. Although we are unable to assess the reorganizational energy, it seems highly unlikely that it would effectively compensate for the energy required in the other processes, and much higher $\Delta(CF_3)$ and $\Delta(CH_3)$ values would be expected. It was on the basis of similar arguments that the $C_6H_5^+$ ion from many benzene derivatives was deduced *not* to be Ph^+ (35), since its appearance potential was much *higher* than expected from simple cleavage of the bond adjacent to the benzene ring and the $C_6H_5^+$ ion was assigned an open chain structure.

In contrast, the ion **6** could possibly be formed from an open chain molecular ion such as **7**.

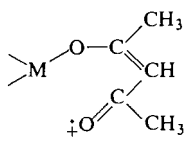

7

However, the formation of this species is also ruled out on energetic grounds. The appearance potential values for the molecular ions of all the chelates are less than those for the corresponding ligands, yet for species such as **7**, the values would be expected to be considerably larger, since their formation involves rupture of a metal–oxygen bond as well as ionization.

We thank the National Research Council of Canada and the Faculty of Graduate Studies, University of Manitoba, for financial assistance. We also thank Dr. H. Gesser and Mr. K. L. Lee for supplying some of the compounds used in this study.

1. C. Reichert and J. B. Westmore. Inorg. Chem. **8**, 1012 (1969).
2. See, for example, J. P. Fackler. Prog. Inorg. Chem. **7**, 361 (1966).
3. D. W. Barnum. J. Inorg. Nucl. Chem. **21**, 221 (1961); **22**, 183 (1961).
4. G. M. Bancroft, C. Reichert, and J. B. Westmore. Inorg. Chem. **7**, 870 (1968).
5. G. M. Bancroft, C. Reichert, J. B. Westmore, and H. D. Gesser. Inorg. Chem. **8**, 474 (1969).
6. C. G. MacDonald and J. S. Shannon. Aust. J. Chem. **19**, 1545 (1966).
7. S. M. Schildcrout, R. G. Pearson, and F. E. Stafford. J. Amer. Chem. Soc. **90**, 4006 (1968).
8. J. D. MacDonald and J. L. Margrave. J. Less-Common Metals, **14**, 236 (1968).
9. H. F. Holtzclaw, R. L. Lintvedt, H. E. Baumgarten, R. G. Parker, M. M. Bursey, and P. F. Rogerson. J. Amer. Chem. Soc. **91**, 3774 (1969).
10. T. Koopmans. Physica, **1**, 104 (1933).
11. W. C. Fernelius and B. E. Bryant. Inorganic synthesis. Vol. 5. McGraw-Hill Book Co., Inc., New York. 1955. p. 105.
12. D. A. Buckingham, R. C. Gorges, and J. T. Henry. Aust. J. Chem. **20**, 281 (1967).
13. F. W. Lossing, A. W. Tickner, and W. C. Bryce. J. Chem. Phys. **19**, 1254 (1951).
14. F. W. McLafferty. Anal. Chem. **31**, 477 (1959).
15. A. L. Clobes, M. L. Morris, and R. D. Koob. J. Amer. Chem. Soc. **91**, 3087 (1969).
16. R. B. King. J. Amer. Chem. Soc. **89**, 6368 (1967).
17. D. R. Stull (*Editor*). JANAF interim thermochemical tables. The Dow Chemical Company, Midland, Mich. revised to Sept. 30, 1963.
18. K. F. Zmbov and J. L. Margrave. J. Inorg. Nucl. Chem. **29**, 673 (1967).
19. R. A. Kent and J. L. Margrave. J. Amer. Chem. Soc. **87**, 3582 (1965).
20. R. A. Kent and J. L. Margrave. J. Amer. Chem. Soc. **87**, 4754 (1965).
21. L. Brewer, G. R. Somayajula, and E. Brackett. Chem. Rev. **63**, 111 (1963).
22. K. F. Zmbov, O. M. Uy, and J. L. Margrave. J. Amer. Chem. Soc. **90**, 5090 (1968).
23. J. D. Hawthorne, M. J. Mays, and R. N. F. Simpson. J. Org. Chem. **12**, 407 (1968).
24. M. J. Mays and R. N. F. Simpson. J. Chem. Soc. A, 1936 (1967).
25. J. R. Majer and C. R. Patrick. Advances in Mass Spectrometry, Vol. 2. *Edited by* R. M. Elliot. MacMillan, New York. 1963.
26. R. G. Cooks. Org. Mass Spectrom. **2**, 481 (1969).
27. C. Reichert and J. B. Westmore. Unpublished results.
28. E. A. Magnusson, K. A. Thomson, and A. G. Wedd. Chem. Commun. 842 (1969).
29. A. Streitweiser, Jr. Molecular orbital theory for organic chemists. John Wiley and Sons, Inc., New York. 1961. pp. 247, 392.
30. J. A. Kerr. Chem. Rev. **66**, 465 (1966).
31. M. J. S. Dewar and H. N. Schmeising. Tetrahedron, **11**, 96 (1960).
32. S. Shibata and K. Sone. Bull. Chem. Soc. Jap. **29**, 852 (1956).
33. H. Budzikiewicz, C. Djerassi, and D. H. Williams. Mass spectrometry of organic compounds. Holden-Day Inc., San Francisco. (1967).
34. M. J. Lacey, C. G. MacDonald, and J. S. Shannon. Org. Mass Spectrom. **1**, 115 (1968).
35. P. Natalis and J. L. Franklin. J. Phys. Chem. **69**, 2935 (1965).
36. R. W. Kiser. Introduction to mass spectrometry and its applications: Prentice-Hall Inc., Englewood, Cliffs, N.J. 1965.

Can. J. Chem. Downloaded from www.nrcresearchpress.com by 210.87.254.5 on 09/05/12
For personal use only.

Can. J. Chem. Downloaded from www.nrcresearchpress.com by 210.87.254.42 on 09/05/12
For personal use only.

Studies in isoxazole chemistry. III.[1] The preparation and lithiation of 3,5-disubstituted isoxazoles

R. G. MICETICH AND C. G. CHIN
R & L Molecular Research Ltd., 8045 Argyll Road, Edmonton 82, Alberta

Received October 20, 1969

3-Arylisoxazol-5-ones and 5-arylisoxazol-3-ones were prepared and converted to the *N*-methyl and *O*-methyl derivatives by reaction with diazomethane. The halogen in 3-phenyl-5-chloroisoxazole was replaced by several alkoxy and thioalkoxy groups. The 3,5-disubstituted isoxazoles thus obtained reacted with *n*-butyllithium to form the 4-lithio derivatives, as shown by conversion to 4-carboxylic acids and 4-iodocompounds. 3-Methoxy-5-phenylisothiazole was also lithiated at the 4-position.

Canadian Journal of Chemistry, 48, 1371 (1970)

Reaction of certain isoxazole acid chlorides with 6-aminopenicillanic acid has been shown (1) to give isoxazolylpenicillins with useful antibacterial activity. In an attempt to prepare 3-phenylisoxazole-5-carboxylic acid, 3-phenyl-5-chloroisoxazole (**7***a*) (2) was reacted with *n*-butyllithium and carbon dioxide. The acid isolated from this reaction in 80% yield was, surprisingly, 3-phenyl-5-chloroisoxazole-4-carboxylic acid (**11***a*) (2). The lithio derivative of **7***a* also reacted with methyl iodide to give a 74% yield of 3-phenyl-4-methyl-5-chloroisoxazole (2), and with iodine to give a 73% yield of the previously unknown 3-phenyl-4-iodo-5-chloroisoxazole. The facility of these reactions led us to investigate the feasibility of preparing by similar methods a variety of isoxazole carboxylic acids with potential value in penicillin synthesis.

The lithiation of various five-membered heteroaromatic compounds has been described (3–7), and that of thiophene has been studied in detail (8). Bowden and co-workers have recently reported (9) that 3-methoxy-5-methylisoxazole on reaction with butyllithium and carbon dioxide gave 3-methoxyisoxazole-5-acetic acid as the major product, along with 3-methoxy-5-methylisoxazole-4-carboxylic acid. We have found that the reaction of 3-phenyl-5-alkoxy or -thioalkoxyisoxazoles **8***a–h* or 3-alkoxy-5-phenylisoxazoles **3***a–c* with *n*-butyllithium and carbon dioxide gave the 4-carboxylic acids **10***a–h* and **5***a–c*.

3-Alkoxy-5-phenylisoxazole-4-carboxylic Acids (5a–c)

These acids were prepared by the reactions illustrated in Scheme 1.

The 3-hydroxy-5-phenylisoxazoles **2***a–c* (10) on treatment with diazomethane gave an approximately 1:1 mixture of the —O—CH_3 **3***a–c* and —N—CH_3 **4***a–c* isomers (11). The 3-methoxy-5-phenylisoxazoles **3***a–c* with butyllithium and carbon dioxide formed the 3-methoxy-5-phenylisoxazole-4-carboxylic acids **5***a–c*.

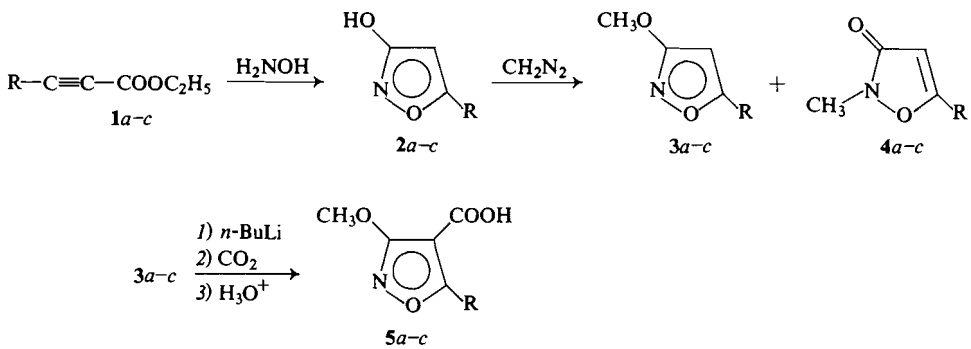

a R = Ph; *b* R = 2-ClPh; *c* R = 2,6-diClPh

SCHEME 1

[1]For paper II in this series see ref. 29.

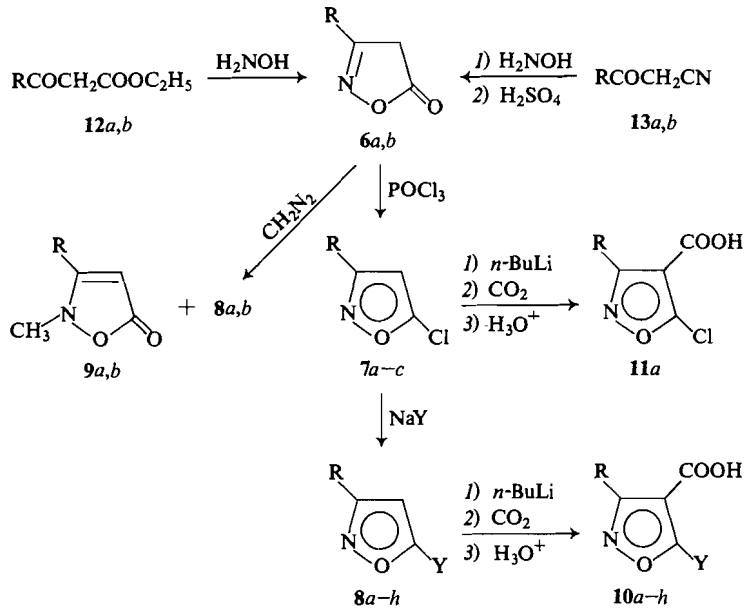

For **8** and **10**

a R = Ph; Y = OCH_3
b R = 2-ClPh; Y = OCH_3
c R = 2,6-diClPh; Y = OCH_3
d R = Ph; Y = OC_2H_5
e R = Ph; Y = $OCH(CH_3)_2$
f R = Ph; Y = $OC(CH_3)_3$
g R = Ph; Y = SC_2H_5
h R = Ph; Y = $SC(CH_3)_3$

SCHEME 2

3-Phenyl-5-alkoxy or thioalkoxyisoxazole-4-carboxylic Acids (10a–h)

Scheme 2 outlines the procedures used in preparing these acids.

The 3-phenylisoxazol-5-ones **6***a,b* were made by the action of hydroxylamine on the β-ketoesters **12***a,b* (12), or by treating the 3-phenyl-5-aminoisoxazoles with sulfuric acid (13). The 3-phenyl-5-aminoisoxazoles were prepared from the benzoylacetonitriles **13***a,b* and hydroxylamine, using the procedure of Obrégia (14). The isoxazol-5-ones **6***a,b* on reaction with diazomethane gave a 6:1 mixture of the —O—CH_3 **8***a,b* and —N—CH_3 **9***a,b* isomers.

The key compounds in the preparation of these acids however were the 3-phenyl-5-chloroisoxazoles **7***a–c*. Compounds **7***a* and **7***b* were made from **6***a,b* by the procedure of Adembri and Tedeschi (2). Subsequently a new method of preparing 5-chloroisoxazoles **7***a–c* was found. This synthesis will be described in a later publication.

Nucleophilic displacement of the chlorine in the 3-phenyl-5-chloroisoxazoles **7***a–c*, produced the 5-alkoxy or -thioalkoxy compounds **8***a–h*, which were converted to the 4-carboxylic acids **10***a–h* by treatment with *n*-butyllithium followed by carbon dioxide. The importance of this method lies in the fact that these acids were not obtained by hydrolysis of the esters. The 5-methoxy group of ethyl 3-phenyl-5-methoxyisoxazole-4-carboxylate, for example, proved to be more acid labile than the ester group (1).

The structure of each acid **5***a–c* and **10***a–h* was confirmed by its infrared (i.r.) and nuclear magnetic resonance (n.m.r.) spectra, its neutralization equivalent, and by its elemental analysis. In addition, the acid obtained by the carboxylation of 3-phenyl-5-methoxyisoxazole was converted to its methyl ester by treatment with diazomethane. This ester was identical (m.p., mixed m.p., i.r. and n.m.r. spectra) with the product from the reaction of diazomethane with methyl 3-phenylisoxazol-5-one-4-carboxylate. The latter compound was made by a procedure similar to that described for the preparation of the ethyl ester (15).

All these acids, except **10***f*, reacted with thionyl

Can. J. Chem. Downloaded from www.nrcresearchpress.com by 210.87.254.42 on 09/05/12
For personal use only.

Can. J. Chem. Downloaded from www.nrcresearchpress.com by 210.87.254.42 on 09/05/12
For personal use only.

chloride at room temperature to form the acid chlorides. The crude acid chlorides were used to make the penicillins by established procedures (1). The lithium salt of 3-phenyl-5-*tert*-butoxyisoxazole-4-carboxylic acid (**10***f*), on standing at room temperature or on heating in aqueous solution, was converted to 3-phenylisoxazol-5-one (**6***a*).

This reaction is not limited to the isoxazoles, since 3-methoxy-5-phenylisothiazole (16) gave a 95% yield of 3-methoxy-5-phenylisothiazole-4-carboxylic acid (17, 18) by this method. The 4-lithio derivatives also reacted with iodine to form the 4-iodo compounds (see ref. 19).

Experimental

Melting points were taken on a Fisher–Johns apparatus and are uncorrected. Infrared spectra (ν_{max} cm^{-1}) were measured on a Perkin-Elmer Model 137 spectrophotometer as Nujol mulls. A Varian Associates Model A-60 spectrometer was used for recording n.m.r. spectra Chemical shifts are given in τ-values and refer to spectra measured in the solvent indicated with TMS as an internal reference. Elemental analysis (C, H, and N) where specified were within ±0.4% of the calculated values, and are filed in the Depository of Unpublished Data, National Science Library, National Research Council of Canada, Ottawa, Canada.

3-Hydroxy-5-phenylisoxazole (2a)

Compound **2***a* m.p. 162–163° ($CHCl_3$), (88%) was prepared as described in the literature (10). The i.r. 2600 (w), 1610, 1516, 1510 (s); n.m.r. (acetone-d_6) 3.53 (s, 1H), 2.15 (m, 2H), 2.49 (m, 3H).

Reported m.p. 163–165° (10).

3-Hydroxy-5-o-chlorophenylisoxazole (2b)

Methyl *o*-chlorophenylpropiolate was made from methyl *o*-chlorocinnamate according to the procedure used for the ethyl ester (20). The fraction boiling at 103–112°/0.4 mm (91%) was used to make 3-hydroxy-5-*o*-chlorophenylisoxazole, m.p. 179–180° ($CHCl_3$), 83%. The i.r. 2600 (w), 1620 (s); n.m.r. (acetone-d_6) 3.37 (s, 1H), 1.9–2.7 (m, 4H). Anal. ($C_9H_6ClNO_2$).

3-Hydroxy-5-(2′,6′-dichlorophenyl)isoxazole (2c)

A solution of 2,6-dichlorobenzaldehyde (21) (58 g, 0.33 mole) and carboethoxymethylenetriphenylphosphorane (22, 23) (118 g, 0.34 mole) in methylene chloride (400 ml) was left at room temperature overnight, then concentrated and the residue extracted with hexane. The hexane extract was concentrated and the residue distilled under reduced pressure to give 70 g (86%) of ethyl 2,6-dichlorocinnamate, b.p. 126°/0.2 mm. This compound was converted to ethyl 2,6-dichlorophenylpropiolate, m.p. 57–57.5° (100%), which gave 3-hydroxy-5-(2′,6′-dichlorophenyl)isoxazole, m.p. 179–183° ($CHCl_3$), (85%) by the procedure used above. The i.r. 2650 (w), 1630, 1530 (s); n.m.r. (acetone-d_6) 3.70 (s, 1H), 2.1–2.7 (m, 3H). Anal. ($C_9H_5Cl_2NO_2$).

3-Phenylisoxazol-5-one (6a)

Compound **6***a*, m.p. 157–158° (benzene), (80%) was prepared as described in the literature (12) except that methanol was used in place of ethanol. The i.r. 1800 (s), 1550 (s); n.m.r. (acetone-d_6) 5.85 (s, 2H), 2.25 (m, 2H), 2.45 (m, 3H).

Reported m.p. 151–152° (12).

3-o-Chlorophenylisoxazol-5-one (6b)

The ethyl *o*-chlorobenzoylacetate (**12***b*) required for this preparation, was made by two routes. Ethyl *o*-chlorobenzoylacetoacetate, made by the action of *o*-chlorobenzoyl chloride on the sodio derivative of acetoacetic ester in tetrahydrofuran, on treatment with ammonical ammonium chloride (25) gave a 25% yield of ethyl *o*-chlorobenzoylacetate, b.p. 110–112°/0.1 mm. Alternatively, this compound could be obtained in 64% yield by the condensation of methyl *o*-chlorobenzoate with ethyl acetate using sodium hydride. The ethyl *o*-chlorobenzoylacetate was converted to 3-*o*-chlorophenylisoxazol-5-one, m.p. 65–67° (ethyl acetate – hexane) in 81% yield by reaction with hydroxylamine hydrochloride in the presence of 2 equ. of sodium methoxide in methanol. The i.r. 1800 (s), 1580 (w), 1560 (w); n.m.r. ($CDCl_3$) 5.97 (s, 2H), 2.1–2.8 (m, 4H). Anal. ($C_9H_6ClNO_2$).

3-o-Chlorophenyl-5-aminoisoxazole

The *o*-chlorobenzoylacetonitrile (**13***b*) required for this preparation was obtained in 30% yield by the procedure of Long (26). The following modification however raised the yield to 61.5%.

A mixture of methyl *o*-chlorobenzoate (341 g, 2 moles) and dry acetonitrile (82 g, 2 moles) was added dropwise to a stirred suspension of sodium hydride (50% in oil, 115.2 g, 2.4 moles, prewashed in hexane) in refluxing dry tetrahydrofuran (600 ml), and the heating continued for 1 h after the gas evolution had ceased. Ether was added to the cooled reaction mixture and the resulting solid filtered off, washed with ether, and dried. The solid was dissolved in water, the solution acidified to ca. p*H* 6 with 6 *N* hydrochloric acid and the precipitated solid filtered and dried to give 221 g of *o*-chlorobenzoylacetonitrile, m.p. 55–56°.

Obrégia's procedure (14) gave 3-*o*-chlorophenyl-5-aminoisoxazole, m.p. 75–75.5° (CH_2Cl_2), (62%). The i.r. 1620 (s), 1580 (m), 1560 (w); n.m.r. ($CDCl_3$) 2.2–3.0 (m, 4H), 4.52 (s, 1H), 5.30 (broad, 2H). Anal. ($C_9H_7ClN_2O$).

3-o-Chlorophenylisoxazol-5-one (6b) from 3-o-Chlorophenyl-5-aminoisoxazole

3-*o*-Chlorophenyl-5-aminoisoxazole (39 g, 0.2 mole), 6 *N* sulfuric acid (200 ml), and methanol (200 ml) were heated under reflux for 1/2 h. The mixture was then concentrated to half its volume, extracted with ethyl acetate (3 × 100 ml), and the combined ethyl acetate layers back extracted with 6 *N* sodium hydroxide (50 ml). The alkaline solution was brought to p*H* ca. 1 with concentrated hydrochloric acid and extracted with ethyl acetate (4 × 50 ml). The combined ethyl acetate layers were dried with magnesium sulfate, filtered, and solvent removed under reduced pressure, when 29.5 g, (75%) of 3-*o*-chlorophenylisoxazol-5-one, identical to the compound made by the alternate route, was obtained.

Can. J. Chem. Downloaded from www.nrcresearchpress.com by 210.87.254.42 on 09/05/12
For personal use only.

Increasing the period of reflux resulted in an increase in the formation of a by-product, *o*-chloroacetophenone oxime, m.p. 103–104°, identical with an authentic sample.

*General Procedure for Preparing —O—CH_3 (**3a–c**, **8a,b**) and —N—CH_3 (**4a–c**, **9a,b**) Isoxazoles*

An ethereal solution of diazomethane (0.30 mole) was added slowly to a stirred mixture of the isoxazolone (**2a–c**, **6a,b**) (0.25 mole) in dry tetrahydrofuran or ether (100 ml), cooled in an ice-bath. The reaction mixture was stirred for 1/2 h after the gas evolution ceased, concentrated under reduced pressure, and chromatographed on an alumina column (2.5 l, Fisher grade adsorption alumina). The —O—CH_3 isomers (**3a–c**, **8a,b**) were eluted with benzene, while the —N—CH_3 isomers were eluted with ethyl acetate – methanol (1:1) (**4a–c**) or methanol (**9a,b**).

*3-Methoxy-5-phenylisoxazole (**3a**)* The m.p. 67–68° (hexane), (51%). The i.r. 1610 (s), 1590 (s), 1570 (s), 1510 (s); n.m.r. ($CDCl_3$) 3.88 (s, 1H), 6.00 (s, 3H), 2.30 (m, 2H), 2.58 (m, 3H).

Reported m.p. 69–71° (24).

*3-Methoxy-5-o-chlorophenylisoxazole (**3b**)* The m.p. 33.5–34° (hexane), (54%). The i.r. 1610 (s), 1590 (s), 1560 (m), 1510 (s); n.m.r. ($CDCl_3$), 3.43 (s, 1H), 5.97 (s, 3H), 2.05 (m, 1H), 2.60 (m, 3H). Anal. ($C_{10}H_8ClNO_2$).

*3-Methoxy-5-(2′,6′-dichlorophenyl)isoxazole (**3c**)* The m.p. 34.5–35° (hexane), (53%). The i.r. 1625 (s), 1570 (sh), 1550 (s), 1510 (s); n.m.r. (CCl_4) 4.00 (s, 1H), 5.97 (s, 3H), 2.70 (m, 3H). Anal. ($C_{10}H_7Cl_2NO_2$).

*3-Phenyl-5-methoxyisoxazole (**8a**)* The m.p. 69–71° (CCl_4), (84%). The i.r. 1600 (s), 1570 (sh); n.m.r. ($CDCl_3$) 4.52 (s, 1H), 6.05 (s, 3H), 2.32 (m, 2H), 2.61 (m, 3H).

Reported m.p. 65–67° (27, 28).

*3-o-Chlorophenyl-5-methoxyisoxazole (**8b**)* The m.p. 58.5–59° (hexane), (84%). The i.r. 1610 (s), 1560 (w-sh); n.m.r. ($CDCl_3$) 4.42 (s, 1H), 6.05 (s, 3H), 2.20–2.90 (m, 4H). Anal. ($C_{10}H_8ClNO_2$).

*2-Methyl-5-phenylisoxazol-5-one (**4a**)* The m.p. 115–116° (benzene–hexane), (44%). The i.r. 1660 (s); n.m.r. ($CDCl_3$) 4.00 (s, 1H), 6.43 (s, 3H), 2.48 (m, 5H).

Reported m.p. 114° (11).

*2-Methyl-5-o-chlorophenylisoxazol-5-one (**4b**)* The m.p. 68–68.5° (ether), (40%). The i.r. 1650 (s); n.m.r. ($CDCl_3$) 3.62 (s, 1H), 6.40 (s, 3H), 2.15–2.75 (m, 4H). Anal. ($C_{10}H_8ClNO_2$).

*2-Methyl-5-(2′,6′-dichlorophenyl)isoxazol-5-one (**4c**)* The m.p. 110–111° (ether–hexane), (42%). The i.r. 1650 (s); n.m.r. ($CDCl_3$) 4.05 (s, 1H), 6.40 (s, 3H), 2.57 (s, 3H). Anal. ($C_{10}H_7Cl_2NO_2$).

*2-Methyl-3-phenylisoxazol-5-one (**9a**)* The b.p. 139°/0.1 mm, m.p. 39–40° (hexane), (14%). The i.r. 1740 (s), 1600, 1580 (m); n.m.r. (CCl_4) 4.57 (s, 1H), 6.72 (s, 3H), 2.48 (s, 5H).

Reported m.p. 43–45° (28).

*2-Methyl-5-o-chlorophenylisoxazol-5-one (**9b**)* The b.p. 142–145°/0.08 mm, (16%). The i.r. (film) 1750 (s), 1610 (m); n.m.r. (CCl_4) 4.68 (s, 1H), 6.81 (s, 3H), 2.30–2.70 (m, 4H). Anal. ($C_{10}H_8ClNO_2$).

*3-Phenyl-5-chloroisoxazole (**7a**)*

The procedure of Adembri and Tedeschi (2) was simplified as follows. A mixture of 3-phenylisoxazol-5-one (145 g, 0.9 mole) and phosphorous oxychloride (805 g, 482 ml) was stirred in an ice-bath and triethylamine (140 ml, 1 mole) added slowly, maintaining the temperature below 25°. After the addition was completed, the stirred mixture was heated on an oil bath at 120° for 2½ h, after which the excess phosphorous oxychloride was removed under reduced pressure. The brown residue was triturated with ice-water (3 l) and the resulting yellow solid filtered, taken up in ethyl acetate, and dried over magnesium sulfate. After filtration and removal of solvent, the brown residue was distilled under reduced pressure to give 135.6 g (84%) of a light yellow oil, b.p. 100°/1 mm, which crystallized, m.p. 45–47° on scratching.

Reported m.p. 51–52°, yield 48% (2).

It is necessary to keep the temperature of the bath below ca. 120° during the distillation otherwise decomposition of the 3-phenyl-5-chloroisoxazole takes place.

*3-o-Chlorophenyl-5-chloroisoxazole (**7b**)*

The b.p. 90–91°/0.5 mm, m.p. 27–28°, 35%. Anal. ($C_9H_5Cl_2NO_2$).

General Procedure for Preparing 3-Phenyl-5-alkoxy (or -Thioalkoxy) Isoxazoles

The alcohol or mercaptan (0.072 mole) was added to a suspension of sodium hydride (50% in oil, 3.1 g, 0.072 mole prewashed with hexane) or potassium (2.8 g, 0.072 g atom) in dry tetrahydrofuran (150 ml) and the mixture heated under reflux until the reaction was complete. (Excess of the respective alcohol could also be used as solvent in place of tetrahydrofuran.) The reaction mixture was cooled to room temperature, 3-phenyl-5-chloroisoxazole **7a–c** (0.06 mole) added, and the mixture left at room temperature for 50 h, after which it was heated under reflux for 6 h and concentrated under reduced pressure. The residue was shaken with ice-water (100 ml) and extracted with ether (3 × 60 ml). The combined ether extracts were dried over magnesium sulfate, filtered and the solvent removed. The residue if solid was crystallized from hexane, and if liquid was distilled under reduced pressure. The i.r. spectra of the alkoxy compounds showed a strong band at 1590–1610 with a shoulder at 1550–1570, while the thioalkoxy compounds had a band at 1530–1540 with a shoulder at 1500. The n.m.r. parameters were consistent with the assigned structures.

*3-(2′,6′-Dichlorophenyl)-5-methoxyisoxazole (**8c**)* The m.p. 124–126°, (93%). Anal. ($C_{10}H_7Cl_2NO_2$).

*3-Phenyl-5-ethoxyisoxazole (**8d**)* The m.p. 75–77°, (75%). Anal. ($C_{11}H_{11}NO_2$).

*3-Phenyl-5-isopropoxyisoxazole (**8e**)* The m.p. 35–36°, (98%). Anal. ($C_{12}H_{13}NO_2$).

*3-Phenyl-5-tert-butoxyisoxazole (**8f**)* The b.p. 120°/0.8 mm, (81%). Anal. ($C_{13}H_{15}NO_2$).

*3-Phenyl-5-thioethoxyisoxazole (**8g**)* The b.p. 120–122°/0.5 mm, m.p. 22°, (96%). Anal. ($C_{11}H_{11}NOS$).

*3-Phenyl-5-thio-tert-butoxyisoxazole (**8h**)* The b.p. 120–122°/0.4 mm, m.p. 51–53°, (65%). Anal. ($C_{13}H_{15}NOS$).

*General Procedure for Preparing Acids, (**5a–c**, **10a–h**, **11a**)*

n-Butyllithium (12.5 ml of 1.6 *M* solution in hexane, 0.02 mole) was added slowly to a solution of the isoxazole (0.018 mole) in dry tetrahydrofuran (50 ml) at −70 to −65° in a nitrogen atmosphere. The mixture was stirred for 30 min, poured onto excess Dry Ice and allowed to warm to room temperature. The solvent was removed at reduced pressure, the resultant powder

Can. J. Chem. Downloaded from www.nrcresearchpress.com by 210.87.254.42 on 09/05/12
For personal use only.

triturated with dry ether, filtered, and dried. The lithium salt thus obtained was dissolved in water (50 ml) and the acid precipitated by acidification with hydrochloric acid. The cooled solution was filtered, the acid dissolved in hot ethyl acetate, the solution dried with magnesium sulfate, and the solvent removed. The acid thus obtained in certain instances was pure, since recrystallization did not raise the melting point. Equivalent weights of the acids were within 1% of the theoretical values. The n.m.r. parameters were consistent with the assigned structures.

3-Methoxy-5-phenylisoxazole-4-carboxylic Acid (5a) The m.p. 227–228° decomposition (ethyl acetate), (99%). The i.r. 1700 (s), 1580, 1570, 1550, 1510 (s). Anal. ($C_{11}H_9NO_4$).

3-Methoxy-5-o-chlorophenylisoxazole-4-carboxylic Acid (5b) The m.p. 204–205° (ethyl acetate), (62%). The i.r. 1730 (s), 1630, 1580, 1530 (s). Anal. ($C_{11}H_8ClNO_4$).

3-Methoxy-5-(2′,6′-dichlorophenyl)isoxazole-4-carboxylic Acid (5c) The m.p. 180–181° (benzene), (75%). The i.r. 1725 (s), 1640 (s), 1575 (m), 1560 (w), 1520 (s). Anal. ($C_{11}H_7Cl_2NO_4$).

3-Phenyl-5-methoxyisoxazole-4-carboxylic Acid (10a) The m.p. 166–167° decomposition (ethyl acetate), (99%). The i.r. 2700 (broad), 1720 (s), 1600 (s). Anal. ($C_{11}H_9NO_4$).

3-o-Chlorophenyl-5-methoxyisoxazole-4-carboxylic Acid (10b) The m.p. 180–182° (ethyl acetate – hexane), (97%). The i.r. 2700 (broad), 1710 (s), 1590 (s). Anal. ($C_{11}H_8ClNO_4$).

3-(2′,6′-Dichlorophenyl)-5-methoxyisoxazole-4-carboxylic Acid (10c) The m.p. 176–178° (benzene), (89%). The i.r. 2700 (broad), 1720 (s), 1610 (s), 1550 (sh). Anal. ($C_{11}H_7Cl_2NO_4$).

3-Phenyl-5-ethoxyisoxazole-4-carboxylic Acid (10d) The m.p. 167–169° decomposition (ethyl acetate), (81%). The i.r. 2700 (broad), 1690 (s), 1600 (doublet). Anal. ($C_{12}H_{11}NO_4$).

3-Phenyl-5-isopropoxyisoxazole-4-carboxylic Acid (10c) The m.p. 176–180° decomposition (benzene), (77%). The i.r. 2600 (broad), 1680 (s), 1580 (doublet). Anal. ($C_{13}H_{13}NO_4$).

3-Phenyl-5-tert-butoxyisoxazole-4-carboxylic Acid (10f) The m.p. 124–125° gas evolution and remelts at 142° (benzene), (75%). The i.r. 2600 (broad), 1680 (s), 1570 (doublet). Anal. ($C_{14}H_{15}NO_4$).

3-Phenyl-5-thioethoxyisoxazole-4-carboxylic Acid (10g) The m.p. 180–182° (CCl_4), (73%). The i.r. 2600 (broad), 1650 (s), 1500 (s). Anal. ($C_{12}H_{11}NO_3S$).

3-Phenyl-5-thio-tert-butoxyisoxazole-4-carboxylic Acid (10h) The m.p. 187–188° (CCl_4), (85%). The i.r. 2600 (broad), 1660 (s), 1500 (doublet). Anal. ($C_{14}H_{15}NO_3S$).

3-Phenyl-5-chloroisoxazole-4-carboxylic Acid (11a) The m.p. 176–179° ($CHCl_3$), (80%). The i.r. 2600 (broad), 1690 (s), 1550 (s). Reported m.p. 168–170° (2).

Methyl 3-phenylisoxazol-5-one-4-carboxylate The procedure of d'Alcontres and co-workers (15) was modified as follows.

Dimethyl malonate (327.4 g, 2.48 moles) was added slowly to a well-stirred suspension of sodium hydride (58% in oil, 102.7 g, 2.48 moles, prewashed with hexane) in dry tetrahydrofuran (1400 ml). After ca. 3/4 of the malonate had been added, the reaction mixture became a voluminous, white, spongy mass. The rest of the malonate was added and the mixture heated under reflux on a water bath for 30 min and then cooled to room temperature and enough methanol added to facilitate stirring. Benzohydroxamyl chloride (192 g, 1.24 moles) dissolved in methanol (600 ml) was added slowly to the reaction mixture, when the temperature rose to 50°. The mixture was stirred at ambient temperature for a further 30 min and concentrated under reduced pressure. Ice-water (ca. 500 ml) was added, the resulting solid filtered, washed with ether, and dried, when 260.4 g (78%) of a white solid (the probable intermediate sodium salt) was obtained. The solid was stirred with water (2 l) and ca. 1.3 l of the water removed by distillation. The hot solution was made acid with hydrochloric acid, and extracted with ethyl acetate (5 × 200 ml). The combined ethyl acetate layers were dried over magnesium sulfate, filtered, and solvent removed, when 190.2 g (70%) of methyl 3-phenylisoxazol-5-one-4-carboxylate, m.p. 155–160° decomposition was obtained. The i.r. spectrum was similar to that of the ethyl ester (15) and had two strong bands at 1700 and 1650 and a broad band at ca. 2600 cm^{-1}; n.m.r. (DMSO-d_6) −2.33 (s, 1H), 2.35 (s, 5H), 6.37 (s, 3H).

Methyl 3-phenyl-5-methoxyisoxazole-4-carboxylate

(1) From Methyl 3-Phenylisoxazol-5-one-4-carboxylate

Ethereal diazomethane (1.7 equ.) was added to a stirred suspension of this compound (1 equ.) in tetrahydrofuran and after 1 h the mixture was concentrated and the residue crystallized from methanol. White microneedles, m.p. 102–104°, (80%) were obtained. The i.r. 1710 (s), 1600 (s); n.m.r. ($CDCl_3$) 2.57 (m, 5H), 5.78 (s, 3H), 6.30 (s, 3H). Anal. ($C_{12}H_{11}NO_4$).

(2) From 3-Phenyl-5-methoxyisoxazole-4-carboxylic Acid

Ethereal diazomethane (1.1 equ.) was added to a stirred solution of the compound (1 equ.) in methanol, the resulting solution concentrated, and the residue crystallized from methanol. White microneedles, m.p. 104–105°, (93%) were obtained. This compound was identical (mixed m.p., i.r., and n.m.r. spectra) with the product by route *1*.

General Procedure for the Preparation of the 4-Iodo Compounds

The 4-lithio compounds were made in the same way as described before. Iodine (1.1 equ.) dissolved in dry tetrahydrofuran was added in one lot and the reaction mixture allowed to warm to room temperature. The solvent was removed under reduced pressure, water added, and the mixture extracted with ethyl acetate. The combined ethyl acetate layers were washed with aqueous sodium thiosulfate, followed by water, and dried over magnesium sulfate. Removal of solvent gave the 4-iodo compounds which were crystallized from hexane.

3-Phenyl-5-chloro-4-iodoisoxazole The m.p. 129–130°, (73%). Anal. (C_9H_5ClINO).

3-Methoxy-5-phenyl-4-iodoisoxazole The m.p. 95–97°, (87%). Anal. ($C_{10}H_8INO_2$).

3-Phenyl-5-methoxy-4-iodoisoxazole The m.p. 89–91°, (88%). Anal. ($C_{10}H_8INO_2$).

3-Methoxy-5-phenyl-4-iodoisothiazole The m.p. 86–88°, (90%). Anal. ($C_{10}H_8INOS$).

3-Phenyl-4-methyl-5-chloroisoxazole The 4-lithio compound was made as described before and methyl iodide

(2 equ.) added in one lot. The reaction mixture was concentrated under reduced pressure, water added, and extracted with ethyl acetate. The organic layer was dried over magnesium sulfate, filtered, concentrated, and the residue distilled under reduced pressure to give 3-phenyl-4-methyl-5-chloroisoxazole, b.p. 103°/1 mm, (74%).

Reported b.p. 85°/0.5 mm (2).

The authors wish to thank Professor R. U. Lemieux for his guidance and encouragement and Messrs. R. A. Fortier, R. Thomas, S. Cherwonka and A. Vanson for their technical assistance. We also wish to thank Hooker Chemical Corp. for very generous supplies of thionyl chloride and phosphorus oxychloride, F. M. C. Corporation for ethyl benzoylacetate, and Heyden Newport Chem. Corporation for samples of *o*-chlorobenzaldehyde and *o*-chlorobenzoic acid.

1. F. P. Doyle, J. C. Hanson, A. A. W. Long, and J. H. C. Nayler. J. Chem. Soc. 5845 (1963).
2. G. Adembri and P. Tedeschi. Estralto Boll. Sci. Fac. Chim. Ind. Bologna, **23**, 203 (1965); Chem. Abstr. **63**, 13234*h* (1965).
3. V. Ramanathan and R. Levine. J. Org. Chem. **27**, 1216, 1667 (1962).
4. J. Berand and J. Metzger. Bull. Soc. Chim. France, 2072 (1962).
5. M. P. L. Caton, D. H. Jones, R. Slack, and K. R. H. Wooldridge. J. Chem. Soc. 446 (1964).
6. R. Hüttell and M. E. Schön. Ann. **625**, 55 (1959).
7. D. A. Shirley and P. W. Alley. J. Amer. Chem. Soc. **79**, 4922 (1957).
8. S. Gronowitz. *In* Advances in heterocyclic chemistry. Vol. I. Academic Press, New York, N.Y. 10003. 1963. p. 73.
9. K. Bowden, G. Crank, and W. J. Ross. J. Chem. Soc. 172 (1968).
10. Sankyo Co. Ltd., Japan, Neth. Pat. Appl. 6 511 925 March 25 (1966), 6 516 871 June 27 (1966); C.A. **65**, 15383*c*, 16974*g* (1966).
11. S. Cabiddu, G. Gaudiano, and A. Quilico. Gazz. Chim. Ital. **92**, 501 (1962).
12. A. O. Fitton and R. K. Smalley. Practical heterocyclic chemistry. Academic Press, New York, N.Y. 10003. 1968. p. 29.
13. H. D. Stachel. Chem. Ber. **96**, 1088 (1963).
14. A. Obrégia. Ann. **266**, 328 (1891).
15. G. Stagno d'Alcontres, G. LoVecchio, and G. Lamonica. Gazz. Chim. Ital. **91**, 1005 (1961).
16. J. G. Goerdeler and W. Mittler. Chem. Ber. **96**, 944 (1963).
17. R. G. Micetich and R. Raap. J. Med. Chem. **11**, 159 (1968).
18. R. U. Lemieux and R. G. Micetich. R & L Molecular Research Ltd., U.S. Patent 3 311 611 (1967).
19. P. E. Iversen. Acta Chem. Scand. **22**, 1690 (1968).
20. M. S. Newman and S. H. Merril. J. Amer. Chem. Soc. **77**, 5549 (1955).
21. G. Stork and W. N. White. J. Amer. Chem. Soc., **78**, 4609 (1956).
22. O. Isler, H. Gutmann, M. Montavon, R. Rüegg, G. Ryser, and P. Zeller. Helv. Chim. Acta. **40**, 1242 (1957).
23. H. O. House, U. K. Jones, and G. A. Frank. J. Org. Chem. **29**, 3327 (1964).
24. P. Bravo, G. Gaudiano, A. Quilico, and A. Ricca. Gazz. Chim. Ital. **91**, 47 (1961).
25. Organic synthesis. Coll. Vol. IV. John Wiley and Sons, Inc., New York. p. 415.
26. R. S. Long. J. Amer. Chem. Soc. **69**, 992 (1947).
27. R. Scarpati and G. Speroni. Gazz. Chim. Ital. **89**, 1511 (1959).
28. F. DeSarlo, L. Fabbrini, and G. Renji. Tetrahedron, **22**, 2989 (1966).
29. R. G. Micetich. Can. J. Chem. **48**, 467 (1970).

Can. J. Chem. Downloaded from www.nrcresearchpress.com by 210.87.254.42 on 09/05/12
For personal use only.

Can. J. Chem. Downloaded from www.nrcresearchpress.com by 210.87.254.6 on 09/05/12
For personal use only.

Preparation of antidotes for anticholinesterase poisoning. IV. Synthesis and protective effectiveness of 2′-(*cis*- and *trans*-2″-hydroxycyclohexyl)aminoethyl 1-phenylcyclopentanecarboxylate hydrochlorides[1]

R. A. B. Bannard and J. H. Parkkari
Defence Research Establishment Ottawa, Ottawa, Canada

Received November 14, 1969

The syntheses of *cis*- and *trans*-2-aminocyclohexanols and of *cis*- and *trans*-2-ethylaminocyclohexanols are described. The *cis* isomers were prepared by treatment of the corresponding *trans*-2-acetamidocyclohexanols with thionyl chloride followed by hydrolysis of the resulting intermediate oxazolines. The 2-aminocyclohexanols were converted to 2′-(*cis*- and *trans*-2″-hydroxycyclohexyl)aminoethyl 1-phenylcyclopentanecarboxylate hydrochlorides (**1** and **2**, R = H) by treatment with 2′-bromoethyl 1-phenylcyclopentanecarboxylate, but attempts to convert the 2-ethylaminocyclohexanols to **1** and **2** (R = C_2H_5) by a similar reaction were unsuccessful. The anticholinesterase activities of several of the compounds are discussed, as are the potencies of **1** and **2** (R = H) in protecting mice and rats from sarin poisoning.

Canadian Journal of Chemistry, **48**, 1377 (1970)

In connection with our continuing studies on the effectiveness of Parpanit (2′-diethylaminoethyl 1-phenylcyclopentanecarboxylate hydrochloride) and its analogues as substitutes for, or adjuncts to, atropine in the treatment of rodents which have been poisoned with organophosphorus anticholinesterases (1–5) it was desired to examine compounds containing a hydroxyl group close to and in known stereochemical relationship with the amino group in Parpanit. To this end the synthesis of compounds of the type **1** and **2** (R = C_2H_5 or H) has been briefly examined and the in vivo protective effectiveness of compounds **1** and **2** (R = H) was determined. It was hoped by the use of these compounds to obtain an indication of whether intramolecular interactions between the hydroxyl and amino groups would affect the activity or whether the hydroxyl group would contribute to secondary binding to the receptor. Friess and co-workers (6, 7) have shown that *cis*-2-hydroxycyclohexyltrimethylammonium iodide is almost twice as potent a reversible cholinesterase inhibitor as its *trans* analogue and it was thus also of interest to examine the anticholinesterase activity of several of the compounds prepared in this work.

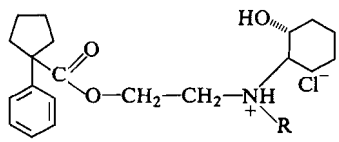

1

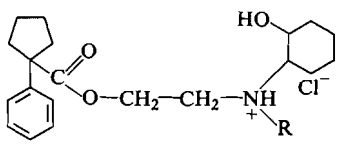

2

We have previously examined methods for the synthesis of Parpanit and its analogues (8–10) and considered that the most expedient route to the desired compounds would likely be provided by the interaction of a 2′-haloethyl 1-phenylcyclopentanecarboxylate with the requisite *trans*- and *cis*-2-aminocyclohexanol. Before embarking on the synthesis of the desired compounds, optimum conditions for the reaction between 2′-bromoethyl 1-phenylcyclopentanecarboxylate and diethylamine in benzene were determined and the resultant yield of Parpanit was 80%.

trans-2-Aminocyclohexanol was prepared from 1,2-epoxycyclohexane and ammonia following the method of Hawkins and Bannard (11). The hydrochloride of the *cis* isomer was obtained by acid hydrolysis of the oxazoline salt which is formed in much improved yield by the addition of a solution of *trans*-2-acetamidocyclohexanol in anhydrous chloroform to thionyl chloride in the same solvent at 0° (cf. 12, 13). Attempted preparation of the same compound under the same reaction conditions, but using *trans*-2-acetamidoacetoxycyclohexane (13) as the starting material, led to recovery of 90% of the latter after removal of the solvent and excess reagent *in vacuo*. This result indicates that the acetoxy group is not a sufficiently good leaving group to

[1]Issued as DREO Report No. 615.

Can. J. Chem. Downloaded from www.nrcresearchpress.com by 210.87.254.6 on 09/05/12
For personal use only.

permit the formation of an oxazoline salt with inversion of configuration at the oxygen-substituted carbon atom, and has important implications from the standpoint of the selective inversion of hydroxyl groups in polyhydroxylated aminoalcohols by partial esterification.

The interaction of 1,2-epoxycyclohexane and ethylamine in ethanol in a stainless steel bomb at 110° for 4 h furnished 92% of *trans*-2-ethylaminocyclohexanol (cf. Brunel (14) and Taguchi and Nakayama (15)). Attempted preparation of the *N*-acetyl derivative of the latter compound by treatment with acetic anhydride at room temperature (cf. Hawkins and Bannard (11)) led to a mixture of *O*- and *N*-acetyl derivatives judging from its infrared (i.r.) spectrum. Since an attempted inversion of *trans*-2-ethylacetamidoacetoxycyclohexane by means of thionyl chloride in chloroform led to quantitative recovery of the starting material, the successful preparation of *cis*-2-ethylaminocyclohexanol by the inversion route selected required the development of a method of preparation for *trans*-2-ethylacetamidocyclohexanol, substantially uncontaminated with the *O*-acetyl or *O*,*N*-diacetyl derivatives. This result was achieved in three ways: (*a*), by the treatment of *trans*-2-ethylaminocyclohexanol with acetyl chloride in dry benzene (67%); (*b*), by the selective hydrolysis of *trans*-2-ethylacetamidoacetoxycyclohexane with aqueous sodium hydroxide (77%); and (*c*), by the alkali-induced O → N migration of the acetyl group in *trans*-2-ethylaminoacetoxycyclohexane hydrochloride (98%, cf. Fodor and Kiss (16)). The last mentioned of these methods was the most satisfactory. The inversion of *trans*-2-ethylacetamidocyclohexanol with thionyl chloride furnished *cis*-2-ethylaminocyclohexanol hydrochloride in 83% yield, a method which is clearly superior to that described by Taguchi and Nakayama (15) in which *cis*-2-aminocyclohexanol was alkylated with ethyl bromide.

2′-Bromoethyl 1-phenylcyclopentanecarboxylate was prepared in 85% yield by the interaction of 1-phenylcyclopentanecarbonyl chloride (8) and 2-bromoethanol in anhydrous benzene. This compound is unstable on storage even under anhydrous conditions, slowly decomposing to form 1-phenylcyclopentanecarboxylic acid (8). The chloro analogue was prepared in a similar manner in 82% yield and is not nearly so prone to decomposition on storage.

The preparation of 2′-(*trans*-2′′-hydroxycyclohexyl)aminoethyl 1-phenylcyclopentanecarboxylate hydrochloride (**1**, R = H) by the interaction of 2′-bromoethyl 1-phenylcyclopentanecarboxylate and *trans*-2-aminocyclohexanol was examined. Optimum conditions were provided by the use of four moles of amine per mole of ester, heating the reactants in 95% ethanol in a sealed tube at 110° for 20 h, and furnished the compound in 39% yield. Identical experimental conditions with the substitution of *cis*-2-aminocyclohexanol for the *trans*-isomer gave 2′-(*cis*-2′′-hydroxycyclohexyl)aminoethyl 1-phenylcyclopentanecarboxylate hydrochloride (**2**, R = H) in 37% yield. Numerous changes in molar ratios, solvent, reaction times, and temperatures failed to improve the yield. Attention was then turned briefly to the reaction of *cis*- and *trans*-2-ethylaminocyclohexanol with 2′-bromoethyl 1-phenylcyclopentanecarboxylate. However, under a variety of experimental conditions, in our hands, the desired Parpanit analogues were not obtained, presumably due to unfavorable steric factors involved in the alkylation reaction since dicyclohexylamine under similar reaction conditions also failed to yield a Parpanit analogue.

The cholinesterase-inhibitory potencies of compounds **1** and **2** (R = H) were determined by a method described earlier (17, 18) together with those of *cis*- and *trans*-2-aminocyclohexanol hydrochloride, *cis*- and *trans*-2-ethylaminocyclohexanol hydrochloride and *cis*- and *trans*-2-aminocyclopentanol hydrochloride. The results, which are shown in Table 1, indicate that compounds **1** and **2** and the hydrochlorides of other *cis*-2-aminocyclanols display the approximately twofold greater cholinesterase-inhibitory potencies over their *trans* analogues previously observed by Friess and co-workers (7) for the trimethylammonium quaternary analogues. It should also be noted that conversion of the 2-aminocyclohexanols to **1** and **2** has little effect on the cholinesterase-inhibitory potency, although substitution of an ethyl group on the nitrogen atom decreases the activity approximately fivefold. The compounds are weak cholinesterase inhibitors (cf. physostigmine, $I_{50} = 6.1 \times 10^{-8}$ (17)).

The in vivo effectiveness of compounds **1** and **2** (R = H) as substitutes for or adjuncts to atropine sulfate and *N*-methylpyridinium-2-aldoxime methanesulfonate in the treatment of mice and rats poisoned with sarin was evaluated by

TABLE 1

Cholinesterase inhibitory potencies of aminocyclanols and Parpanit analogues

Compound	$I_{50} \times 10^4$	Effectiveness as substitutes for atropine*		Effectiveness as adjuncts to atropine*	
		Mouse	Rat	Mouse	Rat
cis-2-Aminocyclohexanol hydrochloride	6.1				
trans-2-Aminocyclohexanol hydrochloride	11.0				
cis-2-Ethylaminocyclohexanol hydrochloride	30.1				
trans-2-Ethylaminocyclohexanol hydrochloride	53.7				
cis-2-Aminocyclopentanol hydrochloride	71				
trans-2-Aminocyclopentanol hydrochloride	150				
cis-2-Hydroxycyclohexyltrimethylammonium iodide†	1.1				
trans-2-Hydroxycyclohexyltrimethylammonium iodide†	2.1				
2′-Diethylaminoethyl 1-phenylcyclopentanecarboxylate‡ hydrochloride	1.5	3.2§	6.1‖	4.6	14.7
2′-(*cis*-2′′-Hydroxycyclohexyl)aminoethyl 1-phenylcyclopentanecarboxylate hydrochloride	6.8	1.2	1.0	4.2	6.3
2′-(*trans*-2′′-Hydroxycyclohexyl)aminoethyl 1-phenylcyclopentanecarboxylate hydrochloride	13.5	1.7	1.6	4.8	15.0

*Given as Protective Ratio where PR = $\frac{LD_{50} \text{ sarin in treated animal}}{LD_{50} \text{ sarin in untreated controls}}$ (see refs. 1, 2).

†See ref. 7.
‡See refs. 1, 18.
§PR atropine = 2.03.
‖PR atropine = 4.2.

methods described previously (1, 2). The results given in Table 1 show that the substitution of a *cis*- or *trans*-2-hydroxycyclohexyl moiety on the nitrogen atom of Parpanit produces compounds which are, at best, marginally effective as substitutes for atropine and that their activities as adjuncts to atropine are no better than that of Parpanit. However, the results suggest that the more potent anticholinesterase (**1**) provides poorer protection as both a substitute for and an adjunct to atropine than does the less potent inhibitor. Because of the low protective activity of both compounds it was not possible to draw any definite conclusion about the effect of the orientation of the hydroxyl group relative to that of the amino group on biological activity.

Experimental[2,3]

D,L-*trans-2-Ethylaminocyclohexanol*

A solution of 1,2-epoxycyclohexane (25.6 g, 0.26 mole) and ethylamine (100 g, 2.2 mole) in ethanol (100 ml) was heated in a stainless steel bomb at 110° for 4 h. After cooling to room temperature, the solution was transferred quantitatively to a flask and distilled to remove the ethanol and unreacted ethylamine. Fractionation of the residue *in vacuo* gave 34.2 g (92%) of *trans*-2-ethylaminocyclohexanol, b.p. 106°/14 mm; m.p. 43–44°. Brunel (14) reports b.p. 220–223°.

trans-2-Ethylaminocyclohexanol hydrochloride was prepared in 94% yield, m.p. 157–158°, after recrystallization from methanol – petroleum ether. Mousseron and Granger (19) report m.p. 155°.

Anal. Calcd. for $C_8H_{18}ONCl$: C, 53.47; H, 10.10; N, 7.79; Cl, 19.73. Found: C, 53.45; H, 9.97; N, 7.73; Cl, 19.78.

D,L-*trans-2-Ethylacetamidocyclohexanol*

(*a*) A solution of acetyl chloride (1.96 g, 0.025 mole) in sodium-dried benzene (10 ml) was added dropwise with stirring to a solution of *trans*-2-ethylaminocyclohexanol (7.16 g, 0.05 mole) in dry benzene (20 ml) in an apparatus protected from entry of moisture. The reaction mixture was heated with stirring for 3 h during which massive precipitation occurred. The precipitate, *trans*-2-ethylaminocyclohexanol hydrochloride, 4.20 g (93%) was collected and washed with ether. The filtrate was distilled to remove ether and benzene. A solid, unreacted *trans*-2-ethylaminocyclohexanol, appeared in the residue and was removed by sublimation. The residue, *trans*-2-ethylacetamidocyclohexanol, contaminated with a small amount of an acetoxy compound (as shown by a small band at 1734 cm^{-1} in its i.r. spectrum (20)), was twice distilled *in vacuo*, yielding 3.13 g (67%) of colorless oil, b.p. 116–117°/0.1 mm.

Anal. Calcd. for $C_{10}H_{19}O_2N$: C, 64.83; H, 10.34; N, 7.56. Found: C, 64.74; H, 10.33; N, 7.46.

(*b*) A solution of *trans*-2-ethylacetamidoacetoxycyclohexane (2.27 g, 0.01 mole) in carbonate-free distilled water (10 ml) and carbonate-free 1 *N* sodium hydroxide (11 ml, 10% excess) was shaken for 1 h then taken to dryness *in vacuo*. The residue was extracted with ether in a Soxhlet extractor for 16 h. The extract was dried ($MgSO_4$), filtered and taken to dryness *in vacuo*. The residue was distilled *in vacuo*, yielding 1.42 g (77%) of a colorless, viscous oil, b.p. 116–117°/0.1 mm, which was

[2]All melting points and boiling points are uncorrected.
[3]Microanalyses were performed by J. G. Helie of these laboratories.

Can. J. Chem. Downloaded from www.nrcresearchpress.com by 210.87.254.6 on 09/05/12
For personal use only.

Can. J. Chem. Downloaded from www.nrcresearchpress.com by 210.87.254.6 on 09/05/12
For personal use only.

shown by i.r. analysis to be the pure *N*-acetyl derivative (strong band at 1620 cm^{-1} but none at 1734 cm^{-1}).

(*c*) A solution of *trans*-2-ethylaminoacetoxycyclohexane hydrochloride (2.22 g, 0.01 mole) in carbonate-free water (10 ml) was shaken with 1 *N* aqueous sodium hydroxide (11 ml, 0.011 mole) for 1 h. The reaction mixture was taken to dryness *in vacuo*, Celite and absolute ethanol were added to the oily residue, and the evaporation was repeated. The residue was extracted with ether in a Soxhlet extractor for 16 h. The extract was dried ($MgSO_4$), filtered, and taken to dryness *in vacuo*. The residue was shown by comparison of i.r. spectra to be *trans*-2-ethylacetamidocyclohexanol uncontaminated with the O-acetyl analogue. Yield 1.82 g (98%).

(*d*) Acetic anhydride (50 ml) was added rapidly with stirring to *trans*-2-ethylaminocyclohexanol (7.16 g, 0.047 mole) and the resultant solution was stirred until the temperature had returned to ca. 25° (20 min). Water (25 ml) was added and the solution was evaporated to dryness *in vacuo*. Absolute ethanol was added to the residue and the evaporation was repeated. This process was repeated twice more, following which the residue was distilled *in vacuo*. The distillate, b.p. 116–117°/0.1 mm, was shown by i.r. analysis to be a mixture of *O*- and *N*-acetyl compounds, since it showed strong bands at 1734 cm^{-1} and 1620 cm^{-1} (20, 21).

Attempts to prepare the pure *N*-acetyl compound by the action of aqueous alkali or Amberlite IRA-400 (OH^-) resin on the mixture of *O*- and *N*-acetyl compounds obtained by method (*d*) were not as successful in our hands as method (*c*).

D,L-*trans-2-Ethylacetamidoacetoxycyclohexane*

A mixture of *trans*-2-ethylaminocyclohexanol (14.3 g, 0.10 mole) and acetic anhydride (50 ml) was heated under reflux with stirring for 3 h. Water (25 ml) was added with stirring and the solution was taken to dryness *in vacuo*. The residue was taken up in absolute ethanol and the solution was again taken to dryness. This process was repeated twice and the dark residue was distilled *in vacuo*, yielding 20.4 g (90%) of *trans*-2-ethylacetamidoacetoxycyclohexane, b.p. 83–84°/0.03 mm, as a colorless oil.

Anal. Calcd. for $C_{12}H_{21}O_3N$: C, 63.41; H, 9.31; N, 6.16. Found: C, 63.64; H, 9.47; N, 6.28.

D,L-*trans-2-Ethylaminoacetoxycyclohexane Hydrochloride*

A solution of acetyl chloride (3.92 g, 0.05 mole) in sodium-dried benzene (20 ml) was added to a mixture of *trans*-2-ethylaminocyclohexanol hydrochloride (8.99 g, 0.05 mole) in benzene (40 ml) in an apparatus protected against the entry of moisture. The mixture was heated under reflux with stirring for 2 h, during which the solid dissolved. The benzene was removed by distillation and the residue crystallized on standing. Recrystallization from methanol–ether furnished 9.67 g, (87%) of *trans*-2-ethylaminoacetoxycyclohexane hydrochloride, m.p. 158–159°.

Anal. Calcd. for $C_{10}H_{20}O_2NCl$: C, 54.16; H, 9.09; N, 6.34; Cl, 15.99. Found: C, 54.12; H, 9.11; N, 6.33; Cl, 15.98.

Thionyl Chloride Inversion Reactions

(*a*) A solution of *trans*-2-acetamidocyclohexanol (7.84 g, 0.05 mole) in anhydrous chloroform (25 ml) was added to a stirred solution of thionyl chloride (14 ml, ca. 0.19 mole) in chloroform (25 ml) at −5 to 0° over a period of 15 min in an apparatus protected against the entry of moisture. The resultant pale yellow oil was kept at room temperature for 3 h, following which the excess thionyl chloride and chloroform were removed by distillation at 20 mm pressure. The viscous pale pink residue was treated with chloroform (10 ml) and the solution was added dropwise with stirring to anhydrous ether (500 ml). The oil which separated crystallized on standing overnight at 4° and the almost colorless crystals of crude oxazoline hydrochloride (cf. 12, 13), were collected and washed with anhydrous ether, yield 8.64 g (98%), m.p. 98.5–100.5°. The oxazoline salt was hydrolyzed by heating it under reflux with 10% hydrochloric acid (250 ml) for 1 h. Removal of the aqueous phase by distillation *in vacuo*, followed by recrystallization of the residue from ethanol–ether furnished 6.83 g (90%) of *cis*-2-aminocyclohexanol hydrochloride, as colorless platelets, m.p. 189–191° (cf. 13).

(*b*) A solution of *trans*-2-acetamidoacetoxycyclohexane (1.99 g, 0.01 mole) in anhydrous chloroform (5 ml) was added to thionyl chloride (2.8 ml, ca. 0.038 mole) in anhydrous chloroform (5 ml) over a period of 5 min so that the temperature did not rise above 0°. The product was isolated in the usual manner used for the oxazoline intermediate and the resultant solid, on recrystallization from ether, proved to be unchanged *trans*-2-acetamidoacetoxycyclohexane, m.p. 116.5–118°. Yield, 1.79 g (90%).

(*c*) *trans*-2-Ethylacetamidocyclohexanol (1.85 g, 0.01 mole) in anhydrous chloroform (5 ml) was added to thionyl chloride (2.8 ml, ca. 0.038 mole) in anhydrous chloroform (5 ml) at 0° over a period of 10 min. The oxazoline intermediate was not isolated but was hydrolyzed directly to the amine hydrochloride with 10% hydrochloric acid after removal of the excess thionyl chloride and chloroform *in vacuo*. Recrystallization of the crude product from ethanol–ether furnished 1.50 g (83%) of *cis*-2-ethylaminocyclohexanol hydrochloride, as colorless crystals, m.p. 194–195°. Taguchi and Nakayama (15) report m.p. 189°.

Anal. Calcd. for $C_8H_{18}ONCl$: C, 53.47; H, 10.10; N, 7.79; Cl, 19.73. Found: C, 53.18; H, 10.08; N, 7.62; Cl, 19.60.

(*d*) The procedure was identical with that given in (*b*) above except that *trans*-2-ethylacetamidoacetoxycyclohexane (2.27 g, 0.01 mole) was used, and recovered quantitatively on application of the usual method for isolation of the intermediate oxazoline.

D,L-*cis-2-Aminocyclohexanol*

cis-2-Aminocyclohexanol hydrochloride was converted to the free base, m.p. 75.5–77.5°, by the method of Bannard (13).

D,L-*cis*-2-*Ethylaminocyclohexanol*

cis-2-Ethylaminocyclohexanol hydrochloride was converted to the free base in 89% yield by the method referred to above, and was purified by sublimation at 60° at 10^{-3} mm pressure, m.p. 64.5–65°. Taguchi and Nakayama (15) report m.p. 63–65°.

2′-Bromoethyl 1-Phenylcyclopentanecarboxylate

A solution of 1-phenylcyclopentanecarbonyl chloride

Can. J. Chem. Downloaded from www.nrcresearchpress.com by 210.87.254.6 on 09/05/12
For personal use only.

(8.34 g, 0.04 mole) prepared by the method of Bannard *et al.* (9) and freshly-distilled 2-bromoethanol (12.5 g, 0.10 mole) in sodium-dried benzene (25 ml) was heated under reflux with stirring for 3 h in an apparatus protected against the entry of moisture. The solvents were removed by distillation, the residue was stirred for 10 min with a small amount of potassium carbonate and Celite, then filtered, and the residue was washed with anhydrous ether. The ether was removed *in vacuo* during which operation a small amount of 1-phenylcyclopentanecarboxylic acid, 0.34 g (4.5%) separated. The latter substance was collected and identified by its i.r. spectrum. The filtrate was fractionated *in vacuo*. After a small forerun, which was discarded, 2′-bromoethyl 1-phenylcyclopentanecarboxylate, b.p. 114–115°/0.1 mm; n_D^{25} 1.5398, was collected as a colorless oil. Yield, 10.1 g (85%).

Anal. Calcd. for $C_{14}H_{17}O_2Br$: C, 56.58; H, 5.77; Br, 26.89. Found: C, 56.70; H, 5.78; Br, 26.94.

This compound is unstable even on storage under anhydrous conditions. 1-Phenylcyclopentanecarboxylic acid was identified as one of the decomposition products by i.r. spectroscopy and a mixed m.p. determination with an authentic sample.

2′-Chloroethyl 1-Phenylcyclopentanecarboxylate

1-Phenylcyclopentanecarbonyl chloride (8.34 g, 0.04 mole) in sodium-dried benzene (25 ml) was added dropwise, with stirring, to redistilled 2-chloroethanol (8.04 g, 0.10 mole) in benzene (25 ml). The reaction mixture was heated under reflux with stirring for 1 h. The benzene was removed by distillation and the residue was dissolved in ether (25 ml). The ether solution was extracted with water (10 ml), separated, dried over potassium carbonate, filtered, and the ether was removed *in vacuo*. The residue was fractionated yielding 2′-chloroethyl 1-phenylcyclopentanecarboxylate as a colorless oil, b.p. 170–171.5°/10 mm, n_D^{25} 1.5268. Yield, 8.27 g (82%).

Anal. Calcd. for $C_{14}H_{17}O_2Cl$: C, 66.53; H, 6.78; Cl, 14.03. Found: C, 66.72; H, 6.74; Cl, 14.00.

This compound was stable even after storage for 4 years as indicated by no change in either its i.r. spectrum or its refractive index.

Esters of 1-Phenylcyclopentanecarboxylic Acid

(a) Parpanit

A mixture of 2′-bromoethyl 1-phenylcyclopentanecarboxylate (1.49 g, 0.005 mole), redistilled diethylamine (1.46 g, 0.02 mole), and benzene (2 ml) was heated in a sealed tube at 110° for 16 h. The resultant solution was taken to dryness *in vacuo* and the crystalline residue was recrystallized from methanol–acetone–ether. The i.r. analysis of the product suggested the presence of Parpanit hydrobromide and diethylammonium bromide, and the mixture was stirred with water (20 ml), the solution was made basic (to p*H* 10) with sodium hydroxide, and extracted with ether (2 × 25 ml). The extract was dried ($MgSO_4$ and Celite), filtered, and taken to dryness *in vacuo*. The residue was dissolved in methanol (5 ml), saturated with hydrogen chloride, and taken to dryness *in vacuo*. Recrystallization from methanol–ether furnished 2′-diethylaminoethyl 1-phenylcyclopentanecarboxylate hydrochloride, m.p. 144–145°. Yield, 1.31 g (80%).

(b) 2′-(trans-2″-Hydroxycyclohexyl)aminoethyl 1-Phenylcyclopentanecarboxylate Hydrochloride (1, R = H)

A mixture of 2′-bromoethyl 1-phenylcyclopentanecarboxylate (1.49 g, 0.005 mole) and *trans*-2-aminocyclohexanol (2.30 g, 0.02 mole) in 95% ethanol (25 ml) was heated in a sealed tube at 110° for 20 h. The light brown reaction mixture was decanted and taken to dryness *in vacuo*. The residue was stirred with water (25 ml) and ether (25 ml). The layers were separated and the aqueous phase was extracted with ether (2 × 10 ml). The aqueous layer was taken to dryness *in vacuo* and recrystallization of the residue from methanol–ether furnished *trans*-2-aminocyclohexanol hydrobromide, m.p. 192–193°, 0.66 g (67% of theoretical bromide ion). Hawkins and Bannard (11) report m.p. 191–192°.

The ether extract was dried ($MgSO_4$), filtered, and taken to dryness *in vacuo*, during which the small amount of residual *trans*-2-aminocyclohexanol was removed by sublimation. The residue was taken up in methanol, treated with charcoal, filtered through Celite, saturated with anhydrous hydrogen chloride, and again taken to dryness *in vacuo*. Two recrystallizations from methanol–ether furnished 2′-(*trans*-2″-hydroxycyclohexyl)aminoethyl 1-phenylcyclopentanecarboxylate hydrochloride, as colorless needles, m.p. 171.5–172°. Yield, 0.72 g (39%).

Anal. Calcd. for $C_{20}H_{30}O_3NCl$: C, 65.29; H, 8.22; N, 3.81; Cl, 9.64. Found: C, 65.33; H, 8.01; N, 3.89; Cl, 9.91.

(c) 2′-(cis-2″-Hydroxycyclohexyl)aminoethyl 1-Phenylcyclopentanecarboxylate Hydrochloride (2, R = H)

The procedure was identical with that given in (*b*) above except that *cis*-2-aminocyclohexanol was used instead of the *trans* isomer. The product was also isolated as described in (*b*) and 0.75 g (76%) of *cis*-2-aminocyclohexanol hydrobromide, m.p. 167.5–168.5°, was isolated as by-product.

Anal. Calcd. for $C_6H_{14}ONBr$: C, 36.75; H, 7.20; N, 7.19; Br, 40.75. Found: C, 37.26; H, 7.04; N, 7.18; Br, 40.80.

2′-(*cis*-2″-Hydroxycyclohexyl)aminoethyl 1-phenylcyclopentanecarboxylate hydrochloride was obtained as discolored needles, m.p. 147.5–149°. Yield, 0.70 g (37%).

Anal. Calcd. for $C_{20}H_{30}O_3NCl$: C, 65.29; H, 8.22; N, 3.81; Cl, 9.64. Found: C, 65.50; H, 8.34; N, 3.70; Cl, 9.50.

The i.r. spectra of the *trans* and *cis* isomers were distinctly different in the fingerprint region.

We are indebted to Mr. J. G. Helie for measuring the in vitro cholinesterase inhibitory potencies reported in Table 1 and to Dr. I. W. Coleman and Mr. G. Patton for determining the in vivo protective effectiveness of the compounds.

1. I. W. Coleman, P. E. Little, and R. A. B. Bannard. Can. J. Biochem. Physiol. **40**, 815 (1962).
2. I. W. Coleman, P. E. Little, and R. A. B. Bannard. Can. J. Biochem. Physiol. **40**, 827 (1962).
3. I. W. Coleman, P. E. Little, and R. A. B. Bannard. Can. J. Biochem. Physiol. **41**, 2479 (1963).

4. I. W. COLEMAN, P. E. LITTLE, G. E. PATTON, and R. A. B. BANNARD. Can. J. Physiol. Pharmacol. **44**, 745 (1966).
5. I. W. COLEMAN, G. E. PATTON, and R. A. B. BANNARD. Can. J. Physiol. Pharmacol. **46**, 109 (1968).
6. S. L. FRIESS and W. J. MCCARVILLE. J. Amer. Chem. Soc. **76**, 1363 (1954).
7. H. D. BALDRIDGE, W. J. MCCARVILLE, and S. L. FRIESS. J. Amer. Chem. Soc. **77**, 739 (1955).
8. R. A. B. BANNARD, J. H. PARKKARI, and I. W. COLEMAN. Can. J. Chem. **40**, 1909 (1962).
9. R. A. B. BANNARD, J. H. PARKKARI, and I. W. COLEMAN. Can. J. Chem. **41**, 2108 (1963).
10. J. H. PARKKARI, R. A. B. BANNARD, and I. W. COLEMAN. Can. J. Chem. **43**, 3119 (1965).
11. L. R. HAWKINS and R. A. B. BANNARD. Can. J. Chem. **36**, 220 (1958).
12. (*a*) W. S. JOHNSON and E. N. SCHUBERT. J. Amer. Chem. Soc. **72**, 2187 (1950). (*b*) G. E. MCCASLAND and D. A. SMITH. J. Amer. Chem. Soc. **72**, 2190 (1950).
13. R. A. B. BANNARD. Can. J. Chem. **42**, 744 (1964).
14. L. BRUNEL. Ann. Chim. (Paris) [8], **6**, 257 (1905).
15. T. TAGUCHI and M. NAKAYAMA. J. Amer. Chem. Soc. **73**, 5679 (1951).
16. G. FODOR and J. KISS. J. Amer. Chem. Soc. **72**, 3495 (1950).
17. D. NACHMANSOHN and I. B. WILSON. Advan. Enzymol. **12**, 259 (1951).
18. R. A. B. BANNARD, J. G. HELIE, JOAN E. PRICE, and I. W. COLEMAN. Can. J. Physiol. Pharmacol. **47**, 1036 (1969).
19. M. MOUSSERON and R. GRANGER. Bull. Soc. Chim. France, 850 (1947).
20. L. J. BELLAMY. The infrared spectra of complex organic molecules. Second Edition. John Wiley and Sons Inc., New York, 1958. Chapter 11.
21. L. J. BELLAMY. The infrared spectra of complex organic molecules. Second Edition. John Wiley and Sons Inc., New York, 1958. Chapter 12.

Can. J. Chem. Downloaded from www.nrcresearchpress.com by 210.87.254.6 on 09/05/12
For personal use only.

Can. J. Chem. Downloaded from www.nrcresearchpress.com by 210.87.254.105 on 09/05/12
For personal use only.

Synthesis of the substituted and crosslinked glucoses corresponding to the structural units in a cotton cellulose modified with *N*-methylbis(2-chloroethyl)amine

E. J. Roberts and S. P. Rowland

Southern Regional Research Laboratory, Southern Utilization Research and Development Division, Agricultural Research Service, U.S. Department of Agriculture, New Orleans, Louisiana 70119

Received November 4, 1969

The syntheses of simple substituted glucoses (i.e., 2-*O*-, 3-*O*-, and 6-*O*-[(*N*-methyl-*N*-2-hydroxyethylamino)ethyl]-D-glucopyranoses) and simple crosslinked glucoses (i.e., *N*-methylaminobis[*O*-(*N*-2-ethyl)-D-glucopyranoses]) with glucose linkages at 2,2′-*O*-, 3,3′-*O*-, 6,6′-*O*-, 2,6′-*O*-, and 3,6′-*O*-positions are described. These result from the reactions of "blocked" glucoses with *N*-methylbis-(2-chloroethyl)amine. The new derivatives were characterized by gas–liquid chromatography and electrophoresis. Cotton cellulose modified with *N*-methylbis(2-chloroethyl)amine to incorporate 0.034 mole of reagent per D-glucopyranosyl unit was hydrolyzed to glucose and substituted glucoses; the substituted glucoses were identified by chromatographic and electrophoretic comparisons with the foregoing authentic glucose derivatives. The relative distribution of (*N*-methyl-*N*-2-hydroxyethylamino)-ethyl groups among the 2-*O*-, 3-*O*-, and 6-*O*-positions was 2.30:0.28:1.00. The distribution of crosslinkages among the 2,2′-*O*-, 2,6′-*O*-, and 6,6′-*O*-positions was 2.10:3.72:1.00; these are the only crosslinked derivatives found. The monofunctionally substituted fraction (having a single reagent unit in the substituent group) accounted for 42.6% of the nitrogen; the crosslinked fraction (having a single reagent unit in the crosslink) accounted for 25.8%; complex products accounted for the remainder of the nitrogen of the crosslinked cotton.

Canadian Journal of Chemistry, **48**, 1383 (1970)

Introduction

The crosslinking of cotton cellulose by reactions with di- or poly-functional reagents is probably the most important reaction involved in the production of wash-wear or permanent press cotton fabric. The literature on the effect of crosslinking of cotton cellulose upon the performance properties of the finished fabric is voluminous. However, no information is available on the efficiency of difunctional reagents as crosslinking agents or on the sites of reaction and distribution of linkages among the 2-*O*-, 3-*O*-, and 6-*O*-positions of the D-glucopyranosyl units of the cotton cellulose.

This paper describes the preparation of simple substituted glucoses and simple crosslinked glucoses (each containing a single reagent residue) which correspond to the structures expected in crosslinked cotton cellulose. Cotton cellulose was crosslinked with *N*-methylbis(2-chloroethyl)-amine and the disposition of reagent residues in the hydrolyzed product was determined: i.e., the extent of simple crosslink formation versus simple substituent formation versus complex product formation. In addition, the distribution of linkages between the reagent and glucose was determined for both the simple substituted and simple crosslinked glucoses.

Experimental

Preparation of Simple Substituted and Simple Crosslinked Glucoses

Step 1. The appropriately blocked glucose was dissolved in 250 ml of dry dioxane. The required amount of reagent, *N*-methylbis(2-chloroethyl)amine, a quantity of powdered potassium hydroxide equal to the weight of the blocked glucose and 10 g of Drierite were added. The mixture was refluxed with stirring for 5 h. The solid material was removed by filtration and was washed with dioxane. The combined filtrate and washings were evaporated under reduced pressure.

Step 2. Benzyl and benzylidene blocking groups were removed by hydrogenolysis as described by Roberts and Rowland (1).

Step 3. Acid labile blocking groups were removed with 2 *N* sulfuric acid as described by Roberts and Rowland (1). The products were freeze-dried yielding amorphous solids.

Results. A summary of the preparation of the simple substituted and simple crosslinked glucoses along with yields and analyses of the reaction products are shown in Table 1.

Reduction of Substituted and Crosslinked Glucoses to the Corresponding Sorbitols

To 0.50 g of the substituted or crosslinked glucose dissolved in 20 ml of water was added 0.20 g of sodium borohydride in 10 ml of water. The solution was allowed to stand overnight. To this solution was added 10 ml of 50% (v/v) acetic acid. The solution was evaporated to dryness below 60°. Then 100 ml of absolute methanol was added and the solution was evaporated to dryness under reduced pressure. This procedure was repeated with five

Can. J. Chem. Downloaded from www.nrcresearchpress.com by 210.87.254.105 on 09/05/12
For personal use only.

TABLE 1

Preparation of simple substituted and simple crosslinked glucoses

Derivative*	Starting compound: Name	Starting compound: Moles	Reagent (moles)	Reaction (steps)	Results: Yield weight (%)	Results: N (%)	Results: Cl (%)	Results: Yield of crosslinked product based on N (%)	Results: Yield of chlorine terminated product (%)
I	Methyl 3-*O*-benzyl-4,6-*O*-benzylidene-α-D-glucopyranoside	0.043	0.024	1,2,3	100	2.30	1.53	73	13
II	1,2;5,6-Di-*O*-isopropylidene-α-D-glucofuranose	0.50	0.027	1,3	100	3.03	1.10	97	10
III	6-*O*-Acetyl-1,2;3,5-di-*O*-methylene-α-D-glucofuranose†	0.50	0.027	1,3	100	2.53	1.10	80	10
IV	1,2;5,6-Di-*O*-isopropylidene-α-D-glucofuranose 6-*O*-Acetyl-1,2;3,5-di-*O*-methylene-α-D-glucofuranose†	0.50 0.50	0.054	1,3	87	1.53	0.15	48	2
V	Methyl 3-*O*-benzyl-4,6-*O*-benzylidene-α-D-glucopyranoside 6-*O*-Acetyl-1,2;3,5-di-*O*-methylene-α-D-glucofuranose†	0.25 0.25	0.027	1,2,3	100	1.79	0.11	57	1

*I = 2-*O*-substituted and 2,2′-*O*-crosslinked glucoses. II = 3-*O*-substituted and 3,3′-*O*-crosslinked glucoses. III = 6-*O*-substituted and 6,6′-*O*-crosslinked glucoses. IV = 3,6′-*O*-crosslinked glucoses. V = 2,6′-*O*-crosslinked glucoses.

†This compound was prepared by the method of Hough *et al.* (2). The acetyl group was removed prior to reaction as described by Roberts and Rowland (1).

Can. J. Chem. Downloaded from www.nrcresearchpress.com by 210.87.254.105 on 09/05/12
For personal use only.

additional 100 ml portions of absolute methanol to remove the borate. The residue was then dissolved in 5–10 ml of water and freeze dried to yield an amorphous product.

Modification of Cotton Cellulose with N-Methylbis-(2-chloroethyl)amine

The fabric used in this study was a desized, scoured, bleached, 80 × 80 print cloth (ca. 3.5 oz/yd^2). An 8″ × 16″ sample weighing 7.7 g was treated in a 1 *M* solution of *N*-methylbis(2-chloroethyl)amine hydrochloride. The sample of fabric was given two immersions and two passes between squeeze rolls to a weight gain of 120%. The wet fabric was then immersed in 100 ml of 2 *N* sodium hydroxide for 45 min with occasional agitation. The fabric was then washed free of reagents with flowing tap water and was allowed to dry in air. The fabric showed a weight gain of 3.9% and contained 0.29% of nitrogen and 0.08% of chlorine. The nitrogen content corresponds to a degree of substitution of 0.034, calculated as if the reagent reacted as a monofunctional agent (i.e., 0.034 mole of agent per D-glucopyranosyl unit of the cotton).

Hydrolysis of the Chemically Modified Cotton Cellulose to Substituted and Crosslinked Glucoses

The sample of fabric was ground in a Wiley Mill to pass a 20-mesh screen and was hydrolyzed by the procedure described by Roberts and Rowland (1). The removal of sulfuric acid and the isolation of the mixture of glucose, substituted glucoses, and crosslinked glucoses was carried out as described in the same reference. There was obtained an amorphous solid containing 0.22% nitrogen and approximately 0.10% chlorine.

Separation of Glucose, Simple Substituted Glucoses, and Simple Crosslinked Glucoses by Electrophoresis

The paper electrophoresis separations were carried out on Whatman 3MM paper in 0.75 *M* formic acid at 75 V per cm for 30 min as described by Roberts and Rowland (3).

Separation of Glucose, Simple Substituted Glucoses, and Simple Crosslinked Glucoses by Gas–liquid Chromatography

The gas–liquid chromatograms (g.l.c.) were obtained with an Aerograph model 1520 instrument equipped with a hydrogen flame ionization detector.[1] The column used for the separations of the simple substituted glucoses was 1% SE-30 on Chromosorb W (hexamethyldisilizane treated, 80–100 mesh); the column was 1/8″ o.d. × 6′ in stainless steel tubing and was obtained from the Perkin–Elmer Instrument Company.[1] It was operated isothermally at 185° with a carrier gas flow of 20 ml/min.

The column employed for the separation of simple crosslinked glucoses was composed of 2% OV-3 on Chromosorb W (60–80 mesh); this was 1/8″ o.d. × 5′ in stainless steel tubing. The column was operated isothermally at 245° with a carrier gas flow of 20 ml/min.

[1]Mention of a company and/or product by the U.S. Department of Agriculture does not imply approval or recommendation of the company or product to the exclusion of others which may also be suitable.

All glucose derivatives to be analyzed were equilibrated overnight in pyridine prior to trimethylsilylation.

Results

Preparation and Identification of Simple Substituted and Simple Crosslinked Glucoses

In order to identify the structure of the reagent residues in cotton cellulose modified with *N*-methylbis(2-chloroethyl)amine, it is necessary to prepare a series of authentic derivatives of glucose to serve as the basis of comparison (through electrophoresis and g.l.c.) with the components of the hydrolyzate from the modified cotton. All of these derivatives of glucose were obtained as mixtures of the simple substituted glucose (for example, 3-*O*-[(*N*-methyl-*N*-2-hydroxyethylamino)ethyl]-D-glucopyranose, **1** of Fig. 1) together with the crosslinked glucose (for example, *N*-methylaminobis[3-*O*-(*N*-2-ethyl)-D-glucopyranose], **2** of Fig. 1).

The preparation of the simple substituted and simple crosslinked glucoses is illustrated in Fig. 1 in the case of the 3-*O*-substituted glucose and the 3,3′-*O*-crosslinked glucose.

The Simple Substituted Glucoses

A paper electrophoregram of the mixture of 3-*O*-substituted and 3,3′-*O*-crosslinked glucoses is reproduced in Fig. 2, electrophoregram *A*. Three spots other than glucose were shown by spraying the paper with aniline phosphate solution. Spot *2* appeared in a position very similar to that of *O*-(2-diethylaminoethyl)-D-glucopyranoses, which were studied previously (1), an indication that this spot represents the 3-*O*-substituted glucose (**1** of Fig. 1). Elution of the component in spot *2* followed by g.l.c. of the trimethylsilyl derivative (prepared from the freeze-dried sample) confirmed this.

The mixture of 3-*O*-substituted and 3,3′-*O*-crosslinked glucoses was converted to trimethylsilyl derivatives for g.l.c. under the conditions employed in preceding studies of 3-*O*-(2-diethylaminoethyl)-D-glucopyranose (1). Each of the products designed to prepare a simple substituted glucose and a symmetrically crosslinked glucose yielded two peaks on the SE-30 column. These pairs of peaks are interpreted to be the alpha and beta anomers of each of the 2-*O*-, 3-*O*-, and 6-*O*-[(*N*-methyl-*N*-2-hydroxyethylamino)-ethyl]-D-glucopyranoses. This is confirmed by the ratios of these peaks (alpha/beta) which are

Can. J. Chem. Downloaded from www.nrcresearchpress.com by 210.87.254.105 on 09/05/12
For personal use only.

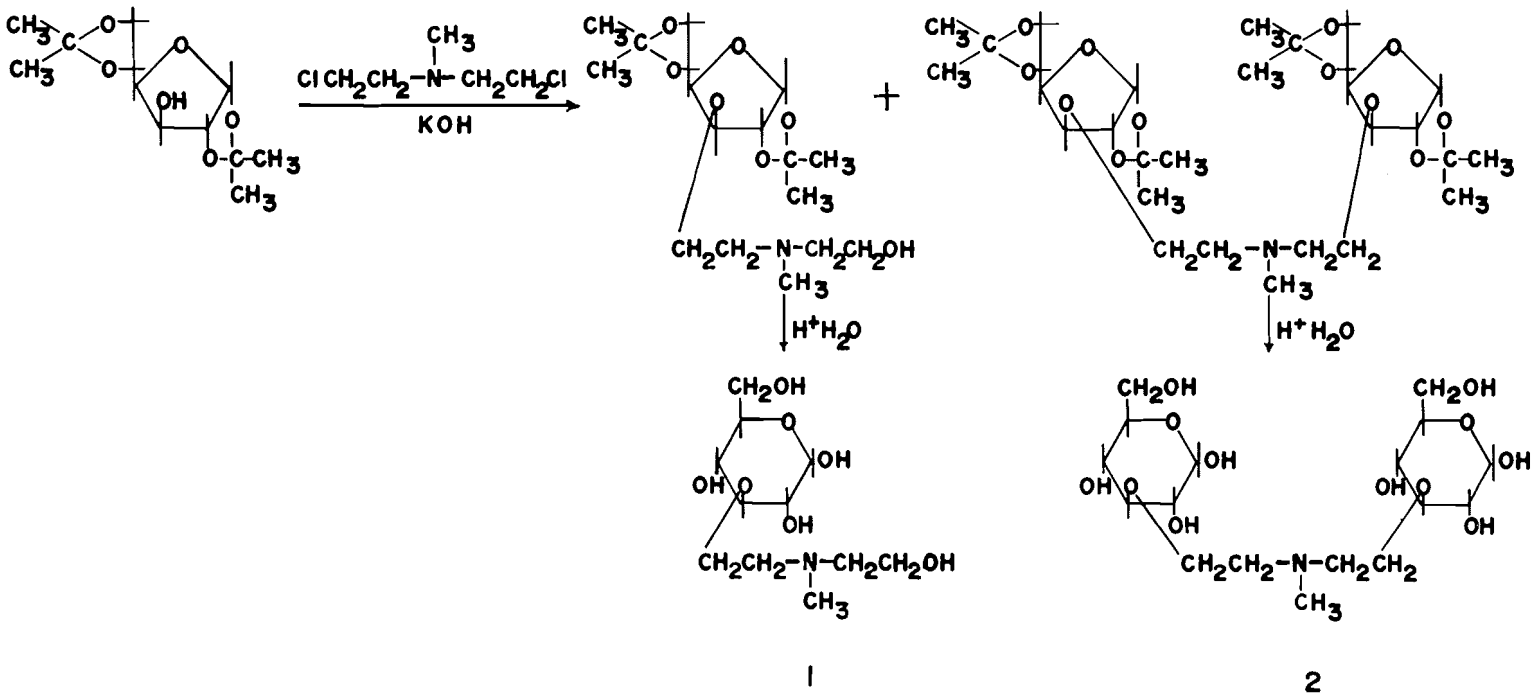

FIG. 1. Major products of the reaction of 1,2;5,6-di-*O*-isopropylidene-α-D-glucopyranose and *N*-methylbis-(2-chloroethyl)amine.

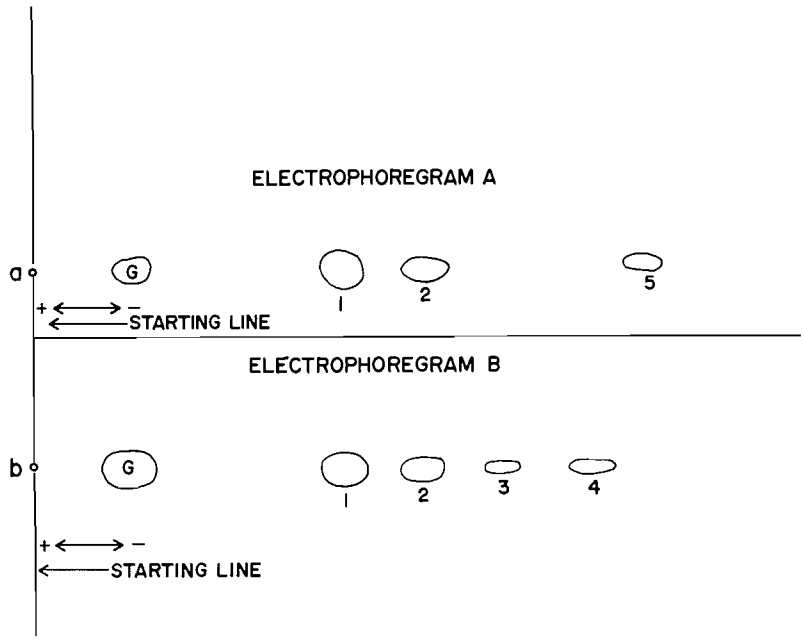

FIG. 2. Electrophoregrams of samples which were applied along the starting line as follows: (*a*) the hydrolyzed product from the reaction of 1,2;5,6-di-*O*-isopropylidene-α-D-glucopyranose and *N*-methylbis(2-chloroethyl)amine; (*b*) the hydrolyzate of the chemically modified cotton from reaction with *N*-methylbis(2-chloroethyl)amine.

TABLE 2

Anomer ratios of the isomers of *O*-[(*N*-methyl-*N*-2-hydroxyethylamino)ethyl]-D-glucopyranose (I) and other substituted glucoses*

	2-*O*-		3-*O*-		6-*O*-		
Substituted glucose	1st anomer	2nd anomer	1st anomer	2nd anomer	1st anomer	2nd anomer	Reference
I	0.35	0.65	0.48	0.52	0.43	0.57	—
II	0.34	0.66	0.48	0.52	0.43	0.57	1
III	0.39	0.61	0.50	0.50	0.43	0.57	7
IV	0.38	0.62	0.50	0.50	0.43	0.57	7

*I is identified in the title; II = *O*-[2-(diethylamino)ethyl]-D-glucopyranose; III = *O*-(2-aminoethyl)-D-glucopyranose; and IV = *O*-(2-hydroxyethyl)-D-glucopyranose.

summarized in Table 2. It is evident that the ratios of the anomer pairs for these new substituted glucoses are identical to those of a series of related substituted glucoses, which have been studied and described previously.

The Simple Crosslinked Glucoses

Spot *1* in electrophoregram *A* of Fig. 2 appears in a location consistent with that expected for a crosslinked glucose: i.e., less mobile than the simple substituted glucose due to higher molecular weight with the same single amine group per molecule. Elution of this spot from the paper followed by freeze drying, silylation, and g.l.c. showed the presence of only the 3,3′-*O*-crosslinked glucose, as discussed in the following paragraph.

By operating at higher temperatures in g.l.c. there were obtained additional peaks from the trimethylsilyl derivatives of the 3-*O*-substituted and 3,3′-*O*-crosslinked glucoses. These were best observed on an OV-3 column operated at 245°, indicating that these components were substantially higher in molecular weight than the simple substituted glucoses which have been described in the preceding section. Three peaks were obtained for each of the symmetrically crosslinked glucoses. This is consistent with expectation of

Can. J. Chem. Downloaded from www.nrcresearchpress.com by 210.87.254.105 on 09/05/12
For personal use only.

Can. J. Chem. Downloaded from www.nrcresearchpress.com by 210.87.254.105 on 09/05/12
For personal use only.

three anomers in these cases: i.e., alpha–alpha, alpha–beta (same as beta–alpha), and beta–beta. These are expected to elute in the order indicated. The predominance of the second peak (a combination of alpha–beta and beta–alpha) provides some confirmation of this. The elution time for these peaks increased, as is normal with glucose derivatives, from the 3,3′-*O*- to the 2,2′-*O*- to the 6,6′-*O*-compound. The number and pattern of anomeric peaks which were the same for all of these isomeric compositions, are considered positive evidence that the reagent residue is linked to two independent glucose units. The total evidence indicates that these are crosslinked glucoses.

The product of the reaction designed to prepare the 2,6′-*O*-crosslinked glucose contained considerable quantities of the 2,2′-*O*- and 6,6′-*O*-isomers with the 2,6′-*O*-crosslinked glucose predominating. The product of the reaction for preparation of the 3,6′-*O*-crosslinked glucose contained considerable quantities of 3,3′-*O*- and 6,6′-*O*-isomers with the 3,3′-*O*-crosslinked glucose predominating in this instance.

In order to facilitate the analysis of mixtures of these crosslinked glucoses, each reaction product was subjected to reduction with sodium borohydride to obtain the corresponding sorbitol derivative. The number of peaks for each crosslinked glucose was reduced to one.

More Complex Substituted or Crosslinked Glucoses

While more complicated derivatives of glucose are expected to be formed in the reactions involving cotton cellulose, they are not likely to be formed in the reactions of the blocked glucoses with *N*-methylbis(2-chloroethyl)amine in anhydrous media. Nevertheless, a faint spot was observed in some electrophoregrams (see spot *5* of electrophoregram *A* of Fig. 2) of these products. These faint spots were not identified, but it is considered that they may represent a glucose unit bearing an extended chain substituent composed of two reagent residues.

Analysis of the Chemically Modified Cotton Cellulose

The Simple Substituted Glucose Fraction

The cotton fabric which had been reacted with *N*-methylbis(2-chloroethyl)amine was hydrolyzed to a mixture of glucose, substituted glucoses, and crosslinked glucoses. The trimethylsilylated derivatives of this mixture of materials in g.l.c. showed the presence of simple 2-*O*-, 3-*O*-, and 6-*O*-substituted glucoses. These were identified by comparison of retention times and by peak enhancement with the corresponding known derivatives.

The ratio of peak areas, calculated by triangulation and the sum of the areas of the anomeric peaks, is expressed in terms of unity for the amount of substitution at the 6-*O*-position. The ratio of substituents at the 2-*O*-, 3-*O*-, and 6-*O*-positions was found to be 2.30:0.28:1.00.

The ratio of 2-*O*- to 6-*O*-substitution, as noted above, is considerably higher than has been found for reactions of cotton cellulose with most monofunctional reagents. 2-Chloroethyldiethylamine, which is closely related to the reagent employed in this study, reacted at the 2-*O*-, 3-*O*-, and 6-*O*-positions in the ratio of 2.05:0.21:1.00 under comparable conditions employing 2 *N* sodium hydroxide (4).

The Simple Crosslinked Glucose Fraction

Chromatographic analysis for simple crosslinked glucoses (following borohydride reduction and silylation of the hydrolyzate) on the OV-3 column showed 3 peaks. These peaks were identified as the 2,2′-*O*-, 2,6′-*O*-, and 6,6′-*O*-crosslinked products by retention times and peak enhancement with the corresponding known crosslinked glucoses. Although the 2,6′-*O*- and 3,6′-*O*-crosslinked glucoses exhibited very similar retention times, the second peak in the hydrolyzate was identified as the 2,6′-*O*-compound by the fact that only this authentic crosslinked glucose in peak enhancement showed no change in retention time and no broadening or distortion of the peak. Chromatographic analysis of the second peak of the hydrolyzate on several columns showed no evidence of the presence of more than one component in the peak.

The area of each peak in the crosslinked fraction of the components from the chemically modified cellulose was determined by triangulation. On this basis, the distribution of the crosslinkages among the 2,2′-*O*-, 2,6′-*O*-, and 6,6′-*O*-positions is indicated to be 2.10:3.72:1.00. The substitution in the 6,6′-*O*-position serves as the basis for comparison (and unity in the above ratio).

Fractions of Reagent Residues in the Various Structural Forms

A paper electrophoregram of the components

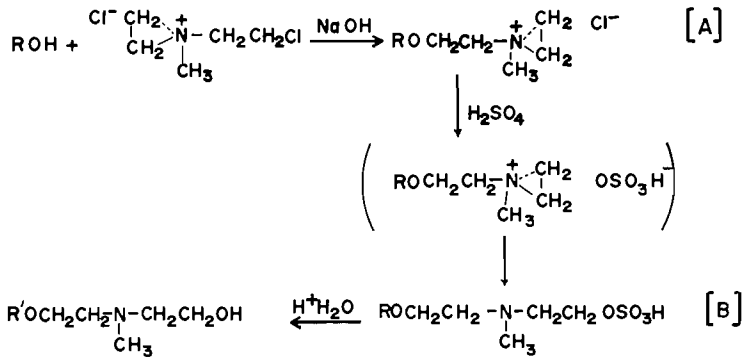

FIG. 3. Proposed mechanisms of reaction of *N*-methylbis(2-chloroethyl)amine with cellulose or blocked glucose. R represents the remaining portion of the blocked glucose or R represents cellulose in which the OH indicated is one of many. R′ represents the glucose after removal of the blocking groups or cellulose after hydrolysis to glucose units.

from the chemically modified cotton cellulose (refer to Fig. 2, Electrophoregram *B*) shows 5 spots. In addition to the spot representing glucose (*G*), spot *1* was identified as the simple crosslinked glucose fraction (all isomers). Spot *2* was identified as the simple substituted glucoses (all isomers containing a single reagent residue). The identities were established by comparison of mobilities of the unknowns with those of the authentic materials described earlier. The structures of the compounds responsible for spots *3* and *4* were not identified; these could represent glucose units containing more than one substituent group, glucose units bearing an extended-chain substituent group from more than one unit of reagent, and/or crosslinked glucose units where the crosslink is composed of more than one reagent residue. These are referred to as "complex glucose derivatives" throughout this paper.

For information regarding the amount of reagent residues in the form of simple substituent, simple crosslink, or complex structures, separations were obtained by electrophoresis and spots *1* and *2* were eluted separately. The quantities of simple substituted glucoses and simple crosslinked glucoses were determined by the hypoiodite oxidation procedure of Hirst *et al.* (5). The simple substituted glucose fraction accounted for 42.6% of the total nitrogen, and the simple crosslinked glucoses accounted for 25.8% of the total nitrogen. The remaining 31.6% of the nitrogen is attributed to complex glucose derivatives.

Discussion

The crosslinking of cotton cellulose with *N*-methylbis(2-chloroethyl)amine is believed to proceed in two steps: one end of the reagent molecule undergoes conversion to the aziridinium ion form and this reacts with a hydroxyl group of a D-glucopyranosyl unit of the cellulose. At this point the other end of the reagent has opportunity to form the aziridinium ion through the same nitrogen atom and this may react with another hydroxyl group of cellulose. These steps are illustrated in eq. [A] of Fig. 3. It may be noted that if both aziridinium ions react with the hydroxyl groups of cellulose, a simple crosslink is formed; if one of the aziridinium groups reacts with water, a simple substituent is formed, and if one end of the reagent fails to react, a chloro-terminated substituent group may result.

It might be expected that the simple substituent groups in cotton cellulose would contain chloroethyl groups on the unreacted end of the reagent. Some chlorine was detected in the chemically modified cellulose, but the chlorine was not found in the simple substituted glucoses after the hydrolysis of the chemically modified cellulose to glucose, substituted glucoses, and crosslinked glucoses. It has been shown that *N*-methylbis(2-chloroethyl)amine is converted to *N*-methyl-*N*-2-chloroethylaziridinium chloride (the reactive species) in aqueous solution (6). Since the *O*-[(*N*-methyl-*N*-2-hydroxyethylamino)ethyl]-D-glucopyranoses were the only products found in the monofunctionally reacted fraction, it is proposed that the chloro groups that may be present in the cotton on the unreacted end of the reagent prior to acid hydrolysis are converted to hydroxyl groups as shown in Fig. 3.

Can. J. Chem. Downloaded from www.nrcresearchpress.com by 210.87.254.105 on 09/05/12
For personal use only.

The chloride ion is probably replaced by a sulfate ion, which forms a sulfato group that is subsequently hydrolyzed to a hydroxyl group.

In the preceding section it was shown that the reagent residues were present in the chemically modified cotton cellulose as follows: 42.6% as simple substituents, 25.8% as simple crosslinkages, and 31.6% in more complex structures. It may then be calculated from other foregoing data that the percentages of reagent residues as simple 2-*O*-, 3-*O*-, and 6-*O*-substituents are 27.4, 3.3, and 11.9; that the percentages as simple 2,2′-*O*-, 2,6′-*O*-, and 6,6′-*O*-crosslinks are 7.9, 14.0, and 3.8; and that the percentage as complex structures is 31.6. The predominance of the simple substituted glucoses and especially of the 2-*O*-substituted glucose is impressive. Among the simple crosslinked glucoses, the predominance of the 2,6′-*O*-structure is generally consistent with the fact that the hydroxyl groups at C-2 and C-6 are substantially more reactive than those at C-3. However, the predominance of 2,6′-*O*-crosslinks over 2,2′-*O*-crosslinks suggests that there is a spatial factor in the cotton cellulose structure which favors crosslink formation in the 2,6′-*O*-location. The general predominance of the substituted glucoses may be a further reflection of spatial requirements which must be satisfied in order to complete a crosslinkage.

1. E. J. Roberts and S. P. Rowland. Can. J. Chem. **45**, 261 (1966).
2. L. Hough, J. K. N. Jones, and M. S. Magson. J. Chem. Soc. 1525 (1952).
3. E. J. Roberts and S. P. Rowland. Carbohyd. Res. **5**, 1 (1967).
4. S. P. Rowland, E. J. Roberts, and C. P. Wade. Text. Res. J. **39**, 530 (1969).
5. E. J. Hirst, L. Hough, and J. K. N. Jones. J. Chem. Soc. 928 (1949).
6. J. R. Sowa and C. C. Price. J. Org. Chem. **34**, 474 (1969).
7. E. J. Roberts and S. P. Rowland. Can. J. Chem. **47**, 1571 (1969).

Can. J. Chem. Downloaded from www.nrcresearchpress.com by 210.87.254.105 on 09/05/12
For personal use only.

Can. J. Chem. Downloaded from www.nrcresearchpress.com by 210.87.254.5 on 09/05/12
For personal use only.

Reactions of norbornen-7-one with Grignard reagents

J. WARKENTIN
Department of Chemistry, McMaster University, Hamilton, Ontario

Received December 3, 1969

The relative importance of addition and reduction, as well as the *syn*:*anti* selectivity of those processes, were determined for the reactions of five Grignard reagents with norbornen-7-one. Reduction is important or dominant in the reactions of Grignard reagents having β-hydrogen and there is a strong preference for the hydride transfer to occur from the *syn* face of the carbonyl group. Addition shows the analogous stereochemical preference with higher selectivity than reduction.

Canadian Journal of Chemistry, **48**, 1391 (1970)

Introduction

In connection with other work a number of 7-alkylnorbornen-7-ols were required. Treatment of the readily-available norbornen-7-one (1) with the appropriate alkyl lithium or Grignard reagents looked attractive as a route to such compounds. Although it was recognized that bulky Grignard reagents are prone to reduce ketones by hydride transfer from the β-position (2, 3), the fate of norbornen-7-one could not be predicted readily. The high reactivity (4) of that strained ketone and the lack of free rotation might make it relatively insensitive to steric factors and therefore less prone to reduction than, for example, diisopropyl ketone. A second interesting question concerned the stereochemistry of addition and reduction. A general preference for reaction from the *syn* face was anticipated, based on the report that the *syn*:*anti* product ratio from reduction of the ketone with borohydride is 15:85 (4).

To determine the selectivities of some of its reactions, norbornen-7-one was treated with four alkyl Grignard reagents in which the extent of α-branching varied, and with a β-branched Grignard reagent.

Results and Discussion

The products of carbonyl reduction of norbornen-7-one are known compounds which were readily characterized from their physical and spectral properties (4, 5). Addition products obtained in this study were readily identified as 7-alkylnorbornen-7-ols from the close resemblance of their nuclear magnetic resonance (n.m.r.) spectra to those of the known products of reduction. Assignment of "*anti*-ol" stereochemistry to the major product from methyl Grignard and norbornenone was supported by converting the alcohol to the bromide with thionyl bromide under conditions which normally lead to retention of configuration.[1] The product was shown (n.m.r.) to be the isomer of the known *syn*-7-bromo-7-methylnorbornene (6).[2] Other addition products were assigned the same stereochemistry on the basis of their n.m.r. spectra and analogy, for there is no reason to expect a change in structure of the Grignard reagent to reverse the sense of the stereochemical selectivity of addition. Proton resonance spectra and other properties of the products are recorded in Table 1.

Table 2 lists the product distributions from the reactions of Grignard reagents with norbornenone in ether at 35°. It is noteworthy that the ethyl and isopropyl reagents are both less selective, as expected for reactions with a highly reactive ketone, than they are in reactions with an unstrained model, diisopropyl ketone (7). For the latter the addition:reduction ratio from ethyl Grignard reagent is 3.7 (7) while isopropyl Grignard fails to add (7). The high stereoselectivity of reduction makes tertiary butyl Grignard reagent, for example, a better choice than borohydride (4) for the synthesis of *anti*-norbornen-7-ol from the ketone. As a synthetic route to tertiary, *anti*-norbornen-7-ols, addition of Grignard reagents is clearly most effective if the latter lack β-hydrogen.

The high preference for attack on the *syn* face may be the result of smaller non-bonded interactions between reagent and two carbon

[1]The alcohol was refluxed for 3 h with $SOBr_2$ in carbon tetrachloride. I am indebted to Mr. F. R. S. Clark for the conversion of alcohol to bromide.

[2]A gift of the *syn* bromide, from Dr. E. C. Sanford, is gratefully acknowledged.

TABLE 1

syn-7-R-Norbornen-7-ols (**1**) and *anti*-7-R-norbornen-7-ols (**2**)

Compound	Melting point (°C)	%C*	%H*	Proton magnetic resonance (δ, CCl_4, internal TMS)†‡							
				H_1	H_2	H_5	H_6	H_7	H_8	H_9	H_{10}
1 R = H	114–116			2.48	5.94	1.80	0.97	3.48	—	—	—
2 R = H				2.71	6.03	1.72	0.92	3.64	—	—	—
1 R = CH_3	77–78	77.37	9.74	2.30	5.96	2.01	0.93	—	1.30	—	—
		77.49	9.50								
2 R = CH_3§				2.47	6.06			—	1.17	—	—
1 R = CH_2CH_3	oil	78.21	10.21	2.37	5.94	1.98	0.94	—	1.67	0.88	—
		78.24	10.32							($J_{8,9}$ = 7.5 Hz)	
1 R = $CH(CH_3)_2$	oil	78.89	10.59	2.43	5.92	1.96	0.92	—	2.29	0.82	—
		78.09	10.54							($J_{8,9}$ = 7.0 Hz)	
1 R = $CH_2C(CH_3)_3$	51–51.5	79.94	11.18	2.53	5.97	2.01	0.98	—	1.73	—	1.03
		79.58	11.09								

*Calculated values in upper rows; analytical results in lower rows.
†Determined with a Varian HA-100 instrument.
‡The numbering system is: H_1 = H_4 = bridgehead, H_2 = H_3 = vinyl, H_5 = *exo*, H_6 = *endo*, H_7 = C_7—H, etc. Signals from the OH group are not tabulated.
§Tentative assignment of this structure is based on the n.m.r. spectrum of the mixture of methyl compounds. Some of the signals expected for 2 (R = CH_3) were probably obscured by the spectrum of 1 (R = CH_3).

bridge in the transition states from *syn* attack. Although partial rate factors for reduction of norbornen-2-one led to the postulate that the etheno bridge has a larger steric requirement than the ethano bridge (4), there are at least two thermodynamically-controlled systems in which the larger 7-substituent of a norbornene prefers the *syn* configuration (8, 9). Addition may have a larger steric requirement than reduction because addition appears to be bimolecular in Grignard reagent (10).[3] Weak complexing between the metal and the π-system is not excluded as a factor determining the preferred *syn* attack.

Experimental

Product Analyses

Crude product mixtures were analyzed by gas–liquid partition chromatography (g.l.p.c.), using a 5′ × 1/4″ column packed with 15% Carbowax 20M on 60–80 mesh Chromosorb W (column A) and a 5′ × 1/4″ column packed with 20% SE-30 on the same support (column B). With column A (125°, helium flow rate = 50 cc min^{-1}) relative retention volumes were (7-substituent other than OH listed): *anti*-H, 0.51; *anti*-CH_3, 0.35; *syn*-CH_3, 0.58; *syn*-CH_2CH_3, 0.78; *syn*-$CH(CH_3)_2$, 0.82; *syn*-$CH_2C(CH_3)_3$, 1.40; *syn*-H, 1.00 (reference). From column B the 7-alkylnorbornenols were eluted after the products of reduction. Analytical samples were obtained by preparative g.l.p.c., using column A. An Aerograph 90P-3 instrument, with thermal conductivity detector, was used throughout.

[3]The molecularity of the corresponding reduction has not been established, it seems. The effects of large changes in concentration and temperature on the distribution of products from norbornenone are under investigation.

TABLE 2

Products from norbornen-7-one and RMgX

R of RMgX*	Product distribution (relative %)†‡			
	Addition		Reduction	
	syn§	*anti*§	*syn*§	*anti*§
CH_3	4‖	96	none	none
CH_3CH_2	—	51	4	45
$(CH_3)_2CH$	—	10	2	88
$(CH_3)_3C$	—	—	2	98
$(CH_3)_3CCH_2$	—	>98	none	1¶

*Grignard reagents are written as RMgX although R_2Mg is usually present also in such solutions.
†A dash is used where the compound in question, an unknown, was not indicated in the n.m.r. spectrum of the crude product. Without an authentic sample with which to calibrate the chromatogram it was not possible to rule out a small quantity of such a compound.
‡The errors in the small numbers are probably at least 50% of their values. Higher percentages (> 40) are subject to an uncertainty of about 5 parts per 100, except the entries for R = CH_2CH_3 and $CH(CH_3)_2$, which have about twice that error. The uncertainty was estimated from the scatter of the results of two to four runs.
§Labels (*syn*, *anti*) refer to the hydroxyl group.
‖Identity inferred from the n.m.r. spectrum of the mixture.
¶Reduction was probably caused by traces of other Grignard reagents. The neopentyl chloride had two impurities in it, totalling about 3%.

Relative yields were determined by integration of the g.l.p.c. traces with a Dupont Model 310 Curve Resolver.[4] Thermal conductivities of isomers were assumed to be the same. Peak areas corresponding to the ethyl and isopropyl addition products were reduced by the factor 1.2. That factor was determined with weighed mixtures prepared from pure *anti*-norbornen-7-ol and *syn*-7-ethylnorbornen-7-ol and it was assumed to apply adequately to the isopropyl compound also.

[4]The peaks did not overlap and the instrument was used as an integrating device only.

Can. J. Chem. Downloaded from www.nrcresearchpress.com by 210.87.254.5 on 09/05/12
For personal use only.

Grignard Reagents

The following description is typical of all preparations except that involving neopentyl Grignard reagent.

Ethyl iodide (0.31 g, 2.0 mmoles) was added all at once to Grignard-quality magnesium turnings (0.24 g, 10.0 mg atom) covered with 10 ml of anhydrous ether. The mixture was stirred and refluxed for one hour before norbornen-7-one (0.11 g, 1.0 mmoles) in 2 ml of ether was added by drops to the boiling solution. When all the ketone had been added heating was continued for 15 min more before the solution was cooled and saturated, aqueous ammonium chloride solution was added gradually. The ether layer was decanted and dried over $CaSO_4$ before it was concentrated with a rotary evaporator. Care was taken not to evaporate the last traces of ether, to minimize loss of product components.

In a run on 4.63 times the above scale the yield of ether-free alcohols was 0.51 g (89%, calculated on the basis of the product distribution in Table 2).

Neopentyl chloride (4.34 g, 45.0 mmoles), in 20 ml of ether, was heated at 60° in a sealed tube with magnesium (1.08 g, 45.0 mg atom). After about 8 h the solution became grey and turbid, suggesting that reaction had begun. In a further 16 h period about half of the metal reacted. The solution above the residue was pipetted from the tube into a flask fitted with magnetic stirrer and heater. The solution was brought to reflux and norbornen-7-one (1.0 g, 9.3 mmoles) in 5 ml of ether was gradually added. After addition was complete the mixture was stirred and heated for 1 h. Hydrolysis with saturated NH_4Cl solution was strongly exothermic, indicating the presence of excess Grignard reagent. Drying the ether layer and evaporation of ether left an oil which crystallized spontaneously in a few minutes. The yield of crude *syn*-7-neopentyl-*anti*-norbornen-7-ol was 1.47 g (88.5%). It contained, in addition to a small amount of *anti*-norbornen-7-ol, about 6% (assuming comparable thermal conductivity) of an impurity which was not identified but which was shown by infrared to be free of OH groups. Purification to m.p. 51–51.5° was accomplished by sublimation.

Financial assistance was provided by the National Research Council of Canada. Brian Sayer and Ian Thompson obtained the n.m.r. spectra for the author.

1. P. G. GASSMAN and P. G. PAPE. J. Org. Chem. **29**, 160 (1964).
2. M. S. KHARASCH and O. REINMUTH. Grignard reactions of nonmetallic substances. Prentice–Hall, Inc., 1954.
3. G. E. DUNN and J. WARKENTIN. Can. J. Chem. **34**, 75 (1956).
4. H. C. BROWN and J. MUZZIO. J. Amer. Chem. Soc. **88**, 2811 (1966).
5. (*a*) E. I. SNYDER and B. FRANZUS. J. Amer. Chem. Soc. **86**, 1166 (1964); (*b*) P. LASZLO and P. VON R. SCHLEYER. J. Amer. Chem. Soc. **86**, 1171 (1964).
6. L. SKATTEBÖL. Tetrahedron **23**, 1107 (1967).
7. F. C. WHITMORE and R. S. GEORGE. J. Amer. Chem. Soc. **64**, 1239 (1942).
8. P. G. GASSMAN, J. ZELLER, and J. L. LUMB. Chem. Commun. 69 (1968).
9. R. R. SAUERS. Chem. Ind. 176 (1960).
10. E. C. ASHBY. Quart. Rev. (London), **21**, 259 (1967).

Can. J. Chem. Downloaded from www.nrcresearchpress.com by 210.87.254.5 on 09/05/12
For personal use only.

Can. J. Chem. Downloaded from www.nrcresearchpress.com by 210.87.254.105 on 09/05/12
For personal use only.

Reactions of some 2-aminophenyl- and 2- and 4-nitrophenyl sulfones in aqueous sodium hydroxide solution[1]

K. B. SHAW AND R. K. MILLER
Defence Research Establishment Ottawa, Defence Research Board, Ottawa 4, Ontario

Received November 6, 1969

When 2-aminophenylsulfonylacetic acid (**3**) was heated under reflux in an excess of dilute sodium hydroxide solution, the only product identified was 2-methylsulfonylaniline (**6**). When 2-nitrophenylsulfonylacetic acid was treated under the same conditions, the major products identified were 2-methylsulfonylnitrobenzene (**7**), 2-nitrophenol (**8**), and orthanilic acid (**13**); minor products of this reaction were **6** and 3-methylsulfonyl-3′-nitro-4-amino-4′-hydroxybiphenyl (**12**). The same products were obtained although the yields were different when **7** was boiled with alkali, but the reaction of 4-methylsulfonylnitrobenzene (**15**) with alkali was less complex and 4-nitrophenol (**16**) was the only major product. The biphenyl **12** was also formed in small yield when *N*-(2-methylsulfonylphenyl)hydroxylamine (**19**) was treated with alkali and its formation in these reactions was investigated in detail. It was concluded that **12** arises from **7** and **19**, but it could also be prepared from **19** and 2-chloro- or better, 2-fluoronitrobenzene, in alkaline solution, and based on all these observations, a mechanism for its formation is suggested. The genesis of the various other products is also discussed. Reference is made to the infrared spectra of sulfones.

Canadian Journal of Chemistry, **48**, 1394 (1970)

Introduction

It has been reported (1) that certain cyclic hydroxamic acids, among them **1** and **2**, are powerful reactivators in vitro of acetylcholinesterase inhibited by diisopropylphosphorofluoridate (DFP). All the compounds were said to be more potent reactivators than pyridine 2-aldoxime methiodide (2-PAM), and **1** was said to be more than twice as potent as 2-PAM and less than half as inhibitory. In view of these claims, it was necessary to extend the reactivation

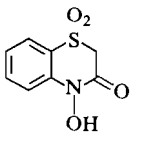

1

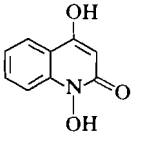

2

studies to cholinesterase inhibited by other organophosphorus compounds. However, we[2] were unable to demonstrate any significant reactivation by **1** or **2** of acetylcholinesterase or serum cholinesterase after inhibition by isopropyl methylphosphonofluoridate (Sarin), although these compounds, in conjunction with atropine, were found to afford some protection to mice against poisoning by Sarin above that afforded by atropine alone.[3]

Because of this protection afforded against Sarin poisoning, it was of interest to study the chemistry of some of these hydroxamic acids and the benzothiazine derivative **1**, was selected for this work. Compound **1** was unaffected by refluxing 10% hydrochloric acid, but when a solution of **1** in dilute sodium hydroxide was heated under reflux for several hours a multitude of products was formed. Before this reaction was investigated further, it seemed desirable to study the action of sodium hydroxide on some related sulfones in order to gain background information which might help in understanding the reaction of **1** with alkali. In this respect however, the information gained from these reactions, some of which were also rather complex, was of limited value. Nevertheless, interesting results were obtained and these form the subject of this and another paper (2). The reaction of **1** with sodium hydroxide is imperfectly understood and is not reported here.

Results and Discussion

It was decided initially to study the action of sodium hydroxide on 2-aminophenylsulfonylacetic acid (**3**). Although **3** could be prepared in solution, the acid could not be isolated owing to the ease with which it cyclized to the lactam, 3,4-dihydro-3-oxo-2*H*-1,4-benzothiazine-1,1-dioxide (**4**) (3, 4). Several attempts to prepare **3** by the published method ((5) reduction of 2-nitrophenylsulfonylacetic acid (**5**) with ferrous sulfate and ammonia) or by reduction of **5** with sodium

[1]Issued as DREO Report No. 612.
[2]K. B. Shaw and R. K. Miller. Unpublished work.
[3]I. W. Coleman. Personal communication.

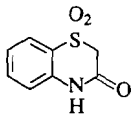

4

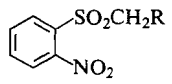

5 R = CO_2H
7 R = H

borohydride and palladium charcoal (6) gave **4** as the only identifiable product. The lactam **4** was also obtained in poor yield by the reduction of **5** with iron and hydrochloric acid (7) but could be prepared in good yield by this method from the methyl ester of **5** since this avoided difficulties arising from the formation of iron salts. The lactam has maxima in the ultraviolet (u.v.) (in water) at 251 and 295 mμ in the p*H* range 1 to about 10. At higher p*H* however, the maxima are at 257 and 305 mμ, when **4** presumably exists as the salt of **3**. The lactam **4** was recovered in high yield after being heated for 4 h with 1 molar equivalent of 0.1 *N* sodium hydroxide, but when the experiment was repeated using 2 molar equivalents of alkali, 2-methylsulfonylaniline (**6**) (7, 8, 9) was obtained in about 20% yield. The yield of **6** was increased to about 30% after a 7 h reaction period and to about 75% after 24 h. In addition, **4** was also recovered and another product appeared (u.v.) to be present but there was no evidence that orthanilic acid was formed in this reaction (see below).

When 2-nitrophenylsulfonylacetic acid (**5**) was heated under reflux in 1 molar equivalent of *N* sodium hydroxide the sole product isolated, in 50–60% yield, was 2-methylsulfonylnitrobenzene (**7**) (8) and this decarboxylation in alkaline solution is a general reaction of 2-nitrophenylsulfonylacetic acids (10). A somewhat cleaner product was obtained in rather higher yield when the decarboxylation was carried out in 0.1 *N* sodium hydroxide for 3 h, but **7** was not the only product of this reaction (cf. (10)), since the reaction mixture showed maxima in the u.v., whereas neither **5** nor **7** shows a maximum in the u.v. Subsequently, it was found that the decarboxylation of **5** takes place almost quantitatively when the acid is heated under reflux for 3 h with only 10% of 1 molar equivalent of dilute sodium hydroxide solution; but when the reaction was carried out in water for the same time, the yield of **7** was less than 20% and the remaining **5** was recovered. It is apparent from these results that in alkaline solution, the nitro acid **5** loses carbon dioxide much more readily than the amino acid **3**. Compound **7** could also be prepared in very high yield by heating under reflux for 20 h a solution of **5** in methanol containing a little piperidine, the method used by Coutts and Smith (11) for the preparation of **7** from the methyl ester of **5**.

The reaction of **5** with two molar equivalents of alkali was complex. Although in a number of runs the yields of the various products were not exactly reproducible, the variations were not large and the same products were obtained. The reaction was carried out by heating a solution of **5** in 0.1 *N* sodium hydroxide under reflux for 7 h. During this time, ammonia was evolved and the solution became deep red (cf. (10)). From this solution **7** could be isolated in about 20% yield by extraction with ether and a very small quantity of **6** was also detected in this fraction. After the solution had been acidified, steam distillation gave a yellow solid which was readily identified as 2-nitrophenol (**8**) (10%), and then extraction with ether gave a semi-solid which was not completely soluble in methanol.

Although no pure compound could be isolated from the methanol-soluble part of this fraction, the methanol-insoluble portion was an orange–red solid which crystallized readily from ethanol–acetone. Elemental analysis indicated an empirical formula $C_{13}H_{12}N_2O_5S$ which was confirmed as the molecular formula by a mass spectrum (mol. wt. 308). The infrared (i.r.) spectrum was very informative and showed peaks ascribable to NH_2, bonded OH, aromatic NO_2 and SO_2Me. In addition, peaks at 1580, 1505, 850, and 815 cm^{-1} were suggestive of a 1,2,4-substituted benzene (12*a*). The sharp NH stretching bands and the slightly broad and weak OH stretching band were well defined, and it seemed unlikely that the amino and hydroxyl groups in the unknown were ortho, since 2-aminophenol (**9**) shows broad absorption between about 3200 and 2300 cm^{-1}. The position and intensity of the OH absorption in the unknown resembled that in 2-nitrophenol. The presence of nitro and methylsulfonyl groups was further confirmed by peaks at *m/e* 292 (M – 16) and 262 (M – 46) and at *m/e* 229 (M – 79) in the mass spectrum, which was consistent with a substituted biphenyl. Hence the part structure **10** accounts for all the atoms present. The nuclear magnetic resonance (n.m.r.) spectrum of the aromatic

Can. J. Chem. Downloaded from www.nrcresearchpress.com by 210.87.254.105 on 09/05/12
For personal use only.

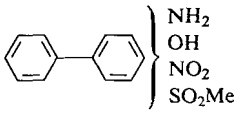

10

protons in the unknown (Fig. 1) showed peaks in the regions A, B, and C (total 5.3 H); not shown in Fig. 1 are a peak at 6.78 τ (3.0H) assigned to the protons in a methylsulfonyl group and a broad peak centered at 3.7 τ (1.9H), assigned to an amino group. The spectrum was also consistent with a biphenyl structure and an inspection of the line positions and coupling patterns allowed the following conclusions to be drawn: (*i*) Each ring contains an electron-withdrawing and an electron-donating substituent. (*ii*) In each ring there is a proton adjacent to the electron-donating substituent, and it is

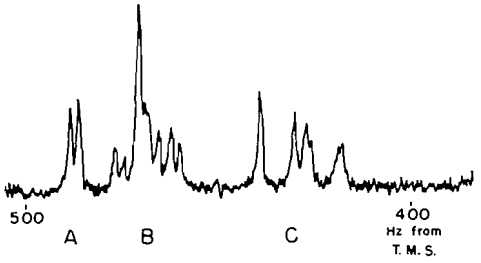

FIG. 1. The nuclear magnetic resonance spectrum of the aromatic protons in the biphenyl **12**.

split by an ortho proton but not by a meta proton (region C). (*iii*) In each ring, there is a proton adjacent to the electron-withdrawing substituent, but it is split only by a meta proton (regions A and B). The only structures which satisfy these requirements, and which are in accord with the previous observations are **11** and **12**. However, **11** may be rejected since the starting material did not contain adjacent nitrogen atoms and thus **12** is the structure of the biphenyl. The yield of **12** was about 2%.

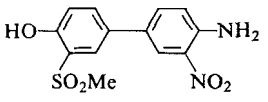

11

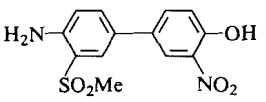

12

After the dark aqueous solution remaining after removal of the ether-soluble material had been decolorized, it showed maxima in the u.v. at 238 and 295 mμ, unchanged when the solution was made alkaline. This spectrum recalled that of 2-aminobenzenesulfonic acid (orthanilic acid) (**13**) (13) and the yield of this acid was estimated from the u.v. spectrum to be about 27%. In one experiment **13** was isolated and its identity was confirmed by u.v. and i.r. spectra and by elemental analysis.

When 2-methylsulfonylnitrobenzene (**7**) was treated with dilute sodium hydroxide solution, the products identified above were again obtained, but the yields (allowing for recovered starting material, ca. 10%) were different. It appeared that more ammonia was evolved during the reaction, and the yields of **6** (ca. 5%), **8** (22%), and **12** (8%) were all higher than in the reaction of **5** with alkali whereas the yield of **13** (13%) was lower. The methanol-soluble fraction from which **12** was isolated was shown by chromatography on alumina to be a mixture of several compounds. Although no pure compound was isolated, there was compelling evidence (comparison of i.r. and u.v. spectra in neutral and in alkaline solution with those of an authentic sample) that one fraction was 2-methylsulfonylphenol (**14**) (about 1% yield) and another fraction which showed NH_2, OH, SO_2Me, and possibly NO_2 absorptions in the i.r. may have been an isomer of **12** (see below).

The course of the reactions which occur when **5** or **7** is treated with alkali is not completely clear but a number of points can be made. The fact that the same products were isolated from **5** and **7** suggests that the decarboxylation of **5** is the first step in the reaction of that compound but, since the yields of the various products of the two reactions were dissimilar, this may not be completely true. In any event, **5** should be susceptible to the same reactions which lead to **8** and **13** from **7** (see below) and the different yields of **8** in particular, in relation to the quantity of **7** recovered, may be a reflection of the different concentrations of hydroxide ion throughout the two reactions. Thus it seems unwise to emphasize these differences in yields unduly and the discussion will be concerned with the reactions of **7**. Although it is well known

Can. J. Chem. Downloaded from www.nrcresearchpress.com by 210.87.254.105 on 09/05/12
For personal use only.

Can. J. Chem. Downloaded from www.nrcresearchpress.com by 210.87.254.105 on 09/05/12
For personal use only.

that certain substituents, e.g. nitro and chloro ortho to a nitro group, are susceptible to nucleophilic attack (14), it was uncertain whether or not the methylsulfonyl group in **7** could be displaced by a nucleophile. However the formation of **8** in the reaction of **7** with alkali indicates that such a reaction can occur and the ready displacement of the methylsulfonyl group in a number of nitrogen heterocycles by various nucleophiles, has been demonstrated recently (15). The vulnerability of a substituent ortho to a methylsulfonyl group to nucleophilic attack is very much less than that of the same substituent ortho to a nitro group (16), and 2-methylsulfonylphenol (**14**) was only a very minor product of the reaction of **7** with alkali. The formation of **14** generates nitrite ion, reduction of which would give ammonia (cf. 17); it is unlikely that ammonia was formed as a result of displacement of an aromatic amino group since both **13** and **6** were unaffected by dilute sodium hydroxide solution.

The activating effect of the ortho-nitro group in **7** is apparent in the formation of **8** (and in the ease of decarboxylation of **5** compared to **3**) and the genesis of **8** is straightforward. However, the formation of orthanilic acid (**13**) is less easily explained. Although several routes to **13** can be envisaged, it seems likely that ortho-substituent interactions (18) are involved in the formation of **13**, and also the numerous unidentified products obtained after treatment of **7** with alkali.

The ready reduction of nitro compounds under alkaline conditions is unexceptional (18 and references therein) but it is often debatable whether an external reducing agent is involved, and if so, what that agent is. A possible reducing agent in the reaction of **7** with alkali was methylsulfinate ion but this idea seemed improbable after an examination of the action of alkali on 4-methylsulfonylnitrobenzene (**15**, prepared by a series of reactions analogous to that used for **7**). In **15**, ortho-substituent interactions are not possible and the reaction of this compound with alkali was much less complex than that of **7**. The sole product isolated ($> 70\%$ yield) was 4-nitrophenol (**16**), and there was no evidence that sulfanilic acid (**17**) or other primary amines, e.g. 4-methylsulfonylaniline (**18**), were formed. In view of the high yield of **16**, and hence presumably methylsulfinate ion, **17** and **18** might have been expected if methylsulfinate ion was acting as a reducing agent.

The formation of the biphenyl **12** during the reaction of **5** or **7** with sodium hydroxide was quite unexpected and some experiments were performed in an effort to understand its mechanism of formation. The biphenyl **12** was not formed when **8** and **6** were boiled in sodium hydroxide solution for several hours (both compounds were recovered in high yield), and, when the reaction of **7** in alkali was carried out in the presence of one mole of **6**, the yield of **12** was again about 8% and **6** was recovered quantitatively. Hence it seemed unlikely that **6** was involved directly in the formation of **12**. If it is assumed that two different molecules are implicated in the formation of **12** (rather than, for example, dimerization of **7** with subsequent elaboration of the substituents) and considering what other compounds might be formed, but which could not be isolated during the reaction of **7** with alkali, one of the possible intermediates in the formation of **12** was *N*-(2-methylsulfonylphenyl)-hydroxylamine (**19**). Furthermore **19** is a part structure of the hydroxamic acid **1**, thus it was relevant to know what products were obtained when **19** was treated with dilute sodium hydroxide solution.

N-(2-Methylsulfonylphenyl)hydroxylamine (**19**), prepared by Claasz (8) by reduction of **7** with zinc and 40% acetic acid, was described as an oil. However, when **7** was reduced with zinc and ammonium chloride (19), **19** was obtained as a solid which crystallized readily. The reactions of **19** in alkali were studied in some detail and are reported elswhere (2). Here it is sufficient to state that **12** was one of several products obtained when **19** was treated with alkali, although the highest yield was about 6%. The isolation of **12** from this reaction did not prove that **19** itself was involved in the formation of **12**, in view of the numerous oxidation – reduction reactions which occur when **7** or **19** is treated with alkali but the result was at least suggestive. The nitro compound **7** was isolated in some cases after treatment of **19** with alkali (2), and since in all likelihood **19** might be formed when **7** was treated with alkali, there seemed a good possibility that these two compounds were the precursors of **12**, especially since the more obvious possibilities had been eliminated. This idea was strengthened by two facts. First, **19** is soluble in alkali in which presumably it is present in large part as the anion which might be a good nucleophile, and second,

TABLE 1
Experiments on the formation of **12***

Experiment no.	**19** (mmoles)	**7** (mmoles)	Aqueous 0.1 *N* NaOH (mmoles)	**12** Isolated (mmoles)
1	0.3	0	0.3	0†
2	0	0.3	0.3	0
3	0.3	0.3	0.3	0.052
4	0.3	0.3	0.3	0.033‡
5	0.3	0.3	0.6	0.040
6	0.3	0.6	0.3	0.049
7	0.3	0.6	0.6	0.034
8	0.6	0.3	0.3	0.039
9	0.6	0.3	0.3 + 3 ml H_2O	0.046
10	0.6	0.3	0.6	0.098

*All reaction mixtures contained 3 ml of ethanol (to increase the solubility of 7) and were heated under reflux 15 min.
†On 10 times the scale, the yield of 12 was 0.072 mmoles.
‡Reaction done in presence of 0.3 mmoles of potassium acetate.

the carbon atom bearing the methylsulfonyl group in **7** is susceptible to nucleophilic attack. Thus, attack by the anion, $RNHO^-$, of **19** on **7** would lead to a reaction intermediate (**20**) which is resonance-stabilized. If this intermediate then rearranges in the manner indicated in Scheme 1, the biphenyl is produced. Alternatively, if **20** merely lost the methylsulfonyl group, an *N*,*O*-diphenylhydroxylamine (a type of compound which does not appear to be known, see below) would result, and this might also rearrange to **12**. Although other modes of joining the two rings are probably less favorable for steric reasons, it might be expected that isomers of **12**, e.g. a 2,2′- or a 2,4′-biphenyl, would also be formed. Such a possibility cannot be ruled out. In one experiment (reaction of **7** with sodium hydroxide), chromatography of the methanol-soluble fraction from which **12** was isolated, gave a fraction which had a similar i.r. spectrum to that of **12** but which could not be crystallized.

In an attempt to acquire some support for the foregoing ideas, numerous small-scale experiments were carried out using **7** and **19**. These experiments are summarized in Table 1. In each case the reaction mixture was worked up to isolate **12** only and no attempt was made to identify the other products. The following points about these results can be made: (*a*) Both **7** and **19** are involved in the formation of **12** (experiments 1–3).[4] (*b*) When one equivalent of sodium hydroxide was used, the yield of **12** was approximately the same when the quantities of **19** and **7** were 1:1 (experiment 3), 1:2 (experiment 6), or 2:1 (experiments 8 and 9). (*c*) When two equivalents of sodium hydroxide were used, and the quantities of **19** and **7** were 1:1 (experiment 5) or 1:2 (experiment 7) the yield of **12** was almost the same as in the experiments mentioned under (*b*). However, when the quantities of **19** and **7** were 2:1 (experiment 10) the yield of **12** was about twice that obtained in the other experiments. This marked difference in yield between experiments 8 and 9, and experiment 10, clearly demonstrates that the anionic form of **19** is the important one in the formation of **12**. In addition, if the first stage of the above mechanism is correct, **19** should react with other appropriate 2-substituted nitrobenzenes in alkaline solution to give **12**, and indeed, when 2-chloronitrobenzene (**22**) was used instead of **7** under the con-

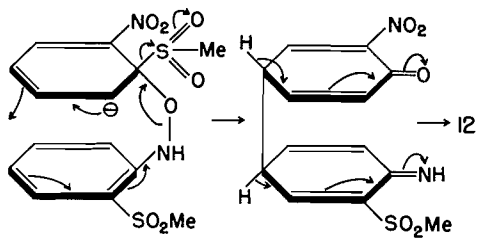

20 21

SCHEME 1

[4]It should be noted that although **12** is one of the products obtained when **19** (3 mmoles) is boiled in dilute sodium hydroxide solution for 15 min (2), the amount expected (by extrapolation) on a 0.3 mmole scale (experiment 2) would be too small to isolate. However **12** was not isolated from any experiment in which **7** was boiled in alkali for only 15 min.

Can. J. Chem. Downloaded from www.nrcresearchpress.com by 210.87.254.105 on 09/05/12
For personal use only.

Can. J. Chem. Downloaded from www.nrcresearchpress.com by 210.87.254.105 on 09/05/12
For personal use only.

ditions of experiment 3, **12** was obtained, but the yield was lower than in experiment 3. However, when 2-fluoronitrobenzene (**23**) was used instead of **7** in experiments analogous to 3, 6, and 10, the yields of **12** were 0.068, 0.068, and 0.14 mmoles respectively, and in addition, because of the more favorable solubility of **23** compared with **7**, it was possible to carry out a reaction involving **23** (experiment 3) at room temperature (48 h) when the yield of **12** was 0.077 mmoles.

In an attempt to prepare *N,O*-diphenylhydroxylamine via its *N*-acetyl derivative (**24**), Cox and Dunn (20) treated *N*-acetylphenylhydroxylamine (**25**) with diphenyliodonium hydroxide, but the main product of this reaction was 4-acetyl-4′-hydroxybiphenyl (**26**) containing some of the 2′-hydroxy isomer. Cox and Dunn considered that the most likely explanation of their results was that **25** was phenylated to give **24** which then spontaneously rearranged intramolecularly to the observed products. The experiments discussed above provide good evidence that the first stage in the formation of **12** is nucleophilic attack by the anion of **19** on the carbon atom bearing the methylsulfonyl group in **7** (and that bearing the halogen atom in **22** and **23**) and an intermediate analogous to **20**, is also likely in the formation of **26**. In the absence of any evidence for the formation of an *N,O*-diphenylhydroxylamine, either in this or the earlier (**20**) work, we prefer to regard the rearrangement as proceeding in the manner outlined above. We also obtained some evidence that **12** is formed in the alkaline solution and not (e.g. by an acid-catalyzed process) during workup (cf. (20)). After completion of the reaction between **19** and **7** (e.g. experiment 3 above) the alkaline reaction mixture had a maximum in the u.v. at 286 mμ, changing to 276 mμ after acidification, and the peak at 286 mμ persisted after extraction of the alkaline solution with chloroform. In aqueous alkali **12** has a peak at 288 mμ, changing to 278 mμ on acidification. However, the reaction cannot be quite as straightforward as outlined above. If this was so, it would be expected that, in the small-scale experiments described above, doubling the quantity of **7** (experiments 6 and 7), or **19** and sodium hydroxide (experiment 10), would lead to an increase in the yield of **12** over that obtained when the reactants were 1:1 (experiment 3), whereas only when 2 parts of **19** and sodium hydroxide were used, was an increase in the yield of **12** observed. A possible explanation of this is that the anion of **19** functions as a base in some other manner e.g. by facilitating the removal of the protons from **21** (cf. (21)). However, other bases e.g. hydroxyl ion (experiment 5) and acetate ion (experiment 4) do not act similarly.

Infrared Spectra

During the course of this and other work, 30 sulfones were available for study. In all these compounds, the sulfur atom was attached to a benzene ring. Nineteen of these compounds contained a methylsulfonyl group, nine contained the group $—SO_2CH_2—$, either in a six-membered ring (e.g. as in **4**) or as in **3**, and the remaining two compounds contained the group $—SO_2CH=$. All the compounds were solids and their i.r. spectra were recorded in potassium bromide disks, and in some cases also in solution. Of the 19 compounds containing the methylsulfonyl group, 18 showed a medium to strong band in the region 950–970 cm^{-1} (very fine splitting was observed with two compounds) and one compound showed two bands in this region. Eight compounds showed a medium-strong to strong band in the region 950–960 cm^{-1} in solution. Of the 11 compounds not containing a methylsulfonyl group four showed a weak band in the region 945–970 cm^{-1}, one showed a band of medium intensity at 980 cm^{-1} and six did not show any absorption between 910 and 1000 cm^{-1}. As an extension of these observations, an inspection of the i.r. spectra of more than 60 sulfones recorded on DMS cards revealed that of 20 compounds containing a methylsulfonyl group, 18 also showed a medium to strong band in the 950–970 cm^{-1} region and two compounds showed a band 5 cm^{-1} outside this range. Of the remaining compounds, only one (a salt) showed any significant absorption in this region.

Sheppard has stated (22) that the CH_3 rocking modes in compounds containing the group $CH_3—X$, in which the atom X is in Period III or higher of the Periodic Table, give rise to strong bands in the region 700–1000 cm^{-1}; and Momose *et al.* (23) have assigned bands in the 950–980 cm^{-1} region of the i.r. spectra of phenyl methylsulfones to methyl rocking vibrations in methylsulfonyl groups. This assignment is clearly supported by the observations recorded here. Furthermore, the spectra on DMS cards indicate

Can. J. Chem. Downloaded from www.nrcresearchpress.com by 210.87.254.105 on 09/05/12
For personal use only.

that the assignment may be extended to include also alkyl methylsulfones. Since all sulfones show strong SO_2 stretching vibrations in the region 1350–1290 and 1160–1100 cm^{-1} (12*b*), the presence of an additional medium to strong band in the 950–970 cm^{-1} region of the spectrum of a sulfone of unknown structure is strong evidence for the presence of a methylsulfonyl group, although it should be noted that aliphatic *N*-oxides and *trans*-1,2-disubstituted olefines also absorb in this region (12*c*, 12*d*).

Experimental

Infrared spectra are for potassium bromide disks except where noted otherwise. The micro analyses were performed by J. G. Helie and the mass spectrum was by Morgan–Schaffer Corporation, Montreal.

2-Nitrophenylsulfonylacetic Acid (5)

This compound was prepared by oxidation of (2-nitrophenylthio)acetic acid (24, cf. also 25) (25 g) in glacial acetic acid (200 ml) with 30% hydrogen peroxide (75 ml) for 5 h at 70°. (When less peroxide was used the product was not readily purified). The reaction mixture was concentrated to small volume, the crude product was separated, washed with water, and then crystallized from water to give the pure acid (80–85%), m.p. 175–176° (lit. (3) m.p. 173–174°); ν_{max} 1720 (C=O), 1535 and 1355 (NO_2), 1335 and 1145 cm^{-1} (SO_2).

Anal. Calcd. for $C_8H_7NO_6S$: C, 39.18; H, 2.86; N, 5.71; S, 13.07. Found: C, 39.36; H, 2.97; N, 5.66; S, 13.04.

Methyl (2-Nitrophenylsulfonyl)acetate

This ester, prepared by the method of Coutts *et al.* (25) in > 90% yield, was recrystallized (thimble) from methanol, m.p. 121–122° (lit. (27) m.p. 119–120°; (11) m.p. 120–121°); ν_{max} 1745 (C=O), 1530 and 1360 (NO_2), 1330 and 1150 cm^{-1} (SO_2).

Anal. Calcd. for $C_9H_9NO_6S$: C, 41.71; H, 3.51; N, 5.40. Found: C, 41.82; H, 3.71; N, 5.15.

2-Methylsulfonylnitrobenzene (7)

(*a*) A mixture of 2-nitrophenylsulfonylacetic acid (2.45 g) and 0.1 *N* sodium hydroxide (10 ml, 10% of 1 molar equ.) was heated under reflux for 3 h and then cooled in ice. The solid was separated and crystallized from 25% (v/v) ethanol–water giving 7 as pale yellow plates (1.86 g, 93%), m.p. 106–107° (lit. (7, 8, 9) m.p. 105–106°); ν_{max} 1540 and 1355 (NO_2), 1300, 1150 and 955 cm^{-1} (SO_2Me).

Anal. Calcd. for $C_7H_7NO_4S$: C, 41.78; H, 3.51; N, 6.96. Found: C, 41.97; H, 3.48; N, 7.15.

(*b*) A solution of 2-nitrophenylsulfonylacetic acid (32.8 g) in 95% methanol (300 ml) containing piperidine (5 ml) was heated under reflux for 20 h. The hot solution was poured into water (600 ml) at ca. 60° and then left to cool. The crystalline solid was separated and washed with dilute methanol, (25.0 g, 93%), m.p. and mixed m.p. 105–106°.

3,4-Dihydro-3-oxo-2H-1,4-benzothiazine-1,1-dioxide (4)

A mixture of methyl (2-nitrophenylsulfonyl)acetate (5 g) and iron powder (12.5 g) in 50% (v/v) aqueous methanol (150 ml) containing concentrated hydrochloric acid (1 ml) was heated under reflux with stirring, for 21 h. The hot solution was filtered (Celite), the filtrate was adjusted to p*H* 1 and then concentrated to small volume. The white solid was separated (2.6 g, 68%, m.p. 206–208°) and crystallized from ethyl acetate – hexane and then, for analysis, from aqueous methanol, m.p. 208.5–209.5° (lit. (3) m.p. 207–208°; (4, 28) m.p. 208–209°); λ_{max} (H_2O) (*a*) p*H* 1: 251 and 295 mμ (log ε 3.91 and 3.67); (*b*) p*H* > 10: 257 and 305 mμ (log ε 3.92 and 3.49); ν_{max} 3290 (NH), 1695 (C=O), 1295 and 1155 and 1120 cm^{-1} (SO_2).

Anal. Calcd. for $C_8H_7NO_3S$: C, 48.72; H, 3.58; N, 7.10; S, 16.26. Found: C, 48.93; H, 3.80; N, 6.72; S, 16.33.

2-Methylsulfonylaniline (6)

(*a*) 2-Methylsulfonylnitrobenzene (5 g) was reduced following the method of Cava and Blake (7). When the concentrated reaction mixture was cooled, the product separated (80–90%, m.p. 83–84°) and extraction with chloroform was unnecessary. Recrystallization from benzene – light petroleum gave white prisms, m.p. 84.5–85.5° (lit. (7) m.p. 53.5–54.5°; (8) m.p. 85–92°; (29) m.p. 65–66°; (9) m.p. 84–85°); λ_{max} (EtOH) 245 and 313 mμ (log ε 3.93 and 3.58); ν_{max} 3470 and 3370 (NH_2), 1280, 1125 and 955 cm^{-1} (SO_2Me).

Anal. Calcd. for $C_7H_9NO_2S$: C, 49.10; H, 5.30; N, 8.18. Found: C, 49.09; H, 5.42; N, 7.96.

(*b*) 3,4-Dihydro-3-oxo-2*H*-1,4-benzothiazine-1,1-dioxide (1 g) in 0.1 *N* sodium hydroxide (100 ml) was heated under reflux for 24 h. Extraction of the solution with chloroform gave an oil (660 mg, 76%) which solidified, m.p. and mixed m.p. with the foregoing product, 83–84°.

N-(2-Methylsulfonylphenyl)hydroxylamine (19)

2-Methylsulfonylnitrobenzene (5 g) in ethanol (140 ml) and water (10 ml) was reduced with zinc (17 g) and ammonium chloride (3 g) following the method of Martinez *et al.* (19). The crude product (4.0 g) was crystallized twice from benzene giving nearly white crystals, m.p. 102–104°. Further recrystallization from benzene (charcoal) gave white needles m.p. 103.5–105°; λ_{max} (H_2O) 241 and 303 mμ (log ε 3.78 and 3.49), unchanged when the solution was acidified; λ_{max} (NaOH) 296 mμ (log ε 3.74), the peak disappeared in 15 min; ν_{max} 3400 (OH), 3280 (NH), 1300, 1140 and 1125, and 960 cm^{-1} (SO_2Me); ν_{max} ($CHCl_3$) 3610 (OH), 3315 (NH), 1310 and 1290, 1140 and 1130, 960 cm^{-1} (SO_2Me).

Anal. Calcd. for $C_7H_9NO_3S$: C, 44.91; H, 4.85; N, 7.48; S, 17.13. Found: C, 44.90; H, 4.98; N, 7.26; S, 17.14.

2-Methylsulfonylphenol (14)

2-(Methylmercapto)phenol (Aldrich) (5 g) in glacial acetic acid (50 ml) containing 30% hydrogen peroxide (25 ml) was kept at 60–70° for 3 h. The mixture was concentrated to small volume, diluted with water, and extracted with ether to give hydrated 2-methylsulfonylphenol as pale yellow prisms (3.7 g, 60%), m.p. 87–90.5° (lit. (30) m.p. 87.5°). A sublimed sample was still partly hydrated and was exposed to a moist atmosphere, giving the pure monohydrate, white prisms, m.p. 85–87°; λ_{max}

Can. J. Chem. Downloaded from www.nrcresearchpress.com by 210.87.254.105 on 09/05/12
For personal use only.

(EtOH) 285 mμ (log ε 3.60); λ_{max} (EtOH + 1 drop NaOH solution) 245 and 318 mμ (log ε 3.99 and 3.81). This spectrum in alkaline solution is rather similar to that of **6** in neutral solution (cf. (31)). ν_{max} 3200–2500 (broad, hydrogen bonded OH), 1280, 1140 and 1120, and 970 (SO_2Me), 3530, 3490, and 1640 cm^{-1} (H_2O); ν_{max} ($CHCl_3$) 3350 (OH), 1315 and 1295, 1130 and 1120, and 955 cm^{-1} (SO_2Me).

Anal. Calcd. for $C_7H_8O_3S \cdot H_2O$: C, 44.20; H, 5.30. Found: C, 44.00; H, 5.00.

(4-Nitrophenylthio)acetic Acid

This compound was prepared from 4-chloronitrobenzene and thioglycolic acid by the method used (24, 25) for the 2-isomer. The crude product was heated with ethanol, the mixture was filtered (the insoluble material was mainly di-(4-nitrophenyl)disulfide and the filtrate was diluted with water to turbidity. The product was obtained as yellow crystals (50%) m.p. 151–153°, raised to 155.5–156.5° after 2 recrystallizations from aqueous ethanol (lit. (26) m.p. 149–151°; (32) m.p. 156.7°); ν_{max} 1695 (C=O), 1575 and 1330 cm^{-1} (NO_2).

Anal. Calcd. for $C_8H_7NO_4S$: C, 45.08; H, 3.31; N, 6.57; S, 15.02. Found: C, 45.13; H, 3.42; N, 6.53; S, 15.13.

4-Nitrophenylsulfonylacetic Acid

This compound was made by oxidation of the foregoing thioacid by the method used for the preparation of **3**. The product (80–90%) after crystallization from water had m.p. 172–173° (lit. (33) m.p. 167°; (26) m.p. 171–172°); ν_{max} 1730 (C=O), 1530 and 1350 (NO_2), 1310 and 1145 cm^{-1} (SO_2).

Anal. Calcd. for $C_8H_7NO_6S$: C, 39.19; H, 2.86; N, 5.71; S, 13.07. Found: C, 39.33; H, 2.94; N, 5.69; S, 12.93.

*4-Methylsulfonylnitrobenzene (**15**)*

The foregoing acid was decarboxylated using method (*b*) described above for the preparation of **7**. The product (ca. 90%), m.p. 140–142°, crystallized from the reaction mixture and it was not necessary to add water. Recrystallization from methanol gave pale yellow needles, m.p. 142–143° (lit. (34) m.p. 139°; (11) m.p. 143°); ν_{max} 1525 and 1345 (NO_2), 1300, 1150, and 960 cm^{-1} (SO_2Me).

Anal. Calcd. for $C_7H_7NO_4S$: C, 41.78; H, 3.51; N, 6.96. Found: C, 41.91; H, 3.70; N, 6.97.

Reactions of 2-Nitrophenylsulfonylacetic Acid in Sodium Hydroxide Solution

A solution of 2-nitrophenylsulfonylacetic acid (4.9 g) in 0.1 *N* sodium hydroxide (400 ml, 2 molar equ.) was heated under reflux 7 h, during which time the solution became deep red and ammonia was evolved (Nessler's Reagent). The cooled solution was extracted several times with ether, giving a pale yellow solid which was crystallized from 25% aqueous ethanol giving 2-methylsulfonylnitrobenzene (**7**) (850 mg), m.p. and mixed m.p. 104–105.5°. The mother liquors from the crystallization were evaporated to dryness and the remaining solid (80 mg) was shown by u.v. and i.r. spectra to be **7** containing ca. 10% of 2-methylsulfonylaniline (**6**). The total yield of **7** was 23%. The aqueous solution was then acidified with concentrated hydrochloric acid and steam distilled. The distillate was extracted with ether giving a yellow solid (276 mg) shown by m.p. and mixed m.p., 45–46°, (lit. (35*a*) m.p. 45°), and i.r. to be 2-nitrophenol (10%). The aqueous solution was then extracted repeatedly with ether giving a sticky orange-red solid (368 mg), to which was added 2–3 ml of methanol. The insoluble material was separated (68 mg; 2.2%), and crystallized from ethanol–acetone giving 3-methylsulfonyl-3′-nitro-4-amino-4′-hydroxybiphenyl (**12**) as orange-red rods, m.p. 213–215°; λ_{max} (EtOH) 282 and ca. 447 mμ (log ε 4.47 and 3.34); λ_{max} (EtOH + 1 drop NaOH solution) 292 and ca. 458 mμ (log ε 4.51 and 3.79); ν_{max} 3420 and 3340 (NH_2), 3210 (bonded OH), 1530 and 1310 (NO_2) 1285, 1130, and 960 cm^{-1} (SO_2Me); n.m.r. (60 MHz)(DMSO-d_6) τ 2.18 (H-2), 2.96 (H-5), and 2.25 p.p.m. (H-6), $J_{2,5}$ 0.2, $J_{2,6}$ 2.4, $J_{5,6}$ 8.0 Hz. τ 1.88 (H-2′), 2.76 (H-5′), and 2.15 p.p.m. (H-6′), $J_{2',5'}$ 0.2, $J_{2',6'}$ 2.3, $J_{5',6'}$ 8.8 Hz.

Anal. Calcd. for $C_{13}H_{12}N_2O_5S$: C, 50.64; H, 3.92; N, 9.09; S, 10.40. Found: C, 50.50; H, 3.91; N, 9.18; S, 10.27.

The acetate of **12** (pyridine and acetic anhydride, overnight at room temperature, the use of elevated temperature gave a mixture of the acetate and its *N*-acetyl derivative) crystallized from ethanol as yellow needles, m.p. 162–163°; ν_{max} 3465 and 3370 (NH_2), 1770 (C=O), 1535 and 1345 (NO_2), 1180 (C—O), 1290, 1135, and 955 cm^{-1} (SO_2Me).

Anal. Calcd. for $C_{15}H_{14}N_2O_6S$: C, 51.42; H, 4.03; N, 8.00; S, 9.15. Found: C, 51.48; H, 4.33; N, 7.95; S, 9.31.

The original aqueous solution was treated several times with charcoal until it was pale yellow. It was estimated by u.v. spectroscopy to contain 960 mg of orthanilic acid (27%).

In one experiment the orthanilic acid was isolated as follows. The aqueous solution was evaporated to dryness *in vacuo*, the resulting dark sticky solid was rubbed well with absolute ethanol (20 ml) and the mixture was filtered giving a brown solid (3.08 g). (The filtrate, after removal of the solvent, gave a dark tar which was not investigated further.) The brown solid was dissolved in water (40 ml) and passed through a column of AG 50W-X8 cation exchange resin, hydrogen form, (Bio. Rad. Laboratories, Richmond, Calif.) (30 ml) which had been previously washed with water, dilute hydrochloric acid, and then water. The column was developed with water and 10 ml fractions were collected. Fractions 2, 3, and 4 showed λ_{max} 238 and 295 mμ and were combined and taken to dryness, giving a brown solid (740 mg). A portion of this solid was dissolved in water and treated three times with charcoal. The solvent was removed leaving a pale yellow solid which crystallized from a small volume of water giving orthanilic acid m.p. > 300° (lit. (35*b*) decomposition 325°), i.r. spectrum identical to that of an authentic sample.

Anal. Calcd. for $C_6H_7NO_3S$: C, 41.62; H, 4.08; N, 8.09; S, 18.55. Found: C, 41.47; H, 4.06; N, 7.79; S, 18.52.

Reactions of 2-Methylsulfonylnitrobenzene in Sodium Hydroxide Solution

A mixture of 2-methylsulfonylnitrobenzene (5 g) and 0.1 *N* sodium hydroxide (550 ml, 2.2 molar equ.) was

heated under reflux 7 h. Ammonia was detected within 15 min of the start of the reaction and was still being evolved at the end when the solution was deep red. The reaction mixture was worked up as described for the reaction of **5** in sodium hydroxide to give: (*a*) A sticky yellow solid (768 mg) which was crystallized from 25% aqueous ethanol, giving starting material **7** (475 mg), m.p. 104–106°. The mother liquors from the crystallization were taken to dryness giving a pale yellow solid (215 mg), shown by u.v. and i.r. spectra to be 2-methylsulfonylaniline (**6**), containing ca. 10% of **7**. Thus the recovery of **7** was ca. 10% and the yield of **6** (allowing for recovered **7**) ca. 5%; (*b*) 2-nitrophenol (680 mg, 22%) m.p. and mixed m.p. 45–46°; and (*c*), the biphenyl **12**, (275 mg, 8%), m.p. 213–215°, after crystallization from ethanol–acetone. The aqueous solution remaining, after treatment as before with charcoal, was estimated by u.v. spectroscopy to contain 500 mg of orthanilic acid (13%).

One attempt was made to purify the methanol-soluble part of the fraction from which **12** was isolated. The mixture (a red oil, 370 mg) was chromatographed in chloroform on alumina (acid 2). The major orange band passed rapidly through the column and was collected in 3 fractions which were combined (230 mg, fraction A), λ_{max} 278 and 320 mμ. Following the major band, 2 fractions were obtained (total 46 mg), which showed λ_{max} 285 mμ; λ_{max} (EtOH + 1 drop NaOH solution) 245 and 318 mμ; ν_{max} ($CHCl_3$) 3340 (OH or NH), 1315 and 1295, 1130 and 1120, and 955 cm^{-1} (SO_2Me). These spectral data are identical with those of **14**. Fraction A was rechromatographed on alumina (acid 2) in benzene. From the appearance of the column and the spectroscopic properties of the various fractions collected, it was clear that fraction A was a mixture of several compounds, and no pure compound was isolated. Most fractions contained SO_2Me (i.r.), and some also showed the presence of NH_2, OH, and possibly NO_2 and may have been (an) isomer(s) of **12**.

Reactions of 4-Methylsulfonylnitrobenzene in Sodium Hydroxide Solution

A mixture of 4-methylsulfonylnitrobenzene (2.0 g) and 0.1 *N* sodium hydroxide (220 ml, 2.2 molar equ.) was heated under reflux 6½ h and then left overnight. The solid which had separated was filtered off and washed with water giving starting material (**15**) (359 mg) m.p. 141–142°. A further quantity (101 mg) of rather less pure **15** was obtained from the alkaline reaction mixture by extraction with ether. The reaction mixture was then acidified and extracted with ether to give an orange solid (977 mg) whose spectral properties closely resembled those of 4-nitrophenol, but which did not melt sharply. The material was therefore chromatographed on alumina (Acid 3) in acetone–hexane (1:3) and the main yellow band was collected giving 4-nitrophenol (764 mg, 72% allowing for recovered **15**), m.p. and mixed m.p. 109–111°, (lit. (35*a*) m.p. 114°). The remaining aqueous solution showed only weak absorption in the u.v. and was not investigated further.

*Preparation of **12***

The experiments summarized in Table 1 were carried out as follows. A mixture of the appropriate quantities of **7**, **19**, 0.1 *N* sodium hydroxide, and ethanol (3 ml) was heated under reflux 15 min. The deep red solution was cooled, diluted with sodium hydroxide solution, filtered, and washed with chloroform. The solution was then acidified and extracted with ether giving a mixture of red solid and oil, which was treated with a little methanol and filtered, giving **12** as a red solid, m.p. in the range 206–212°. The i.r. spectra of the various crude samples of **12** were virtually the same as the spectrum of the pure compound.

We are particularly grateful to Dr. M. A. Weinberger for recording and interpreting the nuclear magnetic resonance spectrum of the biphenyl. We would also like to thank Professor R. T. Coutts for useful discussions, and Dr. R. M. Heggie for his interest and wise counsel throughout the course of this work.

1. D. Bickerton, R. T. Coutts, and W. J. Johnson. Proc. Can. Fed. Biol. Soc. **8**, 44 (1965).
2. K. B. Shaw, R. M. Heggie, and R. K. Miller. Can. J. Chem. This issue.
3. M. Claasz. Ber. **45**, 747 (1912).
4. R. N. Prasad and K. Tietje. Can. J. Chem. **44**, 1247 (1966).
5. A. Ricci and M. Negri. Ann. Chim. (Rome), **50**, 1066 (1961).
6. T. Neilson, H. C. S. Wood, and A. G. Wylie. J. Chem. Soc. 371 (1962).
7. M. P. Cava and C. E. Blake. J. Amer. Chem. Soc. **78**, 5444 (1956).
8. M. Claasz. Ber. **45**, 1015 (1912).
9. J. Bolssens, J. A. C. Th. Brouwers, J. H. Choufoer, A. Kats, P. E. Verkade, and B. M. Wepster. Rec. Trav. Chim. **73**, 819 (1954).
10. K. Schimmelschmidt and H. Thomae. U.S. Patent No. 1 939 416. December 12, 1933.
11. R. T. Coutts and E. M. Smith. Can. J. Chem. **45**, 975 (1967).
12. K. Nakanishi. Infrared absorption spectroscopy. Holden–Day, Inc., San Francisco, 1962. (*a*) p. 167; (*b*) p. 54; (*c*) p. 51; (*d*) p. 24.
13. Organic electronic spectral data. Vol. 2. *Edited by* H. E. Ungrade. Interscience Publishers, Inc., New York, 1960. p. 67.
14. L. F. Fieser and M. Fieser. Advanced organic chemistry. Rheinhold Publishing Corp., New York, 1961. p. 678.
15. G. B. Barlin and W. V. Brown. J. Chem. Soc. *C*, 2473 (1967) and references therein.
16. H. R. Todd and R. L. Shriner. J. Amer. Chem. Soc. **56**, 1382 (1934).
17. V. Gold and C. H. Rochester. J. Chem. Soc. 1710 (1964).
18. J. D. Loudon and G. Tennant. Quart. Rev. London, **18**, 389 (1964).
19. A. P. Martinez, W. A. Skinner, W. W. Lee, L. Goodman, and B. R. Baker. J. Org. Chem. **26**, 860 (1961).
20. J. R. Cox, Jr. and M. F. Dunn. Tetrahedron Lett. **15**, 985 (1963).
21. J. F. Bunnett and J. J. Randall. J. Amer. Chem. Soc. **80**, 6020 (1958).
22. N. Sheppard. Trans. Faraday Soc. **51**, 1465 (1955).
23. T. Momose, Y. Ueda, and T. Shoji. Chem. Pharm. Bull. Tokyo, **7**, 734 (1959). Chem. Abstr. **54**, 14948 (1960).

Can. J. Chem. Downloaded from www.nrcresearchpress.com by 210.87.254.105 on 09/05/12
For personal use only.

24. G. M. BADGER, D. J. CLARK, W. DAVIES, K. T. H. FARRER, and N. P. KEFFORD. J. Chem. Soc. 2624 (1957).
25. R. T. COUTTS, H. W. PEEL, and E. M. SMITH. Can. J. Chem. **43**, 3221 (1965).
26. W. J. KENNEY, J. A. WALSH, and D. A. DAVENPORT. J. Amer. Chem. Soc. **83**, 4019 (1961).
27. R. T. COUTTS and D. G. WIBBERLEY. J. Chem. Soc. 4610 (1963).
28. R. T. COUTTS, D. L. BARTON, and E. M. SMITH. Can. J. Chem. **44**, 1733 (1966).
29. P. BRAND. Ber. **42**, 3466 (1909).
30. M. E. HEPPENSTALL and S. SMILES. J. Chem. Soc. 899 (1938).
31. E. A. FEHNEL and M. CARMACK. J. Amer. Chem. Soc. **72**, 1292 (1950).
32. O. BEHAGHEL. J. Prakt. Chem. **114**, 287 (1926).
33. A. V. SUNTHANKAR, B. D. TILAK, and K. VENKATARAMAN. Proc. Indian Acad. Sci. **38A**, 23 (1953).
34. P. OXLEY, M. W. PARTRIDGE, T. D. ROBSON, and W. F. SHORT. J. Chem. Soc. 763 (1946).
35. A. I. VOGEL. A text-book of practical organic chemistry. Longmans, Green and Co., Toronto. 1951. (*a*) p. 656; (*b*) p. 565.

Can. J. Chem. Downloaded from www.nrcresearchpress.com by 210.87.254.105 on 09/05/12
For personal use only.

Can. J. Chem. Downloaded from www.nrcresearchpress.com by 210.87.254.6 on 09/05/12
For personal use only.

Reactions of *N*-(2- and 4-methylsulfonylphenyl)hydroxylamines and 2-methylsulfonylnitrosobenzene in dilute aqueous sodium hydroxide solution[1]

K. B. SHAW, R. M. HEGGIE, AND R. K. MILLER
Defence Research Establishment Ottawa, Defence Research Board, Ottawa 4, Ontario

Received November 6, 1969

When *N*-(2-methylsulfonylphenyl)hydroxylamine (**4**) was treated with dilute sodium hydroxide solution the major product was always 2,2′-di(methylsulfonyl)azoxybenzene (**5**). At room temperature other significant products were 2-hydroxy-2′-methylsulfonylazoxybenzene (**6***a*) and 2-methylsulfonylnitrobenzene (**2**), while **6***a* was also formed at reflux together with small amounts of 2-hydroxy-2′-methylsulfonylazobenzene (**8**), 2-methylsulfonylaniline (**7**), 3-methylsulfonyl-3′-nitro-4-amino-4′-hydroxybiphenyl (**3**), and **2**. The compounds **5**, **6***a*, and **7** were also obtained when 2-methylsulfonylnitrosobenzene (**9**) was boiled with alkali. The decomposition of *N*-(4-methylsulfonylphenyl)hydroxylamine (**16**) in dilute alkali at room temperature gave a quantitative yield of 4,4′-di(methylsulfonyl)azoxybenzene (**17**) and at reflux, mixtures of **17** and 4,4′-di(methylsulfonyl)azobenzene (**18**) were obtained. The modes of formation of the various products from the two hydroxylamines are discussed.

Canadian Journal of Chemistry, 48, 1404 (1970)

Introduction

In an earlier paper (1) the reactions of 2-nitrophenylsulfonylacetic acid (**1**) and 2-methylsulfonylnitrobenzene (**2**) in dilute sodium hydroxide solution were described. In connection with the genesis of the most unusual product of these reactions, i.e. 3-methylsulfonyl-3′-nitro-4-amino-4′-hydroxybiphenyl (**3**), the effect of alkali on *N*-(2-methylsulfonylphenyl)hydroxylamine (**4**) was studied. The biphenyl **3** was one of the products obtained when **4** was treated with alkali and as a result of this observation, and some additional work, a mechanism for the formation of **3** was suggested. However the reactions of **4** were not described in detail earlier (1) and are reported here. Although the experiments with the nitrosulfones were carried out at 100° (**1** was unaffected by dilute alkali, and **2** was insoluble in dilute alkali, at room temperature) **4** was soluble in, and decomposed by, cold alkali, and the reactions occurring under these conditions, as well as those at 100°, were studied.

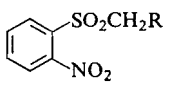

1 R = CO_2H
2 R = H

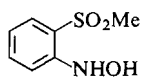

4

Results and Discussion

The decomposition of **4** in 0.1 *N* sodium hydroxide yielded a number of products. Those identified were 2-methylsulfonylnitrobenzene (**2**), the biphenyl (**3**), 2-methylsulfonylaniline (**7**), and three other compounds. The first of these other compounds was shown by elemental analysis and by infrared (i.r.) and nuclear magnetic resonance (n.m.r.) spectra to be 2,2′-di(methylsulfonyl)azoxybenzene (**5**) (2). The i.r. spectrum of the second indicated that it was probably a 1,2-disubstituted benzene containing a hydroxyl group and a methylsulfonyl group, and its color suggested an azoxybenzene. The empirical formula $C_{13}H_{12}N_2O_4S$ was shown by mass spectrometry to be the molecular formula (mol. wt. 292) and thus it was probable that the compound was a 2(2′)-hydroxy-2′(2)-methylsulfonylazoxybenzene i.e. **6***a* or **6***b* (other isomers can be neglected since the starting material was ortho-disubstituted). In a recent paper (3) it was concluded that the position of the *N*-oxide link in unsymmetrically substituted azoxybenzenes can always be determined because base peaks in the mass spectra of such compounds are produced by C—*N* cleavage α to the *N*-oxide group. The base peak in the mass spectrum of **6** was at *m/e* 93 (C_6H_5O) and the peak at *m/e* 155 ($C_6H_4SO_2Me$)

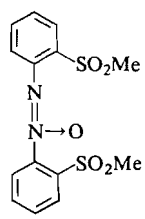

5

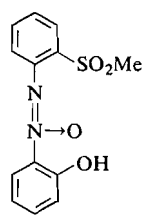

6*a*

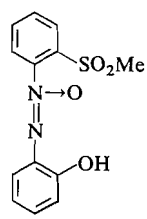

6*b*

[1]Issued as DREO Report No. 617.

TABLE 1

Yields of various products after decomposition of **4** in 0.1 *N* sodium hydroxide

4 (moles)	Reaction time (h)	Reaction temperature	% Yield					
			2	**3**	**5**	**7**	*6a*	**8**
0.0029	6.5	Room	20	<1	41	—	25	—
0.0029	6.5	100°	—	6	35	Trace	ca. 18	ca. 3.5
0.0029	0.25	100°	Trace	6	48	Trace	ca. 18	ca. 3.5
0.005	6.5	100°	—	3	28	Trace	22	

was very weak suggesting that *6a* was the correct structure. The spectral data on the third compound indicated that it was the azo compound corresponding to **6** and this structure (**8**) was confirmed by synthesis from 2-methylsulfonylnitrosobenzene (**9**) and 2-aminophenol. Some evidence (ultraviolet (u.v.) and i.r.) was obtained for the presence of orthanilic acid (**10**) after the decomposition of **4** at 100°. The yields obtained of these various products under different conditions are summarized in Table 1.

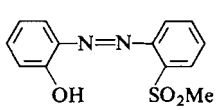

8

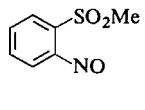

9

It is well known that phenylhydroxylamine (and its homologues) is easily oxidized by air in aqueous solution (*4a*, *5a*). The main product is azoxybenzene, formed by condensation of nitrosobenzene, the first oxidation product, with phenylhydroxylamine, and hydrogen peroxide is also formed. In alkaline solution, azoxybenzene and nitrobenzene but no hydrogen peroxide are obtained; the last compound is used up in the oxidation which leads to the nitro compound (*5a*), although peroxide may also oxidize phenylhydroxylamine to azoxybenzene (6). Thus in the reaction of **4** in alkali in air, the initial transformation product must be **9**; reaction of this intermediate with **4** gives **5** and, at room temperature, further oxidation of **9** gives **2**. At 100° any hydrogen peroxide formed presumably decomposes readily and only a small quantity of **2** was detected after a 15 min reaction time. However, another possible source of **9**, which is potentially important in the reaction under reflux when air has less access to the reaction mixture, is the disproportionation reaction of phenylhydroxylamines (*5a*): 2 RNHOH → RNO + RNH_2 + H_2O. It is possible in the case of **4** that this reaction requires an elevated temperature because the amine **7** was not formed from **4** at room temperature, but even at 100° the yield of **7** was small and unless some was lost by reaction with other compounds in the mixture it seems likely that the disproportionation reaction was not a significant source of **9**. Hence the formation of **2** and **5** was unexceptional but the same cannot be said of *6a*. There appear to be four possible modes of formation of *6a*: (*1*) displacement of a methylsulfonyl group in **5** by hydroxide ion; (*2*) from **9** and 2-hydroxyaminophenol (**11**); (*3*) from **4** and 2-nitrosophenol (**12**), and (*4*) loss of a methylsulfonyl group from a 'bimolecular' precursor of **5**.

The first and most obvious route to *6a* is untenable. The azoxy compound **5** was unaffected by dilute alkali at room temperature and when the suspension was boiled for several hours **5** was recovered (80%), the u.v. spectrum of the aqueous solution, alkaline or acid, differed from that of *6a* in alkali or acid and *6a* was not isolated (the products of this reaction were not identified). In addition when **5** was boiled for 15 min with dilute alkali containing sufficient ethanol or *n*-propanol to ensure that all solid was in solution at the boiling point, **5** was again recovered (80–90%) and *6a* was not isolated. It should also be noted (Table 1) that the main difference between the reaction mixtures obtained when **4** was boiled in alkali for 15 min and 6 h was that, in the latter reaction, the yield of **5** was only about 75% of that obtained in the former, whereas the yield and composition of the mixture of *6a* and **8** were approximately the same in both cases.

The mechanism of formation of azoxybenzenes from a nitrosobenzene and a phenylhydroxylamine in alkali (7) involves a one electron transfer (eq. [1]) and the formation of free radicals (eq. [2]). If the hydroxylamine and the nitroso

Can. J. Chem. Downloaded from www.nrcresearchpress.com by 210.87.254.6 on 09/05/12
For personal use only.

Can. J. Chem. Downloaded from www.nrcresearchpress.com by 210.87.254.6 on 09/05/12
For personal use only.

[1] $RNHOH + 2\,OH^- \rightleftharpoons (RNO)^{2-} + 2\,H_2O$

[2] $(RNO)^{2-} + RNO \rightleftharpoons 2\,(RNO\cdot)^-$

compound are differently substituted (e.g. **11** and **9**), two different anion-radicals are produced (eq. [2]). The same pair is also produced if the substituents in the reactants are transposed (e.g. as in **4** and **12**) and thus it might seem that routes *2* and *3* to **6***a* are indistinguishable. This is of course true in the later stages of the formation of **6***a*, but initially, two different pairs of reactants must be involved and the real problem is whether **11** or **12** is formed. There appeared to be two possible pathways to **11** and **12** from **4** or **9** and these are depicted in Scheme 1. It was realized however that since both **4** and **9** were present in the reaction mixture it would not be possible to differentiate between routes *2* and *3*, or between the various pathways to **11** and **12**, in the absence of additional experimental results.

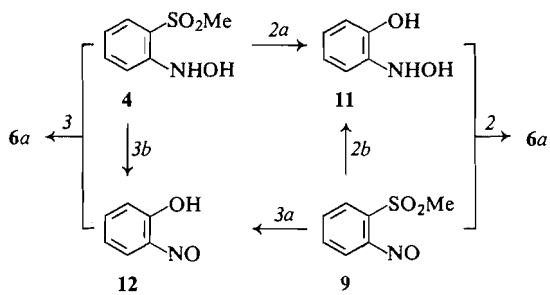

SCHEME 1

Reaction *2a* (Scheme 1) was thought to be feasible through an intramolecular general base-catalyzed mechanism. However, when nitrogen was passed through a solution of **4** in dilute alkali for several hours and the solution then acidified, **4** was recovered (ca. 85%) and the u.v. spectrum of the aqueous solution was the same as that of **4**. Thus reaction *2a* was improbable.

The formation of **12** directly from **4** (reaction *3b*, Scheme 1) would involve a simultaneous oxidation and hydrolysis, and although a precise mechanism for such a reaction was difficult to formulate it could not be ruled out. Thus it was relevant to know what happened when **4** was treated with alkali at 100° in the absence of oxygen when an alternative means of formation of **9**, i.e. by disproportionation of **4** was available. Unfortunately this reaction was unexpectedly complex. The major product was again **5** (ca. 20%) although this time it did not separate from solution during the reaction and it was more deeply colored than all previous samples. The extract which in earlier experiments had contained only **6***a* and **8** was a mixture of several compounds from which **6***a* and **8** were isolated in small yield by chromatography. Several other colored fractions had u.v. spectra which had not been encountered before in this or earlier (1) work. One fraction was tentatively identified (i.r., u.v., and mass spectra) as 2′-methylsulfonylazoxybenzene (**13**) and there was spectroscopic evidence that azoxybenzene was also formed during the reaction. The mode of formation of

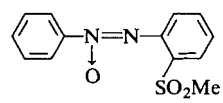

13

these compounds in which a methylsulfonyl group has apparently been replaced by a hydrogen atom posed additional problems (see below). A likely reason for the lower yield of **5** in the present reaction compared with the corresponding one in air is that **9** is formed less readily by disproportionation than by aerial oxidation. As a result, more of **4** would be lost by other modes of decomposition (cf. the many unidentified transformation products). The formation of **6***a* under conditions where oxidation is excluded implies that reaction *3b* is not followed. However the yield of **6***a* was low and thus the result was not conclusive (although **6***a* was difficult to isolate and may have been formed in higher yield) and it was felt that an examination of the behavior of **9** in dilute alkali might be rewarding.

The oxidation of phenylhydroxylamine to nitrosobenzene by chromic acid is carried out at 0° (8) but **4** was too insoluble in dilute sulfuric acid at this temperature and the oxidation to **9** was carried out at about 25°. When **9** was heated under reflux with dilute alkali for several hours the products identified were **5** (34%), **7** (ca. 6%), and **6***a* (ca. 20%) containing only a trace of **8**. No biphenyl (**3**), nitro compound (**2**), or orthanilic acid (**10**) was isolated but there was spectroscopic evidence that **10** was formed (ca. 6%). When the reaction was repeated under nitrogen a similar mixture of products was obtained in comparable yield although **8** was not detected in the fraction containing **6***a*.

Nitroso compounds are dimeric in the solid

Can. J. Chem. Downloaded from www.nrcresearchpress.com by 210.87.254.6 on 09/05/12
For personal use only.

state and although reversion to the monomer usually occurs on dissolution, some compounds, particularly those with ortho-substituents, can exist as dimers in solution (*5b*). A chloroform solution of **9** was deep green demonstrating that a considerable part of it was monomeric in this solvent. When **9** was boiled with water the liquid was pale green but in dilute alkali at 100° no green color was detected, indicating either that **9** dissolved as the dimer or that, more probably, the monomer was converted into other compounds as it was formed. The dimeric form of **9** (**14**) is analogous to **5** which, as noted earlier, is rather insoluble in boiling dilute alkali and there is no reason to expect that **14** would be any

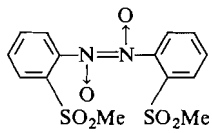

14

more soluble. In addition, the extent of dissociation to monomer increases with temperature (*9*) and at 100° would be very high. Thus it seems more reasonable to interpret the reactions of 2-methylsulfonylnitrosobenzene on the basis of the monomeric structure **9**.

Clearly, at 100° in dilute alkali, **9** is readily reduced to **4** (cf. the formation of **5**) although the mechanism of this reduction is obscure. Nitrosobenzene is reduced to phenylhydroxylamine, or its anion, by alcohol and a base and the mechanism of this reduction has been established (*10*), but alcohol was absent in the present reactions. When **9** was boiled in water alone **5** was not produced (**9** was recovered (> 90%)), and when **9** was stirred in dilute alkali for 14 days at room temperature, ca. 50% of it was recovered and the only other identifiable product was **2**. There was no evidence that **5** or **6***a* was formed, and thus it appeared that the reduction of **9** to **4** requires alkali and an elevated temperature. The reduction should not be affected by an inert atmosphere, and this was apparently the case, but even more important, in contrast to reaction *3b*, reactions *3a* and *2b*, Scheme 1, should not be affected either, and as noted, the yield of **6***a* was, within experimental error, the same in air or under nitrogen. This is good evidence that **9** is the precursor of **11** or **12**. The formation of **11** from **9** (reaction *2b*) would involve two steps and a mechanism for this reaction is difficult to visualize and thus the formation of **12** from **9** (*3a*) seems most likely. In view of the formation of **6***a* when **4** was treated with dilute alkali at room temperature, the reaction **9** → **12** must be facile and it might be expected in the reaction of **9** with alkali, in which **4** was formed, that the yield of **6***a* would be higher than actually observed. However, the relative ease of the numerous reactions which occur when **9** (or **4**) is treated with alkali is unknown and the insolubility of **9** in dilute alkali at room temperature, together with the apparent ease of the reaction **9** → **4** at 100°, prevented any assessment of the facility of the reaction **9** → **12**.

It has been noted already that **9** is unaffected by boiling water, and when a mixture of **9** and **4** was refluxed in water, **5** was obtained (82%) and **6***a* was not isolated. Thus hydroxide ion has a role in the formation of **6***a* that involves more than the catalysis of the reaction between a nitrosobenzene and a phenylhydroxylamine and clearly such a role could be in the conversion of **9** into **12**. The precise mechanism of this reaction is not known, but methylsulfonyl is a good leaving group (*11*) and it is likely that the reaction involves nucleophilic attack by hydroxide ion on the carbon atom bearing the methylsulfonyl group in **9**. Good evidence that the methylsulfonyl group in **9** can be displaced by a nucleophile was obtained when benzofurazan (**15**), identified by u.v. (*12*) and n.m.r. spectra (*13*) was isolated in small yield after treatment of **9** with sodium azide in water at 100° (cf. (*14*)). This reaction clearly

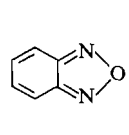

15

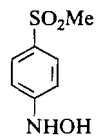

16

involved attack by azide ion on **9** to give 2-azidonitrosobenzene, which then cyclized with loss of nitrogen to give **15**; however the reaction was not investigated in detail and the optimum conditions for the formation of **15** were not established.

In order to determine to what extent ortho effects were important in the reactions of **4** and **9**, the effect of alkali on *N*-(4-methylsulfonylphenyl)hydroxylamine (**16**) was studied. When a solution of **16** in 0.1 *N* sodium hydroxide was stirred at room temperature for several hours,

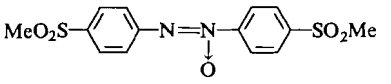

17

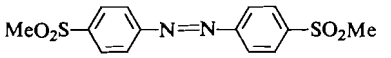

18

the solution became pale yellow and a solid gradually separated. This solid was identified as 4,4′-di(methylsulfonyl)azoxybenzene (**17**) (15) (96%) and no other compound was isolated. When **16** was treated with alkali at 100°, mixtures of **17** and 4,4′-di(methylsulfonyl)azobenzene (**18**) were obtained in high yield (80–90%) together with traces of 4-methylsulfonylaniline (**19**) (16), but, as in the experiment at room temperature, compounds analogous to **6***a* and **8** were not isolated. The constitutions of the mixtures of **17** and **18** depended somewhat on the experimental conditions, and were estimated by u.v. spectroscopy. Thus, when a cold solution of **16** in dilute alkali was heated to 100° and then boiled for 15 min, the solid obtained, after removal of a small amount of ethanol-soluble material, was a mixture of **18** and **17** in the approximate ratio 3:1. On the other hand, when **16** was added to dilute alkali at > 90° and the solution then boiled for 15 min the ratio of **18** to **17** in the solid obtained was about 5:1. In all experiments the ethanol-soluble solid had spectroscopic properties very similar to those of the mixture of **17** and **18**, but it melted considerably lower and was not identified. Similar mixtures to those just described were obtained when the respective experiments were carried out under nitrogen but the combined yield of **17** and **18** was slightly lower (ca. 75%). The formation of **18** is considered below but 4-methylsulfonylnitrosobenzene (**20**) must be an intermediate in the formation of **17**. Since 4-nitrosophenol was apparently not formed from **20** the inference is that an ortho effect was operating in the formation of **12** from **9**. However the evidence is inconclusive because condensation reactions (e.g. azoxybenzene formation) probably proceed so readily in the para series owing to the absence of steric hindrance, that other reactions e.g. displacement of a methylsulfonyl group (or oxidation of **20** to 4-methylsulfonylnitrobenzene (**21**)) cannot occur to any significant extent.

Two further points which merit comment are that the azoxybenzene (**6***a*) was apparently not contaminated with its isomer **6***b* and that 2,2′-di(hydroxy)azoxybenzene (**22**) was not isolated after treatment of **4** or **9** with alkali. The mechanism of azoxybenzene formation (7) mentioned above readily explains why condensations between a nitrosobenzene and a differently substituted phenylhydroxylamine usually yield mixtures of azoxybenzenes (e.g. (17)), since each anion-radical can react with itself as well as with the other. However the yields of the various possible products probably depend on several factors, particularly the nature of the reactants (cf. (18)) and their relative concentrations. Thus the apparent absence of one possible product, e.g. **22**, is not surprising, and indeed **22** may have been formed when **4** or **9** was treated with alkali, although at room temperature especially, it could only have been formed in very small yield. The combination of the anion-radicals referred to above gives the intermediate (**23**) which then loses hydroxide ion after protonation of one of the oxygen atoms. If $R_1 \neq R_2$, two azoxybenzenes should result. However in the intermediate (**24**) from **9** and **12**, hydrogen-bonding between one oxygen atom and the hydroxyl group favors

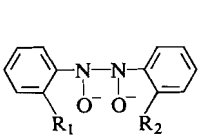

23

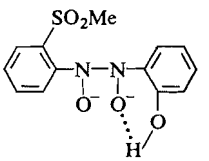

24

elimination of the other oxygen atom. The presence of hydrogen-bonding in **6***a* was indicated by the appearance of the hydroxyl absorption in its i.r. spectrum and by the fact that it was extracted with chloroform from the alkaline solution in which it was formed.

The fourth possible mode of formation of **6***a* considered at the beginning of the discussion was the loss of a methylsulfonyl group from a bimolecular precursor of **5**; the only such precursors are **23**, $R_1 = R_2 = SO_2Me$ and its protonated form. This possibility is difficult to prove or disprove and is probably not excluded by the experimental results. A mechanism for such a reaction, especially one which was inapplicable in the para case, is difficult to envisage (e.g. a reaction in which **23**, $R_1 = R_2 = SO_2Me$,

Can. J. Chem. Downloaded from www.nrcresearchpress.com by 210.87.254.6 on 09/05/12
For personal use only.

Can. J. Chem. Downloaded from www.nrcresearchpress.com by 210.87.254.6 on 09/05/12
For personal use only.

functions as a general base is excluded since **6***a* was not formed from **4** and **9** in water) and although this reaction route to **6***a* cannot be rejected, it does seem improbable.

The mode of formation of the azo compounds **8** and **18** will now be considered. The known (5*a*) disproportionation reaction of phenylhydroxylamines to nitrosobenzenes and anilines, with subsequent condensation of these products to azobenzenes would appear to be a feasible route for the formation of **18**. Although unsymmetrical azo compounds are usually prepared from a nitrosobenzene and an aniline in acetic acid (4*b*), the reaction between nitrosobenzene and aniline apparently does proceed in alkali [quote in ref. (7)]. In view of the high yields of **18** obtained when the hydroxylamine (**16**) was boiled in alkali azobenzene formation appears to be a more facile reaction than azoxybenzene formation. However this may be only a reflection of the ease with which **16** disproportionates (cf. the similar mixtures of **17** and **18** obtained in air or under nitrogen). The yield of **17** in the reaction in which **16** was heated from room temperature to reflux was higher than in the reaction carried out from ca. 90° to reflux because **17** was formed from the nitroso compound (**20**), produced by aerial oxidation of **16**, before the temperature was reached at which disproportionation (and hence formation of **18**) became significant.

A similar explanation cannot be accepted a priori for the formation of the hydroxyazobenzene (**8**) which was formed in small yield when the hydroxylamine (**4**) was treated with alkali at 100° but not at room temperature. The reaction between a nitroso compound and an aniline is inhibited by bulky groups in the ortho positions of the reactants, and the amine (**7**) and the nitroso compound (**9**) did not yield 2,2′-di(methylsulfonyl)azobenzene under optimum conditions, i.e. in glacial acetic acid. In addition, when **7** and a molar equivalent of **9** [a precursor of 2-nitrosophenol (12)] were boiled in dilute alkali very little, if any, **8** was formed. These results contraindicated condensation of a nitrosophenol with an aniline as the mechanism of formation of **8** although it should be noted that **8** was formed by condensation of **9** and 2-aminophenol (**25**) in acetic acid. An alternative route for the formation of **8** is the reduction of the azoxybenzene (**6***a*). The possibility was considered that the hydroxylamine acted as the reducing agent and was itself oxidized to the nitroso compound. However, the hydroxylamine (**16**) did not reduce azoxybenzene itself (**26**). When **16** was boiled in alkali in the presence of a molar equivalent of **26**, the mixture of **17** and **18** produced was the same as that in the absence of **26**; **26** was recovered in high yield and no azobenzene was detected. This result does not completely exclude reduction of **6***a* as a source of **8**. The reduction may be facilitated by the presence of the hydroxy function in the ortho position or may be due to a reducing agent formed by unknown decomposition pathways of the hydroxylamine (**4**). It is probably significant that **8** was virtually absent after the treatment of **9** with alkali at 100° when **4** was not present in excess.

2-Methylsulfonylazoxybenzene (**13**) and azoxybenzene (**26**) were the only compounds isolated during the work described in this, or the earlier report (1) in which a methylsulfonyl group had apparently been replaced by a hydrogen atom. However, **26**, azobenzene (**27**), and 2-methylsulfonylazobenzene (**28**) (19) were obtained in small yield after treatment of 3,4-dihydro-4-hydroxy - 3 - oxo - 2*H* - 1,4 - benzothiazine - 1,1-dioxide (**29**) (cf. (1)) with alkali[2] but their modes of formation were not elucidated, although it was concluded that they were products of the action of sodium hydroxide on **29** and, for example, had not been formed from impurities, e.g. nitrobenzene or phenylhydroxylamine, in the hydroxamic acid. It seems inconceivable in experiments carried out in alkaline solution that a substituent, e.g. a methylsulfonyl group, on an aromatic ring, could be displaced, and replaced by a hydrogen atom, and a seemingly more reasonable route to compounds such as **13**, **26**, **27**, and **28** in the above reactions, was that an intermediate sulfinic acid lost sulfur dioxide in a reaction analogous to the decarboxylation of a carboxylic acid. Although the desulfination of sulfinic acids is a known reaction (20) it does not appear to have been carried out in alkaline solution, and indeed 2-aminobenzenesulfinic acid and azobenzene-2-sulfinic acid are stable in refluxing ethanolic sodium hydroxide solution (19, 21). However, the formation of sulfinic acids themselves in the above reactions poses problems, and hence the modes of formation of **13** and **26**,

[2]K. B. Shaw and R. K. Miller. Unpublished work.

Can. J. Chem. Downloaded from www.nrcresearchpress.com by 210.87.254.6 on 09/05/12
For personal use only.

and **26**, **27**, and **28** in the respective reactions remain a mystery.

Summary

In dilute sodium hydroxide solution, *N*-(2-methylsulfonylphenyl)hydroxylamine (**4**) is readily oxidized by air to 2-methylsulfonylnitrosobenzene (**9**) and at room temperature the hydrogen peroxide produced in this reaction converts **9** into 2-methylsulfonylnitrobenzene (**2**). In addition, **9** is also produced, together with 2-methylsulfonylaniline (**7**) by the disproportionation of **4** at 100°. The hydroxylamine **4** reacts with **2** to give the biphenyl (**3**)(1), and with **9** to give 2,2′-di(methylsulfonyl)azoxybenzene (**5**). The displacement of the methylsulfonyl group in **9** by hydroxide ion gives 2-nitrosophenol (**12**) which reacts with **4** to give 2-hydroxy-2′-methylsulfonylazoxybenzene (**6***a*). The corresponding hydroxy azo compound (**8**) is also formed, perhaps by reduction of **6***a*, but the reaction of **7** and **9** to give 2,2′-di(methylsulfonyl)azobenzene is not observed (steric hindrance). At 100° in dilute alkali **9** is readily reduced to **4**, and then **5** and **6***a* are formed as before.

N - (4 - Methylsulfonylphenyl)hydroxylamine (**16**) in dilute alkali is readily oxidized by air to 4-methylsulfonylnitrosobenzene (**20**), which is also formed, together with 4-methylsulfonylaniline (**19**), by the facile disproportionation of **16** at 100°. The nitroso compound **20** reacts with **16** to give 4,4′-di(methylsulfonyl)azoxybenzene (**17**), and with **19** to give 4,4′-di(methylsulfonyl)-azobenzene (**18**); neither the oxidation of **20** to 4-methylsulfonylnitrobenzene (**21**), nor the loss of the methylsulfonyl group from **20**, with the subsequent formation of a compound analogous to **6***a*, is observed.

Experimental

Infrared spectra are for potassium bromide disks. Microanalyses were performed by J. G. Helie and the mass spectra were by Morgan–Schaffer Corporation, Montreal.

Reactions of N-(2-Methylsulfonylphenyl)hydroxylamine (4) in Aqueous Sodium Hydroxide Solution

The preparation of **4** has been described (1). The experiments were carried out as indicated below and the reaction mixtures were worked up as follows. The solid was filtered off (fraction A) and the solution was washed once with ether (fraction B), and then several times with chloroform (fraction C). The aqueous solution was acidified with hydrochloric acid and again washed with ether (fraction D). Each experiment was carried out more than once and after pure **6***a* and **8** had been obtained, the constitutions of some of the mixtures of **6***a* and **8**, and the purity of **6***a* obtained in the reaction at room temperature, were estimated from the intensity of the peak at 330 mμ in the u.v. (**6***a* and **8** had E_1^1 308 and 612 respectively at 330 mμ). Thin-layer chromatography (t.l.c.) of the mixtures of **6***a* and **8** was carried out on activated (220–230° for 3 h) Gelman Type A absorbent (alumina gel and micro glass fibers) with the solvent system chloroform–hexane (2:1). Spots were detected with *N* sodium hydroxide.

(*a*) A solution of **4** (540 mg) in 0.1 *N* sodium hydroxide (60 ml; 2.1 molar equ.) was stirred at room temperature for 6 h. Fraction A (269 mg, m.p. ca. 180–210°) was washed well with ether and the solid was filtered off giving 2,2′-di(methylsulfonyl)azoxybenzene (**5**) (202 mg, 40%), m.p. 229–231°, which crystallized from ethanol containing a little acetone, as very pale yellow prisms, m.p. 232–233° (lit. (2) m.p. 222°); λ_{max} (EtOH) 307 mμ (log ε 4.02); ν_{max} 1310, 1150 and 1120, and 950 cm^{-1} (SO_2Me); n.m.r. (60 MHz) (DMSO-d_6) 500–450 Hz, max at 480 Hz from TMS (intensity 8H), τ 6.73 and 6.57 (each intensity 3H).

Anal. Calcd. for $C_{14}H_{14}N_2O_5S_2$: C, 47.44; H, 3.98; N, 7.91; S, 18.09. Found: C, 47.38; H, 4.10; N, 7.74; S, 17.91.

The ether-soluble portion of fraction A (59 mg, m.p. 101–104°) and fraction B (60 mg, m.p. 99–103°) were slightly impure **2** (ca. 20%). Fraction C (113 mg) was a yellow solid, m.p. 106–109°, estimated to be > 95% **6***a* (26%), but **8** was absent. It was crystallized three times from ethanol giving 2-hydroxy-2′-methylsulfonylazoxybenzene (**6***a*) as yellow needles, m.p. 111–112°; λ_{max} (EtOH) 243, 282, and 330 mμ (broad) (log ε 3.91, 3.85, and 3.95); (EtOH + 1 drop NaOH solution) 234 and 288 mμ (log ε 4.32 and 3.90); ν_{max} ca. 3200–3100 (weak, bonded OH), 1295, 1165, and 970 (SO_2Me), and 750 cm^{-1} (1,2-disubstituted benzene).

Anal. Calcd. for $C_{13}H_{12}N_2O_4S$ (mol. wt. 292): C, 53.42; H, 4.14; N, 9.59; S, 10.97. Found (292 (mass spectrum)): C, 53.64; H, 4.36; N, 9.79; S, 11.23.

Fraction D (35 mg) was treated with a few drops of methanol and filtered giving the biphenyl **3** (3.5 mg, 0.8%), m.p. 209–211°, i.r. spectrum identical with that of an earlier sample (1).

(*b*) A stirred solution of **4** (540 mg) in 0.1 *N* sodium hydroxide was heated under reflux 6 h. Fraction A was **5** (180 mg, 35%), m.p. 230–232° and was not contaminated with **2**. Fraction B was a pale yellow oil (15 mg) containing some 7. Fraction C was an orange solid (94 mg), m.p. ca. 106–108°, which was a mixture of **6***a* and **8** (ca. 22%) in the approximate ratio 5:1. The solid, after crystallization to constant m.p., 110–112°, was **6***a* containing a trace of **8** (elemental analysis and t.l.c.). Fraction D was a sticky red solid (97 mg), which after treatment with methanol as before gave **3** (26 mg, 6%), m.p. 207–212°, raised to 211–214° after crystallization from ethanol. The methanol-soluble material (70 mg) was a mixture of several compounds, none of which was identified.

(*c*) A stirred solution of **4** (540 mg) in 0.1 *N* sodium hydroxide was heated under reflux 15 min. Fraction A (261 mg, m.p. 227–230° with previous softening) was

Can. J. Chem. Downloaded from www.nrcresearchpress.com by 210.87.254.6 on 09/05/12
For personal use only.

washed with ether giving **5** (247 mg, 48%), m.p. 231–233°. Fraction B (27 mg) was an orange oil containing **2** and **7**. Fraction C (84 mg), m.p. 102–107°, was a mixture of **6***a* and **8** similar to that obtained under (*b*). Fraction D (93 mg) after treatment with methanol as before gave **3** (22 mg, 5%), m.p. 209–212°.

(*d*) A stirred solution of **4** (935 mg) in 0.1 *N* sodium hydroxide (105 ml) was heated under reflux 6 h. Fraction A was washed with ethanol giving **5** (253 mg, 28%) m.p. 231–233°. Fraction B (52 mg) was an orange oil containing **6***a*, **7**, and **8**. Fraction C was an orange solid (154 mg) m.p. ca. 125–130°, and was chromatographed on alumina (Neutral 2) in chloroform–hexane (4:1). A fast moving red band which was closely followed by, and not cleanly separated from, a light orange band, was collected giving an orange solid (93 mg) m.p. ca. 142–148°, which was a mixture of **8** and **6***a* in the approximate ratio 4:1. The column was extruded and a broad yellow band was washed off the alumina with 10% acetic acid in methanol. The resulting solid, in chloroform–hexane (1:2), was chromatographed on alumina (acid 3) and the main yellow band was collected, giving a yellow solid (29 mg) m.p. 110–111°, which was a mixture of **6***a* and **8** in the approximate ratio 13:1. The solid was crystallized from methanol but its melting point and constitution were not changed. The main fraction above was rechromatographed on alumina (Neutral 2) but the various fractions were still mixtures of **8** and **6***a*. The solid from the combined fractions was crystallized three times from methanol giving 2-hydroxy-2′-methylsulfonylazobenzene (**8**) as small orange needles, m.p. 149.5–150°; λ_{max} (EtOH) 246, 330, and 388 mμ (log ε 3.99, 4.23, and 3.92); (EtOH + 1 drop NaOH solution) 236 and 335 mμ (log ε 4.17 and 4.03); ν_{max} 1290, 1140, and 950 (SO_2Me), 760 cm^{-1} (1,2-disubstituted benzene).

Anal. Calcd. for $C_{13}H_{12}N_2O_3S$ (mol. wt. 276): C, 56.51; H, 4.38; N, 10.14; S, 11.60. Found (276 (mass spectrum)): C, 56.52; H, 4.50; N, 9.99; S, 11.86.

Fraction D (143 mg) after treatment with methanol as before gave **3** (25 mg, ca. 3%), m.p. 211–213° after crystallization from ethanol–acetone. The remaining aqueous solution was decolorized (charcoal) and evaporated to dryness and the residue (in water) was passed through a column of AG 50W-X8 cation exchange resin (15 ml). The first three fractions collected (30 ml) had similar u.v. spectra and were evaporated giving a sticky solid (108 mg). The u.v. and i.r. spectra of this material were very similar to those of orthanilic acid (cf. (1)).

(*e*) Reaction (*b*) above was repeated under nitrogen. A yellow material (ca. 15 mg) in the condenser was washed out with ethanol and appeared (u.v. and i.r.) to be azoxybenzene. Virtually no solid separated from the aqueous solution hence there was no fraction A. Fraction B (30 mg) contained some **7**. Fraction C was a sticky red solid (367 mg) which was rubbed well with ether and filtered giving a yellow solid (117 mg) m.p. 216–226°, with an i.r. spectrum very similar to that of **5**. The solid was crystallized twice from ethanol containing a little acetone giving golden yellow prisms, m.p. 230–232°, mixed m.p. with **5**, 231–233°, i.r. and u.v. spectra identical with those of **5**. Found: C, 47.37; H, 4.16; N, 7.78. It was not clear why this product did not separate during the reaction or why it was more deeply colored than previous samples. The ether-soluble material (209 mg) was chromatographed on alumina (Neutral 2) in chloroform–hexane (1:1) and the following fractions were collected: (*i*) An orange oil (52 mg) which solidified when rubbed with a little ethanol, m.p. 82.5–83.5, raised to 83.5–84.5° after crystallization from methanol; λ_{max} (EtOH) 239 and 326 (E^1_1 423 and 587 respectively); ν_{max} 1300, 1150, and 955 (SO_2Me), 760 cm^{-1} (1,2-disubstituted benzene); molecular formula (mass spectroscopy) $C_{13}H_{12}N_2O_3S$ (mol. wt. 276). This compound was tentatively identified as 2′-methylsulfonylazoxybenzene (**13**). (*ii*) A yellow oil (68 mg) which was a mixture of at least 3 compounds none of which was identified. (*iii*) A red-brown solid (35 mg), λ_{max} 244 and 319 mμ, ν_{max} 1300, 1150, and 950 cm^{-1}, which was not identified. (*iv*) An orange-red solid (15 mg) which did not melt sharply but which had u.v. and i.r. spectra similar to those of **8**. The column was extruded and treated in the same way as under (*d*) above giving **6***a* (ca. 7 mg) m.p. 108–111°.

*2-Methylsulfonylnitrosobenzene (**9**)*

N-(2-Methylsulfonylphenyl)hydroxylamine (2 g) was dissolved with gentle warming in a mixture of water (300 ml) and concentrated sulfuric acid (27 ml). The vigorously stirred solution was cooled to 25 °C, a solution of sodium dichromate dihydrate (1.07 g) in water (1 ml) was added and then the mixture was cooled (ice bath) for 15 min. The precipitate was filtered off, washed well with cold water (1.63 g, m.p. 162–163°), and crystallized from methanol containing a little chloroform giving **9** as very pale tan prisms (1.2 g, 61%), m.p. 163.5–165° (green liquid), unchanged on recrystallization; λ_{max} ($CHCl_3$) 288, 311, and ca. 775 mμ (log ε 3.82, 3.65, and 1.45); ν_{max} 1320 and 1280, 1155 and 965 cm^{-1} (SO_2Me).

Anal. Calcd. for $C_7H_7NO_3S$: C, 45.39; H, 3.81; N, 7.56; S, 17.31. Found: C, 45.59; H, 3.92; N, 7.52; S, 17.38.

*2-Hydroxy-2′-methylsulfonylazobenzene (**8**)*

A solution of recrystallized 2-aminophenol (44 mg) in glacial acetic acid (15 ml) was added to a solution of 2-methylsulfonylnitrosobenzene (74 mg) in acetic acid (15 ml) and the mixture, which became deep red in ca. 5 min, was stirred at room temperature 48 h. The mixture was poured into water, adjusted to p*H* 8–9 and extracted several times with chloroform, giving a red oil (101 mg) which was chromatographed on alumina (acid 3) in chloroform–hexane (1:1). The main orange band which was not completely separated from faster moving material was collected and the resulting oil was rechromatographed as before, again giving an oil which crystallized from aqueous methanol as orange needles (55 mg, 50%), m.p. 144–146°. Four recrystallizations from the same solvent system raised the m.p. to 148.5–149.5°, mixed m.p. with **8** obtained from **4** 149–150°; λ_{max} (EtOH) 246, 330, and 388 mμ (log ε 4.02, 4.24, and 3.93); (EtOH + 1 drop NaOH solution) 236 and 335 mμ (log ε 4.18 and 4.03); i.r. spectrum identical with that of the earlier sample.

Anal. Found: C, 56.78; H, 4.12; N, 9.91.

Reactions of 2-Methylsulfonylnitrosobenzene in Aqueous Sodium Hydroxide Solution

The reaction mixtures were worked up as described

Can. J. Chem. Downloaded from www.nrcresearchpress.com by 210.87.254.6 on 09/05/12
For personal use only.

above under the reactions of **4** in alkali, except that the solution was adjusted to p*H* 8–8.5 before it was washed with chloroform.

(*a*) A vigorously stirred mixture of 2-methylsulfonylnitrosobenzene (555 mg) and 0.1 *N* sodium hydroxide (60 ml, 2 molar equ.) was heated under reflux 4 h. Fraction A was **5** (181 mg, 34%), m.p. 231–232°. Fraction B (34 mg) was mainly **7** and did not contain any **2**. Fraction C (85 mg), m.p. 99–104°, was mainly **6***a* (ca. 20%) containing only a trace of **8**. Fraction D (24 mg) was not investigated. The remaining aqueous solution was treated 3 times with charcoal, when it showed λ_{max} (NaOH) 236 and 294 mμ, and probably contained orthanilic acid (ca. 6%) (cf. (1)).

(*b*) The foregoing experiment was repeated under nitrogen. Fraction A was **5** (201 mg, 38%), m.p. 228–230°. Fraction B (34 mg) was mainly **7**. Fraction C (82 mg), m.p. 100–106° was mainly **6***a* (ca. 19%). There was a trace of another compound (which did not move on t.l.c.) but **8** was not detected. Fraction D (18 mg) was not investigated. The aqueous solution probably contained orthanilic acid (ca. 3%).

(*c*) A mixture of **9** (555 mg) and 0.1 *N* sodium hydroxide (60 ml) was stirred at room temperature 14 days. Fraction A (366 mg) was clearly a mixture (i.r., wide m.p. range) and was rubbed well with ether. The insoluble portion (238 mg), m.p. 162–165° (green liquid) was **9** (43% recovery). The ether-soluble portion (117 mg), m.p. 101–105° was **2**. Fraction B (60 mg) was **2** (total yield ca. 50% based on recovered **9**) containing a trace of **7**. Fraction C (13 mg) was also a mixture (white solid (**2**) and yellow oil). Fraction D (< 5 mg) was not investigated.

Reaction of N-(2-Methylsulfonylphenyl)hydroxylamine (4) and 2-Methylsulfonylnitrosobenzene (9) in Water

A mixture of **4** (170 mg), **9** (165 mg), and water (20 ml) was heated under reflux 2 h. The solid was filtered off giving slightly impure **5** (265 mg, ca. 82%), m.p. 225–227°. The yellow aqueous solution was washed with chloroform (aqueous now colorless) giving a mixture of white solid and yellow oil (29 mg), λ_{max} 245 and 308 mμ, which was not investigated further.

When **9** (250 mg) was heated under reflux 2 h in water (20 ml) the liquid was pale green at the boiling point, and after the mixture had cooled, **9** was recovered (228 mg, 91%), m.p. 164–166°. The aqueous solution was washed with chloroform giving a mixture of yellow and white solids (9 mg), u.v. spectrum similar to that of **9**. The remaining aqueous solution showed no maximum in the u.v.

The Formation of Benzofurazan from 2-Methylsulfonylnitrosobenzene

(*a*) A stirred mixture of 2-methylsulfonylnitrosobenzene (**9**) (500 mg) and water (50 ml) containing sodium azide (1 g) was distilled for ca. 50 min. The distillate was washed with ether, giving a pale yellow solid (A, 18 mg). The reaction mixture was cooled giving a brown solid (292 mg), m.p. 165–168°, identified as **9**.

(*b*) A mixture of **9** (100 mg) and water (25 ml) containing sodium azide (200 mg) was heated under reflux several minutes. The solid which collected in the condenser was washed out with ether, then the reaction was continued and the solid removed in the same way. The material from four such experiments (18.9 mg) together with solid A above, was identified as benzofurazan (**15**), m.p. 51.5–52° (lit. (22) m.p. 53°; (23) m.p. 51.5–52°); λ_{max} (cf. (12)) (H_2O) 254 sh, 259, 264, 269, 275, 280, 287, and 302 mμ (log ε 3.28, 3.38, 3.51, 3.55, 3.65, 3.59, 3.64, and 3.49); n.m.r. (cf. (13)) (CCl_4) AA′BB′ spectrum, τ 2.20 (2H), 2.65 (2H), $J + J' = 10.0$ Hz. The yield of **15** under (*a*) above, allowing for recovered **9**, was 13%; no attempt to recover starting material was made in experiment (*b*).

N-(4-Methylsulfonylphenyl)hydroxylamine (16)

4-Methylsulfonylnitrobenzene (1) (5 g) was reduced by the method described earlier (1) for the 2-isomer. The crude product (4.1 g) was crystallized from ethyl acetate – hexane giving pale pink crystals (2.53 g, 54%), m.p. 154° (decomp.). Two further crystallizations from the same solvent mixture gave small pale pink needles, m.p. 157.5–158.5° (decomp.); λ_{max} (H_2O) 263 mμ (log ε 4.14); λ_{max} (NaOH) 252 mμ (log ε 3.79); ν_{max} 3360 (OH), 3295 (NH), 1280, 1135, and 970 cm^{-1} (SO_2Me).

Anal. Calcd. for $C_7H_9NO_3S$: C, 44.91; H, 4.85; N, 7.48; S, 17.13. Found: C, 45.10; H, 5.12; N, 7.39; S, 17.11.

Reactions of N-(4-Methylsulfonylphenyl)hydroxylamine (16) in Aqueous Sodium Hydroxide Solution

(*a*) A solution of **16** (540 mg) in 0.1 *N* sodium hydroxide (60 ml; 2.1 molar equ.) was stirred at room temperature for 6 h. The initial pale yellow solution did not change color during the reaction period but a solid gradually separated. The mixture was filtered giving 4,4′-di(methylsulfonyl)azoxybenzene (**17**) (494 mg, 96%), m.p. 295–297° (decomp.). Crystallization from ethanol–dimethylformamide (DMF) gave **17** as pale orange needles, m.p. 295–296° (decomp.), (lit. (15) m.p. 264°); λ_{max} (DMF) 325 mμ (log ε 4.20); ν_{max} 1295, 1140, 960, and 955 cm^{-1} (SO_2Me).

Anal. Calcd. for $C_{14}H_{14}N_2O_5S_2$: C, 47.44; H, 3.98; N, 7.91; S, 18.09. Found: C, 47.63; H, 3.89; N, 7.94; S, 18.21.

(*b*) Compound **16** (270 mg) was added to 0.1 *N* sodium hydroxide (30 ml) at 95° and the mixture was heated under reflux 15 min and then cooled. The pale orange solid which separated (216 mg, m.p. ca. 280–290°) was crystallized four times from DMF giving 4,4′-di(methylsulfonyl)azobenzene (**18**) as orange prisms (75 mg), m.p. 305–306° (decomp.). λ_{max} (DMF) 323 mμ (log ε 4.37); ν_{max} 1295, 1140, 960, and 955 cm^{-1} (SO_2Me). The i.r. spectrum of **18** differed slightly from that of **17**. In particular the intensities of the bands near 960 cm^{-1} in **18** (955 > 960) were reversed in **17** (955 < 960), and although both compounds showed a band at 1455 cm^{-1}, it was much more intense in **17**.

Anal. Calcd. for $C_{14}H_{14}N_2O_4S_2$: C, 49.68; H, 4.17; N, 8.28; S, 18.95. Found: C, 49.52; H, 4.10; N, 8.18; S, 19.22.

When (*b*) was repeated on twice the scale the crude product (442 mg) was washed with ethanol leaving an orange solid (404 mg), m.p. ca. 295–299°, E_1^1 654, which was a mixture of **18** and **17** in the estimated ratio 5:1. The ethanol solution, which showed λ_{max} 322 mμ, unchanged when the solution was made alkaline, gave a

pale orange solid (31 mg), m.p. ca. 135–140° (decomp.). Its i.r. spectrum was rather similar to that of the mixture of **17** and **18** but it was not identified. The same reaction under nitrogen gave a similar mixture of **17** and **18** (E_1^1 651) in somewhat lower yield (369 mg after removal of the ethanol-soluble portion, 50 mg). The mixture was crystallized from aqueous DMF giving an orange solid (326 mg), m.p. 304–306°, E_1^1 680, which was mainly **18**.

(*c*) A solution of **16** (540 mg) in 0.1 *N* sodium hydroxide (60 ml) was heated under reflux 15 min and then cooled and filtered. The crude product was washed with ethanol leaving an orange solid (444 mg), m.p. 298–299° (decomp.), E_1^1 625, which was a mixture of **18** and **17** in the estimated ratio 3:1. The ethanol-soluble material (28 mg) was similar to that obtained earlier. The original aqueous solution was washed with chloroform giving a yellow oil (12 mg) whose u.v. and i.r. spectra were the same as those of 4-methylsulfonylaniline (16). The aqueous solution was acidified and washed with chloroform giving an oil (6 mg), λ_{max} 268 and 360 mμ, which was not identified.

(*d*) **16** (540 mg) was added to a vigorously stirred mixture of azoxybenzene (580 mg) and 0.1 *N* sodium hydroxide (60 ml) at > 80° and the whole was heated under reflux, under nitrogen, 2 h. The mixture was cooled, shaken well with ether (which had also been used to wash out the condenser), and the contents of the separatory funnel were filtered giving an orange solid (369 mg), m.p. 302–305°, E_1^1 654, which was crystallized from aqueous DMF giving **18** (331 mg, 68%) m.p. 305–306°, raised to 306–307° after recrystallization. Anal. Found: C, 49.68; H, 4.13; N, 8.20; S, 19.19. The ether solution gave an orange oil (580 mg) which was chromatographed on alumina (Basic 3) in benzene–hexane (2:1). A yellow band passed rapidly through the column and was collected giving azoxybenzene (517 mg, 90% recovery). An orange band was eluted with benzene giving a pale orange solid (33 mg) m.p. ca. 137–145°, which was similar to the ethanol-soluble material obtained in the earlier experiments.

Thanks are offered to Dr. M. A. Weinberger for the nuclear magnetic resonance spectra and to Professor R. T. Coutts for useful discussions.

1. K. B. Shaw and R. K. Miller. Can. J. Chem. This issue.
2. M. Claasz. Ber. **45**, 1015 (1912).
3. J. H. Bowie, R. G. Cooks, and G. E. Lewis. Aust. J. Chem. **20**, 1601 (1967).
4. Chemistry of carbon compounds. Vol. 3A. *Edited by* E. H. Rodd. Elsevier Publishing Co., New York. 1954. (*a*) p. 153; (*b*) p. 320.
5. N. V. Sidgwick. The organic chemistry of nitrogen. *Revised and rewritten by* T. W. J. Taylor and W. Baker. Clarendon Press, Oxford. 1942. (*a*) p. 163; (*b*) p. 206 ff.
6. E. Bamberger. Ber. **33**, 119 (1900).
7. G. A. Russell and E. J. Geels. J. Amer. Chem. Soc. **87**, 122 (1965).
8. G. H. Coleman, C. M. McCloskey, and F. A. Stuart. Organic syntheses. Coll. Vol. 3. *Edited by* E. C. Horning, John Wiley and Sons, Inc., New York. 1955. p. 668.
9. C. K. Ingold and H. A. Piggott. J. Chem. Soc. 168 (1924).
10. J. Hutton and W. Waters. J. Chem. Soc. *B*, 191 (1968).
11. G. B. Barlin and W. V. Brown. J. Chem. Soc. *C*, 2473 (1967) and references therein.
12. A. J. Boulton, P. B. Ghosh, and A. R. Katritzky. J. Chem. Soc. *C*, 971 (1966).
13. R. K. Harris, A. R. Katritzky, S. Øksne, A. S. Bailey, and W. G. Paterson. J. Chem. Soc. 197 (1963).
14. A. J. Boulton, P. B. Ghosh, and A. R. Katritzky. J. Chem. Soc. *B*, 1004 (1966); Tetrahedron Lett. **25**, 2887 (1966).
15. Th. Zincke and P. Jörg. Ber. **44**, 614 (1911).
16. E. A. Fehnel and M. Carmack. J. Amer. Chem. Soc. **72**, 1292 (1950).
17. Y. Ogata, M. Tsuchida, and Y. Takagi. J. Amer. Chem. Soc. **79**, 3397 (1957) and references therein.
18. W. Anderson. J. Chem. Soc. 1722 (1952).
19. M. P. Cava and C. E. Blake. J. Amer. Chem. Soc. **78**, 5444 (1956).
20. N. Kharasch, W. King, and T. C. Bruice. J. Amer. Chem. Soc. **77**, 931 (1955).
21. G. Bulmer and F. G. Mann. J. Chem. Soc. 680 (1945).
22. R. J. Gaughran, J. P. Picard, and J. V. R. Kaufman. J. Amer. Chem. Soc. **76**, 2233 (1954).
23. J. M. Prokipcak, P. A. Forte, and D. D. Lennox. Can. J. Chem. **47**, 2482 (1969).

Can. J. Chem. Downloaded from www.nrcresearchpress.com by 210.87.254.6 on 09/05/12
For personal use only.

Can. J. Chem. Downloaded from www.nrcresearchpress.com by 210.87.254.5 on 09/05/12
For personal use only.

Study of iron(II) complexes with halides and thiocyanate in acetonitrile

BYRON KRATOCHVIL AND ROBERT LONG[1]
Department of Chemistry, University of Alberta, Edmonton, Alberta

Received September 11, 1969

In acetonitrile, iron(II) forms stable 1:1 complexes with chloride, bromide, and iodide and both 1:1 and 1:2 complexes with thiocyanate. Stepwise formation constants for the complexes were determined spectrophotometrically by a mole-ratio method. The log K values are: $FeCl^+$, 5.8; $FeBr^+$, 5.5; FeI^+, 4.3; $Fe(SCN)^+$, 5.5; and $Fe(SCN)_2$, 3.7.

Canadian Journal of Chemistry, 48, 1414 (1970)

The stability of metal complexes in solution is greatly affected by the nature of the solvent. According to present theories of nonaqueous coordination chemistry, nonaqueous complexation is considered to be primarily a competition between solvent and ligand for bonding sites on the cation (ref. 1, pp. 12–20). In this picture the major considerations are the relative donor strengths of the solvent and ligand; other properties of the solvent, such as the dielectric constant, are neglected. Although this simplification appears to be generally useful in predicting trends, it is susceptible to variations caused by specific solvent effects such as hydrogen bonding, polarizability, and steric hindrance arising from the size and shape of the solvent molecule.

With few exceptions, accurate quantitative data on the formation of metal complexes in nonaqueous solvents are lacking. As part of a study of iron(III) and iron(II) in acetonitrile, the formation constants of iron(II) with chloride, bromide, iodide, and thiocyanate were measured. The observed values are reported here and compared with trends predicted on the basis of solvent effects and the relative donor strengths of the ligands.

Experimental

Acetonitrile was purified by the method of O'Donnell, Ayres, and Mann (2) and Long (3) with minor modifications. The product from the final distillation was monitored spectrophotometrically; the absorbance of the fraction used was less than 0.01 at 225 mμ and less than 0.1 at 200 mμ. The water content as determined by Karl Fischer titration was about 2×10^{-4} M. The solvent was deaerated with argon immediately before use to avoid air oxidation of iodide or iron(II) in the presence of chloride or bromide. Anhydrous hexakisacetonitrile iron(II) perchlorate, $Fe(ClO_4)_2 \cdot 6CH_3CN$, was prepared by azeotropic distillation of solutions of hydrated iron(II) perchlorate in acetonitrile under reduced pressure in the presence of Linde 3A molecular sieve, followed by removal of excess solvent under vacuum at room temperature. The product, white with a pale-blue cast, is stable to 125 °C; above this temperature it slowly decomposes. Solutions of iron(II) perchlorate in acetonitrile are stable to at least 50 °C. (NOTE: Safety precautions should always be taken when heating perchlorate salts in the presence of organic material.) Analysis of the salt by titration with aqueous potassium dichromate gave a purity of 100.3%.

Tetrabutylammonium perchlorate was precipitated from a boiling aqueous saturated solution of tetrabutylammonium iodide. Deaeration of the solutions was necessary to prevent air oxidation of iodide to triiodide, the tetrabutylammonium salt of which is insoluble. (Use of the bromide salt instead of the iodide would avoid this problem.) The precipitated perchlorate salt was recrystallized from water until an approximately 1 M solution did not absorb above 200 mμ.

Tetraethylammonium chloride, tetrabutylammonium bromide, and tetrabutylammonium iodide (Eastman Organic Chemicals, white label) were recrystallized or extracted once, dried under vacuum over magnesium perchlorate, and analyzed gravimetrically by precipitation of the silver halide. Tetraethylammonium chloride, because of its low solubility in organic solvents, was purified by extraction with acetone in a Soxlet extractor; analysis gave a purity of 99.9%. Tetrabutylammonium bromide was recrystallized from ethyl acetate with stirring to prevent supersaturation; analysis gave a purity of 100.0%. Tetrabutylammonium iodide was recrystallized from a deaerated solution of 10% acetonitrile in water and found to be 99.9% pure. Potassium thiocyanate (Fisher Certified Reagent Grade) was dried for 2 h at 100 °C and found to be 100.1% pure by Volhard titration with silver nitrate.

A Unicam SP800 ultraviolet–visible spectrophotometer was used for the spectrophotometric measurements. The absorbance accuracy of the instrument was ± 0.02 and the reproducibility ± 0.005 absorbance units. All solutions were prepared by weight in a drybox, removed in closed containers, and thermostatted at 25 ± 0.1 °C during measurement. All were made 0.01 M in tetrabutylammonium perchlorate to maintain constant ionic strength, and concentrations were converted to molarities on the basis of the density of 0.01 M tetrabutylammonium perchlorate in acetonitrile, 0.7785 g/ml.

To mix separate anhydrous solutions and make

[1]Present address: Analytical Laboratory, Sylvania Electric Products, Towanda, Pennsylvania 18848.

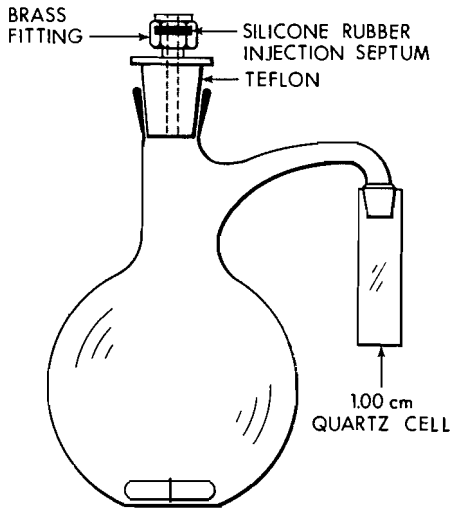

FIG. 1. Spectrophotometric cell used in determination of formation constants.

spectral measurements on the resulting mixtures without exposure to the atmosphere, the apparatus shown in Fig. 1 was constructed. A 200-ml volumetric flask was modified by addition of a side arm to which a conventional 1-cm rectangular quartz cell was connected by a lapped standard-taper joint. The flask stopper was machined with a standard taper from Teflon and contained a silicone-rubber septum through which solutions could be injected. A 100-μl Hamilton gas-tight syringe with a Teflon-tipped plunger, Chaney adapter, and platinum needle was used for the injections. With thermostatted solutions the reproducibility of delivery for the syringe was ± 2 parts per 1000.

Treatment of Data

The formation constants were determined by a mole-ratio method. Absorbance measurements were taken at the wavelength of maximum absorbance of the complex species and a plot of absorbance vs. ligand concentration was made. The molar absorptivity of the first complex was calculated from the slope of the straight-line portion obtained at small ligand-to-metal ratios, and the concentration of the complex at large ratios. An IBM 360/67 computer program was written to calculate concentrations from the experimental data, fit the best straight line to the first portion of the curve by a linear least-squares method, and calculate the molar absorptivity and formation constant for each complex.

Since the absorption maxima of the 1:1 bromide, iodide, and thiocyanate complexes were well separated from those of free iron(II) and ligand, correction for absorbance of these species was not necessary. For chloride, however, the wavelength of maximum absorbance for the $FeCl^+$ complex, 227 mμ, fell on the shoulder of a broad iron(II) absorption maximum at 205–215 mμ and a correction for free iron(II) absorption became necessary.

The formation constant for the second thiocyanate complex was determined in the same general way as for the first except that the thiocyanate concentration was held constant while that of the iron(II) was slowly increased by injections of a solution of iron(II) perchlorate. The second stepwise formation constant was obtained from the expression

$$K_2 = \frac{[Fe(SCN)_2]}{([Fe(II)_{total}] - [Fe(SCN)_2])([SCN^-_{total}] - [Fe(SCN)_2] - [Fe(II)_{total}])}$$

The data were handled by computer in the same general way as before.

TABLE 1

Data for determination of formation constants

(*a*) $FeCl^+$ complex (λ = 227 mμ)

$\frac{[Fe(II)]}{[Cl^-]}$	A	log K	$\frac{[Fe(II)]}{[Cl^-]}$	A	log K	$\frac{[Fe(II)]}{[Cl^-]}$	A	log K
$[Fe(II)] = 2.44 \times 10^{-4}$ Molar absorptivity = 4700			$[Fe(II)] = 2.55 \times 10^{-4}$ Molar absorptivity = 4700			$[Fe(II)] = 2.78 \times 10^{-4}$ Molar absorptivity = 4710		
19.4	0.061		17.8	0.067		16.2	0.080	
9.69	0.117		8.91	0.134		8.08	0.163	
6.46	0.179		5.94	0.205		5.38	0.247	
4.85	0.238		4.45	0.272		4.04	0.324	
3.88	0.296		2.97	0.406		3.23	0.406	
2.77	0.416		2.23	0.541		2.02	0.650	
2.15	0.536		1.78	0.674		1.61	0.806	6.07
1.76	0.650		1.48	0.805	6.26	1.34	0.954	5.81
1.49	0.760	5.98	1.27	0.921	5.82	1.15	1.099	5.84
1.21	0.919	5.83	1.11	1.037	5.86	1.01	1.228	6.03
1.02	1.068	6.08	0.989	1.142	6.13			

Can. J. Chem. Downloaded from www.nrcresearchpress.com by 210.87.254.5 on 09/05/12
For personal use only.

Can. J. Chem. Downloaded from www.nrcresearchpress.com by 210.87.254.5 on 09/05/12
For personal use only.

Results and Discussion

Data obtained for the systems are given in Table 1, and the formation constants calculated from these data in Table 2. The error estimates are standard deviations of values for two to five trials. The mole-ratio method was found to be a satisfactory quantitative technique as long as the formation constants do not exceed about 10^8. Beer's law was followed for all of the systems studied. Although the method used here is somewhat tedious and not highly precise, a direct measurement of the free ligand or metal concentrations by spectrophotometric or potentiometric methods was not possible for these systems.

Iron(II)–Chloride System

Evidence for only one chloride complex,

TABLE 1 (*Continued*)

(*b*) $FeBr^+$ complex (λ = 265 mμ)

[Fe(II)]/[Br⁻]	A	log K	[Fe(II)]/[Br⁻]	A	log K	[Fe(II)]/[Br⁻]	A	log K
[Fe(II)] = 3.04×10^{-4} Molar absorptivity = 3150			[Fe(II)] = 4.75×10^{-4} Molar absorptivity = 3170			[Fe(II)] = 3.14×10^{-4} Molar absorptivity = 3120		
26.8	0.037		25.0	0.062		20.53	0.049	
13.41	0.071		12.5	0.120		10.26	0.095	
8.94	0.106		8.32	0.180		6.84	0.140	
6.70	0.140		6.24	0.244		4.10	0.243	
5.36	0.179		4.99	0.304		2.93	0.335	
4.47	0.219		4.16	0.376		2.28	0.429	
3.83	0.257		3.57	0.426		1.86	0.477	
2.98	0.323		3.12	0.498		1.59	0.602	5.43
2.44	0.392		2.77	0.544		1.37	0.685	5.38
2.06	0.461		2.27	0.660		1.21	0.761	5.35
1.79	0.526	5.67	1.92	0.794		1.08	0.831	5.38
1.58	0.589	5.51	1.66	0.898		0.977	0.891	5.48
1.41	0.651	5.45	1.47	0.990	5.27	0.892	0.946	5.84
1.28	0.712	5.45	1.31	1.064	5.00			
1.12	0.796	5.48	1.25	1.108	4.98			
0.993	0.870	5.62	1.13	1.188	4.96			
			1.04	1.270	5.02			
			0.959	1.338	5.10			
			0.891	1.405	5.28			
			0.831	1.46	5.64			

(*c*) FeI^+ complex (λ = 326 mμ)

[I⁻]/[Fe(II)]	A	log K	[I⁻]/[Fe(II)]	A	log K	[Fe(II)]/[I⁻]	A	log K
[I⁻] = 8.61×10^{-4} Molar absorptivity = 1500			[I⁻] = 1.03×10^{-3} Molar absorptivity = 1870			[Fe(II)] = 1.25×10^{-3} Molar absorptivity = 1290		
18.1	0.073		35.5	0.055		31.9	0.052	
9.04	0.140		17.8	0.108		16.0	0.101	
6.02	0.216		11.8	0.164		10.6	0.149	
4.52	0.277	4.66	8.89	0.221		7.98	0.206	
3.62	0.334	4.35	7.11	0.266	4.67	6.39	0.256	
3.01	0.387	4.19	5.92	0.313	4.42	5.32	0.303	
2.26	0.487	4.03	5.08	0.361	4.33	3.55	0.449	
1.81	0.577	3.95	3.95	0.448	4.13	2.66	0.588	4.56
1.51	0.660	3.91	3.23	0.525	3.98	2.13	0.732	4.59
1.29	0.734	3.88	2.73	0.601	3.90	1.77	0.868	4.55
1.06	0.827	3.85	2.37	0.668	3.83	1.52	0.999	4.54
0.903	0.907	3.85	2.09	0.739	3.80	1.33	1.127	4.56
0.785	0.978	3.87	1.87	0.805	3.78			
0.633	1.081	3.94	1.62	0.887	3.72			
			1.42	0.961	3.68			
			1.27	1.041	3.67			
			1.11	1.129	3.65			
			0.987	1.201	3.63			
			0.888	1.281	3.64			

TABLE 1 (*Concluded*)

(*d*) $Fe(SCN)^+$ complex (λ = 299 mμ)

$\frac{[Fe(II)]}{[SCN^-]}$	A	log K	$\frac{[Fe(II)]}{[SCN^-]}$	A	log K
$[Fe(II)] = 5.65 \times 10^{-4}$ Molar absorptivity = 5130			$[Fe(II)] = 4.96 \times 10^{-4}$ Molar absorptivity = 5290		
40.1	0.070		26.1	0.101	
17.2	0.171		13.0	0.205	
10.9	0.263		8.69	0.304	
8.02	0.360		6.52	0.397	
6.68	0.435		5.22	0.501	
5.73	0.505		4.35	0.603	
5.01	0.580		3.73	0.706	
4.46	0.652		3.26	0.815	
4.01	0.729		2.90	0.906	
3.64	0.801		2.37	1.101	
3.34	0.869		2.01	1.293	5.60
3.08	0.939		1.86	1.385	5.46
2.86	1.011		1.63	1.552	5.16
2.67	1.081		1.45	1.739	5.21
2.51	1.152				
2.36	1.221	5.76			
2.23	1.288	5.56			
2.11	1.357	5.51			
2.00	1.418	5.30			

(*e*) $Fe(SCN)_2$ complex (λ = 289 mμ)

$\frac{[SCN^-]}{[Fe(II)]}$	A	log K	$\frac{[SCN^-]}{[Fe(II)]}$	A	log K
$[SCN^-] = 1.50 \times 10^{-2}$ Molar absorptivity = 10 620			$[SCN^-] = 1.23 \times 10^{-2}$ Molar absorptivity = 10 980		
1090	0.147		340	0.398	
545	0.295		272	0.497	
363	0.440		226	0.595	
272	0.582		194	0.697	
218	0.735		170	0.797	
198	0.810		151	0.894	
182	0.883		136	0.993	
168	0.953		124	1.082	3.91
156	1.025		113	1.182	3.98
145	1.097		104	1.277	3.86
136	1.165	4.04	97.0	1.368	3.70
128	1.248	—	90.5	1.454	3.52
121	1.323	—	84.9	1.541	3.42
115	1.401	—			
109	1.441	3.63			
104	1.500	3.44			
99.1	1.573	3.47			

$FeCl^+$, was found spectrophotometrically in acetonitrile. However, the presence of further complexes with weak absorption maxima hidden under the uncomplexed iron(II) or chloride peaks cannot be ruled out. In this work exclusion of oxygen was found necessary, as chloride lowers the potential of the iron(III)–(II) couple by strongly complexing iron(III). The presence of iron(III)–chloride species is readily detected by their intense ultraviolet absorption spectra in acetonitrile (4, 5).

From the log formation constant of $FeCl^+$ in water, 2.81 (6), a qualitative prediction of the formation constant in acetonitrile can be made based on the nonaqueous coordination model of Gutmann (ref. 1, pp. 12–20). Such a prediction

Can. J. Chem. Downloaded from www.nrcresearchpress.com by 210.87.254.5 on 09/05/12
For personal use only.

TABLE 2

Summary of spectrophotometric data for iron(II)–anion complexes in acetonitrile

Complex	log of stepwise formation constant	Wavelength of maximum absorption of complex (mμ)	Molar absorptivity at λ_{max} (l/mole cm)
$FeCl^+$	5.8±0.1	227	4 705±8
$FeBr^+$	5.5±0.1	261	3 148±26
FeI^+	4.3±0.2	326	1 553±294
$Fe(SCN)^+$	5.5±0.1	299	5 252±57
$Fe(SCN)_2$	3.7±0.1	289	10 802±308

requires estimation of the relative donor strength of acetonitrile and water toward iron(II). Spectrophotometric measurements of the crystal field splitting energy of iron(II) in acetonitrile and in water indicate that acetonitrile has greater donor strength toward iron(II) than has water; therefore the predicted formation constant in acetonitrile would be less than 2.8. We postulate that the larger value found experimentally arises in that a simple coordination model does not take into account the effect of the difference in the dielectric constants of water, 81, and of acetonitrile, 36. A solvent of lower dielectric constant cannot stabilize an ion of plus-two charge so well as one of higher dielectric constant. Complexation of a solvated cation with a neutral ligand would not be expected to depend significantly on the dielectric constant of the solvent. However, coordination of a cation of plus-two charge with an anion will result in partial neutralization of the charges that should make a significant contribution to the stabilization energy of the complex. Thus, the extent of complexation depends not only on the relative donor strength of the solvent but also on the dielectric constant of the solvent and the charge on the ions. As a result, significant complexation may be observed even in solvents in which solvent–cation interaction is large.

Iron(II)–Bromide System

Only one bromide complex, $FeBr^+$, was observed spectrophotometrically in acetonitrile. No evidence for complexes of higher order was seen. Again a distinctive intense spectrum similar to that observed with the iron(II)–chloride system is obtained when oxygen is not rigorously excluded; apparently a stable iron(III)–bromide species is formed.

Values of the formation constant for $FeBr^+$ in water are not available for comparison, but the log formation constant of 5.5 found in acetonitrile correlates with the weaker donor strength of bromide relative to chloride found for other metal–halide complexes in water.

Iron(II)–Iodide System

Only one iodide complex, FeI^+, was observed. The formation constant was determined from both directions, that is, from measurements taken by adding iodide to iron(II) and *vice versa*. The results obtained by both methods were identical, so iodide complexes of higher order, and polynuclear iron species, are not significant. Again traces of oxygen caused relatively large experimental deviations because of air oxidation of iodide to the stable triiodide ion (the formation constant for I_3^- from I_2 and I^- in acetonitrile is $10^{7.40}$ (7)). Spectral interference from triiodide was not completely eliminated despite efforts to minimize oxygen contamination. The value of the formation constant for this system also fits the expected trend in halide-donating power.

Iron(II)–Thiocyanate System

This was the only system for which two complexes, $Fe(SCN)^+$ and $Fe(SCN)_2$, were found. No evidence for further complex formation was observed.

The log of the first iron(II)–thiocyanate formation constant, 5.5, is slightly lower than that of the chloride complex. By comparison, in water iron(II) appears to complex with thiocyanate either only slightly or not at all (8). The second thiocyanate complex, calculated from spectrophotometric measurements at 289 mμ, has a stepwise log formation constant of 3.7.

A check for formation of polynuclear iron(II)–thiocyanate complexes was made by repeating the mole-ratio measurements over iron(II) concentrations from 0.50×10^{-3} to 2.15×10^{-3}

Can. J. Chem. Downloaded from www.nrcresearchpress.com by 210.87.254.5 on 09/05/12
For personal use only.

M. The molar absorptivities remained constant throughout, indicating polynuclear species were absent.

In summary, iron(II) forms 1:1 complexes in acetonitrile with chloride, bromide, and iodide with formation constants of appreciable magnitude. A 2:1 complex is also formed with thiocyanate. No evidence for anionic complexes was seen with any of the ligands studied. This is somewhat unexpected, for anionic species have been reported in acetonitrile for chloride and thiocyanate with nickel(II) and cobalt(II) and for chloride with iron(III), copper(II), manganese(II), and chromium(III) (ref. 1, pp. 161–168).

1. V. GUTMANN. Coordination in nonaqueous solutions. Springer-Verlag, Vienna, Austria. 1968.
2. J. F. O'DONNELL, J. T. AYRES, and C. K. MANN. Anal. Chem. **37**, 1161 (1965).
3. R. LONG. Ph.D. Thesis, University of Alberta, Edmonton, Alberta. 1969.
4. B. J. HATHAWAY and D. G. HOLAH. J. Chem. Soc. 2408 (1964).
5. V. GUTMANN and W. LUX. Monatsh. Chem. 98, 276 (1967).
6. J. DAUPHIN, S. DAUPHIN, D. CHATONIER, and M. T. VIALATTE. Bull. Soc. Chim. France, 2588 (1964).
7. J. DESBARRES. Bull. Soc. Chim. France, 502 (1961).
8. L. G. SILLEN and A. E. MARTELL. Stability constants of metal ion complexes. 2nd ed. Special Publication No. 17, The Chemical Society, London, 1964. p. 119.

Can. J. Chem. Downloaded from www.nrcresearchpress.com by 210.87.254.5 on 09/05/12
For personal use only.

Can. J. Chem. Downloaded from www.nrcresearchpress.com by 210.87.254.105 on 09/05/12
For personal use only.

A physical and chemical investigation of the nature and properties of the species formed in the $Hg(6^3P_1)$–CO system

G. LONDON, A. C. VIKIS, AND D. J. LE ROY
Lash Miller Chemical Laboratories, University of Toronto, Toronto, Ontario

Received November 3, 1969

An investigation of the $Hg(6^3P_1)$–CO system by physical measurements (emission, pressure studies) relevant to the reported Hg*CO species have yielded no additional evidence of its formation.

Chemical experiments on the decomposition of ethylene and H_2 are in accord with formation of a long lived ($> 10^{-5}$ s) species. The relative quenching rate constants of the species by C_2H_4, H_2, and CO are 1:0.10–0.18:0.023, respectively.

The reliability of the "carbon monoxide effect" as a criterion for distinguishing the nature of the quenching process is discussed in the light of a CO enhancement effect ($\sim 30\%$) observed in the $Hg(6^3P_1)$ photosensitized decomposition of hydrogen in the presence of CO and at conditions of incomplete quenching. An alternative to Hg*CO excimer formation is also discussed. This approach is based on the possible formation of $Hg(6^3P_0)$ atoms in quantities in excess of those currently accepted, when Hg–CO mixtures are irradiated with 2537 Å light.

Canadian Journal of Chemistry, 48, 1420 (1970)

Introduction

In a number of recent reports, various authors (1–8) have emphasized the importance of complex formation as an intermediate in the quenching of excited metal atoms, primarily $Hg(6^3P_1)$ and $Na(3^2P)$, by a ground state molecule, M,

$$[1]\quad Hg(6^3P_1) + M \underset{k_{-1}}{\overset{k_1}{\rightleftharpoons}} (HgM) \xrightarrow{k_q} Hg(6^1S_0) + M'$$

where M′ indicates a physically excited or a dissociated molecule.

The proposed lifetimes of these complexes, often called excimers, vary from 10^{-13} to 10^{-5} s. They have been mainly deduced on the basis of theoretical considerations, pressure dependence, quenching of emission, and product distribution studies. Complex formation of an unspecified lifetime was also assumed in the early theoretical attempts to explain the mechanism of the quenching process. The work of Laidler (9), Magee (10*a*), and Magee and Ri (10*b*) on excited sodium and mercury atoms is a typical example. However, it is only recently that attempts have been made towards a more quantitative interpretation. Some of these latter attempts are discussed in the present work.

The conditions for long-lived complex formation have been discussed by Nikitin (1). Such complexes are anticipated when the potential energy surface for the excited atom and the quencher are characterized by significant attraction, such as chemical bond formation. Assuming that the rate of crossing into products is the slow process, an order of magnitude estimation of the complex lifetime, τ_{-1}, is obtained (1) by eq. [2].

$$[2]\qquad 1/\tau_{-1} = \xi\nu\left[\frac{E-D}{E}\right]^{S+(P/2)-1}$$

where ξ is the probability that excimer will cross from the reactant state into the complex state (or the reverse), ν may be approximated to the Hg*—M vibrational frequency, E and D are the excimer energy and bond dissociation energy respectively, and S, P are the active vibrational, rotational degrees of freedom. A long lifetime is thus predicted for complex molecules (high S) that exhibit significant bonding with the excited atom. An investigation (2) of the $Na(3^2P) + N_2$ system showed that although a significant attraction between $Na(3^2P)$ and N_2 could exist ($Na^+N_2^-$ formation), energy transfer could occur within the lifetime of a collision. In the $Hg(6^3P_{1,0})$–CO and $Hg(6^3P_{1,0})$–NO systems, studied by Karl *et al.* (3) by observing the infrared chemiluminescence of the quencher, evidence for long-lived complex formation is discussed. The high cross sections for electronic to vibrational transfer were attributed to formation of a long-lived complex that permits the system to make, during its lifetime, several approaches to the crossing point leading into products. A Hg*CO excimer of a lifetime of the order of 10^{-5} s was postulated by Homer and Lossing (4) as the species responsible for the enhancement in the $Hg(6^3P_1)$ photosensitized decomposition of ethylene in the presence of small

Can. J. Chem. Downloaded from www.nrcresearchpress.com by 210.87.254.105 on 09/05/12
For personal use only.

amounts of CO. The CO effect was observed when the reactions were carried out at incomplete quenching conditions.

Penzes *et al.* (5) were able to observe Hg*HR excimer emission in the quenching of $Hg(6^3P_1)$ atoms by the alkanes. The excimer emission appears at the long wavelength side of the 2537 Å $Hg(6^3P_1)$ emission line, indicating significant attraction between the alkanes and $Hg(6^3P_1)$. The lifetime of the $Hg^*C_3H_8$ excimer was estimated to be $< 10^{-9}$ s on the basis of pressure studies. The Hg*HR emission studies constitute the first direct evidence of excimer formation and of a lifetime estimate.

Based on the latter and also on the apparent dependence of the quenching cross section on the alkane structure and C—H bond strength (cf. isotope effects, $\sigma^2_{prim} < \sigma^2_{sec} < \sigma^2_{tert}$), Vikis and Moser (6) have looked for a correlation between the quenching cross sections of $Hg(6^1P_1)$, $Hg(6^3P_1)$, and $Hg(6^3P_0)$ by the alkanes and the unimolecular HgH—R decomposition lifetimes calculated by the R.R.K.M. method. Their approach was also based on formation of a long-lived complex on an intermediate surface connecting the initial reactant and the final product surface

[3] $$Hg^* + HR \rightarrow Hg^*HR \rightarrow HgH + R$$

An interesting aspect of their studies was the fact that good correlations among structurally differed alkanes, as well as various C—H bond strengths, were obtained only when the energetics of the Hg*HR excimer were adjusted such that decomposition lifetimes of $< 10^{-9}$ s were obtained. This corresponded to Hg*HR potential minima with respect to $Hg(6^3P_1) + HR$ of < 20 kcal/mole.

Homer and Lossing's (4) finding of a rather long-lived ($\sim 10^{-5}$ s) Hg*CO excimer appears surprising and worthy of further investigation. It was observed (4) that the postulated Hg*CO excimer would have to possess a minimum energy in excess of 90 kcal/mole in order to induce the decomposition of C_2H_4 into H_2 and C_2H_2. The problem of stabilization of the excimer to lifetimes of the order of 10^{-5} s at overall pressures of a few Torr of He remains unsolved. Normally one would expect lifetimes with respect to decomposition to the original reactants to be of the order of $< 10^{-8}$ s for a triatomic molecule such as Hg*CO, at Hg*—CO bond dissociation energies of 10–20 kcal/mole. A lifetime of 10^{-5} s with respect to emission is also very long in comparison with Hg*HR lifetimes of the order of $< 10^{-9}$ s.

In addition, the Hg*CO excimer appeared to exhibit a peculiarity in its reactivity. It was observed by Homer and Lossing (4) and Jones and Lossing (11) that molecules known to quench via a triplet mechanism, e.g. ethylene

[4] $$Hg(6^3P_1) + C_2H_4 \rightarrow Hg(6^1S_0) + C_2H_4^*(\text{triplet})$$

showed an enhancement in the rate of decomposition in the presence of a few microns of CO, when the reactions were run at incomplete quenching conditions. Molecules known to quench via a chemical mechanism, e.g. the saturated hydrocarbons

[5] $$Hg^* + RH \rightarrow HgH + R \rightarrow Hg + H + R$$

[6] $$Hg^* + RH \rightarrow Hg + H + R$$

did not show an enhancement effect or showed a decrease in their rate of decomposition under similar conditions. The regularity of the phenomenon with known reactions was extended (11, 12) to a number of reactions in which the "carbon monoxide effect" was used as a criterion in distinguishing the nature of the quenching process.

In the present work we report a number of independent attempts to obtain additional evidence regarding the physical and chemical properties of the assumed Hg*CO excimer. These attempts are centered about five types of experiments: *A*, an investigation into the pressure dependence of the quenching cross section of $Hg(6^3P_1)$ by CO; *B*, pressure broadening of the $Hg(6^1S_0) \rightarrow Hg(6^3P_1)$ absorption in the presence of CO, Ar, N_2, and He; *C*, attempts to observe spontaneous or resonance emission from the Hg*CO excimer; *D*, a reinvestigation of the CO enhancement effect of the ethylene decomposition; *E*, the $Hg(6^3P_1)$ photosensitized decomposition of hydrogen in the presence of CO.

Experimental

The experiments were carried out in flow systems employing Ar or He as the carrier gas at flow rates varying from 4 to 27 cc/min as stated in each individual experiment. Small partial pressures (10^{-3}–2 Torr) of added gases (C_2H_4, H_2, CO, N_2) were introduced to the main flow through calibrated capillaries. The gases were saturated with mercury at the desired pressure by passage

Can. J. Chem. Downloaded from www.nrcresearchpress.com by 210.87.254.105 on 09/05/12
For personal use only.

through a thermostated mercury saturator. The temperature of the latter was controlled to ±0.2 °C and could be varied from −10 to 30 °C. With the exception of the type *B* experiments, the light sources used were low-pressure, d.c. operated, cold cathode, U-shaped mercury resonance lamps. The electrode temperature of the lamps was maintained at 31 ± 0.2 °C by circulating water.

The gases employed and their purity were as follows: Matheson ultra pure argon (99.999%) and carbon monoxide (99.95%); Matheson high purity helium (99.995%), Matheson prepurified nitrogen (99.997%). With the exception of the type *B* experiments, the above gases were passed through quartz tubes packed with copper turnings and heated to a temperature of ~ 500 °C, in order to eliminate any oxygen impurity. Liquid nitrogen or dry ice – acetone traps followed the above treatment. In type *B* experiments the above gases were used without further purification. The rest of the gases were hydrogen (Linde, 99.95%) passed through a Deoxo catalytic purifier before use, and Phillips research grade (99.98%) ethylene additionally degassed by freezing at 77 °K and pumping.

The procedure pertaining to each individual kind of experiment, *A* through *E*, is outlined below.

Type A

A cylindrical quartz cell, 5.0 cm in length, 3.1 cm i.d. was used for these studies. The irradiations were carried out by two U-shaped lamps, placed parallel to the cell. The mercury saturation pressures were 1.66×10^{-4} and 6.76×10^{-5} Torr. The carrier gas flow rates were varied from 10 to 27 cc/min. Emission was observed perpendicularly to the direction of irradiation. Radiation scattered from the lamps in the direction of the phototube was eliminated by a series of slits and collimator lenses. A Westinghouse type WL-775 photodiode at a 90 V potential was used as a detector of the emitted 2537 Å radiation. The photodiode wavelength response, as stated by the manufacturers, was maximum at 2400 Å with upper and lower limits of 3000 and 2000 Å, respectively. The photodiode current was measured with a Keithley model 417 high speed picoammeter.

Type B

The cell was a cylindrical quartz tube, 5.0 cm i.d. and 6.3 cm in length (6.0 cm path length). A circular beam of 2537 Å light (1.0 cm in diameter) was obtained from a GE G4T4.1 germicidal lamp which was maintained at 31.1 ± 0.1 °C in a thermostated distilled water bath. The ratio, α, of the emission half-width to the Doppler half-width of the lamp was 2.28. The light beam was split into two, an analytical beam passing through the cell, and a reference beam. Light intensities were measured by two Westinghouse type WL-775 photodiodes coupled to a Hewlett–Packard Model 740B d.c. standard/differential voltmeter. The mercury saturation pressure in these studies was 1.7×10^{-4} Torr. The cell temperature was that of the room (~ 24 °C).

Type C

A Hilger and Watts Model E517 spectrograph was used in these experiments. Kodak type 103-F and 103-O spectroscopic plates were used interchangeably. The resonance cell was a quartz tube 2.2 cm i.d. and 25 cm in length, ending in a light trap on the end remote from the spectrograph. Besides the low pressure mercury light sources, a low pressure argon–mercury cold cathode discharge was employed. The latter was constructed so that argon and carbon monoxide could be flowed through at various partial pressures. Mercury saturation pressures of 10^{-4} to 10^{-3} Torr were employed in this section.

Types D and E

The experiments were run in a flow system employing Ar as the carrier gas at flow rates of 27 cc/min and a total pressure of 20 Torr. The H_2 reactions were carried out in a quartz tube 2.2 cm i.d. and 11 cm in length (irradiated portion). A single U-shaped mercury resonance lamp, placed parallel to the reaction vessel, was employed as the source of 2537 Å radiation, for the experiments on the decomposition of hydrogen. The experiments on the decomposition of ethylene were carried out in a cylindrical quartz cell consisting of an inner tube, 20 cm long and 3.1 cm i.d., surrounded by an outer tube, 28 cm long and 5.5 cm o.d. Nickel sulfate filter solution at 25 °C was circulated in the outer tube in order to remove radiation in the 4000 Å region. The central region of this cell, 14 cm in length, was illuminated by two U-shaped mercury resonance lamps placed parallel to the reaction cell. The gases were saturated with mercury at a temperature of −3 °C, corresponding to a mercury pressure of 1.3×10^{-4} Torr, before entering the reaction cell.

The analyses were performed with a katharometer type detector consisting of two matched thermistors embedded in a copper block which was maintained at 0 °C with an ice slush bath. One of the thermistors was connected to the reaction cell inlet and served as a reference (sensing everything entering the cell); the other was connected to the outlet (sensing everything leaving the cell). This detector was found to be particularly sensitive to hydrogen due to its high thermal conductivity. Thus the progress of the reaction was monitored by following the rate of hydrogen production in the experiments on the decomposition of ethylene, or the rate of hydrogen consumption upon irradiation in the presence of ethylene, which served as an H-atom scavenger, in the experiments on the decomposition of hydrogen. In the latter experiments, the ethylene partial pressure was maintained at 2% of that of the hydrogen, so quenching by ethylene was negligible. The detector response was found to be linear with the rate of H_2 production or consumption over the concentration ranges used in the present work.[1]

Type A, the Pressure Dependence of the Quenching Cross Section of $Hg(6^3P_1)$ by CO

The quenching of $Hg(6^3P_1)$ by diatomic molecules can be assumed (1, 13) to proceed via formation of a complex

[1]The sensitivity of the detector to ethylene or acetylene is expected to be ~ 10% of the sensitivity to hydrogen, based on their respective thermal conductivities. Also, addition of hydrogen atoms to ethylene in the H_2 decomposition experiments is expected to give primarily the lower hydrocarbons (C_2–C_4) that are of comparable sensitivity to that of ethylene. Therefore the change in the detector response can, to a good approximation, be attributed to the change in hydrogen concentration.

Can. J. Chem. Downloaded from www.nrcresearchpress.com by 210.87.254.105 on 09/05/12
For personal use only.

of some duration in equilibrium with the reactants. For instance, the quenching of $Hg(6^3P_1)$ by CO may be represented by eq. [7]

$$[7] \quad Hg(6^3P_1) + CO \underset{k_{-1}}{\overset{k_1}{\rightleftharpoons}} (Hg^*CO)$$

$$\xrightarrow{k_q} Hg(6^1S_0) + CO\ (v \geqslant 1 + \text{k.e.})$$

The slow step in the quenching process is assumed to be the decomposition of the complex into products, which are in this case a ground state mercury atom and a vibrationally and translationally excited CO molecule. The relevant potential energy surfaces shown in Fig. 1 are in accord with refs. 2 and 13.

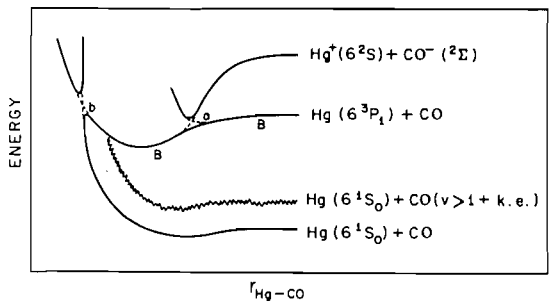

FIG. 1. Schematic potential energy surfaces for the quenching of $Hg(6^3P_1)$ by CO.

On the basis of the above, eq. [8] can be derived for the overall quenching rate constant, k_Q,

$$[8] \quad k_Q = \frac{\xi k_1 \xi' k_q}{\xi k_{-1} + \xi' k_q} \approx k_1 \xi' k_q / k_{-1}$$

where ξ and ξ' are the probabilities that the system would remain on surface B at the crossing points *a* and *b* (see Fig. 1), respectively. A similar equation was proposed by Yang (14) to explain the quenching of $Hg(6^3P_1)$ by the alkanes. An equation of this form was also employed by Vikis and Moser (6) in establishing a relationship between HgH–R decomposition lifetimes and quenching rate constants. Thus one should expect to see a pressure dependence in the quenching cross section if the lifetime of the excimer, $1/\xi k_{-1}$ in this case, is within the range of kinetic collision lifetimes (10^{-7}–10^{-9} s) attainable at ordinary pressures. A pressure dependence can be realized in terms of collisional deactivation of the excimer to the bottom of the potential well, whence the rate of crossing into the products or the reactants would be slower.[2] Because quenching cross sections are usually obtained at low pressures (1 to 2 Torr in the case of CO), any pressure dependence in the quenching cross section would not have become apparent previously.

An order of magnitude estimation of the rate constant k_{-1} can be obtained from eq. [2]. For a triatomic molecule formed by an excited atom and a ground state diatomic molecule, such as Hg*CO, k_{-1} is given by (1) eq. [9]

$$[9] \quad k_{-1} \sim \nu (D/kT)^{-5/2}$$

where v is a frequency factor and D is the dissociation energy of the excimer into Hg* and CO. Considering a reasonable set of v and D, of $10^{12 \sim 13}$ s^{-1} and 10 to 20 kcal/mole, respectively, lifetimes of the order of 10^{-8} to 10^{-10} s are obtained.[3] This seemed encouraging in the search for a pressure dependence in the quenching cross section, despite Homer and Lossing's (4) conclusion that lifetimes of the order of 10^{-5} s are involved (i.e. a collisionally stabilized complex at pressures of a few microns).

Results and Discussion

The results of this study are shown in Fig. 2. The quenching rate constant at each individual pressure was determined by varying the CO partial pressure while maintaining the overall pressure constant. This was done in order to eliminate any pressure broadening effects that might have appeared as an increase or a decrease of the quenching cross section with pressure. The Stern–Volmer type expression for the ratio I_0/I of the 2537 Å emission in the absence to the presence of CO is given by eq. [10]

$$[10] \quad I_0/I = 1 + k_Q(CO)/[1/\tau + k_{Q,P}(P)]$$

where k_Q is the quenching rate constant by CO, τ is the effective $Hg(6^3P_1)$ lifetime, and $k_{Q,P}$ is the quenching rate constant by the rare gas or any impurities in it.

In order to eliminate the remote possibility that quenching by the rare gas (expected to be negligible) or impurities in it would counter-act a possible increase in the quenching rate constant (k_Q) with pressure, two rare gases, He and Ar, were used as carriers (variation of $k_{Q,P}$) at two different mercury concentrations (variation of the effective τ by radiation imprisonment).

The results in Fig. 2 do not indicate any apparent pressure dependence. The somewhat larger deviations in Curve *A* may have been coincidental with a slight variation in the experimental conditions over the length of time that these data were obtained. The slopes of the curves in Fig. 2 are consistent with a k_Q of $5.78 \pm 0.06 \times 10^{13}$ and $5.95 \pm 0.22 \times 10^{13}$ cm^3 $mole^{-1}$ s^{-1} for the cases where helium and argon are used as pressure gases. These values are to be compared with the generally accepted k_Q of 5.59×10^{13} cm^3 $mole^{-1}$ s^{-1} (15). The effective $Hg(6^3P_1)$ lifetime was calculated by eq. [11] shown to be a good approximation at low imprisonment conditions (16).

$$[11] \quad \tau = \tau_0(1 + 0.284 \times 10^{-4} P_{Hg} \rho)$$

where τ_0 is the $Hg(6^3P_1)$ lifetime (1.09×10^{-7} s), P_{Hg} is

[2]A lack of pressure dependence could also be realized in this mechanism if both the forward and the reverse steps are accidentally equally influenced by pressure. A comparison of the quenching cross section, 5.8 Å², with the gas-kinetic cross section, 10.8 Å², would indicate that $\xi' k_q/k_{-1} \approx 0.5$. So a lack of pressure dependence could occur if $\xi' \approx 0.5$.

[3]The lifetime of the complex with respect to dissociation to the reactants is given by $1/\xi k_{-1}$. However, the minimum value of ξ should be ~ 0.5 according to eq. [8] and a comparison of the gas kinetic cross section with the quenching cross section.

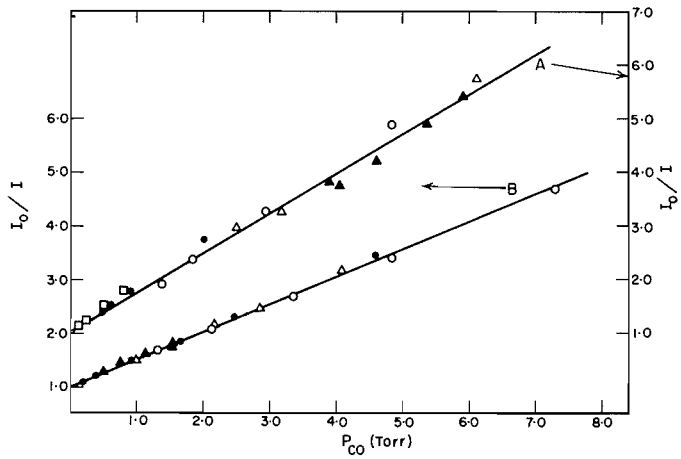

FIG. 2. Stern-Volmer plots of the 2537 Å $Hg(6^3P_1)$ emission as a function of CO at various rare gas total pressures. (*A*, the carrier gas was argon and the Hg saturation pressure was 1.66×10^{-4} Torr; the total pressures were: □, 10 Torr; ●, 50 Torr; ○, 100 Torr; △, 150 Torr; ▲, 200 Torr. *B*, the carrier gas was helium and the Hg saturation pressure was 6.76×10^{-5} Torr; the total pressures were: ▲, 10 Torr; ●, 50 Torr; △, 100 Torr; ○, 200 Torr.)

the partial pressure of mercury in Torr, and ρ (2.5 cm in the present case) is the average distance the 2537 Å photons travel before escaping the cell in the direction of the phototube.

In conclusion, within the limitations of our assumptions, we can exclude a Hg*CO lifetime in the range of 10^{-7} to 10^{-9} s. An alternative approach would have been that $\xi' k_q \gg \xi k_{-1}$, with $\xi \approx 0.5$ and k_Q independent of pressure. At the present there is no evidence that would exclude this latter possibility.

Type B, the Pressure Broadening Cross Section of the $Hg(6^1S_0) \rightarrow Hg(6^3P_1)$ Absorption

Zemansky's method of obtaining Lorentz's halfwidths, $\Delta\nu_L$, has been described elsewhere (17, 18) and it will be omitted here for the sake of brevity. Pressure broadening cross sections, σ_L^2, are obtained from eq. [12]

$$[12] \qquad \sigma_L^2 = (n/\pi\Delta\nu_L)\,(8\pi k\,T/\mu)^{1/2}$$

where n is the number of foreign gas atoms per cm^3 and the rest of the symbols have their conventional meaning.

Pressure broadening cross sections have been correlated by a number of theories (18, 19) to the nature of the foreign gas-excited atom potential. Assuming a potential $V(r)$ of the form, $V(r) = -C/r^s$, $s > 2$, Yang (18) related σ_L^2 to the force constant C in the form of eq. [13]

$$[13] \qquad \sigma_L^2 = \beta(s)(8\pi)^{1/2}\,(kT)^{-2/s}C^{2/s}$$

where $\beta(s)$ is a function of s only. A linear correlation between σ_L^2 and $C^{2/s}$ was obtained (18) for $s = 6$ for a variety of molecules. The pressure broadening cross section of CO which was reinvestigated with He, Ar, and N_2 serving as standards is shown in Table 1. It is evident that there is nothing unusual about the CO pressure broadening cross section (too high for instance) to suggest a much stronger intermolecular potential in the upper state than would correspond to a simple van der Waals attraction, at least over the intermolecular distances in which σ_L^2 is effective. Any long-lived Hg*CO complex would probably be formed at very close intermolecular distances of the order of the quenching radius of the $Hg(6^3P_1)$–CO system and most likely on a different potential energy surface than the initial $Hg(6^3P_1)$–CO surface.

TABLE 1

Pressure broadening cross sections

Gas	Cross section ($cm^2 \times 10^{16}$) This work	Reference 18	Reference 17
N_2	85±10	—	51
A	95–120	108	61.5
CO	60±10	—	44.5
He	33±4	37	15

*Type C, an Attempt to Observe Spontaneous or Resonance Emission from Hg*CO*

A close search was made for a Hg*CO emission continuum in the range of 2000 to 4000 Å, particularly in the region of 2500 to 3000 Å, over a range of CO pressures (10^{-3} to a few Torr), in the presence and in the absence of Ar or He carrier gases. The experiments were of three types: (*a*) Observation of the emission from the reaction cell under illumination with 2537 Å light; (*b*) observation of the emission spectrum of a low pressure mercury lamp designed so that the carrier gas (Ar) could be flowed through at various CO partial pressures; (*c*) observation of the emission spectrum of the reaction cell under simultaneous illumination with a low pressure mercury lamp and flow lamp employed in (*b*). A range of CO pressures (10^{-3}–10^{-2} Torr for the lamp, and 10^{-3} to 1 Torr for the reaction cell) were employed. The latter experiments were done in an attempt to obtain Hg*CO

Can. J. Chem. Downloaded from www.nrcresearchpress.com by 210.87.254.105 on 09/05/12
For personal use only.

Can. J. Chem. Downloaded from www.nrcresearchpress.com by 210.87.254.105 on 09/05/12
For personal use only.

emission from any allowed state(s) populated by resonance excitation from the flow lamp.

All three types of experiments failed to give any evidence of Hg*CO formation. Hg*Ar and Hg*He excimer emission previously observed by a number of workers (20, 21, 5), was also observed strongly in our spectra. The Hg*Ar emission extended from a few angstroms before the 2537 Å $Hg(6^3P_1)$ emission up to 2600 Å, while the Hg*He emission, which was much less intense, was distributed within a few angstroms about the 2537 Å $Hg(6^3P_1)$ emission line. The Hg*Ar emission at ~ 2560 Å was studied in the type (*a*) experiments as a function of CO. The results shown in Fig. 3 gave a normal Stern–Volmer plot with the absence of any second power dependence in CO and a slope of 2.7 $Torr^{-1}$ accounted for in terms of quenching of the $Hg(6^3P_1)$ precursor of Hg*Ar by CO. A Hg*Ar lifetime $< 10^{-7}$ s can be estimated from this experiment.

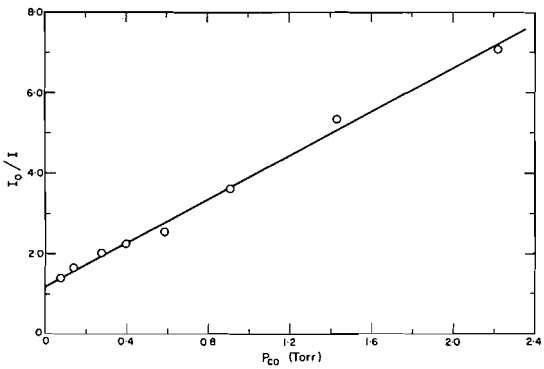

FIG. 3. Stern-Volmer plot of the Hg*Ar emission at 2650 Å vs. CO pressure.

The absence of any excimer emission of the type seen in the $Hg(6^3P_1)$ – rare gas systems could suggest the lack of any significant equilibrium concentration, $Hg(6^3P_1) + CO \rightleftarrows Hg^*CO$, because of a fast depletion by process [14]

$$[14] \quad Hg^*CO \xrightarrow{k_q} Hg(6^1S_0) + CO \ (v \geq 1 + \text{k.e.})$$

This could also explain the lack of a pressure dependence in the quenching cross section, i.e. $k_Q \sim \xi k_1 \sim 0.5k_1$, discussed in case *A*. The limited number of $Hg(6^3P_1)$ or Hg*CO emitters, because of fast quenching by CO, cannot account for the lack of any observed Hg*CO emission. No emission was observed with much longer exposure times, sometimes of the order of 10^3 times longer than the Hg* – rare gas emission exposures, which were obtained within a few minutes.

Type D, a Reinvestigation of the CO Enhancement Effect in the $Hg(6^3P_1)$ Photosensitized Decomposition of Ethylene

The failure to obtain any independent evidence of Hg*CO formation in the experiments described led us to reinvestigate the ethylene decomposition reaction studied by Homer and Lossing (4). An attempt is made to confirm their results under different experimental conditions and also to obtain a more quantitative fit of the proposed mechanism.

In addition, the properties of the Hg*CO excimer regarding its relative specificity towards ethylene and the alkanes (4, 11) were very reminiscent of $Hg(6^3P_0)$ properties studied by Vikis and Moser (6) in comparison with $Hg(6^3P_1)$, namely, a relatively high quenching cross section for the alkenes, and a relatively low quenching cross section for the alkanes. Homer and Lossing's (4) exclusion of $Hg(6^3P_0)$ as the species responsible for the enhancement effect observed in the presence of CO was on the basis of Scheer and Fine's (22) determination of the $Hg(6^3P_1) \rightarrow Hg(6^3P_0)$ quenching rate constant of CO.[4] The latter concluded on the basis of relative experiments with N_2 and CO, that CO is 1.35 times as efficient as N_2 in quenching $Hg(6^3P_1)$ atoms to the $Hg(6^3P_0)$ state. Since the total quenching rate constant for $Hg(6^3P_1)$ is much greater for CO than for N_2, one would conclude that the relative efficiency of CO to quench $Hg(6^3P_1)$ atoms to the ground state as opposed to quenching to the $Hg(6^3P_0)$ state is favored ~ 10:1. Before Scheer and Fine's determination, it was considered that both N_2 and CO quench primarily to the $Hg(6^3P_0)$ state (24). Karl *et al.* (3*a*) have measured absolute $Hg(6^3P_0)$ and $Hg(6^3P_1)$ concentrations in N_2 and Ar, in the presence of equal amounts of CO, by following the absorption of 4047 and 4358 Å light. Their data (cf. Table 3, ref. 3*a*) indicate that the $Hg(6^3P_0)$ concentration is only a factor of 7.1 higher in 2.38 Torr of N_2 than in 2.54 Torr of Ar. The $Hg(6^3P_1)$ concentration was the same in both gases. The CO pressure was $\leq 1.0 \times 10^{-2}$ Torr (25). Argon does not quench $Hg(6^3P_1)$ or $Hg(6^3P_0)$ (3*a*, also see type *A* experiments). On the basis of the above it would follow that $[k_N(N_2) + k_{CO}(CO)]/k_{CO}(CO) \approx 7.1$, where k_N and k_{CO} are the N_2 and CO rate constants of quenching to the $Hg(6^3P_0)$ state. Thus one can obtain $(k_{CO}/k_N) \approx 39$. This order of magnitude would be more than adequate to explain the "CO effect" in terms of $Hg(6^3P_0)$ rather than Hg*CO. The authors of ref. 3*a* estimate that their absorption concentration relationship should be reliable within a factor of two.[5]

We have also investigated the decomposition of ethylene in the presence of nitrogen under the same experimental conditions in an attempt to determine a $Hg(6^3P_0)$ lifetime with which to compare the lifetime of the species present in CO.

Results and Discussion

The results on the decomposition of ethylene in the presence of CO and N_2 are shown in Figs. 4 and 5. The mechanism which fits our data with CO is similar to the

[4]The peculiarities of metal detectors used to detect $Hg(6^3P_0)$ atoms reported by a number of workers (22, 23) is perhaps one of the reasons to be cautious of Scheer and Fine's (22) result. Pressure broadening effects as well as radiation imprisonment effects (15) in their system could have also been more effective than as discussed by ref. 22.

[5]In view of the factors discussed above we considered it worthwhile to compare the properties of the X* species in parallel with the expected properties of $Hg(6^3P_0)$ in the work that follows.

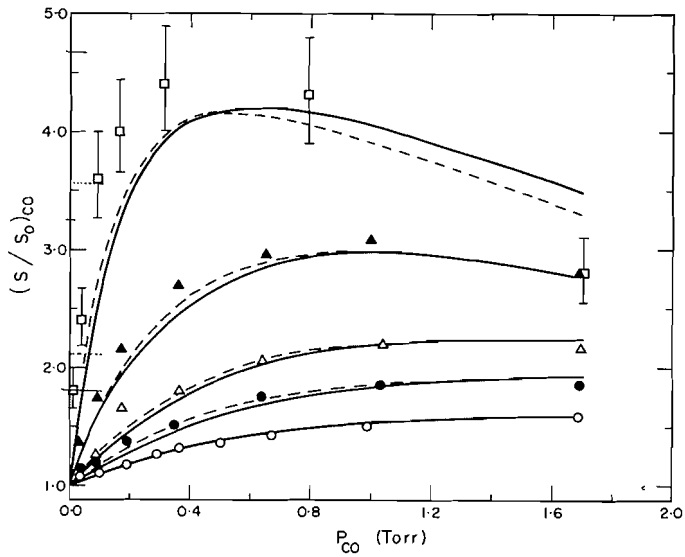

FIG. 4. The rate of H_2 production as a function of CO pressure at various C_2H_4 pressures. (The C_2H_4 pressures were: □, 3.7 ± 0.6 × 10^{-3} Torr; ▲, 18.4 ± 1.0 × 10^{-3} Torr; △, 43.2 ± 1.5 × 10^{-3} Torr; ●, 67.8 ± 1.8 × 10^{-3} Torr; ○, 108 ± 2 × 10^{-3} Torr. The solid line was obtained from eq. [25]; the dotted line from eq. [26].)

one proposed by Homer and Lossing (4) with the exception that Hg*CO is labelled X* and the addition of reaction [20] which is required by our data.

[15] $\quad Hg + h\nu\,(2537\text{ Å}) \rightarrow Hg^*$

[16] $\quad Hg^* \xrightarrow{1/\tau} Hg + h\nu\,(2537\text{ Å})$

[17] $\quad Hg^* + C_2H_4 \xrightarrow{k_E} Hg + C_2H_2 + H_2$

[18] $\quad Hg^* + CO \xrightarrow{k_{CO}} X^*\,(+Hg + CO)$

[19] $\quad X^* + C_2H_4 \xrightarrow{k_E'} (Hg + CO) + C_2H_2 + H_2$

[20] $\quad X^* + CO \xrightarrow{k_{CO}'} (Hg + CO) + CO$

[21] $\quad X^* \xrightarrow{1/\tau'} (Hg + CO) + h\nu'$

where, Hg and Hg* denote $Hg(6^1S_0)$ and $Hg(6^3P_1)$, respectively. The rate constants for the excimer are primed. Step [21] includes in addition to emission any reaction that would appear first order under our experimental conditions, i.e., collisional deactivation in the gas phase or on the walls, quenching by Hg, Ar, or impurities in Ar, which are held fixed. The ratio $(S/S_0)_{CO}$ of the rate of H_2 formation in the presence to the rate in the absence of CO is given by eq. [22]

$$[22] \qquad (S/S_0)_{CO} = \frac{1 + \dfrac{\phi_E'k_E'}{\phi_E k_E} \cdot \dfrac{k_{CO}^x(CO)}{[k_E'(C_2H_4) + k_{CO}'(CO) + (1/\tau')]}}{1 + \dfrac{k_{CO}(CO)}{(1/\tau) + k_E(C_2H_4)}}$$

where ϕ_E and ϕ_E' are factors <1 which allow for the possible deactivation of the excited ethylene initially formed in reactions [17] and [19], respectively, and k_{CO}^x is the rate constant for quenching to the state X*, as opposed to k_{CO} which represents the total quenching rate constant of $Hg(6^3P_1)$ by CO. The denominator of eq. [22] is comprised of known quantities. The effective lifetime, τ, of $Hg(6^3P_1)$ for the cell and mercury concentration employed in these studies was 1.83×10^{-7} s, determined by the photosensitization of ethylene in the absence of CO and in accord with eq. [23]

$$[23] \qquad S_0^{-1} = (1/\phi_E I_a)[1 + 1/\tau k_E(C_2H_4)]$$

where S_0 is the rate of H_2 formation and I_a is the rate of 2537 Å light absorption by $Hg(6^1S_0)$. A value of 3.6×10^{14} cm^3 mole^{-1} s^{-1} (15) was used for k_E. To determine the unknown rate constants in the numerator of eq. [22], the following procedure was adopted. Equation [22] was rearranged to

$$[24] \qquad \frac{(CO)}{(S/S_0)\left[1 + \dfrac{k_{CO}(CO)}{(1/\tau) + k_E(C_2H_4)}\right]^{-1}} = A(C_2H_4) + B(CO) + C$$

Can. J. Chem. Downloaded from www.nrcresearchpress.com by 210.87.254.105 on 09/05/12
For personal use only.

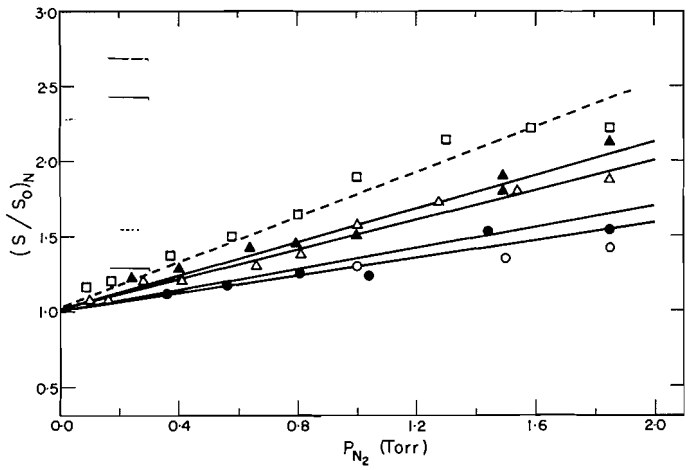

FIG. 5. The rate of H_2 production as a function of N_2 at various C_2H_4 pressures. (The ethylene pressures were: □, $3.7 \pm 0.6 \times 10^{-3}$ Torr; ▲, $5.0 \pm 0.7 \times 10^{-3}$ Torr; △, $6.3 \pm 0.7 \times 10^{-3}$ Torr; ●, $11.0 \pm 0.8 \times 10^{-3}$ Torr; ○, $13.6 \pm 0.9 \times 10^{-3}$ Torr. The solid lines were obtained from eq. [34]; see discussion in the text for dotted line.)

where

$$A = (\phi_E k_E)/(\phi_E' k_{CO}^x),$$

$$B = (\phi_E k_E k_{CO}')/(\phi_E' k_E' k_{CO}^x)$$

and

$$C = (\phi_E k_E)/(\phi_E' k_E' k_{CO}^x \tau')$$

The left hand side of eq. [24], called F, consisted of known or experimentally determined quantities; $k_{CO} = 5.59 \times 10^{13}$ cm^3 mole^{-1} s^{-1}, (15); $\tau = 1.83 \times 10^{-7}$ s, determined experimentally by taking $k_E = 3.6 \times 10^{14}$ cm^3 mole^{-1} s^{-1} (15). Plots of F vs. C_2H_4 at constant CO, and F vs. CO at constant C_2H_4 gave the constants A, B, and C. The averaged (over all CO and all C_2H_4) constants A, B, and C are given in the numerator of eq. [25] which was used to obtain the solid lines in Fig. 4.

$$[25] \quad (S/S_0)_{CO,calcd.} = \frac{1 + \dfrac{(CO)}{6.5(C_2H_4) + 0.15(CO) + 0.02}}{1 + \dfrac{3.0(CO)}{5.47 + 19.4(C_2H_4)}}$$

where the partial pressures are in Torr. A better fit at low CO pressures (dotted line) was obtained by using a 17% lower k_E (also increasing τ by 17% since τ was determined on the basis of k_E). The expression for the latter fit is

$$[26] \quad (S/S_0)_{CO,calcd.} = \frac{1 + \dfrac{(CO)}{5.7(C_2H_4) + 0.15(CO) + 0.02}}{1 + \dfrac{3.0(CO)}{17.0(C_2H_4) + 4.80}}$$

In both eqs. [25] and [26] the results at 3.7×10^{-3} Torr of C_2H_4 are ignored, because our analytical technique was introducing significant errors. Thus, the constants of the best fit and the estimated tolerances given in parenthesis are

$$A = 5.7 \quad (30\%)$$

$$B = 0.15 \quad (20\%)$$

and

$$C = 0.02 \quad (100\%)$$

The large error in C comes as a result of errors in determining A and B. Assuming that $\phi_E/\phi_E' \approx 1$, then $A = k_E/k_{CO}^x = 5.7$, which is comparable to 6.44 (15). Thus CO must quench $Hg(6^3P_1)$ almost totally (within the experimental errors) to the X* state.

The decomposition of ethylene as a function of N_2 pressure was studied previously (6). At low nitrogen pressures (< 2 Torr), the following reactions are of importance

$$[27] \quad Hg + h\nu\,(2537\text{ Å}) \longrightarrow Hg^*$$

$$[28] \quad Hg^* \xrightarrow{1/\tau} Hg + h\nu\,(2537\text{ Å})$$

$$[29] \quad Hg^* + C_2H_4 \xrightarrow{k_E} Hg + C_2H_2 + H_2$$

$$[30] \quad Hg^* + N_2 \xrightarrow{k_N} Hg^0 + N_2$$

$$[31] \quad Hg^0 + C_2H_4 \xrightarrow{k_E^0} Hg + C_2H_2 + H_2$$

$$[32] \quad Hg^0 \xrightarrow{1/\tau^0} Hg + h\nu^0 \quad \text{etc.}$$

where Hg^0 denotes $Hg(6^3P_0)$. The relevant $Hg(6^3P_0)$ rate constants are denoted by superscript 0. Step [32] includes again the equivalent of step [21] in the CO mechanism.

The ratio, $(S/S_0)_N$, of the rate of H_2 production in the presence of N_2 to that in the absence of N_2, is given by eq. [33], an expression similar to eq. [22].

Can. J. Chem. Downloaded from www.nrcresearchpress.com by 210.87.254.105 on 09/05/12
For personal use only.

Can. J. Chem. Downloaded from www.nrcresearchpress.com by 210.87.254.105 on 09/05/12
For personal use only.

[33] $$(S/S_0)_N = \frac{1 + \frac{\phi_E{}^0 k_E{}^0}{\phi_E k_E} \cdot \frac{k_N(N_2)}{[k_E{}^0(C_2H_4) + (1/\tau^0)]}}{1 + \frac{k_N(N_2)}{k_E(C_2H_4) + (1/\tau)}}$$

A similar procedure to that adopted for the experiments with CO was also used here for the determination of the unknown constants in the numerator of eq. [33]. The value of 0.39×10^{13} cm^3 mole^{-1} s^{-1} (26) was used for k_N. This value is a factor of 1.5 higher than the one given in ref. 15, proc. II. However, either value introduces no significant changes because the term $k_N(N_2)/[k_E(C_2H_4) + (1/\tau)]$ is less than 0.10 at the nitrogen pressures used here. The solid curves in Fig. 5 were obtained from eq. [34]

[34] $$(S/S_0)_{N,calcd.} = \frac{1 + \frac{N_2}{160(C_2H_4) + 0.83}}{1 + \frac{0.21\,N_2}{5.47 + 19.4(C_2H_4)}}$$

where the partial pressures are in Torr. The results at 2.7×10^{-3} Torr of C_2H_4 agree with a 14% lower value (which is within the experimental error) for the coefficients in the numerator of eq. [34] (dotted curve). The unknown constants in the present case are: $A' = (\phi_E k_E/\phi_E{}^0 k_N) = 160$ (30%) and $C' = (\phi_E k_E/\phi_E{}^0 k_E{}^0 k_N \tau^0) = 0.83$ (20%). The ratio, $\phi_E/\phi_E{}^0$, is unity at a total pressure of 20 Torr of Ar (6); therefore, A' should be equal to k_E/k_N. The presently determined ratio is closer to a ratio of 138 obtained from the data of ref. 15, proc. II, than the ratio of 92 obtained using k_N of ref. 26.

Assuming that the X* species formed in the presence of CO is Hg(6^3P_0), the following ratios should be comparable: $A'/C' = \tau^0 k_E{}^0 = 1.93 \times 10^2$ Torr^{-1}, $A/C = \tau' k_E' = 2.85 \times 10^2$ Torr^{-1}. This latter ratio is comparable to the one determined by ref. 4, i.e. if the same assumption is made that $k_E' = k_E$, $\tau' = 1.5 \times 10^{-5}$ s. A value of $\tau' = 3.0 \times 10^{-5}$ s was determined by ref. 4. Also the ratio $A/B = k_E'/k_{CO}' = 38.0$, which is least in error from our experimental results, should be comparable to $k_E{}^0/k_{CO}{}^0 = 21.4$, determined by Callear and Williams (27). These values are comparable within a factor of two, and while this does not confirm the identification of X* with Hg(6^3P_0) (even if the values were in exact agreement), it makes it worthy of consideration. Additional results that probe more into this comparison are outlined in Case *E*.

Type E, the Enhancement of the Hg(6^3P_1) Photosensitized Decomposition of H_2 in the Presence of CO.

The relative trends in $(S/S_0)_{CO}$ obtained by ref. 11 for ethylene and some alkanes are shown in Table 2. These values are compared to calculated $(S/S_0)_{CO}$ values assuming that X* = Hg(6^3P_0) and using the Hg(6^3P_0) quenching data of ref. 6. The experimental conditions are those of refs. 4 and 11. On the basis of these results, which indicate a rough correlation of X* with Hg(6^3P_0), it was decided to test the applicability of a Hg(6^3P_0)

TABLE 2

A comparison of calculated $(S/S_0)_{CO}$ ratio* with those obtained by the CO method

M	$k_M/k_M{}^0$†	$(S/S_0)_{CO}$ Calculated‡	$(S/S_0)_{CO}$ Observed§
C_2H_4	16	2.62	2.5
C_2H_6	176	0.68	slight decrease
C_3H_8	224	0.58	"
i-C_4H_{10}	140	0.81	"
n-C_4H_{10}	352	0.45	"
c-C_3H_6	3800	0.24	"
n-C_7H_{16}	363‖	0.48	"

Assuming X = Hg (6^3P_0).
†Reference 6.
‡Calculated on the basis of refs. 4, 11 experimental conditions.
§Reference 11.
‖This ratio is not available experimentally. It was estimated from the Hg(6^3P_0) quenching cross section of n-C_4H_{10} assuming quenching cross section additivity ($\sigma_{n\text{-}C_4H_{10}} = 4\sigma_{sec\text{-}C-H}$ and $\sigma_{n\text{-}C_7H_{10}} = 10\,\sigma_{sec\text{-}C-H}$).

proposition in the case of hydrogen. Under our experimental conditions,[6] it was calculated that a relatively large (20 to 60%) increase in the decomposition of hydrogen was to be expected in the presence of small amounts of CO and under conditions of incomplete quenching, if the X* species were a Hg(6^3P_0) atom.

Hydrogen is also known to quench Hg(6^3P_1) atoms via a chemical mechanism (28–31)

[35] $$Hg(6^3P_1) + H_2 \rightarrow HgH + H \rightarrow Hg(6^1S_0) + 2H$$

or

[36] $$Hg(6^3P_1) + H_2 \rightarrow Hg(6^1S_0) + 2H$$

rather than by a physical mechanism

[37] $$Hg(6^3P_1) + H_2 \rightarrow Hg(6^1S_0) + H_2^* \text{ (triplet)}$$

Thus one would not expect an enhancement effect if X* has a specificity towards molecules that are known to quench via an excited molecule mechanism (4, 11), a conclusion which was used as diagnostic of the nature of the quenching process in a number of cases (11, 12).

Results and Discussion

The results of this study are shown in Figs. 6 and 7. A mechanism similar to the one proposed for the decomposition of ethylene is also employed here

[38] $$Hg + h\nu\,(2537\text{ Å}) \longrightarrow Hg^*$$

[39] $$Hg^* \xrightarrow{1/\tau} Hg + h\nu\,(2537\text{ Å})$$

[40] $$Hg^* + H_2 \xrightarrow{k_H} Hg + 2H$$

[6]On the basis of an expression similar to eq. [22], for a general quencher M, one can show that at conditions of (M) → 0, $(S/S_0)_{CO} > 1$ if $\tau'/\tau > k_M/k_M'$, where the notation is the one used in text. Thus, it can be seen that the magnitude of $(S/S_0)_{CO}$ is also a function of τ which can be varied by radiation imprisonment to achieve a maximum $(S/S_0)_{CO}$.

Can. J. Chem. Downloaded from www.nrcresearchpress.com by 210.87.254.105 on 09/05/12
For personal use only.

[41] $$Hg^* + CO \xrightarrow{k_{CO}} X^* (+ Hg + CO)$$

[42] $$X^* + H_2 \xrightarrow{k_H'} (Hg + CO) + 2H$$

[43] $$X^* + CO \xrightarrow{k_{CO}'} (Hg + CO) + CO$$

[44] $$X^* \xrightarrow{1/\tau'} (Hg + CO) + h\nu' \quad \text{etc.}$$

[45] $$H + sc \xrightarrow{k_{sc}} Hsc$$

where sc is the ethylene scavenger, always 2% of the hydrogen pressure so that quenching of X* or Hg* by ethylene could be neglected. The rest of the symbols have the same meaning as in type *D* experiments.

This mechanism yields the following steady state equation for the rate of H_2 consumption $(-S)$

[46] $$(-S)^{-1} = \left[\frac{(1/\tau) + k_{CO}(CO) + k_H(H_2)}{I_a(H_2)}\right] \times \left[\phi_H k_H + \frac{\phi_H' k_H' k_{CO}^x(CO)}{(1/\tau') + k_H'(H_2) + k_{CO}'(CO)}\right]^{-1}$$

where, ϕ_H and ϕ_H' are factors ≤ 2 which allow for the possible production of hydrogen species other than atomic hydrogen in eqs. [40] and [42], respectively. I_a is the rate of excitation of Hg(6^1S_0) to Hg(6^3P_1).

In the absence of CO the above expression reduces to eq. [47]

[47] $$(-S_0)^{-1} = (1/I_a\phi_H)[1 + 1/\tau k_H(H_2)]$$

A plot of $(-S_0)^{-1}$ vs. $(H_2)^{-1}$ should give a straight line assuming linearity of the detector response and efficient H atom scavenging. This is indeed the case, as shown in Fig. 6. The ratio of the slope to the intercept of this plot, 0.288 Torr is $1/\tau k_H$. The value of $1/\tau = 4.75 \times 10^6$ s^{-1} was determined under identical conditions, but employing the Hg(6^3P_1) photosensitized decomposition of ethylene to yield C_2H_2 and H_2, and following the rate of H_2 production, S_0, with the same detector. A value of 3.6×10^{14} cm^3 mole^{-1} s^{-1} (15) was used for the quenching rate constant, k_E. The rate constant k_H is thus determined to be 3.07×10^{14} cm^3 mole^{-1} s^{-1}, in good agreement with the accepted value of 2.90×10^{14} cm^3 mole^{-1} s^{-1} (15).

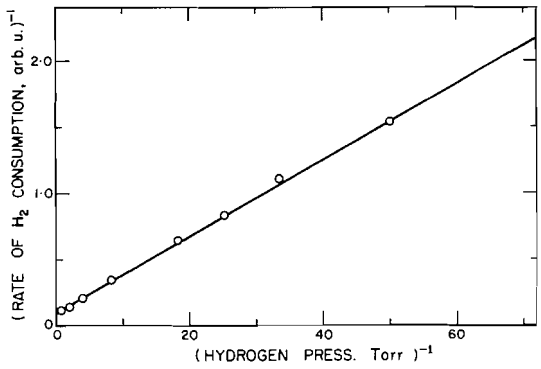

FIG. 6. A plot of the reciprocal of the rate of hydrogen consumption vs. the reciprocal of hydrogen pressure in the absence of CO.

The results at three different carbon monoxide concentrations are shown in Fig. 7. It can be seen that at the low hydrogen pressures (incomplete quenching by hydrogen), there is a small net increase in the rate of

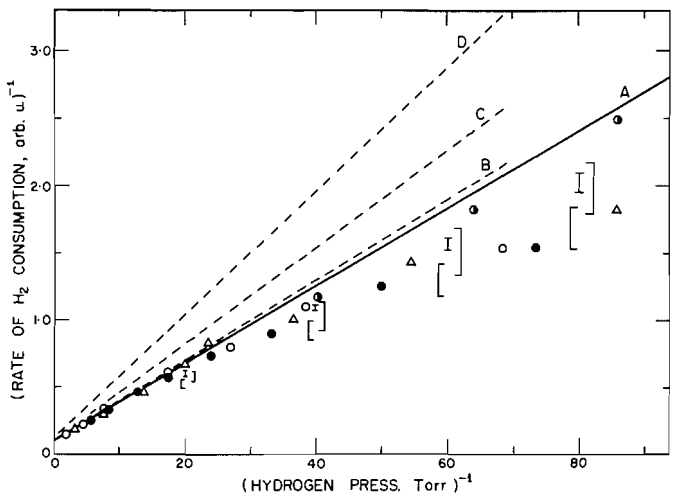

FIG. 7. Experimental and calculated plots of the reciprocal of the rate of hydrogen consumption vs. the reciprocal of hydrogen pressure, at various CO partial pressures. Curve *A* is taken from Fig. 6 and corresponds to zero CO; to estimate the reproducibility a few extra points ◑ were taken at a later date. Curves *B*, *C*, and *D* are calculated reciprocal rates assuming competitive quenching by CO but no X* formation eq. [48] for 0.045, 0.365, and 0.924 Torr of CO, respectively; I,], and [show the CO effect predicted on the assumption that X* = Hg(6^3P_0) at 0.045, 0.305, and 0.924 Torr of CO, respectively. The corresponding experimental points are shown by △, ●, and ○.

Can. J. Chem. Downloaded from www.nrcresearchpress.com by 210.87.254.105 on 09/05/12
For personal use only.

hydrogen decomposition even when there is competitive quenching by CO. When we compare the observed rates with the calculated rates of hydrogen decomposition (see Fig. 7), assuming competitive quenching of $Hg(6^3P_1)$ by H_2 and CO, but no X* formation (eq. [48])

$$[48] \quad (-S)^{-1} - (1/I_a\phi_H)\{1 + [(1/\tau) + k_{CO}(CO)]\,[1/k_H(H_2)]\}$$

it leaves no doubt that there is a definite CO effect in the $Hg(6^3P_1)$ photosensitized decomposition of hydrogen.

It has been previously pointed out by Scheer and Fine (22) that CO can add H atoms to form formaldehyde and glyoxal in the $Hg(6^3P_1)$ photosensitized decomposition of CO—H_2 mixtures, although the rate constant for this reaction is not known. This however cannot be the reason for the observed increase in H_2 consumption, because the phenomenon appears only at incomplete quenching conditions. Also the ethylene scavenger was shown to be quite efficient in removing H atoms in the experiments with no CO.[7]

Also shown in Fig. 7 are the calculated reciprocal rates assuming that the X* is a $Hg(6^3P_0)$ atom. These values were obtained by substituting k_Ek_{CO}'/k_E' and $k_E/k_E'\tau'$, obtained from the decomposition of ethylene, with k_Hk_{CO}'/k_H^0 and $k_H/k_H^0\tau'$, assuming $\phi_E = \phi_E'$ and $\phi_H = \phi_H^0$. The upper limits were obtained using $k_Hk_E^0/k_Ek_H^0 = 8.05$ (27), and the lower limits using $k_Hk_E^0/k_Ek_H^0 = 4.7$ (6). The experimental results lie within these limits.

An alternative would be to postulate a Hg*CO excimer which is quenched by H_2 with a small but finite quenching cross section, in line with the conclusions of Homer and Lossing (4, 11). A physical type of energy transfer, as in the case of ethylene, would require that the species possess a minimum energy in excess of 104 kcal/mole. A minimum energy of 90 kcal/mole was previously estimated from the decomposition of ethylene (4). Thus the probability of stabilization of Hg*CO to lifetimes of the order of 10^{-5} s in a potential well of ~ 8 kcal/mole at pressures of 10 to 20 Torr becomes more remote. However, it is more likely that in the present case, the quenching proceeds via a chemical mechanism

$$[49] \quad X^* + H_2 \rightarrow XH + H \rightarrow (Hg + CO) + 2H$$

in analogy to the $Hg(6^3P_1)$–H_2 system.[8]

Regarding the dependability of the "CO enhancement effect" in predicting the nature of the quenching process the following can be said. First, the method is dependent on the experimental conditions (cf. footnote 6). Second, an enhancement effect is observed in molecules that possess a low k_M/k_M' ratio, which can be due to either a high k_M' (most probable) or a low k_M. An examination of the quenching cross sections of various excited species by a number of molecules would reveal that, in general, molecules which are good quenchers for one excited species are usually good quenchers for another. Thus the "CO enhancement effect" observed by ref. 4 for molecules that are known to quench via physical mechanism, e.g., the olefins, may have been coincidental. It is perhaps worthwhile in this regard to look for enhancement effects in other molecules known to be good quenchers. For instance, the RCl molecules which are known to be good quenchers of $Hg(6^3P_1)$ (15), but quench via a chemical mechanism (8) (Cl abstraction), offer a good test of this proposition.

Conclusions

The limited number of physical measurements described (pressure dependence of the quenching cross section, pressure broadening, emission) have failed to give any indication of long-lived Hg*CO formation. However, this cannot be considered as evidence for its exclusion, because there is always a possibility that the species may not respond to these probes.

The chemical results on the decomposition of ethylene and hydrogen at incomplete quenching conditions and in the presence of CO are in accord with Homer and Lossing's (4) conclusion of a long-lived species formation. In addition, we have obtained quenching rate constants of X* by CO and H_2 relative to C_2H_4. A comparison

---

[7]The linearity of the plot in Fig. 6 as well as the correct value of k_H are the best indications that efficient scavenging is achieved over the range of C_2H_4 and H_2 pressures employed here. The efficiency, e, of scavenging by C_2H_4 vs. wall first order recombination and second order gas phase recombination, is

$$e = k_{sc}(C_2H_4)/[k_{sc}(C_2H_4) + k_c(Ar)(H) + k_w]$$

Since the C_2H_4 pressure was 2% of H_2, one can write

$$e = 2 \times 10^{-2}k_{sc}(H_2)/[2 \times 10^{-2}k_{sc}(H_2) + k_c(Ar)(H) + k_w]$$

The plot of Fig. 6 is in accord with e not being a function of H_2 and thus $e = 1$. One can realize this by comparison of the various rates of H consumption. The rate of scavenging is $1.94 \times 10^2(H_2)\ s^{-1}$, where H_2 is in Torr. A value of $1.8 \times 10^{11}\ cm^3\ mole^{-1}\ s^{-1}$ (32) was used for k_{sc}. The rate of recombination in the gas phase in the presence of 20 Torr of argon is $1.22 \times 10^2(H)\ s^{-1}$. A value of $23 \times 10^{14}\ cm^6\ mole^{-2}\ s^{-1}$ (33) was used for k_c. The calculation of k_w is perhaps the least dependable. A value of $5 \times 10^{-3}\ s^{-1}$ can be estimated for a first order diffusion controlled wall recombination rate constant, employing a recombination coefficient of 1.8×10^{-5} (34). Values as high as 10^{-3} and as low as 10^{-7} were reported in the literature. At the lowest hydrogen pressures, 1.2×10^{-2} Torr, where scavenging by ethylene would be the least efficient, wall recombination could thus be neglected, and

$$e = 1.9 \times 10^2(H)/1.9 \times 10^2(H_2) + 1.3 \times 10^2(H) = 1$$

because $H \ll H_2$. A maximum H atom pressure of 10^{-4} Torr was estimated based on the light intensities employed and

$$H_{max} = [R/k_c(Ar)]^{1/2}$$

where R is the rate of H atom production.

[8]The authors are indebted to Dr. F. P. Lossing for pointing out to them this latter alternative.

of the reactivity of the excimer towards C_2H_4, RH, CO, and H_2, indicates that the species behaves like a $Hg(6^3P_0)$ atom. This similarity plus other evidence mentioned in conjunction with a high $Hg(6^3P_0)$ population in the $Hg(6^3P_1)$–CO system, we feel, is enough to warrant a re-examination of the quenching rate constant for the process

$$Hg(6^3P_1) + CO \rightarrow Hg(6^3P_0) + CO$$

It was furthermore shown by the enhancement effect of CO in the decomposition of H_2 that the "carbon monoxide effect" may not be a dependable means of predicting the nature of the quenching process.

Addendum

It has come to our attention since originally submitting this paper that Horiguchi and Tsuchiya (35) have re-examined the quenching of $Hg(6^3P_1)$ to form $Hg(6^3P_0)$ and $Hg(6^1S_0)$ with both N_2 and CO using an optical method. Their results differ considerably from those of Scheer and Fine (22): CO quenches $Hg(6^3P_1)$ predominantly (78%) to the $Hg(6^3P_0)$ level rather than to the $Hg(6^1S_0)$ level. Their results therefore give substantial support for X* being $Hg(6^3P_0)$ rather than Hg*CO.

The authors gratefully acknowledge the financial support received from the National Research Council of Canada.

1. E. E. NIKITIN. J. Quant. Spectry. Radiat. Transfer, **5**, 435 (1965).
2. A. BJERRE and E. E. NIKITIN. Chem. Phys. Lett. **1**, 179 (1967).
3. (*a*) G. KARL, P. Kruus, and J. C. POLANYI. J. Chem. Phys. **46**, 224 (1967). (*b*) G. KARL, P. KRUUS, J. C. POLANYI, and I. W. M. SMITH. J. Chem. Phys. **46**, 244 (1967).
4. J. B. HOMER and F. P. LOSSING. Can. J. Chem. **44**, 143 (1966).
5. S. PENZES, O. P. STRAUSZ, and H. E. GUNNING. J. Chem. Phys. **45**, 2322 (1966).
6. (*a*) A. C. VIKIS and H. C. MOSER. To be published. (*b*) A. C. VIKIS. Ph.D. Thesis, Kansas State University, Manhattan, Kansas. 1969.
7. K. YANG. J. Amer. Chem. Soc. **89**, 5344 (1967).
8. H. E. GUNNING and O. P. STRAUSZ. Advan. Photochem. **1**, 209 (1963).
9. (*a*) K. J. LAIDLER. J. Chem. Phys. **10**, 34 (1942); **10**, 43 (1942).
10. (*a*) J. L. MAGEE. J. Chem. Phys. **8**, 687 (1940). (*b*) J. L. MAGEE and T. RI. J. Chem. Phys. **9**, 638 (1941).
11. A. JONES and F. P. LOSSING. Can. J. Chem. **45**, 1685 (1967).
12. (*a*) A. JONES, S. YAMASHITA, and F. P. LOSSING. Can. J. Chem. **46**, 833 (1968). (*b*) *S.* YAMASHITA and F. P. LOSSING. Can. J. Chem. **46**, 2925 (1968). (*c*) A. JONES and F. P. LOSSING. Can. J. Chem. **47**, 1391 (1969).
13. J. C. POLANYI. J. Quant. Spectry. Radiat. Transfer, **3**, 471 (1963).
14. K. YANG. J. Amer. Chem. Soc. **89**, 5344 (1967).
15. R. J. CVETANOVIĆ. Progr. Reaction Kinet. **2**, 41 (1964).
16. K. YANG. J. Amer. Chem. Soc. **88**, 4575 (1966).
17. A. C. G. MITCHELL and M. W. ZEMANSKY. Resonance radiation and excited atoms. Cambridge University Press, New York. 1961.
18. K. YANG. J. Amer. Chem. Soc. **86**, 3941 (1964).
19. R. G. BREENE, Jr. The shift and shape of spectral lines. Pergamon Press, New York. 1961.
20. H. KUHN and O. OLDENBERG. Phys. Rev. **41**, 72 (1932).
21. W. M. PRESTON. Phys. Rev. **51**, 298 (1937).
22. M. D. SCHEER and J. FINE. J. Chem. Phys. **36**, 1264 (1962).
23. B. DE B. DARWENT and F. G. HURTUBISE. J. Chem. Phys. **20**, 1684 (1952).
24. M. W. ZEMANSKY. Phys. Rev. **36**, 919 (1930).
25. G. KARL. Ph.D. Thesis. The University of Toronto. Toronto, Ontario. 1964.
26. C. G. MATLAND. Phys. Rev. **92**, 637 (1953).
27. A. B. CALLEAR and G. J. WILLIAMS. Trans. Faraday Soc. **60**, 2158 (1964).
28. A. B. CALLEAR and J. C. ROBB. Trans. Faraday Soc. **51**, 638 (1955).
29. O. P. STRAUSZ and H. E. GUNNING. Trans. Faraday Soc. **60**, 347 (1964).
30. A. B. CALLEAR and R. E. M. HEDGES. Nature, **218**, 163 (1968).
31. T. L. POLLOCK, E. JAKUBOWSKI, H. E. GUNNING, and O. P. STRAUSZ. Can. J. Chem. **47**, 3474 (1969).
32. K. YANG. J. Amer. Chem. Soc. **84**, 719 (1962); **84**, 3795 (1962).
33. B. A. THRUSH. Progr. Reaction Kinet. **3**, 65 (1965).
34. M. GREEN, K. R. JENNINGS, J. W. LINNET, and D. SCHOFIELD. Trans. Faraday Soc. **55**, 2152 (1959).
35. H. HORIGUCHI and S. TSUCHIYA. In press.

Can. J. Chem. Downloaded from www.nrcresearchpress.com by 210.87.254.105 on 09/05/12
For personal use only.

Modification of Pascal's triangle for calculating size distributions in polymers[1]

S. G. WHITEWAY
Atlantic Regional Laboratory, National Research Council of Canada, Halifax, Nova Scotia
Received December 10, 1969

Pascal's triangle, which is well known to yield all solutions to the factorial part of the Bernoulli binomial probability function, is modified to yield the correct factorial term in expressions for the molecular size distribution in polymers. This approach provides an alternative concept of the meaning of these factorial numbers.

Canadian Journal of Chemistry, 48, 1432 (1970

Can. J. Chem. Downloaded from www.nrcresearchpress.com by 210.87.254.6 on 09/05/12
For personal use only.

It has been shown recently (1) that for multichain polymers formed by self-condensation of the monomer RA_f the mole fraction of x-mer, N_x, is given by

$$[1] \quad N_x = \frac{(fx - x)!}{(fx - 2x + 1)!x!} \times (p_{AA})^{x-1}(1 - p_{AA})^{fx-2x+1}$$

where $p_{AA} = \alpha f/2(f - 1)$, and α is defined as the fraction of A groups, originally present, that have condensed to form AA groups. Equation [1] was obtained from the Bernoulli binomial probability function, modified to take into account conditions peculiar to the process of polymerization. The unmodified probability function is

$$[2] \quad P = \frac{n!}{r!(n - r)!} p^{n-r}(1 - p)^r$$

where P is the probability that in n trials an event will be favorable $(n - r)$ times and unfavorable r times, the probability that each trial is favorable being p. All solutions to the factorial part of eq. [2] are contained in Pascal's triangle, which becomes a convenient mnemonic for these solutions.

One purpose of this paper is to describe modifications to Pascal's triangle so that it provides numbers equal to the factorial part of eq. [1]. This factorial part was derived also by Flory (2), and in his terminology, represents the number of configurations of an x-mer; the second purpose of this paper is to provide an alternative concept of the meaning of these factorial numbers.

Unmodified Pascal's Triangle

A portion of an unmodified Pascal's triangle is shown in Fig. 1. Arranged diagonally below the starting position at the apex are two numbered

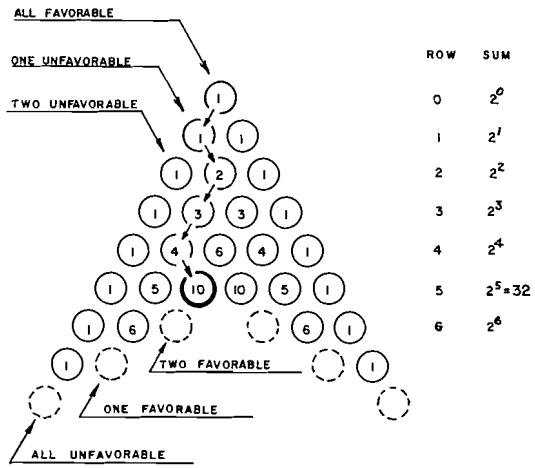

FIG. 1. Unmodified Pascal's triangle.

positions, each of which, in turn, has numbered positions diagonally below it, and so on. Each number is the sum of the two diagonally above, positions outside the triangle being counted zero. Horizontal rows are numbered 0, 1, 2, 3, $\cdots$ starting at the apex. The sum of the numbers in the mth row, S_m, is 2^m.

This triangle is used commonly to predict the results of coin-tossing, and other games of chance. To illustrate, the numbers in row 5 give the probabilities that a coin, if tossed 5 times, will behave in stipulated ways. For example, the probability that 2 heads (favorable) and 3 tails (unfavorable) will occur is 10 in 32. This result agrees with eq. [2] as, when $p = 1/2$

$$P = \frac{5!}{3!2!}(1/2)^3(1/2)^2 = \frac{10}{32}$$

The factorial part, $5!/3!2! = 10$ is given by the number in Fig. 1 which is in the position boldly outlined. It should be noted that, beginning at the apex, there are 10 different pathways, each of

[1]NRCC No. 11 224.

Can. J. Chem. Downloaded from www.nrcresearchpress.com by 210.87.254.6 on 09/05/12
For personal use only.

5 steps, by which this position may be reached. One of these is shown by arrows in Fig. 1. It is a property of Pascal's triangle that the number attached to a position represents the number of pathways from the apex to that position.

In the derivation (1) of eq. [1], it was noted that a simulated x-mer results from a decision-making game, analogous to coin-tossing, which involves choices between A and AA groups. For example, a chain molecule built from RA_3 structural units is specified as a trimer if in such a game it is decided by 6 trials in succession that it contains 2 AA groups and 4 A groups. (These are in addition to the one A group known to start the molecule; its existence is not subject to the vagaries of the game, for without it there is no molecule to consider. In this respect it resembles the apex of Pascal's triangle.)

We may now establish the rules of a game which corresponds to the building of multichain polymers. To obtain all information relevant to an x-mer, $(fx - x)$ trials must be made. We define a favorable outcome to be that of selecting an AA group in a choice between AA and A groups. Polymers which contain no rings are specified by $x - 1$ favorable and $fx - 2x + 1$ unfavorable outcomes. The example given above ($f = 3$, $x = 3$) is shown in Fig. 2. The six positions where decisions were made are lettered; the four established by unfavorable outcomes are denoted by U, and the two by favorable outcomes F.

The specifications given above correspond to definite locations in Pascal's triangle. Our object is to find the number associated with each, for these numbers are the factorial part of eq. [1].

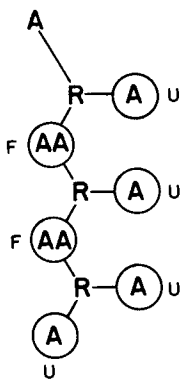

FIG. 2. Trimeric molecule, $f = 3$, specified by 2 favorable (F) and 4 unfavorable (U) trials.

Modified Pascal's Triangle

At this point we note a fundamental difference between the coin-tossing problem solved by Fig. 1, and our polymer-building problem. A "head" that occurs once can occur again; however, structural units that are incorporated in, for example, trimer molecules are never available for possible incorporation in tetramer, and larger, molecules. Hence in the modified Pascal triangle pathways can extend up to, but not beyond, positions which correspond to molecules. *Numbers which occur in such positions must be considered as zero when calculating numbers for positions diagonally below.*

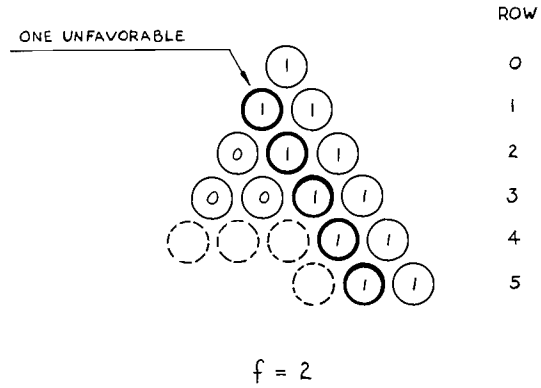

FIG. 3. Modified Pascal's triangle, $f = 2$, for chain polymers.

Figure 3 shows the modified triangle for the trivial case when $f = 2$. For each x-mer x trials must be made, so that positions for monomer, dimer, trimer, $\cdots$ occur in rows 1, 2, 3, $\cdots$, respectively. Within each of these horizontal rows the required position is that corresponding to $x - 1$ favorable (or 1 unfavorable) outcomes. The positions that correspond to these specifications are boldly outlined. The numbers in these positions are the sum of the two numbers diagonally above, *except that numbers in outlined positions are counted as zero.* Thus for $f = 2$ the numbers are always unity, an elementary result that agrees with the factorial part of eq. [1].

Figure 4 shows the modified triangle for $f = 3$. For each x-mer $2x$ trials are required, so that positions for monomer, dimer, trimer, $\cdots$ occur in rows 2, 4, 6, $\cdots$. Within each of these horizontal rows the required position is that corresponding to $x - 1$ favorable (or $x + 1$ unfavorable) outcomes. Again these positions are boldly outlined, and numbers are assigned according to

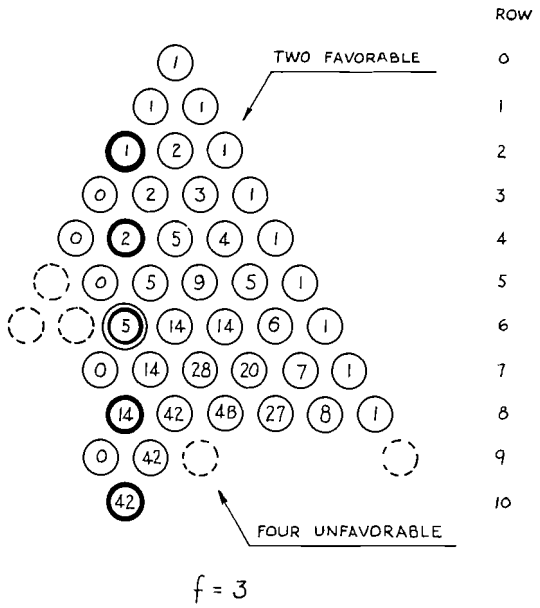

FIG. 4. Modified Pascal's triangle, $f = 3$, for chain polymers. The location for trimer is doubly outlined.

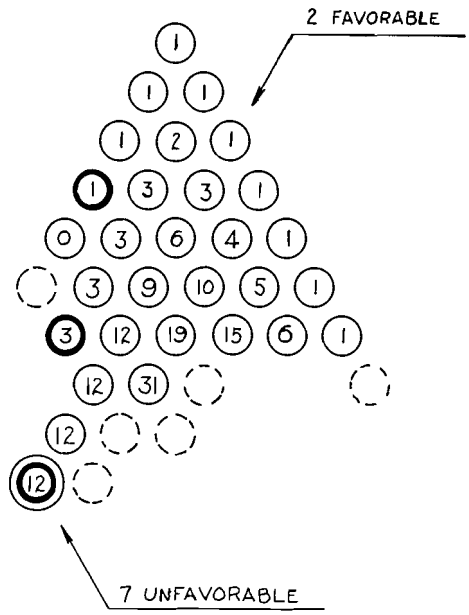

FIG. 5. Modified Pascal's triangle, $f = 4$, for chain polymers. The location for trimer is doubly outlined.

the above scheme. The location for trimer is doubly outlined. Figure 5 shows the modified triangle for $f = 4$. Again, the location for trimer is doubly outlined. In each case the numbers in the outlined positions equal those given by the factorial part of eq. [1]. In addition any such number is equal to the number of pathways from the apex to that position, with the restriction that pathways cannot extend through a boldly-outlined position but must terminate there.

We see that simulated chain polymers of the systems $f = 2, 3, 4, \cdots$ occupy only a few positions of Pascal's triangle, and it is interesting to note that cyclic polymers correspond to some of the others. For example, when $f = 3$, molecules with a single ring are specified by $2x - 1$ trials comprised of x favorable and $x - 1$ unfavorable outcomes. Positions which correspond to these specifications alone are shown in Fig. 6, and the trimer position is doubly outlined. Numbers have been assigned in the usual manner although they have little practical significance, as chain polymers have been artificially excluded from consideration. In addition it should be noted that, although formally present in Fig. 6, a cyclic monomer is not possible; similarly the existence of a cyclic dimer is questionable. Also it has been suggested (3) that cyclization of chains becomes more difficult as they become long, because of the decreased opportunity for interaction between two ends of a molecule.

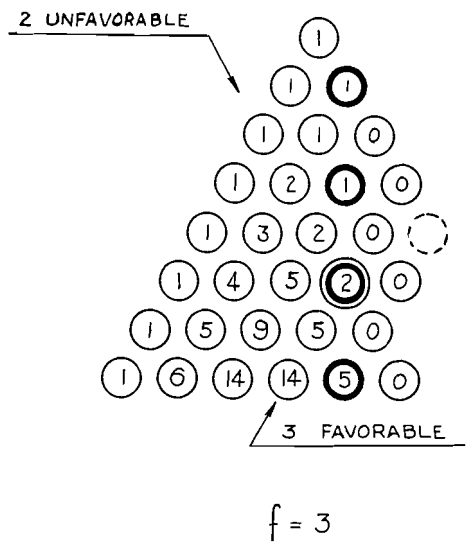

FIG. 6. Modified Pascal's triangle, $f = 3$, for polymers that contain one ring. The location for trimer is doubly outlined.

The simple schemes shown in Figs. 4 and 6 may be combined provided assumptions are made re-

Can. J. Chem. Downloaded from www.nrcresearchpress.com by 210.87.254.6 on 09/05/12
For personal use only.

Can. J. Chem. Downloaded from www.nrcresearchpress.com by 210.87.254.6 on 09/05/12
For personal use only.

garding the above points. Figure 7 shows the effect of superimposing on the triangle for chain polymers the possibility of having cyclic trimers and tetramers. The numbers in the outlined positions, obtained as before, are solutions to a composite factorial term. If we assume that p_{AA} for cyclization is equal to p_{AA} for chain extension, then mole fractions can be obtained by an obvious application of eq. [1]

$$N_{\text{monomer}} = (1 - p_{AA})^2$$

$$N_{\text{dimer}} = 2(p_{AA})(1 - p_{AA})^3$$

$$N_{\text{cyclic trimer}} = 9(p_{AA})^3(1 - p_{AA})^2$$

$$N_{\text{chain trimer}} = 5(p_{AA})^2(1 - p_{AA})^4$$

$$N_{\text{cyclic tetramer}} = 10(p_{AA})^4(1 - p_{AA})^3$$

$$N_{\text{chain tetramer}} = 5(p_{AA})^3(1 - p_{AA})^5$$

Mole fractions for these molecules are shown in Fig. 8 as functions of p_{AA}. (Calculations were not performed for values of $p_{AA} > 0.5$ because at this point, the summation of mole fractions becomes

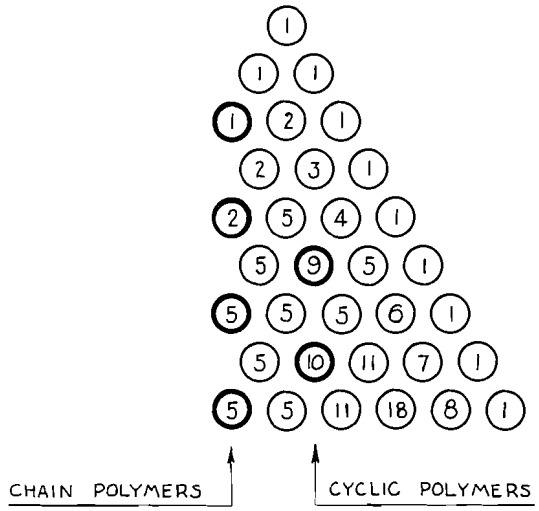

FIG. 7. Modified Pascal's triangle, $f = 3$, for chain polymers along with trimers and tetramers that contain one ring.

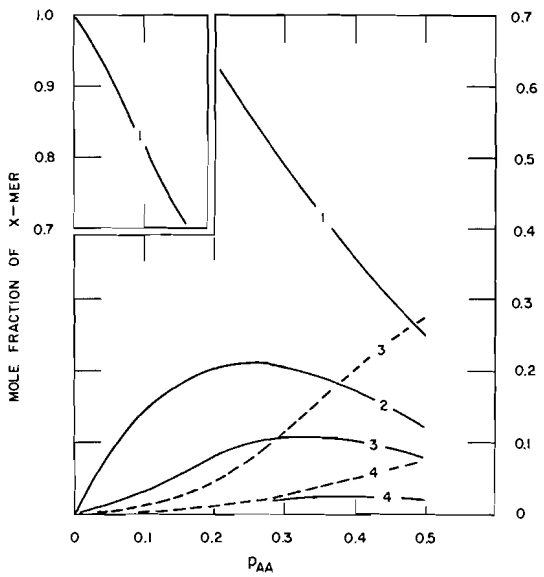

FIG. 8. Mole fractions of polymer species as a function of p_{AA}, when $f = 3$. The numbers of the curves refer to x. Trimers and tetramers that contain one ring occur along with chain polymers. Solid curves are for chain molecules, dashed curves are for ring.

divergent; for $f = 3, p_{AA} = 1/2$ is a critical point.) It is interesting to note that chain polymers are predicted to predominate over cyclic polymers of the same size at low values of p_{AA}, while the situation is reversed at high values of p_{AA}. Such predictions, of course, depend upon the relative values of p_{AA} for the two processes, chain extension and cyclization, and should not be regarded as general. The obvious complexity of ring-chain equilibria (for example, ref. 4) makes it likely that each system would have to be considered as a particular case. It is possible that specific experimental data might be usefully interpreted on the basis of the diagrams shown here.

The author is grateful to Drs. A. G. McInnes and I. B. Smith for helpful comments and discussions.

1. S. G. WHITEWAY, I. B. SMITH, and C. R. MASSON. Can. J. Chem. **48**, 33 (1970).
2. P. J. FLORY. Principles of polymer chemistry. Cornell University Press, Ithaca, New York. 1953.
3. P. J. FLORY. Chem. Rev. **39**, 137 (1946).
4. M. GORDON and G. R. SCANTLEBURY. Proc. Roy. Soc. **A292**, 380 (1966).

Can. J. Chem. Downloaded from www.nrcresearchpress.com by 210.87.254.105 on 09/05/12
For personal use only.

Cyclobutanes in organic synthesis. Part I. Fragmentation to 1,4-dicarbonyl compounds. General considerations

N. R. HUNTER, G. A. MACALPINE, H. J. LIU, AND Z. VALENTA
Department of Chemistry, University of New Brunswick, Fredericton, New Brunswick

Received October 15, 1969

Photo-cycloaddition of vinyl acetates to 2-cyclohexenones followed by hydrolysis of the acetate group and by oxidative fragmentation leads to 2-alkyl-2-cyclohexenones in which the newly introduced alkyl group bears a 2′-carbonyl group. A similar, less generally applicable method, involving photo-cycloaddition, bromination, and heterolytic fragmentation is also described. Possible applications of this sequence in organic synthesis are discussed.

Canadian Journal of Chemistry, **48**, 1436 (1970)

Intramolecular photo-cycloaddition of a double-bond to a cyclohexenone by Ciamician and Silber (1), Sernaggiotto (2), and Büchi and Goldman (3), followed by an extension of this cyclobutane formation to an intermolecular case by Eaton (4), introduced an important new reaction into the field of organic synthesis. In recent years, many relatively difficult syntheses of natural products and strained compounds of theoretical interest have been accomplished in a significantly simplified manner by the use of this method; some of these have been achieved with retention (5–10) and some with modification (11–15) of the cyclobutane ring. We now wish to report a fragmentation of suitably substituted cyclobutanes which promises to have wide synthetic utility.

In the course of our studies on the synthesis of *Ormosia* alkaloids (15) it became necessary to transform **1** into **2** in which the newly introduced side-chain would possess a reactive function at its terminus and in which the cyclohexenone double-bond would be retained. Clearly, a normal alkylation could not be used since the cycloalkenone function in **1** does not possess an enolizable γ-hydrogen atom. Bearing in mind the mode of photo-cycloaddition of unsymmetrical olefins to cyclohexenones (16, 17), and anticipating an easy fragmentation (18, 19) of a suitably substituted cyclobutane ring, we have been able to convert **1** into **2** in the following simple manner.

Irradiation of keto lactam (**1**) in vinyl acetate and tetrahydrofuran gave a 60% yield of crude keto acetate (**3**), which proved to be homogeneous on silica thin-layer chromatography (t.l.c.). Subsequent transformations revealed **3** to be a mixture of four stereoisomers, the major one of which could be recrystallized to a constant m.p. of 200–201 °C. Since none of the keto alcohols obtained by a basic hydrolysis of **3** underwent a reverse aldol reaction to a keto aldehyde, and since all of them gave a cyclobutanone on oxidation, it became clear that all components of the mixture possess structure **3**. Bromination of **3** with pyridinium bromide perbromide in glacial acetic acid gave a mixture of four stereoisomeric bromo ketones (**4**) in 78% yield. These could be chromatographically resolved and characterized; since all four stereoisomers could, however, potentially give the desired product, the mixture was used in the subsequent reaction.

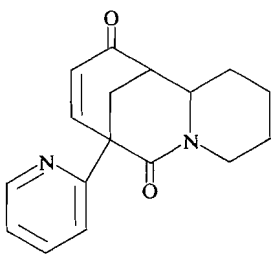

1

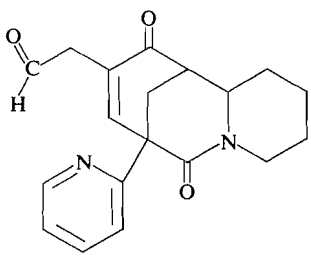

2

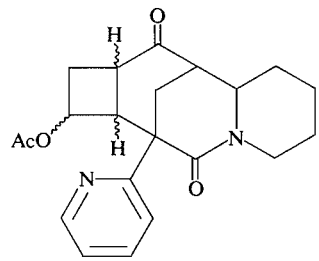

3

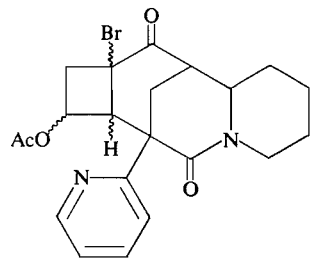

4

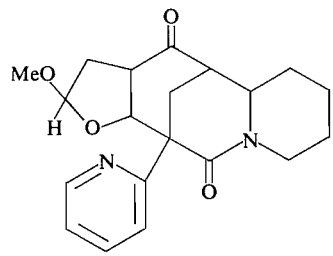

5

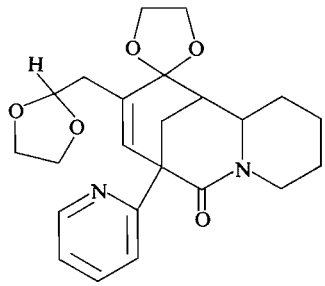

6

Treatment of **4** with aqueous sodium carbonate in methanol at room temperature, followed by chromatography on silica gel, gave the pure keto aldehyde (**2**) in 76% yield and the corresponding acetal (**5**) in 15% yield. The structures of **2** and **5** follow unambiguously from spectroscopic data (see Experimental), from the conversion of pure **2** into **5** on prolonged treatment with methanolic sodium carbonate, and from further conversions of **2** (15).[1] The fragmentation could also be achieved in acidic media. Treatment of **4** in boiling benzene with ethylene glycol and *p*-toluenesulfonic acid gave the bisdioxalane (**6**) in 70% yield.

Photoaddition

The success and ease of these initial transformations led us to consider the general applicability of the reaction sequence **A** → **B** → **C** → **D**. Concerning first the nature of **A**, it is well known that 2-cyclopentenones and 2-cyclohexenones normally undergo smooth cycloaddition and that substitution at various positions of **A**, with the exception of C-2, does not

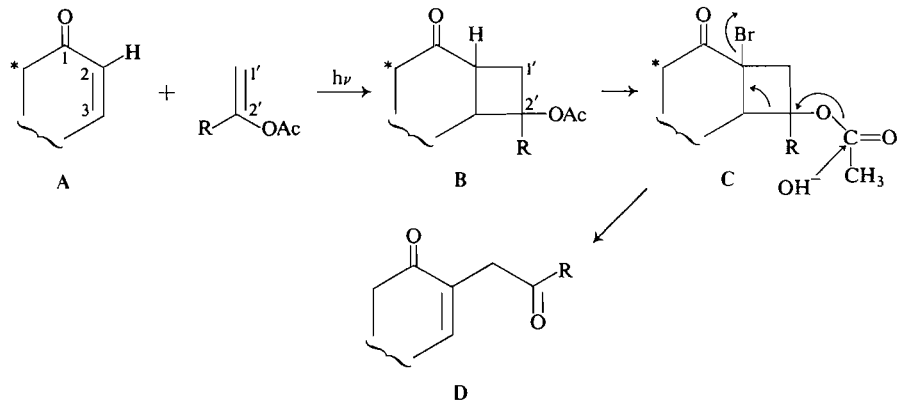

A B C D

[1]Totally synthetic alkaloid ormosanine has now been prepared from **2** in our laboratory.

Can. J. Chem. Downloaded from www.nrcresearchpress.com by 210.87.254.105 on 09/05/12
For personal use only.

TABLE 1
Photo-cycloadditions

Cyclohexenone	Enol acetate	Photo adducts and yields (%)
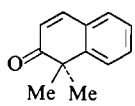	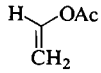	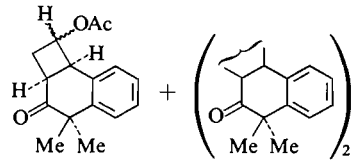 (2 isomers 63%) (11%)
	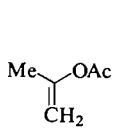	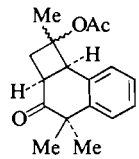 (2 isomers 96%)
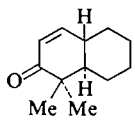	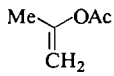	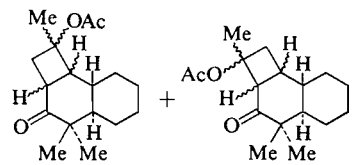 (4 isomers 55%) (~10%)
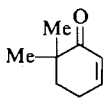	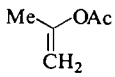	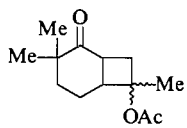 (64%)
	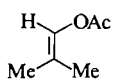	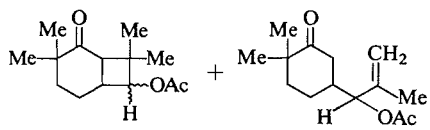 (~34%) (~31%)
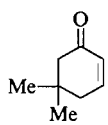	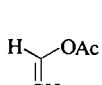	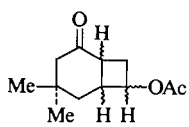 (2 isomers after hydrolysis, 90%)
	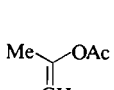	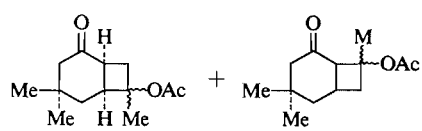 (2 isomers 55% after hydrolysis and extensive chromatography) (~5%)

Can. J. Chem. Downloaded from www.nrcresearchpress.com by 210.87.254.105 on 09/05/12
For personal use only.

Can. J. Chem. Downloaded from www.nrcresearchpress.com by 210.87.254.105 on 09/05/12
For personal use only.

seriously affect the addition (16, 20, 21). It is also known that vinyl acetate adds preferentially in the desired sense (16, 17); as far as its substitution is concerned, our preliminary evidence listed below indicates that the cycloaddition takes place in good yields with a methyl group at C-2′ and lower yields with two methyl groups at C-1′ (see Table 1). The yields of photo adducts from the cycloaddition vary considerably and we have not made a systematic study to optimize conditions. In general, low concentrations of cycloalkenone and the use of aprotic solvents gives little or no cycloalkenone dimer and leads to cleaner photo products. Work described in this communication deals exclusively with cyclohexenones; extension to cyclopentenones will be reported later.

Activation for Fragmentation

The bromination step **B** → **C** proved to be highly efficient in all cases in which enolization of the keto group towards C* was not possible because of substitution or because of strain (cf. **3** → **4**). However, we have so far been unable to achieve a preferential introduction of a leaving group into the desired position in **B** when C* was also reactive. This is clearly a serious limitation to the generality of the above sequence since most synthetic intermediates of the type **B** will obviously have a reactive C*. This difficulty can furthermore not be circumvented by the photoaddition of vinyl acetates to α-bromocycloalkenones. Our results in this respect are completely negative, although such an addition, in an intramolecular case, has been achieved (8) and although α-acetoxycycloalkenones have been found to react (22–24).[2]

One can, however, ask the interesting question whether the presence of a leaving group is in fact essential for the desired transformation **B** → **D**. Formally, at least, one can readily visualize an oxidative fragmentation indicated in **E**, operating by an electron flow opposite to that encountered in the heterolytic fragmentation **C** → **D** and leading directly to **D** without the benefit of a conventional leaving group.

We now find that a number of methods are in fact available for this transformation and that the oxidative fragmentation of the keto alcohols (**E**) thus represents a general solution to the problem. Table 2 summarizes our findings and

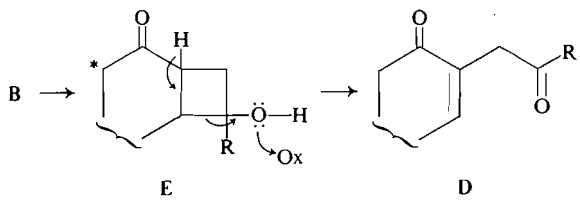

E D

gives yields of fragmentation products obtained on treatment of three keto alcohols with various oxidizing agents. Our results using Ce^{4+} are particularly encouraging. Thus, reaction of keto alcohol **7** with ceric ammonium nitrate in 75% acetic acid solution, until the characteristic reddish color due to the Ce^{4+}–alcohol complex (25) had disappeared, followed by treatment with aqueous mineral acid for several hours, gave an 86% yield of diketone **9**, while a similar oxidation of **8** furnished the desired keto aldehyde **10** in a 71% yield. Additional oxidation results make it clear that the method works equally well with unblocked substrates without oxidation of the resulting cyclohexenone to a phenol.

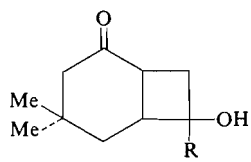

7 R = Me
8 R = H

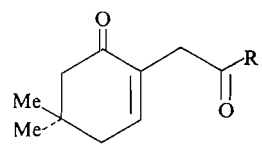

9 R = Me
10 R = H

Published work on oxidations with ceric ion (26, 27) makes it very likely that two consecutive one-electron oxidations are involved, the first leading to radical **11**, the second creating a carbonium ion at position C-3 to give **12**.[3] Experimentally, we have found varying amounts of nitrate esters (**13**) (33) in the reaction product mixture, but this mixture was cleanly converted to **9** (or **10**) by treatment with aqueous mineral acid without requiring separation.

The recent observation of Roček and Radkowsky (28) on the oxidative cleavage of cyclobutanol with Cr^{4+} offers an alternative procedure to the Ce^{4+} oxidation but suffers from

[2]We thank Professors de Mayo and Eaton for a useful exchange of correspondence on this topic.

[3]During the preparation of this manuscript, the Iowa State University group reported further results of their general study of oxidations with cerium(IV). In their interesting new report (33), the successful fragmentation of bicyclo[2.2.1]-2-heptanols and of bicyclo[2.2.2]-2-octanol, as well as the mechanism involving two one-electron processes and the formation of nitrate esters, are discussed.

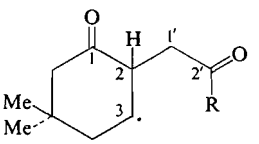

11

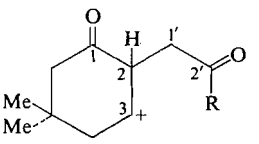

12

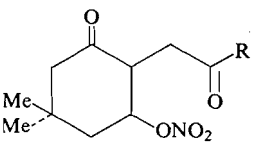

13

the requirement of *in situ* generation of Cr^{4+} and the acidic medium used.

We are presently studying the question whether the following additional methods could be applied in special circumstances for an efficient transformation **B** → **D**. In analogy to rearrangements encountered with α-substituted ketones (29, 30), a vinylogous fragmentation of ketones **F** through the corresponding enol or enolate could take place as indicated in **G**. We have so far not

TABLE 2

Homolytic fragmentations

Keto alcohol	Method	Product(s)	Yield (%)	Reference
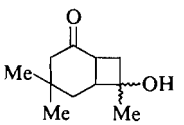	$Pb(OAc)_4/CaCO_3/C_6H_6$ at reflux		18	34, 35
	$HgO/I_2/h\nu/CCl_4$ at reflux	"	49	36
	$Pb(OAc)_4$/pyridine at room temperature	"	67	37
	Ceric sulfate/75% CH_3CN at reflux	"	66	38
	$Ce(NH_4)_2(NO_3)_6$/75% CH_3CN at reflux	"	65–75	26
	$Ce(NH_4)_2(NO_3)_6$/75% HOAc at room temperature	"	86	27
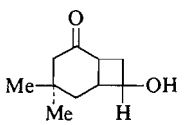	$Pb(OAc)_4$/pyridine	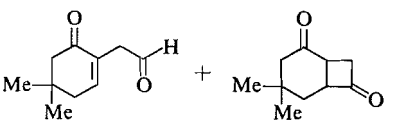 ~2:1	65	37
	$HgO/I_2/h\nu/CCl_4$	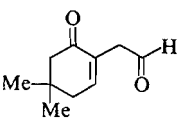	~45	36
	$Ce(NH_4)_2(NO_3)_6$/75% CH_3CN	"	73	26
	$Ce(NH_4)_2(NO_3)_6$/75% HOAc	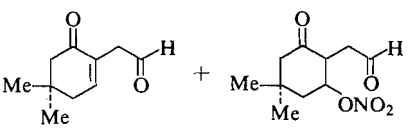 ~1:1	75	27
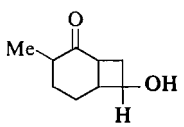	$Ce(NH_4)_2(NO_3)_6$/75% HOAc	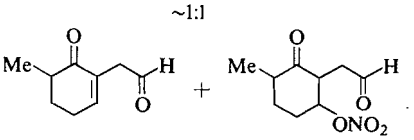 ~1:1	70	27

Can. J. Chem. Downloaded from www.nrcresearchpress.com by 210.87.254.105 on 09/05/12
For personal use only.

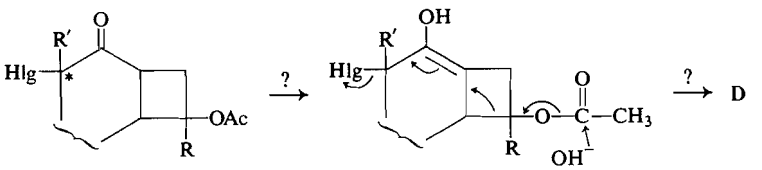

F G

been able to achieve this transformation with haloketones **F** in which R′ = H. The study of systems with R′ = alkyl in which the enolization must take place in the required direction will show whether the geometry of the relevant orbitals in **G** allows the desired fragmentation.

Based on reported reactions (21, 31), **D** could furthermore possibly be prepared by the sequence **A** → **H** → **I** → **J** → **D** in which the required "leaving group" is introduced into the olefin rather than into the alkenone.

In summary, a large variety of dicarbonyl compounds of the type **D** can now be produced often in very high yields, by photo-cycloaddition followed by an oxidative fragmentation of the corresponding keto alcohols **E** with ceric ion. A second high-yield method, bromination followed by a heterolytic fragmentation, is available for photo adducts **B** which do not enolize in the direction of C*.

Direction of Fragmentation

The somewhat surprising fact that all fragmentations studied by us so far proceeded in only one sense, although two pathways, (*a*) and (*b*), are in fact available, must now be discussed.

Considering first the probable intermediate **11** of the one-electron oxidative methods, the formation of the more stable secondary radical can be used as a plausible explanation. Further study involving additional substitution at C-1′ and at C-3 should provide important information in this connection. Specifically, higher substitution at C-1′ should make pathway (*b*) more favorable if this explanation is correct.

The heterolytic fragmentation **C** → **D** was studied on a large number of *cyclohexanones* (Table 3) and was found to proceed invariably in a very high yield. No detectable trace of fragmentation product **K** was found in any of the studied cases, including one with a *gem*-dimethyl group at C-1′. Furthermore, study of pairs epimeric at C-2′ has shown that **D** is formed exclusively, regardless of the relative configuration of the bromine and the acetoxyl group in **C**. Although this specificity is of obvious preparative

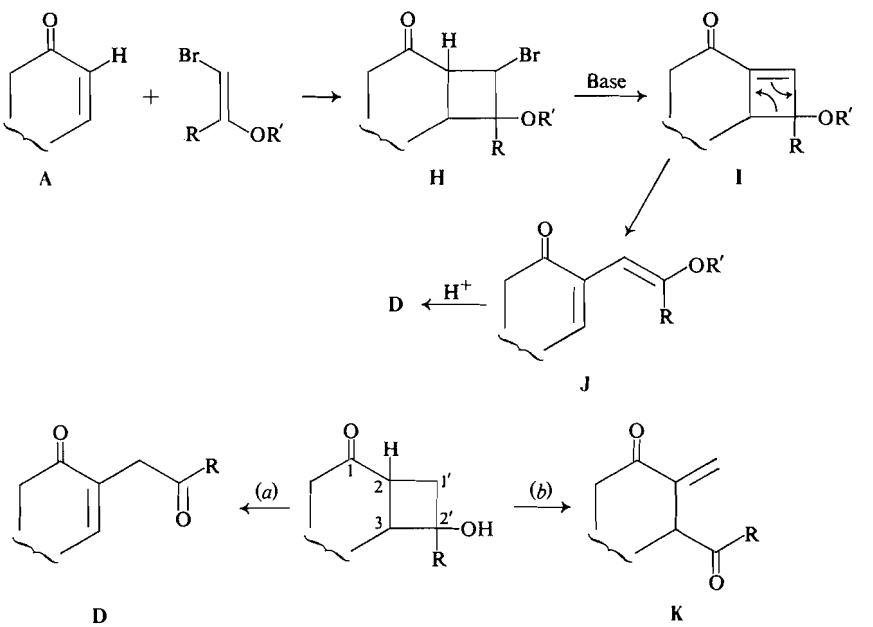

A H I J D K

Can. J. Chem. Downloaded from www.nrcresearchpress.com by 210.87.254.105 on 09/05/12
For personal use only.

value, the full explanation for it has to await further study. It appears unlikely that the cyclobutane ring would in all cases possess an unsymmetrical conformation fulfilling the geometrical requirements for a concerted fragmentation reaction (18, 32) in only one direction. Rather, it can probably be assumed that both pathways are geometrically allowed and that pathway (*a*), involving the formation of an *endo* double-bond, proceeds via a transition state of lower energy. In this connection, the behavior of *cyclopentanones* and strained ring-systems will be of special interest.

Potential Applications

In most general terms, the reactions described above provide a synthetically attractive method for the addition, to the α-position of an α,β-unsaturated cyclohexanone (and presumably also cyclopentanone), of a single carbon chain possessing a carbonyl function. The position of double-bond in the cycloalkenone fully deter-

TABLE 3

Heterolytic fragmentations

Substrate	Fragmentation media	Product	Yields (%)
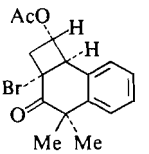	Na_2CO_3/aqueous MeOH	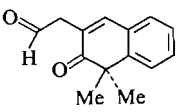	92 (From keto acetates)
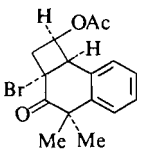	"		98
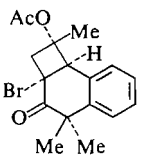	NaOH/aqueous MeOH	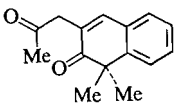	83
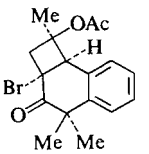	"		97
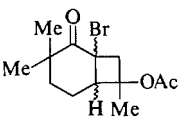 (Mixture of isomers)	KOH/aqueous MeOH	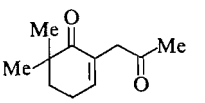	98
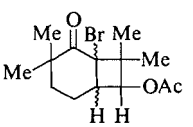 (Mixture of isomers)	KOH/aqueous MeOH	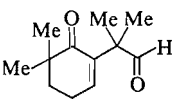	95

Can. J. Chem. Downloaded from www.nrcresearchpress.com by 210.87.254.105 on 09/05/12
For personal use only.

TABLE 3 (*Concluded*)

Substrate	Fragmentation media	Product	Yield (%)
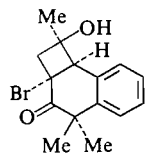	NaOH/aqueous MeOH	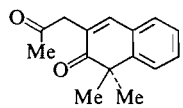	89 (From keto alcohol)
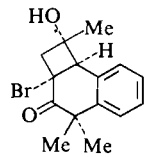	Spontaneous loss of HBr	"	92 (From keto alcohol)
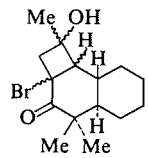 (Mixture of isomers)	Na_2CO_3/aqueous MeOH	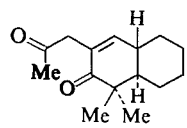	80 (From crude bromo keto alcohols)

mines the site of addition and, rather importantly, an enolizable hydrogen atom in the γ-position of the starting ketone is not required. Unsaturated and, after appropriate reduction, saturated 1,4-dicarbonyl compounds are thus produced.

In principle, chains of arbitrary length (longer than one-carbon) and branching can be added either directly or by subsequent reactions of the side-chain carbonyl group. The relative position of the carbonyl groups furthermore permits a wide variety of special applications.

Five-membered carbocyclic rings can, for instance, be formed by aldol condensations while the corresponding saturated 1,4-dicarbonyl compounds are immediately suited for the preparation of furanes, pyrroles, and thiophenes. We furthermore find that a conversion of the side-chain carbonyl group in **D** into a leaving group followed by an attack with a suitable nucleophile leads to a high-yield production of α-cyclopropyl ketones.

Special applications of the sequence as well as mechanistic and stereochemical details of the described reactions are under further study and will be reported later.

Experimental

General

The infrared (i.r.) spectra were recorded on Perkin–Elmer Infracord or Perkin–Elmer model 237B spectrophotometers. The mass spectra were determined on a Hitachi Perkin–Elmer model RMU-6D spectrometer. The nuclear magnetic resonance (n.m.r.) spectra were recorded on a Varian Associates 56.4 Mc.p.s. instrument using tetramethylsilane as internal standard. A Kofler hot stage apparatus was used to determine the melting points which are uncorrected. Photolysis was carried out using one of the following lamps depending on the reaction scale: Hanovia High-Pressure Quartz Mercury Vapour Lamps, 100 W, Type SOL:608A36; 200 W, Type S:654A36 or 450 W, Type L:679A36.

General Procedure for Photo-cycloadditions

The apparatus used for the photochemical reactions consisted of a cylindrical Pyrex reaction vessel with a nitrogen bubbler which served to agitate the solution, a side-arm for a condenser, and a neck to accommodate a quartz-jacketed water-cooled immersion well which could be fitted with Pyrex or Corex filters and any of the lamps used in the procedure. The cycloalkenone used for the photoaddition was dissolved in hexane (or other appropriate, aprotic solvents) such that the concentration of alkenone was less than 0.05 *M*. The enol acetate to be used for the photoaddition was usually added in a large excess (20 to 50% of the solvent used). The vessel was covered with aluminum foil and, with a good flow of water through the water-jacket, the reaction vessel was immersed in an ice-bath. The system was flushed by bubbling

Can. J. Chem. Downloaded from www.nrcresearchpress.com by 210.87.254.105 on 09/05/12
For personal use only.

Can. J. Chem. Downloaded from www.nrcresearchpress.com by 210.87.254.105 on 09/05/12
For personal use only.

nitrogen through and then irradiated under a nitrogen flow to facilitate mixing. The progress of the reaction was followed by evaporating aliquots and measuring the i.r. absorption. In some cases, t.l.c. was also used.

At the completion of photolysis, the solvent was removed by distillation under reduced pressure and the photo adducts were purified either by distillation under reduced pressure or by chromatography on silica gel. In some cases, the best purification was achieved by hydrolysis of the keto acetate photo adducts to the corresponding alcohol followed by chromatography on silica gel.

Photoaddition of Vinyl Acetate to Keto Lactam (1)

To a solution of the keto lactam (**1**) (1.37 g) in tetrahydrofuran (65 ml), was added vinyl acetate (65 ml). The solution was irradiated with a 100 W lamp, using a Pyrex filter, for 1 h at 0 °C and 2 h at 20 °C. The solution was evaporated to dryness under reduced pressure to give a viscous oil which contained polymeric compounds. The oil was chromatographed on silica gel; the polymeric compounds were eluted with benzene and the photo adduct **3** (1.073 g) was eluted with ether. The photo adduct crystallized from ether to give colorless crystals, m.p. 200–201 °C. The i.r. spectrum showed acetate absorption at 1735 and ketone stretching at 1710 cm^{-1}. The n.m.r. spectrum was completely consistent with the assigned structure.

Anal. Calcd.: C, 68.46; H, 6.56; N, 7.60. Found: C, 68.95; H, 6.60; N, 7.59.

Bromination of Photo Adduct 3

To a solution of the four-membered ring acetate (**3**) (1.66 g) in glacial acetic acid (50 ml) was added pyridinium bromide perbromide (1.71 g) and 46% aqueous hydrobromic acid (1.5 ml). The solution was stirred at room temperature for 16 h. The solution was then basified with saturated aqueous sodium bicarbonate and extracted with chloroform. After drying over magnesium sulfate, filtration, and evaporation *in vacuo* to dryness, the chloroform solution afforded an oil (1.72 g) which by t.l.c. showed mainly four compounds. Column chromatography on silica gel resulted in separation of these four compounds (total 1.58 g). They showed identical i.r. spectra and the mass spectra gave *m/e* 448 and 446. These four compounds were thus four stereoisomers of the bromo acetate (**4**). The isomeric mixture was used in the subsequent reaction.

General Procedure for Bromination of the Photo Adducts

The keto acetate photo adduct (1 mmole) was treated with bromine (1.1 mmole) in 20 ml of Reagent Grade carbon tetrachloride. The time required for bromination varied considerably (usually several hours); the progress of the reaction could be conveniently followed by t.l.c. on silica gel. The organic solution was washed with water, dried over sodium sulfate, and evaporated to dryness *in vacuo* to give the bromo keto acetate in high yield and purity. The bromo keto acetates were homogeneous on t.l.c. and gave i.r., n.m.r., and mass spectra completely consistent with the structures assigned in Table 3.

Heterolytic Fragmentation of Bromo Acetate (4)

To a solution of the isomeric mixture of bromo acetates (**4**) (4.244 g) in methanol (50 ml) was added saturated aqueous sodium carbonate (10 ml). After stirring at 0 °C for 1 h, the mixture was poured into water (500 ml) and extracted with chloroform. The chloroform solution was dried over magnesium sulfate, filtered, and evaporated *in vacuo* to dryness yielding an oil (3.31 g). Column chromatography of the crude product on silica gel gave, in addition to recovered starting material (0.825 g), two new products. The acetal (**5**) (0.408 g) was obtained on elution with ether as a foam; its i.r. spectrum showed a saturated ketone stretching absorption at 1725 cm^{-1}. Elution with methanol–ether (1:50) gave the unsaturated keto aldehyde (**2**) as a foam. Molecular weight (by mass spectrometry): 324. The i.r. spectrum indicated characteristic aldehyde absorptions at 2730 and 1730 cm^{-1} and unsaturated ketone stretching absorption at 1680 cm^{-1}. In the n.m.r. spectrum, the aldehydic proton was recorded at 0.32 τ.

In general, the heterolytic fragmentation proceeded cleanly on base treatment of the bromo keto photo adducts to give the corresponding dicarbonyl compounds (Table 3) in high yield and purity. The dicarbonyl compounds could be further purified by chromatography on silica gel when necessary. Their spectral and analytical data were completely consistent with the assigned structures.

Preparative Scale Ceric Ammonium Nitrate Oxidation of Keto Alcohol (7)

To the keto alcohol (7) (1.1199 g; 6.15 mmole) in 40 ml of 75% aqueous acetic acid at room temperature was added ceric ammonium nitrate (8.439 g; 15.4 mmole) in one portion. The initial red color of the Ce^{4+}–alcohol complex disappeared after several minutes and the reaction mixture was stirred an additional 1.5 h. To this reaction mixture was added concentrated hydrochloric acid (2 ml) and the solution was allowed to stand at room temperature for 3.5 h. Saturated salt solution (150 ml) was added to the reaction mixture and the resulting solution was extracted with methylene chloride (2 × 50 ml) and ether (2 × 50 ml). The combined organic extracts were washed with 10% sodium bicarbonate and saturated salt solution, dried ($MgSO_4$) and evaporated to dryness to yield the diketone (**9**) as a pale yellow oil (0.9584 g; 5.27 mmole; 85.7%). The i.r. spectrum indicated carbonyl absorptions at 1720 and 1677 cm^{-1}. The n.m.r. spectrum showed signals at 8.9 (6H), 7.88 (3H), 7.8 (2H), 7.75 (2H, d), 6.85 (2H), and 3.45τ (1H, t). The mass spectrum gave the molecular ion peak at *m/e* 180.

Oxidative Preparation of Diketone 9 and Nitrate 13 ($R = CH_3$)

The keto alcohol (7) (0.6793 g; 3.73 mmole) was dissolved in 75 ml of 75% aqueous acetonitrile at reflux and ceric ammonium nitrate (4.110 g; 7.50 mmole) was added in one portion. The mixture was stirred at reflux for 25 min during which time the color changed from orange to pale yellow. The solvent was partially removed under reduced pressure and water was added; the mixture was then extracted with ether and methylene chloride. The organic extract was washed with 10% sodium bicarbonate and saturated salt solution, dried ($MgSO_4$) and the solvent removed under reduced pressure. The mixture of diketone (**9**) and nitrate (**13**) (0.6484 g) was obtained as a pale yellow oil. Chromatography on silica gel (60 g) gave on

elution, with 2% ether in benzene, compound **13** (R = CH_3) (0.0651 g; ~10%). The i.r. spectrum of **13** indicated strong absorptions at 1720, 1640, 1280, and 860 cm^{-1}. The n.m.r. spectrum showed a characteristic methyl absorption at 7.80 τ. Further chromatography yielded the diketone (**9**), the spectra of which were superimposable with those of **9** obtained in the preparative scale reaction.

Oxidation of Keto Alcohol (7) in Lead Tetraacetate/ Pyridine Solution

The keto alcohol (**7**) (1.9816 g; 10.88 mmole) was dissolved in 10 ml of benzene and 40 ml of pyridine. To this solution was added lead tetraacetate (9.659 g; 21.8 mmole) and the mixture was heated under reflux for 3.5 h (the oxidation at room temperature was about five times slower), 1.5 ml of ethylene glycol was added to destroy the excess lead tetraacetate and the mixture was stirred until it had cooled to room temperature. The p*H* was adjusted to ≃2 with 10% HCl and the flocculent precipitate was filtered off and washed with water, ether, and chloroform. The acidic aqueous filtrate was extracted with ether (3 × 100 ml) and chloroform (3 × 100 ml). The ether and chloroform extracts were combined, washed with 10% sodium bicarbonate and water, dried ($MgSO_4$), and evaporated *in vacuo* to dryness to give 1.2312 g of product. The acidic solution was continuously extracted with ether for 16 h. This ether extract upon similar work-up yielded an additional 0.2906 g of product. The i.r. spectrum of the product indicated that some β-acetoxy ketone was present, probably from addition of acetate anion or radical to the carbonium ion **12** or radical **11**. When these fractions were combined and treated overnight in a 50:50 solution of 10% hydrochloric acid:tetrahydrofuran, and worked-up in the usual way, the diketone **9** (1.3136 g; 7.30 mmole; 67.1%) was obtained as a dark yellow oil. The spectra of **9** obtained from **7** by this method were identical in all respects to those of **9** obtained by ceric ion oxidation of **7**.

Support of this work by the National Research Council of Canada in the form of scholarships to N. R. H. (1967–1970), G. A. MacA. (1968–1970), and H. J. L. (1967–1968) is gratefully acknowledged.

1. G. Ciamician and P. Silber. Chem. Ber. **41**, 1928 (1908).
2. E. Sernaggiotto. Gazz. Chim. Ital. **47**, I, 153 (1917); **48**, I, 52 (1918).
3. G. Büchi and I. M. Goldman. J. Amer. Chem. Soc. **79**, 4741 (1957).
4. P. E. Eaton. J. Amer. Chem. Soc. **84**, 2454 (1962).
5. E. J. Corey, R. B. Mitra, and H. Uda. J. Amer. Chem. Soc. **86**, 485 (1964); **85**, 362 (1963).
6. J. D. White and D. N. Gupta. J. Amer. Chem. Soc. **88**, 5364 (1966); **90**, 6171 (1968).
7. M. Brown. Chem. Commun. 340 (1965); J. Org. Chem. **33**, 162 (1968).
8. P. E. Eaton and T. W. Cole. J. Amer. Chem. Soc. **86**, 3157 (1964); **86**, 962 (1964).
9. P. E. Eaton. 155th National Meeting of the American Chemical Society, San Francisco, California, April 1968. p. 1.
10. K. Wiesner, Lizzie Poon, I. Jirkovsky, and M. Fishman. Can. J. Chem. **47**, 433 (1969).
11. R. W. Guthrie, Z. Valenta, and K. Wiesner. Tetrahedron Lett. 4645 (1966).
12. E. J. Corey and S. Nozoe. J. Amer. Chem. Soc. **86**, 1652 (1964); **87**, 5733 (1965).
13. B. D. Challand, H. Hikino, G. Kornis, G. Lange, and P. de Mayo. J. Org. Chem. **34**, 794 (1969) and earlier work quoted therein.
14. Z. Valenta, B. Balenovic, P. Cavanagh, and W. L. Wilson. Synthetic work on a ryanodine reduction product completed in this Department.
15. H. J. Liu, Z. Valenta, J. S. Wilson, and T. T. J. Yu. Can. J. Chem. **47**, 509 (1969).
16. E. J. Corey, J. D. Bass, R. Lemahieu, and R. B. Mitra. J. Amer. Chem. Soc. **86**, 5570 (1964).
17. Y. Yameda, H. Uda, and K. Nakanishi. Chem. Commun. 423 (1966).
18. C. A. Grob and P. W. Schiess. Angew. Chem. Internat. Ed., **6**, 1 (1967).
19. C. F. Wilcox, Jr., and D. L. Nealy. J. Org. Chem. **28**, 3450 (1963); L. J. Dolby and C. L. Wilkins. Tetrahedron, **25**, 2381 (1969).
20. P. E. Eaton. Accounts Chem. Res. **1**, 50 (1968) and references quoted therein.
21. T. S. Cantrell, W. S. Haller, and J. C. Williams. J. Org. Chem. **34**, 509 (1959).
22. P. de Mayo. Private communication.
23. S. Kagawa, S. Matsumoto, S. Nishida, S. Yu, J. Morita, A. Ichihara, H. Shirahama, and T. Matsumoto. Tetrahedron Lett. 3913 (1969).
24. T. Matsumoto, H. Shirahama, A. Ichihara, S. Kagawa, and S. Matsumoto. Tetrahedron Lett. 4103 (1969).
25. See reference 4 in the paper by P. M. Nave and W. S. Trahanovsky. J. Amer. Chem. Soc. **90**, 4755 (1968).
26. P. M. Nave and W. S. Trahanovsky. J. Amer. Chem. Soc. **90**, 4755 (1968).
27. W. S. Trahanovsky, L. H. Young, and M. H. Bierman. J. Org. Chem. **34**, 869 (1969).
28. J. Roček and A. E. Radkowsky. J. Amer. Chem. Soc. **90**, 2986 (1968).
29. R. A. Bell and M. B. Gravestock. Can. J. Chem. **47**, 3661 (1969).
30. F. G. Bordwell and R. M. Wellman. J. Org. Chem. **28**, 2544 (1963).
31. C. H. Krauch and W. Metzner. Chem. Ber. **99**, 88 (1966).
32. C. A. Grob, H. R. Kiefer, H. J. Lutz, and H. J. Wilkens. Helv. Chim. Acta, **50**, 416 (1967).
33. W. S. Trahanovsky, P. J. Flash, and L. M. Smith. J. Amer. Chem. Soc. **91**, 5068 (1969).
34. R. E. Partch. J. Org. Chem. **28**, 276 (1963).
35. M. Amorosa, L. Cogliotti, G. Cainelli, H. Immer, J. Keller, H. Wehrli, M. LJ. Mihailovic, K. Schaffner, D. Arigoni, and O. Jeger. Helv. Chim. Acta, **45**, 2674 (1962).
36. M. Akhtar and D. H. R. Barton. J. Amer. Chem. Soc. **86**, 1528 (1964).
37. R. E. Partch and J. Monthony. Tetrahedron Lett. 4427 (1967).
38. G. Mino, S. Kaizerman, and E. Rasmussen. J. Amer. Chem. Soc. **81**, 1494 (1959).

Can. J. Chem. Downloaded from www.nrcresearchpress.com by 210.87.254.105 on 09/05/12
For personal use only.

Can. J. Chem. Downloaded from www.nrcresearchpress.com by 210.87.254.6 on 09/05/12
For personal use only.

Synthesis of 1,2,3,4,7,8,9,10-octahydrodicyclohepta[*de*,*ij*]naphthalene

A. Fischer and D. R. A. Leonard
Department of Chemistry, University of Victoria, British Columbia

and

D. A. R. Happer

Department of Chemistry, University of Canterbury, Christchurch, New Zealand

Received July 24, 1969

Benzosuberone (**5**) has been converted via the tricyclic ketone 3-oxo-1,2,3,7,8,9,10,10*a*-octahydrocyclohepta[*de*]naphthalene (**7**) and the tetracyclic ketone 1-oxo-1,2,3,4,4*a*,5,6,6*a*,7,8,9,10-dodecahydrodicyclohepta[*de*,*ij*]naphthalene (**14**) into 1,2,3,4,7,8,9,10-octahydrodicyclohepta[*de*,*ij*]naphthalene (**16**).

Canadian Journal of Chemistry, **48**, 1446 (1970)

Gilmore and Horton (1) synthesized tetrahydrocyclohepta[*de*]naphthalene (**4**) in two ways (Scheme 1). In the preferred method the seven-membered ring was built up by adding a four-carbon side chain to α-tetralone via a Reformatsky reaction with methyl γ-bromocrotonate; subsequent dehydration, hydrogenation, ester hydrolysis, and ring closure of the acid gave the tricyclic seven-membered ring ketone **2**. Reduction of the ketone to the octahydrocycloheptanaphthalene **3**, followed by dehydrogenation, gave the tetrahydrocycloheptanaphthalene **4** in 35% overall yield. The alternative synthesis started with benzosuberone (**5**) as the functional bicyclic compound and the required six-membered ring was built up via a Reformatsky reaction using ethyl bromoacetate; subsequent dehydration, reduction, conversion to halide, extension of the chain via Grignard formation and carbonation, and ring closure, gave the tricyclic six-membered ring ketone **7**. Reduction of this ketone gave the same octahydrocycloheptanaphthalene as obtained above and dehydrogenation of this gave the tetrahydronaphthalene in 3.8% overall yield. Our synthesis of the octahydrodicyclohepta[*de*,*ij*]naphthalene (**16**) (Scheme 2) started with benzosuberone **5** as the key bicyclic compound. Construction of the six-membered ring gave the tricyclic six-membered ring ketone **7**. The second seven-membered ring was built on through the tricyclic ketone following the general method used by Gilmore and Horton in synthesizing the tricyclic seven-membered ring ketone **2**. Two points were clear at the start. First the synthesis required substantial quantities of benzosuberone. This was obtained from cinnamaldehyde by aldol condensation with acetone, followed by oxidation with hypochlorite to cinnamylideneacetic acid (2), then hydrogenation to δ-phenylvaleric acid and subsequent ring closure. Second, a much improved method of obtaining the tricyclic ketone **7**

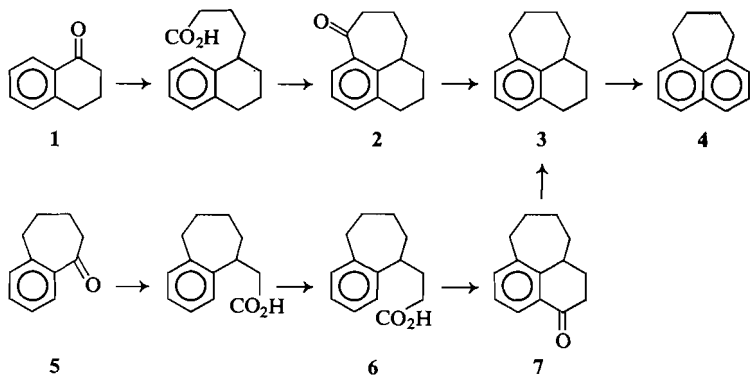

Scheme 1

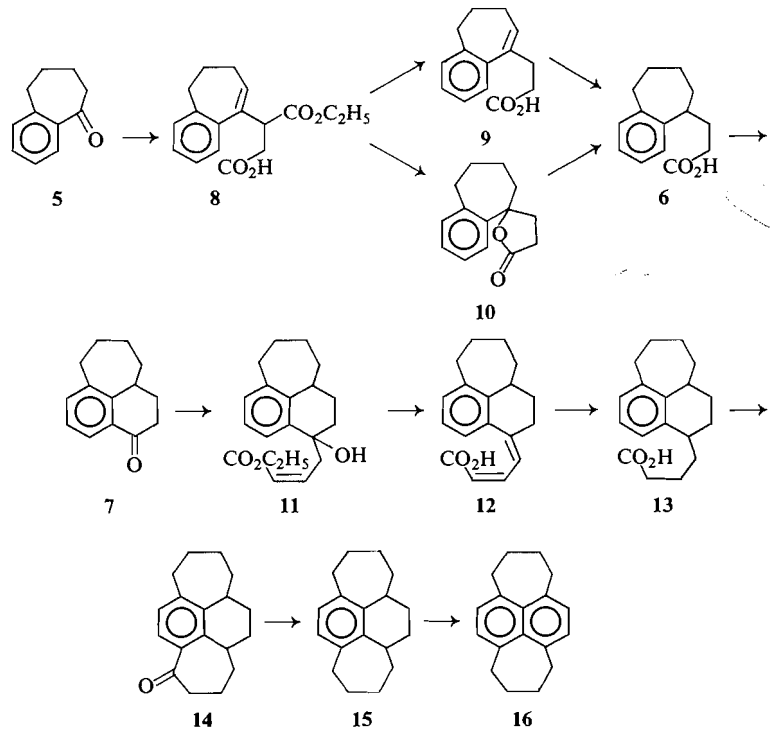

SCHEME 2

was required since Gilmore and Horton's method gave it in only an 11% overall yield. The poorest yielding steps in their synthesis were those associated with extending the length of the side chain of the acid and we chose to insert the required three-carbon side chain in a single step.

Stobbe condensation (3) of benzosuberone with diethyl succinate gave the olefinic half-ester **8** in good yield when potassium *t*-butoxide was used as the condensing agent. Use of sodium hydride gave lower yields of **8**. Hydrolysis and simultaneous decarboxylation of **8** gave a mixture of the olefinic acid **9** (48%) and the isomeric lactone **10** (36%). The olefinic acid **9** was hydrogenated to the acid **6**. Acid **6** was also obtained by reduction of the lactone **10** with red phosphorus and iodine. Polyphosphoric acid-catalyzed cyclization of the acid **6** gave the tricyclic ketone **7**, 61% from benzosuberone. Reformatsky reaction of ketone **7** with ethyl γ-bromocrotonate gave crude unsaturated carbinol ester **11** which underwent dehydration when it was hydrolyzed to give the diene-acid **12**. The diene-acid **12** was hydrogenated to acid **13** and the latter was cyclized with polyphosphoric acid to the tetracyclic ketone **14**. Dodecahydrodicyclohepta[*de*,*ij*]naphthalene (**15**) was obtained from ketone **14** by Clemmensen reduction and was then aromatized to form 1,2,3,4,7,8,9,10-octahydrodicyclohepta[*de*,*ij*]naphthalene (**16**). The octahydrodicycloheptanaphthalene was obtained in 7.3% overall yield from benzosuberone. Clemmensen reduction of the tricyclic ketone **7** gave the octahydrocyclohepta[*de*]naphthalene **3** which was aromatized to the tetrahydrocycloheptanaphthalene **4**, obtained in 44% overall yield from benzosuberone.

Cook *et al.* (4) cited the m.p. 170–173° for the olefinic half-ester **8** but they added that they could not obtain a satisfactory analysis. We could not induce the half-ester to crystallize. From the ratio of the integrated intensity of the triplet at 3.95 τ, attributed to the single olefinic proton of the *endo* isomer **8**, to that of the multiplet at 2.85 τ, attributed to the aromatic protons of both **8** and its *exo* isomer, we calculated that *exo* isomer could have constituted up to one-third of the mixture. We confirmed that the

Can. J. Chem. Downloaded from www.nrcresearchpress.com by 210.87.254.6 on 09/05/12
For personal use only.

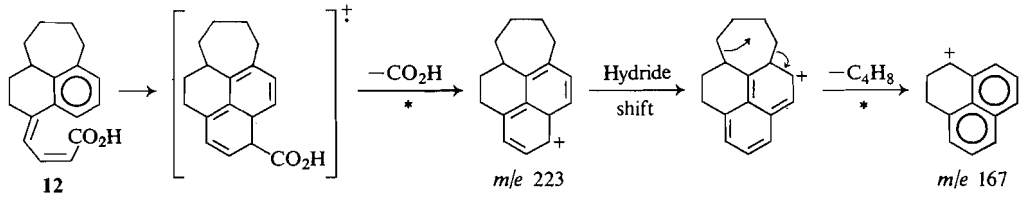

SCHEME 3

predominant product was the *endo* olefinic half-ester by hydrolysis of the carbethoxy group and isolation of the *endo* olefinic diacid. The nuclear magnetic resonance (n.m.r.) spectrum of the hydrolysis product, which showed a triplet at 3.8 τ which integrated for one proton, a multiplet at 5.96 τ (one proton), and a multiplet at 8.16 τ (two protons) established that it was the *endo* diacid. The absorption at 3.8 τ was assigned to the vinylic proton split into a triplet by the adjacent methylenic protons. The absorption at 5.96 τ was assigned to the proton at C-2 which is both allylic and α to a carboxyl group. The absorption at 8.16 τ was attributed to an alicyclic methylene. The *exo* isomer has no vinylic protons. It has two protons both allylic and α to a carboxyl group and has four alicyclic methylene protons. Although the *exo* isomer has the double bond α,β to a carbethoxy group which also brings the carbethoxy group into conjugation with the benzene ring, it is apparently less stable than the *endo* isomer which has the double bond β,γ to carbethoxy. Presumably the dominant factor is the greater relative stability of the seven-membered ring containing the *endo* double bond.

In the mass spectrum of the acids **6** and **13** the predominant cleavage of the molecular ion was that in which the side chain was lost and a secondary cyclic carbonium ion, of mass 145 and 185 respectively and stabilized by the adjacent aromatic ring, was formed. A similar favored cleavage to give a fragment of mass 143 occurred in the unsaturated acid **9** even though, formally, this would lead to a carbonium ion with the charge located on an unsaturated carbon atom. The lactone **10** also underwent cleavage to generate an assumed similar carbonium ion of mass 143 and in this case a hydrogen atom was eliminated with the lactone "side chain". The spectra of acids **6** and **9** also showed the loss of a fragment of mass 60. In the case of **6** this was demonstrated by precise mass measurement to be acetic acid and its formation may be explained as a McLafferty rearrangement product in which the charge remained with the larger (hydrocarbon) fragment. The predominant fission in the molecular ion of ketone **7** was that in which a fragment of mass 42 (ketene) was lost. Ketone **7** has the required substituent at the γ-carbon atom (5). Ketone **14** has a δ rather than a γ substituent and did not show a marked loss of mass 42 from the molecular ion. Loss of a mass 42 (C_3H_6) unit occurred from the molecular ion of hydrocarbon **15**. Fission of one of the seven-membered rings at a bond one removed from the benzene ring and at a second bond attached to the six-membered ring seems likely. A similar fission occurred in the fragment of mass 185 in the spectrum of **13**. Loss of fragments of mass 42 also occurred from the ion of mass 183 in the spectrum of **14** and from the ion of mass 221 in the spectrum of **16**. Appropriate metastables were observed for all of the cited transitions. A proposed fragmentation of the unsaturated acid **12** is depicted in Scheme 3.

Experimental

Infrared (i.r.) spectra were determined on a Perkin–Elmer model 337 spectrometer calibrated with polystyrene. The n.m.r. spectra were determined on Varian A-60 or HA-60-IL spectrometers using tetramethylsilane as internal standard. Mass spectra were determined on AEI MS-902 instruments. Microanalyses were by Dr. A. D. Campbell, University of Otago, Dunedin, New Zealand.

3-Carbethoxy-3-(1′,2′-benzocyclohepta-1′,3′-dien-3′-yl)-propanoic Acid (8) and 1′,2′-Benzocyclohepta-1′,3′-dien-3′-yl-butandioic Acid

Benzosuberone (160 g, 1.0 mole) and diethyl succinate (261 g, 1.5 mole) were added to a solution of potassium *t*-butoxide, prepared from potassium (43 g, 1.1 mole) and *t*-butyl alcohol (1.2 dm^3), under nitrogen. The solution was heated under reflux for 40 min and then allowed to stand at room temperature for 24 h. The mixture was acidified with hydrochloric acid, the solvent removed, and the residue taken up in ether. After washing with water, the product half-ester was extracted into bicarbonate and the bicarbonate solution washed with ether. The product was extracted back into ether from the acidified bicarbonate solution and the ether removed yielding the

Can. J. Chem. Downloaded from www.nrcresearchpress.com by 210.87.254.6 on 09/05/12
For personal use only.

Can. J. Chem. Downloaded from www.nrcresearchpress.com by 210.87.254.6 on 09/05/12
For personal use only.

carbethoxybenzocycloheptadienylpropanoic acid **8** (4) presumably contaminated with the *exo* isomer, as a clear oil (261 g, 90%); i.r. 1740 (ester C=O), 1710 cm^{-1} (acid C=O); n.m.r. (CCl_4) τ 2.85 (m, 4, C_6H_4), 5.95 (t, 0.6, CH=C). Benzosuberone (13 g, 8%) was recovered.

The carbethoxypropanoic acid **8** (2 g) dissolved in methanol (50 g) and water (50 g) containing potassium hydroxide (50 g) was stirred at room temperature for 10 days. The solution was acidified with hydrochloric acid and the diacid was extracted with dichloromethane. After treating the extract with norite the solvent was removed and the residue was recrystallized from aqueous methanol and then sublimed. The sublimate, which melted and resolidified at about 70° and then remelted at 159–161°, was recrystallized from benzene containing a little methanol to give 1′,2′-benzocyclohepta-1′,3′-dien-3′-yl-butandioic acid; m.p. 159–159.5°; i.r. (KBr) 1710 (shoulder), 1700 cm^{-1} (acid C=O); n.m.r. ($CDCl_3$) τ −1.75 (s, 2, CO_2H), 2.72 (m, 4, C_6H_4), 3.8 (t, 1, CH=C), 5.96 (m, 1, C=C—C(H)CO_2H), 7.05 (m, 2, $C_6H_4CH_2$), 7.5 (m, 2, CH_2CO_2H), 7.8 (m, 2, C=CH—CH_2), 8.16 (m, 2, $CH_2CH_2CH_2$); mass spectrum (70 eV) *m/e* (relative intensity) 260.1046 (27, M_r ($^{12}C_{15}{}^{1}H_{16}{}^{16}O_4$) = 260.1049), 242.0942 (28, $C_{15}H_{14}O_3$), 214 (23), 201 (38), 155 (47), 143 (100), 141 (42).

Anal. Calcd. for $C_{15}H_{16}O_4$: C, 69.21; H, 6.20. Found: C, 69.16; H, 6.29.

3-(1′,2′-Benzocyclohepta-1′,3′-dien-3′-yl)propanoic Acid (9) and the Lactone of 3-(1′,2′-Benzo-3′-hydroxycyclohepta-1′-en-3′-yl)propanoic Acid (10)

The carbethoxypropanoic acid **8** (516 g, 1.79 mole) was heated under reflux for 48 h in a solution of acetic acid (3 dm^3), hydrochloric acid (1.5 dm^3), and water (2.2 dm^3) (3). The mixture was concentrated by distillation under reduced pressure and the acid taken up in benzene. The benzene solution was washed with water and the acid was extracted with saturated carbonate solution which was in turn extracted with dichloromethane and the dichloromethane and benzene solutions were then combined. The carbonate solution was acidified and the liberated acid extracted with dichloromethane. The solution was dried, the solvent removed, and the residue recrystallized from 5% benzene–ligroin to yield the unsaturated acid **9** (98 g, 25%); m.p. 71.5–72°; i.r. (nujol) 1705 cm^{-1} (acid C=O); n.m.r. (CCl_4) τ −1.83 (s, 1, CO_2H), 2.89 (m, 4, C_6H_4), 4.03 (t, 1, CH=C), 7.0–8.2 p.p.m. (m, 10); mass spectrum (70 eV) *m/e* (relative intensity) 216.1124 (40, M_r ($^{12}C_{14}{}^{1}H_{16}{}^{16}O_2$) = 216.1152), 156 (31), 143 (100), 141 (43), 115.0546 (43, C_9H_7).

Anal. Calcd. for $C_{14}H_{16}O_2$: C, 77.75; H, 7.46. Found: C, 77.60; H, 7.52.

A residual acidic oil (171 g) was also obtained.

The combined benzene–dichloromethane neutral solution was dried, the solvent removed, and the residue recrystallized from 5% benzene–ligroin to yield the lactone **10** (79 g, 21%); m.p. 132–132.5° (lit. (6) 134°); i.r. (nujol) 1775 cm^{-1} (lactone C=O); n.m.r. ($CDCl_3$) τ 2.83 (m, 4, C_6H_4), 7.13 (m, 2, $CH_2C_6H_4$), 7.53 (s, 4), 7.93 (m, 6); mass spectrum (70 eV) *m/e* (relative intensity) 216.1161 (100, M_r($^{12}C_{14}{}^{1}H_{16}{}^{16}O_2$) = 216.1161), 187.0737 (15, $C_{12}H_{11}O_2$), 161.0972 (50, $C_{11}H_{13}O$), 143.0861 (59, $C_{11}H_{11}$), 141 (9).

Anal. Calcd. for $C_{14}H_{16}O_2$: C, 77.75; H, 7.46. Found: C, 77.73, H, 7.47.

A residual fraction (53 g) was obtained which was combined with the residual acid fraction and rehydrolyzed for 5 days and the olefinic acid **9** and the lactone **10** isolated as described above. The residues were subjected to a third hydrolysis and at this stage the total yield was 84% consisting of acid and lactone in the ratio of 4:3.

3-(1′,2′-Benzocyclohept-1′-en-3′-yl)propanoic Acid (6)

(a) From the Benzocycloheptadienylpropanoic Acid 9

The acid (28.3 g, 0.13 mole) was dissolved in acetone (150 cm^3) and hydrogenated over 5% palladium-on-carbon (2 g) in a shaking autoclave at 8 MN m^{-2} for 4 h. The catalyst was filtered off and the solvent removed under reduced pressure to give the benzocycloheptenylpropanoic acid **6** (25.8 g, 90.5%) as a clear oil.

(b) From the Lactone 10

The lactone (79 g, 0.37 mole) was heated under reflux for 6 h in acetic acid (1 dm^3) with red phosphorus (60 g, 1.9 mole), iodine (20 g, 0.16 mole), and water (20 cm^3) (7). The phosphorus was filtered off, the solution concentrated by distillation under reduced pressure and poured into 5% sodium bisulfite solution (2 dm^3). The organic layer was taken up in benzene–ether and the acid extracted with saturated sodium carbonate solution which was then acidified and extracted with dichloromethane. The dichloromethane solution was dried and the solvent removed yielding the benzocycloheptenylpropanoic acid **6** (66 g, 82%). The residual benzene–ether solution was dried and the solvent removed to leave unreacted lactone **10** (12 g, 16%).

The acid **6** was distilled under reduced pressure and recrystallized from methanol; b.p. 164–168°/0.7 mm (lit. (8) 140–147°/0.3 mm); m.p. 52.5–53.5°; i.r. 1705 cm^{-1} (acid C=O); n.m.r. (CCl_4) τ −1.98 (s, 1, CO_2H), 3.03 (m, 4, C_6H_4), 7.20 (m, 3, $CH_2C_6H_4CH$), 7.74 (m, 4), 8.24 p.p.m. (m, 6); mass spectrum (70 eV) *m/e* (relative intensity) 218.1310 (100, M_r ($^{12}C_{14}{}^{1}H_{18}{}^{16}O_2$) = 218.1307), 200 (2), 158.1080 (29, $C_{12}H_{14}$), 145.1012 (100, $C_{11}H_{13}$), 143.0852 (26, $C_{11}H_{11}$), 129.0694 (28, $C_{10}H_9$), 117.0698 (27, C_9H_9), 115.0546 (36, C_9H_7), 91.0530 (C_7H_7).

Anal. Calcd. for $C_{14}H_{18}O_2$: C, 77.03; H, 8.31. Found: C, 77.06; H, 8.37.

3-Oxo-1,2,3,7,8,9,10,10a-octahydrocyclohepta[de]-naphthalene (7)

The benzocycloheptenylpropanoic acid **6** (116 g, 0.53 mole) was heated on a steam bath, with a solution of phosphorus pentoxide (1.5 kg) in 95% orthophosphoric acid (780 cm^3) for 2 h. The mixture was poured into ice-water (3 dm^3) and the ketone **7** extracted with benzene (4 × 250 cm^3). The benzene extract was washed with saturated sodium carbonate solution, dried, and the solvent removed. On distillation of the residue the oxo-octahydrocycloheptanaphthalene **7** was obtained as an oil (99.6 g, 93.5%) which was crystallized from methanol at −70°; b.p. 160–170°/1.3 mm; m.p. 59–60° (lit. (1) 43–44°); i.r. 1685 cm^{-1} (aromatic C=O); n.m.r. (CCl_4) τ 2.25 and 2.89 (m, 1 and 2, C_6H_4), 7.12 (m, 3, $CH_2C_6H_4CH$), 7.55 (m, 2, CH_2CO), 8.16 p.p.m. (m, 8,

Can. J. Chem. Downloaded from www.nrcresearchpress.com by 210.87.254.6 on 09/05/12
For personal use only.

$CH_2CH_2CH_2CH_2CHCH_2CH_2CO$); mass spectrum (70 eV) *m/e* (relative intensity) 200.1204 (73, M_r ($^{12}C_{14}$-$^1H_{16}{}^{16}O$) = 200.1201), 172 (11), 158.1109 (100, $C_{12}H_{14}$).

Anal. Calcd. for $C_{14}H_{16}O$: C, 83.96; H, 8.05. Found: C, 83.84; H, 8.21.

4-(1',2',3',7',8',9',10',10'a-Octahydrocyclohepta[de]-naphthalen-3'-ylidene)but-2-enoic Acid (12)

Ethyl γ-bromocrotonate (95 g, 0.48 mole) was added to a mixture of zinc dust (50 g) and the tricyclic ketone **7** (96 g, 0.48 mole) dissolved in benzene (250 cm^3) and ether (250 cm^3), and a crystal of iodine added to initiate the reaction. More crotonate (70 g, 0.36 mole) and zinc dust (140 g) was added over 24 h. The mixture was stirred and heated under reflux for the initial 12 h and stirred at room temperature for a further 48 h. The reaction mixture was added to ice and dilute acetic acid and the aqueous and organic layers separated. The aqueous layer and the zinc remaining in the reaction flask were extracted with ether–benzene and the combined organic layers washed successively with 1% ammonia, water, and saturated brine. The solution was dried and the solvent removed giving crude hydroxy ester **11**; i.r. 3505 cm^{-1} (OH). The ester was dissolved in ethanol (2 dm^3) and stirred overnight with 50% potassium hydroxide solution (600 cm^3). The solution was then diluted with water and extracted with benzene–ether which was in turn extracted with saturated sodium carbonate solution. The combined aqueous layers were acidified and extracted with benzene–ether. After removal of the solvent from the acidic extract the residue was repeatedly recrystallized from methanol to give the yellow octahydrocycloheptanaphthalenylidenecrotonic acid **12** (35 g, 26%); m.p. 215–217° (with sublimation); i.r. (nujol) 1675 cm^{-1} (conjugated acid C=O); mass spectrum (70 eV) *m/e* (relative intensity) 268 (61, M_r ($C_{18}H_{20}O_2$) = 268), 223 (100), 167 (49).

Anal. Calcd. for $C_{18}H_{20}O_2$: C, 80.56; H, 7.51. Found: C, 80.62; H, 7.51.

4-(1',2',3',7',8',9',10',10'a-Octahydrocyclohepta[de]-naphthalen-3'-yl)butanoic Acid (13)

In a typical reduction the diene-acid **12** (5.1 g) was dissolved in warm acetic acid – benzene solution (150 cm^3) and shaken in an atmosphere of hydrogen at 5 MN m^{-2} for 4 h. The catalyst was filtered off and the solvent evaporated. The residue was taken up in hot ligroin and filtered. The crystals which were deposited on cooling were recrystallized (×3) yielding the octahydrocycloheptanaphthalenylbutanoic acid **13** (4.7 g, 91%); m.p. 111.5–112.5°; i.r. (nujol) 1690 cm^{-1} (acid C=O); n.m.r. (CCl_4) τ 3.12 (m, 3, C_6H_3), 7.28 (m, 4, $CH_2C_6H_3$-(CH)CH), 7.66 (m, 2, CH_2CO_2H), 8.28 p.p.m. (m, 14, alicyclic and acyclic CH_2); mass spectrum (70 eV) *m/e* (relative intensity) 272 (27, M_r ($C_{18}H_{24}O_2$) = 272), 185 (100), 143 (15).

Anal. Calcd. for $C_{18}H_{24}O_2$: C, 79.37; H, 8.88. Found: C, 79.47; H, 8.95.

1-Oxo-1,2,3,4,4a,5,6,6a,7,8,9,10-dodecahydrodicyclohepta[de,ij]naphthalene (14)

The acid **13** (7.1 g) was heated with a solution of phosphorus pentoxide (250 g) in 95% orthophosphoric acid (240 g) for 2 h. The mixture was worked-up as described above for the tricyclic ketone **7**. The distilled tetracyclic ketone (6.0 g, 90%) was recrystallized from pentane; b.p. 210–220°/2 mm; m.p. 73.5–74.5°; i.r. 1678 cm^{-1} (aromatic ketone C=O); n.m.r. (CCl_4) τ 2.92 (q, 2, J = 8 Hz) 6.9–7.5 (m, 6, $CH_2C_6H_2(CH)CH$, CH_2CO) 7.9–8.7 p.p.m. (m, 14, alicyclic CH_2); mass spectrum (70 eV) *m/e* 254 (100, M_r ($C_{18}H_{22}O$) = 254), 236 (24), 226 (30), 198 (30), 183 (46), 141 (46).

Anal. Calcd. for $C_{18}H_{22}O$: C, 84.86; H, 8.72. Found: C, 85.05; H, 8.87.

1,2,3,4,4a,5,6,6a,7,8,9,10-Dodecahydrodicyclohepta-[de,ij]naphthalene (15)

Zinc dust (5 g) and mercuric chloride (0.5 g) were swirled with dilute hydrochloric acid for a few minutes and the acid then decanted off. The tetracyclic ketone **14** (1.0 g) in toluene (5 cm^3) was added to the amalgamated zinc followed by acetic acid (30 cm^3) and concentrated hydrochloric acid (12 cm^3) and the mixture heated under reflux for 24 h. The reaction mixture was diluted with water and extracted with ether (5 × 25 cm^3). The ethereal extract was washed with saturated sodium bicarbonate solution, dried, and the solvent removed. The residue was chromatographed on alumina (Brockmann 1) with petroleum ether as eluant. Benzene was used to elute a trace (0.03 g) of the ketone. The hydrocarbon **15** (0.85 g, 91%) obtained from the eluate was recrystallized from pentane; m.p. 52–52.5°; n.m.r. (CCl_4) τ 3.33 (s, 2, C_6H_2), 7.27 (m, 6, $CH_2(CH)C_6H_2(CH)CH_2$), 7.9–8.7 p.p.m. (16, alicyclic CH_2); mass spectrum (70 eV) *m/e* 240 (100, M_r ($C_{18}H_{24}$) = 240), 198 (21), 183 (34).

Anal. Calcd. for $C_{18}H_{24}$: C, 89.94; H, 10.06. Found: C, 90.00, H, 10.29.

1,2,3,4,7,8,9,10-Octahydrodicyclohepta[de,ij]-naphthalene (16)

The dodecahydro compound **15** (4.1 g) was heated under an atmosphere of nitrogen with 30% palladium-on-carbon (0.3 g) in a Claisen flask fitted with a cold finger and placed in a silicone-oil bath. Hydrogen evolution started at 260° and continued for about 4 h as the temperature was slowly raised to 310°. At the latter temperature hydrogen evolution was minimal and heating was discontinued. Polymerization occurred above this temperature. The products were isolated by taking the reaction mixture up in a small amount of benzene and chromatographing it through a short (17 × 2.5 cm) column of alumina using petroleum ether as eluant. Under ultraviolet (u.v.) light three bands were revealed. The first fraction obtained was unreacted dodecahydro compound **15** (1.48 g, 36%), the second the desired octahydro compound **16** (2.45 g, 61%), and the third an unidentified high molecular weight compound which was eluted with benzene. The octahydrodicycloheptanaphthalene was recrystallized from pentane; m.p. 143–144°; n.m.r. (CCl_4) τ 3.15 (s, 4, aromatic CH) 6.90 (broad, 8, benzylic CH_2), 8.04 p.p.m. (m, 8, alicyclic CH_2); mass spectrum (70 eV) *m/e* 236 (100, M_r ($C_{18}H_{20}$) = 236), 221 (8), 208 (4), 207 (5), 179 (9).

Anal. Calcd. for $C_{18}H_{20}$: C, 91.47; H, 8.53. Found: C, 91.34; H, 8.75.

1,2,3,7,8,9,10,10a-Octahydrocyclohepta[de]naphthalene (3)

The tricyclic ketone **7** (10 g) was reduced by the Clemmensen procedure described for the reduction of

the tetracyclic ketone **14** and gave hydrocarbon **3** (7.8 g, 84%); b.p. 78–80°/0.3 mm (lit. (2) 155–158/23 mm), i.r. 3065 and 3020 (aromatic C—H), 2920 and 2850 (alicyclic C—H), 1590 (aromatic ring) 1465 and 1445 (CH_2), 785, 778, 768, 746 cm^{-1}.

Some unchanged tricyclic ketone (0.7 g, 7%) was recovered.

7,8,9,10-Tetrahydrocyclohepta[de]naphthalene (4)

The hydrocarbon **3** (7 g) was heated at 300°, under nitrogen, with 30% palladium-on-charcoal (0.4 g) for 4 h. The product was taken up in benzene, the catalyst filtered off, and the benzene removed. The residue, obtained in essentially quantitative yield, was shown to consist of the product tetrahydro **4** and reactant octahydro **3** compounds in the ratio of 85:15. The tetrahydrocycloheptanaphthalene **4** was obtained on recrystallization from ethanol as rhombic crystals; m.p. 54.5–55.5° (lit. (1) 55.5–57°); i.r. (nujol) 3060 and 3035 (aromatic C—H), 1595 and 1580 (aromatic ring), 832, 819, 794, 771 cm^{-1}; n.m.r. ($CDCl_3$) τ 2.7 (m, 6, aromatic C*H*) 6.77 (m, 4, benzylic CH_2) 7.95 (m, 4, alicyclic CH_2).

We thank the Research Committee of the University Grants Committee (New Zealand), the National Research Council of Canada, and the University of Victoria (Canada) for grants, and Dr. R. Hodges and Dr. G. J. Wright for mass spectrometric measurements.

1. R. C. GILMORE, JR., and W. J. HORTON. J. Amer. Chem. Soc. **73**, 1411 (1951).
2. J. T. PLATI, W. H. STRAIN, and S. L. WARREN. J. Amer. Chem. Soc. **65**, 1274 (1943).
3. W. S. JOHNSON, H. C. E. JOHNSON, and J. W. PETERSEN. J. Amer. Chem. Soc. **67**, 1360 (1945).
4. J. W. COOK, R. PHILIP, and A. R. SOMERVILLE. J. Chem. Soc. 169 (1948).
5. H. BUDZIKIEWIEZ, C. DJERASSI, and D. H. WILLIAMS. Mass spectrometry of organic compounds. Holden-Day, Inc., San Francisco, 1967. p. 151.
6. T. A. CRABB and K. SCHOFIELD. J. Chem. Soc. 4282 (1958).
7. B. RIEGEL and J. G. BURR, JR. J. Amer. Chem. Soc. **70**, 1070 (1948).
8. W. J. HORTON and F. E. WALKER. J. Amer. Chem. Soc. **74**, 759 (1952).

Can. J. Chem. Downloaded from www.nrcresearchpress.com by 210.87.254.6 on 09/05/12
For personal use only.

Can. J. Chem. Downloaded from www.nrcresearchpress.com by 210.87.254.5 on 09/05/12
For personal use only.

Kinetic deuterium isotope effect in the reaction of methyl iodide with thiosulfate ion in aqueous solution[1]

ALFRED V. WILLI AND CHONG MIN WON
College of Pharmaceutical Sciences, Columbia University, 115 West 68th Street, New York, New York 10023

Received November 18, 1969

The kinetic deuterium isotope effect in the reaction of methyl iodide with thiosulfate ion in aqueous solution has been determined as follows: k_H/k_D (per 3D) = 0.966 (+0.02°), 0.968 (+10.00°), 0.970 (+19.98°). Kinetic experiments have been carried out in reaction vessels with no gas phase. The experimental data are compared with results of model calculations of isotope effects from force constants. Excellent agreement between experimental and calculated isotope effects may be obtained with the following values of the transition state bending force constants: $f_{HCI} = 0.295$ mdyn Å, $f_{HCS} = 0.300$ to 0.320 mdyn Å. These values are equal to 50–65% of the corresponding bending force constants in stable molecules.

Canadian Journal of Chemistry, **48**, 1452 (1970)

Introduction

In a previous publication (1), the authors of this paper reported results of deuterium isotope effect determinations for the reaction of methyl iodide with cyanide ion in aqueous solution from 0 to 40°.[2] The work was done in comparison to computer calculations of isotope effects from vibrational force constants, with the purpose of gaining information on the transition state of the reaction (2). Reasonable assumptions were made concerning the CC and CI stretching force constants and the interaction force constant f_{12} (interaction between the CC and CI stretches) in the transition state. The sum of the transition state bending force constants, $f_{HCI} + f_{HCC}$, was adjusted to fit the experimental isotope effect at one temperature, and good agreement between experimental and calculated isotope effects then was obtained for the whole temperature range of the experimental data.

It may be expected that the bond orders of the reacting bonds in the transition state are affected by the nucleophilic power of the attacking reagent (3, 4). Force constants referring to reacting bonds are dependent on the bond orders. According to the Swain-Scott scale (5), thiosulfate ion is the nucleophilic reagent with the greatest nucleophilic power. Therefore, it may be interesting to study kinetic isotope effects in the reaction of methyl iodide with thiosulfate ion and to try to evaluate transition state force constants from the experimental data. Alpha-deuterium isotope effects for this reaction in aqueous solution are reported in this work. In the same way as in the previous work on the reaction of methyl iodide with cyanide ion, the kinetic experiments have been done in reaction vessels with no gas phase.

The kinetics of the reaction of CH_3I with $S_2O_3^{2-}$ have been investigated previously by Slator (6) and by Prasad and Godbole (7). It was found that the reaction follows the second order law and essentially goes to completion.[3]

Starting materials and solvent were purified as described in the previous paper (1).

Also, the reaction vessels with no gas phase were identical with those described previously (1). In a similar way as in the previous study, kinetic experiments of the reactions of CH_3I with $S_2O_3^{2-}$ and of CD_3I with $S_2O_3^{2-}$ were done simultaneously, in two equal apparatuses immersed in the same thermostated water bath. Samples were taken out at suitable time intervals, and unreacted thiosulfate ion was titrated with iodine solution. The initial methyl iodide concentration was computed from the initial thiosulfate concentration and the thiosulfate concentration at "infinity time".

Second order rate constants were calculated

[1]Taken from a part of the thesis of Chong Min Won, to be submitted to the Faculty of Pure Science of Columbia University, New York, New York, in partial fulfillment of the requirements for the degree of Doctor of Philosophy.

[2]Brief reviews on previous isotope effect work on S_N2 reactions of alkyl halides are given in refs. 1 and 2.

[3]Unfortunately, a comparison of the rate constants with those found in this study is not possible as the dimension of the rate constants in ref. 7 is unclear.

Can. J. Chem. Downloaded from www.nrcresearchpress.com by 210.87.254.5 on 09/05/12
For personal use only.

from the experimental data with the aid of the equation

$$[1]\quad \log [(S_2O_3^{2-})/(CH_3I)] = \log [(S_2O_3^{2-})_0/(CH_3I)_0] + [(S_2O_3^{2-})_0 - (CH_3I)_0]k_2t/2.303$$

For each kinetic run, the best straight line was fitted to the experimental points of log $[(S_2O_3^{2-})/(CH_3I)]$ vs. t, using an electronic digital computer with a least squares program.

Results and Discussion

In all experiments, the initial concentration of methyl iodide or methyl-d_3 iodide, respectively, is ca. 1×10^{-2} M and that of thiosulfate ion is ca. 2×10^{-2} M. Results of second order rate constants and isotope effects, obtained at three different temperatures, are collected in Table 1.

TABLE 1

Rate constants and isotope effects in the reaction of methyl iodide (RI) with thiosulfate ion in water

Temperature (°C)	$10\,k_2$ (s^{-1} M^{-1}) R = CH_3	$10\,k_2$ (s^{-1} M^{-1}) R = CD_3	k_H/k_D
+0.02	0.01375	0.01424	0.966±0.0043
+10.00	0.05065	0.05283	0.968±0.0045
+19.98	0.1768	0.1824	0.970±0.0031

Each rate constant or isotope effect value is the average of 5 determinations. At temperatures higher than 20°, the reaction is too fast for precise measurement with the equipment used in this work, since the reaction vessels require a relatively long filling time.

Arrhenius parameters and their estimated errors are given as follows

$CH_3I + S_2O_3^{2-}$

$$A = 2.73 \times 10^{13}(\pm 20\%)$$
$$E_a = 20.38(\pm 0.25)\ \text{kcal}$$

$CD_3I + S_2O_3^{2-}$

$$A = 2.69 \times 10^{13}(\pm 20\%)$$
$$E_a = 20.35(\pm 0.25)\ \text{kcal}$$

Isotope effect

$$A_H/A_D = 1.026(\pm 0.030)$$
$$E_{aH} - E_{aD} = 33\ \text{cal}$$

As these experiments are extended over a temperature interval of 20° only, the results of the temperature dependence of the isotope effect are not as precise as those of the previous work on the reaction with cyanide ion (1).

According to the results of this study, the reaction of methyl iodide with thiosulfate ion exhibits a small inverse deuterium isotope effect. An inverse deuterium isotope effect has been found previously for the reaction of methyl iodide with cyanide ion ($k_H/k_D = 0.913$ per 3D at 20°). For the reactions of methyl bromide and methyl p-toluenesulfonate with thiosulfate ion, however, Leffek (8) and Jackson and Leffek (9) observed normal deuterium isotope effects ($k_H/k_D = 1.03$ and 1.12, respectively per 3D at 25°.

Some model calculations of the deuterium isotope effect in the reaction of methyl iodide with thiosulfate ion have been carried out in this work, using the cut-off method suggested by Stern and Wolfsberg (10). In these calculations, the geometry and the force constants of the model of the reactant are the same as in previous calculations (1) (2). In the model for the transition state, the central CH_3 group is planar, with $\angle HCH = 120°$, $\angle HCI = \angle HCS = 90°$, and the following bond lengths and angles

$$r_{CH} = 1.08\ \text{Å}$$
$$r_{CI} = 2.14\ \text{Å} + 10\% = 2.35\ \text{Å}$$
$$r_{CS} = 1.82\ \text{Å} + 10\% = 2.00\ \text{Å}$$
$$r_{SS} = 2.03\ \text{Å}$$
$$\angle CSS = 107°$$

The S_2O_3 moiety is represented by two points, the one being the outer S atom, the other one the SO_3 group whose mass is located in the model at the position of the inner S Atom (cut-off method). Transition state force constants are chosen as follows

$$f_{SS} = 2.5\ \text{mdyn/Å (11)}$$
$$f_{CSS} = 0.1\ \text{mdyn Å}$$

and

$$f_{HCSS} = 0.1\ \text{mdyn Å (torsion)}$$

The values of the force constants for the CH stretching ($f_{CH} = 5.05$ mdyn/Å in all calculations in this paper), HCH bending, and CH_3 out-of-plane bending motions, as well as interactions among these motions are the same as in previous

TABLE 2
Calculated isotope effects*

f_{CI}	f_{CS}	f_{12}	f_{HCI}	f_{HCS}	k_H/k_D 0 °C	k_H/k_D +10 °C	k_H/k_D +20 °C
0.20	0.20	1.50	0.295	0.320	0.964	0.968	0.973
1.18	1.42	3.20	0.295	0.310	0.960	0.965	0.969
1.26	1.32	3.62	0.295	0.300	0.964	0.968	0.972
Experimental results					0.966	0.968	0.970

*Stretching force constants are given in mdyn/Å and bending force constants are given in mdyn Å.

TABLE 3
Transition state bending force constants

Reaction	Reference	Transition state $f_{HCI} + f_{HCY}$	Transition state f_{HCY}	Stable molecule F_{HCY}
$CH_3I + {}^*I^-$	2	0.590	0.295	0.55 (15)
$CH_3I + CN^-$	1	0.695	0.400	0.64 (11)
$CH_3I + S_2O_3^{2-}$	This work	0.595	0.300	0.525 (16)

calculations for other transition state models of the type $I\cdots CH_3\cdots Y$ (1, 2).

The remaining 5 force constants are related to reacting bonds. Sample calculations are done with 3 different sets of values for f_{CS}, f_{CI}, and f_{12} (interaction between the CS and CI stretches, see Table 2). The bending force constant f_{HCI} is kept constant at 0.295 mdyn Å (the value found for the transition state $I\cdots CH_3\cdots I$) while for each of the 3 sets of f_{CS}, f_{CI}, and f_{12} the bending force constant f_{HCS} is adjusted to fit the experimental isotope effect.

The 3 sets of stretching force constants have been selected on the following bases

(*1*) $f_{CS} = f_{CI} = 0.2$ mdyn/Å, $f_{12} = 1.5$ mdyn/Å (no particular theoretical model).

(*2*) The force constants are calculated from a semi-empirical model of the energy barrier with the aid of an equation which corresponds to that suggested by Johnston (12). The model has been described recently (13). Starting from $V_1 = V_2 =$ 37.2 kcal, $p_1 = 2.26$, $p_2 = 1.717$, the following values are obtained: $n = 0.526$ (bond order of bond to be broken) and $F^* = 1.87$ mdyn/Å (force constant describing the curvature of the energy barrier).

(*3*) The same model is applied, but it is assumed that $V_2 > V_1$, as the equilibrium of the reaction is far on the side of the products. The values of $V_1 = 37.2$ kcal, $V_2 = 45.7$ kcal, $p_1 = 2.26$ lead to $p_2 = 1.978$, $n = 0.560$, and $F^* = 2.22$ mdyn/Å.

The force constants of sets (*2*) and (*3*) are calculated from n and F^* with the aid of eqs. [2] and [3]

$$[2a] \qquad f_{CS} = F_{CS}(1 - n)$$

$$[2b] \qquad f_{CI} = F_{CI}n$$

$F_{CS} = 3.00$ mdyn/Å (14) and $F_{CI} = 2.25$ mdyn/Å (15) are the values of the stretching force constants in stable molecules.

$$[3] \qquad f_{12} = [f_{CI}C^2 + f_{CS} + (1 + C^2)F^*]/2C$$
$$C = (1 - n)/n$$

According to the results of isotope effect calculations collected in Table 2, the experimental value for k_H/k_D is obtained if the transition state bending force constant f_{HCS} is adjusted to a value in the range 0.300–0.320 mdyn Å. In all 3 examples, calculated and experimental isotope effects agree within experimental error, at all 3 temperatures.

In Table 3, transition state bending force constants involving one reacting bond are compared with bending force constants for the same bonds in stable molecules. In all 3 examples which are available today, the transition state

Can. J. Chem. Downloaded from www.nrcresearchpress.com by 210.87.254.5 on 09/05/12
For personal use only.

bending force constant is equal to 50–65% of the bending force constant for the stable molecule.

NOTE ADDED IN PROOF: Previous kinetic work on the reaction of methyl iodide with this sulfate ion has been done by Moelwyn-Hughes (17) and Hasty and Sutter (18). The agreement with the results of this work is good.

The authors are pleased to acknowledge financial support of this work by the U.S. Atomic Energy Commission through Contract No. AT(30-1)-3796.

1. A. V. WILLI and C. M. WON. J. Amer. Chem. Soc. **90**, 5999 (1968).
2. A. V. WILLI. Can. J. Chem. **44**, 1889 (1966); Z. Naturforsch, **21a**, 1377 (1966); **21a**, 1385 (1966).
3. G. S. HAMMOND. J. Amer. Chem. Soc. **77**, 334 (1955).
4. C. G. SWAIN and E. R. THORNTON. J. Amer. Chem. Soc. **84**, 817 (1962).
5. C. G. SWAIN and C. B. SCOTT. J. Amer. Chem. Soc. **75**, 141 (1953).
6. A. SLATOR. J. Chem. Soc. London, **85**, 1285 (1904).
7. M. PRASAD and R. D. GODBOLE. J. Indian Chem. Soc. **7**, 127 (1930).
8. K. T. LEFFEK. Can. J. Chem. **42**, 851 (1964).
9. G. E. JACKSON and K. T. LEFFEK. Can. J. Chem. **47**, 1537 (1969).
10. M. J. STERN and MAX WOLFSBERG. J. Chem. Phys. **45**, 4105 (1966).
11. G. HERZBERG. Infrared and Raman spectra of polyatomic molecules. Van Nostrand, New York. 1945.
12. H. S. JOHNSTON. Advan. Chem. Phys. **3**, 131 (1961).
13. A. V. WILLI. Z. Phys. Chem. Frankfurt, **66**, 317 (1969).
14. K. W. F. KOHLRAUSCH. Monatshefte Chem. **68**, 349 (1936).
15. P. F. FENLON, F. F. CLEVELAND, and A. G. MEISTER. J. Chem. Phys. **19**, 1561 (1951).
16. H. SIEBERT. Z. Anorg. Allg. Chem. **271**, 65 (1952).
17. E. A. MOELWYN-HUGHES. Proc. Roy. Soc. London, Ser. A, **196**, 540 (1949).
18. R. A. HASTY and S. L. SUTTER. Can. J. Chem. **47**, 4537 (1969).

Can. J. Chem. Downloaded from www.nrcresearchpress.com by 210.87.254.5 on 09/05/12
For personal use only.

Can. J. Chem. Downloaded from www.nrcresearchpress.com by 210.87.254.5 on 09/05/12
For personal use only.

Activities and ionic distributions in liquid silicates: application of polymer theory[1]

C. R. MASSON, I. B. SMITH, AND S. G. WHITEWAY
Atlantic Regional Laboratory, National Research Council of Canada, Halifax, Nova Scotia

Received December 15, 1969

Theoretical expressions derived previously for molecular size distributions in multichain polymers are applied to binary silicate melts. The treatment is an extension of a previous approach which was limited to the consideration of linear chains. When all configurations of the chain molecules are taken into consideration, the predicted variation of thermodynamic activity with composition agrees with experiment for all binary systems for which data are available. The effect of allowing for all chain configurations is largely to improve the fit between theory and experiment at high silica contents. Calculated ionic distributions for the system 'FeO'–SiO_2 do not differ markedly from those previously reported. The mean chain length is unaffected. The results support previous views that principles of polymer chemistry can be applied usefully to silicate melts and glasses.

Canadian Journal of Chemistry, **48**, 1456 (1970)

Introduction

In a previous paper (1) theoretical expressions were derived for the most probable distribution of molecular sizes in branched polymers formed by the self-condensation of a multifunctional monomer. We now apply this theory to the calculation of activities and ionic distributions in binary silicate melts. Knowledge of the constitution of these melts is important in understanding the thermodynamic behavior of metallurgical slags and interpreting the physical and chemical properties of glasses.

General

Consider a binary silicate melt MO–SiO_2. Apparently such melts contain, in addition to cations M^{2+} and free oxygen ions O^{2-}, a distribution of monomeric and polymeric silicate anions in dynamic equilibrium. The distribution may be calculated approximately by polymer theory from the thermodynamic properties of the melt.

In the following treatment it is considered that liquid silicates may be treated as condensation polymers derived from the "monomer" SiO_4^{4-}. All configurations of the polyionic chains are considered to be allowed. The assumptions in this treatment are identical with those made in conventional polymer theory. These are (*a*) that intramolecular condensation may be neglected and (*b*) that all functional groups of the same kind are chemically equivalent (principle of equal reactivity). In addition it is assumed (*c*) that ion fractions may be related to thermodynamic activities by the Temkin equation, as discussed below.

The first assumption implies that the silicate ions consist exclusively of linear and branched chains of general formula $Si_nO_{3n+1}^{2(n+1)-}$. As shown previously (2) the distribution of anions in such a system may be considered in terms of the equilibrium between the ion SiO_4^{4-} and any species of chain length n to yield the next higher member and a free oxygen ion

$$[1]\quad SiO_4^{4-} + Si_nO_{3n+1}^{2(n+1)-} \rightleftarrows Si_{n+1}O_{3n+4}^{2(n+2)-} + O^{2-}$$

In previous work the approximation was made that the equilibrium ratios k_{1n} for reaction [1] were independent of n. This treatment resembled a theoretical approach first outlined by Graner and Sillen (3). A similar treatment was developed also by Tobolsky and Eisenberg (4) and Tobolsky (5). Although an oversimplification for silicate melts, the method proved valuable in interpreting activity–composition relationships for many binary systems in regions of high basicity. It also allowed ionic distributions to be calculated approximately from thermodynamic activities and showed how they were related to the standard free energies of formation of the pure crystalline silicates.

It is now clear that this simple approach holds only for a system comprised exclusively of linear polymers, as would be derived from a bifunctional monomer. For linear polymers, chain growth by reaction of monomer can occur at only two sites, namely the ends of the chain. Similarly, depolymerization by scission of monomer from

[1]NRCC No. 11 225.

Can. J. Chem. Downloaded from www.nrcresearchpress.com by 210.87.254.5 on 09/05/12
For personal use only.

the chain can occur at only two locations. Hence the equilibrium constant for reaction [1] is independent of chain length, equal reactivity of functional groups being assumed. For multifunctional condensations, however, the number of sites available for growth and degradation by reaction [1] varies with n. Hence the equilibrium ratios k_{1n} are not identical, but depend on the chain length. Calculating how k_{1n} varies with n is equivalent to calculating the configurational aspect of the molecular size distribution in polyfunctional condensations.

When intramolecular condensation is neglected, the correct theoretical expression (1) for the molecular size distribution in polymers derived from a tetrafunctional monomer is

$$[2] \quad N_x = \frac{(3x)!}{(2x+1)!x!}\left(\frac{2\alpha}{3}\right)^{x-1}\left(1-\frac{2\alpha}{3}\right)^{2x+1}$$

where N_x is the mole fraction of x-mer and α is the fraction of functional groups that have reacted. The factorial term in this expression refers to the number of configurations (6, 7) of an x-mer. Strictly, eq. [2] was derived for addition polymers, whose repeating unit is that of the monomer itself, or to condensation polymers in which the product of condensation is removed from the system and is therefore neglected in the expression for mole fractions. In the self-condensation of silicate ions, however, the product of condensation, free oxygen ion O^{2-}, accumulates in the system until equilibrium is attained and its presence cannot be ignored in the evaluation of ion fractions. In this case the exact theoretical expression (1) for the size distribution becomes

$$[3] \quad N_x = \frac{(3x)!}{(2x+1)!x!}\left(\frac{2\alpha}{3}\right)^{x-1}\left(1-\frac{2\alpha}{3}\right)^{2x+1} \times (1 - N_{O^{2-}})$$

where $N_{O^{2-}}$ is the ion fraction[2] of free oxygen ions in the system at equilibrium and N_x is that of any silicate ion of chain length x.

Activities

To calculate activities, we need consider only one of the equilibria represented by reaction [1], and choose the simplest, for $n = 1$. If the value of k_{11} is known, or can be determined, the equilibrium ratio for any other reaction is defined. These remarks apply, of course, for the ideal situation in which the principle of chemical equivalence of functional groups is assumed to hold.

From reaction [1] with $n = 1$, we have, by definition

$$[4] \quad k_{11} = N_2 N_{O^{2-}}/N_1^2$$

where ion fractions are used in place of activities. As shown previously (9), this does not necessarily imply ideal mixing of anions but, more logically, ideal mixing of polyionic segments.

Substituting for N_1 and N_2 from eq. [3] and simplifying, we obtain

$$[5] \quad k_{11} = \frac{N_{O^{2-}}}{1 - N_{O^{2-}}} \cdot \frac{2\alpha}{1 - \frac{2\alpha}{3}}$$

Now the mole fraction of silica may be expressed in terms of the ion fractions of the constituents of the melt by the equation

$$[6] \quad N_{SiO_2} = \frac{\text{moles } SiO_2 \text{ from silicates}}{\text{moles "free" MO} + \text{moles MO from silicates} + \text{moles } SiO_2 \text{ from silicates}} = \frac{N_1 + 2N_2 + 3N_3 + \cdots}{N_{O^{2-}} + 3N_1 + 5N_2 + \cdots} = \frac{\sum x N_x}{N_{O^{2-}} + \sum(2x+1)N_x}$$

[2]As in previous work, the Temkin (8) method of representing ion fractions is used, whereby anions and cations are considered separately. Thus $N_{O^{2-}}$ is given by

$$N_{O^{2-}} = \frac{n_{O^{2-}}}{\sum n_{anions}} = \frac{n_{O^{2-}}}{n_{O^{2-}} + n_{SiO_4^{4-}} + n_{Si_2O_7^{6-}} + \cdots}$$

where n is the number of ions of the species indicated. Similarly, for the anions SiO_4^{4-}, $Si_2O_7^{6-}$, etc.

$$N_1 = \frac{n_{SiO_4^{4-}}}{\sum n_{anions}}$$

$$N_2 = \frac{n_{Si_2O_7^{6-}}}{\sum n_{anions}}$$

For the cations etc.

$$N_{M^{2+}} = \frac{n_{M^{2+}}}{\sum n_{cations}}$$

and, for a binary system MO–SiO_2, $N_{M^{2+}}$ is unity.

Can. J. Chem. Downloaded from www.nrcresearchpress.com by 210.87.254.5 on 09/05/12
For personal use only.

Dividing numerator and denominator by $\sum N_x$ and noting that the mean chain length $\bar{x}_n$ is given by $\sum xN_x/\sum N_x$, eq. [6] becomes

$$[7] \qquad N_{SiO_2} = \frac{\bar{x}_n}{1 + \frac{N_{O^{2-}}}{\sum N_x} + 2\bar{x}_n}$$

As silicate and oxygen are the sole anionic species in the melt, the sum of their ion fractions equals unity

$$[8] \qquad N_{O^{2-}} + \sum N_x = 1$$

Substituting for $\sum N_x$ from eq. [8] in eq. [7], one obtains

$$[9] \qquad N_{SiO_2} = \frac{\bar{x}_n}{\frac{1}{1 - N_{O^{2-}}} + 2\bar{x}_n}$$

Introducing the general expression (6) for the mean chain length in an f-functional condensation

$$[10] \qquad \bar{x}_n = \frac{1}{1 - \frac{\alpha f}{2}}$$

we obtain, for $f = 4$

$$[11] \qquad N_{SiO_2} = \frac{1 - N_{O^{2-}}}{3 - 2(\alpha + N_{O^{2-}})}$$

Equation [11] can be expressed in terms of the activity of MO by introducing the Temkin equation

$$[12] \qquad a_{MO} = (N_{M^{2+}})(N_{O^{2-}})$$

As $N_{M^{2+}}$ is unity for a binary system, we obtain, from eqs. [11] and [12]

$$[13] \qquad \frac{1}{N_{SiO_2}} = \frac{1 - 2\alpha}{1 - a_{MO}} + 2$$

From eqs. [5] and [12]

$$[14] \qquad \frac{1}{\alpha} = 2\left\{\frac{1}{3} + \frac{a_{MO}}{k_{11}(1 - a_{MO})}\right\}$$

Substituting for α in eq. [13]

$$[15] \qquad \frac{1}{N_{SiO_2}} = \frac{1 - \frac{1}{\frac{1}{3} + \frac{a_{MO}}{k_{11}(1 - a_{MO})}}}{1 - a_{MO}} + 2$$

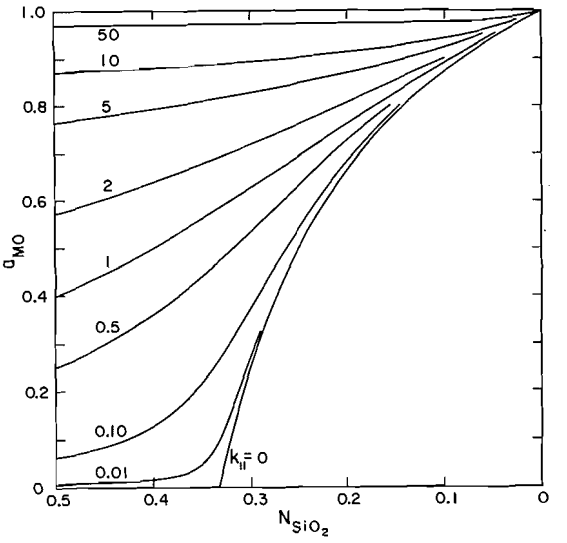

FIG. 1. Theoretical curves of activity of MO against mole fraction of SiO_2 for various values of k_{11}.

Equation [15] is our desired expression for the activity of MO as a function of composition. Theoretical curves of a_{MO} against N_{SiO_2} for various values of k_{11} are presented in Fig. 1.

In contrast to the curves derived previously (2), and as a consequence of allowing for all configurations of the silicate chains, the curves in Fig. 1 no longer pass through zero activity of MO at the metasilicate composition ($N_{SiO_2} = 0.5$). The differences are most marked for high values of k_{11}, as expected.

Comparison with Experiment

In the following, a value of k_{11} was chosen to fit experimental data at one composition. Arbitrarily, a value was chosen which gave the best fit in the region $0.45 > N_{SiO_2} > 0.3$. The theoretical curve for the selected value of k_{11} was then compared with the data for other compositions. Deviations at lower silica contents may be due to the inadequacy of the principle of chemical equivalence of functional groups for the smallest anions; deviations at high silica contents might be due to our neglect of intramolecular condensation.

(1) The System CaO–SiO_2

Due to the low value of k_{11} and consequently the almost complete absence of polymeric species in melts more basic than the orthosilicate, there is little difference between the curve based on eq. [15] and that derived in previous work. As shown

Can. J. Chem. Downloaded from www.nrcresearchpress.com by 210.87.254.5 on 09/05/12
For personal use only.

in Fig. 2, the curve for $k_{11} = 0.0016$ fits the data at all compositions. The experimental points were obtained from Darken's (10) free energy of mixing curve by the method of intercepts, as described previously (2), and the deviations from the line in Fig. 2 are within the error in drawing the tangents.

(2) The System PbO–SiO_2

Activities of PbO in this system were measured recently by Charette and Flengas (11). Their results are in reasonable agreement with the earlier data of Richardson and Webb (12) and of Sridhar and Jeffes (13). The data of all three sets of investigators are reproduced in Fig. 3. The solid line corresponds to eq. [15] with $k_{11} = 0.196$ and fits the data over the entire range up to silica saturation.

Included in Fig. 3 is the line based on the previous treatment for linear chains, using the same value of k_{11}. The curves do not differ significantly

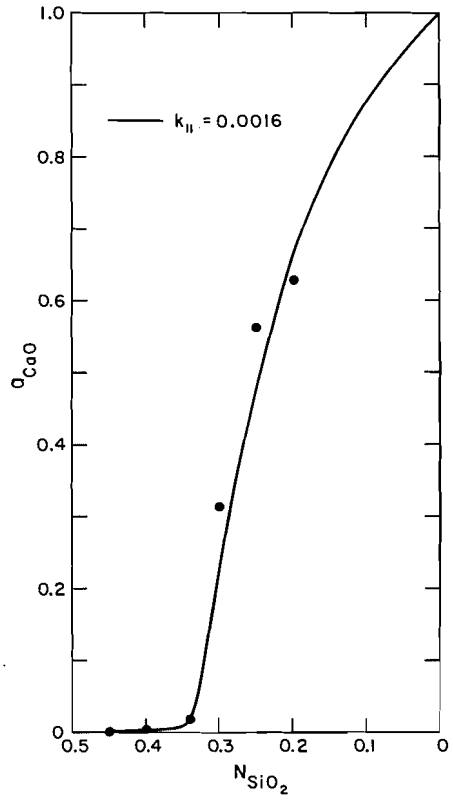

FIG. 2. Activity of CaO plotted against mole fraction of SiO_2 for the system CaO–SiO_2 at 1600 °C. ●, from integral molar free energies of mixing (Darken). The line corresponds to eq. [15] with $k_{11} = 0.0016$.

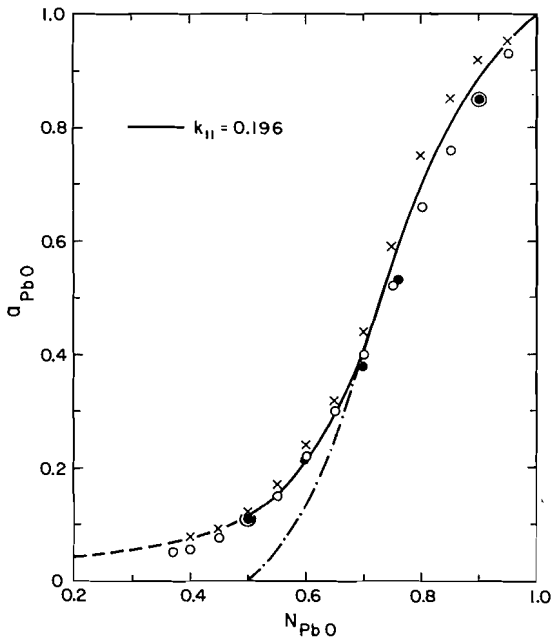

FIG. 3. Activity plotted against mole fraction of PbO for the system PbO–SiO_2 at 1000 °C. ○, Richardson and Webb; ●, Sridhar and Jeffes; ×, Charette and Flengas. The solid line corresponds to eq. [15] with $k_{11} = 0.196$; for $N_{PbO} < 0.5$ it is shown as a broken line, as eq. [15] is not valid in this region. The line –·–·– is the theoretical line for linear chains, using the same value of k_{11}.

for $N_{PbO} > 0.7$, and in this range both treatments fit the data equally well.

(3) The System MnO–SiO_2

Figure 4 is derived (2) from the experimental data of Abraham, Davies and Richardson (14). The curve for $k_{11} = 0.25$ fits the data reasonably well. In particular, the modified theory yields a better representation of the data at high silica contents.

(4) The System 'FeO'–SiO_2

This system is not a true binary but is more properly regarded as the ternary, FeO–Fe_2O_3–SiO_2, with Fe^{2+} and Fe^{3+} cations. As $N_{Fe^{2+}}$ is not unity, a_{FeO} cannot be substituted directly for $N_{O^{2-}}$ in eq. [11]. Instead, $N_{O^{2-}}$ is replaced by $a_{FeO}/N_{Fe^{2+}}$, as given by eq. [12], and a_{MO} in eq. [15] becomes $a_{FeO}/N_{Fe^{2+}}$. The ion fraction of ferrous iron, $N_{Fe^{2+}}$, is determined experimentally by chemical analysis.

A further complication is the necessity for converting the measured activities to stoichiometric FeO as the standard state. As discussed previously (2) this requires a knowledge of $N^0_{Fe^{2+}}$, the

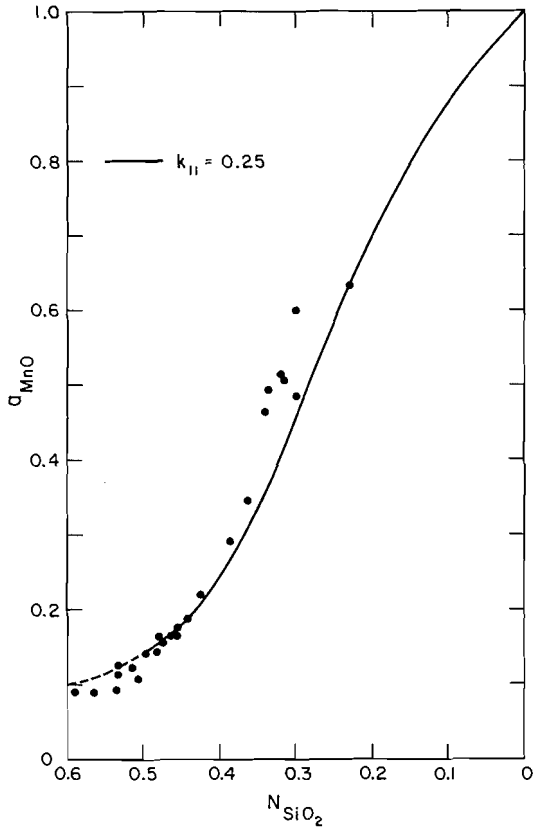

FIG. 4. Activity of MnO plotted against mole fraction of SiO_2 for the system MnO–SiO_2 at 1500–1600 °C. ●, Abraham, Davies, and Richardson, calculated to liquid MnO as standard state. The line corresponds to eq. [15] with $k_{11} = 0.25$.

ion fraction of Fe^{2+} in the non-stoichiometric oxide of composition corresponding to the standard state.

Activities of 'FeO' in this system were measured by Schuhmann and Ensio (15) and Bodsworth (16). Both authors chose, as standard state, supercooled liquid 'FeO' in equilibrium with γ-Fe at the temperature of the melt. The composition of this standard state is most readily visualized as an extrapolation of the line CN in the phase diagram of Darken and Gurry (17). It varies with temperature.

In Table III of ref. (17), Darken and Gurry give values of $r = (Fe^{2+} + Fe^{3+})/Fe^{2+}$ at various temperatures for liquid "FeO" in equilibrium with liquid iron, i.e. for compositions along the line CN. These, along with values of r calculated from the exact compositions at points C, G, and N of the phase diagram, were extrapolated linearly to the temperature of interest to yield values of $N^0_{Fe^{2+}}$ for the standard state at each temperature

$$[16] \qquad r = \frac{Fe^{2+} + Fe^{3+}}{Fe^{2+}} = \frac{n_{Fe^{2+}} + n_{Fe^{3+}}}{n_{Fe^{2+}}} = \frac{1}{N^0_{Fe^{2+}}}$$

These values of $N^0_{Fe^{2+}}$ were used to convert the measured activities to stoichiometric FeO as standard state in the manner described previously.

In Fig. 5, $a_{FeO}/N_{Fe^{2+}}$ is plotted against N_{SiO_2} for both sets of data. The line corresponds to eq. [15] with $k_{11} = 0.7$. Again there is a good fit be-

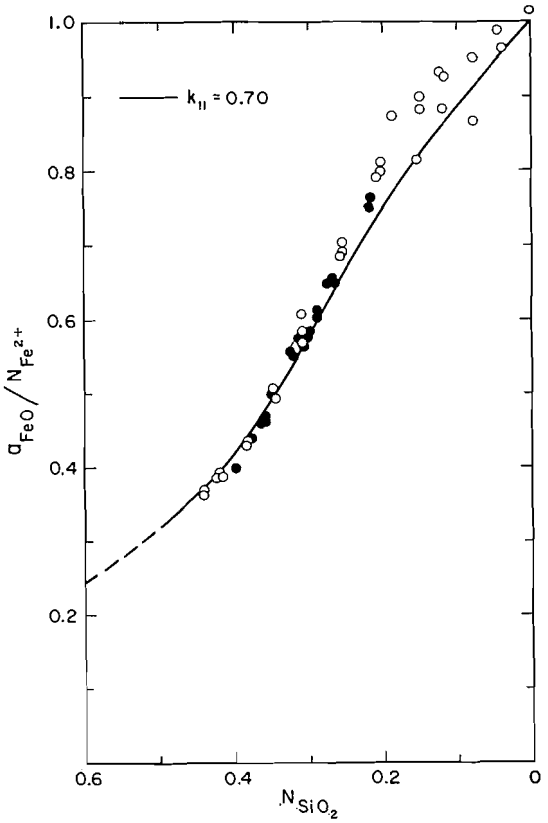

FIG. 5. Values of $a_{FeO}/N_{Fe^{2+}}$ plotted against mole fraction of SiO_2 for the system 'FeO'–SiO_2 at 1257–1406 °C. ○, Schuhmann and Ensio; ●, Bodsworth. The experimental points were recalculated to stoichiometric FeO as standard state. The line corresponds to eq. [15] with a_{MO} replaced by $a_{FeO}/N_{Fe^{2+}}$ and $k_{11} = 0.70$.

Can. J. Chem. Downloaded from www.nrcresearchpress.com by 210.87.254.5 on 09/05/12
For personal use only.

Can. J. Chem. Downloaded from www.nrcresearchpress.com by 210.87.254.5 on 09/05/12
For personal use only.

tween theory and experiment over a wide range of silica contents. The slightly poorer fit at low levels of SiO_2 is in the direction expected if the principle of chemical equivalence of functional groups did not hold exactly and the smaller ions were more reactive.

(5) The system CoO–SiO_2

Activities in this system have not been measured experimentally. Approximate values of a_{CoO} were calculated (9) from the phase diagram (18) using an assumed value for the heat of fusion of CoO. These are plotted in Fig. 6 along with the curve for $k_{11} = 2.0$. In view of the uncertainties, the fit is as good as can be expected for this system.

(6) The System SnO–SiO_2

Activities of SnO in this system were determined by Kozuka, Siahaan, and Moriyama (19). Their results are compared in Fig. 7 with the curve for $k_{11} = 2.55$. The excellent fit over a wide range of silica contents confirms the theory for a system with a high value of k_{11}.

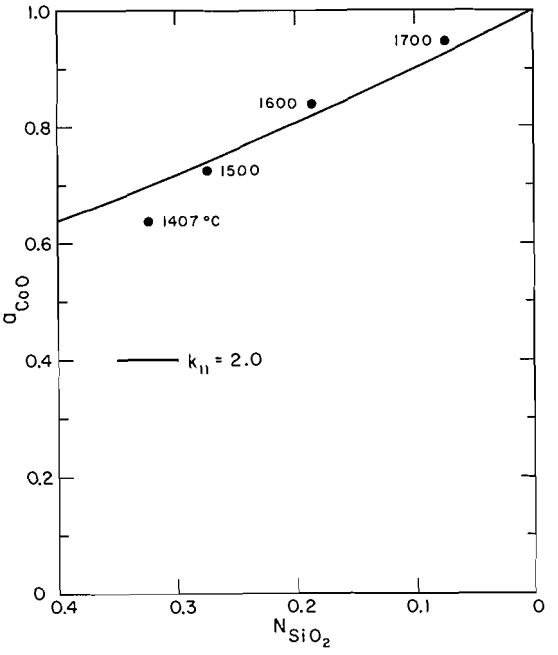

FIG. 6. Activity of CoO plotted against mole fraction of SiO_2 for the system CoO–SiO_2 at 1407–1700 °C. The points were calculated from the phase diagram of Masse and Muan. The line corresponds to eq. [15] with $k_{11} = 2.0$.

Ionic Distributions

Expressions may be derived readily for N_x in terms of any pair of the dependent variables k_{11}, a_{MO}, N_{SiO_2}, and α. Thus, from eqs. [3] and [12] we obtain N_x in terms of α and a_{MO}

$$[17] \quad N_x = \frac{(3x)!}{(2x+1)!x!}\left(\frac{2\alpha}{3}\right)^{x-1} \times \left(1 - \frac{2\alpha}{3}\right)^{2x+1}(1 - a_{MO})$$

If α is expressed in terms of a_{MO} and N_{SiO_2}, we can obtain N_x as a function of a_{MO} and N_{SiO_2}. Thus from eq. [13]

$$[18] \quad \alpha = \frac{1 - (1 - a_{MO})\left(\frac{1}{N_{SiO_2}} - 2\right)}{2}$$

Substituting for α in eq. [17]

$$[19] \quad N_x = \frac{(3x)!}{(2x+1)!x!} \times \left\{\frac{3 - \frac{1 - a_{MO}}{N_{SiO_2}} - 2a_{MO}}{3}\right\}^{x-1} \times \left\{\frac{\frac{1 - a_{MO}}{N_{SiO_2}} + 2a_{MO}}{3}\right\}^{2x+1}(1 - a_{MO})$$

Equation [19] may be used to evaluate ion fractions directly from activity–composition relationships.

A third useful expression is obtained by solving for N_x in terms of k_{11} and a_{MO}. Substituting for α from eq. [14] in eq. [17]

$$[20] \quad N_x = \frac{(3x)!}{(2x+1)!x!} \times \left\{\frac{1}{1 + \frac{3a_{MO}}{k_{11}(1 - a_{MO})}}\right\}^{x-1} \times \left\{\frac{1}{1 + \frac{k_{11}(1 - a_{MO})}{3a_{MO}}}\right\}^{2x+1}(1 - a_{MO})$$

Equations [17], [19], and [20] are of equal utility for calculating ionic distributions. The equation for N_x in terms of k_{11} and N_{SiO_2} is less useful as it involves solution of a quadratic expression.

As illustration of these equations, ionic distributions were calculated for the system 'FeO'–

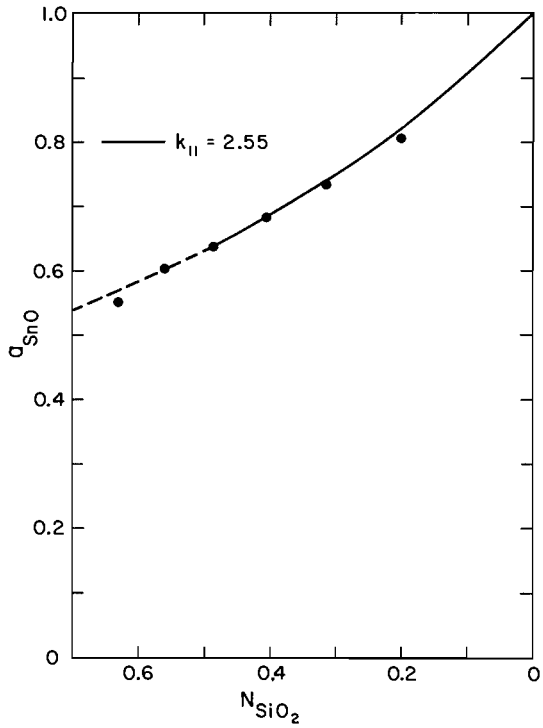

FIG. 7. Activity of SnO plotted against mole fraction of SiO_2 for the system SnO–SiO_2 at 1100 °C. ●, Kozuka, Siahaan and Moriyama. The line corresponds to eq. [15] with $k_{11} = 2.55$.

SiO_2 at 1530–1680 °K. Values of a_{MO} corresponding to various values of N_{SiO_2} were calculated from eq. [15] with $k_{11} = 0.70$. These were inserted in eq. [20] to yield the ion fractions of various species up to the decamer, $Si_{10}O_{31}^{22-}$, at each silica content. The results are presented in Fig. 8.

The distributions closely resemble those calculated previously (2). In particular, each of the ion fractions of SiO_4^{4-}, $Si_2O_7^{6-}$, $Si_3O_{10}^{8-}$, ··· passes through a maximum at compositions corresponding to the formulae Fe_2SiO_4, $Fe_3Si_2O_7$, $Fe_4Si_3O_{10}$, ···, respectively. The refinement of allowing for all configurations results in slightly higher values for $N_{SiO_4^{4-}}$ at all compositions and slightly lower values for the other species. As shown in the following, the mean chain length is unaffected.

Mean Chain Lengths

For the mean chain length, $\bar{x}_n$, of silicate ions we have, from eq. [10]

$$[21] \qquad \bar{x}_n = 1/(1 - 2\alpha)$$

Substituting for α from eq. [14]

$$[22] \qquad \frac{1}{\bar{x}_n} = 1 - \frac{1}{\frac{1}{3} + \frac{a_{MO}}{k_{11}(1 - a_{MO})}}$$

Equation [22] allows the mean chain length to be evaluated directly from the activity if k_{11} is known.

Alternatively, the mean chain length may be expressed in terms of a_{MO} and N_{SiO_2} by substituting for α from eq. [18] in eq. [21]

$$[23] \qquad \frac{1}{\bar{x}_n} = (1 - a_{MO})\left(\frac{1}{N_{SiO_2}} - 2\right)$$

This is identical with the expression derived previously (9).

It should be noted that $\bar{x}_n$ as defined above refers to the silicate ions only. The oxygen ions, which are in general also present in the system, are not included in the expression for the mean chain length. Of course, if oxygen ions are included, the mean chain length of all anions is independent of the degree of polymerization and

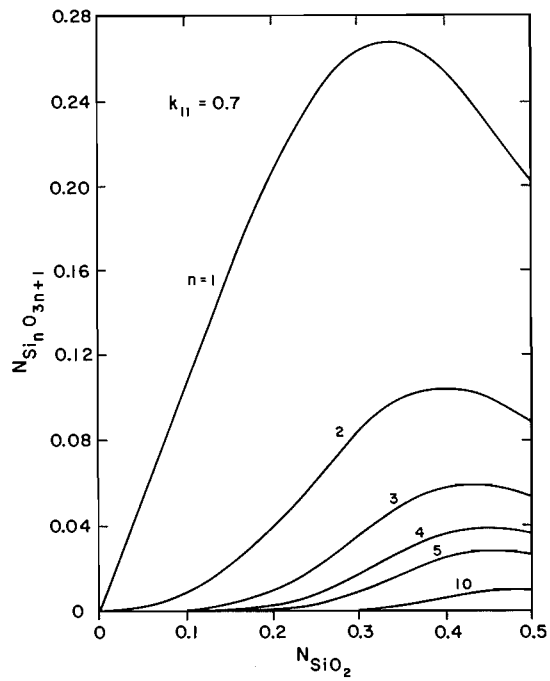

FIG. 8. Ion fractions of SiO_4^{4-}, $Si_2O_7^{6-}$, $Si_3O_{10}^{8-}$, $Si_4O_{13}^{10-}$, $Si_5O_{16}^{12-}$, and $Si_{10}O_{31}^{22-}$ plotted against mole fraction of silica for the system 'FeO'–SiO_2 at 1530–1680 °K.

Can. J. Chem. Downloaded from www.nrcresearchpress.com by 210.87.254.5 on 09/05/12
For personal use only.

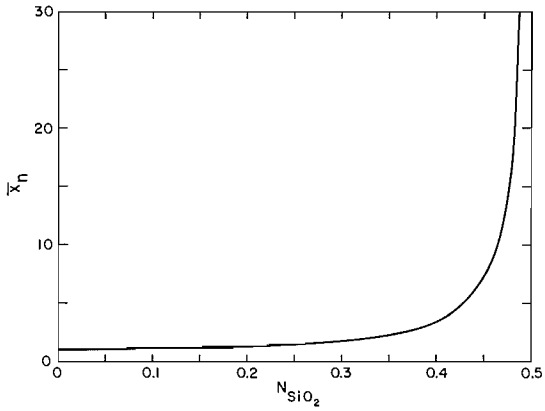

FIG. 9. Mean chain length $\bar{x}_n$ of silicate ions plotted against mole fraction of SiO_2 for the system 'FeO'–SiO_2 at 1530–1680 °K.

is determined solely by the composition of the melt

$$[24] \qquad \frac{1}{(\bar{x}_n)_{\text{all anions}}} = \frac{1}{N_{SiO_2}} - 2$$

The mean chain length of silicate ions in the system 'FeO'–SiO_2, as calculated by eq. [23], is plotted against the mole fraction of silica in Fig. 9. These values may be used in conjunction with the ion fractions in Fig. 8 to calculate distributions as percentages by weight as described previously (9).

Variation of k_{1n} with n

Using ion fractions in place of activities, the equilibrium ratio k_{1n} is given by

$$[25] \qquad k_{1n} = N_{n+1}N_{O^{2-}}/N_1N_n$$

Substituting for N_1, N_n, and N_{n+1} from eq. [3] and simplifying, we obtain

$$[26] \qquad k_{1n} = \frac{2\alpha/3}{1 - 2\alpha/3} \cdot \frac{N_{O^{2-}}}{1 - N_{O^{2-}}} \times \frac{3(3n + 1)(3n + 2)}{2(2n + 3)(n + 1)}$$

Substituting for $N_{O^{2-}}/(1 - N_{O^{2-}})$ from eq. [5]

$$[27] \qquad \frac{k_{1n}}{k_{11}} = \frac{(3n + 1)(3n + 2)}{2(2n + 3)(n + 1)}$$

Equation [27] allows the value of k_{1n} to be calculated for any value of n if k_{11} is known.

TABLE 1

Variation of k_{1n} with n for various binary systems

Oxide	k_{11}	k_{12}	k_{13}	k_{14}	$k_{1\infty}$
CaO	0.0016	0.0021	0.0024	0.0026	0.0036
PbO	0.196	0.261	0.299	0.324	0.441
MnO	0.25	0.33	0.38	0.41	0.56
FeO	0.70	0.93	1.07	1.16	1.575
CoO	2.0	2.7	3.1	3.3	4.5
SnO	2.55	3.40	3.89	4.22	5.74

Values of k_{11}, k_{12}, k_{13}, k_{14}, and $k_{1\infty}$ for the experimental systems are presented in Table 1. The limiting ratio $k_{1\infty}/k_{11}$ is 9/4.

It is interesting to evaluate also the equilibrium ratios[3] $k_{n,n,n+1}$ for redistribution reactions of the type

$$[28] \qquad Si_nO_{3n+1}^{2(n+1)-} + Si_nO_{3n+1}^{2(n+1)-} \rightleftarrows Si_{n+1}O_{3n+4}^{2(n+2)-} + Si_{n-1}O_{3n-2}^{2n-}$$

Substituting for N_n, N_{n+1}, and N_{n-1} from eq. [3] in the expression for the equilibrium constant we obtain

$$[29] \qquad k_{n,n,n+1} = \frac{(3n + 2)(3n + 1)(2n + 1)n}{(3n - 2)(3n - 1)(2n + 3)(n + 1)} \qquad (n > 1)$$

The values of $k_{n,n,n+1}$ rapidly converge to unity as n increases. This may be contrasted with the situation for linear polymers, where $k_{n,n,n+1}$ is, in theory, equal to unity for all values of n.

Discussion

It must be emphasized that the ionic distributions derived above represent "ideal" distributions based on the simplifying assumptions outlined initially. Of these, the principle of chemical equivalence of functional groups, widely used in polymer theory, should not be expected to hold rigorously, particularly for the smallest species. This limitation probably accounts for much of the deviation between theory and experiment for the melts of high basicity in Figs. 4 and 5.

[3]Note on terminology: as discussed elsewhere (9), we use either $k_{n,n,n+1}$ or $k_{n,n,n-1}$ to indicate the equilibrium ratio for reaction [28]. In general, three subscripts are required to indicate precisely the equilibrium ratios of redistribution reactions of this type. We reserve the use of k_{nn} for the special case in which an oxygen ion is eliminated

$$Si_n + Si_n \rightleftarrows Si_{2n} + O^{2-}$$

Can. J. Chem. Downloaded from www.nrcresearchpress.com by 210.87.254.5 on 09/05/12
For personal use only.

The assumption that Temkin's law is valid for binary silicate melts is probably less serious as this law holds for many systems with a common cation or anion.

A significant feature of the results is that, for those systems for which experimental data are available, the theory provides a good representation of the activity vs. composition data over the entire range of applicability of the theory in spite of the neglect of intramolecular condensation. Thus, eq. [15] was derived for melts more basic than $N_{SiO_2} = 0.5$. At this composition, the value of α is 1/2. (That this is true for all values of k_{11} and hence for all values of a_{MO} may be verified directly from eq. [13].) The value of $\alpha = 1/2$ corresponds, in the theory, to $\alpha_{max} = 2/f$ and is the maximum allowable value of α for a tetrafunctional condensation if intramolecular condensation is postulated not to occur.

The close agreement between theory and experiment over the entire range of polymerization up to α_{max} suggests that intramolecular condensation, although it must occur to some extent, does not occur extensively in binary silicate melts, even close to silica saturation. In some instances (Figs. 3, 4, 7) theoretical activities in good agreement with experiment were derived beyond $N_{SiO_2} = 0.5$, i.e., strictly beyond the range of applicability of the theory. These portions of the theoretical curves are indicated by broken lines. The stoichiometry requires that intramolecular condensation *must* occur in these regions.

It is tempting to conclude that silica saturation, with the appearance of a solid phase, corresponds to the onset of extensive intramolecular condensation. This is, however, an oversimplification. Thus, for the system 'FeO'–SiO_2 at 1350 °C, silica saturation occurs at $N_{SiO_2} = 0.43$ whereas for SnO–SiO_2, with a higher value of k_{11}, saturation occurs at $N_{SiO_2} > 0.6$ at the same temperature. Hence the cation must influence the solubility of SiO_2 beyond its effect in determining the magnitude of k_{11}.

1. S. G. WHITEWAY, I. B. SMITH, and C. R. MASSON. Can. J. Chem. **48**, 33 (1970).
2. C. R. MASSON. Proc. Roy. Soc. **A287**, 201 (1965).
3. F. GRANER and L. G. SILLEN. Acta Chem. Scand. **1**, 631 (1947).
4. A. V. TOBOLSKY and A. EISENBERG. J. Amer. Chem. Soc. **82**, 289 (1960).
5. A. V. TOBOLSKY. Properties and structure of polymers. John Wiley and Sons, Inc., New York. 1960.
6. P. J. FLORY. Principles of polymer chemistry. Cornell University Press, Ithaca, New York. 1953.
7. S. G. WHITEWAY. Can. J. Chem. This issue.
8. M. TEMKIN. Acta Physicochim. U.R.S.S. **20**, 411 (1945).
9. C. R. MASSON. J. Amer. Ceram. Soc. **51**, 134 (1968).
10. L. S. DARKEN and R. W. GURRY. Physical chemistry of metals. McGraw-Hill Book Co. Inc., New York. 1953. p. 340.
11. G. G. CHARETTE and S. N. FLENGAS. Can. Met. Quart. **7**, 191 (1968).
12. F. D. RICHARDSON and L. E. WEBB. Trans. Inst. Mining Met. **64**, 529 (1955).
13. R. SRIDHAR and J. H. E. JEFFES. Trans. Inst. Mining Met. **76**, C44 (1967).
14. K. P. ABRAHAM, M. W. DAVIES, and F. D. RICHARDSON. J. Iron Steel Inst. London, **196**, 82 (1960).
15. R. SCHUHMANN, JR. and P. J. ENSIO. J. Metals, **3**, 401 (1951).
16. C. BODSWORTH. J. Iron Steel Inst. London, **193**, 13 (1959).
17. L. S. DARKEN and R. W. GURRY. J. Amer. Chem. Soc. **68**, 798 (1946).
18. D. P. MASSE and A. MUAN. Trans. A.I.M.E. **233**, 1448 (1965).
19. Z. KOZUKA, O. SIAHAAN, and J. MORIYAMA. Trans. Jap. Inst. Met. **9**, 200 (1968).

Can. J. Chem. Downloaded from www.nrcresearchpress.com by 210.87.254.5 on 09/05/12
For personal use only.

Can. J. Chem. Downloaded from www.nrcresearchpress.com by 210.87.254.42 on 09/05/12
For personal use only.

Etude spectroscopique de l'intermédiaire des migrations d'acyle $O \rightarrow N$ dans le β-éthyl triacétyl-3,4,6 désoxy-2 amino-2 D-glucoside

GABOR FODOR,[1] FRANCINE LETOURNEAU, ET NAGABHUSHANAM MANDAVA[2]
Département de Chimie, Université Laval, Québec, Qué.

Reçu le 12 septembre 1969

La migration d'acyle du β-éthyl triacétyl-3,4,6 désoxy-2 amino-2 D-glucoside (**1**) en β-éthyl triacétyl-2,4,6 désoxy-2 amino-2 D-glucoside **3** passe par un intermédiaire (**2**). La structure orthoester-amide de celui-ci fut prouvée par spectroscopie infrarouge et résonance magnétique nucléaire, et confirmée par la dispersion optique rotatoire.

Canadian Journal of Chemistry, **48**, 1465 (1970)

La migration réversible d'acyle $O \rightleftharpoons O$ intensément étudiée dans le domaine des sucres indique la présence d'un orthoester comme intermédiaire (1). La stéréospécificité de la migration de groupements acyles $N \rightleftharpoons O$, connue en outre chez les pseudo-éphédrines (2), les aminocyclanols (3, 4), et les tropanes (5) a également confirmé l'hypothèse (2, 4, 6, 7) d'un orthoacide-ester-amide à savoir (meso-) (μ) hydroxy oxazolidine ou un état de transition semblable comme intermédiaire. Un essai de synthèse (8) d'un tel intermédiaire en partant de (±) thréo méthyl-4 phényl-5 oxazolidone-2 et de bromure phénylmagnésien a en effet donné un produit d'addition dont le comportement (action d'un acide donne un aminoester, celle d'une base par contre, une benzamide) était en harmonie avec celui qu'on avait prévu pour un sel d'un tel orthoacide avec l'organomagnésien. Une lacune de ces travaux est l'étude spectroscopique du sel ; étude devant confirmer que le métal est attaché à l'oxygène et non à l'azote. Plus récemment Welsh (9) a comparé la migration d'acyle $N \rightarrow O$ avec inversion et celle avec retention de configuration dans $H_2{}^{18}O$. Il a pu démontrer qu'il y a incorporation de l'oxygène dans l'aminoester seulement dans le premier cas, ce qui prouve que la réaction avec retention est intramoléculaire et que les mêmes oxygènes restent dans la molécule.

Un autre fait à considérer comme preuve circonstantielle (10) pour l'existence d'un orthoacide-ester-amide comme intermédiaire est le changement considérable du pouvoir rotatoire spécifique (α_D $+3.5° \rightarrow -31.8°$) de l'éthyl triacétyl-3,4,6 désoxy-2 amino-2 D-glucoside (**1**) dans l'acétone ; le produit obtenu par évaporation du solvant se comportait comme le produit de départ ; par exemple, il formait une base Schiff avec l'anisaldehyde etc. D'autre part, par chauffage avec le toluène, le même composé a pu être transposé en β-éthyl *N*-acétyl-diacétyl-4,6 désoxy-2 amino-2 glucoside (**3**), produit final d'une migration d'acyle. Dans la référence 10 nous avons confirmé les valeurs α_D et les points de fusion des composés mentionnés.

Lorsque les glycosides ne montrent aucune mutarotation (ils ne peuvent pas s'anomériser) on en conclu que dans l'acétone l'équilibre entre l'orthoester-amide (**2**) et l'amino-ester (**1**) est déplacé vers l'intermédiaire (**2**) mais, qu'il est inversé par des réactifs tel le phénylisocyanate vers **1**. Une étude spectroscopique du produit supposé être **2** nous paraît nécessaire d'autant plus qu'une étude résonance magnétique nucléaire (r.m.n.) tout récemment publiée par Horton *et al.* (11) concernant la migration d'acétyl $O_1 \rightarrow N$ du tétraacétyl-1,3,4,6 glucosamine en dérivé tétraacétyl-2,3,4,6 n'a pas fourni la preuve de l'existence d'un orthoester comme intermédiaire lors de la migration d'acyle. La mise au point de nos résultats actuels semble donc encore plus justifiée.

(1) Mesures de la dispersion optique rotatoire

La courbe dispersion optique rotatoire (d.o.r.) du dérivé (**1**) triacétylé en 3,4,6 montre, dans le chloroforme une courbe positive sur laquelle se superpose un effet Cotton fortement positif (maximum à 270, minimum à 238 mμ). Le produit intermédiaire, également soluble dans le même solvant, donne par contre une courbe négative ayant un minimum à 280 mμ. L'amide (**3**) et le dérivé tétraacétylé en 2,3,4,6 (**5**) (obtenu

[1]Présente adresse: Department of Chemistry, West Virginia University, Morgantown, W.Va. 26506.
[2]Présente adresse : U.S. Department of Agriculture, Crops Research Division, Beltsville, Maryland.

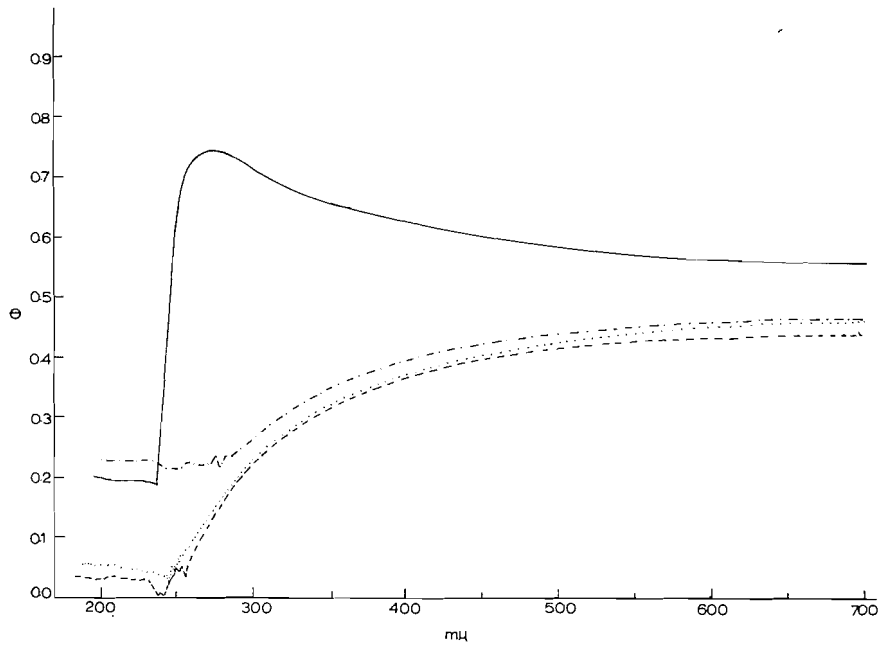

FIG. 1. Courbes d.o.r. dans le chloroforme : **1** triacétyl-3,4,6 β-éthyl désoxy-2 amino-2 D-glucoside, *c* : 4.180% ; **2** intermédiaire diacétyl-4,6 β-éthyl désoxy-2 amino-2 D-glucoside 2,3-orthoacetate, *c* : 1.288% ; **3** triacétyl-2,4,6 β-éthyl désoxy-2 amino-2 D-glucoside, *c* : 0.974% ; **5** tétraacétyl-2,3,4,6 β-éthyl désoxy-2 amino-2 D-glucoside, *c* : 3.985%.

par l'action de l'anhydride acétique sur **1** dans la pyridine) sont solubles dans le chloroforme et montrent des courbes négatives ayant des minima à 244 mμ pour **3** et à 258 et 240 mμ pour **5** (Fig. 1). Kiss et Burkhardt (12) ont aussi trouvé un effet Cotton négatif à 257 mμ pour certains *N*-acétyl glucosamines lorsque l'hydroxyle glycosidique est libre. Listowsky *et al.* ont observé une courbe négative (minimum 220, maximum 200 mμ) pour le méthylacetamido-2 désoxy-2 β-D-glucopyranoside (13).

La différence entre les quatre courbes d.o.r. prouve que les 3 composés ont des structures distinctes.

On a pris la courbe d.o.r. du produit de départ dans l'acétone 2 min après dissolution complète, puis à des intervalles réguliers pendant une période de 150 min. Les courbes sont presque parallèles. L'absorption de l'acétone dans l'ultraviolet (u.v.) a empêché l'observation de la courbe au-dessous de 300 mμ mais le changement est tout de même rapide et considérable.

(2) Spectres infrarouge

L'amino-ester (**1**) montre une absorption à 1605 cm^{-1} (NH déformation) et l'amide (**3**) à 1630 (CO—N). Par contre, l'intermédiaire ne montre pas d'absorption dans la région 1570–1640 cm^{-1}. Ceci semble indiquer que **1** s'est transformé en un nouveau dérivé cyclique. De plus, l'absorption à 3480 cm^{-1} montre une seule bande assez large, ce qui correspondrait à une structure cyclique présentant une seule liaison N—H et une liaison O—H type acide. Se basant sur les valeurs α_D de la solution acétonique, on pourrait encore supposer que c'est un mélange de 77% d'amide et 23% d'ester. Mais, il a été prouvé que le spectre infrarouge (i.r.) d'un tel mélange est tout à fait différent de celui de l'intermédiaire.

(3) Spectres r.m.n.

Le spectre r.m.n. de l'intermédiaire (tableau 1 et Fig. 2) montre quatre signaux dans la région 1.9–2.07 δ au lieu des trois signaux observés pour les 9 protons de **1**. De plus, nous avons un couplage de 2 Hz qu'on peut attribuer au couplage d'un des méthyls avec un autre proton. Ce couplage peut être éliminé par adjonction d'une quantité minime de D_2O à la solution dans

Can. J. Chem. Downloaded from www.nrcresearchpress.com by 210.87.254.42 on 09/05/12
For personal use only.

TABLEAU 1

Résonance magnétique des protons*

β-Ethyl désoxy-2 amino-2 D-glucoside	Méthyl dans éthyl	Méthyl dans acétyle	OH et NH†
1 Triacétyl-3,4,6	1.27 (t) J = 6.5 Hz	2.00 (s) (3H) 2.07 (s) (6H)	1.55 (s) pour NH_2
2 Intermédiaire	1.28 (t) J = 6.0 Hz	1.90 (d) (3H) J = 2 Hz	1.60‡ pour NH
		2.00 (s) (3H) 2.07 (s) (3H)	4.20 pour OH
3 Triacétyl-2,4,6	1.09 (t) J = 6.5 Hz	1.82 (s) (3H) 2.01 (s) (3H) 2.08 (s) (3H)	4.05 (m)§ pour NH et OH
4 Diacétyl-4,6	1.25 (t) J = 7.0 Hz	2.07 (s) (3H) 2.10 (s) (3H)	2.58 (m) pour NH_2 et OH
5 Tétraacétyl-2,3,4,6	1.21 (t) J = 7.0 Hz	1.96 (s) (3H) 2.02 (s) (6H) 2.07 (s) (3H)	6.69 (d) pour NH (J = 9 Hz)

*Les spectres r.m.n. de **1**, **2**, **3**, **4** et **5** furent mesurés dans le chloroforme-d; pour **3** on a aussi utilisé l'acétone-d_6 et le DMSO-d_6. Les valeurs rapportées pour **3** sont celles obtenues dans le DMSO-d_6.

†Singulet = s; doublet = d; triplet = t; multiplet = m.

‡Ce signal est très large (9 Hz, base); il montre plusieurs petites inflexions qui ne sont pas présentes dans le spectre de **1** et **3**.

§Le composé **3** montre les hydrogènes de NH et OH à 2.8 dans l'acétone-d_6.

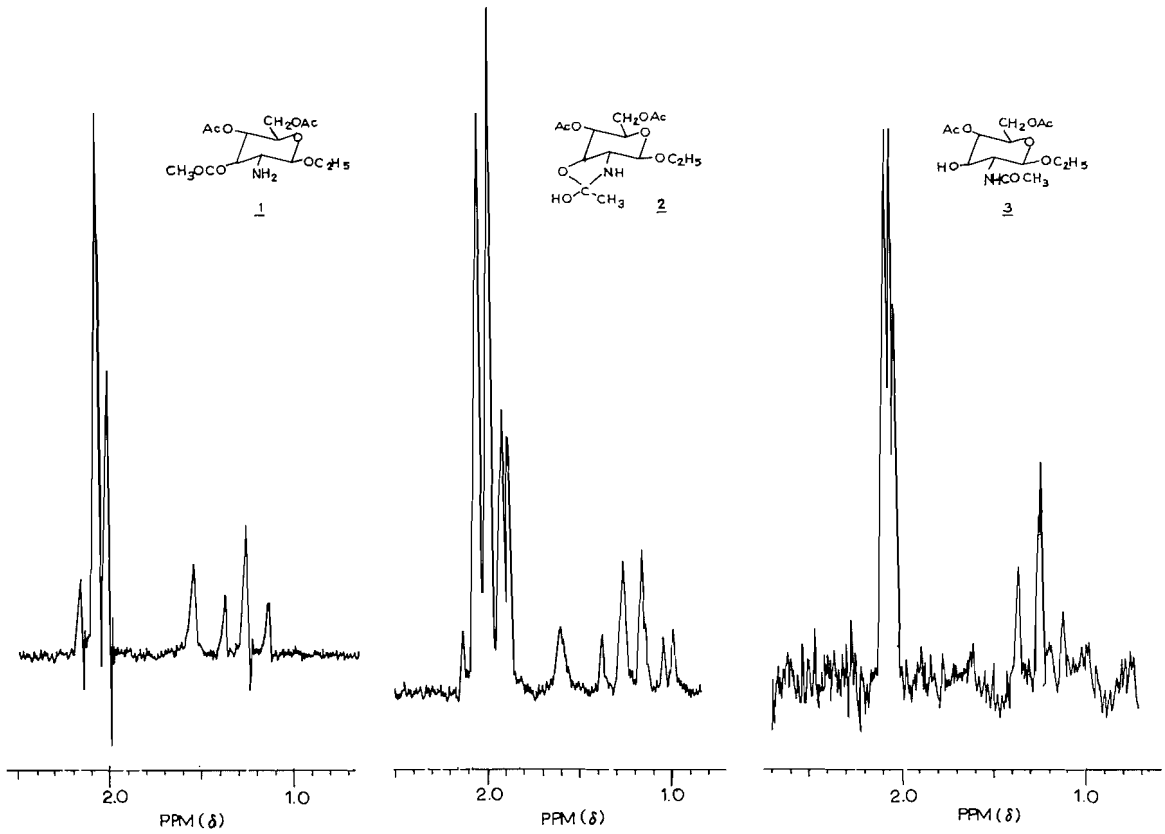

FIG. 2. Spectres r.m.n. des composés **1**, **2**, **3** (dans $CDCl_3$).

Can. J. Chem. Downloaded from www.nrcresearchpress.com by 210.87.254.42 on 09/05/12
For personal use only.

Can. J. Chem. Downloaded from www.nrcresearchpress.com by 210.87.254.42 on 09/05/12
For personal use only.

le chloroforme-*d*. Pour un orthoacétate cyclique le OH ou le NH devrait être couplé avec le méthyle adjacent ce qui s'est avéré exact. Un tel fait n'est pas observé pour les amino-esters **1** et **4** et les amides **3** et **5**.

Il est difficile de découvrir la multiplicité de OH ou de NH qu'on attendrait s'il y avait un tel couplage. Le signal NH est très large (9 Hz) dans **2** et il y a plusieurs inflexions ce qui indique en effet une multiplicité (Fig. 2). Le NH doit être couplé avec H-2 et encore avec le méthyl pour former un sextet. Mais dans les composés **1** et **4** le signal NH_2 ne montre pas un couplage appréciable avec H-2.

Si par contre on accepte la proposition[3] que ce signal méthyl consiste en effet de deux singulets diastéréotopiques due à la formation d'un nouveau centre d'asymétrie, on devrait prévoir l'apparition de 2 signaux eux-mêmes diastéréotopiques pour l'hydroxyl, attaché au même carbone, même s'ils ne sont pas couplés avec les protons méthyl. Donc la multiplicité de l'hydroxyle ne permettrait pas de choisir entre les deux explications pour la duplicité du signal méthyl. De plus, la coalescence du méthyl dans **2** sous l'action de l'eau lourde semble favoriser la première interprétation—sauf si l'eau cause le clivage du cycle.

Le méthyle de l'acétyle primaire est observé à 2.00 p.p.m. et celui de l'acétyle secondaire à 2.07 p.p.m. L'hydrogène de la liaison N—H à 1.60 p.p.m. disparaît après addition de D_2O. La position de cet hydrogène est sensiblement voisine de celle pour les 2 hydrogènes du NH_2 observée à 1.55 p.p.m. du β-éthyl triacétyl-3,4,6 amino-2 désoxy-2 glucoside (**1**). Le signal d'un hydrogène à 4.20 p.p.m. disparaît après addition de D_2O ; ce glissement chimique est attribuable à l'hydrogène du groupe hydroxyle.

Un autre produit de type voisin : un orthodiester-amide fut isolé (14). Sa structure fut vérifiée également par r.m.n. Ce composé ne contient pas de méthyle attaché au carbone de l'orthoester-amide cycliques. Donc le seul glissement chimique du *C*-méthyl que l'on peut comparer avec le nôtre est celui de l'orthoacétate de méthyle (δ 1.35).

[3]Les auteurs aimeraient exprimer leur reconnaissance à l'un des examinateurs pour sa suggestion de cette deuxième alternative.

(4) Observations chimiques et spectrométrie de masse

Ainsi que nous l'avons déjà mentionné (10), l'ester aminé **1** donne dans l'alcool méthylique ou éthylique un produit désacétylé en C-3. Cette sélectivité de l'alcoolyse peut être interprétée comme étant facilitée par une liaison de l'acétyle en C-3 avec la fonction amine en C-2 dans la formation d'un orthoester-monoamide cyclique qui est beaucoup plus facilement susceptible à l'action du méthanol ou de l'éthanol que l'est un ester « normal ».

A partir de l'amino-ester **1** ou de l'intermédiaire, on peut synthétiser la même phénylurée, à savoir le β-éthyl triacétyl-3,4,6 *N*-phénylcarbamyle désoxy-2 amino-2 D-glucoside (**6**).

Par distillation sous 0.1 mm, l'intermédiaire a donné **1** comme seul produit. La fragmentation du produit intermédiaire dans le spectromètre de masse a montré le même schéma que l'ester aminé de départ. Le β-éthyl triacétyl-2,4,6 désoxy-2 amino-2 D-glucoside (**3**) a donné par contre avec le phénylisocyanate un dérivé β-éthyl triacétyl-2,4,6 phénylcarbamyle-3 D-glucoside (**7**) dont le point de fusion, la valeur α_D et les spectres i.r. et de masse étaient différents de ceux du β-éthyl triacétyl-3,4,6 *N*-phénylcarbamyle désoxy-2 amino-2 D-glucoside (**6**) trouvés précédemment.

En travaillant avec l'acétone comme solvant, on a fait les constatations suivantes : (*a*) si le produit n'était pas séché suffisamment, on observait dans i.r. une bande d'absorption à 1680 cm^{-1} ; (*b*) l'analyse élémentaire correspondait à la formule brute $C_{17}H_{29}O_{29}N$, soit **1** contenant une mole d'acétone. Afin d'élucider ce point, on a préparé l'intermédiaire dans l'acétone deutérée et on a étudié le spectre i.r. après des intervalles réguliers de séchage. On a constaté que, si le produit n'est pas séché suffisamment, il y a incorporation d'acétone deutérée. Ceci a été mis en évidence par l'absorption à 1680 (C=O) et à 2100 cm^{-1} (C—D). Mais, ces bandes disparaissent progressivement en séchant plus longtemps et, sous 10^{-2} mm, le produit obtenu de cette manière donne une courbe d.o.r. totalement différente de celle du produit (**1**) de départ.

Discussion et conclusions

Les mesures d.o.r. indiquent un changement fondamental de structure lors de la dissolution

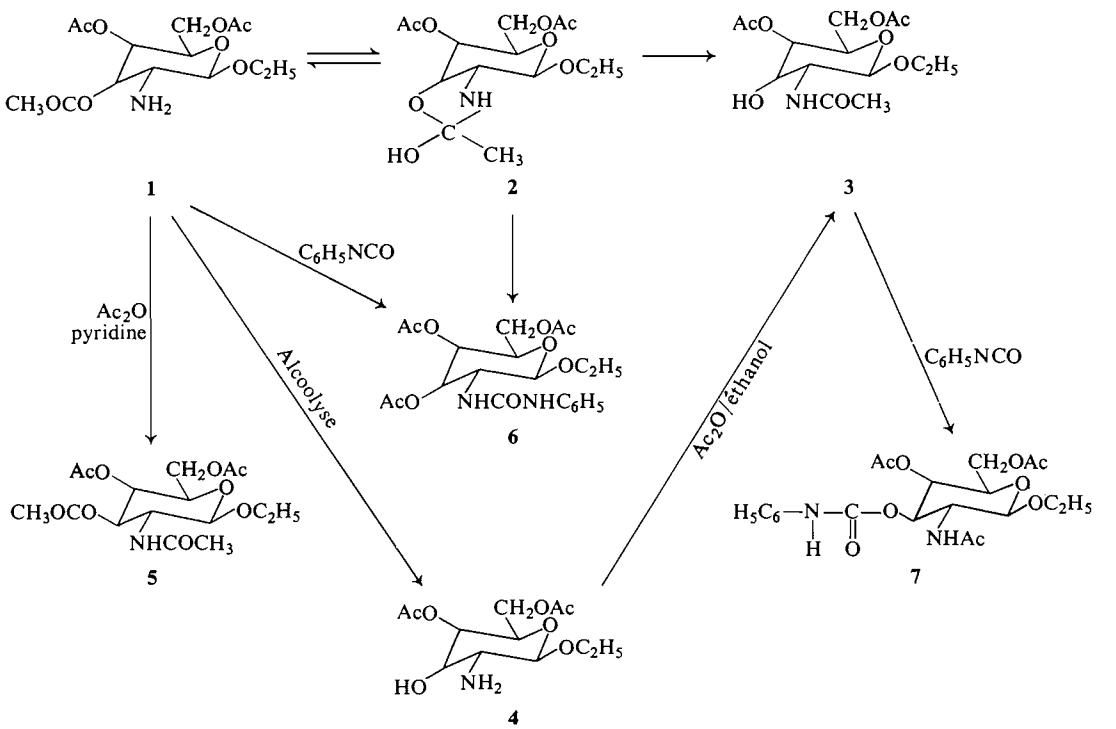

1 2 3 4 5 6 7

de l'ester aminé **1** dans l'acétone, changement qui devient plus important après 150 min. La ressemblance de l'allure des courbes de **2** et **3** indique la participation de l'azote par formation d'une liaison C—N. Le produit obtenu après évaporation complète de l'acétone présente un spectre i.r. dépourvu de NH_2 ou $NHCOCH_3$. Le spectre r.m.n. également montre un des méthyls comme étant couplé avec le NH (ou OH), ou bien deux signaux diastéréotopiques ; l'une et l'autre de ces 2 explications militent en faveur de la structure **2** d'un orthoacide-ester-amide. La transformation de celui-ci en amide **3**, par chauffage avec le toluène (10) et la transposition en ester aminé **1** par distillation, bien que très surprenante, confirment la structure de cet intermédiaire. On a essayé d'y ajouter une preuve chimique supplémentaire ; celle de la méthylation de l'orthoacide par le diazométhane. Malheureusement on n'a pas pu obtenir un produit *O*-méthylé bien défini.

C'est la première fois qu'on a isolé un ortho-ester-acide-amide, composé qu'on avait souvent supposé être l'intermédiaire de la transposition intramoléculaire d'acyles. La réversibilité **1**⇌**2** est probablement due à la position diéquatoriale-trans de l'hydroxyle acétylé en C-3 et de la fonction amine en C-2.

On va étendre cette observation à d'autres modèles de squelettes différents, en utilisant des dérivés acétylés [17]OC.

Partie expérimentale

Hydrobromure de l'acétobromo-glucosamine

L'hydrobromure de l'acétobromo-glucosamine a été préparé suivant la méthode de Irvine *et al.* (15), en traitant le (+) D-glucosamine-hydrochlorure (1 mole) par le bromure d'acétyle (5 moles) pendant 3 jours à environ 40 °C. La masse solide a été dissoute dans le chloroforme et le bromo-triacétyl-3,4,6 désoxy-2 amino-2 D-glucoside-hydrobromure (80.4%) p.f. 150–151 °C est précipité par l'éther anhydre; α_D +147.8° dans l'acétone.

β-*Ethyl triacétyl-3,4,6 désoxy-2 amino-2 D-glucoside-hydrobromure*

Une solution de 20.4 g (0.0440 mole) d'acétobromo-glucosamine-hydrobromure (10, 15) dans 300 ml d'éthanol absolu et 4 ml de pyridine anhydre est maintenue sous vide pendant 1 h à température ambiante et à l'abir de l'humidité. Après 10 h, la solution est mise au réfrigérateur pour une journée. Le β-éthyl triacétyl-3,4,6 D-glucosaminide-hydrobromure (66.4%) est ensuite filtré et recristallisé de l'éthanol. Le produit devient brun à

Can. J. Chem. Downloaded from www.nrcresearchpress.com by 210.87.254.42 on 09/05/12
For personal use only.

Can. J. Chem. Downloaded from www.nrcresearchpress.com by 210.87.254.42 on 09/05/12
For personal use only.

254 °C et forme des stalactites à 275 °C ; α_D + 13.6° (*c*, 0.76 dans l'éthanol).

β-Ethyl triacétyl-3,4,6 désoxy-2 D-*glucoside (1)*

A une solution de 8.285 g (0.02 mole) du β-éthyl triacétyl-3,4,6 D-glucosaminide-hydrobromure dans 75 ml de chloroforme absolu, on ajoute 11.75 ml d'éthylate de sodium 1.70 *N* (0.01975 mole) en agitant. On centrifuge le bromure de sodium et on recristallise dans l'éther anhydre. Rendement 50%, p.f. 136° ; α_D +8.25 (*c*, 3.925 dans le chloroforme), α_D + 3.5 (*c*, 2.020 dans l'acétone). Spectre de masse 333 (M^+), 273 (M-60), 255 (M-78), 212 (M-121), 185 (M-148), 171 (M-162), 166 (M-167), 140 (M-193), 126 (M-207), 114 (M-219), 101 (M-232), 98 (M-235), 80 (M-253), 72 (M-261), 59 (M-274), 43 (M-290).

Transposition du β-éthyl 3,4,6 triacétyl désoxy-2 amino-2 D-*glucoside (1) dans l'acétone*

Une solution de 2% de β-éthyl 3,4,6 triacétyl désoxy-2 amino-2 D-glucoside (**1**) dans l'acétone est agitée pendant 2 jours et le pouvoir rotatoire mesuré régulièrement par l'appareil de d.o.r. On évapore ensuite le solvant, on lave le résidu plusieurs fois avec du chloroforme et de l'éther et on sèche le produit pendant 12 h sous vide à 25° p.f. 92°. L'analyse correspond à un produit contenant une molécule d'acétone de cristallisation.

Anal. calculé pour $C_{17}H_{29}NO_9$: C, 52.0 ; H, 7.4 ; O, 36.8. Trouvé : C, 52.2 ; H, 7.0 ; O, 36.7.

On ajoute du toluène à ce produit et on chasse le solvant à l'évaporateur rotatif. On précipite le produit de départ par l'éther, et évapore le solvant. Si on répète deux fois cette opération et si on maintient le ballon à 25° sous vide (2.10^{-2} mm) pendant 48 h on obtient un produit qui ne contient plus de solvant.

Anal. calculé pour $C_{14}H_{23}NO_8$: C, 50.5 ; H, 6.9 ; O, 38.4. Trouvé : C, 50.5 ; H, 7.2 ; O, 37.7.

Bandes i.r. : 3480 (NH, OH, élongation), 1760 (C=O), pas d'absorption à 1605 ; 1460 (déformation), 1240 cm^{-1} (C—O). Les glissements chimiques sont compris dans le tableau 1 et dans la Fig. 2, la courbe d.o.r. dans la Fig. 1 ; ils montrent qu'il s'agit d'un produit différent de celui de départ. Spectre de masse : identique à celui obtenu pour **1**.

Transformations de l'orthoacétate-2,3 du diacétyle-4,6 amino-2 désoxy-2 β-éthyl D-*glucoside*

(a) En amino-ester 1 par distillation

L'intermédiaire est distillé sous vide (0.1 mm Hg 90 °C). On obtient un solide blanc, p.f. 135°. Les spectres i.r. et r.m.n. coincident avec ceux du β-éthyl triacétyl-3,4,6 désoxy-2 amino-2 D-glucoside (**1**).

Anal. trouvé : C, 50.9 ; H, 7.1 ; O, 37.7.

(b) En phénylurée 6

Comme décrit (10) précédemment, 0.3 g de **2** dans 4 ml acétone anhydre donne avec 0.2 ml de phényl-isocyanate pendant 24 h (87%) de β-éthyl triacétyl-3,4,6 *N*-phénylcarbamyl D-glucosaminide, p.f. 233°. Le même produit fut obtenu avec le même rendement (6) à partir de 0.50 g de l'amino-ester **1** et de 0.18 ml de phényl-isocyanate.

The i.r. : 3300 (m), 2950 (f), 1760 (F), 1660 (m), 1560 (m), 1500 (f), 1445 (m), 1320 (m), 1240 (F), 1050 (F) cm^{-1}.

L'action du phényl-isocyanate provoque une ouverture du cycle de **2** donnant un dérivé de l'amino-ester "libre"; cette réaction est analogue à la scission thermique.

(c) En triacétyl-2,4,6 désoxy-2 amino-2 β-éthyl D-*glucoside (3)*

L'opération décrite auparavant (10) semble être très délicate. Pour compléter cette transposition on procède de la manière suivante. Le même produit *N*-acétylé a été préparé selon (10), en partant du triacétate **1**, dont l'alcoolyse partielle a conduit au β-éthyl diacétyl-4,6 D-glucoside (**4**) p.f. 161° ; spectres i.r. : 3300, 3350, 3100 (NH_2OH) 1755 (CO ester), 1580 cm^{-1} (NH). Spectres r.m.n. voir Fig. 2 et tableau 1.

Spectre de masse : 291 (M), 245 (M-46), 218 (M-73), 204 (M-87), 199 (M-92), 185 (M-106), 176 (M-115), 148 (M-143), 145 (M-146), 130 (M-161), 126 (M-165), 114 (M-177), 101 (M-190), 72 (M-219), 59 (M-232).

Celui-ci fut *N*-acétylé, selon le procédé décrit (10) à l'aide d'anhydride acétique dans l'alcool. Le produit triacétylé-2,4,6 a un p.f. 186° et un α_D −41.9° ; les spectres infrarouge 3400, 3300 (NH, OH), 1740 (CO ester) 1630 (CO—N), 1260 cm^{-1} (C—O), les spectres r.m.n. dans le tableau 1 de même que la fragmentation dans le spectromètre de masses sont complètement différents de ceux de l'amino-ester **1** et de l'orthoacétate **2**.

Spectre de masse de **3** 288 (M-45), 274 (M-59), 260 (M-73), 241 (M-92), 218 (M-115), 214 (M-119), 199 (M-134), 181 (M-152), 172 (M-161), 157 (M-176), 141 (M-192), 130 (M-203), 116 (M-217), 101 (M-232), 84 (M-249), 59 (M-274), 43 (M-290).

Le dérivé phénylcarbamylé

Préparé selon la méthode décrite (10) montre p.f. 182° et un spectre i.r. différent du dérivé *N*-phénylcarbamylé (**5**), 3425 (F), 3300 (F), 3100 (f), 2950 (f), 2850 (f), 1630 (F), 1565 (F), 1450 (m), 1370 (F), 1320 (f), 1255 (F), 1230 (F), 1170 (m), 1130 (m), 1090 (f), 1040 cm^{-1} (F).

β-Ethyl tétraacétyl-2,3,4,6 D-*glucosaminide*

Le composé p.f. 165°, α_D^{20} −19.8 (chloroforme) qui sert de comparaisons spectroscopiques, fut préparé selon Fodor et Ötvös (10) par *N*-acétylation de **1**. Les spectres i.r. : 3300, 3150, 3000 (OH, NH), 1770 (CO-ester), 1670 (CO, amide) 1250 cm^{-1} (C—O). Les spectres r.m.n. sont compris dans le tableau 1, la courbe d.o.r. dans la Fig. 1.

Spectre de masse : 375 (M), 316 (M-59), 302 (M-73), 256 (M-119), 242 (M-133), 214 (M-161), 199 (M-176), 183 (M-192), 165 (M-210), 143 (M-232), 140 (M-235), 114 (M-261), 101 (M-274), 59 (M-316), 43 (M-332).

Les spectres de masse ont été mesurés avec l'appareil Varian M-66 les mesures d.o.r. ont été faites avec l'appareil JASCO Model 5 ORD/UV, et les spectres r.m.n. avec le Varian A-60. Les microanalyses ont été faites par Mme E. Beetz, Germany.

Nous désirons remercier la compagnie Chemcell pour l'aide financière apportée en accordant une bourse à un des auteurs (F.L.) pendant la réalisation de ces travaux et le Conseil National de Recherches du Canada (Bourse No. 2839) sur laquelle Dr. N. M. fut engagé.

1. A. B. Foster et M. Stacey. Advan. Carbohyd. Chem. **7**, 266 (1962).

2. G. FODOR et J. KISS. Nature **163**, 287 ; **164**, 917 (1949).
3. G. FODOR et J. KISS. J. Amer. Chem. Soc. **72**, 3495 (1950); J. Chem. Soc. 1589 (1952).
4. E. E. VAN TAMELEN. J. Amer. Chem. Soc. **73**, 5773 (1951).
5. G. FODOR et K. NADOR. J. Chem. Soc. 721 (1953).
6. A. P. PHILLIPS et R. BALTZLY. J. Amer. Chem. Soc. **69**, 200 (1947).
7. L. H. WELSH. J. Amer. Chem. Soc. **71**, 3500 (1949).
8. K. KOCZKA et G. FODOR. Acta Chim. Hung. **13**, 89 (1951).
9. L. H. WELSH. J. Org. Chem. **32**, 119 (1967).
10. G. FODOR et L. ÖTVÖS. Chem. Ber. **89**, 702 (1956).
11. D. HORTON, W. E. MAST, et K. D. PHILIPS. J. Org. Chem. **32**, 1471 (1967).
12. J. KISS et F. B. BURKHARDT. Helv. Chim. Acta. **52**, 2622 (1969).
13. I. LISTOWSKY, G. AVIGAD, et S. ENGLARD. Carbohyd. Res. **8**, 205 (1968).
14. H. E. ZAUGG, V. PEPENDICK, et J. R. MICHAELIS. J. Amer. Chem. Soc. **86**, 1399 (1964).
15. J. C. IRVINE et A. HYND. J. Chem. Soc. **103**, 48 (1913).

Can. J. Chem. Downloaded from www.nrcresearchpress.com by 210.87.254.42 on 09/05/12
For personal use only.

Can. J. Chem. Downloaded from www.nrcresearchpress.com by 210.87.254.40 on 09/05/12
For personal use only.

Influence of Lewis acids on the Diels–Alder reaction. III. Rearrangement of dimethyl *N*-carbomethoxy-7-azabicyclo[2.2.1]2,5-heptadiene-2,3-dicarboxylate adducts to dimethyl *N*-carbomethoxy-3-aminophthalates[1,2]

R. C. BANSAL,[3] A. W. MCCULLOCH, AND A. G. MCINNES
Atlantic Regional Laboratory, National Research Council of Canada, Halifax, Nova Scotia

Received December 16, 1969

Aluminum chloride accelerates the Diels–Alder reactions of 2- or 2,5-substituted *N*-carbomethoxypyrroles with dimethyl acetylenedicarboxylate, and also catalyzes rearrangement of the *N*-carbomethoxy-7-azanorbornadiene adducts to 6- and 4,6-substituted dimethyl *N*-carbomethoxy-3-aminophthalates. Aromatization of the corresponding adduct of *N*-carbomethoxypyrrole only occurs on prolonged treatment with BF_3. The procedure promises to be a convenient route for the synthesis of polysubstituted anilines.

Canadian Journal of Chemistry, **48**, 1472 (1970)

We have previously reported (1) that Lewis acids accelerate the formation of 7-oxabicyclo-[2.2.1]2,5-heptadiene-2,3-dicarboxylate adducts, and also catalyze their rearrangement to alkyl- and aryl-substituted 3-hydroxyphthalates. Since the latter were obtained in high yield this procedure offers a promising synthetic route to polysubstituted phenols. In this note we wish to report the analogous accelerated formation of alkyl-substituted 7-azabicyclo adducts **2**, and their rearrangement to the *N*-carbomethoxy-3-aminophthalates, **3**. This procedure likewise promises to be of value in the synthesis of polysubstituted anilines.

We have prepared both **2***b* and **2***c* thermally (ca. 75% yield) by refluxing **1** with dimethyl acetylenedicarboxylate for 7–8 days in benzene (solution 0.125 *M* in addends); they can be

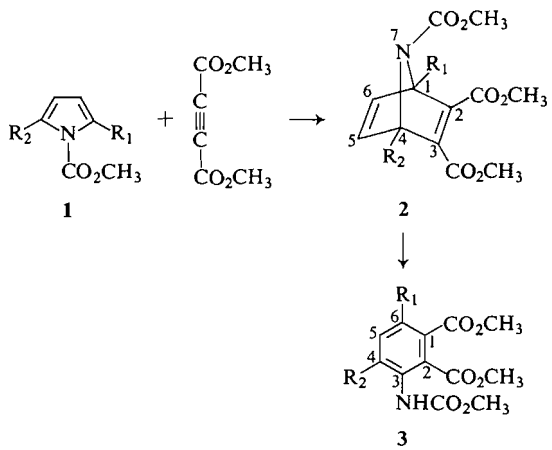

1 **2** **3**

a) $R_1 = R_2 = H$
b) $R_1 = CH_3$; $R_2 = H$
c) $R_1 = R_2 = CH_3$

TABLE 1
Conditions for conversion of 0.03 *M* solutions of **2** in CH_2Cl_2 to **3**

Compound	Yield (%) based on **2**	Lewis acid	Temperature	Time
3*a*	90	BF_3 (saturated)	25°	5 days
3*b*	85	$AlCl_3$ (0.09 *M*)	40°	4 h
3*c*	90	$AlCl_3$ (0.03 *M*)	40°	30 min

[1]Issued as NRCC No. 11206.
[2]This work was reported at the 52nd Annual Conference of the Chemical Institute of Canada, which was held in Montreal on May 25–28th, 1969.
[3]NRCC Postdoctorate Fellow, 1967–1969.

Can. J. Chem. Downloaded from www.nrcresearchpress.com by 210.87.254.40 on 09/05/12
For personal use only.

TABLE 2

Physical constants and spectral data for **2** and **3**

Compound	Melting point (°C) or n_D^{24}	Molecular ion *m/e*	ν_{max} cm^{-1} (CCl_4)	$\lambda\lambda_{max}$ mμ (ε) (EtOH)	τ and J_{pq}($CDCl_3$)				
					CO_2CH_3	N—CO_2CH_3	CH_3	NH	H_4, H_5, H_6
2b	1.5794	—	—	—	6.15, 6.23	6.34	8.01	—	$A(H_5)$ $B(H_6)$ $X(H_4)$ H_5H_6 octet centered at 3.0 τ; H_4 quartet centered at 4.47 τ. $\Delta\nu_{56}$ = 13.7, J_{56} = 5.3, J_{45} = 2.8, J_{46} = 0.8 Hz
*2c**	81–82	—	—	—	6.20 (6H)	6.34	8.00 (6H)	—	H_5, H_6 3.20 τ (s)
3a†	50–51	267	3370 (NH), 1740 (C=O), 1713 (C=O···HN)	240 (50 000), 302 (3300)	6.12 (6H)‡	6.23	—	1.28	$A(H_5)$ $B(H_4)$ $X(H_6)$ H_4H_5 octet centered at 2.59 τ; H_6 quartet centered at 1.64 τ. $\Delta\nu_{45}$ = 10.4, J_{45} = 7.8, J_{56} = 8.5, J_{46} = 1.2 Hz
3b†	68–69	281	3340 (NH), 1739 (C=O), 1703 (C=O···HN)	243 (50 000), 312 (4100)	6.13 (6H)‡	6.24	7.72	0.45	$A(H_5)$ $B(H_4)$ Quartet centered at 2.18 τ. $\Delta\nu_{45}$ = 56.3, J_{45} = 8.7 Hz H_4 at lower field than H_5
3c†	80–81	295	3400 (NH), 1740 (C=O), 1720 (C=O···HN)	234 (65 000), 286 (1850)	6.17 (6H)‡	6.30	7.66, 7.73	2.82	H_5 2.80 τ (broad s) H_5 long-range coupled to CH_3 groups at C-4 and C-6

*Crystallized from ethyl acetate – petroleum ether (b.p. 60–80°).
†Crystallized from ether – petroleum ether (b.p. 60–80°).
‡Ester OCH_3 fortuitously magnetically equivalent; separate resonances were observed in benzene-d_6.

prepared, however, in only 30 min at 0° by interaction of the addends in the presence of five molar equivalents of $AlCl_3$ in CH_2Cl_2 (**2***b*, 50–60%; **2***c*, 85–90% yield), as previously described for the preparation of **2***a* (2).

Compounds **3***b* and **3***c* can be formed either directly by a one-step synthesis (i.e. $AlCl_3$-promoted formation of **2***b* and **2***c* at 0° followed by *in situ* rearrangement at 40°) or indirectly by first isolating the adducts and then rearranging them under the conditions outlined in Table 1. Aromatization of **2***a*, as with the corresponding oxanorbornadiene (1), is more difficult and can only be carried out by the two-step procedure and use of a solution saturated with BF_3 (Table 1).

Derivatives **2** and **3** were purified by preparative thin-layer chromatography on silica gel G [ethyl acetate – petroleum ether (b.p. 60–80°) = 3:7]. Their structures were readily deduced from their mode of formation and proton magnetic resonance (p.m.r.) spectra (Table 2) which were analogous to those reported for the correspondingly substituted 7-oxanorbornadienes and 3-hydroxyphthalates (1, 3). Infrared (i.r.), ultraviolet, and mass spectral data for **3** are also given in Table 2.

The detailed mechanism of the Lewis acid-promoted formation of **2** and the applicability of this procedure to the preparation of compounds of type **2** and **3** carrying substituents other than those reported in this note are under investigation.

We thank D. J. Embree for the mass spectra, P. F. Seto for i.r. spectra, and J. van Ingen for p.m.r. measurements.

1. A. W. McCulloch, B. Stanovnik, D. G. Smith, and A. G. McInnes. Can. J. Chem. **47**, 4319 (1969).
2. R. C. Bansal, A. W. McCulloch, and A. G. McInnes. Can. J. Chem. **47**, 2391 (1969).
3. P. Vogel, B. Willhalm, and H. Prinzbach. Helv. Chim. Acta, **52**, 584 (1969).

Some reactions of 4,4′-dimercaptooctafluorobiphenyl

K. Langille and M. E. Peach
Department of Chemistry, Acadia University, Wolfville, Nova Scotia

Received October 16, 1969

The reactions of 4,4′-dimercaptooctafluorobiphenyl, $HSC_6F_4C_6F_4SH$, have been studied and compared with those of other thiols. Various metallic and non-metallic derivatives have been prepared and characterized. Polymerization occurred on oxidation or reaction with a multifunctional group or multivalent atom.

Canadian Journal of Chemistry, **48**, 1474 (1970)

While the properties of pentafluorothiophenol (1) and tetrafluorobenzene-1,2-dithiol (2) have been studied, this paper continues our studies on fully halogenated aromatic thiols and describes the reactions of 4,4′-dimercaptooctafluorobiphenyl, $HSC_6F_4C_6F_4SH$. This thiol differs from the other thiols investigated in having the two SH groups in the para positions on biphenyl rings and polymerization can occur readily. Oxidation causes polymerization. Polymerization can also occur when the thiol reacts with a multifunctional group or a multivalent atom, forming presumably a macromolecular polymeric species, e.g. attempts to prepare a derivative of phosphorus(III) always resulted in the formation of a polymeric product.

The thiol reacts with a variety of heavy metal ions in acetone–water mixtures to form precipitates of the corresponding metal mercaptides, analogous reactions are observed with pentafluorothiophenol (1); it was possible to prepare, in this way, derivatives of Ag(I), Tl(I), Cu(I) (from Cu(II)), Pd(II), Hg(II), Pb(II), and Cd(II). All these mercaptides can be assumed to be polymeric as they are insoluble in common solvents and the extent of polymerization cannot be estimated due to their insolubility. The pentafluoro-phenylthio derivatives of Ag(I), Tl(I), Cu(I), and Pd(II) are considered to be polymeric containing M—S—M bridges, whereas the derivatives of Hg(II), Pb(II), and Cd(II) are somewhat more soluble and are ionized in various solutions (1).

The thiol is weakly acidic and will react with a suspension of tri-*n*-butyltin oxide in acetone to form the compound $(n\text{-}Bu_3SnSC_6F_4)_2$; this is a

Can. J. Chem. Downloaded from www.nrcresearchpress.com by 210.87.254.40 on 09/05/12
For personal use only.

prepared, however, in only 30 min at 0° by interaction of the addends in the presence of five molar equivalents of $AlCl_3$ in CH_2Cl_2 (**2***b*, 50–60%; **2***c*, 85–90% yield), as previously described for the preparation of **2***a* (2).

Compounds **3***b* and **3***c* can be formed either directly by a one-step synthesis (i.e. $AlCl_3$-promoted formation of **2***b* and **2***c* at 0° followed by *in situ* rearrangement at 40°) or indirectly by first isolating the adducts and then rearranging them under the conditions outlined in Table 1. Aromatization of **2***a*, as with the corresponding oxanorbornadiene (1), is more difficult and can only be carried out by the two-step procedure and use of a solution saturated with BF_3 (Table 1).

Derivatives **2** and **3** were purified by preparative thin-layer chromatography on silica gel G [ethyl acetate – petroleum ether (b.p. 60–80°) = 3:7]. Their structures were readily deduced from their mode of formation and proton magnetic resonance (p.m.r.) spectra (Table 2) which were analogous to those reported for the correspondingly substituted 7-oxanorbornadienes and 3-hydroxyphthalates (1, 3). Infrared (i.r.), ultraviolet, and mass spectral data for **3** are also given in Table 2.

The detailed mechanism of the Lewis acid-promoted formation of **2** and the applicability of this procedure to the preparation of compounds of type **2** and **3** carrying substituents other than those reported in this note are under investigation.

We thank D. J. Embree for the mass spectra, P. F. Seto for i.r. spectra, and J. van Ingen for p.m.r. measurements.

1. A. W. McCulloch, B. Stanovnik, D. G. Smith, and A. G. McInnes. Can. J. Chem. **47**, 4319 (1969).
2. R. C. Bansal, A. W. McCulloch, and A. G. McInnes. Can. J. Chem. **47**, 2391 (1969).
3. P. Vogel, B. Willhalm, and H. Prinzbach. Helv. Chim. Acta, **52**, 584 (1969).

Some reactions of 4,4′-dimercaptooctafluorobiphenyl

K. Langille and M. E. Peach
Department of Chemistry, Acadia University, Wolfville, Nova Scotia

Received October 16, 1969

The reactions of 4,4′-dimercaptooctafluorobiphenyl, $HSC_6F_4C_6F_4SH$, have been studied and compared with those of other thiols. Various metallic and non-metallic derivatives have been prepared and characterized. Polymerization occurred on oxidation or reaction with a multifunctional group or multivalent atom.

Canadian Journal of Chemistry, **48**, 1474 (1970)

While the properties of pentafluorothiophenol (1) and tetrafluorobenzene-1,2-dithiol (2) have been studied, this paper continues our studies on fully halogenated aromatic thiols and describes the reactions of 4,4′-dimercaptooctafluorobiphenyl, $HSC_6F_4C_6F_4SH$. This thiol differs from the other thiols investigated in having the two SH groups in the para positions on biphenyl rings and polymerization can occur readily. Oxidation causes polymerization. Polymerization can also occur when the thiol reacts with a multifunctional group or a multivalent atom, forming presumably a macromolecular polymeric species, e.g. attempts to prepare a derivative of phosphorus(III) always resulted in the formation of a polymeric product.

The thiol reacts with a variety of heavy metal ions in acetone–water mixtures to form precipitates of the corresponding metal mercaptides, analogous reactions are observed with pentafluorothiophenol (1); it was possible to prepare, in this way, derivatives of Ag(I), Tl(I), Cu(I) (from Cu(II)), Pd(II), Hg(II), Pb(II), and Cd(II). All these mercaptides can be assumed to be polymeric as they are insoluble in common solvents and the extent of polymerization cannot be estimated due to their insolubility. The pentafluoro-phenylthio derivatives of Ag(I), Tl(I), Cu(I), and Pd(II) are considered to be polymeric containing M—S—M bridges, whereas the derivatives of Hg(II), Pb(II), and Cd(II) are somewhat more soluble and are ionized in various solutions (1).

The thiol is weakly acidic and will react with a suspension of tri-*n*-butyltin oxide in acetone to form the compound $(n\text{-}Bu_3SnSC_6F_4)_2$; this is a

Can. J. Chem. Downloaded from www.nrcresearchpress.com by 210.87.254.6 on 09/05/12
For personal use only.

Can. J. Chem. Downloaded from www.nrcresearchpress.com by 210.87.254.6 on 09/05/12
For personal use only.

standard method for the preparation of thiol derivatives of organotin compounds (3). Similar experiments starting with di-*n*-butyltin oxide resulted only in the formation of a polymer. The derivatives of triphenyl-tin and -lead could not be formed from the corresponding oxide and the thiol, but were prepared by treating an acetone solution of the triphenylmetal chloride with the lead mercaptide, $Pb(SC_6F_4)_2$. Attempts to prepare the sodium salt from sodium hydroxide in ethanol with the thiol or the lithium salt from the thiol and *n*-butyllithium always gave a product that was very readily hydrolyzed, as would be expected from the salt of a weak acid and a strong base.

Various non-metallic derivatives of the thiol have been prepared. Simple derivatives were formed of the type $RSC_6F_4C_6F_4SR$, where R = Me, MeCO, PhCO, and Cl. Attempts to prepare derivatives where R was multifunctional, e.g. $P_2(SC_6F_4C_6F_4S)_3$ always resulted in the formation of intractable polymers; such reactions were observed with PCl_3, $POCl_3$, or $AsCl_3$ and the thiol in the presence of triethylamine to act as a hydrogen chloride catcher.

The ^1H and ^{19}F nuclear magnetic resonance (n.m.r.) spectra of the thiol have been examined. The proton n.m.r. spectrum shows a single resonance in acetone solution at −4.43 p.p.m., using tetramethylsilane (TMS) as an internal standard; this is of the same order of magnitude as the proton n.m.r. spectrum of pentafluorothiophenol (neat) where the resonance occurs at −3.70 relative to TMS as an internal standard. The fluorine n.m.r. in acetone solution has two multiplet chemical shifts at 137.6 and 139.4 p.p.m. relative to CCl_3F as internal standard. An assignment of these two resonances is impossible without a complete analysis of the spectrum. The chemical shifts of the ortho fluorines in decafluorobiphenyl occur at 137.9 p.p.m. ($CHCl_3$ solvent) (4) and in pentafluorothiophenol the ortho fluorines have a chemical shift of 138.1 p.p.m. (neat) (3) or 135.8 p.p.m. ($CHCl_3$ solution) (4), making it impossible to assign by inference the two chemical shifts in 4,4′-dimercaptooctafluorobiphenyl.

The infrared (i.r.) spectrum of the thiol is similar to that of pentafluorothiophenol (3). The C—S frequency may appear as a shoulder at 708 cm^{-1} on a stronger peak at 720 cm^{-1}, or it may be masked by this stronger peak. The S—H stretching frequency appears at 2602 (m) cm^{-1}, although there is also a weak doublet present at 2580, 2570 cm^{-1}, which could be the S—H frequency. The C—S and S—H frequencies in pentafluorothiophenol have been assigned at 716 and 2620 cm^{-1} respectively (5). It is difficult to assign any M—S frequencies in the metal derivatives with confidence, as there are several peaks in the 500—300 cm^{-1} region where these would be expected. In the acetyl and benzoyl derivatives the carbonyl frequencies occur at 1720(s), 1741(s) (doublet) and 1694(s) cm^{-1} respectively. These are very different from the carbonyl frequencies in the corresponding acid chloride, and are similar to those in the corresponding aldehydes; the carbonyl frequencies are

TABLE 1

Main frequencies characteristic of the $-SC_6F_4C_6F_4S-$ group in $RSC_6F_4C_6F_4SR$

R = H	Cl	Me	MeCO	*n*-Bu_3Sn	Ag	Hg
432 w	438 w	445 w	435 m	435 m	432 w	436 w
596 m	608 m	606 m	607 s		598 w	
721 s	723 s	721 s	723 s	720 s	719 s	722 s
755 w				738 w	760 w	760 w
903 s	895 w	896 w	901 s	896 s	895 m	896 m
1020 s	966 s	978 s	960 s	954 s	949 m	950 s
1028 s	993 m	990 s	988 s	983 m	980 m	976 m
1241 s	1250 s	1242 s	1247 s	1230 m	1232 w	1241 w
1372 w	1371 w		1359 m		1369 w	1360 w
1441 m	1431 m	1438 m	1445 sh	1438 m	1440 m	1440 m
1466 s	1468 s	1468 s	1465 s	1469 s	1460 s	1451 s
1472 s	1482 s	1478 s	1468 s	1475 s	1469 s	1465 s
1486 s	1490 sh		1484 s			1480 m
1500 sh	1500 sh	1502 sh	1500 sh	1504 w	1474 sh	1495 sh
1506 sh	1510 sh	1510 sh	1510 sh	1510 sh	1485 sh	1506 sh
1642 m		1638 w	1628 w	1634 m	1632 w	1632 m

Can. J. Chem. Downloaded from www.nrcresearchpress.com by 210.87.254.6 on 09/05/12
For personal use only.

TABLE 2
Products and analyses

Product	Color	Melting point (°C)	Found (%)			Calculated (%)			Solubility*	Yield	Method
			C	H	S	C	H	S			
$AgSC_6F_4C_6F_4SAg$	White	> 300	25.9	0.0	11.0	25.0	0.0	11.1	Nil	64	A
$TlSC_6F_4C_6F_4STl$	Yellow	> 300	18.7	0.0	8.4	18.7	0.0	8.3	Nil	48	A
$Pd(SC_6F_4C_6F_4S)$	Brown	> 300	30.3	0.0	14.4	30.9	0.0	13.7	Nil	38	A
$Hg(SC_6F_4C_6F_4S)$	White	> 300	26.0	0.0	11.3	25.7	0.0	11.4	Nil	33	A
$Pb(SC_6F_4C_6F_4S)$	Yellow	> 300	26.0	0.0	11.0	26.4	0.0	11.3	Nil	92	A
$Cd(SC_6F_4C_6F_4S)$	Yellow	> 300	31.0	0.0	13.4	30.5	0.0	13.6	Nil	33	A
n-$Bu_3SnSC_6F_4C_6F_4SSn$$n$-$Bu_3$	Yellow	b.p. 130/0.1 mm	46.4	5.7	—	46.0	5.8	—	2, 5	75	B
$Ph_3SnSC_6F_4C_6F_4SSnPh_3$	Yellow	135.5–137.0	54.6	2.6	—	54.4	2.8	—	2, 3, 4, 5	21	C
$Ph_3PbSC_6F_4C_6F_4SPbPh_3$	Yellow	185–187	46.0	2.4	—	46.6	2.4	—	2, 3, 4, 5	31	C
$ClSC_6F_4C_6F_4SCl$	Yellow	85.5–87.0	33.4	0.0	16.5†	33.4	0.0	16.4†	3, 4, 5	93	D
$MeSC_6F_4C_6F_4SMe$	White	92–94	42.8	1.4	16.0	43.1	1.5	16.4	1, 2, 3, 4, 5	64	C
$MeCOSC_6F_4C_6F_4SCOMe$	Yellow	136–141	43.6	1.5	14.0	43.1	1.4	14.4	2, 3, 4, 5	41	E
$PhCOSC_6F_4C_6F_4SCOPh$	Yellow	204–207	53.5	1.7	11.5	52.8	1.8	11.7	2, 3, 4, 5	58	C

*Solubilities: 1 = methanol; 2 = acetone; 3 = diethyl ether; 4 = chloroform; 5 = benzene.
†Percentage Cl.

similar to those observed in other thiolesters (6). In other respects the i.r. spectra of the new compounds contain peaks characteristic of the $-SC_6F_4C_6F_4S-$ group, which are tabulated in Table 1 (only relatively intense peaks) and of their functional groups.

Experimental

All reagents were available commercially. Infrared spectra were recorded on a Perkin–Elmer 457, either as mulls with Nujol or hexachlorobutadiene, or as liquid films. The n.m.r. spectra were recorded on a Varian A60. Microanalyses were performed by Mikroanalytisches Laboratorium Beller, Göttingen, Western Germany. Analytical data for the new compounds are shown in Table 2.

Method A

A solution of approximately 1 mmole of the thiol in acetone was added to a stoichiometric amount of the metal ion in aqueous solution. The precipitated mercaptide was filtered off, washed with acetone, water or dilute acid to remove excess of the reactants, and dried.

Method B

1.0 mmoles of $(n\text{-}Bu_3Sn)_2O$ and 1.0 mmoles of the thiol in acetone were stirred and refluxed for 3 h. After removal of the solvent the oily product was purified by distillation, b.p. 130°/0.1 mm. A similar reaction starting with $n\text{-}Bu_2SnO$ yielded an intractable gum.

Method C

Approximately 1 mmole of $Pb(SC_6F_4)_2$ was added to an acetone or ethanol solution of the stoichiometric amount of the appropriate metal or non-metal halide. After filtering off the lead chloride the solvent was evaporated and the residue recrystallized from *i*-BuOH, or sublimed (Me derivative).

Method D

One mmole of the thiol was allowed to react with 2.2 mmoles of chlorine in a sealed tube. Rapid reaction ensued at room temperature and the tube was opened after 1 h. The HCl and the excess chlorine were removed by vacuum distillation, leaving the pale yellow sulfenyl chloride.

Method E

An excess of acetyl chloride was added to a solution of 3 mmoles of the thiol in ether and refluxed for 2 h. An excess of Et_3N was added and refluxing continued for 3 h. The $Et_3NH\cdot HCl$ was filtered off, and the pale yellow solid left after evaporation of the solvent was purified by sublimation.

Attempts to prepare derivatives from PCl_3, $POCl_3$, and $AsCl_3$, using modifications of method E, or the bromine oxidation of the thiol in carbon tetrachloride resulted in the formation of an intractable gummy polymer.

The i.r. spectrum of the thiol has the following peaks in the 4000–250 cm^{-1} region (KBr disc): 2924 w, 2602 m, 2578 w, 2571 w, 1731 w, 1642 m, 1560 w, 1506 sh, 1500 sh, 1486 s, 1472 s, 1466 s, 1452 sh, 1441 m, 1407 w, 1384 w, 1372 w, 1241 s, 1231 sh, 1178 w, 1131 w, 1044 w, 1034 sh, 1028 s, 1020 s, 976 w, 931 m, 903 s, 850 w, 759 w, 755 w, 721 s, 706 w, 596 m, 432 w, 365 w, 321 m, 310 w, 286 w.

The National Research Council of Canada is thanked for generous financial assistance.

1. M. E. Peach. Can. J. Chem. **46**, 2699 (1968).
2. A. Callaghan, A. J. Layton, and R. S. Nyholm. J. Chem. Soc. D, 399 (1969).
3. M. E. Peach. Can. J. Chem. **46**, 211 (1968).
4. M. I. Bruce. J. Chem. Soc. A, 1459 (1968).
5. P. Robson, M. Stacey, R. Stephens, and J. C. Tatlow. J. Chem. Soc. 4754 (1960).
6. L. J. Bellamy. Advances in infrared group frequencies. Methuen and Co. Ltd., London, 1968. pp. 170–172.

Can. J. Chem. Downloaded from www.nrcresearchpress.com by 210.87.254.6 on 09/05/12
For personal use only.

Can. J. Chem. Downloaded from www.nrcresearchpress.com by 210.87.254.105 on 09/05/12
For personal use only.

COMMUNICATION

Novel electrophilic reaction of dichlorodicyanobenzoquinone

HANS REIMANN AND ROBERT S. JARET
Natural Products Research Department, Schering Corporation, Bloomfield, New Jersey 07003

Received February 16, 1970

The reaction of some steroid 1,3,5-trien-3-ol benzoates with dichlorodicyanobenzoquinone affords 6β-(4′-benzoyloxy-2′,3′-dichloro-5′,6′-dicyanophenoxy)-1,4-dien-3-ones in addition to the expected 1,4,6-trien-3-ones.

Canadian Journal of Chemistry, 48, 1478 (1970)

We wish to report the observation of an electrophilic C—O bond formation involving quinone oxygen in the reaction of some steroid 1,3,5-trien-3-ol benzoates (1) with dichlorodicyanobenzoquinone (DDQ) (2). When 16α-methyl-9α,11β-dichloro-1,3,5-pregnatriene-3,17α,21-triol-20-one 21-acetate 3-benzoate (**1**) (m.p. 169–173°; $[\alpha]_D$ −81°; λ_{max}(MeOH) 229 (ε 20 100), 311 nm (ε 6200); λ(Nujol) 2.80, 5.72, 5.76, 6.11, 6.21, 6.28, 7.86, 8.05 μ),[1] prepared from 16α-methyl-9α,11β-dichloro-1,4-pregnadiene-17α,21-diol-3,20-dione 21-acetate (3), was heated with DDQ in dioxane, two major steroidal products were isolated. The first of these was the expected (4) 1,4,6-trien-3-one **2** (m.p. 215–216° dec.; $[\alpha]_D$ + 93°; λ_{max}(MeOH) 223 (ε 10 800), 248 (ε 8800), 298 nm (ε 11 100); λ(Nujol) 3.04, 5.70, 5.75, 6.04, 6.13, 6.23, 8.05 μ), while the novel structure **3**, 6β-(4′-benzoyloxy-2′,3′-dichloro-5′,6′-dicyanophenoxy)-16α-methyl-9α,11β-dichloro-1,4-pregnadiene-17α,21-diol-3,20-dione 21-acetate, was assigned to the second product[2] on the basis of the following evidence.

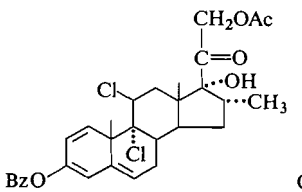

1

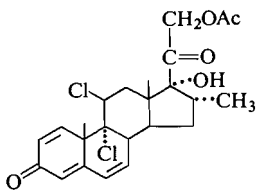

2

Compound **3** (m.p. 232–234°; $[\alpha]_D$ + 25°; λ_{max}(MeOH) 230 (ε 62 700), 322 nm (ε 3700), λ_{max}(NaOH) 250 nm) showed bands in the infrared (i.r.) at 2.82, 5.68, 5.75, 8.1 (corticoid side chain), 5.98, 6.12, 6.25 (conjugated dienone), 4.47 (nitrile), 7.96, 8.20 μ (benzoate ester) and an additional low wavelength carbonyl superimposed on the 5.68 μ band (phenol benzoate). The n.m.r. spectrum exhibited peaks at δ 0.96 (d, J = 7 Hz, 16α-CH_3), 1.23 (s, 18-H_3), 2.05 (s, 19-H_3), 2.16 (s, $COCH_3$), 4.5–5.3 (6α-H, 11α-H, 21-H_2), 6.45 (q, J = 10 and 1.5 Hz, 2-H), 6.53 (4-H), 7.29 (d, J = 10 Hz, 1-H) and 7.5–8.4 (COC_6H_5). The presence of the intact corticoid side chain in **3** was supported by perchloric acid catalyzed methanolysis to give the 21-alcohol **4** (m.p. 192–194°; $[\alpha]_D$ + 16°; λ_{max}(MeOH) 230 (ε 59 800), 322 nm (ε 3400); λ(Nujol) 2.85, 4.45, 5.65, 5.85, 5.99, 6.16, 6.22, 7.95, 8.17 μ). Treatment of **3** with zinc in methanolic acetic acid resulted in elimination of the 9α,11β-dichloro system as well as in reductive deconjugation of the 1,4-dien-3-one with elimination of the 6-substituent (5) to afford the 1,5,9(11)-trien-3-one **5** (acetone solvate, m.p. 189–190°; $[\alpha]_D$ + 69°; λ_{max}(MeOH) 223 nm (ε 12 500); λ(Nujol) 2.84, 5.72, 5.77, 5.90 (acetone), 5.98, 6.20, 8.1 μ) and the monobenzoate of dihydro-DDQ (m.p. 219–221°; λ_{max}(MeOH) 224 (ε 36 000), 235 (ε 36 000), 335 nm (ε 5600); λ(Nujol) 3.10, 4.44, 5.67, 7.92, 8.22 μ) which was prepared independently from

[1]New compounds gave satisfactory microanalytical values. Rotations are in chloroform. Nuclear magnetic resonance (n.m.r.) spectra are recorded for deuteriochloroform solutions in p.p.m. downfield from TMS internal standard on a Varian A-60 A instrument. Physical measurements were under the direction of Mr. M. Yudis.

[2]Compounds **2** and **3** were isolated in yields of 19 and 45%, respectively.

dihydro-DDQ. Acid-catalyzed isomerization of **5** gave 16α-methyl-1,4,9(11)-pregnatriene-17α, 21-diol-3,20-dione 21-acetate, identical with an authentic sample (6).

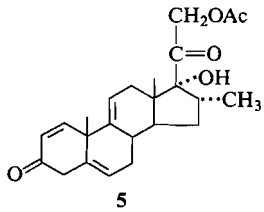

5

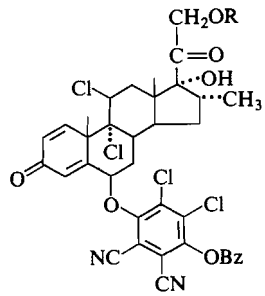

3 R = Ac
4 R = H

Oxidation of **4** with manganese dioxide in chloroform[3] afforded the 17-ketone **6** (m.p. 185–188°; $[\alpha]_D$ + 60°; λ_{max}(MeOH) 230 (ε 65 400), 321 nm (ε 4200); λ(Nujol) 4.46, 5.65, 5.73, 5.98, 6.12, 6.24, 7.97, 8.17 μ) whose n.m.r. spectrum permitted a further assignment of pertinent protons, δ 1.11 (d, J = 7 Hz, 16α-CH_3), 1.37 (s, 18-H_3), 2.06 (s, 19-H_3), 4.83 (q, J = 2.5 and 4 Hz, 11α-H), 5.15 (mult., $J_{w/2} \sim 6$ Hz, 6α-H), 6.47 (q, J = 10 and 1.5 Hz, 2-H), 6.52 (4-H), 7.25 (d, J = 10 Hz, 1-H), 7.5–8.4 (COC_6H_5). The assignment of the β-configuration to the substituent at C-6 is supported by the downfield shift (about 20 Hz) of the C-19 methyl protons vs. the parent structure, and is consistent with the usual β-attack on steroid 3,5-dien-3-ol derivatives.

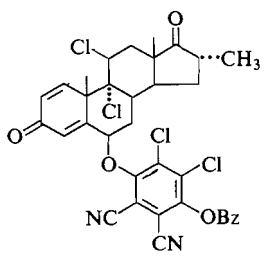

6

The formation of **3**, which involves an unusual benzoyl transfer, presumably proceeds via a species such as **A**, produced either in one step or by coupling of a prior charge-transfer complex (7).

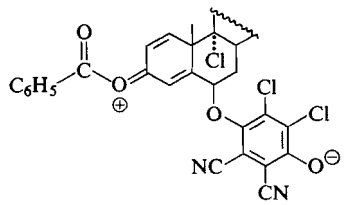

A

Similar results were obtained with 9α,11β-dichloro-1,3,5-pregnatriene-3,17α,21-triol-20-one 21-acetate 3-benzoate and 9α-fluoro-16β-methyl-1,3,5-pregnatriene-3,11β,17α,21-tetrol-20-one 21-acetate 3-benzoate.

We thank Dr. Leon Mandell for helpful advice in the interpretation of the n.m.r. spectra.

[3]H. Reimann and O. Z. Sarre. Manuscript in preparation.

1. Cf. Belg. Pat. 596 946 (1960).
2. For a comprehensive review on DDQ and its reactions, see: D. Walker and J. D. Hiebert. Chem. Rev. **67**, 153 (1967).
3. C. H. Robinson, L. E. Finckenor, R. Tiberi, and E. P. Oliveto. J. Org. Chem. **26**, 2863 (1961).
4. Cf. S. K. Pradhan and H. J. Ringold. J. Org. Chem. **29**, 601 (1964).
5. A. L. Nussbaum, G. Brabazon Topliss, T. L. Popper, and E. P. Oliveto. J. Amer. Chem. Soc. **81**, 4574 (1959).
6. E. P. Oliveto, R. Rausser, L. Weber, A. L. Nussbaum, W. Gebert, C. T. Coniglio, E. B. Hershberg, S. Tolksdorf, M. Eisler, P. L. Perlman, and M. M. Pechet. J. Amer. Chem. Soc. **80**, 4431 (1958).
7. Cf. H.-D. Becker. J. Org. Chem. **34**, 1203 (1969).

Can. J. Chem. Downloaded from www.nrcresearchpress.com by 210.87.254.105 on 09/05/12
For personal use only.

Can. J. Chem. Downloaded from www.nrcresearchpress.com by 210.87.254.40 on 09/05/12
For personal use only.

Canadian Journal of Chemistry

Published by THE NATIONAL RESEARCH COUNCIL OF CANADA

VOLUME 48 MAY 15, 1970 NUMBER 10

Synthesis and characterization of cyclam complexes of rhodium(III)

E. J. BOUNSALL AND S. R. KOPRICH

Department of Chemistry, University of Windsor, Windsor, Ontario

Received November 26, 1969

A series of complexes of the type Rh(cyclam)X_2^+ and Rh(cyclam)XY^{n+} have been prepared and characterized, where cyclam represents 1,4,8,11-tetraazacyclotetradecane and X and Y represent OH^-, H_2O, Cl^-, Br^-, I^-, N_3^-, NCS^-, and NO_2^-. The infrared and electronic spectra are discussed with respect to assignment of the *cis* and *trans* isomers, the linkage isomers, and the Rh–ligand stretching frequencies above 250 cm^{-1}. The thermodynamic *trans* effect is related to shifts in the Rh–ligand stretching frequencies. The intensities of the d–d transitions are related to distortion of the octahedral field to support the *cis* and *trans* assignments, and compared to show the decrease in bond constraint for propylene linkages in place of ethylene. Steric constraint accounts for the single case of stereoisomerization by *cis*-Rh(cyclam)I_2^+.

Canadian Journal of Chemistry, 48, 1481 (1970)

Introduction

Macrocyclic quadridentate ligands such as 1,4,8,11-tetraazacyclotetradecane (cyclam) and 1,4,7,10-tetraazacyclododecane (cyclen) have become important since they provide a substrate for octahedral substitution mechanistic studies with some advantages over the more commonly studied bis(ethylenediamine) systems, and they are also much simpler than naturally occurring cyclic ligands such as the porphyrins. Several *trans*-Co(cyclam)X_2^+ complexes (1) and a few Ni(cyclam)X_2 complexes (2) were prepared by Tobe and co-workers. Collman and Schneider (3) prepared some *cis*-Co(cyclen)X_2^+ complexes and *cis*-Rh(cyclen)Cl_2^+. *cis*-Cr(cyclam)Cl_2^+, as well as the cyclam complexes of several other metals, Cu(II), Zn(II), Cd(II), and Pd(II) have been prepared by Allen and Pedwell (4). Poon and Tobe (5) have recently prepared more *cis*- and *trans*-Co(cyclam)X_2^+ and some Co(cyclam)-XY^+ complexes and have used them to study the mechanism and steric course of octahedral acid hydrolysis. The linear quadridentate analogs of cyclam have also received recent study. The triethylenetetramine (trien) complexes of Co(III) and Rh(III) were reported by Gillard and Wilkinson (6) and also by Sargeson and co-workers (7). 1,4,8,11-Tetraazaundecane (2,3,2-tet), an even more similar analog of cyclam, was studied by Hamilton and Alexander (8) and Gillard and co-workers (9). Gillard and co-workers termed these open-chain ligands as facultative, based on their ability to assume different configurations. The two possible *cis* configurations, as opposed to one for cyclam, make these systems more complicated and less desirable as a simple substrate for mechanistic studies.

The rigidity of the quadridentate cyclic structure is a barrier to isomerization, and for Rh(III) only the *cis*-diiodo complex isomerizes at reflux temperatures. This is due to the steric preference of the large iodo ligands for the *trans* configuration.

The greater number of different Rh(III) complexes of cyclam compared to the bis(ethylenediamine), $(en)_2$, analogs enlarges the scope for *trans* effect and mechanistic studies which will be reported in a later paper. The cyclam complexes are more inert than the bis(ethylenediamine) analogs and the substitution reactions can be measured by conventional spectrometric techniques. The larger enthalpies of activation for cyclam complexes support the prediction that their increased rigidity resists stereochemical rearrangement in the transition state, relative to

Can. J. Chem. Downloaded from www.nrcresearchpress.com by 210.87.254.40 on 09/05/12
For personal use only.

$(en)_2$. Another factor causing the destabilization of the transition state is the decrease in solvation with increasing chelation (10).

Results and Discussion

Stereoisomers

The *cis* and *trans* isomers of the Rh(cyclam)-XY^{n+} series were assigned on the basis of a comparison of the wavelengths and extinction coefficients of the absorption maxima of their electronic spectra (Tables 1 and 2). It is readily apparent that the *trans* isomers exhibit electronic transitions of lesser energy and lesser intensity than those for the *cis* compounds. This observation was used to assign the cyclam complexes for which there is no $(en)_2$ analog.

The *cis*-Rh(cyclam)Cl_2^+ isomer was confirmed by the resolution of the racemic mixture with *d*-α-bromocamphor-π-sulfonate. An optical rotary dispersion (o.r.d.) spectrum showed a very small specific rotation (cf. resolution of *cis*-[Rh(cyclam)Cl_2]Cl, below). Racemic *cis*-[Rh-$(en)_2Cl_2$]Cl has been successfully resolved (11) and the optical rotation of the *l-cis* isomer was measured ($[\alpha]_{535m\mu} = -58°$). The relatively small rotation of the cyclam optical isomer could have been the result of poor separation of the diastereoisomers or the increased symmetry of the cyclam *cis* isomer over the corresponding *cis*-$(en)_2$.

The relative extinction coefficients of the stereoisomers provide further evidence for the assignments. Distortion of the octahedral field around the central metal ion tends to remove the center of symmetry with respect to vibrations and the d^6 states lose some of their *g* character through vibronic coupling (12). This provides a mechanism for increasing the intensity of the d–d

TABLE 1

Electronic spectra of Rh(cyclam)XY^{n+} (absorption maxima)

Complex	λ (mμ)*	ε (l cm^{-1} $mole^{-1}$)
cis-Cl_2^+	354, 299, 207	223, 308, 33900
trans-Cl_2^+	406, 310sh, 242sh, 204	78, 80, 3300, 37100
cis-Br_2^+	367, 309	243, 871
trans-Br_2^+	429, 285, 235	97.3, 2520, 34600
cis-I_2^+	407, 295sh, 260sh, 228	1210, 5300, 17500, 38400
trans-I_2^+	515sh, 466, 353, 275, 226	64, 204, 13100, 34500, 22800
cis-$(N_3)_2^+$	339sh, 262	1250, 11800
trans-$(N_3)_2^+$	377, 286, 208	892, 12700, 27100
cis-$(NO_2)_2^+$	293sh	1030
trans-$(NO_2)_2^+$	320sh, 260sh, 213	535, 2100, 30800
cis-$(NCS)_2^+$	322, 244	1110, 3630
trans-$(NCS)_2^+$	377, 258	882, 3330
trans-$Cl(OH)^+$	363, 276	101, 180
trans-$Cl(H_2O)^{2+}$	385, 296sh, 224sh	55, 101, 4420
trans-$Br(OH)^+$	373, 277sh	113, 384
trans-$Br(H_2O)^{2+}$	468, 403, 310sh, 204	37, 63, 106, 25600
trans-$I(OH)^+$	443, 393, 275, 230	153, 158, 5330, 26300
trans-$I(H_2O)^{2+}$	494, 341sh, 301sh, 271, 230	222, 763, 1290, 2240, 24400
trans-$N_3(OH)^+$	357, 256	525, 6320
trans-$N_3(H_2O)^{2+}$	420sh, 363, 261	79, 715, 5640
cis-$(OH)(H_2O)^{2+}$	328, 291	251, 192
trans-$(OH)(H_2O)^{2+}$	342, 274	118, 222
trans-$ClBr^+$	418, 312sh, 260sh, 221	89, 95, 1950, 32700
trans-ClI^+	493, 445sh, 308, 245	230, 138, 3620, 31300
trans-$Cl(N_3)^+$	382, 270, 207	697, 9390, 23000
trans-$Cl(NCS)^+$	368, 252	340, 8080
trans-BrI^+	497, 459, 321, 256	151, 152, 6200, 33900
trans-$Br(N_3)^+$	393, 281, 214	698, 11900, 21400
trans-$Br(NCS)^+$	368, 262	355, 8980
trans-$I(N_3)^+$	465sh, 417, 300, 280sh, 225	283, 654, 10100, 8970, 20900
trans-$I(NCS)^+$	434, 412, 296, 274, 224	393, 413, 4220, 5660, 30600
trans-$(N_3)(NCS)^+$	352, 270	861, 7330
trans-$(OH)_2^+$	341, 277	101, 163
trans-$(H_2O)_2^{3+}$	352	65
cis-$(OH)_2^+$	331, 278	226, 202
cis-$(H_2O)_2^{3+}$	296, 251	249, 230

*sh = shoulder.

TABLE 2

Electronic spectra of $[Rh(en)_2XY]^+$ (absorption maxima)

Complex	λ (mμ)*	ε (l cm^{-1} $mole^{-1}$)	Reference
cis-Cl_2	352, 295	155, 180	11
trans-Cl_2	406, 286	75, 130	11
cis-Br_2	362, 276	210, 900	11
trans-Br_2	425, 276, 231	100, 2300, 30800	13
cis-I_2	375	1200	11
trans-I_2	462, 340, 269, 222	260, 14300, 31000, 20000	13
trans-$(N_3)_2$	375, 282	740, 13000	13
cis-$(NO_2)_2$	290, 245sh	660, 3500	11
trans-$(NO_2)_2$	300sh, 255sh	590, 2400	11
trans-ClI	440, 300, 242	154, 4350, 38500	13
trans-Cl(N_3)	377, 263	560, 9600	14
trans-Cl(NCS)	363	340	11
trans-BrI	455, 311, 253	260, 7500, 41500	13
trans-Br(N_3)	388, 272	580, 15100	14

*sh = shoulder.

TABLE 3

Electronic spectra (maxima) of some $[Rh(amine)Cl_2]^+$ complexes

Complex	λ (mμ)	ε (l cm^{-1} $mole^{-1}$)	Reference
trans-$[Rh(NH_3)_4Cl_2]^+$	412	66	11
trans-$[Rh(en)_2Cl_2]^+$	406	75	11
trans-$[Rh(cyclam)Cl_2]^+$	406	78	This work
cis-$[Rh(en)_2Cl_2]^+$	352	155	11
cis-$[Rh(cyclam)Cl_2]^+$	354	223	This work
cis-$[Rh(trien)Cl_2]^+$	352	250	11
cis-$[Rh(trien)Cl_2]^+$	370	300	3
cis-$[Rh(cyclen)Cl_2]^+$	365	535	3

transitions. The two spin-allowed bands ($^1T_{1g} \leftarrow {}^1A_{1g}$, $^1T_{2g} \leftarrow {}^1A_{1g}$) are easily observed and are obscured by charge-transfer bands only for nitro complexes with their large ligand field strengths. An increase in steric constraint would be expected to cause greater distortions and thereby greater intensities in the visible absorption of the complexes. Collman and Schneider (3) discuss this principle with respect to a *cis*-Rh(amine)X_2^+ series. The center of symmetry is removed in a *cis* isomer relative to a *trans*, considering the primary effects of the N donors and ignoring the secondary effects of the ethylene and propylene linkages. As a result, larger extinction coefficients for the d–d transitions are predicted for the *cis* isomers. Table 1 shows that this prediction is consistent with the assignment of stereoisomers. It is especially clear in the case of *cis*-[Rh(cyclam)I_2]I, which has the additional distortion resulting from the size of the iodo ligands. The lower energy d–d transition is about 20 times as intense for the *cis* isomer. In addition, as noted, the steric effect of the iodo ligands make this the only complex in the series which undergoes stereoisomerization at reflux temperature.

A comparison of some of the Rh(amine)Cl_2^+ complexes shows this trend very clearly (Table 3). This effect is more pronounced in the *cis* series than the *trans*. The table also shows that the larger size and greater flexibility of the cyclam ring relative to the cyclen ring results in less distortion of the octahedral field. The d–d transition intensity is less than that of complexes with only ethylene linkages. Therefore, the presence of the two propylene bridges in cyclam removes some of the steric constraint in the *cis* series of isomers.

The infrared (i.r.) spectra also provide evidence for the increased distortion of the octrahedral field in the *cis* series. The lower symmetry of the *cis* complexes results in greater detail in the spectrum (Table 4). The ν(N—H) and ν(Rh—N) modes and the CH_2 rocking modes appear as single bands in the *trans* and double bands in the *cis* series. In addition, the bands due to ν(NO_2) and ν(NCS) are resolved in the *cis* complexes.

Can. J. Chem. Downloaded from www.nrcresearchpress.com by 210.87.254.40 on 09/05/12
For personal use only.

TABLE 4

Some details of the infrared spectra of diacidocyclamrhodium(III) complexes*

Complex	Frequency, cm^{-1}				
	ν(NH), s	r(CH_2), m	ν(CN or CC), s	ν(Rh—N), m	Other
cis-Cl_2	3060 3175	840 855	1053 1017 1001	505 459	
trans-Cl_2	3105	875	1020	493	
cis-Br_2	3065 3160	840 855	1052 1019 1001	477 450	
trans-Br_2	3135	890	1020	487	
cis-I_2	3065 3140	840 855	1052 1019 1000	470 423	
trans-I_2	3100	865	1018	482	
cis-$(N_3)_2$	3080 3180	845 860	1053 1029 1005	490 459	351 (Rh—N_3)
trans-$(N_3)_2$	3110	875	1048 1025	501	370 (Rh—N_3)
cis-$(NO_2)_2$	3050 3215	840 855	1055 1027 1002	479 412	815, 830 (NO_2^-)
trans-$(NO_2)_2$	3180	880	1055 1030	499	825 (NO_2^-)
cis-$(NCS)_2$	3125 3210	845 860	1056 1034 1010	533 480	2100, 2080; 835, 820 (NCS^-)
trans-$(NCS)_2$	3105	875	1045 1035	500	2090; 830 (NCS^-)
cis-(OH)(H_2O)	3090 3220	830 850	1040 1028	500 450	546 (Rh—OH)
trans-(OH)(H_2O)	3220	870	1040 1025	493	
trans-Cl(OH)	3225	880	1047 1018	501	523, 487 (Rh—OH)
trans-Cl(H_2O)	3225	875	1040	499	
trans-Br(OH)	3220	875	1050 1017	500	521, 482 (Rh—OH)
trans-Br(H_2O)	3225	875	1034	496	
trans-I(OH)	3220	875	1050 1020	501	516, 484 (Rh—OH)
trans-I(H_2O)	3220	870	1035	497	
trans-(N_3)(OH)	3230	880	1028 1010	502	533, 487 (Rh—OH); 343 (Rh—N_3)
trans-(N_3)(H_2O)	3230	875	1050 1030	499	370 (Rh—N_3)
trans-ClBr	3215	875	1040 1018	497	
trans-ClI	3180	875	1022	496	
trans-Cl(N_3)	3200	875	1021	499	362 (Rh—N_3)
trans-Cl(NCS)	3200	875	1047 1020	499	2090; 835 (NCS^-)
trans-BrI	3180	870	1040 1017	490	
trans-Br(N_3)	3190	875	1045	497	352 (Rh—N_3)
trans-Br(NCS)	3200	875	1040 1024	498	2090; 835 (NCS^-)
trans-I(N_3)	3200	870	1040 1021	491	347 (Rh—N_3)
trans-I(NCS)	3200	870	1045	493	835 (NCS^-)
trans-(N_3)(NCS)	3215	870	1040	499	2090; 833 (NCS^-); 357 (Rh—N_3)

*r = rocking vibration, s = strong, m = medium, assigned according to ref. 15.

Can. J. Chem. Downloaded from www.nrcresearchpress.com by 210.87.254.40 on 09/05/12
For personal use only.

Can. J. Chem. Downloaded from www.nrcresearchpress.com by 210.87.254.40 on 09/05/12
For personal use only.

Linkage Isomers

The thiocyanate ion was bonded in the isothiocyanato form (N-bonded) as determined from its spectra. A medium band near 835 cm^{-1} was observed for each thiocyanate complex (Table 4). Turco and Pecile (16) reported the range 780–860 cm^{-1} for the C—S stretching frequency in isothiocyanato complexes, as opposed to 690–720 cm^{-1} in thiocyanato complexes. In this work, no i.r. bands were observed in the 690–720 cm^{-1} range. A more reliable assignment can be made on the basis of the δ(NCS) fundamental mode, which occurs in the 460–490 cm^{-1} range for M—NCS, while the corresponding band for M—SCN occurs from 410 to 440 cm^{-1} (16). In this work, a single weak band was present near 460 cm^{-1}, which supports the isothiocyanato assignment. This is a necessary confirmation, since the first overtone of the δ(NCS) fundamental, which would occur for both M—SCN and M—NCS, is a band between 800 and 880 cm^{-1} with an intensity comparable to the ν(C—S) mode, and therefore may be mistaken as diagnostic of isothiocyanato. The most reliable criterion for M—NCS bonding is a broad band in the vicinity of 2000 cm^{-1}, while M—SCN gives a very sharp band in the same region in the spectrum of the solid (17). Again, the isothiocyanato assignment for all the complexes prepared, involving the thiocyanato ion, was indicated by a characteristically broad band in the range 2080–2100 cm^{-1}.

The electronic spectrum was in agreement with this assignment. According to Schaffer (18) and Jorgensen (19), thiocyanato should fit close to chloro and bromo in the spectrochemical series, while isothiocyanato should fit along with stronger ligands, such as azido, at lower wavelengths. Comparing the lower energy d–d transition of the thiocyanato, azido, and halo complexes (Table 1), it is evident that thiocyanato has a ligand field strength very close to that of azido.

The ultraviolet (u.v.) spectra of the dinitro complexes show that the linkage isomers contain nitro rather than nitrito ligands. Nitrito has a ligand field strength near that of hydroxo, whereas nitro is close to the strongest ligands in the spectrochemical series. The absorption maxima for the nitro complexes are the farthest in the u.v. and are observed as shoulders, due to the proximity of the charge transfer peaks. All the comparable hydroxo maxima are further in the visible region.

The sharp infrared band near 820 cm^{-1} is diagnostic of a nitro isomer (20). It should not be confused with a broad peak near 860 cm^{-1} found in both nitro and nitrito isomers.

The greater stability of the isothiocyanato and the nitro isomers over the thiocyanato and nitrito isomers tends to indicate the hardness (21) or "class *a*" character (22) of the Rh(cyclam) substrate. This principle is clearly illustrated by the triad Zn(II), Cd(II), and Hg(II): class *a* Zn(II) bonds with N, borderline Cd(II) bonds with N or S, and class *b* Hg(II) bonds with S (ref. 10, p. 297).

Trans Bond Weakening

The σ-inductive theory of the *trans* effect accounts for *trans* activation through competition for the σ_x molecular orbital (ref. 10, p. 372), or repulsion of electrons in the metal p_x orbital. Therefore, the theory predicts that *trans* destablization is related to *trans* labilization, provided π effects are not important. The assumption that the changes in ν(Rh—X) can be correlated with changes in bond strength is probably safe for a series of related compounds. Although there is no necessity that this assumption be so, due to the more complex bond strength relationships of coupled modes, the decrease in ν(Pt—X) in *trans*-$Pt(PEt_3)_2LCl$ (23) was found to be related to the increasing *trans* effect of L, provided that π bonding is not a complicating factor. In addition, a similar correlation has been found for ν(Pt—N) in *cis*-$PtX_2(NH_3)_2$ (24) and in *trans*-$Pt(NH_3)LCl_2$ (25); and for ν(Pt—H) in *trans*-PtA_2LH, where A is $As(Et)_3$ and a series of substituted phosphines (26). Similarly, the *trans* destabilization effect can be inferred from the shifts in the ν(Rh—X) frequencies. In each of the *cis* complexes, a different group is *trans* to a cyclam nitrogen. Therefore, shifts in the ν(Rh—N) frequencies provide a basis for ordering the *trans* ligands according to their bond weakening influence. From the data in Table 4, it is clear that the order of *trans* bond weakening ability is

$$NO_2^- > I^- > Br^- > Cl^- \sim N_3^- > N(cyclam) > NCS^-$$

N(cyclam) was positioned on the basis of the *trans* complexes in which N(cyclam) is *trans* to each Rh—N bond. The order is expected on comparison with the *trans*-effect orders of other octahedral systems, except for azido. However, azido is a good π donor, and as such has an

Can. J. Chem. Downloaded from www.nrcresearchpress.com by 210.87.254.40 on 09/05/12
For personal use only.

additional mechanism for *trans* activation, which is related more to the transition state than the ground state (27). The same relative order of *trans* bond weakening is observed for $\nu(Rh—N_3)$ in *trans*-$Rh(cyclam)L(N_3)^+$ and for $\nu(Rh—OH)$ in *trans*-$Rh(cyclam)L(OH)^+$, where L is a halo or azido ligand.

Preparations

The preparation of cyclam was carried out according to the method of Tobe and co-workers (1) with two modifications which simplified the procedure and improved the yield. The product was precipitated directly from the reaction solution rather than being sublimed along with an added amount of 1,9-diamino-3,7-diazanonane. Secondly, the crude product was purified by vacuum sublimation rather than recrystallization from dioxane. The method of Stetter and Mayer (28) is more elegant but was not used because of its length and similar yield. However, the m.p. of 186–188 °C (sealed tube) was closer to that reported by Stetter and Mayer (185 °C) than that by Tobe and co-workers (173 °C). Recrystallization from dioxane was also used by Stetter and Mayer for purification.

Cyclam was observed to be very stable in air. It was quite soluble in water, in contradiction to the observation of Stetter and Mayer. However, the infrared spectrum corresponded exactly with their spectrum.

The preparation of the 1,5,9,13-tetraazacyclohexadecane analog of cyclam was attempted, since it is a more symmetric ring with four propylene linkages. While a crude product was isolated, it was not stable in air, turning brown, and it was quite viscous. Apparently the stability and high m.p. of cyclam are not shared by this analog. Other close analogs also have low melting points (1,3,7,10-tetraazacyclododecane, 35 °C; 1,4,8,11-tetraazacyclotridecane, 41 °C).

The stability of cyclam is explained by Tobe as the result of diagonal hydrogen bridging by two of the amine hydrogens. This structure leaves two lone pairs available for direct protonation, which agrees with the two pairs of steps involved in the protonation according to Curtis (29). In comparison, the protonation of the open chain follows a regular four-step sequence.

The preparation of the dichloro complex from $RhCl_3 \cdot 3H_2O$ and cyclam in water gave almost entirely the *cis* isomer. On the other hand, if the same preparation was carried out in methanol, the *trans* isomer predominated (60% *trans*, 30% *cis* isolated). When the reaction was carried out in a NaBr solution, sufficient *trans* isomer was produced to be separated, but the impure yield (17%) was much lower than the reaction of the dichloro complex with Br^- reported below. A NaI solution gave an even greater percentage of *trans* isomer, however, it could not be separated from the *cis*.

All the *cis*- and *trans*-$Rh(cyclam)X_2^+$ complexes were prepared from the respective *cis* or *trans* dichloro complex by heating at reflux temperature in an aqueous solution of the desired anion for extended periods of time. This was possible since only the *cis*-diiodo complex showed any tendency to isomerize. However, even the *cis*-diiodo complex could be prepared by carefully limiting the reflux period.

Since these preparations were time consuming, a catalytic approach was attempted. Gillard *et al.* (30) have suggested several catalysts for Rh(III) reactions. $NaBH_4$ was found to be ineffective. The solutions of $NaBH_4$ were basic, causing interference by the predominating base hydrolysis reaction. No further work was done with catalysis since base hydrolysis itself was found to be a convenient pathway for the desired mixed complexes.

The cyclam complexes of Rh(III) were very sensitive to base hydrolysis and gave complete dihydroxo formation in less than 1 h in approximately 0.1 *M* NaOH, with indications of the usual second-order rate dependence. The bis-(ethylenediamine) analogs, on the other hand, were not as susceptible to base hydrolysis and formed the dihydroxo complex at rates slower than the usual substitution rates, which are limited by the acid hydrolysis rate. The rapid formation of hydroxo complexes provided an excellent pathway for the preparation of $Rh(cyclam)XY^{n+}$. By carefully limiting the reflux period from 3 to 10 min, it was found that the solution contained only the mono- and dihydroxo products, and the monohydroxo product could be precipitated in very pure form (yields: approximately 50%) since the dihydroxo could not be precipitated with perchlorate. The monohydroxo complex was acidified to give the monoaquo, which was readily anated with several different anions to give the desired mixed XY complexes.

Can. J. Chem. Downloaded from www.nrcresearchpress.com by 210.87.254.40 on 09/05/12
For personal use only.

Experimental

$RhCl_3 \cdot 3H_2O$ from J. Bishop and Co. Platinum Works was used without further purification. Pure methanol (99.9 mole %) and ion-exchanged distilled water were used as solvents. Reagent grade sodium salts were used as a source of the anions for substitution and precipitation.

Electronic spectra were recorded on a Bausch and Lomb Spectronic 505, using water as the solvent for all samples except those with a hydroxo ligand. Hydroxo complexes were recorded in 0.1 *M* NaOH. Infrared spectra were recorded on a Beckman IR 10 using approximately 1% KBr pellets. The o.r.d. spectra were recorded on a Cary 60 instrument.

1,4,8,11-Tetraazacyclotetradecane (Cyclam)

The open-chain intermediate, 1,9-diamino-3,7-diazanonane, was prepared according to the method of Van Alphen (31). 1,3-Dibromopropane (250 g, 1.2 moles, 126 ml) was added dropwise to ethylenediamine (360 g, 6.0 moles, 400 ml) in 300 ml ethanol. The yellow solution was heated under reflux for 1 h. KOH (300 g, 5.3 moles) was added and the reaction mixture was stirred for 30 min. The KBr and excess KOH were removed by filtration. The ethanol and excess ethylenediamine were removed by distillation (116–117 °C). The 1,9-diamino-3,7-diazanonane was separated by vacuum distillation (138 °C, 4 mm Hg) as a clear viscous liquid (90 g, 0.56 mole, 47% yield).

Cyclam was prepared according to Tobe and coworkers (1) with some modifications. 1,3-Dibromopropane (50 g, 0.25 mole) and 1,9-diamino-3,7-diazanonane (40 g, 0.25 mole) were added to 4 l ethanol and heated under reflux for 24 h, during which the solution turned yellow. Three liters of ethanol were removed by distillation. KOH (35 g, 0.62 moles) was added and the volume was reduced to about 500 ml by distillation. The solution was cooled and the KBr was removed by filtration. The volume was reduced to 150 ml, during which the excess KOH was removed by decantation. The viscous yellow solution was cooled overnight to precipitate the white product (3.0 g, 6%), which was filtered, washed with acetone, and purified by vacuum sublimation (120 °C, 2 mm Hg). The melting point in a sealed tube was 186 °C.

Anal. Calcd. for $C_{10}H_{24}N_4$: C, 59.95; H, 12.08; N, 27.97. Found: C, 59.93; H, 12.24; N, 27.93.

cis-[Rh(cyclam)Cl_2]Cl

$RhCl_3 \cdot 3H_2O$ (7.5 g, 28 mmoles) and cyclam (7.5 g, 37 mmoles) were dissolved in 300 ml methanol and heated under reflux for 5 min, during which the red mixture turned to a yellow solution with a yellow precipitate. The reaction mixture was cooled and filtered. The yellow product (3.1 g, 27%) was washed with ethanol and ether and dried under vacuum for 2 h.

Anal. Calcd. for $[Rh(C_{10}H_{24}N_4)Cl_2]Cl$: C, 29.32; H, 5.91; N, 13.68; Cl, 25.97. Found: C, 29.26; H, 5.99; N, 14.02; Cl, 25.80.

trans-[Rh(cyclam)Cl_2]Cl

The filtrate from the preparation of *cis*-[Rh(cyclam)Cl_2]Cl in methanol was treated with 25 ml concentrated HCl to precipitate the excess cyclam as the tetrahydrochloride (analyzed as 3.5 HCl), and any *cis* isomer left in the solution. After filtration, the yellow solution was evaporated to dryness. The yellow residue was recrystallized from 75 ml water and 25 ml concentrated HCl, washed with acetone and ether and dried under vacuum for 2 h (5.8 g, 50%).

Anal. Calcd. for $[Rh(C_{10}H_{24}N_4)Cl_2]Cl$: C, 29.32; H, 5.91; N, 13.68; Cl, 25.97. Found: C, 29.38; H, 5.89; N, 13.68; Cl, 26.17.

cis-[Rh(cyclam)Cl_2]ClO_4

$RhCl_3 \cdot 3H_2O$ (2.0 g, 7.6 mmoles), cyclam (1.5 g, 7.6 mmoles), and NaCl (2.0 g, 34 mmoles) were added to 50 ml water and heated under reflux for 30 min, during which the red mixture changed to a yellow solution. $HClO_4$ (5 ml, 70%) was added to precipitate the product. The yellow product (2.4 g, 70%) was recrystallized by repeating the procedure.

Anal. Calcd. for $[Rh(C_{10}H_{24}N_4)Cl_2]ClO_4$: C, 25.36; H, 5.11; N, 11.83; Cl, 22.46. Found: C, 25.57; H, 5.29; N, 11.91; Cl, 22.47.

cis-[Rh(cyclam)Br_2]Br

cis-[Rh(cyclam)Cl_2] (500 mg, 1.22 mmoles) and NaBr (2.5 g, 24 mmoles) were dissolved in 50 ml water and heated under reflux for 3 h. The solution turned from yellow to orange, with the formation of an orange precipitate. The reaction mixture was cooled to precipitate the orange product, which was recrystallized by repeating the procedure (450 mg, 68%), washed with ethanol and ether and dried under vacuum for 2 h.

Anal. Calcd. for $[Rh(C_{10}H_{24}N_4)Br_2]$: C, 22.12; H, 4.46; N, 10.32; Br, 44.15. Found: C, 22.26; H, 4.47; N, 10.34; Br, 43.86.

trans-[Rh(cyclam)Br_2]Br

Using the *trans*-dichloro compound, the procedure was the same as for the *cis* isomer with a 5 h reflux period and NaBr (4.6 g, 44 mmoles) in 50 ml water. The *trans* isomer (240 mg, 41%) was also orange.

Anal. Calcd. for $[Rh(C_{10}H_{24}N_4)Br_2]Br$: C, 22.12; H, 4.46; N, 10.32; Br, 44.15. Found: C, 22.28; H, 4.43; N, 10.50; Br, 43.92.

cis-[Rh(cyclam)I_2]I

cis-[Rh(cyclam)Cl_2]Cl (500 mg, 1.22 mmoles) was dissolved in 0.33 *M* NaI and heated under reflux for 30 min. The solution turned from yellow to orange. It was cooled to precipitate the orange product, which was recrystallized by repeating the procedure twice. The orange product (370 mg, 45%) was washed with ethanol and ether and dried under vacuum for 2 h.

Anal. Calcd. for $[Rh(C_{10}H_{24}N_4)I_2]I$: C, 17.56; H, 3.54; N, 8.19; I, 55.66. Found: C, 18.07; H, 3.77; N, 8.43; I, 55.66.

trans-[Rh(cyclam)I_2]I

trans-[Rh(cyclam)Cl_2]ClO_4 (504 mg, 1.06 mmoles) and NaI (3.2 g, 21 mmoles) were added to 150 ml water and heated under reflux for 3 h, during which a brown precipitate was formed. The solution was cooled and the brown product was recrystallized by heating in 2 l water and NaI (3.2 g, 21 mmoles) for 3 days, followed by slow evaporation to 200 ml. The product (610 mg, 84%) was washed with ethanol and ether and dried under vacuum for 2 h.

Can. J. Chem. Downloaded from www.nrcresearchpress.com by 210.87.254.40 on 09/05/12
For personal use only.

Anal. Calcd. for $[Rh(C_{10}H_{24}N_4)I_2]I$: C, 17.56; H, 3.54; N, 8.19; I, 55.66. Found: C, 17.38; H, 3.54; N, 8.20; I, 55.74.

cis-[Rh(cyclam)(N$_3$)$_2$]ClO$_4$

cis-[Rh(cyclam)Cl$_2$]Cl (500 mg, 1.22 mmoles) and NaN_3 (1.0 g, 15 mmoles) were dissolved in 25 ml water and heated under reflux for 3 h. The yellow solution became golden. $HClO_4$ (5 ml, 70%) was added to precipitate the yellow product, which was recrystallized by repeating the procedure. The product (460 mg, 78%) was washed with ethanol and ether and dried under vacuum for 2 h. The product was protected from light to prevent decomposition to a brown compound.

Anal. Calcd. for $[Rh(C_{10}H_{24}N_4)(N_3)_2]ClO_4$: C, 24.68; H, 4.97; N, 28.78; Cl, 7.28. Found: C, 24.70; H, 5.12; N, 29.02; Cl, 7.40.

trans-[Rh(cyclam)(N$_3$)$_2$]ClO$_4$

The *trans* isomer was prepared using the same procedure as for the *cis* compound. The yellow product (390 mg, 73%) was protected from light.

Anal. Calcd. for $[Rh(C_{10}H_{24}N_4)(N_3)_2]ClO_4$: C, 24.68; H, 4.97; N, 28.78. Found: C, 24.88; H, 4.96; N, 28.73.

cis-[Rh(cyclam)(NO$_2$)$_2$]ClO$_4$

cis-[Rh(cyclam)Cl$_2$]ClO$_4$ (500 mg, 1.05 mmoles) and $NaNO_2$ (1.7 g, 24 mmoles) were dissolved in 50 ml water and heated under reflux for 3 h. The solution turned paler yellow. $HClO_4$ (5 ml, 70%) was added to precipitate the product, which was recrystallized by repeating the procedure. The pale yellow product (400 mg, 76%) was washed with ethanol and ether and dried under vacuum.

Anal. Calcd. for $[Rh(C_{10}H_{24}N_4)(NO_2)_2]ClO_4$: C, 24.28; H, 4.89; N, 16.99. Found: C, 24.44; H, 4.93; N, 16.64.

trans-[Rh(cyclam)(NO$_2$)$_2$]ClO$_4$

trans-[Rh(cyclam)Cl$_2$]Cl (719 mg, 1.75 mmoles) and $NaNO_2$ (3.5 g, 51 mmoles) were added to 50 ml water and heated under reflux for 20 h. $HClO_4$ (5 ml, 70%) was added to precipitate the product, which was recrystallized by repeating the procedure. The white powder (484 mg, 58%) was washed with ethanol and ether and dried under vacuum.

Anal. Calcd. for $[Rh(C_{10}H_{24}N_4)(NO_2)_2]ClO_4$: C, 24.28; H, 4.89; N, 16.99; O, 25.87. Found: C, 24.56; H, 4.97; N, 17.00; O, 25.59.

cis-[Rh(cyclam)(NCS)$_2$]ClO$_4$

trans-[Rh(cyclam)(OH)(H$_2$O)](ClO$_4$)$_2$ (375 mg, 0.697 mmole), NaSCN (2.0 g, 25 mmoles), and $NaClO_4 \cdot H_2O$ (10 g, 72 mmoles) were dissolved in 25 ml water and heated under reflux for 2 h during which the solution became darker yellow. The solution was cooled to precipitate the product. The yellow-white product (165 mg, 46%) was washed with ethanol and ether and dried under vacuum.

Anal. Calcd. for $[Rh(C_{10}H_{24}N_4)(NCS)_2]ClO_4$: C, 27.78; H, 4.66; N, 16.20; S, 12.36. Found: C, 27.84; H, 4.57; N, 16.20; S, 12.29.

trans-[Rh(cyclam)(NCS)$_2$]ClO$_4$

trans-[Rh(cyclam)(OH)(H$_2$O)](ClO$_4$)$_2$ (218 mg, 0.405 mmole) and NaSCN (1.0 g, 12 mmoles) were added to 25 ml water and 5 drops of dilute $HClO_4$. The yellow solution was heated under reflux for 50 h. $NaClO_4 \cdot H_2O$ (10 g, 72 mmoles) was added to precipitate the product. The pale yellow complex was added to 50 ml 1.0 *M* NaSCN, heated under reflux for 10 h, and precipitated with $NaClO_4$. The product (72 mg, 34%) was washed with ethanol and ether and dried under vacuum.

Anal. Calcd. for $[Rh(C_{10}H_{24}N_4)(NCS)_2]ClO_4$: C, 27.78; H, 4.66; N, 16.20; S, 12.36. Found: C, 27.56; H, 4.57; N, 15.96; S, 12.44.

trans-[Rh(cyclam)Cl(OH)]ClO$_4$

trans-[Rh(cyclam)Cl$_2$]Cl (306 mg, 0.747 mmole) and NaOH (1 pellet, ~2.5 mmoles) were dissolved in 20 ml water and heated under reflux for 5 min. $NaClO_4 \cdot H_2O$ (5.0 g, 36 mmoles) was added to precipitate the white complex (153 mg, 45%), which was washed with ethanol and ether and dried under vacuum.

Anal. Calcd. for $[Rh(C_{10}H_{24}N_4)Cl(OH)]ClO_4$: C, 26.39; H, 5.54; N, 12.31; Cl, 15.58. Found: C, 26.36; H, 5.48; N, 12.07; Cl, 15.71.

trans-[Rh(cyclam)Cl(H$_2$O)](ClO$_4$)$_2$

trans-[Rh(cyclam)Cl$_2$]Cl (510 mg, 1.24 mmoles) and NaOH (1 pellet, ~2.5 mmoles) were dissolved in 25 ml water and heated under reflux for 4 min. The pale yellow solution was cooled on ice and slightly acidified with dilute $HClO_4$. $NaClO_4 \cdot H_2O$ (10 g, 72 mmoles) was added to precipitate the yellow product (387 mg, 56%), which was washed with ethanol and ether and dried under vacuum for 2 h.

Anal. Calcd. for $[Rh(C_{10}H_{24}N_4)Cl(H_2O)](ClO_4)_2$: C, 21.62; H, 4.72; N, 10.08; Cl, 19.14. Found: C, 21.46; H, 4.35; N, 10.07; Cl, 19.30.

trans-[Rh(cyclam)Br(OH)]ClO$_4$

trans-[Rh(cyclam)Br$_2$]Br (203 mg, 0.374 mmole) and NaOH (1 pellet, ~2.5 mmoles) were dissolved in 15 ml water and heated under reflux for 3 min, during which the solution turned paler yellow. $NaClO_4 \cdot H_2O$ (5.0 g, 36 mmoles) was added to precipitate the pale yellow complex (95 mg, 51%), which was washed with 1:1 ethanol and ether and dried under vacuum.

Anal. Calcd. for $[Rh(C_{10}H_{24}N_4)Br(OH)]ClO_4$: C, 24.04; H, 5.04; N, 11.21; Br, 15.99; Cl, 7.10. Found: C, 24.23; H, 4.94; N, 11.12; Br, 16.04; Cl, 7.08.

trans-[Rh(cyclam)Br(H$_2$O)](ClO$_4$)$_2$

trans-[Rh(cyclam)Br$_2$]Br (214 mg, 0.394 mmole) and NaOH (1 pellet, ~2.5 mmoles) were dissolved in 15 ml water and heated under reflux for 3 min. The yellow solution was cooled and acidified with dilute $HClO_4$. $NaClO_4 \cdot H_2O$ (5.0 g, 36 mmoles) was added to precipitate the pale orange complex (127 mg, 54%), which was washed with 1:1 ethanol and ether and dried under vacuum.

Anal. Calcd. for $[Rh(C_{10}H_{24}N_4)Br(H_2O)](ClO_4)_2$: C, 20.01; H, 4.37; N, 9.34; Br, 13.32; Cl, 11.82. Found: C, 20.42; H, 4.18; N, 9.49; Br, 12.94; Cl, 11.66.

trans-[Rh(cyclam)I(OH)]ClO$_4$

trans-[Rh(cyclam)I$_2$]I (268 mg, 0.392 mmole) and NaOH (1 pellet, ~2.5 mmoles) NaOH were added to 15 ml water and heated under reflux for an additional 5 min. $NaClO_4 \cdot H_2O$ (5.0 g, 36 mmoles) was added to precipitate the orange complex (51 mg, 24%), which was

Can. J. Chem. Downloaded from www.nrcresearchpress.com by 210.87.254.40 on 09/05/12
For personal use only.

washed with 1:1 ethanol and ether and dried under vacuum.

Anal. Calcd. for $[Rh(C_{10}H_{24}N_4)I(OH)]ClO_4$: C, 21.97; H, 4.61; N, 10.25; I, 23.22; Cl, 6.49. Found: C, 22.12; H, 4.49; N, 10.10; I, 23.16; Cl, 6.39.

trans-[Rh(cyclam)I(H₂O)](ClO₄)₂

trans-[Rh(cyclam)I_2]I (292 mg, 0.427 mmole) and NaOH (1 pellet, ~2.5 mmoles) were added to 25 ml water and treated according to the *trans* iodohydroxo preparation. The yellow solution was cooled on ice and slightly acidified with dilute $HClO_4$, which made the solution red. $NaClO_4 \cdot H_2O$ (5.0 g, 36 mmoles) was added to precipitate the red complex (75 mg, 27%), which was washed with 1:1 ethanol and ether and dried under vacuum.

Anal. Calcd. for $[Rh(C_{10}H_{24}N_4)I(H_2O)](ClO_4)_2$: C, 18.56; H, 4.05; N, 8.65; I, 19.61; Cl, 10.96. Found: C, 18.31; H, 4.11; N, 7.99; I, 19.55; Cl, 11.04.

trans-[Rh(cyclam)(N₃)(OH)]ClO₄

trans-[Rh(cyclam)$(N_3)_2$]ClO_4 (203 mg, 0.417 mmole) and NaOH (1 pellet, ~2.5 mmoles) were dissolved in 25 ml water and heated under reflux for 10 min, which made the solution paler yellow. $NaClO_4 \cdot H_2O$ (5.0 g, 36 mmoles) was added to precipitate the pale yellow complex (76 mg, 36%), which was washed with 1:1 ethanol and ether, dried under vacuum, and protected from light.

Anal. Calcd. for $[Rh(C_{10}H_{24}N_4)(N_3)(OH)]ClO_4$: C, 26.01; H, 5.46; N, 21.24. Found: C, 26.17; H, 5.39; N, 20.96.

trans-[Rh(cyclam)(N₃)(H₂O)](ClO₄)₂

trans-[Rh(cyclam)$(N_3)_2$]ClO_4 (233 mg, 0.458 mmole) was treated with NaOH as described for the hydroxo preparation. The yellow solution was cooled on ice and slightly acidified with dilute $HClO_4$. $NaClO_4 \cdot H_2O$ (5.0 g, 36 mmoles) was added to precipitate the yellow complex (140 mg, 54%) which was washed with 1:1 ethanol and ether, dried under vacuum, and protected from light.

Anal. Calcd. for $[Rh(C_{10}H_{24}N_4)(N_3)(H_2O)](ClO_4)_2$: C, 21.36; H, 4.66; N, 17.44. Found: C, 21.45; H, 4.42; N, 17.27.

cis-[Rh(cyclam)(OH)(H₂O)](ClO₄)₂

cis-[Rh(cyclam)Cl_2]Cl (496 mg, 1.21 mmoles) and NaOH (2 pellets, ~5 mmoles) were added to 25 ml water and heated under reflux for 5 min, during which the solution turned paler yellow. $NaClO_4 \cdot H_2O$ (10 g, 72 mmoles) was added and the solution was neutralized with dilute $HClO_4$ to precipitate the very pale yellow product (429 mg, 0.798 mmole, 66%), which was washed with ethanol and ether and dried under vacuum.

Anal. Calcd. for $[Rh(C_{10}H_{24}N_4)(OH)(H_2O)](ClO_4)_2$: C, 22.32; H, 5.24; N, 10.41; Cl, 13.18. Found: C, 22.42; H, 5.15; N, 10.44; Cl, 13.20.

trans-[Rh(cyclam)(OH)(H₂O)](ClO₄)₂

trans-[Rh(cyclam)Cl_2]Cl (698 mg, 1.70 mmoles) and NaOH (5 pellets, ~12 mmoles) were dissolved in 20 ml water and heated under reflux for 100 min during which the solution became very pale yellow. $NaClO_4 \cdot H_2O$ (10 g, 72 mmoles) was added and the solution was neutralized with dilute $HClO_4$. The pale yellow precipitate (610 mg, 67%) was washed with ethanol and ether and dried under vacuum.

Anal. Calcd. for $[Rh(C_{10}H_{24}N_4)(OH)(H_2O)](ClO_4)_2$: C, 22.32; H, 5.24; N, 10.41; Cl, 13.18. Found: C, 22.09; H, 5.19; N, 10.21; Cl, 13.10.

trans-[Rh(cyclam)ClBr]ClO₄

trans-[Rh(cyclam)Cl_2]Cl (218 mg, 0.531 mmole) and NaOH (1 pellet, ~2.5 mmoles) were dissolved in 25 ml water and heated under reflux for 5 min, during which the solution turned paler yellow. Concentrated HBr (10 ml, 87 mmoles) and 10 ml 70% $HClO_4$ were added and the solution was heated at 55 °C for 20 h, during which a yellow precipitate was formed. The product (118 mg, 43%) was recrystallized from water, washed with ethanol and ether, and dried under vacuum.

Anal. Calcd. for $[Rh(C_{10}H_{24}N_4)ClBr]ClO_4$: C, 23.19; H, 4.67; Br, 15.42; Cl, 13.69. Found: C, 23.36; H, 4.70; Br, 15.35; Cl, 13.76.

trans-[Rh(cyclam)ClI]ClO₄

trans-[Rh(cyclam)I_2]I (200 mg, 0.292 mmole) was dissolved in 400 ml 0.1 *M* NaCl and heated at 60 °C in a constant-temperature bath for 2 days. $HClO_4$ (25 ml, 70%) was added to precipitate the complex, which was purified by repeating the procedure. The orange product was washed with ethanol and ether and dried under vacuum.

Anal. Calcd. for $[Rh(C_{10}H_{24}N_4)ClI]ClO_4$: C, 21.26; H, 4.28; I, 22.46; Cl, 12.55. Found: C, 21.55; H, 4.60; I, 22.39; Cl, 12.84.

trans-[Rh(cyclam)Cl(N₃)]ClO₄

trans-[Rh(cyclam)$(N_3)_2$]ClO_4 (232 mg, 0.476 mmole) was added to 50 ml 1.0 *M* HCl and heated at 85 °C for 6 h. $HClO_4$ (5 ml, 70%) was added to precipitate the complex, which was recrystallized from 40 ml water and 2 ml 70% $HClO_4$. The yellow product (140 mg, 61%) was washed with ethanol and ether and dried under vacuum.

Anal. Calcd. for $[Rh(C_{10}H_{24}N_4)Cl(N_3)]ClO_4$: C, 25.10; H, 5.16; N, 20.42; Cl, 14.76. Found: C, 25.15; H, 4.95; N, 20.29; Cl, 14.81.

trans-[Rh(cyclam)Cl(NCS)]ClO₄

trans-[Rh(cyclam)$Cl(H_2O)](ClO_4)_2$ (134 mg, 0.242 mmole) and NaSCN (1.0 g, 12 mmoles) were dissolved in 15 ml water and heated under reflux for 15 min. $NaClO_4 \cdot H_2O$ (5.0 g, 36 mmoles) was added to precipitate the yellow complex (73 mg, 61%), which was washed with ethanol and ether and dried under vacuum.

Anal. Calcd. for $[Rh(C_{10}H_{24}N_4)Cl(NCS)]ClO_4$: C, 26.62; H, 4.88; N, 14.11; Cl, 14.29; S, 6.46. Found: C, 26.56; H, 4.81; N, 13.84; Cl, 14.33; S, 6.46.

trans-[Rh(cyclam)BrI]ClO₄

trans-[Rh(cyclam)I_2]I (280 mg, 0.410 mmole) and NaOH (1 pellet, ~2.5 mmoles) were added to 50 ml water and heated under reflux for 15 min. The yellow solution was filtered, concentrated HBr (4.0 ml, 35 mmoles) was added, and the solution was heated at 70 °C for 5 min. The volume was increased to 500 ml to dissolve the bromide. $HClO_4$ (50 ml, 70%) was added to precipitate the perchlorate. The orange crystals (158 mg, 63%) were

Can. J. Chem. Downloaded from www.nrcresearchpress.com by 210.87.254.40 on 09/05/12
For personal use only.

washed with ethanol and ether and dried under vacuum.

Anal. Calcd. for $[Rh(C_{10}H_{24}N_4)BrI]ClO_4$: C, 19.71; H, 3.97; N, 9.19; Br, 13.11; I, 20.82. Found: C, 19.70; H, 3.80; N, 9.01; Br, 12.90; I, 20.92.

trans-[Rh(cyclam)Br(N_3)]ClO_4

trans-[Rh(cyclam)$(N_3)_2$]ClO_4 (149 mg, 0.306 mmole) was added to 25 ml 1.0 *M* $HClO_4$ and heated under reflux for 5 h. NaBr (2.6 g, 25 mmoles) was added and the yellow solution was heated at 70 °C for 1 h. $HClO_4$ (5 ml, 70%) was added to precipitate the product, which was recrystallized from 25 ml water and 2 ml 70% $HClO_4$. The orange crystals (110 mg, 69%) were washed with ethanol and ether, dried under vacuum, and protected from light.

Anal. Calcd. for $[Rh(C_{10}H_{24}N_4)Br(N_3)]ClO_4$: C, 22.90; H, 4.61; N, 18.69; Br, 15.23; Cl, 6.76. Found: C, 22.76; H, 4.74; N, 18.55; Br, 15.08; Cl, 6.78.

trans-[Rh(cyclam)Br(NCS)]ClO_4

trans-[Rh(cyclam)Br(H_2O)]$(ClO_4)_2$ (214 mg, 0.340 mmole) and NaSCN (1.0 g, 12 mmoles) were dissolved in 15 ml water and heated under reflux for 10 min, which made the solution turn from orange to yellow. $NaClO_4 \cdot H_2O$ (10 g, 72 mmoles) was added to precipitate the yellow complex (144 mg, 78%), which was washed with ethanol and ether and dried under vacuum.

Anal. Calcd. for $[Rh(C_{10}H_{24}N_4)Br(NCS)]ClO_4$: C, 24.64; H, 4.47; N, 12.95; Br, 14.78; Cl, 6.56. Found: C, 24.82; H, 4.39; N, 12.97; Br, 14.59; Cl, 6.70.

trans-[Rh(cyclam)I(N_3)]ClO_4

trans-[Rh(cyclam)I_2]I (306 mg, 0.447 mmole) and NaOH (1 pellet, ~2.5 mmoles) were added to 200 ml water and heated under reflux for 5 min. The yellow solution was filtered and NaN_3 (20 g, 310 mmoles) was added. Then the solution was neutralized with dilute $HClO_4$, during which it turned orange. $HClO_4$ (50 ml, 70%) was added to precipitate the orange product (81 mg, 32%), which was washed with ethanol and ether and dried under vacuum.

Anal. Calcd. for $[Rh(C_{10}H_{24}N_4)I(N_3)]ClO_4$: C, 21.01; H, 4.23; N, 17.15; I, 22.20. Found: C, 21.26; H, 4.21; N, 17.09; I, 22.31.

trans-[Rh(cyclam)I(NCS)]ClO_4

trans-[Rh(cyclam)I(H_2O)]$(ClO_4)_2$ (289 mg, 0.466 mmole) and NaSCN (1.0 g, 12 mmoles) were dissolved in 25 ml water and heated under reflux for 15 min, which made the solution turn from red to orange. $NaClO_4 \cdot H_2O$ (10 g, 72 mmoles) was added to precipitate the pale orange complex (227 mg, 87%), which was washed with ethanol and ether and dried under vacuum.

Anal. Calcd. for $[Rh(C_{10}H_{24}N_4)I(NCS)]ClO_4$: C, 22.48; H, 4.12; N, 11.92; I, 21.59; Cl, 6.03. Found: C, 22.60; H, 4.03; N, 11.95; I, 21.74; Cl, 5.94.

trans-[Rh(cyclam)(N_3)(NCS)]ClO_4

trans-[Rh(cyclam)$(N_3)(H_2O)$]$(ClO_4)_2$ (243 mg, 0.432 mmole) and NaSCN (1.0 g, 12 mmoles) were dissolved in 20 ml water and heated at 70 °C for 75 min, during which the solution remained yellow. $NaClO_4 \cdot H_2O$ (10 g, 72 mmoles) was added to precipitate the yellow complex (142 mg, 64%), which was washed with ethanol and ether and dried under vacuum.

Anal. Calcd. for $[Rh(C_{10}H_{24}N_4)(N_3)(NCS)]ClO_4$: C, 25.77; H, 4.72; N, 21.85; S, 6.25. Found: C, 25.97; H, 4.72; N, 21.97; S, 6.27.

Resolution of cis-[Rh(cyclam)Cl_2]Cl

cis-[Rh(cyclam)Cl_2]Cl (500 mg, 1.22 mmoles) and *d*-ammonium α-bromocamphor-π-sulfonate (0.90 g, 2.7 mmoles) were dissolved in 15 ml water and frozen for 1 week. The mixture was melted and filtered. The pale yellow precipitate was washed with a few drops of ice cold water and ground thoroughly with 2 ml of 1:1:1 ethanol, concentrated HCl, and ether. The *l-cis*-[Rh(cyclam)Cl_2]Cl was filtered (149 mg, 60%).

Using a mercury and sodium lamp, the rotation of a 0.58% solution was too small to measure on a Rudolph polarimeter.

The o.r.d. spectrum of a 1.13% solution was recorded and exhibited zero rotation at 353 and 300 mμ, which corresponds to the absorption maxima of the *cis* isomer. There was a positive rotation (0.0007°) at 325 mμ and a negative rotation (0.0007°) at 370 mμ.

$$[\alpha]_{325\ m\mu} = +6°$$
$$[\alpha]_{370\ m\mu} = -6°$$

The authors are grateful to the National Research Council of Canada for financial assistance in the form of Operating Grant No. A2897 (E. J. Bounsall) and a Scholarship (S. R. Koprich). We are also grateful to Dr. Kirschner (Wayne State University, Michigan) for the use of a Cary 60 spectrometer.

1. B. Bosnich, C. K. Poon, and M. L. Tobe. Inorg. Chem. **4**, 1102 (1965).
2. B. Bosnich, M. L. Tobe, and G. A. Webb. Inorg. Chem. **4**, 1109 (1965).
3. J. P. Collman and P. W. Schneider. Inorg. Chem. **5**, 1380 (1966).
4. A. D. Allen and D. R. Pedwell. Private communication.
5. C. K. Poon and M. L. Tobe. J. Chem. Soc. 2069 (1967); 1549 (1968); 2398 (1968).
6. R. D. Gillard and G. Wilkinson. J. Chem. Soc. 3193 (1963).
7. D. A. Buckingham, P. A. Marzilli, and A. M. Sargeson. Inorg. Chem. **6**, 1032 (1967). A. M. Sargeson and G. H. Searle. Inorg. Chem. **6**, 787 (1967).
8. H. G. Hamilton and M. D. Alexander. J. Amer. Chem. Soc. **89**, 5065 (1967).
9. B. Bosnich, R. D. Gillard, E. D. McKenzie, and G. A. Webb. J. Chem. Soc. 1331 (1966).
10. Fred Basolo and R. G. Pearson. Mechanism of inorganic reactions. 2nd ed. John Wiley and Sons, Inc., New York. 1967. p. 161.
11. S. A. Johnson and Fred Basolo. Inorg. Chem. **1**, 925 (1962).
12. F. A. Cotton. Chemical applications of group theory. Interscience Publishers, Inc., New York. 1963. p. 231.
13. E. J. Bounsall. Ph.D. Thesis, Imperial College, University of London, London, England. 1964.
14. E. J. Bounsall and A. J. Poe. J. Chem. Soc. 286 (1966).
15. H. A. Szymanski. Interpreted infrared spectra. Plenum Press, New York. 1964; R. M. Silverstein and G. C. Bassler. Spectrometric identification of

organic compounds. John Wiley and Sons, Inc., New York. 1963; K. NAKANISHI. Infrared absorption spectroscopy. Holden-Day, Inc., San Francisco. 1962; D. M. ADAMS. Metal–ligand and related vibrations. Edward Arnold and Co., London. 1967, and references therein.
16. A. TURCO and C. PECILE. Nature, **191**, 66 (1961).
17. A. SABATINI and I. BERTINI. Inorg. Chem. **4**, 1665 (1965); C. PECILE. Inorg. Chem. **5**, 210 (1966).
18. C. E. SCHAFFER. Abstracts of International Conference on Coordination Chemistry. The Chemical Society, London. 1959. p. 153.
19. C. K. JORGENSEN. Absorption spectra and chemical bonding in complexes. The Pergamon Press, Ltd., Oxford. 1962.
20. R. B. PENLAND, F. J. LANE, and J. V. QUAGLIANO. J. Amer. Chem. Soc. **78**, 887 (1956).
21. R. G. PEARSON. J. Amer. Chem. Soc. **85**, 3533 (1963).
22. S. ARHLAND, J. CHATT, and R. R. DAVIES. Quart. Rev. London, **12**, 265 (1958).
23. D. M. ADAMS, J. CHATT, J. GERRATT, and A. D. WESTLAND. J. Chem. Soc. 734 (1964).
24. K. NAKAMOTO, P. J. MCCARTHY, J. FUJITA, R. A. CONDRATE, and G. T. BEHNKE. Inorg. Chem. **4**, 36 (1965).
25. D. B. POWELL. J. Chem. Soc. 4495 (1956).
26. J. CHATT and B. L. SHAW. J. Chem. Soc. 5075 (1962).
27. C. K. INGOLD, R. S. NYHOLM, and M. L. TOBE. Nature, **187**, 477 (1960).
28. J. STETTER and K. H. MAYER. Chem. Ber. **94**, 1410 (1961).
29. N. F. CURTIS. J. Chem. Soc. 2644 (1964).
30. R. D. GILLARD, J. A. OSBORN, and G. WILKINSON. J. Chem. Soc. 1951 (1965); R. D. GILLARD, E. D. MCKENZIE, and M. D. ROSS. J. Inorg. Nucl. Chem. **28**, 1429 (1966).
31. J. VAN ALPHEN. Rec. Trav. Chim. **55**, 835 (1936).

Can. J. Chem. Downloaded from www.nrcresearchpress.com by 210.87.254.40 on 09/05/12
For personal use only.

Free-radical reaction of cyanogen bromide with alkanes

DENNIS D. TANNER, G. LYCAN, AND N. J. BUNCE[1]
Department of Chemistry, University of Alberta, Edmonton, Alberta
Received September 15, 1969

The photolysis of cyanogen bromide with cyclohexane yielded cyclohexyl bromide, hydrogen cyanide, and small amounts of cyanogen, while the benzoyl-peroxide-promoted reactions of cyanogen bromide with various alkanes yielded approximately equal amounts of alkyl bromides and alkyl cyanides, often in high yields. Both hydrogen cyanide and hydrogen bromide were shown to react with benzoyl peroxide and an added hydrocarbon to yield the corresponding alkyl cyanide and alkyl bromide. Possible reaction mechanisms for these reactions are discussed.

Canadian Journal of Chemistry, 48, 1492 (1970)

Can. J. Chem. Downloaded from www.nrcresearchpress.com by 210.87.254.42 on 09/05/12
For personal use only.

Introduction

In a recent paper (1) we reported the results of some studies of the free-radical cyanation of alkanes by cyanogen chloride. The mechanism of the reaction was shown to be the reversible sequence shown in Scheme 1

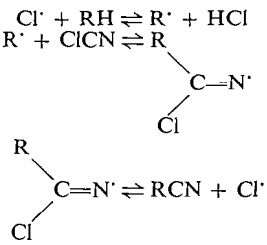

SCHEME 1

As a preparative method for nitriles, however, the following difficulties were encountered. Photochemical initiation of the reaction gave only low yields of cyanides, for the products are themselves sensitive to the short wavelength light necessary to excite cyanogen chloride and initiate the reaction. When benzoyl peroxide was used as a free-radical chain initiator, mixtures of alkyl cyanides and alkyl chlorides were produced; the chlorides were subsequently shown to arise through the oxidation by benzoyl peroxide of the hydrogen chloride formed by hydrogen abstraction (2). This side reaction makes the isolation of the desired alkyl cyanides difficult on a preparative scale.

Müller and Huber (3), however, have reported that cyanogen bromide may also be used as a reagent for free radical cyanation. Their report gives no details about the reaction except that it may be photoinitiated. We decided therefore to investigate the reaction of cyanogen bromide with alkanes, both to study the mechanism of the reaction, and in the hope that it would lead to a preparative method for alkyl cyanides superior to that of using cyanogen chloride.

[1]Killam Memorial Postdoctoral Fellow, 1967–1969.

Results and Discussion

Our first experiments were an attempt to reproduce the conditions used for cyanation by Müller and Huber (3). The photolyses were conducted in quartz equipment using a full mercury arc to excite the absorption of cyanogen bromide (λ_{max}, 229 mμ). In our hands, however, the reaction between cyanogen bromide and cyclohexane failed to yield any cyclohexyl cyanide, but gave cyclohexyl bromide instead. Among the gaseous products were found hydrogen cyanide and small quantities of cyanogen, but much cyanogen bromide remained unreacted even after a prolonged irradiation.

The reaction between cyanogen bromide and cyclohexane was repeated, using benzoyl peroxide as a free-radical initiator. Preliminary experiments indicated the formation of both alkyl bromides and alkyl cyanides in comparable amounts, together with considerable quantities of benzoic acid. Initiation of the reaction with catalytic quantities of benzoyl peroxide allowed the chain length of the reaction to be determined; for cyclohexane the chain length was very short, approximately 2. A series of reactions using ratios of benzoyl peroxide to cyanogen bromide in the range 0–4.5 indicated that at high initial concentrations of benzoyl peroxide, very good yields (>80%) of both alkyl bromides and alkyl cyanides could be obtained. At all initiator concentrations, approximately equal quantities of the bromide and the cyanide were produced (see Fig. 1).

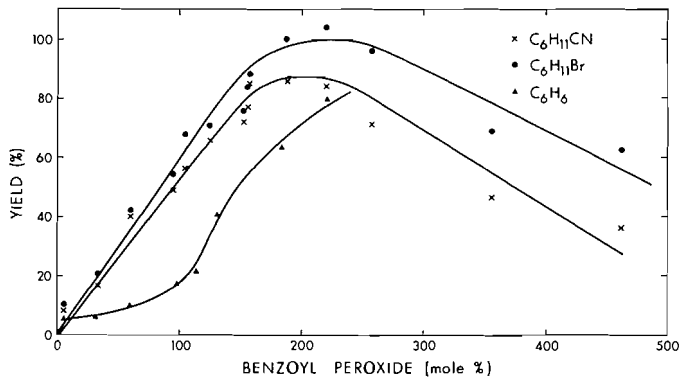

FIG. 1. The reaction between benzoyl peroxide, cyanogen bromide, and cyclohexane at 95 °C.

Very similar results were obtained when 2,3-dimethylbutane was the substrate, and once again approximately equal quantities of alkyl bromides and alkyl cyanides were produced. Of the possible isomeric bromides and cyanides, those produced as a result of abstraction of tertiary hydrogen atoms were formed almost exclusively, suggesting that a very selective radical was involved in the hydrogen abstraction step. The yields of alkyl bromides and alkyl cyanides formed under optimum conditions from various hydrocarbon substrates are collected in Table 1.

Although the data in Table 1 shows that *n*-butane gives rise to both possible isomeric bromides and cyanides, it is not possible to obtain meaningful selectivity data concerning the radical involved in hydrogen abstraction in this reaction. This is because the short chain length of the reaction necessitates having such large quantities of initiator that abstraction by radicals derived from the initiator contributes significantly to the total abstraction. This suggestion was validated by the observation that appreciable amounts of benzene (see Fig. 1) and traces of bromobenzene were formed under the reaction conditions necessary for high conversion of cyanogen bromide to products.

Mechanism of the Reaction

The reaction of cyanogen chloride with alkanes in the presence of benzoyl peroxide (1) takes the overall course shown in Scheme 2 (X = Cl).

$$RH + XCN \rightarrow RCN + HX$$

$$RH + HX + (PhCO_2)_2 \rightarrow 2PhCO_2H + RX$$

SCHEME 2

The evidence for this scheme was that photoinitiation of the reaction gave only alkyl cyanides

TABLE 1

Reaction of cyanogen bromide with alkanes at 95 °C in the presence of benzoyl peroxide

BrCN (*M*)	Benzoyl peroxide (Mole %)*	Substrate	Products (%)†
0.29	190	Cyclohexane	Cyclohexyl cyanide (86) Cyclohexyl bromide (100)
0.35	210	*n*-Butane	1-Cyanobutane (2) 2-Cyanobutane (50) 1-Bromobutane (2) 2-Bromobutane (58)
0.27	290	2,3-Dimethylbutane	2-Bromo-2,3-dimethylbutane (75) 1-Bromo-2,3-dimethylbutane (4) 2-Cyano-2,3-dimethylbutane (92)
0.79	80	Toluene	Benzyl bromide (12) Benzyl cyanide (3)

*Benzoyl peroxide necessary to produce optimum yields of products.
†Based upon initial moles BrCN.

Can. J. Chem. Downloaded from www.nrcresearchpress.com by 210.87.254.42 on 09/05/12
For personal use only.

Can. J. Chem. Downloaded from www.nrcresearchpress.com by 210.87.254.42 on 09/05/12
For personal use only.

and that hydrogen chloride may be oxidized quantitatively to alkyl chlorides in the presence of benzoyl peroxide and an alkane. With cyanogen bromide, however, the photoreaction gives alkyl bromide rather than the cyanide, and so a second overall mechanism must be considered (Scheme 3).

$$RH + XCN \rightarrow RX + HCN$$

$$HCN + RH + (PhCO_2)_2 \rightarrow 2PhCO_2H + RCN$$

SCHEME 3

Because of the divergence between the observed behavior of cyanogen chloride and cyanogen bromide with alkanes, it was decided to investigate the mechanism of the reaction of the latter reagent in more detail.

In an attempt to distinguish between the alternative reaction schemes 2 and 3, hydrogen bromide and hydrogen cyanide were each allowed to interact with benzoyl peroxide and cyclohexane under the conditions used for the reaction of cyanogen bromide. In the case of hydrogen bromide, a quantitative yield of cyclohexyl bromide was obtained, together with 2 moles of benzoic acid per mole of cyclohexyl bromide. It is presumed that this oxidation follows a course analogous to that recently proposed for the corresponding reaction of hydrogen chloride (2)

[1] $HBr + (PhCO_2)_2 \rightarrow PhCO_2H + PhCO_2Br$

[2] $HBr + PhCO_2Br \rightarrow Br_2 + PhCO_2H$

[3] $R^{\cdot} + Br_2 \rightarrow RBr + Br^{\cdot}$

[4] $Br^{\cdot} + RH \rightarrow R^{\cdot} + HBr$

When hydrogen cyanide was oxidized by benzoyl peroxide under similar conditions, either in pure cyclohexane or with acetonitrile as cosolvent, cyclohexyl cyanide was produced, but in no case was the yield ($<20\%$) as great as that obtainable with cyanogen bromide. The limited success of this oxidation reaction suggests a similar intermediate to that formed in the oxidation of the halogen acids, namely, an acyl cyanate

[5] $HCN + (PhCO_2)_2 \rightarrow PhCO_2H + PhCO_2CN$

[6] $R^{\cdot} + PhCO_2CN \rightarrow RCN + PhCO_2^{\cdot}$

Reaction [6] is suggested by analogy with the displacement of an alkyl radical on cyanogen chloride (Scheme 1), while the isolation of benzonitrile and cyclohexyl cyanide from reactions of hydrogen cyanide, benzoyl peroxide, and cyclohexane supports the feasibility of this reaction. Although we have also found that hydrogen bromide reacts rapidly and completely with cyanogen bromide (reaction [7])

[7] $HBr + BrCN \rightarrow Br_2 + HCN$

this cannot be a very important pathway in the reaction of cyanogen bromide, benzoyl peroxide, and cyclohexane because of the demonstrated inefficiency of the oxidation of the hydrogen cyanide produced in the reaction. This would not give the observed high yields of alkyl cyanides. The failure to obtain high yields of alkyl cyanides from these reactions eliminates Scheme 3 as a major pathway for the benzoyl-peroxide-promoted reaction of cyanogen bromide with alkanes. However, the fact that photochemical initiation of the reaction gives alkyl bromide rather than alkyl cyanide equally excludes Scheme 2.

To try to resolve this difficulty, the reaction between cyanogen bromide and cyclohexane was studied in the presence of another initiator, phenylazotriphenylmethane, to determine whether, in the absence of an oxidizing initiator, alkyl bromide or alkyl cyanide would form. Unexpectedly, the reaction with cyclohexane gave no products that were not directly derived from the initiator; namely, nitrogen, triphenylmethane, tetraphenylmethane, and benzene. None of these products appears to involve cyanogen bromide at all.

On the basis of this evidence and considering the extreme inefficiency of the photochemical bromination, it seems questionable whether cyanogen bromide itself undergoes any free-radical chain reaction with alkanes. Since cyanation reactions are observed only in the presence of benzoyl peroxide, the possibility that benzoyl peroxide reacts directly with cyanogen bromide was investigated. This proposal involves benzoyl peroxide as a reactant, rather than merely as a free-radical initiator.

Cyanogen bromide and benzoyl peroxide were therefore allowed to interact in cyclohexane solution at 60 °C. If, for example, reaction [8] occurred, it was hoped that the products would be trapped by addition to cyclohexene (2).

[8] $BrCN + (PhCO_2)_2 \rightarrow PhCO_2Br + PhCO_2CN$

At 60 °C, the thermal decomposition of benzoyl peroxide is relatively slow, and neither benzoyl

Can. J. Chem. Downloaded from www.nrcresearchpress.com by 210.87.254.42 on 09/05/12
For personal use only.

peroxide nor cyanogen bromide reacts with the solvent. It was found that after 1 h at 60 °C, almost all the initial quantity of benzoyl peroxide could be recovered from the reaction mixture. A similar result was obtained when acetic acid was added as a possible acid catalyst for the reaction. These experiments indicate that if an (ionic) reaction between benzoyl peroxide and cyanogen bromide occurs, it must have an activation energy comparable with that for the thermal decomposition of benzoyl peroxide.

Control experiments show that only traces of benzoic acid are produced when benzoyl peroxide is decomposed in a hydrocarbon solvent. Bearing in mind the high yield of benzoic acid obtained in the reaction between cyanogen bromide, benzoyl peroxide, and an alkane, the intermediary of an acyl hypobromite and/or acyl hypocyanite can be speculatively proposed as intermediate in this reaction. Unfortunately, at this time no detailed mechanism for this reaction can be given until further work is completed.

In the photoreaction of cyanogen bromide with cyclohexane, hydrogen cyanide is a major product. However, knowing that reaction [7] is a favorable reaction, we propose that, rather than the reaction sequence [9]–[11]

$$\text{[9]} \qquad \text{BrCN} \xrightarrow{h\nu} \text{Br}^{\cdot} + \text{CN}^{\cdot}$$

$$\text{[10]} \qquad \text{CN}^{\cdot} + \text{RH} \rightarrow \text{HCN} + \text{R}^{\cdot}$$

$$\text{[11]} \qquad \text{R}^{\cdot} + \text{BrCN} \rightarrow \text{RBr} + \text{CN}^{\cdot}$$

being the mechanism of photobromination by cyanogen bromide, the sequence seen in Scheme 4 is more likely to represent the reaction mechanism.

$$\text{BrCN} \xrightarrow{h\nu} \text{Br}^{\cdot} + \text{CN}^{\cdot}$$

$$\text{Br}^{\cdot} + \text{RH} \rightarrow \text{HBr} + \text{R}^{\cdot}$$

$$\text{HBr} + \text{BrCN} \rightarrow \text{Br}_2 + \text{HCN}$$

$$\text{R}^{\cdot} + \text{Br}_2 \rightarrow \text{RBr} + \text{Br}^{\cdot}$$

$$2\text{CN}^{\cdot} \rightarrow \text{C}_2\text{N}_2$$

SCHEME 4

This is compatible with the observation that the phenylazotriphenylmethane-initiated reaction of cyanogen bromide with cyclohexane gives no products derived from cyanogen bromide, indicating that an alkyl radical is capable of displacing neither the cyano nor the bromine moiety of cyanogen bromide.[2]

Bromination has previously been found to follow a similar course when N-bromosuccinimide is the brominating agent (5). The participation of reaction [7] represents another divergence from the chemistry of cyanogen chloride, in which the analogous process is not observed. This is, however, in keeping with the fact that whereas cyanogen chloride is a positive cyano-compound and does not react with potassium iodide solutions, cyanogen bromide is a positive halogen compound and can be estimated iodometrically (6).

Experimental

Materials

The hydrocarbons cyclohexane, 2,3-dimethylbutane, and *n*-butane were Phillips research grade and were used as supplied. Toluene (Fisher Scientific Co.) and acetonitrile (J. T. Baker Chemical Co.) were distilled from phosphoric oxide. Cyanogen bromide was supplied by Eastman Kodak or, alternatively, was prepared by the action of bromine on aqueous sodium cyanide solution (7). Hydrogen cyanide was prepared by the action of sulfuric acid on sodium cyanide, and dried by passing it through a column of granular calcium chloride. Benzoyl peroxide (Fisher Scientific Co.) was used as supplied (assay by iodometric titration >98%).

Procedures and Analytical

Solutions of hydrogen bromide and hydrogen cyanide were estimated by titration with standard base; cyanogen bromide was analyzed iodometrically (6). Experimental procedures have been described previously (1). Gas–liquid phase chromatographic (g.l.p.c.) analyses were carried out using an Aerograph Model 1520 instrument, equipped with 10 ft × 1/4 in. stainless steel columns, and a suitable stationary phase supported on acid-washed 60/80 Chromosorb W. Quantitative g.l.p.c. analyses were carried out in the usual manner (2). In this work, all g.l.p.c. analyses were carried out with temperature programing, usually from 50 to 200 °C. Gas chromatography in conjunction with mass spectrometry (g.c./m.s.) has been described previously (2). Products were isolated from the reaction mixtures by preparative g.l.p.c. and were identified by comparison of their infrared (i.r.) and nuclear magnetic resonance (n.m.r.) spectra with those of authentic samples, wherever possible.

---

[2]Bond energy calculations (ref. 4; see also ref. 1) suggest that displacement on cyanogen bromide to give alkyl bromide should be endothermic by about 4 kcal/mole for cyclohexane, whereas alkyl cyanide formation should be highly exothermic ($\Delta H \approx -30$ kcal/mole). However, in the case of the attack of an alkyl radical on cyanogen chloride (Scheme 1), it was deduced (1) that the activation energy for this process must be quite high. Similar reasoning would explain the inability of an alkyl radical and cyanogen bromide to produce alkyl cyanide.

TABLE 2

Reaction of cyanogen bromide with 2,3-dimethylbutane and benzoyl peroxide at 95 °C

BrCN (M)	Benzoyl peroxide (mole %)	(%)	(%)	(%)
0.31	3	1.0	—	2.2
0.31	3	0.9	—	2.4
0.31	10	3.2	—	6.6
0.31	17	4.8	—	9.0
0.31	48	13.6	—	28.6
0.31	95	24.8	0.5	42.4
0.31	95	27.0	0.7	40.4
0.27	158	55.4	2.2	63.9
0.27	166	51.6	2.1	62.0
0.27	219	63.8	—	77.4
0.27	223	50.1	2.2	59.3
0.27	276	72.3	3.2	84.8
0.27	285	74.5	3.9	91.8

Reaction of Cyanogen Bromide with Cyclohexane

A solution of cyanogen bromide (0.62 M) in cyclohexane (6 ml) was irradiated in a quartz ampoule for 17 h. The gaseous products of the reaction (38.3 ml at 294 °K, 221 mm) were vacuum transferred out of the solution, which was maintained at −41 °C with an acetonitrile slush bath. Mass spectral examination of this fraction showed it to be mainly hydrogen cyanide (exact mass, 27.0109; found, 27.0107) with a smaller quantity of cyanogen (exact mass, 52.0062; found, 52.0061). Gas–liquid phase chromatographic analysis of the residual liquid (10% SE30) showed that cyclohexyl bromide (11%) was present. It was identified by g.l.p.c. retention time and comparison of the i.r. spectrum of an isolated sample with that of authentic material. Repetition of the reaction using a 0.42 M solution of cyanogen bromide in cyclohexane (10 ml) gave the same gaseous products, together with cyclohexyl bromide (7%) and unreacted cyanogen bromide (81%). Photosensitization with benzene or benzophenone likewise gave low yields of cyclohexyl bromide as the only liquid product.

A solution of cyanogen bromide (0.24 M) in cyclohexane (10 ml) with benzoyl peroxide (0.27 mmole) was heated to 75 °C for 50 h. After the reaction, cyanogen bromide (0.18 M) remained. Gas–liquid phase chromatographic analysis showed that cyclohexyl bromide (12%) and cyclohexyl cyanide (8%) had been produced. Isolated samples of these compounds were identified by i.r. and n.m.r. spectra.

In a preparative-scale reaction, cyanogen bromide (3.46 mmoles), benzoyl peroxide (4.00 mmoles), and cyclohexane (20 ml) were heated to 95 °C for 18 h. A similar analytical procedure gave cyclohexyl bromide (84%) and cyclohexyl cyanide (81%; both yields were determined by g.l.p.c.), and samples of the products were isolated and identified spectroscopically. The reaction mixture could be extracted with a solution of sodium bicarbonate, and upon acidification, benzoic acid (5.74 mmoles) was isolated by filtration.

Solutions (5 ml) of cyanogen bromide (0.17 M or 0.29 M) in cyclohexane with quantities of benzoyl peroxide in the range 4–460 mole % were heated to 95 °C for 2½ h. The products, cyclohexyl bromide and cyclohexyl cyanide, were quantitated by g.l.p.c., and the results are plotted in Fig. 1.

Reaction of Cyanogen Bromide with 2,3-Dimethylbutane

Solutions of cyanogen bromide in 2,3-dimethylbutane (5 ml) with varying quantities of benzoyl peroxide were heated to 95 °C for 4½ h. G.l.p.c. analysis (5% Ucon polar 50 HB 2000) indicated the presence of both isomeric bromo-2,3-dimethylbutanes, and of 2-cyano-2,3-dimethylbutane, in the yields indicated in Table 2. Samples of the major products (2-substituted-2,3-dimethylbutanes) were isolated by preparative g.l.p.c. and identified spectroscopically.

Reaction of Cyanogen Bromide with n-Butane

Mixtures of cyanogen bromide, *n*-butane (4 ml), and benzoyl peroxide in thick-walled ampoules were heated to 76 °C for 17 h. An analytical procedure similar to that above gave the isomeric bromobutanes and cyanobutanes in the quantities indicated by Table 3. Samples of the major components were isolated and identified spectroscopically.

Reaction of Cyanogen Bromide with Toluene

A solution of cyanogen bromide (0.88 M) in toluene (10 ml) was irradiated at 0 °C in a quartz ampoule for 17 h. After the reaction, cyanogen bromide (0.50 M) remained. The reaction mixture was examined by g.l.p.c. (10% neopentylglycol succinate); benzyl bromide (0.21 M) was present; a sample was isolated and identified by i.r.

A solution of cyanogen bromide (0.88 M) in toluene (10 ml) with benzoyl peroxide (0.30 mmole) was heated to 75 °C for 55 h. After the reaction cyanogen bromide (0.74 M) remained. Gas–liquid phase chromatographic analysis as above indicated that benzyl bromide (0.081 M) and benzyl cyanide (0.019 M) were present; samples were isolated and identified by i.r.

At high concentrations of benzoyl peroxide, large amounts of the decomposition products of benzoyl peroxide were formed, and, in particular, 2-methylbiphenyl could not be separated from benzyl cyanide on any column used. In a typical experiment, cyanogen bromide

Can. J. Chem. Downloaded from www.nrcresearchpress.com by 210.87.254.42 on 09/05/12
For personal use only.

TABLE 3

Reaction of cyanogen bromide with *n*-butane and benzoyl peroxide at 76 °C

BrCN (mmole)	Benzoyl peroxide (mmole)	Br (%)	Br (%)	CN (%)	CN (%)
1.42	3.18	58	1.7	50	1.8
1.93	3.20	31	1.0	24	1.0
2.14	3.18	34	1.2	30	0.8
2.60	4.10	31	2.5	22	1.4

(0.79 *M*) in toluene (5 ml) and benzoyl peroxide (3.14 mmoles) were heated to 95 °C for 19 h. The reaction mixture was maintained at −15 °C (ice–salt mixture) and the gaseous products were vacuum transferred and examined by i.r. Carbon dioxide (2.14 mmoles) was present, but neither cyanogen nor hydrogen cyanide was detected. Gas–liquid phase chromatographic analysis of the involatile material showed that benzyl bromide (12%) was present. A sample of the mixture of benzyl cyanide and 2-methylbiphenyl was isolated, and was shown by n.m.r. to be 37% benzyl cyanide (3% of initial BrCN).

Oxidation of Hydrogen Bromide

A solution of anhydrous hydrogen bromide (0.26 *M*) in cyclohexane (10 ml) was heated to 95 °C for 10 h in the presence of benzoyl peroxide (3.99 mmoles). Gas–liquid phase chromatographic analysis (SE30) indicated the formation of cyclohexyl bromide (0.28 *M*), while base extraction of the reaction mixture followed by re-acidification gave benzoic acid (4.99 mmoles), m.p. 119–120 °C.

Oxidation of Hydrogen Cyanide

Measured volumes of hydrogen cyanide (0.865, 2.11 mmoles) were condensed onto mixtures of cyclohexane (5 ml) and benzoyl peroxide (2.97, 2.90 mmoles). The mixtures were sealed in degassed ampoules and heated to 92 °C for 16 h. Analysis by g.l.p.c. showed that cyclohexyl cyanide (0.13, 0.22 mmole) was the only product. A sample was isolated for identification, and checked by g.c./m.s.

Solutions of hydrogen cyanide (0.24 *M*) in acetonitrile (10 ml) with cyclohexane (4 ml) and benzoyl peroxide were heated to 75 °C for 10 h. Cyclohexyl cyanide was formed; the amounts are shown in Table 4. In some, but not all, of the reactions carried out in acetonitrile, benzonitrile was also a product. Its yield was variable, but always less than that of cyclohexyl cyanide.

Preparation of Phenylazotriphenylmethane

This compound was prepared from triphenylmethyl chloride by the method of Cohen and Wang (8), with the modification that the intermediate hydrazocompound was oxidized with 30% hydrogen peroxide, rather than with nitrous fumes.

TABLE 4

Reaction of hydrogen cyanide with benzoyl peroxide in acetonitrile at 75 °C*

Benzoyl peroxide (mmole)	Cyclohexyl cyanide (mmole)
2.69	0.16
2.72	0.13
4.05	0.24
4.05	0.24

*Hydrogen cyanide 0.40 *M*, 2.11 mmoles.

Phenylazotriphenylmethane-initiated Reaction of Cyanogen Bromide with Cyclohexane

Solutions of cyanogen bromide (0.28 *M*) in cyclohexane (5 ml) with phenylazotriphenylmethane (0.766, 0.669 g) were heated to 77 °C for 4 h. The reaction mixtures were analyzed by g.l.p.c. (5% Carbowax 20 M) and were found to contain benzene, triphenylmethane, and tetraphenylmethane as the only volatile products other than nitrogen. Neither cyclohexyl bromide nor cyclohexyl cyanide was produced. The identities of the products were ascertained by g.c./m.s.

Interaction of Cyanogen Bromide, Benzoyl Peroxide, and Cyclohexene

A mixture of benzoyl peroxide (2.5 g), cyanogen bromide (1.15 g), and cyclohexene (30 ml) was stirred at 60 °C for 1 h. The reaction mixture was cooled, and the precipitated white crystals (2.1 g) were collected (m.p. 105.5–106 °C with evolution of gas). The reaction was repeated on twice the scale in the presence of acetic acid (0.05 ml); benzoyl peroxide (4.50 g, m.p. 105–106 °C) was recovered.

Interaction of Hydrogen Bromide and Cyanogen Bromide

A solution of cyanogen bromide in benzene (0.19 *M*) was saturated with anhydrous hydrogen bromide (0.31 *M*). The solution immediately turned reddish brown, and ultraviolet (u.v.) analysis showed that bromine (λ_{max}, 412 mμ) had been formed quantitatively.

The authors wish to thank the University of Alberta and the National Research Council of Canada for financial support of this work.

1. D. D. TANNER and N. J. BUNCE. J. Amer. Chem. Soc. **91**, 3028 (1969).
2. N. J. BUNCE and D. D. TANNER. J. Amer. Chem. Soc. In press.
3. E. MÜLLER and H. HUBER. German Patent 1,129,157; C. A. **57**, 13627g (1962).
4. G. GLOCKE. J. Phys. Chem. **63**, 828 (1959).
5. C. WALLING, A. L. RIEGER, and D. D. TANNER. J. Amer. Chem. Soc. **85**, 3129 (1963) and references cited therein.
6. V. MIGRDICHIAN. The chemistry of organic cyanogen compounds. Reinhold Publ. Corp., New York. 1947. p. 113.
7. W. W. HARTMAN and E. E. DREGER. Org. Syn. Collect. Vol. **2**, 150 (1943).
8. S. G. COHEN and C. H. WANG. J. Amer. Chem. Soc. **75**, 5504 (1953).

Can. J. Chem. Downloaded from www.nrcresearchpress.com by 210.87.254.42 on 09/05/12
For personal use only.

Can. J. Chem. Downloaded from www.nrcresearchpress.com by 210.87.254.105 on 09/05/12
For personal use only.

Kinetic laws for solid-supported enzymes

P. V. SUNDARAM, A. TWEEDALE,[1] AND K. J. LAIDLER
Department of Chemistry, University of Ottawa, Ottawa, Canada

Received November 24, 1969

Enzymes behave differently when attached to solid supports for four main reasons: (*1*) their conformations when they are supported may differ from those in free solution, (*2*) they act upon substrates in a different environment, (*3*) there will be partitioning of substrate between the support and the free solution, and (*4*) there will be effects due to diffusion of the substrate in the support. The present paper examines effects (*3*) and (*4*) and shows how rates will vary with substrate concentration. If factors (*1*) and (*2*) do not enter, rates in the limit of high substrate concentrations will be the same for the supported enzyme as in free solution. At low substrate concentrations, rates will be less for the supported enzyme if the substrate is less soluble in the support than in free solution, and the apparent Michaelis constant, K_m(app.), will be greater; conversely, for higher solubility in the support, rates will be greater and K_m(app.) smaller. Effect (*4*) leads to lower rates and higher K_m(app.) values, except in the limit of high substrate concentrations. At a sufficiently low thickness of the support, depending upon the activity of the enzyme, the kinetic behavior becomes identical with that in free solution.

Canadian Journal of Chemistry, **48**, 1498 (1970)

Introduction

During recent years there has been considerable interest in the kinetic behavior of enzymes which are not in free solution but are attached to solid supports (1–4). Aside from certain practical applications, studies of these systems are of importance in leading to an understanding of the *in vivo* behavior of enzymes, where they are attached to membranes and other supporting materials. It is of importance to develop theoretical treatments of the way in which such supports affect the kinetics.

There are four main reasons why an enzyme may behave differently when supported than when present in free solution:

(*1*) The enzyme may be conformationally different. Kinetic behavior depends very critically on enzyme conformation, certain changes leading to a complete loss of activity.

(*2*) In the support, the interaction between the enzyme and the substrate takes place in a different environment from that existing in free solution. Studies of enzyme reactions in different solvents have shown that environmental effects can be very profound (5–7). Some of these effects have been explained satisfactorily (8) in terms of the influence of the dielectric constant of the medium on the electrostatic interactions; such explanations are, however, undoubtedly too simple.

(*3*) There will be partitioning of the substrate between the support and the free solution, so that the substrate concentration in the neighborhood of the enzyme may be different from what it is in free solution. For example, a relatively non-polar substrate will be more soluble in a support which contains a number of non-polar groups than in aqueous solution. In addition, profound effects may arise if both the substrate and the support are electrically charged; this particular situation has been considered in some detail by Goldstein, Levin, and Katchalski (9).

(*4*) The reaction in the solid support may be to some extent diffusion-controlled. In homogeneous aqueous solution even the fastest of enzyme-catalyzed reactions are usually not diffusion-controlled, but this is no longer the case when the substrate has to diffuse towards the enzyme through the solid support. Only in the case of an exceedingly slow enzyme reaction or a sufficiently thin membrane will the reaction be other than diffusion-controlled.

Little information is at present available about factors *1* and *2* for solid-supported enzymes. The kinetic effects of partitioning of substrate between support and solution have been considered by Katchalski and co-workers (9), but only for the case of electrostatic interactions. These workers have also given a treatment of the diffusion problem in a number of special cases; they did not, however, consider the limiting behavior at high substrate concentrations.

The present paper is concerned with the theory of the overall kinetics obtained with an enzyme-containing membrane with a substrate solution at each surface. To a good approximation this treatment will also apply to disks suspended in the substrate solution, provided that the diameter

[1]Present address: Computing Centre, University of Victoria, Victoria, British Columbia.

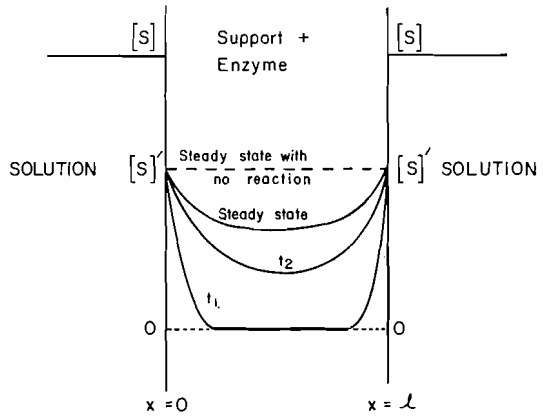

FIG. 1. Schematic representation of the variations in substrate concentration when an enzyme-containing support, of thickness l, is immersed in a substrate solution of concentration [S].

is large compared with the thickness. Computer solutions are given for special cases which illustrate some important general principles. Explicit solutions are given for the limiting behavior at low and high substrate concentrations.

Once the partitioning and diffusional situations are properly understood for a given enzyme system, the way will be open for an understanding of factors *1* and *2*, and ultimately to an understanding of the factors influencing enzyme behavior in the living cell.

Theoretical

The variation of substrate concentration through an enzyme-containing support is shown schematically in Fig. 1. The substrate concentration in the free solution is [S]; the ratio [S]′/[S] is the partition coefficient P for the substrate between the two phases. After a short period of time t_1, the concentration will fall sharply to zero close to each interface; after a longer period of time, the variation may be as shown by the curve marked t_2. Eventually a steady state will be reached. If no reaction were occurring, the steady state would correspond to a horizontal line, and this situation is approached if the enzyme is extremely inactive or the membrane very thin.

Attainment of the Steady State

We consider first the time it takes for steady state to be essentially established. An exact solution of the pre-steady-state diffusion equations, for the case in which reaction is occurring as well as diffusion, does not seem to be possible. A reasonably reliable estimate of the time for the establishment of equilibrium will, however, be given by a treatment in which only diffusion is occurring. The non-steady-state solution (10) for the system represented in Fig. 1 is that the concentration s of substrate within the membrane varies with distance from the surface x and the time t according to the equation

$$[1] \quad s = [S]'\left[1 - \frac{2}{\pi}\sum_{n=1}^{\infty}\frac{1-\cos n\pi}{n} \times \sin\left(\frac{n\pi x}{l}\right)\exp\left(-\frac{Dn^2\pi^2 t}{l^2}\right)\right]$$

where D is the diffusion constant. At the larger t values at which the steady state is more or less established, the leading term, with $n = 1$, will be most important, so that approximately

$$[2] \quad s = [S]'\left[1 - \frac{4}{\pi}\sin\left(\frac{\pi x}{l}\right)\exp\left(-\frac{D^2\pi^2 t}{l^2}\right)\right]$$

where l is membrane thickness. In order to have an arbitrary criterion for the establishment of the steady state, we ask at what time, at $x = l/2$, does the concentration s differ by 10% from the steady-state value [S]′. This time τ is defined by

$$[3] \quad \frac{4}{\pi}\exp\left(\frac{D\pi^2\tau}{l^2}\right) = \frac{9}{10}$$

which reduces to

$$[4] \quad \tau = 0.257\frac{l^2}{D}$$

A typical value of D for a low-molecular-weight substrate is 3×10^{-6} cm^2 s^{-1}, whence

$$[5] \quad \tau = 8.5 \times 10^4 l^2 \text{ s}$$

If the membrane is 1 cm thick, the time to come within 10% of steady-state conditions is thus of the order of 10^5 s, or $\sim$ 28 h. For a membrane 1 mm thick, the time required is 10^3 s, or $\sim$ 17 min.

When chemical reaction is occurring as well, the times will not be as great, since the steady-state concentrations that are attained in the membrane are not so high. It seems safe to conclude that under ordinary circumstances, with membranes less than 1 mm thick, steady state will be essentially established within a few minutes. With membranes much thicker than

Can. J. Chem. Downloaded from www.nrcresearchpress.com by 210.87.254.105 on 09/05/12
For personal use only.

Can. J. Chem. Downloaded from www.nrcresearchpress.com by 210.87.254.105 on 09/05/12
For personal use only.

this, however, it is unsafe to assume that steady-state conditions apply.

Slow Enzymatic Reaction

If the enzymatic reaction is slow (i.e. the enzyme is very inactive, or is present in low concentrations) there will be little depletion of substrate through the support and the reaction will not be diffusion-controlled. The rate of reaction per unit volume of support is

$$[6] \qquad v = \frac{k_c'[E]_m[S]'}{K_m' + [S]'} \quad \text{moles } l^{-1}\ s^{-1}$$

where $[E]_m$ is the number of moles of enzyme present per liter of support, and k_c' and K_m' are the true catalytic constant and Michaelis constant, respectively, for the reaction within the membrane (they may differ from the values of k_c and K_m in the free solution because of factors *1* and *2*. Suppose that E is the total number of moles of enzyme present in a support of thickness l cm and cross-sectional area A cm^2; $[E]_m$ is then $10^3E/Al$ moles l^{-1}, and the total rate of reaction in the support of volume Al cm^3 is given by

$$[7] \qquad v' = \frac{k_c'[E]_m[S]'Al/10^3}{K_m' + [S]'} = \frac{k_c'E[S]'}{K_m' + [S]'} \text{ moles } s^{-1}$$

The concentration $[S]'$ is equal to P $[S]$, where P is the partition coefficient; the rate is thus

$$[8] \qquad v' = \frac{k_c'E[S]}{\frac{K_m'}{P} + [S]} \quad \text{moles } s^{-1}$$

The apparent Michaelis constant is thus K_m'/P. The rate at low substrate concentration is

$$[9] \qquad v_{low}' = \frac{Pk_c'}{K_m'}E[S]$$

If the same amount of enzyme were distributed in 1 l of free solution, the rate at low substrate concentrations would be $k_cE[S]/K_m$; the rate on the support thus differs by the factor P, the partition coefficient, apart from differences between k_c' and k_c, and between K_m' and K_m, brought about by factors *1* and *2*.

At high substrate concentrations, on the other hand, eq. [8] leads to the result that

$$[10] \qquad v_{high}' = k_c'E$$

so that the rate will be the same on the supported enzyme as in free solution, provided that k_c' is the same as k_c.

Systems of this kind, where the enzyme is of low activity (this can always be realized by having it at sufficiently low concentrations), will be valuable for studying the influence of factors *1* and *2* on the activity of the enzyme.

More Active Enzyme Systems

If the rate of the enzymatic reaction is greater (enzyme more active, or present at higher concentrations), there will be a significant variation in substrate concentration through the support, and the effects of diffusion will then be more important. According to Fick's second law of diffusion, the rate of accumulation of substrate at any cross-section, due to diffusion, is given by

$$[11] \qquad v_d = D\left(\frac{\partial^2 s}{\partial x^2}\right)_t \quad \text{moles } l^{-1}\ s^{-1}$$

where D (cm^2 s^{-1}) is the diffusion constant, and the concentration s is in moles per liter. In the steady state this must exactly balance the rate of removal of substrate by reaction, which is equal to

$$[12] \qquad v_r = \frac{k_c'[E]_m s}{K_m' + s} \quad \text{moles } l^{-1}\ s^{-1}$$

The equation to be solved is therefore

$$[13] \qquad D\left(\frac{\partial^2 s}{\partial x^2}\right)_t = \frac{k_c'[E]_m s}{K_m' + s}$$

An explicit solution of this equation cannot be obtained except in the limiting cases $s \ll K_m'$ and $s \gg K_m'$. These limiting solutions will be obtained first, after which some numerical solutions will be given.

Case I. Low Substrate Concentrations

When $s \ll K_m'$ eq. [13] may be written as

$$[14] \qquad \frac{\partial^2 s}{\partial x^2} = \alpha^2 s$$

where α (units of cm^{-1}) is equal to $(k_c'[E]_m/DK_m')^{1/2}$. The solution of this, subject to the boundary conditions $x = 0$, $s = [S]'$ and $x = l$, $s = [S]'$, is

$$[15] \qquad s = [S]'\frac{\sinh \alpha x + \sinh \alpha(l - x)}{\sinh \alpha l}$$

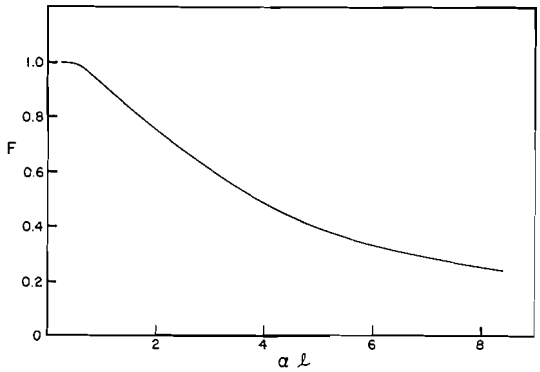

FIG. 2. The function $F = 2(\cosh \alpha l - 1)/\alpha l \sinh \alpha l$ plotted against αl.

The gradients ds/dx at $x = 0$ and $x = l$ are

$$[16] \qquad \frac{ds}{dx} = \mp d[S]' \frac{\cosh \alpha l - 1}{\sinh \alpha l}$$

The rate of entry of substrate at *each* of the surfaces is therefore

$$[17] \qquad v = -AD\left(\frac{ds}{dx}\right)_{x=0} = AD\left(\frac{ds}{dx}\right)_{x=l}$$

$$[18] \qquad = \alpha AD[S]' \frac{\cosh \alpha l - 1}{\sinh \alpha l}$$

This is equal to the rate of exit of product, since in the steady state there is no accumulation of substrate or product within the membrane; the net rate of formation of product in a membrane of cross-sectional area A is thus

$$[19] \qquad v' = 2\alpha AD[S]' \frac{\cosh \alpha l - 1}{\sinh \alpha l}$$

The rate per unit volume of support is

$$[20] \qquad \frac{v'}{Al} = \frac{2\alpha D[S]'}{l} \frac{\cosh \alpha l - 1}{\sinh \alpha l}$$

$$[21] \qquad = \frac{k_c' [E]_m}{K_m'} [S]' \frac{2}{\alpha l} \frac{\cosh \alpha l - 1}{\sinh \alpha l}$$

An equivalent equation has previously been obtained, in a different way, by Goldman, Kedem, and Katchalski (11). The function $F = 2(\cosh \alpha l - 1)/\alpha l \sinh \alpha l$ is shown plotted in Fig. 2; it has its maximum value of unity when αl approaches zero. The maximum rate attainable when a given amount of enzyme is present in unit volume of support is thus obtained when the thickness l approaches zero, and is equal to

$$[22] \qquad v' = \frac{k_c' E[S]'}{K_m'} = \frac{k_c' EP[S]}{K_m'}$$

If, instead, this amount of enzyme were present in unit volume of free solution, and the substrate concentration were sufficiently low that the kinetics were first order, the rate would be

$$[23] \qquad v = \frac{k_c E[S]}{K_m} \text{ moles s}^{-1}$$

The limiting rate for the supported enzyme, when the membrane is made thinner, therefore differs from that in homogeneous solution by the factors

$$\frac{k_c'}{k_c}, \quad \frac{K_m}{K_m'}, \quad P = \frac{[S]'}{[S]}$$

The value of F is very close to unity (within 1%) for αl values less than about 0.3, after which there is a substantial fall. The value of 0.3 for αl therefore represents something of a critical value, below which the rates on the supported enzyme will correspond closely to those in free solution (apart from factors *1* and *2*), and above which they will have substantially lower values. The quantitative significance of this is discussed below.

Case II. High Substrate Concentrations

When $s \gg K_m'$, eq. [13] becomes

$$[24] \qquad \frac{\partial^2 s}{\partial x^2} = \beta$$

where β (units of moles cm^{-5}) is equal to $10^{-3} k_c' [E]_m/D$. The solution of this subject to the boundary condition $x = 0$, $s = [S]'$ and $x = l$, $s = [S]'$ is

$$[25] \qquad s = [S]' - \tfrac{1}{2}\beta x(l - x)$$

The concentration gradients at $x = 0$ and $x = l$ are

$$[26] \qquad \frac{ds}{dx} = \pm \tfrac{1}{2}\beta l$$

The rate of entry of substrate through area A at each side of the support is therefore

$$[27] \qquad v' = \tfrac{1}{2}\beta ADl$$

The total rate of product formation in a membrane of cross-sectional area A cm^2 is thus

Can. J. Chem. Downloaded from www.nrcresearchpress.com by 210.87.254.105 on 09/05/12
For personal use only.

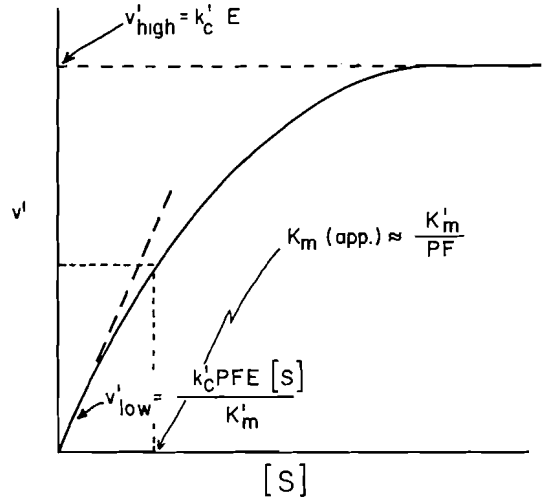

FIG. 3. Plot of v' against substrate concentration in the free solutions. The rate v' is the rate when E moles of enzyme are present in unit volume of support. F is the function $2(\cosh \alpha l - 1)/\alpha l \sinh \alpha l$; it approaches unity as the thickness of the membrane is decreased (cf. Fig. 2).

[28] $v' = \beta ADl$ moles s^{-1}

[29] $= 10^{-3} k_c' [E]_m Al$ moles s^{-1}

The rate per liter of support is thus

[30] $v' = k_c' [E]_m = k_c' E$ moles $l^{-1} s^{-1}$

If the same amount of enzyme is present in 1 l of solution, the rate is

[31] $v = k_c E$ moles $l^{-1} s^{-1}$

The limiting high-substrate-concentration rates now differ only by the factor k_c'/k_c. Experimental studies at high substrate concentrations will thus reveal this factor, uncomplicated by the partitioning effect.

The General Case

Solutions of the general eq. [13] can only be obtained by numerical means. One can, however, infer the approximate form of the dependence of the rate on the substrate concentration, on the basis of the solutions for Cases I and II. This is shown schematically in Fig. 3. The limiting rate at high substrate concentrations is $k_c' E$ (eq. [30]) and that at low is $k_c' PFE[S]/K_m'$, where P is the partition coefficient and F the function plotted in Fig. 2. If Michaelis–Menten kinetics are obtained for the supported enzyme, the rate expression will therefore be

[32] $$v' = \frac{k_c(\text{app.})E[S]}{K_m(\text{app.}) + [S]}$$

where

[33] $$k_c(\text{app.}) = k_c'$$

and

[34] $$K_m(\text{app.}) = \frac{K_m'}{PF}$$

The K_m(app.) extrapolated to low membrane thickness is thus K_m'/P, and if P is measured directly, K_m' can be evaluated and compared with the value in free solution.

Numerical Solutions

Solution of eq. [13] can be carried out numerically by reducing the equation to two first-order equations. The equation can be written as

[35] $$\frac{d^2s}{dx^2} = \frac{as}{b + s}$$

where a is $k_c'[E]_m/D$ and b is K_m'. Making the substitution $z = ds/dx$ leads to

[36] $$\tfrac{1}{2}z^2 = \int \frac{as}{b + s}\,ds + I$$

where I is a constant of integration. This equation can be integrated directly and gives

[37] $$z = \frac{ds}{dx} = \pm 2^{1/2}\left[as - ab \ln\left(1 + \frac{s}{b}\right) + I\right]^{1/2}$$

This can be integrated numerically over the required interval of x, subject to the boundary conditions

$$x = 0, s = [S]' \quad \text{and} \quad x = l, s = [S]'$$

Since these do not permit the evaluation of A in eq. [37], a rough estimate of ds/dx at $x = 0$ is made, and eq. [37] is integrated until $x = l$. The initial value ds/dx can then be adjusted, by trial and error, until $[S]'_{x=l} = [S]'_{x=0}$ to the desired degree of accuracy.

For computational purposes the negative sign in eq. [37] is taken until $ds/dx = 0$, after which the positive sign is used; the changeover point is taken as that value of x at which the argument of the square-root term in eq. [37] becomes negative.

Can. J. Chem. Downloaded from www.nrcresearchpress.com by 210.87.254.105 on 09/05/12
For personal use only.

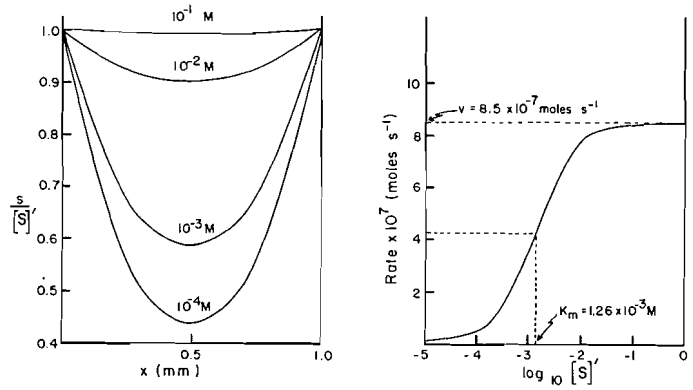

FIG. 4. Computer solutions for a membrane 1.0 mm thick, and using the constants given in the text. The left-hand curves show substrate concentration variations through the membrane, for the four surface concentrations indicated. The rates in the right-hand figure correspond to 1 l of support containing 10^{-7} mole of enzyme.

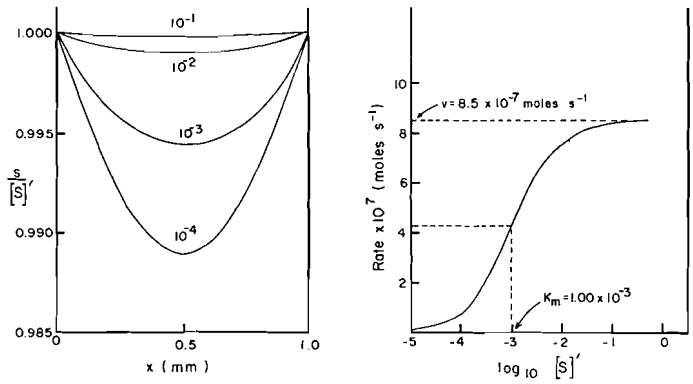

FIG. 5. Similar plots to those shown in Fig. 4, for a membrane 0.1 mm thick.

A number of computer calculations have been carried out, and they confirm the general conclusions drawn above. Examples are shown in Figs. 4 and 5; the left-hand curves show concentration–distance profiles, and the right-hand curve is a plot of rate against the logarithm of [S]', the substrate concentration just inside the surface. Figure 4 relates to the following conditions

$$l = 1 \quad \text{mm}$$
$$K_m' = 10^{-3} \quad M$$
$$a = 0.85 \quad \text{moles cc}^{-5}$$

The latter condition corresponds, for example, to the following

$$k_c' = 8.5 \quad \text{s}^{-1}$$
$$[E]_m = 10^{-7} \quad M$$
$$D = 10^{-6} \quad \text{cm}^2\,\text{s}^{-1}$$

It is to be seen from this figure that if the substrate is equally soluble in the support and in the solution, the K_m(app.) value would be $1.26 \times 10^{-3}\,M$, i.e. slightly greater than K_m'. The k_c(app.) value, however, is 8.5 s^{-1}, exactly the same as k_c'. The rate constant at low substrate concentrations, k_c(app.)/K_m(app.) is $6.75 \times 10^3\,M^{-1}\,s^{-1}$, slightly less than the value of 8.5×10^3 for the enzyme in free solution. If the partition coefficient is not unity but is P, the K_m(app.) values will be reduced by the factor P, and the k_c(app.)/K_m(app.) values raised by the factor P.

Figure 5 shows the results of similar calculations for a membrane of thickness 0.1 mm, but with other conditions the same. In line with the earlier discussion, the K_m(app.) value (for $P = 1$) is now much closer to the K_m' value; it is indeed almost exactly $10^{-3}\,M$. Similarly, the k_c(app.) and k_c(app.)/K_m(app.) values are indistinguishable from the values for the enzyme in free

Can. J. Chem. Downloaded from www.nrcresearchpress.com by 210.87.254.105 on 09/05/12
For personal use only.

solution. Again, if P is other than unity, the k_c(app.) value remains unchanged, but K_m(app.) is reduced and k_c(app.)/K_m(app.) increased by the factor P.

The computer solutions confirm the general conclusion that $\alpha l = 0.3$ represents something of a critical value. The value of α for the parameters used in the examples given above is about 30 cm^{-1}, so that the critical l value should be about $0.3/30 = 0.01$ cm. The computer calculations did in fact show that at 0.1 cm the limit had not quite been reached, but that at 0.01 cm it had been reached.

Significance of the Partition Coefficient, P

Two situations are to be distinguished with reference to the partition coefficient P: that in which the support can be regarded as homogeneous; and that in which it is heterogeneous, the enzymatic action taking place in only one part of the support (e.g. in pores).

No particular problem arises in the homogeneous case. The magnitude of P can be determined directly by separate experiments with the support to which no enzyme has been attached. The importance of electrostatic effects has been emphasized, with examples, by Goldstein, Levin, and Katchalski (9); this and other aspects will be discussed in a forthcoming review (12).

When the support is heterogeneous, certain complications arise. Suppose that a fraction θ of the support consists of pores and the remainder of inert material. If E moles of enzyme are attached to Al cc of support, the effective concentration will be $10^3 E/\theta Al$. This factor alone will produce an enhancement in rate, as compared with the homogeneous case, by a factor of $1/\theta$. However, the fact that the substrate is present only in the pores leads to a reduction in rate by the factor θ. The two effects exactly cancel. Thus, the rate in a porous support will be the same as in a homogeneous support of the same dimensions if the composition of the material in the pores is the same as that in the homogeneous support.

The partition coefficient P to be used, however, must relate to the distribution between the solution and the pore phase, and not between the bulk solution and the support as a whole. The effective coefficient P_{eff} will be equal to θP; P can therefore be found if P_{eff} and θ are measured.

We are grateful to Professor E. M. Crook for reading the manuscript and for valuable discussions.

1. W. E. Hornby, M. D. Lilly, and E. M. Crook. Biochem. J. **98**, 420 (1966).
2. H. I. Silman and E. Katchalski. Annu. Rev. Biochem. **35**, 873 (1966).
3. M. D. Lilly and A. K. Sharp. Chem. Eng. London, No. 215, CE 12 (1968).
4. C. W. Wharton, E. M. Crook, and K. Brocklehurst. Eur. J. Biochem. **6**, 572 (1968).
5. M. L. Barnard and K. J. Laidler. J. Amer. Chem. Soc. **74**, 6099 (1952).
6. K. J. Laidler and M. C. Ethier. Arch. Biochem. Biophys. **44**, 338 (1953).
7. D. Findlay, A. P. Mathias, and B. R. Rabin. Biochem. J. **85**, 139 (1963).
8. K. J. Laidler. The chemical kinetics of enzyme action. The Clarendon Press, Oxford. 1958. pp. 205–209.
9. L. Goldstein, Y. Levin, and E. Katchalski. Biochem. **3**, 1913 (1964).
10. R. M. Barrer. Diffusion in and through solids. Cambridge Univ. Press, London. 1941. p. 15.
11. R. Goldman, O. Kedem, and E. Katchalski. Biochem. **7**, 4518 (1968).
12. K. J. Laidler and P. V. Sundaram. *In* The chemistry of the cell interface. *Edited by* H. D. Brown. Academic Press, Inc., New York. To be published.

Can. J. Chem. Downloaded from www.nrcresearchpress.com by 210.87.254.105 on 09/05/12
For personal use only.

Can. J. Chem. Downloaded from www.nrcresearchpress.com by 210.87.254.42 on 09/05/12
For personal use only.

Radiation chemistry of gaseous oxygen: experimental and calculated yields[1]

C. WILLIS, A. W. BOYD, AND M. J. YOUNG
Physical Chemistry Branch, Chalk River Nuclear Laboratories, Atomic Energy of Canada Limited, Chalk River, Ontario

AND

D. A. ARMSTRONG
Department of Chemistry, University of Calgary, Calgary, Alberta

Received December 12, 1969

The yield of ozone from the radiolysis of gaseous oxygen has been measured at 10^{26}–10^{27} eV g^{-1} s^{-1} to be $G(O_3) = 12.8 \pm 0.6$, in reasonable agreement with the value of 13.8 of Ghormley, Hochanadel, and Boyle (2*a*). At 10^{16} eV g^{-1} s^{-1}, our results and re-examination of previous data give $G(O_3) = 6.2 \pm 0.6$. The same value is obtained at the high dose rates by the addition of electron scavengers. The difference in yields on going from high to low dose rates and the decrease with electron scavengers at the high dose rate is explained by differences in ion neutralization processes. These are supported by computer calculations. The mechanism of the neutralization steps is discussed in terms of the applicability of the electron jump theory and the effect of clustering of the ions.

The proportion of energy lost to ionization, excitation, and subexcitation electrons is calculated. This is based on the *W* value, relative cross sections for ionization, and the potential energy curves for O_2^+ ions. A predicted yield on this basis is $G(O_3) = 14.0 \pm 0.9$, in fairly good agreement with the experimental yield.

Canadian Journal of Chemistry, **48**, 1505 (1970)

Introduction

We have recently given a preliminary report of measurements of ozone yields from the radiolysis of oxygen at low and high dose rates and a mechanism for these yields (1). This paper extends the results and the mechanism, and presents calculations of the yield of ozone from oxygen based on ionization cross sections and the known potential energy levels of the excited and ionic states of oxygen.

This work was undertaken to confirm and explain the yield of ozone of $G(O_3) = 13.8$ obtained at high dose rates ($\sim 10^{26}$ eV g^{-1} s^{-1}) by Ghormley, Hochanadel, and Boyle (2*a*).[2] These workers suggested that their result is not significantly different from the low dose rate (10^{16} eV g^{-1} s^{-1}) value. The most reliable values for gaseous oxygen at low dose rates appear to be those of Kircher *et al.* (3), Johnson and Warman (4), and Sears and Sutherland (5). Kircher *et al.* obtained a maximum yield of $G(O_3) = 9$ at temperatures of 195 and 283 °K using ferrous sulfate dosimetry. Johnson and Warman obtained an initial yield of $G(O_3) = 10.2$ at both 90 and 200 °K using N_2O dosimetry (taking $G(N_2) = 10.0$ instead of the value they used of $G(N_2) = 12.5$). Sears and Sutherland also used ferrous sulfate dosimetry and obtained a maximum differential yield of $G(O_3) = 10.5$ at 77 °K, but at this temperature and also at 195 and 283 °K their initial yield is $G(O_3) \approx 6$. In refs. 3 and 4, O_3 was determined by the iodide method, assuming one molecule of I_3^- is produced per molecule of ozone. However, we have shown that one molecule of ozone produces 1.53 ± 0.11 molecules of I_3^- at p*H* 7.0 (1) and the yield reported in ref. 3 should therefore be $G(O_3) = 5.9$; and in ref. 4, $G(O_3) = 6.7$. In ref. 5, ozone was determined by absorption spectrophotometry using the well-established value for the extinction coefficient of O_3 at 254 nm (6, 7). The best value for low dose-rate irradiations then appears to be $G(O_3) \approx 6$. We have also obtained values in agreement with this at low dose rates at 77 °K. At high dose rates, we obtained $G(O_3) = 12.8$, in reasonable agreement with the value of Ghormley *et al.* (2*a*).

As we have pointed out, the difference between the low and high dose-rate yields can be attributed to the contribution of ionic neutralization processes (1). It is therefore of interest to compare

[1]AECL No. 3574.

[2]An isolated value of $G(O_3) = 10.5$ for the pulse radiolysis of pure oxygen at 560 Torr has been reported by Meaburn *et al.* (2*b*) for dose rates of $\sim 2 \times 10^{25}$ eV g^{-1} s^{-1}. This value was based on $G(N_2) = 10.0$ for nitrous oxide dosimetry. Correcting this to $G(N_2) = 12.4$ gives $G(O_3) = 13.0$, in good agreement both with the present work and that of Ghormley *et al.* (2*a*).

Can. J. Chem. Downloaded from www.nrcresearchpress.com by 210.87.254.42 on 09/05/12
For personal use only.

calculations of the contributions of ions and excited molecules with these experimental yields.

To do this we have used the recent electron impact cross section data of Watson *et al.* (8) and the potential energy curves of Gilmore (9), and combined these with the mechanisms proposed by Fueki and Magee (10), Johnston *et al.* (11), and Johnson and Warman (4).

Experimental

The high dose-rate irradiations were done with a Febetron 705 pulsed electron source and the low dose-rate irradiations with a Gammacell 220.

The procedure and quartz cells used in the Febetron irradiations have been already described (12, 13). The dose absorbed in the cells was determined by nitrous oxide dosimetry, taking $G(N_2) = 12.4$ for Febetron dose rates (14–16). With the Febetron, oxygen was irradiated at three different dose rates. The highest, 1.6 Mrad per pulse $\approx 2 \times 10^{27}$ eV g^{-1} s^{-1}, was obtained with the window of the quartz cell 2 cm from the Febetron tube window. The two lower dose rates were obtained by putting a 0.005 cm tantalum foil at 1 cm from the Febetron tube and varying the distance between the cell and the foil. At 2.0 cm, the dose was 0.7 Mrad per pulse and at 6.0 cm, 0.06 Mrad per pulse.

The low dose-rate irradiations were done at 77 °K. The absorbed dose was determined by nitrous oxide dosimetry, taking $G(N_2) = 10.0$ (17).

The amount of ozone formed was determined both by the optical method used by Sears and Sutherland (5) and the iodide method used by Johnson and Warman (4).

In the optical method, the irradiation cell was connected to an evacuated 10 cm absorption cell. The ozone concentration was determined with a Perkin–Elmer Model 450 spectrophotometer, using the extinction coefficient of 135 cm^{-1} S.T.P. at 254 nm. This was established absolutely by DeMore and Raper (6) and confirmed by Griggs (7), who obtained 132 cm^{-1} S.T.P. It was found that the ozone concentration was the same with either Kel F (halogenated hydrocarbon) or Dow Corning (silicone) grease in the stopcocks. It was also the same for times of 5 to 15 min allowed for mixing and for diffusion between the irradiation and absorption cells.

Irradiations of oxygen with added SF_6 and perfluorocyclobutane (c-C_4F_8) were carried out at high dose rates. The SF_6 and perfluorocyclobutane (Matheson) were used as received after thorough outgassing. The iodide method gave much lower values for O_3 in the mixtures with SF_6 than did the optical method. This was attributed to reduction of I_3^- due to the presence of sulfur compounds (perhaps SO_3^{2-}).

Relative yields of O_3 with these additives were obtained by irradiations in an optical absorption cell. The cell, the light source, the optical system, and the detection system have been described (18). The ozone absorption at 254 nm was measured several milliseconds after the pulse, when the absorption had reached a limiting value. The absorbed dose in this cell was ~ 0.2 Mrad per pulse.

Results

The data from the Febetron irradiations of pure oxygen are given in Fig. 1. Each value is for a single Febetron pulse and therefore the total absorbed energy for a given dose rate is directly proportional to pressure. The maximum absorbed energy is for 800 Torr of oxygen at a dose per pulse of 1.6 Mrad. As can be seen, the ozone yield is independent of pressure from 30–800 Torr and of dose rate from 10^{26} to 10^{27} eV g^{-1} s^{-1}. The straight line in this figure gives $G(O_3) = 12.8 \pm 0.6$. This yield was also independent of dose at the lowest dose rate (10^{26} eV g^{-1} s^{-1}) between 0.05 and 0.35 Mrad (1–7 pulses).

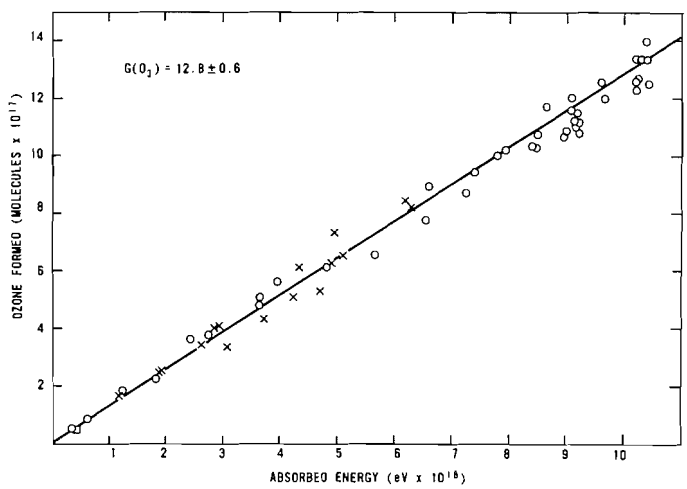

FIG. 1. Ozone production in Febetron irradiation of oxygen by single pulses: ○, 2×10^{27} eV g^{-1} s^{-1}, oxygen pressure 30–800 Torr; ×, 0.8×10^{27} eV g^{-1} s^{-1}, oxygen pressure 200–800 Torr; □, 0.08×10^{27} eV g^{-1} s^{-1} (this point is the average of 10 determinations at 800 Torr).

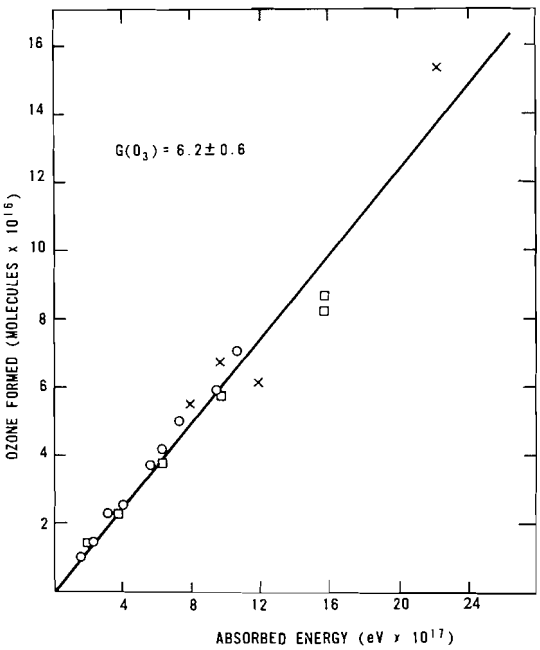

FIG. 2. Ozone production in low dose rate irradiation of oxygen: ○, results taken from ref. 4 both for 77 and 195 °K; □, results taken from ref. 5 both for 77 and 195 °K; ×, present work at 77 °K.

Our low dose-rate values are compared with those of Sears and Sutherland (5) and Johnson and Warman (4) in Fig. 2. The values given in ref. 4 have been corrected using $G(N_2) = 10.0$ and 1.53 molecules of I_3^- formed per molecule of O_3 absorbed. In all these irradiations the pressure was 100–760 Torr and the range of absorbed dose is from 0.05 to 0.3 Mrad.

Sears and Sutherland (5) found little or no effect of electron scavengers on O_3 yields at low dose rates. The effect of the additives SF_6 and c-C_4F_8 at $\sim 10^{27}$ eV g^{-1} s^{-1} is shown in Fig. 3. The plateau value of $G(O_3) = 6.3$ is the same within experimental error as the low dose-rate yield in pure oxygen.

Discussion

There is a large and significant difference between the measured ozone yields in the high and low dose-rate radiolysis of gaseous oxygen. Between 10^{26}–10^{27} eV g^{-1} s^{-1}, $G(O_3) = 12.8 \pm 0.6$ and at 10^{16} eV g^{-1} s^{-1} $G(O_3) = 6.2 \pm 0.6$. There is also a significant difference in the effects of electron scavengers. At high dose rates the yield of ozone is reduced from $G(O_3) = 12.8$ to $G(O_3) = 6.3 \pm 0.6$ by the addition of SF_6 and c-C_4F_8, while at low dose-rates electron scavengers have little or no effect.

In pulse radiolysis studies at 10^{26} eV g^{-1} s^{-1}, the ozone is observed to grow in over a period of $\sim$ 10 μs (2, 19). The mean lifetime of the ions at this dose rate is $\sim 10^{-8}$ s (see below). Therefore ozone cannot be formed in appreciable yields from ion–molecule or ion-neutralization reactions, and the immediate precursor of ozone in irradiated oxygen is almost certainly an atom of oxygen in the ^3P or ^1D state, as in the vacuum-ultraviolet photolysis of oxygen (20)

[1] $$O + 2O_2 \rightarrow O_3 + O_2$$

These oxygen atoms must result from neutralization reactions of ionic precursors or dissociative excitation.

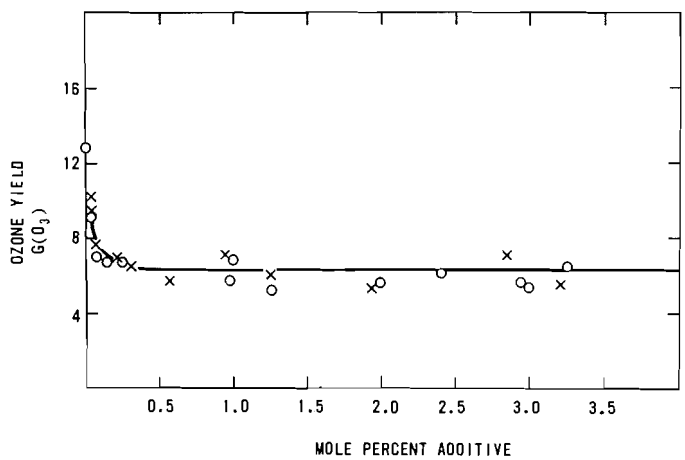

FIG. 3. Effect of electron scavengers on ozone yield: ○, SF_6; ×, c-C_4F_8. All points below 0.5% additive are for 700 Torr oxygen. Above 0.5%, points are for both 400 and 700 Torr.

Can. J. Chem. Downloaded from www.nrcresearchpress.com by 210.87.254.42 on 09/05/12
For personal use only.

Can. J. Chem. Downloaded from www.nrcresearchpress.com by 210.87.254.42 on 09/05/12
For personal use only.

Ion-Neutralization Reactions

We have suggested (1, 16) that the difference in ozone yields at high and low dose rates is due to a difference in the yield of oxygen atoms from ionic processes. At low dose rates the ion-recombination time is of the order of 10^{-2} s, and simple, straightforward calculations show that for any significant absorbed dose reaction [2*a*], which is highly exothermic, can occur prior to ion-combination.

$$[2a]\quad O_2^- + O_3 \rightarrow O_2 + O_3^- \qquad \Delta H = -56 \text{ kcal mole}^{-1}$$

Therefore the predominant neutralization is probably reaction [3]

$$[3]\quad O_2^+ + O_3^- \rightarrow O + 2O_2 \qquad \Delta H = -187 \text{ kcal mole}^{-1}$$

which makes no net contribution to the ozone yield.

Clustering of the oxygen ions may also affect the extent of dissociative neutralization. As n increases in reaction [2*b*]

$$[2b]\quad O_2^+ \cdot (O_2)_n + O_2^- \cdot (O_2)_n \rightarrow \text{products}$$

dissociative neutralization becomes less likely. At low dose rates there is sufficient time for clusters to reach equilibrium size, and recent data from high-pressure mass spectrometry (21–23) imply that at 77 °K, both the positive and the negative ions will be clustered on the average by four oxygen molecules.

To determine the lifetime and the extent of clustering of the ions at Febetron dose rates, we have done computer calculations at two pressures. In these, the concentrations of the possible species are obtained as a function of time during and following the Febetron pulse, using the known reactions for the species present.[3] The rate constants for the reactions which were included in the program are given in Table 1.

The primary yields assumed for these calculations are: $G(O^+) = 0.10$, $G(O_2^+) = 3.17$, $G(e) = 3.27$, and $G(O) = 6.10$. The electron yield is derived from the W value, which is 30.6 eV per ion pair in oxygen (35, 36). The mass-spectral abundance of O^+ relative to 1.00 for O_2^+ with 70 V ionizing electrons is 0.03–0.05 (37, 38). High values in the range 0.15–0.25 have been reported (11, 39). However, these are not consistent with photoionization measurements, which imply a fractional abundance of less than 0.05 for O^+ (40–43). We have used 0.03.

The yield of O atoms is the experimental low dose-rate value of $G(O_3) = 6.2$ less the small contribution of O^+.

The computer program is based on that of Schmidt (44). The Febetron pulse was approximated by a step function with 2 ns steps (16). The dose used of 1.061×10^{20} eV g^{-1} is the maximum dose averaged over the cell volume.

The calculated time dependence of the concentrations of both neutral and ionic species for irradiation at 830 and 83 Torr is shown in Figs. 4 and 5, respectively. These exhibit large differences in the concentrations of the ionic species between the two pressures. Table 2 gives results of detailed calculations of the contributions of the various ion neutralization reactions. The

TABLE 1

Reactions of importance in irradiated oxygen

	Reaction	Rate constant M^{-1} s^{-1}
[5]	$O_2^+ + O_2 \rightarrow O_4^+$	4.2×10^{10}[a]
[6]	$O^+ + O_2 \rightarrow O_2^+ + O$	1.2×10^{10}[b]
[7]	$e + 2O_2 \rightarrow O_2^- + O_2$	2.0×10^{10}[c]
[8]	$O_2^- + O_2 \rightarrow O_4^-$	4.2×10^{10}[d]
[9]	$O^+ + e \rightarrow O$	$\sim 2.0 \times 10^{13}$[e]
[10]	$O^+ + O_2^- \rightarrow O + O_2$	1.2×10^{15}[f]
[11]	$O^+ + O_4^- \rightarrow O + 2O_2$	1.2×10^{15}[f]
[12]	$O_2^+ + e \rightarrow 2O$	1.0×10^{14}[e]
[2]	$O_2^+ + O_2^- \rightarrow 2O + O_2$	1.2×10^{15}[f]
[13]	$O_2^+ + O_4^- \rightarrow 2O + 2O_2$	1.2×10^{15}[f]
[14]	$O_4^+ + e \rightarrow 2O + O_2$	1.0×10^{14}[e]
[15]	$O_4^+ + O_2^- \rightarrow 2O + 2O_2$	1.2×10^{15}[f]
[16]	$O_4^+ + O_4^- \rightarrow 2O + 3O_2$	1.2×10^{15}[f]
[2*a*]	$O_2^- + O_3 \rightarrow O_3^- + O_2$	1.8×10^{11}[g]
[4]	$O_3^- + O_4^+ \rightarrow O_3 + 2O_2$	1.2×10^{15}[f]
[1]	$O + 2O_2 \rightarrow O_3 + O_2$	8.0×10^{6}[h]
[17]	$O + O \rightarrow O_2$	4.0×10^{7}[i]
[19]	$O + O_3 \rightarrow 2O_2$	6.0×10^{6}[j]

[a] A rate constant for $O_2^+ + nO_2$ is given in ref. 10 as 7.4×10^{-10} cm^3 molecule^{-1} s^{-1}; these authors discuss this as an equilibrium reaction with a very fast rate constant for the dissociation of the complex. Reference 24 gives 7×10^{-12} cm^3 molecule^{-1} s^{-1} as the limiting two-body rate constant at 1.0 Torr with helium as third body.

[b] The rate constants for this reaction are summarized in ref. 25.

[c] This is a two-body equivalent rate constant for 830 Torr O_2 at 25 °C. The three-body rate constant is given as $1.4 \pm 0.2 \times 10^{-29}(300/T)\exp(-600/T)$cm^6 molecule^{-2} s^{-1} for oxygen as the third body (26, 27).

[d] This is assumed to be equal to the rate constant for reaction [5] as suggested in ref. 10.

[e] See refs. 28 and 29.

[f] See refs. 30 and 31.

[g] See ref. 32.

[h] This is the two-body equivalent rate constant for 830 Torr O_2 at 25 °C. See refs. 33 and 34 for discussion of values of this rate constant.

[i] This is the two-body equivalent rate constant for 830 Torr O_2 at 25 °C. See refs. 33 and 34 for discussion of values of this rate constant.

[j] See refs. 33 and 34.

[3] Clustering of positive and negative ions beyond O_4 has not been explicitly considered. Preliminary calculations have shown that for 83 Torr oxygen at 298 °K, ions of a molecular weight greater than O_4 make no contribution to the neutralization reactions, and even at 830 Torr the contribution is not large. We have not included ions above O_4 in the present calculations.

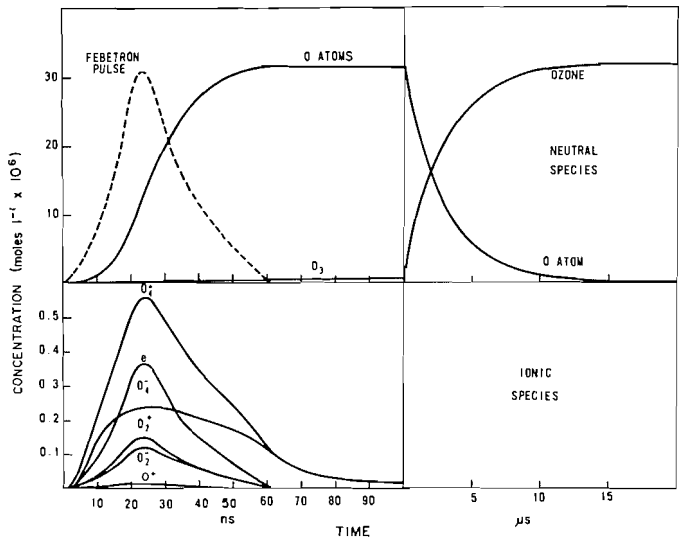

FIG. 4. Calculated ionic and neutral concentration during and following Febetron pulse at 830 Torr pressure and 25 °C. Total dose = 1.06×10^{20} eV g^{-1}. The upper half of the figure gives concentration of neutral species and the lower half, concentrations of ionic species. The pulse intensity can be taken from the ordinate axis. Ten units correspond to 2×10^{27} eV l^{-1} s^{-1}, so that the maximum intensity is 6.16×10^{27} eV l^{-1} s^{-1}.

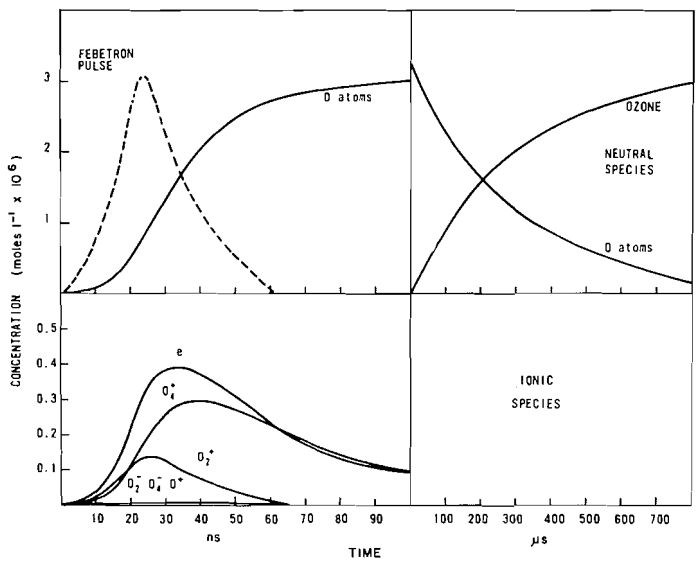

FIG. 5. Calculated ionic and neutral concentration in oxygen during and following a Febetron pulse at 83 Torr pressure and 25 °C. The upper half of the figure gives concentration of neutral species and the lower half, concentrations of ionic species. The pulse intensity units are the same as given in Fig. 4.

main change in going from 830 to 83 Torr pressure is the neutralization of the positive ions by electrons instead of by O_2^- and O_4^-. Reaction [16], which accounts for over 50% of the charge neutralization at 830 Torr, is largely replaced by reaction [14] at 83 Torr. Similarly, direct neutralization of O_2^+ by an electron increases from an almost negligible amount at 830 Torr to nearly 15% at 83 Torr. Finally, as can be seen from the figures, reaction [2*a*] can be neglected at Febetron dose rates, since for single pulses virtually no ozone is present during the lifetime

Can. J. Chem. Downloaded from www.nrcresearchpress.com by 210.87.254.42 on 09/05/12
For personal use only.

TABLE 2

Ion recombination reactions at a mean dose rate of 2×10^{27} eV g^{-1} s^{-1}

Reaction	ΔH, kcal $mole^{-1}$, to form two O atoms	Proportion of neutralization processes, %	
		830 Torr	83 Torr
[16] $O_4^+ + O_4^-$	−131	57.13	9.68
[15] $O_4^+ + O_2^-$	−143	19.64	12.18
[13] $O_2^+ + O_4^-$	−181	11.64	1.06
[14] $O_4^+ + e$	−151	4.74	58.90
[2] $O_2^+ + O_2^-$	−151	4.42	2.42
[12] $O_2^+ + e$	−161	1.08	14.34
[11]* $O^+ + O_4^-$		0.92	0.09
[10]* $O^+ + O_2^-$		0.34	0.20
[9]* $O^+ + e$		0.09	1.13

*Of the 3% O^+ in the system, at both pressures, about half is neutralized in reactions [9]–[11] and about half undergoes the ion–molecule reaction

[6] $O^+ + O_2 = O_2^+ + O$

of the ions and the rate of the reaction is much too slow for it to compete with the neutralization reactions.

If the neutralization reactions [2] and [12] to [16] gave different products, for example, if

[14*a*] $O_4^+ + e \rightarrow 2O + O_2$

and

[16*a*] $O_4^+ + O_4^- \rightarrow 4O_2$

the decrease in pressure from 830 to 83 Torr would be reflected by a significant increase in the experimental ozone yield. This was not observed. Consequently one must conclude that these reactions each give two O atoms, as shown in Table 1. Only on this basis do the computed limiting concentrations of ozone at both pressures correspond to the experimental yield of $G(O_3) = 12.8$ molecules per 100 eV.

The above conclusion regarding the formation of oxygen atoms from combinations of O_4^+ and O_4^- is perhaps a little unexpected. However, the exothermicity of each of the reactions is large and there is no problem on this basis. Chan (45) has considered reactions [2] and [12] from a theoretical point of view. He concludes that highly excited O_2^* molecules are produced from the positive ion in both cases. For reaction [2], the electron has a high probability of tunnelling across from O_2^- to O_2^+ while the ions are orbiting each other at an appreciable distance. The excited oxygen molecules are in dissociative states and once they are formed neutralization is complete. If one assumes that O_4^+ splits up on accepting an electron to produce one oxygen molecule in a dissociative state, reactions [15] and [14] can be looked upon as occurring in a similar way to reactions [2] and [12].

The electron jump mechanism envisaged above for neutralizations involving O_2^- is not likely to be as facile with more complex ions, where the molecular configurations of the negative ion and parent molecule differ. (Note the long lifetimes for autodetachment from SF_6^- (46) and fluorocarbon negative ions (47).) Under these circumstances, neutralization may not be complete until the negative and positive ions coalesce to the point where energy transfer can occur. This is almost certain to be the case for the combination of clustered $O_2^+ \cdot (O_2)_n$ and $O_3^- \cdot (O_2)_n$ ions at low dose rates. Indeed, spectroscopic evidence shows that the equilibrium bond angles of $O_3(\theta = 117°)$ and $O_3^-(\theta = 100°)$ (48) differ, and even without clustering this would make the electron jump process much more difficult than for O_2^-. Hence reaction [20]

[20] $O_2^+(O_2)_n + O_3^-(O_2)_m \rightarrow O_2^* + O_3 + (n + m)O_2 \rightarrow 2O + O_3 + (m + n)O_2$

is very unlikely.

To summarize, since at high dose rates the much shorter ion lifetimes preclude reaction [2*a*] and limit the extent of clustering, recombination reactions such as

[2] $O_2^+ + O_2^- \rightarrow 2O + O_2$

and

[12] $O_2^+ + e \rightarrow 2O$

Can. J. Chem. Downloaded from www.nrcresearchpress.com by 210.87.254.42 on 09/05/12
For personal use only.

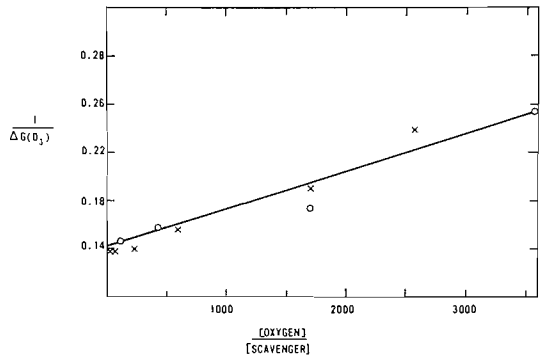

FIG. 6. Stern–Volmer plot for reduction in ozone yields as a function of electron scavenger: ○, SF_6; ×, c-C_4F_8.

replace combinations of clustered species like $O_3^- \cdot (O_2)_n$, $O_2^- \cdot (O_2)_n$, and $O_2^+ \cdot (O_2)_n$, causing the increase in the ozone yield of $\Delta G(O_3) = 6.6 \pm 0.9 \simeq 2G(e)$ on going from 10^{16} to 10^{26} eV g^{-1} s^{-1}.

Effects of Electron Scavengers

A reduction of the ozone yield at high dose rates was observed when the electron scavengers SF_6 and c-C_4F_8 were added, its magnitude being equal to $2G(e)$.

[21] $$e + SF_6 \rightarrow SF_6^-$$

[22] $$e + c\text{-}C_4F_8 \rightarrow c\text{-}C_4F_8^-$$

Again this is consistent with the view that reactions [23] and [24]

[23] $$O_2^+ + SF_6^- \rightarrow [O_2^* + SF_6] \rightarrow 2O + SF_6$$

[24] $$O_2^+ + c\text{-}C_4F_8^- \rightarrow [O_2^* + c\text{-}C_4F_8] \rightarrow 2O + c\text{-}C_4F_8$$

do not occur, due to reduced ability of the electron to tunnel across to O_2^+. Neutralization probably involves bond breaking and the formation of oxygen-containing products from the SF_6^- and c-$C_4F_8^-$ ions.

In Fig. 6, $1/\Delta G(O_3)$ is plotted against the ratios of $[O_2]/[SF_6]$ and $[O_2]/[c\text{-}C_4F_8]$. From the slope of the straight line in this figure, the ratio of rate constants is obtained from the expression

$$\frac{1}{\Delta G(O_3)} = \frac{1}{2G(e)}\left[1 + \frac{k_{e+O_2}[O_2]}{k_{e+scav.}[scav.]}\right]$$

for 700 Torr O_2. This is based on the assumption that no secondary electron transfer or other reactions between O_2^- and the scavengers are occurring.

The ratio of rate constants for both electron scavengers to that of oxygen, i.e. $(k_{e+scav.})/(k_{e+O_2})$ obtained from the slope in this figure and the Stern–Volmer equation, is $(5 \pm 2) \times 10^3$ for both SF_6 and c-C_4F_8. This is in fairly good agreement with the values reported for $k_{e+SF_6} = 1.8 \times 10^{14}$ M^{-1} s^{-1} (49) and $k_{e+O_2} = 1.8 \times 10^{10}$ M^{-1} s^{-1} (26, 27) at 700 Torr and 25 °C.

Electron Balance Calculations

The data required from any fundamental calculation of ozone yields in the radiolysis of oxygen are basically the yields of ions and neutral excited species. An independent calculation from first principles would require precise knowledge of the spectrum of the ionizing radiation and the energy dependence of the cross sections for all possible processes. At the present time these data are not available. However, from the W value, the ion-pair yield is immediately available. In oxygen this can be equated to a part of the observed product yield at high dose rates as we have shown. Also, there are fairly detailed electron

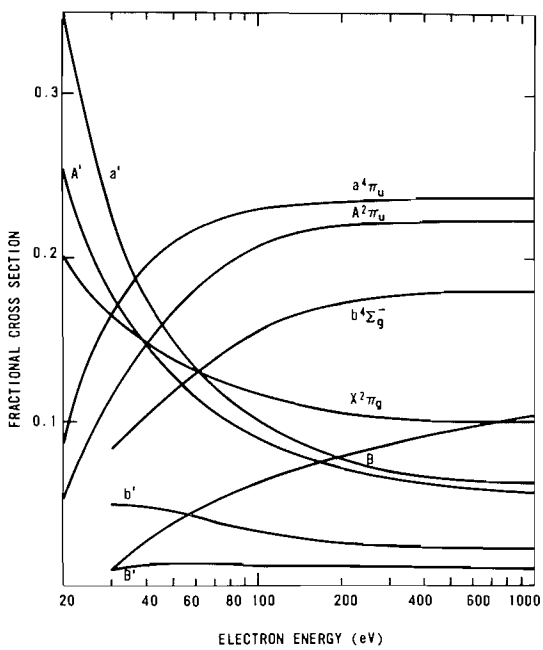

FIG. 7. Fractional cross sections for production of various electron states of O_2^+ in electron bombardment of oxygen, calculated from the data of Watson *et al.* (8). The curves quoted by electronic states are due to direct ionization. Those quoted with the prime notation are for pre-ionization (auto-ionization) where a' is equivalent to $a^4\Pi_u$ state and so on.

Can. J. Chem. Downloaded from www.nrcresearchpress.com by 210.87.254.42 on 09/05/12
For personal use only.

TABLE 3

Calculation of average ionization energy, $\bar{E}_{ion}$, for O_2

Electronic state of ion	Fractional cross section at 100 eV	Energy of state: Vibrational level, v	Energy of state: Energy eV	Energy fraction eV
$a^4\pi_u$	0.229	4	16.7	3.82
$A^2\pi_u$	0.207	6	17.6	3.64
$b^4\Sigma_g^-$	0.155	1	18.3	2.84
$X^2\pi_g$	0.117	2	12.4	1.45
B state (Probably $C^4\Sigma_u^-$ and $C^2\Sigma_g^-$)	0.063	0	24.6	1.55
Sub-total neglecting pre-ionization	0.771			
Average ionization energy based on above values, $\bar{E}_{ion}$, = 17.3 eV				

Pre-ionization contributions	Fractional cross section	Energy of state, assumed to be as above	Energy fraction eV
a' $(=a^4\pi_u)$	0.101	16.7	1.69
A' $(=A^2\pi_u)$	0.090	17.6	1.58
b' $(=b^4\Sigma_g^-)$	0.033	18.3	0.60
B' $(=B$ state)	0.012	24.6	0.30
Average ionization energy based on all above values, $\bar{E}_{ion}$ = 17.5 eV			

impact cross sections for the production of various states of the ions. From these and the potential energy curves for these states, it is possible to calculate an average energy of ionization. By subtracting this average energy of ionization from the W value, we have the energy per ion pair available for excitation. This can be compared with the experimentally observed yield attributable to non-ionic processes.

The relative electron impact cross sections for the known states of O_2^+ are given as a function of electron energy in Fig. 7. These values are calculated from the data of Watson *et al.* (8).

From theoretical considerations (50), it has been shown that over 80% of all ionizations in a typical gas-phase radiolysis are caused by electrons in the "optical energy range" above 100 eV. Reference to Fig. 7 shows that above this energy the variations in the relative ionization cross sections are small. Therefore, we have combined the relative ionization cross sections for an electron energy of 100 eV with the potential energy curves of Gilmore (9) to estimate the average ionization energy $\bar{E}_{ion}$ as shown in Table 3. This estimate is based on the equation

$$E_{ion} = \sum_i \sigma_i E_i / \sum \sigma_i$$

where σ_i is the cross section for the ith electronic level and E_i is the energy required to form it. Rigorously, σ_i is a function of energy, however, as we have discussed above, for the important optical energy range, $\sigma_i/\sum_i \sigma_i$ is virtually independent of energy. The fractional cross section to each given state summed over all energies is given by Watson *et al.* (8). Using their values to calculate a mean ionization energy gives $\bar{E}_{ion} = 17.18$, which is not significantly different to that given in Table 3.

The high Rydberg states of oxygen are presumably responsible for the formation of O_2^+ states by pre-ionization. At the present time the potential energy curves of these Rydberg states are not known. In Table 3 we have therefore assumed that the mean energy for pre-ionization to a given ionic state is the same as that for direct ionization. The minimum average ionization energy may be slightly lower than the value obtained in this way. The maximum average ionization energy, i.e. that calculated assuming pre-ionization to the highest vibrational level of each state below the dissociation energy to O^+ and O, is 17.8 eV. Thus, provided no emission occurs concurrently with ionization, the range of values of 17.3–17.8 eV for the average ionization energy should be correct. The value of $\bar{E}_{ion}$ does depend upon the cross sections of Watson *et al.*

Can. J. Chem. Downloaded from www.nrcresearchpress.com by 210.87.254.42 on 09/05/12
For personal use only.

Can. J. Chem. Downloaded from www.nrcresearchpress.com by 210.87.254.42 on 09/05/12
For personal use only.

(8). However, these are supported by a recent publication of independent measurement of the cross-section for formation of $O_2^+(b^4\Sigma_g^-)$ (51).

The total amount of energy remaining for excitation is then

$$W - \bar{E}_{ion} = 30.6 - 17.5 \pm 0.3 = 13.1 \pm 0.3 \text{ eV}$$

The average energy of subexcitation electrons, E_s, has been estimated for oxygen to be 2.5 ± 0.5 eV (10).

The energy available to produce excitation, $\bar{E}_{ex}, = W - (\bar{E}_{ion} + \bar{E}_s) = 10.6 \pm 0.8$ eV. Taking the average energy required to produce dissociative excitation by transition to the $^3\Sigma_u^+$ and $^3\Sigma_u^-$ states of oxygen as 9.0 ± 0.5 eV (52), the yield of O atoms per 100 eV should be

$$2 \times \frac{10.6 \pm 0.8}{9.0 \pm 0.5} \times G(e) = 2 \times 1.15 \pm 0.15 \times 3.27 = 7.5 \pm 0.9$$

This is consistent with the observed yield attributable to non-ionic processes. The total yield of ozone from all processes is then

$$2(1 + 1.15 \pm 0.15)\,(100/W) = 14.0 \pm 0.9$$

This is in good agreement with the observed high dose-rate yield, to which both ions and excited molecules contribute.

Comparison with High Dose-Rate Radiolysis of Other Gases

We have previously reported anomalously high yields at low pressures for the very high dose-rates available with the Febetron (53). These were attributed to acceleration of secondary electrons by the transient electric fields present at the high charge-density in the electron pulse. Over the range of pressure 500–50 Torr, increases between 40% and >100% for N_2O, HCl, HBr, and NH_3 were observed. No dependence on pressure down to 30 Torr was observed in the present work on oxygen.

We have no explanation for the lack of an increase in $G(O_3)$ at low pressures in oxygen, except possibly that secondary electrons lose their energy in the excitation of $a^1\Delta_g$ and $b^1\Sigma_g^+$ states of oxygen. Transitions to these levels are spin forbidden, but could occur near threshold energy by spin-exchange excitation. An important difference between these and the lowest levels of the hydrogen halides is that they are bound states, while the lowest levels of the other gases are repulsive.

Conclusions

The difference in yields between high and low dose rates can be explained in terms of differing ion neutralization reactions. At high dose rates, the ion neutralization reactions give two molecules of ozone per ion pair. At low dose rates, where the predominant negative ion is expected to be O_3^-, neutralization leads to no net ozone production. If this is due merely to the predominance of O_3^- as the negative ion in the neutralization complex, the initial yield (when the ozone concentration is very small) at all dose rates should be $G(O_3) = 12.8$, and then the absorbed dose at which the yield change from 12.8 to 6.2 occurs would depend upon the ion-recombination time and hence the one-half power of the dose rate. If the reduction in yield is due to more extensive clustering of the ions, then this would not depend on the absorbed dose but upon pressure and the mean ion lifetime with respect to neutralization, and hence dose rate.

For the foregoing reasons, an estimate of the low dose-rate limit of 12.8 is not at present possible. However, the suggestion made by Ghormley *et al.* (2*a*) that the ozone yield is a good optical dosimeter appears valid for the dose-rate range $6 \times 10^{25} - 2 \times 10^{27}$ eV g^{-1} s^{-1} and probably to higher dose rates.

Computer calculations indicate that clustering of the ions does not affect the yields at high dose rates where all of the important neutralization reactions give two oxygen atoms per ion pair. This must be so since the ozone yield is independent of pressure, and at 400–700 Torr the reduction in yield on addition of electron scavengers is equal to $2G(e)$.

Energy balance calculations based on the cross sections for ion yields for the average ionization energy and on electron scattering spectra for the average excitation energy give a calculated yield of $G(O_3) = 14.0 \pm 0.9$, in good agreement with the experimentally measured yield of $G(O_3) = 12.8 \pm 0.6$.

1. A. W. Boyd, C. Willis, R. Cyr, and D. A. Armstrong. Can. J. Chem. **47**, 4715 (1969).
2. (*a*) J. A. Ghormley, C. J. Hochanadel, and J. W. Boyle. J. Chem. Phys. **50**, 419 (1969). (*b*) G. M. Meaburn, D. Perner, J. LeCalve, and M. Bourene. J. Phys. Chem. **72**, 3920 (1968).

3. J. F. KIRCHER, J. S. MCNULTY, J. L. MCFARLING, and A. LEVY. Radiat. Res. **13**, 452 (1960).
4. G. R. A. JOHNSON and J. M. WARMAN. Discuss. Faraday Soc. **37**, 87 (1964).
5. J. T. SEARS and J. W. SUTHERLAND. J. Phys. Chem. **72**, 1166 (1968).
6. W. B. DEMORE and O. RAPER. J. Phys. Chem. **68**, 412 (1964).
7. M. GRIGGS. J. Chem. Phys. **49**, 857 (1968).
8. C. E. WATSON, V. A. DULOCK, JR., R. S. STOLARSKI, and A. E. S. GREEN. J. Geophys. Res. **72**, 3961 (1967).
9. F. R. GILMORE. J. Quant. Spectrosc. Radiat. Transfer, **5**, 369 (1965).
10. K. FUEKI and J. L. MAGEE. Discuss. Faraday Soc. **36**, 19 (1963).
11. W. A. JOHNSTON, F. W. LAMPE, M. L. VESTAL, and E. R. WEINER. U.S.A.E.C. Rep. JLI-2901-0-1 (1963).
12. C. WILLIS, A. E. ROTHWELL, O. A. MILLER, and A. W. BOYD. Radiat. Res. **35**, 428 (1968).
13. C. WILLIS, A. W. BOYD, and O. A. MILLER. Can. J. Chem. **47**, 3007 (1969).
14. C. WILLIS, O. A. MILLER, A. E. ROTHWELL, and A. W. BOYD. Advan. Chem. Ser. **81**, 539 (1968).
15. A. W. BOYD, C. WILLIS, and O. A. MILLER. Can. J. Chem. **47**, 351 (1969).
16. C. WILLIS, A. W. BOYD, and D. A. ARMSTRONG. Can. J. Chem. **47**, 3783 (1969).
17. F. T. JONES and T. J. SWORSKI. J. Phys. Chem. **70**, 1546 (1966).
18. C. WILLIS, W. A. SEDDON, and M. J. YOUNG. AECL Report. To be published.
19. C. J. HOCHANADEL, J. A. GHORMLEY, and J. W. BOYLE. J. Chem. Phys. **48**, 2416 (1968).
20. See review article: J. R. MCNESBY and H. OKABE. Advan. Photochem. **3**, 157 (1964).
21. D. A. DURDEN, P. KEBARLE, and A. GOOD. J. Chem. Phys. **50**, 805 (1969).
22. D. C. CONWAY and L. E. NESBITT. J. Chem. Phys. **43**, 2900 (1965).
23. D. C. CONWAY and L. E. NESBITT. J. Chem. Phys. **48**, 509 (1968).
24. D. K. BOHME. Can. J. Chem. **47**, 1809 (1969).
25. W. L. FITE. Can. J. Chem. **47**, 1797 (1969).
26. J. L. PACK and A. V. PHELPS. J. Chem. Phys. **44**, 1870 (1966).
27. L. M. CHANIN, A. V. PHELPS, and M. A. BIONDI. Phys. Rev. **128**, 219 (1962).
28. E. E. FERGUSON. Advan. Electron. Elect. Phys. **24**, 1 (1968).
29. L. B. LOEB. Basic process of gaseous electronics. Univ. Calif. Press, Berkeley and Los Angeles. 1961.
30. M. A. BIONDI. Can. J. Chem. **47**, 1711 (1969).
31. A. VON ENGEL. Ionized gases. 2nd ed. Oxford Univ. Press, London. 1965.
32. F. C. FEHSENFELD, A. L. SCHMELTEKOPF, H. I. SCHIFF, and E. E. FERGUSON. Planet. Space Sci. **15**, 373 (1967).
33. F. KAUFMAN. Progr. React. Kinet. **1**, 1 (1961).
34. H. I. SCHIFF. Can. J. Chem. **47**, 1903 (1969).
35. G. G. MEISELS. J. Chem. Phys. **41**, 51 (1964).
36. R. COOPER and R. A. MOORING. Aust. J. Chem. **21**, 2417 (1968).
37. Index of mass spectral data. Amer. Soc. Test. Mater. Philadelphia. 1963.
38. A. CORNU and R. MASSOT. Compilation of mass spectral data. Heyden and Sons, London. 1966.
39. P. H. DOOLITTLE, R. I. SCHOEN, and K. E. SCHUBERT. J. Chem. Phys. **49**, 5108 (1968).
40. V. H. DIBELER and J. A. WALKER. J. Opt. Soc. Amer. **57**, 1007 (1967).
41. F. J. COMES, F. SPEIER, and A. ELZER. Z. Naturforsch. **23a**, 114 (1968).
42. D. RAPP and P. ENGLANDER-GOLDEN. J. Chem. Phys. **43**, 1464 (1965).
43. R. I. SCHOEN. Can. J. Chem. **47**, 1879 (1969).
44. K. H. SCHMIDT. U.S.A.E.C. Res. Develop. Rep. ANL-7199 (1966).
45. F. T. CHAN. J. Chem. Phys. **49**, 2533, 2540 (1968).
46. R. N. COMPTON, L. G. CHRISTOPHOROU, G. S. HURST, and P. W. REINHARDT. J. Chem. Phys. **45**, 4634 (1966).
47. W. T. NAFF, C. D. COOPER, and R. N. COMPTON. J. Chem. Phys. In press.
48. R. H. LEE, F. A. COTTON, and G. WILKINSON. Advan. Inorg. Chem. 2nd ed. Interscience Publishers, Inc., New York. 1966.
49. B. H. MAHAN and C. E. YOUNG. J. Chem. Phys. **44**, 2192 (1966).
50. I. SANTAR and J. BEDNAR. Collect. Czech. Chem. Commun. **34**, 1 (1969).
51. J. W. MCCONKEY and J. M. WOOLSEY. J. Phys. B (At. Mol. Phys.) Ser. 2, **2**, 529 (1969).
52. E. N. LASSETTRE. Can. J. Chem. **47**, 1733 (1969).
53. A. W. BOYD, C. WILLIS, O. A. MILLER, and D. A. ARMSTRONG. Radiat. Res. **40**, 255 (1969).

Can. J. Chem. Downloaded from www.nrcresearchpress.com by 210.87.254.42 on 09/05/12
For personal use only.

Can. J. Chem. Downloaded from www.nrcresearchpress.com by 210.87.254.42 on 09/05/12
For personal use only.

Radiolysis of air and nitrogen–oxygen mixtures with intense electron pulses: determination of a mechanism by comparison of measured and computed yields[1]

C. Willis, A. W. Boyd, and M. J. Young

Physical Chemistry Branch, Chalk River Nuclear Laboratories, Atomic Energy of Canada Limited, Chalk River, Ontario

Received January 6, 1970

Air and other mixtures of nitrogen and oxygen containing from 0.1 to 100% oxygen have been irradiated with single, 0.12 Mrad electron pulses at a dose rate of 2×10^{26} eV $g^{-1}s^{-1}$. The major product formed in these irradiations is ozone. For air from 400–1500 Torr, $G(O_3) = 10.3 \pm 0.5$, the addition of SF_6 reduces this by 5.8 ± 0.5 G units. The yield of ozone from other nitrogen–oxygen mixtures varies with the concentration of oxygen. At both 700 and 1500 Torr total pressure for 1 Torr of O_2, $G(O_3) \approx 4$. This increases with oxygen concentration to a maximum of $G(O_3) = 12.8$ for pure oxygen. For all the above conditions the yield of nitrogen dioxide is below the limits of detection.

A mechanism is proposed based on known possible ionic and neutral reactions and their rate constants. Detailed computer calculations using this mechanism give results which compare well with the experimental yields. These results are consistent with an assumed yield of $G(N) = 6$ from processes involving neutral species in the radiolysis of pure nitrogen.

Canadian Journal of Chemistry, 48, 1515 (1970)

Introduction

In previous work we have shown that single pulse irradiations of gases and liquids at high dose rates give results that can generate an understanding of the mechanism involved without the added complication of product interference (1–6). This paper is a report of the application of this technique to the radiolysis of air and other nitrogen–oxygen mixtures.

There have been many studies of the low dose rate radiolysis of nitrogen–oxygen systems including extensive work by Harteck and Dondes (7–12), Dmitriev (13), and Dmitriev and Pshezhetskii (14–18). The major product observed by these workers was nitrogen dioxide with $G(NO_2) \approx 0.72$ for 1:1 N_2–O_2 mixture at 1 atm, increasing with pressure to $G(NO_2) \approx 5.6$ above 100 atm. (16). Smaller amounts of O_3, NO, and N_2O have also been reported.

Some complex pressure changes as a function of absorbed dose were observed in early work by Cloetens (19). These have been explained in terms of NO_3 and N_2O_5 both by Harteck and Dondes (11) and, in a more complete theoretical treatment, by Moseley (20). The latter author gave a general overall mechanism and this has been developed and discussed in various reviews (12, 21–23). A detailed mechanism has been difficult to establish due to lack of knowledge of specific rate constants. Recently, with the large increase of interest in aeronomy, many of the rates of reactions in ionized and non-ionized nitrogen–oxygen systems have been measured. These, coupled with the simplified conditions of single pulse irradiations, have allowed us to do detailed computer calculations and compare the results of these with our experimental measurements.

[1]AECL No. 3575.

Experimental

The pulsed radiation source used is a Febetron 705. The irradiation procedures have been reported elsewhere (3, 4, 24). Single pulses from this accelerator irradiated the gaseous mixtures contained in a multiple reflection cell fitted with a White mirror system. The cell arrangement is capable of better than 100 light passes but a maximum of four were used in the present experiments. The ozone was determined optically using the standard pulse radiolysis technique. The analyzing light was a 1600 W xenon arc which was pulsed to increase its intensity and enhance its stability. Ozone was analyzed by the light absorbed at 254 nm. The light from the xenon arc, after passage through the cell, was dispersed by a 3/4 m Spex Czerny-Turner monochromator. The appropriate wavelength was monitored by a 1P28 photomultiplier (R.C.A. Corp.). An interference filter with transmission peak at 250 nm was used to eliminate scattered light from the monochromator. The light absorbed at 254 nm was measured 10–20 ms after the irradiation pulse. More complete details of the apparatus are given elsewhere (25).

The mean dose absorbed over the cell volume was determined using oxygen at various pressures. The yield of ozone in pure oxygen is $G(O_3) = 12.8 \pm 0.6$ (5, 6, 26). For the conditions of the present experiment, the mean absorbed dose measured in this way was about 0.12 Mrad per pulse delivered at a dose rate of approximately 2×10^{26} eV g^{-1} s^{-1}. The extinction coefficient for ozone used (27, 28) was

$$\varepsilon_{254nm} = 135 \text{ cm}^{-1} \text{ S.T.P.}$$

The oxygen used was Matheson C.P. grade. The nitrogen was Matheson prepurified grade. The air was Linde

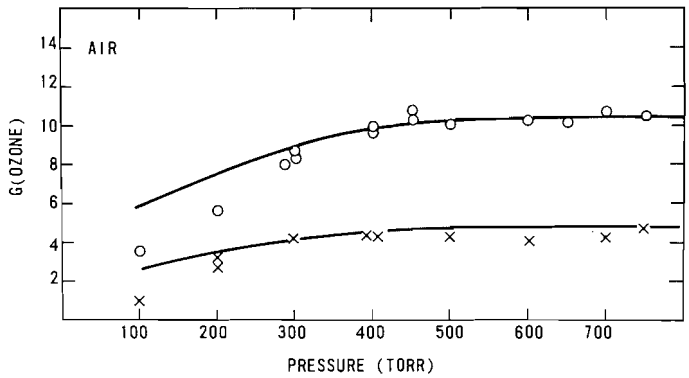

FIG. 1. Ozone yields in irradiated air: ○, pure air; ×, air + 0.5–2.0% SF_6; —, calculated yield.

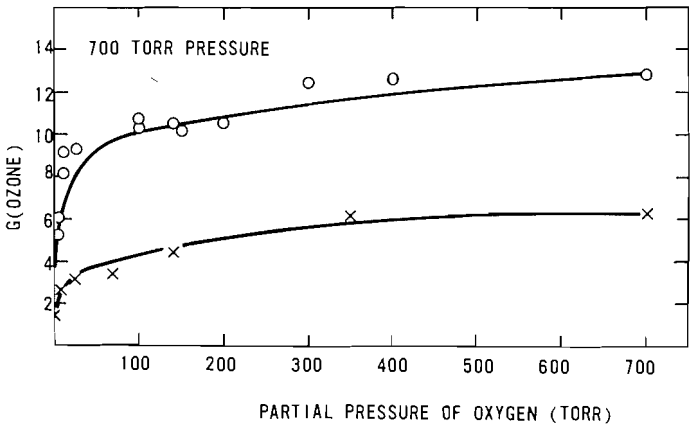

FIG. 2. Ozone yields in irradiated oxygen–nitrogen mixtures at 700 Torr pressure: ○, N_2–O_2 mixtures; ×, N_2–O_2 mixtures + 0.5–2.0% SF_6; —, calculated yield.

dry pumped, oil-free quality. All these gases were used directly from the cylinder. Sulfur hexafluoride (Matheson C.P. grade) was degassed prior to use. All gas mixtures were thoroughly mixed by thermal cycling before irradiation.

Nitrogen dioxide was measured by the method of Shinn (29). The NO_2 was converted to nitrate–nitrite by 0.1 *N* NaOH and the nitrite determined by aqueous sulfanilamide and N-(1-napthyl) ethylene-diamine hydrochloride reagents. The red azo dye color was measured at 540 nm using an equivalent molar extinction coefficient for nitrite of 53 200 cm^{-1}.

Results

Figure 1 shows the ozone yield for single pulse irradiations of air as a function of pressure. The effect of 0.5–2% SF_6 on this yield is also shown. Above 400 Torr, for pure air, $G(O_3) = 10.3 \pm 0.5$. Addition of SF_6 reduces this yield to $G(O_3) = 4.5 \pm 0.5$. Below 400 Torr, the yield of ozone from air both with and without SF_6 decreases as the pressure is reduced.

Figure 2 shows the ozone yield for single pulse irradiations of nitrogen–oxygen mixtures at a total pressure of 700 Torr as a function of the partial pressure of oxygen. The ozone yield slowly decreases from $G(O_3) = 12.8$ for pure oxygen to $G(O_3) \approx 10.0$ for 50 Torr oxygen (i.e. $N_2/O_2 = 13/1$). Below $\sim$ 20 Torr partial pressure of oxygen, the ozone yield decreases more rapidly and drops to $G(O_3) \approx 5$ for 1 Torr O_2 (i.e. $N_2/O_2 = 700/1$). The ozone yield in the presence of SF_6 shows a similar trend as a function of oxygen partial pressure, in all cases being about 50% lower than the yield observed in its absence.

The solid lines drawn in Figs. 1 and 2, both with and without SF_6, are the results from the computer calculations discussed below.

Figure 3 shows the ozone yield for single pulse irradiations of nitrogen–oxygen mixtures at a total pressure of 1500 Torr as a function of the

Can. J. Chem. Downloaded from www.nrcresearchpress.com by 210.87.254.42 on 09/05/12
For personal use only.

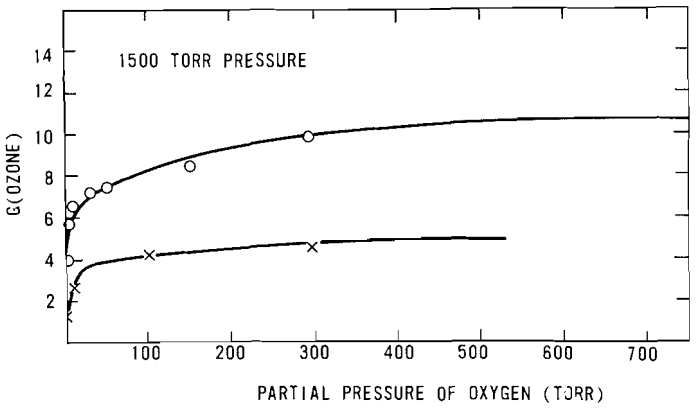

FIG. 3. Ozone yields in irradiated oxygen–nitrogen mixtures at 1500 Torr pressure: ○, N_2–O_2 mixtures, ×, N_2–O_2 mixtures plus 0.5–2.0% SF_6.

partial pressure of oxygen. The results are qualitatively similar to those observed at 700 Torr.

In all cases any nitrogen dioxide formed was below the limits of detection of the analytical procedure. Irradiations for these determinations were carried out in quartz cells (3). At a dose of 1.6 Mrad per pulse (i.e. 10 times that obtained in the optical cell), a limiting yield was estimated to be $G(NO_2) \leqslant 0.15$. Multiple pulse irradiations gave yields considerably larger but these will be reported elsewhere.

Discussion

For single pulse experiments the yields of nitrogen dioxide are very low and the yields of ozone large. This is in contrast to the yields observed from continuous irradiations at low dose rates. There is a large ionic contribution to the observed ozone yield, demonstrated by the decrease in yield on the addition of sulfur hexafluoride.

Ionic Processes

Possible ion reactions[2] that are of importance in irradiated air and nitrogen–oxygen mixtures are given in Table 1.

The predominant primary ions in irradiated nitrogen–oxygen mixtures will be N_2^+ and O_2^+. Formed with these ions will be an equivalent yield of electrons. The yield of O^+ ions from oxygen is small (6) and the yield of N^+ ions from nitrogen will probably also be small (12).

The N_2^+ ion, depending on the dose rate and oxygen concentration can, in single pulse experiments, either undergo charge exchange with oxygen as in reaction [1], or be neutralized by an electron or a negative ion as in reactions [9] and [10].

[1] $$N_2^+ + O_2 \rightarrow N_2 + O_2^+$$

[9] $$N_2^+ + e \rightarrow N + N$$

[10] $$N_2^+ + O_2^- \rightarrow N + N + O_2$$

The products of neutralization of N_2^+ by O_2^- are not known. We have assumed these to be nitrogen atoms and O_2 rather than two NO molecules or oxygen atoms and N_2. This assumption is based on the electron jump mechanism for which the products of neutralization are largely independent of the nature of the negative ion. As we have discussed elsewhere (6), O_2^- can neutralize in this way.

Reactions of N_2^+ or O_2^+ to yield other ionic species, e.g., NO^+ or NO_2^+ will not be important for single pulse experiments. Reactions of the type

[2] $$N_2 + O_2^+ \rightarrow NO^+ + NO$$

[2] N_2^+, O_2^+, and O_2^- can all react to yield N_4^+, O_4^+, and O_4^-, and also more heavily clustered species. Preliminary calculations for oxygen (6) have shown that clustering beyond O_4^+ and O_4^- can be neglected for Febetron pulse-type irradiations. N_4^+, O_4^+, and O_4^- will be formed in quantities depending upon the prevailing conditions. In general, however, for reactions pertinent to the present work, those of the X_4 type ions are similar in both stoichiometry and reaction rate to those of the X_2 type ions. N_2^+ and N_4^+ undergo almost identical charge exchanges with oxygen as shown by reactions [1] and [4]. The neutralization reactions of O_4^+ and O_4^- are apparently indistinguishable from those of O_2^+ and O_2^- (6).

No further discussion of X_4 type ions will be presented. A more complete discussion of these and also of the more heavily clustered species is given for oxygen in ref. 6.

Can. J. Chem. Downloaded from www.nrcresearchpress.com by 210.87.254.42 on 09/05/12
For personal use only.

TABLE 1

Ion–molecule reactions in N_2–O_2 irradiated mixtures

	Reaction	Rate constant (cm^3 molecule^{-1} s^{-1})	Reference
[1]	$N_2^+ + O_2 \rightarrow N_2 + O_2^+$	4.9×10^{-10}	30
		2.0×10^{-10}	31
		1.0×10^{-10}	32
		1.1×10^{-10}	33
		6.5×10^{-11}	34
		8.6×10^{-11}	35,36
[2]	$O_2^+ + N_2 \rightarrow NO^+ + NO$	$< 1\times10^{-15}$	33,37,38
		$< 2\times10^{-16}$	30
[3]*	$N_2^+ + 2N_2 \rightarrow N_4^+ + N_2$	1×10^{-28}	39
[4]	$N_4^+ + O_2 \rightarrow O_2^+ + 2N_2$	1×10^{-10}	30
[5]	$N_2^+ + NO \rightarrow NO^+ + N_2$	5×10^{-10}	33,37,38,40
[6]	$O_2^+ + NO \rightarrow NO^+ + O_2$	8×10^{-10}	33,37,38
[7]	$NO^+ + e \rightarrow N + O$	4×10^{-7}	41
[8]	$O_2^+ + e \rightarrow O + O$	2×10^{-7}	41
[8*a*]	$O_2^+ + O_2^- \rightarrow O + O + O_2$	2×10^{-6}	41
[9]	$N_2^+ + e \rightarrow N + N$	1×10^{-7}	41
[10]	$N_2^+ + O_2^- \rightarrow N + N + O_2$	2×10^{-6}	41
[11]*	$e + 2O_2 \rightarrow O_2^- + O_2$	$1.4\times10^{-29}\left(\frac{300}{T}\right)\exp\left(\frac{-600}{T}\right)$	42
[12]*	$e + O_2 + N_2 \rightarrow O_2^- + N_2$	1.0×10^{-31}	43,44,45
[13]†	$e + NO_2 + N_2 \rightarrow NO_2^- + N_2$	4×10^{-11}	46,47
[14]*	$e + NO + M \rightarrow NO^- + M$	1.3×10^{-31}	48,49
[15]	$O_2^- + O_3 \rightarrow O_3^- + O_2$	3×10^{-10}	50
		4×10^{-10}	51
[16]	$O_3^- + NO \rightarrow NO_2^- + O_2$	8×10^{-10}	51
[17]	$O_3^- + NO_2 \rightarrow NO_2^- + O_3$	7×10^{-10}	52
[18]	$NO_2^- + O_3 \rightarrow NO_3^- + O_2$	1×10^{-11}	50,51
[19]	$NO^- + O_2 \rightarrow O_2^- + NO$	9×10^{-10}	53

*The rate constants for these reactions have three body units, i.e., cm^6 molecule^{-2} s^{-1}.
†This is the "limiting" two body rate constant, see ref. 41.

involving coalescence of the two molecules and considerable rearrangement, are very much slower than charge transfer reactions and will not compete. When products are present during irradiation, such as for multiple pulse experiments or continuous irradiation, other ions can be formed by charge transfer reactions, e.g.

[6] $O_2^+ + NO \rightarrow NO^+ + O_2$

In fact, for low dose rate continuous irradiation the stationary state concentration of NO should be sufficient for NO^+ to be the predominant positive ion participating in the neutralization reaction in nitrogen–oxygen mixtures, even at very low concentrations of oxygen.

In the absence of significant amounts of NO and NO_2 then, the only fate of N_2^+ is charge exchange with O_2 or neutralization, the only fate of the O_2^+ is neutralization

[8] $O_2^+ + e \rightarrow 2O$

[8*a*] $O_2^+ + O_2^- \rightarrow 2O + O_2$

Thus the reactive products of all ionic reactions are N atoms and O atoms.

Neutral Processes and Computer Calculations

Table 2 shows reactions of N atoms and O atoms in nitrogen–oxygen mixtures. Under continuous irradiation all of the listed reactions probably occur and it is not immediately apparent which are really important to the radiolysis mechanism even for single pulse experiments. To determine this we have used computer calculations to investigate the importance of the various reactions.

The program used was that originally written as WR 16 by Schmidt (73). We have previously used this program in other extensive calculations of this type (2, 4, 6). The input data required are the yields of the various initial species, the rate constants of all reactions and the radiation pulse shape. We included both ionic and neutral reactions. The Febetron pulse was approximated by a step function with 2 ns steps. The yield input

Can. J. Chem. Downloaded from www.nrcresearchpress.com by 210.87.254.42 on 09/05/12
For personal use only.

TABLE 2
Neutral–neutral reactions in N_2–O_2 irradiated mixtures

	Reaction	Rate constant (cm^3 molecule^{-1} s^{-1})	Reference
[20]	$N + O + M \rightarrow NO + M$	9×10^{-33}	54
		1.1×10^{-32}	55
[21]	$N + N + N_2 \rightarrow 2N_2$	2.1×10^{-33}	54
		2.25×10^{-32}	56
		3.8×10^{-33}	57
		7.4×10^{-33}	58
[22]	$N + O_2 \rightarrow NO + O$	$1.4 \times 10^{-11} \exp\left(-\frac{7100}{RT}\right)$	59
		$6.5 \times 10^{-12} \exp\left(-\frac{7000}{RT}\right)$	60
		$2.33 \times 10^{-11} \exp\left(-\frac{7900}{RT}\right)$	61
		$1.2 \times 10^{-11} \exp\left(-\frac{6200}{RT}\right)$	62
[23]	$N + O_3 \rightarrow NO + O_2$	$5.7 \pm 1.4 \times 10^{-13}$	63
[24]	$N + NO \rightarrow N_2 + O$	2.2×10^{-11}	63
[25]	$N + NO_2 \rightarrow N_2O + O$	7.7×10^{-12}	64
[26]	$N + NO_2 \rightarrow 2NO$	5.9×10^{-12}	64
[27]	$N + NO_2 \rightarrow N_2 + O_2$	1.8×10^{-12}	64
[28]	$N + NO_2 \rightarrow N_2 + 2O$	2.3×10^{-12}	64
[29]*	$O + 2O_2 \rightarrow O_3 + O_2$	2.8×10^{-34}	65,66
		8.9×10^{-34}	67
[30]*	$O + O + O_2 \rightarrow 2O_2$	2.0×10^{-33}	55
[31]	$O + O_3 \rightarrow 2O_2$	1.0×10^{-14}	68
[32]*	$O + NO + O_2 \rightarrow NO_2 + O_2$	8.1×10^{-32}	69,70
[33]*	$O + NO + N_2 \rightarrow NO_2 + N_2$	1.1×10^{-31}	70
[34]	$O + NO_2 \rightarrow NO + O_2$	$3.2 \times 10^{-11} \exp\left(-\frac{600}{RT}\right)$	70
		$1.5 \times 10^{-11} \exp\left(-\frac{600}{RT}\right)$	63
[35]*	$O_2 + 2NO \rightarrow 2\ NO_2$	1×10^{-33}	71
[36]	$O_3 + NO \rightarrow NO_2 + O_2$	$0.95 \times 10^{-12} \exp\left(-\frac{2460}{RT}\right)$	63,72

*The rate constants for these reactions have three-body units.

data used were: for pure nitrogen, $G(N_2^+) = 2.9$, $G(N) = 6.0$; for pure oxygen, $G(O_2^+) = 3.3$, $G(O) = 6.1$. This gives for air; $G(N_2^+) = 2.40$, $G(O_2^+) = 0.66$, $G(e) = 3.06$, $G(N) = 4.80$, $G(O) = 1.24$, assuming the absorbed dose in each of the constituents is proportional to its electron density. $G(N)$ and $G(O)$ are the yields of these atoms formed by dissociation of excited molecules. The values of $G(N_2^+)$ and $G(O_2^+)$ are derived from the W values; $W_{N_2} = 34.7$ eV per ion pair (74) and $W_{O_2} = 30.6$ eV per ion pair (75). The value of $G(N) = 6.0$ is that recommended by Harteck and Dondes (12). The yield of N atoms given from experiments on the radiation induced isotopic exchange of N_2 (76–78) is ambiguous since the exchange mechanism is not clearly established. However, using the arguments given by Anbar and Perlstein (78), a value of $G(N) = 5.8$ can be obtained from the work of Dawes and Back (77). The agreement which we obtain below between experiment and calculation substantiates a value of close to $G(N) = 6.0$. The value of $G(O) = 6.1$ for oxygen radiolysis is that given by us from pulsed experiments with oxygen (6).

The calculated concentrations of species as a function of time for a single pulse in air are given in graphical form in Fig. 4. As can clearly be seen, the predominant charged species are O_2^+ and the electron with smaller concentrations of N_2^+ and O_2^-. The right hand side of the figure shows the concentrations of neutral species after

Can. J. Chem. Downloaded from www.nrcresearchpress.com by 210.87.254.42 on 09/05/12
For personal use only.

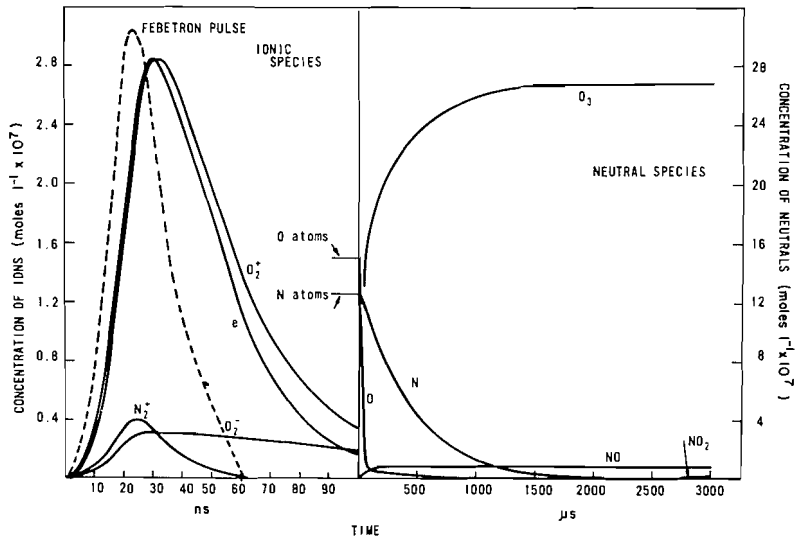

FIG. 4. Calculated concentrations of ionic and neutral species during and after a Febetron pulse in air at 830 Torr: total dose, 1.06×10^{19} eV g^{-1}; Febetron pulse intensity can be taken from ordinate axis with units 0.5×10^{-26} eV l^{-1} s^{-1}, i.e. peak intensity 6.2×10^{26} eV l^{-1} s^{-1}.

the pulse. The concentration of O atoms existing immediately after the pulse decreases very rapidly whereas the concentration of N atoms falls much more slowly. This slower decrease in N atom concentration controls the build up of ozone in the later stages. The concentrations of NO and NO_2 are small. On a time scale longer than that of the figure the NO concentration decreases by reaction with ozone

[36] $$NO + O_3 \rightarrow NO_2 + O_2$$

and the ozone concentration decreases and the NO_2 concentration increases appropriately. The yield of ozone calculated when the NO concentration has fallen to zero can then be compared with the experimentally observed values.

The calculated yields of ozone and nitrogen dioxide do not depend critically upon the rate constants used for the reactions of the ionic species. The value of k_1 relative to both k_9 and k_{10} does affect the yield to some extent, particularly under other conditions of dose rate as we shall see, but all of these rate constants are fairly well established. The value of k_1 used was 1.5×10^{-10} cm^3 $molecule^{-1}$ s^{-1} as given in a review by Fite (79).

The calculated yields are more dependent on the rate constants chosen for the reactions of both N atoms and O atoms. The reactions of N atoms which most affect the calculations, at least for the dose rates used in our experiments are

[22] $$N + O_2 \rightarrow NO + O$$

[24] $$N + NO \rightarrow N_2 + O$$

and

[23] $$N + O_3 \rightarrow NO + O_2$$

Using the rate constants given in Table 2, a good fit cannot be obtained. For example, the calculated ozone yield for 700 Torr air is $G(O_3) = 8.6$. This is too low even considering the experimental errors involved. Changing any one of the rate constants for the above three reactions can give a fit for $G(O_3)$ in 700 Torr air. The value for the rate constant for reaction [22], however, is well established for 298 °K and although this reaction does have a significant activation energy, our knowledge of the ambient temperature during irradiation is almost certainly better than ± 10 °C. Reaction [24] is the standard for N atom determinations and the rate constant must be accepted. The weight of evidence for k_{23} is less and we have chosen to vary it. Phillips and Schiff (63) give $k_{23} = 5.7 \pm 1.4 \times 10^{-13}$ cm^3 $molecule^{-1}$ s^{-1}. Taking a value one third of this, i.e. 2×10^{-13} cm^3 $molecule^{-1}$ s^{-1}, at 25 °C, the fit shown by the solid lines in Figs. 1 and 2 is obtained. The fit to $G(O_3) = 10.3$ for air above 400 Torr is very good. This uses $k_{21} = 5.0 \times 10^{-33}$ cm^3 $molecule^{-1}$ s^{-1}.

An alternative to decreasing k_{23} is to decrease the rate of ozone formation by decreasing k_{29}

Can. J. Chem. Downloaded from www.nrcresearchpress.com by 210.87.254.42 on 09/05/12
For personal use only.

TABLE 3

Importance of various reactions in irradiated N_2–O_2 mixtures as a function of O_2 partial pressure*

	% of N_2^+ reaction when P_{O_2} (Torr) =						
Reaction	1	10	50	100	140	250	450
[1] $N_2^+ + O_2$	14.3	69.1	88.3	93.2	95.3	96.8	97.6
[9] $N_2^+ + e$	85.6	35.2	8.6	3.9	2.1	1.0	0.4
[10] $N_2^+ + O_2^-$	0.1	3.9	3.1	2.9	2.6	2.2	2.0
	% of N atom reaction when P_{O_2} (Torr) =						
Reaction	1	10	50	100	140	250	450
[22] $N + O_2$	5.8	16.4	31.1	38.2	43.3	50.2	60.0
[24] $N + NO$	23.7	44.3	47.0	46.7	45.6	42.2	34.1
[23] $N + O_3$	8.5	25.0	17.7	12.7	9.6	6.9	5.5
[21] $N + N$	52.4	10.4	3.1	1.7	1.0	0.5	0.2
[20] $N + O$	9.6	3.8	1.2	0.6	0.4	0.2	0.1
	% of O atom reaction when P_{O_2} (Torr) =						
Reaction	1	10	50	100	140	250	450
[29] $O + O_2$	70.3	96.2	99.3	99.7	99.8	99.9	100.0
[20] $O + N$	29.7	3.8	0.7	0.3	0.2	0.1	0.0
	Value when P_{O_2} (Torr) =						
Parameter	1	10	50	100	140	250	450
$G(NO_2)$ (calculated)	0	0.02	0.2	0.3	0.4	0.6	0.8
$G(O_3)$ (calculated)	2.0	6.0	9.0	10.0	10.3	11.2	12.0
$G(O_3)$ (observed)	5.0	8.0	—	10.2	10.3	12.2	12.6

*Pressure of system = 700 Torr.

[29] $O + 2O_2 \rightarrow O_3 + O_2$

However, in our calculations we have used the value of Sauer (65) and Sauer and Dorfman (66) which is probably a lower limit.

To help in understanding the mechanism involved in pulse irradiated nitrogen–oxygen mixtures, Table 3 gives the results of detailed calculations of the contributions of the most important reactions as a function of O_2 partial pressure in N_2–O_2 mixtures at 700 Torr.

Conditions for maximum ozone production would be: (*1*) complete charge transfer from all N_2^+ to O_2; (*2*) neutralization of the O_2^+ ion to yield two O atoms; (*3*) half the N atoms reacting with O_2 by reaction [22] and the other half with the NO by reaction [24], thus preventing reaction [36]; (*4*) the O atoms forming ozone via reaction [29]. This would give for air $G(NO_2) = 0$ and $G(O_3) = 2G(e) + G(N) + G(O) = 2(3.06) + 4.80 + 1.24 = 12.16$. As can be seen, the conditions of 140 Torr O_2 nearly approximate to this and account for the large yield of $G(O_3) = 10.3$ observed.

As the partial pressure of O_2 is reduced, less charge transfer to oxygen occurs and more N_2^+ is directly neutralized giving N atoms. At the same time fewer N atoms react with O_2 by reaction [22] and more undergo atom combination reactions [20] and [21]

[20] $N + O + N_2 \rightarrow NO + N_2$

[21] $N + N + N_2 \rightarrow 2N_2$

These changes lead to reduced ozone yields.

Other neutral reactions given in Table 2 but not referred to in Table 3 contribute less than 1% to the reaction mechanism for single pulse, Febetron-type experiments.

The effect of SF_6 addition is presumably due to electron capture and subsequent suppression of dissociative neutralization reactions (6). In general this will not be a direct function of the W value since not all charge neutralizations lead to ozone (since not all N atoms yield ozone). However for air, at 700 Torr, this is near enough the case and it is encouraging to see that for 0.5–2% SF_6, for air between 400 and 760 Torr, $\Delta G(O_3) =$

Can. J. Chem. Downloaded from www.nrcresearchpress.com by 210.87.254.42 on 09/05/12
For personal use only.

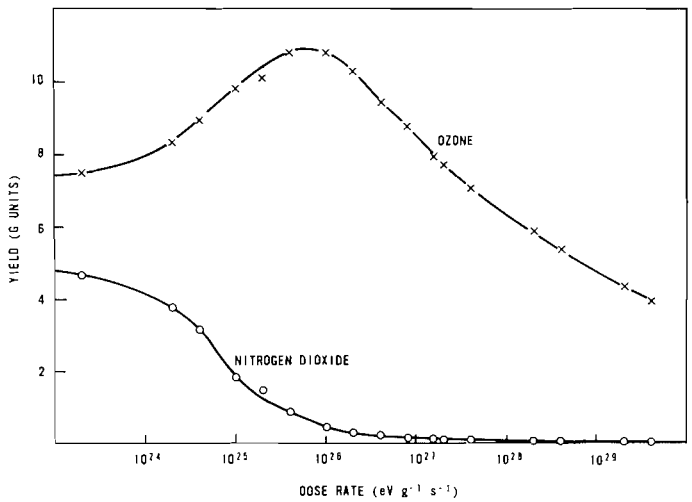

FIG. 5. Calculated yields of ozone and nitrogen dioxide in single pulse irradiations of air at 700 Torr.

$(10.3 \pm 0.5) - (4.5 \pm 0.5) = 5.8$; which is slightly less than $2\ G(e) = 6.12$, in agreement with the proposed mechanism.

A reasonable fit of experimental results to the calculated yields has been obtained for the variety of conditions given in Figs. 1, 2, and 3 and this gives fair confidence in both the mechanism and the specific rate constants used. The fit to low pressures of air, Fig. 1, is not as good as elsewhere and we have no explanation for this. However, experiments in this region do encounter experimental problems which could enlarge the errors.

Calculation of Yields as a Function of Dose Rate

There are obvious dose rate dependent reactions in single pulse irradiations of air (and nitrogen–oxygen mixtures) and it would be very interesting to investigate these. Unfortunately it is difficult to do this experimentally, but it can be done by calculation. Figure 5 shows the calculated yields of ozone and nitrogen dioxide in air at 700 Torr as a function of dose rate for single irradiation pulses from 10^{23}–4×10^{29} eV $g^{-1}\ s^{-1}$. Each is for a constant pulse length and therefore as the dose rate increases the dose per pulse increases proportionately.

At the low dose rates, the ozone yield is tending to $G(O_3) = 7.4$ and the nitrogen dioxide yield to $G(NO_2) = 4.8$. Here, all N_2^+ ions undergo the charge transfer reaction [1] and the O_2^+ ions are neutralized by O_2^-. The yield of O atoms from these reactions will be $2G(e) = 6.12$ and all will yield ozone. All initially formed O atoms will also yield ozone. The N atoms in the system will all react with O_2 by reaction [22] to give equal amounts of NO and O.

[22] $$N + O_2 \rightarrow NO + O$$

The O atoms formed in this reaction will yield ozone which will then react with the NO in reaction [36] giving only NO_2 and no net ozone yield from N atoms. The limiting yields should be

$$G(O_3) = 2G(e) + G(O) = 7.36$$

and

$$G(NO_2) = G(N) = 4.80$$

As the dose per pulse is increased, reaction [24] will compete with reaction [22] for N atoms; the ozone yield should increase to a maximum and the nitrogen dioxide yield should decrease as shown in Fig. 5.

Further increase of the dose rate reduces the yields by the introduction of two types of competition which are the same as those occurring at low partial pressures of oxygen. Direct neutralization of N_2^+ to yield N atoms will compete with the charge transfer reaction [1]. At the same time less ozone will be produced by the N atoms due to the increase in atom combination reactions [21] and [20].

The useful dose rate range available with the Febetron using our optical techniques for ozone is $1–30 \times 10^{25}$ eV $g^{-1}\ s^{-1}$. This corresponds to the region of the maximum in Fig. 5 and thus does not allow us to test our proposed mechanism.

Can. J. Chem. Downloaded from www.nrcresearchpress.com by 210.87.254.42 on 09/05/12
For personal use only.

Can. J. Chem. Downloaded from www.nrcresearchpress.com by 210.87.254.42 on 09/05/12
For personal use only.

An additional test of the mechanism would be provided by measurement of the initial NO_2 yields at lower dose rates and also by measurement of NO_2 yields in multiple pulse irradiations at Febetron dose rates. This work is being carried out and will be reported later.

Low Dose Rate Mechanism

(a) Ionic Processes

At low dose rates, where ion recombination is slow, the neutralization processes will involve the thermodynamically most stable positive and negative ions. Table 4 gives the ionization potentials and electron affinities of the appropriate molecular species that can be present in irradiated nitrogen–oxygen mixtures. The species with the lowest ionization potential is NO and that with the highest electron affinity is NO_2. None of the reaction rates given in Table 1 preclude formation of these and thus the predominant ion neutralization process under continuous low dose rate irradiation will probably be reaction [37].

[37] $$NO^+ + NO_2^- \rightarrow \text{products}$$

We do not know the products of this neutralization reaction. In all probability it will lead to no net yield of ozone or nitrogen dioxide. Moreover, neutralization steps at low dose rates involve clustered ions with reduced probability of dissociative neutralization. We have discussed this with regard to neutralization steps in the radiolysis of oxygen (6) and the argument given there can be applied to nitrogen–oxygen mixtures.

(b) Neutral Processes

As soon as a low stationary state concentration of ozone has built up and some nitrogen dioxide has been produced, the predominant N atom reactions occurring will be

[23] $$N + O_3 \rightarrow NO + O_2$$

[25] $$N + NO_2 \rightarrow N_2O + O$$

[26] $$N + NO_2 \rightarrow 2NO$$

[27] $$N + NO_2 \rightarrow N_2 + O_2$$

[28] $$N + NO_2 \rightarrow N_2 + 2O$$

with

[36] $$NO + O_3 \rightarrow NO_2 + O_2$$

and

[35] $$O_2 + 2NO \rightarrow 2NO_2$$

accounting for final removal of nitric oxide. Production of NO_3 and N_2O_5 transients has been discussed elsewhere (11, 20).

Thus, with no ionic contribution to the nitrogen dioxide yield, the maximum yield should be close to $G(N) + G(O) = 6$, for air. The maximum yield observed by Dmitriev (16) at pressure in excess of 150 atm. of $G(NO_2) \approx 5.0$ is in fair agreement with this. Lower values of $G(NO_2)$ were observed at lower pressures. This pressure effect can be explained by the reactions involving oxygen atoms.

[29] $$O + O_2 + N_2 \rightarrow O_3 + N_2$$

[34] $$O + NO_2 \rightarrow NO + O_2$$

Higher pressures will favor reaction [29] yielding O_3 for reaction [23]. Reaction [34] gives no net NO_2 for the loss of an oxygen atom.

Comparison with Previous Ozone Determinations

There have been no other directly parallel studies published. Most irradiations of nitrogen and nitrogen–oxygen mixtures have been carried out at low dose rates and usually, in the case of nitrogen–oxygen mixtures, to relatively high absorbed doses to explore the possibilities of nitrogen fixation by radiation.

One yield of ozone at low doses for low dose rates has been reported. Johnson and Warman (85) give an initial yield of $G(O_3) = 12$ for nitrogen–oxygen mixtures at about 800 Torr pressure. This yield is numerically incorrect, as we have discussed elsewhere (5), and must be corrected for the dosimetry and also for the stoichiometry used for the ozone analysis. A corrected yield is $G(O_3) \approx 6$. This is very close to the yield of $G(O_3) = 7.4$ for initial yields at low

TABLE 4

Ionization potentials and electron affinities of molecular species present in irradiated N_2–O_2 mixtures

Species	Ionization potentials	Electron affinities
N_2	15.58*	—
O_2	12.2*	0.43 ± 0.02‡
O_3	12.8†	1.9 ± 0.4‡
NO	9.25*	< 0.43‡§
NO_2	9.78†	~ 4.0‡§
N_2O	12.89†	< 1.60‖

*See ref. 80.
†See ref. 81.
‡See ref. 82.
§See ref. 83.
‖Since SF_6 reduces the yields in irradiated nitrous oxide (see ref. 4), the electron affinity of N_2O must be less than that of SF_6 (84).

dose rates predicted in Fig. 5. However, most of this calculated yield is due to ionic precursors and, as we have pointed out (5, 6) for oxygen systems in low dose rate irradiations no ozone is produced from ionic processes (at any significant dose). Thus the predicted measurable yield at low dose rates is only that formed from O atoms, i.e. $G(O_3) = 7.4 - 6.1 = 1.3$. The high value of $G(O_3) = 6$ of Johnson and Warman can perhaps be explained in terms of the iodide analytical procedure used for ozone determinations. The NO_2 interferes with the iodide method and must be eliminated by the addition of sulfanilic acid reagent (86). The authors do not report that this is done.

We should like to thank Professor D. A. Armstrong, University of Calgary, for his critical review of the manuscript and his helpful comments.

1. A. W. Boyd, C. Willis, O. A. Miller, and A. E. Rothwell. Advan. Chem. Ser. **82**, 456 (1968).
2. C. Willis, A. W. Boyd, A. E. Rothwell, and O. A. Miller. Intern. J. Rad. Phys. Chem. **1**, 373 (1969).
3. C. Willis, A. W. Boyd, and O. A. Miller. Can. J. Chem. **47**, 3007 (1969).
4. C. Willis, A. W. Boyd, and D. A. Armstrong. Can. J. Chem. **47**, 3783 (1969).
5. A. W. Boyd, C. Willis, R. Cyr, and D. A. Armstrong. Can. J. Chem. **47**, 4715 (1969).
6. C. Willis, A. W. Boyd, M. J. Young, and D. A. Armstrong. Can. J. Chem. This issue.
7. P. Harteck and S. Dondes. Nucleonics, **14**, 22 (1956).
8. P. Harteck and S. Dondes. J. Chem. Phys. **27**, 546 (1957).
9. P. Harteck and S. Dondes. J. Chem. Phys. **28**, 975 (1958).
10. P. Harteck and S. Dondes. Proc. 2nd Intern. Conf. Peaceful Uses of Atomic Energy U. N. Geneva, **29**, 415 (1958).
11. P. Harteck and S. Dondes. J. Phys. Chem. **63**, 956 (1959).
12. P. Harteck and S. Dondes. Science, **146**, 30 (1964).
13. M. T. Dmitriev. Zh. Fiz. Khim. **32**, 2418 (1958).
14. M. T. Dmitriev and S. Ya. Pshezhetskii. Intern. J. Appl. Rad. Isotopes, **5**, 67 (1959).
15. M. T. Dmitriev and S. Ya. Pshezhetskii. Russ. J. Phys. Chem. **34**, 418 (1960).
16. M. T. Dmitriev. Russ. J. Phys. Chem. **35**, 495 (1961); At. Energ. **15**, 52 (1963); **16**, 282 (1964).
17. M. T. Dmitriev. Russ. J. Phys. Chem. **40**, 819 (1966); **40**, 939 (1966).
18. M. T. Dmitriev. Russ. J. Phys. Chem. **40**, 1467 (1966).
19. R. Cloetens. Bull. Soc. Chim. Belg. **45**, 97 (1936).
20. F. Moseley. AERE report C/R 2802 (1959).
21. S. Ya. Pshezhetskii. Radiation Chemistry, Moscow Conference. 1955 AEC Translation Vol. 1. 1957. pp. 23–28.
22. S. C. Lind. Radiation chemistry of gases. ACS Monograph Rheinhold Publishing Corp. 1961. p. 232.
23. A. R. Anderson. Fundamental processes in radiation chemistry. Interscience Publishers, Inc., New York. 1968. p. 311.
24. A. W. Boyd, D. A. Armstrong, C. Willis, and O. A. Miller. Radiation Res. **40**, 255 (1969).
25. M. J. Young, W. A. Seddon, and C. Willis. AECL Report. To be published.
26. J. Ghormley, C. Hochandel, and J. Boyle. J. Chem. Phys. **50**, 419 (1969).
27. W. B. DeMore and O. Raper. J. Phys. Chem. **68**, 412 (1964).
28. M. Griggs. J. Chem. Phys. **49**, 857 (1968).
29. M. B. Shinn. Ind. Eng. Chem. Anal. Ed. **13**, 33 (1941).
30. M. M. Shanin. J. Chem. Phys. **47**, 4392 (1967).
31. W. L. Fite. J. A. Rutherford, W. R. Snow, and V. A. J. Van Lint. Discuss. Faraday Soc. **33**, 264 (1962).
32. F. C. Fehsenfeld, A. L. Schmeltekopf, and E. E. Ferguson. Planet. Space Sci. **13**, 919 (1965).
33. P. Warneck. J. Geophys. Res. **72**, 1651 (1967).
34. V. Aguilanti and G. G. Volpi. Ric. Sci. **36**, 359 (1966).
35. D. E. Golden, G. Sinnott, and R. W. Varney. Phys. Rev. Lett. **20**, 239 (1968).
36. M. A. Biondi. Can. J. Chem. **47**, 1812 (1969).
37. P. Warneck. Planet. Space Sci. **15**, 1349 (1967).
38. E. E. Ferguson. J. Geophys. Res. **70**, 4323 (1965).
39. P. Warneck. J. Chem. Phys. **46**, 502 (1967).
40. J. W. McGowan. Can. J. Chem. **47**, 1779 (1969).
41. E. E. Ferguson. Advan. Electron. Electron Phys. **24**, 1 (1968).
42. J. L. Pack and A. V. Phelps. J. Chem. Phys. **48**, 3070 (1968).
43. L. M. Chanin, A. V. Phelps, and M. A. Biondi. Phys. Rev. **128**, 219 (1962).
44. M. A. Biondi. Phys. Rev. **84**, 1072A (1951).
45. M. Hirsh, P. Eisner, J. Slerin, and G. Halpern. Bull. Amer. Chem. Soc. **11**, 495 (1966).
46. B. H. Mahan and I. C. Walker. J. Chem. Phys. **47**, 3780 (1967).
47. A. V. Phelps. Can. J. Chem. **47**, 1783 (1969).
48. C. S. Weller and M. A. Biondi. Bull. Amer. Chem. Soc. **11**, 495 (1966).
49. C. S. Weller and M. A. Biondi. Phys. Rev. **172**, 198 (1968).
50. F. C. Fehsenfeld, A. L. Schmeltekopf, H. I. Schiff, and E. E. Ferguson. Planet. Space. Sci. **15**, 373 (1967).
51. E. E. Ferguson. Can. J. Chem. **47**, 1815 (1969).
52. J. A. Rutherford and B. R. Turner. J. Geophys. Rev. **72**, 3795 (1967).
53. F. C. Fehsenfeld, E. E. Ferguson, and A. L. Schmeltekopf. J. Chem. Phys. **45**, 1844 (1966).
54. C. B. Kretschmer and H. L. Petersen. J. Chem. Phys. **39**, 1772 (1964).
55. I. M. Campbell and B. A. Thrush. Proc. Roy. Soc. London, Ser. A, **296**, 222 (1967).
56. K. M. Evanson and D. S. Burch. J. Chem. Phys. **45**, 2450 (1966).
57. I. M. Campbell and B. A. Thrush. Proc. Roy. Soc. London, Ser. A, **296**, 201 (1967).
58. M. A. A. Clyne and D. H. Stedman. J. Phys. Chem. **71**, 3071 (1967).
59. F. Kaufman. DASA Reaction Rate Handbook 14-1 (1967).
60. A. S. Vlastaras and C. A. Winkler. Can. J. Chem. **54**, 2837 (1967).
61. W. E. Wilson. J. Chem. Phys. **46**, 2017 (1967).
62. G. B. Kistiakowsky and G. G. Volpi. J. Chem. Phys. **15**, 237 (1961).
63. L. F. Phillips and H. I. Schiff. J. Chem. Phys. **36**, 1509 (1962).

Can. J. Chem. Downloaded from www.nrcresearchpress.com by 210.87.254.42 on 09/05/12
For personal use only.

64. L. F. PHILLIPS and H. I. SCHIFF. J. Chem. Phys. **42**, 3171 (1965).
65. M. C. SAUER. J. Phys. Chem. **71**, 3311 (1967).
66. M. C. SAUER and L. M. DORFMAN. J. Amer. Chem. Soc. **87**, 3801 (1965).
67. M. F. R. MALCAHY and D. J. WILLIAMS. Trans. Faraday Soc. **64**, 59 (1968).
68. H. I. SCHIFF. Can. J. Chem. **47**, 1903 (1969).
69. A. A. WESTENBERG and N. DEHAAS. J. Chem. Phys. **40**, 3087 (1964).
70. F. S. KLEIN and J. T. HERRON. J. Chem. Phys. **41**, 1285 (1964).
71. P. G. ASHMORE, M. G. BURNETT, and B. J. TYLER. Trans. Faraday Soc. **58**, 685 (1962).
72. M. A. A. CLYNE, B. A. THRUSH, and R. P. WAYNE. Trans. Faraday Soc. **60**, 359 (1964).
73. K. H. SCHMIDT. AEC Research and Development Report ANL 7199 (1966).
74. R. J. WEISS and W. BERNSTEIN. Radiation Res. **6**, 603 (1957).
75. G. G. MEISELS. J. Chem. Phys. **41**, 51 (1964).
76. M. ANBAR and P. PERLSTEIN. J. Phys. Chem. **68**, 1234 (1964).
77. D. H. DAWES and R. A. BACK. J. Phys. Chem. **69**, 2385 (1965).
78. M. ANBAR and P. PERLSTEIN. J. Phys. Chem. **70**, 2052 (1966).
79. W. L. FITE. Can. J. Chem. **47**, 1797 (1969).
80. V. I. VEDENEYEV et al. Bond energies, ionization potentials and electron affinities. Edward Arnold Publishers, London. 1962.
81. G. HERZBERG. Spectra of polyatomic molecules. D. Van Nostrand Co. Inc., New York. 1968.
82. A. V. PHELPS. Can. J. Chem. **47**, 1783 (1969).
83. A. L. FARRAGHER, F. M. PAGE, and R. C. WHEELER, Discuss. Faraday Soc. **37**, 203 (1964).
84. J. KAY and F. M. PAGE. Trans. Faraday Soc. **60**, 1042 (1964).
85. G. R. A. JOHNSON and J. M. WARMAN. Discuss. Faraday Soc. **37**, 87 (1964).
86. D. H. BYERS and B. E. SALTZMAN. Advan. Chem. Ser. **21**, 93 (1959).

Can. J. Chem. Downloaded from www.nrcresearchpress.com by 210.87.254.42 on 09/05/12
For personal use only.

Can. J. Chem. Downloaded from www.nrcresearchpress.com by 210.87.254.42 on 09/05/12
For personal use only.

Acetone-sensitized photodimerization of 3-carene-2,5-dione[1]

IAN W. J. STILL,[2] C. J. MACDONALD, AND (MRS.) Y.–N. OH
Department of Chemistry, University of Toronto, Toronto 181, Ontario, Canada

Received August 15, 1969

Ultraviolet irradiation of 3-carene-2,5-dione **1** in acetone has been found to yield three cyclobutane-type photodimers. A detailed spectroscopic study of these compounds has shown that the two most abundant dimers possess the *head-to-head* orientation. The *head-to-head* dimers have been shown to possess the *anti–anti–anti* and *syn–anti–syn* structures **10** and **8** respectively, while the minor, *head-to-tail* product has one of the corresponding structures **9** or **11**. In all three cases, the cyclobutane and cyclohexane rings are *cis*-fused. Nuclear Overhauser effects enable structures **8** and **10** to be specifically assigned to dimer *B* and dimer *A*, respectively.

Canadian Journal of Chemistry, **48**, 1526 (1970)

As part of a general study of the reactions of 3-carene-2,5-dione **1** and related bicyclo[4.1.0]-heptane derivatives (cf. ref. 1), we earlier observed that photochemical addition reactions between the title compound and various alkenes and alkynes led almost exclusively to the formation of cyclobutane (and cyclobutene) adducts (2). That is, the preferred mode of addition is to the carbon–carbon double bond of the enedione system. We now wish to report the isolation of three crystalline photodimers of 3-carene-2,5-dione, all of which are of the cyclobutane type (**2** or **3**), and to describe the detailed orientational and stereochemical assignment for these photodimers.

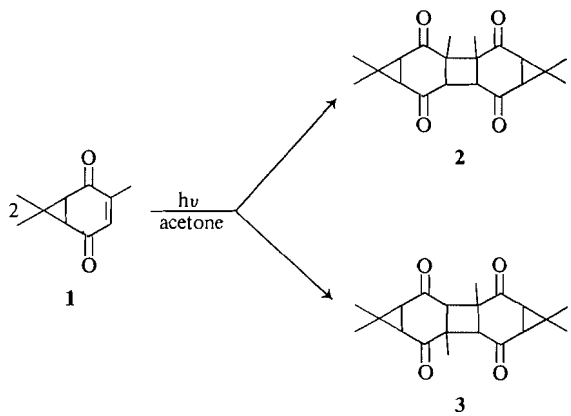

The formation of such cyclobutane-type dimers is now a well established phenomenon in the case of olefins, α,β-unsaturated ketones and carboxylic acid derivatives, and quinones (3, 4) but has not previously been reported to our knowledge for an enedione system such as is present in 3-carene-2,5-dione. This enedione system also incorporates the structural feature of a cyclopropane ring in conjugation with the carbonyl groups. The photochemistry of conjugated cyclopropyl ketones has also been the subject of considerable study (5, 6) but we have obtained no evidence for photochemical opening of the cyclopropane ring either in the starting monomer **1** or in its photodimers.

The irradiation of a 10% solution of 3-carene-2,5-dione in acetone in a quartz vessel could conveniently be monitored by the disappearance of the characteristic infrared (i.r.) bands of the enedione at 6.00 and 6.15 μ, and the appearance of a new, unconjugated carbonyl band at 5.93 μ, indicative of dimer formation. The reaction was stopped after 33 h, and the solid mixture obtained on evaporation was separated by chromatography into three pure components: photodimer *A* (25%), m.p. 250–251°; photodimer *B* (21%), m.p. 248–249°; and photodimer *C* (6%), m.p. 325–326°. In addition, appreciable quantities of **1** were recovered. A fourth product was also obtained, the nuclear magnetic resonance (n.m.r.) spectrum of which clearly showed it to be different from dimers *A*, *B*, and *C*. However, all attempts to further purify this material have so far been without success, and the extreme complexity of the n.m.r. spectrum, as well as serving to distinguish it from those of *A*, *B*, and *C*, is strongly suggestive of a mixture, rather than a single substance.

Before proceeding to discuss the gross structural assignments of *A*, *B*, and *C*, it should be mentioned that several previous attempts to

[1]The work described in this paper is based on the M.Sc. thesis of Y.–N. Oh, University of Toronto, May, 1969.

[2]Author to whom all correspondence should be addressed.

Can. J. Chem. Downloaded from www.nrcresearchpress.com by 210.87.254.42 on 09/05/12
For personal use only.

photodimerize **1** by direct or sensitized irradiation in solvents such as methanol or 1,4-dioxan were unsuccessful.[3] The irradiation of **1** in benzene containing acetophenone, on the other hand, has been found to produce small quantities of photodimers *B* and *C* (but no *A*) in a ratio different to that obtained in acetone. Although Liu *et al.* (7) have reported similar effects in flexible systems, the much greater rigidity of the present system might require a more subtle explanation,[4] such as ground-state complexing.

Turning to the gross structural features of the present dimers, attempts were made to lactonize the carbonyl-containing rings present in structures such as **2** and **3**, as has been carried out successfully for some other cyclobutane dimers (8). However, this technique, and other degradative procedures, did not afford useful products in the present instance, and we have thus relied mainly on spectral data for establishing the structures of *A*, *B*, and *C*. All three dimers showed the expected molecular ion peaks at *m/e* 328 in the mass spectra. Their i.r. spectra each showed a single carbonyl band, in the range 5.90 to 5.93 μ, while the ultraviolet (u.v.) spectrum of *B*, λ_{max}(MeOH) 213 (ε, 15 100) and 300 (ε, 420) nm typifies all three dimers, and is in accord with expectation for a compound containing four saturated carbonyl groups, each conjugated with a cyclopropane ring (9). The n.m.r. spectra of *A*, *B*, and *C* also showed marked general similarities. Dimer *A*, for example, revealed singlets of equal intensity at δ (in $CDCl_3$) 1.30, 1.33, and 1.37 p.p.m., each corresponding to a pair of methyl groups; an AB quartet ($\Delta\nu$ = 3.0 Hz, J = 7.3 Hz) centered at 2.39 p.p.m., corresponding to the four cyclopropyl bridgehead protons; and a singlet at 3.03 p.p.m., representing the two cyclobutyl methine protons. The n.m.r. spectra of *B* and *C* are reported in full in the Experimental. The relative simplicity of all three n.m.r. spectra, indicative of a high degree of symmetry and the absence of vinyl proton signals in all three cases, along with the u.v. spectral data clearly rule out other, less symmetrical dimeric structures, such as those involving oxetane ring formation, for *A*, *B*, and *C*. In addition, the absence of molecular rearrangement during the photodimerization of **1** was revealed by the fact that all three dimers could be reconverted to 3-carene-2,5-dione in more than 85% yield, by heating briefly at temperatures slightly above their melting points.

Thus, having established that *A*, *B*, and *C* have structures conforming to the general types represented by **2** and **3**, we turned our attention to the more complex problems associated with the orientation (*head-to-head* vs. *head-to-tail*) and stereochemistry of the dimers.

The question of the stereochemistry at the cyclobutane ring junctions was simplified by the finding that all three photodimers were recovered completely unchanged after refluxing with sodium methoxide in methanol. The absence of epimerization in such cases has been generally accepted (10, 11) as requiring *cis*-fusion of the cyclobutane and cyclohexane rings. This interpretation was substantiated by noting the disappearance of the low field cyclobutane proton signals in the n.m.r. spectra (and an approximately 20% reduction in intensity of the cyclopropyl bridgehead proton signals) on refluxing the dimers in D_2O–pyridine, thus confirming that enolate ion formation actually occurred on base treatment of *A*, *B*, and *C*.

The important question of orientation in *A*, *B*, and *C* was now considered, i.e. which dimers are represented by gross structure **2** and which by **3**. Examination of the natural abundance ^{13}C satellite signals of the low field (cyclobutane) protons in the n.m.r. spectra at high concentrations (12, 13) led to $J_{^{13}C-H}$ coupling constants of 138, 142, and 143 Hz for *A*, *B*, and *C* respectively. These values lie within the range 126 to 153 Hz reported for a variety of cyclobutane systems (13, 14). Proton–proton coupling constants of J = 6.0, 3.0, and < 1.5 Hz were observed for *A*, *B*, and *C*, respectively. These results, in addition to confirming the existence of the cyclobutane ring in each dimer, enable us to conclude that *A* and *B* possess vicinal cyclobutane protons (J values ranging from 2–11 Hz have been reported (15)) and are therefore *head-to-head* dimers of the type indicated by **2**. Dimer *C* on the other hand, which does not reveal a coupling constant within the above range must necessarily be a *head-to-tail* dimer as indicated by **3**. The reasons for the heavy preponderance (*A* + *B*/*C* = 46/6) of *head-to-head* orientation are not immediately obvious.

[3]I. W. J. Still and D. T. Wang, unpublished findings.
[4]We are indebted to one of the referees for this suggestion.

TABLE 1

Possible symmetric products of photodimerization of 3-carene-2,5-dione

Cyclopropyl–cyclobutyl rings situated	Structure	Symmetry element
A. Syn fusion of cyclohexane rings		
Head-to-head Syn–syn–syn	**4** 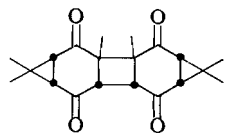	Plane
Head-to-tail Syn–syn–syn	**5** 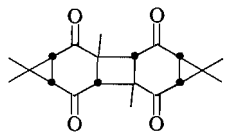	C_2 Axis
Head-to-head Anti–syn–anti	**6** 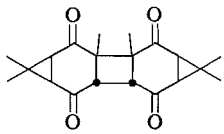	Plane
Head-to-tail Anti–syn–anti	**7** 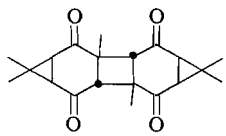	C_2 Axis
B. Anti fusion of cyclohexane rings		
Head-to-head Syn–anti–syn	**8** 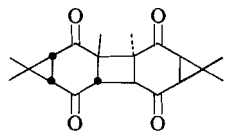	C_2 Axis
Head-to-tail Syn–anti–syn	**9** 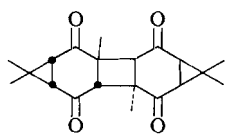	Center
Head-to-head Anti–anti–anti	**10** 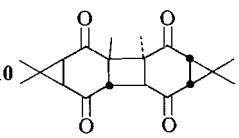	C_2 Axis
Head-to-tail Anti–anti–anti	**11** 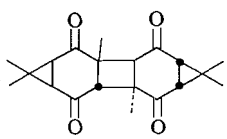	Center

Can. J. Chem. Downloaded from www.nrcresearchpress.com by 210.87.254.42 on 09/05/12
For personal use only.

TABLE 2
Nuclear Overhauser effects in dimer *B* (**8***a*)

Observed protons	δ (p.p.m.)*	Irradiated protons	δ (p.p.m.)	% Area increase†	Internuclear distance (Å)‡
Cyclobutyl	2.91	CH_3 (A)	1.49	24	2.2
Cyclobutyl	2.91	CH_3 (B)	1.28	0	5.5
Cyclobutyl	2.91	CH_3 (C)	1.11	0	2.8
Cyclopropyl	2.19	CH_3 (A)	1.49	0	2.9
Cyclopropyl	2.19	CH_3 (B)	1.28	18	2.3
Cyclopropyl	2.19	CH_3 (C)	1.11	0	3.6

*Tetramethylsilane as internal standard.
†Reproducibility ≤ ± 2%.
‡Closest distance of approach as measured from Dreiding molecular models.

In Table 1 are shown the eight possible *cis*-fused structures available for *A*, *B*, and *C*. (Other, less symmetrical arrangements, such as *anti–anti–syn* were ruled out by virtue of the degree of symmetry implied by the n.m.r. spectra.) From the evidence presented in the previous paragraph, *A* and *B* must be assigned two of the structures **4**, **6**, **8**, or **10**. The size of the vicinal proton coupling constants for the cyclobutane rings in *A* and *B* (J = 6.0 and 3.0 Hz, respectively) is an indication that they are in the *trans*-relationship, since Fleming and Williams (15) have reported values around J = 11 Hz for vicinal cyclobutane protons having a *cis*-relationship. This observation, together with evidence obtained from a study of Dreiding models of the various conformations of **4**, **6**, **8**, and **10** provides a very strong argument in favor of an *anti*-relationship about the central cyclobutane ring in *A* and *B*. It was found with respect to the models of structures **4** and **6** that the presence of severe strain or the absence of the necessary elements of symmetry in a particular conformation made these structures unlikely. Thus, we have assigned structures **8** and **10** to the *head-to-head* dimers *A* and *B*. A similar process of reasoning leads us to suggest structure **9** or **11** for the *head-to-tail* dimer *C*.

The foregoing having established the compounds *A* and *B* as possessing structures **8** and **10**, further discrimination was sought from steady-state nuclear Overhauser effect (n.O.e.) data (16, 17). In the case of compound *B*, the methyl signals are sufficiently well separated to allow unequivocal identification of all these signals. For compound *A*, the closeness of the resonances necessitated additional data from offset irradiations.

Table 2 records the n.O.e. data for compound *B*, together with the internuclear distances between observed and irradiated protons in structure **8***a*. Area changes, found for a carefully degassed ~0.2 *M* solution in $CDCl_3$, are expressed as a percentage of the total area for each signal. Table 3 records similar data for compound *A* and structures **10***a* and **10***b* (other conformations were eliminated on symmetry considerations).

Since the n.O.e. is a function of internuclear distance, it is apparent that in compound *B*, the methyl resonances at δ = 1.49, 1.28, and 1.11 are due to the cyclobutyl, and the *cisoid* and *transoid*[5] cyclopropyl methyl resonances respectively. The data also indicate no intramolecular relaxation effects between the *transoid* cyclopropyl methyls and the cyclobutyl methine protons.

The data for compound *A* indicate that the resonance at δ = 1.30 p.p.m. is due to the *cisoid* cyclopropyl methyls. No relaxation effects on the cyclopropyl ring protons due to the other types of methyl protons are apparent (regular fall off of area change on each side of the signal at δ = 1.30 p.p.m.). Similar considerations indicate that the methyl groups with signals at δ = 1.33 and 1.37 p.p.m. both contribute to the relaxation of the cyclobutyl ring protons. Specific assignment of these signals to the cyclobutyl methyls and the *transoid* cyclopropyl methyls does not appear possible.

Reference to molecular models indicates that in **8**, only the linearly spread conformer **8***a* is

[5]The terms *cisoid* and *transoid* describe the relationship of the cyclopropyl bridgehead protons and the cyclopropyl methyl groups about the plane of the cyclopropane ring in each case.

Can. J. Chem. Downloaded from www.nrcresearchpress.com by 210.87.254.42 on 09/05/12
For personal use only.

TABLE 3

Nuclear Overhauser effects in dimer *A* (**10***a* and **10***b*)

Observed protons	δ (p.p.m.)*	Irradiated protons	δ (p.p.m.)	% Area increase†	Internuclear distance‡ **10***a*	Internuclear distance‡ **10***b*
Cyclobutyl	3.03	—	1.45	6	—	—
Cyclobutyl	3.03	—	1.40	20	—	—
Cyclobutyl	3.03	CH_3 (A)§	1.37	28	2.2	2.2
Cyclobutyl	3.03	CH_3 (B)§	1.33	32	3.6	0.9
Cyclobutyl	3.03	CH_3 (C)	1.30	11	4.7	4.3
Cyclobutyl	3.03	—	1.25	5	—	—
Cyclopropyl	2.39	—	1.45	2	—	—
Cyclopropyl	2.39	—	1.40	6	—	—
Cyclopropyl	2.39	CH_3 (A)§	1.37	8	1.1	3.7
Cyclopropyl	2.39	CH_3 (B)§	1.33	14	3.6	3.6
Cyclopropyl	2.39	CH_3 (C)	1.30	20	2.3	2.3
Cyclopropyl	2.39	—	1.25	10	—	—

*Tetramethylsilane as internal standard.
†Reproducibility ≤ ± 2%.
‡Closest distance of approach as measured from Dreiding molecular models.
§As pointed out in the discussion, the n.O.e. evidence does not permit the unambiguous distinction of methyl groups (A) and (B).

likely, severe non-bonded interactions precluding other conformers. On the other hand, Dreiding models of structure **10** suggest the possibility of two conformers, **10***a* and **10***b*. Since the n.O.e. data on compound *A* show that the *transoid* cyclopropyl methyl groups do approach the cyclobutyl ring protons closely, compound *A* must be represented by structure **10**. The two instances in Table 3 where the internuclear distances vary widely from conformer **10***a* to conformer **10***b*, together with the n.O.e. actually observed, strongly suggest a preference for the latter.

This assignment is compatible with the single resonance spectra, and helps to explain some of its features. For example, if the dimers existed as the linearly spread conformers **8***a* and **10***a*, in which the chemical environments of corresponding protons are very similar, the significant variations in chemical shifts actually found would be hard to explain. The observed variations are consistent with the assignment given above. It is perhaps worth noting that the *cisoid* cyclopropyl methyls in conformer **10***b* have environments practically identical to the corresponding methyl groups in conformer **8***a* in agreement with the observed chemical shifts (δ = 1.30 and 1.28 p.p.m. respectively), whereas the *transoid* cyclopropyl methyls in **10***b* and **8***a* are in substantially different environments (δ = 1.33 or 1.37, and 1.11 p.p.m., respectively). The chemical shift difference in this latter case is in the direction expected (18, 19) since in **10***b* the *transoid* methyls are held substantially in the plane of the adjacent carbonyl groups, whereas the *transoid* cyclopropyl methyl groups in **8***a* are held above the carbonyl groups and would thus be significantly shielded in the n.m.r.

In summary, consideration of the evidence available from Dreiding model studies, chemical shift data, and n.O.e. enables us to assign structure **8** to dimer *B* and structure **10** to dimer *A*, and to predict that **8***a* and **10***b* will be the preferred conformations.

Unfortunately, since only one *head-to-tail* dimer (*C*) is available, it is not possible to use such methods in arriving at a definite decision between structures **9** and **11** for this dimer. Both the *syn–anti–syn* structure **9** and the *anti–anti–anti* structure **11** have a high degree (center) of symmetry as the high melting point (325°) and insolubility observed for *C* would suggest, and we feel that no distinction can be made on the basis of the evidence available.

The photodimerization of 3-carene-2,5-dione has been found to proceed with an unexpected degree of regiospecificity to produce a preponderance of *head-to-head* dimers. No evidence has been found for the presence of *trans*-fused dimer, although at least one instance of this has been reported previously (13). Each of the three photodimers obtained undergoes ready thermal decomposition to regenerate the starting enedione.

Can. J. Chem. Downloaded from www.nrcresearchpress.com by 210.87.254.42 on 09/05/12
For personal use only.

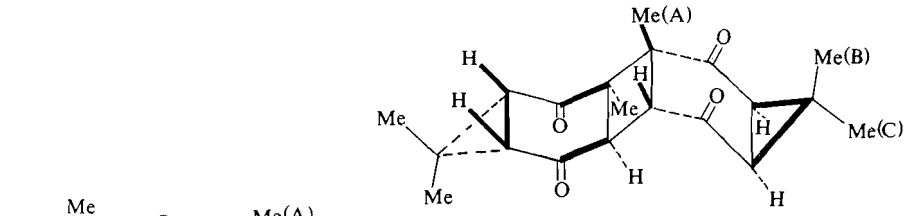

10*a*

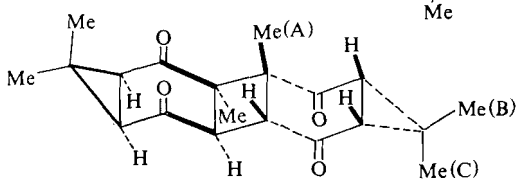

8*a*

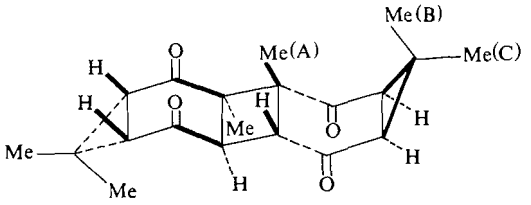

10*b*

Experimental

Infrared spectra were recorded (in $CHCl_3$) on Perkin–Elmer 237B or 257 spectrophotometers, and the u.v. spectra were recorded on a Unicam SP800 spectrophotometer. Nuclear magnetic resonance spectra were obtained on Varian HA-100 instruments, with tetramethylsilane as the internal standard. Mass spectra were obtained using an AEI MS-902 spectrometer. The elemental analyses were carried out in the Microanalytical Laboratory of A. B. Gygli, Toronto.

Silica gel used for chromatography was Davison Chemical Grade 923, 100–200 Mesh. All irradiations were carried out in degassed solvents, under nitrogen, using a 125 W Engelhard–Hanovia medium-pressure mercury arc lamp. Melting points were determined on a Fisher–Johns microhot stage, or in capillary tubes in a Gallenkamp m.p. apparatus, and are uncorrected.

3-Carene-2,5-dione (1)

This compound was prepared starting from carvone and proceeding via eucarvone and 3-carene-2,5-dione 5-oxime in a modification of the original method of Corey and Burke (20, 21).

Photodimerization of 3-Carene-2,5-dione

A 10% solution of 3-carene-2,5-dione in acetone (50 ml) was irradiated at 25° for 33 h. Evaporation of the solvent led to the appearance of a sticky solid mass which was then subjected to chromatography. Starting monomer (68% recovery) was first eluted with 3% acetone in methylene chloride.

Dimer *A* (**10**) was obtained on elution with 5 to 6% acetone in methylene chloride as a white crystalline solid (25% based on monomer consumed), m.p. 250–251° (95% EtOH). The i.r. spectrum showed a carbonyl band at 5.93 μ. The n.m.r. spectrum ($CDCl_3$) showed signals at δ 1.30, 1.33, and 1.37 (singlet, each 6H), 2.39 (4H, AB quartet, $\Delta\nu = 3.0$ Hz, $J = 7.3$ Hz), and 3.03 (2H, s) p.p.m. The mass spectrum revealed a molecular ion at *m/e* 328 and all the fragment ion peaks from *m/e* 164 downwards characteristic of 3-carene-2,5-dione, indicating considerable reversion to monomer in the mass spectrometer. The u.v. spectrum showed λ_{max}(MeOH) 212 (ε, 15 370) and 295 nm (ε, 244).

Anal. Calcd. for $C_{20}H_{24}O_4$: C, 73.18; H, 7.32. Found: C, 73.41; H, 7.56.

Closely following dimer *A* was the mixture referred to in the Discussion. Attempts to purify this mixture by recrystallization from a variety of solvents failed due to decomposition, poor recovery, or a combination of both. Dimer *C* (**9** or **11**) was eluted with 6% acetone in methylene chloride as a white solid (6%), m.p. 325–326° ($CHCl_3$). The i.r. spectrum showed a strong carbonyl band at 5.92 μ, while the u.v. spectrum revealed λ_{max}(MeOH) 212 (ε, 17 450) and 300 nm (ε, 525). The n.m.r. spectrum (CF_3COOH) had signals at δ 1.36, 1.43, and 1.55 (singlets, each 6H), 2.67 (4H, AB quartet, $\Delta\nu = 4.5$ Hz, $J = 6.4$ Hz), and 3.51 (2H, s) p.p.m. The mass spectrum showed the expected molecular ion peak at *m/e* 328 and a fragmentation pattern characteristic of **1** below *m/e* 164.

Anal. Calcd. for $C_{20}H_{24}O_4$: C, 73.18; H, 7.32. Found: C, 72.86; H, 7.17.

The third dimer *B* (**8**) was isolated from the fractions containing 7–10% acetone in methylene chloride as a white crystalline solid (21%), m.p. 248–249° (95% EtOH).

Can. J. Chem. Downloaded from www.nrcresearchpress.com by 210.87.254.42 on 09/05/12
For personal use only.

The i.r. spectrum showed a carbonyl band at 5.90 μ and the u.v. spectrum absorptions at λ_{max}(MeOH) 213 (ε, 15 088) and 300 nm (ε, 415). The expected molecular ion peak at *m/e* 328 was present in the mass spectrum, which was again, as with dimers *A* and *C*, virtually identical with that of 3-carene-2,5-dione **1** in the region below *m/e* 164. Indeed, in this case, the base peak (*m/e* 164) was that corresponding to reversion to monomer. The n.m.r. spectrum ($CDCl_3$) showed signals at δ 1.11, 1.28, and 1.49 (singlets, each 6H), 2.19 (4H, AB quartet, $\Delta\nu = 2.5$ Hz, $J = 6.8$ Hz) and 2.91 (2H, s) p.p.m.

Anal. Calcd. for $C_{20}H_{24}O_4$: C, 73.18; H, 7.32. Found: C, 73.10; H, 7.30.

Pyrolysis of Photodimer A

Dimer *A* (20 mg) in a narrow bore glass tube was inserted into the thermometer socket of a Gallenkamp melting point apparatus, after the temperature had been raised to 270°. Heating for 3 min at this temperature produced a yellow liquid which solidified on cooling to 25°. Pure 3-carene-2,5-dione was obtained in 85% yield by sublimation of the yellow solid at 77° under reduced pressure. The identity of the monomer thus obtained with an authentic sample of **1** was shown by i.r., m.p., and mixture m.p. comparisons. Similar procedures gave monomer in high yield from dimers *B* and *C* also.

Attempted Base-catalyzed Epimerization of Photodimers A, B, and C

The method used was similar to the procedure employed in a similar situation by Yates *et al.* (*8a*).

Enolization of Photodimer A with Base

A saturated solution of dimer *A* in 10% D_2O/pyridine was refluxed for 2 h. The n.m.r. spectrum showed complete disappearance of the cyclobutane proton signal at δ 3.03 p.p.m. and partial disappearance of the cyclopropane proton signal at δ 2.39 p.p.m. The relative intensity of the cyclopropane proton signal and the methyl proton signal was 3:18, compared to 4:18 in the starting material. This experiment confirms that anion formation does occur on base treatment, predominantly on the cyclobutane side of the carbonyl groups. Again, similar results were observed with *B* and *C*.

We wish to acknowledge generous support of this work by the National Research Council of Canada. It is a pleasure to record our thanks to Dr. R. A. Bell of McMaster University for valuable assistance in interpreting the nuclear Overhauser effects.

1. I. W. J. Still and D. T. Wang. Can. J. Chem. **46**, 1583 (1968).
2. I. W. J. Still, M.-H. Kwan, and G. E. Palmer. Can. J. Chem. **46**, 3731 (1968).
3. R. O. Kan. Organic photochemistry. McGraw-Hill, New York, 1966. Chapter 5.
4. A. Schönberg. Preparative organic photochemistry. Springer-Verlag, New York, 1968. Chapter 8.
5. W. G. Dauben, L. Schutte, and R. E. Wolf. J. Org. Chem. **34**, 1849 (1969).
6. L. D. Hess, J. L. Jacobsen, K. Schaffner, and J. N. Pitts, Jr. J. Amer. Chem. Soc. **89**, 3684 (1967).
7. R. S. H. Liu, N. J. Turro, and G. S. Hammond. J. Amer. Chem. Soc. **87**, 3406 (1965).
8. (*a*) P. Yates, S. N. Ege, G. Büchi, and D. Knutsen. Can. J. Chem. **45**, 2927 (1967). (*b*) P. Yates and M. J. Jorgenson. J. Amer. Chem. Soc. **85**, 2956 (1963).
9. W. G. Dauben and G. Berezin. J. Amer. Chem. Soc. **89**, 3449 (1967).
10. P. E. Eaton. J. Amer. Chem. Soc. **84**, 2344 (1962).
11. P. Yates and D. J. McGregor. Tetrahedron Lett. 453 (1969).
12. R. Anet. Tetrahedron Lett. 3713 (1965).
13. H. Ziffer, N. E. Sharpless, and R. O. Kan. Tetrahedron, **22**, 3011 (1966).
14. C. S. Foote. Tetrahedron Lett. 579 (1963).
15. I. Fleming and D. H. Williams. Tetrahedron, **23**, 2747 (1967).
16. F. A. L. Anet and A. J. R. Bourn. J. Amer. Chem. Soc. **87**, 5250 (1965).
17. J. K. Saunders, R. A. Bell, C.-Y. Chen, D. B. MacLean, and R. H. F. Manske. Can. J. Chem. **46**, 2876 (1968), and references therein.
18. D. H. Williams and I. Fleming. Spectroscopic methods in organic chemistry. McGraw-Hill, New York, 1966. pp. 83–85.
19. L. M. Jackman. Applications of n.m.r. spectroscopy in organic chemistry. Pergamon, London, 1959. pp. 114, 122–124.
20. E. J. Corey and H. J. Burke. J. Amer. Chem. Soc. **78**, 174 (1956).
21. G. L. Buchanan, R. A. Raphael, and I. W. J. Still. J. Chem. Soc. 4372 (1963).

Can. J. Chem. Downloaded from www.nrcresearchpress.com by 210.87.254.42 on 09/05/12
For personal use only.

Can. J. Chem. Downloaded from www.nrcresearchpress.com by 210.87.254.40 on 09/05/12
For personal use only.

Anodic oxidation of organic compounds. V. Electrochemical oxidation of *t*-butyl hydroperoxide in presence of tetracyclone[1]

N. L. WEINBERG

Chemical Department, Central Research Division, American Cyanamid Company, Stamford, Connecticut 06904

Received November 18, 1969

A ring expanded lactone is obtained on electrochemical oxidation of *t*-BuOOH in presence of tetracyclone. The same product is formed on chemical oxidation of a mixture of *t*-BuOOH and tetracyclone with ceric ammonium sulfate or on heating the mixture to dryness.

Canadian Journal of Chemistry, 48, 1533 (1970)

The electrochemical oxidation of hydroperoxides has not been reported previously, although their chemical oxidation and thermal decomposition reactions are well-known (2–4). A study of the anodic electrochemistry of hydroperoxides should supplement our knowledge of the oxidation reactions of these compounds.

Electrochemical oxidation of *t*-BuOOH in presence of tetracyclone (**1**) has been found to give a lactone in a Baeyer–Villiger-type reaction. The infrared (i.r.) spectrum of this product exhibited carbonyl absorption at 1780 cm^{-1} (unsaturated lactone). Elemental and nuclear magnetic resonance (n.m.r.) analyses were consistent with structure **2** or **3**.

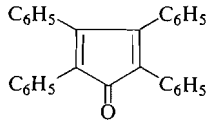

1

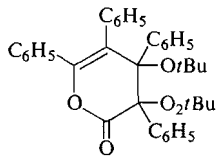

2

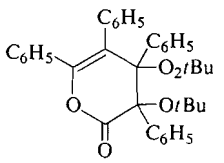

3

It was shown that the reaction product was not formed as a result of electro-oxidation of tetracyclone by carrying out an electrolysis at a stirring rate such that two distinct layers were formed (*t*-BuOOH is only slightly soluble in the reaction medium). The upper layer, containing the tetracyclone, was not in contact with the electrode. Again the lactone was formed. In addition, controlled potential electrolysis of a homogeneous solution of tetracyclone in acetonitrile containing *t*-BuOOH at 2.0 V vs. s.c.e. did not give the lactone product.[2]

Some evidence for provisional assignment of **2** as the structure of the product was derived from the mass spectrum. Scheme 1 indicates two routes of decomposition of **2** which provide the observed ions of higher mass. Thus while **4** could readily undergo concerted fragmentation to *cis*-dibenzoylstilbene (**5**) a similar reaction of the analogous intermediate derived from **3** could not give **5**.

In an effort to determine the relative positions of the *t*-butyl hydroperoxy groups by chemical means, the lactone product was heated in refluxing xylene solution. *cis*-Dibenzoylstilbene was obtained in 79% yield. Reduction of the lactone with Zn/HOAc gave a 72% yield of the hydrogen-bonded alcohol **6** (i.r., 3542 cm^{-1}). The latter compound is probably derived from the lactone by reduction to the epoxide **7** and subsequent hydrolysis. An attempt to reduce the peroxide linkage with KI/HOAc proved unsuccessful, perhaps because of the highly hindered position of the peroxide group.

It is interesting that the lactone could be readily generated from a mixture of *t*-BuO_2H and tetracyclone in 60% yield by chemical oxidation with ceric salt, and in 31% yield on prolonged heating of a mixture of the two reactants to dryness. The lactone was not formed, however,

[1]For part IV see ref. 1.

[2]Tetracyclone in acetonitrile containing 0.1 *M* $(n\text{Bu})_4\text{NClO}_4$ exhibits an anodic wave at $E_{1/2}$ = 1.52 V vs. s.c.e. at a rotating platinum microelectrode. Attempts to determine the oxidation potential of *t*-BuOOH were unsuccessful.

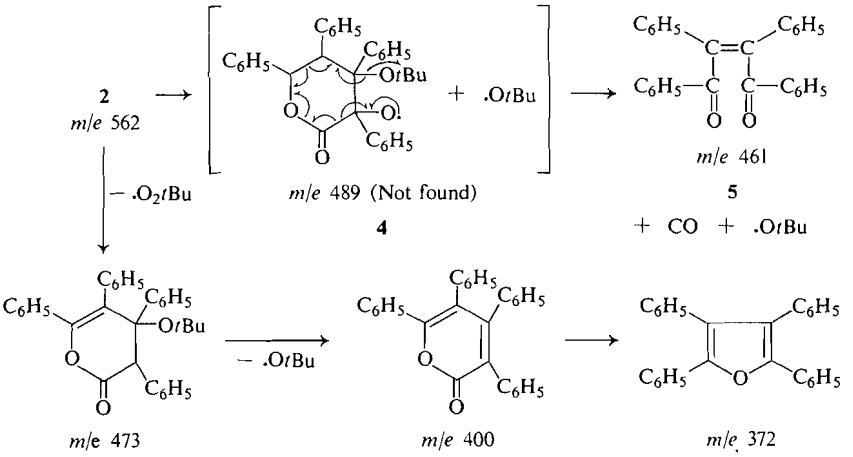

SCHEME 1

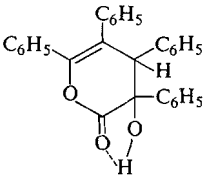

6

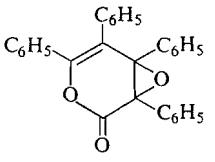

7

when treated under conditions similar to those employed in the electrochemical procedure, but without passage of current.

Hiatt *et al.* (4) have reviewed the subject of homolytic decomposition of hydroperoxides. They conclude that metal ion-catalyzed decomposition of hydroperoxides proceed via one electron transfer of the metal ion with the hydroperoxide, forming radicals (eqs. [1] and [2]). Radical induced chains are thus initiated (eqs. [3] and [4]). Electrochemical oxidation as well as homolytic decomposition of t-BuO_2H at higher temperatures (eq. [5]) would be expected to lead to similar products if t-butyl hydroperoxy radicals are common to all three methods of producing **2**. On this basis, the mechanism of formation of **2** could proceed through the adduct **8** (eq. [5]), which could undergo a free radical displacement on the O—O bond in a reaction of the type that results in epoxides from olefins and hydroperoxides (5).

[1] $Ce^{+4} + RO_2H \rightarrow Ce^{+3} + RO_2\cdot + H^+$

[2] $Ce^{+3} + RO_2H \rightarrow Ce^{+4} + RO\cdot + OH^-$

[3] $RO\cdot + RO_2H \rightarrow ROH + RO_2\cdot$

[4] $RO_2\cdot + RO_2\cdot \rightarrow 2RO\cdot + O_2$

[5]

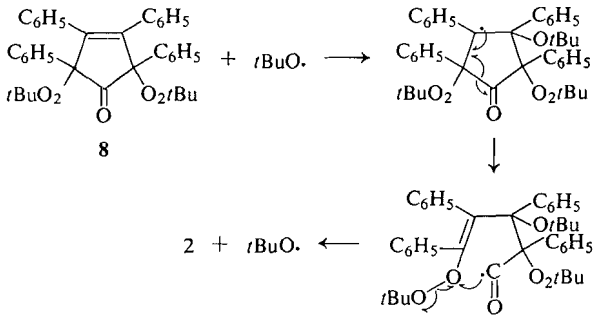

Can. J. Chem. Downloaded from www.nrcresearchpress.com by 210.87.254.40 on 09/05/12
For personal use only.

Can. J. Chem. Downloaded from www.nrcresearchpress.com by 210.87.254.40 on 09/05/12
For personal use only.

Experimental

The electrochemical equipment has been described previously (6). Melting points are uncorrected.

1) Preparation of the Lactone

(a) By Electrochemical Synthesis

The anode compartment of a 3-compartment cell was charged with a mixture of 120 ml of 90% *t*-BuO_2H (Lucidol), 80 ml of water, 18 g of tetramethylammonium hydroxide pentahydrate (Eastman), and 3.845 g (0.0100 mole) of tetracyclone (Aldrich). Electrolysis was carried out at 15° at a pyrolytic carbon anode (mercury pool cathode) at 2.9 V vs. s.c.e., and the mixture was stirred magnetically.[3] After 3150 C had been passed the original color of the deeply wine-colored solution was almost completely discharged and a colorless solid was suspended in solution. After a total of 4800 C, the anolyte was concentrated *in vacuo* at 35–40° (15 mm Hg) to a volume of about 75 ml. To this were added 200 ml of water and the mixture was extracted with 4 × 100 ml of benzene. The combined organic extract was washed with water, dried over anhydrous $MgSO_4$, filtered, and concentrated leaving about 50 ml of an oil smelling strongly of *t*-BuO_2H. This was taken up in 150 ml of ethanol and treated with water until cloudy. After several hours a colorless solid was filtered off and dried in air, 4.7 g; m.p. 110–117°. After two recrystallizations from ethanol–water, 2.11 g (0.0038 mole; 38%) of the lactone **2** was obtained, m.p. 140–140.5°.

Anal. Calcd. for $C_{37}H_{38}O_5$: C, 79.00; H, 6.82. Found: C, 78.78, 78.93; H, 6.79, 6.88.

The n.m.r. spectrum showed aromatic and *t*-butyl group (a single band) hydrogens in a ratio of 20:18 respectively, while the i.r. spectrum in Nujol exhibited a strong absorption at 1780 cm^{-1}, consistent with the unsaturated lactone structure. A mass spectrum of the compound obtained at 130° had a weak molecular ion at m/e = 562 and other major fragments at m/e = 73, 77, 105, 146, 178, 255, 267, 283, 372, 388, 400, 461, and 473.

A blank run was carried out by magnetically stirring a mixture of the same composition as above for 48 h at 10–15° without passage of current. The mixture was not decolorized and work-up gave only tetracyclone.

(b) By Chemical Oxidation

A magnetically stirred mixture of 100 ml of 90% *t*-BuO_2H and 40 ml of water containing 0.22 g (0.00057 mole) of tetracyclone was cooled with an ice-bath, while a slurry of ceric ammonium sulfate (150 g in 300 ml of water) was added over a period of 1½ h by means of a long-stem funnel extending to the bottom of the flask. After a further 1/2 h of stirring, 200 ml of benzene were added and the organic layer was separated, washed with water, dried over anhydrous $MgSO_4$, filtered, and concentrated *in vacuo* at 50–60°, 15–20 mm Hg. The residual oil was taken up in 15 ml of ethanol and treated dropwise with water until just cloudy. The solid which slowly precipitated was filtered and recrystallized from ethanol–water to give 0.19 g (0.00034 mole, 60%) of lactone, m.p. 138.5–140° (decomposition). The i.r. spectrum was identical to that of the solid obtained in section *1a*.

[3]The electrolysis current, about 30 mA, remained almost constant throughout the reaction.

(c) By Heating to Dryness

Into a mixture of 20 ml of 90% *t*-BuO_2H, 40 ml of 1 *N* aqueous NaOH solution, and 1.0 g (0.0026 mole) of tetracyclone was bubbled a finely dispersed stream of air. The mixture was heated for 4 days on a steam bath until evaporation was complete. The colorless solid residue was taken up in 50 ml of water and extracted with 100 ml of chloroform. From the organic extract, a solid was isolated, which on crystallization from ethanol–water gave 0.45 g (0.00080 mole; 31%) of the lactone **2**, m.p. 142–142.5°. A mixed melting point was undepressed and the i.r. spectrum was identical to that of the product of section *1a*.

2) Thermal Decomposition of the Lactone

A solution of 0.530 g (0.00094 mole) of the lactone in 50 ml of purified *p*-xylene was refluxed under nitrogen for 1 h. The solution was cooled to room temperature and treated with 50 ml of hexane. The solid, which slowly crystallized, was filtered, washed with hexane, and dried in air, giving 0.288 g (0.00074 mole; 79%) of *cis*-dibenzoylstilbene, m.p. 213–214.5°. The i.r. spectra of this and an authentic sample were identical.

Anal. Calcd. for $C_{28}H_{20}O_2$: C, 86.58; H, 5.19. Found: C, 86.87; H, 5.18.

3) Reduction with Zinc in Acetic Acid

A mixture of 0.180 g (0.00032 mole) of lactone in 25 ml of glacial acetic acid containing 1.1 g of zinc dust was magnetically stirred at room temperature for 24 h. The mixture was filtered, concentrated to 5 ml *in vacuo*, and diluted with 200 ml of water depositing a solid. Crystallization from ethanol–water afforded 0.095 g (0.00023 mole; 72%) of the alcohol **6**.

Anal. Calcd. for $C_{29}H_{22}O_3$: C, 83.22; H, 5.30. Found: C, 83.28, 83.13; H, 5.37, 5.33.

The i.r. (a solution in methylene chloride exhibits a band at 3542 cm^{-1} for —OH in agreement with a hydrogen-bonded lactone structure) and n.m.r. spectra were consistent with the proposed structure **6**.

4) Reaction of the Lactone with Potassium Iodide in Acetic Acid

A mixture of 0.164 g of the lactone in 40 ml of glacial acetic acid containing 1.0 g of potassium iodide was stirred magnetically at room temperature for 24 h. The strongly iodine colored solution was concentrated *in vacuo* at 50° to about 5 ml. The residue was treated with a little aqueous sodium thiosulfate, diluted with water and the precipitate filtered, and dried in air. Crystallization from ethanol–water provided 0.11 g of starting material, m.p. 143–144° (decomposition).

The author is indebted to Dr. Balwant Singh for participating in several useful discussions, and to Professor R. Hiatt of Brock University for his valuable comments.

1. N. L. Weinberg. J. Org. Chem. **33**, 4326 (1968).
2. M. S. Kharasch and A. Fono. J. Org. Chem. **24**, 72 (1959).
3. J. A. Howard and K. U. Ingold. J. Amer. Chem. Soc. **90**, 1056 (1968).
4. R. Hiatt, T. Mill, and F. R. Mayo. J. Org. Chem. **33**, 1416 (1968).
5. D. E. Van Sickle, F. R. Mayo, E. S. Gould, and R. M. Arluck. J. Amer. Chem. Soc. **89**, 977 (1967); W. F. Brill. J. Amer. Chem. Soc. **85**, 141 (1963).
6. N. L. Weinberg and T. B. Reddy. J. Amer. Chem. Soc. **90**, 91 (1968).

Can. J. Chem. Downloaded from www.nrcresearchpress.com by 210.87.254.6 on 09/05/12
For personal use only.

Infrared study of the state of water in the hydration shell of DNA[1]

MICHAEL FALK, A. G. POOLE,[2] AND C. G. GOYMOUR[3]
Atlantic Regional Laboratory, National Research Council of Canada, Halifax, Nova Scotia

Received November 24, 1969

The state of water in the hydration shell of DNA was studied by infrared spectroscopy. The stretching bands of isotopically dilute HDO adsorbed on DNA have nearly the same band profiles as those of HDO in liquid water. This indicates a distribution of hydrogen-bond strengths similar to that in liquid water. At low temperatures, the spectra show that an inner layer of about 10 water molecules per nucleotide is incapable of crystallization, even when the surrounding water crystallizes into ice I. The biopolymer hydration shells are not "ice-like" in the sense of crystalline ordering into an ice-like structure.

Canadian Journal of Chemistry, 48, 1536 (1970)

Introduction

The state of water which surrounds DNA and other biopolymers is of interest as this water often controls the biopolymer conformation. An additional interest arises from the practical problems connected with the biological effects of desiccation and freezing, intimately connected with the state of the water layer next to the biopolymer surface.

The object of the present study was to obtain information on the state of the hydration shell surrounding DNA at room temperature, the ability of this water to crystallize at lower temperatures, and the identity of the crystalline phase or phases. Our study was based on the OH and OD stretching bands of isotopically dilute HDO in the infrared (i.r.) spectra of hydrated and partially deuterated films of DNA. The profiles of these bands were studied as a function of water content and temperature. The advantages of studying the bands of isotopically dilute HDO in preference to those of isotopically pure H_2O or D_2O are: (*i*) HDO bands have simple profiles related to the distribution of energies (1, 2) and geometries (3) of hydrogen bonds; (*ii*) HDO bands of liquid water are very different from those of ice (Fig. 1); (*iii*) The HDO bands have characteristic frequencies and half-widths for various crystalline forms of ice (4, 5) and of amorphous ice (6). These advantages allowed us to detect and follow the crystallization of a *part* of the hydration shell and to establish the nature of the water phases present at low temperature.

Experimental

DNA Films

Several samples of calf-thymus DNA and salmon sperm DNA were purchased from Sigma Chemical Company as the sodium salt. The purity and molecular integrity of the samples were checked by spectroscopic means (7–9). Films of 5 to 10 μm thickness were prepared by spreading about 3 mg of dry DNA on an i.r.-transparent window of silver chloride or calcium fluoride, adding a drop of distilled water, and allowing the DNA to form a gel covering about 1 cm × 2 cm. The excess of water was evaporated overnight at 4°.

Room Temperature Study

The calcium fluoride plate with the DNA film was cemented into a hygrostatic cell shown in Fig. 2A. The reservoir was filled with about 1 g of a solution made up of D_2SO_4, D_2O, and H_2O so as to maintain both the relative humidity and the H:D ratio at the desired level. The exposure to the vapors above the sulfuric acid solutions did not appear to have any adverse effect on the DNA films. After a period of equilibration of about 24 h, during which the hygrostatic cell was gently shaken, it was inserted into the spectrophotometer (Perkin–Elmer model 521). An identical compensating cell, containing the same D_2SO_4–D_2O–H_2O mixture, was placed in the reference beam. The spectrum was scanned in small sections, spaced about 15 min apart, so as to avoid local heating of the film by the i.r. beam, which would cause the evaporation of a part of the water (8).

The mixtures of sulfuric acid and water were prepared by weight so as to possess vapor pressures (10) corresponding to 100, 93, 82, 62, 33, and 3% relative humidity and at the same time to contain 94.0 mole % D and 6.0 mole % H. The possible slight differences between the relative humidities over H_2SO_4–H_2O and D_2SO_4–D_2O mixtures were neglected. The H:D ratios for stock D_2SO_4 and for all the mixtures were determined by proton magnetic spectroscopy. A Varian A-60 nuclear magnetic resonance (n.m.r.) spectrometer was used, with benzene as an external standard.

The spectra in the OH stretching region were taken in sequence, starting with the film exposed to 100% relative humidity (i.e. to an H_2O–D_2O mixture with no sulfuric acid added), and progressing to lower humidities.

Low Temperature Study

In the low-temperature experiments we used low degrees of deuteration and observed the OD stretching band of HDO. This minimized the effect of hydrogen-deuterium exchange with atmospheric moisture during film transfer. Also, any traces of H_2O ice which some-

[1]Issued as NRCC No. 11190.
[2]I.A.E.S.T.E. Scholar, summer 1967.
[3]I.A.E.S.T.E. Scholar, summer 1968.

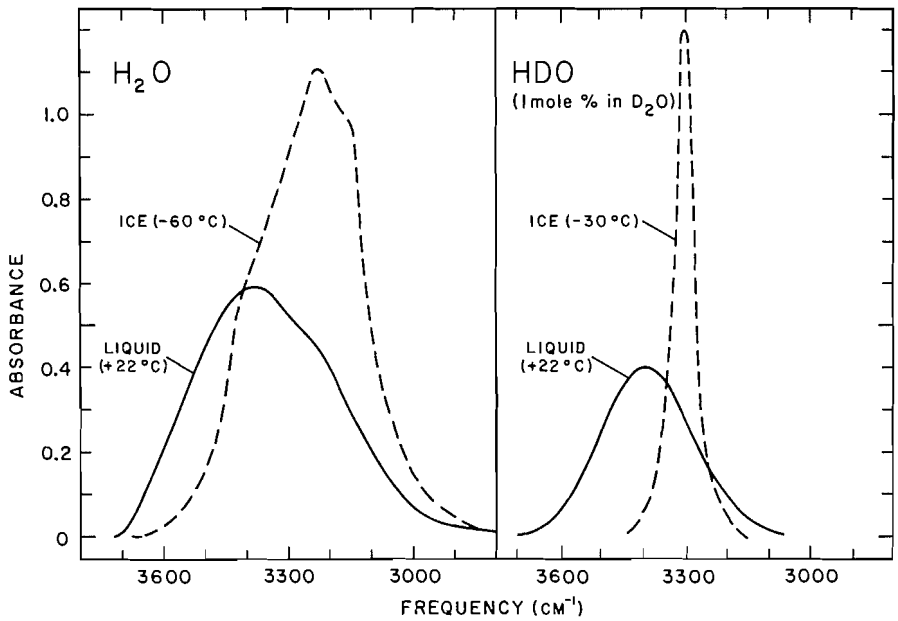

FIG. 1. Comparison of the absorbance profiles of H_2O and of isotopically dilute HDO in the OH stretching region in water and ice. Spectra recorded as in refs. 1 and 2 and replotted to linear absorbance.

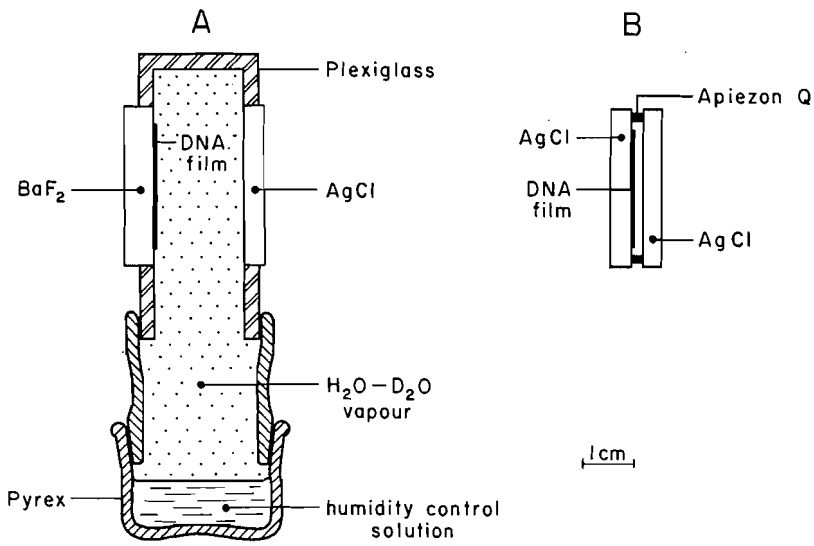

FIG. 2. A, Hygrostatic cell for room-temperature studies. B, The sealed-plate arrangement for low-temperature studies.

times condensed on the cold AgCl windows would affect the base line, but not the shape of the OD bands.

A silver chloride plate with the DNA film was cemented to the hygrostatic cell as before and exposed to a saturated solution of one of the salts listed in ref. 7 in a mixture of about 95 mole % H_2O and 5 mole % D_2O. When the i.r. spectrum showed that the hydrogen–deuterium equilibrium had been attained, usually within 24 h, the plate was quickly withdrawn from the hygrostatic cell and sealed with a gasket of Apiezon Q grease to another silver chloride plate. This transfer was performed in an atmosphere of 100% relative humidity. The sealed plates, shown schematically in Fig. 2B, were inserted into the inner holder of a low-temperature i.r. cell, model VLT-2, manufactured by the Research and Industrial Instruments Company, London. Two or three silver chloride plates were placed in the reference beam. The cell was evacuated and cooled at a controlled rate by

Can. J. Chem. Downloaded from www.nrcresearchpress.com by 210.87.254.6 on 09/05/12
For personal use only.

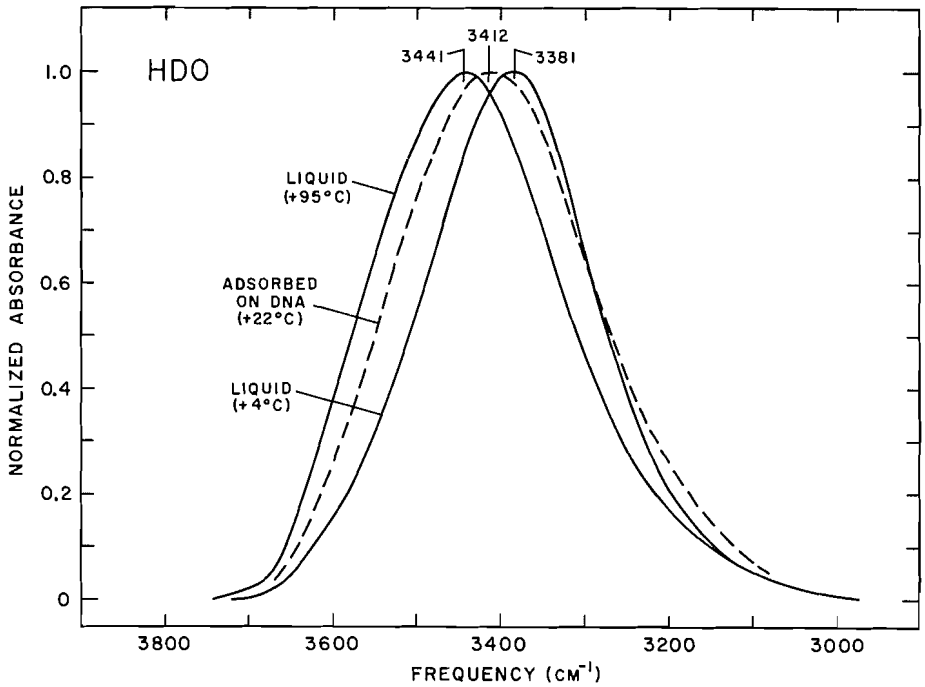

FIG. 3. Comparison of the OH stretching profiles of 1 mole % of HDO in D_2O: (*a*) liquid water at 4 and 95°, (*b*) adsorbed water on DNA at room temperature (difference profile corresponding to HDO desorbed between 93 and 3% relative humidity).

small additions of Dry Ice or liquid nitrogen. The rate of cooling was about 1° per min. The tightness of the seal was tested by recording the i.r. spectrum of the sample before and after leaving it in the evacuated cell for a few hours at room temperature. Any leaks would cause the evaporation of some of the water, detected as a diminution of the OH and OD stretching bands. Provided the seal was vapor-tight, the room-temperature spectrum was reproduced when the cell was reheated after the low-temperature experiments.

The water content of DNA films at relative humidities below 84% was calculated from the relative humidity values, assuming that hydration equilibrium had been attained and using the data of Fig. 1 in ref. 7. For DNA exposed to relative humidities above 84%, small losses of water often occurred during the film transfer after the equilibration. The water content of these films was determined from the measured absorbances at 3400 (due to OH groups), at 2500 (due to OD groups), and at 1220 cm^{-1} (due to phosphate groups of DNA). We have used the linear relation

$$n = 4.52(R - 0.86)$$

which we found to hold to within about 5% for DNA films of several origins and of varying thickness. In the above equation n is the number of water molecules per nucleotide and for undeuterated films $R = A_{3400}/A_{1220}$, where A's are the observed absorbances. For partly deuterated films the value of R was taken to be $R = (A_{3400} + 1.23A_{2500})/A_{1220}$. The factor 1.23 is the ratio of absorptivity at 3400 cm^{-1} to that at 2500 cm^{-1} in liquid HDO (11).

Results and Discussion

State of Water in the Hydration Shell at Room Temperature

Differences between spectra of a DNA film at two values of relative humidity yield the spectral profile of the water desorbed from DNA in that range of relative humidity (r.h.). The only other i.r. absorption in the OD stretching region arises from the stretching of ND groups of the partially deuterated DNA. This absorption is small because DNA contains an average of about 2 NH groups per nucleotide, compared with about 6 OH groups of adsorbed H_2O at 33% r.h. and 40 OH groups at 93% r.h. (7). Also, the i.r. intensity is greater for OH (or OD) stretching than for NH (or ND) stretching vibrations. Thus only a very drastic change in the hydrogen bonding scheme of the NH_2 and NH groups of DNA upon dehydration would have an appreciable effect on the difference spectrum.

In Fig. 3 a typical difference profile in the OH stretching region of DNA between 93 and 3% r.h. is compared with the corresponding absorbance profiles of HDO in liquid water recorded by the method of ref. 1. The difference spectrum

Can. J. Chem. Downloaded from www.nrcresearchpress.com by 210.87.254.6 on 09/05/12
For personal use only.

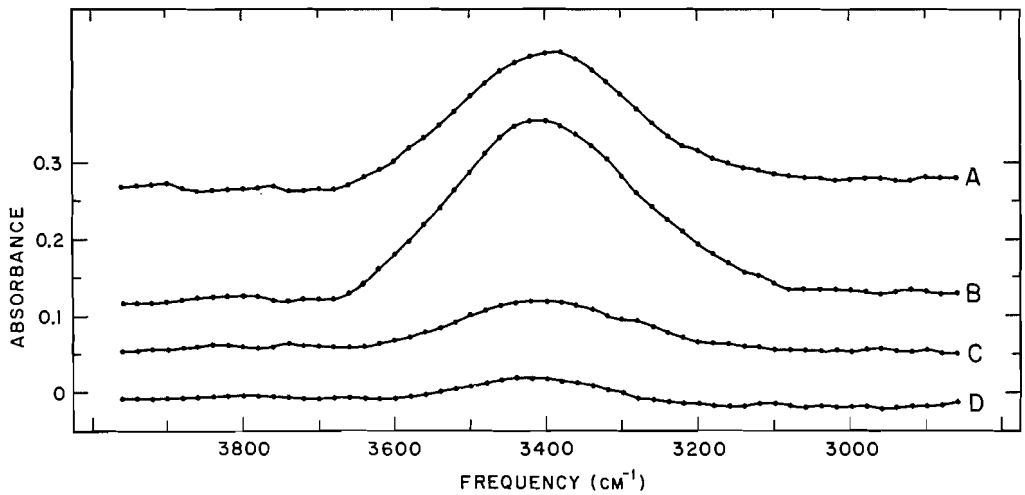

FIG. 4. Difference profiles in the OH stretching region, corresponding to HDO desorbed from DNA in the relative humidity ranges of 93 to 82% (A), 82 to 62% (B), 62 to 33% (C), and 33 to 3% (D). A, B, and C have been displaced upward by 0.05, 0.1, and 0.25 absorbance units, respectively.

for DNA between 93 and 3% relative humidity corresponds to a cross-section of the hydration shell, including water molecules closely associated with the biopolymer and others removed by several molecular diameters from the biopolymer surface. The general similarity between the spectral profiles of water of hydration and of liquid water confirms the absence of regions of ordered water in the hydration shell of DNA (8). The distribution of OH stretching frequencies of HDO is related to the distribution of hydrogen-bond strengths (1). Evidently these distributions differ very little for the bulk of water of hydration and for liquid water at the corresponding temperature.

In Fig. 4 we have plotted the sequence of four difference profiles corresponding to the spectrum of HDO desorbed in the intervals between 93, 82, 62, 33, and 3% r.h. The peak frequencies of these difference profiles, averaged from measurements on four DNA films, are 3411 ± 11, 3417 ± 6, 3414 ± 7, and 3399 ± 11 cm^{-1}. The large standard deviations are due to the uncertainty in the peak position of these broad bands. Within the experimental uncertainty, the peak frequencies are the same for the different r.h. intervals, and so are the band widths. This shows that consecutive layers of water surrounding the macromolecule have similar distributions of hydrogen-bond strengths. It should be noted that even at 3% r.h. DNA still holds one molecule of water per nucleotide and possibly more (12). We had no way of recording a difference spectrum of HDO corresponding to this innermost hydration layer, as it was not possible to hold DNA at 0% r.h. without altering the H:D ratio. However, the residual OH band at 3% r.h. is similar to that at higher humidities. Thus the hydrogen bonding of the water remaining on DNA at 3% r.h. cannot differ greatly from that of the succeeding layers of adsorbed water. The bonding may be somewhat stronger, as shown by a small (30 ± 14 cm^{-1}) downward frequency shift of the peak of the OH stretching band of adsorbed H_2O (8).

We must stress that the i.r. spectra provide information on the strength of intermolecular bonding but not on molecular mobility. Even though hydrogen-bond energies of water–biopolymer and water–water interactions are comparable, the mobility of water molecules near the biopolymer surface may be expected to be lower than in bulk water, because the biopolymer surface will act as a momentum sink for thermal fluctuations.

State of Water in the Hydration Shell at Low Temperature

Figure 5A shows the effect of slow cooling on the spectrum in the OD stretching region for a typical film of partially deuterated DNA of *low water content* (about 9 water molecules per nucleotide). The band shape varies gradually and

Can. J. Chem. Downloaded from www.nrcresearchpress.com by 210.87.254.6 on 09/05/12
For personal use only.

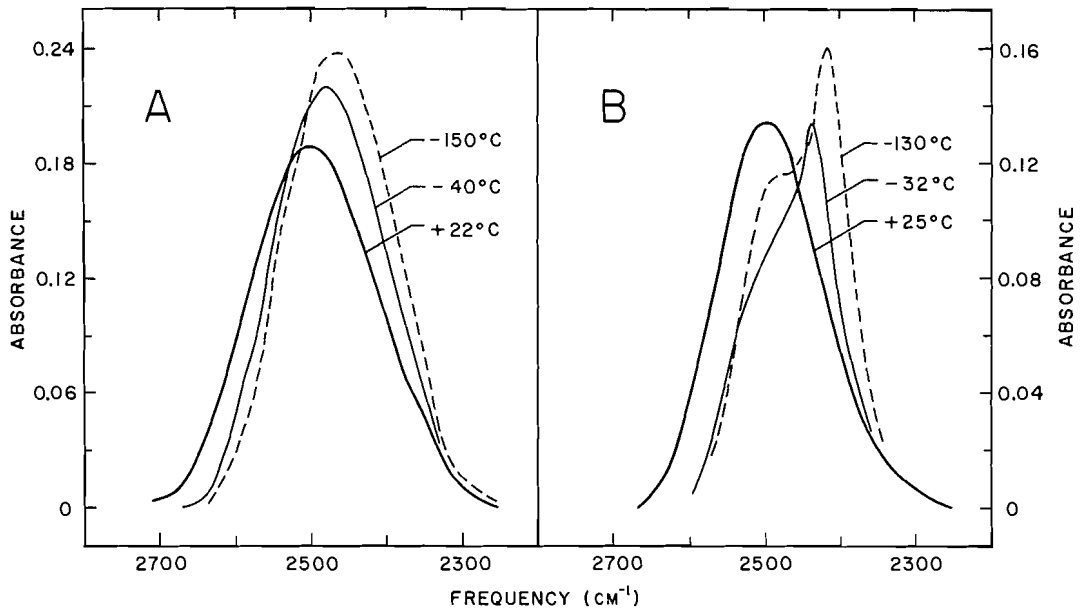

FIG. 5. Effect of slow cooling on the OD stretching band of HDO adsorbed on DNA. A, Sample of lower water content (76% relative humidity, about 9 water molecules per nucleotide). B, Sample of higher water content (86.5% relative humidity, about 14 water molecules per nucleotide).

reversibly with temperature, showing *complete absence* of *crystallization*. The peak intensity increases, the half-width decreases, and the peak frequency shifts downward with decreasing temperature. These changes are in the usual direction for water in condensed phases. The peak frequency is about 50 cm^{-1} higher than that of ice at corresponding temperatures (Fig. 6). This implies average hydrogen-bond strength considerably weaker than in ice. The half-widths are about 160 to 190 cm^{-1} in the temperature region studied, compared with 20 to 40 cm^{-1} for ice (Fig. 7). This suggests a wide distribution of hydrogen-bond strengths, characteristic of the liquid and amorphous states of water.

Figure 5B shows the effect of cooling on the spectrum of a DNA film of a *somewhat higher water content* (about 14 water molecules per nucleotide). In this case, the band shape undergoes a sudden change upon cooling, usually between -10 and $-20°$, corresponding to crystallization of a part of the water. A new sharp band appears at the expense of the broad band, with a peak frequency corresponding within a few cm^{-1} to that of pure ice I at the corresponding temperature (Fig. 6). The half-width of the sharp band is difficult to estimate because of the overlap with the broad band, but it appears to be about the same as for ice I (Fig. 7). This indicates that the crystalline regions correspond to local pockets of ice I. The ice band appeared upon cooling for all DNA films with a water content greater than about 13 molecules of water per nucleotide, the relative intensity of the band being approximately proportional to the water present in excess of that amount. The residual broad band, corresponding to uncrystallized water, had the same frequency and half-width at low or high water contents, i.e. independent of whether the ice band appeared.

Spectra of DNA with less than 10 molecules of water per nucleotide never showed the ice band, even after standing for several weeks at Dry-Ice temperature. Those of DNA with more than 13 molecules of water per nucleotide always showed the ice band, regardless of the rate of cooling. Spectra of DNA with intermediate water contents of 10 to 13 molecules per nucleotide usually showed no ice band, but sometimes a small ice band appeared when the films had been cooled very slowly or if they had been left at Dry-Ice temperature for several days. The above water contents are accurate to about one water molecule per nucleotide.

These results suggest that an inner hydration layer of about 10 water molecules per nucleotide

Can. J. Chem. Downloaded from www.nrcresearchpress.com by 210.87.254.6 on 09/05/12
For personal use only.

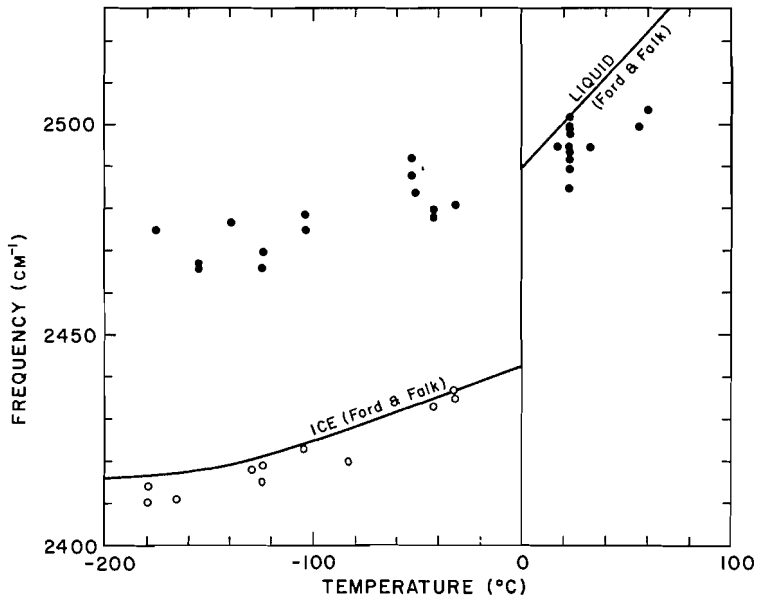

FIG. 6. Frequencies of the broad band (full circles) and of the sharp band (open circles) in the OD stretching region of HDO adsorbed on DNA as a function of temperature. The solid lines are for HDO in liquid water (1) and in ice (2).

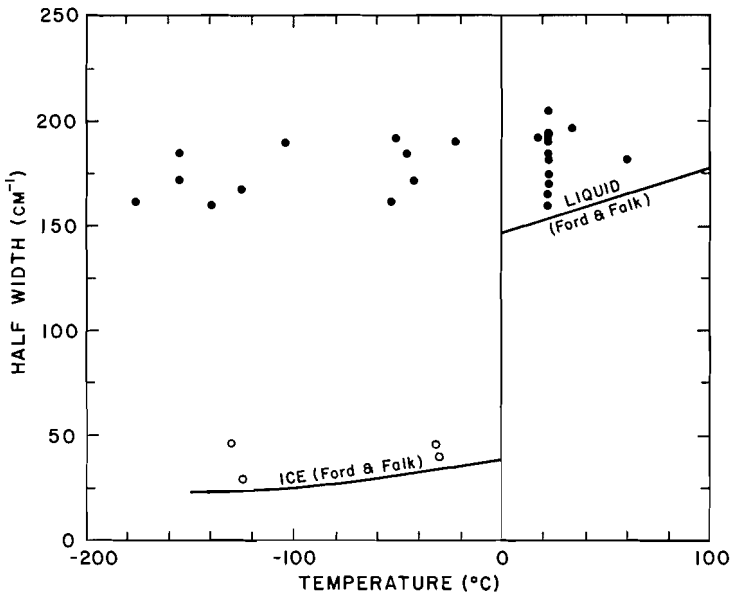

FIG. 7. Half-widths of the broad band (full circles) and of the sharp band (open circles) in the OD stretching region of HDO adsorbed on DNA as a function of temperature. The solid lines are for HDO in liquid water (1) and in ice (2).

is incapable of crystallization, *even when the surrounding water crystallizes into ice I.* An additional intermediate layer of about 3 water molecules per nucleotide crystallizes with difficulty and tends to supercool if the cooling rate is high.

In What Sense are Biopolymer Hydration Shells "Ice-like"?

The hydration shells surrounding macromolecules are often described as "ice-like" (13–19). This may lead to some confusion since there are distinct aspects of ice-likeness that have

Can. J. Chem. Downloaded from www.nrcresearchpress.com by 210.87.254.6 on 09/05/12
For personal use only.

not been always clearly distinguished (20). Ice differs from water in the *reduced molecular motion* and in the perfect *order of its crystal lattice*. The *motion* and the *order* of water molecules are largely independent. This is best shown by the example of vitreous ice (6), which preserves the molecular disorder of liquid water in spite of a drastic reduction in molecular motion.

There is n.m.r. (14, 21–26) and dielectric (13, 17–19, 27) evidence that the translatory and rotatory motion of water molecules in the hydration shells of biopolymers, including DNA, is reduced with respect to that in liquid water. A reduction of molecular motion is to be expected because of the interaction of water molecules with the polar sites on the surface of the biopolymer. On the other hand, the term "ice-like" also seems to imply to many authors a quasi-crystalline ordering of the hydration shell into a lattice corresponding to ice I structure. The formation of such a lattice has been specifically postulated by some authors (13–15), even though there appears to be no direct evidence for it (23). The present results demonstrate that, at least for DNA, there is no such ordering. The innermost, least mobile part of the hydration shell is in fact entirely incapable of crystallizing into the ice structure. Evidently, the preferred configuration of water next to the biopolymer is incompatible with the structure of ice. There is no spectral evidence of "quasi-crystallization" of any part of the hydration shell at room temperature, and at low temperatures it is the water *far* from the biopolymer surface which freezes into ice. The hydration shell of DNA is definitely not "ice-like" in the structural sense.

Haly and Snaith recently concluded from their calorimetric studies of keratin (28) and of polyethyleneterephthalate (29) that sorbed water consists of "freezing water" and "non-freezing water". The existence of an inner, non-crystallizable, and an outer, crystalilzable, hydration shell may thus be a general phenomenon, not limited to DNA. To test this, we intend to apply the present technique to the study of hydration of other biopolymers.

We wish to acknowledge the technical help of Mr. P. F. Seto.

1. M. Falk and T. A. Ford. Can. J. Chem. **44**, 1699 (1966).
2. T. A. Ford and M. Falk. Can. J. Chem. **46**, 3579 (1968).
3. T. T. Wall and D. F. Hornig. J. Chem. Phys. **43**, 2079 (1965).
4. B. Kamb. *In* Structural chemistry and molecular biology. *Edited by* A. Rich and N. Davidson. W. H. Freeman, San Francisco. 1968. p. 507. See especially Fig. 12 on p. 527.
5. E. Whalley. Develop. Appl. Spectrosc. **6**, 277 (1968). See especially Fig. 8 on p. 287.
6. S. I. Ikawa and S. Maeda. Spectrochim. Acta, **24A**, 655 (1968).
7. M. Falk, K. A. Hartman, and R. C. Lord. J. Amer. Chem. Soc. **84**, 3843 (1962).
8. M. Falk, K. A. Hartman, and R. C. Lord. J. Amer. Chem. Soc. **85**, 387 (1963).
9. M. Falk, K. A. Hartman, and R. C. Lord. J. Amer. Chem. Soc. **85**, 391 (1963).
10. Handbook of chemistry and physics. 21st. ed. Chemical Rubber Publishing Co., Cleveland, Ohio. 1949. p. 1952.
11. H. R. Wyss and M. Falk. Can. J. Chem. **48**, 607 (1970).
12. P. J. Killion and L. H. Reyerson. J. Colloid Interface Sci. **22**, 582 (1966).
13. B. Jacobson. J. Amer. Chem. Soc. **77**, 2919 (1955).
14. B. Jacobson. Sv. Kem. Tidskr. **67**, 1 (1955).
15. A. Szent-Györgyi. Bioenergetics. Academic Press, Inc., New York. 1957.
16. I. M. Klotz. Sci. **128**, 815 (1958).
17. S. Takashima. J. Polym. Sci. **62**, 233 (1962).
18. H. P. Schwan. Ann. N.Y. Acad. Sci. **125**, 344 (1965).
19. E. H. Grant. Ann. N.Y. Acad. Sci. **125**, 418 (1965).
20. Anonymous. The Science World, June 23, 1969. p. 9.
21. H. J. C. Berendsen. J. Chem. Phys. **36**, 3297 (1962).
22. R. E. Dehl. J. Chem. Phys. **48**, 831 (1968).
23. R. E. Dehl and C. A. J. Hoeve. J. Chem. Phys. **50**, 3245 (1969).
24. I. D. Kuntz, Jr., T. S. Brassfield, G. D. Law, and G. V. Purcell. Sci. **163**, 1329 (1969).
25. C. F. Hazlewood, B. L. Nichols, and N. F. Chamberlain. Nature, **222**, 747 (1969).
26. F. W. Cope. Biophys. J. **9**, 303 (1969).
27. S. H. M. El-Sabeh. Can. J. Phys. **43**, 1312 (1965).
28. A. R. Haly and J. W. Snaith. Biopolym. **7**, 459 (1969).
29. A. R. Haly and J. W. Snaith. Text. Res. J. **39**, 906 (1969).

Can. J. Chem. Downloaded from www.nrcresearchpress.com by 210.87.254.6 on 09/05/12
For personal use only.

Can. J. Chem. Downloaded from www.nrcresearchpress.com by 210.87.254.105 on 09/05/12
For personal use only.

Reactions of iron pentacarbonyl with compounds containing the N—O linkage

HOWARD ALPER[1]
Department of Chemistry, State University of New York at Binghamton, Binghamton, New York 13901

AND

J. T. EDWARD
Department of Chemistry, McGill University, Montreal, Quebec

Received September 9, 1969

Amine oxides, azoxybenzenes, and nitrones are deoxygenated in good yields by iron pentacarbonyl in hot butyl ether. Substituted nitro- and nitrosobenzenes are reduced under these conditions to azo and/or amino compounds, depending on the nature and location of the substituents; some evidence for nitrene or nitrene-like intermediates in these reactions is presented.

On a enlevé l'oxygène des molécules d'oxydes d'amines, des composés azoxy, et des nitrones par le pentacarbonyl de fer dans l'éther butylique chaud. Les nitro- et nitroso-benzènes substitués donnent les composés azo ou amino ou les deux, moyennant la nature et la position des substituants; on présente l'évidence pour les intermédiaires nitrènes ou semblable aux nitrènes dans ces réactions.

Canadian Journal of Chemistry, **48**, 1543 (1970)

Oximes react with iron pentacarbonyl in boiling butyl ether containing a catalytic amount of boron trifluoride to give the parent carbonyl compounds (1); the fate of the nitrogen atom is not known. This unusual reaction has prompted us to study the reaction of iron pentacarbonyl with six other types of compounds (amine oxides, azoxybenzenes, nitrones, nitro- and nitroso-compounds, and nitrosamines) containing the nitrogen–oxygen band.

In all cases deoxygenation of the compounds took place, sometimes followed by other reactions; in no case was any reaction resembling the enigmatic reaction of oximes encountered.

Amine oxides (aliphatic, aromatic, and heterocyclic[2]) are deoxygenated by iron pentacarbonyl in boiling butyl ether to amines, azoxybenzenes to azobenzenes, and α-phenyl-*N*-phenylnitrone to *N*-benzylidene aniline. The general applicability of the method was shown in the deoxygenation of brucine *N*-oxide hydrate; evidently the presence of water and of the lactam and olefin functional groupings did not interfere with the reaction. Yields were good, although no systematic study of optimum conditions was made, and the method is more convenient than many others reported in the literature (3) for recovering amines from amine oxides.

It was found that one mole of carbon dioxide was formed for each mole of pyridine *N*-oxide or azoxybenzene deoxygenated. A plausible mechanism for the reaction is shown in eq. [1].

The attack of nucleophilic oxygen upon the carbonyl group, shown as the first step in the reaction, finds analogy in the reaction of hydroxide (4) (eq. [2]) or methoxide ion (followed by water) (5) (eq. [3]) with iron pentacarbonyl. Other nucleophiles (e.g., ammonia (6), piperidine

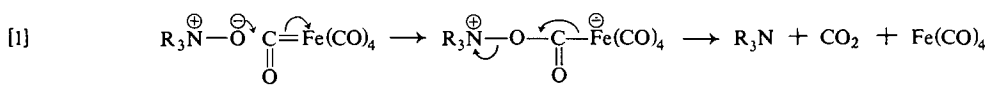

[1]

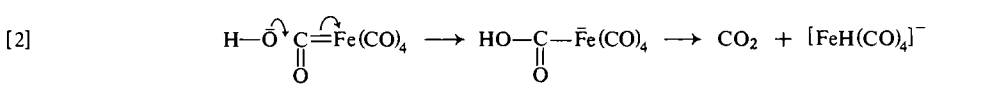

[2]

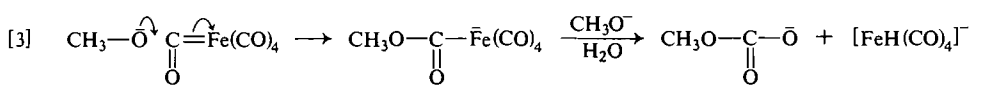

[3]

[1]Holder of NRCC Studentships, 1965–1967.
[2]Hieber and Lipp (2) mentioned briefly that pyridine *N*-oxide reacts with iron pentacarbonyl at a high temperature to form pyridine and iron oxide, but have never published experimental details.

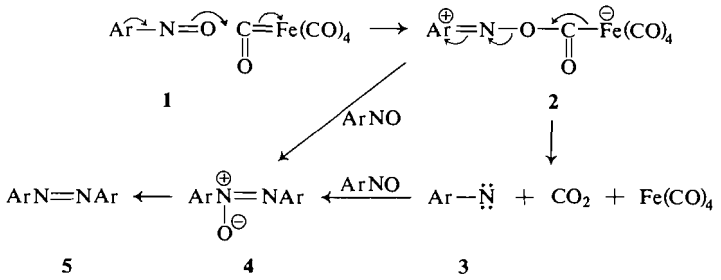

SCHEME 1

(7), and other amines (8), organolithium compounds (9)) react with iron pentacarbonyl by attacking a carbonyl carbon, and mechanisms similar to those of eqs. [1]–[3] may be written for the reactions.

Nitrosobenzene (**1**; Ar = Ph) reacted with one molar equivalent of iron pentacarbonyl in boiling butyl ether to give one mole of carbon dioxide and a 75% yield of azobenzene (**5**; Ar = Ph). At room temperature nitrosobenzene (**1**; Ar = Ph) exists to a minute extent in equilibrium with its dimer ($\bar{O}$—NPh—$\overset{+}{N}$Ph=O) (10), deoxygenation of which could give successively azoxybenzene and azobenzene. However, the concentration of dimer is likely to be extremely small at the temperature of the reaction, and in any case deoxygenation takes place from nitroso compounds which are little dimerized (see below). Consequently, it seems more likely that reaction of the monomeric nitroso compound (**1**; Ar = Ph) with iron pentacarbonyl (Scheme 1) generates a nitrene (cf. ref. 11) (either free (**3**; Ar = Ph) or complexed (**2**; Ar = Ph)). This intermediate can react with more nitrosobenzene to give the azoxy compound (**4**; Ar = Ph), which (as was shown above) can be deoxygenated in turn to azobenzene (**5**; Ar = Ph).

p-Nitrosophenol exists only to the extent of 14–17% in the nitroso form (**6**; $R_1 = R_2 = H$) in dioxan solution, the remainder being in the

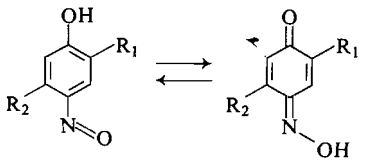

6 **7**

quinone–monoxime tautomeric form **7** ($R_1 = R_2 = H$) (12); dimerization of the nitroso form should be negligible (13). However, reaction of this compound with iron pentacarbonyl in boiling dioxane (in the presence or absence of a small amount of boron trifluoride (1)) gave 4,4′-dihydroxyazobenzene as the only isolable product, no *p*-benzoquinone from deoximation of **7** ($R_1 = R_2 = H$) (cf. ref. 1) being detected. Evidently deoxygenation of the nitroso group proceeded much more rapidly than deoximation of the oxime group. However, from 5-methyl-4-nitroso-2-isopropylphenol (**6**; R_1 = *i*-Pr, R_2 = Me), which exists almost solely in the quinone monoxime form **7** (R_1 = *i*-Pr, R_2 = Me) (14) two products were obtained: 5-isopropyl-2-methyl-1,4-benzoquinone (11% yield), from deoximation of **7** (R_1 = *i*-Pr, R_2 = Me), and 5-methyl-4-amino-2-isopropylphenol (18% yield), from reduction of **6** (R_1 = *i*-Pr, R_2 = Me). No azo compound was obtained, possibly because concentration of the nitroso tautomer **6** (R_1 = *i*-Pr, R_2 = Me) is so low that the reaction: **2** or **3** + nitroso compound → **4**, becomes no longer competitive with hydrogen abstraction from the solvent (cf. ref. 15) by **2** or **3** to give the substituted aniline. When a small amount of boron trifluoride was present in the reaction mixture, the yield of quinone increased and that of amine dropped.

Nitrosobenzene reacted with diiron nonacarbonyl to give a complex, probably **8**, previously prepared by Pauson *et al.* (16) by ultraviolet (u.v.) irradiation of azobenzene with iron pentacarbonyl, and shown to have the structure **8** by Baikie and Mills (17).

The deoxygenation of nitrosamines (**9**) would be expected, from analogy with the reactions of

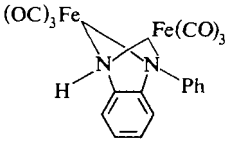

8

Can. J. Chem. Downloaded from www.nrcresearchpress.com by 210.87.254.105 on 09/05/12
For personal use only.

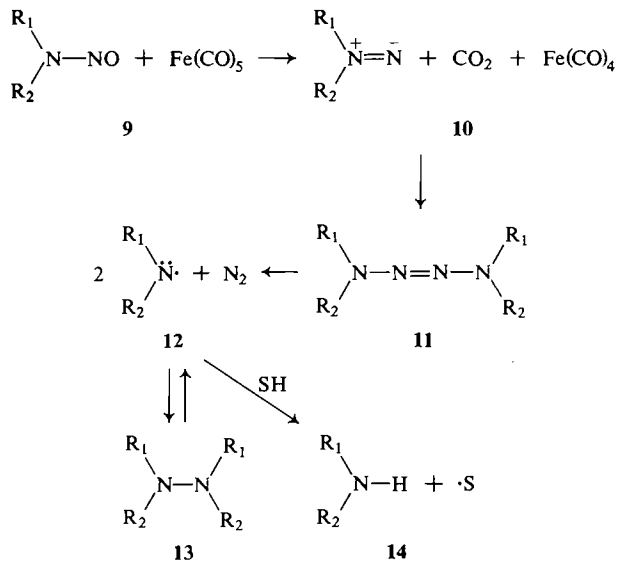

SCHEME 2

C-nitroso compounds, to give tetrazenes (**11**) via the intermediate azamine (**10**) (18) (Scheme 2). Tetrazenes are decomposed at 80–120° to secondary amino radicals (**12**) (19); and diphenylnitrosamine (**9**; $R_1 = R_2 = Ph$) when treated with a boiling solution of iron pentacarbonyl in isooctane gave tetraphenylhydrazine (**13**; $R_1 = R_2 = Ph$) in 52% yield, presumably from the coupling of the diphenylamino radicals **12** ($R_1 = R_2 = Ph$). Diphenylamine (**14**; $R_1 = R_2 = Ph$) was also obtained in this reaction (27% yield), by hydrogen abstraction from the solvent (SH). When the reaction was conducted in butyl ether, from which hydrogen abstraction should occur more readily than from isooctane (20), only diphenylamine was obtained.[3] Several other aromatic nitrosamines were converted by iron pentacarbonyl in butyl ether into secondary amines in 85–92% yields (see Experimental). However, under these conditions the aliphatic nitrosamines, *N*-nitrosopiperidine and *N*-nitrosomorpholine, gave the tetrasubstituted ureas **15**

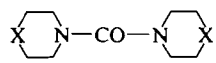

15

(X = CH_2 and O). It is probable that the secondary amines were first formed and then reacted with iron pentacarbonyl to form the ureas, a reaction observed previously with ammonia itself (6).[4]

From the u.v. or ^{60}Co-γ-radiation of various substituted nitrobenzenes in iron pentacarbonyl, von Gustorf *et al.* (21) obtained monomeric or dimeric complexes of the nitrosobenzene and iron tricarbonyl, but up to now the thermal reaction of nitrobenzenes with iron pentacarbonyl seems not to have been investigated. We found that 1.0 mole of nitrobenzene was reduced by 1.0 mole of iron pentacarbonyl to azoxybenzene (containing a little azobenzene), and by 1.4 mole of iron pentacarbonyl to azobenzene in 76% yield. Using the latter proportions, good yields of azobenzenes were obtained from several nitrobenzenes substituted with meta or para electron-releasing substituents, as shown in Table 1. However, ortho-substituents favored the formation of anilines, perhaps because of their steric effect in retarding the competing reaction leading to the azo compound (see Scheme 1). Anilines were also favored by electron-attracting para substituents. (The dimethylamino group probably falls in this

[3]Tetraphenylhydrazine (**13**; $R_1 = R_2 = Ph$), which is known to be partially dissociated into diphenylamino radicals **12** ($R_1 = R_2 = Ph$) (19), abstracted hydrogen from boiling butyl ether to give diphenylamine in 88% yield.

[4]At room temperature, piperidine reacts slowly with iron pentacarbonyl, by nucleophilic attack at the carbonyl carbon, to give *N*-formylpiperidine and other compounds (7).

Can. J. Chem. Downloaded from www.nrcresearchpress.com by 210.87.254.105 on 09/05/12
For personal use only.

TABLE 1
Products from the reaction of substituted nitrobenzenes (1.0 mole) with iron pentacarbonyl (1.4 mole) in hot butyl ether

Substituent	Product	Yield (%)	Melting point (boiling point) (°C)*
(H)	Azobenzene	76	66–68†
o-CH_3	2,2′-Dimethylazobenzene	67	55–56†
	o-Toluidine	13	(196–198)†
m-CH_3	3,3-Dimethylazobenzene	48	52.5–53.5†
	m-Toluidine	6	(199–201)†
p-CH_3	4,4′-Dimethylazobenzene	67	142–144†
o-C_2H_5	2,2′-Diethylazobenzene	39	47–48‡
	o-Ethylaniline	35	(213–216)†
o-OCH_3	*o*-Methoxyaniline	74††	(222–224)†
m-OCH_3	3,3′-Dimethoxyazobenzene	37	74.5–75.5§
p-OCH_3	4,4′-Dimethoxyazobenzene	43	161–163‖
p-F	4,4′-Difluoroazobenzene	67	100–101¶
p-CN	4,4′-Dicyanoazobenzene	20	266–268**
	p-Aminobenzonitrile	11	86–89†
o-NO_2‡‡	2,2′-Diaminoazobenzene	11	118–120†
m-$N(CH_3)_2$	3-Amino-*N*,*N*-dimethylaniline	60	(265–267)†
p-$N(CH_3)_2$	4-Amino-*N*,*N*-dimethylaniline	77	38–41†
o-C_6H_5	2-Aminobiphenyl	58	47–49†
	Carbazole	15	244–246†

*Melting and boiling points are in good agreement with literature values given in the indicated references.
†Reference 30.
‡Reference 35.
§Reference 32*b*.
‖Reference 32*c*.
¶Reference 36.
**Reference 37.
††Yield reduced to 58% when *n*-octane used instead of butyl ether as solvent.
‡‡Mole ratio of iron pentacarbonyl:*o*-dinitrobenzene was 3.0:1.

class because of complexing with iron pentacarbonyl).

2-Nitrobiphenyl gave 2-aminobiphenyl as the major product, together with a small amount of carbazole (Table 1). The formation of the latter can be considered as evidence for a nitrene intermediate (cf. refs. 11, 15). 2,2-Dinitrobiphenyl, on the other hand, gave benzo[*c*]cinnoline (the azo compound) and no amine. 1-Nitronaphthalene (sterically fairly hindered) gave a 70% yield of 1-aminonaphthalene, but 1,8-dinitronaphthalene gave only a trace of 1,8-diaminonaphthalene.

Most of the products obtained from these reactions of nitro compounds with iron pentacarbonyl are also obtained from their reaction with carbon monoxide, at higher temperatures and very much higher pressures, in the presence of a catalytic amount of iron pentacarbonyl (22), and Buckley and Ray (23) reduced nitrosobenzene, nitrobenzene, and azoxybenzene with carbon monoxide alone at 250 °C and 3000 atm to azobenzene. (The possibility of small amounts of iron carbonyls being formed from the steel apparatus under these conditions cannot be excluded).

4-Nitropyridine 1-oxide gave 4,4-azoxypyridine in 22% yield and traces of 4,4-azoxypyridine 1,1-dioxide and 4-nitropyridine. Evidently the metal carbonyl exhibits no great selectivity between the amine oxide and nitro groups of this compound.

When treated with a large excess of iron pentacarbonyl in hot butyl ether, or with 1.4 mole of diiron nonacarbonyl in dioxane, nitrobenzene gave the complex **8**.

Experimental

Materials

N,*N*-Dimethyldodecylamine *N*-oxide (m.p. 127–129°) and *N*,*N*-dimethylaniline *N*-oxide (m.p. 150–153°) were prepared by oxidation of the corresponding amines with *t*-butyl hydroperoxide in *t*-butanol using molybdenum hexacarbonyl as catalyst (24). Brucine *N*-oxide hydrate was prepared by oxidation of brucine according to Hirayama (25). *N*-Nitrosomorpholine was prepared according to Zimmer *et al.* (26). *N*-Nitrosodiphenylamine, *N*-nitroso-*N*-phenylbenzylamine, and *N*-nitroso-*N*-methylaniline were prepared by standard procedures (27); other chemicals were commercial products. All had melting points agreeing closely with reported values. For general procedures, see ref. 28.

General Procedure for N-Oxides

A mixture of the *N*-oxide (20–60 mmole) and iron pentacarbonyl (1:1 mole/mole of *N*-oxide)[5] in dry butyl

[5]1.4:1 mole/mole of brucine *N*-oxide.

Can. J. Chem. Downloaded from www.nrcresearchpress.com by 210.87.254.105 on 09/05/12
For personal use only.

Can. J. Chem. Downloaded from www.nrcresearchpress.com by 210.87.254.105 on 09/05/12
For personal use only.

ether (35–60 ml) was refluxed with stirring under nitrogen for 17 h.[6] The mixture was filtered to remove insoluble inorganic matter, and the amine isolated (*a*) by distillation, when the boiling point of the amine was substantially different from that of butyl ether, as in the case of quinoline, or (*b*) by bubbling in dry hydrogen chloride and collecting the crystalline hydrochloride by filtration. The hydrochloride was then treated with aqueous bicarbonate, and the amine taken up in ethyl ether, dried, and distilled. In the case of brucine, the reaction mixture was filtered through Celite 545, and the amine precipitated by addition of petroleum ether (b.p. 30–60°) to the filtrate; a small additional amount of brucine was obtained by washing the Celite with methanol.

The amines were identified by m.p. or b.p. and by spectral comparison with authentic samples. Yields of pure amines from their *N*-oxides were: pyridine, 79%; 2-picoline, 62%; 4-picoline, 78%; 4-methoxypyridine, 52%; quinoline, 60%; *N,N*-dimethyldodecylamine, 46%; *N,N*-dimethylaniline, 66%; brucine, 51%.

The evolution of one equivalent of carbon dioxide in the deoxygenation of pyridine *N*-oxide was shown by bubbling the nitrogen stream through barium hydroxide, removing barium carbonate by filtration, and titrating the excess barium hydroxide with standard acid.

General Procedure for Azoxy-Compounds

A mixture of the azoxy compound (30–65 mmole) and iron pentacarbonyl (0.8–1.0 mole/mole of azoxy compound) in dry butyl ether (50–60 ml) was refluxed with stirring under nitrogen for 24 h. The mixture was cooled and filtered and the solvent removed from the filtrate at 30 mm. The residue was dissolved in petroleum ether (b.p. 38–54°) and chromatographed on Florosil. The azo compound formed a colored band which was eluted with ether, recovered by evaporation, and identified by m.p. and mixed m.p. with an authentic specimen. Azobenzene was obtained in 77% yield, and 2,2-dimethylazobenzene in 65% yield.

Deoxygenation of α-Phenyl-N-phenylnitrone

A mixture of the nitrone (1.52 g; 7.73 mmole) and iron pentacarbonyl (1.14 ml; 8.50 mmole) in dry butyl ether was refluxed as above for 24 h. Work-up by the procedure described for azoxy compounds gave an oil which crystallized from carbon disulfide as pale yellow needles of *N*-benzylideneaniline (0.85 g; 61%), m.p. 50–52° (lit. m.p. 51–52°) having an infrared (i.r.) spectrum identical to that reported by Nakanishi (29).

Reaction of Nitrosobenzenes with Iron Pentacarbonyl

A mixture of nitrosobenzene (3.13 g, 29.2 mmole) and iron pentacarbonyl (3.93 ml, 29.2 mmole) in dry butyl ether (55 ml) was refluxed for 24 h while being stirred under nitrogen. The solution was cooled, filtered, and concentrated at 30 mm. The residue, recrystallized twice from 95% ethanol, gave azobenzene (2.01 g; 75%), m.p. and mixed m.p. 66–68°. By bubbling the nitrogen stream through barium hydroxide solution it was found that about 2 moles of carbon dioxide were evolved per mole of azobenzene formed.

p-Nitrosophenol (2.43 g, 19.7 mmole), treated in the same way with iron pentacarbonyl in anhydrous dioxane (65 ml), gave a solid from which, by chromatography in ether on Florosil, 4,4-dihydroxyazobenzene was obtained as green crystals (0.86 g, 41%), m.p. 212–214° (lit. m.p. 216° (30)). Further elution with ether gave *p*-nitrosophenol; however, the yield of azo compound was not improved by increasing the reaction time, using more iron pentacarbonyl, or adding a catalytic amount of boron trifluoride etherate.

Similar treatment of 5-methyl-4-nitroso-2-isopropylphenol (3.11 g) in dry butyl ether (50 ml) gave a solid which partially dissolved in petroleum ether. The insoluble residue, crystallized from benzene, gave white needles of 5-methyl-4-amino-2-isopropylphenol (0.50 g, 18%), m.p. 177–179° (lit. m.p. 178–179° (31)), ν_{max} (KBr) 3455, 3390 cm^{-1} (N—H). The petroleum ether extract on concentration deposited yellow plates (0.31 g, 11%) of 5-isopropyl-2-methyl-1,4-benzoquinone, m.p. 42–44° (lit. m.p. 45.5° (30)). When the reaction was repeated in the presence of 0.15 g of boron trifluoride etherate, the aminophenol was obtained in 6% yield and the quinone in 19% yield.

Diiron Hexacarbonyl Complex **8**

(a) From Nitrosobenzene and Diiron Nonacarbonyl

A mixture of nitrosobenzene (1.49 g, 13.9 mmole) and diiron nonacarbonyl (5.08 g, 13.9 mmole) in anhydrous tetrahydrofuran (55 ml) was stirred under nitrogen for 12 h at room temperature. The solution was filtered and concentrated at 30 mm, and the residue extracted with petroleum ether. The extract was chromatographed on Florosil. Elution with petroleum ether gave the complex **8** (0.35 g, 11%), m.p. 158.5–159°, ν_{max} (KBr) 3375 cm^{-1} (ν N—H), 2070, 2035, 1996, 1971, 1956 cm^{-1} (ν C=O), 774 and 687 cm^{-1} (out-of-plane bending of five adjacent C—H on Ph) and 743 cm^{-1} (four adjacent C—H on benzo ring). Pauson *et al.* (8) report m.p. 163–164°, ν_{max} (CCl_4) 3362 cm^{-1} (ν N—H), ν_{max} (KCl) 2072, 2040, 1998, 1975, and 1960 cm^{-1} (ν C=O).

Further elution with petroleum ether gave traces of azobenzene.

(b) From Nitrobenzene and Diiron Nonacarbonyl

The same procedure was used with nitrobenzene, except that the mole ratio of diiron nonacarbonyl:nitrobenzene was 1.4:1, and gave the same yield of complex.

Reaction of N-Nitrosoamines with Iron Pentacarbonyl in Butyl Ether

Reaction was carried out essentially as described for nitrosobenzene, using a mole ratio of iron pentacarbonyl: nitrosamine of 1.1:1 and a reaction time of about 16 h. Solid amines were identified by m.p. and mixture m.p.; liquid amines by b.p.; and ureas by m.p. and i.r. spectrum (ν_{max} (KBr) 1645–1660 cm^{-1}). *N*-Nitrosodiphenylamine gave diphenylamine in 91% yield; *N*-nitroso-*N*-phenylbenzylamine gave *N*-phenylbenzylamine, 85% yield; *N*-nitroso-*N*-methylaniline gave *N*-methylaniline, 90% yield; *N*-nitrosocarbazole gave carbazole, 92% yield;

[6]In the case of *N,N*-dimethyldodecylamine *N*-oxide, *N,N*-dimethylaniline *N*-oxide, and brucine *N*-oxide hydrate, 4 h. It is possible that a shorter time would suffice.

Can. J. Chem. Downloaded from www.nrcresearchpress.com by 210.87.254.105 on 09/05/12
For personal use only.

N-nitrosopiperidine, carbonyldipiperidine, 48% yield;[7] and *N*-nitrosomorpholine, carbonyl dimorpholine, 57% yield.[7]

Reaction of N-Nitrosodiphenylamine with Iron Pentacarbonyl in Isooctane

The reaction was carried out as above, with substitution of isooctane for butyl ether. Filtration of the mixture after reaction removed a solid which dissolved partially in benzene. Concentration of the benzene solution gave crystals of tetraphenylhydrazine, m.p. 147° (decomposition) (lit. m.p. 147–149° (decomposition) (19)) in 56% yield. The isooctane filtrate on concentration deposited diphenylamine, obtained in 27% yield after recrystallization from aqueous ethanol, m.p. 52–54° (lit. m.p. 52.8° (30)).

Reaction of Tetraphenylhydrazine with Butyl Ether

A solution of tetraphenylhydrazine (1.78 g) in anhydrous butyl ether (40 ml) was boiled under reflux while being stirred in a nitrogen atmosphere for 18 h. The solution was cooled, filtered, and concentrated at 30 mm. The residue was treated with petroleum ether, the resultant suspension filtered, and the filtrate concentrated to give diphenylamine (1.57 g, 88%), m.p. 52–54°.

Reaction of Nitro Compounds with Iron Pentacarbonyl in Butyl Ether

The yields shown in Table 1 were obtained by essentially the same procedure as described above for the reduction of nitrosobenzene. In some cases (e.g., from the reaction of *o*-methoxy- and of *m*-dimethylamino-nitrobenzene), a substituted aniline was obtained by distillation of the reaction mixture after filtration. In other cases the residue from this filtrate was taken up in petroleum ether or (if insufficiently soluble, as in the case of the *p*-cyano compounds) in benzene, and chromatographed on Florosil. The azo compound was eluted first, followed by the amino compound; the latter, when liquid, was further purified by distillation. The u.v. absorption peaks of the azo compounds in ethanol were at the wavelengths, and had intensities agreeing with values reported in the literature when these were available (32); 4,4′-dicyanoazobenzene showed λ_{max} (log ε_{max} in parentheses) at 230 (4.13), 375 (4.37), 340 (shoulder) (4.29) and 441 nm (2.98), and 2,2′-diaminoazobenzene at 450 nm (4.05).

The following cases are additional to those reported in Table 1.

(a) Reaction of Equimolar Quantities of Nitrobenzene and Iron Pentacarbonyl in Butyl Ether

The product was chromatographed on Florosil. Elution with petroleum ether gave first 3% of azobenzene, m.p. and mixed m.p. 66–68°, and then 64% of azoxybenzene, m.p. and mixed m.p. 35–36° (lit. m.p. 36° (30)).

(b) Reaction of 2,2-Dinitrobiphenyl

Reaction of 2,2-dinitrobiphenyl (3.55 g, 14.6 mmole) and iron pentacarbonyl (5.87 ml, 43.7 mmole) in butyl ether (55 ml), under the usual conditions, gave yellow blades of benzo[*c*]cinnoline (1.70 g, 65%), m.p. 155–156° (lit. m.p. 155–157° (30)), λ_{max} (EtOH) at 282 (log ε 4.58), 308 (log ε 3.98) and 355 nm (log ε 3.28), in agreement with reported spectrum (33).

[7]Obtained by chromatography of reaction products on Florosil, and elution with petroleum ether – benzene (1:1) and then with benzene–acetone (5:1).

(c) Reaction of 1-Nitronaphthalene

Reaction of 1-nitronaphthalene (3.20 g, 19.5 mmole) with iron pentacarbonyl (3.48 ml, 25.9 mmole) in butyl ether (50 ml) under the usual conditions gave a solid which was chromatographed in acetone on Florosil to give crude 1-aminonaphthalene (2.05 g, 77%), m.p. 44–46°. This was decolorized with charcoal and recrystallized from aqueous ethanol to give 1-aminonaphthalene (1.85 g, 70%) melting at 49–50° (lit. m.p. 49–50° (30)).

(d) Reaction of 1,8-Dinitronaphthalene

1,8-Dinitronaphthalene (3.02 g, 13.8 mmole) was reduced by iron pentacarbonyl (5.59 ml, 41.5 mmole) in butyl ether to give 1,8-diaminonaphthalene (0.02 g), m.p. 63–65° (lit. m.p. 66.5° (30)). Yields were not improved by using a smaller amount of iron pentacarbonyl, by shortening the reaction time to 10 h, or by increasing it to 50 h.

(e) Reaction of 4-Nitropyridine 1-Oxide

4-Nitropyridine 1-oxide (3.00 g, 21.4 mmole) was treated with iron pentacarbonyl (3.17 ml, 23.6 mmole) in butyl ether (40 ml) for 17 h under the usual conditions. The reaction product in benzene was chromatographed on Florosil and gave orange-yellow needles of 4,4-azoxypyridine (0.47 g, 22%), m.p. 123–125° (lit. m.p. 125–126° (31)), λ_{max} 291 nm (log ε 4.20 in ethanol). Further elution removed traces of 4,4-azoxypyridine 1,1-dioxide and 4-nitropyridine, identified by comparison of their u.v. spectra with those reported by den Hertog *et al.* (34).

We are grateful for assistance from Edmund Che–Hoi Keung, a National Science Foundation Undergraduate Research Participant, Binghamton, Summer 1969. The financial support of the National Research Council of Canada and of the Research Foundation of the State of New York (Grant 40-7126A) is gratefully acknowledged.

1. H. ALPER and J. T. EDWARD. J. Org. Chem. **23**, 2938 (1967).
2. W. HIEBER and A. LIPP. Chem. Ber. **92**, 2085 (1959).
3. F. A. DANIKER and B. E. HACKLEY. J. Org. Chem. **31**, 4267 (1966), and references therein.
4. W. HIEBER and F. LEUTERT. Z. Anorg. Allg. Chem. **204**, 145 (1932). A. A. BLANCHARD and G. W. COLEMAN. Inorg. Syn. **2**, 243 (1946).
5. F. FIEGL and R. KRUMHOLZ. Monatsh. **59**, 314 (1932).
6. H. BEHRENS and H. WAKAMATSU. Z. Anorg. Allg. Chem. **320**, 30 (1963).
7. W. F. EDGELL, M. T. YANG, B. J. BULKIN, R. BAYER, and N. KOLZUMI. J. Amer. Chem. Soc. **87**, 3080 (1965).
8. W. F. EDGELL and B. J. BULKIN. J. Amer. Chem. Soc. **88**, 4839 (1966).
9. M. RYANG, Y. SAWA, and H. MASADA. Kogyo Kagaku Zasshi **66**, 1086 (1963); Chem. Abstr. **62**, 7670 *h* (1965); M. RYANG, I. RHEE, and S. TSUTSUMI. Bull. Chem. Soc. Japan, **37**, 341 (1964).
10. P. A. S. SMITH. Open-chain nitrogen compounds. Vol. II. W. A. Benjamin Inc., New York, 1965. pp. 358.
11. M. DEKKER and G. R. KNOX. Chem. Commun. 1243 (1967).
12. H. UFFMANN. Tetrahedron Lett. 4631 (1966). R. K. NORRIS and S. STERNHELL. Aust. J. Chem. **19**, 841 (1966).

13. R. R. HOLMES, R. P. BAYER, L. A. ERREDE, H. R. DAVIS, A. W. WIESENFELD, P. M. BERGMAN, and D. L. NICHOLAS. J. Org. Chem. **30**, 3837 (1965).
14. P. RAMART-LUCAS and M. M. MARTYNOFF. Bull. Soc. Chim. Fr. **16**, 53 (1967).
15. R. J. SUNDBERG. J. Amer. Chem. Soc. **88**, 3871 (1966). L. HORNER, A. CHRISTMASS, and A. GROSS. Chem. Ber. **96**, 399 (1963). P. A. S. SMITH and B. B. BROWN. J. Amer. Chem. Soc. **73**, 2435 (1951). J. I. G. CADOGAN, M. CAMERON-WOOD, R. K. MACKIE, and R. J. G. SEARLE. J. Chem. Soc. 4831 (1965). P. J. BUNYAN and J. I. G. CADOGAN. J. Chem. Soc. 42 (1968).
16. M. M. BAGGA, P. L. PAUSON, F. J. PRESTON, and R. I. REED. Chem. Commun. 543 (1965). M. M. BAGGA, W. T. FLANNIGAN, G. R. KNOX, and P. L. PAUSON. J. Chem. Soc. (C) 1534 (1969).
17. P. E. BAIKIE and O. S. MILLS. Chem. Commun. 707 (1966).
18. D. M. LEMAL and T. W. RAVE. J. Amer. Chem. Soc. **87**, 393 (1963).
19. B. R. CONLEY and W. A. WATERS. J. Chem. Soc. 1228 (1961). W. SCHLENK and E. BERGMANN. Ann. **463**, 281 (1927).
20. R. S. DAVIDSON. Quart. Rev. **21**, 249 (1967).
21. E. K. VON GUSTORF, M. C. HENRY, R. E. SACHER, and C. DIPIETRO. Z. Naturforsch. **21B**, 1152 (1966).
22. J. E. KMIECIK. J. Org. Chem. **30**, 2014 (1965).
23. G. D. BUCKLEY and N. H. RAY. J. Chem. Soc. 1154 (1949).
24. M. N. SHENG and J. G. ZAJACEK. J. Org. Chem. **33**, 588 (1968).
25. K. HIRAYAMA. J. Inst. Polytech. Osaka City University Ser. C **2**, 49 (1951); Chem. Abstr. **46**, 6131*f* (1952).
26. H. ZIMMER, L. F. AUDRIETH, M. ZIMMER, and R. A. ROWE. J. Amer. Chem. Soc. **77**, 790 (1955).
27. A. I. VOGEL. Elementary practical organic chemistry. Part 2, Qualitative organic analysis. Longmans, Green & Co., London, 1959. p. 449.
28. H. ALPER and J. T. EDWARD. Can. J. Chem. **46**, 3112 (1968).
29. K. NAKANISHI. Infrared absorption spectroscopy. Holden-Day. San Francisco, 1964. p. 222.
30. Handbook of chemistry and physics. 46th Edn. *Edited by* C. D. Hodgman. The Chemical Rubber Publishing Co., Cleveland, Ohio, 1966.
31. Dictionary of organic compounds. *Edited by* I. M. Heilbron, A. H. Cook, H. M. Bunbury and D. H. Hey. Eyre & Spottiswoode Publishers, Ltd., London, 1965.
32. (*a*) P. GRAMMATICAKIS. Bull. Soc. Chim. Fr. **15**, 979 (1948); (*b*) **18**, 951 (1951). (*c*) C. J. PEDERSON. J. Amer. Chem. Soc. **79**, 5014 (1957). (*d*) R. B. CARLIN and G. S. WICK. J. Amer. Chem. Soc. **80**, 4023 (1958). (*e*) P. H. GORE and O. H. WHEELER. J. Org. Chem. **26**, 3295 (1961). (*f*) O. H. WHEELER and D. GONZALEZ. Tetrahedron, **20**, 189 (1964). (*g*) B. T. NEWBOLD and D. TONG. Can. J. Chem. **92**, 836 (1964).
33. G. M. BADGER, R. S. PEARCE, and R. PETTIT. J. Chem. Soc. 3199 (1951).
34. H. J. DEN HERTOG, C. H. HENKENS, and J. H. VAN ROON. Rec. Trav. Chim. **71**, 1145 (1952).
35. G. SCHULTZ. Ber. **17**, 473 (1884).
36. J. LICHTENBERGER and R. THERMET. Bull. Soc. Chim. Fr. **18**, 318 (1951).
37. J. N. ASHLEY and S. S. BERG. J. Chem. Soc. 3089 (1957).

Can. J. Chem. Downloaded from www.nrcresearchpress.com by 210.87.254.105 on 09/05/12
For personal use only.

Can. J. Chem. Downloaded from www.nrcresearchpress.com by 210.87.254.105 on 09/05/12
For personal use only.

Pyrrole chemistry. X. Friedel–Crafts alkylation of some pyrrole and furan derivatives

HUGH J. ANDERSON AND C. W. HUANG
Department of Chemistry, Memorial University of Newfoundland, St. John's, Newfoundland

Received November 19, 1969

The Friedel–Crafts *t*-butylation of methyl 2-pyrrolecarboxylate and of 2-acetylpyrrole have been investigated. The results are found to be consistent with the mechanistic pathway suggested in earlier isopropylation papers. Evidence is presented that alkylation of similarly substituted furans may be interpreted in the same way.

Canadian Journal of Chemistry, **48**, 1550 (1970)

Earlier papers in this series (1, 2) described the Friedel–Crafts isopropylation of methyl 2-pyrrolecarboxylate, 2-pyrrolecarbaldehyde, and 2-acetylpyrrole under a variety of experimental conditions. A mechanistic pathway was proposed where 4-isopropylation was sometimes followed by a rearrangement to the 5-position and dialkylation.

It seemed likely that the *t*-butyl group might rearrange more readily than the isopropyl from the 4- to the 5-position of the 2-ester. It might also rearrange in alkylation reactions with the 2-ketone or the 2-aldehyde when the isopropyl group did not.

Methyl 2-pyrrolecarboxylate was *t*-butylated under the same conditions used for the isopropylation experiments but at room temperature. The reaction mixture was worked up in the usual way and, after separation and identification of the products, most subsequent mixtures were analyzed by gas–liquid partition chromatography (g.l.p.c.). Even the use of a large excess of *t*-butyl chloride did not produce any of the dialkylated ester. However, both 4- and 5-*t*-butyl-2-ester were formed.

The results of a series of alkylation experiments are shown in Table 1. The behavior observed appeared consistent with the proposed mechanistic pathway. At ice-bath temperature alkylation was too slow to be useful. When the $AlCl_3$ concentration was low the 4-:5-ratio was greater than 1:1 but the overall alkylation was also less.

Methyl 4-*t*-butyl-2-pyrrolecarboxylate was found to rearrange very easily to the 5-isomer in carbon disulfide in the presence of $AlCl_3$ and HCl gas, and even in the absence of the HCl gas and at room temperature (Table 2). Under HCl/$AlCl_3$/refluxing conditions the 5-*t*-butyl isomer was unchanged after 21 h.

When attempts were made to dialkylate either the 2-ester or the 5-*t*-butyl-2-ester a small amount of 4-*t*-butyl-2-ester was formed. Thus, in the presence of a large amount of the *t*-butyl carbonium ion, an equilibrium may arise between the 4- and 5-isomers which disappears when this ion is used up.

The results of the *t*-butylation of 2-acetylpyrrole are shown in Table 1. This compound was similar in reactivity to the 2-aldehyde but less susceptible to destruction (2). A 4- to 5-isomer rearrangement took place but much less readily than for the corresponding ester derivative above.

This rearrangement was markedly influenced by the aluminum chloride used in these experiments. Aluminum chloride from a partly empty bottle promoted rearrangement much more than $AlCl_3$ of the same manufacture and quality from a freshly opened bottle. The usual preparation involved rapid weighing of catalyst in the laboratory. When dry-box weighing, anhydrous conditions, and aluminum chloride from a freshly opened bottle were used, the alkylation almost ceased. However, experiments where small amounts of water were added produced no consistent results. The "ageing" of the $AlCl_3$ depends not only on the absorption of water but on other factors such as the amount of HCl present.

The results of these *t*-butylation and isopropylation experiments with pyrrole derivatives are similar to earlier observations made in the furan series and may be used to explain the latter. Thus, while isopropylation of furfural gave only the 4-isomer (3, 4) in low yield, *t*-butylation gave only the 5-isomer (5). Both isopropylation and *t*-butylation of methyl 2-furancarboxylate also gave only the 5-isomer (3*a*, 6). 2-Acetylfuran was also 5-*t*-butylated (7). All these alkylations were

TABLE 1
t-Butylation of 2-substituted pyrroles*

Compound	Catalyst†	Temperature (°C)	Time (min)	Conversion (mole%)	Product (mole%) 4-	5-
2-Ester	2.2	0	60	trace	—	trace
	2.2	20	10	5	2.5	2.5
	2.2	20	20	56	15	41
	2.2	20	25	68	11	57
	2.2	20	40	76	9‡	67‡
	2.2	20	60	80	11	70
	2.2	50	3	7	3.5	3.5
	2.2	50	10	76	7.5	68.5
	2.2	50	60	88	—	88
	1.5	20	60	25	14	11
	1.5	50	60	80	4	76
	3.0	20	30	76	6	70
2-Ketone	2.2	50	30	66	22	44
	2.2	50	60	71	19	52
	2.2	50	240	78	6	72
	2.2	50	1800	83	—	83

*Molar ratio of substrate/*t*-butyl chloride was 1:1.
†Molar ratio of substrate/catalyst.
‡Product isolated by column chromatography and weighed: 4-isomer 7%, 5-isomer 64%.

carried out using similar conditions and over long periods (18–24 h). Acheson has remarked that isopropylation of furfural "is perhaps the only recorded case of a substituent entering the furan ring entirely at a 3- or 4-position when there is a free 5-position available" (8). These results may be explained by the same mechanistic pathway described for the pyrrole derivatives. The rearrangement of entering isomeric butyl groups to the *t*-butyl isomer (5, 9) is also in agreement with the carbonium ion mechanism.

The isopropylation of methyl 2-furoate (3*a*, 6) has been repeated and the products analyzed by g.l.p.c. Three products were found, together with unreacted starting material. Samples of these products were collected and identified by proton magnetic resonance (p.m.r.), and by hydrolysis to the corresponding acids, as methyl 4- and 5-isopropyl-2-furoate and methyl 4,5-diisopropyl-2-furoate. The amount of 4-isopropyl-2-ester fell, and that of the 5-isopropyl isomer rose as the reaction proceeded. The behavior of the 2-ester during Friedel–Crafts alkylation appears similar to that observed for the corresponding pyrrole ester reactions. It has been reported that 4-*t*-butyl-2-furancarbaldehyde does not rearrange with aluminum chloride in carbon disulfide at room temperature (5), although no conditions were given. It may be that very dry aluminum chloride was used and no HCl was admitted. In many of the early alkylation experiments in the furan series several products probably were present in the reaction mixture, but only the predominant one was isolated. Yields were often very low.

TABLE 2
4-*t*-Butyl isomer rearrangement experiments

Compound	Time (min)	HCl	Isomer (%) 4-	5-
2-Ester	0	No	100	0
	30		47	53
	90		22	78
	150		1.5	98.5
	270		trace	100
	1	Yes	48	52
	3		19	81
	5		10	90
	30		trace	100
2-Ketone	0	Yes	95	5
	5		81	19
	10		51	49
	30		20	80
	60		1	99

The only comparable alkylations in the thiophene series were the isopropylation of the 2-acetyl derivative (10) and, under somewhat different conditions, of the 2-acid (11). The former gave a mixture which was usually 90% 4-isopropyl-2-acetothienone while only the 5-isomer was obtained in the latter experiment. As these results appeared to fall into the same pattern it seemed useful to see whether *t*-butylation would produce mostly 5-alkylation with

Can. J. Chem. Downloaded from www.nrcresearchpress.com by 210.87.254.105 on 09/05/12
For personal use only.

Can. J. Chem. Downloaded from www.nrcresearchpress.com by 210.87.254.105 on 09/05/12
For personal use only.

thiophene derivatives. However, a preliminary trial showed that, under similar conditions, *t*-butylation of 2-acetylthiophene gave almost the same ratio of 4- to 5-isomers as reported for isopropylation and it did not seem to alter with time. Separation problems have prevented further experiments in this field.

Experimental

General

Melting points are uncorrected. Elemental analyses were determined by Alfred Bernhardt, Mülheim (Ruhr), Germany.

The p.m.r. spectra were determined on a Varian A-60 spectrometer at 60 Mc.p.s. The chemical shifts are in p.p.m. from tetramethylsilane as internal reference and are recorded on the τ scale. The proton on the pyrrole nitrogen was decoupled by addition of a few drops of deuterium oxide.

Analyses of reaction mixtures were carried out by (g.l.p.c.) using an 18 in. column packed with Apiezon L on firebrick. Analyses were accurate to about 2%. Reference 2 gives data on the pyrrole substrates. Aluminum chloride was Fisher Reagent Grade.

General Procedure for Pyrrole Alkylation

(*a*) A mixture of methyl 2-pyrrolecarboxylate (0.625 g, 0.005 mole) and aluminum chloride (as in Table 1) was stirred in carbon disulfide (10 ml) for 1 h at 50°. The temperature was then adjusted and *t*-butyl chloride (0.45 g, 0.005 mole) in 5 ml carbon disulfide was added at once. After stirring for the required period the reaction was quenched in ice and worked-up as described in reference 2.

(*b*) A mixture of 2-acetylpyrrole (2.18 g, 0.02 mole) and aluminum chloride (as in Table 1) was stirred in carbon disulfide (10 ml) for 30 min at 50°. The temperature was then adjusted and *t*-butyl chloride (1.85 g, 0.02 mole) added at once. After stirring for the required period the reaction was quenched and worked-up as in reference 2.

Isolation of Alkylation Products

As in reference 2, structures of the isomeric *t*-butylated esters and ketones were established by p.m.r. spectra. Correspondence with the spectra of the analogous isopropyl derivatives (1, 2) was unequivocal in each case.

Methyl 4-*t*-butyl-2-pyrrolecarboxylate, m.p. 121.5–122° from chloroform–cyclohexane; p.m.r. (CCl_4): H-3 and H-5, 3.3; CH_3O—, 6.18; $(CH_3)_3C$—, 8.77, $J_{3,5}$ ($CDCl_3$), 1.7 c.p.s.

Anal. Calcd. for $C_{10}H_{15}NO_2$: C, 66.27; H, 8.34; N, 7.73. Found: C, 66.49; H, 8.44; N, 7.74.

Methyl 5-*t*-butyl-2-pyrrolecarboxylate, m.p. 128–128.5° from chloroform–cyclohexane; p.m.r. (CCl_4): H-3, 3.32; H-4, 4.12; CH_3O—, 6.18; $(CH_3)_3C$—, 8.66, $J_{3,4}$ 3.8 c.p.s.

Anal. Calcd. for $C_{10}H_{15}NO_2$: C, 66.27; H, 8.34; N, 7.73. Found: C, 66.34; H, 8.55; N, 7.85.

4-*t*-Butyl-2-acetylpyrrole, m.p. 133–134° from hexane; p.m.r. (CCl_4): H-3, 3.28; H-5, 3.10; CH_3CO—, 7.62; $(CH_3)_3C$—, 8.78, $J_{3,5}$ 1.6 c.p.s.

Anal. Calcd. for $C_{10}H_{15}NO$: C, 72.69; H, 9.15; N, 8.48. Found: C, 72.94; H, 9.01; N, 8.68.

5-*t*-Butyl-2-acetylpyrrole, m.p. 88–89° from aqueous methanol; p.m.r. (CCl_4): H-3, 3.34; H-4, 4.12; CH_3CO—, 7.68; $(CH_3)_3C$—, 8.65, $J_{3,4}$ 4.0 c.p.s.

Anal. Calcd. for $C_{15}H_{10}NO$: C, 72.69; H, 9.15; N, 8.48. Found: C, 72.69; H, 9.15; N, 8.38.

Rearrangement of Methyl 4-t-Butyl-2-pyrrolecarboxylate

(*a*) Methyl 4-*t*-butyl-2-pyrrolecarboxylate (1.0 g, 0.0055 mole) was added at once to a stirred mixture of aluminum chloride (2.21 g, 0.0165 mole) in 15 ml carbon disulfide at room temperature. After the appropriate time the reaction mixture was worked-up in the usual manner and analyzed by g.l.p.c. See Table 2 for results.

(*b*) As in (*a*), but a stream of dry hydrogen chloride gas was admitted throughout the course of the reaction. See Table 2 for results.

(*c*) The rearrangement was attempted using dry hydrogen chloride gas in the absence of aluminum chloride. There was no observable change in the starting material after 60 min.

Attempted Rearrangement of Methyl 5-t-Butyl-2-pyrrolecarboxylate

Methyl 5-*t*-butyl-2-pyrrolecarboxylate (2.0 g, 0.011 mole) and aluminum chloride (4.42 g, 0.033 mole) in 20 ml carbon disulfide was stirred at 50° for 21 h while passing through it a stream of dry hydrogen chloride gas. After working-up in the usual manner no change was found in the starting material.

Rearrangement of 4-t-Butyl-2-acetylpyrrole

This rearrangement was carried out in the same manner as procedure (*b*) for the 4-*t*-butyl-2-ester. The results are given in Table 2. Attempts to carry out the rearrangement by procedures (*a*) and (*c*) failed.

Attempted Rearrangement of 5-t-Butyl-2-acetylpyrrole

Attempts to accomplish this rearrangement by the various procedures used for the 4-*t*-butyl-2-ester all failed.

Attempted Preparation of Methyl 4,5-Di-t-butyl-2-pyrrolecarboxylate

(*a*) A mixture of methyl 2-pyrrolecarboxylate (2.5 g, 0.02 mole) and aluminum chloride (8.65 g, 0.065 mole) in 40 ml carbon disulfide was stirred at 50° for 1 h. *t*-Butyl chloride (4.6 g, 0.05 mole) was added at once. After 2 h the reaction mixture was worked-up and analyzed in the usual manner. About 3% of methyl 4-*t*-butyl-2-pyrrolecarboxylate was present, but the remainder was entirely the 5-*t*-butyl isomer.

(*b*) Using methyl 5-*t*-butyl-2-pyrrolecarboxylate as substrate and proceeding as in (*a*) the mixture was analyzed at several time intervals and showed no dialkyl product. An amount of 4-*t*-butyl isomer, rising from a trace after 10 min to a roughly constant 3–4% after 1 h, was present.

Attempted Preparation of 4,5-Di-t-butyl-2-acetylpyrrole

Attempts were made using an excess of *t*-butyl chloride to dialkylate: (*a*) 2-acetylpyrrole (*b*) 5-*t*-butyl-2-acetylpyrrole (*c*) 4-*t*-butyl-2-acetylpyrrole.

None were successful in producing any of the dialkylated compound.

Can. J. Chem. Downloaded from www.nrcresearchpress.com by 210.87.254.105 on 09/05/12
For personal use only.

Isopropylation of Methyl 2-Furoate

(*a*) Using the method of Gilman and Calloway (3*a*), a solution of methyl 2-furoate (0.010 mole) and isopropyl chloride (0.010 mole) was added dropwise to aluminum chloride (0.0125 mole) in 40 ml carbon disulfide. After stirring 24 h at room temperature the mixture was worked-up as described in the pyrrole alkylation section above. The product was analyzed by g.l.p.c.

Starting material, 28%; 5-isopropyl-2-ester, 32%; 4-isopropyl-2-ester, 20%; 4,5-diisopropyl-2-ester, 20%.

(*b*) The method was modified by using the same volume of methylene chloride as solvent.

Starting material, 26%; 5-isopropyl-2-ester, 27%; 4-isopropyl-2-ester, 20%; 4,5-diisopropyl-2-ester, 27%.

(*c*) The same as method (*a*) but refluxed during addition and for 30 min, then worked-up.

Starting material, 51%; 5-isopropyl-2-ester, 10%; 4-isopropyl-2-ester, 16%; 4,5-diisopropyl-2-ester, 22%.

Product identification was obtained by collecting samples of the effluent gas corresponding to each peak of the g.l.p.c. These samples were dissolved in carbon tetrachloride and examined by p.m.r. Each sample was then hydrolyzed (3*a*) and the melting point of the corresponding acid was determined.

Methyl 5-isopropyl-2-furoate; p.m.r. (CCl_4): H-3, 3.03; H-4, 3.98; CH_3O—, 6.20; =CH—, 7.1; $(CH_3)_2C$—, 8.69; $J_{3,4}$ 3.5 c.p.s. See reference 12 for p.m.r. spectrum of ethyl 5-methyl-2-furoate. Corresponding acid m.p. 65–67°, literature m.p. 66–67° (13).

Methyl 4-isopropyl-2-furoate; p.m.r. (CCl_4): H-5, 2.74; H-3, 3.02; CH_3O—, 6.19; =CH—, 7.1; $(CH_3)_2C$—, 8.78, $J_{3,5}$ 0.9 c.p.s. Corresponding acid m.p. 75–76°, literature m.p. 76–77° (3*a*).

Preparation of Methyl 4,5-Diisopropyl-2-furoate

As in (*c*) above, but used 3 molar equi. of isopropyl chloride and 2 molar equi. of aluminum chloride while heating for 6 h. Product was 63% diisopropyl derivative and the rest unreacted. Distillation gave methyl 4,5-diisopropyl-2-furoate, b.p. 116–118° at 6 mm; p.m.r. (CCl_4): H-3, 3.07; CH_3O—, 6.21; =CH—, 7.1; 5-$(CH_3)_2C$—, 8.70; 4-$(CH_3)_2C$—, 8.81. Corresponding 4,5-diisopropyl-2-furoic acid m.p. 107–107.5° (hexane).

Anal. Calcd. for $C_{11}H_{16}O_3$: C, 67.32; H, 8.22. Found: C, 67.56; H, 8.45.

Rearrangement of Methyl 4-Isopropyl-2-furoate

The product ratio from isopropylation reaction of type (*a*) was determined by analysis of a small sample after 8 h. Then a further 0.0125 mole aluminum chloride was added to the product mixture and, while keeping at reflux for a further 2 h, dry hydrogen chloride gas was admitted. A further analysis showed that the ratio of 4-isopropyl- to 5-isopropyl-2-furoate changed from 0.72 to 0.49 during this period while the proportions of starting material and diisopropyl-2-ester did not change greatly.

The authors acknowledge with thanks the continued financial support of the National Research Council of Canada. They are also indebted to Mr. F. D. Smallwood for technical assistance in preparations.

1. H. J. Anderson and L. C. Hopkins. Can. J. Chem. **42**, 1279 (1964).
2. H. J. Anderson and L. C. Hopkins. Can. J. Chem. **44**, 1831 (1966).
3. (*a*) H. Gilman and N. O. Calloway. J. Amer. Chem. Soc. **55**, 4197 (1933). (*b*) H. Gilman, N. O. Calloway, and R. R. Burtner. J. Amer. Chem. Soc. **57**, 906 (1935).
4. N. Elming. Acta Chem. Scand. **6**, 605 (1952).
5. H. Gilman and R. R. Burtner. J. Amer. Chem. Soc. **57**, 909 (1935).
6. T. Reichstein, H. R. Rosenberg, and R. Eberhardt. Helv. Chim. Acta, **18**, 721 (1935).
7. Y. L. Goldfarb and L. D. Tarasova. Izv. Akad. Nauk. S.S.S.R. 1304 (1960). Chem. Abstr. **55**, 504 (1961).
8. R. M. Acheson. An introduction to the chemistry of heterocyclic compounds. Interscience Publishers, New York. 1967. p. 114.
9. C. D. Hurd and G. L. Oliver. J. Amer. Chem. Soc. **76**, 50 (1954).
10. E. C. Spaeth and C. B. Germain. J. Amer. Chem. Soc. **77**, 4066 (1955).
11. V. Weinmayr. J. Amer. Chem. Soc. **72**, 913 (1950).
12. J.-P. Morizur and Y. Pascal. Bull. Soc. Chim. France, 2296 (1966).
13. T. Reichstein, H. Zschokke, R. Gehring, and G. Rona. Helv. Chim. Acta, **15**, 1118 (1932).

Can. J. Chem. Downloaded from www.nrcresearchpress.com by 210.87.254.6 on 09/05/12
For personal use only.

Synthesis of pinosylvin and related heartwood stilbenes

F. W. BACHELOR
Department of Chemistry, University of Calgary, Calgary 44, Alberta

AND

A. A. LOMAN AND L. R. SNOWDON[1]
Canadian Forestry Service, Forest Research Laboratory, Calgary 21, Alberta

Received November 27, 1969

Pinosylvin dimethyl ether and three other stilbene ethers were prepared by condensing the appropriate diethylbenzylphosphonates with an aromatic aldehyde. Cleavage of pinosylvin dimethyl ether with boron tribromide gave in good yield the monomethyl ether, while fusion with pyridine hydrochloride yielded pinosylvin.

Canadian Journal of Chemistry, **48**, 1554 (1970)

Introduction

The heartwood tissues of members of the genus *Pinus* L., (1) as well as sapwood cells which have died slowly as a result of mechanical injury to the cambium (2) or of fungal attack (3) contain variable amounts of pinosylvin (**1***a*) and pinosylvin monomethyl ether (**1***b*). Both of these stilbenes are known to have fungistatic and fungitoxic properties (4–7). However, the extracellular fungal enzyme laccase is not sensitive to pinosylvin monomethyl ether and catalyzes its transformation into presumably non-inhibitory compounds (8).

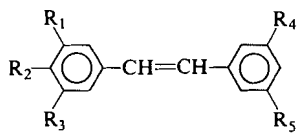

1

a $R_1 = R_3 = OH$; $R_2 = R_4 = R_5 = H$
b $R_1 = OH$; $R_3 = OCH_3$; $R_2 = R_4 = R_5 = H$
c $R_1 = R_3 = OCH_3$; $R_2 = R_4 = R_5 = H$
d $R_2 = OCH_3$; $R_1 = R_3 = R_4 = R_5 = H$
e $R_2 = OH$; $R_1 = R_3 = R_4 = R_5 = H$
f $R_1 = R_2 = R_3 = OCH_3$; $R_4 = R_5 = H$
g $R_1 = R_2 = R_4 = R_5 = OCH_3$; $R_3 = H$

Pinosylvin (**1***a*), pinosylvin monomethyl ether (**1***b*), and pinosylvin dimethyl ether (**1***c*) occur together in the hard pine group with other heartwood constituents such as pinocembrin (**2**) and pinobanksin (**3**) and are rarely obtained in a pure state. We wished to obtain larger quantities of the pure pinosylvin for fungicidal studies. In particular we wished a good synthetic method which we could later apply to the synthesis of labelled compounds in order to trace the fate of pinosylvin and pinosylvin monomethyl ether after transformation by laccase. We have achieved this goal and applied it to the synthesis of a number of other naturally occurring heartwood stilbenes or their methyl ethers.

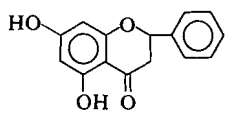

2

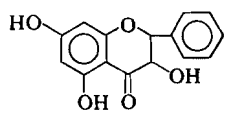

3

In 1941 Späth reported multi-step syntheses for pinosylvin (9) and pinosylvin monomethyl ether (10) based on Perkin condensations and decarboxylation of the α-phenylcinnamic acids formed. His yields were of the order of 6% in both cases. Aulin-Erdtman and Erdtman reported a similar synthesis of pinosylvin dimethyl ether (11).

Attempts to prepare pinosylvin dimethyl ether via a Wittig reaction between triphenylbenzylphosphonium bromide and 3,5-dimethoxybenzaldehyde were singularly unsuccessful. We therefore turned to the modified Wittig reaction using the phosphonate intermediate (12, 13). Diethylbenzylphosphonate (**4**), prepared from benzyl bromide and triethyl phosphite reacted with 3,5-dimethoxybenzaldehyde (**5**) in dimethylformamide under forcing conditions to give pinosylvin dimethyl ether (**1***c*) in good yield (eq. [1]).

The use of the phosphonate esters has the advantage of giving exclusively the *trans* isomer (12) in contrast to the phosphonium ylids which give mixtures of isomers (14). Only one product was detected in the above synthesis. The reverse

[1]Canadian Forestry Service summer research assistant.

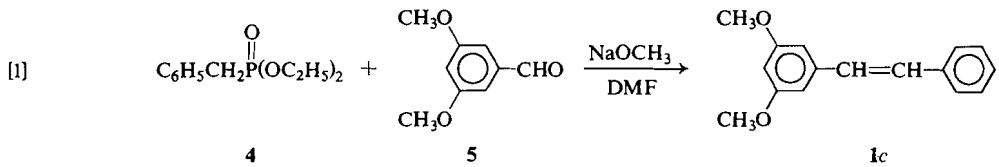

4 5 1c

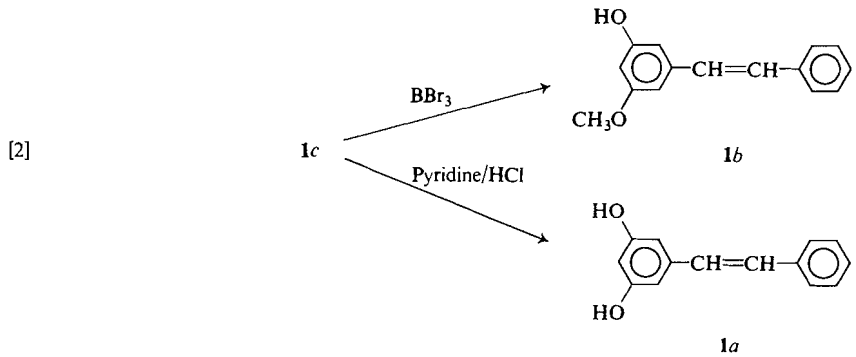

1b 1a

addition of 3,5-dimethoxybenzyldiethylphosphonate to benzaldehyde gave the same product but in poorer yield.

An attempt to demethylate the dimethyl ether with boron tribromide gave a 90% yield of the monodemethylated product (eq. [2]). Further attempts to cleave the second ether with boron tribromide gave only good yields of recovered ether. Although examples of selective cleavage of polyethers on aromatic nuclei with boron trihalides are known, (15, 16) these have always involved the participation of a neighboring carbonyl group. The use of boron tribromide to completely demethylate polymethoxy aromatics apparently only gives good yields when the methoxyl groups are adjacent or in different rings (17–19). However, when the methoxyls are separated and in the same ring poor yields are obtained. For example, the demethylation of 3,5-dimethoxybenzyl cyanide gives the diphenol in only 39% yield (18).

Complete demethylation of pinosylvin dimethyl ether was accomplished by fusing with pyridine hydrochloride, a superior reagent for cleaving aromatic ethers (20), to give pinosylvin in good yield (eq. [2]). This compound was identical in all respects to an authentic sample.

We have applied this synthesis to the preparation of 4-methoxystilbene (**1***d*) and 4-hydroxystilbene (**1***e*), which occur in *Pinus griffithii* (21), as well as 3,4,3′,5′-tetramethoxystilbene (**1***g*) which occurs as the unmethylated phenol in *Vouacapoua macropetala* (22). We have also prepared 3,4,5-trimethoxystilbene (**1***f*) from 3,4,5-trimethoxybenzyl bromide and benzaldehyde. It is suspected that the parent phenol of this compound may be the first product in detoxification by laccase.

Experimental

Melting points are uncorrected. Analyses were performed on a Hewlett–Packard Model 185 CHN analyzer. Gas chromatographic analyses were done on a Hewlett–Packard Model 402 Biochemical Gas Chromatography Instrument using a 4 ft analytical column containing 3.8% SE-30 on Chromosorb W.

3,5-Dimethoxybenzylbromide

An ether solution (500 ml) of 3,5-dimethoxybenzoic acid (25 g) was stirred with lithium aluminum hydride (5.2 g in 250 ml ether) for 20 h at room temperature. After this time the excess LAH was decomposed with wet ether and the suspension acidified with dilute HCl. The layers were separated and the ether layer washed with water and dilute $NaHCO_3$. The ether solution was dried ($MgSO_4$) and the solvent removed *in vacuo* leaving a pale yellow oil which crystallized on addition of a small amount of petroleum ether. The white crystals of 3,5-dimethoxybenzyl alcohol collected by filtration amounted to 20.5 g (89% yield), m.p. 44–47°, and were used without further purification.

The alcohol (20 g) was dissolved in dry benzene (250 ml) and excess dry HBr was bubbled into the solution with stirring over a 20 min period and the solution was refluxed for 2 h. Evaporation of the benzene gave a quantitative yield of slightly colored crystals of 3,5-dimethoxybenzylbromide. Recrystallization from aqueous methanol gave pure material melting at 71–72° [lit. 71–72° (23)].

3,4,5-Trimethoxybenzylbromide

Gallic acid (7.0 g) in 250 ml of dry acetone was treated

Can. J. Chem. Downloaded from www.nrcresearchpress.com by 210.87.254.6 on 09/05/12
For personal use only.

Can. J. Chem. Downloaded from www.nrcresearchpress.com by 210.87.254.6 on 09/05/12
For personal use only.

with an excess of diazomethane in ether at room temperature for 24 h. Removal of the ether and acetone *in vacuo* gave a quantitative yield of 3,4,5-trimethoxymethylbenzoate. Yield 9.3 g (100%); m.p. 82–83° [lit. 80–82° (24)].

The ester (6.6 g) was reduced with excess LAH as above to give 3,4,5-trimethoxybenzyl alcohol. Yield, 5.1 g (84%). The alcohol was converted directly to 3,4,5-trimethoxybenzylbromide with HBr in dry benzene. Yield, 6.35 g (95.5%). Analysis by gas chromatography indicated the bromide was better than 99% pure. Attempts to crystallize this compound were unsuccessful and it was used without further purification.

3,5-Dimethoxystilbene (1c) (Pinosylvin Dimethyl Ether)

Benzyl bromide (3.1 g) was heated with excess triethylphosphite (5 ml) to 130° until the evolution of ethyl bromide had ceased. Excess triethylphosphite was removed by distillation *in vacuo* and the residual diethylbenzylphosphonate (4.1 g) used directly. The diethylbenzylphosphonate was added to 25 ml of dry dimethylformamide containing 1 g of sodium methoxide and cooled to 0°. To this was added 3,5-dimethoxybenzaldehyde (2.0 g) and the mixture allowed to stand at room temperature for 1 h. The reaction mixture was then heated on a steam bath for 1 h and then allowed to stand overnight at room temperature. Water–methanol (2:1; 40 ml) was added and the precipitated stilbene was collected by filtration and washed with water. A second crop was obtained from the combined filtrate and wash water. The 3,5-dimethoxystilbene was recrystallized from methanol–water. Yield, 2.65 g (91.5%); m.p. 55–56° [lit. 56–57° (11)].

3-Hydroxy-5-methoxystilbene (1b) (Pinosylvin Monomethyl Ether)

Boron tribromide (2 g) was dissolved in 10 ml of dry dichloromethane and a solution of 3,5-dimethoxystilbene (1.1 g in 10 ml of CH_2Cl_2) added at −80°. The mixture was allowed to come to room temperature and stand overnight. The yellow borate ester was decomposed by shaking the suspension with 10% KOH. The reaction was then acidified with HCl and the mixture extracted with dichloromethane. The dichloromethane solution was dried ($MgSO_4$) and the solvent removed *in vacuo* to leave a solid residue which was approximately 80% 3-hydroxy-5-methoxystilbene by gas chromatography analysis. Two crystallizations from benzene yielded 3-hydroxy-5-methoxystilbene. Yield 0.5 g, (50%); m.p. 118.5–119.5° [lit. 122–123° (10)].

Purification by column chromatography on silica gel also readily separated the dimethyl ether and pinosylvin from the monomethyl ether.

3,5-Dihydroxystilbene (1a) (Pinosylvin)

Excess pyridine hydrochloride (5.0 g) and 3,5-dimethoxystilbene (1.0 g) were mixed and heated to 190° for 3 h. The hot dark syrup was poured into 25 ml of 2 *N* HCl and the reaction mixture extracted with ether. The ether solution was dried ($MgSO_4$) and the solvent removed *in vacuo*. Two crystallizations from benzene gave pinosylvin as shiny plates. Yield, 441 mg (50%); m.p. 155–155.5° [lit. 155.5–157° (9)].

4-Methoxystilbene (1d)

4-Methoxystilbene was prepared from 2.1 g of 4-methoxybenzaldehyde and 3.3 g of benzyldiethylphosphonate in the same manner as 3,5-dimethoxystilbene. The product was recrystallized from methanol to give 2.6 g (84%) of colorless crystals, m.p. 135–136° [lit. 136–137° (21)].

4-Hydroxystilbene (1e)

4-Methoxystilbene (1.0 g) and pyridine hydrochloride (5.0 g) were heated together at 180° for 5 h. The melt was poured into 200 ml of ice water containing 25 ml of concentrated HCl. A precipitate was formed which was extracted into ether. The acidic layer was washed with two additional portions of ether. The combined ether extracts were extracted twice with 2 *N* NaOH and the basic extracts neutralized with 250 ml of cold dilute HCl. The precipitate was collected by filtration and dried. The yield of 4-hydroxystilbene was 441 mg (77% based on recovered 4-methoxystilbene); m.p. 182–185° [lit. 185–186° (21)].

Concentration of the ether extracts yielded 386 mg of unreacted 4-methoxystilbene.

3,4,3′,5′-Tetramethoxystilbene (1g)

Condensation between 3,5-dimethoxybenzyl bromide (3.7 g) and excess triethylphosphite (5 ml) yielded 3,5-dimethoxybenzyldiethylphosphonate which was then coupled with 3,4-dimethoxybenzaldehyde (3.2 g) as described above. The crude product was purified by chromatography on silica gel and crystallized from petroleum ether (30–60°)/methanol to give 2.1 g (41%), m.p. 66–67° [lit. 68–69° (22)] of 3,4,3′5′-tetramethoxystilbene.

3,4,5-Trimethoxystilbene (1f)

3,4,5-Trimethoxybenzyl bromide (4.0 g) was treated with triethylphosphite (10 ml) as above and the phosphonate coupled with benzaldehyde (2.0 g) according to the described procedure. The dark oily product crystallized on scratching and was collected by filtration. Recrystallization from methanol yielded 2.1 g of white crystals (50%); m.p. 108.5–109.5°; nuclear magnetic resonance (n.m.r.) ($CDCl_3$) τ 6.12 (s) 9H (OCH_3), 2.5–3.25 (m) 9H (aromatic and olefinic CH).

Anal. Calcd. for $C_{17}H_{18}O_3$: C, 75.54; H, 6.71. Found: C, 75.96; H, 6.93.

We wish to thank the Canadian Department of Fisheries and Forestry for the support of this work.

1. H. ERDTMAN in K. KRATZL and G. BILLEK. Biochemistry of wood. Pergamon Press, London, 1959. p. 1.
2. E. VON RUDLOFF and E. JORGENSEN. Phytochem. **2**, 297 (1963).
3. L. SHAIN. Phytopathol. **57**, 1034 (1967).
4. H. ERDTMAN and E. RENNERFELT. Sv. Papperstidn. **47**, 45 (1944).
5. E. RENNERFELT. Sv. Bot. Tidskr. **37**, 83 (1943).
6. E. RENNERFELT. Sv. Bot. Tidskr. **39**, 311 (1945).
7. E. RENNERFELT and G. NACHT. Sv. Bot. Tidskr. **49**, 419 (1955).
8. H. LYR. Flora, **152**, 570 (1962).
9. E. SPÄTH and F. LIEBHERR. Ber. **74**, 869 (1941).
10. E. SPÄTH and K. KROMP. Ber. **74**, 1424 (1941).
11. G. AULIN-ERDTMAN and H. ERDTMAN. Ber. **74**, 50 (1941).

12. W. S. WADSWORTH, JR., and W. D. EMMONS. J. Amer. Chem. Soc. **83**, 1733 (1961).
13. E. J. SEUS and C. V. WILSON. J. Org. Chem. **26**, 5243 (1961).
14. U. SCHÖLLKOPF. Angew. Chem. **71**, 260 (1959).
15. W. SCHÄFER and B. FRANCK. Ber. **99**, 160 (1966).
16. A. J. BIRCH and J. J. WRIGHT. Chem. Commun. 788 (1969).
17. F. L. BENTON and T. E. DILLON. J. Amer. Chem. Soc. **64**, 1128 (1942).
18. J. F. W. MCOMIE and M. L. WATTS. Chem. Ind. 1658 (1963).
19. D. L. MANSON and O. C. MUSGRAVE. J. Chem. Soc. 1011 (1963).
20. R. FILLER, B. T. KHAN, and C. W. MCMULLEN. J. Org. Chem. **27**, 4660 (1962).
21. V. B. MAHESH and T. R. SESHADRI. J. Sci. Ind. Res. (India), **13***B*, 835 (1954).
22. F. E. KING, T. J. KING, D. H. GODSON, and L. C. MANNING. J. Chem. Soc. 4477 (1956).
23. A. BHATI. Tetrahedron, **18**, 1519 (1962).
24. M. U. TSAO. J. Amer. Chem. Soc. **73**, 5495 (1951).

Can. J. Chem. Downloaded from www.nrcresearchpress.com by 210.87.254.6 on 09/05/12
For personal use only.

Can. J. Chem. Downloaded from www.nrcresearchpress.com by 210.87.254.40 on 09/05/12
For personal use only.

Application of proton magnetic resonance to rotational isomerism in halotoluene derivatives. II. α,α,2,4,6-Pentachlorotoluene

B. J. FUHR,[1] B. W. GOODWIN,[1] H. M. HUTTON,[2] AND T. SCHAEFER
Chemistry Department, University of Manitoba, Winnipeg, Manitoba

Received November 3, 1969

At temperatures below −40 °C the proton magnetic resonance of α,α,2,4,6-pentachlorotoluene in toluene-d_8 or methylcyclohexane is an ABX spectrum where X is the methine proton. The C—H bond of the dichloromethyl group lies in the plane of the ring and its proton couples to one ring proton only. As the temperature increases the mean lifetime before interconversion of the "mirror image" isomers decreases and at 70 °C the proton spectrum is A_2X. A density matrix formalism is used to calculate the line shape as a function of the lifetime before exchange. The free energy barrier to rotation of the dichloromethyl group is 15.0 ± 0.1 kcal/mole in both solvents. In toluene-d_8 the entropy of activation is near zero. The high energy transition state is very likely one in which the C—Cl bonds of the ring and the dichloromethyl groups are eclipsed.

Canadian Journal of Chemistry, 48, 1558 (1970)

Introduction

Extensive nuclear magnetic resonance (n.m.r.) studies of the rotational isomers of halogenated ethanes are described in the recent literature (1–4). Reliable thermodynamic parameters for the isomers in their ground state as well as rotational barriers are only obtainable if the n.m.r. spectra of the individual isomers can be observed (1, 2). In common with the halogenated ethanes, toluene derivatives present the problem of rotation about an essentially single carbon–carbon bond. In toluene itself the sixfold barrier to rotation of the methyl group lies well below 200 cal/mole in the gaseous and solid states (5, 7) but it has become clear that in toluene derivatives containing halogen atoms both in the methyl groups and in the ortho ring positions (7),[3] the barrier to rotation can be large enough for convenient study by dynamic n.m.r. (d.n.m.r.) methods (4).

In this laboratory a series of such compounds are under investigation. Previous studies were confined to fluoromethyl toluene derivatives in which the n.m.r. spectra of individual rotamers were not observed (8). In this paper we describe the analytical techniques involved in our studies and report the barriers to rotation about the C—C bond of α,α,2,4,6-pentachlorotoluene (PCT) in toluene-d_8 (C_7D_8) and in methyl cyclohexane ($C_6H_{11}CH_3$).

Experimental

1) Synthesis of α,α,2,4,6-Pentachlorotoluene

Meta toluidine was chlorinated by passing a continuous stream of chlorine into an acetic anhydride solution for 6 to 8 h (9). 2,4,6-Trichloro-3-amino toluene was prepared from the acetylated product by addition of sulfuric acid, followed by steam distillation. A solution of ethanolic sodium nitrite was added to the trichloro-*m*-toluidine and, after several hours, the mixture was steam distilled (10). The purity of the 2,4,6-trichlorotoluene, m.p. 25–27 °C, was checked by the appearance of the n.m.r. spectrum in carbon disulfide. The methyl group of this compound was chlorinated by passing chlorine gas through the liquid in the presence of ultraviolet (u.v.) light until its weight indicated the completion of dichlorination. The PCT was triply distilled and its proton resonance spectrum indicated a small amount of α,α,α,2,4,6-hexachlorotoluene (HCT).[4] Its presence aided the rate study because its proton resonance peak provided a convenient estimate of effective T_2 values at most temperatures.

2) Preparation of Solutions and Nuclear Magnetic Resonance Measurements

Fifteen mole % solutions in C_7D_8 and $C_6H_{11}CH_3$, respectively, containing small amounts of tetramethylsilane (TMS) and cyclopentane (C_5H_{10}) were thoroughly degassed by the freeze–pump–thaw technique. The concentrations were dictated by considerations of signal to noise problems and of solubility limits at low temperatures.

Proton magnetic resonance (p.m.r.) spectra were measured on a DA60I Varian spectrometer in the frequency sweep mode. Peak positions relative to the TMS lock signal were repeatedly measured by counting manual and sweep oscillator frequencies. Radiofrequency intensities in the analytical channel were kept well below saturation levels and sweep rates were never larger than 0.02 Hz/s. Excessive filtering at the dc stage was avoided. Linewidths at half height ($W_{\frac{1}{2}}$) were determined for all peaks, including that due to cyclopentane. The solutions contained very small amounts of α,α,α,2,4,6-hexachlorotoluene and the $W_{\frac{1}{2}}$ was measured for this peak as well.

[1]Holder of an NRCC bursary, 1968–1969.
[2]Brandon University, Brandon, Manitoba.
[3]Reference 7 is paper I of this series.

[4]An increase in chlorination time led to an increase in intensity of the single peak assigned to HCT and to a decrease in the intensity of the peaks due to PCT.

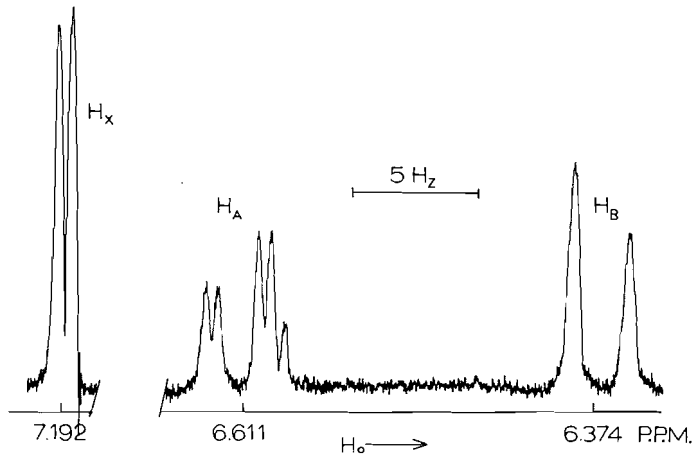

FIG. 1. The proton magnetic resonance spectrum at 60 MHz of a 15 mole % solution of α,α,2,4,6-pentachlorotoluene in toluene-d_8 at −40 °C. Shifts are given in p.p.m. to low field of internal tetramethylsilane. The peak assignment is given with respect to I in the text. The smallest peak near the pair of doublets at 6.6 p.p.m. arises from a small amount of α,α,α,2,4,6-hexachlorotoluene.

The sample temperature was calibrated using methanol in the usual way. The temperatures found in this way were checked by thermocouple measurements on a dummy sample of C_7D_8 and are absolutely accurate to ±1 °K. Temperature intervals between dial settings on the temperature controller (V4343) are more accurate, however, because of the linear relationships between thermocouple readings and dial readings. This means that in Arrhenius plots the slope, which determines the activation energy, is obtained more reliably than the intercept which yields the frequency factor. In other words, enthalpies of activation probably suffer less from systematic errors in our experiments than do entropies of activation.

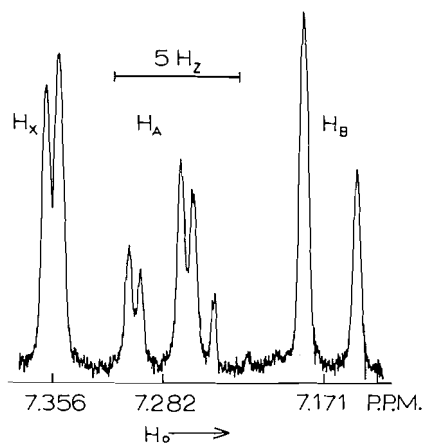

FIG. 2. As in Fig. 1 but for a 15 mole % solution in methylcyclohexane at −37 °C.

Results and Discussion

1) Peak Assignments

In Figs. 1 and 2 the low temperature spectra of PCT are displayed. They are understandable in terms of I or II. There exists a coupling between H_A and H_X, $J_{AX} = 0.52 \pm 0.02$ Hz while J_{BX} is undetectable. The magnitude of J_{AX} is very similar to that found for hydroxyl (11), amino (12), and aldehydic protons (13) situated in bonds whose stereochemical relationship to a meta C—H bond is defined by I (extended zig-zag rule). The H_A is deshielded relative to H_B very probably because of the steric interaction between the C—Cl bonds in the ring and in the dichloromethyl group of I. The deshielding must arise in a way very similar to the deshielding of ring protons caused by ortho–ortho interactions in 1,2-dihalobenzenes (14, 15). The resonance of H_X in I occurs over 1 p.p.m. to low field from its resonance in dichloromethyl toluene and can be understood in terms of the diamagnetic effect of the aromatic ring on the shift of a coplanar proton and in terms of the deshielding caused by perturbations arising from time-dependent electric fields originating in the proximate C—Cl bond in the ring (in I the $H_X \cdots Cl$ distance is less than the sum of the van der Waals radii of hydrogen and chlorine).

At high temperature the proton spectra appear as in Fig. 3. The mean lifetime before rotation of

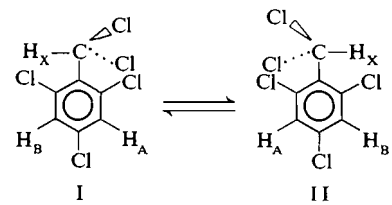

Can. J. Chem. Downloaded from www.nrcresearchpress.com by 210.87.254.40 on 09/05/12
For personal use only.

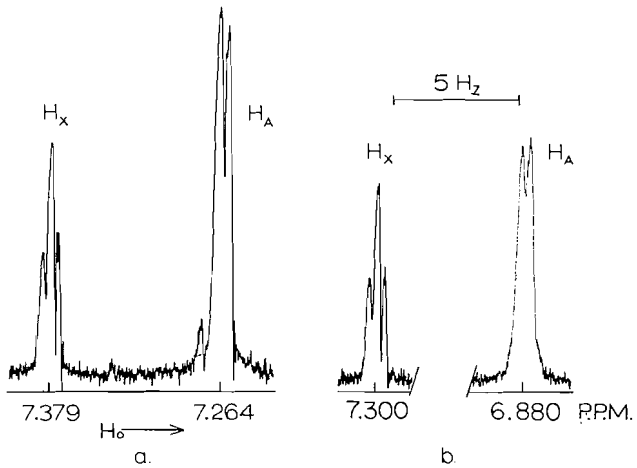

FIG. 3. As in Figs. 1 and 2 but at (*a*) 72 °C in methylcyclohexane and (*b*) at 73 °C in toluene-d_8.

the dichloromethyl group in I or II is now much shorter than the reciprocal of the chemical shift between H_A and H_B. In the resultant A_2X spectrum $J_{AX} = 0.31 \pm 0.02$ Hz. Comparison of J_{AX} at low and high temperatures suggests $J_{BX} \leq 0.1$ Hz in I (the tacit assumption is made that only I and II are appreciably populated at all temperatures under study). In Table 1 the results of the ABX and A_2X analyses are presented.

2) Derivation of Preexchange Lifetimes

At intermediate temperatures the characteristic broadening of the ring proton resonance caused by exchange processes is observed (see Fig. 4). Of course, in the present instance, the ring protons do not exchange sites. They exchange Larmor frequencies each time the dichloromethyl group rotates through π radians. In contrast the methine proton does move from site I to site II but has the same Larmor frequency in both sites. Therefore its resonance peaks remain sharp as the temperature increases. The 1:1 doublet at low temperatures is transformed into a 1:2:1 triplet at high temperatures.[5]

TABLE 1

Proton chemical shifts* and coupling constants for the high and low temperature spectra of 15 mole % solutions of α,α,2,4,6-pentachlorotoluene in toluene-d_8 and in methylcyclohexane

Spectrum	Toluene-d_8	Methylcyclohexane
ABX	−40 °C	−37 °C
ν_A (p.p.m.)	6.611±0.003	7.282
ν_B	6.374	7.171
ν_X	7.192	7.356
J_{AB} (Hz)	2.14 ±0.04	2.14±0.04
J_{AX}	0.52 ±0.02	0.50±0.02
J_{BX}	0.01	0.01
A_2X	72 °C	73 °C
ν_A (p.p.m.)	6.880	7.264
ν_X	7.300	7.379
J_{AX} (Hz)	0.30 ±0.02	0.33±0.02

*In p.p.m. to low field of internal tetramethylsilane. Parameters are quoted with r.m.s. errors.

(a) Line Shape Analysis

The Bloch equations cannot be used here because the A and B nuclei are not even approximately independent of one another. Therefore the density matrix method (16–18) was used to derive the line shape function for the ABX case. The exchange and relaxation terms were introduced in the usual way (4). Terms in T_2, defining the effective linewidth determined by magnetic inhomogeneity, were carried through the derivation of the line shape function. Slow passage conditions were assumed.

The imaginary part of the final expression gives the absorption spectrum. A program in Fortran IV was written (B.W.G.) for an IBM 360/65 computer. It calculates peak positions by searching the line shape function for maxima. The positions of the half-heights of each peak (on either side of the peak) are located and the half-height linewidths are calculated on both sides of the peak. Provision is made for overlapping peaks.

[5]These changes are not reproduced here because the very small peak separations do not allow a reliable fit to spectra computed as a function of exchange rate.

Can. J. Chem. Downloaded from www.nrcresearchpress.com by 210.87.254.40 on 09/05/12
For personal use only.

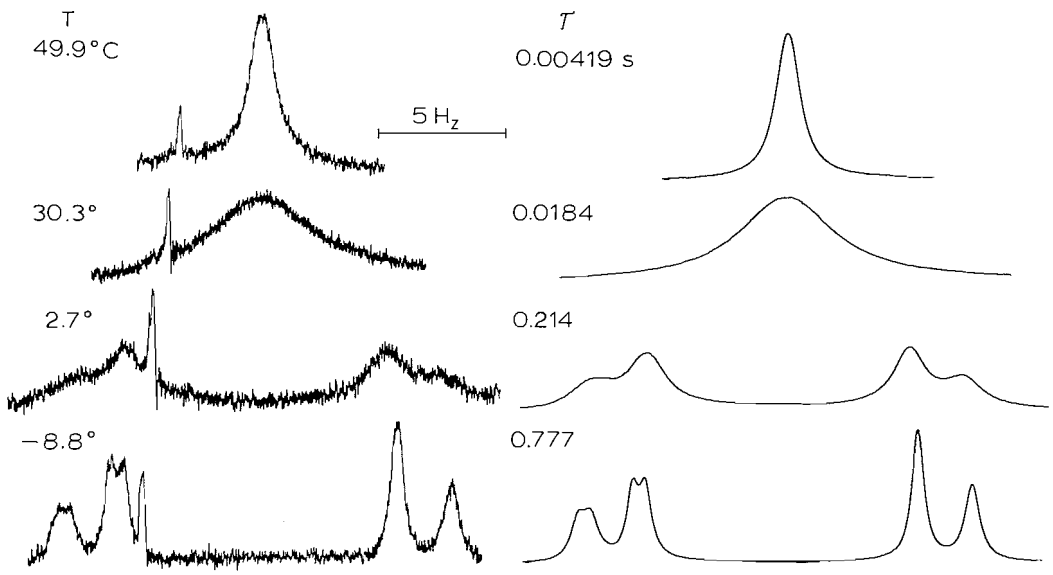

FIG. 4. Experimental and calculated resonance spectra of the ring protons of α,α,2,4,6-pentachlorotoluene in toluene-d_8 solution at various representative temperatures and preexchange lifetimes, τ. The sharp impurity peak due to hexachlorotoluene indicates the homogeneity of the external magnetic field.

The input parameters include τ, T_2, J, and shift values, the scale in Hz and a scaling factor for peak heights to be plotted. Optional parameters of stepsize in τ and number of steps are included. For example, if stepwise = 0.01 and number of steps = 10, ten spectra are output with lifetimes ranging from τ −0.05 to +0.05 s. In this way an optimum τ value for a given experimental width is obtained. The resulting spectrum is plotted on a Calcomp plotter and can be compared with the experimental one.

The maxima are located to an accuracy of 0.001 frequency units. The half-heights are accurate to at least 0.5%. If peaks overlap the half-heights of the overlapping peaks are calculated. The values of the peaks, peak-heights, and half-heights as well as the overlap heights and widths are output and can be compared with experimental data. As the simplest example the printed output, after searching, for the toluene solution of PCT (discussed below) at temperatures where only a single broad peak exists is 5.81 (5.82), 4.42 (4.43), 3.63 (3.64), 1.14 (1.14), 0.83 (0.83), and 0.70 (0.70) Hz. The experimental linewidths are given in brackets and, in this case, correspond to τ values of 0.0227, 0.0184, 0.0157, 0.00419, 0.00200, and 0.00071 s, respectively. Thus, time-consuming plotting procedures can be minimized. Storage required is about 26 K. Total execution time required for 500 trial values of τ is about 1.5 min.

(b) Chemical Shift and T_2 Effects on Line Shapes

The computed spectrum is a function of the internal shift, ν_{AB}, in the absence of exchange; of the linewidths in the absence of exchange, given by the "effective" T_2; of J_{AB}, J_{AX}, and J_{BX}; and of τ, the mean lifetime before exchange. The coupling constants were assumed to be independent of temperature. For example, $J_{AB} = J_m^{H,H}$ in 3,5-dichlorosalicylaldehyde is independent of temperature over 100° within experimental error in nonpolar solvents (19). The temperature independence of J_{AX} and J_{BX} is not proven but the high temperature value of their mean (Table 1) shows that a negligible error will be introduced by the assumption (an increase of J_{BX} by 0.1 Hz had no significant effect on most of the computed spectra).

The $W_{\frac{1}{2}}$ values for cyclopentane were always about 0.1 Hz larger than those for HCT, showing that their application in the determination of T_2 values is incorrect. On the other hand, the small peak due to the ring protons of the HCT arises from protons whose relaxation times must be very nearly equal to those of the PCT. The use of $W_{\frac{1}{2}}$ for this peak in determining effective T_2

Can. J. Chem. Downloaded from www.nrcresearchpress.com by 210.87.254.40 on 09/05/12
For personal use only.

Can. J. Chem. Downloaded from www.nrcresearchpress.com by 210.87.254.40 on 09/05/12
For personal use only.

TABLE 2

Temperature dependence of the internal chemical shift* of the ring protons of α,α,2,4,6-pentachlorotoluene in toluene-d_8 solution (15 mole %)

Temperature (°C)	Shift (Hz)	Temperature (°C)	Shift (Hz)
−39.7	14.17	10.0	12.17
−24.9	13.54	27.2	11.48
−8.8	12.99	30.3	11.35
−3.2	12.62	34.2	11.20
2.7	12.48	49.9	10.57
		58.8	10.21
		72.6	9.65

*Shifts were measured in the left hand column and were obtained by linear extrapolation in the right hand column. These numbers were used in fitting the experimental spectra to calculated spectra.

values seems fully justified. In C_7D_8 solution $W_{\frac{1}{2}}$ of HCT was equal to 0.23 Hz within experimental error for all spectra used in the line shape analysis. Its corresponding value in $C_6H_{11}CH_3$ was 0.20 Hz. In other words the resolution of the spectrometer could be held nearly constant over the important temperature range.

The internal ring proton shift in $C_6H_{11}CH_3$ solution was *apparently* independent of temperature in the region of slow exchange. In C_7D_8, the well known solvent effects (20) can clearly have a different temperature dependence for H_A and H_B. The ring proton shifts were measured as a function of temperature in the region of slow exchange and the internal shift was a linear function of temperature. Extrapolation procedures gave the "true" internal shifts in the absence of exchange at all temperatures of interest and are given in Table 2.[6]

(c) Fitted Spectra

In Fig. 4 the experimental and computed spectra for the C_7D_8 solution are displayed for a representative set of temperatures. The agreement is apparently satisfactory. A constant T_2 was assumed over the whole temperature region in each solution (1.38 s for C_7D_8 and 1.59 s for $C_6H_{12}CH_3$). This assumption is consistent with constant $W_{\frac{1}{2}}$ values for the impurity peak. The mean preexchange lifetimes are given in Table 3.

3) Activation Parameters and Errors

The pseudo first order rate constants $k = 1/\tau$ were used to obtain activation parameters in a variety of ways. In Fig. 5, an Arrhenius plot of $\log k$ vs. $1/T$ is shown for the C_7D_8 solution. The activation energies and frequency factors are given in Table 4. Activation enthalpies and entropies were derived from plots of $\ln(k/T)$ vs. $1/T$ as well as from the equivalent plots of activation free energies[7] vs. T (4). These quantities are also given in Table 4.

The errors in the activation parameters in Table 1 were estimated in a number of ways. The standard errors and the 90% confidence limits in E_A and ΔH^* were based on the standard error in estimating the slope of the straight line in the least squares analysis. The statistical errors in $\log A$ and ΔS^* were based on the standard error in the intercept while those in ΔG^* depended upon the standard error in estimating $\log k$.

In an attempt to account for systematic errors, the maximum and minimum slopes of the straight lines which can be drawn through a set of error bars were estimated as follows. Assuming that all input parameters are correct, the error in the lifetime, τ, would arise from errors in obtaining the widths of the various peaks in the experimental spectra. These standard deviations in the experimental widths gave the maximum uncertainty in $\log k$ values needed to fit calculated to experimental line shapes. The temperature was assumed to be accurate to ±1 °C (in Fig. 4, error bars obtained in this way are indicated). The total uncertainty is represented by a rectangle. Two straight lines, pivoting about the coalescence temperature and passing through the rectangles, gave two different slopes and intercepts. The

TABLE 3

Preexchange lifetimes, τ, from fitted spectra for α,α,2,4,6-pentachlorotoluene

Toluene-d_8		Methylcyclohexane	
Temperature (°C)	τ (s)	Temperature (°C)	τ (s)
72.6	0.00071	52.8	0.00520
58.8	0.0020	43.5	0.00790
49.9	0.00419	30.7	0.0196
34.2	0.0157	23.5	0.0387
30.3	0.0184	14.4	0.0671
27.2	0.0227	7.3	0.0840
10.0	0.116	−0.8	0.0333
2.7	0.214	−8.5	1.01
−3.2	0.347	−17.0	1.72
−8.8	0.777		

[6]In a 10 mole % solution of 3,5-dichlorosalicylaldehyde the internal shift of the ring protons is a linear function of temperature between 30 and 95° C (21).

[7]A transmission coefficient of 1/2 was assumed in calculating ΔG^*. See below.

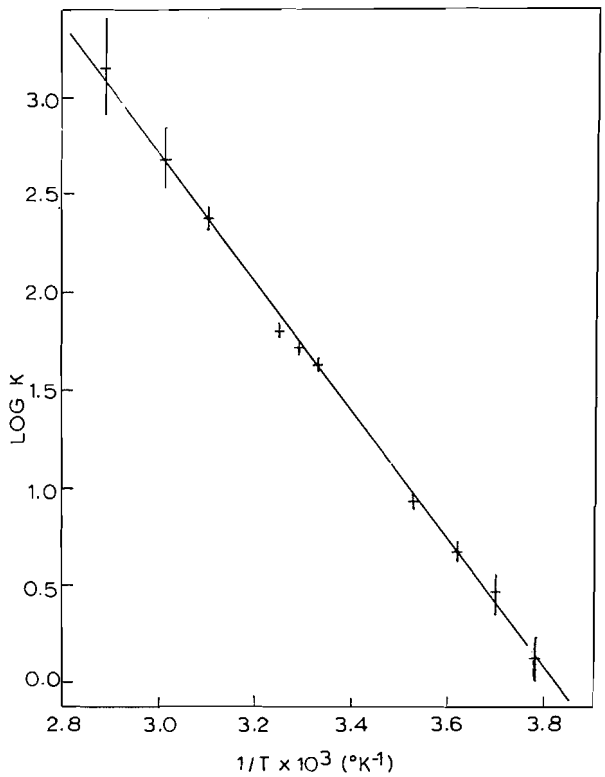

FIG. 5. A plot of log k vs. the reciprocal absolute temperature for the toluene-d_8 solution of α,α,2,4,6-pentachlorotoluene. The error bars were obtained as discussed in the text.

difference in these parameters was taken as a "maximum" error and is given in Table 4.

Variation of T_2 values over a reasonable range (20%) led to line shape fits from which we concluded that T_2 errors generally fall within the "maximum" errors for spectra of good quality (inhomogeneity in magnetic field not much different from 5×10^{-5} G, proper phase settings in detector stages etc.).

Given the nature of straight-line plots derived from n.m.r. line shapes (relatively small range of temperatures and relatively large errors in log k values at either extreme) we feel that our "maximum" errors are more reliable estimates than are the statistical ones.

4) Barrier to Rotation in α,α,2,4,6-Pentachlorotoluene

The rotational barrier is best discussed in terms of the conformations **1** to **5** (**1** and **5** have

TABLE 4
Activation parameters for α,α,2,4,6-pentachlorotoluene

Parameter	Toluene-d_8		Methylcyclohexane	
	Value	Errors*	Value	Errors*
E_A (kcal/mole)	15.2	0.2, 0.5, 1.4	14.3	0.6, 1.2, 1.3
log A	12.7	0.2, 1.0	12.0	0.5, 1.7
ΔG^* (kcal/mole)	14.9 (304 °K)	0.1, 0.1	15.0 (304 °K)	0.1, 0.1
ΔH^* (kcal/mole)	14.6	0.2, 0.5, 1.4	13.7	0.6, 1.2, 1.3
ΔS^* (cal/degree mole)	−1.1	0.7, 4.4	−4.4	2.2, 7.8

*When three errors are given for a parameter the first one refers to the standard error in the linear least squares fit, the second to the 90% confidence limit, the third to the "maximum" error as discussed in the text. When only two errors are given the 90% confidence limit has been omitted.

Can. J. Chem. Downloaded from www.nrcresearchpress.com by 210.87.254.40 on 09/05/12
For personal use only.

Can. J. Chem. Downloaded from www.nrcresearchpress.com by 210.87.254.40 on 09/05/12
For personal use only.

been differently portrayed above). The low temperature spectra of PCT were interpreted above in terms of **1** and its mirror image **5**. That **1** (or **5**) and not **3** is the stable rotational isomer is obvious from the ABX spectra obtained at low temperature (**3** would give an A_2X spectrum). In view of the stereospecificity of the five-bond coupling discussed above it is also likely that **4** is not energetically favored over **1** or **5**. This likelihood is borne out by preliminary potential energy calculations[8] based on modified Bucking-

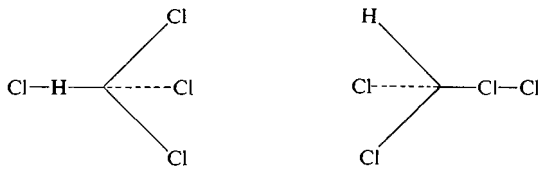

1

2

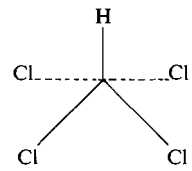

3

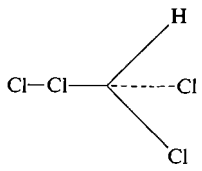

4

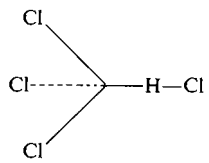

5

ham and/or van der Waals potential functions (22, 23). Conformation **4** is very clearly indicated to be of highest energy (transition state) because of steric interactions between the eclipsed C—Cl bonds. Relative to **1**, conformation **3** has 0.7 of the potential energy of **4**. Identification of **4** with the barrier of between 14 and 15 kcal/mole derived from the n.m.r. studies, rationalizes the absence of a detectable population of **3** at the temperatures involved in these studies and also justifies the use of a transmission coefficient of 1/2 in our calculations of ΔG^* (24).

Evidence favoring **4** as the transition state also comes from the existence of the strongly destabilizing "parallel 1:3 interactions" of C—Cl bonds in chlorinated propanes (25). The steric relationship of the eclipsed C—Cl bonds in **4** is very similar to that in the relevant conformers in the chloropropanes.

5) Solvent Effects on the Barrier

The activation parameters in the two nonpolar solvents are equal within "maximum" experimental error.[9] There appears to be no very good reason why ΔS^* for internal rotation should be significantly different from zero (4). On that basis the parameters in C_7D_8 might be slightly preferred. However, there exists evidence (20) for the presence of solute–solvent interactions amounting to about 1 kcal/mole in aromatic solvents and it is tempting to speculate that the somewhat larger E_A and smaller ΔS^* magnitudes in the C_7D_8 solution are caused by solvation effects. This temptation should be firmly resisted, in our opinion, even if our statistical errors were the correct ones.

An attempt to study the effect of a polar solvent (26) like acetone on the activation parameters was unsuccessful because solubility problems prevented the measurement of the internal shift as a function of temperature. In carbon disulfide solution, the proton resonance of PCT is a very tightly coupled ABC spectrum at -50 °C (and would be so at 220 MHz). The temperature dependence of this spectrum presents a challenge to the analytical procedures recently developed by Binsch (27). We are attempting to fit calculated and experimental spectra by his methods.

We thank Dr. C. J. Macdonald for help with the synthesis of PCT, Dr. A. Mannschreck for helpful correspondence, and the National Research Council of Canada for financial assistance.

1. R. A. Newmark and R. E. Graves. J. Phys. Chem. **72**, 4299 (1968).
2. G. Govil and H. J. Bernstein. J. Chem. Phys. **47**, 2818 (1967); **48**, 285 (1968); **49**, 911 (1968).
3. J. Jonas, A. Allerhand, and H. S. Gutowsky. J. Chem. Phys. **42**, 3396 (1965).
4. G. Binsch. *In* Topics in stereochemistry. *Edited by* E. L. Eliel and N. L. Allinger. Interscience Publishers. New York. Volume 3. 1968.
5. H. D. Rudolph, H. Dreizler, A. Jaeschke, and P. Wendling. Z. Naturforsch. **22a**, 940 (1967).
6. J. Haupt and W. Müller-Warmuth. Z. Naturforsch. **24a**, 1066 (1969).

[8]We are grateful to Mr. Brian Barber for these calculations.

[9]If the temperature dependence of the internal shift of the ring protons in C_7D_8 is ignored one obtains $E_A = 17.3 \pm 0.3$ kcal/mole, log $A = 14.4 \pm 0.2$ (standard errors). The frequency factor appears to be "more reasonable" but the change in internal shift is very clearly present.

7. T. SCHAEFER, R. SCHWENK, C. J. MACDONALD, and W. F. REYNOLDS. Can. J. Chem. **46**, 2187 (1968).
8. J. JONAS, L. BOROWSKI, and H. S. GUTOWSKY. J. Chem. Phys. **47**, 2441 (1967).
9. J. WHITE and R. ADAMS. J. Amer. Chem. Soc. **54**, 2104 (1932).
10. F. D. CHATTAWAY and R. C. T. EVANS. J. Chem. Soc. **69**, 848 (1896).
11. S. FORSÉN and R. A. HOFFMAN. J. Mol. Spectrosc. **20**, 168 (1966).
12. J. A. WEIL, A. BLUM, A. H. HEISS, and J. K. KINNAIRD. J. Chem. Phys. **46**, 3132 (1967).
13. D. G. DEKOWALEWSKI and S. CASTELLANO. Mol. Phys. **17**, 567 (1969).
14. P. DIEHL. Helv. Chim. Acta, **44**, 829 (1961).
15. (*a*) J. S. MARTIN and B. P. DAILEY. J. Chem. Phys. **39**, 1722 (1963). (*b*) B. RICHARDSON and T. SCHAEFER. Can. J. Chem. **46**, 2195 (1968).
16. U. FANO. Rev. Mod. Phys. **29**, 74 (1957).
17. G. M. WHITESIDES. Ph.D. thesis. California Institute of Technology, Pasadena, California, 1964.
18. R. M. LYNDEN-BELL. *In* Progress in nuclear magnetic resonance spectroscopy. *Edited by* J. W. Emsley, J. Feeney, and L. H. Sutcliffe. Pergamon Press. Oxford, 1967. Volume 2.
19. T. SCHAEFER, G. KOTOWYCZ, H. M. HUTTON, and J. W. S. LEE. Can. J. Chem. **46**, 2531 (1968).
20. P. LASZLO. *In* Progress in nuclear magnetic resonance spectroscopy. *Edited by* J. W. Emsley, J. Feeney, and L. H. Sutcliffe. Pergamon Press. Oxford, 1968. Volume 3.
21. G. KOTOWYCZ. Ph.D. thesis. University of Manitoba, Winnipeg, Manitoba. 1967.
22. R. A. SCOTT and H. A. SCHERAGA. J. Chem. Phys. **42**, 2209 (1965).
23. K. E. HOWLETT. J. Chem. Soc. 1055 (1960).
24. D. HOUALLA, R. WOLF, D. GAGNAIRE, and J. B. ROBERT. Chem. Commun. 443 (1969).
25. A. B. DEMPSTER, K. PRICE, and N. SHEPPARD. Spectrochim. Acta, **25A**, 1381 (1969).
26. R. J. ABRAHAM. J. Phys. Chem. **73**, 1192 (1969).
27. G. BINSCH. J. Amer. Chem. Soc. **91**, 1304 (1969).

Can. J. Chem. Downloaded from www.nrcresearchpress.com by 210.87.254.40 on 09/05/12
For personal use only.

Can. J. Chem. Downloaded from www.nrcresearchpress.com by 210.87.254.6 on 09/05/12
For personal use only.

Carcinogenicity of lactones. IV.[1] Alkylation of analogues of DNA guanine groups such as imidazole, *N*-methylimidazole, and guanosine by α,β-unsaturated acids[2]

J. Bryan Jones and John M. Young[3]

Lash Miller Chemical Laboratories, Department of Chemistry, University of Toronto, Toronto 181, Ontario

Received October 30, 1969

Studies on the reactions of carcinogenic γ-lactones and related compounds with analogues of guanine DNA residues indicate that the lactones themselves will not effect permanent alkylation of the guanine N-7 position since the Michael addition reactions involved would be readily reversible. In contrast, the α,β-unsaturated acids resulting from hydrolysis of such lactones are effective guanine N-7 alkylating agents owing to zwitterionic stabilization of the corresponding Michael addition products.

Canadian Journal of Chemistry, **48**, 1566 (1970)

Previous studies (1) have shown that, of a number of γ-lactones which have been tested for carcinogenicity (2), a distinction of possible in vivo significance between active and inactive lactones can be made in that carcinogenic lactones such as 4-hydroxypent-2-enoic acid lactone (**1**) and 4-hydroxyhexa-2,4-dienoic acid lactone (**2**) behave as *alkylating* agents whereas noncarcinogenic lactones are *acylating* agents (1).

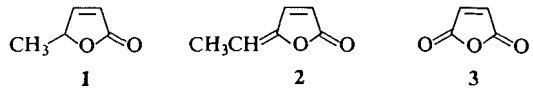

1 **2** **3**

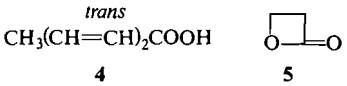

4 **5**

It is now generally accepted (3, 4)[4] that one of the properties of carcinogenic alkylating agents responsible for their cancer-inducing effects is their capacity to effect genetic mutation by alkylating selectively at the N-7 positions of guanine residues of deoxyribonucleic acid (DNA). Accordingly it became of interest to determine whether or not the reactions of the alkylating carcinogenic lactones and related compounds with DNA would follow the same pattern.

Guanosine (**6**) has been widely used as a model compound for the guanine residues of DNA (5–7) but, to our surprise, our attempts to effect reaction of the lactones **1** and **2** and of structurally related carcinogens such as maleic anhydride (**3**) and sorbic acid (**4**) with guanosine under a wide variety of conditions[5] were all unsuccessful. That the above failures to effect alkylation were not the result of a defective experimental technique was demonstrated by the successful repetition of the reaction, carried out earlier by Roberts and Warwick (5) of β-propiolactone (**5**) with guanosine; this gave, after hydrolytic work-up, the reported *N*-7-(2-carboxyethyl)guanine (**8**) in 71% yield (see Chart 1). Attempts to isolate the intermediate nucleoside **7** in a pure form were unsuccessful since it appeared from paper chromatographic analysis that some β-propiolactone modification of the ribose moiety had also occurred.

From a detailed study of the above reaction and of the limits of detectability of compounds such as **7** and **8** by paper chromatographic analysis, the possibility that the reactions of **1** and **2** with guanosine were producing significant amounts of the N-7 alkylated products was excluded.

In view of the facility with which the carcinogenic lactones **1** and **2** had previously effected alkylation of various nucleophiles (1) their inability to modify guanosine was at first somewhat disturbing. However, a consideration of the pathways and intermediates which would be involved in such a reaction provided a rationale for the ineffectiveness of the lactones as alkylating agents of the guanine tertiary N-7 atom. As

[1]For Paper III see ref. 1.

[2]Abstracted from ref. 20. Presented in part at the 52nd Canadian Chemical Conference, Montreal, June, 1969.

[3]Research Fellow of the National Cancer Institute of Canada, 1966–1969.

[4]A more complete discussion of the evidence is contained in ref. 20.

[5]These included heating in aqueous solution at several hydrogen ion concentrations in the p*H* range 5–9 and in dimethylformamide at 150° for several hours. In all cases guanosine, or guanine in the case of a reaction carried out at acid p*H*, was recovered almost quantitatively.

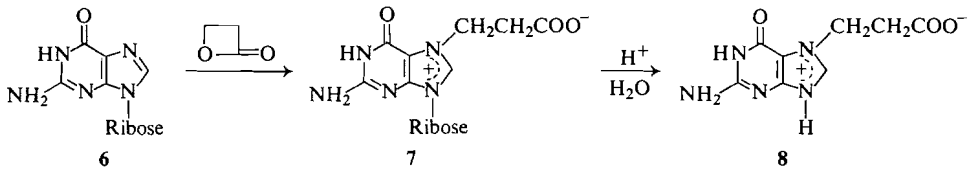

6 7 8

CHART 1

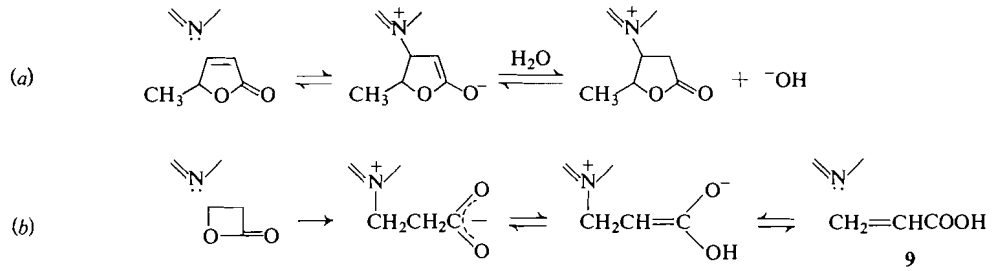

CHART 2

Chart 2*a* indicates, the Michael reaction of lactones such as **1** (or **2**) with a tertiary base would be expected to be unfavorable to product formation when the equilibrium is considered in terms of the relative acidities and basicities of the starting compounds and products involved. On the other hand, with other alkylating agents (5, 6), including β-propiolactone as illustrated in Chart 2*b*, formation of the product would be favored by its stabilization as a normal or zwitterionic salt. Furthermore it was noted that the zwitterionic product stabilization factors operating in the S_N2 reaction of β-propiolactone with tertiary amines would also obtain for the addition of such nucleophiles to α,β-unsaturated acids such as acrylic acid (**9**) (see Chart 2*b*) and that such stabilization might well be sufficient to ensure the accumulation of significant amounts of the Michael addition product.

In view of the difficulties experienced with the guanosine reactions with respect to product purification, spectral interpretations etc., it was decided to test the validity of the above stabilization hypotheses with simpler model compounds containing the guanine N-7 type of function. Purine was considered first but was discarded since its reaction with β-propiolactone led to a multiplicity of products. Fortunately however, the even simpler guanine model compounds, imidazole (**10***a*) and *N*-methylimidazole (**10***b*), proved satisfactory and initially attention was concentrated on the reactions of these two compounds. Unfortunately, *N*-methylimidazole, which is the better model of the latter two since it has one nitrogen atom substituted in a manner analogous to N-9 of guanine nucleotides, effected polymerization of both β-propiolactone and acrylic acid, and it was necessary to use the less satisfactory model imidazole in order to obtain any characterizable products.

That the tertiary nitrogen atom of imidazole was in fact a suitable model for N-7 in guanosine was demonstrated by its facile reaction with one equivalent of β-propiolactone (**5**) in diethylether to give the products of mono- and bis-alkylation, **11** (54%) and **12** (16%) respectively (Chart 3). When acetonitrile, in which **11** is soluble, was used as the solvent the yield of **12** was increased to 50% and on addition of a second equivalent of β-propiolactone the yield of **12** became quantitative.[6]

The charged nature of the imidazolium ring of **11** and **12** was confirmed by the downfield shift in the proton magnetic resonance (p.m.r.) spectra of both compounds of the vinylic protons of the imidazole rings (δ 7.51, C-4 and C-5 H and 8.75 p.p.m., C-2 H) relative to those of imidazole (δ 7.15 and 7.71 p.p.m.) and *N*-methylimidazole (δ 7.23 and 7.77 p.p.m.) respectively.

Extension of the model work to acrylic acid (**9**) (Chart 3) confirmed that zwitterionic stabilization

[6]Similar reactions of this lactone have been observed with pyridine (8), 2-aminopyridine (9), and trialkylamines (10).

Can. J. Chem. Downloaded from www.nrcresearchpress.com by 210.87.254.6 on 09/05/12
For personal use only.

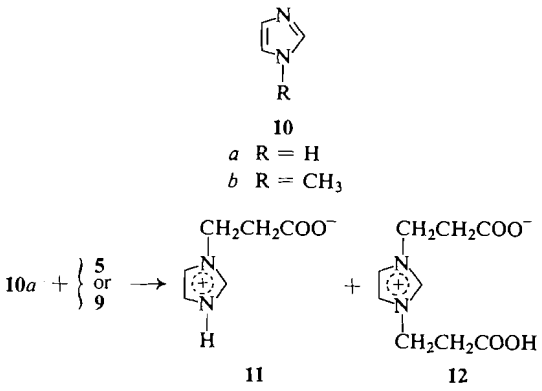

CHART 3

of the Michael addition products of reactions of α,β-unsaturated acids as illustrated in Chart 2*b* was important since the bis-adduct **12** was indeed formed when imidazole was treated with two equivalents of acrylic acid in methanolic or aqueous solution. Although the reaction proceeded somewhat more slowly than with β-propiolactone, a good (54%) yield of **12** was obtained after several hours reaction at steam bath temperature.

This demonstration of the importance of zwitterionic stabilization in the Michael addition of the guanine N-7 type of nucleophile to α,β-unsaturated compounds raised the possibility that, since the carcinogenic lactones and related compounds did not react with DNA, their carcinogenic properties might obtain from their initial in vivo hydrolysis to α,β-unsaturated acids which could then effect alkylation of DNA at the guanine N-7 position.

The discovery of the literature report that maleic acid (**13**, B = OH), the hydrolysis product of the carcinogenic maleic anhydride, reacted with pyridine in aqueous ethanol (11) to give the betaine **14***a* provided a further indication that such a rationale for the in vivo carcinogenic action was reasonable and the subsequent investigations were designed to evaluate the generality of such reactions and of the likelihood of their occurring in vivo.

The reaction of *N*-methylimidazole with maleic acid proceeded smoothly in methanol solution to give 2-(*N*-methylimidazolium)succinic acid betaine **14***b* in 65% yield. In the p.m.r. spectrum of the compound the succinic acid protons appeared as an ABX system and the imidazolium vinylic protons again showed the

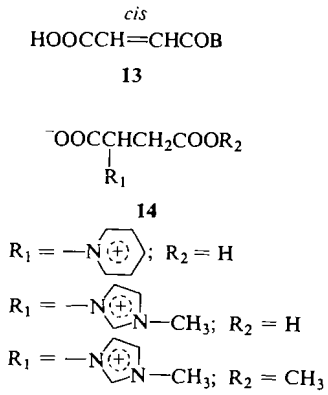

downfield shifts to be expected if the ring was positively charged.

3-Carbomethoxyacrylic acid (maleic acid monomethyl ester; **13**, B = OCH_3) was evaluated next since this could be regarded as a model for the products of in vivo attack of maleic anhydride by any in vivo nucleophiles other than water. Again a ready reaction with *N*-methylimidazole was observed and the product **14***c* was isolated in 57% yield. The p.m.r. spectrum included the characteristic patterns noted above for **14***b*. The assignment of structure **14***c* to the compound, rather than that of the isomeric product which would have resulted from Michael addition in the opposite sense, was made on the assumption that the carbomethoxy group would have a greater directing influence than carboxyl particularly since under the reaction conditions the latter would exist predominantly as the conjugate base. However, the isomeric structure cannot be rejected entirely.

In order to evaluate the influence of the stereochemistry of the double bond on such Michael additions the reaction of fumaric acid with *N*-methylimidazole in aqueous solution was examined. In contrast to the facile room temperature addition observed with the *cis* isomer maleic acid, with fumaric acid the product **14***b* was formed much less readily and even after heating the reactants for several hours at temperatures in excess of 100°, a yield of 18% only was obtained. Nevertheless, although the *trans* acid is clearly much less reactive, significant addition does occur.[7]

[7]This estimate of the effect on this particular type of Michael reaction of the geometry of the ethylenic linkage was valuable since some subsequent reactions were carried out on the more conveniently prepared *trans* analogues of in vivo compounds in which the corresponding unsaturation would be *cis*.

Can. J. Chem. Downloaded from www.nrcresearchpress.com by 210.87.254.6 on 09/05/12
For personal use only.

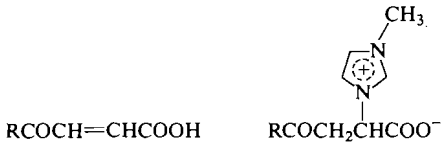

RCOCH=CHCOOH — **15**

a R = CH_2CH_3
b R = CH_3
c R = C_6H_5

RCOCH$_2$CHCOO$^-$ — **16**

a R = CH_2CH_3
b R = CH_3
c R = C_6H_5

The compounds considered next were those related to the hydrolysis product, *cis*-4-oxohex-2-enoic acid (**15***a*), of carcinogenic lactone **2**.[8] *trans*-Acetylacrylic acid (**15***b*), being readily prepared from levulinic acid, was selected as a suitable analogue of **15***a* but unfortunately its reaction with *N*-methylimidazole produced only intractable gums from which none of the desired compound **16***b* could be isolated. Accordingly *trans*-benzoylacrylic acid (**15***c*) was substituted[9] and from the reaction with *N*-methylimidazole in methanol solution the expected zwitterionic product was obtained in 66% yield. The structure was assigned as **16***c*, although again the isomeric formula could not be wholly excluded on the basis of the available data. The p.m.r. spectrum was as expected for **16***c* but unlike those of **14***b* and **14***c* the C-2 and C-3 protons appeared as an A_2X pattern.

Compounds **14***b*, **14***c*, and **16***c* were extremely hygroscopic and satisfactory elemental analyses could only be obtained for the succinic acid derivatives **14***b* and **14***c*.[10] As a result of these difficulties the structural assignment of **16***c* rests primarily on the similarities of the infrared (i.r.) and p.m.r. spectra of the three compounds. Recourse was had to mass spectroscopy in an attempt to establish molecular weights for the three compounds but in no case was a molecular ion observed. However, the spectra (70 eV) of **14***b*, **14***c*, and **16***c* were strikingly similar showing base peaks at *m/e* 82 for **14***b* and **14***c* and a 40% of the base peak for **16***c*. This corresponds to ionized *N*-methylimidazole and its subsequent fragmentation pattern was common to all three spectra. In addition the total mass spectrum of each was compatible with thermal decomposition, involving a reverse Michael reaction, into the respective reactants having occurred prior to ionization.[11]

That Michael reactions with unsaturated acids are not facile for all conjugated unsaturated acids was demonstrated by the total failure of the carcinogen sorbic acid (**4**), or of *trans*-but-2-enoic acid (crotonic acid), to react with *N*-methylimidazole even at temperatures in excess of 150°. In these cases, however, the lack of reaction may be ascribed to the *trans*-stereochemistry of the ethylenic linkages and also to the fact that the adverse electronic effects of the methyl vinyl and methyl groups respectively serve to increase the electron density at the β-carbon atom thereby making nucleophilic attack less facile than on acrylic acid itself. For acetyl- and benzoylacrylic acids the electron-withdrawing β-substituents facilitate Michael addition in the opposite direction.

Although the above results with imidazole and *N*-methylimidazole provide a strong indication that the α,β-unsaturated acid hydrolysis products of the carcinogenic lactones are capable of alkylating guanine N-7 positions, the data are obviously not extrapolatable to nuclear DNA without many reservations. Accordingly the experiments were repeated using guanosine in aqueous solution as a closer model for the in vivo situation and the results obtained are summarized in Chart 4.

The first reaction attempted was that with acrylic acid since it was expected that the products would be identical with those obtained with β-propiolactone and for which isolation and purification procedures had been established. Guanosine and acrylic acid were heated[12] in aqueous solution at 80° for 3 h and after hydrolytic work-up of the reaction mixture a 59% yield[13] of *N*-7-(2-carboxyethyl)guanine (**8**) was obtained which was identical with the β-propiolactone product obtained previously. As in the previous imidazole studies the reaction of acrylic acid with

[8]The acid derived from lactone **1** itself was not studied at this stage since it was felt that the reactions of acrylic acid were sufficiently representative of this type of function. Furthermore analogues of the hydrolysis product of the more potent carcinogen **2** were of more immediate interest.

[9]Ease of preparation was again a factor in the choice of *trans*-benzoylacrylic acid as an appropriate model. In addition, its Michael reactions with, for example, cysteine (12) had been studied previously. Although it possesses considerable biological activity in its own right (13) it has not yet been evaluated as a carcinogen.

[10]This compound formed a hydrate which was relatively stable.

[11]A detailed analysis of the mass spectral data and fragmentation pathways is given in ref. 20, p. 119–124.

[12]Heating was necessary in order to bring the guanosine into solution.

[13]Based on reacted guanosine.

Can. J. Chem. Downloaded from www.nrcresearchpress.com by 210.87.254.6 on 09/05/12
For personal use only.

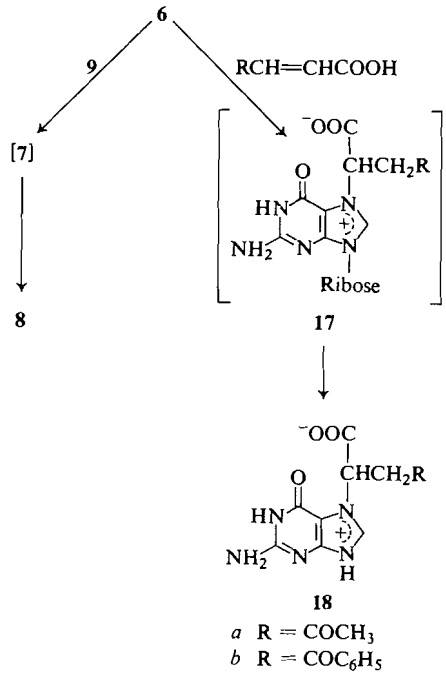

CHART 4

guanosine was much slower than for β-propiolactone but nevertheless proceeded quite readily.

Equally encouraging results were obtained when guanosine was reacted under similar aqueous conditions with the model of the hydrolysis acid of lactone **2**, acetylacrylic acid (**15***b*), and a 29% yield[13] of the N-7 alkylated guanine **18***a* was obtained following the hydrolytic work-up procedure. The material proved somewhat difficult to handle and no satisfactory elemental analyses were obtained. The structural assignment was made on the basis of the i.r. and p.m.r. spectra and of the relative ultraviolet (u.v.) absorptions in 1 *N* aqueous hydrochloric acid, 1 *N* aqueous sodium hydroxide, and p*H* 7 phosphate buffer solutions which were as required for an N-7 alkylated guanine (5, 6).

The reaction of benzoylacrylic acid with guanosine was also investigated but a trace only of the desired product **18***b* was detectable.[14] Although the compounds **18** are undoubtedly produced *via* the intermediacy of compounds **17**, no attempt was made to isolate the latter since such zwitterionic guanosine derivatives are known to be very susceptible to hydrolysis of the glycosidic linkage (6).

Disappointingly, maleic acid appeared to be such an excellent catalyst for the hydrolysis of the guanosine glycoside link that no guanine N-7 alkylation could be achieved prior to the formation of the insoluble hydrolysis product guanine.[15]

Not unexpectedly, in view of the negative *N*-methylimidazole results, sorbic acid and crotonic acid failed to react with guanosine even under the forcing conditions of heating under reflux in *N*,*N*-dimethylformamide solution.

Summary and Conclusions

The total data suggest that for lactones analogous to **1** and **2**, and for related compounds such as maleic anhydride, it may well be the unsaturated acids, or their derivatives, resulting from in vivo hydrolysis that are the proximate carcinogens. This suggestion is still in accord with the *alkylating–acylating* distinction (1) drawn between carcinogenic and non-carcinogenic lactones and on this basis a plausible, albeit at the present time speculative, rationale of their possible in vivo effects can be presented.

Acylation damage by inactive lactones to protein and other cellular nucleophiles should be, in general, non-specific[16] and thus no one site should be selectively or extensively attacked. Furthermore such acyl derivatives, and also the lactones themselves, are susceptible to hydrolysis[17] to give readily metabolizable ketoacids. In the cases of the alkylating carcinogenic lactones it is envisaged that they also will react initially with protein nucleophiles since our experience (1) is that such Michael additions should be more rapid than any other in vivo process.[16] However, the reversible nature of these reactions will allow at least some of the active lactone to proceed, under thermodynamic control, from one nucleo-

[14]The much poorer yields obtained with acetyl- and benzoylacrylic acids compared with acrylic acid itself are probably largely due to the presence of the less favorable *trans* double bond geometry in **15***b* and *c*.

[15]However, this evidence does not exclude the possibility of alkylation of DNA by maleic acid under in vivo conditions. Furthermore, attack by a cellular nucleophile other than water would give rise to compounds such as **13** which are analogous to the oxoacrylic acids for which the reactions with guanosine *were* observed.

[16]Studies with other carcinogenic alkylating agents have given similar indications (5, 14).

[17]A broad spectrum of proteolytic enzymes could assist in this hydrolytic repair process.

Can. J. Chem. Downloaded from www.nrcresearchpress.com by 210.87.254.6 on 09/05/12
For personal use only.

Can. J. Chem. Downloaded from www.nrcresearchpress.com by 210.87.254.6 on 09/05/12
For personal use only.

philic site to another and in this way it could eventually reach the nucleus of the cell. (Further nucleophilic attack at the carbonyl group of the Michael addition products is also a possibility). Hydrolysis at any stage during such migration would produce the corresponding α,β-unsaturated acid which if formed in the vicinity of the nuclear DNA would be capable of effecting its essentially irreversible alkylation.

The somewhat circuitous route to DNA that the above hypothesis implies may account in part for the relatively low carcinogenic potencies and non-cumulative effects of many of the lactone group of compounds evaluated by Dickens *et al.* (2) since it provides ample opportunity for the compounds or their derivatives to enter the normal metabolic or detoxification pathways. Thus conjugated unsaturated acids, or their derivatives or precursors, are likely to be potent carcinogens only if their structures are such that metabolic degradation etc. does not provide for their adequate elimination from the cell prior to reaching the nucleus. Many further studies involving biological testing of selected compounds of this type are required and these are to be carried out.

Sorbic Acid

An important exception to the above rationale is sorbic acid which has been recorded (2) as a fairly potent carcinogen. Our current and previous (1) inability to demonstrate any alkylating capacity for sorbic acid[18] indicates strongly that it is not itself a carcinogen. Its acceptance as a food additive following thorough testing on dogs (16) is also interesting in this regard. Without further testing (which would now appear to be very desirable) it will not be possible to rationalize these conflicting data (2, 16). However, it appears very likely that upon oral administration sorbic acid is metabolized via the normal fatty acid pathway. On the other hand, when subcutaneously injected, sorbic acid probably does not enter the normal metabolic pathways but remains in the region of application where it exerts its carcinogenic effect either because of its unsaturated acid nature or possibly as a result of its conversion to other carcinogenic compounds. This latter possibility deserves further investigation since it has been shown (17) that sorbic acid can undergo autooxidation at the C-4,5 double bond, giving rise to 4-acylacrylic acids of a type expected to be carcinogenic on the basis of the data presented in this communication.

[18]Under very forcing conditions (150° under pressure) sorbic acid does react with amines (15).

Experimental

The instruments and conditions used for spectral, m.p., etc. determinations are as listed previously (1). Paper chromatography was carried out on Whatman #1 filter paper with 1-propanol–water (5:2) as the ascending developing solvent. A Mineralight UVS-11 lamp was used for the detection of fluorescent compounds on paper chromatograms.

Compounds

4-Hydroxypent-2-enoic acid lactone (**1**) and 4-hydroxyhexa-2,4-dienoic acid lactone (**2**) were prepared as described previously (1). Maleic anhydride, maleic acid, fumaric acid, sorbic acid, β-propiolactone, acrylic acid, imidazole, and *N*-methylimidazole were obtained from Fisher or Aldrich and guanosine was purchased from Sigma. Where necessary the commercially supplied compounds were recrystallized or redistilled immediately prior to use. 3-Acetylacrylic acid, m.p. 124–126° (lit. (18) m.p. 125–126°), and 3-benzoylacrylic acid, m.p. 95–96° (lit. (19) m.p. 96–97°), were prepared according to the literature methods.

Attempted Reactions of 4-Hydroxypent-2-enoic Acid Lactone (1) and 4-Hydroxyhexa-2,4-dienoic Acid Lactone (2) with Guanosine (6)

Solutions of guanosine (1 mole equ.) and the lactones (1–5 mole equ.) in water or 50% aqueous *N,N*-dimethylformamide of different p*H*'s in the range 5–9 (adjusted with aqueous hydrochloric acid or sodium hydroxide respectively) were kept for varying periods (2–24 h) at temperatures ranging from 25 to 100°. In all cases unreacted guanosine or its hydrolysis product guanine were recovered to the extent of > 95%.

Reaction of β-Propiolactone with Guanosine

A mixture of guanosine (0.4 g, 1.4 mmole) and β-propiolactone (0.5 g, 7 mmole) in water (4.5 ml) was warmed to 80° at which temperature complete solution took place. The solution was then rotary evaporated at 25° to give a colorless viscous oil. (No attempt was made to purify this material further since paper chromatographic analysis indicated the presence of five compounds, including guanosine (R_f 0.43; dark blue fluorescence) and **8** (R_f 0.5 (light blue fluorescence)). Hydrolysis with 1 *N* hydrochloric acid (10 ml) at 100° for 1 h followed by neutralization with concentrated aqueous ammonium hydroxide, afforded a precipitate which was filtered, washed with water, and dried *in vacuo* over P_2O_5. Paper chromatographic analysis of the solid obtained showed only a single spot (light blue fluorescence) of R_f 0.5 and recrystallization from 40% aqueous *N,N*-dimethylformamide (70 ml) gave 7-(2-carboxyethyl) guanine, (0.23 g), m.p. > 290° (lit. (6) m.p. > 290°), i.r. (Nujol) 1741 (sh), 1725, 1695, and 1650 cm^{-1}; p.m.r. (2 *N* NaOD) δ 2.77 (2H, t, J = 7 Hz, CH_2COO^-), 4.50 (2H, t, J = 7 Hz,

Can. J. Chem. Downloaded from www.nrcresearchpress.com by 210.87.254.6 on 09/05/12
For personal use only.

$CH_2CH_2COO^-$), 5.00 (*H*OD) and 7.83 p.p.m. (1H, s, guanine C-8 *H*).

Reaction of β-Propiolactone with Imidazole

(a) In Diethyl Ether

β-Propiolactone (1.0 g, 13.9 mmole) was added dropwise with stirring to imidazole (1.0 g, 14.7 mmole) in diethyl ether (40 ml) at 20°. Within 10 min a crystallizing oil began to separate and after keeping overnight the mixture was filtered. The solid obtained (1.71 g) was fractionally recrystallized from methanol–chloroform solution to give *1-(2-carboxyethyl)imidazole* (**11**) as leafy plates (1.06 g) m.p. 152.5–153°; i.r. (Nujol) 3180, 2400, 1900 and 1715 cm^{-1}; p.m.r. (D_2O) δ 2.81 (2H, t, J = 6.5 Hz, $CH_2CH_2COO^-$), 4.50 (2H, t, J = 6.5 Hz, $CH_2CH_2COO^-$), 4.89 (*H*OD), 7.50 (2H, broad s, NC*H*=C*H*N) and 8.75 p.p.m. (1H, broad s, N=C*H*N).

Anal. Calcd. for $C_6H_8N_2O_2$: C, 51.25; H, 5.75; N, 19.99. Found: C, 51.23; H, 5.92; N, 19.89.

Also obtained was *1,3-bis(2'-carboxyethyl)imidazolium betaine* (**12**) as fine needles (0.24 g) m.p. 203–204°; i.r. (Nujol) 3180, 3100, 1710 and 1640 cm^{-1}; p.m.r. (D_2O) δ 2.90 (4H, t, J = 6.5 Hz, $CH_2CH_2COO^-$), 4.49 (4H, t, J = 6.5 Hz), $CH_2CH_2COO^-$), 4.82 (*H*OD), 7.56 (2H, d, J = 1.5 Hz, NC*H*=C*H*N) and 8.85 p.p.m. (1H, broad s, N=C*H*N).

Anal. Calcd. for $C_9H_{12}N_2O_4$: C, 50.94; H 5.70; N, 13.20. Found: C, 51.00; H, 5.80; N, 13.06.

(b) In Acetonitrile

When the above reaction was repeated in acetonitrile (50 ml), the bis-addition product **12** was obtained in 50% yield. When two equ of β-propiolactone were used, the recrystallized yield of **12** was increased to 92%.

The Reaction of Acrylic Acid with Imidazole

Acrylic acid (4 g, 55 mmole) and imidazole (2.0 g, 29 mmole) were dissolved in methanol (40 ml) and the solution was slowly concentrated to 10 ml during 3 h by heating on a steam bath. Rotary evaporation of the concentrate afforded a solid which on recrystallization from aqueous methanol gave 3.13 g of 1,3-bis(2-carboxyethyl)-imidazolium betaine (**12**) identical in all respects to that obtained previously from the β-propiolactone reaction.

The Reaction of Maleic Acid with N-Methylimidazole

Maleic acid (2.32 g, 20 mmole) was dissolved in a mixture of diethylether (50 ml) and methanol (10 ml) and *N*-methylimidazole (1.62 g, 20 mmole) was then added with stirring. An oil began to separate which became crystalline following removal of the solvent at 90°. Recrystallization of the solid from 50% aqueous ethanol (40 ml) gave *2-N-(N'-methylimidazolium)succinic acid betaine* (**14***b*) as needles, (2.53 g) m.p. 232–233° (decomposition); i.r. (Nujol) 3300–2400, 1700 (COOH) and 1650–1550 cm^{-1} (COO^-); p.m.r. (2 *N* NaOD) δ 2.94 (H_A, d of d, J_{AB} = 16.5 Hz, J_{AX} = 10 Hz, $CH_XCH_AH_B$-COOH), 3.18 (calcd.) (H_B, d of d, J_{BA} = 16.5 Hz, J_{BX} = 5 Hz, $CH_XCH_AH_BCOOH$), 3.92 (3H, s, CH_3N), 4.70 (HOD), 5.23 (H_X, d of d, J_{XA} = 10 Hz, J_{XB} = 5 Hz, $CH_XCH_AH_BCOOH$), 7.52 (2H, AB q, NC*H*=C*H*N), and 8.84 p.p.m. (1H, broad s, N=C*H*N).

Anal. Calcd. for $C_8H_{10}N_2O_4$: C, 48.49; H, 5.09; N, 14.14. Found: C, 48.33; H, 5.18; N, 14.04.

The Reaction of Maleic Acid Monomethyl Ester with N-Methylimidazole

A solution of maleic anhydride (2.0 g, 20 mmole) in methanol (50 ml) was refluxed for 10 min and *N*-methylimidazole (1.62 g, 20 mmole) was then added. The solution was evaporated slowly on the steam bath during 3 h and the resulting solid was recrystallized from chloroform–ethanol. *2-N-(N'-Methylimidazolium)-3-carbomethoxypropionic acid betaine* (**14***c*) separated as needles (2.42 g), m.p. 157–158° (decomposition); i.r. (Nujol) 3530, 3190, 3075, 1730 ($COOCH_3$), and 1645–1600 cm^{-1} (COO^-); p.m.r. (D_2O), δ 3.35 (H_AH_B, approaching d, J_{AX} = 8 Hz, J_{BX} = 6 Hz, $CH_XCH_AH_B$-$COOCH_3$), 3.74 (3H, s, OCH_3), 4.00 (3H, s, NCH_3) 4.70 (*H*OD), 5.37 (H_X, d of d, J_{XA} = 8 Hz, J_{XB} = 6Hz, NCH_X-CH_AH_B), 7.60 (2H, m, NC*H* = C*H*N), and 8.96 p.p.m. (1H, broad s, N=C*H*N).

Anal. Calcd. for 2 $C_9H_{12}N_2O_4 \cdot 1\ H_2O$: C, 48.86; H, 5.92; N, 12.66. Found: C, 48.73; H, 6.14; N, 12.84.

The Reaction of 3-Benzoylacrylic Acid with N-Methylimidazole

A solution of *N*-methylimidazole (1.62 g, 20 mmole) and 3-benzoylacrylic acid (3.52 g, 20 mmole) in methanol (50 ml) was kept at 50° for 1.5 h and was then rotary evaporated. The residue was recrystallized from chloroform–methanol (10:1, 40 ml) and *2-N-(N'-methylimidazolium)-4-oxo-4-phenylbutanoic acid betaine* (**16***c*) separated as a microcrystalline powder (3.40 g) m.p. 95–106°; i.r. (Nujol) 3450, 3375, 3260, 3130, 3050 (sharp bands), 1685 (CO), and 1640–1625 cm^{-1} (COO^-); p.m.r. (D_2O) δ 4.12 (3H, s, NCH_3), 4.20 (2H, d, J = 6Hz, $CHCH_2COPh$), 5.00 (*H*OD), 5.72 (1H, t, J = 6Hz, $CHCH_2COPh$), 7.5–8.2 (5H, 2H, complex m, C_6H_5-NC*H*=C*H*N), and 9.20 p.p.m. (N=C*H*N).

Reaction of Acrylic Acid with Guanosine

Guanosine (0.40 g, 1.4 mmole) and acrylic acid (0.53 g, 7 mmole) were dissolved in water (6 ml) at 80°. The temperature was maintained at this level for 1.5 h and the solution was then kept at room temperature overnight. The unreacted guanosine (0.17 g) was removed by filtration and the filtrate was diluted with an equal volume of 2 *N* aqueous hydrochloric acid and heated under reflux for 1 h. After cooling the solution and neutralization with concentrated aqueous ammonium hydroxide, 7-(2-carboxyethyl)guanine (0.11 g) separated which was identical in all respects with the material obtained from the guanosine-β-propiolactone reaction.

The Reaction of 3-Acetylacrylic Acid with Guanosine

Guanosine (2.83 g, 10 mmole) in water (50 ml) was heated on a steam bath (90°) until complete solution had occurred. 3-Acetylacrylic acid (1.78 g, 15 mmole) was then added and the mixture was maintained at a temperature of 90°. The progress of the reaction was monitored by paper chromatographic analysis which indicated that several compounds were formed and that the optimum reaction time was 5 h. After this time the guanine (0.36 g) which had precipitated was filtered off from the hot solution and the filtrate was cooled and seeded with guanosine. After keeping overnight at 0°, the mixture was again filtered to give guanosine (0.86 g) and the colored filtrate was treated with charcoal and

TABLE 1

Ultraviolet data for 7-(2′-acetyl-1′-carboxyethyl) guanine

Solvent	λ_{max}	ε	λ_{min}	$\varepsilon_{280}/\varepsilon_{260}$
1 *N* HCl	251 270	7610 5760	230.5	0.68
1 *N* NaOH	244 279	5050 5820	257	1.55
0.1 *M* PO_4^{2-}, p*H* 7	245 283	5720 6120	237 264	1.50

was then evaporated. The solid residue obtained was digested with ethanol (75 ml) under reflux and the ethanolic solution obtained was kept at 0° until precipitation of the product was complete (12 h). Filtration afforded *7-(2′-acetyl-1′-carboxyethyl)guanine* (0.36 g), m.p. > 200° (decomposition); i.r. (Nujol) 3500–2500 and 1725–1550 cm^{-1} (broad, diffuse bands); p.m.r. (2 *N* D_2SO_4) δ 2.28 (3H, s, CH_3CO), 3.52–3.78 (3H, AA′X d of d, J_{AX} = 7.3 Hz, $J_{A'X}$ = 5 Hz, $J_{AA'}$ not observed, $CH_3COCH_AH_BCH_XN$-7), 5.16 (*H*OD), 5.97 (H_X, d of d, J_{XA} = 7.3 Hz, $J_{XA'}$ = 5 Hz, N-7$CH_XCH_AH_BCOCH_3$), and 8.60 p.p.m. (1H, s, guanine C-8H). The u.v. data are tabulated in Table 1.

The generous support of the National Cancer Institute of Canada is gratefully acknowledged.

1. J. B. Jones and J. M. Young. J. Med. Chem. **11**, 1176 (1968) and references therein.
2. F. Dickens, H. E. H. Jones, and H. B. Waynforth. Brit. J. Cancer, **20**, 134 (1966) and references therein.
3. e.g. P. Brookes. Cancer Res. **26**, 1994 (1966) and references therein.
4. e.g. N. H. Colburn and R. K. Boutwell. Cancer Res. **28**, 653 (1968) and references therein.
5. J. J. Roberts and G. P. Warwick. Biochem. Pharmacol. **12**, 1441 (1963) and previous papers.
6. P. Brookes and P. D. Lawley. J. Chem. Soc. 3923 (1961); 1348 (1962).
7. N. H. Colburn, R. G. Richardson, and R. K. Boutwell. Biochem. Pharmacol, **14**, 1113 (1965).
8. T. L. Gresham, J. E. Jansen, F. W. Shaver, R. A. Bankert, and F. T. Fiedorek. J. Amer. Chem. Soc. **73**, 3168 (1951).
9. C. D. Hurd and S. Hayao. J. Amer. Chem. Soc. **77**, 117 (1955).
10. R. Tsuzuki, K. Ichikawa, and M. Kase. J. Org. Chem. **26**, 1808 (1961).
11. L. H. Flett and W. H. Gardner. Maleic anhydride derivatives. J. Wiley and Sons, New York, N.Y., 1952. p. 120.
12. F. H. Kirchner, J. H. Bailey, and C. J. Cavallito. J. Amer. Chem. Soc. **71**, 1210 (1949).
13. B. J. Cramer, W. Schroeder, W. J. Moran, C. H. Nield, M. Edwards, C. I. Jarowski, and B. Puetzer. J. Amer. Pharm. Ass. Sci. Ed. **37**, 439 (1948).
14. W. C. J. Ross. Biological alkylating agents. Butterworth and Co. (Publishers) Ltd., London, 1962.
15. A. J. Verbiscar and K. N. Campbell. J. Org. Chem. **29**, 2472 (1964).
16. K. Lang. Arzneimittel-Forsch. **10**, 997 (1960).
17. M. Hamada. J. Agr. Chem. Soc. (Japan), **16**, 181 (1940).
18. W. G. Overend, L. M. Turton, and L. G. Wiggins. J. Chem. Soc. 3500 (1950).
19. G. Baddeley, G. Holt, and S. M. Makar. J. Chem. Soc. 3289 (1952).
20. J. M. Young, Ph.D. Thesis. University of Toronto, Toronto, Ontario. 1969.

Can. J. Chem. Downloaded from www.nrcresearchpress.com by 210.87.254.6 on 09/05/12
For personal use only.

Carcinogenicity of lactones. V.[1] The reactions of 4-hydroxypent-2-enoic acid lactone with α-toluenethiol, benzylamine, methylamine, imidazole, and guanidine[2]

J. Bryan Jones and Jill N. Barker

Lash Miller Laboratories, Department of Chemistry, University of Toronto, Toronto 181, Ontario

Received October 30, 1969

The Michael additions of α-toluenethiol, methylamine, and benzylamine to 4-hydroxypent-2-enoic acid lactone have been confirmed to be facile. The analogous additions of imidazole and glycine amide are much less readily accomplished and no stable Michael addition product could be detected with guanidine as the base. In the p*H* range 6–9, subsequent lactone ring opening reactions of the Michael addition products were observed only when methylamine (pK_a 9.3) and benzylamine (pK_a 10.6) were used as nucleophiles.

Canadian Journal of Chemistry, **48**, 1574 (1970)

Introduction

During previous investigations related to the carcinogenicity of lactones (1) it was noted that all the carcinogenic γ-lactones studied chemically (1, 2), of which **1** may be regarded as representative, had proven to be alkylating agents and it was concluded (1) that the most probable initial in vivo sites of alkylation would be the nucleophilic functional groups of proteins. It was also noted that the products of such Michael addition reactions, for example **2***a–f*, still allowed the possibility of subsequent in vivo nucleophilic attack at the lactone carbonyl group to give products of the type **3***a–d* (eq. [1]).

The amino acid residues which were considered to be the most readily alkylatable by the lactones were those containing the thiol (cysteine), imidazolium (histidine), and primary amino (*N*-terminal and lysine etc.) functions. As a preliminary step towards delineating the types and selectivities of the permutations and combinations possible for such carcinogen-nucleophile reactions we have examined the reactions of lactone **1** with some simple model compounds containing the above functional groups. Since a purely chemical survey only was intended at this stage little effort was made to duplicate physiological conditions except that whenever feasible reactions were carried out in aqueous solution within the p*H* range 6–9.

[1]For Part IV see ref. 1.

[2]Abstracted from the M.Sc. thesis of J.N.B., University of Toronto, Toronto, Ontario, 1968.

Results and Discussion

(a) Michael Addition Reactions

Attention was first directed towards the reaction of lactone **1** with α-toluenethiol. Selection of the latter as a simple model for a cysteine thiol residue was dictated largely by its easy recognition in the proton magnetic resonance (p.m.r.) spectra of the expected products (3). However, its low solubility in the preferred solvent, water, required the reactions to be carried out in ethereal or alcoholic media. As expected, the Michael addition of α-toluenethiol to lactone **1**

[1] 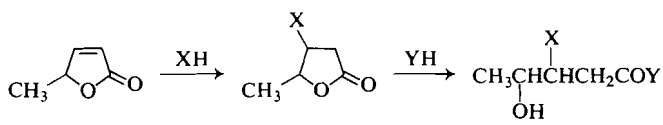

1 **2** **3**

a X = SCH_2Ph — *a* X = SCH_2Ph, Y = $NHCH_3$

b X = 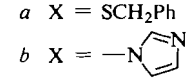 — *b* X = SCH_2Ph, Y = $NHCH_2Ph$

c X = $NHCH_2Ph$ — *c* X = 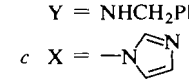 , Y = $NHCH_2Ph$

d X = $NHCH_3$ — *d* X = $NHCH_2Ph$, Y = $NHCH_3$

e X = $NHCH_2CONH_2$

f X = $NHC(=NH)NH_2$

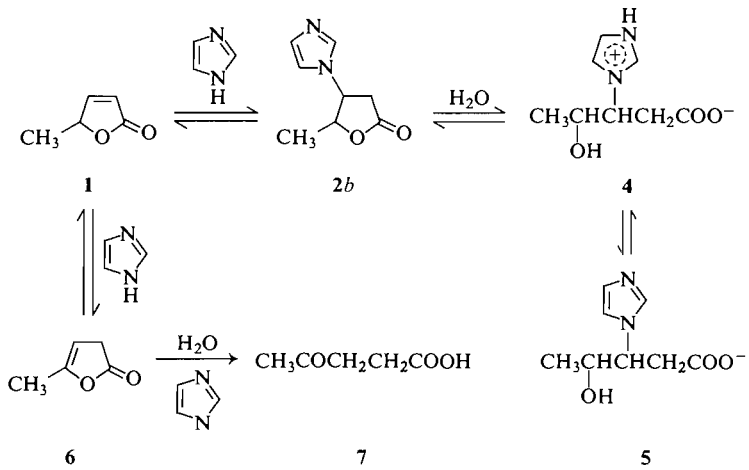

CHART 1

proceeded extremely smoothly in ether solution (containing triethylamine as catalyst) at room temperature to give 3-benzylthio-4-hydroxypentanoic acid lactone (**2***a*) in 89% yield. This result confirmed the earlier data (2) that reactions of carcinogenic δ-lactones with cysteine-like thiol groups are facile.

The reaction considered next, of the histidyl analogue imidazole with **1**, proved more complex than in the above and related studies (3). On mixing lactone **1** with one equivalent of imidazole in aqueous solution at 20°, Michael addition to give **2***b* did occur but owing to the relatively lengthy reaction times required at room temperature to ensure significant conversion of the starting compounds to products, several further and competitive reactions took place. The total situation, which was deduced mainly from periodic p.m.r. analyses, is summarized in Chart 1.

The desired product **2***b* and the zwitterionic compound **4** were both isolable from the reaction mixture. The carboxylate **5** and levulinic acid (**7**) were not isolated but were identified in the mixture by comparison of the relevant p.m.r. peaks with those of authentic spectra.

The complications encountered with imidazole can be largely attributed to its well documented assistance of ester and lactone hydrolysis and to its general base catalytic properties (4). Thus the rate of hydrolysis of **2***b* to **4** would be expected to be enhanced by the presence of imidazole as also would the equilibration of **1** and its isomeric lactone **6**. Although the latter is much less favored thermodynamically, its greater susceptibility to nucleophilic attack (3) by water, either alone or assisted by imidazole, would ensure a steady accumulation of levulinic acid (**7**). Some representative p.m.r. data indicating the composition of the mixture as the reactions proceeded are recorded in Table 1. A further p.m.r. monitored study showed that treatment of either the Michael product **2***b* or the zwitterion **4** with dilute hydrochloric acid afforded a 1:1 equilibrium mixture of both compounds together with a trace of levulinic acid. The use of more concentrated hydrochloric acid as a catalyst resulted only in the formation of increased amounts of levulinic acid. Dilute sodium hydroxide solution effected the conversion of both **2***b* and **4** into the imadazolium carboxylate **5**.

TABLE 1

Yields of products of the reaction of imidazole with 4-hydroxypent-2-enoic acid lactone (**1**) as a function of time*

Product	δ (p.p.m.)† of C-5 CH_3	Percentage present in reaction mixture‡ 24 h	45 h	250 h	500 h
1	1.45	33	29	25	6
2*b*	1.55	30	27	<1	—
4	1.17	10	20	60	67
5	1.10	16	13	—	—
7	2.10	8	11	15	27

*Reactions carried out at 20° in aqueous solution 1.5 *M* in each reagent.
†With sodium 3-(trimethylsilyl)propane sulfonate as the internal standard.
‡Calculated from the area of the C-5 CH_3 peak in the 60 MHz p.m.r. spectrum.

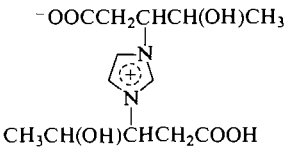

8

Owing to the difficulties encountered during the work-up procedures for compounds **2***b* and **4**, the isolated yields were not as high as might have been expected from the concentrations known to be present in the reaction mixture (cf. Table 1). Furthermore, during the work-up process secondary reactions, including reverse Michael processes, occurred and in addition a certain amount of artefactual material, for which the chemical shifts of the imidazolium vinylic protons in the p.m.r. spectrum at δ 7.6 and 9.14 p.p.m. were considered indicative of the hydrolyzed bis-addition product **8**, was always formed.[3]

The complexity of the reaction of **1** with imidazole under the conditions surveyed make it impossible to draw any conclusions pertinent to the in vivo situation. However, it is apparent that alkylation of histidine residues by carcinogenic γ-lactones is a distinct possibility.

Attention was next directed towards the reactions of the primary amino group. The facile Michael reactions of amines analogous to lysine side chains (pK_a 9.4–10.6 (5)) such as benzylamine (pK_a 9.3 (6)) and methylamine (pK_a 10.6 (6)), with lactone **1** to give **2***c* and **2***d* respectively had been well documented previously (3) and no further work in this area was carried out.

It is of interest to compare the ease with which the Michael addition product can be isolated from the primary amine reactions with the situation encountered with the secondary amine of markedly less basicity and nucleophilicity, imidazole. In the latter case the attainment of equilibrium in the Michael addition reaction appears to be relatively slow, thereby allowing significant isomerization of **1** to the β,γ-unsaturated lactone **6** to occur. In contrast to the apparently sluggish Michael addition capabilities of such secondary amines, their capacity for nucleophilic attack at the carbonyl group of **6**, once the latter is formed, is much superior and accordingly the products of the latter reactions build up under conditions of kinetic control (7).

It was noted that the above primary amines could not be regarded as good models for *N*-terminal amino groups (pK_a 7.6–8.4 (5)). A more suitable model for the latter appeared to be glycine amide and accordingly a study of its reaction with **1** in aqueous solution was carried out. The reactions which occurred turned out to be similar to, but much less facile than, those encountered with imidazole as a nucleophile and in view of the very slow rate of formation of the Michael addition product **2***e* it may be concluded that extensive in vivo alkylation of *N*-terminal amino groups by **1** would be improbable.

Of the remaining amino acid functions known to be readily susceptible to chemical modification (8) only the guanidinium (of arginine) group was considered further in this preliminary survey. It was included on the basis of the abundance of arginine residues in many histones although, in view of its quoted pK_a range of 11.6–12.6 (5), it was not regarded as a serious in vivo lactone alkylation possibility.

Guanidine (pK_a 13.65 (6)) was taken as the simplest analogue. The reagents, guanidine hydrochloride and **1**, were mixed in aqueous solution and in order to achieve reasonable rates of reaction it was found necessary to maintain the p*H* of the solution at values > 10. None of the hoped for Michael addition product **2***f* could be isolated from the reaction mixture and on the basis of a combination of p.m.r. and infrared (i.r.) analyses of the amide products it was concluded that the sequence of reactions indicated in Chart 2 was occurring with the initial step again being guanidine base-catalyzed isomerization of **1** to the β,γ-unsaturated lactone **6**. That the latter compound would in fact then react very rapidly with guanidine was established by mixing guanidine with **6** in either aqueous or methanolic solution. The product from the aqueous reaction showed an i.r. red carbonyl absorption at 1660 cm^{-1} compatible with the amide structure **9** but, presumably as a result of its susceptibility to subsequent nucleophilic attack, it could not be purified. However, the structure assignment was corroborated by the observation that on treatment with aqueous hydrochloric acid, the product hydrolyzed very rapidly to give levulinic acid and guanidinium hydrochloride. Furthermore, on attempted prep-

[3]The formation of such a product would not be unexpected in view of the ease with which β-propiolactone and acrylic acid are known to form such bis-adducts on reaction with imidazole (1).

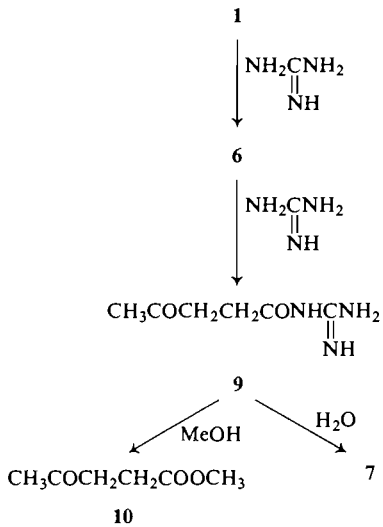

CHART 2

aration of the same compound **9** under anhydrous methanolic conditions the expected products, methyl levulinate (**10**) and guanidinium hydrochloride, were isolated.

(b) Subsequent Reactions of the Initially Formed Michael Products

As outlined at the beginning of this communication, in principle each of the Michael addition products obtained above is susceptible to further attack at the carbonyl group by each of the nucleophiles evaluated. However, of the complete permutation of possible reactant combinations of the Michael products **2***a–d* with all of the above model protein nucleophiles, very few ring opening reactions were observed. In fact at 20° in aqueous or aqueous methanolic solutions in the p*H* range 6–9, the only compounds for which formation of compounds **3** could be satisfactorily[4] demonstrated were for the primary amine analogues of the ε-amino group of lysine; the products **3***a–d* of reaction of **2***a–d* with benzylamine and methylamine were produced in 50–80% yields.

Experimental

The instruments used for spectral etc. determinations, were as listed previously (9).

[4]Guanidine also reacted with compounds **3** and although spectral data indicated that attack at the carbonyl group was occurring, this could not be fully substantiated.

Compounds

4-Hydroxypent-2-enoic acid lactone (**1**) and 3-benzylamino-4-hydroxypentanoic acid lactone (**2***c*) were prepared by the literature methods (3); all other materials used were purchased from Fisher or Aldrich.

The Reaction of 4-Hydroxypent-2-enoic Acid Lactone with α-Toluene Thiol

A solution of 4-hydroxypent-2-enoic acid lactone (2.0 g, 20 mmole), α-toluene thiol (2.54 g, 20 mmole), and triethylamine (2.06 g, 20 mmole) in diethyl ether was stirred for 1 h at 20°. The solvent was then removed by rotary evaporation at 20° and the residual oil distilled to give *3-benzylthio-4-hydroxypentanoic acid lactone* (**2***a*) (4.0 g), b.p. 160–161° (0.7 mm); i.r. ($CHCl_3$) 1780 cm^{-1}; p.m.r. ($CDCl_3$) δ 1.26 (3H, d, J = 6.5 Hz, CH_3CH), 2.6 (2H, m, $CHCH_2CO$), 2.9 (1H, m, $CHCH(S)CH$), 3.73 (2H, s, $SCH_2C_6H_5$), 4.3 (1H, m, $CH_3CH(O)CH$), and 7.30 p.p.m. (5H, s, C_6H_5).

Anal. Calcd. for $C_{12}H_{14}O_2S$: C, 64.90; H, 6.30; S, 14.40. Found: C, 65.29; H, 6.08; s, 14.53.

The Reaction of 3-Benzylthio-4-hydroxypentanoic Acid Lactone with Methylamine and Benzylamine

(a) With Methylamine

A solution of 3-benzylthio-4-hydroxypentanoic acid lactone (2.04 g, 9 mmole), aqueous methylamine (1 ml, 9 mmole CH_3NH_2) in 85% aqueous methanol (14 ml) was stirred for 16 h at 20° and was then rotary evaporated. The p.m.r. analysis indicated the presence of 80% of *3-benzylthio-4-hydroxy-N-methylpentanoamide* (**3***a*) at this stage but all attempts, including distillation, to effect further purification resulted in a reverse Michael reaction. The spectral data obtained were: i.r. ($CHCl_3$) 1668 cm^{-1}; p.m.r. ($CDCl_3$) δ 1.21 (3H, d, J = 6.5 Hz, CH_3CH), 2.47 (2H, m, $CHCH_2CO$), 2.75 (3H, d, J = 4.5 Hz, $CONHCH_3$), 3.2 (1H, m, $CH.CH(S)CH_2$), 3.42 (1H, s, OH), 3.78 (1H, m, $CH_3CH(OH)CH$), 3.80 (2H, s, $SCH_2C_6H_5$), 6.2 (1H, m, $CONHCH_3$), and 7.3 p.p.m. (5H, s, C_6H_5).

(b) With Benzylamine

3-Benzylthio-4-hydroxypentanoic acid lactone (0.51 g, 2 mmole), benzylamine (0.25 g, 2 mmole), and 85% aqueous methanol (3 ml) were stirred together for 24 h at 20° and the solution was then rotary evaporated. The residual solid was chromatographed on Florisil (75 g, column prepared in chloroform) and chloroform–acetone (1:1) elution gave a fraction containing *3-benzylthio-4-hydroxy-N-benzylpentanoamide* (**3***b*). Recrystallization from benzene–cyclohexane afforded 0.38 g of material m.p. 76–77°; i.r. ($CHCl_3$) 1668 cm^{-1}; p.m.r. ($CDCl_3$) δ 1.17 (3H, d, J = 6.5 Hz, CH_3CH), 2.42 (2H, m, $CHCH_2CO$), 3.05 (2H, m, OH and $CHCH(S)CH_2$), 3.75 (2H, s, $SCH_2C_6H_5$), 3.75 (1H, m, $CH_3CH(OH)CH$), 4.38 (2H, d, J = 6.0 Hz, $CONHCH_2C_6H_5$), 6.1 (1H, m, $CONHCH_2$), 7.22 (5H, s, $SCH_2C_6H_5$), and 7.25 p.p.m. (5H, s, $NHCH_2C_6H_5$).

Anal. Calcd. for $C_{19}H_{23}NO_2S$: C, 69.30, H, 7.02; N, 4.25; S, 9.72. Found: C, 69.38; H, 7.20; N, 4.29; S, 9.72.

The Reaction of 4-Hydroxypent-2-enoic Acid Lactone with Imidazole

(a) A solution of 4-hydroxypent-2-enoic acid lactone (1.44 g, 15 mmole) and imidazole (1.01 g, 15 mmole) in

water (10 ml) was kept for 3 weeks at 20°. The precipitate (0.55 g) of *3-imidazolyl-4-hydroxypentanoic acid betaine* (**4**) was collected and the aqueous filtrate concentrated by rotary evaporation at 20°. Trituration of the residue with chloroform–benzene afforded a further 0.47 g of the zwitterion **4**. Recrystallization of a portion from water–acetone afforded a sample, m.p. 185°,[5] i.r. (KBr) 1600 cm^{-1} (COO^-); p.m.r. (D_2O) δ 1.17 (3H, d, J = 6.5 Hz, CH_3CH), 2.9 (2H, m, $CHCH_2CO$), 4.15 (1H, m, $CHCH$-$(N)CH_2$), 4.65 (1H, m, $CH_3CH(OH)CH$), 7.54 (2H, m, $NCH{=}CHN$), and 8.88 p.p.m. (1H, m, $N{=}CHN$).

Anal. Calcd. for $C_8H_{12}N_2O_3$: C, 52.16; H, 6.57; N, 15.21. Found: C, 52.36; H, 6.68, N, 15.14.

No further compounds could be isolated in a pure form from this reaction (see Discussion).

(b) 4-Hydroxypent-2-enoic acid lactone (1.5 g, 15 mmole) and imidazole (3.3 g, 45 mmole) were dissolved in water (15 ml) and the solution was stirred for 21 h at 20°. Water (10 ml) was then added and the aqueous solution was extracted with chloroform (4 × 25 ml). The dried ($MgSO_4$) chloroform extracts were evaporated (20°) and 2 *N* aqueous hydrochloric acid (10 ml) was added to the glassy product. Rotary evaporation at 20° afforded *3-imidazolyl-4-hydroxypentanoic acid lactone hydrochloride* which on recrystallization from aqueous methanol gave needles (0.4 g), m.p. 162–164°; i.r. (KBr) 1784 cm^{-1}; p.m.r. (D_2O) δ 1.53 (3H, d, J = 6.5 Hz, CH_3CH), 3.35 (2H, m, $CHCH_2CO$), 5.12 (2H, m, $CH_3CHC(O)CH$ and $CHCH(N)CH_2$), 7.65 (2H, m, $NCH{=}CHN$), and 8.96 p.p.m. (1H, m, $N{=}CHN$).

Anal. Calcd. for $C_8H_{11}ClN_2O_2$: C, 47.41; H, 5.47; Cl, 17.49; N, 13.82. Found: C, 47.48; H, 5.62; Cl, 17.44; N, 13.82.

3-Imidazolyl-4-Hydroxypentanoic Acid Lactone Hydrochloride from the Zwitterion 4

3-Imidazolyl-4-hydroxypentanoic acid betaine (**4**, 0.38 g, 2 mmole) was treated with 2 *N* aqueous hydrochloric acid at 60° for 30 min and the solution was then rotary evaporated. Recrystallization of the residue from aqueous methanol gave the desired lactone hydrochloride m.p. 162–164° which was identical in all respects with the product obtained above.

The Reaction of 3-Imidazolo-4-hydroxypentanoic Acid Lactone with Benzylamine

A solution of 3-imidazolo-4-hydroxypentanoic acid lactone hydrochloride (0.17 g, 9 mmole) and benzylamine (0.25 g, 27 mmole) in water (5 ml) was stirred for 3 h at 20° and was then filtered. (The filtrate was evaporated and the solid obtained recrystallized from acetone – petroleum ether (b.p. 40–60°) to give benzylamine hydrochloride (0.11 g, 8 mmole) m.p. 245–248°). The residue was recrystallized from aqueous acetone to yield *3-imidazolyl-4-hydroxy-N-benzylpentanoamide* (**3***c*) (0.17 g), m.p. 156–158°; i.r. (KBr) 1635 cm^{-1}; p.m.r. (D_2O) δ 1.18 (3H, d, J = 6.5 Hz, CH_3CH), 2.88 (2H, m, $CHCH_2$-CO), 4.22 (2H, s, $NDCH_2C_6H_5$), 4.25 (1H, m, $CHCH$-CH_2), 5.15 (1H, m, CH_3CHCH), 7.50 (2H, m, $NCH{=}CHN$), 7.51 (5H, s, C_6H_5), and 8.67 p.p.m. (1H, m, $N{=}CHN$).

Anal. Calcd. for $C_{15}H_{19}N_3O_2$: C, 65.91; H, 7.01; N, 15.37. Found: C, 65.82; H, 7.20; N, 15.37.

Reaction of 4-Hydroxypent-3-enoic Acid Lactone (6) with Guanidine

(a) In Aqueous Solution

To a solution of 4-hydroxypent-3-enoic acid lactone (1.74 g, 18 mmole) and guanidine hydrochloride (1.65 g, 18 mmole) in water (3 ml) was added 1 *N* aqueous sodium hydroxide solution (18 ml, 18 mmole). Spectroscopic analysis after 15 min at 20° indicated that complete reaction had occurred to give mainly *N-guanidyl-4-oxopentanoamide* (**8**)[6] [i.r. 1660 cm^{-1}, p.m.r. (H_2O), δ 2.20 (3H, s, CH_3CO), 2.41 (2H, m, $CH_3COCH_2CH_2CO$), and 2.74 p.p.m. (2H, m, $CH_3COCH_2CH_2CO$)]. The mixture was concentrated at 20°, ethanol (10 ml) added, and the precipitated sodium chloride filtered off. Aqueous hydrochloric acid 2*N* (10 ml) was added to the filtrate and the solution was again rotary evaporated and the residue was extracted with acetone. The remaining solid (0.86 g) m.p. 184–186° was identified as guanidine hydrochloride and the acetone solution, after evaporation and distillation, gave levulinic acid (7) (0.89 g), b.p. 84–86° (0.12 mm) which was identical with an authentic sample.

(b) In Methanol Solution

When the above reaction was carried out in anhydrous methanol (5 ml) solution[6] containing sodium methoxide (19 mmole, from sodium 0.45 g), the products isolated were guanidine hydrochloride (0.51 g), m.p. 184–186° and methyl levulinate (**10**, 0.72 g), b.p. 44–45° (15 mm) identical with an authentic sample.

Gratitude is expressed to the National Cancer Institute of Canada for their generous financial support and to the National Research Council of Canada for the award (to J.N.B.) of a Bursary.

1. J. B. Jones and J. M. Young. Can. J. Chem. This issue and references therein.
2. F. Dickens and J. Cooke. Brit. J. Cancer, **19**, 404 (1965) and references therein.
3. J. B. Jones and J. M. Young. Can. J. Chem. **44**, 1059 (1965).
4. T. C. Bruice and S. Benkovic. Bioorganic mechanisms. Vol. 1, W. A. Benjamin Inc., New York, N.Y., 1966. pp. 46–66.
5. W. C. J. Ross. Biological alkylating agents. Butterworth and Co. (Publishers) Ltd., London, 1962.
6. D. D. Perrin. Dissociation constants of organic bases in aqueous solution. Butterworth and Co. (Publishers) Ltd., London, 1965.
7. R. Lukes and Z. Linhartova. Coll. Czech. Chem. Commun. **25**, 502 (1960).
8. B. L. Vallee and J. F. Riordan. Ann. Rev. Biochem. **38**, 707 (1969).
9. J. B. Jones and J. M. Young. J. Med. Chem. **11**, 1176 (1968).

[5]At this temperature a change of crystalline form occurred which was followed by sublimation at 200°.

[6]All attempts to isolate **8** from this solution were unsuccessful owing to its extreme susceptibility to further nucleophilic attack.

Can. J. Chem. Downloaded from www.nrcresearchpress.com by 210.87.254.5 on 09/05/12
For personal use only.

Heats of mixing in the system acetone – acetic anhydride – carbon disulfide, and the corresponding binary systems, at room temperature

A. N. CAMPBELL, E. M. KARTZMARK, AND (IN PART) S. C. ANAND
Department of Chemistry, University of Manitoba, Winnipeg, Manitoba

Received September 25, 1969[1]

A simple calorimeter has been devised by means of which the heats of mixing (molar excess heats) of the following systems have been determined at 22 °C: acetone – acetic anhydride; acetone – carbon disulfide; acetic anhydride – carbon disulfide; and a pseudo-binary section of the ternary system acetone – acetic anhydride – carbon disulfide. From these data the partial molar excess heats have been obtained. All systems are very non-ideal except the system acetone – acetic anhydride, which is almost ideal.

For the partially miscible system acetic anhydride – carbon disulfide, the excess thermodynamic quantities of mixing, G^E, H^E, and TS^E, have been calculated,

Canadian Journal of Chemistry, **48**, 1579 (1970)

Introduction

In a previous paper (1), we have dealt with various physical properties of the system acetone – acetic anhydride – carbon disulfide at 25 °C, and we now report on the heats of mixing. In our previous paper, we reported that the large values of excess volume of mixing, V^E, and excess molar polarizations led us to conclude that the system acetone – carbon disulfide was very non-ideal and might be expected to exhibit a miscibility gap, an expectation which was realized at −73°. The system acetone – acetic anhydride is almost ideal, and exhibits small negative V^E values. The system acetic anhydride – carbon disulfide exhibits a solubility gap at 25°, as does the ternary system acetone – acetic anhydride – carbon disulfide; these systems are therefore very non-ideal and exhibit large, positive V^E values. In conformity with this, one would expect, and indeed it is thermodynamically necessary, that the system acetone – acetic anhydride would exhibit small negative heats of mixing and all the other systems, large positive heats of mixing. In order to deal with the ternary system, we considered it as a pseudo-binary system and we always used solutions lying on a straight line parallel to the tie-lines in the heterogeneous area (*cf.* ref. 1). As, however, the temperature during an experiment sometimes fell as much as 5° in the calorimeter, as a result of the large positive heats of mixing, and because the miscibility gap widens rapidly with fall of temperature, it was impossible for us to work along the straight line touching, or almost touching, the gap at the plait point. In other words, the fall of temperature caused the mixture in the calorimeter to become heterogeneous. We were therefore obliged to study a pseudo-binary system containing much more acetone than in our previous work (1).

Experimental

The sources and purification of our materials are described in a previous communication (1).

Our previous work (2) was done with a somewhat crude calorimeters that did not entirely prevent evaporation. We have therefore designed a new, but still very simple, calorimeter which obviates the error due to evaporation. This calorimeter is not to be compared with those of Watts, Clarke, and Glew (3) or of Bennett and Benson (4). The advantages of our calorimeter are its extreme simplicity and cheapness of construction. Figure 1 shows the construction of the calorimeter, which is in two parts, with a ground-glass joint at *e*. The right-hand compartment *A* contains a magnetic stirrer, heating coil, and tubulure for the insertion of a thermistor. One of the pure liquids is forced into the right-hand chamber, previously weighed, and the apparatus weighed again. The second liquid is placed in the left-hand chamber, *B*, which is fitted only with a thermistor well. The capacities of both chambers are about 200 cm^3. The two chambers are then connected by the ground-glass joint *e*. The air trapped in *e* is then removed by opening cocks *k* and *g*, keeping cock *h* closed, and applying suction at *k*. Both chambers are then placed in a 3-l Dewar flask, packed with cotton wool and left overnight. The amount of the second liquid in the mixture is obtained at the end of the experiment by weighing chamber *A*.

Because of the practical impossibility of obtaining completely matched thermistors, we use only one thermistor, which is transferred from one to the other chamber, to determine whether identity of temperature has been attained. Our thermistor had a sensitivity such that one small division of the chart paper of a Brown–Minneapolis recorder corresponded to 0.01°. The range of the recorder was 10 mV and the chart paper was

[1]Revision received January 19, 1970.

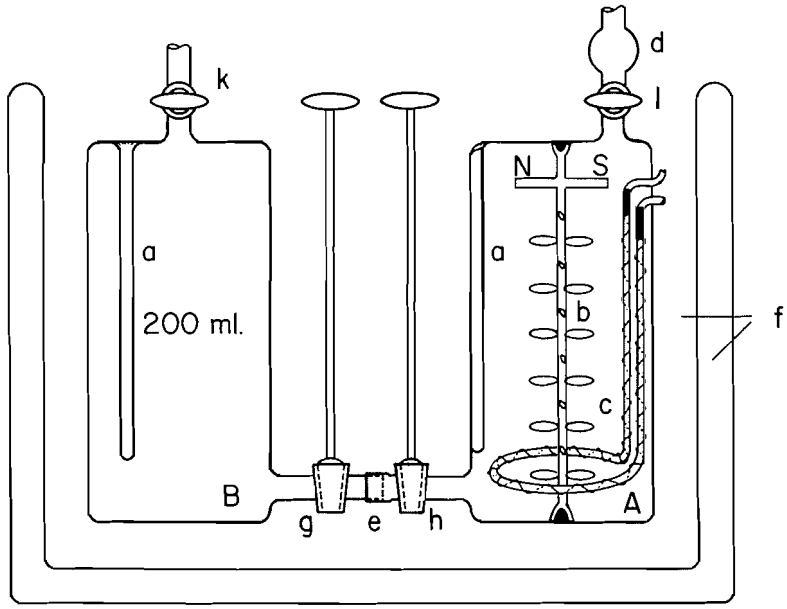

FIG. 1. Construction of the mixing calorimeter: *a*, thermistor wells; *b*, magnetic circulator; *o*, resistance coil; *d*, overflow trap; *e*, ground-glass joints to allow filling from bottom; *f*, cotton wool and 3-l Dewar.

graduated in 300 divisions; in other words, 1 division corresponded to 0.033 mV. It is unlikely that complete temperature identity will be obtained, but it is allowable to apply a small correction, knowing the difference in temperature of the two chambers (which should not exceed 0.05 °C), the specific heat, and the weight of liquid involved.

Some of the liquid in *B* is forced into *A* by air pressure until it is completely full. In the short time (10 s) required for this operation, no evaporation of the entering liquid can occur. The water equivalent of mixture and calorimeter was determined electrically, in the usual way. The temperature was returned to approximately its original value by electrical heating. The source of electrical energy was a 12-V storage battery, current was determined as the drop in potential over a standard resistance, and the potential drop over the heating coil potentiometrically. A standard 2-to-1 shunt was used to reduce the values to the potentiometer range. The radiation correction was made graphically by the usual method. The small expansion chamber *d* allows for expansion during the electrical heating; alternatively, a small bubble of vapor-saturated air can be left below the (closed) cock.

To test our apparatus, we repeatedly determined the heat of mixing of carbon tetrachloride – benzene. The variation from the literature value amounted ±3 J in 100 J, for mixtures around 0.5 mole fraction. In some of the mixtures dealt with in this paper, the heat of mixing amounted to 1500 J, and here the experimental error is very slight, but with the system acetone – acetic anhydride, where the maximum value of the heat of mixing amounts to ~25 J, the error is proportionately greater. In separate (blank) experiments, we investigated the heat developed by the action of the stirrer. This is barely detectable, and should be practically the same in the mixing and in the determination of water equivalent. It is true that the error appears in a ratio

$$\Delta H/CEt = (\Delta T_1 + dT_1)/(\Delta T_2 + dT_2)$$

but dT is neglible in comparison with ΔT. The temperature of measurement was that of the room (air-conditioned), which is fairly constant at about 22 °C.

Results and Discussion

Our direct experimental results are to be found in the Depository of Unpublished Data.[2] The heats of mixing can be represented by the Redlich and Kister equation (5), viz.

$$H^E = X_1X_2[A + B(X_1 - X_2) + C(X_1 - X_2)^2 + \cdots]$$

where X_1 equals the mole fraction of the component first named. The constants for the above equation were determined from our data, using a least-squares fit, on the computer. The program was essentially that of Myers and Scott (6). The constants, together with the σ values (deviations of the constants), are given in Table 1. While the accuracy of the experimental work permits the

[2]Photocopies may be obtained free of charge, upon request, from Depository of Unpublished Data, National Research Council of Canada, Ottawa, Canada.

Can. J. Chem. Downloaded from www.nrcresearchpress.com by 210.87.254.5 on 09/05/12
For personal use only.

TABLE 1

Calculated constants, A, B, and C, of the Redlich and Kister equation and their deviations, σ

System	Subscript 1 stands for	A		B		C	
		Value	σ	Value	σ	Value	σ
1. Acetone – acetic anhydride	Acetone	−91.38	7.34	—	—	—	—
2. Carbon disulfide – acetic anhydride	Carbon disulfide	7067	327	−1103	376	1887	814
3. Acetone – carbon disulfide	Acetone	2822	56.4	790.9	140	1633	294
4. Pseudo-binary **A** 34.15 mole % acetone, 65.85 mole % acetic anhydride ($H^E = -22$ J/mole) **B** 4.95 mole % acetone, 95.05 mole % carbon disulfide ($H^E = 260$ J/mole)	Carbon disulfide in absence of acetone	6197	159	−2884	420	—	—

use of three constants for the systems acetic anhydride – carbon disulfide and acetone – carbon disulfide, the system acetone – acetic anhydride, where the heat of mixing is very small, allows only one. In calculating the results for the pseudo-binary system, the heats of mixing of the pseudo-binary components (**A** and **B**) were added algebraically to the experimental effect. Figures 2, 3, and 4 show the plots of the Redlich and Kister equation, as continuous curves, together with the individual experimental values.

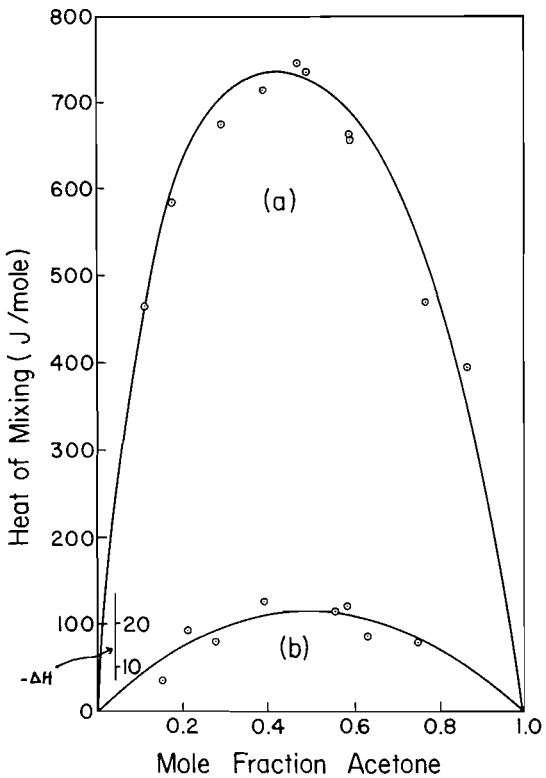

FIG. 2. Molar heat of mixing (J/mole). (*a*) Acetone – carbon disulfide. (*b*) Acetone – acetic anhydride (ΔH = negative).

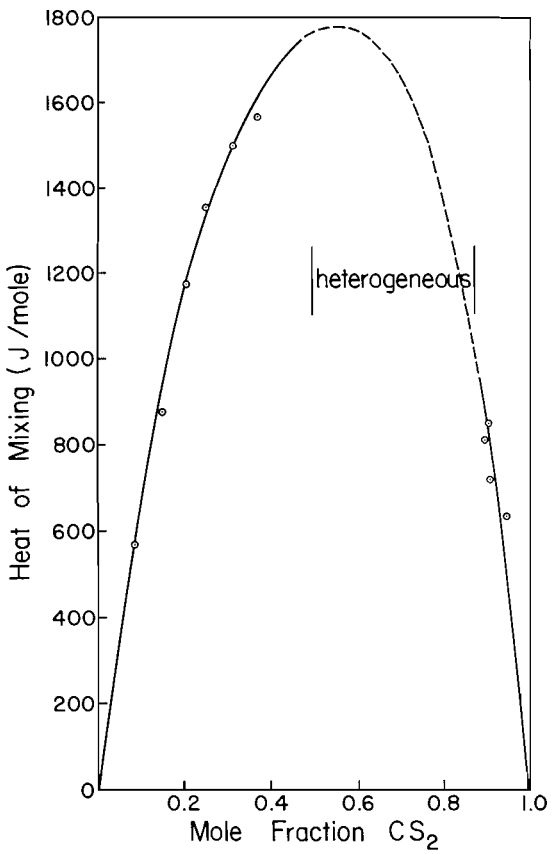

FIG. 3. Molar heat of mixing (J/mole), carbon disulfide – acetic anhydride.

Can. J. Chem. Downloaded from www.nrcresearchpress.com by 210.87.254.5 on 09/05/12
For personal use only.

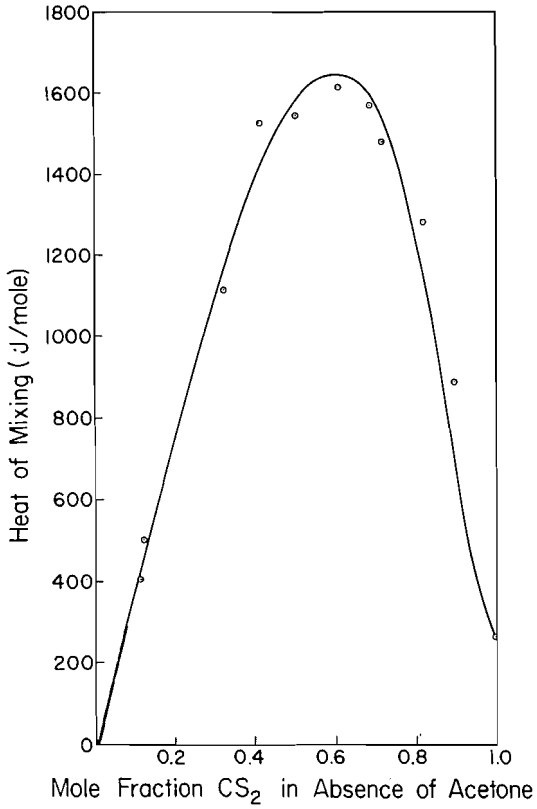

FIG. 4. Molar heat of mixing (J/mole), pseudo-binary system (A + B).

Using the Redlich and Kister constants, the partial molar excess heats can be calculated from the equations

$$\bar{H}_1^E = (1 - X_1)^2[A + B(4X_1 - 1) + C(2X_1 - 1)(6X_1 - 1) + D(2X_1 - 1)^2(8X_1 - 1)]$$

and

$$\bar{H}_2^E = X_1^2[A + B(4X_1 - 3) + C(2X_1 - 1) \times (6X_1 - 5) + D(2X_1 - 1)^2(8X_1 - 7)]$$

The results are expressed graphically in Figs. 5, 6, 7, and 8.

All heats of mixing are strongly positive, except those of the system acetone – acetic anhydride, which are very slightly negative. The results of our previous study (1) show that acetone – acetic anhydride is an almost ideal system. The treatment of Hildebrand and Scott (7), shows that a positive ΔV must be associated with a positive ΔH and conversely, and this is borne out by our

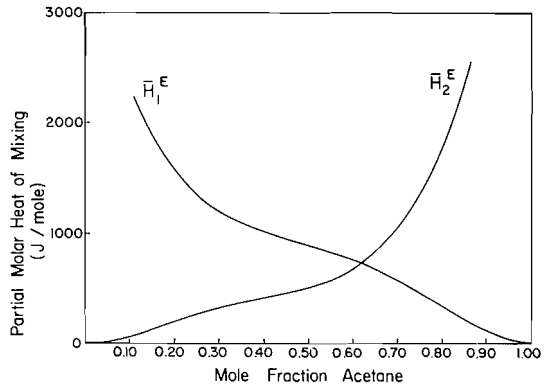

FIG. 5. Partial molar heat of mixing (J/mole), acetone – carbon disulfide.

results. A quantitative relation between these quantities cannot, however, be expected, since these liquid pairs are far from normal. The large positive H^E value for the system acetic anhydride – carbon disulfide is to be expected, since this system is known to show a miscibility gap at 25 °C, and this large positive value of H^E persists even in the presence of rather large amounts of acetone (pseudo-binary system). We were not surprised to find a large positive H^E for the system acetone – carbon disulfide, since we had previously found (1) a large excess molar polarization for this system and an extensive miscibility gap at −73 °C.

We have utilized the data of this paper on heats of mixing, together with that of a previous paper on the compositions of congruent solutions (8) to calculate G^E and TS^E for the system acetic

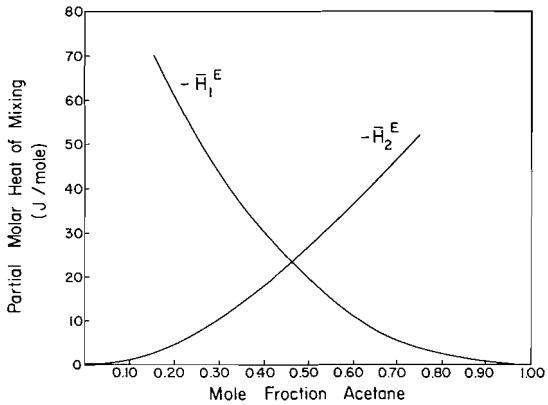

FIG. 6. Partial molar heat of mixing, acetone – acetic anhydride.

Can. J. Chem. Downloaded from www.nrcresearchpress.com by 210.87.254.5 on 09/05/12
For personal use only.

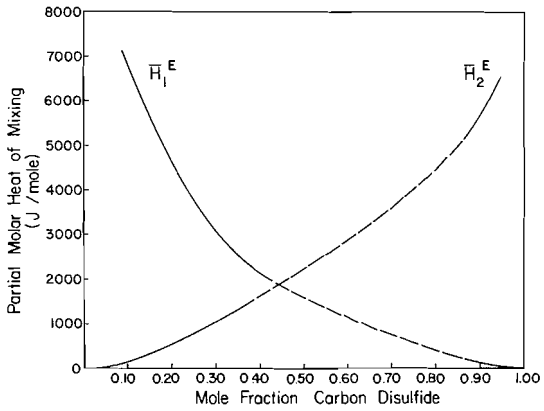

FIG. 7. Partial molar heat of mixing, carbon disulfide – acetic anhydride.

anhydride – carbon disulfide. To calculate G^E, we have used three methods (all to the third order) due to van Laar (9), to Margules (10), and to Scatchard and Hamer (11). The equations are

van Laar

$$G^E = 2.303RT\left[X_1 + X_2\left(\frac{B}{A}\right)\right]k_1(1 - k_1)$$

where

$$k_1 = \frac{1}{1 + \left(\frac{B}{A}\right)\left(\frac{X_2}{X_1}\right)}$$

Margules

$$G^E = 2.303RTX_1X_2[BX_1 + AX_2]$$

Scatchard and Hamer

$$G^E = 2.303RT\left[X_1 + \frac{X_2V_2}{V_1}\right]z_1z_2 \times\left[Bz_1\frac{V_1}{V_2} + Az_2\right]$$

All the above equations can be derived from Wohl's equation (12). We have calculated the A and B constants, using our data for congruent compositions, from equations due to the above authors and reproduced in ref. 13; these equations are too long and cumbrous to reproduce here. The symbols have their usual significance, z_1 and z_2 being the volume fractions. In the calculation of the values of A and B, we used our data for 25.3 °C. Our data for 26.4 °C give somewhat different values for A and B, but, as pointed out by Hala *et al.* (ref. 13, p. 96), the effect

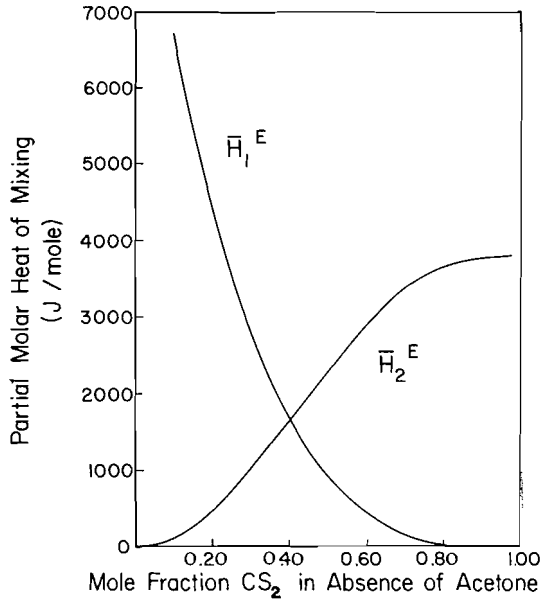

FIG. 8. Partial molar heat of mixing, pseudo-binary system (**A** + **B**).

on the calculated quantity, in this case G^E, is not great. The formulae for A and B become inaccurate in the neighborhood of the critical region and, since the critical temperature for this system is 29.7 °C, it may well be that our values of G^E, and therefore of TS^E, have only qualitative significance.

We have calculated the values of H^E from the Redlich and Kister equation (5), using the constants given in our previous paper (1). Both the G^E and H^E calculations have been made for mole fractions x_1 of 0.1, 0.2, . . . , 0.9, 0.95. Knowing G^E and H^E, TS^E follows at once. These results are reproduced in Table 2, and shown graphically in Fig. 9. For the purposes of the derived quantities and the graph, we have used the results according

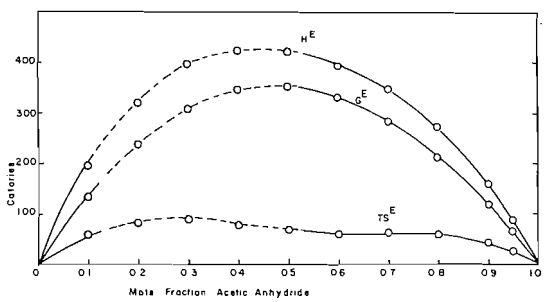

FIG. 9. Thermodynamic quantities calculated for mole fraction X_1 = 0.1, 0.2, . . . , 0.9, 0.95, at 25.3 °C.

Can. J. Chem. Downloaded from www.nrcresearchpress.com by 210.87.254.5 on 09/05/12
For personal use only.

TABLE 2

Thermodynamic functions of the system acetic anhydride – carbon disulfide, at 25.3 °C

Mole fraction acetic anhydride	G^E, cal, derived from equation of			H^E, cal	TS^E, cal§
	van Laar (9)*	Margules (10)†	Scatchard and Hamer (11)‡		
0.10	136.7	124.9	136.9	197.0	60.1
0.20	224.8	205.8	239.5	321.5	82.0
0.30	275.9	245.7	308.6	399.7	91.1
0.40	295.0	259.5	345.9	422.5	76.6
0.50	288.2	244.6	352.9	422.4	69.5
0.60	260.9	210.2	331.7	391.3	59.6
0.70	215.9	162.3	284.0	347.8	63.8
0.80	155.7	107.2	211.7	270.6	58.9
0.90	83.9	51.1	116.5	159.0	42.5
0.95	43.2	24.5	60.7	86.3	25.6

*$A = 1.207$, $B = 0.649$.
†$A = 1.093$, $B = 0.341$.
‡$A = 1.129$, $B = 0.927$.
§Calculated using value of G^E derived from Scatchard and Hamer equation.

to Scatchard and Hamer. Had we used the G^E values from the equations of van Laar or of Margules, the TS^E results would not have been greatly different (Table 2). These equations differ only in the approximations they make. According to these results, the maximum value of G^E lies at $x_1 = 0.5$. For H^E, we find a flat maximum lying between $x_1 = 0.4$ and $x_1 = 0.5$. The maximum in the TS^E curve is displaced to the left of $x_1 = 0.5$ and lies at $x = 0.3$. TS^E is positive throughout.

If one considers Scatchard's formula for the excess free energy of mixing, viz.

$$G^E = x_1 RT \ln \gamma_1 + x_2 RT \ln \gamma_2$$

it is obvious that, since G^E is positive, γ_1 and γ_2 must be greater than unity; in other words, the observed partial vapor pressures must be greater than those calculated by Raoult's law, and this is demonstrably true.

1. A. N. CAMPBELL and E. M. KARTZMARK. Can. J. Chem. **48**, 904 (1970).
2. A. N. CAMPBELL and E. M. KARTZMARK. Can. J. Chem. **47**, 619 (1969).
3. H. WATTS, E. C. W. CLARKE, and D. N. GLEW. Can. J. Chem. **46**, 815 (1968).
4. J. E. BURNETT and G. C. BENSON. Can. J. Chem. **43**, 1912 (1965).
5. O. REDLICH and A. T. KISTER. Ind. Eng. Chem. **40**, 345 (1948).
6. D. B. MEYERS and R. L. SCOTT. Ind. Eng. Chem. **55**, 431 (1963).
7. J. H. HILDEBRAND and R. L. SCOTT. The solubility of non-electrolytes. 3rd ed. Dover Publications, New York. 1964. pp. 138–139.
8. A. N. CAMPBELL and E. M. KARTZMARK. Can. J. Chem. **45**, 2433 (1967).
9. J. J. VAN LAAR. Z. Phys. Chem. Leipzig, **185**, 35 (1929).
10. M. MARGULES. S. B. Akad. Wiss. Wien. Math, Naturwiss. Kl II, **104**, 1243 (1895).
11. G. SCATCHARD and W. J. HAMER. J. Amer. Chem. Soc. **57**, 1805 (1935).
12. K. WOHL. Trans. Amer. Inst. Chem. Eng. **42**, 215 (1946).
13. E. HALA, J. PICK, V. FRIED, and O. VILIM. Vapour–liquid equilibria. 2nd ed. The Pergamon Press, Ltd., New York. 1958. pp. 94–96.

Can. J. Chem. Downloaded from www.nrcresearchpress.com by 210.87.254.5 on 09/05/12
For personal use only.

Can. J. Chem. Downloaded from www.nrcresearchpress.com by 210.87.254.42 on 09/05/12
For personal use only.

A structural model for magnesium chloride-containing melts

A. D. PELTON AND W. T. THOMPSON[1]

Department of Metallurgy and Materials Science, University of Toronto, Toronto 181, Ontario

Received October 23, 1969

A structural model for $MgCl_2$-containing melts has been developed, based upon the assumption of $MgCl_4^{2-}$ complex anions. For the five $MgCl_2$ – alkali chloride and for the $MgCl_2$–AgCl systems, the model gives quantitative, or nearly quantitative, agreement to the experimental enthalpies of mixing in all six systems; to the partial entropies of mixing of alkali chloride in the four systems for which data are available; and to both sides of the phase diagrams in the three systems for which data are available. This is accomplished with the use of only one adjustable parameter for each system, and one other adjustable parameter for all the systems taken together. The same model also quantitatively accounts for the enthalpies of mixing in the five $NiCl_2$ – alkali chloride systems.

Canadian Journal of Chemistry, 48, 1585 (1970)

Introduction

There has recently been much interest in the concept of complex ions in molten salts. The $MgCl_2$ – alkali chloride systems have received much attention as prototypes of complex-forming systems.

Flood and Urnes (1) obtained good fits to the liquidus lines on the alkali chloride-rich sides of the $MgCl_2$–NaCl, $MgCl_2$–KCl, and $MgCl_2$–RbCl systems by assuming that these melts were ideal Temkin solutions of the four ionic species: Mg^{2+}, Alk^+, Cl^-, and the tetrahedral complex anions $MgCl_4^{2-}$. Kleppa and McCarty (2) measured the enthalpies of mixing in all the $MgCl_2$ – alkali chloride systems, and in all but the LiCl case they found a very marked dip in the "interaction parameter", $\Delta H/X(1 - X)$, at $X_{MgCl_2} = 1/3$, which is the concentration corresponding to the formula $Alk_2^+MgCl_4^{2-}$. This was taken to indicate that there is a stabilization of these melts due to the formation of $MgCl_4^{2-}$ complexes. In a more recent publication (3) on the $NiCl_2$ – alkali chloride systems which exhibit the same behavior, Papatheodorou and Kleppa semi-quantitatively explain the dip at $X_{MgCl_2} = 1/3$ on the basis of the existence of these complexes.

Recent electromotive force (e.m.f.) data of Østvold (4) show that there is a most unusual behavior of the partial entropies of mixing in the $MgCl_2$ – alakali chloride systems at $X_{MgCl_2} = 1/3$. This also suggests the possibility of a stabilization of the melts due to the formation of $MgCl_4^{2-}$ complexes. The very low ionic mobility of magnesium in the $MgCl_2$–KCl system (5), can be taken to suggest the existence of complexes. Also, positive excess molar volumes of mixing peaking at about $X_{MgCl_2} = 1/3$ have been observed (6) in the $MgCl_2$–KCl system, and this is also consistent with the assumption of large tetrahedral complexes.

As the alkali cation is changed up the periodic table from Cs^+ to Li^+ in these systems, the tendency in all the experimental data (enthalpy, entropy, phase diagrams) is for the stabilization effect at $X_{MgCl_2} = 1/3$ to become less pronounced, and for ideality to be approached. This has been explained qualitatively by all authors (1–4, 7) as being indicative of the progressive dissociation of the $MgCl_4^{2-}$ complexes as the field strength of the alkali cation increases. This effect was not quantitatively taken into account, however, by Flood and Urnes (1), or by Papatheodorou and Kleppa (3) who assumed complete complexing. Neil *et al.* (7) wrote an equilibrium constant for the dissociation reaction

$$[1] \qquad MgCl_4^{2-} \rightarrow Mg^{2+} + 4Cl^-$$

They estimated equilibrium constants from their partial free energy data in the $MgCl_2$–NaCl and $MgCl_2$–KCl systems, and then proceeded to calculate partial free energies for $MgCl_2$ over the entire composition range by assuming an ideal Temkin model for the entropy, and by ignoring the enthalpy of mixing. In a qualitative way, the data could be fitted in this manner, but in view of the large enthalpies measured by Kleppa and McCarty (2), the value of the treatment is now questionable.

In the present study, a structural model for these melts will be developed, based upon the

[1]Present address: Department of Metallurgy, McGill University, Montreal, Quebec.

TABLE 1

Amounts of ionic species present in magnesium chloride – alkali chloride melts, based on the "discrete complex anion" model*

Ion	Moles of ion per mole solution	Cationic or anionic fraction, N
Mg^{2+}	$X_{MgCl_2}(1 - \alpha/2)$	$\dfrac{X_{MgCl_2}(1 - \alpha/2)}{(1 - \alpha X_{MgCl_2}/2)} = N_{Mg^{2+}}$
A^+	X_{ACl}	$\dfrac{X_{ACl}}{(1 - \alpha X_{MgCl_2}/2)} = N_{A^+}$
$MgCl_4^{2-}$	$\alpha X_{MgCl_2}/2$	$\dfrac{\alpha X_{MgCl_2}}{2(1 + X_{MgCl_2} - 3\alpha X_{MgCl_2}/2)} = N_{MgCl_4^{2-}}$
Cl^-	$X_{ACl} + 2X_{MgCl_2}(1 - \alpha)$ $= (1 + X_{MgCl_2} - 2\alpha X_{MgCl_2})$	$\dfrac{(1 + X_{MgCl_2} - 2\alpha X_{MgCl_2})}{(1 + X_{MgCl_2} - 3\alpha X_{MgCl_2}/2)} = N_{Cl^-}$

*Where A represents Cs, Rb, K, Na, Li, or Ag; X is mole fraction.

assumption of tetrahedral complex formation. This model gives quantitative, or nearly quantitative, agreement with all the experimental data. Furthermore, only one adjustable parameter for each system, and one other adjustable parameter for all the systems taken together, are required.

Discrete Complex Anion Model

Partial complexing to form $MgCl_4^{2-}$ complex anions is assumed. The concept of "complex formation" as used here is taken to mean that at any time a certain fraction of the magnesium present forms strong bonds to a fixed number of chlorines to form a "complex anion" which may be considered to be a statistical entity. The remainder of the magnesium is not preferentially bonded to any fixed number of chlorines, and for the purpose of statistical calculations exists as independent Mg^{2+} cations.

This situation is taken to hold true at all concentrations up to and including pure $MgCl_2$. Some of the magnesium in the pure molten salt exists as independent cations, and some is bonded preferentially to four chlorines to form complex $MgCl_4^{2-}$ anions.

Let n_{MgCl_2} and n_{ACl} be the number of moles of $MgCl_2$ and ACl (where A = Cs, Rb, K, Na, Li, or Ag) present in solution. Let X_{MgCl_2} and X_{ACl} be the corresponding mole fractions. That is

$$[2] \qquad X_{MgCl_2} = n_{MgCl_2}/(n_{MgCl_2} + n_{ACl}) \qquad X_{ACl} = n_{ACl}/(n_{MgCl_2} + n_{ACl})$$

Let $\alpha/2$ be the fraction of magnesium which is present in the $MgCl_4^{2-}$ complexes, and $(1 - \alpha/2)$ the fraction which is present as independent Mg^{2+} cations. In Table 1 are listed the four ionic species present, and the number of moles of each in one mole of solution.

Let $\sum X_+$ and $\sum X_-$ be the number of moles of cations and of anions, respectively, in one mole of solution. That is

$$[3] \qquad \sum X_+ = 1 - \alpha X_{MgCl_2}/2$$

$$[4] \qquad \sum X_- = 1 + X_{MgCl_2} - 3\alpha X_{MgCl_2}/2$$

The cationic or anionic fractions ($N_{Mg^{2+}}$, N_{A^+}, $N_{MgCl_4^{2-}}$, N_{Cl^-}) of the four ionic species are also listed in Table 1.

The maximum possible value of α, α_{max}, may be calculated as follows: for $X_{MgCl_2} \leqslant 1/3$, $\alpha_{max} = 2$. That is, α_{max} is the value of α for which all the magnesium is complexed. For $X_{MgCl_2} \geqslant 1/3$, α_{max} is the value of α at which all the chlorine is complexed, and may be found by setting $N_{Cl^-} = 0$. Thus

$$[5] \qquad \alpha_{max} = 2 \qquad [X_{MgCl_2} \leqslant 1/3]$$

$$\alpha_{max} = (1 + X_{MgCl_2})/2X_{MgCl_2} \qquad [X_{MgCl_2} \geqslant 1/3]$$

In pure $MgCl_2$, for instance, $\alpha_{max} = 1$.

Can. J. Chem. Downloaded from www.nrcresearchpress.com by 210.87.254.42 on 09/05/12
For personal use only.

Random Mixing Approximation

As a first approximation, random mixing was assumed. The Temkin (8) model is used, in which the Mg^{2+} and A^+ cations are randomly arranged over $\sum X_+$ cation "sites", and the Cl^- and $MgCl_4^{2-}$ anions are randomly distributed over the $\sum X_-$ anion "sites". As discussed by Førland (9), the Temkin model has been found to work much better for charge-asymmetric molten salt systems than other models such as "vacancy" models and "equivalent fraction" models. The configurational entropy of one mole of solution (which contains $\sum X_+$ moles of positive ions and $\sum X_-$ moles of negative ions) is then given by

$$[6]\quad S_r = -R(\sum X_+)(N_{Mg^{2+}} \ln N_{Mg^{2+}} + N_{A^+} \ln N_{A^+}) - R(\sum X_-)(N_{MgCl_4^{2-}} \ln N_{MgCl_4^{2-}} + N_{Cl^-} \ln N_{Cl^-})$$

where the subscript r on S_r refers to the fact that this is for the random mixing approximation.

Equation [6] may be expanded as follows

$$[7]\quad S_r = -R\left[X_{MgCl_2}(1-\alpha/2)\ln\left(\frac{X_{MgCl_2}(1-\alpha/2)}{1-\alpha X_{MgCl_2}/2}\right) + X_{ACl}\ln\left(\frac{X_{ACl}}{1-\alpha X_{MgCl_2}/2}\right) + (1 + X_{MgCl_2} - 2\alpha X_{MgCl_2})\ln\left(\frac{1 + X_{MgCl_2} - 2\alpha X_{MgCl_2}}{1 + X_{MgCl_2} - 3\alpha X_{MgCl_2}/2}\right) + (\alpha X_{MgCl_2}/2)\ln\left(\frac{\alpha X_{MgCl_2}/2}{1 + X_{MgCl_2} - 3\alpha X_{MgCl_2}/2}\right)\right]$$

If α^0 is the value of α in pure $MgCl_2$, then the molar configurational entropy, $S^0_{MgCl_2}$, of pure $MgCl_2$ is given by setting $X_{MgCl_2} = 1$ in eq. [7], with the result that

$$[8]\quad S^0_{MgCl_2} = -R\left[(2-2\alpha^0)\ln\left(\frac{2-2\alpha^0}{2-3\alpha^0/2}\right) + (\alpha^0/2)\ln\left(\frac{\alpha^0/2}{2-3\alpha^0/2}\right)\right]$$

For pure ACl, the configurational entropy, S^0_{ACl}, is zero. Assuming that vibrational contributions to the entropy of mixing may be neglected, the entropy of mixing, ΔS_r, in the random mixing approximation, is given by

$$[9]\quad \Delta S_r = S_r - X_{MgCl_2} S^0_{MgCl_2}$$

The enthalpy of mixing can be separated into two terms: a term related to the changes in number and energy of formation of the complex ions, and a term resulting from residual coulombic and polarization interactions not accounted for in the previous term. Papatheodorou and Kleppa (3) have discussed this with respect to the $NiCl_2$ – alkali chloride systems, but only for the case of total complexing, and with no account taken of the effect of the alkali cation upon the energy of formation of the complexes.

An expression for that part of the enthalpy of mixing resulting from complexing may be determined as follows. Let Δe_1 be the energy of formation of a mole of $MgCl_4^{2-}$ complexes in pure $MgCl_2$, and let Δe_2 be the energy of formation of a mole of $MgCl_4^{2-}$ complexes at infinite dilution in pure ACl,

$$[10]\quad Mg^{2+} + 4Cl^- \rightarrow MgCl_4^{2-} \quad (\text{in } MgCl_2) \quad \Delta e_1$$

$$[11]\quad Mg^{2+} + 4Cl^- \rightarrow MgCl_4^{2-} \quad (\text{in ACl}) \quad \Delta e_2$$

Δe_1 and Δe_2 are different because the energy of formation of a complex depends upon its surroundings. The major factor affecting the energy of formation of a complex anion will be the type of cation in its first coordination shell. In pure $MgCl_2$, each $MgCl_4^{2-}$ ion is surrounded only by Mg^{2+} ions. In pure ACl, each complex

Can. J. Chem. Downloaded from www.nrcresearchpress.com by 210.87.254.42 on 09/05/12
For personal use only.

Can. J. Chem. Downloaded from www.nrcresearchpress.com by 210.87.254.42 on 09/05/12
For personal use only.

is surrounded only by A^+ ions. Thus, if A^+ is a large cation such as Cs^+ with a low field strength and, therefore, good ligand donor properties, it would be expected that $\Delta e_2 < \Delta e_1$. If A^+ is a small cation like Li^+ with a high field strength, or if A^+ is an ion like Ag^+ which has a tendency to form covalent bonds, then A^+ is a poor ligand donor, and it is expected that Δe_2 would be approximately equal to, or even greater than, Δe_1.

In general, the energy of formation of a mole of complex ions should vary between Δe_1 and Δe_2, depending upon the cationic fractions of Mg^{2+} and A^+. As a first approximation, a linear variation was assumed. That is

$$[12] \qquad \Delta e = (N_{Mg^{2+}}\Delta e_1 + N_{A^+}\Delta e_2)$$

Since the pressure–volume work of mixing is negligible, the enthalpy of mixing, ΔH, may be taken to be equal to the change in internal energy on mixing. Since there are $\alpha X_{MgCl_2}/2$ moles of complexes in one mole of solution, and $\alpha^0/2$ moles in one mole of pure $MgCl_2$

$$[13] \quad \Delta H_r = \left(\frac{\alpha X_{MgCl_2}}{2}\right)(N_{Mg^{2+}}\Delta e_1 + N_{A^+}\Delta e_2) - \left(\frac{\alpha^0 X_{MgCl_2}}{2}\right)\Delta e_1$$

where the subscript r again refers to the fact that the calculation has been made on the assumption of random mixing. Let us define

$$[14] \qquad b_1 = \Delta e_1 \qquad b_2 = \Delta e_2 - \Delta e_1$$

where b_1 and b_2 are the adjustable parameters in the model, and are taken to be independent of temperature and concentration. The parameter b_1 is independent of the nature of A^+. The parameter b_2 will have a different value for each binary system. Equation [13] can be rearranged as follows

$$[15] \quad \Delta H_r = \left(\frac{X_{MgCl_2}}{2}\right)(\alpha - \alpha^0)b_1 + \left(\frac{\alpha X_{MgCl_2}N_{A^+}}{2}\right)b_2$$

It is also advantageous for the purpose of later calculations to define H_r and $H^0_{MgCl_2}$ as the portions of the molar enthalpies of the solution and of pure $MgCl_2$ resulting from the formation of the complexes. That is

$$[16] \qquad H_r = \frac{\alpha X_{MgCl_2}}{2}b_1 + \frac{\alpha X_{MgCl_2}N_{A^+}}{2}b_2$$

$$[17] \qquad H^0_{MgCl_2} = \frac{\alpha^0}{2}b_1$$

$$[18] \qquad \Delta H_r = H_r - X_{MgCl_2}H^0_{MgCl_2}$$

Much of the energy changes upon mixing due to coulombic and polarization interactions will be included in the energy of complex formation as in eq. [15]. It is difficult to determine an expression for the residual changes in coulombic and polarization interaction energies not included in eq. [15]. A major difficulty in any such calculation is the fact that anion and cation coordination numbers change with concentration in an unknown manner in these charge-asymmetric systems. A basic physical assumption of the present model is that these residual effects are small, and that the total enthalpy of mixing is well represented by eq. [15]. The justification for this assumption in the final analysis, of course, is that, as will be shown, good agreement with experiment is obtained when it is made.

Calculation of α

Equation [7] gives an expression for S_r as a function of α, and eq. [16] gives H_r as a function of α, b_1, and b_2. The value of α which actually occurs is that which minimizes the free energy of the system. That is, the value of α may be calculated from

$$[19] \quad \frac{\partial G_r(\alpha, b_1, b_2)}{\partial \alpha} = \frac{\partial H_r(\alpha, b_1, b_2)}{\partial \alpha} - T\frac{\partial S_r(\alpha)}{\partial \alpha} = 0$$

Substituting eqs. [7] and [16] into eq. [19], performing the differentiations, and rearranging terms yields the equation

$$[20] \quad \ln\left(\frac{(1 - \alpha X_{MgCl_2}/2)(1 + X_{MgCl_2} - 3\alpha X_{MgCl_2}/2)^3\alpha}{2(1 - \alpha/2)(1 + X_{MgCl_2} - 2\alpha X_{MgCl_2})^4}\right) = \frac{-b_1}{RT} - \frac{b_2 X_{ACl}}{RT(1 - \alpha X_{MgCl_2}/2)^2}$$

Can. J. Chem. Downloaded from www.nrcresearchpress.com by 210.87.254.42 on 09/05/12
For personal use only.

If values of b_1 and b_2 are chosen, eq. [20] may be solved numerically with the aid of a digital computer to give a numerical value of α. This value may then be substituted back into eqs. [7] and [16] to give numerical solutions for S_r and H_r. This method of obtaining α is, in effect, the Lagrange multiplier technique.

Similarly, for pure $MgCl_2$, α^0 may be found by setting

$$[21] \quad \frac{\partial G^0_{MgCl_2}(\alpha^0, b_1)}{\partial \alpha^0} = \frac{\partial H^0_{MgCl_2}(\alpha^0, b_1)}{\partial \alpha^0} - T\frac{\partial S^0_{MgCl_2}(\alpha^0)}{\partial \alpha^0} = 0$$

Upon differentiation and rearrangement of terms, an equation exactly the same as eq. [20] with $\alpha = \alpha^0$ and $X_{MgCl_2} = 1$ is obtained

$$[22] \quad \ln\left(\frac{(2 - 3\alpha^0/2)^3}{2(2 - 2\alpha^0)^4}\right) = \frac{-b_1}{RT}$$

This equation may be solved numerically, and the value of α^0 obtained can be substituted into eqs. [8] and [17] to give numerical solutions for $H^0_{MgCl_2}$ and $S^0_{MgCl_2}$.

Complete numerical solutions for ΔS_r and ΔH_r at all compositions can, therefore, be obtained.

It may be noted that eq. [20] may be written

$$[23] \quad \ln\left(\frac{N_{MgCl_4^{2-}}}{N_{Mg^{2+}} N_{Cl^-}{}^4}\right) = \frac{-b_1}{RT} - \frac{b_2 N_{A^+}}{RT \sum X_+}$$

The argument of the logarithm is the ionic concentration ratio for the formation of complex ions according to reaction [1]. This ratio will be a constant independent of concentration (as Neil *et al.* (7) assumed) only if $b_2 = 0$. Only in this case can the ionic activities in the "equilibrium constant" for reaction [1] be equated to ionic concentrations.

Comparison to Enthalpy of Mixing Data

Numerical solutions for ΔH_r and ΔS_r were obtained in the manner discussed above. Good fits to the enthalpy of mixing data of Kleppa and McCarty (2) were obtained with $b_1 = -3.0$ kcal, and with the values of b_2 listed in Table 2. These values of b_1 and b_2 may be seen to be quite reasonable in view of the physical significance attached to these parameters by the model.

In Fig. 1, experimentally measured "interaction parameters", $\Delta H/X_{MgCl_2}X_{ACl}$, as measured by Kleppa and McCarty (2) for six binary systems, are plotted. Curves calculated using the present random mixing approximation are also plotted. In the AgCl, LiCl, and NaCl systems, the agreement is very good. In the KCl, RbCl, and CsCl systems, the agreement is very good on the ACl sides of the systems over to about $X_{MgCl_2} = 0.6$. For higher values of X_{MgCl_2}, the calculated interaction parameters fail to "drop off" as do the experimental curves. This dropping off, however, may be explained as being due to deviations from random mixing, and this problem may be treated by the quasi-chemical approximation, as will be discussed shortly.

Recently, Papatheodorou and Kleppa (3) have measured enthalpies of mixing in the $NiCl_2$–ACl systems (where A = Li, Na, K, Rb, Cs) for concentrations from $X_{NiCl_2} = 0$ to about 0.5. The experimental interaction parameters are nearly exactly the same as those for the corresponding $MgCl_2$ systems. Experimental curves are shown in Fig. 2. Curves calculated from the present model using the parameters $b_1 = -3.0$ kcal; and $b_2 = -16.0$, -13.5, -11.0, -4.5, and -1.5 kcal for the CsCl, RbCl, KCl, NaCl, and LiCl systems, respectively, are also shown.

The Quasi-chemical Approximation

In the $MgCl_2$–KCl, $MgCl_2$–RbCl, and $MgCl_2$–CsCl systems, the substitution of an A^+ ion for an Mg^{2+} ion in the first coordination shell of an $MgCl_4^{2-}$ complex would stabilize the complex and thus would lower the enthalpy of mixing. Such a substitution would also give a negative contribution to the entropy of mixing. The actual extent to which the first coordination shell of a complex is preferentially occupied by A^+ ions is that which gives the best balance between the two

TABLE 2

Values of b_1 and b_2 which give best fit to experimental data in the six $MgCl_2$–ACl systems

System	Temperature, °C	b_2 (kcal)*
$MgCl_2$–CsCl	730	−15.0
$MgCl_2$–RbCl	730	−12.5
$MgCl_2$–KCl	800	−10.5
$MgCl_2$–NaCl	810	−5.5
$MgCl_2$–LiCl	730	−1.0
$MgCl_2$–AgCl	730	+1.5

*$b_1 = -3.0$ kcal.

Can. J. Chem. Downloaded from www.nrcresearchpress.com by 210.87.254.42 on 09/05/12
For personal use only.

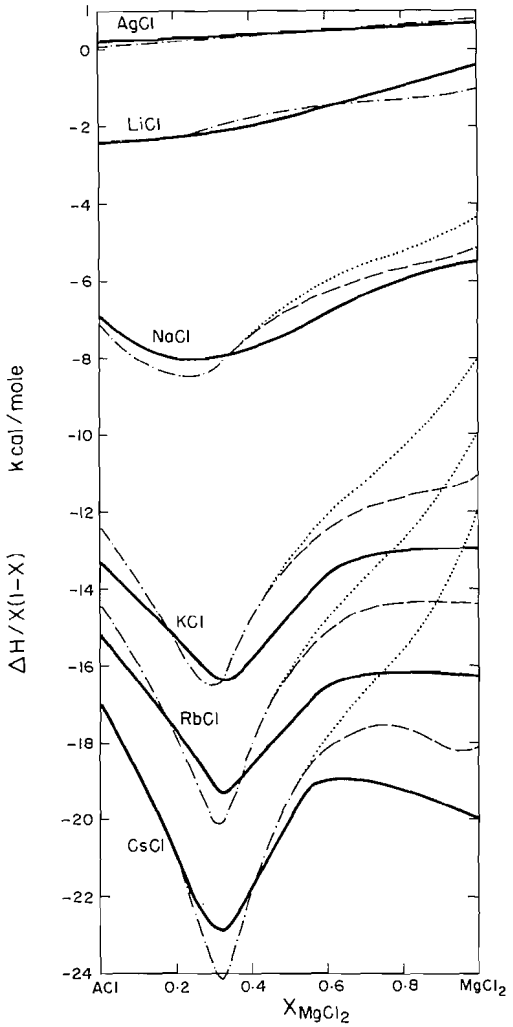

FIG. 1. Interaction parameters, $\Delta H/X_{MgCl_2}X_{ACl}$, in $MgCl_2$–ACl systems. —— from experimental data of Kleppa and McCarty (2), at temperatures as shown in Table 2; ... calculated from model using random mixing approximation; – – –, calculated from model using quasi chemical approximation with $z_- = 6$.

effects. (That is, that which minimizes the free energy.) In the KCl, RbCl, and CsCl systems, ΔH is very negative, and so a large stabilization would be achieved by the non-randomness mentioned above. Therefore, this non-randomness should occur to an appreciable extent, making ΔH lower than the calculated ΔH_r for random mixing. However, on the ACl side of these systems, for $X_{MgCl_2} < 1/3$, it will be shown later that the model predicts that α is nearly equal to its maximum possible value of 2. That is, virtually all the magnesium is complexed. Therefore, virtually all the cations in the first coordination sphere of a complex ion are A^+ ions anyway, and so no further stabilization due to non-randomness is possible. On the ACl side of these systems, then, ΔH_r should be a good approximation to the actual ΔH. It may be seen that these arguments qualitatively explain the observations in the KCl, RbCl, and CsCl systems.

In the NaCl, LiCl, and AgCl systems, ΔH is not so negative, and so the random mixing approximation should be quite good, even for large values of X_{MgCl_2}, as, in fact, it seems to be.

A general approach to obtain a quantitative estimate of the effect of this type of non-randomness is the quasi-chemical approximation of Guggenheim (10). The applications of this method to simple molten salt systems have been discussed by Førland (11). A variation of this approach may be applied to the present problem.

Consider the following equation, which represents the exchange of one mole of nearest-neighbor ions

$$[24]\quad (MgCl_4^{2-} - Mg^{2+})_{pair} + (A^+ - Cl^-)_{pair} \rightarrow (MgCl_4^{2-} - A^+)_{pair} + (Mg^{2+} - Cl^-)_{pair}$$

The molar energy change for this exchange is b_2/z_- where z_- is the anion coordination number. This is obvious if it is realized that b_2 is the energy change when all z_- nearest neighbors of a complex are changed from Mg^{2+} to A^+.

In the random mixture, the probability of a pair of nearest neighbors being an ($MgCl_4^{2-}$ – A^+) pair is ($N_{MgCl_4^{2-}}N_{A^+}$). In the non-random mixture, the number of such pairs is taken to be ($N_{MgCl_4^{2-}}N_{A^+} + y$) where y defines the deviation from the random distribution. The mass action law is now applied to reaction [24]. This gives

$$[25]\quad K = \frac{(N_{MgCl_4^{2-}}N_{A^+} + y)(N_{Mg^{2+}}N_{Cl^-} + y)}{(N_{MgCl_4^{2-}}N_{Mg^{2+}} - y)(N_{A^+}N_{Cl^-} - y)} = e^{-b_2/z_-RT}$$

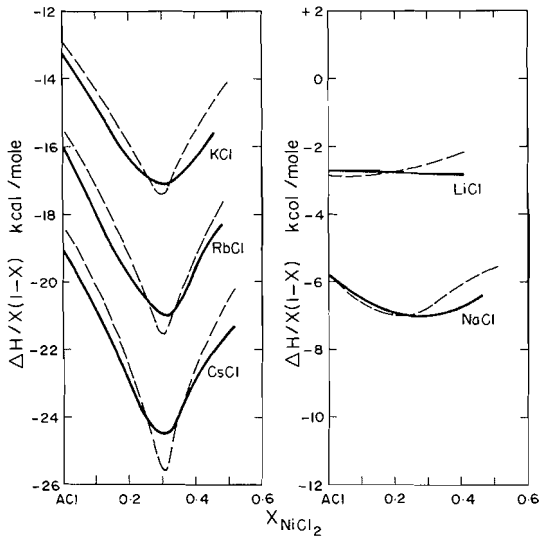

FIG. 2. Interaction parameters, $\Delta H/X_{NiCl_2}X_{ACl}$, in $NiCl_2$–ACl systems. ——, from experimental data of Papatheodorou and Kleppa at 810 °C (3); – – –, calculated from model.

If y is not too large compared to any of the products of a cationic and an anionic fraction, it has been shown by Førland (11) that an approximate solution for y is

$$[26] \quad y = -N_{A^+}N_{Mg^{2+}}N_{Cl^-}N_{MgCl_4^{2-}}\left(\frac{b_2}{z_-RT}\right)$$

In the following calculations, this equation for y was used, but calculated values of y were always checked against eq. [25]. Equation [26] was found to give satisfactory results in all cases except for small values of X_{MgCl_2} ($X_{MgCl_2} < 0.25$ or so) in the KCl, RbCl, and CsCl systems. But for low values of X_{MgCl_2} in these systems, as will be shown, the entire correction for non-randomness is negligible anyway.

The fraction of nearest neighbor cations of a complex which are A^+ ions is now seen to be $(N_{A^+} + y/N_{MgCl_4^{2-}})$, and the fraction which are Mg^{2+} ions is now $(N_{Mg^{2+}} - y/N_{MgCl_4^{2-}})$. Thus

$$[27] \quad \Delta H = \left(\frac{\alpha X_{MgCl_2}}{2}\right) \times [(N_{Mg^{2+}} - y/N_{MgCl_4^{2-}})\Delta e_1 + (N_{A^+} + y/N_{MgCl_4^{2-}})\Delta e_2] - \left(\frac{\alpha^0 X_{MgCl_2}}{2}\right)\Delta e_1$$

That is:

$$[28] \quad \Delta H = \Delta H_r + \Delta H'$$

where

$$[29] \quad \Delta H' = yb_2\left(\frac{\alpha X_{MgCl_2}}{2}\right)\left(\frac{1}{N_{MgCl_4^{2-}}}\right) = yb_2\sum X_- = -\left(\sum X_-\right)N_{A^+}N_{Mg^{2+}}N_{Cl^-}N_{MgCl_4^{2-}} \times \left(\frac{b_2^2}{z_-RT}\right)$$

$\Delta H'$ is the additional enthalpy of mixing due to non-randomness, and is always negative.

Similarly, $\Delta S'$ may be defined

$$[30] \quad \Delta S = \Delta S_r + \Delta S'$$

From the Gibbs–Helmholtz relation, it is easily shown that

$$[31] \quad \Delta S' = \Delta H'/2T = -\tfrac{1}{2}\left(\sum X_-\right)N_{A^+}N_{Mg^{2+}}N_{Cl^-}N_{MgCl_4^{2-}} \times \left(\frac{b_2^2}{z_-RT^2}\right)$$

$\Delta S'$ is also always negative.

Equations [29] and [31] may be used directly to account for the non-randomness. To be strictly correct, however, it must be noted that the non-randomness affects the value of α. That is

$$[32] \quad \frac{\partial G}{\partial \alpha} = \left(\frac{\partial H}{\partial \alpha} - T\frac{\partial S}{\partial \alpha}\right) = \left(\frac{\partial H_r}{\partial \alpha} - T\frac{\partial S_r}{\partial \alpha}\right) + \left(\frac{\partial(\Delta H')}{\partial \alpha} - T\frac{\partial(\Delta S')}{\partial \alpha}\right) = 0$$

Analytical expressions for $\partial(\Delta H')/\partial\alpha$ and $\partial(\Delta S')/\partial\alpha$ are easily calculated. The final result is that there is an additional small, but rather complicated, term on the right-hand side of eq. [20]. This extra complication can be shown to produce negligible difference in the final result, and is probably meaningless anyway in view of the oversimplified nature of the quasi-chemical approximation. In the following calculations, the correction was employed, however, for the sake of completeness.

Can. J. Chem. Downloaded from www.nrcresearchpress.com by 210.87.254.42 on 09/05/12
For personal use only.

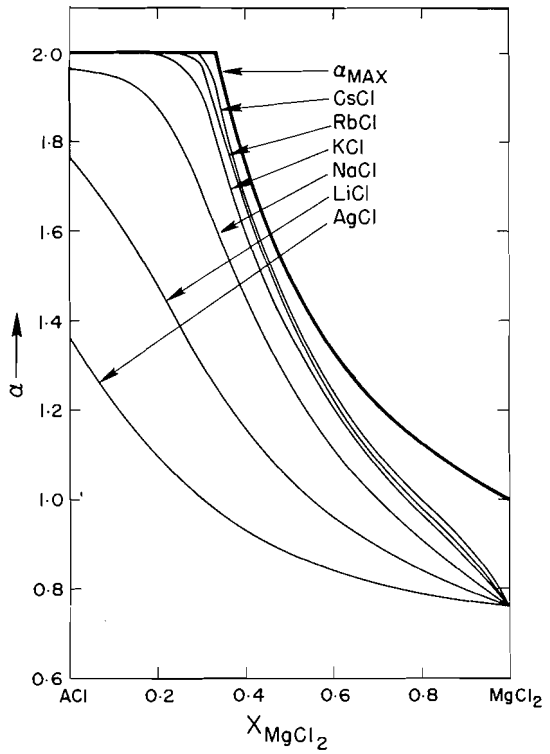

FIG. 3. Plot of α vs. composition, using b_1 and b_2 parameters from Table 2 and $z_- = 6$.

The only additional adjustable parameter introduced by the quasi-chemical approximation is z_-. A reasonable value for z_- is probably about $z_- = 6$. Using $z_- = 6$ and the same parameters b_1 and b_2 as in Table 2, the interaction parameters were recalculated. Results are shown in Fig. 1. It is seen that for the AgCl, LiCl, and NaCl systems, negligible difference from the random mixing case has occurred. To an increasingly greater extent in the KCl, RbCl, and CsCl systems, the quasi-chemical approximation has accounted for the "dropping off" of the curves at large values of X_{MgCl_2}, while leaving the curves essentially unchanged for small values of X_{MgCl_2}. The results are thus in agreement with the qualitative predictions made earlier. (For the $NiCl_2$–ACl systems shown in Fig. 2, the correction for non-randomness made negligible difference in the ACl-rich composition range where $X_{NiCl_2} < 0.5$, where measurements were available.)

The curves were recalculated for $z_- = 4$, 8, and 10. It was found that the results were reasonably insensitive to the choice of z_- over this range. Undoubtedly, z_- varies with concentration. It is impossible to say exactly what effect this has upon the calculations. However, it seems reasonable to presume that this would not qualitatively affect the predictions greatly.

The entire quasi-chemical correction for non-randomness is, of course, fraught with many such approximations. However, it is meant only to explain small second-order effects, and it is presented here as only a qualitative explanation of the observed trends.

In Fig. 3, the calculated values of α for the six systems are plotted vs. composition for the case where $z_- = 6$. A similar plot for the random mixing case showed negligible difference for the AgCl, LiCl, and NaCl systems, and a very slight difference for the KCl, RbCl, and CsCl systems at larger values of X_{MgCl_2}. Also shown in Fig. 3 is a plot of α_{max} from eq. [5]. There are several noteworthy features of this plot. Firstly, α^0 for pure $MgCl_2$ is about 0.75, which means that 3/4 of the chlorine and 3/8 of the magnesium in pure $MgCl_2$ is complexed. Secondly, in the KCl, RbCl, and CsCl systems, virtually complete complexing occurs for $X_{MgCl_2} < 1/3$, but in the NaCl system there is marked dissociation of the complexes even at very low values of X_{MgCl_2}. Thirdly, even in the AgCl system in which b_2 is positive and ΔH is nearly ideal, α nevertheless is seen to increase significantly with added ACl.

Comparison to Partial Entropy Data

Østvold (4) has recently measured the partial free energies of mixing of ACl in the NaCl, KCl, RbCl, and CsCl systems using e.m.f. concentration cells with glass membranes. Using these free energies and the partial enthalpies of mixing calculated from Kleppa and McCarty's data (2), Østvold calculated the partial entropies of mixing of ACl in these systems. His results are shown in Fig. 4. The ideal partial entropies of mixing, $-R \ln X_{ACl}$, are also shown. Very unusual behavior is seen near $X_{MgCl_2} = 1/3$ in all but the NaCl system.

Partial entropies of mixing were calculated using the present model and using the values of b_1 and b_2 in Table 2. (It was found that the best way to calculate partial entropies of mixing was to do so "graphically" on the computer from the calculated integral entropy of mixing curves, since the analytical formula for $\Delta\bar{S}_{ACl}$ turned out to be quite unwieldy.) Calculated curves are also

Can. J. Chem. Downloaded from www.nrcresearchpress.com by 210.87.254.42 on 09/05/12
For personal use only.

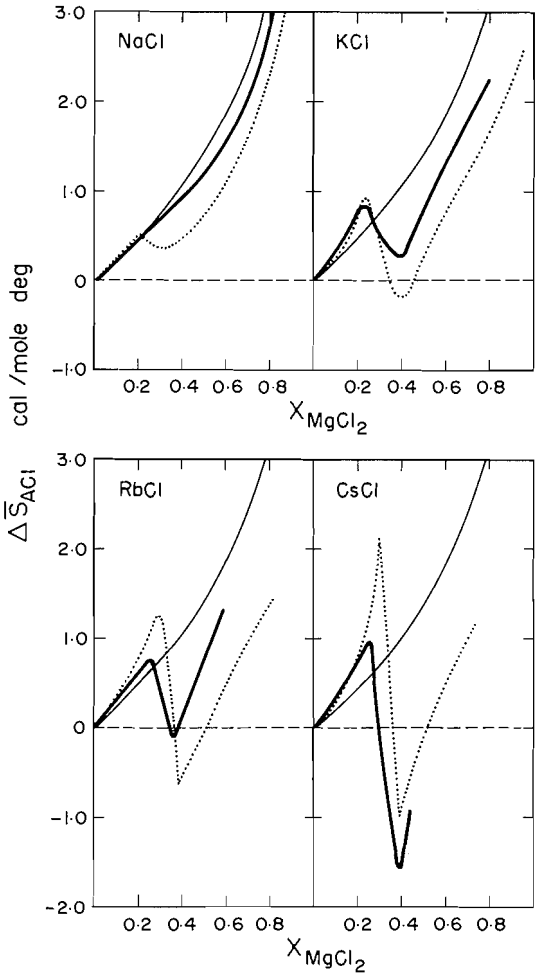

FIG. 4. Partial molar entropies of mixing of ACl in $MgCl_2$–ACl systems. ——, from experimental data of Østvold (4); ..., calculated from model; ——, ideal curves.

shown in Fig. 4. There was negligible difference between the random-mixing and the non-random cases over the composition range of interest. The fits are seen to be very good in all cases.

Partial free energies of mixing of $MgCl_2$ in some of the systems have been measured by Neil *et al.* (7) using formation cells, and by Markov *et al.* (12) using both concentration cells and formation cells. The two sets of data are in poor agreement with one another and it is difficult to assess the errors in partial entropies calculated from these data. The experimental partial entropies and those calculated on the basis of the present model are in good qualitative agreement, however. The general tendency is for the calculated values to be somewhat less positive than the experimental.

Comparison to Phase Diagram Data

Phase diagrams for the $MgCl_2$–NaCl, $MgCl_2$–KCl, and $MgCl_2$–RbCl systems have been determined by Klemm *et al.* (13, 14). No solid solubility is evidenced anywhere in these systems, and so the van't Hoff relationship in the following form holds along the ACl and $MgCl_2$ liquidi

$$[33] \quad \Delta\bar{G}_{solvent} = -T_L \int_{T_f}^{T_L} \Delta H_f \mathrm{d}\left(\frac{1}{T}\right)$$

where $\Delta\bar{G}_{solvent}$ is the partial molar free energy of mixing of the solvent at T_L, ΔH_f is the heat of fusion of the solvent at T, T_L is the liquidus temperature, T_f is the fusion temperature of pure solvent.

Analytical expressions for $\Delta\bar{G}_{ACl}$ and $\Delta\bar{G}_{MgCl_2}$ are derived in the Appendix. Using these expressions, numerical solutions for $\Delta\bar{G}_{ACl}$ and $\Delta\bar{G}_{MgCl_2}$ could be obtained at any T_L.

Values of fusion temperatures, heats of fusion, and liquid and solid heat capacities for the alkali chlorides were taken from Blander's (15) tabulation, which is based mainly upon the measurements of Dworkin and Bredig (16). For $MgCl_2$, the data was taken from the compilation of Wicks and Block (17). The dependence of ΔH_f upon temperature was taken into account in all cases except for RbCl, for which heat capacity data are lacking.

Equation [33] could then be solved numerically to give calculated liquidi.

In Fig. 5 are shown the calculated liquidi on the ACl sides of the phase diagrams. The values of b_1 and b_2 from Table 2 were used. The effect of non-randomness was negligible in these ACl-rich solutions. Also shown in Fig. 5 are the experimental points of Klemm *et al.* (13, 14) and the ideal liquidi calculated using $\Delta\bar{G}_{ACl} = RT \ln X_{ACl}$. The fit is seen to be good in all cases, although at higher concentrations the fit to the RbCl liquidus is somewhat in error.

Flood and Urnes (1) calculated these liquidi on the assumption that $\alpha = \alpha_{max} = 2$ (i.e., complete complexing), and that $\Delta\bar{H}_{ACl} = 0$. Their fit was not too good for the NaCl case. As shown by the present model, this results from the fact that there is not complete complexing in this case. For the KCl and RbCl liquidi, Flood

Can. J. Chem. Downloaded from www.nrcresearchpress.com by 210.87.254.42 on 09/05/12
For personal use only.

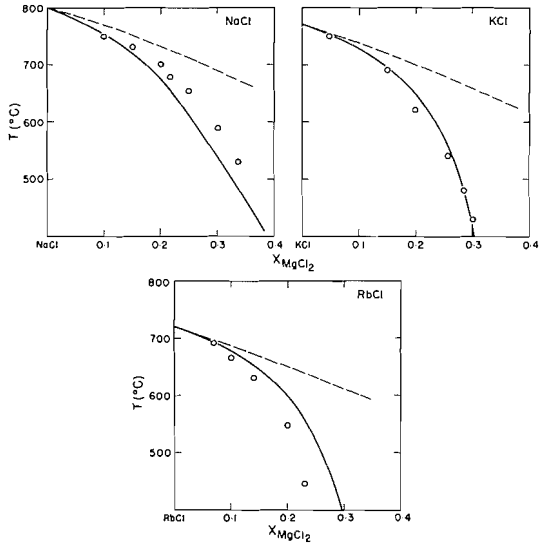

FIG. 5. ACl sides of phase diagrams of $MgCl_2$–ACl systems. Points shown are experimental, from data of Klemm *et al.* (13, 14). ——, calculated from model; – – –, ideal liquidus.

and Urnes obtained fits nearly coincident with those shown in Fig. 5. (In the RbCl case they used a heat of fusion of RbCl of 4400 cal. If the more recent value of 5670 cal (15) had been used, their calculated liquidus would have been about the same as the one calculated by the present model.) As shown in Fig. 3, the present model predicts that α is nearly equal to its maximum value of 2 up to $X_{MgCl_2} = 1/3$ in both these systems. Also, up to $X_{MgCl_2} = 0.2$, $\Delta\bar{H}_{ACl}$ is indeed very small, as shown by experiment (ref. 2) and also as predicted by the present model. This, then, explains why Flood and Urnes obtained good agreement up to $X_{MgCl_2} = 0.2$. For $X_{MgCl_2} > 0.2$, however, $\Delta\bar{H}_{ACl}$ rapidly becomes very negative (as shown both by experiment (ref. 2) and by the present theory.) At the same time, $\Delta\bar{S}_{ACl}$ drops off rapidly (4), whereas the model of Flood and Urnes predicts that $\Delta\bar{S}_{ACl}$ should continue increasing markedly with increasing X_{MgCl_2}. The agreement obtained by Flood and Urnes for $X_{MgCl_2} > 0.2$ must thus be regarded as fortuitous.

In Fig. 6 are shown the experimental liquidus points of Klemm *et al.* (13, 14) on the $MgCl_2$ sides of the three phase diagrams. Also shown are liquidi calculated using values of b_1 and b_2 from Table 2, and a value of $z_- = 6$. In the NaCl case, there was negligible difference between the random mixing and the non-random cases, but in the KCl and RbCl cases, there was a difference, the correction for non-randomness giving somewhat better fits. Also shown in Fig. 6 is the "ideal" liquidus calculated using

$$\Delta\bar{G}_{MgCl_2} = RT \ln X_{MgCl_2}$$

The fit is very good in the NaCl case, and is reasonable in the KCl and RbCl cases.

Flood and Urnes (1) also calculated these liquidi. Although their model was based upon the assumption of $MgCl_4^{2-}$ complexes, their treatment differed substantially from the present model. The liquidus calculated by Flood and Urnes for the NaCl case was not particularly good. For the KCl and RbCl cases, they obtained good agreement with experiment but only by introducing what was essentially an adjustable heat of mixing parameter for each case.

Calculations of the partial enthalpy of mixing, $\Delta\bar{H}_{MgCl_2}$, from the data of Kleppa and McCarty (2) indicate that the negative deviations from ideality in these liquidi are mainly an enthalpy, and not an entropy, effect. (That is, using the ideal partial entropy and the experimental partial enthalpies will give quite good fits to the liquidi.) The present calculations can be shown to be consistent with this. Calculated partial entropies of $MgCl_2$, $\Delta\bar{S}_{MgCl_2}$, are actually even somewhat less than ideal in this composition region. Flood and Urnes treatment, however, takes the major portion of the negative deviations

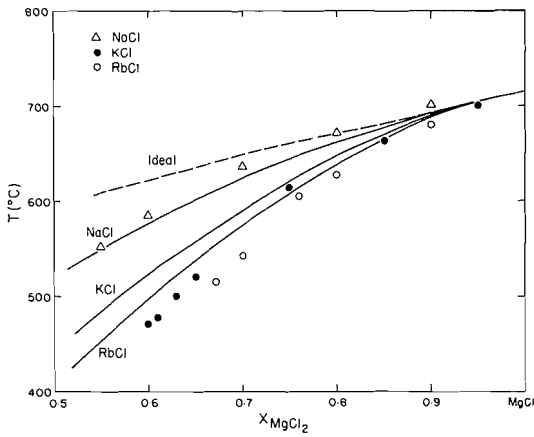

FIG. 6. $MgCl_2$ sides of phase diagrams of $MgCl_2$–ACl systems. Points shown are experimental, from data of Klemm *et al.* (13, 14). ——, calculated from model; – – –, ideal liquidus.

Can. J. Chem. Downloaded from www.nrcresearchpress.com by 210.87.254.42 on 09/05/12
For personal use only.

Can. J. Chem. Downloaded from www.nrcresearchpress.com by 210.87.254.42 on 09/05/12
For personal use only.

to be due to a positive excess entropy of mixing, and their treatment is thus not consistent with the experimental enthalpy data.

It may also be noted that the present model predicts a limiting slope at $X_{MgCl_2} = 1$ equal to the ideal slope. Flood and Urnes (1) claim that the experimental liquidus in the NaCl case exhibits this limiting slope, but that the liquidi in the KCl and RbCl cases exhibit twice this slope. This statement does not seem justified on the basis of the experimental data, however. Accurate cryoscopic data in the very dilute region could be revealing.

Discussion

It does not seem possible at present to decide which of the assumptions in the model is most responsible for the remaining discrepancies with the experimental data. Since any attempts to improve the fits will necessitate the introduction of additional adjustable variables, the validity of such attempts cannot be demonstrated.

One such correction, however, which probably has some validity and is worth mentioning, is a correction to account for the residual part of the enthalpy of mixing due to changes in coulombic interactions upon mixing not included in eq. [15]. This additional term might, to a first approximation, be expected to be of the form $\Delta H_{coulombic} = X_{MgCl_2} X_{ACl} b_3$. The parameter b_3 would be expected to be of the order of -2 or -3 kcal, which is about the value of interaction parameters found for mixtures of simple ionic salts. For example, in the $MgCl_2$–RbCl system with $b_1 = -3.0$, $b_2 = -10.5$, and $b_3 = -3.0$ kcal, substantial improvements in the fits with all the experimental data (enthalpy, entropy, phase diagrams) were found. The correction is small, however, and the data are well fitted without the necessity of introducing the additional adjustable parameter.

The fact that a structural model explains experimental data does not, of course, prove that the physical assumptions of the model are correct. Possibly the data could be explained on the basis of other physical assumptions. It must be left to the reader to decide, on the basis of the accuracy of the fits, the diversity and complexity of the data explained, and the number of assumptions and adjustable parameters required, how much reality he wishes to attach to the model.

Summary

A structural model for $MgCl_2$–ACl liquid solutions (where A = alkali or Ag) has been proposed. A fraction, $\alpha/2$, of the magnesium is considered to form strong bonds to four chlorines to form the complex anions, $MgCl_4^{2-}$, which may be considered as statistical entities. This occurs at all concentrations up to and including pure $MgCl_2$. Entropies are calculated using the Temkin model in which Cl^- and $MgCl_4^{2-}$ anions are randomly distributed over anion "sites", and Mg^{2+} and A^+ cations are randomly distributed over cation "sites". The enthalpies of mixing are considered to result mainly from the changes in number and energy of formation of the complexes. The energy of formation of a complex is taken to vary linearly as the cationic fraction of Mg^{2+} and A^+ ions in the first coordination shell of the complex.

One overall adjustable parameter related to the energy of formation of complexes in pure $MgCl_2$; and one other adjustable parameter for each binary system, related to the stabilization of the complexes by added A^+ ions, are all that are required in the model. These parameters are independent of concentration and temperature. The value of α actually assumed by the melt may be calculated as that which minimizes the free energy. Thus, no "equilibrium constant" is required. The quasi-chemical theory may be used to yield a small correction for non-randomness. This introduces no further adjustable parameters except an anion coordination number. The results are quite insensitive to the value of this coordination number.

The model yields quantitative or nearly quantitative fits to the enthalpies of mixing, partial entropies of mixing, and to both sides of the phase diagrams for all $MgCl_2$–ACl systems for which data are available, and also to the enthalpies of mixing in the $NiCl_2$–alkali chloride systems.

The authors wish to thank Professor S. N. Flengas for his encouragement and for many helpful discussions. Maintenance fellowships from Shell Canada and from the National Research Council of Canada are also gratefully acknowledged.

1. H. Flood and S. Urnes. Z. Elektrochem. **59**, 834 (1955).
2. O. J. Kleppa and F. G. McCarty. J. Phys. Chem. **70**, 1249 (1966).

3. G. N. PAPATHEODOROU and O. J. KLEPPA. J. Inorg. Nucl. Chem. In press.
4. T. ØSTVOLD. Acta Chem. Scand. **23**, 688 (1969).
5. Y. V. BAIMAKOV and B. I. HALFIN. Tsvetn. Metal. **8**, 81 (1939).
6. J. N. REDING. J. Chem. Eng. Data, **10**, 1 (1965).
7. D. E. NEIL, H. M. CLARK, and R. H. WISWALL. J. Chem. Eng. Data, **10**, 21 (1965).
8. M. TEMKIN. Acta Physicochim. URSS, **20**, 411 (1945).
9. T. FØRLAND. Norg. Tek. Vitenskapsakad. Ser. 2, **4**, (1957).
10. E. A. GUGGENHEIM. Mixtures. Oxford University Press, N.Y. (1952).
11. T. FØRLAND. *In* Fused salts. B. Sundheim (Editor). McGraw-Hill Book Co., Inc., New York. 1964. pp. 89–90.
12. B. F. MARKOV, I. K. DELIMARSKII, and I. D. PANCHENKO. Zh. Fiz. Khim. **29**, 51 (1955).
13. W. KLEMM and P. WEISS. Z. Anorg. Allg. Chem. **245**, 279 (1940).
14. W. KLEMM, K. BEYERSDORFER, and J. ORYSCHKEWITSCH. Z. Anorg. Allg. Chem. **256**, 25 (1948).
15. M. BLANDER. *In* Molten salt chemistry. M. Blander (Editor). Interscience Publishers, Inc., New York. 1964. p. 141.
16. A. S. DWORKIN and M. A. BREDIG. J. Phys. Chem. **64**, 269 (1960).
17. C. E. WICKS and F. E. BLOCK. U.S. Bur. Mines Bull. 605 (1963).

Appendix

In this Appendix, analytical expressions for $\Delta\bar{G}_{ACl}$ and $\Delta\bar{G}_{MgCl_2}$ will be calculated. If ΔG is the extensive integral free energy of mixing, then

[A-1] $$\Delta\bar{G}_{ACl} = \left(\frac{\partial(\Delta G)}{\partial n_{ACl}}\right)_{n_{MgCl_2}} = \left(\frac{\partial(\Delta G)}{\partial n_{ACl}}\right)_{n_{MgCl_2},\alpha} + \left(\frac{\partial(\Delta G)}{\partial \alpha}\right)_{n_{ACl},n_{MgCl_2}} \cdot \left(\frac{\partial \alpha}{\partial n_{ACl}}\right)_{n_{MgCl_2}}$$

But, by eq. [19]

[A-2] $$(\partial(\Delta G)/\partial\alpha)_{n_{ACl},n_{MgCl_2}} = 0$$

Therefore

[A-3] $$\Delta\bar{G}_{ACl} = \left(\frac{\partial(\Delta G)}{\partial n_{ACl}}\right)_{n_{MgCl_2},\alpha}$$

and by a similar argument

[A-4] $$\Delta\bar{G}_{MgCl_2} = \left(\frac{\partial(\Delta G)}{\partial n_{MgCl_2}}\right)_{n_{ACl},\alpha}$$

That is, the derivatives of the integral property may be taken at constant α.

Let $\Delta\bar{G}_{ACl(r)}$ and $\Delta\bar{G}_{MgCl_2(r)}$ be the partial molar free energies of mixing calculated on the assumption of random mixing, and let $\Delta\bar{G}'_{ACl}$ and $\Delta\bar{G}'_{AgCl_2}$ be the corrections resulting from non-randomness. That is

[A-5] $$\Delta\bar{G}_{ACl} = \Delta\bar{G}_{ACl(r)} + \Delta\bar{G}'_{MCl}$$
$$\Delta\bar{G}_{MgCl_2} = \Delta\bar{G}_{MgCl_2(r)} + \Delta\bar{G}'_{MgCl_2}$$

Using the relationship

[A-6] $$\Delta G = (n_{ACl} + n_{MgCl_2})[(\Delta H_r + \Delta H') - T(\Delta S_r + \Delta S')]$$

the differentiations in eqs. [A-3] and [A-4] may be performed with the results shown below

[A-7] $$\Delta\bar{G}_{ACl(r)} = \frac{\alpha N_{Mg^{2+}}{}^2 b_2}{2(1-\alpha/2)} + RT(\ln N_{A^+} + \ln N_{Cl^-})$$

[A-8] $$\Delta\bar{G}_{MgCl_2(r)} = \frac{(\alpha-\alpha^0)b_1}{2} + \frac{\alpha N_{A^+}{}^2 b_2}{2} + RT[(1-\alpha/2)\ln N_{Mg^{2+}} + (2-2\alpha)\ln N_{Cl^-} + (\alpha/2)\ln N_{MgCl_4{}^{2-}}] + TS^0_{MgCl_2}$$

[A-9] $$\Delta\bar{G}'_{ACl} = -\frac{\alpha X_{MgCl_2} N_{Mg^{2+}} b_2{}^2}{4z_- RT} \cdot \left[\frac{N_{A^+} N_{MgCl_4{}^{2-}}}{\sum X_-} + \frac{N_{Cl^-}(N_{Mg^{2+}} - N_{A^+})}{\sum X_+}\right]$$

Can. J. Chem. Downloaded from www.nrcresearchpress.com by 210.87.254.42 on 09/05/12
For personal use only.

$$[A\text{-}10] \qquad \Delta\bar{G}'_{MgCl_2} = -\frac{\alpha N_{A^+} N_{Mg^{2+}} b_2^{\,2}}{4z_- RT} \cdot \left[2N_{A^+} N_{Cl^-} - \frac{X_{ACl} N_{MgCl_4^{2-}}}{\sum X_-} \right]$$

It may be noted that analytical expressions for partial molar enthalpies and entropies are not as easily calculated as the partial free energy expressions, since relationships analogous to eq. [A-2] cannot be written for enthalpies and entropies.

Can. J. Chem. Downloaded from www.nrcresearchpress.com by 210.87.254.42 on 09/05/12
For personal use only.

Can. J. Chem. Downloaded from www.nrcresearchpress.com by 210.87.254.6 on 09/05/12
For personal use only.

Etude quantitative des réactions d'ozonolyse. XIII. Sur la structure du zwitterion de Criegee

G. KLUTSCH, J. GRIGNON, J. RENARD, ET S. FLISZÁR
Département de Chimie, Université de Montréal, Montréal, Québec

Reçu le 3 décembre 1969

Les hydroxyperoxydes $R_2CH(OOR_1)OH$ avec $R_1 = CH_3$, C_2H_5; $R_2 = CH_3$, $i\text{-}C_3H_7$, examinés en polarographie, peuvent être facilement reconnus à côté de leurs alcoxyhydroperoxydes $R_2CH(OOH)OR_1$ isomères. Ces hydroxyperoxydes ne se retrouvent pas parmi les produits d'ozonolyse, en présence de méthanol ou d'éthanol, du *trans* méthyl-4 pentène-2. On en conclut à la non-participation de la structure zwitterionique $\rangle C(O^+)O^-$ au mécanisme de formation des ozonides.

The hydroxyperoxides $R_2CH(OOR_1)OH$ ($R_1 = CH_3$, C_2H_5; $R_2 = CH_3$, $i\text{-}C_3H_7$) and their isomeric alkoxyhydroperoxides $R_2CH(OOH)OR_1$ can be differentiated by their polarographic behavior. These hydroxyperoxides are not produced in the ozonolysis of *trans* 4-methyl-2-pentene in the presence of methanol or ethanol. It is concluded that the zwitterionic structure $\rangle C(O^+)O^-$ does not participate in the mechanism of ozonide formation.

Canadian Journal of Chemistry, 48, 1598 (1970)

D'après le mécanisme d'ozonolyse proposé par Criegee et Wenner (1), l'ozonide primaire (trioxolane-1,2,3) engendré par l'addition d'une molécule d'ozone sur une double liaison carbone–carbone se scinde en zwitterion (**1**–**3**) et composé carbonylé. A côté des structures (**1**–**2**) généralement admises pour les zwitterions, Criegee (2) a aussi envisagé la structure **3**.

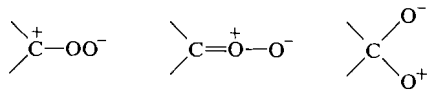

1 **2** **3**

(*syn* et *anti*)

De récents travaux ont montré que la stoechiométrie de la réaction procède bien selon le schéma de Criegee en établissant dans de nombreux cas (3–5), que l'ozonolyse d'une mole d'oléfine, en présence de méthanol ou d'éthanol, conduit à la formation d'une mole de mélange d'alcoxyhydroperoxydes (**4***a*, *b*), issus de **1** ↔ **2**, et d'une mole du mélange d'aldéhydes (eq. [1]).

La publication de nouvelles vues concernant le mécanisme de formation des ozonides a induit divers laboratoires à étudier l'incorporation d'oxygène-18 dans les ozonides produits lors d'ozonolyses d'oléfines en présence d'aldéhyde-^{18}O (6, 7). D'une part l'ozonolyse d'une série de phényléthylènes en présence d'aldéhyde benzoïque-^{18}O a montré sans ambiguïté que l'oxygène aldéhydique est incorporé exclusivement dans la position éther des ozonides produits, en accord avec le mécanisme de Criegee (6); la non-participation de la forme **3** du zwitterion est clairement démontrée dans ce cas, car l'intervention d'une telle structure aurait dû conduire à une incorporation d'oxygène aldéhydique (^{18}O) en position peroxyde dans le cycle ozonique. D'autre part, l'ozonolyse du *trans* diisopropyléthylène en présence d'acétaldéhyde semble conduire à une incorporation partielle de l'oxygène-18 en position peroxyde (7). Ce résultat est interprété par Story *et al.* en faveur du mécanisme, résumé dans le schéma 1, proposé par ces auteurs (8). Un autre mécanisme a cependant été récemment envisagé, capable d'expliquer l'incorporation d'oxygène aldéhydique en position peroxyde dans l'ozonide final (9).

En raison de l'intérêt des techniques de marquage avec l'oxygène-18 en relation avec les études mécanistiques sur l'ozonolyse, il apparaît souhaitable que la non-participation de la struc-

[1]

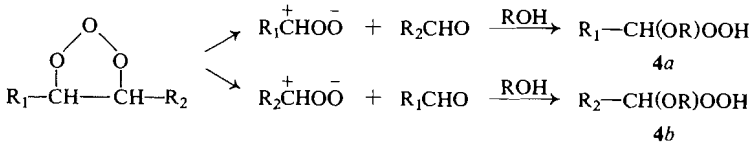

4*a*

4*b*

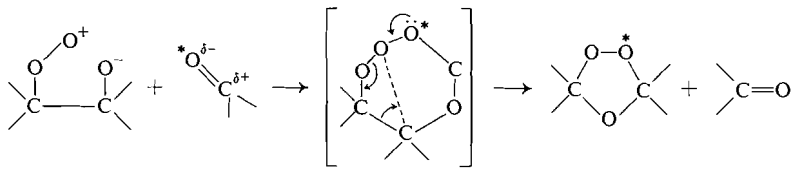

SCHÉMA 1

ture **3** soit clairement établie. Bien que n'ayant pas joui de la faveur des divers auteurs, cette forme n'a pas été réfutée de manière convaincante.

Le principe du présent travail peut être résumé comme suit: par analogie avec la réaction aboutissant à la formation d'alcoxyhydroperoxyde à partir de zwitterion et d'alcool, on suppose que la présence (parmi les produits d'ozonolyse) d'un zwitterion de structure **3** se manifesterait par la formation d'hydroxyperoxyde **5** (eq. [2]). L'absence d'hydroxyperoxyde **5** parmi les produits d'ozonolyse, en présence d'alcool, serait, dès lors, interprétée en termes de la non-participation d'une structure **3** au mécanisme d'ozonolyse.

[2] 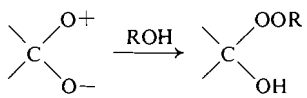

5

Propriétés des hydroxyperoxydes

Les hydroxyperoxydes

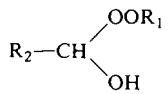

$R_1 = CH_3, C_2H_5$
$R_2 = CH_3, i\text{-}C_3H_7$

ont été préparés et identifiés par leurs spectres de résonance magnétique nucléaire (r.m.n.) (tableau 1).

Les spectres r.m.n. ne permettent cependant pas de différencier de façon certaine les alcoxyhydroperoxydes **4** des hydroxyperoxydes **5**. En raison de la faible solubilité de ces composés dans le tétrachlorure de carbone, les spectres r.m.n. ont été étudiés en solution dans le chloroforme deutéré. Dans ce solvant les protons des groupements OH et OOH sont rapidement échangés et ne peuvent donc pas être observés dans les spectres. Par ailleurs, les protons qui correspondent aux groupements OR et OOR ne sont séparés que de 0.1 p.p.m., ce qui rend l'interprétation des spectres malaisée.

La polarographie s'étant révélée un moyen efficace pour distinguer les hydroxyperoxydes de leurs isomères, les alcoxyhydroperoxydes, une brève étude de la réduction polarographique des hydroxyperoxydes a été effectuée. Les alcoxyhydroperoxydes ont déjà fait l'objet d'une récente étude (5) polarographique.

Processus d'électrode

Par analogie avec le mécanisme de réduction à l'électrode des alcoxyhydroperoxydes (5) et des hydroperoxydes d'alcoyle (10), le mécanisme suivant, impliquant 2 électrons lors du processus de réduction à l'électrode, paraît raisonnable (schéma 2).

L'examen des oscillo-polarogrammes $i = f(E)$ montre bien, pour tous les hydroxyperoxydes

TABLEAU 1

Spectres de résonance magnétique nucléaire et températures d'ébullition de quelques hydroxyperoxydes

			Température d'ébullition (°C/mm Hg)	
R_1	R_2	Déplacements chimiques (δ)*	Trouvé	Litt.†
CH_3	CH_3	3.90 (s); 5.35 (q); 1.2 (d)	42–44/55	25–27/17
	$i\text{-}C_3H_7$	3.90 (s); 4.95 (d); 1.8 (m); 1.0 (d)	42–44/50	—
C_2H_5	CH_3	4.10 (q); 5.35 (q); 1.2 (d); 1.0 (t)	36–38/18	48–52/65
	$i\text{-}C_3H_7$	4.10 (q); 4.95 (d); 1.8 (m); 1.0‡	45–46/43	—

*s = Singulet, d = doublet, t = triplet, q = quadruplet et m = multiplet.
†Voir les réfs. 20 et 21, indiquées dans la partie expérimentale.
‡On distingue, à côté d'un doublet, également un triplet qui lui est presque superposé, à δ 1.0.

Can. J. Chem. Downloaded from www.nrcresearchpress.com by 210.87.254.6 on 09/05/12
For personal use only.

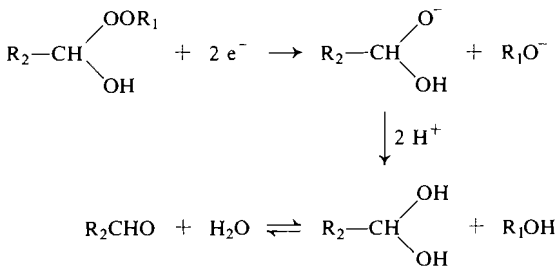

SCHÉMA 2

étudiés, l'irreversibilité complète du processus d'électrode, tout au moins en ce qui concerne le phénomène *global* de la réduction polarographique. On ne saurait, cependant, conclure à partir de ces données expérimentales à l'irreversibilité complète du processus d'électrode lui-même. Ce résultat est confirmé par l'analyse logarithmique des courbes intensité-potentiel au moyen de l'équation

$$E = E_{1/2} - (RT/\alpha nF) \ln [I/(I_l - I)]$$

Pour les hydroxyperoxydes avec $R_1 = C_2H_5$ on observe deux droites. Le coefficient de transfert, α, qui a été calculé à partir des valeurs des pentes des droites est, compte tenu des deux électrons mis en jeu, de 0.06. Par contre, avec les hydroxyperoxydes où $R_1 = CH_3$ on observe une légère courbure (Fig. 1) qui permet néanmoins de conclure à une irreversibilité, du moins partielle, du processus d'électrode.

Influence du pH

L'influence du p*H* sur les potentiels de demi-vague et les courants limites a été étudiée, au moyen du Tampon McIlvaine, dans le domaine de p*H* compris entre 3 et 8. Le p*H* n'a pratiquement pas d'effet sur le potentiel de demi-vague. En effet, par rapport au potentiel de demi-vague observé au p*H* 7, les variations des potentiels n'atteignent que 0.1 V aux limites de p*H* considérées (p*H* 3 et 8). La sensibilité au p*H* est, par contre, bien marquée en ce qui a trait aux intensités des courants limites (Fig. 2). Dans le tampon McIlvaine, les intensités des courants limites accusent une diminution de l'ordre de 25 à 30 % aux p*H* 3 et 8, par rapport aux intensités observées au p*H* 7. Les polarogrammes des hydroxyperoxydes enregistrés à p*H* 7, après un repos de plusieurs heures dans le tampon McIlvaine, n'accusent pas de modification.

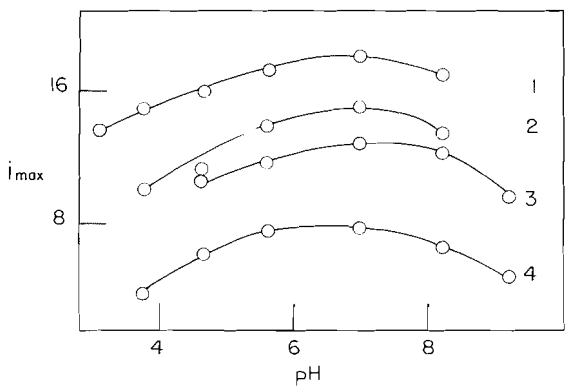

FIG. 2. Influence du p*H* sur l'intensité du pic polarographique, dans le tampon McIlvaine, à 23 °C. (1) $R_1 = C_2H_5$, $R_2 = i\text{-}C_3H_7$; (2) $R_1 = C_2H_5$, $R_2 = CH_3$; (3) $R_1 = R_2 = CH_3$; (4) $R_1 = CH_3$, $R_2 = i\text{-}C_3H_7$.

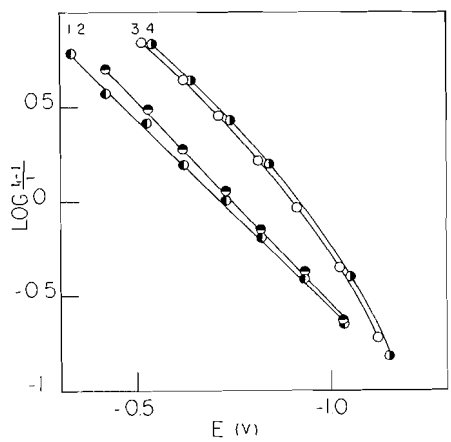

FIG. 1. Courbes intensité-potentiel: $\log[(I_l - I)/I]$ vs. potentiel *E*. (1) $R_1 = C_2H_5$, $R_2 = i\text{-}C_3H_7$; (2) $R_1 = C_2H_5$, $R_2 = CH_3$; (3) $R_1 = CH_3$, $R_2 = i\text{-}C_3H_7$; (4) $R_1 = CH_3$, $R_2 = CH_3$. McIlvaine, p*H* 7, 25°.

Influence de la vitesse de balayage

Les courants maximums des oscillo-polarogrammes $i = f(E)$ ont été étudiés pour des vitesses de balayage comprises entre 1.0 et 20.0 V/s. Ainsi que l'indique la Fig. 3, une relation linéaire est obtenue, pour tous les hydroxyperoxydes examinés, entre i_{max} et la racine carrée de la vitesse de balayage. D'après Delahay (11) et Matsuda et Ayabe (12), un tel comportement est caractéristique pour un courant de diffusion d'un processus irréversible

$$i_{max} = k_2 \, qn(\alpha n_a)^{1/2} C D^{1/2} v^{1/2}$$

Influence de la température

La dépendance du courant maximum observé en polarographie en courant alternatif en fonction

Can. J. Chem. Downloaded from www.nrcresearchpress.com by 210.87.254.6 on 09/05/12
For personal use only.

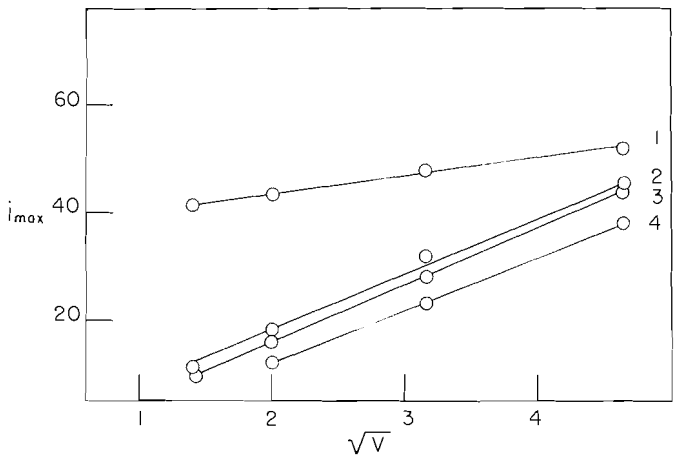

FIG. 3. Variation du courant maximum i_{max} (μA) en fonction de la racine carrée de la vitesse de balayage $(Vs^{-1})^{1/2}$. (1) $R_1 = R_2 = CH_3$; (2) $R_1 = C_2H_5$, $R_2 = i\text{-}C_3H_7$; (3) $R_1 = C_2H_5$, $R_2 = CH_3$; (4) $R_1 = CH_3$, $R_2 = i\text{-}C_3H_7$.

de la température a été étudiée dans le domaine de 10 à 40 °C. Pour tous les hydroxyperoxydes étudiés, l'intensité du courant limite croît linéairement avec la température (Fig. 4). Les pentes observées pour les divers hydroxyperoxydes sont indiquées au tableau 2.

TABLEAU 2
Coefficients de température

R_1	R_2	Coefficient de température (%/°C)
CH_3	CH_3	0.83
	$i\text{-}C_3H_7$	0.80
C_2H_5	CH_3	1.06
	$i\text{-}C_3H_7$	1.13

Ainsi que l'indiquent les résultats du tableau 2, dans tous les cas les coefficients de température sont inférieurs à 1.8% par °C, cette dernière valeur étant, d'après Zuman (13), la valeur du coefficient de température caractéristique d'un courant contrôlé par diffusion. Cette faible valeur, par rapport à 1.8% par degré, pourrait être expliquée en considérant que le processus global est contrôlé partiellement par la réaction d'électrode (coefficient de température nul) et par la vitesse de diffusion du dépolariseur (coefficient de température : 1.8% par °C).

Influence de la concentration en dépolariseur

L'intensité des courants limites a été étudiée en fonction de la concentration en hydroxyperoxyde, dans le tampon McIlvaine au p*H* 7. Ainsi que l'indique la Fig. 5, les intensités des courants enregistrés en polarographie en courant alternatif sont linéairement reliées aux concentrations en hydroxyperoxyde. Dans le tampon McIlvaine au p*H* 7 les résultats sont très reproductibles et se prêtent à des fins analytiques. Les courbes de calibration représentées par la Fig. 5 ont été obtenues en ajoutant 1 ml de solution d'hydroxyperoxyde dans le méthanol, de concentration comprise entre 0.01 et 0.12 *M*, à 25 ml de solution tampon.

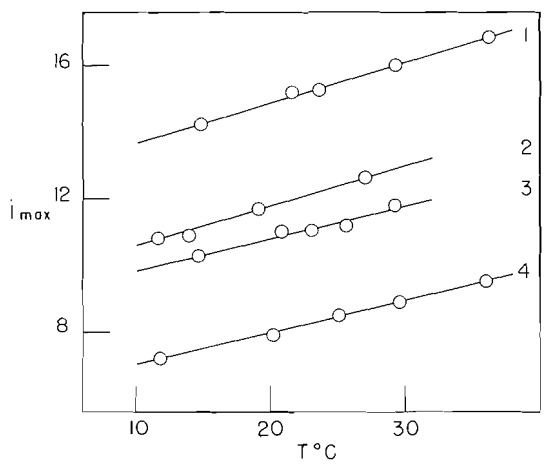

FIG. 4. Influence de la température sur l'intensité du pic polarographique (i_{max}, μA) dans le tampon McIlvaine, p*H* 7, à 25°. (1) $R_1 = CH_3$, $R_2 = i\text{-}C_3H_7$; (2) $R_1 = C_2H_5$, $R_2 = CH_3$; (3) $R_1 = R_2 = CH_3$; (4) $R_1 = C_2H_5$, $R_2 = i\text{-}C_3H_7$.

Can. J. Chem. Downloaded from www.nrcresearchpress.com by 210.87.254.6 on 09/05/12
For personal use only.

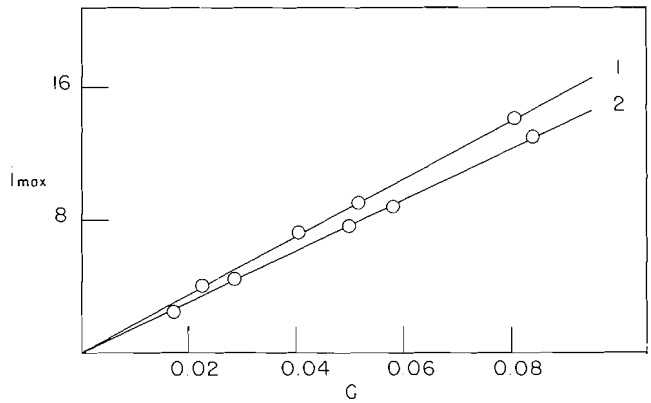

FIG. 5. Intensité des pics polarographiques (μA) vs. concentration c (M) des hydroxyperoxydes, dans le méthanol. Tampon McIlvaine, pH 7, à 25 ± 0.1 °C. (1) $R_1 = C_2H_5$, $R_2 = i\text{-}C_3H_7$; (2) $R_1 = C_2H_5$, $R_2 = CH_3$. Les courbes des composés avec $R_1 = CH_3$ et $R_2 = CH_3$ ou $i\text{-}C_3H_7$ sont pratiquement identiques à la courbe (1).

Ozonolyse du trans méthyl-4 pentène-2 en présence d'alcool

La comparaison des résultats obtenus avec les hydroxyperoxydes **5** et les alcoxyhydroperoxydes **4** (5) montre que la polarographie en courant alternatif est une méthode analytique appropriée en vue d'une distinction entre ces composés isomères. En effet, la réduction du groupement OOH s'effectue à des potentiels beaucoup moins négatifs que celle des groupements OOR. Le tableau 3 permet la comparaison des potentiels de demi-vague, mesurés dans le tampon McIlvaine au pH 7 à 25 °C, des hydroxyperoxydes **5** avec ceux des alcoxyhydroperoxydes **4**.

Les Figs. 6 et 7 illustrent bien, avec $R_2 = CH_3$ ou $i\text{-}C_3H_7$, la possibilité de mettre en évidence les hydroxyperoxydes à côté des alcoxyhydroperoxydes correspondants. A l'aide des courbes de calibration (Fig. 5) établies pour les hydroxyperoxydes avec $R_1 = C_2H_5$ et $R_2 = CH_3$ ou $i\text{-}C_3H_7$, ainsi que des courbes de calibration établies pour les alcoxyhydroperoxydes correspondants (5), il est facile de vérifier que la présence, dans le mélange réactionnel, d'une proportion de 1% d'hydroxyperoxyde à côté de 99% d'alcoxyhydroperoxyde peut être facilement décelée. Cette observation est, par ailleurs, également valable en ce qui a trait à la différenciation des hydroxyperoxydes avec $R_1 = CH_3$ des méthoxyhydroperoxydes correspondants.

L'examen polarographique des solutions de *trans* méthyl-4 pentène-2 ozonées en solution dans le tétrachlorure de carbone, en présence de méthanol ou d'éthanol 3 M, à 25 °C, n'a en aucun cas permis de déceler les pics polarographiques pouvant correspondre aux hydroxyperoxydes attendus. Cette observation semble permettre, dès lors, de conclure à la non-participation d'une forme zwitterionique **3**.

Il a été observé, cependant, qu'une diminution de la concentration en alcool dans le solvant utilisé lors de l'ozonolyse se traduit par la formation de quantités insuffisantes d'alcoxyhydroperoxydes, par rapport à la quantité d'oléfine consommée (tableau 4).

L'effet de la diminution de la concentration

TABLEAU 3

Potentiels de demi-vague ($E_{1/2}$) dans le tampon McIlvaine, pH 7, à 25 °C

		$E_{1/2}$ (V)	
R_1	R_2	R_2—CH(OOH)—OR_1	R_2—CH(OOR_1)—OH
CH_3	CH_3	−0.68	−1.14
	$i\text{-}C_3H_7$	−0.21	−1.13
C_2H_5	CH_3	−0.5	−0.94
	$i\text{-}C_3H_7$	−0.3	−0.92

Can. J. Chem. Downloaded from www.nrcresearchpress.com by 210.87.254.6 on 09/05/12
For personal use only.

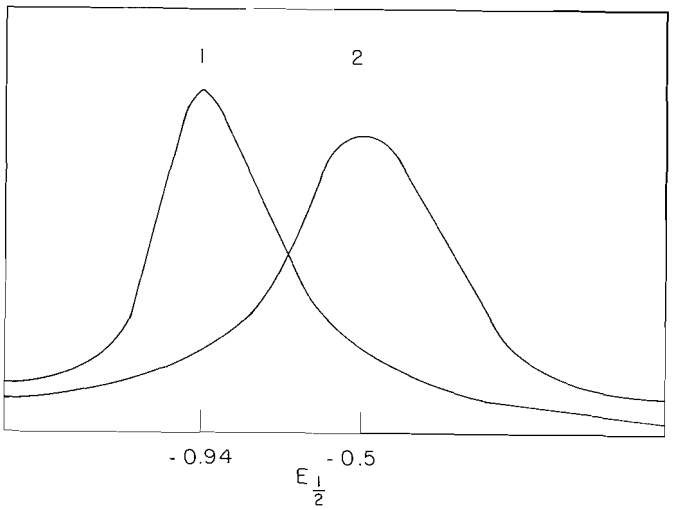

FIG. 6. Comparaison polarographique des hydroxyperoxydes et des alcoxyhydroperoxydes. (1) $CH_3CH(OOC_2H_5)$-OH; (2) $CH_3CH(OOH)OC_2H_5$. Concentrations (M): 0.051 (1) et 0.024 (2), dans le méthanol. Tampon McIlvaine, pH 7, à 25°.

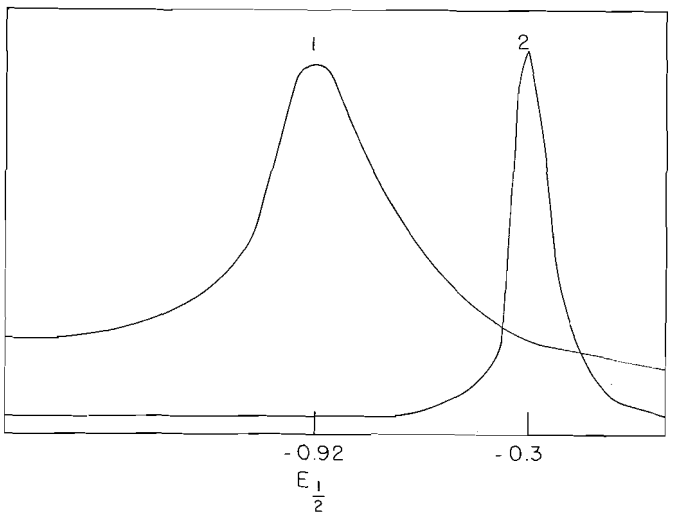

FIG. 7. Comparaison polarographique des hydroxyperoxydes et des alcoxyhydroperoxydes. (1) i-$C_3H_7CH(OOC_2H_5)OH$ (0.047 M); (2) i-$C_3H_7CH(OOH)OC_2H_5$ (0.09 M). Tampon McIlvaine, pH 7, à 25°.

d'alcool sur la distribution des produits d'ozonolyse a été étudié en envisageant la possibilité qu'une augmentation de la durée de vie du zwitterion dans le mélange réactionnel pouvait éventuellement entraîner la formation de la forme zwitterionique **3**. Cependant, même dans ces conditions expérimentales, aucune trace d'hydroxyperoxyde n'a pu être décelée, par voie polarographique, dans les mélanges réactionnels.

A cet égard, il paraît intéressant de relever le point suivant. L'ozonolyse d'une solution 0.1 M de *trans* méthyl-4 pentène-2 dans l'acétate d'éthyle – méthanol (3 M) à 25 °C conduit à la formation d'un total de 1 mole de méthoxyhydroperoxyde par mole d'oléfine ozonée. La distribution des deux méthoxyhydroperoxydes, ainsi qu'elle a été déterminée par analyse polarographique (5), est indiquée par le schéma 3. Par ailleurs, ces proportions de clivage ne dépendent ni de la température d'ozonolyse, ni du solvant utilisé (CCl_4, hexane, acétate d'éthyle, éther, méthanol, ou éthanol) (14).

Can. J. Chem. Downloaded from www.nrcresearchpress.com by 210.87.254.6 on 09/05/12
For personal use only.

TABLEAU 4

Ozonolyse de 1 mmole de *trans* méthyl-4 pentène-2, en présence de méthanol ou d'éthanol

ROH	(*M*)	Température (°C)	Oléfine consommée (mmole)	Hydroperoxyde formé (mmole)	Hydroperoxyde / Oléfine (%)
CH_3OH	0.5	0	0.367	0.290	79.0
			0.560	0.445	79.0
	1.0		0.243	0.200	82.3
			0.534	0.440	82.4
		25	0.427	0.350	82.0
			0.725	0.595	82.0
C_2H_5OH	1.0	0	0.450	0.360	80.0
			0.610	0.485	79.5
		25	0.250	0.200	80.0
			0.629	0.503	80.0
CH_3OH	3.0	25	0.349	0.350	100.3
			0.351	0.350	99.7
			0.375	0.371	98.9

Les rendements en alcoxyhydroperoxydes, observés lors des ozonolyses présentant un défaut dans la quantité totale d'alcoxyhydroperoxyde, peuvent donc être calculés par rapport aux quantités attendues d'après les proportions indiquées dans le schéma 3. Dans une première expérience, 1.0 mmole de *trans* méthyl-4 pentène-2 en solution dans 10 ml d'acétate d'éthyle – méthanol 0.5 *M* a été ozonée partiellement, à 0 °C. D'après le dosage de l'oléfine non consommée, en chromatographie en phase gazeuse (c.p.g.), 0.56 mmole d'oléfine a été consommée. La quantité totale du mélange des deux méthoxyhydroperoxydes, d'après le dosage iodométrique selon Lohaus (15), s'est élevée à 0.445 mmole, soit 79% par rapport à l'oléfine consommée. D'après le dosage polarographique des méthoxyhydroperoxydes, 0.352 mmole de $CH_3CH(OCH_3)OOH$ et 0.090 mmole de i-$C_3H_7CH(OCH_3)OOH$, soit un total de 0.442 mmole, ont été engendrés, ce qui est en bon accord avec la valeur trouvée par iodométrie. D'après le schéma 3, les quantités attendues pour l'ozonolyse de 0.56 mmole d'oléfine sont 0.398 mmole de $CH_3CH(OCH_3)OOH$ et 0.162 mmole de i-$C_3H_7CH(OCH_3)OOH$. On conclut, d'après cette expérience, que 88% du zwitterion $CH_3C^+HOO^-$ se retrouvent dans le mélange final sous forme de son méthoxyhydroperoxyde, mais seulement 55.5% du zwitterion i-$C_3H_7C^+HOO^-$. Une expérience similaire a été effectuée à 25 °C, dans une solution 1 *M* en méthanol dans l'acétate d'éthyle. L'analyse iodométrique des méthoxyhydroperoxydes a conclu à la formation de 0.395 mmole (0.398 mmole par polarographie) pour l'ozonolyse de 0.481 mmole d'oléfine, soit 82% de la quantité attendue. L'analyse polarographique a montré la formation de 0.304 mmole de $CH_3CH(OCH_3)OOH$ (attendu : 0.341 mmole) et de 0.094 mmole de i-$C_3H_7CH(OCH_3)OOH$ (attendu : 0.140 mmole). Ainsi, 89% du méthoxyhydroperoxyde $CH_3CH(OCH_3)OOH$ et 67% de i-$C_3H_7CH(OCH_3)OOH$ ont été retrouvés dans le mélange réactionnel final.

L'examen, en c.p.g., de ces solutions n'a pas permis de déceler l'alcool isobutyrique. Dès lors, le défaut marqué en zwitterion i-$C_3H_7C^+HOO^-$ ne semble pas devoir être attribué à une ozonolyse "anormale". Il a été également établi qu'il ne se forme pas d'isobutyrate de méthyle, qui aurait pu se produire selon un processus de Pasero (16), comme cela a déjà été décrit par Diaper (17) dans certains cas particuliers. Par contre, l'ozonide normal ainsi que l'ozonide de croisement correspondant au diisopropyléthylène ont pu être mis en évidence. Il n'a cependant pas été possible de déceler l'ozonide de croisement correspondant

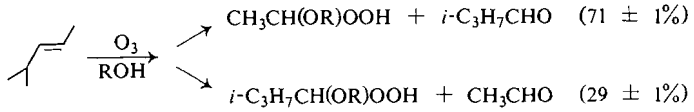

SCHÉMA 3

Can. J. Chem. Downloaded from www.nrcresearchpress.com by 210.87.254.6 on 09/05/12
For personal use only.

Can. J. Chem. Downloaded from www.nrcresearchpress.com by 210.87.254.6 on 09/05/12
For personal use only.

au butène-2. Il est, par ailleurs, probable que la formation d'ozonides impliquant la réaction de l'isobutyraldéhyde est favorisée par rapport à celle impliquant l'acétaldéhyde car, d'après le schéma 3, l'isobutyraldéhyde est formé de façon prépondérante lors du clivage de l'ozonide primaire.

En conclusion, l'ensemble des résultats exposés, notamment en ce qui a trait à l'absence d'hydroxyperoxyde dans tous les mélanges réactionnels, conduit à rejeter la participation d'une forme zwitterionique autre que **1** et **2** au mécanisme d'ozonolyse. Il semble, en effet, difficile d'admettre que la structure **3** puisse contribuer seulement à la formation d'ozonide, donc réagir uniquement avec l'aldéhyde, sans être capable de réagir également avec l'alcool pour engendrer l'hydroxyperoxyde.

Partie expérimentale

Technique d'ozonation

La technique d'ozonation a été décrite précédemment (4). Des débits d'ozone compris entre 0.07 et 0.2 mmole/min ont été utilisés, en limitant l'ozone à moins de 80% de la quantité théorique pour éviter l'autoxydation des aldéhydes.

Dosage iodométrique des hydroperoxydes

Les hydroperoxydes engendrés lors des ozonolyses effectuées en présence d'alcool ont été dosés en suivant une méthode approchant celle décrite par Lohaus (15).

Dosages en chromatographie en phase gazeuse

Lors des ozonolyses du *trans* méthyl-4 pentène-2 en présence d'alcool, les proportions d'oléfine n'ayant pas réagi, ainsi que les traces d'ozonide qui ont été formées dans certains cas, ont été déterminées au moyen d'un c.p.g. F et M, modèle 5750, avec un détecteur à flamme ionisante, comprenant une colonne de 6 pieds de silicone rubber UCW 98 ou de nitrile-silicone (10%) sur chromosorb P. La température du four a été maintenue à 30 °C, ce qui a prévenu la décomposition des alcoxyhydroperoxydes. Après chaque ozonation le solvant évaporé a été soigneusement remplacé et 5 µl d'échantillon ont été injectés dans le chromatographe. Les intensités des pics chromatographiques ont été mesurées au moyen d'un planimètre et les surfaces ainsi obtenues ont été comparées à celles obtenues dans les mêmes conditions par injection de solutions de référence appropriées. Il a été également vérifié que la présence, parmi les produits d'ozonolyse, d'alcool isobutyrique ou d'isobutyrate de méthyle aurait pu être décelée facilement.

Analyse polarographique

Les courbes intensité-potentiel ont été enregistrées à l'aide d'un polarographe Metrohm E-261-R qui offre la double possibilité d'une analyse par voltage continu croissant linéairement ou d'une analyse à l'aide d'une tension alternative de faible amplitude, superposée au voltage continu d'analyse (18, 19). La fréquence de la tension alternative a été de 60 Mc/s et son amplitude de 50 mV. L'électrode à goutte de mercure était constituée par un capillaire assurant un temps de goutte de 1/6 s pour un flux de mercure de 0.9 mg/s. L'électrode de référence était une électrode Ag/AgCl commerciale et l'électrode auxiliaire, une électrode de tungstène. Un oscillo-polarographe Chemtrix SSP-2, utilisant un balayage simple par tension triangulaire, a permis l'enregistrement des oscillo-polarogrammes; les électrodes étaient les mêmes que celles décrites ci-dessus. Le temps de goutte avait été amené à 3 s.

Pour les mesures, 1 ml de la solution ozonée dans l'acétate d'éthyle – méthanol (ou éthanol) a été ajouté à 25 ml de solution tampon McIlvaine au p*H* 7. La solution a été dégazée par un courant d'azote pendant 10 min, puis agitée énergiquement afin d'assurer une bonne homogénéité de la solution, à l'aide d'un agitateur magnétique. Lors de l'utilisation du CCl_4–méthanol (ou éthanol) comme solvant, la solution ozonée a été soumise à une évaporation. Le résidu a été ensuite dissous dans le méthanol (ou l'éthanol) et analysé comme il est indiqué ci-dessus.

Spectres de résonance magnétique nucléaire

Les spectres r.m.n. ont été déterminés au moyen d'un spectromètre Jeolco 60 H, en solution dans le chloroforme, en utilisant du tétraméthylsilane comme référence interne.

Préparation des hydroxyperoxydes

Les synthèses ont été effectuées en deux étapes selon la méthode décrite par Rieche (20, 21). La première étape consiste en une alkylation du peroxyde d'hydrogène par du sulphate de diméthyl ou de diéthyl, qui conduit à la formation des hydroperoxydes d'alcoyle ROOH correspondants. Les rendements ont été améliorés à 40–50% [litt. (20, 21) : 18–20%] probablement grâce à l'utilisation d'un appareil à extraction continue, pendant une semaine, lors de l'extraction des hydroperoxydes de leurs mélanges réactionnels.

Les hydroxyperoxydes ont été obtenus par la condensation des hydroperoxydes d'alcoyle avec les aldéhydes appropriés, en agitant pendant 24 h une solution des réactifs dans l'éther, à la température de la pièce. Les rendements sont faibles (10 à 15%), mais l'hydroperoxyde d'alcoyle n'ayant pas réagi peut être facilement récupéré. Ce mode de préparation évite les réactions secondaires, notamment des réactions de polymérisation. La condensation d'hydroperoxyde d'alcoyle avec l'aldéhyde benzoïque a échoué, même en prolongeant le temps de réaction à 3 jours. Les hydroxyperoxydes ont été purifiés par distillation sous pression réduite. Leurs points d'ébullition, ainsi que leurs spectres r.m.n. sont exposés au tableau 1.

Nous remercions le Conseil National de Recherches du Canada pour un octroi qui a permis ces recherches.

1. R. CRIEGEE and G. WENNER. Ann. **564**, 9 (1949); R. CRIEGEE. Ann. **583**, 1 (1953).
2. R. CRIEGEE. Rec. Chem. Progr. **18**, 111 (1957); R. CRIEGEE. *Dans* Peroxide reaction mechanisms. J. O. Edwards, *Editor* Interscience Publ., Inc., New York, N. Y., 1962. p. 29.

3. S. FLISZÁR. Tetrahedron Lett. 6083 (1966); S. FLISZÁR, CZ. BELŽECKI, and J. B. CHYLIŃSKA. Can. J. Chem. **45**, 221 (1967); P. S. BAILEY, S. B. MAINTHIA, and C. J. ABSHIRE. J. Amer. Chem. Soc. **82**, 6136 (1960); W. P. KEAVENEY, M. G. BERGER, and J. J. PAPPAS. J. Org. Chem. **32**, 1537 (1967).
4. S. FLISZÁR and J. RENARD. Can. J. Chem. **45**, 533 (1967); S. FLISZÁR and M. GRANGER. J. Amer. Chem. Soc. **91**, 3330 (1969).
5. J. RENARD and S. FLISZÁR. Can. J. Chem. **47**, 3333 (1969).
6. S. FLISZÁR and J. CARLES. J. Amer. Chem. Soc. **91**, 2637 (1969); S. FLISZÁR, J. CARLES, and J. RENARD. J. Amer. Chem. Soc. **90**, 1364 (1968).
7. P. R. STORY, C. E. BISHOP, J. R. BURGESS, R. W. MURRAY, and R. D. YOUSSEFYEH. J. Amer. Chem. Soc. **90**, 1907 (1968).
8. P. R. STORY, R. W. MURRAY, and R. D. YOUSSEFYEH. J. Amer. Chem. Soc. **88**, 3144 (1966); R. W. MURRAY, R. D. YOUSSEFYEH, and P. R. STORY. J. Amer. Chem. Soc. **89**, 2429 (1967).
9. S. FLISZÁR and J. CARLES. Can. J. Chem. **47**, 3921 (1969); S. FLISZÁR and J. CARLES. Symp. Oxidation of Hydrocarbons, ACS meeting, Minneapolis, April 1969. Preprints of papers p A59.
10. D. A. SKOOG and A. B. H. LAUWZECHA. Anal. Chem. **28**, 825 (1956).
11. P. DELAHAY. J. Amer. Chem. Soc. **75**, 1190 (1953).
12. H. MATSUDA and Y. AYABE. Z. Elektrochem. **59**, 494 (1955); J. HEYROVSKÝ and J. KŮTA. Principles of polarography, Academic Press, Inc., New York, 1966. p. 505.
13. P. ZUMAN. *Dans* Progress in physical organic chemistry. Vol. 5. Interscience Publishers, Inc., New York, 1967. p. 134.
14. J. RENARD and S. FLISZÁR. A paraître.
15. G. LOHAUS. Ann. **583**, 4 (1953).
16. J. PASERO. Thèse, Université de Marseilles, Marseilles, France, 1963; J. PASERO and M. NAUDET. Rev. Franc. Corps Gras, **7**, 189 (1960); **10**, 453 (1963); J. PASERO, L. COMEAU, and M. NAUDET. Bull. Soc. Chim. France, 493 (1965).
17. D. G. M. DIAPER. Can. J. Chem. **44**, 2822 (1966).
18. B. BREYER, F. GUTMANN, and S. HACOBIAN. Aust. J. Sci. Res. Ser. A, **3**, 558 (1950).
19. B. BREYER, F. GUTMANN, and H. H. BAUER. Oesterr. Chem. Ztg. **57**, 67 (1956).
20. A. RIECHE. Chem. Ber. **62**, 2458 (1929).
21. A. RIECHE and F. HITZ. Chem. Ber. **63**, 2692 (1930)

Can. J. Chem. Downloaded from www.nrcresearchpress.com by 210.87.254.6 on 09/05/12
For personal use only.

Can. J. Chem. Downloaded from www.nrcresearchpress.com by 210.87.254.105 on 09/05/12
For personal use only.

Spectrofluorometric studies. VIII. The effect of CO_2 and $CHCl_3$ on the photochemistry of monofluorobenzene

M. E. MacBeath and I. Unger

Department of Chemistry, University of New Brunswick, Fredericton, New Brunswick

Received November 26, 1969

The sensitized emission of biacetyl technique was used to study the effect of $CHCl_3$ and CO_2 on the triplet quantum yields of both benzene and monofluorobenzene.

The monofluorobenzene was studied at λ excitation (λ_{ex}) of 2470, 2590, and 2670 Å. At 2470 Å, the triplet yield increased by over 40% with both added gases; at λ_{ex} 2590 Å, by around 30%; and at λ_{ex} 2670 Å, about 20%. $CHCl_3$ is slightly more effective than CO_2 in enhancing the biacetyl phosphorescent yield. The quantum yield of fluorescence was unchanged with these added gases. Using a slightly improved technique, the comparison irradiation of a benzene–biacetyl mixture at λ_{ex} 2540 Å with added $CHCl_3$ was repeated. The results confirmed that the biacetyl phosphorescent yield decreased with increasing pressures of $CHCl_3$, but suggest that the effect is not as great as previously reported. At the same wavelength, the triplet yield is unaffected by the addition of CO_2. The quantum yield of fluorescence of benzene is virtually unaffected by the added gases. The data suggest that in the monofluorobenzene case the CO_2 and $CHCl_3$ are quenching vibrationally excited triplet fluorobenzene molecules.

Canadian Journal of Chemistry, **48**, 1607 (1970)

Introduction

Of the several techniques for detecting and estimating the triplet yield of organic molecules that do not exhibit phosphorescence, the two most commonly used in vapor-phase studies are the sensitized emission of biacetyl (BiA) technique (1) and the isomerization of olefins technique, first described by Cundall *et al.* (2, 3). Both techniques have certain limitations (4). In addition to the limitations discussed in ref. 4, the isomerization of olefins technique may have other drawbacks, thus it was recently reported that *cis*-butene-2 at low pressures will isomerize due to direct absorption (5) of 2537 Å radiation. Similarly, it has been shown that the irradiation of either isomer of 1,3-pentadiene at 3660 Å leads to isomerization with quantum yields greater than unity (6). In the present study the sensitized emission of BiA technique was used to monitor the triplet yield of monofluorobenzene (FB) excited at various wavelengths. When applying this technique to molecules which absorb more strongly than benzene, it is often desirable to use lower total pressures than those used by Ishikawa and Noyes (1). The method should still yield reliable results provided a sufficient quantity of some transparent inert quencher is added to the system to deactivate vibrationally hot FB molecules. If this precaution is not taken, the FB molecules in high vibrational levels of the triplet state can, on collision, create BiA molecules with enough energy to dissociate (7). In a previous study of the photochemistry of FB (8), this precaution was not taken and hence we believe the triplet yields given in ref. 8 to be artificially low. The vibrational quenchers employed were $CHCl_3$ and CO_2.

It has been reported that triplet benzene is quenched by $CHCl_3$ (9), since the present study shows that the addition of $CHCl_3$ increases the triplet yield of FB, a molecule whose basic photochemistry is very similar to that of benzene (10–13), the effect of $CHCl_3$ as well as that of CO_2 on the singlet and triplet yields of benzene excited at 2540 Å was re-examined.

Experimental

Monofluorobenzene, obtained from the Aldrich Chemical Company, was used without purification after a vapor phase chromatography (v.p.c.) check showed it to contain less than 0.03% impurities. The biacetyl, obtained from the same company, was stored in a dark reservoir and purified by bulb-to-bulb distillation in vacuo prior to use. Both the chloroform and benzene were fluorometric grade obtained from the Hartmann–Leddon Company. Chromatographic analysis showed the chloroform to be 99.7% pure and the benzene, 99.95% pure. The CO_2 was obtained by allowing Dry Ice to sublime from one bulb to another in vacuo, only the middle portion being retained; all materials were thoroughly outgassed prior to use.

A grease- and mercury-free high vacuum system employing Hoke packless diaphragm metal valves was used in this study. A cuvette type flow-through cell 1 cm × 1 cm × 4.5 cm high and polished on four sides

Can. J. Chem. Downloaded from www.nrcresearchpress.com by 210.87.254.105 on 09/05/12
For personal use only.

was used. The mixtures of gases were circulated through the cell by means of an all-glass pump constructed at the National Research Council of Canada in Ottawa.

When mixing was complete, as evidenced by a constant reading for light intensity passing through the cell, the pump was turned off during the recording of the phosphorescent emission spectrum. Unless this precaution was taken, an artificially low phosphorescent yield was observed. This effect is undoubtedly due to the relatively long lifetime of biacetyl triplet (1.8×10^{-3} s) (14). A certain fraction of the triplet biacetyl species being formed in the cell was being swept past the viewing slit before it had time to emit, this fraction being a function of pump efficiency. A spiral gauge, also made at NRCC, was used in conjunction with a silicone oil manometer in taking pressure measurements. Pressures below 3 Torr were obtained by expansion into previously calibrated sections of the vacuum line.

A modified (15) Aminco–Bowman spectrophotofluorometer (s.p.f.), obtained from the American Instrument Company, Inc., was employed for emission and absorption measurements. Experimental details concerning light source, absorption measurements, and correction factors have been given previously (15, 8).

The intensity of emission was measured using an E.M.I. 9652B photomultiplier tube whose response was displayed on a Kiethly Instruments' 610A electrometer. The response was recorded on a Mosely Autograph X–Y Recorder, Model 7030AM.

The entrance slit of the excitation monochromator was set at 0.5 mm and the exit slits were 1.0, 0.5, and 1.0 mm. This slit arrangement gave excitation spectra with the following characteristics for the wavelengths used in this study

Setting (Å)	Range (Å)	Maximum intensity at	Half band width (Å)
2470	2455–2500	2481 Å	22
2590	2565–2625	2597 Å	32
2670	2650–2700	2655 Å	10

The two entrance slits to the emission monochromator were both 1 mm and the exit slit was also 1 mm. A relative method, described elsewhere (11), was used to obtain the quantum yields of fluorescence and intersystem crossing. In order to obtain sufficient light intensity to give satisfactory results for the calibration, it was found necessary to use a 1.0 mm entrance slit to the excitation monochromator. An analysis of the exciting light with λ excitation set at 2540 Å (the λ excitation used in previous studies reported from our laboratory) (8, 11) showed that the wavelengths ranged from 2500 to 2535 Å, peaking at 2524 Å, and that 53% of the light was below 2520 Å, with 13% below 2510 Å. Since the fluorescent efficiency of benzene is constant from 2520 to 2610 Å (16), the λ excitation (λ_{ex}) for calibration was changed to 2580 Å where, with a 1 mm excitation slit, the spectral distribution of the exciting light was from 2550 to 2630 Å, with 11% above the 2610 Å limit. With a 0.5 mm excitation slit the distribution is between 2557 and 2607 Å, peaking at 2580 Å. Both 1 and 0.5 mm excitation slits were used for calibration at 2580 Å, and results were the same within experimental error.

Results and Discussion

The addition of CO_2 or $CHCl_3$ to mixtures of 20 Torr of benzene and 0.15 Torr of BiA has no effect on the fluorescent yield of benzene; $CHCl_3$ does, however, reduce the triplet yield of benzene, while CO_2 has no effect on this yield (Fig. 1). These results confirm the previously reported work on the $CHCl_3$–benzene system (9), although the data indicate that the reduction in the triplet yield is somewhat smaller than that given in the earlier work.

The singlet and triplet yields for mixtures of 10 Torr of FB and 5 Torr of BiA excited at 2470, 2590, and 2670 Å were redetermined using the improved calibrating technique given in the experimental section of this paper. The data are summarized below

λ_{ex}, Å	Φ_f	Φ_t
2470	0.13	0.39
2590	0.16	0.47
2670	0.17	0.48

where Φ_f is fluorescence quantum yield and Φ_t is triplet quantum yield.

The addition of $CHCl_3$ to 10 Torr of FB or to mixtures of 10 Torr of FB and 5 Torr of BiA excited at various wavelengths has no effect on the singlet yield of FB (Table 1). It does, however, increase the triplet yield of FB; the increase is 47, 36, and 28% at λ_{ex} = 2470, 2590, and 2670 Å, respectively; the data are shown graphically in Fig. 2. Plots of $1/\Phi_t$ vs. $1/M$, where M represents total pressure, are linear (Fig. 3).

The effect of CO_2 on the photochemistry of FB is remarkably similar to that of $CHCl_3$. Thus CO_2 has no effect on the fluorescence yield of FB when that material is present alone, nor does it have any effect on the fluorescence yield of FB in mixtures of FB and BiA at any of the exciting wavelengths examined (Table 2). Addition of CO_2 does, however, increase the triplet yield of FB; the percent increase is dependent on the exciting wavelength, and is found to be 42, 29, and 20% when λ_{ex} = 2470, 2590, and 2670 Å, respectively (Fig. 3). Plots of M/Φ_t vs. M are again found to be linear (Fig. 4). The equations of the lines given in Fig. 3 are summarized in tabular form (Table 3). Using the maximum increases in triplet yield given for $CHCl_3$, the total

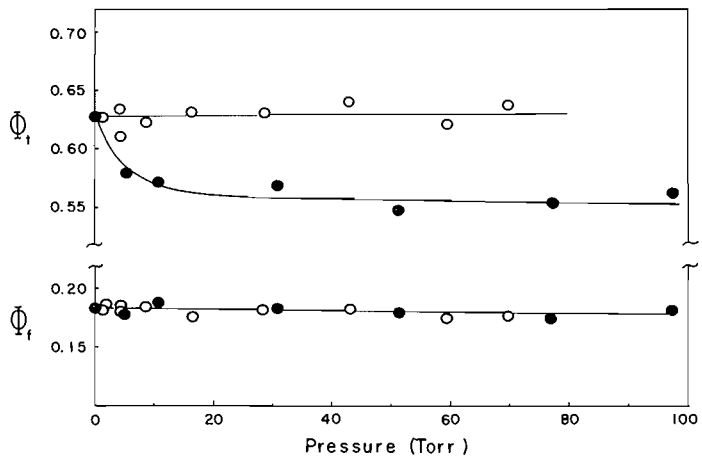

FIG. 1. The effect of $CHCl_3$, ●, and CO_2, ○, on the fluorescence and triplet yields of benzene excited at 2540 Å. Benzene pressure = 20 Torr, BiA pressure = 0.15 Torr.

TABLE 1

Effect of chloroform on the fluorescent quantum yield of FB and on that of FB–BiA mixtures at various exciting wavelengths

λ_{ex} 2470 Å		λ_{ex} 2590 Å		λ_{ex} 2670 Å	
$CHCl_3$ pressure, Torr*	Φ_f	$CHCl_3$ pressure, Torr*	Φ_f	$CHCl_3$ pressure, Torr*	Φ_f
0.0	0.134	0.0	0.165		
5.1	0.131	0.0	0.167	0.0	0.172
10.5	0.129	5.0	0.173	5.1	0.172
20.5	0.126	10.3	0.167	10.2	0.171
30.8	0.134	19.9	0.164	19.9	0.172
41.3	0.134	35.2	0.167	34.7	0.168
51.8	0.128	50.9	0.168	49.8	0.164
62.5	0.135	71.7	0.164	68.3	0.163
77.7	0.132	92.7	0.165	90.3	0.163
93.2	0.134	114.3	0.161	112.5	0.163
108.9	0.132				

λ_{ex} 2470 Å		λ_{ex} 2590 Å		λ_{ex} 2670 Å	
$CHCl_3$ pressure, Torr†	Φ_f	$CHCl_3$ pressure, Torr†	Φ_f	$CHCl_3$ pressure, Torr†	Φ_f
0	0.105	0	0.137	0	0.129
2.2	0.105	3.1	0.140	2.8	0.127
4.7	0.104	6.3	0.141	5.8	0.129
7.5	0.105	9.5	0.137	9.1	0.126
10.5	0.102	13.0	0.140	12.5	0.128
13.8	0.105	16.6	0.143	16.1	0.131
19.2	0.106	21.9	0.141	21.3	0.130
29.5	0.106	32.2	0.142	31.3	0.129
40.1	0.106	42.7	0.142	41.6	0.130
50.9	0.106	53.2	0.138	52.0	0.130
62.0	0.108	63.9	0.142	62.7	0.134
77.5	0.107	78.8	0.140	78.0	0.133
93.2	0.106	93.9	0.137	93.4	0.137

*FB pressure = 10 Torr, no BiA added.
†FB pressure = 10 Torr, BiA pressure = 5.0 Torr.

Can. J. Chem. Downloaded from www.nrcresearchpress.com by 210.87.254.105 on 09/05/12
For personal use only.

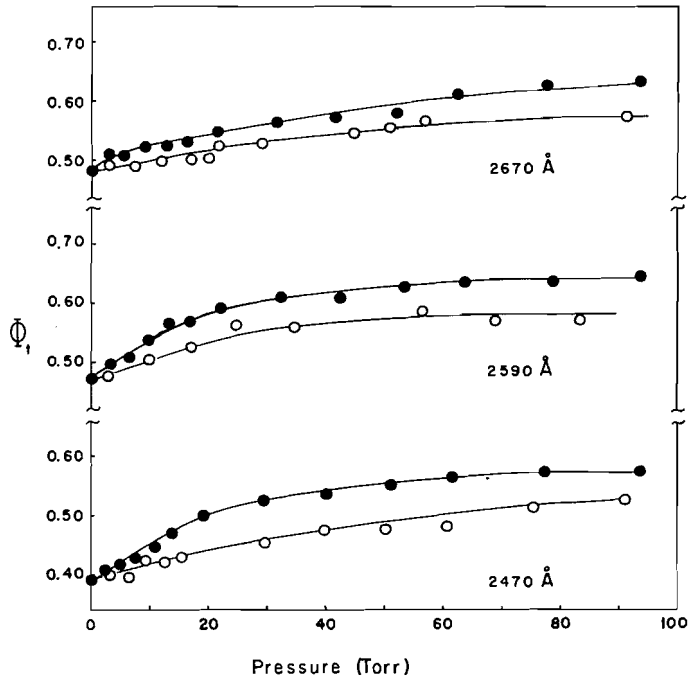

FIG. 2. The effect of $CHCl_3$, ●, and CO_2, ○, on the triplet yield of FB at excitation wavelengths of 2470, 2590, and 2670 Å. FB pressure = 10 Torr, BiA pressure = 5 Torr.

quantum yield of singlet plus triplet at λ_{ex} 2470 Å is 0.70; at λ_{ex} 2590 Å, 0.80; and at λ_{ex} 2670, 0.78.

The mechanism given below is consistent with our experimental observations and known photochemistry of BiA (17)

$$FB + h\nu \rightarrow {}^1FB_z^I \quad I_a$$

[1] $${}^1FB_z^I + N \rightarrow {}^1FB_x^I + N$$

[2] $${}^1FB_z^I + BiA \rightarrow FB + {}^1BiA^{II}$$

[3] $${}^1FB_x^I + BiA \rightarrow FB + {}^1BiA^{II}$$

[4] $${}^1FB_x^I \rightarrow {}^3FB_z^I$$

[5] $${}^1FB_x^I + N \rightarrow {}^1FB_0^I + N$$

[6] $${}^1FB_0^I + FB \rightarrow 2FB$$

[7] $${}^1FB_0^I \rightarrow FB + h\nu_f$$

[8] $${}^1BiA^{II} \rightarrow \text{Dissociation}$$

[9] $${}^3FB_z^I + M \rightarrow {}^3FB_x^I + M$$

[10] $${}^3FB_z^I + BiA \rightarrow {}^3BiA_z^I + FB$$

[11] $${}^3FB_x^I + BiA \rightarrow {}^3BiA_x^I + FB$$

[12] $${}^3FB_x^I (+ M) \rightarrow FB (+ M)$$

[13] $${}^3BiA_z^I \rightarrow \text{Dissociation}$$

[14] $${}^3BiA_x^I + N \rightarrow {}^3BiA_0^I + N$$

[15] $${}^3BiA_0^I \rightarrow BiA + h\nu_p$$

[16] $${}^3BiA_0^I \rightarrow BiA$$

In the above mechanism, Arabic numerals denote spin multiplicity while Roman numerals are used to represent first or second excited states, z is a vibrational level which is higher than the vibrational level x which is in turn higher than the ground vibrational level 0. The energy gap between z and 0, and between x and 0, will depend on the wavelength used for excitation. M is any molecule which can act as a vibrational quencher, while N is total FB and BiA. In this mechanism, some steps such as intramolecular rearrangement of either singlet or triplet FB, which are known to occur (18–20) for benzene and substituted benzenes, have been omitted since these steps have very small quantum yields (21). Application of the steady-state treatment to the mechanism yields

[17] $$[M]/\Phi_t = \frac{(k_{15} + k_{16})(k_{11}[BiA] + k_{12})(k_3[BiA] + k_4 + k_5[N])(k_1[N] + k_2[BiA])(k_9[M] + k_{10}[BiA])}{k_{15}k_{11}[BiA]k_9k_4k_1[N]}$$

Can. J. Chem. Downloaded from www.nrcresearchpress.com by 210.87.254.105 on 09/05/12
For personal use only.

TABLE 2

Effect of carbon dioxide on the fluorescent quantum yield of FB and on that of FB–BiA mixtures at various exciting wavelengths

λ_{ex} 2470 Å		λ_{ex} 2590 Å		λ_{ex} 2670 Å	
CO_2 pressure, Torr*	Φ_f	CO_2 pressure, Torr*	Φ_f	CO_2 pressure, Torr*	Φ_f
0.0	0.134	0.0	0.165	0.0	0.172
5.7	0.133	6.0	0.165	5.4	0.173
11.6	0.132	12.0	0.162	11.0	0.173
21.8	0.144	22.1	0.160	21.3	0.170
30.9	0.137	32.3	0.161	32.0	0.171
51.7	0.132	52.2	0.159	52.0	0.170
77.0	0.135	78.2	0.160	78.0	0.169
102.6	0.137	103.4	0.161	101.6	0.170
λ_{ex} 2470 Å		λ_{ex} 2590 Å		λ_{ex} 2670 Å	
CO_2 pressure, Torr†	Φ_f	CO_2 pressure, Torr†	Φ_f	CO_2 pressure, Torr†	Φ_f
0.0	0.109	0.0	0.137	0.0	0.129
3.1	0.105	2.8	0.136	3.0	0.123
6.4	0.104	9.9	0.138	7.3	0.123
9.4	0.103	16.8	0.137	11.8	0.120
12.2	0.102	24.2	0.140	16.6	0.118
14.7	0.103	34.7	0.138	21.6	0.116
20.0	0.101	45.5	0.138	32.8	0.116
29.9	0.102	56.5	0.137	44.6	0.119
39.9	0.102	68.6	0.136	56.6	0.126
50.1	0.102	83.7	0.130	56.6	0.128
60.6	0.102			69.6	0.133
75.6	0.102			82.5	0.133
90.8	0.102				
140.1	0.103				

*FB pressure = 10 Torr, no BiA added.
†FB pressure = 10 Torr, BiA pressure = 5.0 Torr.

For constant pressures of FB and BiA, eq. [17] predicts that plots of $1/\Phi_t$ vs. $1/M$ should be linear; this prediction is confirmed experimentally (Figs. 3 and 4). Equation [17] also allows the evaluation of k_9/k_{10} at various wavelengths

[18] $$\text{intercept/slope} = k_9/k_{10}[B]$$

Values of these ratios are listed below

	k_9/k_{10}	
λ_{ex}, Å	$CHCl_3$ added	CO_2 added
2470	0.517	0.918
2590	0.696	1.04
2670	1.31	2.56

Our data indicate, then, FB intersystem crossover from the first singlet to the triplet may occur from a variety of vibrational levels, depending on the wavelengths of the incident radiation. Consequently, the triplet BiA molecules, produced by energy transfer between triplet FB and ground state BiA, will have a range of vibrational energies also dependent on the excitation wavelength. Thus, unless some inert gas is present in the system which can deactivate hot triplet FB molecules, vibrationally hot triplet BiA molecules will be produced, some of which may dissociate (17), which will in turn lead to artificially low triplet yields. Our data also show that singlet and triplet energy transfer from FB to either CO_2 or $CHCl_3$ is not significant. This is somewhat surprising, at least for the FB and $CHCl_3$ system, in view of the work of Denschlag and Lee (22) on the benzene–cyclobutanone system, wherein it was shown that singlet benzene transfers 96 kcal/mole of energy to cyclobutanone and that the triplet transfers between 80 and 85 kcal/mole.

Can. J. Chem. Downloaded from www.nrcresearchpress.com by 210.87.254.105 on 09/05/12
For personal use only.

Can. J. Chem. Downloaded from www.nrcresearchpress.com by 210.87.254.105 on 09/05/12
For personal use only.

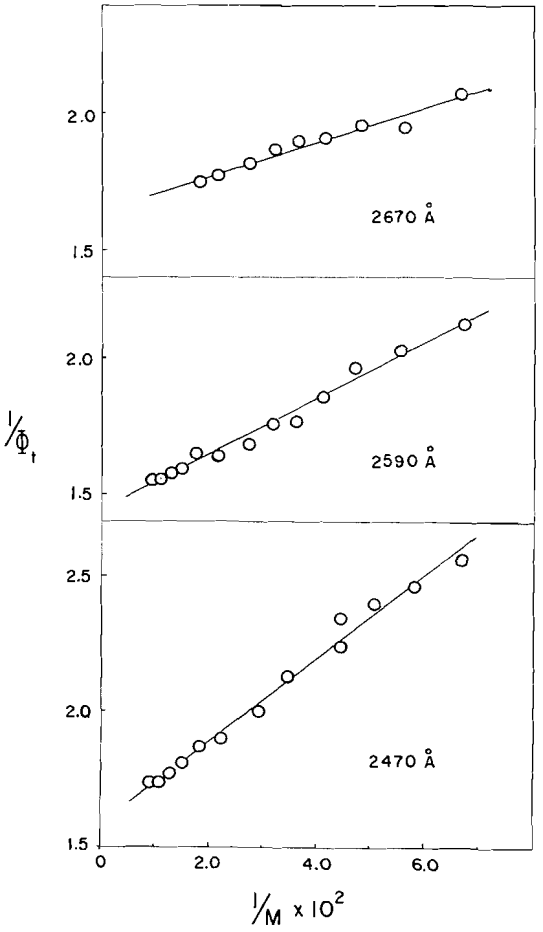

FIG. 3. Plots of $1/\Phi_t$ vs. $1/M$. FB pressure = 10 Torr, BiA pressure = 5 Torr, M = total pressure of FB + BiA + $CHCl_3$.

In the benzene–CO_2 and benzene–$CHCl_3$ systems studied in this report, the benzene pressure was sufficiently large and the BiA pressure so small that most benzene triplets would be quickly deactivated to fairly low vibrational levels before energy transfer collisions with BiA could occur. Rough calculations (considering only the relative numbers of molecules present in the two systems) indicate that the collision frequency of triplet benzene with benzene is ~200 times that for triplet benzene with BiA molecules. On the other hand, in the FB–BiA system the collision frequency of triplet FB with FB is only two times that for triplet FB with BiA. Hence reactions of type [13] and [10] would be unimportant for the benzene systems. Also, our data indicate that reactions of the type

$$^3\text{Benzene} + CO_2 \rightarrow (\text{Benzene—}CO_2)$$

TABLE 3

Equations of lines of $1/\Phi_t$, reciprocal quantum yield of triplet, vs. $1/M$, reciprocal total pressure, at various exciting wavelengths, for FB–BiA mixtures with added $CHCl_3$ or CO_2*

	$CHCl_3$ added	
λ_{ex}, Å	Pressure range $CHCl_3$, Torr	Equation,† $1/\Phi_t$ =
2470	0–93	1.58 + 15.29(1/M) ± 1.09%, max. 3.76%
2590	0–94	1.44 + 10.34(1/M) ± 0.92%, max. 2.46%
2670	0–52	1.64 + 6.28(1/M) ± 0.97%, max. 2.22%
	CO_2 added	
λ_{ex}, Å	Pressure range CO_2, Torr	Equation,† $1/\Phi_t$ =
2470	0–61	1.94 + 10.56(1/M) ± 1.79%, max. 3.77%
2590	0–84	1.63 + 7.84(1/M) ± 1.63%, max. 2.58%
2670	0–33	1.84 + 3.60(1/M) ± 1.22%, max. 2.40%

*FB pressure = 10 Torr, BiA pressure = 5 Torr.
†The first percentage (±) is the average difference of experimental values from values at each corresponding pressure on a least square plot. The second percentage (max.) is the difference of the experimental value whose deviation is greatest from its corresponding point (at the same pressure) on the least square plot.

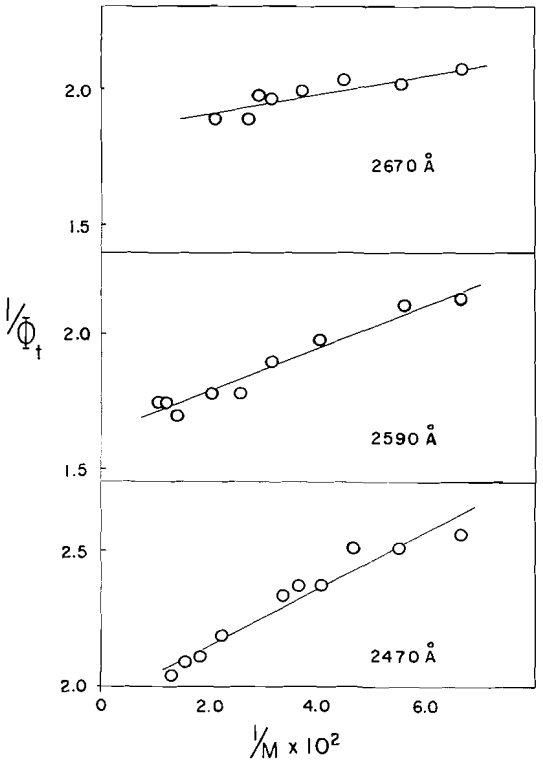

FIG. 4. Plots of $1/\Phi_t$ vs. $1/M$. FB pressure = 10 Torr, BiA pressure = 5 Torr, M = total pressure of FB + BiA + CO_2.

which have been recently shown to occur for the SO_2–CO_2 system (23) cannot be significant here. The reduction in the triplet yield of benzene on the addition of $CHCl_3$ is likely due to energy transfer from the triplet of benzene to $CHCl_3$ with the resulting decomposition of the latter (9).

The authors wish to thank Dr. G. P. Semeluk of this department for many useful discussions.

1. H. ISHIKAWA and W. A. NOYES, JR. J. Chem. Phys. **37**, 583 (1962).
2. R. B. CUNDALL and T. F. PALMER. Trans. Faraday Soc. **56**, 1211 (1960).
3. R. B. CUNDALL and J. R. VOSS. Chem. Commun. 902 (1968).
4. W. A. NOYES, JR., and I. UNGER. Advan. Photochem. **4**, 49 (1966).
5. E. M. ANDERSON and G. B. KISTIAKOWSKY. J. Chem. Phys. **51**, 182 (1969).
6. R. L. DANBENDIEK and G. R. MCMILLAN. 5th Int. Conf. Photochem. Yorktown Heights, N.Y. September 2–5, 1969.
7. S. H. NG, G. P. SEMELUK, and I. UNGER. Ber. Bunsenges. Phys. Chem. In press.
8. M. E. MACBEATH, G. P. SEMELUK, and I. UNGER. J. Phys. Chem. **73**, 995 (1969).
9. S. H. NG, G. P. SEMELUK, and I. UNGER. Can. J. Chem. **46**, 2461 (1968).
10. D. F. EVANS. J. Chem. Soc. 2753 (1959).
11. I. UNGER. J. Phys. Chem. **69**, 4284 (1965).
12. D. PHILLIPS. J. Phys. Chem. **71**, 1839 (1967).
13. R. B. CUNDALL, A. S. DAVIES, K. DUNNICLIFF. The triplet state, Proc. Int. Symp. Beirut, Lebanon. 1967. pp. 183–94 (discuss. 207–10).
14. H. O. OKABE and W. A. NOYES, JR. J. Amer. Chem. Soc. **79**, 801 (1957); W. E. KASKAN and A. B. F. DUNCAN. J. Chem. Phys. **18**, 427 (1950); C. S. PARAMENTER and H. M. POLAND. J. Chem. Phys. **51**, 1551 (1969).
15. F. W. AYER, F. GREIN, G. P. SEMELUK, and I. UNGER. Ber. Bunsenges. Phys. Chem. **72**, 282 (1967).
16. W. A. NOYES, JR., and D. A. HARTER. J. Chem. Phys. **46**, 674 (1967).
17. J. G. CALVERT and J. N. PITTS, JR. Photochemistry. John Wiley and Sons, Inc., New York. 1966. pp. 324–335 and p. 421.
18. K. E. WILZBACH and L. KAPLAN. J. Amer. Chem. Soc. **86**, 2307 (1964).
19. E. M. ARNETT and I. M. BOLLINGER. Tetrahedron Lett. **50**, 3803 (1964).
20. K. E. WILZBACH, A. L. HARKNESS, and L. KAPLAN. J. Amer. Chem. Soc. **90**, 1116 (1967).
21. N. LERAY. J. Chim. Phys. **64**, 1390 (1967).
22. H. O. DENSCHLAG and E. K. C. LEE. J. Amer. Chem. Soc. **90**, 3628 (1968).
23. T. RAO, S. S. COLLIER, and J. G. CALVERT. J. Amer. Chem. Soc. **91**, 1616 (1969).

Can. J. Chem. Downloaded from www.nrcresearchpress.com by 210.87.254.105 on 09/05/12
For personal use only.

Can. J. Chem. Downloaded from www.nrcresearchpress.com by 210.87.254.42 on 09/05/12
For personal use only.

Nuclear recoil reactions in organomanganese compounds. IV. Fulvalenehexacarbonyldimanganese

I. G. DEJONG AND D. R. WILES
Chemistry Department, Carleton University, Ottawa, Canada

Received December 2, 1969

The chemical effects of neutron capture have been studied in fulvalenehexacarbonyldimanganese, in order to determine whether or not the ring–ring bond survives nuclear recoil. Retention in the parent form (9.1%) is comparable to that in other organomanganese compounds, while the radiochemical yield of $CpMn(CO)_3$, the "monomer", is very much lower (0.2%). This suggests that the inter-ring bond is not broken under the conditions in the reaction zone. The formation of radiomanganese compounds with several carbonyl ligands (4.7%) is in accord with mass spectrometric evidence, which suggests that CO may be readily available in the reaction zone.

Canadian Journal of Chemistry, 48, 1614 (1970)

Our study of nuclear recoil reactions in organometal compounds (1–5) has led us to the conclusion that the nuclear reaction often causes fragmentation, but not atomization, of the molecule. The reconstitution of the molecules, incorporating the radioactive metal atom, must then occur by a process of reassembling the fragments. The question then is: To what extent does fragmentation occur?

Studies of methylcyclopentadienylmanganese tricarbonyl ($CH_3CpMn(CO)_3$) showed (2, 3, 5) that the parent compound is reformed, and also $CH_3Mn(CO)_5$ is formed. From this, two important conclusions can be drawn: the CH_3—Cp bond is sometimes, but not always, broken; the Mn—CO bond is frequently also broken in neighboring molecules to give a carbonyl-rich medium.

Further to our previous studies, we now report on recent experiments on fulvalenehexacarbonyldimanganese. This compound was recently reported by Rausch, Kovar, and Kraihanzel (6), who deduced it to have the following configuration

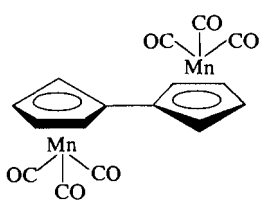

It seemed possible that the manganese atom, recoiling following neutron capture, might cause rupture of the bond joining the two rings. This would then give rise to the formation of $CpMn(CO)_3$ rather than of the fulvalene compound.

Experimental

A sample of fulvalene-$Mn_2(CO)_6$ was kindly supplied by Professor Rausch, and was used without further purification. The irradiated sample (~20 mg) was dissolved in 2 ml of a 4:1 petroleum ether–chloroform solution which contained about 5 mg of I_2 (to scavenge $HMn(CO)_5$ and $Mn(CO)_5$). Carriers were added for $IMn(CO)_5$, $CpMn(CO)_3$, and $Mn_2(CO)_{10}$, and the solution was chromatographed on silica gel to separate the components. $Mn_2(CO)_{10}$ was removed with 1% benzene in petroleum ether, $CpMn(CO)_3$ with 10% benzene in petroleum ether, and $IMn(CO)_5$ with 20–25% benzene in petroleum ether. The fulvalene-$Mn_2(CO)_6$ was finally removed with chloroform. In one case some of the fulvalene compound came along with the $IMn(CO)_5$ and was leached out with petroleum ether, in which the fulvalene compound is not soluble. Determination of chemical recovery was done spectrophotometrically, except for the fulvalene compound, which was weighed directly.

Separate tests showed that no reaction occurs between I_2 and fulvalene-$Mn_2(CO)_6$ in petroleum ether within 30 min. In particular, no conversion (i.e., $\ll 1\%$) to $IMn(CO)_5$ was detectable.

Neutron irradiations were done using the Sb–Be neutron source (7) at the Commercial Products Division, A.E.C.L. Measurement of the radioactivity was done by NaI scintillation counting, using the 0.84 MeV photopeak of ^{56}Mn.

Results and Discussion

The results of the measurements are given in Table 1, which also quotes corresponding data for $CpMn(CO)_3$. The data show clearly that while some radioactive $CpMn(CO)_3$ is formed, it

TABLE 1
Retention and yield data for neutron irradiated fulvalene-$Mn_2(CO)_6$ and corresponding data for $CpMn(CO)_3$*

	Yield of (%)		
Retention (%)	$CpMn(CO)_3$	$Mn_2(CO)_{10}$	$IMn(CO)_5$†
Fulvalene-$Mn_2(CO)_6$			
11.2	0.20	0.40	—
9.1	0.15	0.16	2.34
9.8	0.27	0.19	2.60
8.0	0.20	0.27	6.4
7.5	0.16	0.21	6.1
Ave. 9.1	0.20	0.25	4.4
$CpMn(CO)_3$‡			
7.0		0.3	7.0

*Retention and yield refer to the fraction of the total radioactivity found in the parent compound and in other species, respectively.
†The reason for the large deviations in these data is not immediately known, but doubtless lies in the difficulty of recovering the $IMn(CO)_5$ free from the fulvalene complex.
‡Data from ref. 3.

occurs only to a small extent, indeed the yield of this compound is only about 1/50 of the retention in the parent compound. This observation suggests that the inter-ring bond is not easily broken under the conditions prevailing in the recoil zone, or perhaps that the inter-ring bond may be broken and rapidly re-formed by a radical-cage recombination process. The mass spectrometric evidence (6) is in keeping with the former.

The yields of $I^{56}Mn(CO)_5$ and $^{56}Mn_2(CO)_{10}$ compare reasonably well with the corresponding yields in $CpMn(CO)_3$. This comparison shows that the formation of these carbonyl-rich species is not particularly sensitive to the structure of the target compound. The evident ready availability of CO is also in keeping with the mass spectrometric data (6, 8) for both the fulvalene and the simple cyclopentadienyl complexes, which show that the carbonyl groups are very easily removed from the molecules. The high retention of ^{56}Mn in the parent molecule is perhaps surprising. One would expect that the greater bulk of the fulvalene would give rise to a much smaller reformation of this molecule than is found (3) for the simpler $CpMn(CO)_3$. That this is not the case suggests, then, that the reformation may in both cases depend on the mobility of the Mn atom rather than on that of the ring ligand.

A further question is as to the detailed origin of the fragmentation, whether it is caused primarily by thermal effects ("impulse pyrolysis") resulting from the atom's recoil following high-energy γ emission or rather as a result of the extensive Auger ionization which follows internal conversion of low-energy γ transitions. Both processes occur, but it is not known which gives rise to those radioactive atoms which remain in chemical surroundings suited to the reconstitution of the observed molecules. The experiment of Carlson and White (9) showed that in gaseous $Pb(CH_3)_4$, ionization by X-rays bombardment led to subsequent multiple ionization and to virtually complete atomization of the molecule with almost no recoil energy being given to the lead atom. This is contrary to our observations on various manganese compounds; hence we believe that the fragments occurring in our system result from primarily thermal effects.

We are very grateful to Professor Rausch for giving us his last 100 mg of the fulvalene complex, and to the Commercial Products Division, A.E.C.L. for the use of their neutron source. The work was supported in part by the National Research Council of Canada.

1. T. Costea, I. Negoescu, P. Vasudev, and D. R. Wiles. Can. J. Chem. **44**, 885 (1966).
2. I. C. Yang and D. R. Wiles. Can. J. Chem. **45**, 1357 (1967).
3. I. G. deJong, S. C. Srinivasan, and D. R. Wiles. Can. J. Chem. **47**, 1327 (1969).
4. W. H. Wong and D. R. Wiles. Can. J. Chem. **46**, 3201 (1968).
5. S. C. Srinivasan, D. R. Wiles, and I. C. Yang. Inorg. Nucl. Chem. Lett. **2**, 399 (1966).
6. M. D. Rausch, R. F. Kovar, and C. S. Kraihanzel. J. Amer. Chem. Soc. **91**, 1259 (1969).
7. W. E. Downs and M. W. Davis. Nucl. Appl. Technol. 7, 466 (1969).
8. J. Müller and M. Herberhold. J. Organometal. Chem. **13**, 399 (1968).
9. T. A. Carlson and R. M. White. J. Chem. Phys. **48**, 5191 (1968).

Can. J. Chem. Downloaded from www.nrcresearchpress.com by 210.87.254.42 on 09/05/12
For personal use only.

Nuclear magnetic resonance study of proton exchange in the water – 2-propanol system

K. C. TEWARI AND N. C. LI
Department of Chemistry, Duquesne University, Pittsburgh, Pennsylvania 15219

Received October 28, 1969

The specific rate constants for the reaction

$$ROH + {}^*HOH \rightarrow ROH^* + HOH$$

where ROH is 2-propanol, have been determined at four different temperatures. The activation energy has been calculated to be 10.4 kcal/mole. In addition, the effect of the presence of several electron donors on the kinetics of the reaction has been noted.

Canadian Journal of Chemistry, **48**, 1616 (1970)

Can. J. Chem. Downloaded from www.nrcresearchpress.com by 210.87.254.6 on 09/05/12
For personal use only.

Nuclear magnetic resonance (n.m.r.) measurements on proton-exchange kinetics in aliphatic alcohol – water solutions have been reported by several authors (1–5). The protolysis reaction is found to be both acid and base catalyzed. Recently, Fukumi *et al.* (5) have reported specific rate constants for different processes in the water–2-propanol system. They calculated a value of 2.0 l mole^{-1} s^{-1} at 28 °C for the rate constant, k, of proton exchange between 2-propanol and water with no externally added acid or base

[1] $$ROH + {}^*HOH \rightarrow ROH^* + HOH$$

where R = i-C_3H_7. This value is to be compared with k = 0.35 ± 0.06 l mole^{-1} s^{-1} at 42°, reported by Paterson (3*b*). In view of the wide disagreement, we report here the specific rate constants for reaction [1], determined at four different temperatures, as well as the energy of activation. In addition, the effects of the presence of several electron donors on the kinetics of reaction [1] are reported.

Experimental

Materials

All reagents used were Fisher reagent grade, dried and doubly distilled by the usual methods. De-ionized, doubly distilled water was prepared; its pH varied between 6.7 and 7.0. The alcohol–water solutions were prepared by weight and the concentrations in moles/l calculated from the known density data at various temperatures (6). Since the solutions slowly leach impurities from the glass (3), a given set of n.m.r. measurements were done on the same day that the materials were distilled.

Nuclear Magnetic Resonance Measurements

Spectra were obtained with a Varian A-60 spectrometer. Care was taken to keep the radiofrequency power level well below saturation and the field homogeneity such that a resolution of 0.3 Hz or better was attained. During the recording of the spectra the temperature remained constant to ±1°. The precision in the n.m.r. measurements varied from 0.02 to 0.05 Hz, depending on signal shape. All measurements were an average of at least six determinations.

Results and Discussion

In neat 2-propanol at 31°, the —OH signal was a sharp doublet with spacing 4.22 Hz. In the alcohol–water solutions used in the present study, the —OH signals in 2-propanol and water are quite well separated; thus at 31°, for [H_2O] = 7.2 M, [2-propanol] = 11.2 M, the two —OH signals are separated by 44.6 Hz. The linewidth of the water signal, however, could not be measured accurately because of interference from the methine proton signal, and this has also been reported by Paterson (3*b*).

The specific rate constant, k, for reaction [1] was calculated from the relation (1, 3)

[2] $$\tau_{ROH} = \frac{[ROH]}{d[ROH]/dt} = \frac{1}{k[H_2O]}$$

where τ_{ROH} is the mean lifetime of a hydroxyl proton on a 2-propanol molecule ROH before exchange with a proton on a water molecule.

In order to evaluate successfully the mean lifetimes, it is necessary to know two experimentally determinable parameters: (*1*) the transverse relaxation time, T_2, in the absence of exchange and (*2*) the peak separation of the OH doublet in neat 2-propanol, which is due to spin–spin interaction, $\delta\omega$. Transverse relaxation time, T_2, was considered to be governed chiefly by magnetic field inhomogeneities, and was estimated from the linewidth of a degassed spectrograde

Can. J. Chem. Downloaded from www.nrcresearchpress.com by 210.87.254.6 on 09/05/12
For personal use only.

cyclohexane or purified water sample, by the equation

$$[3] \qquad T_2 = 2/\delta\omega_{\frac{1}{2}}$$

where $\delta\omega_{\frac{1}{2}}$ is the full width, rad s^{-1}, of the signal at half-height. As has been found by Paterson (3), the cyclohexane and water samples gave identical T_2 values within experimental error. The values of $\delta\omega$ and T_2 are slightly temperature-dependent and are listed in Table 1.

The theoretical spectra were calculated from eq. [4] (7)

$$[4] \qquad \frac{\delta\omega_e}{\delta\omega} = \left\{\left[4Q\left(\frac{2}{t}+\frac{1}{Q}\right)^3 + (Q^2+8)\left(\frac{2}{t}+\frac{1}{Q}\right)^2 + (Q^2+2)\left(\frac{2}{t}+\frac{1}{Q}\right)\frac{2}{Q}+1\right]^{\frac{1}{2}} - 4\left(\frac{2}{t}+\frac{1}{Q}\right)^2 - \left(\frac{2}{t}+\frac{1}{Q}\right)Q\right\}^{\frac{1}{2}}$$

where $\delta\omega_e$ is the peak separation of the O*H* doublet in the presence of water, under conditions of slow exchange, and the other terms are

$$[5] \qquad Q = T_2\,\delta\omega \qquad t = \tau\delta\omega$$

The values of τ were evaluated by interpolating from graphs of $\delta\omega_e/\delta\omega$ vs. $1/\tau\delta\omega$. Figure 1 gives plots of $1/\tau$ vs. $[H_2O]$, moles/l, at four different temperatures. From eq. [2], the slopes of the lines are the specific rate constants, k. These values are listed in the last column of Table 1. The point scatter in Fig. 1 is probably due to small traces of impurity, to which the exchange process is very susceptible (3*b*).

TABLE 1
Experimentally determined exchange parameters for 2-propanol and specific rate constants for proton exchange with water

Temperature, °C	$\delta\omega$, rad s^{-1}	T_2, s	k, l $mole^{-1}s^{-1}$
31.0	26.5	0.36	0.31±0.02
38.0	26.7	0.40	0.44±0.04
40.5	26.8	0.42	0.52±0.02
47.5	27.0	0.46	0.73±0.01

Our value of k at 40.5° is in fair agreement with ref. 3*b*, where the temperature is 42 ± 1°. The

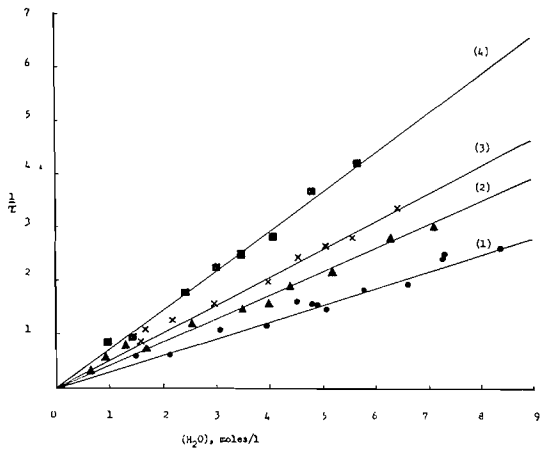

FIG. 1. Plots of $1/\tau$ vs. $[H_2O]$, mole/l at (*1*) 31.0, (*2*) 38.0, (*3*) 40.5, (*4*) 47.5 °C.

activation energy, E_a, for 2-propanol is calculated from a log k vs. $1/T$ plot to be 10.4 kcal/mole. It is interesting to compare this value with the approximate values of 10.0 and 7.6 kcal/mole quoted by Paterson (3) for the activation energy of proton transfer between ethanol and water. Paterson (3*b*) has shown that on the basis of inductive effects, ethanol is more acidic than 2-propanol and that the rates of proton exchange are actually in the order C_2H_5OH–H_2O > *i*-C_3H_7OH–H_2O. The larger activation energy found for the *i*-C_3H_7OH–H_2O system, therefore, is in line with the above.

The identification of k as the specific rate constant for reaction [1] is valid only if there is no other exchange process. Paterson (3*b*) has shown this to be true for R = *n*-C_3H_7 and *i*-C_3H_7, in view of the extremely small ionic concentrations in neutral alcohol–water solutions and the fact that there is no observable proton exchange in pure alcohols.[1] In our experiments, the p*H* of the water varied between 6.7 and 7.0, and suggests that the solutions used were approximately neutral.

[1]Dr. E. Grunwald has suggested the possibility that reaction [1] is catalyzed by a weakly buffered species at low concentrations, presumably the lyonium ion that results from the self-ionization of the solvent, and therefore the rate constants are pseudo constants and the activation energy is a composite quantity. Studies of the p*H* dependence of the exchange rate would throw more light on the interesting suggestion. The qualitative interpretation of Table 2, however, remains unchanged, since the effects of different electron donors would presumably be in the same relative order.

Can. J. Chem. Downloaded from www.nrcresearchpress.com by 210.87.254.6 on 09/05/12
For personal use only.

Effects of Electron Donors

It is known that hydrogen bonding of alcohol and water with electron-donors increases the lifetime of the —OH proton in the molecule. The phenomenon has been used in the detection of spin–spin multiplets in methanol containing acetone (8). Chapman and King (9) have used dimethyl sulfoxide as a solvent for the classification of alcohols in n.m.r. studies. Table 2 gives the effects of different electron-donors in decreasing values of $1/\tau$. The data show that of the three electron-donors used, the ability to depress $1/\tau$ increases in the order acetone, tetrahydrofuran, and dimethyl sulfoxide. This order is the same as the order of increasing electron-donor strength. Thus, for the reaction $OH_2.D + D = OH_2.D_2$, the equilibrium constants in mole fraction units are 0.9 (36° in cyclohexane (10)), 1.4 (35° in cyclohexane (10)), and 2.9 (35° in CCl_4 (11)) for D = acetone, tetrahydrofuran, and dimethyl sulfoxide, respectively.

TABLE 2

Values of $1/\tau$ in 2-propanol – H_2O systems at 32 °C

Concentration of H_2O, *M*	Electron donor and concentration, *M*	$1/\tau$
8.4	None	2.80
8.4	Acetone, 5.0	2.28
8.4	Tetrahydrofuran, 5.0	1.96
8.4	Dimethyl sulfoxide, 5.0	1.27

The —OH proton signal is shifted to higher field when neat 2-propanol is diluted with an electron donor. The extent of the over-all upfield shift caused by the presence of electron donors increases in the order: dimethyl sulfoxide, tetrahydrofuran, and acetone. Since shift to higher field indicates a decrease in hydrogen bonding, this order is in line with the order of decreasing hydrogen-bond strength

$$\overset{R}{HO}\ldots\overset{R}{HO} > (CH_3)_2SO\ldots\overset{R}{HO}$$

$$> \overline{CH_2(CH_2)_2CH_2O}\ldots\overset{R}{HO} > (CH_3)_2CO\ldots\overset{R}{HO}$$

Drinkard and Kivelson (12) have reported the same phenomena for methanol and water as hydrogen donors to acetone and dimethyl sulfoxide.

The authors thank the National Institute of General Medical Sciences, U.S. Public Health Service, for support under PHS Research Grant No. GM-10539-07.

1. Z. Luz, D. Gill, and S. Meiboom. J. Chem. Phys. **30**, 1540 (1959).
2. E. Grunwald, C. F. Jumper, and S. Meiboom. J. Amer. Chem. Soc. **84**, 4664 (1962).
3. (*a*) W. G. Paterson. Can. J. Chem. **41**, 714 (1963); (*b*) W. G. Paterson. Can. J. Chem. **41**, 2472 (1963).
4. W. G. Paterson and H. Spedding. Can. J. Chem. **41**, 2477 (1963).
5. T. Fukumi, Y. Fujiwara, Y. Arata, and S. Fujiwara. Bull. Chem. Soc. Jap. **41**, 41 (1968).
6. International critical tables. Vol. III. McGraw–Hill Book Co., Inc., New York. 1928. pp. 119–120.
7. M. Takeda and E. D. Stejskal. J. Amer. Chem. Soc. **82**, 25 (1960).
8. P. L. Corio, R. L. Rutledge, and J. R. Zimmerman. J. Amer. Chem. Soc. **80**, 3163 (1958).
9. O. L. Chapman and R. W. King. J. Amer. Chem. Soc. **86**, 1256 (1964).
10. F. Takahashi and N. C. Li. J. Amer. Chem. Soc. **88**, 1117 (1966).
11. S. F. Ting, S. M. Wang, and N. C. Li. Can. J. Chem. **45**, 425 (1967).
12. W. Drinkard and D. Kivelson. J. Phys. Chem. **62**, 1494 (1958).

Erratum: Pulse radiolysis of nitric oxide in aqueous solution[1]

W. A. Seddon and M. J. Young

Physical Chemistry Branch, Atomic Energy of Canada Limited, Chalk River Nuclear Laboratories, Chalk River, Ontario

Received March 3, 1970

(Ref.: Can. J. Chem. **48**, 393 (1970))

Canadian Journal of Chemistry, **48**, 1618 (1970)

On p. 393, second column, the ordinate of Fig. 1 should read $G\varepsilon \times 10^{-3}$ and not $\varepsilon \times 10^{-3}$.

[1]A.E.C.L. No. 3491.

The $CdO–CdF_2$ system: X-ray diffractogram, infrared spectrum, and density of $CdO.2CdF_2$

P. RAMAMURTHY AND E. A. SECCO
Chemistry Department, St. Francis Xavier University, Antigonish, Nova Scotia

Received January 5, 1970

The $CdO–CdF_2$ system has been studied by differential thermal analysis (DTA), X-ray powder diffraction, and infrared spectroscopy.

The results show a distinct X-ray diffractogram and infrared spectrum for the $CdO–CdF_2$ mole ratio 1:2, prefused and annealed, suggesting the existence of the compound $CdO.2CdF_2$. The compound undergoes a transformation at 690 °C, characterized by a low heat absorption suggesting an order–disorder phenomenon.

Canadian Journal of Chemistry, **48**, 1619 (1970)

Can. J. Chem. Downloaded from www.nrcresearchpress.com by 210.87.254.40 on 09/05/12
For personal use only.

Introduction

No study of the reaction between CdO and CdF_2 has been reported in the literature to date. A recent study (1) on the decomposition of CdOHF by DTA revealed an unknown endotherm at 687 °C which was tentatively assigned to CdF_2–quartz interaction, analogous to ZnF_2 behavior, forming a silicate. This endotherm was later observed to be present in CdOHF decomposition carried out in platinum lined sample tubes and furthermore, appeared sporadically in curves of prefused $CdO–CdF_2$ mixtures.

The purpose of this note is to clarify the origin of the 687 °C endotherm and report on a study of the $CdO–CdF_2$ reaction over an extended composition range.

Experimental

CdO and CdF_2 use in this work were Fisher Certified reagent grade and A. D. MacKay, Inc. C. P. grade, respectively. The physical mixtures of various compositions were prepared by thorough manual grinding. Each composition sample was prefused at 1000 °C in a platinum crucible in a well-type electric furnace with an ambient atmosphere of dry N_2 (Matheson Prepurified Grade with stated impurity of 0.003% oxygen). The fusion pretreatment enhanced the reproducibility of our measurements and dry N_2 precluded the oxidation of CdF_2. The fused mass was recovered by drilling; samples of this drilled powder were subjected to investigation.

All DTA curves were recorded on a duPont thermal analyzer, d.t.a.-900 using the 1200 °C cell with platinum-lined platinum cup holders and at a heating rate of 20 °C/min. The $CdO–CdF_2$ system is very reactive in the molten state; the liquid attacks the ceramic sleeve of the Pt thermocouple, and reduces the lifetime of the thermocouple.

The X-ray diffractograms and infrared spectra of the specimens were recorded as previously described (2).

Results and Discussion

Heating and cooling DTA curves at selected compositions to illustrate the pertinent features of thermal behavior with composition are shown in Fig. 1. The peak temperatures obtained from such curves were used to construct the reduced phase diagram given in Fig. 2. The diagram as presented resembles a binary system with partial miscibility in the liquid state with a monotectic evident at 970 °C and 20% CdO.

The appearance of the 690 °C endotherm for $CdO–CdF_2$ mixtures is dependent on the thermal history of the sample. This novel endotherm will *only* appear in the curve of $CdO–CdF_2$ mixtures after prefusion of the mixture at 1000 °C as shown in Fig. 3; the corresponding exothermic effect near 690 °C is absent on the cooling cycle. After prefusion of the mixture at 1000 °C, the DTA curve shows a broad exotherm in the region of 550–650 °C which is always followed by the endotherm at 690 °C. The broad exothermic effect is interpreted in terms of a sluggish rearrangement of the oxide–fluoride components leading to an ordered structure. The ordered structure may resemble (*i*) a defect-type compound, (*ii*) anionic substitution compound, or (*iii*) a super-lattice structure of the Au–Cu alloy type. The breakdown of the ordered structure is accompanied by the endothermic effect at 690 °C. The low heat effect involved in this breakdown is taken as strong evidence for an order–disorder phenomenon.

It should be reiterated that the decomposition DTA curve of CdOHF or CdODF *always* showed the 690 °C endotherm, suggesting that the ordered structure is a direct product of decomposition.

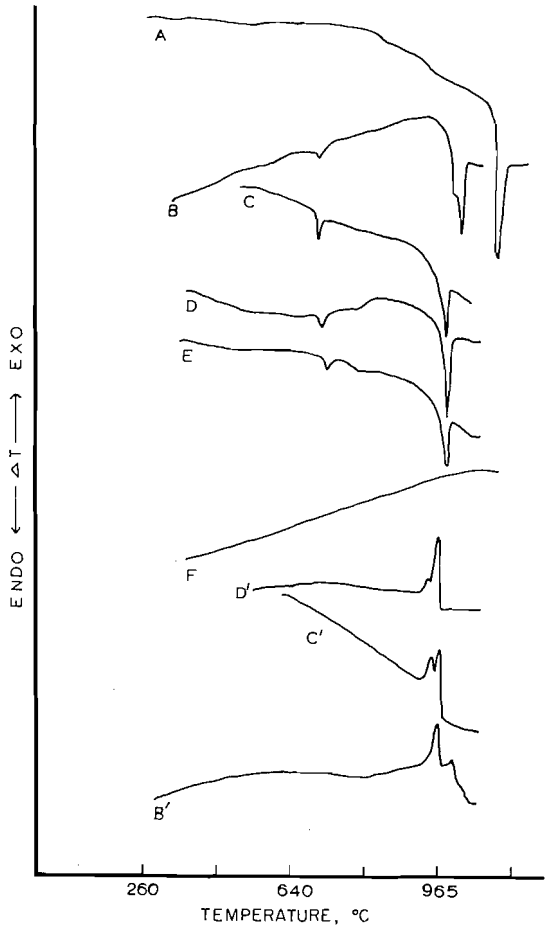

FIG. 1. Heating curves of CdO–CdF_2 mixtures, prefused at 1000 °C, at different compositions to illustrate pertinent features as a function of composition (% by weight). *A*, 100% CdF_2; *B*, 90% CdF_2, 10% CdO; *C*, 50% CdF_2, 50% CdO; *D*, 30% CdF_2, 70% CdO; *E*, 20% CdF_2, 80% CdO; *F*, 10% CdF_2, 90% CdO. *D'*, *B'*, *C'* are cooling curves for the given compositions.

The X-ray diffractogram of the residue immediately after the dehydroxylation step, 400 °C, confirmed the presence of the satellite peaks identified with the ordered structure, Fig. 4.

The X-ray diffractograms and infrared spectra in Figs. 4 and 5 reveal novel features, which attain a maximum for mixtures of 2:1 mole ratio of CdF_2–CdO suggesting the existence of the compound $CdO.2CdF_2$. Untreated room temperature preparations exhibit only CdO and CdF_2 characteristics as do samples pretreated at 1000 °C. Further annealing of the 1000 °C pretreated powder, however, at 500–600 °C for 1 h yields a novel infrared spectrum and a maximum in the diffractogram characteristics. The

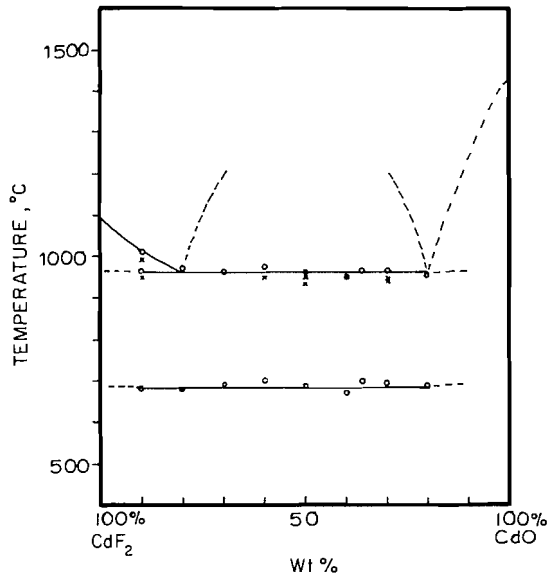

FIG. 2. Reduced phase diagram for the CdO–CdF_2 system determined by differential thermal analysis. O, heating cycle; ×, cooling cycle.

low temperature annealing, below the melting point of the sample, identifies the formation of the compound as a solid-state reaction.

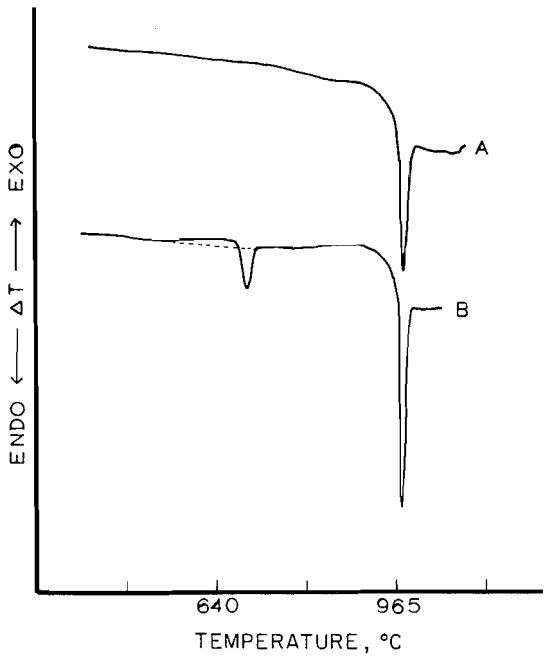

FIG. 3. Heating and cooling curves for 2:1 mole ratio CdF_2–CdO mixture. *A*, first heating cycle; *B*, second heating cycle. The dotted portion in *B* represents a broad exotherm preceding the 690 °C endotherm.

Can. J. Chem. Downloaded from www.nrcresearchpress.com by 210.87.254.40 on 09/05/12
For personal use only.

Can. J. Chem. Downloaded from www.nrcresearchpress.com by 210.87.254.40 on 09/05/12
For personal use only.

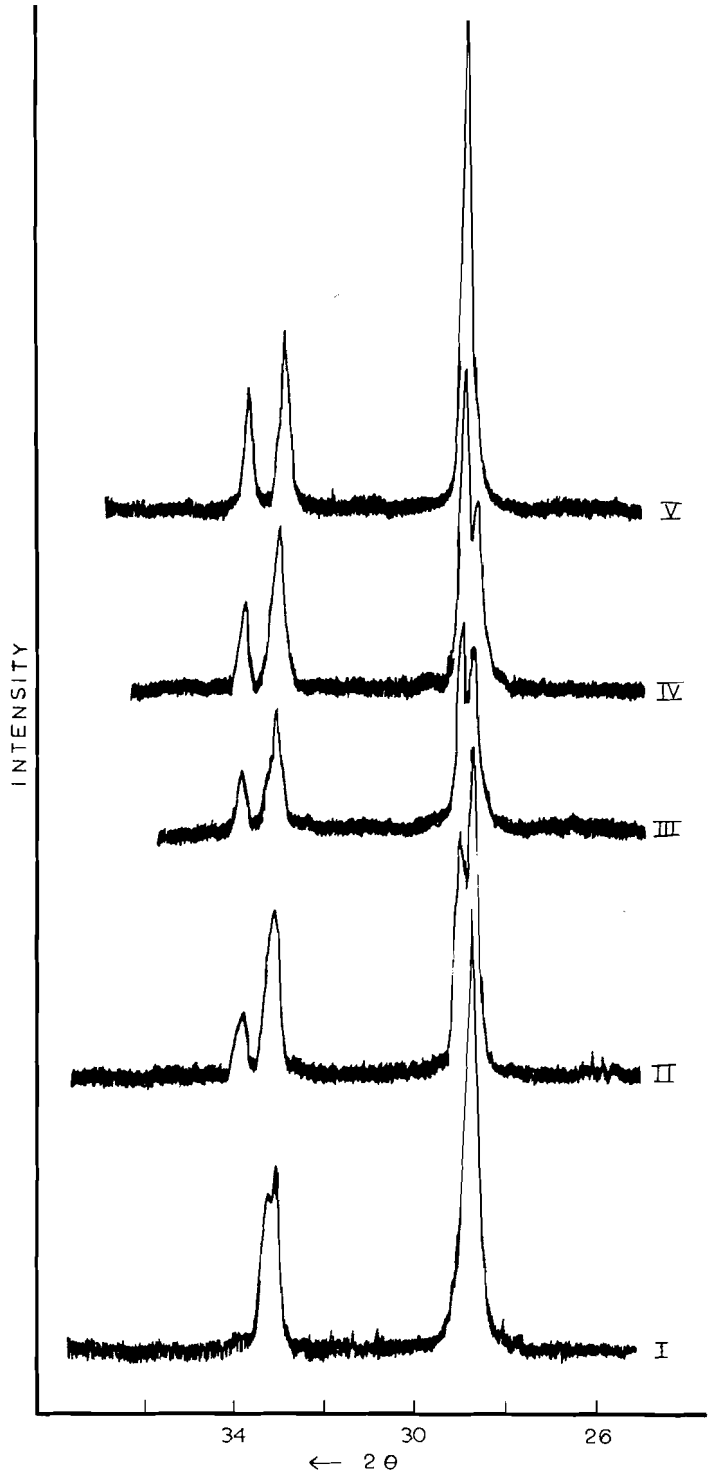

FIG. 4. X-Ray powder diffractograms of 2:1 CdF_2–CdO molar mixture, recorded at room temperature following heat treatment. *I*, fused at 1000 °C; *II*, after heating at 500 °C for 1/2 h; *III*, after heating at 500 °C for 1 h; *IV*, after heating at 500 °C for 1½ h; *V*, after heating at 500 °C for 2 h.

Can. J. Chem. Downloaded from www.nrcresearchpress.com by 210.87.254.40 on 09/05/12
For personal use only.

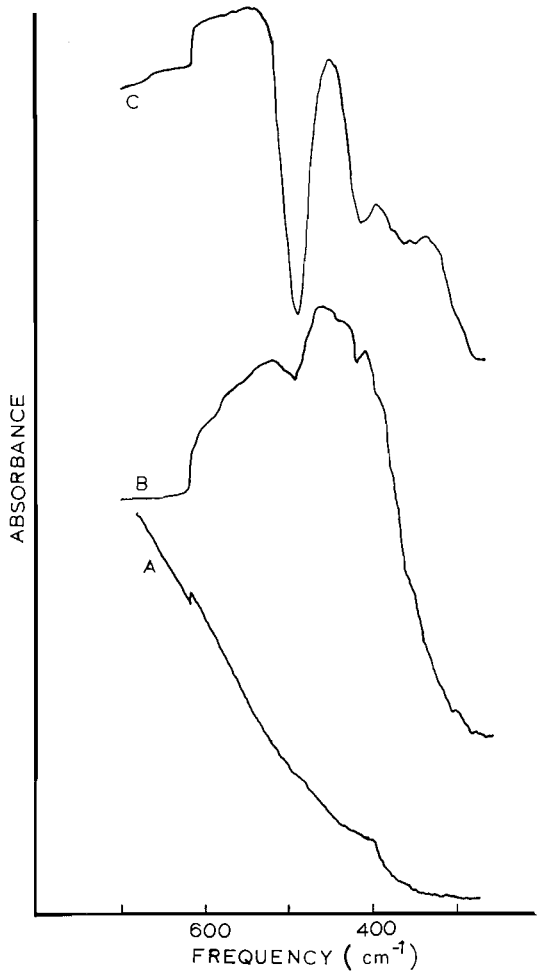

FIG. 5. Infrared spectra: *A*, CdF_2; *B*, 2:1 molar ratio of CdF_2–CdO mixture after fusion at 1000 °C in N_2 atmosphere; *C*, fused sample (*B*) after annealing at 600 °C for 30 mins.

The X-ray diffractograms for the compound and for the physical mixture are strikingly similar; compound peaks appear as satellites to the original peaks of CdF_2 and CdO until the latter are completely replaced for the 2:1 mole ratio of CdF_2–CdO. These satellites originate because (*i*) both CdO and CdF_2 crystallize in a cubic lattice structure, (*ii*) the radii of O^{2-} and F^- are reported as 1.40 and 1.36 Å, respectively (3), (*iii*) both ions are isoelectronic, with equal values for the scattering factors $f_{O^{2-}}$ and f_{F^-}. These structural similarities can be expected, from above considerations, to permit the substitution of O^{2-} for F^- in a predominant fluoride lattice with a minimum of distortion or alteration of the original lattice structure.

The densities of the 2:1 CdF_2–CdO samples at various stages of treatment are presented in Table 1. The density of the sample was determined by the displacement method at 25 °C using benzene as displacing fluid. The calculated density for untreated mixture was from 6.64 and 8.15 g/ml for CdF_2 and CdO, respectively. The density decrease in Table 1 furnishes strong support to the occupancy of normal anion F^- sites by O^{2-}, but for every O^{2-} in the crystal there must be incorporated also an anion vacancy (F^- omission) to maintain charge neutrality in the crystal as a whole, i.e.

TABLE 1

Densities of 2:1 CdF_2–CdO samples at various stages of treatment

Stage of treatment	Density (g/ml)
Physical mixture (untreated)	7.14 (calcd.)
Mixture heated at 1000 °C for 1 h	6.89±0.02
Fused mass annealed at 550 °C for 1 h	6.07±0.03

F^-	Cd^{2+}	F^-	Cd^{2+}
Cd^{2+}	O^{2-}	Cd^{2+}	F^-
F^-	Cd^{2+}		Cd^{2+}
Cd^{2+}	F^-	Cd^{2+}	F^-

The alternative lattice interpretation of O^- occupying F^- sites to maintain charge neutrality cannot be accommodated to the density decrease. If the compound $CdO.2CdF_2$ is, in fact, a defect-type compound, it is expected to possess semiconductor properties. Conductivity measurements of this compound is to be the subject of a future study in this laboratory.

The authors are indebted to the National Research Council of Canada for financial support and to Dr. Michael Falk, of Atlantic Regional Laboratory, Halifax, for providing infrared facilities.

1. O. K. SRIVASTAVA and E. A. SECCO. Can. J. Chem. 45, 1375 (1967).
2. P. RAMAMURTHY and E. A. SECCO. Can. J. Chem. 47, 1045 (1969).
3. L. PAULING. Nature of chemical bond. 3rd ed. Cornell University Press. Ithaca, New York. 1959. p. 514.

Reactions of acid chlorides with ethers in the presence of iron pentacarbonyl

HOWARD ALPER[1] AND J. T. EDWARD
Department of Chemistry, McGill University, Montreal, Quebec

Received September 9, 1969

Iron pentacarbonyl catalyzes the cleavage of alkyl ethers by acid chlorides to form alkyl chlorides and alkyl esters.

On catalyse avec le pentacarbonyle du fer la rupture des éthers alkyliques par les chlorures des acides carboxyliques, pour donner les chlorures et les esters alkyliques.

Canadian Journal of Chemistry, **48**, 1623 (1970)

Can. J. Chem. Downloaded from www.nrcresearchpress.com by 210.87.254.105 on 09/05/12
For personal use only.

Iron pentacarbonyl has proved a remarkably versatile reagent in organic chemistry, effecting deoximation (1), diene rearrangement (2), dehydration (3), and deoxygenation (4), and we have now found it to be effective in catalyzing the cleavage of alkyl ethers by acid chlorides. The last reaction is more effectively catalyzed by Lewis acids such as titanium, stannic, or zinc chlorides (5), but occasionally it may prove advantageous to use iron pentacarbonyl as a slower but milder catalyst.

Butyl ether was cleaved by octanoyl, benzoyl, and *p*-methoxybenzoyl chlorides in the presence of an equimolar amount of iron pentacarbonyl to give the corresponding butyl esters. (No attempt was made to isolate *n*-butyl chloride, presumably the other reaction product.) In similar fashion, benzoyl chloride (**1**; X = H) and *p*-methoxybenzoyl chloride (**1**; X = OMe) reacted with tetrahydrofuran (**2**; R = H) to give the chloroesters **3** (R = H, X = H, and OMe), and *p*-methoxybenzoyl chloride reacted with 2-methyltetrahydrofuran (**2**; R = Me) to give the chloroester **3** (R = Me, X = OMe). No

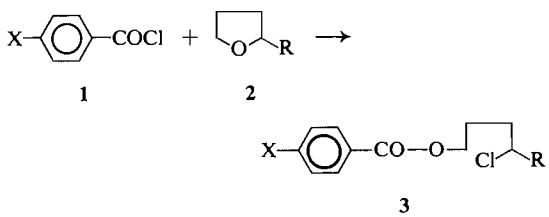

1 **2**

3

attempt was made to study the mechanism of these reactions; however, it was shown that it did not involve catalysis by ferric chloride, produced in some way from iron pentacarbonyl, because in the presence of anhydrous ferric chloride tetrahydrofuran reacted with *p*-methoxybenzoyl chloride to give not the chloroester **3** (R = H, X = OMe), but a high-boiling oligomer. This was shown by its nuclear magnetic resonance (n.m.r.) spectrum to be produced by the reaction of several tetrahydrofuran molecules for each acid chloride molecule. In the absence of the acid chloride, tetrahydrofuran was unaffected by ferric chloride (cf. ref. 6).

Experimental

Reaction of Acid Chlorides with Butyl Ether in Presence of Iron Pentacarbonyl

A mixture of the acid chloride (20–40 mmole) and iron pentacarbonyl (1.1 mole/mole of acid chloride) in dry butyl ether (40 ml) was boiled under reflux while being stirred under nitrogen for 17 h. The mixture was cooled, filtered to remove insoluble inorganic material (shown to contain ferrous chloride by a blue coloration with potassium ferricyanide), and concentrated at 30 mm. Distillation of the residue gave the butyl ester, identified by b.p. and infrared (i.r.) spectrum; yields and b.p.'s were: butyl octanoate, 75%, b.p. 243–245° (lit. b.p. 245° (7)); butyl benzoate, 67%, b.p. 248–250° (lit. b.p. 247° (7)); butyl *p*-methoxybenzoate, 66%, b.p. 165–167° at 20 mm (lit. b.p. 186–187° at 40 mm (7)).

Reaction of Acid Chlorides with Tetrahydrofuran and 2-Methyltetrahydrofuran in Presence of Iron Pentacarbonyl

A mixture of benzoyl chloride (5.25 g; 37.3 mmole) and iron pentacarbonyl (5.52 ml; 41.1 mmole) in dry tetrahydrofuran (40 ml) was refluxed while being stirred under nitrogen for 40 h. The mixture was worked up as above, and yielded 4-chlorobutyl benzoate (**3**; X = R = H) (7.98 g; 86%), b.p. 142–144° at 5 mm (lit. b.p. 140–143° at 5 mm (5)).

By the same procedure, *p*-methoxybenzoyl chloride in tetrahydrofuran gave 4-chlorobutyl *p*-methoxybenzoate (**3**; R = H, X = OMe) (78%), b.p. 160–162° at 1 mm, positive test for Cl, ν_{max} 1717 cm^{-1} (neat liquid). Nuclear

[1]Holder of NRCC Studentships, 1965–1967. Present address: Department of Chemistry, State University of New York at Binghamton, Binghamton, New York 13901, U.S.A.

magnetic resonance spectrum (in CCl_4):[2] triplet at δ 4.20 (CH_2 adjacent to —OCOR); triplet at δ 3.50 (CH_2 adjacent to Cl); multiplet at δ 1.82 (remaining CH_2CH_2).

Anal. Calcd. for $C_{12}H_{15}O_3Cl$: C, 59.4; H, 6.2. Found: C, 59.8; H, 6.4.

Similarly, *p*-methoxybenzoyl chloride in 2-methyltetrahydrofuran gave 4-chloro-1-pentyl *p*-methoxybenzoate (**3**; R = Me, X = OMe) (76%), b.p. 147–149° at 0.5 mm, positive test for Cl, ν_{max} 1720 cm^{-1} (neat). Nuclear magnetic resonance spectrum:[2] triplet at δ 4.17 (CH_2 adjacent to OCOR); multiplet at δ 4.05 (CHCl); doublet at δ 1.43 (CH_3); multiplet at δ 1.77 (remaining CH_2CH_2).

Anal. Calcd. for $C_{13}H_{17}O_3Cl$: C, 60.8; H, 6.7. Found: C, 61.1; H, 6.8.

Reaction of p-Methoxybenzoyl Chloride with Tetrahydrofuran in Presence of Ferric Chloride

A mixture of *p*-methoxybenzoyl chloride (43.9 mmole) and anhydrous ferric chloride (48.3 mmole) in dry tetrahydrofuran (40 ml) was refluxed for 40 h with stirring under nitrogen and then worked up by the usual procedure. A liquid boiling at 295–298° (0.4 mm) was obtained showing an n.m.r. spectrum similar to that of **3** (R = H, X = OMe), but having weaker aromatic and OMe signals.

[2]Aromatic and OMe protons gave signals at the expected frequencies.

We are grateful to the National Research Council of Canada for financial support.

1. H. Alper and J. T. Edward. J. Org. Chem. **32**, 2938 (1967).
2. H. Alper and J. T. Edward. J. Organometal. Chem. **14**, 411 (1968).
3. H. Alper and J. T. Edward. Can. J. Chem. **46**, 3112 (1968).
4. H. Alper and J. T. Edward. Can. J. Chem. In press.
5. M. G. Synerholm. Organic synthesis. Coll. Vol. III. *Edited by* E. C. Horning. J. Wiley and Sons, New York, 1955. p. 187.
6. J. Saegasa, H. Imai, and J. Furukawa. Macromol. Chem. **54**, 218 (1962).
7. C. D. Hodgman (*Editor*). Handbook of chemistry and physics. Chemical Rubber Publishing Co. Cleveland, 1966.

On the occurrence of ononin in *Thermopsis rhombifolia* (Nutt.) Richards

M. H. Benn and Churai Watanatada
Environmental Sciences Centre: Kananaskis, The University, Calgary 44, Alberta

Received December 2, 1969

Ononin, formononetin-*O*-β-D-glucopyranoside, was isolated from *Thermopsis rhombifolia* (Nutt.) Richards. It seems very probable that this is the substance A which Marion and Manske isolated from this plant, and that their substance B was formononetin itself.

Canadian Journal of Chemistry, 48, 1624 (1970)

The legume *Thermopsis rhombifolia* (Nutt.) Richards, known commonly as Buffalo- or Golden-bean,[1] is a conspicuous early-flowering prairie plant the seeds of which have long been recognized as poisonous (1), a property due to the presence of toxic quinolizidine alkaloids (2, 3).

In the course of their pioneering studies of the alkaloids of this plant, Marion and Manske described two crystalline, non-basic substances, A and B, which they isolated from dried plant tops. The two substances were characterized (2) by their solubility properties, melting points, and microanalytical data; thus A was sparingly soluble in water, but could be conveniently recrystallized from aqueous-dioxane or -pyridine, had m.p. 218–220°, and was assigned the composition $C_{19}H_{20}O_{10}$ (no methoxyl groups); B was similarly very sparingly soluble in water, but was more soluble than A in cold dioxane, and recrystallization from aqueous dioxane afforded colorless needles, m.p. 257°, with apparent composition $C_{22}H_{16}O_6$ (one methoxyl group).

In an attempt to establish the identity of these substances,[2] we reexamined *Thermopsis rhombifolia*, and from fresh plant tops we isolated material which seems to correspond to Marion and Manske's substance A; we comment here on its nature, as well as on the probable identity of substance B.

Our compound, like substance A, was spar-

[1]The plant blooms in spring at the time when the buffalo used to leave their wintering grounds and move out across the prairie and it is said that the Blackfoot Indians named it wudzi-eh-kay: the buffalo-flower (1).

[2]We hoped that, taken together with the alkaloid pattern, these compounds might provide chemical coordinates for use in a study of the effect of environment on *Thermopsis rhombifolia* populations.

Can. J. Chem. Downloaded from www.nrcresearchpress.com by 210.87.254.105 on 09/05/12
For personal use only.

magnetic resonance spectrum (in CCl_4):[2] triplet at δ 4.20 (CH_2 adjacent to —OCOR); triplet at δ 3.50 (CH_2 adjacent to Cl); multiplet at δ 1.82 (remaining CH_2CH_2).

Anal. Calcd. for $C_{12}H_{15}O_3Cl$: C, 59.4; H, 6.2. Found: C, 59.8; H, 6.4.

Similarly, *p*-methoxybenzoyl chloride in 2-methyltetrahydrofuran gave 4-chloro-1-pentyl *p*-methoxybenzoate (**3**; R = Me, X = OMe) (76%), b.p. 147–149° at 0.5 mm, positive test for Cl, ν_{max} 1720 cm^{-1} (neat). Nuclear magnetic resonance spectrum:[2] triplet at δ 4.17 (CH_2 adjacent to OCOR); multiplet at δ 4.05 (CHCl); doublet at δ 1.43 (CH_3); multiplet at δ 1.77 (remaining CH_2CH_2).

Anal. Calcd. for $C_{13}H_{17}O_3Cl$: C, 60.8; H, 6.7. Found: C, 61.1; H, 6.8.

Reaction of p-Methoxybenzoyl Chloride with Tetrahydrofuran in Presence of Ferric Chloride

A mixture of *p*-methoxybenzoyl chloride (43.9 mmole) and anhydrous ferric chloride (48.3 mmole) in dry tetrahydrofuran (40 ml) was refluxed for 40 h with stirring under nitrogen and then worked up by the usual procedure. A liquid boiling at 295–298° (0.4 mm) was obtained showing an n.m.r. spectrum similar to that of **3** (R = H, X = OMe), but having weaker aromatic and OMe signals.

[2]Aromatic and OMe protons gave signals at the expected frequencies.

We are grateful to the National Research Council of Canada for financial support.

1. H. Alper and J. T. Edward. J. Org. Chem. **32**, 2938 (1967).
2. H. Alper and J. T. Edward. J. Organometal. Chem. **14**, 411 (1968).
3. H. Alper and J. T. Edward. Can. J. Chem. **46**, 3112 (1968).
4. H. Alper and J. T. Edward. Can. J. Chem. In press.
5. M. G. Synerholm. Organic synthesis. Coll. Vol. III. *Edited by* E. C. Horning. J. Wiley and Sons, New York, 1955. p. 187.
6. J. Saegasa, H. Imai, and J. Furukawa. Macromol. Chem. **54**, 218 (1962).
7. C. D. Hodgman (*Editor*). Handbook of chemistry and physics. Chemical Rubber Publishing Co. Cleveland, 1966.

On the occurrence of ononin in *Thermopsis rhombifolia* (Nutt.) Richards

M. H. Benn and Churai Watanatada
Environmental Sciences Centre: Kananaskis, The University, Calgary 44, Alberta

Received December 2, 1969

Ononin, formononetin-*O*-β-D-glucopyranoside, was isolated from *Thermopsis rhombifolia* (Nutt.) Richards. It seems very probable that this is the substance A which Marion and Manske isolated from this plant, and that their substance B was formononetin itself.

Canadian Journal of Chemistry, 48, 1624 (1970)

The legume *Thermopsis rhombifolia* (Nutt.) Richards, known commonly as Buffalo- or Golden-bean,[1] is a conspicuous early-flowering prairie plant the seeds of which have long been recognized as poisonous (1), a property due to the presence of toxic quinolizidine alkaloids (2, 3).

In the course of their pioneering studies of the alkaloids of this plant, Marion and Manske described two crystalline, non-basic substances, A and B, which they isolated from dried plant tops. The two substances were characterized (2) by their solubility properties, melting points, and microanalytical data; thus A was sparingly soluble in water, but could be conveniently recrystallized from aqueous-dioxane or -pyridine, had m.p. 218–220°, and was assigned the composition $C_{19}H_{20}O_{10}$ (no methoxyl groups); B was similarly very sparingly soluble in water, but was more soluble than A in cold dioxane, and recrystallization from aqueous dioxane afforded colorless needles, m.p. 257°, with apparent composition $C_{22}H_{16}O_6$ (one methoxyl group).

In an attempt to establish the identity of these substances,[2] we reexamined *Thermopsis rhombifolia*, and from fresh plant tops we isolated material which seems to correspond to Marion and Manske's substance A; we comment here on its nature, as well as on the probable identity of substance B.

Our compound, like substance A, was spar-

[1]The plant blooms in spring at the time when the buffalo used to leave their wintering grounds and move out across the prairie and it is said that the Blackfoot Indians named it wudzi-eh-kay: the buffalo-flower (1).

[2]We hoped that, taken together with the alkaloid pattern, these compounds might provide chemical coordinates for use in a study of the effect of environment on *Thermopsis rhombifolia* populations.

Can. J. Chem. Downloaded from www.nrcresearchpress.com by 210.87.254.5 on 09/05/12
For personal use only.

Can. J. Chem. Downloaded from www.nrcresearchpress.com by 210.87.254.5 on 09/05/12
For personal use only.

ingly soluble in water but could be recrystallized from aqueous dioxane to yield fine, felted needles, m.p. 218–219°. An analysis of spectroscopic data, provided in the Experimental section, rapidly established that our compound was an isoflavone hexoside, almost certainly ononin, formononetin-O-β-D-glucopyranoside (4); a conclusion that was verified by comparison of our compound with authentic ononin.

We did not encounter anything resembling substance B, but acid hydrolysis of ononin gives formononetin, m.p. 257°, and we find the correspondence of m.p. and solubility properties of B and formononetin most suggestive.

Unfortunately the original specimens of substances A and B are no longer available so we lack the unequivocal test of their identity which comparison with authentic materials would have provided; however, we believe that Marion and Manske's substance A was ononin, and that their substance B was formononetin possibly formed, or increased in amount, by enzymatic hydrolysis of the glucoside during the drying process.[3]

The occurrence of ononin in *Thermopsis rhombifolia* is not untoward: isoflavones are now considered to be a phytochemical characteristic of the sub-family Papilionatae, to which *Thermopsis* belongs.

Experimental

Melting points are corrected. Infrared (i.r.) and ultraviolet spectra were recorded on Perkin–Elmer 337 and 202 spectrophotometers, respectively. Proton magnetic spectra were recorded on a Varian A-60 spectrometer with tetramethylsilane as an internal standard. The mass-spectrum was measured at the University of Alberta, Edmonton, using an AEI-MS9 spectrometer.

Isolation of Ononin

Fresh above-ground parts of *T. rhombifolia*, collected at the commencement of blossoming, were macerated in methanol (Waring blender) and the slurry filtered. The residue was similarly thrice reextracted with methanol, and after being air-dried amounted to 235 g.

The combined methanol extracts were evaporated (Cyclone) to small bulk, then diluted to ca. 1 l with 1 *N* aqueous sulfuric acid and extracted with hexane (3 × 250 ml). The acid solution was then brought to p*H* ca. 13 with ammonium hydroxide and extracted with chloroform (5 × 150 ml). The aqueous solution was then brought to p*H* ca. 8 with 6 *N* aqueous sulfuric acid and allowed to stand at room temperature.

The yellowish solid which separated was collected, washed with water, and recrystallized from aqueous dioxane to yield fine colorless felted needles, m.p. 218–219° (370 mg); ν_{max} (KBr) 3400 (br., str.), 1645 and 1630 cm^{-1} (d., str.); τ (pyridine-d_5) 6.27 (3H) (s) (OCH_3), 5.65 (ca. 7H) (br. m.) (glucose C—H), 4.20 (1H) (br. d., *J* ca. 7Hz) (anomeric H), 2.97 and 2.82 (2H) (d, *J* = 9Hz) (H-3′ and -5′, partly obscured by a solvent peak at τ 2.75), 2.60 (ca. 2H) (br. m.) (H-6 and H-8, part of the H-6 signal was also masked by the solvent peak at τ 2.75), 2.31 and 2.16 (2H) (d, *J* = 9Hz) (H-2′ and -6′) 1.85 (1H) (s) (H-2), and 1.70 and 1.55 (1H) (d, *J* = 9Hz) (H-5); λ_{max} (90% v/v aqueous EtOH) 265 (ε ca. 22 000) and 293 nm (inflex., ε ca. 12 000).[4] The i.r. spectrum was superimposable upon that of authentic ononin and the mixed melting point was undepressed.

Acetylation (pyridine – acetic anhydride) of our glucoside gave a *tetraacetate*, m.p. 180° (lit. (5, 7) m.p. 183–184°), colorless needles from ethanol; *m/e* 598 (M^+, $C_{30}H_{30}O_{13}$) (45%) (base peak, *m/e* 331, tetraacetylhexopyranosyl cation); τ ($CDCl_3$) 7.93 (12H) (4 × CH_3COO—), 6.17 (3H) (s) (OCH_3), 5.90 (1H) (br. s.) (glucose H-5), 5.75 (2H) (m) (glucose H-6), 4.70 (4H) (br. s.) (glucose H-1,2,3,4), 3.0 (4H) (br. m.) (H-3′,-5′,-6 and -8), 2.55 and 2.40 (2H) (d, *J* = 9Hz) H-2′ and -6′), 2.05 (1H) (s) (H-2), and 1.83 and 1.68 (1H) (d, *J* = 9Hz) (H-5).

Hydrolysis of our glucoside (50 mg) was achieved by dissolving it in methanol (5 ml) to which concentrated hydrochloric acid (1.5 ml) had been added and refluxing the solution for 3 h. The crystals which separated had m.p. 257–258°, undepressed on admixture with authentic formononetin; the i.r. spectra of these two compounds were superimposable.

We are grateful to Dr. Gernot Schultz and Professor Ph. Lebreton for samples of authentic ononin and formononetin, as well as spectroscopic data.

1. A. JOHNSTON. Man's utilisation of the flora of the northwestern plains. *In* Post-pleistocene man and his environment on the northern plains. *Edited by* R. G. Forbis, L. B. Davis, O. A. Christensen, and G. Fedirchuk. University of Calgary, Archeological Society, Calgary, 1969. p. 109. E. V. A. MURPHY. Indian uses of native plants. Desert Printers Inc., Palm Desert, Calif., 1959. A. C. BUDD and K. F. BEST. Wild plants of the Canadian prairie. The Queen's Printer, Ottawa, 1964.
2. L. MARION and R. H. F. MANSKE. Can. J. Res. **B21**, 144 (1943).
3. T. A. HENRY. The plant alkaloids. 4th edition. J. A. Churchill Ltd., London, 1949. p. 151.
4. W. BAKER, R. ROBINSON, and N. M. SIMPSON. J. Chem. Soc. 274 (1933). G. ZEMPLÉN, L. FARKAS, and A. BIEN. Ber. **77**, 452 (1944). L. FARKAS and J. VARADAY. Ber. **92**, 819 (1959).
5. J. B. HARBORNE. Comparative biochemistry of the flavanoids. Academic Press, New York, 1967. p. 168, in footnote 2 to Table 5.8.
6. P. LEBRETON, K. R. MARKHAM, W. T. SWIFT III, OUNG-BORAN, and T. J. MABRY. Phytochem. **6**, 1675 (1967).

[3]Interestingly, Harborne has noted that he has found formononetin to be present in five (unidentified) species of *Thermopsis* (5), but it is not clear whether fresh, or dried, plant material was used in these studies.

[4]This spectroscopic data may be compared with that reported for ononin by Lebreton *et al.* (6).

Can. J. Chem. Downloaded from www.nrcresearchpress.com by 210.87.254.40 on 09/05/12
For personal use only.

Reaction of conjugated enones with divinylcopperlithium tri-*n*-butylphosphine complex. A new preparation of γ,δ-unsaturated ketones

JOHN HOOZ AND ROBERT B. LAYTON[1]

Department of Chemistry, University of Alberta, Edmonton, Alberta

Received February 16, 1970

A new synthesis of γ,δ-unsaturated ketones is reported, based on the reaction of α,β-unsaturated ketones with a vinyl ate complex.

Canadian Journal of Chemistry, **48**, 1626 (1970)

The discovery of lithium dimethylcuprate, $(CH_3)_2CuLi$, by Gilman and coworkers (1) has sparked renewed interest in the properties and reactions of ate complexes (2). Reagents of the type R_2CuLi, or analogs in which an alkyl (or aryl) copper reagent is stabilized by complexation with phosphorus- or sulfur-containing ligands possess considerable synthetic value for the construction of new carbon–carbon bonds (3–6). Recently, several vinyl ate complexes have also been prepared and demonstrated to undergo a coupling reaction with organic halides (5, 7), as well as oxidative and thermally-induced dimerization to dienes (8).

We wish to report that vinyl ate complexes efficiently transfer a vinyl group to the β-carbon atom of conjugated enones to provide good yields of γ,δ-unsaturated ketones. The reagent, formulated (merely for convenience)[2] as $(CH_2{=}CH)_2CuLiP(n\text{-}C_4H_9)_3$, is easily and rapidly prepared by the addition of two equivalents of a solution of vinyllithium in tetrahydrofuran (THF) to one equivalent of tetrakis[iodo-(tri-*n*-butylphosphine)copper (I)] (9) dissolved in THF at −78° under nitrogen.[3] Addition of a conjugated enone to the resultant deeply colored mixture gives, after suitable processing, good yields (65–89%) of the conjugate addition product. The reaction is usually complete in ca. 30 min at −78°, although β,β-disubstituted enones react more slowly. Some typical transformations are depicted in eqs. [1]–[6]. In all instances the products were analyzed by gas–liquid partition chromatography (g.l.p.c.), isolated, and characterized by infrared (i.r.), nuclear magnetic resonance (n.m.r.), and mass spectroscopy, as well as satisfactory combustion analysis.

Of particular note is the high yield obtained in the case of isophorone (eq. [6]). Although we have not undertaken any detailed systematic comparisons between the efficiency toward conjugate addition of vinylic copper ate complexes vs. the Kharasch–Michael[4] procedure (copper-catalyzed Grignard reaction), we have observed a maximum of 8% yield of 1,4-addition product when isophorone was treated with vinylmagnesium chloride using cuprous iodide catalysis.[5] This striking difference not only illustrates that different intermediates are involved in each case, but also points to the possible synthetic advantages of employing pre-formed ate complexes in certain structural situations.

Although the mechanistic details of either process are not yet fully understood, recent work has discounted the intermediacy of free radicals, carbanions, or a pathway involving a cyclic

[1]Holder of a 1967 Science Scholarship.

[2]We intend no structural implications by employing this designation; rather, this formulation is used for simplicity and by consideration of stoichiometry and analogy (2, 5).

[3]Alternatively, the phosphine-free species, $(CH_2{=}CH)_2CuLi$, may be prepared by treating vinyllithium (two equivalents) with cuprous iodide (one equivalent). The rate of formation of this reagent, and its rate of reaction with enones, however, is considerably slower than the phosphine-complexed species.

[4]We suggest this name combination as a succinct way of expressing "the copper-catalyzed 1,4-addition of Grignard Reagents to α,β-unsaturated carbonyl compounds", without any implications regarding mechanism.

[5]Also, mesityl oxide gives a maximum of 7% yield of conjugate addition product under similar conditions.

[1] 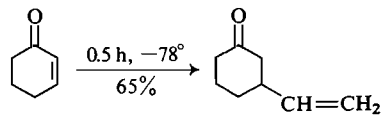

[2] 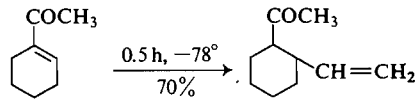

[3] 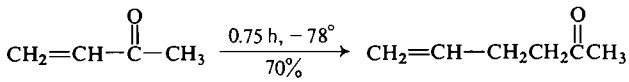

[4] 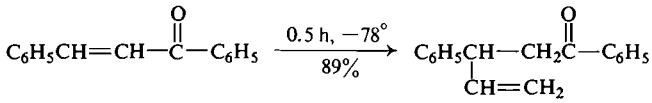

[5] 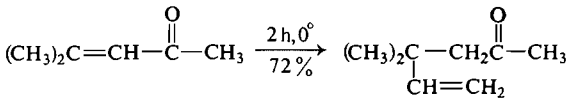

[6] 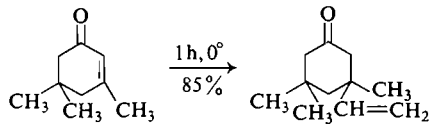

six-centered transition state (3). The current hypothesis is that either partial or complete electron transfer from organometallic to enone occurs to give rise to, respectively, either a charge-transfer complex, or an ion radical (3). An observation we have made which lends some credence (but certainly offers no definitive proof) to the validity of this notion is the isolation, using the Kharasch–Michael reaction on isophorone, of ca. 7% of the dimer **1**.

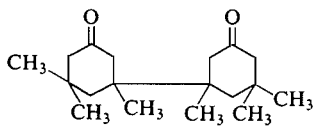

1

The experimental procedure is illustrated for the preparation of 3-vinyl-3,5,5-trimethylcyclohexanone. A solution of vinyllithium[6] (90 mmole) in THF was slowly added to a cooled (−78°), stirred, THF solution of 45 mmole tetrakis[iodo-(tri-*n*-butylphosphine)copper(I)] (9) to yield a blue–black mixture. A solution of isophorone (22 mmole) in THF was added (20 min), the resultant solution was allowed to warm to 0°, then maintained at 0° for 1 h. The mixture was poured into a saturated ammonium chloride solution, and extracted with ether (3 × 50 ml). After removal of solvent from the combined, dried (Na_2SO_4) extracts, g.l.p.c. analysis indicated an 85% yield of product. Chromatography of the crude mixture on silicic acid (elution with chloroform), and subsequent distillation of the carbonyl-containing fraction afforded 1.56 g (60%) of 3-vinyl-3,5,5-trimethylcyclohexanone, b.p. 132–135°(34 mm); n_D^{25} 1.4655; i.r. (liquid film) 1710 (C=O), 910, 1635, 3080 cm^{-1} (—CH=CH_2); n.m.r. ($CDCl_3$) 4.2(—C*H*=CH_2, 1,m), 5.1(—CH=CH_2,2,m), 7.62(—COCH_2C(CH_3)-CH=CH_2, 2, q), 7.85(—COCH_2C(CH_3)$_2$, 2,s), 8.31 ((CH_3)$_2$C—CH_2C(CH_3)CH=CH_2, 2, s), 8.92 (—CH_3—CCH=CH_2, 3,s), 8.99 ((CH_3)$_2$C, 3,s),

[6] Obtained from Alfa Inorganics, Inc.

Can. J. Chem. Downloaded from www.nrcresearchpress.com by 210.87.254.40 on 09/05/12
For personal use only.

9.02 τ ($(CH_3)_2C$, 3,s); mass spectrum (70 eV) M^+ 166.

We wish to thank the National Research Council of Canada for financial support of this work.

1. H. GILMAN, R. D. JONES, and L. A. WOODS. J. Org. Chem. **17**, 1630 (1952); H. GILMAN and G. M. STRALEY. Rec. Trav. Chim. **55**, 821 (1936).
2. W. TOCHTERMANN. Angew. Chem. Int. Ed. Engl. **5**, 351 (1966); G. WITTIG. Quart. Rev. (London), **20**, 191 (1966). Recent reviews of ate complexes.
3. H. O. HOUSE, W. L. RESPESS, and G. M. WHITESIDES. J. Org. Chem. **31**, 3128 (1966); H. O. HOUSE and W. J. FISCHER, JR. J. Org. Chem. **33**, 949 (1968).
4. E. J. COREY and G. H. POSNER. J. Amer. Chem. Soc. **89**, 3911 (1967); **90**, 5615 (1968).
5. G. M. WHITESIDES, W. F. FISCHER, JR., J. SAN FILIPPO, JR., R. W. BASKE, and H. O. HOUSE. J. Amer. Chem. Soc. **91**, 4871 (1969).
6. E. J. COREY and J. A. KATZENELLENBOGEN. J. Amer. Chem. Soc. **91**, 1851 (1969).
7. G. BÜCHI and J. A. CARLSON. J. Amer. Chem. Soc. **90**, 5336 (1968).
8. G. M. WHITESIDES, J. SAN FILIPPO, JR., C. P. CASEY, and E. J. PANEK. J. Amer. Chem. Soc. **89**, 5302 (1967); G. M. WHITESIDES and C. P. CASEY. J. Amer. Chem. Soc. **88**, 4541 (1966).
9. G. B. KAUFFMAN and L. A. TETER. Inorg. Syn. **7**, 9 (1963).

Can. J. Chem. Downloaded from www.nrcresearchpress.com by 210.87.254.40 on 09/05/12
For personal use only.

Can. J. Chem. Downloaded from www.nrcresearchpress.com by 210.87.254.5 on 09/05/12
For personal use only.

Canadian Journal of Chemistry

Published by THE NATIONAL RESEARCH COUNCIL OF CANADA

VOLUME 48 JUNE 1, 1970 NUMBER 11

Cycloaddition reactions. Thermal addition of dimethyl acetylenedicarboxylate to 1-methoxyindene

TERRENCE W. DOYLE

Bristol Laboratories of Canada Limited, 100 Industrial Boulevard, Candiac, Quebec

Received November 26, 1969

The cycloaddition of 1-methoxyindene **2** to dimethyl acetylenedicarboxylate to form a fused cyclobutene system **3** is discussed. Photochemical ring enlargement of **3** leads to a benzocycloheptatriene system **5** while reduction yields a dihydro derivative **4**. Saponification of **3** followed by photochemical ring expansion yields the diacid **7** which is subsequently hydrolyzed and decarboxylated to ketoacid **8**.

Canadian Journal of Chemistry, 48, 1629 (1970)

Introduction

The reactions of cyclic enamines with activated acetylenes to form fused cyclobutenes, which subsequently ring expand, have been extensively studied (1). The corresponding reactions of enol ethers have not been examined in the same detail (2). Recently the photochemical cycloadditions of diphenylacetylene (3*a*) and dimethyl acetylenedicarboxylate (3*b*) to dihydropyran have been reported. Several groups have shown that benzyne reacts with enol ethers to form benzocyclobutenes (4).

We would now like to report on the thermal 2 + 2 cycloaddition[1] of dimethyl acetylenedicarboxylate to 1-methoxyindene and some subsequent transformations of the adduct.

[1]In their original form the Woodward–Hoffman rules forbid 2 + 2 multicenter cycloadditions (5). However, cycloaddition reactions of acetylenes and heterocumulenes with olefins may also be regarded as 2 + 2 + 2 cycloadditions which are thermally allowed processes (2, 6) e.g.

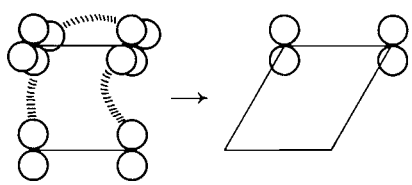

Results and Discussion

1-Methoxyindene (**2**) was prepared in 87% yield from 2-bromo-1-methoxyindane[2] by dehydrobromination with potassium *t*-butoxide (Scheme 1).

Equivalent amounts of **2** and dimethyl acetylenedicarboxylate were refluxed in toluene for 5 h. The reaction course was readily followed by monitoring the disappearance of the olefinic proton of 1-methoxyindene at 4.68 τ in the nuclear magnetic resonance (n.m.r.) spectrum. Distillation of the residue after evaporation of the toluene afforded 1-methoxy-6,7-dicarbomethoxybenzo[2,3]bicyclo(3.2.0)hepta-2,6-diene (**3**) in 73% yield.

The adduct **3** absorbed one equivalent of hydrogen on hydrogenation over platinum to yield 1-methoxy-6,7-dicarbomethoxybenzo[2,3]-bicyclo[3.2.0]hept-2-ene (**4**) in 93% yield. The stereochemistry of this dihydro product has not been determined.

The Woodward–Hoffmann rules (6*b*) governing electrocyclic reactions predict that ring opening in **3** should be photochemically allowed and thermally forbidden. Our results are in accord

[2]The 2-bromo-1-methoxyindane was prepared in 84% yield from the sulfuric acid catalyzed reaction of indene, methanol, and *N*-bromosuccinimide according to Iovchev (7).

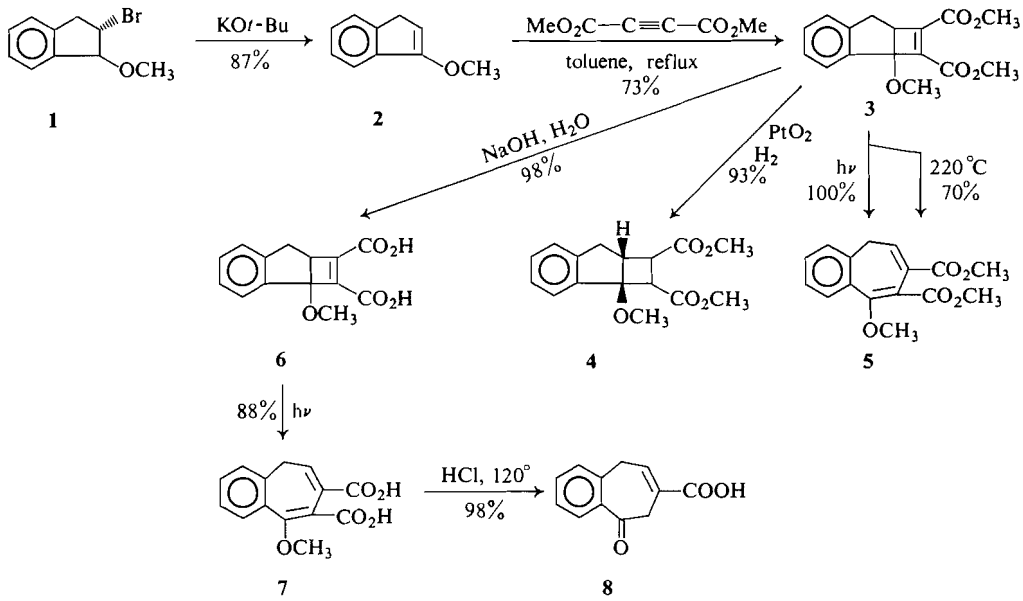

1 2 3 6 4 5 7 8

SCHEME 1

with this prediction. We have found that when **3** was irradiated at room temperature a smooth conversion of **3** to its ring-expanded isomer **5** resulted. In contrast, the thermal conversion of **3** to **5** required temperatures in excess of 200 °C.

Saponification of the adduct **3** gave 1-methoxybenzo[2,3]bicyclo(3.2.0)hepta-2,6-dien-6,7-dicarboxylic acid (**6**) in 97% yield. Irradiation of the diacid **6** converted it into the isomeric acid 1-methoxybenzo(6,7)-5-*H*-cycloheptatrien-2,3-dicarboxylic acid (**7**) in 88% yield again in accord with the prediction that such a photochemical ring opening should occur (6*b*). Attempts to prepare diacid **7** by the saponification of diester **5** failed.

Acid treatment of dicarboxylic acid **7** afforded the decarboxylated product benzo(6,7)cyclohepta-3,6-dien-1-one-3-carboxylic acid (**8**) in 98% yield. The position of the double bond out of conjugation with the ketone was shown by the n.m.r. spectrum of **8** (Table 1).

Summary

We have shown that 1-methoxyindene (**2**) undergoes a thermal 2 + 2 cycloaddition reaction with dimethyl acetylenedicarboxylate to form a fused cyclobutene **3**. Irradiation of this adduct led to the ring-expanded product **5**. These reactions may prove of synthetic utility in the preparation of multifunctional medium ring compounds.

Experimental

The infrared (i.r.) spectra were recorded on a Unicam SP-200G grating i.r. spectrometer. The n.m.r. spectra were determined on a Varian A60-A spectrometer using tetramethylsilane as an internal standard. Melting points are uncorrected and were determined on a Gallenkamp melting point apparatus. The analyses were performed by Micro-Tech Laboratories, Skokie, Illinois.

1-Methoxyindene (2)

To 41 g (1.05 g atoms) potassium metal dissolved in 750 ml of *t*-butanol was added 226.0 g (1.0 mole) 2-bromo-1-methoxyindane (7) at such a rate as to maintain a vigorous reflux (as the bromo compound was added a deep blue–black color developed). When all of the bromide had been added, the *t*-butanol was removed by distillation. To the residual slurry was added 500 ml of methylene chloride. The suspension was filtered and the filter cake washed with methylene chloride. The filtrate was distilled to yield 126.0 g of **2** (87%), b.p. 101–104°/15 mm.

Anal. Calcd. for $C_{10}H_{10}O$: C, 82.16; H, 6.89. Found: C, 82.30; H, 6.85.

The i.r. spectrum (neat) $\rangle C{=}C \langle$ 1620, 1605, 1578 cm^{-1}.

1-Methoxy-6,7-dicarbomethoxybenzo(2,3)bicyclo[3.2.0]-hepta-2,6-diene (3)

In 500 ml of toluene were placed 73.0 g (0.5 mole) of 1-methoxyindene and 71 g (0.50 mole) dimethyl acetylene-

Can. J. Chem. Downloaded from www.nrcresearchpress.com by 210.87.254.5 on 09/05/12
For personal use only.

TABLE 1

Nuclear magnetic resonance chemical shifts in τ-units relative to internal TMS*

Compound	Benzene hydrogens	Vinyl hydrogen	Benzylic and allylic hydrogens	Methyl ether hydrogens	Methyl ester hydrogens
2	2.2–2.9 (m, 4H)	4.68 (t, 1H) J = 2.5 Hz	6.70 (d, 2H) J = 2.5 Hz	6.14 (s, 3H)	
3	2.2–2.9 (m, 4H)		6.1–6.25 (m, 1H) 6.8–7.0 (m, 2H)	6.63 (s, 3H)†	6.18 (s, 6H)‡
4	2.2–2.9 (m, 4H)	§	6.8–7.0 (m, 2H)	6.95 (s, 3H)	6.49 (s, 3H) 6.56 (s, 3H)
5‖	2.3–3.0 (m, 4H)	3.17 (t, 1H) J = 7.5 Hz	6.91 (d, 2H) J = 7.5 Hz	6.31 (s, 3H)	6.43 (s, 3H) 6.46 (s, 3H)
6¶	2.3–3.0 (m, 4H)		6.5–7.0 (m, 2H) 6.22 (q, 1H) J_1 = 7 Hz J_2 = 4 Hz	6.67 (s, 3H)	
7**††	2.3–2.8 (m, 4H)	3.08 (t, 1H) J = 7.5 Hz	6.83 (d, 2H) J = 7.5 Hz	6.46 (s, 3H)	
8‡‡§§	1.90 (m, 1H) 2.35–2.75 (m, 3H)	2.33 (t, 1H) J = 7.2 Hz partly obscured by aromatic protons	5.90 (s, 2H) 5.96 (d, 2H) J = 7.2 Hz		

*Recorded in $CDCl_3$ unless otherwise noted.
†Shifted to 6.86 τ in benzene.
‡In benzene two signals are seen at 6.62 and 6.65 τ.
§The three aliphatic protons appear as a multiline pattern at 6.0–6.7 τ.
‖In CCl_4.
¶Acid proton at −0.85 τ (s).
**In DMSO-d_6.
††Acid protons at −0.40 τ (s).
‡‡In acetone-d_6.
§§Acid proton at 4.8 τ (broad band).

dicarboxylate. The solution was refluxed for 5 h at the end of which time all of the 1-methoxyindene **2** had been consumed (as determined by n.m.r.). The toluene was removed at reduced pressure (15 mm) and the residue was distilled to yield 105 g of **3** (73%), b.p. 160–175°/0.1 mm.

Anal. Calcd. for $C_{16}H_{16}O_5$: C, 66.66; H, 5.59. Found: C, 66.20; H, 5.58.

The i.r. spectrum (neat) C=O 1725 cm^{-1}, C=C 1640 cm^{-1}.

1-Methoxy-6,7-dicarbomethoxybenzo(2,3)bicyclo-[3.2.0]hept-2-ene (4)

To 0.5 g of prehydrogenated platinum oxide in 50 ml of methanol was added 2.88 g (0.01 mole) 1-methoxy-6,7-dicarbomethoxybenzo(2,3)bicyclo[3.2.0]hepta-2,6-diene. The sample was stirred under hydrogen at atmospheric pressure. After 30 min, 0.01 mole of hydrogen had been absorbed. The solution was filtered and evaporated. Distillation of the resultant oil gave 2.70 g of the dihydro derivative **4** (93%), b.p. 140–145°/0.05 mm.

Anal. Calcd. for $C_{16}H_{18}O_5$: C, 66.19; H, 6.25. Found: C, 65.85; H, 6.20.

The i.r. spectrum (neat) C=O 1725 cm^{-1}.

Ring Expansion of 1-Methoxy-6,7-dicarbomethoxy-benzo(2,3)bicyclo[3.2.0]hepta-2,6-diene (3)

(a) Photochemical

A solution of 2.88 g (0.01 mole) of cycloadduct **3** in 1 l of cyclohexane was irradiated at room temperature under nitrogen with a 450 W Hanovia high pressure lamp through a pyrex filter. After 3 h all of the starting material had been consumed (as determined by monitoring the disappearance of the ether methyl protons of **3** at 6.63 τ in the n.m.r. spectrum). The cyclohexane was evaporated at reduced pressure to yield 2.88 g of essentially pure product. Distillation proceded with some decomposition to yield 2.0 g (70%) of 1-methoxy-2,3-dicarbomethoxybenzo(6,7)-5-*H*-cycloheptatriene **5**, b.p. 170–180°/0.05 mm.

Anal. Calcd. for $C_{16}H_{16}O_5$: C, 66.66; H, 5.59. Found: C, 66.74; H, 5.42.

The i.r. spectrum (neat) $\rangle C{=}O$ 1725 cm^{-1}, $\rangle C{=}C\langle$ 1595, 1582 cm^{-1}.

(b) Thermal

A vial containing 2.88 g (0.01 mole) of cycloadduct **3** was placed into a sand bath maintained at 220 °C. After 30 min isomerization was essentially complete (as determined by n.m.r.). Distillation yielded 1.90 g (66%) of the desired ring-enlarged compound, b.p. 175–185°/0.10 mm.

1-Methoxybenzo[6,7]-5-H-cycloheptatriene-2,3-di-carboxylic Acid (7)

(a) Saponification of 3

To 5.70 g (0.142 mole) sodium hydroxide in 100 ml of water was added 20.4 g (0.0708 mole) pure cyclo-

Can. J. Chem. Downloaded from www.nrcresearchpress.com by 210.87.254.5 on 09/05/12
For personal use only.

adduct **3** in 20 ml methanol. The solution was heated at 80 °C for 20 min after which time all of the oil had gone into solution. The solution was cooled and acidified to p*H* 2 with concentrated hydrochloric acid. The mixture was extracted with 150 ml of methylene chloride in three portions. The extracts were dried over magnesium sulfate and concentrated to yield 18.00 g (97%) of an oil. The n.m.r. spectrum of this oil was compatible with that to be expected from 1-methoxybenzo(2,3)bicyclo[3.2.0]hepta-2,6-diene-6,7-dicarboxylic acid **6** (Table 1). The i.r. spectrum ($CHCl_3$) C=O 1740, 1680 cm^{-1}, >C=C< 1635 cm^{-1}.

(b) Ring Expansion of ***6***

The oil from the saponification of **3** (18.0 g) was taken up in 1 l of methylene chloride. It was irradiated at room temperature with a 450 W Hanovia high pressure lamp through pyrex for 16 h. As photolysis proceeded a white precipitate formed. At the end of the reaction, the suspension was filtered yielding 16.5 g of a cream colored solid. Evaporation of the mother liquor to 50 ml and filtration yielded an additional 1.7 g, m.p. 195–197 °C, (87%). The n.m.r. spectrum indicated this compound to contain methylene chloride of crystallization.

Anal. Calcd. for $C_{14}H_{12}O_5.1/2\ CH_2Cl_2$: C, 57.53; H, 4.33. Found: C, 57.25; H, 4.24.

The i.r. spectrum (Nujol mull) >C=O 1670 cm^{-1}.

*Benzo[6,7]cyclohepta-3,6-dien-1-one-3-carboxylic Acid (****8****)*

To 20 ml of concentrated hydrochloric acid was added 18.1 g (0.06 mole) of the 1-methoxybenzo[6,7]-5-*H*-cycloheptatriene-2,3-dicarboxylic acid containing methylene chloride of crystallization. The suspension was heated on a steam bath until carbon dioxide evolution ceased. To this, 100 ml of water was added and the solution was heated for 1 h and then cooled. The suspension was filtered and the filter cake washed five times with 20 ml portions of water and then air dried to yield 11.90 g of acid (98%), m.p. 186–187 °C, recrystallized from methanol.

Anal. Calcd. for $C_{12}H_{10}O_3$: C, 71.28; H, 4.98. Found: C, 70.95; H, 4.82.

The i.r. spectrum (KBr) >C=O 1675 cm^{-1}, >C=C< 1635, 1590 cm^{-1}.

1. For reviews see: (*a*) C. D. GUTSCHE and D. REDMORE. Carbocyclic ring expansion reactions. Academic Press Inc., New York, 1968. (*b*) E. WINTERFELDT. Angew. Chem. Int. Ed. **6**, 423 (1967).
2. For a review of cycloadditions to enol ethers see: F. EFFENBERGER. Angew. Chem. Int. Ed. **8**, 295 (1969).
3. (*a*) H. M. ROSENBERG and P. SERVE. J. Org. Chem. **33**, 1653 (1968). (*b*) R. P. GANDHI and V. K. CHADHA. Indian J. Chem. **6**, 402 (1968).
4. L. FRIEDMAN, R. J. OSIEWICZ, and P. Q. RABIDEAU. Tetrahedron Lett. 5735 (1968) and references therein.
5. R. HOFFMANN and R. B. WOODWARD. J. Amer. Chem. Soc. **87**, 2046 (1965).
6. See also: (*a*) R. B. WOODWARD and R. HOFFMANN. J. Amer. Chem. Soc. **87**, 395 (1965). (*b*) R. HOFFMANN and R. B. WOODWARD. Accounts Chem. Res. **1**, 17 (1968).
7. A. IOVCHEV. Izv. Inst. Org. Khim. Bulg. Akad. Nauk., **2**, 67 (1965), Chem. Abstr. 64: 11076*a*.

Can. J. Chem. Downloaded from www.nrcresearchpress.com by 210.87.254.5 on 09/05/12
For personal use only.

Can. J. Chem. Downloaded from www.nrcresearchpress.com by 210.87.254.6 on 09/05/12
For personal use only.

Cycloaddition reactions. Addition of dimethyl acetylenedicarboxylate to 1-dimethylaminoindene

TERRENCE W. DOYLE
Bristol Laboratories of Canada Limited, 100 Industrial Boulevard, Candiac, Quebec

Received November 26, 1969

The cycloaddition of 1-dimethylaminoindene (**2**) to dimethyl acetylenedicarboxylate to form a fused cyclobutene system **3** is discussed. Compound **3** underwent two modes of ring opening to yield either the indene–maleate system **4** or the benzocycloheptatriene system **5** depending on reaction conditions. The synthesis of a number of multifunctional benzotropones from **5** is discussed.

Canadian Journal of Chemistry, **48**, 1633 (1970)

Introduction

In the accompanying paper (1) the thermal cycloaddition of dimethyl acetylenedicarboxylate to 1-methoxyindene has been reported. This reaction gave a fused cyclobutene system which was subsequently ring expanded.

We would now like to report on the corresponding reaction between 1-dimethylaminoindene (**2**) and dimethyl acetylenedicarboxylate. The reactions of enamines with activated acetylenes (2) have been extensively studied in the past several years (3–6). The usual reaction course in the case of enamines derived from cyclic ketones is the formation of ring expanded products via the fused cyclobutene systems. In a number of cases it has been possible to isolate the cyclobutene intermediate (3, 4).

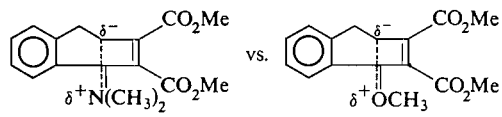

(*i*) (*ii*)

Results and Discussion

1-Dimethylaminoindene (**2**) was prepared in 77% yield from 1-indanone (**1**) according to the method of White and Weingarten (7). Treatment of the enamine **2** with one equivalent of dimethyl acetylenedicarboxylate at −15 °C in benzene gave on evaporation of the benzene 1-dimethylamino-6,7-dicarbomethoxybenzo(2,3)bicyclo-[3.2.0]hepta-2,6-diene (**3**) in quantitative yield (as determined by nuclear magnetic resonance (n.m.r.)). When the reaction between the enamine **2** and dimethyl acetylenedicarboxylate was al-

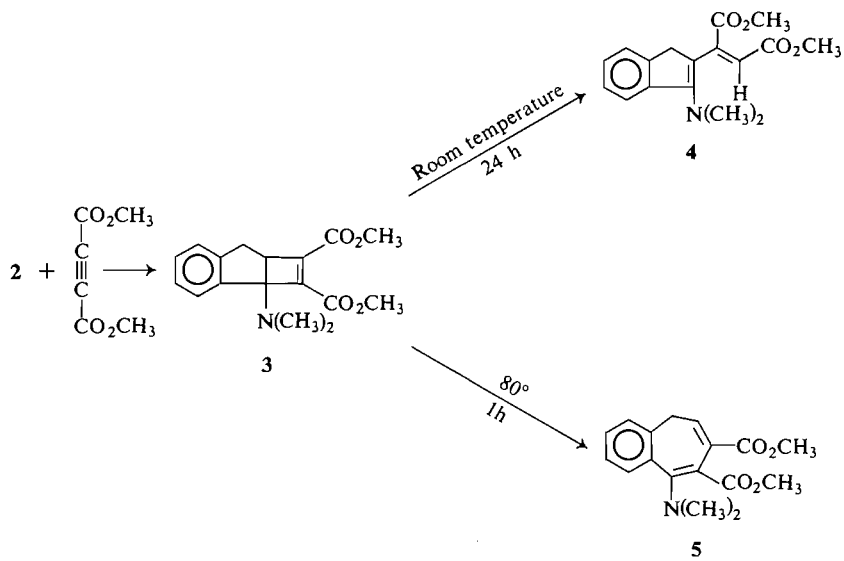

SCHEME 1

Can. J. Chem. Downloaded from www.nrcresearchpress.com by 210.87.254.6 on 09/05/12
For personal use only.

lowed to proceed at reflux in benzene the ring expanded product dimethyl 1-dimethylamino-benzo(6,7)-5-*H*-cycloheptatriene-2,3-dicarboxylate (**5**) was obtained in 90% yield after chromatography of the crude reaction mixture. Alternatively **5** could be prepared by refluxing the fused cyclobutene **3** in benzene for 1 h.

The ease with which **3** undergoes thermal ring expansion to yield **5** (Scheme 1) is in contrast to the difficulty with which the related methoxy compound (*ii*) ring expands (1); this latter reaction requiring temperatures in excess of 200 °C for completion. One explanation of this difference could be that the transition state leading to product involves a polarization of the bond being broken and that the amino compound is better able to stabilize this transition state (*i*). Some recent results reported by Huisgen (8) on the addition of ketenes to vinyl ethers and enamines may lend some support to this hypothesis; e.g. the authors report a relative rate difference of 10^6 for the reactions of 1-ethoxyisobutene and 1-pyrrolidino-isobutene with diphenylketene presumably due to the ability of the amino group to stabilize positive charge in the transition state.

When an attempt to purify compound **3** by column chromatography was made **3** was inadvertently converted into the isomeric dimethyl 1-dimethylamino-2-indenemaleate (**4**) by standing for 24 h at room temperature on the column (Scheme 1). The n.m.r. spectrum of compound **4** showed a singlet at 4.11 τ for the olefinic proton and a singlet at 6.55 τ for the benzylic protons (Table 1). The ultraviolet (u.v.) spectrum of **4** was also consistent with the assigned structure.[1] Hydrolysis of compound **4** gave dimethyl indan-1-one-2-ylidenesuccinate (**6**) in 73% yield (eq. [1]). The n.m.r. spectrum of **6** showed two singlets at 5.67 and 5.80 τ for the two methylenes. The position of the double bond was further confirmed by the u.v. spectrum of **6**.[2]

Hydrolysis of compound **5** (eq. [2]) gave dimethyl 1-hydroxybenzo(6,7)-5-*H*-cycloheptatriene-2,3-dicarboxylate (**7**) in 98% yield. Compound **7** exists entirely in the enolic form (as determined by integration of the enolic proton in the n.m.r. spectrum of **7**) and gives a deep purple color on treatment with ferric chloride solution. The compound is quite acidic and dissolved readily in sodium bicarbonate.

[1] 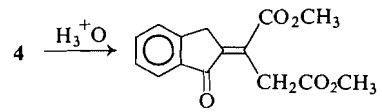

6

[2] 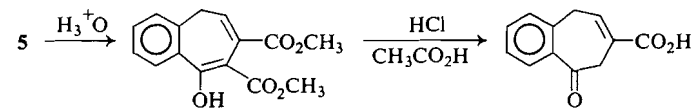

7 **8**

All attempts to hydrolyze the ester functions in compound **7** under basic conditions failed. Bose (6) has reported failure to hydrolyze a similar enolic diester. Treatment of **7** under acidic conditions yielded benzo(6,7)cyclohepta-3,6-dien-1-one-3-carboxylic acid **8** in low yield (25%).[3] The position of the double bond out of conjugation with the ketone function was shown by the n.m.r. spectrum of **8** (1).

Attempted conversion of compound **7** to the

[1]Brannock and co-workers (4*c*) report a similar ring opening reaction for methyl 1-dimethylaminobicyclo[3.2.0]hept-6-en-7-carboxylate (*iii*) to methyl 2-dimethylamino-1-cyclopenten-1-acrylate (*iv*).

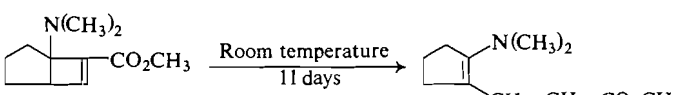

(*iii*) (*iv*)

[2]Huebner *et al.* (3) have shown that hydrolysis of ethyl 1-dimethylaminobicyclo[3.2.0]hept-6-ene-7-carboxylate gave ethyl cyclopentan-1-one-2-ylidenepropionate.

[3]A more convenient synthesis of **8** is reported in the accompanying communication (1).

TABLE 1

The n.m.r. chemical shifts in τ-units relative to internal TMS*

Compounds	Benzene hydrogens	Vinyl hydrogen	Benzylic and allylic hydrogens	Methyl amine hydrogens	Methyl ester hydrogens
2	2.35–2.90(m, 4H)	4.58(t, 1H) J = 2.5 Hz	6.71(d, 2H) J = 2.5 Hz	7.20(s, 6H)	
3	2.25–2.90(m, 4H)		6.80–6.95(m, 2H) 6.0–6.4(m, 1H)	7.73(s, 6H)	6.25(s, 3H) 6.27(s, 3H)
4	2.30–2.90(m, 4H)	4.11(s, 1H)	6.55(s, 2H)	7.14(s, 6H)	6.14(s, 3H) 6.28(s, 3H)
5†	2.30–2.90(m, 4H)	3.32(t, 1H) J = 7.5 Hz	6.83(d, 2H) J = 7.5 Hz	7.03(s, 6H)	6.30(s, 3H) 6.38(s, 3H)
6	2.10–2.80(m, 4H)		5.67(s, 2H) 5.80 (s, 2H)		6.15(s, 3H) 6.30(s, 3H)
7	2.0–2.2(m, 1H) 2.5–3.0(m, 3H)	3.3(t, 1H) J = 7.7 Hz	6.7–7.0(m, 2H)	‡	6.21(s, 3H) 6.41(s, 3H)
9	2.0–2.2(m, 1H) 2.4–2.9(m, 3H)		6.33(s, 2H)	§	6.20(s, 3H) 6.33(s, 3H)
13	1.85–2.1(m, 1H) 2.2–2.8(m, 3H)	3.28(d, 1H) J = 6.0 Hz	5.49(d, 1H) J = 6.0 Hz	‖,¶	6.30(s, 3H) 6.43(s, 3H)
10	1.60–1.80(m, 1H) 2.0–2.4(m, 3H)	2.47(d, 1H) J = 12.5 Hz 2.91(d, 1H) J = 12.5 Hz			6.01(s, 6H)
11††	1.35–1.50(m, 1H) 1.70–2.0(m, 3H)	1.71(d, 1H) J = 11.5 Hz 2.67(d, 1H) J = 11.5 Hz			
12††	1.2–1.4(m, 1H) 2.0–2.35(m, 3H) 2.64(s, 5H)	2.7(d, 1H) J = 11.5 Hz 2.2(d, 1H) J = 11.5 Hz		**	

*All spectra were determined in $CDCl_3$ unless otherwise stated.
†In CCl_4.
‡Enolic proton at −3.10 τ.
§Enolic proton at −3.33 τ.
‖Enolic proton at −3.33 τ.
¶Ether methyl at 6.13 τ.
**Methylene resonance centered at 6.03 (m, 2H) and 6.95 τ (m, 2H).
††Recorded in DMSO-d^9.

corresponding benzotropone **10** by treatment with chloranil failed. The conversion was effected by treating **7** with *N*-bromosuccinimide followed by base induced elimination of hydrogen bromide to give **10** in 94% yield (Scheme 2). In addition, a small amount of a monobromination product **9** was isolated from the mother liquors from several preparations of **10**. The benzotropone **10** could be reconverted smoothly to the enol diester **7** by hydrogenation over 10% Pd/C.

Hydrolysis of compound **10** under either basic or acidic conditions gave the anhydride **11** as the sole product in each case. Attempts to effect decarboxylation of **10** failed, the anhydride formation being favored. When the anhydride was treated with β-phenethylamine the corresponding imide **12** was produced in moderate yield (Scheme 2).

Treatment of the benzotropone diester **10** with sodium methoxide gave the Michael addition product **13**. This compound existed in the enol form. It gave a strong purple color with ferric chloride. The n.m.r. spectrum of **13** further bears out this structural assignment showing the enolic proton at −3.13 τ (integrates for 1H) and the olefinic and benzylic protons as doublets at 3.28 and 5.49 τ respectively.

Experimental

The infrared (i.r.) spectra were recorded on a Unicam SP-200G grating i.r. spectrometer. The n.m.r. spectra were determined on a Varian A60-A spectrometer using

Can. J. Chem. Downloaded from www.nrcresearchpress.com by 210.87.254.6 on 09/05/12
For personal use only.

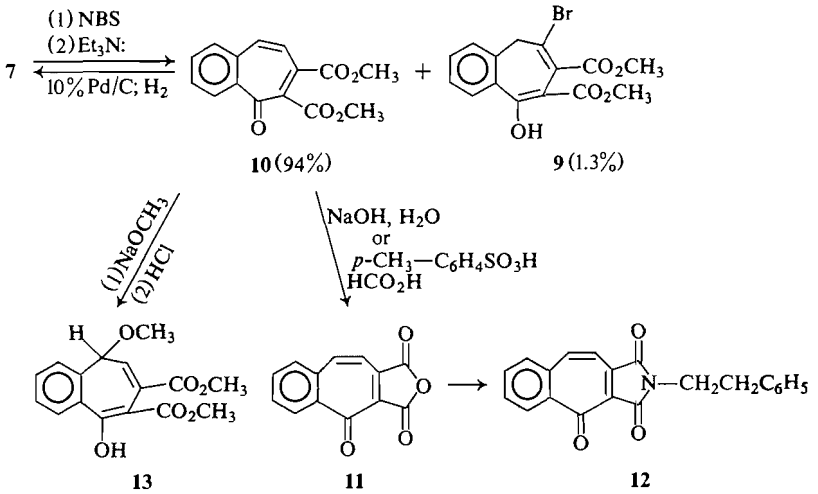

SCHEME 2

tetramethylsilane as an internal standard. Melting points are uncorrected and were determined on a Gallenkamp melting point apparatus. The analyses were performed by Micro-Tech Laboratories, Skokie, Illinois.

Addition of Dimethyl Acetylenedicarboxylate to 1-Dimethylaminoindene (2)

(a) 1-Dimethylaminoindene (2)

To 6.60 g (0.05 mole) of 1-indanone in 300 ml of dry benzene was added 18 g (0.40 mole) dimethylamine in 50 ml of benzene. The solution was cooled to ice bath temperature (0–5 °C). To this a solution of 0.95 g (0.05 moles) of titanium tetrachloride in 50 ml of benzene was added dropwise. The solution was stirred for 18 h at room temperature and filtered through Celite. The solution was concentrated at reduced pressure to yield an oil which was distilled to yield 6.1 g (77%) of **2**, b.p. 126–128 °C/16 mm. The oil was unstable and rapidly darkened on standing. The i.r. spectrum (neat), C=C 1610, 1600, 1575 cm^{-1}. The n.m.r. spectrum was compatible with the assigned structure (Table 1).

(b) 1-Dimethylamino-6,7-dicarbomethoxybenzo(2,3)-bicyclo[3.2.0]hepta-2,6-diene (3)

A solution of 6.1 g (0.0384 mole) 1-dimethylaminoindene (**2**) in 250 ml of benzene was cooled to −15 °C (the solution became a slurry at this temperature). To this was added 5.46 g (0.0384 mole) dimethyl acetylenedicarboxylate in 50 ml of dry benzene over 10 min. A deep red–brown color developed. The solution was allowed to come to room temperature and was stirred under nitrogen for 4 h. The benzene was removed at reduced pressure yielding 12.0 g of **3**. The i.r. spectrum (neat) C=O 1725, C=C 1650 cm^{-1}. The n.m.r. spectrum of this oil was compatible with the assigned structure (Table 1).

Isomerization of 1-Dimethylamino-6,7-dicarbomethoxy-(2,3)bicyclo[3.2.0]hepta-2,6-diene (3)

(a) To Dimethyl 1-Dimethylaminobenzo(6,7)-5-H-cycloheptatriene-2,3-dicarboxylate (5)

A solution of 8 g (0.0292 mole) of crude **3** in 50 ml of dry benzene was refluxed for 1 h. The n.m.r. spectrum of a small aliquot of the solution indicated the complete disappearance of **3** at the end of this interval. The remainder of the solution was evaporated at reduced pressure. Trituration of the oil which resulted gave an oily crystalline solid. This solid was redissolved in 20 cc of benzene and chromatographed on Florisil (Fisher Scientific Co., 60–100 mesh, 40 g) with benzene. Evaporation of the eluent yielded 7.205 g (90%) of **5**, pale yellow needles from benzene–hexane, m.p. 124–126 °C.

Anal. Calcd. for $C_{17}H_{19}NO_4$: C, 67.76; H, 6.36; N, 4.65. Found: C, 67.75; H, 6.47; N, 4.33.

The i.r. spectrum ($CHCl_3$) C=O 1715, 1685 cm^{-1}; C=C 1630, 1601, 1580 cm^{-1}. The u.v. (EtOH, 7.3×10^{-5} *M*); λ 349 mμ (ε_{max} = 10 500); 258 mμ (s) (ε_{max} = 13 400); 239 mμ (s) (ε_{max} = 16 200); 211 mμ (ε_{max} = 20 400). See Table 1 for the n.m.r. spectrum.

(b) To Dimethyl 1-Dimethylamino-2-indenemaleate (4)

A mixture of 9.0 g of compounds **3** and **5** (isomer ratio ~7:3 as determined by n.m.r.) was chromatographed on 300 g Florisil using hexane and thereafter hexane–benzene as eluent (the solvent was changed 2% in composition every 200 ml until a 1:1 mixture had been achieved and 5% thereafter until pure benzene was being used). The first fractions from the column yielded 3.0 g of **5**. The chromatography was then stopped and the compound allowed to stand on the column for 20 h at room temperature. When elution was continued 5.2 g of dimethyl 1-dimethylamino-2-indenemaleate were collected, intense yellow crystals from benzene–cyclohexane, m.p. 121–123 °C.

Anal. Calcd. for $C_{17}H_{19}NO_4$: C, 67.76; H, 6.36; N, 4.65. Found: C, 67.71; H, 6.21; N, 4.53.

The i.r. spectrum ($CHCl_3$) C=O 1725; C=C 1590 cm^{-1}. The u.v. (EtOH, 7×10^{-5} *M*) 332 mμ (ε_{max} = 16 800); 254 mμ (ε_{max} = 7150); 246 mμ (ε_{max} = 7700), 208 mμ (ε_{max} = 16 550).

Hydrolysis of Dimethyl 1-Dimethylamino-2-indenemaleate (4)

To a solution of 2.0 g (0.0066 mole) of **4** in methanol (10 ml) was added 1 ml of concentrated hydrochloric acid in 20 ml of water at room temperature. After 2 h the

Can. J. Chem. Downloaded from www.nrcresearchpress.com by 210.87.254.6 on 09/05/12
For personal use only.

Can. J. Chem. Downloaded from www.nrcresearchpress.com by 210.87.254.6 on 09/05/12
For personal use only.

solution was poured into 100 ml of water and extracted with three 20 ml portions of ether. The extracts were washed once with water, dried over anhydrous magnesium sulfate, and concentrated to yield 1.3 g of dimethyl indan-1-one-2-ylidenesuccinate (**6**) (73%), m.p. 101–103 °C.

Anal. Calcd. for $C_{15}H_{14}O_5$: C, 65.69; H, 5.15. Found: C, 65.74; H, 5.19.

The i.r. spectrum ($CHCl_3$) C=O 1740, 1725, 1690 cm^{-1}; C=C 1635, 1610, 1590 cm^{-1}. The u.v. (EtOH, 4.5×10^{-5} *M*) 275 mμ (ε_{max} = 14 200), 209 mμ (ε_{max} = 11 900).

*Hydrolysis of Dimethyl 1-Dimethylaminobenzo(6,7)-5-H-cycloheptatriene-2,3-dicarboxylate (**5**)*

A solution of 52.0 g (0.17 mole) of **5** in 100 ml of methanol was treated with 100 ml of hydrochloric acid (6 *N*). The solution became warm and changed from deep to pale yellow in color. The solution was stirred an additional 30 min. An oil separated which solidified. Extraction with ether and evaporation of the extracts yields 43.0 g (98%) of pure crystalline dimethyl 1-hydroxybenzo(6,7)-5-*H*-cycloheptatriene-2,3-dicarboxylate (**7**), m.p. 92.5–94 °C. The compound **7** could be recrystallized from ethanol.

Anal. Calcd. for $C_{15}H_{14}O_5$: C, 65.69; H, 5.15. Found: C, 66.01; H, 5.24.

The i.r. spectrum ($CHCl_3$) C=O 1715, 1727 cm^{-1}, C=C 1659, 1635, 1610, 1590, 1565 cm^{-1}. The u.v. (EtOH, 7×10^{-5} *M*) 293 mμ (ε_{max} = 9700); 237 mμ (ε_{max} = 13 600); 215 mμ (ε_{max} = 12 800).

*Benzo(6,7)cyclohepta-3,6-dien-1-one-3-carboxylic Acid (**8**)*

A solution of 5.08 g (0.02 mole) dimethyl 1-hydroxybenzo(6,7)-5-*H*-cycloheptatriene-2,3-dicarboxylate (**7**) in 50 ml of glacial acetic acid and 10 ml of concentrated hydrochloric acid was refluxed for 24 h. The acetic acid was removed at reduced pressure and the residue was extracted with methylene chloride. The extracts were dried over anhydrous magnesium sulfate and concentrated to yield 3.0 g of a brown gum. Trituration of this gum with toluene and filtration gave 1.0 g (25%) of **8**, m.p. 184–186 °C. The sample could be recrystallized from toluene, m.p. 186–187 °C [literature m.p. 186–187 °C (1)].

*Dimethyl Benzo(6,7)tropone-2,3-dicarboxylate (**10**)*

A solution of 13.6 g (0.05 mole) dimethyl 1-hydroxybenzo(6,7)-5-*H*-cycloheptatriene-2,3-dicarboxylate (**7**) and 8.90 g (0.05 mole) *N*-bromosuccinimide in 125 ml of carbon tetrachloride was refluxed for 1 h. A rapid evolution of hydrogen bromide gas was observed. The solution was cooled and filtered to yield 4.9 g (95%) of succinimide. The solution was then evaporated at reduced pressure and the resultant oil taken up in 100 ml of ether. To this, 5.05 g (0.05 mole) triethylamine was added. There was an immediate formation of triethylamine hydrobromide which was removed by filtration. The mother liquor was washed with 10% hydrochloric acid and then water. The extracts were dried over magnesium sulfate and concentrated to yield 13.5 g of a pale yellow solid. Trituration of this solid with 20 ml of ether and filtration gave 12.8 g (94%) of pure **10**, m.p. 92.5–94 °C.

Anal. Calcd. for $C_{15}H_{12}O_5$: C, 66.17; H, 4.44. Found: C, 65.93; H, 4.41.

The i.r. spectrum ($CHCl_3$) C=O 1728, 1738 cm^{-1}, C=C 1634, 1620, 1593, 1573, 1550 cm^{-1}.

*Dimethyl 4-Bromo-1-hydroxy-benzo(6,7)-5-H-cycloheptatriene-2,3-dicarboxylate (**9**)*

After the mother liquors from five runs of the above preparation of compound **10** had been standing for 3 months, it was observed that the oil had partially crystallized. The crystals were filtered and carefully washed with ether to give 1.15 g (1.3% based on 68.0 g of starting material **7**) of **9**, m.p. 134–134.5 °C.

Anal. Calcd. for $C_{15}H_{13}BrO_5$: C, 51.01; H, 3.71; Br, 22.62. Found: C, 51.28; H, 3.77; Br, 22.44.

The i.r. spectrum (melt) C=O 1743, 1730 cm^{-1}, C=C 1661, 1620, 1592, 1560 cm^{-1}.

*Benzo(6,7)tropone-2,3-dicarboxylic Acid Anhydride (**11**)*

Method A

To 10 ml of 4 *N* sodium hydroxide and 50 ml of water were added 2.72 g (0.01 mole) of dimethyl benzo(6,7)-tropone-2,3-dicarboxylate (**10**). The solution was heated at reflux until all of the solid material had gone into solution (5 min). The solution was cooled to 50 °C and acidified with hydrochloric acid to p*H* 2 at which time a suspension of orange crystals formed. Filtration gave 1.60 g of an orange solid (73%), m.p. 184–186 °C. The sample could be recrystallized from acetonitrile, m.p. 198–201 °C (decomposition).

Anal. Calcd. for $C_{13}H_6O_4$: C, 69.08; H, 2.99. Found: C, 68.92; H, 2.94.

The i.r. spectrum (KBr disc) C=O 1885, 1848, 1770 cm^{-1}.

Method B

A solution of 500 mg (0.00184 mole) dimethyl benzo(6,7)tropone-2,3-dicarboxylate (**10**) and 600 mg of *p*-toluenesulfonic acid hydrate in 10 ml of formic acid was heated for 15 min at reflux then at 100 °C for 1 h. The solution was let stand 18 h. The excess formic acid was removed at reduced pressure. The residue was taken up in 50 ml of methylene chloride and washed with water. The extract was dried over magnesium sulfate and concentrated. Trituration of the residue with 5 ml of ether and filtration yielded 300 mg (72%) of the anhydride, m.p. 194–195 °C. The i.r. and n.m.r. spectra were identical with those of the previously prepared material.

*N-Phenethylimide of Benzo(6,7)tropone-2,3-dicarboxylic Acid (**12**)*

A solution of 226 mg (0.001 mole) of compound **11** and 121 mg (0.001 mole) β-phenethylamine in 25 ml of benzene was refluxed for 1 h. The solvent was removed at reduced pressure to give 325 mg of a yellow solid. Recrystallization from benzene gave 150 mg (45%) of compound **12** m.p. 173–174 °C.

Anal. Calcd. for $C_{21}H_{15}NO_3$: C, 76.58; H, 4.25; N, 4.59. Found: C, 76.26; H, 4.15; N, 4.56.

The i.r. spectrum (Nujol) C=O 1780, 1710 cm^{-1}.

*Dimethyl 1-Hydroxy-5-methoxybenzo(6,7)-5-H-cycloheptatriene-2,3-dicarboxylate (**13**)*

To 0.55 g (0.002 mole) of compound **10** in 20 ml of methanol was added 10 ml of a solution of sodium methoxide (0.2 g sodium added to 10 ml of methanol). The solution was acidified with dilute hydrochloric acid and extracted into 100 ml of ether. The extracts were dried over magnesium sulfate and concentrated to yield

0.50 g of compound **13** (84%). The sample was recrystallized from methanol, m.p. 143–144 °C.

Anal. Calcd. for $C_{16}H_{16}O_6$: C, 63.15; H, 5.30. Found: C, 62.84; H, 5.08.

The i.r. spectrum ($CHCl_3$), C=O 1725, 1660 cm^{-1}, C=C 1610, 1590, 1567 cm^{-1}.

*Reduction of Dimethyl Benzo(6,7)tropone-2,3-dicarboxylate (**10**)*

A solution of 2.72 g (0.01 mole) of compound **10** in 50 ml of methanol was stirred under hydrogen over 0.3 g of 10% Pd/C at atmospheric pressure and temperature. When 0.01 mole of hydrogen had been absorbed the solution was filtered and concentrated to give 2.75 g of pure dimethyl 1-hydroxybenzo(6,7)-5-*H*-cycloheptatriene-2,3-dicarboxylate (**5**), m.p. 92–94 °C.

1. T. W. Doyle. Can. J. Chem. This issue.
2. E. Winterfeldt. Angew. Chem. Int. Ed. **6**, 423 (1967).
3. C. F. Huebner, L. Dorfman, M. M. Robison, E. Donoghue, W. G. Pierson, and P. Strachan. J. Org. Chem. **28**, 3134 (1963).
4. K. C. Brannock, R. D. Burpitt, V. W. Goodlett, and J. G. Thweatt. (*a*) J. Org. Chem. **28**, 1464 (1963); (*b*) J. Org. Chem. **29**, 813 (1964); (*c*) J. Org. Chem. **29**, 818 (1964).
5. G. A. Berchtold and G. F. Uhlig. J. Org. Chem. **28**, 1459 (1963).
6. A. K. Bose, G. Mina, M. S. Manhas, and E. Rzucidlo. Tetrahedron Lett. 1467 (1963).
7. W. A. White and H. Weingarten. J. Org. Chem. **32**, 213 (1967).
8. R. Huisgen, L. A. Feiler, and P. Otto. Chem. Ber. **102**, 3444 (1969).

Can. J. Chem. Downloaded from www.nrcresearchpress.com by 210.87.254.6 on 09/05/12
For personal use only.

Can. J. Chem. Downloaded from www.nrcresearchpress.com by 210.87.254.5 on 09/05/12
For personal use only.

The kinetics of formation of ruthenium(II) nitrogen complexes

CLIVE M. ELSON, I. J. ITZKOVITCH, AND JOHN A. PAGE
Department of Chemistry, Queen's University, Kingston, Ontario

Received January 19, 1970

The formation of nitrogen monomers by the reaction of $Ru(NH_3)_5(H_2O)^{2+}$ and *cis*-$Ru(NH_3)_4(H_2O)_2^{2+}$ with N_2 has been shown to be first order in N_2 and second order overall. The formation of bridging N_2 dimers by the reaction of the ruthenium(II) pentaammine and tetraammine with the monomers has been shown to be second order overall.

The reactions were studied in a H_2SO_4–K_2SO_4 electrolyte pH 3.3, $\mu = 0.30$. The ruthenium(II) species were prepared by controlled potential reduction of known ruthenium(III) species at -0.50 V at a Hg cathode. The reactions of the reduced species with N_2 or the monomers were followed spectrophotometrically.

The second order rate constant at 25 °C and the activation energy for the substrate $Ru(NH_3)_5(H_2O)^{2+}$ with the respective nucleophiles are: N_2, 8.0×10^{-2} M^{-1} s^{-1}, 22.0 ± 0.1 kcal/mole; $Ru(NH_3)_5N_2^{2+}$, 3.6×10^{-2} M^{-1} s^{-1}, 19.9 ± 0.5 kcal/mole; $Ru(NH_3)_4(H_2O)N_2^{2+}$, 2.7×10^{-2} M^{-1} s^{-1}, 20.4 ± 0.8 kcal/mole. For the substrate *cis*-$Ru(NH_3)_4(H_2O)_2^{2+}$ the values are: N_2, 1.0×10^{-1} M^{-1} s^{-1}, 20.4 ± 0.2 kcal/mole; $Ru(NH_3)_5N_2^{2+}$, 6.8×10^{-2} M^{-1} s^{-1}, 18.2 ± 0.1 kcal/mole; $Ru(NH_3)_4(H_2O)N_2^{2+}$, 7.2×10^{-2} M^{-1} s^{-1}, 17.1 ± 0.2 kcal/mole.

Canadian Journal of Chemistry, **48**, 1639 (1970)

Introduction

In a previous study (1), the formation of ruthenium(II) nitrogen complexes was examined at a single temperature. In this paper we report on an extended study of the rate and energetics of the formation of the mono- and bi-nuclear nitrogen complexes of ruthenium pentaammine and tetraammine, and of the mixed pentaammine–tetraammine binuclear nitrogen complexes.

The only other work of direct interest reported since the initial paper was a study of the formation and decomposition of nitrogen complexes of ruthenium(II) chloride by Shilova and Shilov (2). This study was carried out over a range of temperature in a tetrahydrofuran solvent. In addition, Armour and Taube (3) reported on the kinetics of substitution of a number of ligands, other than N_2, into ruthenium(II) aquopentaammine.

Experimental

The starting material for the preparation of the pentaammines and tetraammines was pure $Ru(NH_3)_6Cl_3$ obtained from Johnson Matthey Chemicals Limited (Lot B/8). The salt $Ru(NH_3)_5Cl.Cl_2$ was prepared from the hexaammine by the method of Gleu and Rehm (4), while the *cis*-$Ru(NH_3)_4Cl_2.Cl$ was prepared from the pentaammine by the method of Gleu and Cuntze (5). The ruthenium(II) nitrogen pentaammine was prepared in turn from the chloropentaammine ruthenium(III) using sodium azide according to the procedure of Allen *et al.* (6), while the *cis*-$Ru(NH_3)_4(H_2O)N_2.Cl_2$ was prepared from the dichlorotetraammine, again using azide according to the method of Allen *et al.* (7). These nitrogen products were found to contain about 10% unreacted ruthenium(III); this was separated by forming the soluble ruthenium(III) hydroxy complexes. This was accomplished by dissolving the solid complexes in a minimum of warm (50 °C) 1 M NH_3 in the case of the pentaammine or warm (50 °C) 1 M NaOH in the case of the tetraammine. The complexes were then reprecipitated by the addition of solid KCl and cooling, and were then recrystallized from warm water until the pink tinge of the hydroxy species was not apparent upon dissolution of the nitrogen complexes.

The purity of the products was established by infrared spectra, by the coulometric results on the reduction of dissolved ruthenium(III) ammine salts, and by agreement with published extinction coefficients where available. The extinction coefficients actually used in this work are reported in Table 1.

The studies were carried out in a base electrolyte that was 0.099 M in K_2SO_4 and 0.001 M in added H_2SO_4 giving a pH of 3.3 at 25 °C (other anions absorbed

TABLE 1

Extinction coefficients of ruthenium(II) species*

Species	Extinction coefficient 222 nm	Extinction coefficient 262 nm
$Ru(NH_3)_5(H_2O)^{2+}$	0.068×10^4	0.055×10^4
cis-$Ru(NH_3)_4(H_2O)_2^{2+}$†	0.061×10^4	0.046×10^4
$Ru(NH_3)_5N_2^{2+}$	1.64×10^4	0.084×10^4
cis-$Ru(NH_3)_4(H_2O)N_2^{2+}$‡	1.74×10^4	0.067×10^4
$(Ru(NH_3)_5)_2N_2^{4+}$	0.30×10^4	4.8×10^4
$(Ru(NH_3)_4(H_2O))_2N_2^{4+}$	0.31×10^4§	5×10^4‖

*In K_2SO_4–H_2SO_4 electrolyte, pH = 3.3, values for pentaammine species from ref. 1.
†Coulometric reduction of *cis*-$[Ru(NH_3)_4Cl_2]Cl$.
‡Pure *cis*-$[Ru(NH_3)_4(H_2O)N_2]Cl_2$.
§Equated to extinction coefficient of dimer at 302 nm.
‖Derived from ratio of decrease in absorbance at 222 nm to increase in absorbance at 262 nm when monomer reacted with reduced species.

Can. J. Chem. Downloaded from www.nrcresearchpress.com by 210.87.254.5 on 09/05/12
For personal use only.

strongly at the wavelengths of interest). In some cases, the pH was varied by adding H_2SO_4 or KOH to the electrolyte but the ionic strength was maintained constant (μ = 0.30). The controlled potential reductions were carried out in a H-type double diaphragm cell. The working electrode was a mercury pool (13 cm^2) and the total volume of solution electrolyzed was 75 ml. A Wenking 61 RS potentiostat was used to control the electrode potential relative to a Metrohm EA 402A saturated calomel reference electrode. The electrolysis current was integrated using an operational amplifier with capacitance feedback (8). Spectra were recorded on a Bausch and Lomb Spectronic 505 using the flow system previously described (1). The electrolysis cell and flow system were water jacketed and the cell compartment of the spectrophotometer was equipped with a constant temperature block. Temperature regulation to $\pm$ 0.1 °C was achieved by circulating water from a thermostat.

Dissolved air was purged from the solutions using argon (Linde, high purity). The nitrogen and mixed nitrogen–argon gases used in the kinetic runs (Linde, less that 10 p.p.m. oxygen) were purified by passage over hot (100 °C) BASF catalyst R-3-11. The gases were then saturated with vapor by bubbling through base electrolyte before use.

In the experiment designed to follow the displacement of Cl^- on reduction of the $Ru(NH_3)_4Cl_2^+$, an Orion Model 94-17-00 Chloride Specific Ion Electrode was used in a cell with an Orion Model 90-02-00 Double Junction Reference Electrode. The K_2SO_4–H_2SO_4 electrolyte was used in the bridge and the potentials were measured on an Orion Model 801 meter.

Kinetics

The reactions were studied by first preparing the Ru(II) species by a controlled potential reduction of the appropriate Ru(III) ammine at −0.50 V under Ar. The reduction was clean and rapid and the mercury electrode was maintained at this potential throughout the subsequent reactions.

Monomer Formation

The formation of the pentaammine and tetraammine monomers (M) was studied by working with relatively low concentrations of the Ru(II) species (A) and saturating the solution with N_2 gas

$$A + N_2 \xrightarrow{k_M} M$$

$$\frac{dC_M}{dt} = k_M C_A C_{N_2} = k_M' C_A \ (N_2 \text{ saturated})$$

The formation of the monomer was simply followed by the increase in absorbance at 222 nm. The first order rate constant, k_M' was determined from plots of ln (C_A^0 − C_M) vs. time. The plots were linear for the first 30% conversion of A to M but showed a positive curvature at long times due to the formation of significant amounts of dimer. Least squares fits were made over the initial linear portion. Values of the second order rate constants were then calculated using tabulated values for the solubility of N_2 at 1 atm pressure (9). The reactions of both the tetraammine and pentaammine were demonstrated to be first order with respect to N_2 by determining k_M' with a fixed C_A^0 at various concentrations of dissolved N_2 at 25 °C (Fig. 1). The effect of temperature on k_M was examined and the results are given in Table 2. The Arrhenius plots were found to be linear (Fig. 2) and the parameters, determined by least squares fitting, are listed in Table 3.

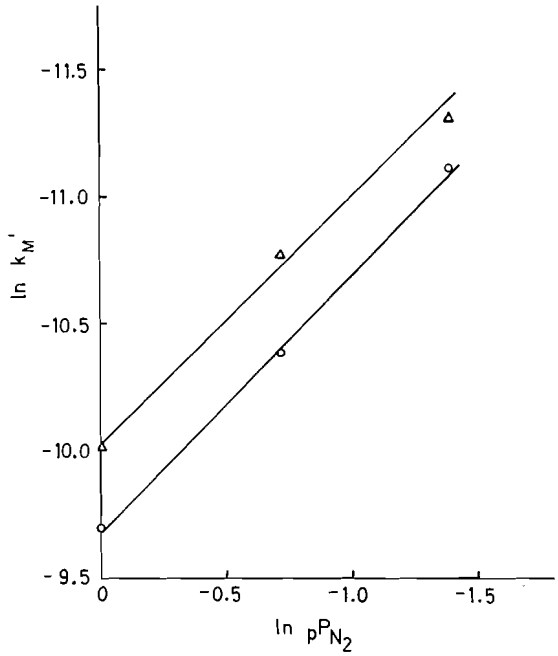

FIG. 1. Rate of reaction with N_2 at 25 °C. Reaction at 1 atm with pure N_2, 49% N_2 – 51% Ar, or 25% N_2 – 75% Ar. △, $Ru(NH_3)_5(H_2O)^{2+}$, $C_A^0 = 1.76 \times 10^{-4}$ M; ○, *cis*-$Ru(NH_3)_4(H_2O)_2^{2+}$, $C_A^0 = 1.18 \times 10^{-4}$ M.

Dimer Formation

The formation of the pentaammine–pentaammine, tetraammine–tetraammine, and mixed pentaammine–tetraammine dimers (D) were studied by adding pure solid monomer to the Ru(II) species

$$A + M \xrightarrow{k_D} D$$

$$\frac{dC_D}{dt} = k_D C_A C_M$$

The formation of the dimer was followed by the decrease in absorbance at 222 nm. The second order rate constant was evaluated from plots of $(C_A^0 - C_M^0)^{-1}$ ln $[(C_A^0 - C_M) C_M^0/(C_M^0 - C_M)C_A^0]$ vs. time. The plots were linear over about 30% conversion of M to D, but showed curvature past this point as the back reaction became significant. Least squares fits were made on the initial linear portion. The value of k_D for the reaction of each of the two monomers with each of the two Ru(II) substrates was determined over a range of temperature and the results are given in Table 4. The Arrhenius plots were linear (Fig. 3) and the parameters are listed in Table 3.

The effect of pH on k_M and k_D for each of the pentaammine and tetraammine was also examined at 25 °C.

TABLE 2

Rate constants for monomer formation*

Temperature (°C).	C_A^0 $M \times 10^4$	C_{N_2} $M \times 10^4$	k_M $M^{-1}\,s^{-1} \times 10$	Number of points	Correlation coefficient
$Ru(NH_3)_5(H_2O)^{2+} + N_2$					
12.2	3.84	7.65	0.16	21	0.999
25.0	1.79	5.69	0.79	15	1.000
25.1	0.752	5.69	0.81	21	0.999
34.9	0.752	4.67	2.72	9	1.000
44.0	0.752	3.87	7.63	18	0.998
cis-$Ru(NH_3)_4(H_2O)_2^{2+} + N_2$					
6.4	3.52	8.61	0.11	16	0.999
15.4	2.99	6.90	0.31	13	1.000
25.0	1.18	5.69	1.06	18	0.999
25.0	0.733	5.69	1.02	10	1.000
35.0	0.733	4.67	3.35	14	0.999
45.2	0.515	3.80	9.03	8	0.999

*In K_2SO_4–H_2SO_4 electrolyte, pH = 3.3.

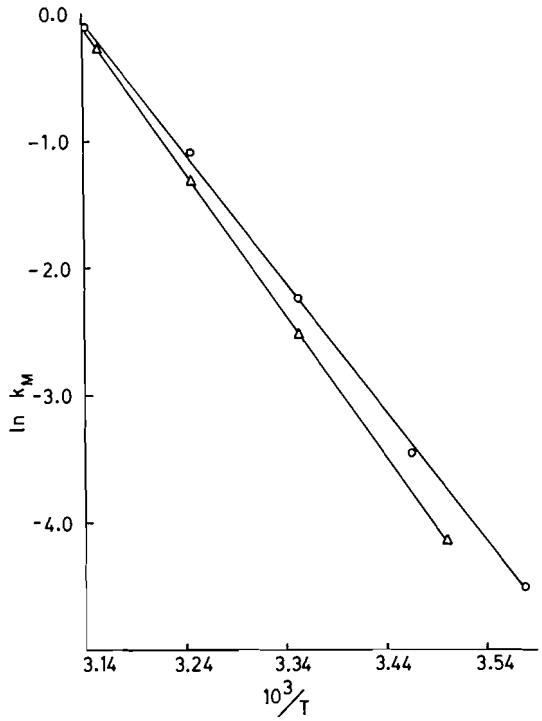

FIG. 2. Effect of temperature on rate of formation of monomers. △, $Ru(NH_3)_5(H_2O)^{2+} + N_2$; ○, *cis*-$Ru(NH_3)_4(H_2O)_2^{2+} + N_2$; N_2 at 1 atm.

Over the pH range 2.3 to 10.7 it was found that the rate constants decreased only slightly with increasing pH; the change being less than 15%.

Discussion

The composition and stereochemistry of the reactants is relatively clear. In the case of the pentaammine, the reacting Ru(II) species would appear to be $Ru(NH_3)_5(H_2O)^{2+}$. Endicott and Taube (10) have reported that the reduction of both $Ru(NH_3)_5(H_2O)^{3+}$ and $Ru(NH_3)_5Cl^{2+}$ with Cr(II) in aqueous media give the same product. The Ru—NH_3 bonds were shown to remain intact and the product was considered to be $Ru(NH_3)_5(H_2O)^{2+}$. In the case of the electrolytic method used to prepare the Ru(II) in this work, the reduction of the $Ru(NH_3)_5Cl^{2+}$ in the sulfate electrolyte gave a solution with an absorption spectrum identical to that reported by Armor and Taube (2) for $Ru(NH_3)_5(H_2O)^{2+}$. The reduction was carried out at various pH values, ranging from 2 to 11, and the spectrum of the reduced species was identical in each case and characterized by a broad weak absorption band centered at 260 nm. The reduction was also carried out in an aqueous $NaBF_4$ electrolyte and this again yielded a solution with an absorption spectrum identical to that of the product formed in the presence of sulfate. While these observations do not eliminate the possibility of a sulfate species in the sixth coordination site of the Ru(II), water should be preferred since sulfate is not a strong π acceptor ligand.

In the case of the tetraammine, the reacting species would appear to be *cis*-$Ru(NH_3)_4(H_2O)_2^{2+}$. Experimentally, the complete displacement of both chlorides from the inner coordination sphere of the starting *cis*-$Ru(NH_3)_4Cl_2^{+}$ was observed during the electrolytic reduction in the sulfate media. This was found by using a specific ion electrode to follow the increase in the free Cl^- concentration during the electrolysis. This displacement is in agreement with the work

Can. J. Chem. Downloaded from www.nrcresearchpress.com by 210.87.254.5 on 09/05/12
For personal use only.

TABLE 3

Arrhenius parameters for monomer and dimer formation at 25.0 °C

System	k_M or k_D M^{-1} s^{-1} × 10	E_a* kcal/mole	log A	$\Delta S^{\ddagger}$† e.u.
$Ru(NH_3)_5(H_2O)^{2+} + N_2$	0.80	22.0±0.1	15.0	10±1.5
cis-$Ru(NH_3)_4(H_2O)_2^{2+} + N_2$	1.04	20.4±0.2	14.0	6±1
$Ru(NH_3)_5(H_2O)^{2+} + Ru(NH_3)_5N_2^{2+}$	0.36	19.9±0.5	13.1	2±0.5
$Ru(NH_3)_5(H_2O)^{2+} +$ *cis*-$Ru(NH_3)_4(H_2O)N_2^{2+}$	0.27	20.4±0.8	13.4	3±0.5
cis-$Ru(NH_3)_4(H_2O)_2^{2+} + Ru(NH_3)_5N_2^{2+}$	0.68	18.2±0.1	12.2	−3±0.5
cis-$Ru(NH_3)_4(H_2O)_2^{2+} +$ *cis*-$Ru(NH_3)_4(H_2O)N_2^{2+}$	0.72	17.1±0.2	11.4	−7±1

*Uncertainty in E_a is standard deviation in least squares fit.
†Uncertainty in $\Delta S^{\ddagger}$ based on 5% error in k.

TABLE 4

Rate constants for dimer formation

Temperature °C	C_A^0 $M \times 10^4$	C_M^0 $M \times 10^4$	k_D M^{-1} s^{-1} × 10	Number of points	Correlation coefficient
$Ru(NH_3)_5(H_2O)^{2+} + Ru(NH_3)_5N_2^{2+}$					
12.0	5.19	0.597	0.070	14	0.999
25.0	4.21	0.570	0.36	11	1.000
35.0	0.947	0.557	0.91	20	1.000
44.1	0.547	0.572	2.52	8	1.000
$Ru(NH_3)_5(H_2O)^{2+} +$ *cis*-$Ru(NH_3)_4(H_2O)N_2^{2+}$					
12.0	3.44	0.881	0.068	18	0.998
18.0	2.24	0.869	0.16	18	0.999
25.0	1.03	0.862	0.27	10	1.000
35.0	0.796	0.761	0.94	17	0.999
44.1	0.608	0.296	2.73	16	0.998
cis-$Ru(NH_3)_4(H_2O)_2^{2+} + Ru(NH_3)_5N_2^{2+}$					
11.4	2.96	0.898	0.17	19	0.999
25.0	1.09	0.950	0.68	9	1.000
35.0	0.850	0.787	1.89	18	1.000
45.0	0.580	0.490	4.88	14	0.997
cis-$Ru(NH_3)_4(H_2O)_2^{2+} +$ *cis*-$Ru(NH_3)_4(H_2O)N_2^{2+}$					
5.7	3.57	1.03	0.099	25	0.999
15.2	2.16	0.857	0.26	23	0.997
25.0	1.08	0.871	0.72	28	1.000
25.2	1.26	0.979	0.76	19	0.998
35.1	1.09	0.871	1.87	20	0.999
44.9	0.637	0.485	4.25	18	0.998

of Movius and Linck (11) who state that the reduction of *cis*-$Ru(NH_3)_4Cl_2^+$ with Cr(II) in an aqueous *p*-toluenesulfonic acid electrolyte gives $Ru(NH_3)_4(H_2O)_2^{2+}$. It is again possible that sulfate from the electrolyte may replace the chloride in the electrolytic reduction, but this can be discounted, for it was observed that a product with an identical absorption spectrum was obtained when the reduction was carried out in a sulfate free methanesulfonic acid electrolyte. The reduced species was characterized by a broad weak absorption band centered at 258 nm. With regard to stereochemistry, Ford and Sutton (12) have shown that there is no isomerization in the reduction of either *cis*- or *trans*-Ru(III) tetraammines with zinc amalgam. This was confirmed in this work by a cyclic experiment. The starting *cis*-$Ru(NH_3)_4Cl_2^+$ was electrolytically reduced at −0.50 V then reoxidized at −0.10 V. The absorption spectrum of the resultant Ru(III) after chloride anation indicated only a *cis*-Ru(III) tetraammine. Thus the Ru(II) species in the kinetic runs would be the *cis*-isomer.

In the case of the nitrogen complexes, the pentaammine monomer is $Ru(NH_3)_5N_2^{2+}$ (6), while Allen *et al.* have shown that the tetraammine nitrogen monomer formed in either aqueous methanesulfonic or sulfuric acid electrolytes is $Ru(NH_3)_4(H_2O)N_2^{2+}$ (7). Since the substitution reactions of Ru(II) are highly

Can. J. Chem. Downloaded from www.nrcresearchpress.com by 210.87.254.5 on 09/05/12
For personal use only.

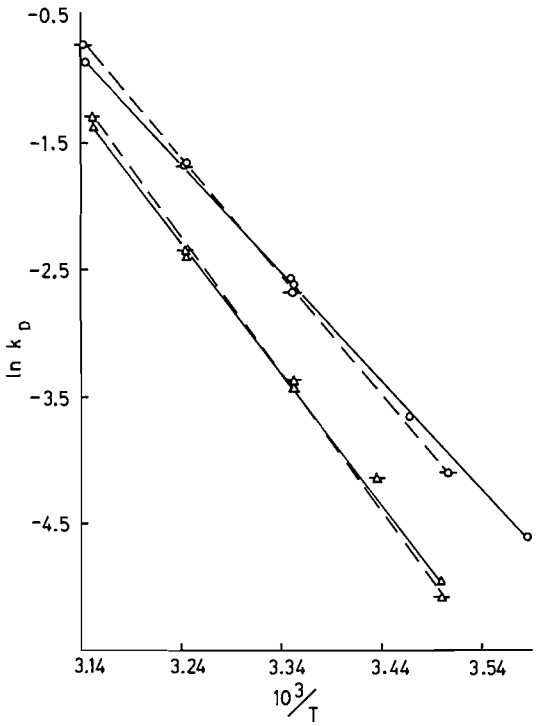

FIG. 3. Effect of temperature on rate of formation of dimers, △, $Ru(NH_3)_5(H_2O)^{2+} + Ru(NH_3)_5N_2^{2+}$; -△- $Ru(NH_3)_5(H_2O)^{2+} + cis\text{-}Ru(NH_3)_4(H_2O)N_2^{2+}$; ○, $cis\text{-}Ru(NH_3)_4(H_2O)_2^{2+} + cis\text{-}Ru(NH_3)_4(H_2O)N_2^{2+}$; -○- $cis\text{-}Ru(NH_3)_4(H_2O)_2^{2+} + Ru(NH_3)_5N_2^{2+}$.

stereospecific (12), the *cis*-nitrogen compound is probably formed from the starting *cis*-tetraammine. This also follows in that *cis*-$Ru(NH_3)_4Cl_2^+$, after reduction with zinc in a dilute aqueous sulfuric acid electrolyte reacts with CO to give *cis*-$Ru(NH_3)_4(H_2O)(CO)^{2+}$ (7).

The formation of both the pentaammine and tetraammine monomers was found to be first order in both Ru(II) and dissolved N_2. This can be interpreted in terms of either a second order displacement mechanism (S_N2), such as

$$Ru(NH_3)_5(H_2O)^{2+} + N_2 \xrightarrow{k_M} Ru(NH_3)_5N_2^{2+} + H_2O$$

or as a dissociative mechanism (S_N1)

$$Ru(NH_3)_5(H_2O)^{2+} \underset{k_{-1}}{\overset{k_1}{\rightleftharpoons}} Ru(NH_3)_5^{2+} + H_2O$$

$$Ru(NH_3)_5^{2+} + N_2 \xrightarrow{k_2} Ru(NH_3)_5N_2^{2+}$$

In the latter case, the reaction will not appear to be second order unless $k_{-1} \gg k_2 \cdot C_{N_2}$ and then $k_M = (k_1/k_{-1})k_2$ (13). Shilova and Shilov (2) have previously stated that Ru(II) chlorides react with N_2 by an S_N1 mechanism involving a five coordinate Ru(II) species but their arguments are not clear.

Armor and Taube (3) have investigated the reaction of $Ru(NH_3)_5(H_2O)^{2+}$ with a variety of other substituents including N_2O, CO, pyridine, and isonicotinamide. These authors also found overall second order kinetics, but their values for the specific rate constants in each case do not differ much from those observed here with N_2. This does not distinguish between the two possible mechanisms, but indicates that all the ligands have about the same nucleophilicity for Ru(II), be it in the S_N2 displacement or the k_2 step of the S_N1 dissociation. In the formation of the tetraammine monomer, the stereospecificity observed in other Ru(II) substitution reactions (12) would require either a square pyramidal intermediate in the dissociative pathway or a *cis* attack in the associative mechanism.

The formation of the dimers was also found to follow second order kinetics, with the rate constants significantly smaller than those for the reaction of the given substrate with N_2. It can be argued that N_2 has two equivalent nucleophilic sites, while a monomer species has only one nucleophilic site. This is in qualitative agreement with the fact that (except for 6 °C) the rate constants for monomer formation were found to be 1.5 to 3.0 times greater than those for dimer formation on a given substrate.

Another feature of the dimer results is the grouping of the Arrhenius plots according to the substrate with the *cis*-$Ru(NH_3)_4(H_2O)_2^{2+}$ reacting twice as fast with either monomer as the $Ru(NH_3)_5(H_2O)^{2+}$. While a statistical argument (14) could be made to explain this result, the corresponding ratio of rates was not found in the case of monomer formation, although the $Ru(NH_3)_4(H_2O)_2^{2+}$ did react somewhat faster than the $Ru(NH_3)_5(H_2O)^{2+}$.

It was also found that for a given substrate, the activation energy for monomer formation was somewhat greater than that for dimer formation, but the entropy of activation for dimer formation was more negative than that for monomer formation. This is consistent with a more highly charged activated complex in dimer formation involving a higher degree of solvation with respect to reactants than is the case in monomer formation (15).

Can. J. Chem. Downloaded from www.nrcresearchpress.com by 210.87.254.5 on 09/05/12
For personal use only.

In the preparation of the tetraammines, the authors are indebted to the mystical preparative talents of Dr. T. Eliades. We also wish to express our gratitude to Caroline B. Elson for her assistance with the computer programming. A fellowship (C.M.E.) from the Province of Ontario and both a scholarship (I.J.I.) and grant from the National Research Council of Canada are gratefully acknowledged.

1. I. J. ITZKOVITCH and JOHN A. PAGE. Can. J. Chem. **46**, 2743 (1968).
2. A. K. SHILOVA and A. E. SHILOV. Kinet. Catal. **10**, 267 (1969).
3. JOHN N. ARMOR and H. TAUBE. J. Amer. Chem. Soc. **91**, 6874 (1969).
4. K. GLEU and K. REHM. Z. Anorg. Allgem. Chem. **227**, 237 (1936).
5. K. GLEU and W. CUNTZE. Z. Anorg. Allgem. Chem. **237**, 197 (1938).
6. A. D. ALLEN, F. BOTTOMLEY, R. O. HARRIS, V. P. REINSALU, and C. V. SENOFF. J. Amer. Chem. Soc. **89**, 5595 (1967).
7. A. D. ALLEN, T. ELIADES, R. O. HARRIS, and V. P. REINSALU. Can. J. Chem. **47**, 1605 (1969).
8. JOHN A. PAGE. Talanta, **9**, 365 (1962).
9. H. STEPHEN and T. STEPHEN (*Editors*). Solubilities of inorganic and organic compounds. Vol. 1, Part 1. Pergamon Press, Ltd., New York. 1963. p. 85.
10. J. ENDICOTT and H. TAUBE. J. Amer. Chem. Soc. **84**, 4984 (1962).
11. WILLIAM G. MOVIUS and R. G. LINCK. J. Amer. Chem. Soc. **91**, 5394 (1969).
12. P. C. FORD and CHRIS SUTTON. Inorg. Chem. **8**, 1544 (1969).
13. F. BASOLO and R. G. PEARSON. Mechanisms of inorganic reactions. 2nd ed. John Wiley and Sons, Inc., New York. 1967. p. 194.
14. JOHN A. BROOMHEAD and LEON KANE-MAGUIRE. Inorg. Chem. **7**, 2519 (1968).
15. A. A. FROST and R. G. PEARSON. Kinetics and mechanism. 2nd ed. John Wiley and Sons, Inc., New York. 1961. pp. 143, 149.

Can. J. Chem. Downloaded from www.nrcresearchpress.com by 210.87.254.5 on 09/05/12
For personal use only.

Pulse radiolysis of ethanol[1]

J. W. FLETCHER, P. J. RICHARDS, AND W. A. SEDDON
Physical Chemistry Branch, Chalk River Nuclear Laboratories, Atomic Energy of Canada Limited, Chalk River, Ontario

Received November 18, 1969

The radiation chemistry of ethanol has been investigated by pulse radiolysis with emphasis on the decay kinetics and yield of the solvated electron, e^-_{EtOH}, in neutral and alkaline solution. Computer calculations show that the experimental data are most consistent with a yield $G(e^-_{EtOH}) = 1.7$ molecules/100 eV, and a pseudo first-order half life for e^-_{EtOH}, $t_{\frac{1}{2}} \approx 6$ μs, which corresponds to a second-order rate constant $k(e^- + EtOH) = 7 \times 10^3\ M^{-1}\ s^{-1}$.

Rates of reaction of the electron with acetaldehyde and C_6F_{12} have been determined to be $4.0 \pm 0.5 \times 10^9$ and $2.5 \pm 0.5 \times 10^9\ M^{-1}\ s^{-1}$, respectively.

The empirical square root formula for spur scavenging kinetics

$$G(e^-_{obs}) = G_{(fe)} + G_{(gc)}\left(\frac{\sqrt{\alpha s}}{1 + \sqrt{\alpha s}}\right)$$

is obeyed for scavenging of the radiation produced positive ion.

Canadian Journal of Chemistry, **48**, 1645 (1970)

Introduction

Much effort has been devoted to determining the natural lifetime of the hydrated electron in the pulse radiolysis of water (1), but very little research in this direction has been done using less polar media such as ethanol. In part, this is due to the lack of relevant rate constant and yield data in ethanol compared to that which is available in the aqueous system.

Pulse radiolysis data (2) have indicated that the electron decay ($t_{\frac{1}{2}} \approx 3$ μs) is faster by a factor of 10^4 in ethanol than in water. However, electrons produced in the alcohols by other than radiation chemical methods have a much longer half life. Feldman *et al.* (3) have found that with ethylenediamine as solvent the reaction rate of the solvated electron with alcohol is not very different from that with water ($t_{\frac{1}{2}} \approx$ ms). In this case the electron was produced by the reaction of sodium with ethylenediamine. Photolytically produced electrons (4) have been found to have a half life of ≈30 μs in ethanol which is a factor of 10 larger than that previously found by pulse radiolysis (2). Walker and co-worker (5) have suggested that if the electron decays by proton abstraction from the solvent, the rate of decay would decrease with decreasing acid strength of the solvent. The relative acid strengths of the polar solvents are $CH_3OH \approx H_2O > CH_3CH_2OH > NH_3$ (6). On this basis the half life for the electron in ethanol should be between that of water and ammonia. This has not been found experimentally.

The pulse radiolysis value for the half life (2) was determined without special purification techniques or removal of the radiolytically formed positive ion. In view of these apparent discrepancies, a further look at the factors affecting the electron decay seemed desirable. High solvent purity was ensured by special techniques. Alkaline solutions were used to remove the radiolytically formed positive ion and prevent its reaction with the electron. Computer calculations have been used to take into account the effect of dose and dose rate on the experimentally observed half life, and to obtain an accurate rate constant for the decay of the electron.

Experimental

(a) Sample Preparation

The anhydrous ethanol was obtained from Commercial Alcohols Ltd. with the following specifications: <0.1 volume % H_2O, $< 2 \times 10^{-4}\ M$ aldehyde, $< 5 \times 10^{-5}\ M$ benzene.

Acetaldehyde is the impurity of most concern and although less than 2×10^{-4} as received, its concentration will be higher if the ethanol has been exposed to oxygen. The acetaldehyde as determined by gas chromatography was reduced to less than $5 \times 10^{-7}\ M$ with a high efficiency spinning band distillation column. The distillation flask was continuously purged through a sinter with hydrogen which had been purified by a palladium catalyst "Deoxo" unit and the head of the still continuously flushed with a stream of 99.97% nitrogen. To prevent oxygen contamination, ethanol samples which

[1]AECL No. 3533.

Can. J. Chem. Downloaded from www.nrcresearchpress.com by 210.87.254.42 on 09/05/12
For personal use only.

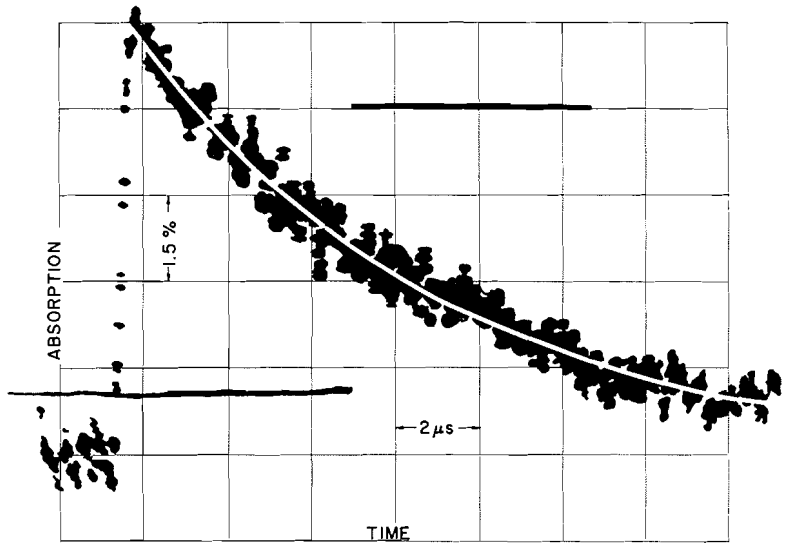

FIG. 1. Oscilloscope trace of the electron decay in ethanol; the solid line superimposed on the trace shows the computed first order decay. The difference between the horizontal traces corresponds to the light intensity (100 mV/div). Dose = 6×10^{19} eV/l, $[EtO^-] = 5 \times 10^{-3}$ *M*, and $t_{\frac{1}{2}} = 5$ μs.

did not contain electron scavengers were transferred directly from the distillation flask to the pulse radiolysis cell in a completely air-tight glass system.

When electron scavengers were added, the ethanol was transferred for sample preparation via a glass line to an oxygen-free dry box. Alkaline samples were prepared by the addition of sodium metal to form the ethoxide negative ion. Samples containing acetaldehyde were prepared just prior to irradiation, since in neutral solutions acetaldehyde slowly decomposes to hemiacetal and acetal which have slower rates of reaction with electrons, and in alkaline solutions decomposes by the aldol condensation reaction. The acetaldehyde was obtained from Eastman Organic Chemicals and the C_6F_{12} from Aldrich Chem. Co.

(b) Pulse Radiolysis System

The techniques used were similar to those adequately described in the literature (7). Samples contained in a 2 cm (optical path length) cell were irradiated at room temperature (25 °C) with 0.5 μs pulses of electrons from a 2 MeV Van de Graaff accelerator. Most samples were given a dose of 6×10^{19} eV/l in ethanol. Dosimetry was done using an oxygen-saturated, 2×10^{-3} *M* KSCN aqueous solution as a primary standard ($G_{(OH)} = 2.9$, $\varepsilon_{475} = 7350$, the average of ref. 8). The charge collected either on a platinum wire in solution or on a metal back plate was used as a secondary standard.

(c) Treatment of Pulse Radiolysis Decay Curves

The original oscilloscope photograph was enlarged, traced on graph paper, and analyzed by computer calculations. This computer program has been written to give the rate constant and yield, from a weighted least-squares treatment of the experimental decay curve. In addition the program presents a calculated decay curve, which can be compared directly with the experimentally obtained curve, to check for self-consistency of the data.

Results and Discussion

The absorption spectrum of the electron in ethanol has been previously determined (9) and has a maximum of 700 nm. The electron decay was monitored at 625 nm and obeyed good first-order decay kinetics except when the sample was irradiated to a higher dose ($>3 \times 10^{20}$ eV/l). A typical decay curve is shown in Fig. 1 with the solid line being the calculated first-order decay curve.

(a) Dose Study

The observed electron half life in pure solution is dependent on the dose per pulse as shown in Fig. 2. The half life decreases with increasing dose per pulse. At the higher doses where the decay curve is not completely first order, the half life is determined from the initial part of the decay curve. The points shown are all individual determinations with fresh solutions for each pulse.

Only an approximate zero dose half life can be estimated by inspection of the half life vs. dose curve (Fig. 2), however, a more precise value can be derived by computer calculation. The solid line in Fig. 2 is calculated from a computer program based on one written by Schmidt (10). The program uses the reactions and rate constants given in Table 1, yields per 100 eV given in Table 2, and the dissociation constant of ethanol = 2.4×10^{-19} (19). It is found that the

Can. J. Chem. Downloaded from www.nrcresearchpress.com by 210.87.254.42 on 09/05/12
For personal use only.

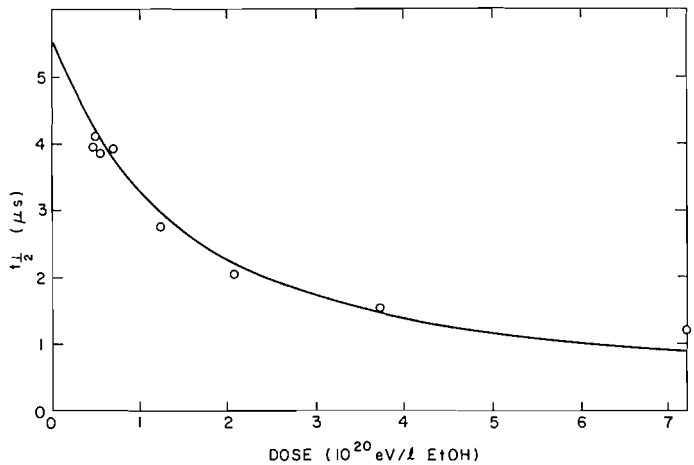

FIG. 2. Effect of dose on electron half life in pure ethanol; points are single measurements on fresh solutions, the solid line is calculated assuming the pseudo first-order rate constant is $1.2 \times 10^5\ s^{-1}$.

TABLE 1

Reactions and rate constants of species in irradiated liquid ethanol

Reaction*	Rate constant ($M^{-1}\ s^{-1}$)	Reference
$e^-_{EtOH} + EtOH_2^+ \rightarrow H + EtOH$	2×10^{10}	11
$e^-_{EtOH} + acet \rightarrow acet^-$	4×10^{9}†	
$e^-_{EtOH} + EtOH \rightarrow EtO^- + H$	7×10^{3}†	
$H + EtOH \rightarrow H_2 + EtO$	2×10^{7}	12
$e^-_{EtOH} + e^-_{EtOH} \rightarrow H_2 + 2EtO^-$	5×10^{9}‡	
$EtO^- + EtOH_2^+ \rightarrow 2EtOH$	7×10^{10}§	
$EtO + EtO \rightarrow acet + EtOH$	4.4×10^{8}‖	
$EtO + EtO \rightarrow dimer$	5.6×10^{8}‖	
$acet^- + EtOH_2^+ \rightarrow EtO + EtOH$	10^{10}¶	
$acet + EtOH_2^+ \rightarrow acetal$	1.6×10^{0}	13

*EtOH = CH_3CH_2OH, EtO = CH_3CHOH, acet = CH_3CHO.
†Determined in this work.
‡High dose rate studies (17).
§Briere and Gaspard (14) have calculated the rate of recombination in ethanol to be one half that in water. Eigen and de Maeyer (15*a*) have found the rate in water to be 1.43×10^{11}. This value has recently been checked by Schmidt (15*b*).
‖The rate constant for the disappearance of the ethanol radical was determined by Dorfman and co-workers (16). The relative rate of disproportionation to dimerization was determined from the yield of acetaldehyde and 2,3-butanediol determined in steady-state radiolysis (17).
¶Estimated (18).

two predominant reactions which affect the electron decay are

[1] $e^-_{EtOH} + EtOH_2^+ \rightarrow H + EtOH$

[2] $e^-_{EtOH} + CH_3CHO \rightarrow CH_3CHO^-$

The best fit is obtained using a second order rate constant $k_{(e^- + EtOH)} = 7 \times 10^3\ M^{-1}\ s^{-1}$. This value is approximately one half the rate previously obtained by pulse radiolysis (2), and earlier conventional steady-state competition studies (20), but similar to a more recent value

TABLE 2

Primary homogeneous radiolytic yields in ethanol

Species	G	Reference
e^-_{EtOH}	1.7*	
$EtOH_2^+$	1.7	
Acetaldehyde (unscavengable)	1.8	(20)
CH_3CHOH	6.5†	
H_2 (unscavengable)	4.2	(20)

*This work and γ-radiolysis steady state values to be published.
†Deduced from chemical analyses of products after γ-radiolysis, using G(dimer) = 2.3 and G(scavengable acetaldehyde) = 1.9 (17).

Can. J. Chem. Downloaded from www.nrcresearchpress.com by 210.87.254.42 on 09/05/12
For personal use only.

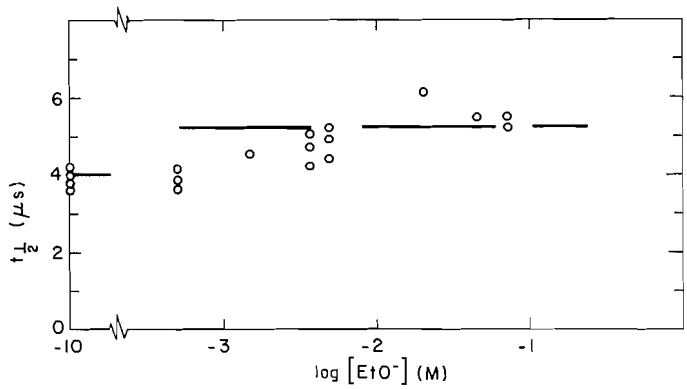

FIG. 3. Effect of ethoxide ion on electron half life; points are single measurements on fresh solutions, the solid line is calculated (dose = 6×10^{19} eV/l).

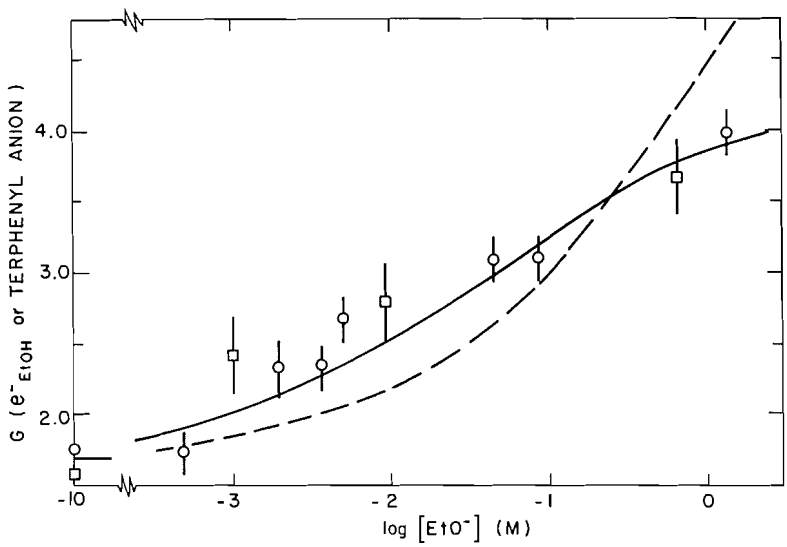

FIG. 4. Effect of ethoxide ion on electron and terphenyl anion yield; solid line calculated assuming $G_{(fe)} = 1.7$, $G_{(ge)} = 2.6$, $\alpha = 6$; dotted line calculated assuming $G_{(fe)} = 1.0$, $G_{(ge)} = 3.3$, $\alpha = 1$; points on this curve are the average of several measurements, ○, electron yield, □, terphenyl anion yield.

calculated from steady-state competition studies (21). On this basis the calculated dose dependence curve (solid line, Fig. 2) gives a very good fit with the experimental values. This dose dependence cannot be explained if the true half life is in fact of the order of milliseconds as found by Feldman *et al.* (3). The long half lives found by Feldman *et al.* may arise from the electron being initially solvated in ethylenediamine.The rate of reaction of the electron solvated in ethylenediamine will be less than in ethanol. Walker (*5b*) has suggested that the rate controlling step could be the rate of alcohol solvation.

$$e^-_{\text{ethylenediamine}} \rightarrow e^-_{EtOH}$$

(b) Effect of Addition of Ethoxide Ion

The normally observed half life and electron yield are both increased by the presence of sodium ethoxide as shown in Figs. 3 and 4. Similar effects have been observed in methanol (22).

The observed half life is increased due to the removal of the radiation produced positive ion in the bulk of the solution.

[3] $$EtOH_2^+ + EtO^- \rightarrow 2EtOH$$

The solid line in Fig. 3 is obtained from computer calculated decay curves using the reaction data and yields in Tables 1 and 2.

Can. J. Chem. Downloaded from www.nrcresearchpress.com by 210.87.254.42 on 09/05/12
For personal use only.

Can. J. Chem. Downloaded from www.nrcresearchpress.com by 210.87.254.42 on 09/05/12
For personal use only.

The yield of the electron as a function of ethoxide concentration, shown in Fig. 4, is approximately doubled. This increase is attributed to scavenging of the geminate positive ion by ethoxide (square brackets indicate that the reaction is in the spur).

[4] $$[EtOH_2^+ + EtO^-] \rightarrow 2EtOH$$

by reducing the importance of reaction [5]

[5] $$[e^- + EtOH_2^+] \rightarrow H + EtOH$$

and allowing a larger percentage of the electrons to become solvated

[6] $$[e^-] \rightarrow e^-_{EtOH}$$

As expected, a similar increase in yield is noted when a scavenger anion is observed instead of the electron. The results obtained in a 5×10^{-4} *p*-terphenyl solution with added ethoxide are also shown in Fig. 4. The terphenyl anion (23) was observed at the absorption maximum 467 nm. The majority of the electrons are solvated before reaction with the terphenyl, therefore the yield curve should be identical to that observed for the electron.

The curve in Fig. 4 fits an empirical square root spur scavenging equation similar to that originated at the Mellon Institute (24).

$$G(e^-_{EtOH_{obs}}) = G_{(fe)} + G_{(ge)}\left(\frac{\sqrt{\alpha s}}{1 + \sqrt{\alpha s}}\right)$$

where $G_{(fe)}$ = yield of free electron, $G_{(ge)}$ = yield of geminate electron, s = scavenger concentration, and α = a fitting constant. The empirical square root relationship has been applied to electron scavengers in which the electron yield is followed by measuring the yield of a stable anion or a secondary

[7] $$e^- + \text{scavenger} \rightarrow \text{scavenger}^- \rightarrow SP$$

stable product SP formed from the transient anion (scavenger$^-$). However, in this paper the electron or the transient anion are observed directly. The kinetics of scavenging a positive or a negative species in the spur should be of the same type, so that one would expect a similar equation to describe both cases. Freeman (25, 26) has considered that the mathematical treatment for scavenging of positive and negative ions would be very similar. The solid curve in Fig. 4 which gives the best fit with the data is obtained by using the following values

$$G_{(fe)} = 1.7,\ G_{(ge)} = 2.6, \text{ and } \alpha = 6$$

The total electron yield = $G_{(fe)} + G_{(ge)} = 4.3$ gave a good fit and has been used by others (24*b*, 26).

An attempt to fit this data using $G_{(fe)} = 1.0$, the lower value that is often quoted (24*b*, 26), and $G_{(ge)} = 3.3$ (24*b*), is shown as a dotted line in Fig. 4 and is not as good a fit as the solid line. It requires that an α value of 1 be used in the calculation.

The α value is related to the relative rate of reaction of the scavenger (24*a*). Values of α between 20 and 2 are found (24), with the larger values being related to reactions having the larger rate constants. The rate of reaction [4] is faster than the rate of reaction [7] for any of the usually used electron scavengers. This would lead to a large value of α as is found when we take $G_{(fe)} = 1.7$. Conversely, the small value of α and the poor fit with the experimental values associated with $G_{(fe)} = 1$ would indicate that $G_{(fe)} > 1$. The higher value of $G_{(fe)}$ is also substantiated by the recently reported values with ethanol (21*b*, 26) or methanol (21*a*, 27) as the solvent and using N_2O as the scavenger.

Freeman (21*b*, 26) has incorporated spur scavenging kinetics in the treatment of the results using N_2O as a scavenger. The spur scavenging curve obtained at high N_2O concentrations is similar to our scavenging curve shown in Fig. 4. In order to observe the spur scavenging kinetics for electrons in neutral solution the N_2O^- must be short lived in comparison with the neutralization reaction [8] in the spur

[8] $$[N_2O^- + EtOH_2^+] \not\rightarrow N_2$$

If the negative ion is long-lived with respect to charge neutralization, then spur scavenging kinetics will not be observed in the form of an increase in ion or SP yield but will give a plateau value of $G_{(fe)}$ with increasing scavenger concentration due to the neutralization reaction

[9] $$[R^- + EtOH_2^+] \rightarrow [RH + EtOH]$$

The latter type of result was observed for R = biphenyl by Sauer *et al.* (9).

The absolute rate constants for reaction of acetaldehyde and C_6F_{12} with solvated electrons in ethanol were determined in the usual manner by pulse radiolysis for application in the computer calculations and to compare with those obtained by steady-state competition kinetics.

TABLE 3

Absolute rate constants

Method	Absolute rate constants $\times 10^{-9}$ CH_3CHO	C_6F_{12}	Reference
Pulse radiolysis	4 ± 0.5	2.5 ± 0.5	This work
Steady state	4	4	To be published
	1.6		(28)
Pulse radiolysis in H_2O	5.4		(12)

The results are given in Table 3. The rate constant obtained by Adams and Sedgewick in the competition scavenging experiments (28) might be low due to the slow removal of acetaldehyde to form hemiacetal (17). The rate constant obtained for C_6F_{12} by steady-state competition kinetics was outside expected experimental error. The reason for this is not known but the higher scavenger concentrations used in steady-state competition kinetic studies sometimes lead to high values.

Conclusions

These data indicate that the yield of the free electron $G_{(fe)} = 1.7$, and that the second order electron decay constant is $7 \times 10^3\ M^{-1}\ s^{-1}$. These conclusions are substantiated further by steady-state radiolysis studies in preparation for publication.

The results indicate that scavenging of the positive ion in the spur obeys the same type of kinetics as are observed for the electron. These results for spur scavenging can be compared with the results obtained in solutions containing nitrous oxide where the N_2O^- is short-lived. No scavenging of the electron in the spur will be observed in neutral solution when the anion is relatively long-lived and reactive with $EtOH_2^+$.

The assistance of Mr. M. J. Young in the design and operation of the electronics in the pulse radiolysis system is greatly appreciated.

1. (*a*) E. J. Hart, S. Gordon, and E. M. Fielden. J. Phys. Chem. **70**, 150 (1966). (*b*) E. J. Hart and E. M. Fielden. J. Phys. Chem. **72**, 577 (1968).
2. I. A. Taub, D. A. Harter, M. C. Sauer, and L. M. Dorfman. J. Chem. Phys. **41**, 979 (1964).
3. L. H. Feldman, R. R. Dewald, and J. L. Dye. Advan. Chem. Ser. **50**, 163 (1965).
4. G. Dobson and L. I. Grossweiner. Rad. Res. **23**, 290 (1964).
5. (*a*) E. A. Shaede and D. C. Walker. Chem. Soc. London, Special Publication **22**, 277 (1967). (*b*) D. C. Walker. Quart. Rev. **21**, 79 (1967).
6. E. J. King. Acid–base equilibria. The MacMillan Co., New York. 1965. p. 293.
7. (*a*) C. L. Greenstock, M. Ng, and J. W. Hunt. Advan. Chem. Ser. **81**, 397 (1968). (*b*) W. A. Seddon. Report in preparation, Atomic Energy of Canada Ltd., Chalk River, Ontario.
8. (*a*) G. E. Adams, J. W. Boag, J. Currant, and B. D. Michael. Pulse radiolysis. The Academic Press, Inc., New York. 1965. p. 117. (*b*) J. H. Baxendale, P. L. T. Bevan, and D. A. Scott. Trans. Faraday Soc. **64**, 2389 (1968).
9. M. C. Sauer, S. Arai, and L. M. Dorfman. J. Chem. Phys. **42**, 708 (1965).
10. K. H. Schmidt. A.E.C. Research and Development Report, ANL 7199 (1966).
11. L. M. Dorfman. Advan. Chem. Ser. **50**, 36 (1965).
12. M. Anbar and P. Neta. Int. J. Appl. Rad. Isotopes, **18**, 493 (1967).
13. A. J. Deyrup. J. Amer. Chem. Soc. **56**, 60 (1934).
14. G. Briere and F. Gaspard. J. Chim. Phys. **64**, 1071 (1967).
15. (*a*) M. Eigen and L. de Maeyer. Z. Elektrochem. **59**, 986 (1955). (*b*) K. H. Schmidt and S. M. Ander. J. Phys. Chem. **73**, 2486 (1969).
16. (*a*) I. A. Taub and L. M. Dorfman. J. Amer. Chem. Soc. **84**, 4053 (1962). (*b*) L. M. Dorfman and I. A. Taub. J. Amer. Chem. Soc. **85**, 2370 (1963).
17. J. W. Fletcher. To be published.
18. K. D. Asmus, A. Henglein, A. Wigger, and G. Beck. Ber. Bunsenges. **70**, 756 (1966).
19. (*a*) G. Briere, B. Crochon, and N. Felici. C.R. **254**, 4458 (1962). (*b*) G. Briere, N. Felici, and E. Piot. C.R. **255**, 107 (1962).
20. J. J. Myron and G. R. Freeman. Can. J. Chem. **43**, 381 (1965).
21. (*a*) K. N. Jha and G. R. Freeman. J. Chem. Phys. **48**, 5480 (1968). (*b*) J. C. Russell and G. R. Freeman. J. Phys. Chem. **71**, 755 (1967). (*c*) J. C. Russell and G. R. Freeman. J. Phys. Chem. **72**, 816 (1968).
22. P. J. Wardman. Private communication.
23. S. Arai and L. M. Dorfman. J. Chem. Phys. **41**, 2190 (1964).
24. (*a*) J. M. Warman, K. D. Asmus, and R. H. Schuler. Advan. Chem. Ser. **82**, 25 (1968). (*b*) J. H. Fendler and S. J. Rzad. Mellon Institute Quarterly Report, RRL-2310-276, July, 1969. p. 11.
25. G. R. Freeman. J. Chem. Phys. **46**, 2822 (1967).
26. G. R. Freeman. Actions chemiques et biologiques des radiations. Series 14, 1969. In press.
27. K. Suryanarayanan and N. N. Lichtin. J. Phys. Chem. **73**, 1384 (1969).
28. G. E. Adams and R. D. Sedgwick. Trans. Faraday Soc. **60**, 865 (1964).

Can. J. Chem. Downloaded from www.nrcresearchpress.com by 210.87.254.42 on 09/05/12
For personal use only.

Can. J. Chem. Downloaded from www.nrcresearchpress.com by 210.87.254.6 on 09/05/12
For personal use only.

Some further reactions of pyrrylthiol esters

E. BULLOCK, T.-S. CHEN, C. E. LOADER, AND A. E. WELLS
Department of Chemistry, Memorial University, St. John's, Newfoundland

Received November 6, 1969

Reduction of pyrrylthiol esters with Raney nickel will yield, under specified conditions, the corresponding hydroxymethyl- or methylpyrroles. Evidence for at least two reduction mechanisms is presented. A convenient synthesis of a previously difficultly accessible pyrrole (**1***f*) related to the coproporphyrins is described.

Canadian Journal of Chemistry, **48**, 1651 (1970)

Desulfurization of thiol esters by Raney nickel normally gives the corresponding formyl or hydroxymethyl derivatives (**1***a*, *b*). The conversion of pyrrylthiol esters to aldehydes has been described (2), and recently the catalytic decarbonylation of pyrrylthiolcarboxylates has been reported (3). In this paper, conditions are described (Scheme 1) which will convert pyrrylthiol esters to hydroxymethyl- or methylpyrroles in high yield.

At room temperature, using W-2 Raney nickel (4) the pyrrylthiol ester **1***a* may be converted almost quantitatively to the hydroxymethyl derivative **1***c*. As conditions are made more severe (especially at higher temperatures) an impurity can be detected by thin-layer chromatography (t.l.c.). This proved to be the methylpyrrole **1***f*. High yield conversion of **1***a* to **1***f* can be achieved with a very active Raney nickel (W-5) used at high temperature and pressure. Similar reductions were observed for the thiolester **2***a*.

Pyrrole **1***f* was also prepared in high yield from the hydroxymethyl compound **1***c* by conversion of the latter to the chloromethyl derivative **1***e* followed by reductive removal of the halogen atom over palladium black.

Since the reduction of acylpyrroles (including aldehydes) to the corresponding alkyl derivatives is well-known (see e.g. 5, 6) attempts were made to see if a sequential reduction (viz. Scheme 2)

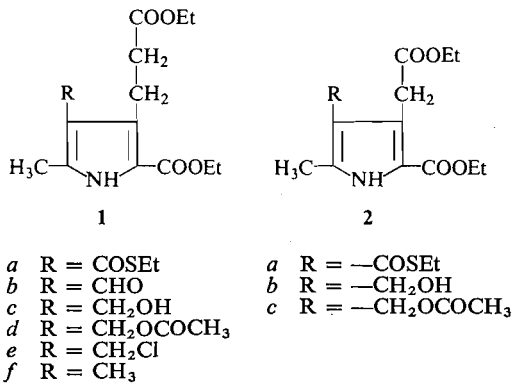

a R = COSEt
b R = CHO
c R = CH_2OH
d R = CH_2OCOCH_3
e R = CH_2Cl
f R = CH_3

a R = —COSEt
b R = —CH_2OH
c R = —CH_2OCOCH_3

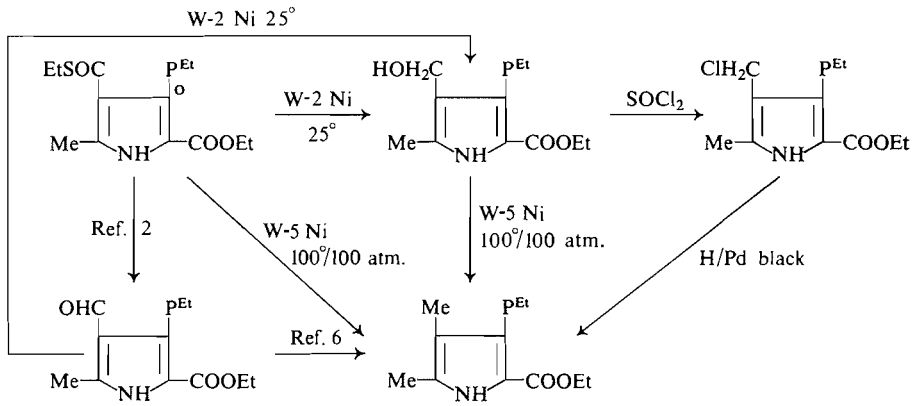

SCHEME 1

$$\text{—COSEt} \xrightarrow{(a)} \text{—CHO} \xrightarrow{(b)} \text{—CH}_2\text{OH} \xrightarrow{(c)} \text{—CH}_3$$

SCHEME 2

Can. J. Chem. Downloaded from www.nrcresearchpress.com by 210.87.254.6 on 09/05/12
For personal use only.

was occurring. In separate experiments, each of the reduction steps envisaged above can be accomplished with Raney nickel and hydrogen (e.g. **1***a* → **1***b* → **1***c* → **1***f*). However, a high yield conversion at step (*c*) requires vigorous conditions. Table 1 shows that even under mild conditions, with an active catalyst, very rapid desulfurization occurs. Not surprisingly, the aldehyde is rapidly removed, but the initial yield of the hydroxymethyl compound slowly declines also, achieving a nearly constant level after about $1\frac{1}{2}$ h. Although the activity of the catalyst has clearly declined as the desulfurization proceeds, separate experiments to test step (*c*) suggest that even with active catalysts, only a very slow conversion of hydroxymethyl to methyl occurs at 70° and 4 atm. Thus, the rapid formation of the methyl compound initially (Table 1) probably represents either direct reduction of the thiol ester, or a pathway from the aldehyde which does not involve a primary alcohol intermediate.

In the Experimental section (Table 2) conditions for formation of **1***c* and **1***f* in good yield are given. The conversions shown in the figure are described. No evidence of decarbonylation under the conditions given in (3) has been observed.

Experimental

Infrared (i.r.) spectra were recorded on a Perkin–Elmer 237B instrument, ultraviolet (u.v.) spectra on a Perkin–Elmer 202 and nuclear magnetic resonance (n.m.r.) spectra on a Varian A-60 spectrometer.

Ethyl 2-Methyl-4-(2′-carbethoxyethyl)-5-carbethoxypyrrole-3-thiolcarboxylate (1a)

A solution of methyl β-oxoadipate (21.6 g) (7) in glacial acetic acid (30 ml) was cooled in ice whilst sodium nitrite (6.9 g as saturated water solution) was added, with stirring, keeping the temperature below 20°. After warming to room temperature (3 h) the solution was added dropwise to a mixture of ethyl acetothiolacetate (14.6 g), glacial acetic acid (45 ml) and zinc dust (6 g) with stirring. The temperature was kept at about 70° during the addition of more zinc dust (15 g). The mixture was held at 80° for 1 h then poured into iced water (2 l) and allowed to stand for 4 h. The precipitate was collected and recrystallized from ethanol to give colorless prisms (16.8 g, 49%), m.p. 94–95°. The u.v. absorption (95% ethanol), maxima at 231, 285 mμ ($\log_{10}\varepsilon_{max}$ 4.33, 4.22). The i.r. spectrum ($CHCl_3$) maxima at (inter alia) 1725 (C=O, CH_2CH_2-COOEt), 1682 (C=O, CO.OEt), 1639 cm^{-1} (C=O, COSEt). The n.m.r. spectrum (CCl_4) showed absorptions at τ −0.5 (broad, NH), 5.68 and 5.89 (quartets —OCH_2—), 7.01 (quartet, —SCH_2—), 6.68 and 7.49 (A_2B_2 multiplet, —CH_2CH_2CO—), 7.42 (singlet —CH_3), and 8.62, 8.68, 8.75 (triplets, ester CH_3).

Anal. Calcd. for $C_{16}H_{23}NO_5S$: C, 56.30; H, 6.79; N, 4.10; S, 9.39. Found: C, 56.47; H, 6.75; N, 4.27; S, 9.45.

Progressive Reduction of Thiol Ester

(*a*) Ethyl 2-methyl-4-(2′-carbethoxyethyl)-5-carbethoxypyrrole-3-thiolcarboxylate (2 g; **1***a*) in absolute ethanol (100 ml) was reduced with Raney nickel (10 g; W-5) in a Parr hydrogenator in an atmosphere of hydrogen at 55 p.s.i. and 70 °C. Samples were removed every 30 min for 3 h and a final sample after 11 h. The samples were analyzed on an Aerograph 1520 gas chromatograph under the following conditions: column, Apiezon L; flow rate, 24 ml/min of He; column temperature, 230 °C; detector temperature, 305 °C; injection temperature, 275 °C; sample volume, 3 μl. Results are shown in Table 1.

(*b*) Table 2 gives results of separate experiments using **1***a* in attempts to define the best preparative conditions for the formation of **1***c* and **1***f*. The pyrrole (0.5 g) in ethanol (75 ml) was reduced under the specified conditions.

Ethyl 2-Methyl-3-hydroxymethyl-4-carbethoxymethylpyrrole-5-carboxylate (2b)

Ethyl 2-methyl-4-carbethoxymethyl-5-carbethoxypyrrole-3-thiolcarboxylate (**2***a*, 4 g), Raney nickel (30 g, W-2), and ethanol (100 ml) were shaken together for 6 h at room temperature. The catalyst was removed (over Celite) and the filtrate evaporated to dryness *in vacuo*. The residue was recrystallized from benzene–ligroin to give colorless needles (2.76 g, 84%) m.p. 116.5–117°. The u.v. absorption (95% ethanol), maxima at 210, 282 mμ ($\log_{10}\varepsilon_{max}$ 3.78, 4.26 respectively). The i.r. spectrum ($CHCl_3$) showed strong bands at 3432, 1711, 1684, 1144 inter alia. The n.m.r. spectrum ($CDCl_3$): 0.31 (broad, NH), 5.55 (singlet, CH_2OH), 5.70 and 5.84 (quartets, O—CH_2—), 6.08 (singlet —CH_2CO), 7.12 (OH), 7.72 (singlet —CH_3), 8.66 and 8.74 (triplets, ester CH_3).

Anal. Calcd. for $C_{13}H_{19}NO_5$: C, 57.98; H, 7.11; N, 5.20. Found: C, 57.85; H, 7.12; N, 5.27.

The acetate **2***c*, m.p. 100–101 °C, was formed from **2***b* by treatment with acetic anhydride/pyridine. It was recrystallized from ether – petroleum ether.

Anal. Calcd. for $C_{15}H_{21}NO_6$: C, 57.87; H, 6.80; N, 4.50. Found: C, 57.90; H, 6.84; N, 4.49.

Ethyl 2-Methyl-3-hydroxymethyl-4-(2′-carbethoxyethyl)-pyrrole-5-carboxylate (1c)

(*a*) This substance was prepared according to the method for **2***b* above. The compound (**1***c*), m.p. 94–94.5° was recrystallized from benzene/petroleum ether. The u.v. absorption (95% ethanol) maxima at 210, 282 mμ ($\log_{10}\varepsilon_{max}$ 3.89, 4.29). The i.r. spectrum ($CHCl_3$), maxima (inter alia) at 1720 (C=O, —CH_2CH_2COOEt) and 1683 (C=O, COOEt). The n.m.r. spectrum ($CDCl_3$) τ, 0.50 (broad, NH), 5.50 (singlet —CH_2OH), 5.69 and 5.91 (quartets, —OCH_2—), 6.96 and 7.24 (A_2B_2 multiplets, —$CH_2.CH_2CO$—), 7.22 (singlet, —OH), 7.71 (singlet, CH_3), 8.65 and 8.80 (triplets, ester —CH_3).

Anal. Calcd. for $C_{14}H_{21}NO_5$: C, 59.36; H, 7.47; N, 4.95. Found: C, 59.18; H, 7.30; N, 4.75.

The acetate (see preparation of **2***c* above) formed colorless needles from ether, m.p. 126–127°.

Anal. Calcd. for $C_{16}H_{23}NO_6$: C, 59.08; H, 7.12; N, 4.31. Found: C, 59.38; H, 7.22; N, 4.23.

(*b*) A mixture of the aldehyde **1***b*, Raney nickel (W-2, 5 g), and ethanol (30 ml) was shaken under hydrogen at

TABLE 1

Progressive reduction of the pyrrylthiol ester (**1***a*)

Time (min)	3-COSEt (**1***a*)	3-CHO (**1***b*)	3-CH_2OH (**1***c*)	3-CH_3 (**1***f*)
0	100			
30	8	23.5	21	47.5
60	4	5.5	15.5	75
90		8*	14	78
120		< 5	12	86
150		trace	12	88
180		trace	10	90
660		trace	10	90

*Retention times of these two products are so similar that resolution is lost at low concentrations.

TABLE 2

Reduction of **1***a* under specified conditions.

Ni added (g)	Temperature (°C)	H_2 pressure (atm)	Time (h)	Products (%)	
				3-CH_2OH	3-CH_3
5 (W-2)	25	4	3	> 95	trace
5 (W-2)*	70	4	3	64	36
1.5 (W-5)	100	100	2	undetected	> 95

*Pretreated with acetone at room temperature for 3 h. Optimum conditions for formation of the aldehyde (**1***b*) have been reported (2).

55 p.s.i. and 70° for 3 h. The catalyst was filtered off and the solvent removed *in vacuo*. The product (from which **1***c* m.p. 94–95.5° was readily isolated) contained at least 90% of **1***c* with some **1***f* (less than 10% as the minor product).

Ethyl 2-Methyl-3-chloromethyl-4-(2′-carbethoxyethyl)-pyrrole-5-carboxylate (1e)

Thionyl chloride (8 ml) was added dropwise to a cooled solution of the hydroxymethyl pyrrole (**1***c*) (15 g) in dry ether (100 ml) with stirring. The solvent and excess thionyl chloride were removed *in vacuo* below 20°, and three 50 ml portions of dry ether were successively added and removed in the same way. The residual solid was recrystallized from dry ether – petroleum ether to give almost colorless needles (15.6 g, 94%), m.p. 126–129°. The compound was unstable in moist air, but the n.m.r. spectrum ($CDCl_3$) confirms its identity: τ, −0.04 (broad, NH), 5.36 (singlet, CH_2Cl), 5.62 and 5.81 (quartets, $—OCH_2$), 6.90 and 7.34 (A_2B_2 multiplet, $—CH_2CH_2-CO—$), 7.66 (singlet, CH_3), 8.62, 8.74 (triplets, ester, $—CH_3$).

Ethyl 2,3-Dimethyl-4-(2′-carbethoxyethyl)-pyrrole-5-carboxylate (1f)

(*a*) Ethy l2-methyl-4-(2′-carbethoxyethyl)-5-carbethoxy-pyrrole-3-thiolcarboxylate was reduced under conditions specified in Table 2.

After cooling at 200 p.s.i., the residual solution was filtered through Celite and the solvent removed to give an almost colorless crystalline residue. Recrystallization from aqueous ethanol gave **1***f* (3.4 g, 87%) as colorless plates, m.p. 89.5°–91° (lit. m.p. 88–89° (6)).

(*b*) Ethyl 2-methyl-3-hydroxymethyl-4-(2′-carbethoxy-ethyl)-pyrrole-5-carboxylate (**1***c*) (0.75 g) in ethanol (150 ml) was reduced over Raney nickel (15 g, W-5) as in (*a*) above. Recrystallization of the product from aqueous ethanol yielded **1***f* (0.52 g, 72%) as colorless plates, m.p. 89.5–91 °C.

(*c*) Ethyl 2-methyl-3-chloromethyl-4-(2′-carbethoxy-ethyl)-pyrrole-5-carboxylate (6 g, **1***e*) and anhydrous sodium acetate (1.7 g) in glacial acetic acid (40 ml) was reduced by hydrogen over palladium black (300 mg) at 55 p.s.i. and 50–60 °C for 3 h. The reaction mixture was poured into iced water (400 ml). The precipitate was washed with water after filtration, then recrystallized from aqueous methanol to give colorless crystals (5.2 g, 92%), m.p. 87–88°, of the corresponding 3-methyl pyrrole derivative **1***f*.

The authors are grateful to Memorial University and the Province of Newfoundland for Fellowships (to C.E.L. and A.E.W.) and to the National Research Council of Canada for financial support.

1. (*a*) A. V. McIntosh, Jr., A. M. Searcy, E. M. Meinzer, and R. H. Levin. J. Amer. Chem. Soc. **71**, 3317 (1949). (*b*) G. B. Spero, A. V. McIntosh, Jr., and R. H. Levin. J. Amer. Chem. Soc. **70**, 1907 (1948).
2. E. Bullock, T.-S. Chen, and C. E. Loader. Can. J. Chem. **44**, 1007 (1966).
3. H. J. Anderson and C. E. Loader. Tetrahedron, **25**, 3879 (1969).
4. R. M. Mozingo. Organic syntheses. Coll. Vol. III. E. C. Horning, *editor*. Wiley, New York, 1947. p. 181.
5. H. Fischer and H. Hofelmann. Ann. **533**, 216 (1938).
6. F. Morsingh and S. F. MacDonald. J. Amer. Chem. Soc. **82**, 4377 (1960).
7. M. Viscontini and N. Merckling. Helv. Chim. Acta, **35**, 2280 (1952). M. Viscontini and H. Kohler. Helv. Chim. Acta, **37**, 41 (1954).

Can. J. Chem. Downloaded from www.nrcresearchpress.com by 210.87.254.6 on 09/05/12
For personal use only.

Can. J. Chem. Downloaded from www.nrcresearchpress.com by 210.87.254.5 on 09/05/12
For personal use only.

Stability constants for some 1:1 metal–carboxylate complexes

JOHN W. BUNTING AND KAIN MEN THONG
Department of Chemistry, University of Toronto, Toronto 181, Ontario

Received October 1, 1969

Stability constants have been measured for the formation of 1:1 complexes between eight divalent metal ions and six carboxylate anions. For each anion the stabilities of the complexes follow the order $Pb^{2+} > Cu^{2+} > Cd^{2+} > Zn^{2+} > Ni^{2+} \sim Co^{2+} > Ca^{2+} \sim Mg^{2+}$. The stabilities of the complexes with each metal ion are directly related to the basicities of the anions, and little or no bidentate chelation occurs between these metal ions and acetoxyacetic acid or *N*-acetylglycine.

Canadian Journal of Chemistry, 48, 1654 (1970)

In connection with another study, we wished to compare stability constants for 1:1 complex formation between various divalent metal ions and carboxylate anions. While stabilities of metal ion – acetate complexes have been well studied (1), comprehensive data are not available for complexes involving other carboxylate anions. The data that are available come from a number of different sources, and are often not directly comparable since widely differing conditions of temperature and ionic strength have been used in their determination. In particular, we were interested in the possibility that *N*-acetylglycine and acetoxyacetic acid might act as bidentate ligands when entering into complex formation with some divalent metal ions. Such bidentate complex formation would be expected to result in greater stabilities for these complexes than would be predicted from the basicities of the carboxylate anions.

We wish to report stability constants, which were measured under constant experimental conditions, for the formation of 1:1 complexes between eight divalent metal ions (lead, cadmium, copper, zinc, nickel, cobalt, calcium, and magnesium) and the anions of six carboxylic acids (acetic, benzoic, formic, chloroacetic, and acetoxyacetic acids and *N*-acetylglycine).

Experimental

Metal Salts

Solutions of divalent metal ions were made up from the best commercially available grade of the metal nitrates. These solutions were standardized by titration with EDTA by the usual procedures (2).

Carboxylic Acids

Acetoxyacetic acid, chloroacetic acid, benzoic acid, and *N*-acetylglycine were recrystallized to constant melting point. Acetic and formic acid solutions were standardized by titration with standard aqueous alkali.

Experimental Procedure

Dissociation constants of the carboxylic acids and stability constants of the 1:1 metal–carboxylate complexes were determined by potentiometric titration at 30° and ionic strength 0.4. The ionic strength was adjusted with suitable concentrations of sodium nitrate.

An aqueous solution (40 ml) containing the metal nitrate (0.1 *M*) and carboxylic acid (0.01 *M*) was titrated with one equivalent (ten aliquots; each 0.4 ml) of potassium hydroxide solution (0.1 *M*). The p*H* of the solution was noted, after the addition of each aliquot of alkali, on a Corning Model 12 p*H* Meter, which had been previously standardized against 0.05 *M* potassium hydrogen phthalate solution (error in p*H* reading ± 0.002). The titration was carried out in a water-jacketed reaction vessel, thermostated at 30°, and nitrogen was continuously bubbled through the solution.

Acid dissociation constants were determined by a similar titration in the absence of divalent metal ions.

The concentrations of free metal ion $[M^{2+}]$, free carboxylate anion $[L^-]$ and 1:1 metal–ligand complex $[ML^+]$, were calculated from equations for the total concentration of metal-containing species, total concentration of ligand-containing species, electroneutrality and the dissociation constant of the carboxylic acid. Hence at each point in the titration, a value for the stability constant

$$K = \frac{[ML^+]}{[M^{2+}][L^-]}$$

for the formation of a 1:1 complex could be calculated. All reported values for log *K* are averages of 7–10 values, and the reported error is the greatest deviation from this value.

Since the stabilities of these complexes are quite low, relatively large concentrations of the metal ions were required in order to shift the equilibria towards the complex species. Although this makes possible the formation of 2:1 metal–ligand complexes, it is considered extremely unlikely that such complexes will occur to any appreciable extent in the systems which are reported in this work. This assumption that only 1:1 complexes are present, is supported by the constancy of the stability constants for these complexes over the ten-fold variation in ligand concentration which occurs during the course of the titrations.

TABLE 1

Values of log K for 1:1 metal–carboxylate complexes*

Metal ion	Acetic acid	Benzoic acid	Formic acid	*N*-Acetyl-glycine	Acetoxy-acetic acid	Chloro-acetic acid
H^+†	4.56±0.03	3.97±0.04	3.53±0.03	3.43±0.02	2.81±0.03	2.63±0.01
Pb^{2+}	1.93±0.04	1.99±0.04	1.65±0.06	1.40±0.05	1.17±0.05	~1.1‡
Cd^{2+}	1.30±0.02	1.15±0.03	1.15±0.03	1.13±0.03	~1.1‡	0.99±0.06
Cu^{2+}	1.76±0.06	1.51±0.03	1.38±0.03	1.30±0.03	1.22±0.04	1.07±0.02
Zn^{2+}	0.91±0.03	0.74±0.04	0.73±0.04	0.71±0.04	0.67±0.04	0.56±0.02
Ni^{2+}	0.72±0.05	0.55±0.04	0.67±0.02	0.58±0.03	0.63±0.05	0.23±0.07
Co^{2+}	0.71±0.05	0.55±0.04	0.68±0.03	0.54±0.02	0.39±0.05	0.23±0.07
Ca^{2+}	0.50±0.04	~0.2‡	0.27±0.03	0.29±0.02	0.32±0.04	0.14±0.05
Mg^{2+}	0.47±0.03	~0.1‡	0.34±0.03	0.32±0.03	0.31±0.04	0.23±0.05

*At 30°, ionic strength 0.4.
†For H^+, log $K = pK_a$.
‡Maximum deviation greater than ±0.1.

Results and Discussion

Stability constants (as log K) for 1:1 complexes of divalent metal ions and carboxylate anions are given in Table 1. The acid dissociation constants for each of the carboxylic acids are also included in this table. In general, the order of the stability constants for a particular metal ion with the carboxylate anions is the same as the order for the basicities of these anions.

Stability constants which have been reported previously for complex formation between these metal ions and carboxylate anions are collected in Table 2. These constants were measured under a variety of conditions, temperatures range between 15 and 35°, and ionic strengths from 0 to 3.0. A literature search did not reveal any reports of stability constants for the association of divalent metal ions with *N*-acetylglycine or acetoxyacetic acid. In general, the stability constants in Tables 1 and 2 are in reasonable agreement. Deviations between the two sets of constants can be traced to different experimental conditions. We believe that Table 1 represents the most comprehensive data that are available on the stabilities of these metal–carboxylate complexes under constant experimental conditions.

For each ligand, the stabilities of the metal complexes follow the order $Pb^{2+} > Cu^{2+} > Cd^{2+} > Zn^{2+} > Ni^{2+} \approx Co^{2+} > Ca^{2+} \approx Mg^{2+}$. The order of the stabilities of the complexes of cobalt, nickel, copper, and zinc is as expected on the basis of the Irving–Williams order (Co < Ni < Cu > Zn) (3).

Abnormally high stability constants for association of substituted carboxylate anions with metal ions have been used by other workers as indications of chelate formation, which involves both the carboxylate group and another ligating center in the same molecule. Examples of such bidentate chelation by the anions of carboxylic acids are:

(*a*) α-oxy-substituted carboxylic acids with divalent manganese, copper and zinc ions, e.g. hydroxyacetic acid, tetrahydrofuran-2-carboxylic acid (4);

(*b*) α-thio-substituted carboxylic acids with the cupric ion, e.g. *S*-carboxymethyl ethyl mercaptan (4);

(*c*) some dicarboxylic acids with divalent lead, copper, cadmium, zinc, and nickel ions, e.g. malonic acid, maleic acid (5).

In each case the stability constants for complex formation are much greater than would be expected from the basicity of the anion.

The data in Table 1 indicate that the association

TABLE 2

Literature values for log K for 1:1 complexes between divalent metal ions and some carboxylate anions*,†

Metal ion	Acetic acid	Benzoic acid	Formic acid	Chloro-acetic acid
Pb^{2+}	1.39–2.70	2.0	0.74–0.78	1.52
Cd^{2+}	1.30–2.0	1.4		1.2
Cu^{2+}	1.61–2.40	1.6–1.92	1.53–2.02	0.9–1.61
Zn^{2+}	0.76–1.59	0.9	0.60	
Ni^{2+}	0.41–1.81	0.9		
Co^{2+}	0.32–1.36			
Ca^{2+}	0.53–0.77		0.48–0.80	
Mg^{2+}	0.51–0.82			

*From ref. 1, p. 357, 364, 374, 530.
†Temperature range 15–35°; ionic strength range 0–3.0.

Can. J. Chem. Downloaded from www.nrcresearchpress.com by 210.87.254.5 on 09/05/12
For personal use only.

constants for the anions of acetoxyacetic acid and *N*-acetylglycine with these metal ions are of the order expected from the basicities of these ligands. This indicates that association of the metal ions with these two ligands probably takes place only with the carboxylate group and does not involve appreciable bidentate chelation, such as would result from the association of the metal ions with both the carboxylate group and the acetoxy or acetamido groups through oxygen or nitrogen atoms. However, the presence of small amounts of chelated species, in equilibrium with the major monodentate complex, are not excluded by these data.

Investigations of various peptide – metal ion complexes have revealed that some metal ions are capable of co-ordinating with peptide ligands via a deprotonated amide nitrogen atom (6–9). Ionization constants for deprotonation of an amide nitrogen atom in a complexed peptide range from $pK_a = 3.90$ in Cu^{2+}–glycylglycine (6) to $pK_a = 9.35$ in Ni^{2+}–glycylglycine (9).

An attempted investigation of the abilities of various metal ions to form species of the type I (M = divalent metal ion) was not productive. The insolubilities of the metal hydroxides and the low stabilities of the metal–carboxylate monodentate complexes precluded the study of the formation of I by the titration procedures used in this study. Even at low metal ion concentrations (0.001 *M*), attempts to show the presence of these species by p*H*-titrations were foiled by the precipitation of the metal hydroxides.

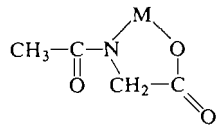

I

We thank the National Research Council of Canada for a research grant in support of this work.

1. L. G. Sillen and A. E. Martell. Stability constants of metal-ion complexes. Special Publication No. 17. The Chemical Society, London, 1964. P. 364.
2. H. Flaschka. EDTA titrations—An introduction to theory and practice. Pergamon Press, Oxford, 1964.
3. H. Irving and R. J. P. Williams. J. Chem. Soc. 3192 (1953).
4. H. Sigel, R. Griesser, B. Prijs, D. B. McCormick, and M. G. Joiner. Arch. Biochem. Biophys. **130**, 514 (1969).
5. M. Yasuda, D. Yamasaki, and H. Ohtaki. Bull. Chem. Soc. Japan, **33**, 1067 (1960).
6. W. L. Koltun, M. Fried, and F. R. N. Gurd. J. Amer. Chem. Soc. **82**, 233 (1960).
7. W. L. Koltun, R. H. Roth, and F. R. N. Gurd. J. Biol. Chem. **238**, 124 (1963).
8. R. B. Martin and J. T. Edsall. J. Amer. Chem. Soc. **82**, 1107 (1960).
9. R. B. Martin, M. Chamberlin, and J. T. Edsall. J. Amer. Chem. Soc. **82**, 495 (1960).

Can. J. Chem. Downloaded from www.nrcresearchpress.com by 210.87.254.5 on 09/05/12
For personal use only.

Can. J. Chem. Downloaded from www.nrcresearchpress.com by 210.87.254.5 on 09/05/12
For personal use only.

Yield of free-ions in the radiolysis of formamide, a liquid of very high dielectric constant

D. A. HEAD[1] AND D. C. WALKER
Chemistry Department, University of British Columbia, Vancouver, British Columbia

Received January 20, 1970

Solutions of N_2O in liquid formamide (dielectric constant 109) gave a yield of N_2 during γ-radiolysis of $G(N_2) = 3.3 \pm 0.3$. Competition between N_2O and other scavengers, including water, ethanol, acids, $AgNO_3$, and CdI_2 strongly resembled the pattern of reactivity characteristic of solvated electrons found in other polar liquids. Furthermore, the yield obtained (3.3) was consistent with the high dielectric constant and predicted for the free-ion yield by Freeman's model assuming a total ionization of 4.7. However, the absence of an absorption band in nanosecond pulse radiolysis experiments suggests that solvated electrons were not present 10^{-9} s after the passage of the ionizing radiation. It is quite possible that in this system "solvent anions" (or other reactive reducing ions) were formed in yield equal to the "free-ion" yield. This presupposes that formamide anions readily reduce N_2O and Ag^+, are inactivated by H^+ and do not react with water and alcohols.

The high dielectric constant apparently leads to large yields of comparatively long-lived ($> 10^{-7}$ s) reducing ions (free-ion yield of 3.3) accompanied by rather small yields of H atoms and simple molecular decomposition products. In these respects the radiolysis decomposition of formamide resembles that of water.

Canadian Journal of Chemistry, 48, 1657 (1970)

Introduction

Of the several molecular properties which govern the radiolysis yield of solvated electrons (e_s^-) the static dielectric constant (ε) is probably the most important. A high dielectric constant will tend to increase the free solvated electron yield, firstly, by diminishing the coulombic attraction between positive ions and thermalized electrons and thus reducing geminate recombination (and random neutralization) and secondly by, in general, facilitating the solvation process. These dependences have been recognized and treated theoretically by several authors and in a variety of ways (e.g. 1–7). Furthermore, the general trends found for $G(e_s^-)$ and $E_{\lambda max}$ (the energy of the optical absorption band maximum of the solvated electron) as a linear function of ε have been reviewed respectively by Holroyd (8) and Dorfman (9).

However, water ($\varepsilon = 78$) is the only liquid having a dielectric constant greater than about 40 for which data are currently available. Thus we have endeavoured to obtain the yield of solvated electrons for a liquid of much higher ε. Of the four common liquids with $\varepsilon > 78$ at 25 °C, formamide, which has $\varepsilon = 109$, seemed best suited to this study.

Recently, two other studies on aspects of the radiation chemistry of formamide ($HCONH_2$, referred to as FA for brevity) have been reported briefly but neither presents an evaluation of the yield of solvated electrons. Fel' *et al.* (10) have investigated the absorption spectra of transient species produced in FA by pulse radiolysis and by irradiation as a glassy solid (containing 15% water) at 77 °K. They found an absorption band centered at 550 nm attributed to e_s^- but concluded it had a very small yield in the aqueous glass, $G \sim 0.03$. Lichtin and Matsumoto (11) have examined the gaseous and high-boiling stable products formed in the γ-radiolysis of FA and deuteroformamide and their results for H_2 and CO are compatible with our data. We know of no study of solutions of alkali metals in formamide which could be of significance here. Boden and Back (12) have investigated the photochemistry and free-radical reactions in formamide vapor and there are reports on the sensitized photodissociation of the liquid (13). *N,N*-Dimethylformamide is a much more commonly studied liquid, for which radiation chemical data are available (14), but not $G(e_s^-)$ unfortunately. However, since its physical and chemical properties (e.g. $\varepsilon = 38$) are widely different from FA any close correspondence in products or yields would be entirely unexpected.

Holroyd (8) has drawn attention to the observation that with electron scavengers at very high concentrations even non-polar liquids such as cyclohexane and benzene, as well as the polar

[1]Present address: Materials Science Division, Atomic Energy of Canada Ltd., Whiteshell Nuclear Research Establishment, Pinawa, Manitoba.

Can. J. Chem. Downloaded from www.nrcresearchpress.com by 210.87.254.5 on 09/05/12
For personal use only.

ones, tend to show total electron yields of $\sim 4.5 \pm 0.5$. High yields for very short periods of time are also implied by certain nanosecond pulse radiolysis experiments (15, 16). It should be noted that this high concentration limit of $G(e_s^-)$ is significantly greater than $100/W_{(gas)}$ for many of these liquids. In some environments the electrons will remain essentially free, in others they will interact to varying extents with the solvent to become quasi-free, solvated, or trapped species. In any of these states a fraction of the electrons will undergo neutralization with their concomitant positive ion or ions originating in the same spur, these being termed "geminate" ions, whilst others will escape to participate in random diffusion and reaction, these being termed "free" ions. An important difference between these two types of electrons is their mean lifetime and hence the scavenger concentration needed to capture them. Media of high dielectric constant might be expected to produce a high ratio of "free" to "geminate" electrons.

In cases where the solvent molecule has a suitable electron affinity the electron formed by radiation may become attached to one molecule and thus form a solvent anion. This attachment may precede or follow solvation of the electron by the bulk solvent and could involve only the electrons destined to become "free" rather than the total ion yield. Little is known about reactivity of these anions towards N_2O and other commonly used solvated electron scavengers.

Experimental

Irradiations were performed on samples of the pure liquid and dilute solutions of various solutes in deoxygenated liquid formamide. Purification of FA (obtained from B.D.H. Ltd.) was performed by drying over 4 Å molecular sieves and anhydrous magnesium sulfate and by low pressure fractional distillation. The consequences of remnant impurities on the radiation chemical yields were examined by studying the dose dependence of the yields and by deliberately adding small amounts of suspected impurities, in particular ammonia, formic acid, ammonium formate, and water (for details see ref. 17). FA is undoubtedly difficult to obtain in high purity; but our results show no indication of interference by impurities and since our conclusions are based on absorption spectra taken within 3 ns and the results of competition between pairs of scavengers at high concentrations, we feel that the purity of our material was adequate. N_2O was purified by trap-to-trap distillation under vacuum; the other chemicals were Reagent Grade or better.

Irradiations were performed on a 4000 Ci ^{60}Co Gammacell at a dose rate of $\sim 6.4 \times 10^{15}$ eV g^{-1} s^{-1} and total doses up to about 10^{20} eV g^{-1}. Typically 20 ml liquid samples were irradiated in a cell similar to that sketched in Fig. 1. By bubbling high purity helium through the sintered glass disc the FA could be deoxygenated prior to irradiation and after irradiation volatile products could be flushed directly into a sensitive vapor phase chromatograph (v.p.c.) for analysis. Generally a Poropak Q pre-column at 25 °C was used to trap out N_2O and FA ahead of the 20 ft 13X molecular sieve column at 95 °C which was used for separation of permanent gases. The working lower limits (corresponding to about 10% errors) by this technique were approximately H_2 10^{-6} mole, N_2 10^{-7} mole, O_2 5×10^{-8} mole, CH_4 10^{-7} mole and CO 10^{-7} mole. Although NH_3 was detectable as a radiation product difficulty was experienced in extracting and estimating it quantitatively. Higher molecular weight products were not analyzed. During the v.p.c. injection various flushing times were adopted so that it was possible to estimate with known reproducibility the fraction of each gas which would be extracted by 3 min of the bubbling (normally 90–95%). For N_2O solutions, after flushing with He to remove oxygen the liquid was equilibrated with N_2O at a predetermined pressure. Dosimetry was performed in the cell sketched in Fig. 1 using the Fricke solution, taking for Fe^{3+} ions $\alpha_{(304)} = 2174$ and $G(Fe^{3+}) = 15.5$, and converting to the appropriate dose-rate expected in FA by multiplying by 1.05, the ratio of electron densities of the FA and dosimeter solutions.

Some pusle radiolysis experiments were performed on pure liquid formamide using the 3 ns pulse of 0.5 MeV electrons from a Febetron accelerator. Absorption spectroscopy studies included the use of laser photometry (16) and nanosecond spectrographic analysis by a technique which will be described elsewhere (18).

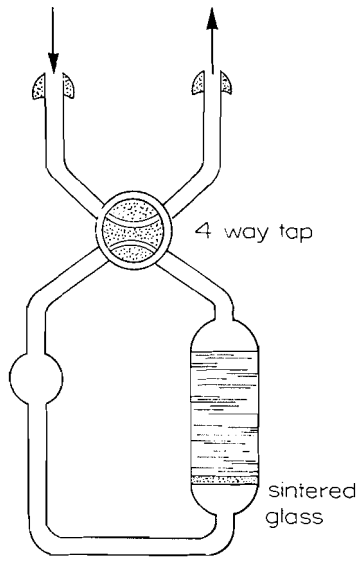

FIG. 1. Irradiation cell, also used for deoxygenation and injection of volatile products into v.p.c. column.

Can. J. Chem. Downloaded from www.nrcresearchpress.com by 210.87.254.5 on 09/05/12
For personal use only.

Results

Purified liquid formamide under γ-irradiation produced H_2 and CO as the principal volatile products. For doses $< 5 \times 10^{19}$ eV g^{-1} the amount was proportional to the dose and gave $G(H_2) = 0.94 \pm 0.08$ and $G(CO) = 0.77 \pm 0.06$. At much larger doses the radiation yield decreased significantly. However these same yields (0.94 and 0.77) were obtained during a small dose following a very large one (at the end of which volatile products were removed), suggesting that an inhibition is caused by the build up of volatile radiation products. Of the other products for which we have meaningful data $G(N_2) < 0.004$, $G(O_2) < 0.002$, and $G(CH_4) < 0.01$.

N_2O concentrations were evaluated from the partial pressure used for equilibration and the measured solubility of N_2O in FA which was found to be 6.8×10^{-5} molar per Torr partial pressure at 25 °C. Figure 2 shows the gas yields as a function of dose for a N_2O concentration of 0.04 *M*. From these linear plots the following values were obtained: $G(N_2) = 3.2 \pm 0.3$, $G(H_2) = 0.75 \pm 0.05$, and $G(CO) = 0.75 \pm 0.05$. Thus addition of N_2O was seen to decrease $G(H_2)$ slightly, leave CO unaffected, and produce copious quantities of N_2. The dependence of these yields upon N_2O concentration is shown in Fig. 3. N_2O at <0.01 *M* was enough to reduce $G(H_2)$ by its full 0.2 diminution.

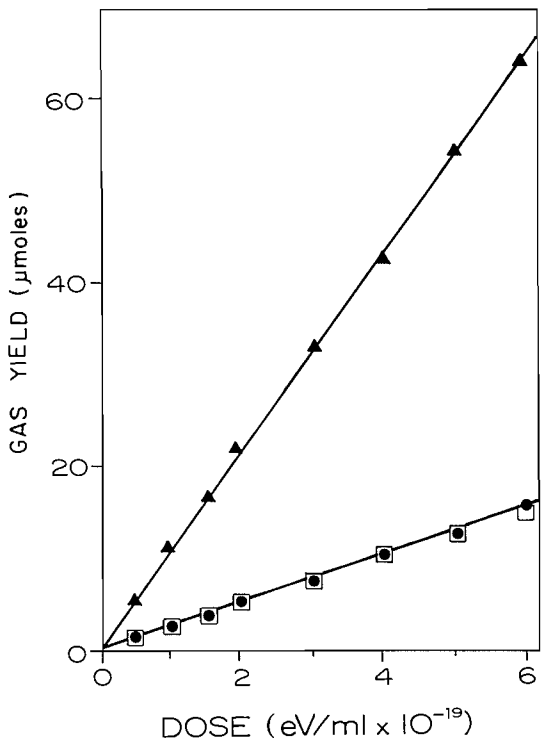

FIG. 2. Gas yields as a function of radiation dose: 0.04 *M* N_2O solution in formamide. ▲, N_2; □ H_2; and ●, CO.

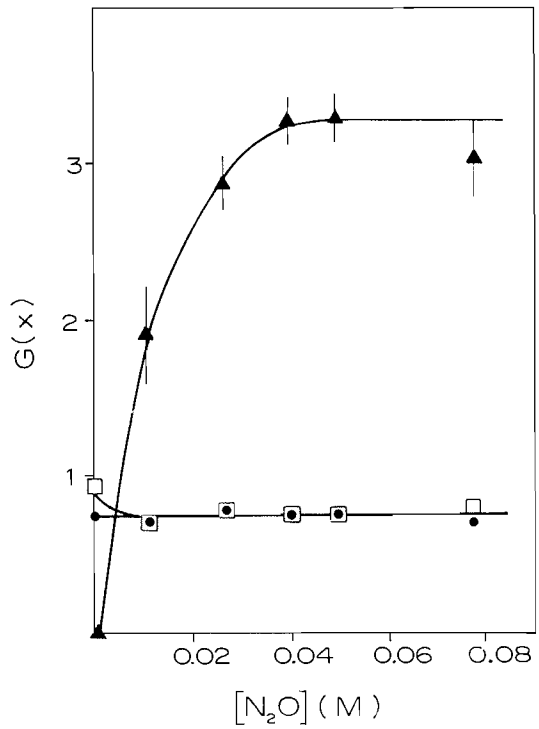

FIG. 3. Radiation yields of N_2, H_2, and CO as a function of N_2O concentration in formamide solutions irradiated to doses $< 5 \times 10^{19}$ eV g^{-1}; ▲, N_2; □, H_2; and ●, CO.

In order to determine the nature of the species with which N_2O was reacting, various second scavengers were added to a 0.04 *M* solution of N_2O in formamide. The data obtained for the radiation yields of N_2, H_2, and CO are reported in Table 1. Each entry represents the mean of at least two experiments and the maximum possible errors are about 10%. Thus it is seen that none of the second scavengers affect $G(H_2)$ significantly whereas $G(CO)$ increased with high concentrations of all scavengers other than water and ethanol, in fact whenever the $G(N_2)$ was reduced appreciably. H_2O (0.19 *M*) did not affect any of the yields in the N_2O solution suggesting either

Can. J. Chem. Downloaded from www.nrcresearchpress.com by 210.87.254.5 on 09/05/12
For personal use only.

TABLE 1

Radiation yields from irradiated formamide containing 0.04 M N_2O plus the second scavenger indicated in column 1 at concentration given in column 2

2nd Scavanger	Concentration (M)	$G(N_2)$	$G(H_2)$	$G(CO)$
None	—	3.3	0.75	0.75
Water	0.19	3.2	0.77	0.68
Ethanol	0.103	2.9	0.75	0.75
HCOOH(anhydrous)	0.133	0.22	0.75	1.08
HCl	0.28	0.06	0.84	1.10
H_2SO_4(anhydrous)	0.18	0.04	0.77	1.70
	0.02	0.07	0.75	1.24
	0.01	0.22	0.68	0.83
	0.002	0.82	0.69	0.90
	0.0005	2.02	0.71	0.79
	0.00025	2.85	0.70	0.70
$AgNO_3$	0.0116	0.13	0.58	1.37
	0.0039	0.22	0.65	1.46
	0.0021	0.29	0.69	1.36
	0.0012	0.59	0.72	1.28
	0.0008	1.80	0.79	0.97
	0.0006	2.38	0.71	0.78
	0.0004	3.10	0.71	0.51
CdI_2	0.219	2.64	0.77	1.34
	0.097	2.61	0.73	1.15
	0.044	2.82	0.75	1.02
	0.023	3.05	0.71	0.94
	0.0088	3.18	0.80	0.88

that it cannot compete with the precursors of N_2, H_2, and CO or that even the driest sample of FA used contained enough water for its effect to be fully felt.

No optical absorption was observed in either pulse radiolysis experiment. The product of radiation yield times optical extinction coefficient throughout the wavelength range 450 to 850 nm for species produced during the pulse must have been less than about 5000, a limit set by comparable observations on glycol (18). Using laser photometry at 632.8 nm, any absorption during the instant of the pulse and up to 450 ns thereafter must have had an optical density of <0.07.

Discussion

In a study of the nature of an intermediate through inferential evidence, as in this case, one is confronted with the need to draw one's conclusions from general analogies with systems which are well understood. Drawing, in particular, on the aqueous system one might expect the scavengers used to behave in the following ways: N_2O to react very much more efficiently with solvated electrons than H atoms, that H_2O might react only with positive ions, ethanol to react only with H atoms, H^+ with e_s^-, Ag^+ and NO_3^- with e_s^-, Cd^{2+} with e_s^- and I^- to react with oxidizing species, be they positive ions or free-radicals.

It certainly appears that $G(H_2) = 0.75$ can be attributed to "molecular" processes which may include molecular detachment of H_2, ion–molecule or hot-atom reactions occurring on every collision or a high probability thermal radical reaction involving the solvent molecules. If the reaction of H atoms with FA to give H_2 is as fast in the liquid as found in gas phase photolyis (12), then this might be the source of non-scavengable H_2, in which case $G(H) < 0.75$. $G(CO) = 0.75$ appears also to be non-scavengable. The increase in CO with many of the second scavengers suggests that they react with a species which otherwise inhibits the formation of CO; perhaps they interfere with a back reaction such as that between NH_2 and HCO, thus permitting HCO to lead to CO. These yields compare quite well with the results of Lichtin and Matsumoto (11) who find $G(H_2) = 0.87 \pm 0.16$ and $G(CO) = 0.61 \pm 0.14$.

Nitrogen could be formed in the N_2O solutions by one or more of the reactions [1] to [4], the analogues of which are known to occur in other polar media

[1] $e_s^- + N_2O \rightarrow N_2 + O^-$

[2] $H + N_2O \rightarrow N_2 + OH$

[3] $R\cdot + N_2O \rightarrow N_2 + RO\cdot$

[4] $FA^* + N_2O \rightarrow N_2 +$ other species

where R· is a free radical species and FA* an electronically excited formamide molecule. In water the ratios k_1/k_2 and k_1/k_3 exceed 10^4 and in several other solvents these ratios are known to be quite large. Thus one would expect reaction [1] to occur at much lower concentrations of N_2O than reaction [2] (19). The following arguments can be advanced, based on the data of Table 1, to support the view that the yield of N_2 of 3.3 could arise predominantly, if not entirely, from reaction [1], and consequently that this yield could represent $G(e_s^-)$.

(*i*) The fact that excess ethanol reduced $G(N_2)$ by only 10% suggests that at most $G(N_2) = 0.4$ arises from reaction [2] or [3]. It should also be noted that just 0.3% acetone impurity in the ethanol would probably cause a decrease in $G(N_2)$

Can. J. Chem. Downloaded from www.nrcresearchpress.com by 210.87.254.5 on 09/05/12
For personal use only.

of 0.4 by reaction with e_s^-, so that too much significance should not be attached to the small drop observed.

(*ii*) All three acids, HCOOH, HCl, and H_2SO_4, strongly inhibit N_2 formation, indeed essentially eliminate it completely. Such an effect is quite contrary to expectation if reactions [2] and [3] were involved but entirely consistent with reaction [1] because of the competitive reaction [5].

[5] $$e_s^- + H_s^+ \rightarrow \text{"H"}$$

a reaction which is well authenticated and known to have very high rate constants in many systems. It also implies that the N_2 which ethanol could inhibit did not arise from "H", the product of reaction [5]. It should be noted that for the sulfuric acid mixture a nuclear magnetic resonance (n.m.r.) examination revealed that a proton was formed in these solutions, probably in the solvated form $HCONH_3^+$. For a simple competition between reactions [1] and [5] and assuming that e_s^- reached a steady-state concentration, the following equation would apply

$$1/G(N_2) = (1 + k_5[H^+]/k_1[N_2O])/G(e_s^-)$$

Figure 4 presents a plot of $1/G(N_2)$ against $2[H_2SO_4]/[N_2O]$ which is seen to be linear. From the intercept and slope the following data could be obtained

$$G(e_s) = 3.5 \pm 0.3 \quad k_5/k_1 = 30 \pm 2$$

This value of $G(e_s^-)$ is in good agreement with the data of Fig. 3. The ratio k_5/k_1 is about 10 times larger that the equivalent ratio of rate constants in water (20). This could mean that k_1 is substantially less than the diffusion controlled limit in FA, or it may represent an argument against solvated electrons being involved.

(*iii*) Ag^+ and/or NO_3^- compete successfully with N_2O for the precursor of N_2. This is also in accord with reaction [1] being largely responsible for N_2 because in aqueous solution both Ag^+ and NO_3^- react very much more efficiently with e_{aq}^- than with H.

(*iv*) Apparently CdI_2 does not compete with N_2O for the precursor of N_2 in a simple manner. This is at first sight another argument against solvated electrons because in aqueous solution the analogue of reaction [7]

[7] $$Cd^{2+} + e_s^- \rightarrow Cd^+$$

has a very fast, diffusion controlled, rate constant.

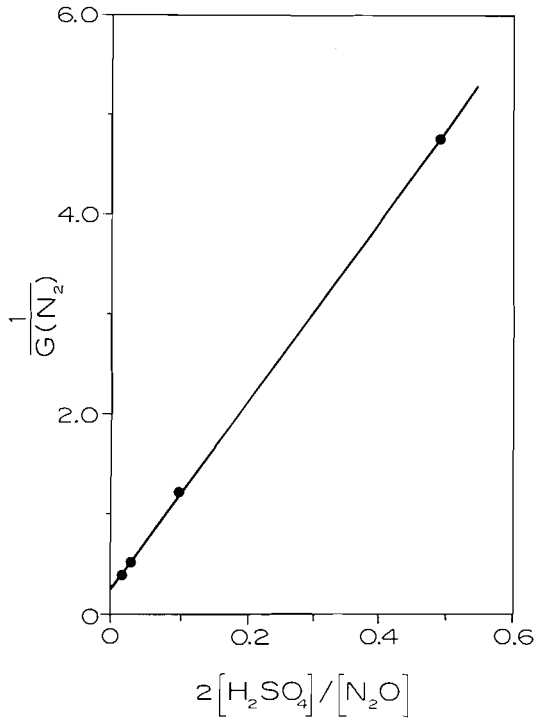

FIG. 4. Plot of $1/G(N_2)$ as a function of $2[H_2SO_4]/[N_2O]$. Data taken from Table 1.

However, the transient monovalent Cd^+ ion formed in reaction [7] could have a high expectation of reacting with N_2O according to reaction [8], when the latter is present at 0.04 *M*.

[8] $$Cd^+ + N_2O \rightarrow N_2 + Cd^{2+} + O^-$$

In fact, the concentration data presented in Table 1 are consistent with a reaction scheme involving reactions [1], [7], [8], and [9]

[9] $$Cd^+ \rightarrow \text{products}$$

in which $k_9/k_8 = 1.0 \times 10^{-2}$ *M*. (A similar charge transfer mechanism involving reactions [10] and [11]

[10] $$e_s^- + Ag^+ \rightarrow Ag$$

[11] $$Ag + N_2O \rightarrow N_2 + Ag^+ + O^-$$

can also account well for the concentration dependence of the $AgNO_3$ data.) Clearly the detailed features of these systems may be rather complex and certainly involve many unknowns; however, the fact that excess I^- did not drastically diminish the N_2 yield is important because it means that N_2 is probably not generated by reaction of N_2O with the concomitant oxidizing

species, be it positive ion or free radical, nor from the O^- formed in reaction [1]. Buxton and Dainton (21) have shown that in aqueous solution I^- scavenges O^- and OH very efficiently. Thus the CdI_2 data strongly suggest that reaction [12]

[12] $$O^- + N_2O \rightarrow N_2 + O_2^-$$

does not contribute to the N_2 formed in this system and consequently each e_s^- does not lead to the generation of two N_2 molecules.

There are no compelling reasons to suspect contributions to $G(N_2)$ from reaction [4], but within the limitations of the experiments, excited formamide molecules could contribute a G of about 0.4 providing the second scavengers which react effectively with e_s^- also react with FA*.

Applying the model and method of Freeman and Fayadh (6, 22) one can calculate an expected solvated electron yield for formamide. According to Freeman's scheme for calculating the fraction of ion pairs which become free, it is necessary to know the distribution of initial separations, in particular the number of ion pairs $N(y)$ with initial separation y since

$$\frac{G(e_{f.i.}^-)}{G(\text{total ions})} = \frac{\int N(y)\phi(y)\,dy}{\int N(y)\,dy}$$

where $\phi(y)$ is the probability that an ion will escape geminate recombination as given by the Onsager relation $\phi(y) = e^{-r/y}$ (r is the effective recombination distance equal to $q^2/\varepsilon kT$ for ions each of charge q in a medium of dielectric constant ε). We have computed a separation spectrum of $N(y)$ as a function of y using the step function for water (22) but correcting the electron range in FA relative to that in water. Taking $\varepsilon = 109$, the values reported in Table 2 were calculated for various values of G (total ionization). Since 4.7 seems to be a reasonable yield of total electrons (8), it is evident that an observed free electron yield of 3.3 would be entirely consistent with this model. Figure 5 shows the general trend of $G(e_s^-)$ as a function of dielectric constant for a number of liquids for which data are available, including 3.3 for formamide.

Our pulse radiolysis results with FA are all negative and hence must be viewed with some reservations. The absorption spectrum taken *during* the 3 ns radiation pulse places an upper limit of $G \times \alpha < 5000\ M^{-1}\ cm^{-1}\ (100\ eV)^{-1}$ on species which may absorb light within the range 450 to 850 nm, where α is the molar decadic extinction coefficient. Kinetic studies by laser photometry also show that at 633 nm $G \times \alpha < 1300$. If one assumes that $G(e_s^-) = 3.3$, then either (*i*) the maximum extinction coefficient of e_s^- within this wavelength range is $< 1500\ M^{-1}\ cm^{-1}$ or (*ii*) that only a small fraction of the solvated electrons are formed during the pulse. Scavenger studies showed that e_s^- would not decay measurably within 3×10^{-9} s and hence to accept (*ii*), one must conclude they were being *formed* only slowly. Conclusion (*i*) would be contrary to the findings of others (10, 11*b*) and to general analogies with other solvents and theoretical or semi-empirical predictions (9). Conclusion (*ii*) would be rather startling and thus must await more direct evidence since it implies that solvated electrons were produced slowly in formamide; perhaps as a result of secondary reactions during the chemical stage of interaction, $> 10^{-9}$ s after passage of the charged particle.

TABLE 2

Calculated values of $G(e_{f.i.}^-)$ for various values of G(total ionization) using the model and method of Freeman and Fayadh (6, 22)

G(total ionization)	$G(e_{f.i.}^-)$
4.0	2.8
4.3	3.0
4.5	3.2
4.6	3.25
4.7	3.3

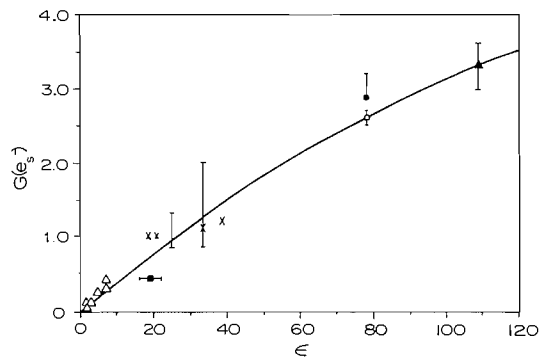

FIG. 5. Plot of the published values of "free" electron yields, $G(e_s^-)$, as a function of static dielectric constant for a variety of liquids. Data taken largely from refs. 6 and 8 but including error bars to cover the spread of experimental data: △ refers to hydrocarbons, alkyl halides, and ethers, ■ is liquid ammonia at various temperatures, × represents aliphatic alcohols, ○ is H_2O, ● is D_2O and ▲ is the formamide data of this work.

Can. J. Chem. Downloaded from www.nrcresearchpress.com by 210.87.254.5 on 09/05/12
For personal use only.

Can. J. Chem. Downloaded from www.nrcresearchpress.com by 210.87.254.5 on 09/05/12
For personal use only.

Although the pattern of reactivity shown in Table 1 conforms very well to the behavior of hydrated electrons, for whose identity there is overwhelming evidence, one cannot be sure that formamide anions ($HCONH_2^-$, or some other reactive reducing species which may be a dissociation product of this ion) were not responsible for our data.[2] Such anions would probably *not* have a strong absorption band in the visible but might nevertheless easily reduce N_2O and Ag^+ and may be inactivated by H^+. They may arise rather rapidly (half-life $< 10^{-10}$ s) through capture and stabilization in a molecular orbital of FA, but perhaps only from solvated electrons or "free" electrons, thus accounting for the N_2 yield fitting to the Freeman picture. Perhaps further pulse radiolysis and electron spin resonance (e.s.r.) studies will reveal their true identity.

Conclusions

In many respects this highly polar liquid shows a close resemblance to water in its general pattern of decomposition under high energy radiations: a large yield ($G = 3.3 \pm 0.3$) of comparatively long-lived reducing ions (either solvated electrons or solvent anions), little evidence of much decomposition into small neutral free radical species ($G(H)$ was very probably < 0.75), and small yields of simple non-scavengable molecular decomposition products. The yield of N_2 produced in irradiated N_2O solutions may be equated with the free-ion yield and fits the Freeman model adequately for a total ionization yield of about 4.7. The pattern of reactivity towards scavengers suggested the free negative ions appeared as solvated electrons, but this was not in accord with the absence of an absorption band during nanosecond pulse radiolysis. Since 0.01 M N_2O scavenged just 50% of the reducing ions it follows that their half-life must exceed 10^{-7} s, because H^+ was shown to be 30 times more reactive than N_2O and the reaction of H^+ would be restricted to the diffusion controlled limit $\sim 3 \times 10^{10}\ M^{-1}\ s^{-1}$. Evidently the alternative fate of these ions was neither geminate recombination (they were too long-lived for this) nor charge neutralization by homogeneous reaction with positive ions produced by the radiation (they were too short-lived for this at the dose rates used).

[2]Comments on this point made by a referee and by Dr. N. N. Lichtin are very much appreciated.

The authors are most grateful to Dr. N. N. Lichtin for providing unpublished data, to Miss G. A. Kenney and Mr. S. C. Wallace for performing the pulse radiolysis experiments reported, to the National Research Council of Canada for financial support, and to the H. R. MacMillan Family for the award of a Graduate Fellowship to D.A.H.

1. A. H. Samuel and J. L. Magee. J. Chem. Phys. **21**, 1080 (1953).
2. R. L. Platzman. N.A.S./N.R.C. Rep. No. 305, 21 (1953).
3. A. Mozumber. J. Chem. Phys. **48**, 1659 (1968).
4. A. Hummel. J. Chem. Phys. **49**, 4840 (1968).
5. W. H. Hamill. J. Phys. Chem. **73**, 1341 (1969).
6. G. R. Freeman. Rad. Res. Rev. **1**, 1 (1968).
7. F. Williams. J. Amer. Chem. Soc. **86**, 3954 (1964).
8. R. A. Holroyd. *In* Fundamental processes in radiation chemistry. *Edited by* P. Ausloos, Interscience Publishers, 1968. p. 413.
9. L. M. Dorfman. Advan. Chem. Ser. **50**, 36 (1965).
10. (*a*) N. S. Fel', P. I. Dolin, and V. I. Zolotarevskii. Khim. Vys. Energ. **1**, 154 (1967). (*b*) N. S. Fel', P. I. Dolin, and V. A. Sharpatyi. Khim. Vys. Energ. **2**, 189 (1968).
11. (*a*) A. Matsumoto and N. N. Lichtin. Oral presentation to the International Conference on Radiation Chemistry, Argonne National Laboratory, Illinois, 1968. (*b*) N. N. Lichtin. Private communication.
12. J. C. Boden and R. A. Back. Trans. Faraday Soc. In press.
13. D. Elad. Angew. Chem. Int. Ed. **5**, 255 (1966).
14. N. Colebourne, E. Collinson, and F. S. Dainton. Trans. Faraday Soc. **59**, 886 (1963).
15. J. K. Thomas and R. V. Bensasson. J. Chem. Phys. **46**, 4147 (1967).
16. G. A. Kenney and D. C. Walker. J. Chem. Phys. **50**, 4074 (1969).
17. D. A Head. Ph.D. Thesis, University of British Columbia, 1969.
18. D. C. Walker and S. C. Wallace. To be published.
19. (*a*) D. A. Head and D. C. Walker. Nature, **207**, 517 (1965). (*b*) D. A. Head and D. C. Walker. Can. J. Chem. **45**, 2051 (1967).
20. See M. Anbar and P. Neta. Intern. J. Appl. Rad. Isotop. **18**, 493 (1967).
21. G. V. Buxton and F. S. Dainton. Proc. Roy. Soc. A **287**, 427 (1965).
22. G. R. Freeman and J. M. Fayadh. J. Chem. Phys. **43**, 86 (1965).

Can. J. Chem. Downloaded from www.nrcresearchpress.com by 210.87.254.5 on 09/05/12
For personal use only.

Photochemistry of nitroso compounds in solution.[1] XV. Configuration and conformation of the enone oximes obtained from photoaddition of *N*-nitrosopiperidine to conjugated dienes

Y. L. Chow, C. J. Colón, and D. W. L. Chang
Department of Chemistry, Simon Fraser University, Burnaby 2, British Columbia

Received November 27, 1969

In the presence of an acid, *N*-nitrosopiperidine photolytically adds to conjugated dienes to give 1:1 adducts in excellent yield. While the major products are the *syn*- and *anti*-isomers of piperidino α,β-unsaturated oxime derived from 1,4-addition, similar types of oximes derived from 1,2-addition are also obtained. The ratio of *syn*- and *anti*-oximes is determined by the relative configurational and the conformational stabilities of the two forms. The nuclear magnetic resonance (n.m.r.) chemical shifts and coupling constants provide useful information for the determination of the configuration and conformation of the oximes. A comparison of the n.m.r. data from α,β-unsaturated oximes indicates that the α-proton generally resonates at a lower field than the β-proton in contrast to the chemical shifts of α,β-unsaturated carbonyl compounds. The photoaddition of nitrosopiperidine to cycloheptatriene gave tropone oxime, probably through the elimination of piperidine from the 1:1 adduct.

Canadian Journal of Chemistry, 48, 1664 (1970)

Results

When a mixture of *N*-nitrosopiperidine and a conjugated diene was irradiated in a methanol solution in the presence of hydrochloric acid, 1:1 adducts of the nitrosamine to the diene were obtained in a good yield. As in the photoaddition to an olefin (2, 3), the reaction was carried out in a Pyrex apparatus at the vicinity of 0° and its progress was traced by following the disappearance of the nitrosamine absorption at 340 mμ. The control experiments showed that in the absence of an acid or of irradiation, this absorption band remained unchanged, demonstrating the similarity of the present photoaddition to that of an olefin (2).

The photoadditions were investigated using symmetrical conjugated dienes, such as butadiene, cyclopentadiene, 1,3-cyclohexadiene, and *cis,cis*-1,3-cyclooctadiene, as the substrate. In every case, the 1,4-adduct was produced in a major amount. Two of the 1,4-adducts further gave pairs of *syn–anti* isomers (**1** and **2**, and **5***c* and **6***c*) while others (**5***a* and **5***b*) gave only one isomer. The minor components of the photoadditions were *syn*- (**4** and **8**) and *anti*-isomers (**3** and **7**) of the 1,2-adducts which could be separated on a silicic acid column. The primary photoadduct to an olefin has been shown to be a *C*-nitroso compound (2, 3). Since the tautomerization of a *C*-nitroso compound yields *syn*, *anti*, or both oximes in a secondary process (2), the formation of the oximes is controlled by the stabilities of the transition states leading to these oximes (3, 4) and will be discussed below.

The structural elucidation of those adducts were greatly facilitated by the analyses of their nuclear magnetic resonance (n.m.r.) spectra. A set of examples is given in Fig. 1. In addition the infrared (i.r.) spectra of all these adducts exhibited a set of multiple absorptions in 900–1000 cm^{-1} range which were the typical N–O stretching modes for the oximino group. While all the 1,4-adducts (**1**,**2**,**5**, and **6**) showed that the H_c signal (the proton at carbon carrying piperidino ring) was coupled to the olefinic protons (H_a and H_b), it was established, either by visual analysis of the coupling pattern or by decoupling experiments, that H_c was not coupled to H_a and H_b in the 1,2-adducts (**3**,**4**,**7**, and **8**). This information provided an unequivocal decision between 1,2- and 1,4-adducts. Where both *syn*- and *anti*-isomers were obtained, the assignments of *syn*- and *anti*-configuration were readily decided by the differences in the n.m.r. chemical shifts in which the *cis* protons to the oximino group were more deshielded by the well-understood anisotropic effects of an oximino group (5–7). Thus H_a and H_b signals of the *syn*-oxime of 1,4-adducts (**2** and **6***c*) generally resonate at a lower field than H_a and H_b of the corresponding *anti*-oxime (**1** and **5***c*). In the 1,2-adducts, the signals due to H_c of *syn*-oximes (**4** and **8**) resonate at a lower field than that due to the corresponding H_c of the *anti*-oxime (**3** and **7**) and the chemical shifts of the

[1]For Part XIV of this series, see ref. 1.

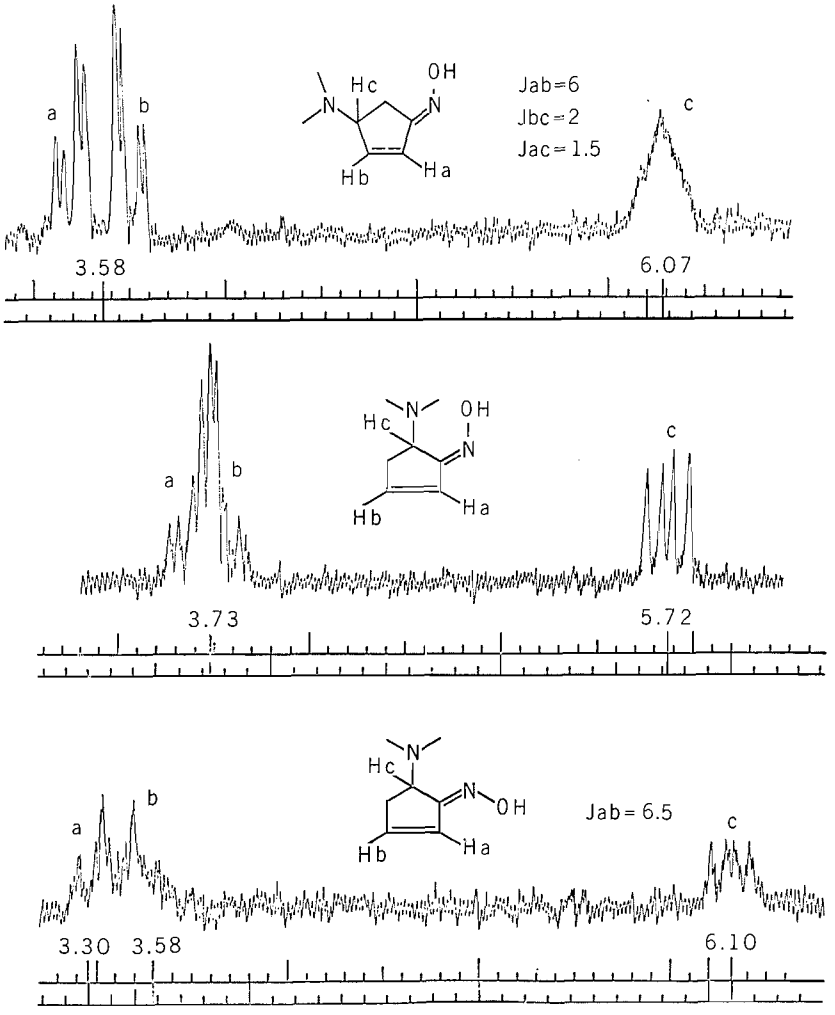

FIG. 1. The n.m.r. spectra of **5***a*, **7***a*, and **8***a* in $CDCl_3$ (60 MHz).

corresponding olefinic protons (H_a and H_b) displayed the opposite trend in agreement with the anisotropic effects of an oximino group (5–7).

The 1,4-adduct from butadiene gave predominantly the *anti*-oxime (**1**) and some *syn*-oxime (**2**); the latter could not be isolated in pure form but was detected by n.m.r. spectroscopy. That both isomers **1** and **2** have *trans*-configuration at the olefinic bond was shown by the coupling constants, 15.5 and 14 Hz respectively for J_{ab}, which were obtained by the analysis of the spectra with first order approximation. The 1,4-adducts from *cis,cis*-1,3-cyclooctadiene contained nearly equal amounts of two isomers, from which only the *syn*-oxime (**6***c*), but not the *anti*-oxime (**5***c*), was isolated in pure state. A small amount of 4-piperidino-2-cyclooctenone (**9**), apparently derived from hydrolysis of **5***c* and **6***c*, was also isolated. The 1,4-adducts to cyclopentadiene and 1,3-cyclohexadiene gave only, in each case, one isomer to which *anti*-configuration (**5***a* and *b*) was assigned for steric reasons (*vide infra*).

The 1,2-adducts from butadiene, **3** and **4**, exhibited well defined 12 line ABX signals for the olefinic protons in their n.m.r. spectra. Further, a mixture of **3** and **4** was hydrogenated to a mixture of *syn*- and *anti*-1-piperidino-2-butanone oximes which showed the ethyl groups as two sets of triplets and quartets in the n.m.r. spectrum. In the photoaddition to cyclic dienes, both *syn*- (**8**) and *anti*-oximes (7) of the 1,2-adducts were isolated in every case and were assigned on the basis of the chemical shifts of the

Can. J. Chem. Downloaded from www.nrcresearchpress.com by 210.87.254.5 on 09/05/12
For personal use only.

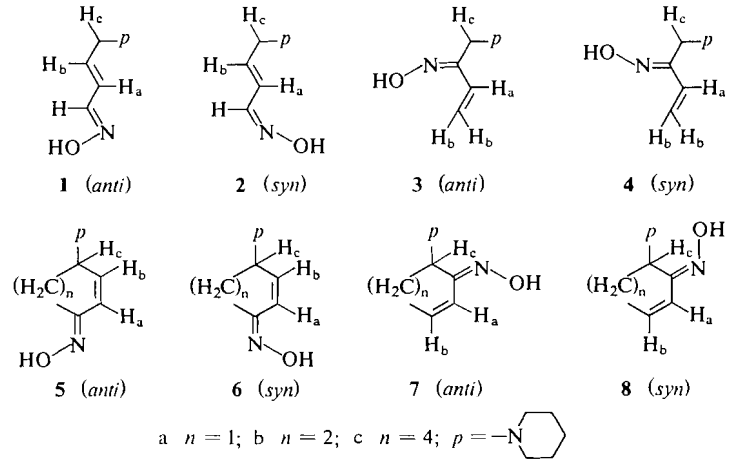

1 (*anti*) **2** (*syn*) **3** (*anti*) **4** (*syn*)

5 (*anti*) **6** (*syn*) **7** (*anti*) **8** (*syn*)

a $n = 1$; b $n = 2$; c $n = 4$; $p = -N$

olefinic (H_a,H_b) and the methine (H_c) protons as discussed above.

Adducts **5**–**8** showed an AB coupling pattern for the olefinic protons and each signal was further coupled to H_c in the 1,4-adducts and to a methylene group in the 1,2-adducts. Since the higher field signal was coupled more strongly to either H_c or the methylene proton than the lower field proton (except in **5***a* and *b*), the former is assigned to H_b and the latter to H_a. From the splitting pattern of the olefinic protons in the adducts 1–4, it is also clear that the higher field signal corresponds to H_b and the lower field signal to H_a. It appears to be a general tendency that the β-hydrogen (H_b) resonates at a higher field than the α-hydrogen (H_a) in an α,β-unsaturated oxime system. This is exactly the reverse to the chemical shift pattern of a conjugated enone system (8). That this reversal of the chemical shifts was due to the anisotropic effects of the oximino group but not to the piperidine ring was verified by the n.m.r. data of 4-piperidino-2-cyclooctenone (**9**). The corresponding β-olefinic proton now showed a chemical shift at a lower field (τ 3.7) than that of the corresponding α-proton (τ 3.98).

When the photoaddition of *N*-nitrosopiperidine (eq. [1]) was run with cycloheptatriene under the same conditions, a strong new absorption peak at 300–500 mμ developed rapidly, interfering with further irradiation. The product was found to be tropone oxime (**10**) (9) and what appeared to be a mixture of 1:1 adducts. The adducts gradually decomposed to give tropone oxime which was identified as the picrate and hydrochloride.

The mass spectra of these adducts usually showed a strong peak equivalent to an elimination of a molecule of water or OH group which appeared to be the major fragmentation pathway. The mass spectra of a pair of *syn*- and *anti*-isomers, where they were available, showed a similar pattern except the relative intensity of the major peaks, e.g., the mass peaks of 176, 111, 110, 96, and 94 in **7***b* and **8***b* and those of 204, 164, and 124 in **7***c* and **8***c*. Certain oximes, such as **1** and **7***b*, exhibit unusually strong $M^+ + 1$ mass peak in comparison to the respective molecular ion peak. It is believed that the $M^+ + 1$ peak is derived from the reaction of $M^+ + M \rightarrow (M^+ + 1) + (M^+ - 1)$ in the ionization chamber. This reaction as well as the fragmentation pathways require some careful studies that may lead to a correlation between structure of oximes and the fragmentation patterns.

Discussion

It is generally recognized that a conjugated diene undergoes addition reaction more readily than does an isolated double bond (10). In the present case, *N*-nitrosopiperidine also shows a remarkable facility to add to a conjugated diene system similar to the general reactivity pattern. Thus the reaction exhibits a potential utility for the synthesis of α,β-unsaturated oximes. The photoaddition is regiospecific (11) in its orientation in which the piperidino group always attaches itself to the 1-position of the symmetrical diene system while the nitroso group goes to either the 2-position or the 4-position. A free radical addition to a conjugated diene generally gives more 1,4-adducts than 1,2-adducts (12–14), while the

Can. J. Chem. Downloaded from www.nrcresearchpress.com by 210.87.254.5 on 09/05/12
For personal use only.

[1] 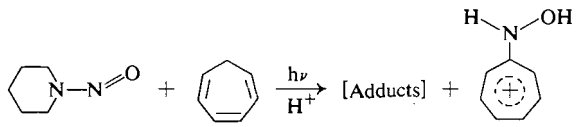

10

trend is reversed if a metal ion is involved during the addition (15, 16). However, there is no predictable pattern on the mode of addition in an ionic mechanism (10). Although nitrosopiperidine preferentially adds to the symmetrical conjugated dienes in a 1,4-mode, this information alone does not allow a decision to be made on the reaction mechanism.

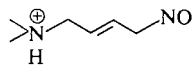

11

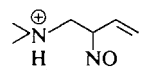

12

That the *C*-nitroso compounds (**11** and **12**) are the primary photoadducts is shown by the typical blue color developed during the photoaddition to cyclopentadiene. An attempt to trap the *C*-nitroso compounds **11** and **12** as the corresponding dimers (3) by performing the photoaddition at −70° gave a dark blue solution which turned to a tar on continuing irradiation. When the photolysis was run at room temperature the oximes **5***a*, **7***a*, and **8***a* were obtained in good yields although a pale blue color was still observed during the reaction. At this temperature **11** and **12** probably tautomerize very rapidly due to the allylic nature of the migrating hydrogen (2), which may account for the good yields of **5**–**8**. A similar situation has been encountered in the photoaddition to simple olefins (3). With a high concentration of **11** and **12** at a low temperature and under the photolysis conditions, an unknown secondary reaction of **11** and **12**, probably photolytic in nature,[2] prevails leading to a tar formation. Although the photolysis condition was varied in order to divert the *C*-nitroso compound **11** and **12** to the corresponding *N*-nitrosohydroxylamine[3] by reacting with HNO (generated *in situ*), such attempts have not met with success.

The tautomerization of the *C*-nitroso compounds to *syn*- or *anti*-oximes is governed by the energetics of the transition states along the reaction axis to the respective oximes (4) and very much related to conformational problems in α,β-unsaturated oximes. The requirement of coplanarity in the cyclohexenone oxime system in **6***b* causes the OH group to experience a severe interaction with C-2 olefinic proton (H_a) and thus destabilizes the *syn*-oxime **6***b* greatly in comparison to the *anti*-oxime (see **13**). The only 1,4-adduct obtained is therefore assigned the *anti*-configuration (**5***b*). In agreement, the C-6 equatorial proton resonates at τ 6.78 which is comparable to the chemical shift of the *cis*-α-equatorial proton (τ 6.61) in *t*-butylcyclohexanone oxime (7). The sole 1,4-adduct obtained from cyclopentadiene is also assigned the *anti*-configuration **5***a* for similar but even more severe steric reasons.

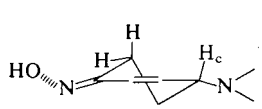

13

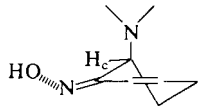

14

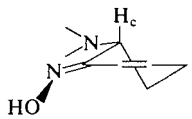

15

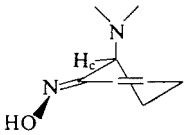

16

The *syn*-cyclohexenone oxime **8***b* must have the forced conformation **14** with the axial orientation of the piperidine ring since a severe $A^{1,3}$ interaction (17, 18) would not allow an equatorial orientation of piperidine ring in the alternative conformation. Though the severe $A^{1,3}$ interaction no longer exists in *anti*-oxime **7***b*, the coupling constants of H_c (τ 6.98) do not clearly indicate the orientation of this proton. It is possible that **7***b* possesses two rapidly equilibrating conformers **15** and **16** which results in an average coupling constant. An analogous situation can be found in *anti*-2-piperidinocyclohexanone oxime[4] which exhibited the proton corresponding to H_c as a

[2]For the reactions of *C*-nitroso compounds see ref. 3 and references cited therein.

[3]A *C*-nitroso compound (R—NO) reacts with HNO to form *N*-nitrosohydroxylamine [R—N(NO)OH] if R—NO can be accumulated in a reasonably high concentration (see ref. 3).

[4]The corresponding proton in *anti*-2-piperidinocyclohexanone oxime shows the chemical shift at τ 7.24 (see ref. 4).

Can. J. Chem. Downloaded from www.nrcresearchpress.com by 210.87.254.5 on 09/05/12
For personal use only.

Can. J. Chem. Downloaded from www.nrcresearchpress.com by 210.87.254.5 on 09/05/12
For personal use only.

narrow band ($W_{\frac{1}{2}}$ = 10 Hz)(4). This appears to indicate an overwhelming contribution of the conformation with the piperidine ring in the axial position (conformation **16** with saturated double bond). Conformation **15** is probably destabilized by an interaction of the two long pair electrons of the amine and oxime nitrogen. Such interaction is very similar to the anomeric effect observed in carbohydrate chemistry (19). It should be pointed out that there exists an interaction between the OH group and C-2 olefinic proton (H_a). Due to these unfavorable strains imposed on the configurations, the actual shapes of **7***b* and **8***b* are probably distorted to relieve the strains. The distortion is indicated by the coupling pattern of the C-6 proton in **7***b* (6 and 3 Hz) and **8***b* (5 and 3 Hz) which are far from the expected values for axial and equatorial protons.

The coupling constants between H_c and two olefinic protons **5***a* and **5***b* merit a discussion in connection with the conformations. If the assignments of the olefinic n.m.r. signals to H_a and H_b are accepted from the correlation shown above, the allylic coupling J_{ac} in **5***b* and *a* (2.5 and 2 Hz, respectively) turns out to be equal to or larger than the vicinal coupling constant J_{ab} (2.5 and 1.5 Hz, respectively). Such a situation can arise only where the C—H_c bond orients itself perpendicular, or nearly so, to the plane defined by C_2—C_3—C_4 in **13**. In this case the maximum allylic coupling and the minimum vicinal coupling are achieved (20, 21). An analogous situation is conceivable in **5***a*.

It is also interesting to mention that *cis,cis*-1,3-cyclooctadiene is not isomerized to *cis,trans*-1,3-cyclooctadiene by a sensitization of photoexcited nitrosopiperidine either in the presence or in the absence of an acid during photolysis. This rules out the possibility that nitrosopiperidine adds to the strained and reactive *cis,trans*-diene in the dark (22).

Experimental

General Procedure

Unless specified otherwise the n.m.r. spectra were recorded with a Varian A56/60 spectrometer in $CDCl_3$ solution using TMS as the internal standard. Some n.m.r. spectra were taken with a Varian HA-100 spectrometer through kind assistance from Dr. K. R. Kopecky, The University of Alberta, Edmonton, Alberta. A Perkin–Elmer RMU-6E mass spectrometer was used to record the mass spectra. The i.r. spectra were recorded with a Perkin–Elmer 457 in Nujol mulls. A Unicam SP-800 UV visible spectrophotometer was used to follow the progress of the reaction. Butadiene of CP grade (Matheson) was used as supplied. The cyclic dienes were freshly distilled before the reactions.

The procedure described for the photoaddition involving a simple olefin in the previous report (2) was followed. The adducts were separated by silicic acid column chromatography using thin-layer chromatography (t.l.c.) to check the purity of each fraction. The t.l.c. also aided in identifying the *syn*- and *anti*-oximes of 1,2-adducts in which the *anti*-oximes moved slower and stained with iodine darker than the *syn*-oximes (4).

Photoadducts

trans,anti-4-Piperidino-2-butenal oxime (**1**, 57%) was recrystallized from cyclohexane and was sublimed: m.p. 97–99°; i.r. 3200, 1620, 1150, 1108, 1046, 990, 960, and 870 cm^{-1}; n.m.r. (100 MHz) τ, −1.0(OH), 2.28 (—CH=N, d, J = 8.5 Hz), 3.18 (H_a, J = 15.5 and 8.5 Hz), 3.62 (H_b, J = 15.5, 6.1 and 1 Hz), 6.91 (H_c, d, J = 6 Hz), 7.54 (4H, m), and 8.47 (6H, m); mass spectrum *m/e* (%) 169(6), 168(M^+,4), 167(13), 151(38), 149(77), 134(24), 122(100), 110(42) and 98(85).

Anal. Calcd. for $C_9H_{16}N_2O$: C, 64.25; H, 9.59; N, 16.65. Found: C, 64.35; H, 9.60; N, 16.84.

A crude 1,4-adduct fraction from chromatograph showed a weak doublet at τ 2.9 (J = 8 Hz) and another set of multiplet at τ 2.70–3.30 (J = 14.5, 8 and 5 Hz) in the 100 MHz n.m.r. spectra. The minor component was *trans,syn*-4-piperidino-2-butenal oxime (**2**).

anti-1-Piperidino-3-buten-2-one oxime (**3**, 16%) was distilled in small scale at 110°/0.1 mm to give an oil; i.r. 3300, 1610, 1120, 1040, 1020, 995, 950, 918, and 870 cm^{-1}; n.m.r. τ 2.0 (OH, broad), 3.02, 4.02, 4.50 (H_a and H_b 12 lines ABX system, J = 11, 18 and 1.5 Hz), 6.82 (H_c, s), 7.60 (m,4H), and 8.54 (m,6H).

syn-1-Piperidino-3-buten-2-one oxime (**4**, 10%) was sublimed to white crystals: m.p. 87–90°; i.r. 3150, 1630, 1110, 1040, 985, 925, 908, and 890 cm^{-1}; n.m.r. τ −1.80 (OH, broad), 3.50, 4.60, and 4.72 (H_a and H_b 12 lines ABX system, J = 17, 11 and 0.5 Hz), 6.56 (H_c,s), 7.52 (m,4H) and 8.48 (m,6H); mass spectrum *m/e* (%) 168 (M^+,51), 167(30), 151(34), 99(49), 98(53), 85(38), and 84(100).

anti-4-Piperidino-2-cyclopentenone oxime (**5***a*, 56%) was recrystallized from a mixture of benzene – petroleum ether: m.p. 101–104°; i.r. 3200, 1648, 1000, 960, and 950 cm^{-1}; n.m.r. τ 1.6 (OH, broad), 3.42 (H_a, d of d, H = 5.5 and 2 Hz), 3.74 (H_b, d of d, J = 5.5 and 1.5 Hz), and 6.07 (H_c,m); mass spectrum, *m/e* (%) 194(M^+,47), 193(16), 179(25), 178(16), 177(65), 149(15), 139(9), 138(11), 137(24), 122(100), 110(16).

Anal. Calcd. for $C_{10}H_{16}N_2O$: C, 66.62; H, 8.95; N, 15.55. Found: C, 66.52; H, 8.98; N, 15.41.

anti-2-Piperidino-4-cyclopentenone oxime (**7***a*, 18%) was recrystallized from 2-propanol to give white crystals: m.p. 130–132°; i.r. 3200, 1630, 1100–918 (multiple peaks), 870, and 750 cm^{-1}; n.m.r. τ 1.0 (OH), 3.30 (H_a, t of d, J = 6 and 2 Hz), 3.54 (H_b, m of d, J = 6 Hz), and 6.09 (H_c, d of d, J = 6.5 and 3.5 Hz).

syn-2-Piperidino-4-cyclopentenone oxime (**8***a*, 7%) was recrystallized from cyclohexane: m.p. 103–105°; i.r. 3200, 1625, 1000–905 (multiple peaks), 875, and 750 cm^{-1}; n.m.r. τ −2.0 (OH), 3.62 (H_a, d of d, J = 6 and 2

Can. J. Chem. Downloaded from www.nrcresearchpress.com by 210.87.254.5 on 09/05/12
For personal use only.

Hz), 3.84 (H_b, m of d, J = 6 Hz), and 5.72 (H_c, J = 7 and 4 Hz).

anti-4-Piperidino-2-cyclohexenone oxime (**5***b*, 61%) was recrystallized from 2-propanol: m.p. 140–142°; i.r. 3150, 1618, 1166, 1050–880 (multiple peaks), and 8.15 cm^{-1}; n.m.r. (in pyridine at 100 MHz) τ 3.53 (H_a, d of d, J = 10 and 2.5 Hz), 3.88 (H_b, d of d, J = 10 and 2.5 Hz), 6.58 (1H, t of d, J = 17 and 4.5 Hz), 6.78 (H_c, q of d, J = 2.5 and 5 Hz), 7.60 (m, 4H), and 8.61 (m, 6H).

Anal. Calcd. for $C_{11}H_{18}N_2O$: C, 68.01; H, 9.34; N, 14.42. Found: C, 68.13; H, 9.12; N, 14.01.

anti-2-Piperidino-5-cyclohexenone oxime (**7***b*, 2%) was sublimed to give white crystals: m.p. 132–134°; i.r. 3290, 1638, 1100, 985, 978, 937, and 778 cm^{-1}; n.m.r. τ 2.53 (OH, broad), 3.28 (H_a, t of d, J = 10 and 1.5 Hz), 3.78 (H_b, t of d, J = 10 and 4.5 Hz), and 6.98 (H_c, d of d, J = 6 and 3 Hz); mass spectrum *m/e* (%), 194 (M^+,1), 176(82), 160(7), 111(32), 110(34), 96(36), 94(55), and 84(100).

syn-2-Piperidino-5-cyclohexenone oxime (**8***b*. 2%) was recrystallized from petroleum ether and was sublimed: m.p. 111–113°; i.r. 3130 1635, 1095, 998, 970, 958, 943, 920, and 870 cm^{-1}; n.m.r. (in pyridine) τ 3.61 (H_a, m of d, J = 11 Hz, each signal was further broadened), 4.00 (H_b, t of d, J = 11 and 4.5 Hz), 5.95 (H_c, d of d, J = 5 and 3 Hz); n.m.r. τ −4.1 (OH); mass spectrum *m/e* 194(M^+,9), 177(16), 176(100), 164(1), 147(1), 111(41), 110(22), 96 (28), and 84(13).

syn-4-Piperidino-2-cyclooctenone oxime (**6***c*), was recrystallized from 2-propanol and was sublimed: m.p. 153–156°; n.m.r. (in pyridine) τ 3.42 (H_a, d, J = 12.5 Hz, each peak was slightly broadened), 4.22 (H_b, d of d, J = 12.5 and 7 Hz), and 6.34 (H_c, m); mass spectrum *m/e* (%) 204 (9), 186(32), 119(53), and 84(100).

Anal. Calcd. for $C_{13}H_{22}N_2O$: C, 70.23; H, 9.97; N, 12.60. Found: C, 70.33; H, 10.08; N, 12.75.

From a column chromatograph, a mixture of *syn* (**6***c*) and *anti* (**5***c*) isomers was obtained as crystals which could not be separated by various methods. The n.m.r. of this mixture showed, in addition to the signal described above, the ABX system at τ 3.79 (H_a, d, J = 12.5 Hz), 4.12 (H_b, d of d, J = 12.5 and 6 Hz), and 6.5 (H_c, m). Total yield of **5***c* + **6***c* is 85% and *syn*:*anti* ratio is about 1:1.

anti-2-Piperidino-7-cyclooctenone oxime (**7***c*, 9%) was recrystallized from 2-propanol: m.p. 162–164°; i.r. 3080, 1660, 1620, 1080, 980, 960, 940, and 870 cm^{-1}; n.m.r. (in pyridine) τ 3.81 (H_a, t of d, J = 13 and 1.5 Hz), 4.18 (H_b, t of d, J = 13 and 3.5 Hz), and 6.57 (H_c, m); mass spectrum *m/e* (%) 222 (M^+, 1), 204 (22) and 164 (100).

syn-2-Piperidino-7-cyclooctenone oxime (**8***c*, 2%) was recrystallized from 2-propanol: m.p. 111–115°; i.r. 3200, 1620, 1100, 1090, 980, 940, and 760 cm^{-1}; mass spectrum *m/e* (%) 222 (M^+, 1), 204 (31), 164 (30), and 124 (100); n.m.r. τ 3.9 and 6.1.

4-Piperidino-2-cyclooctenone (**9**) was obtained as an oil and was distilled at 100°/0.1 mm: i.r. 1665, 1460, 1100, and 760 cm^{-1}; n.m.r. 3.71 (1*H*, d of d, J = 10 and 5 Hz), 3.98 (1*H*, d, J = 10 Hz, each signal was slightly broadened), and 6.38 (1*H*, m, J = 5 Hz); mass spectrum *m/e* (%) 207 (M^+, 10), 178 (25), and 150 (100).

Hydrogenation of a Mixture of **2** *and* **3**

A chromatographic fraction containing **2** and **3** (350 mg) was hydrogenated in ethanol in the presence of 5% Pd/C (50 mg) for 1 h. The crude product was distilled at 120°/0.01 mm to give an oil: n.m.r. τ 8.91 (t, J = 7.5 Hz, CH_3CH_2), 6.71 and 7.65 (q, J = 7.5 Hz, CH_3CH_2), and 6.71 and 7.05 (s, CH_2—N).

Photolysis of N-Nitrosopiperidine in the Presence of Cycloheptatriene

A solution of the nitrosamine (5 g) and a freshly distilled cycloheptatriene (b.p. 112–113°) and concentrated hydrochloric acid in methanol (200 ml) was photolyzed for ½ h. The photolysate turned to a dark red color and a strong absorption appeared at the 300–500 mm region. The basic fraction (1.88 g) was chromatographed to afford a red oil and a fraction which showed the presence of piperidine ring and oximino group in its i.r. and n.m.r. spectra. On sublimation of the latter fraction, it gave the red oil which gave crystalline tropone oxime hydrochloride, m.p. 142–145°, and picrate, m.p. 173–176° (lit. m.p. 149 and 179°) (9).

The authors are grateful to the National Research Council of Canada for its generous support of this project.

1. Y. L. Chow and J. N. S. Tam. J. Chem. Soc. In press.
2. Y. L. Chow, C. J. Colon, and S. C. Chen. J. Org. Chem. **32**, 2109 (1967).
3. Y. L. Chow, S. C. Chen, and D. W. L. Chang. Can. J. Chem. **48**, 157 (1970).
4. Y. L. Chow and C. J. Colon. J. Org. Chem. **33**, 2598 (1968).
5. G. J. Karbatsos, R. A. Taller, and F. M. Vane. J. Amer. Chem. Soc. **85**, 2327 (1963).
6. Y. L. Chow and C. J. Colon. Can. J. Chem. **46**, 2827 (1968).
7. W. F. Trager and A. C. Huitric. Tetrahedron Lett. 825 (1966).
8. L. M. Jackman. Application of nuclear magnetic resonance spectroscopy. Pergamon Press, New York, 1959.
9. T. Nozoe, T. Mukai, K. Takase, and T. Nagase. Proc. Japan Acad. **28**, 477 (1952).
10. M. Cais. *In* The chemistry of alkenes. S. Patai, *Editor*, Interscience Publishers, New York, N.Y., 1964. Chapter 12.
11. A. Hassner. J. Org. Chem. **33**, 2684 (1968).
12. A. A. Oswald, K. Griesbaum, W. A. Thaler, and B. E. Hudson. J. Amer. Chem. Soc. **84**, 3897 (1962).
13. W. P. Newmann and R. Sommer. Ann. **701**, 28 (1967).
14. C. S. Hsia Chen and R. T. Stamm. J. Org. Chem. **28**, 1580 (1963).
15. J. K. Kochi and F. F. Rust. J. Amer. Chem. Soc. **84**, 3946 (1962).
16. J. K. Kochi and H. E. Maino. J. Org. Chem. **30**, 1862 (1965).
17. Y. L. Chow, C. J. Colon, and J. N. S. Tam. Can. J. Chem. **46**, 2821 (1968).
18. F. Johnson. Chem. Rev. **68**, 375 (1968).
19. E. L. Eliel, N. L. Allinger, S. J. Angyal, and G. A. Morrison. "Conformational Analysis." Interscience Publishers, New York, 1966. Chap. 6.
20. G. P. Newsoroff and S. Sternhell. Tetrahedron Lett. 6117 (1968).
21. S. Sternhell. Rev. Pure Appl. Chem. **14**, 15 (1964).
22. R. S. H. Liu. J. Amer. Chem. Soc. **84**, 112 (1967).

Can. J. Chem. Downloaded from www.nrcresearchpress.com by 210.87.254.5 on 09/05/12
For personal use only.

2-Aminomethyl-benzhydrols

KURT FRETER AND MANFRED GÖTZ
Pharma-Research Canada Ltd., Pointe Claire, Montreal 730, P.Q.

Received December 18, 1969

A series of 2-aminomethyl-benzhydrols (**3**) was prepared by different methods; starting with substituted isoindolines (**1**), phthalides (**4**), or cyanobenzophenones (**7**).

Canadian Journal of Chemistry, **48**, 1670 (1970)

In the course of our studies on the ring cleavage of suitably substituted heterocycles, we investigated the reaction of 1-aryl-*N*-alkylisoindolines (**1**) with acetic anhydride (eq. [1]).

[1] 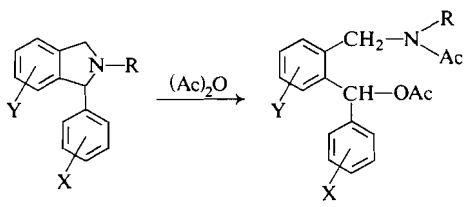

1 **2**

In line with the results obtained with 1-aryl-tetrahydro-β-carbolines (1), 1-aryl-tetrahydro-isoquinolines (2), and 1-aryl-dihydroisobenzofurans (3) this reaction yielded *O*,*N*-diacetyl-2-aminomethylbenzhydrols (**2**). Rather unexpectedly, these compounds exhibited anorexigenic activity (4) which was especially pronounced in the secondary amines (**3**) resulting from saponification of **2**. This property was so far attributed only to derivatives of phenethylamine (5). This interesting finding caused a detailed study of alternate pathways of synthesis (see Scheme 1) as well as a study of structural modifications.

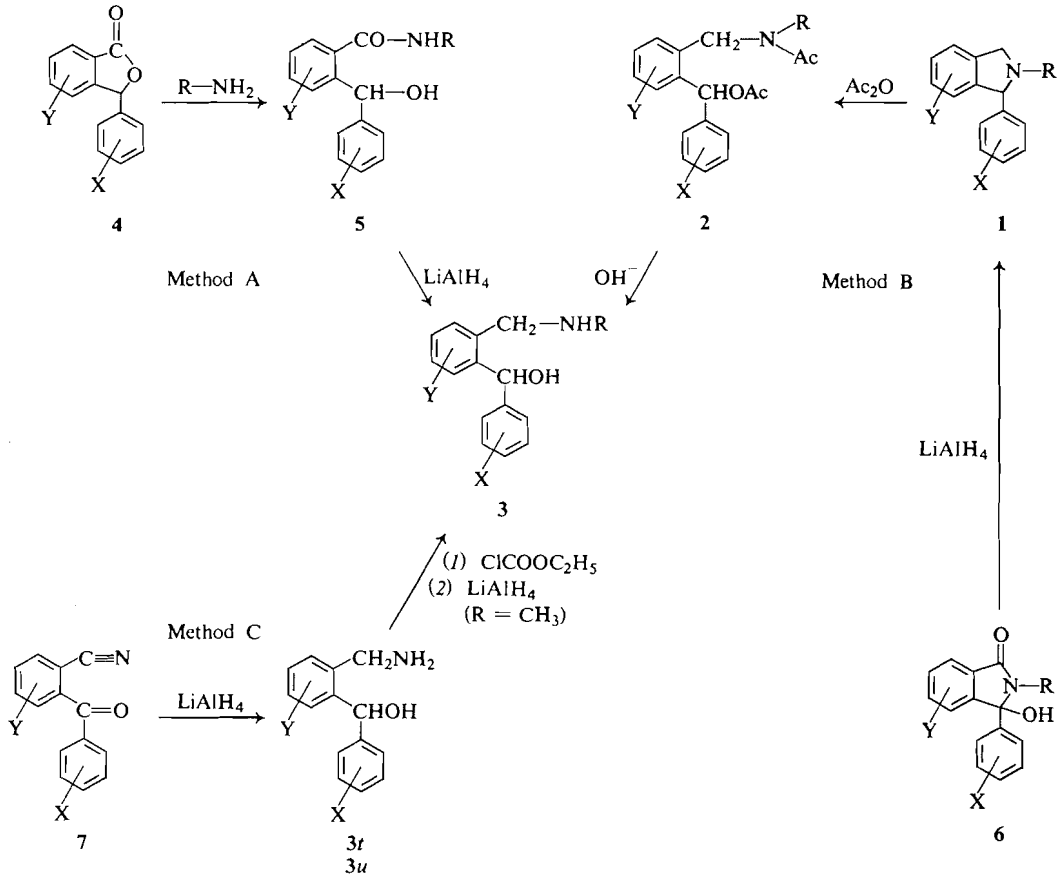

SCHEME 1

Can. J. Chem. Downloaded from www.nrcresearchpress.com by 210.87.254.5 on 09/05/12
For personal use only.

A rather general method for the preparation of **3** comprises the reaction of phenylphthalides (**4**) with amines and subsequent reduction of the amides (**5**) with lithium aluminum hydride (method A). This procedure fails, however, with ammonia.

In cases where the benzoylbenzoic acid necessary for the preparation of the phthalide (**4**) was not easily accessible, as for example, for the preparation of **3***i*, (X = $3CF_3$, 4-Cl; Y = H) the original isoindoline cleavage proved advantageous (method B). The isoindolines (**1**) were obtained via standard procedure from phthalimides and phenylmagnesium halides, followed by reduction of the 1-aryl-1-hydroxy-3-oxoisoindolines (**6**). On refluxing with acetic anhydride, the isoindoline ring was opened to the *N*,*O*-diacetyl compounds (**2**), which were generally saponified with potassium hydroxide without purification to yield **3**. Ring cleavage could not be achieved with the unsubstituted 1-phenyl-2-methylisoindoline.

Method B is also unsuitable for the preparation of the primary amines (**3***t* and *u*).

These compounds were obtained via Sandmeyer reaction of *o*-amino-*p*'-chlorobenzophenone and lithium aluminum hydride reduction of the nitrile (**7**) (method C). Compound **3***t* could be converted to **3***c* with chloroformate and subsequent reduction.

Table 1 indicates the methods used for the preparation of a number of substituted aminomethyl-benzhydrols (**3**).

Recently, a further method for the preparation of similar compounds was described (10); this procedure is limited to the preparation of tertiary amines, which exhibit anti-inflammatory properties according to the patent claims.

Compound **3***c* was separated into the enantiomers with di-*p*-toluoyl tartaric acid as described in the experimental section.

On partial saponification of **8** the carbamate **9** was obtained.

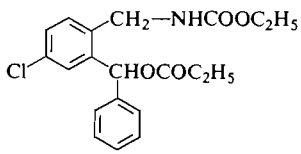

8

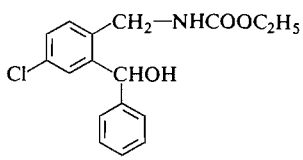

9

[2]

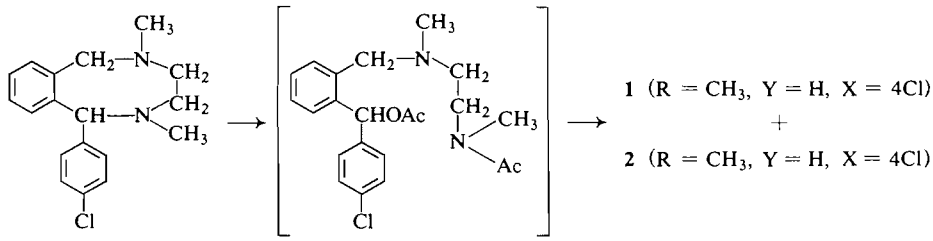

10 **11**

Ring cleavage of the diazocine (**10**) did not yield the acetylaminoethyl derivative (**11**); instead, **2** and the isoindoline (**1**) were isolated as the only reaction products (eq. [2]), most likely due to a Hoffman-Type elimination of *N*-vinyl-*N*-methylacetamide.

Compounds **12** to **15** were prepared by standard procedures to obtain information on the structure-activity relationship, which will be discussed elsewhere (4).

Experimental

Melting points were taken on a Fisher–Johns apparatus and are uncorrected. The microanalyses were performed by Dr. C. Daesslé, Montreal, and Dr. A. B. Gygli, Toronto.

Method A

(*a*) The appropriate phthalide **4** (8) (0.05 mole) was dissolved in 500 ml of benzene, saturated with methylamine, or containing a 5 times molar excess of the corresponding larger amine. The mixture remained at room temperature until no more starting material could be identified on thin-layer chromatography (t.l.c.), generally 48 h, and was then evaporated to dryness *in vacuo*. The residue was crystallized.

(*b*) The amide **5** (0.05 mole), dissolved in 100 ml of tetrahydrofuran/50 ml of ether, was added to a refluxing suspension of 0.1 mole of lithium aluminum hydride in 200 ml of ether. After 3 h of reflux, sodium hydroxide and water were added and the liquid phase removed by suction. The cake was repeatedly washed with ether. The ether was dried over potassium carbonate and evaporated to dryness *in vacuo*. The ethanol solution of the residue

Can. J. Chem. Downloaded from www.nrcresearchpress.com by 210.87.254.5 on 09/05/12
For personal use only.

TABLE 1

Preparation and properties of 2-aminomethyl-benzhydrols

3*	R	X	Y	Method	Yield† (%)	Melting point (°C)	Crystallization solvent	Formula	Analysis											
									Calculated						Found					
									C	H	N	Cl	F	S	C	H	N	Cl	F	S
a	CH_3	H	H	A	73	224–225	Ethanol	$C_{15}H_{17}NO \cdot HCl$	68.30	6.88	5.31	13.44	—	—	68.54	7.06	5.44	13.50	—	—
b	CH_3	4F	H	A B	72 60	231	Ethanol	$C_{15}H_{16}FNO \cdot HCl$	63.94	6.08	4.97	12.58	6.74	—	63.87	6.12	4.82	12.89	6.68	—
c	CH_3	4Cl	H	A B C	71 60 92‡	226–227	Ethanol/ Ether	$C_{15}H_{16}ClNO \cdot HCl$	60.42	5.75	4.70	23.78	—	—	60.56	5.69	4.63	23.80	—	—
d	CH_3	2Cl	H	B	61	205	Ethanol/ Ether	$C_{15}H_{16}ClNO \cdot HCl$	60.42	5.75	4.70	23.78	—	—	61.05	5.81	4.79	23.70	—	—
e	CH_3	3Cl	H	B	15	174	Ethanol/ Ether	$C_{15}H_{16}ClNO \cdot HCl$	60.42	5.75	4.70	23.78	—	—	60.57	5.90	4.70	23.94	—	—
f	CH_3	4Br	H	A	65	206–207	Methanol/ Ether	$C_{15}H_{16}BrNO \cdot HCl$	52.57	5.00	4.09	—	—	—	52.09	5.42	4.11	—	—	—
g	CH_3	$3CF_3$	H	A	53	160–162	Ethanol/ Ether/ Pet. ether	$C_{16}H_{16}F_3NO \cdot HCl$	57.92	5.16	4.22	10.69	17.18	—	57.94	5.29	4.36	11.15	17.48	—
h	CH_3	$4CH_3S$	H	A	62	184	Ethanol/ Ether	$C_{16}H_{19}NOS \cdot HCl$	62.02	6.51	4.52	11.44	—	10.35	62.05	6.44	4.48	11.45	—	10.60
i	CH_3	4Cl $3CF_3$	H	B	45	253	Ethanol/ Ether	$C_{16}H_{15}ClF_3NO \cdot HCl$	52.48	4.40	3.82	19.36	15.56	—	52.58	4.48	3.66	19.53	15.50	—
k	CH_3	$4CH_3$	H	B	40	218–219	Ethanol/ Ether	$C_{16}H_{19}NO \cdot HCl$	69.18	7.26	5.04	—	—	—	69.55	7.38	5.07	—	—	—
l	CH_3	$4CH_3O$	H	B	81	179	Ethanol/ Ether	$C_{16}H_{19}NO_2 \cdot HCl$	65.41	6.86	4.78	—	—	—	65.17	6.98	5.05	—	—	—
m	C_2H_5	4Cl	H	A	65	209	Methanol/ Ether	$C_{16}H_{18}ClNO \cdot HCl$	61.55	6.13	4.48	22.71	—	—	61.21	6.11	4.39	22.60	—	—
n	n-C_4H_9	4Cl	H	B	24	102–105	Ethanol/ Ether	$C_{18}H_{22}ClNO \cdot HCl$	63.53	6.81	4.12	20.84	—	—	63.67	6.86	4.31	20.78	—	—
o	$CH_2CH(CH_3)_2$	4Cl	H	B	15	154	Ethanol/ Ether	$C_{18}H_{22}ClNO \cdot HCl$	63.53	6.81	4.12	20.84	—	—	63.86	7.05	4.30	20.46	—	—

Can. J. Chem. Downloaded from www.nrcresearchpress.com by 210.87.254.5 on 09/05/12
For personal use only.

TABLE 1 (*Concluded*)

3*	R	X	Y	Method	Yield† (%)	Melting point (°C)	Crystallization solvent	Formula	Analysis											
									Calculated						Found					
									C	H	N	Cl	F	S	C	H	N	Cl	F	S
p	$HOCH_2CH_2$	4Cl	H	A	42	157–161	Ethanol/ Ether	$C_{16}H_{18}ClNO_2 \cdot HCl$	58.55	5.84	4.27	21.60	—	—	58.38	6.39	4.42	21.37	—	—
q	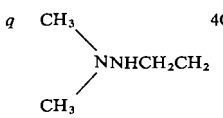	4Cl	H	A	40	184–187	Ethanol/ Ether	$C_{18}H_{24}ClN_3O \cdot HCl$	53.15	6.43	10.33	26.15	—	—	53.39	6.79	10.16	25.78	—	—
	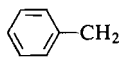	4Cl	H	A	42	200–202	Ethanol/ Petroleum ether	$C_{21}H_{20}ClNO \cdot HCl$	67.39	5.65	3.74	18.94	—	—	67.65	5.84	3.81	18.70	—	—
s		4Cl	H	A	47	198–201	Ethanol/ Petroleum ether	$C_{20}H_{24}ClNO \cdot HCl$	65.63	6.88	3.82	19.37	—	—	65.64	7.16	3.81	19.29	—	—
t	H	4Cl	H	C	82	194–196	Ethanol/ Ether	$C_{14}H_{14}ClNO \cdot HCl$	59.17	5.32	4.93	24.95	—	—	59.11	5.21	5.10	24.85	—	—
u	H	H	5Cl	C	54	169–170	IPA/ Ether	$C_{14}H_{14}ClNO \cdot HCl$	59.17	5.32	4.93	24.95	—	—	59.18	5.42	5.03	25.03	—	—
v	CH_3	H	5Cl	C	81§	190–192	Ethanol/ Ether	$C_{15}H_{17}ClNO \cdot HCl$	60.42	5.75	4.70	23.78	—	—	60.69	5.68	4.68	23.68	—	—
w	CH_3	Cl	4′,5′ di-OCH_3	A	60	190–192	Ethanol/ Ether	$C_{17}H_{20}ClNO_3 \cdot HCl$	51.00	5.91	3.91	19.80	—	—	51.20	5.89	3.67	19.61	—	—
x	H	H	H	‖	59‖	216	Ethanol/ Ether	$C_{14}H_{15}NO \cdot HCl$	67.30	6.47	5.61	14.20	—	—	67.36	6.50	5.70	14.08	—	—

*The general structure is 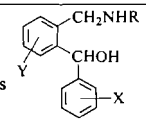

3

†Calculated for the sequences 5 → 3 (Method A), 1 → 3 (Method B) and 7 → 3 (Method C).
‡92% from 3*t* → 3*c*.
§81% from 3*u* → 3*v*.
‖Hydrogenolysis of 3*r*; see experimental section.

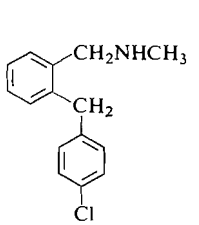

12

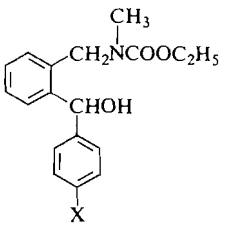

13*a* (X = Cl)
13*b* (X = F)

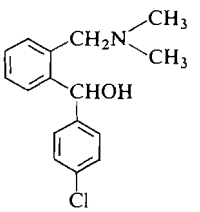

14

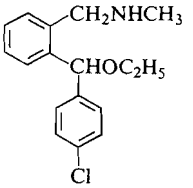

15

was acidified with hydrogen chloride in ether. The material was recrystallized from appropriate solvents (see Table 1).

Method B

(*a*) The appropriate 1-aryl-*N*-methylisoindoline (**1**) (7) (0.2 mole) was refluxed in 500 ml of acetic anhydride for 16 h. The solution was concentrated *in vacuo* and left to crystallize at 0 °C. The diacetate was filtered by suction, washed with ether, and dried.

(*b*) The diacetate (0.1 mole) was refluxed for 1 h in 125 ml of 50% aqueous potassium hydroxide/250 ml of ethylene glycol. The solution was cooled, diluted with 1000 g of ice and extracted five times with 200 ml of ether. The combined extracts were washed with sodium carbonate solution, dried over magnesium sulfate, and evaporated to dryness *in vacuo*. The ethanol solution of the residue was acidified with hydrogen chloride in ether. The material was recrystallized from appropriate solvents.

Method C

The substituted 2-cyanobenzophenone (**7**) (9) (0.02 mole), dissolved in 125 ml tetrahydrofuran, was added dropwise to a refluxing suspension of 0.05 mole of lithium aluminum hydride in 150 ml of ether. After 2 h refluxing, sodium hydroxide solution (2 *N*) was added and the liquid phase removed by suction. The cake and the aqueous phase were repeatedly washed with ether. The ether extracts were combined, dried over potassium carbonate, and evaporated to dryness *in vacuo*. The residue was dissolved in ethanol and acidified with hydrogen chloride in ether. The material was recrystallized from ethanol/ether.

4-Chloro-2′-methylaminomethyl-benzhydrol (3c) from 3t and 5-Chloro-2-methylaminomethyl-benzhydrol (3v) from 3u

(*a*) Ethyl chloroformate (0.1 mole) was added dropwise, with external cooling, to the solution of 0.01 mole of the primary amines **3***t* and *u*, as free bases, in 200 ml of pyridine. After 2 h at room temperature the pyridine was removed *in vacuo* and the residue chromatographed on silicic acid. The major fractions eluting with 2.5% chloroform in benzene were combined, filtered through a glass sinter funnel, evaporated to dryness, and dried in high vacuum. The oil was homogeneous on t.l.c., and analyzed properly.

(*b*) The carbonate-urethane (0.03 mole) in 100 ml of ether was added dropwise to a refluxing suspension of 0.1 mole of lithium aluminum hydride in 200 ml of ether. After 4 h of refluxing, the hydrochloride was isolated in the usual way (properties see Table 1).

Separation of 4-Chloro-2′-methylaminomethyl-benzhydrol (3c) into Enantiomers

The hot concentrated solution of 90 g of di-*p*-toluoyl-*l*-tartaric acid in ethanol was added to a hot concentrated solution of 61 g of 4-chloro-2′-methylaminomethyl-benzhydrol in ethanol. The mixture was left to crystallize overnight at room temperature. The crystals were filtered by suction and the mother liquors were concentrated. A second crystalline fraction was obtained. The first fraction was recrystallized from ethanol. The mother liquors of this fraction were used for the recrystallization of the second fraction.

This procedure was systematically repeated 4 times. The final two crystalline fractions were combined and the free base was liberated with 2 *N* sodium hydroxide solution and extracted with ether. After drying and evaporation of the ether, the residue was recrystallized 4 times from ether/petroleum ether. Yield: 13 g (43%), m.p. 71–74°; $[\alpha]_D^{25°} = +78.4°$ (ethanol).

Anal. Calcd. for $C_{15}H_{16}ClNO$: C, 68.81; H, 6.16; N, 5.35. Found: C, 69.36; H, 6.46; N, 5.60.

The mother liquors of the above recrystallizations were combined, evaporated to dryness, and the base was liberated with 2 *N* sodium hydroxide solution and extracted with ether. The ether solution was dried over potassium carbonate and evaporated to dryness, 27 g of resin remained as residue.

The hot concentrated solution of 40 g di-*p*-toluoyl-*d*-tartaric acid in ethanol was added to the hot concentrated solution of 27 g resin in ethanol. The same procedure was repeated as described for the first enantiomer. Yield: 10.6 g (35%), m.p. 71–74 °C; $[\alpha]_D^{25°} = -80.1°$ (ethanol).

Anal. Calcd. for $C_{15}H_{16}ClNO$: C, 68.81; H, 6.16; N, 5.35. Found: C, 68.55; H, 6.43; N, 5.43.

2-Aminomethyl-benzhydrol (3x)

Palladium-on-charcoal (5%), (2 g), was added to a solution of 8 g 4-chloro-2′-(benzylaminomethyl)-benzhydrol (**3***r*). The mixture was shaken in an atmosphere of hydrogen at room temperature. When the hydrogen uptake came to a standstill after about 48 h, the catalyst was removed by filtration and the solution was evaporated *in vacuo* to dryness. The resulting residue was chromatographed on a silica column using chloroform–methanol–ammonia (90:9.5:0.5) as eluant. The main fraction was converted to the hydrochloride and recrystallized from ethanol/ether (properties see Table 1).

5-Chloro-2-ethoxycarbonylaminomethyl-benzhydrol (9)

5-Chloro-O-ethoxycarbonyl-2-ethoxycarbonylaminomethyl-benzhydrol (17.3 g) (**8**) (preparation see **3***v* from **3***u*, step (*a*)), was dissolved in 25 ml of 95% ethanolic

Can. J. Chem. Downloaded from www.nrcresearchpress.com by 210.87.254.5 on 09/05/12
For personal use only.

Can. J. Chem. Downloaded from www.nrcresearchpress.com by 210.87.254.5 on 09/05/12
For personal use only.

2 *N* sodium hydroxide solution. After 2 h at room temperature the mixture was diluted with water, adjusted to p*H* 6 with 1 *N* hydrochloric acid, and extracted 3 times with chloroform. The combined chloroform extracts were dried over sodium sulfate and evaporated to dryness *in vacuo*. The residue was chromatographed on silicic acid. The major fractions eluting with 1% methanol/benzene were combined, treated with charcoal, filtered through a glass sinter funnel, evaporated to dryness, and dried in high vacuum. 10.7 g (76%) of a colorless oil remained.

Anal. Calcd. for $C_{17}H_{18}ClNO_3$: C, 63.84; H, 5.67; N, 4.38; Cl, 11.08. Found: C, 64.05; H, 6.13; N, 4.27; Cl, 10.81.

*1-(p-Chlorophenyl)-2,5-dimethyl-1,2,3,4,5,6-hexahydro-2,5-benzodiazocine (**10**)*

A mixture of 2.7 g 1-(*p*-chlorophenyl)-1,2,3,4,5,6-hexahydro-2,5-benzodiazocine (6), 4 ml 40% formaldehyde solution, and 10 ml formic acid was heated to reflux for 6 h. The solution was poured over ice and made basic with concentrated ammonia. The mixture was extracted with three 100 ml portions of ether. The combined ether extracts were washed, dried over magnesium sulfate, and evaporated to dryness. The residue was converted to the dihydrochloride by addition of ethereal hydrochloric acid and recrystallized from ethanol/water. Yield: 2.4 g (65%), m.p. 265–266°.

Anal. Calcd. for $C_{18}H_{21}ClN_2 \cdot 2HCl$: C, 57.85; H, 6.21; Cl, 28.45; N, 7.50. Found: C, 58.16; H, 6.52; Cl, 27.99; N, 7.45.

The free base, liberated from the dihydrochloride, could be crystallized from hexane and melted at 83°.

*4-Chloro-2′-(N-methyl-N-acetylaminomethyl)-O-acetylbenzhydrol (**2**, R = CH_3, Y = H, X = 4-Cl)*

The free base **10** (10 g) was heated to reflux in 100 ml of acetic anhydride for 12 h. The mixture was poured on ice–ammonia and extracted with three 200 ml portions of ether. The combined ether extracts were washed with 4 *N* hydrochloric acid. The aqueous, acidic layer yielded, after basification and extraction, a small amount of crystals which were identical in all respects with 1-(4-chlorophenyl)-2-methylisoindoline (**1**, R = CH_3, Y = H, X = 4-Cl). The ether layer was dried over magnesium sulfate and evaporated to dryness. The oily residue crystallized from ethanol. Yield: 8 g (69%), m.p. 132–135°.

Anal. Calcd. for $C_{19}H_{20}ClNO_3$: C, 66.01; H, 5.78; N, 4.05. Found: C, 66.07; H, 5.75; N, 4.20.

*4-Chloro-2′-methylaminomethyl-diphenylmethane (**12**)*

o-(*p*-Chlorobenzyl)-benzoic acid (49 g) was refluxed for 2 h with 75 ml of thionyl chloride. Excess reagent was removed *in vacuo* and the residue dissolved in 500 ml of benzene. Methylamine was introduced in excess under ice cooling. The mixture remained at room temperature for 2 h and was then distributed between water and benzene/chloroform. The organic layer was washed with water, dried over sodium sulfate, and evaporated *in vacuo* to a crystalline slurry. The amide was recrystallized from ethanol. Yield: 36.5 g (70%).

The above amide (29 g) was dissolved in 250 ml of tetrahydrofuran and added dropwise into a refluxing suspension of 12 g lithium aluminum hydride in 350 ml of tetrahydrofuran. The mixture was refluxed for 8 h. Excess lithium aluminum hydride was destroyed with 2 *N* sodium hydroxide. The solids were filtered by suction and washed repeatedly with tetrahydrofuran. The filtrate and the washings were combined and dried over potassium carbonate and evaporated to dryness *in vacuo*. The resulting resin was dissolved in ethanol, and hydrogen chloride was introduced under ice cooling. On addition of ether, crystals separated, which were recrystallized from ethanol/ether. Yield: 17.4 g (63.5%), m.p. 201–205°.

Anal. Calcd. for $C_{15}H_{16}ClN \cdot HCl$: C, 63.82; H, 6.07; N, 4.96; Cl, 25.13. Found: C, 64.00; H, 6.17; N, 5.03; Cl, 25.18.

*4-Chloro-2′-[(N-methyl-N-ethoxycarbonylamino)-methyl]-benzhydrol (**13a**)*

4-Chloro-2′-(methylaminomethyl)-benzhydrol (**3***c*) (5.1 g) was dissolved in 50 ml of dry pyridine and ethyl chloroformate (2.1 g) was added under external cooling. The mixture was allowed to stand at room temperature for 24 h and was then evaporated to dryness. The residue was dissolved in ethyl acetate and the solution was washed with dilute hydrochloric acid, water, sodium carbonate solution, and finally dried over magnesium sulfate. The solvent was removed *in vacuo*. The oily residue crystallized from cyclohexane/petroleum ether, (b.p. 40–60°). Yield: 3.6 g (55%), m.p. 87–88°.

Anal. Calcd. for $C_{18}H_{20}ClNO_3$: C, 64.69; H, 6.05; N, 4.19; Cl, 10.63. Found: C, 64.59; H, 5.93; N, 4.27; Cl, 10.62.

*4-Fluoro-2′-[(N-methyl-N-ethoxycarbonylamino)-methyl]-benzhydrol (**13b**)*

This compound was prepared in the same way as **13***a*. Pure material (4 g) was obtained from 5.8 g of compound **3***b* (53%). The oil did not crystallize but showed the expected properties in the infrared (i.r.) (3330 cm^{-1}, 1675 cm^{-1}) and nuclear magnetic resonance (n.m.r.) spectrum, which were known from the chloro analogue.

Anal. Calcd. for $C_{18}H_{20}FNO_3$: C, 68.15; H, 6.32; N, 4.42; F, 6.00. Found: C, 68.51; H, 6.48; N, 4.44; F, 6.17.

*4-Chloro-2′-(dimethylaminomethyl)-benzhydrol (**14**)*

A mixture of 4-chloro-2′-(methylaminomethyl)-benzhydrol, (**3***c*) (12 g), 5 ml 40% aqueous formaldehyde solution and 40 ml 98% formic acid was heated to reflux for 15 min. After cooling, the mixture was poured over ice/concentrated ammonia and the reaction product extracted with three 100 ml portions of ether. The combined ether extracts were washed with water, dried over magnesium sulfate, and evaporated to dryness. The residue was transformed into the hydrochloride with ethereal hydrochloric acid and recrystallized from ethanol/ether. Yield: 11.5 g (80%), m.p. 203°.

Anal. Calcd. for $C_{16}H_{18}ClNO \cdot HCl$: C, 61.55; H, 6.09; N, 4.48. Found: C, 62.03; H, 6.20; N, 4.42.

*4-Chloro-2′-(methylaminomethyl)-benzhydrol Ethyl Ether (**15**)*

The solution of 4-chloro-2′-(methylaminomethyl)-benzhydrol hydrochloride (**3***c*) (6 g) in 200 ml of ethanol was saturated with hydrogen chloride at room temperature and then heated to reflux for 1 h. The solution was

kept at 0° for 12 h and the crystalline precipitate collected and recrystallized from water. Yield: 4.5 g (69%), m.p. 231°.

Anal. Calcd. for $C_{17}H_{20}ClNO \cdot HCl$: C, 62.65; H, 6.45; N, 4.29. Found: C, 62.80; H, 6.20; N, 4.42.

The authors are indebted to Mrs. A. Thomas, Miss E. Dubois, and Mr. K. Grozinger for their enthusiastic assistance.

1. K. FRETER, H. H. HÜBNER, H. MERZ, H. D. SCHROEDER, and K. ZEILE. Liebigs Ann. Chem. **684**, 159–187 (1965).
2. K. FRETER. Unpublished results.
3. K. FRETER, E. DUBOIS, and A. THOMAS. J. Heterocycl. Chem. **7**, 159 (1970).
4. K. FRETER, M. GÖTZ, and J. T. OLIVER. J. Med. Chem. In press.
5. C. K. CAIN. Annual Reports in Medicinal Chemistry, 1967, page 47, Academic Press, N.Y. 1968. See, however, page 50.
6. T. S. SULKOWSKI, M. A. WILLE, A. MASCITTI, and J. L. DIEBOLD. J. Org. Chem. **32**, 2180 (1967).
7. G. WITTIG and H. STREIB. Liebigs Ann. Chem. **584**, 1 (1953).
8. G. E. RISINGER and J. A. THOMSON. Rec. Trav. Chem. **82**, 801 (1963).
9. F. BELL and J. A. GIBSON. J. Chem. Soc. 3560 (1955).
10. A. G. SANDOZ. Fr. Pat. 1 549 342, December 13, 1968.

Can. J. Chem. Downloaded from www.nrcresearchpress.com by 210.87.254.5 on 09/05/12
For personal use only.

Can. J. Chem. Downloaded from www.nrcresearchpress.com by 210.87.254.42 on 09/05/12
For personal use only.

Mössbauer spectra and electric dipole moments of organotin(IV) complexes with organic ligands

F. PATRICIA MULLINS

Department of Chemistry, Mount St. Vincent University, Halifax, Nova Scotia

Received December 18, 1969

Mössbauer spectra, electric dipole moment, and infrared data are reported for several complexes of the type (*i*) $RSnX_3(AA)$ and (*ii*) $RSnX(AB)_2$ (where R = C_4H_9, C_6H_5; X = Cl, NCS; AA = α,α'-dipyridyl, *o*-phenanthroline, 8-aminoquinoline; AB = oxinate, 2-pyridinethiol 1-oxide). Quadrupole splittings and dipole moments indicate a similar octahedral structure is present in all the complexes studied; in type (*i*) two X groups are *trans* and in type (*ii*) the R and X groups are *cis* to each other. Isomer shifts reveal an order of bond polarity Sn—O ≈ Sn—NCS > Sn—Cl > Sn—S.

Canadian Journal of Chemistry, **48**, 1677 (1970)

Introduction

In recent years, many Mössbauer studies have been undertaken on organotin complexes of the type R_2SnX_2, several on R_3SnX complexes, but to date little seems to have been published on $RSnX_3$ complexes (1, 2). A follow-up of some of the di-*n*-butyltin, diphenyltin dichloride, and diisothiocyanate complexes with nitrogen, oxygen, and sulfur donor ligands was undertaken, using, as before (3, 4), a comparison of Mössbauer data indicating the relative polarities of the Sn—ligand bonds and the electron asymmetry surrounding the tin nucleus and electric dipole moments which are a measure of the molecular electron distribution, including the unshared electrons. It had been noticed in some of the compounds that substitution of phenyl for the *n*-butyl group effected a change from the *trans*-butyl to a *cis*-phenyl configuration (4). Therefore, it was of interest to ascertain the position of the R group in $RSnX_3(AA)$ complexes, whether the R—Sn bond is in the plane of the chelating ligand or perpendicular to it. It is also of interest to ascertain the configuration of $RSnX(AB)_2$ type compounds, as well as the relative electron releasing properties of various donor atoms. Since this investigation was completed, Mössbauer data have been reported on a number of organotin oxinates (1), in excellent agreement with the results reported in Table 3. Four of the complexes were too insoluble in benzene to allow for dielectric constant measurements; the low solubilities of several of the other compounds limit the precision of the dipole moments to ± 0.1 and ± 0.2 D. The Mössbauer spectra of $C_4H_9SnCl_3$ and $C_6H_5SnCl_3$ have been included for purposes of comparison as previous parameters reported for these compounds are not in agreement (2, 5–9).

Experimental

Preparation of Compounds

Phenyltin and *n*-butyltin trichloride were obtained from Alfa Inorganics Inc. With the exception of the sodium salt of 2-pyridinethiol 1-oxide, purchased from Matheson, Coleman and Bell, all ligands and solvents were Baker Analyzed Reagents. Thiophene-free benzene was refluxed over phosphorus pentoxide for several hours before being distilled.

The method of Seyferth and Rochow (10) was followed for the preparation of *n*-butyltin and phenyltin triisothiocyanate by mixing hot absolute ethanol solutions of *n*-butyltin and phenyltin trichloride and potassium or sodium thiocyanate in a 1:3 ratio. The α,α'-dipyridyl and *o*-phenanthroline complexes of $RSnX_3$ (R = C_4H_9, C_6H_5; X = Cl, NCS) were prepared by mixing absolute ethanol solutions of $RSnX_3$ and the ligand in a 1:1 ratio. White precipitates formed quickly. Absolute ether was used as the solvent for the 8-aminoquinoline (8-AQ) ligand, and in this case a buff precipitate was obtained. These and the other precipitates were filtered under vacuum, washed with absolute ethanol and petroleum ether (b.p. 30–60°), and dried under vacuum at 56° for several hours.

The bisoxinate complexes of $RSnX_3$ were obtained by adding stoichiometric amounts of $RSnX_3$ to absolute ethanol (for R = C_4H_9) or absolute methanol (for R = C_6H_5) solutions of 8-hydroxyquinoline to which an alcoholic solution of sodium hydroxide had been previously added. In all cases yellow crystals were obtained either from evaporation of a benzene solution of the filtrate (for the butyl complexes) or as precipitates.

The bis(2-pyridinethiol 1-oxide) (2-SPyO) complexes of $RSnCl_3$ were prepared similarly by adding $RSnCl_3$ to alcoholic solutions of the sodium salt of 2-pyridinethiol 1-oxide. The butyl complex was obtained as a creamy powder from an evaporated benzene solution of the filtrate; the phenyl complex formed as a white precipitate.

Analytical data and melting points for the complexes are given in Table 1.

Mössbauer Spectra

These were obtained with an Austin Science Associates Model S3, constant acceleration transducer type Mössbauer spectrometer drive with S4 flyback module, a Reuter Stokes Model RSG-61 counting tube with

TABLE 1

Analyses and melting points of $RSnX_3$ complexes

Complex	Analysis (%) Found C	Found H	Found S	Calcd. C	Calcd. H	Calcd. S	Melting points Experimental	Melting points Literature*
$C_4H_9SnCl_3(C_{10}H_8N_2)$	38.61	4.05		38.35	3.91		219–d	227–8 (28)
$C_6H_5SnCl_3(C_{10}H_8N_2)$	41.80	3.06		41.92	2.86		274–d	
$C_4H_9SnCl_3(C_{12}H_8N_2)$	41.33	3.89		41.57	3.71		229–d	
$C_6H_5SnCl_3(C_{12}H_8N_2)$	44.85	2.95		44.82	2.72		287–d	
$C_4H_9Sn(NCS)_3(C_{10}H_8N_2)$	39.34	3.58		40.33	3.39		150–51	
$C_6H_5Sn(NCS)_3(C_{10}H_8N_2)$	43.55	2.79		43.36	2.49		212–13	
$C_4H_9Sn(NCS)_3(C_{12}H_8N_2)$	42.80	3.40		43.03	3.23		168–69	
$C_6H_5Sn(NCS)_3(C_{12}H_8N_2)$	45.60	2.45		45.83	2.38		248–50	
$C_6H_5Sn(NCS)(C_9H_6NO)_2$	55.11	3.31	5.86	55.38	3.16	5.91	230–31	
$C_4H_9Sn(NCS)(C_9H_6NO)_2$	53.78	4.17	5.61	52.90	4.05	6.14	70–d	
$C_4H_9SnCl(C_9H_6NO)_2$	52.83	4.35		52.90	4.24		182–83	182–3 (20)
$C_6H_5SnCl(C_9H_6NO)_2$	55.73	3.47		55.46	3.30		215–17	218–9 (29)
$C_4H_9SnCl(C_5H_4NOS)_2$	36.47	3.81		36.27	3.70		123–25	
$C_6H_5SnCl(C_5H_4NOS)_2$	39.97	2.67		39.75	2.71		159–60	
$C_4H_9SnCl_3(C_9H_8N_2)$	36.36	3.96		36.62	4.02		200–d	

*Reference numbers in parentheses.

krypton – carbon dioxide fill gas, a Tetronix oscilloscope, Model 531A, a Nuclear Chicago modified Model 31-24A preamplifier, Model 5315 single channel analyzer, Model 55-6 time base generator with a 1 MHz scaler, Model 24-2 four hundred channel analyzer with Model 23-4 analog digital converter with buffer, Model 99-24-A punch type matrix with Model 80016 typewriter drive for teletype readout. A 5 mC $Ba^{119m}SnO_3$ source obtained from New England Nuclear Corporation was used at room temperature. The finely divided solid absorbers were placed between mylar windows covered with silicone grease or between collodion-coated aluminum foil; the liquid samples were mixed to form a silicone grease mull and placed between collodion-coated aluminum foil. The samples were then mounted in a copper sample holder suspended in a glass Dewar automatically filled with liquid nitrogen. Data were accumulated until at least 4×10^5 counts per channel were collected to minimize statistical error. The data thus obtained were treated by computer analysis to better fit a theoretical Lorentzian curve, using NBS Mössbauer Spectra Program, Technical Notes No. 404, September 30, 1966, in which *ER* (ratio convergence criteria) was set to normal value of 0.001.

The spectrometer was calibrated periodically against a New England Nuclear 80% enriched SnO_2 (5 mg/cm^2) and an NBS Reference $Na_2Fe(CN)_5NO.2H_2O$. The parameters were read from the plotted curves and the error between replicate measurements was less than 0.05 mm s^{-1}.

Dielectric Constants

These were obtained as in previous investigations (11) using an oscillator similar to that described by Estok (12). The relative precision for the values listed in Table 2 is considered to be $\pm$ 0.0005. The $\Delta\varepsilon/wf_2$ ratios listed in Table 3 are average values for the concentrations studied. Electric moments were calculated by the method of Higasi (13), using a value of 0.8481 for β (14).

Infrared spectra of potassium bromide discs were obtained with a Perkin–Elmer 521 spectrometer.

TABLE 2

Dielectric constants of benzene solutions at 25 °C

$1000wf_2$	ε	$100wf_2$	ε
$C_4H_9(NCS)_3$(dipy)		$C_6H_5(NCS)_3$(dipy)	
0.00	(2.273)	0.00	(2.273)
2.80	2.3340	1.41	2.3010
4.61	2.3737	2.08	2.3171
6.57	2.4216	2.42	2.3217
		2.77	2.3313
$C_4H_9(NCS)_3$(*o*-phen)		$C_6H_5(NCS)_3$(*o*-phen)	
2.16	2.3168	0.51	2.2810
5.02	2.3812	0.68	2.2833
7.67	2.4360	1.46	2.2955
$C_4H_9SnCl(ox)_2$		$C_6H_5SnCl(ox)_2$	
5.29	2.3403	10.08	2.3910
6.19	2.3531	19.46	2.4943
8.69	2.3846	28.34	2.5883
$C_4H_9(NCS)(ox)_2$		$C_6H_5(NCS)(ox)_2$	
4.46	2.3479	2.42	2.3068
5.15	2.3628	4.11	2.3313
6.24	2.3794	5.49	2.3486
9.53	2.4327		
$C_4H_9SnCl(2\text{-}SPyO)_2$		$C_6H_5SnCl(2\text{-}SPyO)_2$	
9.67	2.4055	4.84	2.3345
17.88	2.5173	7.97	2.3720
26.87	2.6363	9.42	2.3919
$C_4H_9SnCl_3$(dipy)			
0.75	2.2912		
0.94	2.2949		
1.14	2.3003		

Discussion of Results

The isomer shifts relative to SnO_2, quadrupole splittings, and dipole moments obtained for the compounds studied are listed in Table 3. A small Goldanski effect was noted in the Mössbauer

Can. J. Chem. Downloaded from www.nrcresearchpress.com by 210.87.254.42 on 09/05/12
For personal use only.

TABLE 3

Isomer shifts (δ) relative to SnO_2, quadrupole splittings (ΔE_Q), and electric moments (μ) at 25 °C

Compound	No.	δ* (mm/s)	ΔE_Q* (mm/s)	% absorption	$\Delta\varepsilon/wf_2$	μ_H (D)
$C_4H_9SnCl_3$	**1**	1.37	1.95	5.0		4.32†
$C_6H_5SnCl_3$	**2**	1.20	1.78	7.4		4.23†
$C_4H_9SnCl_3$(dipy)	**3**	1.01	1.65	14.7	23.9	9.8 ±0.2
$C_6H_5SnCl_3$(dipy)	**4**	0.87	1.50	5.3		
$C_4H_9SnCl_3$(*o*-phen)	**5**	1.03	1.67	4.6		
$C_6H_5SnCl_3$(*o*-phen)	**6**	0.87	1.48	3.3		
$C_4H_9Sn(NCS)_3$(dipy)	**7**	0.84	1.75	10.8	22.1	10.2 ±0.1
$C_6H_5Sn(NCS)_3$(dipy)	**8**	0.58	1.55	2.2	20.6	10.0 ±0.2
$C_4H_9Sn(NCS)_3$(*o*-phen)	**9**	0.77	1.80	3.9	21.0	10.1 ±0.2
$C_6H_5Sn(NCS)_3$(*o*-phen)	**10**	0.57	1.56	3.3	15.5	8.9 ±0.2
$C_4H_9SnCl_3$(8-AQ)	**11**	1.02	1.88	9.2		
$C_4H_9Sn(NCS)(ox)_2$	**12**	0.76	1.73	14.2	17.0	9.1 ±0.1
$C_6H_5Sn(NCS)(ox)_2$	**13**	0.58	1.57	7.3	14.0	8.4 ±0.1
$C_4H_9SnCl(ox)_2$	**14**	0.83	1.71	7.0	12.8	7.69±0.03
$C_6H_5SnCl(ox)_2$	**15**	0.68	1.48	2.2	11.4	7.4 ±0.1
$C_4H_9SnCl(2\text{-}SPyO)_2$	**16**	1.09	1.72	6.3	13.6	7.63±0.03
$C_6H_5SnCl(2\text{-}SPyO)_2$	**17**	0.95	1.52	2.2	12.6	7.49±0.05

*±0.05 mm/s.
†Literature values from ref. 30.

spectra of five compounds. The programmed data yielded intensity ratios (area of peak *1*/peak *2*); **6**(1.12), **8**(1.20), **10**(1.11), **13**(1.15), and **16**(0.87). All line widths were less than 0.7 mm/s. Previous comparisons of dipole moments obtained by calculations of Higasi with those from the LeFevre and Vine modification of the Hedestrand equation indicate that density and index of refraction measurements are unnecessary (3, 4).

$RSnX_3$ Compounds

Thiocyanates (M—SCN) are expected to have sharp, well-formed CN stretching frequencies above 2100 cm^{-1}, CS stretching frequencies between 690–720 cm^{-1}, and several NCS bending vibrations from 400–460 cm^{-1}; isothiocyanates (M—NCS) have relatively broad, more intense CN stretching frequencies around or below 2100 cm^{-1}, CS stretching frequencies from 780–860 cm^{-1}, and a single NCS bending vibration from 450–490 cm^{-1}. Bridging NCS groups have CN frequencies 30–80 cm^{-1} higher than terminal groups (15–18). According to these criteria, complexes **7–10** and **12–13** are isothiocyanates. All have absorptions which can be assigned as follows: (*i*) broad CN stretching frequencies in the 2025–2037 cm^{-1} region, (*ii*) stretching frequencies for CS between 828–852 cm^{-1}, and (*iii*) NCS bending vibrations between 465–482 cm^{-1}. The relatively low CN stretching frequencies eliminate the possibility of bridging NCS groups which for similar compounds have been found above 2065 cm^{-1} (4, 18). The 8-aminoquinoline complex is the only one in this series of investigations with tin(IV) having a neutral bidentate ligand containing an NH_2 group. The ligand shows NH_2 stretching frequencies at 3450 and 3345 cm^{-1}. Coakley (19) found that these absorptions shifted to lower frequencies in complexes of the type MCl_2.8-AQ; for example, in $ZnCl_2$.8-AQ peaks at 3270 and 3170 cm^{-1} are assigned to NH_2 stretching vibrations and one at 1080 cm^{-1} to NH_2 wagging, not found in the ligand. In the $BuSnCl_3$.8-AQ complex, absorptions found at 3180 sh and 3160 cm^{-1} are attributed to NH_2 stretching and one at 1082 cm^{-1} to NH_2 wagging.

The quadrupole splittings obtained are interpreted according to the conclusions of Parish and Platt (9), who suggest that (*a*) the magnitude of the quadrupole splitting in tin compounds is governed primarily by imbalance in the polarity of the tin–ligand σ-bonds, (*b*) that structural effects may in some cases supplement this effect, and (*c*) that π-bonding is a secondary factor. This same trend in the various factors controlling the quadrupole splitting in tin compounds had been noticed in previous work (3, 4). The decrease in isomer shift and quadrupole splitting of $RSnX_3$ compounds on replacing butyl by phenyl groups reflects the greater electron releasing power of the former, resulting in (*i*) greater electron density around the tin in butyl compounds and (*ii*) decreasing asymmetry of the electron cloud

Can. J. Chem. Downloaded from www.nrcresearchpress.com by 210.87.254.42 on 09/05/12
For personal use only.

Can. J. Chem. Downloaded from www.nrcresearchpress.com by 210.87.254.42 on 09/05/12
For personal use only.

about the tin atom in the phenyl compounds as the difference in the polarity of the C—Sn and Sn—ligand bonds is reduced. As expected from a study of the diisothiocyanates (4), the triisothiocyanates have lower isomer shifts and larger quadrupole splittings than the corresponding trichlorides, revealing the greater polarity of the Sn—NCS bond. Comparison of the isomer shifts in **3** and **5** with **11** indicates equivalent electron release by pyridine nitrogen and the NH_2 group.

Electric moments were calculated for configurations of $RSnX_3$(*o*-phen) and also for $RSnX(ox)_2$, assuming 90° bond angles, although it is recognized that there is a distortion from a regular octahedral arrangement. Values of bond and group moments derived previously for similar octahedral configurations were used (3, 4, 25, 26): 2.8 D for Sn—O, 5.0 D for Sn—NCS, 4.2 D for the oxine–Sn resultant (exclusive of the Sn—O moment), 3.4 D for octahedral Sn—Cl, and 6.5 D for the phenanthroline–Sn resultant. The contribution of the small Sn—C bond moment was neglected and a difference of approximately $\pm$ 0.4 D for butyl vs. phenyl was expected, enhanced in some cases by varying distortions from octahedral symmetry. Calculations for the phenanthroline complexes of $RSn(NCS)_3$ gave a value of 10.5 D for a configuration having two NCS groups *trans*, and 16 D for one having three *cis* NCS groups. The *trans* configuration is indicated by the experimental dipole moments. From the moment obtained for $BuSn(NCS)_3$(dipy), 10.2 D, a value of 9.1 D is calculated for $BuSnCl_3$-(dipy) with two chlorine atoms *trans*. The estimated value for the *cis* configuration is 11.8 D. A comparison with the experimental value, 9.8 D, suggests a *trans* configuration for this compound also.

A comparison of the electric dipole moments and quadrupole splittings for R_2SnX_2 complexes with *o*-phenanthroline and dipyridyl (3, 4) indicates similar configurations in benzene solution and in the solid state. The configurations of the corresponding $RSnX_3$ complexes cannot at present be inferred from the magnitude of the quadrupole splittings; by analogy they are considered to be similar to the configurations in solution. The similarity of the quadrupole splittings obtained for the four $RSnCl_3$ complexes suggests a similar configuration for all four complexes; it is concluded that they have a *trans* configuration.

$RSnX(AB)_2$ Compounds

In their studies on organotin oxinates, Okawara and co-workers (20, 21) have assigned a strong infrared absorption at about 520 cm^{-1} to Sn—O vibrations and a band of medium intensity near 400 cm^{-1} to Sn—N stretching frequencies. Compounds **12–15** have strong absorptions at about 523 cm^{-1} and broader medium bands at 397 cm^{-1}. This latter absorption is also present in the dipyridyl and phenanthroline complexes of the triisothiocyanates, but was not present in the corresponding trichloride complexes. In a study of tin(IV) pyridine N-oxide complexes, Kawasaki and co-workers (22) have assigned a strong band in the 300–400 cm^{-1} region to the Sn—O vibration and have suggested that the frequency depends considerably on the substituents of the tin atom, with greater values denoting increasing covalent character to the Sn—O bond. Medium strong bands in the spectra of the 2-pyridinethiol 1-oxide complexes at 355 cm^{-1} are attributed to Sn—O stretching vibrations. The N—O stretching vibrations of similar compounds (23) have been compared to the value of 1248 cm^{-1} reported for 2-benzylthiopyridine 1-oxide (24) and values significantly lower than this, about 1197 cm^{-1} for **16**, **17**, taken as indicative of O $\rightarrow$ Sn dative bonding. If the oxygen atoms have a *cis* arrangement about the tin atom in a bis complex, two peaks are anticipated in this region associated with the antisymmetric and symmetric stretching vibrations. Although a barely resolved doublet is present in the strong absorption in **15** and a broad band in **17**, no positive consistent spectroscopic evidence for a *cis*-oxygen configuration for the $RSnX(AB)_2$ complexes can be deduced.

Differences in the polarity of the Sn—S bonds in the bis(2-pyridinethiol 1-oxide) complexes and the N $\rightarrow$ Sn bonds in the bisoxinates could explain the more positive isomer shifts in the former compounds, but similar electron asymmetry around the tin atom in (*i*) the solid state and (*ii*) in benzene solution is suggested by the very small differences in (*i*) quadrupole splittings and (*ii*) dipole moments in the two sets of compounds. A comparison of isomer shifts in **7–10** and **12–13** indicates that the Sn—O and Sn—NCS bonds have about the same polarity in complexes of $RSnX_3$; this contrasts with the values obtained for R_2SnX_2 complexes which indicated that the Sn—O bond was more polar (4).

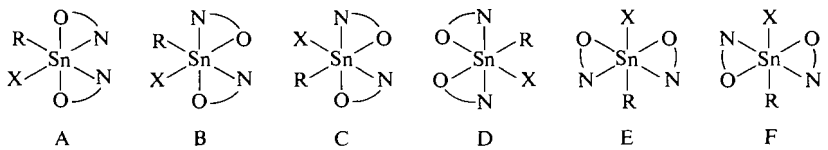

FIG. 1. Possible configurations for $RSnX(ox)_2$.

The dipole moment of $Bu_2Sn(2\text{-}SPyO)_2$, 5.0 D, together with a quadrupole splitting of 3.18 mm s^{-1} (23), indicates a *trans* arrangement for the butyl groups and a *cis* arrangement of the S and O groups. Infrared data for $SnX_2(2\text{-}SPyO)_2$ complexes indicate that the X groups are *cis*. The moment calculated for $RSnCl(2\text{-}SPyO)_2$ with R—Sn—Cl linear and S and O *cis* is 6.0 D. A comparison with the observed moment suggests that the R and Cl groups are probably *cis*.

Calculated dipole moments for the possible configurations of bisoxinates shown in Fig. 1 are 8.7, 8.4, 11.1, 2.8, 10.6, and 3.6 D, respectively for X = Cl and 10, 8.4, 12.2, 3.1, 10.9, and 5.2 D for X = NCS. The observed moments indicate *A* and *B* as likely configurations for both the chloride and isothiocyanate complexes. Schlemper (27) in a structural study of $Me_2Sn(ox)_2$ found the arrangement of atoms about the central tin atom to be that of a highly distorted octahedron, with an N—Sn—O angle of about 74°, a *cis* arrangement of the R groups and an angle of 157° for O—Sn—O, placing the oxygens in approximately *trans* positions (as in configuration *A*). This structure, together with the greater moments obtained for the isothiocyanates than the chlorides, suggests that configuration *A* is the most probable for $RSnX(ox)_2$.

The author is grateful to the National Research Council of Canada for financial support and to the director and staff of the Atlantic Regional Laboratory in Halifax for the use of research facilities; special thanks are due to Dr. M. Falk and his assistants. Gratitude is extended to Dr. B. V. Liengme of Saint Francis Xavier University for the use of his Mössbauer spectrometer and computer program. Appreciation is expressed to Br. C. Curran of the University of Notre Dame for helpful discussions.

1. R. C. POLLER and J. N. R. RUDDICK. J. Chem. Soc. A, 2273 (1969).
2. N. W. G. DEBYE, E. ROSENBERG, and J. J. ZUCKERMAN. J. Amer. Chem. Soc. **90**, 3234 (1968).
3. M. A. MULLINS and C. CURRAN. Inorg. Chem. **6**, 2017 (1967).
4. M. A. MULLINS and C. CURRAN. Inorg. Chem. **7**, 2584 (1968).
5. A. Y. ALEKSANDROV, N. N. DELYAGIN, K. P. MITROFANOV, L. S. POLAK, and V. S. SHPINEL. Dokl. Akad. Nauk. SSSR, Engl. Transl. **148**, 1 (1963).
6. V. A. BRYUKHANOV, V. I. GOLDANSKII, N. N. DELYAGIN, L. A. KORYTKO, I. P. SUZDALEV, and V. S. SHPINEL. Sov. Phys. JETP, **16**, 321 (1963).
7. V. I. GOLDANSKII, V. V. KHRAPOV, O. Y. OKHLOBYSTIN, and V. Y. ROCHEV. *In* Chemical applications of Mössbauer spectroscopy. Academic Press, Inc., New York. 1968. p. 347.
8. H. A. STOCKLER and H. SANO. Trans. Faraday Soc. **64**, 577 (1968).
9. R. V. PARISH and R. H. PLATT. J. Chem. Soc. A, 2145 (1969).
10. D. SEYFERTH and E. G. ROCHOW. J. Amer. Chem. Soc. **77**, 1302 (1955).
11. C. CURRAN, P. A. MCCUSKER and H. S. MAKOWSKI. J. Amer. Chem. Soc. **79**, 5188 (1957).
12. G. K. ESTOK. J. Chem. Educ. **39**, 478 (1962).
13. K. HIGASI. Bull. Inst. Phys. Chem. Res. Tokyo, **22**, 805 (1943).
14. E. CLAEYS, G. VAN DER KELEN and Z. EECKHAUT. Bull. Soc. Chim. Belges, **70**, 462 (1961).
15. J. LEWIS, R. NYHOLM, and P. SMITH. J. Chem. Soc. 4590 (1961).
16. P. MITCHELL and R. WILLIAMS. J. Chem. Soc. 1912 (1960).
17. A. SABATINI and I. BERTINI. Inorg. Chem. **4**, 959, 1665 (1965); **5**, 1025 (1966).
18. M. WADA and R. OKAWARA. J. Organometal. Chem. Amsterdam, **8**, 261 (1967).
19. M. P. COAKLEY. App. Spectrosc. **18**, 149 (1964).
20. T. TANAKA, M. KOMURA, Y. KAWASAKI, and R. OKAWARA. J. Organometal. Chem. Amsterdam, **1**, 484 (1964).
21. K. KAWAKAMI and R. OKAWARA. J. Organometal. Chem. Amsterdam, **6**, 249 (1966).
22. Y. KAWASAKI, M. HORI, and K. UENAKA. Bull. Chem. Soc. Jap. **40**, 2463 (1967).
23. D. PETRIDIS, F. P. MULLINS, and C. CURRAN. Inorg. Chem. In press.
24. A. R. KATRITZKY and A. R. HANDS. J. Chem. Soc. 2195 (1958).
25. J. W. SMITH. *In* Electric dipole moments. Butterworth and Co. Ltd. London, 1955. p. 275.
26. P. E. FIELDING and R. J. LEFEVRE. J. Chem. Soc. 1811 (1951).
27. E. O. SCHLEMPER. Inorg. Chem. **6**, 2012 (1967).
28. D. L. ALLESTON and A. G. DAVIES. J. Chem. 2050 (1962).
29. G. FARAGLIA, L. RONCUCCI and R. BARBIERI. Ric. Sci. Rend. Sez(A), **8**, 205 (1965).
30. H. H. HUANG, K. M. HUI, and K. K. CHIU. J. Organometal. Chem. Amsterdam, **11**, 515 (1968).

Can. J. Chem. Downloaded from www.nrcresearchpress.com by 210.87.254.42 on 09/05/12
For personal use only.

Can. J. Chem. Downloaded from www.nrcresearchpress.com by 210.87.254.40 on 09/05/12
For personal use only.

Thermal [2 + 3] cycloaddition of *N*-trichloroacetyldiphenylcyclopropenimine to 3-aroylaziridines and 3-carbomethoxyaziridines

J. W. LOWN, R. WESTWOOD,[1] AND J. P. MOSER
Department of Chemistry, University of Alberta, Edmonton, Alberta

Received October 20, 1969

N-Trichloroacetyldiphenylcyclopropenimine reacted with either *cis*- or *trans*-3-benzoyl-1-cyclohexyl-2-*m*-nitrophenylaziridine in a [2 + 3] cycloaddition to the C=N bond of the imine to form (*a*) 5-benzoyl-2-*m*-nitrophenyl-4-(spirodiphenylcyclopropene)-3-(trichloroacetylhydrate)-imidazolidine and (*b*) 1-cyclohexyl-4-(*cis*-1,2-diphenylvinyl)-3-dichloroacetyl-2-*m*-nitrophenylimidazoline. Similar reactions with other 3-aroylaziridines gave analogous imidazolidines and imidazolines. Isolation of an unhydrated imidazolidine of type (*a*) in the corresponding addition with 3-carbomethoxy-1-cyclohexyl-2-phenylaziridine gave direct spectroscopic proof for the cyclopropene moiety in these adducts. The orientation of the 1,3 dipolar additions was confirmed by a reaction using a specifically 3-deuterated aziridine.

The isolation of these adducts of type (*a*) strongly supports the previously suggested intermediacy of an oxazolidine in the analogous addition of 3-aroylaziridines to diphenylcyclopropenone.

Canadian Journal of Chemistry, **48**, 1682 (1970)

Diphenylcyclopropenone reacts with 3-aroylaziridines to form 4-aroyl-4-oxazolines (1). This reaction is most plausibly interpreted as proceeding by an initial [2+3] cycloaddition of an azomethine ylide (derived from the thermal cleavage of the aziridine (2–6)) to the carbonyl group of the diphenylcyclopropenone, followed by rearrangement (eq. [1]). Although [2+3] cycloaddition of bicyclic aziridines to the carbonyl group of *p*-nitrobenzaldehyde has been reported (7) and addition of activated aromatic aldehydes to 3-aroylaziridines gives 4-aroyloxazolidines **3** in good yield (8) (eq. [2]), more direct evidence for the intermediacy of the oxazolidine species **1** was lacking. The preparation of iminocyclopropenes was recently reported by Paquette *et al.* (9, 10). We have shown that the C=N double bond of imines and sulfonylimines reacts readily with aroylaziridines to form imidazolidines (11). When the C=N bond of the imine is activated by an electron-withdrawing group in the latter reaction, the product is obtained quantitatively with only one orientation of addition (eq. [3]). Therefore the *N*-trichloroacetyldiphenylcyclopropenimine was reacted with an equimolar quantity of 1-cyclohexyl-3-*p*-nitrobenzoyl-2-phenylaziridine in refluxing acetonitrile for 24 h (eq. [4]). Chromatographic separation afforded two crystalline products to which structures **5** and **6** have been assigned in 50 and 6% yields respectively. Compound **5** analyzed for $C_{38}H_{34}N_3O_5Cl_3$, corresponding to a 1:1 addition product plus a molecule of H_2O. By comparison with product **6** and other products in this series it is evident that the water molecule has added to the trichloro-

[1] 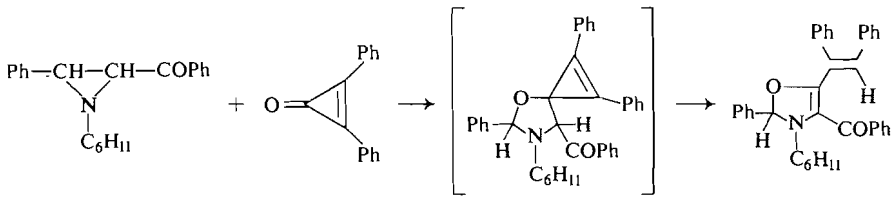

1 **2**

[2] 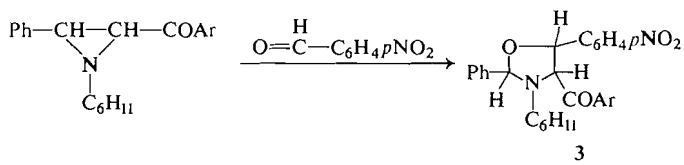

3

[1] NRCC Postdoctoral Fellow, 1967–1969.

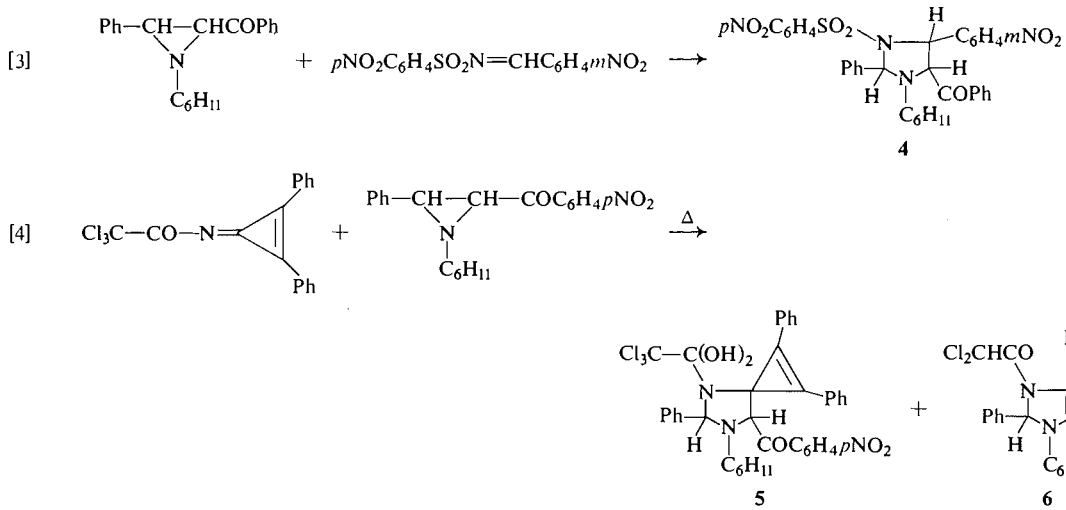

4

5 6

acetyl carbonyl group. The infrared (i.r.) spectrum showed one sharp OH band at 3360 cm^{-1} (unaffected by dilution and therefore assigned to an *intra*molecular hydrogen bond) and a broad OH band at 3440 cm^{-1} (diminished by dilution and therefore assigned to *inter*molecular hydrogen bonding) (12). These assignments were supported by the nuclear magnetic resonance (n.m.r.) spectrum which showed two (1H) singlets at δ 5.8 and 8.5 both exchangeable with deuterium oxide and assigned to *inter*- and *intra*molecularly bonded OH protons respectively. The n.m.r. spectrum also showed two non-exchangeable singlets at δ 4.2 and 5.9 due to the 5- and 2-imidazolidine protons respectively (vide infra).

The imidazolidine **7** was prepared by the reaction of *N*-trichloroacetyldiphenylcyclopropenimine with 3 - carbomethoxy - 1 - cyclohexyl - 2-phenylaziridine in anhydrous acetonitrile. The product analyzed for $C_{33}H_{31}N_2O_3Cl$; i.e. a 1:1 adduct without hydration of the trichloroacetyl

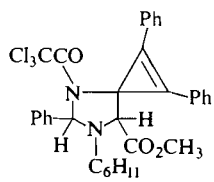

7

carbonyl. The compound showed a normal cyclopropene ultraviolet (u.v.) absorption spectrum with maxima at 292 mμ (ε, 8790) and 222 mμ (ε, 14 870). The i.r. spectrum confirmed that no hydration of the amide carbonyl had taken place and showed a band at 1735 cm^{-1} due to the saturated ester carbonyl and at 1725 cm^{-1} due to the free amide carbonyl (13). The n.m.r. spectrum of **7** showed two singlets at δ 5.47 and 4.95 assigned to the 2- and 5-imidazolidine protons respectively.

The u.v. spectra of **5** and the similar compounds **8** and **10** in this series unlike **7** show two principal maxima in the range (267–260) mμ and at 225 mμ (sh). The u.v. spectra of some related cyclopropenes illustrated in Table 1 show two major absorptions in the region 306–297 and 228–223 mμ with additional shoulder bands.

TABLE 1

Ultraviolet spectra of some cyclopropene derivatives

Compound	Solvent	λ_{max}	ε	Reference
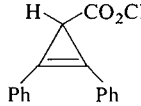	C_2H_5OH	323 306 232 224	26 400 33 900 19 500 21 900	14
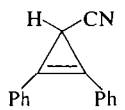	C_2H_5OH	318 303 295 287 231 223	29 400 38 400 28 700 26 800 20 200 22 100	15
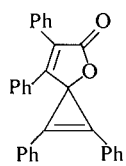	C_2H_5OH	313 297 284 sh 228 222	28 600 39 300 35 200 38 400 37 300	16

Can. J. Chem. Downloaded from www.nrcresearchpress.com by 210.87.254.40 on 09/05/12
For personal use only.

N-Trichloroacetyldiphenylcyclopropenimine shows a principal absorption maximum at 278–286 mμ in isooctane and at 288 mμ in acetonitrile (9) compared with the principal maximum in diphenylcyclopropenone at 297 mμ in acetonitrile (16). Therefore we anticipated a principal maximum in **5** around 290–285 mμ as observed in 7. The observed lower value of 267–260 mμ of the principal absorption in **5** and **9** may possibly be associated with the effects of *intra*molecular hydrogen bonding of the type shown in structure **5** (17–19). Precedents exist in

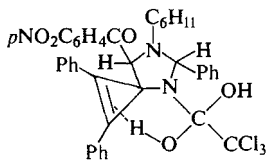

5

the literature of *intra*molecular hydrogen bonds between hydroxyl groups and π-electrons as bases from (*i*) olefins (20) (*ii*) acetylenes (21*a*), and (*iii*) aromatic sextets (21). While the observed lack of hydration of the chloroacetyl group in **6** and similar structures would tend to support this proposal, its tentative nature must be emphasized.

Reaction of *N*-trichloroacetyldiphenylcyclopropenimine separately with stereoisomerically pure *cis*- and *trans*-3-benzoyl-1-cyclohexyl-2-*m*-nitrophenylaziridine afforded the identical imidazolidine **8** and imidazoline **9**. Similar lack of stereospecificity with respect to the aziridine was observed in the addition of *cis*- and *trans*-2-aryl-3-aroylaziridines (with *N*-alkyl substituents) to imines and sulfonylimines to form imidazolidines

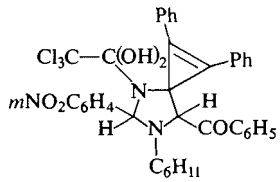

8

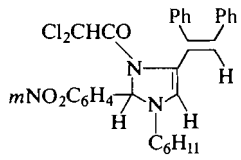

9

(11) and to aryl aldehydes and chloral to form oxazolidines (8). This may be attributed to equilibration of the *cis*- and *trans*-azomethine ylide intermediates (22) (derived from the thermal conrotatory ring opening of the *trans*- and *cis*-aziridines respectively (5)) prior to addition leading to 1,3-dipolar addition exclusively via the more stable *trans*-azomethine ylide (22).

The u.v. spectrum of compound **6**, $C_{31}H_{30}Cl_2N_2O$, shows a band at 280 mμ (ε, 17 450) typical of *cis*-stilbene absorption and at 238 mμ (ε, 35 800). The n.m.r. spectrum showed the 2-imidazoline proton at δ 5.55 and the side-chain vinyl proton at the characteristic position of δ 7.95 (23). The i.r. confirms that the side-chain aroyl group has been removed.

Compound **6** may arise from base-catalyzed elimination of the aroyl group of **5** either during the reaction or during the work up procedure as shown in Scheme 1. The reaction is analogous to the deacylation involved in the last step of the Knorr pyrrole synthesis (24) (eq. [5]), and also the observed dehydrogenative elimination of an aroyl group from a 2-iminothiazolidine by the action of quinones in acetic acid (25), which resembles decarboxylative dehydrogenation (26) (eq. [6]).

In support of Scheme 1, in similar reactions

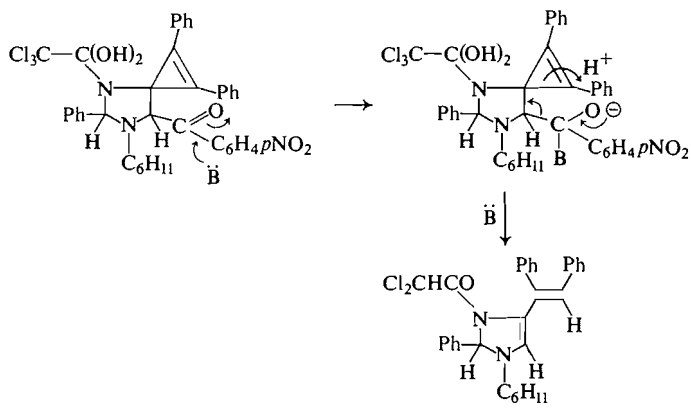

6

SCHEME 1

Can. J. Chem. Downloaded from www.nrcresearchpress.com by 210.87.254.40 on 09/05/12
For personal use only.

[5] 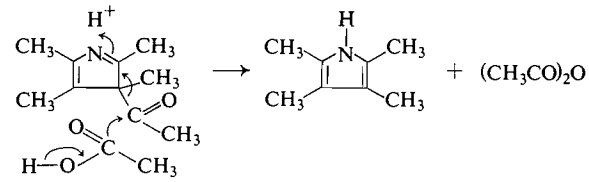

[6] 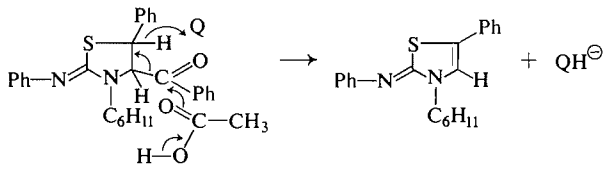

between *N*-trichloroacetyldiphenylcyclopropenimine and 3-benzoyl-1-cyclohexyl-2-phenylaziridine, the products were **10**, a new imidazolidine analogous to **5**, and **11**, the imidazoline which was identical in all respects to the second product **6** obtained in the first reaction. Compound **10** just like **5** also showed hydration of the trichloroacetyl carbonyl and *intra*molecular hydrogen

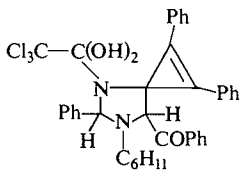

10

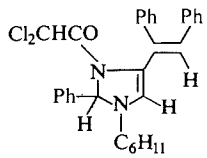

11 ≡ 6

bonding. In a similar reaction of 1-cyclohexyl-2-phenyl-3-*p*-toluoylaziridine and *N*-trichloroacetyldiphenylcyclopropenimine, compound **6** was the only product isolated, confirming that in all these reactions the 5-aroyl group of the intermediate imidazolidine has been removed.

When the 2-aryl substituent on the aziridine ring is not common, then the imidazoline obtained is different from **6**, as in the case of **9** above, as expected. While this interpretation appears plausible, the exact conditions for the above conversion of **5** to **6** have not as yet been established.

The orientation of the thermal [2+3] cycloaddition of sulfonylimines to 3-aroylaziridines to produce 24 imidazolidines with structures like **4** was always in the direction indicated (11). It is reasonable therefore to assume a similar orientation in the addition of the iminocyclopropene to the 3-aroylaziridines to form **5** and **10** and their elimination product **6**. The 2-imidazolidine proton in **4** appears in the n.m.r. at δ 5.8, so the two singlets in the n.m.r. of **5** observed at δ 5.82 and 4.18 were tentatively assigned to the 2- and 5-imidazolidine protons respectively. The above assumption was justified and the line positions confirmed by reaction of the specifically 3-deuterated aziridine **12** (11) with the iminocyclopropene to form **13** (eq. [7]). Examination of the n.m.r. spectrum of **13** after deuterium oxide exchange showed singlets at δ 5.82 (1H) and 4.18 (0.5H). The reduction in the integral of the latter proton due to partial deuteration confirmed the line position assignments proposed above.

In conclusion, it may be stated that the observed [2+3] cycloaddition of 3-substituted aziridines (via the azomethine ylide) to the C=N bond of iminocyclopropenes and isolation of the resulting imidazolidine lends credence to the previously suggested intermediacy of an oxazolidine in the analogous addition of 3-aroylaziridines to diphenylcyclopropenone.

Experimental

Melting points were determined on a Fisher–Johns apparatus and are uncorrected. The i.r. spectra were recorded on a Perkin–Elmer model 421 spectrophotometer, and only the principal, sharply defined peaks are reported. The n.m.r. spectra were recorded on Varian A-60 and A-100 analytical spectrometers. The spectra were measured on approximately 10–15% (w/v) solutions in $CDCl_3$, with tetramethylsilane as a standard. Line positions are reported in parts per million (p.p.m.) from the reference. Absorption spectra were recorded in "spectro"-grade solvents on a Beckman DB recording spectrophotometer. Mass spectra were determined on an Associated Electrical Industries MS-9 double-focusing high resolution mass spectrometer. The ionization energy, in general, was 70 eV. Peak measurements were made by comparison with perfluorotributylamine at a resolving power of 15000. Kieselgel DF-5 (Camag, Switzerland) and Eastman Kodak precoated sheets were used for thin-layer chromatography (t.l.c.) Microanalyses were carried out by Dr. C. Daesslé, Organic Microanalysis Ltd., Montreal, Quebec and by Mrs. D. Mahlow of this department.

Can. J. Chem. Downloaded from www.nrcresearchpress.com by 210.87.254.40 on 09/05/12
For personal use only.

[7] 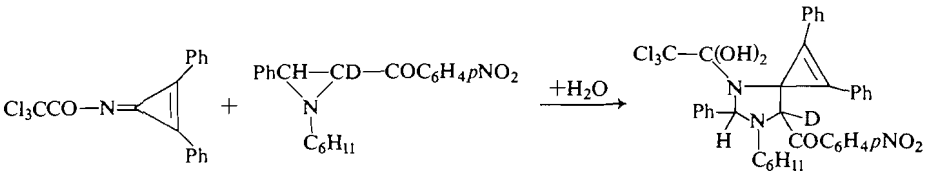

12 13

Synthesis of Aziridines

The 3-aroylaziridines and 3-carbomethoxyaziridine required in this work were prepared by the Gabriel synthesis employing standard procedures described by Cromwell and Caughlan (27).

N-Trichloroacetyldiphenylcyclopropenimine

N-Trichloroacetyldiphenylcyclopropenimine was prepared in 70% yield by the method of Paquette and Horton (10) and had a m.p. 171°–174° (lit. (10) m.p. 169–171°).

Reaction between 3-Benzoyl-1-cyclohexyl-2-phenylaziridine and N-Trichloroacetyldiphenylcyclopropenimine

A solution of 3.06 g (0.01 mole) of 3-benzoyl-1-cyclohexyl-2-phenylaziridine (28) and 3.4 g (0.01 mole) of *N*-trichloroacetyldiphenylcyclopropenimine in 50 ml of acetonitrile was heated under reflux for 24 h. The solvents were removed from the resulting dark red solution *in vacuo* leaving a deep red oil. Chromatography of this oil on alumina (BDH) with benzene gave as the first fraction (*a*) 5-benzoyl-1-cyclohexyl-2-phenyl-4-(spirodiphenylcyclopropene)-3-(*N*-trichloroacetylhydrate)-imidazolidine, 0.551 g (10% yield as a white solid m.p. 153–155° (from hexane)).

Anal. Calcd. for $C_{38}H_{35}Cl_3N_2O_3$: C, 67.70; H, 5.25; N, 4.15. Found: C, 67.80; H, 5.30; N, 4.10.

Mol. Wt. Calcd. (mass spectrum) for $C_{38}H_{35}{}^{35}Cl_3N_2O_3$, 672.1715. Found 672.1710.

The i.r. spectrum: ν_{max} ($CHCl_3$), 3450 (broad, *inter*molecularly bonded (OH), 3370 (sharp, *intra*molecularly bonded OH), 1720 cm^{-1} (C=O). The n.m.r. spectrum: δ_{TMS} ($CDCl_3$): 0.7–1.3, and 3.8 (11H, multiplet, cyclohexyl protons); 4.2 (1H, singlet, 5-imidazolidine proton); 5.9 (1H, singlet, 2-imidazolidine proton); 8.5 and 5.8 (1H each, singlets, exchangeable with deuterium oxide, *intra*- and *inter*molecularly bonded OH protons respectively), 7.2–8.0 (20H, multiplet, aromatic protons). Absorption spectrum (CH_3OH): λ_{max} 260 mμ (sh) (ε, 12 620), 225 mμ (ε, 19 700).

(*b*) Further elution of the column with chloroform gave 0.283 g (5% yield) of a dark red solid, which was purified by recrystallization from ethyl acetate/hexane to give white crystals m.p. 252–253° of 1-cyclohexyl-4-(*cis*-1,2-diphenylvinyl)-3-*N*-dichloroacetyl-2-phenyl-imidazoline.

Anal. Calcd. for $C_{31}H_{30}Cl_2N_2O$: C, 71.95; H, 5.84; N, 5.41. Found: C, 71.99; H, 5.43; N, 5.28.

The i.r. spectrum ν_{max} ($CHCl_3$) 1625 cm^{-1} (amide). The n.m.r. spectrum δ_{TMS} ($CDCl_3$): 1.8–2.0 (10H, multiplet, cyclohexyl protons), 4.0 (1H, multiplet, C*H*—N—); 5.65 (1H, singlet, 2-imidazoline proton), 7.0–7.8 (16H, aromatic and vinyl protons); 8.05 (1H, singlet, *cis*-1,2-diphenylvinyl proton). Absorption spectrum (CH_3OH): λ_{max} 320 mμ (ε, 9250); 280 mμ (ε, 17 450), and 238 mμ (ε, 35 800).

Reaction between 1-Cyclohexyl-3-p-nitrobenzoyl-2-phenylaziridine and N-Trichloroacetyldiphenylcyclopropenimine

A solution of 3.50 g (0.01 mole) of 1-cyclohexyl-3-*p*-nitrophenyl-2-phenylaziridine (25) and 3.49 g (0.01 mole) of *N*-trichloroacetyldiphenylcyclopropenimine in 50 ml of acetonitrile was heated under reflux for 24 h. The dark red solution obtained was evaporated to dryness to give a viscous red oil. Column chromatography of this oil on BDH alumina using benzene as eluant gave

(*a*) 3.6 g (50% yield) of 1-cyclohexyl-5-*p*-nitrobenzoyl-2-phenyl-4-(spirodiphenylcyclopropene)-3-(trichloroacetylhydrate)-imidazolidine, as a pale yellow solid. Recrystallization of this product from benzene/hexane gave white crystals, m.p. 177–180°.

Anal. Calcd. for $C_{38}H_{34}Cl_3N_3O_5$: C, 63.5; H, 4.75; N, 5.85. Found: C, 63.9; H, 5.05; N, 5.65.

Mol. Wt. Calcd. (mass spectrum) for $C_{38}H_{34}{}^{35}Cl_3N_3O_5$: 717.1564. Found, 717.1550.

The i.r. spectrum ν_{max} ($CHCl_3$), 3440 (broad, *inter*molecularly bonded OH); 3360 (sharp, *intra*molecularly bonded OH); 1710 (aroyl C=O), 1500, 1345 cm^{-1} (aromatic NO_2). The n.m.r. spectrum: δ_{TMS} ($CDCl_3$): 0.8–1.6 (10H, multiplet, cyclohexyl protons); 4.0 (1H, multiplet, C*H*N—); 4.2 (1H, singlet, 5-imidazolidine proton); 5.82 (1H, singlet, 2-imidazolidine proton); 8.45 and 5.7 (1H each, singlets, exchangeable with D_2O *intra*- and *inter*molecularly bonded OH respectively); 7.2–8.2 (19H, multiplet, aromatic protons). Absorption spectrum (CH_3OH): λ_{max} 265 mμ (ε, 18 600); 225 mμ (sh) (ε, 19 620).

(*b*) Further elution of the column with chloroform gave 0.339 g (6% yield) of a white solid, m.p. 248–250° of 1-cyclohexyl-4-(*cis*-1,2-diphenylvinyl)-3-*N*-dichloroacetyl-2-phenylimidazoline which had a superimposable i.r. spectrum and was otherwise identical with the compound similarly obtained in the previous reaction with 3-benzoyl-1-cyclohexyl-2-phenylaziridine described above.

Reaction between 1-Cyclohexyl-2-phenyl-3-p-toluoylaziridine and N-Trichloroacetyldiphenylcyclopropenimine

A solution of 3.505 g (0.01 mole) of *N*-trichloroacetyldiphenylcyclopropenimine and 3.19 g (0.01 mole) of 1-cyclohexyl-2-phenyl-3-*p*-toluoylaziridine (28) in 50 ml of acetonitrile was heated under reflux for 24 h. The dark red solution obtained was evaporated to dryness and the residual red oil subjected to chromatography on BDH alumina. Elution of the column with benzene gave a yellow oil which resisted all attempts at crystallization. Elution of the column with chloroform gave a red oil which solidified on trituration with hexane, 1.345 g (24% yield). Recrystallization from ethyl acetate gave 1-cyclohexyl-4-(*cis*-1,2-diphenylvinyl)-3-*N*-dichloroacetyl-2-phenylimidazoline, m.p. 252–253°.

Can. J. Chem. Downloaded from www.nrcresearchpress.com by 210.87.254.40 on 09/05/12
For personal use only.

Can. J. Chem. Downloaded from www.nrcresearchpress.com by 210.87.254.40 on 09/05/12
For personal use only.

Anal. Calcd. for $C_{31}H_{30}Cl_2N_2O$: N, 5.41. Found: N, 5.28.

This material was identical in all respects to that obtained in the previous experiments described above.

Reaction of 1-Cyclohexyl-3-deutero-2-phenyl-3-p-nitrobenzoylaziridine and N-Trichloroacetyldiphenylcyclopropenimine

The reaction of 1.17 g (0.0033 mole) of 1-cyclohexyl-3-deutero-2-phenyl-3-*p*-nitrobenzoylaziridine (11) (60% deuterium incorporation at position 3 by n.m.r.) and 1.17 g (0.0033 mole) *N*-trichloroacetyldiphenylcyclopropenimine was carried out in exactly the manner described for the protium compound above affording 0.749 g (31% yield) of 1-cyclohexyl-5-deutero-5-*p*-nitrobenzoyl-2-phenyl-4(spirodiphenylcyclopropene)-3-(trichloroacetylhydrate)-imidazolidine which recrystallized from hexane as a white solid m.p. 177–180°. Examination of the n.m.r. spectrum showed the position and extent of deuterium incorporation. The product was identical in all other respects to the protium analogue described above.

The n.m.r. spectrum δ_{TMS} ($CDCl_3$): 0.8–1.6 (10H, multiplet, cyclohexyl protons); 4.0 (1H, multiplet, C*H*N—); 4.2 (0.54 H, singlet, 5-imidazolidine proton); 8.45 and 5.7 (1H each, singlets, exchangeable with D_2O *intra-* and *inter*molecularly bonded OH respectively, 7.2–8.2 (19H, multiplet, aromatic protons).

Reaction of 3-Carbomethoxy-1-cyclohexyl-2-phenylaziridine and N-Trichloroacetyldiphenylcyclopropenimine

A solution of 1.33 g (0.00514 mole) of 3-carbomethoxy-1-cyclohexyl-2-phenylaziridine (25) and 1.80 g (0.00514 mole) of *N*-trichloroacetyldiphenylcyclopropenimine in 50 ml of anhydrous acetonitrile was heated under reflux for 16 h. The solvents were removed *in vacuo* (< 40°) and the residual brown oil subjected to chromatography on 100 g of BDH alumina in hexane. Elution with hexane afforded 1.35 g of a yellow oil which upon dissolution in 5 ml of heptane and chilling gave 5-carbomethoxy-1-cyclohexyl-4-(spirodiphenylcyclopropene)-2-phenyl-3-trichloroacetylimidazolidine 0.363 g (44% yield based on unrecovered aziridine), m.p. 179–181° (from heptane).

Anal. Calcd. for $C_{33}H_{31}Cl_3N_2O_3$: C, 64.98; H, 5.12; N, 4.59; Cl, 17.44. Found: C, 65.01; H, 5.34; N, 4.51; Cl, 18.08.

Mol. Wt. Calcd. (mass spectrum) for $C_{33}H_{31}N_2O_3{}^{35}Cl_3$: 608.1402. Found: 608.1399.

The i.r. spectrum: ν_{max} ($CHCl_3$) 1738 (ester C=O); 1725 cm^{-1} (amide C=O (13)), no OH bonds in the region 3400 cm^{-1}. The n.m.r. spectrum: δ_{TMS} ($CDCl_3$): 0.33–2.67 (11H, multiplet cyclohexyl protons), 3.77 (3H, singlet, $COOCH_3$), 4.95–5.46 (1H each, singlets, 5- and 2-imidazolidine protons respectively), 6.68–8.0 (15H, multiplet, aromatic protons). Absorption spectrum (CH_3OH) λ_{max} 292 mμ (ε, 8790), 222 mμ (sh) (ε, 14 870).

Evaporation of the solvents from the filtrate of this fraction gave unreacted 3-carbomethoxy-1-cyclohexyl-2-phenylaziridine (0.98 g) identified by the n.m.r. spectrum.

Reaction between cis- and trans-3-Benzoyl-1-cyclohexyl-2-m-nitrophenylaziridines and N-Trichloroacetyldiphenylcyclopropenimine

A solution of 1.70 g (0.005 mole) of *N*-trichloroacetyldiphenylcyclopropenimine and 1.70 g (0.005 mole) of *trans*-3-benzoyl-1-cyclohexyl-2-*m*-nitrophenylaziridine in 25 ml of acetonitrile was heated under reflux for 21 h. The dark red solution obtained was concentrated *in vacuo* and the residual oil subjected to chromatography on 110 g of BDH alumina. Elution of the column with benzene gave

(*a*) 1.85 g (54.5 yield) of 1-cyclohexyl-5-benzoyl-2-*m*-nitrophenyl-4-(spirodiphenylcyclopropene)-3-(trichloroacetylhydrate)-imidazolidine, as a tan solid m.p. 90–92° from ethyl acetate – hexane.

Anal. Calcd. for $C_{38}H_{34}Cl_3N_3O_5$: C, 63.5; H, 4.75; N, 5.85. Found: C, 63.28; H, 4.77; N, 5.72.

Mol. Wt. Calcd. (mass spectrum) for $C_{38}H_{32}{}^{35}Cl_3N_3O_4$: 699.1459. Found: 699.1443.

The i.r. spectrum ν_{max} ($CHCl_3$), 3440 (broad, *inter*molecularly bonded OH); 3360 (sharp, *intra*molecularly bonded OH), 1710 (aroyl C=O), 1530, 1352 cm^{-1} (aromatic NO_2). The n.m.r. spectrum: δ_{TMS} ($CDCl_3$): 0.64–2.22 (11H, multiplet, cyclohexyl protons), 4.2 (1H, singlet, 5-imidazoline proton); 5.85 (1H, singlet, 2-imidazoline proton); 8.47 and 5.68 (1H each, singlet, exchangeable with D_2O *intra* and *inter*molecularly bonded OH respectively); 6.7–8.4 (19H, multiplet, aromatic protons). Absorption spectrum (CH_3CN): λ_{max} 262 mμ (sh) (ε, 20 300), 248 mμ (ε, 22 200).

(*b*) Further elution of the column with chloroform gave 0.183 g (5.4% yield) of a tan solid, m.p. 243–247° of 1-cyclohexyl-4-(*cis*-1,2-diphenylvinyl)-3-dichloroacetyl-3-*m*-nitrophenylimidazoline.

Anal. Calcd. for $C_{31}H_{29}Cl_2N_3O_3$: C, 66.20; H, 5.19; N, 7.47; Cl, 12.60. Found: C, 66.28; H, 4.68; N, 7.40; Cl, 12.55.

The i.r. spectrum ν_{max} (Nujol) 1625 cm^{-1} (amide). The n.m.r. spectrum δ_{TMS} [$(CD_3)_2SO$]: 0.7–2.4 (10H, multiplet, cyclohexyl protons), 3.5–4.0 (1H, multiplet, C*H*—N—); 5.64 (1H, singlet, 2-imidazoline proton); 6.8–8.8 (14H, multiplet aromatic protons). Absorption spectrum ($CHCl_3$): λ_{max} 312 mμ (ε, 9130) 352 mμ (ε, 9600).

A similar reaction between 1.70 g (0.005 mole) of *N*-trichloroacetyldiphenylcyclopropenimine and 1.70 g (0.005 mole) of *cis*-3-benzoyl-1-cyclohexyl-2-*m*-nitrophenylaziridine in 25 ml of acetonitrile, refluxed for 21 h gave after chromatographic separation on alumina 1.78 g (52.3% yield) of the identical 1-cyclohexyl-5-benzoyl-2-*m*-nitrophenyl-4-(spirodiphenylcyclopropene)-3-(trichloroacetylhydrate)-imidazolidine m.p. 91° and as the second component 1-cyclohexyl-4-(*cis*-1,2-diphenylvinyl)-3-dichloroacetyl-2-*m*-nitrophenylimidazoline 0.403 g (11.8% yield) m.p. 245–248°. Both compounds were identical in all respects to those obtained in the reaction with the *trans* aziridine.

This research was supported by a National Research Council of Canada grant to J. W. Lown. We thank Mr. R. Swindlehurst and Dr. A. Hogg for the n.m.r. and mass spectra, respectively.

1. J. W. Lown, R. K. Smalley, and G. Dallas. Chem. Commun. 1543 (1968).
2. H. W. Heine, R. E. Peavy, and A. J. Durbetaki. J. Org. Chem. **31**, 3924 (1966).
3. R. V. von Capeller, R. Griot, M. Haring, and T. Wagner-Jauregg. Helv. Chim. Acta, **40**, 1652 (1957).

4. H. W. HEINE, A. B. SMITH, and J. D. BOWER. J. Org. Chem. **33**, 1097 (1968).
5. R. HUISGEN, W. SCHEER, and H. HUBER. J. Amer. Chem. Soc. **89**, 1753 (1967).
6. A. PADWA and L. HAMILTON. J. Heterocycl. Chem. **4**, 118 (1967).
7. H. W. HEINE and R. P. HENZEL. J. Org. Chem. **34**, 171 (1969).
8. G. DALLAS, J. W. LOWN, and J. P. MOSER. Chem. Commun. 278 (1970).
9. L. A. PAQUETTE, T. J. BARTON, and N. HORTON. Tetrahedron Lett. 5039 (1967).
10. L. A. PAQUETTE and N. HORTON. Tetrahedron Lett. 2289 (1968).
11. J. W. LOWN, J. P. MOSER, and R. WESTWOOD. Can. J. Chem. **47**, 4335 (1969).
12. A. D. CROSS. Introduction to practical infra-red spectroscopy. Butterworths, London, 1960. p. 37.
13. L. J. BELLAMY. The infra-red spectra of complex molecules. Methuen publishers, 1958. page 211.
14. R. BRESLOW, R. WINTER, and M. BATTISTE. J. Org. Chem. **24**, 415 (1959).
15. R. BRESLOW, J. LOCKHART, and H. W. CHANG. J. Amer. Chem. Soc. **83**, 2375 (1961).
16. R. BRESLOW, T. EICHER, A. KREBS, R. A. PETERSON, and J. POSNER. J. Amer. Chem. Soc. **87**, 1320 (1965).
17. M. ITO. J. Mol. Spectrosc. **4**, 125 (1960).
18. M. ITO and N. HATA. Bull. Chem. Soc. Japan, **28**, 260 (1955).
19. T. KUBOTA. J. Pharm. Soc. Japan, **74**, 831 (1955).
20. (*a*) R. J. OUELLETTE, K. LIPTAK, and G. E. BOOTH. J. Org. Chem. **32**, 2394 (1967). (*b*) F. A. L. ANET and P. M. G. BAVIN. Can. J. Chem. **34**, 1756 (1956). (*c*) J. A. BERSON and M. JONES. J. Amer. Chem. Soc. **86**, 5019 (1964). (*d*) R. WEST. J. Amer. Chem. Soc. **81**, 1614 (1959). (*e*) R. R. SAUERS and R. M. HAWTHORNE. J. Org. Chem. **29**, 1685 (1964).
21. (*a*) G. C. PIMENTEL and A. L. MCCLELLAN. The hydrogen bond. W. H. Freeman publishers, San Francisco, 1960. p. 190. (*b*) D. S. TRIFAN, J. L. WEINMANN, and L. P. KUHN. J. Amer. Chem. Soc. **79**, 6566 (1957).
22. R. HUISGEN, W. SCHEER, H. MADER, and E. BRUNN. Angew. Chem. Intern. Ed. **8**, 604 (1969).
23. J. W. LOWN and R. K. SMALLEY. Tetrahedron Lett. 169 (1969).
24. L. A. PAQUETTE. Principles of modern heterocyclic chemistry. Benjamin Publishers, New York, 1968. p. 112.
25. J. W. LOWN, G. DALLAS, and T. W. MALONEY. Can. J. Chem. **47**, 3557 (1969).
26. L. M. JACKMAN. *In* Advances in organic chemistry. Vol. II. Interscience Publishers Inc., New York, 1960. p. 344.
27. N. H. CROMWELL and J. A. CAUGHLAN. J. Amer. Chem. Soc. **67**, 2235 (1945).
28. N. H. CROMWELL, N. G. BARKER, R. A. WANKEL, P. J. VANDERHORST, F. W. OLSON, and J. H. ANGLIN. J. Amer. Chem. Soc. **73**, 1044 (1951).

Can. J. Chem. Downloaded from www.nrcresearchpress.com by 210.87.254.40 on 09/05/12
For personal use only.

Can. J. Chem. Downloaded from www.nrcresearchpress.com by 210.87.254.40 on 09/05/12
For personal use only.

The Hantzsch pyrrole synthesis[1]

M. W. ROOMI[2] AND S. F. MACDONALD
Biochemistry Laboratory, National Research Council of Canada, Ottawa, Canada

Received November 27, 1969

Ethyl esters of 2-alkyl- and 2,4-dialkylpyrrole-3-carboxylic acids are obtained generally by extensions of the Hantzsch synthesis, benzyl and *t*-butyl esters when the 2-alkyl group is methyl. Hemopyrrole is obtained from butanal and ethyl acetoacetate in three steps. Pyrroles bearing higher alkyl groups or carbobenzoxy groups are reductively alkylated like the corresponding methylpyrroles and carbethoxy derivatives; *t*-butyl esters do not survive.

Canadian Journal of Chemistry, **48**, 1689 (1970)

Introduction

Numerous alkyl pyrroles were required to identify by gas–liquid partition chromatography (g.l.p.c.) those resulting from the reduction of porphyrins and their meso-alkyl derivatives cf. (1). Many of the pyrroles are now easily obtained (2) but the assembly suggested some deficiencies in the methods of pyrrole ring synthesis and a review of their possibilities.

The most generally useful pyrrole synthesis is that form of Knorr's which gives 2,4-dialkylpyrrole-3,5-dicarboxylic esters from two acylacetic esters, one of them nitrosated (3*a*); this will be referred to simply as the Knorr synthesis. Both alkyl groups are frequently desired but, if other than methyl, derive from less accessible acylacetates.

The other pyrrole ring syntheses (3*a*, 3*b*, 4), including other forms of Knorr's, are used when the above Knorr products are not appropriate intermediates, and in special, although important, cases. Their limitations are usually inherent: the intermediates may be less accessible (α-aminoketones), must be symmetrical to avoid ambiguity (1,3-diketones), or the products may be too specialized (2,5-dialkylpyrroles, *N*-substituted pyrroles).

As the Hantzsch pyrrole synthesis (3*a*) was an exception among these, having the formal generality of the Knorr synthesis, we questioned its apparent limitations. In it, ammonia and ethyl acetoacetate condensed with α-halo derivatives of acetaldehyde (5, 6) or of ketones (7, 8) giving 2-methyl-3-carbethoxypyrrole (the only generally useful product (6, 9)) or its 5-alkyl- and 4,5-dialkyl derivatives. The 5-position was thus an embarrassment: permanently blocked if alkylated or, if not, complicating the introduction of a 4-alkyl group. Further, the 2-methyl group seemed virtually obligatory for, when acylacetates other than methyl or ethyl acetoacetate had been used, the expected product was isolated in only one case: in 2% yield from oxalacetic ester, 2-chlorocyclohexanone and ammonia (10; cf. 5, 8, 11, 12). Apparently only eight or nine pyrroles had been made by the Hantzsch synthesis (contrast (3*a*)).

We find that neither of these limitations exists in principle, first because α-halo derivatives of aldehydes other than acetaldehyde may be used, and second because acylacetates other than methyl or ethyl acetoacetate may be used if, as in Hantzsch's original procedure (7), the crude products are purified by washing with both acid and alkali. Ethyl esters of 2-alkyl- and of 2,4-dialkylpyrrole-3-carboxylic acids are then obtained generally, benzyl and *t*-butyl esters, when the 2-alkyl group is methyl, eq. [1].

[1] 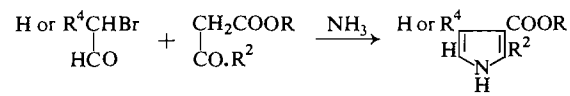

Using chloroacetone, we also obtained the analogous ethyl and benzyl but not *t*-butyl esters of 2-alkyl-5-methylpyrrole-3-carboxylic acids. Aldehydes, however, are in all respects more appropriate components than the ketones used heretofore. Normal aldehydes to C_{12} are commercial products, they are halogenated unambiguously, and their halo-derivatives give both more useful pyrroles and higher yields than do halo-ketones.

[1]Issued as NRCC No. 11229.
[2]NRCC Postdoctoral Fellow 1968–1970.

Can. J. Chem. Downloaded from www.nrcresearchpress.com by 210.87.254.40 on 09/05/12
For personal use only.

TABLE 1

Pyrroles by the Hantzsch synthesis

Components	Yield (%)	Code	Product: Substituents 2	3	4	5	Melting point (°C)	Melting point lit. (°C)	Anal. Calcd. (Found) C	H	N
Chloroacetone and											
ethyl acetoacetate	50 (7)	1.1	Me	COOEt		Me					
methyl acetoacetate	25 (8)	1.2	Me	COOMe		Me					
t-butyl acetoacetate	0										
benzyl acetoacetate	8	1.3	Me	$COOCH_2C_6H_5$		Me	89–91		73.34 (73.48)	6.59 (6.67)	6.11 (6.09)
ethyl propionylacetate	9	1.4	Et	COOEt		Me	55–57		66.27 (66.45)	8.34 (8.27)	7.73 (7.70)
ethyl butyrylacetate	2	1.5	$CH_2CH_2CH_3$	COOEt		Me	73–75		67.66 (67.47)	8.78 (8.61)	7.17 (7.38)
MeCHBrCOEt and ethyl acetoacetate	7	2.1	Me	COOEt	Me	Et	107.5–108	106–107 (15, 2)	67.66 (67.53)	8.78 (8.86)	7.17 (7.23)
$ClCH_2CHCl(OEt)$ and ethyl acetoacetate	40 (5)	5.1	Me	COOEt							
$BrCH_2CHBr(OAc)$ and											
ethyl acetoacetate	45 (6)	5.1	Me	COOEt							
t-butyl acetoacetate	36	5.2	Me	$COOCMe_3$			112–114		66.27 (66.13)	8.34 (8.42)	7.73 (7.65)
benzyl acetoacetate	12	5.3	Me	$COOCH_2C_6H_5$			57–59		72.54 (72.64)	6.09 (6.16)	6.51 (6.61)
ethyl propionylacetate	29	5.4	Et	COOEt			<20		64.65 (64.39)	7.84 (7.71)	8.38 (8.14)
ethyl butyrylacetate	20	5.5	$CH_2CH_2CH_3$	COOEt			33–35		66.27 (66.10)	8.34 (8.32)	7.73 (7.65)
EtCHClCHO and ethyl acetoacetate	30	6.1	Me	COOEt	Et		77–79				
EtCHBrCHBr(OAc) and											
ethyl acetoacetate	40	6.1	Me	COOEt	Et		77–79				
EtCHBrCHO and											
ethyl acetoacetate	45	6.1	Me	COOEt	Et		77–79		66.27 (66.12)	8.34 (8.21)	7.73 (7.86)
t-butyl acetoacetate	32	6.2	Me	$COOCMe_3$	Et		73–75		68.86 (68.68)	9.15 (9.01)	6.67 (6.83)
benzyl acetoacetate	25	6.3	Me	$COOCH_2C_6H_5$	Et		63–65		74.05 (74.16)	7.07 (7.24)	5.76 (5.57)
ethyl propionylacetate	15	6.4	Et	COOEt	Et		43–45		67.66 (67.84)	8.78 (8.86)	7.17 (7.26)
ethyl butyrylacetate	16	6.5	$CH_2CH_2CH_3$	COOEt	Et		56–58		68.86 (68.76)	9.15 (9.20)	6.69 (6.61)
$CH_3(CH_2)_4CHBrCHBr(OAc)$ and											
ethyl acetoacetate	45	6.6	Me	COOEt	$(CH_2)_4CH_3$		69–71		69.92 (69.86)	9.48 (9.61)	6.27 (6.31)
$CH_3(CH_2)_4CHBrCHO$ and											
ethyl acetoacetate	55	6.6	Me	COOEt	$(CH_2)_4CH_3$		69–71				
ethyl propionylacetate	49	6.7	Et	COOEt	$(CH_2)_4CH_3$		52–53		70.85 (70.85)	9.77 (9.61)	5.90 (5.75)

Can. J. Chem. Downloaded from www.nrcresearchpress.com by 210.87.254.40 on 09/05/12
For personal use only.

It will be noted that the principal limitation on the related pyrrole synthesis of Feist could not be avoided in this way for 2,5-dimethyl-3-carbethoxypyrrole resulted when β-aminocrotonic ester was condensed with either hydroxyacetone or lactaldehyde in hot acetic acid (13).

Table 1[3] shows some products of conventional Hantzsch syntheses, 1.1, 1.2, 2.1, and 5.1 and those now obtained by the above extensions, using one mole of each organic component under uniform conditions. Particularly when the yields were low, these conditions were not ideal, for when the mixtures were refluxed for 1 h after the spontaneous reaction was over, the yield of 6.5 was 24% instead of 16% although that of 6.1 (45%) was unchanged (cf. (8)). Also, the cheaper component should presumably be in excess.

To choose between equivalent halo-aldehydes and derivatives, all were first condensed with ethyl acetoacetate and ammonia. Neither 2-bromo-1,1-diethoxybutane nor 1,2-dibromo-1-ethoxybutane gave pyrroles whether or not the mixtures were heated. The best yields (45–55%) were obtained using 1,2-dibromoethyl acetate, 2-bromobutanal, and 2-bromoheptanal. These three, also obtained directly and more easily than their alternatives, were then used with other acylacetates. The yields were then more various (12–49%) and no pyrroles were obtained using benzyl propionylacetate, ethyl pivalylacetate, 2,4-pentanedione, nor the sodium salt of oxalacetic ester or of ethyl acetopyruvate. Chloroacetone (except when used with ethyl acetoacetate) and 2-bromo-3-pentanone both gave lower yields of pyrroles than did the three preferred halo-aldehyde derivatives (Table 1); similarly, the yield of the pyrrole from 3-chloro-2-butanone and ethyl acetoacetate was only 26% (8).

Scheme 1 represents the Hantzsch products (1, 2, 5, 6), related Knorr products (7), the more useful pyrroles derived from these (9, 10, 11, 14), and some reactions connecting them. As specified in Table 2 we have carried out many of these reactions on the Hantzsch products to confirm the structures of the new ones of types 1 and 6, to provide a basis for comparing the Hantzsch products 5 and 6 with the Knorr products 7 as intermediates, and to further define the scope of reductive alkylation. These reactions were carried out under standardized conditions and the only failures encountered are discussed below.

Discussions of the Hantzsch synthesis have emphasized that pyrroles are formed from halo-ketones as in eq. [1] (R^5 for H on 5) rather than with R^4 and R^5 interchanged, and all our products were formulated accordingly. The only evidence in support of this was that 2,5-dimethyl-3-carbethoxypyrrole, 1.1, was obtained from chloroacetone, ethyl acetoacetate, and ammonia (7). In the 2,4-dimethyl-3-carbethoxyfuran formed concurrently, R^4 and R^5 were interchanged (11). The only other evidence was that ethyl β-bromolevulinate, ethyl acetoacetate, and ammonia give the diethyl ester of 2,4-dimethyl-3-carboxypyrrole-5-acetic acid, a pyrrole in which R^4 and R^5 are interchanged (14). In view of this, all the doubtful structures of new Hantzsch products (types 1, 2, and 6) were confirmed, and eq. [1] evidently does represent the products from uncomplicated halo-aldehydes and -ketones. The pyrrole 2.1 was known (15, 2); although it is confused in the literature with its isomer 2.14 of the same m.p. (15, 3*c*), their mixture m.p. is depressed. The remainder, of types 1 and 6, were systematically related to products of the Knorr synthesis, 7, including the new 7.7. With two exceptions, 6.6 and 6.7, ethyl and benzyl esters 6 were authenticated by conversion to Knorr products, 7 (Scheme 1). Pyrroles 1 and 6 with R and R^2 in common were then related through 2. When two pyrroles, 6, differed only in R^4 (6.1 and 6.6, or 6.4 and 6.7), only one was confirmed through 7 for both could be related to the same 1 through a pyrrole of type 2. Less systematically, the structure of 6.1 also follows from its conversion to the known pyrroles 2.14, 3.1, 10.1, 15.1, 14.4 and 14.5, and that of 6.4 from its conversion to 14.2. To avoid a Knorr synthesis, the structure of the *t*-butyl ester 6.2 was confirmed by reducing it to 10.1 which was identified as the solid 14.4, a known pyrrole also obtained from the corresponding ethyl and benzyl esters, 6.1 and 6.3. Similarly, although without the structural significance, the ethyl and benzyl esters 5 were related to 6 and, except in one instance, to 1 through pyrroles of type 2. The *t*-butyl ester 5.2 could not be reductively alkylated, but it was reduced like the corresponding ethyl and benzyl esters, 5.1 and 5.3, to 9.1 which was identified as the solid 13.1.

[3]In Table 1 and Table 2 the units figure in the code identifies the pyrrole type, as defined in Scheme 1, and the decimal numbers distinguish individual pyrroles within it.

Can. J. Chem. Downloaded from www.nrcresearchpress.com by 210.87.254.40 on 09/05/12
For personal use only.

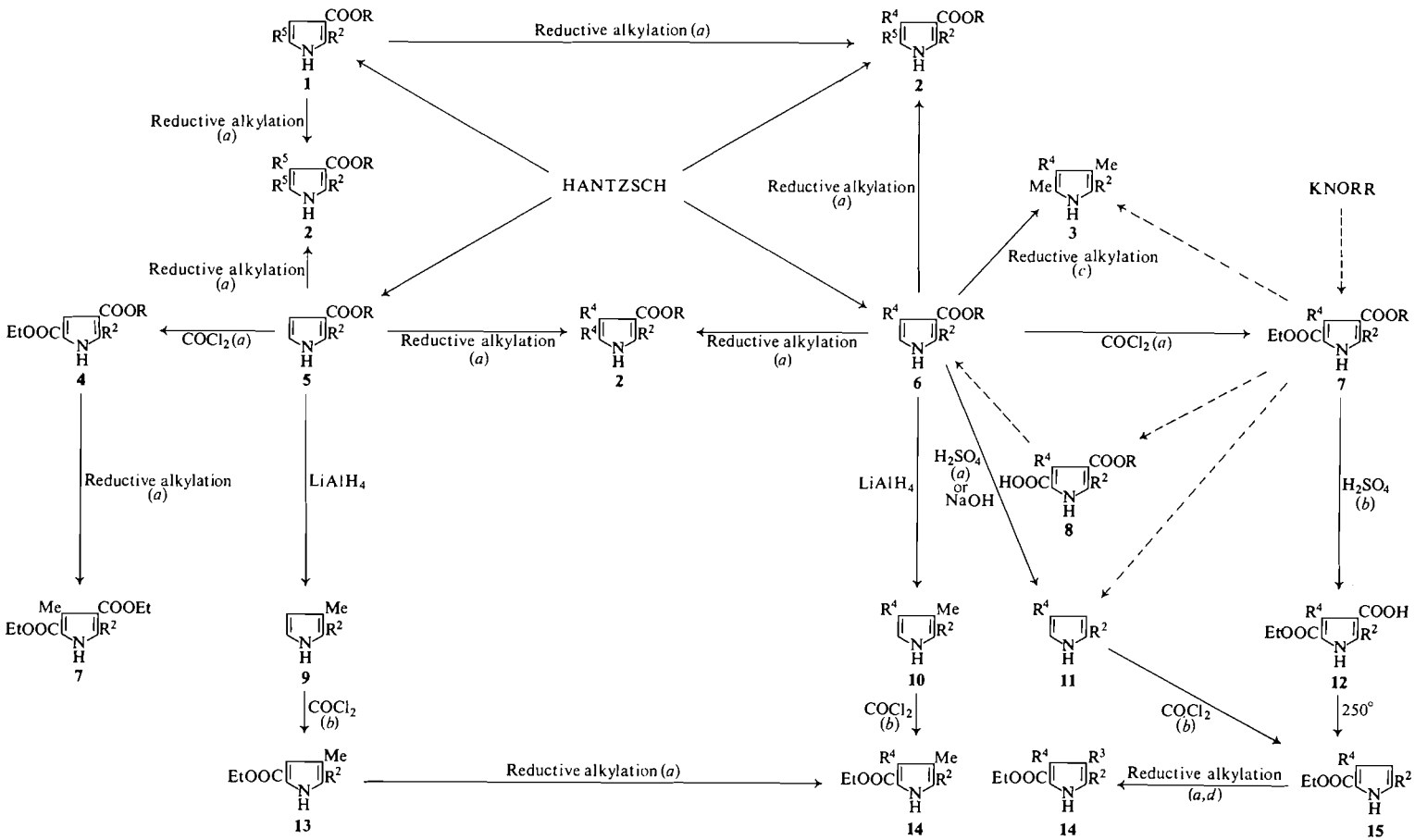

SCHEME 1

Can. J. Chem. Downloaded from www.nrcresearchpress.com by 210.87.254.40 on 09/05/12
For personal use only.

TABLE 2

Pyrroles from Hantzsch products

Starting pyrrole	Method	Code	Substituents 2	3	4	5	Yield (%)	Melting point (°C)	Melting point lit. (°C)	Anal. Calcd. (Found) C	H	N
		1.2	Me	COOMe		Me						
1.2	Reductive alkylation (*a*)	2.2	Me	COOMe	Me	Me	63	124–126		64.65 (64.80)	7.84 (7.98)	8.38 (8.21)
1.2	Reductive alkylation (*a*)	2.3	Me	COOMe	Et	Me	45	142–144		66.27 (66.09)	8.34 (8.22)	7.73 (7.58)
		1.3	Me	$COOCH_2C_6H_5$		Me						
1.3	Reductive alkylation (*a*)	2.4	Me	$COOCH_2C_6H_5$	Me	Me	65	86–88		74.05 (73.92)	7.04 (7.16)	5.76 (5.61)
1.3	Reductive alkylation (*a*)	2.5	Me	$COOCH_2C_6H_5$	Et	Me	20	90–91		74.68 (74.81)	7.44 (7.43)	5.44 (5.33)
		1.4	Et	COOEt		Me						
1.4	Reductive alkylation (*a*)	2.6	Et	COOEt	Me	Me	76	99–101		67.66 (67.56)	8.78 (8.70)	7.17 (7.35)
1.4	Reductive alkylation (*a*)	2.7	Et	COOEt	Et	Me	45	119–121		68.86 (68.99)	9.15 (9.32)	6.67 (6.70)
1.4	Reductive alkylation (*a*)	2.8	Et	COOEt	$(CH_2)_4CH_3$	Me	40	74–76	Below	—	—	—
		1.5	$CH_2CH_2CH_3$	COOEt		Me						
1.5	Reductive alkylation (*a*)	2.9	$CH_2CH_2CH_3$	COOEt	Et	Me	38	111–113		69.92 (70.16)	9.48 (9.55)	6.27 (6.38)
		5.2	Me	$COOCMe_3$								
5.2	$COCl_2$ (*a*)	4.1	Me	$COOCMe_3$		COOEt	86	166–167		61.64 (61.47)	7.56 (7.39)	5.53 (5.39)
5.2	$LiAlH_4$	9.1	Me	Me			60		(3*d*, 9)	75.74 (75.82)	9.54 (9.69)	14.72 (14.88)
9.1	$COCl_2$ (*b*)	13.1	Me	Me		COOEt	67	113–115	114 (3*e*)			
		5.3	Me	$COOCH_2C_6H_5$								
5.3	Reductive alkylation (*a*)	2.4	Me	$COOCH_2C_6H_5$	Me	Me	46	86–88	Above	74.05 (74.22)	7.04 (7.10)	5.76 (5.68)
5.3	Reductive alkylation (*a*)	2.10	Me	$COOCH_2C_6H_5$	Et	Et	11	103–105		75.24 (75.42)	7.80 (7.96)	5.16 (5.29)
5.3	$COCl_2$ (*a*)	4.2	Me	$COOCH_2C_6H_5$		COOEt	78	154–156		66.88 (67.03)	5.96 (6.08)	4.88 (5.07)
5.3	$LiAlH_4$	9.1	Me	Me			77		Above	75.74 (75.88)	9.54 (9.67)	14.72 (14.83)
9.1	$COCl_2$ (*b*)	13.1	Me	Me		COOEt	63	113–115	Above			
		5.4	Et	COOEt								
5.4	Reductive alkylation (*a*)	2.6	Et	COOEt	Me	Me	67	99–101	Above	67.66 (67.88)	8.78 (8.53)	7.17 (7.29)
5.4	Reductive alkylation (*a*)	2.11	Et	COOEt	Et	Et	31	105–107		69.92 (69.79)	9.48 (9.63)	6.27 (6.45)
5.4	$COCl_2$ (*a*)	4.3	Et	COOEt		COOEt	89	116–118		60.24 (60.41)	7.16 (7.30)	5.85 (5.69)
4.3	Reductive alkylation (*a*)	7.1	Et	COOEt	Me	COOEt	80	114–116	116 (3*f*)	61.64 (61.81)	7.56 (7.72)	5.53 (5.35)
5.4	$LiAlH_4$	9.2	Et	Me			70		(3*g*, 16)	77.01 (77.11)	10.16 (10.03)	12.83 (12.88)
9.2	$COCl_2$ (*b*)	13.2	Et	Me		COOEt	87	75–77	79 (16)	66.27 (66.11)	8.34 (8.45)	7.73 (7.81)
13.2	Reductive alkylation (*a*)	14.1	Et	Me	Me	COOEt	63	75–76	78 (17)	67.66 (67.56)	8.78 (8.81)	7.17 (7.33)
13.2	Reductive alkylation (*a*)	14.2	Et	Me	Et	COOEt	42	60–62	62–63 (18)	68.86 (68.68)	9.15 (9.25)	6.69 (6.74)
		5.5	$CH_2CH_2CH_3$	COOEt								
5.5	Reductive alkylation (*a*)	2.12	$CH_2CH_2CH_3$	COOEt	Me	Me	67	80–82	82–83 (19)	68.86 (69.02)	9.15 (9.31)	6.69 (6.51)
5.5	Reductive alkylation (*a*)	2.13	$CH_2CH_2CH_3$	COOEt	Et	Et	43	94–96		70.85 (71.03)	9.77 (9.67)	5.90 (5.74)
5.5	$COCl_2$ (*a*)	4.4	$CH_2CH_2CH_3$	COOEt		COOEt	75	112–114		61.64 (61.48)	7.56 (7.37)	5.53 (5.40)
4.4	Reductive alkylation (*a*)	7.2	$CH_2CH_2CH_3$	COOEt	Me	COOEt	72	116–117		62.90 (63.07)	7.92 (8.04)	5.24 (5.12)
5.5	$LiAlH_4$	9.3	$CH_2CH_2CH_3$	Me			78			77.99 (77.84)	10.64 (10.78)	11.37 (11.44)
9.3	$COCl_2$ (*b*)	13.3	$CH_2CH_2CH_3$	Me		COOEt	82	64–66		67.66 (67.77)	8.78 (8.75)	7.17 (7.29)
13.3	Reductive alkylation (*a*)	14.3	$CH_2CH_2CH_3$	Me	Me	COOEt	84	79–81		68.86 (69.03)	9.15 (8.98)	6.69 (6.69)
		6.1	Me	COOEt	Et							
6.1	Reductive alkylation (*a*)	2.14	Me	COOEt	Et	Me	76	105–107	105–107 (2)	67.66 (67.55)	8.78 (8.83)	7.17 (7.28)
6.1	Reductive alkylation (*a*)	2.15	Me	COOEt	Et	Et	52	105–107	104–106 (1)	68.86 (68.68)	9.15 (9.29)	6.67 (6.81)
6.1	Reductive alkylation (*c*)	3.1	Me	Me	Et	Me	48	62–65	69 (3*h*)	78.77 (78.63)	11.02 (11.30)	10.21 (10.30)
6.1	$COCl_2$ (*a*)	7.3	Me	COOEt	Et	COOEt	77	112–114	115 (3*f*)	61.64 (61.76)	7.56 (7.59)	5.53 (5.39)
6.1	$LiAlH_4$	10.1	Me	Me	Et		75		(3*i*)	77.99 (78.17)	10.64 (10.49)	11.37 (11.23)
6.1	NaOH	11.1	Me		Et		60		(3*j*)	77.01 (77.19)	10.16 (10.04)	12.83 (12.95)
6.1	H_2SO_4	11.1	Me		Et		70		Above			
11.1	$COCl_2$ (*b*)	15.1	Me		Et	COOEt	76	83–85	86 (3*k*)	66.27 (66.15)	8.34 (8.23)	7.73 (7.58)
10.1	$COCl_2$ (*b*)	14.4	Me	Me	Et	COOEt	70	95–97	97 (3*l*)	67.66 (67.60)	8.78 (8.76)	7.17 (7.13)
15.1	Reductive alkylation (*a*)	14.4	Me	Me	Et	COOEt	70	95–97	Above			
15.1	Reductive alkylation (*d*)	14.5	Me	Et	Et	COOEt	41	72–74	75 (3*m*)	68.86 (68.70)	9.14 (9.15)	6.67 (6.51)

Can. J. Chem. Downloaded from www.nrcresearchpress.com by 210.87.254.40 on 09/05/12
For personal use only.

TABLE 2 (*concluded*)

Starting pyrrole	Method	Code	Substituents 2	3	4	5	Yield (%)	Melting point (°C)	Melting point lit. (°C)	Anal. Calcd. (Found) C	H	N
		6.2	Me	$COOCMe_3$	Et							
6.2	$COCl_2$ (*a*)	7.4	Me	$COOCMe_3$	Et	COOEt	86	91–93		64.03 (63.91)	8.24 (8.41)	4.98 (5.10)
6.2	$LiAlH_4$	10.1	Me	Me	Et		55		Above	77.99 (77.80)	10.64 (10.49)	11.37 (11.53)
10.1	$COCl_2$ (*b*)	14.4	Me	Me	Et	COOEt	68	95–97	Above			
		6.3	Me	$COOCH_2C_6H_5$	Et							
6.3	Reductive alkylation (*a*)	2.5	Me	$COOCH_2C_6H_5$	Et	Me	83	89–91	Above	74.68 (74.51)	7.44 (7.35)	5.44 (5.26)
6.3	Reductive alkylation (*a*)	2.10	Me	$COOCH_2C_6H_5$	Et	Et	34	104–106	Above	75.24 (75.42)	7.80 (7.69)	5.16 (5.37)
6.3	$COCl_2$ (*a*)	7.5	Me	$COOCH_2C_6H_5$	Et	COOEt	86	126–128	127–129 (18)	68.55 (68.41)	6.71 (6.80)	4.44 (4.28)
6.3	$LiAlH_4$	10.1	Me	Me	Et		65		Above	77.99 (78.10)	10.64 (10.25)	11.37 (11.21)
10.1	$COCl_2$ (*b*)	14.4	Me	Me	Et	COOEt	71	95–97	Above			
		6.4	Et	COOEt	Et							
6.4	Reductive alkylation (*a*)	2.7	Et	COOEt	Et	Me	80	119–121	Above	68.86 (68.88)	9.15 (9.32)	6.67 (6.76)
6.4	Reductive alkylation (*a*)	2.11	Et	COOEt	Et	Et	35	105–107	Above	69.92 (70.10)	9.48 (9.32)	6.27 (6.41)
6.4	$COCl_2$ (*a*)	7.6	Et	COOEt	Et	COOEt	72	94–96	97 (3*n*)	62.90 (63.07)	7.92 (7.76)	5.24 (5.36)
6.4	$LiAlH_4$	10.2	Et	Me	Et		79		(3*o*)	78.77 (78.83)	11.02 (11.16)	10.21 (10.55)
10.2	$COCl_2$ (*b*)	14.2	Et	Me	Et	COOEt	67	63–65	Above	68.86 (69.03)	9.15 (9.32)	6.67 (6.69)
		6.5	$CH_2CH_2CH_3$	COOEt	Et							
6.5	Reductive alkylation (*a*)	2.9	$CH_2CH_2CH_3$	COOEt	Et	Me	87	111–113	Above	69.92 (70.03)	9.48 (9.60)	6.27 (6.23)
6.5	Reductive alkylation (*a*)	2.13	$CH_2CH_2CH_3$	COOEt	Et	Et	42	94–96	Above	70.85 (70.93)	9.77 (9.89)	5.90 (5.78)
6.5	$COCl_2$ (*a*)	7.7	$CH_2CH_2CH_3$	COOEt	Et	COOEt	80	84–86	See Experimental	64.03 (64.19)	8.24 (8.42)	4.98 (5.11)
		6.6	Me	COOEt	$(CH_2)_4CH_3$							
6.6	Reductive alkylation (*a*)	2.16	Me	COOEt	$(CH_2)_4CH_3$	Me	70	77–79	78–79 (2)	70.85 (70.68)	9.77 (9.60)	5.90 (6.02)
6.6	Reductive alkylation (*a*)	2.17	Me	COOEt	$(CH_2)_4CH_3$	Et	68	60–61		71.67 (71.85)	10.03 (9.91)	5.57 (5.66)
6.6	Reductive alkylation (*c*)	3.2	Me	Me	$(CH_2)_4CH_3$	Me	45			80.38 (80.31)	11.81 (11.65)	7.81 (7.88)
6.6	$LiAlH_4$	10.3	Me	Me	$(CH_2)_4CH_3$		74			79.94 (80.11)	11.59 (11.43)	8.48 (8.49)
6.6	$COCl_2$ (*a*)	7.8	Me	COOEt	$(CH_2)_4CH_3$	COOEt	75	83–85		65.06 (65.04)	8.53 (8.46)	4.74 (4.69)
7.8	H_2SO_4 (*b*)	12.1	Me	COOH	$(CH_2)_4CH_3$	COOEt	71	224		62.90 (62.79)	7.92 (7.84)	5.24 (5.11)
12.1	250°	15.2	Me		$(CH_2)_4CH_3$	COOEt	45	64–66		69.92 (69.88)	9.48 (9.48)	6.27 (6.39)
15.2	Reductive alkylation (*a*)	14.6	Me	Me	$(CH_2)_4CH_3$	COOEt	74	83–85		70.85 (71.02)	9.77 (9.69)	5.90 (6.01)
10.3	$COCl_2$ (*b*)	14.6	Me	Me	$(CH_2)_4CH_3$	COOEt	67	83–85	Above			
		6.7	Et	COOEt	$(CH_2)_4CH_3$							
6.7	Reductive alkylation (*a*)	2.8	Et	COOEt	$(CH_2)_4CH_3$	Me	70	74–76	Above	71.67 (71.71)	10.03 (10.06)	5.57 (5.70)

Can. J. Chem. Downloaded from www.nrcresearchpress.com by 210.87.254.40 on 09/05/12
For personal use only.

We had used methylpyrroles and their carbethoxy derivatives to determine sets of conditions suitable for the reductive alkylation of representative types of pyrroles, and the limitations of these methods (2). The alkylations now carried out (Scheme 1 and Table 2) now show that the generalizations made then are equally applicable to pyrroles bearing higher alkyl groups, and to their carbethoxy or carbobenzoxy derivatives. The only exception was the dicarboxylic ester 4.2 which was too insoluble to be methylated at room temperature, and its carbobenzoxy group was displaced by a methyl group at 45° (see Experimental). The *t*-butyl esters, however, did not survive at room temperature. In detail, the ethyl esters 1.4, 4.3, 4.4, 5.4, 5.5, 6.1, 6.4, 6.5, 6.6, 6.7, 13.2, 13.3, 15.1, 15.2 were methylated, 1.4, 1.5, 5.4, 5.5, 6.1, 6.4, 6.5, 6.6, 13.2, 15.1 were ethylated, and 1.4 was converted into its *n*-pentyl derivative; like their lower homologue (2), 4.3 and 4.4 were not ethylated. The benzyl esters 1.3, 5.3, and 6.3 were both methylated and ethylated; the methylation of 4.2 is discussed above and its ethylation, like that of 4.3 and 4.4 was not to be expected. At 100°, when no difficulty was expected as carbalkoxy groups are replaced, both 6.1 and 6.6 were completely *C*-methylated.

In conclusion, the Hantzsch synthesis and the Knorr synthesis in its various forms have the same formal generality but that of the latter is more fully realized, particularly because 4-acetic and 4-propionic acids are obtained directly, the choice of acylacetates providing the 2- and 3-substituents is wider, and 1,3-diketones may replace acylacetates. The Hantzsch synthesis has advantages when its use permits a commercial aldehyde (halogenated) to replace a higher acylacetate (nitrosated), and also when 4-free pyrroles are required or when the final products are to be 3-methyl derivatives. Thus the 2-alkyl- and 2,4-dialkyl-3-methylpyrroles 9.2, 9.3, 10.1 (hemopyrrole), 10.2, 10.3 are now obtained (as was 2,3-dimethylpyrrole, 9.1 (9)) in three steps from aldehydes and acylacetates, hemopyrrole (12%) from butanal and ethyl acetoacetate.[4] The Hantzsch synthesis also provides attractive routes to 14 (R^3 = Me): 10.1, 10.2, 10.3 → 14.4, 14.2, 14.6 respectively, 13.2 → 14.1 and 14.2, or 13.3 → 14.3. More generally, 14 (R^3 = Me) was obtained through 6.1 → 11.1 → 15.1 → 14.4 and 14.5, or 6.6 → 7.8 → 12.1 → 15.2 → 14.6.

It was necessary to clear up confusion over the m.p. of 2,3-dimethyl-5-carbethoxypyrrole, 13.1 (16, 4). Fischer and Fink applied their "modified Knorr" synthesis (eq. [2*b*]) to 3-formyl-2-butanone and identified the product, m.p. 128°, as 13.1. They concluded, without further evidence, that the lower m.p., 114° (3*e*), of earlier preparations was due to the presence of some of the *N*-carbethoxypyrrole. The *N*-carbethoxy derivative may contaminate products from pyrrylmagnesium halides and ethyl chloroformate (3*a*), and its presence here would reflect on the purity of all the products we obtained by the phosgene method. We found,[5] however, that Fischer and Fink's product is a mixture of 13.1, m.p. 114–116°, with 10–30% of 2,3,4-trimethyl-5-carbethoxypyrrole, m.p. 126–129°, into which it was resolved by preparative g.l.p.c.; conversely, mixtures of these two pyrroles had the same nuclear magnetic resonance (n.m.r.) spectrum and m.p. (128–130°) as the product of Fischer and Fink. Evidently, Knorr syntheses with 1,3-dicarbonyl compounds can take a third course (eq. [2*c*]) (possibly six if the dicarbonyl compound is unsymmetrical) which was foreshadowed by the equivalence of acetylacetone and its oxymethylene derivative in the normal Knorr synthesis (eq. [2*a*]) (16).

Experimental

Melting points are corrected. The assigned structures were consistent with the n.m.r. spectra. Pyrroles gave negative Beilstein tests for halogen and positive Ehrlich reactions. Those encountered more than once had identical n.m.r. spectra and their mixture m.p.'s were not depressed.

The following were obtained by methods in the literature: *t*-butyl acetoacetate (20), benzyl acetoacetate (21), ethyl and benzyl propionylacetate, ethyl butyrylacetate (18), 2-bromo-3-pentanone (22), 1,2-dibromo-1-ethoxybutane (23), 2-chlorobutanal (24), 2-bromobutanal and 2-bromoheptanal (25), and 1,2-dibromo-1-acetoxyheptane (26). 2-Bromo-1,1-diethoxybutane, $b.p._{20}$ 86–88°, and 1,2-dibromo-1-acetoxybutane were obtained like the corresponding pentane (27) and heptane (26) respectively. Hydriodic acid (d = 1.94) and 50% hypophosphorous acid were used.

Standard (not Optimal) Conditions for the Hantzsch Syntheses in Table 1

Aqueous ammonia (50 ml of 28%, 50 ml of water) was added to the acylacetate and halo-compound (0.1 mole of each) and the mixture was stirred for 2 h while the tem-

[4]The bromine required costs six times as much as these cabalistic starting materials.

[5]With D. T. Krajcarski.

[2a] 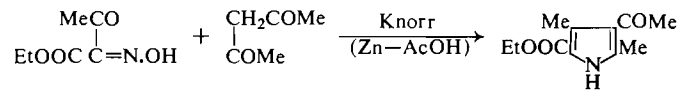

[2b] 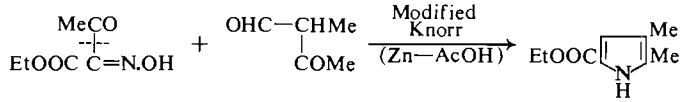

13.1

[2c] 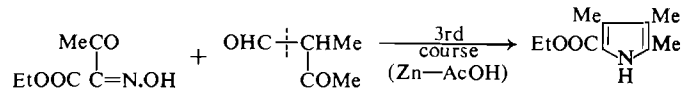

perature rose to about 60° then fell. Next day the product was extracted into ether and the extract was washed with 10% NaOH, with water, with 5% HCl, and again with water. Ether was removed from the dried (Na_2SO_4) extract *in vacuo*. The products 1.3, 1.4, 2.1, 5.2, 5.3, 6.1, 6.2, 6.3, 6.4, 6.5, 6.6, 6.7 crystallized from the residues after a few hours at room temperature and 1.5 crystallized at 0°. These were recrystallized from ether–pentane and then, if necessary, decolorized by sublimation (ca. 90°, 0.5 mm). In the case of 5.4 and 5.5, the distilled residues crystallized at 0°; 5.4 was then drained on cold tile and redistilled, 5.5 was recrystallized from pentane.

Standard Conditions for the Reactions Detailed in Table 2 as Designated There and in Scheme 1

$LiAlH_4$. 3-Methylpyrroles from 3-Carbethoxypyrroles: 9 and 10 from 5 and 6 cf. (9)

A solution of the pyrrole (0.01 mole) in 20 ml of dry tetrahydrofurane was dropped into a stirred solution of $LiAlH_4$ (0.8 g) in 20 ml of tetrahydrofurane over 1/2 h. The solution was then refluxed for 18 h, cooled, and ordinary ether (20 ml) added followed by enough 10% NaOH (ca. 100 ml) to redissolve the initial precipitate. The mixture was extracted with ether, the dried (Na_2SO_4) extract was evaporated (rotary), and the residue was distilled at ca. 90° (10 mm).

$COCl_2$. 5-Carbethoxypyrroles

(a) From 3-Carbethoxypyrroles: 4 and 7 from 5 and 6

A solution of the pyrrole (0.01 mole) in 25 ml of toluene and 1.2 g of dimethylaniline was cooled in an ice–salt bath and stirred while a solution of phosgene (1 g) in toluene (10 ml) was dropped in over 15 min. After standing overnight, the mixture was refluxed for 2 h. Absolute ethanol (10 ml) containing dimethylaniline (1.2 g) was then dropped in at room temperature and the mixture stirred and heated for 1 h. Toluene was removed at room temperature *in vacuo* (rotary), and the residue poured into dilute hydrochloric acid (10 ml concentrated and 100 ml water). The solid which separated was crystallized from ether–pentane.

(b) From Purely Alkyl Pyrroles, cf. (6): 13, 14, and 15.1 from 9, 10, and 11.1

The pyrrole (0.01 mole), in dry ether (25 ml) and dimethylaniline, was treated as in (*a*) but without any heating.

Reductive Alkylation cf. (1, 2)

(a) Using Hydriodic Acid at Room Temperature: 2 from *1, 5, or 6; 7(R^4 = Me, R = Et) from 4(R = Et); 14 from 13; 14(R^3 = Me) from 15*

The pyrrole (0.004 mole) in acetic acid (10 ml), hydriodic acid (10 ml), hypophosphorous acid (2 ml), and the aldehyde (1*x* − 5*x* theory) were stirred for 2 h at room temperature. The solution was poured into 200 ml of water, the mixture made alkaline with ammonia, and the precipitate was recrystallized from ether – *n*-pentane.

(b) Using Hydriodic Acid at 45°, with Loss of Benzyloxycarbonyl Groups: 2,3,4-Trimethyl-5-carbethoxypyrrole from 2-Methyl-3-benzyloxycarbonyl-5-carbethoxypyrrole, 4.2, or from its 4-Methyl Derivative (28)

The pyrrole (0.574 g) in acetic acid (10 ml), hydriodic acid (5 ml), and hypophosphorous acid (1 ml) was stirred for 2 h at 45° with 0.3 g of paraformaldehyde. The product (75%), m.p. 127–129°, was isolated as under (*a*) above.

Anal. Calcd. for $C_{10}H_{15}NO_2$: C, 66.27; H, 8.34; N, 7.73. Found: C, 66.44; H, 8.51; N, 7.57.

(c) Using Hydriodic Acid at 100°, with the Loss of Carbethoxy Groups: 3 from 6

The pyrrole (0.01 mole), 25 ml of acetic acid, 25 ml of hydriodic acid, 5 ml of hypophosphorous acid, and 0.6 g of paraformaldehyde were heated for 3 h under nitrogen at 100°. The cooled solution was poured into water, the mixture was made alkaline with ammonia, and the product was extracted into ether. Ether was removed from the extract and the residue was distilled at ca. 95° (10 mm).

(d) Using HCl–AcOH–Zn: 14.5 (i.e. $R^3 \neq$ Me) from 15.1

Acetic anhydride (20 ml) was added to 5 ml of concentrated hydrochloric acid with cooling. The pyrrole 15.1 (0.004 mole), paraldehyde (0.008 mole) and 10 g of zinc amalgam (20 mesh) were added to this at 25° and stirred for 25 min. The zinc was then separated and the product was isolated as under (*a*) above.

H_2SO_4

(a) Removal of Carbethoxy Groups cf. (3p): 11.1 from 6.1

2-Methyl-4-ethyl-3-carbethoxypyrrole (9.05 g) in 24 ml of concentrated sulfuric acid and 10 ml of water was

Can. J. Chem. Downloaded from www.nrcresearchpress.com by 210.87.254.40 on 09/05/12
For personal use only.

heated for 3 h on the steam bath. The mixture was then made alkaline with 20% NaOH at ≤15°. The product, 2-methyl-4-ethylpyrrole, was extracted into ether then distilled at ca. 86° (20 mm).

(b) Partial Hydrolysis cf. (3g): 12.1 from 7.8

2-Methyl-4-*n*-pentyl-3,5-dicarbethoxypyrrole (7.8) (2 g) was stirred for 1 h at 40° in 4 ml of concentrated sulfuric acid. The product was precipitated by water and dissolved in aqueous NaOH which was then washed with ether. The product, 2-methyl-4-*n*-pentyl-5-carbethoxypyrrole-3-carboxylic acid (12.1) was reprecipitated by acid and recrystallized from ethanol as tiny colorless plates.

NaOH. Removal of Carbethoxy groups cf. (3i): 11.1 from 6.1

2-Methyl-4-ethyl-3-carbethoxypyrrole (9.05 g) was heated for 6 h at 175° with 40 ml of 10% aqueous NaOH in a Teflon lined screw-capped metal tube. The product, 2-methyl-4-ethylpyrrole, was extracted into ether then distilled at ca. 86° (20 mm).

250°. Decarboxylation cf. (3q): 15.2 from 12.1

2-Methyl-4-*n*-pentyl-5-carbethoxypyrrole-3-carboxylic acid (12.1) was decarboxylated at 250°. The product, 2-methyl-4-*n*-pentyl-5-carbethoxypyrrole, 15.2, was sublimed at ca. 60° (0.05 mm) then recrystallized from ether–pentane as prisms.

Knorr. Ring Synthesis of 7.7 cf. (3r)

Ethyl propionylacetate (5.12 g) in 25 ml of acetic acid was nitrosated at ≤5° with 2.46 g of sodium nitrite in a little water. After 15 h at 0°, 5.63 g of ethyl *n*-butyrylacetate in 25 ml of acetic acid were added. The solution was stirred while 10 g of zinc dust were added at 65° Then, after 1 h at 85° the solution was decanted into water. The 2-*n*-propyl-4-ethyl-3,5-dicarbethoxypyrrole which separated was recrystallized from 50% ethanol then twice from *n*-pentane as long colorless needles (25%), m.p. 84–86° and 99–101°.

Anal. Calcd. for $C_{15}H_{23}O_4N$: C, 64.03; H, 8.24; N, 4.98. Found: C, 64.20; H, 8.41; N, 5.02.

1. B. V. Gregorovich, K. S. Y. Liang, D. M. Clugston, and S. F. MacDonald. Can. J. Chem. **46**, 3292 (1968).
2. M. W. Roomi and S. F. MacDonald. Can. J. Chem. **48**, 139 (1970).
3. H. Fischer and H. Orth. Chemie des Pyrrols. Vol. 1. Akademischer Verlag, Leipzig, 1934. (*a*) pp. 2 ff, 231 ff; (*b*) p. 177 ff; (*c*) p. 248; (*d*) p. 41; (*e*) p. 238; (*f*) p. 257; (*g*) p. 47; (*h*) p. 54; (*i*) p. 51; (*j*) p. 46; (*k*) p. 240; (*l*) p. 242; (*m*) p. 243; (*n*) p. 258; (*o*) p. 57; (*p*) p. 42; (*q*) p. 239; (*r*) p. 255 ff.
4. R. A. Nicholaus and R. Scarpati. Sugli Acidi Pyrrolici. Stabilimento Tipografico Guglielmo Genovese, Naples, 1962. p. 13.
5. E. Benary. Chem. Ber. **44**, 495 (1911).
6. A. Treibs and W. Ott. Ann. Chem. **615**, 137 (1958).
7. A. Hantzsch. Chem. Ber. **23**, 1474 (1890).
8. G. Korschun. Chem. Ber. **37**, 2196 (1904); **38**, 1125 (1905).
9. R. L. Hinman and S. Theodoropulos. J. Org. Chem. **28**, 3052 (1963).
10. A. Treibs. Ann. Chem. **524**, 285 (1936).
11. F. Feist. Chem. Ber. **35**, 1539, 1545 (1902).
12. H. Fischer and H. Höfelmann. Z. Physiol. Chem. **251**, 218 (1938).
13. C. D. Nenitzescu, I. Necsoiu, and M. Zalmon. Comun. Acad. Rep. Sop. Rom. **7**, 421 (1957).
14. H. Kondo, S. Ono, and S. Irie. J. Pharm. Soc. Japan, **57**, 78 (German) (1937).
15. L. Knorr and K. Hess. Chem. Ber. **44**, 2762 (1911); **45**, 2626 (Footnote) (1912).
16. H. Fischer and E. Fink. Z. Physiol. Chem. **283**, 152 (1948).
17. H. Fischer and H. Höfelmann. Ann. Chem. **533**, 216 (1938).
18. J. L. Archibald, D. M. Walker, K. B. Shaw, A. Markovac, and S. F. MacDonald. Can. J. Chem. **44**, 345 (1966).
19. Endo Laboratories Inc. (by K. Schoen and I. J. Pachter) Belg. Pat. 670, 796; cf. Chem. Abstr. **65**, 16943 (1966).
20. A. Treibs and K. Hintermeier. Chem. Ber. **87**, 1167 (1954).
21. R. F. Bacon. Amer. Chem. J. **33**, 68 (1905).
22. H. Pauli. Chem. Ber. **34**, 1771 (1901).
23. H. Seifert. Monatsh. Chem. **79**, 198 (1948).
24. A. Krattiger. Bull. Soc. Chim. France, **20**, 222 (1953).
25. J. J. Riehl. C. R. **245**, 1321 (1957).
26. P. Z. Bedoukian. J. Amer. Chem. Soc. **66**, 1325 (1944).
27. R. Kühn and C. Grundman. Chem. Ber. **70**, 1898 (1937).
28. S. F. MacDonald. J. Chem. Soc. 4176 (1952).

Can. J. Chem. Downloaded from www.nrcresearchpress.com by 210.87.254.40 on 09/05/12
For personal use only.

Can. J. Chem. Downloaded from www.nrcresearchpress.com by 210.87.254.42 on 09/05/12
For personal use only.

Appareil pour la mesure de moments dipolaires

C. Barbeau, L. Ricard et J. Turcotte
Département de Chimie, Université Laval, Québec

Reçu le 31 décembre 1969

On décrit un système qui permet la mesure d'un moment dipolaire à partir d'aussi peu que 10^{-4} mole d'une substance de moment dipolaire égal à 1.0 D. La constante diélectrique d'une solution est mesurée à ± 0.000008 unité. Un système de dilution permet d'effectuer la détermination de μ à partir d'une seule pesée. Les différentes méthodes de calcul du moment dipolaire ont été comparées et il est proposé une méthode, déduite de celle de Guggenheim, qui permet d'obtenir, de la seule mesure des constantes diélectriques, une valeur de moment dipolaire très voisine de celle donnée par la méthode classique.

A system is described which enables the determination of dipole moments of magnitude 1.0 D from as little as 10^{-4} mole of substance. The dielectric constant can be measured with a precision of ± 0.000008 unit. Only one weighing is necessary. A modified Guggenheim method, in which only the values of the dielectric constant are required, is used to calculate the dipole moments.

Canadian Journal of Chemistry, 48, 1698 (1970)

Introduction

Les appareils pour la mesure de moments dipolaires en solution exigent normalement une quantité de soluté de l'ordre de 10^{-3} mole et ne sont pas pourvus d'un système de dilutions successives ou de protection contre l'oxygène atmosphérique et l'humidité. L'emploi d'un solvant tel que le cyclohexane, pour éviter des effets de solvant, ne permet pas généralement des concentrations élevées en soluté lorsqu'il s'agit de composés organo-métalliques. Nous avons élaboré un système pour la détermination des moments dipolaires de ces composés organo-métalliques, qui sont très sensibles à l'oxygène atmosphérique, dont la solubilité est très faible et qui ne sont obtenus qu'en très petite quantité.

Les difficultés reliées à la mesure de densité des solutions et l'imprécision sur la mesure de l'indice de réfraction de solutions très diluées nous ont poussés à comparer les méthodes de calcul des moments dipolaires, selon Guggenheim (1), Higasi (2), et Halverstadt–Kumler (3). Nous désirions vérifier si le terme relié à la polarisation électronique, P_E, dans l'équation de Guggenheim, pouvait s'obtenir à partir de la mesure des indices de réfraction dans le benzène ou pouvait être calculé à partir des réfractions atomiques.

Partie expérimentale

Description du Système

Le système utilisé dans la détermination du moment dipolaire consiste, en un appareil pour la mesure de la constante diélectrique ε, en un réfractomètre, et en un circuit permettant d'effectuer, sous atmosphère d'azote, les dilutions et les montées des solutions dans le condensateur liquide.

L'appareil pour la mesure de la constante diélectrique se fonde sur la méthode dite "hétérodyne" et emploie deux oscillateurs Franklin (4), l'un fixe, piloté par un quartz piézo-électrique oscillant à 1.5 MHz, l'autre variable, constitué par quatre condensateurs (C_1–C_4) en parallèle et une bobine d'induction. C_1 et C_2 sont deux condensateurs variables à air, General Radio 1422, de 1100 pF et 250 pF respectivement. C_3 est un condensateur cylindrique constitué par une tête de micromètre pénétrant à l'intérieur d'une gaine de laiton et dont la capacité maximale est de 2.5 pF. Les condensateurs C_1 et C_2 sont gradués à l'aide du condensateur C_3 qui présente 2500 divisions. C_4 est le condensateur liquide qui sert de cellule à constante diélectrique. Il a été construit d'après le modèle de Meredith et Wright (5). La constante de la cellule à 25 °C est de 270 pF. Grâce aux nombreuses divisions des condensateurs C_1, C_2, et C_3, on peut mesurer ε sur une gamme de quatre unités avec une précision de ± 0.000008 unité. Les condensateurs sont placés dans une cage hermétique en plexiglas dont la température est maintenue à 25.0 ± 0.05 °C grâce à un élément chauffant de 500 W et un système de refroidissement à l'eau. La cellule est placée dans un manchon métallique dont la température est rigoureusement maintenue à ± 0.01 °C à l'aide de deux bains thermorégularisés. La tension de 250 V aux bornes des condensateurs de même que la source d'alimentation de 6.3 V nécessaire aux différentes lampes du circuit sont stabilisées de façon à éviter toute fluctuation au cours d'une mesure. Deux condensateurs variables à air C_5 et C_6 dont la capacité maximale est de 800 pF peuvent être substitués au condensateur C_4 au moyen d'un relais actionné par un interrupteur sans capacitance. En cours de mesure, cette substitution permet de vérifier la stabilité du circuit électrique et d'effectuer, si nécessaire, une correction sur la lecture du condensateur liquide C_4.

Le réfractomètre est du type "Bausch & Lomb Dipping Refractometer" auquel on a ajouté une cellule permettant l'entrée et la sortie du liquide. Cette cellule est également

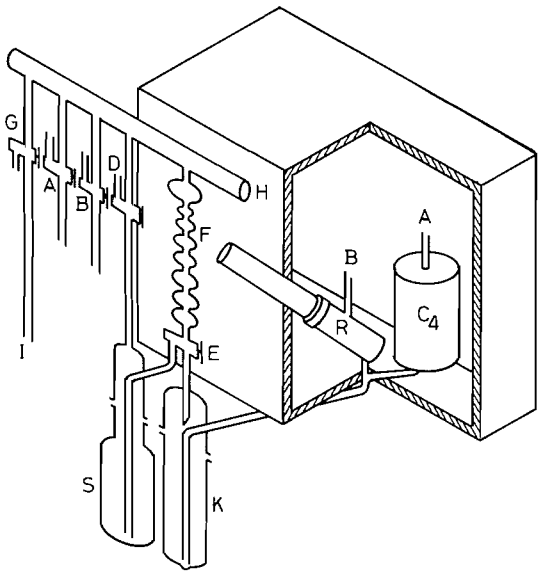

FIG. 1. Système de dilution sous atmosphère inerte.

maintenue à ± 0.01 °C grâce à deux bains thermorégularisés. L'indice de réfraction peut être mesuré à ± 0.00004 unité. La lunette du réfractomètre est située à l'extérieur de la cage de plexiglas et la cellule ainsi que la lampe au sodium se retrouvent à l'intérieur de la cage (Fig. 1).

Toutes les dilutions sont réalisées en transférant, sous pression d'azote, une quantité connue de solvant, d'un réservoir au récipient contenant le soluté. Grâce à une colonne de sphères graduées, reliées entre elles par des tubes capillaires, la quantité de solvant introduite dans la solution est précise à $\pm 0.02\%$. Le courant d'azote, qui pousse la solution dans le réfractomètre et le condensateur liquide, entraîne les gouttelettes restant sur les parois des sphères. Pour que les montées vers les cellules soient uniformes et reproductibles, le courant d'azote est rigoureusement contrôlé par un débitmètre (Matheson, No. 610) relié à un cylindre d'azote.

Lors d'une mesure on procède de la façon suivante. La substance pesée est placée dans le récipient *K* (Fig. 1); l'ensemble du système est complètement purgé d'air et rempli d'azote; le robinet à voie double *E* est placé de façon à permettre au solvant de monter en *F* sous la pression d'azote arrivant en *D*; la colonne remplie au niveau désiré, le robinet *E* est inversé en direction de *K*; sous la poussée d'azote arrivant en *H*, la solution monte dans les cellules C_4 et *R* qui sont reliées aux robinets *A* et *B* ouverts à l'air lors des montées; les cellules remplies, la poussée de l'azote est interrompue et les robinets *B* et *C* sont fermés; après lectures des valeurs de ε et *n*, la pression de l'azote est libérée en dirigeant les robinets *B* et *A* vers *H* et en ouvrant le robinet *G* sur un barboteur *I* relié à l'air.

Le volume minimum requis est de 40 ml. La montée dure environ 3 min et 4 ou 5 mesures par dilution sont suffisantes. Un agitateur magnétique placé au fond de *K* permet un mélange très rapide et un manchon chauffant placé au-dessus du niveau du liquide dans *K* évite toute condensation de solvant sur les parois.

Résultats et discussion

(*a*) *Système de mesure*

La mesure de la constante diélectrique de solutions très diluées est facilement faussée par un léger changement soit dans la température des composantes électriques de l'appareil, soit dans le remplissage de la cellule liquide, soit dans la préparation des solutions. Ainsi nous avons constaté qu'une variation de ± 0.5 °C dans l'enceinte contenant les condensateurs diminuait la précision sur la mesure de ε à ± 0.0001 unité. D'autre part, la montée non-uniforme du liquide dans le condensateur résulte en une baisse appréciable de la reproductibilité des mesures. Finalement, nous avons constaté que la valeur ε_1, obtenue en changeant le récipient *K* pour la mesure du solvant pur, était toujours différente de la valeur obtenue par extrapolation à dilution infinie. On peut donc conclure que la préparation des solutions à différentes concentrations s'effectue dans des conditions identiques seulement dans un système fermé. La technique de dilution continue présente d'autre part le double avantage de permettre la détermination, dans un temps court, d'un moment dipolaire d'une substance peu soluble ou d'une substance disponible en très faible quantité.

Les résultats du tableau 1 montrent qu'en dépit d'une variation d'un facteur 10 dans les dilutions initiales, la valeur $d\varepsilon_{12}/df_2$ de la biphénylamine dans le cyclohexane demeure inchangée. Cette valeur donne la pente de la droite obtenue par moindres carrés lorsqu'on porte graphiquement la constante diélectrique de la solution ε_{12} en fonction de la fraction molaire f_2 du soluté. Les condensateurs de référence se sont avérés très importants lors de la mesure effectuée à partir de 14.7 mg et ont permis d'obtenir une valeur de $d\varepsilon_{12}/df_2$ ($= \alpha$) précise à 10%. Dans la région de très faible dilution nous n'avons constaté aucune variation significative sur la valeur $d\varepsilon_{12}/df_2$ comme en font foi les résultats de la mesure effectuée sur 0.2699 g de biphénylamine.

Les mesures effectuées dans le benzène montrent, qu'en dépit d'une faible polarisation totale P_T et d'une polarisation électronique P_E élevée

Can. J. Chem. Downloaded from www.nrcresearchpress.com by 210.87.254.42 on 09/05/12
For personal use only.

TABLEAU 1

Moment dipolaire (D) de la biphénylamine, $C_{12}H_{11}N$ à 25 °C

Benzène				Cyclohexane			
$f_2 \times 10^3$	$\Delta\varepsilon_{12} \times 10^2$	ε_{12}	$n_{D12}{}^2$		$f_2 \times 10^3$	$\Delta\varepsilon_{12} \times 10^2$	ε_{12}
*A**				*A*†			
19.211	4.683	2.31172	2.26268	I	3.5645	0.684	2.02195
14.884	3.636	2.30125	2.25885		2.3693	0.441	2.01952
10.825	2.638	2.29127	2.25528		1.7744	0.337	2.01848
7.908	1.909	2.28398	2.25290		1.4183	0.276	2.01786
5.966	1.439	2.27928	2.25142	II	1.0339	0.197	2.01684
4.691	1.121	2.27610	2.25049		0.8353	0.159	2.01646
B‡					0.7536	0.144	2.01631
3.8366	0.982	2.28173	2.24978		0.6211	0.118	2.01605
2.9621	0.755	2.27946	2.24899	III	0.6211	0.118	2.01605
2.1471	0.567	2.27758	2.24833		0.4498	0.080	2.01576
1.5649	0.401	2.27592	2.24779		0.3052	0.057	2.01553
1.1737	0.293	2.27484	2.24751		0.2059	0.038	2.01534
				B§			
					0.1949	0.040	2.01539
					0.1294	0.027	2.01526
					0.0969	0.022	2.01521
					0.0774	0.012	2.01511

*Quantité de $C_{12}H_{11}N$ = 1.1301 g; valeurs extrapolées: ε_1 = 2.26489; $n_{1D}{}^2$ = 2.24644; γ = 0.83 ± 0.02; α = 2.43 ± 0.02; μ_G = 1.07 ± 0.01; γ' = 0.84; P_E = 51.73 cm³; μ_H = 1.32; μ_G' = 1.07; μ_C = 1.08.
†Quantité de $C_{12}H_{11}N$ = 0.2699 g; valeurs extrapolées: $\varepsilon_1{}^I$ = 2.01511; $\varepsilon_1{}^{II}$ = 2.01487; $\varepsilon_1{}^{III}$ = 2.01496; α^I = 1.87 ± 0.01; α^{II} = 1.87 ± 0.01; α^{III} = 1.81 ± 0.04; γ' = 0.60; P_E = 51.73 cm³; $\mu_H{}^I$ = 1.36; $\mu_H{}^{II}$ = 1.36; $\mu_H{}^{III}$ = 1.33; $\mu'_G{}^I$ = 1.12; $\mu'_G{}^{II}$ = 1.12; $\mu'_G{}^{III}$ = 1.09.
‡Quantité de $C_{12}H_{11}N$ = 0.2221 g; valeurs extrapolées: ε_1 = 2.27191; $n_{1D}{}^2$ = 2.24648; γ = 0.85 ± 0.02; α = 2.56 ± 0.04; μ_G = 1.11 ± 0.03; γ' = 0.84; P_E = 51.73 cm³; μ_H = 1.35; μ_G' = 1.11; μ_C = 1.08.
§Quantité de $C_{12}H_{11}N$ = 0.01473 g; valeur extrapolée: ε_1 = 2.01499; α = 2.0 ± 0.2; γ' = 0.60; P_E = 51.73 cm³; μ_H = 1.40; μ_G' = 1.17.

pour la biphénylamine, la limite de confiance sur les lectures de n_{12} est atteinte bien avant celle sur les lectures de ε_{12}. En effet la quantité initiale minimale pour observer une variation $dn_{12}{}^2/df_2 = (\gamma)$ est dix fois supérieure à celle permettant une détermination acceptable de $d\varepsilon_{12}/df_2$.

(b) Méthodes de calcul

La méthode d'Higasi (2) telle que vérifiée et décrite par Krishna et Srivastava (6, 7) permet le calcul de μ à partir de $d\varepsilon_{12}/df_2$.

$$[1] \qquad \mu_H{}^2 = \frac{27kTM_1}{4\pi Nd_1(\varepsilon_1 + 2)^2}(\alpha)$$

où k = constante de Boltzmann; T = température absolue; M = masse moléculaire; N = nombre d'Avogadro; d = densité à 25 °C.

La méthode de Guggenheim (1) a été présentée sous plusieurs versions par Smith (8) et une équation modifiée peut se lire

$$[2] \qquad \mu_G{}^2 = \frac{27kTM_1}{4\pi Nd_1(\varepsilon_1 + 2)(n_1{}^2 + 2)}(\alpha - \gamma)$$

où

$$[3] \qquad \gamma = dn_{12}{}^2/df_2$$

Pour les solvants tels que le cyclohexane et le benzène où $n_1{}^2 \cong \varepsilon_1$, la différence entre les équations [1] et [2] réside dans le terme γ qui exprime le degré de polarisation électronique P_E.

La polarisation électronique d'un soluté peut s'obtenir à partir de la somme des polarisations électroniques de liaison telles que compilées par Le Fèvre et Steel (9). Nous avons trouvé que la relation [4]

$$[4] \qquad 0.85P_E = \frac{1}{n_1{}^2 + 2}\frac{M_1}{d_1}\frac{dn_{12}{}^2}{df_2} + \frac{n_1{}^2 - 1}{n_1{}^2 + 2}\frac{M_1}{d_1}$$

donnait des valeurs de $dn_{12}{}^2/df_2 = (\gamma')$ très voisines de celles mesurées.

A défaut d'obtenir la pente expérimentale γ, nous avons introduit la valeur γ' dans l'équation [2].

$$[5] \qquad \mu_G{}^2 = \frac{27kTM_1}{4\pi Nd_1(\varepsilon_1 + 2)(n_1{}^2 + 2)}(\alpha - \gamma')$$

Dans le benzène, on constate (tableau 2), que les valeurs des moments dipolaires calculés selon [5] et [2] sont très semblables et voisines des valeurs μ_C obtenues à partir de données sur les

Can. J. Chem. Downloaded from www.nrcresearchpress.com by 210.87.254.42 on 09/05/12
For personal use only.

Can. J. Chem. Downloaded from www.nrcresearchpress.com by 210.87.254.42 on 09/05/12
For personal use only.

TABLEAU 2

Comparaison des moments dipolaires, à 25 °C, calculés selon les équations [1], [2] et [5]*

Composés	Solvant	α	γ	γ'	P_E (cm^3)	eq. [1] μ_H	eq. [2] μ_G	eq. [5] μ_G'	μ_C	$\mu_G - \mu_G'$	$\mu_C - \mu_G'$	Référence
Diméthyl-3,4 méthoxy-5 isoxazole	Benzène	8.34	−0.20	0.08	32.82	2.44	2.48	2.44	2.46	0.04	0.02	10
Diméthyl-3,4 *N*-méthylisoxazoline one-5	Benzène	45.09	0.04	0.07	32.55	5.67	5.71	5.70	5.68	0.01	−0.02	10
Méthyl-3 phényl-4 *N*-méthylisoxazoline one-5	Benzène	45.30	0.64	0.08	51.11	5.69	5.65	5.67	5.66	−0.02	−0.01	10
Biphénylamine	Benzène	2.43	0.85	0.84	51.73	1.32	1.07	1.07	1.08†	0.00	0.01	—
Cyclohexanone	Benzène	12.97	—	−0.02	30.34	3.04	—	3.06	3.06	—	0.00	11
Chloropyridine-4	Benzène	1.02	0.08	−0.05	29.47	0.85	0.82	0.88	0.84	−0.06	−0.04	12
Cyanopyridine-2	Benzène	38.17	0.13	−0.07	29.08	5.22	5.25	5.26	5.24	−0.01	−0.02	12
Chlorobenzène	Benzène	3.57	0.09	0.01	31.02	1.60	1.59	1.60	1.59	−0.01	−0.01	12
Tribromopyridine-3,4,5	Benzène	1.12	0.73	0.68	7.78	0.89	0.53	0.56	0.58	−0.03	0.02	12
Tribromopyridine-2,3,6	Benzène	14.04	0.76	0.68	47.78	3.17	3.10	3.11	3.11	−0.01	0.00	12
p-Dichlorobenzène chrome tricarbonyle	Benzène	24.53‡	1.03‡	0.98‡	55	4.11‡	4.05‡	4.06‡	4.00‡	−0.01	−0.06	13
Hexaméthyl benzène chrome tricarbonyle	Benzène	58.50‡	0.91‡	1.67‡	72	6.34‡	6.35‡	6.30‡	6.27‡	0.05	−0.03	13
p-Xylène molybdène tricarbonyle	Benzène	55.15	1.13	1.18	60	6.17	6.15	6.14	6.06	0.01	−0.08	14
Molybdène pentacarbonyle triphénylphosphine	Benzène	43.59	3.01	3.27	112	5.57	5.42	5.40	—	0.02	—	14
Benzène molybdène dicarbonyle triphénylphosphine	Benzène	32.05	3.48	3.60	120.5	4.79	4.55	4.54	—	0.01	—	14
Hexaméthyl benzène molybdène tricarbonyle	Benzène	75.57	1.32	1.82	76	7.35	7.33	7.30	—	0.03	—	14
Cyclopentadiényl manganèse dicarbonyle diméthyl-sulfoxyde	Benzène	14.17	0.77	0.79	50.5	3.13	3.12	3.11	3.01	0.01	−0.10	15
Iodoforme	Benzène	2.02‡	—	0.51‡	43.4	1.16‡	—	1.03‡	0.99‡	—	−0.04	7
Dibromoéthylène	Benzène	1.98	—	−0.22	25.35	1.17	—	1.26	1.40	—	0.14	7
Dichloro acétamide	Dioxanne	16.76	—	0.10	23.87	3.45	—	3.45	3.46	—	0.01	16
Trichloro acétamide	Dioxanne	21.74	—	0.03	28.59	3.93	—	3.94	3.94	—	0.00	16
Trifluoro acétamide	Dioxanne	25.53	—	−0.45	14.16	4.26	—	4.31	4.33	—	0.02	16
Chloroacétaldéhyde	Dioxanne	4.79	—	−0.43	14.79	1.84	—	1.93	1.99	—	0.06	16
Diméthyl-3,4 méthylisoxazoline one-5	Dioxanne	48.41	0.25	0.28	32.55	5.86	5.97	5.97	5.84	0.00	−0.07	10
Phényl-3 méthoxy-5 isoxazole	Dioxanne	22.15	0.74	0.85	46.84	3.97	3.98	3.97	3.90	0.01	−0.07	10
Diméthyl-3,4 méthoxy-5 isoxazole	Dioxanne	9.01	0.11	0.29	32.82	2.53	2.60	2.54	2.52	0.04	−0.02	10

*ε_1: dioxanne = 2.2090, benzène = 2.2740; n_1: dioxanne = 1.4246, benzène = 1.4982; d_1: dioxanne = 1.0280, benzène = 0.8738; α: pente de la courbe donnant ε_{12} en fonction de la fraction molaire f_2; γ: pente de n_{12}^2 en fonction de f_2; γ': valeur de dn_{12}^2/df_2 obtenue selon [4]; P_E: somme des polarisations de liaison; μ_C: moment dipolaire calculé selon la méthode d'Halverstadt–Kumler; μ: moment dipolaire exprimé en D.

†Valeur tirée de (17).

‡Valeurs à 20 °C.

indices de réfraction, les densités et les constantes diélectriques.

La méthode d'Higasi donne par contre un moment dipolaire plus éloigné du moment dipolaire μ_C calculé selon Halverstadt–Kumler. Il est intéressant de noter que les deux composés qui faisaient exception dans la série calculée par Krishna et Srivastava (7) présentent des moments dipolaires acceptables si le calcul s'effectue selon [5].

La méthode basée sur un calcul grossier de la polarisation électronique permet d'obtenir avec une précision satisfaisante le moment dipolaire de composés organo-métalliques contenant des groupements volumineux.

Dans un solvant tel que le dioxanne, où n_1^2 est différent de ε_1, on remarque également une grande similitude entre les moments dipolaires calculés selon [2], [5] et la méthode classique.

Nous nous croyons donc justifiés d'employer, lorsqu'il s'agit de moments dipolaires élevés, la polarisation électronique P_E obtenue soit par addition des polarisations de liaison, soit par l'équation [4] (si la valeur γ est connue dans un solvant), pour calculer le moment dipolaire d'une substance à partir de la seule mesure de α.

Puisqu'il est généralement admis (18) que les valeurs de μ obtenues à partir de solutions sont imprécises à ± 0.05 D, l'équation [5] permet donc de déterminer un moment dipolaire dont la valeur est aussi acceptable que celle obtenue par la méthode classique.

Nous remercions le Conseil National de Recherches du Canada pour une subvention et une bourse (L.R.).

1. E. A. GUGGENHEIM. Trans. Faraday Soc. **45**, 714 (1949).
2. K. HIGASI. Bull. Inst. Phys. Chem. Res. Tokyo, 22805 (1963).
3. I. F. HALVERSTADT et W. O. KUMLER. J. Amer. Chem. Soc. **64**, 2988 (1942).
4. C. S. FRANKLIN. Brit. Pat. No. 335, 526 et 369, 575.
5. C. C. MEREDITH et G. F. WRIGHT. Can. J. Technol. **33**, 182 (1955).
6. B. KRISHNA et K. K. SRIVASTAVA. J. Chem. Phys. **27**, 835 (1957).
7. B. KRISHNA et K. K. SRIVASTAVA. J. Chem. Phys. **32**, 663 (1960).
8. J. W. SMITH. Trans. Faraday Soc. **46**, 394 (1950).
9. R. J. W. LE FÈVRE et K. D. STEEL. Chem. Ind. 670 (1961).
10. R. CENCIONI, P. F. FRANCHINI, et M. ORIENTI. Tetrahedron, **24**, 151 (1968).
11. P. F. FRANCHINI. J. Chem. Phys. **48**, 2610 (1967).
12. A. I. VOGEL et C. W. N. CUMLER. J. Chem. Soc. 4723 (1960).
13. W. STROHMEIER et H. HELLMANN. Ber. Bunsenges. Phys. Chem. **67**, 190 (1965).
14. C. BARBEAU ET S. TURCOTTE. Résultats non-publiés.
15. W. STROHMEIER et H. HELLMANN. Ber. Bunsenges. Phys. Chem. **68**, 482 (1964).
16. E. G. CLAYES, G. P. VAN DER KELEN, et Z. EECKHAUT. Bull. Soc. Chim. Belg. **70**, 462 (1961).
17. A. L. MCLELLAN. Tables of experimental dipole moments. W. H. Freeman and Co., London et San Francisco. 1963.
18. H. B. THOMPSON. J. Chem. Ed. **43**, 66 (1966).

Can. J. Chem. Downloaded from www.nrcresearchpress.com by 210.87.254.42 on 09/05/12
For personal use only.

Can. J. Chem. Downloaded from www.nrcresearchpress.com by 210.87.254.6 on 09/05/12
For personal use only.

The silver–indium system: thermal analysis, photomicrography, electron microprobe, and X-ray powder diffraction results

A. N. CAMPBELL AND R. WAGEMANN
Department of Chemistry, University of Manitoba, Winnipeg, Manitoba

AND (in part)

R. B. FERGUSON
Department of Earth Sciences, University of Manitoba, Winnipeg, Manitoba

Received[1] June 18, 1969

In the system Ag–In, the isothermal phase transformation at 281 °C previously assumed by Weibke and Eggers has been found not to exist. Metastability of the γ phase and of the indium phase is persistent at room temperature. The boundaries of the intermediate phases have been redetermined. At room temperature, the equilibrium γ phase (hexagonal) exists between 71.0 and 70.3% silver. At 325 °C and higher temperatures, the γ-phase region extends to higher indium concentrations than those given by Weibke and Eggers. The order–disorder transformation of the γ phase, postulated by Hellner, does not appear to exist. The liquidus is found to lie approximately 8 °C higher than that determined by Weibke and Eggers.

At room temperature, the ε phase exists between 67.5 and 65.0% silver. At these compositions, the cubic cell edges of the ε phase are $a = 9.878 \pm 0.004$ and 9.887 ± 0.004 Å, respectively. The $\gamma/(\gamma + \varepsilon)$ phase boundary has been redetermined and extended.

A new α′ phase is claimed to exist at approximately 73.8 wt. % silver. It is formed by a peritectoid phase reaction at 187°. In the α′ phase the silver atoms occupy the face-centered positions and the indium atoms, the corner positions of the cubic lattice. The intensities of diffraction lines were calculated using such a model and were found to be in reasonable agreement with the observed intensities of the α′ phase. The cell edge of the α′ phase is 4.144 ± 0.004 Å, at room temperature, and this is identical, within experimental error, with that of the α phase.

A new phase diagram for the Ag–In system has been constructed.

Canadian Journal of Chemistry, **48**, 1703 (1970)

Introduction

As a preliminary to an experimental investigation of the ternary alloy Al–In–Ag, we examined the literature of the component binary systems. The system Al–Ag is well established and we saw no reason to doubt the results for the relatively simple Al–In system. The system Ag–In, however, is complicated and the literature conflicting, and we therefore thought it advisable to re-examine this system as a preliminary to work on the ternary system. A very brief survey of the existing literature follows.

Goldschmidt (1) found a hexagonal close-packed phase (Ag_3In, γ or γ′, having lattice constants $a = 2.950$ kx, $c = 4.769$ kx). Frevel and Ott (2) found three intermediate phases at room temperature, in addition to the two terminal solid solutions. Two of these intermediate phases they reported to be hexagonal and the third, face-centered cubic and "very rich in indium". Weibke and Eggers (3) were the first to investigate the system completely and systematically by means of X-ray powder diffraction, photomicrography, and thermal analysis. Hume-Rothery *et al.* (4) investigated the silver-rich region only, with the primary aim of establishing more precisely the solubility limit of indium in silver as a function of temperature. Morris and Williams (5) determined the lattice parameter of the β phase by high-temperature X-ray diffraction and found it to be 3.3682 Å at 684 °C. Hellner (6) and Hellner and Laves (7), who investigated the system to determine the crystal structure and the extent of the regions of homogeneity of the intermediate phases, found that an alloy of 26.6 wt. % of indium, corresponding to Ag_3In, was homogeneous both at 600 and 150 °C with no fundamental difference in crystal structure occurring. The equilibrium diagram of Weibke and Eggers is given in Fig. 1.

According to Weibke and Eggers, and ourselves, thermal analysis shows a heat effect occurring at 204 °C without, however, any change occurring in the X-ray pattern. To explain this, Weibke and Eggers (3) postulated without experimental proof an order–disorder transformation $\varepsilon' \leftrightarrows \varepsilon$ and this supposition was retained by Hellner and Hellner and Laves, (6, 7). The

[1]Revision received November 20, 1969.

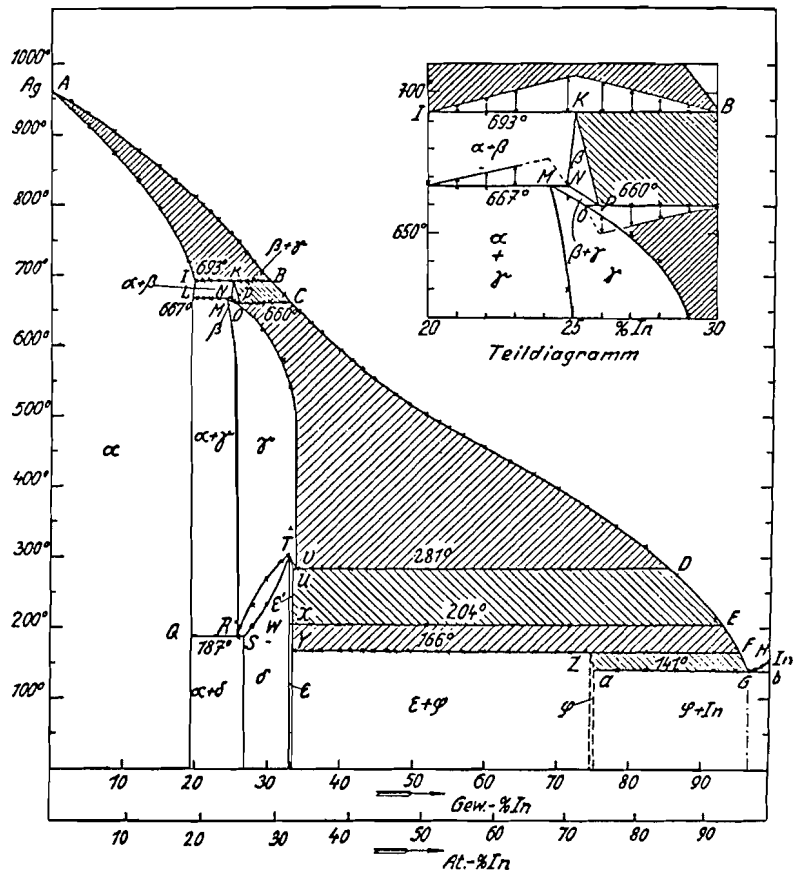

FIG. 1. Phase diagram of Ag–In system by Weibke and Eggers (3).

α-phase boundary (Fig. 1) was very carefully determined by Owen and Roberts (8) over the entire temperature range; their results are in good agreement with those of Hume-Rothery (4) and of Weibke and Eggers (3), so that this part of the system can be considered as well established, but in the composition range 23 to 40 atom % indium, the data of the previous investigations (3, 6) are in conflict in several respects.

Experimental

The techniques used in this work were differential thermal analysis (DTA), X-ray powder diffraction, photomicrography, and electronmicroprobe analysis. All, except perhaps the last, are well known and little need be said, except insofar as the methods have been modified to suit the exigencies of our work.

Silver was obtained from the Matheson, Coleman, and Bell Company and was claimed to be 99.999% pure. Indium, claimed to be 99.99% or better, was presented to us by the Consolidated Mining and Smelting Company of Canada. All compositions are expressed in wt. % unless otherwise stated. Alloys of the desired composition were prepared by accurately weighing the pure components in the required proportions. Prior to any heat treatment or DTA, all alloys were homogenized in an electrical induction coil under helium atmosphere in the cell shown in Fig. 2. The alloy samples were contained in a quartz thimble within a boron nitride cylinder; quartz has no action on silver or indium under the conditions in question. In the molten state, at approximately 1000 °C, the alloy was stirred vigorously by induced currents; this could be observed clearly when the supporting cylinder was not covered. After 5 to 10 min of stirring in this fashion, the alloy was allowed to cool, after which it was subjected to heat treatment or DTA. In the latter case the alloy was transferred to the DTA cell shown in Fig. 3. The copper cylinder served as the reference body. It contained the smaller boron nitride cylinder which in turn contained the small quartz thimble with the sample. Prior to DTA analysis the cell was evacuated, filled with helium, evacuated again, and finally filled with purified helium. Water, if present as an impurity, was removed from the gas by passing it through liquid nitrogen traps. The same procedure was followed in filling the homogenization cell with helium.

Alloys to be used for X-ray diffraction and photomicrography were melted as described. The small ingot was cut into three or four pieces which were sealed

Can. J. Chem. Downloaded from www.nrcresearchpress.com by 210.87.254.6 on 09/05/12
For personal use only.

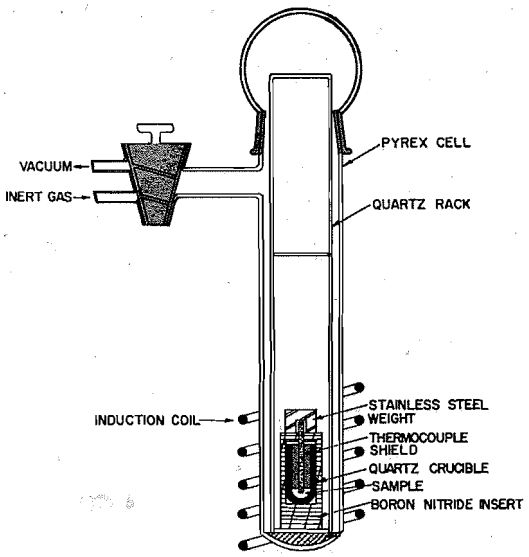

FIG. 2. Homogenization cell.

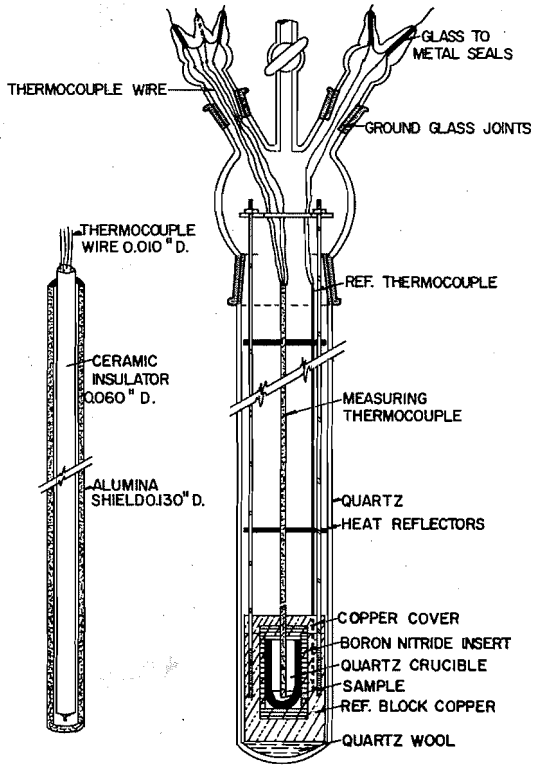

FIG. 3. Differential thermal analysis cell.

individually into evacuated quartz ampoules and annealed. Differential thermal analyses and annealing were carried out in a well-insulated, vertical-tube furnace within a 4 in. central zone which had a temperature variation of less than 0.5 °C over this distance. Composition change within the alloy due to a temperature gradient was considered to be negligible. The main source of variation in composition was volatilization of alloy during melting and DTA. Two representative alloys were subjected to ten repeated melting and DTA cycles and were then analyzed for silver by the Vollhard method. The change in composition was only 0.03 to 0.04%; therefore the weighed-in compositions are considered to be the compositions of the alloy, to a sufficient degree of accuracy.

Microsections were prepared by grinding with a successively finer grit of diamond paste and briefly polished with chromic oxide. Considerable difficulty was experienced in obtaining scratch-free surfaces of heterogeneous alloys, due to the large difference in hardness of the constituents of such alloys, which consisted of hard and brittle intermetallic phases embedded in a very soft matrix of nearly pure indium. Similar difficulties were encountered in etching these alloys. The soft matrix was attacked by all etching reagents tried, while the intermetallic phases showed great chemical resistance to most reagents. The most suitable etching reagent for heterogeneous alloys was an ammonium persulfate solution, which had the property of coloring the ϕ phase brown whenever it was present, and it thus served to identify this phase under the microscope. Alloys which did not contain the soft indium matrix were dip-etched in nitric acid.

The sample temperature and temperature difference were measured with chromel–alumel thermocouples and a Honeywell Electronic 15 two-pen multirange recorder. All external cables in the measuring circuit were metal shielded to minimize interference from stray potentials. Prior to each experiment the recorder was checked against accurately known potentials. The thermocouple was recalibrated after each four to eight DTA cycles, depending on the working temperature. The principal errors in temperature measurement were estimated to be $\pm$ 1.0 °C due to uncertainty in measuring potential and $\pm$ 0.5 °C due to uncertainty in reading the calibration graph, giving a total estimated error of $\pm$ 1.5 °C.

The furnace temperature was varied with an autotransformer which was driven by an electric motor at an appropriately slow rate. The current for the furnace coil was drawn from the autotransformer. The rate of temperature change in DTA work was 0.8 to 0.5 °C per min, giving a very nearly linear variation of temperature with time.

For X-ray work, the hard and brittle alloys were ground in an agate mortar. Filings were taken from other alloys, using a new file for each alloy. Diffraction patterns were obtained with a cylindrical Debye–Scherrer camera of 114 mm diameter, using Cu K_α radiation. The film used was KK industrial X-ray film. The samples were mounted on a thin glass fiber which had been dipped in silicone grease and rolled in the alloy filings or powder.[2] For high temperature work, a Unicam (19 cm radius) camera was used. The samples were sealed into evacuated quartz capillaries of 0.3 mm diameter, to prevent oxidation. The samples were equilibrated in the camera for at least 24 h, at the desired temperature, prior to diffraction.

Where calculated intensities were compared with

[2]The powder data for the different phases are to be found in ref. 10.

Can. J. Chem. Downloaded from www.nrcresearchpress.com by 210.87.254.6 on 09/05/12
For personal use only.

TABLE 1

Annealing history and composition of indium–silver alloys

Alloy No.	Composition (% Ag)	Time annealed (h)	Annealing temperature (°C)	Quenched* from temperature of (°C)
11	76.69	168	325	
		336	165	165
12	70.15	168	325	
		336	165	165
13	68.68	168	325	
		336	165	165
14	76.69	168	325	
		504	129	
15	73.82	168	325	
		504	129	
16	72.11	168	325	
		504	129	
17	70.15	168	325	
		504	129	
18	68.68	168	325	
		504	129	
19	66.50	168	325	
		504	129	
20	65.28	168	325	
		504	129	
21	62.85	336	135	
22	66.50	336	135	
24	34.00	336	135	
29	55.63	168	325	325
31	55.63	168	225	225
32	55.63	336	135	
26	33.89	672	135	
27	31.97	672	135	

*Samples were quenched in liquid nitrogen. Where no quenching temperature is indicated, the samples were allowed to come to room temperature by spontaneous cooling in air, after they were removed from the furnace.

observed intensities, the multifilm technique was employed. The intensities were assigned values of 1 to 100 and were normalized to the same exposure time. These intensities are thus all relative to the same basis and are self-consistent. Table 1 gives the annealing history and composition of In–Ag alloys used.

Results and Discussion

Differential Thermal Analysis

The system was investigated in the region of composition lying between pure indium and 75% silver. The region 75–100% silver was well established previously and was not investigated by us. In order to be able to present the phase diagram on a sufficiently expanded scale, it is reproduced in two parts, in the temperature ranges 700 to 400 °C and from 300 °C to room temperature, in Figs. 4 and 5, respectively.

Our liquidus agrees very well with that of Weibke and Eggers (3) below 450 °C. At high temperatures, the agreement is not so good, our liquidus lying approximately 8 °C above that of Weibke and Eggers. Points indicated by × in Fig. 4 are those of Weibke and Eggers.

The homogeneous γ-phase region was found to extend to much higher indium concentration than was previously claimed by Weibke and Eggers. The high-temperature γ solidus was established by DTA and the low-temperature γ solidus on the basis of X-ray work and by extrapolation of the high-temperature data.

No temperature arrest was observed at 281 °C. This is in agreement with the X-ray diffraction data, which show that the γ phase continues to exist as an equilibrium phase below 281 °C. If the 281 °C "isotherm" really existed (3) but was not observed by us, then the phase rule would require the existence of a new fourth intermediate phase in the composition range in question; such a phase appears not to exist. Examination of the data of Weibke and Eggers shows that almost all the heat effects they observed, and which they attributed to a constant temperature reaction at 281 °C, occur close to the ε-phase region. We also observed these heat effects but they did not occur at a constant temperature, independent of composition; neither were the peaks on the DTA curves characteristic of an isothermal transformation. These heat effects are due to the phase transformation $\gamma \rightarrow \varepsilon$, as was shown by X-ray diffraction. No experimental basis exists for the assumption of a constant-temperature transformation at 281 °C.

On the silver-rich side of the ε phase, Weibke and Eggers (3) observed similar heat effects, which they attributed to an order–disorder transformation of the γ phase. We also observed these heat effects, but again X-ray diffraction showed that they were due to the $\gamma \rightarrow \varepsilon$ phase transformation. Above the temperature at which these effects occurred, only γ phase was present, while below it, both γ and ε phases were present. No experimental evidence exists to justify the claim for an order–disorder transformation.

We redetermined all the other "isotherms" (halt points) of Weibke and Eggers, except one. Our results agree within 3 °C (Table 2).

Can. J. Chem. Downloaded from www.nrcresearchpress.com by 210.87.254.6 on 09/05/12
For personal use only.

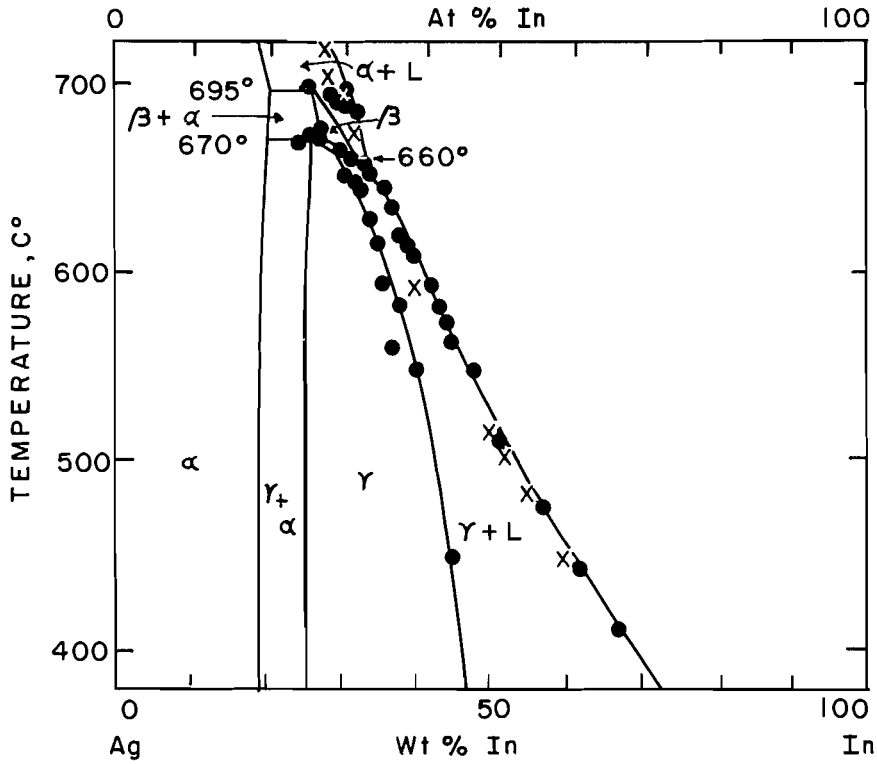

FIG. 4. Phase diagram of Ag–In system in the range 400–700 °C.

TABLE 2

Comparison of isotherms with those of Weibke and Eggers

Temperature (°C)		
This work	Weibke and Eggers	Nature of transformation
144	141	Eutectic
166	166	Peritectic
205	204	Metatectic
660	660	Metatectic
670	667	Peritectoid
695	693	Peritectic

The transformation at 205 °C is a rare case, found in few metal systems. The transformation is, in general, as follows

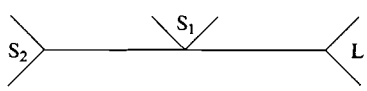

i.e. a solid melts partially as the temperature falls. We call such a transformation "metatectic" (9), but the name has sometimes been applied to a peritectoid reaction. This relatively rare metatectic reaction occurs twice in this system. The 205 °C metatectic reaction manifests itself as intergrain liquefaction of alloys which are cooled rapidly from above 205 °C.

We observed the eutectic temperature arrest, which occurs at 144 °C, at compositions at which it should not occur, viz. at compositions lying between the ε- and ϕ-phase regions. These effects were due to the presence of metastable liquid, which finally froze at the eutectic temperature. The occurrence of these DTA peaks in alloys of compositions such that they should not be present under equilibrium conditions leads to an apparent lengthening of the 144 °C eutectic isotherm; this occurs even with very slow cooling rates. The photomicrograph (Plate 1) shows the trapped eutectic (surrounded by ϕ phase). Plate 2 shows an alloy that was subjected to DTA only, without heat treatment. The substantial amount of γ phase (metastable) surrounded by a narrow rim of ϕ phase (grey) and the large amount of dark-grey indium-rich matrix are clearly visible. After annealing at a temperature of 135 °C (Plate 3), the amount of γ phase has clearly

Can. J. Chem. Downloaded from www.nrcresearchpress.com by 210.87.254.6 on 09/05/12
For personal use only.

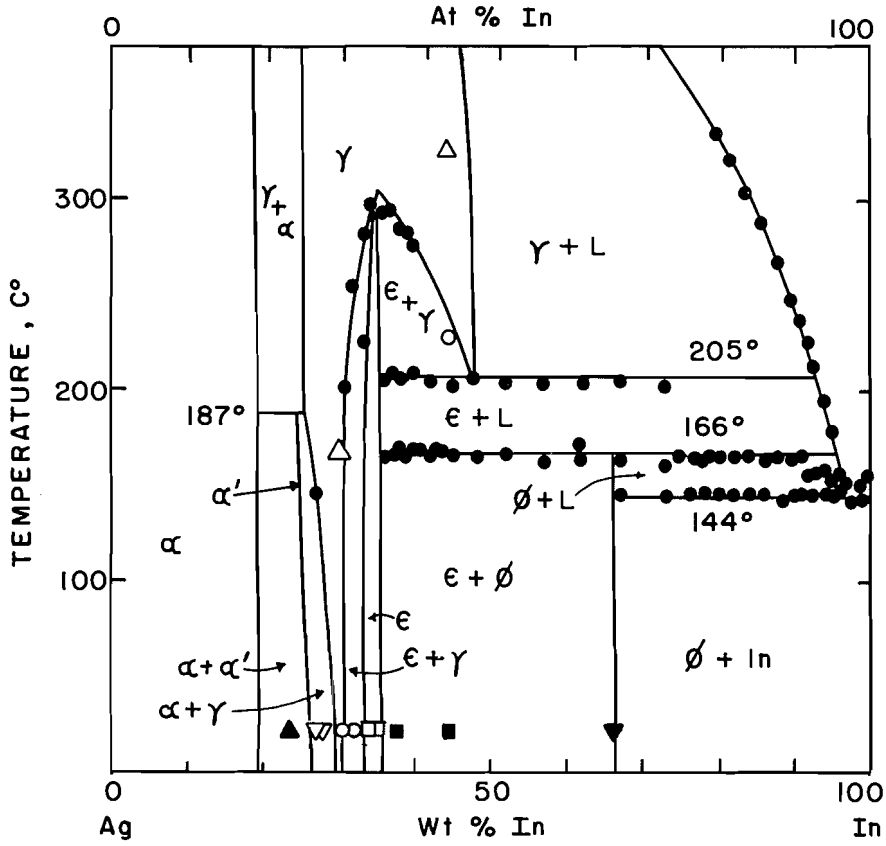

FIG. 5. Phase diagram of Ag–In below 300 °C: ▽, α + γ; ○, ε + γ; □, ε; ■, ε + ϕ; △, γ; ▲, α + α′ (γ phase metastable); ▼, ϕ; ●, DTA.

diminished, as well as that of the indium-rich matrix, while the ϕ phase has increased in amount. Since the γ phase is disappearing with time, and since it is not in physical contact with the matrix, it is metastable with respect to the matrix and the ϕ phase.

Plate 4 reproduces the electron microprobe analysis of an alloy of overall composition 34.00% silver. The areas *AB*, *EF*, *GH*, and *KL* had the same composition, viz. 33.2% silver. The reaction zones *BC*, *DE*, and *HJ* had essentially the same composition as the areas surrounding them, viz. 33.0% silver. The "islands" *CD* and *JK* had an average composition of 70.6% silver. Due to heterogeneity and surface unevenness, the area *FG* (matrix) could not be analyzed quantitatively, but qualitatively it was established that it was nearly pure indium. Within experimental error, the compositions of the areas *AB*, *EF*, *GH*, and *KL* and reaction "rims" corresponded to the composition of the ϕ phase ($AgIn_2$) and the islands had an average composition corresponding to the γ phase.

Plate 5 gives the electron microprobe analysis of an alloy of overall composition 62.50% silver. Areas *AB* and *EF* had the same composition, viz. 66.1% silver; areas *BC* and *DE* both contained 32.3% silver. Within experimental error, the areas *AB* and *EF*, and *BC* and *DE*, corresponded to ε phase and ϕ phase, respectively.

Plate 6 is a photomicrograph of the same alloy as shown in Plate 5. The traverse of the electron beam is shown. The distinct brown color exhibited by the ϕ phase, after etching with ammonium persulphate solution, is characteristic and confirms the electron probe results.

The electron probe analysis showed that an alloy of overall composition 62.50% silver consisted at room temperature of the stable phases ε and ϕ and that an alloy of overall composition 34.00% silver consisted of the stable phase ϕ, an indium-rich matrix, and metastable γ phase,

Can. J. Chem. Downloaded from www.nrcresearchpress.com by 210.87.254.6 on 09/05/12
For personal use only.

PLATE 1. Composition, 61.04% Ag; magnification, ~100×. "Trapped" In phase (dark grey at top) can be seen surrounded by ϕ phase. Major constituent is ε phase.

PLATE 2. Composition, 34.00% Ag; after DTA with no further annealing; magnification ~80×. Reaction rim of the ϕ phase surrounding the "islands" of γ phase (light area) can be seen.

which exists at room temperature even after prolonged annealing at a temperature at which this phase is not stable. The metastable γ phase ("island" of Plate 4) is surrounded by a zone of ϕ phase. The latter phase increases with time, while the γ phase decreases.

Within the range of error of the electron probe, the composition of the ϕ phase can be designated by the formula $AgIn_2$ (31.97% Ag), as suggested by Hellner (6).

The ε Phase and Adjoining Regions

An alloy containing 68.68% Ag is heterogeneous, consisting of γ and ε phases, since lines from both phases appear strongly in the diffraction pattern. An alloy of 66.50% Ag is homogeneous ε phase. From the intensities of diffraction lines of ε and γ phases, respectively, we estimated that the boundary of the ε phase lies at 67.5% Ag, on the silver-rich side. An alloy containing 70.15% Ag contains small amounts of ε phase, since the four strongest lines of the ε phase still appear, but the amount of ε phase is near the limit of detection; we estimate the amount to be 4 or 5% and this places the indium-rich boundary of the γ phase at approximately 70.3% Ag, at room temperature. Alloys containing 65.28 and 66.50% Ag were both homogeneous ε phase. Photomicrographs also failed to reveal any second phase in these alloys.

An alloy containing 62.85% Ag is heterogeneous and consists of ϕ and ε phases. Plate 7, a photomicrograph, shows a small amount of ϕ phase. Therefore, the indium-rich boundary of the ε phase must lie between 65.28 and 62.85% Ag. We estimate it to lie at 65.0% Ag. These boundary compositions are valid for 135° but, since the boundaries are very nearly vertical between 135° and room temperature, they apply fairly accurately at room temperature. The extent of the homogeneous ε phase is approximately 2.5% at room temperature. The compound Ag_2In corresponds to 65.28% Ag and this is within the homogeneous ε-phase range, as Hellner (6) had previously found. Weibke and Eggers (3) estimated the range of homogeneous ε phase to lie between 66.9 and 66.5% Ag, as against our 67.5

Can. J. Chem. Downloaded from www.nrcresearchpress.com by 210.87.254.6 on 09/05/12
For personal use only.

PLATE 3. Composition, 34.00% Ag; annealed 2 weeks at 135 °C; magnification, ~100×. Metastable γ phase (speckled islands) within the ϕ phase (bright areas) can be seen; the black area is In phase.

PLATE 4. Characteristic X-ray picture of electron microprobe scan; magnification, ~350×; composition, 34.00% Ag.

and 65.0% Ag. If the ε phase is assumed to be the stoichiometric compound Ag_2In, then obviously the basic primitive cubic lattice will tolerate a variation in concentration of indium and silver atoms without a fundamental change of lattice, but with cell edge variation. To obtain the cell edges of the limiting phases, viz. at 67.5 and 65.0% Ag, the d values in the range 1.645 Å $\geqslant d \geqslant$ 0.9252 Å of two heterogeneous alloys of 68.68 and 62.85% Ag, respectively, were used to calculate a_0 from the equation $a_0 = d(h^2 + k^2 + l^2)^{\frac{1}{2}}$. The resultant values at room temperature are

$$a_0 = 9.887 \pm 0.004 \text{ Å at } 65.0\% \text{ Ag}$$

$$a_0 = 9.878 \pm 0.004 \text{ Å at } 67.5\% \text{ Ag}$$

Hellner's value of $a_0 = 9.885 \pm 0.005$ Å at Ag_2In (65.28% Ag) falls within the range of our values.

The maximum temperature at which the ε phase is stable, viz. 312 °C, as found by Weibke and Eggers, is in agreement with our observation of the phase transformation ε → γ taking place between 250 and 350 °C. High-temperature X-ray powder diffraction photos of alloys containing 66.50 and 65.28% Ag showed that at 250 °C only the ε phase was present and at 350 °C only the γ phase was present. Thus, heat effects observed by DTA in this composition and temperature range are due to the phase transformation γ → ε. These heat effects were previously attributed by Weibke and Eggers to an order–disorder transformation of the ε phase, although, as they themselves pointed out, X-ray diffraction did not support this explanation. Our work has shown that these heat effects observed by Weibke and Eggers are due to a phase transformation and not an order–disorder transformation of the ε phase.

The α′ Phase

We have discovered a primitive cubic phase, which we designate α′, existing below 187°, at approximately 73.8 wt. % Ag. In the X-ray powder diffraction photographs, weak reflections with (*hkl*) indices not all even or all odd as required by the F lattice of the α phase definitely

Can. J. Chem. Downloaded from www.nrcresearchpress.com by 210.87.254.6 on 09/05/12
For personal use only.

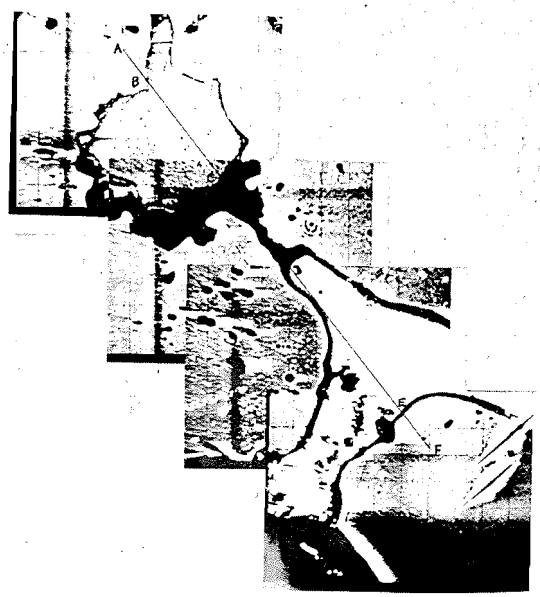

PLATE 5. Characteristic X-ray picture of electron microprobe scan; magnification ~350×; composition, 62.5% Ag.

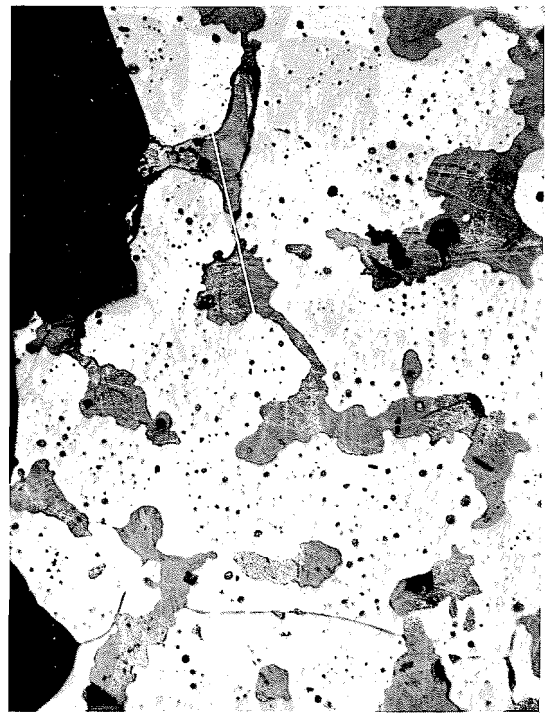

PLATE 6. Composition, 62.5% Ag; magnification, ~100×. Areas of the ϕ phase (dark grey) are traversed by electron beam as indicated.

exist, and therefore this new phase must have a primitive lattice with the same cell edge as the α phase. We were unable to obtain a pure α′ phase. In addition to α′, γ phase and possibly α phase were always present, but the latter phase could not be identified by X-ray diffraction when α′ phase is present, since α and α′ both have the same cell edge. The γ phase is present metastably in the alloy containing 76.69% Ag.

The cell edge of the α′ phase (and of the α phase) is 4.144 ± 0.004 Å, an average calculated from the different diffraction lines in the range 2.395 Å $\geqslant d \geqslant$ 0.7981 Å of the alloy containing 73.82% Ag. The cell edge of the α phase at maximum solution, viz. 4.1447 Å, as given by Owen and Roberts (4), and that of the α′ phase are the same.

We think that the α′ phase is an ordered form of the α solid solution, where one indium atom occupies the corner position (0,0,0) of the cubic cell and the three silver atoms the face-centered positions (0,1/2,1/2, etc.). Such an atomic arrangement results in a primitive cubic lattice and this would account for the observed diffraction lines not allowed by the face-centered lattice. This simple structure could only have the space group *Pm*3*m*. Such an atomic arrangement would also account for the equal lattice parameters of the α and α′ phases. The structure consists of two different types of atoms with different radii. On purely geometric grounds, an interchange of one type of atom from the corner position to the face-centered position and vice versa, would not be expected to change the cell edge, if it is assumed that the spherical atoms touch only in the direction of the face diagonal in each case.

The proposed structure introduces a composition restriction, viz. three silver atoms to one indium atom per unit cell (73.82% Ag). It was at this composition that the diffraction lines with indices *hkl* not all odd or all even were observed to be strongest when compared with the same diffraction lines at other compositions, for example, 76.96 and 72.11% Ag. For this simple structure we calculated the intensities of some of the powder diffraction lines resulting from such an atomic arrangement and compared these calculated intensities with the observed intensities. The results are shown in Table 3, which

Can. J. Chem. Downloaded from www.nrcresearchpress.com by 210.87.254.6 on 09/05/12
For personal use only.

PLATE 7. Composition 62.85% Ag; annealed 2 weeks at 135 °C; magnification ~100×. Small amount of ϕ phase (darker areas) present, main constituent is ε phase.

calls for some explanation. As indicated above, the α′ phase always occurs with the γ phase and possibly also always with the α phase. Thus in Table 3, the X-ray powder data for a sample with composition 73.82% Ag containing α′, γ, and possibly α phases are given, the *d*(obsd.) values in column 1 and the *I*(obsd.) in column 4. The *d*(calcd.) and *hk.l* values for the γ phase are given in column 2, and the *d*(calcd.) and *hkl* values for the (α′ + α) phases in column 3. By comparing columns 1 and 4 with columns 2 and 3, it is possible to ascribe certain of the reflections in the mixed-phase sample to either the (α′ + α) phases or to the α′ phase alone, the latter being those free of γ phase and with *h*, *k*, and *l* not all odd or all even. These reflections are shown in column 3 and are marked with an asterisk. Column 5 then shows, for the α′ phase, the relative intensities, *I*(calcd.), calculated for the first ten possible reflections, assuming the simple ordered primitive structure described above. For the weak reflections due only to the α′ phase (column 3, starred indices), the *I*(calcd.) values (column 5) are in reasonable agreement with the *I*(obsd.) values (column 4). However, for the strong reflections that could be due to both the α and α′ phases, the table shows that the *I*(calcd.) values are all much greater, in relation to the weak reflections, than the *I*(obsd.) values. This suggests that the α′ phase is present without the α phase, but even on this assumption, the *I*(calcd.) values are too great for the strong reflections. We have no explanation for this, but it may relate to the difficulty of estimating by eye the relative intensities on the powder photographs of reflections that differ very widely in intensity. Despite this discrepancy, we feel that the results provide reasonable evidence for our proposed ordered structure for the α′ phase. At 165 °C and 76.69% Ag, the α′ phase still exists but at 325 °C, this phase does not exist as far as could be determined by X-ray diffraction, although the α phase still exists. According to Weibke and Eggers (3), a new phase occurs at 187 °C on cooling. It follows from the above observations that this is the α′ phase. We were unable to establish the extent of the homogeneous existence of the α′ phase, which probably corresponds to Ag_3In, i.e. to approximately 73.8% Ag. The α and α′ phases were indistinguishable microscopically.

The γ Phase and Adjoining Regions

The boundaries of the γ phase were established by DTA and X-ray powder diffraction. The latter technique showed that alloys of 70.50 and 68.68% Ag are both heterogeneous at 129 °C, consisting of (ε + γ) phases, but are both homogeneous (γ) at 165 °C. Therefore, the γ/(γ + ε) boundary must lie between 165 and 129 °C in this composition range. Based on the intensities of the diffraction lines of the two phases (γ + ε) of the heterogeneous alloys, the indium-rich boundary of the γ phase lies at approximately 70.3% Ag. High-temperature X-ray diffraction in the range 300–500 °C showed that these alloys remain single-phased (γ) throughout this temperature range.

At 325 °C, the γ phase has a very wide range of homogeneity. Alloys of 55.63 and 62.85% Ag were heterogeneous when quenched from 225 °C (γ + ε); but were homogeneous (γ) when quenched from 325 and 275 °C. This was evident from photomicrographs of these alloys. Electron microprobe analysis confirmed the identity of these phases. Prior to quenching, the alloys were

Can. J. Chem. Downloaded from www.nrcresearchpress.com by 210.87.254.6 on 09/05/12
For personal use only.

TABLE 3

Comparison of calculated and observed relative intensities (I) for the α′ phase of the Ag–In system

(α′ + γ) phases* d(obsd.), Å	γ phase d(calcd.)†, Å	γ phase $hk.l$	(α′ + α) phases d(calcd.)‡, Å	(α′ + α) phases hkl	(α′ + γ) phases* I(obsd.)	α′ phase I(calcd.)
—	4.794	00.1	—	—	—	—
4.09	—	—	4.144	100§	10	1.25
2.92	—	—	2.930	110§	10	1.11
2.546	2.533	10.0	—	—	200	—
2.395	2.397	00.2	2.393	111	1000	3269
2.255	2.253	10.1	—	—	900	—
2.072	—	—	2.072	200	500	1794
1.786	—	—	1.853	210§	5	0.63
1.748	1.748	10.2	—	—	100	—
—	—	—	1.692	211§	—	0.43
—	1.598	00.3	—	—	—	—
1.466	1.474	11.3	1.465	220	700	1003
—	1.409	11.1	—	—	—	—
—	—	—	1.381	300§	—	0.56
1.353	1.355	10.3	—	—	150	—
—	—	—	1.310	310§	—	0.19
1.270	1.277	20.0	—	—	5	—
1.251	1.256	11.2	1.250	311	750	1162
1.233	1.234	20.1	—	—	40	—
1.196	1.199	00.4	1.196	222	90	—
—	—	—	1.149	320§	—	—
1.129	1.1267	20.2	—	—	20	—
—	—	—	1.108	321§	—	—
—	1.085	10.4	—	—	—	—
1.084	1.084	11.3	—	—	30	—
1.0350	—	—	1.0360	400	20	—
—	—	—	1.0051	410	100	—
0.9963	0.9974	20.3	—	—	—	—
—	—	—	0.9768	411	—	—
—	0.9650	21.0	—	—	—	—
0.9491	0.9507	21.1	0.9507	331	100	—
0.9277	0.9299	11.4	0.9266	420	150	—
0.8969	0.8951	21.2	—	—	80	—

*73.82% Ag.
†d(calcd.) obtained for hexagonal γ phase using $a = 2.961$ Å, $c = 4.778$ Å.
‡d(calcd.) obtained for cubic (α′ + α) phases using $a = 4.144$ Å.
§α′-phase reflections permitted by P lattice but not permitted by the F lattice of the α phase.

equilibrated for 168 h at the respective temperatures. Therefore, in this composition range the γ/(γ + ε) boundary must lie between 275 and 225 °C. The γ → ε transformation was detected in this temperature range by means of DTA. At room temperature these alloys were heterogeneous but the phases were (ε + ϕ) at equilibrium. The γ phase decomposes by a metatectic phase reaction, γ → ε + L, at 205 °C in the composition range of 65.6 to 52.5% Ag, which is followed by the peritectic reaction ε + L → ϕ at 166 °C. Alloys within this composition range which had been quenched from temperatures above 205 °C showed intergrain liquefaction, as can be seen in Plate 8, one of many such. The dark lines between grains and the triangular areas at the grain junctures can be seen clearly as a second phase which is very soft, almost pure indium. When an alloy of such a composition is quenched from above 205 °C, some melting takes place because of the metatectic reaction at this temperature. During the relatively short time required to traverse the temperature interval between 205 and 166 °C, when the alloy is quenched, only a small amount of liquid can form. Melting occurs first at the grain boundaries as in normal melting, as can be seen in Plate 8. As far as we could ascertain, the ϕ phase does not form under these drastic conditions, and the liquid remains as such until it freezes to the indium-rich intergrain phase seen in the photomicrograph. The γ phase solidus was established by DTA and X-ray diffraction, which showed that at 55.63% Ag and 325 °C the alloy is homogeneous (γ), and that it remains as such in the temperature range 325 to 555 °C. These findings, together with DTA data,

Can. J. Chem. Downloaded from www.nrcresearchpress.com by 210.87.254.6 on 09/05/12
For personal use only.

Can. J. Chem. Downloaded from www.nrcresearchpress.com by 210.87.254.6 on 09/05/12
For personal use only.

PLATE 8. Composition 55.63% Ag; quenched from 325 °C; magnification ~100×. Intergrain liquefaction is evident. Dark lines between grains are due to solidified indium phase produced by metatectic reaction.

convince us that the γ solidus must be at a concentration lower than 55.63% Ag at 325 °C, viz. 52.5% Ag, as compared to 66.3% Ag according to Weibke and Eggers (3).

On the silver-rich side of the γ phase, X-ray diffraction of alloys of 76.69, 73.82, and 72.11% Ag, which were annealed at 129 °C for three weeks or longer, showed that these alloys were heterogeneous, consisting of (α′ + γ) phases. The intensities of diffraction lines belonging to the α′ phase were lowest for the 72.11% Ag alloy, though the α′ phase was still present in small amount in this alloy at 129 °C. The silver-rich boundary of the γ phase is estimated to lie at 71.0% Ag at room temperature. Since the indium-rich boundary is at approximately 70.3% Ag, the composition range of the γ phase must be less than 1% at room temperature. At 325 °C the 76.69% Ag alloy contained some α phase but no α′ phase, while the 72.11% Ag alloy consisted of γ phase only. The latter observations are in agreement with those of other investigators (3, 6). The high-temperature phase boundary of the γ phase on the silver-rich side down to 187 °C must be essentially correct as previously established (3).

Hellner (6) had found that an alloy of composition corresponding to Ag_3In (73.82% Ag) was homogeneous (γ) at room temperature. As mentioned previously, we found that an alloy of this composition is heterogeneous at 129 °C, consisting of (α′ + γ), when sufficiently annealed. On the other hand, when this alloy was annealed for only one week at 165 °C, the alloy was homogeneous (γ). The same result was obtained by annealing at 129 °C for one week. The metastable γ phase is thus easily retained at room temperature. Hellner's observation is readily explained in terms of insufficient annealing.

According to our phase diagram, an alloy of 76.69% Ag should not contain γ phase below 187 °C. In practice, even after three weeks of annealing at 129 °C, γ phase was still present. That the γ phase is not stable at this overall composition at room temperature can be seen from a comparison of the photomicrographs in

PLATE 9. Composition 76.69% Ag; annealed 21 days at 129 °C; magnification ~100×. Shows presence of γ phase, α′ phase, and probably also α phase.

TABLE 4

Comparison of cell edges of γ phase at room temperature

Source	Composition	Value (Å)	
		a	*c*
Goldschmidt (1)	Ag_3In	2.956±0.003 (2.950 kx)	4.779±0.005 (4.769 kx)
Hellner (6)	$Ag_{68}In_{32}$ (66.63% Ag)	2.983	4.789
This work	70.3% Ag	2.961±0.002	4.778±0.004

PLATE 10. Same alloy as Plate 9; left for 2 months at room temperature; magnification ~100×, γ phase reacting at grain boundaries.

Plates 9 and 10. Plate 9 is a photomicrograph of the alloy after annealing for three weeks at 129 °C. Plate 10 is a photomicrograph of the same alloy after it had been left for two months at room temperature. It is obvious that the γ phase is slowly transforming, particularly at the grain boundaries, presumably to the (α + α′) phases. (The latter two phases cannot be differentiated by X-ray diffraction when both are present in the alloy.)

The diffraction lines of the hexagonal γ phase were indexed and the best cell dimensions were determined. The *a* and *c* values are

$$a = 2.961 \pm 0.002 \text{ Å}$$

$$c = 4.778 \pm 0.004 \text{ Å}$$

These cell dimensions were calculated from the powder diffraction pattern of an alloy containing 70.15% Ag, using the *d* values in the range 2.263 Å $\geqslant d \geqslant$ 0.9298 Å. This alloy contained some ε phase and therefore the calculated cell edges apply to the indium-rich phase boundary of the γ phase, viz. at 70.3% Ag. Since this phase has a very small composition range at room temperature (less than 1%), the cell edges will be very nearly the same at both boundaries. The cell edges determined by Goldschmidt (1), Hellner (6), and ourselves are given in Table 4.

The substantial difference in the cell dimensions obtained by Hellner and ourselves suggests further that it is difficult to bring the γ phase to thermodynamic equilibrium at room temperature, and that this has not always been realized before. This conclusion is further supported by the fact that we found an alloy of 73.82% Ag to be heterogeneous, consisting of (γ + α′) phases at room temperature, whereas Hellner found the same alloy to be a homogeneous (γ) phase.

1. V. M. GOLDSCHMIDT. Z. Phys. Chem. Leipzig, **133**, 397 (1928).
2. L. L. FREVEL and E. OTT. J. Amer. Chem. Soc. **57**, 228 (1935).
3. F. WEIBKE and H. EGGERS. Z. Anorg. Allg. Chem. **222**, 145 (1935).
4. W. HUME-ROTHERY, G. W. MABBOTT, and K. M. CHANNEL-EVANS. Phil. Trans. Roy. Soc. London, Ser. A, **233**, 1 (1934).
5. D. P. MORRIS and T. WILLIAMS. Acta Cryst. **14**, 74 (1961).
6. E. HELLNER. Z. Metallk. **42**, 17 (1951).
7. E. HELLNER and F. LAVES. Z. Naturforsch. **2a**, 177 (1947).
8. E. A. OWEN and E. W. ROBERTS. Phil. Mag. **27**, 294 (1939).
9. A. PRINCE. Alloy phase equilibria. Elsevier Publ. Co., Inc., New York. 1966. p. 115.
10. R. WAGEMANN. Ph.D. Thesis, University of Manitoba, Winnipeg, Manitoba.

Can. J. Chem. Downloaded from www.nrcresearchpress.com by 210.87.254.6 on 09/05/12
For personal use only.

Can. J. Chem. Downloaded from www.nrcresearchpress.com by 210.87.254.42 on 09/05/12
For personal use only.

Réactions photochimiques de la caféine avec les éthers

S. JERUMANIS ET A. MARTEL
Département de chimie, Université de Sherbrooke, Sherbrooke, Québec

Reçu le 22 juillet 1969

Les auteurs ont étudié la réaction photochimique de la caféine avec le dioxane, le tétrahydrofuranne, le tétrahydropyranne, l'anisol, et l'éther éthylique. Par l'irradiation ultraviolette d'une solution aqueuse de la caféine et d'un éther cyclique en présence de la benzophénone ou de l'acétophénone, on observe la substitution de l'hydrogène en position 8 de la caféine par le radical éther. La réaction photochimique de la caféine avec l'éther éthylique donne la (éthoxy-1 éthyl)-8 caféine et l'éthyl-8 caféine tandis qu'en présence de l'anisol la caféine se révèle inerte. Les structures des composés obtenus ont été déterminées par la spectroscopie infrarouge, la résonance magnétique nucléaire, et la spectrosmétrie de masse.

The photoreaction of caffeine with dioxane, tetrahydrofuran, tetrahydropyran, anisole, and ethyl ether has been studied. Ultraviolet irradiation of aqueous solutions of caffeine and cyclic ethers in the presence of benzophenone or acetophenone using a pyrex filter yields substitution products. Substitution occurs at the 8-position of caffeine. The photoreaction of caffeine with ethyl ether gives 8-(1-ethoxyethyl)-caffeine and 8-ethylcaffeine while in the presence of anisole caffeine has been found to be completely inert. The structures were determined by infrared, nuclear magnetic resonance, and mass spectrometry.

Canadian Journal of Chemistry, **48**, 1716 (1970)

Introduction

Dans la littérature récente, les études de la xanthine et de ses dérivés au point de vue photochimique se retrouvent en nombre restreint. En 1964 M. I. Simon et H. Van Vanukis (1) constatent que l'oxygénation photosensibilisée de la théophylline donne lieu à la formation de la diméthyl-1,3 allantoïne. Egalement, une réaction analogue se présente dans le cas de la xanthine (2) où l'on remarque que cette dernière est dégradée en allantoïne en passant par le peroxyde cyclique.

Dans le cadre d'une étude systématique des réactions photochimiques des dérivés de la xanthine avec divers types de molécules organiques, nous avons concentré notre attention sur les réactions de la caféine avec les éthers cycliques, aliphatiques, et aromatiques tels le dioxane, le tétrahydrofuranne, le tétrahydropyranne, l'anisol, et l'éther éthylique.

Considérant d'une façon générale la réaction photochimique des éthers en présence des composés insaturés, on remarque que l'éther peut s'additionner sur une double liaison carbone–carbone isolée ainsi que sur une double liaison conjuguée pour donner les éthers α alkylés correspondants (3–5).

On observe un autre type de réaction avec la phénanthrènequinone (6) donnant lieu à une addition 1,4 sur des oxygènes quinoniques.

D'autre part, il fut possible récemment d'obtenir un composé de substitution par la réaction d'un éther sur une double liaison conjuguée avec un groupement carbonyle. Ainsi la photolyse de la naphthoquinone-1,4, en utilisant un filtre de verre Wertheimer, en présence de dioxane donne le dioxanyl-2, naphthoquinone-1,4 (7).

Pour étudier le comportement photochimique de la caféine toutes les réactions ont été effectuées en milieu aqueux en présence de la benzophénone ou de l'acétophénone comme initiateur et sous atmosphère d'azote. En général, l'irradiation ultraviolette (u.v.) d'une solution aqueuse de caféine et d'éther cyclique en présence de la benzophénone ou de l'acétophénone donne un produit de substitution (eq. [1]).

[1] 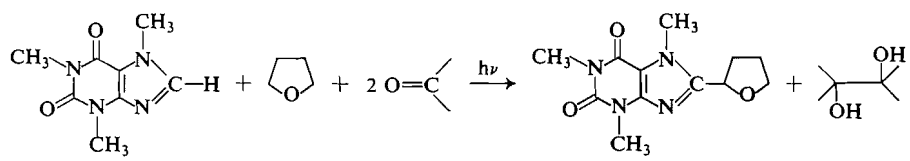

Can. J. Chem. Downloaded from www.nrcresearchpress.com by 210.87.254.42 on 09/05/12
For personal use only.

Au cours de cette réaction l'éther se fixe en position α sur le carbone 8 de la caféine et la cétone subit une réduction en pinacol. Toutefois dans le cas d'éther aliphatique on obtient également le produit de substitution mais aussi un autre produit de réaction l'éthyl-8 caféine, provenant de la rupture de la liaison C—O de l'éther. L'anisol par contre, ne donne pas de réaction avec la caféine quelles que soient les conditions, c'est-à-dire le solvant et l'initiateur utilisé. Toutefois il faut remarquer que l'initiateur employé, soit la benzophénone ou l'acétophénone, est réduit en pinacol. Egalement, la réaction s'avéra négative même dans le cas d'irradiation directe, car l'on retrouve toujours la caféine intacte.

Resultats et discussions

Réaction de la caféine avec le dioxane

Une quantité équivalente de caféine et de benzophénone dissous dans un mélange de dioxane et d'eau, préalablement désoxygéné, est exposée à la lumière u.v. à travers le filtre de pyrex. Après quelques heures d'irradiation un solide blanc se forme dans le milieu réactionnel. La réaction terminée, ce solide blanc est filtré et identifié comme étant le benzopinacol. En effet son point de fusion 186–188 °C, le spectre de masse à *m/e* 366, indiquant un ion moléculaire, le spectre de résonance magnétique nucléaire (r.m.n.), et infrarouge (i.r.) confirment la structure du pinacol. Après l'évaporation du solvant à une température peu élevée le résidu est alors chromatographié sur l'oxyde d'aluminium en couche mince. De cette façon il est possible d'isoler un solide blanc, p.f. 200.5–202 °C, avec un bon rendement. Le même solide blanc est isolé en le faisant précipiter par l'acétone dans les eaux mères concentrées. Détermination de la structure de cette substance par les mesures spectroscopiques montre qu'il y a une substitution d'hydrogène au cours de la réaction sur le carbone 8 de la caféine par le radical dioxanyle pour donner ainsi la dioxanyl-8 caféine. Sur le spectre i.r. on observe toutes les bandes caractéristiques de la caféine et également l'apparition de bandes CH_2 aliphatique dans la région de 2850 à 3000 cm^{-1}. La nouvelle bande prenant naissance à 1115 cm^{-1} confirme la présence du lien C—O—C.

De plus, étant donné que les bandes caractéristiques des carbonyles conjugué et non conjugué de la caféine demeurent inchangées à 1705 et 1660 cm^{-1}, de même que les bandes des liens C=C et C=N à 1605 et 1545 cm^{-1} sont présentes nous pouvons conclure que la caféine a réagi sans subir une transformation appréciable de sa structure.

Par le spectre de r.m.n. on note la disparition de l'hydrogène en position 8 de la caféine, qui apparaissait sous forme de singulet à 7.55 δ. Toutefois, l'apparition d'un multiplet entre 3.75 et 3.95 δ, représente les protons des carbones 6′ et 5′ du dioxanyle, l'intégrale confirmant la présence de quatre protons par rapport aux singulets des méthyles de la caféine; ces derniers étant déplacés de quelques c.p.s. vers les bas champs. Par la suite on remarque un doublet à 4.10 δ (J = 6 c.p.s.) dont l'intégrale confirme les deux hydrogènes en position 3′. Finalement un triplet à 4.80 δ (J = 6 c.p.s.) est interprété comme étant le signal du proton sur le carbone 2′ du dioxanyle.

Dans le spectre de masse on observe un ion moléculaire à *m/e* 280 et l'on peut également identifier le fragment de la caféine à *m/e* 193.

Réaction de la caféine avec le tétrahydrofuranne (THF)

L'irradiation de la caféine dans un mélange d'eau et de tétrahydrofuranne (THF), à l'aide d'une lampe au mercure à pression moyenne, utilisant un filtre de pyrex et en présence de la benzophénone, devrait donner lieu à une réaction déjà observée avec la caféine et le dioxane. En effet, après évaporation totale du solvant et séchage sur le sulfate de magnésium, il est possible d'isoler, par la chromatographie sur alumine, un solide blanc, p.f. 127–128 °C, le tétrahydrofuryl-2′,8 caféine.

En premier lieu, considérant le spectre i.r.,

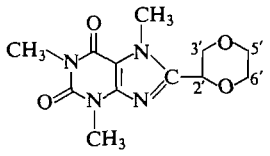

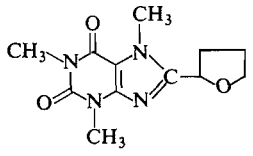

Can. J. Chem. Downloaded from www.nrcresearchpress.com by 210.87.254.42 on 09/05/12
For personal use only.

on doit noter que l'apparition de nouvelles bandes plus fortes entre 2870 et 3000 cm^{-1} confirment la présence du groupe CH_2 aliphatique. Aux environs de 1050 cm^{-1} on remarque les bandes dues aux vibrations du lien C—O—C. Les absorptions correspondant aux vibrations des liens C=C et C=N ainsi qu'aux groupes carbonyles conjugué et non conjugué demeurent inchangées.

L'examen du spectre de r.m.n. dénote la disparition du singulet dû à l'hydrogène en position 8 de la caféine tandis qu'à 5.05 δ apparaît un triplet (J = 6 c.p.s.) qui est causé par le proton en position 2′ de la tétrahydrofurylecaféine. On peut noter, dans le cas du THF, que les protons en α de l'oxygène donnent un signal à 3.92 δ et dans le produit de réaction, le proton en position 2′ subit un déplacement vers les bas champs de 1.13 δ. Une remarque similaire s'effectue pour le proton en α de l'oxygène dans le dioxane qui subit un déplacement de 1.10 δ vers les bas champs lorsqu'il se retrouve en position 2′. Les protons sur le carbone 5′ apparaissent sous la forme d'un triplet à 3.92 δ (J = 6 c.p.s.) et on observe alors un déplacement de 0.19 δ par rapport aux mêmes hydrogènes du THF. Concernant enfin les hydrogènes sur les carbones 3′ et 4′, ces derniers sont indiqués par un multiplet complexe se situant entre 1.75 et 2.80 δ et dont l'intégrale est 4.

La structure de ce produit est confirmée davantage par le spectre de masse révélant l'ion moléculaire à *m/e* 264 de même que le fragment significatif à *m/e* 193.

Réaction de la caféine avec le tétrahydropyranne (THP)

La photolyse d'un mélange de caféine en présence de l'acétophénone et de THP, utilisant l'eau et l'alcool butylique tertiaire comme solvant, est effectuée à travers le pyrex à l'aide d'une lampe au mercure à 450 W grande pression. Au terme de la réaction, on isole un composé blanc, p.f. 156–157 °C, lequel par les méthodes spectroscopiques d'analyse est identifié comme étant le tétrahydropyranyl-8 caféine.

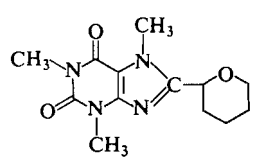

Tout d'abord le spectre i.r. de ce composé fait voir l'apparition de nouvelles bandes à 2990, 2940, et 2820 cm^{-1}, de même qu'une absorption à 1440 cm^{-1} beaucoup plus intense en comparaison à celle de la caféine. Cette série de bandes suggère l'existence de CH_2 aliphatique. De plus, la présence d'une nouvelle bande à 1085 cm^{-1} confirme les vibrations du lien C—O—C.

Le spectre de r.m.n. montre un multiplet complexe entre 1.52 et 2.28 δ dû à l'existence des protons en positions 3′, 4′, et 5′. Les deux protons en position 6′ sont responsables d'une absorption entre les deux singulets dus aux protons des méthyles de la caféine apparaissant respectivement à 3.45 et 3.62 δ. Le signal du proton en position 2′ donne un multiplet situé entre 4.45 et 4.75 δ. Il subit un déplacement de 0.96 δ vers les bas champs par rapport aux hydrogènes en α du THP.

En déterminant le poids moléculaire par la spectrométrie de masse, on distingue l'ion moléculaire à *m/e* 278 et le fragment de la caféine à *m/e* 193.

Réaction de la caféine avec l'éther éthylique

Nous avons constaté que l'éther éthylique, dans les conditions décrites pour la réaction avec le THP réagit avec la caféine de deux façons différentes. Une réaction procédant selon le mode déjà indiqué, à savoir la substitution de l'hydrogène par le radical éther donne la (éthoxy-1 éthyl)-8 caféine (eq. [2]), p.f. 115–116 °C, tandis que la seconde réaction conduit à l'éthyl-8 caféine, p.f. 187–188.5 °C (litt. p.f. 189.5–191 °C) (8). La proportion relative de ces deux produits est 3:1.

1. La (éthoxy-1 éthyl)-8 caféine

Le spectre i.r. de ce composé fait apparaître une bande d'absorption à 2980 cm^{-1}, un épaulement à 2940 cm^{-1}, une bande faible à 2880 cm^{-1} en plus d'une absorption plus intense à 1460 cm^{-1} prouvant ainsi l'existence des groupes CH_3 et CH_2 aliphatiques. Une absorption à 1110 cm^{-1} confirme les vibrations du lien C—O—C.

Un triplet à 1.20 δ (J = 6 c.p.s.) dans le spectre de r.m.n. est dû à l'absorption des protons du méthyle de l'éthoxyle. Le doublet apparaissant à 1.60 δ (J = 7 c.p.s.) suggère l'existence des protons du méthyle 2′ tandis que les protons des deux méthyles de la caféine absorbant à 3.38 et 3.55 δ, masquent partielle-

[2] 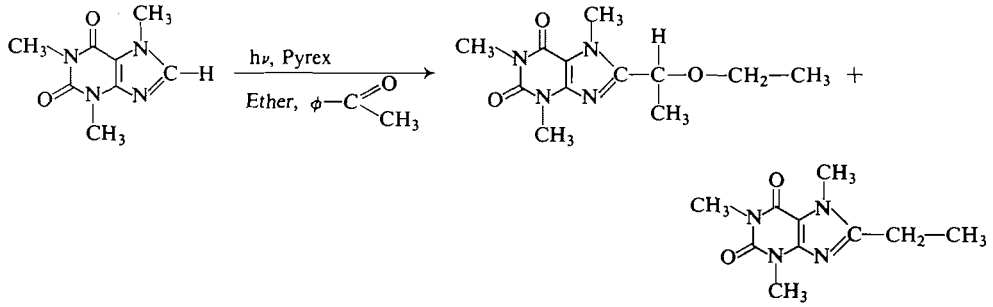

ment le quadruplet (J = 6 c.p.s.) des protons du CH_2 de l'éthoxyle. On remarque également un singulet à 4.08 δ (3 protons) et un quadruplet à 4.76 δ (J = 7 c.p.s.); ce dernier est interprété comme étant dû au proton en position 1 qui set couplé avec les protons du méthyle adjacent.

La spectrométrie de masse révèle un ion moléculaire à *m/e* 266 de même que des fragments très significatifs à *m/e* 251, 221, et 45.

2. Produit secondaire

Ce composé est caractérisé dans i.r. par des bandes d'absorption des CH_3 et CH_2 aliphatiques et par les absorptions des C=O, C=N et C=C dont les positions restent inchangées. Le spectre de r.m.n. montre un triplet à 1.35 δ (J = 7 c.p.s.) correspondant aux protons du méthyle en position 1, lesquels sont couplés avec les hydrogènes du CH_2 apparaissant sous la forme d'un quadruplet à 2.76 δ (J = 7 c.p.s.). Par spectrométrie de masse on note un ion moléculaire à *m/e* 222 et un fragment à *m/e* 193.

Partie expérimentale

Les spectres i.r. ont été pris sur un spectrophotomètre Perkin–Elmer modèle 257 en solution de $CHCl_3$ à 10% dans les cellules de KBr 0.1 mm d'épaisseur.

Les mesures de r.m.n. ont été effectuées à l'aide d'un appareil "Varian" modèle A60. Le tétraméthylsilane servant de référence interne, le solvant utilisé fut le $CDCl_3$.

Les points de fusion ont été déterminés en tubes capillaires au moyen d'un appareil Büchi et ne sont pas corrigés.

Les analyses élémentaires ont été effectuées par "Schwarzkopf Microanalytical Laboratory" de New York.

Les spectres de masse ont été enregistrés par un appareil Hitachi–Perkin–Elmer modèle RMU-6D.

1. Réaction de la caféine avec le dioxane

Dans un ballon de pyrex, on solubilise 1.0 g de caféine et 1.0 g de benzophénone dans une solution composée de 500 ml d'eau et 300 ml de dioxane. Le mélange est alors désoxygéné en faisant barboter durant 30 min, sous bonne agitation, un courant d'azote. Ensuite, ayant constamment une atmosphère d'azote dans le système, on irradie la solution avec une lampe Hanovia "MPL" de 140 W durant 30 jours.

1.1 Identification du benzopinacol

Le précipité blanc formé au cours de la réaction est filtré et recristallisé deux fois dans un mélange benzène – éther de pétrole 2:1. On retrouve ainsi des cristaux blancs, p.f. 185–188 °C, rendement 100%. Spectre i.r.: bandes à 3550, 3050, et 3000 (moyennes), 1590 (faible), 1490 et 1445 (fortes), 1165, 1030, et 700 cm^{-1} (fortes). Le spectre de r.m.n.: doublet aromatique à 7.25 (20H) et singulet à 3.05 δ (2H); le rapport étant 10:1. Le spectre de masse: *m/e* 366: $[(C_6H_5)_2COH—COH(C_6H_5)_2]^+$; *m/e* 348: $(C_6H_5)_2\overset{+}{C}—COH(C_6H_5)_2$; *m/e* 183: $(C_6H_5)_2\overset{+}{C}OH$; *m/e* 77: $C_6H_5^+$.

1.2 Identification du dioxanyl-8 caféine

Le filtrat est alors évaporé presqu'au complet et le résidu dissous dans le chloroforme puis séché sur $MgSO_4$. Après l'évaporation du $CHCl_3$ on retrouve un produit orange. Le spectre de r.m.n. de ce dernier indique qu'environ 50% de la caféine a réagi et on n'observe plus de benzophénone. Ensuite ce produit orange est chromatographié sur la silice en plaque mince en éluant avec le $CHCl_3$. Sur la plaque on observe quatre produits qui sont extraits avec le méthanol. Toutefois il est possible d'en identifier seulement deux: la caféine et la dioxanyl-8 caféine. Le produit de réaction est isolé en évaporant complètement le MeOH puis en solubilisant le résidu dans le $CHCl_3$. Le solide blanc ainsi obtenu est recristallisé dans un mélange d'acétone et de chloroforme. Poudre blanche, p.f. 200.5–202 °C (rendement 60–70% de la théorie, en fonction de la benzophénone utilisée). Spectre i.r.: bandes à 3000, 2970, 2930, et 2860 (moyennes), 1705 et 1660 (très fortes), 1605 (faible), 1545, 1440, et 1340 (moyennes), 1090 et 1075 (fortes), 1040 cm^{-1} (moyenne). Le spectre de r.m.n.: multiplet entre 3.75 et 3.95 (4H), doublet à 4.10, J = 6 c.p.s. (2H), un triplet à 4.80, J = 6 c.p.s. (1H), singulet à 3.40 (3H), 3.57 (3H) et 4.08 δ (3H).

Anal. calculé pour $C_{12}H_{16}N_4O_4$: C, 51.43, H, 5.75; O, 22.83. Trouvé: C, 51.24; H, 5.94; O, 23.00.

Spectre de masse: *m/e* 280: $\overset{+}{I}$-D; *m/e* 251: II-D; *m/e* 223: III-D; *m/e* 193: $\overset{+}{I}$; *m/e* 82: $CH_3—N=\dot{C}—C\equiv\overset{+}{N}—CH_3$; *m/e* 67: $N\equiv C—C\equiv\overset{+}{N}—CH_3$; *m/e* 55: $[N\equiv C\equiv N—CH_3]^+$.

Can. J. Chem. Downloaded from www.nrcresearchpress.com by 210.87.254.42 on 09/05/12
For personal use only.

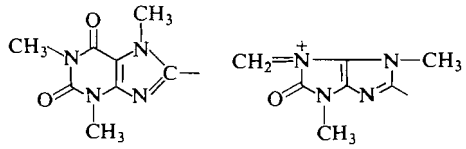

I II

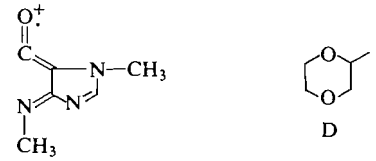

III D

2. Réaction de la caféine avec le tétrahydrofuranne

En utilisant une lampe Hanovia 140 W à pression moyenne et un filtre de pyrex, on irradie durant 30 jours et sous atmosphère d'azote une solution désoxygénée de 400 ml de THF et 450 ml d'eau contenant 1.0 g de caféine et 1.0 g de benzophénone. On remarque que pendant la réaction le pinacol ne précipite pas. Toutefois il est séparé sous forme de gomme insoluble dans l'eau à la fin de la réaction lorsque le THF est évaporé. Le liquide restant est ensuite évaporé puis le résidu est solubilisé dans le $CHCl_3$ et séché sur $MgSO_4$. Le spectre de r.m.n. de ce produit brut indique seulement une trace de caféine non réagie. Par chromatographie en couche mince sur alumine, on visualise avec un mélange d'iode, de KI, de HCl 0.25%, et d'éthanol, deux produits dont l'un n'a pu être identifié. Le second est séparé et isolé par cette méthode à l'échelle préparative, utilisant le $CHCl_3$ comme éluant. Ainsi après l'extraction avec l'alcool méthylique et recristallisation dans l'éther on obtient 0.4 g (66% de rendement théorique) d'un produit blanc, p.f. 127–128 °C. Le spectre i.r.: bandes à 3000, 2950, et 2870 (moyennes), 1705 et 1660 (très fortes), 1605 (faible), 1545 et 1445 (moyennes), 1410 (moyenne), 1053 (épaulement), 1040 cm^{-1} (moyenne). Spectre de r.m.n.: multiplet complexe entre 1.75 et 2.80 (4H), triplet à 3.92, $J = 6$ c.p.s. (2H), triplet à 5.05, $J = 6$ c.p.s. (1H) et les singulets à 3.40, 3.55, et 4.05 δ dont les intégrales respectives représentent 3 protons.

Anal. calculé pour $C_{12}H_{16}N_4O_3$: C, 54.97; H, 6.07. Trouvé: C, 54.45; H, 6.21.

Spectre de masse: *m/e* 264: I-THF; *m/e* 234: II-THF, *m/e* 193: $\overset{+}{I}$; *m/e* 82: $CH_3—N{=}\dot{C}—C{\equiv}\overset{+}{N}—CH_3$; *m/e* 71: $\overset{+}{THF}$; *m/e* 67: $N{\equiv}C—C{\equiv}\overset{+}{N}—CH_3$.

3. Réaction de la caféine avec le tétrahydropyranne

Un mélange réactionnel composé de 475 ml d'eau, 475 ml de butanol tertiaire, 100 ml de THP ainsi que 3 ml d'acétophénone et 1.0 g de caféine est irradié durant 11 jours à l'aide d'une lampe Hanovia 450 W grande pression à travers le pyrex. Après l'évaporation du THP et du butanol tertiaire le pinacol précipite sous forme d'une gomme insoluble dans l'eau et qui est alors séparé par décantation. De la solution restante, le solvant est évaporé et ce qui en résulte est solubilisé dans le $CHCl_3$ et séché sur $MgSO_4$. Par chromatographie en couche mince sur alumine et en éluant avec le $CHCl_3$, on vérifie qu'il n'y a qu'un produit principal. Après le séchage le chloroforme est évaporé et le produit obtenu est recristallisé deux fois dans un mélange méthanol–ether 10:1. Le précipité se présente alors sous la forme d'une poudre blanche, p.f. 156–157 °C, rendement 65%. Le spectre i.r.: bandes à 3005, 2980, et 2860 (moyennes), 1705, 1660 (très fortes), 1545, 1445 (moyennes), 1085, 1040 cm^{-1} (moyennes). Spectre de r.m.n.: multiplet complexe entre 1.52 et 2.28 (6H), singulets à 3.45 (3H), absorption de 3.45 à 3.62 (5H), singulet à 4.10 (3H), multiplet entre 4.45 et 4.75 δ (1H).

Anal. calculé pour $C_{13}H_{18}N_4O_3$: C, 56.09; H, 6.52; N, 20.13. Trouvé: C, 55.65; H, 6.82; N, 19.31.

Spectre de masse: *m/e* 278: $\overset{+}{I}$-THP; *m/e* 221: III-THP; *m/e* 194: IV-THP; *m/e* 193: $\overset{+}{I}$; *m/e* 82: $CH_3—N{=}\dot{C}—C{\equiv}\overset{+}{N}—CH_3$; *m/e* 67: $N{\equiv}C—C{\equiv}\overset{+}{N}—CH_3$; *m/e* 55: $[N{=}\dot{C}{=}N—CH_3]^+$.

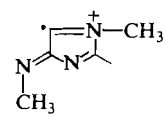

IV

4. Réaction de la caféine avec l'éther éthylique

Un mélange réactionnel comprenant 1 g de caféine, 5 ml d'acétophénone et 150 ml d'éther éthylique est solubilisé dans 950 ml d'eau et de butanol tertiaire 1:1. L'irradiation de la solution est effectuée à l'aide d'une lampe Hanovia 450 W grande pression utilisant un filtre de pyrex. Après 180 h d'exposition à la lumière u.v., on chasse le butanol tertiaire et l'éther sous pression réduite, à température peu élevée. L'acétophénone réduite précipite. On le sépare, et après l'évaporation de l'eau on retrouve un produit blanc qui est alors redissous dans le chloroforme et séché sur $MgSO_4$. Par chromatographie en couche mince sur la silice et éluant avec un mélange acétone – tétrachlorure de carbone 1:1 on observe deux produits qui sont alors isolés en travaillant à l'échelle préparative, rendement global: 50–60%.

4.1 Identification de la (éthoxy-1 éthyl)-8 caféine

Le premier produit est d'abord recristallisé dans un mélange de chloroforme – éther de pétrole – éther éthylique 1:1:10 puis dans un mélange éther éthylique – éther de pétrole 10:1. On obtient ainsi une poudre blanche, p.f. 116–117 °C. Spectre i.r.: bandes à 2970 (moyenne), 2880 (faible), 1705, 1660 (très fortes), 1605 (faible), 1545, 1455 (fortes), 1230 (moyenne), 1110 (forte), 1045 cm^{-1} (moyenne). Spectre de r.m.n.: triplet à 1.20, $J = 6$ c.p.s. (3H), doublet à 1.60, $J = 7$ c.p.s. (3H), singulets à 3.38 (3H), 3.55 (3H), 4.07 (3H), quadruplet à 3.46, $J = 6$ c.p.s. (2H), quadruplet à 4.76 δ, $J = 7$ c.p.s. (1H).

Anal. calculé pour $C_{12}H_{18}N_4O_3$: C, 54.12; H, 6.81; N, 21.04. Trouvé: C, 54.28; H, 6.99; N, 21.19.

Spectre de masse: *m/e* 266: $\overset{+}{I}$-$CH(CH_3)OCH_2CH_3$; *m/e* 251: I-$\overset{+}{C}H—O—CH_2CH_3$; *m/e* 221: I-$\overset{+}{C}HCH_3$; *m/e* 164: III′-$\overset{+}{C}H—CH_3$; *m/e* 82: $CH_3—N{=}\dot{C}—C{\equiv}$

Can. J. Chem. Downloaded from www.nrcresearchpress.com by 210.87.254.42 on 09/05/12
For personal use only.

$\overset{+}{N}—CH_3$; *m/e* 67: $N\equiv C—C\equiv\overset{+}{N}—CH_3$; *m/e* 55: $[N\equiv C—\overset{+}{N}—CH_3]^+$; *m/e* 45: $CH_3—CH_2O^+$; *m/e* 29: $CH_3—CH_2^+$.

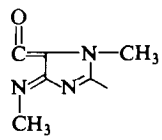

III′

4.2 Identification de l'éthyl-8 caféine

Le second produit est recristallisé dans un mélange éther éthylique – chloroforme 5:1. On retrouve une poudre blanche, p.f. 187–188.5 °C, (litt. (8) p.f. 189.5–191 °C) représentant 25% du rendement global. Spectre i.r.: bandes à 2975 (moyenne), 2875 (faible), 1705, 1660 (très fortes), 1605 (faible), 1545 (forte), 1460 (moyenne), 1380 cm^{-1} (faible). Spectre de r.m.n.: triplet à 1.35, $J = 7$ c.p.s. (3H), quadruplet à 2.76, $J = 7$ c.p.s. (2H), singulet à 3.37 (3H), singulet à 3.55 (3H), singulet à 3.90 δ (3H). Spectre de masse: *m/e* 222: $I\text{-}CH_2CH_3$; *m/e* 207: $I\text{-}\overset{+}{C}H_2$; *m/e* 193: $\overset{+}{I}$ et $II\text{-}CH_2—CH_3$; *m/e* 82: $CH_3—N=\dot{C}—C\equiv\overset{+}{N}—CH_3$; *m/e* 67: $N\equiv C—C\equiv\overset{+}{N}—CH_3$; *m/e* 55: $[N\equiv C—\overset{+}{N}—CH_3]^+$.

5. Réaction de l'anisol avec la caféine

Un mélange réactionnel comprenant 1 g de caféine, 5 ml d'acétophénone et 150 ml d'anisol est dissous dans une solution de 425 ml d'eau et 500 ml de butanol tertiaire. L'irradiation se fait à l'aide d'une lampe Hanovia grande pression 450 W durant 130 h.

L'initiateur étant séparé de façon habituelle, on le retrouve réduit à la fin de la réaction. Après l'évaporation du solvant la présence de la caféine intacte est confirmée par r.m.n. On observe également la formation d'un composé aromatique complexe qui n'est pas identifié.

La même réaction est effectuée par photolyse directe, mais la caféine se révèle inerte.

Les auteurs remercient le Conseil National de Recherches du Canada pour le subside de recherche accordé (S.J. octroi No 4200–4).

L'un de nous (A.M.) exprime sa reconnaissance vis-à-vis du Conseil National de Recherches du Canada, qui lui a alloué une bourse d'études supérieures.

1. M. I. Simon et H. Van Vanukis. Arch. Biochem. Biophys. **105**, 197 (1969).
2. T. Matsuura et I. Soito. Tetrahedron Lett. **24**, 6609 (1968).
3. J. Diekmann et C. J. Pederson. J. Org. Chem. **28**, 2879 (1963).
4. D. Elad et R. D. Youssefyef. J. Org. Chem. **29**, 2031 (1964).
5. I. Rosenthal et D. Elad. Tetrahedron, **23**, 3193 (1967).
6. M. B. Rubin. J. Org. Chem. **28**, 1949 (1963).
7. H. J. Piek. Tetrahedron Lett. **15**, 1169 (1969).
8. H. Goldner, G. Dietz, et E. Carstens. Ann. Chem. **692**, 134 (1966).

Can. J. Chem. Downloaded from www.nrcresearchpress.com by 210.87.254.42 on 09/05/12
For personal use only.

Can. J. Chem. Downloaded from www.nrcresearchpress.com by 210.87.254.105 on 09/05/12
For personal use only.

Vapor absorption spectra of benzoxazole, benzimidazole, and benzothiazole near 2850 Å

R. D. GORDON AND R. F. YANG
Department of Chemistry, Queen's University, Kingston, Ontario

Received January 19, 1970

Sharp vapor absorption spectra, with origins at the frequencies listed, have been observed for benzoxazole (36 493 cm^{-1}), benzimidazole (36 023 cm^{-1}), and benzothiazole (34 327 cm^{-1}). In each case the origin is the strongest band, and excited state fundamentals of approximately 700, 950, and 1225 cm^{-1} are prominent. The vibrational structure is similar to that of related heterocyclic compounds and some substituted benzenes. There is no evidence of a (π^*–n) transition.

Canadian Journal of Chemistry, 48, 1722 (1970)

Introduction

The six benzo-derivatives of five-membered heterocycles listed in Table 1 have similar ultraviolet (u.v.) spectra in solution. Absorption begins with a moderately intense system near 2850 Å, and stronger bands are observed at higher energies. The near u.v. spectra of the compounds **1** must record (π^*–π) transitions. The solution spectra of compounds **2** are similar, and probably of (π^*–π) type, although (π^*–n) transitions might also be expected in these aza-substituted molecules.

In interpreting these spectra, some authors have emphasized analogies to the spectra of substituted benzenes (1, 2). Others have assumed sufficient delocalization over both rings that naphthalene (3) or the indenyl anion (4) is a better model, while some theoretical treatments use both approaches (5, 6).

Hollas (7) has reported a vibrational analysis of the sharp bands observed near 2850 Å in the vapor absorption spectra of the compounds **1**. This paper reports the results of a similar study of compounds **2**. It was carried out to determine whether the vibrational structure typical of the compounds **1** would persist in their "azalogues" **2**; to seek for evidence of a possible (π^*–n) transition; and to see whether a detailed study of the sharp vapor spectra might support one of the interpretive approaches described above.

The spectrum of benzothiazole vapor has been reported previously (8), but under lower resolution than in the present study. A self-consistent field treatment of the electronic spectrum of benzoxazole has recently been published (9).

TABLE 1
Some benzo-derivatives of five-membered heterocycles

Compound	Structure number	
Benzo[*b*]furan	**1**; A = O	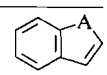
Indole	**1**; A = NH	
Benzo[*b*]thiophene	**1**; A = S	**1**
Benzoxazole	**2**; A = O	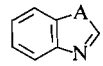
Benzimidazole	**2**; A = NH	
Benzothiazole	**2**; A = S	**2**

Experimental

Benzoxazole and benzothiazole were distilled under reduced pressure, and benzimidazole was recrystallized from alcohol.

The absorption spectra illustrated in the figures were obtained in a 1 m fused silica cell at the lower of the temperatures listed below. Temperatures up to the maxima shown were used to develop the hot bands: benzoxazole, −35 to 100°; benzimidazole, 140 to 170°; benzothiazole, 30 to 100 °C. Spectra were photographed in the second order of a 1.5 m grating spectrograph with a dispersion of 7.4 Å mm^{-1}. The spectrum of an iron hollow cathode lamp was recorded for wavelength calibration. Sharp bands were measured on the films with a J. E. O. L. Comparator, while weaker features were measured less accurately from enlarged prints. The former measurements should be accurate to ± 2 cm^{-1}.

Solution spectra were obtained on a Unicam SP. 800 Spectrophotometer using Spectrograde solvents. The infrared (i.r.) spectra of thin liquid films of benzothiazole and benzoxazole were measured on a Beckman IR 10 Spectrophotometer.

Results

The sharp 2850 Å vapor absorption bands of the three compounds **2** are illustrated in Figs. 1 and 2, and vibrational assignments of some 300 observed bands are given in Tables 2, 3, and 4. Strong bands at 36 493 (benzoxazole), 36 023 (benzimidazole), and 34 327 cm^{-1} (benzothiazole) are assigned as the electronic origins.

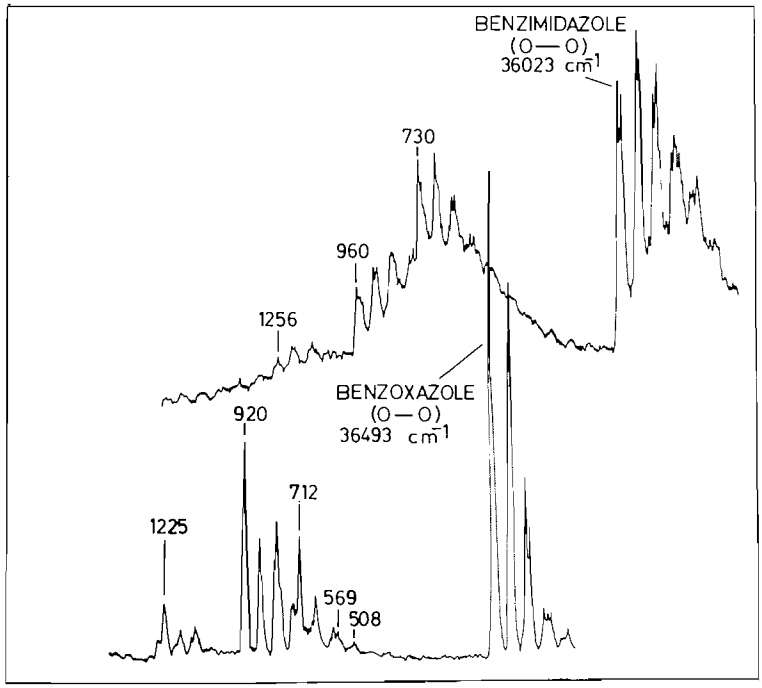

FIG. 1. The 2850 Å vapor absorption bands of benzimidazole and benzoxazole.

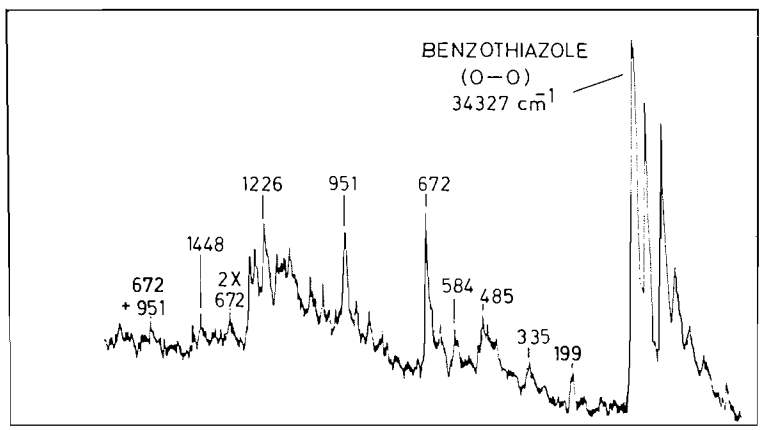

FIG. 2. The 2850 Å vapor absorption bands of benzothiazole. The wavenumber scale is not the same as in Fig. 1.

In each of the spectra the origin band group is the strongest, while other strong bands record excited state fundamentals of approximately 700, 950, and 1225 cm^{-1}. No long progressions are observed, although some weak bands are assigned to (2-0) or (3-0) transitions. The spectra become too diffuse to measure some 2500 cm^{-1} from the origins.

A number of hot bands were observed, and as shown in Table 5 many of the ground state fundamentals agree well with i.r. frequencies. A tentative correlation with excited state modes of similar frequencies and relative intensities has also been made in some cases.

Extensive sequence structure is found on the low energy side of the stronger bands, especially in benzimidazole whose spectrum had to be recorded at a high temperature to obtain sufficient

Can. J. Chem. Downloaded from www.nrcresearchpress.com by 210.87.254.105 on 09/05/12
For personal use only.

TABLE 2

Vibrational analysis of the 2850 Å vapor absorption bands of benzoxazole

Intensity*	Δν†	Assignment‡	Δ§	Intensity*	Δν†	Assignment‡	Δ§
vvw	−2161	*I*, *F*, a, 2c	−2	vw	−1427	*I*, 3c	0
vw	−2140	*I*, *F*, 2c	+4	w	−1379	*I*, a, 2c	+1
vw	−2077	*I*, *F*, c	+5	w	−1364	*I*, 2c	+1
vw	−2016	*I*, *F*	+4	vvw	−1354	*I*, b, c	+1
vvw	−1638	*I*, *B*, 3c	+1	vw	−1316	*I*, a, c	+2
vw	−1590	*I*, *B*, a, 2c	+2	w	−1302	*I*, c	+1
vw	−1575	*I*, *B*, 2c	+2	vvw	−1291	*I*, b	+2
vvw	−1563	*I*, *B*, b, c	+4	vw	−1253	*I*, a	+3
vw	−1555	2*F*	+3	w	*−1241*	*I*	—
vw	−1514	I, B, c	+1	vw	−1213	*H*, a, 2c	−1
vw	−1488	*I*, 4c	+1	w	−1198	*H*, 2c	−1
vw	−1452	*I*, *B*	+1	vw	−1188	*G*, 3c	0
vw	−1148	*H*, a, c	+2	vw	−685	*E*, c	0
w	−1141	*G*, a, 2c	0	vvw	−664	*D*, 2c	0
w	−1135	*H*, c	0	w	*−623*	*E*	—
w	−1126	*G*, 2c	0	w	−601	*D*, c	+1
w	−1087	*H*, a	+1	w	*−540*	*D*	—
w	*−1073*	*H*	—	w	−479	*C*, a, c	+2
w	−1064	*G*, c	0	w	−464	*C*, c	+2
vvw	−1052	*F*, *B*, c	+1	w	−421	*C*, a	−2
vvw	−1042	*F*, *B*, b	+1	w	*−404*	*C*	—
vvw	−1024	*C*, *E*	+3	w	−351	*A*, d	+3
vw	−1015	*G*, a	+2	w	−338	*B*, 2c	−2
w	*−1002*	*G*	—	w	−324	*B*, a, c	+2
w	−990	*F*, *B*	+1	w	−275	*B*, c	−1
w	−982	*F*, a, 3c	−2	w	−267	*A*, c	+1
w	−964	*F*, 3c	+1	w	−248	A, 4c	0
w	−920	*F*, a, 2c	−2	ms	*−212*	*B*	—
w	−903	*F*, 2c	0	w	*−206*	*A*	—
w	−841	*F*, c	0	w	−201	A, a, 3c	0
vvw	−794	*F*, a	0	ms	−187	A, 3c	−1
w	*−779*	*F*	—	vw	−148	A, d	—
vw	−749	*E*, 2c	−2	ms	−139	A, a, 2c	0
vw	−697	*E*, a, c	+3	ms	−124	A, 2c	0
vw	−114	A, b, c	0	vw	575	E, a, 2c	+2
vs	−77	A, a, c	0	w	587	E, 2c	−1
vs	−62	A, c	—	w	596	E, b, c	−2
w	−52	A, b	—	ms	649	E, c	−1
w	−30	A, 2a	0	w	661	F, c	−2
vs	−15	A, a	—	w	671	G, 4c	−1
vs	*(36 493)*	A, Origin	—	s	*712*	E	—
vvw	28	D, *D*	−1	w	*725*	F	—
vvw	47			w	734	G, 3c	0
vw	60			w	747	G, b, 2c	+3
vvw	111			w	783	G, a, 2c	+2
vvw	187	B, 2c	−1	s	796	G, 2c	0
vw	247	B, c	−3	w	807	G, b, c	+1
vw	259	C, 4c	−1	w	844	G, a, c	+1
w	*312*	B	—	s	858	G, c	0
vw	320	C, 3c	−2	w	863	G, b	−5
w	383	C, 2c	−1	ms	907	G, a	+2
vw	399	C, b, c	+5	s	*920*	G	—
w	446	C, c	0	w	943	I, c	−1
vvw	500	E, *B*	0	w	*964*	H	—
w	*508*	C	—	w	*1006*	I	—
vw	556	D, a	+2	w	1040	J, c	−3
w	*569*	D	—	w	1087	J, a.	−3
ms	*1105*	J	—	ms	1635	E, G	+3
ms	*1119*	K	—	w	1641	F, G	−4
ms	1162	L, c	−1	w	1702	2G, a, 2c	+1
w	1179	M, c	−2	w	1717	2G, 2c	+1
w	1188	N, c	+1	w	1726	2G, b, c	0

Can. J. Chem. Downloaded from www.nrcresearchpress.com by 210.87.254.105 on 09/05/12
For personal use only.

TABLE 2—*Continued*

Intensity*	Δν†	Assignment‡	Δ§	Intensity*	Δν†	Assignment‡	Δ§
ms	*1225*	L	—	w	1730	C, L	−3
w	*1243*	M	—	w	1781	2G, c	+3
w	*1249*	N	—	ms	1842	2G	+2
vw	1272	O, c	0	w	1847		
vw	1279	D, E	−2	w	1923		
vw	1314	P, c	+2	w	2029	G, J	+4
w	*1334*	O	—	w	2044	G, K	+5
vw	1359	Q, 2c	+4	vw	2098	G, M, c	−3
w	*1374*	P	—	vw	2108	G, N, c	+1
w	1417	Q, c	0	w	2148	G, L	+3
vw	1437	E, F	0	vvw	2161	G, M	−2
w	*1479*	Q	—	vw	2171	G, N	+2
w	1498	E, G, a, 2c	+5	vvw	2555	E, 2G	+3
w	1505	E, G, 2c	−3	vvw	2761	3G	+1
vw	1538	B, L	+1	vvw	3070	2G, L	+5
w	1572	E, G, c	+2				

*The intensities of the hot bands are relative to others observed at the same elevated temperature.
†Observed separation from the origin in cm^{-1}. Fundamentals are italicized. The wavenumber of the origin is also given in this column.
‡The origin and excited state fundamentals are designated by capital letters, and the ground state fundamentals by italicized capitals. Lower case letters designate the sequence intervals a = −15, b = −52, c = −62, and d = −148 cm^{-1}. Thus, for example, 2G,*A*,a,2c represents $2 \times 920 - 206 - 15 - 2 \times 62 = 1495$ cm^{-1}.
§$\Delta = (\Delta\nu_{obs.} - \Delta\nu_{calcd.})$ in cm^{-1}.

TABLE 3

Vibrational analysis of the 2850 Å vapor absorption bands of benzimidazole*

Intensity	Δν	Assignment	Δ	Intensity	Δν	Assignment	Δ
vw	−1133	*D*, c	0	vs	−63	A, c	—
vw	*−1070*	*D*	—	vw	−54	A, b	—
vvw	*−1009*	*C*	—	vw	−22	A, 2a	0
vvw	−960	*B*, 3c	0	vs	−11	A, a	—
vw	−900	*B*, 2c	−3	vs	*(36 023)*	A, Origin	—
vw	−836	*B*, c	−2	vvw	98	B, 2c	−2
vw	*−771*	*B*	—	vvw	155	B, c	−8
vw	*−421*	*A*	—	vw	*226*	B	—
w	−347	A, 3c, d	−4	vw	*301*	C	—
ms	−281	A, 2c, d	−1	vw	513	D, c, d	0
w	−267	A, a, 4c	−4	vw	537	D, 3c	−4
w	−254	A, 4c	−2	s	594	D, a, 2c	+1
ms	−218	A, c, d	−1	s	602	D, 2c	−2
ms	−204	A, a, 3c	−4	s	656	D, a, c	0
ms	−190	A, 3c	−1	s	666	D, c	−1
vw	−177	A, b, 2c	+3	s	718	D, a	−1
ms	−154	A, d	—	s	*730*	D	—
vs	−137	A, a, 2c	0	w	764	E, 3c	−7
vs	−127	A, 2c	−1	w	804	E, d	−2
vw	−112	A, b, c	+5	w	815	E, a, 2c	−8
vw	−85	A, 2a, c	0	w	828	E, 2c	−6
vs	−74	A, a, c	0	s	883	E, a, c	−3
s	896	E, c	−1	w	1565	D, E, 2c	+1
s	947	E, a	−2	vw	1616	D, E, a, c	0
s	*960*	E	—	w	1627	D, E, c	0
w	1067	F, 3c	0	vw	1675	D, E, a	−4
ms	1130	F, 2c	0	w	1688	D, E	−2
ms	1193	F, c	0	vw	1787	2E, 2c	−7
ms	*1256*	F	—	vw	1853	2E, c	−4
w	1335	2D, 2c	+1	vw	1918	2E	−2
w	1398	2D, c	+1	vw	1985	D, F	−1
w	1461	2D	+1	vw	2088	E, F, 2c	−2
vw	*1480*	G	—	vw	2149	E, F, c	−4
vw	1533	D, E, d	−3	vw	2214	E, F	−2
vw	1552	D, E, a, 2c	−1	vw	2416	2D, E	−4

*The notes to Table 2 also apply here. The sequence intervals are a = −11; b = −54; c = −63; and d = −154 cm^{-1}.

Can. J. Chem. Downloaded from www.nrcresearchpress.com by 210.87.254.105 on 09/05/12
For personal use only.

Can. J. Chem. Downloaded from www.nrcresearchpress.com by 210.87.254.105 on 09/05/12
For personal use only.

TABLE 4

Vibrational analysis of the 2850 Å vapor absorption bands of benzothiazole*

Intensity	Δv	Assignment	Δ	Intensity	Δv	Assignment	Δ
w	−1295	*B*, *D*, c	−6	w	−479	*A*, 4c	−8
vw	−1244	*B*, *D*	+1	w	−429	*A*, 3c	−2
vvw	−1188	*A*, *D*, 4c	−1	w	−380	*A*, 2c	+3
vvw	−1146	*A*, *D*, 3c	−3	w	−351	*A*, a, c	0
w	−1106	2*B*, c	−4	w	−340	*A*, c	−1
w	−1100	*A*, *D*, 2c	−1	w	−308	*A*, a	−1
w	−1061	*A*, *D*, c	−6	ms	*−295*	*A*	—
w	−1058	2*B*	0	w	−267	A, 6c	−3
w	−1016	*A*, *D*	−5	ms	−228	A, 5c	−8
w	−955	*A*, *C*	+2	ms	−178	A, 4c	−2
w	−939	*G*, c	−1	ms	−130	A, 3c	+2
ms	*−894*	*G*	—	ms	−101	A, a, 2c	−1
w	−870	*A*, *B*, c	−2	s	−88	A, 2c	0
w	−837	*F*, c	+2	ms	−74	A, b, c	−1
w	−819	*A*, *B*	+5	vs	−56	A, a, c	0
ms	*−795*	*F*	—	ms	−44	A, c	—
w	*−755*	*E*	—	ms	−29	A, b	—
ms	*−716*	*D*	—	sh	−12	A, a	—
w	−706	*C*, c	0	vs	(*34 327*)	A, Origin	—
ms	*−662*	*C*	—	vw	37	D, *A*	−3
w	−617	*B*, 2c	0	vw	84		
w	−575	*B*, c	−2	vw	*109*	B	—
ms	*−529*	*B*	—				
vw	157	C, c	+2	w	986	E, G, 2c	+5
w	*199*	C	—	w	1009	D, H	+2
vw	246	D, 2c	−1	w	1027	E, G, c	+2
vw	293	D, c	+2	w	1068	E, G	−1
w	*335*	D	—	ms	1134	J, 2c	−4
w	399	E, 2c	+2	ms	1160	E, H	+3
ms	443	E, c	+2	ms	1185	J, c	+3
w	461	E, 2a	0	s	*1226*	J	—
w	473	E, a	0	ms	1257	G, H	+1
ms	*485*	E	—	ms	1277	D, I	−9
w	*500*	F	—	w	1351	2H	+7
ms	*584*	G	—	w	1393	E, I, c	+1
w	615	H, a, c	−1	w	1409	K, c	+5
ms	630	H, c	+2	w	1436	E, I	0
ms	658	H, a	−2	w	*1448*	K	—
s	*672*	H	—	w	*1477*	L	—
vvw	739	C, G, c	0	vw	1541	G, I	+6
w	780	C, G	−3	w	1563	D, J	+2
w	821	D, G	+2	w	1618	H, I	−5
ms	865	I, 2c	+2	vw	1655	M, c	+2
ms	910	I, c	+3	w	*1697*	M	—
s	*951*	I	—	vw	1741		
vw	1800	G, J	−10	vw	2146	H, L	−3
vw	1856	H, J, c	+2				
		2I, c	−2	vvw	2178		
w	1901	HJ	+3				
		2I	−1	vvw	2228		
vw	1937	G, 2H	+9	vvw	2235	D, H, J	+2
vw	1958	D, H, I	0	vvw	2252		
vw	1986	G, K, c	−2	vvw	2317		
vw	2033	G, K	+1	vvw	2422	I, L	−6
vw	2097	E, H, I	−11	vvw	2509	D, I, J	−3

*The notes to Table 2 also apply here. The sequence intervals are a = −12; b = −29; and c = −44 cm^{-1}.

Can. J. Chem. Downloaded from www.nrcresearchpress.com by 210.87.254.105 on 09/05/12
For personal use only.

TABLE 5

Comparison of ground state fundamentals with infrared and excited state frequencies (cm^{-1})

Ground state		
Hot bands	Infrared	Excited state
	Benzoxazole	
206	—	—
212	—	—
404	419	—
540	537	508
623	617	569
779	777	712
1002	1007	920
1073	1072	—
1241	1240	1225
	Benzimidazole	
421	425*	—
771	770†	730
1009	1007†	—
1070	—	960
	Benzothiazole	
295	—	—
529	—	485
662	667	—
716	725	672
755	757	—
795	797	—
894	—	—

*The assignment of this mode to out-of-plane torsion (10) may be mistaken.
†Assigned to in-plane ring bending (10).

vapor pressure. The sequence intervals, which are listed at the foot of Tables 2, 3, and 4, are similar in all three molecules.

The spectrum of benzimidazole is simpler than that of the other two compounds; the vibrational analysis requires only three strong and three weak fundamentals. Other weak fundamentals may be hidden by the strong sequence bands, but the simplicity of the spectrum probably reflects the fact that of the three C_s molecules, benzimidazole is the closest to possessing C_{2v} symmetry.

Under the medium resolution conditions used, the bands appear to be sharp, single-headed, and degraded to longer wavelengths. In benzothiazole they are slightly less sharp. The doubling of the benzimidazole peaks which can be seen in Fig. 1 is too great to be attributed to rotational fine structure. Rather it is due to an 11 cm^{-1} sequence.

The solution spectra of the six heterocycles were measured in different solvents to see whether behavior characteristic of (π^*–n) transitions might be found for the compounds **2**. As shown in Table 6, there is a moderate shift to higher energies with increasing solvent polarity in all six compounds. The red shift found for indole between cyclohexane and methanol is reversed when water is the solvent. No appreciable loss of fine structure was observed. Comparable blue shifts are observed for the first (π^*–π) bands of benzene (11), pyrimidine (12*g*), and pyrazine (12*h*), but much larger blue shifts, accompanied by loss of fine structure, are found for the (π^*–n) bands of the latter two compounds.

TABLE 6

Solvent shifts of the origin bands of the 2850 Å systems (cm^{-1})

Compound	ν_{oo} Cyclohexane	Solvent shifts* Methanol	Water
Benzo[*b*]furan	35 525	+40	—
Indole	34 810	−110	+120
Benzo[*b*]thiophene	33 580	+65	—
Benzoxazole	36 025	+180	—
Benzimidazole	35 585	+255	+410
Benzothiazole	33 865	+80	+400

*$\nu_{(methanol\ or\ water)} - \nu_{(cyclohexane)}$

Discussion

The spectra of the aza-substituted heterocycles **2** are strikingly similar to each other and to the spectra of the compounds **1**. The resemblance between their solution spectra extends to the vibrational structure of their sharp vapor bands and to the solvent dependence of their spectra in solution. Where small changes occur, they vary in a regular way with the hetero group. Data for comparison are listed in Tables 6 and 7.

Only (π^*–π) transitions are expected to occur in the near u.v. spectra of the compounds **1**, and contour analysis of the 2850 Å bands in indole (19) and benzo[*b*]thiophene (20) shows that they are polarized in the molecular plane as expected. The similarities noted above leave little doubt that the 2850 Å systems in all six of the heterocycles record (π^*–π) transitions of a similar nature.

No features were observed in the vapor spectra of the aza-substituted compounds **2** which could not be assigned to this (π^*–π) transition.[1] If

[1]A weak band reported at 3275 Å in the solution spectrum of benzothiazole (18*d*) could not be reproduced in this or other (2) studies.

Can. J. Chem. Downloaded from www.nrcresearchpress.com by 210.87.254.105 on 09/05/12
For personal use only.

TABLE 7

Origins, intensities, and prominent totally-symmetric excited state fundamentals of the longest wavelength electronic transitions in some related molecules

Compound	$\nu_{(0-0)}$ (cm^{-1}) (vapor)	ε_{max} (soln)	Prominent fundamentals (cm^{-1})					Reference*
Benzene	38 086	250	—	—	925 S	—	—	13, 12*a*
Phenol	36 352	2000	475 M	783 S	935 S 958 MS 975 MS	1273 M	1566 w	14, 12*b*
Thiophenol	34 980	400	380 M	750 w	970 S	1070 S	—	15, 12*c*
Styrene	34 761	570	—	746 S	948 S 959 S	1209 w	—	16, 12*d*
Aniline	34 032	1400	492 S	798 S	953 S	1307 M	—	17, 12*e*
Benzo[*b*]furan	35 952	2770	—	721 S 732 MS	939 S	1317 MS	1538 MS	7, 18*a*
Indole	35 233	4060	—	718 S 736 MS	907 S	1313 MS	1454 S	7, 18*b*
Benzo[*b*]thiophene	34 058	3050	—	673 S 737 MS	941 S	1184 S	—	7, 18*c*
Benzoxazole	36 493	3240	508 w 569 w	712 S	920 S	1225 MS	—	1†
Benzimidazole	36 023	5200	—	730 S	960 S	1256 MS	—	12*f*†
Benzothiazole	34 327	1350	485 MS 584 MS	672 S	951 S	1226 S	—	2†

*The first reference is to the vapor and the second to the solution spectrum.
†This work.

Can. J. Chem. Downloaded from www.nrcresearchpress.com by 210.87.254.105 on 09/05/12
For personal use only.

(π^*–n) transitions do occur, they must therefore be hidden beneath the intense absorption at shorter wavelengths. This is not surprising. Mason (4) has predicted that a (π^*–n) transition involving a lone pair electron on a nitrogen atom in a five-membered ring should be stronger, and occur at higher energies relative to the (π^*–π) bands than the corresponding transition involving nitrogen in a six-membered ring. No longer being the lowest singlet–singlet transition, a (π^*–n) transition would lose its characteristic sharpness (21), and would easily be buried under other intense transitions.

Many analogies can be pointed out between the 2850 Å transitions of the six heterocycles and the corresponding transitions in a number of substituted benzenes. Relevant features of the latter spectra are included in Table 7.

Relative to the 2600 Å bands of benzene, the first systems in benzoxazole and benzo[*b*]furan are intensified and shifted to lower energies by about the same amount as in phenol. A smaller intensification and a larger bathochromatic shift are found in benzothiazole and benzo[*b*]thiophene as is the case for styrene and thiophenol. The spectra of benzimidazole and indole resemble each other, but are not too closely related to the spectrum of aniline.

In the context of the present work, a comparison between the vibrational structures of the various spectra is more appropriate. The strength of the origin bands, and the absence of long progressions in the spectra of the heterocycles suggest that the geometrical changes accompanying excitation are small. This is consistent with the small decrease in the rotational constants measured for indole (19) and benzo[*b*]thiophene (20).

The similarity of the prominent fundamental frequencies in the six heterocycles, despite large changes in the masses and electronegativities of the hetero groups, suggests that these geometrical changes are similar in each molecule, and are largely confined to the benzene ring, the only common structural unit. In fact these prominent frequencies are close to those which Brand *et al.* (17) has listed as being the most active in the spectra of many substituted benzenes, *viz.* the symmetric ring stretching mode (ca. 950 cm^{-1}) and three substituent-sensitive modes (ca. 480, 750, and 1275 cm^{-1}).

The comparisons above provide a useful framework for a discussion of the spectra of the six heterocycles. They suggest, but by no means prove, the hypothesis that the 2850 Å transitions in these compounds are localized in the benzene ring. Resemblances to the 3200 Å spectra of naphthalene (22) can also be noted. For example, the prominent totally symmetric fundamentals in the latter system (*viz.* 501 S, 702 vw, 987 VS, 1147 M, 1389 M, and 1435 S cm^{-1}) are not unlike those listed in Table 7.

The authors are grateful to the Ontario Department of University Affairs and to the National Research Council of Canada for research grants. One of us (R. F. Y.) thanks the National Research Council of Canada for the award of a Postgraduate Scholarship.

1. R. Passerini. J. Chem. Soc. 2256 (1954).
2. A. Cerniani and R. Passerini. J. Chem. Soc. 2261 (1954).
3. B. Ellis and P. J. F. Griffiths. Spectrochim. Acta, **21**, 1881 (1965).
4. S. F. Mason. Physical methods in heterocyclic chemistry. Vol. II. *Editor* A. R. Katritzky. Academic Press, London, 1963. Chap. 7.
5. F. Momicchioli and A. Rastelli. J. Mol. Spectry. **22**, 310 (1967).
6. J. R. Platt. J. Chem. Phys. **19**, 101 (1951).
7. J. M. Hollas. Spectrochim. Acta, **19**, 753 (1963).
8. P. E. Todesco, A. Trombetti, and P. Vivarelli. Boll. Sci. Fac. Chim. Ind. Bologna, **23**, 79 (1965).
9. S. D. Carson and H. M. Rosenberg. J. Mol. Spectry. **32**, 242 (1969).
10. M. M. Cordes and J. L. Walter. Spectrochim. Acta, **24A**, 1421 (1968).
11. H. McConnell. J. Chem. Phys. **20**, 700 (1952).
12. D. M. S.-U. V. Atlas of organic compounds. Butterworths, London (1966). (*a*) Spectrum D1/1; (*b*) D5/4, 5; (*c*) D8/6; (*d*) D10/1; (*e*) D6/3; (*f*) H11/1, 2; (*g*) G6/2, 3; (*h*) G6/7, 8.
13. G. Herzberg. Molecular spectra and molecular structure. Vol. III. Electronic spectra and electronic structure of polyatomic molecules. Van Nostrand, Princeton, N. J., 1966. p. 666.
14. H. D. Bist, J. C. D. Brand, and D. R. Williams. J. Mol. Spectry. **21**, 75 (1966); **24**, 413 (1967).
15. W. W. Robertson and F. A. Matsen. J. Amer. Chem. Soc. **72**, 5248 (1950).
16. W. W. Robertson, J. F. Music, and F. A. Matsen. J. Amer. Chem. Soc. **72**, 5260 (1950).
17. J. C. D. Brand, D. R. Williams, and T. J. Cook. J. Mol. Spectry. **20**, 359 (1966).
18. L. Lang. Absorption spectra in the ultraviolet and visible region. Academic Press, New York, 1961. (*a*) **2**, spectrum 327; (*b*) **9**, 1664; (*c*) **1**, 138; (*d*) **2**, 334.
19. A. Mani and J. R. Lombardi. J. Mol. Spectry. **31**, 308 (1969).
20. J. R. Lombardi and A. Hartford. 24th Symposium on molecular structure and spectroscopy, Columbus, Ohio, 1969.
21. R. M. Hochstrasser and C. Marzzacco. J. Chem. Phys. **49**, 971 (1968).
22. D. P. Craig, J. M. Hollas, M. F. Redies, and S. C. Wait. Phil. Trans. Roy. Soc. A**253**, 543 (1961). D. S. McClure. J. Chem. Phys. **22**, 1668 (1954).

Can. J. Chem. Downloaded from www.nrcresearchpress.com by 210.87.254.6 on 09/05/12
For personal use only.

Fluorocarbon-bridged ditertiary phosphine derivatives of rhodium carbonyl halides

W. R. CULLEN AND J. A. J. THOMPSON
Department of Chemistry, University of British Columbia, Vancouver 8, British Columbia

Received December 12, 1969

The ditertiary phosphines, $(C_6H_5)_2PC{=}CP(C_6H_5)_2(CF_2)_nCF_2$ (n = 1, 2) react with $[Rh(CO)_2X]_2$ (X = Cl, Br) via unsymmetrical cleavage of the halide bridges to give ionic complexes $[(P{-}P)_2Rh]^+$ $[cis\text{-}(CO)2RhX_2]^-$. However the diarsine, $(CH_3)_2AsC{=}CAs(CH_3)_2CF_2CF_2$ (ffars) reacts in an anomalous manner to give the neutral dimer, $[(ffars)Rh(CO)Cl]_2$. With an excess of the phosphines, (n = 1, 2 *or* 3) the ionic complexes $[(P{-}P)_2Rh]^+Cl^-$ are obtained. The physical and spectroscopic properties of the new compounds and the tendency of the ions, $[(P{-}P)_2Rh]^+$, not to undergo facile oxidative-addition reactions are discussed.

Canadian Journal of Chemistry, 48, 1730 (1970)

Introduction

Recent work in the field of homogeneous catalysis has spurred interest in the synthesis of new complexes of the platinum metals in their lower oxidation states. In particular, phosphine derivatives of Rh(I) have come under a great deal of scrutiny.

Ditertiary phosphine complexes of Rh(I) derived from rhodium carbonyl halides, $[Rh(CO)_2X]_2$, were first reported in 1964 by Sacco and Ugo (1). These were a number of salts of the type $[Rh(diphos)_2]X$ (diphos = 1,2-bisdiphenylphosphinoethane, X = Cl, ClO_4, $B(C_6H_5)_4$) and were obtained by reaction of excess ligand with the carbonyl chloride. Hieber and Kummer (2) found that variation of ligand and/or reaction conditions resulted in bridged, chelated, or polymeric products. For example, under mild conditions, diphos and $[Rh(CO)_2Cl]_2$ provided the bridged complex, **1**, whereas more stringent conditions gave the chelated structure, **2**.

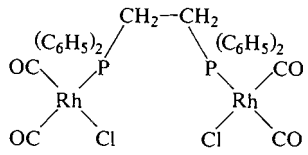

1

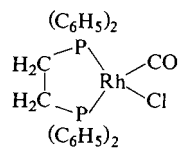

2

Thus, the earlier reports have demonstrated that ditertiary phosphines having saturated hydrocarbon bridging groups react with $[Rh(CO)_2Cl]_2$ to give a symmetric cleavage of the chlorine-bridged dimer. Recently, however, it was shown (3) that 1,2-bisdiphenylphosphino*ethylene* which contains an unsaturated linkage gave complexes of the type $[Rh(P{-}P)_2^+][Rh(CO)_2X_2]^-$ (X = Cl, Br); i.e. complexes derived from asymmetric cleavage of the halide bridges.

As part of our continuing study of the reactions of fluorocarbon-bridged ditertiary phosphines and arsines (4–8), **3**, we have prepared a number of Rh(I) complexes which present some interesting parallels with and differences from earlier studies. Herein we report the results of this work.

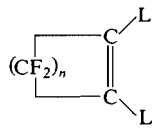

3

(*a*) L = $(C_6H_5)_2P$, n = 2, ffos
(*b*) L = $(C_6H_5)_2P$, n = 3, $f_6$fos
(*c*) L = $(C_6H_5)_2P$, n = 4, $f_8$fos
(*d*) L = $(CH_3)_2As$, n = 2, ffars

Experimental

Physical properties and analytical data for new compounds are given in Table 1.

The carbonyl halides $[Rh(CO)_2X]_2$ were prepared by the method of McCleverty and Wilkinson (9). The ligands ffos (10), $f_6$fos (5), $f_8$fos (8), and ffars (11) (**3** (*a*)–(*d*)), were prepared by published procedures. All reactions were carried out under a nitrogen atmosphere.

Infrared (i.r.) and ^{19}F nuclear magnetic resonance (n.m.r.) spectra were obtained using a Perkin–Elmer 457 Spectrometer and a Varian Associates HA-100 Spectrometer, respectively.

Analyses and molecular weights were performed by Mr. P. Borda of this Department and by the Pascher Mikroanalytisches Laboratorium, Bonn, West Germany.

Conductivity measurements were made using a Wayne–Kerr Universal Bridge, Model B221A. The petroleum ether used had b.p. range 30–60°.

Can. J. Chem. Downloaded from www.nrcresearchpress.com by 210.87.254.6 on 09/05/12
For personal use only.

TABLE 1

Analytical data and physical properties

Compound	Color	Decomposition point (°C)	Found (%)					Calculated (%)					Equivalent conductance‖ (mhos cm^{-1} mole^{-1})
			C	H	Cl	F	P	C	H	Cl	F	P	
$[(ffos)_2Rh]^+[cis\text{-}Rh(CO)_2Cl_2]^-$*	Yellow	> 200	52.8	2.8	5.2	12.0	9.9	52.7	3.1	5.4	11.5	9.4	~24
$[(f_6fos)_2Rh]^+[cis\text{-}Rh(CO)_2Cl_2]^-$†	Yellow	> 195	50.4	2.9	5.1	16.0	8.9	50.7	2.8	5.0	16.0	8.7	24.3
$[(f_6fos)_2Rh]^+[cis\text{-}Rh(CO)_2Br_2]^-$‡	Yellow	> 170	48.1	2.7	—	15.3	8.2	47.7	2.7	—	15.1	8.2	23.9
$[(ffos)_2Rh]^+Cl^-$	Yellow	> 200	59.6	3.6	3.0	13.0	10.9	59.7	3.6	3.1	13.5	11.0	24.3
$[(ffos)_2Rh]^+[B(C_6H_5)_4]^-$	Yellow	200–215	67.9	4.3	—	10.8	9.1	68.1	4.3	—	10.8	8.8	14.3
$[(f_6fos)_2Rh]^+Cl^-$	Yellow	200–215	56.5	3.3	2.7	19.0	9.1	56.8	3.3	2.9	18.6	8.4	24.5
$[(f_6fos)_2Rh]^+[B(C_6H_5)_4]^-$	Yellow	235–245	65.4	3.8	—	14.8	7.4	65.2	4.0	—	15.1	6.8	15.8
$[(f_8fos)_2Rh]^+Cl^-$	Light orange	185–190	53.8	3.3	2.5	23.4	9.1	54.3	3.0	2.7	22.9	9.3	25.4
$[(f_8fos)_2Rh]^+[B(C_6H_5)_4]^-$	Orange	228–230	63.0	4.0	—	19.1	8.1	62.6	3.8	—	18.9	7.7	17.0
$[(ffos)_2RhHCl]^+Cl^-$	Pale yellow	190–195	57.8	4.3	5.8	—	—	57.8	3.6	6.1	—	—	12.2
$[(ffars)Rh(CO)Cl]_2$§	Red	170–180	22.2	2.5	—	15.1	—	21.6	2.4	—	15.2	—	—

*Average molecular weight in acetone: found, 674; calcd. (assuming ionic formulation), 661.
†Average molecular weight in acetone: found, 702; calcd. (assuming ionic formulation), 711.
‡Bromine analysis: found, 11.0; calcd., 10.6.
§Arsenic analysis: found, 29.5; calcd., 29.9. Mol. wt: found (acetone soln.), 990; calcd., 1001.
‖Approximately 10^{-3} *M* nitrobenzene solutions at 25 °C.

Can. J. Chem. Downloaded from www.nrcresearchpress.com by 210.87.254.6 on 09/05/12
For personal use only.

Preparation of $[(f_6fos)_2Rh]^+[cis\text{-}(CO)_2RhCl_2]^-$

To an ethanol solution (20 ml) of $[Rh(CO)_2Cl]_2$ (195 mg, 0.5 mmole) was added 0.54 g (1 mmole) of $f_6$fos. The solution immediately became darker yellow and CO was evolved. Within 2 min a yellow precipitate had formed. The mixture was stirred for 45 min, then filtered by suction. The filtrate (596 mg, 84%) was washed with ethanol and diethyl ether. The crude material was recrystallized from dichloromethane–hexane to give bright yellow crystals. ν(CO) (CH_2Cl_2 solution): 2076 (s) and 1985 (s) cm^{-1}.

Preparation of $[(ffos)_2Rh]^+[cis\text{-}(CO)_2RhCl_2]^-$ and $[(f_6fos)_2Rh]^+[cis\text{-}(CO)_2RhBr_2]^-$

Both complexes were obtained in a manner analogous to that of the above $f_6$fos derivative. The yield of $[(ffos)_2Rh]^+[cis\text{-}(CO)_2RhCl_2]^-$ was 500 mg (76%). It was recrystallized from dichloromethane – petroleum ether and had ν(CO) (KBr disc) at 2076 (s) and 1987 (s) cm^{-1}. The yield of $[(f_6fos)_2Rh]^+[cis\text{-}(CO)_2RhBr_2]^-$ (from $[(CO)_2RhBr]_2$) was 80%. It was recrystallized from dichloromethane – petroleum ether and had ν(CO) (CH_2Cl_2 solution) at 2068 (s) and 1991 (s) cm^{-1}.

Preparation of $[(P—P)_2Rh]^+X^-$ (P—P = ffos and f_6fos; X = Cl, Br, $B(C_6H_5)_4$)

A typical reaction is described. F_6fos (1.09 g, 2 mmoles) was added as the solid to a 95% ethanol solution of $[Rh(CO)_2Cl]_2$ (195 mg, 0.5 mmole). The mixture was stirred while being warmed gently in a water bath. The initial precipitate of $[(f_6fos)_2Rh]^+[cis\text{-}(CO)_2RhCl_2]^-$ dissolved gradually to give an orange solution containing a small amount of suspended solid. The solution was filtered after 1 h and solvent was removed. Yellow crystals formed as the volume decreased and addition of diethyl ether enhanced precipitation. The solid was filtered and washed with ether to give 1.15 g (93%) of the product which was recrystallized from dichloromethane–hexane.

The tetraphenylborate derivative, $[(f_6fos)_2Rh]^+[B(C_6H_5)_4]^-$, was obtained by addition of a methanol solution (5 ml) of excess $Na^+B(C_6H_5)_4^-$ to a solution of the chloride 124 mg (0.1 mmole) in the same solvent (10 ml). Yellow crystals began forming within 30 s. After 1 h the product was filtered and washed with ether. Yield, 128 mg (85%). Recrystallization was accomplished by addition of methanol to a dichloromethane solution (concentrated) of the product.

In the case of $[(f_8fos)_2Rh]^+Cl^-$, 594 mg (1 mmole) of the ligand was added to 98 mg (0.25 mmole) of $[Rh(CO)_2Cl]_2$ in 20 ml of benzene at room temperature. Evolution of CO was rapid and the solution became red-brown. After 25 min, a yellow solid was precipitated. The mixture was warmed briefly (water bath) and petroleum ether was added. Filtration and washing with petroleum ether yielded 574 mg (87%) of the product. Addition of petroleum ether to an acetone solution of the product initially provided an oil which crystallized upon standing.

Preparation of $[(ffars)Rh(CO)Cl]_2$

Ffars (429 mg, 1.3 mmoles) in 10 ml of 95% methanol was mixed with 250 mg (0.65 mmole) of $[Rh(CO)_2Cl]_2$ in 15 ml of the same solvent. The solution immediately became bright cherry red and CO was evolved. Reaction was complete within 5 min after which time solvent was removed at reduced pressure to give 569 mg (78%) of the red, crystalline product. Recrystallization from boiling hexane afforded small dark-red needles, ν(CO) (C_6H_{12} solution): 1971 (s), 1972 (sh), 1959 (w), 1995 (vw) cm^{-1}.

Attempted Preparation of $[(f_8fos)_2Rh]^+[cis\text{-}(CO)_2RhCl_2]^-$

(*A*) A solution of $f_8$fos (596 mg, 1 mmole) in 15 ml of 95% ethanol was added to an ethanol solution (15 ml) of $[Rh(CO)Cl]_2$ (195 mg, 0.5 mmole). The solution quickly became darker and an orange precipitate formed. The mixture was stirred for ~0.5 h then filtered and washed with ether and petroleum ether to yield 500 mg of an orange powder. Attempts at recrystallization resulted in complete decomposition of the complex. ν(CO) (CH_2Cl_2 solution): 2044 cm^{-1}.

(*B*) To a solution of $[Rh(CO)_2Cl]_2$ (195 mg, 0.5 mmole) in hexane (20 ml) was added 600 mg of $f_8$fos as the solid. Carbon monoxide was evolved slowly over a 15 min period during which a fine orange solid was deposited. The mixture was stirred for 0.5 h and warmed gently in the last 5 min. Filtration followed by washing with ether gave 721 mg (~100% assuming $f_8$fosRh(CO)Cl) of a solid whose i.r. spectrum was identical with that of the material obtained in (*A*).

Reaction of $[(ffos)_2Rh]^+Cl^-$ with HCl

The rhodium complex (100 mg, 0.09 mmole) was dissolved in 15 ml of CH_2Cl_2. Anhydrous HCl was bubbled through the stirred solution which rapidly became lighter yellow. After 5 min, the solvent was removed at reduced pressure. The pale yellow solid so obtained was dissolved in HCl-saturated CH_2Cl_2, concentrated under a stream of nitrogen, and finally petroleum ether was added. Fluffy crystals of $[(ffos)_2RhHCl]^+Cl^-$ were obtained. ν(Rh—H) (KBr disc): ~2080 cm^{-1} (vw).

In an identical reaction involving $(f_6fos)_2Rh^+Cl^-$ a similar color change was observed. After work-up, however, the yellow material which was isolated was found to be the starting complex.

Results and Discussion

$[cis\text{-}(CO)_2RhCl_2]^-$ Complexes

The present work involving reactions between the fluorocarbon-bridged chelating ditertiary phosphines **3** (*a*)–(*c*) and $[Rh(CO)_2X]_2$ (X = Cl, Br) was begun in hopes of preparing simple mono-carbonyl complexes of the type **4**; that is, compounds similar to those reported by Hieber and Kummer (2). Subsequently the ability of **4**

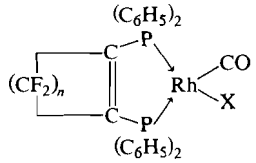

4

n = 2, 3, or 4

TABLE 2

^{19}F n.m.r. data*

Compound	δ (p.p.m.) rel. $CFCl_3$
$[(ffos)_2Rh]^+[(CO)_2RhCl_2]^-$	110 (singlet)
$[(f_6fos)_2Rh]^+[(CO)_2RhCl_2]^-$	108 (triplet), 128 (quintuplet)
$(f_6fos)_2Rh^+B(C_6H_5)_4^-$	109 (triplet), 129 (quintuplet)
$[(ffars)Rh(CO)Cl]_2$†	107 (singlet)

*CH_2Cl_2 Solutions.
†^1H Spectrum: τ_{CH_3} = 8.15 ($CDCl_3$ soln., TMS internal standard).

to undergo oxidative-addition reactions was to be investigated.

Reaction of ffos or $f_6$fos at room temperature with $[Rh(CO)_2X]_2$ in a 2:1 mole ratio in benzene or alcoholic solutions leads to almost immediate precipitation[1] of bright yellow solids, which analyze correctly for the stoichiometry of **4**. However, assignment of this structure is ruled out on the basis of the i.r. and n.m.r. spectroscopic data. In the carbonyl stretching region of the i.r. spectrum two bands (X = Cl: 2076 and 1989 cm^{-1}; X = Br: 2068 and 1991 cm^{-1}) are observed. These values agree with those reported by Vallarino (12) for $[(C_4H_9)_4N]$ [*cis*-$(CO_2RhX_2]$ and by Mague and Mitchener (3) for $\{[cis\text{-}(C_6H_5)_2PCH{=}CHP(C_6H_5)_2]_2Rh\}$ [*cis*-$(CO)_2RhX_2$]. Further, ^{19}F n.m.r. spectra obtained (Table 2) for the chloro-compounds are almost identical with those of the free ligands indicating a symmetrical arrangement of the ligands about the central metal atom. On the basis of the above data we assign the structure, **5**, to the new complexes. The ionic formulation is substantiated by equivalent conductance measurements, which indicated that the compounds are 1:1 electrolytes (~24 mhos cm^{-1} $mole^{-1}$, 10^{-3} *M* nitrobenzene solutions). In addition, reaction in alcoholic suspension of $[(f_6fos)_2Rh][cis\text{-}(CO)_2RhCl_2]$ with sodium tetraphenylborate produced a yellow precipitate of $[(f_6fos)_2Rh]^+[B(C_6H_5)_4]^-$ (vide infra).

The new ionic complexes, **5**, are air-stable, yellow solids which decompose slowly without melting upon heating above 200°. They are readily soluble in chlorinated solvents and acetone but insoluble in alcohols and hydrocarbons. In solution decomposition occurs within 2–3 h. Recrystallization is accomplished by addition of petroleum ether or alcohol to *fresh* solutions of the complexes.

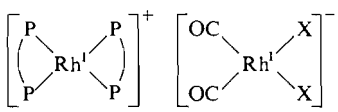

5

In contrast to ffos and $f_6$fos, the ligand $f_8$fos, **3** (*c*) reacts with $[Rh(CO)_2Cl]_2$ under identical conditions to give an orange powder which exhibits only one i.r. absorption in the carbonyl stretching region at 2044 cm^{-1}. All attempts to purify this material were fruitless, apparently because of high instability in any solvent in which it was soluble. Elemental analysis, though not good, would indicate that a complex having the formula $(f_8fos)Rh(CO)Cl$ was present. The insolubility of the solid in alcohol and its lack of volatility suggest a polymeric, **6**, or dimeric structure. Compounds of this type have been formed (3) with *trans*-$(C_6H_5)_2PCH{=}CHP(C_6H_5)_2$ (polymer) and with $(C_6H_5)_2As(CH_2)_2As(C_6H_5)_2$ (possibly a dimer like **7**.) However, in the former case chelation is prevented by the *trans*-structure of the ligand.

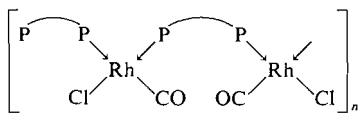

6

A monomeric structure, **6**, for the $f_8$fos complex might be suggested also by the i.r. value which, although somewhat higher (due to the electron withdrawing effect of the fluorocarbon bridge), is near that (2010 cm^{-1}) for the diphos complex, **2**, of Hieber and Kummer (2).

The formation of **5** represents a departure from the normal course of reaction between phosphines or arsines and rhodium(I) carbonyl halides. That is, symmetric cleavage of the chloride bridges usually occurs as in the well known (13) case of $(C_6H_5)_3P$ (reaction [1]).

[1]In the reaction between ffos and $[Rh(CO)_2Cl]_2$ in *benzene* solution the precipitate is slowest in appearing. It is preceded by a clear, dark red solution, possibly due to an intermediate involving coordination of only one phosphorus atom in the ligand.

Can. J. Chem. Downloaded from www.nrcresearchpress.com by 210.87.254.6 on 09/05/12
For personal use only.

Can. J. Chem. Downloaded from www.nrcresearchpress.com by 210.87.254.6 on 09/05/12
For personal use only.

[1] $4(C_6H_5)_3P + [Rh(CO)_2Cl]_2 \rightarrow$ *trans*-$[(C_6H_5)_3P]_2Rh(CO)Cl + 2CO$

Reaction between the fluorocarbon-bridged ditertiary phosphines results in an unsymmetrical cleavage of the bridges as shown in reaction [2].

[2] 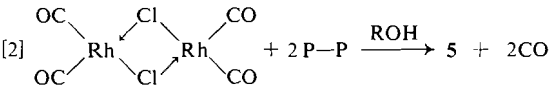

A similar cleavage may be regarded as occurring when, for example, 1,2-bis(dimethylarsino)-benzene (diars) reacts with $PdCl_2$ to give $[(diars)_2Pd][PdCl_4]$ (14). Recently unsymmetrical cleavage reactions have been reported involving a chelating ditertiary phosphine and the *carbonyl*-bridged dimer $[\pi\text{-}C_5H_5Fe(CO)_2]_2$ (15).

A less novel but equally plausible alternative reaction route cannot be ignored. This would involve the formation of two $[Rh(P—P)_2]^+$ ions from one molecule of $[Rh(CO)_2Cl]_2$ followed by attack of the displaced Cl^- on another $[Rh(CO)_2Cl]_2$ to give $[Rh(CO)_2Cl_2]^-$ anions.

The Complex [(ffars)Rh(CO)Cl]$_2$

Reaction of the chelating ditertiary arsine, **3** (*d*) (ffars), with $[Rh(CO)_2Cl]_2$ in ethanol produced a clear, bright red solution. Subsequent work-up provides a red crystalline complex in good yield which bears no resemblance, physically or spectroscopically, to the phosphine complexes discussed above. From elemental analysis and molecular weight measurements (Table 1), i.r. and n.m.r. data (Table 2) we have made a dimeric formulation $[(ffars)Rh(CO)Cl]_2$ to which, because of its similarity to complexes obtained from $(C_6H_5)_2MCH_2M(C_6H_5)_2$ (M = P, As) (3, 16), we can assign the structure **7**.

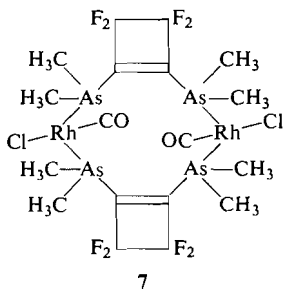

7

In the case of those complexes reported by Mague and Mitchener (3) and Mague (16) the change in function of the ligands (i.e. chelating to bridging) is believed to be a consequence of shortening the length of the hydrocarbon chain, effectively cancelling the chelating ability of the ligand. In the present case, however, the central structure of the molecule remains unchanged but the donor atoms are different. The ligand ffars shows a surprising reluctance to form the chelate complex $(ffars)Fe(CO)_3$ although derivatives of this type are known for ffos, $f_6$fos (6), and $f_8$fos (17). However, all the ligands, **3**, form complexes of the sort $(chelate)Mo(CO)_4$. There is at this time, however, no reasonable explanation for these differences in coordinating properties for the two types of ligand.

The complex $[ffarsRh(CO)Cl]_2$ is air-stable as the solid and in solution. It is quite soluble in most organic solvents and is easily recrystallized from hot hexane.

Because of its greater solubility an infrared spectrum was obtained in cyclohexane solution. Increased resolution in this solvent permitted additional carbonyl bands to be observed. Spectra of $[(C_6H_5)_2MCH_2M(C_6H_5)_2Rh(CO)X]_2$ (M = P, As; X = Cl, Br) (3) were measured as Nujol mulls and they showed one main band ca. 1970 cm^{-1} with a shoulder at ca. 1930 cm^{-1}. The spectrum of **7** shows four bands (two weak) which might be explained by coupling of vibrational modes between the two carbonyl groups.

Both the ^{19}F and ^1H n.m.r. spectra (Table 2) of this complex are compatible with the structure **7**. Single resonances for $—CF_2—$ and $CH_3—$ groups indicate symmetrical environments for the ^{19}F and ^1H nuclei.

[(P—P)$_2$Rh]X Complexes

As part of this study we investigated the reactions of the ligands ffos, $f_6$fos, and $f_8$fos with $[Rh(CO)_2X]_2$ in a 4:1 mole ratio. In warm alcoholic solution, an initial precipitate of the $(CO)_2RhX_2^-$ salt gradually dissolves as the anion reacts with excess of the ligand and a clear orange solution is obtained. Concentration of the solution and addition of ether gives a precipitate of the chloride or bromide, $[(P—P)_2Rh]X$, which is recrystallized from dichloromethane–hexane or acetone–hexane mixtures.

The tetraphenylborate derivatives are obtained by metathetical replacement of the halide ion using $NaB(C_6H_5)_4$ in alcoholic solutions.

The halides and tetraphenylborates are bright yellow crystalline solids which all decompose without melting in the range 200–300°. The

Can. J. Chem. Downloaded from www.nrcresearchpress.com by 210.87.254.6 on 09/05/12
For personal use only.

halides are soluble in all polar solvents whereas the tetraphenylborates are insoluble in alcohols. Their greater stability in solution indicates that the anion $[cis\text{-}(CO)_2RhCl_2]^-$ is the unstable component of **6**. A similar instability was noted by Vallarino (12).

It has been known for some time (18) that cationic square planar Rh(I) complexes with ditertiary phosphines will undergo oxidative-addition reactions with hydrogen chloride to give octahedral Rh(III) species (eq. [4]).

$$[4]\quad [Rh(diphos)_2]Cl + HCl \xrightarrow{CH_2Cl_2} [RhHCl(diphos)_2]Cl$$

More recently, the diarsine complex $[Rh(vdiars)_2{}^+Cl^-$ (vdiars = $cis\text{-}(C_6H_5)_2AsCH{=}CHAs(C_6H_5)_2$) (19) was shown to readily undergo a series of reactions involving hydrogen halides, halogens, allyl chloride or methyl iodide to give *trans* adducts. The complex was found to react reversibly with hydrogen under mild conditions. It was therefore of interest to investigate the ability of the new cations $(P{-}P)_2Rh^+$ to undergo similar reactions and hopefully relate them to catalytic applications.

In dichloromethane solution, anhydrous hydrogen chloride reacts rapidly with $[(ffos)_2Rh]^+Cl^-$ at room temperature and pressure, producing a pale yellow solid which analyzes for $[(ffos)_2RhHCl^+]Cl^-$. The i.r. spectrum shows a very weak absorption at ca. 2080 cm^{-1} which is possibly due to the Rh—H stretch and is just a little higher than values for the analogous diphos compounds (18). Surprisingly, although HCl reacts with $[(f_6fos)_2Rh]^+Cl^-$ in CH_2Cl_2 solution, we were unable to isolate a product which gave the expected analysis and instead obtained only starting material (shown by i.r. spectrum and melting point). This would indicate that the Rh(III) compound if formed is too unstable and reverts easily to the Rh(I) complex.

Further evidence for the high stability of the metal atom in the lower oxidation state was obtained from some hydrogen uptake experiments. These showed that even at 60° in benzene solution, little or no hydrogen was taken up to form the $[(f_6fos)_2RhH_2]^+$ cation (20). Test experiments on a small scale were carried out with CO and allyl chloride. No indication of reaction was noted. Thus it is concluded that under mild conditions, at least, the new Rh(I) cation complexes are highly stable to oxidation. Qualitatively, the stability can be attributed to the electron withdrawing nature of the ligands, which would tend to stabilize rhodium in the lower oxidation state.

The complex $[(f_6fos)_2Rh]^+Cl^-$ does undergo rapid reaction with reducing agents. With $NaBH_4$ in absolute ethanol, or $LiAlH_4$ in tetrahydrofuran a dark green solution is produced. Subsequent work-up provides dark green crystals which are highly unstable even at low temperatures in a vacuum. Attempts to characterize this material further were unrewarding.

We thank the Defence Research Board of Canada for financial support.

1. A. Sacco and R. Ugo. J. Chem. Soc. 3274 (1964).
2. W. Hieber and R. Kummer. Chem. Ber. **100**, 148 (1967).
3. J. T. Mague and J. P. Mitchener. Inorg. Chem. **8**, 119 (1969).
4. W. R. Cullen, P. S. Dhaliwal, and C. J. Stewart. Inorg. Chem. **6**, 2256 (1967).
5. W. R. Cullen, D. A. Harbourne, B. V. Liengme, and J. R. Sams. Inorg. Chem. **8**, 95 (1969).
6. W. R. Cullen, D. A. Harbourne, B. V. Liengme, and J. R. Sams. Inorg. Chem. **8**, 1469 (1969).
7. W. R. Cullen, D. A. Harbourne, B. V. Liengme, and J. R. Sams. J. Amer. Chem. Soc. **90**, 3293 (1968).
8. W. R. Cullen, D. F Dong, and J. A. J. Thompson. Can. J. Chem. **47**, 4671 (1969).
9. J. A. McCleverty and G. Wilkinson. Inorg. Syn. **8**, 211 (1966).
10. W. R. Cullen, D. S. Dawson, and P. S. Dhaliwal. Can. J. Chem. **45**, 683 (1967).
11. W. R. Cullen, P. S. Dhaliwal, and G. E. Styan. J. Organometal. Chem. **6**, 633 (1966).
12. L. M. Vallarino. Inorg. Chem. **4**, 161 (1965).
13. J. A. McCleverty and G. Wilkinson. Inorg. Syn. **8**, 214 (1966).
14. J. Chatt and F. G. Mann. J. Chem. Soc. 1622, (1939).
15. R. B. King, K. H. Pannell, C. A. Eggers, and L. W. Houk. Inorg. Chem. **7**, 2353 (1968).
16. J. T. Mague. Inorg. Chem. **8**, 1975 (1969).
17. W. R. Cullen and J. A. J. Thompson. Unpublished results.
18. A. Sacco and R. Ugo. J. Chem. Soc. 3274 (1964).
19. J. T. Mague and J. P. Mitchener. Chem. Commun. 911 (1968).
20. B. R. James and F. Ng. Unpublished results.

Can. J. Chem. Downloaded from www.nrcresearchpress.com by 210.87.254.40 on 09/05/12
For personal use only.

Basicities in the naphthyl azoxy series[1]

A. Dolenko, K. Mahendran, and E. Buncel
Department of Chemistry, Queen's University, Kingston, Ontario

Received November 10, 1969

The pK_a values of the conjugate acids of the six known phenyl–naphthyl and naphthyl–naphthyl azoxy derivatives have been measured by spectrophotometric methods in sulfuric acid solutions. Trends within the series are discussed in terms of delocalization and structural effects. The azoxy bases deviate slightly from Hammett base behavior.

Canadian Journal of Chemistry, 48, 1736 (1970)

Determination of the base strengths of the series of known phenyl–naphthyl and naphthyl–naphthyl azoxy derivatives has been undertaken as a preliminary to a kinetic study of the rearrangement of these compounds in acidic media, the Wallach rearrangement (1). The compounds investigated are the following:[2] β-1-phenylazoxynaphthalene (**1**), α-2-phenylazoxynaphthalene (**2**), β-2-phenylazoxynaphthalene (**3**), 1,1′-azoxynaphthalene (**4**), β-1,2′-azoxynaphthalene (**5**), and 2,2′-azoxynaphthalene (**6**). Previous studies on the protonation behavior of other aryl azoxy compounds have been confined to azoxybenzene (3–5) and a number of mono- and disubstituted azoxybenzenes (4, 5). The measurements of refs. 3 and 4 refer to aqueous acid while those of ref. 5 to 80% aqueous H_2SO_4 – 20% ethanol.

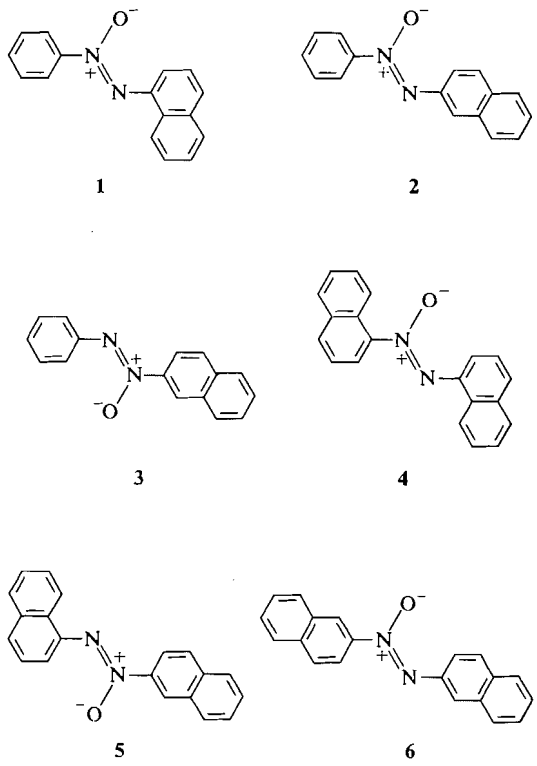

Experimental

Preparation of Azoxy Compounds

The azoxy compounds were obtained upon oxidation of the corresponding azo compounds with *m*-chloroperbenzoic acid or perbenzoic acid, using essentially the procedures outlined in ref. 2. **1**, m.p. 82–83 °C (lit. m.p. 84 °C (2)); **2**, m.p. 124–125 °C (lit. m.p. 125 °C (2)); **3**, m.p. 117.5–118 °C (lit. m.p. 117 °C (2)); **4**, m.p. 124–125 °C (lit. m.p. 127 °C (2)); **5**, m.p. 139.5–140 °C (lit. m.p. 137 °C (2)); and **6**, m.p. 168–168.5 °C (lit. m.p. 164–166 °C (2)). All melting points were obtained on a Fisher–Johns melting point apparatus and are uncorrected. During the preparation and subsequent manipulation of the azoxy compounds precaution was taken to avoid exposure to light in order to prevent a photochemical rearrangement (6).

Sulfuric Acids

Sulfuric acid solutions ranging from 53 to 86% by weight H_2SO_4 were prepared by diluting Fisher or C.I.L. Reagent Grade 96% sulfuric acid and analyzed by standard methods.

Preparation of Solutions for Spectroscopic Examination

Due to the limited solubility of the azoxy compounds in these acid solutions it was necessary to employ an organic co-solvent. As dictated by the solubility characteristics of a particular azoxy compound, the measurements were carried out in aqueous H_2SO_4 containing 0.5% by volume ethanol or 5.0% by volume dioxane. In the former case the small amount of ethanol added was considered to act merely as a diluent (7) and the H_0 values given by Jorgenson and Hartter (8) for purely aqueous acids were employed for the resulting solution. In the latter case the H_0 values due to Noyce and Jorgen-

[1]Part IX in series on the Wallach rearrangement. Part VIII, see ref. 18.

[2]The naming of the compounds is according to ref. 2.

Can. J. Chem. Downloaded from www.nrcresearchpress.com by 210.87.254.40 on 09/05/12
For personal use only.

son (9) applicable to the aqueous dioxane medium were used. Even with the use of these co-solvents solubility difficulties were encountered in the lower acid concentrations thus limiting the range of study. Further restrictions for the 95.0% aqueous H_2SO_4 – 5.0% dioxane medium were imposed due to precipitation of the dioxane sulfate salt in acid concentrations greater than 80% H_2SO_4.

pK_a Determinations

The spectral measurements were performed on a Unicam SP800B spectrophotometer at room temperature (ca. 25 °C). For determination of the pK_a values in 95% aqueous H_2SO_4 – 5.0% dioxane the solutions were prepared by adding 2.25 ml of freshly purified dioxane (10) to a series of 50 ml A Grade volumetric flasks. The flasks were then cooled in an ice–water bath and approximately 40 ml of H_2SO_4 of the appropriate concentrations added. This procedure was followed to dissipate heat developed on mixing and hence minimize decomposition of dioxane under acidic conditions (9). The solutions were allowed to come to room temperature and a 0.25 ml aliquot (lambda pipet) of a 1.00×10^{-3} *M* solution of the substrate in dioxane was added to each. After making up to the mark with the appropriate stock acid solution the contents were transferred immediately to a 10 cm silica cell and the spectrum recorded (usually within 3 to 4 min after the addition of substrate). The 99.5% aqueous H_2SO_4 – 0.5% ethanolic solutions were prepared using 0.25 ml aliquots of a 1.00×10^{-3} *M* stock solution of substrate in ethanol and making up with acid in 50 ml volumetric flasks.

In a number of cases, particularly at the higher acid concentrations, spectral changes (characteristic of rearrangement) were occurring and hence the spectra were recorded at regular time intervals and the desired optical density was obtained by extrapolation to zero time. In the most extreme case, **4** in 79.00% aqueous H_2SO_4 – 5.0% dioxane, the extrapolated optical density (o.d.) value was within 9% of the first recorded value.

In the case of **6** it was required to obtain o.d.'s for some acid concentrations in which the substrate was not completely soluble. Since the substrate appeared to be completely dissolved upon initial preparation of the acid solution (only such solutions were used) the spectrum was recorded as soon as possible after mixing and the decrease in absorption (uniform over the spectral region) which accompanied precipitation of the substrate was followed as a function of time. Extrapolation to zero time gave an estimate of the initial o.d. (within 8% of the value first recorded at the maximum).

Treatment of Data[3]

Plots of ε at $\lambda_{BH^+}{}^{max}$ and at $\lambda_B{}^{max}$ against the appropriate H_0 values gave the usual sigmoid type curve and pK_a values were estimated from the mid-point of the linear portion. The extinction data were also treated by the methods of Davis and Geissman (11) and Arnett and Wu (12).[4] The latter method was particularly applicable to the present study since in addition to a pK_a value it provides an estimate of the molar extinctions ε_B and ε_{BH^+} of the substrate forms, which in most cases could not be obtained experimentally due to the confinement to a relatively narrow acid concentration range for the reasons previously mentioned. Using these values for ε_B and ε_{BH^+} (obtained at $\lambda_{BH^+}{}^{max}$) the ionization ratios were calculated from the relation $I = [BH^+]/[B] = \varepsilon_B - \varepsilon/\varepsilon - \varepsilon_{BH^+}$ for values of log $[BH^+]/[B]$ ranging between +1 and −1.

Results and Discussion

Spectral Features and Hammett Behavior

The spectral characteristics of the azoxy compounds are given in Table 1. It is seen that the neutral forms of the azoxy compounds under consideration show fairly strong absorption maxima in the region 323–390 mμ ($\pi^* \leftarrow \pi$ transition, often referred to as the K band (13)). With the exception of **6** all show a well-defined peak for both the neutral and the protonated form, separated by 50–100 mμ. Whereas the spectrum of neutral **6** showed a more or less symmetrical band at 350 mμ, the spectrum of the protonated form showed an unsymmetrical band with $\lambda_{BH^+}{}^{max}$ at 410 mμ and a broad shoulder at 450 mμ.

Figure 1 for β-1-phenylazoxynaphthalene (**1**) in 99.5% aqueous H_2SO_4 – 0.5% ethanol is illustrative of the spectral changes occurring on protonation in this series. In Fig. 2 the extinctions at $\lambda_B{}^{max}$ and $\lambda_{BH^+}{}^{max}$ are given as a function of H_0. The failure to obtain a well defined isosbestic point in Fig. 1 is probably indicative of a medium effect (14). Due to the very broad shapes of the absorption bands a small shift in the position of the band will not incur a large change in the value of ε.

The slopes of log *I* vs. H_0 plots are given in

[3]The original extinction data obtained for compounds **1** to **6** in the sulfuric acid solutions have been submitted to the Depository of Unpublished Data, National Science Library, National Research Council, Ottawa, Canada. Photocopies may be obtained on request.

[4]The Davis–Geissman procedure (11) consists of plotting the difference in extinctions at two selected wavelengths (usually $\lambda_B{}^{max}$ and $\lambda_{BH^+}{}^{max}$) against H_0; a sigmoid curve is obtained with the pK_a as its inflection point. This method is valuable in minimizing effects due to solvent-induced lateral shifts in the absorption bands.

The Arnett–Wu procedure (12) is an iterative method. An approximate K_a value is used in the equation

$$\varepsilon\,(h_0 + K_a) = \varepsilon_{BH^+} . h_0 + \varepsilon_B . K_a$$

and on plotting $\varepsilon(h_0 + K_a)$ vs. h_0, values of ε_{BH^+} and ε_B are obtained. Using the latter, one plots log(ionization ratio) vs. H_0, which yields an improved value of pK_a. This procedure usually gives a constant pK_a value after one such cycle.

Can. J. Chem. Downloaded from www.nrcresearchpress.com by 210.87.254.40 on 09/05/12
For personal use only.

TABLE 1

Spectral characteristics of aryl azoxy compounds

Compound	Range of acid concentration†	λ_{max}‡ B	λ_{max}§ BH^+	ε_B(expt.)‖ $\times 10^{-3}$	ε_{BH^+}(expt.)‖ $\times 10^{-3}$	ε_B(calcd.)¶ $\times 10^{-3}$	ε_{BH^+}(calcd.)¶ $\times 10^{-3}$	Slope log I vs. H_o**	n††
β-1-Phenylazoxy-naphthalene **1**	59.95–85.50‡‡	390	470	0.940	7.25	0.460	9.22	0.94±0.02	19
	60.54–76.73§§	392	478	0.700	7.61	0.262	9.12	0.86±0.05	11
β-1,2′-Azoxynaphthalene **5**	62.78–76.57§§	396	482	2.40	10.84	0.640	13.14	0.98±0.07	8
1,1′-Azoxynaphthalene **4**	59.85–76.58§§	380	480	1.24	8.68	0.120	9.62	0.93±0.08	8
α-2-Phenylazoxy-naphthalene **2**	52.62–82.59‡‡	344	398	4.84	14.20	4.78	16.38	0.93±0.08	15
β-2-Phenylazoxy-naphthalene **3**	52.62–82.59‡‡	334	398	2.40	14.30	1.92	16.54	0.92±0.09	15
2,2′-Azoxynaphthalene **6**	59.85–76.56§§	350	410	9.70	16.30	5.56	16.94	0.84±0.05	10
Azoxybenzene*	41.1 –96.5	323	383	—	—	—	—	0.97±0.10	—

*Values taken from ref. 3.
†Percent H_2SO_4 after mixing with co-solvent.
‡The λ_{max} observed in lowest acid concentration.
§The λ_{max} observed in highest acid concentration.
‖Experimental values obtained at $\lambda_{BH^+}{}^{max}$.
¶These values are calculated by the method of Arnett and Wu (12) at $\lambda_{BH^+}{}^{max}$. It is noted that in many cases there is a considerable discrepancy between these and the experimental values, which is at least in part the result of the experimental data not being obtained in sufficiently dilute or concentrated acid solutions. This is indicated by the fact that the experimental values for ε_B at $\lambda_{BH^+}{}^{max}$ as obtained in neutral media are closer to the calculated values. A medium effect may also be involved.
**Values of slopes and error limits are obtained from least square plots.
††Number of experimental data points.
‡‡Data obtained in 99.5% aqueous H_2SO_4 – 0.5% ethanol.
§§Data obtained in 95.0% aqueous H_2SO_4 – 5.0% dioxane.

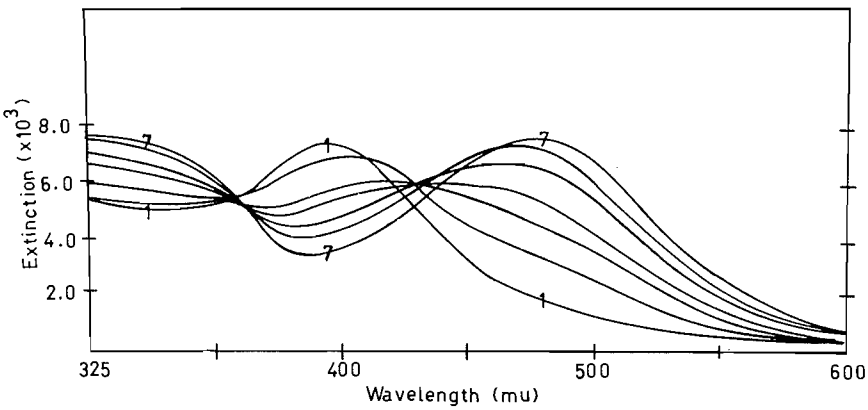

FIG. 1. β-1-Phenylazoxynaphthalene (**1**) in 99.5% aqueous H_2SO_4 – 0.5% ethanol over range of acid concentrations from 64.82 (curve 1) to 76.92% H_2SO_4 (curve 7).

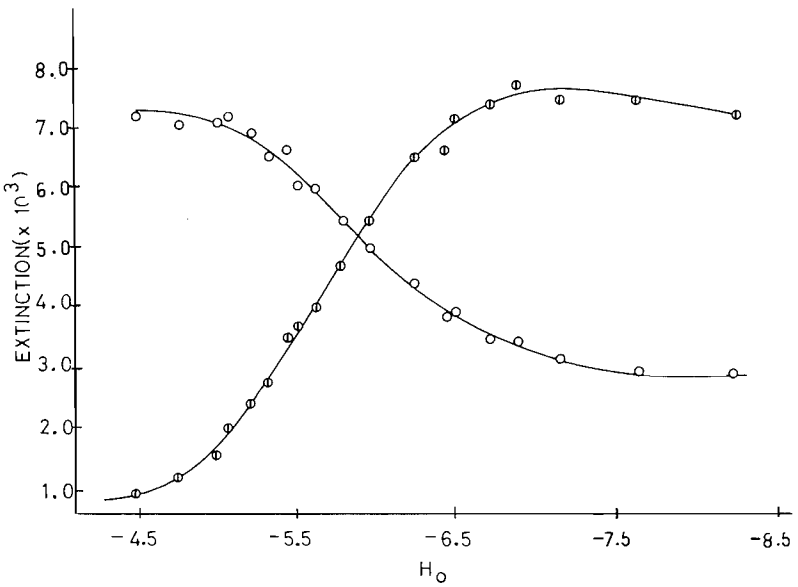

FIG. 2. β-1-Phenylazoxynaphthalene (**1**) in 99.5% aqueous H_2SO_4 – 0.5% ethanol: plots of extinction at 390 mμ (O) and at 470 mμ (Φ) versus H_o.

Table 1 and an illustrative example is shown in Fig. 3. It is seen that the slope values are close to unity, indicating only slight deviation from the H_o acidity function. It is interesting that in determining the basicities of a number of substituted pyridine *N*-oxides, which may be considered somewhat analogous to the azoxy compounds, Johnson *et al.* (15) found that their ionization ratios could be better correlated with the H_A (14) acidity function.

Comparison of pK_a Values

The pK_a values obtained by the methods described are summarized in Table 2. The last column but one (pK_a experimental) records the average of the values obtained by the four methods. Following the practice of Noyce and Jorgenson (16) the pK_a data obtained in 95% aqueous H_2SO_4 – 5% dioxane have been corrected (last column) to purely aqueous acid by an amount (0.15–0.2 H_o units) equivalent to the

Can. J. Chem. Downloaded from www.nrcresearchpress.com by 210.87.254.40 on 09/05/12
For personal use only.

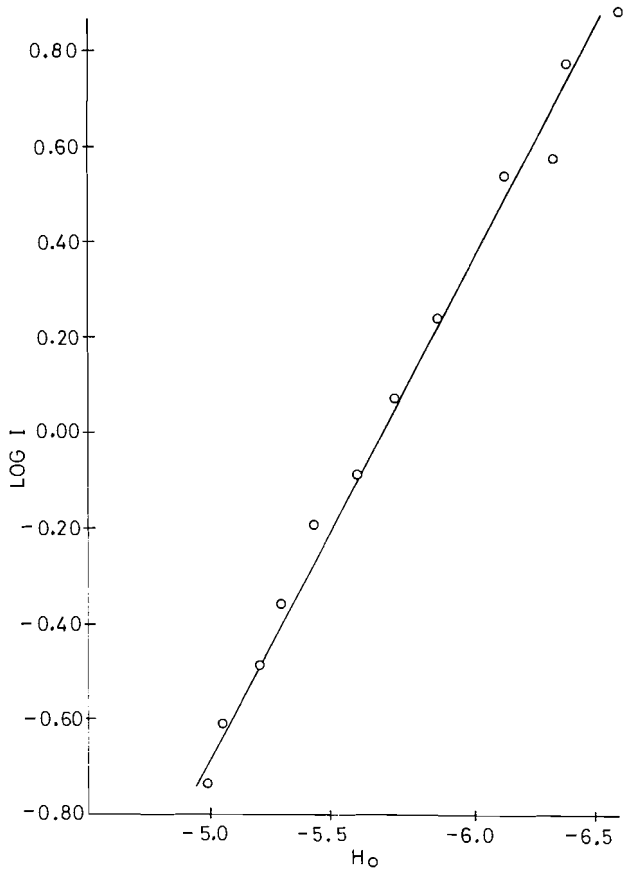

FIG. 3. Plot of log I vs. H_o for β-1-phenylazoxynaphthalene (**1**).

difference in the H_o scales of purely aqueous acid and the 5% dioxane medium at a given concentration of acid. The pK_a data in 99.5% aqueous H_2SO_4 – 0.5% ethanol are assumed (7) to hold in purely aqueous medium. The validity of these assumptions is indicated by the agreement between the experimental and the corrected pK_a values for compound **1**. While structural changes within the series are seen to have only a small effect on the relative basicities of these compounds, nevertheless a definite trend is apparent. Thus azoxy compounds containing a 1-naphthyl group are weaker bases than those containing only 2-naphthyl and/or phenyl groups.

In their study of the basicities of several 4- and 4′-mono- and disubstituted azoxybenzenes in 80% aqueous H_2SO_4 – 20% ethanol Hahn and Jaffé (5) likewise reported a small variation in pK_a values. For the mono-substituted compounds the extremes were −6.04 for 4-methoxyazoxybenzene and −7.01 for 4-bromoazoxybenzene; 4-nitroazoxybenzene was the only exception having a pK_a of −9.83. The pK_a values for the disubstituted azoxy compounds showed a spread of about 2.5 pK_a units. Another interesting feature of these authors' work is the apparent insensitivity of the pK_a values to shifting a substituent from the 4- to 4′-position. For example, pK_a values of −6.04 and −6.14 are reported for 4- and 4′-methylazoxybenzene respectively. Hahn and Jaffé were able to make a satisfactory correlation of the pK_a's with σ and σ^- values ($\rho = 2.5$ for the 4-substituted compounds and $\rho = 1.7$ for the 4′-substituted compounds). The studies of Duffey and Hendley (4) in aqueous H_2SO_4 medium extended to 3- and 3′- substituted azoxybenzenes but in these systems Hammett correlations did not hold well. However there was again only a slight difference in pK_a between 3- and 3′- substituted azoxybenzenes. A similar

Can. J. Chem. Downloaded from www.nrcresearchpress.com by 210.87.254.40 on 09/05/12
For personal use only.

TABLE 2

pK_a Values obtained by various methods

Compound	Method					
	ε_B vs. H_0	ε_{BH+} vs. H_0	Davis–Geissman	Arnett–Wu	pK_a (exptl.)‡	pK_a aqueous H_2SO_4§
β-1-Phenylazoxynaphthalene **1***	−5.77	−5.53	−5.75	−5.80	−5.71	−5.71
β-1-Phenylazoxynaphthalene **1**†	−5.90	−5.78	−5.92	−5.96	−5.89	−5.71
β-1,2′-Azoxynaphthalene **5**†	−6.00	−5.54	−5.80	−5.70	−5.82	−5.64
1,1′-Azoxynaphthalene **4**†	−5.76	−5.69	−5.70	−5.72	−5.72	−5.53
α-2-Phenylazoxynaphthalene **2***	−5.09	−4.90	−5.07	−5.04	−5.03	−5.03
β-2-Phenylazoxynaphthalene **3***	−5.10	−4.88	−5.07	−4.96	−5.00	−5.00
2,2′-Azoxynaphthalene **6**†	−5.12	−5.20	−5.10	−5.08	−5.13	−4.98
Azoxybenzene						−5.15

*Data obtained in 99.5% aqueous H_2SO_4 – 0.5% ethanol.
†Data obtained in 95.0% aqueous H_2SO_4 – 5.0% dioxane.
‡Mean value of four methods.
§pK_a Values corrected for difference between H_0 scale for 95% aqueous H_2SO_4 – 5% dioxane and purely aqueous H_2SO_4. The data for 99.5% aqueous H_2SO_4 – 0.5% ethanol are unchanged.

result is observed in the present work, in that **2** and **3** have closely similar pK_a values.[5]

We are concerned here not with substituent effects as such but with the effects of various aryl rings, and their position of attachment, on the availability of electron density for protonation. The relative basicities of the azoxy compounds should then reflect the extent of delocalization of an unshared electron pair of electrons from the azoxy oxygen throughout the aryl rings. A qualitative estimate of this delocalization may be obtained by examination of the main contributing resonance structures in the series. Considering first β-1-phenylazoxynaphthalene (**1**), an electron pair from the oxygen can be delocalized into the naphthyl system (but not into the adjacent phenyl) and there are two such canonical structures in which aromaticity of one of the fused rings is retained (Chart 1). Corresponding structures can also be written for compounds **4** and **5**. Similar reasoning shows

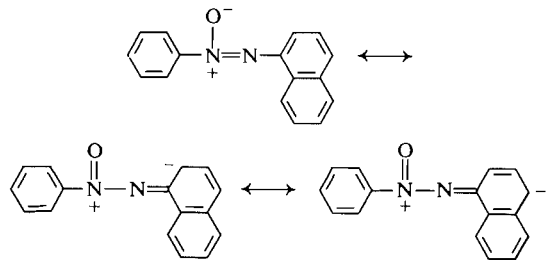

CHART 1

that in **2** and **6** delocalization of the oxygen electron-pair is directed into the removed 2-naphthyl system, but now only one such canonical structure retains aromaticity in one of the fused rings of this 2-naphthyl moiety. Lastly, compound **3** will have the electron-pair delocalized into the phenyl group, analogously to azoxybenzene itself.

According to the above argument one would predict that **1**, **4**, and **5** would have approximately equal basicities, which is closely followed experimentally. The slightly higher basicity of **4** is probably due to steric interactions inhibiting coplanarity and hence conjugation. Further, compounds **2** and **6** should also have about equal base strengths; however, the basicities of **2** and **6** should be greater than of **1**, **4**, and **5**, since the extent of delocalization of the oxygen electron-pair should be smaller with the former two bases. This also is borne out experimentally. Lastly while **3** is observed to have about the same basicity as azoxybenzene, as anticipated, it is perhaps surprising that these pK_a values should

[5]A more stringent test would be to compare the pK_a values of **1** with the isomeric azoxy structure **7**, and of **5** with structure **8** (we thank a referee for drawing this to our attention). However, unfortunately, neither **7** nor **8** have as yet been prepared.

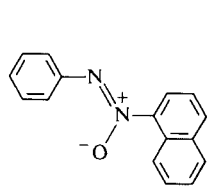

7

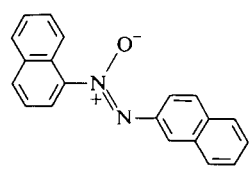

8

Can. J. Chem. Downloaded from www.nrcresearchpress.com by 210.87.254.40 on 09/05/12
For personal use only.

not differ significantly from those of **2** and **6**.[6] Apparently the phenyl and 2-naphthyl moieties have about equal capacity to delocalize the oxygen electron-pair.

Discussion of the basicities of the azoxy compounds would be incomplete without consideration of electronic effects in the conjugate acids of these bases. Now charge delocalization from the protonated oxygen would lead to structures with two adjacent positive charges, which is energetically unfavorable. Hence the base weakening effect in this series is concluded to result from delocalization effects in the neutral substrates as considered above.

The preceding discussion involving delocalization considerations receives support from molecular orbital theory. The conjugative power of a carbon center on an aromatic ring has been defined by Coulson and Longuet–Higgins (17) as equal to β times the self-polarizability of that position, with the following values being assigned (17): phenyl, 0.398; 2-naphthyl, 0.405; 1-naphthyl, 0.443. This leads to the prediction that, in the first order of approximation, the basicities in the present series will fall into two groups: those compounds which allow conjugation between the azoxy-oxygen and a 1-naphthyl group (**1**, **4**, and **5**) and those in which conjugation will occur with a 2-naphthyl or a phenyl group (**2**, **3**, **6**, and azoxybenzene). The former three should be the weaker bases, since increased conjugation will lead to decreased electron density on the oxygen. These predictions coincide almost exactly with the experimental observations. Badger *et al.* (2, 13) were able to make correlations between conjugative ability (17) and electron availability, as reflected in activation parameters in oxidation and in the frequency of the K-absorption band of the aryl azo compounds corresponding to the present azoxy series.

[6]On the analogy that 2-naphthylamine is a weaker base (pK_a 4.11) than aniline (pK_a 4.58) it might have been predicted that **2** and **6** would be weaker bases than **3** or azoxybenzene.

Financial support from the National Research Council of Canada is gratefully acknowledged as is the award of an Ontario Graduate Fellowship to A.D.

1. E. Buncel. *In* Mechanisms of molecular migrations. *Edited by* B. S. Thyagarajan, John Wiley, N.Y. 1968.
2. G. M. Badger and G. E. Lewis. J. Chem. Soc. 2151 (1953).
3. E. Buncel and B. T. Lawton. Can. J. Chem. **43**, 862 (1965).
4. D. Duffey and E. C. Hendley. J. Org. Chem. **33**, 1918 (1968).
5. C. S. Hahn and H. H. Jaffé. J. Amer. Chem. Soc. **84**, 949 (1962).
6. G. M. Badger and R. G. Buttery. J. Chem. Soc. 2243 (1954).
7. R. Stewart and M. R. Granger. Can. J. Chem. **39**, 2508 (1961).
8. M. J. Jorgenson and D. R. Hartter. J. Amer. Chem. Soc. **85**, 878 (1963).
9. D. S. Noyce and M. J. Jorgenson. J. Amer. Chem. Soc. **83**, 2525 (1961).
10. L. F. Fieser. Experiments in organic chemistry. 3rd ed. Heath, Boston, 1955. p. 284.
11. C. T. Davis and T. A. Geissman. J. Amer. Chem. Soc. **76**, 3507 (1954).
12. E. M. Arnett and C. Y. Wu. J. Amer. Chem. Soc. **82**, 5660 (1960).
13. G. M. Badger and R. G. Buttery. J. Chem. Soc. 2156 (1953).
14. K. Yates, J. B. Stevens, and A. R. Katritzky. Can. J. Chem. **42**, 1957 (1964).
15. C. D. Johnson, A. R. Katritzky, and Naeem Shakir. J. Chem. Soc. 1235 (1967).
16. D. S. Noyce and M. J. Jorgenson. J. Amer. Chem. Soc. **84**, 4312 (1962).
17. C. A. Coulson and H. C. Longuet-Higgins. Proc. Roy. Soc. A, **195**, 188 (1948).
18. E. Buncel and W. M. J. Strachan. Can. J. Chem. **48**, 377 (1970).

Can. J. Chem. Downloaded from www.nrcresearchpress.com by 210.87.254.40 on 09/05/12
For personal use only.

"Ideal" intensities of supersonic molecular beams

RODNEY L. LEROY[1]
Department of Chemistry, Yale University, New Haven, Connecticut 06520

AND

THOMAS R. GOVERS[1]
FOM Instituut voor Atoom- en Molecuulfysica, Kruislaan 407, Amsterdam, The Netherlands

Received December 16, 1969

A general equation is derived to predict ideal supersonic beam intensities, allowing for an ellipsoidal local speed distribution at the skimmer. With suitable approximations this is found to reduce to all of the previously derived results. A new approximate equation is presented. This can accurately reproduce the intensities predicted by the general equation, provided only that the speed ratio in the radial direction at the skimmer is much greater than 3/2. It is found that a relatively broad speed distribution in the radial direction can result in an increase in the centerline beam intensity. This increase is only weakly dependent on the nozzle–skimmer separation, and it decreases as the skimmer radius is increased.

Canadian Journal of Chemistry, 48, 1743 (1970)

Can. J. Chem. Downloaded from www.nrcresearchpress.com by 210.87.254.105 on 09/05/12
For personal use only.

Skimmer interference and other non-ideal effects (ref. 1 and references therein) complicate the interpretation of experimental supersonic beam intensities. If such effects are ignored, "ideal" intensities can be readily calculated.

None of the available intensity equations (2–8) allows for a general anisotropic distribution of local velocities in the free jet at the skimmer. However, a relatively broad residual speed distribution is found in the radial direction downstream of the onset of translational freezing (6, 9, 10), and this can influence the centerline beam intensity. To investigate the importance of this effect, we derive here a generalized intensity equation.

The distribution of molecular speeds at the skimmer may be approximated near the centerline by the ellipsoidal function (6, 9, 11)

$$[1] \qquad f(v,\theta)\mathrm{d}v\,\mathrm{d}\omega = \pi^{-3/2}c_{\parallel}^{-1}c_{\perp}^{-2}\,\mathrm{e}^{-v^2\sin^2\theta/c_{\perp}^2}\,\mathrm{e}^{-(v\cos\theta - v_b)^2/c_{\parallel}^2}v^2\,\mathrm{d}v\,\mathrm{d}\omega$$

Here v is the molecular speed, θ is the angle which a particle's trajectory makes with the streamline[2] at the point where it enters the skimmer, v_b is the average velocity of the beam particles in the radial direction, and $\mathrm{d}\omega$ is the element of solid angle. $c_{\parallel}$ and $c_{\perp}$ are reference velocities, defined by

$$c_{\parallel} \equiv (2kT_{\parallel}/m)^{1/2}$$

and

$$c_{\perp} \equiv (2kT_{\perp}/m)^{1/2}$$

where m is the mass of a beam particle, k is the Boltzmann constant, and $T_{\parallel}$ and $T_{\perp}$ are the parallel and perpendicular temperatures respectively, at the skimmer. These temperatures are respectively the "temperatures" of one and two dimensional Boltzmann distribution functions which describe the local speed distributions in the radial direction and in the plane perpendicular to the radial direction.

The flow is assumed to be free molecular downstream of the plane bounded by the skimmer lip. Thus the beam intensity at a centerline detector, due to particles which cross the skimmer opening through a ring of radius r and width $\mathrm{d}r$ (cf. Fig. 1), is

$$[2] \qquad \mathrm{d}I_0 = \int_0^{\infty}\left(2\pi s^2\,\frac{\sin\theta_n}{\cos^3\theta_n}\cos\theta_d\,\mathrm{d}\theta_n\right)\left(\frac{A_d}{l^2}\cos^3\theta_d\right)nvf(v,\theta)\,\mathrm{d}v\Big/A_d/l^2$$

[1]NRCC Postdoctoral Fellow, 1968–1970.

[2]To an excellent approximation the streamlines may be considered to be straight lines radiating from the nozzle throat (12).

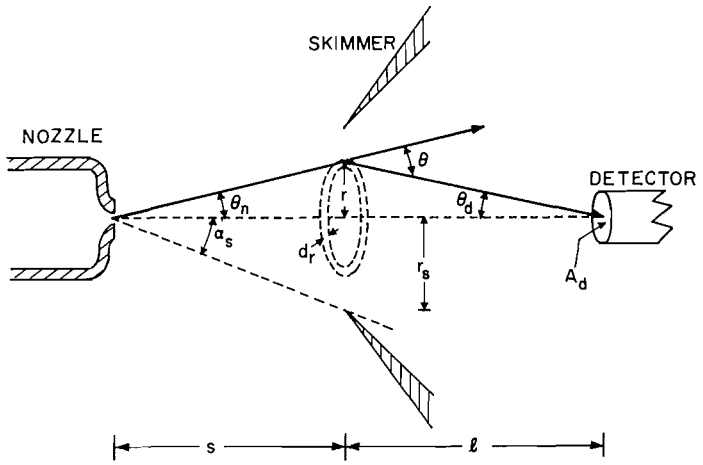

FIG. 1. Schematic representation of the beam defining elements.

n and $f(v,\theta)$ are, respectively, the number density and the velocity distribution function in the plane of the skimmer at a distance r from the centerline. Their values are assumed below to be constant over the skimmer orifice, and are set equal to the values on the centerline at a distance s from the nozzle throat. Other quantities appearing in eq. [2] are defined in Fig. 1. Note that the intensity is expressed per unit of solid angle, where solid angles are measured from the center of the skimmer opening. Substituting $f(v,\theta)$ from eq. [1] and integrating over the skimmer area (from $\theta_n = 0$ to $\theta_n = \alpha_s = \arctan(r_s/s)$), eq. [2] yields the ideal intensity equation

$$[3] \qquad I_0 = \frac{2ns^2}{\pi^{1/2}c_\perp{}^2c_\parallel}\int_0^{\alpha_s}\cos^4\theta_d\,\frac{\sin\theta_n}{\cos^3\theta_n}\cdot\frac{e^{-(S_\parallel{}^2-b^2)}}{a^2}F(b)\,d\theta_n$$

where

$$F(b) \equiv \tfrac{1}{2}(1+b^2)\,e^{-b^2} + \frac{\pi^{1/2}b}{2}(\tfrac{3}{2}+b^2)[1+\mathrm{erf}(b)]$$

$$a \equiv \sin^2\theta/c_\perp{}^2 + \cos^2\theta/c_\parallel{}^2$$

$$b \equiv S_\parallel[1+(c_\parallel\tan\theta/c_\perp)^2]^{-1/2}$$

and

$$S_\parallel \equiv v_b/c_\parallel$$

If the divergence of the flow at the skimmer can be neglected ($\theta_d \approx 0$, $\cos\theta_d \approx \cos\theta_n \approx 1$, and $\sin\theta_n \approx \sin\theta \approx \tan\theta \approx \theta_n \ll 1/S_\perp$, where $S_\perp \equiv v_b/c_\perp$), eq. [3] may be reduced directly to the early intensity equations presented by Parker *et al.* (3) and by French (4). For isentropic flow to the skimmer ($c_\parallel = c_\perp$), eq. [3] becomes equal to the result of Parker *et al.* [3]

$$[4] \qquad I_0 \approx nv_b r_s{}^2(\tfrac{3}{2}+S^2)$$

[3]These results, in common with all simple intensity equations, make use of the assumption that $S_\parallel$ is large enough that $F(b) \approx \pi^{1/2}b(\frac{3}{2}+b^2)$.

where $S = S_\parallel$ is the speed ratio at the skimmer. If for the same skimmer the flow suddenly "freezes" translationally at a distance x_q from the source ($c_\perp/c_\parallel = x_q/s$), eq. [3] reduces to French's expression (5)

$$[5] \qquad I_0 \approx n_q v_b r_s{}^2(\tfrac{3}{2}+S_\parallel{}^2)$$

where

$$n_q = n(s/x_q)^2$$

The intensity equations presented by Anderson and Fenn (6) and by Hagena and Morton (7) take into account the divergence of the flow at the skimmer. The former result

$$[6] \quad I_0 \approx \frac{nv_b s^2}{(1+s/l)^2}\times\left\{1-\exp\left[-\frac{S_\parallel{}^2\left(\frac{r_s(l+s-x_q)}{l}\right)^2}{x_q{}^2-\left(\frac{r_s(l+s-x_q)}{l}\right)^2}\right]\right\}$$

Can. J. Chem. Downloaded from www.nrcresearchpress.com by 210.87.254.105 on 09/05/12
For personal use only.

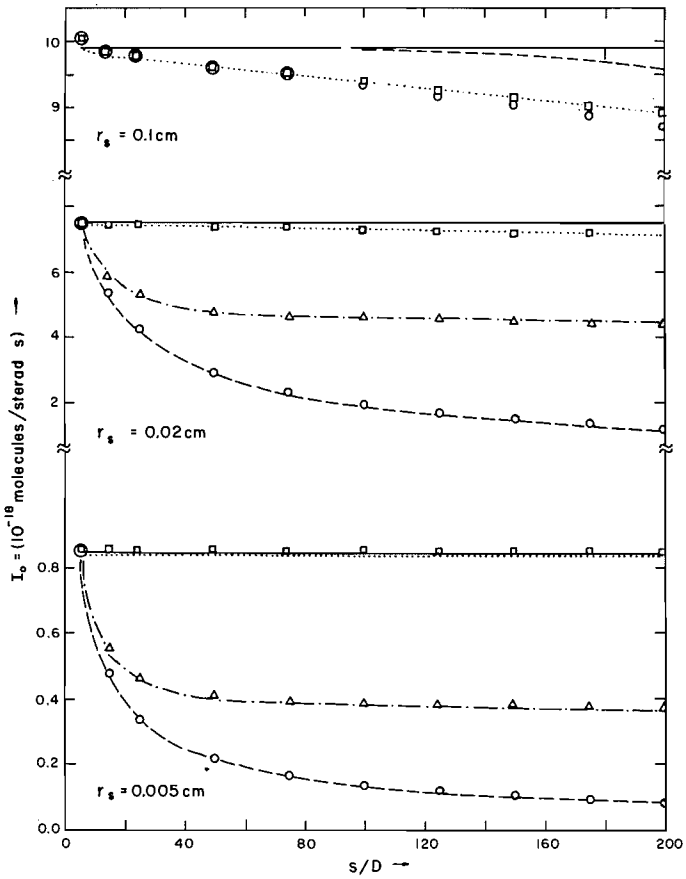

FIG. 2. Comparison of the ideal intensity equations. The points (□, △, ○) are calculated from eq. [3], the solid and broken curves from eq. [7], and the dotted curves from eq. [6]. At each skimmer radius results are presented for (*a*) isentropic flow to the skimmer (○, – – –); (*b*) a sudden translational freezing at x_q (□, ——, · · · · ·), and (*c*) a slow transition from collision dominated to free molecular flow, downstream of the onset of translational freezing (△, –·–·–). The assumed beam parameters are recorded in Table 1.

only applies if the flow suddenly freezes translationally at x_q. However, in this case it reproduces eq. [3] very well, provided only that $S_{\|}^2 \gg 3/2$. Hagena and Morton's equation,[4]

$$[7] \quad I_0 \approx n v_b s^2 (1 - \cos^3 \alpha_s \, e^{-S_\perp^2 \sin^2 \alpha_s})$$

also reproduces eq. [3] very well, provided that $l \gg s$ and the local speed distribution at the skimmer is isotropic.

Intensities calculated from eqs. [6], [7], and the general eq. [3] are compared in Fig. 2. The assumed beam parameters are recorded in Table 1. Intensities are presented as a function of the nozzle–skimmer separation for three values of the skimmer radius, ranging from very small (r_s = 0.005 cm) to large enough (r_s = 0.1 cm) that the skimmer is saturated, i.e. that further increasing r_s does not significantly affect I_0. For each skimmer, intensities were calculated from eq. [3] assuming isentropic flow to the skimmer (circles), free molecular flow downstream of x_q (squares), and a slow transition from isentropic to free molecular flow downstream of x_q (triangles). To obtain these latter results we set $T_{\|} = T_q$, and calculated $T_\perp$ from eq. [2] of ref. 1, using $B = 0.4$ and $C = 2.5$. Hagena and Morton's equation (solid and broken curves) assumes $l \gg s$, and thus overestimates eq. [3] if the skimmer and nozzle–skimmer separation are large. However, when r_s and/or s are small, eqs. [3] and [7] agree quite well. The apparent discrepancies at $s = x_q$

[4]Equation [7] differs slightly from eq. [6] of ref. 7, because of a typographical error in the latter.

Can. J. Chem. Downloaded from www.nrcresearchpress.com by 210.87.254.105 on 09/05/12
For personal use only.

TABLE 1

Beam parameters

Parameter	Value
Geometric nozzle exit diameter (D)*	0.0266 cm
Skimmer–detector distance	99.6 cm
Beam gas	argon
Source pressure	50 Torr
Source temperature	295 °K
Distance from the nozzle at which translational freezing begins (x_q)†	0.16 cm
Density at x_q (n_q)	6.8×10^{15} particles/cc
Local temperature at x_q (T_q)	7.6 °K
Beam velocity downstream of x_q (v_b)‡	5.47×10^5 cm/s

*The nozzle discharge coefficient is assumed to be unity.
†x_q is calculated from the "terminal mach number" M_q, using Ashkenas and Sherman's fitting formula (12) for the centerline mach number in a free jet. M_q is taken from Anderson and Fenn's empirical relation for argon expansions (6).
‡$v_b = M_q[(5/3)kT_q/m]^{1/2}$.

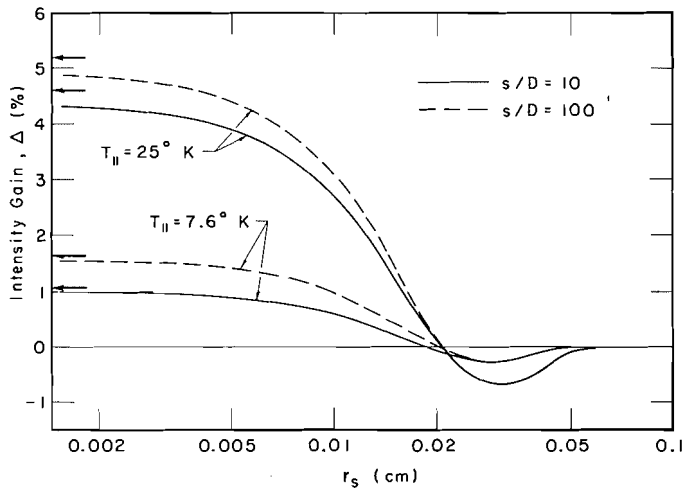

FIG. 3. Increase in centerline beam intensity due to a relatively broad distribution of local speeds in the radial direction at the skimmer. Arrows indicate asymptotic values calculated from eq. [10]. Beam parameters are recorded in Table 1. Perpendicular temperatures (2.9 and 0.029 °K respectively for $s/D = 10$ and 100) were calculated assuming a sudden freeze at x_q.

reflect minor differences in the assumptions used in deriving the two equations. Anderson and Fenn's result (dotted curves) only applies when the flow becomes suddenly free molecular at x_q, but in this case it always agrees with eq. [3] within 2%.

It is convenient to reduce eq. [3] to a simplified expression, which can be used to predict centerline beam intensities in the case of an anisotropic local speed distribution at the skimmer. We assume that α_s is sufficiently small that

$$\cos\theta_d \approx \cos\theta_n \approx 1$$

$$\sin\theta_n \approx \theta_n$$

and

$$\sin\theta \approx \tan\theta \approx \theta \approx \theta_n(1 + s/l)$$

over the whole range of integration. Then if the condition

$$[8] \qquad r_s \ll s\,c_\perp/c_\parallel$$

is satisfied, eq. [3] is accurately approximated by

$$[9] \quad I_0 = \frac{nv_b s^2}{(1 + s/l)^2}\left(1 + \frac{1.5}{S_\parallel^2}\right) \times [1 - e^{-S_\perp^2\alpha_s^2(1+s/l)^2}]$$

This expression reproduces all the predictions of eq. [3] in Fig. 2 within 2%.

We have compared eqs. [3] and [9] for isentropic flow to the skimmer. Here condition [8] becomes $r_s \ll s$, and in agreement with this we find that eq. [9] approaches more and more

Can. J. Chem. Downloaded from www.nrcresearchpress.com by 210.87.254.105 on 09/05/12
For personal use only.

closely to eq. [3] as the nozzle–skimmer separation is increased. However, for such isentropic flow, the two expressions never deviate from one another by more than $\frac{1}{3}\%$, provided that the nozzle–skimmer separation is greater than the skimmer diameter.

In the limit of a very small skimmer ($r_s \to 0$), the effect of a relatively high value of $T_\parallel$ is readily derived from eq. [9]. The centerline beam intensity is increased. Compared to the intensity which would be observed if the local speed distribution were isotropic corresponding to a temperature $T = T_\perp$, this increase is

$$[10] \quad \Delta(r_s \to 0) = 150 \frac{(S_\perp^2/S_\parallel^2 - 1)}{(S_\perp^2 + 1.5)} \%$$

Similarly for a finite skimmer, the percentage change in intensity due to temperature anisotropy is defined as

$$[11] \quad \Delta = 100 \left[\frac{I_0(T_\perp, T_\parallel)}{I_0(T_\perp, T_\parallel = T_\perp)} - 1 \right] \%$$

where intensities are calculated from eq. [3].

Δ is plotted as a function of the skimmer radius in Fig. 3, for two values of $T_\parallel$ and two values of the nozzle–skimmer separation. Perpendicular temperatures are calculated from the parameters of Table 1, assuming a sudden freeze at x_q.

It is apparent from Fig. 3 that eq. [10] represents an upper limit on the effect of anisotropy on centerline molecular beam intensities. The intensity "gain" decreases as the skimmer radius is increased, until it becomes slightly negative, passes through a minimum, and approaches zero. For a very large skimmer ($r_s \to \infty$), the ideal intensities calculated assuming anisotropic and isotropic local speed distributions become identical, as they must.

We are grateful to Dr. Otto Hagena for helping us to understand the ideal intensity equation. This work was supported by the U.S. Atomic Energy Commission (Contract AT(30-1) 1957).

1. R. L. LEROY, T. R. GOVERS, and J. M. DECKERS. Can. J. Chem. **48**, 927 (1970).
2. A. KANTROWITZ and J. GREY. Rev. Sci. Instr. **22**, 328 (1951).
3. H. M. PARKER, A. R. KUHLTHAU, R. ZAPATA, and J. E. SCOTT. *In* Rarefied gas dynamics. *Edited by* F. M. Devienne. Pergamon Press, Inc., New York. 1960. p. 69.
4. J. B. ANDERSON, R. P. ANDRES, and J. B. FENN. *In* Advances in atomic and molecular physics. *Edited by* D. R. Bates and I. Estermann. Academic Press, Inc., New York. 1965. p. 345.
5. J. B. FRENCH. AGARDograph 112, NATO. April, 1966.
6. J. B. ANDERSON and J. B. FENN. Phys. Fluids, **8**, 780 (1965).
7. O. F. HAGENA and H. S. MORTON, JR. *In* Rarefied gas dynamics. Vol. 2. *Edited by* C. L. Brundin. Academic Press, Inc., New York. 1967. p. 1369.
8. E. L. KNUTH, N. M. KULUVA, and J. P. CALLINAN. Entropie, **18**, 38 (1967).
9. B. B. HAMEL and D. R. WILLIS. Phys. Fluids, **9**, 829 (1966).
10. R. H. EDWARDS and H. K. CHENG. A.I.A.A. Journal, **4**, 558 (1966).
11. R. L. LEROY and J. M. DECKERS. Can. J. Chem. **47**, 2161 (1969).
12. H. ASHKENAS and F. S. SHERMAN. *In* Rarefied gas dynamics. Vol. 2. *Edited by* J. H. DeLeeuw. Academic Press, Inc., New York. 1966. p. 84.

Can. J. Chem. Downloaded from www.nrcresearchpress.com by 210.87.254.105 on 09/05/12
For personal use only.

Can. J. Chem. Downloaded from www.nrcresearchpress.com by 210.87.254.6 on 09/05/12
For personal use only.

Application of the Hammett equation to non-aromatic unsaturated systems. VIII. Ionization potentials

MARVIN CHARTON

Department of Chemistry, School of Engineering and Science, Pratt Institute, Brooklyn, New York, 11205

Received October 23, 1969

Ionization potentials of substituted ethylenes, *trans*-1-substituted propenes, and several sets of substituted carbonyl derivatives have been correlated with the extended Hammett equation. The electrical effect in the case of the ethylenes and propenes is characterized by a value of $\varepsilon \approx 2.0$, whereas the carbonyl derivatives show values of ε in the range 0 to 0.4. This difference in the composition of the electrical effect is ascribed to loss of a π electron from the ethylenes and propenes and of an n electron from the carbonyl derivatives. For purposes of comparison, several sets of ionization potentials of substituted benzenes were also correlated with the extended Hammett equation. Values of ε ranged from 1 to 3; thus the substituted benzenes are comparable in their behavior to the ethylenes and propenes.

Canadian Journal of Chemistry, 48, 1748 (1970)

The Hammett equation (1) has previously been shown to apply to equilibrium constants, reaction rates, and dipole moments of *cis*- and *trans*-vinylene, vinylidene, *cis*- and *trans*-heterovinylene and heterovinylidene sets (2–6). In this paper the application of the extended Hammett equation

$$[1] \qquad Q_X = \alpha\sigma_{I,X} + \beta\sigma_{R,X} + h$$

to the ionization potentials of vinylene and heterovinylene sets is considered. Data from the literature have been correlated with eq. [1] by linear multiple regression analysis; data used in the correlations are given in Table 1. The sources of the σ_I and σ_R constants are reported in previous papers of this series.

A number of previous correlations of ionization potentials for substituted benzenes (7–9), benzyl (10), phenoxy (11), and alkyl (12) radicals, and substituted pyridines (13) with the simple Hammett equation

$$[2] \qquad Q_X = \rho\sigma_X + h$$

have been reported. No studies of this type have appeared for substituted ethylenes or carbonyl compounds, however. For purposes of comparison, we have correlated ionization potentials of substituted benzenes and pyridines with eq. [1]. The data used are also given in Table 1.

The justification for the correlation of the ionization potentials of disubstituted carbonyl compounds (set **8**, Table 1) with eq. [1] is set forth in the previous paper of this series (6), in which it was shown that, in general, ignoring interaction terms, the effect of the substituents X^1 and X^2 is given by

$$[3] \qquad Q_X = \alpha_1\sigma_{I,X^1} + \alpha_2\sigma_{I,X^2} + \beta_1\sigma_{R,X^1} + \beta_2\sigma_{R,X^2} + h$$

and as

$$X^1 \equiv X^2$$

then

$$[4] \qquad Q_X = (\alpha_1 + \alpha_2)\sigma_{I,X} + (\beta_1 + \beta_2)\sigma_{R,X} + h$$

equivalent to eq. [1] with

$$[5] \qquad \alpha = \alpha_1 + \alpha_2 \qquad \beta = \beta_1 + \beta_2$$

Results

Results of the correlations of ionization potentials with eq. [1] are presented in Table 2. Very good results were obtained for the substituted ethylenes (set **1**, Table 2). Exclusion of the values for X = C_2H_3, Ac, F, H, OAc from the set gave excellent results (set **1A**). The *trans*-1-substituted propenes gave a very poor correlation. Omission of the value for X = H gave good results.

A very good correlation was obtained for the XCHO (set **3**). Some improvement resulted from the omission of X = H and NH_2 from the set (to give set **3A**). Excellent results were obtained for XMeCO (set **4**). Exclusion of the point for X = H gave some improvement (set **4A**). A very poor correlation was obtained with XEtCO (set **5**). Omission of the value for X = H (set **5A**) gives results which do not seem to be any more meaningful, as is shown by "*t*" tests for the significance of α and β. This is probably due to there being only two types of substituent (alkyl and alkoxy or hydroxy) in the set. The magnitude of *r*, the partial correlation coefficient of σ_I on σ_R, shows that no good separation into localized and

Can. J. Chem. Downloaded from www.nrcresearchpress.com by 210.87.254.6 on 09/05/12
For personal use only.

TABLE 1

Ionization potentials for some aromatic and unsaturated non-aromatic systems

	Ionization potential, eV, for substituted													
Substituent, X, =	Ethylene*	Propene (*trans*-I-X)*	Formyl derivatives*	Acetyl derivatives*	Propionyl derivatives*	Carbethoxyl derivatives*	Benzoyl derivatives*	Carbonyl compounds*	Benzene†	Toluene (4-X)†	Phenol (4-X)†	Aniline (4-X)†	Acetophenone (4-X)‡	Pyridine (4-X)§
Me_2N			9.12	8.81										
NH_2			10.20	9.71					8.32	8.14		7.58	8.36	8.97
CN	10.91								10.09	9.76				
CH_2OH	9.67													
CH_2Cl	10.04			9.71		10.20								
CH_2Br	9.7					10.13								
CF_3	10.90						10.25	11.81						
CCl_3						10.44								
C_2H_3	9.07													
C_2H	9.87													
Me	9.73	9.13	10.21	9.69	9.53	10.10	9.27	9.69	9.18	8.99	8.97	8.14	9.28	9.67
Et	9.58	9.06	9.98	9.53	9.32	10.00		9.32						
Pr		9.16	9.86	9.39										
Bu	9.46		9.82	9.17				9.10						
$BuCH_2$	9.54													
F	10.37		11.40				10.6							
Cl	10.00			11.02			10.6	11.78	9.60	9.21	9.07		9.64	10.15
Br	9.80	9.30		10.55					9.52	9.22	9.04			9.94
H	10.51	9.73	10.87	10.21	9.98	10.61	9.53	10.87	9.56	9.18	9.16	8.32	9.38	9.85
CHO	10.10	9.73												10.12
Ac	9.91			9.23										
CO_2H	10.90													
OH			11.05	10.35	10.24				9.16	8.97			9.27	
OMe	9.93		10.82	10.27	9.87		10.0		8.83			7.52	9.02	
OEt			10.61	10.10	10.00									
OAc	9.19													
Ph							9.45	9.45						
NO_2									10.18	9.82	9.52	8.85	10.24	
Set	**1**	**2**	**3**	**4**	**5**	**6**	**7**	**8**	**9**	**10**	**11**	**12**	**13**	**14**

*Reference 14.
†Reference 7.
‡Reference 8.
§Reference 13.

Can. J. Chem. Downloaded from www.nrcresearchpress.com by 210.87.254.6 on 09/05/12
For personal use only.

delocalized effects is possible in this set. Very poor results were obtained for X(OEt)CO (set **6**); no improvement results from the exclusion of the point for X = H (set **6A**). Excellent correlation was obtained for the XPhCO (set **7**); on omission of the value for X = H no significant improvement in the correlation resulted (set **7A**). The X_2CO gave fair correlation (set **8**); exclusion of the point for X = H resulted in a significant improvement (set **8A**). With the exception of the 4-substituted anilines (set **12**), the results obtained for the substituted benzenes (sets **9–11**, **12**) and pyridines (set **14**) are very good to excellent. Exclusion of the point for X = H not only does not result in any significant improvement in the correlation, but in most of these sets the correlation became poorer (sets **9A–14A**). Those sets which include a hydroxyl substituent are generally very much improved by the omission of the value for this group from the set (sets **9B**, **10B**, **13B**).

Discussion

Composition of the Electrical Effect

To further our discussion of the composition of the electrical effect, we make use of

$$\varepsilon = \beta/\alpha \quad [6]$$

Values of ε for the sets studied are presented in Table 3. The composition of the substituent effect in the substituted ethylenes and propenes includes a significantly larger resonance contribution than is observed for the substituted benzenes and toluenes and very much larger than that for the substituted pyridines. The substituted pyridines and substituted acetophenones could be correlated fairly well with eq. [2] by means of the σ_p constants (for which ε = 1.0); the substituted ethylenes, propenes, toluenes, and benzenes by the σ_p^+ constants (for which ε = 1.6). The substituted anilines and phenols are not well correlated by eq. [2] with any of the available simple σ constants. The substituted formyl, acetyl, and disubstituted carbonyl compounds may be correlated with eq. [2] by means of the σ_m constants (for which ε = 0.33).

The enormous difference in ε between the substituted vinylene and arylene sets on the one hand and the substituted carbonyl compounds on the other is undoubtedly due to the loss of a π electron in the former and an n electron in the latter case. The loss of the π electron makes

TABLE 2

Results of correlations of ionization potentials with eq. [1]

Set[a]	α	β	h	R^b	F^c	r^d	$s_{est}{}^c$	$s_\alpha{}^e$	$s_\beta{}^e$	$s_h{}^e$
1	1.27	1.66	9.75	0.674	7.078	0.0513	0.452	0.491	0.580	0.160
1A	1.32	2.51	9.85	0.936	42.08	0.156	0.218	0.273	0.361	0.0922
2	0.611	2.29	9.46	0.869	4.611	0.0567	0.194	0.380	0.861	0.111
2A	0.769	1.70	9.33	0.989	45.95	0.0379	0.0554	0.112	0.266	0.0387
3	3.58	1.27	10.42	0.849	10.35	0.527	0.390	0.790	0.463	0.192
3A	3.87	1.34	10.31	0.901	12.97	0.560	0.357	0.761	0.517	0.204
4	2.90	0.738	9.71	0.862	15.95	0.297	0.330	0.517	0.323	0.136
4A	3.01	0.589	9.60	0.896	20.43	0.252	0.298	0.471	0.303	0.135
5	3.16	0.996	9.78	0.791	2.516	0.949	0.267	2.37	1.42	0.236
5A	−1.59	−2.51	9.71	0.971	16.64	0.978	0.124	1.77	1.21	0.234
6	−0.190	4.60	10.52	0.867	4.522	0.534	0.149	0.425	1.67	0.137
6A	0.910	−0.174	10.01	0.939	7.499	0.890	0.0801	0.443	2.03	0.191
7	2.27	−0.138	9.38	0.980	48.70	0.342	0.134	0.251	0.249	0.0811
7A	2.42	−0.226	9.29	0.989	68.38	0.213	0.107	0.218	0.206	0.0815
8	4.36	2.32	9.95	0.889	7.571	0.0753	0.658	1.18	2.39	0.353
8A	4.92	0.858	9.58	0.965	20.47	0.163	0.424	0.793	1.64	0.269
9	0.916	1.39	9.46	0.967	42.87	0.381	0.173	0.257	0.212	0.125
9A	1.13	1.24	9.33	0.971	40.66	0.587	0.178	0.335	0.259	0.180
9B	1.04	1.50	9.38	0.998	406.5	0.585	0.0573	0.109	0.0921	0.0585
10	0.826	1.16	9.16	0.957	27.07	0.376	0.180	0.267	0.231	0.129
10A	0.858	1.14	9.14	0.957	21.74	0.593	0.200	0.385	0.310	0.208
10B	0.728	1.48	9.21	0.9996	169.6	0.591	0.0234	0.0456	0.0246	0.0246
11	0.386	1.17	9.14	0.996	122.1	0.593	0.0276	0.0433	0.0953	0.386
11A	0.414	1.13	9.12	0.997	94.94	0.333	0.0303	0.0620	0.123	0.0358
12	0.498	1.28	8.32	0.956	10.65	0.286	0.229	0.406	0.326	0.167
12A	0.504	1.27	8.31	0.953	4.989	0.510	0.323	0.689	0.560	0.345
13	1.12	1.21	9.41	0.954	20.10	0.243	0.211	0.341	0.270	0.153
13A	1.06	1.25	9.45	0.954	15.24	0.497	0.242	0.479	0.381	0.256
14A	1.04	1.12	9.78	0.973	18.11	0.244	0.157	0.358	0.254	0.142

TABLE 2 (*Concluded*)

Set[a]	n^f	C.L.[g]	$t_\alpha{}^h$	C.L.$_\alpha{}^i$	$t_\beta{}^h$	C.L.$_\beta{}^i$	$t_h{}^h$	C.L.$_h{}^i$
1	20	99.0	2.587	98.0	2.862	98.0	70.94	99.9
1A	15	99.9	4.835	99.9	6.953	99.9	106.8	99.9
2	6	<90.0	1.608	50.0	2.660	90.0	95.23	99.9
2A	5	97.5	6.866	95.0	6.391	95.0	241.1	99.9
3	11	99.0	4.532	99.0	2.743	95.0	54.27	99.9
3A	9	99.0	5.085	99.0	2.592	95.0	50.54	99.9
4	14	99.9	5.609	99.9	2.285	95.0	71.40	99.9
4A	13	99.9	6.391	99.9	1.944	90.0	91.11	99.9
5	6	<90.0	1.333	50.0	0.701	20.0	41.44	99.9
5A	5	90.0	0.898	50.0	2.074	80.0	41.50	99.9
6	6	<90.0	0.447	20.0	2.854	90	76.78	99.9
6A	5	<90.0	2.054	80.0	0.086	<20.0	52.41	99.9
7	7	99.5	9.044	99.9	0.554	20.0	115.7	99.9
7A	6	99.5	11.10	99.0	1.097	50.0	114.0	99.9
8	7	95.0	3.695	95.0	0.971	50.0	28.19	99.9
8A	6	97.5	6.204	99.0	0.523	20.0	35.61	99.9
9	9	99.9	3.564	98.0	6.556	99.9	75.68	99.9
9A	8	99.9	3.373	98.0	4.788	99.0	61.83	99.9
9B	7	99.9	9.541	99.9	16.29	99.9	160.3	99.9
10	8	99.5	3.094	95.0	5.022	99.0	71.01	99.9
10A	7	99.0	2.229	90.0	3.677	95.0	53.94	99.9
10B	6	99.9	15.96	99.9	60.16	99.9	374.4	99.9
11	5	99.0	8.915	98.0	12.28	99.0	539.4	99.9
11A	4	90.0	6.677	90.0	9.187	90.0	254.7	99.0
12	5	90.0	1.227	50.0	3.926	90.0	49.82	99.9
12A	4	<90.0	0.731	20.0	2.268	50.0	24.09	95.0
13	7	99.0	3.284	95.0	4.481	98.0	61.50	99.9
13A	6	95.0	2.213	80.0	3.281	95.0	36.91	99.9
14A	6	90.0	2.905	90.0	4.409	95.0	78.87	99.9

[a]See Table 1 and text for compounds included in sets.
[b]Multiple correlation coefficient.
[c]F test for significance of regression.
[d]Partial correlation coefficient of σ_I on σ_R.
[e]Standard error of the estimate, α, β, or h, as indicated by subscript.
[f]Number of points in set.
[g]Confidence level for regression.
[h]"Student's t" test for significance of α, β, or h, as indicated by subscript.
[i]Confidence level for α, β, or h, as indicated by subscript.

TABLE 3

Values of ε for some non-aromatic unsaturated systems*†

Set	ε	Set	ε	Set	ε
1A	1.90	**8A**	0.174	**12**	2.57
2A	2.21	**9B**	1.44	**13**	1.08
3A	0.346	**10B**	2.04	**14A**	1.08
4A	0.196	**11**	3.03		
7	0				

*Values of ε have not been calculated from those sets which do not have significant values of β.
†See Table 1 and text for compounds included in sets.

possible a large resonance effect in comparison with the magnitude of the localized effect.

Magnitude of the Electrical Effect

The value of α (or ρ) serves as a measure of the magnitude of the electrical effect. The substituted ethylenes are more susceptible to substituent effects than are the substituted benzenes or the 4-substituted pyridines, α for the former being 1.32; for both the two latter systems, $\alpha = 1.04$. The value of α for the *trans*-1-substituted propenes is about the same as that obtained for the 4-substituted toluenes.

The values of α obtained for the carbonyl compounds are generally much larger than those for the substituted ethylenes, benzenes, and pyridines, being in the range 2.42–3.81. The only exception is that of the carbethoxyl derivatives, for which $\alpha = 0.910$. Although it seems likely that this difference in magnitude of the electrical effect is due to the ionization of an n electron in the carbonyl compounds as compared with a π electron in the ethylenes, benzenes, and pyridines, we are unable at the present time to propose a detailed explanation for this difference in susceptibility.

It is instructive to compare the values of α for ionization potentials with values observed for other phenomena. To make such comparisons we must multiply the observed α values by a conversion factor from eV to kcal/mole of 23.061. Values of α obtained for sets of rate or equilibrium data must then be multiplied by the conversion

Can. J. Chem. Downloaded from www.nrcresearchpress.com by 210.87.254.6 on 09/05/12
For personal use only.

TABLE 4

Correlations of α_{X^2} and β_{X^2} with eqs. [8] and [9]*

Set	m_1†	m_2‡	m_3§	R‖	F‖	r‖	s‖	s_{m_1}‖	s_{m_2}‖
A	−0.0191	0.731	0.945	0.939	7.497	0.048	0.157	0.525	0.189
B	−0.947	0.117	1.47	0.991	55.25	0.048	0.0289	0.0967	0.0349

Set	s_{m_3}‖	n‖	C.L.‖	t_{m_1}‖	C.L.‖	t_{m_2}‖	C.L.‖	t_{m_3}‖	C.L.‖
A	0.104	5	90.0	0.036	20.0	3.866	90.0	9.08	98.0
B	0.0192	5	97.5	9.795	98.0	3.343	90.0	76.60	99.9

*Data from sets **9B**, **10B**, **11**, **12**, and **13** were used. See Table 1 and text for compounds included in these sets.
†α_{12} or χ_{12}.
‡β_{12} or χ_{21}.
§α_1 or β_1.
‖See footnotes to Table 2 for definition of term.

factor $2.3RT$ if meaningful comparisons are to be made. If α for the ionization potentials of substituted benzenes is compared in this manner with α for the rates of bromination in water – acetic acid at 25 °C of substituted benzenes (15), it is seen that they are comparable in magnitude, the former being about 1.3 times the latter.

Anomalous Substituent Effects

The inclusion of the value for X = H in the ethylene and carbonyl sets leads to poor correlation. This is not true of the substituted benzenes or pyridine sets. We are at present unable to account for this behavior.

The inclusion of the hydroxyl group in substituted benzene sets leads to poorer correlations. The OH group behaves as a much poorer donor than might otherwise have been expected. It may be argued that the σ_I and σ_R values used here for the OH group were determined in protonic solvents and are not applicable to a process occurring in the vapor phase. In that event however, anomalous behavior should have also been observed for the methoxy and, in particular, for the amino groups. The peculiar behavior of the OH group has been reported previously (16, 17).

Effect of Constant Substituents

We have previously shown (18) that for correlations with eq. [2] for sets having a constant substituent X^2 (in addition to a variable substituent X^1)

$$[7] \qquad \rho_{X^2} = \rho_{12}\sigma_{X^2} + \rho_H$$

where ρ_{X^2} is the value of ρ obtained for the set bearing the constant substituent, ρ_H is the value for the unsubstituted set, and ρ_{12} is the coefficient of the interaction term.

For the case of the extended Hammett equation, the corresponding equations are

$$[8] \qquad \alpha_{X^2} = \alpha_1 + \alpha_{12}\sigma_{I,X^2} + \chi_{12}\sigma_{R,X^2}$$

$$[9] \qquad \beta_{X^2} = \beta_1 + \beta_{12}\sigma_{R,X^2} + \chi_{21}\sigma_{I,X^2}$$

Correlations of α_{X^2} and β_{X^2} from sets **9B**, **10B**, **11**, **12**, and **13** were correlated with eqs. [8] and [9]. The results are set forth in Table 4. The correlation of α with eq. [8] is not significant (set **A**, Table 4). The results show that α_{12} is not significant. Correlation with the equation

$$[10] \qquad \alpha_{X^2} = \alpha_1 + \chi_{12}\sigma_{R,X^2}$$

gave the following results: $\alpha_1 = 0.943$, $\chi_{12} = 0.732$, $s = 0.128$, $s_\chi = 0.154$, $r = 0.939$, $t = 4.741$, C.L. = 98.0.

The results obtained for the correlation of β_{X^2} with eq. [9] (set **B**, Table 4) are good. We conclude that in the case of sets of ionization potentials involving a constant substituent, meaningful interaction terms are encountered.

1. H. H. JAFFÉ. Chem. Rev. **53**, 191 (1953); R. W. TAFT, JR. Steric effects in organic chemistry. M. S. Newman (Editor) John Wiley and Sons, Inc., New York. 1956. p. 565; V. A. PALM. Russian Chem. Rev. Engl. Transl. **31**, 471 (1961); P. R. WELLS. Chem. Rev. **63**, 171 (1963); C. D. RITCHIE and W. F. SAGER, JR. Progr. Phys. Org. Chem. **2**, 323 (1963).
2. M. CHARTON and H. MEISLICH. J. Amer. Chem. Soc. **80**, 5940 (1958).
3. M. CHARTON. J. Org. Chem. **30**, 552 (1965).
4. M. CHARTON. J. Org. Chem. **30**, 557 (1965).
5. M. CHARTON. J. Org. Chem. **30**, 969 (1965).
6. M. CHARTON and B. I. CHARTON. J. Org. Chem. **34**, 1871 (1969).
7. G. F. CRABLE and G. L. KEARNS. J. Phys. Chem. **66**, 436 (1962).
8. A. BUCHS, G. P. ROSSETTI, and B. P. SUSZ. Helv. Chim. Acta, **47**, 1563 (1964).
9. H. BABA, I. OMURA, and K. HIGASI. Bull. Chem. Soc. Jap. **29**, 521 (1956).

Can. J. Chem. Downloaded from www.nrcresearchpress.com by 210.87.254.6 on 09/05/12
For personal use only.

10. A. G. HARRISON, P. KEBARLE, and F. P. LOSSING. J. Amer. Chem. Soc. **83**, 777 (1961).
11. J. M. S. TAIT, T. W. SHANNON, and A. G. HARRISON. J. Amer. Chem. Soc. **84**, 4 (1962).
12. A. STREITWEISER, JR. Progr. Phys. Org. Chem. **1**, 1 (1963).
13. M. R. BASILA and D. J. CLANCY. J. Phys. Chem. **67**, 1551 (1963).
14. R. W. KISER. Introduction to mass spectrometry and its applications. Prentice-Hall, Inc., Englewood Cliffs, N.J. 1965.
15. M. CHARTON. Unpublished results.
16. A. FOFFANI, S. PIGNATARO, B. CANTONE, and F. GRASSO. Z. Phys. Chem. Frankfurt, **42**, 221 (1964).
17. S. PIGNATARO, A. FOFFANI, G. INNORTA, and G. DISTEFANO. Z. Phys. Chem. Frankfurt, **49**, 291 (1966).
18. M. CHARTON. Abstr. 145th Nat. Meet. Amer. Chem. Soc., New York. 1963.

Can. J. Chem. Downloaded from www.nrcresearchpress.com by 210.87.254.6 on 09/05/12
For personal use only.

Can. J. Chem. Downloaded from www.nrcresearchpress.com by 210.87.254.6 on 09/05/12
For personal use only.

Remarkable stereoselectivity in the hydrolysis of dioxolenium ions and orthoesters fused to anchored six-membered rings

J. F. KING AND A. D. ALLBUTT
Department of Chemistry, University of Western Ontario, London, Ontario

Received October 2, 1969

Hydrolysis of dioxolenium (acyloxonium) ions fused to anchored six-membered rings gives almost exclusively that hydroxyester in which the ester function is *axial* (and the hydroxyl group equatorial). With the exception of the orthoformate, a group of related orthoesters reacted similarly. The potential utility of these observations in stereoselective synthesis is suggested by the following examples. (*a*) With *trans*-decalin-*cis*-2,3-diol (**21**) formation of the mono-benzoate via the orthoester leads to the axial ester (**23***d*) in good yield; this procedure is complementary to reaction with benzoyl chloride and pyridine, which gives the equatorial ester (**24***d*) as the only isolated product. (*b*) The action of silver acetate and iodine in wet acetic acid (the Woodward–Prévost reaction) on *trans*-Δ^2-octalin gives the axial acetate – equatorial alcohol (**23***b*) again as the only significant product. The generality of this stereoselectivity is further supported by a number of individual examples drawn from the chemistry of carbohydrates. A rationalization is offered which qualitatively accounts for the observed stereoselectivity and its absence in the hydrolysis of the orthoformate, and which is based on the differences in steric strain among the possible transition states that fulfil the stereoelectronic requirements of dialkoxycarbonium ion formation.

Canadian Journal of Chemistry, **48**, 1754 (1970)

Introduction

We have recently described the synthesis of dioxolenium ions fused to anchored six-membered rings (e.g. **1**) and noted their preference for forming the diaxial product (**2**) rather than the diequatorial isomer (**3**) when allowed to react with halide anions (1). A number of nucleophilic reagents, however, form products derived from attack on C-1 rather than C-3 or C-4 of the dioxolenium ring; alcohols yield orthoesters and water gives the hydroxy-ester resulting from opening of the normally unstable "orthoacid" intermediate (e.g. **4**). When the dioxolenium ring is fused to an anchored cyclohexane system one oxygen is in an equatorial configuration and the other axial. As in the cleavage with halide ions, two products may in principle result from the hydrolysis, one from cleavage adjacent to the axial oxygen, the other by breaking of the bond to the equatorial oxygen. This is shown in Scheme 1, in which the dioxolenium salt (**1**) may yield either **5**, in which the hydroxyl group is equatorial and the acyloxy function axial, or **6**, the "axial alcohol – equatorial ester".

In the course of our work with dioxolenium salts we found that the hydrolysis of species such as **1** is remarkably stereoselective, the "axial ester – equatorial alcohol" (e.g. **5**) constituting more than 99.5% of the hydroxy-ester mixture obtained on hydrolysis. In this account we describe our study which rigorously proves the steric course of the hydrolysis, illustrates its scope, considers its ramifications with respect to the hydrolysis of orthoesters and the course of the Woodward–Prévost synthesis of *cis*-1,2-diols, and finally includes a rationalization of the observed stereoselectivity. Some of these results have been outlined already in a preliminary communication (2).

Results and Discussion

Hydrolysis of the Dioxolenium Hexafluoroantimonates

The dioxolenium hexafluoroantimonates (**1**, **7**, and **20**) were prepared by reaction of the corresponding diaxial bromohydrin esters with silver hexafluoroantimonate as described previously (1). The hydrolyses were normally carried out with aqueous acid, though in one experiment with **1**, aqueous base was used with essentially the same result. Examination of the hydrolysis products by thin-layer chromatography (t.l.c.) showed the presence of one major product plus a very small amount of a material running somewhat ahead of the main product. It is commonly, though not invariably, observed that axial alcohols run faster than their equatorial isomers. This suggested that if the two spots corresponded to the two readily derivable esters (e.g. **5** and **6**) then the ester formed in the greater amount had the hydroxyl group equatorial (as in **5**). That this was so was proved by the chemical correlations summarized in Scheme 2.

The essential features of this proof may be

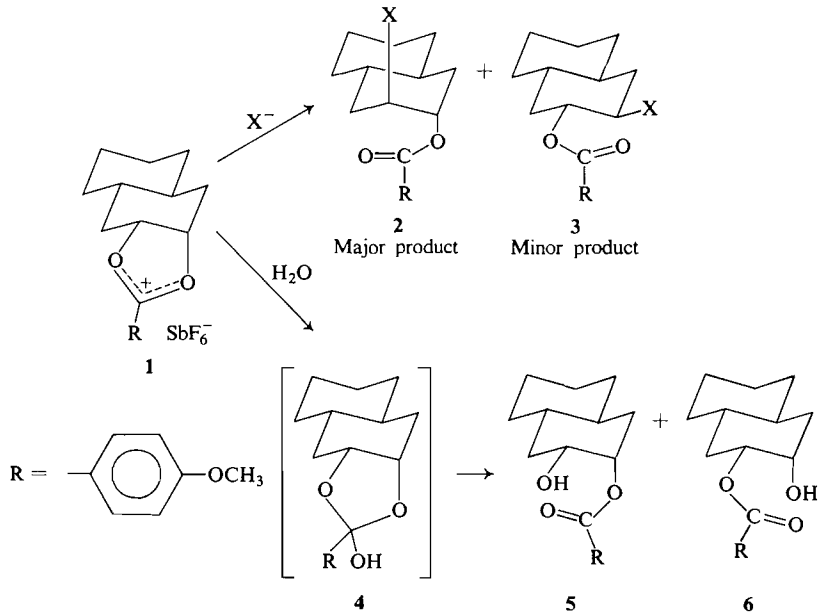

SCHEME 1

summarized with reference to the product (**8**) from the hydrolysis of the 2α,3α-anisoxonium hexafluoroantimonate **7**. Saponification of **8** gave 5α-cholestan-2α,3α-diol (**11**), showing the oxygen functions to be both on the alpha face of the molecule. Oxidation of **8** with Jones' reagent gave the α-anisoxyketone (**9**) which, on reduction with zinc and acetic acid yielded 5α-cholestan-2-one (**10**). Since the keto-function in **10** derives directly from the hydroxyl group in the product from the hydrolysis of the dioxolenium salt **7**, that hydroxyl group must be on C-2 and hence the ester function on C-3. Since the stereochemistry is already known from the formation of **11**, if no rearrangement has occurred the major hydrolysis product from **7** must have structure **8**. Analogous treatment of the major product obtained from the 2β,3β-anisoxonium salt **20**, gave respectively 5α-cholestan-2β,3β-diol (**16**), 2β-anisoxy-5α-cholestan-3-one (**18**), and 5α-cholestan-3-one (**17**), thereby showing it to have very probably the axial ester – equatorial alcohol structure also, in this case structure **19**.

Treatment of the 2α,3α-hydroxyester **8** with camphor-10-sulfonic acid in benzene led to partial conversion to the isomeric ester **12**, derived by migration of the anisoyl function from the 3α- to the 2α-oxygen. This material showed the same behavior on t.l.c. as the faster moving component of the mixture from hydrolysis of **7**. Structure **12** for this product follows from (*a*) the formation of the 2α,3α-diol (**11**) on saponification, and (*b*) production of 2α-anisoxy-5α-cholestan-3-one (**14**) on Jones' oxidation. The same material (**14**) was obtained by acid-catalyzed epimerization of **18**.

Starting with either **8** or **12** we obtained from the camphor-10-sulfonic acid treatment a mixture in which **12** predominated, showing that the equatorial ester–axial alcohol (**12**) is the more stable of the two isomers. This observation also demonstrates that the hydrolysis of the dioxolenium salt (**7**) is subject to kinetic rather than equilibrium control. The acid-catalyzed transesterification reactions **8** → **12** and **12** → **8** were not run to the point of obtaining a true equilibrium mixture owing to formation of by-products, but it can be estimated that **12** would constitute 60–75% of the ester mixture at equilibrium.

Similar acid treatment of the 2β,3β-ester-alcohol (**19**) gave **15**, which also apparently predominates at equilibrium, and which also shows the same behavior on t.l.c. as the faster moving material obtained from the hydrolysis of **20**. Oxidation of **15** gave **13**, identical with a specimen obtained in low yield along with **9** in the Jones' oxidation of **8**. Except for this instance the Jones' oxidation procedure took place without migration or epimerization of the anisoxyl group. Fear of such an occurrence in the usual

Can. J. Chem. Downloaded from www.nrcresearchpress.com by 210.87.254.6 on 09/05/12
For personal use only.

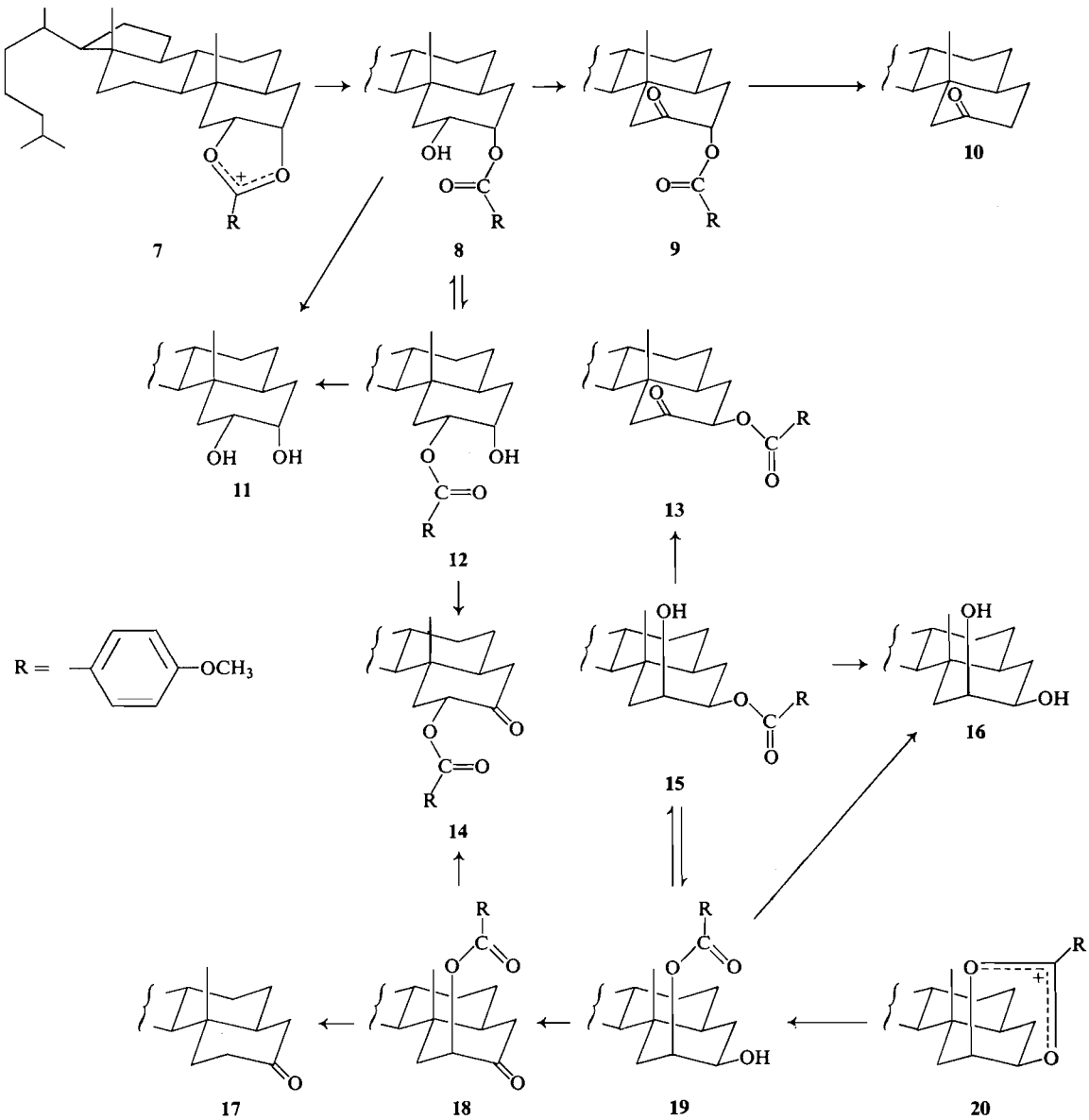

SCHEME 2

media for chromic acid oxidation had prompted us to use dimethyl sulfoxide–acetic anhydride as the oxidizing agent in some of our earlier experiments. This reagent worked well with **15** and **19**, but oxidation of **8** gave in addition to **9** a significant portion of an unidentified material.

The stereochemistry of the four keto-anisates (**9**, **13**, **14**, and **18**) follows not only from their mode of synthesis but also from their optical rotatory dispersion (o.r.d.) and nuclear magnetic resonance (n.m.r.) spectra. The o.r.d. spectra could not be observed below about 280 nm owing to the strong ultraviolet (u.v.) absorption of the anisoxyl group, but enough of the spectrum was measurable to show that the two keto-esters in which the anisoxyl group is axial (**9** and **18**) had large positive Cotton effects (amplitudes greater than 217 and 149, respectively), whereas

Can. J. Chem. Downloaded from www.nrcresearchpress.com by 210.87.254.6 on 09/05/12
For personal use only.

Can. J. Chem. Downloaded from www.nrcresearchpress.com by 210.87.254.6 on 09/05/12
For personal use only.

the two compounds with equatorial anisoxyl functions (**13** and **14**) showed much smaller positive Cotton effects (amplitudes 47 and 23, respectively). These findings are in excellent agreement with predictions based on the octant rule (3), though somewhat different from the observations reported by Williamson and Johnson (4). Because of the low solubility of our keto-esters in methanol, which was the solvent used by Williamson and Johnson, our o.r.d. spectra were obtained with methylene chloride solutions; the two sets of results may not be comparable. The n.m.r. spectra of the keto-anisates, however, were in good agreement with those described for the corresponding keto-acetates (4), the characteristic absorption patterns of the proton on the carbon bearing the ester function[1] being strikingly similar to those observed by Williamson and Johnson and interpreted by them as showing considerable distortion of ring-A from the normal chair conformation in 2β-acetoxy-5α-cholestan-3-one.

It is clear that the chemical interconversions summarized in Scheme 2 taken together with the spectroscopic properties found for compounds **9** to **18** allow no possibility of any kind of rearrangement or epimerization being the major course of any of these reactions, and that structures **8** and **19** are therefore established beyond question. The n.m.r. spectra of **8** and **19** (see Experimental) are in excellent agreement with these formulations and would provide strong independent support for the structures if any were needed. In the compounds derived from the decalin dioxolenium salt (**1**) it should be noted that no chemical proof of structure analogous to that summarized for the steroidal materials is possible owing to the symmetry of the decalin system. The proofs of the structures of the decalin hydroxy-esters rest on a comparison of physical data, notably n.m.r. spectra, with those obtained with the analogous steroids. In view of the virtual identity of the relevant parts of the n.m.r. spectra of the decalin hydroxy-esters to those from the steroid series it can be concluded that the structures of the decalin hydroxy-esters described in both this and subsequent sub-sections are also established beyond doubt. For the reaction which corresponds most directly with that of the steroidal materials, namely the hydrolysis of the decalin dioxolenium salt **1**, the product also proved to be almost entirely the axial ester – equatorial alcohol (**5**) with only a trace of a material presumed to be **6**, which showed the same R_f value on t.l.c. as the compound obtained by acid-catalyzed rearrangement of **5**.

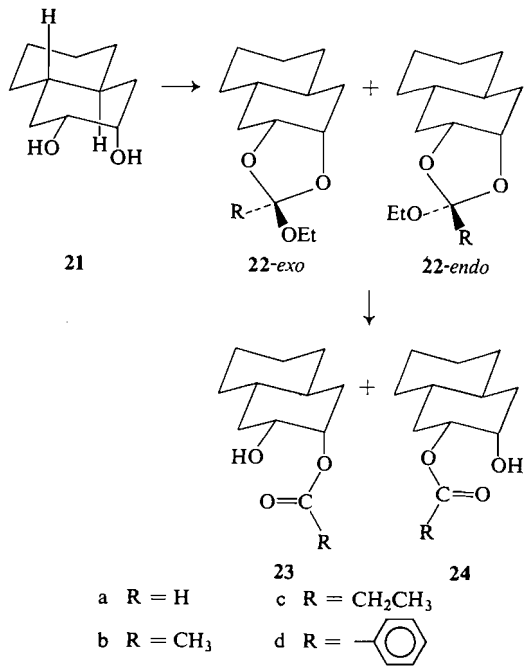

Hydrolysis of Orthoesters of trans-Decalin-2β,3β-diol

Dialkoxycarbonium ions have long been regarded as intermediates in the acid-catalyzed hydrolysis of orthoesters; the evidence supporting this notion has recently been summarized by Cordes (6). For orthoesters derived from *trans*-decalin-2β,3β-diol (**21**) such an intermediate could (though it does not have to) be the dioxolenium ion, and therefore the hydrolysis of the corresponding orthoesters might well be expected to yield the axial ester – equatorial alcohol to the almost complete exclusion of the equatorial ester – axial alcohol. To test this simple extension of the results that we had obtained with the crystalline dioxolenium salts, we prepared the ethyl orthoesters **22***a–c*, by reaction of, respectively, ethyl orthoformate, ethyl orthoacetate, and ethyl orthopropionate with a solution of the diol (**21**) in benzene containing a small amount of camphor-10-sulfonic acid. Upon vacuum distillation the orthoesters were obtained as liquids

[1]This portion of the spectra is reproduced elsewhere (5).

Can. J. Chem. Downloaded from www.nrcresearchpress.com by 210.87.254.6 on 09/05/12
For personal use only.

which gave satisfactory analyses and showed no hydroxyl absorption in their infrared (i.r.) spectra. The n.m.r. spectra were in agreement with the orthoester formulation but suggested that each of the orthoester preparations was in fact a mixture of the two orthoesters epimeric at the orthoester carbon (**22** *exo* and **22** *endo*) in which one epimer was present in much greater amount than the other. In the spectrum of the ethyl orthoformate **22***a*, the orthoformyl proton region showed two singlets, at 5.73 and 5.79 p.p.m. (relative areas roughly 4:1), while the methylene of the ethoxyl group appeared as a quartet at 3.60 p.p.m. (J = 7 Hz) superimposed on a correspondingly smaller quartet at 3.65 p.p.m. (J = 7 Hz). Similarly, the spectrum of the orthoacetate **22***b* shows two methyl singlets, the larger one at 1.61 p.p.m., the smaller at 1.52 p.p.m., and the orthopropionate **22***c* displays a quartet at 3.53 p.p.m. (J = 7 Hz) together with what appears to be another quartet at 3.62 p.p.m.

Perlin has found that formation of orthoacetates under the conditions of the Königs–Knorr synthesis leads to a mixture of epimers as demonstrated both by n.m.r. spectroscopy and actual isolation of the individual epimers (7). The major component of the mixture was suggested to have the alkoxyl group *exo* to the pyranose ring on the basis of the n.m.r. spectra and an earlier suggestion by Lemieux and Cipera (8) that the *exo* product would be expected to predominate because of the more facile approach of the alcohol to the side of the acetoxonium ion remote from the pyranose ring. Lemieux and Morgan (9), in another preparation of orthoesters believed to take place via the dioxolenium ion, also found the predominance of one isomer which was assigned the *exo* structure primarily on the basis of a cogent argument based on an imposing array of n.m.r. data.

Both the mode of preparation and the basic skeleton in our compounds are different from those of these authors, and it would not be surprising if the nature of our orthoester mixture proved to be different from theirs. Nonetheless using their correlations to interpret our n.m.r. data leads to the suggestion that the products that we obtain in the larger amount have the *exo* configuration of the ethoxyl group. This assignment is tentative because it is hard to be certain that the n.m.r. signals described above derive from one and the same minor component.

The hydrolysis of the orthoesters **22***a–c* was effected by dissolving in methanol, adding aqueous acetic acid, and letting the mixture stand at room temperature for 10–15 min. The orthoacetate (**22***b*) and orthopropionate (**22***c*) gave almost quantitative yields of the axial ester – equatorial alcohol (**23**) with only a very small amount of the isomer with the acyl function on the other oxygen (**24**). Both **23***b* and **23***c* underwent the acid-catalyzed transesterification to give **24***b* and **24***c* respectively. The structures of all of these compounds follow from analyses and the close correspondence of their spectra with those of the analogous materials already described (see Experimental).

Hydrolysis of the orthoformate **23***a*, however, gave a distinctly different result. The n.m.r. spectrum of the product showed the characteristic absorption of the axial ester – equatorial alcohol (in this case, **23***a*), but in addition there were equally characteristic bands indicating the presence of about 40% of the equatorial formate – axial alcohol (**24***a*). The axial formate (**23***a*) was obtained crystalline and characterized in the usual way but attempts to obtain a pure specimen of the equatorial formate (**24***a*) failed. Thin-layer chromatography on silica gel led to rapid equilibration of the two esters, a characteristic streaked double spot being obtained starting with either the mixture or with crystalline **23***a*. The ease with which **23***a* is converted to **23***b* on t.l.c. suggested the possibility that the mixture from the hydrolysis of **22***a* might merely be the product of a subsequent equilibration rather than that resulting from kinetic control of the reaction, as was the case with the other hydrolyses. The axial formate (**23***a*), however, was found to be completely stable to the conditions of the original orthoester hydrolysis. The orthoformate (**22***a*) is therefore also giving the kinetically controlled product which contains a much larger proportion of the equatorial ester – axial alcohol than the products of any of the other hydrolyses described in this paper. This observation is believed to be of significance in the rationalization of the steric course of these hydrolyses that is offered later in this account.

In addition to the orthoesters **22***a–c*, we also attempted to obtain the ethyl orthobenzoate **22***d*, following the same procedure as for the others. It was found, however, that distillation of the crude product led to extensive decomposition. The i.r. spectrum of the undistilled reaction prod-

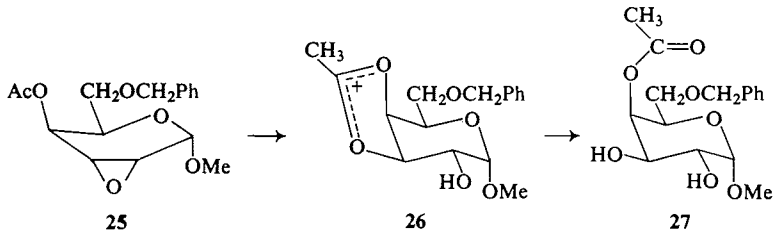

25 26 27

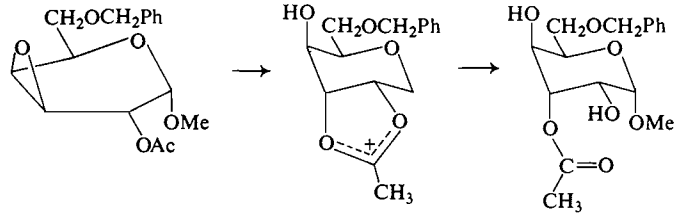

28 29 30

uct indicated that the material consisted primarily of the orthoester (**22***d*), and it was therefore hydrolyzed in the usual way. The t.l.c. showed the only significant components of this product to be the axial ester (**23***d*) and recovered diol (**21**); these were subsequently isolated in yields of 72% (88% based on reacted diol) and 18%, respectively.

It is interesting to compare this method of preparing a monobenzoate ester of **21** with direct esterification. When the diol (**21**) was treated with one equivalent of benzoyl chloride in the presence of pyridine, the other ester (**24***d*), in which the benzoyl group is attached to the *equatorial* oxygen was obtained in 93% yield (based on reacted diol). The complementary stereoselectivity of these methods of forming a mono-ester of such a *cis*-1,2-diol should prove useful in organic synthesis.

Stereoselective Hydrolysis of Carbohydrate Dioxolenium Ions

Reactions proceeding via dioxolenium ions have been used to a considerable extent in carbohydrate synthesis but the generality of the strong preference for forming axial esters on hydrolysis has not been pointed to. The following examples indicate that stereoselective hydrolysis does in fact occur with substituted pyranoses more or less anchored in one conformation. Buchanan and Fletcher (10) found that 80% acetic acid converted the anhydro sugars **25** and **28** to **27** and **30**, respectively, presumably via the acetoxonium ions **26** and **29**. Making the reasonable assumption that **26** and **29** have the C1 conformation as shown, these results are examples of the preferential formation of axial esters by hydrolysis of dioxolenium ions.[2] Perlin (7, 11) has shown that certain mannopyranose 1,2-orthoesters lead to

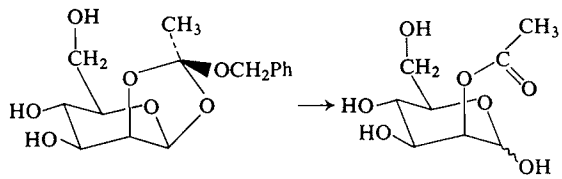

31 32

the axial ester, as for example in the reaction **31** to **32**. It could perhaps be argued that in the case of a dioxolane ring incorporating the anomeric carbon, the reaction may proceed via a different mechanism and that our observations on dioxolenium ions fused to cyclohexane rings are not relevant to the pyranose 1,2-orthoesters. One of the more likely alternative mechanisms would involve cleavage of the bond between the anomeric carbon and the dioxolenium oxygen, assisted by the electrons on the oxygen of the pyranose ring. Lemieux and Morgan (12), however, have shown that tetra-*O*-acetyl-β-D-glucopyranosyl chloride (**33**) with silver acetate in wet acetic acid, gives (presumably via **34**) the 1-acetyl derivative **35**. This result would suggest

[2]NOTE ADDED IN PROOF: The formation of an axial acetate following neighboring group participation of an equatorial acetoxyl function has also been encountered with steroidal systems; S. Julia and R. Lorne have recently (*Comptes Rendus* **268 C**, 1617 (1969)) used the results given in our preliminary communication (2) to help to rationalize these observations.

Can. J. Chem. Downloaded from www.nrcresearchpress.com by 210.87.254.6 on 09/05/12
For personal use only.

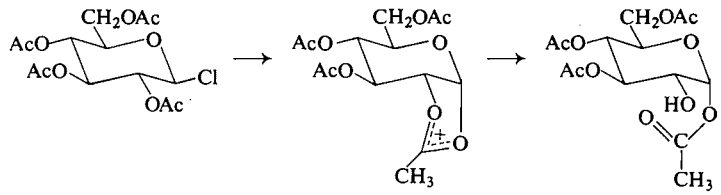

33 34 35

that the direction of cleavage of pyranose 1,2-orthoesters is not controlled by electronic influences associated with the anomeric carbon but rather by the stereochemical factors common to dioxolenium systems fused to six-membered rings. An instance of an unselective opening of an acetoxonium ion has been described by Paulsen and co-workers (13) who report that an acetoxonium derivative of arabinopyranose gives both possible hydroxyacetates. It is unlikely, however, that the arabinopyranose system is anchored, and hence would not be expected to show the stereoselectivity found with species which are.

Stereochemistry of the Hydroxy-ester from the Woodward–Prévost Reaction

The reaction of an olefin with iodine and silver acetate in wet acetic acid (14), often referred to as the Woodward–Prévost reaction, is another process which is believed to proceed via a dioxolenium species, specifically an acetoxonium ion. If this is indeed the case, it would be expected that the hydroxy-acetate obtained as the direct product of the reaction, prior to the usual saponification to the glycol, would have the hydroxyl group equatorial and the acetoxyl function axial. We were unable to find any examples on searching the literature, all such hydroxy-acetates having been hydrolyzed directly to the glycols without any examination of their stereochemistry. We therefore investigated the product of the reaction with *trans*-2-octalin. The t.l.c. of the crude product showed it to consist almost entirely of one compound. After the usual workup we obtained a 79% yield of **23***b*, the major product obtained from hydrolysis of the orthoacetate **22***b*.

Origin of the Stereoselectivity Observed in the Hydrolysis of the Dioxolenium Ions and Orthoesters

According to current informed opinion (6) the hydrolysis of dialkoxycarbonium ions requires at least the steps shown in Scheme 3. In addition to the above minimum number of intermediates, conjugate acid forms of both the "orthoacid" and ester species are probably involved, though proton loss or addition concerted with another bond formation or cleavage is regarded as possible (6). By representing the conjugate acids as discrete species and thereby multiplying the number of steps in the reaction sequence, each individual step becomes simpler and may be represented more easily. The stereochemical argument is essentially the same, however, whether or not addition or loss of a proton is concerted with another process.

Hydrolysis of an orthoester requires, of course, another step leading to formation of a dialkoxycarbonium ion. With the orthoesters incorporating a dioxolane ring, this step may yield either a dioxolenium ion or one in which the dioxolane ring has been opened. In the latter case the ring opening reaction leading to such a species would be stereochemically virtually identical with the second step of the sequence given above, i.e. the formation of the ester (or its conjugate acid). It follows then, that starting with an orthoester the reaction sequence either joins the same path as if it had started at the dioxolenium ion stage, or else it follows a parallel route that is sterically very closely related and which does not require additional special comment.

In our view the origin of the stereoselectivity observed with all of the substrates in this study except the orthoformates, is to be found in a

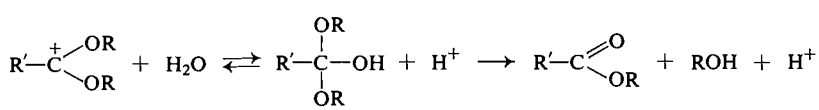

SCHEME 3

Can. J. Chem. Downloaded from www.nrcresearchpress.com by 210.87.254.6 on 09/05/12
For personal use only.

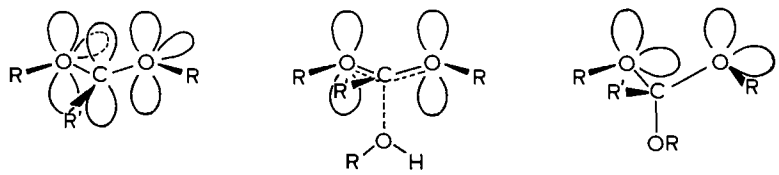

36 37 38

combination of steric and stereoelectronic effects. The latter effect is perhaps most clearly illustrated in terms of a nucleophilic attack on a hydroxyalkoxycarbonium ion, a reaction which is the reverse of the cleavage of an "orthoacid". We will first consider an unstrained system as in **36**, and its reaction with ROH. Simple theoretical considerations which are supported by the results of n.m.r. studies (15–20), require that all six of the atoms indicated in **36** and the localized non-bonding electrons on the oxygen atoms lie in a common plane; structure **36** depicts one of the possible arrangements which satisfies this requirement (the others may be obtained by successive interchange of the positions of the localized non-bonding electrons and the R group on each oxygen). Attack of ROH will take place on a line running through the charged carbon orthogonal to the common plane. This will lead through a transition state imagined to look like **37**, to the product in the conformation shown in **38**. For the reverse reaction **38** to **36**, which is the generalized version of the reaction which forms the basis of this paper, it is evident that in order to achieve maximum stabilization of the positive charge on carbon by the electrons on the two oxygen atoms, one free electron pair on each oxygen must be *anti* (or at least *anti*-periplanar) to the leaving group ROH.[3] If one now considers a specific version of this reaction with the corresponding species derived from a dioxolenium ion fused to an anchored six-membered ring, it is apparent from inspection of molecular models that the fusion of the five- and six-membered rings places restrictions on how to achieve a conformation even approaching one in which a pair of free electrons on each oxygen is *anti*-periplanar with the leaving group (as in **38**). For example, the *endo* electron pair on the axial oxygen (shown in **39**) can become *anti*-periplanar with the equatorial oxygen (which would be the leaving group in the formation of the equatorial alcohol – axial ester by this route) *only* by introducing severe steric strain, either by distorting the five-membered ring or alternatively

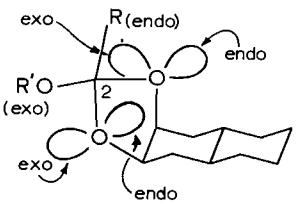

39

by flipping the six-membered ring into a boat conformation. Similarly the *exo* electrons of the equatorial oxygen can also only become *anti*-periplanar to the axial oxygen by introducing a good deal of strain. As is shown in **40**, however, the *exo* electrons of the axial oxygen can comparatively readily become *anti*-periplanar to the equatorial oxygen. Similarly as indicated in **41**, the *endo* electrons of the equatorial oxygen and the axial oxygen can also be so arranged, but in so doing the *endo* substituent on C-2 (shown as R in **41**) moves very close to the nearest axial hydrogen of the cyclohexane ring (H in **41**).[4] It would be expected that all species in which the *endo* function is either an aryl, alkyl, alkoxyl, or

[3]A good example of this requirement has very recently been given by Eliel and Nader (21).

[4]In the mannose derivatives studied by Perlin (7, 11) the non-bonding interaction is not with an axial hydrogen but rather a free electron pair of the pyranose oxygen. This interaction resembles the *syn*-axial non-bonded interaction between a *t*-butyl group and the free electron pairs in 2-alkyl-5-*t*-butyl-1,3-dioxanes, and which has been found by Eliel and Knoeber (22) to be much smaller than the analogous interaction between an axial *t*-butyl group and an axial hydrogen. This would suggest that the stereoselectivity with the mannose derivatives (though *not* with compounds **25**, **28**, and **33**) should be distinctly smaller than that found with the cyclohexane derivatives. Perlin (7) has noted the formation of a little of the 1-acetate from **31**, and has informed us (private communication) that in the hydrolysis of the fully acetylated orthoacetate from mannose he has found "almost equimolar yields of both products". We thank Professor Perlin for telling us of these results and for kindly giving permission to mention them here.

Can. J. Chem. Downloaded from www.nrcresearchpress.com by 210.87.254.6 on 09/05/12
For personal use only.

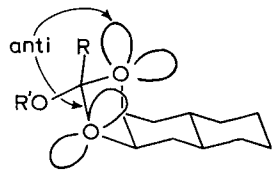

40

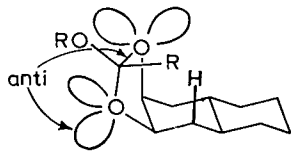

41

hydroxyl group, the interaction of the *endo* group with the neighboring axial hydrogen would make the transition state derived from **41** of much higher energy than the one derived from **40**. It is concluded from this argument that except when the *endo* substituent on C-2 is a hydrogen atom, the route derived directly from **40** would have much the lowest energy of the possible pathways. Such a route, of course, leads to the axial ester – equatorial alcohol, which is found experimentally in these cases to be the predominant product by a large measure.

When one *endo* group on C-2 is a hydrogen atom, the compound is an orthoformate ester (or the derived "orthoacid"). From the work of Lemieux and Perlin described earlier, it would appear that the major portion of a sample of orthoformate or of its derived "orthoacid" should in fact have the C-2 proton in the *endo* configuration. When the *endo* C-2 substituent is hydrogen one would expect that the transition states derived from **40** and **41** be not nearly as different in energy as when the substituent is larger than hydrogen. It is therefore not surprising in the context of this argument to find that the hydrolysis of the orthoformate ester (**22***a*) apparently gives nearly as much of the axial alcohol – equatorial ester (**24**) as of its isomer (**23**).[5]

[5]It might perhaps be mentioned that the mechanism of hydrolysis of orthoformates is believed to be essentially the same as that of the other orthoesters (6), and that any rationalization of the loss of stereoselectivity with the orthoformates must, as is the case here, be in terms of this same mechanism.

Another factor which may contribute in some measure to the stereoselectivity of hydrolysis is the greater ease of protonation of an equatorial oxygen (leading to the equatorial alcohol – axial ester) vs. protonation of an axial oxygen (leading to the axial alcohol – equatorial ester). In general an axial ion is of somewhat higher energy than its equatorial epimer, presumably because of poorer solvation of the axial ion resulting from the less open environment of an axial substituent (cf. ref. 23). An analogous, though perhaps smaller, energy difference would presumably be found between the *transition states* from the axially and the equatorially protonated species as well. Data for the relative basicities of axial and equatorial oxygen do not seem to be at hand but the difference between axial and equatorial amino groups is comparatively small: *cis*-4-*tert*-butylcyclohexylamine (axial NH_2) is less basic than the *trans* (equatorial NH_2) isomer by only 0.25 pK units in 80% methylcellosolve–water (24). Unless oxygen behaves quite differently from nitrogen in such cases, this factor alone could not account for the degree of stereoselectivity observed in the hydrolysis of dioxolenium ions, nor for the behavior of the orthoformates. Its effect, however, may be to increase the amount of the axial ester – equatorial alcohol to some extent.

Experimental

Melting points were determined on a Kofler hot stage and are uncorrected. Infrared spectra were obtained with Beckman IR-5 or IR-10 spectrophotometers using sodium chloride cells, and were determined on chloroform (Fisher Spectranalyzed grade) solutions. Rotations (at the D line) were determined on approximately 1% solutions in chloroform with a Rudolph model 80 polarimeter. Optical rotatory dispersion measurements were carried out with a Jasco ORD/UV-5-CD spectropolarimeter. Nuclear magnetic resonance spectra were run on $CDCl_3$ solutions using a Varian A-60 spectrometer. "Half-width" in the description of n.m.r. bands refers to the width of the band (in Hz) along a line midway between the baseline and the top of the band, cf. ref. (25). Refractive indices were determined with a thermostatically controlled Bausch and Lomb refractometer. Thin-layer chromatography was carried out using Camag silica gel DF 5. Petroleum ether refers to the fraction of boiling range 30–60°. Organic extracts were dried with anhydrous magnesium sulfate.

Acid-catalyzed Hydrolysis of Acyloxonium Hexafluoroantimonates

A solution of the acyloxonium salt in methylene chloride (10 ml) was shaken with aqueous acetic acid (10 ml, 10%) for several minutes. The reaction mixture

Can. J. Chem. Downloaded from www.nrcresearchpress.com by 210.87.254.6 on 09/05/12
For personal use only.

Can. J. Chem. Downloaded from www.nrcresearchpress.com by 210.87.254.6 on 09/05/12
For personal use only.

was then washed with dilute sodium bicarbonate solution, water, dried, the solvent evaporated under reduced pressure, and the residue treated as indicated below.

To obtain a semi-quantitative estimate of the composition of the reaction mixture, the product was dissolved in chloroform to give a suitable concentration for t.l.c. Standard mixtures of the two possible hydrolysis products were prepared, i.e. of the equatorial alcohol – axial ester and axial alcohol – equatorial ester compounds, and were dissolved in chloroform to give the same concentration as that of the hydrolysis product. A standard number of drops of each solution (from the same dropping pipette) were applied to t.l.c. plates which were then eluted with ether–benzene (1:1). The plates were sprayed with 30% sulfuric acid and charred, and the intensities of the resulting spots were compared.

In the products from 5α-cholestan-2α,3α-*p*-anisoxonium, 5α-cholestan-2β,3β-*p*-anisoxonium, and 9β,10α-decalin-2β,3β-*p*-anisoxonium salts the amount of axial alcohol – equatorial ester was in each case estimated at less than 0.5% of the product.

(a) 5α-Cholestan-2α,3α-p-anisoxonium Hexafluoroantimonate (7)

A solution of the salt (1) (370 mg) in methylene chloride was treated as described above. The t.l.c., eluting with ether–benzene (1:1), showed the product (255 mg) to consist of almost entirely one compound (R_f 0.54) together with a trace of a second compound (R_f 0.64), both being visible under u.v. light as well as upon charring. Crystallization from acetone–water gave 2α-hydroxy-5α-cholestan-3α-yl *p*-anisate (**8**); m.p. 146–148°; $[\alpha]_D$ +45°; ν_{max} 3580, 1700 cm^{-1}. The n.m.r. spectrum showed signals at 0.82 (s), 2.47 (s, OH), 3.80 (s), a broad band at 3.87 (half-width 20 Hz), a narrow band at 5.29 (half-width 6 Hz) and a signal interpreted as an AB quartet: δ_A 6.87, δ_B 7.96 p.p.m., J_{AB} 9 Hz. These signals were assigned to the C-19 methyl group, the hydroxyl group, the methoxyl group, the C-2 hydrogen (axial), the C-3 hydrogen (equatorial), and to the aromatic hydrogens respectively.

Anal. Calcd. for $C_{35}H_{54}O_4$: C, 78.01; H, 10.10. Found: C, 77.68; H, 10.08.

(b) 5α-Cholestan-2β,3β-p-anisoxonium Hexafluoroantimonate (20)

A solution of the salt (1) (250 mg) in methylene chloride was treated as above. The t.l.c., eluting with ether–benzene (1:1), showed the product (180 mg) to consist of almost entirely one compound (R_f 0.64), together with a trace of a second compound (R_f 0.85), both spots being visible under u.v. light as well as on charring. Crystallization from acetone – petroleum ether gave 3β-hydroxy-5α-cholestan-2β-yl *p*-anisate (**19**); m.p. 132–133°; $[\alpha]_D$ −22°; ν_{max} 3570, 1700 cm^{-1}. The n.m.r. spectrum had bands at 0.98 (s), 2.48 (s, OH), 3.78 (s), a broad band at 3.87 (half-width 22 Hz), a narrow band at 5.29 (half-width 8 Hz) and a quartet: δ_A 6.82, δ_B 7.93 p.p.m., J_{AB} 9 Hz, assigned to the C-19 methyl group, the hydroxyl group, the methoxyl group, C-3 hydrogen (axial), C-2 hydrogen (equatorial), and the aromatic hydrogens respectively.

Anal. Calcd. for $C_{35}H_{54}O_4$: C, 78.01; H, 10.10. Found: 77.73; H, 9.95.

(c) 9β,10α-Decalin-2β,3β-p-anisoxonium Hexafluoroantimonate (1)

A solution of the salt (1) (500 mg) in methylene chloride was treated with aqueous acetic acid as outlined above. The t.l.c., eluting with ether–benzene (1:1) showed the product (286 mg) to consist of almost entirely one compound (R_f 0.32) together with a trace of a second compound (R_f 0.50). Crystallization from ether – petroleum ether gave 3β-hydroxy-9β,10α-decalin-2β-yl *p*-anisate (**5**); m.p. 92–94°; ν_{max} 3580, 1700 cm^{-1}. The n.m.r. spectrum showed bands at 2.88 (s, OH), 3.71 (broad band, half-width 21 Hz), 3.77 (s), 5.30 (narrow band, half-width 7 Hz), and a quartet δ_A 6.85, δ_B 7.94 p.p.m., J_{AB} 9 Hz. These bands were assigned to the C-3 hydroxyl group, the C-3 hydrogen (axial), the methoxyl group, the C-2 hydrogen (equatorial), and to the aromatic hydrogens respectively.

Anal. Calcd. for $C_{18}H_{24}O_4$: C, 71.03; H, 7.95. Found: C, 70.90; H, 7.87.

(d) 9β,10α-Decalin-2β,3β-benzoyloxonium Hexafluoroantimonate

A solution of the benzoyloxonium salt (1) (100 mg) in methylene chloride (10 ml) was treated with aqueous acetic acid as described above. The t.l.c., eluting with benzene–ether (1:1), showed the product (52 mg) to be almost entirely one compound. Crystallization from ether–pentane gave 3β-hydroxy-9β,10α-decalin-2β-yl benzoate (**23***d*); m.p. 105–107°; ν_{max} 3600, 1705 cm^{-1}. The n.m.r. spectrum had signals at 2.40 (s, OH), 3.78 (broad band, half-width 21 Hz), 5.37 (narrow band, half-width 7 Hz), 7.42, and 8.05 (both multiplets). These signals were assigned to the C-3 hydroxyl group, the C-3 hydrogen (axial), the C-2 hydrogen (equatorial), and the phenyl hydrogens respectively.

Anal. Calcd. for $C_{17}H_{22}O_3$: C, 74.40; H, 8.09. Found: C, 74.34; H, 7.83.

Reaction of 9β,10α-Decalin-2β,3β-p-anisoxonium Hexafluoroantimonate (1) with Base

A solution of the decalin anisoxonium salt (200 mg) in methylene chloride (10 ml) was shaken with aqueous potassium hydroxide solution (10 ml; 5%) for 2 min. The methylene chloride was washed several times with water, dried, and evaporated under reduced pressure. The t.l.c., eluting with benzene–ether (1:1), showed the product to consist of one compound with the same R_f value as 3β-hydroxy-9β,10α-decalin-2β-yl *p*-anisate (**5**). Crystallization from ether – petroleum ether gave 3β-hydroxy-9β,10α-decalin-2β-yl *p*-anisate (112 mg) identified with an authentic specimen by m.p., mixed m.p., and i.r. spectra.

Alkaline Hydrolyses of Hydroxyanisates

A solution of the hydroxyanisate (50–100 mg) and potassium hydroxide (200–300 mg) in methanol (5 ml) and ether (1 ml) was allowed to react overnight at room temperature. The reaction mixture was diluted with water and extracted with ether. The ether extract was washed several times with water, dried, and evaporated under reduced pressure, and further purified as described below for each reaction.

(a) 2α-Hydroxy-5α-cholestan-3α-yl p-Anisate (8)

This compound gave a product which was recrystallized

Can. J. Chem. Downloaded from www.nrcresearchpress.com by 210.87.254.6 on 09/05/12
For personal use only.

from chloroform–acetone; m.p. 222–224°; $[\alpha]_D$ +31°. Henbest and Smith (26) have prepared 5α-cholestan-2α,3α-diol (**11**) and report m.p. 212–214° and $[\alpha]_D$ +32°. Repetition of their procedure gave a sample melting at 214–217° and which on admixture with the material from the saponification, melted at 223–225°.

(b) 3α-Hydroxy-5α-cholestan-2α-yl Anisate (12)

Upon hydrolysis as described above, this anisate gave a material which on recrystallization showed essentially the same properties as the 5α-cholestan-2α,3α-diol (**11**) prepared from **8**: m.p. 225–226°, $[\alpha]_D$ +29°, and mixed m.p. with an authentic specimen 224–226°.

(c) 2β-Hydroxy-5α-cholestan-3p-yl Anisate (15)

Compound **15** was hydrolyzed similarly; the product was recrystallized from ether–methanol; m.p. 174–176°; $[\alpha]_D$ +40°; mixed m.p. with an authentic sample of 5α-cholestan-2β,3β-diol (**16**) (prepared as described below) 177–179°.

(d) 3β-Hydroxy-5α-cholestan-2β-yl Anisate (19)

On hydrolysis as above, **19** gave a product which on recrystallization from ether–methanol melted at 174–176°; $[\alpha]_D$ +42°; mixed m.p. with an authentic specimen of 5α-cholestan-2β,3β-diol (**16**) (see below) 175–177°.

(e) 2β-Hydroxy-9β,10α-decalin-3β-yl Anisate (6)

Compound **6** gave a hydrolysis product which was recrystallized from benzene – petroleum ether to give a sample melting at 140–141°; mixed m.p. 139–140° with an authentic specimen of 9β,10α-decalin-2β,3β-diol (**21**), prepared by the method of Henbest *et al.* (27).

(f) 3β-Hydroxy-9β,10α-decalin-2β-yl Anisate (5)

On similar treatment, **5** gave a product which after recrystallization melted at 141–142°; mixed m.p. with an authentic sample of 9β,10α-decalin-2β,3β-diol (**21**) (27), 141–142°.

5α-Cholestan-2β,3β-diol (16)

This compound was prepared from cholest-2-ene by the method of Henbest and Smith (26), with the exception that the reaction mixture was heated for 3½ h at 80°. The product, after alkaline hydrolysis, was purified by t.l.c., eluting with ether–benzene (1:1); m.p. 177–180° and $[\alpha]_D$ +37°; reported m.p. 174–177° and $[\alpha]_D$ +43° (26).

Oxidation of the Steroid Hydroxyanisates with Dimethyl Sulfoxide and Acetic Anhydride

(a) 3β-Hydroxy-5α-cholestan-2β-yl p-Anisate (19)

A solution of the hydroxyanisate (**19**) (147 mg) in dimethyl sulfoxide (2 ml) and acetic anhydride (2 ml) was allowed to react at room temperature for 36 h. The reaction mixture was diluted with ether and washed with dilute sodium bicarbonate solution, several times with water, dried, and the ether evaporated. Crystallization from ether–pentane gave 5α-cholestan-3-one-2β-yl *p*-anisate (**18**) (124 mg), m.p. 68–74°; $[\alpha]_D$ +51°; ν_{max} 1705 cm^{-1}. The n.m.r. spectrum had bands at 0.95 (s), 3.81 (s), 5.52 (apparent triplet, *J* 7.75 Hz) and a quartet, δ_A 6.88, δ_B 8.00 p.p.m., J_{AB} 9 Hz. These bands were assigned to the C-19 methyl, the methoxyl group, the C-2 hydrogen (equatorial), and to the aromatic hydrogens respectively. Optical rotatory dispersion in methylene chloride (*c*, 0.04): $[\alpha]_{650}$ +25, $[\alpha]_{589}$ +50, $[\alpha]_{307}$ +950, $[\alpha]_{290}$ 0, and $[\alpha]_{280}$ −1825°; amplitude > 149. Ultraviolet spectrum in methylene chloride, λ_{max} 257 nm, log ε 4.35.

Anal. Calcd. for $C_{35}H_{52}O_4$: C, 78.30; H, 9.77. Found: C, 77.96; H, 9.92.

(b) 2α-Hydroxy-5α-cholestan-3α-yl p-Anisate (8)

The hydroxyanisate (**8**) (304 mg) was treated with dimethyl sulfoxide (3 ml) and acetic anhydride (3 ml) as described in (*a*) above. Attempted crystallization of the product from several solvent mixtures failed. The t.l.c., single elution with ether–benzene (1:1), showed only one spot; however, two successive elutions with ether–benzene (5:95) showed two compounds to be present having R_f values of 0.53 and 0.49, respectively, and which were separated by preparative t.l.c.

The slower running of the two proved to be the major product (192 mg) and on recrystallization from ether – petroleum ether gave 5α-cholestan-2-one-3α-yl *p*-anisate (**9**), m.p. 86–88°; $[\alpha]_D$ +88°; ν_{max} 1720 cm^{-1}. The n.m.r. spectrum showed bands at 0.80 (s), 3.83 (s), 5.05 (narrow band, half-width 5 Hz) and a quartet δ_A 6.90, δ_B 7.96 p.p.m., J_{AB} 9 Hz. These bands were assigned to the C-19 methyl group, the methoxyl group, the C-3 hydrogen (equatorial), and to the aromatic hydrogens respectively. Optical rotatory dispersion in methylene chloride (*c*, 0.039): $[\alpha]_{650}$ +100, $[\alpha]_{589}$ +100, $[\alpha]_{320}$ +1715, $[\alpha]_{298}$ 0, and $[\alpha]_{280}$ −2330°; amplitude > 217.

Anal. Calcd. for $C_{35}H_{52}O_4$: C, 78.30; H, 9.77. Found: C, 78.55; H, 9.96.

The material of R_f value 0.53 above (85 mg) was recrystallized from ether – petroleum ether; m.p. 108–110°; $[\alpha]_D$ +65°; ν_{max} 1700 cm^{-1}. The n.m.r. spectrum showed bands at 0.90 (s), 3.83 (s), 4.66 (half-width 11 Hz), 5.50 (half-width 8 Hz) and a quartet: δ_A 6.88, δ_B 7.97 p.p.m., J_{AB} 9 Hz. Qualitative tests for halogen and sulfur were negative.

(c) 2β-Hydroxy-5α-cholestan-3β-yl p-Anisate (15)

The hydroxyanisate (**15**) (134 mg) was treated with dimethyl sulfoxide (2 ml) and acetic anhydride (2 ml) for 72 h, and the product was isolated as described in (*a*) above. This oxidation appeared to be slower than the previous ones as t.l.c., eluting with ether–benzene (1:9) showed that besides the keto-anisate (R_f 0.66) a small amount of starting material was present. The keto-anisate was purified by t.l.c. using ether–benzene (1:9) and the product (77 mg) was recrystallized from chloroform – petroleum ether, giving 5α-cholestan-2-one-3β-yl *p*-anisate (**13**), m.p. 178–179°; $[\alpha]_D$ +45°; ν_{max} 1725, 1705 cm^{-1}. The n.m.r. spectrum had bands at 0.82 (s), 3.80 (s), 5.4 (broad diffuse band), and a quartet: δ_A 6.88, δ_B 8.03 p.p.m., J_{AB} 9 Hz. These signals were assigned to the C-19 methyl group, the methoxyl group, the C-3 hydrogen (axial), and to the aromatic hydrogens respectively. Optical rotatory dispersion in methylene chloride (*c*, 0.04): $[\alpha]_{650}$ +37, $[\alpha]_{589}$ +44, $[\alpha]_{310}$ +700, $[\alpha]_{292}$ 0, $[\alpha]_{285}$ −175, and $[\alpha]_{280}$ 0°; amplitude 47.

Anal. Calcd. for $C_{35}H_{52}O_4$: C, 78.30; H, 9.77. Found: C, 78.52; H, 9.53.

Oxidation of the Steroid Hydroxyanisates with Jones' Reagent

The oxidizing agent used in these experiments consisted of a solution of sodium dichromate (13 g) and concentrated sulfuric acid (8.7 ml) in water (30 ml). To a

Can. J. Chem. Downloaded from www.nrcresearchpress.com by 210.87.254.6 on 09/05/12
For personal use only.

stirred solution of the hydroxyanisate (150–250 mg) in acetone (10–25 ml), at room temperature, was added a few drops of the above oxidizing agent (usually 0.3 ml) so that the solution was a red–orange color. After 3 min a dilute aqueous solution of sodium metabisulfite ($Na_2S_2O_5$) was added to the reaction mixture until a blue–green color was obtained. After dilution with water, the reaction mixture was extracted with ether. The ether extracts were washed with dilute sodium bicarbonate solution and water, and then dried and the ether evaporated under reduced pressure.

(a) 2α-Hydroxy-5α-cholestan-3α-yl p-Anisate (8)

The hydroxyanisate (**8**) (214 mg) in acetone (10 ml) on oxidation as described above gave 195 mg of crude product. The t.l.c., eluting with ether–benzene (5:95) showed that there was very little starting material present and that the product consisted of almost entirely one compound (R_f 0.48) with a small amount of a second product running slightly ahead of the main spot. Preparative t.l.c. separated the material into two fractions weighing respectively 15 mg and 150 mg. Recrystallization from methylene chloride – petroleum ether gave materials identified by melting point, mixed m.p. with an authentic specimen and i.r. spectra as respectively 5α-cholestan-2-one-3β-yl *p*-anisate (**13**) and 5α-cholestan-2-one-3α-yl *p*-anisate (**9**).

(b) 3α-Hydroxy-5α-cholestan-2α-yl p-Anisate (12)

The hydroxyanisate (**12**) (180 mg) in acetone (15 ml) was oxidized as described above. The crude product (176 mg) showed no OH peaks in the i.r. spectrum. Crystallization from pentane gave 5α-cholestan-3-one-2α-yl *p*-anisate (**14**); m.p. 148–150°; $[\alpha]_D$ +105°; ν_{max} 1725, 1705 cm^{-1}. The n.m.r. spectrum had bands at 1.17 (s), 3.78 (s), a doublet of doublets at 5.50 (J_{AB} 6.5 Hz, J_{AC} 12.5 Hz, presumed to be due to coupling with the equatorial and axial protons on C-1, respectively) and a quartet: δ_A 6.88, δ_B 8.00 p.p.m. (J_{AB} 9 Hz). These bands were assigned to the C-19 methyl group, the methoxyl group, C-2 hydrogen (axial), and the aromatic hydrogens respectively. Optical rotatory dispersion in methylene chloride (*c*, 0.04): $[\alpha]_{650}$ +50, $[\alpha]_{589}$ +100, $[\alpha]_{312}$ +550, $[\alpha]_{288}$ +125, and $[\alpha]_{280}$ +625°; amplitude 23.

Anal. Calcd. for $C_{35}H_{52}O_4$: C, 78.30; H, 9.77. Found: C, 77.97; H, 9.68.

(c) 3β-Hydroxy-5α-cholestan-2β-yl p-Anisate (19)

The hydroxyanisate (**19**) (215 mg) in acetone (15 ml) was oxidized as described above. The t.l.c., eluting with ether–benzene (5:95), showed the crude product to consist mainly of one compound (R_f 0.52) together with a small amount of starting material. Purification by t.l.c. gave 5α-cholestan-3-one-2β-yl *p*-anisate (**18**) (139 mg) which was recrystallized from ether–pentane; m.p. 65–75°. The i.r. spectrum was identical to that of the product obtained by oxidation of 3β-hydroxy-5α-cholestan-2β-yl *p*-anisate (**19**) with dimethyl sulfoxide and acetic anhydride.

(d) 2β-Hydroxy-5α-cholestan-3β-yl p-Anisate (15)

The hydroxyanisate (**15**) (233 mg) in acetone (25 ml) was oxidized as described above. The t.l.c., eluting with ether–benzene (1:9), showed the presence of two materials. The slower moving of these was obtained as an oil (60 mg) with bands in the i.r. at 1740 and 1700 cm^{-1} and was not further characterized. The faster running material (130 mg) on recrystallization melted at 180–181°, and was shown by m.p., mixed m.p., and i.r. spectrum to be identical with the specimen of 5α-cholestan-2-one-3β-yl *p*-anisate (**13**) obtained from the dimethyl sulfoxide – acetic anhydride oxidation of 2β-hydroxy-5α-cholestan-3β-yl *p*-anisate (**15**).

Epimerization of 5α-Cholestan-3-one-2β-yl p-Anisate (18) to 5α-Cholestan-3-one-2α-yl p-Anisate (14)

A solution of 5α-cholestan-3-one-2β-yl *p*-anisate (**18**) (35 mg) and D-10-camphorsulfonic acid (5 mg) in benzene (5 ml) was refluxed overnight. The reaction mixture, after dilution with ether, was washed with dilute sodium bicarbonate solution and water, dried, and the solvent removed by evaporation under reduced pressure. The crude product had an i.r. spectrum very similar to that of 5α-cholestan-3-one-2α-yl *p*-anisate (**14**). The product was purified by t.l.c. eluting with ether–benzene (1:9); two recrystallizations from ether–pentane gave 5α-cholestan-3-one-2α-yl *p*-anisate (**14**), m.p. 146–148°; mixed m.p. with an authentic sample 146–148°. The i.r. spectrum was also identical with that of 5α-cholestan-2-one-2α-yl *p*-anisate (**14**).

Reduction of 5α-Cholestan-3-one-2β-yl p-Anisate (18) with Zinc and Acetic Acid

To a solution of the keto-anisate (**18**) (69 mg) in ether (4 ml) and acetic acid (1.5 ml) was added zinc dust (1.0 g); the mixture was refluxed for 4 h. More ether was added to the mixture, which was then filtered through Supercel. The filtrate was washed with dilute sodium carbonate solution and water, dried, and the ether evaporated under reduced pressure. The t.l.c., eluting with ether–benzene (1:9), showed the product to consist of one compound which had the same R_f value as 5α-cholestan-3-one (R_f 0.56) and differed from 5α-cholestan-2-one (R_f 0.66) and from the keto-anisate (R_f 0.61). Recrystallization from ether–methanol yielded 5α-cholestan-3-one, (30 mg), m.p. 128–129°. Mixed m.p. with authentic sample of 5α-cholestan-3-one, 127–129°; mixed m.p. with authentic sample of 5α-cholestan-2-one,[6] 103–118°.

Reduction of 5α-Cholestan-2-one-3α-yl p-Anisate (9) with Zinc and Acetic Acid

2α-Hydroxy-5α-cholestan-3α-yl *p*-anisate (**8**) (150 mg) was oxidized with dimethyl sulfoxide (2 ml) and acetic anhydride (2 ml), as described above. The crude keto-anisate (123 mg) was dissolved in acetic acid, zinc dust (2.5 g) was added, and the mixture was refluxed for 3 h. The product was isolated as described for the 5α-cholestan-3-one-2β-yl *p*-anisate reduction. The t.l.c., eluting with ether–benzene (5:95), showed the product to consist of more than one compound. The major reaction product had the same R_f value (0.45) as 5α-cholestan-2-one, which differed from that of 5α-cholestan-3-one (R_f 0.37). Separation of the major product by t.l.c. yielded 5α-cholestan-2-one (**10**) (42 mg) which on recrystallization from ether–methanol melted at 128–130°; mixed m.p. with authentic 5α-cholestan-2-one 129–131°; mixed m.p. with 5α-cholestan-3-one 103–123°.

---

[6]We thank Professor E. W. Warnhoff for the specimen of 5α-cholestan-2-one.

Can. J. Chem. Downloaded from www.nrcresearchpress.com by 210.87.254.6 on 09/05/12
For personal use only.

9β,10α-Decalin-2β,3β-diyl Ethyl Orthoformate (22a)

A solution of 9β,10α-decalin-2β,3β-diol (**21**), prepared by the method of Henbest *et al.* (27) (2.02 g), triethyl orthoformate (Eastman Practical grade) (1.75 g) together with a few crystals of D-10-camphorsulfonic acid in benzene (10 ml) was refluxed for 15 min. The benzene and alcohol produced by the reaction were distilled off at atmospheric pressure, a few crystals of calcium carbonate were added, and the residue distilled under vacuum. The product (1.75 g) distilled at 108–109° (0.5 mm), n_D^{25} 1.4755. The n.m.r. spectrum showed signals at 1.22 (triplet, *J* 7 Hz), 3.60 (quartet, *J* 7 Hz), 4.2 (broad band), 4.25 (narrow band, half-width 7 Hz), 5.73 (s) and 5.80 p.p.m. (s); the last two peaks were in the ratio 2:7. These signals were assigned to the methyl and methylene of the ethoxyl group, the C-3 and C-2 hydrogens of the decalin ring, and the formyl hydrogens (of the two epimers) respectively.

Anal. Calcd. for $C_{13}H_{22}O_3$: C, 69.05; H, 9.82. Found: C, 68.97; H, 9.65.

9β,10α-Decalin-2β,3β-diyl Ethyl Orthopropionate (22c)

A solution of 9β,10α-decalin-2β,3β-diol (**21**) (27) (2.0 g), triethyl orthopropionate (Eastman practical grade, 2.17 g), and a few crystals of D-10-camphorsulfonic acid in benzene (10 ml) was refluxed for 30 min. The benzene and alcohol were distilled off slowly at atmospheric pressure and, after the addition of a few crystals of sodium carbonate, the residue was distilled under vacuum. The product (1.23 g) distilled over at 112° (0.6 mm), n_D^{25} 1.4735. The n.m.r. spectrum showed in addition to a complex multiplet in the region 0.8 to 1.3 an apparent quartet centered at 3.52 (*J* 7 Hz) with a smaller multiplet (quartet ?) superimposed, a broad band centered at approximately 4.17 (half-width 12 Hz) and a narrow band at 4.38 p.p.m. (half-width 7 Hz). These bands were assigned to the methylenes of the two ethyl groups, and the C-3 and C-2 hydrogens of the decalin ring respectively.

Anal. Calcd. for $C_{15}H_{26}O_3$: C, 70.84; H, 10.30. Found: C, 70.76; H, 10.37.

9β,10α-Decalin-2β,3β-diyl Ethyl Orthoacetate (22b)

This compound was prepared as described above from 9β,10α-decalin-2β,3β-diol (**21**) (27) (1.53 g) and triethyl orthoacetate (Eastman practical grade) (1.62 g). The product (1.77 g), distilled at 106–108° (0.6 mm), n_D^{25} 1.4717. This compound had n.m.r. bands at 1.18 (triplet, *J* 7 Hz), 1.62 (s), 3.57 (quartet, *J* 7 Hz), 4.17 (broad band), and 4.38 (narrow band, half-width 7 Hz). These bands were assigned to the methyl of the ethoxyl group, the acetate methyl, the methylene of the ethoxyl group, and the C-3 and C-2 hydrogens of the decalin ring respectively.

Anal. Calcd. for $C_{14}H_{24}O_3$: C, 69.97; H, 10.07. Found: C, 70.21; H, 10.12.

Hydrolysis of 9β,10α-Decalin-2β,3β-diyl Ethyl Orthoformate (22a)

The orthoformate (150 mg) in methanol (5 ml) was treated with a few drops of aqueous hydrochloric acid (50%). The reaction solution was allowed to stand at room temperature for 10 min, diluted with water and extracted with ether. The ether extract was washed with dilute sodium bicarbonate solution and water, dried, and the ether removed under reduced pressure. The t.l.c., eluting with ether–benzene (1:9), showed the product to be mainly 9β,10α-decalin-2β,3β-diol (**21**).

In a second experiment the orthoformate (**22a**) (829 mg) in methanol (10 ml) was treated with aqueous acetic acid (5 ml, 10%) for 10 min at room temperature. The reaction was diluted with water and extracted with ether, and the ether extract was washed with dilute sodium bicarbonate solution and water, dried, and the solvent removed under reduced pressure. The t.l.c., eluting with ether–benzene (1:1), showed the product (700 mg) to consist of two compounds in roughly equal proportions. The i.r. spectrum had bands at approximately 3580 (m), 1720 (s), 1165 (m), 1145 (m), 1130 (m), 1000 (w), 980 (m), 970 (w), 960 (m), and 938 cm^{-1} (w).

Separation of these two materials was attempted by t.l.c. One half of the hydrolysis product was applied to t.l.c. plates (silica gel) which were then eluted with ether–benzene (1:1). The material was detected on the plates with iodine vapor and showed up as a broad band. This band was divided in half and each half was removed from the plates and extracted with ether. The i.r. spectra of the two fractions were identical to each other and to that of the original hydrolysis product. Upon further t.l.c. using ether–benzene (1:1), each fraction showed two spots, the same as were found in the original material. Thin-layer chromatography upon alumina was also unsuccessful.

The remaining half of the original hydrolysis product was crystallized from pentane and gave 3β-hydroxy-9β,10α-decalin-2β-yl formate (**23a**) (237 mg); m.p. 70–72°; ν_{max} 3580 (m), 1720 (s), 1165 (m), 1145 (m), 1130 (w), 1000 (w), 970 (w), 938 cm^{-1} (w). The n.m.r. spectrum had bands at 2.45 (s, OH), 3.70 (broad multiplet, half-width 21 Hz), 5.22 (narrow multiplet, half-width 6 Hz) and 8.15 (s). These bands were assigned to the C-3 hydroxyl group, the C-3 and C-2 hydrogens, and to the formyl hydrogen respectively.

Anal. Calcd. for $C_{11}H_{18}O_3$: C, 66.65; H, 9.13. Found: C, 66.27; H, 9.14.

A sample of crystalline hydroxyformate (**23a**) was chromatographed upon silica gel as described above. The product was recovered by extraction of the silica gel and was found to have an i.r. spectrum identical to that of the hydrolysis product, and contained the two extra peaks at 980 and 960 cm^{-1}.

In a third experiment the orthoformate (501 mg) was hydrolyzed as above. The product (433 mg) had an i.r. spectrum identical to that obtained previously. The n.m.r. spectrum included the following signals: 3.13 (s, OH), 3.70 (broad band, half-width 22 Hz), 4.07 (narrow band, half-width 7 Hz), 4.87 (broad multiplet), 5.20 (narrow band, half-width 7 Hz), 8.08 and 8.17 (both singlets). The signals at 3.70, 5.20 and 8.17 were assigned to the C-3 (axial) and C-2 (equatorial) hydrogens and to the formyl proton respectively of 3β-hydroxy-9β,10α-decalin-2β-yl formate (**23a**). The signals at 4.07, 4.87, and 8.08 were assigned to the C-2 (equatorial) and C-3 (axial) hydrogens and to the formyl proton respectively of 2β-hydroxy-9β,10α-decalin-3β-yl formate (**24a**).

Stability of 3β-Hydroxy-9β,10α-decalin-2β-yl Formate (23a) to Hydrolysis Conditions

The hydroxyformate (**23a**) (49 mg) in methanol (10 ml) was treated with aqueous acetic acid as described pre-

Can. J. Chem. Downloaded from www.nrcresearchpress.com by 210.87.254.6 on 09/05/12
For personal use only.

viously. The residue had an i.r. spectrum identical with that of the starting material.

9β,10α-Decalin-2β,3β-diyl Ethyl Orthopropionate (22c)

The orthopropionate (**22***c*) (267 mg) in methanol (10 ml) was treated with aqueous acetic acid (5 ml; 10%) for 15 min as described above. The t.l.c., eluting with ether–benzene (1:1), showed that the product (235 mg) consisted of almost entirely one compound (R_f 0.44) with only a slight trace of a second material (R_f 0.53). Crystallization from petroleum ether gave 3β-hydroxy-9β,10α-decalin-2β-yl propionate (**23***c*); m.p. 45–48°; ν_{max} 3580, 1720 cm^{-1}. The n.m.r. spectrum: 1.15 (triplet, *J* 7 Hz), 2.38 (quartet, *J* 7 Hz), 2.57 (s, OH), 3.77 (broad band, half-width 20 Hz), and 5.17 (narrow band, half-width 8 Hz). These bands were assigned to the methyl and methylene of the propionate ethyl group, the C-3 hydroxyl, and to the C-3 (axial) and C-2 (equatorial) hydrogens respectively.

Anal. Calcd. for $C_{13}H_{22}O_3$: C, 68.98; H, 9.81. Found: C, 69.08; H, 9.81.

The second material in the hydrolysis product had the same R_f value as 2β-hydroxy-9β,10α-decalin-3β-yl propionate (**24***c*) (see below).

9β,10α-Decalin-2β,3β-diyl Ethyl Orthoacetate (22b)

The orthoacetate (214 mg) in methanol (5 ml) and ether (1 ml) was treated with a few drops of aqueous acetic acid (50%) as described previously. The t.l.c., eluting with ether–benzene (1:1), showed the product (188 mg) to consist of almost entirely one compound (R_f 0.39) together with a slight trace of a second material (R_f 0.45). Crystallization from ether–pentane gave 3β-hydroxy-9β,10α-decalin-2β-yl acetate (**23***b*), m.p. 73–75°, ν_{max} 3570, 1720 cm^{-1}. The n.m.r. spectrum showed absorption at 2.10 (s), 2.67 (s, OH), 3.70 (broad band, half-width 21 Hz) and 5.13 (narrow band, half-width 7 Hz). These signals were assigned to the acetate methyl group, the C-3 hydroxyl group, and to the C-3 (axial) and C-2 (equatorial) hydrogens respectively.

Anal. Calcd. for $C_{12}H_{20}O_3$: C, 67.89; H, 9.51. Found: C, 68.23; H, 9.45.

Acid-catalyzed Rearrangement of the Hydroxyesters

A solution of the hydroxyester and D-10-camphorsulfonic acid in benzene was refluxed overnight. The products of the reaction were separated by t.l.c., eluting with benzene, the compounds being detected under u.v. light. In all cases, the compounds with an equatorial alcohol group ran slower than the compounds with an axial alcohol group, and were easily separated.

(a) 2α-Hydroxy-5α-cholestan-3α-yl p-Anisate (8)

A solution of the hydroxyester (**8**) (142 mg) and D-10-camphorsulfonic acid (14 mg) in benzene (15 ml) was treated as described above and gave starting material (48 mg) and 3α-hydroxy-5α-cholestan-2α-yl *p*-anisate (**12**) (48 mg), which was recrystallized from chloroform–methanol; m.p. 186–188°; $[\alpha]_D$ +61°; ν_{max} 3590, 1700 cm^{-1}. The n.m.r. spectrum showed signals at 0.90 (s), 2.25 (s, OH), 3.78 (s), 4.13 (narrow band, half-width 6 Hz), 5.1 (broad band, half-width 21 Hz), and a quartet: δ_A 6.82, δ_B 7.93 p.p.m. and J_{AB} 9 Hz. These signals were assigned to the C-19 methyl group, the hydroxyl group, the methoxyl group, the C-3 (equatorial), and C-2 (axial) hydrogens, and to the aromatic hydrogens respectively.

Anal. Calcd. for $C_{35}H_{54}O_4$: C, 78.01; H, 10.10. Found: C, 78.08; H, 9.86.

In two other rearrangements the following results were obtained: (*i*) the hydroxyanisate (372 mg) gave starting material (**8**) (93 mg) and 3α-hydroxy-5α-cholestan-2α-yl *p*-anisate (**12**) (147 mg); (*ii*) from the hydroxyanisate (456 mg) was obtained starting material (155 mg) and the rearranged hydroxyanisate (222 mg).

(b) 3β-Hydroxy-5α-cholestan-2β-yl p-Anisate (19)

The hydroxyester (**19**) (416 mg) and D-10-camphorsulfonic acid (17 mg) in benzene (5 ml) gave starting material (211 mg) and 2β-hydroxy-5α-cholestan-3β-yl *p*-anisate (**15**) (168 mg), which was recrystallized from chloroform–cyclohexane; m.p. 210–212°; $[\alpha]_D$ +27°; ν_{max} 3560, 1700 cm^{-1}. The n.m.r. spectrum had bands at 1.07 (s), 1.87 (s, OH), 3.75 (s), 4.18 (narrow band, half-width 6 Hz), 4.95 (broad band, half-width 21 Hz), and a quartet: δ_A 6.82, δ_B 7.93 p.p.m., J_{AB} 9 Hz. These bands were assigned to the C-19 methyl group, the C-2 hydroxyl group, the methoxyl group, the C-2 hydrogen (equatorial), the C-3 hydrogen (axial), and the aromatic hydrogens respectively.

Anal. Calcd. for $C_{35}H_{54}O_4$: C, 78.01; H, 10.10. Found: C, 78.10; H, 10.37.

(c) 3α-Hydroxy-5α-cholestan-2α-yl p-Anisate (12)

The hydroxyanisate (**12**) (63 mg) plus D-10-camphorsulfonic acid (3 mg), in benzene (3 ml) gave starting material (**12**) (46 mg) and 2α-hydroxy-5α-cholestan-3α-yl *p*-anisate (**8**) (13 mg), both compounds being identified by t.l.c., R_f values, and i.r. spectra.

(d) 2β-Hydroxy-5α-cholestan-3β-yl p-Anisate (15)

From this hydroxyester (**15**) (57 mg) plus D-10-camphorsulfonic acid (3 mg) in benzene (2 ml) was obtained starting material (40 mg) and 3β-hydroxy-5α-cholestan-2β-yl *p*-anisate (**19**) (15 mg), both identified by t.l.c., R_f values, and i.r. spectra.

(e) 3β-Hydroxy-9β,10α-decalin-2β-yl p-Anisate (5)

The hydroxyanisate (**5**) (404 mg) plus D-10-camphorsulfonic acid (67 mg) in benzene (5 ml) gave starting material (130 mg) and 2β-hydroxy-9β,10α-decalin-3β-yl *p*-anisate (**6**) (170 mg), which was recrystallized from ether – petroleum ether; m.p. 96–98°; ν_{max} 3600, 1700 cm^{-1}. The n.m.r. spectrum had signals at 2.62 (s, OH), 3.75 (s), 4.13 (narrow band, half-width 6 Hz), 4.95 (broad multiplet) and a quartet: δ_A 6.81, δ_B 7.94 p.p.m., J_{AB} 9 Hz. These signals were assigned to the methoxyl group, the C-2 (equatorial) and C-3 (axial) hydrogens, and to the aromatic hydrogens respectively.

Anal. Calcd. for $C_{18}H_{24}O_4$: C, 71.03; H, 7.95. Found: C, 70.71; H, 7.80.

In addition to the above two materials, a third fraction (139 mg) was isolated from the t.l.c. plates which ran faster than either of the hydroxyanisates. The i.r. spectrum had absorption at 1745 and 1710 cm^{-1}. Thin-layer chromatography, eluting with benzene, showed this material to consist of at least three compounds; it was not investigated further.

(f) 2β-Hydroxy-9β,10α-decalin-3β-yl p-Anisate (6)

From the hydroxyester (**6**) (59 mg) plus D-10-camphorsulfonic acid (7 mg) in benzene (3 ml) was obtained starting material (**6**) (43 mg) and 3β-hydroxy-9β,10α-decalin-2β-yl *p*-anisate (**5**) (15 mg), both compounds being identified by t.l.c., R_f values, and i.r. spectra.

(g) 3β-Hydroxy-9β,10α-decalin-2β-yl Acetate (23b)

From the hydroxyacetate (**23***b*) (641 mg) and D-10-camphorsulfonic acid (50 mg) in benzene (10 ml) was obtained starting material (225 mg) and 2β-hydroxy-9β,10α-decalin-3β-yl acetate (**24***b*) (236 mg), which was recrystallized from ether–pentane; m.p. 81–83°; ν_{max} 3500, 1720 cm^{-1}. The n.m.r. spectrum: 2.07 (s), 2.38 (s, OH), 4.08 (narrow band, half-width 7 Hz), and 4.8 (broad multiplet). These bands were assigned to the acetate methyl group, the hydroxyl group, the C-2 hydrogen (equatorial) and the C-3 hydrogen (axial), respectively.

Anal. Calcd. for $C_{12}H_{20}O_3$: C, 67.89; H, 9.51. Found: C, 67.89; H, 9.40.

(h) 3β-Hydroxy-9β,10α-decalin-2β-yl Propionate (23c)

The hydroxypropionate (**23***c*) (400 mg) and D-10-camphorsulfonic acid (22 mg) in benzene (4 ml) gave starting material (159 mg) and 2β-hydroxy-9β,10α-decalin-3β-yl propionate (**24c**) (213 mg), which was recrystallized from ether–pentane; m.p. 59–61°; ν_{max} 3590, 1730 cm^{-1}. The n.m.r. showed bands at 1.13 (triplet, *J* 7 Hz), 2.18 (s, OH), 2.35 (quartet, *J* 7 Hz), 4.05 (narrow band, half-width 6 Hz), and 4.8 (broad multiplet). These bands were assigned to the methyl group, the C-2 hydroxyl group, the propionyl methylene group, the C-2 hydrogen (equatorial) and the C-3 hydrogen (axial), respectively.

Anal. Calcd. for $C_{13}H_{22}O_3$: C, 68.98; H, 9.81. Found: C, 69.18; H, 9.74.

(i) 3β-Hydroxy-9β,10α-decalin-2β-yl Benzoate (23d)

The hydroxybenzoate (**23***d*) (820 mg) and D-10-camphorsulfonic acid (40 mg) in benzene (10 ml) gave starting material (345 mg) and 2β-hydroxy-9β,10α-decalin-3β-yl benzoate (**24***d*) (433 mg), which was recrystallized from ether–pentane; m.p. 102–103°; ν_{max} 3580, 1700 cm^{-1}. The n.m.r. showed signals at 2.23 (s, OH), 4.18 (narrow band, half-width 5 Hz) and 5.0 (broad multiplet), assigned to the C-2 hydroxy group, the C-2 hydrogen (equatorial) and to the C-3 hydrogen (axial) respectively, and also complex aromatic absorption centered at 7.47 and 8.03 p.p.m.

Anal. Calcd. for $C_{17}H_{22}O_3$: C, 74.40; H, 8.09. Found: C, 74.53; H, 8.19.

Preparation of 3β-Hydroxy-9β,10α-decalin-2β-yl Benzoate (23d) from the Diol (21) via the Orthoester (22d)

A solution of 9β,10α-decalin-2β,3β-diol (500 mg) and trimethyl orthobenzoate (28) (567 mg) together with a small amount of D-10-camphorsulfonic acid in benzene (5 ml) was refluxed for 30 min. The benzene was distilled off at atmospheric pressure leaving an oily product with only small absorption in the hydroxyl and carbonyl regions of the i.r. spectrum. A solution of the residue in methanol (20 ml) and ether (5 ml) was treated with aqueous acetic acid (5 ml, 20%) for 15 min, after which the reaction mixture was extracted with ether, and the ether solution was washed with dilute sodium bicarbonate solution, water, dried and the solvent removed under reduced pressure. The t.l.c., eluting with ether–benzene (1:1), showed the product (799 mg) to consist mainly of the hydroxybenzoate (**23***d*) together with some decalindiol (**21**). These two materials were separated by column chromatography (B.D.H. silica gel, 3 g), the hydroxybenzoate (**23***d*) (597 mg) being eluted with ether–benzene (1:9) and the diol (93 mg) with ether. The hydroxybenzoate was identified as 3β-hydroxy-9β,10α-decalin-2β-yl benzoate (**23***d*) by m.p., mixed m.p. with authentic sample prepared from the benzoyloxonium salt (above), and i.r. spectrum.

Preparation of 2β-Hydroxy-9β,10α-decalin-3β-yl Benzoate (24d) from the Diol (21)

9β,10α-Decalin-2β,3β-diol (**21**) (250 mg) in pyridine (5 ml) was treated with benzoyl chloride (209 mg) overnight. The t.l.c., eluting with ether–benzene (1:1) showed the crude product (310 mg) to consist of a mixture of the hydroxybenzoate and unreacted diol. Separation by t.l.c. gave 275 mg of the hydroxybenzoate (**24***d*) which was recrystallized from ether–pentane; m.p. 102–104°; mixed m.p. with an authentic sample (prepared by acid-catalyzed rearrangement of **23***d*, above) 101–103°. 9β,10α-Decalin-2β,3β-diol (66 mg) was also recovered from the t.l.c. plates and was identified by m.p. and mixed m.p.

The Woodward-Prévost Reaction with Δ^2-9β,10α-Octalin

To a solution of Δ^2-9β,10α-octalin (2.0 g) in glacial acetic acid (300 ml) was added silver acetate (6.2 g). The mixture was stirred vigorously and powdered iodine (3.3 g) added slowly over 30 min. After a further 30 min, when no iodine was visible, the mixture was treated with aqueous acetic acid (4 ml, 80%) and then stirred overnight. A solution of sodium chloride (6.4 g) in water (20 ml) was added and the stirring stopped. After a few minutes the mixture was filtered and the filtrate evaporated. The residue was dissolved in ether and washed with dilute sodium bicarbonate solution, dilute sodium bisulfite solution, water, dried, and the ether removed by evaporation. The t.l.c., eluting with benzene–ether (1:1), showed the product (2.96 g) to be nearly all one compound, with the same R_f value as 3β-hydroxy-9β,10α-decalin-2β-yl acetate (**23***b*). Column chromatography using silica gel and eluting with ether–benzene gave 3β-hydroxy-9β,10α-decalin-2β-yl acetate (**23***b*) (2.46 g); this was recrystallized from methylene chloride – petroleum ether and identified by m.p., mixed m.p. with authentic sample, and i.r. spectrum.

We gratefully acknowledge the financial support of the National Research Council of Canada and the Alfred P. Sloan Foundation.

1. J. F. KING and A. D. ALLBUTT. Can. J. Chem. **47**, 1445 (1969).
2. J. F. KING and A. D. ALLBUTT. Tetrahedron Lett. 49 (1967).
3. W. MOFFITT, R. B. WOODWARD, A. MOSCOWITZ, W. KLYNE, and C. DJERASSI. J. Amer. Chem. Soc. **83**, 4013 (1961).
4. K. L. WILLIAMSON and W. S. JOHNSON. J. Amer. Chem. Soc. **83**, 4623 (1961).
5. A. D. ALLBUTT. Ph.D. Thesis, University of Western Ontario, London, Ontario, 1967. p. 72.
6. E. H. CORDES. *In* Progress in physical organic chemistry. Vol. 4. *Edited by* A. Streitwieser and R. W. Taft, Interscience Publishers Inc., New York, 1967. p. 1.
7. A. S. PERLIN. Can. J. Chem. **41**, 399 (1963).
8. R. U. LEMIEUX and J. D. T. CIPERA. Can. J. Chem. **34**, 906 (1956).

Can. J. Chem. Downloaded from www.nrcresearchpress.com by 210.87.254.6 on 09/05/12
For personal use only.

9. R. U. LEMIEUX and A. R. MORGAN. Can. J. Chem. **43**, 2199 (1965).
10. J. G. BUCHANAN and R. FLETCHER. J. Chem. Soc. 6316 (1965).
11. C.-S. GIAM, H. R. GOLDSCHMID, and A. S. PERLIN. Can. J. Chem. **41**, 3074 (1963).
12. R. U. LEMIEUX and A. R. MORGAN. Can. J. Chem. **43**, 2190 (1965).
13. H. PAULSEN, W. P. TRAUTWEIN, F. GARRIDO ESPINOSA, and K. HEYNS. Tetrahedron Lett. 4137 (1966); H. PAULSEN, F. GARRIDO ESPINOSA, W. P. TRAUTWEIN, and K. HEYNS. Chem. Ber. **101**, 179 (1968).
14. R. B. WOODWARD and F. V. BRUTCHER, JR. J. Amer. Chem. Soc. **80**, 209 (1958).
15. T. BIRCHALL and R. J. GILLESPIE. Can. J. Chem. **43**, 1045 (1965).
16. H. HOGEVEEN, A. F. BICKEL, C. W. HILBERS, E. L. MACKOR, and C. MACLEAN. Chem. Commun. 898 (1966).
17. M. BROOKHART, G. C. LEVY, and S. WINSTEIN. J. Amer. Chem. Soc. **89**, 1735 (1967).
18. G. A. OLAH and A. M. WHITE. J. Amer. Chem. Soc. **89**, 3591 (1967).
19. H. HART and D. A. TOMALIA. Tetrahedron Lett. 3383 (1966); D. A. TOMALIA and H. HART. Tetrahedron Lett. 3389 (1966).
20. F. M. BERINGER and S. A. GALTON. J. Org. Chem. **32**, 2630 (1967).
21. E. L. ELIEL and F. NADER. J. Amer. Chem. Soc. **91**, 536 (1969).
22. E. L. ELIEL and M. C. KNOEBER. J. Amer. Chem. Soc. **90**, 3444 (1968).
23. C. W. BIRD and R. C. COOKSON. J. Chem. Soc. 2343 (1960).
24. M. TICHÝ, J. JONÁŠ, and J. SICHER. Coll. Czech. Chem. Commun. **24**, 3434 (1959).
25. A. HASSNER and C. HEATHCOCK. J. Org. Chem. **29**, 1350 (1964).
26. H. B. HENBEST and M. SMITH. J. Chem. Soc. 926 (1957).
27. H. B. HENBEST, M. SMITH, and A. THOMAS. J. Chem. Soc. 3293 (1958).
28. S. M. MCELVAIN and J. F. VENERABLE. J. Amer. Chem. Soc. **72**, 1661 (1950).

Can. J. Chem. Downloaded from www.nrcresearchpress.com by 210.87.254.6 on 09/05/12
For personal use only.

Can. J. Chem. Downloaded from www.nrcresearchpress.com by 210.87.254.105 on 09/05/12
For personal use only.

Thermochemistry of copper compounds: $Cu(OH)_2$, $CuCl_2$, $Cu(IO_3)_2 \cdot H_2O$, and $Cu(IO_3)_2$

L. M. GEDANSKY,[1] P. J. PEARCE,[2] AND L. G. HEPLER
Department of Chemistry, The University of Lethbridge, Lethbridge, Alberta

Received January 5, 1970

Calorimetric measurements have led to ΔH_f^0 values for solid $Cu(OH)_2$, $CuCl_2$, $Cu(IO_3)_2 \cdot H_2O$, and $Cu(IO_3)_2$. These ΔH_f^0 values have been used with data from earlier investigations in evaluating ΔG_f^0 and S_{298}^0 values for these compounds. All of these quantities are based on "best" ΔG_f^0, ΔH_f^0, and $\bar{S}_2^0$ values for $Cu^{2+}(aq)$ derived in this paper.

Canadian Journal of Chemistry, **48**, 1770 (1970)

Introduction

Thermodynamic data presently available permit calculation of reliable ΔG_f^0, ΔH_f^0, and $\bar{S}_2^0$ values for $Cu^{2+}(aq)$. We use these values with results of our calorimetric measurements and equilibrium data from the literature to evaluate the thermodynamic properties of solid $Cu(OH)_2$, $CuCl_2$, $Cu(IO_3)_2 \cdot H_2O$, and $Cu(IO_3)_2$.

Experimental

The calorimetric apparatus was similar to that previously described (1). All results are reported in terms of the defined calorie (4.184 J) and refer to 25.00 ± 0.10 °C.

After several trials, the following procedure for preparation of calorimetric samples of $Cu(OH)_2$ was adopted. One liter of 0.1 *M* $CuSO_4$ solution was treated with 150 ml of 5 *M* NH_3 solution, which was sufficient to redissolve the $Cu(OH)_2$ that was initially precipitated. After this solution was warmed to 40–50 °C, 130 ml of 1.5 *M* NaOH solution was slowly added with continuous stirring. The resulting blue precipitate of $Cu(OH)_2$ was allowed to settle and then washed several times by decantation with distilled water. After the washed precipitate was air dried for 1 day, it was further dried under vacuum over concentrated sulfuric acid for several days. During this period the solid was gently ground once. The final blue solid was found by iodometric analysis to contain 97.5 ± 0.2% of the theoretical amount of copper.

Anhydrous $CuSO_4$ was prepared by heating $CuSO_4 \cdot 5H_2O$ at 250 °C for several days.

Two different samples of cupric iodate "monohydrate" were prepared as described by Ramette and Broman (2). After the resulting blue samples were air dried at ~40 °C, iodometric analyses and determination of weight loss on heating indicated stoichiometric composition of both samples to be $Cu(IO_3)_2 \cdot nH_2O$ with $n = 0.90$; that is, a mixture of $Cu(IO_3)_2 \cdot H_2O$ and $Cu(IO_3)_2$. Anhydrous $Cu(IO_3)_2$ was prepared by heating the "monohydrate" at 250 °C for several days. Iodometric analysis indicated a purity of 100.0 ± 0.2%.

All chemicals used in preparation of cupric hydroxide and iodate were reagent grade, as were all chemicals used for preparation of solutions used in subsequent calorimetric measurements.

Cupric chloride was Fisher Certified Reagent. Run 1 was made with a sample taken directly from the reagent bottle. For Runs 2 and 3, samples from the same bottle were dried for 2 and 8 h, respectively, at 115 °C. A sample that was recrystallized from distilled water and then dried for 10 h at 115 °C was used for Runs 4 and 5.

Results and Calculations

Since we use the standard thermodynamic properties of $Cu^{2+}(aq)$ for all calculations with our calorimetric data, we first derive the "best" values for these quantities.

Electrochemical data for the $Cu/Cu^{2+}(aq)$ couple have been reviewed by deBethune, Licht, and Swendeman (3). Reported potentials range from $E^0 = -0.337$ to -0.3448 V, which correspond to ΔG_f^0 values from 15.5 to 15.9 kcal mole^{-1} for $Cu^{2+}(aq)$. Enthalpy and entropy data (4) have led to $\Delta G_f^0 = 15.9$ kcal mole^{-1}, and thence to a calculated $E^0 = -0.34_5$ V. On the basis of estimates of uncertainties in the data and a weighted average, we adopt $E^0 = -0.34_0$ V and the corresponding $\Delta G_f^0 = 15.7$ kcal mole^{-1} for $Cu^{2+}(aq)$.

There are several paths to ΔH_f^0 and $\bar{S}_2^0$ for $Cu^{2+}(aq)$. We choose as best the $\bar{S}_2^0 = -23.6$ cal deg^{-1} mole^{-1} for $Cu^{2+}(aq)$ that has been derived (4) from the thermodynamics of solution of $CuSO_4 \cdot 5H_2O$. Then we obtain $\Delta H_f^0 = 15.6$ kcal mole^{-1} for $Cu^{2+}(aq)$ from this $\bar{S}_2^0$ and the ΔG_f^0 cited above. This value is in good agreement with $\Delta H_f^0 = 15.7$ kcal mole^{-1} derived (4) from the heat of solution of $CuSO_4(c)$ and also with a less certain value from the temperature coefficient of the potential of the copper electrode (3).

Heats of solution of solid $Cu(OH)_2$ in per-

[1]Present address: Scott Paper Co., Philadelphia, Pennsylvania.

[2]Present address: Department of Chemistry, Yale University, New Haven, Connecticut.

Can. J. Chem. Downloaded from www.nrcresearchpress.com by 210.87.254.105 on 09/05/12
For personal use only.

TABLE 1

Heats of solution of $Cu(OH)_2$ in perchloric acid

Moles $Cu(OH)_2$/950 ml $\times 10^3$	$HClO_4$ (M)	$-\Delta H_1$ (kcal mole^{-1})
2.560	0.0238	14.56
4.281	0.0595	14.36
3.801	0.119	14.28

chloric acid of indicated molarity are given in Table 1. We have estimated small heats of dilution (5, 6) to obtain the desired $\Delta H_1^0 = -14.6 \pm 0.5$ kcal mole^{-1} for the reaction represented by eq. [1]

[1] $Cu(OH)_2(s) + 2\ H^+(aq) \rightleftharpoons Cu^{2+}(aq) + H_2O(liq)$

The indicated total uncertainty contains contributions from calorimetric measurements, sample composition, and estimated heats of dilution.

Another approach to the thermodynamic properties of cupric hydroxide is by way of its heat of precipitation, which was determined by adding 2–5 ml of 6 M NaOH to 950 ml of dilute $CuSO_4$ in the calorimeter. A small excess of NaOH was used in each measurement, and the mass of $CuSO_4$ in the solution was accurately known. Separate determination of the (small) total heat due to bulb breaking and dilution of the NaOH permitted calculation of the experimental results in terms of

[2] $CuSO_4(dilute) + 2\ NaOH(dilute) \rightleftharpoons Cu(OH)_2(s) + Na_2SO_4(dilute)$

Heat of dilution data (5, 6) have been used with the ΔH_2 values given in Table 2 to yield the standard heat of reaction values also listed there under ΔH_3^0, which refers to the reaction

[3] $Cu^{2+}(aq) + 2\ OH^-(aq) \rightleftharpoons Cu(OH)_2(s)$

The value $\Delta H_3^0 = -11.2 \pm 0.4$ kcal mole^{-1} is adopted, in which the indicated total uncertainty includes contributions from the calorimetric measurements, heats of dilution, and the state of the precipitated cupric hydroxide. The precipitation reaction in the calorimeter produced a flocculent blue precipitate that later turned green and then black on standing; that is, precipitated hydroxide changed to oxide.

We consider the calorimetric results for $Cu(OH)_2$ in terms of the reaction

[4] $Cu(OH)_2(s) \rightleftharpoons Cu^{2+}(aq) + 2\ OH^-(aq)$

TABLE 2

Heats of precipitation of $Cu(OH)_2$

Moles Cu^{2+}/950 ml $\times 10^3$	Moles OH^- added	$-\Delta H_2$ (kcal mole^{-1})	$-\Delta H_2^0$ (kcal mole^{-1})
6.72	0.018	11.73	11.2
6.42	0.018	11.74	11.2
6.36	0.018	11.73	11.2
3.65	0.018	11.64	11.2
6.29	0.048	11.66	11.1

TABLE 3

Heats of solution of $CuCl_2(c)$

Run	Moles $CuCl_2$/950 ml $\times 10^3$	$-\Delta H$ (kcal mole^{-1})
1	4.891	11.90
2	5.200	12.08
3	5.179	12.12
4	5.310	12.15
5	4.751	12.09

We combine our $\Delta H_1^0 = -14.6$ kcal mole^{-1} with twice the heat of ionization of water (7), $\Delta H^0 = 13.34$ kcal mole^{-1}, to obtain the desired $\Delta H_4^0 = 12.1$ kcal mole^{-1}. Since reaction [4] is the reverse of reaction [3], our heats of precipitation lead to $\Delta H_4^0 = 11.2$ kcal mole^{-1}. We adopt an average $\Delta H_4^0 = 11.6$ kcal mole^{-1} for further calculations. First, combination of this ΔH_4^0 with ΔH_f^0 values for $Cu^{2+}(aq)$ from this paper and for $OH^-(aq)$ (8) gives us $\Delta H_f^0 = -105.9$ kcal mole^{-1} for solid $Cu(OH)_2$. We also use this ΔH_4^0 with $\Delta G_4^0 = 26.3$ kcal mole^{-1} from the solubility product equilibrium constant (9) and entropy values for $Cu^{2+}(aq)$ from this paper and for $OH^-(aq)$ (8) to obtain $S_{298}^0 = 20._7$ cal deg^{-1} mole^{-1} for solid $Cu(OH)_2$. We also calculate $\Delta G_f^0 = -85.8$ kcal mole^{-1} for $Cu(OH)_2(s)$.

Heats of solution of $CuCl_2(c)$ are given in Table 3. Combination of these ΔH values with small heats of dilution estimated from data (5) for other MCl_2 compounds gives us $\Delta H^0 = -12.27 \pm 0.1$ kcal mole^{-1} for the standard heat of solution of $CuCl_2(c)$. Results of earlier workers (5, 10) lead to ΔH^0 values ranging from about -11.9 to about -12.5 kcal mole^{-1}. While our measurements were in progress, we learned of a $\Delta H^0 = -12.29$ kcal mole^{-1} reported by Shchukarev, Vasil'kova, and Barvinok (11), which is in excellent agreement with our value. We combine $\Delta H^0 = -12.3$ kcal mole^{-1} for the

Can. J. Chem. Downloaded from www.nrcresearchpress.com by 210.87.254.105 on 09/05/12
For personal use only.

standard heat of solution of $CuCl_2(c)$ with ΔH_f^0 for $Cu^{2+}(aq)$ from this paper and ΔH_f^0 for $Cl^-(aq)$ (8) to obtain $\Delta H_f^0 = -52.0$ kcal mole^{-1} for $CuCl_2(c)$. This ΔH_f^0 is combined with the third law S_{298}^0 for $CuCl_2(c)$ from Stout and Chisholm (12) to yield $\Delta G_f^0 = -41.4$ kcal mole^{-1} for $CuCl_2(c)$.

In our investigation of the thermodynamics of $Cu(IO_3)_2 \cdot H_2O(c)$ and $Cu(IO_3)_2(c)$ we have studied reactions [5]–[8] calorimetrically and report the results in Tables 4–7.

[5] $Cu(IO_3)_2 \cdot 0.90\ H_2O(c) + 4\ NH_3(0.32\ M) \rightleftharpoons Cu(NH_3)_4^{2+}(M) + 2\ IO_3^-(2\ M) + 0.90\ H_2O(liq)$

[6] $Cu(IO_3)_2(c) + 4\ NH_3(0.32\ M) \rightleftharpoons Cu(NH_3)_4^{2+}(M) + 2\ IO_3^-(2\ M)$

[7] $CuSO_4(c) + 4\ NH_3(0.32\ M) \rightleftharpoons Cu(NH_3)_4^{2+}(M) + SO_4^{2-}(M)$

[8] $CuSO_4(c) \rightleftharpoons Cu^{2+}(M) + SO_4^{2-}(M)$

For the following calculations we need ΔH values for reactions [5]-[8] at some common concentration for which we choose $M = 0.0035$. The data in Tables 4–7 lead to the following: $\Delta H_5 = -10.66$ kcal mole^{-1}, $\Delta H_6 = -13.98$ kcal mole^{-1}, $\Delta H_7 = -33.70$ kcal mole^{-1}, and $\Delta H_8 = -16.97$ kcal mole^{-1}, all for $M = 0.0035$. Although we have written reactions [5]–[7] specifically in terms of $Cu(NH_3)_4^{2+}$, our calculations with ΔH values referring to solutions containing identical concentrations of copper and ammonia make our derived results independent of assumptions about the species in solution. Equilibrium data suggest that $Cu(NH_3)_4^{2+}$ is the principal species, with lesser concentrations of $Cu(NH_3)_3^{2+}$ and $Cu(NH_3)_5^{2+}$ also present.

TABLE 4

Heats of solution of $Cu(IO_3)_2 \cdot 0.90\text{-}H_2O$ in 0.32 M NH_3

Moles Cu^{2+}/950 ml solution $\times 10^3$	$-\Delta H_5$ (kcal mole^{-1})
5.631	10.83
3.940	10.72
3.132	10.63
2.690	10.54
2.499	10.49
2.481	10.35

TABLE 5

Heats of solution of $Cu(IO_3)_2$ in 0.32 M NH_3

Moles Cu^{2+}/950 ml solution $\times 10^3$	$-\Delta H_6$ (kcal mole^{-1})
3.239	13.92
3.332	14.01
3.480	14.00

TABLE 6

Heats of solution of $CuSO_4$ in 0.32 M NH_3

Moles Cu^{2+}/950 ml solution $\times 10^3$	$-\Delta H_7$ (kcal mole^{-1})
3.318	33.71
3.170	33.66
2.371	33.50
1.970	33.31
1.702	33.31
0.9831	32.74
0.7103	32.71
0.6808	32.23

TABLE 7

Heats of solution of $CuSO_4$ in H_2O

Moles Cu^{2+}/950 ml solution $\times 10^3$	$-\Delta H_8$ (kcal mole^{-1})
3.631	16.91
3.781	16.95
3.902	16.94
4.359	16.94

For the heat of solution of the 0.90 hydrate in water we have

[9] $Cu(IO_3)_2 \cdot 0.90\ H_2O(c) = Cu^{2+}(M) + 2\ IO_3^-(2\ M) + 0.90\ H_2O(liq)$

and $\Delta H_9 = \Delta H_5 - \Delta H_7 + \Delta H_8 = 6.07$ kcal mole^{-1} for $M = 0.0035$. Similarly, for the heat of solution of $Cu(IO_3)_2(c)$ at $M = 0.0035$, we have

[10] $Cu(IO_3)_2(c) \rightleftharpoons Cu^{2+}(M) + 2\ IO_3^-(2\ M)$

and $\Delta H_{10} = \Delta H_6 - \Delta H_7 + \Delta H_8 = 2.75$ kcal mole^{-1}. Now the heat of solution of the monohydrate for $M = 0.0035$ as in the equation

[11] $Cu(IO_3)_2 \cdot H_2O(C) = Cu^{2+}(M) + 2\ IO_3^-(2\ M) + H_2O(liq)$

is calculated by way of

[12] $\Delta H_9 = 0.90\ \Delta H_{11} + 0.10\ \Delta H_{10}$

Equation [12] gives us $\Delta H_{11} = 6.43$ kcal mole^{-1}.

Heat of dilution data (5, 6) combined with our ΔH_{10} and ΔH_{11} values for $M = 0.0035$ give us $\Delta H_{10}^0 = 2.5 \pm 0.2$ kcal mole^{-1} and $\Delta H_{11}^0 = 6.2 \pm 0.3$ kcal mole^{-1} corresponding to $M = 0$.

Solubility data cited by Sillen and Martell (13) are in reasonable agreement with results reported by Ramette and Broman (2), from whom we adopt the solubility product $K_{sp} = 7.4 \times 10^{-8}$ for $Cu(IO_3)_2 \cdot H_2O(c)$ at 298 °K. We use the corresponding $\Delta G^0 = 9.73$ kcal mole^{-1} with our ΔG_f^0 of $Cu^{2+}(aq)$ and earlier (8) ΔG_f^0 values for $IO_3^-(aq)$ and $H_2O(liq)$ to obtain $\Delta G_f^0 = -111.9$ kcal mole^{-1} for $Cu(IO_3) \cdot H_2O(c)$. Although K_{sp} values at three temperatures (2) lead to a calculated $\Delta H^0 = 6.8$ kcal mole^{-1} for the standard heat of solution of $Cu(IO_3)_2 \cdot H_2O$ (c), we adopt our $\Delta H_{11}^0 = 6.2$ kcal mole^{-1} to combine with our ΔH_f^0 for $Cu^{2+}(aq)$ and ΔH_f^0 values for $IO_3^-(aq)$ and $H_2O(liq)$ from the N.B.S. (8) to obtain $\Delta H_f^0 = -164.7$ kcal mole^{-1} for $Cu(IO_3)_2 \cdot H_2O(c)$. The ΔH_f^0 and ΔG_f^0 values reported here lead to $S_{298}^0 = 61$ cal deg^{-1} mole^{-1} for $Cu(IO_3)_2 \cdot H_2O(c)$.

Our ΔH_{10}^0 in combination with ΔH_f^0 values for $Cu^{2+}(aq)$ and $IO_3^-(aq)$ gives $\Delta H_f^0 = -92.7$ kcal mole^{-1} for $Cu(IO_3)_2(c)$. We have no low temperature data to lead to S_{298}^0 nor equilibrium data to lead to ΔG_f^0 for this compound, so we follow Latimer's guides (14) and estimate $S_{298}^0 \cong 52$ cal deg^{-1} mole^{-1} and combine with the experimental ΔH_f^0 to obtain $\Delta G_f^0 \cong -53.6$ kcal mole^{-1} for $Cu(IO_3)_2(c)$. The ΔG_f^0 values for $Cu(IO_3)_2 \cdot H_2O(c)$, $Cu(IO_3)_2(c)$, and gaseous water (8) lead to a calculated equilibrium vapor pressure of water equal to about 2×10^{-3} atm at 298 °K, a quantity subject to direct experimental measurement.

We are grateful to the National Science Foundation for support of part of this research done at the University of Louisville.

1. W. F. O'Hara, C. H. Wu, and L. G. Hepler. J. Chem. Educ. **38**, 512 (1961).
2. R. W. Ramette and R. F. Broman. J. Phys. Chem. **67**, 942, 2889 (1963).
3. A. J. deBethune, T. S. Licht, and N. Swendeman. J. Electrochem. Soc. **106**, 616 (1959).
4. J. W. Larson, P. Cerutti, H. K. Garber, and L. G. Hepler. J. Phys. Chem. **72**, 2902 (1968).
5. F. D. Rossini, D. D. Wagman, W. H. Evans, S. Levine, and I. Jaffe. Selected values of chemical thermodynamic properties. National Bureau of Standards Circular 500, U.S. Government Printing Office, Washington, D. C., 1952.
6. E. Lange. The structure of electrolytic solutions *Edited by* W. J. Hamer. John Wiley and Sons, Inc., New York. 1959. E. Lange and W. Miederer. Z. Electrochem. **60**, 34 (1956).
7. J. W. Larson and L. G. Hepler. Solute–solvent interactions. *Edited by* Coetzee and C. D. Ritchie. Marcel Dekker, Inc., New York. 1969. R. N. Goldberg and L. G. Hepler. J. Phys. Chem. **72**, 4654 (1968).
8. D. D. Wagman, W. H. Evans, I. Halow, S. M. Bailey, and R. H. Schumm. Selected values of chemical thermodynamic properties. National Bureau of Standards Technical Note 270-3, U.S. Government Printing Office, Washington, D.C. 1968.
9. P. Schindler, H. Althaus, F. Hofer, and W. Minder. Helv. Chim. Acta, **48**, 1204 (1965); P. W. Schindler. Equilibrium concepts in natural water systems. *Edited by* W. Stumm, Advances in Chemistry Series, No. 67, American Chemical Society, Washington, D.C. 1967.
10. F. R. Bichowsky and F. D. Rossini. The thermochemistry of the chemical substances. Reinhold Publ. Corp., New York. 1936.
11. S. A. Shchukarev, I. V. Vasil'kova, and G. M. Barvinok. Chem. Abstr. **64**, 77, (1966); **65**, 9831 (1966).
12. J. W. Stout and R. C. Chisholm. J. Chem. Phys. **36**, 979 (1962).
13. L. G. Sillen and A. E. Martell. Stability constants of metal-ion complexes. Special Publication No. 17, The Chemical Society, London. 1964.
14. W. M. Latimer. Oxidation potentials. Prentice-Hall, Inc., New York. 1952.

Can. J. Chem. Downloaded from www.nrcresearchpress.com by 210.87.254.105 on 09/05/12
For personal use only.

Can. J. Chem. Downloaded from www.nrcresearchpress.com by 210.87.254.5 on 09/05/12
For personal use only.

NOTES

Reaction of nitrogen atoms with sulfur monoxide[1]

A. JACOB[2] AND C. A. WINKLER
Department of Chemistry, McGill University, Montreal, Quebec

Received[3] June 20, 1969

The reaction sequence of N atoms with SO appears to be SO + N → NO + S, followed by NO + N → N_2 + O, with a rate constant at 27 °C of about 0.8×10^{-12} cc molecule^{-1} s^{-1}.

Canadian Journal of Chemistry, 48, 1774 (1970)

In a previous note from this laboratory, it was reported that SO_2 may be decomposed by active nitrogen from a "poisoned" condensed discharge, but not by that from a microwave discharge (1). Accordingly, the reaction was attributed to energy transfer from excited nitrogen molecules, rather than attack by N atoms. On the other hand, it has been possible to study the reaction of the monoxide, SO, with active nitrogen from a microwave discharge, as outlined in the present study. The intention was to enable its presence during the decomposition of SO_2 to be taken into account in the analysis of further data that have now been obtained for the SO_2 – active nitrogen reaction (2).

Experimental

The apparatus in which the reaction of SO with active nitrogen was studied was essentially similar to that used in the previous study with SO_2 (1). In addition, an auxiliary reactor was provided, in which SO was generated by the quantitative reaction of COS with O atoms at 225 °C (3).[4] The O atoms required for the reaction were obtained by partially dissociating a controlled flow of N_2 in a microwave discharge, and titrating the N atoms so formed with NO near the top of the auxiliary vessel to yield an equivalent flow of O atoms. These reacted with a stream of COS introduced about 3 cm below the NO inlet to form SO, which then passed into the main reactor where its reaction with active nitrogen from a microwave discharge was studied. The reactions involved in the preparation of SO were NO + N → N_2 + O, followed by COS + O → SO + CO. Since CO does not react significantly with active nitrogen (5), any reaction that occurred in the main reactor was attributed to SO.

Results and Discussion

The reaction of COS with O atoms did not seem to occur appreciably at room temperature. When the auxiliary reactor was unheated, and the effluent from it was passed through a liquid nitrogen trap, the condensate appeared to be only COS. When this was introduced into active nitrogen in the main reaction vessel, the yellow afterglow was only slightly weakened. A pale blue flame was then observed for COS flow rates in excess of the active nitrogen flow, and a transparent yellow, non-crystalline product, presumably sulfur nitride, was formed.[5] However, when the auxiliary reactor was heated to 225 °C, and the effluent from it passed directly into a trap at liquid nitrogen temperature, SO was condensed as a yellow-orange solid (6). When the trap was warmed to room temperature, SO_2 was produced, and only a faint yellow deposit remained on the wall of the trap. This deposit was not analyzed, but was almost certainly sulfur, a product of the disproportionation of SO above −50 °C (6, 7)

$$2SO \rightarrow SO_2 + S$$

As with a film of sulfur (8, 9), the deposit could be removed completely by prolonged passage of active nitrogen or atomic oxygen through the system. When the auxiliary reactor was at

[1]This work received financial assistance from the National Research Council of Canada and the Defence Research Board.

[2]Present Address: Trapelo Division of L. F. E. Corporation, 1601 Trapelo Rd., Waltham, Mass.

[3]Revision received January 26, 1970.

[4]Observations by electron spin resonance have indicated that the reaction yields CO and SO in their ground states when neither reactant is in an excited state (4).

[5]By titrating the residual N atoms with NO, a rate constant of the order 4×10^{-13} cc molecule^{-1} s^{-1} was evaluated for the COS + N reaction on the assumption that the probable reaction products, CO + NS, did not react appreciably with N atoms.

Can. J. Chem. Downloaded from www.nrcresearchpress.com by 210.87.254.5 on 09/05/12
For personal use only.

225 °C, and the flow rates of O atoms and COS were adjusted to give an SO flow rate equivalent to one-half the flow rate of N atoms in the main reactor, the yellow afterglow in the main reactor was completely quenched. Presumably the N atoms were entirely removed under these conditions. The yellow afterglow could be made to reappear by merely reducing the O atom or COS flow rate below that corresponding to darkness in the main reactor. When the SO flow was insufficient to quench the yellow afterglow completely, an emission of ill-defined color (mauve?) was observed very close to the SO inlet, possibly a β-band emission of NO and a blue SO_2 emission superimposed on residual yellow afterglow of active nitrogen. An equivalent small flow of CO or COS did not noticeably affect the yellow afterglow.

The yield of SO from the COS + O reaction has been shown mass spectrometrically to be essentially quantitative (10). The same conclusion may be drawn from some experiments in the present study, based on the observation that NO_2 reacts even more rapidly with SO than it does with O atoms (11). Carbonyl sulfide was added to O atoms produced in the auxiliary reactor (at 225 °C) until the emission of the SO_2 afterglow was almost extinguished. The products were then titrated with NO_2 about 2 to 3 cm downstream in the auxiliary reactor, on the assumption of a reaction sequence

[1][6] $$COS + O \rightarrow CO + SO$$

[2] $$SO + O \rightarrow SO_2 + h\nu$$

[3] $$SO + NO_2 \rightarrow SO_2 + NO$$

The flow rate of NO_2 that gave complete extinction of the blue emission from the slow reaction (2) was compared with the NO_2 flow rate required for complete consumption of O atoms in the absence of COS. The two titration values agreed within 5%. It would appear, therefore, that the yield of SO from the COS + O reaction was approximately quantitative, and that the SO was relatively stable at the temperature of 225 °C at which it was prepared. This stability is suggested also by the relatively long duration and intensity of emission of the SO_2 afterglow during oxidation of CS_2 vapor or H_2S gas (12). The essentially quantitative production of SO by reaction (1) suggests that the possible side reaction $COS + O_2 \rightarrow SO + CO_2$ was not significant (the formation of O_2 must have been negligible in the short time between the formation of O atoms and their reaction with COS), and that the reaction $COS + O \rightarrow S + CO_2$ did not occur appreciably at 225 °C, as indicated also by the virtual absence of sulfur on the wall of the auxiliary vessel at this temperature. Mass spectrometric studies have shown that the yields of CO and SO from reaction (1) are about 1000 times more abundant than those of CO_2 and S at room temperature (10).

The reaction of SO with N atoms in the main reactor yielded sulfur in a narrow band close to the SO inlet. This indicated a fairly rapid reaction

[4] $$SO + N \rightarrow NO + S$$

Apparently, the reaction of N atoms with S atoms was not sufficiently rapid to prevent their deposition on the wall (cf. ref. 8).

When the O atom (or COS) flow rate in the auxiliary reactor was less than one-half the N atom flow rate in the main reactor, titration of the residual N atoms with NO showed that their consumption was equal to twice the flow rate of O atoms (or COS), i.e. twice the SO flow rate. On the other hand, the O atom (or COS) flow rate, i.e. the SO flow rate, required to quench the yellow afterglow completely in the main reactor was one-half the flow rate of N atoms in that vessel.

Table 1 summarizes the data obtained at a reaction temperature of 27 °C, for different flow rates of SO, with some variations also in N atom flow rate, in reaction time, in total pressure, and in temperature of the auxiliary reactor and its distance from the main reactor.

Rate constants were calculated for the reaction sequence

[4] $$SO + N \rightarrow NO + S$$

[5] $$NO + N \rightarrow N_2 + O$$

on the assumption that the second step is sufficiently faster than the first that the rate of the overall process may be represented by the second-order rate expression

$$-\frac{d[N]}{dt} = 2k_4[SO][N]$$

Since reaction of each molecule of SO leads to

[6]An activation energy of the order 4.5 to 6 kcal $mole^{-1}$ has been determined for this reaction (15).

TABLE 1

Reaction of active nitrogen with sulfur monoxide*

Auxiliary reactor temperature (°C)	P (Torr)	Reaction time (ms)	Flow rates (mole $s^{-1} \times 10^6$)				$k_4 \times 10^{12}$ (cc molecule^{-1} s^{-1})
			N_2	SO_0	N_0	N_t	
225	2.0	11.5	304	0.33	1.21	0.70	0.70
				0.37	1.42	0.82	0.67
				0.45	1.35	0.65	0.71
				0.46	1.25	0.56	0.73
				0.46	1.02	0.37	0.87
				0.50	1.05	0.34	0.95
400	2.5	7.2	365	0.071	1.52	1.42	0.53
				0.081	1.53	1.40	0.71
				0.12	1.41	1.24	0.59
				0.17	1.35	1.12	0.58
				0.25	1.23	0.95	0.49
				0.30	1.03	0.67	0.71
400†	3.5	7.4	420	0.24	1.38	1.06	0.47
				0.32	1.20	0.80	0.52
				0.43	1.22	0.70	0.52
				0.44	1.17	0.64	0.55
				0.44	1.10	0.57	0.61
				0.45	1.02	0.52	0.58

*Reaction temperature = 27 °C.
†Two-fold change in length of flowline between auxiliary and main reactors.

the consumption of two N atoms

$$-\frac{d[N]_t}{dt} = k_4[N]_t(2[SO]_0 - [N]_0 + [N]_t)$$

and

$$k_4 = \frac{1}{t(2[SO]_0 - [N]_0)} \times \ln \frac{[N]_0(2[SO]_0 - [N]_0 + [N]_t)}{2[SO]_0[N]_t}$$

where the subscripts 0 and t refer to the initial concentration and concentration at time t, respectively. The values of $[N]_0$ and $[N]_t$ were determined by the NO titration. With appropriate conversion of flow rates to concentration units, the values of k_4 in Table 1 were obtained.

The rate constants were satisfactorily concordant with changes in the SO and N flow rates for each temperature at which the SO was prepared and at a given total pressure. The NO titration for stopping the reaction would therefore seem to be vindicated.

On the other hand, it would appear that a decrease in the rate constant did accompany an increase in one or more of the total pressure, the temperature at which SO was prepared, and the distance from the auxiliary to the main reactor. It seems likely that the decrease in k_4 is due mainly to loss of SO as disproportionation becomes significant at the higher temperature (400 °C) in the auxiliary reactor. It was calculated that a decrease in $[SO]_0$ of about 14% would account for the observed decrease in k_4 at 400 °C relative to the value at 225 °C. With a linear velocity of approximately 600 cm s^{-1} through the heated portion (ca. 6 cm) of the auxiliary vessel, it was further estimated that the rate constant for the disproportionation reaction should have an upper limit of about 3×10^{-13} cc molecule^{-1} s^{-1} at 400 °C. This assumes that all the loss of SO is attributable to disproportionation, whereas an increase in the rate of the reaction $COS + O \rightarrow CO_2 + S$, at the higher temperature, might also have contributed to a loss of SO. The upper limit indicated above for the rate constant of the disproportionation reaction at 400 °C may be compared with other recorded values at room temperature, of 4×10^{-12} cc molecule^{-1} s^{-1} (3), an upper limit of 6×10^{-15} cc molecule^{-1} s^{-1} (13), and, quite recently, 1×10^{-13} cc molecule^{-1} s^{-1} (14). It is possible that the highest estimate might be attributed to removal of SO by the large excess of COS used in the earlier investigation, in one or more of several possible exothermic reactions. On the other hand, the lowest estimate is concordant with the rate constant of about 3×10^{-16} cc molecule^{-1} s^{-1} determined for the analogous process, $SO + O_2 \rightarrow SO_2 + O$, which

Can. J. Chem. Downloaded from www.nrcresearchpress.com by 210.87.254.5 on 09/05/12
For personal use only.

is about twice as exothermic as the disproportionation of SO (13).

No attempt was made to determine an activation energy for the SO + N reaction, owing to its high rate even in an unheated vessel. It is likely, however, that this reaction, like the corresponding NO + N reaction, has practically zero activation energy.

1. A. JACOB, MRS. R. A. WESTBURY, and C. A. WINKLER. J. Phys. Chem. **70**, 4066 (1966).
2. A. JACOB and C. A. WINKLER. Unpublished results.
3. J. O. SULLIVAN and P. WARNECK. Ber. Bunsenges. Phys. Chem. **69**, 7 (1965).
4. A. CARRINGTON, D. H. LEVY, and T. A. MILLER. Trans. Faraday Soc. **62**, 2994 (1966).
5. G. B. KISTIAKOWSKY and G. G. VOLPI. J. Chem. Phys. **28**, 665 (1958).
6. P. W. SCHENK and H. PLATZ. Z. Anorg. Allg. Chem. **215**, 113 (1933).
7. E. A. EVANS, A. B. SCOTT, and J. L. HUSTON. J. Amer. Chem. Soc. **74**, 5525 (1952).
8. J. A. S. BETT and C. A. WINKLER. J. Phys. Chem. **68**, 2735 (1964).
9. M. PEYRON and L. T. MY. J. Chim. Phys. **64**, 129 (1967).
10. T. R. ROLFES, R. R. REEVES, and P. HARTECK. J. Phys. Chem. **69**, 849 (1965).
11. B. A. THRUSH and C. J. HALSTEAD. Chem. Commun. **11**, 213 (1965).
12. R. G. W. NORRISH and A. P. ZEELENBERG. Proc. Roy. Soc. **240**, 293 (1957).
13. C. J. HALSTEAD and B. A. THRUSH. Proc. Roy. Soc. **295A**, 363 (1966).
14. R. J. DONOVAN, D. HUSAIN, and P. T. JACKSON. Trans. Faraday Soc. **65**, 2930 (1969).
15. A. A. WESTENBERG and N. DE HAAS. J. Chem. Phys. **50**, 707 (1969). K. HOYERMAN, H. GG. WAGNER, and J. WOLFRUM. Ber. Bunsenges. Phys. Chem. **71**, 603 (1967).

Electric discharge reactions of hydrocarbons

K. L. PACIOREK[1] AND R. H. KRATZER[1]

New Products Division, CCI Aerospace Corporation, Newport Beach, California 92663

Received November 20, 1969

The electric discharge reactions of five hydrocarbons, ethylene, ethane, propylene, cyclopropane, and propane, were investigated in the presence of a rare gas. Three types of products were formed: hydrogen, a mixture of relatively simple hydrocarbons, and polymeric deposits. The deposition of the polymeric films occurred most readily with olefins. The reactions occurring under the influence of an electric discharge appear to be comparable to the processes taking place in radiolysis.

Canadian Journal of Chemistry, **48**, 1777 (1970)

The investigations of the action of an electric discharge on hydrocarbons date back into the eighteenth century, as documented by Glockler and Lind (1). In the present study, a series of five hydrocarbons, ethylene, ethane, propylene, cyclopropane, and propane, was investigated. An attempt was made to select relatively few, simple materials to determine the effects of structural characteristics, such as branching and unsaturation, upon the polymer formation and the composition of the volatile condensibles. The predominant action of the electric discharge was the production of hydrogen, which is to be expected. This note deals mainly with the volatile condensibles; the polymeric materials will be discussed in a later publication. The experimental data and results are summarized in Tables 1 and 2.

[1]Present address: Dynamic Science, 2400 Michelson Drive, Irvine, California 92664.

It is evident from Table 2 that acetylene constituted the bulk of the products obtained from the discharge treatment of ethylene (Exps. 1 and 2). It has been found (2, 3) that excited ethylene decomposes to acetylene by two primary processes without contribution from ionic moieties, i.e.

$$[1] \qquad C_2H_4^* \rightarrow C_2H_2 + H_2$$

$$[2] \qquad C_2H_4^* \rightarrow C_2H_2 + 2H$$

The presence of rare gas should further emphasize this process, due to energy transfer reactions (4). Propane, ethane, and the butanes are most likely derived from radical reactions (5). The relative ease of polymerization of ethylene was shown by the large amount of material deposited on the cold plate. In the case of propylene (Exp. 3), relatively high powers in conjunction with very low hydrocarbon flow rate resulted in a very small quantity of highly cross-

Can. J. Chem. Downloaded from www.nrcresearchpress.com by 210.87.254.5 on 09/05/12
For personal use only.

is about twice as exothermic as the disproportionation of SO (13).

No attempt was made to determine an activation energy for the SO + N reaction, owing to its high rate even in an unheated vessel. It is likely, however, that this reaction, like the corresponding NO + N reaction, has practically zero activation energy.

1. A. JACOB, MRS. R. A. WESTBURY, and C. A. WINKLER. J. Phys. Chem. **70**, 4066 (1966).
2. A. JACOB and C. A. WINKLER. Unpublished results.
3. J. O. SULLIVAN and P. WARNECK. Ber. Bunsenges. Phys. Chem. **69**, 7 (1965).
4. A. CARRINGTON, D. H. LEVY, and T. A. MILLER. Trans. Faraday Soc. **62**, 2994 (1966).
5. G. B. KISTIAKOWSKY and G. G. VOLPI. J. Chem. Phys. **28**, 665 (1958).
6. P. W. SCHENK and H. PLATZ. Z. Anorg. Allg. Chem. **215**, 113 (1933).
7. E. A. EVANS, A. B. SCOTT, and J. L. HUSTON. J. Amer. Chem. Soc. **74**, 5525 (1952).
8. J. A. S. BETT and C. A. WINKLER. J. Phys. Chem. **68**, 2735 (1964).
9. M. PEYRON and L. T. MY. J. Chim. Phys. **64**, 129 (1967).
10. T. R. ROLFES, R. R. REEVES, and P. HARTECK. J. Phys. Chem. **69**, 849 (1965).
11. B. A. THRUSH and C. J. HALSTEAD. Chem. Commun. **11**, 213 (1965).
12. R. G. W. NORRISH and A. P. ZEELENBERG. Proc. Roy. Soc. **240**, 293 (1957).
13. C. J. HALSTEAD and B. A. THRUSH. Proc. Roy. Soc. **295A**, 363 (1966).
14. R. J. DONOVAN, D. HUSAIN, and P. T. JACKSON. Trans. Faraday Soc. **65**, 2930 (1969).
15. A. A. WESTENBERG and N. DE HAAS. J. Chem. Phys. **50**, 707 (1969). K. HOYERMAN, H. GG. WAGNER, and J. WOLFRUM. Ber. Bunsenges. Phys. Chem. **71**, 603 (1967).

Electric discharge reactions of hydrocarbons

K. L. PACIOREK[1] AND R. H. KRATZER[1]

New Products Division, CCI Aerospace Corporation, Newport Beach, California 92663

Received November 20, 1969

The electric discharge reactions of five hydrocarbons, ethylene, ethane, propylene, cyclopropane, and propane, were investigated in the presence of a rare gas. Three types of products were formed: hydrogen, a mixture of relatively simple hydrocarbons, and polymeric deposits. The deposition of the polymeric films occurred most readily with olefins. The reactions occurring under the influence of an electric discharge appear to be comparable to the processes taking place in radiolysis.

Canadian Journal of Chemistry, **48**, 1777 (1970)

The investigations of the action of an electric discharge on hydrocarbons date back into the eighteenth century, as documented by Glockler and Lind (1). In the present study, a series of five hydrocarbons, ethylene, ethane, propylene, cyclopropane, and propane, was investigated. An attempt was made to select relatively few, simple materials to determine the effects of structural characteristics, such as branching and unsaturation, upon the polymer formation and the composition of the volatile condensibles. The predominant action of the electric discharge was the production of hydrogen, which is to be expected. This note deals mainly with the volatile condensibles; the polymeric materials will be discussed in a later publication. The experimental data and results are summarized in Tables 1 and 2.

[1]Present address: Dynamic Science, 2400 Michelson Drive, Irvine, California 92664.

It is evident from Table 2 that acetylene constituted the bulk of the products obtained from the discharge treatment of ethylene (Exps. 1 and 2). It has been found (2, 3) that excited ethylene decomposes to acetylene by two primary processes without contribution from ionic moieties, i.e.

$$[1] \qquad C_2H_4^* \rightarrow C_2H_2 + H_2$$

$$[2] \qquad C_2H_4^* \rightarrow C_2H_2 + 2H$$

The presence of rare gas should further emphasize this process, due to energy transfer reactions (4). Propane, ethane, and the butanes are most likely derived from radical reactions (5). The relative ease of polymerization of ethylene was shown by the large amount of material deposited on the cold plate. In the case of propylene (Exp. 3), relatively high powers in conjunction with very low hydrocarbon flow rate resulted in a very small quantity of highly cross-

Can. J. Chem. Downloaded from www.nrcresearchpress.com by 210.87.254.5 on 09/05/12
For personal use only.

TABLE 1

Summary of reaction data, electric discharge reactions of ethylene, ethane, propylene, cyclopropane, and propane in the presence of rare gas*

Exp. No.	Reaction system	Flow rate (mg/h)	Power (W)	Pressure (μ)		H_2:CH_4	Condensible (%)	
				H_2	Rare gas		Starting materials	Products
1	Ar, C_2H_4	1433	23	90	25	22	72	28
2	He, C_2H_4	453	59	110	38	40	27	73
3	He, C_3H_6	243	81	53	45	108	74	26
4	He, C_3H_6	1477	51	61	42	47	72	28
5	He, cyclo-C_3H_6	1524	53	67	42	73	87	13
6	Ar, cyclo-C_3H_6	2166	42	75	25	52	88	12
7	He, C_2H_6	207	55	69	39	77	82	18
8	He, C_2H_6	595	31	67	35	57	96	4
9	Ar, C_3H_8	1107	35	88	30	36	94	6
10	He, C_3H_8	1351	50	84	50	44	92	8

*For steady-state experimental conditions; the percentages are normalized with respect to the carbon atoms in the starting material.

TABLE 2

Composition of product condensibles, electric discharge reactions of ethylene, ethane, propylene, cyclopropane, and propane in the presence of rare gas*

Exp. No.	Condensible, mole %†									
	C_2H_6	C_2H_4	C_2H_2	C_3H_8	C_3H_6	Cyclo-C_3H_6	C_4H_{10}	C_5H_{12}	C_6H_{14}	Unsaturates
1	17.10	S.m.	53.64	8.75	4.75	0.01	0.86	0.29	0.09	14.43
2	9.87	S.m.	51.66	8.01	8.73	0.07	1.88	0.69	0.13	18.28
3	5.64	1.98	27.59	13.57	S.m.	0.30	5.34	0.30	0.30	44.82
4‡	0.03	0.01	0.01	12.69	S.m.	0.67	21.57	1.05	0.94	39.70
5	0.29	0.23	8.44	3.01	69.36	S.m.	2.25	0.58	0.52	15.03
6§	0.02	0.26	8.32	5.22	59.21	S.m.	3.13	0.61	0.22	13.41
7	S.m.	3.04	77.75	2.58	8.43	Trace	0.01	—	—	7.96
8	S.m.	5.26	27.63	12.66	33.11	Trace	0.01	—	—	—
9	4.93	0.16	0.02	S.m.	50.40	0.79	5.09	3.02	5.72	29.57
10	4.01	0.14	0.29	S.m.	45.42	1.00	6.02	1.43	6.02	29.08

*For experimental conditions, see Table 1.
†Normalized with respect to the starting material (based on carbon, not hydrogen). S.m. = starting material.
‡An additional 23 mole %, which includes C_6 and higher saturates and unsaturates, was obtained by vacuum trap-to-trap distillation. This material, however, was not separated further into its components. It is noteworthy that cyclobutane accounted for 0.36 mole % of the condensible products.
§An additional 9.40 mole % was obtained which includes C_6 and higher saturates and unsaturates.

linked, unsaturated polymer and, under these conditions, acetylene was the major product in the condensible volatiles.

Increasing the propylene flow about six-fold without a change in total pressure (propylene and rare gas), and somewhat decreasing the power (Exp. 4), reduced the proportion of C_2 species to negligible values and gave as the main products butanes, C_5, C_6, and highly unsaturated species. The chromatographic procedure used did not allow the separation of C_5 and C_6 olefinic materials from C_3 acetylenic and allenic compounds, which should be formed in high proportion.

Based on the mass spectral pattern, one would expect cyclopropane and propylene to give the same distribution of products, yet this was found not to be the case (6) in the photolysis studies, where cyclo-C_3H_6 was found to yield ethylene whereas C_3H_6 gave mainly acetylene (6, 7). Our studies with cyclo-C_3H_6 (Exps. 5, 6) afforded C_3H_6 as the major product. Examination of Scala and Ausloos' data (7) shows that radiolysis definitely results in much higher relative yields of propylene (with respect to ethylene) than does photolysis. Secondly, if one compares the yields at 1470 and 1048–67 Å, in the same publication, in the absence of the scavenging agent, the increase in C_3H_6 at the higher energy is two-fold over that at the lower energy. Thus, it would appear that at higher energies more C_3H_6 is formed.

The relative composition of the condensible volatiles obtained on the discharge treatment of

Can. J. Chem. Downloaded from www.nrcresearchpress.com by 210.87.254.5 on 09/05/12
For personal use only.

ethane differs significantly from that reported for the photolysis (8, 9) and radiolysis (10–12) investigations. The most striking difference is the high yield of propylene in the discharge treatment, which seems to be enhanced at lower conversions (higher hydrocarbon flows, lower powers) (cf. Exps. 7, 8). Another surprising fact is the low yield of the butanes. In Exp. 7, conducted at higher power and lower ethane flow rate, acetylene was the main product (in the condensible volatiles).

The predominant formation of propylene from the electric discharge action on propane (Exps, 9, 10), in conjunction with the relatively low yield of ethane, tends to indicate that propylene originates mainly from either the molecular elimination of the superexcited molecule, as postulated by Rebbert and Ausloos (13), or from stepwise hydrogen elimination. The hydride transfer from C_3H_8 to $C_2H_5^+$ (14, 15) followed by neutralization and hydrogen atom elimination does not seem to be of great importance here, in view of the relatively low yield of ethane. It is noteworthy that the yields of hexanes are higher than 10% of the produced propylene. This would imply a high population of propyl radicals. Furthermore, the relatively high yields of butanes (70% isobutane) and pentanes point to the presence of ethyl radicals, since it is safe to assume that these species are produced mainly by free-radical processes.

Experimental

The rare gases, helium and argon, used in these investigations were obtained from Liquid Carbonic Corporation. The purity was 99.995%. The hydrocarbons were Matheson research grade. The gas chromatograms indicated a purity greater than 99.9% for all the hydrocarbons with the exception of cyclopropane, where the purity was 99.6%.

Instrumentation

The apparatus used was a bell jar reactor equipped with two aluminum electrodes separated by 8 cm. Between the electrodes was placed a hollow metal plate (electrically floating, liquid nitrogen cooled) to which glass plates (for polymer film collection) were attached. All the connections and gas inlets were made through a stainless steel header. The chamber was connected to a high-vacuum pumping system via 3 liquid-nitrogen cooled traps (for collection of condensible volatiles) and to a by-pass leading directly to a residual gas analyzer (calibrated for each of the reactant gases and the non-condensible products). The bell jar reactor was situated in an inert atmosphere enclosure to allow, after the conclusion of an experiment, the scraping of the polymeric films without exposure to air or moisture.

The electrical system for establishing and maintaining the a.c. discharge reaction at 60 cps utilized a low impedance, high voltage transformer (Model No. T21-P83 Thordarson Electric Manufacturing Division, Chicago, Illinois) with an output of 1250–0–1250 V at up to 200 ma from a 1 kW constant voltage power supply.

Operation and Product Investigation

To allow for sufficient product accumulation, each discharge reaction was carried out for 3 h. The voltages varied between 450–800 V, whereas the current stayed between 70–80 mA. Thus, the powers given in Table 1 reflect the voltages employed. The volume of the bell jar was 65 l, the average flow of the non-condensible gases (H_2, CH_4, and rare gases) was 195 ± 10 cm^3/h.

In a typical run, first the rare gas, then the reagent gas flow was adjusted. Subsequently, the collection plate and the traps were cooled with liquid nitrogen and the discharge was initiated. Steady-state was usually reached within ca. 20 min. Values given in Table 1 are for the steady state.

The condensible volatiles collected were transferred to a vacuum-line fractionation train, fractionated, and measured. Each fraction was examined by infrared spectroscopy and gas phase chromatography. A Loenco Model 70 chromatograph equipped with a calibrated inlet loop, valve-vacuum assembly, a manometer, and flame ionization detector was employed with a two-column system. (Column 1: 6 ft long, 1/8 in. diameter, packed with 10% NaCl on Al_2O_3; column 2 was the above column in series with 1 ft long, 1/8 in. diameter column packed with 10% $AgNO_3$ on Al_2O_3.)

This investigation was supported by the U.S. Air Force Rocket Propulsion Laboratory under contract F04611-67-C-0084. The authors are indebted to Dr. L. P. Quinn for helpful suggestions and discussions and Miss Jacquelyn Kaufman for technical assistance.

1. G. Glockler and S. C. Lind. The electrochemistry of gases and other dielectrics. John Wiley and Sons, Inc., New York. 1939
2. R. Gordon, Jr., and P. Ausloos. J. Chem. Phys. **47**, 1799 (1967).
3. G. G. Meisels and T. J. Sworski. J. Phys. Chem. **69**, 2867 (1965).
4. G. G. Meisels. Nature, **206**, 287 (1965).
5. G. G. Meisels. Advan. Chem. Ser. **58**, 243 (1966).
6. D. A. Becker, H. Okabe, and J. R. McNesby. J. Phys. Chem. **69**, 538 (1965).
7. A. A. Scala and P. Ausloos. J. Chem. Phys. **49**, 2282 (1968).
8. R. F. Hampson and J. R. McNesby. J. Chem. Phys. **43**, 3592 (1965).
9. W. M. Jackson, J. Faris, and N. J. Buccos. J. Chem. Phys. **45**, 4145 (1966).
10. K. Yang and P. J. Manno. J. Amer. Chem. Soc. **81**, 3507 (1959).
11. K. Yang and P. L. Gant. J. Phys. Chem. **65**, 1861 (1961).
12. N. V. Klassen. J. Phys. Chem. **72**, 1076 (1968).
13. R. E. Rebbert and P. Ausloos. J. Chem. Phys. **46**, 4333 (1967).
14. J. H. Futrell and T. O. Tiernan. J. Chem. Phys. **37**, 1694 (1962).
15. L. W. Sieck, N. K. Blocker, and J. H. Futrell. J. Phys. Chem. **69**, 888 (1966).

Can. J. Chem. Downloaded from www.nrcresearchpress.com by 210.87.254.5 on 09/05/12
For personal use only.

Can. J. Chem. Downloaded from www.nrcresearchpress.com by 210.87.254.42 on 09/05/12
For personal use only.

Electron spin resonance studies of radiation damage. Part III.[1] Gamma irradiated acetonitrile

F. P. SARGENT[2]

Department of Chemistry and Chemical Engineering, The University of Saskatchewan, Saskatoon, Saskatchewan
and
The Cookridge High Energy Radiation Research Center, The University, Leeds, England

Received November 7, 1969

The effects of photobleaching and thermal decay at 77 and 87 °K on the electron spin resonance spectra of gamma irradiated acetonitrile are reported.

Canadian Journal of Chemistry, 48, 1780 (1970)

In an investigation of gamma irradiated acetonitrile Ayscough, Collins, and Kemp (1) found that the main species detected by electron spin resonance (e.s.r.) at 77 °K was $\cdot CH_2CN$ with a small amount of methyl radicals. When the samples were exposed to light an increase in the concentration of methyl radicals was observed, but it was reported that these were removed by continued exposure to light. We wish to report results which are not in total agreement with these but do extend those reported by Bonin, Tsuji, and Williams (2).

Samples of acetonitrile gamma irradiated and examined in the dark at 77 °K gave spectra similar to that in Fig. 1*a*. When the sample was exposed to light the spectrum in Fig. 1*b* was obtained. This spectrum consists of a quartet of intensity ratios approximately 1:3:3:1 with linewidths of 2.6 G and a hyperfine splitting of 21.8 ± 0.2 G. The central peak is due to the $\cdot CH_2CN$ radical previously identified by Ayscough *et al.* (1), having a linewidth of 3.4 G.The line shapes were all gaussian. Clearly there has been a large increase in the intensity of the quartet spectrum when the samples were photobleached. We observed that the quartet decayed thermally at 77 °K and unlike previous workers (1), we could find no enhancement of this decay during exposure to light. The decay was first order with half-lives of 21.4 min at 77 °K and 8.0 min at 87 °K (liquid argon). This decay was paralleled by an increase in the intensity of the central $\cdot CH_2CN$ peak. Since the lines are gaussian and the separations large compared to the linewidths, this increase is real and not due to line overlap effects. The thermal decays were found to be irreversible, i.e., subsequent exposure to light did not regenerate the quartet.

Examination of the gamma irradiated samples in the dark at very low microwave power levels, i.e., less than 50 μW indicated the presence of a singlet in the e.s.r. spectrum which was irreversibly removed by exposure to light; however, this was partially obscured by the $M_I = 0$ $\cdot CH_2CN$ line. Incorporation of electron scavengers such as terbutyl chloride did not produce a very high yield of scavenger radicals and these did not increase when the samples were photobleached. Using thin optical cells it was possible to deduce the optical absorption spectrum of the photobleachable entity in gamma irradiated acetonitrile which had a maximum at about 530 nm.

Discussion

The thermal decays of the quartet at 77 and 87 °K imply an energy activation of 1.3 kcal. Since these decays are paralleled by an increase in the $\cdot CH_2CN$ radical, it is very tempting to assign the quartet to methyl radicals and the decay to reaction [1]

[1] $$CH_3\cdot + CH_3CN \rightarrow CH_4 + \cdot CH_2CN$$

However, the gas phase data (3) indicate an energy of activation of 10 kcal for reaction [1]. In addition the quartet splitting of 21.8 G is lower than the 23 G usually encountered for methyl radicals, although lower values have been reported for some systems, e.g., $CH_3\cdot$ on porous glass surfaces (4). An alternative is that the quartet is not due to methyl radicals but to an acetonitrile anion as proposed by Bonin *et al.* (2) for gamma irradiated deuteroacetonitrile. From the differences in the nuclear magnetic moments the quartet of 21.8 G from three equivalent

[1]For Part II, see ref. 8.

[2]NRCC Postdoctorate Fellow 1965–1967, Science Research Council of Great Britain and Tenovus Fellow at Leeds 1967–1969. Present address: Materials Science Branch, Atomic Energy of Canada Ltd., Whiteshell Nuclear Research Establishment, Pinawa, Manitoba.

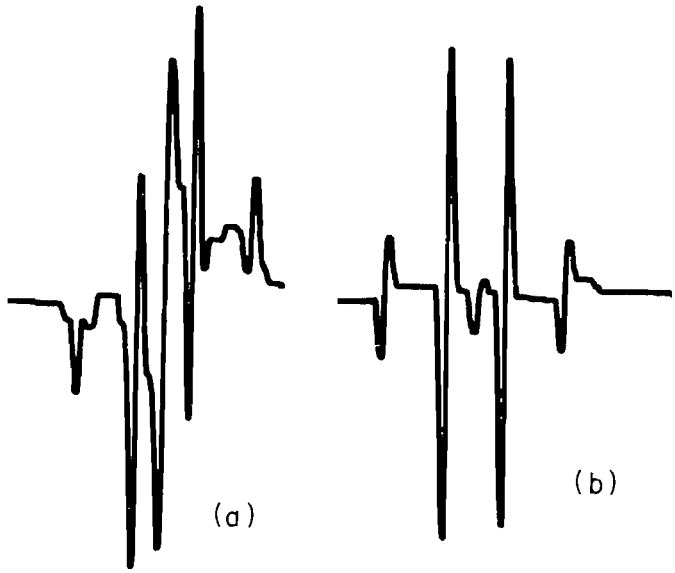

FIG. 1. The e.s.r. spectra of gamma irradiated acetonitrile at 77 °K: (*a*) 5 min after removal from the gamma source, in the dark, gain setting 320, (*b*) immediately after photobleaching, gain setting 160.

protons would correspond to a septet of 3.3 G for the deuterated species, which is in excellent agreement with the value reported for $[CD_3CN]^-$. However, if we assign our quartet to $[CH_3CN]^-$ the methyl group interaction appears to be much larger than expected from the isoelectronic $CH_3CO\cdot$ radical (5.1 G) (5), whereas $H\dot{C}O$ and $[HCN]^-$ have comparable hyperfine interactions (6, 7).

If we assume that the quartet is due to $[CH_3CN]^-$, then the thermal decay leading to a $\cdot CH_2$ containing species could involve a molecular rearrangement where the apparent low energy of activation might well represent a bond rotational barrier. The question arises why this irreversible loss of the anion occurs in acetonitrile but not in deuteroacetonitrile? We suggest that this difference may be explained if a primary kinetic isotope effect is assumed, i.e., $A_D/A_H = 1$ and $E_D - E_H = 1.2$ kcal. The corresponding half-lives for the irreversible loss of the deutero anion in CD_3CN would then be 933 h at 77 °K and 141 h at 87 °K. This process would be much too slow to compete with the reversible process reported by Bonin *et al.* (2).

The photobleachable entity observed in acetonitrile with λ_{max} at 530 nm did not give a distinct e.s.r. spectrum because of the presence of the $\cdot CH_2CN$ radical. With so little evidence it is difficult to conclusively identify this species; we believe it to be an electron associated with more than one acetonitrile molecule, $e(CH_3CN)_N$, where N could quite well be two as shown for the species in CD_3CN (2). Since inclusion of electron scavengers was not particularly effective in removing this entity and since no additive scavenger radicals were produced on photobleaching, we conclude that either photobleaching does not involve the production of a mobile electron or else that the cross section for the reaction of acetonitrile with mobile electron is very high.

Dr. T. E. Lantz is gratefully acknowledged for assistance with the optical spectra and Drs. P. B. Ayscough, G. V. Buxton, F. S. Dainton, F.R.S., and Ffrancon Williams for helpful and constructive discussions.

The National Research Council of Canada, the Science Research Council of Great Britain, and the University of Leeds and Tenovus are acknowledged for financial support.

1. P. B. AYSCOUGH, R. G. COLLINS, and T. J. KEMP. J. Phys. Chem. **70**, 2220 (1966).
2. M. A. BONIN, K. TSUJI, and F. WILLIAMS. Nature, **218**, 946 (1968).
3. M. H. J. WIJNEN. J. Chem. Phys. **22**, 1074 (1954).
4. G. B. GARBUTT, H. D. GESSER, and M. FUJIMOTO. J. Chem. Phys. **48**, 4605 (1968).
5. J. E. BENNETT, B. MILE, and B. WARD. Chem. Commun. 13 (1969).
6. F. J. ADRIAN, E. L. COCHRAN, and V. A. BOWERS. J. Chem. Phys. **36**, 1661 (1962).
7. K. D. J. ROOT, M. C. R. SYMONS, and B. C. WEATHERBY. Mol. Phys. **11**, 161 (1966).
8. P. F. PATRICK and F. P. SARGENT. Can. J. Chem. **46**, 1818 (1968).

FOR ERRATA SEE
V.48#17 1970 P.2790

Can. J. Chem. Downloaded from www.nrcresearchpress.com by 210.87.254.42 on 09/05/12
For personal use only.

Can. J. Chem. Downloaded from www.nrcresearchpress.com by 210.87.254.6 on 09/05/12
For personal use only.

Pyrolysis of ethane in the presence of hydrogen sulfide. Rates of formation of ethylene, hydrogen, and methane[1]

P. R. McLean and D. J. McKenney
Department of Chemistry, University of Windsor, Windsor, Ontario
Received February 24, 1969[2]

Rates of formation of ethylene, hydrogen, and methane have been measured at 630 °C for the thermal decomposition of ethane at pressures between 100 and 620 Torr, with various pressures (approximately 1 to 100 Torr) of added hydrogen sulfide. The effect of the H_2S was to increase the rate of methane formation and to decrease the rate of ethylene and hydrogen formation. Rates of formation of all three of these gases decreased with increasing hydrogen sulfide pressures. The quantitative data obtained and the partial product analysis indicate that a complex mechanism is operative. Possible qualitative explanations for the observations are discussed.

Canadian Journal of Chemistry, 48, 1782 (1970)

Introduction

The H_2S accelerated pyrolysis of various organic compounds can be attributed (1–5) to replacement of the relatively slow reaction

$$R' + RH \xrightarrow{a} R'H + R$$

by the rapid sequence

$$R' + H_2S \xrightarrow{b} R'H + HS$$

$$HS + RH \xrightarrow{c} H_2S + R$$

When olefins are involved, addition reactions complicate the mechanism (5). H_2S has also been used as a free-radical scavenger (reaction *b*) in photolysis and radiolysis experiments (6). HS radicals are removed by recombination processes.

The mechanism of the thermal decomposition of ethane is fairly well understood (7–11). The radicals involved should readily react with H_2S. A few experiments using C_2H_6–H_2S mixtures indicated that the mechanism was very complex and precise estimates of rate constants could not be obtained. Hence work on this system was discontinued. Nevertheless the data revealed several interesting features worth reporting.

Experimental

Two quartz cylindrical reaction vessels were used in a conventional static system. The "unpacked" vessels (277 cm^3) had a surface/volume (s/v) ratio of 1.3 cm^{-1}, while the packed vessel (204 cm^3) had a s/v ratio of 7.8 cm^{-1}. Each had a 1/4 in. i.d. thermocouple well. The furnace, a 5 in. diameter steel, Ni-plated block 12 in. long, was heated electrically (±0.25 °C) by a Sunvic controller. Temperature gradients within the vessel were estimated to be less than ±0.5 °C.

Pressure changes were monitored using a differential pressure transducer in conjunction with a d.c.-converter, amplifier, and recorder.

The purified reactants were mixed ~ 20 min prior to a "run". The reaction vessel was evacuated to $< 5 \times 10^{-5}$ Torr between "runs". Initial conditioning of the reaction vessels involved three rinsings with hot concentrated HNO_3, and pumping for several hours.

Ethane (Matheson c.p. grade [99.0%]) and hydrogen sulfide (c.p. grade [99.6%]) were purified by at least three trap-to-trap distillations under vacuum at liquid nitrogen temperature. Chromatographic analysis of the "purified" ethane showed no evidence of impurities, while the hydrogen sulfide still contained a slight trace ($\ll 1\%$) of CO_2.

After reacting a mixture for a measured time interval, the contents of the reaction vessel were expanded into two traps at liquid nitrogen temperature and the non-condensible products (CH_4, H_2, and a trace of C_2H_4) collected in calibrated volumes using a Toepler pump. H_2 was removed by circulating the mixture through a CuO tube at 285 °C. CH_4 was then analyzed by gas chromatography (g.c.) (Model 700, F and M) using a thermal conductivity detector and a 6 ft, 1/4 in. i.d. column at 30 °C packed with Type Q Porapak. The H_2 yield was obtained by difference. Small corrections were made for the C_2H_4 present. Warming the two traps to −160 °C (isopentane slush bath) allowed the C_2H_6, C_2H_4, and H_2S to evolve. These were analyzed on the same column at 45 °C. An attempt was made to analyze the remaining products on the Porapak column at 100 °C, on a 6 ft column containing 20% 1,2,3-tris(2-cyanoethoxy) propane on a Diatoport S, on a S.E. 30 (silicone oil) 1/8 in. i.d., 8 ft column, and on a Perkin–Elmer R (polypropylene) capillary column 150 ft in length and 0.02 in. i.d. The last two columns were used in a Varian 1200 instrument with an electron capture detector.

---

[1]Based on part of a thesis submitted by P. R. McLean to the Faculty of Graduate Studies at the University of Windsor in partial fulfillment of the requirements for the Master of Science degree.

[2]Revision received January 8, 1970.

Can. J. Chem. Downloaded from www.nrcresearchpress.com by 210.87.254.6 on 09/05/12
For personal use only.

Results

To test for reproducibility, manometric rates were obtained in the unpacked vessel using pure ethane at 582, 610, 624, 635 °C. The rates compared favorably (within ~ 5%) with those obtained by Laidler and Wojciechowski (12) and Quinn (10).

Both in the presence and absence of H_2S, the major products were hydrogen and ethylene. Methane was produced in relatively low yield. These products, and also ethanethiol, ethylene sulfide, and propylene, were identified by coincidence of product and standard sample g.c. peaks. The sulfur-containing compounds were detected on the Varian 1200 instrument using an electron capture detector and R column. A whitish-yellow deposit which accumulated in the traps was assumed to be elemental sulfur. Two other minor products, representing $\ll 1\%$ of the sulfur-containing products were not identified. Six other "peaks" of doubtful significance (~ within the noise level) were observed.

Rates in the packed vessel were lower than in the unpacked vessel. A six-fold increase in s/v ratio decreased the rates of formation of hydrogen and ethylene by a factor of approximately 2.5; the methane rate was reduced by a factor of about 1.3.

Rates of formation of H_2, C_2H_4, and CH_4 at 50 s reaction time were calculated (i.e. $[\text{Product}]_{t=50}/50$). In the case of CH_4 and H_2, these rates differed only slightly from initial rates since the yields were approximately a linear function of time at very low conversions. In the case of ethylene, however, the rate decreased rapidly with increasing reaction time. Plots of (C_2H_4)/time vs. time showed considerable curvature, and extrapolations to determine initial rates involved a rather large uncertainty. As a result, rates at 50 s were used throughout, and these are estimated to be ~ 10–20% lower than the initial rates of production of ethylene.

The rates of formation of C_2H_4, H_2, and CH_4 at varying H_2S pressures and various constant pressures (P) of C_2H_6 at 630 °C, relative to their rates in the absence of H_2S, are shown in Figs. 1, 2, and 3, respectively. Values of v^0 (rate in pure ethane) were calculated from the results of Lin and Back (7). Rates of H_2 and C_2H_4 production are inhibited by H_2S. Hydrogen rates appear to be reduced by approximately the same amount at all pressures of ethane. Probably the same result

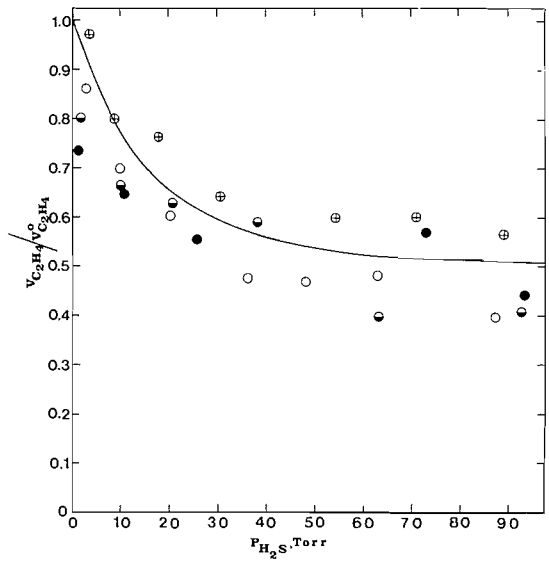

FIG. 1. Relative rate of ethylene formation as a function of hydrogen sulfide pressure. ●, 620 Torr C_2H_6; ◒, 464 Torr C_2H_6; ○, 235 Torr C_2H_6; ⊕, 102 Torr C_2H_6.

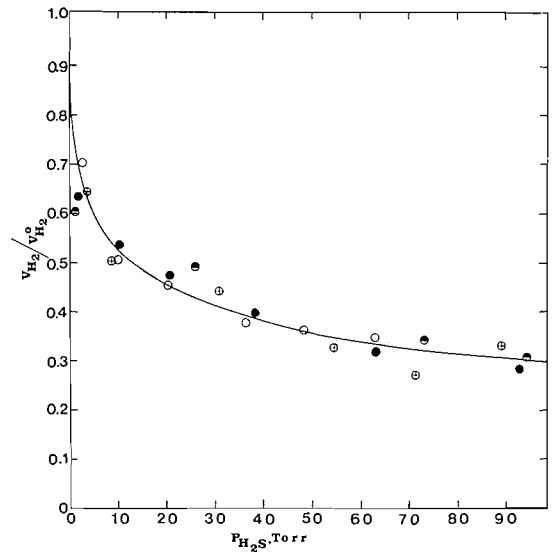

FIG. 2. Relative rate of hydrogen formation as a function of hydrogen sulfide pressure. ◓, 620 Torr C_2H_6; ●, 464 Torr C_2H_6; ○, 235 Torr C_2H_6; ⊕, 102 Torr C_2H_6.

applied to ethylene inhibition, but in this case the data are scattered to a greater extent. Rates of ethylene production are greater than hydrogen production in the presence of H_2S. The ratio $V_{C_2H_4}/V_{H_2}$ is 1.20 ± 0.16 at $P_{C_2H_6}$ = 620 Torr, and 1.88 ± 0.17 at $P_{C_2H_6}$ = 102 Torr (average of

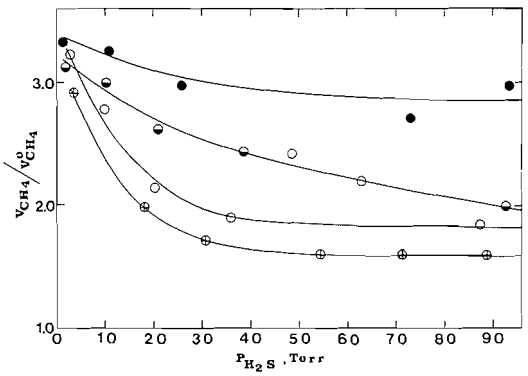

FIG. 3. Relative rate of methane formation as a function of hydrogen sulfide pressure. ●, 620 Torr C_2H_6; ◒, 464 Torr C_2H_6; ○, 235 Torr C_2H_6; ⊕, 102 Torr C_2H_6.

5 runs). There were no clear trends with increasing P_{H_2S}.

The relative rate of methane production *appears* to increase to a sharp maximum at very low H_2S pressures and then decrease to an approximately constant value which depends on the ethane pressure. The scatter in the experimental data in this case is large and there is also a large uncertainty in the ratio v/v^0, since v^0 is calculated from work done elsewhere.

Discussion

Darwent and Roberts (13) have shown that at high temperatures (> 600 °C) the pyrolysis of H_2S is second order and homogeneous. Below 600 °C the reaction was surface dependent. Here, 630 °C was chosen as the working temperature in order to minimize the heterogeneous decomposition of H_2S and yet remain within the temperature range in which the pyrolysis of ethane has recently been studied (7–9).

Results obtained using the packed vessel suggest that methane is produced primarily by homogeneous reactions, but some significant heterogeneous processes effectively inhibit the production of hydrogen and ethylene. This heterogeneous process does not occur to any great extent in the absence of hydrogen sulfide. A surface reaction involving H_2S, or HS, or S with C_2H_5 radicals probably occurs.

Clearly, speculation on a complete mechanism for this system would be premature. Nevertheless, certain qualitative conclusions can be made regarding the homogeneous formation of C_2H_4, H_2, and CH_4.

The main source of ethylene is probably by decomposition of the ethyl radical

[1] $$C_2H_5 \rightarrow C_2H_4 + H$$

In the presence of H_2S, the decrease in the ethyl radical concentration, principally by

[2] $$C_2H_5 + H_2S \rightarrow C_2H_6 + HS$$

would account for the reduction in ethylene yield with increasing pressure of hydrogen sulfide.

The decrease in the rate of H_2 formation with increasing P_{H_2S} (Fig. 2) can also be explained by the decrease in $[C_2H_5]$ by reaction [2]. Because H_2 is produced by abstraction from C_2H_6 and H_2S by H atoms, and because reaction [1] is the predominant source of the atoms, reaction [2] will decrease H_2 formation.

It is more difficult to explain the fact that the rate of production of C_2H_4 is greater than the rate of production of H_2 in the presence of H_2S. Most of the H atoms must yield molecular hydrogen. Combination reactions are not expected to effect the $[H_2]$ significantly. Addition of H atoms to C_2H_4 is clearly not responsible for this effect. This suggests that the disproportionation

[3] $$C_2H_5 + HS \rightarrow C_2H_4 + H_2S$$

is much faster than the corresponding process

[4] $$2C_2H_5 \rightarrow C_2H_4 + C_2H_6$$

and/or that $[HS] \gg [C_2H_5]$ even at low pressures of H_2S.

The rate of formation of CH_4 is increased in the presence of H_2S, but decreases with increasing P_{H_2S}. This effect is more pronounced at low pressures of ethane (Fig. 3).

We have no satisfactory explanation for the increased rate in the presence of H_2S. CH_4 is formed by CH_3 radicals abstracting H atoms from C_2H_6 and H_2S, the only source of methyl radicals initially being decomposition of ethane. Secondary processes producing CH_4 in the absence of H_2S are not very significant at low conversions (10). However, Trenwith (14) found that in the presence of H_2, there was a marked increase in secondary CH_4 formation. Perhaps H_2S behaves in a similar way, but this does not appear to be the case judging from the shapes of our yield–time plots. Since the rates decrease slightly in the packed vessels, the enhanced rate cannot be attributed to heterogeneous effects.

Can. J. Chem. Downloaded from www.nrcresearchpress.com by 210.87.254.6 on 09/05/12
For personal use only.

We are grateful to the National Research Council of Canada for generous financial support. We also wish to thank Mr. J. Trizisky for his very helpful technical assistance and Dr. S. J. Price for the use of the Varian 1200 chromatograph and for useful discussions.

1. N. IMAI and O. TOYAMA. Bull. Chem. Soc. Jap. **33**, 1120 (1960).
2. N. IMAI and O. TOYAMA. Bull. Chem. Soc. Jap. **33**, 1408 (1960).
3. N. IMAI and O. TOYAMA. Bull. Chem. Soc. Jap. **34**, 328 (1961).
4. D. J. MCKENNEY and K. J. LAIDLER. Can. J. Chem. **41**, 2009 (1963).
5. M. NICLAUSE, R. MARTIN, F. BARONNET, and G. SCACCHI. Rev. Inst. Fr. Pétrole Ann. Combust. Liquides, **21**, 1724 (1966).
6. A. A. SCALA and P. AUSLOOS. J. Chem. Phys. **49**, 2282 (1968) and earlier papers, especially P. AUSLOOS and S. G. LIAS. J. Chem. Phys. **44**, 521 (1966).
7. M. C. LIN and M. H. BACK. Can. J. Chem. **44**, 505 (1966).
8. M. C. LIN and M. H. BACK. Can. J. Chem. **44**, 2357 (1966).
9. M. C. LIN and M. H. BACK. Can. J. Chem. **44**, 2369 (1966).
10. C. P. QUINN. Proc. Roy. Soc. London, Ser. A, **275**, 190 (1963).
11. C. P. QUINN. Trans. Faraday Soc. **59**, 2543 (1963).
12. K. J. LAIDLER and B. W. WOJCIECHOWSKI. Proc. Roy. Soc. London, Ser. A, **260**, 91 (1961).
13. B. DEB. DARWENT and R. ROBERTS. Proc. Roy. Soc. London, Ser. A, **216**, 352 (1953).
14. R. B. TRENWITH. Trans. Faraday Soc. **63**, 2452 (1967).

Oxidation products of 2,3,6,7-tetramethoxy-9,10-dimethylphenanthrene

J. M. EDWARDS AND ULRICH WEISS

National Institute of Arthritis and Metabolic Diseases, National Institutes of Health, Bethesda, Maryland 20014

Received October 15, 1969

Depending upon the conditions of solvent and temperature, oxidation of the readily accessible 2,3,6,7-tetramethoxy-9,10-dimethylphenanthrene (**3**) with $Na_2Cr_2O_7$ gave 2,3,6,7-tetramethoxyphenanthrene-9,10-dicarboxylic acid anhydride (**1**), 2,2′-diacetyl-4,4′,5,5′-tetramethoxybiphenyl (**4**), or the new aldehyde **5**. Compounds **1** and **4** have been obtained previously only by oxidative degradation of the alkaloid tylophorine (**2**); their ready availability may be of value for the synthesis of pharmacologically active compounds related to **2**.

Canadian Journal of Chemistry, **48**, 1785 (1970)

For synthetic work in progress in our laboratory, an efficient method for the preparation of 2,3,6,7-tetramethoxyphenanthrene-9,10-dicarboxylic acid anhydride (**1**) was needed; it seemed likely that a simple synthesis of **1** (and perhaps potentially of analogous methoxylated phenanthrene-9,10-carboxylic acid anhydrides) from commercially available reagents might also provide a convenient starting material for the elaboration of alkaloids of the tylophorine type, many of which have powerful and interesting pharmacological properties (1, 2).

A compound assigned structure **1** was obtained by Govindachari *et al.* (3) on oxidative degradation of the alkaloid tylophorine (**2**) (Scheme 1), but attempts by these authors to prepare **1** through oxidation of 2,3,6,7-tetramethoxy-9,10-dimethylphenanthrene (**3**), now readily accessible from veratrole, biacetyl, and 70% H_2SO_4 by the method of Manson and Musgrave (4), were unsuccessful (5). We have now found that **1** is easily obtained, in 54% yield, if **3** is oxidized with $Na_2Cr_2O_7$ in aqueous solution at 180° (Scheme 1); this general method was worked out by Friedman (6) for the oxidation of 2,3-dimethylnaphthalene to 2,3-naphthalenedicarboxylic acid at 250°. The lower temperature required for the oxidation of **3** reflects the greater sensitivity of the methoxylated aromatic system; at 250° a complex mixture of products is formed. The m.p. of our product agrees with that given by Govindachari *et al.* (3), and through this two-step reaction sequence **1** becomes an easily available substance.

Products different from **1** were obtained when **3** was oxidized with $Na_2Cr_2O_7$ in solvents other than H_2O (Scheme 1). Use of a 20% solution of H_2SO_4 in aqueous dioxane (1:1) gave 2,2′-diacetyl-4,4′,5,5′-tetramethoxybiphenyl (**4**), which like **1** has been prepared previously only during the degradation of **2** (3). Finally, oxidation of **3** with $Na_2Cr_2O_7$ in boiling HOAc gave a new compound $C_{22}H_{22}O_7$, m.p. 215–216°, for which the structure **5** was established by chemical and

Can. J. Chem. Downloaded from www.nrcresearchpress.com by 210.87.254.6 on 09/05/12
For personal use only.

We are grateful to the National Research Council of Canada for generous financial support. We also wish to thank Mr. J. Trizisky for his very helpful technical assistance and Dr. S. J. Price for the use of the Varian 1200 chromatograph and for useful discussions.

1. N. IMAI and O. TOYAMA. Bull. Chem. Soc. Jap. **33**, 1120 (1960).
2. N. IMAI and O. TOYAMA. Bull. Chem. Soc. Jap. **33**, 1408 (1960).
3. N. IMAI and O. TOYAMA. Bull. Chem. Soc. Jap. **34**, 328 (1961).
4. D. J. MCKENNEY and K. J. LAIDLER. Can. J. Chem. **41**, 2009 (1963).
5. M. NICLAUSE, R. MARTIN, F. BARONNET, and G. SCACCHI. Rev. Inst. Fr. Pétrole Ann. Combust. Liquides, **21**, 1724 (1966).
6. A. A. SCALA and P. AUSLOOS. J. Chem. Phys. **49**, 2282 (1968) and earlier papers, especially P. AUSLOOS and S. G. LIAS. J. Chem. Phys. **44**, 521 (1966).
7. M. C. LIN and M. H. BACK. Can. J. Chem. **44**, 505 (1966).
8. M. C. LIN and M. H. BACK. Can. J. Chem. **44**, 2357 (1966).
9. M. C. LIN and M. H. BACK. Can. J. Chem. **44**, 2369 (1966).
10. C. P. QUINN. Proc. Roy. Soc. London, Ser. A, **275**, 190 (1963).
11. C. P. QUINN. Trans. Faraday Soc. **59**, 2543 (1963).
12. K. J. LAIDLER and B. W. WOJCIECHOWSKI. Proc. Roy. Soc. London, Ser. A, **260**, 91 (1961).
13. B. DEB. DARWENT and R. ROBERTS. Proc. Roy. Soc. London, Ser. A, **216**, 352 (1953).
14. R. B. TRENWITH. Trans. Faraday Soc. **63**, 2452 (1967).

Oxidation products of 2,3,6,7-tetramethoxy-9,10-dimethylphenanthrene

J. M. EDWARDS AND ULRICH WEISS
National Institute of Arthritis and Metabolic Diseases, National Institutes of Health, Bethesda, Maryland 20014

Received October 15, 1969

Depending upon the conditions of solvent and temperature, oxidation of the readily accessible 2,3,6,7-tetramethoxy-9,10-dimethylphenanthrene (**3**) with $Na_2Cr_2O_7$ gave 2,3,6,7-tetramethoxyphenanthrene-9,10-dicarboxylic acid anhydride (**1**), 2,2′-diacetyl-4,4′,5,5′-tetramethoxybiphenyl (**4**), or the new aldehyde **5**. Compounds **1** and **4** have been obtained previously only by oxidative degradation of the alkaloid tylophorine (**2**); their ready availability may be of value for the synthesis of pharmacologically active compounds related to **2**.

Canadian Journal of Chemistry, **48**, 1785 (1970)

For synthetic work in progress in our laboratory, an efficient method for the preparation of 2,3,6,7-tetramethoxyphenanthrene-9,10-dicarboxylic acid anhydride (**1**) was needed; it seemed likely that a simple synthesis of **1** (and perhaps potentially of analogous methoxylated phenanthrene-9,10-carboxylic acid anhydrides) from commercially available reagents might also provide a convenient starting material for the elaboration of alkaloids of the tylophorine type, many of which have powerful and interesting pharmacological properties (1, 2).

A compound assigned structure **1** was obtained by Govindachari *et al.* (3) on oxidative degradation of the alkaloid tylophorine (**2**) (Scheme 1), but attempts by these authors to prepare **1** through oxidation of 2,3,6,7-tetramethoxy-9,10-dimethylphenanthrene (**3**), now readily accessible from veratrole, biacetyl, and 70% H_2SO_4 by the method of Manson and Musgrave (4), were unsuccessful (5). We have now found that **1** is easily obtained, in 54% yield, if **3** is oxidized with $Na_2Cr_2O_7$ in aqueous solution at 180° (Scheme 1); this general method was worked out by Friedman (6) for the oxidation of 2,3-dimethylnaphthalene to 2,3-naphthalenedicarboxylic acid at 250°. The lower temperature required for the oxidation of **3** reflects the greater sensitivity of the methoxylated aromatic system; at 250° a complex mixture of products is formed. The m.p. of our product agrees with that given by Govindachari *et al.* (3), and through this two-step reaction sequence **1** becomes an easily available substance.

Products different from **1** were obtained when **3** was oxidized with $Na_2Cr_2O_7$ in solvents other than H_2O (Scheme 1). Use of a 20% solution of H_2SO_4 in aqueous dioxane (1:1) gave 2,2′-diacetyl-4,4′,5,5′-tetramethoxybiphenyl (**4**), which like **1** has been prepared previously only during the degradation of **2** (3). Finally, oxidation of **3** with $Na_2Cr_2O_7$ in boiling HOAc gave a new compound $C_{22}H_{22}O_7$, m.p. 215–216°, for which the structure **5** was established by chemical and

Can. J. Chem. Downloaded from www.nrcresearchpress.com by 210.87.254.5 on 09/05/12
For personal use only.

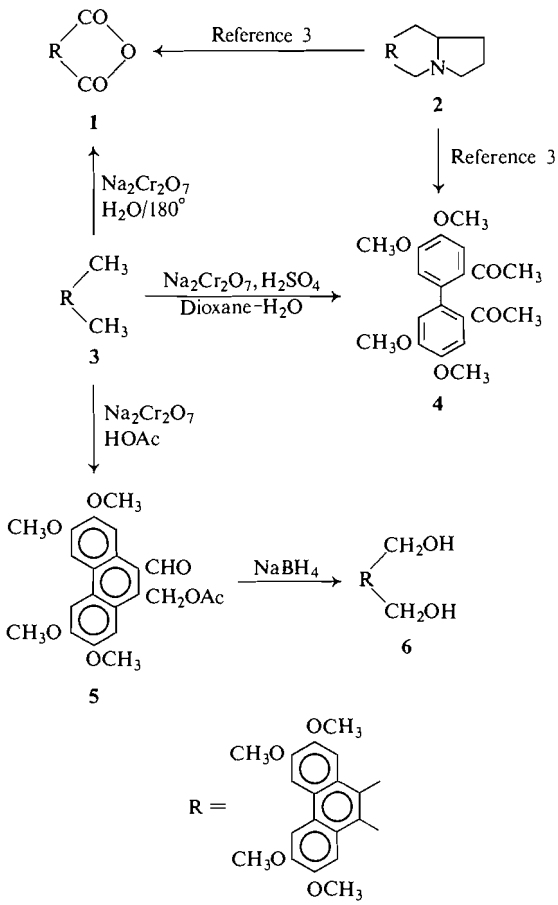

SCHEME 1

spectroscopic observations. Presence of the aldehyde group was suggested by spectroscopic findings (ν = 1678 cm^{-1}, δ 10.90) and confirmed by the formation of an anil, and by BH_4^- reduction (with simultaneous hydrolysis of the acetoxy group) to the diol **6**, further characterized as its diacetate. The other groups in **5** were established by the infrared (i.r.) (ν = 1738 cm^{-1}, acetate) and nuclear magnetic resonance (n.m.r.) spectra (see Experimental).

The strong dependence of the products formed on dichromate oxidation of **3** upon solvent and temperature is unusual, as are the formation of the acetoxy compound (**5**), and the loss of this acetyl group on hydride reduction. In view of the unsatisfactory state of our knowledge of the intimate mechanisms of dichromate oxidations (7), attempts to explain in detail the striking effects of solvent and physical conditions upon the oxidation of **3** would be unjustified. However, the formation of **4** in a strongly acidic medium is consistent with the ring opening which has been observed in similar cases (7); as to **5**, the corresponding alcohol is presumably formed by reaction of **3** with three moles of chromic acid in the normal manner (7), and one could assume that a mixed anhydride of chromic and acetic acids acts as the acetylating species in the subsequent formation of **5**.

Experimental

Melting points, determined on a Reichert hot-stage microscope, are uncorrected. Infrared spectra were recorded in $CHCl_3$ on a Perkin–Elmer 257 instrument; only the major bands are reported. Ultraviolet (u.v.) spectra in absolute methanol were recorded on a Cary 14 spectrophotometer, and n.m.r. spectra in deuteriochloroform with a Varian Associates A-60 instrument. Mass spectra were obtained on a L.K.B. 7000 mass-spectrometer.

2,3,6,7-Tetramethoxy-9,10-dimethylphenanthrene (3)

Compound **3** was prepared in 72% yield by the method of Manson and Musgrave (4); m.p. 224° (lit. (4) 223°).

2,3,6,7-Tetramethoxy-phenanthrene-9,10-dicarboxylic Acid Anhydride (1)

2,3,6,7-Tetramethoxy-9,10-dimethylphenanthrene (0.33 g, 1 mmole) was heated with $Na_2Cr_2O_7 . 2H_2O$ (0.66 g, 2.2 mmole) and water (50 ml) for 18 h at 180° in a steel bomb. After cooling, the mixture was filtered, acidified, and extracted with chloroform. Evaporation gave a yellow solid which was recrystallized from dioxane to give **1** (0.2 g, 54%) as bright orange crystals; m.p. 312–316°; ν_{max} 1820 s, and 1770 s cm^{-1} (anhydride bands), δ 7.62 (2H) and 7.17 (2H), aromatic protons, 4.08 (6H) and 4.00 (6H), —OMe; λ_{max} 408 sh, 365, 320, 287, 262, and 225 nm (log ε 4.0, 4.4, 4.8, 5.4, 5.6, and 5.2).

Anal. Calcd. for $C_{20}H_{16}O_7$ (mol. wt. 368): C, 65.22; H, 4.38. Found (368 (mass spectrometry)): C, 65.38; H, 4.60.

2,2′-Diacetyl-4,4′,5,5′-tetramethoxybiphenyl (4)

A solution of $Na_2Cr_2O_7 . 2H_2O$ (0.94 g, 3.1 mmole) in water (10 ml) was added dropwise over a period of 15 min to a boiling solution of **3** (0.5 g, 1.52 mmole) in 100 ml of a 20% solution of H_2SO_4 in aqueous dioxane (1:1). After refluxing for a further 30 min, the solution was cooled and extracted with $CHCl_3$. Evaporation of the solvent gave **4** in 48% yield; pale-yellow crystals; m.p. 212–213° (lit. (3) 212°) from dioxane–water; ν_{max} 1680 s cm^{-1}; δ 7.30 (2H) and 6.58 (2H), aromatic protons, 3.90 (6H) and 3.80 (6H), —OMe, 2.02 (6H), —$COCH_3$.

Anal. Calcd. for $C_{20}H_{22}O_6$ (mol. wt. 358): C, 67.03; H, 6.19. Found (358 (mass spectrometry)): C, 67.25; H, 6.29.

2,3,6,7-Tetramethoxy-9-formyl-10-acetoxymethyl-phenanthrene (5)

A solution of $Na_2Cr_2O_7.2H_2O$ (0.94 g, 3.1 mmole) in acetic acid (10 ml) was added dropwise over a period of 15 min to **3** (0.5 g, 1.52 mmole) in refluxing acetic

Can. J. Chem. Downloaded from www.nrcresearchpress.com by 210.87.254.5 on 09/05/12
For personal use only.

acid (40 ml). The resulting green solution was cooled, poured into water (200 ml), and extracted with $CHCl_3$. After removal of the solvent the crude yellow product was recrystallized from dioxane–water to yield **5** (0.23 g, 40%); m.p. 215–216°; ν_{max} 1738 s (acetate), 1678 (CHO), and 1620 s cm^{-1}; δ 10.90 (1H) CHO, 8.20 (1H), 7.56 (2H), and 7.42 (1H), aromatic protons, 5.70 (2H), $-CH_2-O$, 4.05, 4.00 (singlets, 6H each) —OMe, 2.02 (3H), $-COCH_3$; λ_{max} 345, 288, 270, and 243 nm (log ε 4.7, 5.2, 5.2, and 5.0).

Anal. Calcd. for $C_{22}H_{22}O_7$ (mol. wt. 398): C, 66.30; H, 5.60. Found (398 (mass spectrometry), 400.3 (osmometric)): C, 66.50; H, 5.90.

The aldehyde (**5**) (0.1 g) was refluxed in ethanol (20 ml) with aniline (0.2 g) for 2 h. On cooling the *anil* was precipitated, which, on recrystallization from ethanol, gave yellow crystals, m.p. 210–213°.

Anal. Calcd. for $C_{28}H_{27}NO_6$ (mol. wt. 373): C, 71.02; H, 5.75; N, 2.96. Found (373 (mass spectrometry)): C, 70.74; H, 6.05; N, 2.89.

2,3,6,7-Tetramethoxy-9,10-dihydroxymethylphenanthrene (6)

The aldehyde (**5**) in methanol was reduced with an excess of sodium borohydride at room temperature. Normal work-up gave **6** as white crystals, m.p. 225–227° from methanol.

Anal. Calcd. for $C_{20}H_{22}O_6$ (mol. wt. 358): C, 67.00; H, 6.20. Found (358 (mass spectrometry)): C, 66.80; H, 6.11.

Compound **6** was acetylated with acetic anhydride and sulfuric acid; normal work-up gave the *diacetate* as white crystals from methanol; m.p. 226–228°; ν_{max} 1738 s (ester), and 1628 s cm^{-1}.

Anal. Calcd. for $C_{24}H_{26}O_8$ (mol. wt. 442): C, 65.15; H, 5.92. Found (442 (mass spectrometry)): C, 65.10; H, 6.20.

1. T. R. GOVINDACHARI. *In* The alkaloids. Vol. 9. R. H. F. Manske, *Editor*, Academic Press, New York and London, 1967. p. 517.
2. G. R. DONALDSON, M. R. ATKINSON, and A. W. MURRAY. Biochem. Biophys. Res. Commun. **31**, 104 (1968).
3. T. R. GOVINDACHARI, M. V. LAKSHMIKANTHAM, K. NAGARAJAN, and B. R. PAI. Tetrahedron, **4**, 311 (1958).
4. D. L. MANSON and O. C. MUSGRAVE. J. Chem. Soc. 1011 (1963).
5. T. R. GOVINDACHARI, M. V. LAKSHMIKANTHAM, B. R. PAI, and S. RAJAPPA. Tetrahedron, **9**, 53 (1960).
6. L. FRIEDMAN. Org. Syn. **43**, 80 (1963).
7. K. B. WIBERG. *In* Oxidation in organic chemistry. K. B. Wiberg, *Editor*, Academic Press, New York and London, 1965. Part A, pp. 69 ff.

Hexanor–cucurbitacin D, a degraded cucurbitacin from *Begonia tuberhybrida* var. *alba*[1]

RAYMOND W. DOSKOTCH AND CHARLES D. HUFFORD[2]

Division of Natural Products Chemistry, College of Pharmacy, The Ohio State University, Columbus, Ohio 43210

Received January 22, 1970

A compound isolated from *Begonia tuberhybrida* has been shown to have the structure of hexanor–cucurbitacin D (**3**). Its diacetate is identical to the periodate cleavage product of cucurbitacin B diacetate.

Canadian Journal of Chemistry, **48**, 1787 (1970)

The cytotoxic activity of the alcoholic extract residue from tubers of *Begonia tuberhybrida* Voss var. *alba* has recently been traced to the presence of cucurbitacin B (**1**) (1). That this unusual tetracyclic triterpene was found in a source botanically removed from its more common producers (2) required further examination of additional constituents. Cucurbitacin D (**2**) and dihydrocucurbitacin B (side-chain double bond reduced) were subsequently isolated and identified. In addition a fourth unknown substance, designated compound A, was obtained in very low yields and was assigned the molecular formula $C_{24}H_{34}O_5$ on the basis of elemental analysis and high resolution mass spectrometry. We wish to report the identification of this material as hexanor–cucurbitacin D (**3**), a new natural occurring degraded cucurbitacin.

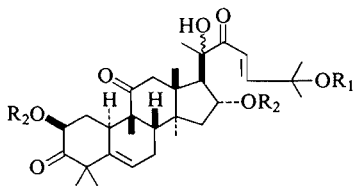

1 R_1 = Ac, R_2 = H
2 R_1 = R_2 = H
5 R_1 = R_2 = Ac

The carbonyl region in the infrared (i.r.) spectrum of hexanor–cucurbitacin D was considerably simplified in comparison with the other iso-

[1]Antitumor Agents. Part V. Previous paper R. W. Doskotch and F. S. El-Feraly. J. Org. Chem. In press.
[2]NIH Predoctoral Fellow.

Can. J. Chem. Downloaded from www.nrcresearchpress.com by 210.87.254.5 on 09/05/12
For personal use only.

acid (40 ml). The resulting green solution was cooled, poured into water (200 ml), and extracted with $CHCl_3$. After removal of the solvent the crude yellow product was recrystallized from dioxane–water to yield **5** (0.23 g, 40%); m.p. 215–216°; ν_{max} 1738 s (acetate), 1678 (CHO), and 1620 s cm^{-1}; δ 10.90 (1H) CHO, 8.20 (1H), 7.56 (2H), and 7.42 (1H), aromatic protons, 5.70 (2H), $-CH_2-O$, 4.05, 4.00 (singlets, 6H each) —OMe, 2.02 (3H), $-COCH_3$; λ_{max} 345, 288, 270, and 243 nm (log ε 4.7, 5.2, 5.2, and 5.0).

Anal. Calcd. for $C_{22}H_{22}O_7$ (mol. wt. 398): C, 66.30; H, 5.60. Found (398 (mass spectrometry), 400.3 (osmometric)): C, 66.50; H, 5.90.

The aldehyde (**5**) (0.1 g) was refluxed in ethanol (20 ml) with aniline (0.2 g) for 2 h. On cooling the *anil* was precipitated, which, on recrystallization from ethanol, gave yellow crystals, m.p. 210–213°.

Anal. Calcd. for $C_{28}H_{27}NO_6$ (mol. wt. 373): C, 71.02; H, 5.75; N, 2.96. Found (373 (mass spectrometry)): C, 70.74; H, 6.05; N, 2.89.

2,3,6,7-Tetramethoxy-9,10-dihydroxymethylphenanthrene (6)

The aldehyde (**5**) in methanol was reduced with an excess of sodium borohydride at room temperature. Normal work-up gave **6** as white crystals, m.p. 225–227° from methanol.

Anal. Calcd. for $C_{20}H_{22}O_6$ (mol. wt. 358): C, 67.00; H, 6.20. Found (358 (mass spectrometry)): C, 66.80; H, 6.11.

Compound **6** was acetylated with acetic anhydride and sulfuric acid; normal work-up gave the *diacetate* as white crystals from methanol; m.p. 226–228°; ν_{max} 1738 s (ester), and 1628 s cm^{-1}.

Anal. Calcd. for $C_{24}H_{26}O_8$ (mol. wt. 442): C, 65.15; H, 5.92. Found (442 (mass spectrometry)): C, 65.10; H, 6.20.

1. T. R. GOVINDACHARI. *In* The alkaloids. Vol. 9. R. H. F. Manske, *Editor*, Academic Press, New York and London, 1967. p. 517.
2. G. R. DONALDSON, M. R. ATKINSON, and A. W. MURRAY. Biochem. Biophys. Res. Commun. **31**, 104 (1968).
3. T. R. GOVINDACHARI, M. V. LAKSHMIKANTHAM, K. NAGARAJAN, and B. R. PAI. Tetrahedron, **4**, 311 (1958).
4. D. L. MANSON and O. C. MUSGRAVE. J. Chem. Soc. 1011 (1963).
5. T. R. GOVINDACHARI, M. V. LAKSHMIKANTHAM, B. R. PAI, and S. RAJAPPA. Tetrahedron, **9**, 53 (1960).
6. L. FRIEDMAN. Org. Syn. **43**, 80 (1963).
7. K. B. WIBERG. *In* Oxidation in organic chemistry. K. B. Wiberg, *Editor*, Academic Press, New York and London, 1965. Part A, pp. 69 ff.

Hexanor–cucurbitacin D, a degraded cucurbitacin from *Begonia tuberhybrida* var. *alba*[1]

RAYMOND W. DOSKOTCH AND CHARLES D. HUFFORD[2]

Division of Natural Products Chemistry, College of Pharmacy, The Ohio State University, Columbus, Ohio 43210

Received January 22, 1970

A compound isolated from *Begonia tuberhybrida* has been shown to have the structure of hexanor–cucurbitacin D (**3**). Its diacetate is identical to the periodate cleavage product of cucurbitacin B diacetate.

Canadian Journal of Chemistry, **48**, 1787 (1970)

The cytotoxic activity of the alcoholic extract residue from tubers of *Begonia tuberhybrida* Voss var. *alba* has recently been traced to the presence of cucurbitacin B (**1**) (1). That this unusual tetracyclic triterpene was found in a source botanically removed from its more common producers (2) required further examination of additional constituents. Cucurbitacin D (**2**) and dihydrocucurbitacin B (side-chain double bond reduced) were subsequently isolated and identified. In addition a fourth unknown substance, designated compound A, was obtained in very low yields and was assigned the molecular formula $C_{24}H_{34}O_5$ on the basis of elemental analysis and high resolution mass spectrometry. We wish to report the identification of this material as hexanor–cucurbitacin D (**3**), a new natural occurring degraded cucurbitacin.

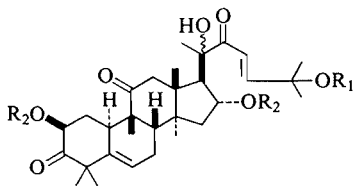

1 R_1 = Ac, R_2 = H
2 R_1 = R_2 = H
5 R_1 = R_2 = Ac

The carbonyl region in the infrared (i.r.) spectrum of hexanor–cucurbitacin D was considerably simplified in comparison with the other iso-

[1]Antitumor Agents. Part V. Previous paper R. W. Doskotch and F. S. El-Feraly. J. Org. Chem. In press.
[2]NIH Predoctoral Fellow.

Can. J. Chem. Downloaded from www.nrcresearchpress.com by 210.87.254.5 on 09/05/12
For personal use only.

Can. J. Chem. Downloaded from www.nrcresearchpress.com by 210.87.254.5 on 09/05/12
For personal use only.

lated cucurbitacins, showing one intense somewhat broadened band at 1710 cm^{-1} in place of the usual multiplicity of peaks. Absorption in the olefin region was restricted to a weak band at 1670 cm^{-1} and strong absorption at 3600 and 3470 cm^{-1} was evidence for hydroxyl groups. The nuclear magnetic resonance (n.m.r.) spectrum exhibited five three-proton singlets at δ 0.69, 1.08, 1.30, 1.37, and 1.43 assigned to tertiary methyl groups and another singlet at δ 2.20 (3H) was due to a methyl ketone. The latter was confirmed by a positive iodoform test and by the presence in the mass spectrum of the base peak at *m/e* 43 ($CH_3C{=}O$).

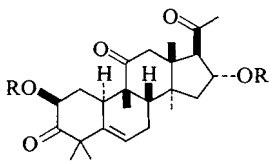

3 R = H
4 R = Ac

Acetylation of hexanor–cucurbitacin D gave a diacetate **4** that lacked absorption in the hydroxyl region of the i.r. spectrum and showed in the n.m.r. spectrum two sharp peaks at δ 2.03 (3H) and 2.15 (3H) in addition to the methyl ketone at δ 2.18. The physical properties of the acetate corresponded very closely with those reported for hexanor–elatericin A (hexanor–cucurbitacin D) diacetate (**4**), obtained by periodate cleavage of cucurbitacin D diacetate (3). We prepared a sample of hexanor–cucurbitacin D diacetate (**4**) by a similar cleavage of cucurbitacin B diacetate (**5**) and the product was identical (ultraviolet (u.v.), i.r., n.m.r., $[\alpha]_D$, mixture m.p.) to the diacetate of the substance isolated from the Begonia tubers. This is the first report of a degraded cucurbitacin found in nature and which bears an analogy to the pregnane skeleton in the steroid series.

Experimental

Melting points are uncorrected. The i.r. spectra were determined in chloroform at 8–10% concentration on a Perkin–Elmer Infracord 237 or 257 spectrophotometer. The u.v. spectra were taken in methanol on a Cary model 15 spectrophotometer. Optical rotations and circular dichroism (c.d.) curves were obtained on a Jasco ORD/UV-5 instrument in methanol. The n.m.r. spectra were taken in deuterochloroform on a Varian A-60A instrument with tetramethylsilane as internal standard and the chemical shifts reported in δ (p.p.m.) values and *J* in Hz units.

Hexanor–cucurbitacin D(3)

The isolation method and some physical properties of hexanor–cucurbitacin D (**3**), m.p. 216–218°, obtained from *Begonia tuberhybrida* Voss var. *alba* in a yield of 0.0003% have been reported (1). The c.d. curve exhibits a maximum at 296 mμ, [Θ] + 19 000. The mass spectrum showed peaks at *m/e* 402 (M^+, 12%), 387 ($M\text{-}CH_3$, 6%), 384 ($M\text{-}H_2O$, 6%), 364 ($M\text{-}CH_3\text{-}H_2O$, 9%), 359 ($M\text{-}COCH_3$, 2%), and 43 ($COCH_3$, 100%).

Hexanor–curcurbitacin D Diacetate (4)

A 10 mg sample of hexanor–cucurbitacin D (**3**) was dissolved in 0.5 ml of pyridine and 0.1 ml of acetic anhydride was added. After 24 h at room temperature the solution was diluted with water and extracted with diethyl ether. The combined ether layer was washed with 3 *N* HCl, 2% $NaHCO_3$, and water, then dried (Na_2SO_4) and evaporated. The residue crystallized from diethyl ether to give 7 mg of the acetate **4**, m.p. 202–204°, $[\alpha]_D^{25}$ + 94° (*c* 0.075); λ_{max} 290 mμ (ε 180); ν_{max} 1730 (broad), 1710, 1695, and 1200–1300 (broad) cm^{-1} [lit. (3), m.p. 202–205°, $[\alpha]_D$ + 112° (*c* 1.06 in $CHCl_3$); λ_{max} 288 mμ (ε 200); ν_{max} 1730 (broad), 1700, and 1240 cm^{-1}]. The compound gave a positive iodoform test (4).

Conversion of Cucurbitacin B (1) to Hexanor–cucurbitacin D Diacetate (4)

Curcurbitacin B (**1**) was acetylated to give the amorphous diacetate **5** in quantitative yields according to Schlegel *et al.* (5), and a 500 mg sample of the product was dissolved in 10 ml of dioxane and treated with 700 mg of periodic acid dissolved in 8 ml of water. After 72 h at room temperature the solution was adjusted to p*H* 7 with $NaHCO_3$ and the dioxane removed by evaporation at reduced pressure. The concentrate containing a white solid was diluted with water, acidified to p*H* 3 with dilute HCl, and extracted with chloroform. The chloroform extract was washed with 2% $NaHCO_3$ and water, then dried (Na_2SO_4). The 397 mg of residue remaining after evaporation of solvent was chromatographed on a partition column (200 g diatomaceous earth) prepared from 100 ml of formamide as stationary phase and benzene – petroleum ether (b.p. 60–70°) (1:1) as mobile phase. The fraction emerging between 150–300 ml of effluent, after the holdup volume, yielded on crystallization from diethyl ether, 107 mg of hexanor–cucurbitacin D diacetate, m.p. 200–201°, undepressed when admixed with the diacetate of hexanor–cucurbitacin D isolated from Begonia. The acetates also showed identical i.r., u.v., and n.m.r. spectra, and specific rotation.

This investigation was supported by Public Health Service Research Grant No. CA-08133 from the National Cancer Institute.

1. R. W. Doskotch, M. Y. Malik, and J. L. Beal. Lloydia, **32**, 115 (1969).
2. G. P. Moss. Planta Med. **14** (Suppl.), 86 (1966).
3. D. Lavie and Y. Shvo. J. Amer. Chem. Soc. **82**, 966 (1960).
4. N. D. Cheronis. Micro and semimicro methods. Vol. VI. *In* Technique of organic chemistry. *Edited by* A. Weissberger, Interscience Publishers, Inc., New York, 1954. p. 465.
5. W. Schlegel, A. Melera, and C. R. Noller. J. Org. Chem. **26**, 1206 (1961).

Can. J. Chem. Downloaded from www.nrcresearchpress.com by 210.87.254.40 on 09/05/12
For personal use only.

The permeation of electrolytic hydrogen through lead[1]

IVAN ČADERSKÝ, BANSI L. MUJU, AND FRANK R. SMITH[2]
Chemistry Department, Memorial University of Newfoundland, St. John's, Newfoundland

Received February 12, 1970

Conclusive evidence is reported for the permeation of electrolytic hydrogen through lead. The diffusion coefficient at 25 °C lies between 10^{-7} and 10^{-6} cm^2 s^{-1} while the bulk concentration of dissolved hydrogen is indicated to be 10^{-6} g-atom cm^{-3} at current densities of 10 to 50 mA cm^{-2}.

Canadian Journal of Chemistry, **48**, 1789 (1970)

Smith (1) in 1948 concluded that hydrogen diffusion through lead occurs only at temperatures close to the melting point, the earlier evidence[3] for diffusion of hydrogen produced by electrolysis being considered too slender to accept. More recently Heath (2) and Wahlin and Naumann (3) both failed to observe electrolytic permeation through lead.

Electrolytic permeation currents of 0.5 to 5 μA cm^{-2} have been observed using lead foils cathodized in hydrogen (Matheson prepurified, BASF-BTS catalyst-treated) stirred 1 *M* $HClO_4$ (Reagent Grade, plus 3 × distilled water) at 10 to 100 mA cm^{-2}, on one side and potentiostatted in hydrogen-saturated 0.2 *M* KOH (Reagent Grade, plus 3 × distilled water) at +200 mV vs. a hydrogen electrode, also in 0.2 *M* KOH. Fisher lead (L27, ca. 99% pure) and Goodfellow Metals (99.9% pure) lead gave comparable results when degreased in boiling benzene, chemically polished in 60% $HClO_4$ and washed with 3 × distilled water before use. Cathodic protection currents of 30 μA cm^{-2} applied to the cathode side were without effect on the diffusion side, where background anodic currents were ca. 1 μA cm^{-2}.

Figure 1 shows typical data plotted according to Devanathan and Stachurski (4) with the experimental points lying on reasonably straight lines which for 10 and 25 mA cm^{-2} have the theoretical intercept of $\log_{10} 2$ at $t = 0$. The diffusion coefficients D_H may be calculated from the experimental slopes (4).

An improved method of treating the data is due to McBreen, Nanis, and Beck (5). A theoretical curve for the ratio of flux, J_t, at time t to the steady state flux, J_∞, was derived by Laplace transformation with appropriate boundary conditions. The first-order approximation is

$$[1] \qquad \frac{J_t}{J_\infty} = \frac{2}{\pi^{1/2}} \frac{1}{\tau^{1/2}} e^{-1/4\tau}$$

where τ is the dimensionless parameter Dt/L^2, L being the foil thickness. This curve, plotted in Fig. 2, and the experimental curves should be of identical shape up to $J_t/J_\infty \approx 0.95$, if the boundary conditions are applicable. D is then calculable from the τ and t values appropriate to the chosen value of J_t/J_∞. Experimental curves for 10 and 25 mA cm^{-2} conform to expectations for $J_t/J_\infty > 0.2$, whereas those for ⩾ 50 mA cm^{-2} are anomalous. Calculated diffusion coefficients for atomic hydrogen in 99.9% pure polycrystalline lead at 25 ± 2 °C are given in Table 1.

Agreement is good between the calculated

TABLE 1
Diffusion coefficient for H in lead at 25 °C

	$D_H \times 10^7$ (cm^2 s^{-1})				
		Fig. 2† for J_t/J_∞ =			
$i_{cathodic}$ (mA cm^{-2})	Fig. 1*	0.2	0.3	0.5	0.8
10	1.22	1.16	1.18	1.19	1.22
25	2.9	—	2.78	2.88	2.87
50	4.7	—	—	8.72	6.82

*$L = 0.15$ mm, $D_H = 2.3L^2K/\pi^2$.
†$L = 0.15$ mm, $D_H = \tau L^2/t$.

[1]This research was supported, in part, by the Defence Research Board of Canada, Grant number 5401/09.
[2]To whom correspondence should be addressed.
[3]References 906, 1091, 1092, 1266, 1268, and 1269 cited in ref. 1.

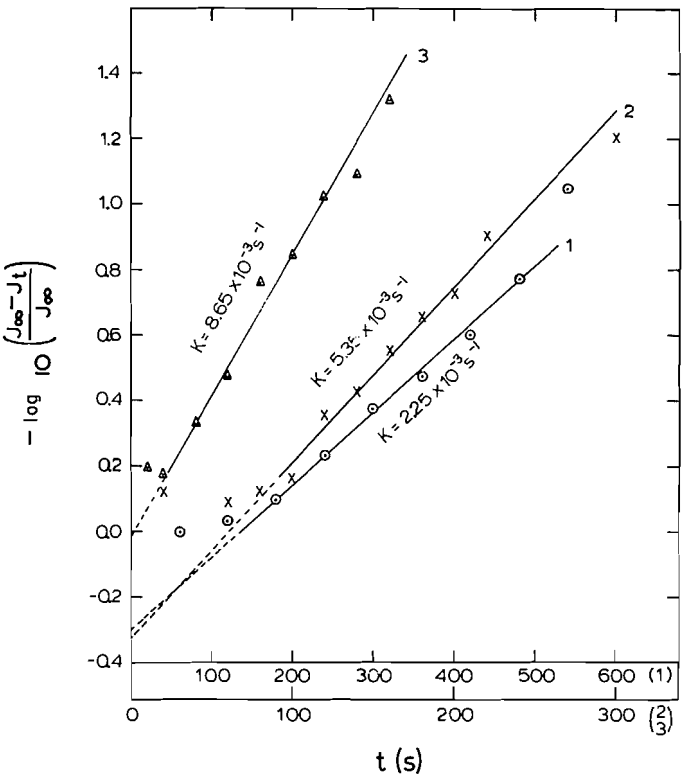

FIG. 1. Successive permeation transients in cathodization at 10 mA cm^{-2} (circles), 25 mA cm^{-2} (crosses), and 50 mA cm^{-2} (triangles), plotted according to Devanathan and Stachurski (4). J_t, J_∞ are anodic current densities (μA cm^{-2}) above background, at time t after application of cathodic current and at steady state, respectively. Transients observed on one foil in order *1*, *2*, *3* with ca. 15 min at 30 μA cm^{-2} between cathodization. K's are best straight line slopes.

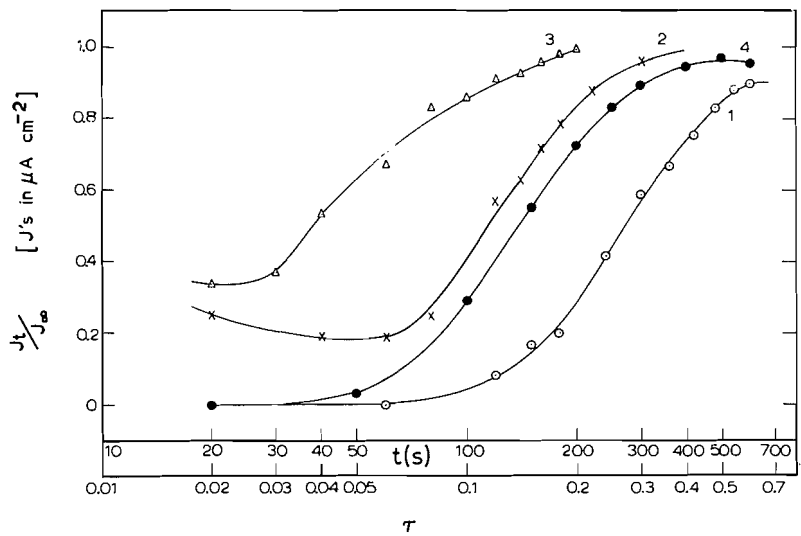

FIG. 2. Rising transients of Fig. 1 treated according to McBreen, Nanis, and Beck (5). J_t and J_∞ as in Fig. 1. Numbers refer to Fig. 1 except *4* which is the theoretical curve of eq. [1].

Can. J. Chem. Downloaded from www.nrcresearchpress.com by 210.87.254.40 on 09/05/12
For personal use only.

values at 10 and 25 mA cm^{-2} but D_H apparently depends on the applied current, presumably because of a dependence on the bulk concentration of hydrogen in the metal (ca. 10^{-6} g-atom cm^{-3}). Gileadi, Fullenwider, and Bockris (6) observed an increasing D_H in successive permeations through platinum. Their suggestion of hydrogen concentrated in regions of strain being less free to diffuse may apply here also. However, the formula $PbH_{0.00002}$ differs by orders of magnitude from Wells and Roberts' $PbH_{0.19}$ achieved by exposure of evaporated lead films to atomic hydrogen (7). Hence the lead is unlikely to have become saturated in the present work.

Thanks are due to the National Research Council of Canada and to the Defence Research Board for their support.

1. D. P. SMITH. Hydrogen in metals, Univ. of Chicago Press. Chicago, Ill. 1948. p. 286.
2. H. R. HEATH. Brit. J. Appl. Phys. **3**, 13 (1952).
3. H. B. WAHLIN and V. O. NAUMANN. J. Appl. Phys. **24**, 42 (1953).
4. M. A. V. DEVANATHAN and Z. O. J. STACHURSKI. Proc. Roy. Soc. London, Ser. A, **270**, 90 (1962).
5. J. MCBREEN, L. NANIS, and W. BECK. J. Electrochem. Soc. **113**, 1218 (1966).
6. E. GILEADI, M. A. FULLENWIDER, and J. O'M. BOCKRIS. J. Electrochem. Soc. **113**, 926 (1966).
7. B. R. WELLS and M. W. ROBERTS. Proc. Chem. Soc. 173 (1964).

Total synthesis of DL-glucose

U. P. SINGH[1] AND R. K. BROWN
Department of Chemistry, University of Alberta, Edmonton, Alberta

Received February 20, 1970

The stereoselective synthesis of DL-glucose has been accomplished in 34% overall yield starting from 1,6:2,3-dianhydro-4-dexoy-β-DL-*ribo*-hexopyranose (**1**), a compound obtainable from the Diels–Alder condensation of acrolein.

Canadian Journal of Chemistry, **48**, 1791 (1970)

The compound 1,6:2,3-dianhydro-4-deoxy-β-DL-*ribo*-hexopyranose (**1**), obtained from acrolein dimer according to published directions (1), was converted into 1,6-anhydro-3,4-dideoxy-β-DL-*erythro*-hex-3-enopyranose (**2**) with *n*-butyllithium at room temperature following the known reaction of oxiranes with the organolithium reagent (2). Treatment of **2** with *m*-chloroperoxybenzoic acid in methylene chloride at room temperature for 24 h gave the expected 1,6:3,4-

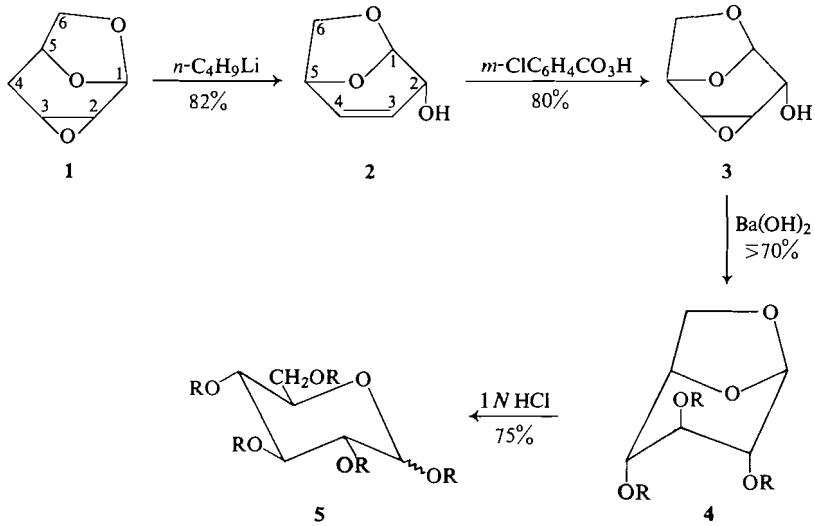

[1]Postdoctoral Fellow 1969–1971.

Can. J. Chem. Downloaded from www.nrcresearchpress.com by 210.87.254.40 on 09/05/12
For personal use only.

values at 10 and 25 mA cm^{-2} but D_H apparently depends on the applied current, presumably because of a dependence on the bulk concentration of hydrogen in the metal (ca. 10^{-6} g-atom cm^{-3}). Gileadi, Fullenwider, and Bockris (6) observed an increasing D_H in successive permeations through platinum. Their suggestion of hydrogen concentrated in regions of strain being less free to diffuse may apply here also. However, the formula $PbH_{0.00002}$ differs by orders of magnitude from Wells and Roberts' $PbH_{0.19}$ achieved by exposure of evaporated lead films to atomic hydrogen (7). Hence the lead is unlikely to have become saturated in the present work.

Thanks are due to the National Research Council of Canada and to the Defence Research Board for their support.

1. D. P. SMITH. Hydrogen in metals, Univ. of Chicago Press. Chicago, Ill. 1948. p. 286.
2. H. R. HEATH. Brit. J. Appl. Phys. **3**, 13 (1952).
3. H. B. WAHLIN and V. O. NAUMANN. J. Appl. Phys. **24**, 42 (1953).
4. M. A. V. DEVANATHAN and Z. O. J. STACHURSKI. Proc. Roy. Soc. London, Ser. A, **270**, 90 (1962).
5. J. MCBREEN, L. NANIS, and W. BECK. J. Electrochem. Soc. **113**, 1218 (1966).
6. E. GILEADI, M. A. FULLENWIDER, and J. O'M. BOCKRIS. J. Electrochem. Soc. **113**, 926 (1966).
7. B. R. WELLS and M. W. ROBERTS. Proc. Chem. Soc. 173 (1964).

Total synthesis of DL-glucose

U. P. SINGH[1] AND R. K. BROWN
Department of Chemistry, University of Alberta, Edmonton, Alberta

Received February 20, 1970

The stereoselective synthesis of DL-glucose has been accomplished in 34% overall yield starting from 1,6:2,3-dianhydro-4-dexoy-β-DL-*ribo*-hexopyranose (**1**), a compound obtainable from the Diels–Alder condensation of acrolein.

Canadian Journal of Chemistry, **48**, 1791 (1970)

The compound 1,6:2,3-dianhydro-4-deoxy-β-DL-*ribo*-hexopyranose (**1**), obtained from acrolein dimer according to published directions (1), was converted into 1,6-anhydro-3,4-dideoxy-β-DL-*erythro*-hex-3-enopyranose (**2**) with *n*-butyllithium at room temperature following the known reaction of oxiranes with the organolithium reagent (2). Treatment of **2** with *m*-chloroperoxybenzoic acid in methylene chloride at room temperature for 24 h gave the expected 1,6:3,4-

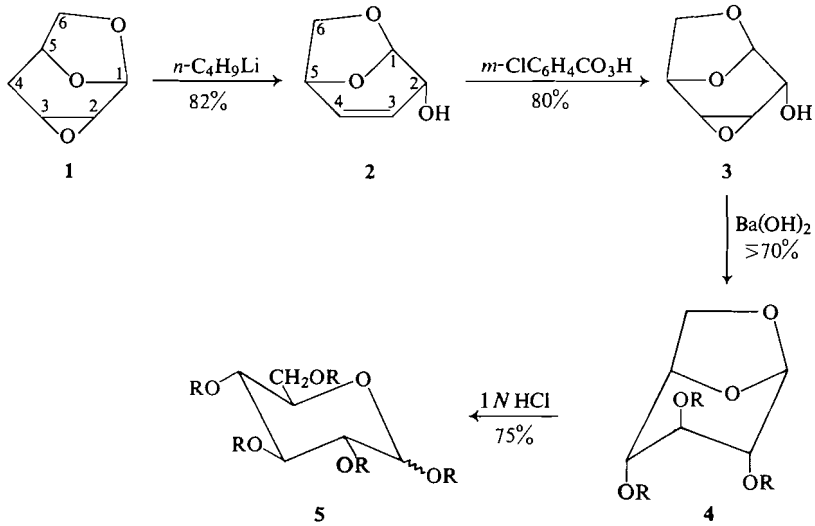

[1]Postdoctoral Fellow 1969–1971.

Can. J. Chem. Downloaded from www.nrcresearchpress.com by 210.87.254.42 on 09/05/12
For personal use only.

dianhydro - β - DL - *allo* - hexopyranose (**3**). The reaction with 10% aqueous barium hydroxide at 80° for 16 h under nitrogen (3) converted **3** into 1,6 - anhydro - β - DL - *gluco* - hexopyranose (**4**, R = H), which yielded the triacetate **4** (R = CH_3CO) with pyridine and acetic anhydride. Hydrolysis of **4** (R = H) with 1 *N* aqueous hydrochloric acid gave α,β-DL-glucose (**5**, R = H) as a solid which shrinks at 44° but melts at 113–115°.[2] Acetic anhydride and pyridine converted **5** (R = H) into its pentacetate **5** (R = CH_3CO) which was an approximately 1:1 mixture of the α and β anomers.

Elemental analyses all agreed very well with the calculated values. The infrared (i.r.) and proton magnetic resonance (p.m.r.) spectra of all of these compounds supported the assigned structures. Furthermore the i.r. and p.m.r. spectra of compounds **4** (R = CH_3CO) and **5** (R = H and CH_3CO) were identical with those of authentic 2,3,4-tri-*O*-acetyl-1,6-anhydro-β-D-glucopyranose, α,β-D-glucose, and α,β-D-glucose pentacetate respectively.

We wish to thank the National Research Council of Canada for the financial support which permitted the pursuit of this work.

1. F. SWEET and R. K. BROWN. Can. J. Chem. **46**, 2289 (1968).
2. H. NOZAKI, T. MORI, and R. NOYORI. Tetrahedron, **22**, 1207 (1966).
3. G. CHARALAMBOUS and E. PERCIVAL. J. Chem. Soc. 2443 (1954).
4. M. L. WOLFROM and B. H. WOOD. J. Amer. Chem. Soc. **71**, 3175 (1949).

[2]Reference 4 reports the melting point of a 1:1 mixture of D- and L-glucose as 112–113.5°.

Can. J. Chem. Downloaded from www.nrcresearchpress.com by 210.87.254.42 on 09/05/12
For personal use only.

Can. J. Chem. Downloaded from www.nrcresearchpress.com by 210.87.254.5 on 09/05/12
For personal use only.

Canadian Journal of Chemistry

Published by THE NATIONAL RESEARCH COUNCIL OF CANADA

VOLUME 48 JUNE 15, 1970 NUMBER 12

Transient-phase studies of a trypsin-catalyzed reaction

H. P. KASSERRA[1] AND K. J. LAIDLER

Department of Chemistry, University of Ottawa, Ottawa, Canada

Received November 6, 1969

The stopped-flow technique has been used to study the pre-steady-state kinetics of the hydrolysis of *N*-carbobenzoxy-L-alanine-*p*-nitrophenyl ester catalyzed by trypsin. By working under conditions such that the enzyme concentration is much greater than that of the substrate, it has been possible to measure $\tilde{k}_2$, the rate constant for the conversion of the enzyme-substrate complex into the acyl enzyme. The p*H* dependence of $\tilde{k}_2$ reveals a pK_b' value of 6.9 for the conversion of complex into acyl enzyme, in agreement with deductions from steady-state investigations. The p*H* dependence of $\tilde{K}^*$ (equal to $(k_{-1} + k_2)/k_1$) has also been determined. The results provide direct evidence for the existence of an enzyme-substrate complex for this reaction.

The work has been done in various mixtures of water and isopropyl alcohol. The logarithms of the rate constants $\tilde{k}_2$ and $\tilde{k}_2/\tilde{K}^*$ vary linearly with $1/D$, showing a decrease with increasing alcohol concentration; $\tilde{K}^*$ increases with alcohol concentration. The solvent results suggest that addition of alcohol affects the hydrophobic bonding in the protein and leads to unfolding of the enzyme.

Canadian Journal of Chemistry, 48, 1793 (1970)

Introduction

Previous work in this laboratory has been concerned with the steady-state kinetics of reactions catalyzed by chymotrypsin (1, 2) and trypsin (3, 4). The present paper describes a study, using the stopped-flow technique, of the pre-steady-state kinetics of the hydrolysis of *N*-carbobenzoxy-L-alanine-*p*-nitrophenyl ester (CANE) catalyzed by trypsin. The work has been done over a range of p*H* values and in various mixtures of isopropyl alcohol and water.

There have been several previous investigations of the transient (pre-steady-state) phase of reactions catalyzed by proteolytic enzymes. Hartley and Kilby (5, 6) studied the hydrolysis of *p*-nitrophenyl acetate by chymotrypsin, and demonstrated for the first time that the mechanism involves three distinct steps

$$E + S \underset{k_{-1}}{\overset{k_1}{\rightleftharpoons}} ES \xrightarrow[P_1]{k_2} ES' \xrightarrow{k_3} E + P_2$$

Later Gutfreund and Sturtevant (7) obtained a value for the rate constant k_1 for the very rapid combination of enzyme and substrate. Step 2 in the above scheme is a rapid liberation of *p*-nitrophenol (P_1), and step 3 is a slow, zero-order, release of acetate ions. Further, more detailed, transient-phase studies of this reaction have been made (8–11) and it has been concluded that the acylation rate constant k_2 is p*H* dependent with a p*K* value of approximately 6.8.

Transient-phase studies on trypsin have been carried out by Stewart and Ouellet (12) who used *p*-nitrophenyl acetate as substrate, and by Bender *et al.* (13) who used the specific substrate α-*N*-carbobenzoxy-L-lysine-*p*-nitrophenyl ester hydrochloride. The former workers concluded that the acylation rate constant k_2 was p*H* independent, in contrast to the situation with chymotrypsin. A value of k_2 at one p*H* (2.66) was obtained by Bender *et al.* (13); however, a p*H* study is difficult to carry out by conventional stopped-flow techniques, because of the high values of the acylation rates with the amino-acid substrates. One of the objectives of the present studies was the elucidation of the p*H*-dependence of acylation in the case of an amino-acid substrate.

Another object of the present work was to verify the reaction order of the acylation process and to obtain direct evidence for a Michaelis

[1]Present address: Central Research Laboratory, DuPont of Canada Ltd., Kingston, Ontario.

Can. J. Chem. Downloaded from www.nrcresearchpress.com by 210.87.254.5 on 09/05/12
For personal use only.

complex. Faller and Sturtevant (14) and Milstein and Fife (15) reported that the acylation of α-chymotrypsin by *p*-nitrophenyl esters followed simple second-order rather than Michaelis–Menten kinetics; i.e., no evidence was obtained for a Michaelis complex. However, as was appreciated by these workers, earlier investigators had analyzed their results on the basis of a pre-steady-state treatment for the case of high substrate concentrations, and in order for the treatment to be applied to the data the following conditions had to be satisfied: (*a*) deacylation is rate-limiting ($k_2 \gg k_3$); (*b*) the substrate concentration is much greater than $(k_{-1} + k_2)/k_1$; this ratio will be referred to as K^*. Condition (*a*) was satisfied, but not (*b*). This second condition is difficult to realize, since the ordinary Michaelis constant, K_m, applicable to steady-state conditions, is large for these systems. The steady-state solution for this mechanism is

$$[1] \qquad v = \frac{\frac{k_2k_3}{k_2 + k_3}[E]_0[S]}{\frac{k_{-1} + k_2}{k_1} \cdot \frac{k_3}{k_2 + k_3} + [S]}$$

and

$$[2] \qquad K_m = \frac{k_{-1} + k_2}{k_1} \cdot \frac{k_3}{k_2 + k_3} = K^* \frac{k_3}{k_2 + k_3}$$

Since for these systems $k_2 \gg k_3$, K^* greatly exceeds K_m, which is large, so that it is virtually impossible to work at substrate concentrations greater than K^*. Failure to meet condition (*b*) means that the Michaelis complex ES becomes experimentally undetectable, so that the acylation is strictly second order. On the other hand, Kédzy and Bender (10) have worked at high enzyme concentrations with *p*-nitrophenyl acetate and have obtained Michaelis–Menten kinetics with a K^* of $\sim 10^{-3}$ *M*.

It is shown in the next section that if the enzyme concentration is in excess of that of the substrate the value of k_2 can be obtained directly without any conditions having to be satisfied. The present stopped-flow studies were therefore made under these conditions.

Transient-Phase Theory for Excess Enzyme Concentration

Treatments of the theory of pre-steady-state kinetics have been given by Laidler (16), Ouellet and Laidler (17), Gutfreund (18), Gutfreund and Sturtevant (8), Ouellet and Stewart (19), Peller and Alberty (20), and Darvey (21). The present treatment is confined to developing the equations relevant to excess enzyme concentration.

If, for the scheme given above, e_0 is the total enzyme concentration, s_0 the total substrate concentration, and y_1, y_2, p_1, and p_2 are the concentrations of ES, ES′, P_1, and P_2 at time t, the concentrations of free enzyme and substrate at time t are

$$[3] \qquad e = e_0 - y_1 - y_2$$

$$[4] \qquad s = s_0 - y_1 - y_2 - p_2$$

When $e_0 \gg s_0$ the concentration of free enzyme, e, is close to e_0 and we may write the following differential equations

$$[5] \qquad \dot{y}_1 = k_1e_0(s_0 - y_1 - y_2 - p_2) - y_1(k_{-1} + k_2)$$

$$[6] \qquad \dot{y}_2 = k_2y_1 - k_3y_2$$

$$[7] \qquad \dot{p}_1 = k_2y_1$$

$$[8] \qquad \dot{p}_2 = k_3y_2$$

Differentiation of eq. [5] and elimination of $\dot{y}_2$ and $\dot{p}_2$ by use of eqs. [6] and [8] leads to

$$[9] \qquad \ddot{y}_1 + P\dot{y}_1 + Qy_1 = 0$$

where

$$[10] \qquad P = k_1(e_0 + K^*)$$

$$[11] \qquad Q = k_1k_2e_0$$

$$[12] \qquad K^* = (k_{-1} + k_2)/k_1$$

The general solution of eq. [9] is, if the roots are real,

$$[13] \qquad y_1 = Me^{Ft} + Ne^{Gt}$$

where F and G are given by

$$[14] \qquad F = \tfrac{1}{2}[-P + (P^2 - 4Q)^{1/2}] \approx -Q/P$$

$$[15] \qquad G = \tfrac{1}{2}[-P - (P^2 - 4Q)]^{1/2} \approx Q/P - P$$

The boundary conditions $t = 0$, $y_1 = 0$ lead to

$$[16] \qquad M = -N = k_1e_0s_0/(F - G)$$

Substitution of eq. [13] into eq. [7], and integration with the boundary condition that at $t = 0$, $p_1 = 0$, gives

Can. J. Chem. Downloaded from www.nrcresearchpress.com by 210.87.254.5 on 09/05/12
For personal use only.

$$[17] \quad p_1 = \frac{k_2M}{F}(e^{Ft} - 1) + \frac{k_2N}{G}(e^{Gt} - 1)$$

When t is sufficiently large this equation reduces to

$$[18] \quad p_1 = -(k_2M/F) - (k_2N/G)$$

Equations [17] and [18] show that for a system in which the enzyme concentration is in excess, and therefore constant, the steady state is never established, p_1 exponentially approaching a constant value at large t.

A schematic plot of the function represented by eq. [17] is shown in Fig. 1. The initial exponential rise is due to the term $(k_2N/G)(e^{Gt} - 1)$, and is followed by an exponential fall-off to zero rate due to the term $(k_2M/F)(e^{Ft} - 1)$. The individual behavior of the two terms is also shown in Fig. 1. Their relative magnitudes depend on the relative magnitudes of F and G. As all the quantities involved are positive, G will usually be larger than F, and e^{Gt} will approach zero more rapidly than e^{Ft}, while the coefficient of e^{Gt} will be smaller than the coefficient of e^{Ft}. This condition suggests that experimentally the e^{Ft} term will be easier to detect than the e^{Gt} term.

Extrapolation of the portion of the curve in Fig. 1 which is due to the term in F (cf. eq. [17]) to the time axis yields a quantity τ which may be conveniently referred to as the induction period

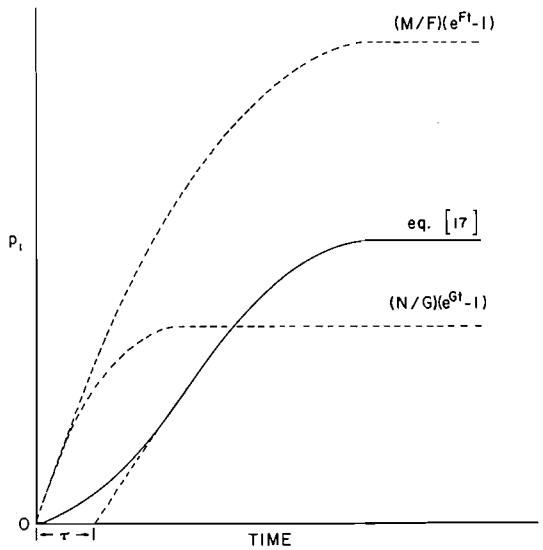

FIG. 1. Schematic plot of the rate of formation of product P_1 according to eq. [17]. The dashed curves show the variations of the functions shown.

of the reaction. For a certain period of time $e^{Gt} \approx 0$ while e^{Ft} is not. A Maclaurin series expansion of e^{Ft}, using the first two terms only (since t is small at the beginning of the reaction), reduces eq. [17] to

$$[19] \quad p_1 = k_2Mt - k_2N/G$$

When $p_1 = 0$, substitution for the value of G yields the expression

$$[20] \quad \tau = \frac{1}{k_1(e_0 + K^*)}$$

This expression for the induction period is the same as that for the system involving a single intermediate (16–18) with e_0 replacing s_0. Thus, provided that τ is measurable, the rate constant k_1 (and k_{-1} if k_2 is known) for the reversible formation of the Michaelis complex can be determined. However, in those cases where the three-step mechanism could apply, the induction period appears to be immeasurably small (7, 22). This result implies that the term e^{Gt} is negligibly small even at the beginning of the reaction.

Substitution of the appropriate values of P and Q into eqs. [14] and [15] gives

$$[21] \quad F = -k_2e_0/(e_0 + K^*)$$

$$[22] \quad G = -k_1(e_0 + K^*)$$

Together with the values for M and N from eq. [16], eq. [17] becomes

$$[23] \quad p_1 = \frac{s_0}{\frac{k_2e_0}{k_1(e_0 + K^*)^2} - 1}(e^{Ft} - 1) + \frac{s_0}{\frac{k_1(e_0 + K^*)^2}{k_2e_0} - 1}(e^{Gt} - 1)$$

It is reasonable to assume that $k_1 \gg k_2$, and for the condition that e_0 is very large, since e^{Gt} approaches zero very rapidly, eq. [23] reduces to

$$[24] \quad p_1 = s_0(1 - e^{Ft})$$

where F is defined by eq. [21]. If therefore p_1 or a physical property proportional to p_1 can be measured, k_2 and K^* can be evaluated from the values of $k_2e_0/(e_0 + K^*)$ at different concentrations of enzyme.

At the beginning of the reaction, the series development of the exponential term in eq. [24] would give a good approximation of the function.

The initial rate of production of the product p_1 is then described by

$$[25] \qquad p_1 = -Fs_0t = \frac{k_2e_0}{e_0 + K^*} s_0t$$

and approximate values of k_2 and K^* can be obtained from initial rate data.

Experimental

Materials

N-Carbobenzoxy-L-alanine-*p*-nitrophenyl ester (Lot No. K-5538-R) was purchased from Cyclo Chemical Corporation and recrystallized from ethyl acetate – hexane, twice in the presence of charcoal and once without, with slight warming. The product was stored dry and frozen, since it tends to decompose on standing. Trypsin (twice crystallized, salt-free, Lot No. TRL 8CA) was obtained from Worthington Biochemical Corporation and used without further purification.

Sodium phosphate buffer solutions were prepared with "Baker Analyzed" Reagent Grade materials. Isopropyl alcohol (Fisher Certified A.C.S. Spectranalyzed) was dried and stored over Linde molecular sieve previously reactivated by heating at 350 °C for several hours. Water was doubly distilled, deionized, and freed of carbon dioxide.

Stopped-Flow Spectrophotometer

The pre-steady-state rates of hydrolysis of *N*-carbobenzoxy-L-alanine-*p*-nitrophenyl ester (CANE) were measured with a Durrum-Gibson Stopped-Flow Spectrophotometer manufactured by the Durrum Instrument Corporation, Palo Alto, California.

Equal volumes of substrate in 2-propanol – water solution and enzyme in an appropriate buffer solution are hydraulically forced through the mixing jet into the cuvette and hence into the stop syringe. Just before the plunger hits a mechanical stop, it makes contact with a trigger switch which actuates the horizontal time-basis sweep for the oscilloscope display. Since the flow of sample is stopped immediately after mixing, the reaction in the cuvette takes place with a minimum of interference caused by turbulence or flow artifacts. The monochromatic light obtained from the monochromator passes through the mixed solution in the cuvette and the resultant variation in light intensity is sensed by the photomultiplier tube. The photomultiplier output, proportional to the instantaneous light intensity transmitted by the reacting solution, is applied to the vertical axis of the oscilloscope. The display on the storage oscilloscope, which indicates percentage transmittance vs. time, in general started just before the reaction began and ended according to a preselected time-base setting. All measurements were made at 400 mμ. The reaction system was maintained at 25.0 ± 0.1 °C by means of a thermostatically controlled water bath.

Kinetic Procedure

Stock solutions of CANE were made up in dry isopropyl alcohol and were stored in sealed bottles in the refrigerator. Just before use the alcohol solution was diluted with gas-free water to a final concentration of 1.0×10^{-5} *M* substrate in 1–20% (v/v) isopropyl alcohol as required. Dilution had to be done slowly and with cooling to avoid aeration of the solution caused by the evolution of heat during mixing. A fresh stock solution of trypsin in 0.1 *M* phosphate buffer was prepared every day. The enzyme solution was first centrifuged for 30 min at 7000 r.p.m. in a Sorvall Superspeed RC2-B refrigerated centrifuge to remove water-insoluble impurities. Protein concentrations were determined with a Perkin Elmer Model 350 Spectrophotometer at 280 mμ using a value of 14.4 for the extinction coefficient (23). The solution was then diluted with the appropriate buffer to give dilutions ranging in concentration from 0.14 to 1.4×10^{-3} *M* enzyme. The p*H* of the trypsin solution was measured to ± 0.05 units at the beginning and end of each series of runs and was found to remain constant for that period of time.

Prior to a typical series of runs, the oscilloscope was calibrated for 100% transmittance with substrate solution and the appropriate buffer solution in the drive syringes. The calibration was repeated for different settings of amplifier gain and zero offset to give a satisfactory record of the reaction to be studied. For this purpose the zero-offset circuit of the Durrum–Gibson Spectrophotometer was modified to include a calibrated ten-turn potentiometer. The buffer solution was then replaced by enzyme solution buffered to the same p*H*, and approximately 0.15 ml each of enzyme and substrate solution were injected into the cuvette. At least 10 min of thermostatting time was allowed each time after the drive syringes had been filled with reactants.

After four of five traces reflecting the rate of hydrolysis of CANE had been reproduced on the oscilloscope screen, a polaroid photograph of the stored display was taken. Runs lasted from 0.5 to 5 s. An oscilloscope photograph from a typical experimental run is shown in Fig. 2.

Analysis of Results

Attempts were made initially to analyze the results using the Guggenheim method (24, 25) but this proved unsatisfactory; the matter is further considered in the Appendix. In view of this, the parameter F in eq. [23] was obtained by a least-squares method, as follows.

If the Lambert–Beer law applies (see below) the product concentration p_1 is related to absorbance A by

$$[26] \qquad A = \varepsilon p_1 l$$

where ε is the molar extinction coefficient and l the thickness of the absorbing medium. Together with eq. [24] this gives

$$[27] \qquad A = \varepsilon s_0 l(1 - e^{Ft})$$

However, base-line instability and electrical drift of the stopped-flow equipment used in this study made it necessary to introduce a correction factor ΔA into eq. [27], which becomes

$$[28] \qquad A - \Delta A = Q(1 - e^{Ft})$$

or

$$[29] \qquad \ln\left(1 - \frac{A - \Delta A}{Q}\right) = Ft$$

Can. J. Chem. Downloaded from www.nrcresearchpress.com by 210.87.254.5 on 09/05/12
For personal use only.

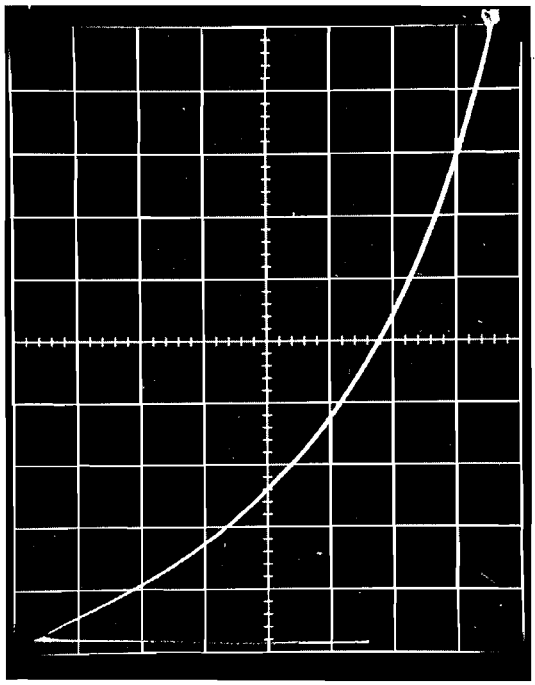

FIG. 2. Typical oscilloscope trace for the trypsin-catalyzed hydrolysis of CANE. Vertical scale: 50–100% transmittance; horizontal scale: 0.5 s/division; time constant: 5 ms.

If the logarithmic term is expressed as B, then

$$[30] \quad \Sigma = \text{sum of (deviations)}^2 = \Sigma(B - Ft)^2$$

Differentiation gives

$$[31] \quad \delta\Sigma/\delta F = \Sigma[-2t(B - Ft)]$$

To satisfy the condition that $\Sigma (B - Ft)^2$ is minimized, eq. [31] is put equal to zero and solved for F, which gives

$$[32] \quad F = \Sigma Bt/\Sigma t^2$$

The restrictions on eq. [29] are that ΔA cannot be larger than the smallest value of A and that Q must be larger than the largest value of $(A - \Delta A)$.

A digital computer program involving multiple iterations with given values of Q and ΔA was written to calculate the best value of F by the method of least squares. It should be noted that two minima in $\Sigma (B - Ft)^2$ exist: (*i*) the desired minimum square deviation for finite values of Q and F, and (*ii*) a trivial solution under the conditions that $A = \infty$ and $F = 0$.

Since the analysis of results depends on the fact that the Lambert–Beer law is obeyed over the full range of product concentrations at all pH values, the relationship was tested directly. Linearity between absorbance and concentration of *p*-nitrophenol existed up to an optical density of 2.0. In this work the highest measured optical densities did not exceed 0.1. The least-squares-fit method does not require conversion of the experimentally measured absorbance data to concentrations of product. It is therefore not necessary to take account of the fact that, over the pH range studied, the product exists partially as *p*-nitrophenol and partially as *p*-nitrophenoxide ion. At 400 mμ the extinction coefficients of these two species are 81.4 and 18 330, respectively.

Input data for the least-squares-fit computer program were obtained from enlargements of the oscilloscope pictures in arbitrary units of transmittance and time. The program was written in Fortran IV for the IBM 360/65 computer. In general an approximate fit for F was first obtained by using intervals of 0.001 and 0.0001 between successive values of Q and ΔA in the iteration procedure. This was followed by a final fit with appropriately smaller intervals for Q and ΔA. The program includes a modification which selects and prints out for every value of Q only those values of ΔA and F which give a minimum in $\Sigma (B - Ft)^2$. The "best" values of Q, ΔA, and F were then chosen from the computer print-out on the basis of the lowest minimum square deviation.

Details of the least-squares-fit computer program will gladly be provided by H.P.K.

Results

*p*H Dependence of the Acylation Process

Typical curves for the pre-steady-state rate of production of product P_1 in terms of rate of change of absorbance are shown in Fig. 3. Only one-half of the 18 experimental points usually

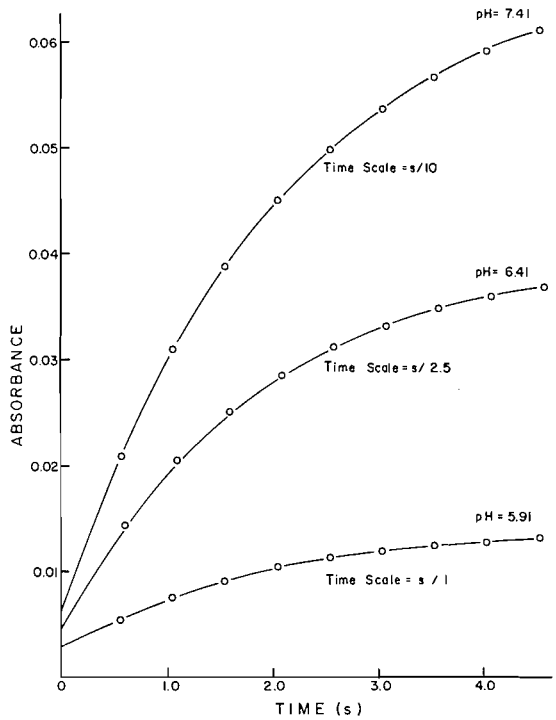

FIG. 3. Experimental curves showing change of absorbance with time for the pre-steady-state hydrolysis of CANE catalyzed by trypsin at high enzyme concentration.

Can. J. Chem. Downloaded from www.nrcresearchpress.com by 210.87.254.5 on 09/05/12
For personal use only.

Can. J. Chem. Downloaded from www.nrcresearchpress.com by 210.87.254.5 on 09/05/12
For personal use only.

TABLE 1

Pre-steady-state data for the trypsin-catalyzed hydrolysis of CANE in 1% (v/v) isopropyl alcohol and 0.05 *M* phosphate buffer at 25.0 °C and $s_0 = 1 \times 10^{-5}$ *M*

$[E] \times 10^4$ (*M*)	Values of F (s^{-1})		
	p*H* = 5.91	p*H* = 6.41	p*H* = 7.41
0.70	0.286	0.705	2.45
0.91	0.367	0.816	2.95
1.19	0.399	0.910	3.13
1.75	0.483	1.10	3.82
3.15	0.543	1.34	4.50
4.90	—	1.48	4.90
7.00	0.678	1.59	5.66

used for the computer fit have been plotted. The intercept on the absorbance axis is equal to the "best" value of ΔA obtained from the least-squares-fit analysis for F. The value of ΔA can safely be assumed to be constant for the duration of an experimental run and therefore does not contribute to any absolute error in F. It does, however, contribute to the precision in fitting F, since it represents a third parameter in eq. [28], which describes the exponential variation of absorbance with time.

The p*H*-dependent constants $\tilde{K}^*$ and $\tilde{k}_2$ corresponding to the formation of the Michaelis complex and the acyl enzyme have been evaluated from Lineweaver–Burk plots (26) of the computer-fitted results for F as a function of enzyme concentration. In Table 1, three representative sets of results for the transient phase of the tryptic hydrolysis of CANE are reported at different p*H* values.[2] These data are plotted in Fig. 4. For this as for all other linear plots in this study the intercepts and slopes have been obtained by a least-squares fit. The values of $\tilde{k}_2$ and $\tilde{K}^*$ obtained in this way from the Lineweaver–Burk plots are given in Table 2. The kinetic parameters are average values based on three runs covering the full range of enzyme concentrations. The p*H* dependencies of these parameters are shown in Figs. 5 and 6.

The curve in Fig. 5 is the theoretical curve

TABLE 2

Kinetic parameters for the trypsin-catalyzed hydrolysis of CANE in 1% (v/v) isopropyl alcohol and 0.05 *M* phosphate buffer at 25.0 °C

p*H*	$\tilde{k}_2$ (s^{-1})	$\tilde{K}^* \times 10^4$ (*M*)
5.91	0.698	0.976
6.08	1.12	1.17
6.41	1.81	1.10
6.62	2.30	1.07
6.90	3.55	1.19
7.10	4.88	1.48
7.41	5.76	1.00
		Mean value = 1.14 ± 0.12

[2]The values of F, $\tilde{k}_2$, and $\tilde{K}^*$ given in the tables are based on the assumption that the enzyme is 100% pure. Studies at high substrate concentrations suggest that it is in fact about 80% pure.

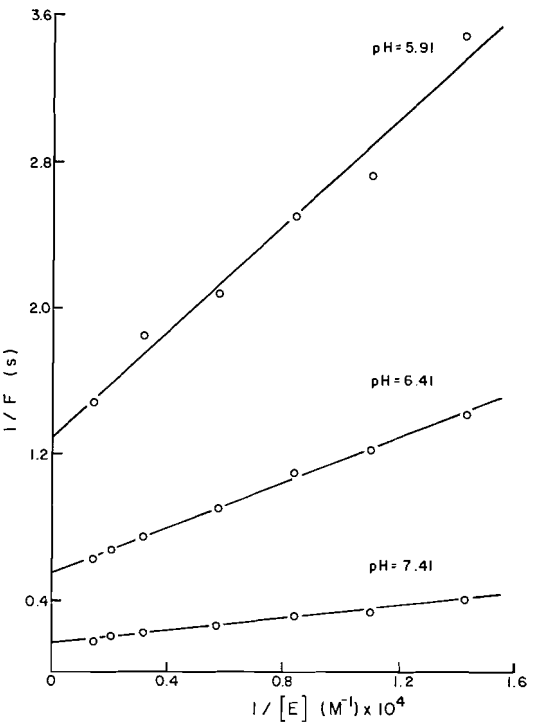

FIG. 4. Lineweaver–Burk plots for the pre-steady-state hydrolysis of CANE catalyzed by trypsin at high enzyme concentration.

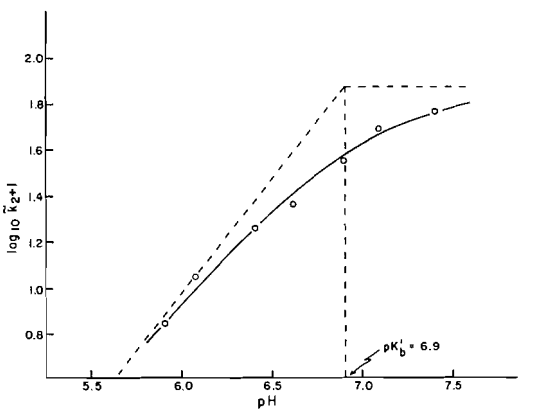

FIG. 5. Variation of $\log_{10} \tilde{k}_2$ with p*H* for the pre-steady-state hydrolysis of CANE in 0.05 *M* phosphate buffer at 25.0 °C.

TABLE 3

Kinetic parameters for the trypsin-catalyzed hydrolysis of CANE in 0.05 M phosphate buffer at 25.0 °C and pH 6.90

[2-Propanol] (%)	[2-Propanol] (M)	Dielectric constant D	$\tilde{k}_2$ (s^{-1})	$\tilde{K}^* \times 10^4$ (M)	$\tilde{k}_2/\tilde{K}^*$ ($M^{-1}\ s^{-1}$)
1	0.130	77.8	3.55	1.19	29 800
8	1.04	72.8	2.40	1.37	17 500
15	1.95	67.7	1.59	1.65	9 600
20	2.60	64.1	1.16	2.13	5 400
Extrapolated for water		78.5	3.66	1.14	32 300

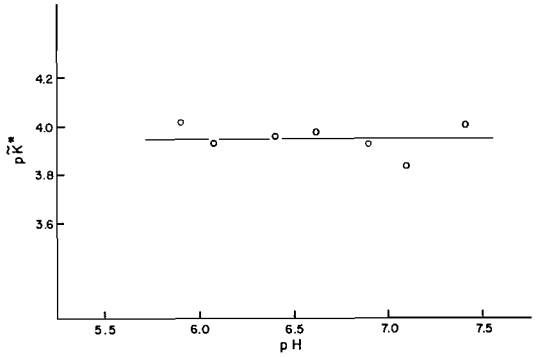

FIG. 6. Variation of p$\tilde{K}^*$ with pH for the hydrolysis of CANE in 0.05 M phosphate buffer at 25.0 °C.

obtained by a reiterative process which gives the closest fit to the experimental points. It corresponds to the equation

$$[33] \qquad \tilde{k}_2 = \frac{k_2}{1 + \frac{[H]}{K_b'}}$$

with $k_2 = 7.5\ s^{-1}$ and p$K_b' = 6.9$. The shape of the $\log_{10}\ \tilde{k}_2$–pH curve in Fig. 5 suggests the participation of a single basic group in the process of acylation, with p$K_b' = 6.9$. The same conclusion was drawn on the basis of the steady-state studies on the trypsin-catalyzed hydrolysis of *N*-benzoyl-L-alanine methyl ester, as described in a previous publication (3).

The constant $\tilde{K}^*$ is shown in Fig. 6 to be constant over the pH range studied, with an average value of $1.14 \times 10^{-4}\ M$. It appears therefore that both k_1 and k_{-1} are pH-dependent quantities in this region; they are, however, too large to be measured by the stopped-flow technique.

Solvent Effects

Table 3 shows the results obtained in the various solvent mixtures; the dielectric constants are taken from Åkerlöf (27).

Discussion

The present results demonstrate without any doubt that the acylation process shows Michaelis–Menten kinetics and not second-order kinetics, and therefore provides direct evidence for the enzyme-substrate complex. As has been noted in the Introduction, Faller and Sturtevant (14) observed second-order kinetics for the acylation process. This result can now be attributed to the fact that condition (*b*), referred to above, could not be satisfied in the studies using excess of substrate. This difficulty has been avoided in the present work with enzyme in excess.

The acylation rates with specific ester substrates of trypsin are so high that they cannot be directly measured by stopped-flow methods at optimum pH values. Although not a specific substrate, since it lacks a positive center on the side chain, CANE is more like a specific substrate than *p*-nitrophenyl acetate, its acylating group resembling that of a specific substrate.

The variation of the acylation rate constant $\tilde{k}_2$ with pH (Fig. 5) demonstrates an ionizing group of p$K \sim 6.9$. This result agrees with the conclusions from the steady-state studies (3). The group involved is undoubtedly the imidazole ring of histidine-46, as we have discussed in a previous paper (4); acylation requires the imidazole residue to be unprotonated. Similar conclusions have been drawn for the acylation of α-chymotrypsin by *p*-nitrophenyl acetate (10, 11).

The present result is, however, at variance with that of Stewart and Ouellet (12) for the trypsin-catalyzed hydrolysis of *p*-nitrophenyl acetate, which suggests an apparent pH independence of $\tilde{k}_2$. However, under the experimental conditions of these authors condition (*b*) was not satisfied.

The present work shows that pK_m is pH independent (Fig. 6) over the range from 5.9 to

Can. J. Chem. Downloaded from www.nrcresearchpress.com by 210.87.254.5 on 09/05/12
For personal use only.

Can. J. Chem. Downloaded from www.nrcresearchpress.com by 210.87.254.5 on 09/05/12
For personal use only.

7.4. This agrees with the conclusion of other workers (10, 11) for trypsin and *N*-benzoyl-L-argininamide. The present results for $\tilde{k}_2$ and $\tilde{K}^*$ require that the pH profile of $\log_{10} \tilde{k}_2/\tilde{K}^*$ would reveal the pK of a basic group (p$K_b \sim 6.9$) which is free to ionize in the free enzyme. Complex formation between trypsin and CANE is therefore unaffected by the protonation of histidine-46 in the free enzyme. This result is again consistent with the steady-state studies (3, 4).

Solvent Effects

It is to be seen from Table 3 that $\tilde{k}_2/\tilde{K}^*$, relating to complex formation, and $\tilde{k}_2$, relating to acylation, both decrease with increasing alcohol concentration. On the other hand $\tilde{K}^*$ increases with increasing alcohol concentration. Faller and Sturtevant (14) noted a similar effect on $\tilde{k}_2/\tilde{K}^*$ for the chymotrypsin-catalyzed hydrolysis of *p*-nitrophenyl acetate.

Plots of the logarithms of these rate parameters against $1/D$ are shown in Figs. 7 to 9 to be essentially linear. Extrapolation of the lines gives a good estimate of the rate constants in pure water, which cannot be obtained directly because of the low solubility of the substrate. These pure-water rate constants are included in Table 3.

It is also possible to regard solvent effects as due to inhibition or activation (see, for example, refs. 14, 28, and 29). However, the kinetic parameters obtained in the present work did not yield straight lines when their reciprocals were plotted

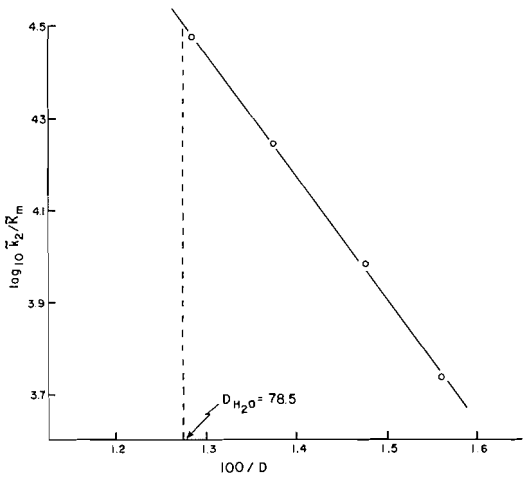

FIG. 7. Variation of $\log_{10} \tilde{k}_2/\tilde{K}^*$ with the reciprocal of the dielectric constant of isopropyl alcohol – water mixtures at pH 6.90 and 25.0 °C.

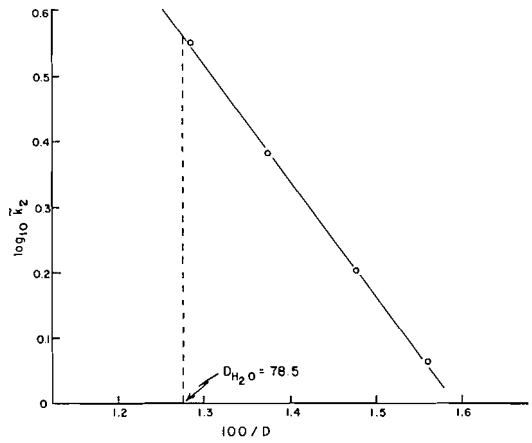

FIG. 8. Variation of $\log_{10} \tilde{k}_2$ with the reciprocal of the dielectric constant of isopropyl alcohol – water mixtures at pH 6.90 and 25.0 °C.

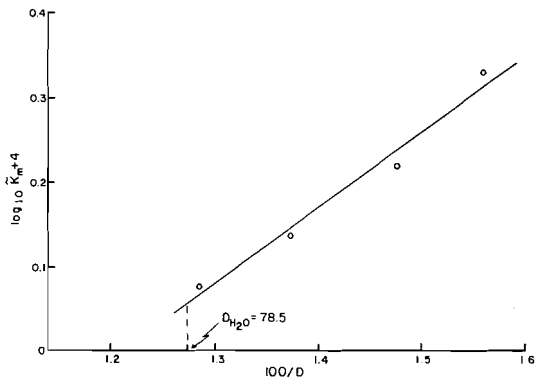

FIG. 9. Variation of $\log_{10} \tilde{K}^*$ with the reciprocal of the dielectric constant of isopropyl alcohol – water mixtures at pH 6.90 and 25.0 °C.

against alcohol concentration, according to Dixon's method (30). On the other hand, plots of the reciprocal rate constants varied quite linearly with the square of the alcohol concentration. Faller and Sturtevant (14) obtained a linear relationship by plotting $(\tilde{K}^*/\tilde{k}_2)^{1/2}$ against alcohol concentration, and suggested an explanation in terms of inhibition by alcohol at two identical but independent sites on the enzyme. However, we prefer to believe that these relationships are fortuitious, and that a more satisfactory explanation for the effects is to be found in terms of the conformation of the enzyme molecule.

Present evidence on the conformations of protein molecules in non-aqueous solvents (31, 32) suggests that three interdependent factors determine protein conformations: (*i*) electro-

Can. J. Chem. Downloaded from www.nrcresearchpress.com by 210.87.254.5 on 09/05/12
For personal use only.

static interactions, (*ii*) hydrogen bonds between peptide linkages, and (*iii*) hydrophobic interactions. In addition, conformational entropy changes may contribute to the total free energy of the protein in solution.

A very simple view of the electrostatic interactions is provided by considering the protein molecule as a sphere of radius r and net charge Ze. According to Debye–Hückel theory its electrostatic free energy is equal to

$$[34] \qquad F_{e.s.} = \frac{Z^2e^2}{2D}\left(\frac{1}{r} - \frac{\kappa}{1 + \kappa a}\right)$$

where κ is the reciprocal of the thickness of the ionic atmosphere and a is the distance of closest approach of the macroion and its counterion. Addition of alcohol reduces D and therefore increases the electrostatic free energy of the protein. This effect would favor some disordering of the molecular structure of the protein.

The effect of solvent on the hydrogen-bonding contribution to the conformation of the protein molecule is probably only slight. Hydrogen bonds play an important role in the formation of helical structures in proteins, but the evidence is that such bonds between protein side chains play only a very minor role (33–36). It therefore seems likely that isopropyl alcohol, which is an "unreactive" organic solvent (37) and has a low proton-donating capacity relative to the N—H group, induces little alteration in intrapeptide hydrogen bonding of the trypsin molecule.

Protein conformations are determined to a considerable extent by hydrophobic interactions, and these will be considerably affected by change in solvent. Conformational stabilization by hydrophobic bonding is considerably reduced in a non-aqueous solvent. By analogy with chymotrypsin (38–40, 4) it is to be expected that most of the non-polar residues in trypsin are in the interior of the molecule. Increasing concentration of organic solvent should therefore lead to substantial unfolding of the enzyme.

It follows from the preceding discussion that the strongest effect of solvent on protein conformation should be related to hydrophobic bonding. The net effect of adding isopropyl alcohol is therefore expected to cause an unfolding of the enzyme. This effect is probably adequate to explain the results of the present work, namely a decrease, on adding alcohol, of the rate constants and an increase in Michaelis constant; the latter corresponds to a decrease in substrate binding.

Appendix

Analysis of Results

Guggenheim Method

The Guggenheim method (24) has previously been used to analyze experimental results obtained for the transient phase of three-step enzymatic reactions (8, 12). This method has been suggested as being useful for reactions for which the initial or final concentrations are unknown, and where the relative readings taken during the course of a reaction cannot be conveniently converted to concentrations. It has been extended to second-order reactions (41).

Applications of the method to a reaction obeying eq. [23] is made as follows. If A_1, A_2, and A_3 are any series of readings directly proportional to the amount of product p_1 at times t_1, $t_1 + \Delta t$, and $t_1 + 2\Delta t$ respectively, where Δt is a fixed interval of time, then

$$[a] \quad A_1 + A_3 - 2A_2 = -s_0(e^{Ft_1})(e^{F\Delta t} - 1)^2$$

and

$$[b] \quad \log (A_1 + A_3 - 2A_2) = \log \text{constant} + Ft_1/2.303$$

With the use of this linear equation it is possible to determine F from the slope of a plot of log $|A_1 + A_3 - 2A_2|$ vs. t_1.

In order to obtain reliable results on the basis of this method it is necessary that the interval Δt be large; it is suggested (24) that Δt should be 3 or 4 times the half-life of the reaction. In addition, however, the magnitude of an acceptable Δt is strongly dependent on the relative precision with which A can be measured. We suggest, in fact, that a more realistic criterion for Δt is that the differences between successive $A_1 + A_3 - 2A_2$ terms should be at least equal to twice the expected precision of the A values.

Our attempts to obtain the rate parameters on the basis of Guggenheim's method were by no means satisfactory. Choice of different Δt values, and shifts in the portion of the curve analyzed, led to quite widely divergent answers. When the data were smoothed on the basis of the least-squares fit, the Guggenheim method gave results which were self-consistent and were consistent with those obtained from the least-squares method.

Can. J. Chem. Downloaded from www.nrcresearchpress.com by 210.87.254.5 on 09/05/12
For personal use only.

It is recommended that considerable caution be taken in applying the Guggenheim method to experimental data, since relatively minor scattering of results can lead to unreliable parameters.

Computer Program Tests

To establish the accuracy and reproducibility of the least-squares fit, the following tests were carried out on the program for a number of experimental runs.

(1) Using the "best" fitted results for Q, ΔA, and F, values of A were recalculated and found to agree with the experimental absorbance values within $\pm$ 2% or better. This is well within the accuracy of the oscilloscope read-out used in this study.

(2) A random 2% variation of some recalculated A values in a given run caused less than 1% change in the least-squares-fit result for F. In contrast, a Guggenheim fit on sets of data altered in a similar way caused up to 40% changes in F; also the results depended on the value of Δt. This again shows the limitations inherent in the Guggenheim method, as discussed earlier.

(3) A systematic or random reduction of data points from 18 to 9 within a given run sometimes caused an increase of up to 4% in the least-squares-fit result for F. Essentially no variation was noted when more than 12 data points were used.

(4) In most runs, F could be fitted to better than 3% precision, by using intervals of 0.0001 and 0.00001 between successive Q and ΔA values respectively for the iteration procedure. To maintain the same precision, these factors were reduced by 10 in those cases where the experimental minimum absorbance values were of the order of 0.005 units.

(5) A lower limit in the precision of fitting F was reached when the "best" fitted results for Q, ΔA, and F and those adjacent to it gave recalculated values of A which agreed within $\pm$ 2%. This situation arose only when the experimental data were restricted to extremely low absorbance values or showed unusually large scatter.

1. H. KAPLAN and K. J. LAIDLER. Can. J. Chem. **45**, 547 (1967).
2. H. KAPLAN and K. J. LAIDLER. Can. J. Chem. **45**, 559 (1967).
3. H. P. KASSERRA and K. J. LAIDLER. Can. J. Chem. **47**, 4021 (1969).
4. H. P. KASSERRA and K. J. LAIDLER. Can. J. Chem. **47**, 4031 (1969).
5. B. S. HARTLEY and B. A. KILBY. Biochem. J. **50**, 672 (1952).
6. B. A. HARTLEY and B. A. KILBY. Biochem. J. **56**, 288 (1954).
7. H. GUTFREUND and J. M. STURTEVANT. Proc. Nat. Acad. Sci. **42**, 719 (1956).
8. H. GUTFREUND and J. M. STURTEVANT. Biochem. J. **63**, 656 (1956).
9. G. H. DIXON and H. NEURATH. J. Biol. Chem. **225**, 1049 (1957).
10. F. J. KÉDZY and M. L. BENDER. Biochem. **1**, 1097 (1962).
11. T. SPENCER and J. M. STURTEVANT. J. Amer. Chem. Soc. **81**, 1874 (1959).
12. J. A. STEWART and L. OUELLET. Can. J. Chem. **37**, 751 (1959).
13. M. L. BENDER, F. J. KÉZDY, and J. FEDER. J. Amer. Chem. Soc. **87**, 4953 (1965).
14. L. FALLER and J. M. STURTEVANT. J. Biol. Chem. **241**, 4825 (1966).
15. J. B. MILSTEIN and T. H. FIFE. Biochem. **8**, 623 (1969).
16. K. J. LAIDLER. Can. J. Chem. **33**, 1614 (1955).
17. L. OUELLET and K. J. LAIDLER. Can. J. Chem. **34**, 146 (1956).
18. H. GUTFREUND. Discuss. Faraday Soc. **20**, 167 (1955).
19. L. OUELLET and J. A. STEWART. Can. J. Chem. **37**, 737 (1959).
20. L. PELLER and R. A. ALBERTY. Progr. React. Kinet. **1**, 236 (1961).
21. I. G. DARVEY. J. Theor. Biol. **19**, 215 (1968).
22. H. GUTFREUND. Discuss. Faraday Soc. **17**, 220 (1954).
23. E. W. DAVIE and H. NEURATH. J. Biol. Chem. **212**, 515 (1955).
24. E. A. GUGGENHEIM. Phil. Mag. **1**, 538 (1926).
25. K. J. LAIDLER. Chemical kinetics. 2nd ed. McGraw-Hill Book Co., New York, 1965. pp. 14–15.
26. H. LINEWEAVER and D. BURK. J. Amer. Chem. Soc. **56**, 658 (1934).
27. G. ÅKERLÖF. J. Amer. Chem. Soc. **54**, 4125 (1932).
28. T. INAGAMI and J. M. STURTEVANT. Biochim. Biophys. Acta, **38**, 64 (1960).
29. G. E. CLEMENT and M. L. BENDER. Biochem. **2**, 836 (1963).
30. M. DIXON. Biochem. J. **55**, 161, 170 (1953).
31. H. A. SCHERAGA. Protein structure. Academic Press, Inc., New York. 1961. p. 177.
32. S. J. SINGER. Advan. Protein Chem. **17**, 1 (1962).
33. W. J. KAUZMANN. Advan. Protein Chem. **14**, 1 (1959).
34. I. M. KLOTZ. *In* Protein structure and function. Brookhaven Symposium in Biology, Brookhaven National Laboratory, New York. 1960. p. 25.
35. I. M. KLOTZ and S. B. FARNHAM. Biochem. **7**, 3879 (1968).
36. C. TANFORD. Physical chemistry of macromolecules. John Wiley and Sons Inc., New York. 1961. Chap. 8.
37. F. SEYDOUX, J. YON, and G. NEMETHY. Biochim. Biophys. Acta, **171**, 145 (1969).
38. D. M. BLOW, J. J. BIRKTOFT, and B. S. HARTLEY. Nature, **221**, 337 (1969).
39. B. W. MATTHEWS, P. B. SIGLER, R. HENDERSON, and D. M. BLOW. Nature, **214**, 652 (1967).
40. P. B. SIGLER, D. M. BLOW, B. W. MATTHEWS, and R. HENDERSON. J. Mol. Biol. **35**, 143 (1968).
41. W. E. ROSEVEARE. J. Amer. Chem. Soc. **53**, 1651 (1931).

Can. J. Chem. Downloaded from www.nrcresearchpress.com by 210.87.254.40 on 09/05/12
For personal use only.

Electron spin resonance studies of irradiated nitrous oxide[1]

D. R. SMITH AND W. A. SEDDON

Physical Chemistry Branch, Atomic Energy of Canada Limited, Chalk River Nuclear Laboratories, Chalk River, Ontario

Received January 7, 1970

The γ-radiolysis of N_2O at 77 °K, or vapor phase irradiation with 1 MeV He^+ ions followed by condensation at 77 °K, results in the formation and trapping of at least 4 paramagnetic species. Using isotopically labelled N_2O these are identified as N_2O^+, NO_2, NO_3, and N. The latter assignment is reasonable on spectroscopic grounds but since this species arises exclusively from the central nitrogen of N_2O it is difficult to describe its formation from established chemical reactions. The addition of H_2O to the vapor phase experiments resulted in the trapping of O^-, while the addition of tetranitromethane or NO indicated the existence of O_2^- and O atoms, respectively. Possible reaction mechanisms are indicated.

Canadian Journal of Chemistry, 48, 1803 (1970)

Introduction

Nitrous oxide has been studied extensively in the field of chemical kinetics, particularly via radiation chemistry of the pure gas (1, 2) or liquid (3), by mass spectrometry (2), and photochemistry (4). In radiation chemistry N_2O has been used predominantly as an electron scavenger (5, 6), and gas phase dosimeter (7, 8), but our knowledge of the overall radiolysis mechanism remains incomplete.[2] To obtain more information on the free radicals involved we have investigated by electron spin resonance (e.s.r.), the paramagnetic species produced directly by γ-radiolysis at 77 °K, and also after vapor phase irradiation followed by rapid condensation at 77 °K. The latter "crossed beam" technique (9–11), has previously demonstrated that species can be trapped in the matrix and are sometimes different from those normally observed by low temperature γ-irradiation. For example, by this method trapped electrons are observed in neutral ice at 77 °K (10, 12–14).

A recent note by ourselves (15) discusses the formation of N_2O^+, while this paper reports in more detail our observations on the other radicals observed in irradiated N_2O.

Experimental

$^{14}N_2O$ and $^{14}N^{15}NO$ (96%) were obtained from Matheson and Merck, Sharpe and Dohme Ltd., (M.S.D.), respectively. $^{15}N^{14}NO$ and $^{15}N_2O$ were synthesized by thermal decomposition (16), from $^{15}NH_4{}^{14}NO_3$ (96.1%) and $^{15}NH_4{}^{15}NO_3$ (96%), obtained from Isotopes Inc. and M.S.D., respectively. After decomposition a trace of oxygen was added to convert any NO to NO_2 and the sample repeatedly distilled to and from traps at −78, −196 °C and molecular sieve (Type 3A), to remove water and NO_2. Solid samples for γ-radiolysis were prepared by slowly condensing N_2O into a 3 mm i.d. spectrosil e.s.r. tube. This did not form a homogeneous sample, the N_2O apparently condensing in regions partly glassy and partly amorphous. Such samples were irradiated in a ^{60}Co Gammacell 220 to a total dose of about 1.4 Mrads. The technique for the "crossed beam" experiments has been described previously (9–11).

X-Band e.s.r. spectra were obtained with a Varian V-4502-04 spectrometer using standard dual cavity techniques and X–Y recording. Spectroscopic g values were obtained by comparison with the Varian "strong pitch in KCl" standard (g = 2.0028), and the aid of a Hewlett-Packard X532-B wavemeter. Samples were thermally annealed, utilizing a Varian variable temperature accessory.

Results

Representative spectra are presented in Figs. 1, 2, 3, and 4. Figure 1 shows a wide scan first derivative spectrum obtained from $^{14}N_2O$. Figures 2, 3, and 4 show second derivative spectra of narrower scan and low modulation amplitude (~0.5 G) to enhance the resolution in the central region of each spectrum. These were obtained from $^{14}N_2O$, $^{15}N^{14}NO$, and $^{15}N_2O$, respectively. Figure 3 was shown in ref. 15 but is repeated in this paper for convenience. Spectral patterns definitely characterized are indicated by stick diagrams and numbered to designate each species. Unfortunately we are unable to assign several strong and weak lines. However, those identified represent the major fraction of the total observed yield of radicals. Table 1 summarizes the e.s.r. data.

[1]AECL No. 3545

[2]References 1–8 are merely recent examples and are not intended to be a comprehensive survey of the literature.

Can. J. Chem. Downloaded from www.nrcresearchpress.com by 210.87.254.40 on 09/05/12
For personal use only.

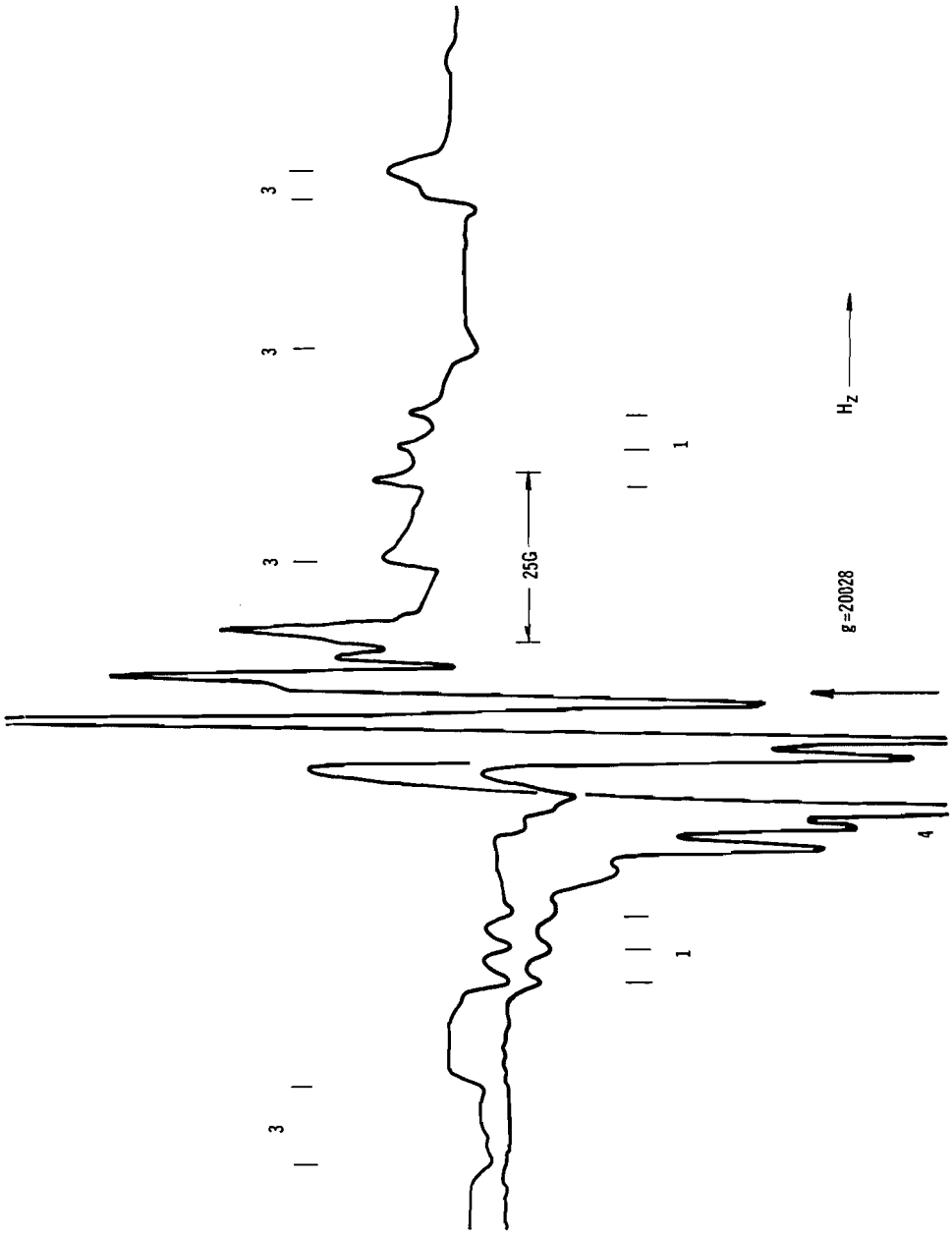

FIG. 1. First derivative e.s.r. spectrum observed at 77 °K from irradiated $^{14}N_2O$. Upper trace, γ-irradiated; lower trace, crossed beam.

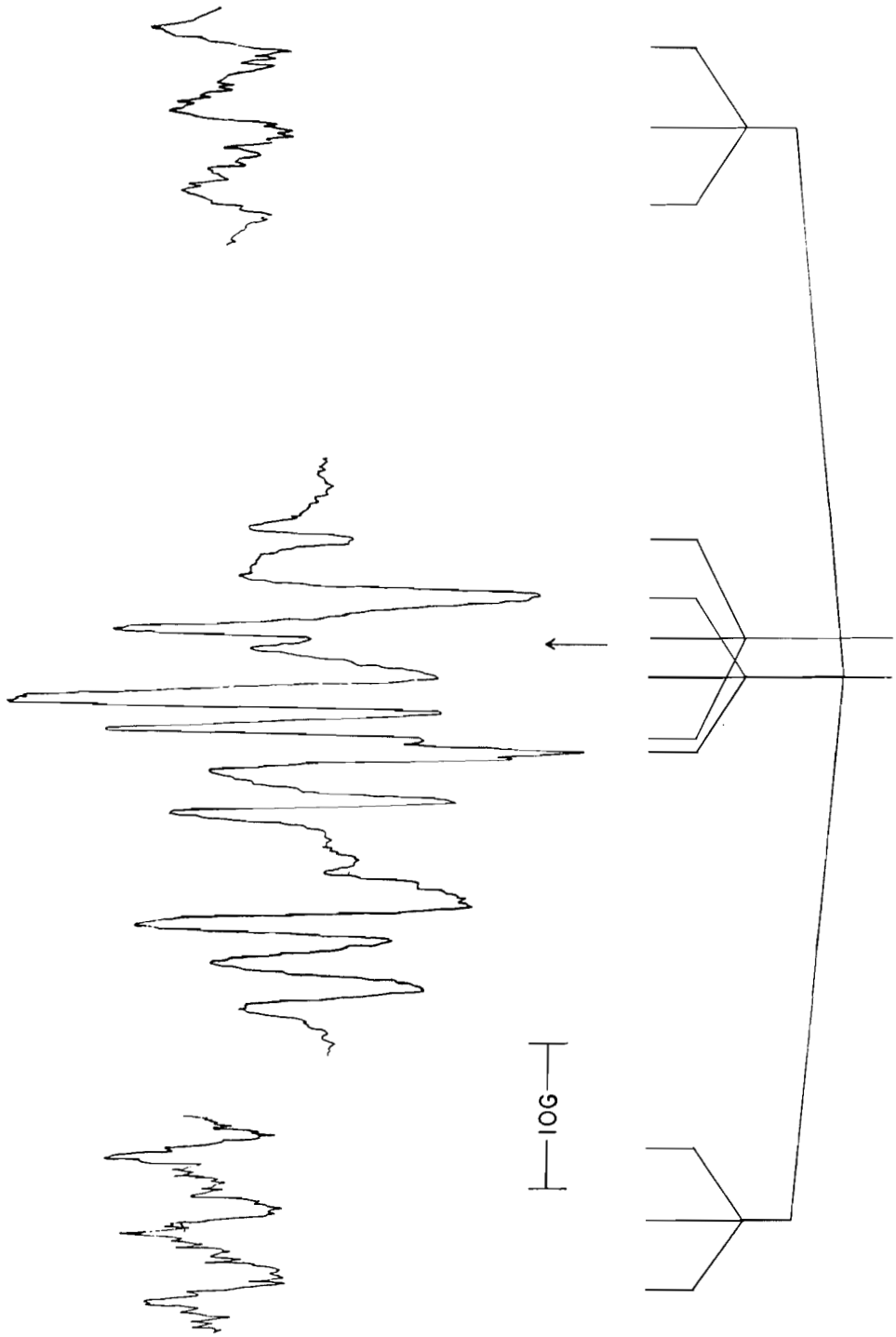

FIG. 2. Second derivative e.s.r. spectrum observed at 77 °K from crossed beam irradiated $^{14}N_2O$. Arrow denotes $g = 2.0028$.

Can. J. Chem. Downloaded from www.nrcresearchpress.com by 210.87.254.40 on 09/05/12
For personal use only.

Can. J. Chem. Downloaded from www.nrcresearchpress.com by 210.87.254.40 on 09/05/12
For personal use only.

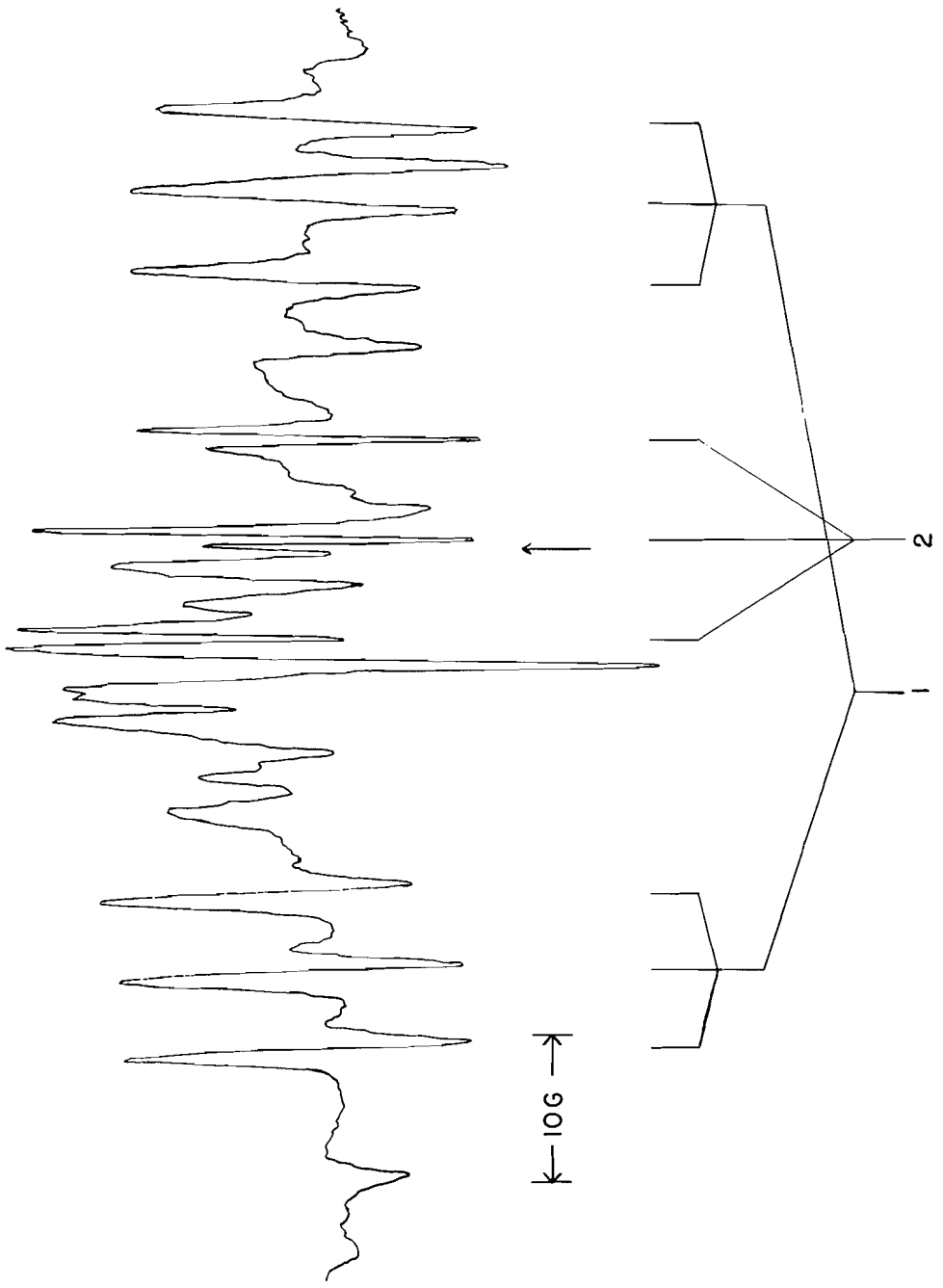

FIG. 3. Second derivative e.s.r. spectrum observed at 77 °K from γ-irradiated $^{15}N^{14}NO$. Arrow denotes $g = 2.0028$.

Can. J. Chem. Downloaded from www.nrcresearchpress.com by 210.87.254.40 on 09/05/12
For personal use only.

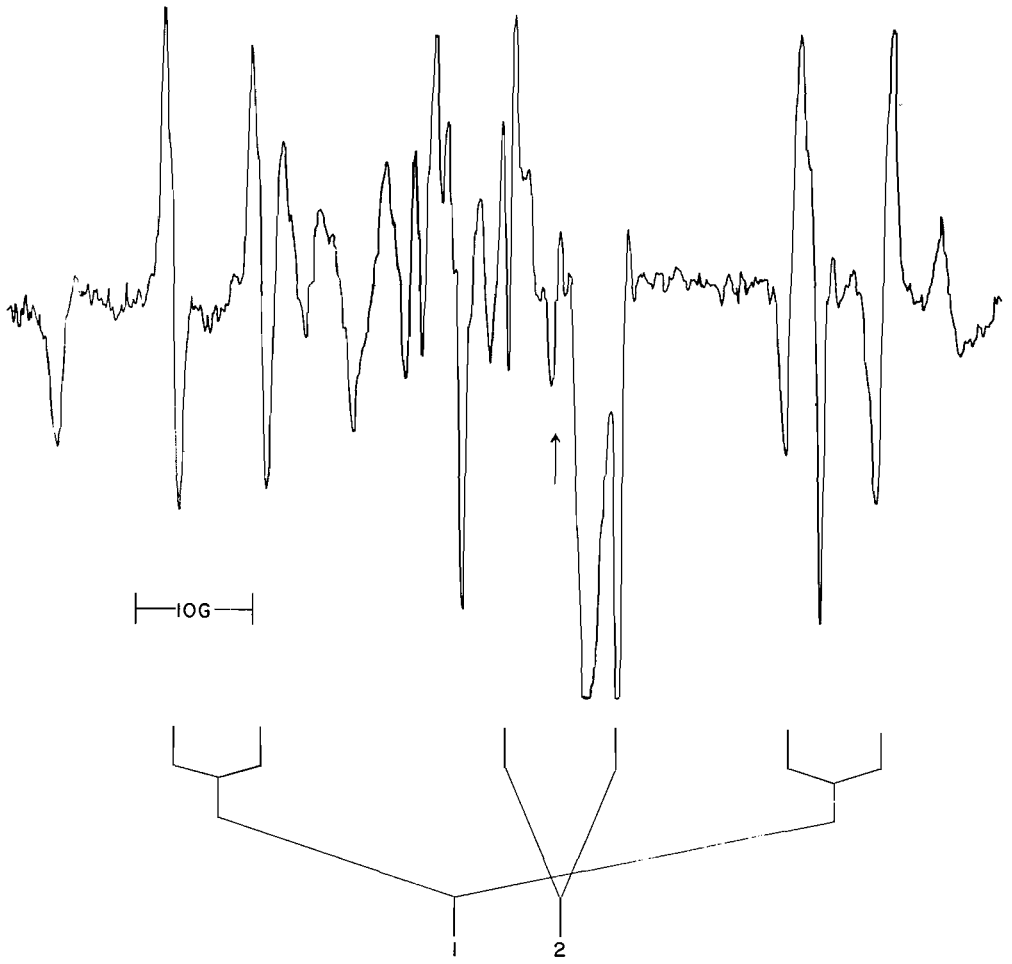

FIG. 4. Second derivative e.s.r. spectrum observed at 77 °K from γ-irradiated $^{15}N_2O$. Arrow denotes $g = 2.0028$.

TABLE 1

Electron spin resonance parameters of radicals trapped in N_2O

	Structure and hyperfine couplings (G)					
g	$^{14}N_2O$	$^{14}N^{15}NO$	$^{15}N^{14}NO$	$^{15}N_2O$	Species	Identity
2.0041	3 triplets 5.3 37.5	3 doublets 7.1 37.5	2 triplets 5.3 52.5	2 doublets 7.1 52.5	**1**	N_2O^{+*}
2.0025	One triplet 6.8	One doublet 9.6	One triplet 6.8	One doublet 9.6	**2**	N
1.9904 2.0013 2.0052	3 triplets 49.5 73.5 53.2	3 doublets and 3 triplets 68.2 102.5 75.6	 49.5 73.5 53.2	3 doublets 68.2 102.5 75.6	**3**	NO_2
2.015	Asymmetric singlet	Asymmetric singlet	Asymmetric singlet	Asymmetric singlet	**4**	NO_3†
2.05	Wide singlet	Wide singlet	Wide singlet	Wide singlet	**5**	O^-

*For N_2O^+, the largest coupling, $A_{\|}$, arises from the terminal nitrogen and the smallest coupling arises from the central nitrogen (15). The g value must be $g_{\|}$. The $A_\perp$, $g_\perp$ features have not been identified.
†This line underlies some resolved but unidentified lines.

Can. J. Chem. Downloaded from www.nrcresearchpress.com by 210.87.254.40 on 09/05/12
For personal use only.

(a) γ-Radiolysis of Solid N_2O at 77 °K

After irradiation the sample was colored red, the glassy regions being more intense in color. Electron spin resonance lines due to species **1**, **2**, and **3** were also observed. Species **3** is readily identified as NO_2 (see later) and radiolysis of $^{14}N^{15}NO$ or $^{15}N^{14}NO$ forms in each case approximately equal amounts of $^{14}NO_2$ and $^{15}NO_2$. Post irradiation ultraviolet (u.v.) photolysis (2537 Å) bleached the red color, removed **1** (N_2O^+) (15), and slowly reduced all spectral intensities. Post irradiation annealing at 100 °K again removed the red color and species **1** in about 10 min.

(b) Crossed Beam Experiments

In this case, species **1**, **2**, **3**, and **4** were observed. The lines due to **3** were significantly weaker relative to the total yield of radicals and could only be detected using high gain and modulation amplitude. Again, however, $^{15}NO_2$ and $^{14}NO_2$ are formed in approximately equal amounts from both $^{15}N^{14}NO$ and $^{14}N^{15}NO$. In contrast to the γ-irradiated samples, the deposit was pale blue in color. Subsequent u.v. photolysis removed species **1** and **2** while species **4** remained and species **3** was greatly enhanced. In the singly ^{15}N labelled samples similar photolysis formed equal quantities of $^{15}NO_2$ and $^{14}NO_2$. Prolonged photolysis gradually diminished all spectral intensities. Annealing at 100 °K again removed species **1**. On warming to 130 °K, species **2–4** also disappear but we are unable to interpret such changes, the spectra becoming poorly resolved and anisotropic.

In the crossed beam method homogeneous mixtures are readily prepared and one can examine the effect of additives. Experiments were conducted with mixtures of N_2O containing either 1% H_2O, D_2O, tetranitromethane (TNM), or 0.7% NO. Both H_2O and D_2O reduced species **4** and at the same time resulted in the formation of species **5**. The latter gave a broad line centered at $g = 2.05$ and is identified as the $g_\perp$ feature of O^-, (17). We have not detected the $g_\parallel$ feature of O^- presumably because it is masked by other spectra and is of lower intensity. No lines attributable to OH or OD were detected. In the presence of NO species **2** increased slightly, **4** disappeared, **1** remained unaffected, and a large yield of **3** was produced. The addition of TNM removed **1** and again produced a large yield of **3**. We were unable to ascertain the effect on **2** and **4**. Deposits containing 0.1 and 2% NO_2 in N_2O were prepared for purposes of identification and gave spectra typical of NO_2, although the lines were broadened due to electron–electron dipolar interaction.

Discussion and Conclusions

Identity of the Radicals

Radical **1** has been identified as N_2O^+ in an earlier publication (15). The largest hyperfine constant represents the maximum value of the hyperfine tensor due to the terminal nitrogen, while the small coupling arises from the central nitrogen due to adjacent atom spin polarization effects. The unpaired electron occupies a π anti-bonding molecular orbital such that p character unpaired spin density is located only on the terminal atoms. Hence the terminal nitrogen splitting is largely anisotropic and the central nitrogen splitting small and isotropic. The unusual line intensities and shapes are explained in terms of a spectral envelope (15). The data for N_2O^+ in Table 1 and in ref. 15 must be $A_\parallel$ for the terminal nitrogen and $g_\parallel$. We have not succeeded in identifying the $A_\perp$, $g_\perp$ features.[3]

Solely on the basis of the spectrum from $^{14}N_2O$ it is reasonable to assign radical **2**, a 6.8 G triplet, to trapped N atoms (18). However, the ^{15}N labelled compounds show that this species always contains the central nitrogen from N_2O, a 6.8 G ^{14}N triplet or 9.6 G ^{15}N doublet being observed with irradiated $^{15}N^{14}NO$ or $^{14}N^{15}NO$. The complete absence of N atom splittings from the terminal nitrogen isotopes suggests alternative assignments, but these are eliminated as follows. The species NO_2, NO_2^{2-}, and NO_3^{2-} are excluded since their ^{14}N isotropic hyperfine couplings are known to be about 55, 14, and 41 G, respectively (19). N_2O^- is possible, but being isoelectronic with NO_2 and CO_2^-, should exhibit hyperfine interaction with both nitrogen nuclei and must also be ruled out. The most logical assignment on chemical grounds is NO. Nitric oxide is a known product of the radiolysis of N_2O (20). Photolysis of N_2O (21) produces NO predominantly by cleavage of the N—N bond. Available e.s.r. data for NO trapped in single crystals of NH_3OHCl (22), gives g_x =

[3]We regret that this point was apparently not clear to readers of ref. 15.

Can. J. Chem. Downloaded from www.nrcresearchpress.com by 210.87.254.40 on 09/05/12
For personal use only.

1.998, $g_y = 1.999$, $g_z = 1.886$, $A_x = 36.4$ G, $A_y = 5.4$ G, and $A_z = 11.5$ G. Our spectrum **2** is in poor agreement with the g_y and A_y values and attempts to prepare "blanks" containing NO in N_2O did not give an e.s.r. spectrum. Furthermore, the narrow lines of spectrum **2** are characteristic of trapped atoms rather than a molecular radical. We must therefore identify radical **2** as the nitrogen atom. The fact that it is formed exclusively from the central nitrogen of N_2O makes it impossible to devise a mechanism based on established chemical reactions.[4]

Radical **3** is easily identified as NO_2. The g and A parameters in Table 1 were derived using the analysis of Schaafsma *et al.* (23). Our data give $A_{\text{isotropic}}$ (^{14}N) = 60.9 G and an ONO bond angle $\theta = 129°$ for NO_2 in N_2O, compared to 55.3 G and 130.5° for NO_2 trapped in N_2O_4 (23). It is interesting to note that Atkins and Symons (24) were unable to detect NO_2 from rapidly frozen solutions of NO_2 in contrast to the work of James and Marshall (25). Our method indicates an easy way of trapping NO_2 in a wide variety of matrices to study the variation in hyperfine parameters.

Species **4** we identify as the NO_3 radical (26–29). The observed $g = 2.015$ is low compared to the values 2.019 (27) and 2.018 (28), but agrees with 2.015 obtained by Ayscough and Collins (29). Spectra obtained from the ^{15}N labelled samples show that the three weak lines superimposed on the wide NO_3 singlet are due to two other unidentified species formed in low yield. Such lines prevent us from identifying any structure due to NO_3 with any certainty. Species **5** as mentioned earlier is identified as the $g_\perp$ feature of O^- (17).

Reaction Mechanisms

Although not all the spectral features have been assigned we believe the major fraction of the radicals have been identified. We will therefore comment briefly on their possible modes of formation using $^{15}N^{14}NO$ as an example where necessary.

The primary processes of ionization and excitation are well accepted and established from mass spectrometry and radiation chemistry.

[1] $$N_2O \rightarrow N_2O^+, e^-, N_2O^*$$

The parent ion N_2O^+ is detected in both the crossed beam and γ-irradiated samples while the electrons are expected to react with N_2O predominantly by the dissociative electron capture process

[2] $$N_2O + e^- \rightarrow N_2 + O^-$$

The O^- ion presumably disappears in pure N_2O via reactions [3] and [4] (30, 31).

[3] $$O^- + N_2O \rightarrow N_2 + O_2^-$$

[4] $$O^- + {}^{15}N^{14}NO \rightarrow {}^{15}NO^- + {}^{14}NO$$

Alternative modes of decomposition of the parent ion or excited molecules as in reactions [5], [6], and [7]

[5] $$^{15}N^{14}NO^* \rightarrow {}^{15}N + {}^{14}NO$$

[6] $$^{15}N^{14}NO^+ \rightarrow {}^{15}N + {}^{14}NO^+$$

[7] $$^{15}N^{14}NO^* \rightarrow {}^{15}N^{14}N + O$$

can occur (2, 21) and subsequent condensed phase radical reactions of N and O are expected in part to give N_2 and O_2. Clearly the different physical circumstances between the two kinds of irradiation (10, 12) can affect the relative ratio and nature of the species finally observed. This is seen in the formation of NO_3 and the very low concentration of NO_2 observed from the crossed beam experiment. Possible reactions for the formation of NO_3 in the condensed phase are reactions [8] and [9]

[8] $$NO_2 + O \rightarrow NO_3$$

[9] $$NO^+ + O_2^- \rightarrow NO_3$$

The addition of NO prevents the formation of NO_3 and at the same time produces a large yield of NO_2 indicating the transient existence of oxygen atoms and the occurrence of reaction [10] to form NO_2. The absence of NO_3 may be explained by reactions [10] and [11] replacing reactions [8] and [9].

[10] $$^{14}NO + O \rightarrow {}^{14}NO_2$$

[11] $$^{14}NO + O_2^- \rightarrow {}^{14}NO_3^-$$

An alternative mode of formation of NO_2 must

---

[4]One referee has made the novel suggestion that a bimolecular or concerted reaction can occur in the condensed phase, with the nitrogen atom arising from the central atom of N_2O, e.g.

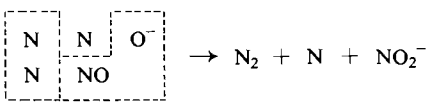

$$\rightarrow N_2 + N + NO_2^-$$

Can. J. Chem. Downloaded from www.nrcresearchpress.com by 210.87.254.40 on 09/05/12
For personal use only.

also exist since roughly equivalent amounts of $^{14}NO_2$ and $^{15}NO_2$ were always observed from either $^{15}N^{14}NO$ or $^{14}N^{15}NO$. We suggest reactions [12] and [13]

[12] $$^{15}N + O_2 \rightarrow {}^{15}NO_2$$

[13] $$^{14}NO^+ + O^- \rightarrow {}^{14}NO_2$$

together with reaction [10] to account for this observation.

The addition of TNM also results in the production of NO_2 and this indicates the presence of O_2^- and occurrence of reaction [14] (32), rather than [15], which should not compete effectively with reaction [2]

[14] $$C(NO_2)_4 + O_2^- \rightarrow C(NO_2)_3^- + NO_2 + O_2$$

[15] $$C(NO_2)_4 + e^- \rightarrow C(NO_2)_3^- + NO_2$$

Clearly, some of our reactions appear contradictory. Our observation of N_2O^+, and of N atoms arising exclusively from the central atom of N_2O, precludes reactions such as [5, 6, 9, 12, 13]. However, formation of $^{15}NO_2$ and $^{14}NO_2$ requires reactions such as [12] and [13]. It is possible that N atoms produced by such processes are simply not trapped. These are interesting problems for future study.

Miscellaneous

The difference in color between the γ-irradiated sample (red) and the crossed beam (pale blue) probably arises from two sources. In the former case significantly higher concentrations of N_2O^+ and NO_2 are present while the latter contains NO_3. Samples containing N_2O^+ might be expected to absorb in the region of 350–400 nm (33). The NO_3 radical absorbs in the 550–650 nm region and should appear blue (34–36).

Photolysis (2537 Å) of the crossed beam sample does not affect NO_3 but removed N_2O^+ and N and produces NO_2. Similar periods of photolysis of the γ-irradiated sample have little effect other than to remove N_2O^+.

Dissociation of N_2O^+, reaction [16], may in each case represent the initial process

[16] $$^{15}N^{14}NO^+ \xrightarrow{h\nu} {}^{15}N + {}^{14}NO^+$$

This might then be followed by reaction [12] along with reactions [17] and [13]

[17] $$^{15}N + {}^{14}NO \rightarrow N_2O$$

[13] $$^{14}NO^+ + O^- \rightarrow {}^{14}NO_2$$

Some reactions such as [10], [12], and [13] are required to explain the formation of $^{14}NO_2$ and $^{15}NO_2$ in approximately equal amounts.

We feel that some O^- is probably present in all samples although undetected in pure N_2O on account of its low concentration and wide e.s.r. line. The radical ion O^- was only easily observed in the presence of added H_2O or D_2O. This is puzzling but may be due to the formation of an inhomogeneous sample with zones of water capable of trapping O^- very efficiently in competition with its reaction with N_2O.

1. C. Willis, A. W. Boyd and D. A. Armstrong. Can. J. Chem. **47**, 3783 (1969).
2. R. Gorden, Jr., and P. Ausloos. J. Res. of the Nat. Bur. of Stand. (A) **69**, 79 (1965).
3. M. G. Robinson and G. R. Freeman. J. Phys. Chem. **72**, 1394 (1968).
4. J. R. McNesby and H. Okabe. Advan. Photochem. **3**, 157 (1964).
5. W. J. Holtslander and G. R. Freeman. J. Phys. Chem. **71**, 2562 (1967).
6. J. M. Warman and R. W. Fessenden. J. Chem. Phys. **49**, 4718 (1968).
7. F. T. Jones and T. J. Sworski. J. Phys. Chem. **70**, 1546 (1966).
8. A. W. Boyd, C. Willis, and O. A. Miller. Can. J. Chem. **47**, 351 (1969).
9. D. R. Smith and J. C. Tole. Can. J. Chem. **45**, 779 (1967).
10. W. A. Seddon, D. R. Smith, and P. E. Bindner. Can. J. Chem. **46**, 1747 (1968).
11. W. A. Seddon and D. R. Smith. Advan. Chem. Ser. No. **82**, Radiat. Chem. II, 163 (1968).
12. P. Wardman and W. A. Seddon. Can. J. Chem. **47**, 2149 (1969).
13. P. Wardman and W. A. Seddon. Can. J. Chem. **47**, 2155 (1969).
14. R. Marx, S. Leach, and M. Horani. J. Chim. Phys. **60**, 726 (1963).
15. D. R. Smith and W. A. Seddon. Chem. Phys. Lett. **3**, 640 (1969).
16. L. Friedman and J. Bigeleisen. J. Chem. Phys. **18**, 1325 (1950).
17. M. J. Blandamer, L. Shields, and M. C. R. Symons. J. Chem. Soc. 4352 (1964).
18. P. B. Ayscough, R. G. Collins, and F. S. Dainton. Nature, **205**, 965 (1965).
19. H. J. Bower, M. C. R. Symons, and D. J. A. Tinling. *In* Radical ions. *Edited by* E. T. Kaiser and L. Kevan. Interscience Publ. Inc., New York. 1968. Chap. 10 and references therein.
20. See G. R. A. Johnson. Strahlenchemie. *Edited by* K. Kaindl and E. H. Gravl. 1967. p. 592.
21. J. P. Doering and B. H. Mahan. J. Chem. Phys. **36**, 1682 (1962).
22. H. Ohigashi and Y. Kurita. J. Phys. Soc. Jap. **24**, 654 (1968).
23. T. J. Schaafsma, G. A. v. d. Velde, and J. Kommandeur. Mol. Phys. **14**, 501 (1968).
24. P. W. Atkins and M. C. R. Symons. *In* The structure of inorganic radicals. Elsevier Publ. Inc., New York. 1967. p. 128.
25. D. W. James and R. C. Marshall. J. Phys. Chem. **72**, 2963 (1968).

26. R. M. GOLDING and M. HENCHMAN. J. Chem. Phys. **40**, 1554 (1964) and references therein.
27. D. E. WOOD and T. M. PIETRZAK. J. Chem. Phys. **46**, 2973 (1967).
28. E. HAYON and E. SAITO. J. Chem. Phys. **43**, 4314 (1965).
29. P. B. AYSCOUGH and R. G. COLLINS. J. Phys. Chem. **70**, 3128 (1966).
30. G. R. A. JOHNSON and J. M. WARMAN. Nature, **203**, 73 (1964).
31. J. M. WARMAN. Nature, **213**, 381 (1967).
32. J. RABANI, W. A. MULAC, and M. S. MATHESON. J. Phys. Chem. **69**, 53 (1965).
33. I. E. DAYTON, F. W. DALBY, and R. G. BENNETT. J. Chem. Phys. **33**, 179 (1960).
34. M. DANIELS. J. Phys. Chem. **70**, 3022 (1966).
35. R. BROSZKIEWICZ. Int. J. App. Radiat. Isotop. **18**, 25 (1967).
36. T. W. MARTIN, A. HENSHALL, and R. C. GROSS. J. Amer. Chem. Soc. **85**, 113 (1963).

Can. J. Chem. Downloaded from www.nrcresearchpress.com by 210.87.254.40 on 09/05/12
For personal use only.

Can. J. Chem. Downloaded from www.nrcresearchpress.com by 210.87.254.5 on 09/05/12
For personal use only.

A determination of W and $G(H_2)$ values for methyl fluoride and fluoroform

MARIO SACA AND R. A. LEE
Puerto Rico Nuclear Center, College Station, Mayaguez, Puerto Rico

Received December 12, 1969

Methyl fluoride and fluoroform have been irradiated with gamma rays from a 1200-Ci ^{60}Co source. Ionization currents were measured using a Pyrex parallel-plate-type ionization chamber. W values of 27.2 and 28.0 eV were determined for the two gases, CH_3F and CHF_3, respectively. The method employed was a comparative one, making use of the Bragg–Gray theory of cavity ionization. $G(H_2)$ yields of 4.20 and 1.25 for CH_3F and CHF_3, respectively, were then calculated from the above W values and the measured ion-pair yields for hydrogen. The formation of hydrogen is probably due to the fact that the C—H bonds in these compounds are weaker than the C—F bonds.

Canadian Journal of Chemistry, **48**, 1812 (1970)

Introduction

There are usually two simple methods available for determining G values (the number of molecules destroyed or formed per 100 eV of energy absorbed) in the radiolysis of gases. One method makes use of the equation

$$[1] \qquad G = M/N \times 100/W$$

where M/N is the ion-pair yield (that is the ratio of the number M of molecules formed or destroyed to the number N of ion pairs produced) and W is the energy required to form an ion pair. The other method involves a comparison of the energy absorbed in a standard gas with the test gas. The G value for the standard gas must have already been well established and correction for the difference in the stopping powers of the test and standard gas must be made.

The method employed in this work is the former, which requires a knowledge of W values for the gases methyl fluoride (CH_3F) and fluoroform (CHF_3). These values are non-existent in the literature; however, they may be determined from the equation

$$[2] \qquad W_t = W_s \sigma_s^t (J_s/J_t)$$

where t refers to either of the gases CH_3F or CHF_3, and s refers to a standard gas whose W value has been well established; J represents the saturation ionization current per unit pressure of gas in the ionization chamber; σ_s^t is the ratio of the energies absorbed per unit pressure in the test and standard gases. At ambient room temperature and pressures below atmospheric, where deviations from ideal gas behavior are negligible, the ratio σ_s^t may be considered as the ratio of the energies absorbed per molecule in the test and standard gases. This approach to the W determination is similar to that described by Armstrong and co-workers (1, 2).

Experimental

Materials

Methyl fluoride and fluoroform, both of at least 99.0% purity, were obtained from Matheson. These were further purified by several bulb-to-bulb distillations in a vacuum line. The middle fraction, obtained by distilling from a Dry Ice – alcohol bath to a liquid nitrogen bath, was collected and used. This fraction submitted to mass spectrometric analysis was found to be free of impurities (< 0.05%).

Air was passed slowly through a U-tube, kept at dry ice temperature to remove water vapor, and used without further purification.

Research grade krypton (99.995% purity) was obtained from Matheson, and used without further purification.

Apparatus

A conventional type vacuum line capable of maintaining 10^{-5} Torr was employed for the purification and preparation of samples for irradiation.

Another vacuum line containing a Toepler pump, McLeod gauge, and a palladium thimble which could be heated, was used for determining hydrogen yields (2).

A detailed description of the Pyrex parallel-plate-type ionization chamber used for measuring ionization currents and hydrogen yields has already been reported (3).

Method

The ionization cell was evacuated for several hours to 10^{-5} Torr and then filled with the test gas at the desired pressure. The pressure was measured by means of a diaphragm gauge by equilibrating the pressure on either side of the diaphragm and reading off the pressure from a mercury manometer. The cell was then placed in a cylindrical steel container lined with a plastic sheet. Coaxial cables, which were connected to the cell, passed through the lid of the steel container into a 1 in. diameter tygon tubing. The whole system was now lowered into a pool type ^{60}Co gamma-ray irradiator. The tygon tubing kept the coaxial cables from getting wet and was connected to the lid in such a way as to prevent water from

Can. J. Chem. Downloaded from www.nrcresearchpress.com by 210.87.254.5 on 09/05/12
For personal use only.

entering the steel container. The gamma-ray irradiator consisted of 12 ^{60}Co pencils (each of about 100 Ci) arranged in a circle. Immediately after the steel container had been lowered into position, ionization currents were read from a Keithley 410C micro-microammeter while the applied voltage (supplied by a Hamner N413 power supply) was varied. After the cell had been irradiated for the desired time, ionization current measurements were again obtained, and the cell connected to a vacuum line for hydrogen analysis.

Results and Discussion

Figure 1 shows typical plots of ionization currents vs. voltages at different gas pressures. It can be seen that saturation is only attained at pressures below 300 Torr, and hence the technique (4) of plotting $1/i$ vs. i/v^2 has been used to obtain the saturation ionization currents (i_s). By an extrapolation of this plot to $i/v^2 = 0$, i_s can be determined. Saturation above 300 Torr has been obtained by decreasing the dose rate appreciably. Figure 2 shows J values plotted as a function of pressure for a roughly constant dose rate.

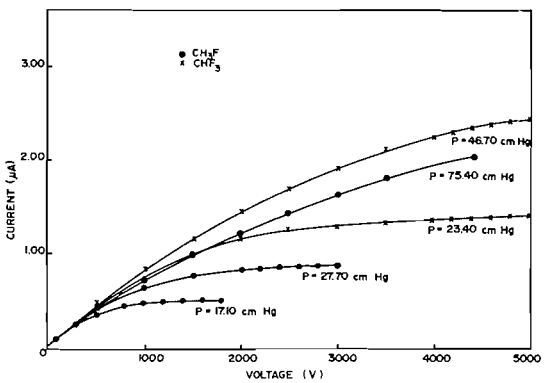

FIG. 1. Plots of ionization currents vs. applied voltage at different pressures.

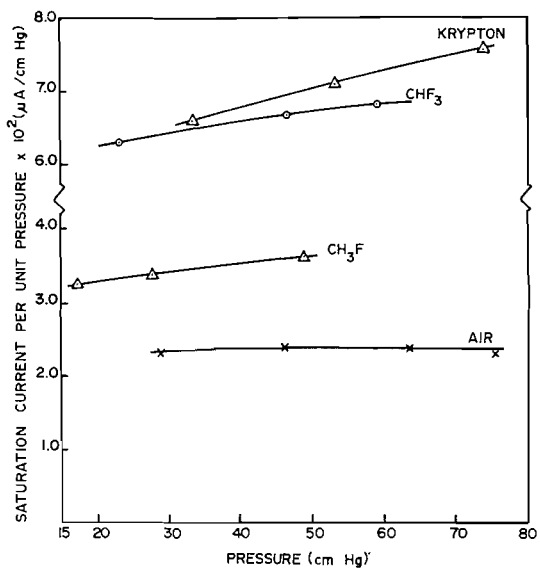

FIG. 2. Variation of I_s per unit pressure with pressure.

In eq. [2], which has been developed from the Bragg–Gray theory of cavity ionization, the value of σ_s^t (calculated from the Bethe (5) stopping power equation) is reasonably constant over the electron energy range from 0.02 to 1.00 MeV (Table 1). The mean energy of electrons emanating from the Pyrex walls is about 0.50 MeV (method of Fano (6)) and values of σ_s^t at this energy have been used.

Since these values vary with pressures (Fig. 2), it was necessary to choose J values at gas pressures equivalent in mean stopping power to air at 650 Torr. The reason for this has been discussed by Davidow and Armstrong (1). W values were calculated for CH_3F and CHF_3 from eq. [2], using $W = 33.8$ and 24.0 eV, respectively, for the standard gases air and krypton. As shown in Table 2 they were quite similar in magnitude.

The ion pair yields (M/N) were obtained by measuring the saturation ionization currents and the total number of hydrogen molecules formed after a given time. These are given in Table 3 along with values of $G(H_2)$ calculated from eq. [1]. The dose rate was purposely varied from one determination to the next. The hydrogen yield for CH_3F is seen to be $\sim$3 times larger than for CHF_3.

In a paper by Fessenden and Schuler (7), which

TABLE 1

Results of the calculation of molecular stopping power ratios of CH_3F and CHF_3 to air and Kr for electrons at different energies

E (Mev)	$\sigma_{Air}^{CH_3F}$	$\sigma_{Kr}^{CH_3F}$	$\sigma_{Air}^{CHF_3}$	$\sigma_{Kr}^{CHF_3}$
0.02	1.366	0.741	2.286	1.240
0.05	1.274	0.659	2.296	1.188
0.10	1.271	0.640	2.302	1.160
0.20	1.270	0.625	2.307	1.137
0.30	1.269	0.618	2.310	1.125
0.40	1.268	0.613	2.312	1.118
0.50	1.267	0.609	2.313	1.112
0.60	1.267	0.606	2.314	1.107
0.70	1.267	0.604	2.315	1.103
0.80	1.266	0.602	2.316	1.100
0.90	1.266	0.600	3.317	1.097
1.00	1.266	0.598	2.317	1.094

TABLE 2

Results of W for CH_3F and CHF_3*

Standard	Pressure (Torr)	$J_s \times 10^3$ (μA/Torr)	$\sigma_{std.}^{CH_3F}$	$\sigma_{std.}^{CHF_3}$	W_{CH_3F} (eV)	W_{CHF_3} (eV)
Air	650	2.30	1.27	2.31	27.4	28.1
Krypton	260	6.65	0.61	1.11	27.1	27.8

*J_t for CH_3F (510) = 3.60×10^{-3} μA/Torr; J_t for CHF_3 (270) = 6.40×10^{-3} μA/Torr.

TABLE 3

Results of $G(H_2)$ for CH_3F and CHF_3

Gas	P (Torr)	i_s (μA)	Total number of ion pairs $\times 10^{-17}$	Total number of H_2 molecules $\times 10^{-17}$	Time (h)	M/N	$G(H_2)$
CH_3F*	420	2.27	1.79	1.90	$3\frac{1}{2}$	1.06	3.92
	420	1.57	1.88	2.22	$5\frac{1}{3}$	1.18	4.35
	240	0.55	1.49	1.74	12	1.17	4.31
CHF_3†	467	2.84	10.20	3.68	16	0.36	1.28
	433	1.46	2.61	0.92	8	0.35	1.25
	264	1.41	0.64	0.22	7	0.34	1.21

*Mean $G(H_2)$ for CH_3F = 4.20 ± 0.2.
†Mean $G(H_2)$ for CHF_3 = 1.25 ± 0.1.

deals with the identification of radicals by electron spin resonance (e.s.r.), they have observed the presence of both the CH_2F and CH_3 radicals, when CH_3F is frozen in a 2% mixture with either Kr or Xe and irradiated at −188 °C with X-rays. In the case of CHF_3, the chief radical observed was CF_3. In these irradiations, these radicals would be expected as a result of either or both excitation and ionization transfer from the inert gas molecules to the fluoride molecules. The radicals observed should be the same as if these fluorides were irradiated individually, since the initial act expected would be ionization and excitation of these molecules. There should be a difference in the subsequent reactions of these radical intermediates due to a difference between gaseous and solid phase irradiations. With this in mind, one would expect hydrogen gas to be formed by the reaction of hydrogen atoms with the original molecules, thus

$$H + CH_3F \rightarrow H_2 + CH_2F$$

and

$$H + CHF_3 \rightarrow H_2 + CF_3$$

The C—H bonds in both of these compounds are weaker than the C—F bonds (8) and hence hydrogen abstraction is preferred to fluorine. These hydrogen atoms may arise from the initial ionization and excitation processes.

This work was supported by the U.S. Atomic Energy Commission through Contract AT(40-1)-1833 to the University of Puerto Rico.

1. R. S. Davidow and D. A. Armstrong. Rad. Res. **28**, 143 (1966).
2. R. A. Lee, R. S. Davidow, and D. A. Armstrong. Can. J. Chem. **42**, 1906 (1964).
3. R. A. Lee and D. A. Armstrong. Int. J. App. Rad. Isotop. **19**, 585 (1968).
4. P. B Scott and J. R. Greening. Phys. Med. Biol. **8**, 1, 51 (1963).
5. H. A. Bethe. Experimental nuclear physics. Vol. 1. *Edited by* E. Segre. 1953. p. 254.
6. U. Fano. Phys. Rev. **92**, 328 (1953).
7. R. W. Fessenden and R. H. Schuler. J. Chem. Phys. **43**, 2704 (1965).
8. (*a*) J. H. Simons. Fluorine chemistry. Vol. 1. Academic Press Inc., New York. 1950. (*b*) G. O. Pritchard and R. L. Thomarson. J. Phys. Chem. **68**, 568 (1964). (*c*) C. M. Sharts. J. Chem. Educ. **45**, 185 (1968).

Can. J. Chem. Downloaded from www.nrcresearchpress.com by 210.87.254.5 on 09/05/12
For personal use only.

Can. J. Chem. Downloaded from www.nrcresearchpress.com by 210.87.254.40 on 09/05/12
For personal use only.

Triethylenetetraaminеruthenium(II) complexes containing bridging molecular nitrogen

R. O. Harris and Miss B. A. Wright

Chemistry Department, Scarborough College, University of Toronto, West Hill, Ontario

Received December 5, 1969

Reaction between a reduced solution of *cis*-$[Ru(trien)Br_2]Br \cdot 2H_2O$ and gaseous nitrogen yields the dimeric species $[(trien)RuXN_2XRu(trien)]X_2$ where X = added anion I, Br and trien = triethylene tetraamine. In solution, the halides undergo solvolysis, before bridge splitting occurs, giving the monomeric $[Ru(trien)N_2H_2O]^{2+}$ ion. The rate of formation of monomer is p*H* dependent, being faster in base.

Canadian Journal of Chemistry, **48**, 1815 (1970)

Introduction

Since the first report of the nitrogen-containing complex ion $[Ru(II)(NH_3)_5N_2]^{2+}$ (1), several similar complexes have been made in which the ammine ligand has been altered (2, 3) to see if this affects the bonding ability of the nitrogen. Preparation of these is by one of two principal methods. The first is by decomposition of a corresponding ruthenium(III) azide complex (4) by a redox mechanism to the ruthenium(II) nitrogen complex. For example, it was earlier reported (5) that *cis*-$[Ru(III)(trien)(N_3)_2]^+$, where trien = triethylenetetraamine, does decompose to a nitrogen complex, which, however, proved difficult to obtain pure. We now report attempts to make this nitrogen complex by the second method, initially reported by Harrison and Taube (6), in which there is direct formation of the required complex in water between molecular nitrogen and a suitable ruthenium(II) species.

Experimental

Materials

Ruthenium trichloride used as starting material for the ruthenium compounds was supplied by Johnson Matthey and Co., Ltd. It was then converted to potassium trisoxalatoruthenium(III) tetrahydrate (7). Triethylenetetraamine, reagent grade, was from Fisher Scientific Co. All other chemicals were reagent grade or better.

cis-Dibromo(triethylenetetraamine)ruthenium(III) Bromide Dihydrate

This salt was prepared in a completely analogous manner to that described for *cis*-dichloro(triethylenetetraamine)ruthenium(III) chloride dihydrate (8). Hydrobromic acid (5 *N*) was added to triethylenetetraamine (3.6 ml) until a p*H* 3 solution was obtained. This was added to $K_3[Ru(Ox)_3] \cdot 4H_2O$ (6.0 g) in 15 ml water and the resulting solution heated on a steam bath for 1 h. The white precipitate was filtered off, and the filtrate allowed to stand for several hours when red-orange crystals of product were deposited. These were filtered off and recrystallized from dilute HBr solution. The crystals were washed with alcohol and ether and dried under vacuum at 80° for 1 h; yield 0.51 g, 10%.

Anal. Calcd. for $C_6H_{22}N_4O_2Br_3Ru$: C, 13.8; H, 4.20; N, 10.7; Br, 45.9; Ru, 19.3. Found: C, 14.2; H, 4.54; N, 10.9; Br, 45.6; Ru, 20.6.

Iodo(triethylenetetraamine)ruthenium(II)-μ-nitrogen-iodo(triethylenetetraamine)ruthenium(II) Di-iodide

Argon gas was bubbled for 1 h through a slurry of $[Ru(trien)Br_2]Br \cdot 2H_2O$ (0.11 g, 2×10^{-4} mole) in 0.1 *M* sulfuric acid (10 ml) containing amalgamated zinc (2 g), during which time the complex dissolved. The zinc was filtered off and then nitrogen gas bubbled through the solution for about 20 h. Addition of solid potassium iodide (1 g) to this solution under argon gave an immediate yellow precipitate which was washed with methanol and ether. The product can be recrystallized from 0.1 *M* sulfuric acid. The light yellow powder was dried under vacuum over P_2O_5 at 61°; yield 0.1 g, 90%.

Anal. Calcd. for $C_{12}H_{36}N_{10}I_4Ru_2$: C, 14.0; H, 3.49; N, 13.6; I, 49.3; Ru, 19.6. Found: C, 14.0; H, 3.57; N, 13.6; I, 49.6; Ru, 19.3.

Bromo(triethylenetetraamine)ruthenium(II)-μ-nitrogen-bromo(triethylenetetraamine)ruthenium(II) Dibromide Dihydrate

The preparation of this salt was exactly the same as that for the iodo complex except that the reaction mixture was concentrated to 5 ml before potassium bromide (4 g) was added to precipitate the product. The yellow powder was washed and dried as before, yield 20%.

Anal. Calcd. for $C_{12}H_{40}N_{10}O_2Br_4Ru_2$: C, 16.4; H, 4.55; N, 15.9; Br, 36.4; Ru, 23.0. Found: C, 16.6; H, 4.53; N, 15.7; Br, 36.6; Ru, 22.7.

Attempts to prepare the corresponding chloro compound by a similar method were unsuccessful, extremely small yields of product being obtained. Addition of potassium thiocyanate at the appropriate stage to give a thiocyanato complex produced an off-white powder whose infrared spectrum showed co-ordinated thiocyanate. Analyses of this product gave consistently low carbon, hydrogen, and nitrogen results. Decomposition of this compound, with loss of molecular nitrogen, took place within 24 h.

Apparatus

Vibrational spectra were recorded on a Perkin–Elmer 521 grating spectrophotometer in the range 4000–200

Can. J. Chem. Downloaded from www.nrcresearchpress.com by 210.87.254.40 on 09/05/12
For personal use only.

cm^{-1}. Solid samples were prepared as Nujol mulls on KRS-5 plates or on polystyrene film. Electronic spectra were measured on a Bausch and Lomb 505 spectrophotometer using 1 cm fused silica cells. Magnetic measurements by the Gouy method were carried out on an Alpha Scientific Laboratories S2 magnetic susceptibility apparatus. Conductivities were recorded at 25° using a Beckmann Model RC-18 bridge system with BB1 dip cell, cell constant 1.0 cm^{-1}.

Gas samples were collected by a method previously described (4). The mass spectra of such samples were analyzed on an AEI-MS10c2 mass spectrometer at 70 eV, trap current 50 μA, and a scan time of 2000 s.

Microanalyses were carried out by A. B. Gygli, Toronto. Halide analyses were determined potentiometrically, and metal by reduction in a stream of hydrogen.

Results

The bromo- and iodo-μ-nitrogen complexes were found to be diagmagnetic, as required for low-spin ruthenium(II) complexes, and relatively air-stable. Loss of molecular nitrogen occurs slowly over a period of days to give ill-defined red-brown products. Dry heating of these compounds produces a non-condensible gas which mass spectra showed to be > 95% nitrogen, the amount collected being > 90% of that expected theoretically.

Infrared (i.r.) spectra of the products are largely similar to that of the starting material, *cis*-$[Ru(trien)Br_2]Br \cdot 2H_2O$. The iodo-complex is slightly different in that it does not contain a band for lattice water which occurs in the starting material at 1635 cm^{-1}, and in the bromo complex at 1647 cm^{-1}. The differences that do occur can be attributed to coordinated nitrogen. Nitrogenruthenium(II) complexes, with one exception, are characterized by a strong absorption in their infrared spectra at about 2150 cm^{-1}, assigned to $\nu(N{\equiv}N)$ (4). The exception is in the bridged nitrogen ion $[(Ru(NH_3)_5)_2N_2]^{4+}$, first reported by Taube and co-workers (9), where only a small, weak absorption occurs at about 2060 cm^{-1} for the fluoroborate salt. This weak absorption is also found in these bridged complexes, at 2068 cm^{-1} in the iodo salt, and at 2060 cm^{-1} in the bromo salt. A new intense band appears in the spectra at 501 cm^{-1} for $[(Ru(trien)Br)_2N_2]Br_2 \cdot 2H_2O$ and at 497 cm^{-1} for $[(Ru(trien)I)_2N_2]I_2$ (Fig. 1). The position and relative intensity of this band are very similar to that reported for $\nu(Ru{-}N_2)$ in monomeric ruthenium(II) complexes (4). For example, it is found at 489 cm^{-1} in $[Ru(NH_3)_5N_2]I_2$. This band was observed to decrease with time as the bridged complexes lose nitrogen.

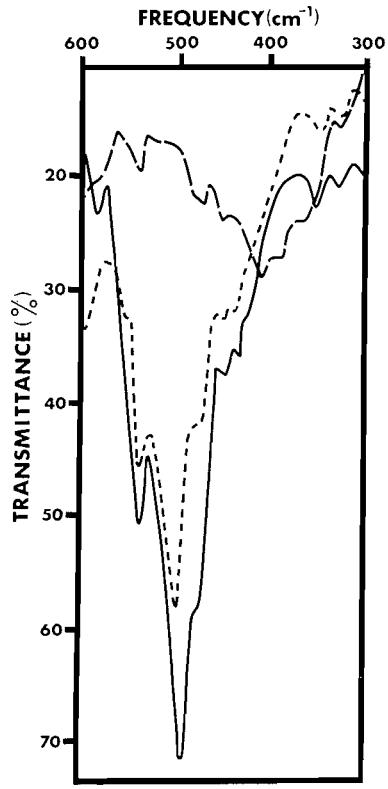

FIG. 1. Infrared spectra in the region 600–300 cm^{-1} of some ruthenium–triethylenetetraamine complexes: – – –, $[Ru(trien)Br_2]Br \cdot 2H_2O$; —, $[(Ru(trien)I)_2N_2]I$; - - -, $[(Ru(trien)Br)_2N_2]Br_2 \cdot 2H_2O$.

The conductivities of these salts were compared against those for similar electrolytes in dimethyl sulfoxide over the concentrations used. It was found that the conductivity of their solutions increased slowly with time (Fig. 2). After a period of about 2 days, a maximum value is obtained. Thereafter, the solutions begin to cloud, the readings becoming erratic. When the maximum conductivity readings are plotted against concentration (Fig. 3), they correspond to an electrolyte greater than 1:3. Complete solution of the two bound halides would give a 1:4 electrolyte. By extrapolation of these conductivity vs. time graphs, it is possible to estimate a conductivity at zero time. The values obtained for the iodo dimer correspond to a 1:2 electrolyte in dimethyl sulfoxide, but those for bromo complex are somewhat high. The high result could be explained by either more rapid hydrolysis in this

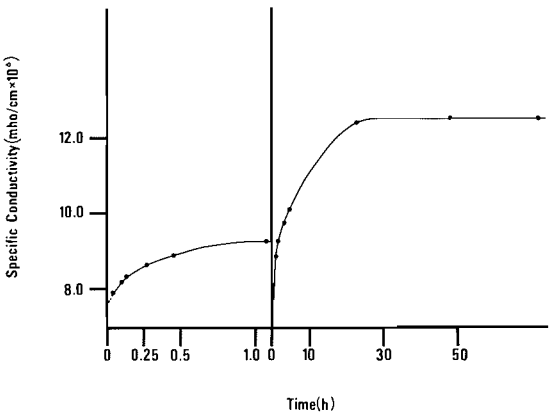

FIG. 2. Changes in specific conductivity with time of a 7.9×10^{-5} M solution of $[(Ru(trien)Br_2N_2]Br_2 \cdot 2H_2O$ in dimethyl sulfoxide at 25 °C.

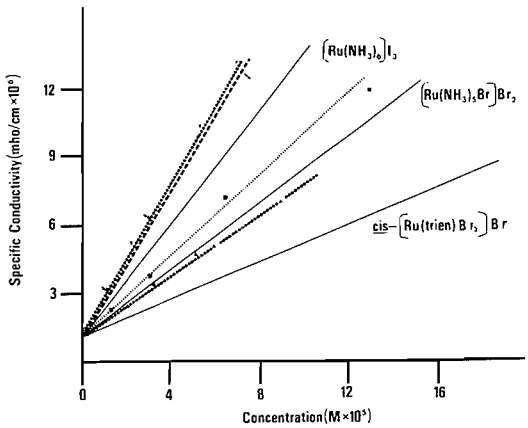

FIG. 3. Conductivity of some complexes of ruthenium in dimethyl sulfoxide at 25 °C. ▲, $[(Ru(trien)I)_2N_2]I_2$, extrapolated values; ■, $[(Ru(trien)Br)_2N_2]Br_2 \cdot 2H_2O$, extrapolated values; ⓘ, $[(Ru(trien)I_2N_2]I_2$, after 4 days; ×, $[(Ru(trien)Br)_2N_2]Br_2 \cdot 2H_2O$, after 4 days.

case, making the error in the extrapolation more significant, or by the salt containing some aquo complex. Both would have the effect of giving a high initial reading; considering the difficulty in preparing the salt, both seem equally likely.

The conductivity results have been explained by a solvolysis reaction

$$2S + [(Ru(trien)X)_2N_2]^{2+} \rightarrow [(Ru(trien)S)_2N_2]^{4+} + 2X^-$$

However, ruthenium-μ-nitrogen complexes have been reported to undergo bridge splitting (9), and the conductivity results could be explained equally well by the following reaction

$$[(Ru(trien)X)_2N_2]^{2+} \rightarrow [Ru(trien)SN_2]^{2+} + [Ru(trien)S_2]^{2+} + 2X^-$$

in which bridge breaking precedes or is concurrent with the solvolysis process. However, spectral work (see later) shows that bridge splitting does occur, but only after solvolysis of the halide ions has taken place.

Data from the electronic spectra of these and similar compounds are collected in Table 1. There are several pieces of evidence that suggest that the spectra of the trien-μ-nitrogen complexes in water are all that of the solvated ion. The first is that bridged complexes are distinguished by a single strong sharp absorption band at 267–268 nm, except in the case of the iodo complex, which has an additional absorption band at 225 with a molar extinction coefficient of 5.4×10^4. Iodide ion has an absorption band at this wavelength. Moreover, most of the absorption at this point is expected to come from free iodide ion in solution since, as is observed in the bromo-complex case, there is minimum absorption at this wavelength from the complex cation. The molar extinction of iodide ion at 225 nm is reported (10) to be approximately $1.35 \times 10^{+4}$ so that the absorption found corresponds to four iodide ions per dimer in solution. Secondly, the band at 267–268 nm in all three complex ions is moved to 273 nm in base (dilute sodium hydroxide or ammonia) and returns to 267–268 on re-acidification of the solution, which strongly suggests an acid–base reaction with coordinated water. Solvolysis in water is therefore much faster than the same reaction in dimethyl sulfoxide.

Data in Table 1 can be used to distinguish

TABLE 1

Visible and ultraviolet absorption maxima (λ) and intensities (ε_{max}) of some ruthenium complex ions in water

Complex	λ, nm	$\varepsilon_{max} \times 10^{-4}$
cis-$[RuBr_2(trien)]^{2+}$	407	0.13
	340	0.12
	306	0.10
$[RuOH_2(trien)N_2]^{2+}$	225	2.2
$[RuOH_2en_2N_2]^{2+}$	220*	~1.3†
$[Ru(NH_3)_5N_2]^{2+}$	221	1.6‡
$[(Ru(trien)Br)_2N_2]^{2+}$	268	4.4
$[(Ru(trien)I)_2N_2]^{2+}$	268	4.5
	225	5.4
$[(Ru(NH_3)_5)_2N_2]^{4+}$	262	4.7‡

*en = ethylenediamine.
†Reference 2.
‡Reference 9.

Can. J. Chem. Downloaded from www.nrcresearchpress.com by 210.87.254.40 on 09/05/12
For personal use only.

Can. J. Chem. Downloaded from www.nrcresearchpress.com by 210.87.254.40 on 09/05/12
For personal use only.

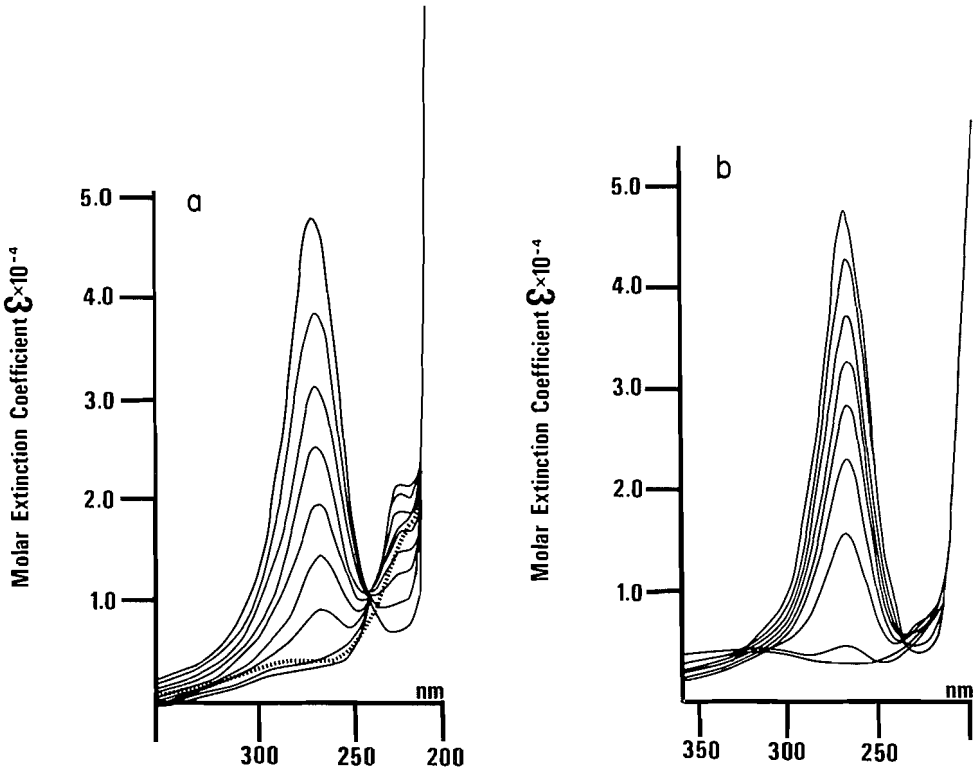

FIG. 4. (*a*) Decomposition of $[(Ru(trien)Br)_2N_2]Br_2 \cdot 2H_2O$ (1.38×10^{-5} *M*, 273 nm) in dilute ammonia at 25 °C. The reaction times for the decreasing absorption at 273 nm are 0, 3, 7, 10, 15, 18, 21, 30, 40 min, respectively. Final reading (---), 2.5 h. (*b*) Decomposition of $[(Ru(trien)Br)_2N_2]Br_2 \cdot 2H_2O$ (1.4×10^{-5} *M*, 268 nm) in water at 25 °C. The reaction times for the decreasing absorption at 268 nm are 0, 0.75, 2.0, 3.0, 4.0, 5.0, 10, 25, 55 h, respectively.

between monomeric and dimeric nitrogen complexes. The spectra of monomers have a less intense band some 50 nm higher in energy than the dimer band, at about 220 nm. Taube and co-workers have already reported (9) that, in solution, there occurs an interconversion between the two species. Itzkovitch and Page (11) have measured the rate of formation of the ammonia dimer from monomer in dilute acid. Figure 4*a* shows the conversion of the trien dimer to monomer under argon at room temperature in dilute ammonia. Disappearance of the dimer band at 273 nm is accompanied by a corresponding increase of the monomer band at 225 nm, the presence of an isosbestic point at 239 nm showing a simple reaction to be taking place. Reaction occurs fairly rapidly, being essentially complete after one hour. The molar extinction coefficient calculated for the monomer at this time is $2.2 \times 10^{+4}$. However, from Fig. 4*a*, it appears as if a position of equilibrium is reached, so that absorption from residual dimer would tend to raise this value from the correct one. Decomposition of the monomer with loss of nitrogen subsequently takes place. The reading taken after 2.5 h clearly shows decrease in monomer absorption and, moreover, it does not pass through the isosbestic point.

This instability of the monomer to loss of coordinated nitrogen is demonstrated more fully when the dimer is allowed to decompose in water under argon at room temperature (Fig. 4*b*). The rate of disappearance of the dimer band at 268 nm is now very much slower. The isosbestic point at 238 nm is maintained for about 4 h but the absorption due to formation of the monomer never fully develops. Eventually, a much weaker band at approximately 320 nm appears.

In their reactions toward acids, the complexes behave similarly to other ruthenium nitrogen complexes. When the dimer is heated in 5 *N* hydrochloric acid in air, the resulting yellow solution contains absorption bands at 352 and 310 nm characteristic of *cis*-$[Ru(trien)Cl_2]^+$ ion

Can. J. Chem. Downloaded from www.nrcresearchpress.com by 210.87.254.40 on 09/05/12
For personal use only.

(8). Similarly, hydrobromic acid produces bands at 407, 339, and 306 nm characteristic of *cis*-$[Ru(trien)Br_2]^+$. This behavior has been used to produce $[Ru(NH_3)_5Cl]^{2+}$ from $[Ru(NH_3)_5N_2]^{2+}$ (4). When the same experiments are carried out under argon, unidentified blue solutions characteristic of ruthenium(II) are obtained. The same reaction was reported for $[Ru(NH_3)_4H_2ON_2]^{2+}$ (3).

Discussion

The presence of halide ions within the coordination sphere of these nitrogen complexes seems to have little effect upon their overall stability in air. The main feature of the halide ligands is their rapid solvolysis before any noticeable disruption of the nitrogen bridge takes place. Solvolysis is complete upon dissolving $[(Ru(trien)I)_2N_2]^{4+}$ in water, whereas in dimethyl sulfoxide, the same reaction takes over a day at room temperature. The same lability of anionic ligands is found in monomeric nitrogen complexes, where it has already been noted (5) in the salts *cis*-$[Ru(trien)N_2N_3]I$ and in other ruthenium(II) ammine complexes that also contain a ligand capable of π bonding with the metal (3, 12, 13). In all these examples, the labilized group is *trans* to the π ligand. In the trien complexes, the replaced halide is assumed to be *cis* to coordinated nitrogen. Supporting evidence that retention of configuration is maintained during reduction is found in the carbonyl ammine series, where *cis*-$[Ru(NH_3)_4Cl_2]^+$ gives rise to *cis*-$[RuCO(NH_3)_4H_2O]^{2+}$ and *trans*-$[Ru(NH_3)_4Cl_2]^{2+}$ gives *trans*-$[RuCO(NH_3)_4H_2O]^{2+}$. For low-spin d^6 octahedral cobalt(III) ammine complexes, Basolo and Pearson have proposed a mechanism (14) of *trans*-ligand labilization when there is a π-accepting ligand in the molecule. Although the mechanism shows the *trans* ligand to be particularly sensitive to replacement, it also requires that a similar but less pronounced effect will occur with the *cis* ligand. If this is the reason for lability of the halide in these nitrogen complexes, then one might also expect complexes of the type *trans*-$[RuN_2(NH_3)_4H_2O]^{2+}$. So far, these have not been reported.

Rate of decomposition of the nitrogen bridge clearly depends upon the p*H* of the solution, faster decomposition taking place in base. Disappearance of the dimer absorption band is about 20 times faster in dilute base than in water. Taube and co-workers (9) also report fairly rapid dissociation of $[(Ru(NH_3)_5)_2N_2]^{4+}$ in a p*H* 10.4 solution. The dissociation of $[(Ru(NH_3)_5)_2N_2]^{4+}$ in acid has not been measured directly. Itzkovitch and Page, who give a value of 4.2×10^{-2} cm^{-1} s^{-1} at 26 °C for the formation of $[(Ru(NH_3)_5)_2N_2]^{4+}$ from $[Ru(NH_3)_5H_2O]^{2+}$ and $[Ru(NH_3)_5N_2]^{2+}$ in a p*H* 2.6 solution, state that the reverse reaction is very slow compared to the rate of dimer formation.

For the monomers, $[RuH_2O(trien)N_2]^{2+}$ loses nitrogen more readily than $[Ru(NH_3)_5N_2]^{2+}$. When the preparation of the latter ion, by direct formation between $[Ru(NH_3)_5H_2O]^{2+}$ and N_2 in neutral solution, is followed by spectral changes (6), the monomer band at 221 nm grows out of the dimer band at 260 nm for up to 6 h. From Fig. 3*b*, it is evident that, under similar conditions, $[RuH_2O(trien)N_2]^{2+}$ is losing nitrogen at almost the same rate that it is being produced in solution. The kinetic behavior of these and similar complexes is being studied further.

Grateful acknowledgment is made to the National Research Council of Canada for support of this research. We should also like to thank Mr. Garfield Purdon for running the mass spectra.

1. A. D. Allen and C. V. Senoff. Chem. Commun. 621 (1965).
2. L. A. P. Kane-Maguire, P. S. Sheridan, F. Basolo, and R. G. Pearson. J. Amer. Chem. Soc. **90**, 5296 (1968).
3. A. D. Allen, T. Eliades, R. O. Harris, and P. Reinsalu. Can. J. Chem. **47**, 1905 (1969).
4. A. D. Allen, F. Bottomley, R. O. Harris, V. P. Reinsalu, and C. V. Senoff. J. Amer. Chem. Soc. **89**, 5595 (1967).
5. T. Eliades, R. O. Harris, and P. Reinsalu. Can. J. Chem. **47**, 3823 (1969).
6. D. E. Harrison and H. Taube. J. Amer. Chem. Soc. **89**, 5706 (1967).
7. R. Charronet. Ann. Chim. Fr. **16**, 6 (1931).
8. J. A. Broomhead and L. A. P. Kane-Maguire. J. Chem. Soc. 546 (1967).
9. D. F. Harrison, E. Weissberger, and H. Taube. Science, **159**, 320 (1968).
10. J. W. Mellor. Comprehensive treatise on inorganic and theoretical chemistry. Vol. II, Suppl. I. Longmans, Green and Co., Ltd., London. 1962. p. 934.
11. J. Itzkovitch and J. A. Page. Can. J. Chem. **46**, 2743 (1968).
12. K. Gleu, W. Breuel, and K. Rehm. Z. Anorg. Allg. Chem. **235**, 201 (1938).
13. K. Gleu and I. Buddecker. Z. Anorg. Allg. Chem. **268**, 208 (1952).
14. F. Basolo and R. G. Pearson. Mechanisms of inorganic reactions. 2nd ed. John Wiley and Sons, Inc., New York. 1967. Ch. 3.

A quantum-chemical study of some properties and reactions of H_2CN^-, H_2CN^+, $H_2CNH_2^+$, H_2CNH, and HCN, using small and intermediate-sized sets of basis functions

J. B. MOFFAT
Department of Chemistry, University of Waterloo, Waterloo, Ontario
Received October 6, 1969

It is suggested that given two molecules potentially capable of being involved in the same reaction, one as a product and one as a reactant, it seems reasonable that the calculated difference in energy between these molecules may become relatively constant with smaller basis sets than the calculated energies themselves. To examine this suggestion, and at the same time to provide information on small molecules containing bonds related to the nitrile bond, a number of linear combination of atomic orbitals-molecular orbitals-self consistent field (l.c.a.o.-m.o.-s.c.f.) calculations using small or intermediate sizes of basis sets of Gaussian orbitals were performed on H_2CNH, H_2CN^-, $H_2CNH_2^+$, H_2CN^+, and HCN. The change of energy in passing from one molecule to another is shown to converge to a reasonably constant value for smaller basis sets than are required for convergence of individual molecular energies.

Canadian Journal of Chemistry, **48**, 1820 (1970)

Can. J. Chem. Downloaded from www.nrcresearchpress.com by 210.87.254.6 on 09/05/12
For personal use only.

Introduction

The chemist is interested not only in the properties of molecules themselves, but also in the reactions of these molecules. Many atoms and molecules are being studied using quantum mechanical methods, but it is only recently that much work has been done on computations involving reactions. Clementi (ref. 1, and subsequent papers in the series) has pioneered in the use of ab initio calculations involving Gaussian functions for the study of chemical reactions. There have been, of course, a number of papers describing semi-empirical calculations on simple reactions.

While on the one hand the semi-empirical studies on reactions are conveniently done with relatively small consumption of machine time, they often suffer from the disadvantage of being unpredictably inaccurate. On the other hand, ab initio calculations on reactions are quite expensive since copious quantities of computer time on relatively sophisticated machines are required. Of course, ab initio calculations on reactions can be made quite accurately provided sufficient care and substantially sized basis sets are employed.

Ideally, for the chemist interested in reactions, some reasonable compromise would be worthwhile. From this point of view, it seemed of value to attempt a study of some simple reactions using a relatively small basis set in an ab initio type of calculation. From earlier studies (see, for example, ref. 2 and references therein) on the effect of size of basis set and exponent optimization on the accuracy of the calculated wavefunction, certain extensions seemed apparent. It was hoped that it might be shown that the *change* in energy involved when one molecule was transformed to another is insignificantly altered by employing larger basis sets and/or different exponents, provided a reasonable size of basis set had been initially chosen. Obviously this cannot be rigorously so, but it was hoped that the size of the basis set would not need to be too large before this was valid to an accuracy reasonable enough for rough chemical work. It seemed not unreasonable to suggest that some, and hopefully a substantial amount, of the deviation from the Hartree–Fock energy would be cancelled out in the calculation of the change in energy in passing from one molecule to another. Consequently, if so, it might well be expected that the calculated change of energy for a particular reaction would become relatively constant for smaller sizes of basis set than would the energies of the reactant or product molecules themselves.

Snyder and Basch (3) have recently published the results of some interesting work in which heats of reaction are calculated on the assumption that correlation energy does not change when closed-shell reactants react to form closed-shell products where the number of electron pairs is conserved. This type of assumption is, of course, implicit in the present work.

As a consequence of the previous work on nitriles in this laboratory (4), it appeared to be desirable to examine reactions involving the C≡N bond or the related C=N bond. Simple reactions involving H_2CNH, H_2CN^+, H_2CN^-,

Can. J. Chem. Downloaded from www.nrcresearchpress.com by 210.87.254.6 on 09/05/12
For personal use only.

and $H_2CNH_2^+$ were selected for study. Some results obtained previously (5) for HCN are also employed here. The first theoretical studies of some of these molecules, namely, the first three listed above, were done by Brown and Penfold (6, 7) who examined the π-electron distributions and reported the total π-electron energies for these molecules. Julg *et al.* (8) applied his improved l.c.a.o. method to a calculation on $H_2CNH_2^+$. The third and most recent theoretical work on any of these molecules appears to be that of Lehn and Munsch (9) who performed l.c.a.o.-m.o.-s.c.f. calculations using Gaussian orbitals on methyleneimine (H_2CNH).

There is a further advantage in the selection of these molecules already mentioned for the present study. Since the previous work in this laboratory has concentrated on organic compounds involving the C≡N group, it appeared reasonable to extend such studies to the C=N and C—N group in order to permit comparisons among these types of bonds. In addition, the results of our work involving energy partitioning of nitrile molecules (9) suggest that it would be desirable to expand these studies to molecules involving bonds closely related to the C≡N bond.

Method

Calculations by the l.c.a.o.-m.o.-s.c.f. method using basis sets of Gaussian orbitals were performed on H_2CNH, H_2CN^-, $H_2CNH_2^+$, and H_2CN^+. The nuclear coordinates chosen for the various molecules are given in Tables 1 and 2. The coordinates for H_2CNH given as set *1* in Table 1 are taken from the work of Brown and Penfold (7), while those of set *2* in Table 1 are those of Lehn and Munsch (9) for their geometrical configuration of lowest total energy. The bond lengths and angles for methyleneimine which were used by the latter workers were taken from those for the molecule H_2CNCH_3 (10).

The nuclear coordinates for H_2CN^+ given in Table 1 represent only part of a complete study of the protonation of HCN which will be reported later (11). The coordinates for HCN are taken from previous work (5), and those for H_2CN^- and $H_2CNH_2^+$ represent estimates obtained from the work of Brown and Penfold (7) and of Lehn and Munsch (9). It should be emphasized that the nuclear coordinates for H_2CN^+, H_2CN^-, and $H_2CNH_2^+$ do not necessarily represent equilibrium configurations. The present molecular geometries have been employed to permit comparison with previous work, and with the realization that the major postulate of the present work may be tested on any nuclear configurations.

The values for the exponents used in this work are displayed in Table 3. Exponent sets *1* to *3* are

TABLE 1

(*a*) Nuclear coordinates (a.u.) for H_2CNH

Set number	Atom	Nuclear coordinate		
		X	*Y*	*Z*
1	H1	4.4863	0.0	0.0
	H2	−1.012	1.7527	0.0
	H3	−1.012	−1.7527	0.0
	C	0.0	0.0	0.0
	N	2.5701	0.0	0.0
2	H1	3.1950	−1.7395	0.0
	H2	−1.0120	1.7527	0.0
	H3	−1.0120	−1.7527	0.0
	C	0.0	0.0	0.0
	N	2.4567	0.0	0.0

(*b*) Nuclear coordinates (a.u.) for H_2CN^+

Set number	Atom	Nuclear coordinate		
		X	*Y*	*Z*
	H1	−2.0967	0.0	0.0
	C	−0.0824	0.0	0.0
	N	2.0967	0.0	0.0
1	H2	+2.5000	0.0	0.0
2	H2	−2.5000	0.0	0.0
3	H2	−3.5000	0.0	0.0
4	H2	−0.0824	2.5000	0.0

TABLE 2

Nuclear coordinates for HCN, H_2CN^-, and $H_2CNH_2^+$

Molecule/ion	Atom	Nuclear coordinate		
		X	*Y*	*Z*
HCN	C	0.0	0.0	0.0
	H	−2.000	0.0	0.0
	N	+2.187	0.0	0.0
H_2CN^-	H1	−1.0120	1.7527	0.0
	H2	−1.0120	−1.7527	0.0
	C	0.0	0.0	0.0
	N	2.5701	0.0	0.0
$H_2CNH_2^+$	H1	+3.1950	−1.7527	0.0
	H2	−1.0120	+1.7527	0.0
	H3	−1.0120	−1.7527	0.0
	H4	+3.1950	+1.7527	0.0
	C	0.0	0.0	0.0
	N	2.4567	0.0	0.0

TABLE 3
Exponents used in the calculations

Function	Exponent			
	Set *1*	Set *2*	Set *3*	Set *4*
HS	0.2015	0.2015	0.2015	0.2015
S	1.3320	1.3320	1.3320	1.3320
CS	5.1477	5.1477	7.0	0.154
S	42.4974	42.4974	56.0	0.608
S	146.0970	146.0970	448.0	2.39
S	634.8813	634.8813	3584.0	9.42
S	1.9665	1.9665	2.0	37.3
S	0.4962	0.4962	—	146.0
S	14.1892	14.1892	—	575.0
CP	0.3595	0.2469	0.2469	0.252
P	1.14	1.4810	1.4810	1.48
NS	7.19	7.19	7.0	0.217
S	59.8	59.8	56.0	0.857
S	204.7	204.7	448.0	3.37
S	887.4509	887.4509	3584.0	13.3
S	2.6860	2.6860	2.0	52.5
S	0.7000	0.7000	—	206.0
S	19.9981	19.9981	—	811.0
NP	0.53	0.2469	0.2469	0.3630
P	1.71	1.4810	1.4810	2.1300

those used previously for HCN (5) and are essentially those of Reeves (12) and Huzinaga (13). Set *4* is taken from the work of Csizmadia *et al.* (14).

Calculations were performed on the molecules mentioned using various sizes of basis sets and various sets of exponents. However, an attempt was made in each case to employ a basis set consistent with one of those used previously for HCN. Thus, for example, previous calculations of HCN had involved a basis set of 24 basis functions (b.f.) of the type (20/56/56) indicating 2 S-type functions on the H atom with 5 S-type and 6 P_q-type on both the C and N atoms. Hence, in the present work, for example, a calculation on H_2CN^- using 26 b.f. of the type (40/56/56) was done for comparison.

In addition, previous work (5) on HCN had shown that a basis set of 28 functions of type (20/76/76) gave a reasonably good energy (−116.1327 a.u. compared with −116.4236 a.u. as obtained with a minimal basis set of Slater orbitals (15)). Although of course larger basis sets produced lower energies in general, the 28 function set appeared to be a reasonable compromise between accuracy and computer time. Hence, the largest calculations on the molecules described in the present work were in general done with basis sets analogous to the 28 function set for HCN.

Results and Discussion

Results of the calculations are presented in Tables 4 to 7. In each of these tables the size of basis set and the numbers and types of Gaussian functions are identified. The exponent set is given, followed by a listing of the orbital energies. The occupied and unoccupied π-orbitals are labelled as π and π*, respectively. All energies shown are reported in Hartree units. The nuclear repulsion energy, electronic energy, and total energy are listed, the latter being the sum of the two former energies. The calculated dipole moment in Debyes and the separation between the occupied and unoccupied π-orbitals are also shown. In the case of Table 6, the position of the second H atom with respect to HCN is identified by means of the number of the nuclear configuration set.

Before examining the later tables it is of interest to comment on some of the features of the results given in Tables 4 to 7. For comparison purposes some results obtained previously (3) for HCN are shown in Table 8. The results given in run 5 of Table 8 have not been reported previously. It should be noted here that no

Can. J. Chem. Downloaded from www.nrcresearchpress.com by 210.87.254.6 on 09/05/12
For personal use only.

attempt was made in any of the present calculations to minimize the individual orbital energies. Further, it must be kept in mind during these discussions that while the wavefunctions which have been obtained in this work are expected to be reasonably good, the energies which are obtained are, of course, not the Hartree–Fock energies. Hence, our considerations must be taken as semi-quantitative at best.

The lowest total electronic energies obtained for each of the molecules studied may be seen from an inspection of Tables 4 to 8. As has been mentioned, ab initio calculations have been performed previously for only one of the present molecules, namely H_2CNH, for which Lehn and Munsch (9) obtained a total energy of −93.9473 a.u. which is substantially lower than the best value reported here. The first ionization potential for H_2CNH was calculated on the basis of Koopmans' Theorem (17) to be 11.63 eV. This

TABLE 4

Orbital energies, electronic energies, and total energies[a] for H_2CN^-

Run No.	Exponent set	Orbital energies	Nuclear repulsion energy	Electronic energy	Total energy	Dipole moment (D)	Energy π–π^*
1 (14 b.f.) (20/33/33)	1	−15.7027 −11.0131 −0.4047 −0.2152 −0.2051 −0.0836 (π) 0.0499 0.2507 0.5159 (π^*)[b]	26.0669	−112.7742	−86.7074	4.6287	0.5995
2 (22 b.f.) (40/36/36)	1	−14.8905 −10.7393 −0.3962 −0.2855 −0.2519 +0.0189 (π) 0.0729 0.2968 0.6390 (π^*)[b]	26.0669	−114.1042	−88.0373	1.6498	0.6201
3 (26 b.f.) (40/56/56)	1	−14.8914 −10.7665 −0.4378 −0.2794 −0.2453 0.0360 (π) 0.1023 0.2635 0.6686 (π^*)[b]	26.0669	−114.8993	−88.8324	1.3370	0.6326
4 (30 b.f.) (40/76/76)	2	−15.4055 −11.0436 −0.8416 −0.5197 −0.3181 −0.1361 (π) −0.0774 0.0126 0.4861 (π^*)[b]	26.0669	−118.7664	−92.6995	4.8435	0.6222
5 (26 b.f.) (40/56/56)	3	−15.2981 −11.1100 −0.1851 −0.4811 −0.4195 −0.1954 (π) −0.1323 −0.0972 +0.3833 (π^*)[b]	26.0669	−116.3010	−90.2342	—	0.5787

Can. J. Chem. Downloaded from www.nrcresearchpress.com by 210.87.254.6 on 09/05/12
For personal use only.

TABLE 4—*Concluded*

Run No.	Exponent set	Orbital energies	Nuclear repulsion energy	Electronic energy	Total energy	Dipole moment (D)	Energy π–π^*
6 (30 b.f.) (40/76/76)	4	−15.2882 −11.0439 −0.8172 −0.5109 −0.3153 −0.1395 −0.0681 (π) 0.0213 +0.5226 (π^*)[b]	26.0669	−118.8797	−92.8128	—	0.5907
7 (22 b.f.) (40/36/36)	3	−15.5131 −11.0170 −0.6665 −0.4668 −0.4370 −0.2270 (π) −0.1446 −0.0962 +0.3496[b]	26.0669	−115.7886	−89.7217	4.2346	0.5766

[a]All energies are in Hartrees.
[b]Energy of the first unoccupied orbital.

TABLE 5

Orbital energies, electronic energies, and total energies[a] for $H_2CNH_2^+$

Run No.	Exponent set	Orbital energies	Nuclear repulsion energy	Electronic energy	Total energy	Dipole moment (D)	Energy π–π^*
1 (16 b.f.) (40/33/33)	1	−16.5704 −12.0393 −1.3776 −1.1692 −1.1074 −0.9696 −0.8707 −0.8652 (π) −0.1753 (π^*)[b]	38.6930	−127.1763	−88.4833	3.997	0.6899
2 (26 b.f.) (80/36/36)	1	−15.8725 −11.6449 −1.2709 −1.1730 −1.0838 −1.0083 −0.9319 −0.8781 (π) −0.1923 (π^*)[b]	38.6930	−128.7615	−90.0685	3.968	0.6858
3 (30 b.f.) (80/56/56)	1	−15.8828 −11.5905 −1.3226 −1.1431 −1.0941 −1.0044 −0.8984 −0.8371 (π) −0.1480 (π^*)[b]	38.6930	−129.5821	−90.8891	—	0.6891

Can. J. Chem. Downloaded from www.nrcresearchpress.com by 210.87.254.6 on 09/05/12
For personal use only.

TABLE 5—*Concluded*

Run No.	Exponent set	Orbital energies	Nuclear repulsion energy	Electronic energy	Total energy	Dipole moment (D)	Energy π–π^*
4 (30 b.f.) (80/56/56)	3	−16.0711 −11.7580 −1.4844 −1.1921 −1.1549 −1.0216 −0.9459 −0.9027 (π) −0.2590 (π^*)[b]	38.6930	−130.1246	−91.4316	2.9673	0.6437
5 (34 b.f.) (80/76/76)	2	−16.1841 −11.7267 −1.6511 −1.2091 −1.0696 −0.9259 −0.8544 −0.7731 (π) −0.1536 (π^*)[b]	38.6930	−132.4291	−93.7361	2.9929	0.6195
6 (34 b.f.) (80/76/76)	4	−16.0341 −11.7197 −1.6057 −1.1902 −1.0496 −0.9225 −0.8449 −0.7636 (π) −0.1362 (π^*)[b]	38.6930	−132.5186	−93.8256	—	0.6277
7 (20 b.f.) (80/33/33)	1[c]	−16.4631 −11.9568 −1.1637 −1.0704 −0.9601 −0.7899 −0.7839 (π) −0.6322 −0.0887 (π^*)[b]	38.6930	−126.4542	−87.7612	4.1937	0.6952
8 (26 b.f.) (80/36/36)	3	−16.2242 −11.7047 −1.4146 −1.2258 −1.1253 −1.0445 −0.9748 −0.9464 (π) −0.2911 (π^*)[b]	38.6930	−129.6229	−90.9299	2.6566	0.6552

[a]All energies are in Hartrees.
[b]Energy of the first unoccupied orbital.
[c]HS exponents 0.8000, 1.3320.

compares quite well with the experimental value of 11.9 eV (18).

It is interesting to note that, in contrast with the other species, where the orbital energies are all negative, the calculation which produced the lowest energy for H_2CN^- displays one antibonding orbital for this molecule. The same run provides an energy of −0.1361 a.u. for the occupied π-orbital, which is quite similar to the value -0.13 ± 0.02 a.u. reported for the highest filled π-orbital energy of OCN^- and SCN^- by Clementi and Klint (16) quite recently. These authors made note of the constancy of the π-orbital energy for molecules containing the nitrile bond while drawing attention to the difference of this energy between charged and

Can. J. Chem. Downloaded from www.nrcresearchpress.com by 210.87.254.6 on 09/05/12
For personal use only.

Can. J. Chem. Downloaded from www.nrcresearchpress.com by 210.87.254.6 on 09/05/12
For personal use only.

TABLE 6

Orbital energies, electronic energies, and total energies[a] for H_2CN^+

Run No.	Exponent set	Nuclear configuration set	Orbital energies	Nuclear repulsion energy	Electronic energy	Total energy	Dipole moment (D)	Energy π–π^*
1 (30 b.f.) (40/76/76)	2	1	−17.3167 −11.8781 −1.8195 −1.3787 −1.1443 −0.9101 (π) −0.9101 (π) −0.1912 (π^*)[b] −0.1912 (π^*)[c]	43.8198	−128.7982	−84.9785	—	0.7189
2 (30 b.f.) (40/76/76)	2	2		30.4062	−117.6930	−87.2868	—	—
3 (30 b.f.) (40/76/76)	2	3	−16.2042 −11.7719 −1.6698 −1.2509 −0.8601 −0.7877 (π) −0.7877 (π) −0.3421[b] −0.0926 (π^*)[c]	27.6410	−119.9251	−92.2841	5.6971	0.6951
4 (30 b.f.) (40/76/76)	2	4	−16.2628 −11.7815 −1.7550 −1.1729 −0.9096 −0.8918 −0.8436 (π) −0.2711[b] −0.1305 (π^*)[c]	28.7442	−121.1335	−92.3893	—	0.7131

[a]All energies are in Hartrees.
[b]Energy of the first unoccupied orbital.
[c]Energy of the second unoccupied orbital.

Can. J. Chem. Downloaded from www.nrcresearchpress.com by 210.87.254.6 on 09/05/12
For personal use only.

TABLE 7

Orbital energies, electronic energies, and total energies[a] for H_2CNH

Run No.	Exponent set	Nuclear configuration set	Orbital energies	Nuclear repulsion energy	Electronic energy	Total energy	Dipole moment (D)	Energy π–π^*
1 (15 b.f.) (30/33/33)	2	1	−16.8688 −12.0475 −1.2907 −0.9300 −0.7235 −0.6929 −0.5629 (π) −0.4029 +0.0173 (π^*)[b]	31.4039	−117.8798	−86.4759	1.6318	0.5802
2 (22 b.f.) (60/53/53)	2	1	−16.5381 −11.9011 −1.4212 −1.0211 −0.6738 −0.6660 −0.4814 (π) −0.3446 +0.0919 (π^*)[b]	31.4039	−119.9346	−88.5307	0.4663	0.5733
3 (22 b.f.) (60/53/53)	2	2	−16.5177 −11.9667 −1.4749 −0.9897 −0.7490 −0.6164 −0.5209 (π) −0.4273 +0.0939 (π^*)[b]	32.6871	−121.1124	−88.4253	1.5896	0.6148
4 (32 b.f.) (60/76/76)	1	2	−15.8223 −11.4012 −1.2874 −0.8874 −0.6780 −0.5951 −0.4370 (π^*) −0.4063 +0.1551 (π^*)[b]	32.6871	−126.0815	−93.3944	2.2804	0.5921

[a]All energies are in Hartrees.
[b]Energy of the first unoccupied orbital.

TABLE 8

Orbital energies, electronic energies, and total energies[a] for HCN

Run No.	Exponent set	Orbital energy	Nuclear repulsion energy	Electronic energy	Total energy	Energy π–π^*
1 (14 b.f.) (20/33/33)	1[d]	−15.9218 −11.3958 −0.7646 −0.4030 −0.3829 (π) −0.3550 (π) +0.0540 (π) +0.3651[b] +0.4099 (π^*)[c]	23.8762	−109.8314	−85.9552	—
2 (20 b.f.) (20/36/36)	3	−15.9308 −11.4382 −1.2191 −0.7555 −0.6651 (π) −0.6651 (π) −0.5184 +0.0648 (π^*)[b] +0.0648 (π^*)[c]	23.8762	−113.2268	−89.3506	0.7299
3 (24 b.f.) (20/56/56)	3	−15.6849 −11.4988 −1.2524 −0.7668 −0.6159 (π) −0.6152 (π) −0.5444 +0.1014 (π^*)[b] +0.1015 (π^*)[c]	23.8762	−113.7758	−89.8996	0.7166
4 (28 b.f.) (20/76/76)	2	−15.8416 −11.4047 −1.3436 −0.8104 −0.5323 −0.4817 (π) −0.4817 (π) +0.2092 (π^*)[b] +0.2092 (π^*)[c]	23.8762	−116.1327	−92.2565	0.6909
5 (28 b.f.) (20/76/76)	4	−15.7599 −11.3801 −1.3054 −0.8074 −0.5555 −0.4814 (π) −0.4813 (π) +0.2258 (π^*)[b] +0.2259 (π^*)[c]	23.8762	−116.2503	−92.3741	0.7071

[a]All energies are in Hartrees.
[b]Energy of first unoccupied orbital.
[c]Energy of second unoccupied orbital.
[d]HS exponents 0.8000, 1.3320.

neutral molecules. In general the occupied π-orbital energies are of the same order of magnitude for all the calculations on a given molecule (at least for the larger basis sets), the major exception being that of H_2CN^- where both the sign and magnitude change. The occupied π-orbital energies are approximately −0.90, −0.76, −0.48, −0.44, and −0.14 a.u. for H_2CN^+, $H_2CNH_2^+$, HCN, H_2CNH, and H_2CN^-, respectively. Clementi and Klint quote a value of −0.49 a.u. for neutral nitriles. It is not unexpected that the π-orbital energies for the molecules, other than HCN, would be considerably different from the value expected for a

Can. J. Chem. Downloaded from www.nrcresearchpress.com by 210.87.254.6 on 09/05/12
For personal use only.

Can. J. Chem. Downloaded from www.nrcresearchpress.com by 210.87.254.6 on 09/05/12
For personal use only.

nitrile since it is immediately obvious that the addition of the hydrogens substantially alters the CN bond in each of these molecules.

With all the molecules examined the π–π^* separations remain relatively unchanged from one calculation to another for a given molecule. These separations are approximately 0.71, 0.71, 0.63, 0.59, and 0.59 a.u. for HCN, H_2CN^+, $H_2CNH_2^+$, H_2CN^-, and H_2CNH, respectively.

In all cases the dipole moments fluctuate substantially from calculation to calculation with a given molecule, reflecting their sensitivity to the "goodness" of the wavefunction.

Brown and Penfold (6, 7) report a total π-electron energy of approximately -23 eV (-0.8 a.u.) and -62.7 eV (-2.3 a.u.) for H_2CN^- and $H_2CNH_2^+$, respectively, based on their π-electron calculations. These may be compared with -0.12 and -1.5 a.u., respectively, from the present work. One may speculate that perhaps the discrepancy between their value and that given here is related to the inaccuracy of the assumption of σ–π separability. In this connection it is interesting to note that the highest occupied orbital is a π-orbital in the case of $H_2CNH_2^+$, but not for H_2CN^-.

The results for H_2CN^+ given in Table 6 represent different nuclear configurations and therefore reflect such differences in the number of occupied π-orbitals. Calculations involving linear structures, that is, where the second H atom is colinear with the HCN molecule, yield results involving two π-orbitals whereas with a planar, but nonlinear, molecule, only one π-orbital exists.

Table 9 illustrates the differences between the total energies (electronic energy plus nuclear repulsion energy) of molecules where the calculations have been done with analogous basis sets and the corresponding sets of exponents. The notation (i, j) will refer to the sizes of the basis sets used in the calculations to obtain the subtracted energies. Thus (28, 30) indicates that an energy obtained with a basis set of 30 functions was subtracted from that found with 28 functions, where the former set was used with H_2CN^-, the latter with HCN, for example.

The differences in total energy between HCN and H_2CN^- are 0.3711, 0.3346, 0.4430, and 0.4387 a.u. with basis sets of (20, 22), (24, 26), (28, 30), and (28, 30) functions, respectively, as seen from the first four rows of Table 9. However, the individual energies calculated with the 24- and 26-function sets are about 2.5 a.u. larger than with the 28- and 30-function sets. Hence, a change of approximately 0.11 a.u. in ΔE is associated here with a change of about 2.5 a.u. in energy itself. It should be noted that the runs whose energies are subtracted involve the same exponent set, but the ΔE values which are compared involved either different sizes of basis sets and/or different exponent sets. It should be recalled that one Hartree (a.u.) is equivalent to 627.7 kcal per mole so that small differences in Hartree units can make substantial differences in kilocalorie units. However, it does appear that, at least for the data presented in the first part of Table 10, the change in ΔE is much less than the change in the energy itself. In addition, there is some evidence that, in the present case, the total energy difference has become relatively constant for the (28, 30) results even though the energy itself is still changing.

As can be seen from second part of Table 9, the differences between the energies of $H_2CNH_2^+$ and HCN are given as 1.4515, 1.4796, 1.5320, 1.5793, and 1.8061 a.u. for basis sets (28, 34), (28, 34), (24, 30), (20, 26), and (14, 20). The energies obtained with the largest basis sets and exponent set *2* for a given molecule are about 2.3 a.u. lower than those with the next smallest basis set. However, the energy differences, as displayed in column 5 are separated only by approximately 0.05 a.u. The total energies obtained for the molecules under discussion as found with the smallest sets are about 3 a.u. higher than those obtained with the next largest basis sets, while the energy difference is about 0.3 a.u. Hence, it may be seen that the ΔE values do appear to be reaching more constant values with much smaller basis sets than the values of total energy.

The last part of Table 9 illustrates the energies obtained for H_2CN^- and $H_2CNH_2^+$ as the size of the basis set is increased. The values of ΔE, the difference in total energy between these two molecules, as shown in the fourth column, change in a manner somewhat different from the cases discussed previously. In the present case the values of ΔE increase as the total energy of either H_2CN^- or $H_2CNH_2^+$ decreases. With further decrease in the energy of either of these molecules, ΔE passes through a maximum and then falls off relatively slowly as the energy continues to decrease. It appears that a further

Can. J. Chem. Downloaded from www.nrcresearchpress.com by 210.87.254.6 on 09/05/12
For personal use only.

TABLE 9

Comparison of total energy differences (a.u.) for the various molecules as a function of size of basis set

Total energy (a.u.)			Total energy difference (a.u.)
HCN	H_2CN^-	$H_2CNH_2^+$	
−89.3506 (20/36/36) Exponent 3	−89.7217 (40/36/36) Exponent 3		0.3711
−89.8996 (20/56/56) Exponent 3	−90.2342 (40/56/56) Exponent 3		0.3346
−92.2565 (20/76/76) Exponent 2	−92.6995 (40/76/76) Exponent 3		0.4430
−92.3741 (20/76/76) Exponent 4	−92.8128 (40/76/76) Exponent 4		0.4387
−85.9552 (20/33/33) Exponent 1[a]		−87.7613 (80/33/33) Exponent 1[a]	1.8061
−89.3506 (20/36/36) Exponent 3		−90.9299 (80/36/36) Exponent 3	1.5793
−89.8996 (20/56/56) Exponent 3		−91.4316 (80/56/56) Exponent 3	1.5320
−92.2565 (20/76/76) Exponent 2		−93.7361 (80/76/76) Exponent 2	1.4796
−92.3741 (20/76/76) Exponent 4		−93.8256 (80/76/76) Exponent 4	1.4515
	−86.7074 (20/33/33) Exponent 1	−88.4833 (40/33/33) Exponent 1	1.7759
	−88.0373 (40/36/36) Exponent 1	−90.0685 (80/36/36) Exponent 1	2.0312
	−88.8324 (40/56/56) Exponent 1	−90.8891 (80/56/56) Exponent 1	2.0567
	−89.7217 (40/36/36) Exponent 3	−90.9299 (80/36/36) Exponent 3	1.2082
	−90.2342 (40/56/56) Exponent 3	−91.4316 (80/56/56) Exponent 3	1.1974
	−92.6995 (40/76/76) Exponent 2	−93.7361 (80/76/76) Exponent 2	1.0366
	−92.8128 (40/76/76) Exponent 4	−93.8256 (80/76/76) Exponent 4	1.0128

[a]HS exponents 0.8000, 1.3320.

TABLE 10

Changes in total electronic energy for various hypothetical reactions[a]

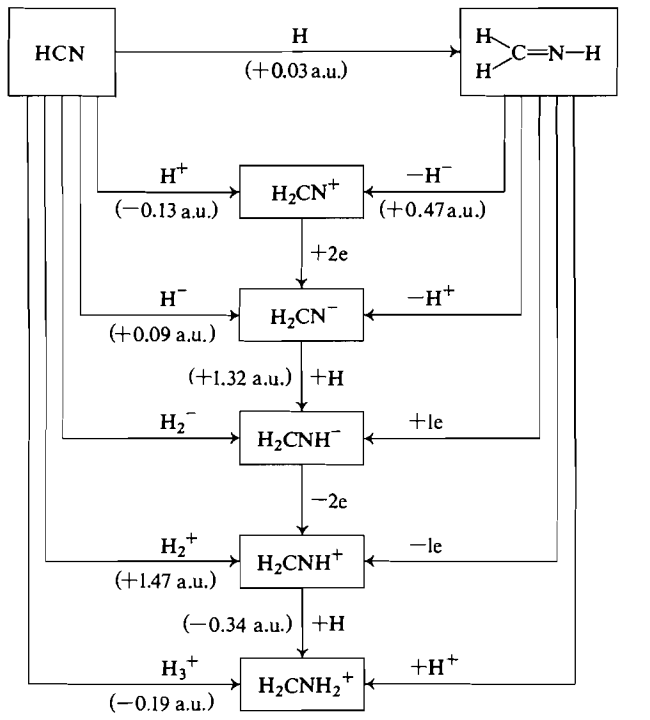

[a]Electronic energies for H^-, H_2^+, H_2, and H_3^+ are taken from refs. 19, 20, 21, and 22, respectively.

increase in the size of basis set is not likely to change ΔE by more than 0.1 a.u. However, a disconcerting feature of the behavior of the energies of the molecules under discussion is the apparently erratic change of ΔE in the region of small basis sets. No convenient method for explaining this is apparent at the moment. However, the results of the calculations using the four largest basis sets show that the value of ΔE changes by only 0.2 a.u. while the energy itself changes by approximately 3 a.u. Hence, with these two molecules H_2CN^- and $H_2CNH_2^+$, the ΔE values again appear to change relatively little as the energy decreases substantially, at least for reasonably sized basis sets.

It is interesting to attempt to calculate the changes in electronic energy which would be associated with some hypothetical processes involving the molecules discussed here. The reactions considered and the energy changes are shown in Table 10. The electronic energies for H^-, H_2^+, H_2, and H_3^+ were taken from the work of various authors, and are listed at the bottom of Table 10. The changes in energy for the reactions are, in general, quite small. Since these changes have been obtained by the subtraction of two relatively large numbers, which may be in error by as much as 0.1 a.u., it is, of course, dangerous to attach much significance to these values. On the other hand, since the present work seems to indicate that changes in ΔE will become small quite rapidly as the size of basis set is increased, it is hoped that the values of ΔE for the complete reactions would at least be of the correct order of magnitude. Of course, the values of ΔE so obtained are relevant only for the particular nuclear configurations used for the various molecules in this work. Further, no energies associated with motions of the nuclei have been considered so that it is not possible to relate the estimated changes in electronic energy with the thermodynamic heats of reaction.

Finally, it has appeared worthwhile to consider the present results in the light of more

Can. J. Chem. Downloaded from www.nrcresearchpress.com by 210.87.254.6 on 09/05/12
For personal use only.

Can. J. Chem. Downloaded from www.nrcresearchpress.com by 210.87.254.6 on 09/05/12
For personal use only.

detailed examination of the paper by Clementi and Klint (16). These authors examined the effect of bringing various positive or negative point charges up to various distances from the carbon atom in CN^-. In all cases the point charges were placed along the CN axis. In addition, the calculations were repeated for the isocyano group, which was simulated by bringing the point charges up to various distances from the nitrogen atom in CN^-. The results of these calculations were displayed in the form of the orbital energies and total energies for each value of the charge selected and for each separation of the point charge involved.

It appears to the present author that an interesting semi-quantitative extrapolation of the results of Clementi and Klint could be made such that some applicability could be seen to the results of the present work. It seems not unreasonable to suggest that, for example, H_2CN^+ might be thought of as a point charge (H_2^{2+}) placed approximately 1 a.u. from the carbon atom of CN^-. In the same way H_2CN^- could perhaps be considered as a point charge (H_2^0) situated approximately 1 a.u. from the carbon atom of CN^-. Finally $H_2CNH_2^+$ might be taken as CN^- with a point charge (H_2^+) approximately 1 a.u. from the carbon of the CN^- and another point charge of H_2^+ approximately 1 a.u. from the nitrogen atom.

Clementi and Klint have performed calculations for point charges of ± 0.2 and ± 0.4 at 2, 3, and 5 a.u. from the carbon atom, and similarly for the point charges placed in respect to the nitrogen atom. The effect of bringing a point charge of ± 0.4 from a distance of 5 a.u. to a distance of 2 a.u. from the carbon atom can then be observed. Variations of the energy of the π-orbital, for example, as a result of such changes can then be considered. From the tables of Clementi and Klint it is estimated that a change of 1 a.u. closer to the carbon atom of CN^- increases the value of the negative of the energy of the π-orbital ($-\varepsilon_\pi$) by 0.013 a.u. For example, a charge of $+0.4$ when brought from 2 a.u. to 1 a.u. from the carbon atom causes $-\varepsilon_\pi$ to increase from 0.3034 to approximately 0.316 a.u., the latter being an extrapolated value. Further, an increase of the positive charge from 0.2 to 0.4 produces an increase of $-\varepsilon_\pi$ by 0.0345, 0.0484, and 0.0561 a.u. for distances of 5, 3, and 2 a.u. of the positive charge from the carbon atom of CN^-. Hence, it is estimated that an increase of the charge by 0.2 at a distance of 1 a.u. from the carbon atom should increase $-\varepsilon_\pi$ by 0.06 a.u. Therefore an increase of the charge from its value of $+0.4$ given above to $+2.0$ (for H_2^+) at a distance of 1 a.u. from the carbon atom should increase $-\varepsilon_\pi$ by 0.48 a.u., which when added to the previous value of 0.316 a.u. yields approximately 0.801 a.u. for $-\varepsilon_\pi$. It is interesting to compare this with the π-orbital energy of -0.84 a.u. obtained for H_2CN^+ in run 4 (Table 6).

In the same way, a value of -0.74 a.u. may be estimated for the π-orbital energy of $H_2CNH_2^+$ to be compared with a value of approximately -0.76 a.u. found in run 6 (Table 5) for $H_2CNH_2^+$. The estimated value was based on a model of a $+1.0$ charge approaching CN^- from both sides. For H_2CN^- a value of -0.19 a.u. can be estimated for the π-orbital energy and may be compared with -0.07 a.u. from run 12 (Table 6). Finally by bringing a charge of $+1.0$ up to H_2CN^- from the right, the π-orbital energy for H_2CNH may be approximated to be -0.46 a.u. which compares favorably with -0.44 a.u. and found in run 4 (Table 7).

It is readily seen that in all the cases discussed here, except that of H_2CN^-, the value of the π-orbital energy estimated from the work of Clementi and Klint agrees with the calculated values reasonably well considering the simplicity of the model employed. Even in the case of H_2CN^- the direction of the change of the π-orbital energy is reproduced. These semi-quantitative calculations suggest that the extension of these ideas to other molecules may well be worthwhile. Of course, assuming the agreement obtained is not fortuitous, such results also lend support to the idea that a significant amount of the variation of orbital energies in series of similar molecules may be ascribed to charge effects. It must be emphasized that the extrapolation of the results of Clementi and Klint are, at best, semi-quantitative. The assumptions that their work can be extrapolated from 2 a.u. to distances of much less than this, and further, that molecularly-sized species may be considered as point charges are obviously difficult to support. However, the justification here lies entirely in the agreement obtained between the results so obtained and the values reported from the calculations in the present work. Finally, it must be recalled that these extrapolations have been

applied to nuclear configurations not all of which have been shown to represent equilibrium structures.

The work discussed in the present paper has presented some calculations on similar molecules using relatively small basis sets and has demonstrated that it may not be unreasonable to suggest that differences between Hartree–Fock energies and those calculated using such small basis sets may indeed to a significant extent cancel out in the calculation of energy changes on reaction.

This suggests that there may be some hope of performing ab initio calculations on chemical reactions with relatively small basis sets. Obviously a substantial amount of additional work is required to support such a contention. Finally, some highly speculative extrapolations of a point charge model produce results which suggest that it may be possible, at least in part, to account for variations in orbital energies through the use of such a model.

The financial support of the National Research Council of Canada and the assistance of the Computer Center of the University of Waterloo are gratefully acknowledged.

1. E. CLEMENTI. J. Chem. Phys. **46**, 3851 (1967).
2. J. B. MOFFAT. Can. J. Chem. **46**, 3893 (1968).
3. L. C. SNYDER and H. BASCH. J. Amer. Chem. Soc. **91**, 2189 (1969).
4. J. B. MOFFAT and H. E. POPKIE. Int. J. Quantum Chem. **11**, 565 (1968).
5. J. B. MOFFAT and R. J. COLLENS. Can. J. Chem. **45**, 655 (1967).
6. R. D. BROWN and A. PENFOLD. J. Chem. Phys. **24**, 1259 (1956).
7. R. D. BROWN and A. PENFOLD. Trans. Faraday. Soc. **53**, 397 (1957).
8. A. JULG and P. CARLES. C. R. **251**, 1782 (1960).
9. J. M. LEHN and B. MUNSCH. Theor. Chim. Acta, Berlin, **12**, 91 (1968).
10. K. V. L. N. SASTRY and R. F. CURL. J. Chem. Phys. **41**, 77 (1964).
11. J. B. MOFFAT. To be published.
12. C. M. REEVES. J. Chem. Phys. **39**, 1 (1963).
13. S. HUZINAGA. J. Chem. Phys. **42**, 1293 (1965).
14. I. G. CSIZMADIA, M. C. HARRISON, J. W. MOSKOWITZ, and B. T. SUTCLIFFE. Theor. Chim. Acta, Berlin, **6**, 191 (1966).
15. A. D. MCLEAN. J. Chem. Phys. **37**, 627 (1962).
16. E. CLEMENTI and D. KLINT. J. Chem. Phys. **50**, 4899 (1969).
17. T. KOOPMANS. Phys. **1**, 104 (1933).
18. J. E. COLLIN and M. J. FRANKLIN. Bull. Soc. Roy. Sci. Liege, **35**, 267 (1966).
19. E. A. HYLLERAS and J. MIDTDAL. Phys. Rev. **103**, 829 (1956).
20. H. WIND. J. Chem. Phys. **42**, 2371 (1965).
21. W. KOLOS and C. C. J. ROOTHAAN. Rev. Mod. Phys. **32**, 219 (1960).
22. B. D. JOSHI. J. Chem. Phys. **44**, 3627 (1966).

Can. J. Chem. Downloaded from www.nrcresearchpress.com by 210.87.254.6 on 09/05/12
For personal use only.

Can. J. Chem. Downloaded from www.nrcresearchpress.com by 210.87.254.105 on 09/05/12
For personal use only.

Stereospecific synthesis of two epimeric 2-chlorodeoxy pentoses involving anomeric chlorine participation[1]

H. J. JENNINGS
Biochemistry Laboratory, National Research Council of Canada, Ottawa, Canada

Received December 4, 1969

A simple procedure has been developed for the stereospecific synthesis of some 2-chloro-2-deoxy pentoses. Treatment of β-D-xylopyranosyl chloride 2,3,4-tri(chlorosulfate) with aluminum chloride (>1 mole equivalent) resulted in specific chloro-displacement of the C-2 chlorosulfate group via a mechanism involving anomeric chlorine migration, which occurred to the extent of almost 100%. The resultant crystalline 2-chloro-2-deoxy-α-D-lyxopyranosyl chloride 3,4-di(chlorosulfate) when treated with sodium iodide yielded crystalline 2-chloro-2-deoxy-D-lyxose. Similarly α-D-lyxpoyranosyl chloride 2,3,4-tri(chlorosulfate) yielded 2-chloro-2-deoxy-α-D-xylopyranosyl chloride 3,4-di(chlorosulfate) from which pure 2-chloro-2-deoxy-D-xylose was obtained by a modified procedure. The structures of these compounds have been confirmed and the mechanism is discussed.

Canadian Journal of Chemistry, **48**, 1834 (1970)

Introduction

Although a number of syntheses of 2-chlorodeoxy glycoses have been reported (1), in no recorded case has a stereospecific synthesis been devised. These syntheses are usually best achieved by the chlorination of 1,2-glycal acetates first carried out by Fischer *et al.* (2). This reaction has recently been shown to yield a diastereoisomeric mixture of 2-chlorodeoxy-glycosyl chlorides (3–5) from which 2-chlorodeoxy glycoses have been obtained by anomeric dechlorination (6) and acid-catalyzed deacetylation (7). Another method that has been utilized is the scission of 2,3-anhydro glycosides with hydrogen chloride (8) which yields a mixture of 2- and 3-chlorodeoxy isomers exclusively in the 2,3-*trans* configuration. The best approach to a stereospecific synthesis would seem to be via a direct displacement (S_N2) of a suitable leaving group at C-2 by chloride ion, but none have been reported presumably due to the inactivity of a leaving group at this site. However, displacements of 2-sulfonate esters have been achieved through the agency of participating epithiosulfide groups (9) whereby the opening of the cyclic epithiosulfonium ion yields a mixture of 2- and 3-chlorodeoxy isomers exclusively in the 2,3-*trans* configuration. The method we now report probably falls into this latter category of chloro-substitution via vicinal group participation but has the attractive feature of involving anomeric chlorine participation. This results in the subsequent migration of anomeric chlorine, in yields of almost 100%, exclusively to C-2 thus avoiding the formation of epimeric and isomeric products. To our knowledge this is the first reported incidence of chlorine migration in carbohydrate chemistry although it is probable that chlorine participation does occur to varying degrees in the chlorination of glycal acetates (3, 5) and in some anomeric exchange reactions involving the 2-chlorodeoxy substituents of glycosyl chloride derivatives (10).

Discussion

Previous attempts to anomerize β-D-xylopyranosyl chloride 2,3,4-trichlorosulfate (**1**) with aluminum chloride (0.25 mole equ.) had given very poor yields of the crystalline α-D-anomer (**2**) (11) (Scheme 1). A study of the proton magnetic resonance (p.m.r.) spectrum at 60 MHz of the crude reaction product indicated that the poor yield was due to both incomplete anomerization, and to the simultaneous formation of another product to which the structure **4** was assigned. By gradually increasing the mole ratio of aluminum chloride in this reaction and following the ratio of products by p.m.r. spectroscopy it was found that with 1.5 mole equ. of aluminum chloride that **4** became the exclusive product of this reaction (Table 1). This was also found to be the case when **2** was treated with aluminum chloride in a similar manner. The structure of crystalline **4** was consistent with its elemental analysis, specific rotation, and p.m.r. parameters. The first order coupling constants $J_{1,2}$ 1.8, $J_{2,3}$ 3.5, $J_{3,4}$ 9.6, $J_{4,5e}$ 5.9, $J_{4,5a}$ 10.0, and $J_{5a,5e}$ 12.0 Hz obtained from

[1]NRCC No. 11244.

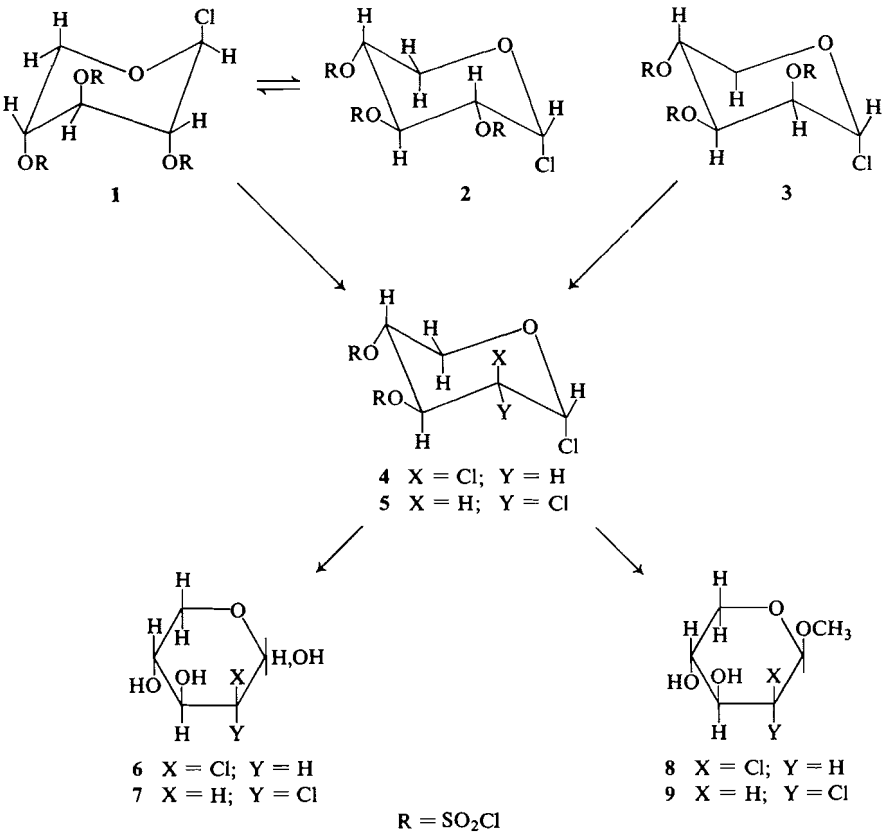

SCHEME 1

TABLE 1

Approximate percentage (%) of **1**, **2**, and **4** obtained by treating **1** with different mole ratios of aluminum chloride and titanium tetrachloride

Reagent	Reaction time (min)	Moles reagent/ moles **1**	% Products in reaction mixtures		
			1	**2**	**4**
$AlCl_3$	45	0.25	26	37	37
$AlCl_3$	45	0.50	—	48	52
$AlCl_3$	45	1.00	—	21	79
$AlCl_3$	45	1.50	—	—	>90
$TlCl_4$	180	8.00	14	72	14

the p.m.r. spectrum of **4** (Fig. 1) are consistent with its α-D-lyxopyranosyl structure (Cl(D) conformation). Also the coupling constants are almost identical to those obtained from the p.m.r. spectrum of **3** (11), a configurational analogue of **4** differing only in the nature of the C-2 substituent. This introduction of the less electronegative chloro-group on C-2 of **4** is probably responsible for the considerable upfield shift (12) of the H-2 signal (quartet at τ 5.15) compared with the signal previously assigned to H-2 in the p.m.r. spectrum of **3** (11). That the H-2 proton of **4** was assigned correctly was confirmed by field swept spin decoupling experiments at 60 MHz. When the quartet at τ 5.15 was irradiated (δ + 78.5 Hz) the low field anomeric doublet at τ 3.83 collapsed to a singlet. Conversely when the anomeric signal was irradiated (δ − 78.5 Hz) the quartet at τ 5.15 collapsed to a doublet with a spacing of 3.6 Hz. This confirmed the value of the $J_{2,3}$ coupling constant which is consistent with the axial orientation of the C-2 chloro-group in **4** (Cl(D) conformation). Further evidence for the structure of **4** was obtained by the methanolysis of **4** and subsequent dechlorosulfation of the product to give a syrupy mono-chloro-methyl glycopyranoside (**8**) (Scheme 1), which slowly consumed 1 mole of periodate with subsequent overoxidation. The uptake of periodate indicated

Can. J. Chem. Downloaded from www.nrcresearchpress.com by 210.87.254.105 on 09/05/12
For personal use only.

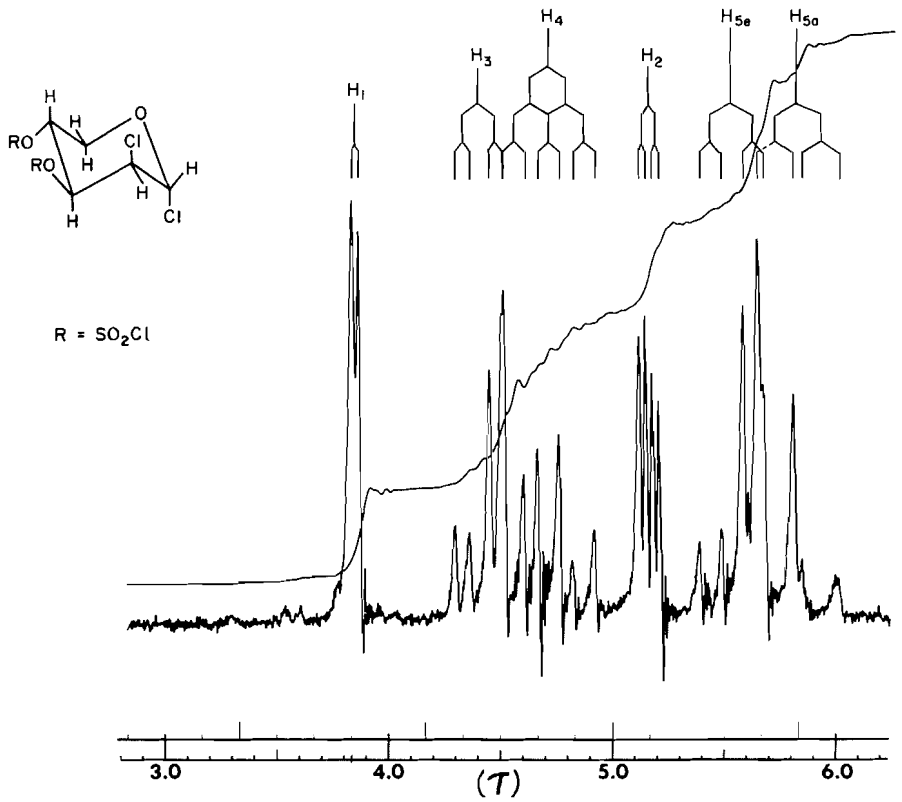

FIG. 1. Proton magnetic resonance spectrum at 60 MHz of 2-chloro-2-deoxy-α-D-lyxopyranosyl chloride 3,4-di(chlorosulfate) (**4**) in deuteriochloroform.

the presence of vicinal hydroxyl groups as it has been previously demonstrated that 3-chlorodeoxy glycopyranosides are resistant to periodate oxidation (13, 14). The β-D-configuration was assigned to **8** by virtue of its high negative specific rotation, but gas–liquid chromatographic (g.l.c.) analysis of the syrupy product revealed the presence of a small quantity of the α-D-anomer. That this small component was in fact the α-D-anomer of **8** was ascertained by the methanolysis of the syrupy product, which yielded the same two components but with a preponderance of the α-D-anomer in this case (g.l.c. analysis). The treatment of **4** with sodium iodide yielded crystalline 2-chloro-2-deoxy-α-D-lyxose (**6**) (Scheme 1) which on methanolysis yielded a mixture of **8** and its α-D-anomer (g.l.c. analysis). The slow mobility of **6** on paper electrophoretograms was indicative of a 2-chloro substituted glycose (15) and also eliminated the only other expected alternative products that could result from the mono-chloro substitution of **1** or **2**, namely, 4-chloro-4-deoxy-L-arabinose (16) or the corresponding D-xylose derivative (15). Authentic samples of these compounds had a considerably faster mobility than **6** on paper electrophoretograms.

The reaction of aluminum chloride with **3** yielded a syrupy product which resisted crystallization. The p.m.r. spectra of the syrupy product at 60 and 100 MHz (Fig. 2) indicated one major component exemplified by its anomeric signal (doublet) at τ 3.84, to which the structure **5** was assigned. Small quantities of impurities in the syrupy product were also detected by other weak signals in the p.m.r. spectra (Fig. 2), some of which were found to be characteristic of the signals of unreacted **3** (11). Despite the extraneous signals a first-order analysis was made of both the 60 and 100 MHz spectra of **5** and the coupling constants ($J_{1,2}$ 3.7, $J_{2,3}$ 9.6, $J_{3,4}$ 9.6, $J_{4,5e}$ 6.0, $J_{4,5a}$ 9.8, and $J_{5a,5e}$ 11.7 Hz) are consistent with its α-D-xylopyranosyl structure in the Cl(D) conformation; and are almost identical to those obtained from the p.m.r. spectrum of a con-

Can. J. Chem. Downloaded from www.nrcresearchpress.com by 210.87.254.105 on 09/05/12
For personal use only.

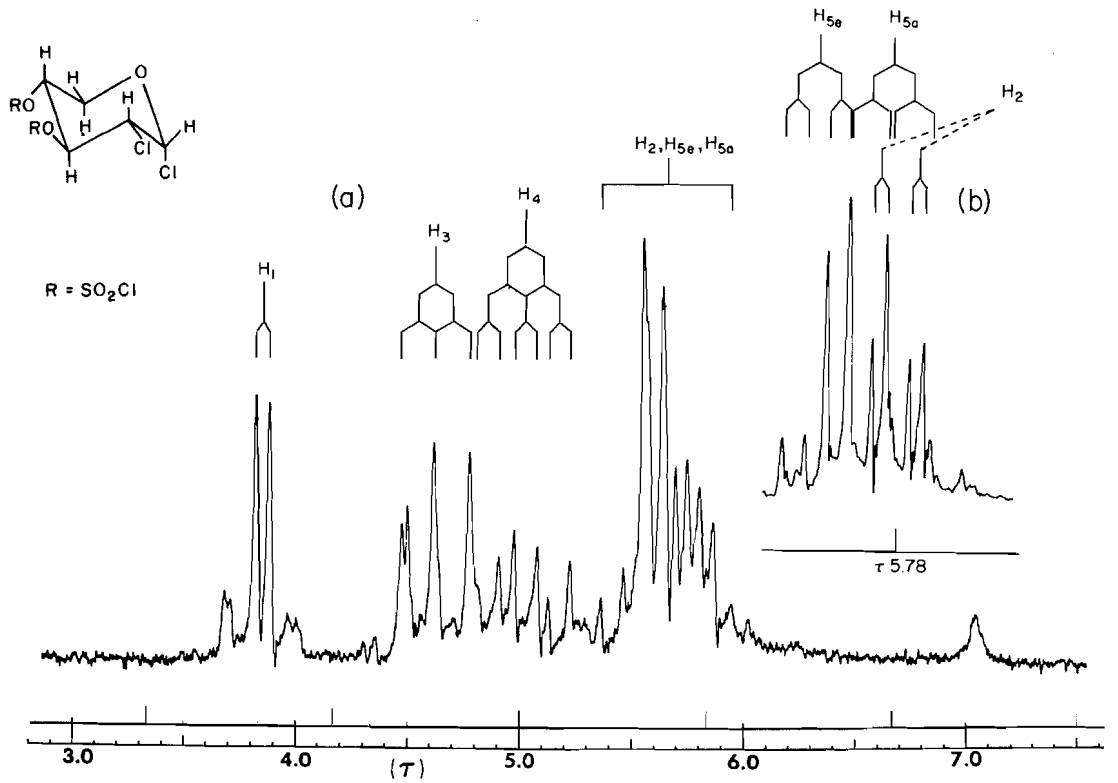

FIG. 2. Proton magnetic resonance spectra of 2-chloro-2-deoxy-α-D-xylopyranosyl chloride 3,4-di(chlorosulfate) (**5**) in deuteriochloroform, (*a*) at 60 MHz, (*b*) high-field part of the 100 MHz spectrum.

figurational analogue (**2**) (11). The quartet centered on τ 5.78 was assigned to H-2 of **5** by analogy with the assignment of the H-2 proton of **4**. That the H-2 signal of **5** was assigned correctly was substantiated by decoupling experiments (100 MHz), when irradiation of the anomeric doublet of **5** (τ 3.84) caused the collapse of the highest field line of the H-2 quartet. The fact that an easily recognizable doublet was not produced was due to the complex overlap of some of the lines of the H-2 and H-5*a* signals (Fig. 2). Methanolysis of **5** and the subsequent dechlorosulfation of the syrupy product gave a syrupy mixture of methyl glycosides from which **9** was obtained crystalline. Crystalline **9** consumed periodate at an almost identical rate to that of **8** and was assigned the β-D-configuration by virtue of its negative specific rotation. Crystalline **9** was shown to be homogeneous by g.l.c. analysis and both **9** and its α-D-anomer were detected in the mother liquors obtained from its recrystallization (g.l.c. analysis). Methanolysis of crystalline **9** gave two components with identical retention volumes to those found in the mother liquors above.

The treatment of **5** with sodium iodide by the same procedure used in the conversion of **4** to **6** yielded an approximately equimolar mixture of the two epimeric 2-chloro-deoxy pentoses (**6** and **7**) (paper electrophoresis and g.l.c. analysis). The loss of asymmetry at C-2 during this procedure can best be explained in this case by the simultaneous dechlorosulfation and dehydrochlorination of **5** to give a 2-chloro-xylal intermediate. This intermediate would then undergo hydroxylation of the double bond yielding a mixture of 2-chlorodeoxy epimers (**6** and **7**). The *trans*-diaxial orientation of the anomeric chloro-group and the proton on C-2 of **5** are a prerequisite for such a facile elimination process (17), whereas this orientation of these substituents cannot be achieved in the case of **4**. The possibility that **5** was originally a mixture of **4** and **5** was discounted by the absence of some of the characteristic p.m.r. signals of **4** in the spectrum of **5** (Fig. 2) and by the fact that methanolysis of **5** did not yield any

Can. J. Chem. Downloaded from www.nrcresearchpress.com by 210.87.254.105 on 09/05/12
For personal use only.

[1]

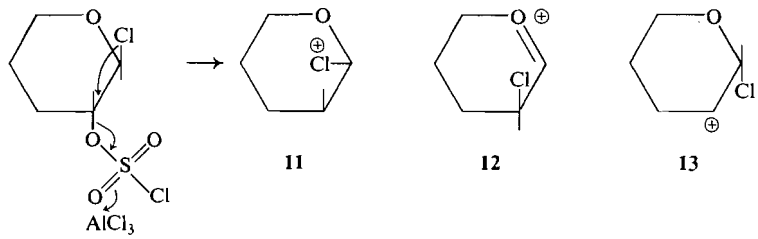

10 11 12 13

detectable quantity of **8** or its α-D-anomer (g.l.c. analysis). A further possibility of epimerization of the product (**7**) during the dechlorosulfation procedure was also discounted because no evidence of this type of elimination was encountered following replacement of the anomeric chlorine of **5** by a hydroxyl group, and this modification enabled pure **7** to be obtained from **5**. The purity of **7** was established by g.l.c. analysis and paper electrophoresis.

It would appear on the evidence obtained by p.m.r. spectroscopy and g.l.c. analysis that the crude reaction products which yielded **4** and **5** were essentially free of their respective 2-chloro epimers. Thus the mechanism of this reaction would have to explain 2-chloro substitution of both **1** and **3** with exclusive inversion of configuration. It would also have to be consistent with the fact that the C-2 chlorosulfate group was preferentially substituted when under normal S_N2 conditions it has been demonstrated that **1** in the presence of chloride ion was preferentially substituted at C-4, to give 4-chloro-4-deoxy-L-arabinopyranosyl chloride 2,3-di(chlorosulfate) (16). The mechanism therefore involves a considerable activation of the C-2 chlorosulfate group as a leaving group coupled with a localization of nucleophilic chlorine in the vicinity of the anomeric center. The simplest mechanistic interpretation would be an intramolecular displacement of the C-2 chlorosulfate group involving participation of anomeric chlorine. The heterolysis of the (C-2)—O bond of **1** probably occurs with the simultaneous participation of the anomeric chlorine as represented in **10** to give the chloronium ion (**11**) (eq. [1]). Then preferential addition of chloride ion to the more highly reactive anomeric center of **11** would result in net inversion of configuration at C-2 of **1** to yield **4**. An analogous argument could be presented for the conversion of **3** to **5** with the minor modification of further anomerization of the initial 1,2-*trans* product discussed below. The chlorosulfate groups are probably activated by the co-ordination of their oxygen atoms with aluminum chloride and this would account for the reagent dependence of the reaction where the weaker Lewis acid ($TiCl_4$) was less efficient in promoting 2-chloro substitution than aluminum chloride (Table 1). Evidence for this type of co-ordination involving adduct molecules of aluminum chloride and sulfonyl chlorides is well established (18). It is interesting to note that exclusive 2-chloro-displacement occurs in **1** and **3** despite the presence of other accessible chlorosulfate groups in both molecules. It seems unlikely that this specificity could be attributed to the enhanced activation of the C-2 chlorosulfate group, and it is more likely that a predominant factor in this specificity is the preference of chlorine to migrate through a 1,2-cyclic ion. Any alternative mechanism involving the direct formation of the β-chlorocarbonium ion (**13**) is highly unlikely as this would again require the enhanced activation of the C-2 chlorosulfate group over the other chlorosulfate groups in these molecules. Also in these circumstances **2** and **3** would have yielded an identical ion (**13**) whereas each gave a different epimerically pure product (**4** and **5** respectively). The fact that chlorine migration occurred to the extent of almost 100% in these reactions is worthy of mention because chlorine has generally been shown to have poor participating properties (3, 19, 20). However, these migrations are not without precedent as it has been more recently established that 1,2-chlorine shifts can be obtained in comparable yields by the trifluoroacetolysis of 2-chloro-propyl *p*-nitrobenzoate-sulfonate (21) and also by the methanol quenching of 1,2-chloronium ions generated in antimony pentafluoride – sulfur dioxide (22). Firm evidence for the existence of the chloronium ion has also been obtained by p.m.r. spectroscopy (23).

The proposed mechanism requires a 1,2-*trans*

Can. J. Chem. Downloaded from www.nrcresearchpress.com by 210.87.254.105 on 09/05/12
For personal use only.

Can. J. Chem. Downloaded from www.nrcresearchpress.com by 210.87.254.105 on 09/05/12
For personal use only.

arrangement of the groups and both **1** and **3** are already in preferred conformations where this requirement is met. The fact that **2** also yielded **4** can readily be explained by the continual equilibration (anomerization) of **2** to a small amount of the reactive β-anomer (**1**) in the presence of a Lewis acid. The proposed mechanism should also yield a 1,2-*trans* product whereas in the case of **3** a 1,2-*cis* product (**5**) was predominant. This is due to the anomerization of the thermodynamically less stable β-anomer of **5** (initial 1,2-*trans* product) to the more stable 1,2-*cis* product (**5**) and demonstrates the contribution of carbonium ions of type **12**.

Experimental

Melting points were determined on a Kofler hot stage and are uncorrected, and optical rotations were measured at 21 ± 3°. Solutions were concentrated below 50° under diminished pressure. Thin-layer chromatography (t.l.c.) was performed on silica gel (Adsorbosil-1) coated plates with solvent systems (v/v); (*a*) chloroform–methanol (9:1), (*b*) light petroleum (b.p. 30–60°) – ether (2:1), (*c*) benzene – *n*-propanol (2:1). Paper electrophoresis was carried out on Whatman 3MM filter paper using 0.05 *M* borate as the buffer solution and the rates of movement of the individual glycoses are given relative to that of D-glucose (M_G). The glycoses were detected on paper electrophoretograms by *p*-anisidine hydrochloride (24) and by alkaline silver nitrate (25) spray reagents.

An F and M (model 420) chromatograph was used for g.l.c. with a 10% Neopentylglycol Sebacate on Gas Chrom A (100–120 mesh) column at 165°. Retention volumes are given relative to that of xylitol (R_X). The p.m.r. spectra were obtained from Varian A-60A and HA-100 spectrometers, using deuteriochloroform as the solvent and tetramethylsilane ($\tau = 10.0$) as the internal standard. Chemical shifts and coupling constants were obtained by first-order analysis and field swept spin decoupling at 60 MHz ($\delta = \pm$ frequency separation in Hz) was carried out using a Varian V-6058 spin decoupler. Decoupling experiments at 100 MHz were carried out with the spectrometer being operated in the frequency-sweep mode.

2-Chloro-2-deoxy-α-D-lyxopyranosyl Chloride 3,4-Di(chlorosulfate) (4)

Crystalline **1** (20 g, 0.043 mole) was dissolved in absolute chloroform (400 ml) and the solution was heated to 60°. Aluminum chloride (9 g, 0.067 mole) was added to the solution in three equal portions at 15 min intervals. Vigorous mechanical stirring was maintained throughout the additions to prevent excessive decomposition, and was continued for a further 15 min following the last addition of aluminum chloride. The chloroform solution was then washed with water, saturated sodium bicarbonate solution, and dried over anhydrous sodium sulfate. Following clarification with charcoal the solution was filtered, and concentrated to a syrup which crystallized. Recrystallization from ether – light petroleum (b.p. 30–60°) gave large crystals (12.0 g, 73%) of m.p. 59–60° and $[\alpha]_D$ +28.6° (*c*, 2.07 in chloroform).

Anal. Calcd. for $C_5H_6O_7Cl_4S_2$: C, 15.64; H, 1.57; Cl, 36.92; S, 16.70. Found: C, 15.81; H, 1.43; Cl, 36.86; S, 16.48.

The p.m.r. spectrum of the crude reaction product was almost identical to that of pure **4** shown in Fig. 1.

Crystalline **2** (0.5 g, 0.0011 mole) was treated with aluminum chloride (0.225 g, 0.0017 mole) using identical conditions to those described above. Crystalline **4** (0.35 g, 85%) was isolated from the reaction mixture by the procedure previously described and identified by its m.p. 59–60°, undepressed on admixture with authentic **4**. The p.m.r. spectrum of the crude reaction product was again almost identical to that of pure **4**.

The quantity of aluminum chloride used in the above reactions that was found to give the best yield of **4** was determined by a previous series of experiments using **1**. The quantity of aluminum chloride was varied in each case but the reaction conditions were otherwise identical to those described above. The only components of all these reaction mixtures were found to be unchanged **1** and compounds **2** and **4** (p.m.r.). The approximate percentage of the individual components in each reaction mixture was determined by integration of the anomeric signals of **1** (τ 3.74) (11), **2** (τ 3.54) (11), and **4** (τ 3.83), in the p.m.r. spectrum of each reaction mixture. These percentages are listed in Table 1 together with similar data obtained from a previous experiment where **1** was treated with titanium tetrachloride (11).

Methyl 2-Chloro-2-deoxy-β-D-lyxopyranoside (8)

Crystalline **4** (10.0 g) was refluxed in anhydrous methanol (50 ml) for 16 h, following which the solution was concentrated to half volume and poured into chloroform (200 ml). The chloroform solution was washed with water, saturated sodium bicarbonate solution, and then dried over anhydrous sodium sulfate. Filtration of the chloroform solution gave a clear filtrate which was concentrated to a syrup which was immediately dechlorosulfated with sodium iodide in aqueous acetone in the presence of barium carbonate (14). The solution was filtered free of insoluble barium salts, concentrated to small volume, and continuously extracted with chloroform for 12 h. Concentration of the chloroform solution yielded syrupy **8** (3.5 g, 74.5%) which was shown to be homogeneous by t.l.c. analysis in solvent (*a*) and had $[\alpha]_D$ − 96° (*c*, 1.3 in chloroform).

Anal. Calcd. for $C_6H_{11}ClO_4$: C, 39.40; H, 6.00; Cl, 19.50. Found: C, 39.31; H, 6.02; Cl, 19.77.

Syrupy **8** (20 mg) was oxidized with 0.012 *M* sodium metaperiodate (25 ml). Samples were withdrawn at intervals and the moles of periodate consumed (26) were as follows: 0.52 (4 h); 0.76 (7 h); 1.13 (11 h); 1.35 (23 h); 1.45 (31 h); 1.75 (48 h). The syrup was shown to contain a small quantity of the α-D-anomer of **8** as it was resolved into two components by g.l.c. analysis of its trimethylsilylated derivative. The major component (R_X 1.60) was assigned to **8** and the minor component (R_X 1.48) to its α-D-anomer by virtue of the large negative value of the specific rotation of the mixture. This was confirmed by refluxing the syrupy mixture in 3% methanolic hydrogen chloride for 10 h (constant specific rotation). The solution

Can. J. Chem. Downloaded from www.nrcresearchpress.com by 210.87.254.105 on 09/05/12
For personal use only.

was neutralized (silver carbonate), filtered, and concentrated to a syrup, the trimethylsilylated derivative of which gave two components (g.l.c. analysis) with identical retention volumes to those quoted above but with a reversal of intensities (major component at R_X 1.48).

2-Chloro-2-deoxy-α-D-lyxopyranose (6)

Crystalline **4** (8 g) was dissolved in aqueous acetone and treated with sodium iodide (100 mg) in the presence of barium carbonate as previously described (14). The solution was filtered, concentrated to dryness, and the residue was left in a desiccator over phosphoric oxide overnight. The residue was then extracted (× 4) with hot acetone and the acetone extracts were combined and concentrated to a syrup which crystallized. Recrystallization from acetone–ether gave crystalline **6** (2.4 g, 68%) of m.p. 157–159° and $[\alpha]_D$ −0.5° (*c*, 1.03 in methanol) → −15.5° (equilibrium).

Anal. Calcd. for $C_5H_9ClO_4$: C, 35.60; H, 5.40; Cl, 21.00. Found: C, 35.40; H, 5.58; Cl, 21.00.

Paper electrophoresis of the above crystals indicated one component at M_G 0.06, whereas 4-chloro-4-deoxy-D-xylopyranose and 4-chloro-4-deoxy-L-arabinopyranose had M_G 0.25 and 0.39 respectively. The trimethylsilyl derivative of the above crystals indicated one component at R_X 1.36 (g.l.c.). The above crystals were equilibrated in methanol solution, and after concentration of the solution the trimethylsilyl derivative of the equilibrated product gave two peaks at R_X 1.36 (α-D-anomer) and 1.70 (β-D-anomer). Methanolysis of the above crystals in 2% methanolic hydrogen chloride and subsequent trimethylsilylation of the product gave two peaks with identical retention volumes to those cited previously for **8** and its methyl α-D-anomer.

2-Chloro-2-deoxy-α-D-xylopyranosyl Chloride 3,4-Di(chlorosulfate) (5)

Crystalline **3** (20 g) (9) was treated with aluminum chloride (9 g) using identical conditions to those described previously in the preparation of **4** from **1**. The chloroform soluble product was a light brown syrup (12 g, 72.3%) which did not crystallize and had $[\alpha]_D$ +79° (*c*, 3.2 in chloroform). The p.m.r. spectrum of the syrup (Fig. 2) indicated that the major component was **5** (anomeric doublet at τ 3.84), but showed the presence of impurities including some of the starting compound (**2**) (anomeric doublet τ 3.69 (11)).

Methyl 2-Chloro-2-deoxy-β-D-xylopyranoside (9)

The syrupy product above (2 g) was shaken for 48 h with silver carbonate (6 g), silver perchlorate (0.2 g), drierite (3 g) in anhydrous methanol (40 ml). The solution was filtered, clarified with charcoal, and concentrated to a clear syrup which did not crystallize. The syrup was dechlorosulfated and the product was continuously extracted from aqueous solution by chloroform using identical procedures to those previously described above in the synthesis of **8**. Concentration of the chloroform solution gave a syrup (0.7 g, 50%) which slowly crystallized. Recrystallization from chloroform – light petroleum (b.p. 30–60°) gave crystalline **9** (0.4 g, 28%) of m.p. 136–137° and $[\alpha]_D$ −21° (*c*, 1.5 in methanol).

Anal. Calcd. for $C_6H_{11}ClO_4$: C, 39.40; H, 6.00; Cl, 19.50. Found: C, 39.13; H, 6.30; Cl, 19.60.

A periodate oxidation of the crystals was carried out as previously described for **8** and the moles of periodate consumed (26) were as follows: 0.45 (4 h); 0.65 (7 h); 0.97 (12 h); 1.40 (23 h); 1.50 (31 h); 1.88 (48 h). The trimethylsilyl derivative of **9** gave one peak at R_X 2.50 (g.l.c. analysis). This peak was also detected in the g.l.c. analysis of the trimethylsilylated residues of the mother liquors of **9** together with another large peak at R_X 1.95 which was assigned to the α-D-anomer of **9**. This assignment was confirmed when a small quantity of **9** was refluxed in 2% methanolic hydrogen chloride for 24 h and g.l.c. analysis of the trimethylsilylated syrupy product indicated two major components with identical retention volumes to those given by the trimethylsilylated residues of the mother liquors of **9** above.

2-Chloro-2-deoxy-D-xylopyranose (7)

Syrupy **5** (10 g) was treated with sodium iodide and the product was isolated by identical procedures described previously in the formation of **6** from **4**. The acetone extracts were concentrated to a syrup (3.5 g) which was shown to be one major product with two minor impurities by t.l.c. in solvent (*c*). The impurities were removed from the major product by silica-gel column chromatography using solvent (*c*). The fraction corresponding to the major component was concentrated to a syrup (2.9 g) of $[\alpha]_D$ +23° (*c*, 1.0 in methanol) which was shown to be an approximately equimolar mixture of both **6** and **7**. Paper electrophoretograms indicated two reducing components of equal intensity which had identical mobilities to **6** and **7**. This was also confirmed by g.l.c. analysis of the trimethylsilylated syrupy product which gave three peaks with identical retention volumes and approximately equivalent areas to those given by an authentic equilibrated mixture (1:1) of **6** and **7**. Therefore a modified procedure was used for the synthesis of **7**.

Syrupy **5** (12 g) was dissolved in chloroform (60 ml) and refluxed for 18 h with silver carbonate (16 g) and water (5 ml) essentially by the method described by Vargha and Kuszmann (7) for the replacement of anomeric chlorine by a hydroxyl group. The reaction was followed by t.l.c. in solvent (*b*) by the gradual disappearance of the faster moving component (**5**). The chloroform solution was filtered, dried over anhydrous sodium sulfate, and concentrated to a syrup. The dechlorinated syrupy product (7.8 g) was then dissolved in aqueous acetone and treated with sodium iodide (100 mg) as described previously in the formation of **6** from **4**. Concentration of the acetone extracts gave a syrup which was shown to contain by t.l.c. analysis in solvent (*c*), one major component, preceded and followed by minor components. These minor components were removed by the application of the mixture to a silica-gel column using solvent (*c*) as the eluant. Concentration of the fraction of the eluant containing the major component gave a colorless syrup (2.5 g, 48%) of $[\alpha]_D$ +63° (*c*, 1.2 in methanol).

Anal. Calcd. for $C_5H_9ClO_4$: C, 35.60; H, 5.40; Cl, 21.00. Found: C, 35.80; H, 5.70; Cl, 21.00.

Paper electrophoresis indicated one component (**7**) at M_G 0.16, and no spot corresponding to **6** (M_G 0.06) could be detected in this case. This was also confirmed by g l.c. analysis of the trimethylsilylated syrupy product which gave two peaks at R_X 1.70 (α-D-anomer) and 2.50 (β-D-

anomer). Although the α-D-anomer of **7** was shown to have an identical retention volume to the β-D-anomer of **6** no peak corresponding to the α-D-anomer of **6** (R_X 1.46) could be detected in the syrupy product above. Syrupy **7** did yield a few crystals on long standing which had $[\alpha]_D$ +103.5° → +63° (equilibrium) (*c*, 1.0 in methanol) but these were shown to be still a mixture of 2-chloro-2-deoxy-α-D-xylopyranose (**7**) and its β-D-anomer, enriched with **7** (g.l.c. analysis as above).

Independent Synthesis of 2-Chloro-2-deoxy-D-lyxose (6)

3,4-Di-*O*-acetyl-D-xylal (14 g) (27) was dissolved in carbon tetrachloride and treated with chlorine (2, 5). The mixture of epimeric mono-chloro-pentoses was then obtained using methods described by Vargha and Kuszmann (7). The mixture of 1,2-dichloro derivatives was dissolved in carbon tetrachloride and refluxed with silver carbonate and water to remove the anomeric chlorine and the resultant mixture of acetates was deacetylated by refluxing them in 0.1 *N* hydrochloric acid. The syrupy product crystallized on seeding with **6** and recrystallization from methanol–ether gave crystals (3.5 g, 29.6%) of m.p. 157° undepressed on admixture with authentic 2-chloro-2-deoxy-α-D-lyxopyranose (**6**). Both **6** and **7** were detected in the mother liquors of the recrystallization by paper electrophoresis and g.l.c. analysis as previously described.

The author wishes to thank Dr. O. E. Edwards for helpful discussions, Mrs. B. McLean for technical assistance and Mr. A. E. Castagne for determination of the microanalyses and the 60 MHz p.m.r. spectra.

1. J. E. G. Barnett. Advan. Carbohyd. Chem. **22**, 177 (1967).
2. E. Fischer, M. Bergmann, and H. Schotte. Chem. Ber. **53**, 509 (1920).
3. R. U. Lemieux and B. Fraser-Reid. Can. J. Chem. **43**, 1460 (1965).
4. M. S. Lefar and C. E. Weill. J. Org. Chem. **30**, 954 (1965).
5. K. Igarashi, T. Honma, and T. Imagawa. Tetrahedron Lett. 755 (1968).
6. A. M. Gakhokidze. J. Gen. Chem. U.S.S.R. **15**, 530 (1945); Chem. Abstr. **40**, 4673 (1946).
7. L. Vargha and J. Kuszmann. Chem. Ber. **96**, 411 (1963).
8. F. H. Newth. Quart. Rev. (London), **13**, 30 (1959).
9. L. Goodman and J. E. Christensen. J. Org. Chem. **28**, 158 (1963).
10. L. D. Hall and J. F. Manville. Can. J. Chem. **47**, 379 (1969).
11. H. J. Jennings. Can. J. Chem. **47**, 1157 (1969).
12. L. M. Jackman. Nuclear magnetic resonance spectroscopy. The Pergamon Press Ltd., New York, 1959.
13. J. G. Buchanan. J. Chem. Soc. 2511 (1958).
14. H. J. Jennings and J. K. N. Jones. Can. J. Chem. **43**, 2372 (1965).
15. H. J. Jennings and J. K. N. Jones. Can. J. Chem. **43**, 3018 (1965).
16. H. J. Jennings and J. K. N. Jones. Can. J. Chem. **40**, 1408 (1962).
17. D. V. Banthorpe. Elimination reactions. Elsevier Publishers Co., Inc., Amsterdam. 1963.
18. I. Lindqvist. Adduct molecules of OXO-compounds. Academic Press Inc., New York. 1963.
19. S. Winstein, E. Grunwald, and R. E. Buckles. J. Amer. Chem. Soc. **70**, 828, 841, 846 (1948).
20. H. C. Brown. Chem. Eng. News, **45**, 87 (Feb. 13, 1967).
21. P. E. Peterson and F. J. Slama. J. Amer. Chem. Soc. **90**, 6516 (1968).
22. G. A. Olah and J. M. Bollinger. J. Amer. Chem. Soc. **90**, 947 (1968).
23. G. A. Olah and J. M. Bollinger. J. Amer. Chem. Soc. **89**, 4744 (1967).
24. L. Hough, J. K. N. Jones, and W. H. Wadman. J. Chem. Soc. 1702 (1950).
25. W. E. Trevelyan, D. P. Procter, and J. S. Harrison. Nature, **166**, 444 (1950).
26. G. Neümoller and E. Vasseur. Ark. Kem. **5**, 235 (1953).
27. F. Weygand. Methods Carbohyd. Chem. **1**, 182 (1962).

Can. J. Chem. Downloaded from www.nrcresearchpress.com by 210.87.254.105 on 09/05/12
For personal use only.

Can. J. Chem. Downloaded from www.nrcresearchpress.com by 210.87.254.6 on 09/05/12
For personal use only.

Photocyclization reactions of aryl polyenes. The photocyclization of 1-substitutedphenyl-4-phenyl-1,3-butadienes

CLIFFORD C. LEZNOFF AND ROGER J. HAYWARD
Department of Chemistry, York University, Downsview, Ontario

Received January 16, 1970

Irradiation of 1-*p*-substitutedphenyl-4-phenyl-1,3-butadienes gave mixtures of 1-*p*-substitutedphenylnaphthalenes and 7-substituted-1-phenylnaphthalenes. Photocyclization of 1-*m*-substitutedphenyl-4-phenyl-1,3-butadienes gave 1-*m*-substitutedphenylnaphthalenes, 6-substituted-1-phenylnaphthalenes, and 8-substituted-1-phenylnaphthalenes. Characterization of the photoproducts was achieved through synthesis by an independent method.

Canadian Journal of Chemistry, 48, 1842 (1970)

The photochemical *cis–trans* isomerization of stilbenes has been extensively investigated in recent years and the detailed mechanism of the reaction has been discussed by several groups (1). The concurrent photochemical cyclizations of stilbene and substituted stilbenes to phenanthrene and substituted phenanthrenes have also been studied both from preparative (2) and mechanistic (3) points of view.[1] Stilbene-like photochemical cyclizations have recently been utilized in the synthesis of a wide variety of interesting polycyclic compounds (4).

Photochemical cyclizations[1] of 1,4-diphenyl-1,3-butadienes have received scant attention since Fonken showed that 1,4-diphenyl-1,3-butadiene undergoes a photochemical cyclization to give 1-phenylnaphthalene (5). The present paper describes the photocyclization of 1-substitutedphenyl-4-phenyl-1,3-butadienes.

The 1-substitutedphenyl-4-phenyl-1,3-butadienes (**1***a–e* and **2***a–e*) were prepared by one of two possible Wittig reactions (6). Either a solution of triphenylcinnamylphosphonium bromide and a monosubstituted benzaldehyde in methanol was reacted with lithium methoxide (method A) or a solution of cinnamaldehyde and a monosubstitutedbenzylphosphonium halide in methanol was treated with lithium methoxide (method B). Although the yields of these reactions were only moderate (Table 1), the ready availability of the starting materials and the simplicity of the reactions favored the use of Wittig reactions in the synthesis of 1,4-diaryl-1,3-butadienes.

[1]The photochemical cyclization reaction of stilbenes gives dihydrophenanthrene intermediates, which are very readily oxidized to phenanthrenes. Hence the term "photocyclization" shall include both the cyclization and oxidation steps.

Compounds **1***a–e* and **2***a–e* were readily characterized by their spectral data (Table 2) and by comparison with known 1,4-diaryl-1,3-butadienes. Mass spectroscopy revealed the presence of strong parent ions for **1***a–e* and **2***a–e*. The ultraviolet (u.v.) and infrared (i.r.) spectra clearly showed the presence of the butadiene moiety.[2]

Irradiation of 1×10^{-3} *M* solutions of 1-*p*-substitutedphenyl - 4 - phenyl - 1,3 - butadienes (**1***a–e*) in dry benzene containing 2×10^{-3} *M* iodine gave, after 3–6 days, mixtures of 1-*p*-substitutedphenylnaphthalenes (**3***a–e*) and 1-phenyl-7-substitutednaphthalenes (**4***a–e*). As shown in eq. [1], photocyclization of **1***a–e* can occur to the unsubstituted phenyl ring to give **3***a–e* and to the substituted phenyl ring to give **4***a–e*.

[1]

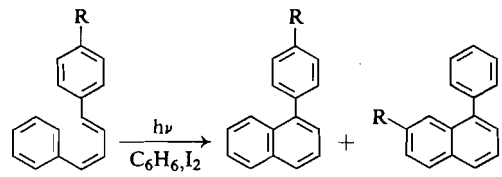

1 **3** **4**

a	R = MeO	*a*	R = MeO	*a*	R = MeO
b	R = Me	*b*	R = Me	*b*	R = Me
c	R = Cl	*c*	R = Cl	*c*	R = Cl
d	R = F	*d*	R = F	*d*	R = F
e	R = CN	*e*	R = CN	*e*	R = CN

Similarly, irradiation of 1 - *m* - substituted - phenyl-4-phenyl-1,3-butadienes (**2***a–e*) gave mixtures of 1-*m*-substitutedphenylnaphthalenes (**5***a–e*), 1-phenyl-6-substitutednaphthalenes (**6***a–e*),

[2]It is assumed that the *trans–trans* butadienes are formed from the method of preparation and the i.r. spectral data of **1***a–e* and **2***a–e* show absorption peaks for *trans* double bonds.

TABLE 1

1-Substitutedphenyl-4-phenyl-1,3-butadienes

Compound	Substituent	Melting point (°C)	Method of synthesis	Yield (%)	Molecular formula	Analysis (%) Found C	Found H	Calculated C	Calculated H
1*a*	*p*-Methoxy	163–164	A	54	$C_{17}H_{16}O$	86.61	6.73	86.41	6.82
1*b*	*p*-Methyl	155–156*	B	50	$C_{17}H_{16}$	—	—	—	—
1*c*	*p*-Chloro	166–167†	A	46	$C_{16}H_{13}Cl$	—	—	—	—
1*d*	*p*-Fluoro	154–155	A	26	$C_{16}H_{13}F$	85.96	5.79	85.72	5.83
1*e*	*p*-Cyano	164–165‡	B	34	$C_{17}H_{13}N$	—	—	—	—
2*a*	*m*-Methoxy	78–79	A	16	$C_{17}H_{16}O$	86.15	6.66	86.41	6.82
2*b*	*m*-Methyl	102–103§	B	38	$C_{17}H_{16}$	—	—	—	—
2*c*	*m*-Chloro	113–114‖	A	29	$C_{16}H_{13}Cl$	—	—	—	—
2*d*	*m*-Fluoro	111–112	A	24	$C_{16}H_{13}F$	85.48	5.77	85.75	5.83
2*e*	*m*-Cyano	115–116	B	43	$C_{17}H_{13}N$¶	88.01	5.99	88.28	5.62

*Lit. (19), m.p. 156°.
†Lit. (20); m.p. 161°.
‡Lit. (21), m.p. 162–163°.
§Lit. (22), m.p. 95–96.5°.
‖Lit. (20), m.p. 114°.
¶Anal. Calcd.: N, 6.06. Found: N, 6.31.

TABLE 2

Spectral characteristics of 1-substitutedphenyl-4-phenyl-1,3-butadienes

Compound	Substituent	Ultraviolet spectra λ_{max}(nm)(ε)			Infrared spectra ν(cm^{-1})	Mass spectra *m/e*, M^+ (% of base peak)
1*a*	*p*-Methoxy	361 (30 500)	342.5 (44 700)	331 (37 500)	—	236 (100)
1*b*	*p*-Methyl	355 (33 800)	337 (54 200)	323 (47 000)	1610, 1020	220 (95)
1*c*	*p*-Chloro	351 (33 400)	336 (53 100)	325 (44 000)	1590, 998	240 (97)
1*d*	*p*-Fluoro	351 (23 500)	332.5 (38 900)	319 (35 000)	1600, 1240, 1160, 991	224 (100)
1*e*	*p*-Cyano	365 (27 100)	347.5 (40 800)	335 (34 200)	2235, 1601, 998	231 (100)
2*a*	*m*-Methoxy	354 (26 100)	337.5 (40 000)	326 (35 400)	1592, 1570, 1157, 992	236 (100)
2*b*	*m*-Methyl	355 (24 300)	335 (39 500)	322.5 (35 400)	—	220 (100)
2*c*	*m*-Chloro	353 (30 200)	335 (48 600)	322 (41 700)	1590, 1562, 994	240 (93)
2*d*	*m*-Fluoro	351.5 (32 100)	333 (48 900)	322 (40 000)	1600, 1256, 1150, 989	224 (81)
2*e*	*m*-Cyano	353 (28 100)	335 (43 100)	326 (39 700)	2280, 1615, 1580, 1010	231 (100)

and 1-phenyl-8-substitutednaphthalenes (**7***a–e*). Photocyclization of **2***a–e* can thus occur to the unsubstituted phenyl ring to give **5***a–e* and to the substituted ring to give **6***a–e* and **7***a–e* (eq. [2]).

The photochemical reactions of **1***a–e* and **2***a–e* gave the substituted-1-arylnaphthalenes in 6 to 12% yield, along with the formation of some dimeric and polymeric products which were not further investigated.

Substituted-1-arylnaphthalenes were synthesized by an independent route and shown to be identical to the photoproducts of **1***a–e* and **2***a–e*, when compared by vapor phase chromatography (v.p.c.) (see Experimental). The syntheses of **3***a–e* and **5***a–e* were accomplished by the reaction of α-tetralone with the appropriate substituted-phenylmagnesium bromide (7). The first-formed tertiary alcohol was readily dehydrated to give 3,4-dihydro-1-arylnaphthalenes, which were not isolated. Subsequent dehydrogenation with dichlorodicyanoquinone (DDQ) gave **3***a–d* and **5***a–d*.

In order to prepare the 7-substituted-1-phenylnaphthalenes (**4***a–d*), it was necessary to synthesize 7-substituted-α-tetralones. The reaction of succinic anhydride with anisole, toluene, chlorobenzene, or fluorobenzene gave the respective 1-*p*-substitutedbenzoylpropionic acids (**8***a–d*) (8). Reduction of the acids, **8***a–d*, with zinc in hydrochloric acid (Scheme 1) gave γ-*p*-substitutedphenylbutyric acids (**9***a–d*) (9). Subsequent treatment of **9***a–d* with thionyl chloride gave the respective acid chlorides, which on cyclization with aluminum chloride yielded 7-methoxy (**10***a*) (10), 7-methyl (**10***b*) (11), 7-chloro (**10***c*) (12),

Can. J. Chem. Downloaded from www.nrcresearchpress.com by 210.87.254.6 on 09/05/12
For personal use only.

[2]

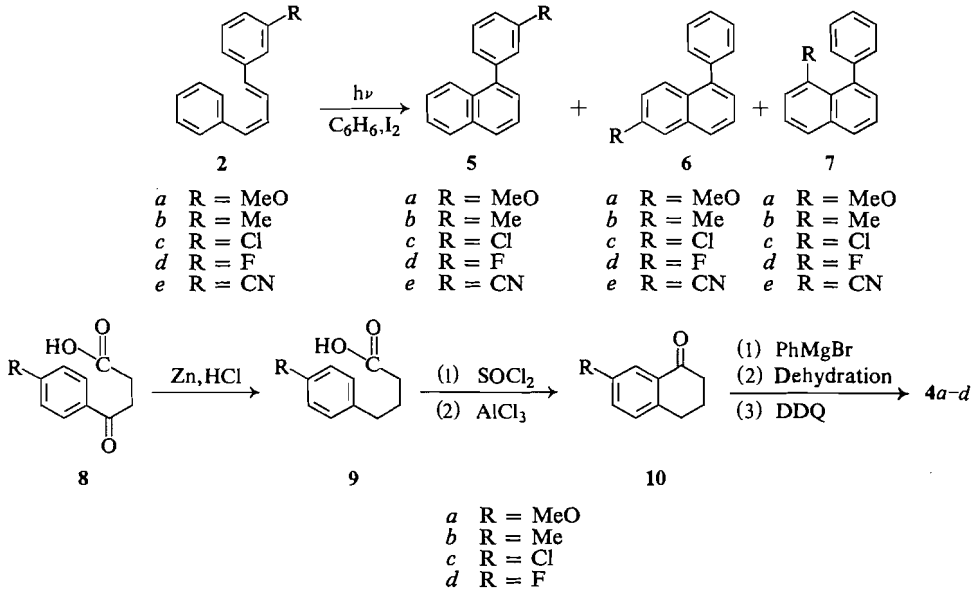

SCHEME 1

and 7-fluoro-α-tetralones (**10***d*) (13). The 7-substituted-α-tetralones, **10***a–d*, were reacted with phenylmagnesium bromide and dehydrated upon workup to give 7-substituted-3,4-dihydro-1-phenylnaphthalenes, which were not characterized but were treated with DDQ to give **4***a–d* directly.

One example of a 6-substituted-1-phenylnaphthalene, **6***a*, was prepared in a similar manner, using the commercially available 6-methoxy-α-tetralone.[3]

The syntheses of 1-*p*-cyanophenylnaphthalene (**3***e*), 7-cyano-1-phenylnaphthalene (**4***e*), and 1-*m*-cyanophenylnaphthalene (**5***e*) were achieved by treatment of the corresponding chloro-1-phenylnaphthalenes, **3***c*, **4***c*, and **5***c* respectively, with cuprous cyanide at 230° (14) (eq. [3]).

The substituted-1-arylnaphthalenes were characterized by their physical and spectral data (Table 3). All substituted-1-arylnaphthalenes exhibited parent ions in their mass spectra and the u.v. absorption spectra were typical of 1-phenylnaphthalene (15). The i.r. spectra were consistent with the assigned structure.

The mixtures of substituted-1-arylnaphthalenes, **3***a–e* and **4***a–e*, formed in the photocyclization of **1***a–e* were analyzed by v.p.c. (Table 4) and shown to be identical to **3***a–e* and **4***a–e* synthesized above. It can be readily seen that the photoproducts having substituents in the phenyl ring, **3***a–e*, have higher retention times than the photoproducts having substituents in the naphthalene ring, **4***a–e*, under the given v.p.c. conditions.

The mixtures of substituted-1-arylnaphthalenes **5***a–e*, **6***a–e*, and **7***a–e*, produced in the irradiation of **2***a–e*, were resolved by v.p.c. into peaks having the retention times shown in

[3]

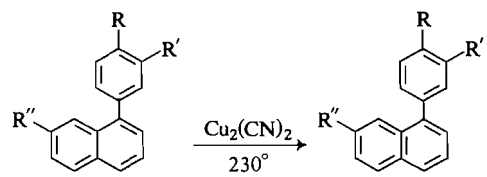

3*c* R = *p*-Cl; R′ = R″ = H
4*c* R = R′ = H; R″ = Cl
5*c* R = R″ = H; R′ = Cl
3*e* R = *p*-CN; R′ = R″ = H
4*e* R = R′ = H; R″ = CN
5*e* R = R″ = H; R′ = CN

[3]Purchased from Aldrich Chemical Co.

Can. J. Chem. Downloaded from www.nrcresearchpress.com by 210.87.254.6 on 09/05/12
For personal use only.

Can. J. Chem. Downloaded from www.nrcresearchpress.com by 210.87.254.6 on 09/05/12
For personal use only.

TABLE 3

Physical and spectral properties of synthesized substituted-1-arylnaphthalenes[k]

Compound	Substituent	Boiling point (°C(mm))	Molecular formula	Analysis (%) Found C	Found H	Calculated C	Calculated H	Spectra: Ultraviolet λ_{max}(nm)(ε)		Mass *m/e* M^+ (% of base peak)
3*a*	*p*-Methoxy	114–115[a,b]	$C_{17}H_{14}O$	—	—	—	—	286 (11 400)	224 (59 600)	234 (100)
3*b*	*p*-Methyl	54–55[a,c]	$C_{17}H_{14}$	—	—	—	—	283 (11 500)	228 (77 100)	218 (100)
3*c*	*p*-Chloro	145–147 (0.2)[d]	$C_{16}H_{11}Cl$	—	—	—	—	284 (16 900)	221.5 (83 800)	238 (70)
3*d*	*p*-Fluoro	71–72[a,e]	$C_{16}H_{11}F$	—	—	—	—	278 (7 300)	220 (49 200)	222 (100)
3*e*	*p*-Cyano	167–171 (0.2)	$C_{17}H_{11}N$	88.70	5.07	89.02	4.84	288 (3 700)	222 (34 900)	229 (89)
4*a*	7-Methoxy	154–156 (0.1)[f]	$C_{17}H_{14}O$	87.08	5.85	87.18	5.98	289 (6 200)	232 (39 800)	234 (100)
4*b*	7-Methyl	109–111 (0.2)[g]	$C_{17}H_{14}$	—	—	—	—	288 (7 900)	228 (53 200)	218 (100)
4*c*	7-Chloro	79–80[a,h]	$C_{16}H_{11}Cl$	—	—	—	—	289 (10 600)	232 (67 200)	238 (91)
4*d*	7-Fluoro	57–59[a]	$C_{16}H_{11}F$	86.08	4.85	86.44	4.96	289 (9 600)	230 (54 400)	222 (100)
4*e*	7-Cyano	81–82[a]	$C_{17}H_{11}N$	89.47	5.11	89.02	4.84	293 (7 500)	239 (59 900)	229 (92)
5*a*	*m*-Methoxy	154–156 (0.2)	$C_{17}H_{14}O$	87.42	6.28	87.18	5.98	287 (8 400)	223 (50 700)	234 (100)
5*b*	*m*-Methyl	165–167 (2.5)[i]	$C_{17}H_{14}$	—	—	—	—	280 (6 000)	221 (37 600)	218 (100)
5*c*	*m*-Chloro	155–157 (0.2)	$C_{16}H_{11}Cl$	80.83	4.48	80.48	4.62	287 (10 000)	221 (55 600)	238 (93)
5*d*	*m*-Fluoro	130–132 (0.2)	$C_{16}H_{11}F$	86.44	5.11	86.44	4.96	285 (10 900)	224 (61 100)	222 (95)
5*e*	*m*-Cyano	161–166 (0.2)	$C_{17}H_{11}N$	88.74	4.99	89.02	4.84	281 (6 380)	219 (36 900)	229 (85)
6*a*	6-Methoxy	156–158 (0.1)[j]	$C_{17}H_{14}O$	—	—	—	—	280 (6 000)	226 (37 600)	234 (12)

[a]Melting point.
[b]Lit. (12) m.p. 116–116.5°.
[c]Lit. (23) b.p. 148–150° (0.15).
[d]Lit. (24) b.p. 151–155° (0.4).
[e]Lit. (24) m.p. 71–72°.
[f]Melting point 25°.
[g]Lit. (25) b.p. 145–150° (1.0).
[h]Lit. (12) m.p. 77–78°.
[i]Lit. (23) b.p. 140–145° (0.15).
[j]Lit. (26) b.p. 158–162° (0.1).

[k]The general structure is:

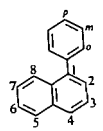

Can. J. Chem. Downloaded from www.nrcresearchpress.com by 210.87.254.6 on 09/05/12
For personal use only.

TABLE 4

The v.p.c. retention times of substituted-1-arylnaphthalenes from photocyclization of **1***a–e*

Compound	Substituent	Retention time (min)	Relative yield (%)
1*a*	*p*-MeO	9.34	—
3*a*	*p*-MeO	8.48	62
4*a*	7-MeO	7.94	38
1*b*	*p*-Me	8.67	—
3*b*	*p*-Me	7.90	41
4*b*	7-Me	7.73	59
1*c*	*p*-Cl	9.38	—
3*c*	*p*-Cl	9.22	50
4*c*	7-Cl	9.02	50
1*d*	*p*-F	7.80	—
3*d*	*p*-F	6.98	92
4*d*	7-F	7.12	8
1*e*	*p*-CN	10.10	—
3*e*	*p*-CN	9.40	33
4*e*	7-CN	9.22	67

TABLE 5

The v.p.c. retention times of substituted-1-arylnaphthalenes from photocyclization of **2***a–e*

Compound	Substituent	Retention time (min)	Relative yield (%)
2*a*	*m*-MeO	9.68	—
5*a*	*m*-MeO	8.60	55
6*a*	6-MeO	8.72	33
7*a*	8-MeO	8.00	12
2*b*	*m*-Me	9.32	—
5*b*	*m*-Me	8.00	52
6*b*	6-Me	8.10	38
7*b*	8-Me	7.22	10
2*c*	*m*-Cl	9.82	—
5*c*	*m*-Cl	8.86	62
6*c*	6-Cl	8.66	25
7*c*	8-Cl	8.22	13
2*d*	*m*-F	8.08	—
5*d*	*m*-F	6.82	87
6*d*	6-F	6.25	7.5
7*d*	8-F	6.20	5.5
2*e*	*m*-CN	10.04	—
5*e*	*m*-CN	8.82	52
6*e*	6-CN	8.75	42
7*e*	8-CN	7.72	6

Table 5. Compounds, **5***a–e*, synthesized above were shown to have identical retention times to one of the long retention time peaks. Compound **6***a* was shown to be identical to the other long retention time peak observed in the v.p.c. of the photoproducts of **2***a*. The short retention time peaks were thus assigned to **7***a–e* (see below).

TABLE 6

Assignment of methoxy and methyl protons in the n.m.r. spectra of substituted-1-arylnaphthalenes

Compound	Substituent	Peak (p.p.m.)
1*a*	*p*-MeO	3.83
3*a*	*p*-MeO	3.78
4*a*	7-MeO	3.65
1*b*	*p*-Me	2.12
3*b*	*p*-Me	2.15
4*b*	7-Me	2.42
2*a*	*m*-MeO	3.80
5*a*	*m*-MeO	3.72
6*a*	6-MeO	3.64
7*a*	8-MeO	3.27
2*b*	*m*-Me	2.36
5*b*	*m*-Me	2.25
6*b*	6-Me	2.32
7*b*	8-Me	1.85

The relative yields of the substituted-1-arylnaphthalenes **5***a–e*, **6***a–e*, and **7***a–e*, were determined by measurement of the areas under the peaks in the v.p.c. The assignments of the peaks having the shortest retention times to **7***a–e* are consistent with the fact that **7***a–e* are produced in the lowest yield. Photocyclization of **2***a–e* ortho to the substituent of the phenyl ring giving **7***a–e* would be sterically unfavorable compared to photocyclization of **2***a–e* para to the substituent of the phenyl ring giving **6***a–e*.[4]

The nuclear magnetic resonance (n.m.r.) spectra of the mixture of substituted-1-arylnaphthalenes produced by the irradiation of **2***a* and **2***b* was extremely informative and aided us in affirming the assignment of **6***a*, **7***a* and **6***b*, **7***b*. From Table 6 it is seen that the n.m.r. spectrum of the mixture of **5***a*, **6***a*, and **7***a* obtained in the photocyclization of **2***a* gives us three absorption peaks representing the methoxy protons of **5***a*, **6***a*, and **7***a*. Two of these peaks have been absolutely assigned to **5***a* and **6***a* by comparison with the pure synthesized products. The third absorption peak at 3.27 p.p.m. has been assigned to the methoxy protons of **7***a*, which thus exhibit an upfield shift of 0.4 p.p.m. relative to the methoxy protons of **6***a*. This upfield shift of the methoxy protons of **7***a* is expected, due to the shielding effect of the phenyl group at the

[4]The yields of **6***d* and **7***d* are very close and hence a firm assignment based on product yield is not possible. The retention times of **6***d* and **7***d* are very similar and thus the given assignments to these peaks are only tentative.

Can. J. Chem. Downloaded from www.nrcresearchpress.com by 210.87.254.6 on 09/05/12
For personal use only.

1-position of **7***a* (16) and substantiates the assignment of the peak at 3.27 p.p.m. to the methoxy protons of **7***a*. Similarly, the absorption peak at 1.85 p.p.m. exhibited in the n.m.r. spectrum of the mixture of **5***b*, **6***b*, and **7***b* obtained from the photocyclization of **2***b* substantiates the presence of **7***b*.

Thus n.m.r., v.p.c., and product yield data strongly indicate the formation of **7***a–e* in the photocyclization reactions of **2***a–e*.

The product distribution data of Table 4, showing the relative yields of **3***a–e* and **4***a–e* from the photocyclization of **1***a–e* and the data from Table 5 showing the relative yields of **5***a–e*, **6***a–e*, and **7***a–e* from the photocyclization of **2***a–e* clearly show that a substituent on a phenyl ring of 1,4-diphenyl-1,3-butadiene does not appreciably influence the direction of photocyclization. The major exception to this finding is the photocyclization of **1***d* and **2***d* which gives mainly photoproducts **3***d* and **5***d*. The fluoro substituents cause cyclization to occur to the unsubstituted phenyl ring. The photocyclization of **1***e* gives a slight preponderance of **4***e* over **3***e* (2:1).

The possibility that some of the substituted-1-arylnaphthalenes were undergoing photo-decomposition could not be overlooked in evaluating the relative yields of the photoproducts. All substituted-1-arylnaphthalenes were irradiated under conditions identical to those for **1***a–e* and **2***a–e* and found to be unchanged even after 6 days irradiation.

Thus selective photo-decomposition of the minor photo-products **4***d*, **6***d*, and **7***d* in the photocyclization reactions **1***d* and **2***d* cannot be the reason for the high relative yield of **3***d* and **5***d* and the correct explanation must await further studies.

Although a detailed mechanistic study of the parent 1,4-diphenyl-1,3-butadiene has not yet been undertaken, the closely related fulgicides have been shown to proceed through a 1,2-dihydronaphthalene intermediate which on dehydrogenation gives a 1-phenylnaphthalene type compound (17). In all probability the mechanism of photocyclization of **1***a–e* and **2***a–e* proceeds through similar intermediates. Further studies on the detailed mechanism of the photocyclization of 1-substitutedphenyl-4-phenyl-1,3-butadienes and related diaryl polyenes are currently in progress.

Experimental

All melting points were determined on a Kofler hot stage and are corrected. The i.r. spectra were recorded on a Perkin–Elmer 257 i.r. spectrophotometer using KBr discs. The u.v. spectra were measured using a Cary 14 u.v. spectrometer and 95% ethanol as solvent. The n.m.r. spectra were measured on a Varian A60 spectrometer using tetramethylsilane as an internal standard ($\delta = 0$ p.p.m.) and deuterochloroform as solvent. Mass spectra were recorded on a Hitachi–Perkin–Elmer RMU-6D mass spectrometer. Column chromatography was performed using Woelm alumina, activity II–III; silica gel was used for thin- and thick-layer chromatography. All photochemical reactions were carried out in a Rayonet photochemical reactor using RPR 3500 Å lamps. Microanalyses were performed by Dr. C. Daesslé of Montreal.

Vapor Phase Chromatography

Vapor phase chromatographic measurements were made under standard conditions. A Hewlett–Packard 700 gas chromatograph equipped with a 6 ft stainless steel column packed with silicone rubber SE-30 810 was used for product analysis. The column temperature was programmed at 30 °C per min from 70 to 250 °C and then maintained at the upper limit until all compounds had been eluted. Flow rate was kept constant at 40 ml per min of helium. The detector and injection port temperatures were maintained at 275 °C. All analyses were run in diethyl ether solution and retention times are measured with reference to the ether peak.

Synthesis of 1-Monosubstitutedphenyl-4-phenyl-1,3-butadienes

Method A

A typical example is given for the preparation of 1-*m*-methoxyphenyl-4-phenyl-1,3-butadiene. To a mixture of 11.5 g of (0.025 moles) triphenylcinnamylphosphonium bromide and 3.5 g (0.026 moles) of *m*-methoxybenzaldehyde in 100 ml methanol, was added 130 ml of 0.2 *M* lithium methoxide. The mixture was allowed to crystallize overnight after which crystals of 1-*m*-methoxyphenyl 4-phenyl-1,3-butadiene were filtered off.

Method B

The remaining 1-substitutedphenyl-4-phenyl-1,3-butadienes were prepared by reacting a monosubstitutedbenzylphosphonium bromide and cinnamaldehyde by a procedure identical to method A (Table 1).

Preparation of Benzyltriphenylphosphonium Bromides

All substitutedbenzyltriphenylphosphonium bromides were synthesized in a manner identical to that of *p*-methylbenzyltriphenylphosphonium bromide described previously (6). A mixture of 25.0 g (0.135 moles) of 4-bromo-*p*-xylene and 44 g (0.17 moles) of triphenylphosphine in 160 ml dimethyl formamide was refluxed overnight. After cooling to room temperature, the salt crystallized out of the solution and was filtered. The physical data for the phosphonium salts used in method B is described in Table 7.

Irradiation of 1-Substitutedphenyl-4-phenyl-1,3-butadienes

The photochemical experiments were carried out at concentrations of 1×10^{-3} *M* in 1,3-butadiene and 2×10^{-3} *M* iodine in 500 ml of dry benzene under a

TABLE 7

Substitutedbenzyltriphenylphosphonium bromides*

Substituents	Melting point (°C)	Yield (%)	Analysis (%) Found C	Found H	Calculated C	Calculated H
R′ = H, R = CN	~350		68.42	4.75	68.26	4.59
R′ = CN, R = H	~350†		68.38	4.53	68.26	4.59
R′ = H, R = Me	293–295‡		—	—	—	—
R′ = Me, R = H	267–269§		—	—	—	—

*The compound has the following general structure:

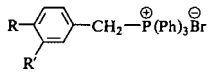

†Lit. (21) m.p. 311–320°.
‡Lit. (6) m.p. 276–277°.
§Lit. (27) m.p. 271–272°.

nitrogen atmosphere. For irradiation of 1-methoxyphenyl-4-phenyl-1,3-butadienes concentrations of 5×10^{-4} *M* were used to minimize polymer formation. The reactions were followed by u.v. spectroscopy, aliquots being taken from the reaction vessel at selected times. The characteristic absorption peaks of the 1-substitutedphenyl-4-phenyl-1,3-butadienes gradually disappeared over 3 days (6 days when the substituents were cyano group) and $\lambda_{max} = 220$ mμ characteristic of phenylnaphthalenes appeared.

After the photochemical reaction was complete the benzene solution was washed with aqueous sodium thiosulfate and dried over anhydrous magnesium sulfate. The benzene solution was concentrated and passed through an aluminum column (20 g) to remove polymers. The phenylnaphthalenes were isolated by preparative thick-layer chromatography (t.l.c.) using hexane as eluant. All phenylnaphthalenes moved faster than the starting 1,3-butadienes on t.l.c. Compounds moving slower than the starting material invariably turned out to be dimeric products as shown by mass spectroscopy. The mixtures of phenylnaphthalenes obtained in this manner were analyzed by v.p.c. to give two substituted-1-arylnaphthalenes in the case of the photocyclization of 1-*p*-substitutedphenyl-4-phenyl-1,3-butadiene (**1***a–e*) and three substituted 1-arylnaphthalenes for the photo products of 1-*m*-substitutedphenyl-4-phenyl-1,3-butadienes (**2***a–e*).

The total yields of phenylnaphthalenes varied from 6–12%.

Preparation of Substituted-α-tetralones

The substituted-α-tetralones were prepared essentially as described in reference 13. A typical synthesis of an α-tetralone is represented by the following synthesis of 7-fluoro-α-tetralone. A mixture of 16.0 g of *p*-fluorophenylbutyric acid (18) and 10 ml (0.13 moles) of redistilled thionyl chloride under dry nitrogen was warmed until the acid melted. The reaction proceeded for 30 min without further heating. The mixture was then heated for 10 min on a steam bath. The excess thionyl chloride was removed by distillation under reduced pressure from a water pump. To the flask, cooled in an ice bath and fitted with a reflux condenser was added 80 ml of carbon disulfide and 15 g (0.115 moles) of anhydrous aluminum chloride. After the rapid evolution of hydrogen chloride had ceased, the mixture was slowly warmed to the boiling point. After heating and shaking for 10 min the reaction was complete. The reaction mixture was cooled to 0 °C and the aluminum chloride complex was decomposed by careful addition of 50 g of ice. To this mixture was now added 12 ml of concentrated hydrochloric acid. The mixture was then separated and extracted with ether. The combined ether – carbon disulfide layer was separated, dried over magnesium sulfate, and vacuum distilled to give 7-fluoro-α-tetralone (**10***d*) b.p. 93–96° (1.4 mm). On cooling the oil crystallized to give **10***d*, m.p. 66–68° in 69% yield.

Anal. Calcd. for $C_{10}H_9FO$: C, 73.18; H, 5.49. Found: C, 73.15; H, 5.55.

Synthesis of Substituted-1-arylnaphthalenes

Substituted-1-arylnaphthalenes were prepared by reaction of a suitably substitutedphenyl Grignard to a suitable α-tetralone as previously described (7, 12) to give a substituted-3,4-dihydro-1-arylnaphthalene. The dihydro compound was dehydrogenated with an equivalent amount of 2,3-dichloro-5,6-dicyanobenzoquinone (DDQ) in refluxing benzene for 15 h. The resulting substituted-1-arylnaphthalene was purified by t.l.c. The cyano substituted phenylnaphthalenes were not prepared by this method.

Preparation of Cyano Substituted Phenylnaphthalenes

A typical procedure is given for the synthesis of 1-*p*-cyanophenylnaphthalene. A mixture of 0.3 g (0.0012 moles) of 1-*p*-chlorophenylnaphthalene and 0.25 g (0.028 moles) of cuprous cyanide was refluxed for 24 h at 230 °C with the exclusion of moisture. The reaction product was purified on preparative t.l.c. on elution with hexane:benzene (1:1) to give 1-*p*-cyanophenylnaphthalene, b.p. 167–171° (0.2 mm) in 58% yield.

The authors wish to acknowledge the support of the National Research Council of Canada for a grant in aid of this research.

1. D. Gegiou, K. A. Muszkat, and E. Fischer. J. Amer. Chem. Soc. **90**, 3907 (1968); J. Saltiel, O. C. Zafiriou, E. D. Megarity, and A. A. Lamola. J. Amer. Chem. Soc. **90**, 4759 (1968).
2. C. S. Wood and F. B. Mallory. J. Org. Chem. **29**, 3373 (1964).

Can. J. Chem. Downloaded from www.nrcresearchpress.com by 210.87.254.6 on 09/05/12
For personal use only.

3. H. GÜSTEN and L. KLASINC. Tetrahedron, **24**, 5499 (1968); K. A. MUSZKAT and E. FISCHER. J. Chem. Soc. (B) 662 (1967); F. B. MALLORY, C. S. WOOD, and J. T. GORDON. J. Amer. Chem. Soc. **86**, 3094 (1964); W. M. MOORE, D. D. MORGAN, and F. R. STEIMETZ. J. Amer. Chem. Soc. **85**, 829 (1963); M. V. SARGENT and C. J. TIMMONS. J. Amer. Chem. Soc. **85**, 2186 (1963).
4. W. H. LAARHOVEN, TH. J. H. M. CUPPEN, and R. J. F. NIVARD. Rec. Trav. Chim. **87**, 687 (1968) and references therein.
5. G. J. FONKEN. Chem. Ind. 1327 (1962).
6. R. N. MCDONALD and T. W. CAMPBELL. J. Org. Chem. **24**, 1969 (1959).
7. F. G. BADDAR, L. S. EL-ASSAL, and M. GINDY. J. Chem. Soc. 1270 (1948).
8. L. F. SOMERVILLE and C. F. H. ALLEN. Organic syntheses. Coll. Vol. II. John Wiley and Sons, Inc., New York, N.Y. 1961. p. 81.
9. E. L. MARTIN. Organic syntheses. Coll. Vol. II. John Wiley and Sons, Inc., New York, N.Y. 1961. p. 499.
10. D. G. THOMAS and A. H. NATHAN. J. Amer. Chem. Soc. **70**, 331 (1948).
11. A. J. M. WENHAM and J. S. WHITEHURST. J. Chem. Soc. 3857 (1956).
12. F. G. BADDAR, L. S. EL-ASSAL, and N. A. DOSS. J. Chem. Soc. 1027 (1959).
13. E. L. MARTIN and L. F. FIESER. Organic syntheses. Coll. Vol. II. John Wiley and Sons, Inc., New York, N.Y. 1961. p. 569.
14. M. S. NEWMAN. J. Amer. Chem. Soc. **59**, 2472 (1937).
15. R. A. FRIEDEL. Appl. Spectrosc. **11**, 13 (1957).
16. L. M. JACKMAN. Nuclear magnetic resonance spectroscopy. Pergamon Press Ltd., London, 1959. p. 125.
17. A. SANTIAGO and R. S. BECKER. J. Amer. Chem. Soc. **90**, 3654 (1968).
18. L. F. FIESER, M. T. LEFFLER, and co-workers. J. Amer. Chem. Soc. **70**, 3197 (1948).
19. A. V. DOMBROVSKII. Dokl. Akad. Nauk. S.S.S.R. **111**, 827 (1956).
20. F. BERGMANN, J. WEIZMAN, and D. SCHAPIRO. J. Org. Chem. **9**, 408 (1944).
21. B. R. BAKER and E. H. ERICKSON. J. Med. Chem. **12**, 408 (1969).
22. B. M. MIKHAILOV, L. S. POVAROV, and G. S. TER-SARKISYAN. Chem. Abstr. **56**, 4443 (1963).
23. F. BERGMANN and A. WEIZMANN. J. Org. Chem. **9**, 352 (1944).
24. F. BERGMANN and J. SZMUSZKOWICZ. J. Amer. Chem. Soc. **70**, 2748 (1948).
25. A. OHTA, Y. OGIHARA, K. NEI, and S. SHIBATA. Chem. Pharm. Bull. **11**, 754 (1963).
26. F. BERGMANN, J. SZMUSZKOWICZ, and G. FAWAZ. J. Amer. Chem. Soc. **69**, 1773 (1947).
27. C. E. GRIFFIN and M. GORDON. J. Organometal. Chem. **3**, 414 (1965).

Can. J. Chem. Downloaded from www.nrcresearchpress.com by 210.87.254.6 on 09/05/12
For personal use only.

Can. J. Chem. Downloaded from www.nrcresearchpress.com by 210.87.254.42 on 09/05/12
For personal use only.

Some potentially physiologically active β,β-diphenylethylamines derived from adrenaline[1,2,3]

JANET E. FORREST, S. KAŠPÁREK,[4] AND R. A. HEACOCK
Atlantic Regional Laboratory, National Research Council of Canada, Halifax, Nova Scotia

AND

T. P. FORREST
Department of Chemistry, Dalhousie University, Halifax, Nova Scotia

Received December 16, 1969

The reaction that occurs between adrenaline (**1**) and phenols, in the presence of hydrochloric acid, to form potentially physiologically active β,β-diphenylethylamine derivatives, is described. The products obtained include adrepine (**7**), formed from **1** alone, and others obtained by the interaction of **1** with a second phenolic component, such as epinine or 4-methylcatechol. The nuclear magnetic resonance and mass spectroscopic data obtained for these products and a number of related compounds are presented and discussed.

Canadian Journal of Chemistry, 48, 1850 (1970)

It has been suggested (1, 2) that two of the new compounds which are formed by treating adrenaline (**1**) with 10 *N* hydrochloric acid and then detected by chromatography (in a phenol – 0.1 *N* HCl system) were identical with the compounds previously described as "diadrenaline ether" (**2**) (3, 4) and adnamine (i.e. 5-methylaminomethyl-2,3,7,8-tetrahydroxydibenzo[*a,e*]cycloheptatriene, **3**) (5). The compounds **2** and **3** have been obtained as crystalline solids by the action of hydrochloric acid on **1** under the appropriate conditions (3–5). The formation of different types of products including β-phenylnaphthalene derivatives (6, 7) and phenylacetaldehyde and phenylacetone derivatives (8–10) by the action of strong mineral acids on β-phenylethanolamines in general has also been reported. Furthermore it is well known that in the presence of acids, aliphatic alcohols form ethers with the secondary alcohol function of some β-phenylethanolamines (3, 4, 11–14).

In view of the large number of products which can possibly be formed from **1** by the action of hydrochloric acid it was decided to investigate further the nature of some of these compounds.

The compound described as "diadrenaline ether" (i.e. **2**), which was identified chromatographically as one of the products formed by the action of 10 *N* HCl on **1** (1) was synthesized by one of the methods described in the literature (cf. 4). The nuclear magnetic resonance (n.m.r.) spectrum of this compound indicated that the previously assigned symmetrical ether structure (i.e. **2**) (3, 4) could not possibly be correct. Microanalytical data confirmed that the empirical formula of this compound (which is usually isolated as its dihydrochloride), for which we have proposed the trivial name *adrepine*, (cf. footnote 3) was $C_{18}H_{24}O_5N_2 \cdot 2HCl$. The compound was, in fact, isomeric with **2**, i.e. it was derived from two molecules of **1** by the elimination of one molecule of water. All attempts to observe the molecular ion in the mass spectrum of this compound were, however, unsuccessful; the highest mass fragment ion was observed at *m/e* 299.

Adrepine forms two different acetyl derivatives depending on the conditions of acetylation used. Acetylation with acetic anhydride and pyridine gives a heptaacetate ($C_{32}H_{38}N_2O_{12}$), whilst with acetic anhydride in aqueous sodium bicarbonate a hexaacetate ($C_{30}H_{36}N_2O_{11}$) is obtained. The hexaacetate can be converted to the heptaacetate on further acetylation with acetic anhydride and pyridine. It is known that by acetylation with acetic anhydride and pyridine, adrenaline (**1**) gives a tetraacetate (**4**) (15), however, a triacetate of **1** (i.e. **5**), in which the β-OH group in the side chain is not acetylated is obtained with acetic anhydride and aqueous sodium bicarbonate (16). The above evidence suggested that an adrenaline

[1]Issued as NRCC No. 11239.
[2]Presented in part at the 52nd Annual Conference of the Chemical Institute of Canada, Montreal, Quebec, May 1969.
[3]For a brief preliminary report of part of this investigation see reference 23.
[4]NRCC Postdoctorate Fellow 1965–1967.

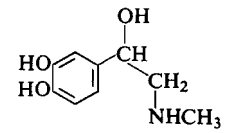

1

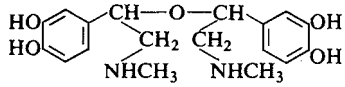

2

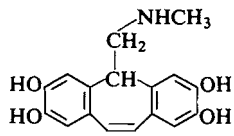

3

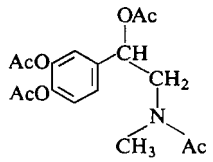

4

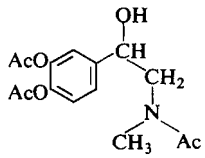

5

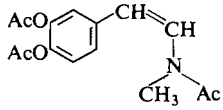

6

Ac = CH_3CO

type β-ethanolamine side chain, containing a free secondary alcoholic OH group, is present in the adrepine molecule and that this OH group is not acetylated in the hexaacetate. The infrared (i.r.) spectrum of adrepine hexaacetate shows a broad absorption at ca. 3300 cm^{-1} due to the aliphatic OH group, and peaks are observed in the carbonyl region at 1770 and 1630 cm^{-1} due to the phenolic ester and amide carbonyl groups respectively. Adrepine heptaacetate however exhibits no absorption in the OH/NH stretching region, but shows an extra carbonyl peak at 1735 cm^{-1}, presumably due to the aliphatic ester carbonyl group.

In the mass spectrum of hexaacetyladrepine the highest mass peak was observed at *m/e* 582 (i.e. [M-H_2O]). The mass spectrum of heptaacetyladrepine also showed the presence of an ion at *m/e* 582 (i.e. [M-60]), due in this case to the loss of acetic acid, which was observed as a strong peak at *m/e* 60. The peak at *m/e* 60 was absent in the mass spectrum of the hexaacetyl derivative. The mass spectra of these two compounds are shown in Figs. 1 and 2. Similar fragmentations were observed in the mass spectra of tri- and tetraacetyladrenaline (i.e. **5** and **4**) as shown in Fig. 3. The strong peak at *m/e* 60 [CH_3COOH] is visible in the spectrum of **4**, but absent in the spectrum of **5**. The decomposition of tetraacetyladrenaline (**4**) on attempted high vacuum distillation has been described (15). Acetic acid is eliminated from the side chain with the reported formation of *N*-[2-(3,4-diacetoxyphenyl)vinyl]-*N*-methylacetamide (**6**) (15). It is not unreasonable to assume that analogous decompositions would occur under the conditions used to obtain the mass spectra of **4** and heptaacetyladrepine. The mass spectral evidence obtained from these four acetyl derivatives confirms the presence of an adrenaline-type side chain in adrepine.

The n.m.r. spectra of the tri- and tetraacetyl derivatives of adrenaline and the hexa- and heptaacetyl derivatives of adrepine also suggest that an adrenaline-type side chain is present in adrepine. The signal due to the methine proton in triacetyladrenaline (**5**) (i.e. a compound where the benzylic OH group is not acetylated) is observed as a multiplet at τ 5.10. However, on acetylation of this OH group, i.e. in the tetraacetyl derivative **4**, the signal due to the methine proton is observed at τ 4.05. A similar difference of approximately 1 p.p.m. is observed between the peaks due to the corresponding methine protons in the n.m.r. spectra of hexaacetyladrepine (τ, 4.75) and heptaacetyladrepine (τ, 3.75).

Can. J. Chem. Downloaded from www.nrcresearchpress.com by 210.87.254.42 on 09/05/12
For personal use only.

Can. J. Chem. Downloaded from www.nrcresearchpress.com by 210.87.254.42 on 09/05/12
For personal use only.

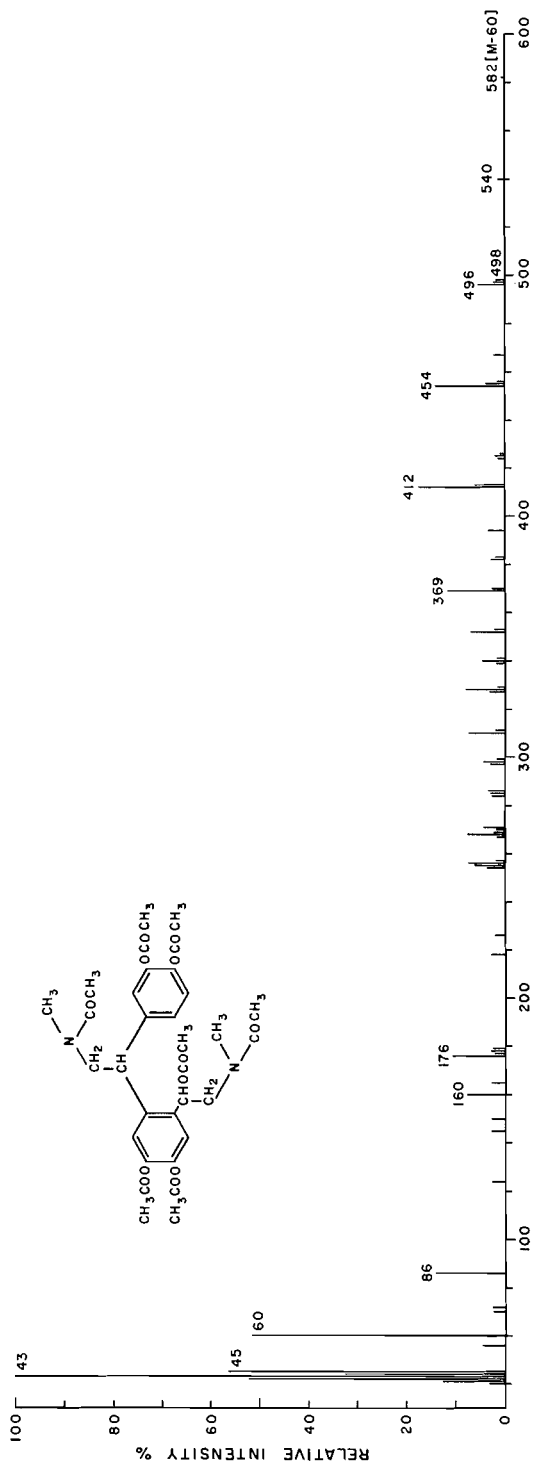

FIG. 1. Mass spectrum of hexaacetyladrepine.

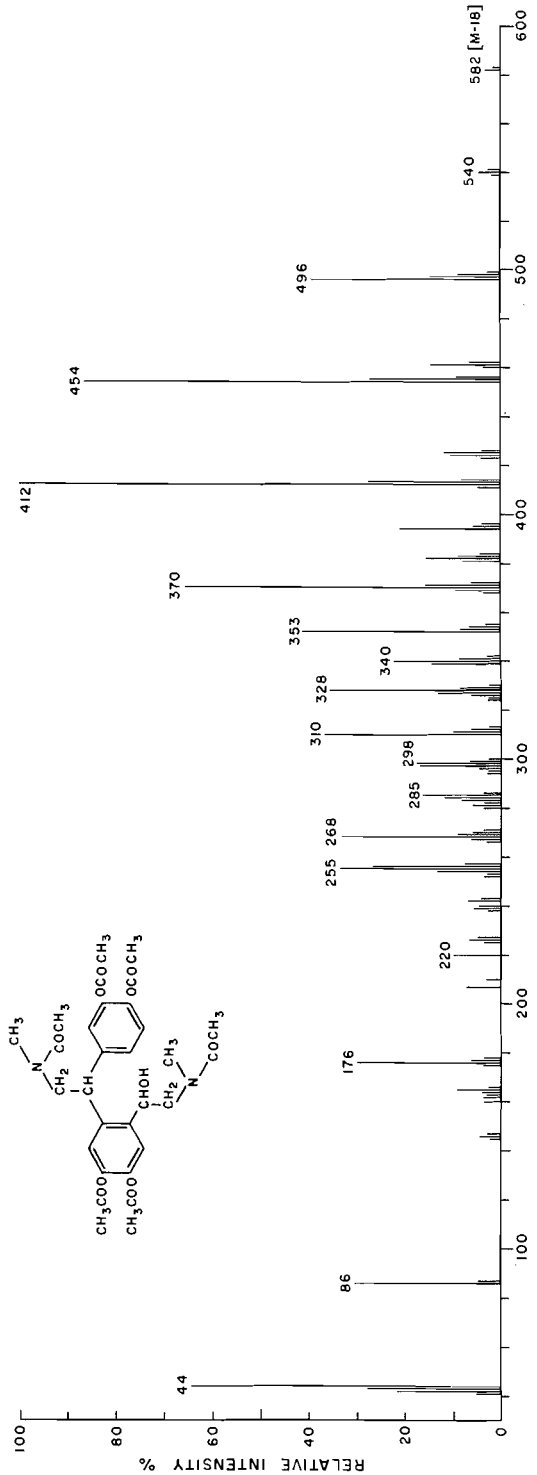

FIG. 2. Mass spectrum of heptaacetyladrepine.

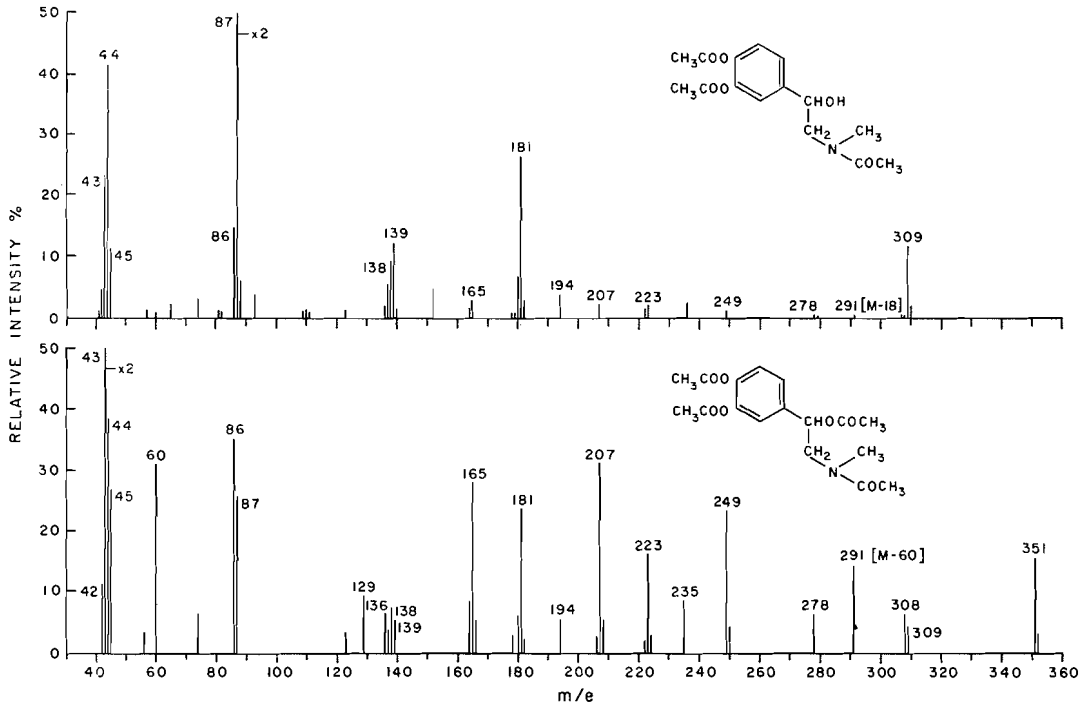

FIG. 3. Mass spectra of triacetyladrenaline (**5**) and tetraacetyladrenaline (**4**).

The n.m.r. spectrum of adrepine in D_2O/DCl showed the presence of five aromatic protons between τ 2.85 and 3.30; two *N*-methyl groups at τ 7.12 and 7.32 respectively; an A_2X system, containing a two proton doublet at τ 6.28 (J_{AX} = 8.0 Hz) and a one proton triplet at τ 5.40 and an ABX system with the A and B protons seen at τ 7.56 and 6.91 and the X proton at τ 4.70 (J_{AB} = 13.0 Hz; J_{AX} = 3.5 Hz; J_{BX} = 10.0 Hz).

In the light of the above evidence the molecule must contain two different $\rangle CH—CH_2—$ systems, one of which, on the basis of the evidence presented above for the acetates, must form part of an adrenaline-type side chain. This is the ABX system. Evidence in support of this assignment will be presented later in the discussion.

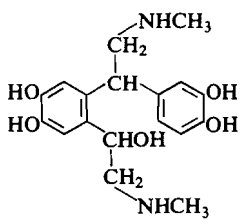

7

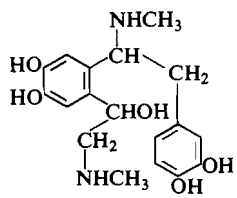

8

The presence of only five aromatic protons indicates that one of the aromatic rings in adrepine is tetrasubstituted. The problem of the structure of adrepine is, therefore, reduced to deciding firstly between a one carbon linkage joining the two aromatic rings, as in **7**, or a two carbon linkage, as in **8**, and secondly to deciding the substitution pattern of the tetrasubstituted aromatic ring. Analysis of the mass spectra of adrepine and its acetyl derivatives permitted the assignment of a structure of type **7** to this compound.

The most intense peak in the mass spectrum of adrepine (see Fig. 4) occurred at *m/e* 44 [$CH_2{=}\overset{+}{N}HCH_3$]. This ion could theoretically arise from cleavage β to either nitrogen atom. The relatively large peak which is observed at *m/e* 286 [M-H_2O-44] could however only arise from a structure of the type **7** and not from structure **8**. The formation of a fragment ion by the loss of water and the —CH_2NHCH_3 group (*m/e* 44) from the same side chain is not possible. In the mass spectrum of adrenaline (17) the base peak was observed at *m/e* 44, arising from fragmentation occurring β to the nitrogen atom. The

Can. J. Chem. Downloaded from www.nrcresearchpress.com by 210.87.254.42 on 09/05/12
For personal use only.

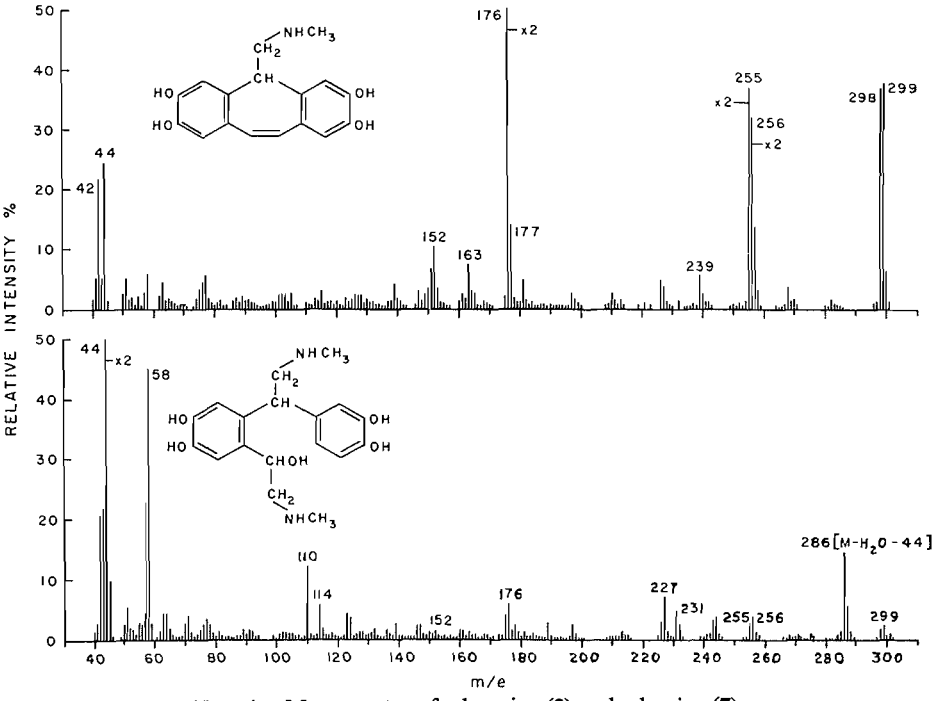

FIG. 4. Mass spectra of adnamine (3) and adrepine (7).

[M-44] peak at *m/e* 139 and the [M-18] peak at *m/e* 165 were observed but no peak was present at *m/e* 121 [M-H_2O-44] due to the loss of both water and the —CH_2NHCH_3 fragment. The ion at *m/e* 286 in the mass spectrum of adrepine is therefore due to the elimination of water from the adrenaline-type side chain and loss of the —CH_2NHCH_3 group from another part of the molecule. Structure **7** would permit the ready loss of —CH_2NHCH_3 from the $\rangle CHCH_2$-$NHCH_3$ system including the bridge carbon atom, but structure **8** would not. Analogous fragmentation patterns were observed in the mass spectra of the two adrepine acetates. In these cases, fragmentation β to the nitrogen atom gave rise to peaks at *m/e* 86 [$CH_2{=}\overset{+}{N}$-$(COCH_3)CH_3$] and at *m/e* 496 i.e. [M-H_2O-86] in the case of the hexaacetate and [M-CH_3COOH-86] in the heptaacetate.

Supporting evidence for the assignment of a one carbon, as opposed to a two carbon, linkage between the two aromatic rings in adrepine was obtained by consideration of the major fragmentations of two simple model compounds: 2,2-diphenylethylamine and 1,2-diphenylethylamine. The mass spectrum of the former showed strong peaks at *m/e* 30 [$CH_2{=}\overset{+}{N}H_2$] and *m/e* 167 [M-30] due to fragmentation β to the nitrogen atom. These ions were not observed in the latter case. The mass spectrum of 2,2-diphenylethylmethylamine showed the expected peaks at *m/e* 44 and *m/e* 167 due to an analogous fragmentation.

The dibenzocycloheptatriene derivative adnamine (**3**), a substance with an established structure (5, 18, 19), can be readily obtained from adrepine either by heating the solid above its melting point or by heating it in solution in 10% hydrochloric acid at 90–95° for several hours (20). This easy conversion of adrepine into adnamine (**3**) strongly indicates that the free ethanolamine side chain in adrepine must be in a position *ortho* to the carbon atom linking the two aromatic rings.

The cumulative evidence presented above proved that adrepine has the structure **7** [i.e. 6 - (3′,4′ - dihydroxy - α - methylaminomethylbenzyl)adrenaline].

Solid products were often obtained when solutions of adrenaline in 20% hydrochloric acid, containing an excess of a second phenolic

Can. J. Chem. Downloaded from www.nrcresearchpress.com by 210.87.254.42 on 09/05/12
For personal use only.

Can. J. Chem. Downloaded from www.nrcresearchpress.com by 210.87.254.42 on 09/05/12
For personal use only.

component, were allowed to stand at 40° for 24 h or more. In this manner crystalline compounds were obtained by the interaction of adrenaline and the following phenolic components: phenol, 4-methylcatechol and epinine.

The product obtained from phenol and adrenaline is derived from one molecule of each and has been shown to be β-(*p*-hydroxyphenyl)-epinine, i.e. 4-hydroxyphenyl-3′,4′-dihydroxyphenylmethylaminomethylmethane (**9**) (21), i.e. the same product as one of the solvent derived artifact spots observed when solutions of adrenaline in hydrochloric acid are chromatographed in solvents containing phenol (21).

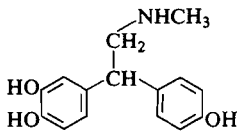

9

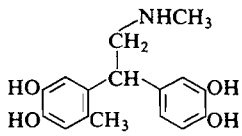

10

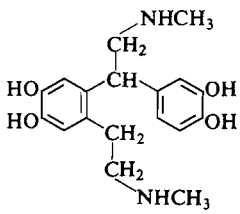

11

The analogous products **10** and **11** were obtained by the interaction of adrenaline with 4-methylcatechol and epinine respectively. All the spectral data obtained for these compounds were consistent with the structures indicated. The mass spectra of the products **9**, **10**, and **11** all showed intense peaks at *m/e* 44 due to the expected cleavage β to the nitrogen atom.

The assignment of the ABX system in the n.m.r. spectrum of adrepine **7** to the ethanolamine (i.e. adrenaline-type) side chain is confirmed by comparison with the n.m.r. spectra of the compounds **3**, **10**, and **11** all of which contain an analogous β,β-diphenylethylamine system but no ethanolamine side chain. The ABX system which can be clearly seen in the spectrum of **7** is absent in the spectra of the others. The n.m.r. spectra of **7** and **11** (i.e. the product obtained by the interaction of adrenaline and epinine in the presence of hydrochloric acid) are shown in Fig. 5.

With regard to possible explanations of the mode of formation of adrepine and the related

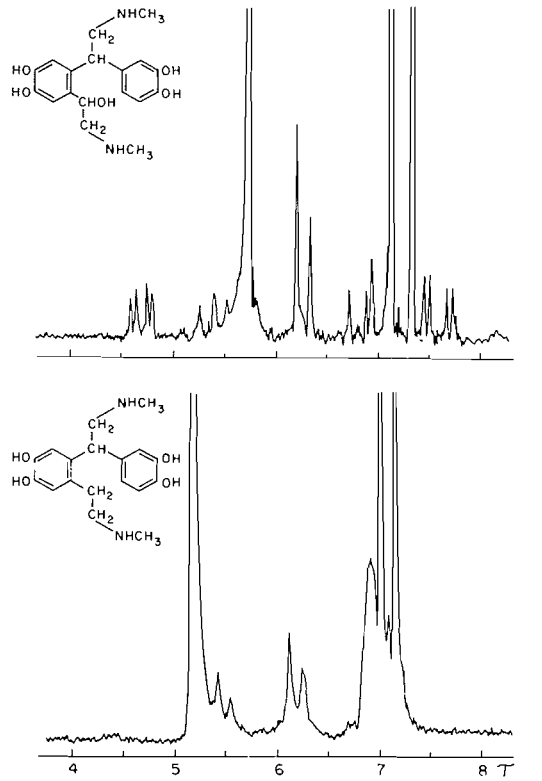

FIG. 5. The n.m.r. spectra of adrepine (**7**) hydrochloride and epinine (**11**) hydrochloride in D_2O with TMS as an external reference.

products, described in this paper, it is most probable that the carbonium ion **12** is formed by the action of strong mineral acids on adrenaline (see Scheme 1) and that compounds of the adrepine type and other β,β-diphenylethylamines are formed by electrophilic attack on a second aromatic ring by this cation.

The reactions discussed here are examples of those which occur when β-3,4-dihydroxyphenylethanolamines, such as adrenaline, are dissolved in acids, either alone or in the presence of a second phenolic component. The basic reaction appears to be of a general nature, in which various phenols may be used, thus permitting the synthesis of a large variety of potentially physiologically active compounds.

Experimental

The melting points were determined on a Thomas-Hoover capillary melting point apparatus and are uncorrected. The i.r. and ultraviolet (u.v.) spectra were recorded on Perkin–Elmer model 237 and Beckman DK-2

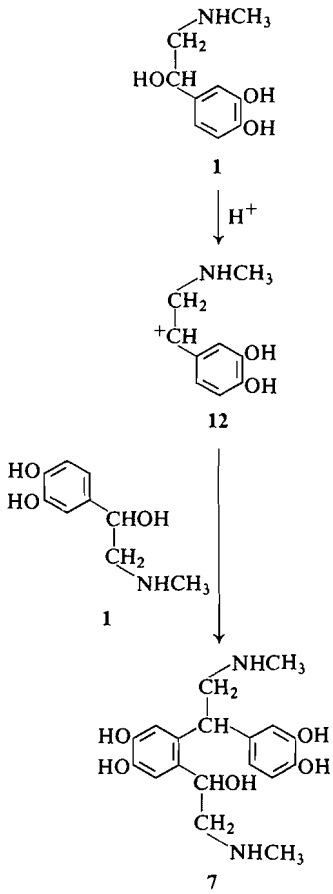

SCHEME 1

recording spectrophotometers respectively. The n.m.r. spectra were obtained on a Varian A-60-A instrument using tetramethylsilane as an internal (or external) reference. The mass spectral data were obtained on Bell and Howell/C.E.C. instruments (Models 21-110[5] or 21-104[6]).

Adrepine Hydrochloride [i.e. 6-(3',4'-Dihydroxymethyl-aminomethylbenzyl)adrenaline (7) Hydrochloride]

A solution of DL-adrenaline (20 g) in 20%[7] aqueous hydrochloric acid (200 ml) was maintained at 40° for 24 h. The white crystalline precipitate which formed was removed by filtration and washed in turn with ice-cold water and ice-cold ethanol. A second crop of crystalline material was obtained after the mother liquors had been maintained at 40° for a further 24 h. A total yield of 14 g of crude product (m.p. 180–182° with decomposition) was obtained. Pure adrepine hydrochloride dihydrate (m.p. 185°, with decomposition) was obtained in colorless prisms on repeated recrystallization of the crude product from 70% ethanol.

Anal. Calcd. for $C_{18}H_{26}N_2O_5Cl_2 \cdot 2H_2O$: C, 47.40; H, 6.61; N, 6.13; Cl, 15.50. Found: C, 47.59; H, 6.39; N, 6.48; Cl, 15.45.

Anhydrous adrepine hydrochloride (m.p. 212°, with decomposition) was obtained when the hydrate was dried *in vacuo* at 120° for 1 h; λ_{max}(EtOH): 285 mμ; ε_{max}(EtOH): 6800.

Anal. Calcd. for $C_{18}H_{26}N_2O_5Cl_2$: C, 51.27; H, 6.30; N, 6.62; Cl, 16.87. Found: C, 51.29; H, 6.22; N, 6.68; Cl, 16.83.

The n.m.r., τ(D_2O): 2.80–3.30 (5H, m, aromatic); 4.70 (1H, dd, X of ABX, J_{AX} = 3.5 Hz, J_{BX} = 10.0 Hz, methine H of —CH(OH)CH_2—); 6.91 (1H, dd, B of ABX, J_{AB} = 13.0 Hz); 7.75 (1H, dd, A of ABX, J_{AB} = 13.0 Hz); 5.40 (1H, t, X of A_2X, J_{AX} = 8.0 Hz, methine H of $\diagdown$CHCH_2—); 6.28 (2H, d, A of A_2X, J_{AX} = 8.0 Hz); 7.12 (3H, s, $\diagdown$*N*—CH_3); 7.32 (3H, s, $\diagdown$*N*—CH_3).

Heptaacetyladrepine [cf. Acetylation of Adrenaline (15)]

A solution of adrepine hydrochloride (0.4 g) in a mixture of anhydrous pyridine (4 ml) and acetic anhydride (4 ml) was heated at 70°, under reflux, for 1 h. The solution was then poured dropwise, with stirring, into ice–water. The resulting aqueous reaction mixture, was neutralized with solid sodium bicarbonate and extracted with chloroform (5 × 50 ml). The combined chloroform extracts were washed with water, dried (Na_2SO_4), and evaporated to dryness *in vacuo* below 40°. The resulting oil was treated with 2 *N* hydrochloric acid until the p*H* reached 5. The solution was then reextracted with chloroform (5 × 50 ml); the combined chloroform extracts washed with 2% aqueous sodium bicarbonate (2 × 50 ml) and water (2 × 50 ml); dried (Na_2SO_4), and concentrated to dryness *in vacuo* below 40° to give a pale yellow oil which crystallized on trituration with light petroleum (b.p. 35–60°). Pure heptaacetyladrepine was obtained as a white crystalline solid (0.45 g) m.p. 167–170° on recrystallization from ethyl acetate; λ_{max}(EtOH): 268; 274 mμ; ν_{max}(Nujol): (C=O) 1775; 1755; 1735; 1640 cm^{-1}.

Anal. Calcd. for $C_{32}H_{38}N_2O_{12}$ (mol. wt. 642): C, 59.80; H, 5.96; N, 4.36; $COCH_3$, 46.9. Found (645): C, 59.95; H, 6.09; N, 4.27; $COCH_3$, 47.06.

The n.m.r., τ($CDCl_3$): 2.60–3.05 (5H, m, aromatic); 3.85 (1H, m, methine —CH(OAc)CH_2—); 4.95 (1H, m, methine $\diagdown$CHCH_2—), 6.00–6.80 (4H, m, —$CH_2N\diagup$).

Hexaacetyladrepine [cf. Acetylation of Adrenaline (16)]

Acetic anhydride (15 ml) was added in four equal portions to a vigorously stirred suspension of adrepine hydrochloride (0.5 g) in 15% aqueous sodium bicarbonate (200 ml). The vigorous foaming which ensued was controlled by the periodic addition of small quantities of diethyl ether. The solution was stirred until evolution of carbon dioxide ceased, allowed to stand for 5 min, and extracted with chloroform (6 × 100 ml). Evaporation of the combined, dried (Na_2SO_4) chloroform extracts to

[5]Atlantic Regional Laboratory.
[6]Dalhousie University.
[7]Concentrated HCl (570 ml) and water (430 ml).

Can. J. Chem. Downloaded from www.nrcresearchpress.com by 210.87.254.42 on 09/05/12
For personal use only.

Can. J. Chem. Downloaded from www.nrcresearchpress.com by 210.87.254.42 on 09/05/12
For personal use only.

dryness *in vacuo* gave hexaacetyladrepine as a pale yellow oil, which solidified on trituration with light petroleum (b.p. 35–60°). This substance was difficult to purify,[8] however some purification of the product was effected by its repeated precipitation from solution in ethyl acetate by the addition of light petroleum (b.p. 60–80°); λ_{max}(EtOH): 272, 263 mμ; ν_{max}(Nujol): (OH), 3300 (broad); (C=O), 1770, 1630 cm^{-1}.

Anal. Calcd. for $C_{30}H_{36}N_2O_{11}$ (mol. wt. 600.6): C, 59.97; H, 6.00; N, 4.67; $COCH_3$, 43.03. Found (623): C, 59.23; H, 5.80; N, 4.76; $COCH_3$, 43.88.

The n.m.r., τ($CDCl_3$): 2.55–2.98 (5H, m, aromatic); 4.75 (1H, m, methine H —CH(OH)CH_2—); 5.25 (1H, m, methine H, >$CHCH_2$—); 6.13 (2H, m, methylene >$CHCH_2N$<); 6.72 (2H, m, methylene, —CH(OH)-CH_2—).

β-*(2-Methyl-4,5-dihydroxyphenyl)*-β-*(3′,4′-dihydroxyphenyl)ethylmethylamine (10) Hydrochloride*

A solution of 4-methylcatechol (13.2 g) and L-adrenaline (6.8 g) in 20% aqueous hydrochloric acid (200 ml) was maintained at 40° for 48 h. The crystalline precipitate which formed afforded β-(2-methyl-4,5-dihydroxyphenyl)-β-(3′,4′-dihydroxyphenyl)ethylmethylamine hydrochloride (14 g, m.p. 282°, with decomposition) in colorless prisms on recrystallization from 70% aqueous alcohol; λ_{max}(EtOH): 285 mμ, ε_{max}(EtOH): 7100.

Anal. Calcd. for $C_{16}H_{20}NO_4Cl$: C, 58.96; H, 6.18; N, 4.24; Cl, 10.88. Found: C, 58.94; H, 6.03; N, 4.20; Cl, 10.67.

The n.m.r., τ(D_2O): 2.90–3.25 (5H, m, aromatic); 5.54 (1H, t, methine, J = 8.0 Hz); 6.34 (2H, d, methylene); 7.17 (3H, s, >N—CH_3); 7.78 (3H, s, >C—CH_3).

β-*(6-Epinyl)epinine*[9] *Hydrochloride [i.e. β-(2-β′-Methylaminoethyl-4,5-dihydroxyphenyl)-β-(3′,4′-dihydroxyphenyl)-N-methylethylamine (11) Hydrochloride]*

A suspension of epinine hydrochloride (0.75 g) and L-adrenaline (0.25 g) in 20% aqueous hydrochloric acid was maintained at 40° for 48 h. During this time the initially insoluble epinine hydrochloride slowly dissolved and a clear solution resulted. The colorless crystalline precipitate (platelets; 0.23 g; m.p. 144–146°) which subsequently slowly formed in the reaction mixture was removed by filtration. L-Adrenaline (250 mg) was added to the mother liquors and the reaction mixture was allowed to stand at 40° for a further 24 h. A second crop of impure crystalline product (257 mg; m.p. 140–142°) was obtained.

A pure sample of β-(6-epinyl)epinine hydrochloride was obtained in colorless plates (m.p. 144–146°) on recrystallization of the crude material from 70% aqueous ethanol.

Anal. Calcd. for $C_{18}H_{26}N_2O_4Cl_2$: C, 53.34; H, 6.47; N, 6.91; Cl, 17.49. Found: C, 53.06; H, 6.44; N, 6.84; Cl, 17.52.

The n.m.r., τ(D_2O): 2.80–3.15 (6H, m, aromatic); 5.41 (1H, t, methine H, J = 8.0 Hz); 6.19 (2H, d, —CH_2— of —CH_2CH<); 6.93 (4H, broad s, —CH_2—CH_2—); 7.04 (3H, s, >N—CH_3); 7.17 (3H, s, >N—CH_3).

Tetraacetyladrenaline (4)

Tetraacetyladrenaline (**4**) was prepared by the method of Bretschneider (15). The n.m.r., τ($CDCl_3$): 2.80 (3H, broad s); 4.05 (1H, m, methine); 6.40 (1H, m, methylene); 7.10 (3H, s, >N—CH_3); 7.26 (6H, s, aromatic —O—$COCH_3$); 7.95 (3H, s, side chain —O—$COCH_3$); 8.00 (3H, s, >N—$COCH_3$).

O^3,O^4,N-Triacetyladrenaline (5)

O^3,O^4,N-Triacetyladrenaline (**5**) was prepared by the method of Welsh (16). The n.m.r., τ($CDCl_3$): 2.70–2.82 (3H, m, aromatic); 5.08 (1H, m, methine); 5.40 (1H, broad s, OH); 6.45 (1H, m, methylene); 7.17 (3H, s, >N—CH_3); 7.25 (6H, s, —O—$COCH_3$); 7.96 (3H, s, >N—$COCH_3$).

Adnamine (3)

Adnamine (**3**) was prepared by the method of Forrest *et al.* (20). The n.m.r., τ(D_2O): 3.18 (4H, d, aromatic); 3.42 (2H, s, olefinic); 5.98 (1H, t, methine, J = 8.5 Hz); 6.94 (2H, d, methylene); 7.53 (3H, s, >N—CH_3).

Thin-layer Chromatography

The R_f values of a number of the compounds described in this investigation were determined on Eastman "Chromagram" Cellulose sheets, using *n*-butanol saturated with 3 *N* HCl as running solvent. The spots were located on the developed chromatograms either by exposing them to ammonia fumes or by spraying with the 4-aminoantipyrene reagent (cf. 22). The R_f values obtained are as follows: **1** (0.35); 7 (0.14); **3** (0.56); **10** (0.60); **9** (0.70); **11** (0.22).

The authors wish to express their thanks to: (*a*) Mr. J. van Ingen (A.R.L.) for recording some of the n.m.r. spectra; (*b*) Mr. D. Embree (A.R.L.) for recording some of the mass spectra and to Dr. W. D. Jamieson (A.R.L.) for useful discussions of the mass spectroscopic data and (*c*) Dr. R. Baltzly of the Wellcome Research Laboratories (New York) for a generous gift of epinine hydrochloride.

1. D. J. ROBERTS and K. J. BROADLEY. J. Chromatogr. **27**, 407 (1967).
2. P. H. REDFERN and D. J. ROBERTS. Biochem. Pharmacol. **16**, 1281 (1967).
3. C. FUNK and L. FREEDMAN. J. Amer. Chem. Soc. **45**, 1792 (1923).
4. H. ÖPPINGER and H. VETTER. Med. Chem. Abh. Med. Chem. Forschungsstaetten I. G. Farbenind. **4**, 343 (1942).

[8]Possibly due to the fact that DL-adrenaline was originally used and the product was a mixture of isomers.

[9]The trivial name "*epepinine*" is suggested for this compound.

5. M. KAWAZU. J. Pharm. Soc. Japan, **78**, 407 (1958); Chem. Abstr. **53**, 318 (1959).
6. H. E. CARTER and E. J. VAN LOON. J. Amer. Chem. Soc. **60**, 1077 (1938).
7. M. KAWAZU. J. Pharm. Soc. Japan, **78**, 978 (1958). Chem. Abstr. **53**, 4295 (1959).
8. J. H. FELLMAN. Nature (London), **182**, 311 (1958).
9. H. AUTERHOFF and H. J. ROTH. Arch. Pharm. **289**, 470 (1956).
10. A. CHATTERJEE, S. K. SRIMANY, and B. CHAUDHURY. J. Chem. Soc. 4576 (1961).
11. B. F. TULLAR. J. Amer. Chem. Soc. **70**, 2067 (1948).
12. I. SERLIN and M. GOLDENBERG. Biochem. J. **54**, 483 (1953).
13. F. F. BLICKE and W. K. JOHNSON. J. Amer. Pharm. Ass. (Sci. Ed.), **45**, 437 (1956).
14. I. STEWART and T. A. WHEATON. J. Org. Chem. **33**, 471 (1968).
15. H. BRETSCHNEIDER. Monatsh. Chem. **76**, 355 (1947).
16. L. WELSH. J. Amer. Chem. Soc. **74**, 4967 (1952).
17. J. REISCH, R. PAGNUCCO, H. ALFES, N. JANTOS, and H. MÖLLMANN. J. Pharm. Pharmacol. **20**, 81 (1968).
18. M. KAWAZU. J. Pharm. Soc. Japan, **78**, 399 (1958); Chem. Abstr. **53**, 317 (1959).
19. M. KAWAZU. J. Pharm. Soc. Japan, **78**, 401 (1958); Chem. Abstr. **53**, 317 (1959).
20. J. E. FORREST, D. ROBERTS, and R. A. HEACOCK. J. Pharm. Pharmacol. **21**, 786 (1969).
21. J. E. FORREST, R. A. HEACOCK, D. ROBERTS, and T. P. FORREST. In preparation.
22. T. A. LARUE and E. R. BLAKLEY. Anal. Chim. Acta, **31**, 400 (1964).
23. J. E. FORREST, S. KAŠPÁREK, R. A. HEACOCK, and T. P. FORREST. **47**, 2118 (1969).

Can. J. Chem. Downloaded from www.nrcresearchpress.com by 210.87.254.42 on 09/05/12
For personal use only.

Can. J. Chem. Downloaded from www.nrcresearchpress.com by 210.87.254.40 on 09/05/12
For personal use only.

Preparation of an aromatic hydroxylamine and some cyclic hydroxamic acids, and their reaction with hydrochloric acid

R. T. COUTTS AND N. J. POUND
Faculty of Pharmacy and Pharmaceutical Sciences, University of Alberta, Edmonton, Alberta

Received November 18, 1969

The reduction of 2,3-dimethyl-4-(*o*-nitrophenylthio)-1-phenyl-3-pyrazolin-5-one by sodium borohydride and palladium–charcoal gave the corresponding hydroxylamine. The action of hydrochloric acid on this hydroxylamine gave the *p*-chloroamine. In a similar manner, treatment of some 2*H*-1,4-benzothiazine and -benzoxazine hydroxamic acids with hydrochloric acid resulted in the formation of 7-chloro-2*H*-1,4-benzothiazine and -benzoxazine lactams.

Canadian Journal of Chemistry, 48, 1859 (1970)

Reduction of aromatic nitro-compounds by sodium borohydride catalyzed by palladium–charcoal gives the corresponding amines rapidly, and in good yields (1). No intermediate compounds are isolated (1) although evidence is available that the reduction proceeds via the hydroxylamine; reduction of various (*o*-nitrophenylthio)acetates and related compounds by means of sodium borohydride and palladium–charcoal gives derivatives of the *N*-hydroxy compound, 3,4-dihydro-4-hydroxy-2*H*-1,4-benzothiazine (2–4).

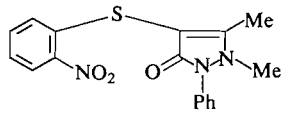

1

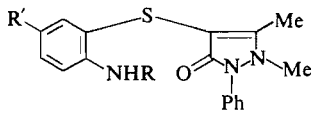

2

	R	R′
a	H	H
b	Ac	H
c	H	Cl
d	Ac	Cl
e	OH	H

In the present study an aromatic nitro-compound, with a bulky substituent in the ortho-position, was reduced with catalyzed sodium borohydride and an aromatic hydroxylamine has been isolated. Reduction of 2,3-dimethyl-4-(*o*-nitrophenylthio)-1-phenyl-3-pyrazolin-5-one (**1**) gave two products of which the amine (**2***a*) was the minor one. In contrast, the same amine was the only product obtained when **1** was reduced using iron and ferrous ammonium sulfate. The major product of the catalyzed sodium borohydride reduction of **1** was a chlorine-containing compound, $C_{17}H_{16}ClN_3OS$. The introduction of the chlorine atom occurred during the work-up procedure in which hydrochloric acid was added to decompose the unreacted sodium borohydride. A structure (**2***c*) has been assigned to this product. Its formation suggested that the reduction of **1** had proceeded only as far as the hydroxylamine, **2***e*, which was subsequently attacked by the chloride ion to yield **2***c* as illustrated in Scheme 1.

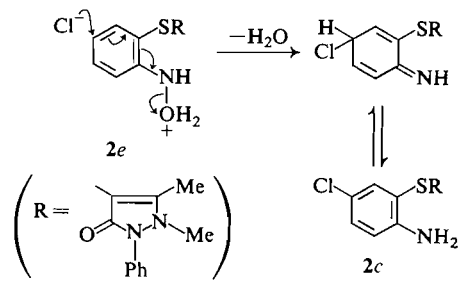

SCHEME 1

The location of the chlorine atom in **2***c* was inferred (*a*) from the ample literature evidence that when hydrochloric acid and other nucleophilic reagents react with aromatic hydroxylamines, *p*-substituted amines are the major products (5–7); (*b*) from the nuclear magnetic resonance (n.m.r.) spectrum of the aromatic protons in the chlorinated ring (Fig. 1), (*c*) from the observation that only *p*-substitution was observed in related reactions described below; and (*d*) from the report (8) that 6-chloro-1-hydroxy-4-quinolones are formed when *o*-nitrobenzaldehyde reacts with ethyl acetoacetate and

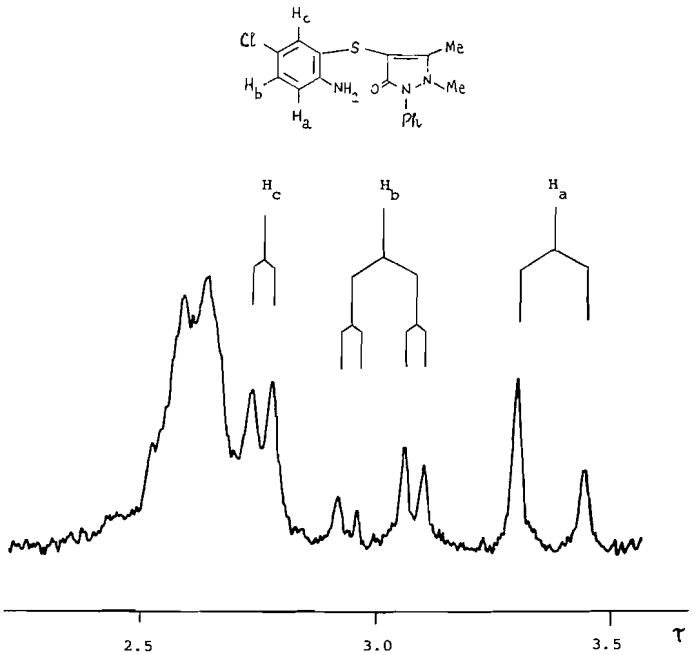

FIG. 1. The n.m.r. spectrum (aromatic ring protons) of 4-(2-amino-5-chlorophenylthio)-2,3-dimethyl-1-phenyl-3-pyrazolin-5-one (**2***c*).

related compounds in the presence of hydrochloric acid.

It was apparent that if hydrochloric acid was excluded from the reaction, reduction of **1** should yield **2***e*. Reduction of **1**, therefore, was repeated except that acetic acid was used in the work-up procedure, and 4-(*o*-hydroxylaminophenylthio)-2,3-dimethyl-1-phenyl-3-pyrazolin-5-one (**2***e*) was obtained. This structure was assigned for the following reasons. The compound analyzed satisfactorily for $C_{17}H_{17}N_3O_2S$; its mass spectrum showed weak M^+ and $[M-2]^+$ ions and an $[M-16]^+$ ion of appreciable abundance, characteristic of an aromatic hydroxylamine (9); NH and OH stretching bands were observed in the infrared (i.r.) spectrum, and the product readily reduced Tollen's reagent.

Another reduction of the pyrazolone (**1**) by means of sodium borohydride and palladium–charcoal was performed in which the filtrate from the reaction was *not* acidified. The major product isolated then was the azoxy compound, namely 2,2′-bis[4-(2,3-dimethyl-1-phenyl-3-pyrazolin-5-onyl)thio]azoxybenzene (**3**), the structure of which was confirmed by means of elemental analysis and i.r. and mass spectra. The same compound (**3**) was the product of the oxidation of the hydroxylamine (**2***e*) by hydrogen peroxide.

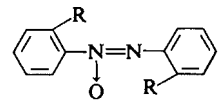

3

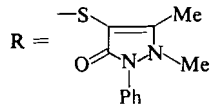

In view of the findings just described, the reduction of (*o*-nitrophenylthio)acetic acid (**4**) by means of sodium borohydride and palladium–charcoal was reinvestigated. Previously (3) we had concluded that an unexpected product of this reduction was the sulfone, 3,4-dihydro-3-oxo-2*H*-1,4-benzothiazine-1,1-dioxide (**5**). Its melting point, i.r. spectrum, and analytical data were all

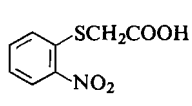

4

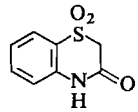

5

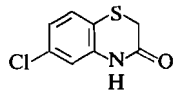

7

Can. J. Chem. Downloaded from www.nrcresearchpress.com by 210.87.254.40 on 09/05/12
For personal use only.

Can. J. Chem. Downloaded from www.nrcresearchpress.com by 210.87.254.40 on 09/05/12
For personal use only.

consistent with such a conclusion. However, the possibility of the product being a chloro-compound was not considered at that time. A mass spectrum of this product has now been recorded and this has revealed that the compound was not **5**; it had a molecular formula $C_8H_6ClNO_2S$. Its n.m.r. spectrum showed a complex signal for the aromatic protons, the pattern of which (Fig. 2) was consistent with a 1,2,4-trisubstituted benzene derivative. The product, therefore, was suspected to be 7-chloro-3,4-dihydro-3-oxo-2*H*-1,4-benzothiazine (**6**). The possibility that the product was the isomer (**7**) was very unlikely but as the m.p. of the product isolated by us and that of **7** were identical, it was necessary to prepare a sample of 6-chloro-3,4-dihydro-3-oxo-2*H*-1,4-benzothiazine (**7**) for direct comparison with our product. Reduction of (4-chloro-2-nitrophenylthio)acetic acid with sodium hydrosulfite, using the reported (10) method, gave the required lactam (**7**) which was shown by a comparison of i.r. and n.m.r. spectra (Figs. 2 and 3) and a mixed melting point to differ from **6**.

The formation of **6** can be explained in a manner similar to that described for **2***c*. It apparently involves the nucleophilic attack of a chloride ion on the protonated hydroxamic acid as illustrated in Scheme 2. The authenticity of this mechanism was substantiated when it was found that the lactam (**6**) was the product isolated in 81% yield when 3,4-dihydro-4-hydroxy-3-oxo-2*H*-1,4-benzothiazine (**8**) was treated with hydrogen chloride.

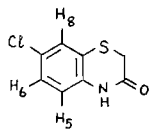

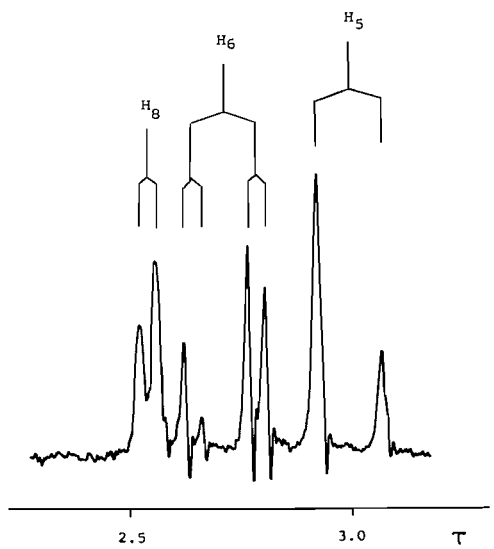

FIG. 2. The n.m.r. spectrum (aromatic ring protons) of 7-chloro-3,4-dihydro-3-oxo-2*H*-1,4-benzothiazine (**6**).

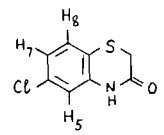

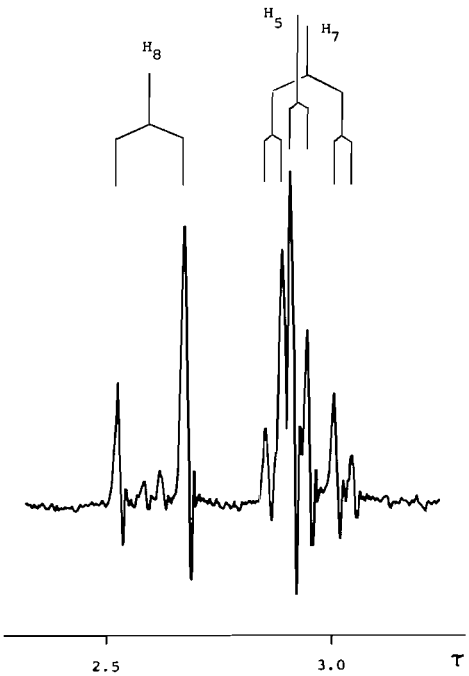

FIG. 3. The n.m.r. spectrum (aromatic ring protons) of 6-chloro-3,4-dihydro-3-oxo-2*H*-1,4-benzothiazine (**7**).

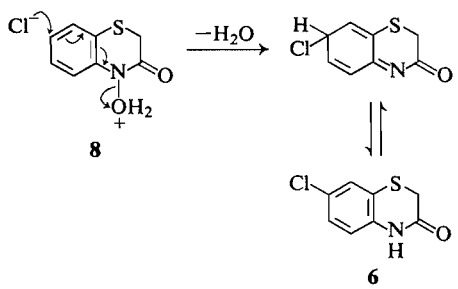

SCHEME 2

Can. J. Chem. Downloaded from www.nrcresearchpress.com by 210.87.254.40 on 09/05/12
For personal use only.

This novel reaction offers a means of preparing 7-chlorobenzothiazines which are not readily available by conventional reductive methods of synthesis. Such methods would require (2-nitro-5-chlorophenylthio)acetic acid as a starting material for the preparation of **6**, but this acid is not available by the action of thioglycolic acid on 2,4-dichloronitrobenzene, because of the reactivity of both chlorine atoms.

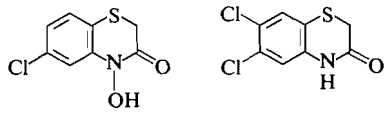

9 **10**

In the same way, the action of hydrogen chloride on 6-chloro-3,4-dihydro-4-hydroxy-3-oxo-2*H*-1,4-benzothiazine (**9**) gave an excellent yield of 6,7-dichloro-3,4-dihydro-3-oxo-2*H*-1,4-benzothiazine (**10**). The structure of **10** was readily deduced from its n.m.r. spectrum which indicated the absence of ortho- and meta-coupling in the aromatic signal (1-proton singlets at τ 2.80 and 2.32) and which verified that the attack of the chloride ion was at the ring position para to the nitrogen function.

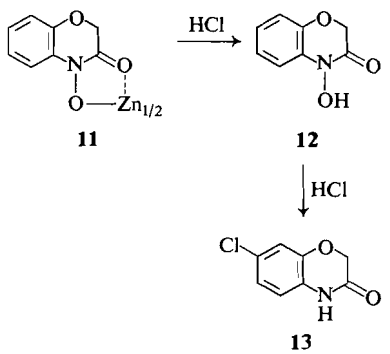

11 **12** **13**

SCHEME 3

This new synthetic method is not restricted to the preparation of benzothiazines. Related benzoxazines can also be obtained in the same way. Thus, reduction of methyl *o*-nitrophenoxyacetate gave the zinc complex of 3,4-dihydro-4-hydroxy-3-oxo-2*H*-1,4-benzoxazine (**11**). Treatment of this complex with hydrochloric acid gave the expected hydroxamic acid (**12**) (Scheme 3) but, in addition, a neutral compound was isolated. Its mass and i.r. spectra and elemental analysis were consistent with this compound being 7-chloro-3,4-dihydro-3-oxo-2*H*-1,4-benzoxazine (**13**). The same product (**13**) is formed in 79% yield by the action of hydrochloric acid on the hydroxamic acid (**12**). Similarly, a solution of 2-ethyl-3,4-dihydro-4-hydroxy-3-oxo-2*H*-1,4-benzoxazine (**14**) in sodium carbonate solution, on acidifying with hydrochloric acid, gave a chloro-compound, presumably 7-chloro-2-ethyl-3,4-dihydro-3-oxo-2*H*-1,4-benzoxazine (**15**).

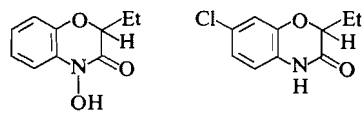

14 **15**

Experimental

Melting points are uncorrected. The i.r. spectra were recorded as Nujol mulls. Mass spectra were measured with an A.E.I. MS-9 spectrometer, and n.m.r. spectra were recorded on a Varian A-60 spectrometer using DMSO-d_6 as solvent. Chemical shifts are expressed in τ units with TMS as standard.

Reduction of 2,3-Dimethyl-4-(o-nitrophenylthio)-1-phenyl-3-pyrazolin-5-one (1)

(*i*) A solution of sodium borohydride (1.02 g) in water (15 ml) was added in three equal portions at 5 min intervals to a suspension of the title compound (**11**) (2.01 g) and 10% palladium-on-charcoal (0.11 g) in dioxane (100 ml) through which nitrogen gas was bubbled. After 15 min, the suspension was filtered and the colorless filtrate was acidified with dilute hydrochloric acid, then reduced in volume to near dryness. Chloroform (50 ml) was added and the resulting pale brown solution was extracted repeatedly with dilute hydrochloric acid. The combined acid extract (250 ml) was made alkaline with 50% sodium hydroxide solution over ice then extracted with chloroform. Evaporation of the dried chloroform solution gave a pale brown solid (1.41 g) which, when crystallized from benzene then ethanol, gave *4-(2-amino-5-chlorophenylthio)-2,3-dimethyl-1-phenyl-3-pyrazolin-5-one* (**2***c*) as a colorless solid, m.p. 180–181°. The i.r. spectrum: 3400, 3320 (NH_2); 1642 (C=O); 812 (CH) cm^{-1}. The n.m.r. spectrum: 7.58 and 6.80 (3-proton singlets) (CH_3); 4.26 (2-proton broad singlet) (NH_2); 2.30–3.50 (8-proton aromatic signal) (Fig. 1). Mass spectrum: 345 (M^+, 62%) 347 (25%).

Anal. Calcd. for $C_{17}H_{16}ClN_3OS$: C, 59.04; H, 4.66; N, 12.15. Found: C, 59.41; H, 5.12; N, 11.60.

Treatment of **2***c* (0.17 g) with acetic anhydride in the usual manner gave the *acetate* (**2***d*) (0.14 g) which crystallized from benzene as a colorless solid, m.p. 202–203°. The i.r. spectrum: 3320 (NH); 1700 and 1641 (C=O); 812 (CH) cm^{-1}.

Anal. Calcd. for $C_{19}H_{18}ClN_3O_2S$: C, 58.83; H, 4.68; Cl, 9.14; N, 10.83. Found: C, 59.08; H, 5.09; Cl, 8.90; N, 10.41.

(*ii*) Reduction (*i*) was repeated on the title compound

Can. J. Chem. Downloaded from www.nrcresearchpress.com by 210.87.254.40 on 09/05/12
For personal use only.

(2.24 g) except that the filtrate was acidified with acetic acid. Evaporation of the acidified filtrate gave a brown oil which, when triturated with ethanol then washed with water, left a yellow solid (1.5 g). Crystallization from ethanol gave *4-(o-hydroxylaminophenylthio)-2,3-dimethyl-1-phenyl-3-pyrazolin-5-one* (**2e**) as a bright yellow solid, m.p. 156–158° (dec.) which reduced Tollen's reagent. The i.r. spectrum: 3245 (broad, NH and OH); 1619 (C=O) cm^{-1}. Mass spectrum: 327 (M^+, 1%), 325 (5%), 311 (25%).

Anal. Calcd. for $C_{17}H_{17}N_3O_2S$: C, 62.36; H, 5.23; N, 12.84. Found: C, 62.28; H, 5.34; N, 12.92.

(*iii*) Reduction (*i*) was repeated on the title compound (1.01 g). The filtrate was not acidified. It was evaporated to dryness and the resulting semi-solid extracted with hot ethanol (3 × 10 ml). On concentration of the ethanol solution, *2,2'-bis[4-(2,3-dimethyl-1-phenyl-3-pyrazolin-5-onyl)thio]azoxybenzene* (**3**) (0.48 g) separated as an orange solid and had m.p. 272–273.5° (dec.) when crystallized from dimethylsulfoxide–ethanol. The i.r. spectrum: 1668 (C=O) cm^{-1}. Mass spectrum: 634 (M^+, 0.3%), 618 (2%).

Anal. Calcd. for $C_{34}H_{30}N_6O_3S_2$: C, 64.33; H, 4.76; N, 13.24. Found: C, 63.63; H, 4.39; N, 12.71.

(*iv*) Powdered iron (2.07 g) and ferrous ammonium sulfate (0.57 g) were suspended in a solution of the title compound (1.01 g) in ethanol (80 ml) and the mixture was heated under reflux for 90 min. The hot solution was filtered with the aid of Celite. Evaporation of the colorless filtrate gave an off-white solid (0.82 g). Crystallization from ethanol gave *4-(o-aminophenylthio)-2,3-dimethyl-1-phenyl-3-pyrazolin-5-one* (**2a**) as a colorless solid, m.p. 204–207°, which on diazotization and coupling with β-naphthol gave a red dye. The i.r. spectrum: 3400, 3318 (NH_2); 1642 (C=O) cm^{-1}. Mass spectrum: 311 (M^+, 63%).

Anal. Calcd. for $C_{17}H_{17}N_3OS$: C, 65.57; H, 5.50; N, 13.50. Found: C, 65.55; H, 5.84; N, 13.41.

Treatment of **2a** (1.05 g) with acetic anhydride in the usual way gave the *acetate* (**2b**) (0.89 g), m.p. 162–164° (from ethanol). The i.r. spectrum: 3250 (NH); 1700 and 1650 (C=O) cm^{-1}.

Anal. Calcd. for $C_{19}H_{19}N_3O_2S$: C, 64.52; H, 5.42; N, 11.89. Found: C, 64.49; H, 5.81; N, 11.48.

Oxidation of Hydroxylamine (2e)

4-(*o*-Hydroxylaminophenylthio)-2,3-dimethyl-1-phenyl-3-pyrazolin-5-one (0.48 g) was suspended in dioxane (30 ml) and 30% hydrogen peroxide solution (5 ml) was added gradually with stirring. Reaction was continued for 18 h during which time the starting material dissolved and a yellow precipitate (0.17 g) formed. Recrystallization from DMSO–ethanol gave the *azoxy compound* (**3**), m.p. 272–275° (dec.), the i.r. spectrum of which was superimposable on that of the product obtained in the reduction of **1** (method (*iii*)).

*6,7-Dichloro-3,4-dihydro-3-oxo-2H-1,4-benzothiazine (**10**)*

Hydrogen chloride was bubbled through a methanolic solution (10 ml) of 6-chloro-3,4-dihydro-4-hydroxy-3-oxo-2*H*-1,4-benzothiazine [prepared by the literature (3) method] (0.22 g) for 2 min at 5°. The solution was set aside at room temperature for 3 h then evaporated to dryness. The resulting grey solid (0.23 g) was crystallized from ethanol to yield the *title compound*, m.p. 249–251°. The i.r. spectrum: 3170 (NH), 1678 (C=O) cm^{-1}. The n.m.r. spectrum: 6.47 (2-proton singlet) (CH_2); 2.80 (1-proton singlet) (C_5-H); 2.32 (1-proton singlet) (C_8-H); −0.75 (1-proton broad singlet) (NH).

Anal. Calcd. for $C_8H_5Cl_2NOS$: C, 41.04; H, 2.15; N, 5.98. Found: C, 40.94; H, 2.42; N, 5.99.

Reduction of (o-Nitrophenylthio)acetic Acid (4)

The title compound was reduced with sodium borohydride and palladium–charcoal in dioxane as described previously (3). The product, m.p. 208–209° was 7-chloro-3,4-dihydro-3-oxo-2*H*-1,4-benzothiazine (**7**), lit. (12) m.p. 206°. The i.r. spectrum: 3180 (NH), 1688 (C=O) cm^{-1}. Mass spectrum: 199 (M^+, 100%), 201 (35%). The n.m.r. spectrum: 6.50 (2-proton singlet) (CH_2); 2.45–3.10 (3-proton aromatic signal) (Fig. 2); −0.68 (1-proton broad singlet) (NH).

Anal. Calcd. for C_8H_6ClNOS: C, 48.13; H, 3.03; N, 7.02; S, 16.06. Found: C, 48.55; H, 3.03; N, 6.92; S, 16.00.

6-Chloro-3,4-dihydro-3-oxo-2H-1,4-benzothiazine (7)

This compound was prepared by the reported method (10). The i.r. spectrum: 3185 (NH), 1670 (C=O) cm^{-1}. The n.m.r. spectrum: 6.50 (2-proton singlet) (CH_2); 2.48–3.10 (3-proton aromatic signal) (Fig. 3); −0.67 (1-proton broad singlet) (NH).

Action of Hydrochloric Acid on the Zinc Complex of 3,4-Dihydro-4-hydroxy-3-oxo-2H-1,4-benzoxazine (11)

The crude zinc complex was prepared from ethyl *o*-nitrophenoxyacetate by a previously reported method (14). The sample was purified by dissolving it in dimethylsulfoxide, filtering off the insoluble zinc, then reprecipitating the complex by pouring the filtrate into ethanol. Crystallization from ethanol gave a flocculent white precipitate, m.p. >360°. The i.r. spectrum: 1631 cm^{-1} (chelated C=O).

Anal. Calcd. for $C_{16}H_{12}N_2O_6Zn$: C, 48.82; H, 3.07; N, 7.12. Found: C, 48.99; H, 2.81; N, 7.04.

A suspension of the zinc complex (0.15 g) in dilute hydrochloric acid (5 ml) was stirred for 2 h and the resulting light brown suspension was extracted with chloroform. Evaporation of the chloroform gave a brown solid (71 mg) which was redissolved in chloroform. This solution was extracted with 10% aqueous sodium carbonate, dried and evaporated to yield *7-chloro-3,4-dihydro-3-oxo-2H-1,4-benzoxazine* (**13**) (40 mg), as a white solid, m.p. 197–200° when crystallized from methanol. Infrared spectrum: 3175 (NH), 1684 (C=O), 800 (CH) cm^{-1}. Mass spectrum: 183 (M^+, 100%), 185 (35%). The n.m.r. spectrum: 5.42 (2-proton singlet) (CH_2); very broad signal centered at 4.25 (NH); 2.90–3.12 (3-proton aromatic signal).

Anal. Calcd. for $C_8H_6ClNO_2$: C, 52.34; N, 3.29; N, 7.63. Found: C, 52.67; H, 3.52; N, 7.67.

The aqueous sodium carbonate solution described above was acidified with glacial acetic acid and extracted with chloroform. Evaporation of the chloroform extract gave 3,4-dihydro-4-hydroxy-3-oxo-2*H*-1,4-benzoxazine (**12**) (15 mg) as a white solid, m.p. 165–166° [lit. (13)

m.p. 168–169°]. Its infrared spectrum was superimposable on that of an authentic sample.

The benzoxazine (**13**, 0.61 g) was also obtained by heating under reflux a suspension of 3,4-dihydro-4-hydroxy-3-oxo-2*H*-1,4-benzoxazine (**12**) (0.7 g) in dilute hydrochloric acid (15 ml) for 2.5 h. The cooled mixture was extracted with chloroform; the latter was washed with sodium carbonate solution, then water, and evaporated to give **13**, m.p. 195–199°.

*Action of Hydrochloric Acid on 2-Ethyl-3,4-dihydro-4-hydroxy-3-oxo-2H-1,4-benzoxazine (**14**)*[1]

A solution of the title compound (10 mg) in aqueous sodium carbonate (20 ml) was acidified with concentrated hydrochloric acid and allowed to stand for 15 h. The crystalline product (5 mg), m.p. 143–144°, was *7-chloro-2-ethyl-3,4-dihydro-3-oxo-2H-1,4-benzoxazine* (**15**). The i.r. spectrum: 3190 (NH), 1696 (C=O), 798 (CH) cm^{-1}. Mass spectrum: 211 (M^+, 67%), 213 (20%).

Anal. Calcd. for $C_{10}H_{10}ClNO_2$: N, 6.62. Found: N, 6.30.

The award of a Medical Research Council of Canada Studentship (to N.J.P.) and other M.R.C. financial assistance (grant No. MA 2993) is greatly appreciated.

[1]K. W. Hindmarsh carried out this reaction.

The authors acknowledge meaningful discussions with Dr. R. A. Abramovitch, and thank Mrs. S. Li, Mr. E. Mah, and Mr. W. F. Dylke for technical assistance.

1. T. Neilson, H. C. S. Wood, and A. G. Wylie. J. Chem. Soc. 371 (1962).
2. R. T. Coutts, H. W. Peel, and E. M. Smith. Can. J. Chem. **43**, 3221 (1965).
3. R. T. Coutts, D. L. Barton, and E. M. Smith. Can. J. Chem. **44**, 1733 (1966).
4. R. T. Coutts and E. M. Smith. Can. J. Chem. **45**, 975 (1967).
5. E. Bamberger. Ann. **424**, 233 and 297 (1921).
6. E. Bamberger. Ann. **441**, 297 (1925).
7. G. R. Robertson and R. A. Evans. J. Org. Chem. **5**, 142 (1940).
8. J. D. Loudon and I. Wellings. J. Chem. Soc. 3470 (1960).
9. R. T. Coutts and Gita Mukherjee. Org. Mass Spectrom. **3**, 63 (1970).
10. R. N. Prasad and K. Tietje. Can. J. Chem. **44**, 1247 (1966).
11. R. T. Coutts and S. J. Storey. Can. J. Pharm. Sci. **2**, 22 (1967).
12. G. Vasiliu, O. Maior, and N. Arsenescu. An. Univ. Bucuresti, Ser. Stiint. Nat. **12**, 47 (1963); Chem. Abstr. **64**, 17581 (1966).
13. E. Honkanen and A. I. Virtanen. Acta Chem. Scand. **14**, 1214 (1960).

Can. J. Chem. Downloaded from www.nrcresearchpress.com by 210.87.254.40 on 09/05/12
For personal use only.

Studies on the decomposition of tetra-alkylammonium salts in solution. Part III. Interpretation of Hammett correlations

E. C. F. Ko AND K. T. LEFFEK
Department of Chemistry, Dalhousie University, Halifax, Nova Scotia

Received October 31, 1969

Hammett free energy correlations are reported for the decomposition reactions of tetra-alkylammonium halides in chloroform and acetone solution. All the salts contained a substituted benzyl group attached to the nitrogen atom and decomposed to yield a benzyl iodide and dimethylaniline as the only products.

The curved Hammett plots for para-substituted benzyl compounds are compared to the linear plot found previously for a series of salts each containing a para-substituted phenyl group, and it is concluded that curved Hammett plots cannot be used as evidence for a change of mechanism, unless direct conjugative effects between substituent and reaction site are absent.

Canadian Journal of Chemistry, 48, 1865 (1970)

Can. J. Chem. Downloaded from www.nrcresearchpress.com by 210.87.254.105 on 09/05/12
For personal use only.

Introduction

In the previous paper of this series (1) a ρ value of +1.4 was found for para-substituted phenyl groups for the decomposition reaction of phenylbenzyldimethylammonium iodides. These salts all decompose completely and cleanly to yield benzyl iodide and a tertiary amine and follow first-order kinetics when the calculations are made with respect to the concentration of the ammonium ion (2). Therefore, the reaction is considered to be a decomposition of the ammonium ion involving a transfer of the charge from the nitrogen atom to the benzyl carbon atom, to yield a tertiary amine and a carbonium ion, which is probably associated as an ion-pair, since it is most likely that the original ammonium ion is associated as a triple-ion in poorly ionizing solvents (2). The carbonium ion-pair then collapses to yield the benzyl halide. By an extension of the current terminology, this mechanism was called an ionic internal nucleophilic substitution (2).

In this paper the Hammett correlation for the same reaction is studied for para-substituted benzyl groups. In this case, in contrast to the para-substituted phenyl group, the electrons move away from the benzene ring during the reaction, so that a negative value of ρ would be expected (3). The decomposition reaction is really a nucleophilic substitution of a substituted benzyl compound with a $C_6H_5N^+(CH_3)_2$ leaving group. Jaffe has reported a number of Hammett correlations for this type of reaction of benzyl compounds (4), based on data most of which was obtained in the 1930's. Nearly all of these correlations gave negative ρ values, although a few gave positive values. Some of these correlations have been recalculated by Wells (5) who imposed further restrictions to improve the fit, but the benzyl compound correlations have as their common feature quite low correlation coefficients. Thus the ρ values obtained for benzyl compounds have large uncertainties and these are transferred from the experimental results to the interpretation. For example, Swain and Langsdorf (6) discussed Hammett correlations for benzyl compounds and reached the conclusion that there is a single concerted mechanism for nucleophilic substitutions, whereas Wiberg (3) used the ρ value of −2.2 for benzyl chloride solvolyses as evidence for the S_N2 nature of the reaction. These different conclusions are made from essentially the same experimental data.

Since the decomposition of benzyl containing tetra-alkylammonium salts is not an S_N2 reaction (2), it provides a good test case for the interpretation of the Hammett correlations.

Results and Discussion

Rate constants at 40 °C for the decomposition of a series of ammonium bromides and iodides containing para-substituted benzyl groups in two solvents are given in Table 1 and are plotted as $\log_{10} k_1$ vs. σ, the Hammett substituent constant, in Fig. 1. Also included in Fig. 1 is a similar graph for a series of iodides containing para-substituted phenyl groups. The rate constants for this series and the value of ρ equal to +1.4 are taken from the previous paper of this series (1).

The curvature of the plot (concave upwards)

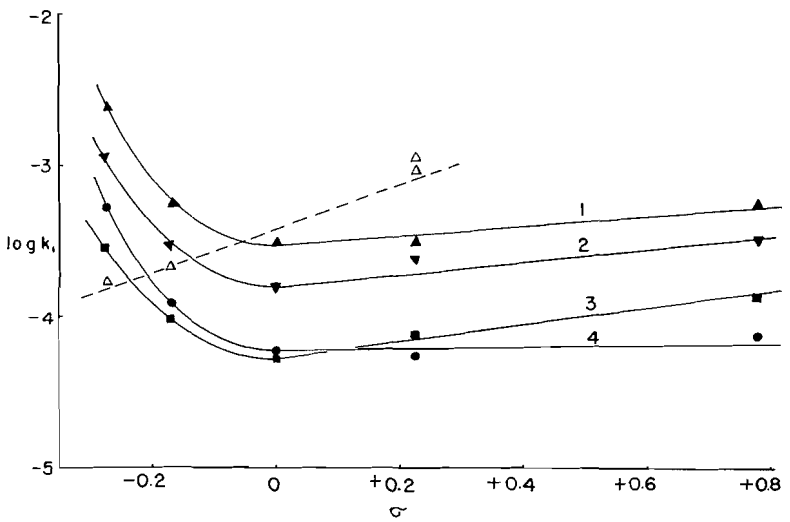

FIG. 1. Correlation of the logarithm of the first order specific rate of the decomposition of 4-X,benzylphenyldimethylammonium salts and the Hammett σ constant; *1*) iodide in chloroform solution; *2*) iodide in acetone solution; *3*) bromide in acetone solution; *4*) bromide in chloroform solution. The dashed line (open triangles) represents a similar graph for para-substituted-phenylbenzyldimethylammonium iodide in chloroform solution (1).

TABLE 1

Specific first-order rate constants for the decomposition of tetra-alkylammonium halides in solution at 40 °C

p-Substituted benzylphenyldimethylammonium halide	10^4k_1 (s^{-1})	
	Chloroform	Acetone
Bromide		
p-MeO	5.30	2.90
p-Me	1.25	0.960
p-H	0.607	0.553
p-Br	0.556	0.803
p-NO_2	0.782	1.37
Iodide		
p-MeO	24.7	11.4
p-Me	6.04	2.91
p-H	3.18	1.59
p-Br	3.25	2.51
p-NO_2	5.94	3.28

for the para-substituted benzyl series is qualitatively very similar to that obtained by other workers for nucleophilic substitutions on benzyl compounds (6), although the present results show a definite minimum. Swain and Langsdorf explained the curved plots in terms of resonance interaction and argued for a single mechanism of reaction. On the other hand, Jaffe (4) considered the same results to indicate the presence of two reaction mechanisms with different ρ values which combined to yield the curved plot. In the present study, the nature of the transition state is deduced by means of a Hammett correlation in which the substitution of different groups is made in two separate benzene rings, within the parent compound, which are chemically different but symmetrically arranged with respect to the bond which is breaking during the reaction. The two separate results which are obtained from substitution in the benzyl ring in the one case and in the phenyl ring in the other, should give essentially consistent indications of the type of transition state occurring in the reaction because the kinetics, which clearly indicate the major aspects of the mechanism (2), are the same for all the compounds studied. This, together with the fact that the substituents on the phenyl ring apparently do not change the mechanism, leads to the conclusion that the curved plot obtained for the para-substituted benzyl series does not indicate a change of mechanism.

Therefore, an explanation of the curvature similar to that of Swain and Langsdorf is preferred. The Hammett σ values refer to reactions in which the electron transfer process from the aromatic ring to the reaction site is governed by the inductive effect alone. In a reaction such as the decomposition under study, in which a positive charge is being developed on the benzyl carbon atom, a para-substituted methoxy group may release electrons by direct conjugation,

Can. J. Chem. Downloaded from www.nrcresearchpress.com by 210.87.254.105 on 09/05/12
For personal use only.

Can. J. Chem. Downloaded from www.nrcresearchpress.com by 210.87.254.105 on 09/05/12
For personal use only.

which would be a much stronger effect than its inductive electron withdrawal. Similarly, a para-methyl group may release electrons by hyperconjugation in addition to its inductive electron release. Thus, compounds with these substituents would be expected to give abnormally fast rate constants, if the Hammett plot is assumed to be the normal specific rate. Therefore, although a precise estimate of ρ cannot be made, it may be estimated to be 0.25 ± 0.2 from the right-hand side of the plots in Fig. 1. Alternatively, the Hammett plot could be constructed using σ^+ values for the substituents which release electrons by direct conjugation. This has the effect of spreading out the σ scale on the negative side and thus gives a curve which is more U-shaped. It is then possible to calculate a ρ value from either arm using three points in each case, so that either a negative value of about -1.2 may be obtained for ρ or the positive quoted above.

According to the usual interpretation of Hammett ρ values, this parameter measures the sensitivity to change of electron availability at the reaction center. The sign of the substituent σ values is such that in a reaction in which positive charge accumulates adjacent to the benzene ring, ρ is negative, and when negative charge accumulates it is positive. Thus, the value of $+1.4$ found (1) for the substituted phenyl series confirmed the fact that the central nitrogen atom adjacent to the phenyl ring had a reduced positive charge in the transition state. The U-shaped curve for the substituted benzyl series is not inconsistent with this, but because of the conjugative electron release of some substituents and of the almost zero value obtained from the plots in Fig. 1, it might be concluded that very little positive charge accumulates on the benzyl carbon atom during the activation process. Therefore, either this positive charge is extensively dispersed from the central nitrogen atom on to the benzyl carbon atom in the initial state, or the transition state is reached very early on the reaction co-ordinate, or both of these effects are present. When added to the evidence obtained from the activation parameters of the para-substituted phenyl reactions (1), the reaction is most easily envisaged as involving both effects simultaneously.

In conclusion, it may be seen that the evidence from the study of tetra-alkylammonium salt decompositions shows that curved Hammett plots may result from direct conjugative effects. Therefore, such curved plots should not be used as evidence for a change of mechanism, unless direct conjugative effects are clearly absent from the system under study.

Experimental

Materials

The tetra-alkylammonium bromides and iodides were made as outlined previously (1). Excess (3- to 4-fold) of purified dimethylaniline was added dropwise, with stirring, to the appropriate cold benzyl halide without any solvent. The stirring was continued for 2 h at room temperature, after which the solid product was filtered, washed a few times with ether, and dried under vacuum. The salts were purified by repeated recrystallization until their purities, determined by potentiometric titration of halide ions with standard silver nitrate solution, were 99% or better. The yield was quantitative. For the hygroscopic salts, the whole operation of purification was carried out in an atmosphere of dry nitrogen. A summary of the recrystallization conditions and the melting points of the products is given in Table 2.

Commercial benzyl bromide was distilled, b.p. 82–83 °C at 3 mm and 4-nitrobenzyl bromide was recrystallized from ethanol, m.p. 98.5 °C. 4-Methoxybenzyl bromide, b.p. 110–112 °C at 2 mm, was made by bubbling dry hydrogen bromide into a solution of 4-methoxybenzyl alcohol in AR benzene as described by Lapworth and Shoesmith (7). 4-Bromobenzyl bromide, m.p. 60–61 °C (recrystallized from ethanol), was prepared by bromination of 4-bromotoluene (8). 4-Methylbenzyl bromide, m.p. 33–36 °C (recrystallized from benzene), was made from *p*-xylene and *N*-bromosuccinimide in carbon tetrachloride containing a trace of benzoyl peroxide (9).

4-Nitrobenzyl iodide was purchased from Koch–Light Laboratories and used without further purification. Benzyl iodide, m.p. 24–25 °C (from ether), 4-methoxybenzyl iodide, m.p. 32–33 °C (from ether), 4-methylbenzyl iodide, m.p. 49–50 °C (from ether), and 4-bromobenzyl iodide, m.p. 70–71 °C (from ethanol), were made from

TABLE 2

Recrystallization and physical data for 4-X,benzylphenyldimethyl N^+Y^- compounds

X	Y	Medium for recrystallization (by volume)	Melting point (°C)
MeO	Br	Methanol/ether (1:10)	Hygroscopic
	I	Ethanol/petroleum ether (1:15)	Hygroscopic
Me	Br	Ethanol/ether (1:20)	127–128
	I	Ethanol/ether (1:10)	121–123
H	Br	Ethanol/acetone (1:2)	154–156
	I	Ethanol	148–150
Br	Br	Ethanol/ether (1:5)	145–146
	I	Ethanol	129–131
NO_2	Br	Ethyl acetate	146–147
	I	Ethanol	136–137

the corresponding benzyl bromides or chlorides by the action of sodium iodide in acetone as described by Gardner and Noyes (10).

The chloroform solvent was Matheson, Coleman, and Bell chromatoquality reagent as used previously (1). Acetone was purified by refluxing first with potassium permanganate, then over anhydrous calcium sulfate, followed by fractional distillation, b.p. 57.5 °C, according to the method of Taft *et al.* (11).

Kinetics

The procedure for the kinetic measurements was, in general, as described in earlier papers (1, 2). Resistances were measured on a Wayne–Kerr conductivity bridge. The precision and accuracy of the rate constants are the same as those reported in part I of this series (2) in which a number of experimental comparisons were made and illustrative runs quoted from which these figures of merit may be estimated.

Because of solubility limitations, the concentration range of the solution was 0.005–0.09 *M* in chloroform and 0.002–0.035 *M* in acetone. Solutions were made by weight dilution and in the case of sparingly soluble salts, saturated solutions were used.

Reaction Products

Reaction mixtures of the decomposition reactions in chloroform, after equilibration for 15 to 20 half-lives, were analyzed by vapor-phase chromatography on an A-700 Autoprep chromatograph. The column (20′ × ¼″ o.d.) was packed with silicone gum rubber SE 30 on HMDS chromosorb mesh size 80–100. Dimethylaniline and the appropriate benzyl halide were identified with authentic samples in each case and no other products were found. Dimethylaniline and most of the 4-substituted benzyl halides were conveniently determined at column temperatures 200–225 °C, but 4-bromo, 4-methyl, and 4-methoxybenzyl iodides were found to be unstable at such high temperatures. Good separations for these compounds were achieved at column temperatures 150–170 °C.

The authors are grateful for financial support by the National Research Council of Canada.

1. J. T. Burns and K. T. Leffek. Can. J. Chem. **47**, 3725 (1969).
2. K. T. Leffek and F. H-C. Tsao. Can. J. Chem. **46**, 1215 (1968).
3. K. B. Wiberg. Physical organic chemistry. J. Wiley & Son, Inc., New York, 1964. p. 404.
4. H. H. Jaffe. Chem. Rev. **53**, 191 (1953).
5. P. R. Wells. Linear free energy relationships. Academic Press Inc., London, 1968. p. 13.
6. C. G. Swain and W. P. Langsdorf. J. Amer. Chem. Soc. **73**, 2813 (1951).
7. A. Lapworth and J. B. Shoesmith. J. Chem. Soc. 1391 (1922).
8. M. Weizman and S. Patai. J. Amer. Chem. Soc. **68**, 150 (1946).
9. R. A. W. Johnstone and T. S. Stevens. J. Chem. Soc. 3346 (1960).
10. I. J. Gardner and R. M. Noyes. J. Amer. Chem. Soc. **83**, 2409 (1961).
11. R. W. Taft, E. Price, I. R. Fox, I. C. Lewis, K. K. Anderson, and G. T. Davis. J. Amer. Chem. Soc. **85**, 709 (1963).

Can. J. Chem. Downloaded from www.nrcresearchpress.com by 210.87.254.105 on 09/05/12
For personal use only.

Reactions of pentachlorothiophenol. I. Preparation of some simple metallic and non-metallic derivatives

C. R. Lucas and M. E. Peach
Department of Chemistry, Acadia University, Wolfville, Nova Scotia
Received January 12, 1970

The preparation and properties of simple metal derivatives of pentachlorothiophenol are described: MSC_6Cl_5 (M = Na, K, Rb, Cs, Tl, Cu, Ag, Au, Ph_3Sn, *n*-Bu_3Sn, Ph_3Pb, Ph_4As), $M(SC_6Cl_5)_2$ (M = Zn, Cd, Hg, Ni, Pd, Pb, *n*-Bu_2Sn, Sn), $Ge(SC_6Cl_5)_4$, and $Pt(SC_6Cl_5)_3Cl$. Non-metallic derivatives of group V, $M(SC_6Cl_5)_3$ (M = P, As, Sb) and $PhP(SC_6Cl_5)_2$ have also been prepared from $Pb(SC_6Cl_5)_2$ and the corresponding non-metallic chloride. The infrared spectra of these compounds and the mass spectra of C_6Cl_5SH and $(C_6Cl_5S)_2$ have been examined.

Canadian Journal of Chemistry, **48**, 1869 (1970)

Can. J. Chem. Downloaded from www.nrcresearchpress.com by 210.87.254.5 on 09/05/12
For personal use only.

This paper is an extension and amplification of work described previously in a short communication (1). The preparation and properties of various derivatives of the main group elements and transition metals are described.

While the chemistry of pentafluorothiophenol and its derivatives has been studied in some detail (2, 3) little is known about the chemistry of pentachlorothiophenol (4). Commercially available pentachlorothiophenol contains about 40% of bis(pentachloro-phenyl)disulfide, from which it may be separated by dissolution in basic solution. Pure pentachlorothiophenol has a m.p. 241.5–242°. In basic solution thiols are readily oxidized to disulfides. Polymerization is observed to occur in basic solutions of pentafluorothiophenol in air, but not in a nitrogen atmosphere (3, 5); pentachlorothiophenol in air will not polymerize in basic solution. The polymerization of pentafluorothiophenol probably involves initial oxidation, giving bis(pentafluoro-phenyl)disulfide, which is subsequently attacked nucleophilically by the $C_6F_5S^-$ ion. That a similar reaction does not occur with pentachlorothiophenol must be due either to the poor properties of the $C_6Cl_5S^-$ ion as a nucleophile, or to the low susceptibility to nucleophilic attack of the C_6Cl_5 nucleus. Pentachlorothiophenol is readily oxidized to the disulfide.

Simple Derivatives

The thiols, in general, show properties of the type classified as hydrogen pseudohalide, and are somewhat acidic. The pK_a of pentachlorothiophenol is 5.21 ± 0.04 in 50% dioxane–water. The acidity can be utilized in various synthetic reactions. Pentachlorothiophenol reacted in ethanol with some oxides, such as ZnO, PbO, PbO_2, and Cu_2O, but did not react with MnO_2 and GeO_2; similar reactions have been observed with pentafluorothiophenol (3). The thiol dissolves in aqueous sodium or potassium hydroxides, from which the sodium or potassium salt can be isolated on removal of the solvent. The thiol also forms salts with rubidium and cesium carbonates. The acidic properties of the thiol were shown in its reaction with *n*-butyllithium forming *n*-butane and the lithium salt. All the alkali metal salts are soluble in water forming basic solutions, as would be expected from the salt of a weak acid and a strong base.

Several metal mercaptides are insoluble in water or ethanol (6). Using pentachlorothiophenol, ethanol is a more convenient solvent as both the thiol and some metal salts are soluble. Precipitation is effected by mixing the two solutions; in this way derivatives were prepared of Tl(I), Ph_3Sn, Ph_3Pb, Pb(II), Ag(I), Cu(I), Cd(II), Hg(II), and Pt(IV). In a similar reaction (7) palladium(II) mercaptide, $Pd(SC_6Cl_5)_2$, was prepared by shaking a benzene solution of the thiol with an aqueous solution of the metal ion causing precipitation of the metal mercaptide in the aqueous phase.

Thiol derivatives of the non-metals may be prepared by two general techniques (8). In one, the thiol is allowed to react with a non-metallic halide in a suitable solvent; when the product is susceptible to attack by the hydrogen halide generated, a hydrogen halide acceptor, such as triethylamine is added. In the other technique the reaction of a lead mercaptide with a non-metallic halide totally eliminates the need for a hydrogen halide acceptor as lead(II) halide is formed

Can. J. Chem. Downloaded from www.nrcresearchpress.com by 210.87.254.5 on 09/05/12
For personal use only.

(eqs. [1] and [2]). Using these methods it was

[1] $GeCl_4 + 4\ Et_3N + 4\ C_6Cl_5SH \rightarrow Ge(SC_6Cl_5)_4 + 4\ Et_3NHCl$

[2] $2\ PCl_3 + 3\ Pb(SC_6Cl_5)_2 \rightarrow 2\ P(SC_6Cl_5)_3 + 3\ PbCl_2$

possible to prepare derivatives of Ge(IV), Sn(II) (from $SnCl_4$), P(III), PhP(III), As(III), Sb(III), and Bi(III). The triethylamine method can be applied to some of the earlier transition metal halides, such as titanium tetrachloride where a very unstable product was isolated. No reactions were observed with trimethylchlorosilane, phosphoryl chloride, and vanadium and tungsten trichlorides, but partial reaction occurred with silicon tetrachloride and boron trichloride.

The Sn—S bond in organotin compounds such as $R_2Sn(SR')_2$, is susceptible to fracture by metal halides in methanol (9) and has been found to be fractured by germanium tetrachloride, but not silicon tetrachloride (eq. [3]). This type of reaction is of more synthetic utility than a similar one

[3] $2\ n\text{-}Bu_2Sn(SC_6Cl_5)_2 + GeCl_4 \rightarrow 2\ n\text{-}Bu_2SnCl_2 + Ge(SC_6Cl_5)_2$

involving the fracture of the Si—S bond in the alkyl(alkylthio)silanes (10) as the corresponding organotin thiol derivatives are not hydrolytically sensitive and are easily prepared from the organotin oxide and the thiol (11). Trimethyl-(pentafluoro-phenylthio)silane can be prepared by refluxing hexamethyldisilazane and pentafluorothiophenol in benzene (5) (eq. [4]). A

[4] $Me_3SiNHSiMe_3 + 2\ C_6F_5SH \rightarrow 2\ Me_3SiSC_6F_5 + NH_3\uparrow$

similar reaction did not occur with pentachlorothiophenol and hexamethyldisilazane. The inability to prepare fully substituted derivatives of silicon parallels observations noted in the chemistry of pentafluorothiophenol (5), and may be due to the inherent thermal instability of the higher molecular weight orthothiosilicates (12), or due to their extreme hydrolytic sensitivity. This latter is undoubtedly the reason for the inability to prepare $B(SC_6Cl_5)_3$ since several orthothioborates are known (13).

Triphenylbismuthine reacts with thiophenol in refluxing xylene to form $Bi(SPh)_3$ (14). Little reaction was observed to occur in refluxing benzene between pentachlorothiophenol and triphenylbismuthine and none with triphenylstibine.

Redox Reactions

If pentachlorothiophenol acts as a hydrogen pseudohalide it ought to be fairly readily oxidized to the disulfide. Conversely the disulfide should act as an oxidizing agent. No oxidizing properties of bis(pentachloro-phenyl) disulfide have been observed, and only very few reactions are known in which an organic disulfide acts as an oxidizing agent (15).

Pentachlorothiophenol is similar to other thiols in being readily oxidized by iron(III), copper(II), and gold(III) ions and lead dioxide; except with iron(III) ions an insoluble mercaptide is formed with the metal ion in its lower valence state (3). Phosphorus pentachloride oxidizes the thiol forming the disulfide and $P(SC_6Cl_5)_3$. Two features are different from those observed with other thiols; no tin(IV) mercaptide was formed, and a platinum(IV) mercaptide was prepared. Tin(IV) mercaptides are generally stable (16), but all successful attempted preparations of tin(IV) mercaptide yielded tin(II) mercaptide and the disulfide, the reaction probably proceeding via an unstable tin(IV) mercaptide, (eq. [5]). The

[5] $Sn(SC_6Cl_5)_4 \rightarrow Sn(SC_6Cl_5)_2 + (C_6Cl_5S)_2$

reaction of a solution of platinum(IV) chloride with a thiol usually produces platinum(II) mercaptide and the corresponding disulfide, the reaction presumably proceeding via an unstable platinum(IV) mercaptide. In the reaction of platinum(IV) chloride with pentachlorothiophenol $Pt(SC_6Cl_5)_3Cl$ was isolated and showed no signs of thermal instability.

Chlorine and bromine react with the thiol in an inert solvent to give pentachlorobenzenesulfenyl chloride and bromide respectively (4).

Structures

Various nickel mercaptides have a polymeric structure involving

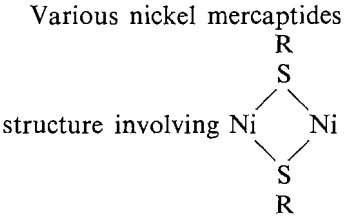

bridges (17). This type of structure is fairly general in the insoluble transition metal mercaptides, where bridges of the type —M—S—M— may also be formed. It

TABLE 1

Assignment of some i.r. frequencies (cm^{-1})

Compound	C—C ring	C—C ring	C—S stretching	C—Cl stretching
C_6Cl_5SH	1338 s	1288 m	872 w	668 s; 679 s
$(C_6Cl_5S)_2$	1330 s	1308 s	870 m	672 m; 688 s
$Ge(SC_6Cl_5)_4$	1335 s	1306 s	masked	681 s; 692 s
$P(SC_6Cl_5)_3$	1332 s	1305 s	872 m	680 s; 691 s
$NaSC_6Cl_5$	1325 s	1280 s	870 vw	678 s
KSC_6Cl_5	1320 s	1288 s	872 vw	688 s
$CuSC_6Cl_5$	1328 s	1290 s	870 vw	678 m; 688 m
$NiSC_6Cl_5$	1330 s	1300 s	870 m	678 m; 692 m
$[Ph_4As]_2[Co(SC_6Cl_5)_4]$*	1322 s	1308 s	865 w	681 s
$K_2[Pt(SC_6Cl_5)_4]$*	1325 s	1291 s	870 w	682 s

*See ref. 1.

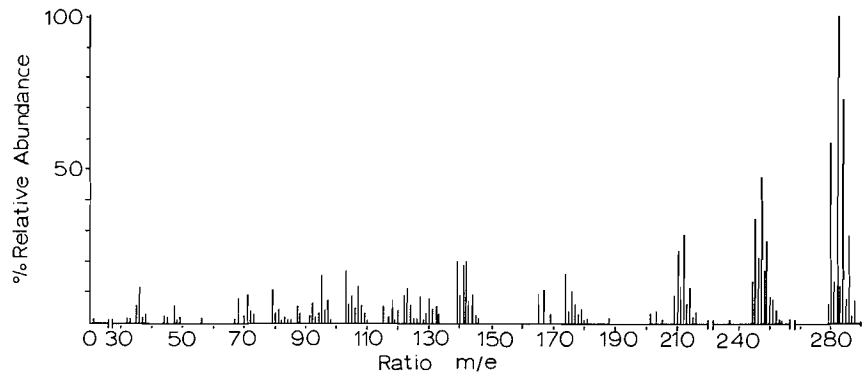

FIG. 1. Mass spectrum of pentachlorothiophenol: direct introduction, block temperature 143°.

would be expected with the class B metals (18) where the partially filled d orbitals on the metal atom can form back π bonds by overlapping with the empty d orbitals on the sulfur.

The effect of the d orbitals of the metal ion may account for the non-preparation of the mercaptides, by the methods described, of titanium(III and IV), vanadium(III), chromium(III), manganese(II), and iron(II and III), where the d orbitals are only partially occupied. The actual stable transition metal mercaptides and complex ions prepared (1, 2) are restricted to the latter transition elements, which have d^7, d^8, and d^{10} configurations and the d orbitals involved in metal to ligand π bonding are filled. Chromium and molybdenum mercaptides, $M(SR)_3$, have recently been prepared from the carbonyls and the disulfides (19, 20), both presumably having d^3 configurations. The two slightly different nickel mercaptides formed may be different types of polymer.

It can be assumed that the alkali metal mercaptides, and the tetraphenylarsonium salt, are all ionic in the solid state; they are partially hydrolyzed in aqueous solution. The non-metallic derivatives have properties that are typical of covalent compounds, i.e. solubility in organic solvents and ease of hydrolysis.

Spectra

The infrared (i.r.) spectra of all the products have been recorded; various frequencies characteristic of the C_6Cl_5S group are shown in Table 1. The ionic species show a relatively strong adsorption between 1215 and 1200 cm^{-1}, that is either weaker or totally absent in compounds with other types of bonding. The detailed spectra of a selection of compounds are tabulated in the Experimental section.

The mass spectra of the thiol and the disulfide are shown diagrammatically in Figs. 1 and 2. No metastable peaks were observed, so it is not possible to predict a specific decomposition mechanism. The mass spectra of $(C_6F_5S)_2$ (indirect introduction, sample sublimation $\leqslant 84°$, inlet reservoir 100°, ionization chamber 205°) (5)

Can. J. Chem. Downloaded from www.nrcresearchpress.com by 210.87.254.5 on 09/05/12
For personal use only.

Can. J. Chem. Downloaded from www.nrcresearchpress.com by 210.87.254.5 on 09/05/12
For personal use only.

TABLE 2

Products and analyses

Product	Melting point* (°C)	Color	Found (%)				Calculated (%)				Yield (%)*	Solubility†
			C	H	M	S	C	H	M	S		
$LiSC_6Cl_5 \cdot 2H_2O$	> 300	none	22.4	2.0			22.2	1.3			94	5, 6
$NaSC_6Cl_5$	> 300	none	24.3	0.0			23.7	0.0			75	1, 2, 6
KSC_6Cl_5	> 300	none	22.1	0.0			22.5	0.0			60	1, 2, 6
$RbSC_6Cl_5$	> 300	none	19.2	0.0			19.6	0.0			63	1, 2, 6
$CsSC_6Cl_5$	> 300	none	17.8	0.0			17.4	0.0			25	1, 2, 6
$TlSC_6Cl_5$	> 300	pale yellow	15.1	0.0		6.2	14.8	0.0		6.6	60	nil
$Ge(SC_6Cl_5)_4$	> 300	none	23.8	0.0		10.4	24.1	0.0		10.7	58(*a*), 67(*b*)	nil
$Ph_3SnSC_6Cl_5$	218–219	none	45.9	2.3			45.7	2.4			24	4, 5, 6
n-$Bu_3SnSC_6Cl_5$	b.p. 195/0.4 mm	none	38.1	4.8			37.8	4.8			95	3, 4, 5, 6
n-$Bu_2Sn(SC_5Cl_5)_2$	104–105	none	30.4	2.5			30.2	2.3			80	3, 4, 5, 6
$Sn(SC_6Cl_5)_2$	> 300	light yellow	21.3	0.0	16.8		21.2	0.0	17.4		74	nil
$Ph_3PbSC_6Cl_5$	214 (decomp.)	none	40.7	2.1			40.0	2.1			62	3, 5, 6
$Pb(SC_6Cl_5)_2$	> 300	yellow	18.7	0.0			18.7	0.0			75(*c*), 93(*d*)	nil
$P(SC_6Cl_5)_3$	223–224	none	24.6	0.0		10.6	24.7	0.0		11.0	96	3, CCl_4
$PhP(SC_6Cl_5)_2$	249–250	none	31.4	0.7		9.6	32.2	0.7		9.6	49	3, 5, CCl_4
$As(SC_6Cl_5)_3$	260 (decomp.)	pale yellow	22.5	0.0		10.5	23.5	0.0		10.5	82(*e*), 94(*f*)	3, CCl_4
$Ph_4AsSC_6Cl_5$	> 300	orange	53.4	2.9			54.2	3.0			99	2, 3, 6
$Sb(SC_6Cl_5)_3$	245 (decomp.)	yellow	22.3	0.0		10.1	22.4	0.0		10.0	47(*b*), 73(*f*)	3
$Zn(SC_6Cl_5)_2$	> 300	none	22.8	0.0			22.9	0.0			88	2
$Cd(SC_6Cl_5)_2$	> 300	none	21.7	0.0			21.4	0.0			89	nil
$Hg(SC_6Cl_5)_2$	> 300	none	19.6	0.0			18.9	0.0			88(*e*), 97(*d*)	nil
$CuSC_6Cl_5$	> 300	grey–green	20.4	0.0			20.9	0.0			35(*e*), 86(*d*)	nil
$AgSC_6Cl_5$	> 300	yellow	18.6	0.0			18.5	0.0			48	nil
$AuSC_6Cl$	265 (decomp.)	brown	15.8	0.0			15.1	0.0			74	nil
$Ni(SC_6Cl_5)_2$	282(*d*), > 300(*g*)	black	23.3	0.0			23.2	0.0			39(*d*), 43(*g*)	6
$Pd(SC_6Cl_5)_2$	> 300	brown	21.1	0.0			21.5	0.0			22	nil
$Pt(SC_6Cl_5)_3Cl$	> 300	flesh	20.1	0.0	18.1	9.3	20.1	0.0	18.1	9.0	65	nil

*(*a*) = from n-$Bu_2Sn(SC_6Cl_5)_2$; (*b*) = from $C_6Cl_5SH + Et_3N$; (*c*) = from PbO_2; (*d*) = from M^{n+}; (*e*) = from MO_x; (*f*) = from $Pb(SC_6Cl_5)_2$; (*g*) = anhydrous media.
†Solubilities: 1 = water; 2 = ethanol (95%); 3 = benzene; 4 = petroleum ether; 5 = ether; 6 = acetone.

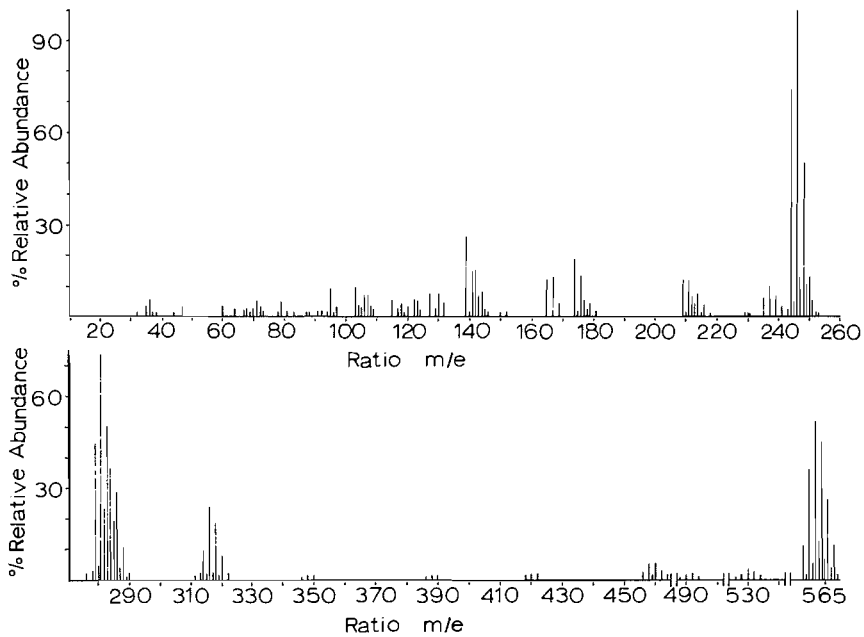

FIG. 2. Mass spectrum of bis(pentachloro-phenyl)disulfide: direct introduction, block temperature 152°.

and $(C_6Cl_5S)_2$ (direct introduction, block temperature 152°) are quite different. In the chloro-compound the C-6 nucleus is retained and Cl, or multiples thereof, are split off, whereas in the fluoro-compound the C-6 nucleus is only found in the $C_6F_4S^+$ ion with molecular weight less than $C_6F_5S^+$ and is decomposed by loss of CF, CSF, etc.; metastable peaks indicate the decompositions $C_6F_5S^+ \rightarrow C_5F_5^+ + CS$ and $C_6F_5S^+ \rightarrow C_5F_3S^+ + CF_2$. The chloro-compound rearranges with loss of sulfur, i.e. ions such as $C_{12}Cl_8S^+$ and $C_6Cl_6S^+$ are found; there are no corresponding ions formed in the decomposition of the fluoro-compound. In the fluoro-compound the S—S bond is retained in various ions, $C_{12}F_9S_2^+$, $C_6F_5S_2^+$, $C_5F_4S_2^+$, $C_5F_3S_3^+$, but there is only one ion, other than the parent ion, containing two S in the chlorocompound, $C_6Cl_3S_2^+$. Similarly a comparison of the spectra of the thiols C_6F_5SH (indirect introduction, sample sublimation $\leqslant 105°$) and C_6Cl_5SH (direct introduction, block temperature 143°) shows that the C-6 nucleus is retained and sulfur lost in many more ions from the chloro-thiol than from the fluoro-thiol.

Experimental

All reagents were available commercially. Microanalyses were performed by Mikroanalytisches Laboratorium Beller, Göttingen, Western Germany. Analytical data for the new compounds prepared are shown in Table 2. All experiments were performed using approximately 1 to 2 mmoles of reagents; products were purified, where possible, by recrystallization or distillation. The i.r. spectra were recorded as mulls with Nujol or hexachlorobutadiene, or as thin films, on a Perkin–Elmer 457. Mass spectra were recorded on a Consolidated Electrodynamics Corporation 21-110B high resolution mass spectrograph.

Pentachlorothiophenol and Bis(pentachloro-phenyl)-disulfide

Technical grade pentachlorothiophenol was extracted three times with aqueous caustic soda; the insoluble residue was mainly bis(pentachloro-phenyl)disulfide, together with traces of hexachlorobenzene. Acidification of the filtrate precipitated the thiol, which was filtered off, washed with water, and dried. The thiol was further purified by decolorizing with charcoal in benzene and recrystallizing. Any disulfide formed in this step was removed by dissolving the product in ammoniacal 50% aqueous ethanol and filtering; the thiol reprecipitated on acidification. The white thiol has a m.p. 241.5–242° and sublimes readily at 100°/0.4 mm. Its molecular weight was confirmed from its mass spectrum. It was soluble in organic solvents such as carbon tetrachloride, chloroform, petroleum ether, ethanol, methanol, and aromatic hydrocarbons. In hot or basic solutions it is susceptible to air oxidation to the disulfide.

Bis(pentachloro-phenyl)disulfide was obtained from the insoluble residue left after dissolution of the impure thiol in aqueous base; it was further purified by recrystallization from benzene or chlorobenzene. It is an orange solid, m.p. 234–235°, soluble in petroleum ether and sublimes at 170°/0.4 mm; its molecular weight was confirmed from its mass spectrum.

Can. J. Chem. Downloaded from www.nrcresearchpress.com by 210.87.254.5 on 09/05/12
For personal use only.

Can. J. Chem. Downloaded from www.nrcresearchpress.com by 210.87.254.5 on 09/05/12
For personal use only.

The pK_a of pentachlorothiophenol in 50% dioxane–water was found, by conventional spectroscopic techniques (21), to be 5.21 ± 0.04 at ionic strength 0.5 and 22.5°.

Attempts to polymerize the thiol by fusing with solid sodium hydroxide in a platinum crucible produced a violent reaction at about 300° giving off a pungent gas and leaving a black solid. The water extract of this solid contained Cl^- ions, and on acidification H_2S was evolved; the black solid remaining was carbon.

Reactions Due to the Acidity of the Thiol

A 95% ethanol solution of the thiol was stirred with suspensions of various oxides (Cu(I), Zn, Hg(II), *n*-Bu_3Sn(IV) (in C_6H_6), *n*-Bu_2Sn(IV), Pb (II and IV) and As(III) (NH_3 added)). The precipitated mercaptide was isolated. The Zn, As(III), and *n*-Bu_3Sn(IV) products were isolated after removal of the solvent. In the Pb(IV) oxide reaction $Pb(SC_6Cl_5)_2$ precipitated leaving the disulfide in solution. Under similar conditions GeO_2 and MnO_2 did not react. $LiSC_6Cl_5 \cdot 2H_2O$ precipitated on mixing stoichiometric amounts of *n*-butyllithium (hexane) and the thiol (benzene); the water was not removed by drying *in vacuo* over P_2O_5 at room temperature, but thermogravimetric analysis showed the loss of 2.3 ± 0.1 moles of water per mole of thiol at $203 \pm 5°$.

The MSC_6Cl_5 was obtained either from the thiol and the hydroxide in ethanol (Na, K) and isolated on removal of the solvent, or precipitated on shaking a saturated aqueous carbonate solution (Rb, Cs) in a nitrogen atmosphere with the thiol in benzene. On standing in air the alkali metal mercaptides slowly decomposed to the hydroxide and the disulfide.

Precipitation of Mercaptides

Various insoluble metal mercaptides were formed by mixing ethanol solutions of the thiol and a metal salt (Tl(I), Ag(I), Pb(II), Cd(II), Pt(IV) (10% in 1 *M* HCl → $Pt(SC_6Cl_5)_3Cl$), Ph_3M (M = Sn, Pb, from Ph_3MCl)). Oxidation occurred and precipitation of the metal in its lower valence state as its mercaptide with Cu(II) → Cu(I), Au(III) → Au(I); Fe(III) was reduced to Fe(II), but no mercaptide formed. No reaction was observed with salts of the metals Mg, Ca, Sr, Ba, Al, Cr(III), Mn(II) and Be (in C_6H_6). A product of uncertain composition was obtained from Ph_2PbCl_2; the compounds $Ph_2Pb(SR)_2$ are known to be unstable (22), decomposing to $Pb(SR)_2$, RSSR, and Ph_3PbSR.

Two somewhat different Ni mercaptides were obtained from Ni(II) in ethanol through which dry NH_3 was bubbled, or in ethanol to which aqueous NH_3 had been added; on evaporation of the solvent black crystals were recovered in each case. Under similar conditions Fe(II) did not react, but Co(II) gave an impure green product.

Reactions Using $Pb(SC_6Cl_5)_2$

The reaction of a non-metallic chloride, MCl_x, with suspension of $Pb(SC_6Cl_5)_2$ in refluxing benzene formed $PbCl_2$ and $M(SC_6Cl_5)_x$ (M = P(III) (from PCl_3, or PCl_5 → $P(SC_6Cl_5)_3$ + $(C_6Cl_5S)_2$), PhP(III), As(III), and Sb(III)). With BCl_3 in a sealed tube with no solvent a very hydrolytically sensitive white product was extracted with CCl_4; analysis for boron, after complete hydrolysis, via the mannitol method, was about half that required for $B(SC_6Cl_5)_3$. No reaction was observed with Me_3SiCl, $SnCl_2$, or $SnCl_4$.

Reactions Involving Triethylamine

A chloride (MCl_x) was reacted with the thiol in a suitable solvent to which Et_3N had been added, forming Et_3NHCl (removed by washing with $HCCl_3$) and $M(SC_6Cl_5)_x$ (M = Ge(IV), Sn(II) (from Sn(IV)), and Sb(III)). The $BiO(SC_6Cl_5)$ formed using $BiCl_3$ and $TiCl_4$ gave an extremely air and water sensitive red product, m.p. about 184°. No reaction was observed when M = Al, PO, V(III), and Ti(III).

Miscellaneous Preparations

Hydrolytically sensitive $Ge(SC_6Cl_5)_4$ precipitated from a mixture of $GeCl_4$ and *n*-$Bu_2Sn(SC_6Cl_5)_2$ in ether, but no reaction occurred using $SiCl_4$ in place of the $GeCl_4$.

No reaction occurred between $(Me_3Si)_2NH$ and C_6Cl_5SH in refluxing benzene, or Sn and $(C_6Cl_5S)_2$ in benzene through which HCl gas was bubbled (a standard technique for the preparation of $Sn(SR)_2$ (23)). The Ph_3Sb did not react with the thiol in refluxing benzene, but partial reaction occurred with Ph_3Bi.

The $M(SC_6Cl_5)$ (M = Ph_4As^+, Et_3NH^+) precipitated on addition of Ph_4AsCl or Et_3N to a solution of the thiol in aqueous base or benzene respectively.

Infrared Data

The i.r. absorption peaks in the region 4000 to 250 cm^{-1} of a selection of compounds are listed below:

C_6Cl_5SH: 2582 w, 2573 w, 1338 s, 1288 m, 1229 w, 1100 w, 945 w, 934 w, 921 w, 872 w, 688 s, 679 s, 608 w, 390 vw, 375 vw.

$C_6Cl_5SSC_6Cl_5$: 1510 m, 1330 s, 1308 s, 1215 w, 1205 w, 1170 m, 1100 s, 870 m, 688 s, 672 m, 599 w, 399 w, 319 w.

KSC_6Cl_5: 1505 w, 1470 w, 1320 s, 1288 s, 1278 m, 1202 s, 1170 m, 1085 vw, 969 vw, 920 vw, 872 vw, 688 s, 394 vw, 370 vw, 320 w.

$Ge(SC_6Cl_5)_4$: 1508 w, 1335 s, 1306 s, 1210 vw, 1180 w, 1120 vw, 1100 m, 692 s, 681 s, 422 m, 400 w, 348 w, 318 w.

$Sn(SC_6Cl_5)_2$: 1330 s, 1300 m, 688 m, 679 m, 385 w, 335 w, 309 vw.

$As(SC_6Cl_5)_3$: 1505 vw, 1330 s, 1299 s, 1210 vw, 1170 vw, 1095 w, 965 vw, 935 vw, 870 w, 688 s, 678 s, 590 vw, 380 m, 338 m, 312 m.

$CuSC_6Cl_5$: 1328 s, 1318 vw, 1290 s, 870 vw, 688 m, 678 m, 590 vw.

$[(C_6H_5)_4As]_2[Cd(SC_6Cl_5)_3Cl]$ (1): 3045 w, 1505 w, 1479 m, 1435 s, 1322 s, 1290 s, 1210 m, 1181 w, 1160 w, 1080 s, 1020 w, 995 s, 930 vw, 870 w, 835 w, 740 s, 680 s, 610 vw, 478 m, 460 m, 395 vw, 350 m, 320 w.

Mass Spectra

In the mass spectra the ions with relative abundance greater than 5% are:

C_6Cl_5SH: $C_6Cl_5SH^+$, $C_6Cl_5S^+$, $C_6Cl_5H^+$, $C_6Cl_5^+$, $C_6Cl_4SH^+$, $C_6Cl_4S^+$, $C_6Cl_4H^+$, $C_6Cl_4^+$, $C_6Cl_3SH^+$, $C_6Cl_3S^+$, $C_6Cl_3^+$, $C_6Cl_2S^+$, $C_5Cl_3^+$, $C_6Cl_2H^+$, $C_6Cl_2^+$, $C_6Cl_6^{2+}$, C_6ClSH^+, C_6ClS^+, $C_5Cl_2H^+$, $C_5Cl_2^+$, C_5ClS^+, $C_6Cl_4SH^{2+}$, $C_6Cl_4S^{2+}$, $C_4Cl_2^+$, C_4ClS^+, C_6ClH^+, C_6Cl^+, $C_3Cl_2^+$, C_6SH^+, C_6S^+, C_3ClS^+, C_5Cl^+, C_5S^+, $C_6Cl_2S^{2+}$, $CClS^+$, C_3Cl^+, C_3S^+, C_5^+, CCl^+.

$(C_6Cl_5S)_2$: $C_{12}Cl_{10}S_2^+$, $C_{12}Cl_8S^+$, $C_{12}Cl_4S^+$, $C_6Cl_6S^+$,

$C_6Cl_6^+$, $C_6Cl_5S^+$, $C_6Cl_4S^+$, $C_6Cl_3S_2^+$, $C_5Cl_5^+$, $C_6Cl_4^+$, $C_6Cl_3S^+$, $C_6Cl_3^+$, $C_6Cl_2S^+$, $C_5Cl_3^+$, $C_6Cl_2^+$, $C_3Cl_3^+$, C_6ClS^+, C_5ClS^+, $C_6Cl_4S^{2+}$, C_4ClS^+, C_6Cl^+, $C_3Cl_2^+$, C_3ClS^+, C_5Cl^+, C_3Cl^+.

The authors wish to thank Dr. W. D. Jamieson (NRCC, Halifax) and Dr. O. Knop (Dalhousie University) for their help in obtaining mass spectra and thermogravimetric analyses respectively. The generous financial assistance of the National Research Council of Canada for an operating grant and a studentship (C. R. L.) is acknowledged.

1. C. R. Lucas and M. E. Peach. Inorg. Nucl. Chem. Lett. **5**, 73 (1969).
2. W. Beck, K. H. Stetter, S. Trados, and K. E. Swarzhans. Chem. Ber. **100**, 3944 (1967).
3. M. E. Peach. Can. J. Chem. **46**, 2699 (1968).
4. N. Kharasch, C. M. Buess, and R. B. Langford. Quart. Rep. Sulfur Chem. **2**, 249 (1967).
5. M. E. Peach and H. G. Spinney. Unpublished observations.
6. E. E. Reid. Organic chemistry of bivalent sulfur. Vol. I. The Chemical Publ. Co., Inc., New York, 1958. pp. 107–169.
7. W. E. Duncan, E. Ott, and E. E. Reid. Ind. Eng. Chem. **23**, 381 (1931).
8. A. Haas. Angew. Chem. Int. Ed. **4**, 1014 (1965).
9. E. W. Abel, D. B. Brady, and B. C. Crosse. J. Organometal. Chem. Amsterdam. **5**, 260 (1966).
10. E. W. Abel and C. R. Jenkins. J. Organometal. Chem. Amsterdam, **14**, 285 (1968).
11. M. E. Peach. Can. J. Chem. **46**, 211 (1968).
12. M. Schmeisser and H. Mueller. Angew. Chem. **69**, 781 (1957).
13. J. Goubeau and H. W. Whittmeier. Z. Anorg. Allg. Chem. **270**, 16 (1952).
14. H. Gilman and H. L. Yale. J. Amer. Chem. Soc. **73**, 4770 (1951).
15. T. Saegusa, S. Kobayashi, Y. Ito, and N. Yasuda. J. Amer. Chem. Soc. **90**, 4181 (1968).
16. R. C. Mehrota, V. D. Gupta, and D. Sukhani. J. Inorg. Nucl. Chem. **29**, 1577 (1967).
17. E. W. Abel and B. C. Crosse. J. Chem. Soc. A, 1377 (1966).
18. S. Ahrland, J. Chatt, and N. R. Davies. Quart. Rev. **12**, 265 (1958).
19. D. A. Brown, W. K. Glass, and B. Kumar. J. Chem. Soc. A, 1510 (1969).
20. R. N. Jowitt and P. C. H. Mitchell. Inorg. Nucl. Chem. Lett. **4**, 39 (1968).
21. A. Albert and E. P. Serjeant. Ionization constants of acids and bases. Methuen and Co., Ltd., London, 1962.
22. W. E. Davidson, K. Hills, and M. C. Henry. J. Organometal. Chem. Amsterdam, **3**, 285 (1965).
23. H. Wuyts and A. Vangindertalen. Bull. Soc. Chem. Belges, **30**, 323 (1921).

Can. J. Chem. Downloaded from www.nrcresearchpress.com by 210.87.254.5 on 09/05/12
For personal use only.

Reaction of carbon disulfide with nickel(II)–amine complexes

B. JACK MCCORMICK AND ROY I. KAPLAN
Department of Chemistry, West Virginia University, Morgantown, W.Va. 26506
Received January 27, 1970

The reaction of carbon disulfide with a variety of nickel(II)–amine complexes has been carried out. It has been found that dithiocarbamate complexes are readily formed under the proper conditions, and the synthetic procedures presented provide a convenient and direct route to such compounds. Complexes having hydroxyl and mercaptide groups in addition to amine groups have been found to give exclusively dithiocarbamate complexes, rather than xanthates or trithiocarbonates. The infrared and optical spectra of the complexes have been measured and are discussed in terms of the proposed structures of the complexes.

Canadian Journal of Chemistry, **48**, 1876 (1970)

Introduction

While N,N-dialkyldithiocarbamate complexes of nickel(II) and other transition metal ions have been known for many years (1), most of them have been prepared by metathetical reactions between a salt of a transition metal and that of a N,N-dialkyldithiocarbamic acid. Very recently there have been a few reports on the preparation of dithiocarbamate complexes by carbon disulfide insertion reactions, viz.

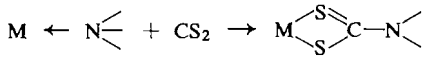

Bradley and Gitlitz (2, 3) have made use of the carbon disulfide insertion reaction to prepare a number of interesting complexes of early transition metals. In a review (4) Lappert has summarized the results of studies concerned with the insertion of carbon disulfide into several types of metal–nitrogen bonds.

In view of the possible synthetic utility of carbon disulfide insertion reactions, we have investigated the reaction of CS_2 with a variety of nickel(II)–amine complexes involving: (I), a monodentate amine; (II), bidentate primary amines; (III), bidentate amines in which one donor nitrogen atom is in a pyridine ring; (IV), bidentate amines containing hydroxyl and mercaptide functional groups; and (V), a tridentate amine. Six of the complexes prepared have not been reported previously. Studies of selected properties of the complexes have been made, and the results are discussed in relation to the structures of the complexes.

Experimental

All of the amine complexes were prepared by known or modifications of known procedures (5). Dimethyl sulfoxide was distilled under nitrogen before use, and solution spectra were measured in Fisher "Spectro-analyzed" solvents.

Reaction Procedures

Several solvents for the insertion reactions were examined. Among these were water, methanol, ethanol, acetone, and N,N-dimethylformamide. While the reactions did proceed in these solvents, they were very slow, requiring 3 to 4 days. In many cases the slow rate of reaction undoubtedly was due to the lack of mutual solubility of the metal amine and carbon disulfide in the solvent. The most suitable solvent found was dimethyl sulfoxide (DMSO), in which most of the reactions were complete in 30 min. The reactions were done under an atmosphere of N_2, and the reaction products were not exposed to air until they had been partially dried. In general, the reactions were carried out by dissolving and/or suspending 0.05 mole of the amine complex in 50 ml of DMSO, to which was added 0.5 mole of carbon disulfide dissolved in 10 ml of DMSO. Typically the solutions underwent a series of color changes, and after 30 min, 250 ml of water was added to the reaction mixture, whereupon a precipitate formed immediately. The precipitate was separated by filtration, washed with 500 ml of warm water and 200 ml of methanol, dried in a stream of nitrogen, and then dried at 64° in vacuo over P_4O_{10}. The yields were high in all cases except system I*a*.

The reaction with bis(2-mercaptoethylamine)nickel(II) proceeded very slowly at room temperature owing to the insolubility of the complex in DMSO, and the above general procedure was modified in that the reaction was carried out in a sealed, heavy walled glass tube at 70°. Under these conditions the reaction was complete in 6 h. The analytical sample was recrystallized from DMSO. Special procedures also were necessary for the reaction of dichloro(1,1,7,7-tetraethyldiethylenetriamine)nickel(II) with carbon disulfide. In this reaction, 0.03 mole of the amine complex in 50 ml of absolute ethanol was treated with 0.03 mole of CS_2. The solution quickly turned from a deep red to a bright green color. After 20 min a green precipitate was filtered off, washed with ethanol, and air dried. Recrystallization from absolute ethanol followed by drying over P_4O_{10} provided an analytically pure sample.

Given in Table 1 are the systems studied and the products formed from each system. The systems are

TABLE 1
Reactants and products

System	Reaction	Amine (symbol)	Starting complex	Product*
I	*a*	NH_3	$Ni(NH_3)_6Cl_2$	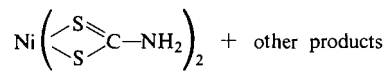 + other products
II	*a*	$H_2N(CH_2)_2NH_2$ (en)	$Ni(en)_3Cl_2$	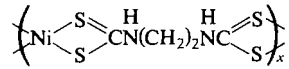
II	*b*	$H_2N(CH_2)_2NH_2$ (en)	$Ni(en)_2Cl_2$	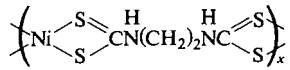
II	*c*	$H_2N(CH_2)_3NH_2$ (tn)	$Ni(tn)_3Cl_2$	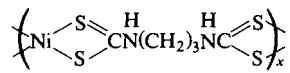
II	*d*	$H_2NCH_2CH(CH_3)CH_2NH_2$ (pn)	$Ni(pn)_3Cl_2$	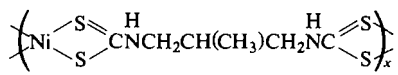
III	*a*	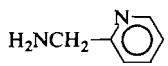 (amp)	$Ni(amp)_3Cl_2$	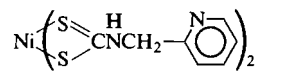
III	*b*	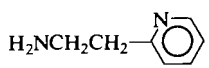 (aep)	$Ni(aep)_2Cl_2$	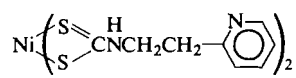
IV	*a*	$H_2NCH_2CH(OH)CH_2NH_2$ (tnOH)	$Ni(tnOH)_3Cl_2$	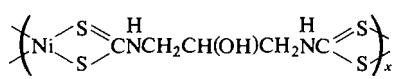
IV	*b*	$H_2NCH_2CH_2S^-$ (mea)	$Ni(mea)_2$	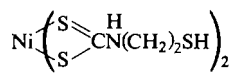
V	*a*	$((C_2H_5)_2NCH_2CH_2)_2NH$ (tedt)	$Ni(tedt)Cl_2$	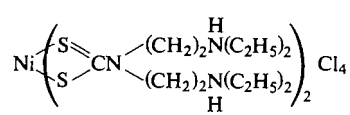

*For convenience, only one of several possible canonical forms is shown.

TABLE 2
Analytical data for dithiocarbamate complexes

	Carbon		Hydrogen		Nitrogen		Sulfur		Nickel	
Product*	Calcd.	Found	Calcd.	Found	Calcd.	Found	Calcd.	Found	Calcd.	Found
II*a*	17.9	18.2	2.25	2.51	10.4	10.5	—	—	21.8	21.5
II*b*	17.9	18.5	2.23	2.70	—	—	—	—	—	—
II*c*	21.2	21.6	2.83	3.22	9.90	9.84	—	—	20.8	20.3
II*d*	21.2	21.8	2.83	3.12	9.90	9.94	—	—	20.8	20.4
III*a*	39.5	39.1	3.32	3.41	—	—	30.2	29.6	—	—
III*b*	42.4	42.5	4.01	4.11	12.4	12.6	—	—	13.0	12.8
IV*a*	20.1	20.2	2.68	2.89	9.37	9.59	—	—	19.6	19.2
IV*b*	19.8	20.0	3.33	3.57	7.71	7.37	—	—	—	—
V*a*	39.8	39.7	7.70	7.89	10.7	10.5	—	—	—	—

*The product numbers correspond to the systems and reactions given in Table 1.

designated by numbers which correspond to those given in the Introduction for the various types of amines.

Elemental analyses for all of the compounds are given in Table 2. Carbon, hydrogen, nitrogen, and sulfur analyses were done by Galbraith Laboratories, Knoxville, Tenn., but the nickel analyses were done in our laboratory by conductometric titrations with EDTA (5).

Measurements

Infrared spectra were recorded with Beckman IR-8 and IR-12 spectrometers using the Nujol mull technique. Solution spectra were measured with a Cary Model 14 Spectrophotometer; diffuse reflectance spectra were measured with the same instrument and a Model 1411 reflectance attachment. The proton nuclear magnetic resonance (n.m.r.) spectrum was obtained with a Varian Model HA-60 Spectrometer using TMS as a reference. Spectral data are summarized in Table 3.

Results and Discussion

General Aspects of Reactions

Reaction of carbon disulfide with amine complexes of nickel(II) provides a direct and convenient route to nickel(II) dithiocarbamate complexes. This technique also should be suitable for the preparation of complexes of other transition metals. In many cases it is synthetically advantageous to use the direct method rather than a metathetical reaction, since the latter procedure requires the preparation of a dithiocarbamate salt, which frequently is unstable or difficult to prepare and isolate.

While the detailed mechanism is not known, two mechanistic aspects of the reactions deserve comment. First, there is some indication that DMSO serves as a reactant, as well as a solvent. In all cases the initial product from the reactions is soluble in DMSO, and the addition of water is required for the precipitation of the desired complex. However, in several cases the complex precipitated is not soluble in DMSO. This may indicate that the initial species formed is a mixed ligand complex involving coordinated DMSO as well as dithiocarbamate. The second point concerns the fate of the proton displaced from the amine during the course of the reaction. In systems I*a* through IV*a*, the protons, no doubt, react with excess amine displaced during the reaction, viz.

$$\overset{H}{Ni(NR_2)_4}^{2+} + 2\,CS_2 \rightarrow Ni(S_2CNR_2)_2 + 2\,R_2NH_2^+$$

R = alkyl, hydrogen

In the case of $Ni(mea)_2$ and $Ni(tedt)Cl_2$, basic sites are maintained on the coordinated dithiocarbamate which accommodate the displaced protons.

Specific Reactions, Properties, and Structures

Ia. The reaction of carbon disulfide with $Ni(NH_3)_6^{2+}$ is, in principle, the most simple system studied, and it was established from infrared studies that $Ni(S_2CNH_2)_2$ is formed. However, the product obtained was not pure. This finding is not surprising since dithiocarbamic acid, its salts, and complexes are not stable (1).

IIa–IId. The four starting complexes in this group involve bidentate diamine ligands, and there are two conceivable types of reaction products. Reaction can occur at one amine group of a given ligand, with the released proton reacting with the remaining amine group to give a zwitterion, or both amine groups can react to give a bisdithiocarbamate. Ethylenediamine forms a monodithiocarbamate zwitterion in the absence of added base (6) and a bisdithiocarbamate in the presence of sodium hydroxide (7). In the four cases studied here, bisdithiocarbamate

TABLE 3

Infrared and electronic spectral data*

Compound	$\bar{\nu}$(C⋯N)	$\bar{\nu}_{max}$ Reflectance	$\bar{\nu}_{max}$ DMSO†
II*a*(= II*b*)	1496	15.7	16.3 (127)
		23.3 sh	23.5 (1320) sh
		26.1	26.1 (4520)
		—	31.1 (23000)
II*c*	1500	15.9	15.8 (126)
		24.0 sh	24.1 (1530) sh
		26.3	26.1 (3590)
		—	31.5 (23200)
II*d*	1494	15.9	15.8 (68)
		22.6 sh	23.3 (1620) sh
		25.8	26.0 (5560)
		—	30.9 (28200)
III*a*	1543	15.9	15.7 (85)
		20.8	20.8 (234)
		23.4 sh	23.8 (1400) sh
		26.3	25.9 (5820)
		—	30.5 (28200)
III*b*	1551	15.6	16.0 (113)
		20.8	20.8 (220)
		24.4 sh	23.8 (1420) sh
		25.1	25.9 (4790)
		—	30.7 (28200)
IV*a*	1520	15.9	16.1 (68)
		24.2 sh	23.5 (1390) sh
		26.5	26.0 (3860)
		—	31.1 (23600)
IV*b*	1502	16.3	15.9 (85)
		21.7	21.7 (550)
		23.9 sh	23.8 (1900) sh
		26.3	25.8 (6200)
		—	31.1 (25200)
V*a*	1510	16.1	15.9 (48)
		23.3	23.2 (316) sh
		25.9	25.5 (1180)
		—	30.5 (26000)

*Electronic data is in kilokaysers (kK); sh indicates a shoulder. Infrared data is in cm^{-1}.
†Extinction coefficients (l $mole^{-1}$ cm^{-1}) are given in parentheses.

ligands are formed, and the resulting insoluble, green complexes are undoubtedly polymeric, as indicated in Table 1. If zwitterionic ligands were involved, the complexes should show a degree of solubility in water, as well as infrared frequencies characteristic of quaternary ammonium groups. Similar complexes prepared by metathetical reactions have been reported previously (8).

The structures given in Table 1 are idealized in the sense that only chelating dithiocarbamate groups are shown. Bridging ligands may be important, but such detailed structural features cannot be ascertained at this time. Aside from their polymeric nature, the complexes appear to be very similar to the many nickel(II) dithiocarbamates that have been previously studied. The complexes are diamagnetic and show a characteristic (9) C⋯N stretching frequency in the 1495–1500 cm^{-1} region. The electronic spectra, as given in Table 3, are identical to that reported previously by Jorgensen (10) for bis(N,N-diethyldithiocarbamato)nickel(II), except that the band at ca. 21 kK is not resolved.

IIIa,b. In these chelating diamines there is one amine group that can react with carbon disulfide and one ring nitrogen atom that is not expected to enter into reaction with carbon disulfide. It was of interest to determine whether the pyridine nitrogen atom would remain coordinated after the primary amine had undergone reaction with carbon disulfide. The results indicate that the pyridine moiety is displaced from the coordination sphere by the dithiocarbamate formed from the primary amine group to give the usual type of dithiocarbamate complex. In contrast to the polymeric complexes formed in system II, these green, diamagnetic monomers are somewhat soluble in a variety of polar organic solvents. The magnitude of the C⋯N stretching frequency suggests that double bond character increases in the (S_2)C—N bond (11) in going from system II to system III. Electronic spectra measured at room temperature are identical to those that have been reported previously (10) for nickel(II) dithiocarbamates.

Since Coucouvanis and Fackler (11) have shown that certain nickel(II) dithiocarbamates form adducts at low temperatures with nitrogenous bases, it was of interest to determine whether the present complexes enter into *intra-* or *inter*-molecular association with the uncoordinated pyridine groups. That such association can take place in solution with the concomitant formation of pseudo-octahedral nickel(II) complexes was indicated by low temperature spectral studies. An acetone solution of system III*b* at room temperature exhibited the same absorption bands as those given in Table 3. As the solution was cooled to −12°, the color became lighter and a weak absorption band appeared at 10.2 kK. Further cooling to −80° resulted in a very pale green solution (no precipitation) with a moderately intense band at 10.2 kK. These spectral changes are in close agreement with those reported by Coucouvanis and Fackler (10) for bis(N,N-diethyldithiocarbamato)nickel(II) in pyridine at temperatures from −80 to 20°.

IVa. Ethanolamine, $HOCH_2CH_2NH_2$, reacts with carbon disulfide under room conditions to provide the dithiocarbamate rather than the xanthate, $HS_2COCH_2CH_2NH_2$, which goes to 2-mercaptooxazoline on standing (12). Hence, it was of interest to determine the course of reaction of carbon disulfide with a coordinated amine containing an —OH group. In principle, it is possible to form a dithiocarbamate, a xanthate, or a mixed dithiocarbamate–xanthate complex. The results indicate that reaction takes place exclusively at the nitrogen atoms to provide a polymeric complex having the structure shown in Table 1. The color, solubility, magnetic, and electronic spectral properties of the complex were essentially identical to those shown by the complexes in Group II. The C···N and OH stretching frequencies were located at 1520 and 3375 cm^{-1}, respectively, and there were no bands in the 1000–1250 cm^{-1} region that could be attributed to a xanthate group (13). The compound was stable and did not decompose to provide a 2-mercaptooxazoline.

IVb. 2-Mercaptoethylamine is known to react with carbon disulfide to give the trithiocarbonate zwitterion (14), but it was found in this work that coordinated mea reacts to give the dithiocarbamate. Upon displacement from the coordination sphere the mercapto group becomes protonated to provide a monomer of the type shown in Table 1. This reaction represents a distinct example of the mediation of an organic reaction by a metal ion. Complex IV*b* is green, slightly soluble in polar organic solvents, and diamagnetic. Strong C···N and weak S—H stretching frequencies were found at 1502 and 2350 cm^{-1}, respectively. Further evidence for the presence of a sulfhydryl group was provided by an n.m.r. study in DMSO-d_6, where a resonance due to the proton on the sulfur atom was located at 6.60 τ.

Va. The tedt complex reacted quite readily to give a complex of a positively charged dithiocarbamate ligand. This complex, prepared by an alternate route, has been discussed elsewhere (15).

This work was supported by the National Science Foundation through Grant No. GP-6671 and through a grant that supported the purchase of the IR-12 Spectrometer.

1. G. D. THORN and R. A. LUDWIG. The dithiocarbamates and related compounds. Elsevier Publ. Co., New York. 1962.
2. D. C. BRADLEY and M. H. GITLITZ. Chem. Commun. 289 (1965).
3. D. C. BRADLEY and M. H. GITLITZ. J. Chem. Soc. A, 1152 (1969).
4. M. F. LAPPERT. Advances in organometallic chemistry. *Edited by* F. G. A. Stone and R. West. Academic Press, Inc., New York. pp. 291–292.
5. R. I. KAPLAN. Ph.D. Thesis, West Virginia University, Morgantown, West Virginia. 1969.
6. A. W. HOFMAN. Ber. **5**, 240 (1872).
7. A. Y. YAKUBOVICH and V. A. KLIMOVA. J. Gen. Chem. U.S.S.R., **9**, 1777 (1939).
8. L. C. A. THOMPSON and R. O. MOYER. J. Inorg. Nucl. Chem. **27**, 2225 (1965).
9. J. CHATT, L. A. DUNCANSON, and L. M. VENANZI. Suomen Kem. **B29**, 75 (1956).
10. C. K. JORGENSEN. J. Inorg. Nucl. Chem. **24**, 1571 (1962).
11. D. COUCOUVANIS and J. P. FACKLER, JR. Inorg. Chem. **6**, 2047 (1967).
12. P. G. SERGEEV and S. N. IVANOVA. J. Gen. Chem. U.S.S.R., **7**, 1495 (1937).
13. G. W. WATT and B. J. MCCORMICK. Spectrochim. Acta, **21**, 753 (1965).
14. W. O. FOYE, J. R. MARSHALL, and J. MICKLES. J. Pharm. Sci. **52**, 406 (1963).
15. B. J. MCCORMICK, B. P. STORMER, and R. I. KAPLAN. Inorg. Chem. **8**, 2522 (1969).

Can. J. Chem. Downloaded from www.nrcresearchpress.com by 210.87.254.42 on 09/05/12
For personal use only.

Asymmetric syntheses of optically active α-amino acids by hydrocyanic acid addition to the optically active Schiff base[1]

MAHENDRA S. PATEL AND MICHAEL WORSLEY
Research Council of Alberta, 11315 87 Avenue, Edmonton, Alberta

Received August 5, 1969

The syntheses of L(+) and D(−) enantiomers of α-amino acids, norvaline, norleucine, and leucine, as their hydrochloride salts have been achieved in almost 100% optical purity and 40–60% overall yield.

Canadian Journal of Chemistry, 48, 1881 (1970)

Nonenzymatic asymmetric syntheses of α-amino acids from the corresponding α-keto acids have been described previously (1–8). However, all these syntheses involve a method of catalytic hydrogenation of the optically active Schiff bases of α-keto acids with L(−) and D(+)α-alkylbenzylamine. The optical purities of the α-amino acids produced by this method range between 12 and 91%. The catalytic addition of hydrogen to the Schiff bases has not yet led to optically pure amino acids.

Harada and Fox (9, 10) have reported the asymmetric synthesis of optically active alanine by the Strecker synthesis. Their method involved the reaction of optically active L(−)α-methylbenzylamine with a racemic aldehyde cyanohydrin, followed by hydrolysis and subsequent hydrogenolysis of the resulting α-amino nitrile. The overall yield of amino acid produced was 17%, and optical purity ranged from 86–99%, after one recrystallization.

We now report the alternative Strecker synthesis, i.e., the asymmetric synthesis of optically active α-amino acids by the addition of hydrocyanic acid (HCN) to the optically active Schiff bases. Good yields of amino acids in high optical purity were obtained.

Our total method of asymmetric synthesis involves: (*a*) preparation of a Schiff base from optically active L(−) and D(+)α-methylbenzylamine and aliphatic aldehydes, (**1**); (*b*) addition of hydrocyanic acid to the Schiff base obtained from (*a*), (**2**); (*c*) acid hydrolysis of the amino nitrile obtained from (*b*), (**3**); and finally, (*d*) removal of α-methylbenzyl residue by catalytic hydrogenation over 10% palladium on carbon catalyst, (**4**). These four steps for the synthesis are schematically represented in Fig. 1. The L(+) and D(−) isomers of α-amino acids, norvaline, norleucine, and leucine, have been synthesized by this method. The crude products as isolated from the reaction solution were used in the successive steps of the synthesis.

The overall yields of these synthesized amino acids were 40–60% (based on starting amine) and the optical purities were >98% without recrystallization. It has been observed that the addition of hydrocyanic acid (HCN) to the Schiff base has resulted in the exclusive formation of one isomer. The possibility of selective elimination of the minor isomer during the isolation of the intermediate compound (**3**) is excluded by the fact that D(−) and L(+) isomers of α-amino acids have been obtained in high optical purity from the corresponding D(+) and L(−) isomers of the starting amine.[2] Furthermore, the amino acids produced had the same configuration as that of the starting amine. Thus, D(+)α-methylbenzylamine gave D(−) amino acids and L(−)α-methylbenzylamine gave L(+) amino acids. The reaction mechanism of this synthesis has not been studied.

[1]Contribution No. 477 from the Research Council of Alberta, Edmonton, Alberta.

[2]The possibility of fractionation having occurred is extremely unlikely, since in the case of L(+)leucine, when the intermediate compound (**3**) and final amino acid were isolated using ion exchange resin (AG50, H^+ form) column, rather than precipitation, the results were very similar to those obtained using precipitation as an isolation procedure. [e.g., The desalted crude mixture was applied to resin column (2 × 25 cm), washed with water, then **3** was eluted with 1 *N* aqueous ammonia, eluate evaporated to dryness under reduced pressure at 30–40 °C, residue suspended in absolute alcohol, filtered, washed with anhydrous ether, dried, and specific rotation measured. L(−)*N*-(α-Methylbenzyl)-leucine $[\alpha]_D^{25}$ −23.0° (cf. −22.2°); L(+)leucine $[\alpha]_D^{25}$ −15.0° (cf. −15.6°)].

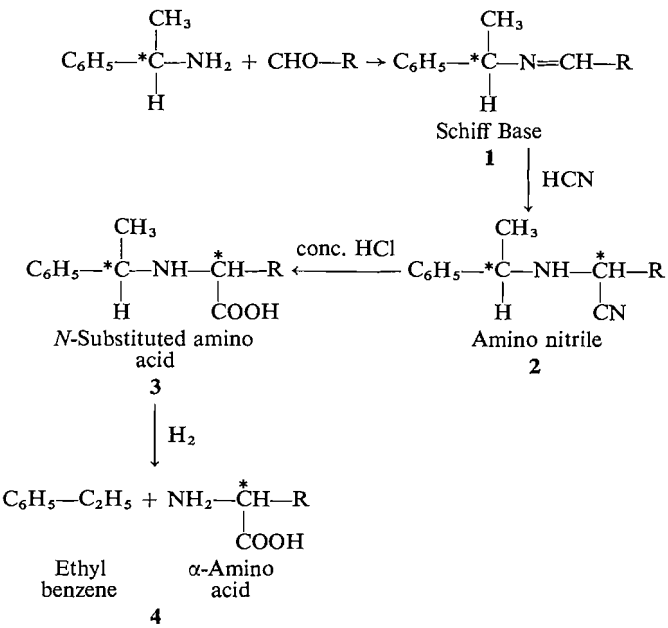

FIG. 1. Asymmetric syntheses of optically active α-amino acids. *Asymmetric carbon; R = alkyl.

TABLE 1

Elemental analysis for intermediate *N*-(α-methylbenzyl) amino acid and final amino acid hydrochloride salt

Name of acid		% C	% H	% N	% Cl
L(−)*N*-(α-Methylbenzyl)-norvaline	Calcd.	70.55	8.65	6.33	—
	Found	70.45	8.46	6.34	—
D(+)*N*-(α-Methylbenzyl)-norvaline	Calcd.	70.55	8.65	6.33	—
	Found	70.43	8.52	6.55	—
L(+)Norvalinehydrochloride	Calcd.	39.09	7.88	9.12	23.08
	Found	38.99	7.78	8.99	22.97
D(−)Norvalinehydrochloride	Calcd.	39.09	7.88	9.12	23.08
	Found	38.92	7.72	9.06	23.07
L(−)*N*-(α-Methylbenzyl)-norleucine	Calcd.	71.45	9.00	5.95	—
	Found	71.28	8.82	6.12	—
D(+)*N*-(α-Methylbenzyl)-norleucine	Calcd.	71.45	9.00	5.95	—
	Found	71.23	8.84	6.01	—
L(+)Norleucinehydrochloride	Calcd.	42.99	8.42	8.36	21.14
	Found	43.16	8.24	8.51	21.04
D(−)Norleucinehydrochloride	Calcd.	42.99	8.42	8.36	21.14
	Found	43.16	8.41	8.49	21.02
L(−)*N*-(α-Methylbenzyl)-leucine	Calcd.	71.45	9.00	5.95	—
	Found	71.31	8.80	6.10	—
D(+)*N*-(α-Methylbenzyl)-leucine	Calcd.	71.45	9.00	5.95	—
	Found	71.48	8.82	6.11	—
L(+)Leucinehydrochloride	Calcd.	42.99	8.42	8.36	21.14
	Found	43.09	8.23	8.51	21.06
D(−)Leucinehydrochloride	Calcd.	42.99	8.42	8.36	21.14
	Found	43.06	8.58	8.58	21.23

Can. J. Chem. Downloaded from www.nrcresearchpress.com by 210.87.254.42 on 09/05/12
For personal use only.

Can. J. Chem. Downloaded from www.nrcresearchpress.com by 210.87.254.42 on 09/05/12
For personal use only.

TABLE 2

Asymmetric syntheses of α-amino acids

R in R—CHO	Amine*	Schiff base: Overall yield (%)	Schiff base: $[\alpha]_D^{25°}(\pm 2°)$ [*c*, 3–4, in CH_3OH]†	α-Amino nitrile: Overall yield (%)	α-Amino nitrile: $[\alpha]_D^{25°}(\pm 2°)$ [*c*, 3–4, in CH_3OH]	*N*-(α-Methylbenzyl) amino acid: Overall yield (%)	*N*-(α-Methylbenzyl) amino acid: $[\alpha]_D^{25°}$ [*c*, 2–3, in 6 *N* HCl]	α-Amino acid hydrochloride: Name	Overall yield (%)	$[\alpha]_D^{25°}(\pm 2°)$ [*c*, 2–3, in 6 *N* HCl]‡	Optical purity§ (%)
C_3H_7—	Me (+)	96.4	+82	94.5	+148	46.1	+16	D(−)Norvaline	41.4	−23.0 (−23.3)‖	99
C_3H_7—	Me (−)	99.0	−84	98.6	−150	47.7	−17.6	L(+)Norvaline	42.6	+23.2 (+23.3)	99
C_4H_9—	Me (+)	95.8	+79	93.7	+148	47.0	+ 8.2	D(−)Norleucine	42.7	−22.3 (−22.4)	99
C_4H_9—	Me (−)	94.8	−80	94.3	−150	48.8	−10	L(+)Norleucine	42.8	+20.9 (+21.3)	98
i-C_4H_9—	Me (+)	97.5	+79	97.4	+155	64.3	+21.1	D(−)Leucine	58.4	−15.0 (−15.2)	99
i-C_4H_9—	Me (−)	95.1	−79	94.3	−160	56.1	−22.2	L(+)Leucine	49.3	+15.0 (+15.2)	99

*Me(+), D(+)α-Methylbenzylamine $[\alpha]_D^{25°}$ +39.7° (neat); Me(−), L(−)α-methylbenzylamine $[\alpha]_D^{25°}$ −40.6° (neat) [Lit. (*i*) $[\alpha]_D^{25°}$ −39.2–39.7° (11); (*ii*) $[\alpha]_D^{25°}$ −40.3°, Theilacker and Winkler (13)].

†Spectroscopic grade methanol has been used.

‡Percentage concentration is calculated for neutral amino acid.

§Optical purity = $[\alpha]_D$ observed/$[\alpha]_D$ literature. NOTE: Specific rotations for the intermediate Schiff base and α-amino nitrile are given for the crude products as isolated from the reactions without further purification.

‖Numbers in brackets indicate the literature values used for calculation of the optical purity.

Can. J. Chem. Downloaded from www.nrcresearchpress.com by 210.87.254.42 on 09/05/12
For personal use only.

Experimental[3]

The D(+) and L(−)α-methylbenzylamine were obtained from commercial racemic amine (11).[4] The commercial aldehydes, *n*-butyraldehyde, *n*-valeraldehyde, and isovaleraldehyde were dried over anhydrous magnesium sulfate ($MgSO_4$) and distilled prior to use.

Preparation of Schiff Base: L(−)α-Methylbenzylamine, N-Butylidene (1)

To 2.425 g (0.020 mole) of L(−)α-methylbenzylamine (b.p. 184–185 °C), precooled to 15 °C, was added 1.442 g (0.020 mole) of *n*-butyraldehyde (b.p. 75 °C) with stirring over a period of 15–20 min. During the addition of aldehyde the reaction temperature was maintained at 0 °C. The stirring was discontinued, and the reaction solution was cooled to −10 °C prior to the addition of ca. 15–20 g of anhydrous calcium sulfate as a desiccant. (Note: Addition of $CaSO_4$ raises the temperature from −10 °C to 10 °C.) The reaction mixture was allowed to stand at room temperature overnight (15–20 h), anhydrous ether (25 ml) was added, ether solution was filtered, and the desiccant washed with ether (4 × 25 ml). Evaporation of the filtrate under reduced pressure (rotary evaporator) at room temperature yielded **1**, 3.50 g. The infrared (i.r.) spectrum (neat, liquid film) of the product showed a strong absorption band at 1660 cm^{-1}, attributed to $\rangle C{=}N$, and absence of primary $-NH_2$ band at 3500–3400 cm^{-1}. The product was used for the next reaction without further purification.

Preparation of α-Amino Nitrile: L(−)2-Amino-N(α-methylbenzyl)-valeronitrile (2)

The Schiff base ((**1**), 3.07 g) in absolute alcohol (50 ml) at −10 °C was treated with an excess (3 g) of HCN gas (12) under constant stirring. The reaction mixture was stirred overnight (20 h) at room temperature and excess reagent and solvent were removed under reduced pressure at room temperature to yield **2**, 3.50 g. The i.r. spectrum (neat, liquid film) of the product showed absorption bands at 2210 cm^{-1}, attributed to $-C{\equiv}N$, at 3310 cm^{-1}, due to secondary $\rangle NH$, and absence of $\rangle C{=}N$ band at 1660 cm^{-1}. This product was used in the next experiment.

Acid Hydrolysis: L(−)N-(α-Methylbenzyl)-norvaline (3)

The α-amino nitrile ((**2**), 3.40 g) in concentrated HCl[5] (50 ml, sp. gr. 1.38) was stirred at room temperature (2–4 h) and finally heated under reflux on a steambath for 16–20 h. The excess hydrochloric acid was removed under reduced pressure, water (3 × 10 ml) was added to the residue and the solution evaporated to dryness to remove last traces of HCl. The residue in absolute alcohol (50 ml) was kept at 0 °C (3 h) and filtered to remove ammonium chloride (NH_4Cl). The filtrate was neutralized to p*H* 6 with pyridine, and evaporated to dryness under reduced pressure. The residue was dissolved in water and **3** was precipitated by addition of an equal volume of absolute alcohol, kept at 5 °C (ca. 15 h), filtered, washed with water followed by alcohol and dried. Yield, 1.80 g. The i.r. spectrum (0.3% KBr) of the product showed a strong absorption band at 1550–1600 cm^{-1} and also at 1280–1300 cm^{-1}, due to ionized carboxyl, C=O stretching, and a series of continuous bands at 3030–3500 cm^{-1}, attributed to $\overset{+}{N}H_3$. The m.p., sublimed above 228 °C.

Hydrogenolysis: Preparation of L(+)Norvaline-hydrochloride (4)

L(−)*N*-(α-Methylbenzyl)-norvaline ((**3**), 1.23 g) in absolute ethanol (20 ml) containing 1 equ. of concentrated hydrochloric acid was hydrogenolyzed over 10% palladium on carbon catalyst (250 mg), at 1000 p.s.i. and 30 °C for 6 h. The catalyst was filtered off, washed with absolute alcohol, the filtrate evaporated to dryness under reduced pressure, 1 *N* HCl (5 ml) was added to the residue and the solution evaporated to dryness. The resulting solid was dissolved in absolute alcohol, filtered, and **4** was precipitated by addition of anhydrous ether, collected under suction, washed with ether, and dried. Yield, 0.76 g. The melting point and i.r. spectrum of the amino acid were identical to those of the authentic sample.

The experimental results for the synthesis of the D(−) isomer of norvalinehydrochloride and other amino acids are summarized in Tables 1 and 2.

[3]All temperature measurements were uncorrected. All optical rotations were performed with a Perkin–Elmer polarimeter, Model 141. Elemental analyses were carried out by Alfred Bernhardt Microanalytical Laboratory, West Germany. Hydrogenolysis experiments were carried out by using a high-pressure hydrogenator (rocking type).

[4]The values of overall yields, specific rotations, and the elemental analyses are omitted from the experimental text and are reported only in Tables 1 and 2.

[5]During initial addition of the HCl, the reaction mixture should be maintained at 0–5 °C.

1. F. Knoop and C. Martius. Z. Physiol. Chem. **258**, 238 (1939).
2. (*a*) R. G Hiskey and R. C. Northrop. J. Amer. Chem. Soc. **83**, 4798 (1961). (*b*) ibid. **85**, 1753 (1965).
3. A. Kanai and S. Mitsui. J. Chem. Soc. Japan, Pure Chem. Sec. **87**, 183 (1966).
4. K. Harada and K. Matsumoto. J. Org. Chem. **32**, 1794 (1967).
5. K. Matsumoto and K. Harada. J. Org. Chem. **31**, 1956 (1966).
6. K. Harada. J. Org. Chem. **32**, 1790 (1967).
7. K. Harada. Nature, **212**, 1571 (1966).
8. K. Matsumoto and K. Harada. J. Org. Chem. **33**, 4526 (1968).
9. K. Harada. Nature, **200**, 1201 (1963).
10. K. Harada and S. W. Fox. Naturwiss. **51**, 106 (1964).
11. A. H. Blatt. Organic syntheses. Coll. Vol. II. John Wiley and Sons, Inc., New York, N.Y., 1943. p. 506.
12. A. H. Blatt. Organic syntheses. Coll. Vol. I. John Wiley and Sons, Inc., New York, N.Y., 1941. p. 314.
13. W. Theilacker and H. Winkler. Chem. Ber. **87**, 690 (1954).

Can. J. Chem. Downloaded from www.nrcresearchpress.com by 210.87.254.105 on 09/05/12
For personal use only.

Reaction of bis(trifluoromethyl)diazomethane with trimethyl-3,3,3-trifluoropropynyltin, trimethyltin hydride, and related compounds

W. R. CULLEN AND M. C. WALDMAN

Chemistry Department, University of British Columbia, Vancouver, British Columbia

Received January 30, 1970

Bis(trifluoromethyl)diazomethane (**1**) reacts with the compounds $(CH_3)_3MC{\equiv}CCF_3$ (M = Ge, Sn) to give the cyclopropenes $(CH_3)_3MC{=}C(CF_3)C(CF_3)_2$. Cyclopropenes are also obtained from the reaction of **1** with the acetylenes $RC{\equiv}CCF_3$ (R = H, CF_3) but the main products are the isopyrazoles $RC{=}C(CF_3)N{=}N{-}C(CF_3)_2$. Compound **1** reacts easily with $(CH_3)_3SnH$ to give $(CH_3)_3SnC(CF_3)_2H$ and a similar insertion reaction takes place with $(CH_3)_2AsH$. Compound **1** does not insert into Si—H, Ge—H, Ge—Br, Ge—Ge bonds. It reacts with $(CH_3)_2As{-}As(CH_3)_2$ to give $(CH_3)_2AsC(CF_3)_2H$. Bis(trifluoromethyl)diazirine also reacts with $(CH_3)_3GeC{\equiv}CCF_3$ to give the cyclopropene.

Canadian Journal of Chemistry, 48, 1885 (1970)

The reaction of a diazomethane $RR'CN_2$ with an inorganic compound has proved to be a useful means of inserting a one-carbon fragment into an M—X bond (X = H, halogen, oxygen) (eq. [1]).

$$[1] \qquad M{-}X + RR'CN_2 \rightarrow M{-}\underset{\displaystyle R}{\overset{\displaystyle R'}{\overset{|}{\underset{|}{C}}}}{-}X + N_2$$

The earlier literature has been reviewed by Seyferth (1), and since 1955 a number of investigations of this "insertion" reaction have been made (e.g. 2–7). Moreover, there has been considerable interest in the reactions of diazomethanes with organometallic systems in the hope of preparing novel compounds (e.g. 6, 8–10).

Bis(trifluoromethyl)diazomethane (**1**) has recently been reported (11) and a few of its reactions have been studied (6, 7, 11–14). Those reactions that have been investigated have been interpreted in three ways: (*a*) as attack by the diazo compound acting as a 1,3-dipolar reagent, (6, 12); (*b*) as involving bis(trifluoromethyl)carbene (6, 11, 12) the main intermediate in both the thermal and photolytic decompositions of **1**; or (*c*) as radical attack on the terminal nitrogen of **1** (13). The diazo compound was of primary interest in the present investigation as a 1,3-dipolar reagent and as a source of the carbene $C(CF_3)_2$.

Experimental

Volatile reactants and products were manipulated in a vacuum system. Unless otherwise indicated reactions were carried out in thick-walled Pyrex Carius tubes. Vapor-phase chromatography (v.p.c.) separations were carried out using an Aerograph A-90-P gas chromatograph. The columns used for a particular separation are given in the experimental details below. Molecular weights were determined using Regnault's method. Nuclear magnetic resonance (n.m.r.) spectra were run using Varian A-60 (^1H spectra in p.p.m. with respect to external TMS), and Varian HA-100 (^{19}F spectra in p.p.m. with respect to internal $CFCl_3$) spectrometers; positive values of chemical shift being to higher field. Infrared (i.r.) spectra were recorded using a PE 457 spectrometer.

Microanalyses were performed by Mr. Peter Borda of this Department.

Bis(trifluoromethyl)diazomethane and bis(trifluoromethyl)diazirine were prepared from hexafluoroacetone (the kind gift of the Allied Chemical Company) according to the methods described by Gale *et al.* (11). The purity of the diazomethane was checked by i.r. spectroscopy and by its molecular weight of 177 (Calcd. for $C_3F_6N_2$: 178). The diazirine was found to be only 95% pure on the basis of its ^{19}F n.m.r. spectrum but was used without further purification.

1) Reaction with 3,3,3-Trifluoropropyne

3,3,3-Trifluoropropyne (1.395 g, 14.8 mmoles) and bis(trifluoromethyl)diazomethane (1.187 g, 6.66 mmoles) were heated for 20 h at 150°. The v.p.c. separation (20% SE-30 at 55°) of the volatile fraction which condensed at −78° showed five components but only the second and third fractions could be collected and identified. The first eluted major component was identified as 3,3,5-tris(trifluoromethyl)isopyrazole (0.776 g), micro b.p. 52° (atm).

Anal. Calcd. for $C_6HF_9N_2$: C, 26.45; H, 0.37; F, 62.90. Found: C, 26.58; H, 0.43; F, 62.50.

The i.r. spectrum (vapor): 3060 (w), 2009 (w), 1738 (vw), 1323 (m), 1300 (m), 1281 (s), 1271 (s), 1231 (w), 1200 (s), 1180 (m), 1120 (m), 978 (m), 973 (m), 852 (w), 805 (vw) cm^{-1}. The ^1H n.m.r. spectrum showed a complex but well defined multiplet at −5.99 p.p.m. (see Fig. 1). The ^{19}F n.m.r. spectrum showed two peaks, each a doublet, centered at 61.39 ($=\underset{|}{C}CF_3$) (J_{F-H} = 5.7 c.p.s.) (area 1) and 61.81 p.p.m. ($-\underset{|}{C}(CF_3)_2$) (J_{F-H} = 2.4 c.p.s.) (area 2).

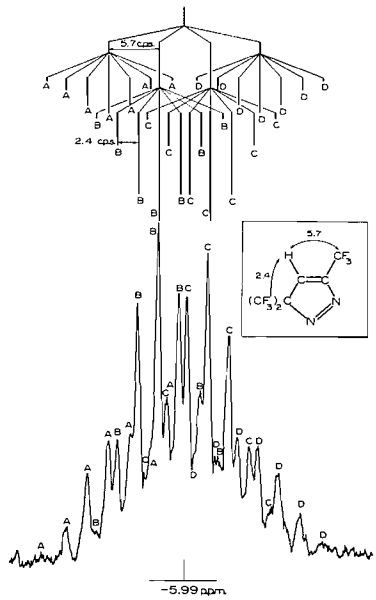

FIG. 1. The ^1H n.m.r. spectrum of the isopyrazole obtained from the reaction of $HC{\equiv}CCF_3$ with $(CF_3)_2CN_2$.

The second component was identified as 1,3,3-tris(trifluoromethyl)cyclopropene (0.201 g), micro b.p. 56.9° (atm).

Anal. Calcd. for C_6HF_9: C, 29.53; H, 0.41; F, 70.01. Found: C, 29.55; H, 0.62; F, 69.66.

The i.r. spectrum: 3185 (w), 1814 (w), 1321 (s), 1291 (m), 1262 (s), 1246 (m(sh)), 1215 (s), 1195 (s), 1005 (w), 961 (m), 772 (w), 708 (m) cm^{-1}. The ^1H n.m.r. spectrum showed a poorly defined complex multiplet at −7.02 p.p.m. The ^{19}F n.m.r. spectrum showed two multiplets centered at 62.0 p.p.m. ($=CCF_3$) (J_{F-H} = 1.3 c.p.s.; J_{F-F} = 1.2 c.p.s.) (area 1) and 67.65 p.p.m. ($-C(CF_3)_2$) (J_{F-H} = 1.0 c.p.s.) (area 2) (see Fig. 2).

The fraction which passed through the −78° bath was identified as slightly impure 3,3,3-trifluoropropyne (0.728 g).

In another reaction, the trifluoropropyne and the diazo compound were heated at 150° for 21 h and then examined to determine the ratio of the products. From the v.p.c. and ^1H n.m.r. integrations of the −78° fraction, it was determined that the isopyrazole and the cyclopropene together comprised 30% of the products based on propyne consumed, and that the ratio isopyrazole:cyclopropene was 2.45:1.

When the reaction was carried out under ultraviolet (u.v.) light (450 W u.v. source) for 21 h the n.m.r. spectrum indicated that the isopyrazole and cyclopropene comprised 65.5% of the products, based on propyne consumed, and that the ratio isopyrazole:cyclopropene was 2.04:1.

2a) Reaction with Hexafluorobutyne-2

Hexafluorobutyne-2 (0.424 g, 2.66 mmoles) and bis(trifluoromethyl)diazomethane (0.466 g, 2.62 mmoles) were heated at 150° for 20 h. A small amount of the starting butyne (0.086 g) was recovered. The fraction which condensed at −78° was separated by v.p.c. into 5 components (20% silicone GE-SS-96 at 51°). Only the first and third eluted fractions were identified. The first (~0.07 g) was identified as tetrakis(trifluoromethyl)-cyclopropene (see section 2*b* below).

The second fraction was identified as 3,3,4,5-tetrakis-(trifluoromethyl)isopyrazole (0.262 g, 35% yield) micro b.p. 81° (atm).

Anal. Calcd. for $C_7F_{12}N_2$: C, 24.72; F, 67.04. Found: C, 24.92; F, 66.6.

The i.r. spectrum (vapor): 2392 (vw), 1672 (vw), 1356 (s), 1302 (s), 1269 (vw), 1227 (vw), 1197 (vs), 1149 (m), 1050 (w), 1004 (w), 980 (m), 952 (s), 941 (w), 772 (w), 755 (vw), 737 (m), 672 (w) cm^{-1}. The ^{19}F n.m.r. spectrum showed an $A_3M_3X_6$ pattern where A_3 was the 4-position CF_3 group (δ(A) = 56.2 p.p.m.), M_3 was the 5-position CF_3 group (δ(M) = 63.25 p.p.m.), and X_6 was the two, 3-position CF_3 groups (δ(X) = 64.45 p.p.m.) (J_{A-M} = 8.5 c.p.s.; J_{A-X} = 6 c.p.s.) (see Fig. 3).

2b) Pyrolysis of 3,3,4,5-Tetrakis(trifluoromethyl)pyrazole

The pyrazole (0.903 g, 2.68 mmoles) was heated at 300° for 72 h. The product, tetrakis(trifluoromethyl)-cyclopropene (0.764 g, 92% yield), was purified by repeated passes through a trap at −78°.

Anal. Calcd. for C_7F_{12} (mol. wt. 312): C, 26.93; F, 72.90. Found (308): C, 27.23; F, 72.60.

The i.r. spectrum: 1919 (w), 1321 (s), 1303 (s(sh)), 1246 (s), 1225 (s), 1200 (s), 1030 (m), 961 (m), 765 (vw), 709 (m), 666 (m), 641 (w) cm^{-1}. The ^{19}F n.m.r. spectrum showed two septets, at 61.2 p.p.m. ($CF_3C{=}CCF_3$) and 67.5 p.p.m. ($-C(CF_3)_2$) (J_{F-F} = 1.15 c.p.s.). A linear plot of log *p* against $10^3/T$ was extrapolated to give a b.p. of 34.9° (760 mm).

3) Reaction with 3,3,3-Trifluoropropynyltrimethylgermane

3,3,3-Trifluoropropynyltrimethylgermane (0.779 g, 3.69 mmoles) and bis(trifluoromethyl)diazomethane (1.076 g, 6.05 mmoles) were heated at 150° for 29 h. A non-condensible gas, presumably nitrogen, was produced. The fraction which condensed at −78° was examined by v.p.c. (20% Kel-F grease at 72°). The two major components were identified as, in order of their elution: 3,3,5-tris(trifluoromethyl)isopyrazole, of known i.r. spectrum (see 1 above) and 2,3,3-tris(trifluoromethyl)-cyclopropenyltrimethylgermane (0.179 g, 12.3% yield), micro b.p. 124.5° (atm).

Anal. Calcd. for $C_9H_9F_9Ge$: C, 29.95; H, 2.50. Found: C, 29.37; H, 2.46.

The i.r. spectrum (vapor): 2995 (w), 2915 (w), 1837 (w), 1420 (vw), 1358 (w), 1320 (vs), 1295 (s), 1269 (vs), 1228 (s(sh)), 1209 (vs), 1183 (vs), 1163 (s(sh)), 1104 (vw), 1080 (vw), 997 (w), 958 (s), 841 (s), 841 (m), 768 (w), 710 (m) cm^{-1}. The ^1H n.m.r. spectrum showed a singlet at −0.35 p.p.m. The ^{19}F n.m.r. spectrum showed a septet and quartet centered at 62.0 p.p.m. and 66.9 p.p.m. with J = 1.2 c.p.s. in both splitting patterns. The area ratio of the low field to high field absorptions was 1:2 (Calcd. 1:2).

Can. J. Chem. Downloaded from www.nrcresearchpress.com by 210.87.254.105 on 09/05/12
For personal use only.

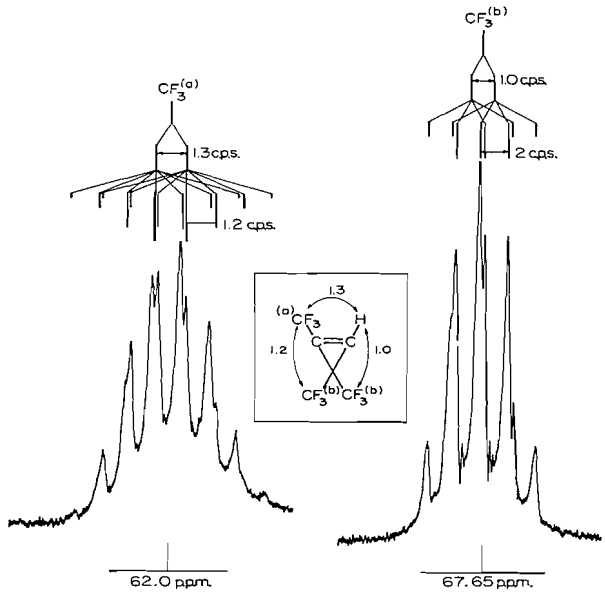

FIG. 2. The ^{19}F n.m.r. spectrum of the cyclopropene obtained from the reaction of $HC{\equiv}CCF_3$ with $(CF_3)_2CN_2$.

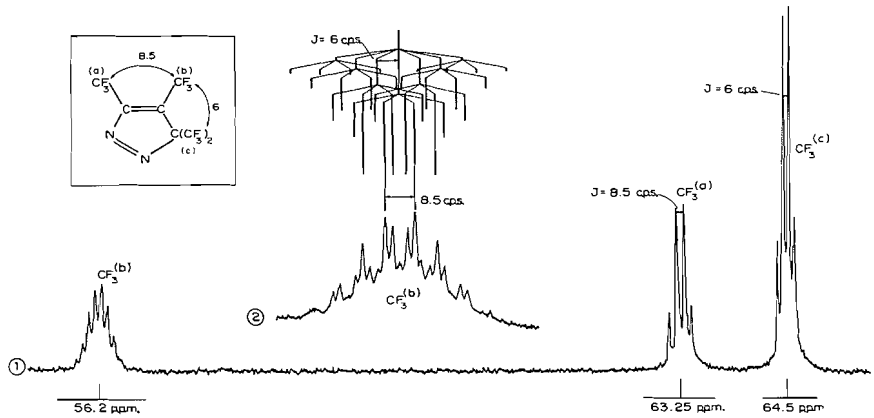

FIG. 3. The ^{19}F n.m.r. spectrum of the isopyrazole obtained from the reaction of $CF_3C{\equiv}CCF_3$ with $(CF_3)_2CN_2$.

4) Reaction with 3,3,3-Trifluoropropynyltrimethyltin

3,3,3-Trifluoropropynyltrimethyltin (1.178 g, 4.59 mmoles) and bis(trifluoromethyl)diazomethane (1.424 g, 8.02 mmoles) were heated at 165° for 29 h. There was considerable decomposition. No free propyne was detected but a non-condensible gas, presumably nitrogen, was produced. The −78° fraction was separated by v.p.c. (20% Kel-F grease at 100°) into many components but only the last eluted component could be collected as a single, uncontaminated product. It was identified as 2,3,3-tris(trifluoromethyl)cyclopropenyltrimethyltin (0.140 g, 7% yield). The i.r. spectrum (vapor): 3000 (vw), 2925 (vw), 1820 (w), 1358 (w), 1321 (s), 1290 (m), 1266 (s), 1209 (s), 1181 (s), 1000 (vw), 982 (vw), 958 (m), 788 (vw), 763 (vw) cm^{-1}. The ^1H n.m.r. spectrum showed a singlet at −0.3 p.p.m. with tin satellite peaks ($J_{117_{Sn-CH_3}}$ = 58.2 c.p.s.; $J_{119_{Sn-CH_3}}$ = 61.0 c.p.s.). The ^{19}F n.m.r. spectrum showed two sets of peaks: a septet at 62.55 p.p.m. ($-CF_3$) and a quartet at 66.9 p.p.m. ($-\underset{|}{C}(CF_3)_2$) (J_{F-F} = 1.25 c.p.s.), (area ratio, septet:quartet = 1:2 (Calcd. 1:2)). The compound decomposed in a glass isotenoscope at ~67°. The b.p. is estimated from the data collected below this temperature to be ~99°.

5) Reaction with Trimethylsilane

Trimethylsilane (0.40 g, 5.4 mmoles) and bis(trifluoromethyl)diazomethane (0.250 g, 1.4 mmoles) did not

Can. J. Chem. Downloaded from www.nrcresearchpress.com by 210.87.254.105 on 09/05/12
For personal use only.

Can. J. Chem. Downloaded from www.nrcresearchpress.com by 210.87.254.105 on 09/05/12
For personal use only.

appear to react after 1 day at 20°. The mixture was heated at 100° for 72 h after which the volatiles were examined by ^{1}H n.m.r. spectroscopy. The spectrum showed only one multiplet at −3.25 p.p.m. (J = 3.7 c.p.s.) which corresponded with the original trimethylsilane.

6) Reaction with Trimethylgermane

Trimethylgermane (0.356 g, 3.0 mmoles) and bis(trifluoromethyl)diazomethane (0.761 g, 4.27 mmoles) did not appear to react after 1 day at 20°. The mixture was heated at 135° for 50 h. The ^{1}H n.m.r. spectrum of the volatiles showed three high field absorptions and a septet centered at −2.64 p.p.m. (J = 9.5 c.p.s.). However, the ^{1}H n.m.r. spectra of the major v.p.c. separated products (20% Kel-F grease at 90°) showed that the septet was due to a compound which did not have any high field methyl absorptions and thus, not due to $(CH_3)_3GeC(CF_3)_2H$. The v.p.c. separated products were not further studied.

7) Reaction with Trimethyltin Hydride

Trimethyltin hydride (0.633 g, 4.0 mmoles) and bis(trifluoromethyl)diazomethane (0.741 g, 4.2 mmoles) reacted upon warming to 20° with evolution of gas and loss of color. A white precipitate had formed after 2 h. After 3 days a brown decomposition product was observed. After 3 weeks at 20° the volatiles were fractionated by trap-to-trap distillation. The fraction which condensed at −78° was purified by v.p.c. (20% Kel-F grease at 95°) and identified as 1,1,1,3,3,3-hexafluoroisopropyltrimethyltin (0.611 g, 51% yield), micro b.p. 129.5° (atm).

Anal. Calcd. for $C_6H_9F_7Sn$: C, 22.89; H, 3.20; F, 36.21. Found: C, 23.06; H, 3.20; F, 35.91.

The i.r. spectrum (vapor): 3000 (w), 2939 (w), 1766 (w), 1363 (s), 1282 (vs), 1250 (m), 1220 (vs(br)), 1195 (s), 1130 (w), 1079 (m), 1050 (m), 970 (vw), 900 (w), 870 (w), 787 (m), 674 (w) cm^{-1}. The ^{1}H n.m.r. spectrum showed a singlet at −0.30 p.p.m. (—CH_3) with tin satellite peaks ($J_{^{117}Sn-CH_3}$ = 51.5 c.p.s.; $J_{^{119}Sn-CH_3}$ = 56.5 c.p.s.) and a septet at −2.54 p.p.m. (—$CH(CF_3)_2$) (J_{F-H} = 11.5 c.p.s.). The two absorptions integrated in the ratio 9.3:1, respectively (Calcd. 9:1). The ^{19}F n.m.r. spectrum showed a doublet of septets centered at 56.1 p.p.m. (J_{F-CH_3} = 0.5 c.p.s.).

The material which passed through the −78° bath was identified as mostly perfluoropropene by its known i.r. spectrum.

8) Reaction with Trimethylgermanium Bromide

Trimethylgermanium bromide (0.713 g, 3.60 mmoles) and bis(trifluoromethyl)diazomethane were miscible at 20°. The mixture was opaque after 1 day. After 48 h at 100° a brown decomposition product had formed. A small amount of perfluoropropene (<0.1 g) was isolated. The fraction which condensed at −78° was separated into two major components by v.p.c. (20% silicone GE-SS-96 at 90°). The first fraction (0.110 g) showed i.r. absorptions at 7.9, 8.05, and 13.81 μ.[1] It was not identified. The second component was identified as trimethylgermanium bromide (0.278 g) by comparison of its i.r. and ^{1}H spectra with that of a known sample.

9) Reaction with Dimethylarsine

Dimethylarsine (0.374 g, 3.54 mmoles) and bis(trifluoromethyl)diazomethane (0.799 g, 4.48 mmoles) were miscible at 20°. No evidence of reaction was observed after two days. After 48 h at 100° a brown decomposition product had formed. The fraction which condensed at −78° was purified by v.p.c. (20% Kel-F grease at 95°) and identified as the insertion product, 1,1,1,3,3,3-hexafluoroisopropyldimethylarsine (0.605 g, 67% yield), micro b.p. 110.5° (atm).

Anal. Calcd. for $C_5H_7F_6As$: C, 23.45; H, 2.75; F, 44.52. Found: C, 23.63; H, 2.84; F, 44.22.

The i.r. spectrum (vapor): 3025 (w), 3000 (w), 2939 (w), 1424 (w(br)), 1358 (s), 1296 (vs), 1241 (vs), 1213 (s), 1142 (m), 1090 (s), 1075 (s(sh)), 909 (m), 975 (w), 960 (w), 679 (m) cm^{-1}. The ^{1}H n.m.r. spectrum showed a broad singlet and a septet at −1.0 p.p.m. (CH_3) and −2.67 p.p.m. (—$CH(CF_3)_2$), respectively (J_{F-H} = 10 c.p.s.). The ^{19}F n.m.r. spectrum displayed a doublet of septets centered at 55.90 p.p.m. (J_{F-CH_3} = 0.95 c.p.s.). The lower boiling fraction was identified by i.r. spectroscopy as a mixture of starting diazo compound and perfluoropropene.

10) Reaction with Hexamethyldigermane

Hexamethyldigermane (0.726 g, 3.09 mmoles) and bis(trifluoromethyl)diazomethane (0.742 g, 4.17 mmoles) were miscible at 20°. There was no visible evidence of any reaction after one day at 20°. The mixture was heated at 100° for 24 h. The fraction which condensed at −78° was examined by v.p.c. (20% silicone GE-SS-96 at 132°), and found to be 82% hexamethyldigermane.

Anal. Calcd. for $C_6H_{18}Ge$: C, 30.85; H, 7.72. Found: C, 30.63; H, 7.65.

The fraction which passed through the −78° bath was found by its i.r. spectrum to be a mixture of tetramethylgermane, perfluoropropene, and the starting diazo compound.

11) Reaction with Tetramethyldiarsine

Tetramethyldiarsine (0.940 g, 4.5 mmoles) and bis(trifluoromethyl)diazomethane (0.893 g, 5.0 mmoles) were miscible at 20°. No evidence of reaction was observed after two days at 20°. The mixture was heated at 100° for 48 h. The volatile fractions which condensed at −63° were combined and separated by v.p.c. (20% Kel-F grease at 100°). One of the two major components was identified as 1,1,1,3,3,3-hexafluoroisopropyldimethylarsine (0.185 g). This was the last compound to elute from the column and was characterized by comparing its i.r. spectrum with that of a known sample (see section 9 above).

Reaction of Bis(trifluoromethyl)diazirine with 3,3,3-Trifluoropropynyltrimethylgermane

Bis(trifluoromethyl)diazirine (0.924 g, 5.17 mmoles) and 3,3,3-trifluoropropynyltrimethylgermane (0.683 g, 3.24 mmoles) were heated at 165° for 13 h. The fraction of the reaction mixture which condensed at −78° was examined by v.p.c. (20% Kel-F grease at 72°). The major component was identified as 2,3,3-tris(trifluoromethyl)-cyclopropenyltrimethylgermane (0.241 g, 20% yield) by its i.r. spectrum (see section 3 above). A small amount of 3,3,5-tris(trifluoromethyl)isopyrazole was also identified by its known i.r. spectrum (see section 1 above).

[1]This spectrum was run on a Perkin–Elmer Infracord.

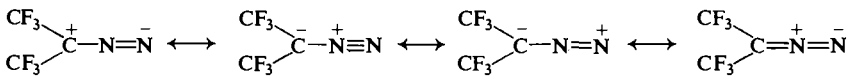

1a **1b** **1c** **1d**

Results and Discussion

Reactions with Acetylenes

The 1,3-dipolar nature of diazo compounds in general, and of **1** in particular, arises from the fact that the structure of a diazo compound can be represented as a number of canonical forms, **1a–1d**. In the case of **1** it is predicted that the canonical forms **1b** and **1c** (a 1,3-dipole) will predominate due to the stabilizing effect of the strongly electron-withdrawing trifluoromethyl groups.

Numerous investigations of 1,3-dipolar additions of diazo compounds to alkynes have been reported (15); however, only one reaction of **1** with an alkyne has been described (12) (eq. [2]).

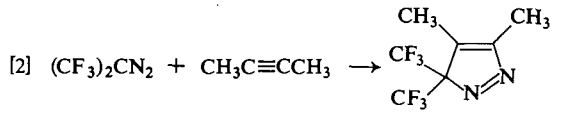

[2] $(CF_3)_2CN_2 + CH_3C{\equiv}CCH_3 \rightarrow$

The isopyrazole[2] eliminates nitrogen at 400° to give the cyclopropene according to eq. [3].

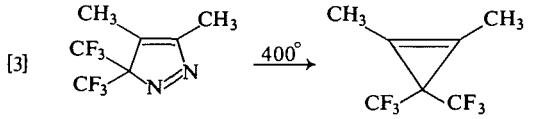

[3]

We have now found that bis(trifluoromethyl)-diazomethane reacts with 3,3,3-trifluoropropyne either at 150° or under the influence of u.v. light ($\lambda > 2850$ Å) to give as major products: 3,3,5-tris(trifluoromethyl)isopyrazole (**2**) and 1,3,3-tris(trifluoromethyl)cyclopropene (**3**) (eq. [4]). When the reactants are heated at 150°, **2** and **3** together comprise 30% of the products based on propyne consumed and are in the ratio **2**:**3** = 2.45:1. Under photolytic conditions a slightly lower ratio, 2.04:1, is obtained; however, the overall yield is higher, namely, 65.5%.

The structure of the isopyrazole **2** is indicated mainly by its n.m.r. spectra. Thus by using the coupling constants derived from the ^{19}F spectrum the complex multiplet displayed in the ^1H spectrum can be satisfactorily assigned as shown in Fig. 1. This isopyrazole is apparently the only one formed (1,3-addition (15) could take place in the opposite direction to give a second isomer) and the direction of addition corresponds with addition of **1c** to the acetylene polarized in the direction $H\overset{\delta+}{C}{\equiv}\overset{\delta-}{C} \rightarrow CF_3$. This polarization has been observed in other studies (19). It is interesting to note that 3,3,3-trifluoropropyne reacts with 2,2,2-trifluorodiazoethane to give two isomeric pyrazoles, the predominant one corresponding to addition in the same sense as **2** (16).

The structure of the cyclopropene **3** is confirmed by its i.r. and n.m.r. spectra. The ^1H n.m.r. spectrum shows a single complex peak at -7.02 p.p.m. similar to that of $H\overset{\frown}{C{=}C(CF_3)CF_2}$ (-7.37 p.p.m.) (20). A small upfield shift might be expected in the present case since the vinylic fluorine atoms have been replaced by less electron-withdrawing CF_3 groups. The ^{19}F n.m.r. spectrum shows two sets of peaks as shown in Fig. 2 and the coupling constants can all be assigned on a first order basis.

In a similar way **1** reacts with hexafluorobutyne-2 to give 3,3,4,5-tetrakis(trifluoromethyl)-isopyrazole (**4**) and a small amount of tetrakis-(trifluoromethyl)cyclopropene (**5**) (eq. [5]). Under the conditions studied, **4** and **5** comprise 50% of the products (based on butyne consumed) and are in the ratio **4**:**5** = 3.8:1. As in the reaction described by eq. [3], **4** loses nitrogen on heating (300°) to give the cyclopropene **5**. The structure of **4** is shown immediately by its ^{19}F n.m.r. spectrum, Fig. 3, and confirmed by elemental analysis for carbon and fluorine. The three peaks in the ^{19}F n.m.r. spectrum integrate in the ratio 1:1:2, as expected, and the splitting patterns can be completely analyzed on a first order basis. The structural proof of the cyclopropene **5** is provided by its ^{19}F n.m.r. spectrum which shows two septets ($J = 1.15$ c.p.s.) of

[2]The ring structure has the parent name "pyrazole"; however, no systematic nomenclature has yet been accepted for the ring structure . This latter structure has been called $\Delta^{1,3}$-pyrazole (16), pyrazolenine (17), 3-*H*-pyrazole (12), and isopyrazole (18). In this paper the parent name isopyrazole will be used.

Can. J. Chem. Downloaded from www.nrcresearchpress.com by 210.87.254.105 on 09/05/12
For personal use only.

TABLE 1
Infrared spectra of cyclopropene derivatives $RC\overline{=C(CF_3)C(CF_3)_2}$*

Derivative	Peak values (cm^{-1})											
R/H	3185	1814	1321	1291	1262	1215	1195	1005	961	772	708	
CF_3		1919	1321	1303	1246	1225	1200	1030	961		709	666
$(CH_3)_3Ge$		1837	1320	1295	1269	1209	1183	997	958	841	710	
$(CH_3)_3Sn$		1820	1321	1290	1266	1209	1181		958			

*Main bands only.

[4] $(CF_3)_2\bar{C}-N=\overset{+}{N} + HC\equiv CCF_3 \longrightarrow$ 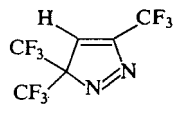 + 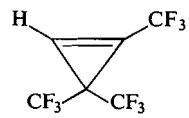

2 3

[5] $(CF_3)_2\bar{C}-N=\overset{+}{N} + CF_3C\equiv CCF_3 \longrightarrow$ 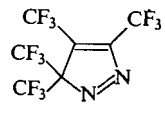 + 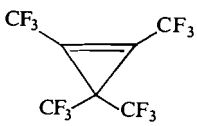

4 5

[6] $(CF_3)_2CN_2 + (CH_3)_3MC\equiv CCF_3 \longrightarrow$ 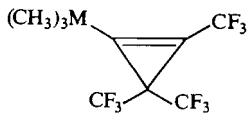
M = Ge, Sn

6

equal intensity at chemical shift values similar to those of the cyclopropene **3** (Table 2). The i.r. frequency associated with the C=C stretching vibration occurs at 1914 cm^{-1} and is the second highest recorded C=C frequency of a cyclopropene. The highest frequency, 1945 cm^{-1}, occurs in perfluorocyclopropene (21). These i.r. spectra are further discussed below.

The reaction of **1** with the Group IV trifluoropropynyl derivatives at 165° gives the corresponding Group IV 2,3,3-tris(trifluoromethyl)cyclopropenyl derivative (eq. [6]). A small amount of **2** is also produced in the reaction involving the propynyl germanium derivative which probably results from the reaction of **1** with $HC\equiv CCF_3$. The latter has been detected in the products of thermal reactions involving $(CH_3)_3GeC\equiv CCF_3$ (22).

The proposed structures of the compounds **6** (M = Ge, Sn) are based primarily on the similarity of their i.r. and n.m.r. spectra to those of $H\overline{C=C(CF_3)C(CF_3)_2}$ (Tables 1 and 2). Analytical data for the germanium compound are somewhat over the margin of experimental error. However the proposed structure is confirmed by the finding that the i.r. spectrum of the major product of the reaction of $(CH_3)_3GeC\equiv CCF_3$ and bis(trifluoromethyl)diazirine $(CF_3)_2\overline{C-N=N}$ is identical with the spectrum of the germanium derivative produced in the reaction given by eq. [6]. Thermal decomposition of the diazirine at temperatures $\geqslant 150°$ is known to produce only $C(CF_3)_2$ as a reactive species (12) and thus $(CH_3)_3Ge\overline{C=C(CF_3)C(CF_3)_2}$ is the expected product. It is notable that some of the isopyrazole **2** is also produced in the reaction of $(CH_3)_3GeC\equiv CCF_3$ with the diazirine. This is surprising since the diazirine is not expected to produce isopyrazole products; however, the diazirine used was only 95% pure and one of the impurities may have been **1**.

The cyclopropenes **3**, **5**, and **6**, could have been formed either by elimination of nitrogen from the corresponding isopyrazoles or by the direct addition of $C(CF_3)_2$ to the C≡C bonds. Neither

Can. J. Chem. Downloaded from www.nrcresearchpress.com by 210.87.254.105 on 09/05/12
For personal use only.

TABLE 2
Nuclear magnetic resonance parameters of some cyclopropene derivatives

	^1H (δ)	^{19}F $\delta(F^a)$	^{19}F $\delta(F^b)$	$J_{F^a-F^b}$
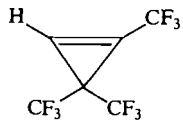	−7.02	62.0	67.65	1.2
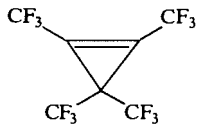		61.2	67.5	1.15
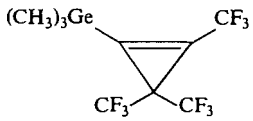	−0.35	62.0	66.9	1.2
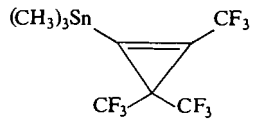	−0.30	62.55	66.9	1.25

possibility can be excluded with the present experimental results. However, in one experiment which we have been unable to repeat, the product from the reaction of **1** with the trifluoropropynylgermane was the isopyrazole (14) which suggests that this might be the intermediate.

The i.r. spectra of all the cyclopropenes show a weak high frequency C=C stretching band and a very similar pattern of bands in the C—F stretching region (Table 1). Although it is recognized that the C=C stretching vibration of cyclopropenes is not a very "pure" vibration (23) it is worth noting the frequency increase of this vibration as more electronegative groups are substituted in the vinylic positions. Thus we have for series $(CF_3)_2\overline{C—CX=CY}$: X = Y = CH_3, 1745 cm^{-1} (12); X = H, Y = CF_3, 1814 cm^{-1}; X = Y = CF_3, 1919 cm^{-1}; and for the series $F_2\overline{C—CX=CY}$: X = H, Y = CF_3, 1730 cm^{-1} (20); X = Y = CF_3, 1820 cm^{-1} (20); X = Y = F, 1945 cm^{-1} (21). This is probably due to coupling with the C—F or C—CF_3 stretching vibrations.

The n.m.r. parameters listed in Table 2 also show a high degree of internal consistency.

"Insertion" Reactions

Bis(trifluoromethyl)diazomethane (**1**) reacts easily with dimethylarsine and trimethyltin hydride (eqs. [7] and [8]). Nitrogen is eliminated and the $C(CF_3)_2$ group is inserted into the M—H bond giving the 1,1,1,3,3,3-hexafluoroisopropyl

[7] $(CH_3)_2AsH + (CF_3)_2CN_2 \rightarrow (CH_3)_2AsC(CF_3)_2H + N_2$
7

[8] $(CH_3)_3SnH + (CF_3)_2CN_2 \rightarrow (CH_3)_3SnC(CF_3)_2H + N_2$
8

derivatives. The ^1H n.m.r. spectra of both products show broad singlets due to the CH_3 groups and a septet ($J_{H-F} \approx 11$ c.p.s.) due to the isopropyl hydrogen atoms. The broadness of the CH_3 absorption is due to coupling with the fluorine atoms since the ^{19}F spectra show a doublet of septets for **7** ($J_{CH_3-F} \approx 1$ c.p.s.) and a doublet of multiplets (at least 7) ($J_{CH_3-F} \approx$

Can. J. Chem. Downloaded from www.nrcresearchpress.com by 210.87.254.105 on 09/05/12
For personal use only.

[9] 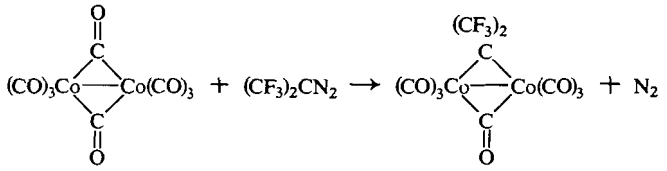

[10] 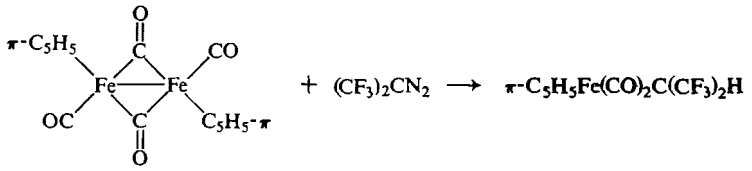

0.5 c.p.s.) for **8**. Similar insertion products have been obtained from the reaction of **1** with pentacarbonyl(hydrido)manganese (20°) and a platinum hydride (120°) (6). The low temperature reactions (20°) probably proceed via attack of a molecule of **1** to form an intermediate complex which then rearranges with elimination of nitrogen to give the final product (1). It is possible that the platinum and arsenic hydride reaction involves the free carbene (6). Compound **1** does not react with trimethylsilane (100°), trimethylgermane (135°), or trimethylgermanium bromide (110°) with insertion into the Si—H, Ge—H, or Ge—Br bonds. It does, however, insert into the Pd—Cl bond of $(C_6H_5CN)_2PdCl_2$ (7). The carbene CF_3CH, from CF_3CHN_2, inserted into the Si—H and C—H bonds of $(CH_3)_3SiH$ (3).

Dicobaltoctacarbonyl reacts with **1** at 20° as indicated by eq. [9] (6). This reaction can be regarded as an initial addition of **1** across the Co—Co bond followed by loss of CO and N_2 and formation of a new Co—Co bond. Therefore it was of interest to see what would happen if a compound such as tetramethyldiarsine which contains a very reactive As—As bond (24) were mixed with **1**. One of the main products of this facile reaction is the isopropyl derivative **7**, indicating that any intermediate adduct is not very stable. A similar reaction occurs when **1** is heated with $[\pi\text{-}C_5H_5Fe(CO)_2]_2$ (eq. [10]). In this case the additional hydrogen atom comes from the solvent (6). Hexamethyldigermane does not react easily or cleanly with **1** at 100°. The analogous ditin compound would be expected to be more easily cleaved.

We thank the National Research Council of Canada for financial assistance and Mr. Bruce Hodgson for performing some preliminary experiments. We are indebted to Dr. D. E. McGreer for many helpful discussions.

1. D. SEYFERTH. Chem. Rev. **55**, 1155 (1955).
2. A. PADWA and D. EASTMAN. J. Org. Chem. **34**, 2728 (1969).
3. J. H. ATHERTON and R. FIELDS. J. Chem. Soc. C, 2277 (1968).
4. K. A. W. KRAMER and A. N. WRIGHT. J. Chem. Soc. 3604 (1963).
5. T. SAEGUSA, S. TOMITA, and T. UESHIMA. J. Organometal. Chem. **10**, 360 (1967).
6. J. COOKE, W. R. CULLEN, M. GREEN, and F. G. A. STONE. Chem. Commun. 170 (1968); J. Chem. Soc. A, 1872 (1969).
7. J. ASHLEY-SMITH, J. CLEMENS, M. GREEN, and F. G. A. STONE. J. Organometal. Chem. **17**, P23 (1969).
8. M. F. LAPPERT and J. S. POLAND. Chem. Commun. 1061 (1969).
9. H. WERNER and J. H. RICHARDS. J. Amer. Chem. Soc. **90**, 4976 (1968).
10. M. M. BAGGA, P. E. BAIKIE, O. S. MILLS, and P. L. PAUSON. Chem. Commun. 1106 (1967).
11. D. M. GALE, W. J. MIDDLETON, and C. G. KRESPAN. J. Amer. Chem. Soc. **87**, 657 (1965).
12. D. M. GALE, W. J. MIDDLETON, and C. G. KRESPAN. J. Amer. Chem. Soc. **88**, 3617 (1966).
13. W. J. MIDDLETON, D. M. GALE, and C. G. KRESPAN. J. Amer. Chem. Soc. **90**, 6813 (1968).
14. W. R. CULLEN and M. C. WALDMAN. Inorg. Nucl. Chem. Lett. **4**, 205 (1968).
15. R. HUISGEN. Angew. Chem. Int. Ed. **2**, 565 (1963).
16. J. H. ATHERTON and R. FIELDS. J. Chem. Soc. C, 1507 (1968).
17. J. D. LONDON. *In* The chemistry of carbon compounds. Vol. IV[A]. E. H. RODD, *Editor*, Elsevier, Amsterdam, 1957. p. 208.
18. R. FUSEO. *In* Heterocyclic compounds: pyrazoles, pyrazolines, indazoles and condensed rings. R. H. Wiley, *Editor*, Interscience, New York, 1967. p. 1.
19. W. R. CULLEN and M. I. Bruce. Advan. Fluorine Chem. **4**, 79 (1969).
20. W. R. CULLEN and M. C. WALDMAN. Can. J. Chem. **47**, 3093 (1969).
21. P. B. SARGEANT and C. G. KRESPAN. J. Amer. Chem. Soc. **91**, 415 (1969).
22. W. R. CULLEN and M. C. WALDMAN. Unpublished results.
23. G. L. CLOSS. Advan. Alicyclic. Chem. **1**, 53 (1963).
24. W. R. CULLEN. Advan. Organometal. Chem. **4**, 145 (1966).

Can. J. Chem. Downloaded from www.nrcresearchpress.com by 210.87.254.105 on 09/05/12
For personal use only.

Can. J. Chem. Downloaded from www.nrcresearchpress.com by 210.87.254.5 on 09/05/12
For personal use only.

Biosynthesis of lycopodine from lysine and acetate. The pelletierine hypothesis[1]

M. Castillo, R. N. Gupta, D. B. MacLean, and Ian D. Spenser
Department of Chemistry, McMaster University, Hamilton, Ontario

Received January 28, 1970

The biosynthesis of lycopodine (**5**) was studied in intact plants and in excised shoots of the clubmoss *Lycopodium tristachyum* Pursh. Specific incorporation of label from lysine and from acetate was demonstrated by partial degradation. The observed distribution of activity was incompatible with a polyketide origin of lycopodine. The incorporation pattern is consistent with the hypothesis that lycopodine is a modified dimer of pelletierine (**4**), which, in turn, is derivable from lysine and acetate.

Canadian Journal of Chemistry, 48, 1893 (1970)

Introduction

Of the various structural types found amongst the Lycopodium alkaloids (2), it is the $C_{16}N_2$ skeletons (**1** and **2** respectively) of the lycodine–obscurine and of the cernuine groups which are most revealing from a biogenetic point of view. These structures lend themselves to visual dissection (dotted lines) into two halves whose skeleton, in turn, corresponds to that of the C_8N piperidine alkaloids, of which coniine (**3**) and pelletierine (**4**) are prominent examples.

If structural relations be a guide to biogenesis, the $C_{16}N_2$ skeletons of the lycodine–obscurine group and of the cernuine group of alkaloids might be thought to originate by dimerization of a suitably functionalized C_8N monomer.

The $C_{16}N$ Lycopodium alkaloids might, in turn, be derived from $C_{16}N_2$ intermediates by loss of nitrogen. A $C_{16}N_2$ intermediate of the lycodine–obscurine type (**1**) may give rise (1), by C—N cleavage, followed by extrusion of nitrogen and recyclization, to the lycopodine (**5**) skeleton, $C_{16}N$, from which other $C_{16}N$ skeletal types (e.g. annotinine (3) and serratinine (4)), might be derived by oxidative C—C cleavage and recyclization.

It is suggestive that in every one of the structural variants of the $C_{16}N$ group of alkaloids an oxygen function is present at C-5, the site of attachment of a nitrogen atom in the $C_{16}N_2$ skeleton of the lycodine–obscurine type.

If lycopodine (**5**) and the other $C_{16}N$ Lycopodium alkaloids were indeed derived from a $C_{16}N_2$ intermediate with a lycodine–obscurine skeleton, all the bases could be regarded as modified dimers of a precursor related in structure to

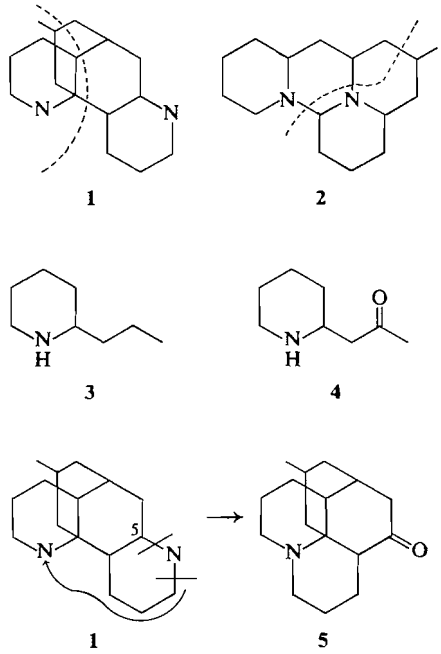

C_8N piperidine alkaloids such as coniine (**3**) or pelletierine (**4**).

The biosynthesis of these piperidine alkaloids has been studied during the past five years, and precursor–product relationships have been established. Even though the carbon–nitrogen skeletons of coniine and pelletierine are identical, the two alkaloids originate by entirely different routes.

Coniine (**3**) (5) and related hemlock alkaloids (5, 6) are of polyketide origin. This conclusion rests on the results of unambiguous degradation of a sample of coniine, isolated from hemlock plants which had been infused with 1-^{14}C-acetate. One-quarter of the activity of the intact alkaloid was located at each of C-2, -4, and -6 of the

[1]A preliminary report of part of this work has been published (1).

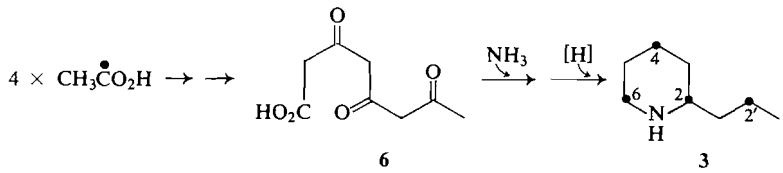

SCHEME 1

Biosynthesis of coniine

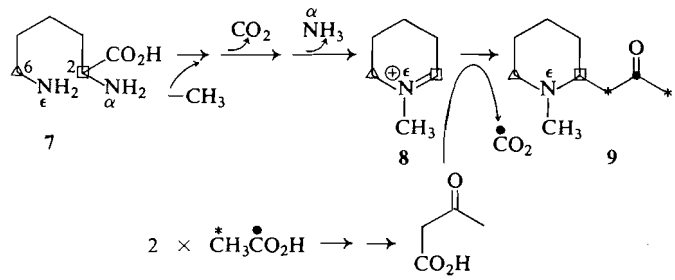

SCHEME 2

Biosynthesis of *N*-methylpelletierine

piperidine nucleus and C-2′ of the sidechain. The other four carbon atoms were unlabelled. This result suggests that a tetraacetyl chain (**6**) is an intermediate on the route between acetate and the C_8N skeleton of coniine (Scheme 1). Biosynthesis of a Lycopodium alkaloid by dimerization of a coniine type monomer, i.e. derivation from two tetraacetyl chains, as postulated by Conroy (7), would be predicted to lead to a characteristic incorporation pattern of label from 1-^{14}C- and 2-^{14}C-acetate (Scheme 3*a*).

The C_8N skeleton of *N*-methylpelletierine (**9**) is formed in an entirely different fashion. Its piperidine nucleus is derived from a C_5N chain which originates from lysine (**7**) in a nonsymmetrical manner (8, 9). A derivative (**8**) of Δ^1-piperideine (**14**) is a likely intermediate. The propanone sidechain is specifically derived from acetate (9–11) (Scheme 2). Biosynthesis of a Lycopodium alkaloid by dimerization of a pelletierine (**4**) type monomer would be predicted to lead to non-random entry of label from lysine, as well as to specific incorporation of activity from 1-^{14}C- and 2-^{14}C-acetate in a manner (Scheme 3*b*) entirely different from that demanded by the coniine–polyketide hypothesis.

In the present investigation of the biosynthesis of lycopodine it was our objective to test these alternative hypotheses.

Methods and Results

The species chosen for experiment was *Lycopodium tristachyum* Pursh. We are indebted to Dr. J. S. Pringle, Royal Botanical Gardens, Hamilton, Ontario, for the taxonomic identification of the species used in our experiments. A voucher specimen of the experimental plant is deposited in the herbarium of Algonquin Provincial Park, Ontario. It is unfortunate that an erroneous designation of the species used in our work was reported in our preliminary communication (1). Lycopodine (**5**) is the major alkaloid (12) and lycodine has now been found to be a minor component of *L. trystachyum*. This species, having a subterranean stem, is firmly rooted and therefore suitable for wick-feeding (13).

This method for the administration of labelled compounds to intact plants was employed in all but three of the present experiments. In the other experiments cuttings of the plant were kept in contact with tracer solution (14). These methods, outlined in the Experimental, were used to study the mode of incorporation of activity from specifically labelled samples of acetate, lysine, and cadaverine into lycopodine. A summary of these experiments is presented in Table 1.

The labelled samples of lycopodine obtained from individual feeding experiments were degraded, by reactions fully described in the Experi-

Can. J. Chem. Downloaded from www.nrcresearchpress.com by 210.87.254.5 on 09/05/12
For personal use only.

Can. J. Chem. Downloaded from www.nrcresearchpress.com by 210.87.254.5 on 09/05/12
For personal use only.

SCHEME 3*a*

If lycopodine were a coniine–polyketide type dimer:

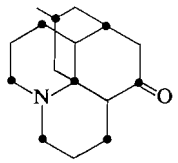

Each of eight carbon atoms derived from 1-^{14}C-acetate (●) should carry 12.5% of the activity of the intact alkaloid.

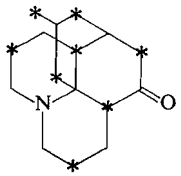

Each of eight carbon atoms derived from 2-^{14}C-acetate (*) should carry 12.5% of the activity of the intact alkaloid.

SCHEME 3*b*

If lycopodine were a pelletierine-type dimer:

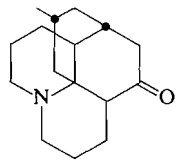

Each of two carbon atoms derived from 1-^{14}C-acetate (●) should carry 50% of the activity of the intact alkaloid.

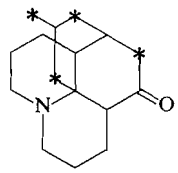

Each of four carbon atoms derived from 2-^{14}C-acetate (*) should carry 25% of the activity of the intact alkaloid.

SCHEME 3

Predicted incorporation patterns of 1-^{14}C-acetate (●) and 2-^{14}C-acetate (*) into lycopodine

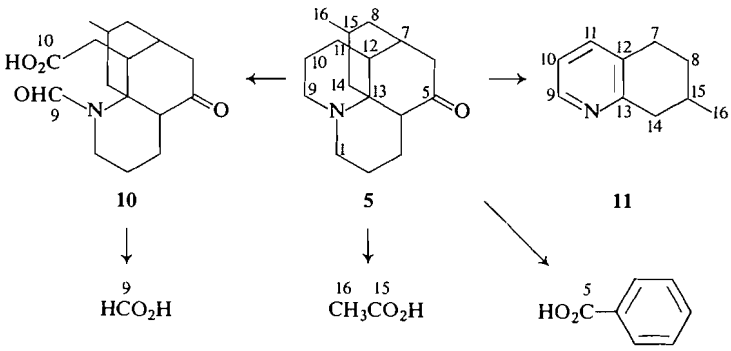

SCHEME 4

Degradation of lycopodine (numbers refer to carbon atoms of lycopodine)

mental, into the degradation products shown in Scheme 4. The specific activities of the degradation products are listed in Tables 2, 3, and 4 (indicated limits are standard deviation of the mean).

The samples of lycopodine, derived from 1-^{14}C-acetate (experiment 1) and from 3-^{14}C-acetoacetate (experiment 8), yielded acetic acid (corresponding to C-15, -16) which, within experimental error, contained one-half of the activity of the intact lycopodine. Benzoic acid (C-5) derived from 1-^{14}C-acetate lycopodine was inactive. Lycopodine samples obtained from 2-^{14}C-acetate (experiment 2) and from 4-^{14}C-β-hydroxybutyrate (experiment 9), gave acetic acid (C-15, -16) which contained a little less than one-quarter of the activity of the intact alkaloid (Table 2).

One-quarter of the activity of the lycopodine samples derived from 2-^{14}C-lysine (experiments 3 and 6), from 6-^{14}C-lysine (experiments 4 and 5), and from 1,5-^{14}C-cadaverine (experiment 11) was recovered in benzoic acid (C-5), and one-quarter in formic (C-9). One-half of the total activity was recovered in 7-methyl-5,6,7,8-tetrahydroquino-

Can. J. Chem. Downloaded from www.nrcresearchpress.com by 210.87.254.5 on 09/05/12
For personal use only.

TABLE 1

Incorporation of labelled compounds into lycopodine

Experiment no.	Compound administered	Nominal specific activity (mCi/mmole)	Mode of administration	Date	Weight of dry plant (g)	Yield (mg)	Lycopodine specific activity (counts min^{-1} $mmole^{-1}$) $\times 10^{-3}$
1	Sodium 1-^{14}C-acetate*	2.0	Wick	July 1966	160	81‖	6.12 ± 0.11
2	Sodium 2-^{14}C-acetate*	2.0	Wick	July 1966	450	350‖	1.84 ± 0.07
8	Sodium 3-^{14}C-acetoacetate*§	4.2	Wick	June 1968	35	95	16.9 ± 0.65
9	Sodium 4-^{14}C-DL-β-hydroxybutyrate†	8.6	Wick	August 1968	95	205	8.61 ± 0.22
3	2-^{14}C-DL-Lysine*	3.3	Wick	September 1967	300	540‖	2.88 ± 0.05
6	2-^{14}C-DL-Lysine*	3.3	Cuttings	September 1967	70	230	13.0 ± 0.29
4	6-^{14}C-DL-Lysine‡	9.2	Wick	September 1967	220	380	0.91 ± 0.03
5	6-^{14}C-DL-Lysine‡ 4,5-$^{3}H_2$-DL-Lysine*	9.2 2.9×10^3	Cuttings	September 1967	430 (Fresh weight)	350	12.2 ± 0.29 (^{14}C)
11	1,5-^{14}C-Cadaverine*	3.2	Cuttings	June 1969	36	100	728 ± 15

*New England Nuclear Corporation.
†Radiochemical Centre.
‡Commissariat a l'Energie Atomique, France.
§See Experimental.
‖Isolated by column chromatography (see Experimental).

Can. J. Chem. Downloaded from www.nrcresearchpress.com by 210.87.254.5 on 09/05/12
For personal use only.

TABLE 2

Incorporation of polyketide precursors into lycopodine

Precursor	Experiment no.	Product: Lycopodine SA*	Product: Lycopodine RSA†	Product: Acetic acid (as α-naphthylamide) (C-15, -16) SA*	Product: Acetic acid (as α-naphthylamide) (C-15, -16) RSA†	Predicted RSA† of acetic acid on the basis of: Polyketide hypotheses (c.f. Scheme 3*a*)	Predicted RSA† of acetic acid on the basis of: Pelletierine hypotheses (c.f. Scheme 3*b*)	Predicted RSA† of acetic acid on the basis of: Intact incorporation of C_3-unit
1-^{14}C-Acetate	1	6.12±0.11	100±2	2.89±0.10	47±2	12.5	50	
2-^{14}C-Acetate	2	1.84±0.07	100±4	0.39±0.02	21±1	12.5	25	
3-^{14}C-Acetoacetate	8	8.89±0.34‡	100±4	4.56±0.14	51±3			50
4-^{14}C-β-Hydroxybutyrate	9	8.61±0.22	100±3	1.75±0.06	20±1			50

*Specific activity (counts min^{-1} mmole^{-1}) × 10^{-3}.
†Relative specific activity: percent (lycopodine = 100).
‡Obtained by recrystallizing a mixture of 66 mg lycopodine, specific activity (16.89 ± 0.65) × 10^3 counts min^{-1} mmole^{-1}, and 50 mg carrier lycopodine.

TABLE 3

Incorporation of lysine into lycopodine

Precursor	2-^{14}C-DL-Lysine						6-^{14}C-DL-Lysine			
Experiment no.	3		6				4		5	
Product	SA*	RSA†	SA	RSA	SA	RSA	SA	RSA	SA	RSA
Lycopodine	2.88±0.05	100±2	13.01±0.29	100±2	2.87±0.08‡	100±3	0.91±0.03	100±3	12.20±0.29	100±2
Benzoic acid (C-5)	0.69±0.02	24±1	3.34±0.07	26±1	—		—		3.08±0.09	25±1
Formic acid (as α-naphthylamide) (C-9)	—		—		0.63±0.02	22±1	0.23±0.01	25±1	—	
7-Methyltetrahydroquinoline hydrochloride (C-7 to -16)	1.35±0.08	47±3	—		—		—		—	

*Specific activity (counts min^{-1} mmole^{-1}) × 10^{-3}.
†Relative specific activity: percent (lycopodine = 100).
‡Obtained by recrystallizing a mixture of 56 mg lycopodine, specific activity (13.01 ± 0.29) × 10^3 counts min^{-1} mmole^{-1}, and 197 mg carrier lycopodine.

TABLE 4

Incorporation of cadaverine into lycopodine. Experiment 11

	SA*	RSA†
Lycopodine	30.76±6.20‡	100±2
Benzoic acid (C-5)	7.73±0.38	25±1
Formic acid (as α-naphthylamide) (C-9)	7.55±0.21	24±1

*Specific activity (counts min^{-1} $mmole^{-1}$) × 10^{-3}.
†Relative specific activity: percent (lycopodine = 100).
‡Obtained by approximately 25-fold dilution of the lycopodine, specific activity (7.28 ± 0.15) × 10^5 counts min^{-1} $mmole^{-1}$, with inactive lycopodine.

line (**11**) (C-7 to -16) (Tables 3 and 4). Lycopodine, derived from a sample of 4,5-$^3H_2$, 6-^{14}C-lysine ($^3H/^{14}C$ 10.7 ± 0.2) (experiment 5) showed a ^3H:^{14}C ratio ($^3H/^{14}C$ 8.4 ± 0.1) which was 22% lower than that of the doubly labelled precursor.

Discussion

Incorporation of Polyketide Precursors

Biosynthesis of lycopodine, by the polyketide or by the pelletierine route, is expected to lead to incorporation of acetate into the alkaloid. The distribution pattern of radioactivity within the lycopodine samples derived from Lycopodium plants to which 1-^{14}C- and 2-^{14}C-acetate had been administered should be characteristic of the biosynthetic route (Scheme 3).

Kuhn–Roth oxidation of lycopodine yields acetic acid from C-15 and C-16. The fraction of the activity within the Kuhn–Roth acetate, obtained from the labelled lycopodine samples derived from 1-^{14}C- and 2-^{14}C-acetate, is diagnostic of the labelling pattern of these lycopodine samples, and hence indicative of the biosynthetic route whereby they originate.

According to the polyketide hypothesis the Kuhn–Roth acetic acid should carry one-eighth (12.5%) of the activity present in lycopodine, regardless of whether 1-^{14}C-acetate or 2-^{14}C-acetate were the precursors (Scheme 3*a*). The pelletierine hypothesis predicts an entirely different labelling pattern. The Kuhn–Roth acetate should contain one-half or one-quarter, respectively, of the activity of the labelled lycopodine, depending on whether the latter had been derived from 1-^{14}C-acetate or from 2-^{14}C-acetate (Scheme 3*b*). The results of experiments 1 and 2, presented in Table 2, are in agreement with the predictions of the pelletierine hypothesis. The Kuhn–Roth acetate from 1-^{14}C-acetate-derived lycopodine contained 47±2%, that from 2-^{14}C-acetate-derived lycopodine 21±1% of the activity of the intact alkaloid. Since the pelletierine hypothesis demands that the non-acetate derived carbon atoms of lycopodine originate from lysine, and since acetate can serve as a precursor of lysine (15), the slight deviation of the observed from the predicted values is not inconsistent with the hypothesis.

Additional experiments with 3-^{14}C-acetoacetate and 4-^{14}C-β-hydroxybutyrate (experiments 8 and 9) complement the results obtained with acetic acid. The pelletierine hypothesis demands the intact incorporation into lycopodine of two C_3-units derived by decarboxylation of acetoacetate (Scheme 2), and predicts entry of label from 3-^{14}C-acetoacetate exclusively and equally into C-7 and C-15, and of label from 4-^{14}C-acetoacetate (and therefore also from 4-^{14}C-β-hydroxybutyrate) exclusively and equally into C-8 and C-16 of lycopodine.

Whereas the predicted pattern of incorporation of activity from 3-^{14}C-acetoacetate is thus expected to be identical with that from 1-^{14}C-acetate and cannot therefore serve to establish intact incorporation of a C_3-unit, the predicted mode of incorporation of 4-^{14}C-β-hydroxybutyrate differs from that of 2-^{14}C-acetate and would thus be diagnostic for intact entry of a C_3-moiety (Table 2). The results of experiments 8 and 9 (Table 2) show that, as expected, the pattern of incorporation of activity from 3-^{14}C-acetoacetate (experiment 8) is identical with that of 1-^{14}C-acetate (experiment 1), but that contrary to expectation, the pattern of incorporation of 4-^{14}C-β-hydroxybutyrate (experiment 9) was identical with that of 2-^{14}C-acetate (experiment 2). This result indicates that direct incorporation of a C_3-unit derived from acetoacetate had not occurred, but that, prior to incorporation, the precursor had suffered degradation to acetate. Similar observations have been made in an investigation of the origin of the three-carbon sidechain of *N*-methylpelletierine (9).

Incorporation of Lysine and Cadaverine

The observed mode of incorporation of acetate into lycopodine is inconsistent with the polyketide route (Scheme 3*a*) but follows the predictions of the pelletierine pathway (Scheme 3*b*).

Can. J. Chem. Downloaded from www.nrcresearchpress.com by 210.87.254.5 on 09/05/12
For personal use only.

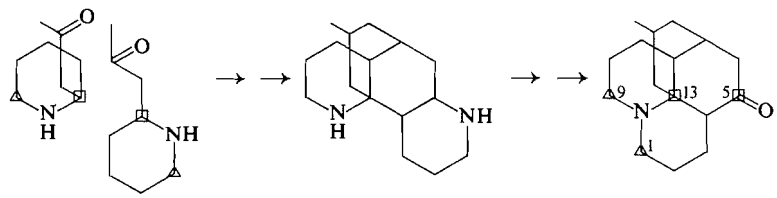

4 1 5

SCHEME 5

Expected incorporation pattern of 2-^{14}C-lysine (□) and 6-^{14}C-lysine (△) into lycopodine, as predicted by the pelletierine hypothesis

This pathway demands the incorporation of lysine into lycopodine (Scheme 5). The distribution, in lycopodine, of radioactivity from 2-^{14}C- and 6-^{14}C-lysine may be predicted on the basis of two premises: that entry of lysine into the pelletierine, serving as the lycopodine precursor, follows the pathway (Scheme 2) established for the incorporation of lysine into *N*-methylpelletierine in *Sedum sarmentosum* (9); and that, since lycopodine is regarded as a modified dimer of pelletierine, the two "halves" of lycopodine should be equally labelled. The hypothesis thus demands that one half of the activity of lycopodine derived from 2-^{14}C-lysine (□) should reside at C-5, and hence be recovered in benzoic acid, whereas C-9 (i.e. formic acid) from this lycopodine should be inactive. Conversely, one-half of the activity of lycopodine derived from 6-^{14}C-lysine (△) should be localized at C-9, and hence be recovered in formic acid, whereas C-5 (i.e. benzoic acid) from this sample should be inactive (c.f., Scheme 4).

The results of experiments 3–6 (Table 3) indicate that even though lysine is incorporated into lycopodine in a specific manner, the observed distribution of activity differs from that predicted: formic acid (i.e. C-9 of lycopodine) as well as benzoic acid (C-5 of lycopodine) contained, within experimental error, one-quarter of the activity of the intact alkaloid, regardless of whether 2-^{14}C-lysine (experiments 3 and 6) or 6-^{14}C-lysine (experiments 4 and 5) had been the precursor.

In each case the rest of the activity would then be expected to reside at C-1 (25%) and C-13 (25%). Neither of these carbon atoms could be extracted individually. A degradation product containing one of them, C-13, was obtained: lycopodine, derived from 2-^{14}C-lysine (experiment 3) yielded 7-methyl-5,6,7,8-tetrahydroquinoline (**11**) (C-7 to -16) (Scheme 4) which contained approximately one-half of the activity of the intact alkaloid (Table 3). It is thus demonstrated that a fragment which contains all carbon atoms predicted to arise from one lysine moiety (C-9 to -13) and none predicted to arise from the other (C-1 to -5), does indeed account for 50% of the activity of lycopodine. Since C-9 (formic acid) contains approximately 25% of the activity of the alkaloid (experiment 6), it is likely that the remaining 25% resides at C-13, the predicted site. The observed distribution of activity leads to the inference that two C_5-units comprising C-2 to -6 of lysine are, indeed, incorporated into lycopodine with equal efficiency, as predicted, but that contrary to prediction, these units are derived from lysine by way of a symmetrical intermediate such as cadaverine (1,5-diaminopentane) (**12**), and not in a non-symmetrical manner. This conclusion is substantiated by the observation that 1-^{14}C-cadaverine is incorporated into lycopodine[2] (experiment 11) and yields the expected pattern of radioactivity (Table 4).

The Pelletierine–dimer Hypothesis

The experimental results demonstrate that lysine and acetate serve as specific precursors of lycopodine. Even though the total activity of the molecule could not be accounted for in its entirety in terms of the individual radioactive sites and the evidence is therefore incomplete, it is significant that predictable positions of the alkaloid contained one-half (experiments 1 and 8)

[2]It is significant to note, in this context, that incorporation of radioactivity from cadaverine into lycopodine is approximately 100 times more efficient than incorporation of label from lysine (Table 1). It is also of interest that the specific activity of pipecolic acid ($\sim 2 \times 10^6$ counts min^{-1} $mmole^{-1}$), isolated from *L. tristachyum*, after administration of 2-^{14}C-lysine (experiment 3), was much higher than the specific activity of lycopodine (see Table 1) from the same plants.

Can. J. Chem. Downloaded from www.nrcresearchpress.com by 210.87.254.5 on 09/05/12
For personal use only.

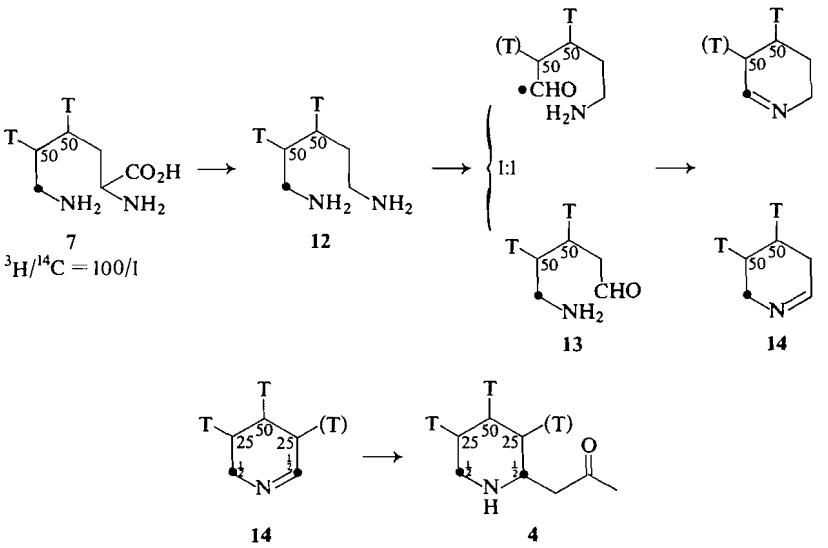

SCHEME 6

Predicted mode of incorporation of 4,5-$^3H_2$,6-^{14}C-lysine into lycopodine

or one-quarter (experiments 2–6, 9, 11) of the total activity, consistent with the view that lycopodine is derived from two identical precursor units.

The labelling pattern which is observed is that predicted by the hypothesis that lycopodine is generated from two pelletierine units whose side-chains are derived from acetate and whose piperidine nucleus arises from lysine via a symmetrical intermediate, cadaverine (**12**).

The observation that incorporation of 4,5-$^3H_2$,6-^{14}C-lysine ($^3H/^{14}C$ 10.7 ± 0.2) into lycopodine ($^3H/^{14}C$ 8.4 ± 0.1) (experiment 5) is accompanied by a loss of 22% tritium, relative to ^{14}C, is consistent with this hypothesis.

A possible mode of incorporation into lycopodine of this doubly labelled lysine is illustrated in Scheme 6. Since several of the reactions involving tritium loss could be accompanied by primary hydrogen–tritium isotope effects or stereochemical discrimination of hydrogen and tritium, only maximum tritium loss can be predicted. It is clear however that loss of tritium would occur only from C-5 of lysine and would be due entirely to the incorporation of the precursor via a symmetrical intermediate. Incorporation of this lysine in a non-symmetrical manner would not place a tritium atom at a sensitive position.

If pelletierine is indeed the monomer, whose dimerization leads to the Lycopodium alkaloids, several questions which cannot yet be answered arise. Of these, the most intriguing is why the mode of incorporation of lysine into this putative intermediate in *Lycopodium tristachyum* differs

Can. J. Chem. Downloaded from www.nrcresearchpress.com by 210.87.254.5 on 09/05/12
For personal use only.

Can. J. Chem. Downloaded from www.nrcresearchpress.com by 210.87.254.5 on 09/05/12
For personal use only.

from the manner in which lysine enters *N*-methylpelletierine in *Sedum sarmentosum*.

Direct evidence in support of the pelletierine hypothesis is being sought. Radioactive lycopodine has been isolated from *L. tristachyum* to which singly and multiply labelled samples of pelletierine (16) had been administered. Degradation of these samples is in progress.

Experimental

Administration of Labelled Compounds to Lycopodium tristachyum Pursh

Lycopodium tristachyum Pursh, ground cedar, a clubmoss whose creeping stem is buried 3–5 in. below ground, was found in the vicinity of Huntsville, Ontario, near Algonquin Provincial Park. Attempts to propagate the plant in the greenhouse were unsuccessful.

Labelled compounds were administered to intact plants (experiments 1–4, 8, 9) and to excised shoots (experiments 5, 6, and 11). The first experiments were carried out in the bush. A circular clump of the clubmoss, approximately 2 ft in diameter, was isolated by means of a narrow 1 ft deep trench. Cotton thread was inserted into approximately 20 shoots, and the ends of each thread were placed into a small glass receptacle. The labelled compound was dissolved in glass-distilled water (10 ml) and the solution was distributed among the receptacles, and was absorbed into the plant through the cotton wicks. After the original tracer solution had been absorbed the receptacles were repeatedly refilled with glass-distilled water. The plants were kept in contact with the tracer for 48 h, and were then collected. Shoots and subterranean stems were dried separately and the material was then taken to the laboratory for extraction and work-up.

This procedure, entertaining and enjoyable though it was when employed in the first experiments in midsummer 1966, was unsuitable for routine use, since it demanded experimental skills of a type not usually taught in Departments of Chemistry, as well as physical endurance and devotion to science far beyond the normal call of academic duty.

More recent wick feeding experiments were carried out in the greenhouse. Pieces of turf (approximately 3 ft × 2 ft × 8 in. deep), containing a clump of the clubmoss, were collected in the bush and transported to McMaster University in plywood boxes designed for the purpose. The wick-feeding experiments were carried out in the greenhouse on the following day.

In another feeding method (experiments 5, 6, and 11) shoots 2 to 3 in. in length from a 3 × 2 ft clump of clubmoss were cut and packed, cut surfaces downward, into three 100 ml beakers. The aqueous solution containing the radioactive tracer was divided among the beakers. Glass-distilled water (3 ml) was added to each beaker after 24 h, when most of the original solution had been absorbed, and the experiment was continued for a further 24 h.

A summary of the feeding experiments which were carried out is presented in Table 1. Tracers for experiments 1–6, 9, and 11 were commercial products (Table 1). Sodium 3-^{14}C-acetoacetate (experiment 8) was prepared by hydrolysis (c.f. ref. 16) of ethyl 3-^{14}C-acetoacetate (Radiochemical Centre). The nominal total activity administered in experiments 1–4, 6, 8, 9, and 11 was 0.1 mCi. The nominal total activity administered in experiment 5 was 0.1 mCi ^{14}C and 1 mCi ^{3}H.

Isolation and Degradation of Labelled Samples of Lycopodine

Labelled lycopodine was isolated, as outlined below, from each of the feeding experiments. Yield and specific activity of the samples are summarized in Table 1. The samples were partially degraded, by methods to be described below, to determine the sites of radioactivity. The results of these degradations are given in Tables 2, 3, and 4. Each labelled product was purified to constant activity.

Isolation of Lycopodine

Preliminary experiments indicated that the subterranean stems of *L. tristachyum* contained little alkaloid. Labelled lycopodine was obtained from the aerial parts of the plant.

Green shoots of *L. tristachyum* were dried and ground to a fine powder in a blendor (Osterizer Galaxie 10). The powder was moistened with 1 *M* ammonia (50–100 ml), and was continuously extracted with ether for 48 h. The ether solution was extracted with hydrochloric acid (0.5 *M*, 4 × 25 ml), the aqueous extract was washed with ether, and was then basified with 1 *M* ammonia. The alkaloids were extracted into ether (3 × 30 ml), the ether extract was dried (Na_2SO_4) and the solvent evaporated. The residue was extracted with warm hexane. The hexane extract was concentrated to dryness and the residue was sublimed at 110° and 1×10^{-3} mm, yielding a crystalline sublimate which consisted of lycopodine containing not more than 1–5% lycodine, as shown by gas–liquid chromatography (g.l.c.) (5% SE 30 on Chromosorb W, 1/8 in. × 4 ft, 200°, 15 ml per min of helium). The sublimate was dissolved in a little boiling hexane, and the solution was kept overnight. Lycopodine which crystallized (m.p. 115°) was sublimed at 90° and 1×10^{-3} mm. The purity of the product was checked by g.l.c. and by radiochromatography (Radiochromatogram Scanner, Model 7201, Packard Instrument Co.) of a thin-layer chromatogram (t.l.c.) (Silica Gel coated with 0.1 *N* sodium hydroxide, developed with chloroform/methanol 1:1, R_f 0.48).

Even though g.l.c. indicated a single component, in several instances the product required further purification to remove a radiochemical contaminant whose presence was detected by t.l.c. and radioscanning.

Lycopodine was dissolved in ether and the solution was mixed with an ether solution of perchloric acid. Solvent was evaporated, and the lycopodine perchlorate so obtained was recrystallized from hot methanol. Melting point 276–278° (reported melting point 279° (12)).

Several variations of the above procedure were employed in early experiments. In experiment 5 the shoots of the plant were homogenized in methanol, the methanol solution was filtered and concentrated, the residue was extracted with hydrochloric acid (1 *M*, 3 ×, 10 ml), and the acid solution was basified with ammonia. The

Can. J. Chem. Downloaded from www.nrcresearchpress.com by 210.87.254.5 on 09/05/12
For personal use only.

alkaloidal fraction was then extracted into ether and worked-up as already described.

In experiments 1–3 the basic fraction was separated into its components by column chromatography on alumina. Lycopodine and lycodine were separated from the other basic components by elution with benzene.

Degradation of Lycopodine

Carbon-5 as Benzoic Acid (cf. Ref. 17)

Lycopodine (100 mg) dissolved in dry ether (50 ml) was added dropwise to a solution of phenyl lithium (1.9 *M*, 5.8 ml) in ether, and the mixture was refluxed 4 h in an atmosphere of nitrogen. The solution was cooled and poured into concentrated hydrochloric acid (5 ml) to which crushed ice (10 g) had been added. The ether layer was discarded, the aqueous layer was washed with ether (2 × 30 ml), and was basified with ammonia. The product was extracted into ether (5 × 30 ml), the ether solution was dried (Na_2SO_4), the solvent was evaporated and the residue (105 mg) was recrystallized from *n*-hexane, yielding phenyldihydrolycopodine, melting at 150–153° (reported melting point 154–155° (17)). The g.l.c. (5% SE 30 on Chromosorb W, 200°, 1/8 in. × 4 ft, 15 ml per min of helium) revealed the presence of traces of lycopodine. The product was oxidized without final purification.

Finely ground potassium permanganate (500 mg) was added in small portions to a suspension of phenyldihydrolycopodine (80 mg) in hot water (25 ml). The mixture was refluxed 8 h with vigorous stirring, and was then acidified with 0.5 *M* hydrochloric acid and decolorized by addition of sodium bisulfite. The solution was extracted with ether (3 × 40 ml), the extract dried (Na_2SO_4), solvent evaporated, and the residue sublimed to yield benzoic acid (14–20 mg, 40–50% yield), melting at 119–120°.

Carbon-9 as Formic Acid (cf. Ref. 18)[3]

A solution containing lycopodine (250 mg) and oxalic acid (125 mg) in water (25 ml) was cooled in an ice bath. Finely powdered potassium permanganate (525 mg) was added in small portions over 2 h with vigorous stirring. After addition was complete, stirring of the solution was continued for 4 h at 0° and for 2 h at room temperature. Sulfur dioxide was passed through the suspension, resulting in a clear yellow solution. The solution was extracted with chloroform (6 × 20 ml). To remove acidic products, the chloroform layer was extracted with 2 *M* ammonia (2 × 30 ml), the ammoniacal extract was acidified with dilute hydrochloric acid, and extracted with chloroform. The chloroform solution was evaporated and the residue sublimed to yield the *N*-formylamino acid (**10**) (70–78 mg; 24–30% yield).

The *N*-formylamino acid (**10**) (70 mg) was converted into the methyl ester by reaction with diazomethane. After sublimation at 140° and 1×10^{-3} mm the methyl ester (56 mg) melted at 114–116° (reported m.p. 117° (18)).

The methyl ester (55 mg) was dissolved in 1 *M* sulfuric acid (10 ml) and the mixture was refluxed 2 h. Steam was then passed through the reaction mixture until 50 ml of the distillate, containing volatile acids, had been collected. The distillate was neutralized with 0.1 *M* sodium hydroxide (~ 1 ml), and the solution was evaporated to dryness. The residue was dissolved in water (2 ml) containing α-naphthylamine hydrochloride (20 mg) and 1-ethyl-3-(3-dimethylaminopropyl)-carbodiimide hydrochloride (50 mg). *N*-Formyl-α-naphthylamide precipitated after a few minutes. After sublimation at 120° and 1×10^{-3} mm, recrystallization from benzene, and resublimation, the product melted at 137–138° (reported melting point 139° (19)), and was identical (mass spectrum, melting point, mixture melting point) with an authentic specimen.

Carbons-15 and -16 as Acetic Acid

A solution of chromic acid (2 g) in water (3 ml) was added to a solution of lycopodine (100 mg) in 2 *M* sulfuric acid (5 ml). The mixture was refluxed for 2 h. Steam was then passed through the mixture until 50 ml distillate had been collected. The distillate was neutralized with 0.1 *M* sodium hydroxide (~ 2.5 ml), the solution was evaporated, and the sodium acetate so obtained converted into acetyl-α-naphthylamide (50–60% yield) (20).

Carbons-7 to -16 as (+)-7-Methyl-5,6,7,8-tetrahydroquinoline

An intimate mixture of lycopodine (250 mg) and zinc powder (8 g) was placed into a Carius tube (15 × 1 cm) and more zinc powder (8 g) was added. The tube was evacuated and sealed, and was heated at 290–310° for 24 h. A yellow liquid condensed in the cold end of the tube which protruded from the furnace. Gas–liquid chromatography of the reaction product showed it to be a mixture of 7-methylquinoline, 7-methyl-5,6,7,8-tetrahydroquinoline (**11**), a 7-methyldecahydroquinoline, an unidentified dimethylquinoline (presumably 5,7-dimethylquinoline), and several other unidentified products. The relative amounts of the different components varied from run to run. The g.l.c. (20% Carbowax 20M on Chromosorb W coated with 5% KOH, 3/8 in. × 10 ft, 175°, 15 ml per min of helium) gave 7-methyl-5,6,7,8-tetrahydroquinoline with a retention time of 51 min. This oily product (α_D + 18°, in ether) was further purified by conversion to the hydrochloride, m.p. 153–156° after high vacuum sublimation. The mass spectrum of a sample of the free base was identical with that of a synthetic specimen of (±)-7-methyl-5,6,7,8-tetrahydroquinoline (21).

Determination of Radioactivity

Radioactivity was assayed on samples of finite thickness on aluminum planchets with a gas-flow system (Model 4342 Nuclear Chicago). The usual corrections for background and self-absorption were applied. For plating, a 1% solution of collodion in dimethylformamide was used as the solvent. In the case of benzoic acid, a drop of a 5% solution of sodium hydroxide in 50% aqueous methanol was added to prevent loss by evaporation.

The $^3H/^{14}C$-ratios were measured by liquid scintillation counting (Mark 1 liquid scintillation computer, Model 6860, Nuclear Chicago). Activity due to ^3H and ^{14}C was determined simultaneously, by external standardization counting with ^{133}Ba. Samples were dissolved in methanol or methanol–water and the solution was dispersed in a solution of Liquifluor (Nuclear Chicago) diluted 25 times with toluene. Duplicate samples of each compound were

[3]We are indebted to Dr. W. A. Ayer for informing us of this work.

counted under comparable conditions of quenching. For highly quenched samples the confidence limits of the quench correction curves were ±5%.

Confidence limits shown in the tables are standard deviation of the mean.

This work was supported by the National Research Council of Canada.

1. R. N. GUPTA, M. CASTILLO, D. B. MACLEAN, I. D. SPENSER, and J. T. WROBEL. J. Amer. Chem. Soc. **90**, 1360 (1968).
2. D. B. MACLEAN. *In* The alkaloids. Vol. 10. *Edited by* R. H. F. Manske. Academic Press Inc., New York, 1968. p. 305.
3. K. WIESNER. Fortschr. Chem. Org. Naturst. **20**, 271 (1962).
4. Y. INUBUSHI, H. ISHII, B. YASUI, and T. HARAYAMA. Tetrahedron Lett. 1551 (1966); Chem. Pharm. Bull. Tokyo, **16**, 101 (1968).
5. E. LEETE. J. Amer. Chem. Soc. **85**, 3523 (1963); **86**, 2509 (1964).
6. E. LEETE and N. ADITYACHAUDHURY. Phytochem. **6**, 219 (1967).
7. H. CONROY. Tetrahedron Lett. No. 10, 34 (1960).
8. R. N. GUPTA and I. D. SPENSER. Chem. Commun. 85 (1968).
9. R. N. GUPTA and I. D. SPENSER. Phytochem. **8**, 1937 (1969).
10. D. G. O'DONOVAN and M. F. KEOGH. Tetrahedron Lett. 265 (1968).
11. H. W. LIEBISCH, N. MAREKOV, and H. R. SCHÜTTE. Z. Naturforsch. **23**B, 1116 (1968).
12. L. MARION and R. H. F. MANSKE. Can. J. Res. **22**B, 1 (1944).
13. J. R. GEAR and I. D. SPENSER. Can. J. Chem. **41**, 783 (1963).
14. R. N. GUPTA and I. D. SPENSER. Can. J. Chem. **45**, 1275 (1967).
15. A. MEISTER. Biochemistry of the amino acids. 2nd Ed., Vol. 2. Academic Press Inc., New York, 1965. Chapter 6P.
16. R. N. GUPTA and I. D. SPENSER. Can. J. Chem. **47**, 445 (1969).
17. D. B. MACLEAN, R. H. F. MANSKE, and L. MARION. Can. J. Res. **28**B, 460 (1950).
18. D. A. LAW. Ph.D. Thesis, University of Alberta, Edmonton, Alberta. 1963.
19. A. I. VOGEL. A textbook of practical organic chemistry. 3rd Ed. Longmans, Green and Co. Ltd., London, 1956. p. 656.
20. E. LEETE, H. GREGORY, and E. G. GROS. J. Amer. Chem. Soc. **87**, 3475 (1965).
21. C. K. YU and D. B. MACLEAN. Unpublished results.

Can. J. Chem. Downloaded from www.nrcresearchpress.com by 210.87.254.5 on 09/05/12
For personal use only.

Can. J. Chem. Downloaded from www.nrcresearchpress.com by 210.87.254.40 on 09/05/12
For personal use only.

Alkali metal adducts of benzophenone azine. I. The sodium and potassium adducts

E. J. MacPherson and James G. Smith
Department of Chemistry, University of Waterloo, Waterloo, Ontario

Received September 29, 1969

Contrary to previous reports, the reaction between benzophenone azine and sodium or potassium produces an adduct containing 2 g-atoms of alkali metal per mole of azine. The chemical reactions of this dianion have been examined and a 1,2-dianionic structure is most consistent with its chemical behavior.

Treatment of the adduct with methyl iodide, 1,3-dibromopropane, or 1,4-dibromobutane results in alkylation on the benzylic carbon and adjacent nitrogen. However, regeneration of benzophenone azine occurred with methylene iodide, 1,2-dibromoethane, and benzyl chloride.

With ethyl chloroformate, reaction occurred at the carbanionic center to form an intermediate unstable anion. This anion could be protonated or alkylated but if allowed to stand, decomposed to diphenyldiazomethane and the anion of ethyl diphenylacetate.

Reaction of the benzophenone azine dianion with methyl benzoate is quite complicated and leads to substantial amounts of benzophenone azine being regenerated by electron transfer. That portion of the dianion which is not converted to azine reacts with methyl benzoate to produce the anion of α-benzamido-α,α-diphenylacetophenone.

The possibility that an adduct of *N*-benzoyl benzophenone imine is an intermediate in this last reaction is examined and rejected.

Canadian Journal of Chemistry, **48**, 1904 (1970)

During their original extensive survey of alkali metal addition reactions, Schlenk and Bergmann (1) reported that benzophenone azine (**1**) reacted with sodium in diethyl ether (DEE) to give the tetrasodio derivative. The nature of the adduct was based on the isolation of a compound identified as *N*,*N*′-dibenzhydrylhydrazine after treatment of the adduct with water.

A repetition of this study was felt worthwhile since the formation of a molecule with four anionic centers is quite unusual. In addition, our studies of the reaction of azomethines with alkali metals, (2–6) have not yet included a molecule with two such groups in conjugation. Our observations to date are incompatible with the earlier report. Indeed, with sodium or potassium metal in tetrahydrofuran (THF) or in DEE, **1** clearly forms a dianion, **2**.

Protonation and Alkylation of the Dianion

Titration of a solution of the adduct at various time intervals during its formation demonstrated that the reaction in either THF or DEE was quite rapid and formation of the adduct was essentially complete after 4 h (Scheme 1). At this point the adduct contained 2 g-atoms of alkali metal per mole of azine and no further uptake of sodium was detected even when the reaction was allowed to run for 24 h.

While a dianion was evidently formed, several possibilities existed for its structure. Since our interests were in the synthetic utility of these alkali metal compounds, these structural possibilities were investigated by means of the reactions of the adduct.

Hydrolysis of a solution of the dianion produced a material which was identified as *N*-benzhydryl benzophenone hydrazone (**3**) (Scheme 1). This identification was based on the nuclear magnetic resonance (n.m.r.) and infrared (i.r.) spectra, upon its analysis, and upon the similarity in its melting point behavior to that described by Cohen and Wang for **3** (7). However, the melting point of this compound also resembled that of the hydrolysis product reported by Schlenk and Bergmann (1) who identified it as *N*,*N*′-dibenzhydrylhydrazine.

The rather unsatisfactory physical properties of this product led to alkylation of **2** with various alkyl halides. Two equivalents of methyl iodide reacted with the dianion (**2**) in either THF or DEE to produce a product showing two nonequivalent methyl groups in the n.m.r. spectrum. This, together with the analysis, suggested that alkylation had occurred both on the benzylic carbon and on the nitrogen. However, the i.r. spectrum showed no absorption band attributable to an azomethine group. Evidence for the presence of this last functional group was obtained through acid hydrolysis of the product in the presence of 2,4-dinitrophenylhydrazine when benzophenone 2,4-dinitrophenylhydrazone was

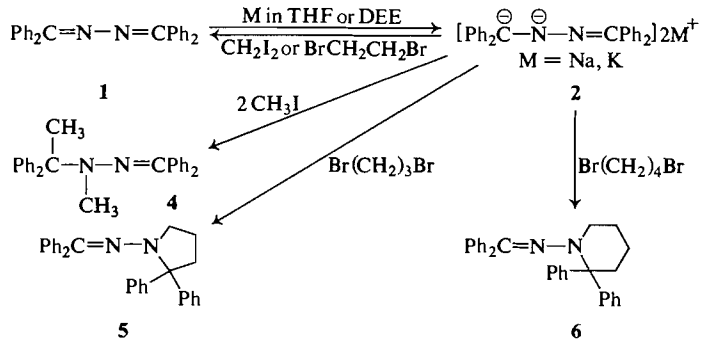

SCHEME 1

Alkylation of the dianion of benzophenone azine

obtained. Thus, the structure of the methylation product is *N*-(1,1-diphenylethyl)-*N*-methyl benzophenone hydrazone (**4**).

Treatment of THF or DEE solutions of **2** with 1,3-dibromopropane or THF solutions of **2** with 1,4-dibromobutane gave the analogous products *N*-(2,2-diphenyl-1-pyrrolidinyl) benzophenone imine (**5**) and *N*-(2,2-diphenyl-1-piperidyl) benzophenone imine (**6**) respectively (Scheme 1). The structures of these alkylation products were consistent with their spectral properties, their analyses and with the formation of benzophenone on acid hydrolysis.

An interesting feature of these alkylation products is their tendency to form different crystalline modifications. Both compound **4** and compound **5** exhibited this behavior and in both cases one crystalline form was yellow and the other white. Each such pair of polymorphs showed distinct differences in their i.r. spectra as solids but gave identical spectra as solutions. As expected, the melting point of a mixture of the two crystalline forms gave only the melting point of the more stable polymorph.

The ultraviolet (u.v.) spectra of these three compounds **4**, **5**, and **6** are characterized by three bands. Two of these bands were found at the same wavelength, 233–234 and 253–254 mμ, but the third was variable both in wavelength and extinction coefficient and is tabulated on Table 1 together with other compounds of interest.

In the reference compound, *N*-benzhydryl benzophenone hydrazone, the band appears at 303 mμ as a shoulder on another band at 288 mμ. When additional alkyl groups are attached to the amino nitrogen, the band shifts to longer wavelengths of 325–350 mμ. Presumably this band is

TABLE 1

Ultraviolet spectra of various hydrazones

Compound	λmμ*	ε
$Ph_2C{=}N{-}NH{-}CHPh_2$	288,303	14 000
$Ph_2C{=}N{-}N(CH_3){-}CPh_2$	332	6 000
$Ph_2C{=}N{-}N(C_4H_8){-}CPh_2$	325	11 500
$Ph_2C{=}N{-}N(C_5H_{10}){-}CPh_2$	346	3 400
$Ph_2C{=}N{-}NH{-}CPh_2(CO_2Et)$	293	15 600
$Ph_2C{=}N{-}N(CH_3){-}CPh_2(CO_2Et)$	331	4 900

*Measured in ethanol.

due to the $n \rightarrow \pi^*$ transitions of the unshared electron pair on the azomethine nitrogen:

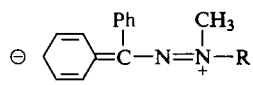

Electron donating alkyl groups would stabilize contributing forms such as the one shown with the result that the absorption band is shifted to longer wavelengths.

It must be concluded from these reactions, which are summarized in Scheme 1, that the dianion of benzophenone azine behaves chemically as if it had structure **2**, i.e. the 1,2-dianion.

It is attractive to rationalize the observed

Can. J. Chem. Downloaded from www.nrcresearchpress.com by 210.87.254.40 on 09/05/12
For personal use only.

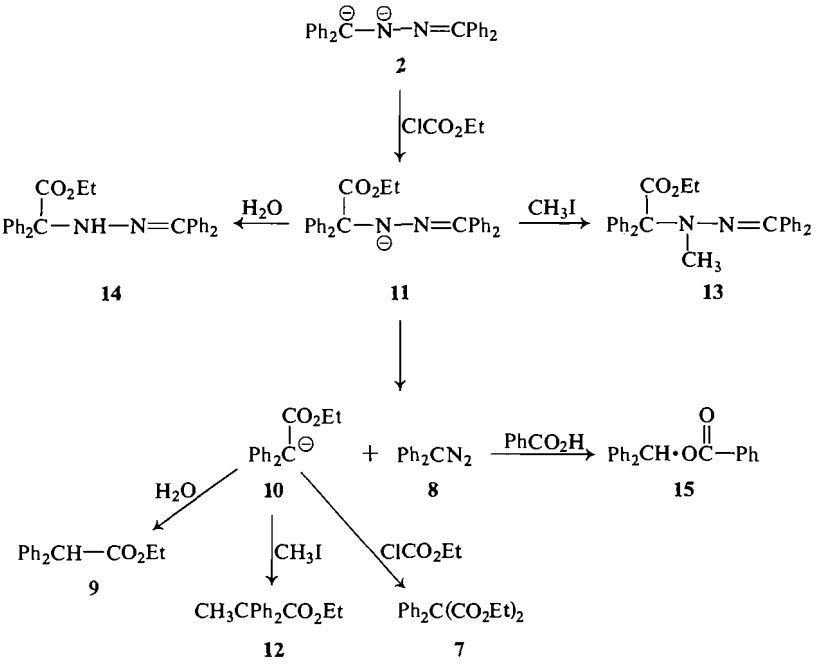

SCHEME 2

Reactions involving ethyl chloroformate

stability of this dianion towards an excess of alkali metal by considering resonance hybridization of the anionic center and the adjacent azomethine group.

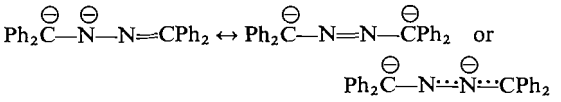

If this is the case, alkylation of the "allylic" anionic portion of the dianion **2** occurs predominantly on the nitrogen. Attempts were made to induce bis-carbon alkylation of the dianion (a possibility suggested by the resonance hybrid structure) using methylene iodide or 1,2-dibromoethane. Only regeneration of the benzophenone azine was observed and, indeed, a similar behavior occurred with benzyl chloride. Such a behavior is reminiscent of other vicinal dianions, e.g. the vicinal dianion of stilbene (13).

Since no significant difference was observed between the dipotassio and the disodio adducts, subsequent studies were confined to the disodio adduct.

Reaction with Ethyl Chloroformate

As an extension of the alkylation reactions, the behavior of the dianion **2** towards ethyl chloroformate was examined. The gross aspects of this reaction have been described in a preliminary publication (8). When 2 equ of ethyl chloroformate were added to a solution of the dianion in THF, diethyl diphenylmalonate (**7**) and diphenyldiazomethane (**8**) were obtained. Compound **7** was identified by mixture melting point with an authentic sample while **8** was converted to benzhydryl benzoate **15** (9, 10) on treatment with benzoic acid and identified by comparison with an authentic sample.

Seemingly, some decomposition of the dianion or a partially reacted species occurred during the course of the reaction. In order to elucidate the details of this decomposition, 1 equ of ethyl chloroformate was used followed by an aqueous work-up after 24 h. Ethyl α,α-diphenylacetate (**9**) and **8**, were obtained. Compound **9** was identified by comparison to an authentic sample and by hydrolysis to diphenylacetic acid.

The formation of **7** and **9** from these two reactions implicated the anion **10** as an intermediate. The decomposition appeared to occur (see Scheme 2) through the initial formation of

Can. J. Chem. Downloaded from www.nrcresearchpress.com by 210.87.254.40 on 09/05/12
For personal use only.

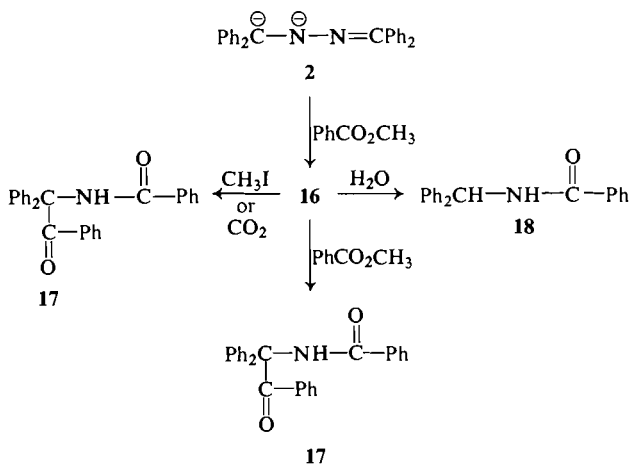

SCHEME 3

Reaction with methyl benzoate

anion **11** followed by its decomposition to anion **10** and diphenyldiazomethane (**8**). Additional evidence for the existence of the anion **10** was obtained by treatment of the reaction product of the dianion **2** and 1 mole of ethyl chloroformate (reaction time 24 h) with one mole of methyl iodide. From the reaction products, ethyl α,α-diphenylpropionate (**12**) was isolated and identified by hydrolysis to and comparison with an authentic sample of the acid.

The decomposition of the half reacted dianion **2** i.e. anion **11**, did not appear to be instantaneous. On the contrary, **11** had a definite temporal existence. This was demonstrated by decreasing the time interval between the addition of the second reagent (methyl iodide or water) and the addition of the first mole of ethyl chloroformate. Under these conditions the intermediate anion, **11**, was captured as its alkylated product *N*-methyl-*N*-carbethoxydiphenylmethyl benzophenone hydrazone (**13**) or its protonated product *N*-carbethoxydiphenylmethyl benzophenone hydrazone (**14**). The structure of these two products was established through their spectral data, chemical analyses, and the formation of benzophenone on acid hydrolysis.

It is puzzling that the intermediate monoanion, **11**, which reacts with methyl iodide without difficulty does not react with ethyl chloroformate when 2 moles of this reagent are added. Possibly, the anionic center on **11** is somewhat sterically hindered by the groups attached to it. While the hindrance is not sufficient to prevent a nucleophilic substitution of methyl iodide, it is sufficient to slow its reaction with the second mole of ethyl chloroformate. Consequently, fragmentation of the anion **11** to diphenyldiazomethane and anion **10** is observed.

Reaction with Methyl Benzoate

The reaction of the benzophenone azine dianion **2** with methyl benzoate proved to be the most difficult reaction to understand. It was investigated since studies (5) of the related dianion from benzophenone anil indicated that only the anionic center on the nitrogen atom should react. Our observations are summarized in Scheme 3.

From the reaction of the dianion **2** with 2 moles of methyl benzoate, considerable benzophenone azine was formed and some methyl benzoate remained unreacted. An additional product was isolated and identified as α-benzamido-α,α-diphenylacetophenone (**17**). This identification was based on the chemical analysis and spectral properties of the compound. Treatment of the dianion with 1 mole of methyl benzoate produced *N*-benzhydrylbenzamide (**18**) identified by comparison with an authentic sample.

These results implied that the reaction of 1 mole of methyl benzoate with **2** resulted in fragmentation of the product to some intermediate, **16**. This intermediate then reacted with

Can. J. Chem. Downloaded from www.nrcresearchpress.com by 210.87.254.40 on 09/05/12
For personal use only.

Can. J. Chem. Downloaded from www.nrcresearchpress.com by 210.87.254.40 on 09/05/12
For personal use only.

additional methyl benzoate to give **17** or, in the absence of excess benzoate, with the water added during isolation to give **18**. At the time, the most logical structure for **16** appeared to be **16***a*.

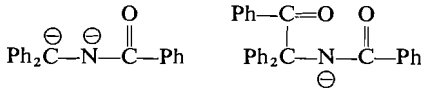

16*a* **16***b*

Two experiments were designed to test this hypothesis, both based on the formation of **16** with 1 mole of methyl benzoate followed by its reaction with either carbon dioxide or methyl iodide. From both these reactions, the only product besides benzophenone azine was the dibenzoyl compound, **17**. These experiments established that the structure of **16** could not be **16***a* but must be **16***b*.

The anion, **16***b*, was formed whether 1 or 2 moles of methyl benzoate were used. The formation of the monobenzoyl product **18** from the dibenzoyl anion **16***b* was shown by a control experiment to be due to hydrolysis of the dibenzoyl product **17** during the aqueous work-up (eq. [1]). In neutral or acidic media, this hydrolysis was not observed at room temperature.

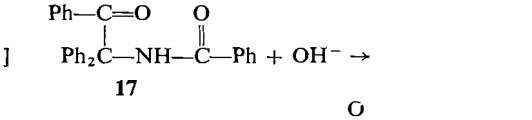

[1] **17** **18**

However, in the presence of sodium hydroxide (formed from the sodium methoxide present among the reaction products) hydrolysis occurred during the isolation. The presence of the dibenzoyl product **17** in the reaction products from 1 mole of methyl benzoate was readily demonstrated by treating the reaction mixture with dilute aqueous acid rather than water, thereby neutralizing the base and so preventing the hydrolysis of the dibenzoyl product.

Methyl iodide, carbon dioxide, and excess methyl benzoate all served to reduce the basicity of the reaction mixture after hydrolysis. Methyl iodide undoubtedly alkylated the methoxide ion present in the reaction mixture and prevented formation of hydroxide on hydrolysis. The action of carbon dioxide needs no comment while methyl benzoate appeared to reduce the basicity by forming benzoate ion on addition of water.

The reaction with carbon dioxide afforded a small yield of an alkali soluble product which was identified as *N*-benzoyl-α,α-diphenylglycine (**20**) (11) by decarboxylation to **18**. Its formation suggested that the reaction product from methyl benzoate and the dianion, **2**, was an equilibrating system of the anions of both the monobenzoyl and dibenzoyl products (eq. [2]) with the equilibrium favoring the mono anion **16***b*.

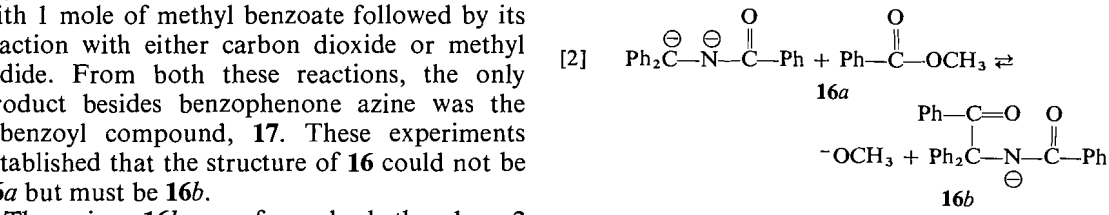

[2] **16***a* **16***b*

Two reaction paths seemed possible for the formation of the dibenzoyl anion, **16***b*, from the dianion of benzophenone azine, **2**. Both are shown in Scheme 4 and both involve the transfer of electrons from the dianion **2** to a recipient molecule (indicated by transfer) with regeneration of benzophenone azine. This transfer must be occurring since at least half the starting material is recovered from any of these reactions.

In both reaction paths, non-anionic intermediates are suggested: in path A, a tetrabenzoyl derivative; in path B, *N*-benzoyl benzophenone imine. While path A could not be tested directly, path B could and was. *N*-Benzoyl benzophenone imine (**19**) was synthesized (12) and found to form an adduct with sodium in tetrahydrofuran. However, the adduct contained 1.5 atoms of sodium per mole rather than 2 and in its reactions with water and methyl benzoate, the *N*-benzoyl benzophenone imine adduct showed a different behavior than that required for the intermediate.

Treatment of the adduct of *N*-benzoyl benzophenone imine with water did, indeed, produce the mono-benzoyl product, **18**, *N*-benzhydryl benzamide. However, accompanying this product was a second amide which at no time appeared among the reaction products of benzophenone azine dianion. Methyl benzoate and the sodium adduct of *N*-benzoyl benzophenone imine produced a rather complex reaction product which contained both the mono benzoyl compound **18** and the dibenzoyl derivative **17** in a ratio of

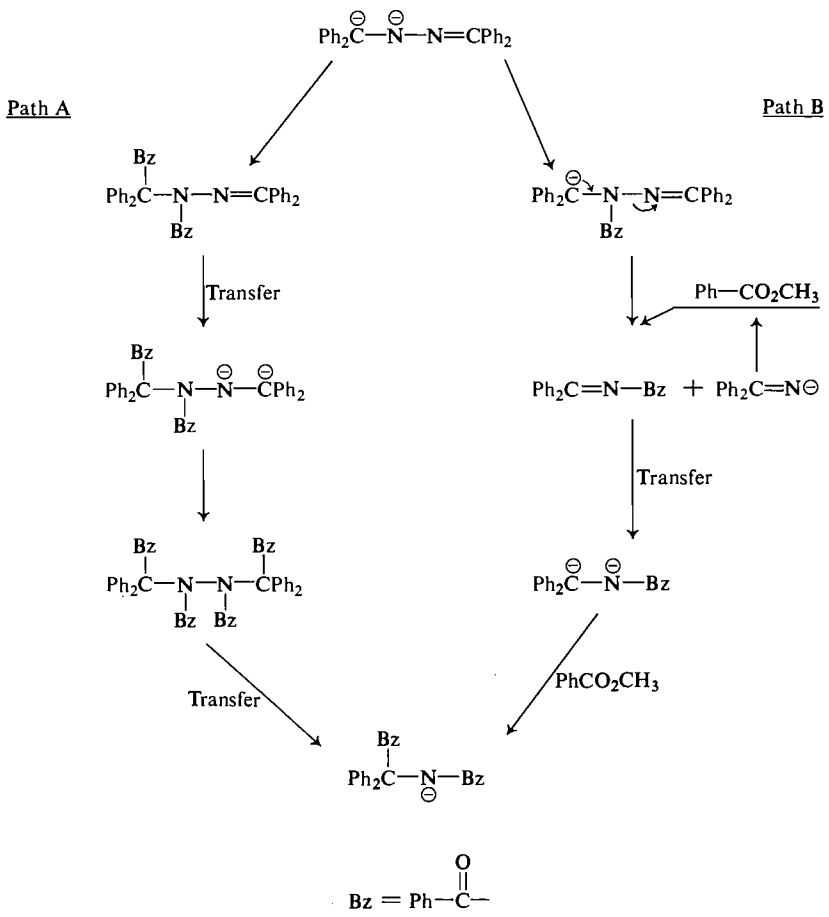

SCHEME 4

approximately 2:1, in addition to other unidentified products. It must be concluded that *N*-benzoyl benzophenone imine **19**, (i.e. path B) is an unlikely intermediate in the reaction of the dianion with methyl benzoate.

Both reaction paths are unsatisfactory in one respect. They predict that the reaction mixture from 1 mole of the dianion and 1 mole of methyl benzoate (followed by a water quench) should contain a half mole of benzophenone azine **1**, a half mole of the dibenzoyl compound, **17**, and a quarter mole of the reduction product, **3**. This last compound was not detected but benzophenone azine was often recovered in greater than the half mole quantity predicted. Two explanations are possible. First, there is still the possibility of an additional transfer reaction between the dianion and a carbonyl group on the excess methyl benzoate to regenerate the benzophenone azine, **1**. Second, even in the alkylation reactions, some benzophenone azine was recovered in 10–25% yield due to the inadvertent admittance of oxygen into the system during handling of the reagents. Either (or both) of these reasons may account for our inability to detect any **3**, among the reaction products.

Experimental

The melting points are uncorrected and were determined in an open capillary using a Mel-temp melting point apparatus. The n.m.r. spectra were recorded on a Varian T-60 or Jeol C-60 spectrometer, using 10–15% solutions of the compound in chloroform-*d*. Chemical shifts are reported in p.p.m. downfield from tetramethylsilane as an internal reference. The i.r. spectra were re-

Can. J. Chem. Downloaded from www.nrcresearchpress.com by 210.87.254.40 on 09/05/12
For personal use only.

Can. J. Chem. Downloaded from www.nrcresearchpress.com by 210.87.254.40 on 09/05/12
For personal use only.

corded on a Beckman IR-10 spectrophotometer, with solutions or thin films. The u.v. spectra were recorded on a Beckman DB-G spectrophotometer in ethanol. Thin-layer chromatography (t.l.c.) was carried out with Eastman Kodak silica gel precoated sheets. For column chromatography, silica gel (70-325 mesh A.S.T.M.) purchased from E. Merck (Germany) was utilized. Microanalyses were performed by A. Gygli, Toronto, Ontario.

Preparation of Benzophenone Azine (1)

The procedure of Cohen and Wang (7) proved unsatisfactory for our purposes. The required azine was prepared by refluxing a solution of 11.6 g (0.05 mole) of freshly prepared dry benzophenone hydrazone hydrochloride and 9.1 g (0.05 mole) of benzophenone in 500 ml of ethanol for 2 h. Cooling precipitated the crude azine (17 g, m.p. 160–163 °C, 95% yield) and recrystallization from carbon tetrachloride gave 15 g (83% yield) of benzophenone azine, m.p. 164–165 °C.

The required benzophenone hydrazone was prepared according to reference 18.

Preparation of the Disodio and Dipotassio Adducts

The alkali metal adducts were prepared by shaking THF or DEE solutions of benzophenone azine with excess alkali metal in modified Schlenk tubes. Details of this procedure and of the measurement of metal uptake have been reported elsewhere (1–5).

The composition of both the sodium and potassium adducts in THF reached two atoms of metal per mole of azine within 2 h and remained constant for the next 24. Both adducts proved insoluble in DEE but estimates of the composition of the adducts were made by quenching and titrating entire runs. Again the same ratio of alkali metal to azine was observed.

The preparative procedure was standardized using 3.6 g (0.01 mole) of **1**, 0.08 atoms of alkali metal, and 100 ± 10 ml of solvent with 4 h of agitation. The adduct, once formed, was drained under nitrogen from the excess metal into the reaction flask.

Hydrolysis of the Adduct. Preparation of N-Benzhydryl Benzophenone Hydrazone (3)

A solution of 0.01 mole of the dianion **2** at −65 °C was treated with 0.02 mole (0.36 g) of freshly distilled water. The mixture decolorized almost immediately and was allowed to stir until it had warmed to room temperature.

The mixture was poured into water and the product isolated by ether extraction. After removal of the solvent, the residue (a solid weighing 3.5 g) was chromatographed on a 65 × 2.8 cm silica gel column with petroleum ether (30–60 °C) and chloroform as eluants. The first fraction, 1.95 g (54%), of **3** melted at 110–120 °C with some decomposition, and recrystallization from ethanol did not improve the melting point. This material appeared to be identical to that isolated by Cohen and Wang (7). The i.r. spectrum showed a broad band centered at 3300 cm^{-1} (NH) and a strong band at 1655 cm^{-1} (C=N). The n.m.r. had absorption at 5.75 (1H, CH), 7.25 (20H, aromatics) but no N—H absorption was apparent. This product formed an 80% yield of benzophenone 2,4-dinitrophenylhydrazone (m.p. and mixture m.p. 238 °C) on refluxing 3 h with a methanol solution of 5 equ of 2,4-dinitrophenylhydrazine hydrochloride.

The second fraction, 1.55 g (43%), melted at 160 °C and did not depress the m.p. of benzophenone azine, **1**.

When the reaction was run in diethyl ether and hydrolyzed, 1.6 g of the reaction mixture on chromatography yielded 1.2 g (75%) of **3**, m.p. 110–135 °C, and 0.4 g (25%) of benzophenone azine. The i.r. and n.m.r. spectra of the material melting at 110–135 °C were identical with those of the corresponding material isolated from the reaction run in THF.

Anal. Calcd. for $C_{26}H_{22}N_2$: C, 86.25; H, 6.08; N, 7.75. Found: C, 85.87; H, 5.96; N, 7.61.

Reactions with Methyl Iodide. Preparation of N-(1,1-Diphenylethyl)-N-methyl Benzophenone Hydrazone (4)

A solution of the dianion prepared from 0.01 mole of benzophenone azine (**1**) in 100 ml of THF was cooled to −65 °C and treated with 2.82 g (0.02 mole) of methyl iodide. The mixture decolorized within 1 h and was allowed to warm to room temperature. After stirring for 24 h, the THF was removed *in vacuo* and the residue triturated with anhydrous diethyl ether. The solid sodium iodide was filtered off and the solvent removed *in vacuo* leaving 4.2 g of a yellow oil which was chromatographed on silica gel with chloroform. Fraction one consisted of *N*-(1,1-diphenylethyl)-*N*-methyl benzophenone hydrazone (**4**), a white solid (yellow in solution), weight 3.0 g (77%), m.p. 103–110 °C. Recrystallization from ethanol raised the m.p. to 112–114 °C. The i.r. spectrum (in chloroform) showed bands at 2800 (N—Me), 2865, and 2940 cm^{-1} (C—Me). No absorption at 1640 cm^{-1} (C=N) was observed. The n.m.r. showed absorption at 7.4 (20H, aromatics) and at 2.15 and 2.25 (6H, C—Me, N—Me).

This material on acid hydrolysis in the presence of excess 2,4-dinitrophenylhydrazine (see above) gave a 90% yield of benzophenone 2,4-dinitrophenylhydrazone.

Anal. Calcd. for $C_{28}H_{26}N_2$ (mol. wt. 390): C, 86.25; H, 6.67; N, 7.18. Found (393): C, 86.25; H, 6.92; N, 7.04.

The second fraction, benzophenone azine, amounted to 0.9 g (25% recovery) and did not depress the melting point of an authentic sample.

In one experiment, chromatography of the crude product yielded a yellow solid melting at 101–102 °C. While the solution spectra (i.r. and n.m.r.) were identical to the material melting at 112–114 °C, the i.r. spectra of mulls of these two solids showed several discrete differences. When the lower melting solid was boiled in ethanol and allowed to crystallize, the m.p. increased to 112–114 °C. For the material melting at 101–102 °C:

Anal. Calcd. for $C_{28}H_{26}N_2$ (mol. wt. 390): C, 86.25; H, 6.67; N, 7.18. Found (405): C, 86.00; H, 6.69; N, 7.17.

This alkylation procedure and isolation was repeated with two different solvents and alkali metals. The results (together with those of the experiment just described) are summarized in Table 2.

Reaction with 1,3-Dibromopropane. Preparation of N-(2,2-Diphenyl-1-pyrrolidinyl) Benzophenone Imine (5)

The sodium adduct **2** (0.01 mole) in THF was treated with 2.02 g (0.01 mole) of 1,3-dibromopropane at −65 °C. Subsequent work-up was essentially the same as employed in the experiments with methyl iodide.

Can. J. Chem. Downloaded from www.nrcresearchpress.com by 210.87.254.40 on 09/05/12
For personal use only.

TABLE 2

Methylation of benzophenone azine adduct

Alkali metal	Solvent	% Yield alkylation product(4)	Recovered azine (1)
Na	THF	77	25
Na	DEE	62	33
K	THF	85*	—
K	DEE	69	31

*Crude product recrystallized only.

On chromatographing, the first fraction, **5** (2.7 g, 67% yield) was obtained as a white solid, m.p. 164–165 °C. Recrystallization from ethanol did not raise the melting point. The i.r. spectrum (in solution) showed aliphatic CH bands at 2890 and 2980 cm^{-1} but no C=N-absorption in the 1640 cm^{-1} region. The n.m.r. spectrum had a multiplet at 7.2 (20H, aromatics), a triplet at 2.85 (2H, CH_2—N, J = 7.0 c.p.s.), a triplet at 2.45 (2H, —CH_2—, J = 7.0 c.p.s.) and a quintet at 1.8 (2H, —CH_2—, J = 7 0 c.p s.).

Hydrolysis of this material in the presence of 2,4-dinitrophenylhydrazine as described above gave benzophenone 2,4-dinitrophenylhydrazone in 99% yield.

Anal. Calcd. for $C_{29}H_{26}N_2$ (mol. wt. 402): C, 86.52; H, 6.52; N, 6.96. Found (414): C, 86.60; H, 6.69; N, 6.86.

The second product, 0.9 g (25% recovery) of **1** was eluted from the column with methylene chloride. This material did not depress the m.p. of an authentic sample.

In a second experiment, chromatography of the crude product gave 2.8 g (70%) of a yellow solid which melted at 133–134.5 °C. Recrystallization from ethanol did not raise the m.p. The i.r. (in solution) and the n.m.r. spectra were identical to that of the material previously isolated, which melted at 164–165 °C. The mixture m.p. of these two polymorphs, was 164 °C. The i.r. spectra of the two products taken as Nujol mulls, showed several discrete differences. For the compound melting at 133–134.5 °C:

Anal. Calcd. for $C_{29}H_{26}N_2$ (mol. wt. 402): C, 86.52; H, 6.52; N, 6.96. Found (411): C, 86.56; H, 6.51; N, 6.82.

This reaction was repeated using various combinations of solvents and alkali metals. The results are summarized in Table 3 together with the results just described.

Reaction of the Adduct with 1,4-Dibromobutane. Preparation of N-(2,2-Diphenyl-1-piperidyl) Benzophenone Imine (5)

The sodium adduct from 0.01 mole of benzophenone azine in THF was treated at −65 °C with 2.16 g (0.01 mole) of 1,4-dibromobutane. The crude product was isolated and chromatographed as described in the experiments using methyl iodide. The first fraction 3.6 g (86%) of yellow crystalline material, m.p. 141–142 °C, was **5**. Recrystallization from ethanol gave a slightly yellow material melting at 142–143 °C. The i.r. spectrum had aliphatic absorptions at 2870 and 2950 cm^{-1}. No C=N absorption in the region of 1640 cm^{-1} was observed. The n.m.r. spectrum (Jeol C-100) had a multiplet at 7.25 (20H, aromatics), triplets at 2.87 and 2.71 (4H, —CH_2—N and —CH_2—, J = 5 c.p.s.), and 2 broad multiplets at 1.58 and 1.25 (4H, —CH_2—CH_2—).

Hydrolysis of this material in the presence of excess 2,4-dinitrophenylhydrazine as described above gave a 95% yield of benzophenone 2,4-dinitrophenylhydrazone.

Anal. Calcd. for $C_{30}H_{28}N_2$ (mol. wt. 419): C, 86.57; H, 6.75; N, 6.68. Found (419): C, 86.69; H, 6.99; N, 6.63.

TABLE 3

Reaction with 1,3-dibromopropane

Alkali metal	Solvent	% Yield alkylation product (5)	Recovered azine (1)
Na	THF	69	25
Na	DEE	40	53
K	THF	80	17

TABLE 4

Reaction of disodio adduct with halides

Halide	Amount g (moles)	% Yield azine 1
CH_2I_2	5.36 (.02)	95*
$BrCH_2CH_2Br$	3.76 (.02)	98
$C_6H_5CH_2Cl$	2.52 (.02)	95

*39% CH_2I_2 was also recovered.

Miscellaneous Attempted Alkylations

The disodio adduct (0.01 mole in THF) was treated with other halides under the conditions described for the reaction with methyl iodide. Isolation of the products by column chromatography on silica gel produced chiefly benzophenone azine identified by melting point and mixture melting point. The results are summarized in Table 4.

Reaction of the Adduct with Ethyl Chloroformate. Formation of Diphenyldiazomethane (8) and Ethyl Diphenylacetate (9)

A THF solution of 0.01 mole of the adduct **2** at −65 °C was treated with 1.08 g (0.01 mole) of ethyl chloroformate. The reaction mixture underwent a color change from purple through dark brown to a deep red. After warming to room temperature with stirring for 24 h, the mixture was poured into water and the reaction product isolated by ether extraction.

This product was a red oil whose i.r. spectrum had a very strong absorption at 2050 cm^{-1} as well as a carbonyl band at 1725 cm^{-1} and was found to decolorize with gas evolution in the presence of mineral acid. The red material was tentatively identified as **8**.

On placing the crude product on a silica gel column decomposition with gas evolution occurred. Chromatography of the resulting material gave 1.7 g (m.p. 53–55 °C) of a white solid which on recrystallization from ethanol gave ethyl diphenylacetate, m.p. 56–57 °C. No depression of m.p. was observed on mixing with an authentic sample (m.p. 57–58 °C). The i.r. spectrum (thin film from chloroform) was identical to that of the reference sample and showed aliphatic bands from 2880 to 3000 cm^{-1} and a strong ester carbonyl absorption at 1725 cm^{-1}. The n.m.r. spectrum had bands at 7.2 (10H, aromatics), 5.0 (1H, singlet, CH), 4.2 (2H, quartet —O—CH_2—, J = 7.0 c.p.s.), and 1.3 (3H, triplet, —CH_3, J = 7.0 c.p.s.). Further confirmation of this compound's structure was

Can. J. Chem. Downloaded from www.nrcresearchpress.com by 210.87.254.40 on 09/05/12
For personal use only.

obtained by hydrolysis in boiling 40% NaOH solution to diphenylacetic acid, m.p. and mixture m.p. with an authentic sample 147–148 °C (19).

A second fraction obtained from the same chromatographic separation was identified as benzophenone azine by mixture m.p. (0.9 g, 25% recovery).

Formation of Diethyl Diphenylmalonate (7) and Diphenyldiazomethane (8)

Treatment of a 0.01 mole solution of the dianion **2** in THF at −65 °C with 2.7 g (0.02 mole) of ethyl chloroformate gave a rapid color change from purple to red brown. After warming to room temperature and stirring 24 h the mixture was quenched in water and extracted with diethyl ether. The red–pink ether solution was dried ($MgSO_4$) and concentrated *in vacuo*. The i.r. of this crude mixture showed a strong absorption at 2050 cm^{-1} and a second strong band at 1730 cm^{-1}. Preliminary experiments with this material demonstrated that it consisted of a mixture of 7 and **8**. For example, the former compound crystallized from a solution of the reaction product in 30–60° petroleum ether at −10 °C. The latter compound was converted to benzhydryl benzoate on heating with benzoic acid (9, 10).

The reaction between the disodio adduct of benzophenone azine and 2 equ of ethyl chloroformate was repeated except that after 12 h reaction at room temperature, 3.66 g (0.03 mole) of benzoic acid was added. After an additional 8 h the color had faded from deep red to a light yellow. The reaction product was diluted with water, extracted with diethyl ether, and the ether extracts washed with 10% sodium hydroxide, water, dried ($MgSO_4$), and concentrated. Chromatography of the residue on silica gel using carbon tetrachloride and chloroform gave two fractions.

The first fraction, 2.0 g (74% yield) m.p. 87–89 °C, was identified as benzhydryl benzoate (**15**) by mixture melting point with an authentic sample (m.p. 87–89 °C, lit. (19) 89 °C) prepared from benzhydrol and benzoyl chloride in pyridine. The i.r. spectrum had a strong carbonyl band at 1720 cm^{-1} and the n.m.r. spectrum had absorptions at 7.4 and 8.2 (aromatics), the expected methine proton presumably being lost in the aromatics.

The second fraction (2.8 g, 90% yield) melted at 56–58 °C and was identified as 7. It did not depress the m.p. of an authentic sample (m.p. 57–58 °C, lit. (15) 57–58 °C) prepared by treating the anion of ethyl diphenylacetate with ethyl chloroformate, a synthetic extension of ref. 14. Spectral properties (i.r. and n.m.r.) of the fraction and an authentic sample were identical. The i.r. spectrum showed aliphatic absorption bands at 2910 and 2942 cm^{-1} and a strong ester carbonyl band at 1730 cm^{-1}. The n.m.r. spectrum had absorptions at 7.4 (10H, multiplet, aromatics), 4.3 (4H, quartet, $—CH_2—$, J = 7.0 c.p.s.), and 1.3 (6H, triplet, $—CH_3$, J = 7.0 c.p.s.).

Formation of Ethyl α,α-Diphenylpropionate (12) and Diphenyldiazomethane (8)

Ethyl chloroformate (1.08 g, 0.01 mole) was added to 0.01 mole of **2** in THF at −65 °C. After warming to room temperature and stirring for 8 h the mixture was recooled to −65 °C and 0.01 mole (1.42 g) of methyl iodide was added. The solution was stirred an additional 12 h and then quenched in water and extracted with diethyl ether. The ether layer was dried ($MgSO_4$) and concentrated *in vacuo*. The i.r. of this crude mixture had a strong band at 2050 cm^{-1} due to the diazo group and an ester absorption at 1733 cm^{-1}. No band at 2800 cm^{-1} for N—Me was observed. The mixture was taken up in benzene and treated with 2 equ of benzoic acid to decompose **8**. After extraction with 10% sodium hydroxide solution to remove the excess benzoic acid, the solution was dried and concentrated *in vacuo*. Chromatography of the residue on silica gel with chloroform gave two fractions: 3.8 g of an oil, and 0.8 g (22% recovery) of benzophenone azine (identified by mixture m.p. with an authentic sample). The oil was taken up in *n*-hexane and on cooling deposited 1.8 g (62%) of benzhydryl benzoate, **15**, (9, 10) m.p. 87–89 °C, identified by mixture m.p. The filtrate on evaporation left 2.0 g (79%) of an oil which resisted crystallization and which was identified as **12** (14). The i.r. spectrum contained a strong band at 1733 cm^{-1} indicative of an ester group. The n.m.r. spectrum had absorptions at 7.25 (10H, aromatics), 4.2 (2H quartet, J = 7.0 c.p.s., $—CH_2—$), 1.93 (3H singlet, CH_3), and 1.2 (3H, triplet, J = 7.0 c.p.s., $CH_3—$). A 1.0 g sample of this material was hydrolyzed by boiling with 30% aqueous potassium hydroxide solution. The final solution was cooled and acidified to precipitate 0.85 g of α,α-diphenylpropionic acid, m.p. 170–172 °C. After recrystallization from a water–ethanol mixture, it melted at 172 °C and did not depress the m.p. of an authentic sample (m.p. 172–173 °C) prepared according to (14).

Preparation of N-Methyl-N-(Carbethoxydiphenylmethyl) Benzophenone Hydrazone (13)

The preceding reaction was repeated a second time except that the mixture was treated with 0.01 mole (1.42 g) of methyl iodide at −65 °C only 10 min after the addition of the ethyl chloroformate. After allowing to warm to room temperature the mixture was stirred for 24 h, and then quenched in water, extracted with diethyl ether, the extracts dried ($MgSO_4$), and concentrated *in vacuo*. The i.r. spectrum of this crude residue had a weak absorption at 2050 cm^{-1} indicative of a small quantity of **8**. Accordingly, the mixture was treated with 1 equ of benzoic acid in benzene and then extracted with 10% sodium hydroxide to remove the excess acid. The solvent was removed and the product chromatographed on silica gel with chloroform. Three fractions were collected, the first, 50 mg of a yellow oil, could not be resolved, the second 3.1 g (69%) of a yellow solid identified as **13**, m.p. 120–123 °C, and the third 0.85 g (24%) of benzophenone azine (**1**) identified by mixture m.p. with an authentic sample. The second fraction after recrystallization from diethyl ether melted at 122–123 °C. The i.r. spectrum (in carbon tetrachloride) had several aliphatic bands from 2880 to 2990 cm^{-1} in addition to a weak band at 2805 cm^{-1} (N—Me) and a strong ester absorption at 1740 cm^{-1}. No band in the region of 1640 cm^{-1} (for a C=N—) was apparent. The n.m.r. spectrum had absorptions of 7.35 (20H, multiplet, aromatics), 4.1 (2H, quartet, J = 7.0 c.p.s., $CH_2—O—$), 1.95 (3H, singlet, N—Me), and 1.0 (3H, triplet, J = 7.0 c.p.s., $—CH_3$).

Anal. Calcd. for $C_{30}H_{28}N_2O_2$ (mol. wt. 449): C, 80.33; H, 6.29; N, 6.25. Found (455): C, 80.29; H, 6.38; N, 6.34.

Can. J. Chem. Downloaded from www.nrcresearchpress.com by 210.87.254.40 on 09/05/12
For personal use only.

This material was hydrolyzed in the presence of excess 2,4-dinitrophenylhydrazine hydrochloride as described earlier to produce benzophenone 2,4-dinitrophenylhydrazone in 97% yield.

*Preparation of N-(Carbethoxydiphenylmethyl) Benzophenone Hydrazone (**14**)*

The above reaction was repeated and within a few minutes after the initial addition of ethyl chloroformate the mixture was treated at −65 °C with 5.0 ml of freshly distilled water. The cooling bath was removed and the mixture allowed to warm to room temperature. After stirring for 2 h, more water was added and the mixture treated with a few drops of concentrated hydrochloric acid to discharge the red color of diphenyldiazomethane (**8**). The mixture was extracted with diethyl ether, the extracts dried ($MgSO_4$), and evaporated *in vacuo*. Chromatography on silica gel gave 4.1 g of an oil as a first fraction and as a second fraction, 0.5 g (14%) of benzophenone azine, identified by mixture m.p. Trituration of the first fraction with ethanol gave a solid 3.1 g (71%) of **14**, m.p. 85–89°. After recrystallization from a minimum of diethyl ether, **14** melted at 89–91 °C. The i.r. spectrum had absorptions at 3300 (NH), and 1730 cm^{-1} (ester). No band in the region of 1640 cm^{-1} (C═N—) was apparent. The n.m.r. spectrum had absorptions at 7.3 (20H, multiplet, aromatics), 6.4 (1H, singlet, exchangeable with D_2O, NH), 4.2 (2H, quartet, J = 7.0 c.p.s., —CH_2—O) and at 1.1 (3H, triplet, J = 7.0 c.p.s., CH_3—).

Anal. Calcd. for $C_{29}H_{26}N_2O_2$ (mol. wt. 435): C, 80.18; H, 6.03; N, 6.44. Found (465, 447): C, 80.29; H, 5.95; N, 6.55.

This material was hydrolyzed in the presence of excess 2,4-dinitrophenylhydrazine hydrochloride as described above to give a 98% yield of benzophenone 2,4-dinitrophenylhydrazone.

Compound **14** on storage became oily over a two week period. However, on sealing in an ampoule, samples have been stored unchanged over a 6 month period.

*Reactions of the Adduct, **2**, with Methyl Benzoate. Preparation of α-Benzamido-α,α-diphenylacetophenone (**17**)*

The disodium adduct from 0.01 mole of azine, **1**, in 100 ml of THF at −65 °C was treated with 0.02 mole (2.72 g) of methyl benzoate. The reaction was allowed to warm to room temperature and stand for 18 h after which time the mixture was quenched in water and extracted with chloroform. The extracts were dried and evaporated *in vacuo* leaving a yellow solid. This, on chromatography on silica gel with chloroform, gave 1.8 g (50% recovery) of benzophenone azine (**1**), identified by mixture m.p., 1.0 g (37% recovery) of methyl benzoate identified by means of its i.r. spectrum, and 2.0 g (51%) of a white solid, **17**, m.p. 185–187.5 °C. Recrystallization from ethanol did not change the m.p. The i.r. spectrum had absorptions at 3400 (N—H) and 1662 cm^{-1} (amide I). This latter band had a shoulder at 1720 cm^{-1} (carbonyl). The n.m.r. spectrum had absorptions at 7.4 (20H, complex multiplet, aromatics) and 8.5 (1H, broad singlet, NH).

Anal. Calcd. for $C_{27}H_{21}NO_2$ (mol. wt. 392): C, 82.83; H, 5.42; N, 3.58. Found (396): C, 82.55; H, 5.36; N, 3.68.

*Preparation of N-Benzhydryl Benzamide (**18**) Using one Equivalent of Methyl Benzoate*

The disodium adduct **2** from 0.01 mole of benzophenone azine in 100 ml of THF at −65 °C was treated with 1.36 g (0.01 mole) of methyl benzoate. The mixture was allowed to warm to room temperature, stirred for 24 h, and then quenched in water. After extraction with diethyl ether in the usual manner, the product was chromatographed on silica gel with chloroform giving 2.3 g (64% recovery) of **1** identified by mixture m.p. and 1.85 g (65%) of a white solid **18**, m.p. 170–172 °C. After recrystallization from ethanol this material melted at 174 °C and did not depress the m.p. of an authentic sample (16, 19). The i.r. spectrum had bands at 3450 (NH) and 1660 cm^{-1} (amide I). The n.m.r. spectrum (20) had absorption at 7.96 (3H, multiplet NH and ortho protons), 7.35 (13H, multiplet, aromatics) and 6.50 (1H, doublet, methine).

*Formation of α-Benzamido-α,α-diphenylacetophenone (**17**) Using one Mole of Methyl Benzoate*

The reaction with 0.01 mole of methyl benzoate was repeated as before. After warming to room temperature and stirring for 24 h the mixture was quenched by the addition of 15 ml of 20% hydrochloric acid, stirred for an additional 5 min, diluted with water, and extracted with diethyl ether. After drying ($MgSO_4$) the extracts were evaporated and the residue was chromatographed on silica gel with chloroform giving 2.0 g (55% recovery) of benzophenone azine, identified by mixture m.p., and 1.85 g (47%) of **17** identified by mixture m.p. with a reference sample.

*Hydrolysis of α-Benzamido-α,α-diphenylacetophenone (**17**) with Sodium Methoxide*

A solution of 0.5 g (0.0013 mole) of α-benzamido-α,α-diphenylacetophenone in 25 ml of anhydrous THF was treated with 0.25 g (0.0046 mole) of anhydrous sodium methoxide. Addition of the methoxide caused the solution to become faintly yellow but this color gradually faded. After stirring for 24 h, water was added and the product extracted with diethyl ether. The extracts were dried with $MgSO_4$ and evaporated leaving 0.35 g (94%) of crude **18**, m.p. 164–167 °C. Recrystallization gave material, m.p. 172 °C, which showed no depression of m.p. on mixing with an authentic sample.

*Preparation of α-Benzamido-α,α-diphenylacetophenone (**17**) Using one Equivalent of Methyl Benzoate and Methyl Iodide*

The reaction with 0.01 mole of methyl benzoate was repeated as before except that after 24 h of stirring the mixture was recooled to −65 °C and treated with 2.84 g (0.02 mole) of methyl iodide. The reaction product was isolated and chromatographed as described above giving 1.8 g (50% recovery) of benzophenone azine, identified by mixture m.p., and 2.4 g (61%) of **17**, m.p. 180–183 °C. This material on recrystallization from ethanol melted at 185 °C and did not depress the m.p. of an authentic sample.

*Preparation of α-Benzamido-α,α-diphenylacetophenone (**17**) Using one Equivalent of Methyl Benzoate and Carbon Dioxide*

The reaction with 0.01 mole of methyl benzoate was

Can. J. Chem. Downloaded from www.nrcresearchpress.com by 210.87.254.40 on 09/05/12
For personal use only.

repeated and after allowing to stir for 12 h was poured onto Dry Ice. The reaction product was isolated and chromatographed as already described giving 1.8 g (50% recovery) of benzophenone azine identified by mixture m.p., and 1.6 g (41%) of **17**, m.p. 186 °C, which did not depress the m.p. of an authentic sample. The water layer from the ether extraction was neutralized with 5% hydrochloric acid to precipitate 0.4 g (12%) of an acid, identified as *N*-benzoyl-α,α-diphenylglycine (**20**). This material was recrystallized from a water–ethanol mixture and melted at 198–199 °C (11, 17) with decomposition. The i.r. spectrum of this product had a broad band centered at 2950 cm^{-1} and a second broad band at 1700 cm^{-1}. A sample of this material was decomposed by gentle warming at the m.p. On cooling, the product had a m.p. of 174 °C. Recrystallization from ethanol did not raise the m.p. nor was it depressed on mixing with an authentic sample of **18**.

*Reaction of N-Benzoyl Benzophenone Imine (**19**) (12) with Sodium in THF*

The adduct was prepared by the same method as used for the preparation of dianion, **2**, from benzophenone azine (**1**). Thus 0.01 mole (2.85 g) of **19** was allowed to react with sodium metal in THF. Aliquots of the solution were withdrawn at various time intervals, quenched in water, and titrated with standardized acid. Table 5 summarizes the uptake of sodium observed. The residual solution, representing 0.0055 mole of the original **19** was drained from the excess sodium into water and extracted with diethyl ether. The combined extracts were dried ($MgSO_4$) and reduced in volume. The product, a white oily solid, was chromatographed on silica gel with chloroform giving 0.8 g (55%) of **18**, m.p. 173 °C, identified by mixture m.p. with an authentic sample, and a second fraction, 0.75 g of material, m.p. 130–145 °C, which on t.l.c. was resolved into at least two compounds. The i.r. spectrum of the mixture showed an amide carbonyl at 1650 cm^{-1} and NH at 3300 and 3450 cm^{-1}. This material is presently under study.

*Reaction of the Sodium Adduct of N-Benzoyl Benzophenone Imine (**19**) with Methyl Benzoate*

The adduct prepared from 2.85 g (0.01 mole) of **19**, 100 ml of THF, and an excess of sodium metal was treated with 2.04 g (0.015 mole) of methyl benzoate at −65 °C. The mixture was allowed to warm to room temperature and stirred for 24 h. Twenty milliliters of 20% hydrochloric acid was added and the product extracted with diethyl ether. The combined extracts were washed with 10% sodium bicarbonate solution, dried, and evaporated. Chromatography of the residue on silica gel with chloroform gave 1.6 g (78% recovery) of methyl benzoate identified by its i.r. spectrum, and 1.6 g (55%) of a mixture consisting of **18** and **17**. The third fraction collected was 1.35 g of a complex mixture which by t.l.c. appeared to be the same as the unresolved mixture from the water quenched reaction.

TABLE 5

Reaction of *N*-benzoyl benzophenone imine with sodium

Duration of agitation (h)	Atoms of Na per mole
0.5	1.28
1.0	1.40
2.0	1.50
3.0	1.56
5.0	1.50

The i.r. spectrum of the second fraction had NH absorptions at 3450 (NH, **18**, strong) and 3400 cm^{-1} (NH, **17**, weak). A shoulder at 1720 cm^{-1} (on the amide I band at 1665 cm^{-1}) was also indicative of an aromatic carbonyl due to the presence of **17**. This mixture could not be separated by chromatography but **17** was converted to **18** and benzoic acid, by treatment with sodium methoxide in THF as described previously. Work-up gave 1.3 g of **18** and 0.25 g of benzoic acid which meant that the original mixture had contained 31% of **17**.

The authors are indebted to the National Research Council of Canada for financial support and to the Ontario Government for a fellowship (E.J.M.). We are also grateful to Dr. A. Balasubramanian of this department for helpful discussions of the ultraviolet spectra.

1. W. Schlenk and E. Bergmann. Ann. **463**, 281 (1928).
2. J. G. Smith. Can. J. Chem. **44**, 59 (1966).
3. J. G. Smith and C. D. Veach. Can. J. Chem. **44**, 2497 (1966).
4. J. G. Smith and C. D. Veach. Can. J. Chem. **45**, 1785 (1967).
5. J. G. Smith and C. D. Veach. Can. J. Chem. **44**, 2245 (1966).
6. J. G. Smith. Can. J. Chem. **46**, 2271 (1968).
7. S. G. Cohen and C. H. Wang. J. Amer. Chem. Soc. **77**, 2457 (1955).
8. E. J. MacPherson and J. G. Smith. Tetrahedron Lett. 3159 (1969).
9. H. Staudinger, E. Anthes, and F. Pfenninger. Ber. **49**, 1928 (1916).
10. E. Hardegger *et al.* Helv. Chim. Acta, **31**, 439 (1948).
11. C. W. Bird. J. Org. Chem. **27**, 4091 (1962).
12. O. Exner. Collect. Czech. Chem. Commun. **20**, 1360 (1955); **21**, 1500 (1956).
13. J. W. B. Reesor, J. G. Smith, and G. F. Wright. J. Org. Chem. **19**, 940 (1954).
14. H. E. Zaugg, D. A. Dunnigan *et al.* J. Org. Chem. **26**, 644 (1961). See also: Brit. Pat. No. 768, 563 (July 23, 1958), Chem. Abstr. **53**, p. 2096*i*.
15. A. W. Dox and A. Thomas. J. Amer. Chem. Soc. **45**, 1811 (1923).
16. G. W. H. Cheeseman and R. C. Poller. Anal. **87**, 366 (1962).
17. F. R. Japp and A. Findlay. J. Chem. Soc. 1027 (1899).
18. Organic syntheses. Coll. Vol. III. E. C. Horning, *editor*. John Wiley and Sons, Inc., 1955. 352.
19. R. L. Shriner, R. C. Fuson, and D. Y. Curtin. The systematic identification of organic compounds. John Wiley and Sons, Inc., New York, 1967.
20. L. Skulski, G. C. Palmer, and M. Calvin. Tetrahedron Lett. 1773 (1963).

Can. J. Chem. Downloaded from www.nrcresearchpress.com by 210.87.254.105 on 09/05/12
For personal use only.

Alkali metal adducts of benzophenone azine. II. The lithium adduct

E. J. MacPherson and James G. Smith
Department of Chemistry, University of Waterloo, Waterloo, Ontario

Received October 17, 1969

The behavior of benzophenone azine towards lithium has been studied. Unlike sodium and potassium, lithium effected extensive reduction and cleavage of benzophenone azine; the reaction product being benzhydryl amine. By limiting the amount of lithium to 2 g-atoms per mole of azine, the reaction product was shown to be *N*-lithiobenzophenone imine on the basis of its chemical behavior.

Two reasons are advanced to explain the behavior of lithium in contrast to that of sodium or potassium. One explanation relies upon the greater reducing power of lithium compared with the other two alkali metals. The other relies upon the tendency of organolithium compounds to associate via formation of multi-center bonds.

Canadian Journal of Chemistry, **48**, 1915 (1970)

As a natural extension to our earlier study (1, 2) of the reaction between benzophenone azine and sodium or potassium, the behavior of this compound towards lithium was examined. Unexpectedly, lithium presented a reaction pattern quite different from that of the other two alkali metals.

Results

In the presence of excess lithium, the uptake of the metal by the azine did not stop at the expected level of 2 g-atoms per mole. Instead, the reaction continued until an astonishing total of 5–6 g-atoms of lithium per mole of azine was reached. On quenching this "polylithio" species in water, benzophenone and benzhydrylamine were isolated. The latter compound was identified by its infrared (i.r.) spectrum and its benzamide while the former was identified by its i.r. spectrum. The yield of the benzhydrylamine was somewhat variable and the maximum (76%) was obtained with solutions more dilute than normal.

Attempts were made to obtain alkylation products of this "polylithio" species by treating the reaction mixture with methyl iodide or 1,3-dibromopropane. However, such complex mixtures of products resulted that no definite compound could be isolated.

The investigation was continued by restricting the available lithium to 2 g-atoms per mole of azine. Under these conditions, rupture of the nitrogen–nitrogen bond occurred and the formation of *N*-lithiobenzophenone imine was the only reaction observed. This conclusion was based on several reactions which are summarized in Scheme 1.

Treatment of the *N*-lithiobenzophenone imine with the theoretical amount of methanol produced benzophenone imine, while benzoyl chloride generated *N*-benzoylbenzophenone imine. Hydrolysis of these compounds was avoided by omitting the customary aqueous work-up. Alkylation of the *N*-lithio derivative was also examined. While treatment with methyl iodide produced *N*-methylbenzophenone imine, benzyl chloride generated a product whose nuclear magnetic resonance (n.m.r.) spectrum clearly indicated that it was not the expected *N*-benzylbenzophenone imine. Hydrolysis of the product produced benzophenone and 1,2-diphenylethylamine establishing the product as *N*-(1,2-diphenylethyl)benzophenone imine.

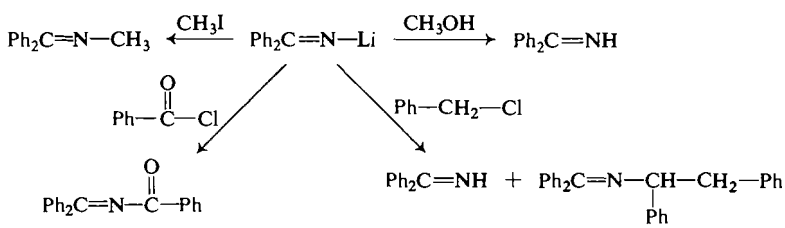

SCHEME 1

Reactions of *N*-lithiobenzophenone imine

Can. J. Chem. Downloaded from www.nrcresearchpress.com by 210.87.254.105 on 09/05/12
For personal use only.

The formation of this derivative reflected the strong basic nature of *N*-lithiobenzophenone imine. Hauser *et al.* (3) demonstrated that strong bases converted benzyl chloride to 1-chloro-1,2-diphenylethane. In the present case, the 1-chloro-1,2-diphenylethane alkylated either the benzophenone imine or the *N*-lithio derivative producing the observed product.

Attempts to alkylate *N*-lithio benzophenone imine with either 1,3-dibromopropane or allyl bromide failed to generate any alkylation product in isolable amounts; only benzophenone imine was detected. Possibly, this behavior was again due to the strong basic nature of the *N*-lithio derivative which effected dehydrohalogenation of the bromo compounds with formation of benzophenone imine.

Discussion

It is clear that lithium has a more extensive effect on benzophenone azine than sodium or potassium. Reduction of the azomethine groups is accompanied by cleavage of the nitrogen–nitrogen bond. From the experiments using a limited amount of lithium, the first step in the reaction is cleavage of the nitrogen–nitrogen bond to form *N*-lithiobenzophenone imine (**1**) (Scheme 2). In the presence of excess lithium, further reaction occurs effecting reduction of the carbon–nitrogen double bond. The "polylithio" species must consist of a mixture of unreacted **1** and perhaps a trilithio compound such as **2**. Protonation of this mixture gives benzhydrylamine from **2** and benzophenone imine from **1**, the last compound hydrolyzing to benzophenone during isolation.

It is tempting to attribute the behavior of lithium towards benzophenone azine (in contrast to sodium (2)) as resulting from the greater reducing power of lithium over sodium which results in cleavage of the nitrogen–nitrogen bond rather than reduction of the carbon–nitrogen

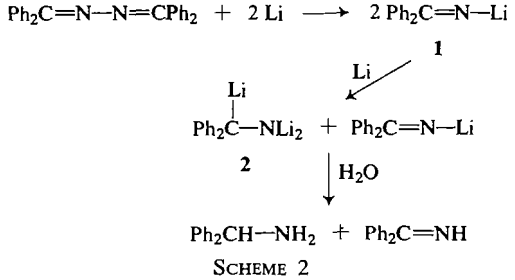

SCHEME 2

double bond. Documentation of this strong reducing power is readily available. For example, the reduction of aromatic rings by lithium and secondary amines is a well-known reaction (4). Again, the formation of a dilithium adduct of naphthalene in contrast to a mono sodium adduct may be cited (5). In situations more analogous to that under discussion, Weyenberg *et al.* (6) have used lithium to obtain monomeric reduction products of aralkenes rather than their dimers. Smith and Veach (7) have cited this ability of lithium to explain the striking differences in behavior of acetophenone anil towards lithium and sodium.

However, a more careful scrutiny of the reaction reveals that this explanation is insufficient. The reaction between an alkali metal and a conjugated system depends on the transfer of an electron from the metal to the conjugated system. In the case of benzophenone azine, a total of two electrons are so transferred and if the transfer is considered stepwise, there is no apparent reason why the first such transfer should be responsible for the differences observed. It is therefore assumed that the first transfer is the same for both sodium and lithium, the product being the radical ion **3** (Scheme 3).

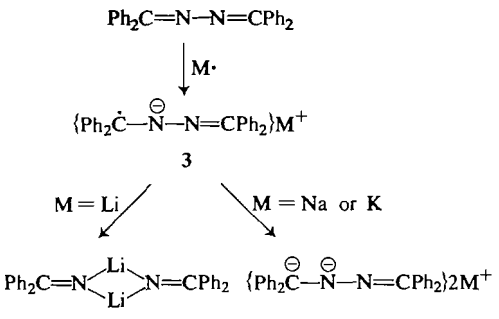

SCHEME 3

Thereafter, the reaction paths diverge depending on the electron source. At present, the reason for this divergence is unclear. One possibility is the relatively greater covalent nature of the bonds formed with lithium (8) compared with sodium. In the case of the lithium radical ion such a covalent bond may localize the odd electron and result in sufficient instability that decomposition occurs to the observed products.

A second possibility evolves from the greater Lewis acidity (9) of organolithium compounds. Such a property explains the recognized tendency

Can. J. Chem. Downloaded from www.nrcresearchpress.com by 210.87.254.105 on 09/05/12
For personal use only.

of organolithium compounds to associate. It is conceivable, then, that this tendency to associate results in rearrangement of the lithium radical ion to an associated dimer **4** before (or during) the transfer of the second electron. Such a reaction path is not accessible to the sodium or potassium analogues and the adduct **5** is formed.

The behavior of other azines towards lithium is presently being investigated.

One minor comment should be made on the reaction of **1** with methyl iodide. Anselme *et al.* (10) have reported that this reaction produced a small yield of a high boiling, presumably dimeric, methylation product and offered this as partial evidence for a dimeric structure of **1**. We did not observe this material in our methylations. However, on repeating the reaction using Anselme's procedure for preparing **1** (phenyl lithium and benzonitrile), this high boiling methylation product was formed. It is suggested that the source of this methylation product is a by-product formed during the preparation of *N*-lithiobenzophenone imine by this latter synthesis and that its appearance does not lend support to a dimeric structure for **1**.

Experimental

The melting points are uncorrected and were determined in an open capillary using a Mel-temp. melting point apparatus. The n.m.r. spectra were recorded on a Varian T-60 spectrometer using 10–15% solutions of the compound in chloroform-d_1. Chemical shifts are reported in p.p.m. downfield from tetramethylsilane as an internal reference. The i.r. spectra were recorded on a Beckman IR-10 spectrophotometer with solutions or thin films. Thin-layer chromatography (t.l.c.) was carried out with Eastman Kodak silica gel precoated sheets. For column chromatography, silica gel (70-325 Mesh A.S.T.M.) purchased from E. Merck (Germany) was utilized.

Preparation of the Lithium Adducts of Benzophenone Azine

The techniques employed for the preparation of the lithium adducts of benzophenone azine have been described elsewhere (11, 12, 13).

TABLE 1

Rate of reaction for the preparation of lithium adducts of benzophenone azine

Agitation time (h)	g-Atoms Li per mole of azine
0.25	3.2
0.5	2.8
1	4.3
2	4.7
4	5.3
8	5.4
24	6.0

The rate of reaction was measured using 3.6 g (0.01 mole) of benzophenone azine, 0.56 g (0.08 g-atoms) and 100 ml of tetrahydrofuran with results as shown in Table 1.

For preparative reactions, more concentrated solutions were used (see Experimental for exact amounts) and either 2 or 6 g-atoms of lithium per mole of azine depending on the type of reaction desired and 100 ± 10 ml of solvent. The mixture was agitated 24 h and transferred under nitrogen to the reaction flask.

Hydrolysis of the Adduct Prepared from Benzophenone Azine with an Excess of Lithium Metal

The adduct prepared from 3.6 g (0.01 mole) of benzophenone azine and 0.42 g (0.06 g-atoms) of lithium was drained into an ice-water mixture and the crude product isolated by an ether extraction. After removing the ether, the residue was chromatographed on silica gel with chloroform. The first fraction obtained was 1.0 g (28%) of benzophenone (presumably formed by hydrolysis of benzophenone imine on the column) identified through its i.r. spectrum. The next fraction was 1.8 g (50%) of benzhydryl amine whose i.r. spectrum was identical to that of a reference sample. Further confirmation was obtained by converting the amine with benzoyl chloride to its benzamide in 93% yield, m.p. 174 °C undepressed on mixing with an authentic sample of benzhydryl benzamide (2, 14). An intermediate fraction of 0.45 g was identified as a mixture of benzophenone and benzhydryl amine from its i.r. spectrum.

In a second experiment the adduct, prepared from 1.7964 g (0.00499 mole) of benzophenone azine and 0.2078 g (0.02995 mole) of lithium metal, was cooled to −65 °C and treated with 2.0 ml of anhydrous methanol. The mixture decolorized rapidly and was allowed to warm to room temperature overnight. Water was added and the product, isolated by an ether extraction, was boiled in aqueous 10% hydrochloric acid to hydrolyze any benzophenone imine which may have been present. After cooling, the water was extracted with ether, the ether dried and evaporated, giving 0.4 g (20%) of benzophenone, identified from its i.r. spectrum. The water layer from this extraction was neutralized with 10% aqueous sodium hydroxide solution and extracted with diethyl ether. After drying, the ether layer was evaporated giving 1.4 g (76%) of benzhydryl amine identified by its i.r. spectrum and by conversion to its benzamide.

Methanolysis of the Adduct from two Equivalents of Lithium

The adduct prepared from 4.933 g (0.0137 mole) of benzophenone azine and 0.1904 g (0.0274 g-atoms) of lithium in THF was treated with 0.90 g (0.0274 mole) of anhydrous methanol at −65 °C. The mixture decolorized immediately and after 15 min was allowed to warm to room temperature. After stirring for 3 h the THF was removed *in vacuo*, anhydrous diethyl ether added, and product filtered. The ether was removed *in vacuo* and the product distilled giving 3.7 g (75%) of benzophenone imine, a clear colorless liquid, b.p. 94–95 °C/0.23 mm Hg. The i.r. spectrum of this oil in chloroform was superimposable upon that of an authentic sample obtained

Can. J. Chem. Downloaded from www.nrcresearchpress.com by 210.87.254.105 on 09/05/12
For personal use only.

from the methanolysis of the addition product (15) prepared from benzonitrile and phenylmagnesium bromide. When this reaction was repeated using diethyl ether instead of THF, benzophenone imine was obtained in 88% yield

Reaction of the Adduct from two Equivalents of Lithium with Methyl Iodide

The adduct prepared from 2.9052 g (0.0081 mole) of benzophenone azine and 0.120 g (0.016 g-atoms) of lithium was treated with 2.3 g (0.0161 mole) of methyl iodide at −65 °C. The mixture was allowed to warm to room temperature and stirred for a further 2 h after which time the color had changed from a deep red to a pale straw yellow. The mixture was poured into water and extracted with diethyl ether. The combined extracts were dried ($MgSO_4$) and evaporated *in vacuo*. The resulting oil gave 2.6 g (83%) of *N*-methylbenzophenone imine on distillation, b.p. 93–94 °C/0.2 mm. The i.r. spectrum was superimposable on that of an authentic sample (10) prepared by treating *N*-lithiobenzophenone imine with methyl iodide.

Reaction of the Adduct Prepared from two Equivalents of Lithium with Benzoyl Chloride

The adduct prepared from 4.49 g (0.0125 mole) of benzophenone azine and 0.1731 g (0.02495 g-atoms) of lithium was treated with 3.5 g (0.0249 mole) of freshly distilled benzoyl chloride at −65 °C. The mixture was allowed to warm to room temperature and stirred overnight. After treatment with 1.5 g (a slight excess) of absolute ethanol, the mixture was stirred a further 1/2 h and the THF removed *in vacuo*. Anhydrous ether was added and the product filtered to remove the solid lithium ethoxide. The ether was removed *in vacuo* and 20 ml of anhydrous cyclohexane was added. On cooling and filtering, 5.5 g (79%) of *N*-benzoylbenzophenone imine was obtained. This material melted at 115–116 °C and did not depress the melting point of an authentic sample prepared by a published procedure (12).

Reaction of the Adduct from two Equivalents of Lithium with Benzyl Chloride

A solution of the adduct prepared from 2.4624 g (0.00684 mole) of benzophenone azine and 0.0950 g (0.0137 g-atoms) of lithium in 100 ml of THF was treated with 1.73 g (0.0147 mole) of benzyl chloride at −65 °C. The red color of the adduct faded slowly. After warming to room temperature the mixture was stirred for 24 h, poured into water, and extracted with diethyl ether. The ether extracts were dried ($MgSO_4$), and evaporated *in vacuo* giving a faintly yellow oil which was chromatographed on silica gel with chloroform. The first fraction consisted of 2.0 g (49%) of *N*-(1,2-diphenylethyl)benzophenone imine m.p. 55–58 °C which was recrystallized from ethanol and melted at 58 °C.

The i.r. spectrum of the second fraction (1.1 g, 45%) indicated that it was a mixture of benzophenone and benzophenone imine.

The i.r. spectrum of *N*-(1,2-diphenylethyl)benzophenone imine showed bands at 2960–2880 cm^{-1} (aliphatics) and a strong absorption at 1620 cm^{-1} (C=N).

Anal. Calcd. for $C_{27}H_{23}N$: C, 89.70; H, 6.43; N, 3.88. Found: C, 89.70; H, 6.40; N, 3.90.

The structure of the imine was established by hydrolysis of 1.0 g in refluxing 20% hydrochloric acid for 2 h. Extraction with ether gave, after removal of the solvent, 0.45 g (90% yield) of benzophenone identified by its i.r. spectrum and confirmed by its 2,4-DNPH derivative. The aqueous acid layer was made basic, extracted with ether, and evaporated to give 0.50 g (90% yield) of an oil whose i.r. spectrum was identical to that of an authentic specimen of 1,2-diphenylethylamine synthesized by a published procedure (16, 17). Further confirmation was obtained by conversion of the amine to its benzamide with benzoyl chloride (93% yield, m.p. 177–178 °C) and comparison (i.r. and mixture m.p.) with authentic *N*-benzoyl-1,2-diphenylethyl amine (18).

The n.m.r. spectrum of *N*-(1,2-diphenylethyl)benzophenone imine showed the aromatic protons in a complex band 6.2 to 7.8 (20H) and the aliphatic protons as a typical ABX pattern; a double doublet centered at 4.52 (CH, 1H, H_X) and two overlapping quartets centered at 3.07 and 3.19 (—CH_2—, 2H, H_A and H_B, J_{AB} = 14.2, J_{AX} = 9.8, J_{BX} = 4.8).

The 1,2-diphenylethyl amine also showed a typical ABX pattern in its n.m.r. spectrum; two overlapping quartets centered at 2.75 and 2.87 (—CH—, 2H, H_A and H_B, J_{AB} = 13, J_{AX} = 10.2, J_{BX} = 3.8), a double doublet at 4.08 (CH, 1H, H_X), as well as the NH absorption at 1.30 (2H) and the aromatic protons between 6.4 and 8.0 (10H).

The authors are indebted to the National Research Council of Canada for financial support and to the Ontario Government for a fellowship (E. J. M.).

1. E. J. MacPherson and J. G. Smith. Tetrahedron Lett. 3159 (1969).
2. E. J. MacPherson and J. G. Smith. This issue.
3. C. R. Hauser, W. R. Brasen, P. S. Skell, S. W. Kantor, and A. E. Brodhag. J. Amer. Chem. Soc. **78**, 1653 (1956).
4. R. A. Benkesser, C. Arnold, Jr., and R. F. Lambert. J. Amer. Chem. Soc. **77**, 6042 (1955).
5. J. Smid. J. Amer. Chem. Soc. **87**, 655 (1965).
6. D. R. Weyenberg, L. H. Toporcer, and A. E. Bey. J. Org. Chem. **30**, 4096 (1965).
7. J. G. Smith and C. D. Veach. Can. J. Chem. **45**, 1785 (1967).
8. G. E. Coates, M. L. H. Green, and K. Wade. Organometallic compounds. Vol. I, 3rd edition. Methuen, London, 1967. p. 32.
9. J. J. Eisch. The chemistry of organometallic compounds. The MacMillan Co., New York, 1967. p. 15 and 86.
10. J. P. Anselme, W. Fischer, and N. Koga. Tetrahedron, **25**, 89 (1969)
11. J. G. Smith. Can. J. Chem. **44**, 59 (1966).
12. J. G. Smith and C. D. Veach. Can. J. Chem. **44**, 2245 (1966).
13. J. G. Smith and C. D. Veach. Can. J. Chem. **44**, 2497 (1966).
14. G. W. H. Cheeseman and R. C. Poller. Anal. **87**, 366 (1962).
15. Org. Syn. **44**, 51 (1964).
16. A. Pohland. U.S. 2 772 311 (November 27, 1956). Chem. Abstr. **51**, P7432C (1957).
17. C. Torres and Y. Gonzales. Bull. Soc. Chim. **37**, 159 (1925).
18. B. B. Dey and V. S. Ramanathan. Proc. Nat. Inst. Sci. India, **9**, 193 (1943); Chem. Abstr. **43**, 5027*a* (1949).

Determination of pK_{BH^+} for aliphatic ketones from nuclear magnetic resonance chemical shift data

DONALD G. LEE
Department of Chemistry, University of Saskatchewan, Regina, Saskatchewan
Received September 29, 1969

The pK_{BH^+} values for 3-pentanone, 2-butanone, and 3-methyl-2-butanone have been determined from chemical shift data. The values (−7.6, −7.1, and −7.2, respectively) are in good agreement with those previously determined for aliphatic ketones by use of ultraviolet–visible and Raman spectroscopy.

Canadian Journal of Chemistry, **48**, 1919 (1970)

Can. J. Chem. Downloaded from www.nrcresearchpress.com by 210.87.254.105 on 09/05/12
For personal use only.

Introduction

The protonation of weak organic bases is a subject of considerable importance since its understanding is essential to an appreciation of a great variety of reactions that are sensitive to acid catalysis. The work of L. P. Hammett and others in the 1930's initiated interest in this area, and in the intervening years a great deal of information regarding the protonation of various types of aromatic compounds has accumulated (1). Unfortunately there has not been a concomitant accumulation of information related to the protonation of aliphatic compounds. The primary reason for the comparative dearth of data on the protonation of aliphatic compounds derives from the fact that most of these substances (with the notable exception of several carbonyl compounds) do not possess suitable chromophores to permit a study of their protonation behavior by use of visible–ultraviolet spectrophotometry. Consequently a number of attempts have been made to use other types of spectral measurements such as nuclear magnetic resonance (n.m.r.) chemical shifts and Raman band intensities to estimate the extent to which aliphatic compounds undergo protonation in aqueous acids. The limitations of these as well as several less direct methods, such as the use of distribution data or the variation in the rates of acid catalyzed reactions, have recently been reviewed (2).

Of all the possible methods that have been suggested for studying the protonation of aliphatic compounds it would seem that the use of n.m.r. chemical shifts appears to be the most attractive. Many aliphatic compounds give simple, nearly first-order n.m.r. spectra that are known, in at least some cases, to respond predictably to changes in acidity (3–5), and the shift of methyl signals relative to an internal standard has been used to determine pK_{BH^+} values for a number of amines, phosphine oxides, phosphine sulfides, and sulfoxides (6–9). Although it has been claimed that chemical shifts are subject to medium effects which greatly diminish the reliability of this method (2), there are no *a priori* reasons to suspect that chemical shifts would be more sensitive to medium effects than any other type of spectroscopy. Indeed, since n.m.r. involves an interaction with molecules in their ground states, it might well be less susceptible to solvent changes than other types of spectroscopy where medium effects on the excited states must also be considered. This reasoning is supported by the fact that Haake *et al.* were able to obtain highly accurate values for the basicity of acetophenone and *N,N*-dimethylacetamide from a study of methyl chemical shifts (relative to an internal standard) as a function of acidity (7). Furthermore, it would seem that any possible medium effects could be sharply reduced if the technique developed by Edward *et al.* was employed (5). These authors estimated the extent of protonation of several aliphatic compounds by measuring the difference between the chemical shifts of α and β hydrogens in the same molecule. (The α hydrogens, since they are closer to the site of protonation, are shifted downfield to a greater extent as the compound is protonated.) Because both the α and β hydrogens in a small molecule should be in approximately the same environment, it is not unreasonable to expect that gross medium effects might be similar for both types of hydrogens and hence minimized in the difference.

As a further test of this method we have undertaken a study of the protonation of a number of aliphatic ketones using chemical shift differences between α and β hydrogens to estimate the degree of protonation. Aliphatic ketones were used in this study for two reasons; (*i*) the pK_{BH^+}

TABLE 1

Differences (Δ) between the chemical shifts for α and β hydrogens of 3-pentanone, 2-butanone, and 3-methyl-2-butanone

	Δ (c.p.s.)		
H_2SO_4 (%)	3-Pentanone	2-Butanone	3-Methyl-2-butanone
0	93.2	72.0	68.2
7.7	93.5	72.4	68.4
29.6	94.1		69.0
37.8	94.5	73.6	69.3
48.0	94.5		
56.3	94.9	75.1	70.5
68.9	96.1	77.4	72.9
72.0	96.7	78.7	74.2
76.9	99.1	81.5	76.8
79.7	101.3	85.2	80.8
83.3	104.5	88.8	84.4
84.5	105.8	90.9	86.5
88.7	109.1	93.3	89.1
91.0	109.7	94.5	90.5
95.8		95.6	
97.0	111.1	95.8	91.9
98.5	112.0	96.1	
100.1	112.4	96.2	92.5
102.9	113.3	96.0	93.0

for several aliphatic ketones has previously been investigated using ultraviolet and Raman spectroscopy (3, 10) and (*ii*) the n.m.r. spectra of the protonated ketones are well known from the work of Olah *et al.* (11). The use of both ultraviolet and Raman spectroscopy gave similar results, indicating that simple ketones were half protonated in about 80% H_2SO_4; i.e. that the pK_{BH^+} is approximately -7.3.[1] In the following paper we will show that the use of n.m.r. chemical shifts also gives pK_{BH^+} values of about the same magnitude, thus establishing that this technique can be used, at least in some cases, to estimate the basicity of aliphatic compounds.

Experimental

All spectra were obtained using a Varian A60A spectrophotometer. Each measurement was made by adding 0.10 ml of ketone to 5.0 ml of standardized acid in a volumetric flask. The flask was inverted several times to insure homogeneity, a small portion was transferred to an n.m.r. tube and the spectrum taken at 37 ± 1 °C. Each spectrum was recorded four times, twice moving upfield and twice moving downfield, with a sweep width of 250 Hz and a sweep time of 250 s. Prior to each determination the chart paper was carefully calibrated using the sideband technique and the chemical shifts were then read directly from the chart paper. Since we were interested only in the difference (Δ) between the chemical shifts of the α and β hydrogens, no internal standard was added. By this method it was possible to obtain average values of Δ that were reproducible to within ± 0.3 c.p.s.

The spectra of all non-protonated ketones were consistent with a first-order analysis and with published spectra. In each case it was observed that increasing the acidity of the medium in which the spectra were obtained caused the difference (Δ) between the chemical shifts of the α and β hydrogens to increase until the ketones became fully protonated. Further increases in acidity beyond this point produced only small increases in the magnitude of Δ. The spectra of the fully protonated ketones were similar to those previously reported at −60 °C in fluorosulfuric acid with one major exception; no evidence of *cis* and *trans* isomers resulting from asymmetric protonation of the oxygen was obtained (11). Presumably at 37 °C, there is a rapid exchange between the two isomers which becomes imperceptibly slow (relative to the n.m.r. time scale) at −60°.

Table 1 lists the Δ values for these ketones in a number of sulfuric acid solutions of varying acidity. For 3-pentanone, Δ was taken as the difference between the chemical shifts of the methyl and methylene groups, while for 2-butanone and 3-methyl-2-butanone it was taken as the difference between the chemical shifts of primary hydrogens α and β to the carbonyl group. Methyl hydrogens were used whenever possible because they give strong, more readily definable signals than the corresponding methylenes.

The ketones were obtained commercially and purified by fractional distillation before use. Acid solutions were prepared by diluting reagent-grade 97% sulfuric acid with de-ionized water. Acids with concentrations greater than 97% were prepared by the addition of fuming sulfuric acid to 97% H_2SO_4. Standardization was achieved through titration against sodium hydroxide

[1]Throughout this paper pK_{BH^+} is taken to be the H_0 of the solution in which the base is half protonated. H_0 scales based on the protonation of primary aromatic amines were taken from refs. 12 and 13.

Can. J. Chem. Downloaded from www.nrcresearchpress.com by 210.87.254.105 on 09/05/12
For personal use only.

Can. J. Chem. Downloaded from www.nrcresearchpress.com by 210.87.254.105 on 09/05/12
For personal use only.

solutions of known concentrations using the phenolphthalein end point.

The H_0 values used up to 99.44% H_2SO_4 are those reported by Jorgenson and Hartter (12). The acidities for solutions containing greater than 99.44% H_2SO_4 were estimated by combining the data of Brand *et al.* (13) for the protonation of aromatic nitro compounds with those reported by Jorgenson and Hartter for the protonation of primary aromatic amines. While it is obvious that this procedure might lead to quite serious errors in the exact acidity values of these solutions, it should not introduce an appreciable error into our work since these highly acidic solutions were used only to obtain Δ for the fully protonated ketones.

Statistical analysis of the data was accomplished with the aid of an IBM 1130 computer.

Results and Discussion

The difference (Δ) between the chemical shifts of hydrogens α and β to the carbonyl groups of three aliphatic ketones have been determined in sulfuric acid solutions of varying concentrations. When these Δ values (which have been compiled in Table 1) are plotted against acidity, well-defined sigmoidal curves are obtained, as indicated in Fig. 1. Assuming that these curves arise as a result of protonation of the ketones, it then follows that the inflection point should correspond to the pK_{BH^+} of each base. A more accurate estimation of the pK_{BH^+} can, however, be obtained from the relationship $\log [BH^+]/[B] = -H + pK_{BH^+}$, where [B] is the concentration of unprotonated ketone, $[BH^+]$ is the concentration of protonated ketone, and H is an appropriate acidity function (14). It can then be shown, if Δ_B represents the difference between the chemical shifts of the α and β hydrogens of the unprotonated ketone, Δ_{BH^+} represents the same parameter for the protonated ketone, and Δ the chemical shift difference when the ketone is partially protonated, that $\log [BH^+]/[B] = \log (\Delta - \Delta_B)/(\Delta_{BH^+} - \Delta)$. Hence a plot of $\log (\Delta - \Delta_B)/(\Delta_{BH^+} - \Delta)$ against $-H$ should give a straight line of unit slope with intercept equal to pK_{BH^+}. The advantage of this method is that the need for an arbitrary choice of the inflection point of the curve is eliminated, since the best straight line and the intercept can be determined by the method of least squares.

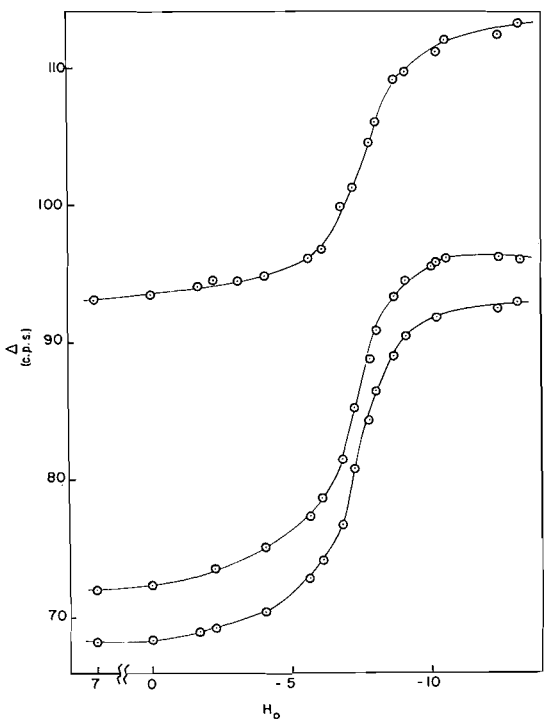

FIG. 1. Titration curves for the protonation of 3-pentanone, 2-butanone, and 3-methyl-2-butanone (top to bottom). Δ is the difference between the chemical shifts of α and β hydrogens. H_0 is the amine acidity function (12).

However, two difficulties are encountered in attempting to prepare linear plots of this type. The first of these is in determining values for Δ_B and Δ_{BH^+}. Ideally, these values could be obtained directly if the sigmoidal plots were all flat at both very high and very low acidities. However, it has previously been found possible to construct linear plots even when the sigmoidal curves are not ideal by choosing values for the free base and the protonated base that are equidistant above and below the estimated inflection point and beyond the steep part of the curve. As has been pointed out by Stewart and Granger (15) and by Yates, Stevens, and Katritzky (16), the use of this method minimizes errors which can result from the non-ideality of the sigmoidal plots. In this work the values of Δ_B and Δ_{BH^+} were arbitrarily chosen to be five H_0 units above and below the estimated inflection points. The value of five H_0 units was chosen because it placed the readings well beyond the steep part of the curve and because it was found to generate good linear plots. Almost identical results were obtained when Δ_B and Δ_{BH^+} were chosen $\pm 7 H_0$ units from the inflection point, but a definite curvature of some of the plots was noted when attempts were made to use Δ_B values obtained in neutral water and Δ_{BH^+} values obtained in fuming sulfuric acid. The failure to obtain good

Can. J. Chem. Downloaded from www.nrcresearchpress.com by 210.87.254.105 on 09/05/12
For personal use only.

linear plots in the latter case is probably a consequence of medium effects on the magnitude of the chemical shift differences.[2] Alternatively, it may simply be a reflection of the possibility that H_0 and the acidity function that properly describes the protonation of ketones are not parallel. Development of such an acidity function for aliphatic ketones remains as a current challenge to physical organic chemists.

Hence the second difficulty encountered in attempting to prepare good linear plots involves the choice of an appropriate available acidity function. We have plotted $\log (\Delta - \Delta_B)/(\Delta_{BH^+} - \Delta)$ against two possible acidity functions which are defined for primary aromatic amines (12) and benzophenones (18), respectively.[3] As the plots in Figs. 2, 3, and 4 indicate, the use of these two functions results in the formation of linear plots with slopes of approximately 0.5 for the amine function and 0.8 for the ketone function. Since the slopes of the latter plots are closer to unity, it would appear that the protonation behavior of aliphatic ketones more closely resembles that of benzophenones than that of amines. This observation of a better correlation between the mode of protonation of the two types of carbonyl compounds than between ketones and amines is to be expected and suggests that we are not wrong in assuming that the changes in Δ are caused primarily by protonation.

One other fact that has greatly encouraged us to believe chemical shift data can be used to determine pK_{BH^+} is the excellent correlation between the values which are obtained from the intercepts of the plots in Figs. 2, 3, and 4 and those previously obtained for aliphatic ketones by use of ultraviolet and Raman spectroscopy (3, 10). All three methods indicate that aliphatic ketones are half protonated in approximately 80% H_2SO_4; i.e. that the pK_{BH^+} for these compounds are

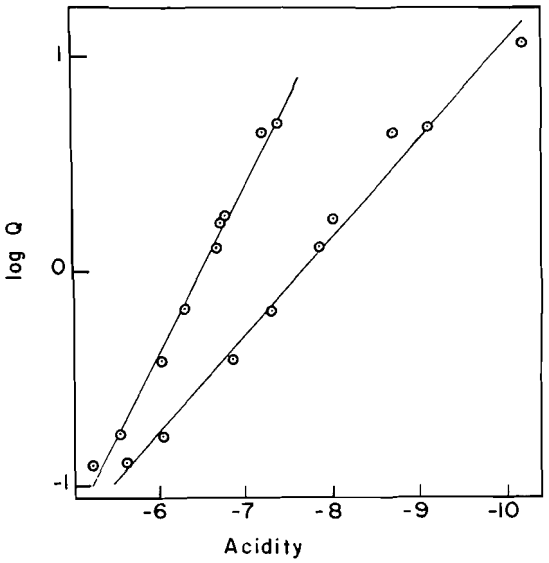

FIG. 2. *3-Pentanone.* $Q = (\Delta - \Delta_B)/(\Delta_{BH^+} - \Delta)$. For the benzophenone acidity function (left), intercept = -6.50 ± 0.08, slope = -0.80, and correlation coefficient = 0.987. For the amine acidity function (right), intercept = -7.63 ± 0.19, slope = -0.46, and correlation coefficient = 0.984.

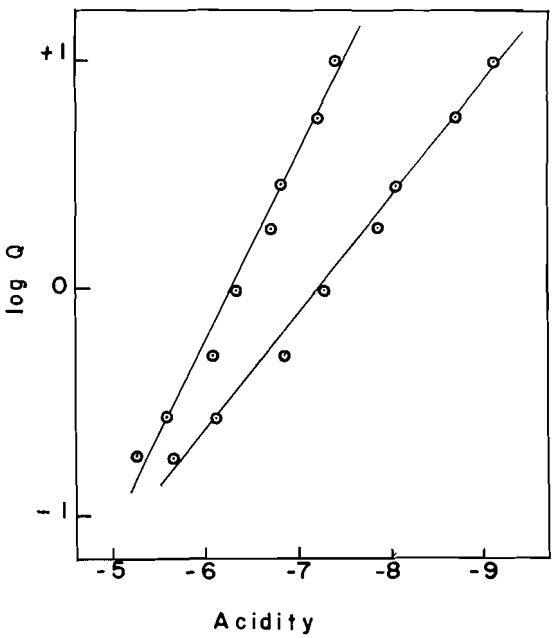

FIG. 3. *3-Methyl-2-butanone.* $Q = (\Delta - \Delta_B)/(\Delta_{BH^+} - \Delta)$. For the benzophenone acidity function (left), intercept = -6.30 ± 0.11, slope = -0.78, and correlation coefficient = 0.980. For the amine acidity function (right), intercept = -7.25 ± 0.13, slope = -0.52, and correlation coefficient = 0.989.

[2]A referee has suggested, in analogy with the work of Peterson (17), that the gradual increase in Δ at low acidities may be related to changes in the extent of hydrogen bonding between the solvent and the carbonyl oxygen. However, a fine distinction cannot be drawn between the situation where a base is extensively hydrogen bonded to an acidic solvent and where it is actually protonated; both cases are merely different aspects of the same process.

[3]Unfortunately the same symbol (H_0) has been used for both of these acidity functions. We have attempted to distinguish between them by referring to one as the "amine acidity function" and the other as the "benzophenone acidity function."

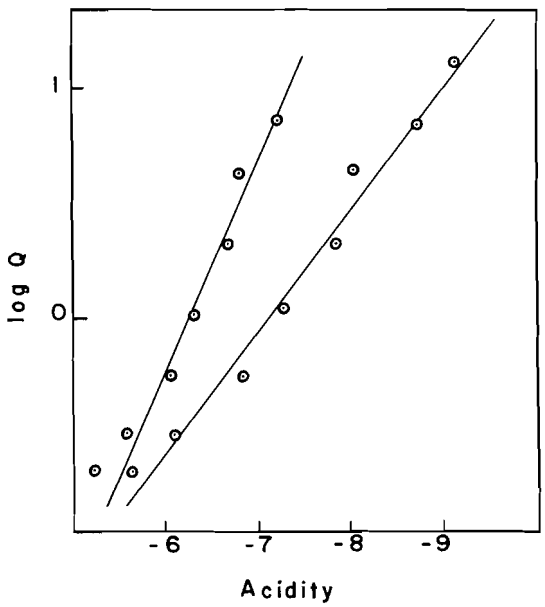

FIG. 4. *2-Butanone.* $Q = (\Delta - \Delta_B)/(\Delta_{BH^+} - \Delta)$. For the benzophenone acidity function (left), intercept = -6.21 ± 0.14, slope = -0.82, and correlation coefficient = 0.967. For the amine acidity function (right), intercept = -7.10 ± 0.18, slope = -0.54, and correlation coefficient = 0.981.

about -7.3 on the H_0(amine) scale. The exact values for the intercepts obtained from the plots in Figs. 2, 3, and 4 are -7.63 ± 0.19 for 3-pentanone, -7.25 ± 0.13 for 3-methyl-2-butanone, and -7.10 ± 0.18 for 2-butanone. As indicated, a least-squares analysis of the data suggests that the probable errors in the intercepts are about $\pm$ 0.2 H_0 units; however, we feel that this statistical error may be too low, primarily because of the assumptions made in estimating Δ_B and Δ_{BH^+}. (On the benzophenone acidity scale, the pK_{BH^+} are -6.50 ± 0.08 for 3-pentanone, -6.30 ± 0.11 for 3-methyl-2-butanone, and -6.21 ± 0.14 for 2-butanone.)

In conclusion, it can be seen that the results of the experiments reported in this paper establish two important facts; (*i*) they show that n.m.r. chemical shifts can be used quantitatively to estimate the pK_{BH^+} values of at least some types of aliphatic compounds, and (*ii*) they confirm previous observations that aliphatic ketones are one-half protonated in approximately 80% H_2SO_4.

The author is grateful to Mrs. Edna Denning and Mr. Ron Cameron for skillful technical assistance and to the National Research Council of Canada for financial support.

1. L. P. HAMMETT. Physical organic chemistry. McGraw–Hill Book Co., Inc., New York. 1940.
2. E. M. ARNETT. Progr. Phys. Org. Chem. **1**, 223 (1963).
3. N. C. DENO and M. J. WISOTSKY. J. Amer. Chem. Soc. **85**, 1735 (1963).
4. R. W. TAFT and P. L. LEVINS. Anal. Chem. **34**, 436 (1962).
5. J. T. EDWARD, J. B. LEANE, and I. C. WANG. Can. J. Chem. **40**, 1521 (1962).
6. E. GRUNWALD, A. LOEWENSTEIN, and S. MEIBOOM. J. Chem. Phys. **27**, 641 (1957).
7. P. HAAKE, R. D. COOK, and G. H. HURST. J. Amer. Chem. Soc. **89**, 2650 (1967).
8. P. HAAKE and R. D. COOK. Tetrahedron Lett. 427 (1968).
9. D. LANDINI, G. MODENA, G. SCORRANO, and F. TADDEI. J. Amer. Chem. Soc., **91**, 6703 (1969).
10. H. J. CAMPBELL and J. T. EDWARD. Can. J. Chem. **38**, 2109 (1960).
11. G. A. OLAH, M. CALIN, and D. H. O'BRIEN. J. Amer. Chem. Soc. **89**, 3586 (1967).
12. M. J. JORGENSON and D. R. HARTTER. J. Amer. Chem. Soc. **85**, 878 (1963).
13. J. C. D. BRAND, W. C. HORNING, and M. B. THORNLEY. J. Chem. Soc. 1374 (1952).
14. M. A. PAUL and F. A. LONG. Chem. Rev. **57**, 1 (1957)
15. R. STEWART and M. R. GRANGER. Can. J. Chem. **39**, 2508 (1961).
16. K. YATES, J. B. STEVENS, and A. R. KATRITZKY. Can. J. Chem. **42**, 1957 (1964).
17. P. E. PETERSON. J. Org. Chem. **31**, 439 (1966).
18. T. G. BONNER and J. PHILLIPS. J. Chem. Soc. B, 650 (1966).

Can. J. Chem. Downloaded from www.nrcresearchpress.com by 210.87.254.105 on 09/05/12
For personal use only.

Can. J. Chem. Downloaded from www.nrcresearchpress.com by 210.87.254.5 on 09/05/12
For personal use only.

Nuclear charge dispersion of light-mass fission products in the fission of ^{235}U and ^{238}U by medium-energy protons

A. H. KHAN,[1] G. B. SAHA,[2] AND L. YAFFE

Radiochemistry Laboratory, Department of Chemistry, McGill University, Montreal, Quebec

Received November 14, 1969

Independent fission yields for $^{90}Y^{m}$, $^{90}Y^{m+g}$, $^{91}Y^{m}$, $^{91}Y^{m+g}$, and ^{92}Y and cumulative yields for ^{91}Sr, ^{92}Sr, and ^{93}Y in the fission of ^{235}U and ^{238}U by protons of energy from 20–85 MeV have been determined. Excitation functions and charge dispersion curves have been obtained. The most probable charge, Z_p, moves closer to stability, Z_A, with increasing energy. The values of $Z_A - Z_p$ for the two fissioning systems are identical, unlike the situation in the heavy-mass region. The values of $Z_A - Z_p$ for the light- and heavy-mass regions differ considerably, showing that the equal charge displacement hypothesis does not hold even at these moderate energies.

Canadian Journal of Chemistry, **48**, 1924 (1970)

Introduction

Very few data regarding the dispersion of nuclear charge in the fission of heavy nuclei as a function of energy have been published. A series of papers from this laboratory (1–9) have dealt mainly with the dispersion in heavy-mass products (A = 129–141). The broadening of the charge dispersion curves as the bombarding energy was increased, as well as the shift of Z_p, the most probable charge, towards Z_A, the charge associated with stability for mass A, were clearly evident from these studies. In addition, the studies pointed out the importance of the neutron-to-proton ratio of the target in determining the fission product distribution (8, 9).

While the amount of information regarding charge dispersion in the heavy-mass region is beginning to mount up, very little information regarding the complementary mass region exists. Hagebø *et al.* (10) investigated light-mass products found in the fission of ^{238}U by 170-MeV protons. They found that the charge dispersion curves were narrower than those found in the heavy-mass region by the previous investigations and were similar to those found in the thermal neutron fission of ^{235}U (11).

The present study was undertaken in order to investigate the nuclear charge dispersion of the light-mass fission products obtained from the fission of ^{235}U and ^{238}U by protons of energies 20–85 MeV. In this paper are reported the yields of some yttrium and strontium nuclides, in the mass region A = 90–93, obtained by radiochemical methods.

In addition to yielding fundamental data germane to the fission process, such a study enables one to estimate the total number of neutrons emitted during the fission process at each bombarding energy. A study based on these and other data will be published shortly.

Experimental

(a) Targets and Irradiations

The target materials were ^{235}U (94%) and natural uranium foils ranging in thickness from 77–122 mg/cm^2. The target foils were cleaned with nitric acid, washed with water, then acetone, and sandwiched between two aluminum catcher foils (9 mg/cm^2) to stop recoiling fission fragments from the target foil during the irradiation.

The proton beam was monitored by the $^{65}Cu(p,pn)^{64}Cu$ reaction for the entire energy region. The copper foil, 21.4 mg/cm^2 thick, was sandwiched between two similar copper foils and placed upstream to the proton beam.

The target, catcher, and monitor foils were carefully aligned to ensure equal exposure to the incident proton beam, wrapped in aluminum foil (0.008 in. thick), and clamped to the target holder which was then fixed to the end of the water-cooled cyclotron probe.

All the irradiations were performed at various radii in the internal circulating proton beam of the McGill Synchrocyclotron. The duration of irradiation varied from 8–20 min depending on the bombarding energy and the beam intensity which varied between 0.5 and 1.0 μA.

(b) Chemical Separations

After irradiation, the uranium foil, along with the aluminum catcher foils, was dissolved by heating in a few milliliters of concentrated hydrochloric acid plus a few drops of nitric acid in the presence of the following carriers: yttrium (20 mg), zirconium (20 mg), and 10 mg each of strontium, barium, lanthanum, and cerium. Since two separations were necessary to determine the yields of some yttrium isotopes, an aliquot of the target solution

[1]Present address: Chemistry Division, Atomic Energy Centre, P.O. Box 164, Ramna, Dacca, East Pakistan.

[2]Present address: Division of Nuclear Medicine, 2nd Floor Medical Wing, Royal Victoria Hospital, Montreal, Quebec.

TABLE 1

Pertinent nuclear data (16) and methods of detection of radioactive nuclides studied

Nuclide	Half-life	Radiation followed	Branch abundance, %	Detection technique*
$^{90}Y^{m}$	3.2 h	0.202 MeV γ	97†	PHA
$^{90}Y^{g}$	64.2 h	β^-	100	β-prop
$^{91}Y^{m}$	50.0 min	0.551 MeV γ	95†	PHA
$^{91}Y^{g}$	59.0 day	β^-	100	β-prop
^{92}Y	3.5 h	β^-	100	β-prop
^{93}Y	10.1 h	β^-	100	β-prop
^{91}Sr	9.7 h	β^-	59 to $^{91}Y^{m}$ 41 to $^{91}Y^{g}$	not measured directly
^{92}Sr	2.7 h	β^-	100	not measured directly
^{64}Cu	12.8 h	0.511 MeV γ	38	PHA

*NaI crystal plus pulse-height analyzer; β-prop = β-proportional counter; PHA = NaI crystal plus pulse-height analyzer.
†The remaining isomeric transitions are internally converted.

was used for the initial quick separation and another portion was used to separate yttrium at a later appropriate time. The chemical procedure was essentially based on that given in ref. 12, while the separation of the copper was done following that of Kraus and Moore (13). A brief description of the methods as adapted follows.

Yttrium

Yttrium was precipitated as the hydroxide with ammonia from an aliquot of the target solution, digested for 1/2 min and the end of digestion taken as the time of separation of yttrium from strontium. Further purification of the yttrium activity was effected by several cycles of fluoride and hydroxide precipitations. Yttrium was then extracted into tributyl phosphate from concentrated nitric acid, back-extracted into water, and precipitated with ammonia. This cycle of extraction and precipitation was repeated, the hydroxide dissolved in 4 *N* hydrochloric acid, made to volume, and an aliquot used for measurement of the activities of $^{90}Y^{m}$ and $^{91}Y^{m}$. Chemical yields were determined spectrophotometrically using sodium alizarin (14) as the complexing agent.

From another aliquot of the purified yttrium solution, a solid source was prepared for β-activity measurements by precipitating yttrium oxalate with oxalic acid. The precipitate was ignited at 850–900 °C for about 1 h. The ignited yttrium oxide was powdered and mounted on a glass fiber filter paper disk for measurement. The chemical yields were determined from the weight of the oxide.

Copper

The copper foil was dissolved in concentrated hydrochloric acid plus a few drops of hydrogen peroxide. The solution was evaporated to dryness, taken up with 4.5 *N* hydrochloric acid, and passed through a Dowex-1 × 8 anion-exchange resin column. The copper was eluted with 1.5 *N* hydrochloric acid, precipitated with ammonium thiocyanate as the thiocyanate, washed, dried at 110 °C, and mounted for activity measurements. The chemical yields were determined from the weight of copper thiocyanate.

(c) Activity Measurements

The pertinent decay characteristics (16) of the various nuclides of interest and the methods of their detection are summarized in Table 1. The γ rays of energies 0.551 and 0.202 MeV from the isomeric transitions of 50-min $^{91}Y^{m}$ and 3.2-h $^{90}Y^{m}$, respectively, as well as the 0.511 MeV annihilation radiation from ^{64}Cu were measured by a calibrated 3 in. × 3 in. NaI(Tl) scintillation crystal coupled to a 400-channel pulse-height analyzer. The β activities of $^{90}Y^{g}$, $^{91}Y^{g}$, ^{92}Y, and ^{93}Y were measured by both an end-window proportional counter and a very low background (~0.5 counts/min) Beckman Wide-Beta II counter. These counters were calibrated against a 4πβ counter with activities of these nuclides obtained from separate bombardments. The activities of all nuclides were measured for several half-lives.

(d) Treatment of Data

The measured activities were resolved into the individual components either graphically or with the aid of the CLSQ computer program (15). The counting rates at the end of bombardment or separation were converted to absolute disintegration rates by correcting for chemical yields, detector efficiencies, dilution factors, and branching ratios. The sources used for β-ray measurements were thin enough and the energies of the β rays high enough so that no self-absorption corrections were necessary.

The independent formation cross-sections of $^{90}Y^{m}$ and $^{90}Y^{m+g}$, and also the cumulative formation cross-section of ^{93}Y, were determined from the disintegration rates at

TABLE 2

Monitor cross sections from Meghir (17)

Proton energy (MeV)	Cross section $^{65}Cu(p,pn)^{64}Cu$ (mb)
20	260
30	390
40	260
50	210
60	180
70	160
77	150
85	140

Can. J. Chem. Downloaded from www.nrcresearchpress.com by 210.87.254.5 on 09/05/12
For personal use only.

TABLE 3

Formation cross sections from ^{235}U fission

E_p (MeV)	No. of measurements	σ (mb)* $^{90}Y^m$ (Ind)	$^{90}Y^{m+g}$ (Ind)	$^{91}Y^m$ (Ind)	$^{91}Y^{m+g}$ (Ind)	^{92}Y (Ind)	^{93}Y (Cum)	^{91}Sr (Cum)	^{92}Sr (Cum)
20	1	0.13±0.02	2.4±0.4	1.3±0.2	3.0±0.7	6.9±1.0	55± 7	43± 7	47± 7
30	1	0.22±0.03	3.4±0.5	2.1±0.3	4.9±1.0	9.9±1.5	53± 7	40± 7	41± 6
40	2	0.32±0.05	4.0±0.5	3.5±0.5	7.5±1.7	14.3±2.4	85±13	69±13	67±11
50	1	0.67±0.10	4.6±0.7	3.9±0.5	9.0±2.0	16.0±2.4	84±11	70±12	75±11
60	2	0.79±0.11	4.7±0.8	5.5±0.8	11.3±2.4	19.7±3.1	88±12	72±13	72±12
70	2	0.98±0.11	5.8±0.9	6.0±1.0	12.2±3.0	16.9±2.7	86±13	78±16	77±12
77	1	1.4 ±0.2	6.1±0.9	5.2±0.7	11.8±2.6	19.5±2.9	92±12	75±13	78±12
85	1	1.3 ±0.2	6.0±1.0	5.0±0.6	11.5±2.5	18.0±2.7	84±11	74±12	75±11

*Ind = independent; Cum = cumulative.

TABLE 4

Formation cross sections from ^{238}U fission

E_p (MeV)	No. of measurements	σ (mb)* $^{90}Y^m$ (Ind)	$^{90}Y^{m+g}$ (Ind)	$^{91}Y^m$ (Ind)	$^{91}Y^{m+g}$ (Ind)	^{92}Y (Ind)	^{93}Y (Cum)	^{91}Sr (Cum)	^{92}Sr (Cum)
20	1	0.12±0.02	2.9±0.4	0.97±0.13	4.5±1.0	7.3±1.1	42± 5	26± 4	31± 5
30	2	0.15±0.02	3.0±0.5	1.6 ±0.2	5.6±1.3	8.9±1.2	67±10	52±10	60± 8
40	2	0.19±0.03	3.5±0.5	1.8 ±0.2	5.4±1.2	11±1.8	70±10	51± 9	66±11
50	2	0.22±0.03	3.9±0.6	1.9 ±0.3	6.2±1.3	10±1.7	75±11	56±10	62±10
60	1	0.22±0.03	3.5±0.6	2.0 ±0.3	6.4±1.4	13±1.9	68± 9	57±10	59± 9
70	1	0.28±0.04	4.1±0.6	1.8 ±0.2	6.7±1.5	13±2.0	62± 8	58±10	64±10
77	1	0.33±0.05	4.4±0.7	1.8 ±0.2	7.6±1.7	13±1.9	67± 9	60±10	52± 8
85	2	0.37±0.05	4.4±0.7	2.0 ±0.3	7.7±1.7	12±1.8	66±10	61±10	60±10

*Ind = independent; Cum = cumulative.

the end of bombardment by the use of standard equations (3). To determine the cross-sections of the parent and daughter nuclides in the ^{91}Sr–$^{91}Y^m$, ^{91}Sr–$^{91}Y^{m+g}$, and ^{92}Sr–^{92}Y pairs, the growth–decay equations, as given by Friedlander *et al.* (3) were used, along with the disintegration rates of the appropriate yttrium isotope, measured at the two separation times. The monitor cross-sections for the $^{65}Cu(p,pn)^{64}Cu$ reaction were those of Meghir (17), and these values are given in Table 2 for ready reference.

Results and Discussion

The measured cross-sections for the various nuclides are shown in Tables 3 and 4 for formation from ^{235}U and ^{238}U, respectively. Because ^{93}Sr, the parent of ^{93}Y, is short-lived ($t_{\frac{1}{2}}$ = 8.3 min), only cumulative cross sections of ^{93}Y were determined. In the case of ^{91}Y, two parent–daughter pairs were studied, i.e. ^{91}Sr–$^{91}Y^m$ and ^{91}Sr–$^{91}Y^{m+g}$, and the appropriate branching-ratio correction made (16). The results agreed very well and the cumulative cross sections for ^{91}Sr are the averages of the two results.

(a) Excitation Functions

Excitation functions of the various nuclides investigated are shown in Figs. 1–11 inclusive. Data obtained by other workers at higher energies are included in the figures. Comparison is made very difficult because in some cases no monitor cross sections have been quoted. In the other cases, different monitors were used at the higher energies. Results obtained by other workers at energies greater than 500 MeV are not included since other mechanisms (e.g. fragmentation) may be taking part in the process.

The uncertainties quoted include both the random errors associated with the decay-curve analysis, chemical yields, dilution factors, etc., as well as systematic errors associated with detector efficiencies, spread in proton beam energy, etc. Errors due to uncertainties in the monitor cross sections and decay-scheme data have not been included. In the case of duplicate measurements the errors quoted are the mean deviations. These

Can. J. Chem. Downloaded from www.nrcresearchpress.com by 210.87.254.5 on 09/05/12
For personal use only.

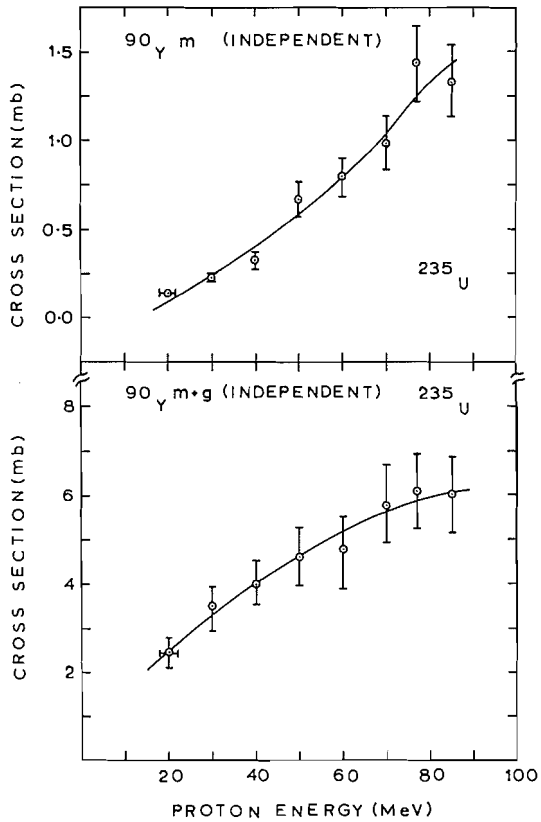

FIG. 1. Excitation functions for the independent formation of $^{90}Y^{m}$ and $^{90}Y^{m+g}$ from ^{235}U.

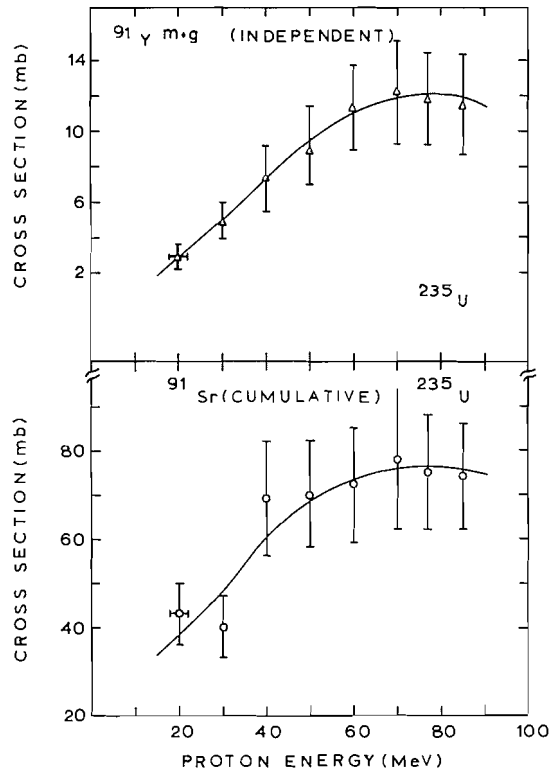

FIG. 2. Excitation functions for the independent formation of $^{91}Y^{m+g}$ and the cumulative formation of ^{91}Sr from ^{235}U.

were less than the total uncertainty quoted, which varied between ± 13 and $\pm 24\%$.

(b) Nuclear Charge Dispersion

The cross-section data for the yttrium and strontium nuclides obtained from both fissioning targets were used to construct charge dispersion curves at each bombarding energy studied. The curves were obtained by plotting the independent formation cross-section as a function of the neutron-to-proton ratio (N/Z), following the procedure described by Friedlander *et al.* (3). In the presentation of data in this manner it is assumed that the mass distribution curve is essentially flat in the narrow mass region $90 \leqslant A \leqslant 93$. In the more neutron-excess regions where independent cross-section data were not available, cumulative cross sections of ^{91}Sr, ^{92}Sr, and ^{93}Y were used to draw the dotted portion of the curve in such a way that the independent formation cross sections read from the curve summed to the measured cumulative cross sections. If one assumes that no gross discontinuities occur in the charge dispersion curves, the above constraint uniquely defines the right-hand portion of the curves. Samples of these curves at 50-MeV bombarding energy are shown in Fig. 12.

Sugarman *et al.* (21) have shown from their results of the 450-MeV proton-induced fission of ^{238}U that the N/Z_p (where Z_p = the most probable charge) values vary with the mass number of the fission products. Recently Hogan and Sugarman (22) observed that, again for fission of ^{238}U with 450-MeV protons, the N/Z_p values initially increase with $A = 70$–90, remain almost constant in the region $A = 100$–125, and then increase for $A = 130$–145. It is very difficult to extrapolate from this high-energy region to the moderate energies under consideration in this paper and expect the same results to hold true. In addition, the mass range being considered here is small enough so that the above objections do not influence the conclusions drawn here.

The values of Z_p at various bombarding

Can. J. Chem. Downloaded from www.nrcresearchpress.com by 210.87.254.5 on 09/05/12
For personal use only.

Can. J. Chem. Downloaded from www.nrcresearchpress.com by 210.87.254.5 on 09/05/12
For personal use only.

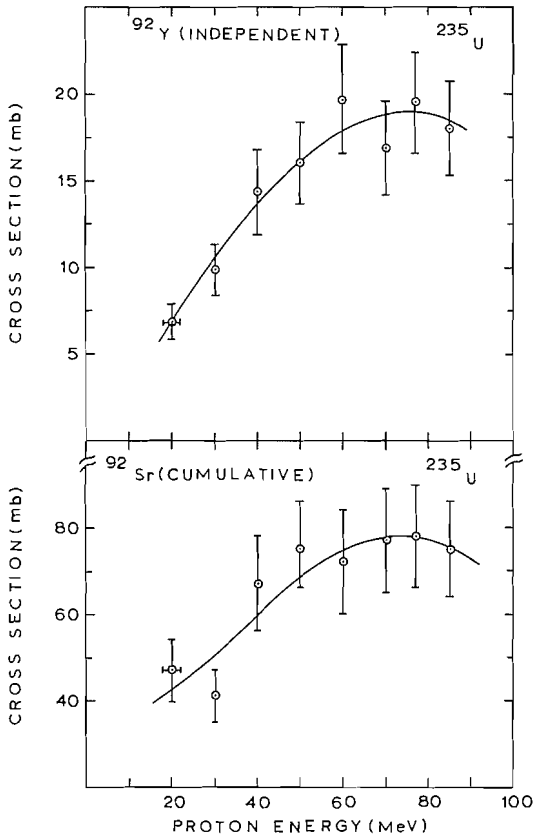

FIG. 3. Excitation functions for the independent formation of ^{92}Y and cumulative formation of ^{92}Sr from ^{235}U.

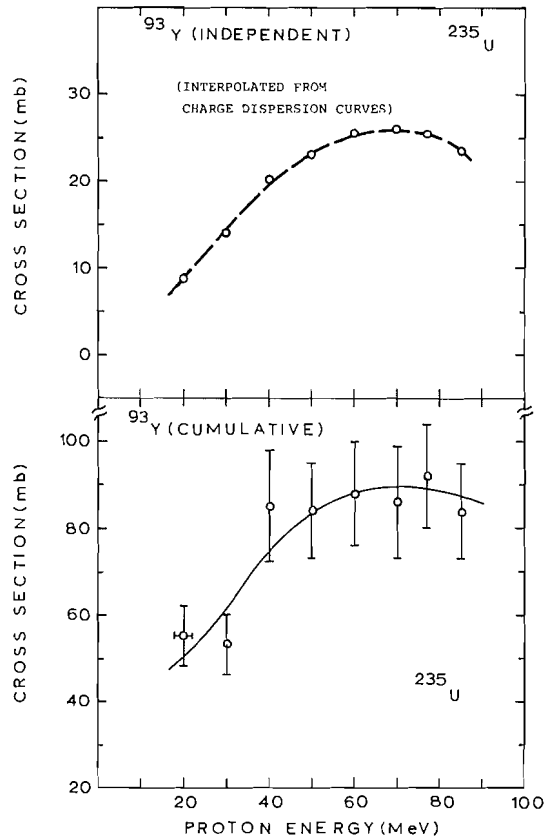

FIG. 4. Excitation functions for the independent formation of ^{93}Y from ^{235}U (interpolated from the charge dispersion curves) and the cumulative formation of ^{93}Y from ^{235}U (directly determined).

energies were obtained from the values of N/Z at the peak of the charge dispersion curves. The values of N/Z at half-maximum were converted to Z values to obtain the full-width at half-maximum (FWHM) of the various curves. These values, as well as that for $Z_A - Z_p$, where Z_A is the most stable charge for mass A, are given in Tables 5 and 6, and their variation with proton bombarding energy is shown in Fig. 13. The values of Z_A are those of Coryell (23).

It can be seen that, as the proton bombarding energy increases, the full-width at half-maximum remains virtually constant at a value of 2.9 Z units for both ^{235}U and ^{238}U, up to about 45 MeV. Above this value, the FWHM values increase by about 0.1 Z unit for every 10 MeV increase in bombarding energy.

The behavior of charge dispersion curves in this energy bombardment range has been studied

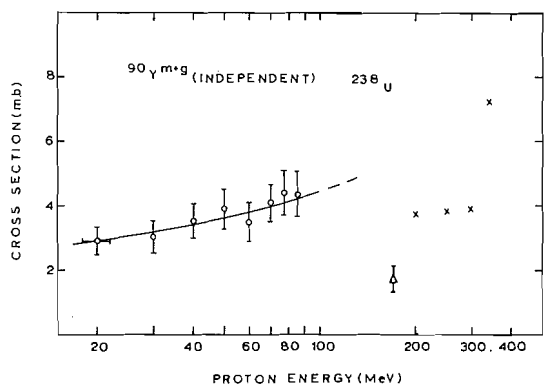

FIG. 5. Excitation function for the independent formation of $^{90}Y^{m+g}$ from ^{238}U. ○, this work; △, Hagebø *et al.* (10); ×, Stevenson *et al.* (18).

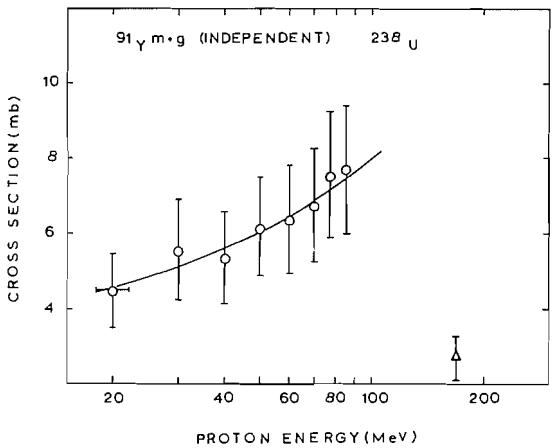

FIG. 6. Excitation function for the independent formation of $^{91}Y^{m+g}$ from ^{238}U. ○, this work; △, Hagebø *et al.* (10).

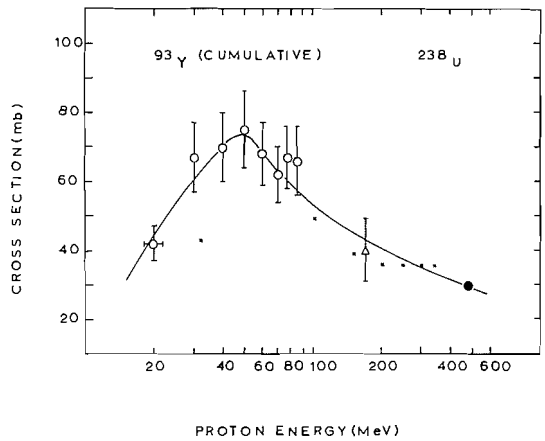

FIG. 8. Excitation function for the cumulative formation of ^{93}Y from ^{238}U. ○, this work; ×, Stevenson *et al.* (18); △, Hagebø *et al.* (10); ●, Vinogradov *et al.* (19).

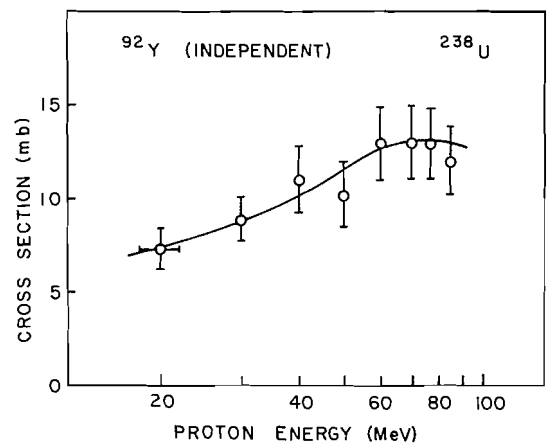

FIG. 7. Excitation function for the independent formation of ^{92}Y from ^{238}U.

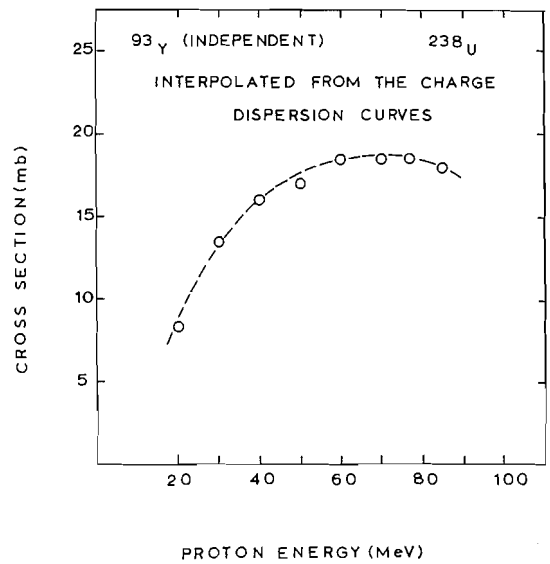

FIG. 9. Excitation function for the independent formation of ^{93}Y from ^{238}U. (Interpolated from charge dispersion curves).

in the mass region of A = 130–138 by Davies and Yaffe (4) for ^{238}U fission, by Benjamin *et al.* (7) for ^{232}Th fission, Tomita and Yaffe (8) for ^{233}U fission, and Saha and Yaffe (9) for ^{239}Pu fission, in the region A = 139–143 for ^{238}U fission by Parikh *et al.* (5), and in the region A = 130–135 by Pate *et al.* (1). In all of these studies dealing with heavy-mass fission products, the full-width at half-maximum values and their energy dependence were almost identical for all the systems. The values remained constant at about 2–2.2 charge units up to a bombardment energy of 40 MeV and then increased with increasing energy up to a value of about 3.2 charge units at 85 MeV. The same trend is shown by the light-mass products observed here, though the widths observed are somewhat larger at the lower energies. Conversely, Hagebø *et al.* (10) reported a smaller value of the FWHM for light-mass products as compared with heavy-mass products in the fission of ^{238}U by protons of 170-MeV energy. This may well be a function of the post-fission behavior of the products (e.g. neutron emission).

Can. J. Chem. Downloaded from www.nrcresearchpress.com by 210.87.254.5 on 09/05/12
For personal use only.

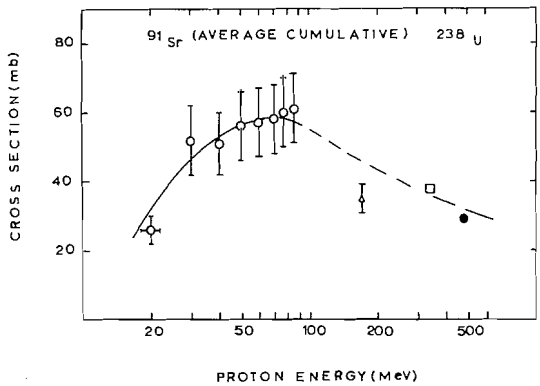

FIG. 10. Excitation function for the cumulative formation of ^{91}Sr from ^{238}U. ○, this work; △, Hagebø *et al.* (10); □, Folger, Stevenson, and Seaborg (20); ●, Vinogradov *et al.* (19).

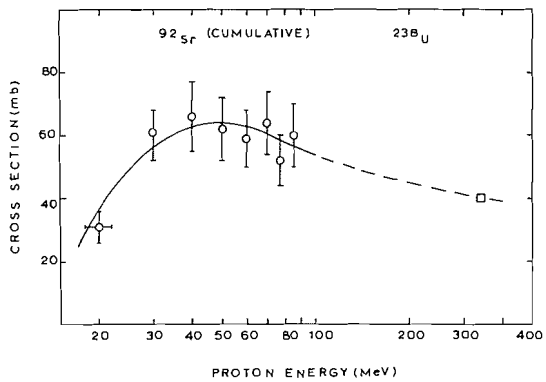

FIG. 11. Excitation function for the cumulative formation of ^{92}Sr from ^{238}U. ○, this work; □, Folger, Stevenson, and Seaborg (20).

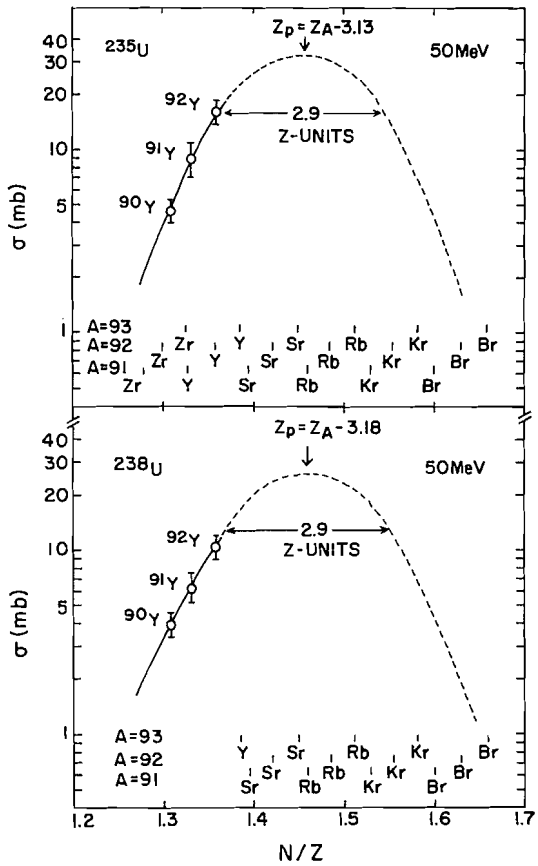

FIG. 12. Charge dispersion at 50 MeV for ^{235}U and ^{238}U. The right-hand (dashed) portion has been drawn so that the sums of the isobaric yields read off the curve approximate the *measured* cumulative yields.

Again, as reported by other workers (1, 4, 5, 7–9), the most probable charge, Z_p, moves slowly towards stability with increasing bombardment energy. In all the above studies, the $Z_A - Z_p$ values varied with energy from about 2.7 Z units at 20 MeV to about 1.6 charge units at 85 MeV. The present studies show a variation from 3.4 to 3.0 Z units for the same energy region. This difference in the behavior of light- and heavy-mass fission products is not yet understood, but the above data show clearly that, even at these moderate energies, the equal charge displacement hypothesis (24) does not hold. This is contrary to the conclusions drawn by Pate (25) for reactions occurring in the same energy region.

Surprisingly, the values of $Z_A - Z_p$ for fission of ^{235}U and ^{238}U are virtually identical at the same bombardment energy and the two curves are indistinguishable. It has been shown by the work on the heavy-mass fission products of ^{233}U (8), ^{239}Pu (9), ^{232}Th (7), ^{238}U (4), and ^{235}U (26) that the value of $Z_A - Z_p$ at any given bombardment energy is a function of the neutron-to-proton ratio of the fissioning target element. Indeed this has been used (9, 26) to predict successfully the $Z_A - Z_p$ values of hitherto unstudied systems. This is obviously not the case with the light-mass products.

The general features of the charge dispersion curves can be explained in terms of the variation of the distribution of fissioning nuclei. As the bombarding energy is increased, the competition between neutron evaporation and fission is enhanced, thus leading to the formation of many possible fissioning nuclei. Accordingly, the possibility for the formation of different fission

Can. J. Chem. Downloaded from www.nrcresearchpress.com by 210.87.254.5 on 09/05/12
For personal use only.

TABLE 5

Parameters of charge dispersion curves for ^{235}U

Proton energy (MeV)	Full-width at half-maximum		Peak position		
	N/Z	Z	N/Z	Z_p	$Z_A - Z_p$*
20	0.170	2.7	1.475	38.78	3.42
30	0.180	2.9	1.466	38.93	3.27
40	0.174	2.8	1.463	38.97	3.23
50	0.186	2.9	1.457	39.07	3.13
60	0.197	3.1	1.453	39.13	3.07
70	0.199	3.2	1.450	39.18	3.02
77	0.204	3.3	1.450	39.18	3.02
85	0.214	3.4	1.446	39.25	2.95

*$Z_A = 42.2$ for $A = 96$ (23).

TABLE 6

Parameters of charge dispersion curves for ^{238}U

Proton energy (MeV)	Full-width at half-maximum		Peak position		
	N/Z	Z	N/Z	Z_p	$Z_A - Z_p$*
20	0.184	2.9	1.470	38.86	3.34
30	0.181	2.9	1.465	38.95	3.25
40	0.184	2.9	1.460	39.02	3.18
50	0.185	2.9	1.460	39.02	3.10
60	0.194	3.2	1.455	39.10	3.10
70	0.201	3.2	1.455	39.10	3.10
77	0.209	3.3	1.455	39.10	3.10
85	0.210	3.4	1.455	39.10	3.10

*$Z_A = 42.20$ for $A = 96$ (23).

products will increase. This would then be seen as a widening of the charge dispersion curves, as observed in the present and previous studies.

The shift of the most probable charge towards stability as the bombarding energy is increased is a direct consequence of the lowering of the N/Z value of the fissioning element because of neutron evaporation giving rise to fission products with lower N/Z values, increasing Z_p and causing it to shift towards stability. Alternatively, evaporation of neutrons from the fission fragments will yield the same result.

From the charge dispersion curves, isobaric yields for mass $A = 93$ were obtained at various bombarding energies for ^{235}U and ^{238}U fission. These are shown in Table 7 and Fig. 14. The yields for the two systems are identical at 20 MeV, but the yields for ^{235}U reach a plateau at a higher level than those for ^{238}U. This is a reflection of the behavior of both the charge dispersion curves and of the gross mass–yield curves. The

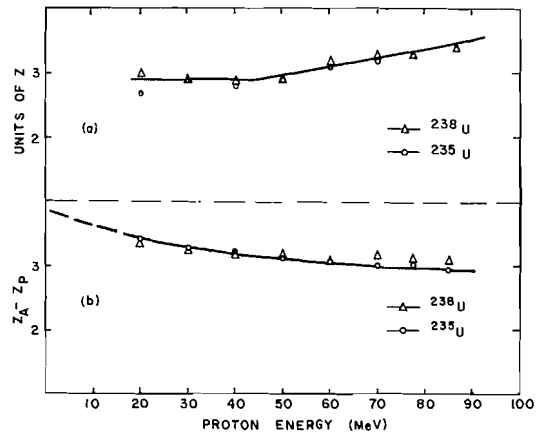

FIG. 13. (*a*) Full-width at half-maximum of charge dispersion curves vs. proton energy. (*b*) Displacement of Z_p towards beta stability, Z_A.

TABLE 7

Total isobaric cross section for $A = 93$ as a function of bombarding energy for fission of ^{235}U and ^{238}U

E_p (MeV)	σ (mb)	
	^{235}U	^{238}U
20	50	48
30	65	70
40	89	76
50	94	79
60	96	75
70	98	76
77	101	76
85	93	75

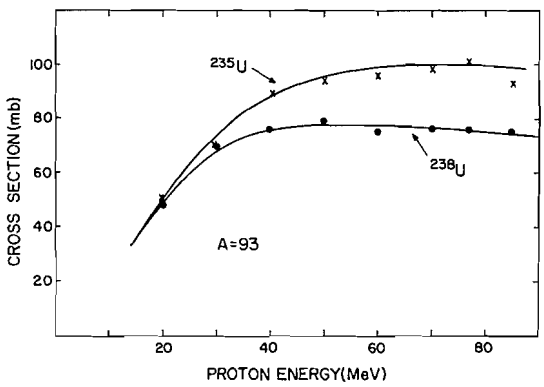

FIG. 14. Total isobaric yields of mass number $A = 93$ calculated from charge dispersion curves for fission of ^{235}U and ^{238}U.

Can. J. Chem. Downloaded from www.nrcresearchpress.com by 210.87.254.5 on 09/05/12
For personal use only.

TABLE 8

Calculation of the most probable charge "Z_p" for $A = 96$ from the fission of ^{238}U

Bombarding energy (MeV)	Fissioning nuclei (Np-isotopes)	Primary fragments	Calculated average Z_p (e.c.d:)	Calculated average Z_p (u.c.d.)	Experimental Z_p
20	239	98			
	238	98, 97	38.72	38.28	38.86
	237	97			
30	239	98			
	238	98			
	237	97	38.81	38.35	38.95
	236	97			
50	239	99			
	238	98			
	237	98	39.17	38.50	39.02
	236	98			
	235	98, 97			
	234	97			

latter can only be synthesized from studies which take charge dispersion into account.

(c) Calculation of the Most Probable Charge, Z_p

Values of Z_p have been calculated by different postulates and compared with experimental values. The method follows that of Saha and Yaffe (9) and is briefly outlined here. The calculation has been made in the fission of ^{238}U for $A = 96$ at bombarding energies of 20, 30, and 50 MeV, where compound nucleus formation would be the main initial reaction mechanism. The features of the calculation are as follows.

(*1*) The excitation energy of the compound nucleus $^{239}_{93}Np$ was calculated, followed by a fission – neutron evaporation competition.

(*2*) The residual excitation energy after neutron evaporation, U'', was calculated as

$$U'' = U' - B_n - 2T$$

where U' is the excitation energy of the preceding nucleus. B_n is the neutron binding energy, and $2T$ is the kinetic energy of the neutron. T is the nuclear temperature, given by $U'' = aT^2 - 4T$, where a is the level-density parameter, taken to be 10.5 MeV^{-1} (27). The odd–even parameter, δ, was taken to be 1.1 MeV. Neutron binding energies and fission barriers were obtained by use of the Myers and Swiatecki tables (28).

(*3*) The fission branching ratio, $G = \Gamma_f/(\Gamma_f + \Gamma_n)$, was then calculated for each fissioning nucleus, using the equations of Huizenga and Vandenbosch (27).

(*4*) A number of fragment pairs were selected with those of the light-mass region corresponding to $A = 96$–100 for each fissioning nucleus. The total energy release was calculated from the mass-excess values (28) of the fragments and the fissioning nuclei.

(*5*) The average kinetic energy of the fragments, as given by Milton and Fraser (29) was subtracted and the remaining excitation energy assumed to be distributed between the fragments in proportion to their masses.

(*6*) Neutron evaporation from the fragments was considered in the same way as described above for the parent nuclei and only those nuclei which, after neutron evaporation, contributed to $A = 96$ were sorted.

(*7*) Z_p was calculated for each product according to the equal charge displacement and unchanged charge displacement hypotheses. These values were then weighted by the fission branching ratio, G.

The parentage of different primary fragments, the calculated Z_p values, and the experimental values are given in Table 8. The calculated values for Z_p differ by only about one-half a charge unit and are both very close to the experimental values, although the values predicted by the e.c.d. hypothesis are closer. This is, of course, contradicted by the experimental fact that $(Z_A - Z_p)_l \neq (Z_A - Z_p)_h$, where l and h refer to the light and heavy fission fragments, respectively.

This research received financial support from the National Research Council of Canada.

1. B. D. Pate, J. S. Foster, and L. Yaffe. Can. J. Chem. **36**, 1691 (1958).
2. A. Kjelberg, H. Taniguchi, and L. Yaffe. Can. J. Chem. **39**, 635 (1961).

Can. J. Chem. Downloaded from www.nrcresearchpress.com by 210.87.254.5 on 09/05/12
For personal use only.

3. G. FRIEDLANDER, L. FRIEDMAN, B. GORDON, and L. YAFFE. Phys. Rev. **129**, 1809 (1963).
4. J. H. DAVIES and L. YAFFE. Can. J. Phys. **41**, 762 (1963).
5. S. S. PARIKH, D. A. MARSDEN, N. T. PORILE, and L. YAFFE. Can. J. Chem. **45**, 1863 (1967).
6. J. H. FORSTER, N. T. PORILE, and L. YAFFE. Can. J. Chem. **44**, 2951 (1966).
7. P. P. BENJAMIN, D. A. MARSDEN, N. T. PORILE, and L. YAFFE. Can. J. Chem. **47**, 301 (1969).
8. I. TOMITA and L. YAFFE. Can. J. Chem. **47**, 2921 (1969).
9. G. B. SAHA and L. YAFFE. J. Inorg. Nucl. Chem. **32**, 745 (1970).
10. E. HAGEBØ, A. C. PAPPAS, and P. AAGAARD. J. Inorg. Nucl. Chem. **26**, 1639 (1964).
11. A. C. WAHL, R. L. FERGUSON, D. R. NETHAWAY, D. E. TROUTNER, and K. WOLFSBERG. Phys. Rev. **126**, 1112 (1962).
12. R. J. PRESTWOOD. Collected radiochemical procedures. (Radiochemistry Group J-11), Los Alamos Sci. Lab. Univ. Calif. Rep. no. LA-1721. 2nd ed. 1958.
13. K. A. KRAUS and G. E. MOORE. J. Amer. Chem. Soc. **75**, 1460 (1953).
14. E. B. SANDELL. Colorimetric determination of traces of metal. 3rd ed. (revised). Interscience Publishers, Inc., New York. 1959. p. 748.
15. J. B. CUMMING. Application of computers to nuclear and radiochemistry. Nat. Acad. Sci., Nat. Res. Counc., Nucl. Sci. Ser. NAS-NS-3107. 1962. p. 25.
16. C. M. LEDERER, J. M. HOLLANDER, and I. PERLMAN. Table of isotopes. 6th ed. John Wiley and Sons, Inc., New York. 1967.
17. S. MEGHIR. Ph.D. Thesis, McGill University, Montreal, Quebec. 1962.
18. P. C. STEVENSON, H. G. HICKS, W. E. NERVIK, and D. R. NETHAWAY. Phys. Rev. **111**, 886 (1958).
19. A. P. VINOGRADOV, I. P. ALIMARIN, V. I. VARANOV, A. K. LAVRUKHINA, T. V. BARANOVA, F. I. PAVOLTSKAYA, A. A. BRAGINA, and Y. YAKOVLEV. Acad. Sci. USSR, Conf. Peaceful Uses At. Energy, Moscow, 1955. USAEC transl. 2435. 1955. p. 65.
20. R. L. FOLGER, P. C. STEVENSON, and G. T. SEABORG. Phys. Rev. **98**, 107 (1955).
21. N. SUGARMAN, H. MÜNZEL, J. A. PANONTIN, K. WIELGOZ, M. V. RAMANIAH, G. LANGE, and O. E. LOPEZ-MANCHERO. Phys. Rev. **143**, 952 (1966).
22. J. J. HOGAN and N. SUGARMAN. Phys. Rev. **182**, 1210 (1969).
23. C. D. CORYELL. Ann. Rev. Nucl. Sci. **2**, 305 (1953).
24. L. E. GLENDENIN, C. D. CORYELL, and R. R. EDWARDS. Phys. Rev. **75**, 337 (1949).
25. B. D. PATE. Can. J. Chem. **36**, 1707 (1958).
26. G. B. SAHA, I. TOMITA, and L. YAFFE. To be published.
27. J. R. HUIZENGA and R. VANDENBOSCH. Nuclear reactions. Vol. II. North–Holland Publishing Co., Amsterdam. 1962. p. 42.
28. W. D. MYERS and W. J. SWIATECKI. Univ. Calif. Radiat. Lab. Rep. UCRL-11980. 1965. Unpublished.
29. J. C. D. MILTON and J. S. FRASER. Can. J. Phys. **40**, 1626 (1962).

Can. J. Chem. Downloaded from www.nrcresearchpress.com by 210.87.254.5 on 09/05/12
For personal use only.

Can. J. Chem. Downloaded from www.nrcresearchpress.com by 210.87.254.42 on 09/05/12
For personal use only.

Effect of thorium on the reactions of iron(II) and iron(III) at a platinum electrode

J. H. BRECKENRIDGE[1] AND W. E. HARRIS
Department of Chemistry, University of Alberta, Edmonton, Alberta

Received[2] January 14, 1969

The effect of thorium perchlorate on the iron(III)–iron(II) couple was studied by the use of current–voltage data and chronopotentiometry. It is suggested that the primary effect of thorium on the ferric–ferrous couple is exclusion of iron from the double layer and the blocking of active sites on the electrode surface with a resultant decrease in the exchange current for the iron couple.

Canadian Journal of Chemistry, **48**, 1934 (1970)

During studies of an amperometric titration utilizing thorium as titrant and iron(III) as an amperometric indicator, the thorium titrant was found to interfere with the reduction of iron(III) at a platinum electrode. A subsequent investigation of this effect is reported here.

Experimental

Distilled water was treated with organic-removal and ion-exchange cartridges and then redistilled. Reagent-grade thorium nitrate was purified by repeatedly precipitating thorium oxalate and redissolving it in hot perchloric acid. Ferric perchlorate solutions were prepared by heating ferric chloride to fuming with perchloric acid until nearly dry. Ferrous perchlorate was prepared according to the method of Lindstrand (1). The platinum electrode consisted of a platinum wire with a nominal surface area of 0.15 cm^2, sealed in soft glass. For chronopotentiometric and current–voltage measurements the counter electrode was a platinum gauze cylinder surrounding the working electrode. Constant current was provided by appropriate calibrated resistors placed in series with two 45-V batteries.

During current–voltage measurements the electrode was rotated to avoid polarization; equivalent anodic and cathodic currents were used alternately. Each measurement was carried out for about 15 s, and the potential displacement resulting from the passage of current was recorded by a Metrohm Polarecord. Usually eleven currents ranging from 5 to 75 μA were used for a set of measurements. The maximum currents were not more than 15% of the diffusion current. The electrode used corresponds to the aged-reduced electrode described by Anson (2).

Results

An irreversible chronopotentiogram can be analyzed to obtain a rate constant for both the electrode reaction and the transfer coefficient. The following equation has been applied (3)

$$[1] \quad \ln\left[1 - \left(\frac{t}{\tau}\right)^{\frac{1}{2}}\right] = \frac{\alpha n F}{RT} E - \ln \frac{nFCk}{i_A}$$

where t is elapsed time in s, τ is transition time in s, α is the transfer coefficient, n is the Faradays per mole of electrode reaction, F is the Faraday (96 493 C), R is the gas constant, T is absolute temperature, E is electrode potential, C is concentration in moles per cm^3, k is the rate constant for the electrode reaction at the potential of the reference electrode in s^{-1} cm^{-2}, and i_A is current density in A per cm^2. A plot of $\ln [1 - (t/\tau)^{\frac{1}{2}}]$ against E should yield a straight line with slope $\alpha nF/RT$ and intercept $-\ln (nFCk/i_A)$. Although the transition time is well defined in theory, the choice of method of experimental measurement becomes arbitrary when the chronopotentiogram is so irreversible that the transition time is not well defined experimentally. The method of measuring transition times ascribed to Kuwana (see ref. 4) was chosen because it gives linear plots of $\log [1 - (t/\tau)^{\frac{1}{2}}]$ against electrode potential. In the system reported here, even though the shapes and transition times of the chronopotentiograms varied widely, the plots obtained of these relations were always linear.

As the thorium concentration of an iron(III) solution was increased, chronopotentiograms

[1]Present address: Selkirk College, Box 1200, Castlegar, British Columbia.

[2]Revision received February 4, 1970.

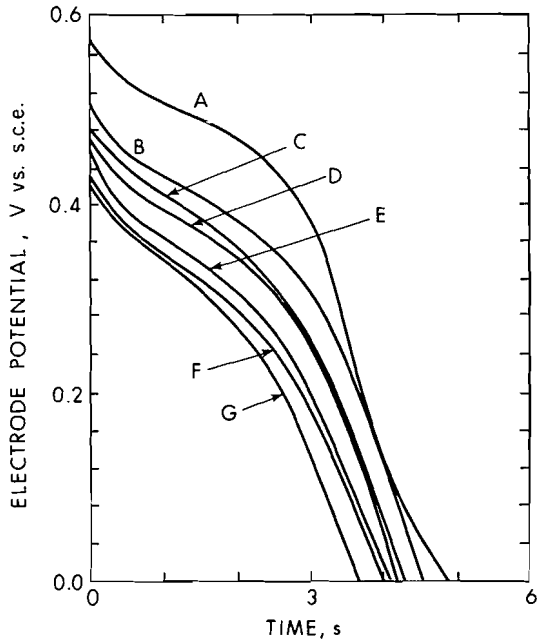

FIG. 1. Chronopotentiograms for the reduction of ferric perchlorate at a platinum electrode with various concentrations of thorium perchlorate and with 3.28×10^{-3} M $Fe(ClO_4)_3$ and 0.1 M $HClO_4$. Nominal current density 300 mA/cm^2. A, 0; B, 1.64×10^{-4}; C, 3.27×10^{-3}; D, 6.54×10^{-3}; E, 1.64×10^{-2}; F, 3.27×10^{-2}; G, 9.80×10^{-2} M thorium perchlorate.

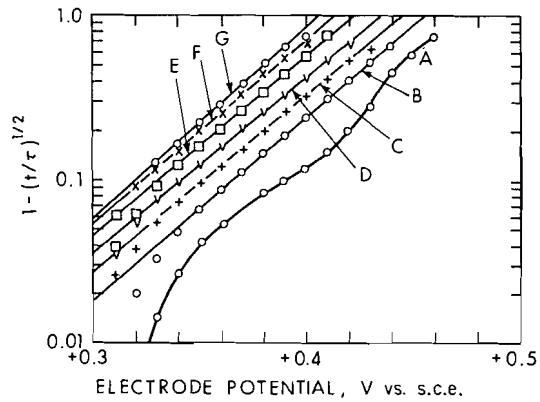

FIG. 2. The relation between $1 - (t/\tau)^{\frac{1}{2}}$ and the electrode potential for the chronopotentiograms in Fig. 1.

for the reduction of iron(III) underwent several changes. Figure 1 indicates that the overvoltage increased steadily with increasing thorium concentration, the shape of the chronopotentiogram changed when thorium was added, and the transition time decreased as the thorium concentration was increased. Theoretically the transition time for a chronopotentiogram does not depend on the reversibility of the electrode reaction. Delahay suggested (5) that the adsorption of an inactive species could reduce the transition time by reducing the amount of electrode surface available for the reaction.

Figure 2 shows plots of $1 - (t/\tau)^{\frac{1}{2}}$ against potential for the chronopotentiograms in Fig. 1. The nearly parallel straight lines in the presence of thorium indicate that the transfer coefficient for the reduction of iron(III) was constant with changing thorium concentration and that the exchange current decreased with increasing thorium concentration. Since the equation

$$[2] \qquad \ln [i/(1 - e^{-nf\eta})] = \ln i_0 - \alpha nf\eta$$

where η is the overvoltage, i is the current in A, and i_0 is the exchange current, applies to an electrode reaction (6), a plot of $\ln [i/(1 - e^{-nf\eta})]$ against overvoltage should result in a straight line with slope equal to $-\alpha nf$ and intercept $\ln i_0$. Equation 2 was applied to data on overvoltages obtained by forcing small currents through the electrode and measuring the change in potential caused by the current. In general, the best straight-line plots of $\ln [i/(1 - e^{-nf\eta})]$ against η resulted when the electrode was aged and the overvoltages were large (0.04 V). These current–voltage measurements indicate that the transfer coefficient does not depend on thorium concentration and that the exchange current is markedly decreased by thorium. For example, in 0.1 M perchloric acid, the 0.01 M iron(III)–iron(II) exchange current in the absence of thorium was 1 mA cm^{-2}; a thorium concentration of 3.0×10^{-3} M reduced it by 50%. The exchange current for the iron(III)–iron(II) couple is a linear function of the logarithm of the thorium concentration. The iron(III)–iron(II) couple became more sensitive to the thorium effect at higher pH values.

We suggest that thorium, possibly because of its high charge, is strongly attracted into the double layer at the electrode surface. The thorium then replaces other cations in the double layer and blocks active sites on the electrode surface, and hence the iron(III)–iron(II) exchange current is reduced. Such an effect should exist with other couples as well. Another investigator re-

Can. J. Chem. Downloaded from www.nrcresearchpress.com by 210.87.254.42 on 09/05/12
For personal use only.

ported (7) that thorium makes the reaction $Cu^{2+} + 2e \rightarrow Cu(s)$ more irreversible at a platinum electrode.

In conclusion, the evidence from both chronopotentiometry and current–voltage measurements is that thorium decreases the exchange current for the iron(III)–iron(II) couple. We suggest that this effect may be caused by the exclusion of iron from the double layer and a blocking of active sites on the electrode surface.

1. F. LINDSTRAND. Z. Anorg. Allg. Chem. **230**, 187 (1936). (Chem. Abstr. **31**, 2115 (1937)).
2. F. C. ANSON. Anal. Chem. **33**, 934 (1961).
3. P. DELAHAY and T. J. BERZINS. J. Amer. Chem. Soc. **75**, 2486 (1953).
4. C. D. RUSSELL and J. M. PETERSON. J. Electroanal. Chem. **5**, 467 (1963).
5. P. DELAHAY. New instrumental methods in electrochemistry. Interscience Publ., Inc., New York. 1959. p. 209.
6. P. DELAHAY. Double layer and electrode kinetics. Interscience Publ., Inc., New York. 1965. p. 163.
7. J. DEAN. Ph.D. thesis, University of Alberta, Edmonton, Alberta. 1967.

Standard heats of formation of two tribromoborazines

B. C. SMITH, LAMBODAR THAKUR,[1] AND (MRS.) MARGUERITE A. WASSEF[2]

Birkbeck College (University of London), Malet Street, London, W.C.1, England, and Department of Chemistry, University of Western Ontario, London 72, Ontario

Received December 16, 1969

The heats of hydrolysis of $B_3Br_3N_3Me_3$ and $B_3Br_3N_3H_3$ are -84.4 ± 0.5 and -120.9 ± 0.5 kcal mole^{-1}, and their standard heats of formation are -246.5 and -215.9 kcal mole^{-1}, respectively. The estimated boron–nitrogen bond energy terms are 113.2 and 105.5 kcal mole^{-1}, respectively.

Canadian Journal of Chemistry, **48**, 1936 (1970)

Introduction

Borazines, $B_3X_3N_3R_3$ (**1**), are isoelectronic with derivatives of benzene. sp^2-Hybridized boron and nitrogen form a σ-bonded framework with superimposed dative π bonding from filled p_z orbitals on nitrogen to vacant p_z orbitals on boron. The strengths of the resulting boron–nitrogen bonds depend on the nature of the exocyclic substituents (1).

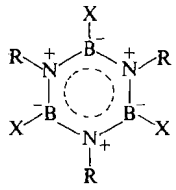

1

The heats of hydrolysis of two tribromoborazines, $B_3Br_3N_3R_3$ (R = Me, H), have been measured in order to determine their standard heats of formation. Boron–nitrogen bond energy terms, estimated from heats of atomization using standard terms for exocyclic bonds on the assumption that thermochemical differences are concentrated in the borazine rings, are compared with data for other borazines (2) and hexagonal boron nitride.

Results

The crystalline tribromoborazoles are hydrolyzed rapidly by water at 25 °C.

$$B_3Br_3N_3R_3(c) + 9H_2O(aq) = 3H_3BO_3(aq) + 3RNH_3Br(aq) \quad (R = Me, H)$$

Heat changes, q, and heats of hydrolysis, ΔH_1, are recorded in Table 1.

The standard heats of formation, ΔH_f^0, heats of atomization, ΔH_a, and boron–nitrogen bond energy terms, E(B—N), for the tribromoborazines, recorded in Table 2, are calculated from the following relationships

$$\Delta H_f^0 = -\Delta H_1 - 9\Delta H_2 + 3\Delta H_3 + 3\Delta H_4$$

$$\Delta H_a(\text{borazine}) = -\Delta H_f^0 + \sum \Delta H_a(\text{elements}) - \Delta H_5$$

$$6E(\text{B—N}) = \Delta H_a - \sum E(\text{exocyclic bonds})$$

ΔH_1 is the mean heat of hydrolysis from Table

[1]Present address: Postgraduate Department of Chemistry, Bhagalpur University, Bhagalpur 7, India.

[2]Present address: A'in Shams University, Cairo, U.A.R.

Can. J. Chem. Downloaded from www.nrcresearchpress.com by 210.87.254.42 on 09/05/12
For personal use only.

ported (7) that thorium makes the reaction $Cu^{2+} + 2e \rightarrow Cu(s)$ more irreversible at a platinum electrode.

In conclusion, the evidence from both chronopotentiometry and current–voltage measurements is that thorium decreases the exchange current for the iron(III)–iron(II) couple. We suggest that this effect may be caused by the exclusion of iron from the double layer and a blocking of active sites on the electrode surface.

1. F. LINDSTRAND. Z. Anorg. Allg. Chem. **230**, 187 (1936). (Chem. Abstr. **31**, 2115 (1937)).
2. F. C. ANSON. Anal. Chem. **33**, 934 (1961).
3. P. DELAHAY and T. J. BERZINS. J. Amer. Chem. Soc. **75**, 2486 (1953).
4. C. D. RUSSELL and J. M. PETERSON. J. Electroanal. Chem. **5**, 467 (1963).
5. P. DELAHAY. New instrumental methods in electrochemistry. Interscience Publ., Inc., New York. 1959. p. 209.
6. P. DELAHAY. Double layer and electrode kinetics. Interscience Publ., Inc., New York. 1965. p. 163.
7. J. DEAN. Ph.D. thesis, University of Alberta, Edmonton, Alberta. 1967.

Standard heats of formation of two tribromoborazines

B. C. SMITH, LAMBODAR THAKUR,[1] AND (MRS.) MARGUERITE A. WASSEF[2]

Birkbeck College (University of London), Malet Street, London, W.C.1, England, and Department of Chemistry, University of Western Ontario, London 72, Ontario

Received December 16, 1969

The heats of hydrolysis of $B_3Br_3N_3Me_3$ and $B_3Br_3N_3H_3$ are -84.4 ± 0.5 and -120.9 ± 0.5 kcal mole^{-1}, and their standard heats of formation are -246.5 and -215.9 kcal mole^{-1}, respectively. The estimated boron–nitrogen bond energy terms are 113.2 and 105.5 kcal mole^{-1}, respectively.

Canadian Journal of Chemistry, **48**, 1936 (1970)

Introduction

Borazines, $B_3X_3N_3R_3$ (**1**), are isoelectronic with derivatives of benzene. sp^2-Hybridized boron and nitrogen form a σ-bonded framework with superimposed dative π bonding from filled p_z orbitals on nitrogen to vacant p_z orbitals on boron. The strengths of the resulting boron–nitrogen bonds depend on the nature of the exocyclic substituents (1).

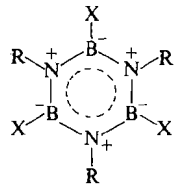

1

The heats of hydrolysis of two tribromoborazines, $B_3Br_3N_3R_3$ (R = Me, H), have been measured in order to determine their standard heats of formation. Boron–nitrogen bond energy terms, estimated from heats of atomization using standard terms for exocyclic bonds on the assumption that thermochemical differences are concentrated in the borazine rings, are compared with data for other borazines (2) and hexagonal boron nitride.

Results

The crystalline tribromoborazoles are hydrolyzed rapidly by water at 25 °C.

$$B_3Br_3N_3R_3(c) + 9H_2O(aq) = 3H_3BO_3(aq) + 3RNH_3Br(aq) \quad (R = Me, H)$$

Heat changes, q, and heats of hydrolysis, ΔH_1, are recorded in Table 1.

The standard heats of formation, ΔH_f^0, heats of atomization, ΔH_a, and boron–nitrogen bond energy terms, E(B—N), for the tribromoborazines, recorded in Table 2, are calculated from the following relationships

$$\Delta H_f^0 = -\Delta H_1 - 9\Delta H_2 + 3\Delta H_3 + 3\Delta H_4$$

$$\Delta H_a(\text{borazine}) = -\Delta H_f^0 + \sum \Delta H_a(\text{elements}) - \Delta H_5$$

$$6E(\text{B—N}) = \Delta H_a - \sum E(\text{exocyclic bonds})$$

ΔH_1 is the mean heat of hydrolysis from Table

[1]Present address: Postgraduate Department of Chemistry, Bhagalpur University, Bhagalpur 7, India.

[2]Present address: A'in Shams University, Cairo, U.A.R.

Can. J. Chem. Downloaded from www.nrcresearchpress.com by 210.87.254.40 on 09/05/12
For personal use only.

Can. J. Chem. Downloaded from www.nrcresearchpress.com by 210.87.254.40 on 09/05/12
For personal use only.

TABLE 1

Heats of hydrolysis of tribromoborazines in water (100 ml) at 25 °C

Compound	Concentration (mmole)	q (cal)	ΔH_1 (kcal mole^{-1})
$B_3Br_3N_3Me_3$	0.0715	−5.99	−83.71
	0.1192	−10.08	−84.60
	0.1853	−15.73	−84.84
$B_3Br_3N_3H_3$	0.0766	−9.30	−121.3
	0.0837	−10.16	−121.4
	0.1100	−13.24	−120.4
	0.1114	−13.46	−120.8
	0.1321	−15.99	−120.8
	0.1330	−16.04	−120.6

TABLE 2

Thermochemical data for tribromoborazines

Parameter	Value, kcal mole^{-1}	
	$B_3Br_3N_3Me_3$	$B_3Br_3N_3H_3$
ΔH_1	−84.4±0.5	−120.9±0.5
ΔH_2	−68.32	−68.32
ΔH_3	−256.5	−256.5
ΔH_4	−58.75	−60.74
ΔH_f^0	−246.5	−215.9
ΔH_5	17.7	20.6
$\Sigma\Delta H_a$ (elements)	1807.5	982.2
ΔH_a (borazine)	2036.3	1177.5
ΣE (exocyclic bonds)	1357.2	544.8
E (B—N)	113.2	105.5

1. ΔH_2, ΔH_3, and ΔH_4, respectively, are the standard heats of formation of water (3), and boric acid (2) and methylammonium bromide or ammonium bromide (3), in dilute aqueous solution. The heats of mixing of the hydrolysis products were shown to be negligible. ΔH_5 is the heat of sublimation, measured for $B_3Br_3N_3H_3$ (4) and estimated for $B_3Br_3N_3Me_3$. Heats of atomization of the elements and bond energy terms are from Cottrell (5), except for the heat of atomization of boron, 135.7 kcal mole^{-1} (2), and E(B—Br), 88.2 kcal mole^{-1}, which is recalculated from the heat of hydrolysis of liquid boron tribromide, −81.0 ± 0.4 kcal mole^{-1} (6).

Discussion

The boron–nitrogen bond energy term is greater in $B_3Br_3N_3Me_3$ than in $B_3Br_3N_3H_3$. Methyl exerts a stronger positive inductive effect than hydrogen, so the supply of electrons to the ring is greater in *N*—Me than *N*—H derivatives. Table 3 shows that the boron–nitrogen bond energy terms decrease along the series X = H > Br > Cl for both sets of borazines (R = Me, H) (2). The electron density of the ring is reduced by negative inductive effects in trihalogenoborazines, and dative π bonding from nitrogen to boron is opposed by positive mesomeric effects of the halogens.

TABLE 3

Electronegativities, e, and bond energy terms, E, for $B_3X_3N_3R_3$ compounds

$B_3X_3N_3R_3$ compound	e_X	e_R	E(B—N), kcal mole^{-1}
$B_3H_3N_3Me_3$	2.1	2.0	121.4
$B_3Br_3N_3Me_3$	2.8	2.0	113.2
$B_3Cl_3N_3Me_3$	3.0	2.0	108.5
$B_3H_3N_3H_3$	2.1	2.1	117.9
$B_3Br_3N_3H_3$	2.8	2.1	105.5
$B_3Cl_3N_3H_3$	3.0	2.1	104.8

The influence of the exocyclic substituents is illustrated by a plot of boron–nitrogen bond energy terms against a suitable function of the electronegativities of the substituents, e.g., $e_X/4 + e_R$, as in Fig. 1. The bond energy terms appear more sensitive to changes in the *N* substituents than the *B* substituents, just as ionization energies of borazines are more sensitive to *N*-methyl than *B*-methyl substitution (7). The boron–nitrogen bonds are expected to be stronger and shorter in $B_3Me_3N_3Me_3$.

Hexagonal boron nitride is also derived from sp^2-hybridized boron and nitrogen. The structure (8) differs from that of graphite, and differences in color, electrical conductivity, dia-

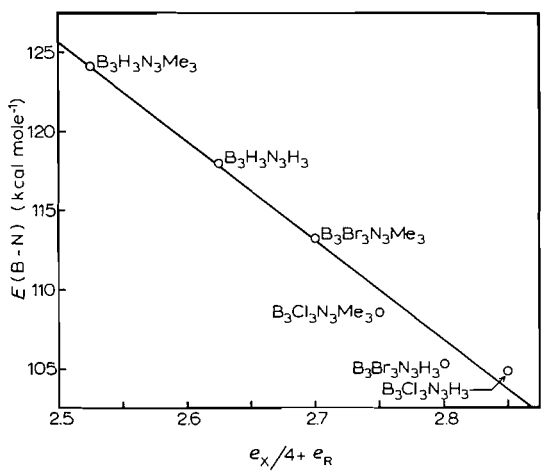

FIG. 1. Effect of electronegativities of substituents on boron–nitrogen bond energy terms. Boron–nitrogen bond energy terms vs. $e_X/4 + e_R$.

magnetic anisotropy, and coefficients of thermal expansion indicate that the bond order is less than 1.33 in boron nitride. The standard heat of formation of hexagonal boron nitride is -59.51 ± 0.72 kcal mole^{-1} (9), which leads to 308.1 kcal mole^{-1} for the heat of atomization. Hence the boron–nitrogen bond energy term is approximately 100 kcal mole^{-1}, allowing for a contribution of 8 kcal mole^{-1} from interlayer attractions. This appears consistent with a bond order of 1.0 for hexagonal boron nitride, although the value 1.22 has also been suggested (10).

Experimental

BB'B'' - Tribromo - *NN'N''* - trimethylborazine, m.p. 145 °C [lit. (11), 143–146°], prepared from boron tribromide and methylammonium bromide in bromobenzene, and *BB'B''*-tribromoborazine, m.p. 128 °C [lit. (4), 128.5–129°], a gift from Dr. P. G. Thompson, were purified by sublimation at $100°/10^{-2}$ mm. Weighed samples were sealed in fragile glass ampoules in an atmosphere of nitrogen and placed in the closed-system calorimeter (2, 12) at 25°. The tribromoborazines reacted completely with water (100 ml) within ½ min when the ampoule was broken. Temperature changes were measured with a 10 kΩ thermistor, and the calorimeter was calibrated electrically. Uncertainties reported for heats of hydrolysis pertain to precision, and not to estimates of accuracy.

We thank Bhagalpur University for leave of absence to L.T. and Imperial Chemical Industries Limited for a grant to construct the calorimeter.

1. J. C. Sheldon and B. C. Smith. Quart. Rev. London, **14**, 200 (1960).
2. B. C. Smith, L. Thakur, and M. A. Wassef. J. Chem. Soc. A, 1616 (1967).
3. Selected values of thermodynamic properties. Nat. Bur. Stand. circ. 500. Washington, D.C., 1952.
4. A. W. Laubengayer and C. W. J. Scaife. J. Chem. Eng. Data, **11**, 172 (1966).
5. T. L. Cottrell. The strengths of chemical bonds. 2nd ed., Butterworth and Co., Publishers, Ltd., London. 1958.
6. H. A. Skinner and N. B. Smith. Trans. Faraday Soc. **51**, 19 (1955).
7. P. M. Kuznesof, F. E. Stafford, and D. F. Shriver. J. Phys. Chem. **71**, 1939 (1967).
8. R. S. Pease. Acta Cryst. **5**, 356 (1952).
9. JANAF thermochemical tables. U.S. Dep. Commer., Springfield, Va. 1965.
10. L. Pauling. Proc. Nat. Acad. Sci. U.S.A. **56**, 1646 (1966).
11. R. F. Riley and C. J. Schack. Inorg. Chem. **3**, 1651 (1964).
12. D. P. Roch, B. C. Smith, and L. Thakur. Chem. Ind. London, 1787 (1965).

Electron spin resonance spectra of ^{15}N labelled amino radicals[1]

D. R. Smith and W. A. Seddon

Physical Chemistry Branch, Atomic Energy of Canada Limited, Chalk River Nuclear Laboratories, Chalk River, Ontario

Received January 16, 1970

Electron spin resonance (e.s.r.) spectra of radiolytically formed $^{15}NH_2$ and $^{15}ND_2$ radicals are presented along with their hyperfine splitting constants and spectroscopic g factors. A comparison with previously observed spectra of $^{14}NH_2$ and $^{14}ND_2$ is briefly discussed and their hyperfine parameters revised as a result of our ^{15}N data. Miscellaneous observations on the effect of additives (water, methyl-iodide, tetranitromethane) are discussed.

Canadian Journal of Chemistry, **48**, 1938 (1970)

Introduction

We have shown previously (1–4) that free radicals and electrons are produced and may subsequently be trapped at 77 °K after the irradiation of water and alcohols in the vapor phase by 1 MeV He^+ ions. Since this "crossed-beam" technique can be used with samples as small as 0.05 g, studies of isotopically enriched molecules become more economical. This note summarizes the data obtained from ^{15}N enriched NH_3 and ND_3 and leads to an improved analysis of the spectra due to $^{14}NH_2$ and $^{14}ND_2$. More accurate hyperfine splitting constants than those presently in the literature were required for amino radicals trapped in ammonia for comparison with related unpublished data in adsorbed systems obtained by D. R. Smith and P. Wardman.

Since, in contrast to water (1), trapped electrons are not formed from pure ammonia, elec-

[1]AECL No. 3587.

Can. J. Chem. Downloaded from www.nrcresearchpress.com by 210.87.254.40 on 09/05/12
For personal use only.

magnetic anisotropy, and coefficients of thermal expansion indicate that the bond order is less than 1.33 in boron nitride. The standard heat of formation of hexagonal boron nitride is -59.51 ± 0.72 kcal mole^{-1} (9), which leads to 308.1 kcal mole^{-1} for the heat of atomization. Hence the boron–nitrogen bond energy term is approximately 100 kcal mole^{-1}, allowing for a contribution of 8 kcal mole^{-1} from interlayer attractions. This appears consistent with a bond order of 1.0 for hexagonal boron nitride, although the value 1.22 has also been suggested (10).

Experimental

BB'B'' - Tribromo - *NN'N''* - trimethylborazine, m.p. 145 °C [lit. (11), 143–146°], prepared from boron tribromide and methylammonium bromide in bromobenzene, and *BB'B''*-tribromoborazine, m.p. 128 °C [lit. (4), 128.5–129°], a gift from Dr. P. G. Thompson, were purified by sublimation at $100°/10^{-2}$ mm. Weighed samples were sealed in fragile glass ampoules in an atmosphere of nitrogen and placed in the closed-system calorimeter (2, 12) at 25°. The tribromoborazines reacted completely with water (100 ml) within ½ min when the ampoule was broken. Temperature changes were measured with a 10 kΩ thermistor, and the calorimeter was calibrated electrically. Uncertainties reported for heats of hydrolysis pertain to precision, and not to estimates of accuracy.

We thank Bhagalpur University for leave of absence to L.T. and Imperial Chemical Industries Limited for a grant to construct the calorimeter.

1. J. C. Sheldon and B. C. Smith. Quart. Rev. London, **14**, 200 (1960).
2. B. C. Smith, L. Thakur, and M. A. Wassef. J. Chem. Soc. A, 1616 (1967).
3. Selected values of thermodynamic properties. Nat. Bur. Stand. circ. 500. Washington, D.C., 1952.
4. A. W. Laubengayer and C. W. J. Scaife. J. Chem. Eng. Data, **11**, 172 (1966).
5. T. L. Cottrell. The strengths of chemical bonds. 2nd ed., Butterworth and Co., Publishers, Ltd., London. 1958.
6. H. A. Skinner and N. B. Smith. Trans. Faraday Soc. **51**, 19 (1955).
7. P. M. Kuznesof, F. E. Stafford, and D. F. Shriver. J. Phys. Chem. **71**, 1939 (1967).
8. R. S. Pease. Acta Cryst. **5**, 356 (1952).
9. JANAF thermochemical tables. U.S. Dep. Commer., Springfield, Va. 1965.
10. L. Pauling. Proc. Nat. Acad. Sci. U.S.A. **56**, 1646 (1966).
11. R. F. Riley and C. J. Schack. Inorg. Chem. **3**, 1651 (1964).
12. D. P. Roch, B. C. Smith, and L. Thakur. Chem. Ind. London, 1787 (1965).

Electron spin resonance spectra of ^{15}N labelled amino radicals[1]

D. R. Smith and W. A. Seddon

Physical Chemistry Branch, Atomic Energy of Canada Limited, Chalk River Nuclear Laboratories, Chalk River, Ontario

Received January 16, 1970

Electron spin resonance (e.s.r.) spectra of radiolytically formed $^{15}NH_2$ and $^{15}ND_2$ radicals are presented along with their hyperfine splitting constants and spectroscopic g factors. A comparison with previously observed spectra of $^{14}NH_2$ and $^{14}ND_2$ is briefly discussed and their hyperfine parameters revised as a result of our ^{15}N data. Miscellaneous observations on the effect of additives (water, methyl-iodide, tetranitromethane) are discussed.

Canadian Journal of Chemistry, **48**, 1938 (1970)

Introduction

We have shown previously (1–4) that free radicals and electrons are produced and may subsequently be trapped at 77 °K after the irradiation of water and alcohols in the vapor phase by 1 MeV He^+ ions. Since this "crossed-beam" technique can be used with samples as small as 0.05 g, studies of isotopically enriched molecules become more economical. This note summarizes the data obtained from ^{15}N enriched NH_3 and ND_3 and leads to an improved analysis of the spectra due to $^{14}NH_2$ and $^{14}ND_2$. More accurate hyperfine splitting constants than those presently in the literature were required for amino radicals trapped in ammonia for comparison with related unpublished data in adsorbed systems obtained by D. R. Smith and P. Wardman.

Since, in contrast to water (1), trapped electrons are not formed from pure ammonia, elec-

[1]AECL No. 3587.

Can. J. Chem. Downloaded from www.nrcresearchpress.com by 210.87.254.5 on 09/05/12
For personal use only.

Can. J. Chem. Downloaded from www.nrcresearchpress.com by 210.87.254.5 on 09/05/12
For personal use only.

tron scavengers were added in an effort to detect the transient presence of electrons.

Experimental

The experimental technique has been described in detail elsewhere (1, 2). Briefly, species which are formed in the gas phase as a result of 1 MeV He^+ ion bombardment, become trapped in a solid deposit at 77 °K. These are studied by e.s.r. after isolating the deposit under vacuum. All spectra shown are first derivative, obtained using a Varian V-4502-04 spectrometer with fieldial sweep control.

Isotopically labelled $^{15}NH_3$ (95 atom % ^{15}N), and $^{15}ND_3$ (95.7% ^{15}N) and $^{14}ND_3$ (98% D) were obtained from Merck, Sharpe and Dohme Ltd. The $^{14}NH_3$ (anhydrous) was obtained from the Matheson Co. Both NH_3 and ND_3 were dried over sodium before use. The $^{15}NH_3$ and $^{15}ND_3$ were used as received. All samples were degassed.

Results and Discussion

Pure Ammonia

Figures 1*A* and 1*B* show the e.s.r. spectra obtained from $^{14}NH_3$ at 77 and 118 °K, respectively, and Figs. 1*C* and 1*D* the corresponding spectra from $^{14}ND_3$. Similar spectra have been obtained by other workers (5–7), but are repeated here to facilitate comparison with spectra from $^{15}NH_3$ and $^{15}ND_3$ and because we have obtained better resolution.

Figures 2*A* and 2*B* show the e.s.r. spectra obtained from $^{15}NH_3$ and $^{15}ND_3$, respectively, at 77 °K.

The spectra presented in Figs. 1*A*–1*D* can be compared to those previously observed in ammonia matrices and assigned to $^{14}NH_2$ and $^{14}ND_2$ radicals by Marx and Maruani (5), Al-Naimy *et al.* (6), and Tupikov *et al.* (7). The resolution in our spectra, though inferior to that for $^{14}NH_2$ and $^{14}ND_2$ spectra observed by Foner *et al.* (8) in an argon matrix at 4.2 °K, is somewhat better than that obtained in the earlier work (5–7). Marx and Maruani (5) attributed this lack of good resolution to a phase effect and restricted rotation of the radicals due to hydrogen bond formation. Al-Naimy *et al.* (6) also suggested that the N splitting of these radicals is "quenched" in aqueous solutions of ammonia at 77 °K as a result of strong hydrogen bonding with the neighboring water molecules. This latter postulate is only partially valid, since in the case of $^{14}ND_2$ the underlying spectrum is composed of 3 groups due to ^{14}N hyperfine interaction and the outer $I_N = \pm 1$ lines, though broadened, have not completely vanished. Substitution of ^{15}N for ^{14}N confirms this (see below). It is possible, however, that the polycrystalline nature of the matrix results in anisotropic hyperfine interactions which can broaden and complicate the spectra. In alkyl radicals Cochran, Adrian, and Bowers (9), have shown that when two α protons have their nuclear spins anti-parallel, the hyperfine anisotropy cancels and results in sharper, more intense hyperfine lines, while parallel orientations of the α protons give broad weak lines. At 77 °K, the $I_N = \pm 1$ lines for $^{14}ND_2$ (Fig. 1*C*) are very broad and of low intensity with no resolved D splittings. The $I_N = 0$ line is much narrower, more intense, and D splittings are resolved. Also at 77 °K, the lines of the $^{14}NH_2$ spectrum (Fig. 1*A*) are very anisotropic, broad, and of low intensity for $I_N = \pm 1$ with the result that the spectrum is dominated by a strong triplet of lines corresponding to $I_N = 0$, $\sum I_H = 0, \pm 1$; the triplet splitting arising from the two equivalent amino protons. This effect is slightly more pronounced in our spectrum at 77 °K than in that of Marx and Maruani at 98 °K (5).

Optimum resolution is obtained at about 118 °K. As expected (8), the $^{14}NH_2$ spectrum (Fig. 1*B*) consists of 3 triplets and the $^{14}ND_2$ spectrum contains 3 quintets, though the quintet splittings due to two equivalent amino deuterons are less clearly resolved. The stick spectrum for $^{14}NH_2$ in Fig. 1*B* is calculated using the measured isotropic values of A_D and $A_{^{15}N}$ (see below) to determine A_H and $A_{^{14}N}$. This model, which is much simpler than that of Marx and Maruani (5), predicts the line positions very closely, though it does not account for line intensity anomalies. We believe that the latter effect arises predominantly from variations in line width combined with variations in the degree of line overlap across the spectrum.

The spectrum in Fig. 2*A* is assigned to the $^{15}NH_2$ radical. No improvement in resolution was obtained on warming. A fully resolved spectrum would consist of 6 lines due to hyperfine interaction from 2 equivalent protons and one ^{15}N atom ($I_{^{15}N} = \pm \frac{1}{2}$). The apparent quartet structure arises from the close similarity of $A_{^{15}N}$ to A_H (see Table 1). This is depicted by the stick diagram in Fig. 2*A*. To calculate this A_H was obtained from A_D and the known ratio A_H/A_D, while $A_{^{15}N}$ was measured directly from the spectrum of $^{15}ND_2$. Again the resolution is incomplete since one expects a spectrum com-

Can. J. Chem. Downloaded from www.nrcresearchpress.com by 210.87.254.5 on 09/05/12
For personal use only.

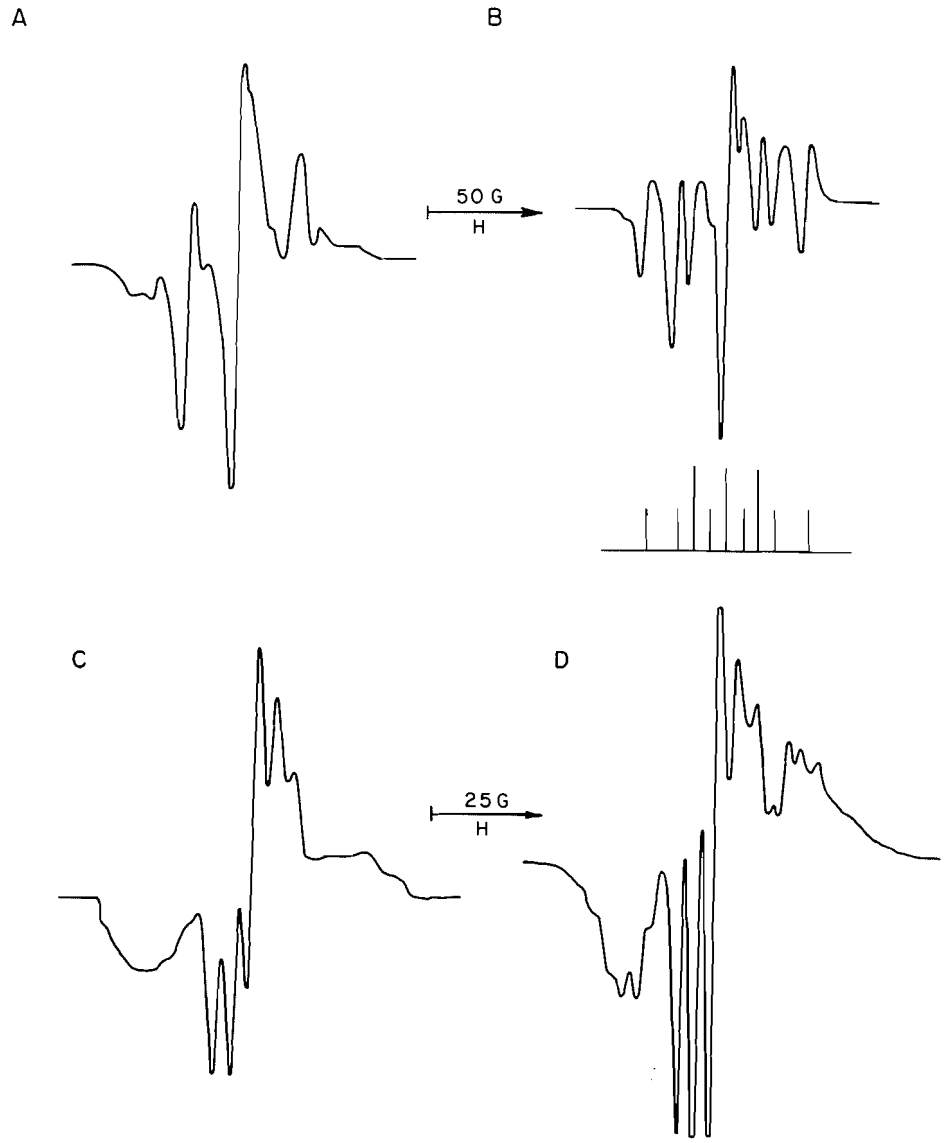

FIG. 1. *A* and *B* show the e.s.r. spectra observed from $^{14}NH_3$ at 77 and 118 °K, respectively; *C* and *D* show the corresponding spectra from $^{14}ND_3$. The "stick" spectrum in *B* is lined up with the derivative maxima.

posed of 2 quintets. The dominant feature is the ^{15}N doublet and there is underlying poorly resolved structure due in part to D splittings. The spectrum appears to be contaminated by some weak lines due presumably to the presence of some $^{15}NH_2$ or ^{15}NHD. Warming clearly resolves D splittings but the presence of weak lines from ^{15}NHD or $^{15}NH_2$ prevents a detailed analysis.

Table 1 summarizes the hyperfine splitting constants A_H, A_D, $A_{^{14}N}$, and $A_{^{15}N}$ along with g factors for the amino radical trapped in an ammonia matrix. A_H and $A_{^{14}N}$ are calculated from the measured values $A_D = 3.9$ and $A_{^{15}N} = 21.3$ G using the known ratios $A_H/A_D = 6.5$ and $A_{^{15}N}/A_{^{14}N} = 1.4$, respectively. As noted above for Fig. 1*B*, these values of A_H and $A_{^{14}N}$ closely predict the line positions for $^{14}NH_2$. Our ^{15}N

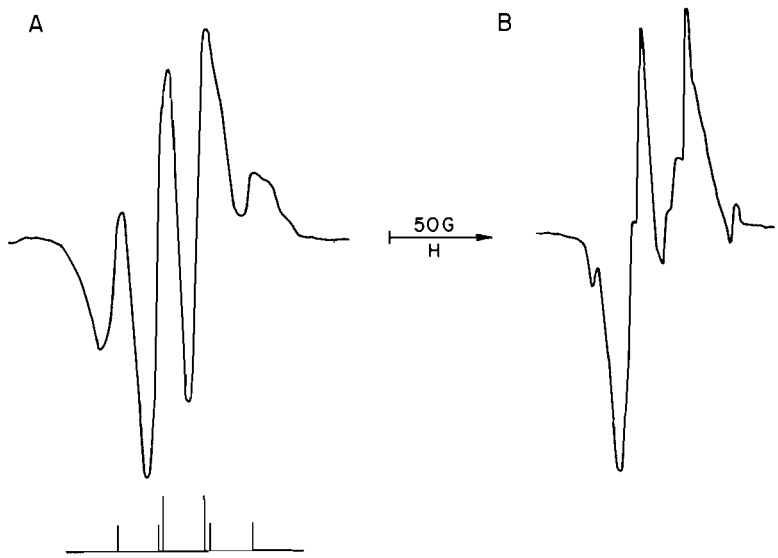

FIG. 2. *A* and *B* show the e.s.r. spectra observed at 77 °K from $^{15}NH_3$ and $^{15}ND_3$, respectively. The "stick" spectrum in *A* is lined up with the derivative maxima.

TABLE 1

Hyperfine splitting constants (G) and *g* factors

Radical	Parameter*	Value					
		This work	Reference 8	Reference 5	Reference 7	Reference 6	Reference 10
$^{14}NH_2$	A_H	25.4	23.8 ±0.1	20.0	24.5	21.0	
	g	2.0046±0.0003	2.0049				
	$A_{^{14}N}$	15.2	10.4 ±0.1	14.5	15–31†	18.0	
$^{14}ND_2$	A_D	3.9 ±0.15	3.7	~4	—		
	g	2.0042±0.0003	2.0049	—	—	—	
	$A_{^{14}N}$	15.2	—	13.5	—	—	
$^{15}NH_2$	A_H	25.4	—	—	—	—	27.3±0.2‡
	g	2.0052±0.0005	—	—	—	—	
	$A_{^{15}N}$	21.3 ±0.7	—	—	—	—	18.6±0.2‡
$^{15}ND_2$	A_D	~4					
	g	2.0052±0.0005	—	—	—	—	
	$A_{^{15}N}$	21.3 ±0.7	—	—	—	—	

*A_H and $A_{^{14}N}$ are calculated from the measured values of A_D and $A_{^{15}N}$, respectively.
†Depends on matrix.
‡In single crystals of $K^{15}NH_2SO_3$.

data qualitatively confirm previous identifications and analyses of spectra (5–7), for the amino radical trapped in an ammonia matrix, but cause a significant revision of hyperfine splitting constants. The difference in our values of A_N compared to those in an argon matrix (ref. 8*a*, also for reinterpretation, see ref. 8*b*), or in a crystalline KNH_2SO_3 matrix (10), is a common phenomenon arising from the different radical environment. Symons (11) has discussed the observation of various values of $A_{^{14}N}$ with changes in medium and suggests the effect is associated with differing bond angles for the amino radical.

Effect of Additives

The NH_3 system differs from water (1) in that trapped electrons were not detected directly. Evidence for the transient existence of electrons is ambiguous in the case of NH_3. Difficulties encountered in scavenging experiments have

Can. J. Chem. Downloaded from www.nrcresearchpress.com by 210.87.254.5 on 09/05/12
For personal use only.

been discussed previously (3). It is clear, however, that the addition of < 0.01 v% of electron scavengers such as tetranitromethane or CH_3I does give the expected radical products NO_2 and CH_3, respectively, but does not affect the yield of amino radicals. A notable result is that the addition of 5 v% D_2O to ND_3 gave a uniformly pale blue deposit and an e.s.r. singlet at $g = 2$ which was very susceptible to microwave saturation. This may be assigned to trapped electrons (1). The role of water in this respect may simply be to provide a suitable trapping site.

1. W. A. SEDDON, D. R. SMITH, and P. E. BINDNER. Can. J. Chem. **46**, 1747 (1968).
2. W. A. SEDDON and D. R. SMITH. Advan. Chem. Ser. **82**, 163 (1968).
3. P. WARDMAN and W. A. SEDDON. Can. J. Chem. **47**, 2149 (1969).
4. P. WARDMAN and W. A. SEDDON. Can. J. Chem. **47**, 2155 (1969).
5. R. MARX and J. MARUANI. J. Chim. Phys. **61**, 1604 (1964).
6. B. S. AL-NAIMY, P. N. MOORTHY, and J. J. WEISS. J. Phys. Chem. **70**, 3654 (1966).
7. V. I. TUPIKOV, V. I. TSIVENKO, S. YA PSHEZHETSKII, A. G. KOTOV, and V. K. MILINCHUK. Russ. J. Phys. Chem. **37**, 65 (1963). V. I. TUPIKOV and S. YA PSHEZHETSKII. Russ. J. Phys. Chem. **37**, 1031 (1963); **37**, 1364 (1963).
8. (*a*) S. N. FONER, E. L. COCHRAN, V. A. BOWERS, and C. K. JEN. Phys. Rev. Lett. **1**, 91 (1958). (*b*) E. L. COCHRAN, F. J. ADRIAN, and V. A. BOWERS. J. Chem. Phys. **51**, 2759 (1969).
9. E. L. COCHRAN, F. J. ADRIAN, and V. A. BOWERS. J. Chem. Phys. **34**, 1161 (1961).
10. J. R. MORTON and D. R. SMITH. Can. J. Chem. **44**, 1951 (1966).
11. M. C. R. SYMONS. Advan. Chem. Ser. **82**, 1 (1968).

Organic and biological spectrochemical studies. XXVIII. Electron spin resonance spectra of some polynuclear aromatic hydrocarbon ions[1]

J. T. COOPER,[2] W. F. FORBES, AND J. C. ROBINSON
Departments of Chemistry and Statistics, University of Waterloo, Waterloo, Ontario

Received September 12, 1969

The electron spin resonance spectra are presented for the anions and cations of the polynuclear aromatic hydrocarbons anthanthrene, benz[*ghi*]perylene, benz[*e*]pyrene, dibenz[*fg,op*]naphthacene, and dibenz[*a,c*]triphenylene. The cation of dibenz[*fg,op*]naphthacene is shown to form a dimer under certain conditions.

The usefulness of a new oxidizing agent for the production of the cations, boron trichloride, has been investigated and was found to afford comparable spectra to boron trifluoride, using sulfur dioxide as solvent.

Canadian Journal of Chemistry, **48**, 1942 (1970)

Introduction

Anions and cations have been prepared for the polynuclear hydrocarbons, **1** to **5**. The anions were prepared by standard techniques, using sodium reduction in tetrahydrofuran. Several different methods were used for the cations as no single approach proved completely satisfactory for all compounds.

Splitting constants for the ions studied are listed in Table 1 and are believed to be correct to ± 0.02 G. All analyses were checked by computer simulation of the experimental spectra and excellent agreement was obtained in each case.

Experimental

Samples of each hydrocarbon, except anthanthrene (**1**), were obtained from two sources: the Aldrich Chemical Company, U.S.A., and the Coal Tar Research Association, Britain. Anthanthrene was obtained from the latter source only. All the anions were prepared by alkali metal reduction using standard high-vacuum techniques. Two approaches were used for oxidation to the cation: dissolution of the hydrocarbon in oxidizing acids, such as sulfuric or methane sulfonic acids, and treatment with a boron trihalide in sulfur dioxide. The use of BF_3 is well established (1, 2), but BCl_3 was also employed in this study.[3] It was found to yield identical results to the trifluoride but, since it has a considerably higher boiling point (12.5° C), it has the advantage of easier handling.

[1]For part XXVII in this series, see ref. 6.

[2]Present address: Biophysics Department, Roswell Park Memorial Institute, Buffalo, New York, 14203.

[3]The authors are indebted to Dr. A. Finch of Royal Holloway College, University of London, England, for suggesting the use of BCl_3.

Can. J. Chem. Downloaded from www.nrcresearchpress.com by 210.87.254.5 on 09/05/12
For personal use only.

been discussed previously (3). It is clear, however, that the addition of < 0.01 v% of electron scavengers such as tetranitromethane or CH_3I does give the expected radical products NO_2 and CH_3, respectively, but does not affect the yield of amino radicals. A notable result is that the addition of 5 v% D_2O to ND_3 gave a uniformly pale blue deposit and an e.s.r. singlet at $g = 2$ which was very susceptible to microwave saturation. This may be assigned to trapped electrons (1). The role of water in this respect may simply be to provide a suitable trapping site.

1. W. A. SEDDON, D. R. SMITH, and P. E. BINDNER. Can. J. Chem. **46**, 1747 (1968).
2. W. A. SEDDON and D. R. SMITH. Advan. Chem. Ser. **82**, 163 (1968).
3. P. WARDMAN and W. A. SEDDON. Can. J. Chem. **47**, 2149 (1969).
4. P. WARDMAN and W. A. SEDDON. Can. J. Chem. **47**, 2155 (1969).
5. R. MARX and J. MARUANI. J. Chim. Phys. **61**, 1604 (1964).
6. B. S. AL-NAIMY, P. N. MOORTHY, and J. J. WEISS. J. Phys. Chem. **70**, 3654 (1966).
7. V. I. TUPIKOV, V. I. TSIVENKO, S. YA PSHEZHETSKII, A. G. KOTOV, and V. K. MILINCHUK. Russ. J. Phys. Chem. **37**, 65 (1963). V. I. TUPIKOV and S. YA PSHEZHETSKII. Russ. J. Phys. Chem. **37**, 1031 (1963); **37**, 1364 (1963).
8. (*a*) S. N. FONER, E. L. COCHRAN, V. A. BOWERS, and C. K. JEN. Phys. Rev. Lett. **1**, 91 (1958). (*b*) E. L. COCHRAN, F. J. ADRIAN, and V. A. BOWERS. J. Chem. Phys. **51**, 2759 (1969).
9. E. L. COCHRAN, F. J. ADRIAN, and V. A. BOWERS. J. Chem. Phys. **34**, 1161 (1961).
10. J. R. MORTON and D. R. SMITH. Can. J. Chem. **44**, 1951 (1966).
11. M. C. R. SYMONS. Advan. Chem. Ser. **82**, 1 (1968).

Organic and biological spectrochemical studies. XXVIII. Electron spin resonance spectra of some polynuclear aromatic hydrocarbon ions[1]

J. T. COOPER,[2] W. F. FORBES, AND J. C. ROBINSON
Departments of Chemistry and Statistics, University of Waterloo, Waterloo, Ontario

Received September 12, 1969

The electron spin resonance spectra are presented for the anions and cations of the polynuclear aromatic hydrocarbons anthanthrene, benz[*ghi*]perylene, benz[*e*]pyrene, dibenz[*fg,op*]naphthacene, and dibenz[*a,c*]triphenylene. The cation of dibenz[*fg,op*]naphthacene is shown to form a dimer under certain conditions.

The usefulness of a new oxidizing agent for the production of the cations, boron trichloride, has been investigated and was found to afford comparable spectra to boron trifluoride, using sulfur dioxide as solvent.

Canadian Journal of Chemistry, **48**, 1942 (1970)

Introduction

Anions and cations have been prepared for the polynuclear hydrocarbons, **1** to **5**. The anions were prepared by standard techniques, using sodium reduction in tetrahydrofuran. Several different methods were used for the cations as no single approach proved completely satisfactory for all compounds.

Splitting constants for the ions studied are listed in Table 1 and are believed to be correct to ± 0.02 G. All analyses were checked by computer simulation of the experimental spectra and excellent agreement was obtained in each case.

Experimental

Samples of each hydrocarbon, except anthanthrene (**1**), were obtained from two sources: the Aldrich Chemical Company, U.S.A., and the Coal Tar Research Association, Britain. Anthanthrene was obtained from the latter source only. All the anions were prepared by alkali metal reduction using standard high-vacuum techniques. Two approaches were used for oxidation to the cation: dissolution of the hydrocarbon in oxidizing acids, such as sulfuric or methane sulfonic acids, and treatment with a boron trihalide in sulfur dioxide. The use of BF_3 is well established (1, 2), but BCl_3 was also employed in this study.[3] It was found to yield identical results to the trifluoride but, since it has a considerably higher boiling point (12.5° C), it has the advantage of easier handling.

[1]For part XXVII in this series, see ref. 6.

[2]Present address: Biophysics Department, Roswell Park Memorial Institute, Buffalo, New York, 14203.

[3]The authors are indebted to Dr. A. Finch of Royal Holloway College, University of London, England, for suggesting the use of BCl_3.

Can. J. Chem. Downloaded from www.nrcresearchpress.com by 210.87.254.40 on 09/05/12
For personal use only.

TABLE 1

Splitting constants of hydrocarbon ions **1** to **5**

Hydrocarbon	Anion			Cation		
	Position	ρ_M*	Splitting†	Position	ρ_M*	Splitting†
Anthanthrene (**1**)	4	−0.03894	0.65	1	0.04076	0.90
	2	0.03872	0.88	4	−0.03709	0.90
	1	0.04260	1.02	2	0.04225	0.99
	3	0.13242	3.37	3	0.12606	4.06
	5	0.15572	3.61	5	0.14431	4.46
	6	0.19981	5.05	6	0.19591	4.94
Benz[*ghi*]perylene (**2**)	3	0.01508	0.49	3	0.01681	0.25
	2	0.01958	0.62	2	0.02905	0.68
	8	−0.03290	0.79	8	−0.03146	0.68
	9	0.12782	2.88	1	0.11637	3.50
	1	0.12854	3.81	9	0.12827	3.50
	7	0.17017	4.09	7	0.16352	4.51
Benz[*e*]pyrene (**3**)	10	0.02791	0.78	9	−0.00490	0.12
	2	−0.04952	1.00	10	0.02100	0.84
	4	0.11691	2.41	2	−0.04911	1.16
	1	0.17220	4.24	4	0.13759	2.62
	3	0.18304	4.58	1	0.15990	4.91
	9	−0.00783	—	3	0.17331	5.08
Dibenz[*fg*,*op*]naphthacene (**4**)	2	−0.04463	0.85	2	−0.04463	1.02 (0.44)‡
	5	0.03769	0.85	5	0.03656	1.02 (0.44)‡
	1	0.16578	4.12	1	0.15781	4.68 (2.30)‡
	4	−0.00984	—	4	−0.00695	— —
Dibenz[*a*,*c*]triphenylene (**5**)	2	−0.02441	0.65	2	−0.02321	0.59
	3	0.07325	1.78	3	0.06901	2.00
	1	0.09481	2.12	1	0.09013	2.26
	4	0.01533	—	4	0.01548	—

*McLachlan unpaired spin density.
†Experimental splitting in G.
‡Splitting constants for dimeric ion.

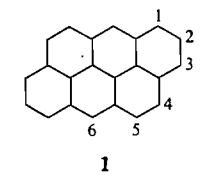

1

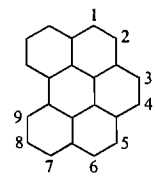

2

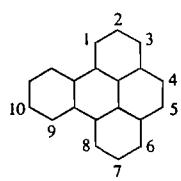

3

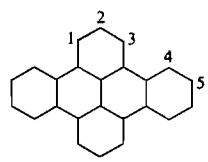

4

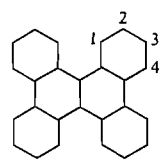

5

Results and Discussion

The results are summarized in Table 1, the hydrocarbons studied will be discussed individually.

Anthanthrene (1)

Dissolution in concentrated sulfuric acid was of limited use with anthanthrene since a well-resolved cation spectrum could not be obtained. Improved resolution was achieved in the SO_2 – boron trihalide system at low temperatures and also by dissolving the hydrocarbon in nitrobenzene and adding a 5- to 10-fold excess of methane sulfonic acid to give an overall concentration of ca. 10^{-2} *M*. This latter method is a modification of that of Malachesky *et al.* (3). Linewidths of ca. 0.08 G were achieved with both methods.

As expected, the anion spectrum analyzes in terms of six groups of two equivalent protons. With the cation, accidental degeneracy occurs at the four positions of lowest spin density, with the

Can. J. Chem. Downloaded from www.nrcresearchpress.com by 210.87.254.40 on 09/05/12
For personal use only.

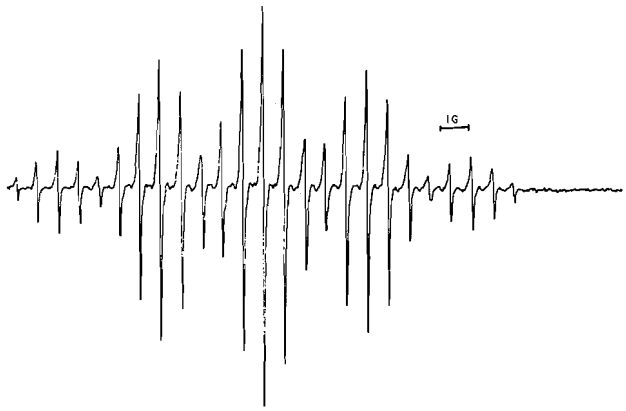

FIG. 1. The e.s.r. spectrum of the dibenz[*fg*,*op*]naphthacene anion.

result that only five splitting constants are detected (see Table 1).

Benz[ghi]perylene (2)

Well-resolved cation spectra were obtained by dissolving the hydrocarbon in nitrobenzene and adding 98% sulfuric acid, analogously to the method described above, and also by the use of SO_2 – boron trihalide.

The anion spectrum shows no unexpected features but, again, the cation displays accidental degeneracy with the spectrum analyzing in terms of only four different splitting constants (see Table 1).

Benz[e]Pyrene (3)

The cation was prepared in the SO_2 – boron trihalide system, the only medium in which it yielded a well-resolved electron spin resonance (e.s.r.) signal. The spectrum was recorded at −20 °C using a dilute, ca. 10^{-4} *M* solution for optimum resolution.

Only five splitting constants can be extracted from the anion spectrum, corresponding to ten protons. It is concluded that the remaining pair of positions have a corresponding splitting constant of less than ca. 0.03 G and, hence, are not observed. This is consistent with the fact that the smallest splitting in the cation is only 0.12 G and splitting constants for a given position in hydrocarbon ions tend to be larger in the cation than in the anion (8–10).

Dibenz[fg,op]naphthacene (4)

Both the anion and cation spectra of this hydrocarbon show considerable anomalies. The anion spectrum is shown in Fig. 1. The lines are sharp and well resolved, with a width of only 0.05 G, and the analysis, in terms of one group of six protons and one of four, is unambiguous. The implications of this are two-fold.

(*a*) The spin density at one set of four equivalent protons corresponds to a splitting constant of less than 0.015 G.

(*b*) The spin density at the pair of equivalent protons corresponds to a splitting constant within a few mG of that due to one of the sets of four protons. If this were not so, each of the heptets apparently due to six protons would show broadening towards the center. This is not observed, none of the five groups shows such line-width trends and the relative intensity distribution within each is close to the theoretical binomial distribution 1:6:15:20:15:6:1.

A weak, poorly-resolved, spectrum of the cation was obtained by dissolving the hydrocarbon in warm nitrobenzene and then adding 98% sulfuric acid. The lines are broad, ca. 0.3 G, but the spectrum can be analyzed in terms of two groups of protons, analogous to the anion. It is possible that the broadness of the lines may be due, in part, to an unresolved quintet splitting arising from the remaining set of four protons.

An attempt was made to prepare the cation in the sulfur dioxide – boron trihalide system, but the result was a spectrum (see Fig. 2) quite different from that obtained in acid solution. This spectrum is readily interpreted in terms of one group of 12 equivalent protons and one group of eight. It is ascribed to the dimeric (dibenz[*fg*,*op*]-naphthacene)$_2^+$ cation, in which two molecules of the hydrocarbon lie in parallel planes, one above the other, with a single electron removed

Can. J. Chem. Downloaded from www.nrcresearchpress.com by 210.87.254.40 on 09/05/12
For personal use only.

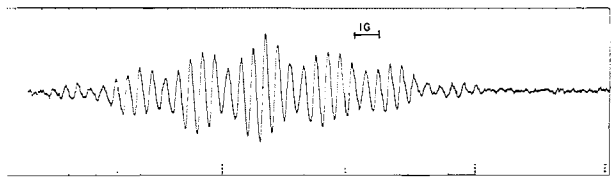

FIG. 2. The e.s.r. spectrum of the dibenz[*fg*,*op*]naphthacene cation dimer.

from the pair. Consistent with this is the observation that the splitting constants for this species are approximately half the values measured for the simple cation in H_2SO_4–nitrobenzene. Analogous dimeric species have been reported previously (4–6), supporting this interpretation.

Dibenz[a,c]triphenylene (5)

Both anion and cation have been reported previously (4); however, for both species only three of the expected four splitting constants could be detected. As the spectra were not well resolved, the hydrocarbon was included in the present study.

No significant improvement on the earlier work was achieved with the anion, but considerably improved spectra were obtained with the cation. Using the SO_2 – boron trihalide system and recording the e.s.r. signal at -70 °C, a well-resolved spectrum was obtained with a linewidth of only 0.06 G. However, the spectrum still analyzes in terms of only three splitting constants, although the upper limit for the remaining one can now be set at 0.015 G. This splitting is probably well below 0.015 G as the lines show no signs of distortion due to an unresolved quintet.

Molecular Orbital Calculations

Molecular orbital calculations were carried out for all the ions studied. In addition to simple Hückel calculations, which predict the same unpaired electron distribution for both anion and cation, modified McLachlan calculations were carried out which predict different spin density distributions for the ions. The results of these latter calculations are included in Table 1. (The assignments can only be considered tentative, confirmation would require studies on selectively-labelled hydrocarbons.)

Theoretically, there should be a linear dependence of proton splitting constant on the unpaired electron spin density at the contiguous carbon atom (7). This is expressed in the McConnell relationship:

$$a_H = Q\rho$$

where a_H = proton splitting constant; ρ = unpaired spin density; and Q = a constant.

Using the McLachlan calculations it is found that for the series of anions

$$a_H = 24.28\rho_M \pm 0.06 \text{ G}$$

and for the cations

$$a_H = 27.39\rho_M \pm 0.15 \text{ G}$$

where the values of Q are estimated from a linear regression analysis and the standard error, the average squared deviation from the fitted line, was calculated from the residual sums of squares.

As expected, if the simple Hückel data are used in place of the McLachlan calculations, a less satisfactory fit to a linear relationship is obtained. The results, using the Hückel calculations, are $a_H = 31.77\rho_H \pm 0.26$ G and $a_H = 35.20 \pm 0.33$ G for the anions and cations, respectively.

This work was supported by the National Cancer Institute of Canada, the Canadian Department of Public Health and Welfare, the National Research Council of Canada, the Defence Research Board of Canada, (Grant No. 1675-04), and by the United States Public Health Service Research Grant RH00392, National Center for Radiological Health.

1. J. P. COLPA and E. DE BOER. Mol. Phys. **7**, 333 (1963).
2. E. DE BOER and A. PRAAT. Mol. Phys. **8**, 291 (1964).
3. P. A. MALACHESKY, L. S. MARCOUX, and R. N. ADAMS. J. Phys. Chem. **70**, 2064 (1966).
4. I. C. LEWIS and L. S. SINGER. J. Chem. Phys. **43**, 2712 (1965).
5. O. W. HOWARTH and G. K. FRAENKEL. J. Amer. Chem. Soc. **88**, 4514 (1966).
6. J. T. COOPER and W. F. FORBES. Can. J. Chem. **46**, 1158 (1968).
7. H. M. MCCONNELL. J. Chem. Phys. **24**, 764 (1956).
8. J. P. COLPA and J. R. BOLTON. Mol. Phys. **6**, 273 (1963).
9. G. GIACOMETTI, P. L. NORDIO, and M. V. PAVAN. Theor. Chim. Acta, **1**, 404 (1963).
10. T. C. SAYETTA and J. D. MEMORY. J. Chem. Phys. **40**, 2748 (1964).

Can. J. Chem. Downloaded from www.nrcresearchpress.com by 210.87.254.40 on 09/05/12
For personal use only.

Benzodiazocines. I. Synthesis of hexahydro-1,4-benzodiazocin-2,5-dione

J. M. MUCHOWSKI
Bristol Laboratories of Canada, Candiac, Quebec
Received January 9, 1970

A three step synthesis of the title compound from isatin is described.
Canadian Journal of Chemistry, 48, 1946 (1970)

Can. J. Chem. Downloaded from www.nrcresearchpress.com by 210.87.254.42 on 09/05/12
For personal use only.

There are nine possible bicyclic benzodiazocines, and representatives of each of the 1,6-, 1,5-, 1,4-, 2,5-, and 3,4-isomers are known.[1] Derivatives of 1,6-, 1,5-, and 2,5-benzodiazocine, have recently become quite numerous (see refs. 1–5, 6–8, and 9–11 respectively, and the papers cited therein), a few 3,4-benzodiazocines are known (12), but only one example of a 1,4-benzodiazocine has appeared in the literature to date (13). This publication describes a simple three step synthesis of a hexahydro derivative of the parent 1,4-benzodiazocine.

The preparation of the title compound was based on a cyclolization reaction identical to that used by Glover *et al.* (14) for the synthesis of some dioxo diazocyclodecanes. Thus, sodioisatin (**1**) was acetylated with azidoacetyl chloride, and the azido compound **2** thus produced, was catalytically hydrogenated in one step (15)[2] to the aminoacetyloxindole **3** (Scheme 1), which was isolated as its crystalline perchlorate salt. Continuous extraction of an aqueous bicarbonate solution of **3** with dichloromethane gave a very insoluble neutral compound isomeric with the starting material. It was assigned the benzodiazocine structure **5**, rather than that of the cyclol **4**, on the basis of the nuclear magnetic resonance (n.m.r.) spectrum (DMSO-d_6), which consisted of singlets at δ 3.57(2H) and 10.15(1H), a doublet at 3.28(2H, J = 5.0 c.p.s.), a triplet at 7.83(1H, J = 5.0), and a complex multiplet (4H) between 7.03 and 7.43. In perdeuteriodimethylsulfoxide containing added deuterium oxide the single proton absorptions at δ 7.83 and 10.15 disappeared, and the two proton doublet at δ 3.28 was replaced by a singlet (2H) at δ 3.32. The low field positions of the single proton absorptions at δ 7.83 and 10.15, as well as the readily observable coupling (19) between the protons on C-3 (δ 3.28) and the N_4H proton, were both more consistent with **5** than with **4**. That **5** was monomeric and not dimeric in nature was proved by the mass spectrum (see Table 1) which had a molecular ion peak at *m/e* 190 with an intensity 42% of that of the base peak (*m/e* 133). The strong (22%) peak at *m/e* 172 indicated that the loss of water via the cyclol **4** was an important fragmentation pathway as has been observed for other compounds of this type (14). Other intense peaks were present at *m/e* 144 (41%, M-HOH-CO), 105 (44%), and 104 (46%). The base peak at *m/e* 133 was probably due, at least in part, to the oxindole molecular ion. This supposition was supported by the prominent peaks at *m/e* 105, 104, and 78, with the appropriate metastable peaks at *m/e* 83 and 103, characteristic (20) of this species.

This synthesis should also be amenable to the preparation of certain derivatives of **5** substituted in the 3-position or in the aromatic ring, and to the homologous 1,5-benzodiazonine.

Several attempts were made to reduce **5** to the corresponding diamine (lithium aluminum hydride or diborane), but mixtures of unidentified carbonyl-containing products were obtained in each case. Since other synthetic routes to derivatives of this diamine had already been devised (21), no further effort was expended along these lines.

Experimental

The melting points were determined in a Gallenkamp melting point apparatus and are not corrected. The infrared (i.r.) spectra were measured with a Perkin–Elmer 237B grating spectrophotometer or a Unicam SP-200G i.r. spectrophotometer. The n.m.r. spectrum was recorded

[1]There are no published examples of the 1,2-, 1,3-, 2,3-, or 2,4-benzodiazocine ring systems.

[2]Recently (15), we erroneously attributed the first instance of the direct catalytic reduction of isatin to oxindole, to Beckett *et al.* (16). This reduction was in actuality first described by Prof. G. Tacconi (University of Pavia, Italy) in 1964 (17). We thank Prof. Tacconi for bringing this point to our attention. Furthermore, in 1965, Walker *et al.* (18) reported that *N*-methylisatin could be reduced catalytically to *N*-methyloxindole.

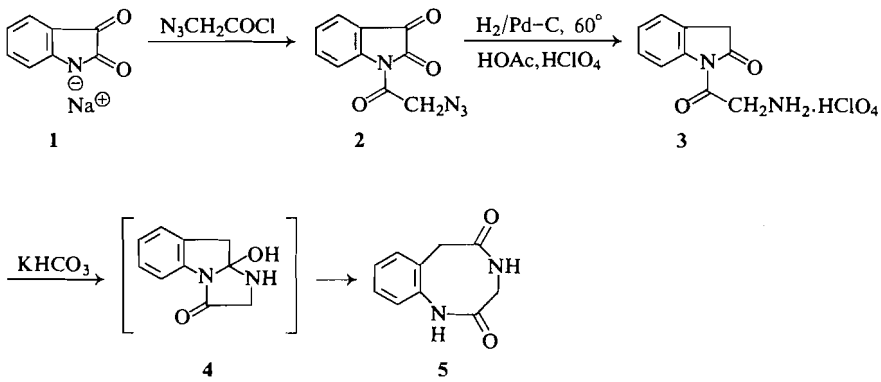

SCHEME 1

TABLE 1

Mass spectrum* of hexahydro-1,4-benzodiazocine-2,5-dione

m/e	Relative intensity†	m/e	Relative intensity	m/e	Relative intensity	m/e	Relative intensity
191	5	117	22	79	5	43	4
190	42	116	10	78	28	42	5
173	3	115	3	77	23	41	3
172	22	114	11	76	6	40	3
162	3	107	4	75	3	39	11
146	4	106	27	72	4	38	3
145	5	105	44	71	8	32	5
144	41	104	46	65	4	30	24
143	7	103	4	64	4	29	5
133	100	91	7	63	9	28	24
132	9	90	12	62	4	27	5
118	5	89	17	53	3	18	4

*Measured with a Hitachi RMμ 6D mass spectrometer using an ionization energy of 70 eV and the direct inlet probe technique (100°).

†Intensities are rounded off to the nearest percent. Peaks with a relative intensity of less than 3% were not tabulated.

with a Varian A-60A spectrometer and is expressed in p.p.m. (δ) from internal tetramethylsilane.

Azidoacetyl chloride was prepared from azidoacetic acid (22) by the method of Bertho and Maier (23).

1-Azidoacetylisatin

Sodium hydride in mineral oil (2.86 g of a 55% suspension) was washed free of the carrier with hexane, and layered with 500 ml of dry toluene. Isatin (8.72 g, 59.2 mmoles) was added, and the vigorously stirred mixture was heated at reflux temperature until gas evolution was complete (1 h). After cooling to room temperature, azidoacetyl chloride (7.13 g, 59.6 mmoles) was added dropwise with stirring over a 10 min period, and after 1/2 h at ambient temperature, the mixture was heated under reflux for 2 h. The hot mixture was filtered; on cooling to room temperature, 3.57 g of impure isatin (m.p. 188–196°) was deposited. The supernatant solution was evaporated *in vacuo* and the solid residue was extracted with boiling 200 ml portions of 10% benzene in petroleum ether (b.p. 90–120°) until only a red gummy material remained. Careful cooling of the extracts gave the azido compound as a lemon yellow solid, m.p. 137–140°. The yield ranged between 49 and 58%, based on isatin consumed. After three crystallizations from benzene:cyclohexane (3:1) the compound had m.p. 139–141°.

Anal. Calcd. for $C_{10}H_6N_4O_3$: C, 52.18; H, 2.63; N, 24.34. Found: C, 52.02; H, 2.68; N, 24.60.

The i.r. spectrum ($CHCl_3$) had strong bands at 2120, 1783, 1749, and 1732 cm^{-1}.

1-Aminoacetyloxindole Perchlorate

The above azido compound (2.30 g, 10 mmoles), and 10% palladium-on-charcoal (460 mg), in acetic acid containing 3 ml of 60–62% perchloric acid (total volume, 100 ml), was hydrogenated at room temperature and an initial hydrogen pressure of 60 p.s.i.g. After 40 min, the reaction temperature was raised to 60° and hydrogenation was continued until the theoretical amount of hydrogen was absorbed (6 h). The mixture was cooled to room temperature, and the product was collected by filtration. The salt was taken up in hot acetonitrile and filtered to remove the catalyst. Upon cooling, the product, m.p. 246–248° dec. (1.746 g, 60.5%) was obtained as a white crystalline solid. Two additional crystallizations did not raise the melting point.

Anal. Calcd. for $C_{10}H_{10}N_2O_2$:$HClO_4$: C, 41.31; H, 3.82. Found: C, 41.43; H, 3.78.

Can. J. Chem. Downloaded from www.nrcresearchpress.com by 210.87.254.42 on 09/05/12
For personal use only.

The i.r. spectrum (Nujol mull) had absorptions at 3206, 3154, 3095, 1741, and 1709 cm^{-1}.

Hexahydro-1,4-benzodiazocin-2,5-dione

A solution of the perchlorate salt (1.74 g, 6 mmoles), in 250 ml of water containing 1.8 g (18 mmoles) of potassium bicarbonate, was continuously extracted with dichloromethane for 20 h. The solvent was removed *in vacuo* and the solid residue was crystallized from acetonitrile. The product, which decomposed at 215–218°, was obtained in two crops in 54–64% yield. Recrystallization of the compound from acetonitrile gave material which decomposed at 216–218° (220–222°, fast heating).

Anal. Calcd. for $C_{10}H_{10}N_2O_2$: C, 63.15; H, 5.30; N, 14.73. Found: C, 62.95; H, 5.32; N, 15.06.

The i.r. spectrum (Nujol mull) had bands at 3294, 3180, 3056, and 1673 cm^{-1}.

The mass spectrum was measured at the Chemistry Department, University of Montreal. We are grateful to Dr. R. Rousseau for making this service available to us.

1. H. Stetter. Chem. Ber. **86**, 197 (1953).
2. G. Wittig, W. Joos, and P. Rathfelder. Ann. **610**, 180 (1957).
3. W. Schroth and B. Streckenbach. Z. Chem. **3**, 465 (1963).
4. T. S. Sulkowski. U.S. Pat. 3293243 (1966); Chem. Abstr. **66**, 46443*n* (1967).
5. W. W. Paudler and A. G. Zeiler. J. Org. Chem. **34**, 2138 (1969).
6. M. E. Dereig, R. M. Schweininger, and R. I. Fryer. J. Org. Chem. **34**, 179 (1969).
7. M. Denzer and H. Ott. J. Org. Chem. **34**, 183 (1969).
8. B. I. Auret, M. F. Grundon, and I. I. McMaster. J. Chem. Soc. (C) 2862 (1968).
9. T. S. Sulkowski, M. A. Willie, A. Mascitti, and J. L. Diebold. J. Org. Chem. **32**, 2180 (1967).
10. D. H. Kim, A. A. Santilli, T. S. Sulkowski, and S. J. Childress. J. Org. Chem. **32**, 3720 (1967).
11. P. Aeberli and W. J. Houlihan. J. Org. Chem. **34**, 1720 (1969).
12. N. L. Allinger and G. A. Youngdale. J. Org. Chem. **25**, 1509 (1960).
13. P. A. Petyunin. Khim. Geterotsikl. Soedin. Akad. Nauk. Latv. SSR. 476 (1965); Chem. Abstr. **63**, 13133 (1965).
14. G. I. Glover, R. B. Smith, and H. Rapoport. J. Amer. Chem. Soc. **87**, 2003 (1965).
15. J. M. Muchowski. Can. J. Chem. **47**, 857 (1969).
16. A. H. Beckett, R. W. Daisley, and J. Walker. Tetrahedron, **24**, 6093 (1968).
17. G. Tacconi. Il. Farmaco, Ed. Sc. **19**, 113 (1964).
18. G. B. Walker, R. T. Smith, and B. N. Weaver. J. Med. Chem. **8**, 627 (1965).
19. R. H. Bible, Jr. Interpretation of n.m.r. spectra. Plenum Press, New York, 1965. p. 59.
20. J. C. Powers. J. Org. Chem. **33**, 2044 (1968).
21. J. M. Muchowski. Unpublished results.
22. J. H. Boyer and J. Horner. J. Amer. Chem. Soc. **77**, 951 (1955).
23. A. Bertho and J. Maier. Ann. **498**, 50 (1932).

Photochemistry of β-bromo-β-nitrostyrene

G. W. Shaffer

Givaudan Corporation, 125 Delawanna Avenue, Clifton, New Jersey 07014

Received December 5, 1969

Ultraviolet irradiation of β-bromo-β-nitrostyrene in hydroxylic solvents gives a good yield of alkyl α-isonitrosophenyl acetates (**1**).

Canadian Journal of Chemistry, 48, 1948 (1970)

In view of the interesting biological activity (1) of β-bromo-β-nitrostyrene (BNS, yellow solid, m.p. 67–68°), it becomes desirable to learn more about the chemistry of this molecule. We had previously observed that yellow solutions of BNS in organic solvents gradually became colorless when exposed to daylight. Consequently, we investigated the photochemistry of BNS and found that irradiation in hydroxylic solvents leads to a rapid disappearance of the BNS ultraviolet (u.v.) absorption at 310 nm and gives a good yield (50–80%) of alkyl α-isonitrosophenyl acetates (**1**).

The methyl ester (**1**, R = CH_3) obtained from irradiation in methanol was identical with a synthetic sample, as also was the methyl ester obtained from treatment of an aqueous dioxane irradiation mixture with diazomethane. The structure of the ethyl ester (**1**, R = C_2H_5) obtained from irradiation in ethanol was unambiguously determined by spectral data and melting point.

Can. J. Chem. Downloaded from www.nrcresearchpress.com by 210.87.254.42 on 09/05/12
For personal use only.

The i.r. spectrum (Nujol mull) had absorptions at 3206, 3154, 3095, 1741, and 1709 cm^{-1}.

Hexahydro-1,4-benzodiazocin-2,5-dione

A solution of the perchlorate salt (1.74 g, 6 mmoles), in 250 ml of water containing 1.8 g (18 mmoles) of potassium bicarbonate, was continuously extracted with dichloromethane for 20 h. The solvent was removed *in vacuo* and the solid residue was crystallized from acetonitrile. The product, which decomposed at 215–218°, was obtained in two crops in 54–64% yield. Recrystallization of the compound from acetonitrile gave material which decomposed at 216–218° (220–222°, fast heating).

Anal. Calcd. for $C_{10}H_{10}N_2O_2$: C, 63.15; H, 5.30; N, 14.73. Found: C, 62.95; H, 5.32; N, 15.06.

The i.r. spectrum (Nujol mull) had bands at 3294, 3180, 3056, and 1673 cm^{-1}.

The mass spectrum was measured at the Chemistry Department, University of Montreal. We are grateful to Dr. R. Rousseau for making this service available to us.

1. H. Stetter. Chem. Ber. **86**, 197 (1953).
2. G. Wittig, W. Joos, and P. Rathfelder. Ann. **610**, 180 (1957).
3. W. Schroth and B. Streckenbach. Z. Chem. **3**, 465 (1963).
4. T. S. Sulkowski. U.S. Pat. 3293243 (1966); Chem. Abstr. **66**, 46443*n* (1967).
5. W. W. Paudler and A. G. Zeiler. J. Org. Chem. **34**, 2138 (1969).
6. M. E. Dereig, R. M. Schweininger, and R. I. Fryer. J. Org. Chem. **34**, 179 (1969).
7. M. Denzer and H. Ott. J. Org. Chem. **34**, 183 (1969).
8. B. I. Auret, M. F. Grundon, and I. I. McMaster. J. Chem. Soc. (C) 2862 (1968).
9. T. S. Sulkowski, M. A. Willie, A. Mascitti, and J. L. Diebold. J. Org. Chem. **32**, 2180 (1967).
10. D. H. Kim, A. A. Santilli, T. S. Sulkowski, and S. J. Childress. J. Org. Chem. **32**, 3720 (1967).
11. P. Aeberli and W. J. Houlihan. J. Org. Chem. **34**, 1720 (1969).
12. N. L. Allinger and G. A. Youngdale. J. Org. Chem. **25**, 1509 (1960).
13. P. A. Petyunin. Khim. Geterotsikl. Soedin. Akad. Nauk. Latv. SSR. 476 (1965); Chem. Abstr. **63**, 13133 (1965).
14. G. I. Glover, R. B. Smith, and H. Rapoport. J. Amer. Chem. Soc. **87**, 2003 (1965).
15. J. M. Muchowski. Can. J. Chem. **47**, 857 (1969).
16. A. H. Beckett, R. W. Daisley, and J. Walker. Tetrahedron, **24**, 6093 (1968).
17. G. Tacconi. Il. Farmaco, Ed. Sc. **19**, 113 (1964).
18. G. B. Walker, R. T. Smith, and B. N. Weaver. J. Med. Chem. **8**, 627 (1965).
19. R. H. Bible, Jr. Interpretation of n.m.r. spectra. Plenum Press, New York, 1965. p. 59.
20. J. C. Powers. J. Org. Chem. **33**, 2044 (1968).
21. J. M. Muchowski. Unpublished results.
22. J. H. Boyer and J. Horner. J. Amer. Chem. Soc. **77**, 951 (1955).
23. A. Bertho and J. Maier. Ann. **498**, 50 (1932).

Photochemistry of β-bromo-β-nitrostyrene

G. W. Shaffer

Givaudan Corporation, 125 Delawanna Avenue, Clifton, New Jersey 07014

Received December 5, 1969

Ultraviolet irradiation of β-bromo-β-nitrostyrene in hydroxylic solvents gives a good yield of alkyl α-isonitrosophenyl acetates (**1**).

Canadian Journal of Chemistry, 48, 1948 (1970)

In view of the interesting biological activity (1) of β-bromo-β-nitrostyrene (BNS, yellow solid, m.p. 67–68°), it becomes desirable to learn more about the chemistry of this molecule. We had previously observed that yellow solutions of BNS in organic solvents gradually became colorless when exposed to daylight. Consequently, we investigated the photochemistry of BNS and found that irradiation in hydroxylic solvents leads to a rapid disappearance of the BNS ultraviolet (u.v.) absorption at 310 nm and gives a good yield (50–80%) of alkyl α-isonitrosophenyl acetates (**1**).

The methyl ester (**1**, R = CH_3) obtained from irradiation in methanol was identical with a synthetic sample, as also was the methyl ester obtained from treatment of an aqueous dioxane irradiation mixture with diazomethane. The structure of the ethyl ester (**1**, R = C_2H_5) obtained from irradiation in ethanol was unambiguously determined by spectral data and melting point.

Can. J. Chem. Downloaded from www.nrcresearchpress.com by 210.87.254.42 on 09/05/12
For personal use only.

Can. J. Chem. Downloaded from www.nrcresearchpress.com by 210.87.254.42 on 09/05/12
For personal use only.

This photoreaction is a variation of that reported by Chapman *et al.* (2) and his mechanism (eq. [1]) will account for the observed products, since the acid bromides **2** are logical precursors for the incorporation of alcoholic solvent. Attempts were unsuccessful to provide evidence of **2** by irradiation of BNS in a hydrocarbon solvent followed by treatment of the mixture with ethanol in the dark; only non-monomeric tar was formed. Failure of **2** to survive the irradiation is not unreasonable in light of the known (3) photolability of the carbon–halogen bond of acyl halides.

[1]

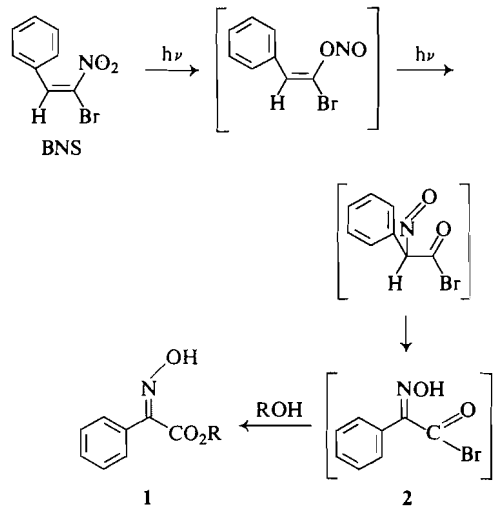

Both the *syn* and *anti* oximes are formed in the photoisomerization but recrystallization appears to give only one isomer. This is most evident for the ethyl ester photoproduct (**1**, R = C_2H_5). The ethyl group nuclear magnetic resonance (n.m.r.) absorption of the crude ester appears as two overlapping quartets and two overlapping triplets (all J's = 7 Hz); these multiplets collapse to a single quartet and a single triplet upon recrystallization.

During the irradiation of BNS there is an additional product formed initially (40–50% by gas–liquid chromatography (g.l.c.)) which then disappears as the oxime is formed. This product could not be isolated as it reconverts to starting material upon standing in the dark or removal of solvent. One possible structure for this product would be the geometrical isomer of BNS where the instability might be explained by the steric interaction of a *cis* phenyl ring and bromine atom.

Experimental[1]

Irradiation of BNS in Methanol

A solution of 3.00 g of BNS (4) in 150 ml of reagent methanol (0.10 *M*) was irradiated for 2 h, after which time g.l.c. on SE-30 showed starting material gone and one new peak (retention time relative to BNS equaled 1.1). The solution was concentrated and the crude oil (3.52 g) was recrystallized once from aqueous ethanol and then from water to yield pure methyl α-isonitrosophenyl acetate, m.p. 149–150° (reported (5) m.p. 138–139°), ν_{max} 2800–3500(broad), 1732(s), 1435(m), 1408(m), 1197(s), 1054(m), 1010(s), 787(m), 770(broad), 716(m), 691(m) cm^{-1}; n.m.r. (acetone-d_6), 11.4–11.5 (1H, broad singlet, oxime H), 7.36–7.66 (5H, aromatic H), 3.81 (3H, singlet, methyl H).

The ester obtained from irradiation was identical (i.r. and n.m.r. spectra, g.l.c. retention time, mixed m.p. 147–149°) to a synthetic sample (m.p. 149–151°) obtained by oximation of methyl benzoylformate (Aldrich).

Irradiation of BNS in Ethanol

A solution of 3.00 g of BNS in 150 ml of absolute ethanol (0.10 *M*) was irradiated for 2 h, after which time g.l.c. on SE-30 showed 17% BNS, 4% minor product, (retention time relative to BNS equaled 0.5–0.6), and 79% major product (retention time relative to BNS equaled 1.3). The solution was concentrated and the major product was isolated by recrystallization of the crude crystalline material (3.40 g) from aqueous ethanol and then from water. This compound was identified as ethyl α-isonitrosophenyl acetate on the basis of the following data: m.p. 112.0–113.5° (reported (5) m.p. 112–113°), ν_{max} 2900–3500(broad), 1730(s), 1198(s), 1059(s), 1013(s) cm^{-1}; n.m.r. ($CDCl_3$), 10.2 (1H, broad absorption, oxime H), 7.35–7.73 (5H, aromatic H), 4.34 (2H, quartet, J = 7 Hz, methylene H), 1.31 (3H, triplet, J = 7 Hz, methyl H).

Mol. Wt. Calcd. for $C_{10}H_{11}NO_3$: 193.0694. Found (high resolution mass spectrum): 193.0682.

The crude ester before recrystallization exhibited n.m.r. absorption for the ethyl group as two overlapping quartets and two overlapping triplets (all J's = 7 Hz) which collapsed to a single quartet and a single triplet upon recrystallization. This was attributed to photochemical formation of both the *syn* and *anti* isomers.

Irradiation of BNS in Aqueous Dioxane

A solution of 0.50 g of BNS in 150 ml of aqueous

[1]Irradiations were carried out with a Pyrex-filtered 450 W medium pressure Hanovia mercury lamp in an immersion probe and were outgassed with argon before and during the reaction. The disappearance of BNS can be monitored by g.l.c. on SE-30 or by u.v. absorption (λ_{max} 310 nm, (ε 14 300)). The yields of the photoproducts varied depending on the run but were generally in the region of 50–80%. The observed photoreactions did not occur in the dark.

The infrared (i.r.) spectra were taken as potassium bromide pellets, n.m.r. spectra were taken on a Varian A-60A and are reported as δ units from TMS, and melting points were taken with a Büchi oil bath apparatus and are uncorrected.

dioxane (50% water by volume) (0.017 *M*) was irradiated 1/2 h, after which time g.l.c. on SE-30 showed the starting material was gone. The solvent was removed and the residual oil (1.10 g) was treated with excess diazomethane. After reaction and decomposition of the diazomethane with acetic acid, the ethereal solution was washed with 5% sodium carbonate, dried, filtered, and concentrated. The crude crystalline material (0.227 g) was recrystallized from water and identified as methyl α-isonitrosophenyl acetate by comparison to a synthetic sample (see above).

Irradiation of BNS in Hydrocarbon Solvents

Irradiation of BNS in isooctane or heptane led to a rapid disappearance of starting material but only non-monomeric tar was formed. This tar was allowed to react with ethanol under reflux but no ethyl α-isonitrosophenyl acetate could be detected by g.l.c. on SE-30.

In each irradiation, including those in alcohols or water, there was an additional product formed initially (40–50% by g.l.c., retention time relative to starting material equaled 0.5–0.6) which then disappeared as the tar in the case of hydrocarbon solvents, or the oxime in the case of hydroxylic solvents, was formed. This product was not isolated as it reconverts to starting material upon standing in the dark or removal of solvent.

The author would like to thank Dr. H. Daeniker for helpful discussion and Messrs. P. Porcaro and P. Shubiak for experimental spectra.

1. TECHNICAL BULLETIN BNS-1, "Giv-Cide® BNS", Givaudan Corporation, Sindar Division, 321 W. 44th St., New York, N.Y. 10036.
2. O. L. CHAPMAN, A. A. GRISWOLD, E. HOGANSON, G. LENZ, and J. REASONER. Pure Appl. Chem. **9**, 585 (1964).
3. U. SCHMIDT. Angew. Chem. Int. Ed. **4**, 146, 239 (1965); J. G. CALVERT and J. N. PITTS, JR. Photochemistry. John Wiley and Sons, Inc., N.Y., 1966. p. 434.
4. Supplied by M. Manowitz, Givaudan Corp.; B. Priebs, Ann. **225**, 319 (1884).
5. J. R. A. POLLOCK and R. STEVENS, *Editors*. Dictionary of organic compounds. Vol. I. Oxford University Press, New York, 1965. p. 359.

Can. J. Chem. Downloaded from www.nrcresearchpress.com by 210.87.254.42 on 09/05/12
For personal use only.

1951-5747

Canadian Journal of Chemistry

Published by THE NATIONAL RESEARCH COUNCIL OF CANADA

VOLUME 48 JULY 1, 1970 NUMBER 13

Carbon monoxide yields in the radiolysis of carbon dioxide at very high dose rates[1]

C. WILLIS, A. W. BOYD, AND P. E. BINDNER

Physical Chemistry Branch, Chalk River Nuclear Laboratories, Atomic Energy of Canada Limited, Chalk River, Ontario

Received February 23, 1970

Carbon dioxide has been irradiated with electron pulses at a dose rate of 2×10^{27} eV g^{-1} s^{-1}. The measured carbon monoxide yield is $G(CO) = 7.8 \pm 0.3$. Addition of SF_6, an electron scavenger, reduces this yield to $G(CO) = 4.8$ which is the same, within the experimental error, as the low dose rate yield $G(CO) = 4.5 \pm 0.5$. The effect of SF_6 and the difference between the high and low dose rate yields is explained by suppression of dissociative neutralization of the $C_2O_4^+$ ion.

Canadian Journal of Chemistry, 48, 1951 (1970)

Introduction

The accepted initial yield for carbon monoxide in the low linear energy transfer (l.e.t.) radiolysis of carbon dioxide at dose rates in the range 10^{16}–10^{20} eV g^{-1} s^{-1} is $G(CO) = 4.5 \pm 0.5$ (for a review of radiolysis of CO_2, see ref. 1*a*). Meaburn *et al.* (2) have reported a value of $G(CO) = 6.0 \pm 0.3$ using a pulsed electron accelerator giving a dose rate of 2×10^{25} eV g^{-1} s^{-1}. This value was reduced to $G(CO) = 4.2$ on the addition of 0.04 to 5% SF_6. Electron scavengers such as NO_2 and N_2O have no effect on the value of $G(CO) = 4.5$ at the above low dose rates.[2]

In the present work, we have determined $G(CO)$ both for pure CO_2 and CO_2–SF_6 mixtures at 2×10^{27} eV g^{-1} s^{-1}. Our results are compared with those of Meaburn *et al.* (2) and a mechanism to account for the dose rate dependence and the effects of electron scavengers is proposed.

[1]AECL No. 3595.

[2]Addition of SF_6 to carbon dioxide at low dose rates $\sim 10^{16}$–10^{18} eV cm^{-3} s^{-1} leads to some net production of carbon monoxide and oxygen in contrast to the situation in pure CO_2 where steady state concentrations of CO and O_2 are established at lower doses (1*b*). However, SF_6 has no effect on the initial carbon monoxide yield as determined by isotopic exchange.

Experimental

The electron pulses were obtained from a Febetron 705. Samples were irradiated in quartz cells and products analyzed by volume measurement in a calibrated McLeod gauge followed by mass-spectrometric determination of the composition. The techniques have been reported several times before (3–5).

The dose from these electron pulses was determined from the yield of nitrogen from nitrous oxide taking $G(N_2) = 12.4$ (6–8).

Ozone was estimated by the iodide method using solutions buffered at pH = 7.0. The stoichiometry of O_3 to I_2 has been shown to be 1 to 1.54 for this pH (9, 10).

The carbon dioxide (Matheson "bone-dry" grade) and sulfur hexafluoride (Matheson C.P. grade) were subjected to several sublimation cycles to remove non-condensible impurities.

Results

The amount of carbon monoxide produced from carbon dioxide as a function of absorbed energy is shown in Fig. 1. As the dose at a fixed pressure is increased (by using several pulses) the rate of production of carbon monoxide decreases. The initial slope, independent of pressure in the range 400–1500 Torr, gives $G(CO) = 7.8 \pm 0.3$. The inset to this figure gives the initial yield to lower pressures where the precision is less, however, the yield appears to be independent of pressure down to at least 50 Torr.

Figure 2 shows the effect of the addition of

Can. J. Chem. Downloaded from www.nrcresearchpress.com by 210.87.254.6 on 09/05/12
For personal use only.

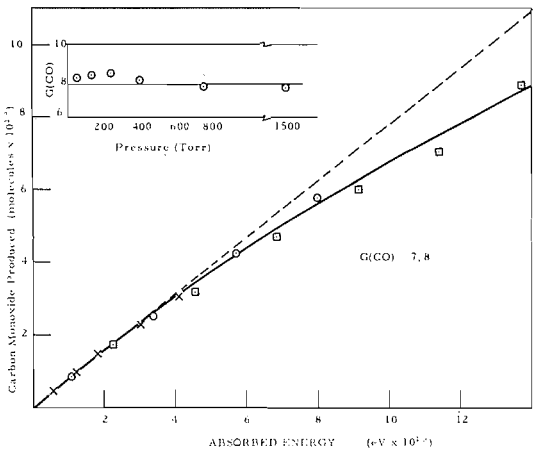

FIG. 1. Carbon monoxide produced as a function of absorbed energy: ×, 400 Torr carbon dioxide; ○, 750 Torr carbon dioxide; □, 1500 Torr carbon dioxide. Inset figure shows carbon monoxide yield as a function of pressure from 50–1500 Torr carbon dioxide.

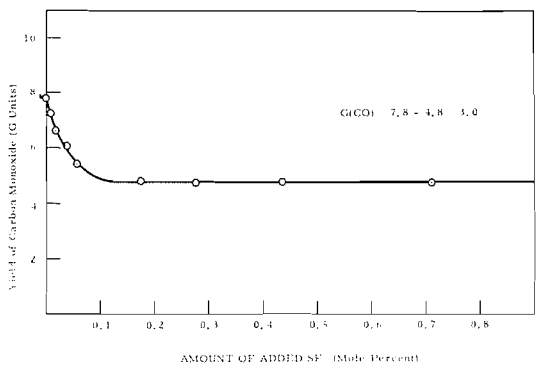

FIG. 2. Carbon monoxide yield as a function of added sulfur hexafluoride at 750 Torr carbon dioxide. Single pulse irradiations.

SF_6. The yield of carbon monoxide decreases from $G(CO) = 7.8 \pm 0.3$, in the absence of SF_6, to $G(CO) = 4.8 \pm 0.2$ above 0.2% added SF_6.

The oxygen yield, in all cases, was approximately half the carbon monoxide yield within experimental error. A limiting yield of ozone for carbon dioxide at 750 Torr for 1–10 pulses was determined to be $G(O_3) \leqslant 0.1$.

Discussion

The yields of Meaburn *et al.* (2) at 2×10^{25} eV g^{-1} s^{-1} were based on $G(N_2) = 10$ in the radiolysis of N_2O at this dose rate. We have shown (6–8) that the yield of N_2 from N_2O at a dose rate of 2×10^{27} eV g^{-1} s^{-1} is $G(N_2) = 12.4$ and, as discussed in ref. 8, it is estimated that the reduction in the yield of nitrogen from N_2O from $G(N_2) = 12.4$ to $G(N_2) = 10.0$ occurs below 10^{25} eV g^{-1} s^{-1}. On this basis, Meaburn *et al.* (2) should have used $G(N_2) = 12.4$. Their corrected yields at 2×10^{25} eV g^{-1} s^{-1} are $G(CO) = 7.4 \pm 0.4$ in pure CO_2 and $G(CO) = 5.2$ (± 0.4?) with 0.04 to 5% SF_6. These are in good agreement with our values at 2×10^{27} eV g^{-1} s^{-1} of $G(CO) = 7.8 \pm 0.3$ and $G(CO) = 4.8 \pm 0.2$.

The high dose rate yield in the presence of an electron scavenger is also in good agreement with the low dose rate yield in pure CO_2 of $G(CO) = 4.5 \pm 0.5$.

The increase in the yield of CO in going to higher dose rates and the effects of electron scavengers at high and low dose rates suggest that at least some of the ionic processes in CO_2 contribute to the yield at high dose rates only.

The predominant ions formed on irradiation of carbon dioxide are CO_2^+, CO^+, O^+, and C^+. The reactions of these ions in carbon dioxide in the absence of oxygen and carbon monoxide are given in Table 1. It can be seen that the yield of carbon monoxide from ionic processes is $G(CO)_{ionic} = G(CO_2^+) + 2G(CO^+) + 2G(O^+) + 3G(C^+)$. There is some disagreement as to the relative abundance of these ions. Anderson *et al.* (1*a*) prefers those of Smyth (15), which are CO_2^+, 76.9%; CO^+, 15.4%; O^+, 5.4%; and C^+, 2.3%. Assuming these abundances and taking the ion pair yield, $G(\text{ion pair}) = 2.99$, from the W value of 33.5 eV/ion pair (16), $G(CO)_{ionic} = 2.30 + 2(0.46) + 2(0.16) + 3(0.07) = 3.75$.

The contribution from non-ionic reactions is then $G(CO)_{excited} = 7.8 - 3.75 = 4.05$. Since this is lower than the reduced yield with SF_6 or the low dose rate yield, ionic reactions must persist under both these conditions. The following arguments show how such contributions from ionic reactions could be explained.

Sulfur hexafluoride will scavenge electrons

[11] $$SF_6 + e \rightarrow SF_6^-$$

and it is generally accepted that neutralization of the positive ion of the parent species by SF_6^- does not result in dissociation of the positive ion. As a result, the neutralization reactions [6] and [10] will be suppressed by the addition of SF_6 though the ion–molecule reactions [5], [7], [8], and [9] will remain unaffected. The reduction in

480219

Can. J. Chem. Downloaded from www.nrcresearchpress.com by 210.87.254.6 on 09/05/12
For personal use only.

TABLE 1

Ionic processes in irradiated carbon dioxide

	Reaction	Rate constant (cm^3 $molecule^{-1}$ s^{-1})	Reference
[1]	$CO_2 \rightsquigarrow CO_2^+ + e$	—	(1)
[2]	$CO_2 \rightsquigarrow CO^+ + O + e$	—	(1)
[3]	$CO_2 \rightsquigarrow O^+ + CO + e$	—	(1)
[4]	$CO_2 \rightsquigarrow C^+ + O + O + e$	—	(1)
[5]	$CO_2^+ + 2CO_2 \longrightarrow C_2O_4^+ + CO_2$	3×10^{-28}*	(11)
[6]	$C_2O_4^+ + e \longrightarrow CO + O + CO_2$	$\sim 3 \times 10^{-7}$†	—
[7]	$CO^+ + CO_2 \longrightarrow CO + CO_2^+$	1.1×10^{-9}	(12)
[8]	$O^+ + CO_2 \longrightarrow O_2^+ + CO$	1.2×10^{-9}	(13)
[9]	$C^+ + CO_2 \longrightarrow CO + CO^+$	1.9×10^{-9}	(12)
[10]	$O_2^+ + e \longrightarrow O + O$	$\sim 2 \times 10^{-7}$	(14)

*The units for this rate constant are cm^6 $molecule^{-2}$ s^{-1}.
†This rate constant is estimated from known electron-neutralization reaction rate constants (see ref. 8).

yield due to SF_6, then, should be $\Delta G(CO) = G(CO_2^+) + G(C^+) + G(CO^+) = 2.83$, in good agreement with the observed value $\Delta G(CO) = 3.0$.

The ionic processes at low dose rates for any appreciable dose will be much more complex (17). For example, it is almost certain that the $C_2O_4^+$ ion will undergo a rapid charge transfer process with oxygen.

[12] $$C_2O_4^+ + O_2 \rightarrow 2CO_2 + O_2^+$$

Thus the ionic contribution to the CO yield would be from reactions [3], [7], [8], and [9].[3] The expected yield at low dose rates is then $G(CO)_{excited} + G(CO^+) + G(O^+) + 2G(C^+) = 4.8$.

It should be pointed out that two assumptions have been made in the above discussion. First, since we do not have values for the abundance of negative ions, we have neglected reactions such as

[13] $$CO_2 \rightsquigarrow CO^+ + O^-$$

In carbon dioxide, the O^- ion will react to give CO_3^- by reaction [14]

[14] $$O^- + 2CO_2 \rightarrow CO_3^- + CO_2$$

$k_{14} = 9 \times 10^{-29}$ cm^6 $molecule^{-2}$ s^{-1} (18) and the neutralization steps will be modified, although the same yield of carbon monoxide may be obtained.

[3]We have performed detailed computer calculations of the type previously described (10) to determine the extent of reaction [12] at our dose rates. This is negligible, even for 20 pulses the calculated change of yield would be less than experimental errors.

[15] $$C_2O_4^+ + CO_3^- \rightarrow CO + O_2 + 2CO_2$$

Second, it is assumed that oxygen atoms formed in the ion–molecule reactions or the neutralization processes do not give rise to any further carbon monoxide. It has been suggested (19–21) that $O(^1D)$ can yield carbon monoxide through a CO_3 complex

[16] $$CO_2 + O(^1D) \rightleftarrows CO_3 \rightarrow CO + O_2$$

However, as was pointed out by Clerc (22), this would predict quantum yields of carbon monoxide in the vacuum u.v. photolysis of carbon monoxide (where $O(^1D)$ atoms are the predominant initial oxidizing species) in excess of unity. These have not been observed (23), so we must assume that reaction [16] does not occur to any great extent. It should be noted that reaction [16] is spin forbidden (to give $O_2{}^3\Sigma$) and is unlikely on these grounds.

The decrease in the carbon monoxide yield with increasing dose shown in Fig. 1 cannot be attributed to the charge transfer reaction [12] as this will not compete with reactions [5] and [6] at our dose rates. It must be due to the back reaction

[17] $$O + CO + CO_2 \rightarrow 2CO_2$$

competing with the recombination reaction

[18] $$O + O + CO_2 \rightarrow O_2 + CO_2$$

However, since detailed knowledge of the electronic states of the oxygen atoms and the reactions of CO_3 are not available, quantitative comparisons cannot be made.

To gain a more complete understanding of the

Can. J. Chem. Downloaded from www.nrcresearchpress.com by 210.87.254.6 on 09/05/12
For personal use only.

radiolysis of carbon dioxide, further high dose rate studies of CO_2–O_2 mixtures are being made and these will be reported later.

1*a*. A. R. ANDERSON and D. A. DOMINEY. Rad. Res. Rev. **1**, 269 (1968). *b*. A. R. ANDERSON and J. V. F. BEST. Advan. in Chem. **82**, 231 (1968).
2. G. M. MEABURN, D. PERNER, J. LECALVE, and M. BOURENE. J. Phys. Chem. **72**, 3920 (1968).
3. C. WILLIS, A. W. BOYD, and O. A. MILLER. Can. J. Chem. **47**, 3007 (1969).
4. A. W. BOYD, D. A. ARMSTRONG, C. WILLIS, and O. A. MILLER. Rad. Res. **40**, 255 (1969).
5. C. WILLIS, A. W. BOYD, A. E. ROTHWELL, and O. A. MILLER. Int. J. Rad. Phys. Chem. **1**, 373 (1969).
6. C. WILLIS, O. A. MILLER, A. E. ROTHWELL, and A. W. BOYD. Advan. Chem. Ser. **81**, 539 (1968).
7. A. W. BOYD, C. WILLIS, and O. A. MILLER. Can. J. Chem. **47**, 351 (1969).
8. C. WILLIS, A. W. BOYD, and D. A. ARMSTRONG. Can. J. Chem. **47**, 3783 (1969).
9. A. W. BOYD, C. WILLIS, R. CYR, and D. A. ARMSTRONG. Can. J. Chem. **47**, 4715 (1969).
10. A. W. BOYD, C. WILLIS, and R. CYR. Anal. Chem. **42**, 670 (1970).
11. J. F. PAULSON, F. DALE, and R. L. MOSHER. Nature, **204**, 377 (1964).
12. F. C. FEHSENFELD, A. L. SCHMELTEKOPF, and E. E. FERGUSON. J. Chem. Phys. **45**, 23 (1966).
13. F. C. FEHSENFELD, E. E. FERGUSON, and A. L. SCHMELTEKOPF. J. Chem. Phys. **44**, 3022 (1966).
14. C. WILLIS, A. W. BOYD, M. J. YOUNG, and D. A. ARMSTRONG. Can. J. Chem. **48**, 1505 (1970).
15. H. D. SMYTH. Rev. Mod. Phys. **3**, 347 (1931).
16. W. P. JESSE and J. SADAUSKIS. Phys. Rev. **97**, 1668 (1965).
17. D. A. DOMINEY and T. F. PALMER. Discuss. Faraday Soc. **36**, 35 (1963).
18. J. L. MORUZZI and A. V. PHELPS. J. Chem. Phys. **45**, 4617 (1966).
19. A. R. ANDERSON. Fundamental processes in radiation chemistry. *Edited by* P. Ausloos. J. Wiley and Sons, Inc., New York. 1968. p. 281.
20. A. V UNG and H. I. SCHIFF. Can. J. Chem. **44**, 1981 (1966).
21. J. W. MCGOWAN. Can. J. Chem. **47**, 1875 (1969).
22. M. CLERC. Can. J. Chem. **47**, 1875 (1969).
23. T. G. SLANGER. Can. J. Chem. **47**, 1875 (1969).

Can. J. Chem. Downloaded from www.nrcresearchpress.com by 210.87.254.6 on 09/05/12
For personal use only.

Can. J. Chem. Downloaded from www.nrcresearchpress.com by 210.87.254.42 on 09/05/12
For personal use only.

Diagramme de phases du système K–K_2O et le monooxyde de potassium K_2O

F. NATOLA ET PH. TOUZAIN
Département de chimie, Université de Montréal, Montréal, Québec

Reçu le 8 janvier 1970

Le diagramme de fusion du système K–K_2O est obtenu par la technique de l'analyse thermique différentielle. La fusion du monooxyde de potassium K_2O se manifeste à 646 ± 5 °C. Des transformations cristallines réversibles de l'oxyde sont observées à 317, 372 et 446 °C. La dismutation de l'oxyde en peroxyde et métal apparait à une température approximativement égale à celle de la dernière des transitions. Le diagramme K–K_2O comporte un eutectique à une température très proche de la température de fusion du potassium et une monotectie à 600 °C (concentration monotectique: 30.5% atomique d'oxygène). Aucune existence de sous-oxyde n'est démontrée.

The potassium–oxygen phase diagram has been determined up to the composition of K_2O by the technique of differential thermal analysis. Potassium monoxide K_2O melts at 646 ± 5 °C. Reversible transitions occur in solid K_2O at 317, 372, and 446 °C. Disproportion of the monoxide into the peroxide and metal occurs at a temperature identical or very near to that of the last transition. The K–K_2O eutectic melts at a temperature very close to the melting temperature of pure K (degenerate eutectic) and the monotectic at 600 °C (monotectic concentration: 30.5 oxygen atomic %). No evidence has been obtained that would indicate the existence of a lower oxide.

Canadian Journal of Chemistry, **48**, 1955 (1970)

L'étude des systèmes M–M_2O dans lesquels M symbolise un métal alcalin a permis de tracer les diagrammes de phases correspondant au césium (1) et au rubidium (2). Ces deux diagrammes mettent en évidence l'existence des cinq sous-oxydes suivants: Cs_7O, Cs_3O à fusion congruente Cs_4O, Cs_7O_2 et Rb_3O à fusion incongruente.

Continuant dans la même voie, nous avons abordé le système potassium – monooxyde de potassium. Gay–Lussac et Thénard (3) avaient observé durant la combustion du potassium dans l'air la formation d'un composé bleu auquel ils attribuèrent la formule d'un sous-oxyde: K_4O. En effectuant l'analyse brute de ce produit bleu, Lupton (4) démontra qu'il s'agissait non pas d'un sous-oxyde mais d'un mélange de monooxyde K_2O et de peroxyde K_2O_2. Besson et Touzain (5) et Touzain (6) montrèrent par études aux rayons X et spectrophotométrie de ce même produit qu'il s'agissait, plus vraisemblablement, d'un mélange de peroxyde K_2O_2 et de métal qui, dispersé à l'état colloïdal au sein de l'oxyde, produisait cette couleur bleue.

Rengade (7), en préparant du K_2O dans un grand excès de potassium métallique, obtient après distillation de cet excès de métal des cristaux transparents de formes très nettes. Cette expérience prouve que l'oxyde est légèrement soluble dans le métal. Cette solubilité est néanmoins beaucoup plus faible que dans le cas du rubidium ou du césium.

Williams *et al.* (8) ont déterminé cette solubilité dans l'intervalle de température 100–305 °C. La solubilité (donnée en g O pour 100 g K) est:

$$S = 0.0865 - 6.09\ 10^{-4}\ t + 7.71\ 10^{-6}\ t^2$$

(t en °C)

Le tableau 1 indique quelques valeurs de cette solubilité calculées à l'aide de cette équation.

TABLEAU 1

Solubilité de l'oxygène dans le potassium

t (°C)	$10^3 \times S$ (g O/g K)	S (% atom. O)
100	1.0	0.24
200	2.7	0.66
300	6.0	1.47

Techniques Expérimentales

Préparation des mélanges potassium–oxygène

Les diverses compositions sont réalisées par union directe des quantités préalablement pesées de potassium et de monooxyde de potassium. Cette opération est effectuée dans une boite à gants sous azote anhydre et exempt d'oxygène. Le monooxyde de potassium est préparé selon la technique indiquée par Rengade (7): oxydation ménagée du métal fondu sous faible pression d'oxygène, suivie de la distillation sous vide à 250–300 °C du potassium en excès. Quant au métal, il est, avant utilisation, distillé deux fois sous vide selon une méthode déjà décrite (6).

Le mélange K–K_2O est homogénéisé en composition, en le portant dans un tube scellé (en verre Pyrex ou en alumine) à une température suffisante pour amener les constituants à la fusion. Il est ensuite refroidi lentement.

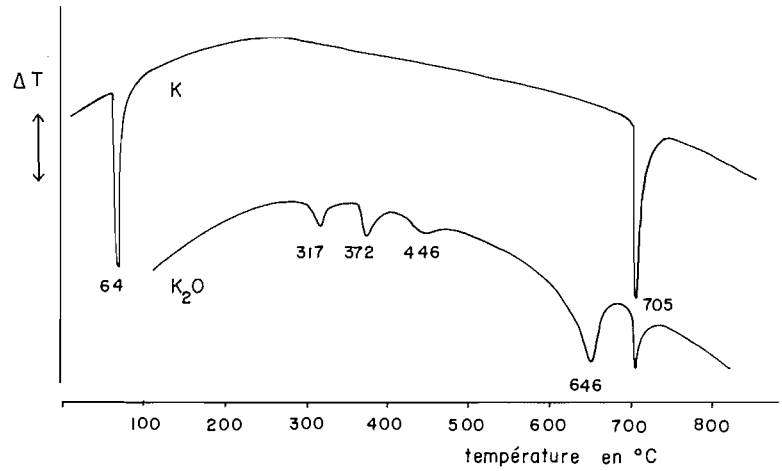

FIG. 1. Courbes d'analyse thermique différentielle du potassium et du monooxyde de potassium.

Analyse thermique différentielle

La détermination des températures du diagramme de phases du système $K–K_2O$ est faite par analyse thermique différentielle (ATD). L'appareillage a été décrit antérieurement (2).

L'échantillon de mélange pesant environ 30 mg est conditionné directement dans un tube en verre Pyrex,[1] scellé sous vide, de 2 mm de diamètre intérieur et haut de 1 cm. Le bas du tube est soufflé de façon à ce qu'il prenne la forme de la coupelle porte-échantillon en platine de l'analyseur thermique différentiel. L'échantillon de référence est un tube de même section mais rempli d'alumine.

Les courbes d'ATD, $\Delta T = f(T)$, sont obtenues par élévation de la température et non par refroidissement. En effet, une surfusion importante des mélanges ne permet pas d'obtenir de précision sur les mesures obtenues par refroidissement bien que le "pic de solidification" soit souvent plus net que le "pic de fusion".

L'élévation de température est maintenue à une vitesse de 8–10 °C par minute. Les sommets des pics des courbes $\Delta T = f(T)$ ont servi à mesurer les températures des diverses transitions observées. La précision du thermocouple est de l'ordre de ± 2 °C. Les mesures sont toutefois moins précises par suite de l'étalement d'un certain nombre de pics (au maximum ± 5 °C).

[1]Des matériaux autres que le verre tels le platine et l'alumine ont été essayés: Les creusets de platine sont attaqués fortement par le mélange à partir de 330 °C. Ils ne peuvent donc pas être utilisés. Par contre, des tubes d'alumine vitrifiée (1.5 mm diamètre interne, 3 mm diamètre externe et 6 cm de hauteur) scellés au chalumeau oxhydrique (sous pression atmosphérique) restent intactes alors que le verre Pyrex est légèrement attaqué par K_2O au moment de sa fusion. Cependant, les résultats d'ATD étant peu changés, le verre Pyrex donnant des résultats plus nets a été utilisé préférentiellement à l'alumine. Les tubes d'alumine ont servi néanmoins pour déterminer le point de fusion de K_2O.

Résultats

Le monooxyde de potassium

Les courbes d'ATD obtenues avec l'oxyde de potassium pur à l'échauffement sont représentées sur la Fig. 1. Quatre phénomènes endothermiques respectivement à 317, 372, 446, 646 °C et un autre, variable entre 690 et 730 °C, sont observés. On retrouve ces pics (exothermiques) à l'abaissement de la température avec un retard pouvant aller jusqu'à 50 °C. Tous ces phénomènes sont donc réversibles.

L'accident à 646 °C est la fusion de l'oxyde. L'observation visuelle dans un tube de verre Pyrex corrobore ce résultat. L'oxyde, blanc à température ordinaire, passe graduellement en élevant la température, par le jaune citron, par l'orange, par le brun puis fond enfin en un liquide rouge foncé vers 650 °C.

Les deux premiers accidents à 317 et 372 °C sont de faible amplitude. Des spectres Debye–Scherrer obtenus avec des échantillons de K_2O en poudre à différentes températures indiquent que les deux phénomènes observés sont des transformations cristallines réversibles.

Le pic étalé, observé vers 446 °C, est lié probablement à la décomposition du produit. En effet, Rengade (7) avait remarqué une décomposition de K_2O sous vide avec libération de métal qu'il signale vers 350–400 °C. Nous avons repris cette expérience avec plus de précision par thermogravimétrie sous vide. Un échantillon de K_2O (environ 20 mg) placé dans

Can. J. Chem. Downloaded from www.nrcresearchpress.com by 210.87.254.42 on 09/05/12
For personal use only.

Can. J. Chem. Downloaded from www.nrcresearchpress.com by 210.87.254.42 on 09/05/12
For personal use only.

un petit creuset d'alumine non scellé est suspendu au fléau d'une thermobalance "Cahn". L'élévation de température se fait à raison de 4 °C par minute. L'oxyde subit une perte de poids très importante à partir de 430–440 °C alors que du potassium métallique se condense sur les parois froides du tube laboratoire. Dans un tube scellé, on n'observe pas l'aspect métallique du potassium libéré mais seulement, à partir de 440–450 °C, la coloration brune probablement due à une dispersion du potassium dans l'oxyde orangé. Le dosage de cet oxyde, après fusion et refroidissement rapide, indique une teneur pondérale en peroxyde[2] de l'ordre de 7%. La réaction débutant à 446 °C correspond donc à la dismutation suivante:

$$2\,K_2O \rightarrow K_2O_2 + 2\,K$$

D'autre part, la diffractométrie de rayons X effectuée à des températures supérieures à 446 °C (450 et 500 °C) indique une extinction notable de l'intensité de quelques raies du spectre Debye–Scherrer par rapport à celle effectuée à la température de 390 °C. Cela laisse supposer que la transition à 446 °C est une transformation ordre–désordre. Dworkin et Bredig (9) laissaient prévoir que la dernière transformation avant fusion des composés AB_2 à structure cubique face centrée (type fluorine ou antifluorine) est une transformation ordre–désordre.

De ce fait, l'atome de potassium devenant plus libre, peut s'échapper plus facilement de sa position cristalline initiale. Ce départ pourrait être ainsi la cause de la dismutation partielle du monooxyde en peroxyde.

Quant au phénomène remarqué à l'ATD aux alentours de 700 °C, il est amputable à la vaporisation du potassium provenant de la décomposition de l'oxyde. La courbe d'ATD obtenue avec du potassium pur présente également un pic très endothermique à la température de 705 °C (Fig. 1). Comme d'une part, les tubes d'alumine utilisés dans ces expériences sont scellés à la pression atmosphérique, et que d'autre part, la température de fusion de l'alumine est élevée (2050 °C), la pression à l'intérieur du tube d'alumine après refroidissement de la soudure se trouve environ de moitié inférieure à la pression atmosphérique. Ceci expliquerait que les températures mesurées soient inférieures à 760 °C, température d'ébullition du potassium sous une pression d'une atmosphère. A 705 °C par exemple, la pression d'ébullition du potassium est de 0.60 atm (10).

[2]Le dosage du peroxyde est effectué par colorimétrie des complexes formés entre l'eau oxygénée provenant de l'hydrolyse de K_2O_2 et le titane(IV). Ou utilise l'éthanol pur pour dissoudre préalablement l'oxyde.

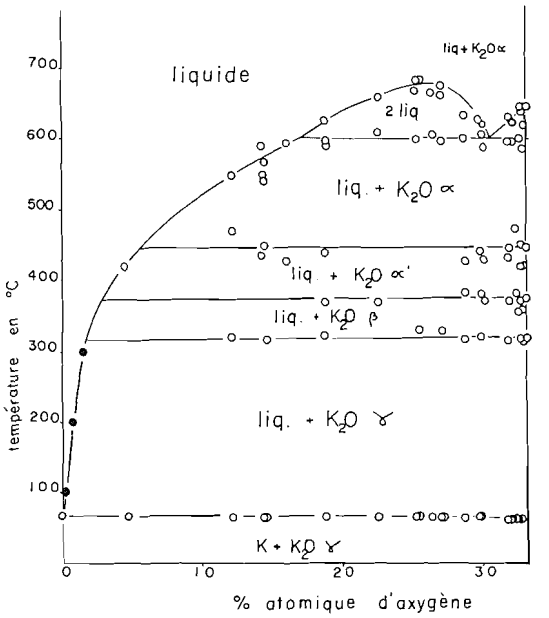

FIG. 2. Diagramme de phases du système K–K_2O (Points expérimentaux: ○, par ATD; ●, par mesure de solubilité (8)).

Diagramme de phases du système K–K_2O

Le mélange K–K_2O, une fois homogénéisé, a une coloration gris-bleue à température ambiante. Par chauffage, il devient jaune-verdâtre, brunâtre puis brun foncé après fusion.

Le diagramme de phases du système est représenté sur la Fig. 2. Pour les % atomiques d'oxygène plus petit que 2%, la pente du liquidus étant très grande, l'ATD ne peut fournir aucun renseignement sur ce liquidus. Les points expérimentaux (ronds noirs) situés dans cette zone correspondent aux résultats de Williams *et al.* (8) obtenus par mesure de solubilité. Le diagramme comporte un eutectique à une température très proche de la température de fusion du potassium et pour un % atomique d'oxygène plus petit que 0.24% (eutectique dégénéré). Il comporte également une monotectie à 600 °C pour le % atomique d'oxygène de 30.5%. La

Can. J. Chem. Downloaded from www.nrcresearchpress.com by 210.87.254.42 on 09/05/12
For personal use only.

température critique de solution est à peu près égale à 680 °C (à 25% atomique d'oxygène) soit environ 35 ° au dessus de la température de fusion de K_2O. La fin de la zone d'immiscibilité des 2 liquides se trouve à environ 17% atomique d'oxygène. Ainsi, ce diagramme ressemble à celui du système $K–K_2S$ (11) bien que la température critique se trouve plus haute proportionellement au point de fusion de l'oxyde ou du sulfure.

Précisons que ce diagramme d'équilibres dépend de conditions expérimentales orthobariques (tubes scellés sous vide ou non, pression de vapeur du potassium fonction de la température, dissociation thermique de K_2O ....) et qu'ainsi, les températures trouvées peuvent être sujettes à des variations importantes.

Discussion

Le diagramme du système $K–K_2O$ au contraire de celui du rubidium et celui du césium ne montre aucune existence de sous-oxyde. Finalement, quatre sous-oxydes ont été découverts pour le césium, un seul pour le rubidium et aucun pour le potassium. Cette évolution de propriétés le long de la famille des alcalins laisse prévoir qu'aucun autre sous-oxyde n'existe dans les systèmes $Na–Na_2O$ et $Li–Li_2O$. Par contre, le système $Fr–Fr_2O$ devrait comporter de nombreuses sous-structures. La radioactivité du francium ainsi que sa période très courte de 21 min empêcheront néanmoins l'étude de ce système par une méthode classique.

Quant au monooxyde de potassium, il se présente sous la forme de trois variétés: (*i*) la forme γ, stable au dessous de 317 °C est cubique faces centrées, structure type antifluorine (12); (*ii*) une forme β stable entre 317 et 372 °C; (*iii*) une forme α′ à structure ordonnée entre 372 et environ 446 °C et une forme α à structure désordonnée au dessus de 446 °C jusqu'au point de fusion de l'oxyde.

Il est à noter que deux transitions cristallines ont été observées aussi dans le cas du monooxyde de sodium Na_2O (13).

L'examen du liquidus du système $K–K_2O$ vers le point de fusion du monooxyde de potassium, tracé en fonction du % atomique de potassium métallique dans le mélange $K–K_2O$, permet d'évaluer approximativement la chaleur de fusion de K_2O à 8.0 kcal $mole^{-1}$ et son entropie de fusion à 8.7 cal $°C^{-1}$ $mole^{-1}$. Remarquons que cette entropie de fusion est du même ordre de grandeur que celle de Na_2O (13) d'environ $11400/1405 = 8.1$ cal $°C^{-1}$ $mole^{-1}$.

En admettant 7% en poids de peroxyde formé au moment de la fusion de l'oxyde, l'abaissement cryoscopique dû au peroxyde et aux deux atomes de potassium libérés par molécule de peroxyde formée, serait:

$$\Delta T = \frac{RT_f^2 n}{\Delta Hf} = \frac{2 \times 920^2 \times (7/110 + 5/39)/((100 - 7 - 5)/94 + 7/110 + 5/39)}{8000}$$

$$= \frac{2 \times 920^2 \times 0.17}{8000} = 36\ °C$$

La température de fusion de K_2O doit donc être relevée de 36 °C. On est alors conduit à proposer pour le point de fusion de l'oxyde pur, une température de l'ordre de 685 °C.

Le Conseil National de Recherches du Canada est remercié pour l'aide financière apportée à ce travail. Nous remercions aussi le Professeur Marcel Bourgon du département de chimie de l'Université de Montréal pour la réalisation de ces expériences ainsi que le Docteur Marcel Caillet du Centre National de la Recherche Scientifique de Grenoble pour les diverses analyses de rayons X qu'il a effectuées.

1. E. Rengade. Bull. Soc. Chim. France, **5**, 994 (1909).
2. Ph. Touzain. Can. J. Chem. **47**, 2639 (1969).
3. J. Gay-Lussac et L. Thénard. Rech. physico-chim. **1**, 125 (1811).
4. S. Lupton. J. Chem. Soc. **30**, 565 (1870).
5. J. Besson et Ph. Touzain. C. R. **260**, 916 (1965).
6. Ph. Touzain. Etude cinétique de l'oxydation des métaux alcalins par l'oxygène sec. Comm. Energ. At. Fr., Rapport CEA R. 3301 (1967).
7. E. Rengade. Ann. Chim. Phys. **11**, 425 (1907).
8. D. D. Williams, J. A. Grand, et R. R. Miller. J. Phys. Chem. **63**, 68 (1959).
9. A. S. Dworkin et M. A. Bredig. J. Phys. Chem. **72**, 1277 (1968).
10. P. Y. Achener. The alkali metals. Chem. Soc. Spec. Publ. **22**, 82 (1967).
11. A. S. Dworkin et M. A. Bredig. J. Phys. Chem. **71**, 764 (1967).
12. E. Zintl, A. Harder, et B. Dauth. Z. Elektrochem. **40**, 588 (1934).
13. R. Bouaziz, G. Papin, et A. P. Rollet. C. R. **262**, 1051 (1966).

Coordination complexes of gallium(III) and indium(III) halides. V. Trialkyl and mixed alkyl–aryl phosphine complexes of indium(III) chloride, bromide, and iodide

A. J. CARTY AND T. HINSPERGER
Chemistry Department, University of Waterloo, Waterloo, Ontario,
AND (IN PART)
P. M. BOORMAN
Chemistry Department, University of Calgary, Calgary, Alberta
Received January 14, 1970

The new complexes InX_3L (X = Cl, Br, I; L = tricyclohexylphosphine), InX_3L_2 (X = Cl, Br, I; L = trimethylphosphine, triethylphosphine, dimethylphenylphosphine), InX_3L_2 (X = Cl, Br, L = diphenylethylphosphine), InX_3L_3 (X = Cl, Br; L = dimethylphenylphosphine) have been prepared and characterized by far-infrared, Raman, and molecular weight studies. Structures of the types *trans* trigonal bipyramidal InX_3L_2 and C_{3v} ψ-tetrahedral InX_3L can be readily characterized by virtue of their typical infrared and Raman spectra. Nuclear magnetic resonance chemical shifts and coupling constants for adducts of trimethylphosphine, triethylphosphine, dimethylphenylphosphine, and diphenylethylphosphine are discussed.

Canadian Journal of Chemistry, 48, 1959 (1970)

Introduction

We have previously reported that gallium trihalides form pseudotetrahedral C_{3v} complexes with triphenylphosphine and para-substituted triarylphosphines (1, 2) whereas the corresponding indium complexes are usually of the type InX_3L_2 (X = Cl, Br, I; L = triarylphosphine) (1, 3). This behavior has now been confirmed by other workers (4, 5). Moreover, far-infrared (4, 6) and Raman (4) measurements on $InCl_3(PR_3)_2$ ($R = C_6H_5$, CH_3) are consistent with *trans* trigonal bipyramidal structures for these adducts. Recent X-ray crystallographic data has shown that the triphenylphosphine complex has this formulation in the solid state (7).

Although five coordination has, in the past, been considered rare in indium chemistry (8) the above results together with the recently determined square pyramidal stereochemistry for the $InCl_5^{2-}$ ion (9) indicate that as in other systems (10), five coordinate structures can be stabilized by suitable choice of ligands, experimental conditions, or cations. In view of the established stereochemistry of $InCl_3(Ph_3P)_2$ we have investigated further the reactions of a variety of trialkyl, alkyl diaryl, and diaryl alkyl phosphines with indium(III) chloride, bromide, and iodide in an attempt to synthesize and characterize further five coordinate adducts. Factors influencing the tendency of phosphines to stabilize pentacoordination are also of interest.

Experimental

General

Anhydrous indium trihalides were prepared as previously described (3). The tertiary phosphines, trimethylphosphine (Me_3P), triethylphosphine (Et_3P), diphenylethylphosphine (Ph_2EtP), dimethylphenylphosphine (Me_2PhP), tn-*n*-butylphosphine (nBu_3P), and tricyclohexylphosphine (Cy_3P) were obtained from Strem Chemical Company Ltd., Andover, Massachusetts or from Orgmet Inc., New Hampstead, New Hampshire in sealed ampoules and were subsequently handled on a vacuum line or in a Vacuum Atmospheres Corporation Dri-Lab. Solvents used in preparations, recrystallizations, and n.m.r. measurements were Spectral Grade and were thoroughly degassed before use.

Microanalyses were carried out by A. B. Gygli, Toronto, Chemalytics Inc., Tempe, Arizona and Alfred Bernhardt, Elsbach über Engelskirchen, West Germany. Indium was determined by titration against 0.005 *M* EDTA using pyridine-2-azo-4-resorcinol as an indicator. Microanalytical data is summarized in Table 1.

Physical Measurements

Melting points were measured in evacuated sealed capillaries in a Mel-Temp apparatus and are uncorrected. Infrared (i.r.) measurements in the range 4000–600 cm^{-1} were made on Beckman IR-10 and IR-9 spectrometers. Samples were examined as Nujol mulls or as solutions in degassed solvents. In the far-infrared a Beckman IR-12 was employed, together with cesium iodide plates. Frequencies are accurate to ± 1 cm^{-1} over the entire range.

Raman measurements on powdered solids were made on a Cary 81 instrument equipped with a He/Ne laser. Frequencies are accurate to $\pm$ 2 cm^{-1}. Nuclear magnetic resonance spectra were run on Varian T-60 and HA-100 spectrometers. An Hitachi – Perkin–Elmer Model 115 vapor pressure osmometer was employed in molecular

Can. J. Chem. Downloaded from www.nrcresearchpress.com by 210.87.254.42 on 09/05/12
For personal use only.

TABLE 1
Analytical data for indium complexes

Compound	Melting point (°C)	C (%)		H (%)		In (%)		Halogen (%)		P (%)	
		Calculated	Found	Calculated	Found	Calculated	Found	Calculated	Found	Calculated	Found
$(Me_3P)_2InCl_3$	227–233	19.29	19.31	4.86	4.81	30.74	30.77	28.48	28.35	16.59	16.47
$(Me_3P)_2InBr_3$	217–220	14.22	14.38	3.58	3.47	22.66	22.58	47.31	47.22		
$(Me_3P)_2InI_3$	169–172	11.10	10.99	2.80	2.80	17.72	17.77	58.79	58.99		
$(Me_2PhP)_3InCl_3$	75–78	45.34	45.04	5.23	5.02	18.06	17.98	16.73	16.60		
$(Me_2PhP)_2InCl_3$	122–124	38.62	38.94	4.44	4.46	23.07	23.39	21.37	21.19		
$(Me_2PhP)_3InBr_3$	79–81	37.48	37.38	4.33	4.20	14.93	14.88	31.17	31.03		
$(Me_2PhP)_2InBr_3$	113–116	30.46	29.92	3.52	3.42	18.20	18.25	38.00	38.20		
$(Me_2PhP)_2InI_3$	124–127	24.81	24.60	2.87	2.96	14.87	14.79	49.32	49.52		
$(Et_3P)_2InCl_3$	138–140	31.49	31.43	6.60	6.44	25.08	25.01	23.24	23.09		
$(Et_3P)_2InBr_3$	93–95	24.39	24.85	5.12	5.26	19.43	19.22	40.57	40.21		
$(Et_3P)_2InI_3$	177–179	19.68	19.97	4.13	4.14	15.69	15.66	52.02	51.58		
$(Ph_2EtP)_2InCl_3$	140–142	51.75	51.75	4.89	4.89	17.67	17.59	16.37	16.18		
$(Ph_2EtP)_2InBr_3$	100–104	42.94	42.72	3.86	3.97	14.66	14.77	30.61	30.77		
$(Cy_3P)InCl_3$	255–258	43.09	42.76	6.63	6.43	22.88	22.94	21.20	21.21		
$(Cy_3P)InBr_3$	273–276	34.09	34.22	5.24	5.35	18.07	18.00	37.75	37.93		
$(Cy_3P)InI_3$	254–258	27.86	28.14	4.29	3.99	49.06	49.16	14.79	14.60		

weight determinations. Molecular weights were measured as $\overline{M}_n$, the number average molecule weight defined as

$$\overline{M}_n = \Sigma N_i M_i / \Sigma N_i$$

where N_i is the number of molecules having molecular weight M_i.

Preparation of Complexes

Two basic methods were used to prepare the complexes. The vacuum distillation technique (method *B*) is preferable for the volatile phosphines Me_3P, Et_3P, and Me_2PhP, since these invariably show traces of ν(P=O) bands in the i.r. after storage for several weeks. The purity of each product was checked by scanning the i.r. region 1250–1100 cm^{-1}. Medium to strong i.r. absorption in this region is characteristic of oxidation products.

Method A

Reaction of indium trichloride (0.5 g) in warm ethyl acetate (25 ml) with excess Me_3P in the same solvent gave an immediate crystalline precipitate, which was washed with degassed diethyl ether and dried in vacuo.

Method B

Approximately 25 ml of degassed ethyl acetate was distilled in vacuo on to indium trichloride (0.5 g) contained in a 100 ml flask. The trichloride dissolved on warming. Excess Me_3P was then vacuum distilled from an ampoule into the reaction vessel and reaction completed by stirring at room temperature. The product was identical with that from method *A* above. A similar product prepared by another method has since been reported by Beattie and Ozin (4) although full analytical data were not given. The far-infrared spectra of the two products are virtually identical.

$(Me_3P)_2InBr_3$, $(Me_3P)_2InI_3$

These compounds were prepared as colorless crystals by methods *A* and *B* above.

$(Me_2PhP)_3InCl_3$

Addition of an acetonitrile solution of indium trichloride to excess Me_2PhP in acetonitrile gave, on evacuation, a white solid. This was dried in vacuo for 2 h. The compound loses phosphine on prolonged evacuation.

$(Me_2PhP)_2InCl_3$

Addition of Me_2PhP (0.02 mole) in acetonitrile to indium trichloride (0.01 mole) in acetonitrile gave the pure bis complex.

Method *B* used in the preparation of the *tris* adduct gave a white solid which partially dissolved in ether. The residue (X) and crystals from the ether extract (Y) were filtered off and dried in vacuo for 2 h. Analyses and far-infrared spectra implied that X was a mixture of bis and tris complexes whereas the crystals Y contained the free phosphine and the tris complex.

Anal. Found: X, C, 41.27; H, 4.91; Y, C, 47.64; H, 5.62.

After pumping in vacuo for 4 days re-analysis indicated the presence of pure bis and tris complexes.

Anal. Found: X, C, 39.64; H, 4.44; Y, C, 45.35; H, 5.27.

$(Me_2PhP)_3InBr_3$, $(Me_2PhP)_2InBr_3$

These were prepared as for the respective chloride complexes. The tris compound loses phosphine on prolonged evacuation.

$(Me_2PhP)_2InI_3$

Methods *A* and *B* gave pale yellow crystals of the bis complex. Attempts to prepare a tris derivative were unsuccessful.

$(Et_3P)_2InX_3$ ($X = Cl, Br, I$)

These complexes were prepared as colorless or pale yellow crystals by methods *A* and *B* above. An excess of Et_3P must be avoided, however, since this results in oils which are difficult to crystallize.

$(Ph_2EtP)_2InCl_3$

Method *A* was used with diethyl ether or acetonitrile as solvent. White crystals were obtained.

$(Ph_2EtP)_2InBr_3$

Method *A* using diethyl ether gave white crystals.

No crystalline complex could be obtained from

Can. J. Chem. Downloaded from www.nrcresearchpress.com by 210.87.254.42 on 09/05/12
For personal use only.

Can. J. Chem. Downloaded from www.nrcresearchpress.com by 210.87.254.42 on 09/05/12
For personal use only.

Ph_2EtP and indium triiodide under a variety of conditions. Oils were formed and they were not further characterized.

$(Cy_3P)InX_3$ (X = Cl, Br, I)

Ethyl acetate solutions of indium trihalides afforded colorless or pale yellow crystals of the complex when treated with tricyclohexylphosphine in ethyl acetate. Even with a large excess of phosphine, pure bis complexes could not be isolated.

Reactions of indium trihalides with *n*-Bu_3P in various solvents gave thick oils which could not be crystallized. Characterization of these oils was not attempted.

Exchange Reactions using Indium Trihalide – Phosphine Complexes

(1) Reactions of InX_3L_n with M_2PdX_4 and M_2PtX_4 (X = Cl, Br, I; L = tertiary phosphine; M = Na, K)

Several reactions of this type were carried out to confirm phosphine transfer from indium. The same halide ion was present in both reactants. A typical procedure is outlined below.

An equimolar mixture of $(Me_2PhP)_3InCl_3$ and $Na_2PdCl_4 3H_2O$ in water was stirred for 3 h, filtered and the pale-orange residue extracted with dichloromethane. On slow evaporation pale-yellow crystals were obtained. A further crop of crystals was obtained by recrystallization of the residue from the dichloromethane extract. The compound was characterized as a mixture of *cis* and *trans* isomers of $(Me_2PhP)_2PdCl_2$, m.p. 191–192° (Lit. 192–194° (11)). In chloroform the n.m.r. corresponded to that reported by Jenkins and Shaw (11). The ^1H (methyl) resonance consisted of a 1:1 doublet at $\tau = 8.25$ ($J = 11.0$ Hz) and a 1:2:1 triplet at $\tau = 8.25$ ($J = 3.80$ Hz) corresponding to the *cis* and *trans* isomers, respectively.

Several other complexes were synthesized and characterized in similar fashion. In each case the reactants contained the same halide ion. Reactions involving the complexes $(Cy_3P)InX_3$ were very slow and gave poor yields of the Pd and Pt derivatives. The following complexes are representative.

trans-$(Me_3P)_2PdCl_2$, m.p. 276–278° (lit. 281–282° (12)).

trans-$(Ph_2EtP)_2PdCl_2$, m.p. 195–198°.

Anal. Calcd.: C, 55.51; H, 4.99. Found: C, 55.37; H, 5.09.

cis- and *trans*-mixture $(Me_2PhP)_2PtBr_2$, m.p. 198–199° (lit. 201–204° (11)).

cis-$(Et_3P)_2PtI_2$, m.p. 130–134° (lit. m.p. 136–137° (13)).

$(Cy_3P)_2Pt_2I_4$, m.p. 237–240°.

Anal. Calcd.: C, 29.59; H. 4.54. Found: C, 28.76; H, 4.44.

In a separate experiment $(Me_3P)_2InCl_3$ was thermally decomposed at 200°. The gaseous decomposition products were passed into a flask containing $HAuCl_4$ in acetone. From the resulting colorless solution crystals of $(Me_3P)AuCl$ were obtained and were characterized by far-infrared spectroscopy (14).

(2) Reactions involving Phosphine and Halogen Exchange from InX_3L_n

Equimolar quantities of $(Et_3P)_2InI_3$ and $Na_2PdCl_4 3H_2O$ were stirred in aqueous ethanol for 3 h. The orange solution was filtered, solvent carefully removed, and then cooled. Large, orange crystals separated out, m.p. 135–138°.

The compound was characterized as *trans*-$(Et_3P)_2PdI_2$ (lit. m.p. 139° (15)).

Anal. Calcd.: C, 24.16; H, 5.05. Found: C, 24.45; H, 5.09.

Although reactions of this type proceeded smoothly when InI_3L_n and M_2PdCl_4 were used, indium bromide complexes gave mixtures of products with M_2PdCl_4.

Results and Discussion

Three types of complex have been synthesized: (*a*) InX_3L_3 (X = Cl, Br; L = Me_2PhP), (*b*) InX_3L_2 (X = Cl, Br, I; L = Me_3P, Et_3P, Ph_2EtP, Me_2PhP), (*c*) InX_3L (X = Cl, Br, I; L = Cy_3P).

The dimethylphenylphosphine complexes of type (*a*) are the first tris phosphine adducts of the indium trihalides to be prepared. They are rather labile, losing one molecule of phosphine on evacuation or washing with diethylether to yield the bis complexes. This contrasts with the behavior of the bis complexes of Me_3P, Et_3P, Ph_2EtP, and Me_2PhP which do not readily lose free ligand under these conditions.

The ease of preparation of complexes of type (*b*) appears to depend somewhat on the solubility of the products in organic solvents. Thus trimethylphosphine complexes, which might have been expected to be difficult to prepare on account of the facile oxidation of the free ligand, crystallize readily from solution in a pure state due to their low solubility. By contrast, complexes of diphenylethylphosphine crystallize with difficulty and have an oily appearance when pure. No crystalline species of formula $(Ph_2EtP)_2InI_3$ could be prepared. Further, tri-*n*-butylphosphine gave only oils with indium trihalides under a variety of conditions. Packing factors and intermolecular forces are clearly of considerable importance in determining the nature of the complexes formed. That such parameters are extremely difficult to predict can be seen from the fact that while $(Et_3P)_2InX_3$ (X = Cl, Br) are moist in appearance, difficult to crystallize, and smell of phosphine, the iodide $(Et_3P)_2InI_3$ precipitates from solution as pure dry crystals. This, however, together with vibrational data (see later), may suggest a different structure for $(Et_3P)_2InI_3$ compared to $(Et_3P)_2InCl_3$ and $(Et_3P)_2InBr_3$.

Cy_3P forms only 1:1 adducts with indium trihalides. These complexes are much less soluble in organic solvents than the bis and tris adducts of other phosphines. $(Cy_3P)InX_3$ (X = Cl, Br, I)

Can. J. Chem. Downloaded from www.nrcresearchpress.com by 210.87.254.42 on 09/05/12
For personal use only.

react sluggishly with CS_2 to give the orange addition complex Cy_3PCS_2 whereas reaction is rapid with the other complexes. Exchange reactions with Na_2PdCl_4 and K_2PtCl_4 are also slow. Although there may be other reasons for the sluggish reactions of Cy_3P complexes, poor dissociation in solution will clearly make a significant contribution, since the reactions depend primarily on the presence of free phosphine in solution.

Stoichiometries

It is of interest to compare the stoichiometries of the phosphine adducts with physical data available for the free ligand (16, 17). Cy_3P is unique in that it has the highest basicity (pk_a 8.69), the highest melting point, and is more bulky[1] than the other ligands.

On the basis of the electroneutrality principle, strong σ donor properties would favor a lower coordination number. Steric effects would also tend to favor a lower coordination number. Thus for Cy_3P both factors may be important in ensuring the formation of 1:1 adducts and strong In—P bonds. Also worth noting is the low basicity of Ph_3P (pk_a 2.73). While $(Ph_3P)_2InCl_3$ is a crystalline solid (3), the In—P bonds are considerably longer than the sum of the covalent radii of In^{3+} and phosphorus (7) and the complex readily dissociates in solution (3). The low basicity of Ph_2EtP (pk_a ca. 4.5) would also favor a five coordinate rather than four coordinate structure. That the stoichiometry is not a simple function of σ donor strength and steric effects can however be seen from the Me_3P, Et_3P, and Me_2PhP complexes. In particular, the formation of both bis and tris complexes with Me_2PhP, a ligand of intermediate basicity (pk_a 6.49) and size, but only bis complexes with Me_3P (pk_a 8.65) and Et_3P (pk_a 8.69) is noteworthy. Also of interest is the high dipole moment of Et_3P (1.84 D). As noted in transition metal chemistry (15) this may well be important in determining the higher solubility of Et_3P complexes than Me_3P complexes and hence in their wider use for physical measurements.

These qualitative observations are, however, clearly insufficient to allow accurate predictions of complex stoichiometry. One can conclude that energy balances in equilibria involving indium complexes are delicate and that small changes in factors such as steric requirements, basicity, and dipole moment of ligand together with packing factors and intermolecular forces are of considerable importance in dictating the eventual reaction product.

Solution Behavior

Molecular weight measurements suggest that the complexes $(Ph_2EtP)_2InCl_3$ (mol. wt. found 461; calcd. 650), $(Ph_2EtP)_2InBr_3$ (mol. wt. found 487; calcd. 784), and $(Me_2PhP)_3InCl_3$ (mol. wt. found 320; calcd. 636) dissociate in benzene solution. Since the observed $\bar{M}_n$ values for $(Ph_2EtP)_2InX_3$ (X = Cl, Br) are greater than half the molecular weight of the undissociated species only partial dissociation occurs in a 10^{-1} M solution. The dissociation is concentration dependent (Fig. 1), the value of $\bar{M}_n$ approaching that of the undissociated monomer at high concentrations. Because of the lability of InX_3L_n in solution, the solid complexes may be used as a source of free phosphine for the preparation of MX_2L_2 (M = Pd, Pt) compounds. AgI.L and $AgNO_3L$ (L = Me_3P) have previously been used for this purpose (12). The indium complexes are useful since reactions occur without the necessity of decomposing the starting material. Thermal decomposition of $(Me_3P)_2InCl_3$ is also an excellent preparative method to liberate free

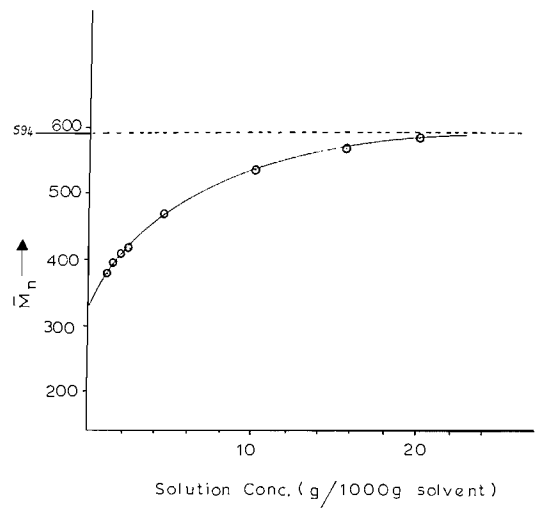

FIG. 1. Plot of number average molecular weight vs. concentration for $(Ph_2EtP)_2InCl_3$ in benzene.

[1]For example, Cy_3P has 18 more H atoms and C—C distances 10% longer than in $(C_6H_5)_3P$. The P—Cu—P angles in $[(C_6H_5)_3P]_2CuNO_3$ and $(Cy_3P)_2CuNO_3$ are 131.2° and 139°, respectively (35).

Can. J. Chem. Downloaded from www.nrcresearchpress.com by 210.87.254.42 on 09/05/12
For personal use only.

Me_3P. As $(Me_3P)_2InCl_3$ is stable for several weeks in air, this complex represents an alternative method of storing the toxic and volatile Me_3P.

In addition to phosphine exchange, halogen exchange occurs. This is best illustrated by the reaction $(Et_3P)_2InI_3 + Na_2PdCl_4 \rightarrow (Et_3P)_2PdI_2$. Whereas halogen transfer from indium iodide complexes goes quickly to completion, only partial displacement of chloride by bromide occurs, giving mixed products. The weakness of In—I bonds, the lower solubility of the transition metal iodide complexes, and the greater covalency of the M—I (M = Pd, Pt) bonds compared to M—Cl and M—Br may all be contributing factors in the observed sequence.

As previously mentioned, complexes of Cy_3P appear to be less labile in solution than the bis and tris adducts. Exchange reactions proceed only slowly to give poor yields of $(Cy_3P)_2MX_2$ (X = Cl, Br; M = Pd, Pt) and $Pt_2I_4(Cy_3P)_2$. The latter complex, a halogen bridged dimer, is probably formed as a result of experimental conditions. Beg and Clark (18) have previously demonstrated conversion of $(Me_3P)_2PtCl_2$ to $(Me_3P)_2Pt_2Cl_4$ on boiling in methanol.

From the above qualitative and quantitative observations, one can conclude that the following equilibria exist in solutions of the complexes InX_3L_n.

$$InX_3L_{n-1} + L \underset{\text{solvents}}{\overset{\text{non-polar}}{\rightleftharpoons}} InX_3L_n \underset{\text{solvents}}{\overset{\text{polar}}{\rightleftharpoons}} InX_2L_n^+X^-$$

Conductance measurements on other indium species suggest similar equilibria (3, 19). The available solution data for indium(III) complexes clearly point out the dangers inherent in the inference of structure in the solid state from physical measurements made on solutions.

Infrared and Raman Spectra

In favorable circumstances far-infrared and Raman measurements on solid complexes can provide unambiguous structural assignments. Phosphine complexes of indium are particularly amenable to study by vibrational spectroscopy in view of the low frequencies and intensities of modes associated with indium–phosphorus stretching. Coupling with ν(In—X) modes is likely to be less important than in the corresponding oxo- or nitrogen-donor complexes. Moreover, the vibrational spectra of several phosphines in the region 500–200 cm^{-1} are well documented and rather simple (20). Success in predicting the *trans* trigonal bipyramidal structure for $(Ph_3P)_2InCl_3$ (6) led us to believe that infrared and Raman spectra of other adducts might be equally useful.

Infrared Spectra, 4000–600 cm^{-1}

Changes in the spectra of tertiary phosphines occur on complexing (21). Spectra were routinely measured in this region to confirm coordination to indium (22) but are not included here to conserve space. In general, changes in ligand vibrational frequencies parallel those observed for transition metal complexes (20, 23).

Infrared and Raman Spectra, 600–200 cm^{-1}

$(Me_3P)_2InX_3$ (X = Cl, Br, I)

Beattie and Ozin (4) have reported far-infrared and Raman results for $(Me_3P)_2InCl_3$ and $(Me_3P)_2InI_3$. Table 2 shows that our data for $(Me_3P)_2InCl_3$ agree well with that of Beattie and Ozin. A *trans* trigonal bipyramidal structure seems likely for this compound with the intense infrared absorption at 283–287 cm^{-1} assigned to the E′ mode. A shoulder at 256 cm^{-1} is presumably due to the infrared forbidden A_1' mode. Interestingly the E′ mode for $(Me_3P)_2InCl_3$ lies 34 cm^{-1} to lower frequency from the corresponding mode for $(Ph_3P)_2InCl_3$ and 38 cm^{-1} lower than in $(Me_3N)_2InCl_3$ (24).

For $(Me_3P)_2InBr_3$, a strong absorption appears at 203 cm^{-1} in the infrared, 40 cm^{-1} lower than ν(In—Br) in $(Me_3N)_2InBr_3$ (24). A weak Raman line at 203 cm^{-1} and a strong band at 170 cm^{-1} suggest a similar *trans* structure for $(Me_3P)_2InBr_3$. Vibrational data for $(Me_3P)_2InI_3$ are complex (4) and an unambiguous assignment cannot be made in this case.

$(Me_2PhP)_nInX_3$

The far-infrared and Raman spectra of Me_2PhP reported by Goubeau and Langhardt (20*c*) and of the complexes $(Me_2PhP)_nInX_3$ are given in Table 3. The i.r. and Raman active vibration at 325 cm^{-1} in Me_2PhP and the bis complexes moves to 336 and 352 cm^{-1} in $(Me_2PhP)_3InBr_3$ and $(Me_2PhP)_3InCl_3$, respectively. The free ligand also has δ(PC) modes at 250 and 280 cm^{-1} in the Raman which do not appear in the i.r. The main features of the spectra of $(Me_2PhP)_2InCl_3$ are a strong broad band incompletely resolved, between 285 and 305 cm^{-1}

TABLE 2

Far-infrared and Raman spectra of solid $(Me_3P)_2InX_3$ complexes*

$(Me_3P)_2InCl_3$			$(Me_3P)_2InBr_3$		$(Me_3P)_2InI_3$		
Infrared		Raman,	Infrared,	Raman,	Infrared		Raman,
This work	Reference 4	reference 4	this work	this work	This work	Reference 4	reference 4
							75 m s
						83 m s	79 m s
	86 m w						90 v w
							98 v w
	120 m s						120 v w br
	125 m s						
		153 m					151 v s†
				120 m		169 s†	
	187 m	195 w		174 m†		186 sh†	190 v w
			203 v s†	203 w†			
256 m sh†	258 sh†	256 v s†	255 v w	255 w	255 v v w		260 w
283–287 s br†	286 s†	283 w†			287 v w		
302 sh			308 v w br	287 w	308 v w		
							318 v w
		327 w					
347 m	350 v w		340 v w	327 w			
410 v w							

*v = very, w = weak, m = medium, s = strong, br = broad, sh = shoulder.
†These bands are probably due to ν(In—X) vibrations.

in the i.r. with a weaker band at 260 cm^{-1} and an intense Raman line at 260 cm^{-1} with a weak satellite at 286 cm^{-1}. These spectra eliminate a covalent halogen bridged dimeric structure where a separation of ca. 100 cm^{-1} in bridging and terminal ν(In—Cl) modes is expected. (See ref. 25 for Ga_2Cl_6 and ref. 26 for In_2I_6.) An ionic dimer formulation $[InCl_2(Me_2PhP)_4][InCl_4]$ is also unlikely since $\nu_1(A_1)$ (321 cm^{-1}) and $\nu_3(F_2)$ (337 cm^{-1}) of $InCl_4^-$ (27) are not observed in the spectra. A structure $InCl_2(Me_2PhP)_2^+Cl^-$ can be excluded since the ν(In—Cl) vibrations of a four coordinate cation would absorb at a higher frequency than that found (compare for example $(Cy_3P)InCl_3$ ν(In—X) at 331 and 323 cm^{-1}).

The selection rules for *cis* trigonal bipyramidal (C_s or C_{2v}) and *cis* or *trans* square-based pyramidal (C_s or C_{2v}) structures do not allow a distinction to be made between five coordinate geometries of this type. However, these structures are unlikely in view of the simplicity of the i.r. and Raman spectra. As for $(Me_3P)_2InCl_3$ and $(Ph_3P)_2InCl_3$, the most reasonable assignment is *trans* trigonal bipyramidal of D_{3h} symmetry with similar assignments for the E′ and A_1' modes. The relative positions and intensities appear to be characteristic for D_{3h} solid state structures.

Similar arguments are relevant for $(Me_2PhP)_2InBr_3$. However, a medium intensity Raman band at 200 cm^{-1} is close to the ν_1 frequency of $InBr_4^-$ at 197 cm^{-1} (27). Although the ionic dimer $[InBr_2(Me_2PhP)_4][InBr_4]$ is therefore a possibility, the absence of ν_3 of $InBr_4^-$ (239 cm^{-1}) in the infrared rules out this structure. We assign the 219 cm^{-1} band to the E′ mode and the 175 cm^{-1} Raman line to the A_1' mode of a *trans* trigonal bipyramidal structure.

Owing to a lack of infrared data for $(Me_2PhP)_2InI_3$, we cannot distinguish between the structures *trans* trigonal bipyramidal and $[InI_2(Me_2PhP)_4][InI_4]$ for this complex. The very strong Raman band at 141 cm^{-1} corresponds to the $\nu_1(A_1)$ frequency for InI_4^- (139 cm^{-1}) but there is no scattering in the region of ν_3 (185 cm^{-1}) (27). The alternative assignment E′ (165 cm^{-1}) and A_1' (139 cm^{-1}) for ν(In—I) of *trans*-$(Me_2PhP)_2InI_3$ is possible.

The complexes $(Me_2PhP)_3InX_3$ (X = Cl, Br) have markedly different i.r. and Raman spectra from the bis complexes. The available data provide conclusive evidence for an increase in coordination number. Thus the strongest ν(In—X) bands of lowest frequency for $(Me_2PhP)_3InX_3$ appear at 245 and 161 cm^{-1}, respectively, for X = Cl and X = Br whereas their counterparts in the bis species are at ca. 300 and 175 cm^{-1}. The ionic structures $InX_2L_3^+X^-$ are therefore unlikely. The known vibrational

Can. J. Chem. Downloaded from www.nrcresearchpress.com by 210.87.254.42 on 09/05/12
For personal use only.

Can. J. Chem. Downloaded from www.nrcresearchpress.com by 210.87.254.42 on 09/05/12
For personal use only.

TABLE 3

Far-infrared and Raman spectra of $(Me_2PhP)_nInX_3$ complexes

Me_2PhP (20*c*)		$(Me_2PhP)_2InCl_3$		$(Me_2PhP)_2InBr_3$		$(Me_2PhP)_2InI_3$		$(Me_2PhP)_3InCl_3$		$(Me_2PhP)_3InBr_3$	
Infrared	Raman	Infrared	Raman	Infrared	Raman	Infrared	Raman	Infrared	Raman	Infrared	Raman
							130 w sh*				120 m
							141 v s*				139–140 v w
							145 m sh*				161 v s*
					175 v s*						
							165 w*				
									182 v w		
					200 m*			215 m*	213 w m*		
				219 v s*	220 w sh*						
								232 sh*	232 v s*		
								245 s*			
	250 s	260 s*	259 v s*	254 w		257 w	261 v w	255 w	255 w	255 w	255 w
	280 s	285 v s*	285 v w*	280 w		285 v w		287 m	293 v w	280 v w	
			287 v w*						295 v w		297 w sh
		‡						‡	300 v w	297 v w	300
		305 v s*	307 w	304 v w	307 w	307 v w	306 w	305 w		304 v w	302 w sh
			318 w		318 w	312 w sh					
325 s	325 s	324 s	328 v w	321 w br	328 v w	324 w	325 w br				
								337 v w	337 m	335 w	335 m
								352 v w	352 w sh	352 v w sh	352 w sh
						375 w					
390 s	390 s	410 s		409 w	—†	407 m	—†	410 m	—†	407 m	—†
434 m		433 w	—†	433 v w	—†	432 sh	—†	435 w	—†	432 w	—†
481 s	481 s	483 s	—†	482 m	—†	482 v s	—†	485 v s	—†	481 v s	—†

*These frequencies are probably due to ν(In—X) vibrations.
†The region was not observed in the Raman spectra.
‡This is a broad envelope with two separate peaks.

TABLE 4

Far-infrared and Raman spectra of Ph_2EtP complexes

Ph_2EtP, infrared	$(Ph_2EtP)_2InCl_3$		$(Ph_2EtP)_2InBr_3$	
	Infrared	Raman	Infrared	Raman
		150 w		137 w
				176 v s*
		222 w br	223 v s*	218–220 w*
250 v v w				
			255 w sh	258 v w
	269 m sh*	271 v s*	267 w	
297 w			296 w	
304 w	307 v s*	300–309 w*		304 v w
337 w				
	353 m	350 w	354 w	367 v w
375 sh			375 w	
398 m	396 w		397 w	Not measured
	423 m w	426 w	424 sh	
436 s			436 s	Above 400 cm^{-1}
	452 s		450 s	
478 v s	475 v s		473 s	
			482 s	
511 v s	510 v s	513 w	514 v s	
542 m				
620 w				
637 w				

*These peaks are probably due to ν(In—X) vibrations.

spectrum of the ion $InCl_6^{3-}$ also argues against the formulation $[In(Me_2PhP)_6][InCl_6]$ (28). Thus the predicted lines $\nu_3(T_{1u})$ (250 cm^{-1}), $\nu_1(A_{1g})$ 277 cm^{-1} and $\nu_4(T_{1u})$ (277 cm^{-1}) cannot be traced in the spectrum of $(Me_2PhP)_3InCl_3$.

The most likely structure for these complexes is an octahedral monomer of *cis* or *trans* configuration. The selection rules for *cis*-C_{3v} (ν(In—X) (A_1 + E)) and *trans*-C_{2v} (ν(In—X) ($2A_1$ + B_2) theoretically allow these configurations to be distinguished by vibrational spectroscopy. In practice, however, this is fraught with difficulty. Thus for *trans*-$SiCl_3(py)_3^+$, only one intense Raman line is observed (29). A single Raman band is also found in $InCl_3(dmso)_3$ of unknown structure (30). We have not therefore attempted to assign the geometry of the adducts $(Me_2PhP)_3InX_3$ until X-ray data becomes available.

$(Ph_2EtP)_2InX_3$ (X = Cl, Br)

Infrared and Raman data (Table 4) for these compounds closely resemble that for $(Me_3P)_2InX_3$ (X = Cl, Br) and $(Me_2PhP)_2InX_3$ (X = Cl, Br). The following assignments are reasonable for *trans* trigonal bipyramidal structures: $(Ph_2EtP)_2InCl_3$, E′ (307 cm^{-1}), A_1′ (269 cm^{-1}); $(Ph_2EtP)_2InBr_3$, E′ (223 cm^{-1}), A_1′ (176 cm^{-1}). The separation of the E′ and A_1′ modes for the chloride and bromide complexes are 30 and 40 cm^{-1} which correspond well with frequency differences in $(Me_3N)_2InCl_3$ and $(Me_3N)_2InBr_3$ (24).

$(Et_3P)_2InX_3$ (X = Cl, Br, I)

ν(In—X) modes appear at 285 cm^{-1} (s) in the i.r. and at 255 cm^{-1} (vs) and 285 cm^{-1} (w) in the Raman (Table 5) for $(Et_3P)_2InCl_3$ again suggesting a *trans* five coordinate stereochemistry. Similarly, for $(Et_3P)_2InBr_3$ a *trans* structure is likely. The iodide complex has a very complicated pattern of bands in the Raman between 191 and 123 cm^{-1} and a simple interpretation is impossible. A similar situation was found for $(Me_3P)_2InI_3$. Clearly X-ray data will be necessary in this case before an assignment can be attempted.

Finally, it is worth noting two further points at this stage. The infrared spectra of *trans* trigonal bipyramidal molecules of the type $InCl_3L_2$ are characterized by the presence of a very strong band in the region 280–320 cm^{-1} and a weaker satellite 30–40 cm^{-1} to lower frequency. In the Raman the same bands appear with the intensities reversed. If the weak i.r. band is due to the A_1′ equatorial stretching mode then the appearance of this band may be some indication of distortion from trigonal bipyramidal geometry. It is noteworthy that in $(Ph_3P)_2InCl_3$, $(p\text{-}Tol_3P)_2InCl_3$, and $(p\text{-}Anis_3P)_2$-

Can. J. Chem. Downloaded from www.nrcresearchpress.com by 210.87.254.42 on 09/05/12
For personal use only.

TABLE 5

Far-infrared and Raman spectra of $(Et_3P)_2InX_3$ complexes

Et_3P (20*a*)		$(Et_3P)_2InCl_3$		$(Et_3P)_2InBr_3$	$(Et_3P)_2InI_3$	
Infrared	Raman	Infrared	Raman	Infrared	Infrared	Raman
						123 sh w*
						140 v s*
						165 w*
						176 w*
						181 v v w*
						191 w*
				209 v s*		
			220 v w	226 m sh		
	249 w					
			255 v s*	253 w		
				265 v w br		
	278 w		280 v w sh	278 w	280 v w br	
		285 v s*	285 w sh*			
	306 w	302 sh	310 v w	313 w	309 v w br	311 w
328 w	333 w		335 v w			336 w
365 w	368 w		368 v w			369 w
		383 s		375 v w br		
408 w	410 w	433 v w br		425 w	423 v w	

*These peaks are probably due to ν(In—X) vibrations.

$InCl_3$ this band is barely visible above the background in the i.r. (31). In $(Ph_3P)_2InCl_3$, the X-ray determination shows little significant distortion from a regular trigonal bipyramidal (7). The decrease in frequency of the E′ mode (compare $(Ph_3P)_2InCl_3$, 319 cm^{-1}; $(p\text{-}Tol_3P)_2InCl_3$, 310 cm^{-1}; $(Me_2PhP)_2InCl_3$, 290 cm^{-1}; $(Et_3P)_2InCl_3$, 285 cm^{-1}; $(Me_3P)_2InCl_3$, 286 cm^{-1}) is also noticeable although whether this is a feature of bonding or coupling in these species cannot be determined.

$(Cy_3P)InX_3$ (X = Cl, Br, I)

Raman and i.r. results for the chloride and bromide complexes (Table 6) are consistent with monomeric C_{3v} structures for these adducts. For both complexes, ν(In—X) vibrations are at higher frequencies than in the five coordinate monomers. The coincidence of infrared and Raman modes and the relative intensities of the bands compare well with data for GaX_3L (32) and suggest the following assignments: $(Cy_3P)InCl_3$, E, 331 cm^{-1}; A_1, 323 cm^{-1}; $(Cy_3P)InBr_3$, E, 236 cm^{-1}; A_1, 212 cm^{-1}. As for the other series, $(Cy_3P)InI_3$ has a more complex Raman spectrum which cannot be unambiguously interpreted although the complexity argues against a simple C_{3v} geometry such as that found for the chloride and bromide. A dimeric formulation $[(Cy_3P)_2InI_2]^+[InI_4]^-$ is possible, in which case bands at 138 and 185 cm^{-1} may arise from ν_1 and ν_3 of InI_4^- (27). This would leave the 162 cm^{-1} to be assigned to a cation mode. X-Ray studies at present underway should provide an unequivocal answer to problems associated with the vibrational spectra of indium iodide species.

Nuclear Magnetic Resonance Spectra

The phenomenon of virtual coupling has proven extremely helpful in inorganic chemistry for the structural characterization of complexes by n.m.r. spectroscopy. Methyl substituted phosphines have been especially valuable for this purpose. Jenkins and Shaw (33) have demonstrated that when two Me_2PhP ligands are in mutual *trans* positions in a complex, virtual coupling between phosphorus nuclei occurs such that the methyl proton resonance of the coordinated ligands appears as a symmetrical 1:2:1 triplet. For the corresponding *cis* compounds, a methyl doublet appears due to coupling to only one phosphorus nucleus. The spectrum then unambiguously establishes the geometry around the metal. Studies of this type have so far been limited to transition metal complexes. We have attempted to apply this technique to the Me_2PhP, Ph_2EtP, and Et_3P complexes described herein in an attempt to obtain further stereochemical information.

$(Me_3P)_2InX_3$ and $(Me_2PhP)_2InX_3$/ $(Me_2PhP)_3InX_3$

Chemical shift and coupling constant data for the free phosphines and complexes are sum-

Can. J. Chem. Downloaded from www.nrcresearchpress.com by 210.87.254.42 on 09/05/12
For personal use only.

TABLE 6

Far-infrared and Raman spectra of Cy_3P complexes

Cy_3P	$(Cy_3P)InCl_3$		$(Cy_3P)InBr_3$†	$(Cy_3P)InI_3$	
Infrared	Infrared	Raman	Infrared	Infrared	Raman
		110 w			138 v s*
		150 w			162 m*
					185 w sh*
		181 m			191 w*
					198 w sh*
208 w sh	208 w sh	208 w sh		202 v w	
			212 m*		
		220 w	224 w*		220 w
228 w	227 w sh			227 v w	
			236 v s*		
247 w	245 v v w				
255 sh	253 v v w				
281 v w	278 v v w				
305–320 v w br	302 w sh		307 v w		
327 v w br	323 sh*	323 v s*	320 sh		320 v v w
			326 w	326 w	
	331 v s*	331 sh*			
376 m	384 w		383 w	381 m	
390 m	393 w		391 w	391 m	
410 m	410 w		410 w	—	
430 sh	428 w		428 sh	425 w	
445 m	445 w		443 w	442 m	
	461 w		455 w	456 m	
463 s					
	475 w		470 w	470 s	
490 v w br					
514 v s	518 m		518 m	515 v s	
537 s					

*These bands are probably due to ν(In—X).
†$(Cy_3P)InBr_3$ prepared from ethyl acetate.

TABLE 7

Nuclear magnetic resonance spectra of $(Me_3P)_2InX_3$ and $(Me_2PhP)_{2\text{ or }3}InX_3$

Compound	Solvent	τ	$^2J_{P-H}$ (Hz)	Remarks
Me_3P (34)	Neat	9.11	2.7	1:1 doublet
Me_3PO (34)	D_2O	8.07	13.4	1:1 doublet
$(Me_3P)_2InCl_3$	Benzene	9.05	10.5	1:1 doublet
$(Me_3P)_2InBr_3$	Benzene	9.05	10.5	1:1 doublet
$(Me_3P)_2InI_3$	Benzene	9.13	11.2	1:1 doublet
Me_2PhP (11)	$CDCl_3$	8.61	1.7	1:1 doublet
Me_2PhPO (11)	$CDCl_3$	8.24	13.0	1:1 doublet
$Me_2PhP^+MeI^-$	$CHCl_3$/MeOH	7.62	13.2	1:1 doublet
$(Me_2PhP)_2InCl_3$	$CHCl_3$	8.23	10.0	1:1 doublet
$(Me_2PhP)_3InCl_3$	$CHCl_3$	8.35	6.7	1:1 doublet
$(Me_2PhP)_2InBr_3$	$CHCl_3$	8.21	10.0	1:1 doublet
$(Me_2PhP)_3InBr_3$	$CHCl_3$	8.34	6.3	1:1 doublet
$(Me_2PhP)_2InI_3$	$CHCl_3$	8.39	10.0	1:1 doublet
ca. 1:1 mixture				Two overlapping
$(Me_2PhP)_2InCl_3$	$CHCl_3$	8.23	11.5	1:1 doublets
and $(Me_2PhP)_3InCl_3$		8.35	5.0	

marized in Table 7. For $(Me_3P)_2InX_3$, chemical shifts and coupling constants are very similar, with 1:1 doublets appearing at $\tau = 9.05$, 9.09, 9.13, respectively, for the chloride, bromide, and iodide. The coupling constants (ca. 10 c.p.s.) are larger than $^2J_{P-H}$ (2.7 c.p.s.) in the free ligand. In general $^2J_{P-H}$ increases markedly on complex formation or quaternization (34) due to an increase in the s character of the phosphorus bonding orbitals.

Can. J. Chem. Downloaded from www.nrcresearchpress.com by 210.87.254.42 on 09/05/12
For personal use only.

TABLE 8

Nuclear magnetic resonance spectra of $(Et_3P)_2InX_3$ and $(Ph_2EtP)_2InX_3$ complexes at 60 Mc/s*

Compound	M	τCH_2	$^2J_{P-H}$	M	τCH_3	$^3J_{P-H}$	J_{H-H}	Solvent
Et_3P (34)	Complex	8.8	0.5	Complex	9.04	13.7	7.6	Neat
Et_3PO (34)	Complex	8.35	11.9	Complex	8.9	16.3	7.8	$CHCl_3$
$Et_4P^+I^-$ (34)	2 × 4	7.38	8.0	2 × 3	8.9	23.0	7.5	$CHCl_3$
$(Et_3P)_2InCl_3$	2 × 4	8.00	8.8	2 × 3	8.76	18.0	8.2	$CHCl_3$
$(Et_3P)_2InBr_3$	2 × 4	7.94	8.5	2 × 3	8.65	19.0	8.3	$CHCl_3$
$(Et_3P)_2InI_3$	2 × 4	8.29	9.0	2 × 3	8.92	18.0	8.2	Benzene
Ph_2EtP	1 × 4	8.09	1.0	2 × 3	9.02	18.8	8.3	Neat
$Ph_3EtP^+I^-$	2 × 4	6.35	14.0	2 × 3	8.70	19.6	7.0	$CDCl_3$
$(Ph_2PEt)_2InCl_3$	2 × 4	7.65	8.60	2 × 3	8.85	19.5	7.9	Benzene
$(Ph_2EtP)_2InBr_3$	2 × 4	7.74	8.40	2 × 3	8.88	18.0	8.2	Benzene

*M = multiplicity, J = values in Hz.

Since only one symmetrical doublet appears in the n.m.r. spectra, two possible conclusions can be drawn. Firstly the complex has a structure with two equivalent phosphine ligands. The n.m.r. data do not disagree, therefore, with the *trans* structure suggested from vibrational spectroscopy. Alternatively, rapid exchange of ligands in solution may be occurring to render both phosphines equivalent on the n.m.r. time scale. The absence of virtual coupling may support the latter alternative.

For the bis-Me_2PhP complexes, a symmetrical doublet is again observed for the CH_3 resonance. The tris compounds, $(Me_2PhP)_3InX_3$ (X = Cl, Br), likewise give rise to only one doublet. These results may imply D_{3h} and C_{3v} structures for the bis and tris adducts. Comparison of chemical shifts and $^2J_{P-H}$ values within the two series shows (*a*) an up-field shift of methyl resonances in the tris adducts and (*b*) a decrease in $^2J_{P-H}$ in the tris adducts. These differences are probably the result of weaker In—P bonding in the *tris* complexes due to the higher coordination number of indium.

$(Ph_2EtP)_2InX_3$ (X = Cl, Br) and $(Et_3P)_2InX_3$

Chemical shift, $^2J_{P-H}$ and $^3J_{P-H}$ values for these complexes are grouped in Table 8. The n.m.r. spectrum of Et_3P is second order (34). The complexes give essentially first-order spectra consisting of two overlapping methylene proton quartets (giving a 1:4:6:4:1 intensity pattern) and two overlapping methyl proton triplets. The effect of the indium trihalide substituent on the chemical shifts of the α and β protons appears to be intermediate between that of an Et^+ group and a P=O group since $Et_4P^+I^-$ has a similar first order spectrum whereas that of Et_3P=O is second order (34). Spectra of Ph_2EtP complexes resemble the first order spectrum of $Ph_3\overset{+}{E}t\overset{+}{P}I^-$ (34). The usual increases in $^2J_{P-H}$, $^3J_{P-H}$ occur on complexing and the α and β resonances are moved to lower field. For structural purposes the spectra give little new information. As for $(Me_3P)_2InX_3$, the presence of only one type of ethyl proton environment implies a symmetrical structure of D_{3h} or C_{2v} symmetry. The absence of virtual coupling might indicate a *cis* trigonal bipyramidal configuration but as we have not observed this behavior in any of these systems, this conclusion must be doubtful. In a separate study we are examining the low temperature n.m.r. spectra of these adducts to throw further light on the apparent absence of virtual coupling and the possibility of chemical exchange.

Conclusions

Several important conclusions can be drawn from this work. Firstly there is now strong evidence from this and previous work that indium prefers five-coordination when phosphorus donors are involved. This contrasts with the many six coordinate complexes prepared with nitrogen and oxygen donor ligands (32). *Trans* trigonal bipyramidal complexes of the type InX_3L_2 appear to give rise to characteristic vibrational spectra thus aiding identification.

Nuclear magnetic resonance measurements at room temperature do not appear to be as useful in the chemistry of non-transition metal – phosphine complexes as in the transition metal field. Theories of bonding, in particular the factors influencing a preference for a given coordination number, remain obscure and less well developed than in transition metal chemistry although

Can. J. Chem. Downloaded from www.nrcresearchpress.com by 210.87.254.42 on 09/05/12
For personal use only.

ligand basicity, size, and melting point are of some importance. Further work, including X-ray and thermochemical studies at present underway in this laboratory, will be necessary before a composite picture of bonding in adducts of this type can be formulated.

We acknowledge the financial support of the Government of Ontario Department of University Affairs, and the National Research Council of Canada.

1. A. J. CARTY. Can. J. Chem. **45**, 345 (1967).
2. A. J. CARTY. Can. J. Chem. **45**, 3187 (1967).
3. A. J. CARTY and D. G. TUCK. J. Chem. Soc. A, 1081 (1966).
4. I. R. BEATTIE and G. A. OZIN. J. Chem. Soc. A, 2373 (1968).
5. A. BALLS, N. N. GREENWOOD, and B. P. STRAUGHAN. J. Chem. Soc. A, 753 (1968).
6. D. M. ADAMS, A. J. CARTY, P. CARTY, and D. G. TUCK. J. Chem. Soc. A, 162 (1968).
7. M. V. VEIDIS and G. PALENIK. Chem. Commun. 586 (1969).
8. D. C. BRADLEY. Progr. Stereochem. **3**, 1 (1963).
9. D. S. BROWN, F. W. B. EINSTEIN, and D. G. TUCK. Inorg. Chem. **8**, 14 (1969).
10. L. SACCONI. Rev. Pure Appl. Chem. **17**, 95 (1968).
11. J. M. JENKINS and B. L. SHAW. J. Chem. Soc. A, 770 (1966).
12. J. G. EVANS, P. L. GOGGIN, R. J. GOODFELLOW, and J. G. SMITH. J. Chem. Soc. A, 465 (1968).
13. G. BOOTH. Advan. Inorg. Chem. Radiochem. **6**, 42 (1964).
14. G. E. COATES and C. PARKIN. J. Chem. Soc. 421 (1963).
15. P. L. GOGGIN and R. J. GOODFELLOW. J. Chem. Soc. A, 1462 (1966).
16. W. A. HENDERSON, JR. and C. A. STREULI. J. Amer. Chem. Soc. **82**, 5791 (1960).
17. L. MAIER. Progr. Inorg. Chem. **5**, 27 (1963).
18. M. A. A. BEG and H. C. CLARK. Can. J. Chem. **38**, 119 (1960).
19. D. G. TUCK. Private communication.
20. (*a*) J. H. S. GREEN. Spectrochim. Acta, **24A**, 137 (1968). (*b*) G. BOUQUET and M. BIGORGNE. Spectrochim. Acta, **23A**, 1169 (1967). (*c*) VON. J. GOUBEAU and D. LANGHARDT. Z. Anorg. Allg. Chem. **338**, 163 (1965).
21. G. B. DEACON and J. H. S. GREEN. Spectrochim. Acta, **24A**, 845 (1968).
22. T. HINSPERGER. M.Sc. Thesis, University of Waterloo, 1969.
23. P. J. D. PARK and P. J. HENDRA. Spectrochim. Acta, **25A**, 227 (1969).
24. I. R. BEATTIE, T. GILSON, and G. A. OZIN. J. Chem. Soc. A, 1092 (1968).
25. I. R. BEATTIE, T. GILSON, and (in part) P. COCKING. J. Chem. Soc. A, 702 (1967).
26. I. R. BEATTIE, T. GILSON, and G. A. OZIN. J. Chem. Soc. A, 813 (1968).
27. D. M. ADAMS. Metal ligand and related vibrations. Arnold, London, 1968.
28. T. BARROWCLIFFE, I. R. BEATTIE, and P. DAY. J. Chem. Soc. A, 1810 (1967).
29. I. R. BEATTIE, T. GILSON, and G. A. OZIN. J. Chem. Soc. A, 2772 (1968).
30. A. J. CARTY, P. M. BOORMAN, and H. A. PATEL. Can. J. Chem. **48**, 492 (1970).
31. A. J. CARTY. Unpublished results.
32. A. J. CARTY. Coord. Chem. Rev. **4**, 29 (1969).
33. J. M. JENKINS and B. L. SHAW. Proc. Chem. Soc. 279 (1963).
34. J. B. HENDRICKSON, M. L. MADDOX, J. J. SIMS, and H. D. KAESZ. Tetrahedron, **20**, 449 (1964).
35. G. J. PALENIK and G. G. MESSMER. Inorg. Chem. **8**, 2750 (1969) and unpublished results.

Can. J. Chem. Downloaded from www.nrcresearchpress.com by 210.87.254.42 on 09/05/12
For personal use only.

Confirmation of the dielectric polarization theory of anodic film formation: a voltage pulse technique for investigating Faradaic-current-driven polarization processes

M. J. DIGNAM AND D. F. TAYLOR
Department of Chemistry, University of Toronto, Toronto 181, Ontario
Received December 23, 1969

Potentiostatic voltage-pulse experiments, carried out on anodically formed tantalum oxide films, show directly the existence of a dielectric polarization process which is driven by the passage of ion-current. Furthermore, quantitative analysis of the data yields a value for the constant coupling the polarization rate to the ion-current density, of the same order as that obtained from galvanostatic field transients, a result expected if the dielectric polarization of the film makes a large contribution to the effective field causing film growth. This experiment provides, therefore, convincing evidence in support of the main tenet of the dielectric polarization theory for anodic film growth (the ion-current-driven polarization process) with some support for the effective-field postulate also provided.

Canadian Journal of Chemistry, **48**, 1971 (1970)

Can. J. Chem. Downloaded from www.nrcresearchpress.com by 210.87.254.6 on 09/05/12
For personal use only.

Introduction

The dielectric polarization theory for anodic film growth (1–4) provides quantitative agreement with data from the literature for the steady-state anodic oxidation of a number of valve metals, but several other theories predict similar results. Steady-state measurements consequently cannot provide a means for distinguishing between the various theories. Even measurement of the "in-situ" a.c. impedance of the electrode system during steady-state film growth cannot differentiate between the dielectric polarization theory and the high-field Frenkel defect theory (5).[1] To date, only constant field transient measurements differentiate effectively between these models, lending substantial support to the dielectric polarization theory (1, 2).

Although certain other unique predictions of this theory were also found to be in agreement with data (1), it has not yet been shown directly that there exists a polarization process whose rate is proportional to the ion-current density, which is the main postulate of the theory.

Values of the various parameters involved in the dielectric polarization theory have been obtained for tantalum and aluminum from measurements of galvanostatic ion-current transients (5). For both systems, the predicted extraordinary polarization current is at most only a few percent of the ion-current producing it.[2] Attempts to detect the extraordinary polarization current in the presence of ion-current, through a.c. impedance measurements, for example, are therefore unsuccessful (7). The anomalous polarization process should be made apparent, however, by monitoring the depolarization current, measured at zero ion-current, following a polarizing pulse during which ion-current flows.

Experimental

Apparatus

A conventional galvanostatic circuit (8) was used for growing oxide films on tantalum. The potential difference between the anode and reference electrode was measured continuously during film growth.

The potentiostatic circuit used for the polarization measurements is shown in Fig. 1. Burr–Brown solid-state amplifiers were used throughout. The 3043/15 control amplifier is capable of delivering ± 100 mA at ± 10 V and the 3013/15 and 3116/12C follower amplifiers both have FET inputs. Four lead–acid storage batteries, each with a nominal output of 12 V, served as the high voltage supply. The advantage of this particular potentiostatic circuit is that low voltage, high performance solid-state amplifiers can contol high voltages. This unit exhibits an offset voltage of less than 1 mV and a net offset current of less than 1 nA with negligible peak-to-peak noise. The time constant is easily adjustable from less than 10 μs to any value that may be required under conditions of heavy capacitive loading and violent voltage fluctuations.

[1]The high-field Frenkel defect theory was originally proposed by Bean *et al.* (6).

[2]The calculated contribution to the effective dielectric constant made by the ion-current-driven polarization process during ion-current transients was shown to be negligible in a previous communication (7).

Can. J. Chem. Downloaded from www.nrcresearchpress.com by 210.87.254.6 on 09/05/12
For personal use only.

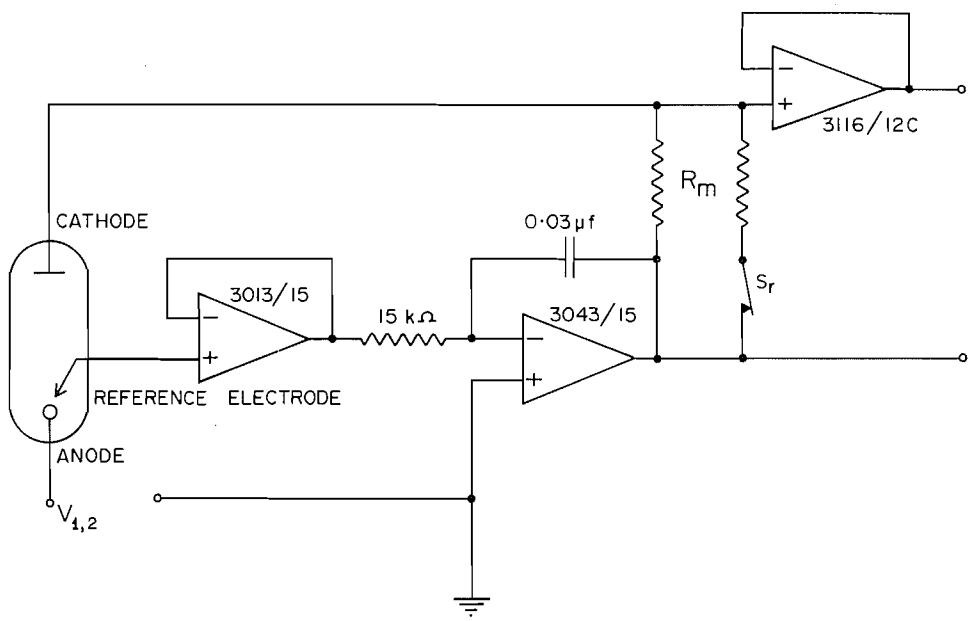

FIG. 1. Potentiostatic circuit. The value of the measuring resistor, R_m, is switched by a mercury-wetted relay, S_r. Model numbers refer to Burr–Brown designations.

Five mercury-wetted contact relays (Clare HGS 1026, Potter and Brumfield JML 5160-81, three JML 1260-81) were connected to provide sequential switching of the cell voltage from V_1 to V_2 to V_1 followed by a change in the potentiostat's measuring resistor. Both the width of the voltage pulse, and the time which elapses before the change in resistance, are easily adjustable, and once set are reproducible to better than 5×10^{-5} s. The voltage drop across the current measuring resistor was monitored by an oscilloscope and camera.

Materials

Rectangular electrodes 1 in. × 0.25 in. with a tab 2.5 in. × 0.06 in. were punched from a sheet of 0.01 in. Metallurgical Grade, annealed tantalum obtained from Fansteel Metallurgical Corporation. These electrodes were cleaned, chemically polished in a standard sulfuric–nitric–hydrofluoric acid bath (9), then leached in boiling water as recommended by Young (10).

The Pyrex electrolysis cell utilized a specially designed Lucite insert (5) for positioning the anode, platinum counter electrodes, and $Hg/Hg_2SO_4/H_2SO_4$ (0.1 *M*) reference electrode. Dilute sulfuric acid (0.1 *M*) was used as electrolyte since excellent steady-state data is available for this system (11).

Procedure

Initially, oxide was formed at constant current to a cell potential in excess of 100 V on a 1 in. segment of the electrode handle just above the blade. This served to define the working area and to eliminate the effects of electrolyte creepage during the experiment. In a typical run, anodic oxidation of the blade was carried out at 22.6 °C with a current density of 2.39×10^{-4} A cm^{-2}. Film growth was halted at 45.18 V.

During the voltage-pulse experiments, the potentiostat maintained the potential at V_1 for a minimum of 2 h after each change. $(V_2 - V_1)$ was held constant at 25.01 V for all the experiments, while V_1 ranged between 0 and 25.01 V. (These values were chosen so that ion-current could flow only during the charging pulse.) The charging pulse width chosen was 7 ms. A small resistance of 50 Ω initially in parallel with a larger resistance (normally 1 kΩ) was switched out of the current measuring circuit 3 ms after returning to V_1. Four oscilloscope pictures, with different time scales and baseline positions, were required for each selected value of V_1. One-half hour was allowed between these measurements for the system to approach its initial polarization state.

Theory

The dielectric polarization theory for the anodic oxidation of the valve metals has been discussed at length in previous publications, with further mechanistic detail forthcoming. We present here only a phenomenological description of the theory and the relevant equations.

The ion-current density, j, is given approximately (3) by

$$[1] \qquad j = \alpha \exp \beta E_c$$

where α and β are temperature dependent constants and E_c is the local field effecting ion transport. As the rate controlling step for ion transport is assumed to occur at an interface

Can. J. Chem. Downloaded from www.nrcresearchpress.com by 210.87.254.6 on 09/05/12
For personal use only.

(probably the oxide–electrolyte interface), E_c is proportional to the electric displacement in the film, $D = \varepsilon_0 E + P$, where E is the field strength in the oxide, P the polarization of the oxide, and ε_0 the permittivity of free space. Ion-current transients are thus predicted to arise as a result of dielectric relaxation. The form of both potentiostatic and galvanostatic transients are accounted for quantitatively (5) on setting

$$[2] \quad \frac{dP}{dt} = \varepsilon_0\chi_1 \frac{dE}{dt} + \sum_{i=2}^{3} B_i\, j(\varepsilon_0\chi_i E - P_i)$$

where $P = \varepsilon_0\chi_1 E + P_2 + P_3$, and for equilibrium (or steady-state) polarization conditions, $P_i = \varepsilon_0\chi_i E$. The final two terms in eq. [2] represent the contentious ion-current-driven polarization processes.[3] Under conditions of zero ion-current, it is well known that there exist thermally activated slow polarization processes. Generalizing eq. [2] to include these, we obtain

$$[3] \quad \frac{dP}{dt} = \varepsilon_0\chi_1 \frac{dE}{dt} + \sum_{i=2}^{3} B_i\, j(\varepsilon_0\chi_i E - P_i) + \sum_{i=4}^{N} (1/\tau_i)(\varepsilon_0\chi_i E - P_i)$$

where the τ_i are relaxation times.

Although the various polarization processes must interact with one another, each can be treated separately to a good approximation *provided* that changes in the $P_i (i = 2 \rightarrow N)$ remain sufficiently small. Then for these conditions we may write

$$[4] \quad \frac{dP_i}{dq_j} + B_i P_i = B_i \varepsilon_0 \chi_i E \quad i = 2, 3$$

$$[5] \quad \frac{dP_i}{dt} = (1/\tau_i)(\varepsilon_0\chi_i E - P_i) \quad i \geqslant 4$$

where q_j is the ion charge passed per unit area. Before the polarizing pulse, $E = E_1$; during the pulse $E = E_2$. At $t = 0$ when $q_j = 0$, $P_i = \varepsilon_0\chi_i E_1$. With these boundary conditions, eqs. [4] and [5] and the expression for P_i can be integrated over the period that V_2 is applied to the cell leading to

$$[6] \quad q_1 = \varepsilon_0(1 + \chi_1)\Delta E$$

$$[7] \quad q_i = \varepsilon_0\chi_i \Delta E(1 - e^{-B_i q_j}) \quad i = 2, 3$$

$$[8] \quad q_i = \varepsilon_0\chi_i \Delta E(1 - e^{-t/\tau_i}) \quad i \geqslant 4$$

where q_i is the charge passed per unit area associated with P_i.

When the cell voltage is returned to V_1, those polarization processes which are not ion-current-driven simply operate in reverse. The charge displacement induced by ion-current, however, must now dissipate using thermally activated mechanisms since the ion-current has ceased to flow. These thermal processes have relatively long relaxation times (2), so augmentation of the discharge current should be clearly distinguishable. The small displacements of P_2 and P_3 relative to $\varepsilon_0\chi_2 E_1$ and $\varepsilon_0\chi_3 E_1$ during the pulse allows a linear approximation in the expression for their sum (i.e. $B_i q_j \ll 1$, $i = 2, 3$) so that eq. [7] leads to

$$[9] \quad q_2 + q_3 = \varepsilon_0 \Delta E(\chi_2 B_2 + \chi_3 B_3) q_j$$

The total charge passed per unit area during the polarizing pulse, Q_+, is given by

$$[10] \quad Q_+ = \sum_{i=1}^{N} q_i + q_j$$

The total charge per unit area passed after the pulse until reestablishment of equilibrium polarization conditions, Q_-, will be given to a good approximation by

$$[11] \quad q_j = Q_+ + Q_-$$

Combining eqs. [7] and [11] leads to the result

$$[12] \quad -Q_- = \varepsilon_0 \Delta E(\chi_2 B_2 + \chi_3 B_3) q_j + \varepsilon_0(1 + \chi_1)\Delta E + \sum_{i=4}^{N} \varepsilon_0\chi_i \Delta E(1 - e^{-t/\tau_i})$$

Provided that ΔE and the polarizing pulse time, t, are maintained the same for a series of values of E_1, a plot of $(-Q_-)$ vs. q_j should therefore yield a straight line with slope $\varepsilon_0 \Delta E(\chi_2 B_2 + \chi_3 B_3)$.

Analysis and Discussion of Results

In Fig. 2 the ion-current-driven polarization phenomenon is clearly illustrated. For the results shown, the oscilloscope settings were selected to show both the charging (positive) and discharging (negative) currents for the three values of the

[3] Previously, only one such B term has been included. However, recent analysis of transient data indicates that two terms provide a considerably better description of the system (ref. 5).

Can. J. Chem. Downloaded from www.nrcresearchpress.com by 210.87.254.6 on 09/05/12
For personal use only.

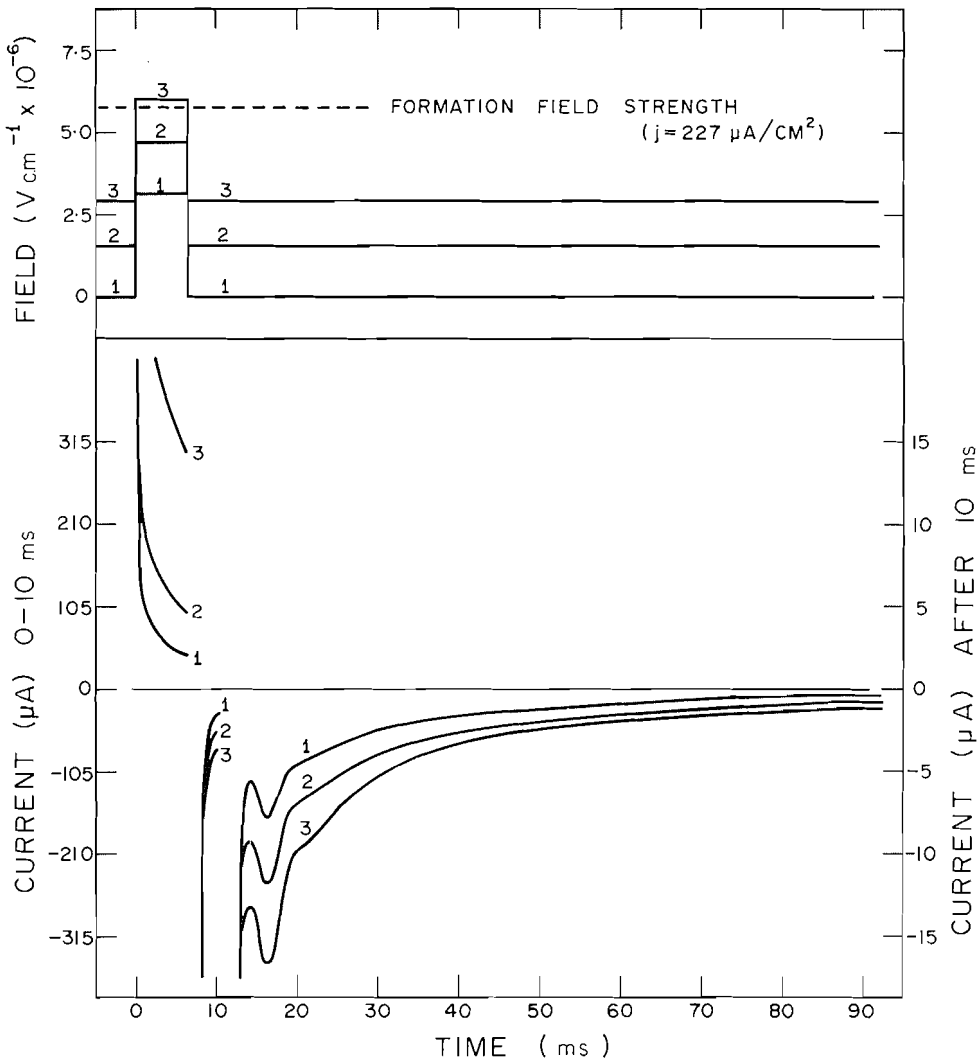

FIG. 2. Current–time curves illustrating increasing rate of dielectric polarization with increasing ion-current for a constant polarizing field increment and time interval. The effect is made apparent through the behavior of the discharge current.

field strength, E_1. Increasing the time constant of the potentiostat to 450 μs did not eliminate ringing following the change in the current measuring resistor. The residual oscillation, however, presents no problem in interpretation.

Quantitative analysis of the results was done by enlarging the photographs, and measuring the total charges with a planimeter, precision being better than 1%. The film thickness d, required to calculate ΔE, was obtained from a computer analysis of the steady-state film-growth data. A least-squares fit of the voltage increments vs. time yielded dV/dt, from which both j and E were determined by iteration using Young's steady-state data (11).

The electrode area could then be calculated from j and the total current. Calculation of d required the overpotential reached before film growth was terminated, and since this oxide system does not attain its equilibrium potential at open circuit, thermodynamic data must be used. The equilibrium potential of the cell

$$\mathrm{Ta}\,|\mathrm{Ta_2O_5}\,|\mathrm{H_2SO_4}(0.1\ M)\,|\mathrm{Hg_2SO_4}\,|\mathrm{Hg}$$

was calculated to be 1.48 V, thus

[13] $$d = (V_{\mathrm{final}} + 1.48\ \mathrm{V})/E$$

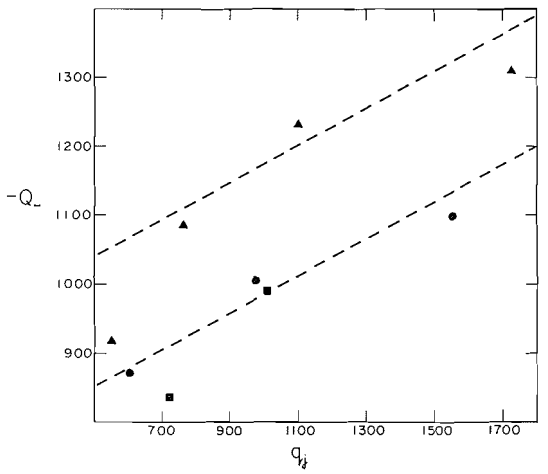

FIG. 3. Dependence of the charge passed during the depolarization process, Q_-, on the charge passed as ion-current during the charging pulse, q_j. (E_1 changing chronologically according to: ▲, 0.19, 1.79, 2.33, 2.85 × 10^6 V cm^{-1}; ■, 2.85, 2.33 × 10^6 V cm^{-1}; ●, 2.33, 2.85, 3.39 × 10^6 V cm^{-1}. ΔE = 3.20 × 10^6 V cm^{-1}. Broken lines represent the expected *slope*.)

The constants χ_2, B_2, χ_3, and B_3 have been obtained from a double exponential fit of galvanostatic transient data published by Dewald (5, 12) ($\chi_2 B_2 + \chi_3 B_3 = 9.48 \times 10^5$ cm^2 C^{-1}). The separate values for $\chi_2 B_2$ and $\chi_3 B_3$ were used with eq. [7] to verify the linear approximation made in eq. [9], for q_j and $(q_2 + q_3)$ values beyond those actually encountered. The experimental results have been plotted in the form $-Q_-$ vs. q_j in order to test the data against eq. [12] (cf. Fig. 3). The expected slope is represented by the broken lines.

Quantitative interpretation of the present results is difficult. The apparent dependence of the results both on whether E_1 was increased or decreased from one run to the next in a sequence, and on elapsed time, would seem to indicate that equilibrium polarization was probably never attained. The curvature of the plots might have resulted from applying inadequate methods for charge measurement. The major difficulty lay in obtaining accurate values for the charge passed in the first few milliseconds after the pulse, and after approximately 1 s had elapsed in the discharge period.[4] The errors arising in this way were quite substantial. For $E_1 = 0$, Q_+ was 1470 planimeter units, and $|Q_-|$, 920 units. Had the initial polarization state been re-established during the discharge measurement, they should have been equal, since essentially no ion-current should flow at $E_2 = 3.39 \times 10^6$ V cm^{-1}. Film growth during the pulse could not have contributed any significant error. q_j was typically less than 10^{-6} C per pulse whereas 0.384 C were required to form the film. Again, any uncertainty in the film thickness, current density, field strength, and electrode area could not have contributed in any significant way to the final results.

Although the present numerical results leave something to be desired on the quantitative side, qualitatively they represent convincing support for the dielectric polarization theory. Within the uncertainty of the present measurement, they are also in quantitative agreement with the theory. That the value of $(\chi_2 B_2 + \chi_3 B_3)$ obtained from the present discharge measurement should be of the same order of magnitude as that obtained from ion-current transients is not likely a coincidence.

[4]Some of the τ_i are apparently of the order of several hours (see ref. 2).

The authors are grateful to the National Research Council of Canada for supporting this research and for a scholarship (D.F.T.).

1. M. J. DIGNAM. J. Electrochem. Soc. **112**, 722 (1965); **112**, 729 (1965).
2. M. J. DIGNAM and P. J. RYAN. Can. J. Chem. **46**, 535 (1968); **46**, 549 (1968).
3. M. J. DIGNAM and D. B. GIBBS. J. Phys. Chem. Solids, **30**, 375 (1969).
4. M. J. DIGNAM. In preparation. Presented at the meeting of the Electrochem. Soc. held in New York, May, 1969.
5. M. J. DIGNAM and D. GOAD. In preparation. Presented at the meeting of the Electrochem. Soc. held in New York, May, 1969.
6. C. P. BEAN, J. C. FISHER, and D. A. VERMILEA. Phys. Rev. **101**, 551 (1956).
7. M. J. DIGNAM and D. F. TAYLOR. Appl. Phys. Lett. **15**, 198 (1969).
8. George A. Philbrick Researches, Inc., Applications Manual for Computing Amplifiers, circuit III. 4, Nimrod Press, Boston. 1966.
9. W. J. MCG. TEGART. The electrolytic and chemical polishing of metals. Pergamon Press, London. 1956.
10. L. YOUNG. Trans. Faraday Soc. **53**, 841 (1957).
11. L. YOUNG. Proc. R. Soc. A, **258**, 496 (1960); **244**, 41 (1958).
12. J. F. DEWALD. J. Phys. Chem. Solids. **2**, 55 (1957).

Can. J. Chem. Downloaded from www.nrcresearchpress.com by 210.87.254.6 on 09/05/12
For personal use only.

Can. J. Chem. Downloaded from www.nrcresearchpress.com by 210.87.254.105 on 09/05/12
For personal use only.

Temperature dependence of the ^{35}Cl nuclear quadrupole resonance in the trimethylamine – boron trichloride complex

D. F. R. GILSON AND R. M. HART
Department of Chemistry, McGill University, Montreal, Quebec

Received December 2, 1969

A ^{35}Cl nuclear quadrupole resonance study of the trimethylamine – boron trichloride complex has revealed line-width and frequency changes which correlate with transitions observed in the wide-line proton magnetic resonance study.

Canadian Journal of Chemistry, **48**, 1976 (1970)

Introduction

In a recent wide-line nuclear magnetic resonance (n.m.r.) study of molecular motions in complexes of trimethylamine with boron trihalides and borane, line-width and second-moment transitions were observed and attributed to methyl group reorientation in the temperature range below 110 °K, followed by rotation of the trimethylamine group about the B—N axis at higher temperatures (1). For the borane and boron trifluoride complexes it is probable that reorientation of these groups occurred prior to the onset of rotation of the trimethylamine group. It was not possible to determine from these studies whether or not motion of the BCl_3 or BBr_3 groups occurred, although the activation energies determined from line-width analyses were about 9 kcal $mole^{-1}$ for trimethylamine rotation compared with about 2 kcal $mole^{-1}$ for the same process in the BF_3 and BH_3 complexes. This suggested that the molecule rotates as a whole rather than uncorrelated motion of the two halves.

We have examined the frequency and "apparent" line widths of the ^{35}Cl nuclear quadrupole resonance as a function of temperature in the trimethylamine – boron trichloride complex to obtain additional information on the molecular motion in these compounds.

The nuclear quadrupole resonance (n.q.r.) frequencies of a series of boron trichloride complexes were first reported by Kaplansky and Whitehead (2). For the trimethylamine complex at 77 °K, two lines were observed, at 21.765 and 21.340 MHz, with an intensity ratio of 2:1.

Experimental

The Dean-type super-regenerative spectrometer and the methods of operation and frequency measurement have been described previously (3, 4). Frequencies are estimated to be within ±2 kHz for broad lines and better than ±1 kHz for the narrow lines. Line widths were measured at half peak height from the recorder traces. The modulation amplitude was reduced as much as possible to avoid artificial line broadening. Temperatures were measured with a copper–constantan thermocouple and a Rubicon potentiometer, and are estimated to be within ±1 °C.

The trimethylamine – boron trichloride complex was prepared by standard methods (5).

Results

The temperature dependence of the resonance frequencies is shown in Fig. 1. The "apparent" line width of the stronger resonance line is shown in Fig. 2 as a function of temperature. Both resonance lines broadened over the temperature range 77 to 100 °K, then narrowed until 230 °K,

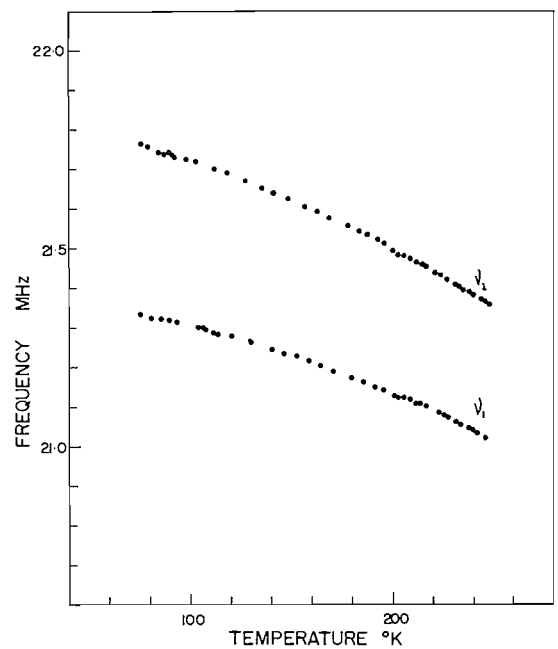

FIG. 1. Temperature dependence of the ^{35}Cl n.q.r. frequencies.

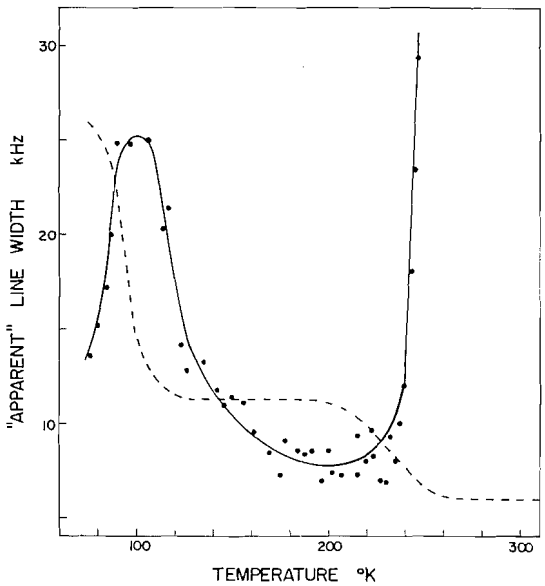

FIG. 2. Apparent line width of ν_2 as a function of temperature. Dotted line is the proton n.m.r. second moment.

when a further broadening occurred. At 247 °K the lines were no longer observable. Also shown in Fig. 2 is the temperature dependence of the proton magnetic resonance second moments. A most obvious feature is the coincidence of the broadening of the n.q.r. line and the onset of the second-moment transitions. The resonances due to ^{37}Cl were observed at the predicted frequencies.

Discussion

The theory of the temperature dependence of n.q.r. frequencies was developed by Bayer (6) and extended by Kushida, Benedek, and Bloembergen (7). Torsional motions of molecules lead to an averaging of the electric field gradient and a consequent reduction in resonance frequency. If the torsional motions are treated as quantum harmonic oscillators, the resonance frequency at temperature T °K can be expressed by

$$[1] \quad \nu(T) = \nu(0)\left[1 - \frac{3}{2}\sum_i \frac{h}{A_i\omega_i} \times \left(\frac{1}{2} + \frac{1}{\exp\left(\frac{h\omega_i}{kT}\right) - 1}\right)\right]$$

where $\nu(0)$ is the frequency at 0 °K, ω_i is the torsional frequency and A_i the moment of inertia about the ith axis. Equation [1] applies under constant-volume conditions, whereas resonance frequencies are usually measured at constant pressure. Thermal expansion effects can be compensated for by allowing the torsional frequencies to vary with temperature

$$[2] \quad \omega_i(T) = \omega_i(0)(1 - \alpha T)$$

For the trimethylamine – boron trichloride complex, only torsion about the molecular axis need be considered; however, two choices exist for the moment of inertia. The BCl_3 group alone could be undergoing torsion against a rigidly held trimethylamine group, or the molecule as a rigid body can oscillate in a potential well defined by the crystal lattice. The moments of inertia were calculated to be 5.25×10^{-38} and 6.81×10^{-38} g cm^2, respectively, using the structural data given for the acetonitrile complex (8).

A least-squares fit to each curve was made for eq. [1] using the McGill IBM 360/75 computer, with $\nu(0)$, α, and ν_t (converting ω_i to cm^{-1}) as variable parameters. The values obtained are given in Table 1, together with the root-mean-square (r.m.s.) deviations. Changing the value of the moment of inertia leads to a compensating change in the torsional frequency, since the exponential term has lesser importance with higher temperature, and no improvement in the r.m.s. deviation. It can be seen in Fig. 1 that changes in slope of the resonance frequency vs. temperature curves occur at 100 and 204 °K. If these changes are real, an improvement might result if the curves were considered in sections. However, in the temperature region around 100 °K the lines are broad with larger errors in frequency measurement. For this reason, and the small number of points below 100 °K, the curves were divided into two parts rather than three. The results of the least-squares fits are given in Table 1. The r.m.s. deviations are improved over the fits to the entire curves. The improvement for the low temperature range is better than indicated because those points with larger error become more heavily weighted.

The change in slope at about 200 °K is real and coincides with the onset of the n.m.r. line narrowing process.

The changes in line width of the quadrupole resonance are more obvious but, due to their mode of operation, super-regenerative oscillator-detectors do not provide true line-shape functions; therefore the line widths are referred to

Can. J. Chem. Downloaded from www.nrcresearchpress.com by 210.87.254.105 on 09/05/12
For personal use only.

TABLE 1

A values obtained from eq. [1]

	A (g cm^2 × 10^{-38})	ν (T) (cm^{-1})	α × 10^{-4}	$\nu(0)$ (MHz)	R.m.s. deviation (kHz)
All points					
ν_1	5.25	69.1	9.0	21.387	2.48
ν_1	6.81	61.1	9.2	21.390	2.47
ν_2	5.25	61.4	8.8	21.830	3.15
ν_2	6.81	54.2	8.9	21.834	3.16
Temperature range 77–200 °K					
ν_1	5.25	70.1	9.7	21.386	2.02
ν_1	6.81	62.2	9.9	21.389	2.01
ν_2	5.25	63.1	9.6	21.826	3.13
ν_2	6.81	55.8	9.8	21.829	3.13
Temperature range 200–248 °K					
ν_1	5.25	125.7	19.5	21.273	1.87
ν_1	6.81	110.6	19.6	21.275	1.87
ν_2	5.25	69.0	10.7	21.782	2.58
ν_2	6.81	60.7	10.7	21.786	2.58

here as "apparent."[1] Although no quantitative significance can be attached to the magnitude of the line widths, important relative changes occur and they do so over temperature ranges where line-width and second-moment transitions were observed in the proton magnetic resonance measurements (Fig. 2). There are several causes of line broadening in quadrupole resonance: magnetic dipole interactions, electrical strains, relaxation effects, and randomization of field gradients by disordering processes. Only the latter two are important in the present case. Torsional oscillations occur in the frequency range 10^{11}–10^{12} s^{-1}, i.e. very much faster than the quadrupole resonance frequency. However, due to fluctuations in torsional frequencies there can be Fourier components at approximately the same range as the resonance frequency, which leads to relaxation between the quadrupolar energy levels. This lifetime-limiting process may occur in the present case. In nuclear magnetic resonance, line narrowing occurs when the frequency of the motion approaches the line width expressed in frequency units, i.e. about 10^4–10^5 Hz. This is approaching the frequency region of the nuclear quadrupole resonance and it is not surprising that the widths of the n.q.r. lines should be affected. This is probably the mechanism operative at 100 °K where the wide-line n.m.r. data indicate reorientation of methyl groups. The quadrupole resonance line narrows when the rate of reorientation becomes too fast for effective direct relaxation.

The same mechanism may be responsible at the high temperature transition but, as mentioned earlier, the activation energy obtained from the n.m.r. data suggests that hindered rotation of the whole molecule occurs. The frequency of this rotation is of a magnitude to cause lifetime broadening by direct interaction, but at a sufficiently rapid rate of rotation an averaging of the field gradient will occur along the axis of rotation and the resonance should be observable again. The new resonance frequency is given by

$$[3] \qquad \nu' = (\nu/2)(3\cos^2\theta - 1)$$

Where θ is the angle between the axis of rotation and the former principal component of the electric field gradient. For the —BCl_3 case the frequency should be reduced to one-third the original value, but attempts to observe resonance at higher temperatures at around 7 MHz were unsuccessful. This failure may be due to the experimental problem of operating the spectrometer in this frequency region.

Although there have been several instances reported where disappearance of the nuclear quadrupole resonance occurs at temperatures well below the melting points, notably for —CCl_3 groups, only in 1,2-dichloroethane (9) and 1,2-dibromoethane (10) has resonance been observed again on the high temperature side of the transi-

[1]The observed broadening of these resonance lines was not an instrumental effect. Other compounds studied under the same experimental conditions showed only narrow lines.

Can. J. Chem. Downloaded from www.nrcresearchpress.com by 210.87.254.105 on 09/05/12
For personal use only.

tion. In 1,2-dichloroethane the line broadening phenomenon also coincides with transitions observed by wide-line n.m.r. methods (11).

The nuclear quadrupole resonance spectrometer was made available for these measurements by Professor M. A. Whitehead, whose generosity is gratefully acknowledged.

1. C. T. YIM and D. F. R. GILSON. Can. J. Chem. **48**, 515 (1970).
2. M. KAPLANSKY and M. A. WHITEHEAD. Mol. Phys. **16**, 481 (1969); Can. J. Chem. **48**, 697 (1970).
3. M. KAPLANSKY and M. A. WHITEHEAD. Can. J. Chem. **45**, 1669 (1967).
4. C. T. YIM, M. A. WHITEHEAD, and D. H. LO. Can. J. Chem. **46**, 3595 (1968).
5. A. R. KATRITZKY. J. Chem. Soc. 2049 (1959).
6. H. BAYER. Z. Phys. **130**, 227 (1951).
7. T. KUSHIDA, G. B. BENEDEK, and N. BLOEMBERGEN. Phys. Rev. **104**, 1364 (1956).
8. B. SWANSON, D. F. SHRIVER, and J. A. IBERS. Inorg. Chem. **8**, 2182 (1969).
9. J. L. RAGLE. J. Phys. Chem. **63**, 1395 (1959).
10. H. W. DODGEN and R. ANDERSON. J. Chem. Phys. **31**, 851 (1959).
11. H. S. GUTOWSKY and G. E. PAKE. J. Chem. Phys. **18**, 162 (1950).

Can. J. Chem. Downloaded from www.nrcresearchpress.com by 210.87.254.105 on 09/05/12
For personal use only.

Can. J. Chem. Downloaded from www.nrcresearchpress.com by 210.87.254.42 on 09/05/12
For personal use only.

Alkaloids of *Shepherdia argentea* and *Shepherdia canadensis*

W. A. AYER AND L. M. BROWNE
Department of Chemistry, University of Alberta, Edmonton, Alberta

Received February 2, 1970

Tetrahydroharmol (**3**) was isolated from *Shepherdia argentea*. Tetrahydroharmol (**3**), serotonin (**12**), and a new alkaloid shepherdine (**2***a*) were isolated from *Shepherdia canadensis*; and evidence was obtained for the presence of 6-hydroxytryptamine in *S. canadensis*.

Canadian Journal of Chemistry, **48**, 1980 (1970)

"You take the root of a cherry tree, boil it, and strain it through a cloth, and you can use it as a cure for diarrhea." So wrote Mike Oka in "A Blood Indian's Story" (1). The tree mentioned was probably buffalo or bullberry, *Shepherdia argentea* Nutt. (Eleagnaceae) (2). Our interest in this report led us to investigate the alkaloidal content of the two species of *Shepherdia* indigenous to Alberta, *S. argentea* (thorny buffalo-berry) and *S. canadensis* (Canadian buffalo-berry).

Shepherdia argentea was extracted with methanol and the crude bases isolated in the usual way; i.e., by acid–base extraction. The crude bases were acetylated, then separated by elution chromatography on deactivated alumina. Two major fractions were obtained: a mixture of non-polar acetylated bases (shown to be simple amines, *N*-acetylpyrrolidine and *N*-acetyl-*p*-anisidine were positively identified) and a crystalline compound (A).

Compound A crystallizes from ethyl acetate (m.p. 202°), is optically inactive, and has a typical indole chromophore in the ultraviolet (u.v.) (λ_{max}(EtOH) 229 (ε = 21 000), and 282 mμ (ε = 3500)) (3). The infrared (i.r.) spectrum shows indolic N—H, as well as carbonyl absorption due to an ester (1745 cm^{-1}) and an amide (1625 cm^{-1}). The nuclear magnetic resonance (n.m.r.) spectrum shows indolic N—H (τ 1.07), an ABX system characteristic of a 1,2,4-trisubstituted benzene ring, a low field methine (τ 4.35, J = 7 c.p.s.) coupled to a methyl group (τ 8.66, J = 7 c.p.s.), an ABCD system of methylene protons and two acetyl groups. The formula $C_{16}H_{18}N_2O_3$ (M^+ 286) was established by high resolution mass spectrometry. The evidence presented is consistent with either structure **1** or structure **2**.

The alkaloid itself was isolated from the crude basic extract of *Shepherdia argentea* by elution chromatography. It melts at 254.5° and the u.v. and i.r. spectra correspond closely to those reported (4) for tetrahydroharmol (**3**).

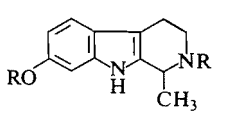

1 R = —$COCH_3$
3 R = H

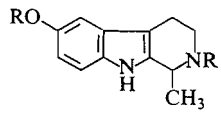

2 R = —$COCH_3$
2*a* R = H

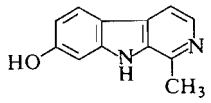

4

An authentic sample of **3** was prepared by reduction of harmol (**4**) (4). Acetylation gave *N*,*O*-diacetyltetrahydroharmol, identical in all respects with the compound isolated from *S. argentea*.

The basic material from *Shepherdia canadensis* was acetylated and separated by chromatography over alumina. Elution with benzene gave a compound $C_{17}H_{20}N_2O_3$, m.p. 212–214°, which is discussed below. Elution with benzene–chloroform gave a crystalline material, which had spectral properties (i.r., u.v., mass spectrometry) very similar to those of *N*,*O*-diacetyltetrahydroharmol (**1**). The n.m.r. spectrum, however, indicated that the material was a mixture (~1:1) of two very similar compounds. Fractional crystallization from methanol separated the two components. One proved to be identical with **1**, while the other, m.p. 192–194° was an isomer of **1**. Since this compound appears not to have been reported previously, we suggest the trivial name shepherdine for the unacetylated base.

N,*O*-Diacetylshepherdine crystallizes from methanol (m.p. 192–194°). The u.v. spectrum shows an indole chromophore while the i.r. spectrum shows indole N—H as well as carbonyl

Can. J. Chem. Downloaded from www.nrcresearchpress.com by 210.87.254.42 on 09/05/12
For personal use only.

absorptions due to an ester and an amide. The n.m.r. spectrum shows indole N—H, an ABX system of aromatic protons, a low field methine coupled to a methyl group, an ABCD system of methylene protons, and two acetyl groups. The molecular formula $C_{16}H_{18}N_2O_3$ (M^+ 286) was established by high resolution mass spectrometry. The evidence presented is consistent with either strucutre **1** or **2**, but since it has been shown (see above) that *N,O*-diacetylshepherdine is different from **1**, structure **2** is indicated for *N,O*-diacetylshepherdine. Recently, another harmala-type alkaloid, plectocomine (**5**), which has an oxygen function at C-6, has been identified (5).

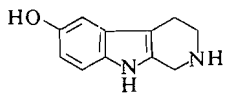

5

Sulfuric acid catalyzed condensation of 5-benzyloxytryptamine with acetaldehyde (6), followed by acetylation, hydrogenolysis (Pd–C), and acetylation gave *N,O*-diacetylshepherdine (**2**). The melting point (192–194°) and i.r. spectrum were identical with those of the acetylated alkaloid. Shepherdine thus has structure **2***a*.

The compound (m.p. 212–214°) referred to above also shows an indole chromophore in the u.v. The i.r. spectrum shows indole N—H as well as carbonyl absorption due to an ester and an amide. The n.m.r. spectrum shows indolic N—H, an ABX system of aromatic protons, an AA′BB′ system of methylene protons, two acetyl groups, and a *gem*-dimethyl group (τ 8.16). The molecular formula $C_{17}H_{20}N_2O_3$ (M^+ 300) was established by high resolution mass spectrometry. The evidence presented is consistent with either structure **6** or **7**.

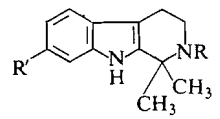

6 R = $COCH_3$; R′ = $OCOCH_3$
8 R = H; R′ = H
9 R = $COCH_3$; R′ = H

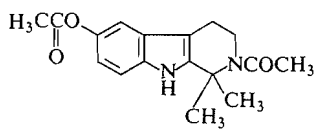

7

Since the signal in the n.m.r. assigned to the *gem*-dimethyl group occurs at lower field than expected, a model compound was prepared to determine whether *N*-acetylation markedly deshields the *gem*-dimethyl group in this situation. *p*-Toluene sulfonic acid catalyzed condensation of tryptamine with acetone to form the Schiff base, followed by phosphorus oxychloride catalyzed ring closure and then hydrolysis yielded compound **8** (7). The n.m.r. spectrum of compound **8** shows a six-proton singlet due to the *gem*-dimethyl group at τ 8.54. Acetylation of compound **8** gives compound **9**, the n.m.r. of which shows the *gem*-dimethyl group at τ 8.09, confirming that *N*-acetylation does cause considerable deshielding.

The hypothesis that indole alkaloids are derived in part from tryptophan is generally accepted (8*a*, *b*). Thus an alkaloid of structure **6** or **7** could be derived either from a suitably oxygenated tryptophan and acetone, or by methylation of a suitable tetrahydroharmol precursor. Acetone or its biological equivalent is not a common biosynthetic building block and we suspected that the compound might be an artifact formed during the isolation. Tryptamines with a C-6 oxygen substituent have been shown to condense readily with acetone under mild conditions to form ring closed condensation products (7). To determine whether or not the acetylated compound was an artifact, *S. canadensis* was extracted with acetone-free methanol. Examination (chromatography, mass spectrometry) of the crude basic extract after acetylation showed no trace of the *gem*-dimethyl compound. Structure **6** is thus suggested on this basis. The precursor which gives rise to **6**, assumed to be 6-hydroxytryptamine, was not isolated.

The last acetylated alkaloid characterized shows an indole chromophore in the u.v. as well as indolic N—H and ester and amide carbonyl in the i.r. The n.m.r. spectrum shows indolic N—H, an ABX system of aromatic protons, an aromatic proton alpha to the indole N—H, an AA′BB′ system of methylene protons, an amide N—H (τ 6.77), and two acetyl groups. The molecular formula $C_{14}H_{16}N_2O_3$ (M^+ 260) was established by high resolution mass spectrometry. The evidence presented is consistent with either structure **10** or **11**.

Serotonin creatinine sulfate was acetylated and creatinine was removed. *N,O*-Diacetylserotonin

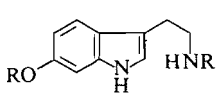

10 R = $COCH_3$

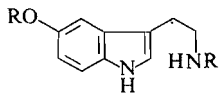

11 R = $COCH_3$
12 R = H

thus formed has an i.r. spectrum superimposable on the i.r. spectrum of the acetylated naturally occurring compound. Thus the acetylated alkaloid has structure **11**. It is assumed that this is present in the plant as serotonin (**12**).

It is interesting to note that spin–spin decoupling experiments with **11** reveal a small coupling between indolic N—H and H-4. To the best of our knowledge, this type of coupling has not previously been reported for indoles.

Both the harmala alkaloids and tryptamines show psychotomimetic activity (*9a*, *b*). Whether this property stimulated the use of these plants in folk medicine is a matter for conjecture. It is also of interest to note that various synthetic ethers of harmol find use in treatment of amebic dysentery (10).

Experimental

Optical rotatory dispersion (o.r.d.) spectra were measured in methanol using a Jasco Optical Rotatory Dispersion Recorder model ORD/UV-5.

The u.v. spectra were measured in 95% ethanol, unless otherwise specified, using a Perkin–Elmer Ultraviolet Spectrophotometer model 202 or a Jasco Optical Rotatory Dispersion Recorder model ORD/UV-5.

The i.r. spectra were measured in chloroform solution, unless otherwise specified, using a Perkin–Elmer model 337 grating i.r. spectrophotometer.

The n.m.r. spectra were measured in deuteriochloroform, unless otherwise specified, using a Varian Associates model HR-100 spectrophotometer with tetramethylsilane as internal standard.

Mass spectra were recorded on an A.E.I. model MS-9 mass spectrometer.

Melting points were determined on a hot-stage Leitz melting point apparatus or a hot-stage Fisher–Johns melting point apparatus and are uncorrected.

Plant Materials

Shepherdia argentea was collected from the Lethbridge area by A. Johnston and from the University of Alberta Experimental Farm by R. H. Knowles.

Shepherdia canadensis was collected near the North Saskatchewan river in the Edmonton area and was identified by R. G. H. Cormack, Department of Botany, University of Alberta.

Extraction and Isolation of the Crude Bases of Shepherdia argentea

The bark of the roots (880 g) of *Shepherdia argentea* was ground, air dried, and extracted with 5% aqueous methanol in a Soxhlet extractor. Excess methanol was removed *in vacuo*, water added, then traces of methanol removed *in vacuo*. Five percent aqueous hydrochloric acid was added until the p*H* was less than 5 and the insoluble material filtered and discarded. The acidic and neutral components were removed from the filtrate by ether extraction. The acidic solution was basified with aqueous ammonia to p*H* 10 and the resultant precipitate filtered. The basic filtrate was continuously extracted with ether for 48 h. The ether extract was dried (anhydrous magnesium sulfate) and excess solvent removed *in vacuo* to give 1.7 g crude bases (0.2%). Further purification of the crude alkaloidal material was achieved by a second acid–base extraction.

Acetylations

The base(s) were dissolved in one part pyridine, two parts acetic anhydride added, and the reaction mixture allowed to stand at room temperature at least 12 h. Excess solvents were removed by azeotropic distillation with toluene *in vacuo*.

Isolation of Acetylated Bases of Shepherdia argentea

Crude acetylated bases were separated by elution chromatography on Woelm alumina, activity 3. Two fractions were obtained: (*1*) non-polar bases, eluted with benzene–chloroform, 10:1 (36%); (*2*) *N,O*-diacetyltetrahydroharmol, eluted with benzene–chloroform, 5:1 (24%).

N,O-Diacetyltetrahydroharmol (1)

Compound **1** was isolated by elution chromatography on deactivated alumina with benzene–chloroform (5:1). Compound **1** crystallizes from ethyl acetate, m.p. 202°. The u.v. spectrum: λ_{max} 229 (ε = 21 000) and 282 mμ (ε = 3500). The i.r. spectrum: ν_{max} 3450, 3300, 1745, 1625 cm^{-1}. The n.m.r. spectrum: τ 1.07, singlet (N—*H*); 2.72, doublet, *J* = 8 c.p.s. (H-5); 3.01, doublet *J* = 2 c.p.s. (H-8); 3.26, doublet of doublets, *J* = 2, 8 c.p.s. (H-6); 4.35, quartet, *J* = 7 c.p.s. (H-1); 6.08, multiplet (H-3e); 6.65, multiplet (H-3a); 7.34, multiplet (H-4e,4a); 7.73, singlet (N—CO—CH_3); 7.82, singlet (O—CO—CH_3); 8.66, doublet, *J* = 7 c.p.s. (C_1—CH_3). Assignments have been verified by spin–spin decoupling experiments. Mass spectrum: *m/e* 286 ($C_{16}H_{18}N_2O_3$; found 286.1317, calculated 286.1317), 271, 244, 229 (base), 201, 187. The o.r.d. spectrum: no rotation.

Tetrahydroharmol (3)

Compound **3** was isolated by elution chromatography of the crude bases of *S. argentea* on deactivated alumina using chloroform–methanol (20:1). Compound **3** thus obtained melted at 254–255°; reported 256° (4). The u.v. spectrum: λ_{max} 229 (log ε = 4.57), 270 (log ε = 3.77), and 299 mμ (log ε = 3.85). The i.r. spectrum: ν_{max}(Nujol) 3380, 3265, 3245, 1620, 1560 cm^{-1}. Mass spectrum: *m/e* 202 ($C_{12}H_{14}N_2O$; found 202.1104, calculated 202.1106), 187 (base), 172, 159.

Tetrahydroharmol was dissolved in a minimum amount of hot methanol and methanolic HCl added until the solution was acidic. Excess solvent was removed. Tetrahydroharmol hydrochloride crystallizes from methanol–ether, m.p. 230° (dec.), reported 235° (4). Several months later, the same sample of tetrahydroharmol hydrochloride melted at 235° without decomposition.

Can. J. Chem. Downloaded from www.nrcresearchpress.com by 210.87.254.42 on 09/05/12
For personal use only.

Can. J. Chem. Downloaded from www.nrcresearchpress.com by 210.87.254.42 on 09/05/12
For personal use only.

Isolation of Non-polar Bases of Shepherdia argentea by Gas Chromatography

The non-polar acetylated bases separated by gas chromatography (g.c.) (Aerograph Manual Temperature Programmed Gas Chromatograph model A-90-P3, equipped with a thermal conductivity detector, 10′ × 1/4″, 5% SE-30 column, column temperature 205°, flow rate (He) 20 ml/min) are shown in Table 1. Apparent molecular formulas as determined by mass spectrometry are given in parentheses.

The compounds with retention time of 6.5 and 23.3 min were identified as *N*-acetylpyrrolidine and *N*-acetyl-*p*-anisidine, respectively, by comparison (g.c., mass spectra) with authentic samples.

Extraction and Isolation of Crude Bases of Shepherdia canadensis

The bark of roots (610 g) was extracted by the procedure reported for *S. argentea*, yielding 2.2 g crude bases (0.36%). The crude bases were acetylated in the usual manner and chromatographed over Woelm alumina, activity 3. Four major fractions were isolated, as shown in Table 2.

7-Acetoxy-2-acetyl-1,1-dimethyl-1,2,3,4-tetrahydro-2-carboline (6)

Compound **6** was isolated by elution chromatography over deactivated alumina using benzene. Compound **6** crystallizes from methanol, m.p. 212–214°. The u.v. spectrum: λ_{max} 227, (ε = 10 300) and 291 mμ, (ε = 2000). The i.r. spectrum: ν_{max} 3455, 3300, 1750, 1640 cm^{-1}. The n.m.r. spectrum: τ 1.58, singlet (N—*H*); 2.60, doublet, *J* = 8 c.p.s. (H-5); 2.94, doublet, *J* = 2 c.p.s. (H-8); 3.20, doublet of doublets, *J* = 2, 8 c.p.s. (H-6); 6.36, triplet (H-3e,3a); 7.22, triplet (H-4e,4a); 7.68, singlet (N—CO—CH_3); 7.75, singlet (OCOCH_3); 8.16, singlet (C(CH_3)$_2$).

TABLE 1

Gas chromatogram of acetylated non-polar bases

Retention time (min)	Molecular ion (*m/e*)
6.5	113 ($C_6H_{11}NO$)
8.8	157 ($C_8H_{15}NO_2$)
9.5	—
10.6	—
16.0	163 ($C_{10}H_{13}NO$)
23.3	165 ($C_9H_{11}NO_2$)

TABLE 2

Chromatogram of acetylated bases

Fraction	Eluent	Contents
1	Benzene	Simple acetylated bases
2	Benzene	Artifact of extraction
3	Benzene–chloroform (5:1)	*N,O*-Diacetyltetrahydroharmol (35%); *N,O*-diacetylshepherdine
4	Chloroform–methanol (100:1)	*N,O*-Diacetylserotonin (17%)

Assignments have been verified by spin–spin decoupling experiments. Mass spectrum: *m/e* 300 ($C_{17}H_{20}N_2O_3$; measured 300.1475, calculated 300.1474), 285, 258, 243 (base), 201, 200.

Synthesis of 2-Acetyl-1,1-dimethyl-1,2,3,4-tetrahydro-2-carboline (9) (7)

Tryptamine (0.9 g), acetone (3.5 ml), and *p*-toluenesulfonic acid (catalytic amount) in anhydrous benzene (30 ml) were refluxed under nitrogen for 3.5 h with azeotropic distillation of water. The solution was cooled, filtered over anhydrous potassium carbonate, and excess solvent removed *in vacuo*. The residue was suspended in anhydrous benzene and freshly distilled phosphorus oxychloride (2.5 ml) added. The mixture was allowed to stand at room temperature 1 h, then refluxed 1 h. Excess solvent was removed *in vacuo* under nitrogen. The residue was heated briefly with water (30 ml), filtered, decolorized with Norit, basified (p*H* 9) with ammonia, then extracted with ether. The ether fraction was dried (anhydrous magnesium sulfate) and excess solvent removed *in vacuo* to give 1,1-dimethyl-1,2,3,4-tetrahydro-2-carboline (**8**). Compound **8** was purified by elution chromatography on Woelm alumina, activity 3. Compound **8** crystallizes from benzene, m.p. 94–96°, reported 111.5–115.5° (7). The n.m.r. spectrum: τ 2.20 singlet (N—*H*); 2.90, multiplet (4 Ar—*H*); 6.80, triplet (H-3e,3a); 7.30, triplet (H-4e,4a); 8.00, singlet (N—*H*); 8.54, singlet (C—(CH_3)$_2$).

Compound **8** was acetylated in the usual manner giving **9** which crystallizes from acetone–water, m.p. 228–229°. The n.m.r. spectrum: τ 1.67, singlet (N—*H*); 2.72, multiplet (4 Ar—*H*); 6.30, triplet (H-3e,3a); 7.16, triplet (H-4e,4a); 7.70, singlet (NCOCH_3); 8.09, singlet (C—(CH_3)$_2$).

Extraction and Isolation of Bases of Shepherdia canadensis Using Reagent Methanol

Dried, ground roots (710 g) of *S. canadensis* were extracted with reagent methanol (free from acetone) in a Soxhlet extractor. Excess solvent was removed *in vacuo*, water added, and traces of methanol removed. The aqueous extract was acidified (p*H* 3) with 5% aqueous hydrochloric acid, then extracted with ether to remove neutral and acidic material. The aqueous acidic fraction was basified (p*H* 9) with sodium carbonate, the precipitate filtered, and the filtrate continuously extracted with ether for 48 h. The ether fraction was dried (anhydrous magnesium sulfate) and excess solvent removed *in vacuo* yielding crude bases (3.3 g). The crude bases (1.3 g) isolated by extraction of *S. canadensis* with reagent methanol were acetylated in the usual manner yielding crude acetylated bases (2.1 g). Mass spectrum: *m/e* 286, 260, 229, 175. The mass spectrum of the crude acetylated bases obtained using technical grade methanol showed an additional peak at *m/e* 300. Elution chromatography of the crude acetylated bases on Woelm alumina, activity 3, showed no trace of compound **6**.

Isolation of N,O-Diacetyltetrahydroharmol from Shepherdia canadensis

N,O-diacetyltetrahydroharmol was isolated by elution chromatography of the crude acetylated bases of *S. canadensis* on deactivated alumina using benzene–chloro-

Can. J. Chem. Downloaded from www.nrcresearchpress.com by 210.87.254.42 on 09/05/12
For personal use only.

form (5:1). It was separated from *N,O*-diacetylshepherdine by fractional crystallization from methanol. It has a melting point 202° and its spectral properties are identical with those reported for compound **1**.

Synthesis of N,O-Diacetyltetrahydroharmol (1) (4)

Sodium (1.5 g) was added to a refluxing solution of harmol (0.1 g) (Aldrich Chemical Co.) in anhydrous ethanol under a nitrogen atmosphere. When all the sodium was dissolved, the solution was acidified (aqueous HCl), the precipitate filtered and washed with ethanol. The ethanol washings and filtrate were combined and excess solvent removed *in vacuo*. The crude residue was dissolved in water, the solution basified with aqueous ammonia, then extracted with ether. The ether was dried (anhydrous magnesium sulfate), then removed *in vacuo* to give tetrahydroharmol (**3**). Tetrahydroharmol was acetylated in the usual manner and the crude acetate purified by elution chromatography over Woelm alumina, activity 3. *N,O*-Diacetyltetrahydroharmol crystallizes from ethyl acetate, m.p. 202°. Its spectral properties are identical with those of the naturally occurring alkaloid.

N,O-Diacetylshepherdine (2)

N,O-diacetylshepherdine was isolated by elution chromatography of the crude acetylated bases of *S. canadensis* on deactivated alumina using benzene–chloroform (5:1). It was separated from *N,O*-diacetyltetrahydroharmol by fractional crystallization from methanol. It crystallizes from methanol, m.p. 192–194° and gives a depressed mixed melting point with *N,O*-diacetyltetrahydroharmol, m.p. 165–175°. The u.v. spectrum: λ_{max} 226 (ε = 31 400) and 281 mμ (ε = 6300). The i.r. spectrum: ν_{max} 3450, 3275, 1745, 1630 cm^{-1}. The n.m.r. spectrum: τ 1.14, singlet (N—*H*); 2.80, doublet, J = 8 c.p.s. (H-8); 2.92, doublet, J = 1 c.p.s. (H-5); 3.22, doublet of doublets, J = 1, 8 c.p.s. (H-7); 4.30, quartet, J = 6 c.p.s. (H-1); 6.07, multiplet (H-3e); 6.64, multiplet (H-3a); 7.34, multiplet (H-4e,4a); 7.71, singlet (NCOC*H*$_3$); 7.80, singlet (OCOC*H*$_3$); 8.62, doublet, J = 6 c.p.s. (C—C*H*$_3$). Assignments have been verified by spin–spin decoupling experiments. Mass spectrum: 286 (base) ($C_{16}H_{18}N_2O_3$; found 286.1317, calculated 286.1317), 271, 244, 229, 201, 187.

Synthesis of N,O-Diacetylshepherdine (2) (6)

5-Benzyloxytryptamine (0.1 g) (Aldrich Chemical Co.), 2 *N* sulfuric acid (5 drops), dioxane (1 ml), and water (1 ml) were cooled under nitrogen and freshly prepared 10% aqueous acetaldehyde (2 ml) added. The mixture was allowed to stand at room temperature. After 0.5 h, a crystalline precipitate formed which was collected and acetylated in the usual manner to give 2-acetyl-6-benzyloxy-1-methyl-1,2,3,4-tetrahydro-2-carboline. It crystallizes from acetone–methanol, m.p. 179.5–181°. The crystalline compound (0.4 g) and 30% palladium–charcoal (catalytic amount) in reagent methanol (15 ml) were hydrogenated at room temperature and atmospheric pressure for 4 h, i.e., until starting material had all reacted (t.l.c.). The solution was filtered, excess solvent removed *in vacuo* and the crude residue acetylated in the usual way. The crude acetyl derivative was purified by elution chromatography on Woelm alumina, activity 3, to give **2** which crystallizes from methanol, m.p. 192–194°. Its melting point, mixed melting point, and i.r. spectrum are identical with those of the naturally occurring *N,O*-diacetylshepherdine.

N,O-Diacetylserotonin (11)

N,O-Diacetylserotonin was isolated by elution chromatography of the crude acetylated bases of *S. canadensis* over deactivated alumina using chloroform. *N,O*-Diacetylserotonin could not be crystallized. The u.v. spectrum: λ_{max} 224 (ε = 27 000) and 287 mμ (ε = 5500). The i.r. spectrum: ν_{max} 3500, 3325, 1750, 1675 cm^{-1}. The n.m.r. spectrum: τ acetone-d_6 −0.20, singlet (N—*H*); 2.68, doublet, J = 8 c.p.s. (H-7); 2.75, doublet, J = 2 c.p.s. (H-4); 2.86, singlet (H-1); 3.21, doublet of doublets, J = 2, 8 c.p.s. (H-6); 6.58, multiplet (H-2′e,2′a); 6.77, broad singlet (N*H*COCH$_3$); 7.15, triplet (H-1′e,1′a); 7.79, singlet (NCOC*H*$_3$); 8.15, singlet (OCOC*H*$_3$). Assignments made have been verified by spin–spin decoupling experiments. In addition, irradiation at 1020 c.p.s. causes sharpening of signals at τ 2.75 and 2.86 indicating a small W coupling between the indole N—H and H-4, and a small coupling between indole N—H and H-1. Irradiation at 716 c.p.s. causes sharpening of the signal at τ 3.21 showing a small para coupling between H-4 and H-7. Mass spectrum: *m/e* 260 ($C_{14}H_{16}N_2O_3$; found 260.1158, calculated 260.1161), 201, 188, 159, 146.

Synthesis of N,O-Diacetylserotonin (11)

Serotonin creatinine sulfate (Aldrich Chemical Co.) (9.1 g) was acetylated in the usual manner. Creatinine was removed by addition of acetone and filtering the precipitate. Excess acetone was removed *in vacuo* and crude **11** purified by elution chromatography on Woelm alumina. *N,O*-Diacetylserotonin has an i.r. spectrum identical with that of the naturally occurring compound.

We wish to thank A. Johnston and R. H. Knowles for supplying *Shepherdia argentea* and the National Research Council of Canada for financial support. We also wish to thank Dr. A. N. Hogg and Messrs. R. N. Swindlehurst and G. Bigam for their help in various phases of this work.

1. M. Oka. Alberta Hist. Rev. **3**, 14 (1955).
2. A. Johnston. Alberta Hist. Rev. **8**, 11 (1960).
3. A. I. Scott. *In* Interpretation of the ultraviolet spectra of natural products. The MacMillan Co., New York, 1964.
4. T. F. Platanova, A. D. Kuzovkov, and P. S. Massagetov. J. Gen. Chem. USSR **26**, 2553 (1956).
5. A. K. Kiang, K. C. Chan, and W. I. Taylor. Lloydia, **30**, 189 (1967).
6. B. Meek, S. S. Szinai, and D. Wallis. Chem. Ind. 622 (1964).
7. J. B. Hester, Jr. J. Org. Chem. **29**, 2864 (1964).
8. (*a*) E. Leete. *In* Biosynthesis of natural products. *Edited by* P. Bernfeld. Pergamon Press, Oxford, 1963. p. 768. (*b*) D. G. O'Donovan and M. F. Kenneally. J. Chem. Soc. (*C*), 1109 (1967).
9. (*a*) C. Naranjo. *In* Ethnopharmacologic search for psychoactive drugs. *Edited by* D. H. Efron. U.S. Public Health Serv. Publ. #1645 (1967). pp. 385. (*b*) B. Holmstedt and J. Lindgren. *In* Ethnopharmacologic search for psychoactive drugs. *Edited by* D. H. Efron. U.S. Public Health Serv. Publ. #1645 (1967). p. 339.
10. C. E. Coulthard. Biochem. J. **28**, 264 (1934).

Can. J. Chem. Downloaded from www.nrcresearchpress.com by 210.87.254.42 on 09/05/12
For personal use only.

2-D-Hydroxyhexadecanoic acid: a metabolic product of the yeast *Hansenula sydowiorum*

R. F. VESONDER, F. H. STODOLA, W. K. ROHWEDDER, AND D. B. SCOTT[1]

Northern Regional Research Laboratory, Agricultural Research Service, United States Department of Agriculture, Peoria, Illinois 61604

Received December 4, 1969

A new species of yeast, *Hansenula sydowiorum*, excreted free α-hydroxy fatty acids when grown on glucose solution. The major component, 2-D-hydroxyhexadecanoic acid, was identified by the mass spectrum of its methyl ester.

Canadian Journal of Chemistry, 48, 1985 (1970)

The occurrence of α-hydroxy fatty acids in plants, animals, yeasts, molds, and bacteria was reviewed by Downing (1) in 1961. Since that time additional reports have appeared on the isolation of these acids from the microorganisms *Claviceps purpurea* (2), *Rhodomicrobium vannielii* (3), a strain of *Streptomyces* (4), and *Streptomyces sioyaensis* (5). These higher α-hydroxy acids always occur as constituents of more complex molecules, usually in the form of esters and amides (6).

We recently observed that free α-hydroxy acids are formed by a new species of yeast, *Hansenula sydowiorum*, isolated (7) in South Africa from the insect *Sinoxylon ruficorne* Fahr., which we examined during our work on the extracellular lipids of yeasts (8). When grown for 12 days on a malt-glucose medium, the bisexual form of this organism produced 1.66 g/l of crude acid, 80% of which was 2-D-hydroxyhexadecanoic acid. The unisexual form secreted only one-half this amount of acid into the culture medium.

The crude acid mixture, obtained by ether extraction of the culture liquor, was converted to methyl esters with diazomethane. Preparative gas–liquid chromatography (g.l.c.) yielded as the main component methyl 2-hydroxyhexadecanoate (m.p. 45–45.5 °C, lit. (9), 45.5–45.7 °C); its levorotation in chloroform (−5.8°; *c*, 6.4) shows the free acid to have the D-configuration, as do all known naturally occurring 2-hydroxy acids. Our value for the rotation of this ester is intermediate between that of Hitchcock *et al.* (10) (−8.0°; *c*, 2.5, $CHCl_3$) and that of Horn *et al.* (9) (−3.6°; *c*, 10, $CHCl_3$), showing the dependence of the value on concentration. Baer and Mahadevan (11) reported a similar effect for 1,2-diglycerides in chlorinated solvents.

The structure of the methyl ester was established by showing the identity of its mass spectrum with that of methyl 2-DL-hydroxyhexadecanoate. Saponification of the pure ester gave 2-D-hydroxyhexadecanoic acid; m.p. 91–92 °C, lit. (9), 93.3–93.5 °C; $[\alpha]_D^{24}$ +4.6 (*c*, 6.1, pyridine), lit. (9), +3.6° (*c*, 6, pyridine). The *p*-bromophenacyl ester melted at 87.5–88 °C.

Experimental

Melting points were determined with a Fisher–Johns[2] apparatus and were not corrected. Mass spectra were recorded on a Nuclide instrument (model 12-90 G). Gas chromatographic analyses were carried out in an F and M laboratory chromatograph (model 700) equipped with a flame ionization detector. The column (4 ft × 1/4 in. o.d. aluminum) was packed with 20% silicone OV-17 on Chromosorb W-HMDS. Temperature was maintained at 300 °C and helium flow was 50 ml/min. Preparative g.l.c. was carried out in an Aerograph Autoprep (model A-700) equipped with a thermoconductivity detector. The column (6 ft × 1/4 in. stainless steel) was packed with 5% Apiezon L on Chromosorb W-AWDMCS. The temperature was maintained at 200 °C.

Production of Crude Acid

Stock cultures of the yeasts [NRRL Y-7128 (unisexual) and NRRL Y-7130 (bisexual) from the ARS Culture Collection here] were maintained at 25 °C on YM agar slants (1% glucose, 0.5% peptone, 0.3% yeast extract, 0.3% malt extract, and 2% agar). A sterilized liquid medium (200 ml), consisting of 5% commercial glucose hydrate and 5% malt extract contained in 500 ml Erlenmeyer flasks, was inoculated with 0.1 ml of a cell suspension prepared from a 1 day old YM slant culture and 2 ml of YM broth. The flasks were incubated at 25 °C on a Gump shaker (180 r.p.m.; 1 in. radius).

[1]Microbiology Research Group, Council for Scientific and Industrial Research, P.O. Box 395, Pretoria, South Africa.

[2]The mention of firm names or trade products does not imply that they are endorsed or recommended by the Department of Agriculture over other firms or similar products not mentioned.

TABLE 1

Lipid formation by *Hansenula sydowiorum*

Days	Yield of crude lipid in mg/l	
	Y-7128 Unisexual	Y-7130 Bisexual
3	550	550
5	675	1000
8	840	1345
12	—	1665
14	575	1300

At intervals the contents of 24 flasks were extracted separately with ether. Yields of crude acid for the unisexual and bisexual yeasts are recorded in Table 1.

Methyl 2-D-Hydroxyhexadecanoate

A composite of crude acid (2.00 g) was esterified with diazomethane. The resulting ester was shown by mass spectral and g.l.c. analyses to consist of 80% methyl 2-hydroxyhexadecanoate, the remainder being C_{15}, C_{17}, and C_{18} homologs. A portion of the crude ester (110 mg, m.p. 41–42.5 °C), subjected to preparative g.l.c., yielded 62.0 mg (m.p. 44.5–45 °C) of the main component, which was crystallized from hexane (m.p. 45–45.5 °C), $[\alpha]_D^{24}$ −5.8° (*c*, 6.4, $CHCl_3$); lit. (9), m.p. 45.5–45.7 °C, $[\alpha]_D$ −3.6° (*c*, 10, $CHCl_3$).

Anal. Calcd. for $C_{17}H_{34}O_3$: C, 71.28; H, 11.96. Found: C, 71.7; H, 12.1.

p-Bromophenacyl 2-D-Hydroxyhexadecanoate

Methyl ester (55 mg), refluxed for 1 h with alcoholic KOH, gave 50 mg of crude hydroxy acid (m.p. 89–92 °C). Crystallization from hexane yielded 23 mg of acid, which was converted to the *p*-bromophenacyl derivative by the DICE procedure (12). The crude product (38 mg, m.p. 77–83 °C) on crystallization from 95% alcohol gave 22 mg of pure *p*-bromophenacyl ester (m.p. 87.5–88 °C).

Anal. Calcd. for $C_{24}H_{37}O_4Br$: C, 61.40; H, 7.94. Found: C, 61.6; H, 8.1.

A second portion of crude ester (500 mg) gave a larger sample of pure 2-D-hydroxyhexadecanoic acid, which melted at 91–92 °C; $[\alpha]_D^{24}$ of +4.6° (*c*, 6.1, pyridine).

1. D. T. Downing. Rev. Pure Appl. Chem. **11**, 196 (1961).
2. J. W. ApSimon, A. J. Hannaford, and W. B. Whalley. J. Chem. Soc. 4164 (1965).
3. C. Park and L. R. Berger. J. Bacteriol. **93**, 230 (1967).
4. M. A. Lanéelle. Exper. **24**, 541 (1968).
5. J. Kawanami, A. Kimura, Y. Nakagawa, and H. Otsuka. Chem. Phys. Lipids, **3**, 29 (1969).
6. N. S. Radin. J. Amer. Oil Chem. Soc. **42**, 569 (1965).
7. D. B. Scott and G. P. van der Walt. Antonie van Leeuwenhoek. In press.
8. F. H. Stodola, M. H. Deinema, and J. F. T. Spencer. Bacteriol. Rev. **31**, 194 (1967).
9. D. H. S. Horn, F. W. Hougen, E. von Rudloff, and D. A. Sutton. J. Chem. Soc. 177 (1954).
10. C. Hitchcock, L. J. Morris, and A. T. James. Eur. J. Biochem. **3**, 473 (1968).
11. E. Baer and V. Mahadevan. J. Amer. Chem. Soc. **81**, 2494 (1959).
12. F. H. Stodola. Microchem. J. **7**, 389 (1963).

Can. J. Chem. Downloaded from www.nrcresearchpress.com by 210.87.254.42 on 09/05/12
For personal use only.

Can. J. Chem. Downloaded from www.nrcresearchpress.com by 210.87.254.105 on 09/05/12
For personal use only.

Reaction of dialkyl phosphonates with hexafluoroacetone

A. F. JANZEN AND R. POLLITT
Department of Chemistry, University of Manitoba, Winnipeg, Manitoba

Received January 26, 1970

The reaction of dialkyl phosphonates, $(RO)_2P(O)H$ where R = CH_3, C_2H_5, and n-C_4H_9, with hexafluoroacetone gives, in each case, two isomeric products, $(RO)_2P(O)OCH(CF_3)_2$ and $(RO)_2P(O)C(OH)(CF_3)_2$. Products are characterized by elemental analyses, infrared, proton and fluorine nuclear magnetic resonance, and mass spectrometry. The relative yield of isomer depends markedly on the alkyl group present. These results are explained in terms of an inductive effect on the polarity of the P—H bond which influences the direction of addition of hexafluoroacetone.

Canadian Journal of Chemistry, 48, 1987 (1970)

The reactions of dialkyl phosphonates, $(RO)_2P(O)H$, with ketones, aldehydes and olefins have been studied for a number of years (1). However, reactions with halogenated ketones have been reported only recently. With hexafluoroacetone, hexafluoroisopropyldialkyl phosphates were formed (2) (cf. isomer A) whereas with chlorofluoroacetones the isolated products were vinyl esters of phosphorus acids (3). Phospholanes containing the grouping $\overline{POC(CF_3)_2C(CF_3)_2O}$ (4) may be converted into phosphinate esters, $R_2P(O)OCH(CF_3)_2$ (5), and addition of hexafluoroacetone and secondary phosphines followed by air oxidation is also reported to give phosphinate esters (6).

We now report the reaction of hexafluoroacetone with dialkyl phosphonates, $(RO)_2P(O)H$ where R = CH_3, C_2H_5, and n-C_4H_9, and find that two isomeric products are formed in each case. Such isomer formation does not appear to have been studied previously.

The reaction of dialkyl phosphonates and hexafluoroacetone under mild conditions (25° or lower, absence of solvent) results in the formation of 1:1 adducts for which several structures are possible, the most likely being isomers A, B, or C.

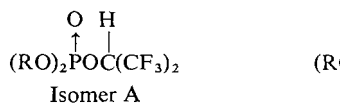

Isomer A

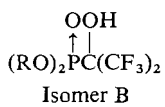

Isomer B

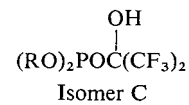

Isomer C

For those dialkyl phosphonates used in this investigation both isomers A and B were formed although the relative yield depended markedly on the alkyl group present. The products are shown in Table 1. Yields of isomers are based on peak areas in the ^{19}F nuclear magnetic resonance (n.m.r.) spectra determined shortly after preparation.

TABLE 1

Products from reaction of dialkyl phosphonates and hexafluoroacetone

R	O H ↑ | $(RO)_2POC(CF_3)_2$ (%)	OOH ↑| $(RO)_2PC(CF_3)_2$ (%)
Methyl	94	6
Ethyl	88	12
n-Butyl	5	95

The products were characterized by elemental analyses, infrared (i.r.), ^1H and ^{19}F n.m.r. spectroscopy, and mass spectrometry. A summary of pertinent results and assignment of structures is found in Table 2.

The ^{19}F n.m.r. spectra of compounds **1**, **3**, and **5** (isomer A) show doublets (J = 6 Hz) at +75.0 ± 0.1 p.p.m. assigned to the six fluorines which couple with the single adjacent hydrogen. Coupling with phosphorus across four bonds appears negligible.

For compounds **2**, **4**, and **6** (isomer B) the ^{19}F n.m.r. spectra show doublets (J = 3 Hz) at +72.5 ± 0.4 p.p.m. assigned to the six fluorines which couple with the phosphorus atom.

The ^1H n.m.r. spectra of compounds **1** and **3** (isomer A) show a nine-line multiplet at about −5.5 p.p.m. assigned to the single hydrogen which couples with six fluorines and one phosphorus.[1] A typical ^1H n.m.r. spectrum of isomer

[1]R. F. Stockel (6) reports a septet for $R_2P(O)OCH(CF_3)_2$ where R = phenyl, cyclohexyl. We assume he did not observe the low intensity lines and hence did not report a doublet of septets.

TABLE 2

Elemental analyses and n.m.r. data

Compound	Analysis		^{19}F n.m.r. (p.p.m.)	^{1}H n.m.r.* (p.p.m.)
	Calculated	Found		
$(CH_3O)_2\overset{\uparrow}{P}O\overset{|}{C}(CF_3)_2$ (O H) **1**	C 21.75 H 2.56 F 41.29	C 21.96 H 2.50 F 41.55	Doublet (J=6 Hz) at +75.1	Nine-line multiplet at −5.43
$(CH_3O)_2\overset{\uparrow}{P}C(CF_3)_2$ (OOH) **2**			Doublet (J=3 Hz) at +72.3	Singlet at −8.00
$(C_2H_5O)_2\overset{\uparrow}{P}O\overset{|}{C}(CF_3)_2$ (O H) **3**	C 27.64 H 3.65 F 37.48	C 27.78 H 3.66 F 38.78	Doublet (J=6 Hz) at +74.9	Nine-line multiplet at −5.56
$(C_2H_5O)_2\overset{\uparrow}{P}C(CF_3)_2$ (OOH) **4**			Doublet (J=3 Hz) at +72.9	Singlet at −8.90
$(C_4H_9O)_2\overset{\uparrow}{P}O\overset{|}{C}(CF_3)_2$ (O H) **5**			Doublet (J=6 Hz) at +74.9	†
$(C_4H_9O)_2\overset{\uparrow}{P}C(CF_3)_2$ (OOH) **6**	C 36.67 H 5.32 F 31.65	C 36.30 H 5.24 F 31.86	Doublet (J=3 Hz) at +72.1	Singlet at −7.21

*Alkyl absorptions omitted.
†Too low concentration for accurate estimation.

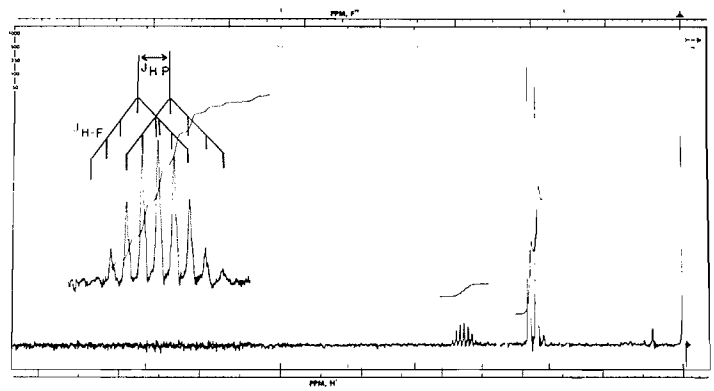

FIG. 1. ^{1}H n.m.r. spectrum of $(CH_3O)_2P(O)OCH(CF_3)_2$ (isomer A) showing doublet of septets due to single hydrogen and doublet due to methyl groups.

A, that of compound **1**, is reproduced in Fig. 1.

The ^{1}H n.m.r. spectra of compounds **2**, **4**, and **6** (isomer B) show singlets at about −7 to −9 p.p.m. assigned to the hydroxyl group.

Infrared spectroscopic examination proved useful in distinguishing between isomers. The i.r. spectrum of compound **1** (isomer A) is shown in Fig. 2 and that of compound **6** (isomer B) in Fig. 3.

The mass spectrum of compound **1** showed strong peaks (M = molecular ion) at *m/e* 276(M), 257(M—F), 256(M—HF), 246(M—CH_2O), 237-(M—HF_2), 226(M—CF_2), 225(M—CF_2H), 110-(M—C_2F_6O), 109(M—C_2F_6HO).

Can. J. Chem. Downloaded from www.nrcresearchpress.com by 210.87.254.105 on 09/05/12
For personal use only.

Can. J. Chem. Downloaded from www.nrcresearchpress.com by 210.87.254.105 on 09/05/12
For personal use only.

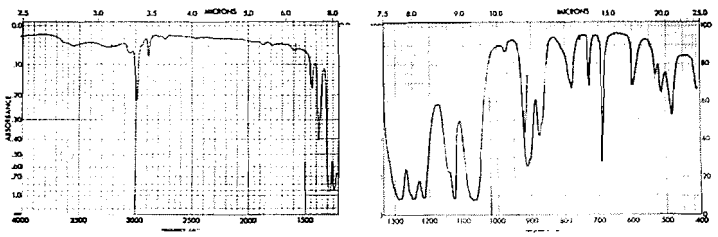

FIG. 2. Infrared spectrum of $(CH_3O)_2P(O)OCH(CF_3)_2$ (isomer A). Recorded as neat film.

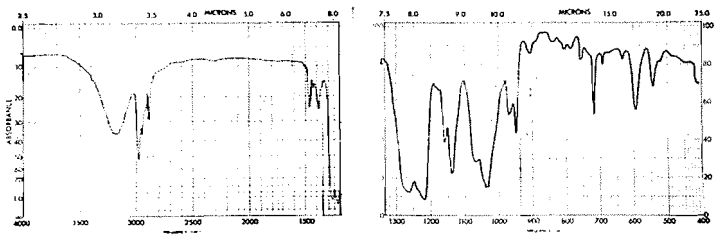

FIG. 3. Infrared spectrum of $(C_4H_9O)_2P(O)C(OH)(CF_3)_2$ (isomer B). Recorded as neat film.

For compound **6** the most intense peak occurred at *m/e* 249(M—C_8H_{15}) assigned to the ion $(HO)_3\overset{+}{P}C(OH)(CF_3)_2$. The parent molecular ion was not observed, but low intensity peaks were found at *m/e* 304(M—C_4H_8), 275(M—C_6H_{13}), 263(M—C_7H_{13}), 261(M—C_7H_{15}), 229(M—$C_8H_{16}F$).

To account for the formation of isomers A and B we assume that hexafluoroacetone adds across a P—H bond of the dialkyl phosphonate and that the direction of addition may be varied (eqs. [1] and [2]).

$$[1]\quad \begin{array}{c} O \\ \uparrow \\ (RO)_2P\text{—}H \\ O{=}C(CF_3)_2 \end{array} \rightarrow \underset{\text{Isomer A}}{\begin{array}{c} O \quad\quad H \\ \uparrow \quad\quad\ \ | \\ (RO)_2P\text{—}O\text{—}C(CF_3)_2 \end{array}}$$

$$[2]\quad \begin{array}{c} O \\ \uparrow \\ (RO)_2P\text{—}H \\ (CF_3)_2C{=}O \end{array} \rightarrow \underset{\text{Isomer B}}{\begin{array}{c} O \quad OH \\ \uparrow \quad\ \ | \\ (RO)_2P\text{—}C(CF_3)_2 \end{array}}$$

As seen from Table 1 isomer A is produced in greater yield if R = CH_3 or C_2H_5 whereas isomer B is the major product if R = C_4H_9. The differences may be explained in terms of an inductive effect of the alkyl groups on the polarity of the P—H bond. The polarization in the sense $^{+\delta}P\text{—}H^{\delta-}$ should decrease in the order $CH_3O > C_2H_5O > C_4H_9O$ since the inductive effect of alkyl groups decreases in the order $C_4H_9 > C_2H_5 > CH_3$. For dibutyl phosphonate the polarization may therefore be in the opposite direction i.e. $^{-\delta}P\text{—}H^{\delta+}$.

Support for the above suggestion comes from similar reactions of hexafluoroacetone and perfluorocyclobutanone with compounds containing metalloid–hydrogen bonds. For example, the B—H bond reacts with perfluorocyclobutanone (7) and the Si—H (8, 9), Ge—H, and Sn—H (9) bonds react with hexafluoroacetone to give alkoxides containing the grouping $M\text{—}O\text{—}\overset{\overset{H}{|}}{C}$. These reactions are seen to be analogous to the formation of isomer A and the polarization of the metalloid–hydrogen bond is generally assumed to be $^{+\delta}M\text{—}H^{\delta-}$.

On the other hand, hexafluoroacetone reacts with C—H, N—H, P—H, As—H, O—H, and S—H bonds to give alcohols (10) containing the grouping $M\text{—}\overset{\overset{OH}{|}}{C}$. These reactions are analogous to the formation of isomer B and the polarization of the metalloid–hydrogen bonds in these compounds is generally assumed to be $^{-\delta}M\text{—}H^{\delta+}$.

Experimental

General

Conventional vacuum line techniques were used for handling volatile materials. Hexafluoroacetone (Matheson of Canada) and the dialkyl phosphonates (Eastman

Organic Chemicals) were purified by trap-to-trap distillation before use. Microanalyses were performed by Galbraith Laboratories, Knoxville. The i.r. spectra were recorded with a Perkin-Elmer 337 spectrophotometer and n.m.r. spectra were obtained on a Varian A-56/60A spectrometer, using 60 MHz and 56.4 MHz for proton and fluorine respectively. ^1H and ^{19}F chemical shifts are relative to internal tetramethylsilane and internal trichlorofluoromethane respectively. Mass spectra were determined on a Hitachi Perkin–Elmer RMU-6D mass spectrometer.

Reaction of Dimethyl Phosphonate with Hexafluoroacetone

Dimethyl phosphonate (1.08 g, 9.83 mmole) and a slight excess of hexafluoroacetone (1.71 g, 10.3 mmole) were sealed in a previously evacuated reaction tube. The reaction mixture at −78° was slowly warmed to 25° and shaken for 3 days. ^1H and ^{19}F n.m.r. spectroscopy showed that two products, **1** and **2**, were formed in ratio 94:6. Compound **1**, the more volatile product, was purified by trap-to-trap distillation and identified as 1,1,1,3,3,3-hexafluoroisopropyldimethyl phosphate, $(CH_3O)_2P(O)OCH(CF_3)_2$ (2.54 g, 9.20 mmole).

Compound **2**, prepared in small yield above, was not purified since it was difficult to remove last traces of compound **1**. It is identified as dimethyl 2-hydoxy-1, 1, 1, 3, 3, 3-hexafluoroisopropylphosphonate, $(CH_3O)_2P(O)C(OH)(CF_3)_2$, on the basis of its spectral properties and by comparison with the reaction of dibutyl phosphonate described below.

Elemental analyses, ^1H and ^{19}F n.m.r. data for compounds **1** to **6** are summarized in Table 2.

Reaction of Diethyl Phosphonate with Hexafluoroacetone

Diethyl phosphonate (1.17 g, 8.46 mmole) and hexafluoroacetone (2.34 g, 14.1 mmole) were reacted according to the method outlined for dimethyl phosphonate.

Two products **3** and **4** were formed in the ratio 88:12. Compound **3**, the more volatile product, was purified by trap-to-trap distillation and identified as 1,1,1,3,3,3-hexafluoroisopropyldiethyl phosphate, $(C_2H_5O)_2P(O)OCH(CF_3)_2$, (2.20 g, 7.25 mmole).

Compound **4** was identified as diethyl 2-hydroxy-1,1,1,3,3,3-hexafluoroisopropylphosphonate, $(C_2H_5O)_2P(O)C(OH)(CF_3)_2$, on the basis of its spectroscopic properties.

Reaction of Di-n-butyl Phosphonate with Hexafluoroacetone

Di-*n*-butyl phosphonate (2.11 g, 10.7 mmole) and hexafluoroacetone (2.56 g, 15.4 mmole) were reacted as above. Two products **5** and **6** were formed in the ratio 5:95. Compound **5**, produced in small yield, was identified as 1,1,1,3,3,3-hexafluoroisopropyldibutyl phosphate, $(C_4H_9O)_2P(O)OCH(CF_3)_2$, on the basis of its ^{19}F n.m.r. spectrum.

Compound **6**, the less volatile product, was purified by trap-to-trap distillation and identified as dibutyl 2-hydroxy-1, 1, 1, 3, 3, 3-hexafluoroisopropylphosphonate, $(C_4H_9O)_2P(O)C(OH)(CF_3)_2$ (3.75 g, 10.4 mmole). No decomposition or isomerization was evident after 6 months in a sealed tube.

The financial assistance of the National Research Council of Canada is gratefully acknowledged.

1. V. S. Abramov. Zh. Obshch. Khim. **22**, 647 (1952); and other papers by Abramov and co-workers. A. N. Pudovik. Zh. Obshch. Khim. **22**, 462 (1952).
2. S. Z. Ivin, V. K. Promonenkov, and E. A. Fokin. J. Gen. Chem. USSR, **37**, 2388 (1967).
3. S. Z. Ivin, V. K. Promonenkov, and E. A. Fokin. Zh. Obshch. Khim. **37**, 1642 (1967).
4. N. P. Gambaryan, Yu. A. Cheburkov, and I. L. Knunyants. Bull. Acad. Sci. USSR, **8**, 1433 (1964). F. Ramirez, C. P. Smith, J. F. Pilot, and A. S. Gulati. J. Org. Chem. **33**, 3787 (1968).
5. F. Ramirez, C. P. Smith, and J. F. Pilot. J. Amer. Chem. Soc. **90**, 6726 (1968).
6. R. F. Stockel. Chem. Commun. 1594 (1968).
7. G. W. Parshall. Inorg. Chem. **4**, 52 (1965).
8. A. F. Janzen and C. J. Willis. Can. J. Chem. **43**, 3063 (1965); Inorg. Chem. **6**, 1900 (1967).
9. W. R. Cullen and G. E. Styan. Inorg. Chem. **4**, 1437 (1965).
10. C. G. Krespan and W. J. Middleton. Fluorine Chem. Rev. Vol. 1. *Edited by* P. Tarrant. M. Dekker, New York, 1967. p. 145.

Can. J. Chem. Downloaded from www.nrcresearchpress.com by 210.87.254.105 on 09/05/12
For personal use only.

Can. J. Chem. Downloaded from www.nrcresearchpress.com by 210.87.254.105 on 09/05/12
For personal use only.

Studies on some 4,5-diacyl-1,3-dithioles

M. AHMED, J. M. BUCHSHRIBER, AND D. M. MCKINNON
Department of Chemistry, University of Manitoba, Winnipeg, Manitoba

Received December 12, 1969

1,2-Dithiole-3-thiones and 1,2,4-dithiazole-3-thiones react with dibenzoylacetylene to provide thioacylmethylene or thioacylimino-1,3-dithiole adducts respectively. Some of these, on sulfurization, provide thieno[3,4*d*]-1,3-dithiole derivatives, but in others a retro-1,3-dipolar reaction predominates. Further reaction of the initial adducts with more dibenzoylacetylene provides spiran compounds.

Canadian Journal of Chemistry, **48**, 1991 (1970)

As part of our studies on heterocyclic sulfur compounds, we wished to examine the conversion of some 4,5-dibenzoyl-2*H*-1,3-dithioles (**1**) to derivatives of the thieno[3,4*d*]-1,3-dithiole system (**2**). Thieno[3,4*d*]-2*H*-1,3-dithiole-2-thione (**3**) is already known (1) and examples of the isomeric thieno-1,2-dithioles have also been prepared recently (2). One approach to these compounds (**1**) appeared to be from suitably substituted 3*H*-1,2-dithiole-3-thiones (**4**) and 3*H*-1,2,4-dithiazole-3-thiones (**5**) by treatment with reactive acetylenes.

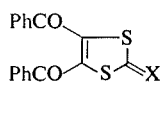

1

a X = CHCSPh
b X = CPhCSPh
c X = CPhCHS
d X = NCSPh
e X = $NCSC_6H_4o$Me
f X = $NCSC_6H_4p$Me
g X = NCS-2-Furyl
h X = NCS-2-Thienyl
i X = S

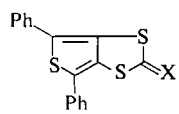

2

a X = NCSPh
b X = $NCSC_6H_4o$-Me
c X = $NCSC_6H_4p$-Me
d X = NCS-2-Furyl
e X = NCS-2-Thienyl
f X = NCOPh

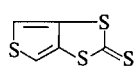

3

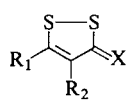

4

a R_1 = Ph; R_2 = H; X = S
b R_1 = Ph; R_2 = Ph; X = S
c R_1 = H; R_2 = Ph; X = S
d R_1 = Ph; R_2 = H; X = NPh

The reactions of these thiones with acetylenic esters have been studied rather extensively (3–9). Initially, 1,3-dipolar reactions provide 2*H*-1,3-dithiole carboxylic esters (4). During our investigations of these reactions, and of the products obtained (8), we were interested in other such cycloaddition reactions, particularly those with acetylenic ketones which would provide the required diacyldithioles (**1**). Dibenzoylacetylene was chosen for our investigations since it is readily prepared (10) and, since it is a highly reactive dienophile (11, 12), it might also be expected to function as a good 1,3-dipolarophile.

Three 3*H*-1,2-dithiole-3-thiones (**4***a–c*) studied reacted readily with dibenzoylacetylene. With the thiones (**4***a*, *b*), stable dibenzoyl-1,3-dithiole mono-adducts (**1***a*, *b*) were obtained when treated with equimolar quantities of the acetylene. Treatment with two equivalents of the acetylene, however, produced di-adducts (**6***a*, *b*) of the type obtained by further 1,4-dipolar reaction of the 2-thioacylmethylene mono-adducts with acetylenic esters (7–9).

With 4-phenyl-3*H*-1,2-dithiole-3-thione (**4***c*) however, the mono-adduct (**1***c*) was formed at room temperature, but this could not be purified satisfactorily since it was extremely unstable. This compound, in contrast to the thiones (**1***a*, *b*) produced above, is a thioaldehyde, and these are notoriously unstable (13). The product probably decomposes by loss of the thial sulfur as has been found for related compounds (14). The nuclear magnetic resonance (n.m.r.) spectrum of the product showed a sharp singlet at $\tau = -0.65$ characteristic of the thioaldehyde proton (15). The di-adduct from this reaction was not obtained. Usually formation of these from the mono-adducts and further 1,3-dipolarophile requires heating (8). Evidently the mono-adduct decomposes before this further addition can take place.

With 5-phenyl-3-phenylimino-3*H*-1,2-dithiole (**4***d*), which has been shown to react with acetylenic esters (8) to provide thiazolecarboxylic ester mono-adducts (**7***a*), dibenzoylacetylene reacted

Can. J. Chem. Downloaded from www.nrcresearchpress.com by 210.87.254.105 on 09/05/12
For personal use only.

fairly rapidly, but the products appeared to be unstable and could not be satisfactorily purified.

Five 3*H*-1,2-4-dithiazole-3-thiones (**5***a–e*) studied reacted readily with dibenzoylacetylene to give substituted-2-thioacylimino-4,5-dibenzoyl-2*H*-1,3-dithiole mono-adducts (**1***d–h*) by 1,3-dipolar reaction. In one of these dithiazoles (**5***d*) there might also have occurred Diels–Alder type addition to the 2,5-positions of the furan ring, similar to known examples (16), but no products of this type were found. The 1,3-dipolar reaction appears to be the more rapid. Subsequent Diels–Alder type addition to the furan nucleus of the mono-adduct product (**1***g*) is unlikely owing to the electron withdrawing thiocarbonyl group attached to the furan ring.

When the thiones (**5***a*, *b*) were treated with two equivalents of dibenenzoylacetylene, di-adducts (**8***a*, *b*) were obtained of the type previously encountered with acetylenic esters (6). These would have arisen by further reaction of dibenzoylacetylene on the initially produced -2-thioacylimino-2*H*-1,3-dithioles (**1***d*, *e*).

These dibenzoyldithioles (**1***a*, *b*, *d–g*) produced above are substituted dibenzoylethylenes, and as such might be expected to give thiophenes on sulfurization, similar to the preparation of isobenzothiophenes from diacyldihydrobenzenes (12) or diacylbenzenes (17). Thus, treatment of the -2-thioacylimino compounds (**1***d–g*) with phosphorus pentasulfide in pyridine gave the desired thieno[3,4*d*]-1,3-dithioles (**2***a–d*) in good yield. The structures of these follow from their analyses and from the absence of any C=O stretching bands in the infrared (i.r.). Bands at 1201–1210 cm^{-1} are probably those for the C=S stretching frequency. These are within the accepted range for this band (18). Reaction of one of these derivatives (**2***a*) with mercuric acetate, which is known (19) to convert a thiocarbonyl function to a carbonyl, gave the corresponding -2-benzoylimino-compound (**2***f*), demonstrating the presence of the thiobenzoylimino group in the original compound. After this treatment the band at 1210 cm^{-1} disappeared and an absorption at 1651 cm^{-1}, assigned to C=O stretch, was obtained.

Treatment of the dibenzoyl-2-thioacylmethylene-1,3-dithioles (**1***a*, *b*) with phosphorus pentasulfide gave rather less successful results. In each case the original 3*H*-1,2-dithiole-3-thiones (**4***a*, *b* respectively) were recovered, probably formed by retro-1,3-dipolar reaction. Apparently with these mono-adducts there is a greater tendency towards this reverse reaction than with the thioacylimino compounds (**1***d–g*). However, sulfurization of a di-adduct (**6***a*) was successful, and a product of the presumed thienothiopyranspirothieno-1,3-dithiole structure (**9**) was obtained. Evidently there is less tendency towards the reverse reactions than with the mono-adducts (**1***a*, *b*).

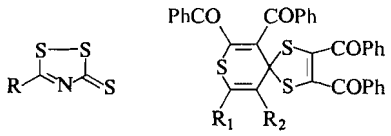

5

a R = Ph
b R = C_6H_4o-Me
c R = C_6H_4p-Me
d R = 2-Furyl
e R = 2-Thienyl

6

a R_1 = Ph; R_2 = H
b R_1 = Ph; R_2 = Ph
c R_1 = H; R_2 = Ph

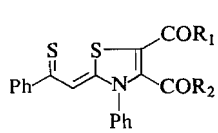

7

a $R_1 = R_2$ = OMe
b $R_1 = R_2$ = Ph

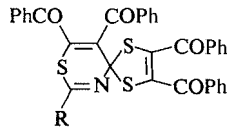

8

a R = Ph
b R = C_6H_4p-Me

To permit the preparation of thieno[3,4*d*]-1,3-dithioles without the 2-thioacylmethylene or 2-thioacylimino side chains, attempts were also made to obtain 4,5-dibenzoyl-2*H*-1,3-dithiole-2-thione (**1***i*) by reaction of dibenzoylacetylene with suitable 1,3-dithioles. The preparation of 2*H*-1,3-dithiole-2-thione-3,4-dicarboxylic esters by reaction of 1,3-dithiolane-2-thione with dimethyl acetylenedicarboxylate is reported (7). However, reaction with dibenzoylacetylene failed. Possibly this may have been due to lack of sufficient dipole character in the thione since it does not have resonance forms comparable to the 2*H*-1,3-dithiole-2-thiones. To test this, 4,5-diphenyl-2*H*-1,3-dithiole-2-thione (**10**) was prepared by acid-catalyzed cyclization of α-phenylphenacyl ethyl trithiocarbonate to the 2-ethylthio-4,5-diphenyl-1,3-dithiolium cation, similar to known methods (20, 21) followed by treatment with sodium hydrogen sulfide. This thione did react with dibenzoylacetylene but the product,

although it possessed benzoyl groups, could not be purified satisfactorily.

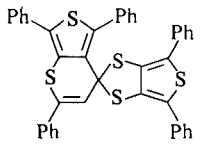

9

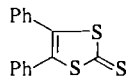

10

Experimental

The i.r. spectra were performed on a Perkin–Elmer model 337 spectrophotometer in liquid paraffin mulls. Nuclear magnetic resonance (n.m.r.) spectra were obtained on a Varian model 56/60A spectrometer, in deuterochloroform solution using tetramethylsilane as an internal standard. Thin-layer chromatography (t.l.c.) was performed using "Camag" silica gel type D.S.F.5 supplied by Mondray Ltd., on glass plates. Development of plates was carried out using benzene with increasing proportions of chloroform.

Reaction of 5-Phenyl-3H-1,2-dithiole-3-thione with Dibenzoylacetylene to form 3-Thiophenacylidene-4,5-dibenzoyl-2H-1,3-dithiole (1a)

The thione (1.04 g) (22) and dibenzoylacetylene (1.34 g) in benzene (25 ml) were stirred together at room temperature for 18 h. The solution rapidly turned dark brown. The solvent was removed under reduced pressure and the crude product recrystallized from nitromethane as a brown powder, m.p. 141–143 °C (75%).

Anal. Calcd. for $C_{25}H_{16}O_2S_3$: C, 67.57; H, 3.60; S, 21.62: Found: C, 67.51; H, 3.48; S, 21.57.

The i.r. spectrum of **1***a*: 1660 (C=O) and 1645 (C=O) cm^{-1}. The n.m.r. of **1***a*; 2.81–2.41 (15H multiplet), and 1.71 τ (1H singlet).

Reaction of 4,5-Diphenyl-3H-1,2-dithiole-3-thione with Dibenzoylacetylene to form 3-(α-Phenylthiophenacylidene)4,5-dibenzoyl-2H-1,3-dithiole (1b)

The thione (179 mg) (23) and the acetylene (134 mg) in benzene (10 ml) were stirred together at room temperature for 2 h. The solution rapidly became dark. The solvent was removed under reduced pressure and the products purified by t.l.c. and crystallized from nitromethane m.p. 209–210 °C (83%).

Anal. Calcd. for $C_{31}H_{20}O_2S_3$: C, 70.98; H, 3.92; S, 18.82. Found: C, 70.76; H, 3.96; S, 18.75.

The i.r. spectrum of **1***b*: 1680 and 1660 (C=O) cm^{-1}. The n.m.r. of **1***b*; 2.09–240 τ (20H multiplet).

Reaction of 4-Phenyl-3H-1,2-dithiole-3-thione with Dibenzoylacetylene to form 2-(α-Thioformylbenzylidene)- 4,5-dibenzoyl-2H-1,3-dithiole (1c)

The thione (70 mg) (24) and the acetylene (90 mg) were stirred together at room temperature for 2 h. The red solution rapidly became dark brown. The solvent was removed under reduced pressure and t.l.c. of the crude material gave 93 mg of a brown paste which could not be purified further, as this compound decomposed in hot solvents or on standing. No attempts were made to have it analyzed.

The i.r. spectrum of **1***c*; 1618 (C=O) cm^{-1}. The n.m.r. of **1***c* 2.99–2.53 (15H multiplet), −0.65 τ (1H singlet).

Treatment of the thione with two equivalents of the acetylene and refluxing led to a complex mixture of products. No satisfactory separation could be effected.

Reaction of 5-Phenyl-3H-1,2-dithiole-3-thione with Dibenzoylacetylene to form 4,5-Dibenzoyl-1,3-dithiole-2-spiro-4-(2-phenyl-5,6-dibenzoylthiopyran) (6a)

The thione (0.52 g) and the acetylene (1.34 g) in benzene (20 ml) were refluxed together for 9 h. The orange solution was evaporated under reduced pressure and the crude product recrystallized from nitrobenzene, m.p. 191–193° (84%).

Anal. Calcd. for $C_{41}H_{20}O_4S_3$: C, 72.57; H, 3.83; S, 14.22. Found: C, 72.47; H, 3.93; S, 14.07.

The i.r. spectrum of **6***a*; 1665 (C=O) cm^{-1}. The n.m.r. of **6***a*, 4.01 (1H singlet), 2.99–2.16 τ (25H multiplet).

Reaction of 4,5-Diphenyl-3H-1,2-dithiole-3-thione with Dibenzoylacetylene to form 4,5-Dibenzoyl-1,3-5,6-dibenzoyl-2,3-diphenylthiopyran (6b)

The thione (179 mg) and the acetylene (300 mg) in benzene (20 ml) were refluxed together for 9 h. The solution was evaporated and the yellow residue purified by t.l.c. The product was recrystallized from ethanol, m.p. 106–108 °C (76%).

Anal. Calcd. for $C_{47}H_{30}O_4S_3$: C, 74.80; H, 31.98; S, 12.73. Found: C, 75.03; H, 3.88; S, 12.68.

The i.r. spectrum of **6***b*; 1660 (C=O) and 1665 (C—O) cm^{-1}. The n.m.r. of **6***b* 1.93–1.41 τ (30H multiplet).

Reaction of 5-Phenyl-3-phenylimino-3H-1,2-dithiole with Dibenzoylacetylene

The imine (268 mg) and dibenzoylacetylene (234 mg) in benzene (10 ml) were refluxed together for 18 h. The solution was evaporated and the residue examined by t.l.c. No proper separation could be effected.

Reaction of 3H-1,2,4-Dithiazole-3-thiones with Dibenzoylacetylene to form 2-Thioacylimino-4,5-dibenzoyl-2H-1,3-dithioles (1d–h)

The thiones (0.5 g) and dibenzoylacetylene (0.6 g) in benzene (20 ml) were boiled for 2 h. The dark-red products were isolated by evaporation and recrystallization from nitromethane. The results are summarized in Table 1.

Reaction of 3H-1,2,4-Dithiazole-3-thiones with Dibenzoylacetylene to form 4,5-Dibenzoyl-1,3-dithiole-2-spiro-4(-5,6-dibenzoyl-1,3-thiazines) (8a–c)

The thiones (0.5 g) and dibenzoylacetylene (1 g) in benzene (20 ml) were boiled for 7 h. The yellow products were isolated by evaporation of the solvent and recrystallization from nitromethane. The results are summarized below.

4,5-Dibenzoyl-1,3-dithiole-2-spiro-4-(5,6-dibenzoyl-2-phenyl-1,3-thiazine) (8a)

This was obtained as yellow plates, m.p. 187–188 °C (70%).

Anal. Calcd. for $C_{40}H_{25}NO_4S_3$: C, 70.68; H, 3.68; N, 2.06; S, 14.15. Found: C, 70.81; H, 3.86; N, 2.22; S, 14.31.

Can. J. Chem. Downloaded from www.nrcresearchpress.com by 210.87.254.105 on 09/05/12
For personal use only.

TABLE 1

Preparation of 2-thioacylimino-4,5-dibenzoyl-2*H*-1,3-dithioles (**1***d–h*)

Compound **1**	Yield (%)	Melting point (°C)	Formula	Calculated (%) C	H	N	S	Found (%) C	H	N	S
d	95	160–161	$C_{24}H_{15}NO_2S_3$	64.71	3.37	3.15	21.58	64.09	3.56	3.25	21.40
e	90	161	$C_{25}H_{17}NO_2S_3$	64.64	3.79	3.05	20.81	64.48	3.92	3.16	20.65
f	90	167	$C_{25}H_{17}NO_2S_3$	64.64	3.79	3.05	20.81	64.59	3.90	3.17	20.95
g	91	145–147	$C_{22}H_{13}NO_3S_3$	59.32	3.13	3.37	21.57	59.62	3.15	3.43	21.73
h	93	197–198	$C_{22}H_{13}NO_2S_4$	58.53	2.88	3.10	28.38	58.58	2.71	3.17	28.35

TABLE 2

Preparation of 2,5-diphenylthieno[3,4*d*]-2-thioacylimino-2*H*-1,3-dithioles

Compound **2**	Yield (%)	Melting point (°C)	Formula	Calculated (%) C	H	N	S	Found (%) C	H	N	S
*a**	45	203–203.5	$C_{24}H_{15}NS_4$	64.71	3.37	3.15	28.76	64.54	3.56	3.26	28.63
b†	47	197–200	$C_{25}H_{17}NS_4$	65.35	3.71	3.05	27.89	65.35	3.88	3.24	27.78
c‡	51	207–207.5	$C_{25}H_{17}NS_4$	65.35	3.71	3.05	27.89	65.40	3.64	3.05	27.64
d§	55	218–220	$C_{22}H_{13}NOS_4$	60.68	3.00	3.21	29.43	60.10	3.12	3.24	29.01
e‖	60	213–214	$C_{22}H_{13}NS_5$	58.55	2.89	3.11	35.48	58.41	2.73	3.12	35.35

*Infrared absorption 1210 cm^{-1} (C═S).
†Infrared absorption 1204 cm^{-1} (C═S).
‡Infrared absorption 1201 cm^{-1} (C═S).
§Infrared absorption 1201 cm^{-1} (C═S).
‖Infrared absorption 1203 cm^{-1} (C═S).

The i.r. spectrum: 1655 (C═O) and 1645 (C═O) cm^{-1}. The n.m.r. 2.86–2.03 τ (25H multiplet).

4,5-Dibenzoyl-1,3-dithiole-2-spiro-4-(5,6-dibenzoyl-2-p-toluyl-1,3-thiazine) (8b)

This was obtained as yellow plates, m.p. 185–188 °C (85%).

Anal. Calcd. for $C_{41}H_{27}NO_4S_3$: C, 70.01; H, 3.90; N, 2.02; S, 13.81. Found: C, 70.82; H, 4.28; N, 2.16; S, 13.81.

The i.r. spectrum: 1650 (C═O) and 1648 (C═O) cm^{-1}. The n.m.r. 7.59 (3H singlet) and 2.85–2.08 τ (24H multiplet).

Sulfurization of the 4,5-Dibenzoyl-2-thioacylimino-2H-1,3-dithioles (1d–h) to form the 2,5-Diphenylthieno [3,4d]-2-thioacylimino-2H-1,3-dithioles (2a–e)

The dibenzoyldithioles (0.5 g) and phosphorus pentasulfide (0.25 g) in pyridine (10 ml) were refluxed for 5 h. The mixtures were thrown into water, and the dried benzene extracts were evaporated. The crude dark-red products were recrystallized from benzene–ethanol 1:1. The results are summarized in Table 2.

2,5-Diphenylthieno[3,4d]-2-benzoylimino-2H-1,3-dithiole (2e) from 2,5-Diphenylthieno [3,4d]-2-thiobenzoylimino-2H-1,3-dithiole (2a)

The thiobenzoyl compound (0.25 g) was added to a solution of mercuric acetate (0.5 g) in acetic acid (15 ml) and the mixture shaken 48 h. Dilution with water and ether extraction afforded a yellow powder, which was crystallized from benzene:ethanol, 1:1. A pale yellow powder, m.p. 214–215 °C was obtained (37%).

Anal. Calcd. for $C_{24}H_{15}NOS_3$: C, 67.13; H, 3.50; N, 3.26; S, 22.38. Found: C, 66.91; H, 3.64; N, 3.30; S, 22.46.

The i.r. spectrum: 1640 (C═O) cm^{-1}.

Sulfurization of the 2-Thioacylmethylene-1,3-dithioles (1a, b)

These dithioles (0.25 g) and phosphorus pentasulfide (1 g) in pyridine (10 ml) were refluxed for 5 h. The mixtures were thrown into water and the dried benzene extracts were examined by t.l.c. The only identifiable products were the thiones (**4***a, b*).

Sulfurization of 4,5-Dibenzoyl-1,3-dithiole-2-spiro-4 (2-phenyl-5,6-dibenzoylthiopyran) (6a)

The tetrabenzoyl compound (240 mg) and phosphorus pentasulfide (160 mg) in pyridine (7 ml) were refluxed for 3 h. The pyridine was removed under reduced pressure and the crude product subjected to t.l.c. The product was finally recrystallized from ethanol:benzene, 2:1 as brown felted needles m.p. 219–221° (33%).

Anal. Calcd. for $C_{41}H_{26}S_5$: C, 72.57; H, 3.83; S, 23.62. Found: C, 72.92; H, 3.66; S, 23.69.

Reaction of 2H-1,3-Dithiolane-2-thione with Dibenzoylacetylene

The thione (0.64 g) and dibenzoylacetylene (1.00 g) in xylene (20 ml) were refluxed 18 h. The dark mixture was examined by t.l.c. but the only identifiable product was unreacted 2H-1,3-dithiolane-2-thione.

Preparation of α-Phenylphenacyl Ethyl Trithiocarbonate

Ethanethiol (25 g) was added to a solution of sodium

Can. J. Chem. Downloaded from www.nrcresearchpress.com by 210.87.254.105 on 09/05/12
For personal use only.

(11 g) dissolved in ethanol (250 ml). Carbon disulfide (26.6) was added with stirring and after 1/2 h α-phenylphenacyl chloride (71 g) in ethanol (350 ml) was added. The mixture was allowed to stand 1 h and poured into water (21) and after 5 h a yellow solid was filtered off (56%). This was used directly in the next stage.

Preparation of 4,5-Diphenyl-2-ethylthio-1,3-dithiolium Perchlorate

α-Phenylphenacyl ethyl trithiocarbonate (1 g) in sulfuric acid (10 ml) was heated at 100° for 10 min. The dark solution was chilled and diluted with water (10 ml) and ethyl acetate (20 ml) added. After standing at 0° for several hours a dark orange paste was obtained which was dissolved in acetic acid (10 ml) and 70% perchloric acid (0.4 ml) added. Cooling deposited pale purple crystals of the salt m.p. 121–123 °C (51%).

Anal. Calcd. for $C_{17}H_{15}ClO_4S_3$; S, 49.16; H, 3.61; Cl, 8.70; S, 23.13. Found: C, 49.20; H, 3.72; Cl, 8.70; S, 23.24.

Preparation of 4,5-Diphenyl-2H-1,3-dithiole-2-thione from 4,5-Diphenyl-2-ethylthio-1,3-dithiolium Perchlorate

The perchlorate (1.0 g) in ethanol (10 ml) was treated with a saturated solution of sodium hydrogen sulfide in ethanol (10 ml) and heated until solution had occurred. Cooling afforded yellow needles which were recrystallized from ethanol, m.p. 112 °C (96%).

Anal. Calcd. for $C_{15}H_{10}S_3$; C, 62.91; H, 3.52; S, 33.59. Found: C, 62.85; H, 3.61; S, 33.68.

The i.r. spectrum: 1061, (tentatively assigned to C=S) cm^{-1}. The n.m.r. 3.01–2.47 τ (10H multiplet).

Reaction of 4,5-Diphenyl-2H-1,3-dithiole-2-thione with Dibenzoylacetylene

The thione (286 mg) and dibenzoylacetylene (242 mg) were refluxed in benzene (20 ml) for 72 h. The evaporated mixture was examined by t.l.c. The only identifiable band consisted of unreacted thione (180 mg). Other slower running bands were eluted. These exhibited C=O absorption in the i.r. but could not be purified satisfactorily.

The authors wish to thank Dr. D. Leaver for helpful suggestions, and Mr. R. Dickinson for the preparation of nuclear magnetic resonance spectra. Financial support by the National Research Council of Canada is gratefully acknowledged.

1. S. Gronowitz and P. Moses. Acta Chem. Scand. **16**, 105 (1962).
2. P. Rioult and J. Vialle. Bull. Soc. Chim. France, 4483 (1968).
3. J. W. MacDonald and D. M. McKinnon. Can. J. Chem. **45**, 1225 (1967).
4. H. Behringer, D. Bender, J. Falkenberg, and R. Weidenmann. Ber. **101**, 1428 (1968).
5. H. Behringer and D. Deichmann. Tetrahedron Lett. 1013 (1967).
6. G. Lang and J. Vialle. Bull. Soc. Chim. France, 2865 (1967).
7. D. B. J. Easton and D. Leaver. Chem. Commun. 585 (1965).
8. J. M. Buchshriber, D. M. McKinnon, and M. Ahmed. Can. J. Chem. **47**, 2039 (1969).
9. H. Davy, M. Demuynck, P. Paquer, A. Roessac, and J. Vialle. Bull. Soc. Chim. France, 2057, (1968).
10. R. E. Lutz and W. R. Smithey. J. Org. Chem. **16**, 51 (1951).
11. W. Ried and K. H. Boeminghausen. Ann. **639**, 61 (1961).
12. M. E. Mann and J. D. White. Chem. Commun. 420 (1968).
13. R. Mayer. Synthesis and properties of thiocarbonyl compounds. *In* Organosulfur chemistry. Interscience, New York, 1967.
14. D. Leaver. Personal communication.
15. J. G. Dingwall, S. McKenzie, and D. H. Reid. J. Chem. Soc. (C) 2543 (1968).
16. K. Alder and H. F. Rickert. Ber. **70**, 1354 (1937).
17. D. M. McKinnon and J. Y. Wong. Unpublished results.
18. C. N. R. Rao, R. Venkataraghavan, and T. R. Kasturi. Can. J. Chem. **42**, 36 (1964).
19. J. Derocque and J. Vialle. Bull. Soc. Chim. France, 1183 (1966).
20. E. Campaigne, R. D. Hamilton, and N. W. Jacobsen. J. Org. Chem. **29**, 1708 (1964).
21. E. Campaigne and R. D. Hamilton. J. Org. Chem. **29**, 1711 (1964).
22. E. Klingsberg. J. Amer. Chem. Soc. **83**, 2936 (1961).
23. M. G. Voronkov, A. S. Brown, and G. B. Karpenko. Dokl. Akad. Nauk. S.S.S.R. **59**, 1437 (1968); J. Gen. Chem. U.S.S.R. Eng. Transl. **19**, 395 (1949).
24. E. K. Fields. J. Amer. Chem. Soc. **77**, 4255 (1955).

Can. J. Chem. Downloaded from www.nrcresearchpress.com by 210.87.254.105 on 09/05/12
For personal use only.

Can. J. Chem. Downloaded from www.nrcresearchpress.com by 210.87.254.40 on 09/05/12
For personal use only.

Radical cations of some substituted pyrenes

J. T. COOPER[1]
Department of Chemistry, University of Waterloo, Waterloo, Ontario

Received December 24, 1969

The electron spin resonance spectra of several substituted pyrene cations, produced by oxidation with boron trifluoride in sulfur dioxide, are reported. The spectra are analyzed and the splitting constants given. With 4-chloropyrene, hyperfine splitting is observed due to the chlorine atom, for the first time in such a species. Molecular orbital calculations (Hückel and McLachlan) are presented for three of the compounds studied.

Canadian Journal of Chemistry, **48**, 1996 (1970)

Introduction

During the course of an electron spin resonance (e.s.r.) study of cation radicals derived from polynuclear aromatic hydrocarbons,[2] the cations of several monosubstituted pyrenes were prepared. The compounds studied were 3-methyl-, 4-chloro-, 4-phenyl-, 4-cyclohexyl-, and

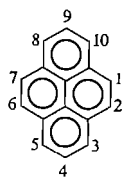

Pyrene

4-methoxypyrene. 4-Cyclohexylpyrene gave a well-resolved but highly complex spectrum under the oxidizing conditions employed which could not be analyzed, while 4-methoxypyrene gave no evidence of cation formation. However, the remaining four compounds yielded interpretable e.s.r. spectra which could be assigned to the respective radical cations.

Experimental

The cations were produced by dissolution of the pyrene derivatives in sulfur dioxide, followed by addition of boron trifluoride, using standard vacuum techniques. This method of oxidation was introduced by deBoer *et al.* (4, 5), and has proved to be a useful general method for the one-electron oxidation of aromatic hydrocarbons and related species. Solutions were prepared at liquid nitrogen temperature in 4 mm o.d. e.s.r. sample tubes attached to a vacuum line via a ball joint. These were then sealed off and inserted into the precooled spectrometer cavity.

The pyrene derivatives were a gift from Professor C. Jutz of the University of Munich and were used without further purification.

The compounds studied will now be discussed individually.

[1]Present address: Biophysics Department, Roswell Park Memorial Institute, Buffalo, N.Y. 14203, U.S.A.

[2]See references 1–3 for previous work in this study.

Results

4-Methylpyrene

This compound dissolves in SO_2–boron trifluoride to give a green solution of the cation, stable below ca. −40 °C but decaying in minutes at room temperature. The e.s.r. spectrum at −50 °C is shown in Fig. 1, together with a computer simulation in terms of the splitting constants given in Table 1. The spectrum superficially resembles that of the pyrene cation (1) but careful analysis shows that it interprets in terms of 12, rather than 10, protons, although there is some overlapping of splitting constants. Thus, the methyl splitting and that due to the single proton at position 9 are, within experimental error, the same; because of this, the spectrum shows, unexpectedly, a central line. Further, the 3-, 5-, 8-, and 10-positions are characterized by a single splitting constant rather than falling into two groups of two. However, the analysis is unambiguous: the spectral linewidth is only 0.08 G and the computer simulation affords excellent agreement with the experimental plot.

3-Methylpyrene

This hydrocarbon also gives a pale green solution of the corresponding cation in SO_2–boron trifluoride and at −40 °C a well-resolved, though complex e.s.r. spectrum is obtained. All 10 splitting constants could be extracted and are given in Table 1. Raising the temperature above −40 °C results in line broadening and at 0 °C analysis is impossible. However, the ion is stable for a period of several hours at room temperature and the effects of warming are reversible, with the lines sharpening again on cooling.

4-Phenylpyrene

On dissolution in SO_2–boron trifluoride a yellow–green paramagnetic solution is obtained. The e.s.r. spectrum of the cation is poorly re-

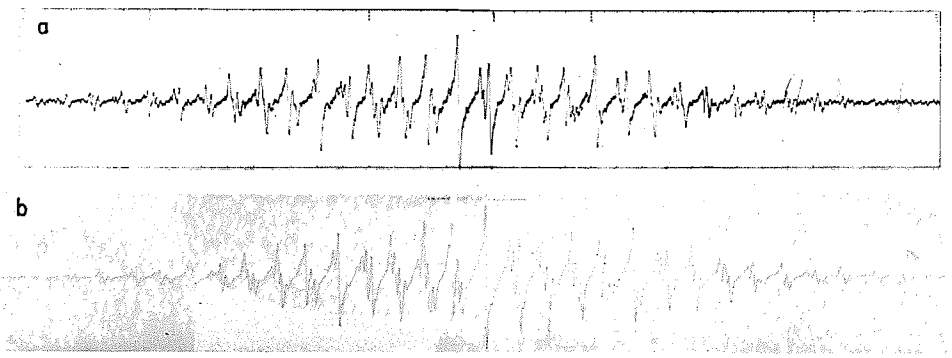

FIG. 1. The e.s.r. spectrum of the 4-methylpyrene cation. (*a*) Experimental. (*b*) Computed.

TABLE 1
Splitting constants for the pyrene cation radicals

Compound	Position	Splitting (G)
Pyrene	1	2.17*
	3	5.39*
	4	1.20*
4-Methylpyrene	Me	1.22
	9	1.22
	3, 5, 8, 10	5.34
	1, 7, or 2, 6	2.10
	1, 7, or 2, 6	2.21
3-Methylpyrene	Me	7.02
	4, or 9	1.06
	4, or 9	1.23
	1, 2, 6, or 7	1.70
	1, 2, 6, or 7	1.90
	1, 2, 6, or 7	2.23
	1, 2, 6, or 7	2.68
	5, 8, or 10	4.95
	5, 8, or 10	5.13
	5, 8, or 10	5.32
4-Phenylpyrene	9	1.2
	1, 2, 6, 7	2.2
	3, 5, 8, 10	5.4
4-Chloropyrene	Cl	0.22
	9	1.18
	1, 7, or 2, 6	1.83
	1, 7, or 2, 6	2.52
	3, 5, 8, 10	5.38

*Reference 1.

solved over the accessible temperature range of −80 to +60 °C; even under optimum conditions of concentration and temperature, the linewidth is almost 0.50 G. The spectrum can be simulated in terms of two groups of four equivalent protons plus a single proton. The most probable explanation of this is that only the protons of the pyrene nucleus can be detected, with the unpaired spin density in the phenyl ring being too small to produce detectable splittings. The broad linewidth may be partially due to unresolved splittings from the phenyl protons.

4-Chloropyrene

The cation of this compound is of particular interest. It appears to be the first chlorine-substituted polynuclear aromatic hydrocarbon from which a radical ion can be prepared showing hyperfine splitting due to the chlorine nucleus. (Other π-radicals which show chlorine hyperfine splitting in solution have recently been summarized by Broze and Luz (6).) The cation was prepared in SO_2–boron trifluoride in which it yields a yellow solution, stable for many hours at low temperatures but decaying slowly above ca. 0 °C. A section of the low field wings of the spectrum at −50 °C under high amplification appears in Fig. 2. In this figure the extreme four lines at low field are due to the chlorine splitting. (Both chlorine-35 and chlorine-37 have a nuclear spin of 3/2, leading to a hyperfine splitting pattern of four equally spaced lines. The natural abundances of the isotopes are 75.4 and 24.6%, respectively. From their relative nuclear magnetic moments, the theoretical ratio of their expected splitting constants, $a_{Cl\text{-}35}$ to $a_{Cl\text{-}37}$ is 1.20. Hence, it is not surprising that splittings due to the two isotopes are not separately resolved; they should differ by no more than 0.03–0.04 G.)

The splitting constants for the cations studied are listed in Table 1. They are believed to be accurate to ±0.02 G with the exception of those for 4-phenylpyrene which are believed accurate to ±0.1 G. For comparison purposes, the parameters for pyrene are also given. From these data, a number of observations can be made regarding the perturbing effect of the substituents on the unpaired spin density distribution in the pyrene cation.

(*a*) The introduction of a methyl or phenyl substituent into the 4-position has little effect on the spin densities at the other positions in the

Can. J. Chem. Downloaded from www.nrcresearchpress.com by 210.87.254.40 on 09/05/12
For personal use only.

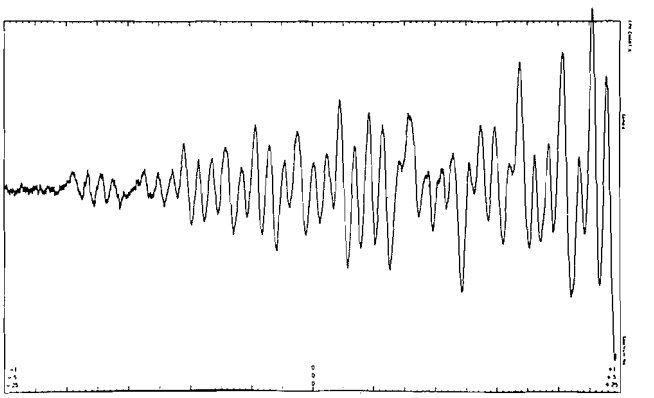

FIG. 2. Low field wings of the 4-chloropyrene cation spectrum at high amplification.

cation over their values in the unsubstituted parent compound. Considering these substituents to exert only a positive inductive effect, this is to be expected for their introduction in a position for which simple Hückel theory predicts a node in the unpaired electron density and McLachlan calculations a small negative spin density (see Table 2).

(*b*) Introducing a methyl substituent into the 3-position, where a high unpaired spin density exists for the parent cation, should result in a rather more pronounced perturbation, and this is observed. The most marked difference between the 3-methyl and 4-methyl cations lies in the methyl splittings which are 7.02 and 1.22 G respectively. The magnitude of the larger splitting is consistent with those observed for the CH_3-protons in the 9-methyl- and 9,10-dimethylanthracene cations (7.79 and 8.00 G respectively (7)), where the substituents are again in positions at which the unpaired spin density in the parent cation is high. The splitting constants due to the nine pyrene protons in the 3-methyl cation fall into three groups as expected, but precise assignment is not possible.

TABLE 2

Summary of molecular orbital calculations

Compound	Position	ρ_H*	ρ_M†	$\lvert a\rvert$‡ (G)
Pyrene	1	0.0873	0.0975	2.67
	3	0.1358	0.1781	4.88
	4	0.0000	−0.0541	1.48
4-Methylpyrene	1	0.0873	0.0975	2.67
	2	0.0873	0.0976	2.67
	3	0.1358	0.1787	4.89
	8	0.1358	0.1781	4.88
	9	0.0000	−0.0540	1.48
3-Methylpyrene	1	0.0933	0.1103	3.02
	2	0.0761	0.0809	2.22
	4	0.0041	−0.0427	1.17
	5	0.1141	0.1519	4.16
	6	0.0710	0.0752	2.06
	7	0.0946	0.1107	3.03
	8	0.1348	0.1790	4.90
	9	0.0000	−0.0540	1.48
	10	0.1331	0.1784	4.88
4-Chloropyrene	1	0.0873	0.0975	2.67
	2	0.0873	0.0976	2.67
	3	0.1358	0.1786	4.89
	8	0.1358	0.1781	4.88
	9	0.0000	−0.0540	1.48
	4	0.0000	−0.0522	—

*ρ_H = Unpaired spin density from simple Hückel theory.
†ρ_M = Unpaired spin density from modified McLachlan calculations.
‡p_a = Calculated splitting constant from $|a| = 27.4|\rho_M|$.

An attempt was made to investigate whether these trends could be rationalized by simple molecular orbital calculations, using a hetero atom model to make allowance for the substituent. Some of the results of these calculations are summarized in Table 2.

An accepted model for chlorine is to consider

(*c*) The splitting due to the chlorine nucleus in 4-chloropyrene is small, as expected; indeed, it is surprising that it is seen at all. The splitting of the single proton in the 9-position and the large splitting of the 3, 5, 8, and 10 protons are virtually identical to their corresponding values in the unsubstituted cation. The main perturbing effect of the chlorine is at the 1-, 2-, 6-, and 7-positions. At two of these the spin density is significantly reduced over the values in the pyrene radical cation, while at the other two it is increased by an approximately equal amount. (A similar situation holds for the methyl pyrenes, with the average splitting constant for the 1-, 2-, 6-, and 7-positions remaining close to the 2.17 G of the unsubstituted radical.)

Can. J. Chem. Downloaded from www.nrcresearchpress.com by 210.87.254.40 on 09/05/12
For personal use only.

Can. J. Chem. Downloaded from www.nrcresearchpress.com by 210.87.254.40 on 09/05/12
For personal use only.

its contributing a p_z-type orbital and two electrons to the π-system, ignoring any possible contribution from the 3d orbitals. However, there is some disagreement in the literature over the appropriate values of the Coulomb integral, α, and resonance integral, β, to be used in conjunction with chlorine (8). Expressing these integrals in the usual way, in terms of the standard values for benzene, α_0 and β_0,

$$\alpha_{Cl} = \alpha_0 + h_{Cl}\beta_0$$
$$\beta_{C-Cl} = k_{C-Cl}\beta_0$$

recommended values of h_{Cl} range from 0.8 to 2.8 and of k_{C-Cl} from 0.3 to 1.0. Because of this, calculations were carried out systematically varying these parameters over a wide range. However, it was found that with both simple Hückel and modified McLachlan (9) calculations, the predicted spin densities are highly insensitive to variation of α and β. This is exemplified by $k_{C-Cl} = 0.6$, $h_{Cl} = 2.00$ for which the data are given in Table 2. An estimate of the chlorine splitting constant can be made using the expression (6),

$$a_{Cl} = Q_{CCl}\rho_C + Q_{ClC}\rho_{Cl}$$

where ρ_{Cl} and ρ_C are the calculated unpaired spin densities at the chlorine atom and adjacent carbon atom respectively, while the Q terms are the sigma–pi interaction parameters, using the notation of Karplus and Fraenkel (10). If the assumption is made that Q_{CCl} and Q_{ClC} are of the same order of magnitude then, to a first approximation, the second term of the above expression can be ignored, (ρ_{Cl} is calculated to be -0.0030), leaving an equation analogous to the McConnell relation (11) for proton splittings. Using a value of 2.5 for $|Q_{CCl}|$, (6), leads to the prediction of $a_{Cl} = 0.13$ G. This is in reasonable agreement with the experimental value of 0.22 G.

Calculations are also given for the two methyl-substituted pyrenes, where the parameters used were $k_{C-Me} = 0.7$, $h_{Me} = 2.00$ (8). Again, for the 4-substituted compound, the calculations predict no significant change in the spin density distribution over that in the parent hydrocarbon. To facilitate comparison with the experimental data, Table 2 also lists the estimated splitting constants, calculated from the McLachlan spin densities, ρ_M, by the McConnell relationship (11),

$$a = Q\rho_M$$

The value of $|Q|$ employed was 27.4 G, taken from an earlier study of a series of hydrocarbon cations (3).

In summary, a more refined type of calculation is clearly needed if the relatively small perturbations to the spin density distribution, induced by a substituent in the 4-position, are to be predicted. However, for a methyl substituent in the 3-position, the McLachlan calculations appear to give a good prediction of the redistribution of spin density in the cation, although the assignment of splitting constants they suggest cannot be confirmed from the present work; studies on selectively-labelled compounds would be required and this has not been undertaken. The chloropyrene results suggest that it would be of considerable interest to study related compounds to investigate more fully chlorine splittings. In particular it should be instructive to study a system in which the splitting of the chlorine and perturbation due to it should be larger. To this end, considerable attention was given to attempting to generate the cations of 9-chloro-, and 9,10-dichloroanthracene. Electron spin resonance spectra were obtained from both compounds under the same conditions as were used for generating the chloropyrene cation but in neither case has analysis been possible.

The substituted pyrenes used in this research were synthesized in the laboratory of Professor C. Jutz at the University of Munich and generously provided by him. The author wishes to thank Dr. W. F. Forbes for his encouragement and guidance at all stages of this work. The research was carried out during the tenure of a National Research Council of Canada studentship, which is gratefully acknowledged, and was supported by grants from the National Research Council of Canada, the National Cancer Institute of Canada, and the Defence Research Board.

1. J. T. Cooper and W. F. Forbes. Can. J. Chem. **46**, 1158 (1968).
2. H. Van Willigan, E. de Boer, J. T. Cooper, and W. F. Forbes. J. Chem. Phys. **49**, 1190 (1968).
3. J. T. Cooper, W. F. Forbes, and J. C. Robinson. Can. J. Chem. **48**, 1942 (1970).
4. J. P. Colpa and E. de Boer. Mol. Phys. **7**, 333 (1963).
5. E. de Boer and A. Praat. Mol. Phys. **8**, 291 (1964).
6. M. Broze and L. Luz. J. Phys. Chem. **71**, 3690 (1967).
7. J. R. Bolton, A. Carrington, and A. D. McLachlan. Mol. Phys. **5**, 31 (1962).
8. A. Streitwieser. Molecular orbital theory for organic chemists. John Wiley and Sons, New York, 1961. Ch. 5.
9. A. D. McLachlan. Mol. Phys. **3**, 233 (1960).
10. M. Karplus and G. K. Fraenkel. J. Chem. Phys. **35**, 1312 (1961).
11. H. M. McConnell. J. Chem. Phys. **24**, 762, (1956).

Can. J. Chem. Downloaded from www.nrcresearchpress.com by 210.87.254.42 on 09/05/12
For personal use only.

Synthesis and polarographic studies of beta-substituted phenylcystine derivatives

R. J. THIBERT AND C. PATEL
Department of Chemistry, University of Windsor, Windsor, Ontario
Received October 29, 1969

The synthesis of *N*-benzoyl-*threo*-β-*p*-substituted phenylcystine ethyl esters via azlactone intermediates is reported. A polarographic method for their determination using 0.1 *M* sodium acetate in anhydrous methanol as the supporting electrolyte was investigated. The relationship between the half-wave potential and the Taft polar substituent constant, σ*, was studied.

Canadian Journal of Chemistry, 48, 2000 (1970)

Introduction

Polarographic investigations of cystines and alpha-substituted cystines (1, 2) have prompted further experiments with substituted cystines because studies with alpha-substituted cystines revealed that no direct correlation with the Taft polar substituent constants existed. This may have been due in part to the differing steric and polar effects of the various groups in the alpha position on the reduction of the disulfide linkage. It became of interest to study only the polar effects of different groups in the beta position of various para-substituted phenylcystine derivatives on the half-wave potentials, the diffusion current, the diffusion coefficient, and on the general shapes of the polarograms, since the para-substituted phenylcystines would have rather constant steric factors. Studies of this type on the effect of the substituent on the half-wave potential have been reported by Zuman (3).

Experimental

Materials and Methods

The Sargent (E. H. Sargent and Co.) model XVI polarograph with a Sargent model A IR compensator was employed for this study. A special type of micro-H-cell (a modification of the H-cell of Arthur and Lyons (4)) was used. All the measurements were carried out in non-aqueous methanol using a methanolic saturated calomel in the working cell and an aqueous saturated calomel reference electrode. The characteristics of the capillary used were: $m = 1.426$ mg s^{-1}; $t = 5.6$ s; $m^{2/3}t^{1/6} = 1.689$ $mg^{2/3}$ $s^{-1/2}$ at -0.640 V. The height of the mercury column was 53.5 cm. A conductivity bridge (model RC 16 B2, Industrial Instruments, Inc.) was used to measure the cell resistance. A Fluke model 825A differential voltmeter was used to measure the potential against the aqueous saturated calomel electrode. The supporting electrolyte used was 0.1 *M* sodium acetate in anhydrous methanol. No maximum suppressor was required. No damping was used in this study.

p-Substituted benzaldehydes used as starting materials for the synthesis of *N*-benzoyl-*threo*-β-*p*-substituted cystine ethyl esters were obtained from Fisher Scientific Co. The substituted azlactones were prepared according to the procedure of Erlenmeyer *et al.* (5–9) from the corresponding substituted benzaldehydes by condensation with hippuric acid in the presence of anhydrous sodium acetate and acetic anhydride. On treatment of the various azlactones with sulfuric acid and ethanol, the corresponding substituted ethyl-α-benzamidocinnamates were obtained. These cinnamates condensed readily with dichlorothioacetic acid according to the method of Sicher *et al.* (10) to the corresponding *N*-benzoyl-*S*-dichloroacetyl-*threo*-β-*p*-substituted phenylcysteine ethyl esters. The reduction of these compounds via the Meerwein–Ponndorf–Verley (11) reaction gave the corresponding *N*-benzoyl-*threo*-β-*p*-substituted cysteine ethyl esters. The phenyl-, *p*-chlorophenyl-, *p*-methoxyphenyl-, and the *p*-nitrophenylcystine derivatives were prepared from the corresponding substituted cysteine derivatives by oxidation. All melting points reported are uncorrected. Infrared (i.r.) spectra used to identify reaction products were obtained on a Beckman IR 10 spectrophotometer. The microanalyses were performed by Schwarzkopf Microanalytical Laboratory, 56-19 37th Avenue, Woodside, N.Y. 11377, U.S.A.

Synthesis

Compounds which had been previously reported were synthesized and characterized using appropriate literature references. Procedures for preparing new compounds are listed with the physical properties, analyses, and yields. The sequence of reactions used for the various syntheses is outlined in Scheme 1. The physical and analytical data for the various compounds are summarized in Table 1.

Previously Prepared Compounds

2-Phenyl-4-benzylidene azlactone, m.p. 164–166 °C; lit. m.p. 165–166 °C (5–9); yield 75%.

2-Phenyl-4-*p*-methoxybenzylidene azlactone, m.p. 155–156 °C; lit. m.p. 156.5 °C (5–9); yield 42%.

Ethyl-α-benzamidocinnamate, m.p. 148–149 °C; lit. m.p. 149 °C (5–9); yield 85%.

Ethyl-α-benzamido-*p*-nitrocinnamate, m.p. 165–166 °C; lit. m.p. 165–166 °C (10); yield 80%.

N-Benzoyl-*S*-dichloroacetyl-*threo*-β-*p*-phenylcysteine ethyl ester, m.p. 128–131 °C; lit. m.p. 128–131 °C (10); yield 40%.

N-Benzoyl-*S*-dichloroacetyl-*threo*-β-*p*-nitrophenylcysteine ethyl ester, m.p. 142–143 °C; lit. m.p. 142 °C (10); yield 38%.

N-Benzoyl-*threo*-β-phenylcysteine ethyl ester, m.p. 125–126 °C; lit. m.p. 125–126 °C (10); yield 70%.

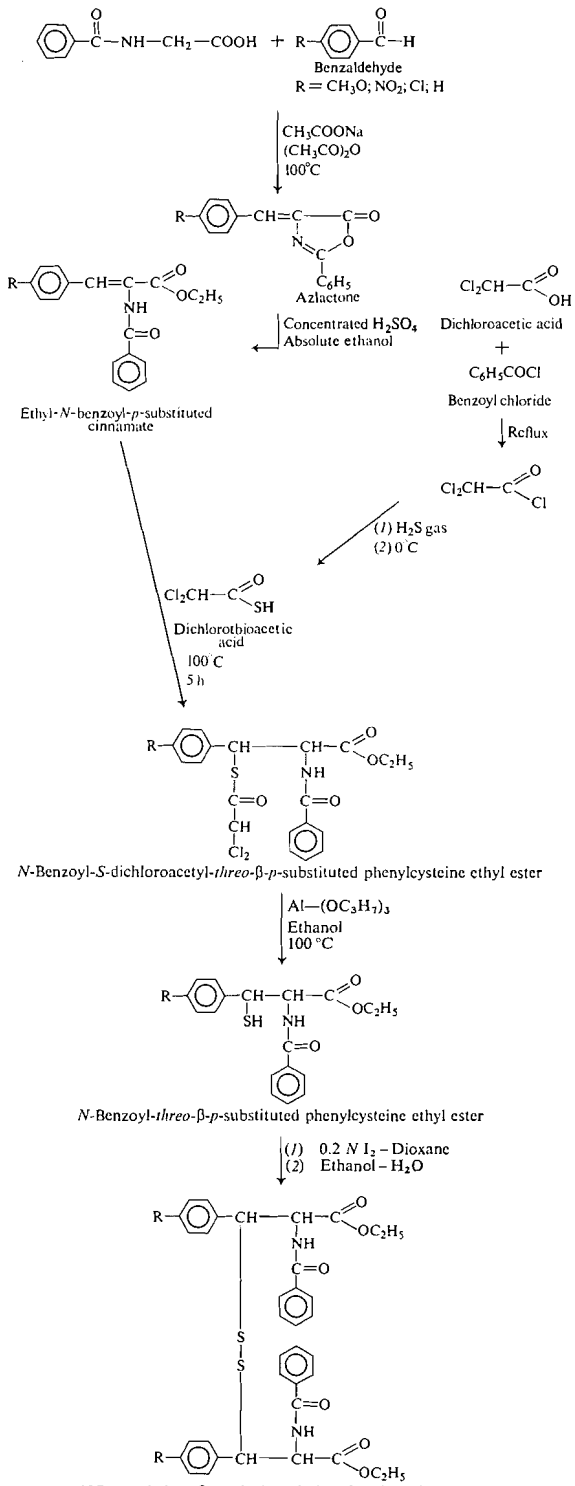

Synthesis of beta-substituted phenylcystine derivatives

SCHEME 1

Can. J. Chem. Downloaded from www.nrcresearchpress.com by 210.87.254.42 on 09/05/12
For personal use only.

Can. J. Chem. Downloaded from www.nrcresearchpress.com by 210.87.254.42 on 09/05/12
For personal use only.

TABLE 1

Properties of compounds prepared*

Type of compound	Group R	Yield (%)	Melting point (°C)	Reference	Analysis									
					Found (%)					Calculated (%)				
					C	H	N	S	Cl	C	H	N	S	Cl
2-Phenyl-4-*p*-benzylidene azlactone	H†	75	165–166	5–9										
	OCH_3†	42	155–156	5–9										
	Cl	55	195–196	—	67.80	3.76	4.92		12.35	67.60	3.87	4.93		12.32
	NO_2	67	235–237 (dec.)	—										
Ethyl-α-benzamido-cinnamates	H†	85	148–149	5–9										
	OCH_3	91.6	146–147	—	70.07	5.80	4.28			70.15	5.84	4.30		
	Cl	73.3	149–150	—	65.45	4.97	4.01		10.56	65.65	4.86	4.25		10.63
	NO_2†	80	165–166	10										
Adduct with dichloro-thioacetic acid	H†	40	128–131	10										
	OCH_3	31	108–109	—										
	Cl	30.9	133–134	—										
	NO_2†	38	142–143	10										
β-Phenylcysteine ethyl esters	H†	70	125–126	10										
	OCH_3	41.6	139–140	—	62.42	6.04	4.06	9.40		62.49	6.02	4.02	9.17	—
	Cl	37	147–148	—	59.16	5.25	4.04	8.87	9.39	59.40	4.95	3.85	8.81	9.78
	NO_2	75	134–135	—	49.22	4.69				48.88	5.18			
β-*p*-Substituted phenyl-cystine ethyl esters	H†	75	135–138	—										
	OCH_3	70	153–155	—										
	Cl	60	198–200	—										
	NO_2	40	230–232	—										

*The analyses reported in this table refer only to the newly synthesized compounds.
†These compounds have been reported in the literature.

Can. J. Chem. Downloaded from www.nrcresearchpress.com by 210.87.254.42 on 09/05/12
For personal use only.

Intermediates

Azlactone Syntheses

Azlactones (2-phenyl-4-*p*-nitrobenzylidene azlactone and 2-phenyl-4-*p*-chlorobenzylidene azlactone) were prepared by the method of Erlenmeyer *et al.* (5–9), which involves the reaction of the appropriate substituted benzaldehydes (0.33 mole) with hippuric acid (0.33 mole) in the presence of anhydrous sodium acetate (0.33 mole) and acetic anhydride (0.83 mole). The mixture was refluxed for 1.5 h, and the resulting crude product was filtered, washed with alcohol, and recrystallized from benzene. The yields obtained were 67 and 55%, respectively. The corresponding m.p. were 235–237 °C (dec.) and 195–196 °C.

Cinnamate Syntheses

The substituted cinnamates (ethyl-α-benzamido-*p*-methoxycinnamate and ethyl-α-benzamido-*p*-chlorocinnamate) were synthesized according to the procedure of Erlenmeyer *et al.* (5–9). A suspension of the appropriate azlactones (0.05 mole) was refluxed with a mixture of absolute ethanol (2.1 moles) and concentrated sulfuric acid (5 ml) for 3–4 h. After removal of the excess ethanol, the white residue was washed with water until free of any traces of sulfuric acid. The product was recrystallized from ethanol. The yield and m.p. were 91.6%, m.p. 146–147 °C for the *p*-methoxy derivative and 73.3%, m.p. 149–150 °C for the *p*-chloro derivative.

Adducts of Dichlorothioacetic Acid with the Ethyl Cinnamates (10)

A mixture of ethyl-α-benzamido-*p*-substituted cinnamate (0.023 mole) and dichlorothioacetic acid (10 ml) was refluxed on a steam bath for 5 h. On addition of ether, scratching immediately induced separation of white crystals. The crystals were washed and recrystallized from ethanol. The yields and melting points of *N*-benzoyl-*S*-dichloroacetyl-*threo*-β-*p*-chlorophenylcysteine ethyl ester and *N*-benzoyl-*S*-dichloroacetyl-*threo*-β-*p*-methoxyphenylcysteine ethyl ester are given in Table 1.

Syntheses of N-Benzoyl-threo-β-p-substituted Phenylcystine Ethyl Esters

The adduct with dichlorothioacetic acid (0.005 mole) was reduced with aluminum isopropoxide (0.005 mole) in ethanol to the corresponding sulfhydryl amino acid derivative, by refluxing for 4 h (11). On evaporation of the excess ethanol and treatment of the residue with 15% tartaric acid (100 ml), a white precipitate was obtained. This was extracted with ether, the ether layer was dried, and on evaporation of the ether a white solid was obtained. This was recrystallized from isopropanol. The yields and melting points for *N*-benzoyl-*threo*-β-*p*-methoxyphenylcysteine ethyl ester, *N*-benzoyl-*threo*-β-*p*-chlorophenylcysteine ethyl ester, and *N*-benzoyl-*threo*-β-*p*-nitrophenyl derivative are reported in Table 1.

Syntheses of N-Benzoyl-β-p-substituted Phenylcystine Ethyl Esters

The appropriate *N*-benzoyl-*threo*-β-*p*-substituted phenylcysteine ethyl ester (250 mg) was dissolved in 40 ml of dioxane and titrated with 0.2 *N* iodine solution. The solution was evaporated to dryness and the resulting residue treated with 5–10 ml of ethanol–water mixture. Filtration and recrystallization yielded the pure cystine derivative in 40–75% yield. The yields and melting points for *N*-benzoyl-*threo*-β-phenylcystine ethyl ester, *N*-benzoyl-*threo*-β-*p*-methoxyphenylcystine ester, *N*-benzoyl-*threo*-β-*p*-chlorophenylcystine ethyl ester, and *N*-benzoyl-*threo*-β-*p*-nitrophenylcystine ethyl ester are listed in Table 1.

Polarographic Procedure

Stock solutions of beta-substituted phenylcystine derivatives were prepared by dilution of solutions made from accurately weighed portions of the appropriate substituted phenylcystines. For polarography, the solutions were prepared using aliquots of the stock solution and diluting to the proper volume with stock electrolyte solution (0.2 *M* sodium acetate in anhydrous methanol). The solutions were transferred to the polarographic cells and nitrogen (purified by passage through a gas-washing bottle containing copper turnings and a 1:1 ammonium hydroxide solution saturated with ammonium chloride and another one containing concentrated sulfuric acid) was bubbled through for 15–20 min. All polarograms were run at 25 ± 0.1 °C. The apparent p*H* of the solutions used for polarography was 9.7.

Results

Effects of Concentration on the Diffusion Current

A linear relation of the diffusion current to the concentration was obtained (Table 2). No prewave was observed as reported by Kalousek *et al.* (12) for the case of the polarographic reduction of cystines and α-substituted cystines as shown by Thibert and Walton in an aqueous medium (2). All of the amino acids gave only one wave except the *p*-nitro derivative, where two waves were observed. The first wave in this case represents the disulfide reduction (this was confirmed by observing the reduction of *p*-nitrobenzaldehyde and ethyl-α-benzamido-*p*-nitrocinnamate). The true half-wave potentials were calculated according to the method of Taylor and Smith (13).

Diffusion Coefficient and Reversibility of the Reaction

By substitution in the Ilkovic equation, the

TABLE 2

Effect of concentration on diffusion current*

Amino acid† concentration (mole/l)	Diffusion current (μA)			
	H	Methoxy	Chloro	Nitro‡
1×10^{-4}	0.541	0.587	0.491	1.192
8×10^{-5}	0.448	0.487	0.402	1.078
5×10^{-5}	0.310	0.304	0.281	0.848
3×10^{-5}	—	—	—	0.626
2×10^{-5}	—	0.141	0.117	—
1×10^{-5}	0.070	—	—	—

*All the values are an average of three determinations and are uncorrected for residual current.
†Amino acid–appropriate *N*-benzoyl-*threo*-β-*p*-substituted phenylcystine ethyl ester.
‡Diffusion current measured from the first wave.

TABLE 3
Properties of some amino acids

Amino acid*	Diffusion coefficient ($cm^2\ s^{-1} \times 10^6$)	Half-wave potential (V)	Slope of plots of E vs. $\log (i_d - i)/i^2$
β-Phenyl-	7.24	−0.638	0.0246
β-*p*-Methoxy-phenyl-	6.33	−0.639	0.0208
β-*p*-Chloro-phenyl-	6.24	−0.638	0.0185
β-*p*-Nitro-phenyl-	50.8	−0.655	0.0212

*Amino acid derivatives–appropriate *N*-benzoyl-*threo*-β-*p*-substituted cystine ethyl ester. The amino acid concentration employed in the polarographic measurements was 5×10^{-5} *M*.

diffusion coefficients for the beta-substituted phenylcystine derivatives were calculated. They were found to be between 6.24 to 50.8 $\times$ 10^{-6} $cm^2\ s^{-1}$. The reversibility of the reaction was tested by plotting E vs. $\log (i_d - i)/i^2$ (1). The slopes of these plots are given in Table 3 (all current values used have been corrected for residual current).

Half-wave Potential

Determination of half-wave potentials was carried out in 0.1 *M* sodium acetate in anhydrous methanol for the phenyl-, *p*-methoxyphenyl-, *p*-chlorophenyl-, and *p*-nitrophenylcystine derivatives. True half-wave potentials were measured from a plot of E vs. $\log (i_d - i)/i$ for a particular polarogram where all current values were corrected for residual current (13).

Discussion

A polarographic method has been developed for the quantitative determination of derivatives of substituted phenylcystines. A quantitative polarographic method was thought to be feasible due to previous work with alpha-substituted cystines (2). Diffusion current plots vs. concentration showed a linear relationship. This indicated that a rapid and accurate polarographic determination can be carried out without any complication using 0.1 *M* sodium acetate in methanol as the supporting electrolyte at an apparent p*H* 9.7.

No p*H* dependency studies were carried out, since a non-aqueous medium was used. Only the apparent p*H* of the supporting electrolyte was measured.

No maxima were observed on the polarograms, therefore no maximum suppressor was used. The shapes of the polarograms were similar to those of cystine and alpha-substituted cystines but different from them in having no prewave (1, 2).

In order to determine whether the reduction of substituted β-phenylcystine derivatives was reversible, plots of E vs. $\log (i_d - i)/i^2$ were made. All of the amino acid derivatives gave a straight line whose slopes are given in Table 3. Values ranging from 0.0246–0.0185 were obtained. The theoretical slope of 0.0295 indicates a reversible reduction reaction involving two electrons. Experimental values are not very close to the theoretical values, and so it cannot be determined whether a reversible or a nonreversible reduction reaction occurs in the case of these substituted amino acids.

Although straight lines were obtained for plots of $\log (i_d - i)/i^2$ vs. E, the data obtained at constant p*H* and constant concentration of the amino acids in no way suggest any variation of $E_{1/2}$ with concentration of the amino acids as would have been predicted by this type of relationship (i.e., $E_{1/2}$ shows no change with concentration as observed from the numerous polarograms run). This type of observation is probably explained by the fact that the mechanism is more complex than anticipated, as based on a comparison with an apparent two-electron reduction step in the case of cystine. Furthermore, the case of the *p*-nitrophenylcystine derivative is particularly difficult to interpret with regards to the abnormally high diffusion current obtained for the reduction of the disulfide. It appears that the nitro group in some way enhances the reduction of the disulfide thereby giving the latter an abnormally high diffusion current. At this stage, therefore, it is not possible to speculate on the complex nature of the reduction for these types of disulfides. The values of $E_{1/2}$ are valid under the experimental conditions reported here.

Diffusion coefficients were calculated by substitution of the experimental values into Ilkovic's equation. Table 3 shows values which lie between 7.24 to 6.24 $\times$ 10^{-6} $cm^2\ s^{-1}$ for phenyl-, *p*-methoxyphenyl-, and *p*-chlorophenylcystine derivatives, while 50.8 $\times$ 10^{-6} $cm^2\ s^{-1}$ was found for the *p*-nitrophenylcystine derivative. The value reported for cystine is 5.70 $\times$ 10^{-6} $cm^2\ s^{-1}$, which is less than that of β-substituted phenylcystine derivatives. Alpha-substituted cystines have diffusion coefficients in the range of 4.87 to

Can. J. Chem. Downloaded from www.nrcresearchpress.com by 210.87.254.42 on 09/05/12
For personal use only.

Can. J. Chem. Downloaded from www.nrcresearchpress.com by 210.87.254.42 on 09/05/12
For personal use only.

3.27×10^{-6} cm^2 s^{-1}, which is less than cystine as well as β-substituted phenylcystine derivatives. This could be due to the difference in structure and the use of a non-aqueous medium.

Thus far, the discussion has been mainly concerned with polarographic determinations. Consideration will now be given to the correlation between the half-wave potential and the structure of the substituent (the substituent constant σ*). Hammett (14) has defined the substituent constant by the following equation:

$$\log k/k^\circ = \sigma\rho$$

where k is the dissociation constant of substituted benzoic acids and k° is the dissociation constant of benzoic acid. Rho equals the reaction constant, which depends on the reaction, the condition, and the nature of the side chain. However, the substituent constants for a particular electron-withdrawing group, applicable to most reactions, does not give good results when used with reactions of other series. Therefore, special substituent constants have been defined by Jaffe (15), Taft and Lewis (16), and several others have been summarized by Swain and Lupton (17).

An attempt was made to correlate the half-wave potentials of the various β-phenylcystine derivatives with several of the substituent constants summarized by Swain and Lupton (17) and the Taft and Lewis constants (16). *p*-Phenyl-, *p*-methoxyphenyl-, *p*-chlorophenyl-, and *p*-nitrophenylcystine ethyl esters show very little difference (ca. 17 mV) between their half-wave potentials. Only a strong electron-withdrawing group (like NO_2) can effect this small (17 mV) change in half-wave potential. One can, therefore, conclude that there is no apparent correlation between half-wave potential and the structure of the substituent (substituent constant e.g. σ*). There is a possibility that the value of the *p*-chloro-derivative is lower than one would expect (possibly due to resonance effects).

In the final analysis, it appears that substitution in disulfides must occur directly on the sulfur for any correlation between $E_{1/2}$ and polar substituent constants (3). Attempts at correlation of polar constants such as σ* in the alpha-substituted cystines was not successful perhaps due to both steric and polar effects since substitution of the alpha carbon did not maintain a constant steric environment (2).

In the beta-substituted cystines, however, the steric factors were kept relatively constant throughout the series. Since no direct correlation of $E_{1/2}$ with any of the various polar substituent constants was obtained, it can be concluded that direct attachment to the sulfur of the disulfide linkage is required for manifestations of polar effects (3). Even one carbon interposed between the electroactive group is enough to obviate the polar effects. In fact, so good is the insulation of the electroactive group from the para-substituent on the phenyl group of the beta-substituted phenylcystines, that only a nitro group with its very large polar effect can cause any change in the half-wave potential.

The authors wish to thank the National Research Council of Canada for financial support of this work. The authors also wish to acknowledge the valuable assistance of Dr. R. J. Walton, of the Chemistry Department at the University of Windsor, for his valuable suggestions throughout this entire work.

1. I. M. Kolthoff and D. Barnum. J. Amer. Chem. Soc. **63**, 520 (1941).
2. R. J. Thibert and R. J. Walton. Can. J. Chem. **45**, 713 (1967).
3. P. Zuman. Substituent effects in organic polarography. Plenum Press, New York, 1963.
4. P. Arthur and H. Lyons. Anal. Chem. **24**, 1422 (1952).
5. E. Erlenmeyer. Ann. Chem. **275**, 3 (1893).
6. E. Erlenmeyer and W. Stadlin. Ann. Chem. **337**, 265 (1904).
7. E. Erlenmeyer and O. Matter. Ann. Chem. **337**, 271 (1904).
8. E. Erlenmeyer. Ann. Chem. **307**, 70 (1899).
9. E. Erlenmeyer and J. T. Halsey. Ann. Chem. **307**, 139 (1899).
10. J. Sicher, M. Svoboda, and J. Farkas. Collection Czech. Chem. Commun. **20**, 1439 (1955).
11. R. J. W. Cremlyn and R. H. Still. Named and miscellaneous reactions in practical organic chemistry. Heineman education books, Ltd., London, 1967.
12. M. Kalousek, O. Grubner, and A. Tochstein. Chem. Listy, **47**, 1143 (1953).
13. J. K. Taylor and S. W. Smith. J. Res. Nat. Bur. Std. **56**, No. 3, 143 (1956).
14. L. P. Hammett. Physical organic chemistry. McGraw–Hill Book Co., Inc., New York, 1940.
15. H. H. Jaffe. Chem. Rev. **53**, 191 (1953).
16. R. W. Taft and I. C. Lewis. J. Amer. Chem. Soc. **80**, 2436 (1958).
17. C. G. Swain and E. C. Lupton. J. Amer. Chem. Soc. **90**, 4328 (1968).

Can. J. Chem. Downloaded from www.nrcresearchpress.com by 210.87.254.40 on 09/05/12
For personal use only.

Lithiation of five-membered heteroaromatic compounds. The methyl substituted 1,2-azoles, oxadiazoles, and thiadiazoles

R. G. MICETICH

R & L Molecular Research Ltd., 8045 Argyll Road, Edmonton 82, Alberta

Received January 20, 1970

The lithiation of various methyl substituted isoxazoles, isothiazoles, pyrazoles, oxadiazoles, and thiadiazoles using *n*-butyllithium has been studied. Three types of reactions, namely, lateral lithiation, ring cleavage, and addition of butyllithium to the ring, have been found. 3,5-Dimethylisoxazole, 3-phenyl-5-methylisoxazole, 3,4-dimethyl-1,2,5-oxadiazole, 2,5-dimethyl-1,3,4-thiadiazole, 3-phenyl-5-methyl-1,2,4-oxadiazole, and 3,5-dimethyl-1,2,4-thiadiazole all undergo lateral lithiation to give the respective acetic acids after carboxylation. 1-Methyl-3,5-disubstituted pyrazoles form the 1-lithiomethyl derivatives, while 1-phenyl-3,5-disubstituted pyrazoles are converted to the 1-ortholithiophenyl-3,5-disubstituted pyrazoles. 4-Methylisothiazole is lithiated mainly at C-5, but also suffers ring cleavage to form 1-*n*-butylthio-2-cyanoprop-1-ene. Heteroaromatic compounds containing an N—S bond, such as 3,4-dimethyl-1,2,5-thiadiazole, 4-methyl-5-phenyl-1,2,3-thiadiazole, and 3,5-dimethylisothiazole, undergo nucleophilic attack at sulfur with resulting ring cleavage. 3,5-Dimethylisothiazole produces 2-*n*-butylthiopent-2-en-4-one. 3-Methyl-5-phenyl-1,2,4-oxadiazole gave 3-methyl-5-phenyl-5-*n*-butyl-1,2,4-dihydroöxadiazole by addition to the azomethine bond. The results of these lithiations are discussed. 3-Methyl-5-lithiomethylisoxazole was converted to various derivatives. Nuclear magnetic resonance spectral analysis was used to establish the identity of the products.

Canadian Journal of Chemistry, 48, 2006 (1970)

In connection with our work on semisynthetic penicillins (1), we required various five-membered heteroarylacetic acids. These acids have usually been made by multistage processes (see for example refs. 1–4). It occurred to us that some of the methyl substituted heteroaromatic compounds would undergo lateral metalation with butyllithium and that these lithioderivatives with carbon dioxide would form the desired acetic acids. These lithiomethyl compounds could also give rise to other derivatives.

Although the lateral metalation of six-membered heteroaryl compounds has been investigated (5–13), this reaction has not been applied to the simple five-membered heteroaromatic compounds, except for the thiazoles (14) and certain isoxazoles (15).

The Isoxazoles

Bowden *et al.* (15) have shown that while 3-methoxy-4,5-dimethylisoxazole is lithiated exclusively at the C_5-methyl group, 3-methoxy-5-methylisoxazole reacts with butyllithium to form both the C_5-lithiomethyl and the C_4-lithio compounds.

We found that 3,5-dimethylisoxazole (16) (**1**) and 3-phenyl-5-methylisoxazole (17) are lithiated at the C_5-methyl group. These lithioderivatives reacted with carbon dioxide to give 3-methylisoxazole-5-acetic acid (**3**) (73%) and 3-phenylisoxazole-5-acetic acid (18) (81%) respectively.

3-Methyl-5-lithiomethylisoxazole (**2**) was used as an example to study further synthesis with this class of compound. Scheme 1 illustrates these reactions.

An Ivanov-type reagent (19) could be obtained from **3** and two equivalents of butyllithium. Reaction with methyl iodide gave 3-methylisoxazole-5-α-methylacetic acid (**4**) in 70% yield. The structure of this acid was established unequivocally by elemental analysis, infrared (i.r.), and nuclear magnetic resonance (n.m.r.) spectral analysis. The thioketeneacetal **6** and the 'dimer' **7** are conveniently prepared from **2**.

The Isothiazoles

The synthetic utility of the 5-lithioisothiazoles has been demonstrated by Caton *et al.* (20). In the case of this ring system however, a competitive ring-cleavage reaction also takes place. Thus, 3-butylthiobuten-2-one (11%) was isolated from the preparation of 3-methylisothiazole-5-aldehyde (50%) starting from 3-methylisothiazole. The formation of this minor compound was explained by the addition of butyllithium to the —N—S-bond of the isothiazole ring, followed by hydrolysis during the work-up (20).

We have found that 3,5-dimethylisothiazole (**23**) undergoes a similar cleavage with butyllithium. On treatment with butyllithium and carbon dioxide, **23** forms a salt (i.r. spectrum shows a strong broad band at 1600 cm^{-1} and the

Can. J. Chem. Downloaded from www.nrcresearchpress.com by 210.87.254.40 on 09/05/12
For personal use only.

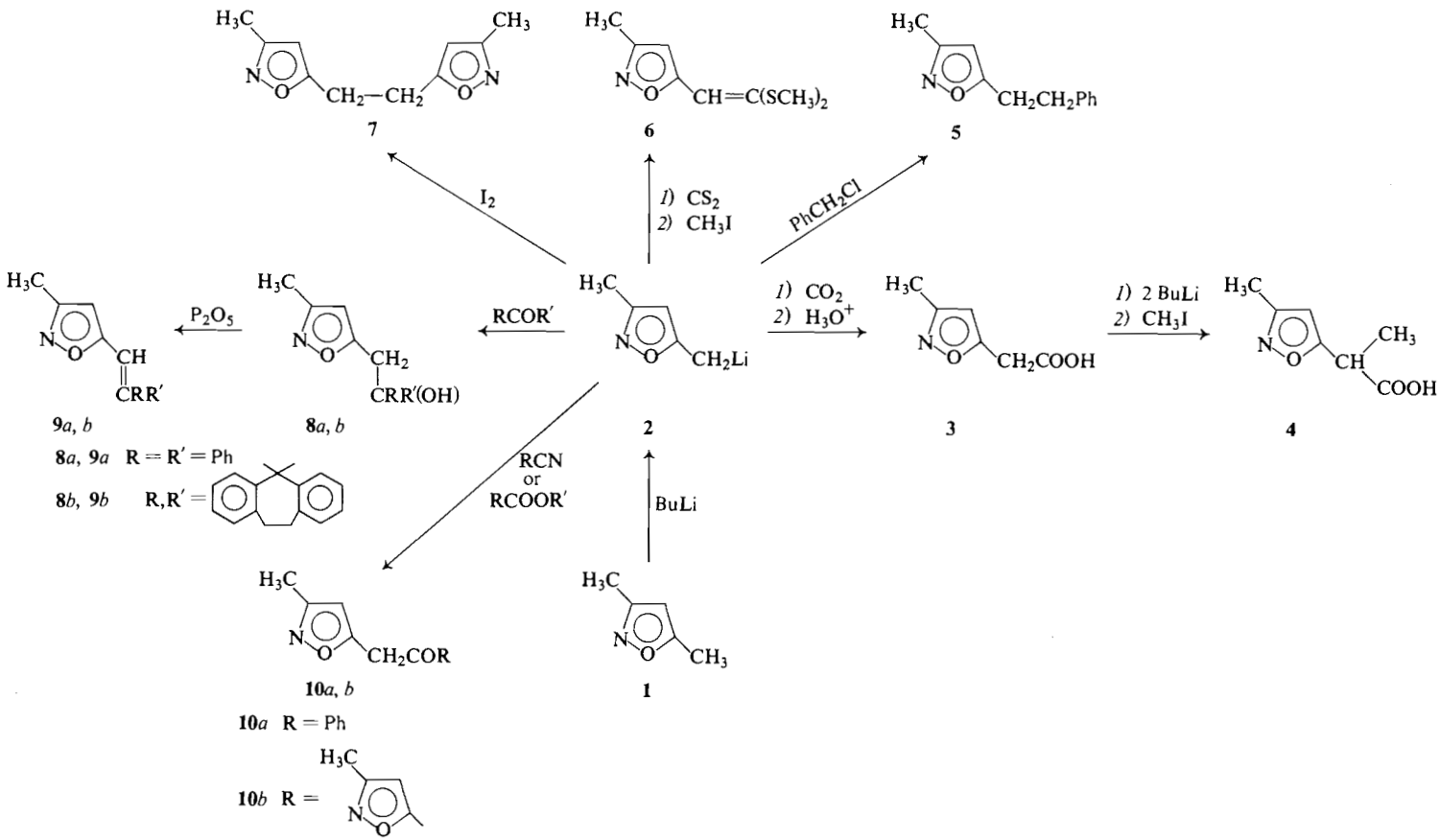

SCHEME 1

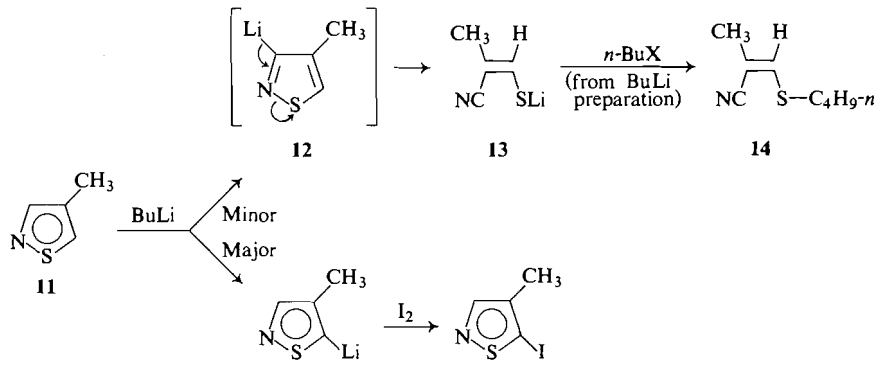

SCHEME 2

compound is insoluble in ether) which evolves gas on treatment with water giving an ether soluble oil. Distillation of this oil gave 2-*n*-butylthiopent-2-en-4-one (**26**) (25%), the structure of which was established from its elemental analysis and i.r. and n.m.r. spectral analysis. A very low yield of acidic material (ca. 1%) was also obtained from this reaction. The n.m.r. spectrum of this fraction showed it to be a mixture. No further work has been done on this material. 4-Methylisothiazole (**11**) was found to cleave in a different manner. On treatment with *n*-butyllithium followed by iodine, 4-methyl-5-iodoisothiazole (**16**) (69%) is formed, along with another product. The i.r. and n.m.r. spectra and elemental analysis of this compound showed it to be 1-*n*-butyl thio-2-cyanoprop-1-ene (**14**) (8.4%). Its formation can be explained by the reactions illustrated in Scheme 2.

The Pyrazoles

The lithiation of various pyrazoles has been reported (21–23). The 1-substituted pyrazoles in which the 5-position is free, gave the 5-lithiopyrazoles. In the case of 1-phenylpyrazole, metalation also occurred at the ortho position of the phenyl group, the ratio of 5- to ortho-substitution products being estimated at ca. 4:1 (21). The 4-lithiopyrazoles were obtained by halogen–lithium exchange. Thus, 4-bromo-1,3,5-trimethylpyrazole, on treatment with butyllithium followed by carbon dioxide, gave an 81% yield of 1,3,5-trimethylpyrazole-4-carboxylic acid (23).

We found that 1,3,5-trimethylpyrazole (**17***a*) (24) and 1-methyl-3-phenyl-5-methoxypyrazole (**17***b*) were lithiated at the 1-methyl group. Treatment of these lithioderivatives with carbon dioxide gave the respective pyrazole-1-acetic acids, **18***a* and **18***b*, in yields of 82 and 93%. The structures of these acids were confirmed from their elemental analysis and their i.r. and n.m.r. spectra. In addition 3,5-dimethylpyrazole-1-acetic acid (**18***a*) was synthesized by an unambiguous route. Ethyl bromoacetate reacted with sodio-3,5-dimethylpyrazole to form ethyl 3,5-dimethylpyrazole-1-acetate, which was converted to the acid. This acid was identical (m.p., mixed m.p., and i.r. spectrum) to the acid **18***a* obtained from the lithio-derivative of **17***a* (Scheme 3).

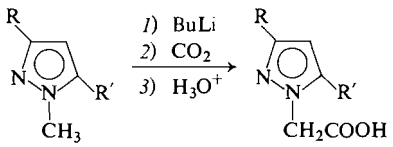

a R = R′ = CH_3
b R = Ph, R′ = —OCH_3

SCHEME 3

In the case of 1-phenyl-3,5-dimethylpyrazole **19***a* and 1-phenyl-3-methyl-5-methoxypyrazole **19***b*, reaction with butyllithium and carbon dioxide gave the respective ortho-benzoic acids **20***a* and **20***b* (Scheme 4). The structure of these acids was confirmed by their n.m.r. spectral analysis. Thus in both the acids **20***a* and **20***b* the pyrazole C_4-proton signal appeared as a singlet at ca. τ 4.25. The signals due to the phenyl protons appeared as two distinct multiplets centered at ca. τ 2.05 and 2.55, with an integrated area ratio of 1:3, indicating ortho-substitution of the phenyl ring (see Experimental for the n.m.r. data).

Can. J. Chem. Downloaded from www.nrcresearchpress.com by 210.87.254.40 on 09/05/12
For personal use only.

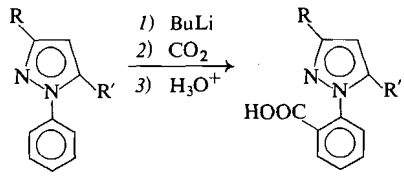

19*a*, *b* **20***a*, *b*

a R = R′ = CH_3
b R = CH_3, R′ = —OCH_3

SCHEME 4

The Oxadiazoles and Thiadiazoles

Although the lithiation of 1,2,3-thiadiazoles (2) and the sydnones (25) have been reported, no instance of lateral lithiation in this series is known. Table 1 summarizes the results of our preliminary experiments in this area. In the case of those compounds **21***b*, *c*, and *h*, where ring cleavage occurred and a mixture of products resulted, no attempt was made to identify the products or investigate the mode of cleavage.

Discussion of Results

The lithiation of five-membered heteroaromatic compounds can give rise to three different types of reaction, viz. substitution or addition reactions and nucleophilic ring cleavage. According to Shirley *et al.*, "it has been long recognized that the principal factor in the metalation reaction which determines the position of the entering lithium atom is the relative 'acidity' of the ring hydrogen as influenced by inductive effects of ring substituents" (26). The inductive effect has been suggested to decrease in the order $SO_2 > O > S > N$ (27). However the relative order of S and N would seem to be dependent on the system under study since Shirley and Jackson have shown that metalation of fused-ring phenothiazines always occurs adjacent to nitrogen (28). Replacement of the most 'acidic' proton by lithium can result in lithiation of the ring or lateral lithiation of a substituent on the ring. In some cases, the lithioderivative thus formed can undergo spontaneous ring cleavage (2).

The lithiation of isoxazoles may be explained by the strong inductive effect of the ring oxygen which also extends to the C_5-methyl group of 3-substituted-5-methylisoxazoles. This effect is however modified by the nature of the C-3 substituent. Thus, in the case of 3-methoxy-5-methylisoxazole, the inductive effect of the C_3-methoxy group increases the 'acidity' of the C-4 proton. As a result, lithiation produces a mixture of compounds as shown by the work of Bowden *et al.* (15). With the 3-phenyl-5-alkoxy, -thioalkoxy, or -chloroisoxazoles or the 3-methoxy-5-phenylisoxazoles, lithiation produces the 4-lithioderivative exclusively (29).

The reaction of butyllithium on the isothiazoles is more complicated. 4-Methylisothiazole is thus attacked at both the C_3- and the C_5-positions and this is probably a result of the comparable inductive effects of the nitrogen and sulfur in this ring. The yields of products indicate that sulfur is more strongly directing in metalation reactions in this ring system.[1]

Another complication in the case of the isothiazoles and other ring systems containing an N—S bond is the susceptibility of this bond to nucleophilic attack (30, 31). The ring cleavage product observed by Caton *et al.* (20) and the formation of 2-*n*-butylthiopent-2-en-4-one (**26**) from 3,5-dimethylisothiazole (**23**) is best explained by a nucleophilic displacement on sulfur as illustrated by Scheme 5.

This same mechanism probably accounts for the ring cleavage observed in the case of 3,4-dimethyl-1,2,5-thiadiazole (**21***b*) and 4-methyl-5-phenyl-1,2,3-thiadiazole (**21***h*). The nucleophilicity of the lithiating agent is also an important factor. Thus as we have found previously 5-phenyl-1,2,3-thiadiazole gave a 64% yield of the 4-lithioderivative with methyllithium, but only a trace of this compound with *n*-butyllithium (2). The greater nucleophilicity of the *n*-butyllithium probably resulted in the preferred nucleophilic attack at the N—S bond with resultant ring cleavage.

The lithiation of the 1-methyl group of 5-substituted-1-methylpyrazoles, the ortho position of 5-substituted-1-phenylpyrazoles, and the lateral lithiation of **21***a*, *d*, *e*, and *g* may be explained by the inductive effects of the ring

[1]The alternate possibility of nucleophilic attack at the N—S bond with expulsion of a hydride ion seems unlikely.

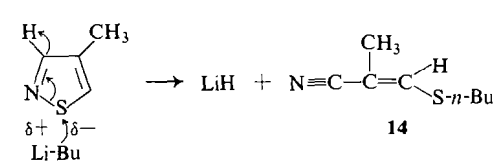

14

Can. J. Chem. Downloaded from www.nrcresearchpress.com by 210.87.254.40 on 09/05/12
For personal use only.

Can. J. Chem. Downloaded from www.nrcresearchpress.com by 210.87.254.40 on 09/05/12
For personal use only.

TABLE 1

The lithiation of methyloxa- and thiadiazoles*

Number	Compound **21**	Boiling point (°/mm)	Reference	Nuclear magnetic resonance τ (solvent)	Product **22**	Melting point (°)	Yield %	Reference	Nuclear magnetic resonance τ (solvent)
a	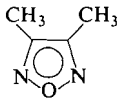	154–158	34	7.72s (CCl_4)	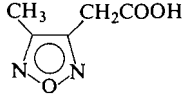	82–83	93	4	—0.45 (s, 1H), 6.12 (s, 2H) 7.63 (s, 3H) ($CDCl_3$)
b	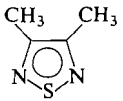	142–144	35	7.55s (CCl_4)	Ring cleavage				
c	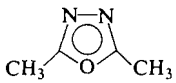	178	36	7.59s (CCl_4)	Ring cleavage				
d	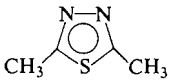	m.p. 64	37	7.28s ($CDCl_3$)	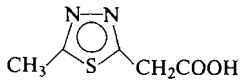	106–107 dec.	80	—	5.28 (s, 2H), 7.30 (s, 3H), 7.33 (s, 1H) (DMSO-d_6)
e	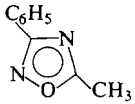	84–86/0.1 m.p. 41	38	1.93 (m, 2H), 2.57 (m, 3H), 7.46 (s, 3H) (CCl_4)	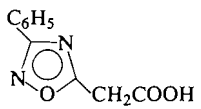	125–127 dec.	67	—	0.14 (s, 1H), 1.92 (m, 2H), 2.50 (m, 3H), 5.98 (s, 2H) ($CDCl_3$ + DMSO-d_6)
f	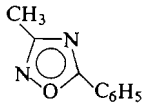	77–79/0.1 m.p. 58–59	38	1.91 (m, 2H), 2.50 (m, 3H), 7.60 (s, 3H) (CCl_4)	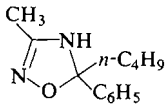	98–100	83	—	2.63 (m, 5H), 4.23 (broad, 1H), 7.95 (broad, 2H), 8.15 (s, 3H), 8.70 (broad, 4H), 9.13 (t, 3H) ($CDCl_3$)
g	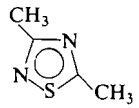	42/13	39	7.29s, 7.47s (CCl_4)	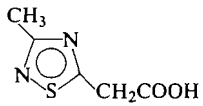	144 dec.	62	39	5.72 (s, 2H), 7.25 (s, 1H) 7.47 (s, 3H) (DMSO-d_6)
h	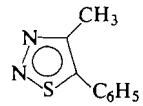	110/0.5	2	2.59 (s, 5H), 7.24 (s, 3H) (CCl_4)	Ring cleavage				

* 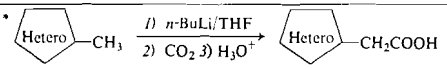

21 **22**

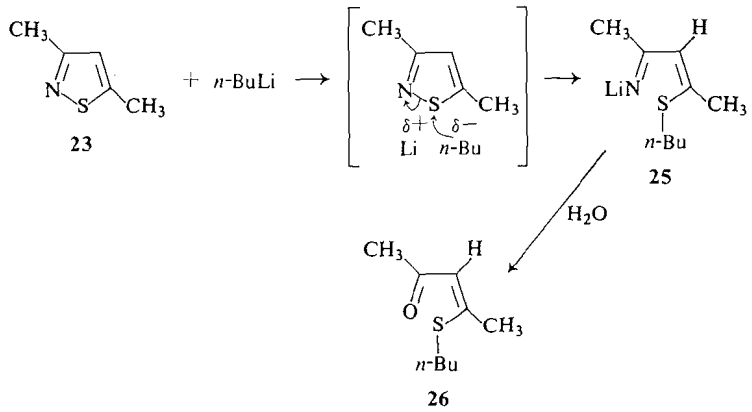

SCHEME 5

heteroatoms contributing to the increased 'acidity' of the protons which are substituted.

It is also apparent that the type of reaction (addition, substitution, or nucleophilic cleavage) is dependent not only on the ring system, but also on the substitution pattern of the ring. Thus, there is a remarkable difference in the reaction of 3-phenyl-5-methyl-1,2,4-oxadiazole (**21***e*) and its isomer 3-methyl-5-phenyl-1,2,4-oxadiazole (**21***f*) with *n*-butyllithium. Compound **21***e* undergoes lateral lithiation, while butyllithium adds to the azomethine bond of **21***f* and after work up gives a compound which has been assigned structure **22***f* from elemental analysis and spectroscopic (i.r. and n.m.r.) data, and from the existence of similar compounds (the dihydro-1,2,4-oxadiazoles) (32, 33). This method thus provides a convenient route to these compounds.

Experimental

Melting points were taken on a Fisher–Johns apparatus and are uncorrected. The i.r. spectra (ν_{max} cm^{-1}) were measured on a Perkin–Elmer model 137 spectrophotometer as Nujol mulls (solids) and films (liquids). A Varian Associates model A-60 spectrometer was used for recording n.m.r. spectra. Chemical shifts are given in τ-values and refer to spectra measured in the solvent indicated with TMS as an internal reference. Elemental analyses where specified were within ±0.4% of the calculated values, and are filed in the Depository of Unpublished Data, National Science Library, National Research Council of Canada, Ottawa, Canada.

*3,5-Dimethylisoxazole (**1**)*

Compound **1**, b.p. 136–140°, (89%) was prepared as described in the literature (16). The n.m.r. (neat) 4.12 (s, 1H), 7.70 (s, 3H), 7.83 (s, 3H). Reported b.p. 140–142° (57–67%) (16).

3-Phenyl-5-methylisoxazole

Was made as described previously (17). The n.m.r. ($CDCl_3$) ca. 2.20 (m, 2H), 2.59 (m, 3H), 3.73 (s, 1H), 7.59 (s, 3H).

*1,3,5-Trimethylpyrazole (**17***a*)*

Methylhydrazine (46 g, 1 mole) was added slowly to a stirred ice-cooled solution of 2,4-pentanedione (100 g, 1 mole) in methanol (500 ml), at such a rate as to keep the reaction temperature at ca. 30°. The mixture was stirred for 2 h after the addition was completed and distilled under reduced pressure to give 94 g (85%) of 1,3,5-trimethylpyrazole, b.p. 80°/35 mm, m.p. 37–38°.

Reported m.p. 37° (24), n.m.r. (40).

*1-Phenyl-3,5-dimethylpyrazole (**19***a*)*

Compound **19***a*, b.p. 135°/15 mm, was obtained in 87% yield from phenylhydrazine and 2,4-pentanedione using the same procedure. The n.m.r. (neat) from 2.50 to 2.92 (m, 5H), 4.12 (s, 1H), 7.74 (s, 3H), 7.91 (s, 3H).

Reported b.p. 237° (41).

3,5-Dimethylpyrazole

The compound, m.p. 107° (CCl_4), was obtained in 80% yield from hydrazine and 2,4-pentanedione using the same procedure.

Reported m.p. 107° (42).

3,5-Dimethylisothiazole

The compound, b.p. 153–155°, was obtained in 39% yield from 3-methylisothiazole using a published procedure (20). The n.m.r. (CCl_4), 3.39 (s, 1H), 7.55 (s, 3H), 7.68 (s, 3H).

Reported b.p. 157° (20).

*1-Methyl-3-phenyl-5-methoxypyrazole (**17***b*)*

A solution of diazomethane in ether (550 ml of a 0.2 *M* solution, 0.11 mole) was added to a stirred suspension of 1-methyl-3-phenylpyrazole-5-one (17.4 g, 0.1 mole) in THF and the mixture left at room temperature overnight. Distillation of the residue gave 17.5 g (93%) of **17***b* as a pale yellow liquid b.p. 116°/0.3 mm, m.p. 35°. The i.r. (mull) 1550 (s), 1500 (m); n.m.r. ($CDCl_3$) ca. 2.33 and 2.75 (m, 5H), 4.27 (s, 1H), 6.19 (s, CH_3), 6.41 (s, 3H). Anal. ($C_{11}H_{12}N_2O$), C, H, N.

*1-Phenyl-3-methyl-5-methoxypyrazole (**19***b*)*

The compound, b.p. 124–126°/0.4 mm, was obtained in 75% yield from 1-phenyl-3-methylpyrazole-5-one using

Can. J. Chem. Downloaded from www.nrcresearchpress.com by 210.87.254.40 on 09/05/12
For personal use only.

Can. J. Chem. Downloaded from www.nrcresearchpress.com by 210.87.254.40 on 09/05/12
For personal use only.

the same procedure. The i.r. 1580, 1550 and 1500 (s); n.m.r. (CCl_4) ca. 2.33 and 2.79 (m, 5H), 4.72 (s, 1H), 6.30 (s, 3H), 7.83 (s, 3H). Anal. ($C_{11}H_{12}N_2O$), C, H, N.

Preparation of Dimethyl- and Phenylmethyloxadiazoles and Thiadiazoles

The following compounds were prepared by procedures described in the literature.

*3,4-Dimethyl-1,2,5-oxadiazole (**21a**)* b.p. 154–158°, 60%. Reported b.p. 154–159° (34).

*3,4-Dimethyl-1,2,5-thiadiazole (**21b**)* b.p. 142–144°, 35%. Reported b.p. 146–148° (35).

*2,5-Dimethyl-1,3,4-oxadiazole (**21c**)* b.p. 178°, 58%. Reported b.p. 65°/12 mm (36).

*3,5-Dimethyl-1,2,4-thiadiazole (**21g**)* b.p. 42°/13 mm, 30%. Reported b.p. 42°/13 mm 92°/125 mm (39).

*2,5-Dimethyl-1,3,4-thiadiazole (**21d**)* was prepared as follows:

Diacetylhydrazine (65.5 g, 0.56 mole), phosphorus pentasulfide (50 g, 0.22 mole), and xylene (b.p. 133–135°, 150 ml) were stirred vigorously and heated under reflux for 1 h by which time the solid had dissolved and gas evolution had ceased. The mixture was cooled in an ice bath and stirred while ice water (200 ml) was added. After stirring for 1/2 h the layers were separated and the aqueous layer extracted with ether (3 × 100 ml). The combined organic layers were discarded. The aqueous layer was made basic (p*H* ca. 10) with aqueous sodium hydroxide and continuously extracted with ether for 24 h. The ether layer was dried over magnesium sulfate, filtered, and solvent removed when 44 g, 68% of white needles were obtained, m.p. 64° (hexane). Reported m.p. 64° (37).

*3-Phenyl-5-methyl-1,2,4-oxadiazole (**21e**)*

The compound was prepared by an extension of a method of preparing 3-aryl-1,2,4-oxadiazoles (32, 43, 44).

Benzamidoxime (104 g, 0.8 mole) and triethylorthoacetate (260 g, 1.6 mole) were stirred and heated for 2 h under reflux on an oil bath at 140°. The ethanol formed was removed by distillation and the residue distilled under reduced pressure using a 12″ Vigreux column. The fraction b.p. 84–86°/0.1 mm, weighed 53.2 g, 42%, and crystallized on scratching, m.p. 41°. Reported m.p. 41° (38).

*3-Methyl-5-phenyl-1,2,4-oxadiazole (**21f**)*

The compound was made following a procedure described by F. Eloy (45).

Triethylamine (5 ml) in benzene (250 ml) was added over ca. 10 min to a stirred solution of nitroethane (41.3 g, 0.55 mole), phenyl isocyanate (119 g, 1.0 mole), and benzonitrile (103 g, 1.0 mole) in benzene (500 ml). About 5 min after the addition was completed the color of the mixture became yellow and after another 5 min a solid began to separate. There was a mild exothermic reaction and the temperature rose to 35°. The mixture was heated with stirring at 50° for 1 h and then under reflux for 3 h and left overnight at room temperature. The white solid was filtered and the filtrate concentrated under reduced pressure. The residue on distillation under reduced pressure using a 12″ Vigreux column gave 17 g of an oil b.p. 77–79°/0.1 mm. The oil was taken up in ether and on cooling gave 10.2 g, 11% of white needles m.p. 58–59°. Reported m.p. 57° (38).

*4-Methyl-5-phenyl-1,2,3-thiadiazole (**21h**)*

Phenyl-2-propionone (67 g, 0.5 mole), carbomethoxyhydrazine (45 g, 0.5 mole), and acetic acid (1 ml) were mixed with warming until homogeneous and left overnight at room temperature. The crude hydrazone thus formed was dried under vacuum, powdered, and added slowly to stirred thionyl chloride (357 g, 3 mole) cooled in an ice bath. There was an immediate reaction with gas evolution. After the addition was completed the mixture was left at room temperature for 3 h and concentrated under reduced pressure. The residue was shaken well with ice-water (300 ml) and extracted with ethyl acetate (3 × 300 ml). The combined ethyl acetate layers were extracted with aqueous sodium carbonate and then water and dried over magnesium sulfate. After filtration and removal of solvent the residue was distilled under reduced pressure and gave 77.5 g, 88% of a light yellow oil b.p. 110°/0.5 mm. Reported b.p. 82–83°/0.1 mm (2).

General Procedure for the Preparation of Acids

A solution of *n*-butyllithium in hexane (18.8 ml of a 1.6 *M* solution, 0.03 mole) was added slowly to a stirred, cold (−70°) solution of the compound (0.03 mole) in dry THF (50 ml) in a nitrogen atmosphere, the temperature of the mixture being maintained below −50°. After 1/2 h at this temperature, the mixture was poured with stirring onto excess of finely powdered Dry-Ice and allowed to reach ambient temperature, after which it was concentrated under reduced pressure. (The lithium salt of the acid (usually a solid) could be washed with ether and isolated if desired.) The residue was dissolved in water and extracted with ether. The aqueous layer was then made acid with concentrated hydrochloric acid, when a solid usually separated. Extraction with ethyl acetate, drying the organic layer ($MgSO_4$), and removal of solvent gave the acid.

*3-Methylisoxazole-5-acetic Acid (**3**)*

The m.p. 104–105°, (73%). The i.r. 1700, 1590, 1480; n.m.r. (DMSO-d_6) 3.80 (s, 1H), 6.15 (s, 2H), 7.82 (s, 3H). Anal. ($C_6H_7NO_3$), C, H, N.

The *methyl ester* (90%) was obtained by reaction with diazomethane, b.p. 67°/0.2 mm. Anal. ($C_7H_9NO_3$) C, H.

3-Phenylisoxazole-5-acetic Acid

The m.p. 131–133°, (81%). The i.r. 1700, 1640 (broad); n.m.r. (DMSO-d_6) ca. 2.18 and 2.51 (m, 5H), 3.12 (s, 1H), 6.05 (s, 2H).

Reported m.p. 129–130° (18).

*3,5-Dimethylpyrazole-1-acetic Acid (**18a**)*

In the case of this acid it was necessary to continuously extract the acidified reaction mixture with ethyl acetate for 36 h. The m.p. 189–190°, (82%). The i.r. 1710, 1530; n.m.r. (DMSO-d_6) 4.21 (s, 1H), 5.28 (s, 2H), 7.88 (s, 3H), 7.95 (s, 3H). Anal. ($C_7H_{10}N_2O_2$), C, H, N.

*3-Phenyl-5-methoxypyrazole-1-acetic Acid (**18b**)*

The m.p. 212–213°, (93%). The i.r. 1710, 1570, 1500; n.m.r. (DMSO-d_6) ca. 2.30 and 2.70 (m, 5H), 3.87 (s, 1H), 5.30 (s, 2H), 6.13 (s, 3H). Anal. ($C_{12}H_{12}N_2O_3$), C, H, N.

*o-(3,5-Dimethyl-1-pyrazole)-benzoic Acid (**20a**)*

The m.p. 151–153°, (44%). The i.r. 1690, 1650 (sh), 1590, 1550; n.m.r. ($CDCl_3$) 2.07 (m, 1H), 2.58 (m, 3H), 4.07 (s, 1H), 7.76 (s, 3H), 7.95 (s, 3H). Anal. (C_6H_6NO), C, H.

*o-(3-Methyl-5-methoxy-1-pyrazole)benzoic Acid (**20b**)*

The m.p. 163–165°, (53%). The i.r. 1700, 1600, 1590,

Can. J. Chem. Downloaded from www.nrcresearchpress.com by 210.87.254.40 on 09/05/12
For personal use only.

1560, 1500; n.m.r. (CCl_4) 2.05 (m, 1H), 2.54 (m, 3H), 4.52 (s, 1H), 6.21 (s, 3H), 7.73 (s, 3H). Anal. ($C_{12}H_{12}N_2O_3$), C, H, N.

*3-Methyl-1,2,5-oxadiazol-4-acetic Acid (**22a**)*

The m.p. 82–83°, (93%). Reported m.p. 83–84° (4).

*2-Methyl-1,3,4-thiadiazol-5-acetic Acid (**22d**)*

The m.p. 106–107° dec., (80%). Anal. ($C_5H_6N_2O_2S$), C, H, N.

*3-Phenyl-1,2,4-oxadiazol-5-acetic Acid (**22e**)*

The m.p. 125–127° dec., (67%). Anal. ($C_{10}H_8N_2O_3$), C, H, N.

*3-Methyl-1,2,4-thiadiazol-5-acetic Acid (**22g**)*

The m.p. 144° dec., (62%). Reported m.p. 144° (39).

*3-Methylisoxazole-5-α-methylacetic Acid (**4**)*

3-Methylisoxazole-5-acetic acid, **3** was treated with 2 equ of butyllithium maintaining the temperature below −20° and after 1/2 h methyl iodide (1.5 equ) was added. On work-up, as described above, an oil was obtained. Distillation gave the acid, b.p. 145°/2 mm, m.p. 56–58° in 70% yield. The i.r. (mull) 1710, 1600; n.m.r. (CCl_4) 3.99 (s, 1H), 6.11 (q, 1H), 7.77 (s, 3H), 8.45 (d, 3H) J = 7 Hz. Anal. ($C_7H_9NO_3$), C, H, N.

Unambiguous Synthesis of 3,5-Dimethylpyrazole-1-acetic Acid

3,5-Dimethylpyrazole (9.6 g, 0.1 mole) was added in portions to a stirred suspension of sodium hydride (4.6 g of a 56% oil suspension, 0.11 mole, prewashed with hexane) in dry THF. The reaction was mildly exothermic. After 1/2 h at room temperature, ethyl bromoacetate (18.4 g, 0.11 mole) was added, and the mixture heated under reflux for 1 h after which the solvent was removed. Water (100 ml) was added to the residue, and the mixture extracted with ethyl acetate (3 × 50 ml). The combined organic layers were dried ($MgSO_4$), filtered, and concentrated. Distillation of the residue gave 12 g, (66%) of ethyl 3,5-dimethylpyrazole-1-acetate, b.p. 80°/0.5 mm.

This ester was hydrolyzed with methanolic sodium hydroxide to give 3,5-dimethylpyrazole-1-acetic acid, m.p. 189–190°, identical (mixed m.p. and i.r. spectra) with the sample obtained by the alternate route.

*General Procedure for the Reactions with 3,5-Dimethylisoxazole (**1**) (Scheme 1) and 4-Methylisothiazole (Scheme 2)*

A solution of *n*-butyllithium in hexane (18.8 ml of a 1.6 *M* solution, 0.03 mole) was added slowly to a stirred cold (−70°) solution of the 1,2-azole (0.03 mole) in dry THF (50 ml) in a nitrogen atmosphere, the temperature being maintained below −50°. After 1/2 h at this temperature, the appropriate reagent (0.033 mole) was added in one lot, the reaction mixture allowed to warm to room temperature, and the solvent removed under reduced pressure. The mixture was shaken with aqueous ammonium chloride and extracted with ether or ethyl acetate. The combined organic layers were dried ($MgSO_4$), filtered, and solvent removed under reduced pressure. The compound was then distilled or crystallized.

*4-Methyl-5-iodoisothiazole (**16**)*

The product from the reaction of iodine on lithiated 4-methylisothiazole was an oil. Distillation gave three fractions. Fraction I, b.p. 34–40°/12 mm, was mainly 4-methylisothiazole. Fraction II, b.p. 94–97°/12 mm, was 4-methyl-5-iodoisothiazole. Redistillation gave 69% of an oil b.p. 73–76°/3 mm. The i.r. 1440; n.m.r. (CCl_4) 1.92 (s, 1H), 7.75 (s, 3H). Anal. (C_4H_4NSI), C, H, N. Fraction III b.p. 75–80°/0.5 mm was a yellow oil. On redistillation it gave 8.4% of *1-n-butylthio-2-cyanoprop-1-ene* (**14**), b.p. 80°/0.5 mm. The i.r. (film) 2200 (strong, sharp), 1660, 1580; n.m.r. (CCl_4) 3.22 (m, 1H), ca. 7.19, 8.42, 9.06 (m, 9H), 8.07 (d, 3H), J = 2 Hz. Satisfactory analyses were obtained only after further purification by gas–liquid chromatography (g.l.c.) ($C_8H_{13}NS$) C, H, N, S.

*3-Methyl-5-β-phenylethylisoxazole (**5**)*

Benzyl chloride gave **5**, b.p. 108°/0.6 mm, (62%). The i.r. 1610, 1490; n.m.r. (CCl_4) 2.88 (s, 5H), 4.38 (s, 1H), 7.10 (s, 4H), 7.88 (s, 3H); n.m.r. (CF_3COOH) 2.80 (m, 5H), 3.63 (s, 1H), 6.90 (m, 4H), 7.47 (s, 3H). In trifluoroacetic acid the C_5—CH_2—CH_2— protons become nonequivalent as a result of quaternization of the isoxazole ring. Anal. ($C_{12}H_{13}NO$), C, H, N.

*3-Methyl-5-isoxazole-(β,β-dithiomethyl)ethylene (**6**)*

This compound was obtained by treating 3-methyl-5-lithiomethylisoxazole, **2**, at 0° with 1/2 equ of carbon disulfide, followed by 1.1 equ of methyl iodide. It was a pale yellow oil b.p. 118°/0.4 mm (75%). The i.r. 1580, 1550 (sh); n.m.r. (CCl_4) 3.61 (d, 2H), 7.57 (s, 3H), 7.62 (s, 3H), 7.78 (s, 3H). Anal. ($C_8H_{11}NOS_2$), C, H, N, S.

*1,2-Di-(3-methyl-5-isoxazole)ethane (**7**)*

Iodine gave **7**, m.p. 89–90°, (48%). The i.r. 1600; n.m.r. ($CDCl_3$) 4.14 (s, 1H), 6.89 (s, 2H), 7.77 (s, 3H). Anal. (C_5H_6NO), C, H, N.

*3-Methyl-5-benzoylmethylisoxazole (**10a**)*

Benzonitrile gave **10***a*, m.p. 70–72°, (71%). The i.r. 1690, 1600, 1580 (sh); n.m.r. ($CDCl_3$) ca. 1.96 and 2.40 (m, 5H), 3.88 (s, 1H), 5.60 (s, 2H), 7.75 (s, 3H). Anal. ($C_{12}H_{11}NO_2$), C, H, N.

*3-Methyl-5-(3′-methyl-5′-isoxazoloylmethyl)isoxazole (**10b**)*

Methyl 3-methylisoxazole-5-carboxylate (17) gave **10***b*, m.p. 105–109°, (75%). The i.r. 1690, 1600, 1570; n.m.r. ($CDCl_3$) 3.13 (s, 1H), 3.82 (s, 1H), 5.61 (s, 2H), 7.62 (s, 3H), 7.73 (s, 3H). Anal. ($C_{10}H_{10}N_2O_3$), C, H, N.

*3-Methylisoxazole-5-(β,β-diphenyl)ethanol (**8a**)*

Benzophenone gave **8***a*, m.p. 92–93°, (51%). The i.r. 3300, 1600, 1480; n.m.r. ($CDCl_3$) 2.65 (m, 10H), 4.40 (s, 1H), 6.32 (s, 2H), 6.80 (s, 1H), 7.94 (s, 3H). Anal. ($C_{18}H_{17}NO_2$), C, H, N.

*3-Methylisoxazole-5-methylene-(1′-hydroxy-1′-dibenzosuberone) (**8b**)*

Dibenzosuberone gave **8***b*, m.p. 113–114°, (60%). The i.r. 3350, 1600; n.m.r. (CCl_4) ca. 2.31 and 2.99 (m, 8H), 4.71 (s, 1H), 6.55 (s, 1H), 6.49 (s, 2H), ca. 6.15 to 7.15 (m, 4H), 7.97 (s, 3H). Anal. ($C_{20}H_{19}NO_2$), C, H, N.

General Procedure for the Dehydration of the Carbinols 8a and 8b

A mixture of the carbinol (0.01 mole), P_2O_5 (0.02 mole) and benzene (25 ml) was stirred and heated on a water bath under reflux. Periodically (every 15 min), an i.r. spectrum was obtained on the benzene solution. When the reaction was over (the —OH band in the i.r. spectrum had disappeared, about 1½ h) the benzene layer was decanted and the residue washed once with hot benzene. The combined benzene layers were washed with water,

Can. J. Chem. Downloaded from www.nrcresearchpress.com by 210.87.254.40 on 09/05/12
For personal use only.

dried ($MgSO_4$), and solvent removed to give the anhydro compound.

3-Methylisoxazole-5-(β,β-diphenyl)ethylene (9a)

The m.p. 93–94°, (70%). The i.r. 1610, 1570; n.m.r. (CCl_4) 2.75 (m, 10H), 3.03 (s, 1H), 5.18 (s, 1H), 7.98 (s, 3H). Anal. ($C_{18}H_{15}NO$), C, H, N.

3-Methylisoxazole-5-methene-1'-dibenzosuberane (9b)

The m.p. 103–106° (95%). The i.r. 1610 1570; n.m.r. (CCl_4) 2.81 (m, 8H), 3.31 (s, 1H), 4.95 (s, 1H), 6.88 (broad, 4H), 7.98 (s, 3H). Anal. ($C_{20}H_{17}NO$), C, H, N.

The Lithiation of 3,5-Dimethylisothiazole

A solution of *n*-butyllithium in hexane (25 ml of a 2 *M* solution, 0.05 mole) was added slowly to a stirred, cold (−70°) solution of 3,5-dimethylisothiazole (5.65 g, 0.05 mole) in dry THF (100 ml) in a nitrogen atmosphere. There was a mildly exothermic reaction and an orange–red color developed. After 1/2 h at −70° the mixture was poured with stirring over excess, powdered Dry-Ice, and allowed to reach ambient temperature, after which it was concentrated under reduced pressure. The residue, a yellow–orange solid, was washed with dry ether (4 × 50 ml) and the ether removed each time by decantation since the fine solid that was present clogged the filter. The solid was dried and weighed 5.9 g. Its i.r. spectrum showed a strong broad band at 1600 cm^{-1} and its n.m.r. spectrum showed strong bands characteristic of *n*-butyl groups. The solid was added to ice water when a gas was evolved and an oil resulted. The oil was extracted with ether (3 × 50 ml) and the ether extract dried ($MgSO_4$), filtered, and ether removed leaving 3.1 g of a brown oil. Distillation gave 1.1 g of a light yellow oil b.p. 85–87°/0.4 mm.

The ether wash of the solid was washed with water, dried ($MgSO_4$), and distilled when 1.1 g of a light yellow oil b.p. 85–89°/0.4 mm was obtained. Since the i.r. and g.l.c. of these two fractions were identical they were combined and redistilled when 2 g of a light yellow oil b.p. 80°/0.2 mm was obtained. The i.r. 1570, 1550; n.m.r. ($CDCl_3$) 4.03 (s, 1H), 7.63 (s, 3H), 7.83 (s, 3H), ca. 7.22, 8.45 and 9.05 (m, 9H). Satisfactory analysis results were obtained only after further purification by g.l.c. Anal. ($C_9H_{16}SO$), C, H, S. (S + 0.5%).

The aqueous layers from the above experiment were combined, made acid with concentrated hydrochloric acid and continuously extracted for 24 h with ethyl acetate. The organic layer on drying and removal of solvent gave 100 mg of a waxy solid. This fraction was discarded since its n.m.r. spectrum showed it to be a mixture.

3-Methyl-5-phenyl-5-n-butyl-1,2,4-dihydroöxadiazole (22f)

n-Butyllithium in hexane (14 ml of a 2 *M* solution, 0.028 mole) was added to a cooled (−70°) stirred solution of 3-methyl-5-phenyl-1,2,4-oxadiazole (**21***f*) (3.2 g, 0.02 mole) in dry THF (25 ml) in a nitrogen atmosphere at such a rate as to keep the reaction temperature below −60°. A dark brown solution resulted. Ten minutes after the addition was completed, the cold reaction mixture was poured with stirring onto excess of well powdered Dry-Ice and the reaction mixture allowed to reach ambient temperature after which concentration under reduced pressure gave an orange foamy solid. This solid was stirred with water and extracted with ether (3 × 30 ml). The combined ether extracts were dried over $MgSO_4$ and taken down to dryness when 3.6 g, 83% of a pink colored solid, m.p. 92–97°, was obtained. Recrystallization from benzene–hexane raised the m.p. to 98–100°. The i.r. spectrum (Nujol mull) showed a strong broad band at ca. 3200 cm^{-1} characteristic of —NH stretching and a strong sharp band at 1620 cm^{-1}. The n.m.r. spectrum is described in Table 1.

In the case of **21***b*, *c*, and *h*, reaction with *n*-butyllithium and carbon dioxide using the procedure described for **21***a* above resulted in neutral and acid fractions. The n.m.r. spectra of these fractions showed that they were mixtures of products. No further work was done on these fractions.

The author thanks Professor R. U. Lemieux, Director of Research, for his advice and interest in this work and Messrs. Ray Thomas and Robert Fortier for their capable technical assistance.

1. R. Raap and R. G. Micetich. J. Med. Chem. **11**, 70 (1968).
2. R. Raap and R. G. Micetich. Can. J. Chem. **46**, 1057 (1968).
3. E. Campaigne and W. M. LeSuer. J. Amer. Chem. Soc. **70**, 1555 (1958).
4. L. B. Crast. Bristol-Myers Co., Brit. Pat. 1 124 920, August 21, 1968; Chem. Abstr. **70**, 4106*g* (1969).
5. S. E. Forman. J. Org. Chem. **29**, 3323 (1964).
6. T. Kato and Y. Goto. Chem. Pharm. Bull. (Tokyo), **11**, 461 (1963).
7. S. K. Chakrabarthy and R. Levine. J. Heterocycl. Chem. **4**, 109 (1967). See also earlier references by R. Levine and co-workers.
8. F. H. Rash, S. Boatman, and C. R. Hauser. J. Org. Chem. **32**, 372 (1967).
9. N. V. Nederlands Combinatie voor Chemische Industrie. Fr. Pat. 1 404 514, July 2, 1965; Chem. Abstr. **64**, 3572*b* (1966).
10. A. J. Nunn and K. Schofield. J. Chem. Soc. 589 (1952).
11. (*a*) J. P. Wibaut and J. W. Hey. Rec. Trav. Chim. **72**, 513, 522 (1953). Also see earlier references by J. P. Wibaut and co-workers. (*b*) A. M. Jones, C. A. Russell, and S. Skidmore. J. Chem. Soc. 2245 (1969).
12. A. D. Cale, Jr., R. W. McGinnis, Jr., and P. C. Teague. J. Org. Chem. **25**, 1507 (1960).
13. B. M. Mikhailov and T. K. Kozminskaya. Izv. Akad. Nauk. SSSR, Otd. Khim. Nauk. 80 (1959); Chem. Abstr. **53**, 16128 (1959).
14. J. Beraud and J. Metzger. Bull. Soc. Chim. (France), 2072 (1962).
15. K. Bowden, G. Crank, and W. J. Ross. J. Chem. Soc. 172 (1968).
16. A. O. Fitton and R. K. Smalley. Practical heterocyclic chemistry. Academic Press, New York, 1968. p. 28.
17. R. G. Micetich. Can. J. Chem. **48**, 467 (1970).
18. Shionogi and Co. Jap. Pat. 6 814 216, June 15, 1968; Chem. Abstr. **70**, 20054*u* (1969).
19. D. Ivanov, Iv. M. Panaiotov, and G. Borisov. C. R. Acad. Bulg. Sci. **9**, 23 (1956); Chem. Abstr. **52**, 7189*b* (1958) and previous papers.
20. M. P. L. Caton, D. H. Jones, R. Slack, and K. R. H. Wooldridge. J. Chem. Soc. 446 (1964).

21. P. W. ALLEY and D. A. SHIRLEY. J. Amer. Chem. Soc. **80**, 6271 (1958).
22. H. R. SNYDER, F. VERBANE, and D. B. BRIGHT. J. Amer. Chem. Soc. **74**, 3243 (1952).
23. R. HÜTTELL and M. E. SCHÖN. Ann. **625**, 55 (1959).
24. L. KNORR. Ann. **279**, 232 (1894).
25. (*a*) T. NAITO, S. NAKAGAWA, K. TAKAHASHI, K. MASUKO, K. FUJISAWA, and H. KAWAGUCHI. J. Antibiot. (Japan), **21**, 290 (1968) and references cited therein. (*b*) C. V. GRECO, M. PERCE, and J. M. FRANCO. J. Heterocycl. Chem. **3**, 391 (1966).
26. D. A. SHIRLEY, J. R. JOHNSON, JR., and J. P. HENDRIX. J. Organometal. Chem. **11**, 209 (1968).
27. J. M. MALLAN and R. L. BEBB. Chem. Rev. **69**, 693 (1969).
28. D. A. SHIRLEY and T. G. JACKSON. J. Organometal. Chem. **2**, 188 (1964) and earlier papers.
29. R. G. MICETICH and C. G. CHIN. Paper submitted to Can. J. Chem.
30. (*a*) W. D. CROW and N. J. LEONARD. J. Org. Chem. **30**, 2660 (1965). (*b*) W. D. CROW and I. GOSNEY. Aust. J. Chem. **22**, 765 (1969), and earlier papers.
31. (*a*) W. R. HATCHARD. J. Org. Chem. **29**, 660, 665 (1964). (*b*) S. WATANABE. Bull. Chem. Soc. (Japan), **42**, 1152 (1969).
32. C. AINSWORTH, W. E. BUTING, J. DAVENPORT, M. E. CALLENDER, and M. C. MCCOWEN. J. Med. Chem. **10**, 208 (1967).
33. F. ELOY and R. LENAERS. Chem. Rev. **62**, 155 (1962).
34. L. C. BEHR and J. T. BRENT. Organic synthesis. Coll. Vol. IV. John Wiley and Sons, N.Y. p. 342, 1963.
35. L. N. WEINSTOCK, P. DAVIS, B. HANDELSMAN, and R. TULL. J. Org. Chem. **32**, 2823 (1967).
36. C. AINSWORTH and R. E. HACKLER. J. Org. Chem. **31**, 3442 (1966).
37. R. STOLLÉ. Ber. **32**, 797 (1899).
38. O. SCHULZ. Ber. **18**, 1085 (1885).
39. J. GOERDELER and H. W. HAMMEN. Chem. Ber. **97**, 1134 (1964).
40. E. E. ZAEV, U. K. VORONOO, M. S. SHVARTSBERG, S. F. VASILEVSKY, YU. N. MOLIN, and I. L. KOTLJAREVSKY. Tetrahedron Lett. **5**, 617 (1968).
41. L. KNORR. Ber. **20**, 1103 (1887).
42. J. THIELE and E. DRALLE. Ann. **302**, 294 (1898).
43. C. AINSWORTH. J. Heterocycl. Chem. **3**, 470 (1966).
44. M. ARBASINO and P. GRUENANGER. Chim. Ind. (Milan), **45** (10), 1238 (1963); Chem. Abstr. **60**, 10672*c* (1964).
45. F. ELOY. Union Carbide Corp., U.S., 3 264 318, August 2, 1966; Chem. Abstr. **65** 15391*f* (1966).

Can. J. Chem. Downloaded from www.nrcresearchpress.com by 210.87.254.40 on 09/05/12
For personal use only.

Can. J. Chem. Downloaded from www.nrcresearchpress.com by 210.87.254.5 on 09/05/12
For personal use only.

Phase relationships in lead sulfide – alkali chloride quasi-binary systems

A. D. PELTON AND S. N. FLENGAS
Department of Metallurgy and Materials Science, University of Toronto, Toronto 181, Ontario

Received February 2, 1970

Phase relationships in PbS–ACl (where A = Na, K, Rb, Cs) quasi-binary systems have been determined. These systems all show very large regions of liquid–liquid immiscibility. Cryoscopic calculations in PbS-rich solutions suggest that the alkali chloride dissolves in PbS partially as dissociated ions and partially as associated ion pairs.

Canadian Journal of Chemistry, **48**, 2016 (1970)

Introduction

Although sulfide ores are very important, there have been very few systematic studies of the thermodynamic properties of molten metal sulfides and their mixtures with other materials. For several years, a series of systematic studies of the properties of sulfide–halide systems has been in progress in this laboratory. Several common cation systems have been studied by a variety of techniques (1–6).

Most of the transition and post-transition metal sulfides are electronic semiconductors in the liquid as well as the solid state. This renders direct electrolysis of the ores impossible. However, when the molten sulfides are mixed with ionic metal halides, the conduction changes from electronic to ionic, and the recovery of metal by fused salt electrolysis becomes possible. The alkali chlorides might be useful solvents in such processes.

In the present investigation, a study of the phase diagrams of PbS – alkali chloride systems was undertaken. The systems all were found to have very large ranges of liquid–liquid immiscibility, and all systems were quasi-binary. Such behavior is to be expected from the large positive heats of the "exchange reactions"

$$[1] \qquad PbS + 2ACl \rightarrow PbCl_2 + A_2S$$

(where A = alkali). Values of ΔH^0_{298} for this reaction range from +44 kcal when A = Na to +78 kcal when A = Cs (7, 8).

Experimental

Preparation of Materials

Lead sulfide was prepared by direct reaction of stoichiometric amounts of lead and sulfur in sealed, evacuated quartz ampoules at 1050 °C. The ampoules were held at 1050 °C for 12 h to ensure completeness of reaction. The lead used was 99.999% pure, and the sulfur was reagent grade sublimed flowers of sulfur which was re-distilled under vacuum. There was no evidence of unreacted lead or sulfur in the lead sulfide. Several batches of PbS prepared in this manner gave the same melting point to within less than 0.5 °C.

Reagent grade NaCl and KCl were used. The RbCl and CsCl (Fisher) were 99+ % pure. All salts were dried under vacuum for 3 days at 300 °C, and were subsequently stored in a vacuum dessicator.

Cryoscopic Measurements

In the PbS-rich solutions, the liquidi could be determined over to the monotectic compositions by cooling curve measurements. Monotectic temperatures could also be measured by this method. All such measurements were carried out on samples of approximately 30 g in sealed, evacuated quartz cells. The cells had to be sealed because of the high vapor pressure of PbS (0.2 atm at the melting point (9)). Such a method yields a true equilibrium liquidus, since the salts are under their own equilibrium vapor pressures.

Thermocouples were sheathed in close-fitting quartz tubes blown into the cells. The cells were placed in an Inconel metal sheath and lowered into a vertical tube furnace. By grounding the Inconel sheath, any spurious voltages induced in the thermocouple by the a.c. field of the furnace windings were entirely eliminated. The use of such a grounded sheath was found to be essential if accurate results were to be obtained. The melt filled the cells to a depth of about 3 cm, and the thermocouple sheath extended about 2 cm below the surface of the melt. Temperature gradients over the depth of the melt were 0.25 °C or less.

The furnace was controlled by a variable auto-transformer. The furnace could be cooled at any desired rate by means of an electric motor which drove down the auto-transformer through a variable-ratio gear reductor. With cooling rates of less than 1 °C per min, supercooling could be kept to a tolerable level of between 0.25 and 2 °C. A rate of 0.75 °C per min was adopted in all experiments. Supercooling was avoided as much as possible by rocking the entire furnace.

The output from the thermocouple was recorded on a 1 mV full scale Sargent SR recorder, with most of the thermocouple output compensated by a Leeds and Northrup K2 potentiometer. A 0.015 in. Pt – Pt, 13% Rh thermocouple, calibrated against the melting points of

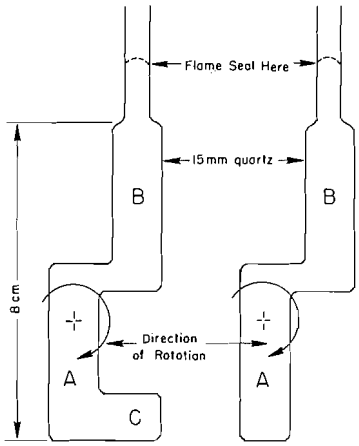

FIG. 1. Decantation cells.

gold and KCl, was used. Reproducibility of liquidus points was of the order of 0.25 to 0.5 °C as will be shown later.

Decantation and Analysis

In the alkali chloride-rich solutions, a method of decantation and analysis was used to measure the solubility of PbS in the alkali chlorides and also to determine the position of the boundary of the liquid–liquid immiscibility gap. Direct sampling of the melts was impossible because of the high vapor pressure of PbS.

For determining the boundary of the 2-liquid region above the monotectic temperature, quartz cells of Type I as shown in Fig. 1 were used. Cells were charged so as to fill compartments A and C with a mixture of alkali chloride and about 10% PbS. The cells were evacuated, and the filling tubes were sealed off. The cells were held tightly in metal containers in a tube furnace. Temperatures were read to ± 1.5 °C with calibrated thermocouples placed in quartz sheaths held tightly against the cells. In a typical experiment, a cell was held at some temperature above the monotectic for 30 min. The entire furnace was then slowly tilted so as to rotate the cell approximately 120° clockwise as shown in Fig. 1. All of the denser PbS-rich liquid phase was trapped in compartment C, while a sample of the less-dense halide-rich phase flowed into compartment B. The furnace was cooled in the tilted position. The cell was removed, and the material in compartment B was analyzed.

For determining the solubility limit of solid PbS in alkali chloride, cells of Type II in Fig. 1 were used. In a typical experiment, a cell was charged so as to fill compartment A with a mixture of alkali chloride and about 10% PbS. The cell was sealed under vacuum, heated above the monotectic, and cooled back to a desired temperature below the monotectic. This procedure gave one solid piece of PbS in the bottom of the cell, and further, it ensured that the liquid phase was saturated with PbS. The cell was held at temperature for 1½ h, and was then tilted 120° clockwise. The liquid phase flowed into compartment B, and the solid remained behind in A. The furnace was cooled, and the sample in B was analyzed. There is, of course, in these experiments the danger that some solid PbS in suspension in the liquid flowed into compartment B during decantation. However, for all systems studied, analyses of liquid phases which were decanted at temperatures just above the eutectic temperatures indicated extremely low solubilities (0.1–0.4 mole%) of PbS at these temperatures, and this then gives the maximum error which this problem might cause.

The samples obtained from the decantation experiments consisted of about 3 g of alkali chloride containing about 0.1 to 5.0 mole% PbS, all securely adhering to the quartz tube. In an analysis, the entire sample compartment of a decantation cell was broken off and crushed. The sample was dissolved in 300 ml of water, heated for 2½ h to dissolve the halide, and then filtered through a fine Pyrex frit. The residue was weighed as PbS + quartz. The frit and residue were then heated in 300 ml of aqua regia for 5 h. A final filtration was performed, and the residue was weighed as quartz. The method was tested for accuracy by analyzing several blank samples of known compositions which had been fused in quartz tubes by heating above the monotectic temperatures. For concentrations of PbS from 0.3 to 15 mole%, the analysis method was found to give the concentration of PbS to within 0.1 mole%.

Results

Cryoscopic Measurements

Results of the cooling curve experiments in PbS-rich solutions are given in Table 1. Temperatures are on the International Temperature Scale of 1948.

The listed melting point of PbS is the average of 10 measurements on 5 different cells. Only one of the 10 values deviated more than 0.4 °C from this mean. This value compares well with previously reported values of 1111.9 (3) and 1110 °C (7).

Experimental liquidus points are shown in Fig. 2. The lines shown are theoretically calculated lines as will be discussed later. The absolute accuracy of all points is estimated at ± 1 °C. However, the freezing point depressions are estimated to be accurate to about ± 0.5 °C since the thermocouple calibration error would be the same for all points over such a short temperature range.

The monotectic temperature listed for the PbS–NaCl system is the average of 6 measurements at 4 overall compositions from 22 to 80 mole% PbS. Only one point deviated more than 0.5 °C from the mean. In the PbS–KCl system, 2 measurements on different cells gave results within 0.1 °C. Only one measurement was made in

Can. J. Chem. Downloaded from www.nrcresearchpress.com by 210.87.254.5 on 09/05/12
For personal use only.

Can. J. Chem. Downloaded from www.nrcresearchpress.com by 210.87.254.5 on 09/05/12
For personal use only.

TABLE 1

Results of cryoscopic measurements

System	Mole % alkali chloride	Liquidus temperature (°C)
Pure PbS	0	1113.4
PbS–NaCl	1.02	1108.8
	1.96	1104.4
	2.92	1100.5
	Monotectic	1096.2
PbS–KCl	0.31	1111.4
	0.50	1109.7
	0.50	1109.8
	0.81	1108.2
	1.01	1107.3
	1.49	1104.6
	1.97	1102.6
	2.43	1100.2
	2.44	1099.3
	2.92	1097.5
	Monotectic	1096.0
PbS–RbCl	0.99	1106.2
	1.72	1102.1
	Monotectic	1095.5
PbS–CsCl	1.00	1106.2
	1.72	1102.0
	Monotectic	1095.3

the RbCl system. In the CsCl system, it was difficult to obtain good reproducibility in determining the monotectic temperature. A scatter of ± 1.2 °C was observed. It is not known why this scatter occurred here. The fact that PbS and the alkali chlorides form true quasi-binary systems is evidenced by the fact that the monotectic temperatures were independent of the overall composition of the samples.

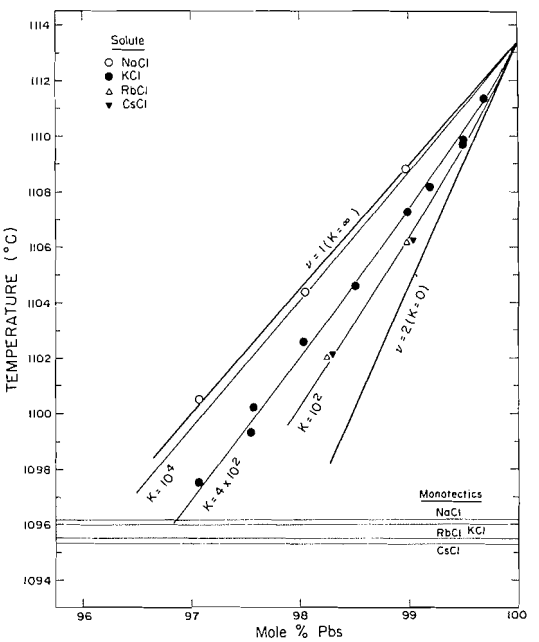

FIG. 2. Liquidi in PbS-rich solutions.

TABLE 2

Results of decantation and analysis experiments

System	Temperature (°C)	Mole % PbS
PbS–NaCl	854	0.14
	920	0.62
	937	0.31
	971	0.54
	1013	0.68
	1028	0.62
	1070	1.02
	1115	1.32
	1135	1.37
	1154	1.14
	1157	1.44
	1181	1.54
PbS–KCl	795	0.58
	874	0.63
	937	0.84
	946	0.58
	1001	1.48
	1028	1.69
	1069	1.60
	1080	1.70
	1111	2.49
	1135	2.50
	1154	2.59
	1162	2.84
PbS–RbCl	795	0.60
	874	1.21
	1001	1.63
	1069	2.16
	1080	2.46
	1162	3.15
PbS–CsCl	854	0.45
	920	0.93
	971	1.23
	1013	2.72
	1070	2.38
	1115	3.78
	1157	4.84
	1181	3.72

Although there is possibly a slight trend in going from NaCl down the series to CsCl, all four monotectic temperatures are within 1 °C of each other.

Decantation and Analysis

Results are listed in Table 2. The alkali chloride-rich sides of the phase diagrams are shown in Fig. 3. A definite trend towards increasing solubility of PbS as the solvent is changed from NaCl down the series to CsCl is evident.

Cooling curves were obtained for the pure

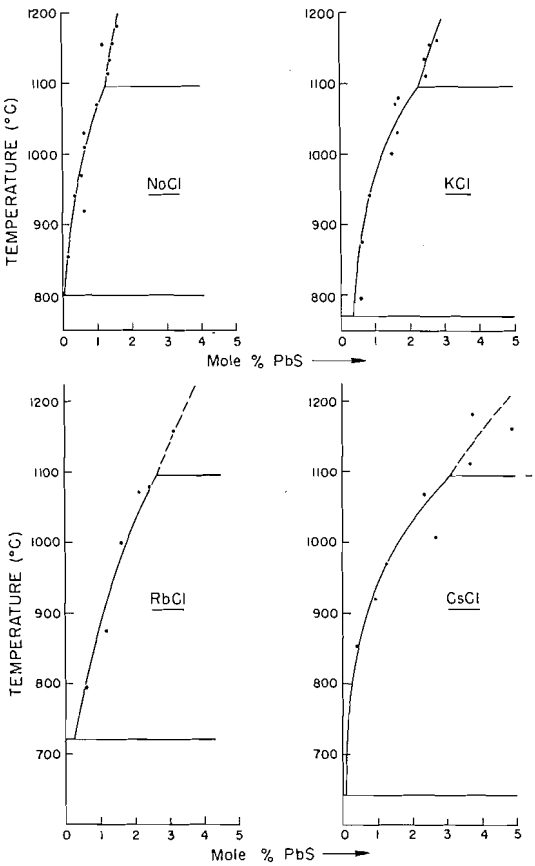

FIG. 3. Alkali chloride-rich sides of phase diagrams.

alkali chlorides and also for mixtures with overall compositions of about 10 mole% PbS in order to determine the eutectic temperatures. In all 4 systems, the eutectic temperature was within 0.5 °C of the melting point of the pure alkali chloride.

Discussion

PbS-rich Solutions

In dilute solutions of alkali chloride, ACl, in PbS, the limiting form of the van't Hoff relationship may be used

$$[2] \qquad \Delta T = \frac{\nu R T_F T_L X_{ACL}}{\Delta H_f}$$

where T_F = melting point of pure PbS, T_L = liquidus temperature, $\Delta T = (T_F - T_L)$ = freezing point depression, X_{ACl} = mole fraction ACl at T_L, ΔH_f = heat of fusion of PbS, R = ideal gas constant, and ν is the average number of particles produced when one "molecule" of ACl enters the solution. The basic assumption in the derivation (10) of this equation is that the depression of the freezing point is primarily an entropy, and not an enthalpy, effect. The use of this equation also requires that solid solubility be negligible. In view of the large regions of liquid immiscibility in these systems, the existence of any appreciable solid solubility is highly unlikely.

Theoretical liquidi calculated from eq. [2] for $\nu = 1$ and $\nu = 2$ are shown in Fig. 2. Such liquidi of constant ν are nearly straight lines. From Fig. 2 it can be seen that the measured liquidus in the PbS–KCl system approaches the $\nu = 2$ line at high dilution, but that ν becomes less as the solutions become less dilute. The same appears to be true for the RbCl and CsCl systems. The PbS–NaCl liquidus is nearly coincident with the $\nu = 1$ line.

The results suggest a simple association scheme such as

$$[3] \qquad A^+ + Cl^- \rightarrow (A^+Cl^-)_{pair}$$

in which the alkali chloride enters solution partially as dissociated A^+ and Cl^- ions, and partially as (A^+Cl^-) ion pairs. If the equilibrium concentration ratio, K, for reaction [2] is defined as

$$[4] \qquad K = \frac{N_{(A^+Cl^-)}}{(N_{A^+})(N_{Cl^-})}$$

where $N_{(A^+Cl^-)}$, N_{A^+}, and N_{Cl^-} are the number of moles of the various species per mole (overall) of solution, then, by means of a simple mass balance, it is easily shown that

$$[5] \qquad K = \frac{(2 - \nu)}{X_{ACl}(\nu - 1)^2}$$

Liquidi were calculated using eqs. [2] and [5]. In these calculations, a value of $\Delta H_f = 8700$ cal (9) was used. With $K = 4 \times 10^2$, a very good fit to the PbS–KCl liquidus was obtained as can be seen in Fig. 2. The measured points for the RbCl and CsCl systems lie very close to the calculated liquidus for $K = 10^2$. A value of $K = 10^4$ gives a liquidus very close to the measured PbS–NaCl points. Varying the value of ΔH_f used between the stated (9) error limits of $\pm$ 800 cal did not change the good agreement between the model and the observations.

In such dilute mixtures of a 1–1 salt, ACl, in a 2–2 salt, PbS, it would be expected that an A^+ ion would act as a negative charge center in the

Can. J. Chem. Downloaded from www.nrcresearchpress.com by 210.87.254.5 on 09/05/12
For personal use only.

divalent lattice, and a Cl^- ion would act as a positive charge center. A tendency towards pair formation might thus be expected to result.

On the model presented here, the tendency for the freezing point depression to decrease on going from CsCl as solute up the series to NaCl is considered to result from an increasing tendency to pair formation. This could be partially the result of an increase in the A—Cl bond strength in a pair as the size of the alkali cation is decreased. However, there are other factors affecting the energy of formation of an ion pair which could also be significant.

Conclusions

The solubility of PbS in the alkali chlorides is small enough that the solutions should not conduct electronically. Recent work in this laboratory (6), in which these solutions were used as electrolytes in formation cells, has confirmed that the saturated solutions conduct purely ionically.

Undoubtedly, other metal sulfide – alkali halide systems should be similar to the PbS – alkali chloride systems. In the Ag_2S – alkali chloride systems, for instance, work in this laboratory has indicated that the solubility of Ag_2S in alkali chlorides is much less than the solubility of PbS. Conceivably, relative solubilities of certain sulfides in alkali halides may be such that these solutions could be used in solvent-extraction processes for separating sulfide ores.

The authors wish to thank the National Research Council of Canada for financial assistance. A maintenance fellowship for one of us (A.D.P.) from the International Nickel Company is also gratefully acknowledged.

1. M. C. Bell and S. N. Flengas. J. Electrochem. Soc. **111**, 569 (1964).
2. M. C. Bell and S. N. Flengas. J. Electrochem. Soc. **111**, 575 (1964).
3. M. C. Bell and S. N. Flengas. J. Electrochem. Soc. **113**, 27 (1966).
4. M. C. Bell and S. N. Flengas. J. Electrochem. Soc. **113**, 31 (1966).
5. A. K. Garbee. Ph.D. thesis. University of Toronto, Toronto, Ontario. 1969.
6. W. T. Thompson. Ph.D. thesis. University of Toronto, Toronto, Ontario. 1969.
7. J. Elliot and M. Gleiser. Thermochemistry for steelmaking. Vol. 1. Addison Wesley, London. 1960.
8. C. E. Wicks and F. E. Block. U.S. Bur. of Mines Bull. 605. 1963.
9. O. Kubaschewski, E. W. Evans, and C. B. Alcock. Metallurgical thermochemistry. 4th ed. Pergamon Press, New York. 1967.
10. M. Blander. Molten salt chemistry. *Edited by* M. Blander. Interscience Publ. Inc., New York. 1964. p. 128–130.

Can. J. Chem. Downloaded from www.nrcresearchpress.com by 210.87.254.5 on 09/05/12
For personal use only.

Effect of pressure on the solvolysis of benzyl chloride in glycerol–water mixtures[1]

D. L. GAY[2] AND E. WHALLEY
Division of Chemistry, National Research Council of Canada, Ottawa, Canada

Received March 4, 1970

The effect of pressure up to 1.6 kbar on the rate of solvolysis of benzyl chloride in 0 to 75% v/v glycerol–water has been measured at 50 °C. The volume of activation is $-10.7 \pm \sim 0.4$ cm^3 mole^{-1}, essentially independent of solvent composition. Therefore, the partial volumes of both benzyl chloride and the transition state depend on solvent composition in the same way. The constant-volume energy and entropy of activation are simple functions of the solvent composition, and resemble the constant-volume parameters in ethanol–water mixtures. It is concluded that constant-volume conditions are probably more appropriate than constant-pressure conditions for discussing the solvent dependence of these solvolyses.

Canadian Journal of Chemistry, 48, 2021 (1970)

Introduction

The constant-pressure enthalpy and entropy of activation for the solvolysis of benzyl chloride vary much less with composition in aqueous glycerol than in aqueous ethanol (1), and in particular, the minima so frequently observed in similar systems are almost absent. The constant-volume energy and entropy of activation for the reaction in aqueous ethanol have no minimum as a function of solvent composition (2), and other reactions behave in similar ways (see ref. 1 for a summary). These and related observations have lead to the suggestion that some of the complexity of the variation of the constant-pressure activation parameters for reactions in aqueous organic solvents is directly connected with the large variation in the thermal expansivity of the solvent with composition. The larger the thermal expansivity, the more the interaction of the initial and transition states with the solvent will change with temperature. This changing interaction with temperature contributes a term to the constant-pressure enthalpy and entropy of activation that is absent in the constant-volume energy and entropy of activation.

The thermal expansivity of aqueous glycerol is almost independent of composition near 60 °C, and consequently there should be no contribution to the composition dependence of the constant-pressure parameters of activation of reactions carried out in it arising from a composition-dependent thermal expansion. This explains why the constant-pressure parameters for the solvolysis of benzyl chloride depend much less on composition in aqueous glycerol than they do in aqueous ethanol (1).

In order to complete this work it is clearly desirable to measure the constant-volume parameters for benzyl chloride in aqueous glycerol, and this paper reports the results.

Experimental

The materials and techniques were those used previously (1) except for the high-pressure techniques. The conductimetric cells were similar to those described by Baliga and Whalley (3) except that they were small enough that two could be fitted into the pressure vessel. They were made of Pyrex glass, about 80 mm long and 20 mm o.d. and had a capacity of about 20 cm^3. The cells had holes at the lower end and were immersed in mercury in a Teflon cup to prevent a short-circuit to ground. Mercury flowed into the cell to transmit the ambient pressure.

Electrode polarization was eliminated by a light deposit of platinum black; the conductance of millimolar hydrochloric acid differed by $\sim 0.02\%$ at 0.4 and 1 kc s^{-1}. The cells were cleaned with hot concentrated nitric acid, washed thoroughly with distilled water, and treated with 0.1 *M* hydrochloric acid at 100 °C until the conductance of millimolar hydrochloric acid at 50 °C remained constant within 0.1% for 2 days. The conductance was measured with a General Radio catalogue number 1680-A automatic capacitance–conductance bridge and digital read-out as described previously (1).

Results

The rate constants are summarized in Table 1 and are plotted in Fig. 1. The volumes of activation were determined both from the slopes of the lines of Fig. 1 and by plotting mean volumes of activation $\Delta V^{\ddagger}$ between two pressures, given by

[1]NRCC No. 11 297.
[2]NRCC Postdoctorate Fellow, 1965–1967; present address: Xavier College, Sydney, Nova Scotia.

TABLE 1

First-order rate constants (10^6 k/s^{-1}) for the solvolysis of benzyl chloride in aqueous glycerol at 50 °C

	Composition, % v/v at 25 °C					
p/bar	0	5.0	12.5	25.0	50.0	75.0
1	219.6	207.5	190.7	163.1	108.3	58.82
	219.4	207.0	191.2	162.5	108.3	58.87
				163.1	108.7	
395	253.5	240.7	223.0	189.5	128.6	68.71
	255.5	240.4	220.2	187.2	125.4	68.40
	255.0	240.9				68.45
792	290.0	276.1	253.7	214.1	146.3	79.77
	288.4	272.2	252.4	214.2	145.8	78.65
		272.6			145.9	
1190	328.2	311.4	287.2	241.2	162.0	—
	329.8	312.5	289.7	239.1	164.0	
	327.0					
1590	361.2	347.7	319.7	270.0	179.6	103.7
	363.4	339.6	318.1	270.3	180.1	102.0
		345.9		263.6		103.2

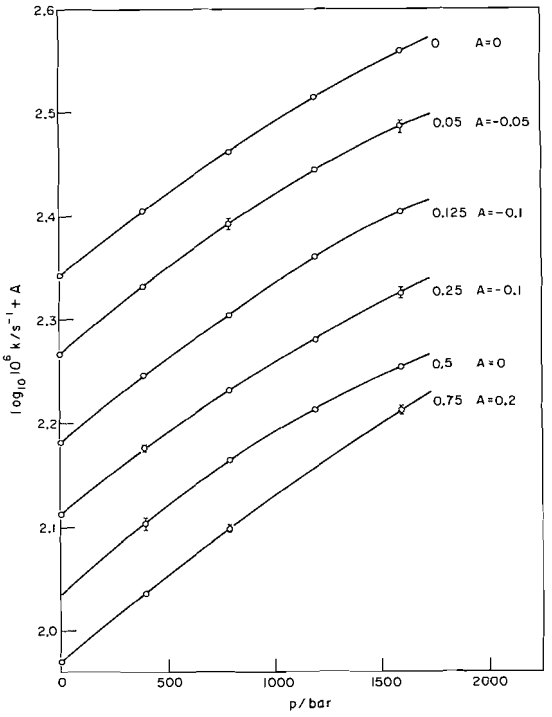

FIG. 1. Rate constants for the solvolysis of benzyl chloride in several glycerol–water mixtures at 50 °C and pressures up to 1.6 kbar. The numbers attached to the curves are the volume fractions of glycerol.

$-(RT \ln k_1/k_2)/(p_1 - p_2)$, where k_1 and k_2 are the rate constants at pressures p_1 and p_2, against the mean pressure and extrapolating to zero pressure. The plots are given in Fig. 2 and the volumes of

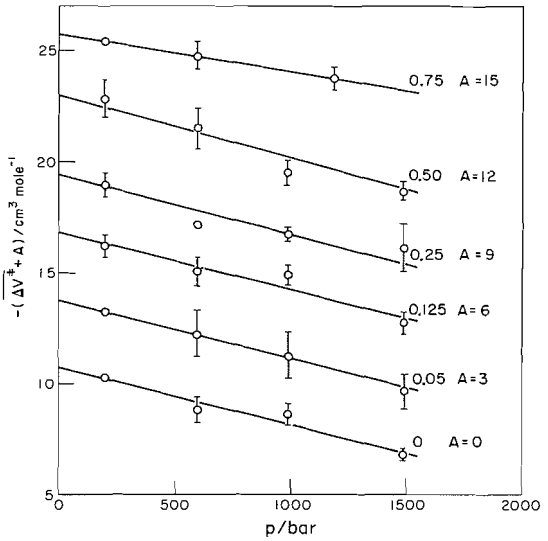

FIG. 2. Mean volumes of activation $\overline{\Delta V^{\ddagger}}$ [$= (RT \ln k_2/k_1)/(p_2 - p_1)$] against $\frac{1}{2}(p_2 + p_1)$ for the solvolysis of benzyl chloride in glycerol–water at 50.0 °C. The numbers attached to the curves are the volume fractions of glycerol.

TABLE 2

Volumes of activation for the solvolysis of benzyl chloride in aqueous glycerol at 50 °C

Volume fraction glycerol	$\Delta V^{\ddagger}$ cm^3 mole^{-1} $\pm \sim 0.4$
0.0	−10.7
0.05	−10.7
0.125	−10.8
0.25	−10.4
0.50	−11.0
0.75	−10.7

activation are summarized in Table 2. The accuracy appears to be about ± 0.3 or 0.4 cm^3 mole^{-1}. The pressure variation of the activation volume is about 2.6 cm^3 mole^{-1} kbar^{-1} for all solvents except perhaps 0.75 volume fraction glycerol, where it appears to be smaller.

The only activation volume for comparison is one by Hyne, Golinkin, and Laidlaw (4) who report -8 ± 1 cm^3 mole^{-1} in water at 50.25 °C based on a least-squares fit of four rate constants to a quadratic of ln k in the pressure. Surprisingly, the pressure coefficient of the volume of activation in water was negative, that is, the activation volume became more negative with increasing pressure, in contrast to the positive values in aqueous ethanol, and the positive value in water

TABLE 3

Constant-volume parameters of activation for the solvolysis of benzyl chloride in aqueous glycerol at 50 °C

Volume fraction glycerol	$10^6\,\alpha$* / deg^{-1}	$T\alpha\Delta V^{\ddagger}/\kappa$ cal mole^{-1} ± ~100	$\Delta\Delta H_p^{\ddagger}$ cal mole^{-1} ± ~100	$T\Delta\Delta S_p^{\ddagger}$ cal mole^{-1} ± ~100	$\Delta U_v\Delta^{\ddagger}$ cal mole^{-1} ± ~140	$T\Delta\Delta S_v^{\ddagger}$ cal mole^{-1} ± ~140
0.0	458	−851				
0.05	460	−882	−157	−194	−126	−163
0.125	475	−962	−231	−327	−120	−216
0.25	490	−1027	−361	−565	−185	−389
0.50	557	−1392	−400	−880	+141	−339
0.75	543	−1501	−300	−1186	+350	−536

*From the data in ref. 5.

found here. If the possibility of a negative $\partial\Delta V^{\ddagger}/\partial p$ is ignored, the best line through Hyne, Golinkin, and Laidlaw's points agrees reasonably well with our value. The reason for the apparent discrepancy is unknown.

In order to calculate the constant-volume energy and entropy of activation according to the equations

$$\Delta U_v^{\ddagger} = \Delta H_p^{\ddagger} - T\alpha\Delta V^{\ddagger}/\kappa$$

$$\Delta S_v^{\ddagger} = \Delta S_p^{\ddagger} - \alpha\Delta V^{\ddagger}/\kappa$$

it is necessary to know the thermal expansivity α and the compressibility κ of the solvent. The thermal expansivity was obtained graphically from data in the literature (5). The compressibility was obtained from measurements in this laboratory (6) at 60 °C. These values were taken as appropriate for 50 °C; the compressibility of pure water at 50 °C is less than 1% smaller than that at 60 °C, and that of pure glycerol is about 4% smaller. The true values of $-T\alpha\Delta V^{\ddagger}/\kappa$ are therefore somewhat larger than the values in Table 3, but are probably within the claimed error. The constant-pressure parameters from ref. 1 and the constant-volume parameters derived from them are listed in Table 3.

Discussion

1. Activation Volume and its Solvent Dependence

The activation volume in water is similar to the values for the hydrolysis of methyl and isopropyl bromides (3). The important contributions probably arise from an increase in the C—Cl bond length, a contraction due to a possible formation of a new C—O bond by incoming water, and a contraction of the solvent and the transition state caused by the increased electrostatic interaction with the solvent due to the electric moments of the transition state. There is no firm evidence about the relative values of the various contributions.

The activation volume does not change significantly with composition in the range 0 to 0.75 volume fraction glycerol in water. For the same reaction in ethanol–water (4) there is a large change of activation volume with solvent composition which appears to be largely caused by a change with solvent composition of the partial volume of the initial state (7). On the basis of the dipole-in-dielectric model of the transition state, no great change in the volume of solvation of the transition state is expected (8). In glycerol–water, the partial volumes of benzyl chloride and the transition state vary with solvent composition in the same way, and both may be almost independent of solvent composition.

2. Energy and Entropy of Activation at Constant Volume

The constant-pressure and constant-volume activation parameters are plotted in Fig. 3. There is a minimum in $\Delta H_p^{\ddagger}$ about 400 cal mole^{-1} deep which is reduced to less than 200 cal mole^{-1} in $\Delta U_v^{\ddagger}$, and may even be zero. $T\Delta S_v^{\ddagger}$ decreases by about 500 cal mole^{-1} from water to 75% v/v glycerol–water compared to a decrease of about 1200 cal mole^{-1} for $T\Delta S_p^{\ddagger}$ under the same conditions.

The question must be asked "which is to be considered the more fundamental, the constant-pressure or the constant-volume parameters, or are they to be considered equally fundamental?" The dependence of the constant-volume parameters on the solvent can be readily understood in the terms used by Baliga and Whalley (2) for the solvolysis of benzyl chloride in ethanol–water.

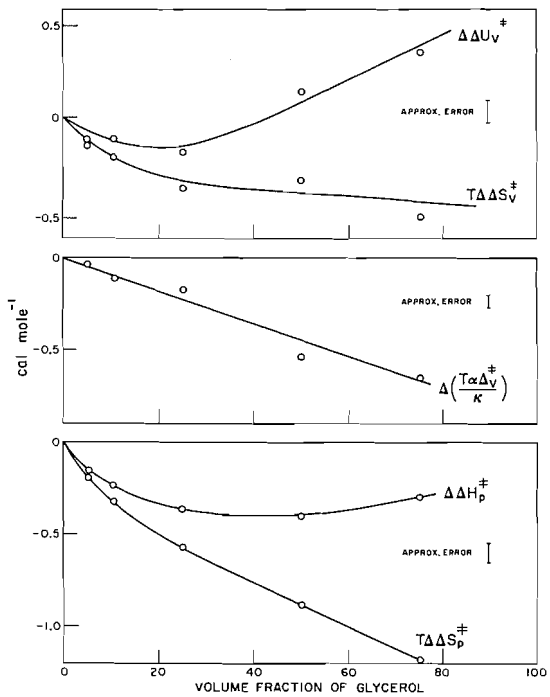

FIG. 3. Parameters of activation at constant pressure and constant volume, as labelled, for the solvolysis of benzyl chloride in glycerol–water mixtures.

Solvolysis of molecules solvated completely by water is faster than that of molecules partly solvated by the less solvating organic component. Consequently, most of the reaction in the dilute organic solution is reaction of molecules solvated by water. The energy required therefore depends little on the composition, but the activation entropy decreases because only a part of the reactant is contributing significantly to the rate. In less aqueous solvents, molecules partly solvated by the organic component contribute appreciably to the reaction, and the activation energy increases.

It appears then that the solvent dependence of the constant-volume parameters are easily and naturally understood. The minimum in the constant-pressure enthalpy is then to be understood in terms of this non-linear variation in the constant-volume energy of activation and a smooth and nearly linear fall in the quantity $T\alpha\Delta V^{\ddagger}/\kappa$.

Further evidence for this conclusion is that the activation parameters for the solvolysis of benzyl chloride in ethanol–water and in glycerol–water behave quite differently at constant pressure (1, 4) in that the minima in $\Delta H_p^{\ddagger}$ and $T\Delta S_p^{\ddagger}$ are several times deeper in ethanol–water. At constant volume, however, they behave in similar ways (2) in that there is little or no minimum in $\Delta U_v^{\ddagger}$.

Conclusions

There is no doubt that the effect of solvent on the activation parameters of several solvolyses is simpler and more easily understood when looked at at constant volume than when looked at at constant pressure. This does not of course prove that the constant-volume viewpoint is the more valid. Nevertheless, science has progressed by adopting the most appropriate viewpoint, and this is usually the one that gives the simplest view. There is no doubt that the simplicity of the constant-volume condition is a strong argument for its adoption at least for the reactions mentioned in this paper.

We are greatly indebted to A. Lavergne for help with the high-pressure apparatus.

1. D. L. GAY and E. WHALLEY. J. Phys. Chem. **72**, 4145 (1968).
2. B. T. BALIGA and E. WHALLEY. J. Chem. Phys. **71**, 1166 (1967).
3. B. T. BALIGA and E. WHALLEY. J. Phys. Chem. **73**, 654 (1969).
4. J. B. HYNE, H. S. GOLINKIN, and W. G. LAIDLAW. J. Amer. Chem. Soc. **88**, 2104 (1966).
5. J. TIMMERMANS. The physico-chemical constants of binary systems in concentrated solutions, Vol. 4. Interscience Publ. Inc., New York. 1960. p. 256.
6. D. L. GAY, J. B. R. HEATH, and E. WHALLEY. To be published.
7. H. S. GOLINKIN, I. LEE, and J. B. HYNE. J. Amer. Chem. Soc. **89**, 1307 (1967).
8. B. T. BALIGA and E. WHALLEY. Can. J. Chem. **42**, 1835 (1964).

Can. J. Chem. Downloaded from www.nrcresearchpress.com by 210.87.254.40 on 09/05/12
For personal use only.

Transition state volumes and solvolysis mechanisms

MOYRA J. MACKINNON, A. B. LATEEF,[1] AND J. B. HYNE
Department of Chemistry, The University of Calgary, Calgary, Alberta

Received January 29, 1970

The transition state partial molal volume behavior, $\bar{V}_t$, as a function of binary solvent composition was obtained for three reactions by dissection of the activation volume, ΔV^*, into initial and transition state components: $\Delta V^* = \bar{V}_t - \bar{V}_g$. The solvolyses of *t*-butyl chloride, benzyl chloride, and *p*-chlorobenzyl chloride represented a gradation of reaction type between S_N1 and S_N2 and the transition state partial molal volume behavior was found to be distinctly different in each case and in agreement with the mechanistic classification of these reactions.

Canadian Journal of Chemistry, 48, 2025 (1970)

Introduction

Golinkin, Lee, and Hyne (1) have reported a method for obtaining partial molal volumes of solutes in binary solvent mixtures, $\bar{V}_g$, and have used these volumes in conjuction with pressure–rate data, ΔV^*, to obtain the partial molal volumes of the transition state, $\bar{V}_t$, in solvolysis reactions by use of the equation $\Delta V^* = \bar{V}_t - \bar{V}_g$. A "roller–coaster" type curve was obtained for the transition state behavior in aqueous ethanol of benzyl chloride, which is generally accepted as solvolyzing by an S_N2 mechanism close to the S_N1 limit (2). The present investigation was undertaken to compare this type of behavior with that for the transition states for solvolysis reactions more distinctly S_N1 and S_N2 in character. A typical S_N1 reaction, the solvolysis of *t*-butyl chloride in aqueous ethanol, was chosen since pressure–rate data were already available (3). Also chosen was the solvolysis of *p*-chlorobenzyl chloride since it reacted at an experimentally suitable rate and represented a reaction more S_N2 in character than benzyl chloride (2). Laidler and Martin (4) have reported a similar dissection for *p*-methylbenzyl chloride in acetone–water mixtures. However, since the solvolyses considered in our analysis were carried out in ethanol–water mixtures, a direct comparison cannot be made with the acetone–water results. These reactions were therefore studied to determine if there existed some regular variation in the transition state partial molal volume behavior in binary solvents with change in mechanism.

Experimental

Materials

Water

House distilled water was first passed through Illco-Way de-ionizing resin and then redistilled in a Pyrex apparatus from which carbon dioxide was excluded. The conductivity of the water was about 8×10^{-7} Ω^{-1} cm^{-1} at 25 °C.

p-Chlorobenzyl Chloride

p-Chlorobenzyl chloride supplied by Eastman Organic Chemicals was analyzed by gas–liquid chromatography and found to contain about 2% impurity. After two recrystallizations from ether, samples obtained from liquor and crystal fractions varied in impurity from almost none to about 15%. Kinetic runs with these different samples yielded perfect straight-line first-order plots and the rate constants obtained were identical to within experimental error (± 0.5%). It was concluded that the impurity did not affect the kinetic results. The crystals with negligible impurity, obtained from two crystallizations from ether, were used throughout the investigation.

t-Butyl Chloride

t-Butyl chloride supplied by British Drug Houses was found to contain about 3% impurity when analyzed by gas–liquid chromatography. After two distillations under vacuum the impurity was reduced to about 0.5%. Partial molal volumes determined with samples containing 0.5 and 3% impurity were identical; it was therefore concluded that the impurity did not seriously affect the partial molal volume determinations.

Benzyl Fluoride

Benzyl fluoride supplied by Pierce Chemicals was used without further purification for partial molal volume determinations.

Ethanol

Absolute alcohol from Reliance Chemicals was dried over magnesium turnings and then distilled (5). Binary mixtures with water were prepared by weight and stored in glass-stoppered bottles.

Kinetics

The rates of hydrolysis of *p*-chlorobenzyl chloride and of *t*-butyl chloride were studied in ethanol–water mixtures over a pressure range from 1 to 4 083 atm. The rate of production of HCl resulting from the hydrolysis was followed conductimetrically. The experimental details have been previously reported (6) except that in this work an automatic balancing a.c. conductance bridge with digital print-out (General Radio type 1680A) was used. Pseudo first-order rate constants were obtained by graphical analysis of the data by the Guggenheim method (7). The high pressure systems and controls have also

[1]Present address: Chemistry Department, Youngstown State University, Youngstown, Ohio, U.S.A.

Can. J. Chem. Downloaded from www.nrcresearchpress.com by 210.87.254.40 on 09/05/12
For personal use only.

TABLE 1

Rate constants for the solvolysis of *p*-chlorobenzyl chloride at 50.25 °C in aqueous ethanol at various pressures

Pressure (atm)	$k \times 10^5$ (s^{-1}) for mole fraction of ethanol =							
	0	0.05	0.10	0.15	0.20	0.25	0.30	0.40
1	12.5 ±0.1	7.19±0.03	3.308±0.008	1.78 ±0.02	0.999±0.007	0.6736±0.0004	0.518±0.005	0.292±0.002
681	16.2 ±0.1	10.03±0.06	5.267±0.001	2.821±0.004	1.740±0.002	1.128 ±0.005	0.833±0.008	0.500±0.008
1361	20.2 ±0.1	13.10±0.01	7.46 ±0.06	4.15 ±0.03	2.67 ±0.01	1.70 ±0.02	1.219±0.006	0.743±0.004
2041	23.88±0.08	16.15±0.09	9.93 ±0.02	5.91 ±0.02	3.76 ±0.03	2.38 ±0.01	1.71 ±0.02	1.034±0.007
2722	26.5 ±0.2	19.1 ±0.1	12.23 ±0.05	7.425±0.008	5.05 ±0.07	3.23 ±0.02	2.40 ±0.01	1.44 ±0.01
4083			16.4 ±0.1	11.10 ±0.03	7.13 ±0.04	5.01 ±0.01	3.62 ±0.02	2.03 ±0.01

TABLE 2

Rate constants for the solvolysis of *t*-butyl chloride at 0.2 °C in aqueous ethanol at various pressures

Pressure (atm)	$k \times 10^5$ (s^{-1}) for mole fraction of ethanol =			
	0.02	0.2	0.3	0.4
1	6.40±0.04	3.00±0.04	0.494±0.003	0.147±0.003
340	7.50±0.05	4.55±0.05	0.847±0.001	0.373±0.006
681	9.13±0.10	5.87±0.10	1.40 ±0.03	
1361		8.10±0.10		0.706±0.003
2041		10.0 ±0.1	2.62 ±0.04	1.02 ±0.01

been previously described (6). The temperature in a thermostatted oil bath was maintained at 50.25 ±0.01 °C in the case of the *p*-chlorobenzyl chloride and at 0.20 ±0.01 °C in the case of the *t*-butyl chloride.

Partial Molal Volumes

The method for determination of partial molal volumes by injection from a microsyringe into a dilatometer as previously reported (1) was used unchanged. Calibration of the dilatometer was done by using the known molal volumes of water and ethanol to obtain apparatus constants when pure water was injected into water, and pure ethanol into ethanol at the temperature of the thermostatted oil bath.

Partial molal volumes were obtained for four solutes in ethanol–water mixtures which were degassed before use by boiling in a flask fitted with a Dry Ice/acetone condenser. Determinations of densities before and after degassing showed no change in composition of the aqueous binary solvents (changes in density were no more than 1 part in 10 000). Partial molal volumes of benzyl chloride, *p*-chlorobenzyl chloride, and benzyl fluoride were measured at 50.25 °C in a thermostatted oil bath. A glycol–water bath at 1.35±0.003 °C was used for *t*-butyl chloride volume determinations.

Calculation of the partial molal volumes required the densities of the solutes at the temperature of injection. The densities of benzyl chloride and *t*-butyl chloride were taken from refs. 8 and 9. The densities of *p*-chlorobenzyl chloride and benzyl fluoride were determined with a micropycnometer calibrated with distilled water. Density of benzyl chloride at 32.5 °C, 1.02_1 g/ml; *p*-chlorobenzyl chloride at 31.0 °C, 1.25_5 g/ml.

Results

Rates

The conductance data yielded the first-order rate constants for *p*-chlorobenzyl chloride in ethanol–water mixtures at 50.25 °C as a function of pressure. These rate constants, presented in Table 1, are the average of at least two, and in many cases four or more, runs with the indicated errors being average deviations. The fourth figure in some of these rates is not significant, but merely a guard figure when the error is quoted to this degree of accuracy. The rate constants for *t*-butyl chloride at 0.2 °C are presented in Table 2. Although there is still considerable discussion as to the most appropriate form of the rate–pressure relationship (3), we believe (10) that for solvolytic systems of this type the quadratic yields a best fit and the solvent dependence of the extracted ΔV^* values differs little from that obtained by use of other forms of the rate–pressure relationship. Whalley and Baliga (3) have obtained some values of ΔV^* for the solvolysis of *t*-butyl chloride at 0 °C and these are presented in Table 3, in addition to our values of ΔV^* for *t*-butyl chloride and *p*-chlorobenzyl chloride. The possible errors given in our ΔV^* values are the standard deviations from the quadratic analysis, although more realistic experimental uncertainties might be ± 0.5 to 1.0 ml/mole. Also included in Table 3 are values of ΔV^* for benzyl chloride as previously reported by Golinkin, Lee, and Hyne (1). The value in pure water for benzyl chloride is a revised value supplied by Mr. S. J. Dickson of this laboratory.

Partial Molal Volumes

The partial molal volumes for benzyl chloride, *p*-chlorobenzyl chloride, *t*-butyl chloride, and benzyl fluoride in ethanol–water mixtures are presented in Table 4. These values are the average of at least four determinations with their average deviations as indicated. The volumes obtained by Golinkin, Lee, and Hyne (1) for benzyl chloride were in reasonable agreement (about 1%) with the present results except for their value at 0.3 mole fraction ethanol of 119.9 ± 0.1 ml/mole as compared to our value of 125.4 ± 0.7 ml/mole.

From the activation volume, ΔV^*, and the partial molal volume of the initial state, $\overline{V}_g$, the partial molal volume of the transition state, $\overline{V}_t$, can be calculated, $\Delta V^* = \overline{V}_t - \overline{V}_g$. Figure 1 represents the dissection of the volume parameters for *p*-chlorobenzyl chloride, benzyl

Can. J. Chem. Downloaded from www.nrcresearchpress.com by 210.87.254.40 on 09/05/12
For personal use only.

TABLE 3

Activation volumes for the solvolysis of *p*-chlorobenzyl chloride, benzyl chloride, and *t*-butyl chloride in ethanol–water mixtures

Mole fraction ethanol	ΔV^* (ml/mole)		
	p-Chlorobenzyl chloride*	Benzyl chloride†	*t*-Butyl chloride
0.000	−11.5±0.3	−9.8±0.1	−2.0±0.5‡
0.020			−9.3±0.3§
0.0338			−7.0±1.0‡
0.0500	−13.8±0.2		
0.0951			−13.2±0.6‡
0.100	−17.9±0.1	−17 ±1.0	
0.150	−18.8±0.2		
0.1725			−21.5±1.0‡
0.200	−21.8±0.1	−20.3±0.2	−24.3±0.2§
0.250	−19.9±0.02		
0.300	−18.9±0.2	−22.9±0.2	−19.9±0.2§
0.400	−20.8±0.1	−17.9±0.9	−17.6±0.1§
0.500			

*Present work, 50.25 °C.
†Hyne, Golinkin, and Laidlaw 50.25 °C (6).
‡Baliga and Whalley, 0 °C (3). The authors wish to thank Drs. Baliga and Whalley for the *t*-butyl chloride ΔV^* data prior to publication.
§Present work, 0.20 °C.

TABLE 4

Partial molal volumes in aqueous ethanol mixtures of benzyl chloride, benzyl fluoride, and *p*-chlorobenzyl chloride at 50.25 °C, *t*-butyl chloride at 1.35 °C

Mole fraction ethanol	Partial molal volume (ml/mole)			
	Benzyl chloride	Benzyl fluoride	*p*-Chlorobenzyl chloride	*t*-Butyl chloride
0.000	114.5±0.5	103.7±0.9	126.0±0.8	
0.020				
0.0338				104.1±0.7
0.0500	115.2±0.3		130.8±0.8	
0.0951		109.0±0.4		104.9±0.6
0.100	116.7±0.6		135.3±0.7	
0.150			138.0±0.6	
0.1725		113.6±0.6		106.7±0.7
0.200	121.4±0.7		144.0±0.8	
0.250			142.5±0.8	
0.300	125.4±0.7	115.5±0.6	138.8±0.6	109.6±0.8
0.400	117.8±0.8	114.1±0.5	137.4±1.5	108.4±1.1
0.500				109.8±0.8

chloride, and *t*-butyl chloride using the data in Tables 1–4. Figure 2 is a plot of our partial molal volumes of benzyl fluoride and those of anilinium chloride, tetraethylammonium chloride, and tetramethylammonium chloride, as reported previously by Lee and Hyne (11, 12), whose figures are included for comparison with our results.

Although we are comparing $\bar{V}_t$ curves obtained at different temperatures for different compounds (*p*-chlorobenzyl chloride and benzyl chloride at 50.25 °C, *t*-butyl chloride at 1.35 °C) the temperature variation should not invalidate a comparative analysis. Millero and Drost-Hansen (13) report that the apparent molal expansibility of tetramethylammonium chloride (0.053 *m*) over 20–40 °C is about 0.11 ml mole^{-1} deg^{-1}. Dickson (14) has found a maximum temperature dependence of ΔV^* for benzyl chloride in aqueous *t*-butanol of −0.25 ml mole^{-1} deg^{-1} and Lateef and Hyne (15) found ΔV^* changed by about −0.08 ml mole^{-1} deg^{-1} for the solvolysis of allyl chloride in aqueous ethanol. These small temperature effects of comparable magnitude on both sides of the equation $\Delta V^* = \bar{V}_t - \bar{V}_g$ should cancel within the accuracy of our experimental results in the calculation of $\bar{V}_t$.

Can. J. Chem. Downloaded from www.nrcresearchpress.com by 210.87.254.40 on 09/05/12
For personal use only.

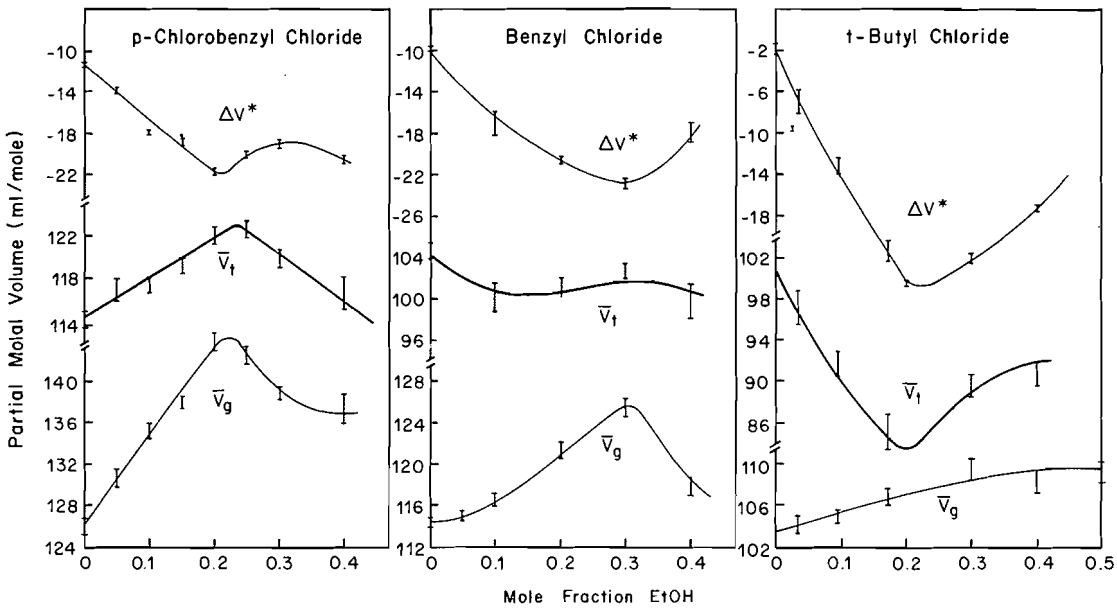

FIG. 1. Volume parameters for the solvolysis of *p*-chlorobenzyl chloride, benzyl chloride, and *t*-butyl chloride in aqueous ethanol.

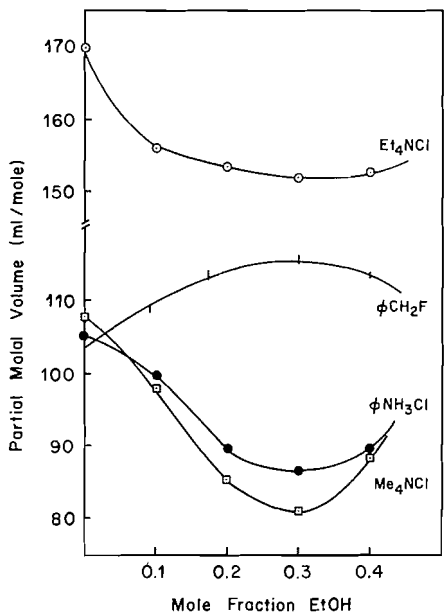

FIG. 2. Partial molal volumes as a function of mole fraction ethanol of benzyl fluoride, tetraethylammonium chloride, tetramethylammonium chloride, and anilinium chloride.

Discussion

The dissection of the observed volume of activation behavior into initial and transition state components for the three solvolysis reactions is presented in Fig. 1. In all these cases ΔV^* passes through a minimum as a function of solvent composition and the initial state partial molal volume passes through a maximum. The transition state volume behavior, however, is distinctly different in each case. A maximum in $\bar{V}_t$ is observed in the more S_N2 type *p*-chlorobenzyl chloride solvolysis while a very distinct minimum characterizes the $\bar{V}_t$ behavior for the S_N1 *t*-butyl chloride solvolysis. The $\bar{V}_t$ behavior for benzyl chloride is clearly intermediate between these two extremes. It would therefore appear that the behavior of the partial molal volume of the transition state as a function of solvent composition is directly related to the position occupied by the reaction in question on the mechanistic scale from S_N2 to S_N1.

The observed maximum in the volume of the transition state for *p*-chlorobenzyl chloride should be compared with the similar behavior for all the initial states, $\bar{V}_g$, and for benzyl fluoride (Fig. 2). This maximum behavior appears to be characteristic of all non-ionic substrates. The very pronounced minimum in volume observed for the transition state of *t*-butyl chloride, however, is characteristic of the behavior of ionic species, as was demonstrated for tetramethylammonium and anilinium chlorides by Lee and Hyne (11, 12) (Fig. 2). The transition state behavior of benzyl chloride was shown by Lee

Can. J. Chem. Downloaded from www.nrcresearchpress.com by 210.87.254.40 on 09/05/12
For personal use only.

and Hyne (11) to be more similar to the partial molal volume curve for tetraethylammonium chloride, indicating less charge development in the transition state than is represented by tetramethylammonium chloride.

The behavior of the transition state volumes $\overline{V}_t$ in the three cases, therefore, is in general agreement with the mechanistic classification of the three reactions. The transition state for *p*-chlorobenzyl chloride is more dipolar than ionic (S_N2); the transition state for *t*-butyl chloride is well simulated by the ionic tetramethylammonium chloride (S_N1); while that for benzyl chloride is intermediate between the two extremes as was previously suggested by the similarity of the $\overline{V}_t$ behavior with that of tetraethylammonium chloride. These findings suggest that the solvent dependence of the partial molal volume of a solvolytic transition state obtained by dissection of the observed activation volume can serve as a useful yardstick in the characterization of reaction mechanism.

The authors wish to thank the National Research Council of Canada for financial assistance in support of this work.

1. H. S. GOLINKIN, IKCHOON LEE, and J. B. HYNE. J. Amer. Chem. Soc. **89**, 1307 (1967).
2. E. T. TOMMILA, E. PAAKKALA, U. K. VIRTANEU, A. ERVA, and S. VARILA. Ann. Acad. Sci. Fenn. **A11** (91), 1 (1959).
3. B. T. BALIGA and E. WHALLEY. Can. J. Chem. **48**, 528 (1970).
4. K. J. LAIDLER and R. MARTIN. Int. J. Chem. Kinetics, **1**, 113 (1969).
5. A. I. VOGEL. A textbook of practical organic chemistry. 3rd ed. Longmans, Green and Co., Ltd., London. 1961. p. 167.
6. J. B. HYNE, H. S. GOLINKIN, and W. G. LAIDLAW. J. Amer. Chem. Soc. **88**, 2104 (1966).
7. E. A. GUGGENHEIM. Phil. Mag. **2** (7), 538 (1926).
8. A. I. VOGEL. J. Chem. Soc. 644 (1948).
9. J. TIMMERMANS. Physico-chemical constants of pure organic compounds. Elsevier Publ. Co., Inc., Amsterdam. 1950.
10. H. S. GOLINKIN, W. G. LAIDLAW, and J. B. HYNE. Can. J. Chem. **44**, 2193 (1966).
11. IKCHOON LEE and J. B. HYNE. Can. J. Chem. **47**, 1437 (1969).
12. IKCHOON LEE and J. B. HYNE. Can. J. Chem. **46**, 2333 (1968).
13. F. J. MILLERO and W. DROST-HANSEN. J. Phys. Chem. **72**, 1758 (1968).
14. S. J. DICKSON. Ph.D. Thesis, University of Calgary, Calgary, Alberta. 1970.
15. A. B. LATEEF and J. B. HYNE. Can. J. Chem. **47**, 1369 (1969).

Can. J. Chem. Downloaded from www.nrcresearchpress.com by 210.87.254.40 on 09/05/12
For personal use only.

Can. J. Chem. Downloaded from www.nrcresearchpress.com by 210.87.254.6 on 09/05/12
For personal use only.

Anionic polymerization of styrene in oxepane (hexamethylene oxide). counter-ion, sodium[1]

G. LÖHR[2] AND S. BYWATER
Division of Chemistry, National Research Council of Canada, Ottawa, Canada

Received March 2, 1970

The propagation reaction in the anionic polymerization of styrene in oxepane has been studied as a function of temperature and concentration of polystyrylsodium. Conductance measurements on polystyrylsodium were also made together with determinations of density, viscosity, dielectric constant, and dipole moment of oxepane itself. The measurements enabled the propagation rate constant to be determined of the polystyryl anion at 30 °C and of the ion-pair over a wide temperature range. The results have been compared with those obtained in tetrahydrofuran and tetrahydropyran.

Canadian Journal of Chemistry, 48, 2031 (1970)

Introduction

The anionic polymerization of styrene has been studied in a series of ethereal solvents of varying dielectric constant, dimethoxyethane (1, 2), tetrahydrofuran (3–5), tetrahydropyran (7–9), and dioxane (9, 10). Evidence has been presented for the presence of three types of active species, the free anion, a solvent-separated ion-pair, and a contact ion-pair, in order of decreasing reactivity. The contribution to the reaction of all but the latter species decreases as the dielectric constant decreases. It is of interest to examine solvents intermediate in dielectric constant between tetrahydropyran ($\varepsilon = 5.5$) and dioxane ($\varepsilon = 2.2$) and it was thought oxepane,

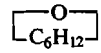

might help in this regard. Little physical data on this compound exists in the literature and so some of its physical properties were measured.

Experimental

Apparatus

A modification of the basic apparatus described earlier (11) was used. This involves a greaseless high vacuum vessel, which is prewashed with polystyrylsodium and rinsed with solvent from the active polymer solution. The same solvent can be later distilled into the reaction cell for use as reaction medium. Monomer was added in fragile bulbs which were crushed with magnetic breakers. Initiation was carried out by contacting a small amount of styrene in the solvent with a sodium mirror.

Polymerization rates were measured in a Cary-14 spectrophotometer by following the disappearance of the styrene absorption at 291.2 mμ. The concentration of polystyryl sodium was measured using its absorption band at 343 mμ. The extinction coefficient used at 30° was 1.35×10^4 as determined in tetrahydropyran (13). There are negligible differences in absorption in a series of cyclic ethers. At 30° and above, the temperature was maintained by means of a heated cell block through which thermostatted water was circulated. This system was backed-up by a controlled air temperature circulation system in the cell compartment. Below room temperature, the reaction cell was immersed in methanol in a quartz Dewar provided with optical windows and maintained at required temperature by circulation of methanol from a low temperature thermostat (Ultra kryostat UK-70W, Lauda Instruments). A comparison of the optical density of a polystyrylsodium solution at various temperatures with the measured densities of oxepane showed that the extinction coefficient at the maximum increased by 0.13_4% per degree as the temperature was lowered. Similar results have been reported in tetrahydropyran (14). An appropriate correction was made for this change in estimating concentrations of active centers at various temperatures.

Materials

Oxepane was obtained from the Aldrich Chemical Co. It contained about 10% of 7-oxa-bicyclo[2,2,1]heptane. It was found impossible to remove this material by conventional physical methods and recourse was made to its easy polymerizability. The commercial material was treated for 30 h at 60–70° with 100 ml $SOCl_2$ + 3.5 g $FeCl_3$ per 1.5 kg of material. The solution was cooled and made basic with concentrated aqueous NaOH and subjected to a simple distillation. Oxepane was recovered as an azeotrope with water boiling around 80°. This often required the addition of extra water. Phase separation occurred at room temperature and the oxepane so obtained was dried and again subjected to the $SOCl_2/FeCl_3$ treatment and distillation until analytical gas chromatography showed no detectable oxabicycloheptane. Two treatments were usually adequate. The final product was refluxed over potassium for 24–48 h and fractionated at high reflux ratio in a 100-plate column retaining only the center third fraction. The material was stored for use on the vacuum line over Na/K alloy.

Sodium tetraphenylboride (Fisher Scientific) was recrystallized from tetrahydrofuran at low temperature.

[1]NRCC No. 11 305.
[2]NRCC Postdoctorate Fellow, 1968–1969.

Can. J. Chem. Downloaded from www.nrcresearchpress.com by 210.87.254.6 on 09/05/12
For personal use only.

Sodium metal was subjected to vacuum distillation to remove traces of potassium. Styrene was purified as described previously (12).

Physical Measurements

For conductance measurements a side-arm which contained a conductance cell with a constant of 0.0101 cm^{-1} was added to the standard apparatus. Conductivities were measured using a Wayne–Kerr universal bridge. Dielectric constants of oxepane were measured on the bulk material at 1 kc, and 10 kc using a General Radio 1615A capacitance bridge and a three-terminal guarded cell. The dipole moment was determined using the same equipment on dilute solutions of oxepane in cyclohexane. The method of Guggenheim (15) was used to evaluate dipole moments from the dielectric constant data. The refractive-index term was determined using a Bryce–Pheonix differential refractometer and found to be small. Figure 1 shows the data obtained, $\Delta\varepsilon/w$ being 1.85. The $(n^2 - n_0^2)/w$ term was about 0.01, the two results leading to a dipole moment of 1.51 D. Viscosity measurements were made in calibrated Cannon–Ubbelohde viscometers (Cannon Instrument Co.). Densities were determined in a pycnometer of standard design. The physical properties of oxepane are summarized in Table 1.

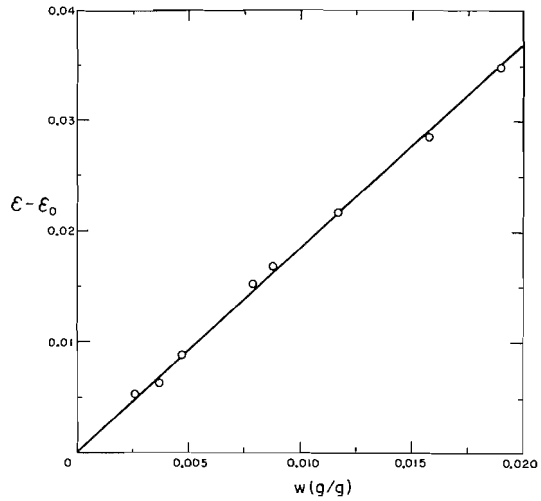

FIG. 1. Dependence of dielectric constant on weight fraction of oxepane for dilute solutions in cyclohexane at 30°.

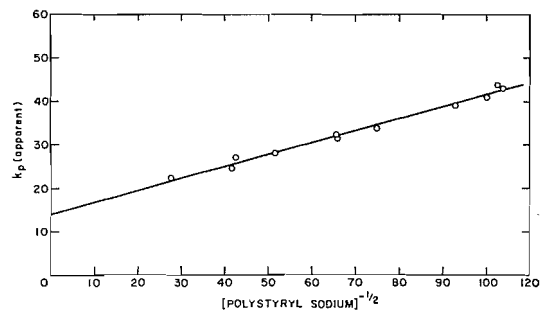

FIG. 2. Apparent k_p ($-d\ln M/dT$/[active centers]) in the polymerization of styrene in oxepane (30°, counter ion, Na^+).

Results

The kinetic measurements at 30.0° are shown in Fig. 2, plotted in the conventional way as apparent k_p vs. [polystyrylsodium]$^{-1/2}$. The intercept gives the ion-pair rate constant ($k_p^{\pm} = 14.0\ M^{-1}\ s^{-1}$) and the slope (0.275), leads to the product $k_p^{-}K_D^{1/2}$ (where k_p^{-} is the free anion rate constant and K_D the ion-pair dissociation constant). Auxiliary measurements on the conductance (Fig. 3) enabled an estimate of K_D to be made. The conductance is plotted according to the simple Kraus and Bray (16) method. More sophisticated treatments are not warranted in the present case. The slope of the line in Fig. 3 (2.1×10^8) is equivalent to $(K_D\Lambda_0^2)^{-1}$. Λ_0 was estimated as 25.5 at 30° by use of Walden's rule and the previously determined Λ_0 of polystyrylsodium in tetrahydrofuran (5, 17). This allows the determination of K_D as $7.3 \times 10^{-12}\ M$ and k_p^{-} as $1.0 \times 10^5\ M^{-1}\ s^{-1}$. Over a wider temperature range the ion-pair constant was measured by carrying out the reaction in presence of sufficient sodium tetraphenylboride ($\sim 1 \times 10^{-3}\ M$) to suppress the ionization of polystyrylsodium. It was established that although the solubility of this salt in oxepane decreases rapidly as the temperature is lowered, even at −60° this amount can be dissolved. The results are shown in Fig. 4. Above room temperature the rates follow, within

TABLE 1

Physical properties of oxepane*

Temperature (deg)	Density (g cm^{-3})	Dielectric constant ε
30.0	0.891	4.97
25.0	0.896	5.06
20.0	0.905	5.15
10.0	0.909	5.36
0	0.918	5.57
−10.0	0.928	5.80
−20.0	0.936	6.05
−30.0	0.946	6.32
−40.0	0.955	6.62
−50.0	0.965	6.95

*$d\ln\varepsilon/d\ln T = -1.096$; $d\ln v/dt = 9.9 \times 10^{-4}$; $\eta \times 10^3 = 10.99$ P at 30.0°.

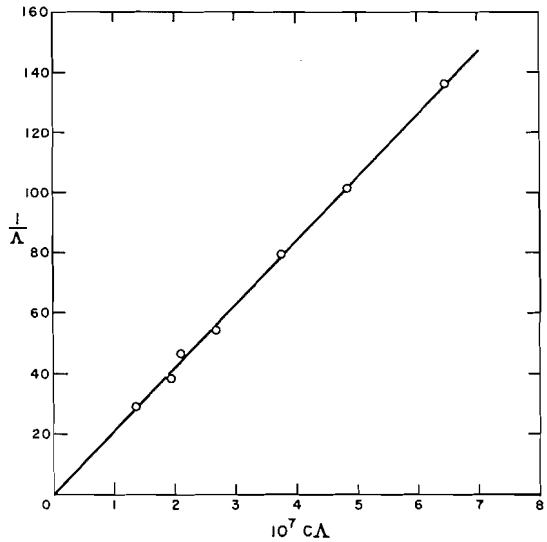

FIG. 3. Fuoss plot of the conductance of polystyrylsodium ($DP \sim 27$) in oxepane at 30°.

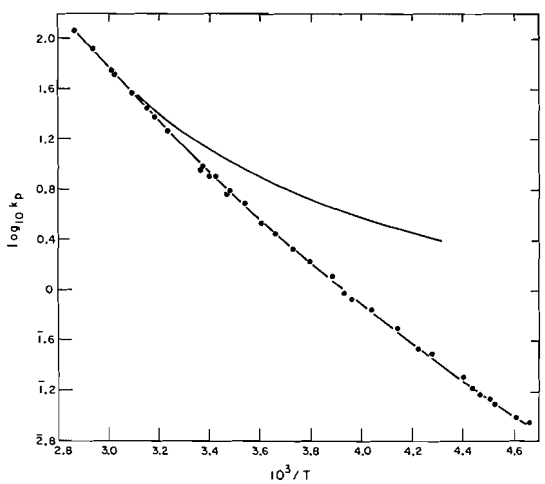

FIG. 4. Ion-pair propagation constant as a function of temperature. (Upper line, tetrahydropyran (7); experimental points, present results in oxepane).

experimental error, an Arrhenius dependence on temperature $k_p^{\pm} = 1.59 \times 10^8 \exp(-9800/RT)$. Below room temperature the reaction rates become progressively higher than that estimated by the above equation and around −50°, the apparent activation energy has dropped to around 6500 cal/mole. Similar deviations have been observed in tetrahydropyran (7), the results being plotted in Fig. 4.

Discussion

The dielectric constant of oxepane is higher than it was hoped to be at the start of this investigation, being only ~10% lower than that of tetrahydropyran (THP) at room temperature. The ion-pair rate constant is about 20% lower under the same conditions, but as the temperature is increased the rates tend to become equal to those in THP within the limits of experimental error but diverge increasingly as the temperature is lowered. If we accept the explanation (7) that the falling activation energy is caused by an increase in the proportion of solvent-separated ion-pairs, then these must be less important in oxepane than in THP. In fact the high temperature rate constants in oxepane are very close to those estimated from experiments in THP for contact ion-pairs (18).

The free ion rate constant at 30° in oxepane is similar to that in THP ($1.3 \times 10^5\ M^{-1}\ s^{-1}$) (13). The difference of about 30% is probably within the limits of experimental error. Even in tetrahydrofuran (THF) the value does not seem significantly different with reported values between 7×10^4 and 1.2×10^5 at 25° (4, 5). We must conclude that the free anion rate constant is not sensitive to the solvent properties.

The ion-pair dissociation constant differs more between the two solvents ($K_D^{THP} = 1.7 \times 10^{-10}$, $K_D^{OXP} = 7.3 \times 10^{-12}$ at 30°) but the values are about those expected on dielectric continuum theory using the Fuoss equation, $K = 3000/4\pi Na^3 \exp - (e^2/a\varepsilon kT)$, and an inter-ionic separation, a, of 4.1 Å. In fact, the dissociation constant in THF can be fitted to this equation using only a slightly larger a value of 4.3 Å. The values of a obtained from this equation are of course not an accurate measure of the interionic separation because of general deficiencies in the theory, and in particular because it does not allow for extra specific solvation of the cation in the dissociated state. The values are, therefore, larger than would be expected from reasonable values of ionic radii. Since increased cation solvation produces an apparently larger effective interionic separation, the similarity of the values obtained suggests that there are no large differences in the degree of cation solvation in these solvents, but that THF may be somewhat more efficient.

The dipole moments of the three solvents do not vary very much ($\mu_{THF} = 1.75$ D (19), $\mu_{THP} =$

Can. J. Chem. Downloaded from www.nrcresearchpress.com by 210.87.254.6 on 09/05/12
For personal use only.

1.55 D (19), $\mu_{OXP} = 1.51$ D)[3] although there seems to be a downward trend with increasing ring size. Ion–dipole interaction of solvent molecules with the cation will, therefore, be similar in all three cases although again slightly stronger with THF.

The importance in the reaction of solvent-separated ion-pairs also decreases markedly in the series THF, THP, and oxepane. In magnitude this effect must be comparable with the decrease in overall dissociation constant. It is unlikely, however, that it can be related to the changes in dielectric constant as can K_D, but more probably is a consequence of increasing molecular volume. The two are of course related in this series. Presumably solvent separated ion-pairs are more easily formed with small solvent molecules since the energy required for partial charge separation will be smaller.

The authors would like to thank Mr. P. E. Black and Mr. P. M. Toporowski for technical help in this work.

1. T. SHIMOMOURA, J. SMID, and M. SZWARC. J. Amer. Chem. Soc. **89**, 5743 (1967).

[3]Variations exist in reported dipole moments depending on the method of measurement and on how the data were treated, particularly some are due to assumptions made regarding atom polarization (e.g. $\mu_{THF} = 1.63 - 1.65$ D) (20). The above values may not be correct absolutely but should be internally consistent as the data were treated in an equivalent manner.

2. G. LÖHR and G. V. SCHULZ. Makromol. Chem. **117** 283 (1968).
3. D. N. BHATTACHARYYA, C. L. LEE, J. SMID, and M. SZWARC. Polym. **5**, 54 (1964); J. Phys. Chem. **69**, 612 (1965).
4. H. HOSTALKA, R. V. FIGINI, and G. V. SCHULZ. Makromol. Chem. **71**, 198 (1964); Z. Phys. Chem. **45**, 286 (1965).
5. T. SHIMOMOURA, K. J. TÖLLE, J. SMID, and M. SZWARC. J. Amer. Chem. Soc. **89**, 796 (1967).
6. W. K. R. BARNIKOL and G. V. SCHULZ. Makromol. Chem. **68**, 211 (1963); Z. Phys. Chem. **47**, 89 (1965).
7. L. BÖHM, W. K. R. BARNIKOL, and G. V. SCHULZ. Makromol. Chem. **110**, 222 (1967).
8. F. S. DAINTON *et al.* Makromol. Chem. **89**, 257 (1965).
9. F. S. DAINTON, K. J. IVIN, and R. T. LAFLAIR. Eur. Polym. J. **5**, 379 (1969).
10. G. ALLEN, G. GEE, and C. STRETCH. J. Polym. Sci. **48**, 189 (1960).
11. D. J. WORSFOLD and S. BYWATER. Can. J. Chem. **38**, 1891 (1960).
12. S. BYWATER and D. J. WORSFOLD. J. Phys. Chem. **70**, 162 (1966).
13. A. PARRY, J. E. L. ROOVERS, and S. BYWATER. Unpublished results.
14. J. COMYN and K. J. IVIN. Eur. Polym. J. **5**, 587 (1969).
15. E. A. GUGGENHEIM. Trans. Faraday Soc. **47**, 373 (1951).
16. C. A. KRAUS and W. C. BRAY. J. Amer. Chem. Soc. **35**, 1315 (1913).
17. D. J. WORSFOLD and S. BYWATER. J. Chem. Soc. 5234 (1960).
18. G. V. SCHULZ. I.U.P.A.C. Macromolecular Symposium, Budapest. 1969.
19. C. W. N. CUMPER and A. I. VOGEL. J. Chem. Soc. 3521 (1959).
20. W. L. GENT. J. Chem. Soc. 58 (1957).
21. D. N. BHATTACHARYYA, J. SMID, and M. SZWARC. J. Phys. Chem. **69**, 624 (1965).

Can. J. Chem. Downloaded from www.nrcresearchpress.com by 210.87.254.6 on 09/05/12
For personal use only.

Can. J. Chem. Downloaded from www.nrcresearchpress.com by 210.87.254.5 on 09/05/12
For personal use only.

The kinetics of oxygen exchange between the sulfite ion and water

R. H. BETTS AND R. H. VOSS
Department of Chemistry, University of Manitoba, Winnipeg 19, Manitoba

Received February 6, 1970

Oxygen of mass 18 was used as a stable tracer to measure the rate of exchange between the sulfite ion and water as a function of p*H* and total sulfite concentration. A value for the rate constant of hydration of SO_2 in aqueous solution was determined. The gross rate constants k_1 and k_{-1} for the overall reaction

$$SO_2 + H_2O \underset{k_{-1}}{\overset{k_1}{\rightleftharpoons}} H^+ + HSO_3^-$$

at 24.7 °C and ionic strength = 0.9 were evaluated from exchange results to be

$$k_{-1} = 2.48 \pm 0.27 \times 10^9 \text{ mole}^{-1}\text{ l s}^{-1}$$

$$k_1 = 1.06 \pm 0.13 \times 10^8 \text{ s}^{-1}$$

Also, for the first time, rate constants for the pyrosulfite equilibrium

$$2\ HSO_3^- \underset{k_{-2}}{\overset{k_2}{\rightleftharpoons}} S_2O_5^{2-} + H_2O$$

were obtained

$$k_2 = 7.00 \pm 0.21 \times 10^2 \text{ mole}^{-1}\text{ l s}^{-1}$$

$$k_{-2} = 10^4 \text{ s}^{-1}$$

at 24.7 °C and ionic strength = 0.9.

Canadian Journal of Chemistry, 48, 2035 (1970)

Introduction

Despite the major importance of aqueous solutions of sulfur dioxide in numerous industrial processes, a surprising uncertainty remains as to the nature of the equilibria between the molecular and ionic species in these solutions. Although the ions H_3O^+, HSO_3^-, and SO_3^{2-} are indeed present in such solutions, the undissociated free acid (presumably H_2SO_3) has never been isolated or shown to exist. Nevertheless, its existence has been taken for granted by most chemists. However, evidence from spectral studies including Raman (1, 2), infrared (i.r.) (3, 4), and ultraviolet (u.v.) absorption (5) techniques, has shown that in aqueous solutions of SO_2 the unionized sulfur species consists mainly of uncombined sulfur dioxide molecules with sulfurous acid (H_2SO_3) molecules present in very minor amounts (if at all). Infrared spectra of aqueous solutions of sulfur dioxide show only bands typical of SO_2 molecules in the liquid and gaseous state. Falk and Giguère (3) set an upper limit for H_2SO_3 of approximately 3% of the total sulfur dioxide present. It is probable that the actual concentration of H_2SO_3 is very much smaller than that, for even at −190 °C where the compound H_2SO_3 would be much more likely to occur, there is no evidence from infrared measurements for an SO_2–H_2O combination (3). From a macroscopic viewpoint, the overall equilibrium may be represented as

$$[1] \qquad SO_2 + H_2O \underset{k_{-1}}{\overset{k_1}{\rightleftharpoons}} H^+ + HSO_3^-$$

An extensive Raman study by Simon and Waldmann (6–8) revealed for the first time in these solutions some lines due to the bisulfite ions, HSO_3^-, as well as pyrosulfite ions, $S_2O_5^{2-}$, pointing to the hitherto unsuspected equilibrium

$$[2] \qquad 2HSO_3^- \underset{k_{-2}}{\overset{k_2}{\rightleftharpoons}} S_2O_5^{2-} + H_2O$$

Golding (9) by u.v. absorption measurements confirmed the preceding equilibrium and determined an approximate value of 7×10^{-2} for the equilibrium constant, $K = [S_2O_5^{2-}]/[HSO_3^-]^2$.

Information on the exchange of oxygen between the sulfite ion and water is highly contradictory. Mills (10) reported no exchange between K_2SO_3 and water after 24 h at 100 °C, whereas Hall and Alexander (11) found complete exchange in 8 h at 95 °C. Winter and Briscoe (12) found the exchange between Na_2SO_3 and water was negligible after 72 h at room temperature.

Can. J. Chem. Downloaded from www.nrcresearchpress.com by 210.87.254.5 on 09/05/12
For personal use only.

On the basis of their proposed mechanism for oxygen exchange between sodium thiosulfate and water, Pryor and Tonellato (13) suggest that their results "demonstrate unequivocably that, in the presence of thiosulfate, sulfite exchanges oxygen with water as slowly as does thiosulfate at 80 °C and p*H* 6" which would suggest a half-life of approximately 780 h. Halperin and Taube (14) passed SO_2 gas into enriched water adjusted to the desired p*H* and then immediately quenched the exchange by oxidizing the sulfite to sulfate with iodine. They found the exchange to be complete in less than 5 min when the aqueous solution was initially 0.1 *M* HCl or 0.4 *M* NaOH. In contrast to the rapid exchange observed by Halperin and Taube in the basic region, Hall and Alexander (11) observed that K_2SO_3 did not exchange with water even after 5 h in 0.2 *N* NaOH at 95 °C, and Brodskii and Vysotskoya (15) obtained half-lives of 2.5 and 210 h at 100 and 20 °C, respectively, under approximately the same conditions.

Eigen *et al.* (16) observed by ultrasonic techniques characteristic relaxation times (of the order of 10^{-6} s) in aqueous solutions of sulfite at p*H* 1 to 5. On the assumption that equilibrium [1] was involved, they deduced values of $k_{-1} = 2.0 \times 10^8$ mole^{-1} l s^{-1} and $k_1 = 3.4 \times 10^6$ s^{-1} (20 °C, ionic strength = 0.1). These values of course depend on the value chosen for the equilibrium constant for reaction [1] above.

A later paper by Wang and Himmelblau (17) reported values of k_1 and k_{-1} deduced from measurements on the rate of transfer of radioactive sulfur dioxide ($^{35}SO_2$) between an aqueous phase and its corresponding vapor. The values given are approximately eight orders of magnitude smaller than those given by Eigen *et al.* (16), to which no reference is made by these authors.

In view of these large uncertainties in the literature, extending over a period of nearly 30 years, the present authors felt that a further investigation of the sulfite–water exchange reaction would be desirable.

Experimental

Materials and Apparatus

Water enriched to about 1.6 atom % (obtained from YEDA Research and Development Co. Ltd.) was distilled once from alkaline permanganate. Water of normal isotopic composition (containing approximately 0.2 atom % ^{18}O) was doubly distilled. ^{18}O-enriched sodium sulfite was prepared by dissolving normal sodium sulfite (certified A.C.S., Fisher) in a large excess of enriched water at room temperature, allowing the mixture to equilibrate overnight (which was found to be sufficient time for complete exchange), and then removing the water by distillation under vacuum. All other chemicals were of reagent grade and used without further treatment.

The p*H* values were measured using an Orion Model 801 digital p*H* meter. Isotopic analyses were made on a Varian-Mat GD 150 isotope ratio mass spectrometer.

Sample Preparation and Isotopic Analysis

Preliminary studies of the oxygen exchange between the sulfite ion and water were carried out using a "freeze–dry" technique. The kinetic runs were followed by measuring either the increase or decrease of the ^{18}O-enrichment of Na_2SO_3. To start the exchange reaction a weighed amount of either normal or ^{18}O-enriched Na_2SO_3 was added to 10 ml of either ^{18}O-enriched or normal water respectively and kept at the desired temperature (24.7 °C for most runs). The p*H* of the solution was adjusted by adding the required quantities of either concentrated NH_4OH or HCl. At timed intervals, aliquots of the mixture were removed, frozen to −196 °C to "stop" the exchange reaction and the water pumped off under high vacuum. This technique was not very satisfactory. The drying of the salt required a long time, and the experimental reproducibility was not better than 4–5%. Furthermore, as it became desirable to control the p*H*, the remainder of the work was carried out with borax buffer solutions. The sulfite was precipitated from solution as the insoluble salt $SrSO_3$ by addition of $SrCl_2$. Argon (Matheson H.P.) was bubbled through the water or borax buffer solutions for approximately 5 min to remove any dissolved oxygen and then slowly bubbled through the exchanging mixture to preclude air oxidation of the sulfite while the reaction was in progress.

The isotopic composition of the sodium sulfite or the strontium sulfite was determined using a technique suggested by Shakhaskiri and Gordon (18). The oxygen in the compound is converted to CO_2 by heating the sample with AgCN for approximately 2 h at 500 °C. The relative abundance of oxygen-18 in the CO_2 samples recovered was determined by measuring the ratio of mass 46 to (mass 44 + mass 45) peaks ($^{12}C^{16}O^{18}O/^{12}C^{16}O^{16}O + {}^{13}C^{16}O^{16}O + {}^{12}C^{16}O^{17}O$) on the isotope ratio mass spectrometer. This ratio was read directly by the double collector procedure and is referred to as the *p*-factor. The half-lives of the exchange reaction ($t_{1/2}$) were derived graphically (allowing for a reproducible zero time or induced exchange of approximately 13–16%) from experimental points (6 points per run) by plotting the logarithm of the fraction $(1 - F)$ vs. time, where F, the fraction exchanged at time t, was evaluated from the relationship

$$[3] \qquad F = \frac{P_t - P_0}{P_\infty - P_0}$$

where P_0, P_t, and P_∞ refer to the isotopic composition (*p*-factors) of the CO_2 samples at time zero, t, and infinity (that is, at isotopic equilibrium), respectively.

The rate of oxygen exchange, R, was then calculated using the equation

$$[4] \qquad R = \frac{a\ b\ 0.693}{(a + b)t_{\frac{1}{2}}}$$

Can. J. Chem. Downloaded from www.nrcresearchpress.com by 210.87.254.5 on 09/05/12
For personal use only.

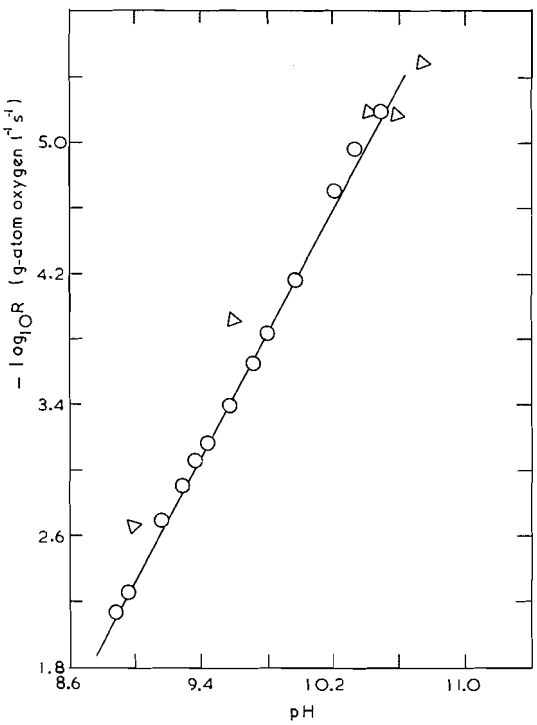

FIG. 1. pH dependence for sulfite–H_2O oxygen exchange at 24.7 °C and $[S_T] = 0.3\ M$ ($\mu = 0.9$): ○, precipitation technique; △, "freeze–dry" technique.

where a and b are the number of g-atoms of oxygen per l in the water and sulfite respectively.

Results

From the preliminary studies carried out in the pH range 3–8 (3.0, 3.8, 5.9, 6.9, 8.2) using the "freeze–dry" technique, it was found to be impossible to "stop" the exchange reaction by freezing before isotopic equilibrium occurred. However, in the pH region 9–11 the exchange was found to be slow enough so that its kinetics could be followed. Further measurements were therefore made in this region.

pH Dependence

The pH dependence of the exchange process was studied in experiments in which the total concentration of "sulfite", $[S_T]$, ($[S_T] = [SO_3^{2-}] + [HSO_3^-] + [SO_2] + 2[S_2O_5^{2-}]$) was maintained constant ($[S_T] = 0.3\ M$, ionic strength = 0.9). A plot of $-\log_{10} R$ vs. pH ($-\log_{10}[H^+]$) was linear (Fig. 1). A linear least squares treatment of these data gave for the slope a value of 1.93 ± 0.05. This is then the kinetic order of the exchange with respect to H^+ ion concentration. Values obtained from the "freeze–dry" experiments are also included in Fig. 1. The half-lives corresponding to the upper (pH 10.50) and lower (pH 8.90) points of Fig. 1 correspond to values of 1518 min (25.3 h) and 1.3 min, respectively. For an experiment carried out at p$H \simeq 12.7$ (0.3 M Na_2SO_3, 0.1 M NaOH), no exchange was observed even after 17 days, as would be expected from extrapolation of the data given in Fig. 1.

Sulfite Dependence

The dependence of rate of oxygen exchange on the total sulfite concentration, $[S_T]$, was determined by measuring the rate of exchange for five different S_T concentrations (0.600, 0.450, 0.300, 0.150, and 0.075 M) maintaining the pH as close as possible to a value of 9.52. A plot of $-\log_{10} R^*$ vs. $-\log_{10}[S_T]$ (Fig. 2) was linear with an approximate slope of 1.2. (R^* represents the rate of exchange at pH 9.52 which was the pH observed for the reaction carried out for $[S_T] = 0.6\ M$; the value of R^* for $[S_T] = 0.3\ M$ was obtained from Fig. 1, and all other values were normalized to pH 9.52 assuming that $R \propto [H^+]^2$).

A least-squares treatment of all R^* values gave

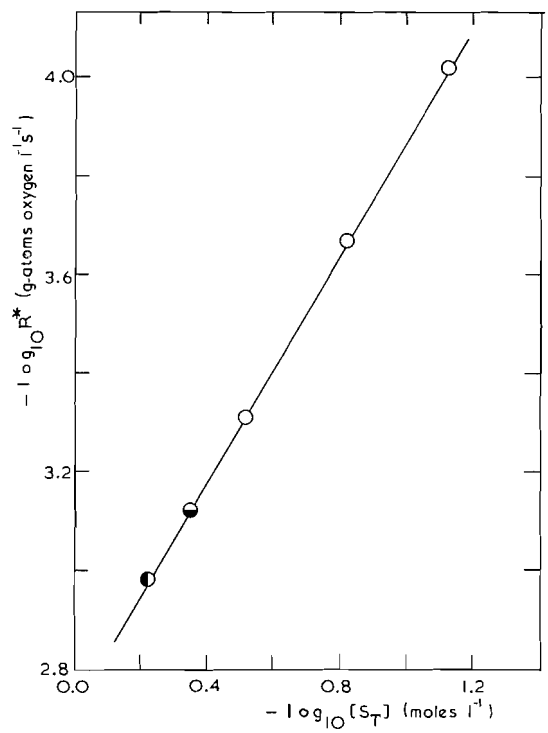

FIG. 2. Total sulfite concentration ($[S_T]$) dependence of the rate of sulfite–H_2O oxygen exchange at 24.7 °C: ○, $\mu = 0.9$; ◒, $\mu = 1.35$; ◐, $\mu = 1.80$.

Can. J. Chem. Downloaded from www.nrcresearchpress.com by 210.87.254.5 on 09/05/12
For personal use only.

for the slope, which is the order with respect to $[S_T]$, a value of 1.15 ± 0.03. The ionic strength for the runs carried out at $[S_T]$ = 0.300, 0.150, and 0.075 *M* was 0.90; that for the latter two points was adjusted by adding potassium nitrate. The ionic strength for the runs corresponding to $[S_T]$ = 0.480 and 0.600 *M* was 1.35 and 1.80, respectively.

Temperature Dependence

The rate of exchange for $[S_T]$ = 0.3 *M* was measured at 10.0, 24.7, 35.9, and 50.3 °C. The corresponding p*H* values of the solutions were 9.62, 9.62, 9.74, and 9.88, respectively. The actual values of the rates at the latter two p*H* values were therefore normalized to 9.62 by assuming $R \propto [H^+]^2$. Values for the Arrhenius parameters were calculated from these data in the usual way: E_A = 8.86 ± 0.8 kcal mole^{-1}, $\log_{10} A$ = 2.64 g-atom oxygen l^{-1} s^{-1} (see Fig. 3).

Discussion

Rate Law and Mechanism for Exchange

From the experimental studies, the empirical rate law (at 24.7 °C and ionic strength = 0.9) was found to be

$$[5] \qquad R = k[H^+]^{2.0}[S_T]^{1.15}$$

where $[S_T]$ represents the total sulfite (= $[SO_2]$ + $[HSO_3^-]$ + $[SO_3^{2-}]$ + 2$[S_2O_5^{2-}]$) in solution.

We now propose mechanisms which are consistent with this result. Exchange of oxygen could occur by the following paths

$$H^+ + SO_3^{2-} \rightleftharpoons HSO_3^- \quad \text{(fast)}$$

followed by the hydration reaction

$$[1] \qquad HSO_3^- + H^+ \underset{k_1}{\overset{k_{-1}}{\rightleftharpoons}} SO_2 + H_2O$$

If process [1] alone were responsible for isotopic exchange, the rate of the exchange would be first order in total sulfite. The observed value of 1.15 suggests that both first and second order processes contribute.

The following process, second order in $[S_T]$, may be postulated

$$[2] \qquad 2HSO_3^- \underset{k_{-2}}{\overset{k_2}{\rightleftharpoons}} S_2O_5^{2-} + H_2O$$

Equilibria [1] and [2] would yield corresponding terms in the overall rate expression

$$[6] \quad R = k_{-1}[H^+][HSO_3^-] + k_2[HSO_3^-]^2$$

Equation [6] predicts, as is observed, that the rate of exchange will be second order with respect to $[H^+]$, since in the p*H* region examined, $[HSO_3^-]$ varies directly with $[H^+]$. Equation [6] is also consistent with the observed dependence of the rate on $[S_T]$, as will now be shown.

In the p*H* region 9 to 10.5, the principal sulfite species are HSO_3^- and SO_3^{2-}, i.e., $[S_T] \simeq [HSO_3^-] + [SO_3^{2-}]$.

In terms of $[HSO_3^-]$ the total sulfite concentration S_T can be written, to a good approximation, as follows

$$[7] \qquad [S_T] = [HSO_3^-]\left(\frac{1 + [H^+]K_2}{[H^+]K_2}\right)$$

where $K_2 = [HSO_3^-]/[H^+][SO_3^{2-}]$. Sillén and co-workers (19) list for K_2 a value of 2.19 × 10^6 for ionic strength = 1.0, T = 25 °C, conditions which are appropriate for the present study.

It is convenient to re-cast eq. [7]

$$[8] \qquad \frac{[HSO_3^-]}{[S_T]} = \frac{[H^+]K_2}{1 + [H^+]K_2}$$

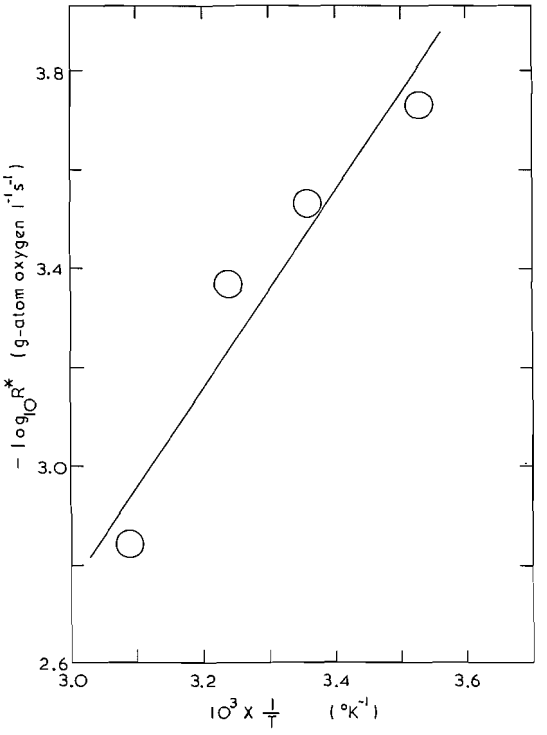

FIG. 3. Arrhenius plot for sulfite–H_2O ^{18}O exchange reaction.

Can. J. Chem. Downloaded from www.nrcresearchpress.com by 210.87.254.5 on 09/05/12
For personal use only.

For experiments made at a fixed pH, eq. [8] shows that the ratio $[HSO_3^-]/[S_T]$ is a constant (given by r in eq. [9] below). Equation [6] then becomes

$$[9] \qquad R = k_{-1}r[H^+][S_T] + k_2r^2[S_T]^2$$

Dividing through eq. [9] by $[S_T]$

$$[10] \qquad \frac{R}{[S_T]} = k_{-1}r[H^+] + k_2r^2[S_T]$$

Clearly, a plot of $R/[S_T]$ vs. $[S_T]$ should give a straight line whose slope is not zero if there is a second order contribution to oxygen exchange. Such a plot is shown in Fig. 4; it is linear with a non-zero slope, indicating participation by processes second order in $[S_T]$. A least-squares analysis of the data in Fig. 4 gave values of $9.1 \pm 2 \times 10^{-4}$ g-atom oxygen mole^{-2} l s^{-1} (slope) and $1.34 \pm 0.04 \times 10^{-3}$ g-atom oxygen mole^{-1} s^{-1} (intercept). Values for the rate constants k_2 and k_{-1} were determined from the slope ($= k_2r^2$) and intercept ($= [H^+]rk_{-1}$) to be $7.00 \pm 0.21 \times 10^2$ mole^{-1} l s^{-1} and $2.24 \pm 0.06 \times 10^9$ mole^{-1} l s^{-1}, respectively ($r = 6.61 \times 10^{-4}$ for pH = 9.52).[1]

A value for k_{-1} can be found in another way by using the data from the pH-dependence series (Fig. 1). If the contribution of the second order process $R_2 = k_2[HSO_3^-]^2$ is subtracted from the total rate of exchange [6] using the value of k_2 deduced from Fig. 4, then k_{-1} can be determined from eq. [11],

$$[11] \qquad k_{-1} = \frac{R - R_2}{[H^+][HSO_3^-]}$$

The average value of this constant was found to be $2.48 \pm 0.27 \times 10^9$ mole^{-1} l s^{-1}, independent of pH, agreeing very well with the value $2.24 \pm 0.06 \times 10^9$ mole^{-1} l s^{-1} found from the intercept of Fig. 4.

Our results are compatible with the qualitative results in refs. 11 and 15. There is, however, disagreement with the results in refs. 10, 12, 13, and 14. Eigen and co-workers' results (16) are in a category by themselves, and are discussed more fully below.

Mills (10) and Winter *et al.* (12) did not observe exchange under conditions where we do. This discrepancy we suggest is probably due to the low sensitivity of the methods used by those workers (who followed the isotopic composition of the solvent) and perhaps also due to the uncertainties inherent in the use of the very slightly enriched water available at that time.

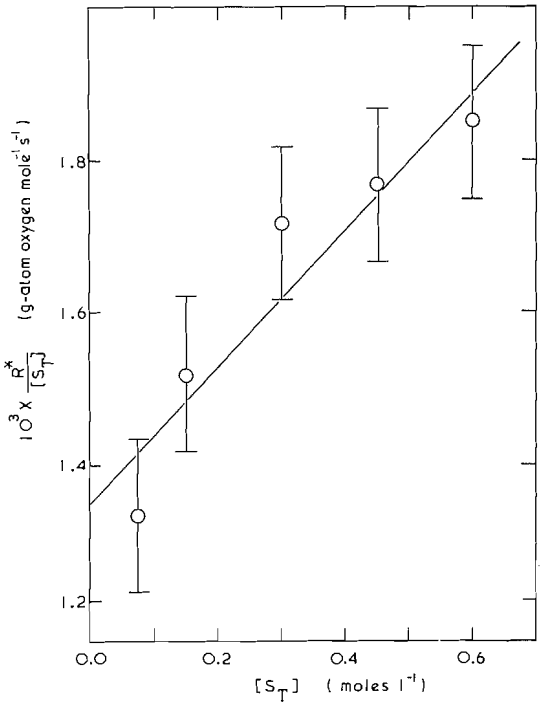

FIG. 4. Determination of the second order contribution to the rate of sulfite–H_2O oxygen exchange.

The conclusion of Pryor and Tonellato (13) that the sulfite–water exchange is very slow at pH 6 is indirect, in the sense that these workers did not actually follow the isotopic composition of the sulfite in the SO_3^{2-}–$S_2O_3^{2-}$–H_2O system. Their concern was primarily with the rate of transfer of oxygen from H_2O to the thiosulfate ion, via the S atom transfer process

$$^{2-}O_3S—\overset{*}{S} + SO_3^{2-} \rightarrow O_3S^{2-} + \overset{*}{S}—SO_3^{2-}$$

which is known to occur (13). If the sulfite—H_2O oxygen exchange were rapid, then the S atom transfer would, in effect, transfer oxygen between H_2O and $S_2O_3^{2-}$. The "catalytic" role of sulfite appeared to be too low in the work reported in ref. 13 and it was concluded on this basis that the sulfite–H_2O exchange must therefore be slow at pH 6.0. It appears possible that the exact relation

[1]One of the referees has suggested that the apparent curvature of the plot in Fig. 4 may be associated with the two forms of bisulfite proposed in ref. 9. We have not been able to devise a quantitative treatment incorporating this suggestion.

between the rate of sulfur atom transfer (SO_3^{2-} + $S_2O_3^{2-}$) and the concomitant rate of oxygen transfer from H_2O to $S_2O_3^{2-}$ is somewhat more complex than allowed for by the previous work (13). Indeed, recent measurements in this laboratory (20), to be published elsewhere, on the $S_2O_3^{2-}$–SO_3^{2-}–H_2O system show no inconsistency as between S and oxygen exchange and support the view that the sulfite–water exchange is rapid at p*H* 6.0.

We do not have, as yet, a convincing explanation which will reconcile our results with those of Halperin and Taube (14). There is no reason to doubt the validity of their observation, which is that when unlabelled sulfite is added to 0.4 *M* NaOH in ^{18}O labelled water, and then oxidized (within 5 min) to sulfate by addition of iodine, the sulfate formed has the isotopic composition of the solvent. A possible explanation would be that both sulfite and sulfate are slow to exchange oxygen with water in alkaline systems. However, one or more transient intermediate species formed by reaction of iodine with sulfite may be very substitution-labile, and the oxygen transfer from water observed by Halperin and Taube takes place at that stage. Further investigation of the I_2–SO_3^{2-} system would be desirable to resolve this question.

As was mentioned above, the results of Eigen *et al.* (16) were deduced from relaxation measurements on aqueous (0.05–0.15 *M*) sulfite solutions in the p*H* region 1 to 5. The relaxation was attributed to the processes involved in equilibrium [1], for which a value of

$$K_1 = k_1/k_{-1} = [H^+][HSO_3^-]/[SO_2] = 0.017$$

was assumed, as appropriate for $T = 20$ °C, $\mu = 0.1$. Values of k_1 and k_{-1} evaluated in this way are given in Table 1. Corresponding values determined in the present work by ^{18}O transfer are also given in Table 1. It will be evident from the earlier discussion that our values of k_1 and k_{-1} depend critically on the value used for the second dissociation constant of the bisulfite ion, $K_2 = 2.19 \times 10^6$, and we have chosen what we believe is a value appropriate to the ionic strength and temperature. The value of k_1 is, in both cases, related to k_{-1} through the relation given above involving K_1. Eigen *et al.* used $K_1 = 0.017$, while we have used $K_1 = 0.0428$, for somewhat different conditions of temperature and ionic strength.

In view of these points, and also the vastly different nature of the experimental methods, we regard the agreement between the values of k_{-1}, 2.48×10^9 (this work) and 2.0×10^8 (Eigen *et al.*), as very satisfactory. The agreement between the k_1 values is not as striking, but this is not unexpected in view of the importance of K_1 values in making such comparisons.

Finally, coincidence of results may be obtained between our work and that of Eigen *et al.* by "selecting" values of $K_1 = 0.017$ and $K_2 = 1.6 \times 10^7$ (values given by Tartar and Garretson (21) for zero ionic strength). We do not, in fact, think that these values are appropriate for our conditions, and refer to them simply to underline the relative ease of reconciling these two sets of data.

TABLE 1

Comparison of rate constants obtained in this study with values derived from other methods

$$H^+ + HSO_3^- \underset{k_1}{\overset{k_{-1}}{\rightleftharpoons}} SO_2 + H_2O$$

k_{-1} (mole^{-1} l s^{-1})	k_1 (s^{-1})	Reference	Temperature (°C)	Ionic strength
2.48×10^9	1.06×10^8*	This work	24.7	0.9
2.0×10^8	3.4×10^6†	16	20	0.1

*The value for k_1 was calculated from k_{-1} using the value reported for the equilibrium constant K_1 ($= [H^+][HSO_3^-]/[SO_2]$) = 0.0428 by Sillén *et al.* (19).
†Assuming $K_1 = 0.017$ (16).

$$2HSO_3^- \underset{k_{-2}}{\overset{k_2}{\rightleftharpoons}} S_2O_5^{2-} + H_2O$$

k_2 (mole^{-1} l s^{-1})	k_{-2}* (s^{-1})	Reference	Temperature (°C)	Ionic strength
7.00×10^2	$\sim 10^4$	This work	24.7	0.9

*k_{-2} was calculated using the value for k_2 and the value reported by Golding (9) for the equilibrium constant $K = [S_2O_5^{2-}]/[HSO_3^-]^2 \simeq 0.07$.

We thank the National Research Council of Canada for financial support of this work, and also for a Scholarship for R.H.V.

1. A. Simon and K. Waldmann. Z. Anorg. Allg. Chem. **283**, 359 (1956).
2. B. P. Rao. Proc. Indian Acad. Sci. **20A**, 292 (1944).
3. M. Falk and P. A. Giguère. Can. J. Chem. **36**, 1121 (1958).
4. L. H. Jones and E. J. McLaren. J. Chem. Phys. **28**, 995 (1958).
5. P. A. D. DeMaine. J. Chem. Phys. **26**, 1036 (1957).
6. A. Simon and K. Waldmann. Z. Anorg. Allg. Chem. **281**, 113 (1955).

Can. J. Chem. Downloaded from www.nrcresearchpress.com by 210.87.254.5 on 09/05/12
For personal use only.

7. A. SIMON and K. WALDMANN. Z. Anorg. Allg. Chem. **284**, 36 (1956).
8. A. SIMON and K. WALDMANN. Chem. Ber. **89**, 2442 (1956).
9. R. M. GOLDING. J. Chem. Soc. 3711 (1960).
10. G. A. MILLS. J. Amer. Chem. Soc. **62**, 2833 (1940).
11. N. F. HALL and O. R. ALEXANDER. J. Amer. Chem. Soc. **62**, 3455 (1940).
12. E. R. S. WINTER and H. V. A. BRISCOE. J. Amer. Chem. Soc. **73**, 496 (1951).
13. W. A. PRYOR and U. TONELLATO. J. Amer. Chem. Soc. **89**, 3379 (1967).
14. J. HALPERIN and H. TAUBE. J. Amer. Chem. Soc. **74**, 375 (1952).
15. A. I. BRODSKII and N. A. VYSOTSKOYA. Zh. Fiz. Khim. **32**, 1521 (1958).
16. M. EIGEN, K. KUSTIN, and G. MAASS. Z. Phys. Chem. Neue Folge, **30**, 130 (1961).
17. J. C. WANG and D. M. HIMMELBLAU. A.I.Ch.E.J. **10** (4), 574 (1964).
18. B. Z. SHAKHASKIRI and G. GORDON. Talanta, **13**, 142 (1966).
19. M. FRYDMAN, G. NILSSON, R. TORSTEN, and L. G. SILLÉN. Acta Chem. Scand. **12**, 878 (1958).
20. R. H. BETTS and S. LIBICH. To be published.
21. H. V. TARTAR and H. H. GARRETSON. J. Amer. Chem. Soc. **63**, 808 (1941).

Can. J. Chem. Downloaded from www.nrcresearchpress.com by 210.87.254.5 on 09/05/12
For personal use only.

Can. J. Chem. Downloaded from www.nrcresearchpress.com by 210.87.254.6 on 09/05/12
For personal use only.

Studies on hydrogen–oxygen systems in the electrical discharge. III. Surface effects

PAUL E. BRUNET, XAVIER DEGLISE, AND PAUL A. GIGUÈRE
Département de Chimie, Université Laval, Québec, Québec

Received December 30, 1969

Surface effects in the reactions of dissociated hydrogen–oxygen systems and the products condensed therefrom have been investigated. Water vapor at about 0.1 Torr was streamed at high velocity through an electrodeless discharge confined in tubes of different materials or with various surface coatings. In all cases the products trapped in liquid nitrogen evolved oxygen gas on warming, but the relative amounts varied considerably from one type of surface to another. In some cases there was clear evidence that the walls of discharge tube were attacked by hydrogen atom bombardment. The decomposition, both thermal and electrical, of pure hydrogen peroxide vapor was studied likewise. The pyrolysis products gave off very little oxygen on warming. By contrast the products from electrical decomposition, even at low power level, evolved much oxygen, most of it above the melting point.

It is concluded that there is always some decomposition of hydrogen peroxide in the trapped products. However, this does not seem sufficient to account for all the evolved oxygen; at least not in the case of dissociated water vapor.

On a étudié le rôle des surfaces dans les réactions entre les produits de dissociation de l'eau et divers autres systèmes oxyhydriques. Un courant de vapeur d'eau sous basse pression (moins de 0.1 Torr) était dissocié par passage très rapide à travers une décharge sans électrode dans des tubes de divers matériaux, puis piégé aussitôt dans l'azote liquide. En se réchauffant ces produits dégageaient toujours de l'oxygène, mais en quantités très variables selon le type de surface. Dans certains cas les parois du tube à décharge étaient visiblement attaquées par l'hydrogène atomique. On a étudié par la même méthode les produits de la dissociation thermique et électrique de la vapeur de peroxyde d'hydrogène pur. Alors que les produits de la pyrolyse ne dégageaient que très peu d'oxygène lors du réchauffement, ceux de la décharge électrique, même à faible puissance, en produisaient toujours beaucoup, surtout après la fusion.

On en conclut qu'il y a toujours une certaine décomposition du peroxyde d'hydrogène piégé. Cependant ce phénomène ne peut rendre compte de tout l'oxygène dégagé; du moins pas dans le cas de la vapeur d'eau dissociée.

Canadian Journal of Chemistry, 48, 2042 (1970)

In Part I of this series (1) the reactions of hydrogen peroxide vapor with electrically dissociated hydrogen gas were studied mainly for the purpose of identifying the source of the oxygen evolved by the condensed products on warming. The results were interpreted as suggesting decomposition of part of the hydrogen peroxide present in this material possibly under the influence of some contaminants introduced through the electrical discharge (2). Various evidence was quoted indicating that a powerful discharge through hydrogen in a glass tube generates traces of unidentified compounds, presumably of silicon. However, the validity of this explanation has been questioned (3). It seemed desirable, therefore, to test it at least qualitatively; for instance, by substituting various materials of surface coatings for the discharge tube. For comparison purposes other related systems were similarly studied, such as hydrogen peroxide vapor dissociated thermally or electrically.

Experimental

The conventional gas flow system featured fast pumping: maximum capacity of about 250 l/min at 0.1 Torr. The flow of water vapor, generally of the order of 3 to 4 m/s in a discharge tube of 1 cm^2 inner section, was produced by evaporation through a calibrated needle valve of a weighed sample of the deaerated liquid in a small bulb. Most of the experiments were carried out with a microwave discharge as described before in Part II (4). The amount of power dissipated in the "load" was kept constant at 100 W. This was more than 10 times the energy required to atomize completely all the input water vapor (5).

For comparison a number of runs were carried out with an electrodeless radio frequency (r.f.) discharge of the type used before in this laboratory (6). However, the other experimental conditions could not be reproduced because of the difficulty of maintaining a steady discharge in a small diameter tube, and of operating the r.f. generator at a power level of less than 200 W. From

Can. J. Chem. Downloaded from www.nrcresearchpress.com by 210.87.254.6 on 09/05/12
For personal use only.

appearance the difference between the two types of discharge was that with the microwave, the red glow (Balmer lines) was confined to a few cm on each side of the cavity, whereas with the r.f. coil, it was much more spread out. In particular with a large (4 cm diameter) discharge tube it extended all the way down to the vacuum pump, except for the zone in the liquid nitrogen trap where it was extinguished. Preliminary runs (7) with a capacitance coupled discharge (using a pair of outer sleeve electrodes some 10 cm apart), confirmed previous findings (8) about the very low efficiency of this type of coupling for dissociating water molecules. The concentration of hydrogen peroxide condensed therefrom was only of the order of 1% as against 40 to 60% with an inductive coupling.

The liquid nitrogen trap was of the conventional, concentric tube type, some 4.5 cm in outer diameter and 15 cm long. It was inserted into the vacuum system through flange joints with Viton O-rings so that it could be used in both directions, with slightly different results. However, no systematic study of the size and shape of traps was attempted. The level of liquid nitrogen in the unsilvered Dewar flask was kept constant to within 2 cm by means of an automatic device (Hereaus-Leybold Vacuum Corp.). After completion of a run (usually 2 h) the section comprising the discharge tube and the cold trap was isolated from the rest of the system and the liquid nitrogen poured out. This allowed the condensate to warm up at an average rate of 3 °C/min. A tiny copper–constantan thermocouple cemented to the outer wall of the trap at the level of the deposit gave the temperature to ±1 °C as displayed on a direct reading Digitec Thermometer (United Systems Corp.). The pressure of evolved oxygen as a function of temperature was read on a Texas Instrument Quartz Spiral Pressure Gage or an aneroid manometer (Wallace and Tiernan, Model M). Upon reaching room temperature the trap was disconnected and weighed to the nearest 5 mg. The titer of the hydrogen peroxide solution was determined to ±0.5% from the refractive index (9). Obviously, the weight of the condensate was known with less accuracy (about ±5%) than that of input water (±1%) and that of evolved oxygen. In a few runs the concentration of oxygen in the exhaust gas (mostly hydrogen) was determined to about 1% with a magnetic oxygen analyzer (Beckman, Model D-2). Also, in a few cases, the ozone content of the evolved oxygen was measured by iodometry.

For the pyrolysis experiments the apparatus was modified as follows: (*a*) The metal needle valve was replaced by a greaseless Pyrex–Teflon stopcock to avoid catalytic decomposition of the hydrogen peroxide vapor. (*b*) An electrical resistance furnace 25 cm long was substituted for the microwave cavity. The temperature of the quartz tube inside the furnace was measured to ± 2 °C with an iron–constantan thermocouple. (*c*) The liquid nitrogen trap, of the Dewar flask type, was located some 15 cm from the end of the furnace. It was sealed directly, through a graded seal, to the quartz tube to avoid the difficulties of a heated ground glass joint. At the end of a run the melted products were condensed in a small flask located at the bottom of the trap, for weighing and analysis. The concentrated (98.6%) hydrogen peroxide was prepared by fractional distillation of BECCO's 80% commercial product. The liquid sample, held in a small flask with a ground glass joint, was kept in ice water during a run.

Discussion of Results

As the behavior of these systems has been described repeatedly in the literature, and again recently in an exhaustive monograph (3), only the new features relevant to surface effects will be reported here. For that purpose the following parameters are defined: yield, the fraction of input oxygen which is converted into hydrogen peroxide in the final products (i.e. after warming up to room temperature); efficiency, the fraction of input oxygen trapped at liquid nitrogen temperature (this is the sum of the water and hydrogen peroxide in the final products plus the evolved oxygen and ozone). The material balance is expressed in mmoles h^{-1}. (*n* units in the tables).

Nature of the Surface

Pyrex glass, the most commonly available material for a discharge tube, is also the one which gives the highest yields of peroxide, as shown by the typical run No. 1, Table 1. Fused quartz, although it has a lower dielectric loss than Pyrex at microwave frequencies (10), always gave appreciably smaller yields (run No. 2 is rather extreme in that respect). This difference in behavior does not seem to have been reported before. It must be related to the effect of the borosilicate components of Pyrex on the surface recombination of the atomic and radical species in the discharge tube. In quartz, water production was slightly favored at the expense of peroxide. However, the relative amount of evolved oxygen remained the same. A soft glass (ordinary soda glass) discharge tube yielded no hydrogen peroxide at first (run No. 3). In subsequent runs some peroxide was found in increasing proportion although always much less than with a Pyrex tube. Surface reactions leading to water formation were prominent as manifested by overheating of the discharge tube. Unless the latter was cooled by a strong air blast the yellow lines of sodium were noticeable. Much more water could be fed into the system with that tube because very little permanent gas was generated, the limiting factor being the capacity

TABLE 1

Influence of various factors on the reactions of dissociated water vapor

Description	Run No.	H_2O input *n*	H_2O_2 produced wt %	H_2O produced *n*	O_2 evolved *n*	O_2/H_2O_2	Yield %	Efficiency %
Surface effects								
Pyrex	1	24.0	67	7.9	1.35	0.16	71	115
Quartz	2	20.6	49	10.5	0.84	0.15	52.5	110
Soda glass	3	85.7	0	31.0	0.25	—	0	37
Soda glass	4	72.6	9	66.0	0.62	0.17	10	102
Teflon	5	80.0	0	65.5	7.3	—	0	100
Teflon	6	97.2	14.5	71.3	3.9	0.61	13	95
H_3PO_4	7	30.5	52	12.7	1.25	0.17	47	97
Packing, carrier gas, etc.								
Raschig	8	9.4	23.2	7.3	0.2	0.17	25	107
Capillary	9	2.1	4.2	2.0	0.01	0.25	4	100
r.f. discharge	10	13.8	63.5	3.6	0.5	0.1	68	111
r.f. discharge*	11	69	40	40.5	4.4	0.31	41	113
r.f. discharge* + Ar	12	40	44	22.4	2.2	0.24	46.5	113
r.f. discharge* + 10 Ar	13	22	25	16.7	1.3	0.45	26.5	114

*Large (4 cm diameter) discharge tube.

of the vacuum pumps. In view of the high flow rates (up to 40 m/s) it is doubtful if all the water vapor could be dissociated.

Teflon has good thermal and chemical stability as well as fairly low dielectric power loss. Its behavior as a discharge tube was roughly the same as soft glass except that much more oxygen was evolved from the trapped products on warming (run No. 6). Furthermore, the latter was found to be contaminated by hydrofluoric acid arising from corrosion of the plastic discharge tube. This could not be due to a thermal reaction as the temperature of the discharge tube never rose above 50 °C. The well-known catalytic decomposition of hydrogen peroxide by strong acids (9) must, therefore, be responsible for the excess of evolved oxygen in this case. Lastly, a coating of orthophosphoric acid on Pyrex reduced somewhat the yield, although more water vapor could be dissociated. This type of "wet" surface is known to minimize recombination of hydrogen atoms, favoring water formation at the expense of peroxide.

An interesting observation relates to the efficiency of trapping, which tended to be greater than 100% with Pyrex and quartz. The excess seems real as it lies outside the uncertainty of our analyses. This means that more oxygen was trapped than was introduced as water. Since analysis of the exhaust gas showed an oxygen content of the order of 10% the overall excess is still larger than shown here. An obvious explanation for this is the formation of water from silicates under bombardment of excited hydrogen atoms. Evidence for this has been reported before in this laboratory (1), and by other workers (11, 12).

Miscellaneous Effects

Packing the discharge tube with tiny Pyrex rings decreased the peroxide yield considerably (run No. 8). This must be the combined result of increased surface reactions and reduced pumping speed (i.e. longer residence time). These effects were further enhanced in a capillary (1 mm diameter) discharge tube, although again in this instance all the water may not have been dissociated because of the very high flow rate (about 150 m/s). The radio-frequency discharge gave roughly the same results as the microwave (comp. runs No. 1 and 10) under comparable conditions, but with a larger tube (4 cm diameter) much more water could be dissociated. It is not easy to disentangle the various factors involved here, namely: higher power (about 200 W), lower surface to volume ratio, longer residence time (flow rate of 0.5 m/s). Incidentally, most of the experiments reported here were done under viscous flow conditions (mean free path/diameter of tube $\sim$ 0.01) after Knudsen.

Varying the distance between the discharge zone and the cold trap altered the yield in the same fashion as reported before (3, 13) but the effect was much less marked with a phosphoric

Can. J. Chem. Downloaded from www.nrcresearchpress.com by 210.87.254.6 on 09/05/12
For personal use only.

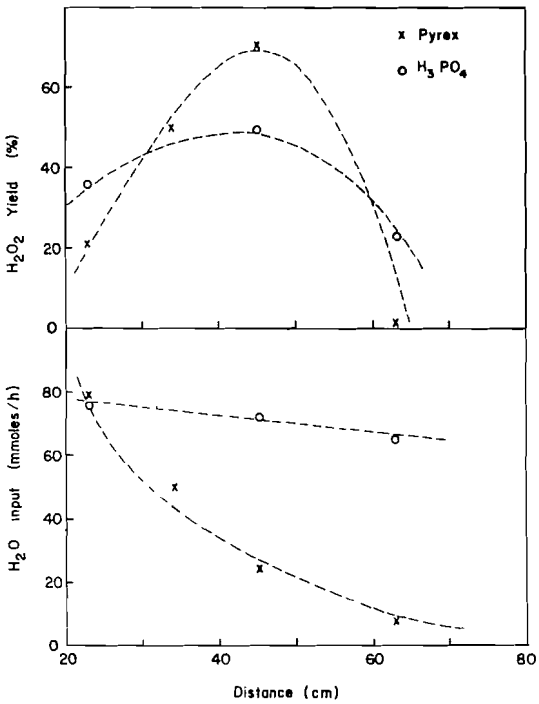

FIG. 1. Effect of distance between discharge zone and cold trap surface on water vapor input and hydrogen peroxide yield.

acid surface (Fig. 1) for the reason already discussed. Addition of a carrier gas (Argon) caused little change at low ratio (1 to 1 as in run No. 12) but the yield decreased rapidly at higher dilution (run No. 13).

Thermal vs. Electrical Dissociation of H_2O_2

In order to bring out some of the specific features of the electrical discharge in these systems it was decided to compare their behavior in thermally and electrically induced dissociation under closely similar conditions. Pure hydrogen peroxide vapor was used for that purpose because dissociation of water requires very high temperatures. The pyrolysis of hydrogen peroxide has been studied before in a flow system (14) but not from the viewpoint of the trapped products. It is well known that the homogeneous decomposition becomes gradually more important above 400 °C (15). Blank runs indicated that the surface decomposition amounted to less than 10% in our apparatus. As for the electrical dissociation, Winkler and co-workers (16) have shown that it gives results somewhat similar to those of water vapor. Therefore, the present comparative study is relevant to the problem at hand.

The trend of the data for the thermal dissociation (Table 2) shows that it was only partial in the temperature range covered. The species present in the dissociated stream then were the molecules H_2O, H_2O_2, and O_2, and in much lower concentrations, the radicals $HO_2^{\cdot}$ and $HO^{\cdot}$. In contrast, in the electrical discharge, only radicals and atoms must exist, even at low power level. This difference was reflected in the physical appearance of the trapped products which were partly crystalline for the thermal decomposition, but vitreous, with the typical yellow color, for the electrical dissociation. However, the major difference for our purpose was in the extent of oxygen evolution from the condensate on warming. Generally speaking this was at least an order of magnitude greater in the products from electrical discharge. Another important observation was that the greater part of this gas evolution took place after the trapped products had begun melting. It could be observed as an active foaming of the liquid as it ran down the walls of the Dewar trap.

TABLE 2

Dissociation of hydrogen peroxide vapor

Reaction type	Run No.	Temperature or power	H_2O_2 input n	H_2O_2 produced n	H_2O_2 produced wt %	H_2O produced n	O_2 evolved 230 °K	O_2 evolved 290 °K	Efficiency %
Thermal dissociation									
	14	1100 °K	22.5	15	75	9.7	—	0.08	85
	15	1200 °K	19.5	11	72	8.2	—	0.09	78
	16	1310 °K	11	2.8	37.5	9.3	—	0.08	67
Electrical dissociation									
	17	25 W	35	4.8	24	14.5	0.9	—	37
	18	37.5 „	27	4.5	38	14.0	0.85	2.0	50
	19	75 „	29	5.3	44.5	12.2	1.15	3.8	53
	20	150 „	19.5	4.0	53.1	6.7	0.75	2.5	51

Can. J. Chem. Downloaded from www.nrcresearchpress.com by 210.87.254.6 on 09/05/12
For personal use only.

A few blank runs were also carried out in which hydrogen peroxide vapor was condensed, without dissociation, in the same apparatus. Also, hydrogen peroxide solutions of various concentrations were quickly chilled by dropwise addition to a liquid nitrogen bath (17). The glassy beads thus produced gave off only traces of oxygen (about one order of magnitude less than the products from pyrolysis) while melting. Therefore, this phenomenon, as well as the reaction between hydrogen peroxide and ozone (never found in more than traces in the evolved oxygen), could only be of minor importance in these systems.

Conclusions

From the above results it may be concluded safely that decomposition of hydrogen peroxide always occur to some extent in the trapped products from all these systems. Therefore, it cannot be ruled out as a possible source of evolved oxygen, even in the case of the liquid ozone – atomic hydrogen system (4). The erratic results reported by various authors (3), and particularly the high values of the ratio O_2/H_2O_2, can thus be understood.

On the other hand the much larger amounts of oxygen given off by the products from the electrical discharge seem to be specific of that process. Kinetics and stoichiometric studies such as the present cannot provide definite evidence for or against the postulated higher oxides, H_2O_3 or H_2O_4. Still they can give some useful indications. For instance, the fairly constant and reproducible values of the O_2/H_2O_2 ratio in a given experimental system cannot be satisfactorily accounted for only in terms of catalytic decomposition of hydrogen peroxide as pointed out recently (18).

NOTE ADDED IN PROOF

This work was completed when the existence of stabilized H_2O_3 molecules in the trapped products from dissociated water vapor was confirmed definitely in this laboratory by means of infrared spectroscopy. Details will be reported in the next paper of this series. It is now clear that the bulk of the evolved oxygen comes from this and other possible metastable intermediates. Nevertheless, the above conclusions are still valid.

The authors are grateful to the National Research Council of Canada for continued financial support of this project.

1. N. HATA and PAUL A. GIGUÈRE. Can. J. Chem. **44**, 869 (1966).
2. P. A. GIGUÈRE. I.C.S.U. Rev. **4**, 172 (1962).
3. M. VENUGOPALAN and R. A. JONES. Chemistry of dissociated water vapor and related systems. Interscience Publ. Inc., New York. 1968. p. 174.
4. K. HERMAN and P. A. GIGUÈRE. Can. J. Chem. **46**, 2649 (1968).
5. E. A. SECCO. J. Chem. Phys. **23**, 1734 (1955).
6. P. A. GIGUÈRE, E. A. SECCO, and R. S. EATON. Discuss. Faraday Soc. **14**, 104 (1963).
7. F. S. LARKIN. Unpublished results.
8. E. A. SECCO. Ph.D. Thesis. Université Laval, Québec, Québec. 1953.
9. W. C. SCHUMB, C. N. SATTERFIELD, and R. I. WENTWORTH. Hydrogen peroxide. Reinhold Publ. Corp. New York. (1955).
10. F. K. MCTAGGART. Plasma chemistry in electrical discharges. Elsevier Publ. Co. New York. 1967. p. 60.
11. F. K. MCTAGGART. Nature, **201**, 1320 (1964).
12. A. A. BERGH. Bell System Tech. J. 261 (1965).
13. L. I. NEKRASOV, N. I. KOBOZEV, and E. N. EREMIN. Vestn. Mosk. Univ. Ser. II, Khim. **15**, 12 (1960).
14. C. K. MCLANE. J. Chem. Phys. **17**, 379 (1949).
15. P. A. GIGUÈRE and I. D. LIU. Can. J. Chem. **35**, 283 (1957).
16. J. S. BATZOLD, C. LUNER, and C. A. WINKLER. Can. J. Chem. **31**, 262 (1953).
17. R. C. SMITH and S. J. WYARD. Nature, **189**, 211 (1961).
18. R. S. JONES, W. CHAN, and M. VENUGOPALAN. J. Chem. Phys. **51**, 1273 (1969).

Can. J. Chem. Downloaded from www.nrcresearchpress.com by 210.87.254.6 on 09/05/12
For personal use only.

Can. J. Chem. Downloaded from www.nrcresearchpress.com by 210.87.254.105 on 09/05/12
For personal use only.

Studies on microcapsules. VI. Effect of variations in polymerization condition on microcapsule size

YOSHIMICHI SHIGERI, MASUMI KOISHI, AND TAMOTSU KONDO
Faculty of Pharmaceutical Sciences, Science University of Tokyo, Funagawara-machi, Shinjuku, Tokyo, Japan

AND

MOTOHARU SHIBA AND SUIICHI TOMIOKA
Research Laboratory, Chugai Pharmaceutical Co., Ltd., Takada, Toshima, Tokyo, Japan

Received January 13, 1970

The effect of variations in polymerization condition on the size of microcapsules prepared by the interfacial polycondensation method was studied. Factors lowering the rate and degree of polymerization, such as a decrease in temperature or monomer concentration, were found to increase the microcapsule size. A mechanism was proposed for the formation of large microcapsules in the polycondensation step.

Canadian Journal of Chemistry, **48**, 2047 (1970)

Introduction

The procedure of preparing microcapsules containing water consists of two steps in the interfacial polycondensation method. That is, for example, the polyphthalamide microcapsules containing water are prepared in the following way (1). An aqueous solution of piperazine (water soluble monomer) is mechanically emulsified with a stirrer in a cyclohexane–chloroform mixture to form a water-in-oil emulsion in the presence of Span 85 as emulsifier, and then a phthaloyl dichloride (oil soluble monomer) solution in the mixed solvent is added to yield the polyphthalamide membrane at the surface of emulsion droplets.

The size of microcapsules thus prepared has been considered to be completely determined by the conditions used in emulsification as reported in the previous paper (1) of this series. Recent works in our laboratory have revealed, however, that the size is also dependent on the conditions for polycondensation. The present paper describes how the variations in polymerization condition affect the microcapsule size.

Experimental

Preparation of Microcapsules

Microcapsules were prepared in a way similar to that described in the previous paper (1). To 7.5 ml of distilled water in a 1 liter round bottom flask immersed in a constant temperature bath controlled at −10, 3, and 30 °C was added an equal volume of 0.4 *M* solution of a water soluble monomer (1,6-hexamethylenediamine or piperazine) in aqueous 0.45 *M* sodium carbonate solution. To this solution was added 75 ml of mixed solvent (chloroform–cyclohexane 1:3, v/v) containing 10% (v/v) Span 85 as emulsifier. The mixed solution was then mechanically emulsified by a Model B-100 Chemistirrer (Tokyo Rika Kikai Co., Tokyo) at 620 r.p.m. for 5 min to give a water-in-oil emulsion. The alkali served to neutralize hydrogen chloride formed during the polycondensation.

Without stopping the stirring, 75 ml of solution of an oil soluble monomer in the mixed solvent was quickly added to the emulsion, and the stirring was further continued for 3 min. The solution of oil soluble monomer was made immediately before use by dissolving 3 moles of either sebacoyl dichloride, phthaloyl dichloride or 2,2′-dichlorodiethyl ether in the mixed solvent. In some cases, the solution was diluted with the same solvent or a part of the difunctional monomer was replaced by monofunctional monomer such as benzoyl chloride.

To the dispersion containing microcapsules was added 100 ml of cyclohexane to slow down the polycondensation reaction. A portion of the dispersion was pipetted into 10 ml of aqueous 50% (v/v) Tween 20 solution in a beaker. Finally, the aqueous dispersion was diluted with an appropriate amount of distilled water for photographing microcapsules under microscope.

The three different microcapsules (Table 1), two polyamides and one polyether, were prepared.

TABLE 1

Monomers used and polymers prepared

Water soluble monomer	Oil soluble monomer	Polymer formed
1,6-Hexamethylenediamine	Sebacoyl dichloride	Polyamide A
Piperazine	Phthaloyl dichloride	Polyamide B
Piperazine	2,2′-Dichlorodiethyl ether	Polyether

Can. J. Chem. Downloaded from www.nrcresearchpress.com by 210.87.254.105 on 09/05/12
For personal use only.

Microcapsule Size

Each sample of microcapsules prepared by the above method was placed on a hemocytometer and photographed under a microscope.

In each photographed strip film, 1500 microcapsule diameters were measured by projecting the film on a large section paper with a Colour Cabin slide projector (Cabin Industry Co., Tokyo). The scales in the hemocytometer were used for calibration. Then, the calculations were made of the mean diameter, size distribution, and standard deviation by using an IBM 1620 electronic computer.

Viscosity

A part of each of the microcapsules prepared under various conditions was washed on the centrifuge and dried by means of freeze drying. The dried sample was dissolved in *m*-cresol as described in the literature (2).

For each of the sample solutions, the relative viscosity was measured with a Ubbelohde viscometer at several concentrations at 30 °C. The reduced viscosity was then plotted against the concentration of sample and the intrinsic viscosity was graphically estimated by extrapolation to zero concentration.

Results and Discussion

Effect of Monomer Combination

The combination of monomers affected the microcapsule size to a surprisingly great extent. Typical photomicrographs are given in Figs. 1–3 for the polyamide A, polyamide B, and polyether microcapsules prepared under exactly the same conditions. The size seems to be the biggest for the polyether microcapsules, and the smallest for the polyamide B microcapsules. This trend is confirmed by the size distribution curves shown in Fig. 4 and by the mean diameters listed in Table 2.

As the conditions for preparation are exactly the same for all of the three kinds of microcap-

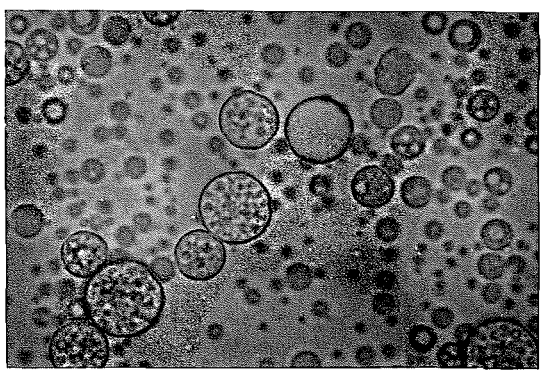

FIG. 1. Photomicrograph (×600) of polyamide A microcapsules prepared at 3 °C.

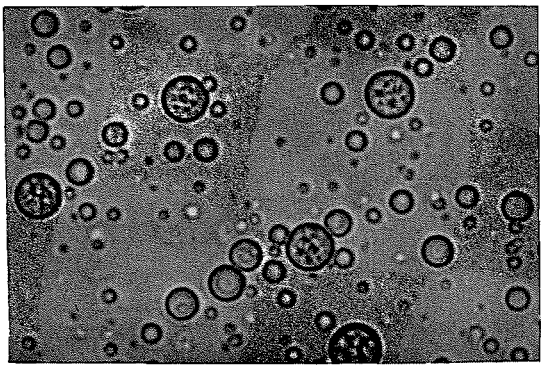

FIG. 2. Photomicrograph (×600) of polyamide B microcapsules prepared at 3 °C.

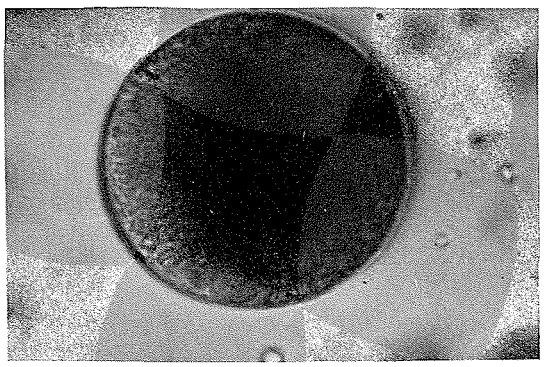

FIG. 3. Photomicrograph (×600) of polyether microcapsules prepared at 3 °C.

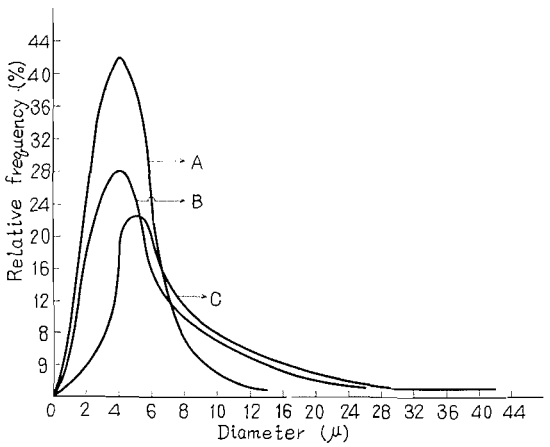

FIG. 4. Size distribution curves of microcapsules prepared at 3 °C. *A*, polyamide B; *B*, polyamide A; *C*, polyether.

Can. J. Chem. Downloaded from www.nrcresearchpress.com by 210.87.254.105 on 09/05/12
For personal use only.

TABLE 2
Mean diameters of microcapsules

Microcapsule	Mean diameter (μ)	Standard deviation
Polyamide A	5.90	5.41
Polyamide B	3.37	2.22
Polyether	9.94	9.39

sules, the difference in size should arise from the different polymerization characteristics for each combination of monomers. However, the comparative study of polymerization characteristics for the three monomer combinations is far beyond the scope of this work. This problem will, therefore, be put aside in the present work.

Effect of Temperature

Figures 5 and 6 show representative photomicrographs of the polyether microcapsules prepared at 30 °C and of the polyphthalamide B microcapsules prepared at −10 °C, respectively. Comparisons of Figs. 3 and 5, and of Figs. 2 and 6 indicate the existence of a remarkable temperature effect, especially for the polyether microcapsules. Figure 7 affirms this indication, showing a significant reduction in the microcapsule size with increasing temperature. The curves *B* and *C* in Fig. 8 are the size distribution curves for the polyamide B microcapsules prepared at 3 and −10 °C, respectively. Temperature effect is rather moderate in this case. This is due to the different temperature dependence of polymerization characteristics for these poly-

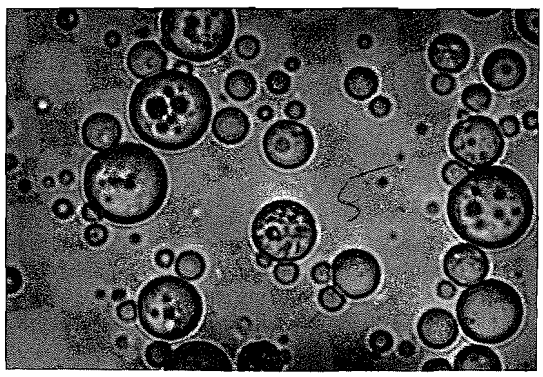

FIG. 5. Photomicrograph (×600) of polyether microcapsules prepared at 30 °C.

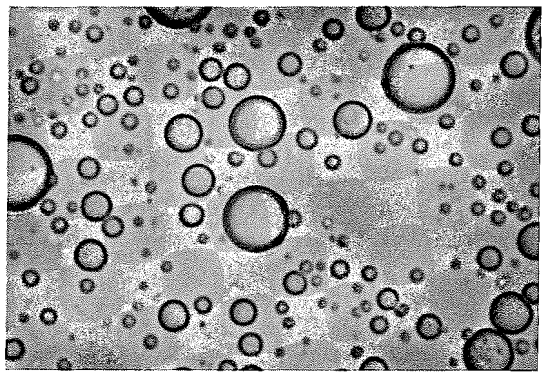

FIG. 6. Photomicrograph (×600) of polyamide B microcapsules prepared at −10 °C.

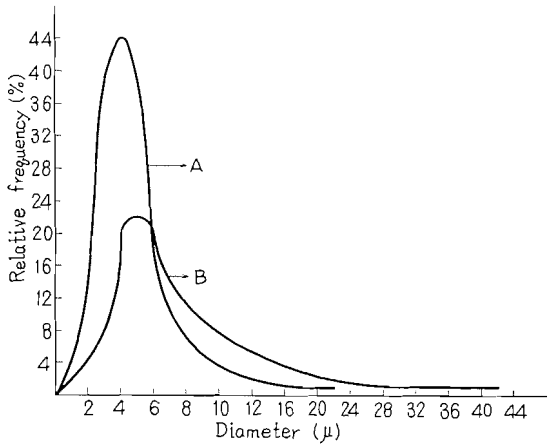

FIG. 7. Size distribution curves of polyether microcapsules prepared at different temperatures. *A*, 30 °C; *B*, 3 °C.

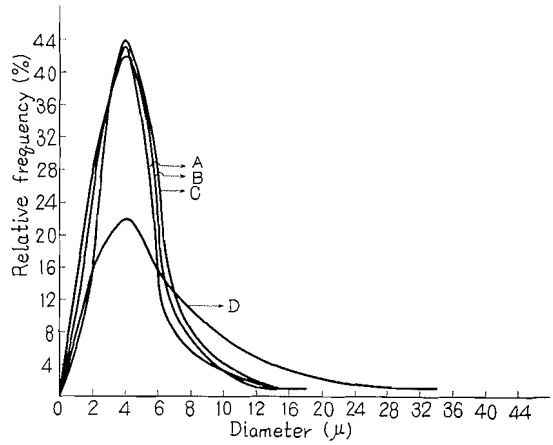

FIG. 8. Size distribution curves of polyamide B microcapsules prepared under various conditions. *A*, monomer diluted, 3 °C; *B*, monomer nondiluted, 3 °C; *C*, monomer nondiluted, −10 °C; *D*, mono- and difunctional monomer used, 3 °C.

TABLE 3
Some characteristics of microcapsules

Microcapsule	Temperature of preparation (°C)	Mean diameter (μ)	Standard deviation	Intrinsic viscosity of membrane polymer
Polyether	3	9.94	9.39	0.012
	30	5.07	5.00	0.022
Polyamide B	3	3.37	2.22	0.055
	−10	3.88	2.55	0.045

mers. Since the effect of temperature on the size of emulsion droplets was found to be inappreciable, the above findings will result from the change in the polymerization characteristics.

In Table 3 are summarized the mean diameters, standard deviations and intrinsic viscosities of membrane polymers for microcapsules prepared at various temperatures.

An inspection of the table indicates that a rise in temperature brings about a decrease in the microcapsule size. The table also suggests that the size is closely related to the intrinsic viscosity of membrane polymer. Thus, the size seems to decrease as the intrinsic viscosity increases. This implies that the membrane strength may determine the microcapsule size, because the intrinsic viscosity of a polymer is a measure of its molecular weight and the membrane strength is expected to be highly dependent on the molecular weight of polymers constituting the membrane.

Effect of Monomer Concentration

The polymerization characteristics may be altered by changing the monomer concentration. Actually, as shown in Fig. 9, a decrease in monomer concentration causes an increase in the microcapsule size, probably through a change in the polymerization characteristics.

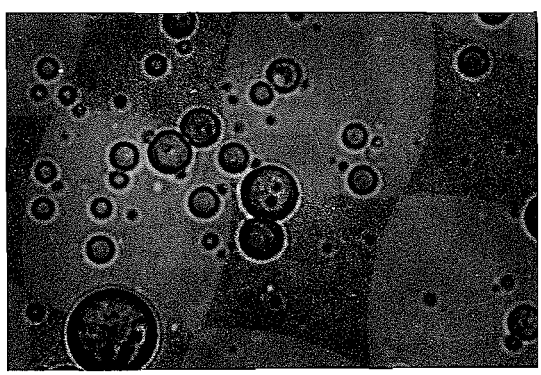

FIG. 9. Photomicrograph (×600) of polyamide B microcapsules prepared using diluted phthaloyl dichloride solution at 3 °C.

The calculated mean diameters differ from each other for the microcapsules prepared using oil soluble monomer solutions of different concentrations though the modal diameters of distribution curve (curves *A* and *B* in Fig. 8) are practically the same in the two cases. Thus, for example, the dilution of oil soluble monomer solution with the mixed solvent to 60% of the original concentration increased the mean diameter from 3.37 to 3.96 μ. Furthermore, the standard deviation also changed from 2.22 to 4.61. This means that the size distribution is broadened to some extent by the dilution. The intrinsic viscosity of membrane polymer was found to decrease from 0.055 to 0.038 through the reduction in the monomer concentration. A similar correlation can be seen, therefore, between the microcapsule size and the intrinsic viscosity of membrane polymer to that observed in the foregoing section, indicating again an important role of the membrane strength in determining the microcapsule size.

Effect of Monofunctional Monomer

Figure 10 illustrates a photomicrograph of polyphthalamide B microcapsules prepared using a mixture of phthaloyl dichloride and benzoyl chloride (2:3 in molar ratio) as oil soluble monomer. The mean diameter of 8.43 μ obtained in this case is more than double that of 3.37 μ for the microcapsules prepared using phthaloyl dichloride alone. The intrinsic viscosity of membrane polymer was drastically lowered by the substitution of benzoyl chloride for a part of phthaloyl dichloride. Namely, it was found to drop from 0.055 for the membrane polymer obtained using phthaloyl dichloride alone to 0.010 for that obtained using the mixture. This

Can. J. Chem. Downloaded from www.nrcresearchpress.com by 210.87.254.105 on 09/05/12
For personal use only.

appears to manifest the role of benzoyl chloride as terminating agent in the polycondensation reaction. A close relation comes out here once again, therefore, between the microcapsule size and the membrane strength.

Mechanism of Formation of Large Microcapsules

As has been mentioned so far, the formation of large microcapsules is closely related to the lowered membrane strength brought about by a decrease in the degree of polymerization of membrane polymer. Moreover, it is worth noting that the factors lowering the rate of polymerization also increase the microcapsule size. Thus, a drop in temperature or a decrease in the monomer concentration caused an increase in the size as described in the foregoing sections. This leads us to a hypothesis that the formation of large microcapsules takes place at an early stage of the polycondensation reaction, through the coalescence of primary emulsion particles with membrane of insufficient strength and coverage to prevent them from uniting each other to form a large secondary particle, provided the rate of polymerization is not so high. Since the polymerization reaction is still going on at this and later stages, the membrane being formed on the secondary particle surface may shortly thicken enough to resist further coalescence from occurring.

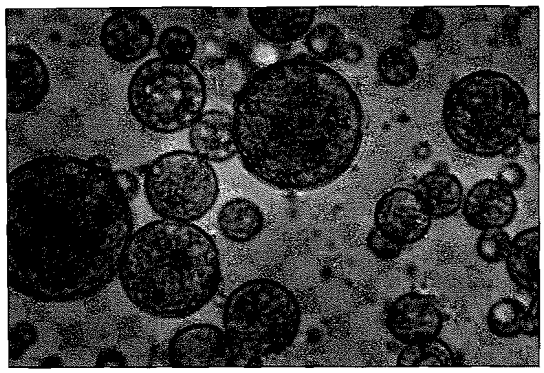

FIG. 10. Photomicrograph (×600) of polyamide B microcapsules prepared using the mixture of phthaloyl dichloride and benzoyl chloride in a molar ratio of 2:3 at 3 °C.

In this connection, it will be of interest to remark that large microcapsules often take the form of double capsules, as are seen in Figs. 1, 3, 5, and 10. These double microcapsules are likely to be formed by the penetration of a number of small capsules, on collision, into a large capsule. The mechanism is discussed elsewhere (3).

1. M. KOISHI, N. FUKUHARA, and T. KONDO. Chem. Pharm. Bull. Tokyo, **17**, 804 (1969).
2. M. KATZ. J. Polymer Sci. **40**, 337 (1959).
3. M. SHIBA, S. TOMIOKA, M. KOISHI, and T. KONDO. Chem. Pharm. Bull. Tokyo. In press.

Can. J. Chem. Downloaded from www.nrcresearchpress.com by 210.87.254.105 on 09/05/12
For personal use only.

Can. J. Chem. Downloaded from www.nrcresearchpress.com by 210.87.254.105 on 09/05/12
For personal use only.

Ultrasonic absorption in the water–2-isobutoxyethanol system[1]

R. J. FANNING[2] AND P. KRUUS
Department of Chemistry, Carleton University, Ottawa, Canada

Received November 7, 1969

Ultrasonic absorption measurements have been carried out on the system 2-isobutoxyethanol–water as a function of composition, temperature, and frequency. The composition and frequency dependence of the absorption show the same general type of behavior as for previously investigated critical binary liquid systems and for alcohol–water systems. The temperature dependence shows a behavior opposite to that for the other systems at the frequency where it was studied in detail. At the lowest experimentally available frequency, however, the temperature dependence is somewhat similar to that in other critical binary liquid systems. Ultrasonic absorption measurements are also reported for water at small temperature intervals. No anomalous behavior in the temperature range 0 to 30 °C is observed.

Canadian Journal of Chemistry, 48, 2052 (1970)

Introduction

Ultrasonic absorption studies have been carried out in a number of binary liquid systems which are partially miscible. At least seven systems with an upper critical solution temperature have been studied: nitrobenzene–*n*-hexane (1, 2), nitrobenzene–*n*-heptane (3), nitrobenzene–isooctane (4), aniline–cyclohexane (3, 5–7), aniline–*n*-hexane (8), and perfluoromethylcyclohexane – carbon tetrachloride (9). However, only two systems with a lower critical solution temperature have been investigated: triethylamine–water (1, 8–10) and butylcellosolve–water (11).

Another binary liquid system with a lower critical solution temperature was investigated in order to see whether the features observed in the systems studied previously are generally present in critical binary liquid systems. The system chosen was 2-isobutoxyethanol (isobutyl cellosolve) – water, which has a lower critical solution temperature near 25 °C (12).

Experimental

Apparatus

Two apparatuses were used for making the measurements. One (apparatus **A**) was useful for measuring the frequency dependence of the absorption, but required a relatively large amount of liquid (50 ml). The second (apparatus **B**) required less liquid (10 ml) and had a better temperature control, but was useful only at one frequency (20.5 Mc).

Figure 1 shows a schematic diagram of apparatus **A** (13). The equipment used was: an Arenberg PG-650-C pulsed oscillator, Arenberg ATT-693 and Weinschel 905 attenuators, an Arenberg PA-620-B tuned preamplifier, an Arenberg WA-600-E amplifier, a Tektronix 546 oscilloscope, a Hewlett–Packard 608D ser. E C.W. generator, and an HP 5245L frequency counter.

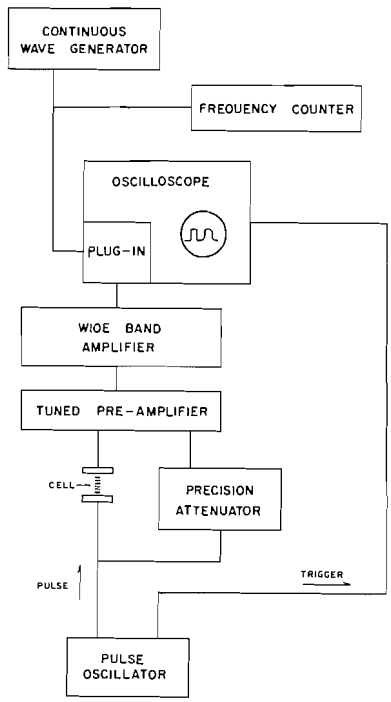

FIG. 1. Schematic diagram of apparatus **A** (range 3.5 to 52 Mc).

A Dow–Key DK60 coaxial relay was at times used at the output of the pulsed oscillator in order to avoid interference between the signal going through the cell and the comparison signal.

The cell used in apparatus **A** is shown in Fig. 2. The transducers were X-cut quartz crystals with a resonant frequency of 3.5 Mc. Both the transducers and the delay rods were supplied by Valpey Corp.

Apparatus **B** was essentially the same as apparatus **A**,

[1]Taken in part from the thesis submitted by R. J. Fanning in partial fulfillment of the requirements for the B.Sc. (Honours) degree.

[2]Present address: Uniroyal Research Laboratories, Guelph, Ontario.

Can. J. Chem. Downloaded from www.nrcresearchpress.com by 210.87.254.105 on 09/05/12
For personal use only.

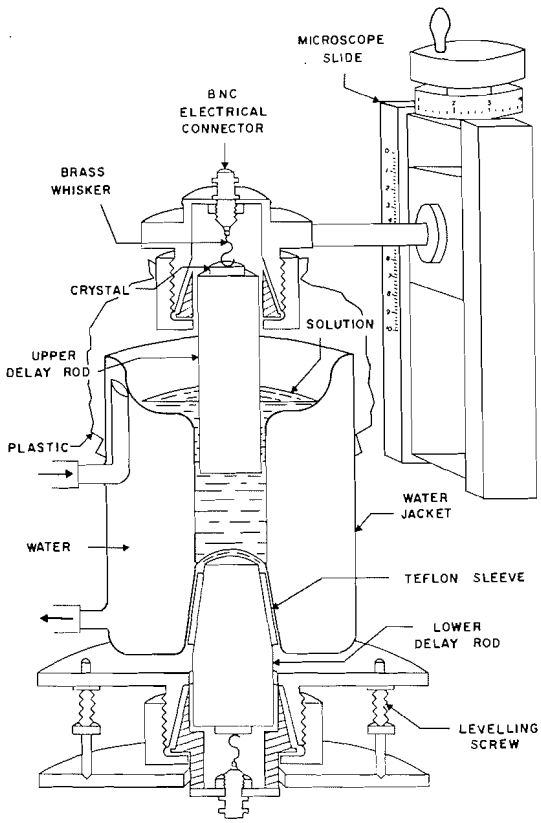

FIG. 2. Diagram of the cell used in apparatus **A**.

except that (*i*) the crystals had a resonant frequency of 20.5 Mc, (*ii*) the cell was smaller and had a thermocouple well in it, (*iii*) the moving delay rod was centrally supported instead of being on an arm, and (*iv*) a specially designed preamplifier–mixer circuit (14) preceded the tuned preamplifier.

The temperature was controlled by circulating water (or water–methanol mixtures) from a temperature bath through the measuring cell. The constant temperature bath had in it a Neslab PB-C2 cooling unit and heaters controlled by a Melab CTC-1A proportional temperature controller. When apparatus **B** was used, the temperature in the cell was measured with an iron–constantan thermocouple and a Fluke 845 A microvoltmeter.

Procedure

The absorption coefficient was measured by dividing (or alternating) the signal from the oscillator to go through the attenuator and the cell. The two signals were then displayed on the oscilloscope, and the separation of the delay rods was altered to make the signals of equal height. This procedure was repeated for a number of attenuator settings, and the absorption coefficient then obtained from the slope of the resulting attenuation vs. delay rod separation curve. Pulses were used which were about 10 μs long and had a repetition rate of 60 s^{-1}.

The frequency was measured by mixing a signal from the C.W. generator with the pulsed radiofrequency (r.f.) signals from the amplifier. The C.W. generator frequency was varied to give a zero beat frequency. This frequency was then measured using the frequency counter.

The wavelength, and thus also the velocity, was measured by an interferometric technique. At small separations of the delay rods, there is interference between the primary signal and that reflected from the surface of the upper delay rod. As the rods are moved apart this interference is alternately constructive and destructive. The wavelength can be calculated as 2 × the change in delay rod separation divided by the number of positive interferences in that change.

Viscosity measurements were made using a Cannon–Fenske viscometer calibrated using distilled water.

Chemicals

The water used was distilled water redistilled from potassium permanganate solution.

The 2-isobutoxyethanol was J. T. Baker D 651 purified by chromatography using a Prep Master 776 chromatograph with a column of 20% sucrose – acetate – isobutyrate on 30/60 mesh chromosorb W.

Fisher A-401 *t*-butanol was used without further purification.

Results

Pure Components

The results of the absorption measurements in water are presented in Fig. 3. The precision in the absorption coefficients is estimated to be at best ± 1.5%, and in the temperature, ± 0.05 °C. For some points, the error in the temperature could be considerably greater. It was noticed after the experiments that sudden changes could occur in the cell temperature due to changes in circulation patterns in the bath caused by icing-up of the cooling coil.

Results of the absorption measurements for pure 2-isobutoxyethanol are given in Fig. 4. Measurements made at 5 different frequencies at 26.6 °C show α/f^2 to be constant with frequency to within experimental error from 10 to 53 Mc.

Composition Dependence

The composition dependence of the absorption is shown in Fig. 5, together with a solubility diagram for the system (12). Additional data is given in Table 1, giving viscosity, velocity, and the classical absorption (15) for the system at 25 °C.

Temperature Dependence

The temperature dependence of the absorption in a mixture 27% by weight of 2-isobutoxyethanol is shown in Fig. 6. As can be seen from Fig. 7,

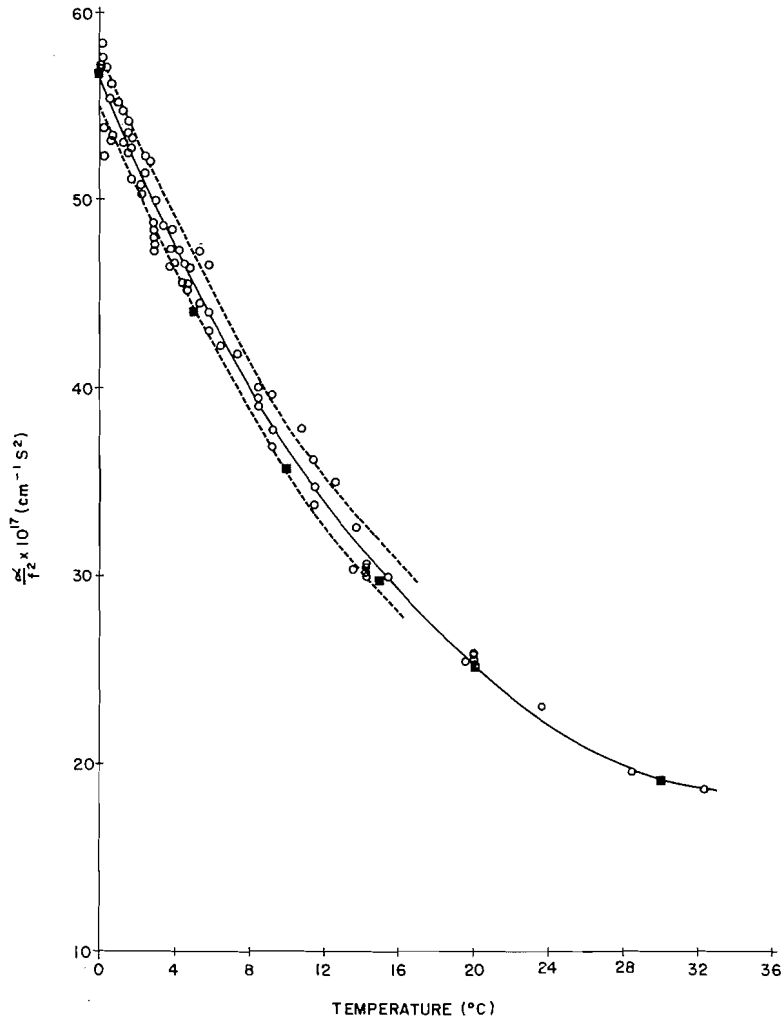

FIG. 3. Ultrasonic absorption as a function of temperature in water, 20.8 Mc. ■, data of Pinkerton (ref. 23); - - -, standard error limits.

the absorption at that composition and frequency keeps rising as the temperature is lowered, as at −4.3 °C the α/f^2 at 20.5 Mc is 3800 × 10^{-17} cm^{-1} s^2. The mixture begins to freeze between −6 and −7 °C.

The two other curves in Fig. 6 show the temperature dependence of the mixtures into which the 27% by weight mixture separates at 26.0 °C. From the solubility diagram (12), the upper phase is estimated to be 44% by weight and the lower 17%. From the absorption at 25.7 °C (Fig. 5) the phases are estimated to be 40 and 17% by weight 2-isobutoxyethanol, respectively.

Frequency Dependence

The frequency dependence of a 27% mixture is shown in Fig. 7 for four temperatures (24.8 to −4.3 °C). Measurements at frequencies higher than 31.8 Mc were difficult to make due to the very high absorption. At 24.8 °C, the value of α/f^2 at 38.8 Mc was estimated to be 930 × 10^{-17} cm^{-1} s^2. This value is estimated to be accurate to within 10%.

The lines drawn in Fig. 7 are the results of a least-squares fit of the experimental data to a single-relaxation equation.

Figure 8 shows the frequency dependence of a

Can. J. Chem. Downloaded from www.nrcresearchpress.com by 210.87.254.105 on 09/05/12
For personal use only.

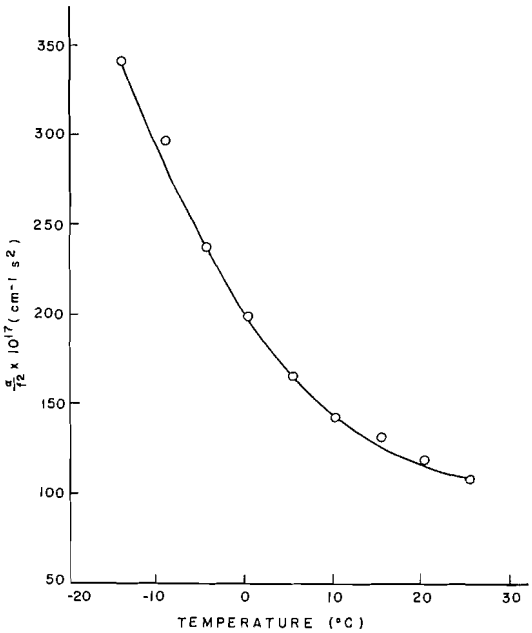

FIG. 4. Ultrasonic absorption as a function of temperature in 2-isobutoxyethanol, 20.8 Mc.

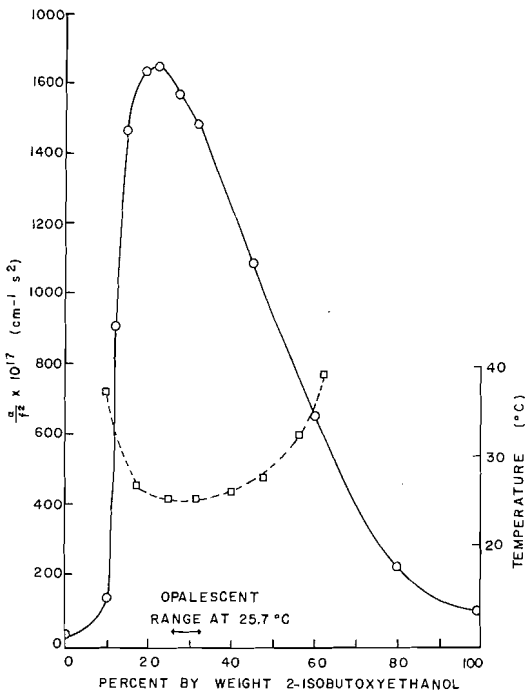

FIG. 5. Ultrasonic absorption as a function of composition in the system water–2-isobutoxyethanol; 20.8 Mc, 25.7 °C. — ○ —, absorption; - - - □ - - -, solubility curve.

TABLE 1

Viscosity, ultrasonic velocity, and classical ultrasonic absorption, α_c/f^2, in the system water–2-isobutoxyethanol at 25 °C

Percent by weight 2-isobutoxyethanol	Viscosity (centistokes)	Velocity ($m\ s^{-1}$)	$10^{17} \times \alpha_c/f^2$ ($cm^{-1}\ s^2$)
100	3.33	1260	44
95.5	3.70	1284	46
70.1	4.40	1359	46
58.5	4.27	1407	40
44.9	3.65	1427	33
29.9	2.70	1473	22
24.4	2.4	1491	19
9.9	1.2	1558	8.4
2.4	0.9	1515	6.8

42% by weight mixture of *t*-butanol in water at three temperatures. The data is fitted by a single-relaxation equation and the equation derived by Fixman (16) for critical binary liquid systems.

Theoretical Considerations

The large ultrasonic absorption in critical binary liquid systems could be present for several reasons.

Brown (17) and Brown and Richardson (6)

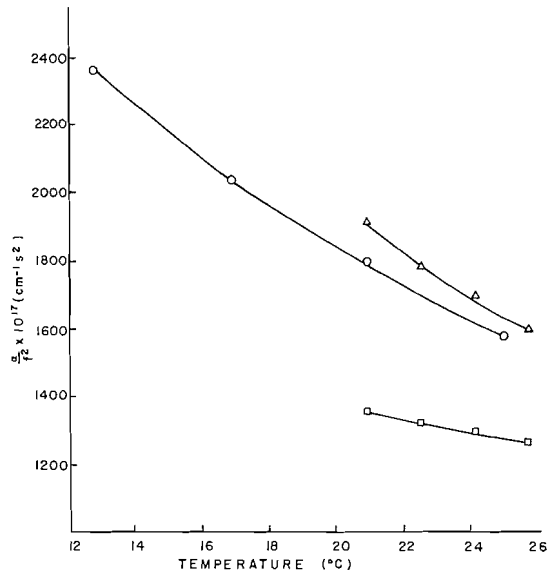

FIG. 6. Ultrasonic absorption as a function of temperature in the system water–2-isobutoxyethanol, 20.8 Mc. ○, 27% by weight 2-isobutoxyethanol; △, lower phase at 26.0 °C (~ 17% by weight 2-isobutoxyethanol); □, upper phase at 26.0 °C (~ 40% by weight 2-isobutoxyethanol).

Can. J. Chem. Downloaded from www.nrcresearchpress.com by 210.87.254.105 on 09/05/12
For personal use only.

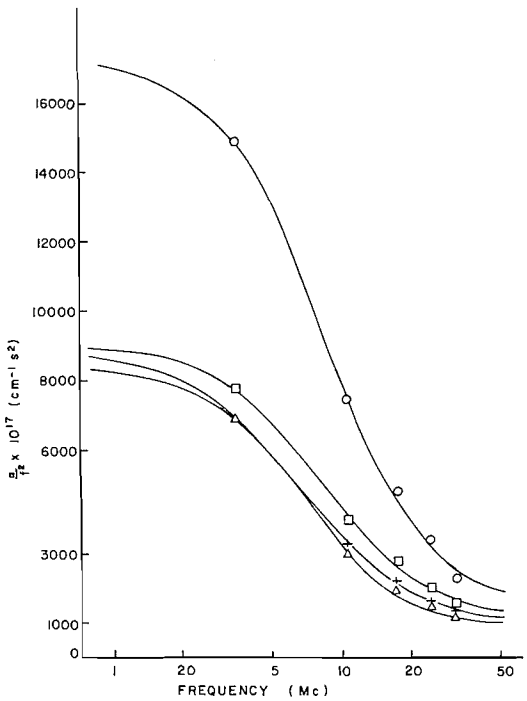

FIG. 7. Ultrasonic absorption as a function of frequency in the system water–2-isobutoxyethanol, 27% by weight isobutoxyethanol. ○, −4.3; □, 12.1; +, 18.2; △, 24.8 °C.

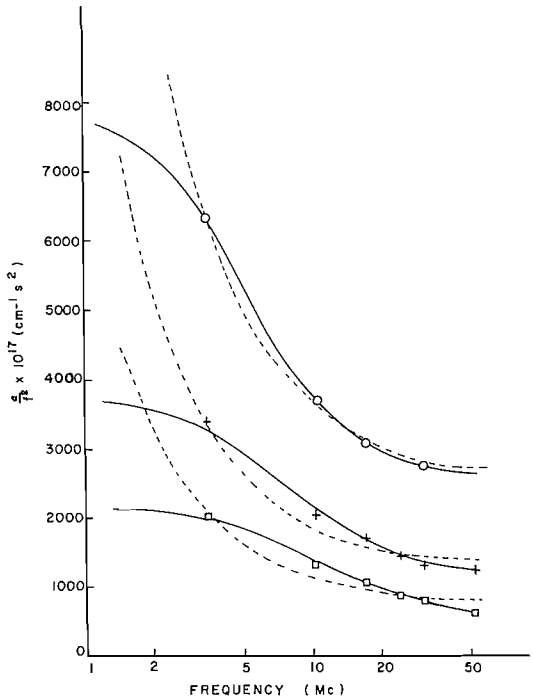

FIG. 8. Ultrasonic absorption as a function of frequency in the system water–*t*-butanol, 42% by weight *t*-butanol. ○, 0.0; +, 12.1; □, 24.9 °C. —, fit with a single-relaxation equation; - - -, fit with Fixman's equation (ref. 16).

explain the large attenuation in terms of scattering of the ultrasonic waves. This explanation is based on (*i*) detection of a significant amount of scattered ultrasound, (*ii*) the agreement in obtaining a scatterer radius of about 0.03 cm from both the frequency exponent method (6) and the angular distribution of the scattered ultrasound (17), and (*iii*) the decrease in the relaxation frequency with a rise in temperature (away from the critical solution temperature) if a single-relaxation fit is applied to the data. It is pointed out that the scattering would account for the major part of the excess attenuation distant from the critical point, but a much smaller part as the critical point is approached. The remaining attenuation is thought to be due to molecular absorption of a structural type.

Fixman (16) explains the large attenuation near the critical point in liquid mixtures as being due to relaxation phenomena occurring due to the disturbance of the composition fluctuations present by the temperature variation caused by the ultrasonic waves. This theory has been successful in interpreting both the temperature and the frequency variation of the absorption (2–4, 9).

The approach in which the excess absorption in liquid mixture is attributed to local concentration fluctuations has been discussed in more general terms by Romanov and Solov'ev (18). If the concentration dependence of the specific volume and enthalpy in the system is nonlinear, then there is a contribution to the specific volume and enthalpy of the system due to local fluctuations in concentration. The equilibrium intensity of these fluctuations is then influenced by the pressure and temperature variations in a sound wave.

The kinetics of the process of establishing a new distribution is described in terms of diffusion. When the concentration fluctuations are expressed in terms of a spatial Fourier series, then each Fourier component exhibits a single relaxation time which is proportional to the inverse square of the wave number of the component. A broad relaxation-time spectrum is then predicted by this theory when a continuous

Can. J. Chem. Downloaded from www.nrcresearchpress.com by 210.87.254.105 on 09/05/12
For personal use only.

Can. J. Chem. Downloaded from www.nrcresearchpress.com by 210.87.254.105 on 09/05/12
For personal use only.

distribution (e.g., the Debye distribution) of wave numbers is assumed.

It is also possible that a large part of the absorption is due not to the critical solution phenomenon, but more directly to the intermolecular interactions which cause the separation into phases in the first place. Systems of water with alcohols (19–22), amines (20, 23), and other non-electrolytes (20) all show excess ultrasonic absorption even though the mixture is far from the critical solution temperature. This absorption is thought to be due to the relaxation of equilibria involving molecules of water, solute, and water–solute complexes (20–23). In the case of amines, the relaxation of a proton transfer equilibrium is thought to contribute (23).

The Romanov–Solov'ev theory outlined above has also been used to explain the excess absorption in liquid systems which show no critical solution phenomena. There is qualitative agreement between the theory and the concentration dependence of the excess absorption in ethanol–water and propanol–water (18). However, well-defined relaxation frequencies are observed in other alcohol–water systems (21) instead of the continuous distribution predicted by the theory. There is reasonable agreement between the theory and the frequency dependence of the excess absorption in a water–acetone mixture over a wide frequency range (24), but again only single relaxation times have been observed in ethanol – ethyl halide systems (25), in conflict with the predictions of the theory.

Discussion

Pure Water

Numerous measurements have been made of the ultrasonic absorption of pure water as a function of frequency (15). The first reliable data was that of Pinkerton (26), using a pulse apparatus. These points are shown in Fig. 3; they are in good agreement with the present data. No detailed work on the temperature dependence of the ultrasonic absorption in water seems to have been done since that time.

There has been controversy regarding the presence of discontinuities of physical properties of water at certain temperatures (27–29). Recent measurements of the viscosity of water as a function of temperature (29) revealed no abrupt changes at discrete temperatures. The authors suggest that some of the thermal anomalies previously reported in bulk properties of water may have been due to structural transitions in ordered water structures near interfaces. High-resolution measurements of the ultrasonic velocity at 9.9 Mc in water from 6 to 81 °C also disclosed no thermal anomalies (30). The existence of "anomalous" water near interfaces (in capillaries) has been reported (31).

The measured values of α/f^2 for water (77 pieces of data) were fitted to polynomials of various degrees using a least-squares program. A polynomial of the third degree gave the smallest standard error (1.28, or about 3%) with a relationship $\alpha/f^2 \times 10^{17} = 56.44 - 2.452T + 5.402 \times 10^{-2}T^2 - 4.662 \times 10^{-4}T^3$, where T is the temperature in degrees centigrade. To within experimental error, there are no thermal anomalies in the ultrasonic data in this temperature range, as seen by the distribution of the experimental points inside the standard error limits in Fig. 3.

Pure 2-Isobutoxyethanol

The second pure component acts as a typical associated liquid (15), as expected. There is no relaxation present, as α/f^2 is constant with frequency, and the ultrasonic absorption is probably due to "volume" viscosity throughout the temperature range investigated (−15 to 25 °C).

Composition Dependence

Several points are noteworthy in the composition dependence of the absorption for the water–2-isobutoxyethanol system as shown in Fig. 5.

(*1*) The absorption is not a maximum when the system is opalescent (i.e., when light scattering is a maximum). There is also no sign of a discontinuity in the absorption over the range of composition where the system is opalescent. Table 1 shows the classical absorption to be negligible in the high-absorption composition region.

(*2*) The behavior of the absorption vs. composition curve at low alcohol concentrations is similar to that in other alcohol–water systems (19–22). The sharp rise in absorption occurs at about 11% by weight alcohol, corresponding to a mole fraction of 0.018, and the maximum at 0.030 mole fraction. For the *t*-butanol–water system, the rise occurs at a mole fraction of 0.05, and the maximum at 0.10 (22). The absorption–composition curve for the water–2-isobutoxyethanol

TABLE 2

Parameters for a single-relaxation equation obtained by fitting ultrasonic absorption data for alcohol–water systems and critical binary liquid systems

System	Temperature (°C)	$A \times 10^{17}$ (cm^{-1} s^2)	$B \times 10^{17}$ (cm^{-1} s^2)	f_c (Mc)	Reference
(*1*) 27.0% by wt. 2-isobutoxyethanol in water	−4.3	15600	1550	8.4	
(*2*)	12.1	7790	1210	8.0	
(*3*)	18.2	7290	1120	6.9	
(*4*)	24.8	7880	914	6.3	
(*5*)*	18.2	7760	1140	6.6	
(*6*)*	18.2	6700	1100	7.4	
(*7*) 42% by wt. (0.15 mole fraction) *t*-butanol in water	0.0	5310	2610	5.3	
(*8*)	12.1	2510	1240	7.6	
(*9*)	24.9	1530	630	10.3	
(*10*) 0.15 mole fraction *t*-butanol in water	5	3680	1970	5.3	21
(*11*)	25	1310	956	6.0	21
(*12*)	45	737	789	5.2	21
(*13*) 56% by volume carbon tetrachloride in perfluoro-*n*-heptane	28.4	1400	460	7.1	9
(*14*)	33.9	850	470	6.4	9
(*15*) 61% by volume *n*-heptane in nitrobenzene	20.0	5510	243	5.8	3
(*16*)	25.0	2780	252	6.1	3

*Same as *3*, with 3.5 Mc point 5% higher.

system is very similar in shape to that for the *t*-butanol–water system (22).

The absorption in this system must therefore in large part be due to the same phenomena as those present in the *t*-butanol–water system. On the basis of the model of the alcohol–water systems described by Franks and Ives (32), the alcohol is first accommodated interstitially by the water. As 2-isobutoxyethanol is larger than *t*-butanol, the interstitial spaces would be filled at a smaller mole fraction of alcohol for the former. When more alcohol is added, the alcohol dissolves by substitution into the water lattice.

The equilibrium between interstitial alcohols and alcohol molecules in the lattice would be very sensitive to pressure, as the interstitial alcohol would take up little volume, while the lattice-substituted alcohol would take up normal volume. The absorption would then be due to the disturbance of this type of equilibrium by the pressure variations in the ultrasonic wave.

An analysis of the concentration dependence of the excess absorption in terms of the Romanov–Solov'ev theory (18) is not possible because of a lack of thermodynamic data for this system.

Temperature Dependence

The temperature dependence of a 27% alcohol (by weight) 2-isobutoxyethanol–water mixture is different from that of all other critical liquid mixtures at the frequency used (20.8 Mc). In the case of critical liquid mixtures, with both an upper and a lower critical solution temperature (including butyl cellosolve – water (11)), the absorption increases as the critical solution temperature is approached (1–11). In this case, the absorption increases regularly as the temperature gets farther from the critical solution temperature (Fig. 6).

The type of behavior noted in Fig. 6 is opposite to the predictions of Fixman's theory (16). However, if the absorption is considered to be due mostly to the equilibria present in all alcohol–water mixtures, then the increase in α/f^2 with a decrease in temperature can be explained.

At the lowest frequency used, however, there is a slight increase in the absorption as the temperature is raised close to the critical solution temperature (Fig. 7). This rise would seem to be due to a contribution to the total absorption from the critical solution phenomenon at lower frequencies. This is another example of the difficulty of evaluating theories in ultrasonic absorption on the basis of limited data.

Frequency Dependence

The relaxation of the concentration fluctuations in a binary liquid mixture near the critical solution temperature has been measured (33, 34). The relaxation times are proportional to $(T - T_c)^{-0.9}$

Can. J. Chem. Downloaded from www.nrcresearchpress.com by 210.87.254.105 on 09/05/12
For personal use only.

Can. J. Chem. Downloaded from www.nrcresearchpress.com by 210.87.254.105 on 09/05/12
For personal use only.

and are of the order of 100 μs in a mixture of nitrobenzene–2,2,4-trimethylpentane. A single relaxation time was sufficient to fit the data. The results of ultrasonic absorption data have also been fitted well with a single-relaxation time curve (7).

Figure 7 shows the experimental data for a mixture of 27% by weight 2-isobutoxyethanol in water fitted by a single-relaxation equation

$$\alpha/f^2 = A/[1 + (f/f_c)^2] + B$$

Figure 8 shows the same type of data for the system *t*-butanol–water at a composition at the corresponding place in the absorption–composition curve (42% by weight *t*-butanol, or a mole fraction of 0.15). The values of A, B, and f_c for the seven curves are given in Table 2.

Table 2 also contains an indication of the sensitivity of the single-relaxation curve to inaccuracies in the lowest frequency points (at 3.5 Mc), which were the least accurate (estimated to be within 5%).

The systems certainly contain more than a single relaxation, as the value of B is high in all cases. If B were of the order of 200×10^{-17} cm^{-1} s^2 at −4.3 °C, and 100×10^{-17} cm^{-1} s^2 at 24.8 °C, then the excess absorption could be due to a single-relaxation phenomenon. However, the values of B are nearly 10 times higher, and considerably higher than the less accurate high-frequency points at 24.8 °C. This would indicate the presence of another relaxation at higher frequencies, as obtained in other alcohol–water mixtures (21).

The theory proposed by Fixman (16) predicts a frequency dependence of the type

$$\alpha/f^2 = Af^{-5/4} + B$$

A least-squares fit of the data using this equation gave results which in no case were as good as a fit with a single-relaxation equation. Examples of the fits are given in Fig. 8 for *t*-butanol–water. It should be noted, however, that this equation has only two adjustable parameters, as compared to three in the single-relaxation equation.

If the attenuation of the ultrasound is due to scattering, then for scattering particles much smaller than the wavelength, the attenuation should rise as f^4. If the scattering particles are of the order of magnitude of the wavelength (17, 6), then the frequency dependence can be different from f^4. In this case, the frequency dependence of α is between f^1 and f^2.

The reasonably good fit of the data in this frequency range to a single-relaxation equation (Fig. 7) would suggest that the continuous distribution predicted by the Romanov–Solov'ev theory (18) is not present in this system. However, the frequency range covered is probably too narrow to be able to conclude definitely that only some discrete relaxation times are present.

An interesting aspect is that the relaxation frequency is of the same order of magnitude in a relatively wide range of temperatures for all the systems listed in Table 2 (in some cases it even decreases with an increase in temperature). This is also true of other alcohol–water mixtures which have been studied (21, 22). On a simple interpretation, this would indicate a zero or even a negative activation energy from some process which is involved. This temperature dependence of f_c could probably be explained only if the relaxation is due to a complex cooperative structural type (21, 32).

Conclusions

No thermal anomalies seem to be present in the ultrasonic absorption data for pure water in the temperature range 0 to 30 °C.

The results indicate that most of the ultrasonic absorption in the system water–2-isobutoxyethanol is due to the structural type of absorption present in all alcohol–water systems. However, there are signs that the critical solution phenomenum contributes appreciably to the absorption at lower frequencies.

Comparison of the temperature dependence of the relaxation frequencies obtained by fitting a single-relaxation equation to the experimental data of alcohol–water systems and of systems showing critical solution phenomena indicates a remarkable similarity. This suggests that the basic phenomena responsible for the ultrasonic absorption may in both cases be of a cooperative structural type.

The authors wish to thank Dr. J. E. Piercey, Mr. D. R. Dickson, and Mr. A. Raffler for assistance in planning and constructing the apparatus, Mr. D. G. Fecchio and Miss V. Lindstrom for technical assistance, and Dr. P. M. Laughton for helpful discussions. The project was supported financially by the National Research Council of Canada and the Inland Waters Branch, Department of Energy, Mines, and Resources.

1. G. F. ALFREY and W. G. SCHNEIDER. Discuss. Faraday Soc. **15**, 281 (1953).
2. G. D'ARRIGO and D. SETTE. J. Chem. Phys. **48**, 691 (1968).
3. P. KRUUS and T. A. BAK. Acta Chem. Scand. **20**, 231 (1966).
4. A. V. ANANTARAMAN, A. B. WALTERS, P. D. EDMONDS, and C. J. PINGS. J. Chem. Phys. **44**, 2651 (1966).
5. M. CEVOLANI and S. PETRALIA. Nuovo Cim. Ser. X 2, 495 (1955).
6. A. E. BROWN and E. G. RICHARDSON. Phil. Mag. **4**, 705 (1959).
7. G. D'ARRIGO, L. MISTURA, D. SETTE, and J. L. HUNTER. Proc. 6th Intern. Congr. Acoust., Tokyo, J-89 1968. J-89.
8. A. G. CHYNOWETH and W. G. SCHNEIDER. J. Chem. Phys. **19**, 1566 (1951).
9. P. KRUUS. Can. J. Chem. **42**, 1712 (1964).
10. S. SHIMAKAWA. J. Phys. Soc. Jap. **16**, 113 (1961).
11. J. E. PIERCEY. Ph.D. thesis, University of London, London, England. 1955.
12. H. L. COX and L. H. CRETCHER. J. Amer. Chem. Soc. **48**, 453 (1926).
13. D. R. DICKSON. M.Sc. thesis, Carleton University, Ottawa, Canada. 1967.
14. R. J. FANNING. B.Sc. thesis, Carleton University, Ottawa, Canada. 1968.
15. K. F. HERZFELD and T. A. LITOVITZ. Absorption and dispersion of ultrasonic waves. Academic Press, Inc., New York. 1959.
16. M. FIXMAN. J. Chem. Phys. **33**, 1357 (1960); **33**, 1363 (1960); **36**, 310 (1962); **36**, 1957 (1962); **36**, 1961 (1962).
17. A. E. BROWN. Acust. **18**, 169 (1967).
18. V. P. ROMANOV and V. A. SOLOV'EV. Sov. Phys. Acoust. Engl. Transl. **11**, 68 (1965); **11**, 219 (1965).
19. C. J. BURTON. J. Acoust. Soc. Amer. **20**, 186 (1946).
20. J. H. ANDREAE, P. D. EDMONDS, and J. F. MCKELLAR. Acust. **15**, 74 (1965).
21. M. J. BLANDAMER, N. J. HIDDEN, M. C. R. SYMONS, and N. C. TRELOAR. Trans. Faraday Soc. **65**, 1805 (1969); **64**, 3242 (1968).
22. M. J. BLANDAMER, D. E. CLARKE, N. J. HIDDEN, and M. C. R. SYMONS. Chem. Commun. 342 (1966). Trans. Faraday Soc. **64**, 2691 (1968).
23. M. J. BLANDAMER, D. E. CLARKE, N. J. HIDDEN, and M. R. C. SYMONS. Trans. Faraday Soc. **62**, 66 (1966).
24. J. M. DAVENPORT, J. F. DILL, V. A. SOLOV'EV, and K. FRITSCH. Sov. Phys. Acoust. Engl. Transl. **14**, 236 (1968).
25. V. A. SOLOVYEV, C. J. MONTROSE, M. H. WATKINS, and T. A. LITOVITZ. J. Chem. Phys. **48**, 2155 (1968).
26. J. M. M. PINKERTON. Nature, **160**, 128 (1947).
27. M. FALK and G. S. KELL. Science, **154**, 1013 (1966).
28. W. DROST-HANSEN. Advan. Chem. Ser. **67**, 70 (1967).
29. L. KORSON, W. DROST-HANSEN, and F. J. MILLERO. J. Phys. Chem. **73**, 34 (1969).
30. W. SENGHAPHAN, G. O. ZIMMERMAN, and C. E. CHASE. J. Chem. Phys. **51**, 2543 (1969).
31. B. V. DERYAGIN and N. V. CHURAYEV. Priroda, **4**, 16 (1968).
32. F. FRANKS and D. I. G. IVES. Quart. Rev. London, **20**, 1 (1966).
33. P. DEBYE and K. KLEBOTH. J. Chem. Phys. **42**, 3155 (1965).
34. P. DEBYE, C. C. GRAVATT, and M. IEDA. J. Chem. Phys. **46**, 2352 (1967).

Can. J. Chem. Downloaded from www.nrcresearchpress.com by 210.87.254.105 on 09/05/12
For personal use only.

Can. J. Chem. Downloaded from www.nrcresearchpress.com by 210.87.254.6 on 09/05/12
For personal use only.

Contribution à l'étude des mélanges liquides $PbCl_2$–PbO

MAURICE RENAUD, EMMANUEL POIDATZ ET JEAN-EDMOND CHAIX
Département de Génie Métallurgique, Ecole Polytechnique, Montréal, Québec

Reçu le 15 octobre, 1969

Le diagramme de solidification des mélanges liquides $PbCl_2$–PbO a été tracé pour les fractions molaires en oxyde de plomb inférieures à 2/3; trois composés définis ont été mis en évidence; ce sont les oxychlorures $3PbCl_2,2PbO$; $PbCl_2,PbO$ et $PbCl_2,2PbO$. Par ailleurs l'étude cryoscopique du liquidus du chlorure de plomb amène les auteurs à envisager l'existence, dans la phase liquide, d'une espèce $PbO,PbCl_2$ ainsi que l'absence presque complète d'ions Cl^- libres.

The solidification diagram of liquid $PbCl_2$–PbO mixtures was determined for molar fractions of lead oxide smaller than 2/3; three compounds were identified: these are the oxychlorides $3PbCl_2,2PbO$; $PbCl_2,PbO$, and $PbCl_2,2PbO$. Furthermore, the cryoscopic study of the liquidus of lead chloride led the authors to suggest the existence of the species $PbCl_2,PbO$ and the almost complete lack of Cl^- ions in the liquid phase.

Canadian Journal of Chemistry, 48, 2061 (1970)

Diagramme de solidification

Le diagramme de phases des mélanges $PbCl_2$–PbO a déjà été étudié par Ruer (1) et Baroni (2) sur toute la gamme des concentrations. Ayant constaté que comme le signale Janz (3) le mélange eutectique se solidifie à une température inférieure de 30 °C à celles signalées par les deux premiers auteurs nous avons entrepris de retracer le diagramme.

Nous avons limité notre étude aux mélanges contenant une fraction molaire en oxyde de plomb inférieure à 2/3. En effet nous avons remarqué que pour les fortes concentrations en PbO les mélanges liquides cristallisent difficilement. Les solides obtenus après refroidissement ont souvent l'aspect de verres et il est alors impossible de parler de changement de phase.

Pour mettre en évidence les températures de début et de fin de cristallisation nous avons opéré par analyse thermique différentielle.

Après avoir préparé le mélange de composition désirée avec des produits conservés à l'étuve, le mélange est fondu. Il est ensuite maintenu à 100 °C au-dessus de sa température de fusion pendant une heure et ce afin d'en assurer l'homogénéité.

Le refroidissement est conduit au rythme de 5 °C par min. Des mesures ont aussi été faites avec un rythme de refroidissement plus rapide : 20 °C par min. Le Tableau 1 regroupe les résultats des diverses mesures.

La Fig. 1 représente le diagramme de phases tel que nous avons pu le tracer à l'aide des mesures effectuées. Le liquide eutectique E contenant 24% de PbO cristallise à 405 °C. Ruer et Baroni donnent 24% à 438 °C alors que Janz (3) signale 30% et 402 °C. Le liquide péritectique P_1 contenant 36% de PbO est la fraction liquide de la fusion non congruente du composé défini $3PbCl_2,2PbO$ (T_F = 450 °C). Ce composé qui a déjà fait l'objet d'une étude cristallographique

TABLEAU 1

X(PbO) ± 0.001	T à 5 °C min^{-1} ± 2 °C	T_F à 5 °C min^{-1} ± 5 °C	T à 20 °C min^{-1} ± 5 °C
0.000	495		
0.050	481		
0.090	477	406	
0.110	462	410	
0.134	459	410	
0.184	434	405	
0.194	428	400	
0.237	407	407	
0.271	422	405	
0.303	434	410	
0.332	438	407	
0.359	453	401	
0.364	468	409	462
0.384	473	407	423
0.406	478	408	478
0.417	520	405	482
0.427	544		480
0.438	586		488
0.448	588		489
0.465	570		493
0.482	615		492
0.500	619		493
0.500	606		
0.530	652		
0.564	652		
0.564	672		
0.579	660		
0.618	672		
0.666	680		

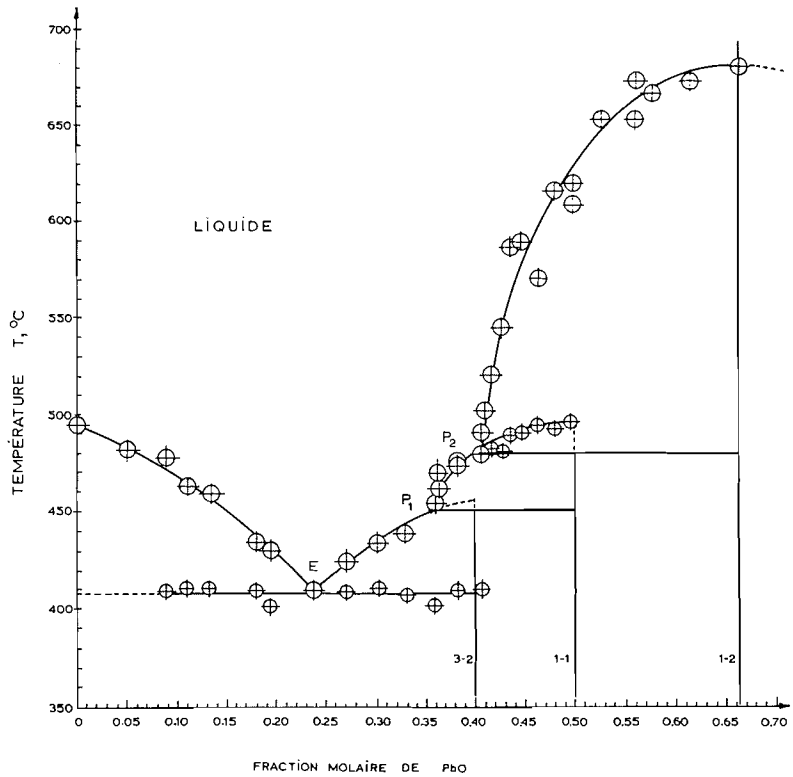

FIG. 1. Diagramme de solidification des mélanges $PbCl_2$–PbO ayant des fractions molaires en PbO inférieures à 2/3.

(fiche ASTM 6–0475) n'avait été remarqué ni par Ruer ni par Baroni. Le liquide péritectique P_2 contenant 40% de PbO est la fraction liquide de la fusion non congruente du composé défini $PbCl_2$,PbO (T_F = 478 °C). Ce composé a été signalé par Ruer et par Baroni avec une température de fusion égale à 525 °C. Cette température étant à 1 °C près celle de la fusion non congruente de la matlockite naturelle (4) de composition $PbCl_2$,$Pb(OH)_2$, nous pensons que les auteurs (1, 2) cités plus haut ont travaillé avec des produits hydratés ce qui a faussé l'ensemble de leurs résultats.

La température de fusion congruente du composé défini $PbCl_2$,2PbO a été trouvée égale à 680 °C soit inférieure de 15 °C à celle citée par les auteurs antérieurs. Ce composé présente souvent une surfusion et lors du refroidissement rapide de mélanges dont la composition est comprise entre 40 et 50% de PbO la température de début de cristallisation se place sur le prolongement du liquidus du composé $PbCl_2$,PbO.

L'étude des spectres de diffraction de rayons X effectués sur des poudres de compositions intermédiaires n'a pas permis de mettre en évidence d'autres composés définis que les trois mentionnés ci-dessus.[1]

Par ailleurs nous avons déterminé les chaleurs de fusion approximatives de ces trois composés. Pour ce faire nous avons comparé l'aire du pic obtenu par analyse thermique différentielle pour la fusion de chacun des oxychlorures, avec l'aire du pic obtenue pour la fusion du chlorure de plomb pur.

Le Tableau 2 résume les principales propriétés des trois oxychlorures mis en évidence par ce travail.

Calculs Cryoscopiques

L'activité du chlorure de plomb dans le mélange liquide peut être déterminée à l'aide de l'abbaissement de son point de cristallisation grâce à la relation [1]

$$[1] \qquad \ln a = -(\Delta H_F^0 - T\Delta S_F^0)/RT$$

[1]Une étude cristallographique détaillée de ces oxychlorures est actuellement en cours et sera publiée ultérieurement.

Can. J. Chem. Downloaded from www.nrcresearchpress.com by 210.87.254.6 on 09/05/12
For personal use only.

TABLEAU 2

Composé	Couleur	Densité à ± 0.02	Fusion, T_F à ± 2 °C	ΔH_F^0 kcal mole^{-1} à ± 10%
$3PbCl_2,2PbO$	Jaune orangé	6.32	non-congruente 450	11.3
$PbCl_2,PbO$	Jaune pâle	6.55	non-congruente 478	6.4
$PbCl_2,2PbO$	Blanc gris	6.73	congruente 680	27.4

TABLEAU 3

T, °C ± 2 °C	X ± 0.001	ln a	ln x_1	ln x_2	ln x_3	ln x_4
495	0.000	0.001	0.000	0.000	0.000	0.000
481	0.050	−0.053	−0.017	−0.051	−0.018	−0.054
477	0.090	−0.068	−0.032	−0.094	−0.036	−0.104
462	0.110	−0.128	−0.040	−0.117	−0.046	−0.132
459	0.134	−0.141	−0.050	−0.144	−0.059	−0.168
434	0.184	−0.248	−0.073	−0.203	−0.093	−0.256
428	0.194	−0.275	−0.077	−0.216	−0.100	−0.275
407	0.237	−0.372	−0.099	−0.271	−0.140	−0.372

où $\Delta H_F^0 = 4.40$ kcal mole^{-1} et $\Delta S_F^0 = 5.73$ cal mole^{-1} deg^{-1} (5).

Pour chaque point expérimental nous avons essayé d'exprimer l'activité du chlorure de plomb dans le mélange liquide en utilisant divers modèles. Pour ce faire nous avons assimilé l'activité de chaque espèce chimique à sa fraction molaire réelle.

Ainsi l'activité du chlorure de plomb est prise égale à la somme des fractions molaires des espèces chimiques constituant le chlorure de plomb liquide.

Les quatre modèles envisagés tiennent compte du fait signalé par d'autres auteurs (6) que l'oxyde de plomb n'est pas dissocié aux températures considérées.

Dans toutes les expressions qui suivent nous désignons par X le nombre de moles d'oxyde de plomb dissoutes dans $1 - X$ mole de chlorure de plomb.

Modèle 1

L'oxyde de plomb est sous la forme PbO. Le chlorure de plomb est entièrement dissocié avec augmentation du nombre des espèces chimiques

$$PbCl_2 \rightarrow Pb^{2+} + 2Cl^-$$

La fraction molaire en chlorure de plomb est alors $x_1 = (3 - 3X)/(3 - 2X)$.

Modèle 2

L'oxyde de plomb est sous la forme PbO. Le chlorure de plomb est dissocié sans augmentation du nombre des espèces chimiques par exemple

$$2PbCl_2 \rightleftarrows PbCl_4^{2-} + Pb^{2+}$$

$$3PbCl_2 \rightleftarrows PbCl_6^{4-} + 2Pb^{2+}$$

De tels complexes ont déjà été signalés par plusieurs auteurs (7, 8). La fraction molaire en chlorure de plomb est alors $x_2 = 1 - X$.

Modèle 3

L'oxyde de plomb est sous la forme PbO, $PbCl_2$. Le chlorure de plomb est entièrement dissocié avec augmentation du nombre des espèces chimiques

$$PbCl_2 \rightarrow Pb^{2+} + 2Cl^-$$

La fraction molaire en chlorure de plomb est alors $x_3 = (3 - 6X)/(3 - 5X)$.

Modèle 4

L'oxyde de plomb est sous la forme $PbO,PbCl_2$. Le chlorure de plomb est dissocié sans augmentation du nombre des espèces chimiques par exemple

$$2PbCl_2 \rightleftarrows PbCl_4^{2-} + Pb^{2+}$$

$$3PbCl_2 \rightleftarrows PbCl_6^{4-} + 2Pb^{2+}$$

La fraction molaire en chlorure de plomb est alors $x_4 = (1 - 2X)/(1 - X)$.

Can. J. Chem. Downloaded from www.nrcresearchpress.com by 210.87.254.6 on 09/05/12
For personal use only.

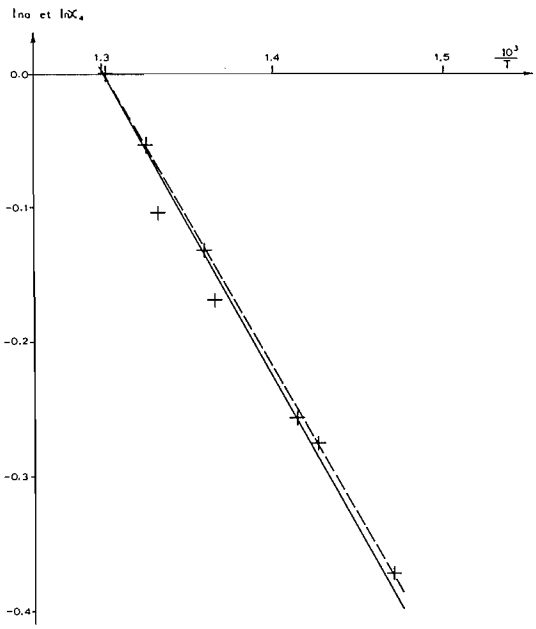

FIG. 2. Logarithmes de l'activité et de la fraction molaire x_4 de $PbCl_2$ vs. l'inverse de la température.

Pour chacun des points expérimentaux (définis par X et T) du liquidus correspondant à la solidification du chlorure de plomb pur, nous avons comparé la valeur donnée par l'expression [1] à celle du logarithme de la fraction molaire en chlorure de plomb calculée avec chacun des 4 modèles précédents.

Le Tableau 3 réunit ces résultats. On peut y remarquer que c'est le Modèle 4 qui donne les valeurs les plus proches de l'expression [1].

Sur la Fig. 2 la droite continue est tracée par la méthode des moindres carrés à partir des valeurs de $\ln (1 - 2X)/(1 - X)$ et la droite discontinue représente l'expression $\ln a = -(\Delta H_F^0 - T\Delta S_F^0)/RT$.

L' enthalpie de fusion calculable à l'aide de la pente de la droite continue est $\Delta H_F^0 = 4.52$ kcal mole^{-1}. Cette valeur est très voisine de la valeur $\Delta H_F^0 = 4.40$ kcal mole^{-1} donnée dans la littérature (5). Ceci tend à confirmer les hypothèses proposées, à savoir, qu'il existe peu d'ions Cl^- libres et que l'oxyde de plomb est maintenu en solution sous forme d'un complexe, probablement $PbO,PbCl_2$.

Par ailleurs le composé $PbCl_2,2PbO$ étant à fusion congruente on peut s'attendre à ce qu'il existe aussi en solution des espèces $PbCl_2,2PbO$ en équilibre avec les $PbCl_2,PbO$, l'une ou l'autre espèce étant prépondérante selon la fraction molaire en PbO et la température considérées.

Pour effectuer ce travail Messieurs E. Poidatz et J. E. Chaix ont bénéficié d'une bourse d'études offerte par la société ALCAN respectivement en 1967–1968 et en 1968–1969.

1. R. RUER. Z. Anorg. Allg. Chem. **49**, 372 (1906).
2. A. BARONI. Atti Accad. Naz. Lincei, Rend. Classe Sci. Fis. Mat. Nat. **20**, 384 (1934).
3. J. JANZ. Molten salts handbook. Academic Press, Inc., New York. 1967. p. 33.
4. C. D. HODGEMAN (*Editor*). Handbook of chemistry and physics. 48th ed. Chemical Rubber Co., Cleveland, Ohio. 1967–1968.
5. J. LUMSDEN. Thermodynamics of molten salt mixtures. Academic Press, Inc., New York. 1966. p. 191.
6. H. FLOOD and T. FORLAND. Acta Chem. Scand. **1**, 592 (1947).
7. J. HILDEBRAND and G. C. RUHLE. J. Amer. Chem. Soc. **49**, 722 (1929).
8. H. BLOOM and S. B. TRICKLEBANK. Aust. J. Chem. **19**, 187 (1966).

Can. J. Chem. Downloaded from www.nrcresearchpress.com by 210.87.254.6 on 09/05/12
For personal use only.

Can. J. Chem. Downloaded from www.nrcresearchpress.com by 210.87.254.6 on 09/05/12
For personal use only.

Synthesis of 7-azabicyclo[2.2.1]heptane, *exo*-2-chloro-7-azabicyclo[2.2.1]heptane, and derivatives[1]

ROBERT R. FRASER AND ROBERT B. SWINGLE
Department of Chemistry, University of Ottawa, Ottawa 2, Ontario

Received February 13, 1970

A synthesis of 7-azabicyclo[2.2.1]heptane (**1**) in five steps and an overall yield of 18% has been achieved. An alternative five-step route which gives **1** in 36% yield but which requires large amounts of platinum oxide has also been developed. In comparison, the only previous synthesis of this compound gave less than a 1% overall yield of an impure product. Several *N*-acyl derivatives and the *N*-nitroso derivative have been prepared, and the barriers to rotation about the N—CO bond of the acetyl derivative and the N—NO bond of the nitroso derivative have been determined. The barriers were found to be 1.2 and 6.5 kcal less, respectively, than in their unstrained analogs. *exo*-2-Chloro-7-azabicyclo[2.2.1]heptane has also been synthesized.

Canadian Journal of Chemistry, 48, 2065 (1970)

Considerable interest has recently developed in the nitrogen analogs of bicyclo[2.2.1]heptane. Reports on the synthesis and reactions of compounds containing nitrogen in the 1-position (1, 2) and in the 2-position (3, 4) have appeared. The 7-azabicyclo[2.2.1]heptane system has perhaps received more attention. In particular, many highly substituted derivatives have been produced by the Diels–Alder reactions of *N*-alkyl and *N*-acyl pyrroles with dimethylacetylene dicarboxylate (5–12). In contrast the parent 7-azabicyclo[2.2.1]heptane (**1**) was reported as synthesized only in impure form and was characterized by conversion to a picrate and a 7,7-dimethiodide derivative (13). Its synthesis from hydroquinone involved seven steps and gave **1** in an overall yield of less than 1%. We wish to report an improvement in the synthesis of **1**, which allows its preparation in yields of up to 36%. The proof of structure of **1** is supported by its conversion to five derivatives, two of which are the subject of a temperature-dependent nuclear magnetic resonance (n.m.r.) investigation. In addition the *exo*-2-chloro derivative of **1** was synthesized and preliminary studies of its reactivity are reported.

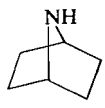

1

[1]This work was presented in part at the 52nd Annual Meeting of the Chemical Institute of Canada, in May 1969.

Synthesis of 1

Three approaches to the synthesis of **1** were considered at the outset. Although the Diels–Alder synthesis of the 7-azabicyclo[2.2.1]heptane skeleton via the reaction of *N*-substituted pyrroles with acetylenic dienophiles had been reported (9), the low yields (< 9%) in all reactions made this route seem unattractive. Recently, Shafi'ee and Hite described improved yields for the Diels–Alder reaction in the synthesis of the *N*-carbobenzoxy derivative of 7-azabicyclo[2.2.1]-hept-2-ene-2-carboxylic acid (12) and in the past year the use of aluminum chloride as a catalyst was shown to improve the yield of the product from reaction of *N*-carbomethoxypyrrole with acetylene dicarboxylic ester to 93% (6).

Formation of the bicyclic structure by ring closure at the C_1—C_2 bond presented obvious difficulties in synthesis of the necessary activated intermediates and so was not investigated. Making the C_1—N bond in the last step seemed most attractive since the analogous ring closure had been successful in producing both 7-oxa and 7-thiabicyclo[2.2.1]heptane in good yields (14,15).

The reactions leading to the synthesis of **1** are outlined in Scheme 1. Catalytic reduction of 4-acetamidophenol (**2**) to a mixture of *cis*- and *trans*-*N*-(4-hydroxycyclohexyl)-acetamide (**3**) has been described by three independent groups. Ferber and Bruckner reported an 80% yield of *trans*-**3** using a 1:10 weight ratio of platinum dioxide to **2** (16). Using Raney nickel at elevated temperature and pressure, Billman and Buehler (17) obtained a 30% yield of *trans*-**3** while Della and Jefferies (18) claimed an 80% yield for the same reduction. In our hands the Raney nickel

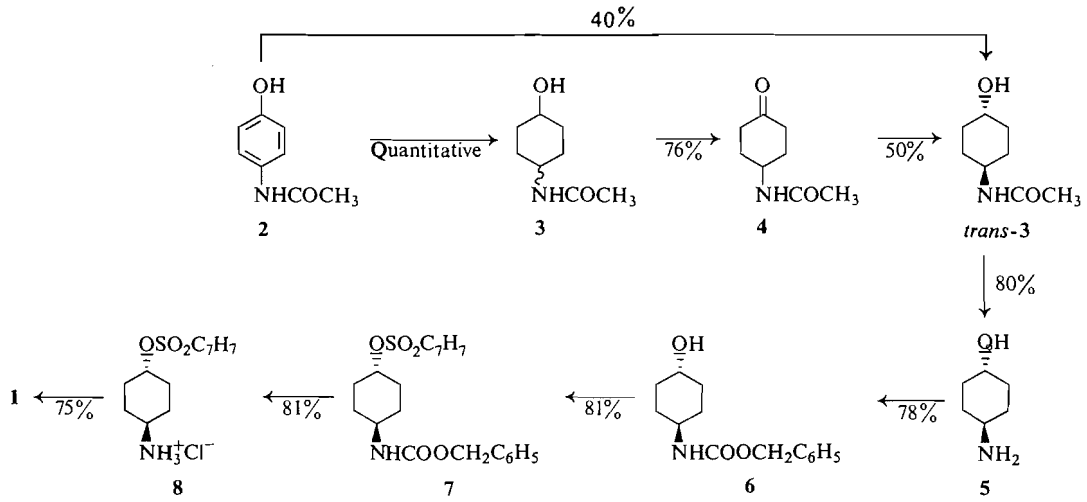

SCHEME 1

procedure gave pure *trans*-**3** in yields of 20 to 25% after four crystallizations from acetone. In view of the length of the Raney nickel procedure and the expense involved in using the platinum dioxide procedure, alternative routes were sought. First a modification in the platinum catalyzed reduction was made. Use of only a 1:60 ratio of catalyst to phenol **2** still gave a 40% yield of *trans*-**3**. A second alternative involved the addition of two extra steps both of which are rapid, easily conducted reactions. A mixture of *cis*- and *trans*-**3** was oxidized to the cyclohexanone **4** in 76% yield using Jones reagent (19). Reduction of **4** with sodium borohydride gave a 35% yield of **3** in isopropyl alcohol solvent and a 50% yield of **3** using methanol as solvent. The greater yield in methanol was anticipated on the basis of Kwart's observations on the influence of the electronegativity of a 4-substituent on competing transition state stabilities in the reduction of various cyclohexanones with sodium borohydride (20). Presumably, in the higher dielectric medium the dipole–dipole interaction between the positively charged C-4 and the negative charge in the transition state leading to *cis* product is made less favorable, allowing "thermodynamic control" to exert a greater influence on the product ratio. This sequence of reactions gave convenient amounts of **3** in the improved yield of 38% from **2**. Furthermore, the *cis* isomer remaining after crystallization of **3** can be recycled to form additional *trans* isomer. One other method for improvement of the yield of **3** was also tried. Direct equilibration of the *cis* and *trans* mixture using either sodium and fluorenone in xylene or aluminum isopropoxide and acetone in isopropyl alcohol failed. The extreme insolubility of **3** in these solvents likely contributed to the failures.

The next step in the synthesis required replacement of the acetyl group by a suitable blocking group. Experiments with the simplest such group, the protonated amine, failed. When **3** was hydrolyzed to **5** and tosylation of its hydrochloride was attempted, only the *N*-tosyl derivative of **5** could be isolated. Direct tosylation of the oxy anion of **5** was also tried in several solvents. In glyme it was possible to form the *O*-tosylate but only in 5% yield. Apparently, either competing displacement of the chlorine in tosyl chloride by attack of alkoxide was occurring (an infrared (i.r.) spectrum of the product indicated some ketonic product was formed) or the sodium salt of **5** was not sufficiently reactive. An attempt at direct cyclization of **5** to **1** using the conditions successfully employed by Gassman and Fentiman in the synthesis of 1-azabicyclo[3.1.0]hexane (21) also failed.

The carbobenzoxy group proved to be a successful protector of the amino function. Tosylation of **6** followed by cleavage of the carbobenzoxy group gave the amino tosylate **8** which cyclized to **1** in 70% aqueous ethanol. The overall yield for the six (or eight) steps was 12%.

Can. J. Chem. Downloaded from www.nrcresearchpress.com by 210.87.254.6 on 09/05/12
For personal use only.

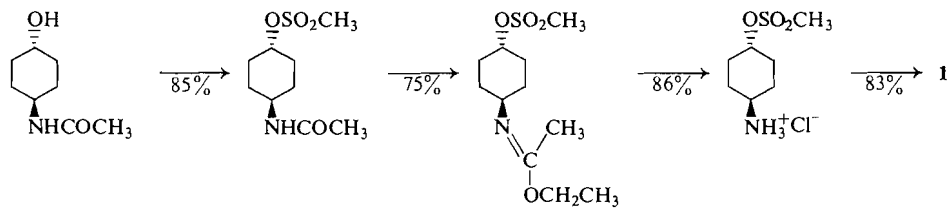

trans-3 9 10 11

SCHEME 2

Although the above sequence succeeded in producing **1**, a decrease in the number of steps was of obvious value. It had been shown by Muxfeldt and Rogalski in their impressive synthesis of a tetracycline (22) that the benzoyl group of an amide could be removed under mild conditions using Meerwein's reagent (23) and hydrolysis of the resultant benzimidate in 5% acetic acid. We therefore examined the possibility of using the acetyl group present in **3** as the blocking group. Since tosylation of **3** gave a viscous oil which resisted crystallization, a reaction with methanesulfonyl chloride was tried which gave the crystalline methanesulfonate **9** in 85% yield. Reaction of **9** with triethyloxonium fluoborate gave a 75% yield of the imido ester **10**. Hydrolysis of **10** at p*H* 1.5 to 2.0 gave the aminomesylate **11** which was cyclized at room temperature in 80% aqueous ethanol to form **1**. This sequence for the synthesis of **1** is given in Scheme 2. The yields in the last two steps were 80 and 83% resulting in an improved yield of 18% (26%, based on oxidation and reduction of recovered *cis*-**3**) for the five (or seven) step synthesis of **1**. Two of the above steps merit comment as they required carefully controlled reaction conditions. If the p*H* was not in the range 1.5 to 2.0, hydrolysis of **10** gave back the amide **9**, and conditions for cyclization of **11** to **1** were stringent in that considerable elimination occurred in 70% aqueous ethanol or even in 80% aqueous ethanol at lower than room temperature.

Finally, it should be noted that use of the large amounts of platinum dioxide (16) to make *trans*-**3** followed by the reaction in Scheme 2 provides a five step synthesis of **1** in the overall yield of 36%.

Proof of Structure

The only physical constant available for comparison of our product with that previously reported for **1** is the melting point of its picrate. Braun and Schwarz (13) state that cyclization of 4-aminocyclohexyl bromide gave a 70% yield of picrate A, m.p. 170–173° to which they assigned the 4-aminocyclohexene structure and a 15% yield of picrate B, m.p. 151–153° to which they assigned the bicyclic structure **1**. We have prepared the picrates of 4-aminocyclohexene and **1** and found their melting points to be 166–168 and 171–174° respectively. It would appear then that the picrate B of Braun and Schwarz was not derived from **1**. Picrate A very likely has the assigned structure, and not that of **1** since it was obtained in such a high yield from the reaction of a mixture of *cis*- and *trans*-4-bromocyclohexylamines using a concentrated solution of reactants. The amine which produced picrate B may well have been the product of an intermolecular reaction. In spite of the doubts regarding the nature of the picrates, some **1** must have been obtained, since conversion of the crude product in unspecified yield to the 7,7-dimethiodide of **1** was effected. The melting point of this derivative agrees with more recent value obtained by Corey and Hertler (24) for the same compound synthesized via the Hoffman–Löffler reaction of *N*-methylcyclohexylamine. In view of the unknown yield in the final step, the overall yield obtained by Braun and Schwarz cannot be precisely determined but has a maximum value of 1%.

The proof of structure of **1** is provided by spectral evidence, its unambiguous method of synthesis, and the synthesis of five derivatives. The n.m.r. spectrum of the hydrochloride of **1** in deuterochloroform shows four sets of absorption in the regions of τ 0.5, 5.8, 7.76, and 8.36 which have relative intensities 1:1:2:2. They are assigned to the NH_2, bridgehead, *exo*, and *endo* protons, respectively. The *exo* and *endo* proton absorption appears as an A_2B_2 pattern whose low field half is broadened, presumably by coupling

Can. J. Chem. Downloaded from www.nrcresearchpress.com by 210.87.254.6 on 09/05/12
For personal use only.

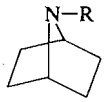

12 R = CH_3
15 R = $COCH_3$
16 R = HCO
17 R = $COCCl_3$
18 R = NO

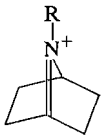

13

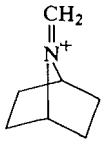

14

19 R = $COCCl_3$
20 R = H·HCl
21 R = H

with the bridgehead protons. Since coupling occurs only between the bridgehead and *exo* protons in norbornanes (25), 7-thianorbornanes (15), and 7-azanorbornanes (12), the broader absorption is assigned to the *exo* protons.

The mass spectrum of the hydrochloride of **1** shows a parent peak for the free base at *m/e* 97 and its i.r. spectrum shows absorption characteristic of a secondary amine hydrochloride (see Experimental for details).

Chemical Properties of 1

7-Azabicyclo[2.2.1]heptane is a secondary amine having the nitrogen atom in a highly strained position. For instance, the internal C_1—C_7—C_4 bond angle in norbornane has been determined to be 96° by electron diffraction (26). In **1** a similar but slightly larger angle would be expected since C—N bonds are shorter than C—C bonds (27). It was of interest to see if this strain affects the chemical behavior of the nitrogen atom. Determination of the pK_A of **1** in water gave a value of 10.8 which appears to be normal when compared with the pK_A's of azetidine (11.3) and pyrrolidine (11.3) (28). Either strain is not influencing the pK or it is being offset by a sterically favorable solvation of the conjugate acid of **1**.

The reactivity of the nitrogen atom in **1** differs from that of monocyclic secondary amines. Most of our acylation reactions required longer reaction times than those required for pyrrolidine or piperidine. The Leuckart reduction (29) of **1** to its *N*-methyl derivative **12**, also appeared to be sluggish requiring 15 h and gave only a 53% yield of product. Both **12** and **1** were subjected to the Leonard oxidation reaction (30) in hopes that perhaps abstraction of a β-hydrogen atom might produce oxidation at C-2. No reaction was observed on prolonged refluxing. The inertness of **12** to alpha oxidation is expected as the iminium salt **13** would be prohibited by Bredt's rule while formation of the alternative product **14** has been found to be a sluggish reaction in previous studies (30).

The acetyl, **15**, trichloroacetyl, **16**, and formyl, **17**, derivatives of **1** as well as the nitrosamine, **18**, have all been synthesized and characterized by the spectral data presented in the Experimental section. Two of these compounds exhibited temperature dependent n.m.r. spectral behavior which differed from that observed previously for secondary amine derivatives. A discussion of this topic is presented at the end of the paper.

Synthesis of exo-2-Chloro-7-azabicyclo[2.2.1]-heptane (21)

One objective of this work was the synthesis of the two epimeric 2-halo or 2-tosyloxy derivatives of **1** whose solvolytic behavior would be of interest in comparison with that exhibited by their norbornyl and 7-oxanorbornyl counterparts. Several attempts at a direct synthesis of such derivatives using an N—C_1 ring closure in the final step failed and these are described in the thesis of R. B. Swingle (31). Finally the free-radical chlorination of **17** was investigated and found to give a mono chlorination product **19** and two other products whose n.m.r. spectra indicate them to contain two chlorine atoms. The choice of **17** as substrate for the chlorination was dictated by the necessity for an inert group on nitrogen. Treatment of **17** with sulfuryl chloride and benzoyl peroxide in refluxing methylene chloride until the appearance of dichlorination products was indicated by thin-layer chromatography (t.l.c.) gave a 31% yield of pure **19** after

Can. J. Chem. Downloaded from www.nrcresearchpress.com by 210.87.254.6 on 09/05/12
For personal use only.

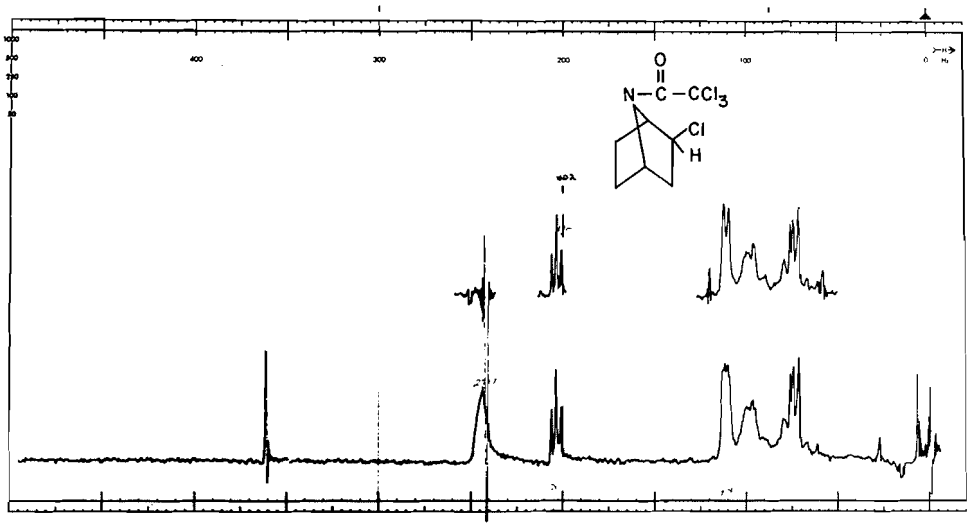

FIG. 1. The 100 MHz spectrum of *exo*-2-chloro-7-trichloroacetyl-7-azabicyclo[2.2.1]heptane. The insert above the regular spectrum shows the effect of irradiation of τ 5.2 on the peak at τ 7.8 and the lack of any other effect.

isolation by column chromatography. The yield based on recovery of **17** is 47%. The proof of structure for **19** is provided by its elemental analysis, n.m.r. spectrum, and hydrolysis to *exo*-2-chloro-7-azabicyclo[2.2.1]heptane, isolated as its hydrochloride, **20**. The n.m.r. spectrum of **19** also provided the evidence for assigning the *exo* configuration to chlorine. This spectrum, shown in Fig. 1, consists of a broad peak at τ 5.10, assigned to the two bridgehead protons, a sharp triplet of spacing 5 Hz at τ 5.9 which is assigned to the proton at C-2, a poorly resolved multiplet at τ 7.75 representing the two protons at C-3, and a complex absorption pattern over the range τ 8.0–8.8 for the remaining four nonequivalent protons on C-5 and C-6. Evidence in support of this assignment is provided by a frequency-sweep double irradiation experiment. Irradiation of the bridgehead protons at τ 5.10 produced only one significant change in the remainder of the spectrum (this is shown in the upper portion of Fig. 1). The multiplet at τ 7.75 became a well-resolved doublet of spacing 5 Hz while the triplet at τ 5.9 was unaffected. Thus the removal of any bridgehead coupling by irradiation has simplified the absorption for the protons on C-2 and C-3 to the XX′ portion of an AXX′ pattern. The observed splitting equals $1/2(J_{AX} + J_{AX'})$ (32) and its magnitude is only slightly lower than values normally observed for bicyclo[2.2.1]-heptanes (33, 34). A decrease is expected on the basis of the smaller vicinal couplings found in the 7-azabicyclo[2.2.1]heptanes of Shafi'ee and Hite (12). Shafi'ee and Hite also observed the lack of vicinal coupling between an *endo* proton and a bridgehead hydrogen but appreciable coupling for the *exo*-bridgehead interaction. Thus the absence of any detectable splitting of the proton at C-2 by the adjacent bridgehead proton established its *endo* configuration. The chlorine on C-2 is thus in the *exo* position. The formation of the *exo* product only in the chlorination reaction parallels the stereochemical result for the chlorination of norbornane under the same conditions which Roberts *et al.* (35) found to give a 20:1 ratio of *exo* to *endo*. In contrast, photochlorination of 7-oxabicyclo[2.2.1]heptane gave a 2.2:1 ratio of *exo* to *endo* products (36). Hydrolysis of **19** with potassium *t*-butoxide in *t*-butanol and treatment with hydrogen chloride gave a 73% yield of **20** whose mass spectrum (parent peaks at *m/e* 131 and 133 in a ratio of 3:1) and n.m.r. spectrum confirmed the assigned structure.

One of the motives for the synthesis of **21** was an intended study of its solvolytic behavior. At this time only a few preliminary experiments in this area have been conducted as the supply of **21** was very limited. Efforts were concentrated on converting **21** to the olefin **22** with a view to hydroboration of the olefin to give the epimeric 2-hydroxy compounds. Surprisingly, heating **21**

Can. J. Chem. Downloaded from www.nrcresearchpress.com by 210.87.254.6 on 09/05/12
For personal use only.

with sodium methoxide in DMF at 110° for 24 h failed to produce any reaction. We are continuing attempts to obtain a pair of epimeric substituents at C-2 before undertaking detailed solvolysis studies.

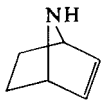

22

23

Variable Temperature Nuclear Magnetic Resonance Studies on 15 and 18

The temperature dependence of the n.m.r. spectra of amines, their amides and nitrosamines has been studied extensively. Amines, as a result of their pyramidal structure have a barrier to inversion whose magnitude is normally small, 6–8 kcal (37) but is enhanced by effects of strain and electronegative substituents (38, 39). Amides and nitrosamines, on the other hand, possess barriers to rotation of 14–18 kcal, which are decreased by the effect of strain in a cyclic amine. A study of these two opposing effects of strain in acyl aziridines has been reported by Anet and Osyany (40). Some of the acyl derivatives (**23**; R = $COOCH_3$; R = $CON(CH_3)_2$) no longer showed a barrier to rotation but rather a barrier to inversion at nitrogen. We have measured the variable temperature spectra of **15** and **18** to examine the effect of the bicyclic structural constraint on the conformational barriers present in the molecules.

The n.m.r. spectrum of **15** at 30° contains two peaks at τ 5.90 and 5.38 each representing one proton, assignable to the bridgehead protons at C-1 and C-4. When spectra were measured at higher temperatures the peaks gradually broadened and coalesced at 75°. From this coalescence temperature, the barrier to rotation is calculated to be 16.7 kcal using the expression $\Delta F\ddagger = RT(\ln kT/h - \ln \pi\Delta\nu/\sqrt{2})$ (41). Although this expression is only strictly applicable to the coalescence of two sharp singlets, the couplings to the bridgehead protons in **15** are small and should not produce any significant error in the calculated $\Delta F\ddagger$. For example in a much more serious deviation from the two-site model, the barrier to inversion in cyclohexane differed by less than 0.2 kcal from that determined using the ideal substrate, cyclohexane-d_{11} (42). The experimental value of 17.1 kcal for **15** is significantly less than that for dimethylacetamide. Most recent work assigns a value for $\Delta F_{348°}\ddagger$ = 18.3 kcal (43). The decreased barrier in **15** is likely caused by steric factors. A more pronounced difference is found for the barrier to inversion in **18** relative to its open-chain analog, *N*,*N*-dimethylnitrosamine. Initial variable temperature studies were made on a solution of **18** in deuterochloroform. In this solvent the two bridgehead protons gave rise to a multiplet at τ 5.06 at room temperature. When the temperature was lowered to −30° a separation into two components occurred whose chemical shifts increased as the temperature was lowered to −70°. Since the coalescence temperature *appeared* to be unusually low,a variable temperature study of **18** in carbon disulfide was also performed. At room temperature in this solvent two triplets representing the bridgehead protons appeared at τ 4.87 and 5.06. When the temperature was raised to 52 °C the two peaks broadened, then coalesced. For this coalescence temperature the barrier to rotation is 16.5 kcal. The apparent coalescence at −30° for the deuterochloroform solution of **18** must have been due to a fortuitous equivalence of the bridgehead protons in this solvent. This explanation is supported by the fact that no broadening at the coalescence temperature was seen. The value of 16.5 kcal for the barrier in **18** is much lower than the 23.0 kcal value reported for *N*,*N*-dimethylnitrosamine (44). We attribute the differences between **15** and **18** relative to the open chain counterparts as being a reflection of differences in steric effects. In both compounds there are unfavorable steric interactions between the bridgehead hydrogen and the oxygen *cis* to it which is held in the same plane by the partial double bond at nitrogen. This interaction is essentially an $A_{1,3}$ strain as defined by Johnson and Malhotra (45). The effect is small in **15** but greater in **18** since an N—N bond is shorter than an N—C bond (27).

It is evident that there is only a qualitative difference in the behavior of **15** and **18** relative to their acyclic counterparts and that the strained bond angles of the nitrogen do not produce any aziridine-like behavior. It might be possible using appropriately deuterated samples to detect a barrier to inversion in **15** or **18** but as Anet and

Can. J. Chem. Downloaded from www.nrcresearchpress.com by 210.87.254.6 on 09/05/12
For personal use only.

Can. J. Chem. Downloaded from www.nrcresearchpress.com by 210.87.254.6 on 09/05/12
For personal use only.

Osyany point out (40) it should be low in compounds possessing hindered rotation.

Experimental

All melting points are corrected. The n.m.r. spectra were recorded on either a Varian T-60, or an HA-100 n.m.r. spectrometer using deuterochloroform as solvent. Spin-decoupling and variable temperature experiments were performed on the 100 MHz instrument. Low temperature calibrations were performed using the internal methanol shift method of Varian. Mass spectra were measured on a Hitachi–Perkin–Elmer RMU-6D spectrometer. The i.r. spectra were determined on either a Beckmann IR-8 or IR-20 instrument using a KBr dispersion of the solid. Unless otherwise specified, magnesium sulfate was used as the drying agent of solutions.

Preparation of N-(4-Hydroxycyclohexyl)-acetamide (3)

The method of Ferber and Bruckner (16) was utilized with the modification that only a 1:60 weight ratio of catalyst to 4-acetamidophenol was employed. Hydrogenation on a 20 g scale in water at 60 p.s.i. and 60° for 15 h in a Parr apparatus gave complete reduction. After removal of catalyst and solvent the residue was treated with acetone. The less soluble *trans* isomer slowly crystallized. A total of 8 g of solid, m.p. 166–167°, was obtained (lit. m.p. 164° (16)). The *cis* isomer crystallized from the mother liquor after it had stood for 2 days at 3°. After two crystallizations from acetone it melted at 134–136° (lit. m.p. 135° (16)).

The procedure of Billman and Buehler (17) was also used. Hydrogenation of 80 g of 4-acetamidophenol in ethanol in an autoclave at 1000 p.s.i. and 190° using 5 g of W-4 Raney nickel catalyst gave, after work-up, 20 g (25%) of *trans*-**3**.

Oxidation of 3 to N-(4-Oxocyclohexyl)-acetamide (4) (19)

A mixture of *cis*- and *trans*-**3** obtained directly from the above hydrogenation was dissolved in acetone which had been distilled from potassium permanganate. This solution was titrated at 20° with a solution of chromic acid prepared from 12.35 g of chromium trioxide, 11.5 ml concentrated sulfuric acid, and 20 ml of water. A persistent orange–brown coloration indicated the end point. The solution was filtered and ethanol added. The precipitated chromium salts were filtered off and the filtrate was concentrated. Chloroform was added to the residue, the solution dried, filtered, and evaporated. The residual ketone m.p. 135–136° was not further purified.

Reduction of 4

(a) In 2-Propanol

A solution of 0.50 g of the above ketone in 5.0 ml of anhydrous 2-propanol was added to 64 mg of sodium borohydride in 20 ml of solvent with stirring. The mixture was left at room temperature overnight and then concentrated. The residue was hydrolyzed with 5.0 ml water and then with 5.0 ml of 10% sodium hydroxide. The resulting mixture was evaporated under reduced pressure and the residue extracted in a Soxhlet using ether as solvent. Evaporation of ether yielded the corresponding alcohol (490 mg) from which 267 mg of crude *trans* alcohol, m.p. 150–154° was isolated (53%).

(b) In Methanol

The above ketone (0.40 g) was dissolved in 25 ml of methanol and a trace of sodium carbonate and 0.4 g (large excess) of sodium borohydride was added slowly to the above stirring solution. After 4 h at room temperature the solution was acidified to p*H* 4 with dilute hydrochloric acid and then concentrated to dryness. The solid obtained was extracted in a Soxhlet using ether as solvent. Evaporation of the solvent yielded 0.40 g of solid from which *trans*-**3** (0.28 g), m.p. 150–154°, was isolated from an acetone solution. Recrystallization from acetone gave 0.20 g of **3**, m.p. 162–164° (50% yield). Further concentration of the acetone solution gave the corresponding *cis* isomer m.p. 130–135°.

trans-4-Aminocyclohexanol (5)

The method of Ferber and Bruckner (16) for the synthesis of **5** proved ineffective and resulted in partial elimination of the hydroxyl group. A more convenient method is described below.

A solution of *trans*-**3** (20 g) in 500 ml of 20% aqueous sodium hydroxide was refluxed for 8 h. The aqueous solution was then placed in a continuous extractor and the mixture was extracted with chloroform for a further 8 h. Compound **5** was obtained in 80% yield after recrystallization from ethyl acetate and melted at 110–111°, the melting point given by Ferber and Bruckner (16).

trans-4-Carbobenzoxyaminocyclohexanol (6)

Following the procedure of Bergman and Zervas (46) a solution of **5** (12 g) in 100 ml of water was placed in an ice bath. Then carbobenzoxy chloride (25 ml; a three-fold excess) was added in 3 to 5 ml portions alternating with portions of 10% aqueous sodium hydroxide. Vigorous shaking by hand was maintained throughout the reaction. After the addition, the mixture was allowed to come to room temperature and the solid product filtered off. This was dissolved in hot ethyl acetate, and pyridine was added until the ethyl acetate no longer clouded upon the addition. The solvent mixture was then washed three times with 25 ml portions of water and dried. After filtration the solution was concentrated under vacuum until **6** began to crystallize. Recrystallization of the product from fresh ethyl acetate yielded white needles in 78% yield melting at 159–160.5°.

Anal. Calcd. for $C_{14}H_{19}O_3N$: C, 67.45; H, 7.68; N, 5.61. Found: C, 67.38; H, 7.65; N, 5.77.

The i.r.: 3615, 3450, 1720, 1515 cm^{-1}. The n.m.r. (60 MHz): τ 2.66 (5H), 4.86 (2H), 5.42 (1H), 6.25 (2H), 7.8–9.0, broad multiplet (9H).

trans-4-Carbobenzoxyaminocyclohexyl p-Toluenesulfonate (7)

To 100 ml of dry pyridine, in a 250 ml flask were added 10 g of **6**. The solution was cooled and stirred in an ice bath while 10 g (20% excess) of *p*-toluenesulfonyl chloride was added slowly. The solution was kept at 0° for 12 h after which time the pyridine was removed under vacuum. The solid residue was dissolved in chloroform, washed three times with water, then with 25 ml of 1 *N* hydrochloric acid. After drying, the solution was filtered,

Can. J. Chem. Downloaded from www.nrcresearchpress.com by 210.87.254.6 on 09/05/12
For personal use only.

the solvent was removed, and the excess toluenesulfonyl chloride was extracted with boiling (30–60°) petroleum ether. The residue which did not dissolve in the ether was recrystallized from ethanol to give **7** in 81% yield. The melting point of the solid obtained was 116–117°.

Anal. Calcd. for $C_{21}H_{25}O_5NS$: C, 62.48; H, 6.24. Found: C, 62.29; H, 6.28.

The i.r.: 3450, 1720, 1600, 1515, 1460, 1365, 1178 cm^{-1}. The n.m.r. (60 MHz): an A_2B_2 at τ 2.04 and 2.66 (4H), 2.67 (5H), 4.90 (2H), 5.30 doublet (1H), 5.50 (1H), 6.50 (1H), 7.55 (3H), broad multiplet 7.7–9.0 (8H).

trans-4-Aminocyclohexyl p-Toluenesulfonate Hydrobromide (8)

To a solution of **7** in 30 ml of glacial acetic acid were added a solution of 3 ml of 48% aqueous hydrobromic acid in 7 ml of acetic acid. Stirring was continued 20 min after the evolution of carbon dioxide had ceased. The solvent was then removed under vacuum. The residue was washed with ether and recrystallized twice from ethyl acetate to give needles melting at 135–136° in 81% yield.

Anal. Calcd. for $C_{13}H_{20}BrO_3NS$: C, 44.58; H, 5.75. Found: C, 44.76; H, 5.95.

The i.r.: (3200–3000), 1365, 1180 cm^{-1}. The n.m.r. (100 MHz): τ 1.77 (3H), an A_2B_2 at 2.13 and 2.67 (4H), 5.58 (1H), 6.88 (1H), 7.51 (3H), 7.7–8.1 (8H).

7-Azabicyclo[2.2.1]heptane Hydrochloride (1)

To 500 ml of a 70% aqueous ethanol solution containing 2 equ of 1 *N* sodium hydroxide (36 ml) were added 6 g of **8**. After the mixture had stood for 14 h at room temperature, hydrogen chloride gas was introduced into the mixture and the solvent was removed under vacuum. The residue was dissolved in 10% aqueous sodium hydroxide and the amine was extracted with ether. The ether was then dried, filtered, and the filtrate dried further over calcium hydride. After the final filtration, dry hydrogen chloride gas was introduced into the ether and the precipitate which formed was filtered off. Recrystallization from a methanol: ethyl acetate mixture gave a solid melting at 261–263°. The yield for the reaction was 77%.

Anal. Calcd. for $C_6H_{12}NCl$: C, 53.95; H, 9.06. Found: C, 53.76; H, 9.23.

The i.r.: 3000–2550, 1605, 1473, 1453, 1363, 1278, 1230, 1090, 975, 908, 884 cm^{-1}. The n.m.r. (60 MHz): τ 5.77 (2H), 7.76, 8.36, 2 broad peaks (8H). The n.m.r. of free amine **1** at 100 MHz: τ 6.37 (2H) 8.40, 8.49, 8.66, 8.68, 4 broad peaks (9H). Mass spectrum: *m/e* (relative intensity) 98 (1.3), 97 (18.0), 96 (3.1), 70 (8.0), 69 (80.5), 68 (100), 43 (10.1), 42 (10.0), 41 (24.2).

The picrate of **1** was formed by reaction with picric acid in aqueous medium and melted at 171–173 °C.

trans-4-Acetamidocyclohexyl Methanesulfonate (9)

The *trans* alcohol **3**, (3 g), was finely powdered and dissolved in a solution composed of 50 ml of dichloromethane and 50 ml of pyridine at a temperature of 30°. Methanesulfonyl chloride (3.5 g) was then slowly added with cooling and the reaction mixture was stirred for 2 h. The solvent was then removed under vacuum and the residue was dissolved in chloroform and washed with 25 ml of 2 *N* hydrochloric acid. The aqueous portion was extracted with ten 25 ml portions of chloroform and the two organic layers were combined and dried. After the drying agent was removed and solvent evaporated, the residue was crystallized from ethyl acetate. The solid amounted to 3.8 g (85%) yield and melted from 150–151°.

Anal. Calcd. for $C_9H_{17}NO_4S$: C, 45.93; H, 7.23. Found: C, 45.56; H, 7.07.

The i.r.: 3310, 1630, 1550, 1374, 1340, 1170, 1000, 970, 945, 855 cm^{-1}. The n.m.r. (60 MHz): τ 4.33 (1H), 5.42 (1H), 6.23 (1H), 7.00 (1H), broad multiplet 7.63–8.80 sharp peak 8.03.

The yield was less than 25% when solvents such as pyridine, chloroform, ethyl acetate, or dimethylformamide were used.

Ethyl-N-(4-mesyloxycyclohexyl)-acetimidate (10)

The Meerwein reagent (1.4 g) was prepared (23) and added to 1 g of *trans*-4-acetamidocyclohexyl methanesulfonate (**9**) in 50 ml of methylene chloride. The reaction mixture was allowed to stand for 8 h and then 10 ml of triethylamine was added. After standing overnight, the mixture was washed with water and dried. The solution was filtered, the solvent removed under vacuum, and the residue extracted with boiling heptane. The solid (0.84 g) which was recovered from the heptane melted at 80–82°. The yield for the reaction was 75%.

Anal. Calcd. for $C_{11}H_{21}NSO_4$: C, 50.16; H, 8.04. Found: C, 50.15; H, 8.06.

The n.m.r. (100 MHz in $CDCl_3$): τ 5.30 broad (1H), 6.01 quartet (2H), (J = 7 Hz), 6.40 broad (1H), 7.00 (3H), broad multiplet 7.7–8.9 (14H), including singlet 8.15, triplet 8.80 (J = 7.0 Hz).

trans-4-Aminocyclohexyl Methanesulfonate Hydrochloride (11)

The imidate ester, **10**, was suspended in water and oxalic acid was added until the p*H* reached 1.5–2. After the mixture has been stirred for a few minutes, all of **10** had dissolved and the acid solution was allowed to stand for 16 h. Chloroform was then added and the aqueous portion was made basic with 1*N* sodium hydroxide. After the aqueous portions were extracted with more chloroform, the chloroform extracts were dried and then hydrogen chloride gas was bubbled in. When the solvent was removed, the residue was recrystallized from a methanol:ethyl acetate mixture. The solid obtained melted at 141–143 °C. The yield varied from 70 to 86%.

Anal. Calcd. for $C_7H_{16}O_3NSCl$: C, 36.59; H, 7.02. Found: C, 36.79; H, 7.20.

7-Azabicyclo[2.2.1]heptane Hydrochloride (1)

The hydrochloride, **11**, obtained from the previous reaction was placed in an 80% aqueous ethanol solution containing 2 equ of 1 *N* sodium hydroxide. After 16 to 18 h the same work-up as described previously gave **1** in a yield of 83%.

Determination of the pK_A of 1 (47)

Samples of 7-azabicyclo[2.2.1]heptane hydrochloride (**1**) weighing 35, 45, and 50 mg, respectively, were dissolved in 50 ml of water in a 250 ml beaker. The solution was stirred with a magnetic stirrer. Titration of **1** using a solution of 0.100 *N* sodium hydroxide (BDH volumetric reagent) was followed with a Radiometer p*H* meter type, 24e, using a glass electrode. The p*H* meter was standard-

Can. J. Chem. Downloaded from www.nrcresearchpress.com by 210.87.254.6 on 09/05/12
For personal use only.

ized at p*H* 8, 10, and 11 before each sample determination. The p*H* of the solution was read after each 0.05 ml of titrant was added and a plot was made of p*H* vs. volume of sodium hydroxide added. The first inflection point was determined and the p*H* noted at this point. This then gave the pK_A for the amine. The average value for the three determinations was 10.8.

*7-Methyl-7-azabicyclo[2.2.1]heptane Hydrochloride (**12**)*

The hydrochloride of **1** (500 mg) was placed in a 100 ml flask fitted with two condensers and a drying tube. Formic acid (15 ml) and 20 ml of a 37% formaldehyde solution was added and the mixture was refluxed for 3 h (48). At this time 0.5 g of paraformaldehyde was carefully introduced and the mixture was refluxed a further 12 h then allowed to stand at room temperature for 10 h. Hydrochloric acid (10 ml of 4 *N*) was added and the solution evaporated to dryness under vacuum. The solid residue was taken up in water and the insoluble portion removed by filtration. The filtrate was made basic and extracted with ether. The ether was dried with magnesium sulfate then calcium hydride and, after removal of the drying agent, hydrogen chloride gas was introduced. The precipitate which formed was collected and recrystallized from an ethyl acetate:methanol mixture to give a solid melting at 255.5 to 257°. The yield was 53%.

Anal. Calcd. for $C_7H_{14}NCl$: C, 56.94; H, 9.56. Found: C, 56.76; H, 9.52.

The i.r.: 3000–2400, 1490, 1460, 1375, 1333, 1230, 1178, 1139, 1069, 1011, 958, 880 cm^{-1}. The n.m.r. (60 Hz): τ 6.03 (2H), 7.21 doublet (3H), 7.33–8.51 broad multiplet (8H).

*7-Acetyl-7-azabicyclo[2.2.1]heptane (**15**)*

A three-necked flask was fitted with a gas outlet, a thermometer, a dropping funnel, and a stirrer. Triethylamine (0.4 ml) and 0.3 ml of acetic acid were added together with 0.5 ml of ethyl chloroformate in 50 ml of methylene chloride. The temperature was maintained at −20° and the mixture was stirred for 1 h. The free base of **1** (400 mg) was added slowly and evolution of carbon dioxide was noted by trapping it under water. After 4 h the mixture was washed with 10 ml of 1 *N* hydrobromic acid and the solvent was dried and carefully evaporated. On bulb-to-bulb distillation of the residual liquid and subsequent recrystallization of the distillate from heptane, a solid melting at 41.0–42.5° was obtained in 40% yield.

Anal. Calcd. for $C_8H_{13}ON$: C, 69.03; H, 9.41. Found: C, 68.92; H, 9.22.

The i.r.: 1640, 1457, shoulder 1425, 1365, 1320, 1157, 975 cm^{-1}. The n.m.r. (100 MHz): τ 4.62 (1H), 4.10 (1H), 2.00 (3H), 1.62 multiplet (8H). Mass spectrum: *m/e* (relative intensity) 139 (31), 69 (100), 68 (75).

A 73% yield of **15** was obtained by refluxing **1** (500 mg) for 2 h in 20 ml of acetic anhydride containing 500 mg of sodium acetate.

*7-Formyl-7-azabicyclo[2.2.1]heptane (**16**)*

In a round-bottom flask were placed 1 g of 98% formic acid and 2 g of acetic anhydride. The mixture was cooled to −15° and after 20 min, 60 mg of **1** were added. The solution was allowed to warm slowly to room temperature and after standing for 24 h it was made basic with 20% sodium hydroxide and extracted with chloroform. After the chloroform was dried and the solvent removed, distillation of the residue under vacuum at 40° gave a liquid (38 mg, 67% yield) of b.p. 60° at 0.06 mm pressure.

Anal. Calcd. for $C_7H_{11}NO$: C, 67.17; H, 8.86. Found: C, 66.98; H, 8.74.

The n.m.r. (100 MHz): τ 1.95 (1H), 5.39 (1H), 5.92 (1H), broad multiplet with four main peaks 8.18, 8.29, 8.46, 8.55 (8H). Mass spectrum: *m/e* (relative intensity) 125 (34.7), 97 (26), 96 (39), 69 (28.5), 68 (100), 41 (44.4).

*7-Trichloroacetyl-7-azabicyclo[2.2.1]heptane (**17**)*

A solution of **1** in 50 ml methylene chloride was added to 50 ml of saturated sodium carbonate. The two phase mixture was cooled and stirred vigorously while 300 mg of trichloroacetyl chloride (49) was rapidly added. After 1 h the two layers were separated and the aqueous portion extracted with methylene chloride. The solution was dried and the solvent evaporated leaving 130 mg (70% yield) of solid which, after recrystallization from heptane, melted at 105.5–106°.

Anal. Calcd. for $C_8H_{10}NOCl_3$: C, 39.62; H, 4.15. Found: C, 39.79; H, 4.21.

The i.r.: 675, 1460, 1420, 1320, 1260, 1160, 985, 830, 800, 725, 650 cm^{-1}. The n.m.r. (100 MHz): τ 5.24 (2H), broad multiplet 2 main peaks centered at 8.06, 8.45 (8H).

*7-Nitroso-7-azabicyclo[2.2.1]heptane (**18**)*

A solution of **1** (235 mg) in 25 ml of water was placed in a round-bottom flask fitted with a condenser. Sodium nitrite (400 mg) was added in one portion along with 1.5 ml of 2 *N* hydrochloric acid. The solution was heated to 70–75° and stirred for 3 h. The product was extracted from the cooled acidic solution with ether, the extracts were dried, and the ether was carefully removed under reduced pressure. The residual yellow needles were recrystallized from heptane to give 160 mg (73% yield) of a solid melting at 85–86°.

Anal. Calcd. for $C_6H_{10}N_2O$: C, 57.10; H, 7.91. Found: C, 56.92; H, 7.86.

The i.r.: 1475, 1465, 1450, 1408, 1335, 1310, 1155, 1130, 990, 870, 717 cm^{-1}. The n.m.r. (100 MHz in $CDCl_3$–CS_2): multiplet τ 5.06 (2H), multiplet 8.30 (8H).

*2-Chloro-7-trichloroacetyl-7-azabicyclo[2.2.1]heptane (**19**)*

To a solution of **17** (300 mg) in 25 ml of methylene chloride were added 100 mg of benzoyl peroxide and 0.5 ml of sulfuryl chloride. The mixture was refluxed for 24 h. The solvent was then removed under vacuum and the residue placed on a chromatographic column containing 30 g of silica gel. A 15% hexane:ethyl acetate mixture was used as eluent. This treatment yielded 150 mg of crude monochloride which after sublimation melted at 70.0–71.5° (107 mg; 31% yield).

Anal. Calcd. for $C_8H_9NOCl_4$: C, 34.68; H, 3.28. Found: C, 34.52; H, 3.28.

The i.r.: 1680, 1425, 1317, 870, 840, 805, 739, 610 cm^{-1}. The n.m.r. (100 MHz): τ 5.10 (2H), 5.90 triplet (1H), 7.76 (2H), 8.03 (2H), 8.50 multiplet (2H).

Recrystallization of the material first eluted from the column produced 110 mg of unreacted **17**. Although some

disubstituted product (45 mg) was also obtained as indicated by n.m.r. it was not purified.

2-Chloro-7-azabicyclo[2.2.1]heptane Hydrochloride (20)

To a solution of **19** (100 mg) in 15 ml of frozen *t*-butanol were added 100 mg of potassium *t*-butoxide. The reaction vessel was sealed and the solid allowed to melt. Fifteen minutes after the bubbles ceased to evolve the mixture was again frozen and the tube unsealed. Hydrogen chloride gas was bubbled through the solution as the solvent melted and the *t*-butanol was removed under vacuum. The residue was extracted with chloroform and filtered to remove the solid potassium chloride. After the chloroform was removed, the residue was recrystallized from a methanol–ether mixture, giving 75 mg of solid which melted with decomposition at 242° (73% yield).

Anal. Calcd. for $C_6H_{11}NCl_2$: C, 42.87; H, 6.59. Found: C, 42.68; H, 6.76.

The i.r.: 3000–2450, 1610, 1581, 1450, 1435, 1369, 1354, 1320, 1050, 880, 670, 500 cm^{-1}. The n.m.r. (100 MHz): τ 5.55 (1H), 5.70 (1H), 5.89 (1H), 7.80 broad (4H), 8.44 broad (2H). Mass spectrum: *m/e* (relative intensity) 133 (2), 131 (5.5), 70 (45), 69 (100), 68 (29.3), 67 (29), 42 (13), 41 (13).

The authors thank the National Research Council of Canada for financial support of this research and for the award of an NRCC studentship to R. B. S. for the period 1967–1969. The assistance of Dr. Y. Y. Wigfield in work on improving the synthesis of *trans*-**3** is greatly appreciated.

1. J. Meisenheimer. Ann. **420**, 196 (1920).
2. S. Wawzonek and T. C. Wilkinson. J. Org. Chem. **31**, 1732 (1966).
3. P. G. Gassman and R. L. Cryberg. J. Amer. Chem. Soc. **91**, 2047 (1969).
4. P. S. Portoghese. J. Med. Chem. **11**, 219 (1968).
5. J. P. Fleury, J. M. Biehler, and M. Desbois. Tetrahedron Lett. 4091 (1969).
6. R. C. Bansal, A. W. McCulloch, and A. G. McInnes. Can. J. Chem. **47**, 2391 (1969).
7. A. Runquist, G. Pierson, and O. Runquist. J. Org. Chem. **34**, 3192 (1969).
8. R. Kitzing, R. Fuchs, M. Joyeux, and H. Prinzbach. Helv. Chim. Acta, **51**, 888 (1968).
9. L. Mandell, J. U. Piper, and C. E. Pesterfield. J. Org. Chem. **28**, 574, (1963).
10. V. Rautenstrauch. Chem. Commun. 1122 (1969).
11. L. A. Carpino and D. E. Barr. J. Org. Chem. **31**, 764 (1966).
12. A. Shafi'ee and G. Hite. J. Org. Chem. **33**, 3435 (1968).
13. J. Braun and K. Schwarz. Ann. **481**, 56 (1930).
14. H. W. Heine. J. Amer. Chem. Soc. **79**, 6268 (1957).
15. E. J. Corey and E. Block. J. Org. Chem. **31**, 1663 (1966).
16. E. Ferber and H. Bruckner. Chem. Ber. **72**, 995 (1939).
17. J. H. Billman and J. A. Buehler. J. Amer. Chem. Soc. **75**, 1345 (1953).
18. E. W. Della and P. R. Jefferies. Austr. J. Chem. **14**, 610 (1961).
19. A. Bowers, T. G. Halsall, E. R. H. Jones, and A. J. Lemin. J. Chem. Soc. 2555 (1953).
20. H. Kwart and T. Takeshita. J. Amer. Chem. Soc. **84**, 2833 (1962).
21. P. G. Gassman and A. Fentiman. J. Org. Chem. **32**, 2388 (1967).
22. H. Muxfeldt and W. Rogalski. J. Amer. Chem. Soc. **87**, 933 (1965).
23. H. Meerwein, H. Ginz, P. Hoffmann, E. Kroning, and E. Pfel. J. Prakt. Chem. (2) **147**, 275 (1936).
24. E. J. Corey and W. R. Hertler. J. Amer. Chem. Soc. **82**, 1657 (1960).
25. R. R. Fraser and Y. S. Lin. Can. J. Chem. **46**, 801 (1968), and references quoted therein.
26. J. F. Chiang, C. F. Wilcox, and S. H. Bauer. J. Amer. Chem. Soc. **90**, 3149 (1968).
27. Tables of interatomic distances. Special Publication #18, The Chemical Society, London, 1965.
28. S. Searles, M. Tamres, F. Block, and L. A. Quarterman. J. Amer. Chem. Soc. **78**, 4917 (1956).
29. Organic reactions. Vol. **5**. John Wiley and Sons, Inc., 1949. p. 301.
30. N. J. Leonard and F. P. Hauck. J. Amer. Chem. Soc. **79**, 5279 (1957).
31. R. B. Swingle. Ph.D. Thesis, University of Ottawa, Ottawa, Ontario, 1969.
32. J. A. Pople, W. G. Schneider, and H. J. Bernstein. High-resolution nuclear magnetic resource. McGraw-Hill Book Co. Inc., New York, 1959. p. 134.
33. F. A. L. Anet, H. H. Lee, and J. L. Sudmeier. J. Amer. Chem. Soc. **89**, 4431 (1967).
34. K. L. Williamson. J. Amer. Chem. Soc. **85**, 516 (1963).
35. J. D. Roberts, L. Urbanek, and R. Armstrong. J. Amer. Chem. Soc. **71**, 3049 (1949).
36. P. D. Bartlett and J. C. Martin. J. Amer. Chem. Soc. **79**, 2533 (1957).
37. J. B. Lambert and W. L. Oliver, Jr. J. Amer. Chem. Soc. **91**, 7774 (1969).
38. S. J. Brois. J. Amer. Chem. Soc. **90**, 506, 508 (1968).
39. J. M. Lehn and J. Wagner. Chem. Commun. 148 (1968).
40. F. A. L. Anet and J. M. Osyany. J. Amer. Chem. Soc. **89**, 352 (1967).
41. J. A. Pople, W. G. Schneider, and H. J. Bernstein. High-resolution nuclear magnetic resource. McGraw-Hill Book Co., Inc., New York, 1959. p. 223.
42. F. A. L. Anet and A. J. R. Bourn. J. Amer. Chem. Soc. **89**, 760 (1967).
43. R. C. Neuman and V. Jonas. J. Amer. Chem. Soc. **90**, 1970 (1968).
44. C. E. Looney, W. D. Phillips, and E. L. Reilly. J. Amer. Chem. Soc. **79**, 6136 (1957).
45. F. Johnson and S. K. Malhotra. J. Amer. Chem. Soc. **87**, 5492, 5513 (1965).
46. M. Bergmann and L. Zervas. Chem. Ber. **65**, 1192 (1932).
47. S. Glasstone. Textbook of physical chemistry. D. Van Nostrand Co., New York, 1946. p. 1002.
48. H. T. Clarke, H. B. Gillespie, and S. Z. Weisshaus. J. Amer. Chem. Soc. **55**, 4571 (1933).
49. R. R Fraser and R. B. Swingle. Tetrahedron, **25**, 3469 (1969).

Can. J. Chem. Downloaded from www.nrcresearchpress.com by 210.87.254.6 on 09/05/12
For personal use only.

Can. J. Chem. Downloaded from www.nrcresearchpress.com by 210.87.254.5 on 09/05/12
For personal use only.

The reaction of 2-butyne with hydrogen catalyzed by nickel, copper, cobalt, iron, and nickel–copper alloys

R. S. Mann and C. P. Khulbe
Department of Chemical Engineering, University of Ottawa, Ottawa, Canada

Received September 12, 1969

The reaction between hydrogen and 2-butyne over unsupported nickel, copper, cobalt, iron, and nickel–copper alloys has been investigated in a static constant volume system between 30 and 250 °C for a wide range of reactant ratios. The reaction over metals and their alloys is simple hydrogenation, the early stages being principally a selective production of *cis*-2-butene with small yields of polymers. The order of reaction with respect to hydrogen was one and independent of temperature. While the order of reaction over cobalt and copper with respect to 2-butyne was zero, it was slightly negative and temperature dependent for nickel and nickel–copper alloys. The selectivity was independent of initial hydrogen pressure for nickel, cobalt, copper and most of the nickel–copper alloys. The overall activation energy for nickel, cobalt, and copper were 9.1, 6.6, 33.5 kcal/mole, respectively. Selectivity and extent of polymerization increased with increasing amounts of copper in the nickel–copper alloy.

Canadian Journal of Chemistry, 48, 2075 (1970)

Introduction

Though recently several papers have appeared on the hydrogenation of acetylene (1, 2), methylacetylene (3, 4), and ethylacetylene (5, 6) over supported and unsupported metals of the eighth group, very little has been reported about the kinetics of the hydrogenation of 2-butyne over metals. While Meyer and Burwell (7) studied the reaction of deuterium with 2-butyne on palladium–alumina, Webb and Wells (8) have reported the kinetics of the reaction over supported ruthenium and osmium, and Phillipson *et al.* (9) investigated the kinetics of the hydrogenation of 2-butyne over alumina supported cobalt, nickel, iron, rhodium, iridium, and platinum catalysts.

In the present study, we have examined the reaction of 2-butyne with hydrogen catalyzed by nickel, copper, cobalt, iron, and nickel–copper alloys. Here we report the kinetics of the reaction and the yields of butenes and butane over a wide range of operating conditions.

Experimental

The apparatus and experimental procedure were essentially the same as described by Mann and Khulbe (3). Homogeneous nickel–copper alloys and pure nickel, copper, cobalt, and iron powders were prepared by the method of Best and Russell (11). The mixed basic carbonates (in case of alloys) or basic carbonates (for pure metal powders), precipitated by ammonium bicarbonate from their nitrate solutions containing the appropriate quantities of the nitrate, were decomposed to the oxides by calcination at 500 °C in a muffle furnace, and then reduced in a hydrogen stream for 24 h at 400 °C. The pumice-supported iron was prepared as described earlier by Mann and Naik (10). 2-Butyne, supplied by Frachan Research Laboratory, was further purified by vacuum distillation. Cylinder hydrogen gas (Linde Co.) was passed through a bed of palladium asbestos (10% Pd) maintained at 200 °C by an electric furnace surrounding it, and then through a trap immersed in liquid nitrogen. Quantitative analysis of the products was carried out by means of a Varian Aerograph, Model A-90 P3, employing a 20 ft long column packed with 30% dimethyl sulfolane supported on 20–60 mesh acid washed Chromosorb-P. The column was maintained at 35 °C, and helium, flowing at a rate of 80 cc per min, was used as the carrier gas.

The amount of polymerization was calculated as the difference between the intial pressures of 2-butyne and the sum of 2-butyne reacted to form butenes and butane and the unreacted 2-butyne in the products. These polymers may have been in the gaseous form, which could not be detected by the dimethyl-sulfolane column under experimental conditions.

X-Ray analysis of the reduced nickel–copper catalysts showed that solid solutions, closely corresponding to the expected composition, were indeed formed. All the alloys contained no detectable free metal, and had face centered cubic structure. The lattice constants and calculated compositions of these are given in Table 1. These checked very well with the expected values within a reasonable accuracy. Surface areas of these catalysts were determined by B. E. T. method and are given in Table 1.

Results

Unsupported nickel, copper, cobalt, and nickel–copper alloy catalysts were found to be quite active and did not get poisoned when 2-butyne or hydrogen was admitted first into the reactor. The activity remained fairly constant for several days. However, unsupported iron was found to be very much less active as a catalyst

Can. J. Chem. Downloaded from www.nrcresearchpress.com by 210.87.254.5 on 09/05/12
For personal use only.

TABLE 1

Characteristic of the catalyst and order of reaction and activation energies*

Catalyst	Weight (g)	Lattice parameter (Å)	Surface area (m^2/g)	Temperature range (°C)	Specific rate, k ($min^{-1}\ m^{-2}$)	Activation energy, E (kcal/mole)	Average order of reaction	
							n	m
Ni–Cu alloy, % Cu								
0	0.075	3.521	1.70	40–83	0.133	9.1	0.980±0.02	−0.155±0.155
10	0.075	3.530	2.0	40–70	0.227	6.5	1.01 ±0.047	−0.025±0.025
20	0.075	3.538	2.29	50–97	0.139	7.7	1.05 ±0.05	−0.05 ±0.05
30	0.075	3.543	0.78	50–81	0.130	7.1	0.98 ±0.02	−0.03 ±0.03
50	0.075	3.570	2.29	50–92	0.028	9.2	1.01 ±0.05	−0.025±0.025
75	0.225	3.590	1.45	59–100	0.008	8.9	1.00 ±0.02	−0.03 ±0.03
100	1.00	3.610	0.40	200–250	0.000	33.5	1.04 ±0.06	0.00 ±0.00
Cobalt	0.075			40–90		6.6	0.99 ±0.01	−0.08 ±0.08

*n = order of reaction with respect to hydrogen; m = order of reaction with respect to 2-butyne; k = specific rate at 60 °C.

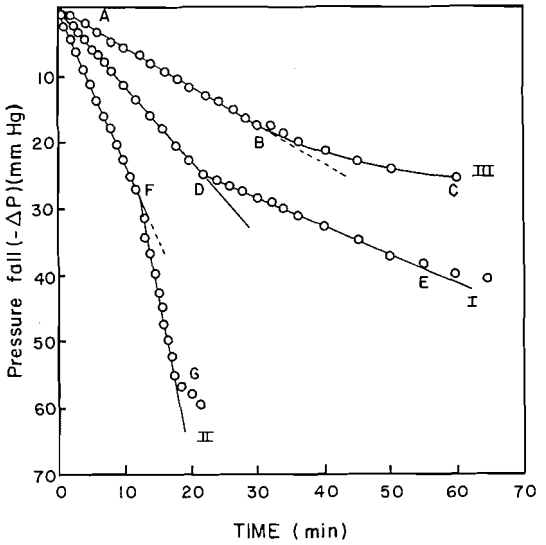

FIG. 1. Pressure–time curve: Temperature = 40 °C; $P_{C_4H_6}$ = 50 mm. Curve ADE, I, Ni = 90%, Cu = 10%, P_{H_2} = 50 mm; curve AFG, II, Ni = 90%, Cu = 10%, P_{H_2} = 120 mm; curve ABC, III, Ni powder, P_{H_2} = 50 mm.

as compared to nickel, cobalt, or copper. It lost its activity rapidly. It was observed that the rate of deactivation decreased with the number of runs, and increased hydrogen/2-butyne ratios and temperatures.

(a) Pressure Fall-time Curves

The various types of pressure fall-time (P–t) curves observed in the hydrogenation of acetylene (12) and methylacetylene (10) over nickel–pumice catalysts have been discussed in considerable detail previously. The P–t curves (Fig. 1) observed in the hydrogenation of 2-butyne for hydrogen/2-butyne ratios of less than two consisted of either two linear portions of different slopes (curve ADE, type I) or a straight line up to a pressure fall of about two thirds of 2-butyne and then a curve (curve ABC, type III). For hydrogen/2-butyne ratios greater than two, either a type III or type II (curve AFG) was observed. Curve AFG is comprised of two linear regions, region AF, in which the reaction was first order and region FG in which the rate of pressure fall accelerated. In the region AF, the main product of the reaction was *cis*-2-butene with a very small amount of butane, whereas after the rapid acceleration (region FG), the main process occurring was the further hydrogenation of 2-butenes to butane. The kinetic forms of the pressure–time curves

TABLE 2
Pressure fall-time curves

Catalysts	Kinetics (type of curves) $H_2: C_2H_6 < 2$	$H_2: C_4H_6 > 2$
Ni 100%, Cu 0%	III	III
Ni 90%, Cu 10%	I	II
Ni 80%, Cu 20%	I	II
Ni 70%, Cu 30%	III	III
Ni 50%, Cu 50%	III	III
Ni 25%, Cu 75%	III	III
Ni 0%, Cu 100%	III	III
Co powder	I	II

observed with different catalysts are summarized in Table 2.

(b) Orders of Reaction with respect to Hydrogen and 2-Butyne

Using a fixed 2-butyne pressure of 50 mm and a wide range of hydrogen pressures (18–200 mm), order in hydrogen was determined at several temperatures. Similarly the order of reaction with respect to 2-butyne was obtained by using 50 mm hydrogen and varying pressures of 2-butyne between 40 and 180 mm at several temperatures.

The orders of reaction with respect to hydrogen (n) was always about one and independent of temperature for all catalysts (Table 1). While the order of reaction with respect to 2-butyne (m) was zero and nearly independent of temperature for copper and cobalt, it was zero for nickel and nickel–copper alloys at lower temperatures and became slightly negative with increased temperatures. Table 3 shows the order of reaction with 2-butyne for nickel, cobalt, and nickel–copper alloys for several temperatures.

(c) Temperature Dependence of Rate Constants

Plots of $\log_{10}$ specific rates against the reciprocal of absolute temperature were good straight lines over a wide temperature range for all the catalysts satisfying the Arrhenius equation. The activation energies for all the catalysts are given in Table 1. There appears to be no direct relationship between the energy of activation and the copper content of the alloy, except that the minimum activation energy was observed for an alloy containing approximately 10% copper.

(d) The Dependence of Activity on Composition of Nickel–Copper Alloys

The hydrogenation of 2-butyne has been

Can. J. Chem. Downloaded from www.nrcresearchpress.com by 210.87.254.5 on 09/05/12
For personal use only.

TABLE 3

Order with respect to butyne-2 (m)

Nickel		20% Cu		50% Cu		Copper		Cobalt	
Temperature (°C)	m	Temperature (°C)	m	Temperature (°C)	m	Temperature (°C)	m	Temperature (°C)	m
40	0.00	50	0.00	50	0.00	230	0.00	49	0.0
54	0.00	60	0.00	63	0.00	240	0.00	60	0.0
67	−0.06	77	0.00	74	0.00	250	0.00	69	0.0
73	−0.16	85	−0.08	82	0.00			80	0.0
83	−0.31	97	−0.10	92	−0.05			90	−0.16

TABLE 4

Effect of copper concentration on product distribution*

% copper in Ni–Cu alloys	2-Butyne intial pressure (mm)		Pressure of products (mm)					Selectivity S	2-Butyne lost	% polymers
	80 °C	Room temperature	Butane	1-Butene	*trans*-2-Butene	*cis*-2-Butene	2-Butyne			
0	52.0	47.75	0.00	0.50	0.25	16.0	31.0	1.000	0.00	0.00
10	52.0	47.75	0.25	0.50	0.25	15.2	28.0	0.985	3.55	7.43
20	52.0	47.75	0.50	1.00	0.00	15.0	26.5	0.970	4.25	8.90
30	50.0	46.0	0.25	1.50	0.25	14.5	25.0	0.985	4.50	9.78
50	49.0	45.2	0.25	1.50	0.00	14.0	26.0	0.984	3.50	7.73
75	52.5	48.2	0.00	2.00	0.50	13.0	25.0	1.000	7.70	16.00
100†	53.0	43.5	0.00	0.00	0.00	11.0	26.5	1.000	6.00	13.80
Co	50.5	46.5	0.50	1.50	0.25	18.5	21.5	0.976	4.25	9.14

*Hydrogen = 50 ± 2 mm ΔP = 20 mm.
†T = 185 °C.

Can. J. Chem. Downloaded from www.nrcresearchpress.com by 210.87.254.5 on 09/05/12
For personal use only.

Can. J. Chem. Downloaded from www.nrcresearchpress.com by 210.87.254.5 on 09/05/12
For personal use only.

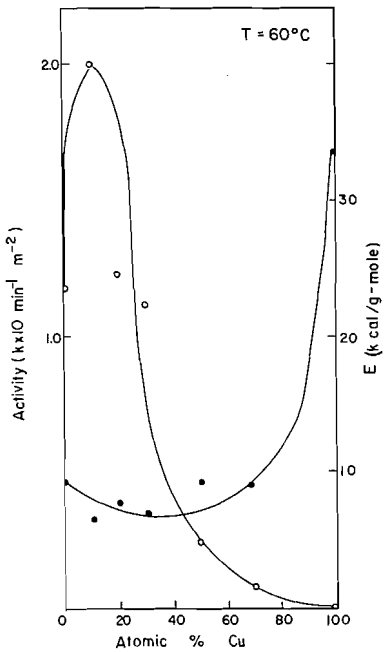

FIG. 2. Energy of activation vs. % copper in alloy.

studied over several different nickel–copper alloys. The results are summarized in Table 1. The striking feature of these results is that the catalytic activity rapidly increases with the slight increase of copper content (up to 10% Cu) in the alloy, and then decreases with increasing copper content, till at about 60% copper, when the activity became nearly zero (Fig. 2). Similar behavior was observed by Mann and Khulbe (3) in the hydrogenation of methylacetylene over nickel–copper alloys. However, Best and Russell (11) observed the maximum activity in the hydrogenation of ethylene over nickel–copper alloys in the copper rich region.

(e) Dependence of Selectivity upon Pressure-fall or Conversion

The course of the reaction and the dependence of the selectivity, S, for the various catalysts, and upon the concentration of copper in the nickel–copper alloys was studied at 80 °C for hydrogen/2-butyne ratios of 1 (P_{H_2} = 50 mm, $P_{C_4H_6}$ = 50 mm) and about 2.4 (P_{H_2} = 120 mm, $P_{C_4H_6}$ = 50 mm) by analyzing the reaction products after various falls in pressure. The selectivity (S) has been defined as the ratio of butenes to butenes plus butane

$$S = \sum P_{\text{butenes}} / \sum (P_{\text{butenes}} + P_{\text{butane}})$$

The distribution of products and the selectivity of the various catalysts for a total pressure fall of about 20 mm is given in Tables 4 and 5. While Fig. 3 *A*, *B*, and *C* show the distribution of products for equimolal amounts of hydrogen and 2-butyne for nickel, cobalt, and copper for different pressure falls (amounts of conversion), Fig. 4 *A*, *B*, and *C* show the distribution of

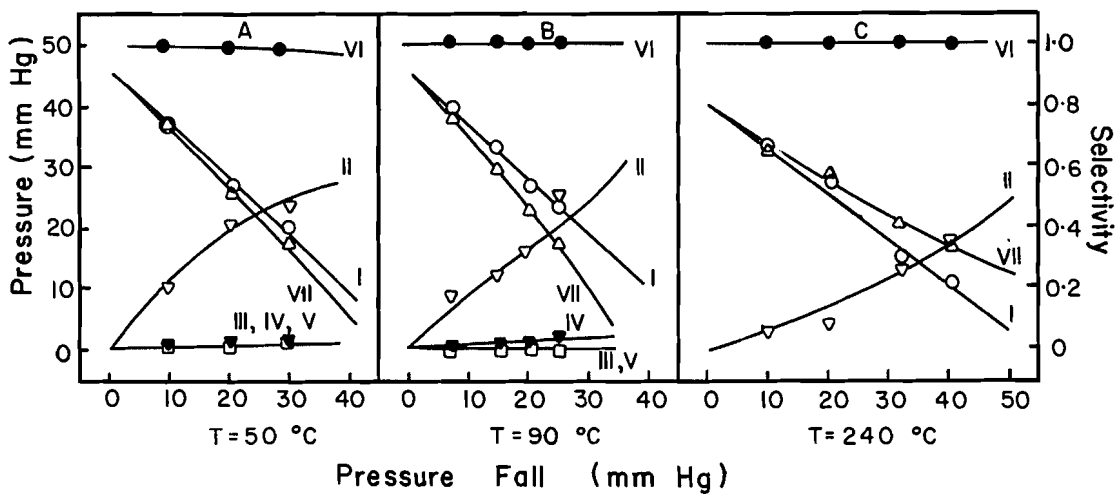

FIG. 3. Distribution of products during the course of reaction P_{H_2} = 50 mm, $P_{C_4H_6}$ = 50 mm. *A*, Ni powder (T = 50 °C); *B*, Co powder (T = 90 °C); *C*, Cu powder (T = 240 °C). Curve I, 2-butyne (○); curve II, *cis*-2-butene (▽); curve III, *trans*-2-butene (□); curve IV, 1-butene (▼); curve V, *n*-butane (□); curve VI, selectivity (●); curve VII, hydrogen (△).

Can. J. Chem. Downloaded from www.nrcresearchpress.com by 210.87.254.5 on 09/05/12
For personal use only.

TABLE 5

Effect of copper concentration on product distribution*

Catalyst	2-Butyne initial pressure (mm)		Pressure of products (mm)					Selectivity *S*	2-Butyne lost	% polymers
	80 °C	Room temperature	Butane	1-Butene	*trans*-2-Butene	*cis*-2-Butene	2-Butyne			
Ni–Cu alloy, % Cu										
0	50.0	46.0	0.75	0.75	0.75	20.3	23.5	0.967	0.0	0.0
10	50.0	46.0	1.00	0.75	1.25	14.5	25.0	0.942	3.5	7.6
20	50.0	46.0	5.00	0.00	3.00	6.0	25.0	0.643	7.0	15.2
30	50.0	46.0	4.00	0.25	1.50	6.5	25.5	0.672	8.25	17.9
50	52.0	47.75	0.00	0.50	0.00	13.2	23.5	1.000	10.55	22.0
75	48.5	44.8	0.00	2.00	0.00	14.0	22.0	1.000	6.80	15.1
100†	54.0	48.0	0.00	0.00	0.00	19.5	21.5	1.000	7.00	14.6
Co	49.0	45.2	0.75	2.00	0.25	20.0	21.5	0.967	0.7	1.55

*Hydrogen = 120 ± 2 mm; ΔP = 20 mm.
†T = 185 °C.

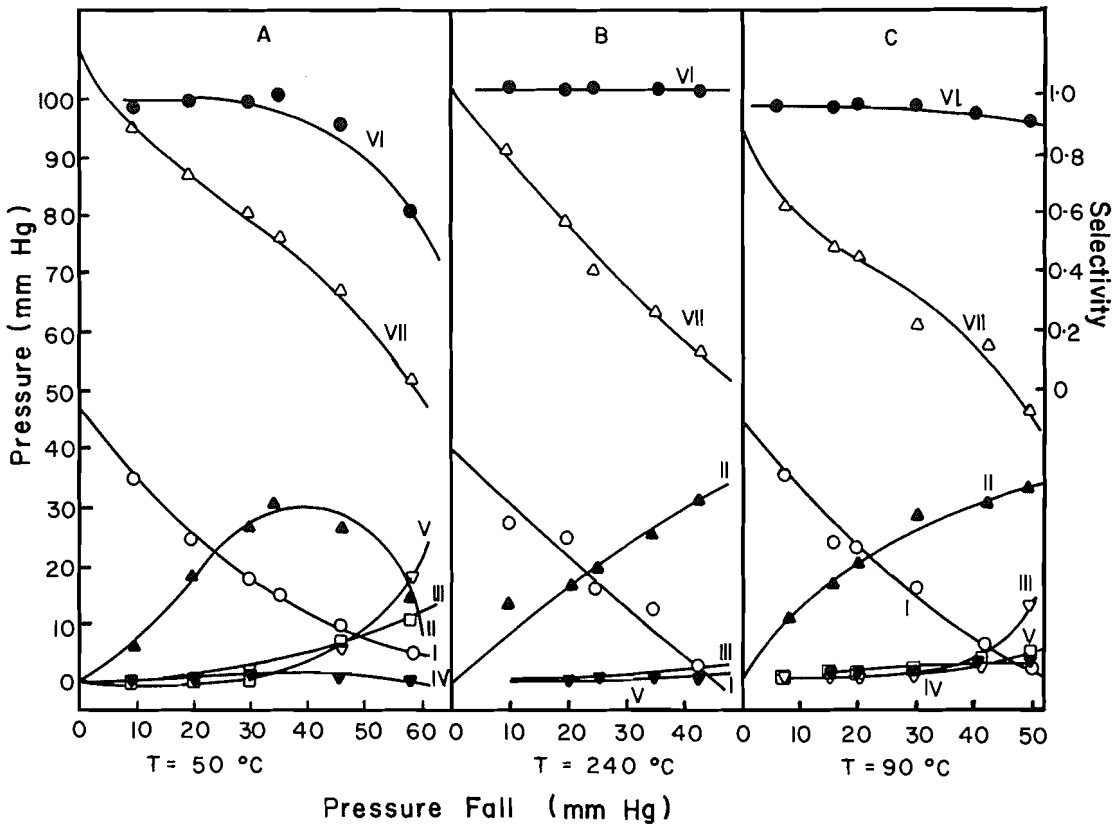

FIG. 4. Course of reaction; $P_{H_2} = 120$ mm, $P_{C_4H_6} = 50$ mm. *A*, Ni powder ($T = 50$ °C); *B*, Cu powder ($T = 240$ °C); *C*, Co powder ($T = 90$ °C). Curve I, 2-butyne (○); curve II, *cis*-2-butene (▲); curve III, *trans*-2-butene (□); curve IV, 1-butene (▼); curve V, *n*-butane (▽); curve VI, selectivity (●); curve VII, hydrogen (△).

products for hydrogen/2-butyne ratios of about 2.4. In the hydrogenation of 2-butyne, the main product was *cis*-2-butene and smaller amounts of other butenes and butane. While for hydrogen/2-butyne ratio of one, the selectivity was independent of pressure fall for nickel, cobalt, and copper catalysts, it decreased with pressure fall for hydrogen/2-butyne ratios greater than two. The dependence of selectivity on the pressure fall for various alloy compositions is shown in Fig. 5 *A* and *B*. While the selectivity was independent of pressure fall for all alloy compositions for hydrogen/2-butyne ratio of one, it decreased with pressure fall for all catalysts for hydrogen/2-butyne ratios of 2.4.

(f) The Dependence of Selectivity upon the Initial Pressures of Hydrogen and 2-Butyne

Measurements were made of the selectivity of nickel, copper, and cobalt, and nickel–copper alloy catalysts at several temperatures as a function of initial hydrogen pressure by using a fixed 2-butyne pressure (50 mm) and varying the hydrogen pressures. Products were analyzed when the total pressure fall was equal to 20 mm. The results are shown in Fig. 6. The selectivity was independent of initial hydrogen pressure for nickel, copper, cobalt, and for all nickel–copper alloys, except those containing 20 and 30% copper. In the case of the alloy containing 20% copper, the selectivity increased with increasing pressures of hydrogen till about 100 mm, beyond which it remained nearly constant. However, for the alloy containing 30% copper, the selectivity remained constant up to a pressure fall of about 80 mm beyond which it decreased with increasing pressures of hydrogen. Similarly the variation of the selectivity with 2-butyne was determined for fixed hydrogen pressure (50 mm) and varying 2-butyne pressure. The selectivity was indepen-

Can. J. Chem. Downloaded from www.nrcresearchpress.com by 210.87.254.5 on 09/05/12
For personal use only.

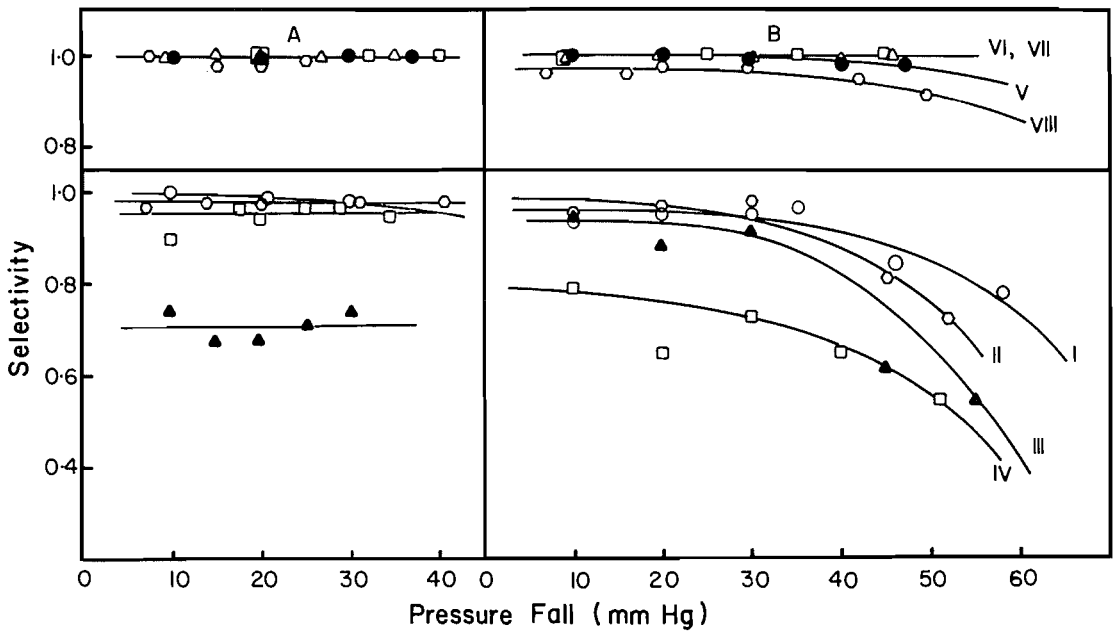

FIG. 5. Dependence of selectivity upon pressure fall: *A*, P_{H_2} = 50 mm, $P_{C_4H_6}$ = 50 mm; *B*, P_{H_2} = 120 mm, $P_{C_4H_6}$ = 50 mm. Curve I, Ni powder (○), T = 50 °C; curve II, Ni = 90%, Cu = 10% (◇), T = 50 °C; curve III, Ni = 80%, Cu = 20% (▲), T = 40 °C; curve IV, Ni = 70%, Cu = 30% (□), T = 70 °C; curve V, Ni = 50%, Cu = 50% (●), T = 130 °C; curve VI, Ni = 25%, Cu = 75% (△), T = 100 °C; curve VII, Cu powder (□); curve VIII, Co powder (●).

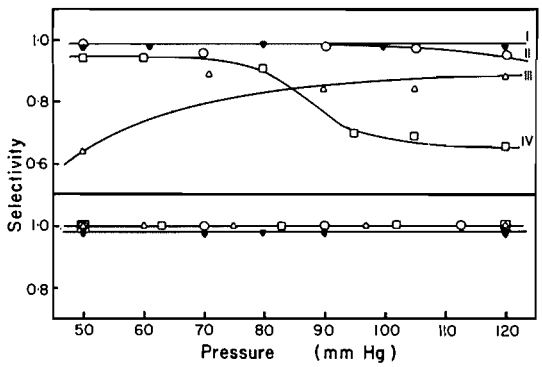

FIG. 6. Dependence of selectivity upon hydrogen pressure: curve I, Ni powder (▼), T = 50 °C; curve II, Ni = 90%, Cu = 10% (○), T = 50 °C; curve III, Ni = 80%, Cu = 20% (△), T = 40 °C; curve IV, Ni = 70%, Cu = 30% (□), T = 70 °C; curve V, Ni = 50%, Cu = 50% (○), T = 130 °C; curve VI, Ni = 25%, Cu = 75% (△), T = 100 °C; curve VII, Co powder (▼), T = 90 °C; curve VIII, Cu powder (□), T = 240 °C.

dent of 2-butyne pressure for nickel, copper, cobalt, and all nickel–copper alloys except the one containing 30% copper, for which the selectivity increased with increasing 2-butyne pressure (Fig. 7).

(g) The Dependence of Selectivity upon Temperature

The temperature dependence of the selectivity for hydrogen/2-butyne ratio of 1 and 2.4 was studied by analyzing the reaction products at several temperatures for a total pressure fall of 20 mm. The results are given in Fig. 8. For equimolal ratio the selectivity was independent of temperature. For hydrogen/2-butyne ratio of 2.4, while the selectivity increased slightly with increasing temperature for the catalyst containing 20% copper, it decreased slightly at higher temperatures for the catalysts containing 10 and 30% copper. For all other catalysts, it was independent of temperature.

(h) Polymerization

The amount of polymerization was calculated from the loss of 2-butyne during the reaction. The amount of polymerization observed at 80 °C for hydrogen/2-butyne ratio of 1 and 2.4 for various catalysts is given in Tables 4 and 5. The amount of polymers increased with increasing amounts of copper, with a maximum of about 22% for the alloy containing 50% copper. No

Can. J. Chem. Downloaded from www.nrcresearchpress.com by 210.87.254.5 on 09/05/12
For personal use only.

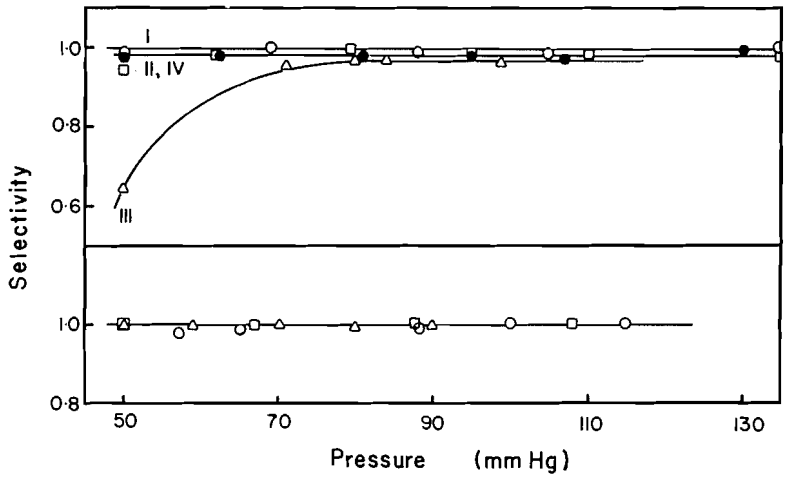

FIG. 7. Dependence of selectivity upon 2-butyne pressure. Curve I, Ni powder (○), T = 50 °C; curve II, Ni = 90%, Cu = 10% (●), T = 50 °C; curve III, Ni = 80%, Cu = 20% (△), T = 40 °C; curve IV, Ni = 70%, Cu = 30% (□), T = 70 °C; curve V, Ni = 50%, Cu = 50% (○), T = 130 °C; curve VI, Ni = 25%, Cu = 75% (△), T = 100 °C; curve VII, Co powder (□), T = 90 °C.

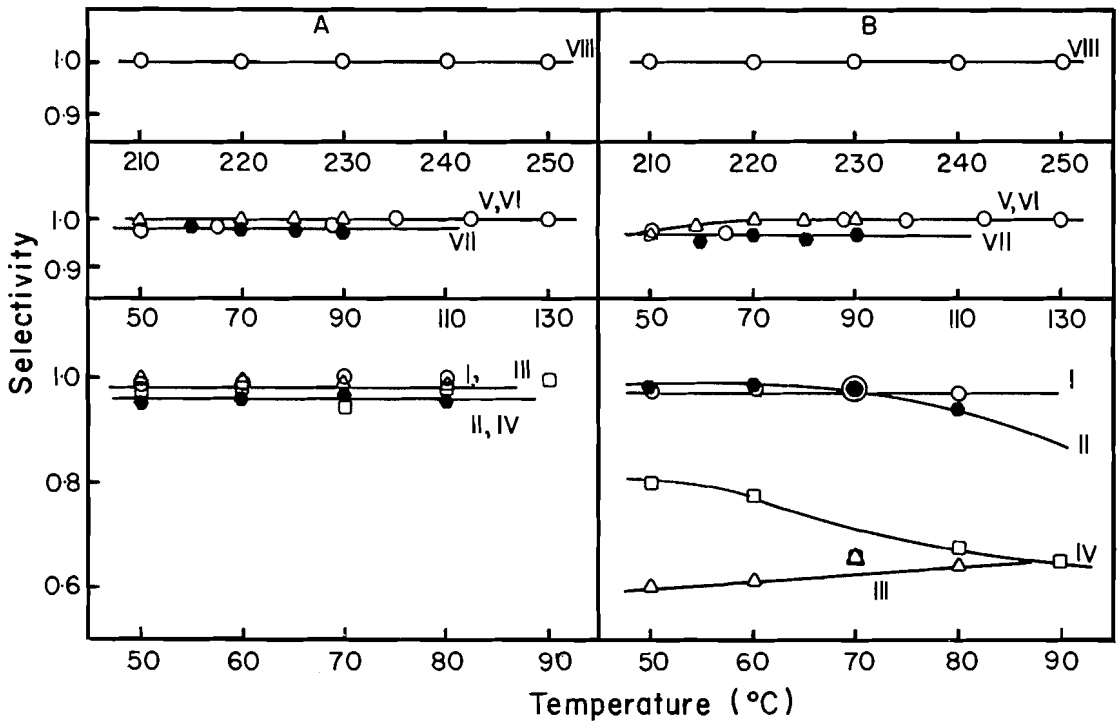

FIG. 8. Dependence of selectivity upon temperature: A, P_{H_2} = 50 mm, $P_{C_2H_6}$ = 50 mm; B, P_{H_2} = 120 mm, $P_{C_4H_6}$ = 50 mm. Curve I, Ni powder (○); curve II, Ni = 90%, Cu = 10% (●); curve III, Ni = 80%, Cu = 20% (△); curve IV, Ni = 70%, Cu = 30% (□); curve V, Ni = 50%, Cu = 50% (○); curve VI, Ni = 25%, Cu = 75% (△); curve VII, Co powder (●); curve VIII, Cu powder (○).

Can. J. Chem. Downloaded from www.nrcresearchpress.com by 210.87.254.5 on 09/05/12
For personal use only.

Can. J. Chem. Downloaded from www.nrcresearchpress.com by 210.87.254.5 on 09/05/12
For personal use only.

polymerization was observed to take place in the presence of nickel catalysts.

Discussions

While the kinetic studies of Meyer and Burwell (7) were limited to the reaction of deuterium with 2-butyne over palladium–alumina, the studies of Webb and Wells (8) and Phillipson *et al.* (9) related to the hydrogenation of 2-butyne over alumina supported ruthenium, osmium, cobalt, nickel, iron, rhodium, iridium, and platinum. Though Bond (12) studied the shape of the pressure–time curves in detail for acetylene hydrogenation over nickel, and Mann and Khulbe (4–6) for methylacetylene and ethylacetylene hydrogenation for several catalysts, no such studies are reported for 2-butyne hydrogenation. Hence, no direct comparison of the pressure–time curves obtained in this work can be made with those of any published work.

Though the order of the reaction with respect to 2-butyne was zero and nearly independent of temperature for copper and cobalt, it was zero for nickel and nickel–copper alloys at low temperatures (40–60 °C), and became slightly negative with increasing temperatures. Similar behavior was observed by Mann and Khulbe (13) in the hydrogenation of methylacetylene over nickel powder. Phillipson *et al.* (9) observed the order of the reaction with respect to 2-butyne over nickel and copper to be -0.3 and zero. However, no mention is made of the temperature dependence of the reaction.

The first order reaction with respect to hydrogen and zero to slightly negative with respect to 2-butyne indicate that the latter was the more strongly adsorbed reactant, and its surface coverage was high, whereas hydrogen was weakly adsorbed by comparison and its surface coverage was correspondingly low. Yates and Lucchesi (14) also reported that 2-butyne was very strongly adsorbed on alumina surface and that the molecules lay parallel to the surface.

Though the main product in the reaction of hydrogen with 2-butyne was *cis*-2-butene, yet in the initial stages, small amounts of *trans*-2-butene, 1-butene, and *n*-butane were also formed over all the catalysts, except copper. The formation of these products may be due to (*a*) addition of atomic or molecular hydrogen to the hydrocarbon, (*b*) isomerization of *cis*-2-butene, and (*c*) isomerization of 2-butyne.

The addition of atomic or molecular hydrogen could give *cis*-2-butene as follows

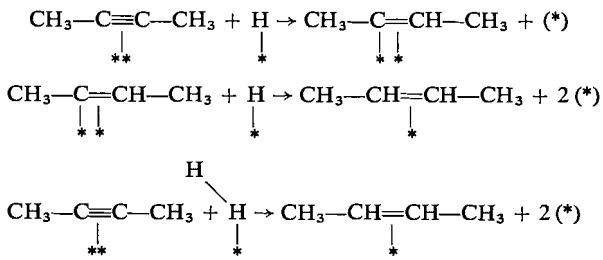

Bond *et al.* (15, 16) proposed a scheme for the isomerization of butenes

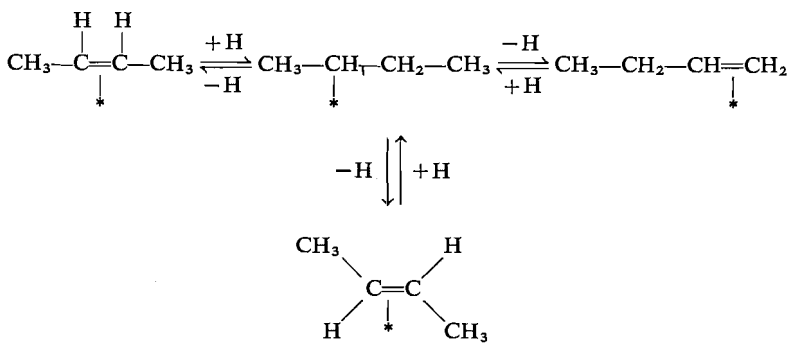

Can. J. Chem. Downloaded from www.nrcresearchpress.com by 210.87.254.5 on 09/05/12
For personal use only.

With few exceptions, it was observed that when *trans*-2-butene was formed, *n*-butane appeared as a product, which provides some evidence for the alkyl reversal mechanism. From the other studies of the hydro-isomerization of butenes (1), one would expect *trans*-2-butene/1-butene ratios greater than one in the product; but in the present study, *trans*-2-butene/1-butene ratios were less than one. It appears therefore that butene isomers were obtained by some other mechanism. It is possible that the half hydrogenated state converts into a radical before it could react with another atom of hydrogen

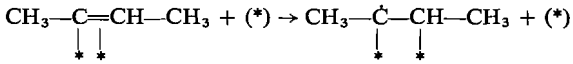

which on further hydrogenation either gives butenes as follows

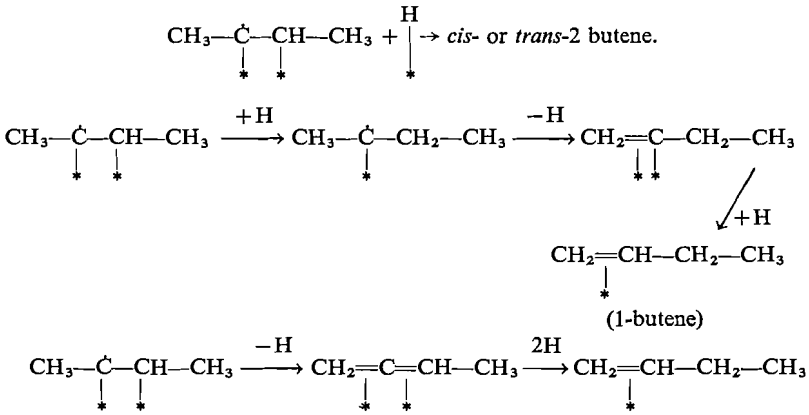

or this radical reacts with adsorbed 2-butyne molecules, giving polymers.

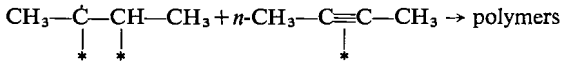

Considering that 2-butyne was strongly adsorbed, its surface coverage was high and that of weakly adsorbed hydrogen correspondingly low, the following mechanism is proposed

[1] 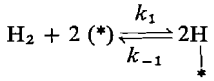

[2] 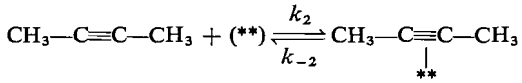

[3] 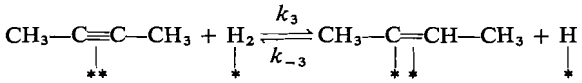

Assuming that $k_1 \gg k_{-1}$ and $k_3 \gg k_{-3}$, as suggested by Bond and Wells (35), from reactions [1] and [3], rate of adsorption of hydrogen = $k_1 P_{H_2}[**] + k_3 P_{H_2}\theta_{C_4H_6}$, where $\theta_{C_4H_6}$ is fraction of surface covered by C_4H_6.

Since $\theta_{C_4H_6} \rightarrow 1$ due to strong adsorption of 2-butyne and the concentration of single and pair of sites remaining constant for a certain pressure of 2-butyne at a particular temperature, the rate of adsorption of hydrogen would be proportional to the fraction of the surface covered by hydrogen (θ_H)

$$\text{as } \theta_H = [k_1[**] + k_3]P_{H_2}$$

$$\theta_H \propto P_{H_2}$$

[4] $CH_3-C\equiv C-CH_3 + H \underset{k_{-4}}{\overset{k_4}{\rightleftharpoons}} CH_3-C=CH-CH_3 + (*)$

[5] $CH_3-C=CH-CH_3 + H \xrightarrow{k_5} CH_3-CH=CH-CH_3 + 2\,(*)$

[6] $CH_3-C=CH-CH_3 + (*) \underset{k_{-6}}{\overset{k_6}{\rightleftharpoons}} CH_3-\dot{C}-CH-CH_3 + (*)$

[7] $CH_3-\dot{C}-CH-CH_3 + H \underset{k_{-7}}{\overset{k_7}{\rightleftharpoons}} CH_3-\dot{C}-CH_2-CH_3 + 2\,(*)$

(unstable)

[8] $CH_3-\dot{C}-CH_2-CH_3 \xrightarrow{k_8} CH_2=CH-CH_2-CH_3 + (*)$

1-butene

Steps [5] and [8] are not shown reversible as (*a*) butene formed in these steps was desorbed and was replaced by 2-butyne and (*b*) adsorbed butene so formed was further hydrogenated to *n*-butane. Rate of formation, R, of C_4H_8 from steps [5] and [8] is therefore

$$[9] \qquad R = k_5\theta_{C_4H_7}\theta_H + k_8\theta_{C_4H_8\cdot}$$

where $\theta_{C_4H_7}$ and $\theta_{C_4H_8\cdot}$ are surface covered by C_4H_7 and $C_4H_8^{\cdot}$, respectively. Applying steady state assumption for C_4H_7, $C_4H_7^{\cdot}$, and C_4H_8

$$[10] \quad k_3\theta_{C_4H_6}P_{H_2} + k_4\theta_{C_4H_6}\theta_H = k_{-3}\theta_{C_4H_7}\theta_H + k_{-4}\theta_{C_4H_7}[*] + k_5\theta_{C_4H_7}\theta_H + k_6\theta_{C_4H_7}[*] - k_{-6}\theta_{C_4H_7\cdot}$$

From reaction [6], [7], and [8]

$$[11] \quad k_6\theta_{C_4H_7}[*] + k_{-7}\theta_{C_4H_8\cdot}[*]^2 = k_{-6}\theta_{C_4H_7\cdot}[*] + k_7\theta_{C_4H_7}\theta_H$$

$$[12] \quad k_7\theta_{C_4H_7\cdot}\theta_H - k_{-7}\theta_{C_4H_8}[*]^2 = k_8\theta_{C_4H_8\cdot}$$

Combining eqs. [11] and [12] with eq. [10], the rate of formation of C_4H_8 is

$$[13] \quad R = k_5\theta_{C_4H_7}\theta_H + k_8\theta_{C_4H_8\cdot} = k_3\theta_{C_4H_6}P_{H_2} - k_{-3}\theta_{C_4H_7}\theta_H + k_4\theta_{C_4H_6}\theta_H - k_{-4}\theta_{C_4H_7}[*]$$

If $\quad k_3\theta_{C_4H_6}P_{H_2} \gg k_{-3}\theta_{C_4H_7}\theta_H$

and $\quad k_4\theta_{C_4H_6}\theta_H \gg k_{-4}\theta_{C_4H_7}[*]$

The rate of reaction $= k_3\theta_{C_4H_6}P_{H_2} + k_4\theta_{C_4H_6}\theta_H$

$\approx k_3P_{H_2} + k_4\theta_H$

$\approx P_{H_2}$, as $\theta_{C_4H_6} \to 1$

The order of reaction reduces to first order, which is in agreement with the experimentally obtained order (Table 1).

The observed negative order in 2-butyne may be due to the fact that at higher pressures, the molecules form a more ordered array on the surface, thus reducing the number of vacant sites, and therefore causing reduced hydrogen adsorption according to reaction [3]. Alternately, an increase in 2-butyne pressure may enable it to compete more effectively with hydrogen for the surface.

The order with respect to 2-butyne was temperature dependent in the case of nickel. Similar results have been obtained by Bond and Wells (2) in acetylene hydrogenation over alumina supported palladium and by Mann and Khulbe (4) for methylacetylene hydrogenation on platinum, palladium, and iridium. An increase in temperature would decrease the amounts of reactants on the surface. Since 2-butyne is generally more strongly adsorbed on the surface than hydrogen, it is possible that with increased temperatures, the desorption of 2-butyne would be less than that of hydrogen resulting in decreased hydrogen/2-butyne ratios on the surface. Hence the order of reaction with respect to 2-butyne becomes more negative with increasing temperatures.

There seems to be no direct relationship between the energy of activation and the copper concentration in the nickel–copper alloys.

However, a "compensation effect" was observed to exist between the various metals and the alloys tested (Fig. 9).

Can. J. Chem. Downloaded from www.nrcresearchpress.com by 210.87.254.5 on 09/05/12
For personal use only.

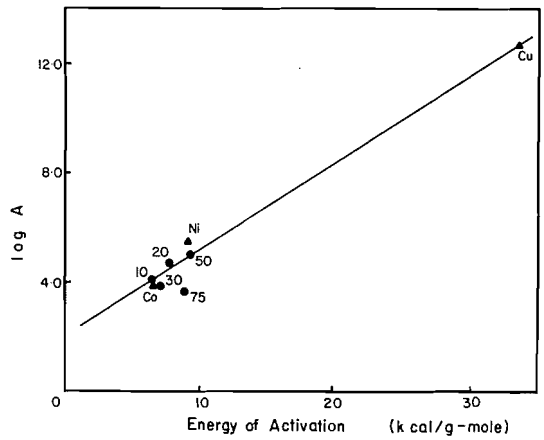

FIG. 9. Energy of activation vs. $\log_{10}$ A (each number shows Cu % in the alloy).

A sudden increase in the activity of the nickel catalyst was observed by the addition of small amounts of copper. The activity seemed to increase with small additions of copper (Fig. 2), pass through a maximum at about 10% copper, and decrease with further addition of copper. Similar phenomenon has been observed by several investigators (3, 11, 17, 18). For pure metals, the activity (specific rate, $min^{-1}g^{-1}$) was in the sequence

$$Ni > Co > Cu$$

According to Dowden *et al.* (19), the catalytic activity of transition metals is due to the holes in the d-band. The most common method to regulate the concentration of holes in d-band is to make alloys. From the X-ray analysis of the alloy catalysts, it was observed that the alloys were homogeneous solid solutions. The catalytic activity of nickel copper alloys in hydrogenation reactions has been the subject of many investigators (20, 21). However, their experimental results have not always agreed with each other. For instance, it has been reported that the catalytic activity decreases progressively, as the concentration of d-holes falls until a sudden decrease marks the filling of the d-band or, in somes cases, it exhibits one or two maxima depending on the catalyst (22). Takai *et al.* (21), who studied the catalytic activities for the liquid phase hydrogenation of maleic acid, allyl alcohol, and acetone over nickel–copper alloys, observed an increase in the catalytic activity on addition of small amounts of copper. They interpreted the activity pattern for the catalysts containing 5–60% copper on the basis of Dowden's theory for maleic acid and allyl alcohol hydrogenation. But in the case of acetone, the activity was independent of d-holes. However, Campbell and Emmett (22), while hydrogenating ethylene over nickel–copper films observed a minimum in the activity – composition curve for the alloy containing approximately 25–30% nickel, which is contradictory to the views of Dowden.

Considering the crystal structure, it was found that the catalytic activity of copper catalyst, having a face centered cubic structure, was nearly zero, whereas nickel having a face centered cubic structure was much more active than copper. Beeck (23) made a systematic study of ethylene hydrogenation on evaporated metals and related the activities of the catalysts to their crystal parameter. Based on the postulation of Beeck, the activity of copper should be much higher than that of nickel, and the activity of the alloy series should increase markedly with increasing copper composition. The results of the present study are contrary to this.

Correlating the catalytic activity with Pauling's % d-character (30) the activity of pure metals should be as follows

$$Ni > Co > Cu$$

The results of the present investigations based on the kinetic studies over pure metals and nickel–copper alloys support the above view except for the appearance of a maximum in the activity – composition pattern at about 10% copper in the alloy.

Takeuchi *et al.* (25) in the hydrogenation of ethylene and benzene observed that though the activity pattern observed over massive nickel–copper alloys was similar to the one predicted by Dowden, it was quite complicated over granular alloys. They have also demonstrated that the heat of adsorption of hydrogen and the catalytic activity of the hydrogenation of ethylene are closely related to the composition of alloys. In another paper (24), Takeuchi tried to correlate the heat of adsorption of hydrogen with the rate of hydrogenation of ethylene and the activation energy. Takai and Yamanaka (21) also observed that the ability of nickel metal to absorb hydrogen increased with increased amount of copper in the nickel copper alloy. Recently, Takeuchi *et al.* (32) measured the electric resistance of the nickel–copper alloys, but they could not get a simple relation between the electric resistance and the catalytic activity. There appears to be no simple

Can. J. Chem. Downloaded from www.nrcresearchpress.com by 210.87.254.5 on 09/05/12
For personal use only.

Can. J. Chem. Downloaded from www.nrcresearchpress.com by 210.87.254.5 on 09/05/12
For personal use only.

relationship between the heats of adsorption of hydrogen and electric resistance with the catalytic activity of metals in 2-butyne hydrogenation.

Sachtler and co-workers (26, 27) studied the surface of nickel–copper alloy films and concluded that there is a general similarity between the work function of alloy films and their catalytic activity. The work of Best and Russell (11), Campbell and Emmett (22), Alexander and Russell (28), Mann and Khulbe (3, 4), and the present work cast some doubt on the general validity of the conclusions of Sachtler and Jongepie. Sachtler and co-workers (26, 27) also observed that the surface composition of the evaporated nickel–copper alloy is not consistent with the over all composition. While Campbell and Emmett (22) observed two phases, one containing pure nickel or copper, and the other nickel–copper alloy containing about 60% copper, Gharpuey and Emmett (33), Best and Russell (11), Mann and Khulbe (3, 4) obtained completely homogeneous alloys. Sachtler and co-workers (26, 27) and Campbell and Emmett (22) prepared evaporated alloy films by depositing metals at less than 200 °C, Best and Russell, and Mann and Khulbe used flow method for the reduction of mixed metal oxides. Takeuchi *et al.* (25) proposed that the concentration of nickel at the surface of the granular alloy differs from that of the interior and the activity is due to the imperfection of the crystal. They have also suggested that the activity factor may best be discussed by taking into account the non-uniform distribution of nickel on the surface. Unfortunately we do not have enough data to support their views.

Considering the concentration of d-holes, Bond and Mann (34) and Mann and Khulbe (3, 4) have suggested three idealized possible forms of activity pattern in the activity composition diagram. In one of the activity patterns, case *B*, it is suggested that as the d-band is filled, the binding strength decreases and the activity increases reaching a maximum before the band is completely filled. As soon as the d-band is completely filled the activity becomes nearly equal to that of copper. This type of pattern has been confirmed by Couper and Eley (31) in the para hydrogen conversion over palladium–gold alloys and by Mann and Khulbe (3) in the methyl acetylene hydrogenation over nickel–copper alloy powders. In the present study, the results are also very similar. However, some of the opposing effects may lead to an earlier maximum. It may be possible that the physical properties of the reactants and their structure also play an important role in the activity pattern besides the method of preparation of the catalysts and the structure of the alloys. Considering d-hole concentration (as in case *B*) for pure metals, the activity pattern should be in the following sequence

$$\text{Ni} > \text{Co} > \text{Cu}$$

This agrees with the results obtained in the present investigations.

It was observed that the selectivity decreased with increasing amounts of copper in the nickel–copper alloy, reaching a minimum at 20% copper, while the activity increased to a maximum at about 10% copper. Generally the selectivity should be dependent on the activity. However, it was not so in this case. It appears that besides activity, some other factors, such as different type of active centers, crystal imperfections, may play an important role in controlling the selectivity.

At equimolal ratio of hydrogen and 2-butyne, while the yield of *cis*-2-butene (Table 4) decreased slightly with increased copper concentration, that of 1-butene increased. The ratio of *trans*-2-butene/1-butene was always less than one, indicating that the formation of 1-butene was not only due to alkyl reversal mechanism. As the concentration of 2-butyne at the surface was greater than that of hydrogen, there is a possibility that the half hydrogenated state converts into a radical before reacting with another adsorbed hydrogen. This radical could give either butenes by reacting with adsorbed hydrogen or polymers by reacting with adsorbed 2-butyne molecule. The absence of *n*-butane in the product at higher copper concentration indicates that the rate of desorption of butenes increased. However, as the rate of adsorption of 2-butyne was greater than the rate of desorption, the rate of free radical formation or polymerization increased.

Cobalt powder was more active than copper, but less active than nickel. The polymerization was highest in the case of copper and least in the case of nickel, which suggests that the extent of polymerization depends on the atomic radius of the metals. The energy of activation was least for cobalt and highest for copper. The kinetics of the hydrogenation of 2-butyne over nickel, cobalt, and copper powder was the same,

suggesting thereby that the reaction mechanism over these metals is the same.

The authors are grateful to the National Research Council of Canada for financial aid (A-1125) for the project and Mr. John F. Rowland and Mr. R. K. Collings of Energy, Mines and Resources, for X-ray and surface area determinations.

1. G. C. Bond and P. B. Wells. Advan. Catal. **15**, 91 (1965).
2. G. C. Bond and P. B. Wells. J. Catal. **6**, 397 (1966).
3. R. S. Mann and K. C. Khulbe. Can. J. Chem. **45**, 2755 (1967).
4. R. S. Mann and K. C. Khulbe. Can. J. Chem. **47**, 215 (1969).
5. R. S. Mann and K. C. Khulbe. J. Catal. **10**, 401 (1968).
6. R. S. Mann and K. C. Khulbe. J. Catal. **13**, 25 (1969).
7. E. F. Meyer and R. L. Burwell. J. Amer. Chem. Soc. **85**, 2881 (1963).
8. G. Webb and P. B. Wells. Trans. Faraday Soc. **61**, 1232 (1965).
9. J. J. Phillipson, P. B. Wells, and D. W. Gray. Proc. Intern. Congr. Catal. 3rd. Amsterdam, **2**, 1250 (1964).
10. R. S. Mann and S. C. Naik. Can. J. Chem. **45**, 1023 (1967).
11. R. J. Best and W. W. Russell. J. Amer. Chem. Soc. **85**, 2881 (1963).
12. G. C. Bond. J. Chem. Soc. 2705 (1968).
13. R. S. Mann and K. C. Khulbe. Can. J. Chem. **46**, 623 (1968).
14. D. J. C. Yates and P. J. Lucchesi. J. Chem. Phys. **35**, 243 (1961).
15. G. C. Bond, J. J. Phillipson, P. B. Wells, and Winterbottom. Trans. Faraday Soc. **62**, 443 (1966).
16. G. C. Bond, G. Webb, and P. B. Wells. Trans. Faraday Soc. **64**, 3077 (1968).
17. G. M. Schwab and W. Brennecke. Z. Phys. Chem. Leipzig, **B24**, 393 (1933).
18. W. K. Hall and P. H. Emmett. J. Phys. Chem. **63**, 1102 (1959).
19. D. A. Dowden and P. W. Reynolds. Discuss. Faraday Soc. **8**, 184 (1950).
20. E. Takai. Sci. Pap. Inst. Phys. Chem. Res. Jap. **62**, 24 (1968).
21. E. Takai and T. Yamanaka. Sci. Pap. Inst. Phys. Chem. Res. Jap. **55**, 194 (1961).
22. J. B. Campbell and P. H. Emmett. J. Catal. **7**, 252 (1967).
23. O. Beeck. Rev. Mod. Phys. **17**, 61 (1945).
24. T. Takeuchi. Bull. Chem. Soc. Jap. **38**, 322 (1965).
25. T. Takeuchi, M. Sakaguchi, I. Miyoshi, and T. Takabatake. Bull. Chem. Soc. Jap. **35**, 1390 (1962).
26. W. M. H. Sachtler and G. J. H. Dorgelo. J. Catal. **4**, 645 (1965).
27. W. M. H. Sachtler and R. Jongepier. J. Catal. **4**, 665 (1965).
28. E. G. Alexander and W. W. Russell. J. Catal. **4**, 184 (1965).
29. W. K. Hall. J. Catal. **4**, 184 (1965).
30. L. Pauling. Phys. Rev. **54**, 899 (1938); Proc. Roy. Soc. London, **A196**, 343 (1938).
31. A. Couper and D. D. Eley. Discuss. Faraday Soc. **8**, 172 (1950).
32 T. Takeuchi, Y. Tezucka, and O. Takayasu. J. Catal. **14**, 126 (1969).
33. M. K. Gharpuey and P. H. Emmett. J. Phys. Chem. **65**, 1182 (1961).
34. G. C. Bond and R. S. Mann. J. Chem. Soc. 3566 (1959).
35. G. C. Bond and P. B. Wells. J. Catal. **4**, 211 (1965).

Can. J. Chem. Downloaded from www.nrcresearchpress.com by 210.87.254.5 on 09/05/12
For personal use only.

Can. J. Chem. Downloaded from www.nrcresearchpress.com by 210.87.254.40 on 09/05/12
For personal use only.

Infrared studies of some *N*-methylacetamide complexes[1]

Y. H. SHAW AND N. C. LI
Chemistry Department, Duquesne University, Pittsburgh, Pennsylvania 15219

Received January 7, 1970

Hydrogen bonding of *N*-methylacetamide (NMA) with dimethylsulfoxide (DMSO) and *N*,*N*-dimethylacetamide (DMA) in carbon tetrachloride and $CCl_4/CHCl_3$ mixed solvent was studied by a near-infrared method, which consists of measuring the effects of various concentrations of DMSO or DMA on the molar absorptivity of 0.06 *M* NMA at 6800 cm^{-1}, corresponding to the first overtone of the uncomplexed NH stretching vibration. The association constants for the formation of 1:1 NMA–DMA and NMA–DMSO complexes in CCl_4 are 10 and 12 l/mole, respectively, at 25°. In order to obtain an association constant for the formation of NMA–DMSO in $CCl_4/CHCl_3$ mixed solvent, it is necessary to have data on association constants of $CHCl_3$–DMSO complexes in CCl_4, and we have obtained these by determining the effects of various concentrations of DMSO on the proton magnetic resonance frequency of 0.05 *M* $CHCl_3$ in CCl_4. The association constants for the formation of NMA–DMSO and NMA–DMA in $CCl_4/CHCl_3$ mixed solvent are slightly higher than in CCl_4, presumably due to hydrogen bonding between Cl_3CH and C=O in NMA. NMA was chosen as the simplest molecule containing the peptide amide group and hence can be regarded as a structural unit of the polypeptide chain. Our results show that DMSO and DMA are effective in disrupting the interamide bonds, by acting as hydrogen acceptors to the NH group.

Canadian Journal of Chemistry, **48**, 2090 (1970)

Introduction

Self-association of *N*-methylacetamide (NMA) has been reported by several investigators (1–3). Li *et al.* (4–7) have studied hydrogen bonding using NMA as a hydrogen acceptor to thiols, 2-propanol, amines, and hindered phenols by nuclear magnetic resonance (n.m.r.) spectroscopy in carbon tetrachloride solutions. These compounds have hydrogen-donor groups which disrupt interamide hydrogen bonds by forming bonds with C=O of NMA. It would be of interest to use NMA as a hydrogen donor and choose several hydrogen acceptors which will compete with the self-association of NMA to form hydrogen bonds and to obtain the equilibrium constants of the hydrogen-bonded complexes. The NMA was chosen as the simplest molecule containing the peptide amide group and hence can be regarded as a model structural unit of the polypeptide chain.

The near-infrared absorption spectra of NMA have been reported (1–3). In CCl_4 solutions, NMA at 0.01 *M* shows a single peak at 1.47 μ (6800 cm^{-1}), corresponding to the first overtone of the NH stretching vibration. The intensity of this band decreases with increasing concentration of NMA and a new double-peaked band appears between 1.5–1.6 μ. In the pure liquid, only bands at 1.52 and 1.58 μ, due to the associated molecules, were observed. In a solution of a given concentration the 1.47 μ band increases in intensity and at the same time the 1.52 and 1.58 μ bands become weaker when the temperature is raised. It was concluded that the first overtone monomeric NH stretching occurs at 1.47 μ, the associated NH at 1.52 and 1.58 μ. Of the two associated NH bands, it is possible that the 1.52 μ band is due to the overtone of the NH stretching vibration, and the 1.58 μ band may be due to a combination between the NH stretching vibration and two quanta of the NH deformation vibration.

In any solvent, the environment of the NH group of NMA changes if it forms a hydrogen bond with a hydrogen acceptor. One would expect therefore that both infrared (i.r.) and n.m.r. methods can be used for the study of hydrogen bonding involving NMA as a hydrogen donor. Unfortunately, the NH proton signal in n.m.r. becomes too broad at concentrations below 0.4 *M*, to be measured accurately. The n.m.r. technique was, therefore, not feasible, and we carried out near-infrared studies in the overtone range (1.36–1.6 μ). *N*,*N*-Dimethylacetamide (DMA) and dimethylsulfoxide (DMSO) were used as hydrogen acceptors, with carbon tetrachloride and $CCl_4/CHCl_3$ as solvents.

Takahashi and Li (7) have reported the hydrogen-bond formation constants of chloroform with NMA and DMA in CCl_4. Based on

[1]This investigation was supported by Public Health Service Grant No. GM 10539-07 and by National Science Foundation Grant No. GB-8237.

Can. J. Chem. Downloaded from www.nrcresearchpress.com by 210.87.254.40 on 09/05/12
For personal use only.

their data, the formation constants are interpolated to be 0.47 and 0.89 l/mole, respectively, at 25°. However, there has been no report on hydrogen bonding between chloroform and DMSO in CCl_4. Since this information is useful for any system containing $CHCl_3$ and DMSO in CCl_4, we have applied the n.m.r. method to study hydrogen bonding between chloroform and DMSO in CCl_4 at different temperatures by using the method described by Mathur *et al.* (8). The results are also included in this paper.

Experimental

Spectroscopic Equipment and Materials

All of the spectra in the first overtone NH stretching band region were obtained with a Cary Model 14 spectrophotometer, using 10 cm cells for solutions containing CCl_4 as solvent, and 5 cm cells for $CCl_4/CHCl_3$ as solvent. The sample and reference cells were placed in jacketed cell holders connected to a constant-temperature bath. The temperature inside the cell compartment was checked with an iron-constantan thermocouple before and after each measurement.

The NMA and DMA, obtained from Eastman Organic Chemicals, were distilled under nitrogen and collected at 205–206° and 164–165°, respectively. Chloroform was purified by shaking with concentrated sulfuric acid, distilled water, and dried over calcium chloride. It was then distilled and the fraction boiling at 60° was collected. The DMSO was treated with sodium hydroxide and distilled under vacuum. All the purified materials were stored over Linde molecular sieve.

Sample Preparation

Stock solutions of NMA, DMA, and DMSO in CCl_4 were prepared. The final concentration of NMA in solutions containing DMSO or DMA was kept at 0.06 *M*, and the concentrations of DMSO or DMA were varied in the range of 0.6–1.3 *M*. The concentration of chloroform in the $CCl_4/CHCl_3$ mixed solvent varied from 6 to 10 *M*. Solutions containing chloroform were always freshly prepared and used within 5 days from the day the chloroform was purified. The sample and reference solutions contained the same concentration of the DMSO and DMA, and for the mixed solvent, the same concentration of $CHCl_3$, except that NMA was placed in the sample cells and not in the reference cells.

Nuclear Magnetic Resonance Measurements

The n.m.r. spectra were obtained with a Varian A-60 spectrometer. Chemical shifts of the CH signal in $CHCl_3$ were measured with respect to tetramethylsilane (TMS) as internal reference. At temperatures below room temperature, the Varian low temperature kit together with the variable temperature controller was used. The temperatures remained constant to within ± 1° during the measurements. The accuracy in measuring the peak position of the CH proton signal is estimated to be ± 0.3 Hz.

Association Constants

In the NMA–D–CCl_4 system, where D = DMSO or DMA, and where the concentration of D is more than ten times greater than the NMA concentration, we have assumed that the significant interaction is the formation of the 1:1 NMA–D complex. Since the band at 1.47 μ corresponds to the free uncomplexed NMA only we, have obtained the molar absorptivity, E_f, for the free monomeric NMA by constructing a graph of apparent absorptivity, E_a, at 1.47 μ vs. concentration of NMA in CCl_4 and extrapolating to zero concentration, at which point all of the solute should be in the monomeric state. The value thus obtained in CCl_4, 2.12 cm^{-1} l $mole^{-1}$, is in good agreement with that reported by Klotz and Franzen (1).

For an equilibrium between a monomeric hydrogen donor, N, and a hydrogen acceptor, D, to form a 1:1 complex, ND, the eq. [1] may be derived when $c_D^\circ \gg$ [ND] and assuming that the Beer–Lambert law holds.

$$[1] \qquad \frac{1}{E_f - E_a} = \frac{1}{E_f} + \frac{1}{E_f}\frac{1}{Kc_D^\circ}$$

In eq. [1], c_D° is the total concentration of D and K is the association constant for the formation of the NMA–D complex. Equation [1] is similar to eq. [1] of Takahashi *et al.* (9), taking the molar absorptivity of the hydrogen-bonded species, ND, to be zero at 1.47 μ. It must be mentioned that Mizushima *et al.* (2), have shown that NMA takes only the *trans* form, so that the calculated association constants are for the *trans* form only.

For mixed solvent of carbon tetrachloride and chloroform, in which $c_{CHCl_3} \gg c_{CHCl_3\text{-}D}$ and $c_D^\circ \gg c_{NMA}^\circ$, a modified form of eq. [1] is obtained, which is similar to eq. [8] of Takahashi *et al.* (9). In eq. [2], K_s is the association constant for the formation of the chloroform–D

$$[2] \qquad \frac{1}{E_f - E_a} = \frac{1}{E_f} + \frac{1}{E_f}\frac{1 + K_s c_{CHCl_3}}{K}\frac{1}{c_D^\circ}$$

complex, and E_f is the molar absorptivity for the monomeric NMA (uncomplexed by D), and was again obtained by constructing a graph of E_a at 1.47 μ vs. concentration of NMA in the $CCl_4/CHCl_3$ mixed solvent and extrapolating to zero concentration. The absorbancy at 1.47 μ for a given NMA concentration in the mixed solvent is independent of the $CHCl_3$ concentration in the range c_{CHCl_3} = 6.90 to 9.85 *M*, and E_f is determined to be 1.88 cm^{-1} l $mole^{-1}$.

Duplicate experiments were carried out and the uncertainty in absorbance values was found to be 0.01. The estimated errors in the calculated association constants are about ± 1 l $mole^{-1}$.

Results and Discussion

Table 1 lists the apparent molar absorptivities of 0.06 *M* NMA in the presence of various concentrations of D in CCl_4 at 25° for 1.47 μ. Linear plots of $1/(E_f - E_a)$ vs. $1/c_D^\circ$ according to eq. [1] are obtained, from which the values of K are determined to be 10 and 12 l $mole^{-1}$, for D =

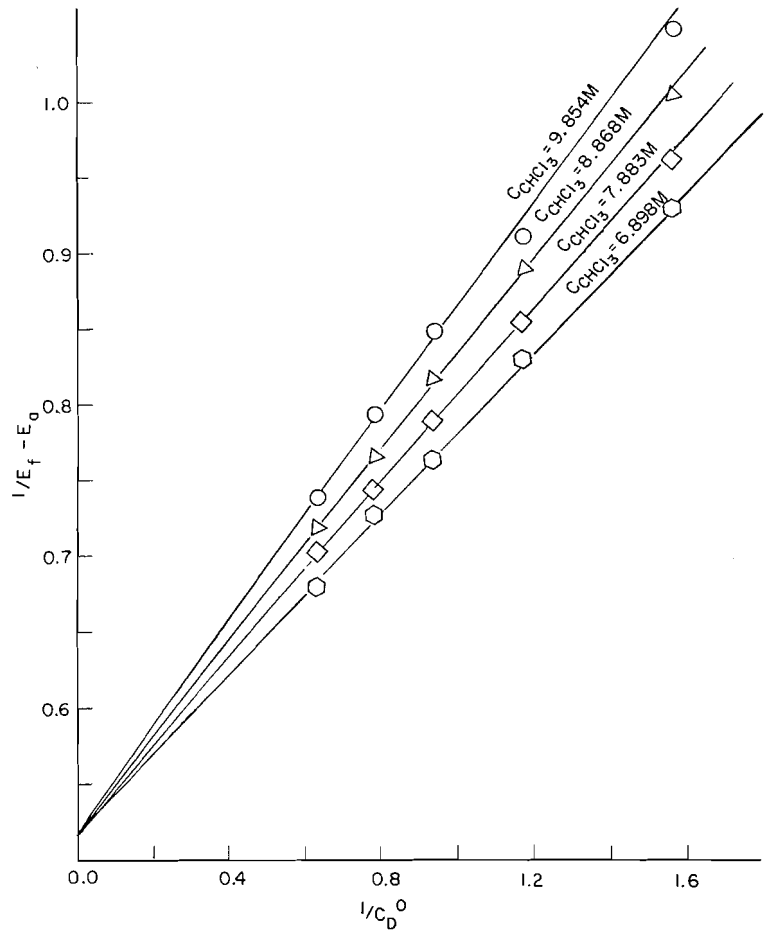

FIG. 1. Plots of $1/(E_f - E_a)$, measured at 1.47 μ and 25° vs. reciprocal concentration of DMA in $CCl_4/CHCl_3$ mixed solvent (c_{CHCl_3} is the concentration of chloroform in the mixed solvent).

DMA and DMSO, respectively. Both plots yield the same intercept, from which E_f is calculated to be 2.1, in excellent agreement with the extrapolated value from a E_a vs. c_{NMA}° (in the absence of D) plot. The apparent absorptivities can be calculated on the basis of eq. [3] which is

$$E_a = E_f/(1 + Kc_D^\circ) \quad [3]$$

equivalent to eq. [1] and are included in Table 1. The agreement in E_a is satisfactory.

Figure 1 gives plots of $1/(E_f - E_a)$ vs. $1/c_D^\circ$ (D = DMA) for different values of c_{CHCl_3} in the

TABLE 1

Absorptivity of NMA (0.06 *M* in CCl_4) in the presence of various concentrations, c_D°, of DMSO or DMA in CCl_4 at 25°, 1.47 μ

	E_a			E_a	
c_D° (DMSO)	Observed	Calculated	c_D° (DMA)	Observed	Calculated
1.139	0.15	0.15	1.285	0.16	0.15
0.978	.18	.17	1.064	.19	.18
.838	.20	.19	0.857	.22	.22
.699	.23	.23	.643	.28	.29

Can. J. Chem. Downloaded from www.nrcresearchpress.com by 210.87.254.40 on 09/05/12
For personal use only.

Can. J. Chem. Downloaded from www.nrcresearchpress.com by 210.87.254.40 on 09/05/12
For personal use only.

TABLE 2

Absorptivity of 0.06 *M* NMA in $CCl_4/CHCl_3$ mixed solvent in the presence of various concentrations, $c_D°$, of DMSO and DMA at 25°, 1.47 μ

		c_{CHCl_3}							
		9.854 E_a		8.868 E_a		7.883 E_a		6.898 E_a	
	$c_D°$	Observed	Calculated*	Observed	Calculated	Observed	Calculated	Observed	Calculated
DMA	1.583	0.52	0.53	0.49	0.50	0.45	0.46	0.40	0.42
	1.284	.62	.62	.57	.58	.53	.54	.50	.49
	1.070	.70	.69	.65	.65	.61	.61	.57	.56
	0.856	.78	.79	.75	.75	.71	.70	.67	.65
	.642	.92	.93	.88	.88	.84	.83	.80	.78
DMSO	1.677	0.55	0.55	0.52	0.51	0.48	0.47	0.43	0.43
	1.285	.67	.66	.63	.62	.59	.57	.54	.53
	0.838	.86	.85	.84	.81	.79	.76	.73	.70

*E_a calculated from eq. [4]. The parameters used were: $E_f = 1.88$, K_s ($CHCl_3$–DMSO) = 1.06, K_s ($CHCl_3$–DMA) = 0.89, K (NMA–DMSO) = 16.5, K (NMA–DMA) = 15.6.

TABLE 3

Observed CH chemical shifts for 0.05 M $CHCl_3$ in the presence of various concentrations of DMSO in CCl_4

Temperature							
30°		19.5°		4.5°		−9.0°	
$c_D°$	Hz from TMS	$c_D°$	Hz from TMS	$c_D°$	Hz from TMS	$c_D°$	Hz from TMS
0	434.3	0	434.7	0	435.1	0	435.5
0.306	448.2	0.310	450.0	0.314	452.4	0.319	454.6
.612	456.5	.616	459.2	.627	461.6	.637	464.2
.765	459.4	.770	462.1	.784	464.7	.796	467.7
.918	461.8	.924	465.0	.941	467.3	.955	470.7
1.376	468.2	1.385	471.0	1.410	473.1	1.433	475.6
$K_s = 0.99$		$K_s = 1.15$		$K_s = 1.30$		$K_s = 1.49$	
$\Delta H = -1.6$ kcal/mole							

TABLE 4

Summary of constants, 25°

Solvents	Constant	D = DMA	D = DMSO
CCl_4	K_{NMA-D}	10	12 l/mole
	K_{CHCl_3-D}	0.89*	1.06 l/mole
	ΔH_{CHCl_3-D}	−1.1*	−1.6 kcal/mole
$CCl_4/CHCl_3$†	K_{NMA-D}	15.6	16.5 l/mole

*Taken from ref. (7).
†In the range $c_{CHCl_3} = 6.9$–9.9 M.

$CCl_4/CHCl_3$ mixed solvent. Table 2 lists the apparent molar absorptivities of 0.06 M NMA in the presence of various concentrations of D in the $CCl_4/CHCl_3$ mixed solvent, in which the chloroform concentration is c_{CHCl_3}. The apparent absorptivities can be calculated on the basis of eq. [4] which is equivalent to eq. [2] and are

$$[4] \qquad E_a = \frac{E_f(1 + K_s c_{CHCl_3})}{K c_D{}^0 + (1 + K_s c_{CHCl_3})}$$

included in Table 2. The values of K_s for the formation of $CHCl_3$–DMA and $CHCl_3$–DMSO complexes in CCl_4 are taken to be 0.89 and 1.06 l $mole^{-1}$, respectively. The former value is taken from ref. 7, and the latter value is obtained from the n.m.r. data to be discussed next. It was found that the values of K which give good agreement between the calculated and observed E_a values are 15.6 and 16.5 l $mole^{-1}$ respectively for the NMA–DMA and NMA–DMSO complexes in the mixed solvent, in the range c_{CHCl_3} = 6.90 to 9.85 M. These association constants are slightly higher than the values obtained in CCl_4, because in the mixed solvent, the $CHCl_3$ proton is hydrogen bonded to C=O in NMA.

The value of K_s for the formation of $CHCl_3$–DMSO in CCl_4 was determined by measuring the chloroform proton signal in CCl_4 solutions containing 0.05 M $CHCl_3$ and various concentrations of DMSO at four different temperatures, and the data treated according to Mathur *et al.* (8). Table 3 lists the results obtained. Linear plots of $1/(\nu - \nu_f)$ vs. $1/c_D°$ at different temperatures (with the same intercept) and linear plots of log K_s vs. $1/T$ were obtained. The values of K_s at the different temperatures and ΔH are included in Table 3. The value of K_s at 25° is interpolated to be 1.06, and was used in the calculation of E_a in NMA–DMSO–$CCl_4/CHCl_3$ system according to eq. [4].

Table 4 summarizes the results obtained for NMA and $CHCl_3$ bonded to DMSO and DMA. It can be seen that in every respect DMSO is a slightly better hydrogen acceptor than DMA. Both DMSO and DMA effectively disrupt the self-association of NMA and serve as acceptors to the NH of NMA.

1. I. M. Klotz and J. S. Franzen. J. Amer. Chem. Soc. **84**, 3461 (1962).
2. S. Mizushima, T. Simanouti, S. Nagakura, K.

Can. J. Chem. Downloaded from www.nrcresearchpress.com by 210.87.254.40 on 09/05/12
For personal use only.

KURATANI, M. TSUBOI, H. BABA, and O. FUJIOKA. J. Amer. Chem. Soc. **72**, 3490 (1950).
3. M. DAVIES, J. C. EVANS, and R. C. JONES. Trans. Faraday Soc. **51**, 761 (1955); M. DAVIES and D. K. THOMAS. J. Phys. Chem. **60**, 767 (1956).
4. R. MATHUR, S. M. WANG, and N. C. LI. J. Phys. Chem. **68**, 2140 (1964).
5. F. TAKAHASHI and N. C. LI. J. Phys. Chem. **68**, 2136 (1964).
6. F. TAKAHASHI and N. C. LI. J. Phys. Chem. **69**, 1622 (1965).
7. F. TAKAHASHI and N. C. LI. J. Phys. Chem. **69**, 2950 (1965).
8. R. MATHUR, E. D. BECKER, R. B. BRADLEY, and N. C. LI. J. Phys. Chem. **67**, 2190 (1963).
9. F. TAKAHASHI, W. J. KAROLY, J. B. GREENSHIELDS, and N. C. LI. Can. J. Chem. **45**, 2033 (1967).

Can. J. Chem. Downloaded from www.nrcresearchpress.com by 210.87.254.40 on 09/05/12
For personal use only.

Can. J. Chem. Downloaded from www.nrcresearchpress.com by 210.87.254.5 on 09/05/12
For personal use only.

Infrared studies of water in crystalline hydrates: $NaClO_4 \cdot H_2O$, $LiClO_4 \cdot 3H_2O$, and $Ba(ClO_4)_2 \cdot 3H_2O$[1]

GEORGE BRINK[2] AND MICHAEL FALK
Atlantic Regional Laboratory, National Research Council of Canada, Halifax, Nova Scotia

Received December 5, 1969

Infrared spectra of undeuterated and partially deuterated $NaClO_4 \cdot H_2O$, $LiClO_4 \cdot 3H_2O$, and $Ba(ClO_4)_2 \cdot 3H_2O$ were examined. Crystallographic data point to a weak hydrogen bond between water molecules and the perchlorate ions in $LiClO_4 \cdot 3H_2O$. This is confirmed by the high HDO stretching frequencies for this compound. The nearly identical HDO stretching frequencies in $LiClO_4 \cdot 3H_2O$, $NaClO_4 \cdot H_2O$, $Ba(ClO_4)_2 \cdot 3H_2O$, and in aqueous solutions of these salts show that similar weak hydrogen bonds occur in all three hydrates and in solution. The hydrogen bond energy is of the order of 2 kcal/mole. In all three compounds the water molecules are symmetric at room temperature. At $-165°$ the water molecules become highly distorted in the sodium compound, slightly distorted in the barium compound, and remain undistorted in the lithium compound. Very narrow OD stretching bands are observed, showing that the hydrogen atom positions are ordered in all three hydrates.

Canadian Journal of Chemistry, 48, 2096 (1970)

Introduction

The broad bands near 3400 cm^{-1} (OH stretching) and near 2500 cm^{-1} (OD stretching) in the infrared (i.r.) spectrum of HDO[3] in solutions of electrolytes differ only slightly from the corresponding bands of HDO in liquid water (1, 4, 6). The solutions of perchlorate salts appear exceptional in that an additional band appears near 3575 cm^{-1} for OH stretching and near 2630 cm^{-1} for OD stretching (4, 7–10). The origin of this high-frequency band is of considerable interest (7–10).

We have now investigated the spectra of HDO in partly deuterated hydrates of sodium, lithium, and barium perchlorate to determine whether the high-frequency stretching band occurs in crystals as well as in solution. In addition, we have examined the spectra to determine the symmetry of the water molecules in the crystal. The previous i.r. studies of these compounds (refs. 11, 12, and references therein) dealt largely with the bands of the perchlorate ion. A Raman study of undeuterated $LiClO_4 \cdot 3H_2O$ has been published by Mathieu and Couture–Mathieu (13, 14).

Experimental

Samples of $NaClO_4 \cdot H_2O$, $LiClO_4 \cdot 3H_2O$, and $Ba(ClO_4)_2 \cdot 3H_2O$ (obtained from G. F Smith Chemical Co., Columbus, Ohio) were recrystallized from aqueous solutions at room temperature. The monohydrate of sodium perchlorate and the trihydrates of lithium perchlorate and barium perchlorate are known to crystallize under these conditions (15).

A solution of 1.5 mole % D_2O in H_2O was used to prepare the crystals for the study of the OD stretching vibration of HDO. The OH stretching vibration of HDO was also studied for $NaClO_4 \cdot H_2O$; for this preparation a solution of 1 mole % of H_2O in D_2O was used. However, because of rapid isotopic exchange with atmospheric moisture, particularly in the preparation of the mulls, this low H:D ratio could not be maintained easily. The higher H:D ratios caused asymmetry and broadening of the OH band profile of HDO; the peak frequencies were not affected. As the OD and OH vibrations of isotopically dilute HDO contain essentially the same information, the OH stretching vibrations of the Li and Ba perchlorate hydrates were not studied. A 30 mole % solution of H_2O in D_2O was used to prepare the crystals for the study of the isolated H—O—H bending vibration of isotopically dilute H_2O in $NaClO_4 \cdot H_2O$. The resulting isotopic concentrations were calculated to be 9 mole % H_2O, 42 mole % HDO, and 49 mole % D_2O, assuming a random distribution of H and D throughout the crystal. The H:D ratios for the hydrated crystals were assumed to be the same as those of the parent solution, and are therefore only approximate.

Crystals were studied as mulls between two CaF_2 or AgCl plates using a perhalocarbon oil (Fluorolube). They could not be studied in a KBr matrix because part of the water of crystallization was lost to the matrix.

We have also obtained spectra of the hydrate crystals prepared by the evaporation of a drop of saturated solution on a CaF_2 plate under a stream of nitrogen. These spectra were of poorer quality than those of mulls, but gave the same frequencies at all temperatures. This shows that the grinding in the preparation of mulls caused no structural changes in the crystals.

Spectra were recorded on a Perkin–Elmer model 521 spectrophotometer purged with dry nitrogen. Use of an automatic frequency marker makes it possible to measure the frequency of sharp peaks to within 0.5 cm^{-1}. A

---

[1]Issued as NRCC No. 11304.
[2]NRCC Postdoctorate Fellow, 1968–1970.
[3]Isotopically dilute HDO has a far simpler vibrational spectrum than H_2O or D_2O, hence is preferable in structural studies (1–5).

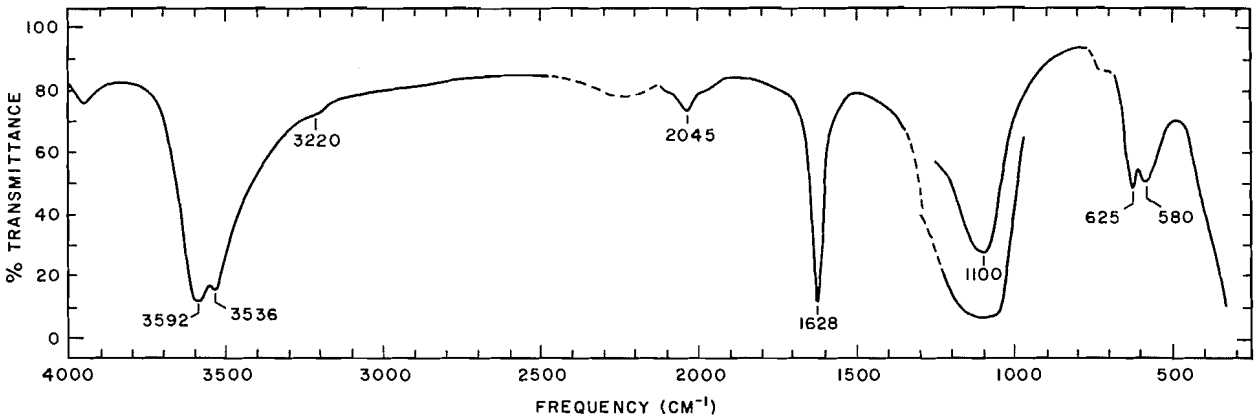

FIG. 1. Spectrum of undeuterated $NaClO_4 \cdot H_2O$. Mull in Fluorolube above 1300 cm^{-1} and in Nujol below 1300 cm^{-1}. Silver chloride windows. Broken lines denote regions of absorption of the mulling agent.

variable temperature cell (model VLT-2, Research and Industrial Company, London) was used for the low temperature spectra. Temperatures were measured with a copper-constantan thermocouple and are accurate to within 2 °C. The effective slit width used for the sharp OD stretching bands was less than 0.5 cm^{-1}.

Results

Spectra of Undeuterated Hydrates

The major features in the spectra of undeuterated $LiClO_4 \cdot 3H_2O$, $Ba(ClO_4)_2 \cdot 3H_2O$, and $NaClO_4 \cdot H_2O$ are very similar. The spectrum in the range 4000 to 300 cm^{-1} consists of bands due to the vibrations of water molecules and perchlorate ions.

Figure 1 shows the spectrum of undeuterated $NaClO_4 \cdot H_2O$ at room temperature. The bands at 3592 and 3536 cm^{-1} are due to the stretching vibrations of H_2O. It is possible that the more intense 3592 cm^{-1} peak corresponds to the ν_3 fundamental and the 3536 cm^{-1} peak to the ν_1 fundamental. However, this assignment is uncertain, since ν_3 and ν_1 may each have several components due to the coupling of vibrations of neighboring H_2O molecules in the crystal. It should be stressed that the stretching fundamentals ν_1 and ν_3 of H_2O in the crystal are not simply the symmetric and antisymmetric stretching vibrations if the H_2O molecule is asymmetric, which is the case for $NaClO_4 \cdot H_2O$ and $Ba(ClO_4)_2 \cdot 3H_2O$ at low temperatures. A detailed discussion of the effect of an asymmetric crystalline site on the fundamental vibrations of the H_2O molecule has been given by Schiffer (16). The band at 1628 cm^{-1} is due to ν_2, the HOH bending vibration. The remaining bands due to H_2O are: ν_R, the band of librational frequencies, centered near 580 cm^{-1}, the overtone band $2\nu_2$ at about 3220 cm^{-1}, and a weak band near 2000 cm^{-1} due to the combination band $\nu_2 + \nu_R$ (overlapped by the perchlorate band at 2045 cm^{-1}). All these bands undergo the usual frequency shifts upon deuteration. At low temperatures (−165°) the HOH bending frequency shifts to about 1615 cm^{-1}; the stretching frequencies shift very slightly. Bands due to the perchlorate ion are observed at 1100 and 625 cm^{-1}; the first overtone of the 1100 cm^{-1} frequency occurs as a weak band at 2045 cm^{-1}. At low temperature additional bands appear at 951 cm^{-1} (singlet) and at 478 and 440 cm^{-1} (doublet). Our band shapes and relative intensities agree with the spectrum of $NaClO_4 \cdot H_2O$ published by Wood (17), who did not report band frequencies. Our frequencies of the perchlorate ion agree reasonably well with those of Hezel and Ross (12), except that these authors resolved four features in the region of the 1100 cm^{-1} band.

The spectra of undeuterated $Ba(ClO_4)_2 \cdot 3H_2O$ and $LiClO_4 \cdot 3H_2O$ are very similar to those of $NaClO_4 \cdot H_2O$ and are not shown. The stretching vibrations of H_2O at room temperature give rise to peaks at 3579 and 3529 cm^{-1} for the Ba compound and at 3560 and 3519 cm^{-1} for the Li compound. The bending vibrations give rise to peaks at 1619 and 1620 cm^{-1}, respectively. The perchlorate bands for the Ba compound are at about 1100 cm^{-1}, and a doublet at 626 and 643 cm^{-1}. For the Li compound the perchlorate bands are at about 1100 and at 622 cm^{-1}. At low temperature additional bands were observed at about

Can. J. Chem. Downloaded from www.nrcresearchpress.com by 210.87.254.5 on 09/05/12
For personal use only.

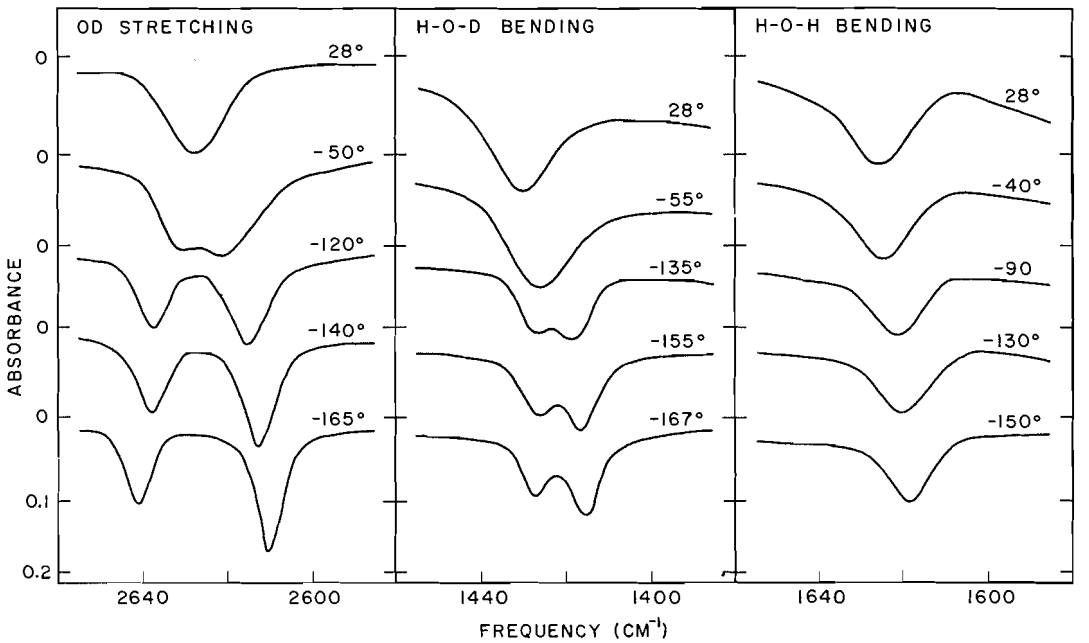

FIG. 2. Spectra of partially deuterated $NaClO_4 \cdot H_2O$ in the OD stretching and H—O—D bending region (H:D = 99:1), and in the H—O—D bending region (H:D = 30:70). Mulls in Fluorolube.

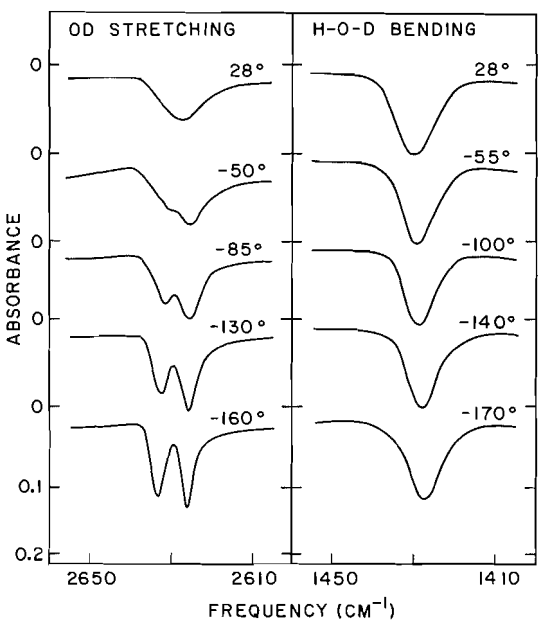

FIG. 3. Spectra of partially deuterated $Ba(ClO_4)_2 \cdot 3H_2O$ in the OD stretching and H—O—D bending regions (H:D = 99:1). Mulls in Fluorolube.

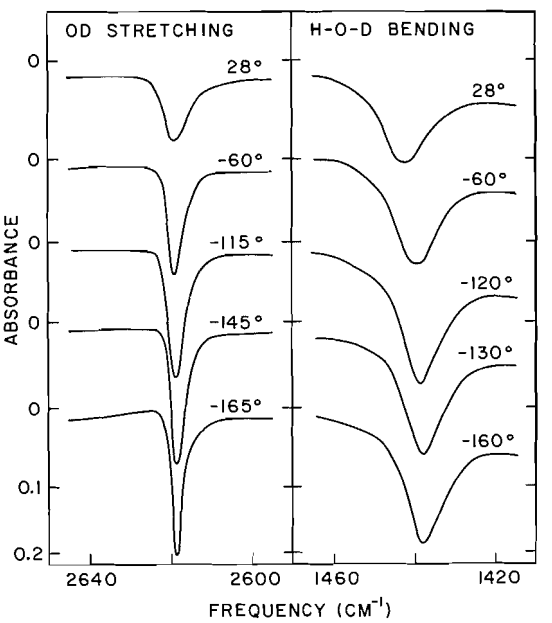

FIG. 4. Spectra of partially deuterated $LiClO_4 \cdot 3H_2O$. OD stretching and HOD bending region (H:D = 99:1). Mulls in Fluorolube.

Can. J. Chem. Downloaded from www.nrcresearchpress.com by 210.87.254.5 on 09/05/12
For personal use only.

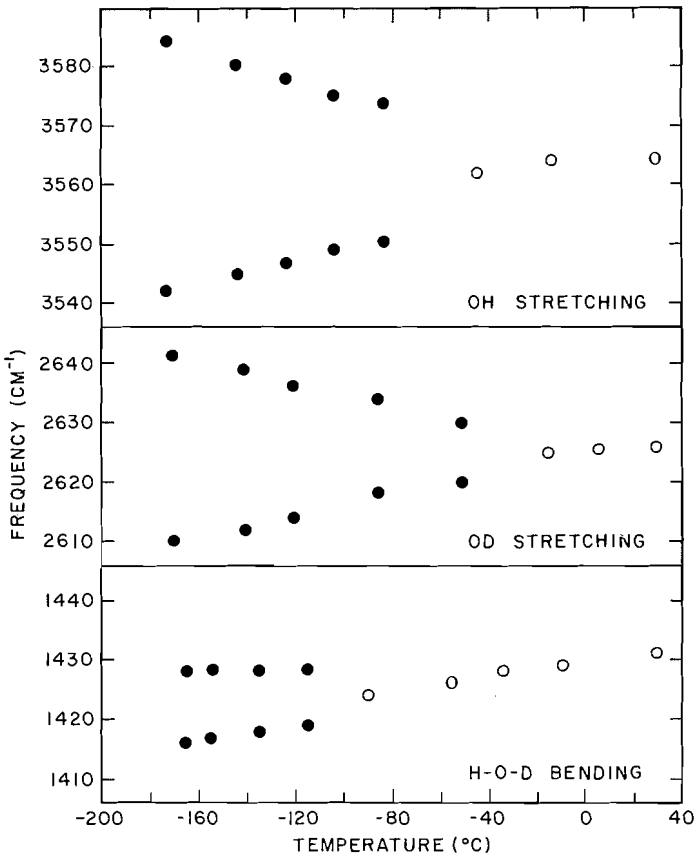

FIG. 5. A plot of peak frequencies of HDO against temperature for $NaClO_4 \cdot H_2O$. Open circles represent single or unresolved peaks, full circles represent resolved components.

950 and 450 cm^{-1} for the Ba compound and at about 450 cm^{-1} for the Li compound. The perchlorate frequencies agree reasonably well with those reported by Ross (11) and Hezel and Ross (12).

Bands of Isotopically Dilute HDO and H_2O

Figure 2 shows the effect of temperature on the spectrum of isotopically dilute HDO in partly deuterated $NaClO_4 \cdot H_2O$, in the region of OD stretching and H—O—D bending, and on the spectrum of isotopically dilute H_2O in the region of the H—O—H bending. All three bands are single at room temperature. Figures 3 and 4 show the corresponding spectra of HDO in $LiClO_4 \cdot 3H_2O$ and $BaClO_4 \cdot 3H_2O$. Again, no splitting is observed at room temperature.

All three fundamentals of isotopically dilute HDO in the sodium compound resolve into two components at lower temperatures, the separation of the two components increasing with decreasing temperature. The isolated H—O—H bending band does not split, and shifts with temperature in the same fashion as the H—O—H bending vibration of the undeuterated hydrate.

Figure 3 shows that the OD stretching fundamental of HDO in the barium compound also resolves into two bands at low temperatures. However, the splitting is smaller than for the sodium compound (31 cm^{-1} for $NaClO_4 \cdot H_2O$ and only 7 cm^{-1} for $Ba(ClO_4)_2 \cdot 3H_2O$ at $-165°$), and there is no detectable splitting in the H—O—D bending band of the barium compound. In the lithium compound no splitting was detected for either the OD stretching or the H—O—D bending band (Fig. 4). The OD stretching band in this compound becomes especially sharp at low temperatures, its half-width being about 2 cm^{-1} at $-170°$.

The details of the temperature-shifts of the HDO peak frequencies of $NaClO_4 \cdot H_2O$ are shown graphically in Fig. 5.

Can. J. Chem. Downloaded from www.nrcresearchpress.com by 210.87.254.5 on 09/05/12
For personal use only.

Can. J. Chem. Downloaded from www.nrcresearchpress.com by 210.87.254.5 on 09/05/12
For personal use only.

Discussion

The Nature of OH–Perchlorate Interactions

Let us first consider what is known from crystallographic studies about the geometry of the water molecules with respect to the perchlorate ions. The structure of $NaClO_4 \cdot H_2O$ does not appear to have been studied. The structures of $Ba(ClO_4)_2 \cdot 3H_2O$ (18), as well as those of $Cu(ClO_4)_2 \cdot 6H_2O$ (19) and $Mg(ClO_4)_2 \cdot 6H_2O$ (20) have been investigated by X-ray crystallography. In each of these structures, water molecules occupy positions adjacent to ClO_4^- ions. However, as the hydrogen positions remain unknown, the details of hydrogen-bond geometry are uncertain.

We shall therefore concentrate our attention on $LiClO_4 \cdot 3H_2O$ for which there is considerable information available. X-Ray crystallographic analysis by West (21) shows that the crystal belongs to the hexagonal space group C_{6v}^4–$P6_3mc$, with two formula units per unit cell. The water oxygens, O_w, are all equivalent and lie on mirror planes. The immediate environment of each water molecule is a distorted tetrahedron, consisting of two lithium atoms, Li′ and Li″, and two oxygens, O′ and O″, which belong to different perchlorate groups (Fig. 6).

The positions of the protons are not known from X-ray analysis but can be calculated as follows. Because of the plane of symmetry, which renders the two protons equivalent, only three independent geometric parameters are required to fix the positions of both protons in the crystal. Couture–Mathieu and Mathieu derived the value of $90 \pm 7°$ for the angle between the H′—O_w—H″ plane and the six-fold axis of the crystal from the intensities of the Raman spectra of oriented single crystals of $LiClO_4 \cdot 3H_2O$ (14). Aleksandrov and Petrzhak derived the H′—H″ distance of 1.58 ± 0.01 Å from proton magnetic resonance measurements (22). This yields two of the three required parameters. The additional parameter could be either the O—H distance, or the H—O—H angle. The H—O—H angle seems relatively insensitive to the molecular environment in hydrates (23, 24) and we have used the mean value obtained from several neutron diffraction investigations, 109° (23). Combining this H—O—H angle with the above X-ray, Raman, and nuclear magnetic resonance (n.m.r.) data on $LiClO_4 \cdot 3H_2O$, we obtain the angles and distances listed in column A of Table 1. Columns B and C of Table 1 list the corresponding angles and distances from the very recent neutron diffraction data of Sequeira and Bernal (25) and of Datt *et al.* (26).[4]

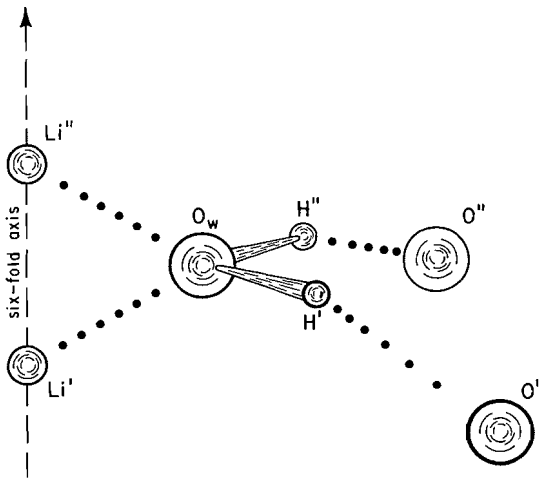

FIG. 6. The environment of a water molecule in $LiClO_4 \cdot 3H_2O$. A mirror plane passes through Li′, Li″, and O_w atoms, making the hydrogen atoms H′ and H″, and the oxygen atoms O′ and O″ equivalent.

Whichever set of geometric parameters one accepts, it is clear that the water–perchlorate interactions in $LiClO_4 \cdot 3H_2O$ satisfy the geometric criteria of hydrogen bonding (24). The relatively long $O_w \ldots O'$ distance of about 2.96 Å points to a rather weak hydrogen bond.

The stretching frequencies of HDO of all three hydrates investigated occur near 3560 cm^{-1} for OH and near 2620 cm^{-1} for OD. This can be taken to indicate that weak hydrogen bonds between water molecules and perchlorate ions, similar to those in $LiClO_4 \cdot 3H_2O$, occur in $NaClO_4 \cdot H_2O$ and $BaClO_4 \cdot 3H_2O$. These stretching frequencies are unusually high for crystalline hydrates, the most common frequency range being 3300–3500 cm^{-1} for OH and 2440–2560 cm^{-1} for OD (5, 16, 27–30). These frequencies correspond closely to the high-frequency peaks in the spectra of HDO in aqueous solutions of perchlorate ions (4, 7–10), showing that very similar weak hydrogen bonds occur in the crystalline hydrates and in solution. If one assumes the shift of the stretching frequency to be proportional to the hydrogen-bond enthalpy [Badger–Bauer rela-

[4]We are grateful to the referees for bringing to our attention refs. 13 and 25.

TABLE 1

Distances (in Å) and angles between an H_2O molecule and its nearest neighbors in $LiClO_4 \cdot 3H_2O$ (cf. Fig. 6)

	A From combined X-ray (21), Raman (14), and n.m.r. (22) data	B From neutron diffraction (25)	C From neutron diffraction (26)*
$O_w \ldots Li'$	2.15	2.112	2.076±0.01
$O_w \ldots Li''$	2.15	2.150	2.170±0.01
$O_w \ldots O'$, $O_w \ldots O''$	2.96†	2.954	2.986±0.004
$O_w \ldots H'$, $O_w \ldots H''$	0.97	0.936	0.933±0.004
$H' \ldots H''$	1.58	‡	1.453±0.004
$H' \ldots O'$, $H'' \ldots O''$	2.033	2.052	2.097
$H—O_w—H$	109°	‡	102.5°
$O' \ldots O_w \ldots O''$	125.5°	‡	128°
$Li' \ldots O_w \ldots Li''$	78.1°	‡	79.3°
$O_w—H' \ldots O'$, $O_w—H'' \ldots O''$	159.5°	161.4°	158°
Φ§	90°	‡	88.4°
Θ‖	111.7°¶	‡	104.4°

*Uncorrected for thermal motion.
†West (21) gives this distance as 2.94 Å, but his atomic coordinates lead to 2.96 Å.
‡Cannot be calculated from the incompletely reported data in ref. 25.
§Φ is the angle between the six-fold axis and the bisector of the H′—O_w—H″ angle.
‖Θ is the angle between the six-fold axis and the bisector of the O′—O_w—O″ angle.
¶The value of Θ has been given as 99° in refs. 14 and 22, apparently due to a miscalculation. It has also been quoted as 90° in ref. 22, apparently by confusion with the angle Φ.

tion (31–33)], then the latter can be roughly estimated. The vapor–crystal shift for ice at 0° is $3705 - 3304 = 401\ cm^{-1}$ for OH and $2719 - 2443 = 276\ cm^{-1}$ for OD (33). The corresponding shifts for $NaClO_4 \cdot H_2O$ at 25° are $3705 - 3564 = 141\ cm^{-1}$ and $2719 - 2626 = 93\ cm^{-1}$. As the enthalpy of sublimation of ice at 0° is 12.2/2 = 6.1 kcal/mole *per hydrogen bond*, the Badger–Bauer relation gives $(141/401) \times 6.1 \simeq (93/276) \times 6.1 \simeq 2.1$ kcal/mole as a rough estimate of the strength of the hydrogen bonds between water and the perchlorate ion.

Environment and Symmetry of Water Molecules $NaClO_4 \cdot H_2O$

The three HDO fundamentals of $NaClO_4 \cdot H_2O$ occur as single bands at room temperature, showing that all of the water molecules are identical and that their two OH groups are identical. At lower temperatures each of the three HDO fundamentals splits into two components. The corresponding OH and OD component frequencies remain in a constant ratio of 1.3562 ± 0.0005, nearly the same as the ratios observed in gypsum (30, 34) and $NaCl \cdot 2H_2O$ (16, 29). This shows that the splitting is not due to proton tunnelling (16, 29, 30, 34) and must be due to the existence of two physically distinct OH groups in the crystal.

The two distinct OH groups may correspond to either the existence of *one* species of asymmetric H_2O molecule or *two* symmetric but distinct species of H_2O molecules in the $NaClO_4 \cdot H_2O$ crystal. The occurrence of two HDO bending peaks is consistent with either of these two possibilities but does not distinguish between them. However, the single H_2O bending peak of isotopically isolated H_2O molecules proves the existence of only *one* type of H_2O molecule, distorted by an asymmetric environment (16, 30). The distortion is greatest at the lowest temperature and *gradually* disappears as temperature increases. At room temperature the two OH groups are spectroscopically identical, apparently by accident rather than as a result of crystal symmetry.

Although the frequencies of the two components of the stretching bands change with temperature, their averages remain unchanged at $3562 \pm 2\ cm^{-1}$ for OH and at $2625 \pm 1\ cm^{-1}$ for OD, between −175 and +30°. This indicates that no *net* change occurs in the average strength of these very weak hydrogen bonds with tem-

Can. J. Chem. Downloaded from www.nrcresearchpress.com by 210.87.254.5 on 09/05/12
For personal use only.

Can. J. Chem. Downloaded from www.nrcresearchpress.com by 210.87.254.5 on 09/05/12
For personal use only.

perature, i.e. one OH group of each water molecule becomes more strongly bonded at low temperatures, while the other OH group becomes more weakly bonded. The HDO bending vibration, on the other hand, undergoes a net shift of about 10 cm^{-1} in the same temperature range, probably indicating changes in the oxygen–sodium interactions.

The small half-widths of the stretching bands (16 cm^{-1} at 0° and 7 cm^{-1} at −165° for the OD band) are comparable with those of other hydrates in which the hydrogen atom positions are ordered (16, 29).

$Ba(ClO_4)_2 \cdot 3H_2O$

The OD stretching fundamental occurs as a single band at room temperature but splits at lower temperatures. This splitting is analogous to that in $NaClO_4 \cdot H_2O$, but is only about one-fourth as great. The phenomenon is clearly the same in the two hydrates, but the asymmetry is much smaller in the Ba compound. If the splitting of the H—O—D bending fundamental due to the distortion is in the same ratio as the splitting of the OD stretching fundamental then a maximum splitting of 12 × (7/31) = 3 cm^{-1} would be expected for the Ba compound at the lowest temperature investigated, −165°. As the half-width of the H—O—D bending band of $Ba(ClO_4)_2 \cdot 3H_2O$ is about 11 cm^{-1} at −165°, a splitting of 3 cm^{-1} would not be detected.

The equivalence of all water molecules is required by either of the two space groups possible for $Ba(ClO_4)_2 \cdot 3H_2O$ as a result of the X-ray study by Mani and Ramaseshan (18). The spectroscopic identity of the two OH groups of each water molecule at room temperature may be accidental, as in $NaClO_4 \cdot H_2O$. The non-equivalence of the two OH groups is consistent with either of the possible space groups for $Ba(ClO_4)_2 \cdot 3H_2O$. The first space group, C_6^6–$P6_3$, requires the water oxygens to occupy sites of symmetry C_1, leading to non-equivalent hydrogens. The second space group, C_{6h}^2–$P6_3/m$, requires the water oxygens to occupy sites of symmetry C_s, which can also lead to non-equivalent hydrogens, provided that the hydrogens lie *on* the mirror plane, in contrast to those of $LiClO_4 \cdot 3H_2O$, which lie *off* the mirror plane.

$LiClO_4 \cdot 3H_2O$

No measurable splitting of HDO fundamentals is observed at any temperature, showing that the water molecules in this hydrate are identical and that they remain effectively undistorted. The identity of the two OH groups is unlikely to be accidental *at all temperatures*, hence they must be related by symmetry, as in Fig. 6. The identity of all the water molecules and the equivalence of the two OH groups of each H_2O are consistent with the space group and with the proposed structure for this hydrate.

We thank Mr. P. F. Seto for checking the calculations of the angles and distances in Table 1.

1. R. D. Waldron. J. Chem. Phys. **26**, 809 (1957).
2. T. T. Wall and D. F. Hornig. J. Chem. Phys. **43**, 2079 (1965).
3. M. Falk and T. A. Ford. Can. J. Chem. **44**, 1699 (1966).
4. K. A. Hartman, Jr. J. Phys. Chem. **70**, 270 (1966).
5. J. Schiffer and D. F. Hornig. J. Chem. Phys. **49**, 4150 (1969).
6. H. R. Wyss and M. Falk. Can. J. Chem. **48**, 607 (1970).
7. Z. Kęcki, P. Dryjański, and E. Kozłowska. Rocz. Chem. **42**, 1749 (1968).
8. P. Dryjański and Z. Kęcki. Rocz. Chem. **43**, 1053 (1969).
9. G. E. Walrafen. Abstracts of Symposium on "Structures of Water and Aqueous Solutions", University of Chicago, June 16–18, 1969.
10. G. Brink and M. Falk. In preparation.
11. S. D. Ross. Spectrochim. Acta, **18**, 225 (1962).
12. A. Hezel and S. D. Ross. Spectrochim. Acta, **22**, 1949 (1966).
13. J. P. Mathieu and L. Couture-Mathieu. J. Phys. Radium, **13**, 271 (1952).
14. L. Couture-Mathieu and J. P. Mathieu. Acta Crystallogr. **5**, 571 (1952).
15. Gmelins Handbuch der anorganischen Chemie. **21**, 411 (1928); **20**, 405 (1960); **30**, 374 (1960).
16. J. Schiffer. Ph.D. Thesis. Princeton University, Princeton, New Jersey, 1963. Diss. Abstr. **25**, 2786 (1964).
17. D. L. Wood. Biochem. J. **58**, 30 (1954).
18. N. V. Mani and S. Ramaseshan. Z. Kristallogr. **114**, 200 (1960).
19. N. V. Mani and S. Ramaseshan. Z. Kristallogr. **115**, 97 (1961).
20. C. D. West. Z. Kristallogr. **91**, 480 (1935).
21. C. D. West. Z. Kristallogr. **88**, 198 (1934).
22. N. M. Aleksandrov and E. Petrzhak. Zh. Strukt. Khim. **6**, 527 (1965).
23. W. C. Hamilton and J. A. Ibers. Hydrogen bonding in solids. W. A. Benjamin, Inc., New York, 1968. p. 213.
24. W. C. Hamilton. *In* Structural chemistry and molecular biology. *Edited by* A. Rich and N. Davidson. W. H. Freeman, San Francisco, 1968. p. 466. See pp. 468 and 469.
25. A. Sequeira and I. Bernal. N.B.S. Spec. Publ. 301, 1969.
26. I. D. Datt, N. V. Rannev, and R. P. Ozerov. Kristallogr. **13**, 261 (1968).
27. R. A. Fifer and J. Schiffer. J. Chem. Phys. **50**, 21 (1969).
28. J. Schiffer and D. F. Hornig. *In* Molecular

dynamics and structure of solids. *Edited by* R. S. Carter and J. J. Rush. N.B.S. Spec. Publ. 301, 1969.
29. T. A. FORD and M. FALK. J. Mol. Struct. **3**, 445 (1969).
30. V. SEIDL, O. KNOP, and M. FALK. Can. J. Chem. **47**, 1361 (1969).
31. R. M. BADGER and S. H. BAUER. J. Chem. Phys. **5**, 839 (1937).
32. K. F. PURCELL and R. S. DRAGO. J. Amer. Chem. Soc. **89**, 2874 (1967).
33. T. A. FORD and M. FALK. Can. J. Chem. **46**, 3579 (1968).
34. R. KLING and J. SCHIFFER. Chem. Phys. Lett. **3**, 64 (1969).

Can. J. Chem. Downloaded from www.nrcresearchpress.com by 210.87.254.5 on 09/05/12
For personal use only.

Can. J. Chem. Downloaded from www.nrcresearchpress.com by 210.87.254.40 on 09/05/12
For personal use only.

Nucleophilic substitution of vinylic halogens in 3-halomethacrylonitriles. Some observations on olefin stabilities

D. V. GARDNER AND D. E. MCGREER

Department of Chemistry, University of British Columbia, Vancouver, British Columbia

Received January 30, 1970

3-Chloro- and 3-bromomethacrylonitrile (*E*- and *Z*-) have been shown to undergo nucleophilic substitution at C-3 with >95% retention of configuration. The configuration of each product has been established by the use of nuclear magnetic resonance spectroscopy. The thermodynamic position of equilibrium for each pair of *E*–*Z* isomers has been determined and the factors which affect this equilibrium are discussed. Some form of *cis* interactions, non-steric in origin, dominates in determining the equilibrium positions.

Canadian Journal of Chemistry, 48, 2104 (1970)

Introduction

Although nucleophilic reactions in activated ethylenic systems have been studied mechanistically in great detail (1–11), few quantitative measurements of the thermodynamic stability of the various reaction products appear to have been made. In the present work the *E* and *Z* isomers (highest priority groups *cis* for *Z* and *trans* for *E* (12)) of 3-bromo- and 3-chloromethacrylonitrile have been synthesized and their reactions with nucleophiles investigated. Both the mechanism of reaction and the stability of the products have been determined.

As a general rule, simple vinylic halides are unreactive, compared to their saturated counterparts, towards nucleophilic attack. When the carbon atom β to the site of substitution bears an electron-withdrawing group, however, e.g. CN (7), $CO_2C_2H_5$ (4, 6, 10), $COCH_3$ (13–15), SO_2Ph (2, 9), F (16), or *p*-nitrophenyl (1, 17), replacement of the vinylic halogen by nucleophiles readily occurs. This replacement usually follows one of two pathways, although others are possible (8, 10, 18), either "direct substitution", eq. [1] or "elimination-addition", eq. [2]. The former

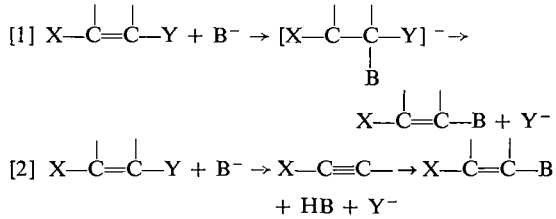

mechanism appears to be the preferred path in the reaction of activated substrates with polarizable, weakly basic nucleophiles (1–11); the latter mechanism is mainly encountered when the nucleophile is an alkoxide ion, particularly when the leaving groups are *trans* orientated (2, 3, 10). Usually direct substitution occurs with retention of configuration although cases are known in which only the thermodynamically stable product has been isolated (2, 5, 7, 17).

Less quantitative information is available on the thermodynamic stability of the various reaction products. It does appear, however, that electronic factors play an important part in determining the relative stability of the *E* and *Z* isomers formed in these reactions. Thus it has been found qualitatively that the β-substituted crotonates (**1**, X = Cl, $N(C_2H_5)_2$, PhS, mesitylthio, C_2H_5O) are all more stable in the *E* configuration (4, 10, 19–21), despite the varying steric requirements of the group X. When X is

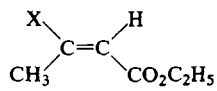

1 (*E*)

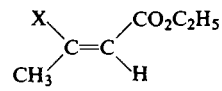

1 (*Z*)

alkylamino, however, the *Z* isomer is the more stable due to internal hydrogen bonding between the amino proton and the carboethoxy group (20, 22). Methyl crotonate itself exists approximately 82% in the *E* form (*trans*) between 200 and 500° (23).

Similar results have been obtained by Stirling (24) with the corresponding sulfones (**2**). When X = OCH_3 or $(PhCH_2)_2N$ the sulfone **2** exists

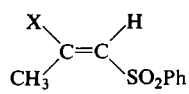

2 (*E*)

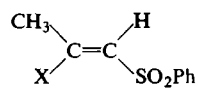

2 (*Z*)

100% in the *E* form whereas when X = $PhCH_2NH$ approximately 34% of the *Z* form is

Can. J. Chem. Downloaded from www.nrcresearchpress.com by 210.87.254.40 on 09/05/12
For personal use only.

present at equilibrium. The reduction in the equilibrium amount of *Z* isomer in the sulfone **2** (X = $PhCH_2NH$) compared with the crotonate **1** (X = RNH) probably reflects a combination of increased steric hindrance and weaker hydrogen bonding in the sulfone.

Mechanistic Studies

Since the 3-halogenomethacrylonitriles do not possess an α hydrogen, they cannot undergo nucleophilic substitution by a simple elimination–addition process. Our observations, that 3-bromomethacrylonitrile (**3**, *E*- and *Z*-, X = Br) gives substitution with sodium methoxide, sodium thioethoxide, and dimethylamine and that 3-chloromethacrylonitrile (**3**, *E*- and *Z*-, X = Cl) gives substitution with diethylamine, indicate that substitution can in all of these cases take place without the requirement of elimination.

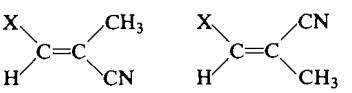

3 (*E*) **3** (*Z*)

In all cases reaction occurred with greater than 95% retention of configuration at C-3, as determined by vapor phase chromatography (v.p.c.) or nuclear magnetic resonance (n.m.r.) spectral analysis, despite the fact that the product is thermodynamically less stable than its isomer in many cases. Where v.p.c. analysis was employed, it was shown that the respective *E* and *Z* isomers did not interconvert under the conditions used. No products resulting from α elimination were detected (8, 18).

The above results are consistent with the direct substitution (addition–elimination) mechanism, eq. [1], proposed by Miller and Yonan (1) and modified by Jones *et al.* (4), in which the attacking nucleophile is assumed to approach at right angles to the plane of the double bond.

The path requiring the least energy is a 60° rotation to place the halogen parallel to the orbital carrying the electron pair followed by *trans* elimination of halide. This path, eq. [3], requires a minimum of eclipsing (H against CN or CH_3) and leads to a product of retained configuration, as observed. It also permits the formation of some product of the opposite configuration as is frequently observed. Scotti and Frazza (7) have proposed a similar mechanism to account for the retention of configuration observed in the reaction of 3-chloroacrylonitrile with ethoxide or *p*-toluene sulfide ion. With piperidine, however, only one product was isolated, starting from either chloronitrile, to which they assigned the *trans* structure (**4**). Furthermore, kinetic evidence was obtained which indicated that both chloronitriles were

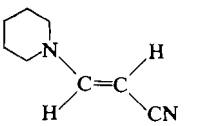

4

reacting by the same mechanism (addition–elimination). The reason for this lack of stereospecificity is not clear, especially as in the present work both 3-chloro- and 3-bromomethacrylonitrile (*E*- and *Z*-) react stereospecifically with diethylamine and dimethylamine respectively, in spite of the ease of isomerization of the products. Pattenden and Walker (11) have observed a similar lack of stereospecificity in the reactions of trisubstituted phosphines with 3-halogenoacrylic acid derivatives, which they attribute to steric crowding in the the transition state.

In the present work, since the mechanism of reaction is based only on product distribution, it was necessary to assign the correct stereochemistry to each pair of *E*–*Z* isomers. This has been achieved by n.m.r. spectroscopy; in all cases the isomer with the more deshielded olefinic proton has been assigned the *E* configuration (Table 1) in which the olefinic hydrogen and the cyano group are *cis* orientated (25–27). In addition, the configurations of the isomeric chloromethacrylonitriles have already been determined by chemical means (28).

3-Methoxymethacrylonitrile-*E* has been prepared previously by Lichty (29) by treatment of

[3] 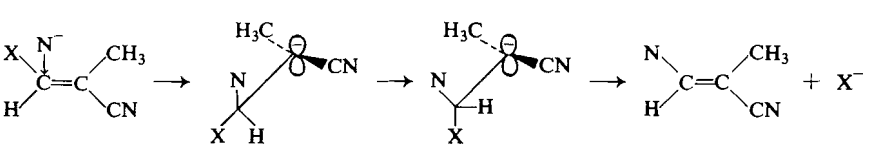

TABLE 1

Chemical shifts and coupling constants for the 3-substituted methacrylonitriles (**3**)

R	*E* isomer*				*Z* isomer*			
	τ_R	τ_{CH_3}	τ_H	*J*(Hz)	τ_R	τ_{CH_3}	τ_H	*J*(Hz)
Br	—	7.99d	2.84q	1.5	—	7.98d	3.13q	1.5
Cl	—	7.98d	3.09q	1.5	—	7.96d	3.31q	2.0
CH_3O	6.20s	8.27d	3.29q	1.5	6.21s	8.24d	3.39q	1.5
CH_3CH_2S	8.65t			1.5	8.64t			
	7.18q	8.17d	3.03q	7.0	7.18q	8.04d	3.28q	7.0
$(CH_3)_2N$	7.04s	8.07s	3.61s	—	6.98s	8.21s	3.77s	—
$(CH_3CH_2)_2N$	8.85t				8.82t			
	6.69q	8.12s	3.59s	7.0	6.69q	8.21s	3.80s	7.0

*s, singlet; d, doublet; t, triplet; q, quartet.

2-cyano-1,2-dichloropropane with methanolic sodium hydroxide. The stereochemistry of the product was not given but a boiling point comparison with the isomers we have prepared shows it to most closely compare with the *E* isomer. The above experiment was repeated under milder conditions and was shown to give the *Z* isomer as the major (82%) product, and thus Lichty's preparation undoubtedly gave the product as the equilibrated mixture which contains 78% of the *E* form.

Equilibration Studies

The positions of equilibrium for the 3-substituted methacrylonitriles, **3**, prepared in this study, are presented in Table 2. It is of interest to consider the factors that determine the position of this equilibrium. Although steric factors have traditionally been emphasized, in recent years the observation that a number of *cis*-1,2-disubstituted olefins are more stable than their *trans* isomers suggests an important stabilization due to

TABLE 2

Equilibration results for the 3-substituted methacrylonitriles (**3**), $XCH{=}C(CH_3)(CN)$

X	% *E* isomer at equilibrium	Method of equilibration*	% *E* predicted from Table 3
Cl	60†	*1*	58
Br	60†	*1*	
CH_3O	78†	*1*	
C_2H_5S	68†	*2a*	
$(CH_3)_2N$	13‡	*2b*	
$(CH_3CH_2)_2N$	13‡	*2b*	
CH_3	20†	*3*	18

*1) Bromine in sunlight at about 30°; *2a*) thermally in sealed tubes at 210°; *2b*) equilibration occurred on v.p.c. columns at 210°; *3*) trace of sodium methoxide in methanol at 25°.
†The v.p.c. analysis.
‡The n.m.r. analysis.

TABLE 3

Position of equilibrium for *cis–trans*-1,2-disubstituted ethylenes

Substituents	% *cis*	Temperature
Cl, CH_3	75.5 (30, 31)	30°
Br, CH_3	68 (33)	0–100°
Cl, CN	69 (30)	30°
CH_3, CN	57 (30), 58 (34)	80°, 400°
CH_3, CH_3	23 (35)	

a van der Waals or electrostatic attraction between many groups. This attractive interaction is illustrated by the percent *cis* isomer at equilibrium as given in Table 3 for compounds related to those of the present study.

For the methacrylonitriles the relative steric requirements of the methyl and the nitrile groups can be evaluated in 3-*t*-butylacrylonitrile (36) where steric factors will clearly be dominant. Equilibration of **5** at 30° with bromine and sunlight gives 8% of the *E* form. Thus as expected from other studies the methyl has a larger steric requirement than the nitrile group.

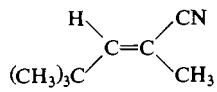

5 (*E*)

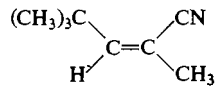

5 (*Z*)

The data in Table 2 indicate that only in the 3-dimethylamino and possibly in the 3-methyl compounds are the steric factors dominant in determining equilibrium positions. The dimethyl amino group, in order to provide conjugation with the nitrile group, would become planar and thereby introduce a steric requirement of an order equivalent to a *t*-butyl group. The equilibrium positions for the other compounds in Table 2 show effects similar to those which con-

Can. J. Chem. Downloaded from www.nrcresearchpress.com by 210.87.254.40 on 09/05/12
For personal use only.

Can. J. Chem. Downloaded from www.nrcresearchpress.com by 210.87.254.40 on 09/05/12
For personal use only.

tribute to the favored *cis* orientations noted in Table 3.

In the range of compounds where steric effects are not dominant we might expect the equilibrium position for a trisubstituted olefin to be equal to that predicted by an additive contribution of the vicinal pairs.[1] It is interesting therefore that the data of Table 3 can be used to predict two of the observed equilibria in Table 2 to within the combined experimental error of the measurements. On the other hand, data from Table 3 predicts the equilibrium position for 2-bromo-2-butene to be 88% *trans*, a value which is close to, but outside, the experimental error for the observed value of 83% (37, 38). It seems, however, that it would be desirable to further evaluate additivity in these systems. It may, for example, be advantageous to only use data at infinite dilution in a common solvent at a common temperature.

Experimental

Vapor phase chromatographic analysis and preparative separation were carried out using commercial (Varian Aerograph) 10 ft × 1/4 in. stainless steel columns containing the appropriate packing. Boiling points were determined by the microcapillary method and are uncorrected. The n.m.r. spectra were recorded on a Varian A60 instrument using 20% by volume samples in carbon tetrachloride. All new compounds gave infrared spectra consistent with their respective structures.

3-Chloromethacrylonitrile (E- and Z-)

The title compounds were prepared from chloroacetone cyanohydrin (28) by the method of Hurd and Rector (39). The product (70%, b.p. 54–80°/40 mm) contained 3-chloromethacrylonitrile (*E*-), (28%), 3-chloromethacrylonitrile (*Z*-) (51%), and 2-cyano-1,2-dichloropropane (21%). Separation was effected by preparative v.p.c. on a 15% QF1 – 5% carbowax 20M column at 145°.

3-Bromomethacrylonitrile (E- and Z-)

Bromine (80 g, 0.5 mole) in carbon tetrachloride (50 ml) was added dropwise over 3 h to methacrylonitrile (33.5 g, 0.5 mole) and the stirred solution was then left overnight at room temperature. Removal of the solvent at room temperature *in vacuo* yielded crude 2-cyano-1,2-dibromopropane (56 g, 49%). To the crude product, dissolved in *t*-butanol (50 ml), was added, with vigorous stirring, potassium hydroxide (18 g) in water (32 ml). After 21 h potassium bromide was removed by filtration and the filtrate was diluted with ether (100 ml). The aqueous layer was further extracted with ether (2 × 100 ml) and the combined ether extracts were dried over magnesium sulfate. Removal of the ether and *t*-butanol, followed by distillation at 50–70°/20 mm yielded 3-bromomethacrylonitrile (*E*:*Z* = 3:5, 25.5 g, 71%). Although thermally labile, the two isomers were readily separable by preparative v.p.c. (15% QF1 – 5% carbowax 20M) at 150° and have the following properties.

3-Bromomethacrylonitrile (*E*-); n_D^{20} 1.4995.

Anal. Calcd. for C_4H_4BrN: C, 32.87; H, 2.74. Found: C, 33.25; H, 3.01.

3-Bromomethacrylonitrile (*Z*-); n_D^{20} 1.4929.

Anal. Found: C, 32.80; H, 2.87.

If methanol was used instead of *t*-butanol in the above experiment, a small amount of 3-methoxymethacrylonitrile (*E*-) was also obtained which could not be separated from the 3-bromomethacrylonitrile (*Z*-).

3-Methoxymethacrylonitrile (E-)

Sodium methoxide (1 equ) in methanol was added dropwise, with stirring, to 3-bromomethacrylonitrile (*E*-) (1 equ), sodium bromide being instantly precipitated. The vigorous exothermic reaction was controlled by external cooling. On completion of the methoxide addition, the solution was stirred for 1.5 h at room temperature, then neutralized with glacial acetic acid and diluted with ether. Removal of the precipitate, followed by evaporation of the solvent under reduced pressure yielded a yellow oil which was distilled under reduced pressure. Final purification was effected by preparative v.p.c. on QF1–carbowax at 180° to give 3-methoxymethacrylonitrile (*E*-), b.p. 182–183° (lit. (29) b.p. 80–83°/27 mm), contaminated with a small amount of 3,3-dimethoxy-2-methylpropionitrile.

3-Methoxymethacrylonitrile (Z-)

This was prepared as above from 3-bromomethacrylonitrile (*Z*-). An analytical sample had b.p. 202–203° and n_D^{20} 1.4498.

Anal. Calcd. for C_5H_7NO: C, 61.86; H, 7.22. Found: C, 61.69; H, 7.33.

Reaction of 2-Cyano-1,2-dichloropropane with Methanolic Sodium Hydroxide (29)

To a stirred solution of 2-cyano-1,2-dichloropropane (0.55 g) in methanol (1 ml) was added sodium hydroxide (0.32 g) in water (1 ml). After 1 h at room temperature the solution was extracted with ether. Analysis of this extract by v.p.c. showed, besides starting material and volatile products, 3-methoxymethacrylonitrile (*E*- and *Z*-), in the ratio 2:9.

[1]Additivity in the free energy term would appear as a product of the equilibrium constants thus for

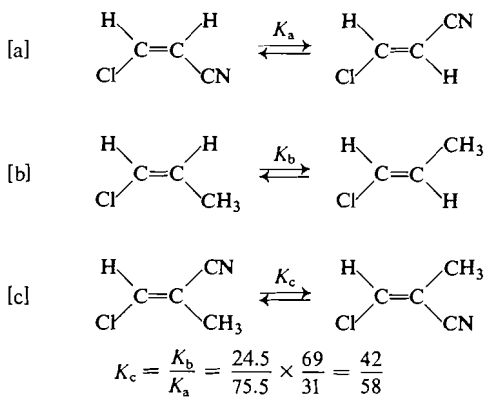

$$K_c = \frac{K_b}{K_a} = \frac{24.5}{75.5} \times \frac{69}{31} = \frac{42}{58}$$

Can. J. Chem. Downloaded from www.nrcresearchpress.com by 210.87.254.40 on 09/05/12
For personal use only.

3-Dimethylaminomethacrylonitrile (E- and Z-)

3-Bromomethacrylonitrile (*E*-) (0.2 g) in ether (2 ml) was treated with dimethylamine (1 ml). The resulting solution was kept, in a screw-cap jar, overnight at room temperature then diluted with ether. After removal of the precipitated dimethylamine hydrobromide by filtration, the ether and excess dimethylamine were evaporated under reduced pressure. Analysis of the crude reaction product by n.m.r. showed that only 3-dimethylaminomethacrylonitrile (*E*-) was present. The *cis–trans* equilibration, however, occurred when an attempt was made to purify the sample by preparative v.p.c. at 210°. The resulting mixture contained both *E* and *Z* isomers in the ratio 13:87.

Anal. Calcd. for C_5H_7NO: C, 61.86; H, 7.22. Found: C, 61.69; H, 7.33.

Starting with 3-bromoethacrylonitrile (*Z*-) only 3-dimethylaminomethacrylonitrile (*Z*-) was present in the crude product. The same equilibrium mixture as above was, however, obtained by v.p.c. purification.

3-Diethylaminomethacrylonitrile

A solution of 3-chloromethacrylonitrile (*E*-) (0.88 g) in ether (6 ml) and diethylamine (6 ml) was boiled under reflux for 39 h. After dilution with ether and removal of the precipitated diethylamine hydrochloride, the solvent was removed to give a mixture of starting material and 3-diethylaminomethacrylonitrile (*E*-) in the ratio 2:3. The latter equilibrated to a mixture of *E* and *Z* forms (88% *Z*) when purified by v.p.c. on Dow Corning 550 at 210°.

The crude product obtained from the reaction of 3-chloromethacrylonitrile (*Z*-) with diethylamine contained 36% starting material and 64% 3-dimethylaminomethacrylonitrile (*Z*-). Purification by v.p.c. as above gave 3-diethylaminomethacrylonitrile (*E*- and *Z*-) in the ratio 14:86.

Anal. Calcd. for $C_8H_{14}N_2$: C, 69.56; H, 10.14. Found: C, 69.81; H, 10.34.

3-Thioethoxymethacrylonitrile (E- and Z-)

Treatment of 3-bromomethacrylonitrile (*E*- and *Z*-) with 1 equ of sodium thioethoxide in methanol (prepared from sodium methoxide (1 equ) and ethanethiol (1.1 equ)) yielded the corresponding 3-thioethoxy compounds. Stereospecific replacement of bromine was shown to have taken place by v.p.c. analysis on QF1–carbowax at 180°. The two isomers, isolated by preparative v.p.c., had the following physical properties.

3-Thioethoxymethacrylonitrile (*E*-): n_D^{18} 1.5281, b.p. 201–202°.

Anal. Calcd. for C_6H_9NS: C, 56.69; H, 7.09. Found: C, 58.45; H, 7.33.

3-Thioethoxymethacrylonitrile (*Z*-): $n_D^{18.5}$ 1.5180, b.p. 216–217° (with 4% *E* present).

Anal. Found: C, 56.59; H, 7.10.

Methods of Equilibration

In every case, except for methyl 3-dimethylaminomethacrylate, the position of equilibrium has been determined by equilibrating each *E* and *Z* isomer separately, the following procedures being used.

(1) Bromine and sunlight: To a neat solution of the nitrile in a sealed or tightly-stoppered tube was added 1–2 mole % of bromine (10% solution in carbon tetrachloride). The tubes were placed in direct sunlight, samples being removed periodically for analysis.

(2) Thermolysis: Small samples (10–50 μl) of the nitrile were sealed in Pyrex tubes (4 mm o.d.) and placed in a furnace at 210°. Although some darkening of the samples occurred, there was no apparent decomposition. Samples were removed and analysed at fixed intervals.

(3) Sodium methoxide in methanol: The nitrile was treated with a trace of sodium methoxide in methanol and the mixture analyzed periodically by v.p.c.

A fellowship to D.V.G. and general support from NRCC is gratefully acknowledged.

1. S. I. Miller and P. K. Yonan. J. Amer. Chem. Soc. **79**, 5931 (1957).
2. G. Marchese, G. Modena, and F. Naso. Tetrahedron, **24**, 663 (1968); J. Chem. Soc. (B), 958 (1968).
3. S. Patai and Z. Rappoport. The chemistry of alkenes. Interscience, London, 1964. Chapt. 8.
4. D. E. Jones, R. O. Morris, C. A. Vernon, and R. F. M. White. J. Chem. Soc. 2349 (1960).
5. F. Montanari. Boll. Sci. Fac. Chem. Ind. Bologna, **16**, 31 (1958), and earlier papers.
6. J. S. Pizey and W. E. Truce. J. Org. Chem. **30**, 4355 (1965).
7. F. Scotti and E. J. Frazza. J. Org. Chem. **29**, 1800 (1964).
8. P. Beltrame, S. Carra, P. Macchi, and M. Simonetta. J. Chem. Soc. 4386 (1964).
9. J. S. Meek and J. S. Fowler. J. Org. Chem. **33**, 985 (1968).
10. F. Theron. Bull. Soc. Chim. France, 278 (1969).
11. G. Pattenden and B. J. Walker. J. Chem. Soc. (C), 531 (1969).
12. J. E. Blackwood, C. L. Gladys, K. L. Loening, A. E. Petrarca, and J. E. Rush. J. Amer. Chem. Soc. **90**, 509 (1968).
13. A. E. Pohland and W. R. Benson. Chem. Rev. **66**, 161 (1966).
14. D. Landini and F. Montanari. Chem. Commun. 180 (1967).
15. D. Landini, F. Montanari, G. Modena, and F. Naso. J. Chem. Soc. (B), 243 (1969).
16. J. D. Park and W. C. Frank. J. Org. Chem. **32**, 1333 (1967).
17. G. Marchese, F. Naso, and G. Modena. J. Chem. Soc. (B), 290 (1969).
18. J. G. Pritchard and A. A. Bothner-By. J. Phys. Chem. **64**, 1271 (1960).
19. J. S. Pizey and W. E. Truce. J. Chem. Soc. 865 (1964).
20. J. Chalchat, F. Theron, and R. Vessiere. C. R. **267**, 426, 1864 (1968).
21. F. Theron and R. Vessiere. Bull. Soc. Chim. France, 2994 (1968).
22. A. Gomez-Sanchez, M. T. Aldave, and W. Scherdegger. J. Chem. Soc. (C), 2570 (1968).
23. J. N. Butler and G. J. Small. Can. J. Chem. **41**, 2492 (1963).
24. C. J. M. Stirling. J. Chem. Soc. 5856, 5863 (1964).
25. G. Descotes and P. Laconche. Bull. Soc. Chim. France, 2149 (1968).
26. A. N. Kurtz, W. E. Billups, R. B. Greenlee, H. F. Hamil, and W. T. Pace. J. Org. Chem. **30**, 3141 (1965).
27. G. S. Reddy, J. H. Goldstein, and L. Mandell. J. Amer. Chem. Soc. **83**, 1300 (1961).

28. A. F. FERRIS and I. G. MARKS. J. Org. Chem. **19**, 1971 (1954).
29. J. G. LICHTY. U.S. Pat. 2 384 106. September 4, 1945; Chem. Abstr. **40**, p. 5947 (1946).
30. J. W. CRUMP. J. Org. Chem. **28**, 953 (1963).
31. M. CRAEN. Dissertation. Univer. Brussels. 1924, p. 45, quoted by Viehe (ref. 32).
32. H. G. VIEHE. Chem. Ber. **93**, 1697 (1960).
33. K. E. HARWELL and L. F. HATCH. J. Amer. Chem. Soc. **77**, 1682 (1955).
34. J. N. BUTLER and R. D. MCALPINE. Can. J. Chem. **41**, 2487 (1963).
35. K. S. PITZER and J. L. HOLLENBERG. J. Amer. Chem. Soc. **76**, 1493 (1954).
36. D. V. GARDNER and D. E. McGREER. Can. J. Chem. This issue.
37. A. S. DREIDING and R. J. PRATT. J. Amer. Chem. Soc. **76**, 1902 (1954).
38. M. LEPINGLE. Bull. Soc. Chim. France, **39**, 741 (1926).
39. C. D. HURD and C. H. RECTOR, JR. J. Org. Chem. **10**, 441 (1945).

Can. J. Chem. Downloaded from www.nrcresearchpress.com by 210.87.254.40 on 09/05/12
For personal use only.

Can. J. Chem. Downloaded from www.nrcresearchpress.com by 210.87.254.40 on 09/05/12
For personal use only.

Influence of steric and polar effects in determining the equilibrium position for *cis–trans*-olefin pairs

D. V. GARDNER AND D. E. MCGREER
Department of Chemistry, University of British Columbia, Vancouver, British Columbia
Received January 30, 1970

A series of α,β-unsaturated nitriles and esters substituted by *t*-butyl or isopropyl groups at the β-position along with methoxyl, thioethoxyl dimethylamino, chloro, and hydrogen at the other β-position have been prepared. Evaluation of the isomer stability from *cis–trans* equilibrations achieved catalytically or thermally supports earlier observations that steric and polar factors maintain a strong tendency for a β-methoxyl group to be *trans* to a nitrile or carbomethoxy group even when opposed by a *t*-butyl group. The tendency for a chloro group to prefer to be *trans* to a carbomethoxy group in methyl β-chlorocrotonate is overcome by replacing the β-methyl by isopropyl or *t*-butyl.

Canadian Journal of Chemistry, 48, 2110 (1970)

In the preceding paper (1) the position of thermodynamic equilibrium for the *E* and *Z* forms (highest priority groups *cis* for *Z* and *trans* for *E* (2)) of several 3-substituted methacrylonitriles was measured. It was noted that interactions non-steric in origin were dominant in determining the position of equilibrium. In a similar interplay of effects it is well recognized that the β-halocrotonic acid derivatives are more stable in the *E* form in which the smaller halogen group is *trans* to the carbonyl containing group (3). To further evaluate the contribution of steric and polar factors in determining the position of equilibrium for *cis–trans* pairs of isomers, we have prepared a number of α,β-unsaturated nitriles and esters for study.

Chart 1 lists the compounds which have been studied along with the equilibrium data. New compounds in Chart 1 were prepared by standard methods. Reaction of α-bromo-β-alkylacrylonitriles with sodium methoxide in methanol gave **1** and **12**. The *Z* form of all of the β-methoxy compounds **1**, **6**, **7**, **10**, and **12** were prepared by addition of diazomethane to the appropriate β-keto-nitrile or ester. The *E* isomers could be obtained by irradiation of the *Z* isomers in a silica flask with a mercury lamp. The chloronitrile **5** and the chloroester **9** were separately obtained from the corresponding aldehyde, 3-chloro-4,4-dimethyl-2-pentenal (4), the former by use of the Corey procedure (5), the latter by dehydration of the aldoxime. The chloro compounds **5** and **9** could not be obtained by reaction of phosphorus pentachloride with the corresponding β-keto-nitrile or ester (6). Under these conditions the β-ketonitrile was recovered essentially unchanged and the β-ketoester underwent chlorination α to the carbonyl groups. Compounds **2–4** and **8** were prepared from the corresponding β-chloro derivatives **5** and **9** by nucleophilic substitution. Attempts to prepare corresponding β-enaminoesters from **9** were unsuccessful. The β-chloroesters **11** and **13** were obtained from the known acids by esterification.

Assignment of Configuration

In some cases it was possible to assign the configuration about the double bond on the basis of chemical evidence. Thus the enol ether **7**, obtained from the reaction of diazomethane with ethyl 4,4-dimethyl-3-ketopentanoate (6) was assigned the *Z* configuration on the following basis. First the β-ketoester, which was shown by nuclear magnetic resonance (n.m.r.) spectroscopy to exist approximately 40% in the enol form, gave a positive ferric chloride test, and secondly, in the absence of methanol only 10% of the β-ketoester reacted with diazomethane. This is in line with earlier studies on the reaction of β-ketoesters with diazomethane which demonstrated that *cis* enols require methanol catalysis and give the *Z* methyl ether (22).

Stereoselective preparation of **1** and **2** from 2-bromo-4,4-dimethyl-2-pentenitrile (*E* or *Z*) is expected to occur by *trans* addition to the acetylene intermediate (7, 8) and thus should lead to product rich in the *Z* isomer. The chloronitrile **5** and the chloroester **9** also may react with nucleophiles via an acetylenic intermediate although this was only definitely confirmed for the reaction of **5** and **9** with sodium methoxide.

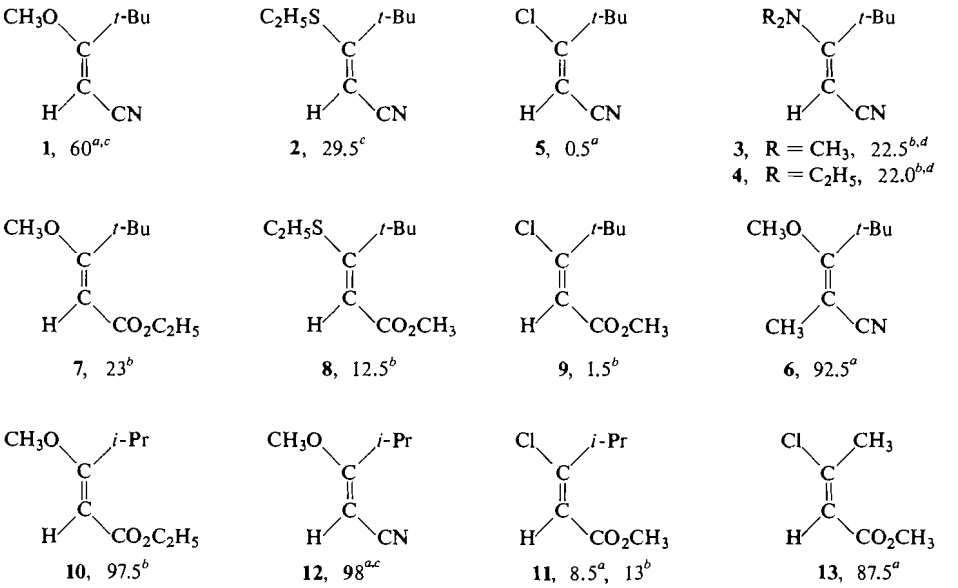

CHART I

Percent composition at equilibrium for the *E* form of the compounds studied.

Procedures used for equilibrations, as described elsewhere (1), were: (*a*) bromine in sunlight at about 30°; (*b*) thermally in sealed tubes at 210°; (*c*) catalytically with 1 equ of sodium methoxide in methanol at 60°; (*d*) equilibrium approached from one isomer only.

Finally, where appropriate, the corresponding isopropyl compounds have been synthesized and comparisons made between the like physical and spectroscopic properties of the two series.

In the majority of cases, where chemical evidence of structure was not available, assignment of configuration has been based on n.m.r. spectroscopic measurements. The data collected is shown in Tables 1 and 2. Assignments were possible because in every case both stereoisomers were available. There is little doubt that a β-hydrogen *cis* to a nitrile or carbomethoxy group will be to lower field (9). For each pair of isomers studied the chemical shift of the *t*-butyl group was assumed to be at lower field in those isomers in which the *t*-butyl group and nitrile group are *cis* orientated. This effect was larger than for the methyls in an isopropyl group due to the necessity of a *t*-butyl group to have at least one methyl in close proximity of the nitrile. Although this appears contrary to the observations of Hayashi *et al.* (10, 11) on alkylidenecyanoacetic esters it is significant that the magnitude of the chemical shift differences for the *t*-butyl groups is more pronounced for most of the nitriles (0.00–0.21 p.p.m.) than for the esters (0.00–0.12 p.p.m.), a situation which is different from that observed for β-methyls. This change in relative effects will be the result of the difference between the form of the shielding cone of a nitrile and a carbonyl and their different relative geometry. A β-methyl is strongly shielded by a carbonyl but weakly shielded by a nitrile. A β-*t*-butyl group will have the methyls placed favorably over the nitrile for stronger shielding than from a carbonyl.

Further supporting evidence was obtained by comparison of the chemical shift of the olefinic protons. Jones *et al.* (12) and Pizey and Truce (13) have shown for a series of 3-substituted crotonates that the α-olefinic proton is more deshielded when it is *trans* to the electron-donating group at position 3 than when it is *cis*. Apart from the chloroesters and chloronitriles where the difference is small the present results are fully in accord with those of the aforementioned workers.

Pizey and Truce (13) further showed that the chemical shift of the α-olefinic proton in the 3-substituted crotonates moves to higher field as the electron-donating ability (14) of the 3-

Can. J. Chem. Downloaded from www.nrcresearchpress.com by 210.87.254.40 on 09/05/12
For personal use only.

TABLE 1

Chemical shifts and coupling constants for the β-*t*-butylacrylonitriles and esters

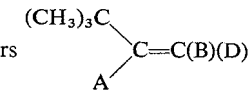

Compound no.	Configuration	A	B	D	Chemical shift (τ)* —C(CH₃)₃	A	B	D	J (Hz)
15	*E*	H	H	CN	8.90	3.34d	4.78d	—	16.5
15	*Z*	H	H	CN	8.75	3.69d	4.82d	—	12.0
16	*E*	H	CH_3	CN	8.82	3.77q	8.02d	—	1.5
16	*Z*	H	CH_3	CN	8.79	3.94q	8.06d	—	1.5
17	*E*	H	Br	CN	8.74	3.32	—	—	—
17	*Z*	H	Br	CN	8.74	3.12	—	—	—
1	*E*	CH_3O	H	CN	8.70	6.40	5.66	—	—
1	*Z*	CH_3O	H	CN	8.91	5.81	5.58	—	—
6	*E*	CH_3O	CH_3	CN	8.70	6.32	8.11	—	—
6	*Z*	CH_3O	CH_3	CN	8.80	6.09	8.03	—	—
2	*E*	CH_3CH_2S	H	CN	8.59	7.32q, 8.67t	5.24	—	7.5
2	*Z*	CH_3CH_2S	H	CN	8.80	6.78q, 8.68t	4.44	—	7.0
5	*E*	Cl	H	CN	8.58	—	4.42	—	—
5	*Z*	Cl	H	CN	8.77	—	4.48	—	—
3	*E*	$(CH_3)_2N$	H	CN	8.58	7.33	5.71	—	—
3	*Z*	$(CH_3)_2N$	H	CN	8.78	6.96	5.64	—	—
4	*E*	$(CH_3CH_2)_2N$	H	CN	8.64	7.11q, 8.96t	5.53	—	7.0
4	*Z*	$(CH_3CH_2)_2N$	H	CN	8.81	6.69q, 8.91t	5.28	—	7.0
7	*E*	CH_3O	H	$CO_2CH_2CH_3$	8.88	6.40	5.13	5.94q, 8.77t	7.0
7	*Z*	CH_3O	H	$CO_2CH_2CH_3$	8.88	6.10	4.97	5.94q, 8.77t	7.0
8	*E*	CH_3CH_2S	H	CO_2CH_3	8.67	7.35q, 8.83t	4.73	6.35	7.0
8	*Z*	CH_3CH_2S	H	CO_2CH_3	8.79	7.18q, 8.83t	4.01	6.39	7.0
9	*E*	Cl	H	CO_2CH_3	8.71	—	4.02	6.35	—
9	*Z*	Cl	H	CO_2CH_3	8.76	—	4.04	6.35	—

*d, Doublet; t, triplet; q, quartet. All resonances are singlets unless otherwise marked.

substituent increases. A similar effect has been found particularly in the *E* series for the nitriles **3** > **1** > **2** > **5** and esters **7** > **8** > **9** presently studied, the chemical shift (τ) of the olefinic proton decreasing in the series $(CH_3)_2N$— > CH_3O— > C_2H_5S— > Cl.

Like the *t*-butyl group, the hydrogens on the carbon C* at the γ position in other β-substituents are also deshielded by the nitrile or ester group to a greater extent than expected. This may suggest an *S-cis* configuration with respect to the double bond for LC^*H_2R' (L = O, S, N; R′ = H, CH_3) as in structure **14**.

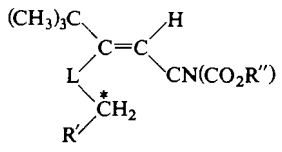

14

Our assignment of the *Z* configuration to the more stable chloro isopropyl ester **11** is based on the position of the methine hydrogen at 7.40 τ in that isomer compared to the less stable isomer with the methine hydrogen at 5.75 τ. This large chemical shift difference is in line with the view that the methine hydrogen is oriented for steric reasons towards the carbomethoxy group in the *E* form and experiences a maximum deshielding effect (11, 15). Pizey and Truce (13) prepared the ethyl ester **21** and assigned the *E* configuration to the more stable isomer by analogy with stabilities in the β-chlorocrotonate series. Our preparation of **11** was from 3-chloro-4-methyl-2-pentenoic acid (16) by esterification with methanol and contained both isomers of **11** as well as small amounts of the β,γ-isomer, methyl 3-chloro-4-methyl-3-pentenoate (**22**). Attempts to obtain the *E* isomer of **11** pure by vapor phase chromatography (v.p.c.) were unsuccessful. In every case samples isolated contained large amounts of a new component identified below. On the other hand a sample of **11** (*Z*-) was isolated containing less than 6% of the β,γ-isomer **22** as

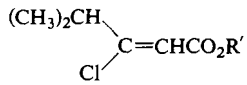

11 R′ = CH_3
21 R′ = C_2H_5

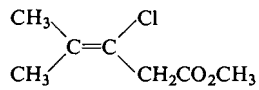

22

Can. J. Chem. Downloaded from www.nrcresearchpress.com by 210.87.254.40 on 09/05/12
For personal use only.

Can. J. Chem. Downloaded from www.nrcresearchpress.com by 210.87.254.40 on 09/05/12
For personal use only.

TABLE 2

Chemical shifts and coupling constants for the β-isopropylacrylonitriles and esters

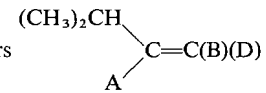

Compound no.	Configuration	A	B	D	Chemical shift (τ)*					J (Hz)
					$(CH_3)_2$—C—(d)	—C—H(m)	A	B	D	
18	*E*	H	H	CN	8.91	7.15–7.95	3.22q	4.73q	—	*trans* = 16.5 CH_1CH = 6.5 CH_1CH_3 = 6.5
18	*Z*	H	H	CN	8.89	6.70–7.50	3.74q	4.82d	—	*cis* = 11.0 CH_1CH = 9.5 CH_1CH_3 = 6.5
19	*E*	H	Br	CN	8.86	6.90–7.40	3.50d	—	—	CH_1CH = 9.5 CH_1CH_3 = 7.0
19	*Z*	H	Br	CN	8.90	6.85–7.50	3.40d	—	—	CH_1CH = 9.0 CH_1CH_3 = 6.5
12	*E*	CH_3O	H	CN	8.86	6.50–7.20	6.36	5.79	—	CH_1CH_3 = 7.0
12	*Z*	CH_3O	H	CN	8.96	7.40–8.15	5.90	5.75	—	CH_1CH_3 = 7.0
20	*E*	H	H	CO_2CH_3	8.91	7.94	3.14q	4.32q	6.34	*trans* = 15.8 CH_1CH = 1.4, 6.5 CH_1CH_3 = 6.7
20	*Z*	H	H	CO_2CH_3	8.99	6.35	4.03q	4.43d	6.36	*cis* = 11.4 CH_1CH = 9.2 CH_1CH_3 = 6.6
10	*E*	CH_3O	H	$CO_2CH_2CH_3$	8.94	6.10	6.39	5.19	5.96, 8.78	CH_2CH_3 = 7.0
10	*Z*	CH_3O	H	$CO_2CH_2CH_3$	8.91	7.30–8.00	6.07	5.10	5.96, 8.78	CH_1CH_3 = 7.0 CH_2CH_3 = 7.0
11	*E*	Cl	H	CO_2CH_3	8.87	5.40–6.10	—	4.07	6.31	CH_1CH_3 = 6.5
11	*Z*	Cl	H	CO_2CH_3	8.80	7.00–7.80	—	4.06	6.32	CH_1CH_3 = 6.5

*d, Doublet; t, triplet; q, quartet or two doublets; m, multiplet. All resonances are singlets unless marked otherwise.

the only impurity. Photolysis of **11** (*Z*-) gave a mixture of isomers in which the n.m.r. spectrum of **11** (*E*-) could clearly be identified.

Equilibration of **11** (*Z*-) at 210° gave, in addition to the three isomers **11** (*Z*- and *E*-) and **22**, substantial quantities of a new component which has been identified as the butenolide **23** by comparison of its n.m.r. spectrum with that recently reported for **23** (17). Formation of **23** from **11** by

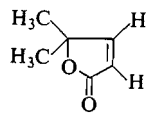

23

loss of methyl chloride is not without precedent and we are examining this reaction further in our laboratories (18, 19). Preliminary results indicate **23** is formed from **22** and not **11**. The equilibration results at 210° are complicated by the side reaction to form **23**, however the fact that the value of 13% *E* is close to the value 8.5% *E* found by the light initiated bromine catalyzed method suggests it is of the right order of magnitude.

Equilibration Studies

The effect of an alkyl group alone at the β-position in acrylonitriles and acrylates is shown in Table 3. In all cases, except where the group is *t*-butyl, there is a significant amount of the *cis*-isomer. For vinyl ketones and aldehydes a β-methyl or β-halogen effectively destabilizes the *cis* form so that less than 2% is present at equilibrium (20, 21). The marked sensitivity of the carbonyl compounds to *cis*-substituents at the β-position is undoubtedly due to the requirement that for maximum conjugation the carbonyl must be in the plane of the double bond and in this form is very sensitive to steric effects. The contribution of the zwitterion form to the stability

TABLE 3

The % of *cis* isomer at equilibrium for β-alkylacrylonitriles and acrylates

β-Substituent	Nitriles	Acrylates
CH_3	58 (24)	18 (25)
CH_3CH_2	—	12.5 (15)
$(CH_3)_2CH$	28 (26), 33*	10 (15)
$(CH_3)_3C$	1.5*	

*Present work.

TABLE 4

The % of *Z*-isomer at equilibrium for β-substituted methacrylates (compare to methacrylonitriles (1))

β-Substituent	% *Z*
CH_3	17 (27)
Br	<1*
CH_3O	<0.2*

*Y. Y. Wigfield, this laboratory.

of aldehydes and ketones would be greater than for esters and thus aldehydes and ketones would show a greater sensitivity to steric inhibition of conjugation. The importance of the zwitterion form in esters is increased when an electron-donating (by resonance) group is attached at the β-position and here also a *trans* configuration is strongly favored (see particularly methyl β-methoxymethacrylate in Table 4).

For compounds of Chart 1 we have an interplay of all these factors. Of particular note is the large % of the *E* form for the β-methoxy compounds **1**, **6**, and **12**. The methoxyl group by conjugation would be in the plane of the double bond and thus may have an effective bulk greater than a *t*-butyl group. Such an argument cannot also explain the equilibrium position for **7**. We feel that coupled with the steric effect there is a repulsive term between the methoxyl and the nitrile or ester groups which is analogous to the interaction between halogen and ester found in **13**. This is in line with the many reports concerning β-methoxy ketones which have those two groups *trans* in the more stable isomer (21, 22).

The repulsive term between halogen and ester is illustrated by the β-chlorocrotonate **13** which is 87.5% in the form with the chlorine (which sterically is expected to be smaller than the methyl) *trans* to the ester and β-bromomethacrylate (Table 4). This repulsive term is more than offset by the isopropyl group in **11** and completely overcome by the *t*-butyl group in **5**.

The positions of equilibrium for the β-dialkyl amino compounds and β-thioethoxy compounds are more nearly where one might predict with the recognition that the dialkyl amino group is held in the plane of the double bond. The importance of conjugation here is noted from the ease with which these and other vinyl amines undergo *cis–trans* isomerization (23).

Can. J. Chem. Downloaded from www.nrcresearchpress.com by 210.87.254.40 on 09/05/12
For personal use only.

Can. J. Chem. Downloaded from www.nrcresearchpress.com by 210.87.254.40 on 09/05/12
For personal use only.

Experimental

The v.p.c. analysis and preparative separation were carried out on commercial (Varian Aerograph) 10 ft × 1/4 in. stainless steel columns containing the appropriate packing. Boiling points were determined by the micro-capillary method and are uncorrected. The n.m.r. spectra in τ values were recorded on a Varian A60 instrument using 20% by volume samples in carbon tetrachloride. All new compounds gave infrared (i.r.) spectra consistent with their respective structures.

*4-Methyl-2-pentenitrile (**18**)*

Condensation of isobutyraldehyde with cyanoacetic acid in pyridine (28) yielded a crude reaction mixture containing *cis*-4-methyl-2-pentenitrile (18%), *trans*-4-methyl-2-pentenitrile (19%), and 4-methyl-3-pentenitrile (63%). After distillation, separation was effected by preparative v.p.c. on a column of 15% QF1 – 5% carbowax-20M at 145°.

*4,4-Dimethyl-2-pentenitrile (**15**)*

A mixture of *cis*- and *trans*-4,4-dimethyl-2-pentenitrile in the ratio 21:79 was obtained from pivaldehyde in an analogous manner to that described above. The physical properties of the *cis*-isomer, b.p. 147–148°, n_D^{20} 1.4328, do not appear to have been reported previously.

Anal. Calcd. for $C_7H_{11}N$: C, 77.07; H, 10.09. Found: C, 77.30; H, 9.92.

3-Keto-2,4,4-trimethylpentanitrile

Condensation of propionitrile with methyl pivalate by means of sodium amide in liquid ammonia (29) yielded the title β-ketonitrile of 93% purity in 75% yield. An analytical sample, b.p. 46°/0.3 mm, $n_D^{17.5}$ 1.4288, was obtained by v.p.c. on S.E. 30 at 155°.

Anal. Calcd. for $C_8H_{13}NO$: C, 69.07; H, 9.35. Found: C, 68.40; H, 9.56.

3-Hydroxy-2,4,4-trimethylpentanitrile

Sodium borohydride reduction of the above β-ketonitrile readily yielded an *erythro–threo* mixture of alcohols (83% yield), b.p. 64–65°/0.3 mm.

Anal. Calcd. for $C_8H_{15}NO$: C, 68.10; H, 10.64; N, 9.93. Found: C, 67.89; H, 10.55; N, 9.93.

*2,4,4-Trimethyl-2-pentenitrile (**16**, E- and Z-)*

(1) To the above mixture of alcohols (2.82 g) dissolved in pyridine (3.2 ml) was added, dropwise with stirring and cooling, thionyl chloride (3 ml). After the addition was complete the reaction mixture was allowed to attain and maintain room temperature for 3 h, then it was heated at 80° for 2 h. After work-up (30) and distillation, a mixture of 2,4,4-trimethyl-2-pentenitrile (*E*- and *Z*-, 1.40 g, 57%) was obtained containing 80% of the *Z* isomer. The two isomers were separated by v.p.c. on QF1-carbowax at 130°, the following physical properties being recorded.

The *E* isomer, b.p. 165–166°, $n_D^{17.5}$ 1.4440.

Anal. Calcd. for $C_8H_{13}N$: C, 78.05; H, 10.57. Found: C, 77.88; H, 10.49.

The *Z* isomer, b.p. 147–148°, $n_D^{17.5}$ 1.4380.

Anal. Found: C, 78.14; H, 10.77.

(2) Dehydration of the cyanohydrin of 4,4-dimethyl-2-pentanone (31) (1.35 g) was effected by means of thionyl chloride (1.46 ml) and pyridine (1.62 ml). The distilled product (0.5 g) contained mainly 85% of a mixture of 2,4,4-trimethyl-2-pentenitrile (*Z*-) and 4,4-dimethyl-2-methylenepentanitrile in the ratio 16:7. Found *M* (mass spectrum) 122. The n.m.r. (CCl_4) on mixture (data only given for the methylenenitrile), 8.99 (singlet, 9 protons), 7.87 (doublet, 3 protons, J = 1.5 Hz), 4.38 (quartet, 1 proton, J = 1.5 Hz), 4.11 (doublet, 1 proton, J = 1.5 Hz).

A minor product (3%), which was not identified, had an identical v.p.c. retention time (QF1-carbowax at 150°) with 2,4,4-trimethyl-2-pentenitrile (*E*-).

*2-Bromo-4-methyl-2-pentenitrile (**19**)*

Crude 2,3-dibromo-4-methylpentanitrile, prepared by the addition of bromine to *cis*-4-methyl-2-pentenitrile, was dehydrobrominated with sodium acetate in acetic acid (32). The crude reaction product contains the *E* and *Z* isomers of 2-bromo-4-methyl-2-pentenitrile in the ratio 47:53. After distillation, the two isomers were separated by v.p.c. on QF1-carbowax at 160°. A correct elemental analysis could not be obtained for either isomer although both isomers appeared to be homogeneous from v.p.c. and n.m.r. analysis. The following physical properties were, however, obtained.

2-Bromo-4-methyl-2-pentenitrile (*E*-), b.p. 160–161°, n_D^{20} 1.4766, *M* (mass spectrum) 173.

2-Bromo-4-methyl-2-pentenitrile (*Z*-), b.p. 168–169°, n_D^{20} 1.4780, *M* (mass spectrum) 173.

The equilibrium mixture, determined from each isomer by irradiation of a sample in carbon tetrachloride containing 1% bromine, contained 42% of the *E* form.

*2-Bromo-4,4-dimethyl-2-pentenitrile (**17**, E- and Z-)*

Treatment of a *cis–trans* mixture of 4,4-dimethyl-2-pentenitrile (containing 88% *trans* isomer) with bromine, followed by dehydrobromination with sodium acetate in acetic acid, yielded the required bromo-nitriles (*E*:*Z* ratio = 2:1). The following physical properties were determined.

2-Bromo-4,4-dimethyl-2-pentenitrile (*E*-), b.p. 179–180°, n_D^{20} 1.4829.

Anal. Calcd. for $C_7H_{10}BrN$: C, 44.68; H, 5.32. Found: C, 44.75; H, 5.32.

2-Bromo-4,4-dimethyl-2-pentenitrile (*Z*-), b.p. 190–191°, n_D^{20} 1.4821.

Anal. Found: C, 44.74; H, 5.22.

In a further experiment, starting from 4,4-dimethyl-2-pentenitrile (79% *trans*), a mixture of 2-bromo-4,4-dimethyl-2-pentenitrile (*E*- and *Z*-) was obtained containing over 85% of the *E* isomer. An attempt to increase the amount of *Z* isomer in this mixture photochemically was unsuccessful. Irradiation of an ether solution of the mixture at 2537 Å through Pyrex caused virtually no isomerization, whilst irradiation through silica for 6 h yielded *trans*-4,4-dimethyl-2-pentenitrile as the major product.

The equilibrium position determined as above contained 81% of the *E* form.

*3-Methoxy-4-methyl-2-pentenitrile (Z-) (**12**)*

(1) Treatment of 2-bromo-4-methyl-2-pentenitrile (either isomer) with sodium methoxide (1.1 equ) in methanol at room temperature for 1.5 h yielded an *E–Z*

Can. J. Chem. Downloaded from www.nrcresearchpress.com by 210.87.254.40 on 09/05/12
For personal use only.

mixture of 3-methoxy-4-methyl-2-pentenitrile containing over 90% of the thermodynamically less stable *Z* isomer. After distillation and purification by v.p.c. on QF1-carbowax at 160° a sample of pure *Z* isomer was obtained, the n.m.r. and i.r. spectra of which were identical with those of a sample prepared as below.

(2) 3-Keto-4-methylpentanitrile was prepared in 80% yield by the sodium amide catalyzed condensation of acetonitrile and methyl isobutyrate (29). The ketonitrile, b.p. 60°/0.1 mm, n_D^{19} 1.4752, is a colorless liquid which decomposes on heating or standing. It is completely stable, however, when stored in the solid form at −78°.

Anal. Calcd. for C_6H_9NO: C, 64.86; H, 8.11; N, 12.61. Found: C, 64.96; H, 8.22; N, 12.75.

The n.m.r. 8.87 (doublet), 7.20 (septet), 6.36 (singlet, J = 7.0 Hz).

Yamashita (33) has previously obtained this compound as a light yellow oil, b.p. 102–104°/12 mm, using sodium ethoxide as condensing agent. The yield, however, was only 45% and the procedure more tedious than that described here.

Treatment of 3-keto-4-methylpentanitrile (4 g) with an ethereal solution of diazomethane (from 12 g of *N*-nitroso-*N*-methylurea) resulted in an instantaneous evolution of nitrogen. After 16 h at room temperature the ether was removed and the residue distilled at 73–85°/15 mm. The resulting white liquid (3.65 g, 81%) contained the *E* and *Z* isomers of 3-methoxy-4-methyl-2-pentenitrile in the ratio 3:97. A sample of pure *Z* isomer, b.p. 184.5–185.5°, $n_D^{17.5}$ 1.4602, was obtained by v.p.c. on QF1-carbowax at 160°.

Anal. Calcd. for $C_7H_{11}NO$: C, 67.20; H, 8.80. Found: C, 67.02; H, 8.92.

3-Methoxy-4-methyl-2-pentenitrile (E-) (12)

Irradiation of an ether solution of the above *Z* isomer through silica at 2537 Å for 3 h yielded a mixture containing 95% of the *E* isomer. Separation was effected by v.p.c. on QF1-carbowax at 160° to give 3-methoxy-4-methyl-2-pentenitrile (*E*-), b.p. 196.5–197.5°, n_D^{15} 1.4553.

Anal. Found: C, 67.44; H, 9.05.

4,4-Dimethyl-3-methoxy-2-pentenitrile (Z-) (1)

This was prepared by analogous methods to those used for the corresponding isopropyl compound, either by treatment of 2-bromo-4,4-dimethyl-2-pentenitrile with sodium methoxide in methanol or, more conveniently, by the reaction of β-cyanopinacolone (34) with diazomethane (35). After purification by distillation and v.p.c. on QF1-carbowax at 160°, 4,4-dimethyl-3-methoxy-2-pentenitrile (*Z*-), b.p. 191–192°, n_D^{20} 1.4572 (lit. (35) b.p. 87–88° at 19 mm, n_D^{30} 1.4482), was obtained.

Anal. Calcd. for $C_8H_{13}ON$: C, 69.07; H, 9.35. Found: C, 69.27; H, 9.45.

4,4-Dimethyl-3-methoxy-2-pentenitrile (E-) (1)

Irradiation of an ether solution of the above *Z* isomer through silica at 2537 Å for 5 h yielded a mixture containing 42% of the *E* isomer. After separation by v.p.c. on QF1-carbowax at 160° pure *E* isomer, b.p. 215–216°, n_D^{20} 1.4630, was obtained.

Anal. Found: C, 68.96; H, 9.51.

3-Methoxy-2,4,4-trimethyl-2-pentenitrile (E-) (6)

3-Keto-2,4,4-trimethylpentanitrile (4 g) was treated with diazomethane (from 10.3 g of *N*-nitroso-*N*-methylurea) in ether (100 ml). As evolution of nitrogen did not occur, methanol (20 ml) was added to the reaction mixture. After 16 h the solvent was evaporated and the distilled residue (3.7 g) examined by v.p.c. Since the distillate contained (v.p.c.) 33% unchanged starting material, it was treated with a further portion of diazomethane (as above). Work-up yielded a colorless liquid (3.34 g) containing 82% of the *E* and 4% of the *Z* isomer of 3-methoxy-2,4,4-trimethyl-2-pentenitrile. An analytical sample of the *E* isomer, b.p. 203–204°, $n_D^{17.5}$ 1.4588, was obtained by v.p.c. on S.E. 30 at 165°.

Anal. Calcd. for $C_9H_{15}NO$: C, 70.58; H, 9.80. Found: C, 68.93; H, 9.90.

3-Methoxy-2,4,4-trimethyl-2-pentenitrile (Z-) (6)

Irradiation of a 2.5% ethereal solution of the distillate from the previous experiment through silica at 2537 Å for 2.5 h increased the amount of *Z* isomer to 15%.

3-Chloro-4,4-dimethyl-2-pentenal (with B. D. Page)

Vilsmeier formylation of pinacolone with phosphorous oxychloride and dimethylformamide was carried out as described by Bodendorf and Mayer (4). A 61% yield of the chloroaldehyde was obtained which was shown (36) by n.m.r. spectroscopy to contain only the *Z* isomer.

Oxime of 3-Chloro-4,4-dimethyl-2-pentenal (Z-)

3-Chloro-4,4-dimethyl-2-pentenal (*Z*, 6.37 g) and hydroxylamine hydrochloride (3.63 g, 1.2 equ) were dissolved in pyridine (25 ml). An exothermic reaction occurred and after 5 min, a second liquid layer (approximately 5 ml) separated at the bottom of the flask. After 17.5 h, water was added and the mixture was extracted twice with ether. The combined ether extracts were washed with three portions of 3 *N* hydrochloric acid then dried over magnesium sulfate. Removal of the ether under reduced pressure yielded the required oxime (95% crude yield) as a viscous oil which was used immediately in the next experiment.

Once, when the liquid oxime was allowed to stand at room temperature for 24 h, it partially solidified with evolution of heat. Dehydration of this semi-solid oxime in an analogous manner to that described below gave, besides the required nitrile, a 30% yield of 5-*t*-butylisoxazole.

3-Chloro-4,4-dimethyl-2-pentenitrile (Z-) (5)

The crude liquid oxime (5.54 g) was dissolved in dry benzene (10 ml) and added to a syrup of ethanol and phosphorus pentoxide (prepared from 2.8 g of ethanol and 6.3 g of phosphorus pentoxide by the method of Mukaiyama and Hata (37)). The reaction mixture was stirred and boiled under reflux for 35 min, then cooled and the benzene layer decanted. The residual syrup was dissolved in water, extracted with ether and the organic layer dried over magnesium sulfate. After removal of the solvent from the combined ether and benzene extracts, the resulting liquid was distilled. The v.p.c. analysis indicated the distillate (4.25 g, 82% based on the chloroaldehyde) to be >98% pure. An analytical sample of

Can. J. Chem. Downloaded from www.nrcresearchpress.com by 210.87.254.40 on 09/05/12
For personal use only.

3-chloro-4,4-dimethyl-2-pentenitrile (*Z*-), b.p. 198–199°, $n_D^{17.5}$ 1.4679, was obtained by v.p.c. purification on Apiezon J at 168°.

Anal. Calcd. for $C_7H_{10}ClN$: C, 58.55; H, 6.97. Found: C, 58.45; H, 7.14.

3-Chloro-4,4-dimethyl-2-pentenitrile (E-) (5)

Irradiation of an ether solution of the above *Z* isomer through silica at 2537 Å for 2.5 h yielded only 4% of the *E* isomer. An enriched sample, containing 15% of the *E* isomer was obtained by v.p.c.

4,4-Dimethyl-3-dimethylamino-2-pentenitrile (3)

To 3-chloro-4,4-dimethyl-2-pentenitrile (*Z*-, 1.5 g) dissolved in ether (2 ml) was added dimethylamine (10 ml) and the reaction mixture was kept in a tightly-stoppered tube for 13 days. More ether was then added and the dimethylamine hydrochloride was removed by filtration. Evaporation of the solvent yielded an oil which was distilled at 120–130°/20 mm to give 4,4-dimethyl-3-dimethylamino-2-pentenitrile (1.5 g, 94%). An analytical sample containing 17% *E* and 83% *Z* isomers was obtained by v.p.c. on Apiezon J at 210°.

Anal. Calcd. for $C_9H_{16}N_2$: C, 71.06; H, 10.53. Found: C, 70.80; H, 10.80.

4,4-Dimethyl-3-diethylamino-2-pentenitrile (13)

Reaction of 3-chloro-4,4-dimethyl-2-pentenitrile with a large excess of boiling diethylamine for 24 h yielded a small amount of unchanged starting material and an *E–Z* mixture of the required enaminonitrile containing >90% of the *Z* isomer.

Anal. Calcd. for $C_{11}H_{20}N_2$: C, 73.33; H, 11.11. Found: C, 73.11; H, 11.21.

The above *E–Z* mixture of enaminonitriles was also prepared, though less conveniently, by reaction of 2-bromo-4,4-dimethyl-2-pentenitrile (*Z*-) with boiling diethylamine. The *E* form of the bromonitrile reacted only very slowly with both diethyl- and dimethylamine.

4,4-Dimethyl-3-thioethoxy-2-pentenitrile (Z-) (2)

To 3-chloro-4,4-dimethyl-2-pentenitrile (*Z*-, 1 g) cooled in ice was added, with stirring, a solution of sodium thioethoxide (2 equ) in methanol. After 1.5 h the reaction mixture was neutralized with acetic acid and diluted with ether. After filtration, the solvent was removed and the residue was distilled under reduced pressure. The v.p.c. analysis of the distillate (0.64 g) showed the presence of both isomers of 4,4-dimethyl-3-thioethoxy-2-pentenitrile (*E*:*Z* ratio = 3:97). Further purification on FFAP at 168° yielded pure *Z* isomer, b.p. 227–228°, n_D^{20} 1.5032.

Anal. Calcd. for C_9H_5NS: C, 63.90; H, 8.88. Found: C, 63.94; H, 9.18.

The above *Z* isomer was also prepared by treating 2-bromo-4,4-dimethyl-2-pentenitrile (*E*- or *Z*-) with 2 equ of sodium thioethoxide in methanol.

4,4-Dimethyl-3-thioethoxy-2-pentenitrile (E-) (2)

The title compound was most conveniently prepared by heating of the *Z* isomer at 210° for 28 h, the resulting equilibrium mixture containing 30% of the *E* isomer. After purification on FFAP at 168° pure *E* isomer, b.p. 231–232°, $n_D^{18.5}$ 1.5228, was obtained.

Anal. Found: C, 64.20; H, 8.67; N, 8.38.

Ethyl-4,4-dimethyl-3-methoxy-2-pentenoate (Z-) (7)

Ethyl 4,4-dimethyl-3-ketopentanoate was prepared by the action of sodium amide in liquid ammonia on a mixture of pinacolone and diethyl carbonate (6). To the ketoester (1.5 g) in methanol (10 ml) was added diazomethane (from 5.2 g of *N*-nitroso-*N*-methylurea) in ether (50 ml). After 6 days the solvent was removed and the residue was distilled under reduced pressure. The resulting distillate (1.5 g) was purified further by v.p.c. on QF1-carbowax at 175° to give ethyl 4,4-dimethyl-3-methoxy-2-pentenoate (*Z*-), b.p. 205–206°, n_D^{20} 1.4490.

Anal. Calcd. for $C_{10}H_{18}O_3$: C, 64.52; H, 9.68. Found: C, 64.27; H, 9.53.

Ethyl-4,4-dimethyl-3-methoxy-2-pentenoate (E-) (7)

Irradiation of a 2.5% ether solution of the above *Z* isomer through silica at 2537 Å for 2 h yielded an *E–Z* mixture containing 46% of the *E* isomer (from n.m.r. spectral analysis). The two isomers were only partially separable by v.p.c.

Ethyl-3-methoxy-4-methyl-2-pentenoate (Z-) (10)

The title compound was prepared from ethyl isobutyrylacetate and diazomethane in an identical fashion to that described above. Attempts to purify the crude *Z* isomer by v.p.c. on QF1-carbowax at 175° resulted in *cis–trans* isomerization, the collected sample containing both *E* and *Z* isomers in the ratio 7:9.

Anal. Calcd. for $C_9H_{16}O_3$: C, 62.79; H, 9.30. Found: C, 62.41; H, 9.37.

Ethyl-3-methoxy-4-methyl-2-pentenoate (E-) (10)

Heating of the above *E–Z* mixture at 210° for 17.6 h yielded a mixture containing approximately 90% of the *E* isomer, 2% of the *Z* isomer, and 8% of the β,γ-isomer ethyl 3-methoxy-4-methyl-3-pentenoate. No attempt was made to purify the *E* isomer.

Ethyl-2-chloro-4,4-dimethyl-3-ketopentanoate

To a suspension of phosphorus pentachloride (8.3 g) in benzene (10 ml) was added dropwise over 1.5 h, with stirring, ethyl 4,4-dimethyl-3-ketopentanoate (3.44 g). After 6 days water (10 ml) was added, with cooling, and the reaction mixture was stirred for a further 24 h. Extraction of the aqueous layer with ether yielded a product identical with that obtained from the benzene layer (total yield 2.7 g after distillation under reduced pressure). An analytical sample, b.p. 230–231°, was obtained by v.p.c. on DC 550 at 200°.

Anal. Calcd. for $C_9H_{15}ClO_3$: C, 52.29; H, 7.26. Found: C, 52.20; H, 7.59.

The n.m.r. (CCl_4): 8.72 (singlet, 9 protons), 8.69 (triplet, J = 7.0 Hz), 3 protons), 5.73 (quartet, J = 7.0 Hz, two protons), 4.90 (singlet, one proton).

Methyl 3-Chloro-4,4-dimethyl-2-pentenoate (Z-) (9)

Active manganese dioxide (38) (20 g) was added to a stirred solution of 3-chloro-4,4-dimethyl-2-pentenal (2 g), sodium cyanide (3.6 g), and acetic acid (2 ml) in methanol (110 ml). After 16.5 h, the manganese dioxide was removed by filtration and the methanol evaporated under reduced pressure. Water and ether were added to the residue and the aqueous layer was then extracted with two further portions of ether. The combined organic

TABLE 5

Pyrolysis of methyl 3-chloro-4-methyl-2-pentenoate (*Z*-) (**11**)

Time (h)	Chloro ester (*E*-) (**11**)	Chloro-ester (*Z*-) (**11**)	*E*:*Z* ratio	β,γ-Chloro-ester (**22**)	Butenolide **23**
0	0.0	95.0	0:95	5.0	0.0
92	9.5	55.6	1:5.9	22.9	12.0
116	8.8	50.2	1:5.7	27.6	13.4
169	6.0	40.7	1:6.8	30.4	22.9
265	2.6	18.65	1:7.2	25.9	52.85

extracts were dried over magnesium sulfate and the solvent was then removed. Distillation of the residue under reduced pressure yielded methyl 3-chloro-4,4-dimethyl-2-pentenoate (*Z*-) as a clear liquid (1.9 g, 79%) which was shown by v.p.c. to be 98% pure. An analytical sample, b.p. 203–204°, n_D^{17} 1.4655, was obtained by v.p.c. on QF1-carbowax at 165°.

Anal. Calcd. for $C_8H_{13}ClO_2$: C, 54.41; H, 7.36. Found: C, 54.70; H, 7.54.

*Methyl 3-Chloro-4,4-dimethyl-2-pentenoate (E-) (**9**)*

Irradiation of a 2% ethereal solution of the above *Z* isomer through silica at 2537 Å for 3.5 h gave an *E*–*Z* mixture containing 20% of the *E* isomer. The two isomers were separated by v.p.c. on QF1-carbowax at 165° to give methyl 3-chloro-4,4-dimethyl-2-pentenoate (*E*-), b.p. 178–179°, n_D^{15} 1.4585.

Anal. Found: C, 54.59; H, 7.48.

*Methyl 3-Chloro-4-methyl-2-pentenoate (Z-) (**11**)*

Crude 3-chloro-4-methyl-2-pentenoic acid (13) was converted to the methyl ester by the method of Scheibler and Voss (16). The crude ester was initially purified by distillation under reduced pressure. The distillate was further separated into its components by v.p.c. on Apiezon J at 150°. The first product isolated was a mixture of methyl 3-chloro-4-methyl-2-pentenoate (*E*-) and an unidentified component (see below). The latter appeared to be a decomposition product formed during the v.p.c. separation as it was not present in the original distillate. The second product isolated was a mixture, b.p. 181–182°, of methyl 3-chloro-4-methyl-2-pentenoate (*Z*-) and methyl 3-chloro-4-methyl-3-pentenoate in the ratio 94:6.

Anal. Calcd. for $C_7H_{11}ClO_2$: C, 51.69; H, 6.77. Found: C, 51.76; H, 7.00.

Pyrolysis of Methyl 3-Chloro-4-methyl-2-pentenoate (Z-)

(1) Pyrolysis of the chloroester (40 ml) at 235° for 88 h gave a dark-brown liquid. Analysis of this liquid by v.p.c. on Apiezon J at 153° indicated the presence of only one non-volatile product. Isolation of this product by v.p.c. yielded a small amount of a clear liquid, the n.m.r. spectrum of which was identical with that recently reported (17) for 5,5-dimethyl-3-butenolide (**23**).

(2) The chloroester (4 × 10 μl) was pyrolyzed in sealed Pyrex tubes at 195°, samples being removed at fixed intervals for v.p.c. analysis (Apiezon J, 153°). The results after different time intervals are shown in Table 5.

Reaction of Methyl 3-Chloro-4,4-dimethyl-2-pentenoate (Z-) with Dimethylamine

To the title chloroester (1.4 g) in ether (3 ml) was added dimethylamine (10 ml) and the reaction mixture was kept in a screw-cap jar at room temperature for 11 days. The v.p.c. analysis (S.E. 30, 205°) of the crude product indicated starting material (6%) together with two minor products (18%) and one major product (76%). Purification of the major product was effected by distillation under reduced pressure, followed by v.p.c. on SE 30 at 205° to give a white solid, m.p. 45–46° after recrystallization from petroleum ether (b.p. 30–60°). Elemental analysis, n.m.r. and mass spectroscopy indicated the solid to be the dimethylamide of 3-chloro-4,4-dimethyl-2-pentenoic acid (*Z*-).

Anal. Calcd. for $C_9H_{16}ClNO$: C, 56.99; H, 8.44; N, 7.39; Cl, 18.74. Found: C, 57.05; H, 8.57; N, 7.12; Cl, 18.51.

The n.m.r. (CCl_4): 8.78 (singlet, 9 protons), 7.09, 7.03 (2 singlets, 3 protons each), 4.07 (singlet, 1 proton).

Methyl 3-chloro-4,4-dimethyl-2-pentenoate (*Z*-) was recovered essentially unchanged after 65 h in boiling diethylamine and 16 h in boiling dimethylformamide (39).

*Methyl 4,4-Dimethyl-3-thioethoxy-2-pentenoate (**8**)*

Treatment of methyl 3-chloro-4,4-dimethyl-2-pentenoate (*Z*-) with sodium thioethoxide (2 equ) in methanol at 0° for 1.5 h gave, after distillation under reduced pressure, a mixture of methyl 4,4-dimethyl-3-thioethoxy-2-pentenoate (*E*- and *Z*-) in the ratio 7:93.

Anal. Calcd. for $C_{18}H_{18}O_2S$: C, 59.40; H, 8.91. Found: C, 59.24; H, 8.89.

A sample of pure *Z* isomer, n_D^{20} 1.4931, was obtained by v.p.c. on FFAP at 165°.

Irradiation of a 2% solution of the above mixture of isomers through silica at 2537 Å for 7 h only increased the amount of *E* isomer to 11%. A mixture containing 20–25% of the *E* isomer was, however, obtained by treating methyl 3-chloro-4,4-dimethyl-2-pentenoate (*E*-) with 1.1 equ of sodium thioethoxide in methanol.

*Methyl 3-Chlorocrotonate (**13**)*

Methylation of 3-chlorocrotonic acid (*E*-) with an ethereal solution of diazomethane yielded methyl 3-chlorocrotonate (*E*-) in 90% yield. The corresponding *Z* isomer was prepared by irradiation of an ethereal solution of the *E* isomer.

A fellowship to D.V.G. and financial support from NRCC are gratefully acknowledged.

Can. J. Chem. Downloaded from www.nrcresearchpress.com by 210.87.254.40 on 09/05/12
For personal use only.

1. D. V. GARDNER and D. E. McGREER. Can. J. Chem. This issue.
2. J. E. BLACKWOOD, C. L. GLADYS, K. L. LOENING, A. E. PETRARCA, and J. E. RUSH. J. Amer. Chem. Soc. **90**, 509 (1968).
3. W. J. LE NOBLE. J. Amer. Chem. Soc. **83**, 3897 (1961).
4. K. BODENDORF and R. MAYER. Chem. Ber. **98**, 3554 (1965).
5. E. J. COREY, N. W. GILMAN, and B. E. GANEM. J. Amer. Chem. Soc. **90**, 5616 (1968).
6. R. LEVINE and C. R. HAUSER. J. Amer. Chem. Soc. **66**, 1768 (1944).
7. W. E. TRUCE and J. A. SIMMS. J. Amer. Chem. Soc. **78**, 2756 (1956).
8. S. I. MILLER. J. Amer. Chem. Soc. **78**, 6091 (1956).
9. U. E. MATTER, C. PASCUAL, E. PRETSCH, A. PROSS, W. SIMON, and S. STERNHELL. Tetrahedron, **25**, 691 (1969).
10. T. HAYASHI, I. HORI, H. BABA, and H. MIDORIKAWA. J. Org. Chem. **30**, 695 (1965).
11. T. HAYASHI, M. IGARASHI, S. HAYASHI, and H. MIDORIKAWA. Bull. Soc. Chem. Japan, **38**, 2063 (1965).
12. D. E. JONES, R. O. MORRIS, C. A. VERNON, and R. F. M. WHITE. J. Chem. Soc. 2349 (1960).
13. J. S. PIZEY and W. E. TRUCE. J. Chem. Soc. 865 (1964).
14. C. K. INGOLD. Structure and mechanism in organic chemistry. Bell, London, 1953. p. 75.
15. D. E. McGREER and N. W. K. CHIU. Can. J. Chem. **46**, 2225 (1968).
16. H. SCHEIBLER and J. VOSS. Chem. Ber. **53**, 379 (1920).
17. G. BUCHI and S. H. FEAIRHELLER. J. Org. Chem. **34**, 609 (1969).
18. Y. Y. WIGFIELD. Ph.D. thesis. The University of British Columbia, Vancouver, B.C., 1969.
19. E. LEWARS, J. K. STOWELL, S. WAWZONEK, and P. YATES. Chem. Ind. 344 (1968).
20. D. E. McGREER and B. D. PAGE. Can. J. Chem. **47**, 866 (1969).
21. D. LANDINI and F. MONTANARI. Chem. Commun. 180 (1967).
22. E. EISTERT, F. ARNDT, L. LOEWE, and E. AYCA. Chem. Ber. **84**, 156 (1951).
23. Y. SHVO and H. SHANAN-ATIDI. J. Amer. Chem. Soc. **91**, 6689 (1969).
24. J. N. BUTLER and R. D. McALPINE. Can. J. Chem. **41**, 2487 (1963).
25. J. N. BUTLER and G. J. SMALL. Can. J. Chem. **41**, 2492 (1963).
26. G. DESCOTES and P. LACONCHE. Bull. Soc. Chim. France, 2149 (1968).
27. D. E. McGREER, W. WAI, and G. CARMICHAEL. Can. J. Chem. **38**, 2410 (1960).
28. G. BAERTS. Bull. Soc. Chim. Belg. **41**, 314 (1932); Chem. Abstr. **27**, 267 (1933).
29. C. J. EBY and C. R. HAUSER. J. Amer. Chem. Soc. **79**, 723 (1957).
30. C. D. HURD and C. H. RECTOR, JR. J. Org. Chem. **10**, 441 (1945).
31. R. HEILMANN, G. DE GAUDEMARIS, and P. ARNAUD. Bull. Soc. Chim. France, 972 (1951).
32. C. F. H. ALLEN and C. O. EDENS, JR. Organic syntheses. Coll. Vol. III. John Wiley and Sons, New York, 1955. p. 731.
33. M. YAMASHITA. J. Org. Chem. **23**, 835 (1958).
34. O. WIDMAN and E. WAHLBERG. Chem. Ber. **44**, 2065 (1911).
35. F. IIMURA. Nippon Kagaku Zasshi. **78**, 48 (1957); Chem. Abstr. **53**, 5185*d* (1959).
36. B. D. PAGE. Unpublished results.
37. T. MUKAIYAMA and T. HATA. Bull. Chem. Soc. Japan, **34**, 99 (1961).
38. J. ATTENBURROW, A. F. B. CAMERON, J. H. CHAPMAN, R. M. EVANS, B. A. HEMS, A. B. A. JANSEN, and T. WALKER. J. Chem. Soc. 1094 (1952).
39. N. D. HEINDEL and P. D. KENNEWELL. Chem. Commun. 38 (1969) and references therein.

Can. J. Chem. Downloaded from www.nrcresearchpress.com by 210.87.254.40 on 09/05/12
For personal use only.

Can. J. Chem. Downloaded from www.nrcresearchpress.com by 210.87.254.6 on 09/05/12
For personal use only.

Transition state analysis. I. Correlation between solvent stretching frequencies and C vs. O product ratios in alkylation of ambient anions. A new explanation for the observed product ratios

DONALD C. WIGFIELD
Department of Chemistry, Carleton University, Ottawa 1, Ontario

Received December 10, 1969

A new explanation is presented for the O to C product ratios observed in alkylation reactions of ethyl acetoacetate and related enolic and phenolic compounds, based on a Hammond postulate analysis of the nature of the transition states involved. The explanation not only covers the effects of solvent and the nature of the metal cation, but also encompasses the previously unexplained effect of the alkyl halide structure. From the latter effect, ground state interaction between solvent and alkyl halide is predicted. Evidence consistent with this interaction is found in linear free energy relationships between the $\Delta\Delta G^{\ddagger}$ (C vs. O) values for various alkyl halides and the stretching frequency of the solvent (S=O of DMSO; P=O of HMPA) when measured as alkyl halide solutions.

Canadian Journal of Chemistry, **48**, 2120 (1970)

Introduction

The experimental factors governing the orientation of attack in alkylation reactions of ethyl acetoacetate and related compounds, whether on oxygen or on carbon, are now well known (1–6). It has become clear that the O to C product ratio is a function of several variables; nevertheless, an adequate and unified explanation of the way in which these factors, particularly the structure of the alkylating agent (4, 6) operates, is lacking.

Alkylation of the anion of ethyl acetoacetate can give four products, which have been termed "O", "C", "CO", and "CC", as shown in Fig. 1.

The three main factors that have a systematic influence on the O to C product ratio have been shown to be (*a*) the solvent, (*b*) the metal cation, and (*c*) the structure of the alkylating agent (1–6). Previous explanations of the effect of the solvent and the cation involve the concepts of freedom (6) and of selective solvation (1, 6) of the ground state enolate anion. Little in the way of explanation has yet been offered to account for the effect of the alkylating agent. In considering product ratios of *kinetically controlled* reactions, such as this, we prefer to examine, as closely as feasible, the structure of the *transition state* rather than that of the *ground state*. In this paper, we wish to present a unified explanation of the product ratios, based on an assessment of the effect that the variable factors are likely to have on the structure of the transition state. Independent evidence consistent with the explanation is presented.

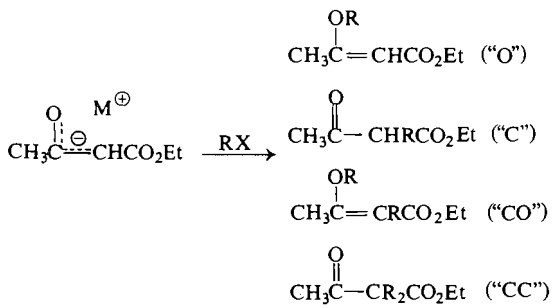

FIG. 1. Products of the alkylation of ethyl acetoacetate.

Experimental

Reagents

Solvents and reagents used in this study were all commercially available. Reagent or spectral grade reagents were used and were freshly distilled prior to making spectral measurements. The DMSO[1] and HMPA[1] were stored over molecular sieves after distillation.

Spectra

Dilute solutions (2%) of DMSO and HMPA in the various alkyl halides were prepared. Infrared (i.r.) spectra were recorded on a Perkin–Elmer model 225 spectrophotometer.

Discussion and Results

Our own interest in this area has stemmed from the intriguing fact that a prediction of whether O-alkylation or C-alkylation would predominate in a given circumstance, would markedly depend on what position the transition state occupied with respect to the reaction coordinate. In other words,

[1]The abbreviations DMSO and HMPA are used for dimethyl sulfoxide and hexamethylphosphoramide respectively.

Can. J. Chem. Downloaded from www.nrcresearchpress.com by 210.87.254.6 on 09/05/12
For personal use only.

considering an alkylation reaction with a transition state occurring very early during the reaction process, and therefore structurally resembling the ground state reactants, it would be anticipated that alkylation would occur predominantly at the site of highest electron density,[2] namely at oxygen. On the other hand, for a reaction proceeding through a transition state that occurred late in the reaction process, the factors affecting the energy of the transition state would be expected to be similar to those affecting the energy of the product, and hence the more stable product would have the energetically more favorable transition state. In this way the *thermodynamically* more stable product is preferentially produced as a result of a purely *kinetic* process. The term "product development control" has been coined for this phenomenon (8). In this case, the thermodynamically more stable product is that of C-alkylation.[3] Thus, for a reaction with a transition state resembling reactants, one expects O-alkylation, whereas if the transition state resembles products, a predominance of C-alkylation is predicted.

In order to evaluate whether this type of reasoning could be a factor underlying the observed product ratios in alkylation of ethyl acetoacetate, it becomes necessary to have a probe to investigate the nature of the transition states involved. For this purpose, the well-established, although not infallible, Hammond postulate (9), which essentially relates the heat of reaction, in a qualitative sense, with the nature of the transition state, was selected.

Solvent Effect

It has become clear that the use of dipolar aprotic solvents, such as dimethyl sulfoxide or hexamethylphosphoramide, causes an increase in the amount of O-alkylation with respect to alkylation reactions performed in hydroxylic solvents (1, 3, 5). Dipolar aprotic solvents of this type are known to solvate cations strongly, but to be poor solvators of anions (10). Thus in DMSO or HMPA the enolate anion is a higher energy species than when heavily solvated in hydroxylic solvents, and the reaction is therefore more exothermic. According to the Hammond postulate, the reaction will be expected, therefore, to proceed via a transition state more closely resembling reactants,[4] giving rise to a greater proportion of O-alkylated product, in agreement with the experimental observation.

Cation Effect

Kurz *et al.* (5) have shown that yields of O-alkylation increase when the cation associated with the enolate anion is varied through the series Li^+, Na^+, K^+, Cs^+, NR_4^+. Similar, although less markedly differentiating, results have also been obtained in other laboratories (3, 4). The series from Li^+ through NR_4^+ is presumably producing enolate anions of greater freedom and therefore of greater energy. Accordingly, the series is proceeding to higher exothermicity, and, from the Hammond postulate, towards transition states bearing more resemblance to reactants. Thus it is to be expected that the series will tend towards greater O-alkylation, as is experimentally observed. Evidence that the energy of the ground state is indeed affected by the nature of the metal cation is furnished by the observation (6) that reaction of the lithium enolate is considerably slower than other members of the series.

Alkyl Halide Effect

We have demonstrated above that evaluation of the effect of solvent and the metal cation on the nature of the transition state by use of the Hammond postulate and extension of this information to assess the effect on the C vs. O product ratio successfully predicts trends that are experimentally observed. This approach to rationalizing product ratios must therefore be regarded as an equally valid explanation to those already put forward (2, 6). We now extend this approach to the effect of alkyl halide structure, which has proved to be a stumbling-block for rationalizations (6). Owing to the careful and systematic work of LeNoble *et al.* (4, 6), a relationship between C to O product ratio and S_N2 reactivity of the alkyl halide has emerged which has been summarized by LeNoble and Puerta (4) in the words, "increased S_N2 reactivity (of the

[2]The concept of ground state electron densities giving a fairly accurate picture of the preferred position of attack is not without precedent. For an example, see ref. 7.

[3]The Claisen rearrangement is an experimental verification of the fact that C-alkylation products are generally more stable than those of O-alkylation.

[4]The effect of solvent on the energy of attacking anions, and its relation to the nature of the transition state using the Hammond postulate, has been used with great success in explaining stereochemical product ratios in the Michael addition (11).

TABLE 1

Sulfoxide stretching frequency of DMSO in various alkyl halides and parameters derived from product ratios in alkylation of ethyl acetoacetate in DMSO

Alkyl halide	ν_{max}(S=O) (cm^{-1})	"O"* (%)	"C" + "CO" + "CC"* (%)	"O"/"C" + "CO" + "CC"	$\Delta\Delta G‡$ (kcal $mole^{-1}$)
2-Chloropropane	1071.5	62	38	1.63	−0.39
1-Chloropropane	1070.0	47	53	0.89	0.09
1-Bromopropane	1068.5	31	69	0.45	0.64
1-Iodopropane	1067.2	14	86	0.16	1.45
Benzyl chloride	1062.7	5	95	0.05	2.36

*Data from ref. 4.

TABLE 2

Phosphoramide stretching frequency of HMPA in various alkyl halides and parameters derived from product ratios in alkylation of ethyl acetoacetate in HMPA

Alkyl halide	ν_{max}(P=O) (cm^{-1})	"O"* (%)	"C" + "CO" + "CC"* (%)	"O"/"C" + "CO" + "CC"	$\Delta\Delta G‡$ (kcal $mole^{-1}$)
2-Chloropropane	1214.9	81	19	4.3	−1.10
1-Chloropropane	1212.9	61	39	1.56	−0.34
Allyl chloride	1209.2	17	83	0.20	1.21
Benzyl chloride	1208.0	13	87	0.15	1.45

*Data from ref. 6.

alkyl halide) is correlated with a decreased O/C product ratio".

In order to explain these results using the approach developed in the present work, it would appear that increased S_N2 reactivity of the alkyl halide must be correlated with a transition state more closely resembling product which implies, by application of the Hammond postulate, a less exothermic reaction for alkyl halides of greater S_N2 reactivity. This result strongly suggests some kind of stabilizing interaction of the alkyl halide by the solvent (DMSO or HMPA) that is dependent on the S_N2 activity of the alkyl halide. This requirement may be met by the formation of complexes of the following type:

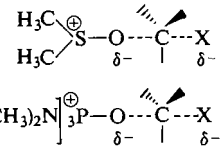

Such complexes involve interaction of the nucleophilic oxygen of DMSO or HMPA with the carbon of the alkyl halide bearing the halogen, to give a system reminiscent of the transition state commonly written for S_N2 displacement reactions. The extent of interaction in complexes of this nature will clearly be dependent on the S_N2 reactivity of the alkyl halide.

Since the above explanation for C vs. O product ratios in alkylation reactions has necessitated invoking the existence of DMSO- and HMPA-alkyl halide complexes, it becomes of paramount importance, as an independent check on the validity of the theory, to obtain independent evidence for the existence or non-existence of these complexes. For this evaluation, an i.r. spectral study was selected, since formation of a partial oxygen–carbon bond will cause the S=O frequency of DMSO or the P=O frequency of HMPA to shift to lower wave number. Accordingly, the spectra of DMSO and of HMPA were measured in a variety of alkyl halides, that had been used in previous studies on product ratio determinations (4, 6), and the S=O and P=O band positions respectively determined. The results are shown in Tables 1 and 2 from which it is clear that a greater degree of C-alkylation is indeed correlated with a longer wavelength band, as predicted, both for DMSO and HMPA.

These results are, therefore, consistent with the postulated existence of solvent – alkyl halide interactions demanded by the explanation ad-

Can. J. Chem. Downloaded from www.nrcresearchpress.com by 210.87.254.6 on 09/05/12
For personal use only.

Can. J. Chem. Downloaded from www.nrcresearchpress.com by 210.87.254.6 on 09/05/12
For personal use only.

vanced for observed product ratios in alkylation reactions.[5]

A further point of interest emerges on converting the product ratios to free energy terms. The alkylation process with respect to ethyl acetoacetate is slightly complex in that four products are formed but since the "CO" and "CC" products must arise from the "C" compound, the O vs. C ratio of the *initial* (mono) alkylation is represented by the ratio of "O" to ("C" + "CO" + "CC"). Calculating this ratio from the data of LeNoble *et al.* (4, 6) enables calculation of the difference in energies ($\Delta\Delta G\ddagger$) between the two transition states leading to the two different products. Plots of $\Delta\Delta G\ddagger$ against ν_{max} of DMSO and HMPA as a function of the alkyl halide are shown in Figs. 2 and 3.

These plots give unexpectedly good linear free energy relationships. The cause of the *linear* relationship is not immediately obvious. We plan to examine further the generality of this phenomenon, which may be of significance in determining the nature of transition states involved in alkylation reactions.

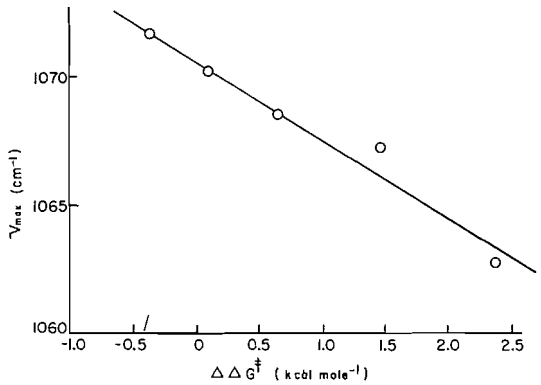

FIG. 2. Plot of S=O stretching frequency of DMSO of solutions of DMSO in various alkyl halides against the difference in free energies of activation between reactions leading to C-alkylation and to O-alkylation of ethyl acetoacetate in DMSO with the alkyl halides.

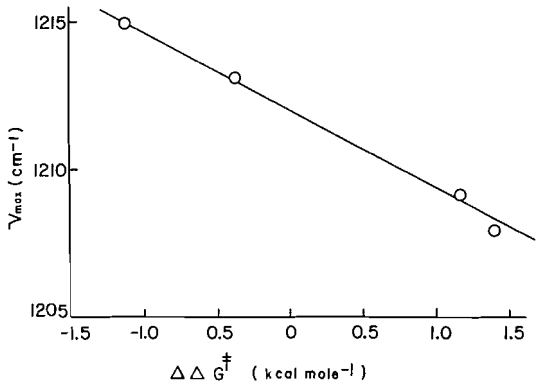

FIG. 3. Plot of P=O stretching frequency of HMPA of solutions of HMPA in various alkyl halides against the difference in free energies of activation between reactions leading to C-alkylation and to O-alkylation of ethyl acetoacetate in HMPA with the alkyl halides.

The author is pleased to acknowledge stimulating discussions with Professors C. H. Langford and E. Piers, the technical assistance of Mr. R. C. J. Sampson, and the financial support of the National Research Council of Canada.

1. N. KORNBLUM, P. J. BERRIGAN, and W. J. LENOBLE. J. Amer. Chem. Soc. **85**, 1141 (1963).
2. S. T. YOFFE, K. V. VATSURO, E. E. KUGUTCHEVA, and M. I. KABACHNIK. Tetrahedron Lett. 593 (1965).
3. G. BRIEGER and W. M. PELLETIER. Tetrahedron Lett. 3555 (1965).
4. W. J. LENOBLE and J. E. PUERTA. Tetrahedron Lett. 1087 (1966).
5. A. L. KURZ, I. P. BELETSKAYA, A. MACIAS, and O. A. REUTOV. Tetrahedron Lett. 3679 (1968).
6. W. J. LENOBLE and H. F. MORRIS. J. Org. Chem. **34**, 1969 (1969).
7. R. A. ABRAMOVITCH and G. A. POULTON. J. Chem. Soc. B 901 (1969).
8. W. G. DAUBEN, G. J. FONKEN, and D. S. NOYCE. J. Amer. Chem. Soc. **78**, 2579 (1956).
9. G. S. HAMMOND. J. Amer. Chem. Soc. **77**, 334 (1955).
10. J. E. PRUE and P. J. SHERRINGTON. Trans. Faraday Soc. **57**, 1795 (1961).
11. R. A. ABRAMOVITCH and D. L. STRUBLE. Tetrahedron, **24**, 357 (1968).

[5]A referee has pointed out that the small interactive effect between alkyl halide and DMSO or HMPA molecules could result from a generalized solvent dielectric effect of the alkyl halide and is not necessarily evidence of the formation of a stable directed bond between the S=O or P=O oxygen and the carbon atom α to the halogen.

On the ionization of isobutyryl chloride

RAM CHAND PAUL, R. D. SHARMA, AND K. C. MALHOTRA
Department of Chemistry, Panjab University, Chandigarh, India

Received[1] October 2, 1968

Conductance, freezing point, and infrared studies of the solutions of isobutyryl chloride in disulfuric acid and in Lewis acids and bases show that it is a feebly self-ionized solvent. This finds further support from solvolytic reactions.

Canadian Journal of Chemistry, 48, 2124 (1970)

Acid halides have been frequently used as reaction media and a large number of acid–base reactions supporting the auto-ionization of these solvents have been studied (1–4). However, some of the acid–base reactions can also be explained by coordination model (5), where Lewis acids form donor–acceptor complexes through carbonyl oxygen (6). Recently a simple method of studying the basic nature of oxygen or the possible ionization of halide ions has been reported (7) for these acid halides. It is of interest to study the nature of isobutyryl chloride which finds many applications in synthetic organic chemistry. Some evidence regarding the ionic nature of isobutyryl chloride is presented here.

Disulfuric acid is molecularly dissociated and a self-ionized solvent. The behavior of various electrolytes in it may be represented by the general equation (8)

$$[1]\quad \text{Solute} + s\text{H}_2\text{S}_2\text{O}_7 \rightarrow a\text{X}^+ + a\text{HS}_3\text{O}_{10}^- + b\text{Y} + c\text{H}_2\text{SO}_4$$

where Y represents uncharged species. Sulfuric acid so formed in the reaction does not contribute significantly to the value of γ, the number of $HS_3O_{10}^-$ ions, or to ν, the number of particles or ions produced per mole of the solute, as it is one of the products of self-dissociation of the acid (9). Isobutyryl chloride may behave according to reactions [2] or [3]

$$[2]\quad (\text{CH}_3)_2\text{CHCOCl} + 2\text{H}_2\text{S}_2\text{O}_7 \rightarrow (\text{CH}_3)_2\text{CHC(OH)}^+\text{Cl} + \text{HS}_3\text{O}_{10}^- + \text{H}_2\text{SO}_4$$

$$[3]\quad (\text{CH}_3)_2\text{CHCOCl} + 3\text{H}_2\text{S}_2\text{O}_7 \rightarrow (\text{CH}_3)_2\text{CHCO}^+ + \text{HSO}_3\text{Cl} + \text{HS}_3\text{O}_{10}^- + 2\text{H}_2\text{SO}_4$$

depending upon whether it has sufficiently basic oxygen to be protonated as in reaction [2] or ionizable chloride ion to form chlorosulfuric acid as in reaction [3]. The conductance and freezing point data in disulfuric acid at interpolated values of molality are given in Table 1, and presented in Figs. 1 and 2. By comparing the observed conductance and freezing point vs. composition curves with the calibrated curves (8) for reactions [2] and [3], it is found that isobutyryl chloride behaves according to the latter. Cryoscopic titrations of the above solutions against sulfur trioxide show that only 2 moles of sulfuric acid are being produced per mole of isobutyryl chloride; this also supports the above conclusion.

Infrared spectrum of the solution of isobutyryl chloride in disulfuric acid shows a sharp band at 2260 cm^{-1}, which is assigned to stretching vibrations of $RC{\equiv}O^+$, confirming that iso-

TABLE 1

Conductance and cryoscopic data of isobutyryl chloride in disulfuric acid

$M \times 10^2$	$K \times 10^3$ (ohm^{-1} cm^{-1})	Freezing point (°C)
1.0	3.9826	34.99
2.0	4.2792	34.88
3.0	4.5580	34.73
4.0	4.8826	34.60
5.0	5.2383	34.46
6.0	5.5626	34.29
7.0	5.9324	34.12
8.0	6.3045	33.96
9.0	6.6098	33.61
10.0	6.9523	33.60
12.0	7.6504	33.22
14.0	8.2866	32.85
16.0	8.8580	32.43
18.0	9.4316	32.03
20.0	9.8958	31.60

[1]Revision received March 16, 1970.

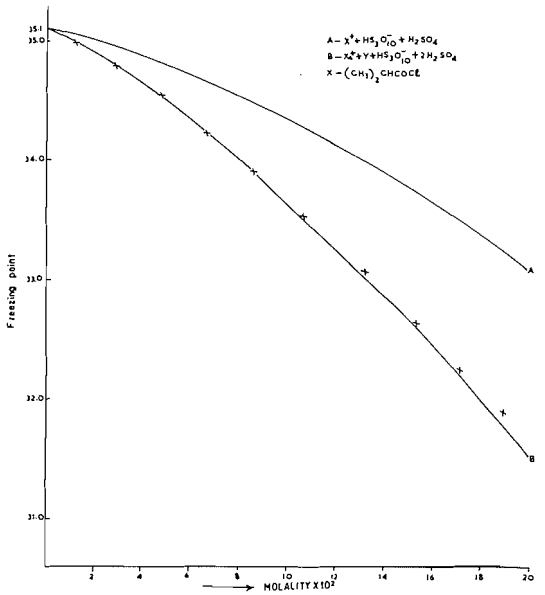

FIG. 1. Freezing point of isobutyryl chloride in disulfuric acid.

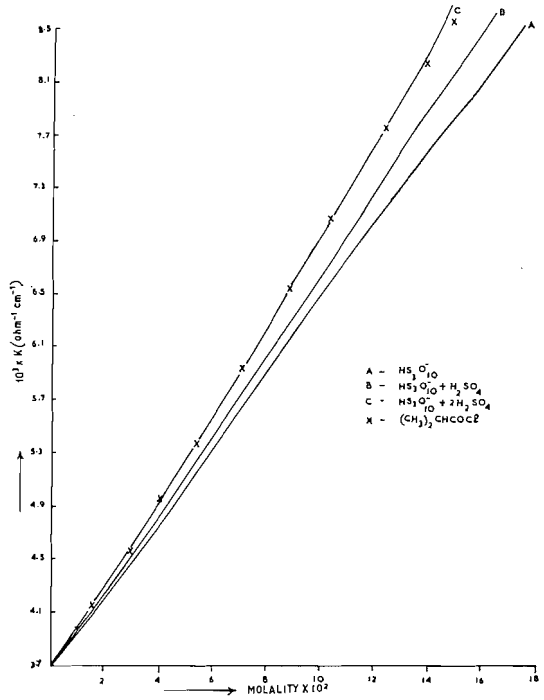

FIG. 2. Specific conductance of isobutyryl chloride in disulfuric acid.

butyryl chloride has ionizable chloride ion as in reaction [3]. Isobutyryl cation, being a strong electrophile, is stable in weakly nucleophilic medium ($H_2S_2O_7$). This behavior of isobutyryl chloride is similar to that of nitryl chloride (10) and acetyl chloride (11), which have been shown to be slightly self-ionized.

Isobutyryl chloride forms solid complexes with organic tertiary bases such as pyridine, quinoline, α-picoline, dimethylaniline, and morpholine which are soluble in an excess of the solvent to give conducting solutions (Table 2), indicating the formation of ions. Though we have isolated and characterized a number of these complexes, only that of pyridine is being reported here for brevity. Its molar conductance in nitrobenzene suggests that it behaves as a uni–univalent electrolyte, this conclusion also finds support from molecular weight determination. Infrared spectrum of pyridine complex shows absorption bands at 1650, 1604, 1540, 1350, 1250, 1170, 1080, 1010, 930, 690, and 650 cm^{-1} due to pyridinium ions, and supports the ionic nature of the complex. Isobutyryl cation, being a strong electrophile, accepts electrons from pyridine which thus acquires a positive charge to form pyridinium ion. By analogy with the structure of the complexes of organic bases with ionic acid halides (12, 13), the ions present in these complexes may be formulated as

$$(CH_3)_2CHCOCl + 2\ Base \rightarrow (CH_3)_2\ CHCOCl{\cdot}2Base$$
$$\Updownarrow$$
$$[(CH_3)_2CHCO{\cdot}B_2]^+ + Cl^-$$

Antimony(V) chloride, zirconium(IV) chloride, titanium(IV) chloride, and tin(IV) chloride form conducting solutions in isobutyryl chloride. Antimony(V) chloride and tin(IV) chloride also form solid complexes with it. Specific conductivity of these solutions at a particular concentration are given in Table 2. As compared to pure components the conductance of these solutions is very high and shows the formation of ions. The reactions occurring in the solution may be represented as

$$(CH_3)_2CHCOCl + SbCl_5 \rightarrow (CH_3)_2CHCOCl{\cdot}SbCl_5$$
$$\Updownarrow$$
$$(CH_3)_2CHCO^+ + SbCl_6^-$$

In the infrared spectrum of the complex $(CH_3)_2CHCOCl{\cdot}SbCl_5$, we confined our interest only to identify the absorption band due to $-C\equiv O^+$. A sharp band at 2280 cm^{-1} shows the presence of $RC\equiv O^+$. Molar conductance of this adduct in acetonitrile suggests that it is a uni–univalent electrolyte, and also supports the above mode of ionization of the Lewis acid adducts with the solvent. This formulation of

TABLE 2

Specific conductance of various solutions in insobutyryl chloride at 25 °C

Substance	Concentration (mole/l)	$K \times 10^4$ (ohm^{-1} cm^{-1})	Substance	Concentration (mole/l)	$K \times 10^4$ (ohm^{-1} cm^{-1})
Tetramethylammonium chloride	0.0062	6.584	Tin(IV) chloride	0.0082	1.056
Tetraethylammonium bromide	0.0048	1.295	Titanium(IV) chloride	0.0050	0.986
α-Picoline	0.0032	3.906	Zirconium(IV) chloride	0.0054	0.468
Quinoline	0.0028	3.588	Antimony(V) chloride	0.0032	0.954
Dimethylaniline	0.0036	3.015	Iron(III) chloride	0.0018	0.152

ions finds support from nuclear magnetic resonance (14) and X-ray (15) studies of this compound.

Conductometric and visual titrations between the solutions of antimony(V) chloride and tetramethylammonium chloride and pyridine have been carried out in isobutyryl chloride and lend support to the ionic nature of the solutions. There are sharp breaks in the conductivity composition curves at the molar ratio acid/base of 1:1. The change in the color of the visual indicator (crystal violet) near the end point is exactly the same as that in water. It has been indicated earlier that ions are present in these acidic and basic solutions, these acid–base titrations therefore can be explained as a reaction between various ions just as in other polar solvents.

The presence of ionizable chloride ion in isobutyryl chloride is further supported by its high solvolyzing power. It reacts with alkali and alkaline earth metal oxides, nitrites, nitrates, carbonates, acetates, oxalates, and formates to form the corresponding chlorides, even at room temperature in some cases. However, in some other cases, the mixture has to be heated for some time to complete the reaction. Silver nitrate when solvolyzed forms silver chloride, which is insoluble in isobutyryl chloride. The other products which have been characterized are nitrosyl chloride and isobutyric anhydride (b.p. 185 °C). Solvolytic reaction may be explained as

$$Ag^+ + NO_3^- + (CH_3)_2CHCO^+ + Cl^- \rightarrow AgCl + (CH_3)_2CHCONO_3$$

Isobutyryl nitrate formed during the reaction decomposes on heating to form isobutyric anhydride and oxides of nitrogen as

$$4(CH_3)_2CHCONO_3 \rightarrow 2[(CH_3)_2CHCO]_2O + 4NO_2 + O_2$$

However, in the presence of excess of isobutyryl chloride, isobutyryl nitrate forms nitrosyl chloride (16) as

$$2(CH_3)_2CHCONO_3 + 6(CH_3)_2CHCOCl \rightarrow 4[(CH_3)_2CHCO]_2O + 2NOCl + Cl_2$$

From all these observations, it may be concluded that isobutyryl chloride is a source of negative chlorine and is feebly ionized as

$$(CH_3)_2CHCOCl \rightleftharpoons (CH_3)_2CHCO^+ + Cl^-$$

Experimental

Isobutyryl chloride was purified in the same manner as acetyl chloride (3). Lewis acids and bases were purified by the usual methods. Solvents for molar conductance were dried by keeping them over molecular sieves for 48 h and were distilled before use. Disulfuric acid of exact composition was prepared by comparing its conductance and freezing point values with the known values. Cryoscopic set up and method of determining freezing point was exactly the same as that used by Gillespie and Malhotra (8). The conductance of the solutions was measured at 25.0 ± 0.02 °C by using a precision measuring bridge type WBR No. 108 with logarithmic indicator amplifier type TAV,IKC. No. 034 (Wissenschaftlich Technische Werkstatten, Wielheim/Oby, Germany).

Preparation of the Complex of Pyridine with Isobutyryl Chloride

To an ice cold solution of pyridine (0.8 g) in carbon tetrachloride, a cold solution of isobutyryl chloride (0.5 g) in carbon tetrachloride was added with constant stirring. A pale yellow compound separated out immediately. The mixture was then allowed to stand at room temperature for 1 h and then filtered in a dry atmosphere. The compound was repeatedly washed with carbon tetrachloride and finally with petroleum ether and was dried in a vacuum desiccator.

Anal. Calcd. $(CH_3)_2CHCOCl.2C_5H_5N$: Cl, 13.42; base, 59.73. Found: Cl, 13.02; base, 58.56.

Molar conductance in nitrobenzene is 22.6 ohm^{-1} cm^2 $mole^{-1}$. Infrared spectra showed important bands at 1650, 1604, 1540, 1350, 1170, 1080, 1010, 930, 690, and 650 cm^{-1}.

Complex of antimony(V) chloride with isobutyryl chloride was prepared in the same manner as suggested by Olah *et al.* (14). It is highly sensitive to moisture and decomposes before melting. Its molar conductance in acetonitrile is 68.4 ohm^{-1} cm^2 $mole^{-1}$.

1. M. Baaz, V. Gutmann, and L. Hubner. Montash, **91**, 557 (1960).
2. J. Jakson and G. B. L. Smith. J. Amer. Chem. Soc. **62**, 544 (1940).
3. B. S. Manhas, R. C. Paul, and S. S. Sandhu. J. Chem. Soc. 325 (1959).
4. R. C. Paul, K. C. Malhotra, and G. Singh. J. Ind. Chem. Soc. **37**, 105 (1960).
5. C. I. Branden and I. Lindquist. Acta Chem. Scand. **17**, 533 (1963).
6. D. W. Meek and R. S. Drago. J. Amer. Chem. Soc. **83**, 4322 (1961).
7. R. C. Paul, V. P. Kapila, and K. C. Malhotra. Chem. Commun. 644 (1968).
8. R. J. Gillespie and K. C. Malhotra. J. Chem. Soc. A, 1933 (1968).
9. R. J. Gillespie and K. C. Malhotra. J. Chem. Soc. A, 1944 (1967).
10. K. C. Malhotra. Chem. & Ind. 1704 (1967).
11. R. C. Paul, D. Singh, and S. S. Sandhu. J. Chem. Soc. 319 (1959).
12. R. C. Paul and S. L. Chadha. Ind. J. Chem. **5**, 272 (1968).
13. R. C. Paul and S. L. Chadha. Spectrochim. Acta, **22**, 615 (1966).
14. G. A. Olah, S. J. Kuhn, W. S. Jolgyesi, and E. B. Baher. J. Amer. Chem. Soc. **84**, 2733 (1962).
15. J. M. Le Carpentier and R. Weirs. Chem. Commun. 596 (1968).
16. O. Diels and H. Okada. Ber. **44**, 3333 (1911).

Osmotic coefficients of benzenesulfonic acid solutions at 25 °C

A. E. MARCINKOWSKY[1]
Department of Chemistry, University of Manitoba, Winnipeg, Manitoba

Received February 23, 1970

Osmotic coefficients of aqueous benzenesulfonic acid solutions from 0.5 to 16 *m* are reported. These results compare well with available literature data over the limited concentration interval 0.5 to 5 *m*. A correlation between the osmotic coefficients and the organic content for benzenesulfonic acid and four substituted aromatic monosulfonic acid solutions at corresponding concentrations above 4 *m* is shown.

Canadian Journal of Chemistry, 48, 2128 (1970)

Can. J. Chem. Downloaded from www.nrcresearchpress.com by 210.87.254.6 on 09/05/12
For personal use only.

Introduction

Interest in the osmotic properties of concentrated aqueous solutions of aromatic sulfonic acids and their salts arises primarily because these systems serve effectively as "models" for studies relating to the ion-exchange properties of sulfonated polystyrene – divinylbenzene copolymers (1–5). For the aromatic monosulfonic acids osmotic and activity coefficient data presently available are: benzenesulfonic acid (1) (0.1–5 *m*); *p*-toluenesulfonic acid (2, 3) (0.1–10 *m*); *p*-ethylbenzensulfonic acid (2, 4) (0.1–8.5 *m*); *p*-xylenesulfonic acid (5) (0.1–5 *m*); and mesitylenesulfonic acid (1) (0.1–5.5 *m*) where *m* is molality (moles of solute per 1000 g of water).

In this note the osmotic coefficients, ϕ, for solutions of benzenesulfonic acid from 0.5 to 16 *m* at 25 °C are reported and discussed. Over the limited concentration range 0.5 to 5 *m* these results are compared with previously reported data (1). In the high solute concentration range ($m \geqslant 4$) the ϕ values of benzenesulfonic acid and four substituted aromatic monosulfonic acid solutions are correlated in terms of the organic content of the solution. This is possible if one considers the organic part of the anion taken as the neutral molecule together with the water as a sort of mixed solvent. The organic content of each solution is determined in accordance with the additivity of volumes, i.e. v % organic = $m\overline{V}_0 \times 100/m(\overline{V}_0 + 0.5\,\overline{V}_{SO_3}) + V_{H_2O}$ where $\overline{V}_0$ and $\overline{V}_{SO_3}$ are the molar volumes of the unsulfonated parent organic compound and SO_3 respectively, and V_{H_2O} is the volume of 1000 g of H_2O. The $\overline{V}_0$ values for benzene, toluene, ethylbenzene, *p*-xylene and mesitylene calculated from density data (6) are 88.7_3, 106.1, 122.3, 123.2, and 139.1 cc mole^{-1}, respectively, and $\overline{V}_{SO_3}$ for the liquid is 40.6 cc mole^{-1}.

[1]Present address: Union Carbide Corporation, Technical Center, South Charleston, W. Va. 25303.

Experimental

The isopiestic apparatus used was similar to that described by Robinson and Sinclair (7). Equilibrated solutions were usually diluted slightly and re-equilibrated a second time before they were discarded in favor of a fresh set. The benzenesulfonic acid solutions were prepared by dilution of a concentrated stock solution which was prepared from reagent grade benzenesulfonic acid recrystallized once from its melt. Solutions of $HClO_4$ and H_2SO_4 were prepared from reagent grade chemicals. Each acid solution was standardized in duplicate by weight titration using standard alkali. The bath temperature was controlled at 25 ± 0.01 °C. Densities of benzenesulfonic acid solutions were obtained by conventional pycnometric methods using as reference (8) the density of water at 25°C, 0.99707 g/ml.

Osmotic coefficients are obtained from the isopiestic data at equilibrium in accordance with the relationship

$$\phi = \frac{\nu_r m_r}{\nu m}\,\phi_r = R\phi_r$$

where ϕ, *m*, ν, and *R* represent the osmotic coefficient of the solution, the molality, the number of ions formed on complete dissociation of the electrolyte, and the isopiestic ratio, respectively, and the subscript r refers to the reference solution. Tabulated ϕ_r values for solutions of H_2SO_4 as a function of *m* are given by Robinson and Stokes (8). The osmotic coefficients of benzenesulfonic acid solutions at rounded concentrations were obtained from a large scale curve of ϕ vs. *m*. The reported ϕ values are accurate to about 0.5%. To insure true equilibration was achieved solutions of $HClO_4$, whose ϕ values are known (8), were always equilibrated along with the benzenesulfonic acid solutions and in every case the measured ϕ_{HClO_4} value agreed with the literature data to better than 0.2%.

Results and Discussion

The osmotic coefficients for benzenesulfonic acid solutions at rounded concentrations over the

TABLE 1

Osmotic coefficients of benzenesulfonic acid solutions at 25 °C

Molality (m)	Volume % organic	Osmotic coefficient ϕ	Molality (m)	Volume % organic	Osmotic coefficient ϕ
0.5		0.939	7.5		1.330
0.6		0.938	8.0	37.96	1.371
0.7		0.937	8.5		1.412
0.8		0.937	9.0	40.36	1.452
0.9		0.938	9.5		1.489
1.0	8.00	0.940	10.0	42.51	1.524
1.5		0.945	10.5		1.561
2.0	14.58	0.960	11.0	44.44	1.590
2.5		0.981	11.5		1.622
3.0	20.07	1.001	12.0	46.20	1.650
3.5		1.026	12.5		1.677
4.0	24.73	1.058	13.0	47.79	1.704
4.5		1.093	13.5		1.728
5.0	28.74	1.132	14.0	49.25	1.752
5.5		1.168	14.5		1.775
6.0	32.22	1.205	15.0	50.59	1.797
6.5		1.246	15.5		1.816
7.0	35.27	1.287	16.0	51.82	1.836

range 0.5 to 16 m along with the calculated v% organic content at whole concentration intervals are given in Table 1. Density data for a selected set of benzenesulfonic acid solutions from 0.7 to to 15.6 m along with the organic contents calculated from these data are given in Table 2. The v% organic content for the benzenesulfonic acid solutions calculated from density data (Table 2) compare well with values obtained by the method of volume additivities (Table 1) when one-half the $\bar{V}_{SO_3}$ value is used. This suggests that if density data were available for the substituted aromatic monosulfonic acids the organic contents would compare equally well with those derived from volume additivity and leads to the conclusion that the organic contents for the substituted aromatic acid solutions used here are reasonably accurate.

TABLE 2

Density data of benzenesulfonic acid solutions at 25 °C

Molality (m)	Density (d)	Volume % organic
0.6918	1.032_9	5.71_5
0.8370	1.038_1	6.81
1.943	1.082_5	14.27
3.219	1.122_0	21.23
4.325	1.150_0	26.20
5.840	1.180_6	31.80
6.879	1.197_5	35.00
7.841	1.211_2	37.61
9.876	1.234_7	42.23
15.58	1.277_1	50.96

Over the concentration interval 0.5 to 5 m, where the benzenesulfonic acid solution ϕ values overlap with those reported by Bonner and Rogers (1), better than 1% agreement is noted. Bearing in mind the limitations in obtaining highly purified solutes, this agreement is considered quite good and appears to be essentially the same or perhaps slightly better than reported for the systems p-toluenesulfonic acid (2, 3) and p-ethylbenzenesulfonic acid (2, 4) for which duplicate sets of data are available.

In Fig. 1 the osmotic coefficients of benzenesulfonic acid, p-toluenesulfonic acid, p-ethylbenzenesulfonic acid, p-xylenesulfonic acid, and mesitylenesulfonic acid solutions at $m = 4$ and higher are plotted on a logarithmic scale as a function of v% organic content at several molalities. The present discussion is restricted to the concentrated region $m \geq 4$ where the ϕ values for all the acids are increasing with increase in m. At $m = 4$ or 5, where data for all five acids are available (1–5), straight lines pass through all the points (Fig. 1) showing that as the organic content of the solution at a fixed m is increasing, the ϕ values decrease.

According to Bonner and Rogers (1) the cause of the decrease in the values of the osmotic coefficients with increase in molecular weight of

Can. J. Chem. Downloaded from www.nrcresearchpress.com by 210.87.254.6 on 09/05/12
For personal use only.

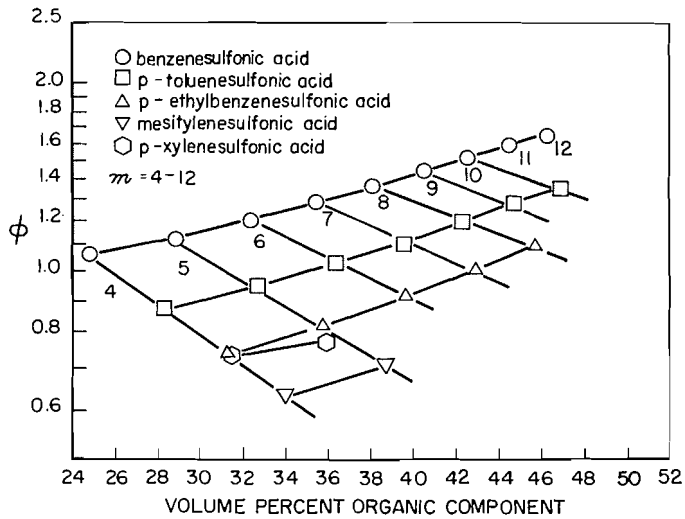

FIG. 1. Osmotic coefficients of aromatic monosulfonic acid solutions as a function of organic content.

the acid, i.e. they mean organic content of the solution, is explainable in terms of a decrease in the effective dielectric constant of the solution. At $m > 5$ less data is available; nevertheless, the correlation appears to hold equally well, although the ϕ vs. organic content slope is decreasing slightly which is probably due to the fact that the sulfonic acids are only moderately strong acids (1) and so the extent of ion-pairing with increase in organic content would be increasing.

It is also of interest to compare the ϕ values of anisolesulfonic acid solutions (4) on this model, even though the acid differs structurally from the other acids in that it contains the ether linkage. The osmotic coefficients for anisolesulfonic acid solutions are significantly higher than those of the corresponding *p*-ethylbenzenesulfonic acid solution concentrations ($m \geqslant 4$) although their molecular weights are almost identical. However, in terms of organic content anisolesulfonic acid ($\overline{V}_0 = 108.7$ cc mole^{-1}) has a much lower organic content than *p*-ethylsulfonic acid at the same *m*. For example at $m = 4$, the v% organic content is 28.7 for anisolesulfonic acid compared to 31.0 for *p*-ethylbenesulfonic acid and at $m = 5$ the values are 33.0 and 35.7, respectively. Thus according to the present correlation, the anisolesulfonic acid ϕ values should be compared with *p*-toluenesulfonic acid (28.2% organic at $m = 4$ and 32.5% organic at $m = 5$) which then fits the correlation reasonably well (at $m = 4$, ϕ (*p*-toluenesulfonic acid) = 0.87 and ϕ (anisolesulfonic acid) = 0.89 and at $m = 5$, ϕ (*p*-toluenesulfonic acid) = 0.94 and ϕ (anisolesulfonic acid) = 0.96).

From these correlations the conclusion follows that the position of the hydrocarbon groups attached to the benzene ring does not affect the ϕ values appreciably, but rather the total organic content of the solution at these high concentrations is the significant quantity. In light of these observations, the view of Bonner *et al.* (1, 4) that the position of the hydrocarbon side chain on the benzene ring has substantial influence on the ϕ values may be relaxed for the region of concentration $m > 4$.

I wish to thank Professor W. J. Biermann for helpful discussions and the National Research Council of Canada for financial support.

1. O. D. BONNER and O. C. ROGERS. J. Phys. Chem. **64**, 1499 (1960).
2. O. D. BONNER, G. D. EASTERLING, D. L. WEST, and V. F. HOLLAND. J. Amer. Chem. Soc. 77, 242 (1955).
3. O. D. BONNER and O. C. ROGERS. J. Phys. Chem. 65, 981 (1961).
4. O. D. BONNER and J. R. OVERTON. J. Phys. Chem. 67, 1035 (1963).
5. O. D. BONNER, V. F. HOLLAND, and L. L. SMITH. J. Phys. Chem. 60, 1102 (1956).
6. Handbook of physics and chemistry. 48th ed. The Chemical Rubber Co., Cleveland, Ohio. 1967.
7. R. A. ROBINSON and D. A. SINCLAIR. J. Amer. Chem. Soc. **56**, 1830 (1934).
8. R. A. ROBINSON and R. H. STOKES. Electrolyte solutions. Butterworths Publ. Ltd., London. 1955.

Can. J. Chem. Downloaded from www.nrcresearchpress.com by 210.87.254.6 on 09/05/12
For personal use only.

Gallium and indium electrode potentials in fused LiCl–KCl eutectic

JOSEPH M. SHAFIR AND JAMES A. PLAMBECK
Department of Chemistry, University of Alberta, Edmonton, Alberta

Received February 11, 1970

Electrode potentials of indium and gallium couples have been measured in dilute solutions of the ionic species in fused LiCl–KCl eutectic at 450 °C. Standard molar electrode potentials of the observed couples are −1.210, −0.944, and −1.136 V against a standard molar platinum reference for the In(I)–In(0), In(III)–In(I), and Ga(III)–Ga(0) couples, respectively. These oxidation states and potentials are compared with previous work in this and other fused salt systems.

Canadian Journal of Chemistry, 48, 2131 (1970)

Introduction

A recent review (1) containing the electromotive force series in anhydrous molten LiCl–KCl eutectic at 450 °C included values (2) for the Ga(III)–Ga(0) and In(III)–In(0) standard potentials. Recent measurements (3) have shown the monovalent oxidation states of gallium and indium to be of importance in fused tetrachloroaluminates, and a Raman study has shown the existence of indium(I) in fused LiCl–KCl (4). It therefore appeared desirable to re-investigate the oxidation states and potentials of gallium and indium in this medium.

Experimental

Materials

Reagent grade lithium chloride and potassium chloride (Fisher Scientific) were purified by the method of Maricle and Hume (5). In addition, the melt was treated with polished magnesium ribbon to remove any remaining traces of chlorine. Platinum wire and foil were used for electrodes (Engelhard Industries of Canada). Gallium (99.99%) was obtained from A. D. MacKay, Inc., New York, and indium (electronic material, 99.999%) from Cominco Ltd., Montreal, in wire form.

Apparatus

The apparatus used was quite similar to that described previously (6, 7) except that the gallium and indium electrodes were designed as cups since both metals are liquid at operating temperature. They consisted of a uranium glass tube with a tungsten wire lead protruding from it. To the end of the tube was blown a small uranium glass cup such that the lead extended into the cup and was completely covered by the molten metal after the cup was filled with metal wire and placed in the cell. The effect of this was to provide a metal pool electrode of 7 mm diameter for the coulometric anodizations.

Potentials were measured with a Hewlett-Packard Model 3400A digital voltmeter.

Procedure

The procedure used for carrying out the coulometric oxidations and measurements under argon has been previously described (6, 7). The oxidation of indium(I) to indium(III) was carried out, after the indium pool electrode had been removed, using a carbon rod such as was used as the counterelectrode (6). Calculations were carried out by computer.[1] The potentials were measured against a Pt(II)–Pt(0) reference electrode (2) and are reported with respect to the appropriate standard platinum electrode on the molar, molal, and mole fraction scales in Table 1. The conventions and standard states used in this Table have been described elsewhere (1).

TABLE 1
Standard potentials of gallium and indium couples

Couple	E_M^0	E_m^0	E_x^0	Standard error
In(I)–In(0)	−1.210	−1.194	−1.104	0.012
Ga(III)–Ga(0)	−1.136	−1.141	−1.171	0.008
In(III)–In(0)*	−1.033	−1.038	−1.068	0.009
In(III)–In(I)	−0.944	−0.960	−1.050	0.005
Ga(III)–Ga(0)†	−0.84	−0.84	−0.88	0.02
In(III)–In(0)†	−0.800	−0.805	−0.835	0.009

*Calculated from experimental free energies.
†Reference 2; otherwise, this work.

Results

Indium(I)–Indium(0) Couple

A total of 35 concentration–potential data points were taken in 4 separate coulometric anodizations of the indium pool electrode at 450 ± 1 °C. The concentration of In(I) ranged from 0.009 to 0.3 *M*. A plot of the electromotive force as a function of the logarithm of coulombs used was linear and had a slope of 0.138 ± 0.010 V/log unit, in good agreement with the theoretical value of 0.143 V/log unit expected for a one-electron process at this temperature. The standard potential obtained from the intercept is given in Table 1. During this oxidation a small amount of a yellow-red substance, probably InCl, condensed in the upper, cool part of the isolation compartment. This unavoidable volatilization decreased

[1]Copy of FORTRAN program used is available in the Appendix of the Ph.D. Thesis of Bodewig (8).

Can. J. Chem. Downloaded from www.nrcresearchpress.com by 210.87.254.105 on 09/05/12
For personal use only.

Can. J. Chem. Downloaded from www.nrcresearchpress.com by 210.87.254.105 on 09/05/12
For personal use only.

the concentration, leading to values of the standard potential which may be too positive. It is estimated, however, that this effect should not be greater than 5 mV.

Indium(III)–Indium(I) Couple

A total of 22 concentration–potential data points were taken in 3 separate coulometric anodizations at a carbon electrode, the solutions of indium(I) being prepared as above. The concentration ratio of In(III)/In(I) ranged from 0.007 to 2.4. The current density was approximately 3 mA/cm^2. A plot of the electromotive force as a function of the logarithm of coulombs used was linear and had a slope of 0.076 $\pm$ 0.004 V/log unit, in good agreement with the theoretical value of 0.072 V/log unit expected for a two-electron process at this temperature. The standard potential obtained from the intercept is given in Table 1, as is the value for In(III)–In(0) calculated from these data.

Gallium(III)–Gallium(0) Couple

A total of 27 concentration–potential data points were taken in 3 separate coulometric anodizations of the gallium pool electrode. The concentration of Ga(III) ranged from 0.002 to 0.07 *M*; at higher concentrations, volatilization of $GaCl_3$ became noticeable. A plot of the electromotive force as a function of the logarithm of coulombs used was linear, with a slope of 0.061 $\pm$ 0.006 V/log unit, in fair agreement with the theoretical value of 0.048 V/log unit expected for a three-electron process. Attempts to further oxidize the resulting solution using a carbon electrode produced only chlorine.

Discussion

Studies of gallium ((9), and references cited therein) and indium ((10), and references cited therein) have left no doubt as to the existence of stable gallium(I) and indium(I) compounds, the "divalent" state turning out to be a I–III compound. The univalent state has been observed, and the standard potentials for its oxidation and reduction measured, in fused tetrachloroaluminates (3). In the previous study (2) in fused LiCl–KCl, the reported potentials for Ga(III)–Ga(0) and In(III)–In(0) were obtained by adding the respective metal *trichloride* to the melt and carrying out a coulometric reduction, presumed to be to the metal. In the present study in which the metals were coulometrically oxidized, the oxidation was to the trivalent state only for gallium. This indicates that the previous gallium trichloride reduction (2) was directly to the metal. Indium, however, was oxidized first to the monovalent state, whose stability in this medium has been confirmed by the Raman study of Clarke and Hester (4), and could not be further oxidized in the presence of metallic indium. It is, therefore, concluded that the indium potential measured previously (2) corresponded to the In(III)–In(I) couple rather than the reported In(III)–In(0). The data of ref. 2 appear to be insufficient to distinguish the oxidation state to which reduction occurred.

It is not surprising that the potentials observed in this study are significantly different from those observed in the previous work, since the trichlorides of gallium and indium are highly volatile at these temperatures. The direct addition procedure of Laitinen and Liu (2) would lead to considerably greater loss of the trichloride than the electrochemical generation used in the present work, and hence to considerably more positive standard potential values. This appears to be true according to data presented in Table 1. It is felt that for these reasons, and because considerably more data were obtained in the present study, that the values of the present study are to be preferred.

Conclusion

The stable oxidation states in fused LiCl–KCl eutectic of gallium are the metal and the trivalent ion, and of indium are the metal, the monovalent ion, and the trivalent ion. The reduction potentials for these states have been established.

The authors are grateful to the National Research Council of Canada for their support of this work through an Operating Grant to J.A.P.

1. J. A. Plambeck. J. Chem. and Eng. Data, **12**, 77 (1967).
2. H. A. Laitinen and C. H. Liu. J. Amer. Chem. Soc. **80**, 1015 (1958).
3. U. Anders and J. A. Plambeck. Can. J. Chem. **47**, 3055 (1969).
4. J. H. R. Clarke and R. E. Hester. Inorg. Chem. **8**, 1113 (1969).
5. D. L. Maricle and D. N. Hume. J. Electrochem. Soc. **107**, 354 (1960).
6. H. A. Laitinen and J. A. Plambeck. J. Amer. Chem. Soc. **87**, 1202 (1965).
7. J. A. Plambeck. Can. J. Chem. **46**, 929 (1968).
8. F. G. Bodewig. Ph.D. thesis, University of Alberta, Edmonton, Alberta. 1970.
9. R. K. McMullan and J. D. Corbett. J. Amer. Chem. Soc. **80**, 4761 (1958).
10. R. J. Clark, E. Griswold, and J. Kleinberg. J. Amer. Chem. Soc. **80**, 4764 (1958).

Recombination of iodine atoms in sulfur dioxide

J. BROWN[1] AND G. BURNS
Department of Chemistry, University of Toronto, Toronto 181, Ontario

Received January 5, 1970

The reaction $2I + SO_2 \rightarrow I_2 + SO_2$ has been studied between 293 and 668 °K. At 293 °K, the recombination rate constant is 2.6×10^{10} l^2 mole^{-2} s^{-1}; it attains 1/10 of this value at 668 °K. Although the infrared and ultraviolet spectra of SO_2, studied previously, suggest the existence of two forms of SO_2 in the temperature range in question, the present recombination studies present no further supporting evidence about the existence of the excited form.

Canadian Journal of Chemistry, 48, 2133 (1970)

Can. J. Chem. Downloaded from www.nrcresearchpress.com by 210.87.254.6 on 09/05/12
For personal use only.

The present work deals with recombination of iodine atoms in excess of sulfur dioxide.

Experimental

The experimental technique of measuring halogen atom recombination rates by flash photolysis over a wide temperature range has been described previously (1, 2).

The reaction vessel was double walled, constructed of quartz tubing, 70 cm in length and 25 mm in internal diameter. The outer compartment of the vessel was filled with sulfur dioxide to a pressure of 720 Torr so that no photodissociation of sulfur dioxide contained in the inner portion of the vessel would occur. The reaction vessel was contained in a furnace; the temperature fluctuation along the length of the cell being less than 2 °C. The flash was generated by discharging through the lamp a 10 μF capacitor at typically 15 kV.

The recombination was monitored using a quartz incandescent lamp, collimating lenses and an RCA 931-A photomultiplier tube. The analyzing beam was rendered monochromatic by employing an interference filter and a Corning Number 3389 cut-off filter. The transmission peak of this combination of filters was at 487 mμ with a peak half-width of 7 mμ. The amplified output of the photomultiplier was displayed on an oscilloscope and photographed. Four photographs were taken and the mean calculated to obtain one value of the rate constant.

The iodine molecule concentration was obtained by determining the optical transmission of the cell before and after filling with the iodine–sulfur dioxide gas mixture. The iodine–sulfur dioxide ratio employed was typically less than 1:100. The variation of extinction coefficient with temperature for our photomultiplier – interference filter combination was obtained by Blake (3).

Results and Discussion

The data obtained for the recombination of iodine atoms over the temperature range 293–668 °K with sulfur dioxide as third body display a typical (2, 4) monotonic negative temperature dependence (Fig. 1). Thus, $k_r^{SO_2}$ for iodine recombination and k_r^{Kr} for bromine recombination differ only by a constant factor (Fig. 1). It may be concluded then that the properties of SO_2 as a chaperon in the recombination reaction do not change in any unusual way between 293 and 668 °K. It is known, however, that the ultraviolet (4) and infrared (5) spectra of SO_2 do change appreciably over this temperature range; and it has been suggested (5, 6) that the change is due to the formation of a new isomeric form of SO_2 (5) or to the existence of a low lying excited electronic state (6). It has also been suggested (7) that the new u.v. spectrum is due to a symmetrical form of sulfur dioxide with a bond angle of 72° and with a somewhat larger S—O bond distance.

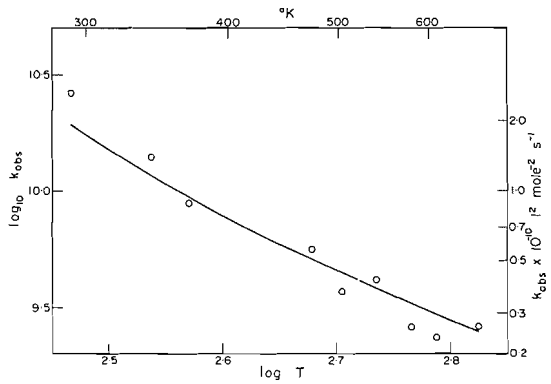

FIG. 1. Experimental points: the logarithm of the recombination rate constants for I atoms in SO_2, vs. temperature. Solid line is the logarithm of the recombination rate constant of Br in krypton multiplied by an arbitrary constant (1.07974).

From earlier experiments (8), it may be concluded that the equilibrium constant for the $SO_2 \rightleftharpoons SO_2$(excited) reaction changes from nearly zero to room temperature to 0.052 at 373 °K and to 0.62 at 673 °K. Therefore, one might expect that a change in SO_2 structure, as

[1]Present address: Ontario Hydro Research Division, 200 Kipling Ave. South, Toronto 18, Ontario.

suggested previously (5, 6), would affect considerably the $k_r^{SO_2}$ and its temperature dependence. This is because the atomic recombination rate constant is generally a fairly sensitive function of the nature of the third body. For example, in the recombination of iodine atoms, the efficiency of NO exceeds (9) that of He by a factor of 10 000. If the excited form of SO_2, either as isomer, or as an electronically excited species, would contain unpaired electrons, an increase in temperature would be likely to result in an appreciable increase of $k_r^{SO_2}$.

Thus, the fact that SO_2 behaves in the present experiments as if its structure does not change between 293 and 668 °K provides no further evidence for the existence of the excited form of SO_2. It may only be said that of the three possibilities suggested previously (5–7), the present work favors the third suggestion (7). This is because in this case (7), van der Waals-type forces between an iodine atom and SO_2, which affect the rate of I atom recombination, would not change drastically with the temperature.

This work was supported by the National Research Council of Canada, The Defence Research Board, Grant No. 9530–54, the Directorate of Chemical Sciences, Air Force Office of Scientific Research, Grant No. 506–64 and Grant No. 506–66 and 69–1965 and Petroleum Research Fund of the American Chemical Society.

1. J. K. K. Ip and G. Burns. Discuss. Faraday Soc. **44**, 241 (1967).
2. J. K. K. Ip and George Burns. J. Chem. Phys. **51**, 3414 (1969).
3. J. A. Blake and George Burns. To be published.
4. R. Engelman and N. R. Davidson. J. Amer. Chem. Soc. **82**, 4770 (1960).
5. R. G. W. Norrish and G. A. Oldershaw. Proc. Roy. Soc. London, Ser. A, **249**, 498 (1959).
6. P. A. Giguère and R. Savoie. Can. J. Chem. **43**, 2357 (1965).
7. E. F. Hayes and G. V. Pfeiffer. J. Amer. Chem. Soc. **90**, 4773 (1958).
8. J. Brown and G. Burns. Can. J. Chem. **47**, 4291 (1969).
9. A. Porter, Z. G. Szabo, and M. A. Townsend. Proc. Roy. Soc. London, Ser. A, **270**, 493 (1962).

Substituent effects on geminal proton–proton coupling constants

Y. L. Chow, S. Black, J. E. Blier, and M. M. Tracey
Department of Chemistry, Simon Fraser University, Burnaby 2, B.C.

Received February 2, 1970

The geminal coupling constants between the non-equivalent benzylic protons of a series of para- and meta-substituted *N*-benzyl-2-methylpiperidines were shown to be proportional to the Hammett σ constants of the substituents with ρ −1.38 in carbon tetrachloride, −1.21 in benzene, and nearly 0 in 1 *N* DCl solutions. The ρ values were compared with those of other series and were discussed in terms of the possible conformations involved. The chemical shifts of the benzylic protons of the piperidine derivatives did not give a good correlation with the Hammett σ constants in these solvents.

Canadian Journal of Chemistry, **48**, 2134 (1970)

A pair of magnetically non-equivalent methylene protons are named as diastereotopic protons and give rise to different chemical shifts in nuclear magnetic resonance (n.m.r.) spectroscopy (1–3). Numerous cases of the non-equivalence of methylene protons as a part of a ring system are readily understandable in terms of rigid conformation and have been well documented (2). The non-equivalence of methylene protons in acyclic systems is, however, sensitive to conformation (4). The most general cases of diastereotopic methylene protons in acyclic systems are those which arise from the presence of a chiral center in the vicinal position or interposed by a hetero atom (3–7), although there are other cases due to reasons other than dissymmetry of the molecule. In such cases the n.m.r. parameters of the magnetic non-equivalence are not just sensitive to conformations but sometimes also to a contribution from the intrinsic diastereomerism (6). We have observed that the benzylic protons in **1** (X = H) and the phenacyl methylene protons of **2** and **3** are non-equivalent while the benzyl protons in **4** are magnetically equivalent (5). The latter case appears to indicate that the chiral center is too remote to induce non-equivalence on the benzyl protons. Subsequently in the n.m.r. study of *N*-benzylpiperazine derivatives, Lyle and Thomas (4) have shown that the conditions necessary and sufficient to

Can. J. Chem. Downloaded from www.nrcresearchpress.com by 210.87.254.6 on 09/05/12
For personal use only.

suggested previously (5, 6), would affect considerably the $k_r^{SO_2}$ and its temperature dependence. This is because the atomic recombination rate constant is generally a fairly sensitive function of the nature of the third body. For example, in the recombination of iodine atoms, the efficiency of NO exceeds (9) that of He by a factor of 10 000. If the excited form of SO_2, either as isomer, or as an electronically excited species, would contain unpaired electrons, an increase in temperature would be likely to result in an appreciable increase of $k_r^{SO_2}$.

Thus, the fact that SO_2 behaves in the present experiments as if its structure does not change between 293 and 668 °K provides no further evidence for the existence of the excited form of SO_2. It may only be said that of the three possibilities suggested previously (5–7), the present work favors the third suggestion (7). This is because in this case (7), van der Waals-type forces between an iodine atom and SO_2, which affect the rate of I atom recombination, would not change drastically with the temperature.

This work was supported by the National Research Council of Canada, The Defence Research Board, Grant No. 9530–54, the Directorate of Chemical Sciences, Air Force Office of Scientific Research, Grant No. 506–64 and Grant No. 506–66 and 69–1965 and Petroleum Research Fund of the American Chemical Society.

1. J. K. K. Ip and G. Burns. Discuss. Faraday Soc. **44**, 241 (1967).
2. J. K. K. Ip and George Burns. J. Chem. Phys. **51**, 3414 (1969).
3. J. A. Blake and George Burns. To be published.
4. R. Engelman and N. R. Davidson. J. Amer. Chem. Soc. **82**, 4770 (1960).
5. R. G. W. Norrish and G. A. Oldershaw. Proc. Roy. Soc. London, Ser. A, **249**, 498 (1959).
6. P. A. Giguère and R. Savoie. Can. J. Chem. **43**, 2357 (1965).
7. E. F. Hayes and G. V. Pfeiffer. J. Amer. Chem. Soc. **90**, 4773 (1958).
8. J. Brown and G. Burns. Can. J. Chem. **47**, 4291 (1969).
9. A. Porter, Z. G. Szabo, and M. A. Townsend. Proc. Roy. Soc. London, Ser. A, **270**, 493 (1962).

Substituent effects on geminal proton–proton coupling constants

Y. L. Chow, S. Black, J. E. Blier, and M. M. Tracey
Department of Chemistry, Simon Fraser University, Burnaby 2, B.C.

Received February 2, 1970

The geminal coupling constants between the non-equivalent benzylic protons of a series of para- and meta-substituted *N*-benzyl-2-methylpiperidines were shown to be proportional to the Hammett σ constants of the substituents with ρ −1.38 in carbon tetrachloride, −1.21 in benzene, and nearly 0 in 1 *N* DCl solutions. The ρ values were compared with those of other series and were discussed in terms of the possible conformations involved. The chemical shifts of the benzylic protons of the piperidine derivatives did not give a good correlation with the Hammett σ constants in these solvents.

Canadian Journal of Chemistry, **48**, 2134 (1970)

A pair of magnetically non-equivalent methylene protons are named as diastereotopic protons and give rise to different chemical shifts in nuclear magnetic resonance (n.m.r.) spectroscopy (1–3). Numerous cases of the non-equivalence of methylene protons as a part of a ring system are readily understandable in terms of rigid conformation and have been well documented (2). The non-equivalence of methylene protons in acyclic systems is, however, sensitive to conformation (4). The most general cases of diastereotopic methylene protons in acyclic systems are those which arise from the presence of a chiral center in the vicinal position or interposed by a hetero atom (3–7), although there are other cases due to reasons other than dissymmetry of the molecule. In such cases the n.m.r. parameters of the magnetic non-equivalence are not just sensitive to conformations but sometimes also to a contribution from the intrinsic diastereomerism (6). We have observed that the benzylic protons in **1** (X = H) and the phenacyl methylene protons of **2** and **3** are non-equivalent while the benzyl protons in **4** are magnetically equivalent (5). The latter case appears to indicate that the chiral center is too remote to induce non-equivalence on the benzyl protons. Subsequently in the n.m.r. study of *N*-benzylpiperazine derivatives, Lyle and Thomas (4) have shown that the conditions necessary and sufficient to

Can. J. Chem. Downloaded from www.nrcresearchpress.com by 210.87.254.5 on 09/05/12
For personal use only.

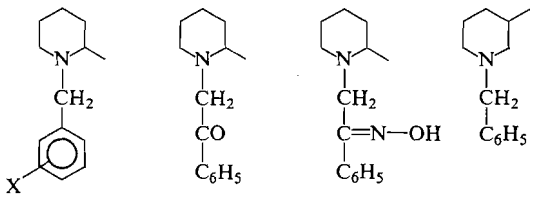

1 2 3 4

afford an observable non-equivalence of the benzyl protons are not only the presence of the chiral center at C-2 position but also an equatorial methyl group. Lyle and Thomas (4) have argued that the respective orientation of the two benzylic protons with respect to the lone pair of electrons of the nitrogen causes the magnetic non-equivalence, and the population of the most stable conformer decides the magnitude of the non-equivalence.

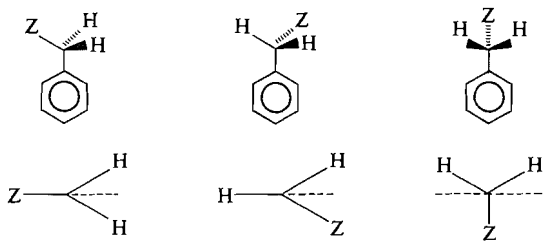

5*a* 5*b* 5*c*

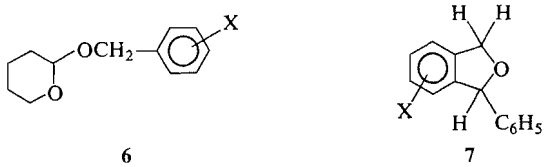

6 7

On the other hand, the magnetic non-equivalence of the benzylic protons of the benzyloxytetrahydropyran (**6**) has also been studied on the basis of the orientations of the benzylic protons with respect to the benzene ring (8–10). Fraser *et al.* (8) have successfully correlated the geminal coupling constants and the chemical shifts of the benzylic protons with Hammett σ constants in para- and meta-substituted 2-benzyloxytetrahydropyrans. The success of the correlation has been attributed to the relative orientation of the benzylic protons with respect to the benzene ring in the conformation **5***a* which transmits the hyperconjugative effect more favorably than other conformers **5***b* and *c* (11).

Thus, it is conceivable that more than one factor contributes to the magnetic non-equivalence in **1**. If the conformation of the benzylic protons is such that the aryl group exerts the dominant effect, the Hammett substitution effect should be significant. On the contrary, if the lone pair electrons of the nitrogen atom orients in such a position as to effect a significant magnetic non-equivalence to the benzylic protons, such correlation should show a small ρ value. The derivatives of *N*-benzylpiperidines (**1**) were synthesized and the correlation of the geminal coupling constants (*J*) and the chemical shifts of the non-equivalent benzylic protons with σ values of the para- and meta-substituents were studied.

Experimental

Material

The *N*-benzyl-2-methylpiperidines (**1**) were prepared by the method described previously (5), except for the *p*-amino derivative. The appropriately substituted para- or meta-substituted benzyl halide was treated with more than 2 moles excess of 2-methylpiperidine in benzene solution. The commercial benzyl halides, without purification, were used except for *p*-methoxybenzyl chloride (b.p. 101–103°/10 mm) which was prepared by the method of Shriner and Hull (12). A hydrogenation of *p*-nitrobenzyl-2-methylpiperidine in the presence of platinum oxide gave an unstable *p*-amino derivative which was purified as the non-crystalline hydrochloride salt by reprecipitation. The free base was liberated immediately before the spectroscopic measurement. The benzylpiperidines were purified by repeated distillation. The *p*-substituted *N*-benzyl-2-methylpiperidines have the following percentage yields and b.p.'s; *m*-chloro, 77%, 130–132°/3 mm; *p*-chloro, 67%, 107–113°/1 mm; *m*-fluoro, 72%, 87–98°/2 mm; *p*-fluoro, 78%, 78–91°/1 mm; *p*-methyl, 58%, 108–112°/2 mm; *m*-nitro, 41%, 167–170°/3 mm; *p*-nitro, 68%, 167–174°/2.5 mm; *p*-bromo, 88%, 124°/1 mm; *p*-methoxy, 120°/1 mm. Each compound produced its corresponding molecular ion peak in mass spectrometric measurements.

Nuclear Magnetic Resonance Spectroscopy

The n.m.r. spectra were measured with a Varian A56/60 spectrometer in 10% solution (w/v) in benzene or carbon tetrachloride using tetramethylsilane as internal standard. The n.m.r. sample was equilibrated to the probe temperature and the standard spectrum was recorded. The AB quartet portion was then recorded at a 100 Hz sweep width. The coupling constant (*J*) and the chemical shift difference (Δν) were calculated from these spectra. The same n.m.r. measurement was repeated in 1 *N* DCl in D_2O using sodium 2,2-dimethyl-2-silapentane-5-sulfonate as the internal standard.

Results and Discussion

The n.m.r. parameters of the non-equivalent benzylic protons are summarized in Table 1. The sharp AB quartets of **1** are generally centered at the τ 6.4–6.8 region. The doublet at the higher

Can. J. Chem. Downloaded from www.nrcresearchpress.com by 210.87.254.5 on 09/05/12
For personal use only.

TABLE 1

The n.m.r. parameters of the substituted *N*-benzyl-2-methylpiperidines* (**1**)

	In CCl_4 solution			In benzene solution			In 10% DCl–D_2O		
—X	J	τ_A	τ_B	J	τ_A	τ_B	J	τ_A	τ_B
p-NH_2	13.2	6.20	7.09	13.2	6.09	7.03	13.1	5.36	6.01
p-CH_3	13.2	6.10	7.02	13.4	6.07	7.02	13.2	5.41	6.02
p-OCH_3	13.1†	6.14	7.05	13.2	6.09	7.02	—	—	—
H	13.4	6.05	6.96	13.6	6.08	7.03	13.2	5.34	6.00
p-F	13.5	6.10	7.00	13.5	6.30	7.23	13.4	5.33	5.98
p-Cl	13.6	6.11	7.01	13.7	6.36	7.19	13.3	5.43	6.06
p-Br	13.5	6.13	7.02	13.8	6.37	7.27	—	—	—
m-F	13.9	6.09	6.97	14.0	6.29	7.14	13.4	5.27	5.93
m-Cl	13.8	6.10	7.00	13.8	6.20	7.20	—	—	—
m-NO_2	14.1	6.04	6.88	14.4	6.36	7.20	—	—	—
p-NO_2	14.5	5.99	6.83	14.5	6.45	7.13	—	—	—
o-CH_3	13.0	6.05	7.08	13.2	6.14	7.11	—	—	—

*The coupling constants (J) are expressed in Hz. The τ_A and τ_B refer to the chemical shifts of the doublets at the lower and higher field signals, respectively. In DCl/D_2O solution, σ-constant (0.41) for $N(CH_3)_3^+$ group is used for the *p*-amino derivative.
†Since the methoxy signal superimposes with the signal of τ_A, the coupling constant of the B-proton is used.

field is generally found to overlap with a part of the signal arising from α-equatorial protons at the C-6 position (broad doublet) in the 2-methylpiperidine ring. For these reasons, the coupling constant (J_{AB}) obtained from the doublet at a higher field may deviate up to 0.5 Hz in some cases from the J_{AB} obtained from the doublet at a lower field. In such cases, J_{AB} of the doublet at the low field is adopted. Broadening of each line of the quartet due to the coupling with benzene protons was observable with spectra of 100 Hz sweep width (10, 13). Measurements of J_{AB} from these runs were done by considering the symmetry of each signal. The deviation in these measurements is probably not larger than 0.3 Hz. The coupling constants (J_{AB}) of para- and meta-substituted **1** are plotted against the Hammett substituent constants (σ) as shown in Fig. 1. The good straight lines can be drawn by visual observation and indicate that the size of J_{AB} correlates well with the electronic effects transmitted to the benzylic protons; the ρ value is −1.38 in carbon tetrachloride and −1.21 in benzene.[1] It is seen that the electron-withdrawing nitro group causes a more negative (and therefore numerically bigger) coupling constant, while the electron-donating methoxy group results in a less negative constant.

A geminal coupling constant in a benzyl group is subjected to hyperconjugative effect, as has been demonstrated by the semi-empirical calculation of Barfield and Grant (11). Further, the molecular orbital theory treatment of the nuclear spin coupling by Pople and Bothner-By (14) has indicated that the geminal coupling constants are affected by inductive and hyperconjugative electron transfers. The prediction that the hyperconjugative effect is maximal (most negative J_{AB}) in the conformation of **5***a* and minimal in the conformation **5***c* has been utilized by Fraser *et al.* (8) to explain the observed size of ρ values in various series of compounds. Since the two benzylic protons in conformation **5***a* are symmetric with respect to the benzene ring, the hyperconjugative effects must render the benzylic protons more susceptible to diastereotopic effect derived from dissymmetry of other parts of the molecule in this conformation.

Fraser *et al.* (8) have proposed that the sensitivity of the correlation is dependent on the population of conformation **5***a* in each series; ρ is largest (−1.80) in the compounds (15) **7** where the benzylic protons are ideally oriented. Other known ρ values are −1.5 for 2-benzyloxytetrahydropyranes (**6**), −1.1 for dibenzylsulfites, and 0 for benzylphenyl sulfoxides (8). The range of ρ values, $-1.38 \sim 1.21$, in the present case places the correlation of the piperidine series in between **6** and dibenzylsulfite. The conformational stability of benzyl derivatives has been investigated by the Kerr effect (16) and theoretical calculation (17) where **5***c* has been shown to be the most stable conformer while **5***a* is the least

[1]It is assumed that the geminal coupling constant has a negative value of analogy to the negative coupling constant observed for most of the geminal coupling of protons attached to sp^3 hybridized carbons (15). The ρ values are therefore negative.

Can. J. Chem. Downloaded from www.nrcresearchpress.com by 210.87.254.5 on 09/05/12
For personal use only.

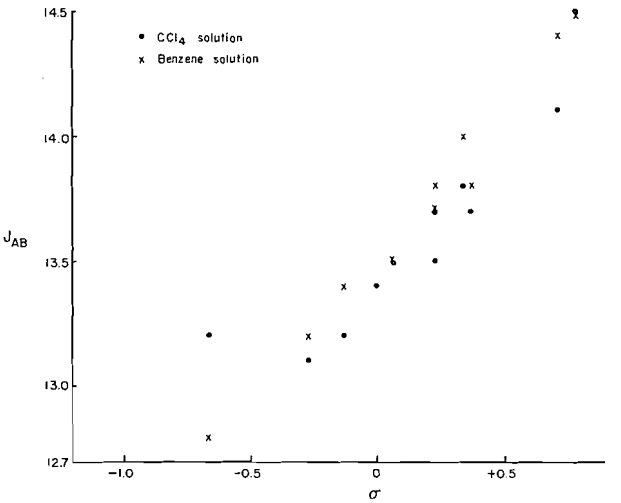

FIG. 1. A plot of the geminal coupling constant (J_{AB}) vs. the Hammett substituent parameter σ for the series of para- and meta-substituted **1**.

stable one. It follows that the contribution of the conformation **5***a* decreases in the order of **6**, **1**, dibenzylsulfite, and benzylphenyl sulfoxide. This is to be expected since the Z group is the 2-methylpiperidine ring which is more bulky than the 2-pyranyloxy group. Although there is no pertinent report concerning the conformation volume of a sulfoxyl group, the size of a sulfoxyl group may be equivalent to or larger than the piperidino group due to the expanded Van der Waals radius of sulfur. It is also clear that there is an additional effect other than a purely steric one operating to stabilize the conformation **5***c* in the sulfoxide and sulfite series. It is speculated that an interaction of the π-electron cloud with the electron deficient sulfur atom may result in stabilization of conformation **5***c*. Alternatively the low ρ-value of this series may be explained by the fact that the benzylic proton is subjected to an overwhelming inductive effect (14) from the vicinal sulfoxide group which offsets the hyperconjugative of the benzene ring. The ρ-value of nearly zero for the piperidinium salt of **1** in DCl–D_2O solution is an analogous case to the sulfoxide series. The piperidinium ion becomes very bulky due to hydration and is not able to assume the eclipsed position as shown in **5***a*.

In conclusion, orientation of the benzene ring undoubtedly contributes to an extent to the magnetic non-equivalence of the benzylic protons in **1**. The extent of this contribution to the magnetic non-equivalence with respect to that from the term dependent on the lone pair electrons and that from the term of the intrinsic asymmetry is, however, not readily estimated from the coupling constant data.

The plot of the chemical shifts of the benzylic protons against the Hammett σ-constant, however, gave considerable scatter and only suggests general trends of slope. Although the scatter was somewhat alleviated when the points of meta-substituted compounds were ignored, the τ value of the *p*-nitro compound still deviates considerably from a straight line defined by all other points of para-substituted compounds. The similar correlations of σ-constants and chemical shifts in other series generally give small negative ρ-values (0–0.21 p.p.m./σ unit) in chloroform solutions (9). It is interesting to point out that in the piperidine series **1**, while the sign of the ρ-value in carbon tetrachloride is negative, the corresponding sign in benzene solution is positive. The reversal of the sign of the ρ-value may be related to the n.m.r. solvent effects (18) since it is well known that an aromatic solvent forms a collision complex with certain solutes. This solvent effect has been said to be stereospecific although the exact geometry of the complexes is less clear. A study of the solvent effects with respect to the ρ-value may reveal more information about the conformation of the solute molecule as well as the complex.

Can. J. Chem. Downloaded from www.nrcresearchpress.com by 210.87.254.5 on 09/05/12
For personal use only.

The authors wish to thank the National Research Council of Canada for financial assistance. We also thank Dr. R. R. Fraser, University of Ottawa, and Dr. T. Schaefer, University of Manitoba for helpful discussions and unpublished results.

1. K. Mislow and M. Raban. *In* Topics in stereochemistry. Vol. 1. *Edited by* N. L. Allinger and E. L. Eliel. Interscience Publishers, New York, N.Y., 1967. Chapt. 1.
2. R. C. Cookson, T. A. Crabb, J. J. Franken, and J. Hudec. Tetrahedron Suppl. **7**, 355 (1966).
3. R. W. Horobin, J. McKenna, and J. M. McKenna. Tetrahedron Suppl. **7**, 35 (1966).
4. R. E. Lyle and J. J. Thomas. Tetrahedron Lett. 897 (1969).
5. Y. L. Chow and C. J. Colon. Can. J. Chem. **45**, 2559 (1967).
6. M. Raban. Tetrahedron Lett. 3105 (1966).
7. W. F. Reynolds and T. Schaefer. Can. J. Chem. **42**, 2119 (1964).
8. R. R. Fraser, P. Hanbury, and C. Reyes-Zamora. Can. J. Chem. **45**, 2481 (1967).
9. R. R. Fraser, R. N. Renaud, C. Reyes-Zamora, and R. B. Swingle. Can. J. Chem. **47**, 2767 (1969).
10. R. W. Franck and J. Auerback. Can. J. Chem. **45**, 2489 (1967).
11. M. Barfield and D. M. Grant. J. Amer. Chem. Soc. **85**, 1899 (1963).
12. R. L. Shriner and C. J. Hull. J. Org. Chem. **10**, 228 (1945).
13. H. Rottendorf and S. Sternhell. Aust. J. Chem. **17**, 1315 (1964).
14. J. A. Pople and A. A. Bothner-By. J. Chem. Phys. **42**, 1339 (1965).
15. R. R. Fraser. Private communication.
16. K. E. Calderman, R. J. W. LeFèvre, and R. K. Pierens. J. Chem. Soc. B, 968 (1969).
17. T. Schaefer. Private communication.
18. T. Ledaal. Tetrahedron Lett. 1683 (1968).

Selective removal of phenolic groups in certain dihydroxytoluenes by tetrazole ether formation and hydrogenolysis

C. F. Barfknecht,[1] R. V. Smith, and V. D. Reif[2]

Division of Medicinal Chemistry, College of Pharmacy, University of Iowa, Iowa City, Iowa 52240

Received February 9, 1970

Selectivity and yield were studied in the reaction of 5-chloro-1-phenyltetrazole with dihydroxytoluene systems. The mono-ethers of 2-methylhydroquinone (**1***a*), 3-methylcatechol (**2***a*), and 4-methylcatechol (**3***a*) were formed in moderate yields with the predominant isomer resulting from attack by the more nucleophilic anion. With **1***a* and **2***a*, steric effects diminished the amount of predominant isomer formed as compared to **3***a*. The di-(1-phenyltetrazole) ethers were formed in good yields. Hydrogenolysis of mono- and di-ethers gave good yields of cresols and toluene as determined by gas chromatography and ultraviolet analysis, respectively.

Canadian Journal of Chemistry, 48, 2138 (1970)

In 1966 Musliner and Gates (1) reported a facile method for the removal of phenolic hydroxyl groups by reaction with 5-chloro-1-phenyltetrazole under basic conditions and subsequent hydrogenolysis with palladium on carbon. By this procedure phenolic hydroxyl groups could be removed in the presence of various functional groups (e.g., amino, carbethoxy, carboxaldehyde, and methoxy). Since many natural products contain phenolic hydroxyl or methoxyl groups, it was of interest to determine the scope and selectivity of this procedure for multi-hydroxyl systems particularly in the absence of strong ring-activating functions. It was proposed that this reaction sequence could be valuable in structure elucidation and degradation if high selectivity or near quantitative removal of phenolic hydroxyls could be demonstrated. This paper reports the results with methyl-substituted catechols and hydroquinone.

The yields of mono-(1-phenyltetrazole) ethers and di-(1-phenyltetrazole) ethers are summarized in Table 1. The di-ethers were formed in excellent yields while the mono-ethers were formed in fair to moderate yields. Thin-layer chromatography (t.l.c.) and nuclear magnetic resonance (n.m.r.) spectroscopy were used in determining product

[1]To whom inquiries and reprint requests should be addressed.
[2]Undergraduate research participant.

Can. J. Chem. Downloaded from www.nrcresearchpress.com by 210.87.254.5 on 09/05/12
For personal use only.

The authors wish to thank the National Research Council of Canada for financial assistance. We also thank Dr. R. R. Fraser, University of Ottawa, and Dr. T. Schaefer, University of Manitoba for helpful discussions and unpublished results.

1. K. Mislow and M. Raban. *In* Topics in stereochemistry. Vol. 1. *Edited by* N. L. Allinger and E. L. Eliel. Interscience Publishers, New York, N.Y., 1967. Chapt. 1.
2. R. C. Cookson, T. A. Crabb, J. J. Franken, and J. Hudec. Tetrahedron Suppl. **7**, 355 (1966).
3. R. W. Horobin, J. McKenna, and J. M. McKenna. Tetrahedron Suppl. **7**, 35 (1966).
4. R. E. Lyle and J. J. Thomas. Tetrahedron Lett. 897 (1969).
5. Y. L. Chow and C. J. Colon. Can. J. Chem. **45**, 2559 (1967).
6. M. Raban. Tetrahedron Lett. 3105 (1966).
7. W. F. Reynolds and T. Schaefer. Can. J. Chem. **42**, 2119 (1964).
8. R. R. Fraser, P. Hanbury, and C. Reyes-Zamora. Can. J. Chem. **45**, 2481 (1967).
9. R. R. Fraser, R. N. Renaud, C. Reyes-Zamora, and R. B. Swingle. Can. J. Chem. **47**, 2767 (1969).
10. R. W. Franck and J. Auerback. Can. J. Chem. **45**, 2489 (1967).
11. M. Barfield and D. M. Grant. J. Amer. Chem. Soc. **85**, 1899 (1963).
12. R. L. Shriner and C. J. Hull. J. Org. Chem. **10**, 228 (1945).
13. H. Rottendorf and S. Sternhell. Aust. J. Chem. **17**, 1315 (1964).
14. J. A. Pople and A. A. Bothner-By. J. Chem. Phys. **42**, 1339 (1965).
15. R. R. Fraser. Private communication.
16. K. E. Calderman, R. J. W. LeFèvre, and R. K. Pierens. J. Chem. Soc. B, 968 (1969).
17. T. Schaefer. Private communication.
18. T. Ledaal. Tetrahedron Lett. 1683 (1968).

Selective removal of phenolic groups in certain dihydroxytoluenes by tetrazole ether formation and hydrogenolysis

C. F. Barfknecht,[1] R. V. Smith, and V. D. Reif[2]

Division of Medicinal Chemistry, College of Pharmacy, University of Iowa, Iowa City, Iowa 52240

Received February 9, 1970

Selectivity and yield were studied in the reaction of 5-chloro-1-phenyltetrazole with dihydroxytoluene systems. The mono-ethers of 2-methylhydroquinone (**1***a*), 3-methylcatechol (**2***a*), and 4-methylcatechol (**3***a*) were formed in moderate yields with the predominant isomer resulting from attack by the more nucleophilic anion. With **1***a* and **2***a*, steric effects diminished the amount of predominant isomer formed as compared to **3***a*. The di-(1-phenyltetrazole) ethers were formed in good yields. Hydrogenolysis of mono- and di-ethers gave good yields of cresols and toluene as determined by gas chromatography and ultraviolet analysis, respectively.

Canadian Journal of Chemistry, 48, 2138 (1970)

In 1966 Musliner and Gates (1) reported a facile method for the removal of phenolic hydroxyl groups by reaction with 5-chloro-1-phenyltetrazole under basic conditions and subsequent hydrogenolysis with palladium on carbon. By this procedure phenolic hydroxyl groups could be removed in the presence of various functional groups (e.g., amino, carbethoxy, carboxaldehyde, and methoxy). Since many natural products contain phenolic hydroxyl or methoxyl groups, it was of interest to determine the scope and selectivity of this procedure for multi-hydroxyl systems particularly in the absence of strong ring-activating functions. It was proposed that this reaction sequence could be valuable in structure elucidation and degradation if high selectivity or near quantitative removal of phenolic hydroxyls could be demonstrated. This paper reports the results with methyl-substituted catechols and hydroquinone.

The yields of mono-(1-phenyltetrazole) ethers and di-(1-phenyltetrazole) ethers are summarized in Table 1. The di-ethers were formed in excellent yields while the mono-ethers were formed in fair to moderate yields. Thin-layer chromatography (t.l.c.) and nuclear magnetic resonance (n.m.r.) spectroscopy were used in determining product

[1]To whom inquiries and reprint requests should be addressed.
[2]Undergraduate research participant.

Can. J. Chem. Downloaded from www.nrcresearchpress.com by 210.87.254.40 on 09/05/12
For personal use only.

TABLE 1

Mono- and di-(1-phenyltetrazole) ethers of dihydroxytoluene systems

Number	Parent compound	Ether	Yield (%)	Melting point (°C)	Calculated analysis (%) C	H	N	Observed (%) C	H	N
1*a*	2-Methyl-1,4-hydroquinone	Mono	29.6	167–182	62.68	4.51	20.88	62.58	4.56	20.81
2*a*	3-Methylcatechol	Mono	26.6	156–158	62.68	4.51	20.88	62.66	4.46	20.76
3*a*	4-Methylcatechol	Mono	57.7	121–132	62.68	4.51	20.88	62.59	4.54	21.01
1*b*	2-Methyl-1,4-hydroquinone	Di	90.3	154–156	61.15	3.91	27.18	60.90	3.92	27.14
2*b*	3-Methylcatechol	Di	87.4	136–138	61.15	3.91	27.18	61.07	3.75	27.10
3*b*	4-Methylcatechol	Di	92.2	196–197	61.15	3.91	27.18	60.98	3.94	27.05

TABLE 2

Nuclear magnetic resonance data*

Compounds	Phenolic protons	Aromatic protons	Methyl protons
1*a*	9.61† (s)‡ (1)§	8.10–7.47 (m) (5); 7.42–6.58 (m) (3)	2.03 (s) (3)
1*b*	—	8.11–7.29 (m) (13)	2.25 (s) (3)
2*a*	9.94 (s) (1)	8.13–7.52 (m) (5); 7.40–6.61 (m) (3)	2.24 (s) (3)
2*b*	—	7.94–7.30 (m) (13)	2.35 (s) (3)
3*a*	9.89 (s) (1)	8.12–7.53 (m) (5); 7.50–6.57 (m) (3)	2.28 (s) (3)
3*b*	—	7.89–7.34 (m) (13)	2.42 (s) (3)

*DMSO-d_6 solutions; 1% tetramethylsilane as internal standard.
†δ values.
‡s, singlet; m, multiplet.
§Number of protons.

composition and purity. The n.m.r. spectra of the mono-(1-phenyltetrazole) ethers (**1***a*, **2***a*, and **3***a*) are characterized by phenolic protons between 9.94 to 9.61 δ; absorption due to aromatic hydrogens is divided into downfield multiplets (8.13 to 7.47 δ) integrating for five protons and three protons upfield between 7.50 to 6.57 δ. The upfield absorptions were assigned to the protons on the phenolic nucleus. This was substantiated by the fact that the aryl protons in the di-ethers (**1***b*, **2***b*, and **3***b*) all appear as downfield multiplets between 8.11 to 7.29 δ. Since the 1-phenyltetrazole ring is an effective electron withdrawing group, it apparently counteracts the shielding (electron donating) effect usually exerted by oxygen substituted on aromatic rings (2). This counter effect may partially be the reason why the methyl resonances of the di-ethers are, in each instance, downfield from those of the mono-ethers (see Table 2).

Following t.l.c. (see Table 3), the di-ethers appeared as single spots and showed higher mobility than the mono-ethers; a negative phenolic test (diazotized sulfanilic acid) was observed with the di-ethers.

The mono-ethers **1***a* and **2***a* appeared as two

TABLE 3

Thin-layer chromatography*

Compound	$R_f \times 10^2$
o-Cresol†	51
m-Cresol†	44
p-Cresol†	46
2-Methylhydroquinone‡	11
3-Methylcatechol‡	22
4-Methylcatechol‡	16
1*a*	26§, 32
1*b*	63
2*a*	32§, 38
2*b*	64
3*a*	33
3*b*	65

*On silica gel GF_{254}; benzene–methanol (95:5) as solvent; detection by fluorescence quenching and diazotized sulfanilic acid.
†Average of 7–16 determinations.
‡Average of 2–4 determinations.
§Predominant spot.

Can. J. Chem. Downloaded from www.nrcresearchpress.com by 210.87.254.40 on 09/05/12
For personal use only.

TABLE 4

Hydrogenolysis reaction and gas chromatography data

Compound	Hydrogenolysis (% yield)	Products	Isomers ratio	Method of analysis	Gas chromatographic retention times (min*)
1*a*	86.6	Cresols	ortho 1 meta 2	Gas chromatography†,‡	10.0 11.8
2*a*	68.2	Cresols	ortho 1 meta 2	Gas chromatography†,‡	10.0 11.8
3*a*	66.8	Cresols	meta 6 para 1	Gas chromatography§	6.46‖ 2.18‖
1*b*	80.1	Toluene	—	Ultraviolet	—
2*b*	84.3	Toluene	—	Ultraviolet	—
3*b*	93.8	Toluene	—	Ultraviolet	—

*Relative to solvent front; average of 6–8 determinations.
†On a 3% OV-17 on 100–120 Gas-Chrom Q column, 6 ft × 1/4 in.
‡Developed at 90 °C; carrier gas (helium), 60 ml/min.
§Developed at 210 °C; carrier gas (helium), 60 ml/min.
‖As 2,4,6-tribromo-3-methylphenol.
¶As 2,6-dibromo-4-methylphenol.

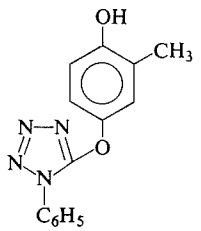

4

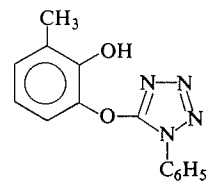

5

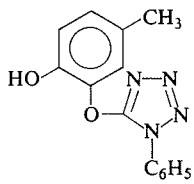

6

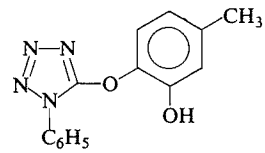

7

spots on t.l.c.; the predominant spots had lower R_f values. The more mobile (minor) materials were believed to be **4** and **5**, respectively (3). This interpretation led to the prediction that *m*-cresol would be the major hydrogenolysis product of **1***a* and **2***a*.

The mono-(1-phenyltetrazole) ether of 4-methylcatechol (**3***a*) showed one spot on t.l.c.; however, this was not considered indicative of homogeneity since the possible isomers (**6** and **7**) should possess similar chromatographic characteristics. Compounds **1***a*, **2***a*, and **3***a* gave positive diazotized sulfanilic acid tests (4).

Hydrogenolysis of all ethers proceeded smoothly with the di-(1-phenyltetrazole) ethers giving better overall yields (see Table 4). The t.l.c. of the hydrogenolysis products of **1***a* and **2***a* revealed major spots corresponding to *m*-cresol and minor spots corresponding to *o*-cresol. Results of the t.l.c. from the hydrogenolysis of **3***a* indicated *m*- and/or *p*-cresol; no thin-layer system was found suitable for the separation of these isomers. Quantitative analysis of *o*- and *m*-cresol was achieved with gas chromatography (g.c.) (see Table 4). Separation and quantitation of *m*- and *p*-cresol by g.c. proved difficult. Success was attained by treating the cresols with bromine to prepare the respective tribromo- and dibromo-derivatives (5), which could be separated and analyzed.

Some selectivity of ether formation was indicated by studies of the composition of the hydrogenolysis products of the mono-ethers. With **1***a* and **2***a* 2:1 meta:ortho cresol ratios were observed. With **3***a* a 6:1 meta:para cresol ratio was observed. In all cases formation of the tetrazole ethers seems to correlate with preferential production of the more nucleophilic anion. Thus, the predominant isomers may result from a difference in the rate of this reaction (6). The smaller ratios observed with **1***a* and **2***a* could be the result of less favorable steric situations during the synthesis of these tetrazole ethers.[3]

[3]One referee has suggested that greater selectivity in mono-etherification of dihydric phenols may be possible by use of aprotic solvents with high dielectric constants (e.g., dimethylsulfoxide and dimethylformamide; see ref. 6).

Can. J. Chem. Downloaded from www.nrcresearchpress.com by 210.87.254.40 on 09/05/12
For personal use only.

Can. J. Chem. Downloaded from www.nrcresearchpress.com by 210.87.254.40 on 09/05/12
For personal use only.

Based upon ultraviolet (u.v.) spectrophotometric analysis of the hydrogenolysis product of the di-ethers, uniformly good yields of toluene were obtained. Apparently steric conditions which influence mono-ether formation do not adversely affect di-ether yield. These results indicate that di-(1-phenyltetrazole) ether formation and hydrogenolysis may be a near quantitative and facile method for the removal of hydroxyl groups.

Experimental

Melting points were determined with a Thomas–Hoover apparatus and are corrected. Elemental analyses were conducted by Galbraith Laboratories, Inc., Knoxville, Tennessee. Infrared spectra were determined in KBr with a Beckman IR-5A spectrophotometer. The u.v. spectra were recorded with a Beckman DK-2 spectrometer. Solvents and reagents employed in spectral and chromatographic work were reagent grade. The n.m.r. spectra were obtained with a Varian T-60 spectrometer from DMSO-d_6 solutions with tetramethylsilane as an internal standard. The t.l.c. was carried out with 250 μ layers of silica gel GF_{254} (Brinkmann) using benzene–methanol (95:5) as solvent. The g.c. was performed with a Hewlett–Packard 5750B gas chromatograph equipped with dual flame ionization detectors and conditions indicated in Table 4. Curves of peak height vs. amount chromatographed were used for quantitative analysis.

*2-Methyl-1,4-hydroquinone Mono-(1-phenyltetrazole) Ether (**1a**)*

To a dry flask equipped with reflux condenser, mechanical stirrer and nitrogen inlet was added 2-methyl-1,4-hydroquinone (4.03 g, 0.0325 mole), 5-chloro-1-phenyltetrazole (4.51 g, 0.025 mole), and potassium *tert*-butoxide (2.8 g, 0.025 mole) in isopropyl alcohol (250 ml). The mixture was stirred and refluxed in a nitrogen atmosphere for 18 h. The mixture was filtered through paper while hot, evaporated under reduced pressure, and recrystallized from isopropyl alcohol–water.

*3-Methylcatechol Mono-(1-phenyltetrazole) Ether (**2a**) and 4-Methylcatechol Mono-(1-phenyltetrazole) Ether (**3a**)*

To a dry three-necked flask equipped with reflux condenser, mechanical stirrer, and nitrogen inlet was added methylcatechol, 5-chloro-1-phenyltetrazole, and potassium carbonate in the molar ratio of 0.05:0.05:0.1. After acetone (250 ml) was added, the mixture was stirred and refluxed in a nitrogen atmosphere for 18 h. The warm reaction mixture was filtered and evaporated under reduced pressure. The residue was suspended in cold water, neutralized with 5% hydrochloric acid, and extracted several times with chloroform. The combined chloroform extracts were dried over anhydrous sodium sulfate, then filtered and evaporated to dryness. The residue was recrystallized from acetone–water.

*2-Methyl-1,4-hydroquinone Di-(1-phenyltetrazole) Ether (**1b**), 3-Methylcatechol Di-(1-phenyltetrazole) Ether (**2b**), and 4-Methylcatechol Di-(1-phenyltetrazole) Ether (**3b**)*

To a dry three-necked flask equipped with reflux condenser, mechanical stirrer, and nitrogen inlet was added the appropriate dihydroxy compound, 5-chloro-1-phenyltetrazole, and potassium carbonate in the molar ratio of 0.025:0.05:0.1. After adding anhydrous acetone, the mixture was stirred and refluxed in a nitrogen atmosphere overnight. Following evaporation of the solvent at reduced pressure, the residue was mixed with cold water and neutralized with 5% hydrochloric acid. The precipitate which formed was extracted with several portions of chloroform. The combined chloroform extracts were dried over anhydrous sodium sulfate. After removal of the solvent, the white solid was recrystallized from acetone–water.

Hydrogenolysis of Mono- and Di-(1-phenyltetrazole) Ethers

The ether (500 mg) and 5% palladium on carbon (100 mg) were placed in a Parr hydrogenation bottle with 100 ml of 95% ethanol. The mixture was shaken with hydrogen overnight, then filtered. An aliquot of the filtrate of the products resulting from **1***a* and **2***a* was evaporated to dryness, dissolved in 1 ml acetonitrile and gas chromatographed. The hydrogenolysis product of **3***a* was treated as indicated under bromo derivatives of *m*- and *p*-cresol and submitted to g.c. The filtrates from the hydrogenolysis of the di-ethers were distilled at atmospheric pressure and the distillate analyzed by u.v. spectroscopy.

Bromo Derivatives of m- and p-Cresol

One to 20 mg of *m*- or *p*-cresol or hydrogenation products of **3***a* was reacted with 1 ml of bromine water (10 g bromine, 10 g potassium bromide, 100 ml water) for 5 min. The mixture was quenched with 0.5 ml of 10% sodium bisulfite solution and extracted with hexane. The hexane solution was used for g.c. analysis. A single and different product was produced upon reaction with *m*- and *p*-cresol, presumably 2,4,6-tribromo-3-methylphenol and 2,6-dibromo-4-methylphenol, respectively (5).

This research was supported by grant MH-16379 from the National Institute of Mental Health.

1. W. J. Musliner and J. W. Gates. J. Amer. Chem. Soc. **88**, 4271 (1966).
2. F. R. Benson. Heterocyclic compounds. Vol. 8. *Edited by* R. C. Elderfield. John Wiley and Sons, Inc., New York, 1967. Chap. 1.
3. W. W. Fike. Anal. Chem. **38**, 1697 (1966).
4. L. R. Axelrod and T. E. Pulliam. Arch. Biochem. Biophys. **89**, 106 (1960).
5. R. L. Shriner, R. C. Fuson, and D. Y. Curtin. The systematic identification of organic compounds. 4th ed. John Wiley and Sons, Inc., New York, 1956. pp. 264 and 325.
6. L. C. Dorman. J. Org. Chem. **31**, 3666 (1966).

Studies on some 1,2,4-dithiazolium salts

M. AHMED AND D. M. MCKINNON
Department of Chemistry, University of Manitoba, Winnipeg, Manitoba

Received January 26, 1970

3-Alkylthio-1,2,4-dithiazolium salts are most conveniently made by alkylation of the corresponding 1,2,4-dithiazole-3-thiones by dimethyl sulfate. These salts readily undergo nucleophilic attack by amines in position 3, with loss of a methylthio group. Hydrogen peroxide oxidation, or chlorination, of the thiones gives the corresponding dithiazole-3-ones.

Canadian Journal of Chemistry, 48, 2142 (1970)

Can. J. Chem. Downloaded from www.nrcresearchpress.com by 210.87.254.42 on 09/05/12
For personal use only.

To provide suitable examples of the 1,2,4-dithiazolium cation (**1**) for study, we have investigated some of their preparations and reactions. One suitable approach to this system appeared to be from the readily accessible (1, 2) 3*H*-1,2,4-dithiazole-3-thiones (**2**), since it was expected that they might react similarly to the 3*H*-1,2-dithiole-3-thiones, which can be converted by several methods (3–5), into examples of the 1,2-dithiolium cation.

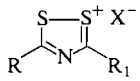

1

a R = Ph; R_1 = Cl; X = Cl
b R = Ph; R_1 = SCl; X = Cl

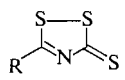

2

a R = Ph
b R = *p*-MeC_6H_4
c R = *o*-MeC_6H_4
d R = 2-Furyl
e R = *p*-$MeOC_6H_4$
f R = 1-Naphthyl
g R = 2-Naphthyl

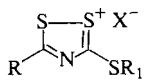

3

a R = Ph; R_1 = Me; X = I
b R = Ph; R_1 = Et; X = BF_4
c R = Ph; R_1 = Me; X = ClO_4
d R = *p*-MeC_6H_4
e R = *o*-MeC_6H_4
f R = 2-Furyl
g R = *p*-$MeOC_6H_4$
h R = 1-Naphthyl
i R = 2-Naphthyl

The first reaction studied was the alkylation of the thiones (**2**), to provide a convenient synthesis of the 3-alkylthio-1,2,4-dithiazolium cations (**3***a–i*). The preparation of one of these (**3***a*) using methyl iodide as the alkylating agent has been reported (1). Also, use of triethyloxonium fluoroborate (6) provides examples of the 3-ethylthio cation (**3***b*). However, the first of these methods is unsatisfactory in that the 3-methylthio-1,2,4-dithiazolium iodide (**3***a*) is insufficiently soluble to provide a convenient study of its properties. The latter method is also inconvenient in that it requires prior synthesis of triethyloxonium fluoroborate.

A much more convenient method utilized dimethyl sulfate at 80°. The thiones, **2***a–g*, were readily alkylated and treatment of the reaction solutions with perchloric acid afforded the 3-methylthio salts, **3***c–i*, as their perchlorates in good yields. These were stable, bright colored, and readily soluble in acetic acid or nitromethane, permitting study of their properties. The reactions of these salts with amines are similar to the reaction of various 1,2-dithiolium salts with amines (7–9). 3*H*-1,2,4-Dithiazole-3-thiones (**2**) are reported to undergo nucleophilic attack by primary amines (1) at position 5 of the ring, with the eventual formation of thioamides. However, nucleophilic attack on the 3-alkylthio salts **3** by primary amines occurs at position 3, with subsequent elimination of methanethiol. The 3-arylimino products **4** appear to be rather reactive, and in two cases, the imines **4***a*, *b*, formed by reaction of aniline with the salts **3***c*, *d* respectively, could not be isolated, although a preparation of the imine **4***a* has been reported recently (10) by another method. Instead, in these experiments, further addition products **5** with the amine were isolated. Only in the reaction of the salt (**3***d*) with *p*-toluidine was the imine **4***c* isolated. These further additions probably occurred at position 5 rather than at position 3 to give the compounds **5***a*, *b* or tautomers rather than the isomeric compounds **6** since nucleophilic attack of amine to the isoelectronic dithiazolethiones **2** takes place at position 5. This structure is also indicated by nuclear magnetic resonance (n.m.r.), which shows that two

quite different NH groups are present. In structure **6** the two NH protons would be expected to be rather similar. No doubt other reactions are competing in the above. Some *N*-methylanilinium iodide was obtained by reaction of the iodide **3***a* with aniline, apparently by transmethylation.

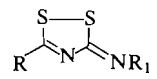

4

a R = R_1 = Ph
b R = *p*-MeC_6H_4; R_1 = Ph
c R = R_1 = *p*-MeC_6H_4

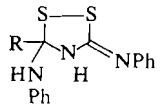

5

a R = Ph
b R = *p*-MeC_6H_4

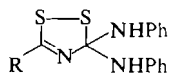

6

a R = Ph
b R = *p*-MeC_6H_4

Reaction of the compound **3***c* with *N,N*-dimethylaniline gave a different type of product, the 3-(4-dimethylaminophenyl)-5-phenyl cation was obtained as its perchlorate, **7***a*. The iodide, **3***a*, reacted similarly, but the cation was obtained as tri-iodide **7***b*. The reaction probably proceeds by nucleophilic displacement of methanethiolate anion by the dimethylaniline. Similar displacements are reported in the reaction of 3-alkylthio-1,2,4-dithiazolium salts with pyrroles (**6**).

Treatment of 3*H*-2-dithiole-3-thiones with hydrogen peroxide in acetic acid or peroxyacetic acid (3, 11) gives 1,2-dithiolium salts. However, similar treatment of the thione **2***a* gave 5-phenyl-3*H*-1,2,4-dithiazole-3-one (**8**). Similar reactions have been reported in the peracetate oxidation of 4*H*-pyran-4-thiones (12). The reason for the difference in reactions is not clear. Although sulfines are probably intermediates in the oxidation of heterocyclic thiones (13, 14), many different types of products are reported.

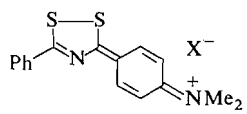

7

a X = ClO_4
b X = I_3

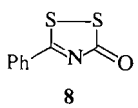

8

Also, treatment of 3*H*-1,2-dithiole-3-thiones with chlorine produces 3-chloro-1,2-dithiolium salts (5, 15). The dithiazolethione, **2***a*, under these conditions once more gave the -3-one **8** along with what appeared to be an adduct of the thione with chlorine. Probably the -3-one compound is derived from the 3-chloro-1,2,4-dithiazolium salt (**1***a*) by hydrolysis. 1,2-Dithiole-3-ones are obtained from dithiolethiones by chlorination in boiling acid (16) and iminochlorides of the type (**1***a*) would be expected to hydrolyze more rapidly. The supposed adduct was a yellow compound, which decomposed in a few days on standing in the air at room temperature to a mixture of dithiazole-3-thione and dithiazolone. Chlorination in carbon tetrachloride provided only this adduct, which, in view of its limited solubility in non-polar solvents, may be 3-chlorothio-1,2,4-dithiazolium chloride (**1***b*). Similar adducts are reported in the halogenation of dithiolethiones (5, 17, 18). Another preparative method of similar halides, the action of oxalyl chloride on dithiole-3-ones, -3-thiones (19), or isothiazolones (20) was also unsuccessful when applied to the dithiazolone or dithiazolethione.

Experimental

Thin-layer chromatography (t.l.c.) was performed on "Camag" silica gel type D.S.F.5. supplied by Mondray Ltd. Development of plates was carried out using benzene with increasing proportions of chloroform. The n.m.r. spectra were obtained on a "Varian" model 56/60A spectrometer in deuteriochloroform solution using tetramethylsilane as an internal standard.

Reaction of 3H-1,2,4-Dithiazole-3-thiones (2a–g) with Dimethyl Sulfate to Form 3-Methylthio-1,2,4-dithiazolium Perchlorates (3c–i)

The freshly recrystallized thiones (1 g) (1) and dimethyl sulfate (3 ml) were heated together at 80° until the mixture was homogeneous. The solution was treated with 70% perchloric acid (0.5 ml) and ether (5 ml) added. The precipitated salts were collected, washed with more ether, and recrystallized from acetic acid. The details are summarized below.

3-Methylthio-5-phenyl-1,2,4-dithiazolium Perchlorate (3c)

This was obtained as pale yellow needles m.p. 165° (82%).

Anal. Calcd. for $C_9H_8NS_3ClO_4$: C, 33.19; H, 2.46; N, 4.30; S, 29.51; Cl, 10.88. Found: C, 32.79; H, 2.51; N, 4.31; S, 29.16; Cl, 11.13.

This compound was also prepared by treatment of 3-methylthio-5-phenyl-1,2,4-dithiazolium iodide (1) (**3***a*) in boiling acetic acid with perchloric acid. The dark solution was decanted off insoluble material and diluted with ether. Recrystallization gave a perchlorate identical to that above.

Can. J. Chem. Downloaded from www.nrcresearchpress.com by 210.87.254.42 on 09/05/12
For personal use only.

Can. J. Chem. Downloaded from www.nrcresearchpress.com by 210.87.254.42 on 09/05/12
For personal use only.

3-Methylthio-5-p-tolyl-1,2,4-dithiazolium Perchlorate (3d)

This was obtained as pale yellow needles m.p. 157° (90%).

Anal. Calcd. for $C_{10}H_{10}NS_3ClO_4$: C, 35.32; H, 2.94; N, 4.13; S, 28.26; Cl, 10.45. Found: C, 35.22; H, 2.89; N, 4.27; S, 28.45; Cl, 10.64.

3-Methylthio-5-o-tolyl-1,2,4-dithiazolium Perchlorate (3e)

This was obtained as bright yellow needles m.p. 164° (87%).

Anal. Calcd. for $C_{10}H_{10}NS_3ClO_4$: C, 35.32; H, 2.94; N, 4.13; S, 28.26; Cl, 10.45. Found: C, 35.22; H, 2.89; N, 4.27; S, 28.45; Cl, 10.64.

3-Methylthio-5-(2 furyl)-1,2,4-dithiazolium Perchlorate (3f)

This was obtained as pale yellow needles m.p. 140.5 (73%).

Anal. Calcd. for $C_7H_6NN_3ClO_5$: C, 26.69; H, 1.91; N, 4.44; S, 30.41; Cl, 11.26. Found: C, 26.76; H, 1.95; N, 4.57; S, 30.25; Cl, 11.14.

3-Methylthio-5-p-methoxyphenyl-1,2,4-dithiazolium Perchlorate (3g)

This was obtained as bright yellow needles m.p. 155° (61%).

Anal. Calcd. for $C_{10}H_{10}NS_3ClO_5$: C, 33.82; H, 2.81; N, 3.94; S, 27.10; Cl, 9.99. Found: C, 33.73; H, 2.75; N, 4.13; S, 27.12; Cl, 9.85.

3-Methylthio-5-(1-naphthyl)-1,2,4-dithiazolium Perchlorate (3h)

This was obtained as light orange needles m.p. 141° (91%).

Anal. Calcd. for $C_{13}H_{10}NS_3ClO_4$: C, 43.45; H, 2.57; N, 3.59; S, 24.69; Cl, 9.12. Found: C, 43.15; H, 2.61; N, 3.85; S, 24.91; Cl, 9.40.

3-Methylthio-5-(1-naphthyl)-1,2,4-dithiazolium Perchlorate (3h)

This was obtained as light orange needles m.p. 141° (91%).

Anal. Calcd. for $C_{13}H_{10}NS_3ClO_4$: C, 43.45; H, 2.57; N, 3.59; S, 24.69; Cl, 9.12. Found: C, 43.15; H, 2.61; N, 3.85; S, 24.91; Cl, 9.40.

3-Methylthio-5-(2-naphthyl)-1,2,4-dithiazolium Perchlorate (3i)

This was obtained as orange needles m.p. 155° (86%).

Anal. Calcd. for $C_{13}H_{10}NS_3ClO_4$: C, 43.45; H, 2.57; N, 3.59; S, 24.69; Cl, 9.12. Found: C, 43.14; H, 2.72; N, 3.74; S, 24.91; Cl, 9.04.

Reaction of 3-Methylthio-5-phenyl-1,2,4-dithiazolium Perchlorate with Aniline to Form the Compound 5a

The perchlorate (0.5 g) and aniline (0.3 g) were heated together in acetic acid (10 ml) until the solution was homogeneous, then the mixture was diluted with water. The dried ether extract was examined by t.l.c. and two bands were eluted. The first band (50 mg) did not crystallize, but the second band crystallized under ethanol. Pale yellow needles m.p. 126° were obtained (62%).

Anal. Calcd. for $C_{20}H_{17}N_3S_2$: C, 66.21; H, 4.68; N, 11.55; S, 17.65. Found: C, 66.00; H, 4.67; N, 11.72; S, 17.64.

The n.m.r. spectrum 3.4 to 2.2 (15H band, from the three aromatic rings); 1.78 (1H singlet, on 5-anilino nitrogen), −4.11 τ (1H singlet, on ring nitrogen). When the above reaction was performed in ethanol and the solution diluted with ether, a small amount (~60 mg) of *N*-methylanilinium iodide was obtained. Work-up as above gave similar results.

Reaction of 3-Methylthio-5-p-tolyl-1,2,4-dithiazolium Perchlorate (3d) with Aniline to Form 5b

This reaction was performed as above. Pale yellow needles m.p. 145–146 were obtained (78%).

Anal. Calcd. for $C_{21}H_{19}N_3S_2$: C, 66.81; H, 5.04; N, 11.07; S, 16.99. Found: C, 66.52; H, 5.17; N, 10.93; S, 16.73.

The n.m.r. spectrum 7.72 (3H singlet methyl group), 3.4 to 2.2 (14H bands from the aromatic rings), 1.20 (1H singlet, on 5-anilino nitrogen), −4.10 τ (1H singlet, on ring nitrogen).

Reaction of 3-Methylthio-5-p-tolyl-1,2,4-dithiazolium Perchlorate (3d) with p-Toluidine

The perchlorate (0.5 g) and *p*-toluidine (0.2 g) in acetic acid (10 ml) were heated until a homogeneous yellow solution was obtained. The solution was diluted with water and the ether extract examined by t.l.c. The first band did not crystallize but the second crystallized on evaporation and was recrystallized from ethanol. Orange-yellow plates m.p. 125–126° were obtained (42%).

Anal. Calcd. for $C_{16}H_{14}N_2S_2$: C, 64.42; H, 4.69; N, 9.39; S, 21.48. Found: C, 64.23; H, 4.75; N, 9.21; S, 21.59.

The n.m.r. spectrum 7.65 (3H singlet) 7.63 (3H singlet), 3.1 to 1.9 τ (8H bands, from aromatic rings).

Reaction of 3-Methylthio-5-phenyl-1,2,4-dithiazolium Perchlorate (3c) with Dimethylaniline to Form 3-Perchlorate (7a)

The perchlorate (0.5 g) and dimethylaniline (0.4 g) in acetic acid (10 ml) were heated together for 10 min. The solution rapidly became deep blue. The crude product obtained on cooling was washed with ether and recrystallized from acetic acid. Dark blue needles with a green reflex were obtained, m.p. 225–226° (70%).

Anal. Calcd. for $C_{16}H_{15}N_2S_2ClO_4$: C, 48.18; H, 3.76; N, 7.03; S, 16.06; Cl, 8.90. Found: C, 47.99; H, 3.86; N, 7.01; S, 16.23; Cl, 9.10.

Reaction of the iodide, **3a**, was performed the same way. Dark blue crystals were obtained of compound **7b** m.p. 240–245° (21%).

Anal. Calcd. for $C_{16}H_{15}N_2S_2I_3$: C, 28.25; H, 2.21; N, 4.13; S, 9.42; I, 56.10. Found: C, 28.60; H, 2.49; N, 4.09; S, 9.35; I, 55.89.

Reaction of 5-Phenyl-3H-1,2,4-dithiazole-3-thione (2a) with Hydrogen Peroxide

To a solution of the thione (1.0 g) in acetic acid (20 ml) at 25°, hydrogen peroxide (0.55 ml, 30% solution in water) was added. The solution became darker, then paler after 30 min. After 1 h the mixture was diluted with ether, but no salt-like material was precipitated. Dilution with water and evaporation of the ether extract gave the dithiazolone (**8**), identical (mixed m.p.) with an authentic sample (2) (25%).

Chlorination of 5-Phenyl-1,2,4-dithiazole-3-thione (2a)

(*a*) In acetic acid. The thione (0.5 g) in acetic acid at room temperature (10 ml) was treated with a stream of chlorine until the red color had disappeared. The mixture, treated with ether, afforded an insoluble yellow precipitate which decomposed in a few days to a mixture of the dithiazolethione and dithiazolone. Evaporation of the ether solution gave dithiazolone.

(*b*) In carbon tetrachloride. The thione (0.5 g) in carbon tetrachloride was treated with chlorine. A yellow precipitate was obtained identical to that above.

Reactions of 5-Phenyl-1,2,4-dithiazol-3-thione (2a) with Oxalyl Chloride and Thionyl Chloride

The thione was treated with an excess of oxalyl chloride or thionyl chloride in boiling benzene for 4 h. Only starting material was isolated.

We would like to thank Dr. T. Schaefer for helpful discussion, Mr. R. Dickinson for the preparation of nuclear magnetic resonance spectra, and the National Research Council of Canada for financial support.

1. J. W. MacDonald and D. M. McKinnon. Can. J. Chem. **45**, 1225 (1967).
2. J. Derocque and J. Vialle. Bull. Soc. Chim. France, 1183 (1966).
3. E. Klingsberg. J. Amer. Chem. Soc. **83**, 2934 (1961).
4. B. Bottcher and F. Bauer. Ann. **568**, 227 (1950).
5. R. S. Spindt, D. R. Stevens, and W. E. Baldwin. J. Amer. Chem. Soc. **73**, 3693 (1951).
6. R. Gompper and R. Weiss. Angew. Chem. Int. Ed. **7**, 297 (1968).
7. A. Luttringhaus and U. Schmidt. Chem. Ztg. **77**, 135 (1955).
8. D. Leaver, D. M. McKinnon, and W. A. H. Robertson. J. Chem. Soc. 4643 (1963).
9. D. M. McKinnon and E. A. Robak. Can. J. Chem. **46**, 1855 (1968).
10. W. Walter and P. M. Hell. Ann. **727**, 22 (1969).
11. D. Leaver, W. A. H. Robertson, and D. M. McKinnon. J. Chem. Soc. 5104 (1962).
12. M. A. Elkaschef and M. H. Nosseir. J. Chem. Soc. 4643 (1963).
13. T. J. Adley, A. K. M. Anisuzamman, and L. N. Owen. J. Chem. Soc. [C] 807 (1967).
14. J. Strating, L. Thijs, and B. Zwanenburg. Tetrahedron Lett. 65 (1966).
15. P. S. Landis and L. A. Hamilton. J. Org. Chem. **25**, 1742 (1960).
16. H. Quinou and N. Losac'h. Bull. Soc. Chim. France, 1167 (1963).
17. A. Luttringhaus, R. Cordes, and U. Schmidt. Angew. Chem. **67**, 275 (1955).
18. Y. Mollier and N. Losac'h. Bull. Soc. Chim. France, 1076 (1952).
19. J. Faust and R. Mayer. Ann. **688**, 150 (1965).
20. J. Faust. Z. Chem. **8**, 170 (1968).

Can. J. Chem. Downloaded from www.nrcresearchpress.com by 210.87.254.42 on 09/05/12
For personal use only.

Can. J. Chem. Downloaded from www.nrcresearchpress.com by 210.87.254.40 on 09/05/12
For personal use only.

Cyclopropylcarbinyl-oxo-carbonium ions. A solvolytic basis for the cyclopropylcarbinyl-oxo-carbonium ion

BERT FRASER-REID AND BRUNO RADATUS
Department of Chemistry, University of Waterloo, Waterloo, Ontario

Received January 28, 1970

Hydrolysis of 4,6-*O*-benzylidene-3-deoxy-3-*C*-(iodomethyl)-D-allal (**1**) in neutral buffered medium with or without silver ion assistance gives the cyclopropyl aldehyde **4** as the only product. Methanolysis of **1** gives an equal mixture of the α and β anomers of methyl 4,6-*O*-benzylidene-2,3-*C*-methylene-2,3-dideoxy-D-allopyranosides (**6** and **7**). These results indicate that the *cyclopropylcarbinyl-oxo-carbonium ion* (**2**), is produced with unit efficiency in solvolyses in neutral media, and the formation of both diasteriomers (**6** and **7**) requires the complete absence of bicyclobutonium ion (**9**) resonance contribution to the stabilized intermediate, and implies a strong contribution from the oxo-carbonium ion **10**. In basic media compound **1** undergoes quantitative dehydroiodination to the conjugated diene, 4,6-*O*-benzylidene-1,2,3-trideoxy-3-*C*-methylene-D-ribo-hex-1-enopyranose (**8**).

Canadian Journal of Chemistry, **48**, 2146 (1970)

In a recent communication from this laboratory it was suggested that the vinyl ether **1** might provide access to the novel ion **2**, named the *cyclopropylcarbinyl-oxo-carbonium ion* in order to denote its composition from two well stabilized ions (1). This communication presents results of some solvolytic studies which confirm the earlier speculation (1) in that they are best rationalized by the carbonium ion **2** rather than by either of the contributing ions operating singly. Additionally, the study has afforded a number of novel carbohydrate structures which appear to be of theoretical and synthetic importance.

Under conditions which left a normal primary iodide 35% unreacted after 18 h, silver-ion assisted hydrolysis of iodide **1** was complete in less than 1 min (1). In the absence of silver ion, the hydrolysis buffered at p*H* 6.98 required refluxing for 2 h. A single product was given in either case and this could also be obtained in quantitative yield by refluxing either **6** or **7** in aqueous dioxan (p*H* 6.23) for 1 h. The substance was judged to be **4**[1] since its nuclear magnetic resonance (n.m.r.) spectrum was devoid of olefinic protons, but indicated an intact benzylidene group, four cyclopropyl protons (τ 7.8–8.8), an aldehyde[2] proton (τ 0.38, J_{12} = 4.0 Hz), and an exchangeable proton. The latter belonged to a secondary hydroxyl group since acetylation at 0° with acetic anhydride/pyridine gave rise to a one-hydrogen multiplet at τ 4.9 (2). It had to be ascribed to H-5 of **5**[3] since the aldehyde group (1704 cm^{-1}; τ 0.23; J_{12} = 3.0 Hz) had been unaffected by the acetylation.

Silver-ion assisted deiodination of **1** evidently led to ion **2** (see Scheme 1) which experienced nucleophilic attack by water at C-1, undoubtedly the site of highest charge density. This rationalization could be tested by using methanol since the resulting acetal would be incapable of such rearrangement. Accordingly, methanolysis[4] of compound **1** gave an equal mixture of two compounds judging from the intensities of their methoxyl n.m.r. signals. They were separated by silica column chromatography, and one was the previously reported cyclopropane **6** (1, 3). The other compound was obviously the β-D-anomer **7** since its n.m.r. spectrum differed from that of **6** only in the two main respects expected for an

[1]For **4**: m.p. 142.5–144.5; $[\alpha]_D^{23}$ −63.9 (*c*, 3.1 in $CHCl_3$).
Anal. Calcd. for $C_{14}H_{16}O_4$: C, 67.72; H, 6.50. Found: C, 67.90; H, 6.46.

[2]The compound gave a positive Schiff's test; μ_{max}: 2793, 2703, 1701 cm^{-1}.

[3]For **5**: m.p. 126–128; $[\alpha]_D^{23}$ − 89.2 (*c*, 2.36 in $CHCl_3$).
Anal. Calcd. for $C_{16}H_{18}O_5$: C, 66.19; H, 6.25. Found: C, 66.45; H, 6.39.

[4]Methanol, silver nitrate, and silver carbonate.

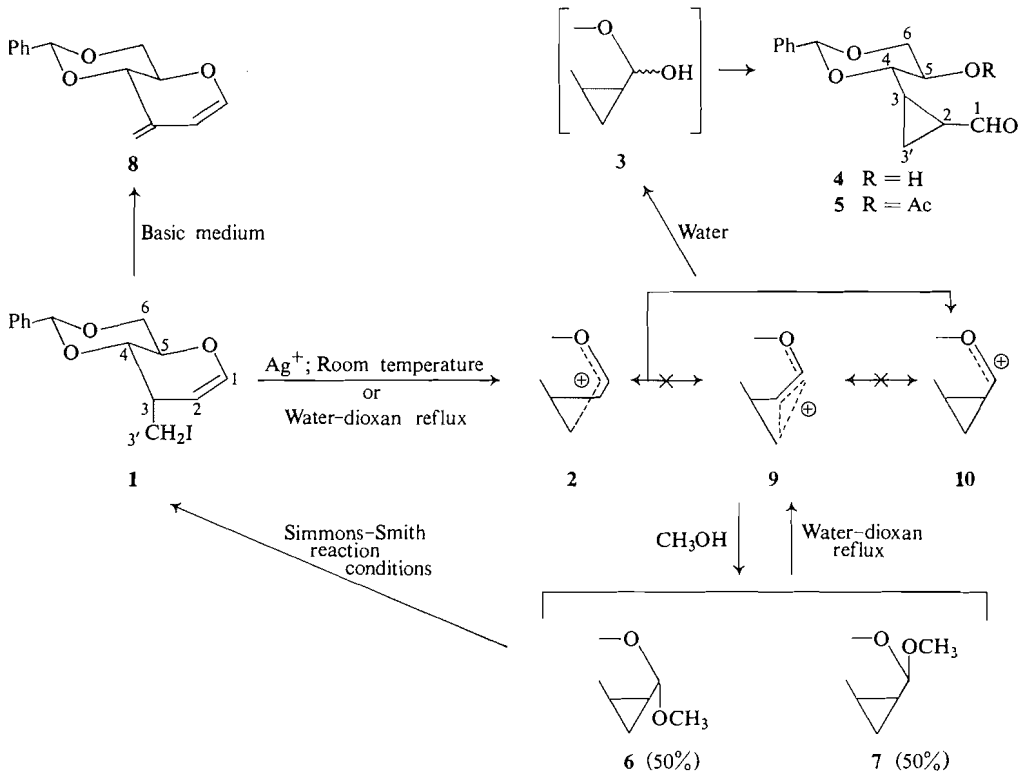

SCHEME 1

anomeric pair (4), namely (*i*) a signal easily recognizable as an anomeric proton (5) at τ 5.27, 0.24 p.p.m. to higher field than the H-1 resonance of **6**[5] and (*ii*) a signal for methoxyl at τ 6.58, 0.09 p.p.m. to lower field than the corresponding signal in **6**. Independent support for this assignment was obtained from the specific rotations[6] which conform to the pattern usually observed for anomeric pairs in the D-series of carbohydrate molecules (6).

When **1** was refluxed in aqueous dioxan containing triethylamine or sodium hydroxide the conjugated diene **8**[7] was the only substance formed. Complete absence of the "normal" hydrolysis product (**4**) suggested that the ion **2** was not involved in the base catalyzed reactions. This was supported by showing that when independently treated with base, **4** was not converted to **8**. Presumably in base the tertiary hydrogen (H-3) is the preferred site for nucleophilic attack and dehydroiodination results.

Solvolyses of **1** in neutral media are therefore seen to lead to cyclopropanated derivatives *exclusively*. This implies total orbital overlap between the —O—C=C— array and the developing carbonium ion at C-3′, an outcome directly attributable to involvement of the vinyl oxygen in the process since in steroidal analogues, cyclopropane derivatives comprise only about 50% of the product (7). Of even greater note is the formation in equal amounts of the anomers **6** and **7** during methanolysis of **1** in contrast to the steroidal models where the rearrangements give only one diasteriomer (8). This result indicates that *the intermediate possess no contribution from*

[5] J_{12} in **6** is 5.0 Hz and in 7 it is < 0.2 Hz.

[6] For **6**: $[\alpha]_D^{23}$, + 115.2 (*c*, 2.86 in $CHCl_3$). For 7: $[\alpha]_D^{23}$, −8.0 (*c*, 3.06 in $CHCl_3$).

[7] Spectral evidence in support of **8** are: μ_{max}: 3012, 2849, 1645, 1600, 878 cm^{-1}; λ_{max}: 243 mμ (ε = 4600). H-1, τ 3.60 (J_{12} = 6.0 Hz, $J_{13'} \leq$ 0.5 Hz); H-2, τ 4.53 (J_{12} = 6.0 Hz; no other coupling).

Anal. Calcd. for $C_{14}H_{14}O_3$: C, 73.02; H, 6.13. Found: C, 72.90; H, 6.38.

Can. J. Chem. Downloaded from www.nrcresearchpress.com by 210.87.254.40 on 09/05/12
For personal use only.

bicyclobutonium resonance forms such as ***9*** *which would protect the α-face of the ion. This presumably reflects the extent to which the charge is delocalized from the α-position to the oxygen, giving added weight to the oxocarbonium* ***(10)*** *contribution.*

Further work on the chemistry of the cyclopropylcarbinyloxo-carbonium ion (**2**) is underway and will be reported upon in due course. In addition the compounds (**4**, **5**, **8**) arising from this study are interesting new members of the branched-chain carbohydrate family, and their elaboration into other novel structures is also being investigated.

We acknowledge generous financial support from the National Research Council of Canada and the Department of University Affairs of Ontario. The accomplishment of this work was greatly facilitated by the presence in the Department of a T-60 n.m.r. spectrometer, generously loaned to us by Varian Associates of Toronto.

1. B. FRASER-REID and B. RADATUS. Can. J. Chem. **47**, 4095 (1969).
2. J. A. ELVIDGE. *In* Nuclear magnetic resonance for organic chemistry. D. W. Mathieson, *Editor*. Academic Press, London, 1967. Table 1.
3. E. L. ALBANO, D. HORTON, and J. H. LAUTERBACH. Carbohydrate Res. **9**, 149 (1969).
4. R. U. LEMIEUX and B. FRASER-REID. Can. J. Chem. **42**, 532 (1964).
5. R. U. LEMIEUX, R. K. KULLNIG, H. J. BERNSTEIN, and W. G. SCHNEIDER. J. Amer. Chem. Soc. **81**, 6098 (1958).
6. C. S. HUDSON. Advan. Carbohydrate Chem. **3**, 1 (1948).
7. G. STORK and J. TSUJI. J. Amer. Chem. Soc. **83**, 2784 (1961); J. J. BONET, H. WEHRLI, and K. SCHAFFNER. Helv. Chim. Acta, **45**, 2615 (1962); J. TADANIER. J. Org. Chem. **31**, 2124 (1966).
8. E. M. KOSOWER and S. WINSTEIN. J. Amer. Chem. Soc. **78**, 4347, 4354 (1956); M. AKHTARAND, D. H. R. BARTON. J. Amer. Chem. Soc., **86**, 1528 (1964); J. TADANIER. J. Org. Chem. **31**, 2124 (1966); K. SYHORA, J. A. EDWARDS, and A. D. CROSS, J. Org. Chem. **31**, 3411 (1966).

Can. J. Chem. Downloaded from www.nrcresearchpress.com by 210.87.254.40 on 09/05/12
For personal use only.

Solvent effect on the conformational preference of the carbanions derived from benzyl methyl sulfoxide

T. DURST, R. R. FRASER, M. R. MCCLORY, R. B. SWINGLE, R. VIAU, AND Y. Y. WIGFIELD
Department of Chemistry, University of Ottawa, Ottawa, Canada

Received April 13, 1970

The effect of solvent on the stereochemical course of deuteration of benzyl methyl sulfoxide has been studied by two methods. In the first, the relative rates of exchange of the diastereotopic methylene protons were found to vary from 14:1 (D_2O/NaOD) to 0.5:1 (*t*-butanol-OD/NaO-*t*-butyl). Experiments on quenching α-lithiobenzyl methyl sulfoxide with D_2O gave the same diastereomers in ratios ranging from 1.7:1 (DMSO) to 0.065:1 (THF). The significance of these findings in relation to previous work on conformational stabilities of α-sulfinyl carbanions is discussed.

Canadian Journal of Chemistry, 48, 2148 (1970)

A number of authors have recently reported the kinetic nonequivalence in the proton exchange of methylene groups α to a sulfoxide (1–5). In particular Wolfe and co-workers (1) found a 16:1 rate difference for the exchange of the methylene protons of benzyl methyl sulfoxide (**1**) in D_2O/NaOD at 15°. Wolfe and Rauk (6) subsequently reported the absolute stereochemistry of the more rapidly exchanging protons as *pro S* when the sulfur chirality was also *S*. They furthermore suggested that the preferred exchange occurred by way of the carbanion bisecting the internal oxygen–sulfur - lone pair angle. Extensive LCAO–MO–SCF calculations (7) on the hypothetical carbanion $^-CH_2S(O)H$ and on methyl sulfinyl carbanion indicated this conformation to be highly favored with the carbanion preferring to be non-planar.

Baldwin and co-workers (8) have recently questioned the application of the theoretical

bicyclobutonium resonance forms such as ***9*** *which would protect the α-face of the ion. This presumably reflects the extent to which the charge is delocalized from the α-position to the oxygen, giving added weight to the oxocarbonium* ***(10)*** *contribution.*

Further work on the chemistry of the cyclopropylcarbinyloxo-carbonium ion (**2**) is underway and will be reported upon in due course. In addition the compounds (**4**, **5**, **8**) arising from this study are interesting new members of the branched-chain carbohydrate family, and their elaboration into other novel structures is also being investigated.

We acknowledge generous financial support from the National Research Council of Canada and the Department of University Affairs of Ontario. The accomplishment of this work was greatly facilitated by the presence in the Department of a T-60 n.m.r. spectrometer, generously loaned to us by Varian Associates of Toronto.

1. B. FRASER-REID and B. RADATUS. Can. J. Chem. **47**, 4095 (1969).
2. J. A. ELVIDGE. *In* Nuclear magnetic resonance for organic chemistry. D. W. Mathieson, *Editor*. Academic Press, London, 1967. Table 1.
3. E. L. ALBANO, D. HORTON, and J. H. LAUTERBACH. Carbohydrate Res. **9**, 149 (1969).
4. R. U. LEMIEUX and B. FRASER-REID. Can. J. Chem. **42**, 532 (1964).
5. R. U. LEMIEUX, R. K. KULLNIG, H. J. BERNSTEIN, and W. G. SCHNEIDER. J. Amer. Chem. Soc. **81**, 6098 (1958).
6. C. S. HUDSON. Advan. Carbohydrate Chem. **3**, 1 (1948).
7. G. STORK and J. TSUJI. J. Amer. Chem. Soc. **83**, 2784 (1961); J. J. BONET, H. WEHRLI, and K. SCHAFFNER. Helv. Chim. Acta, **45**, 2615 (1962); J. TADANIER. J. Org. Chem. **31**, 2124 (1966).
8. E. M. KOSOWER and S. WINSTEIN. J. Amer. Chem. Soc. **78**, 4347, 4354 (1956); M. AKHTARAND, D. H. R. BARTON. J. Amer. Chem. Soc., **86**, 1528 (1964); J. TADANIER. J. Org. Chem. **31**, 2124 (1966); K. SYHORA, J. A. EDWARDS, and A. D. CROSS, J. Org. Chem. **31**, 3411 (1966).

Can. J. Chem. Downloaded from www.nrcresearchpress.com by 210.87.254.5 on 09/05/12
For personal use only.

Solvent effect on the conformational preference of the carbanions derived from benzyl methyl sulfoxide

T. DURST, R. R. FRASER, M. R. MCCLORY, R. B. SWINGLE, R. VIAU, AND Y. Y. WIGFIELD
Department of Chemistry, University of Ottawa, Ottawa, Canada

Received April 13, 1970

The effect of solvent on the stereochemical course of deuteration of benzyl methyl sulfoxide has been studied by two methods. In the first, the relative rates of exchange of the diastereotopic methylene protons were found to vary from 14:1 (D_2O/NaOD) to 0.5:1 (*t*-butanol-OD/NaO-*t*-butyl). Experiments on quenching α-lithiobenzyl methyl sulfoxide with D_2O gave the same diastereomers in ratios ranging from 1.7:1 (DMSO) to 0.065:1 (THF). The significance of these findings in relation to previous work on conformational stabilities of α-sulfinyl carbanions is discussed.

Canadian Journal of Chemistry, 48, 2148 (1970)

A number of authors have recently reported the kinetic nonequivalence in the proton exchange of methylene groups α to a sulfoxide (1–5). In particular Wolfe and co-workers (1) found a 16:1 rate difference for the exchange of the methylene protons of benzyl methyl sulfoxide (**1**) in D_2O/NaOD at 15°. Wolfe and Rauk (6) subsequently reported the absolute stereochemistry of the more rapidly exchanging protons as *pro S* when the sulfur chirality was also *S*. They furthermore suggested that the preferred exchange occurred by way of the carbanion bisecting the internal oxygen–sulfur - lone pair angle. Extensive LCAO–MO–SCF calculations (7) on the hypothetical carbanion $^-CH_2S(O)H$ and on methyl sulfinyl carbanion indicated this conformation to be highly favored with the carbanion preferring to be non-planar.

Baldwin and co-workers (8) have recently questioned the application of the theoretical

Can. J. Chem. Downloaded from www.nrcresearchpress.com by 210.87.254.5 on 09/05/12
For personal use only.

results for $^{-}CH_2S(O)H$ to benzyl methyl sulfoxide and showed that the original stereochemical assignment was in error in that benzyl methyl sulfoxide in D_2O/NaOD exchanges the *pro R* hydrogen more rapidly when sulfur has *S* chirality.[1]

Efforts have been made to verify experimentally the theoretical calculations regarding preferred carbanion conformations using conformationally constrained cyclic sulfoxides (4[2], 5). The results of both studies were in conflict with the theoretical predictions. In addition preliminary results have indicated substantial variations in the relative rates of exchange of diastereotopic protons α to a sulfinyl group with changes in solvent (5, 9).

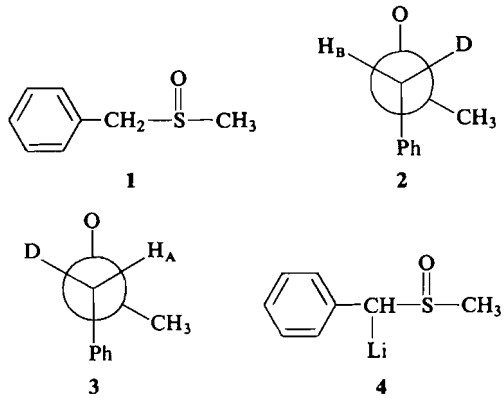

We have investigated the effect of solvent on the stereoselectivity of formation of diastereomeric monodeuterated sulfoxides **2** and **3** produced from benzyl methyl sulfoxide by competitive base-catalyzed exchange in deuterated protic solvents and by rapid quench of the α-lithiosulfoxide (**4**) in aprotic media. Under both sets of conditions the diastereomer **2** having the *R* configuration at carbon (sulfur chirality *S*) is preferentially formed in solvents of high dielectric constant while **3** having the *S* stereochemistry at carbon predominates in low dielectric constant solvents.

The relative rates of exchange of the two diastereotopic protons of **1** are given in Table 1. The rates in D_2O/NaOD were obtained by monitoring deuterium uptake by mass spectrometry and are accurate to within 2% (11); they compare favorably with those obtained by nuclear magnetic resonance (n.m.r.) integration of the benzylic AB quartet as the exchange proceeds (1). The latter method was also used to obtain the data in CD_3OD/CD_3ONa. The simple n.m.r. method could not be used for the exchange in *t*-butanol-O-*d* since the benzylic protons are magnetically equivalent in this solvent.[3] Relative rates were obtained by quenching the reaction after partial exchange and analyzing the n.m.r. spectrum of the material so obtained according to the method described previously (12), the accuracy being ±15%.

TABLE 1

Relative rates of exchange of the diastereotopic protons in benzyl methyl sulfoxide at 24°

Solvent/base	Relative rates H_A	H_B
D_2O/NaOD	14.2	1
CD_3OD/CD_3ONa	5.5	1
*t*BuOD/*t*BuONa	0.50	1
*t*BuOD/*t*BuOLi	0.22	1

The lithio derivative **4** was generated at 24° in DMSO, THF, and benzene and quenched after 1 min by addition of D_2O (D_2O/DOAc in the benzene and DMSO reactions). The ratio of **2** to **3** was determined by n.m.r., the accuracy being ±10% (Table 2). The experiments in THF at 24, −20, and −60° show variations in selectivity consistent with a temperature-dependent equilibrium.

TABLE 2

Relative amounts of monodeuterated species **2** and **3** formed upon quenching of **4** with D_2O

Solvent	Relative amounts **2**	**3**	Temperature (°C)
DMSO	1.7	1	24
Benzene	0.11	1	24
THF	0.13	1	24
THF	0.080	1	−20
THF	0.065	1	−60

[1]S. Wolfe has informed us that his group had independently arrived at the same conclusion.

[2]The tentative stereochemical assignments made in this paper have been shown to be in error and have been corrected (10).

[3]The *pro R* in *S* proton appears at lower field in water, methanol, and DMSO-d_6 but at higher field in deuterochloroform. Similar solvent effects have been noted previously (3).

Can. J. Chem. Downloaded from www.nrcresearchpress.com by 210.87.254.5 on 09/05/12
For personal use only.

Our results can be rationalized on the basis of *either* a single planar carbanion intermediate[4] which protonates preferentially from one side in the high dielectric constant solvents D_2O, CD_3OD, and DMSO and from the other side in the low dielectric constant solvents *t*-BuOD, THF, and benzene *or* two isomeric pyramidal carbanions[4] in which the relative energies of the diastereomers vary greatly with solvent. The latter explanation appears preferable to us at this time. On this basis the above experiments provide evidence that the relative stability of the diastereomeric carbanions derived from **1** is markedly dependent on solvation. The kinetic results provide the relative stabilities of the transition states leading to the carbanions whereas the quenching experiments give the relative stabilities of the lithio carbanions directly. In the latter experiments it is assumed that the ratio of the monodeuterated species reflects the equilibrium between the diastereomeric lithio derivatives, that equilibrium has been reached prior to quenching (14), and that protonation occurs with retention.

Since the detailed steps of all the exchange reactions have not been established we wish to postpone discussion of the conformational preferences for carbanions α to a sulfinyl group until more information becomes available. Regardless of the solution to this problem, it is obvious that our experiments demand inclusion of solvation in any consideration of conformational effects on the stability of these carbanions.

Our results also indicate possibilities for asymmetric synthesis. For instance, a number of reactions involving α-sulfinyl carbanions, e.g. hydroxyalkylations (15) and possibly chlorinations of sulfoxides with positive chlorine species (16–19), give high selectivity. From our results we would prédict that the appropriate solvent change should alter the stereochemical result. These predictions, together with further efforts to establish the nature of the carbanion intermediate or intermediates are being investigated.

[4]The question of planar vs. pyramidal carbanion structure has been more thoroughly discussed for the related α-sulfonyl carbanions (13).

The authors thank the National Research Council of Canada for generous financial support.

1. A. Rauk, E. Buncel, R. Y. Moir, and S. Wolfe. J. Amer. Chem. Soc. **87**, 5498 (1965).
2. E. E. Bullock, J. M. W. Scott, and P. D. Golding. Chem. Commun. 168 (1967).
3. M. Nishio. Chem. Commun. 562 (1967).
4. R. R. Fraser and F. J. Schuber. Chem. Commun. 397 (1969).
5. B. J. Hutchinson, K. K. Andersen, and A. R. Katritzky. J. Amer. Chem. Soc. **91**, 3839 (1969).
6. S. Wolfe and A. Rauk. Chem. Commun. 778 (1966).
7. S. Wolfe, A. Rauk, and I. G. Csizmadia. Can. J. Chem. **47**, 113 (1969); J. Amer. Chem. Soc. **89**, 5712 (1967).
8. J. E. Baldwin, R. E. Hackler and R. M. Scott. Chem. Commun. 1415 (1969).
9. R. R. Fraser and F. J. Schuber. Unpublished observations.
10. R. R. Fraser and F. J. Schuber. Can. J. Chem. **48**, 633 (1970).
11. R. B. Swingle. Ph.D. Thesis, University of Ottawa, Ottawa, Canada, 1969.
12. R. R. Fraser and F. J. Schuber. Chem. Commun. 1474 (1969).
13. (*a*) D. J. Cram and T. A. Whitney. J. Amer. Chem. Soc. **89**, 4651 (1967); (*b*) D. J. Cram, R. D. Trepka, and P. St. Janiak. J. Amer. Chem. Soc. **88**, 2749 (1966); (*c*) E. J. Corey and T. H. Lowry. Tetrahedron Lett. 793, 803 (1965).
14. D. J. Cram and S. H. Pine. J. Amer. Chem. Soc. **85**, 1069 (1963), and references therein.
15. T. Durst. J. Amer. Chem. Soc. **91**, 1034 (1969).
16. S. Iriuchijima and G. Tsuchihashi. Tetrahedron Lett. 5259 (1969).
17. M. Cinquini, S. Colonna, and F. Montanari. Chem. Commun. 607 (1969).
18. R. N. Loeppky and D. C. K. Chang. Tetrahedron Lett. 5415 (1968).
19. M. Hojo and Z. Yoshida. J. Amer. Chem. Soc. **90**, 4496 (1968).

Can. J. Chem. Downloaded from www.nrcresearchpress.com by 210.87.254.40 on 09/05/12
For personal use only.

Canadian Journal of Chemistry

Published by THE NATIONAL RESEARCH COUNCIL OF CANADA

VOLUME 48 JULY 15, 1970 NUMBER 14

The radioactive decay series $^{138}Nd \rightarrow {}^{138}Pr \rightarrow {}^{138}Ce$[1]

JAMES J. HOGAN

Department of Chemistry, McGill University, Montreal, Quebec

Received February 9, 1970

Measurements of the energies and intensities of gamma rays associated with decay of ^{138}Nd, $^{138}Pr^{m}$, and $^{138}Pr^{g}$ have been performed using a Ge(Li) detector. The branching ratio to a previously unreported excited level of ^{138}Pr (328.1 keV) has been measured, thus allowing for direct measurement of the decay of ^{138}Nd. Half-lives of 2.20 ± 0.07 and 5.04 ± 0.09 h have been measured for $^{138}Pr^{m}$ and ^{138}Nd, respectively. Decay schemes for $^{138}Pr^{m} \rightarrow {}^{138}Ce$ and for the decay chain $^{138}Nd \rightarrow {}^{138}Pr^{g} \rightarrow {}^{138}Ce$ are proposed.

Canadian Journal of Chemistry, **48**, 2151 (1970)

Introduction

Until recently, little work had been performed on the neutron-deficient neodymium isotopes since their discovery nearly two decades ago (1). At that time, ^{139}Nd was reported to have a half-life of 5.5 h while that of ^{138}Nd was thought to be 22 min. Twelve years later, Dzhelepov *et al.* (2) suggested, on the basis of measurements of the positron spectra of the five-hour neodymium fraction by Bonch-Osmolovskaya *et al.* (3), that *both* ^{139}Nd and ^{138}Nd had half-lives of about 5 h. It was proposed that ^{138}Nd then decayed to a short-lived isomer of ^{138}Pr, and that this isomer in turn decayed directly to the ground state of ^{138}Ce, by-passing the well-established (1) two-hour isomer of ^{138}Pr. Gromow *et al.* (4) published two studies of the decay chain $^{138}Nd \rightarrow {}^{138}Pr^{g} \rightarrow {}^{138}Ce$, including measurement of the half-life of the short-lived $^{138}Pr^{g}$, based upon studies of positron energy spectra and of conversion electrons. The first measurement of branching ratios and transition energies between excited levels of ^{138}Ce was carried out by Buttsev *et al.* (5) as part of a long-range study of very neutron-deficient neodymium nuclides. These authors are the first to refer to the existence of an excited state of ^{138}Pr lying "about 325 keV" above the ground state, but below the two-hour isomer. They did not measure the branching ratio to this level, however.

It was felt that a further study of this decay chain would be of value for several reasons. First, establishment of the branching ratio and decay energy of this excited state would provide a simple, direct means of studying ^{138}Nd formed in nuclear reactions, by gamma ray spectroscopy. This nuclide was previously thought to decay entirely, and directly, to the ground state of ^{138}Pr with a positron–electron capture half-life indistinguishable from that of $^{139}Nd^{m}$.[2] Second, no accurate (to better than ± 10 keV) determination of the excited energy levels of ^{138}Ce had been performed (6). Third, decay of the aforementioned excited level of ^{138}Pr would provide the first direct measurement of the half-life of ^{138}Nd, with no problems arising from contamination by $^{139}Nd^{m}$. And finally, the system has intrinsic interest. Because of the large difference in the angular momentum of the ground and metastable states of ^{138}Pr, almost no states populated in the decay of one isomer are populated in decay of the other. One therefore has two almost totally unrelated level schemes in ^{138}Ce, each populated entirely by decay of a different level of ^{138}Pr.

[1]Research supported by a grant from the National Research Council of Canada.

[2]The 5-h ^{139}Nd discovered by Stover (1) was later found (4) to be actually a metastable state; therefore it is now properly written $^{139}Nd^{m}$. The 22-min activity was most likely the 29-min ground state, $^{139}Nd^{g}$.

TABLE 1

Gamma rays observed in this work attributed to the decay $^{138}Pr^{m} \rightarrow {}^{138}Ce$

Transition number	Energy (keV)	Relative intensity	Energy of level of origin (keV)*	Fraction of decays to this energy level (%)*
1	306.1±0.6	87.0±0.7	2132.5±0.7	87.0±0.7
2	353.9±0.6	0.8±0.4	2571.5±0.8	0.8±0.4
3	391.2±0.4	5.5±0.5	2217.6±0.5	4.7±0.6
4	547.4±0.5	3.0±0.6†	2373.8±0.6	3.0±0.6
5	788.6±0.2	100.0±0.8*†	788.6±0.2	0.0
6	1037.8±0.3	≡100.0	1826.4±0.4	4.6±1.2

*Calculated from the decay scheme proposed later in this work.
†After correction for a five-hour decay component (see text).

Experimental

The targets, 99.999% pure praseodymium dioxide, were irradiated by 48-MeV protons in the internal beam of the McGill University Synchrocyclotron, for periods ranging from 12–60 s. With a nominal beam current of 1 μA, quantities of the desired ^{138}Nd and ^{138}Pr activities sufficient for the purposes of this work were produced by the ^{141}Pr (p,4n) and ^{141}Pr (p,p3n) reactions, respectively. The powdered target material, typically of the order of 40 mg of PrO_2, was contained in a thin-walled aluminum tube, pinched off at both ends, identical to those used in previous nuclear reaction studies in the McGill Radiochemistry Laboratory (7).

The bombarding energy of 48 MeV was chosen because it is less than the calculated threshold for production of ^{137}Nd by the (p,5n) reaction (8), but also substantially beyond the energy at which the peaks occur in the (p,3n) excitation functions for production of $^{139}Nd^{m}$ and $^{139}Nd^{g}$.[3] This bombarding energy allows then for maximum production of the desired products of mass 138, with minimum contamination from those of masses 137, 139, and 140.

After irradiation, the aluminum tube was slit open and the powder dispersed as evenly as possible over a circular area of approximately 1 cm^2.

The activity of the samples was measured on a 25-cm^3 Ge(Li) detector, at a source-to-detector distance of 8–14 cm, beginning about 15 min after the end of irradiation. In one case, in which a search was carried out for decay periods of 5–30 min, the source was placed less than 1 cm from the detector to maximize the counting rate in the necessarily short counting periods. In the most frequently used counting configuration (8 cm), the detector efficiency and resolution for ^{60}Co was 0.039% with a full-width at half-maximum of 4.7 keV.

A series of International Atomic Energy Agency standard sources were measured in the same geometrical arrangements as the samples to determine both the counter efficiency and an energy calibration curve. These sources provide eleven external (to the neodymium samples) energy calibration points which were used in conjunction with four internal data points arising in the decay of $^{139}Nd^{m,g}$ (9) to calibrate the energy scale.

[3]Measurement of the ^{141}Pr (p,xn) excitation functions is presently in progress in this laboratory.

After the background was subtracted, the data in each channel of a given peak were fitted to a Gaussian-shaped curve which determined the peak position. The fifteen calibration energies, ranging from 113.8 to 1332.5 keV, were then used to determine the energies of the gamma rays arising in the decay of ^{138}Nd and ^{138}Pr.

Decay curves for all peaks were fitted by standard least-squares decay-curve analysis.

Finally, the activity of a source from one irradiation was measured for several hours, making use of a biased amplifier, to search for any peaks at gamma-ray energies from 1600 to 3600 keV. No unidentifiable peaks in this energy region were found.

Results

(a) The Decay $^{138}Pr^{m} \rightarrow {}^{138}Ce$

Gamma rays associated with transitions in ^{138}Ce which are populated from decay of $^{138}Pr^{m}$ are characterized by the parent half-life of approximately 2.2 h. The transitions which are listed in Table 1 arose from the decay in whole, or in part, of a nuclide with a decay period of between 2.0 and 2.5 h. The first column lists the transitions measured. The energy of each transition, in keV, with its associated standard deviation, is listed in the second column. The relative intensity of each gamma transition, normalized to the peak at 1037.8 keV ≡ 100.0 is presented in the third column. The fourth column gives the energy of the level above the ground state of ^{138}Ce from which the transition originates, and the fifth gives the fraction of all decays which lead to the energy level listed in column four. Note that this is the branching fraction *to the level* and not to the transition. The data in the fourth and fifth columns are discussed in the Discussion section.

For two of the measured gamma rays, least-squares analysis of the decay curves revealed the presence of a five-hour component. These have been so noted in Table 1. Three possibilities must

Can. J. Chem. Downloaded from www.nrcresearchpress.com by 210.87.254.40 on 09/05/12
For personal use only.

Can. J. Chem. Downloaded from www.nrcresearchpress.com by 210.87.254.40 on 09/05/12
For personal use only.

be considered as explanation: (*i*) the peak may, purely coincidentally, overlap with a peak associated with the decay of $^{139}Nd^{m}$, (*ii*) the peak may also be associated with the decay of $^{138}Pr^{g}$ which, because of its short half-life, will be in secular equilibrium with ^{138}Nd, and (*iii*) there may be a branch from ^{138}Nd to $^{138}Pr^{m}$ which would introduce a growth component to the decay. One of the purposes of this work was to establish firmly whether, as first suggested by Gromow *et al.* (4), the decay of ^{138}Nd does indeed by-pass completely this isomeric state.

The transition at 547.4 keV was corrected for contamination by the 547.7-keV transition in the decay of $^{139}Nd^{m}$ by means of the known (9) relative intensities of the peaks in $^{139}Nd^{m}$ at 547.7 and 738.1 keV. This method proved more satisfactory than a simple two-component decay-curve analysis because of the statistical uncertainty in the count rates of the peaks at 547 keV and the similarity of the half-lives of the two nuclides. The two methods of correction agree within the limit of error; this is not surprising in the light of the large error associated with the latter procedure.

The peak at 788.6 keV also contains a five-hour component. Since there is no peak of similar energy in the decay of $^{139}Nd^{m}$, and no other peaks in the decay of $^{138}Pr^{m}$ show such a component, one must conclude that the peak arises in decay of both $^{138}Pr^{g}$ and $^{138}Pr^{m}$.

Two methods exist for resolution of the two- and five-hour components: simple decay-curve analysis, feasible in this peak because of higher counting rates, and comparison of the relative intensities of the peaks at 1037.8 and 788.6 keV, suggested to be equal in decay of $^{138}Pr^{m}$ by results of both Gromow (4) and Buttsev (5). The observed difference in the intensities may then be attributed solely to decay of $^{138}Pr^{g}$. The values for the relative intensity as calculated by the two procedures agree within the limits of uncertainty, which unlike the previous case, are quite similar.

The various half-lives determined by least-squares analysis of the decay curves for each of the peaks (except that at 547.4 keV, for which the uncertainty was too great) were than combined and weighted by $1/\sigma^2$ to determine the "best" half-life for $^{138}Pr^{m}$.

The results of the experiments are presented in Fig. 1 as a decay scheme for $^{138}Pr^{m}$. The ordering

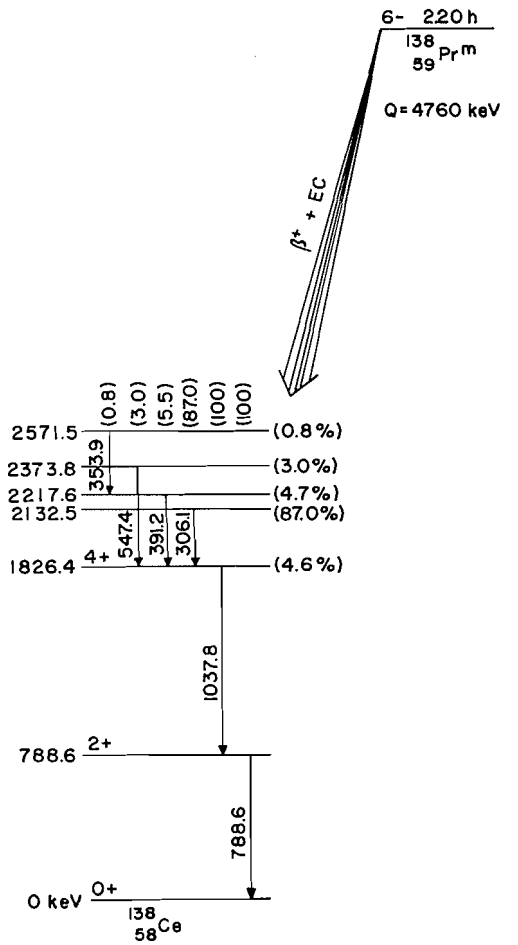

FIG. 1. Proposed decay scheme for $^{138}Pr^{m} \rightarrow {}^{138}Ce$.

of levels is that of Buttsev *et al.* (5). The branching ratios, relative intensities, energies, and half-life are those measured in this work.

(b) The Decay $^{138}Nd \rightarrow {}^{138}Pr^{g} \rightarrow {}^{138}Ce$

Gamma rays associated with this decay chain are characterized by a half-period of about 5 h. Gamma rays measured in this work, having this half-life, and which could not be accounted for as coming from $^{139}Nd^{m}$, are listed in Table 2. In addition, two negative results with their limits of uncertainty are reported for transitions reported by Buttsev *et al.* (5). These will be discussed in the appropriate section. The first three columns of Table 2 report the same quantities as those of Table 1. The fourth column indicates in the excited states of which nuclide in the decay chain the transition occurs. The fifth and sixth

TABLE 2

Gamma rays observed in this work attributed to the decay chain $^{138}Nd \rightarrow {}^{138}Pr^{g} \rightarrow {}^{138}Ce$

Transition number	Energy (keV)	Relative intensity	Transition occurs between levels of	Energy of level of origin (keV)*	Fraction of decays to this energy level (%)*
1	328.1±0.8	9.0±0.3	$^{138}Pr^{g}$	328.1±0.8	6.5±0.8
2	687.8±0.8	3.9±0.4	^{138}Ce	1476.4±0.8‡	3.1±0.4
3	788.6±0.2	≡10.0	^{138}Ce	788.6±0.2	4.4±1.2
4	1476.5±1.5	0.4±0.1	^{138}Ce	1476.5±1.5	3.1±0.4
5	(722)†	0.0±0.02	—	—	<0.1
6	(1510)†	0.0±0.02	—	—	<0.1

*Calculated from the decay scheme proposed later in this work.
†Gamma rays observed by previous workers (see text).
‡This error differs from that for Transition 4 in columns 2 and 5 because it is calculated from the cascade-energy sum. The overall value for this energy level is 1476.5 ± 0.8 keV.

columns are similar to the fourth and fifth of Table 1.

There is no way of indisputably showing that the listed gamma transitions arise in the decay chain under study, rather than from decay of $^{139}Nd^{m}$, in *these* experiments. However, none of the transitions are listed in the extensive work of Beery *et al.* (9) on decay of $^{139}Nd^{m}$, nor have any of them appeared below the calculated threshold for the (p,4n) reaction in the excitation function studies which are in progress. It is therefore reasonable to assume that these transitions all arise in the mass 138 decay chain.

The results of the experiments are shown in Fig. 2 as a decay scheme for these neutron-deficient mass 138 nuclides. It should be noted that the two unobserved transitions which were reported by Buttsev *et al.* both arise from the same state, 1510 keV above the ground state of ^{138}Ce. The first of these (722 keV) is a transition to the 788.6-keV level, and the second (1510 keV) represents de-excitation to the ground state (5).

The four intensities measured, in addition to a normalization requirement (all possible branches must sum up to 100%) provide the five independent data points to determine the five branching ratios given in Fig. 2. It has been assumed that the excited state of ^{138}Pr at 328.1 keV decays in every case to the ground state, never directly to excited levels of ^{138}Ce. This assumption is supported on theoretical grounds in the Discussion; it *is* an assumption, however. Unless it introduced a delay in the decay of the mass 138 chain (that is, unless its half-life were greater than 5–10 min), there would be no way in these experiments to distinguish its decay products from those coming via the ground state.

The ordering of levels is identical with that of Gromow *et al.* (4) and Buttsev *et al.* (5) except that the aforementioned level at 1510 keV in ^{138}Ce reported in the latter work has been omitted.

Discussion

The errors in the determination of transition energies reported in the second column of Tables 1 and 2 are chiefly associated with the ability of the energy calibration curve to reproduce the energies of each "known" standard. Errors arising from uncertainty in the peak position are assumed to be small except in the case of the peak at 1476.5 keV, which had large statistical uncertainty in the counts recorded per channel.

The errors associated with the values of the relative intensities reported in column three of Tables 1 and 2 are determined by the statistical counting error as well as the reproducibility of results from the several experiments. The error in the "negative" results at 722 and 1510 keV is that arising purely from the statistical uncertainty in the measurement of background.

The errors reported in the last column of both tables, the fraction of decays leading to a certain level, arise from two sources: first, the uncertainty in the intensity of decay of each individual peak (column three), and second, from mathematical manipulations involving more than one measured quantity. For example, the errors in the branching ratios reported for the $^{138}Nd \rightarrow {}^{138}Pr^{g} \rightarrow {}^{138}Ce$ decay chain reflect the errors in all of the individual relative intensity measurements because calculation of these values involves simultaneous solution of a series of equations embracing all the measured quantities.

Can. J. Chem. Downloaded from www.nrcresearchpress.com by 210.87.254.40 on 09/05/12
For personal use only.

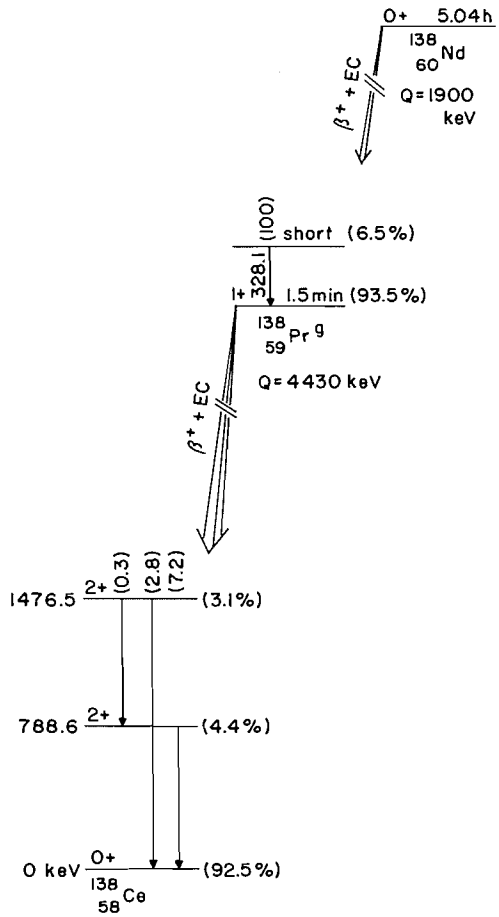

FIG. 2. Proposed decay scheme for $^{138}Nd \rightarrow {}^{138}Pr^{g} \rightarrow {}^{138}Ce$.

(a) The Decay $^{138}Pr^{m} \rightarrow {}^{138}Ce$

There are three principal additions made to the decay schemes originally presented by Buttsev *et al.* (5) in addition to relatively minor changes in the values of the gamma transition energies, energy levels, and branching ratios.

The first of these is a substantial reduction in the fraction of decays of $^{138}Pr^{m}$ leading to the level lying 2374 keV above the ground state of ^{138}Ce. This almost certainly is the product of the 63% reduction in intensity made in this work for contamination by the 547.7-keV transition in the decay of $^{139}Nd^{m}$. It is doubtful that Buttsev *et al.* (5) had the benefit of the decay scheme of Beery *et al.* (9) for $^{139}Nd^{m}$ when their work was performed.

Second, the branch to the level of 2571.5 keV in ^{138}Ce, previously reported as "less than 4%" has been evaluated, primarily as a result of much better statistical data.

Third, the existence of a fairly substantial branch (4.6%) to the level at 1826 keV has been observed. This branch was inferred from the observed excess in intensity of the 1038-keV gamma ray over that expected from the sum of all other transitions leading to this level. It is likely that this branch was missed by the previous workers because of their inability to evaluate with better than 4% uncertainty the small branch to the level at 2571.5 keV mentioned above. While recognizing that evaluation of this new branch involves accurate determination of all other branches, there seems no doubt in the present work that the calculated value lies well outside the limits of error in the calculation.

The half-life determined for the isomer $^{138}Pr^{m}$ (2.20 ± 0.07 h) is essentially the same as those reported previously, with a somewhat reduced level of uncertainty.

(b) The Decay Chain $^{138}Nd \rightarrow {}^{138}Pr^{g} \rightarrow {}^{138}Ce$

The additions to the decay scheme proposed by Buttsev *et al.* (5) for this chain are four-fold: first, the "negative" results for the existence of a level at 1510 keV in ^{138}Ce; second, measurement of the branching ratio to the 328.1-keV level of ^{138}Pr; third, measurement of the half-life of ^{138}Nd without necessity of correction for decay of $^{139}Nd^{m}$; and fourth, measurement of the 1476.5-keV gamma-ray transition.

In each of the several irradiations, gamma-ray peaks at 722 and 1510 keV were sought. In one experiment the hint of a peak at 1510 keV was observed. This "peak", which was not reproducible in other experiments, would have amounted to a branch of less than 0.05%. In every experiment but this one, including those involving long counting periods, and in each individual spectrum in experiments for which decay-curve analyses were performed, there was no evidence for a statistically significant increase in the counting rate in this energy region. And at no time, in any experiment, was there a positive result in the region of 722 keV. It must be concluded that in this work no evidence could be found for the gamma-ray cascade proposed by Buttsev *et al.* (5) beginning at a level 1510 keV above the ground state in ^{138}Ce. Since Beery *et al.* (9) do not report peaks in this energy region in decay of ^{139}Nd, it is impossible to

Can. J. Chem. Downloaded from www.nrcresearchpress.com by 210.87.254.40 on 09/05/12
For personal use only.

Can. J. Chem. Downloaded from www.nrcresearchpress.com by 210.87.254.40 on 09/05/12
For personal use only.

explain this discrepancy in terms of isotopic impurity. As these energy regions are comparatively "clean" of gamma activities, it is highly doubtful that such a peak could have been overlooked in this work.

As discussed in the Results section, the branching ratio for decay of ^{138}Nd to the reported excited level of ^{138}Pr has been determined. As also mentioned previously, it has been assumed that this state decays entirely by gamma emission to the ground state with no direct beta decay to excited levels of ^{138}Ce. This assumption may be justified as follows.

A knowledge of the branching ratio to this excited state allows calculation of the partial half-lives of ^{138}Nd for decay to the two states, which, in addition to knowledge of the total energy difference between the ground states of the two nuclides, provides a means of estimating log (*ft*) values. Taking the total energy of decay of ^{138}Nd to be 1900 keV (8), the calculated values of log (*ft*) are, for decay to the ground and 328.1-keV states, 4.7 and 7.3, respectively. The value of log (*ft*) calculated from the measured branching ratio is consistent with the report of Gromow *et al.* (4) that the ground state of ^{138}Pr is 1+. (This is also the prediction of the Shell Model for a $p(d_{5/2})^3,n(d_{3/2})^1$ configuration.) The excited state at 328.1 keV might be expected on grounds of the log (*ft*) value for decay to it to be either a 1+ state (from an allowed, l-forbidden, beta transition) or 1− state (first-forbidden beta transition). Because no measurements of conversion coefficients have been made in this work, it is pointless to speculate further on the spin and parity of the state. What is of importance, however, is the fact that the gamma transition from the 328.1-keV level to the ground (1+) state must be of low multipole order and therefore fast with respect to any possible beta transitions to excited levels of ^{138}Ce. This supports the assumption that the excited state at 328.1 keV decays entirely to the ground state of ^{138}Pr.

In each of the several irradiations directly related to this work in which the decay of the 328.1-keV level was followed, the least-squares decay-curve analysis was carried out with variable half-life. In addition, data from earlier irradiations performed as part of the ^{141}Pr(p,xn) excitation function studies were also included in the "best" determination of the ^{138}Nd half-life. The half-life determined in this work (5.04 ± 0.09 h) is comparable to those previously measured (5.2 and 5 h, neither with quoted error (4)). Since both of these involved quite indirect measurements, it is felt that the present direct determination of the decay of ^{138}Nd provides substantial improvement in the precision of the measured half-life of this nuclide.

Finally, in light of the spins and parities assigned to the low-lying levels of ^{138}Ce by previous workers, it is puzzling to find the presence of a 1476.5-keV component in the measured gamma ray spectrum. Buttsev *et al.* (5) have assigned a spin and parity of 0+ to this level, precluding the existence of this $0+ \rightarrow 0+$, 1476.5-keV, gamma ray. In light of the fairly good agreement in energies, branching ratios to this level, and branching ratios for decay of this level, between the present work and that of Buttsev *et al.* (5), it is suggested that the 2+ state assigned by Buttsev to the level at 1510 keV (that level which was not observed in this work) is actually at 1476 keV. It is not surprising that the (M1 + E2) transition to the 788.6-keV level is enhanced relative to the E2 transition to the ground state. Rough calculation (see any textbook of nuclear chemistry, e.g. ref. 10) of the probable branching ratio between these two modes of decay predict that decays leading directly to the ground state of ^{138}Ce should account for approximately 6% of all decays. This is certainly comparable to the value of 9.6 ± 1.0% reported in this paper.

It is, at first glance, tempting to suggest that the 1510-keV level does exist as determined by Buttsev *et al.*, but that *it* rather than the level at 1476 keV is the 0+ state. While this would explain the absence of the 1510-keV transition in this work, it would not explain the similar absence of the 722-keV E2 transition. In summary then, it must simply be concluded from this work that no evidence is present for an excited 2+ level lying 1510 keV above the ground state of ^{138}Ce.

The author wishes to thank Mr. R. H. Mills for aid in performing the irradiations, and Mr. S. Murzynski and Dr. S. K. Mark for assistance in the activity measurements. Helpful discussions with Dr. L. Yaffe are also acknowledged with thanks.

1. B. J. Stover. Phys. Rev. **81**, 8 (1951).
2. B. S. Dzhelepov, L. K. Peker, and V. O. Sergeev. Decay schemes of radioactive nuclei. Academy of Sciences (USSR), Moscow. 1963.

3. N. A. BONCH-OSMOLOVSKAYA, B. S. DZHELEPOV, O. E. KRAFT, and CHOU YVEN-WA. Izv. Akad. Nauk SSSR, ser. fiz. **27**, 1357 (1963).
4. K. GROMOW, I. DEMETER, SCH. SCHELEW, W. KALINNIKOW, KIM EN SUE, N. LEBEDEW, F. MOLNAR, W. MOROSOW, G. PFREPPER, W. CHALKIN, E. HERRMAN, and D. CHRISTOW. Nucl. Phys. **88**, 225 (1966); K. GROMOW, A. S. DANAGULYAN, L. K. NIKITYUK, V. V. MURAV'EVA, A. A. SOROKIN, M. Z. SHTAL', and V. S. SHPINEL. Zh. Eksp. Teor. Fiz. **47**, 1644 (1964).
5. V. S. BUTTSEV, Zh. T. ZHELEV, V. G. KALINNOKOW, A. V. KUDRYAVTSEVA, J. LIPTAK, F. MOLNAR, V. NAZAROV, and J. URBANEC. Joint Institute of Nuclear Research Report. (Dubna, USSR) No. P6-3541 (1967) (Unpublished).
6. C. M. LEDERER, J. M. HOLLANDER, and I. PERLMAN. Table of isotopes. Wiley–Interscience, Inc., New York. 1967.
7. J. S. FOSTER, J. W. HILBORN, and L. YAFFE. Can. J. Phys. **36**, 555 (1958).
8. W. D. MYERS and W. J. SWIATECKI. Univ. Calif. Radiat. Lab. Rep. UCRL-11980, 1965. (Unpublished).
9. D. B. BEERY, W. H. KELLY, and W. C. MCHARRIS. Phys. Rev. **188**, 1851 (1969).
10. G. FRIEDLANDER, J. W. KENNEDY, and J. M. MILLER. Nuclear and radiochemistry. John Wiley and Sons, Inc., New York. 1964.

Can. J. Chem. Downloaded from www.nrcresearchpress.com by 210.87.254.40 on 09/05/12
For personal use only.

Can. J. Chem. Downloaded from www.nrcresearchpress.com by 210.87.254.105 on 09/05/12
For personal use only.

The conformation of some biaryl radicals

W. G. LAIDLAW AND R. B. FLEWWELLING
Department of Chemistry, The University of Calgary, Calgary, Alberta

Received November 27, 1969

The conformations of the radicals of biphenyl, diphenylmethyl, and some of their methyl substituted derivatives were investigated by calculating the π-electron delocalization energy and the non-bonded repulsions between the rings. The barriers to rotation are also reported.

Canadian Journal of Chemistry, 48, 2158 (1970)

Introduction

The conformation of biphenyl, diphenylmethyl, or molecules related to them (e.g. benzophenones) have been the subject of numerous investigations (1). More recently the conformation of radicals derived from these species has been studied. The electron spin resonance (e.s.r.) experiments of Falle and Adam (2) suggested that there was a "concerted rotation" of the two rings in methyl substituted biphenyl radicals which averaged out differences in conformation. Takeshita and Hirota (3) measured the e.s.r. spectra of benzophenoneketyls at relatively low temperatures and observed two sets of ortho proton splittings; certainly evidence for a conformation in which these protons were inequivalent. Indeed, the latter workers studied the effect of temperature on the e.s.r. line widths and were able to obtain a measure of the barrier to rotation. Simultaneous to this experimental investigation has come the theoretical investigation of the spin density as a function of conformation. The bulk of such work has been concerned with evaluating the spin density, not with calculating the conformational energy. However, in order to investigate adequately the dynamic processes such as those reported by Falle and Adam and by Takeshita and Hirota, it would seem necessary to evaluate the conformational energy surface as well as the spin density.

The Conformational Energy

The conformational energy E includes the contribution of the π-electron system, E_π, which favors planarity, plus the contribution of the steric interactions E_{Rep}, favoring non-planarity, hence

$$E = E_\pi + E_{\text{Rep}}$$

In biphenyl, E_π and E_{Rep} can be developed as a function of the dihedral angle θ, and for the diphenylmethyl species the angles θ_1 and θ_2 (see Fig. 1) are rather obvious variables. In addition, variations in bond length can be considered; for example, the interannular bond length $R_{6,7}$ in biphenyl may be varied. Other variables, such as bending of the C—H_{ortho} bond or even deformation of the rings, can be invoked. However, in an attempt to keep the problem tractable we considered only $E(\theta,R_{6,7})$ for the biphenyl series and $E(\theta_1,\theta_2)$ for the diphenyl methyl species.

The π-Delocalization Energy

The π-electron energy, E_{el}, was obtained from the self-consistent field (s.c.f.) unrestricted Hartree–Fock (u.H.F.) procedure of Pople and Nesbet (4). The non-zero off-diagonal core integrals, β_{rs}, were taken to be of the form

$$\beta_{rs} = \beta_{rs}^{\,0}\, g(\theta) f(R_{rs})$$

where $\beta_{rs}^{\,0} = -2.39$ eV is the value for the C—C bond in benzene and

$$g(\theta) = |\cos\theta|$$

$$f(R_{rs}) = \exp\,[-1.586(R_{rs} - 1.397)]$$

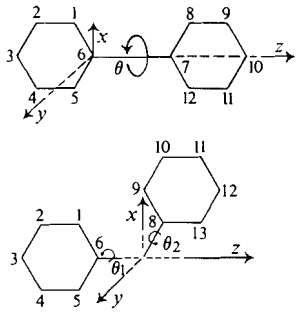

FIG. 1. Geometry of biphenyl and diphenylmethyl species.

TABLE 1

Parameters for repulsion formulae involving hydrogen and carbon centers

Function source	Type of repulsion	Parameter*		
		A (eV Å^6)	B (eV)	C (Å^{-1})
Howlett (11)	H...H*	0.0	4.15×10^1	2.55
Bartell (12)	H...H*	2.14	2.86×10^2	4.08
	C...C†	12 800.	1.41×10^3	—
	H...C‡	5.42	1.94×10^3	2.04
Williams (13)	H...H*	1.56	1.73×10^2	3.74
	C...C*	23.2	3.22×10^3	3.60
	H...C*	6.02	4.07×10^2	3.67
Kitaygorodsky (14)	H...H*	1.86	1.30×10^3	5.00
	C...C*	18.2	1.30×10^3	3.45
	H...C*	6.07	1.30×10^3	4.17

*Parameters are for the functional form
$$V(r) = -Ar^{-6} + B\,e^{-Cr}$$
†Parameters are for the functional form
$$V(r) = Ar^{-12} - Br^{-6}$$
‡Parameters are for the functional form
$$V(r) = (-A + B\,e^{-Cr})r^{-6}$$

The formula for $f(R_{rs})$ is due to Yamaguchi *et al.* (5). The two-electron repulsion integrals γ_{rs} were determined through use of the Ohno (6) formula

$$\gamma_{rs}(R_{rs}) = 14.4/(R_{rs}^2 + 1.674)^{1/2}$$

for all separations $R_{rs} \geqslant 0$. The variation of γ_{rs} with angle of orientation was investigated by both the method of Laidlaw and Adam (7) and the multipole expansion method of Parr (8) and was found to yield differences of less than 5%. Since the variation in other contributions to the energy, for the same conformational change, was much greater, we felt the angle dependence could be ignored. Repulsions between π cores were represented by the formula (9)

$$E_{rs}^{core} = 7.2\left(\frac{1}{R_{rs}} + \frac{1}{(R_{rs}^2 + 3.5)^{\frac{1}{2}}}\right)$$

Hence

$$E_\pi' = E_{core} + E_{el}$$

and the delocalization energies, E_π, can be written

$$E_\pi(R_{6,7},\theta) = E_\pi'(R_{6,7},\theta) - E_\pi'(R_{6,7},90°)$$

for biphenyl species and

$$E_\pi(\theta_1,\theta_2) = E_\pi'(\theta_1,\theta_2) - E_\pi'(90°,90°)$$

for diphenylmethyl species.

The Steric Repulsions

The energy contributions due to steric crowding may be evaluated in terms of pairwise repulsions of atomic centers. In treating the biphenyl molecule, Casalone *et al.* (10) included the repulsions of all atom pairs whose separations depended upon variable conformational parameters. On the other hand, Howlett (11) considered only the repulsions between ortho substituents in studying ortho substituted biphenyl molecules. For the purposes of the present study, interactions of atomic centers beyond the ortho ring positions were ignored and all remaining atom pairs whose separations were angle dependent were taken into account.

The parameter sets used for the unsubstituted radicals are given in Table 1. With the exception of the Bartell C—C and H—C formulae, the parameters are for the functional form

$$V(r) = -Ar^{-6} + Be^{-Cr}$$

The form of the Bartell function for C—C repulsions is given in

$$V(r) = Ar^{-12} - Br^{-6}$$

To treat the repulsions of unlike species, the formula used is made up as the root-mean-square, term by term, of the respective homoatomic

Can. J. Chem. Downloaded from www.nrcresearchpress.com by 210.87.254.105 on 09/05/12
For personal use only.

TABLE 2

Parameters for formulae to be used to represent repulsions involving methyl groups

Function source	Type of repulsion	A (eV Å^6)	B (eV)	C (Å^{-1})
Howlett (11)	Br...Br	0.0	4.24×10^3	3.30
Hill (15)	Br...Br	151	1.58×10^4	3.51
	Br...C	59.2	7.13×10^3	3.55
	Br...H	15.4	1.65×10^3	3.62
Kreevoy–Mason (16)	Kr...Kr	169	2.04×10^3	2.76
	Kr...C	62.6	2.56×10^3	3.18
	Kr...H	16.2	5.94×10^2	3.25
DeRocco–Halford (17)	CH_4...CH_4	128	1.18×10^4	3.33
	CH_4...C	52.4	6.16×10^3	3.47
	CH_4...H	14.1	1.43×10^3	3.53

repulsion formulae. Thus, the Bartell H—C repulsion formula has the form

$$V(r) = (-A + Be^{-Cr})r^{-6}$$

The spurious maxima characteristic of the 6-exponent functions occur at sufficiently high energy such that the conformational energy of the radical becomes large enough to prevent many species approaching close enough to be improperly represented. Thus the planar conformation of diphenylmethyl is not given an appropriate energy by these functions, but this conformation is obviously not energetically favorable and may be ignored.

The parameters of Table 2 were employed to represent the steric repulsions of methyl groups. They are taken from data for bromine, krypton, and methane as indicated. The variety of sources is due to the unavailability of the parameters which represent methyl group repulsions. As bromine atoms are considered (11) sterically equivalent to methyl groups, their choice in this case appears valid. Similarly, the interactions of krypton atoms would be expected to give a reasonable representation of the repulsions of bonded bromine atoms, hence methyl groups. Spherical symmetry of the methyl group is, of course, assumed in the use of these functions and no attempts were made to take the bonds to the phenyl ring into account. Treatment of the methyl group as a single entity rather than as four atoms is reasonable in light of the finding of Falle and Adam (2) that the ortho methyl groups in substituted diphenylmethyls are free to rotate.

Summation of repulsions over each of the pairs of interacting species yields the total repulsive energy, E_{Rep}.

$$E_{Rep} = \sum_{\substack{r,s \\ (r\neq s)}} V(R_{rs})$$

If the assumption of rigid geometry[1] is made, we can immediately calculate E_{Rep}, and with E_π as previously determined, the conformational energy, E, is determined.

Conformational Energy of the Biphenyl Species

Unsubstituted Biphenyl Anions

We shall, in the first instance, consider $R_{6,7}$ to be fixed at 1.48 Å. The features of $E(1.48,\theta) = E(\theta)$ which bear most directly upon the problem at hand are the position and depth of the minima. The values of $E(\theta)$ using the representations of the repulsion discussed in the previous section and E_π calculated by the u.H.F.-s.c.f. method are indicated in Fig. 2. In each case a minimum in the range $\theta = 25$ to 30° is suggested. The value of $\Delta_0 = E(0°) - E_{min}$ is 0.1 eV, while $\Delta_{90} = E(90°) - E_{min}$ is approximately 0.7 eV.

For comparison, the total conformational energies derived from Hückel E_π and Howlett E_{Rep} results for $R_{6,7} = 1.4$ Å, are also shown in Fig. 2; the minimum is found at $\theta \simeq 30°$ with

[1]However, some of the larger repulsions in biphenyl and diphenylmethyl may be relieved by bond bendings and other geometric distortions. Some of these were investigated using a simple Hooke's Law potential energy of distortion. Although the energy of the distorted configuration is substantially decreased, the distortions are really beyond the limits of applicability of a Hooke's Law representation of the distortion force. In any case, the *relative* energies of various conformations are little affected.

Can. J. Chem. Downloaded from www.nrcresearchpress.com by 210.87.254.105 on 09/05/12
For personal use only.

TABLE 3

The conformational energies of the biphenyl anion as a function of interannular bond length, $R_{6,7}$, and dihedral angle, θ*

	Conformational energy, eV, for $R_{6,7}$ =					
θ	1.397	1.42	1.45	1.48	1.51	1.54
0	−1.292	−1.342	−1.400	−1.433	−1.444	−1.425
10	−1.338	−1.382	−1.434	−1.462	−1.469	−1.447
20	−1.407	−1.436	−1.481	−1.503	−1.503	−1.476
30	−1.361	−1.407	−1.479	−1.497	−1.491	−1.466
40	−1.215	−1.281	−1.354	−1.410	−1.418	−1.406
50	−0.995	−1.089	−1.194	−1.275	−1.301	−1.309
60	−0.739	−1.013	−1.004	−1.114	−1.168	−1.193
70	−0.473	−0.777	−0.805	−0.945	−1.023	−1.069
80	−0.220	−0.405	−0.612	−0.767	−0.880	−0.946
90	0.000	−0.206	−0.398	−0.617	−0.746	−0.929

*E (1.397, 90°) is defined as the zero of energy.

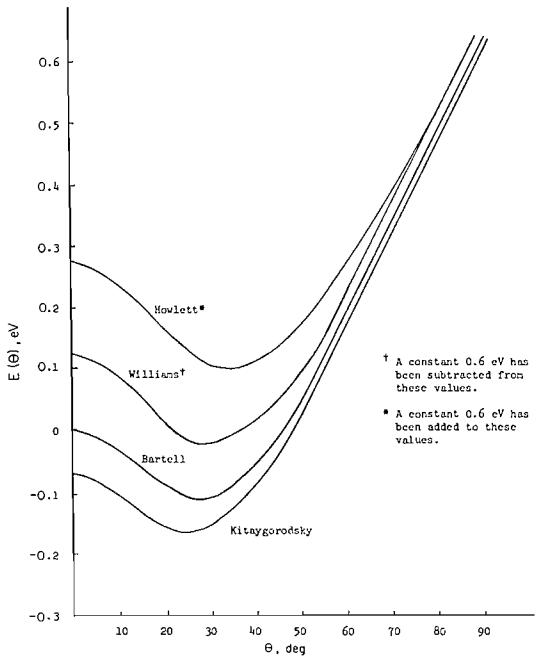

FIG. 2. Conformational energy maps for the biphenyl anion with u.H.F. E_π.

$\Delta_0 = 0.17$ eV and $\Delta_{90} = 0.5$ eV. The differences between these values and those for the u.H.F. determinations may be largely due to the smaller value of $R_{6,7}$ employed in the Hückel calculation, through the assumption $f(R_{rs}) = 1$. These energy descriptions suggest the radical tends toward a non-planar conformation ($\theta \simeq 30°$) yet may readily pass through $\theta = 0$ to an equivalent non-planar conformation $\theta \simeq -30°$. However, conformations with $|\theta| > 60°$ are energetically very unfavorable.

The examination of the $R_{6,7}$ dependence of the conformational energy requires the introduction of variables which were held constant in the preceding step. That is, we consider the total energy $E(R_{6,7},\theta)$ as the sum of the several terms

$$E(R_{6,7},\theta) = E_\pi(R_{6,7},\theta) + E_{Rep}(R_{6,7},\theta) + E_\sigma(R_{6,7})$$

Here $E_\sigma(R_{6,7})$ accounts for the change in energy of the $\sigma_{6,7}$ bond, and, using the formula of Coulson and Dixon (18), is given by

$$E_\sigma(R_{6,7}) = -84\{\exp[-4.056(R_{6,7} - 1.51)] - 2\exp[-2.028(R_{6,7} - 1.51)]\}$$

Nothing new is added to $E_{Rep}(R_{6,7},\theta)$ that was not already involved in $E_{Rep}(\theta)$. However, with respect to the extension from $E_\pi(\theta)$ to $E_\pi(R_{6,7},\theta)$ further considerations are necessary. The delocalization energy must be evaluated as the sum of the π-electron energy of the u.H.F. treatment and the core–core repulsion term, discussed earlier, i.e.

$$E_\pi(R_{6,7},\theta) = E_\pi'(R_{6,7},\theta) + E_{6,7}^{core}(R_{6,7})$$

The values of $E_\pi(R_{6,7},\theta)$ for a number of different values of $R_{6,7}$ and of θ are given in Table 3. It is clear that the minimum with respect to $R_{6,7}$ moves to increasing bond length for θ increasing or decreasing from 25°. That is, as θ increases beyond 30°, the decrease in delocalization energy allows the bond to increase

Can. J. Chem. Downloaded from www.nrcresearchpress.com by 210.87.254.105 on 09/05/12
For personal use only.

Can. J. Chem. Downloaded from www.nrcresearchpress.com by 210.87.254.105 on 09/05/12
For personal use only.

in length. Decreasing θ below 20° introduces sufficient steric repulsions to lengthen the bond at the expense of delocalization energy.[2]

Consequently the energetically most favorable value of $R_{6,7}$ appears to be 1.48 ± 0.01 Å, with which θ = 25 ± 5° must be associated.

Substituted Biphenyl Anions

Introduction of bulky substituents at the ortho positions of the biphenyl anion would be expected to result in a different conformation than that determined for the unsubstituted species. The substituted anion could have a larger interannular bond length and dihedral angle θ.

As an example of the effect of the methyl substituents upon the conformation of the biphenyl anion, several energy maps were determined for the 1,1′,5,5′-tetramethyl biphenyl anion as shown in Fig. 3. These energies were found in the fashion described in employing the bromine, krypton, and methane parameters to represent interactions involving the methyl groups. The value $R_{6,7}$ = 1.48 Å was assumed.

The minima of the $E(\theta)$ in Fig. 3 fall in the region of θ = 80° with a small (Δ ≃ 0.1 eV) barrier to the θ = 90° conformation and a much larger barrier to planarity.[3] Here again the energy map suggests two equivalent conformations (θ = ±80°) separated by a small (0.1 eV) barrier. However, these conformations are near θ = 90° for the substituted anion as opposed to the θ ≃ 25° most favorable conformation for the unsubstituted anion.

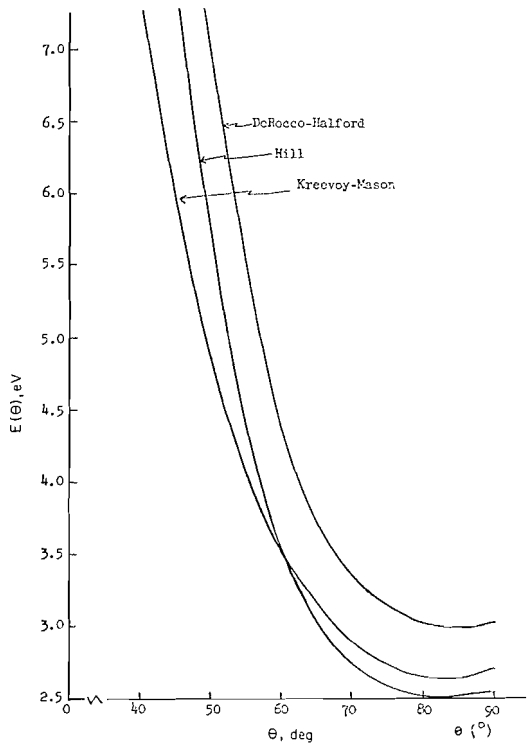

FIG. 3. Conformational energy maps for the tetra-*ortho*-methylated biphenyl anion (determined for constant interannular bond length, $R_{6,7}$ = 1.48 Å, and rigid bond angles).

The Diphenylmethyl Species

Unsubstituted Diphenylmethyl Anions

The conformation of the diphenylmethyl radical was taken as completely defined by the parameter set (θ_1,θ_2). (Other geometric distortions were ignored in the molecular orbital calculations and the phenylmethyl bond lengths were assumed constant at 1.48 Å.)

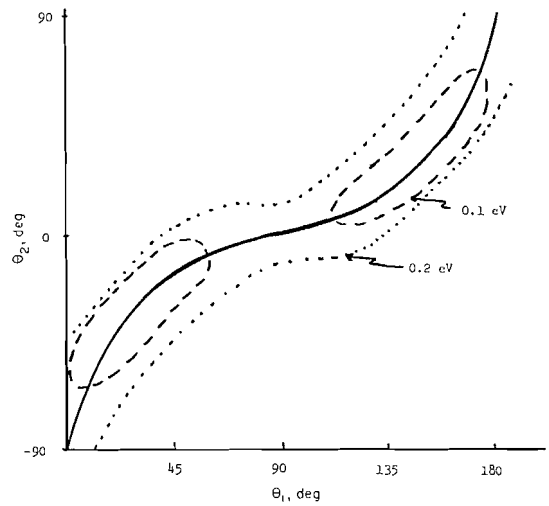

FIG. 4. The conformational energy map for the diphenylmethyl radical.

[2]This result is in accord with that of G. Casalone *et al.* (10) for the biphenyl anion, while Golebiewski and Parezewski (19) found a shorter bond length for the planar molecule than for θ = 40°.

[3]Introducing flexing of the ortho bond angles to minimize the steric energy reduces the barrier height for the planar conformation yet it remains large (approximately 6 eV). As with the unsubstituted biphenyl results, the distortions implied in the minimization calculations go beyond the capabilities of the theory and make the results of only qualitative significance. The large θ implied by these results would also suggest that an interannular bond length of 1.48 Å could be an underestimate.

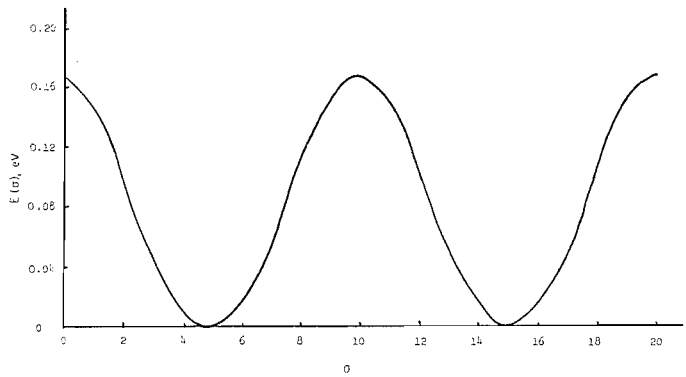

FIG. 5. Conformational energies of the diphenylmethyl radical as a function of the rotation coordinate as determined by use of the Kitaygorodsky repulsion formulae.

Figure 4 indicates the conformational energy map determined with the Kitaygorodsky (14) formulae for non-bonded repulsions and the u.H.F. E_π results. The corresponding results for the other determinations of E_π and E_{Rep} differed only insignificantly from those of Fig. 5. The dashed lines are iso-energic curves defining conformations with energies 0.1 and 0.2 eV greater than the relative minimum energy. The solid line is not an iso-energic curve, but represents the set of (θ_1,θ_2) for which $(\partial E(\theta_1,\theta_2)/\partial\theta_1)_{\theta_2} = 0$, i.e. it is the rotation path for the concerted rotation described by Adam and Falle (2). The rotation coordinate, σ, is defined as zero at (90°,0°) and 20 at (90°,180°), and represents the distance along the rotation curve. The energy $E(\theta_1,\theta_2)$ along the rotation coordinate $E(\sigma)$, is pictured in Fig. 5 where the minimum at $\sigma = 10$ corresponds to the symmetrical conformation $(\theta_1,\theta_2) = (30°, -30°)$. The barrier to the concerted rotation is, in this case, 0.166 eV.

While the general features of the energy map corresponding to Fig. 5 are essentially the same for the various determinations of $E(\theta_1,\theta_2)$, there is some variety in the rotation barriers predicted. Table 4 presents the barriers obtained when the different forms of E_{Rep} are used. All the predictions fall in a narrow range with an average 0.16 eV.

The Substituted Diphenylmethyl Species

Calculations of the conformational energy in methyl substituted diphenylmethyl species have been undertaken. Although only preliminary results are available at this time, the potential barriers appear to be approximately twice that of the unsubstituted species.

TABLE 4

Activation energies for concerted rotation in the diphenylmethyl radical employing s.c.f.-u.H.F. E_π

E_{Rep} formula source	$E = E_{90} - E_{min}$ (eV)
Howlett (11)	0.164
Bartell (12)	0.161
Williams (13)	0.125
Kitaygorodsky (14)	0.166
	Average 0.16 eV = 3.8 kcal

Conclusions

An appropriate interannular bond distance and dihedral angle have been obtained for biphenyl radical as $R_{6,7} = 1.48 \pm 0.1$ Å and $\theta = 25 \pm 5°$, with the barriers to rotation $\Delta_{0°} = 0.1$ and $\Delta_{90°} = 0.7$ eV. For the methyl substituted species, the most favorable dihedral angle was obtained at $80 \pm 5°$ with a small (0.1 eV) barrier to rotation through 90° and a considerably larger barrier to planarity. The energy map for the unsubstituted diphenylmethyl radical contains a pathway $(\theta_1 \simeq -\theta_2)$ for the concerted rotation for which the barrier is approximately 0.16 eV with the minimum at $\theta_1 = -\theta_2 = 30°$. The latter barrier compares with the value 0.19 eV measured by Takeshita and Hirota (3) for the benzophenoneketyl.

The financial support of the National Research Council of Canada and the availability of the computing facilities at the University of Calgary are gratefully acknowledged.

Can. J. Chem. Downloaded from www.nrcresearchpress.com by 210.87.254.105 on 09/05/12
For personal use only.

1. G. ZERBI and S. SANDRONI. Spectrochim. Acta, **24A**, 483 (1968).
2. H. R. FALLE and F. C. ADAM. Can. J. Chem. **44**, 1387 (1966).
3. T. TAKESHITA and N. HIROTA. J. Chem. Phys. **51**, 2146 (1969).
4. J. A. POPLE and R. K. NESBET. J. Chem. Phys. **22**, 571 (1954).
5. H. YAMAGUCHI, T. NAKAJIMA, and T. L. KUNII. Theoret. Chim. Acta Berlin, **12**, 351 (1968).
6. K. OHNO. Theoret. Chim. Acta Berlin, **2**, 219 (1964).
7. W. G. LAIDLAW and F. C. ADAM. Aust. J. Chem. **21**, 2287 (1968).
8. R. G. PARR. J. Chem. Phys. **33**, 1184 (1969).
9. R. B. FLEWWELLING. M.Sc. Thesis, University of Calgary, Calgary, Alberta, 1969.
10. G. CASALONE, C. MARIANI, A. MAGNOLI, and M. SIMONETTE. Mol. Phys. **15**, 339 (1968).
11. K. E. HOWLETT. J. Chem. Soc. 1055 (1960).
12. L. S. BARTELL. J. Chem. Phys. **32**, 827 (1960).
13. D. E. WILLIAMS. J. Chem. Phys. **45**, 3770 (1966).
14. A. I. KITAYGORODSKY. Tetrahedron, **14**, 230 (1961).
15. T. L. HILL. J. Chem. Phys. **16**, 399 (1948).
16. M. M. KREEVOY and E. A. MASON. J. Amer. Chem. Soc. **79**, 4851 (1957).
17. A. G. DEROCCO and J. O. HALFORD. J. Chem. Phys. **28**, 1152 (1958).
18. C. A. COULSON and W. T. DIXON. Tetrahedron, **17**, 215 (1962).
19. A. GOLEBIEWSKI and A. PAREZEWSKI. Theoret. Chim. Acta Berlin, **7**, 171 (1967).

Can. J. Chem. Downloaded from www.nrcresearchpress.com by 210.87.254.105 on 09/05/12
For personal use only.

Can. J. Chem. Downloaded from www.nrcresearchpress.com by 84.22.46.98 on 09/08/12
For personal use only.

Absolute rate constants for hydrocarbon autoxidation. XIX. Oxidation of some α-substituted toluenes[1]

J. A. HOWARD AND S. KORCEK[2]
Division of Chemistry, National Research Council of Canada, Ottawa, Canada

Received February 24, 1970

Absolute propagation and termination rate constants have been measured for the liquid phase autoxidation of some α-substituted toluenes at 30 °C. Rate constants for reaction of α-substituted toluenes with their own peroxy radical and with the *t*-butylperoxy radical have been compared. It would appear that the reactivity of an α-substituted benzylperoxy radical depends on the nature of the α-substituent.

Reactivities of α-substituted toluenes towards the *t*-butylperoxy radical, the bromine atom, and the phenyl radical have been compared.

Canadian Journal of Chemistry, 48, 2165 (1970)

Introduction

The rate controlling propagation reaction for the autoxidation of many organic compounds at ambient temperatures and oxygen partial pressures above about 100 mm of Hg is abstraction of the weakest hydrogen atom from the substrate RH by a peroxy radical ROO·

$$ROO\cdot + RH \xrightarrow{k_p} ROOH + R\cdot$$

It is well known that the magnitude of the propagation rate constant k_p can be influenced by polar effects and that the dipolar structure $ROO^-:H^{\cdot+}R$ plays an important role in the transition state for reaction [1] (1). For example, rates of oxidation of ring-substituted toluenes (2) and cumenes (2, 3) and rate constants for reaction of cumylperoxy radicals with ring-substituted cumenes (4) can be correlated by the Hammett equation using Brown's electrophilic σ^+ substituent constants (5). Polar effects that are transmitted through a benzene ring are relatively small and can be overshadowed by substitution on the α-carbon. Consequently, oxidation of benzyl phenyl ethers and benzyl alkyl ethers (3) are insensitive to ring substitution on the benzyl or phenyl group. Presumably the ether oxygen atom acts as the most powerful electron supplier in both the substituted and unsubstituted compounds.

Russell (2) has measured the rates of oxidation of a number of α-substituted toluenes at 90 °C at a constant initiator concentration. He found that powerful electron-withdrawing groups such as cyano, carbomethoxy, and benzoyloxy and weak electron-withdrawing groups such as chlorine had little effect on the reactivity of the remaining α-hydrogens. If only resonance stabilization of the incipient radical mattered in reaction [1], a considerable increase in reactivity would have been expected for these substituents. Russell, therefore, concluded that polar effects evidently offset the increase in reactivity expected from resonance stabilization of the incipient radical.

It has been suggested that the differences in reactivity of aldehydes towards the same peroxy radical can best be understood in terms of an inductive effect of the group R attached to the CHO group. Increasing the electron donating capacity of R increases the rate constant for hydrogen abstraction by a peroxy radical (6, 7).

Polar effects may play an important role in the reactivity of a peroxy radical as well as in the reactivity of a substrate. Walling and McElhill (6) have reported that *p*-substitution apparently influences the reactivity of benzoylperoxy radicals. Benzoylperoxy radicals have been found to be 500–900 times more reactive than tetralylperoxy radicals (7). This difference in reactivity must be because acylperoxy radicals are more electrophilic than alkylperoxy radicals. Electron attracting groups should increase the electrophilicity of the radical and hence increase the importance of polar contributions to the transition state.

It would, therefore, appear that α-substitution can produce fairly dramatic effects on the propagation rate constant for autoxidations by influencing both the reactivity of the substrate and the reactivity of the peroxy radical. We have, therefore, measured absolute rate constants for the autoxidation of some α-substituted toluenes in an attempt to determine more quantitatively the effect of α-substitution on peroxy radical and substrate reactivity.

[1]NRCC No. 11 319.
[2]NRCC Postdoctorate Fellow, 1968–1970.

TABLE 1

Primary reaction products formed from oxidation of benzyl alcohol, benzyl chloride, benzyl benzoate, benzyl acetate, and α–methylbenzyl alcohol at 30 °C.

Substrate	Substrate concentration (M)	Chain length	Oxygen absorbed $\times 10^2$ (M)	Titratable hydroperoxide $\times 10^2$ (M)	Yield % Hydroperoxide*	H_2O_2*	Carbonyl*
Benzyl alcohol	2.0	16	0.64	0.65	—	93	~120
Benzyl chloride	8.7	16	1.35	1.2	90	—	—
Benzyl benzoate	4.85	10	1.02	0.9	90	—	—
Benzyl acetate	7.0	5	2.6	2.1	80	—	—
α-Methylbenzyl alcohol	8.3	20	45	47	—	104	96

*Based on the concentration of oxygen absorbed in moles.

Experimental

Materials

Benzyl alcohol, benzyl chloride, benzyl bromide, benzyl acetate, benzyl benzoate, benzyl cyanide, benzyl ketone, benzaldehyde, and α-methylbenzyl alcohol were commercial products purified by distillation or crystallization. *t*-Butyl phenyl acetate was prepared from phenyl acetyl chloride and *t*-butyl alcohol (8). *t*-Butyl hydroperoxide was dried and crystallized from pentane.

Kinetic Procedure

Methods used to measure rates of oxidation and rates of chain initiation have been described previously (9). Absolute rate constants were measured by the rotating sector method. Whenever necessary termination rate constants have been corrected for an apparent first order contribution. All rate constants reported in this paper were measured at 30 °C.

Product Analysis

Total hydroperoxide concentrations were determined by iodometric titration. Yields of carbonyl compounds produced from the alcohols were determined by infrared analysis. Hydrogen peroxide yields were determined by titration of an aqueous extract of the oxidized substrate (10). The chain carrying peroxy radical for the oxidation of benzyl alcohol was identified by trapping experiments with 2,6-di-*t*-butyl-4-methyl phenol. The phenolic oxidation products were identified by thin layer chromatography on silica gel eluted with 30% ether in petroleum ether. A spot which developed with 5% KI and 5% acetic acid in isopropanol and had a retention time identical with an authentic sample was assumed to be 2,6-di-*t*-butyl-4-methyl-4-hydroperoxy-2,5-cyclohexadiene-1-one, **1**. It was assumed that 2,6-di-*t*-butyl-4-methyl-4-α-hydroxyalkylperoxy-2,5-cyclohexadien-1-ones would not develop with the KI/acetic acid spray and would have retention times different from that of **1**. Concentrations of **1** were estimated by visual means.

Results and Discussion

α-Substituted toluenes, with the exception of alcohols, oxidize to give hydroperoxides in nearly 100% yield at 30 °C (Table 1). Rates of oxidation are generally independent of oxygen pressure. The rates are proportional to substrate concentration and to the half power of the rate of chain initiation. This means that these autoxidations can be represented by the following free-radical chain process

Initiation

[1] Production of free-radicals

Propagation

[2] $\mathrm{PhCH(X)^{\cdot}} + \mathrm{O_2} \rightarrow \mathrm{PhCH(X)OO^{\cdot}}$

[3] $\mathrm{PhCH(X)OO^{\cdot}} + \mathrm{PhCH_2X} \xrightarrow{k_p} \mathrm{PhCH(X)OOH} + \mathrm{PhC^{\cdot}HX}$

Termination

[4] $\mathrm{2PhCH(X)OO^{\cdot}} \xrightarrow{2k_t}$ Non-radical products

where $\mathrm{PhC^{\cdot}HX}$ is the α-substituted alkyl radical and $\mathrm{PhCH(X)OO^{\cdot}}$ is the α-substituted alkylperoxy radical derived by abstraction of an α-hydrogen from the substrate $\mathrm{PhCH_2X}$. The rate of oxidation R_s is then given by the expression

$$[5] \qquad R_s = \frac{-\mathrm{d}[\mathrm{O_2}]}{\mathrm{d}t} = \frac{k_p[\mathrm{PhCH_2X}]R_i^{1/2}}{(2k_t)^{1/2}}$$

where R_i is the rate of chain initiation and k_p and $2k_t$ are the rate controlling propagation and termination rate constants.

Alcohols do not oxidize to give hydroperoxides as the primary reaction product but give instead hydrogen peroxide and a carbonyl compound. For example, benzyl alcohol gives hydrogen peroxide and benzaldehyde. These products might be due either to the instability of α-hydroxybenzyl hydroperoxide

Can. J. Chem. Downloaded from www.nrcresearchpress.com by 84.22.46.98 on 09/08/12
For personal use only.

Can. J. Chem. Downloaded from www.nrcresearchpress.com by 84.22.46.98 on 09/08/12
For personal use only.

[6] $PhCH(OH)OOH \rightarrow PhCHO + H_2O_2$

or to decomposition of the α-hydroxybenzylperoxy radical to benzaldehyde and the hydroperoxy radical

[7] $PhCH(OH)OO^{\cdot} \rightarrow PhCHO + HO_2^{\cdot}$

In the former case the chain is carried by α-hydroxybenzylperoxy radicals while in the latter case it is carried by hydroperoxy radicals. A hydroperoxy radical chain reaction was found for the oxidation of 1,4-cyclohexadiene which at 30 °C gives benzene and hydrogen peroxide (10). The chain carrying radical for this oxidation was identified by inhibition with 2,6-di-*t*-butyl-4-methylphenol.

The hydroperoxy radical was trapped as 2,6-di-*t*-butyl-4-methyl-4-hydroperoxy-2,5-cyclohexadien-1-one, **1**, via the following reactions

[8] $HO_2^{\cdot}$ + 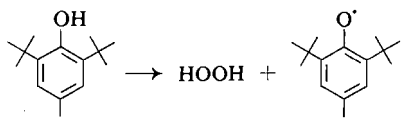 → HOOH +

[9] $HO_2^{\cdot}$ + 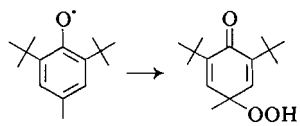

1

Oxidation of benzyl alcohol in the presence of 2,6-di-*t*-butyl-4-methylphenol gave less than 10% of the theoretical maximum of 2,6-di-*t*-butyl-4-methyl-4-hydroperoxy-2,5-cyclohexadien-1-one. This implies that benzyl alcohol at 30 °C is oxidized by means of an α-hydroxybenzyl peroxy radical chain process and it can be described by reactions [1]–[4]. This is supported by the fact that at chain lengths of about 16 the total yield of carbonyl compounds was always greater than 100% based on the oxygen absorbed. This must mean that carbonyl compounds are formed in termination as would be expected if this reaction involves two α-hydroxybenzyl peroxy radicals

[10] 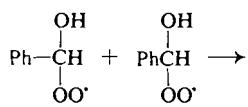

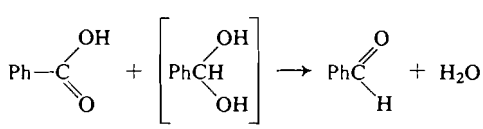

Rates of oxidation of benzyl alcohol, benzyl chloride, benzyl acetate, and benzyl benzoate do not strictly obey eq. [5] since the ratio of the rate of the photochemically initiated oxidation at very high speeds of sector rotation to the rate at steady illumination (R_∞/R_s) is less than 0.5. This is analogous to the situation previously encountered for oxidation of styrene (11) and ring-substituted styrenes (12) where termination rate constants had to be corrected for an apparent first order contribution.

Oxidation of benzyl chloride is further complicated by autocatalysis apparently due to thermal instability of α-chlorobenzyl hydroperoxide. The photochemically initiated oxidation of benzyl alcohol is also autocatalytic because of initiation from photolysis of one of the major reaction products, benzaldehyde (7).

Absolute rate constants for oxidation of some α-substituted toluenes are given in Table 2. In all cases the ratio $k_p/(2k_t)^{1/2}$ is independent of the chain length. Termination rate constants for benzyl alcohol, benzyl chloride, and *t*-butylphenyl acetate are in the range normally found for α-alkyl toluenes such as ethylbenzene and bibenzyl (13) and are also similar to values for benzyl *t*-butyl ether and benzyl phenyl ether (14), i.e. $3–5 \times 10^7$ M^{-1} s^{-1}. Benzyl acetate and benzyl benzoate have termination rate constants similar to toluene (13) and benzyl ether (14), i.e. in the range $1–3 \times 10^8$ M^{-1} s^{-1}. Propagation rate constants for the five secondary α-substituted toluenes are similar and lie in the range $2–5$ M^{-1} s^{-1}. Interpretation of the values of propagation rate constants is, however, complicated by differences in peroxy radical reactivity as well as in substrate reactivity.

The termination rate constant for α-methylbenzyl alcohol is about 5 times the value for isopropyl ether (14) and is larger than values normally found for oxidation of tertiary hydrocarbons, i.e. $10^3–10^5$ M^{-1} s^{-1} (15). The termination reaction for oxidation of substrates which give tertiary peroxy radicals (e.g. cumene) is usually described by the following reaction sequence (ref. 15 and references cited therein, refs. 16, 17)

[14] $ROO^{\cdot} + ROO^{\cdot} \underset{k_{-14}}{\overset{k_{14}}{\rightleftharpoons}} ROOOOR$

$(K = k_{-14}/k_{14})$

[15] $ROOOOR \xrightarrow{k_{15}} [RO^{\cdot}\ O_2\ {}^{\cdot}OR]_{cage}$

TABLE 2

Rate constants for autoxidation of some α-substituted toluenes at 30 °C

Substrate	Substrate concentration (M)	$R_i \times 10^7$ ($M\,s^{-1}$)	$R_s \times 10^6$ ($M\,s^{-1}$)	$k_p/(2k_t)^{1/2} \times 10^3$* ($M^{-1/2}\,s^{-1/2}$)	k_p ($M^{-1}\,s^{-1}$)	$2k_t \times 10^{-7}$ ($M^{-1}\,s^{-1}$)
Benzyl alcohol	4.0	2.2	1.4	1.0	4.0	1.6
	4.0	0.42	5.8	0.83	4.6	3.1
	2.0	1.85	6.25	0.84	4.0	2.2
	2.0	0.38	2.7	0.74	5.6	6.0
Benzyl chloride	1.74	0.41	1.54	0.41	—	—
	3.48	0.49	2.94	0.38	—	—
	8.7	0.47	7.6	0.40	3.0	5.0
	8.7	0.12	3.65	0.40	—	—
	8.7	1.3	15.6	0.50	3.6	5.0
Benzyl benzoate	4.85	0.04	0.11	0.36	—	—
	4.85	0.18	0.2	0.36	5.2	22
Benzyl acetate	7.0	0.06	0.14	0.31	—	—
	7.0	0.24	0.29	0.31	4.4	22
t-Butyl phenyl acetate	5.1	0.15	0.17	0.28	1.6	3.3
α-Methyl benzyl alcohol	8.34	0.91	1.66	0.91	2.13	0.5

*Calculated from k_p and $2k_t$ for autoxidations exhibiting some first order termination.

[16] $[RO^{\cdot}\ O_2\ {}^{\cdot}OR]_{cage} \xrightarrow{k_{16}} ROOR + O_2$

[17] $[RO^{\cdot}\ O_2\ {}^{\cdot}OR]_{cage} \xrightarrow{k_{17}} RO^{\cdot} + O_2 + {}^{\cdot}OR$

where ROO· and RO· represent the cumylperoxy and cumyloxy radicals, respectively. The cumyloxy radicals formed in reaction [17] as well as reacting with cumene may undergo β-scission to give acetophenone and the methyl radical

[18] $PhC(CH_3)_2O^{\cdot} \xrightarrow{k_{18}} PhCOCH_3 + CH_3^{\cdot}$

Methyl radicals will add oxygen to give methylperoxy radicals which can either propagate the chain

[19] $CH_3OO^{\cdot} + RH \rightarrow CH_3OOH + R^{\cdot}$

or terminate the chain

[20] $CH_3OO^{\cdot} + ROO^{\cdot} \xrightarrow{k_{20}}$ Non-radical products

The termination rate constant for oxidation of a neat tertiary hydrocarbon is therefore enhanced by a contribution from k_{20}.

The high value of $2k_t$ for α-methylbenzyl alcohol may be due to a high value of k_{15}, the unimolecular rate constant for tetroxide decomposition, or to a large contribution from terminations such as reaction [20].

The propagation rate constant per α hydrogen for α-methylbenzyl alcohol is similar to the value for benzyl alcohol even though a tertiary hydrogen is removed rather than a secondary hydrogen. This is almost certainly analogous to the situation found in hydrocarbon oxidation where k_p for ethylbenzene is larger than k_p for cumene (13) because the cumylperoxy radical is less reactive than the α-methylbenzylperoxy radical.

Rate constants for oxidation of some α-substituted toluenes in the presence of *t*-butyl hydroperoxide are given in Table 3. We have shown previously that *t*-butyl hydroperoxide concentrations above about 1 M eliminate substrate peroxy radicals from the rate controlling reactions for oxidation of primary and secondary hydrocarbons (18), tetrahydrofuran (9), benzyl ether (14), and isopropyl ether (14). The propagation and termination reactions for these oxidations can be represented by

[21] $BOO^{\cdot} + RH \xrightarrow{k_p^{br}} BOOH + R^{\cdot}$

and

[22] $BOO^{\cdot} + BOO^{\cdot} \rightarrow$ Non-radical products

where BOO· is the *t*-butylperoxy radical and RH is the substrate.

It might be expected that alcohols would be more difficult to study by this technique since hydrogen bonding greatly reduces the rate constant for the transfer reaction

[23] $ROO^{\cdot} + R'OOH \rightarrow ROOH + R'OO^{\cdot}$

Can. J. Chem. Downloaded from www.nrcresearchpress.com by 84.22.46.98 on 09/08/12
For personal use only.

TABLE 3

Rate and rate constant data for oxidation of α-substituted toluenes in the presence of *t*-butyl hydroperoxide at 30 °C

Substrate	Concentration (M)		$R_i \times 10^7$ ($M\,s^{-1}$)	$R_s \times 10^6$ ($M\,s^{-1}$)	$k_p/(2k_t)^{1/2} \times 10^3$ ($M^{-1/2}\,s^{-1/2}$)	k_p^{br}* ($M^{-1}\,s^{-1}$)
	Substrate	Hydroperoxide				
Benzaldehyde	0.5	2.0	0.49	2.7	24.4	0.85
Benzaldehyde	0.5	4.0	0.31	2.15	24.4	0.85
Benzyl alcohol	2.0	1.0	3.1	4.0	3.6	0.12
Benzyl alcohol	2.0	3.0	1.27	2.75	3.9	0.13
Benzyl ketone	0.8	2.0	0.21	0.61	5.3	0.18
Benzyl chloride	5.2	4.0	0.30	0.43	0.48	0.017
Benzyl benzoate	4.2	2.0	0.11	0.21	0.48	0.017
Benzyl acetate	5.6	2.0	0.14	0.3	0.45	0.016
Benzyl bromide	5.05	4.0	0.91	0.53	0.35	0.012
α-Methylbenzyl alcohol	6.7	2.0	0.11	2.0	2.8	0.10
α-Methylbenzyl alcohol	5.8	3.0	0.12	2.0	3.1	0.11
α-Methylbenzyl alcohol	5.0	4.0	0.14	2.0	3.2	0.11

*Calculated using a value of $1.2 \times 10^3\ M^{-1}\,s^{-1}$ for $2k_t$.

TABLE 4

Collected rate constants for autoxidation of α-substituted toluenes at 30 °C

Substrate	$k_p/(2k_t)^{1/2} \times 10^3$ ($M^{-1/2}\,s^{-1/2}$)	k_p per α-H ($M^{-1}\,s^{-1}$)	$2k_t \times 10^{-7}$ ($M^{-1}\,s^{-1}$)	k_p^{br} per α-H for Bu^{t}OO· ($M^{-1}\,s^{-1}$)	k_p/k_p^{br} per α-H
Benzaldehyde	660	33000	250	0.85	~40 000
Benzyl ether	—	7.5*	16	0.3	25
Benzyl *t*-butyl ether	2.75	5.75	2.1	0.55	10.5
Benzyl alcohol	0.85	2.4	3.2	0.065	37
Benzyl ketone	0.55	(0.82)	(3.6)	0.045	18
Benzyl cyanide	0.52	(1.56)	(3.6)	0.01	156
Benzyl chloride	0.42	1.50	5.0	0.008	190
Benzyl benzoate	0.36	2.6	22	0.0085	306
Benzyl acetate	0.31	2.3	22	0.0075	307
Benzyl phenyl ether	0.3	0.75	2.4	0.1	7.5
t-Butyl phenyl acetate	0.28	0.8	3.3	0.03	27
Ethylbenzene	0.21	0.65	4.0	0.1	6.5
Benzyl bromide	0.2	(0.6)	(3.6)	0.006	100
Toluene	0.014	0.08	30	0.009	9

*Propagation rate constant for intermolecular abstraction. Values in parentheses are estimated rate constants.

For example, the rate constant for reaction of cumylperoxy radicals with tetralin hydroperoxide is reduced almost to zero at high *t*-butyl alcohol concentrations (19). We find, however, that the rate of oxidation of benzyl alcohol or α-methylbenzyl alcohol in the presence of greater than 1 M *t*-butyl hydroperoxide is independent of hydroperoxide concentration.

A rate constant has been estimated for reaction of *t*-butylperoxy radicals with benzaldehyde. It is well known that certain hydroperoxides react readily with aldehydes to give α-hydroxy peroxides, for example, *n*-butyl hydroperoxide reacts with *n*-butyraldehyde at room temperature and below to give 1-hydroxybutyl butyl peroxide (20). However, under our experimental conditions *t*-butyl hydroperoxide did not react with benzaldehyde to any appreciable extent.

Individual rate constants for autoxidation of α-substituted toluenes in the absence and presence of *t*-butyl hydroperoxide are summarized in Table 4; the substrates are arranged in order of decreasing ease of oxidation. Included in the table are our previously published data for oxidation of benzyl ether, benzyl phenyl ether, benzyl *t*-butyl ether (9, 14), ethylbenzene, and toluene (18). Absolute rate constants for benzaldehyde oxidation have been calculated from our data at 0 °C. The logarithm of the pre-exponential factor for the propagation reaction ($\log_{10} A$) was taken as 8.5,

Can. J. Chem. Downloaded from www.nrcresearchpress.com by 84.22.46.98 on 09/08/12
For personal use only.

Can. J. Chem. Downloaded from www.nrcresearchpress.com by 84.22.46.98 on 09/08/12
For personal use only.

a typical value for a bimolecular hydrogen atom abstraction reaction. This gave a propagation activation energy of 5.5 kcal/mole. The termination activation energy was taken to be 2 kcal/mole. The difference in reactivity of benzaldehyde towards the benzoylperoxy radical and towards the *t*-butylperoxy radical, $k_p/k_p^{br} \sim 40\,000$, is 40–100 times higher than was previously estimated for the difference in reactivity of benzoylperoxy radicals and tetralylperoxy radicals (7). Tertiary peroxy radicals are generally about 5 times less reactive than secondary peroxy radicals towards a hydrocarbon (19). The much larger difference in reactivity of these radicals towards benzaldehyde may be due to the transition state for the oxidation of aldehydes being much more sensitive to the polar nature of the attacking peroxy radical.

We were not able to measure individual propagation and termination rate constants for the oxidation of benzyl ketone, benzyl bromide, and benzyl cyanide. The ratio R_∞/R_s for benzyl ketone was too low to give reliable data while rate ratios for the oxidation of benzyl bromide were not reproducible. The rate of oxidation of benzyl cyanide in the absence and presence of *t*-butyl hydroperoxide depends on the oxygen concentration up to 1 atm. Values of $k_p/(2k_t)^{1/2}$ for these oxidations were obtained by extrapolation to infinite oxygen pressure. We have assumed a value of $3.6 \times 10^7\ M^{-1}\ s^{-1}$ for $2k_t$ for these three substrates and used this value in conjunction with the ratio $k_p/(2k_t)^{1/2}$ to give propagation rate constants. The value $3.6 \times 10^7\ M^{-1}\ s^{-1}$ is an average of the values of $2k_t$ for benzyl *t*-butyl ether, benzyl alcohol, benzyl chloride, benzyl phenyl ether, *t*-butyl phenyl acetate, and ethylbenzene.

From the rate constants tabulated in Table 4 it is clear that the peroxy radicals derived from α-substituted toluenes are all more reactive than the *t*-butylperoxy radical. It is also apparent that the reactivity of a secondary peroxy radical depends to some extent on the nature of the group attached to the α-carbon.

There is a reasonably good correlation between the ratio k_p/k_p^{br} (i.e. the ratio of the reactivity of an α-monosubstituted toluene towards its own peroxy radical and towards the *t*-butylperoxy radical) and σ-*meta* substituent constants (Fig. 1). It is clear that the reactivity of a peroxy radical increases as the electron-withdrawing capacity of the α-substituent increases. This is not unexpected

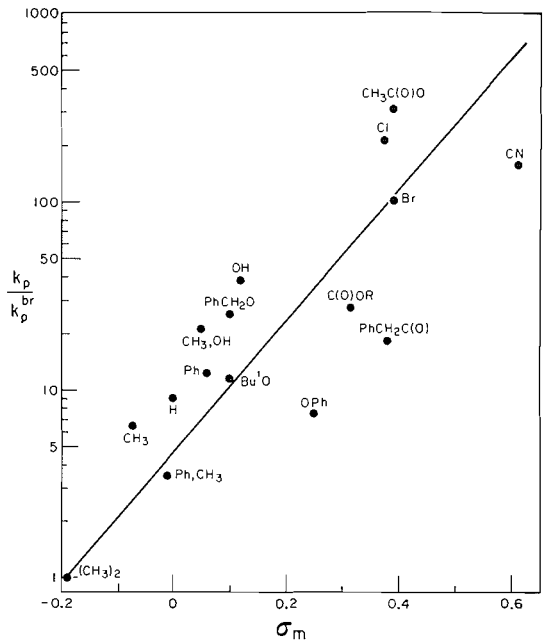

FIG. 1. $\log_{10} k_p/k_p^{br}$ plotted against σ_m for α-monosubstituted benzylperoxy radicals and $\Sigma\sigma_m$ for α,α-disubstituted benzylperoxy radicals.

since acylperoxy radicals, which have a very strong electron-withdrawing substituent on the α-carbon, are considerably more reactive than alkylperoxy radicals (7). The difference in the reactivity of α-acyloxybenzylperoxy radicals and alkylperoxy radicals was confirmed by the fact that tetralin hydroperoxide reduces the rate of oxidation of benzyl acetate and benzyl benzoate even though the termination rate constant for tetralylperoxy radicals is lower than for the peroxy radicals derived from these two esters. This situation is analogous to the inhibiting effect tetralin hydroperoxide has on the oxidation of benzaldehyde (7).

Ratios of k_p/k_p^{br} for oxidation of cumene, 1,1-diphenylethane and α-methylbenzyl alcohol have also been plotted in Fig. 1 and correlate quite well with $\Sigma\sigma_m$ substituent constants. It would, therefore, appear that differences in reactivity between tertiary alkylperoxy radicals and secondary alkylperoxy radicals (4, 19) are mainly due to polar effects.

α-Substitution apparently has little influence on the magnitude of the termination rate constant for α-mono substituted benzylperoxy radicals. Unfortunately, termination rate constants could

Can. J. Chem. Downloaded from www.nrcresearchpress.com by 84.22.46.98 on 09/08/12
For personal use only.

TABLE 5

Rate constants relative to toluene (per α-hydrogen) for reactions of α-substituted toluenes with *t*-butylperoxy radicals, bromine atoms, and phenyl radicals

Toluene derivative		$Bu^tOO^\cdot$ at 30 °C	$Br^\cdot$ at 77 °C	Phenyl
$PhCH_2OCH_2Ph$		33	159*	13
$(Ph)_3CH$	1.	28	102	39
$(Ph)_2CHCH_3$	2.	7.3	66	18
$PhCH(CH_3)_2$	3.	18	57.5	9.7
$PhCH_2OPh$	4.	11	46	11.4
$PhCH_2CH_3$	5.	11	25.2	4.5
$PhCH_2Ph$	6.	9.4	17.6	7.7
$PhCH_2OCOCH_3$	7.	0.75	1.37	—
$PhCH_3$	8.	1.0	1.0	1.0
$PhCH_2Cl$	9.	0.9	0.46	6.2
$PhCH_2COOCH_3(Bu^t)$†	10.	3.0	0.27	3.8
$PhCH_2CN$	11.	1.1	0.22	24
$PhCH_2Br$	12.	0.7	0.18	5.1
$PhCH_2OH$		6.7	—	14
$PhCH_2CH{=}CH_2$		20.5	—	7.2
$PhCH_2COCH_2Ph$		5	—	20
$PhCH_2OCOPh$		0.95	—	3.8
PhCHO		94.5	—	22

*Benzyl methyl ether.
†Methyl phenyl acetate was used for the reactions of bromine atoms and phenyl radicals while *t*-butyl phenyl acetate was used for *t*-butylperoxy radicals.

not be determined for benzylperoxy radicals with strong electron-withdrawing groups such as cyano and nitro on the α-carbon.

The relative rate constants for hydrogen atom abstraction from α-substituted toluenes relative to toluene for *t*-butylperoxy radicals, bromine atoms (21) and phenyl radicals (22) have been compared (Table 5). As expected *t*-butylperoxy radicals correlate much better with the electrophilic bromine atom (Fig. 2) than with phenyl radicals which are only very slightly electrophilic (22).

1,1-Diphenylethane, benzyl acetate, and *t*-butyl phenyl acetate (which has been assumed to have the same reactivity as methyl phenyl acetate) are the only substrates for which the correlation between *t*-butylperoxy radicals and bromine atoms is poor. From the slope of the line in Fig. 2 it is clear that bromine atoms are more selective in hydrogen atom abstraction than *t*-butylperoxy radicals.

Relative rate constants for reaction of bromine atoms with α-mono substituted toluenes have been reported to correlate much better with σ_p^+ than with σ_m or σ_p (21). The ρ value of −2.46 at 77 °C is greater than for reaction of bromine atoms with ring substituted toluenes (ρ = −1.38

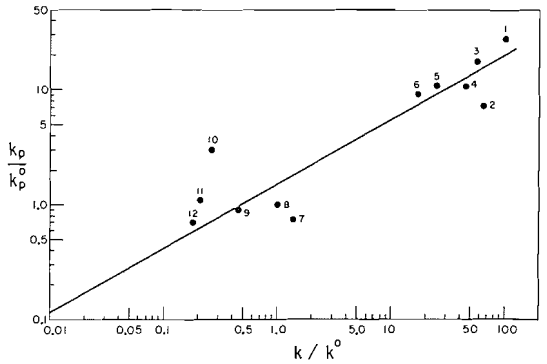

FIG. 2. Plot of $\log k_p/k_p^0$ for reaction of *t*-butylperoxy radicals with α-substituted toluenes against $\log k/k^0$ for reaction of bromine atoms with α-substituted toluenes: (*1*) $(Ph)_3CH$, (*2*) $(Ph)_2CHCH_3$, (*3*) $PhCH(CH_3)_2$, (*4*) $PhCH_2OPh$, (*5*) $PhCH_2CH_3$, (*6*) $PhCH_2Ph$, (*7*) $PhCH_2OCOCH_3$, (*8*) $PhCH_3$, (*9*) $PhCH_2Cl$, (*10*) $PhCH_2C(O)OR$, (*11*) $PhCH_2CN$, (*12*) $PhCH_2Br$.

at 80 °C (23)) presumably because α-substitution has a much greater effect than ring substitution on the polarization of the transition state. Reaction of α-monosubstituted toluenes with *t*-butylperoxy radicals also correlates slightly better with σ_p^+ than with σ_p substituent constants and gives a poor correlation with σ_m. The correlation with σ_p^+ suggests that both inductive and resonance effects influence the reactivity of the labile hydrogens. Similarly the ρ^+ value of −1.2 is higher than the ρ^+ value of −0.6 reported by Russell (2) for oxidation of ring-substituted toluenes at 90 °C and the ρ^+ value of −0.56 for reaction of *t*-butylperoxy radicals with ring-substituted toluenes at 30 °C (24).

The authors wish to thank Dr. K. U. Ingold for his continuing interest and advice throughout the course of this work.

1. K. U. INGOLD. Account. Chem. Res. **2**, 1 (1969).
2. G. A. RUSSELL. J. Amer. Chem. Soc. **78**, 1047 (1956).
3. G. A. RUSSELL and R. C. WILLIAMSON, JR. J. Amer. Chem. Soc. **86**, 2357 (1964).
4. J. A. HOWARD, K. U. INGOLD, and M. SYMONDS. Can. J. Chem. **46**, 1017 (1968).
5. H. C. BROWN and Y. OKAMOTO. J. Amer. Chem. Soc. **80**, 4979 (1958).
6. C. WALLING and E. A. MCELHILL. J. Amer. Chem. Soc. **73**, 2927 (1951).
7. G. E. ZAIKOV, J. A. HOWARD, and K. U. INGOLD. Can. J. Chem. **47**, 3017 (1969).
8. A. I. VOGEL. Practical organic chemistry. Longmans, Green and Co., London. 1948. p. 378.
9. J. A. HOWARD and K. U. INGOLD. Can. J. Chem. **47**, 3809 (1969).
10. J. A. HOWARD and K. U. INGOLD. Can. J. Chem. **45**, 785 (1967).

11. J. A. HOWARD and K. U. INGOLD. Can. J. Chem. **43**, 2729 (1965).
12. J. A. HOWARD and K. U. INGOLD. Can. J. Chem. **43**, 2737 (1965).
13. J. A. HOWARD and K. U. INGOLD. Can. J. Chem. **45**, 793 (1967).
14. J. A. HOWARD and K. U. INGOLD. Can. J. Chem. **48**, 873 (1970).
15. J. A. HOWARD, K. ADAMIC, and K. U. INGOLD. Can. J. Chem. **47**, 3793 (1969).
16. T. G. TRAYLOR and G. A. RUSSELL. J. Amer. Chem. Soc. **87**, 3698 (1965).
17. J. R. THOMAS. J. Amer. Chem. Soc. **89**, 4872 (1967).
18. J. A. HOWARD and K. U. INGOLD. Can. J. Chem. **46**, 2655 (1968).
19. J. A. HOWARD, W. J. SCHWALM, and K. U. INGOLD. Advan. Chem. Ser. **75**, 38 (1968).
20. L. J. DURHAM, C. F. WURSTER, JR., and H. S. MOSHER. J. Amer. Chem. Soc. **80**, 332 (1958).
21. S. S. FRIEDRICH, E. C. FRIEDRICH, L. J. ANDREWS, and R. M. KEEFER. J. Org. Chem. **34**, 900 (1969).
22. G. A. RUSSELL. Private communication.
23. C. WALLING, A. L. RIEGER, and D. D. TANNER. J. Amer. Chem. Soc. **85**, 3129 (1963).
24. J. A. HOWARD. Unpublished data.

Can. J. Chem. Downloaded from www.nrcresearchpress.com by 84.22.46.98 on 09/08/12
For personal use only.

Can. J. Chem. Downloaded from www.nrcresearchpress.com by 210.87.254.42 on 09/05/12
For personal use only.

Photo-initiated reactions of thiols and olefins. V. Inhibition of butene-2 isomerization by oxygen: a new method for determining relative reactivities

D. M. GRAHAM AND J. F. SOLTYS
Department of Chemistry, University of Western Ontario, London, Ontario

Received February 6, 1970

Investigation of the kinetics of oxygen inhibition of the thiyl radical catalyzed isomerization of *cis*-butene-2 has yielded an estimate for the relative rates of oxidation (k_7) and decomposition (k_3) of the CH_3S and olefin adduct radical. At 25 °C, $k_7/k_3 = 7 \times 10^4$ l mole^{-1}, and $E_3 - E_7 = 11.8 \pm 2.5$ kcal. Making use of these results, a new method has been developed for determining relative reactivities of olefins, and some preliminary results have been obtained.

Canadian Journal of Chemistry, 48, 2173 (1970)

Introduction

In previous publications in this series, it has been shown that the rate constant for attack of CH_3S on olefins may be determined only under special circumstances because of the reversibility of the reaction. Where *cis–trans* isomers exist, the rate constant may be obtained directly from the catalyzed rate of isomerization (1). Addition rate measurements, on the other hand, can yield an attack constant only if the rate of decomposition of the adduct radical is competitive with its rate of reaction with thiol (2). Although this was found to occur with acetylene (3), in the case of ordinary olefins, decomposition is generally much faster than dehydrogenation of thiol over the thiol concentration range available to gas-phase studies (2).

It apppeared possible therefore that, by introducing another reaction into the system, which could be capable of competing with decomposition of the adduct radical, a kinetics might be obtained which could yield attack constants. Since oxygen is known to react rapidly with alkyl radicals, this seemed a likely choice, and a study of the kinetics of the catalyzed isomerization of *cis*-butene-2 in the presence of oxygen was undertaken.

Experimental

The apparatus and techniques used were as previously described (1, 2). All gas chromatographic analyses were done on a 300 ft dimethylsulfolane capillary column at 0 °C, using a hydrogen flame ionization detector.

For the determination of relative co-oxidation rates, mixtures of ethylene and one or more olefins were used, together with *n*-butane as an unreactive internal standard for vapor phase chromatographic analysis. The *n*-butane concentration was kept at about 2.94×10^{-4} mole l^{-1}, and the olefin pressures were adjusted by experiment so that the degrees of conversion were all roughly the same, and less than 10%. A high pressure of methanethiol (5.87×10^{-3} mole l^{-1}) was used in order to eliminate any possibility of radical attack on *n*-butane or of peroxy radical attack on olefin. Samples of the reaction mixture were analyzed before and after reaction.

Results and Discussion

Inhibition Kinetics

Some representative isomerization curves are shown in Fig. 1, and all of the rate data obtained are summarized in Table 1.

In the absence of oxygen, the thiyl radical catalyzed isomerization of *cis*-butene-2 (*C*) to the *trans*- form (*T*) has been treated (1) according to the following mechanism

$$CH_3SH \rightarrow CH_3S \qquad (\text{rate} = r_i)$$

[1*c*] $$CH_3S + C \rightarrow X$$

[2] $$X + CH_3SH \rightarrow XH + CH_3S$$

[3] $$X \rightarrow CH_3S + \rho_3 T + (1 - \rho_3)C$$

[4] $$2CH_3S \rightarrow CH_3SSCH_3$$

X is the adduct radical, and ρ_3 is the probability that, when it decomposes, the *trans*-isomer is formed. It has been established that the rate of reaction [2] is negligible compared with that of reaction [3] above 0 °C, and at thiol pressures up to atmospheric.

It would appear likely that inhibition by oxygen occurs through its reaction with the adduct radical, i.e.,

[7] $$X + O_2 \rightarrow XO_2$$

The chain length for isomerization is very long and removal of X radicals could have a large effect on the reaction rate. Photolysis of mixtures of methanethiol and oxygen, at temperatures from 25 to 200 °C, failed to yield any sulfur-

TABLE 1

Inhibited initial rates of isomerization

Temperature (°C)	Oxygen (mole l^{-1}) × 10^5	R_{ic} (mole l^{-1} s^{-1}) × 10^7	$k_7/\rho_3 k_3$ (l $mole^{-1}$) × 10^{-3}
−20*	0.0	2.34	1930
	1.15	0.114	
	2.29	0.0534	
	3.42	0.0379	
25*	0.0	2.47	152
	0.968	1.02	
	1.94	0.599	
	2.90	0.432	
25*	0.0	6.37	107
	0.511	4.33	
	1.02	2.83	
	2.04	1.96	
	3.06	1.52	
125†	0.0	120	0.434
	108	87.7	
	269	54.6	
	538	36.5	

*For −20 and 25 °C, methanethiol = 2.15 × 10^{-4} mole l^{-1}, *cis*-butene-2 = 5.38 × 10^{-4} mole l^{-1}.
†For 125 °C, methanethiol = 5.38 × 10^{-3} mole l^{-1}, *cis*-butene-2 = 1.35 × 10^{-3} mole l^{-1}. (The light intensity was the same only for the first two sets of data.)

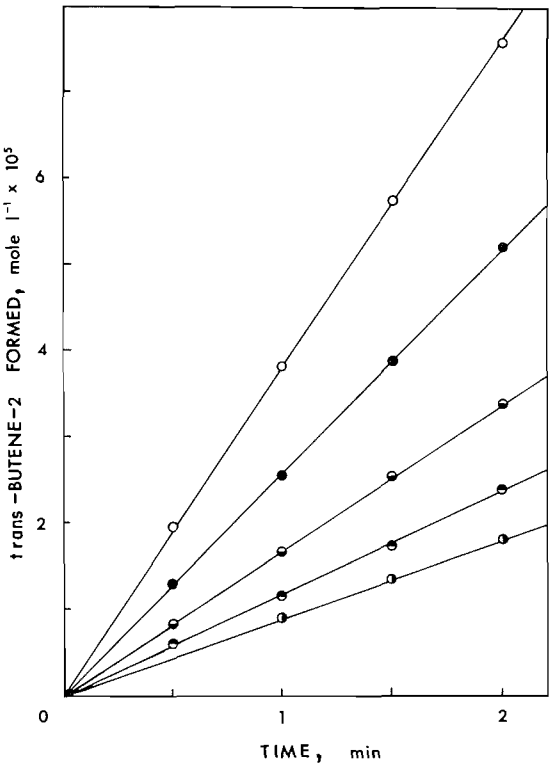

FIG. 1. Isomerization of *cis*-butene at 25 °C. Methanethiol = 2.15 × 10^{-4} l^{-1}; *cis*-butene-2 = 5.38 × 10^{-4} mole l^{-1}; oxygen = 0(○), 0.511(●), 1.02(◒), 2.04(◓), 3.06(◑) × 10^{-5} mole l^{-1}.

containing product other than 2,3-dithiabutane, which results from thiyl combination. Reaction of thiyl radicals and oxygen may, therefore, probably be eliminated from the inhibition mechanism.

The main fate of the peroxy radical that is formed in reaction [7] cannot at this stage be ascertained. Because methanethiol is quite reactive to dehydrogenation by alkyl radicals (4), it might be reasonable to expect that the peroxy radicals may undergo a similar rapid reaction to yield hydroperoxides. Such hydroperoxides have been shown to be the primary product of co-oxidation of thiols and olefins in solution (5), where quite long chain lengths have been observed (6). If this is assumed to be the case, the following expression may be derived for the initial rate of isomerization of *cis*-butene-2.

$$[8] \qquad R_{iC} = \left(\frac{r_i}{2k_4}\right)^{\frac{1}{2}} \frac{\rho_3 k_3 k_{1C}[C]}{k_3 + k_7[O_2]}$$

This equation predicts a linear relation between R_{iC}^{-1} and oxygen concentration. Two such plots obtained at 25 °C are shown in Fig. 2. The initial olefin and thiol concentrations were the same in both cases, only the light intensity was different. Plots of the rest of the data in Table 1 are not shown since they cannot be conveniently fitted on the same scale; the scatter of the experi-

Can. J. Chem. Downloaded from www.nrcresearchpress.com by 210.87.254.42 on 09/05/12
For personal use only.

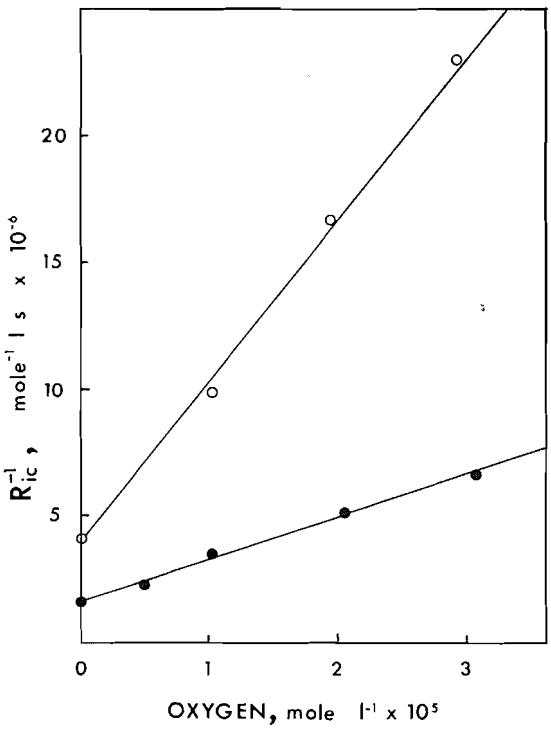

FIG. 2. Inverse plot of 25 °C results from Table 1. High light intensity, ●; low light intensity, ○.

mental points in each case is about the same as in Fig. 2. The ratio of the slopes to intercepts of these plots yields directly the rate constant ratios $k_7/\rho_3 k_3$ which are given in the last column of Table 1.

The difference in the two 25 °C results may be attributed to the appearance of a first order termination reaction at higher oxygen pressures, since the order dependence on light intensity, which may be estimated from the data of Table 1, increases from 0.50 at zero oxygen concentration to 0.68 at the highest oxygen concentration, as shown in Fig. 2. This reaction is most likely the termination of the peroxy radical, XO_2, on the cell wall. Since the relative contribution of this heterogeneous termination should be smaller the higher the thiyl radical concentration, the lower value of $k_7/\rho_3 k_3$, which is obtained at a higher light intensity, is probably more correct. An Arrhenius plot of the rate constant ratios yields $E_3 - E_7 = 11.8 \pm 2.5$ kcal (90% confidence limits). Since E_7 should be very close to zero, these measurements provide the first estimate of the carbon–sulfur bond strength in the adduct radical. Again, it may be argued that this is probably an overestimate, since the thiyl radical concentration should increase with increasing temperature as a result of reaction [3] competing more successfully with reaction [7].

Although these results should be considered as only estimates, they do permit a calculation of the conditions under which the reversibility of the attack step may be made negligible, i.e., where $k_3 \ll k_7[O_2]$. This has led to the development of a new method for determining relative attack constants.

Relative Reactivities from Competitive Co-oxidation

Consider the photolysis of a mixture of methanethiol, two olefins, A and B, and oxygen. Two parallel competitive reactions may occur

$$A + CH_3S \underset{k_{3a}}{\overset{k_{1a}}{\rightleftharpoons}} X_a \xrightarrow{[k_{7a}O_2]} \text{Products}$$

$$B + CH_3S \underset{k_{3b}}{\overset{k_{1b}}{\rightleftharpoons}} X_b \xrightarrow{[k_{7b}O_2]} \text{Products}$$

Under conditions where $k_3 \ll k_7[O_2]$ for each olefin, it follows that

$$[9] \qquad \frac{-d[A]/dt}{-d[B]/dt} = \frac{k_{1a}[A]}{k_{1b}[B]}$$

Hence, if the conversions of both species are kept small, the relative attack constants may be determined from the initial relative rates of disappearance of the two olefins. It is important to note that eq. [9] is independent of the subsequent fate of the peroxy radicals as long as reaction [3] is negligible. The reasoning of course may be extended to a mixture of any number of olefins.

For *cis*-butene-2 it was calculated, using the data given above, that at 0 °C and about 500 Torr oxygen, $k_3/k_7[O_2] < 10^{-3}$. Hence, at this temperature and pressure, eq. [9] should hold reasonably well, even for systems where the rate of reaction [3] is an order of magnitude greater. Relative attack constants have been determined under these conditions, and in all cases when *cis*-butene-2 was present, the amount of isomerization observed was much less than 1% of the butene-2 disappearing by co-oxidation.

The rate constants, obtained from relative co-oxidation rates at 0 °C, are, relative to that for ethylene: methylacetylene, 0.92 ± 0.20 (3); *trans*-butene-2, 1.96 ± 0.75 (3); propylene, 2.42 ±

Can. J. Chem. Downloaded from www.nrcresearchpress.com by 210.87.254.42 on 09/05/12
For personal use only.

0.24(3); *cis*-butene-2, 4.13 ± 0.72(10); isobutene, 4.45 ± 0.84 (4). The errors are 70% confidence limits, and the number of experimental determinations is listed in parentheses. The rather poor precision that is indicated is probably due to fractionation on sampling and transfer to the gas chromatograph. The results do indicate, however, that the relative reactivities of olefins toward thiyl radicals is nowhere near as sensitive to olefin structure as has been observed for $S(^3P)$ or $O(^3P)$ (7), the magnitude of the observed trends more closely resembling that for CF_3 (7). Since a new apparatus is now being developed in which it is hoped that sampling errors may be minimized, further discussion of the relative reactivity data will be postponed until more precise results are forthcoming.

Since isomerization kinetics for butene-2 are complicated by the probability factor in reaction [3], only the products $\rho_3 k_{1C}$ and $(1 - \rho_3)k_{1T}$ could be obtained for the *cis*- and *trans*-isomers, respectively (1). In order to determine the attack constants themselves, the relative reactivity of *cis*- and *trans*-butene-2 was determined directly by the co-oxidation method. Since fractionation errors should be much less in this case, the value obtained $k_{1C}/k_{1T} = 2.07 \pm 0.20$ (70% confidence limits, four experiments) should be reasonably good. The equilibrium constant for the catalyzed isomerizations is (1)

$$K = [T]_{eq}/[C]_{eq} = \rho_3 k_{1C}/(1-\rho_3)k_{1T}$$

using $K = 3.78$ at 0 °C (extrapolated from data given in ref. 8), $\rho_3 = 0.65$. Taking $\rho_3 k_{1C} = 1.6 \times 10^6$ l mole^{-1} s^{-1} (1, 3), the attack constant for *cis*-butene-2 is calculated to be 2.5×10^6 l mole^{-1} s^{-1}. This may be compared with the attack constant for ethylene, 4.8×10^5 l mole^{-1} s^{-1} (3), to yield a relative reactivity for *cis*-butene-2 of 5.1, which is in reasonably good agreement with the value 4.13 given above.

The co-oxidation method appears more generally applicable than the inhibition technique previously developed for butadiene (9), since it may be applied to compounds where attack may be reversible. The use of both methods when possible, however, should prove extremely useful in determining the validity of reactivity data.

We are grateful to the National Research Council of Canada for financial support and to the Province of Ontario for a Fellowship awarded to J.F.S.

1. D. M. Graham, R. L. Mieville, and C. Sivertz. Can. J. Chem. **42**, 2239 (1964).
2. D. M. Graham, R. L. Mieville, R. H. Pallen, and C. Sivertz. Can. J. Chem. **42**, 2250 (1964).
3. D. M. Graham and J. F. Soltys. Can. J. Chem. **47**, 2529 (1969).
4. G. Greig and J. C. J. Thynne. Trans. Faraday Soc. **62**, 379 (1966).
5. D. M. Graham. Unpublished results.
6. A. A. Oswald. J. Org. Chem. **24**, 443 (1959); **26**, 842 (1961).
7. R. J. Cvetanovic and R. S. Irwin. J. Chem. Phys. **46**, 1694 (1967).
8. Natl. Bur. Stand. Circ.: Selected properties of hydrocarbons. A.P.I. Project 44.
9. D. M. Graham and J. F. Soltys. Can. J. Chem. **47**, 2719 (1969).

Can. J. Chem. Downloaded from www.nrcresearchpress.com by 210.87.254.42 on 09/05/12
For personal use only.

Can. J. Chem. Downloaded from www.nrcresearchpress.com by 210.87.254.40 on 09/05/12
For personal use only.

Ligand field splitting energies of the hexaamminecobalt(II) ion and the hexaamminenickel(II) ion measured by a calorimetric method

BADRI MUHAMMAD[1] AND J. W. S. JAMIESON
Department of Chemistry, Dalhousie University, Halifax, Nova Scotia

Received January 28, 1970

Various normal lower ammines and high-energy modifications of the lower ammines of cobalt(II) sulfate and nickel(II) sulfate have been prepared and the heats of solution in dilute ammonia have been measured for both types. For each of these ammine systems the maximum difference in heat of solution, expressed as kcal/mole of each heptaammine, between the high-energy and the normal salts has been found to be in close agreement with the ligand field splitting energy of the hexaamminemetal(II) ion.

Canadian Journal of Chemistry, 48, 2177 (1970)

Introduction

In a recent study (1) of both normal crystalline lower hydrates and high-energy modifications of the lower hydrates of the divalent sulfates of manganese, iron, cobalt, and nickel it was found that the maximum differences in heat of solution, expressed as kcal/mole of each heptahydrate, were empirically equivalent to the ligand field splitting energies of the corresponding hexaaquo cations. Since it seemed desirable to determine whether or not the ligand field splitting energies of other complexes could be measured in the same way, various ammine complexes of cobalt(II) sulfate and nickel(II) sulfate have now been studied.

Experimental

Suitable temperatures for preparation of the anhydrides of cobalt(II) sulfate and nickel(II) sulfate from higher hydrates were determined from experiments in thermogravimetric analysis (TGA) and differential thermal analysis (DTA). Thus anhydrous $CoSO_4$ was obtained by heating $CoSO_4 \cdot 7H_2O$ (J. T. Baker Analyzed Reagent) in an oven at 270 °C for 3 days and anhydrous $NiSO_4$ was similarly prepared from $NiSO_4 \cdot 6H_2O$ of Fisher certified reagent grade at a temperature of 350 °C. Completeness of dehydration was checked by the loss of weight which agreed with the calculated values to within 0.1%.

The anhydrous salts were finely powdered and about 4 g samples were taken for reaction with anhydrous ammonia (supplied by Matheson of Canada, Ltd.) at atmospheric pressure for about 2 days (2, 3). In each case during the initial stage of reaction there was evolution of heat accompanied by increase of volume and change of color (violet to pink for the cobalt complexes; yellow to green to light violet for the nickel complexes). The composition of each product was determined from both the gain in weight and gravimetric sulfate analysis. Cobalt(II) sulfate hexaammine, which was probably pentaamminecobalt(II) sulfate monoammine, was prepared and used as starting material for the preparation of some lower ammines, but as has been reported (4) it was found to be unstable under ordinary conditions in the atmosphere. Thus the starting materials for preparation of most of the samples of the lower ammines were $NiSO_4 \cdot 6NH_3$ and $CoSO_4 \cdot (5.68\text{-}NH_3)$.

Some $CoSO_4 \cdot 6NH_3$ was also prepared essentially as described by Wendlandt and Smith (5) by passing dry ammonia through a suspension of the free salt in absolute ethanol. Samples prepared both directly and by this method were examined by thermogravimetric analysis at a heating rate of about 0.12 deg/min and were found to be virtually identical.

A sample of $NiSO_4 \cdot 6NH_3$, which was probably pentaamminenickel(II) sulfate monoammine, prepared by the method of Werner (6) was shown by thermogravimetric analysis and differential thermal analysis to be essentially identical with both the hexaammine prepared directly and that reported by George and Wendlandt (7), although the colors of the products were different, due presumably to different particle sizes. The infrared spectra of the hexaammines prepared by these methods were found to be identical and in agreement with the spectrum recently reported (8).

Deammoniation of the hexaammines of cobalt(II) sulfate and nickel(II) sulfate was carried out in vacuo or in an oven at various temperatures, after which the glass tubes containing the samples were sealed to prevent water vapor in the air from reacting with the lower ammines.

After partial loss of ammonia, some samples were heated in sealed tubes at different temperatures for various time intervals.

All the ammine complexes prepared appeared to be homogeneous. Duplicate samples prepared in the same way had the same uniform color and gave practically identical heats of solution.

Integral heats of solution were measured as previously described (1) except that the ammines of cobalt(II) sulfate were dissolved in 3 *M* aqueous ammonia and the ammines of nickel(II) sulfate were dissolved in 0.75 *M* aqueous ammonia, to ensure complete solubility.

Results

The results given in Tables 1 and 2 and in Figs. 1 and 2 show that linear relations are obtained by plotting the heats of solution in cal g^{-1} of solute against the percentages of ammonia in the

[1]Colombo Plan Scholar.

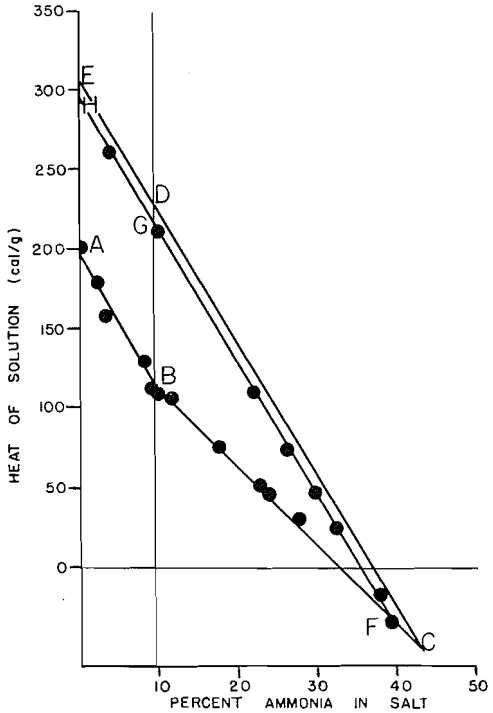

FIG. 1. Heats of solution for various ammines of cobalt(II) sulfate.

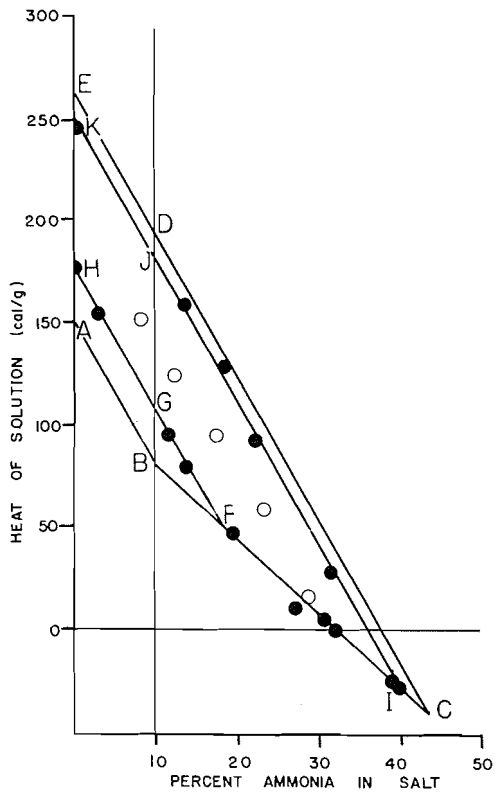

FIG. 2. Heats of solution for various ammines of nickel(II) sulfate.

samples. The vertical lines in Figs. 1 and 2 are at the monoammine compositions. It is assumed that the monoammines are $M(SO_4 \cdot NH_3)$ since the heat of solution lines AB (between the free salt and the monoammine) have different slope than the heat of solution lines BC (between the monoammine and the heptaammine). Thus it is evident that the last NH_3 is bonded differently.

As in the case of the aquo complexes (1) the lines CE, which represent the maximum possible heats of solution for samples which might be prepared from the heptaammines $MSO_4 \cdot 7NH_3$, which are probably $[M(NH_3)_6]^{2+}SO_4^{2-} \cdot NH_3$, have been calculated and drawn through the point C for each heptaammine. Since the readily prepared starting materials were $CoSO_4 \cdot (5.68\text{-}NH_3)$, $CoSO_4 \cdot 6NH_3$, and $NiSO_4 \cdot 6NH_3$ the points C for the heptaammines and the lines CE were obtained by extrapolation of the experimental data.

Cobalt(II) Sulfate

The heat of solution data for the ammines of cobalt(II) sulfate may be expressed as linear

TABLE 1

Heats of solution for various ammines of cobalt(II) sulfate

% Ammonia in sample	Heat of solution (cal/g)	Nature of sample or method of deammoniation
4.39	261	Vacuum
10.3	212	Vacuum
22.2	111	Vacuum
26.2	74.0	Vacuum
30.1	47.2	Vacuum
32.9	24.5	Direct preparation
38.3	−16.8	Direct preparation
10.4	110	Direct preparation
12.1	108	Deammoniation at 130 °C
18.1	76.4	Deammoniation at 80 °C
23.2	51.1	Deammoniation at 80 °C
24.7	46.6	Deammoniation at 40 °C
28.2	18.2	Deammoniation at 100 °C
39.8	−35.6	Direct preparation
0.0	201	Deammoniation over 350 °C
2.15	180	Deammoniation at 300 °C
3.92	158	Deammoniation at 300 °C
8.89	131	Deammoniation at 130 °C
9.78	113	Direct preparation

Can. J. Chem. Downloaded from www.nrcresearchpress.com by 210.87.254.40 on 09/05/12
For personal use only.

Can. J. Chem. Downloaded from www.nrcresearchpress.com by 210.87.254.40 on 09/05/12
For personal use only.

TABLE 2

Heats of solution for various ammines of nickel(II) sulfate

% Ammonia in sample	Heat of solution (cal/g)	Nature of sample or method of deammoniation
0.0	246	Vacuum
12.5	160	Vacuum
18.3	129	Vacuum
22.1	93.2	Vacuum
31.4	28.3	Vacuum
39.9	−27.7	Direct preparation
19.6	48.2	Deammoniation at 253 °C
27.1	11.8	Deammoniation at 77 °C
30.6	6.4	Deammoniation at 10 °C
32.2	0.0	Deammoniation at 70 °C
39.0	−23.9	Direct preparation
39.9	−27.7	Direct preparation
0.0	177	Sealed tube over 350 °C
2.94	155	Sealed tube at 340 °C
11.6	95.8	Sealed tube at 200 °C
13.8	80.0	Sealed tube at 200 °C

equations, calculated by the method of least squares, as

$$y_{BC} = -5.09x + 167$$

$$y_{AB} = -8.26x + 197$$

$$y_{FH} = -8.26x + 296$$

Extrapolation of the line BC gives an estimate of the heat of solution of $CoSO_4 \cdot 7NH_3$ (43.38% ammonia), which is probably $[Co(NH_3)_6]^{2+}SO_4^{2-} \cdot NH_3$, as −54.0 cal/g and that of $CoSO_4 \cdot NH_3$ (9.898% ammonia), which is probably $Co^{2+}SO_4^{2-} \cdot NH_3$, as 117 cal/g. The line CE in Fig. 1 has been drawn through the point C for $CoSO_4 \cdot 7NH_3$, the species which would probably contain the hexaamminecobalt(II) ion, with a slope equal to that of the line FH. The heat of solution of the high-energy modification of $CoSO_4 \cdot NH_3$ (9.898% ammonia) at the point D on the line CE is then calculated as 223 cal/g. Therefore the maximum energy of transition is 223 − 117 = 106 cal/g which is equivalent to 1.02×10^4 cm^{-1} per mole of $CoSO_4 \cdot 7NH_3$.

Nickel(II) Sulfate

Similar linear equations of the heat of solution data for the ammines of nickel(II) sulfate are

$$y_{BC} = -3.06x + 116$$

$$y_{IK} = -6.96x + 250$$

$$y_{FH} = -6.98x + 176$$

Lower ammines of nickel(II) sulfate prepared in vacuo gave heats of solution along the line IK in Fig. 2 but samples prepared by simple heating in an oven gave lower heats of solution, falling between the lines IK and FH as shown by the points marked with open circles. The line FH was obtained for the heats of solution of samples having approximately the desired percentage of ammonia which were heated in sealed tubes at elevated temperatures.

Extrapolation of the line BC gives the heat of solution of $NiSO_4 \cdot 7NH_3$ (43.51% ammonia), which is probably $[Ni(NH_3)_6]^{2+}SO_4^{2-} \cdot NH_3$, as −41.0 cal/g and that of $NiSO_4 \cdot NH_3$ (9.913% ammonia), which is probably $Ni^{2+}SO_4^{2-} \cdot NH_3$, as 79.9 cal/g. The line CE in Fig. 2 through the point C for hexaamminenickel(II) sulfate monoammine has been calculated using the slope of the line IK as

$$y_{CE} = -6.96x + 262$$

The heat of solution for the maximum possible high-energy modification of $NiSO_4 \cdot NH_3$ (9.913% ammonia) at the point D on the line CE can then be estimated as 193 cal/g. Thus the maximum energy of transition can be calculated as 1.08×10^4 cm^{-1} per mole of $NiSO_4 \cdot 7NH_3$.

Discussion

The lower ammine complexes, although apparently homogeneous, were almost certainly mixtures rather than integral lower ammines. According to the phase rule no more than two such solid phases could be present at equilibrium. Frost, Moon, and Tompkins (9) showed that both integral hydrates and two-phase mixtures of hydrates gave heats of solution falling along straight lines (from anhydride to monohydrate and from monohydrate to heptahydrate). Similarly, mixtures of ammines give the same heat of solution lines as integral ammines.

For consistent results it is necessary that all heat of solution samples dissolve to give the same species in aqueous ammonia solution. Since the results are consistent it seems reasonable to assume that this is so. While it seems likely that, in each case, the hexaamminemetal(II) ion is formed, even if it were some other entity such as $[M(NH_3)_x(H_2O)_{6-x}]^{2+}$ the differences in heat of solution such as DB would be unchanged.

The values of the ligand field splitting energies now obtained are in close agreement with the orig-

Can. J. Chem. Downloaded from www.nrcresearchpress.com by 210.87.254.40 on 09/05/12
For personal use only.

inal spectroscopic values of Jørgensen, quoted by Orgel (10) of 1.01×10^4 cm^{-1} for the hexaamminecobalt(II) ion and 1.08×10^4 cm^{-1} for the hexaamminenickel(II) ion (11), just as the maximum differences in heat of solution between the high-energy and normal crystalline hydrates of several transition metal sulfates have previously been shown to be equivalent to the spectroscopically measured ligand field splitting energies for several hexaaquo cations. Thus there appears to be further verification that the present calorimetric method, at least in principle, could be used to give quantitative measurements of the ligand field splitting energies for cations having six ligands in an octahedral field.

The heat of solution of $[M(NH_3)_6]^{2+}SO_4^{2-} \cdot NH_3$ would be the heat of reaction for

$$[M(NH_3)_6]^{2+}SO_4^{2-} \cdot NH_3 + n\underset{\text{aqueous}}{NH_3} \rightarrow [M(NH_3)_6]^{2+} + \underset{\text{solvated}}{SO_4^{2-} \cdot NH_3}$$

and the heat of solution of $M(SO_4 \cdot NH_3)$ would be the heat of the reaction

$$M^{2+}SO_4^{2-} \cdot NH_3 + (n + 6)\underset{\text{aqueous}}{NH_3} \rightarrow [M(NH_3)_6]^{2+} + \underset{\text{solvated}}{SO_4^{2-} \cdot NH_3}$$

so that the heat of solution of the heptaammine minus the heat of solution of the monoammine could be expressed as the standard heat of formation of the monoammine plus 6 × [the standard heat of formation of ammonia$_{(aqueous)}$] minus the standard heat of formation of the heptaammine, which is the heat of the reaction

$$[M(NH_3)_6]^{2+}SO_4^{2-} \cdot NH_3 \rightarrow M(SO_4 \cdot NH_3) + 6NH_{3\ (aqueous)}$$

The standard heat of formation of $NiSO_4 \cdot 7NH_3$ at point C = −408.2 kcal/mole (12), the standard heat of formation[2] of normal or low-energy $NiSO_4 \cdot NH_3$ at point B = −267.2 kcal/mole of monoammine and the standard heat of formation[2] of the high-energy modification of $NiSO_4 \cdot NH_3$ at point D = −247.8 kcal/mole of monoammine. Thus in the thermochemical cycle CBD for the ammines of $NiSO_4$, ΔH from C to B would be the heat of the reaction

$$NiSO_4 \cdot 7NH_3 \rightarrow NiSO_4 \cdot NH_{3\ (low\text{-}energy)} + 6NH_{3\ (aqueous)}$$

or $-267.2 + 6(-19.35) - (-408.2) = +24.9$ kcal, which is equivalent to the difference in heats of solution of the heptaammine (41.0 cal/g or 11.2 kcal/mole of heptaammine) and the monoammine (−79.9 cal/g or −13.7 kcal/mole of monoammine = $11.2 - (-13.7) = +24.9$ kcal. Similarly ΔH from C to D would be the heat of reaction for

$$NiSO_4 \cdot 7NH_3 \rightarrow NiSO_4 \cdot NH_{3\ (high\text{-}energy)} + 6NH_{3\ (aqueous)}$$

or $-247.8 + 6(-19.35) - (-408.2) = +44.3$ kcal, which seems to be a reasonable estimate of the total energy of the six metal—ligand bonds broken.

ΔH from C to B would be composed of a positive term for the energy of the six metal–ligand bonds broken and a negative term for the energy of rearrangement of the structure from the heptaammine lattice to the monoammine lattice. ΔH from B to D would be $193 - 79.9 = 113$ cal/g or 19.4 kcal/mole of monoammine. (This energy expressed as 31.0 kcal/mole of heptaammine is the ligand field splitting energy of 1.08×10^4 cm^{-1}.) Thus ΔH from C to D would be the sum of ΔH_{CB} and ΔH_{BD} or + the energy of the six metal—ligand bonds broken − the energy of rearrangement + 19.4 kcal. Since it seems likely that ΔH_{CD} is just the energy of the six metal–ligand bonds broken, the other terms appear to cancel each other so that the energy of rearrangement would probably be −19.4 kcal. Thus the energy of rearrangement seems to be entirely due to the presence or absence of the ligand field.

It now appears that loss of ligands without a corresponding structural rearrangement would give heats of solution along the line CD and with rearrangement the heats of solution would be along the line BC. The energy difference (measured as a difference in heats of solution) would be the ligand field splitting energy or some fraction of the ligand field splitting energy for fewer than six ligands.

For example, the loss of a single ligand from a heptaammine would involve both rupture of the bond holding the ammonia ligand to the metal and rearrangement to the lattice of the normal hexaammine, which is probably $[M(NH_3)_5]^{2+}SO_4^{2-} \cdot NH_3$. It now seems that if deammoniation is done in vacuo the bond is broken but rearrangement of the lattice does not occur and the heat of solution would fall along the maximum high-energy line CE. If rearrangement to the normal

[2]Heats of formation of the low- and high-energy forms of the monoammine have been estimated from data in ref. 12 and the present heat of solution data.

hexaammine occurred the splitting energy of the *d*-orbitals would decrease and the heat of solution would fall below CE on the minimum low-energy line BC for the normal ammines.

It has been assumed that the metallic ions M^{2+} in the monoammine lattice have no ligands and therefore no ligand field. If sulfato or other ligands formed complexes with these metal(II) ions, this would presumably occur to the same extent with both the high- and low-energy modifications, so that there would be no effect on energy differences such as DB.

In some senses plots of heat of solution in cal or kcal per mole of solute against mole fraction of ammonia (or moles of ammonia per mole of MSO_4) might seem to have greater fundamental significance than the present plots of heat of solution in cal/g of solute against percent ammonia. Unfortunately such plots would not show the lines AB, CE, FH, and IK as parallel. The plot of heat of solution in cal/g of solute vs. percent ammonia is useful not only to make these lines parallel but also to give a self-consistent set of data, e.g., each heat of solution could be multiplied by the molecular weight of the heptaammine to give appropriate values for the system containing one mole of metal(II) ion and one mole of sulfate ion.

It may seem contradictory that heats of formation and heats of solution for integral ammines were used in the thermochemical cycle CBD discussed above. However, the use of different molecular weights for the free salt and the various integral ammines gives different slopes for the lines AB, CE, FH, and IK, which might seem to imply that the bonds holding the ligands in the different lattices have different strengths, but that all ligands in a given normal lattice are held with equal strength. Such implications are absurd, since it is well established that the first few ligands are more readily removed than the last one or two. Consideration of the data in Figs. 1 and 2 (heats of solution at the percentages of ammonia in the various integral ammines) shows that the heats of reaction increase for the successive removal of ligands. Thus for a given mole of ligand removed (e.g., the third), the energy to break the metal–ligand bond would be the same, whether that ligand was originally one of three in the tetraamine, one of four in the pentaammine or one of six in the heptaammine.

Financial assistance from the National Research Council of Canada is gratefully acknowledged. The authors are also grateful to the Canadian International Development Agency for the award of a scholarship to one of us (B.M.).

1. J. W. S. JAMIESON, G. R. BROWN, D. W. GRUENER, R. V. PEILUCK, and R. A. LAMONTAGNE. Can. J. Chem. **43**, 2148 (1965).
2. J. W. MELLOR. A comprehensive treatise on inorganic and theoretical chemistry. Vol. XIV. Longmans, Green & Co., Inc., London. 1936. p. 463.
3. J. W. MELLOR. A comprehensive treatise on inorganic and theoretical chemistry. Vol. XV. Longmans, Green & Co., Inc., London. 1936. p. 770.
4. G. L. CLARK, A. J. QUICK, and W. O. HARKINS. J. Amer. Chem. Soc. **42**, 2483 (1920).
5. W. W. WENDLANDT and J. P. SMITH. J. Inorg. Nucl. Chem. **25**, 985 (1963).
6. A. WERNER. Z. Anorg. Chem. **21**, 199 (1899).
7. T. G. GEORGE and W. W. WENDLANDT. J. Inorg. Nucl. Chem. **25**, 395 (1963).
8. MICHELINE VILTANGE. Mikrochim. Ichnoanal. Acta, **4**, 609 (1965).
9. G. B. FROST, K. A. MOON, and E. H. TOMPKINS. Can. J. Chem. **29**, 604 (1951).
10. L. E. ORGEL. An introduction to transition-metal chemistry: ligand field theory. Methuen, London. 1960. p. 46.
11. C. K. JØRGENSEN. Acta. Chem. Scand. **10**, 887 (1956).
12. FREDERICK D. ROSSINI, DONALD D. WAGMAN, WILLIAM H. EVANS, SAMUEL LEVINE, and IRVING JAFFE. Nat. Bur. Stand. (U.S.) Circ. No. 500. 1952.

Can. J. Chem. Downloaded from www.nrcresearchpress.com by 210.87.254.40 on 09/05/12
For personal use only.

Photoconductivity of γ-irradiated methyltetrahydrofuran glass at 77 °K[1]

K. F. BAVERSTOCK[2] AND P. J. DYNE

Materials Science Branch, Whiteshell Nuclear Research Establishment, Atomic Energy of Canada Limited, Pinawa, Manitoba

Received December 10, 1969

γ-Irradiated glasses of methyltetrahydrofuran at 77 °K exhibit photoconductivity on illumination with visible light. A variety of kinetic effects are observed as the wavelength of the exciting light is changed from blue to the near infrared. It is suggested that, due to the coulombic field of the positive ions in the glass, some electrons can be released by red light while others can be released only by blue light. A thermally unstable red sensitive center can also be formed in the glass during illumination with blue light. This unstable center could be a dielectron.

Canadian Journal of Chemistry, 48, 2182 (1970)

Can. J. Chem. Downloaded from www.nrcresearchpress.com by 210.87.254.40 on 09/05/12
For personal use only.

The processes of solvation and trapping of electrons produced by high energy radiation in condensed media are of considerable current interest. While the existence of solvated electrons in liquids and trapped electrons in organic glasses are well established, the nature of the trapping sites and the mechanism of trapping are not at all well understood.

In a study of the kinetics of bleaching of electrons trapped in γ-ray irradiated 2-methyltetrahydrofuran (MTHF) at 77 °K, Dyne and Miller (1) concluded that electrons could travel distances of 1000 Å or more before being recaptured by positive ions. Other estimates of the ranges gave similar values (2). In these samples positive ions are present at separations of 200 Å or less and it was evident that the range of electron movement was considerably greater than the interionic separation and that coulombic attraction was not an overwhelming driving force for recombination.

If electrons travel such distances in glasses after being released from their traps by the absorption of light, then γ-irradiated organic glasses should also show photoconductivity. This paper describes some exploratory work on the photoconductivity of γ-irradiated MTHF which provides more information on the complexity of the trapping centers in organic glasses and evidence for a dielectron.

It is hoped that photoconductivity measurements will eventually provide a direct measure of the distances thermal electrons can move in a condensed medium. However, a conductivity measurement alone measures the product: No. of moving electrons × distance moved; the distance itself is indeterminate.

In this paper we describe qualitatively the effects of the wavelength of the exciting light on the time dependence of the photocurrents. A quantitative interpretation of currents obtained with different wavelengths of exciting light is, however, difficult since the variations of quantum efficiency of releasing electrons from traps with the wavelength of exciting light is unknown, but is likely to be large. Such problems can only be resolved by measurements of electron mobility (via, for instance, the Hall effect). The qualitative studies described here are an essential prelude to such more detailed studies.

Photoconductivity in closely related systems has been studied in some detail by Albrecht and his collaborators (3–5) and by Willard and his collaborators (6, 7). Albrecht studied glassy solutions of N-N-N′-N′-tetramethylparaphenylenediamine (TMPD) in 3-methylpentane (3-MP). This solute readily photoionizes and the resulting electrons are trapped in the solvent much as they would be after γ-irradiation of pure 3-MP. Wiseall and Willard (6) and Ling and Willard (7) have been principally interested in the electrical conductivity which appears on warming the sample from 77 °K and have briefly studied the photoconductivity in 3-methylpentane. The results in these systems are in many ways closely similar to those reported here on MTHF and detailed comparisons are made in the bulk of this paper. Willard (8) has recently reviewed the work in this and related areas.

Experimental

The Conductivity Cell

The design of the conductivity cell follows that described by Johnson and Albrecht (4) and is shown in

---

[1]AECL No. 3613.

[2]NRCC Postdoctoral Fellow, 1967–1969. Present address: Department of Chemistry, University of Nottingham, Nottingham, England.

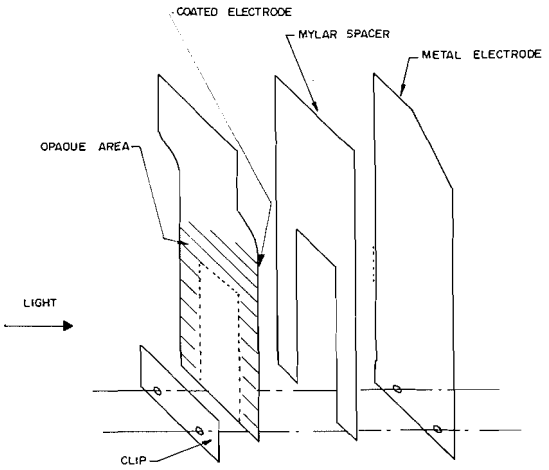

FIG. 1. Exploded schematic view of the photoconductivity cell. The left hand electrode is a microscope slide coated with stannic oxide. The mylar spacer is 0.05 mm thick and liquid MTHF is drawn up into the cut-out portion by capillary attraction.

Fig. 1. The metal electrode was of polished copper. No experimental differences were observed when glass electrodes with surface coatings of various vapor deposited metals were used in its place. The mylar spacer was typically 0.05 mm thick.

The semi-transparent glass electrode was made from a microscope slide which was coated on one side with conducting stannic oxide. Other vapor plated electrodes, gold and platinum, were also used for the transparent electrode but no experimental differences were observed. The resistance of the tin oxide coated electrodes varied from one preparation to another but was typically of the order 50 kohm/cm (point to point). The non-conducting side of the electrode was masked with liquid bright gold to prevent light reaching the mylar film. About 1 cm^2 of the sample was illuminated.

A clip held the assembly in place, and connections were made to the electrodes by spring clips. The electrode assembly was contained in a Pyrex vessel. This outer vessel was coated with liquid bright gold except for a window allowing the illumination of the electrodes; the gold coating was grounded to reduce electrical noise. To prepare a sample the completed cell was attached to a vacuum line and evacuated through a side arm. A small amount of MTHF was then distilled into the cell under vacuum and the sample degassed by freeze–thaw techniques. MTHF was drawn up between the electrodes by capillary attraction. When frozen the cell was filled with dry gas (helium) and removed from the vacuum line in a Dewar. The whole cell was then filled with liquid nitrogen which thus surrounded the electrode assembly. Irradiations were made with ^{60}Co γ-rays at a dose rate of 2×10^{18} eV g^{-1} min^{-1}. For most of the data reported here the dose was 10^{19} eV/g. On completion of the irradiation the cell was transferred to a Dewar having a clear, non-silvered strip. New samples were prepared for each of the experiments reported here. In some preliminary studies samples were re-irradiated after bleaching or after thawing and refreezing. No major effects were observed.

High voltage (negative with respect to ground) was supplied to the metal electrode by a Keithley HV supply. For most experiments a potential of 500 V was used, giving a potential gradient of $\sim 10^4$ V/cm. Signals were amplified by a Keithley Electrometer 610 and the output was displayed either on a Hewlett–Packard Recorder or Tektronix Storage Oscilloscope.

The Optical System

A variety of light sources, filters, or monochromators were used for illuminating the sample after irradiation. Blue illumination at 404 and 436 nm was provided by a 100 W Hg arc source (Oriel Optics) which was filtered with heat absorbing filters and an interference filter transmitting between 380 and 500 nm. Red and infrared light was obtained from a 150 W quartz iodine lamp with a 1 cm filter of 8% H_2O in MTHF which cuts off at wavelengths > 1200 nm, and either an Ealing Special Infrared Pass Filter, or a combination of Corning Filters Nos. 2030 and 2550.

For simultaneous illumination with two wavelengths of light, the two light beams, initially at right angles were combined with a partially aluminized front surface mirror set at 45° to each beam.

Where a greater degree of resolution in wavelength of illumination was required, a Jarrel Ash f.3.5 grating monochromator was used with the quartz iodine lamp. Light intensities were compared with an Eppley Thermopile: the highest intensities were ~ 2 mW/cm^2 over the 1 cm^2 illuminated area for infrared light. For blue light these were $\sim 10^{-2}$ mW/cm^2. The samples are thin so that the optical density (~ 0.02 at 1200 nm) is sufficiently small that the sample is being essentially uniformly illuminated across its thickness.

Materials

2-Methyltetrahydrofuran was supplied by Eastman Organic Chemicals. Sodium wire was placed in the bottle a few days prior to use. The decanted ether was then distilled from the sodium at atmospheric pressure and stored in a vacuum line. Before use the ether was distilled several times over a sodium mirror. Final drying was carried out over a sodium mirror and in the presence of a small amount of naphthalene. The distillate used in the experiments was shown to be naphthalene free.

Results

1. Volt–Ampere and Dose Characteristics

In preliminary experiments we confirmed that for the red light and blue light, for fields between 2 and 80 kV/cm the initial currents were proportional to applied voltage and that the currents or total charge removed were approximately proportional to dose over the range 5×10^{17} to 4×10^{19} eV/g. Some dose effects were observed, the charge extracted being less than proportional to dose at higher doses. The total charge extracted during illumination with red light is in the order of 1% of the total charge stored in the sample after

Can. J. Chem. Downloaded from www.nrcresearchpress.com by 210.87.254.40 on 09/05/12
For personal use only.

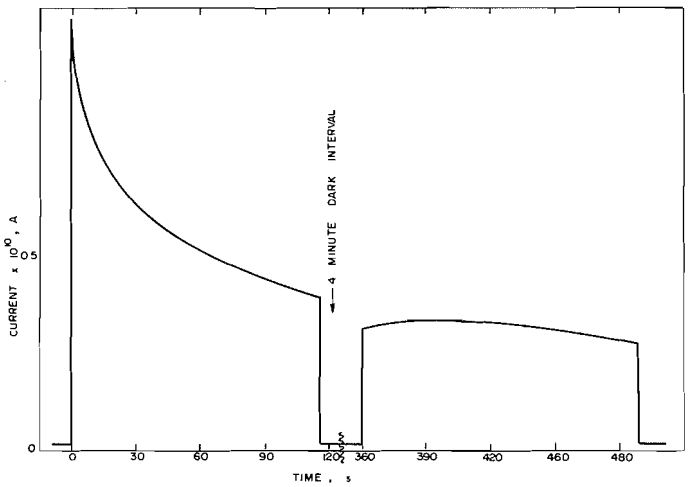

FIG. 2. Current spike obtained on illumination with "red" light. Interruption of the light produces a small thermal decay. Details of the experimental conditions for this and other figures are in the text.

γ-irradiation. This collected charge is equivalent to a movement of the total stored charge through a distance ~ 50 Å. These data do not, however, give any quantitative data on electron ranges in the matrix since all that can be measured without a knowledge of the electron mobility is the product: No. of charges moving × average distance moved. We can conclude only that some electrons can move distances which are significantly larger than the average separation of positive ions at the doses used (50 to 200 Å). The initial currents were proportional to light intensity from the maximum available, to intensities ~ 1/50 of the maximum.

A number of blank experiments, similar to those described by Albrecht, were carried out to show that the observed currents are due to electron transport in the glass, the most significant being that photocurrents were observed only after γ-irradiation. Experiments with blocking electrodes are not feasible since γ-irradiation at 77 °K will almost certainly produce bleachable color centers in any material chosen for blocking electrodes. A suprasil sample gave large photocurrents. Previous workers (3–7) have demonstrated the significance of these photoconductivity techniques.

2. Illumination by Red Light and Infrared Light

Illumination with infrared light (900–1200 nm) or red light (600–800 nm) gave a current spike of the type shown in Fig. 2. The initial rise is fast and essentially instantaneous relative to the time constant of our measuring circuit (~ 10^{-3} s). At the doses used in these experiments, trapped electrons are thermally stable; no significant decay being observable for 3 to 5 h after irradiation. The thermal instability observed by Smith and Pieroni (9) occurs at doses ten times greater than used here and over periods of 10 to 100 h. Because of this short term thermal stability the initial currents are independent of the time between irradiation and illumination when these are of the order of 1 to 2 h. If the light is turned off the current falls instantaneously to its initial value. When the light is turned on again the current does not go back to the value observed when the light was turned off. This difference increases as the dark interval increases. The figure shows an extreme case for a 4 min dark interval. On a simple model the photocurrent at any time will be proportional to the concentration of trapped electrons. However, a rough comparison of the initial rate of decay of the photocurrent with the initial rate of bleaching by light of the same wavelength shows that the current is decaying at a considerably faster rate (as much as a factor of ten) than the concentration of trapped electrons measured spectrophotometrically. Qualitatively similar results are obtained with light in the wavelength range 600–550 nm. With the shorter wavelength the rate of decay of the photocurrent and of the bleaching are more nearly comparable. Accurate comparison of the concentration of trapped electrons and the photocurrent would be of considerable interest but such measurements unfortunately present some formidable technical difficulties.

Can. J. Chem. Downloaded from www.nrcresearchpress.com by 210.87.254.40 on 09/05/12
For personal use only.

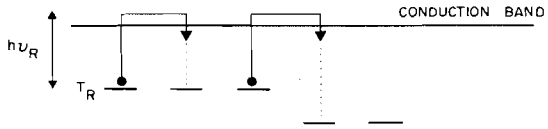

FIG. 3. Red light, quanta $h\nu_R$, releases trapped electrons from shallow traps, T_R, to the conduction band. They may diffuse through the sample being retrapped at other sites, T_R, or may be trapped at deeper sites.

A formal interpretation of the red current spike is given in Fig. 3. Electron traps of varying depth are present. Electrons can be released from shallow centers, T_R, by red light. If they are trapped at the deeper centers they cannot contribute further to the red photocurrent. These deep traps would include positive ions. If positive ions were the only deep traps then the rate of decay of the photocurrent and the rate of bleaching would be proportional to one another. The observation that the rate of decay of photocurrent is greater than the rate of bleaching shows, however, that positive ions cannot be the only deep traps for the process envisaged in Fig. 3. Figure 3 does not provide a rationalization for the apparent thermal decay seen on interruption of the illumination. This is discussed later.

3. Illumination by Blue Light

With "blue" light, the broadened lines from a high pressure mercury arc between 400 and 500 nm, a different current profile is observed (Fig. 4). There is an initial sharp rise, instantaneous in the terms defined in the previous section, followed by a slow rise to a maximum and by a much slower decay. The time taken to reach the maximum varies with several parameters. Figure 4*A* is for a sample which had only been γ-irradiated; Fig. 4*B* is for a similar sample which had previously been illuminated with red light and the red current had decreased to about one tenth its initial value. With prior red illumination the slow rise to a maximum is considerably prolonged. Figure 5 shows the effect of dose on the blue profiles. At low doses the slow rise is hardly apparent.

The distinction between "red" and "blue" current profiles is not simply a matter of the illuminating wavelength. Illumination of the sample at one wavelength can affect the current profile at another wavelength. This is seen in the current profiles shown in Fig. 6. The sample was first illuminated with infrared light of wavelength > 800 nm. Subsequent illumination with red

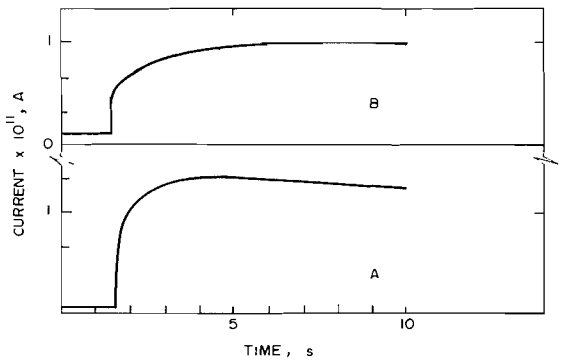

FIG. 4. Current profiles obtained on illumination with blue light. *A*, immediately after γ-irradiation; *B*, after prior red illumination such that the red spike had decayed to about 1/10 its initial value.

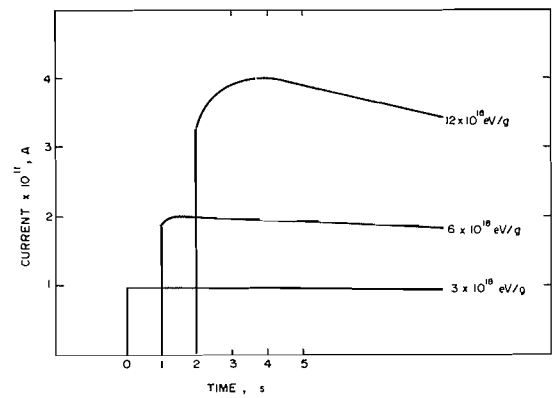

FIG. 5. Blue current profile as a function of γ-ray dose. For clarity the curves are separated along the time axis. The dose rate is 2×10^{18} eV/g min.

light 600–800 nm gave the current profile *A*. The sample was then illuminated with blue light, giving a typical blue current profile *B*. Re-illumination with red light then produced a current profile *C* which is clearly distinct from that originally obtained at *A*.

The photocurrent produced by infrared light decays with illumination. The sensitivity to infrared light can, however, be restored by illumination with blue light as shown in Fig. 7. If there had been no intermediate blue illumination we would have obtained a current profile similar to those shown in Fig. 2. We shall call currents produced under these conditions "induced" red currents.

These induced red currents differ from the red currents described in Fig. 2 in that they are thermally unstable. As already noted, the trapped

Can. J. Chem. Downloaded from www.nrcresearchpress.com by 210.87.254.40 on 09/05/12
For personal use only.

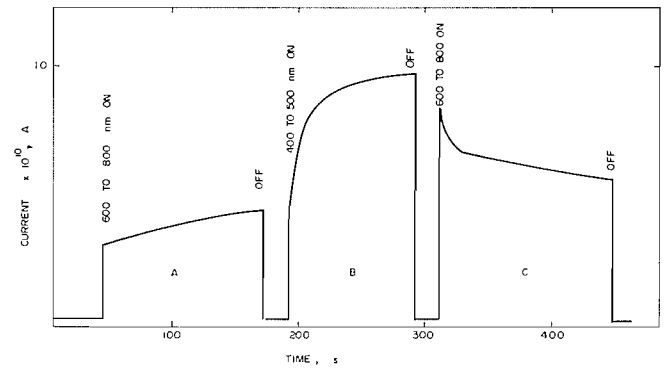

FIG. 6. Effect of illumination on current profiles. The sample is illuminated with infrared light > 800 nm. Illumination with red light, 600–800 nm then gives the profile *A*. After illumination with blue light *B*, the spike profile *C* is observed with red light.

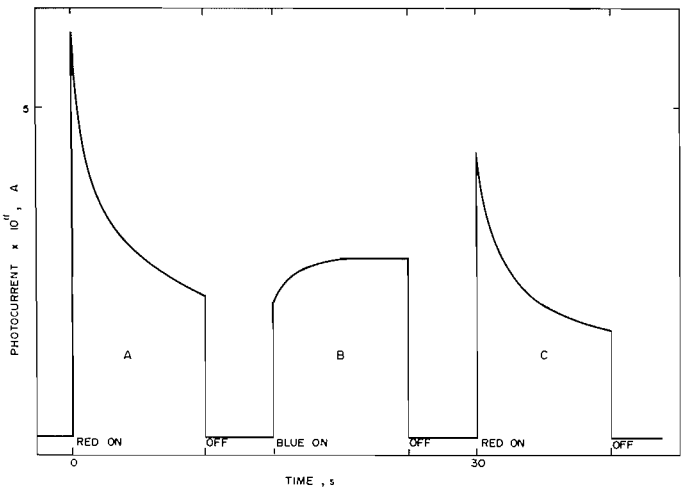

FIG. 7. After illuminating with red light, *A*, blue illumination *B*, induces sensitivity to infrared light and regenerates a spike current *C*.

electron normally observed in MTHF is thermally stable: the optical and electron spin resonance, (e.s.r.) spectra remain unchanged for periods of up to several hours after γ-irradiation. This is also true of the initial red photocurrents and blue photocurrents. The induced infrared current, however, decays quite rapidly with time, independent of any illumination. This is demonstrated by varying the dark period between blue illumination and red illumination. The initial current spike is plotted against dark time in Fig. 8 and shows a half life of the order of 2 min. Induced red currents are only observed after the sample has been bleached with red light. No significant increase in the red current is observed if, after irradiation, the sample is simply illuminated by

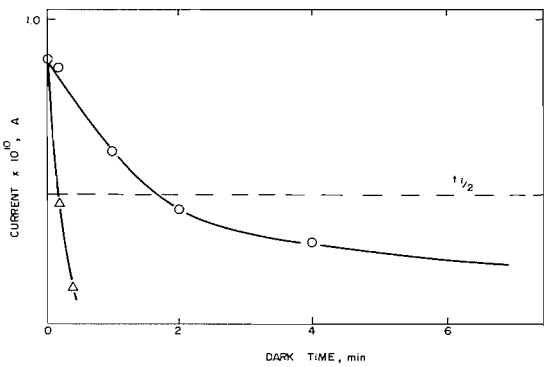

FIG. 8. ○, initial current of regenerated spike *C* (Fig. 7) as a function of dark time after cessation of blue illumination; △, decay of current spike with infrared illumination on the same timescale.

Can. J. Chem. Downloaded from www.nrcresearchpress.com by 210.87.254.40 on 09/05/12
For personal use only.

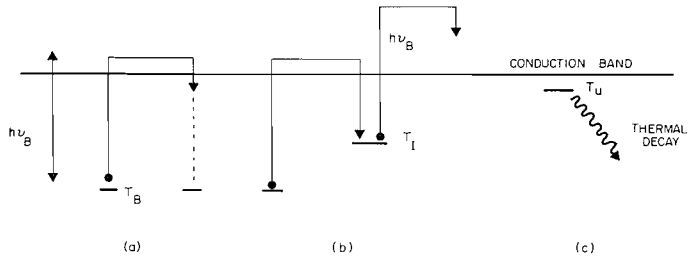

FIG. 9. (*a*), Blue light, quanta $h\nu_B$, releases electrons from traps T_B; (*b*), blue light populates intermediate traps T_I, electrons can also be released from these traps by blue light; (*c*), the shallow thermally unstable center T_u required by the observation of induced currents.

blue light; the current observed on subsequent red illumination is that which would have been observed without blue illumination.

The blue current profile is very similar to that observed for alkali halides at elevated temperatures (125–235 °C) (10, 11). In alkali halides this profile is explained by supposing that electrons are promoted by blue light to the centers just below the conduction band and are released to the conduction band by purely thermal processes. For the MTHF system, however, the effects described above, where the shape of the profile is affected by dose and by prior illumination with red light, are more readily understood by the scheme shown in Fig. 9. The fast current rise is produced by the release of electrons from traps as shown in (Fig. 9*a*) in the left hand side of the diagram and may be retrapped again in blue traps T_B or intermediate traps T_I. Blue light can of course also release electrons from the shallower traps T_I (Fig. 9*b*). Following blue illumination we can expect an increase in the number of electrons in the shallower traps. If we make the reasonable assumption that blue light is more efficient in promoting electrons to the conduction bands from T_I than from T_B traps then the photocurrent will increase with time, as observed. The induced infrared currents require us to postulate a shallow unstable center T_u (Fig. 9*c*).

This model would lead us to expect that these current profiles would also be affected by light intensity. With the small ranges of intensity available to give a conveniently measured current this is true. With red light a decrease in the light intensity flattens the spike. Similar effects have been observed for alkali halides (see Fig. 7.5 in ref. 10). With blue light an increase in intensity tends to shorten the time of the slow rise; with high light intensities an apparent spike profile might be formed but this has not been observed.

The existence of an intermediate trapping level can be seen in another experiment. The induced red spike current can be reformed several times by blue illumination. The size of the induced spike is roughly comparable on each illumination although it does, of course, diminish slowly as the electrons move progressively to deeper trapping sites on prolonged blue illumination. If, then, after the sequence shown in Fig. 7 we illuminate simultaneously with blue and red light a current profile of the type shown in Fig. 10 is seen, where a red current spike is superimposed on the blue current. With simultaneous illumination, however, the red spike decays much more slowly than it does in the absence of blue light. This is shown by the dotted line in the figure. This is to be expected from the scheme shown in Fig. 9 since, with simultaneous illumination, the levels which are being depleted by red light are being simultaneously replenished by blue illumination and a larger current will be obtained than with red illumination alone.

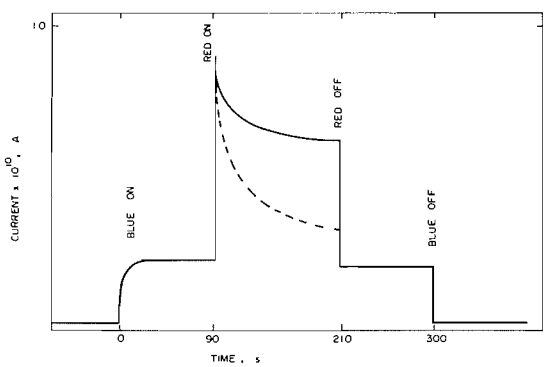

FIG. 10. Current profile during simultaneous red and blue illumination. Dotted line shows the red profile (as in *C*, Fig. 7) which would have been attained without blue light.

Can. J. Chem. Downloaded from www.nrcresearchpress.com by 210.87.254.40 on 09/05/12
For personal use only.

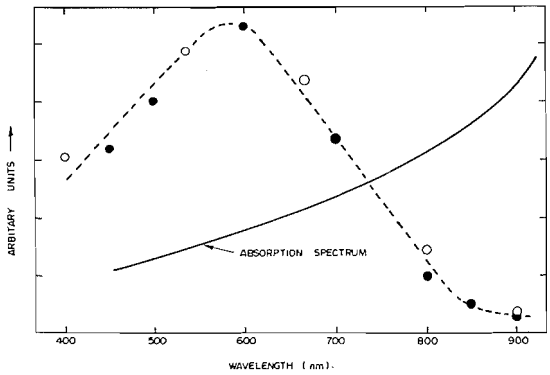

FIG. 11. ○, quantum efficiency of bleaching; ●, initial photocurrent/quanta absorbed. For comparison these have been normalized at 600 nm. The precise values are given in the text. The short wavelength side of the absorption due to the trapped electron is shown by the solid line.

Discussion

The data we have presented can conveniently be discussed in two parts: first, the current profiles produced by red and blue light, second the induced currents excited by infrared light and resulting effects. We suggest that the gross effects of wavelength on the current profiles can be understood on the basis of arguments advanced previously by Albrecht which consider the effect of local coulomb potentials on the trapped electron. We discuss several special configurations of trapped electrons in MTHF glasses to account for the induced currents and their thermal instability.

(a) Electron Traps and Local Coulomb Potentials

Following the discussion in ref. 1 and the theoretical model for the electron in ammonia

FOR ERRATA SEE
V.49#7.1971 p.1149

The initial quantum efficiency at 500 nm was reported as 0.1 ± 25%. The photoconductivity data are for initial (fast) currents per quantum absorbed. Light intensities were obtained from thermopile measurements; absorption data were from the measured absorption spectra. For a sample irradiated to 10^{19} eV/g and illuminated at 500 nm the observed currents are $\sim 3.6 \times 10^{-4}$ A/quantum absorbed with 500 V across the cell. This figure takes no account of reflectance losses at the interfaces in the cell and may be perhaps 20% low because of this. As with the quantum efficiency it would be unwise to assume that uncertainties in this value of A/quantum absorbed are less than 25%. The data differ from those reported earlier (1) in that, from 500 to 400 nm, the bleaching efficiency decreases on going to shorter wavelengths. While we have no explanation for this experimental discrepancy, careful checking leads us to conclude that the present data are reliable. The action spectra for photoconductivity show a similar maximum and we conclude that the bleaching process and the photoconductivity are closely related, the primary light absorption step being the same for both processes.

The effect of the local coulomb potentials on such properties as photoionization and photoconductivity have been discussed by Cadogan and Albrecht (13). In Albrecht's experiments electrons are produced by the photoionization of TMPD and are then trapped in the matrix. The photoionization of TMPD is equivalent to γ-irradiation in our experiments. Current profiles in the red and blue are then observed which are qualitatively identical to those observed by ourselves in MTHF: a small induced red current is observed but its thermal stability is not discussed. The explanations advanced for these current profiles are formally identical to those we have proposed in Figs. 3 and 9.

Albrecht (5, 13) discusses the effect that the coulomb field of a neighboring positive ion can have on the properties of a trapped electron. In MTHF, electrons are released from these traps by light quanta of 1.4 eV or more. They may reach the positive ions and recombine or may be retrapped. Electrons released from traps will, however, contribute to photoconductivity only if they diffuse with the applied field. Close to the positive ion the local coulomb fields are considerably greater than the applied field, so that

Can. J. Chem. Downloaded from www.nrcresearchpress.com by 210.87.254.40 on 09/05/12
For personal use only.

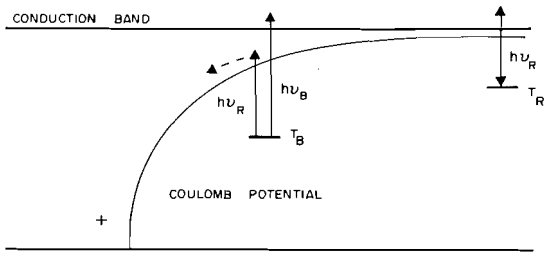

FIG. 12. Red light ionizes electron from trap T_R but mobilizes electrons from trap T_B. Blue light can ionize electrons from both traps.

the average direction of motion of electrons affected by the coulomb field is random. These electrons will not, as a consequence, contribute to a photocurrent. Following Albrecht, we distinguish between electrons which are "ionized", free to move in the conduction band with the applied field, and those which are mobilized, moving only in the coulomb field of the positive ion.

This situation is shown diagrammatically in Fig. 12. Red light, quanta $h\nu_R$, promotes electrons in traps T_R to the conduction band but not from traps T_B where the electrons are only mobilized. Larger quanta, $h\nu_B$, could, however, promote electrons from traps T_B into the conduction band.

In Fig. 13, which now combines Figs. 3 and 7 with the idea summarized in Fig. 12, we see at *A* the levels of the unperturbed electron trap. In the presence of a coulomb field the level of the unperturbed electron trap is, for conductivity experiments, depressed and a continuum of allowed states is formed (*B*). After γ-irradiation, electrons will be found at levels from 1.4 eV below the conduction band to 3.0 eV or more below the conduction band. The simple electrostatic calculation shows that electrons 65 Å from a positive ion have their potential energy reduced by ~ 1.5 eV from electrons an infinite distance away. There is no reason for the absorption spectrum of the electron to be markedly perturbed. All these electron traps are still 1.4 eV below the energy required for mobilization.

We have therefore identified the red, blue, and intermediate traps, T_R, T_B, and T_I, in Figs. 3 and 7 which describe our experimental data in phenomenological terms with traps situated at varying distances from positive ions. T_R, T_B, and T_I are shown at *D* in Fig. 13. With red light, electrons are either retrapped in traps of the same depth where they can continue to contribute with equal

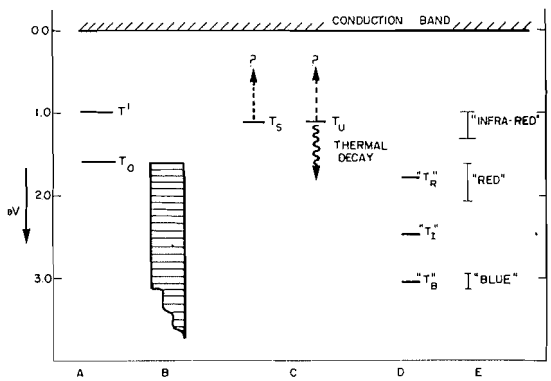

FIG. 13. Summary of trapping sites in MTHF. At *A*, T_0 is the unperturbed electron trap, T′ is its bound excited state. At *B* the levels T_0 are spread into a continuum by the coulomb potential of the positive ions. At *C*, *D*, the shallow infrared sensitive traps T_S and T_u are shown. The traps T_R, T_I, and T_B from Figs. 3 and 9 are shown at *D* and the energies and band widths of the exciting light used are shown at *E*.

efficiency to the photoconductivity on absorption of light or are trapped more deeply where they can at most only be mobilized. With blue light, however, they may be retrapped in shallower traps. With the assumption that blue light is more efficient in promoting electrons to the conduction band from the shallower, intermediate traps, the "blue profile", a slow increase in current after the initial spike, would be observed. From our observation that illumination with blue light only leads to a small increase in the subsequent red current (not the induced infrared spike), we can conclude that during blue illumination most electrons are retrapped in intermediate traps and not in the shallow red sensitive traps.

(b) Infrared and Thermally Unstable Traps

The limited but significant amount of bleaching observed with quanta of less than the ionization energy of 1.4 eV (ref. 1) and the photocurrent with the same excitation require us to postulate a stable infrared sensitive trap T_S. We suggest below that this could be due to a configuration we call the "electron pair". In addition there is the thermally unstable center, responsible for the induced currents which we will designate T_u. This could be an electron associated with the tight dipolar center suggested by Albrecht, or a dielectron.

(c) The Electron Pair

Cadogan and Albrecht (13) have argued that

Can. J. Chem. Downloaded from www.nrcresearchpress.com by 210.87.254.40 on 09/05/12
For personal use only.

Can. J. Chem. Downloaded from www.nrcresearchpress.com by 210.87.254.40 on 09/05/12
For personal use only.

electrons trapped very close to the positive ion would be thermally unstable. When the coulomb gradient is large it provides a major perturbation of the potential holding the electron in its trap. Such electrons could not, however, be responsible for the thermally unstable red currents because, from the arguments given in Section (*a*), while they would be mobilized by red light, they would be "ionized" only by much more energetic quanta. To explain, a small amount of bleaching of electrons observed out to wavelengths of 1600 nm (Fig. 5 of ref. 1), Dyne and Miller suggested that a few electrons were trapped so close to the positive ion that even in the bound excited state they had a finite probability of escape and of being captured by the positive ion. This is another version of the argument given by Albrecht. Since, however, such electrons would not contribute to a red stimulated photoconductivity, another type of trapping environment has to be postulated.

Just as trapped electrons are affected by the attractive field of positive ions, they will also be affected by the repulsive coulomb field of other trapped electrons. We suggest that, in the proximity of another electron, the bound excited state of a trapped electron is predissociated. Absorption of light > 800 nm can then lead to ionization. We suggest that electron pairs are the T_S sites responsible for the bleaching observed at longer wavelengths and for photoconductivity in this wavelength region.

(d) The T_u Site: Dipolar Centers and Dielectrons

With the electron pair we are postulating that the perturbations of coulombic repulsion are sufficient to change the photobleaching properties of the two electrons. This perturbation is, of course, a function of the distance between the electrons. As this distance decreases we can anticipate that the perturbation becomes so large that the center is thermally unstable. At the same time, of course, coulombic repulsion makes the trapping of the second electron less likely and any discussion of the "tight" electron pair must meet this objection. One possibility is via the tight dipolar center postulated by Cadogan and Albrecht, the other is by postulating the stability of the dielectron e_{tr}^{2-}, two electrons in one cavity, whose stability has recently been discussed by Fueki (14).

To explain certain aspects of the photoconductivity of glasses containing TMPD as a solute, Cadogan and Albrecht have postulated a "charge transfer" state. In effect this is an electron trapped close to a positive ion: the combination of the two centers being, for some purposes, equivalent to an excited singlet state of the molecule from which the positive ion was derived. A second electron, trapped close to the center might indeed have the red sensitivity and thermal instability of the T_u center.[3]

(e) The Dielectron

A prima facie case can be made that the T_u center is the dielectron. There are striking similarities between the properties of electrons trapped in polar glasses and between electrons trapped as F-centers in alkali halides where the dielectron, $(e^{2-})_{tr}$ or, F′-center as it is called for the alkali halide systems, is well established.

Quantitative correlations between the properties of electrons in organic glasses and alkali halides have been made by Blandamer *et al.* (15). Photoconductivity due to the detrapping of bound electrons has an action spectrum with a maximum to the short wavelength side of the F-center absorption closely analogous to the data shown in Fig. 11 (16). An induced red stimulated conductivity on illumination with blue light was described by Glaser and Lehfeldt (11). This work is reproduced in detail by Markham (10). The current profiles observed in these studies are strikingly similar to those shown in Fig. 7. This induced red photoconductivity is attributed to the formation of the dielectron or F′-center.

Fueki (14) has recently discussed the stability of the dielectron in glassy media. If the static and optical dielectric constants for the media are such that $D_S > D_{op}/(D_{op} - 1)$ then the dielectron may be stable. We have measured D_S at liquid N_2 temperatures to be 2.88. This criterion requires $D_{op} > 1.53$ and hence the refractive index to be greater than 1.25. Since the refractive index of MTHF at room temperature is 1.43, the refractive index at 77 °K should be significantly greater than this due to the increase in density. Accordingly we can anticipate a measure of stability for the dielectron in glassy MTHF. Kevan and co-workers (17, 18) have optical evidence for the formation of the dielectron in alkaline ices.

[3]We are indebted to Professor Albrecht who pointed out to us the possible relevance of the "charge transfer" state to our observations.

Can. J. Chem. Downloaded from www.nrcresearchpress.com by 210.87.254.40 on 09/05/12
For personal use only.

(f) Infrared and Induced Currents

Immediately after γ-irradiation a sample contains electrons trapped at varying distances from the positive ion, some electrons at T_s sites (electron pairs) and some at T_u sites (dielectrons?).

The electrons in T_u sites decay thermally and their absorption spectrum, which, if they are dielectrons, probably lies to the red of that of single trapped electrons, would be observed only by special techniques. Since the thermal half life is about 2 min, this absorption would not be easily observed in a recording spectrophotometer if the time between irradiation and observation was 2 min or more and might then only appear as a small shoulder on the long wavelength side of the strong absorption of the single electron.

Electron pairs can be ionized by light of wavelength > 800 nm giving a photocurrent and limited amount of bleaching. Some of these electrons, ionized by red or infrared light, may be retrapped as dielectrons. Dielectrons are, however, readily dissociated by infrared light and the steady state concentration of dielectrons will be low. A change in photoconductivity would be observed after a dark period due to the thermal decay of this low steady state concentration of dielectrons; the current would not regain the value it had at the instant the light was cut off. This explains the change in current level after a dark period shown in Fig. 2. The slow buildup on the second illumination occurs as a concentration of dielectrons grows in.

This model would suggest in principle that, even on initial red illumination a slow buildup might be observed rather than the sharp spike which is in fact observed. The observed profile is, however, the resultant of currents which are decaying with time and those which increase. It appears that the initial distribution of electrons and their sensitivity to red light is such that the decaying process always predominates for initial red illumination.

Induced currents are more readily seen if the thermally stable component is bleached out, a state which is produced by the sequence *B* shown in Fig. 7. The observation that large induced currents are only observed after prior red illumination requires a further hypothesis. We suggest that the T_u sites (dielectron) are in some sense unique, a special configuration of solvent molecules (say) being required. These could be the sites of some of the electron pairs which, as we have suggested, are also sensitive to longer wavelength light. High concentrations of sites for the formation of T_u are only available after the T_s sites have been bleached out.

One could expect that the formation of electrons in the different situations we have postulated would be shown up in varying shapes of the absorption band following various sequences of illumination. We have already (1) shown that the absorption is relatively weaker at the short wavelength side of the band after bleaching with blue light. The recent work of Sawai and Hamill (19) shows that partial thermal annealing leads to a weaker absorption on the long wavelength side of the band. It is tempting to ascribe this latter change to the preferential destruction of electron pairs which, like the dielectron, may have strong absorptions in the near infrared. Further study of changes in the infrared spectrum of γ-irradiated MTHF could provide confirmation of some of the suggestions advanced in this paper.

1. P. J. Dyne and O. A. Miller. Can. J. Chem. **43**, 2696 (1965).
2. P. J. Dyne and J. Denhartog. Can. J. Chem. **44**, 461 (1966).
3. G. E. Johnson and A. C. Albrecht. J. Chem. Phys. **44**, 3162 (1966).
4. G. E. Johnson and A. C. Albrecht. J. Chem. Phys. **44**, 2179 (1966).
5. K. D. Cadogan and A. C. Albrecht. J. Phys. Chem. **72**, 929 (1968).
6. B. Wiseall and J. E. Willard. J. Chem. Phys. **46**, 4387 (1967).
7. A. C. Ling and J. Willard. J. Phys. Chem. **73**, 2048 (1969).
8. J. E. Willard. Fundamental processes in radiation chemistry. Ed. P. Ausloos. Publ. John Wiley Inc., New York. 1968. p. 519.
9. D. R. Smith and J. J. Pieroni. Can. J. Chem. **43**, 876 (1965).
10. J. J. Markham. F-centers in alkali halides. Solid state physics supplement 8. Academic Press, Inc., New York. 1966. p. 65 ff.
11. G. Glaser and W. Lehfeldt. Gottinger Nachr. **2**, 91 (1936).
12. J. Jortner. J. Chem. Phys. **30**, 839 (1959).
13. K. D. Cadogan and A. C. Albrecht. J. Chem. Phys. **51**, 2710 (1969).
14. Kenji Fueki. J. Chem. Phys. **50**, 5681 (1969).
15. M. J. Blandamer, R. Catteral, L. Shields, and M. C. R. Symons. J. Chem. Soc. London. 4337 (1966).
16. G. Spinolo and D. Y. Smith. Phys. Rev. **140**, A2117.
17. J. Zimbrick and L. Kevan. J. Amer. Chem. Soc. **89**, 2483 (1967).
18. L. Kevan, D. R. Renneke, and R. J. Friauf. Solid State Commun. **6**, 469 (1968).
19. T. Sawai and W. H. Hamill. J. Phys. Chem. **73**, 3452 (1969).

Can. J. Chem. Downloaded from www.nrcresearchpress.com by 210.87.254.42 on 09/05/12
For personal use only.

Infrared spectra of some alkyl platinum compounds. Part I. Comparison with the spectra of chemisorbed hydrocarbons

B. A. MORROW
Department of Chemistry, University of Ottawa, Ottawa 2, Canada

Received March 24, 1970

A series of triphenylphosphine stabilized platinum dialkyl compounds of the type $(Ph_2P)_3PtR_2$ where R = methyl, ethyl, ethyl-d_3, *n*-propyl, *n*-butyl, and *n*-hexyl have been synthesized and their infrared spectra in the CH stretching region have been obtained. These spectra are discussed in terms of the infrared spectra of hydrocarbons which are chemisorbed on transition metal catalysts.

Canadian Journal of Chemistry, 48, 2192 (1970)

Infrared spectroscopy has been widely used to study the species produced during the chemisorption of hydrocarbons on silica-supported transition metal catalysts (1–5). The interpretation of such spectra has been based mainly on examination of the bands in the C—H stretching region (νCH) between 3300 and 2700 cm^{-1} because the silica support absorbs strongly between 2000 and 1300 cm^{-1} and absorbs totally below 1300 cm^{-1}.

Implicit in the interpretation of such spectra has been the assumption that the infrared spectrum of a hydrocarbon attached to a surface transition metal atom will resemble the spectrum of a pure hydrocarbon (1–3). On this basis, comparisons of the spectra of chemisorbed hydrocarbons with those of pure hydrocarbons have been used to deduce the nature of the surface species present. However, such an interpretive procedure is subject to the criticism that the functional group of a hydrocarbon which is attached to a surface metal atom might not absorb at the same frequency as its pure hydrocarbon counterpart (2, 3).

A major difficulty in interpreting the infrared spectra of chemisorbed hydrocarbons has been the lack of suitable transition metal alkyl compounds with known infrared spectra which can be used as model compounds for purposes of comparison. Chatt and Shaw (6, 7) have synthesized some bis(trimethylphosphine)dialkylplatinum compounds and Adams (8) has published a spectrum of the methyl derivative in the νCH region and has reported some tentative frequencies for the ethyl and *n*-propyl derivatives. However, trimethylphosphine also absorbs in the same spectral region and obscures part of the metal–alkyl spectrum.

In the present work a series of *cis*-platinum dialkyl compounds have been synthesized of the type $(Ph_3P)_2PtR_2$ (Ph = phenyl) where R = methyl, ethyl, ethyl-d_3, *n*-propyl, *n*-butyl, and *n*-hexyl. All of these are new compounds except for the dimethyl derivative which has been reported by Chatt and Shaw (6). The infrared spectra in the νCH region have been obtained and are discussed in terms of the infrared spectra of chemisorbed hydrocarbons. In these compounds, the absorptions due to the phenyl portion of the molecule lie above 3000 cm^{-1} and do not obscure the spectrum of the aliphatic groups whose absorptions lie below 2960 cm^{-1}.

Experimental and Results

The platinous dialkyl compounds were prepared by the reaction of *cis*-dichlorobis(triphenylphosphine)platinum (II), $(Ph_3P)_2PtCl_2$, with an ether solution of the corresponding alkyllithium. The method was essentially the same as that used by Chatt and Shaw (6, 7) for the synthesis of the corresponding trimethylphosphine and triethylphosphine stabilized dialkyl derivatives. *cis*-$(Ph_3P)_2PtCl_2$ was prepared by the reaction of K_2PtCl_4 with Ph_3P as described by Jensen (9). The diethyl derivative was also prepared by the reaction of *cis*-$(Ph_3P)_2PtCl_2$ with CH_3CH_2MgBr with slightly lower yield and the di(ethyl-d_3) derivative was prepared by this method using CD_3CH_2Br as starting material. This contained 98% deuterium in the terminal position and was supplied by Merck, Sharp and Dohme Ltd. of Montreal.

Products were crystallized from light petroleum ether (30–60 °C) except for the dimethyl derivative which was crystallized from benzene. Yields, melting points, and analytical data are shown in Table 1.

Nuclear magnetic resonance spectra were run on a Varian Associates T60 instrument and the ratio of the integrated intensities of the phenyl to alkyl signals agreed to within a few percent of the theoretical. The spectrum of the dimethyl derivative was identical to the published spectrum (10). Infrared spectra were run as dilute solutions in CCl_4 (about 0.01 *M*, path length of 0.5 mm) at low resolution on a Beckmann IR-20 instrument, and at high resolution in the νCH region on a Perkin–Elmer model 13G infrared spectrometer using a spectral slit width of about 2 cm^{-1}. The high resolution spectra of

TABLE 1

Analytical data for $(Ph_3P)_2PtR_2$ compounds

R	Yield (%)	Melting point (°C)	C		H	
			Obsd.	Calcd.	Obsd.	Calcd.
Methyl	87	238–239	60.9	60.87	4.92	4.84
Ethyl	46	147–148	62.0	61.76	5.46	5.18
n-Propyl	43	142–144	62.6	62.63	5.69	5.50
n-Butyl	45	132–134	63.5	63.37	5.96	5.80
n-Hexyl	45	123–124	65.3	64.77	6.93	6.34

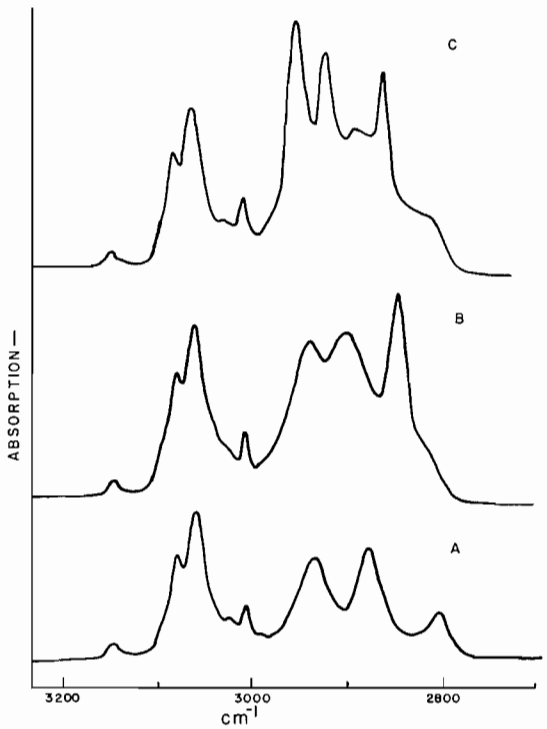

FIG. 1. Infrared spectra in the vCH region of $(Ph_3P)_2PtR_2$: *A*, R = methyl; *B*, R = ethyl; *C*, R = *n*-propyl. All spectra were run as approximately 10^{-2} *M* solutions in CCl_4.

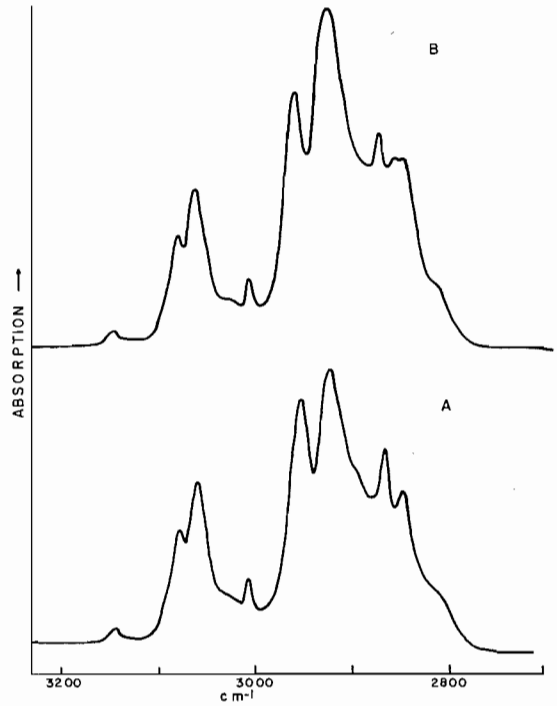

FIG. 2. Infrared spectra in the vCH region of $(Ph_3P)_2PtR_2$: *A*, R = *n*-butyl; *B*, R = *n*-hexyl.

the normal alkyl derivatives in the vCH region between 3200 and 2700 cm^{-1} are shown in Figs. 1 and 2, and the spectrum of the di(ethyl-d_5) derivative is shown in Fig. 3. All of the absorptions above 3000 cm^{-1} are attributable to the CH stretching modes of the phenyl groups and these bands only are observed in the spectrum of $(Ph_3P)_2PtCl_2$. The bands below 3000 cm^{-1} are due solely to the alkyl portion of the molecule and Table 2 lists the observed frequencies and optical densities of these bands.

Discussion

The usual (11, 12) assignments for the observed bands in the infrared spectra of saturated hydrocarbons in the CH stretching region are shown in Table 3. Sheppard and Ward (3) have recently discussed some of the criteria for using these assignments for the qualitative interpretation of the spectra of adsorbed molecules and have concluded that such assignments are generally valid except possibly for the functional group which is attached directly to the metal, which may be shifted to a somewhat lower frequency.

Sheppard and Ward (3) also discuss the validity of using intensity measurements for determining the ratio (*n*) of the number of methylene groups present to the number of methyl groups. In a series of *n*-alkanes, Jones (13) has

Can. J. Chem. Downloaded from www.nrcresearchpress.com by 210.87.254.42 on 09/05/12
For personal use only.

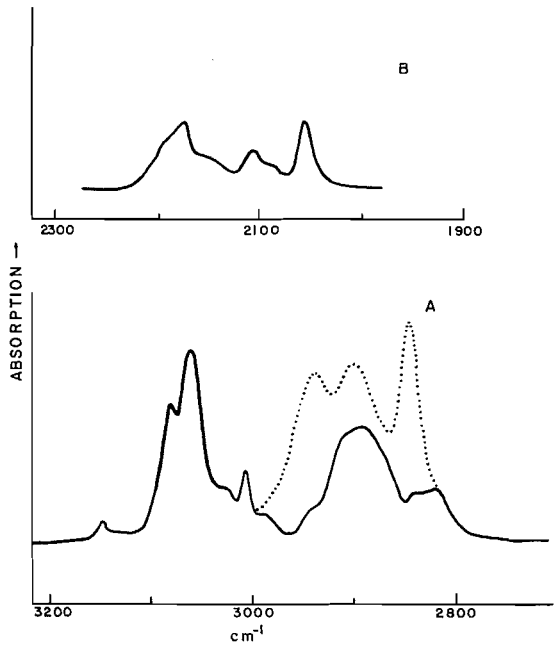

FIG. 3. Infrared spectra of $(Ph_3P)Pt(CH_2CD_3)_2$ in the νCH and νCD regions. The dotted portion of *A* is the spectrum of $(Ph_3P)Pt(CH_2CH_3)_2$ as in Fig. 1*B*.

shown that the intensity of the band near 2960 cm^{-1} [ν(as)CH_3] remains approximately constant as the chain length increases but the intensity of the CH_2 band at 2925 cm^{-1} [ν(as)CH_2] increases in almost direct proportion to the chain length. Therefore, the ratio of the optical density of these bands is a useful measure of the relative proportion of these groups present. From an examination of the infrared spectra of a number of tin and lead alkyl compounds, Sheppard and Ward conclude (3) that the Jones relationship is still approximately valid, although use of the hydrocarbon data may lead to an underestimate of the ratio *n* by one methylene unit.

In the present work the frequencies of the major bands in the spectrum of the *n*-propyl, *n*-butyl, and *n*-hexyl derivatives agree quite well with the Fox and Martin (12) assignments, the agreement improving as the chain length increases (Table 2). Further, the ratio of the optical density of the band near 2925 cm^{-1} also increases with the chain length, and using the Ward and Sheppard (3) criteria, are in quite good agreement with that which would be predicted for each particular case.

It is particularly worth noting that the spectrum of the alkyl portion of the *n*-butyl derivative is almost an exact replica of the spectra which has frequently been observed in studies of ethylene and butene hydrogenation on nickel and platinum (2, 4, 5, 14) and which has always been attributed to a chemisorbed *n*-butyl group. This is the first

TABLE 2

Observed alkyl CH stretching frequencies of $(Ph_3P)_2PtR_2$

R	Frequency (cm^{-1})	Optical density	Ratio of optical density of ν(as)CH_2/ν(as)CH_3*
Methyl	2934	0.110	
	2878	0.125	
	2806	0.05	
Ethyl	2937	0.170	1.06
	2901	0.180	
	2848	0.240	
	2817	sh †	
n-Propyl	2949	0.315	0.83
	2919	0.260	
	2889	0.150	
	2860	0.230	
	2820	sh	
n-Butyl	2952	0.295	1.20
	2923	0.355	
	2900	sh	
	2878	0.220	
	2851	0.160	
	2820	sh	
n-Hexyl	2956	0.318	1.57
	2924	0.490	
	2874	0.245	
	2856	0.210	
	2848	0.210	
	2814	sh	
Ethyl-2,2,2-d_3	2909	sh	
	2893	0.110	
	2841	0.050	
	2817	0.050	
	2174	0.040	
	2107	0.035	
	2055	0.060	

*as = asymmetric stretching mode using the assignments of Fox and Martin (12).
†sh = shoulder.

TABLE 3

Infrared frequency data for saturated hydrocarbons

Group	Frequency cm^{-1} (11, 12)	Assignment (11)*
C—CH_3	2962 ± 10	νCH(as)
	2872 ± 10	νCH(s)
C—CH_2-	2926 ± 10	νCH(as)
	2853 ± 10	νCH(s)
C—CH	2890 ± 10	νCH

*as = asymmetric, s = symmetric.

Can. J. Chem. Downloaded from www.nrcresearchpress.com by 210.87.254.42 on 09/05/12
For personal use only.

Can. J. Chem. Downloaded from www.nrcresearchpress.com by 210.87.254.42 on 09/05/12
For personal use only.

direct piece of experimental evidence which corroborates this assignment.

In a comparison of the spectrum of *trans*-$(Me_3P)_2PtClMe$ [Me = methyl] and $(Me_3P)_2PtClCD_3$, Adams (8) deduced that the νCH absorptions of Pt—CH_3 occurred at about 2930, 2885, and 2815 cm^{-1}. However, the two higher frequency bands only appeared as shoulders on either side of an intense P—CH_3 band. A similar spectrum was obtained for *cis*-$(Me_3P)_2PtMe_2$. The spectrum of the dimethyl platinum derivative in this work agrees very well with that "predicted" by Adams, and its general form is similar to the νCH spectra of other metal—CH_3 compounds in having two strong high frequency bands and a weaker low frequency band (3, 15–17).

Adams (8) assigned the low frequency 2815 cm^{-1} band to the symmetric νCH mode and was unable to decide which of the two high frequency bands was attributable to the asymmetric νCH mode, or indeed, why there were two bands at all. In view of the intensities, it would appear more reasonable to assign the 2934 and 2874 cm^{-1} bands to the asymmetric and symmetric CH stretching modes, respectively, and the lower frequency mode to an overtone of δCH which is brought up in intensity by Fermi resonance interaction (3, 15, 17, 18). However, any assignment can only be speculative at this time and either gas phase band contour data, or the frequencies of the partially deuterated methyl species would be needed to further confirm any assignment. There is increasing evidence in the literature that the traditional Fox and Martin assignments may not be correct (19, 22) and it is anticipated that the data for the isotopic dimethyl platinum derivative will be forthcoming in a later part of this series.

The spectrum of the diethyl platinum derivative in the νCH region (< 3000 cm^{-1}) is not typical of the spectrum to be expected for an ethyl group (3, 18, 20) which normally has a pair of bands near 2960 and 2870 cm^{-1} due to the CH_3, and another pair near 2925 and 2855 cm^{-1} due to CH_2. However, the observed spectrum of the Pt—ethyl group is apparently similar to that observed by Adams (8) for *cis*-$(Me_3P)_2Pt(CH_2CH_3)_2$ which had a strong band at 2840 cm^{-1} and weaker bands near 2933 and 2892 cm^{-1} appearing as shoulders on either side of the intense P—CH_3 band at 2905 cm^{-1}.

In view of the similarity in the spectrum of the Pt—(*n*-butyl) derivative in this work and that of a chemisorbed *n*-butyl group (2, 4) it is worth noting the form of the Pt—ethyl spectrum since a chemisorbed ethyl species has long been postulated as an intermediate during the hydrogenation of ethylene to ethane (2). The spectrum of the ethyl radical has never been unambiguously identified by infrared spectroscopic techniques and conversely, no spectrum similar to that of the Pt—ethyl group in this work has ever been observed (4). However, it is considered that chemisorbed ethyl groups would not necessarily be on the surface under the static reaction conditions generally employed for infrared studies of this reaction (4), but it could exist as a transient under dynamic reaction conditions.

In an attempt to assign the major features in the Pt—ethyl spectrum, the partially deuterated compound *cis*-$(Ph_3P)_2Pt(CH_2CD_3)_2$ was synthesized and its spectrum is shown in Fig. 3. Clearly, the strong bands at 2937 and 2848 cm^{-1} in the spectrum of the Pt—CH_2CH_3 compound have disappeared from the νCH region and probably appear as the two bands at 2174 and 2107 cm^{-1} in the νCD region (νCH/νCD = 1.351 in each case), and are attributable to the methyl group. The spectrum in the νCD region is very similar to that reported by Adams (8) for *cis*-$(Me_3P)_2Pt(CD_3)_2$. However, the remaining features in the νCH region are a broad strong doublet at 2909 and 2893 cm^{-1} and a weak doublet at 2841 and 2817 cm^{-1}, which can possibly be assigned respectively as the asymmetric and symmetric stretching modes of the CH_2 group with the doublet splitting arising from coupling between the two methylenes. This would correspond to the traditional Fox and Martin Assignment. However, it is also possible that the stronger pair of bands near 2900 cm^{-1} might be the asymmetric and symmetric stretching frequencies of the methylene group (19, 21, 22) and that the low frequency bands might be overtone or combination bands. Similar features have been reported by Nolin and Jones (18) who compared the spectrum of diethyl ketone $CH_3CH_2COCH_2CH_3$, with that of diethyl ketone-d_6, $CD_3CH_2COCH_2CD_3$. Again, further work is necessary to confirm the assignments for an ethyl group. In the present context, it will be necessary to synthesize the other partially deuterated derivative and this work will be presented as a later part of this series.

The financial support of the National Research Council of Canada is gratefully acknowledged. The author also wishes to thank Dr. A. D. Westland for many helpful discussions, and Miss M. Flett for assistance with the experimental part of this work.

1. L. H. LITTLE. Infrared spectra of adsorbed molecules. Academic Press Inc., New York. 1966.
2. R. P. EISCHENS and W. A. PLISKIN. Advan. Catal. **10**, 1 (1958).
3. N. SHEPPARD, and J. W. WARD. J. Catal. **15**, 50 (1969).
4. B. A. MORROW and N. SHEPPARD. Proc. Roy. Soc. Ser. A. **311**, 391 (1969).
5. B. A. MORROW and N. SHEPPARD. Proc. Roy. Soc. Ser. A. **311**, 414 (1969).
6. J. CHATT and B. L. SHAW. J. Chem. Soc. 705 (1959).
7. J. CHATT and B. L. SHAW. J. Chem. Soc. 4020 (1959).
8. D. M. ADAMS. J. Chem. Soc. 1220 (1962).
9. K. A. JENSEN. Z. Anorg. Chem. **229**, 237 (1936).
10. E. D. GREAVES, R. BRUCE, and P. M. MAITLIS. Chem. Commun. 860 (1967).
11. L. J. BELLAMY. Infrared spectra of complex molecules. 2nd ed. Methuen, London. 1958.
12. J. J. FOX and A. E. MARTIN. Proc. Roy. Soc. Ser. A. **167**, 257 (1938); **175**, 208 (1940).
13. R. N. JONES. Spectrochim. Acta, **9**, 235 (1957).
14. J. ERKELENS and TH. J. LIEFKENS. J. Catal. **8**, 36 (1967).
15. D. B. POWELL and N. SHEPPARD. Spectrochim. Acta, **21**, 559 (1965).
16. D. E. CLEGG and J. R. HALL. Spectrochim. Acta, **21**, 357 (1965).
17. J. H. S. GREEN. Spectrochim. Acta, **24A**, 863 (1968).
18. B. NOLIN and R. N. JONES. J. Amer. Chem. Soc. **75**, 5626 (1953).
19. F. WINTHER and D. O. HUMMEL. Spectrochim. Acta, **25A**, 425 (1969).
20. B. NOLIN and R. N. JONES. Can. J. Chem. **34**, 1392 (1956).
21. N. SHEPPARD. Private communication.
22. S. C. GRAHAM. Spectrochim. Acta, **26A**, 345 (1970).

Can. J. Chem. Downloaded from www.nrcresearchpress.com by 210.87.254.42 on 09/05/12
For personal use only.

Can. J. Chem. Downloaded from www.nrcresearchpress.com by 210.87.254.105 on 09/05/12
For personal use only.

Anharmonicity, solvent effects, and hydrogen bonding: NH stretching vibrations

A. FOLDES[1] AND C. SANDORFY
Département de Chimie, Université de Montréal, Montréal, Québec

Received February 19, 1970

The influence of solvent effects and hydrogen bond formation on the anharmonicity of the NH stretching vibration of simple secondary amides, lactams, anilides, indole, pyrrole, and imidazole have been studied; and the frequencies of the first and second overtones, their half widths and solvent shifts measured. The validity of Buckingham's theory is established in the case of inert solvents; whereas the second order perturbation treatments are shown to be inapplicable to the case of hydrogen bonding solvents. All NH stretching modes seem to exhibit the same anharmonic behavior which is very different from that of OH vibrations.

Canadian Journal of Chemistry, 48, 2197 (1970)

Introduction

In previous papers from this laboratory (1–5), the influence of hydrogen bond formation and other environmental effects on the anharmonicity of OH and NH vibrations was examined. In order to assess the extent of this influence we have tested the validity of conventional second order perturbation formulas from which anharmonicity constants are usually computed. The following criteria can be used.

(*a*) If $\nu_{01}, \nu_{02}, \nu_{03}, \ldots$ are the frequencies of the fundamental, the first, second, ... overtones, then it follows from second order perturbation theory that the anharmonicity constant for a diatomic vibrator

$$[1] \quad X_{12} = X_{23} = \nu_{01} - \frac{\nu_{02}}{2} = \frac{\nu_{02}}{2} - \frac{\nu_{03}}{3} = X = -\omega_e X_e$$

(*b*) It also follows from second order perturbation theory that the anharmonicity constants of OH and OD, NH, and ND vibrations should be inversely proportional to the reduced masses (6, 7).

(*c*) In Buckingham's theory of solvent effects (8–10), it is shown that the gas to solution shifts of ν_{01}, ν_{02}, ν_{03}, as well as the respective half widths should be in the proportions 1:2:3:... This relation is independent of the actual form of the potential, but it is linked to the validity of a second order perturbation treatment.

In testing (*a*) and (*b*) the perturbation is taken to be the anharmonic part of the intramolecular potential and we examine the changes it undergoes upon hydrogen bond formation or solvent perturbations. In Buckingham's theory an intermolecular potential is introduced, and this together with the anharmonic terms of the intramolecular potential is taken to be the perturbation. The solvent shifts then turn out to depend on products of intramolecular anharmonic potential constants and derivatives of the intermolecular potential. Despite this difference of language and the fact that Buckingham's theory was not meant to be applied to such strong perturbations as hydrogen bonds, it was considered worthwhile to use criteria (*a*), (*b*), and (*c*) together to gain insight into the effect of hydrogen bond formation and solvent effects on vibrational anharmonicity.

Previously (1), N—H ... N type bonds in secondary amines and O—H ... O type bonds in alcohols have been studied. They showed very different anharmonic behavior. For the secondary amines X_{12} showed a marked decrease with respect to the X_{12} of the free N—H stretching vibration, but X_{23} had values similar to those of free N—H. For alcohols (2), X_{12} increased significantly and X_{23} decreased when hydrogen bonds were formed. This indicates that the respective potential surfaces differ significantly, a fact that should be important for an understanding of the nature of these associations.

In the present work we report an investigation of the anharmonic behavior of the N—H stretching vibration of secondary amides, lactams and anilides, pyrrole, indole, and imidazole, some of which have considerable biological importance.

[1]Present address: Delmar Chemicals Ltd., La Salle, Quebec.

Can. J. Chem. Downloaded from www.nrcresearchpress.com by 210.87.254.105 on 09/05/12
For personal use only.

Experimental

(a) Materials

Most compounds were Eastman analytical grade reagents. They were dried in vacuum over phosphorus pentoxide and used without further purification. ε-Caprolactam was purified by sublimation in vacuo (m.p., 69–70 °C). Salicylanilide was recrystallized twice from a benzene–hexane solution (m.p., 134–136 °C). Pyrrole was distilled twice under nitrogen atmosphere. The resulting liquid was colorless. The solvents used were of "spectrograde" quality, from Matheson, Coleman and Bell. They were redistilled from appropriate drying agents and kept over molecular sieves.

Deuteration was accomplished by exchange with deuterium oxide (Merck, Sharpe and Dohme, 99.7 mole%). Usually, about 50 ml of a 0.05 to 0.1 *M* solution of the substance in the particular organic solvent was kept in contact with D_2O overnight. The two phases were then separated and the organic layer passed through a drying column before recording the spectrum. In the case of water-soluble compounds, they were "salted into" the organic solvents by addition of sodium chloride. After separation the organic phase was evaporated to dryness and the deuterated product dried in vacuum over P_2O_5. The absence of D_2O was evident from the spectra.

The concentration of our compounds in "neutral" solvents was approximately 0.05 *M*. Although self-association was observable at this concentration, it was nonetheless necessary to locate the second overtones under our conditions. In no case did we observe any shift of the position of "free" NH bands upon further dilution.

In the case of hydrogen bonding solvents, the concentration had to be increased in order to be able to reduce the path length of the cells. It should be pointed out that throughout our experiments, measurements of fundamental as well as first and second overtone frequencies were all made on the same solution without changing the concentration.

(b) Instrumentation

Fundamental frequencies were recorded on a Perkin–Elmer Spectrometer model 621, which was calibrated using hydrogen bromide, ammonia, and water vapors. First and second overtone frequencies were recorded on a Cary spectrophotometer model 14, calibrated against the emission lines of argon and krypton as well as absorption bands of water and hydrogen bromide vapors. The path lengths of the cells varied between 0.1 mm and 10 cm depending on the vibrational level and the transmittance of the solvents used. The scale-expansion device supplied with the Cary 14 instrument proved useful in measuring the second overtone frequencies.

Results and Discussion

The N—H stretching fundamentals, their first, and, if possible, second overtones were measured at room temperature in a series of solvents varying from "inert" halogenated solvents to strongly associative ones, such as nitromethane, acetonitrile, and dioxane. The NH bands are increasingly affected by associations of the solute–solvent type. Data concerning the related ND vibrations were also obtained where possible. Deuteration also helped in the assignment of the bands. In checking Buckingham's relation, $CF_2Cl—CFCl_2$ was used as a reference solvent since gas phase values of the overtones proved difficult to obtain. This solvent has a slight dipole moment (0.12 D) which improved the solubility of our compounds without impairing the results.

N-Methylpropionamide is a typical example. Table 1 shows the frequencies of the fundamental, the first, and second overtones of the NH stretching vibrations (01, 02, and 03), the half width ($\Delta\nu_{\frac{1}{2}}$), the shift with respect to $C_2Cl_3F_3$ and the ratio $\Delta\nu/\nu_{C_2Cl_3F_3}$.[2] The latter should be constant to the second order in the same approximation (3).

It appears immediately that the 1:2:3 relation of the shifts is well obeyed in $C_2Cl_3F_3$, CCl_4, and C_2Cl_4. The situation is somewhat uncertain for benzene where some of the bands have an asymmetric shape but stronger perturbations are clearly indicated. There are large departures from the rule in the hydrogen bonding solvents CH_3NO_2, CH_3CN, and $C_4H_8O_2$ (dioxane); the relative shifts show a similar behavior. The half widths appear to be less sensitive; although we consider these less accurate than our other data.

Table 2 contains the anharmonicity constants. X_{12} shows a behavior very similar to that of the secondary *amines*. It is hardly affected by the inert solvents, but diminishes drastically in the strongly proton accepting solvents. At the same time X_{23} remains roughly constant or increases for the hydrogen bonded species. This indicates the invalidity of second order perturbation treatments in the case of hydrogen bonding. Y_{123} and X_{123} which correspond to the approximation of the next higher order were computed from

---

[2]The asterisks in the tables denote bands of composite character.

The apparent maximum was used in computing the anharmonicity constants and the shifts. If the number in italics is alongside the respective column it represents the mean value of two partially overlapping bands of comparable intensity. In these cases the half widths were evaluated after graphic resolution. The uncertainties involved in this procedure do not impair the qualitative conclusions.

The values of the frequencies of the fundamentals of the molecules reported in this paper have been measured by us. They have, however, been reported previously by several authors in, at least, some of the solvents; and the large number of relating references is omitted.

TABLE 1

The wave numbers (ν), half widths ($\Delta\nu_{\frac{1}{2}}$), shifts with respect to $C_2Cl_3F_3$ solution, and relative shifts ($\Delta\nu/\nu$) of the fundamental (01), first (02) and second overtones (03) of N-methylpropionamide

Solvent	Concentration (moles/l)	Transition	NH ν	NH $\Delta\nu_{\frac{1}{2}}$	NH $\nu_{C_2Cl_3F_3}-\nu$	NH $\frac{\Delta\nu}{\nu}\times 10^3$	ND ν	ND $\Delta\nu_{\frac{1}{2}}$	ND $\nu_{C_2Cl_3F_3}-\nu$	ND $\frac{\Delta\nu}{\nu}\times 10^3$
$C_2Cl_3F_3$	0.05	01	3480	20			2580	17		
		02	6821	42			5083	37		
		03	10020	72						
CCl_4	0.05	01	3472	18	8	2.30	2574	18	6	2.32
		02	6804	35	17	2.49	5070	37	13	2.55
		03	9996	62	24	2.39				
C_2Cl_4	0.05	01	3469	17	11	3.16	2571	19	9	3.49
		02	6800	34	21	3.08	5066	38	17	3.34
		03	9990	65	30	2.99				
CS_2	0.05	01	3460	21	20	5.75	2566	22	14	5.42
		02	6780	44	41	6.01	5056	40	27	5.31
		03	9958	77	62	6.19				
C_6H_6	0.05	01	3442	32	38	10.92	2552	40	28	10.85
		02	*6761*, 6773 *	67*	60	8.80	5037*	58*	46	9.05
		03	*9920*, 9950 *	114	100	9.98				
CH_3NO_2	0.05	01	3440	40	40	11.49				
		02	6768	79	53	7.77				
		03	9946	125	74	7.38				
CH_3CN	0.3	01	3405	70	75	21.55				
		02	6745	142	76	11.14				
		03	9751, 9887 *9819*	~250*	201	20.06				
$C_4H_8O_2$	0.5	01	3372	90	108	31.03				
		02	*6710*, 6654 sh	200*	111	16.18				
		03	9877							
		03	*9823*	~300*	197	19.66				
			9705							

TABLE 2

The anharmonicity constants, "harmonic" frequencies and isotopic ratios of N-methylpropionamide

Solvent	NH X_{12}	NH X_{23}	NH X_{13}	NH Y	NH X_{123}	NH ω_e	ND X_{12}	ND ω_e	$\frac{\nu_{01}(NH)}{\nu_{01}(ND)}$	$\frac{\nu_{02}(NH)}{\nu_{02}(ND)}$	$\frac{\omega_e(NH)}{\omega_e(ND)}$	$\frac{X(NH)}{X(ND)}$
$C_2Cl_3F_3$	69.5	70.5	70.0	0.5	67.3	3619	38.5	2657	1.3488	1.3419	1.3621	1.8052
CCl_4	70.0	70.0	70.0	0.0	70.0	3612	39.0	2652	1.3489	1.3420	1.3620	1.7949
C_2Cl_4	69.0	70.0	69.5	0.5	66.8	3607	38.0	2647	1.3493	1.3423	1.3627	1.8158
CS_2	70.0	70.7	70.3	0.3	68.5	3600	38.0	2642	1.3484	1.3410	1.3626	1.8421
C_6H_6	61.5	73.8	67.7	6.2	33.8	3565	33.5	2619	1.3487	1.3423	1.3612	1.8358
CH_3NO_2	56.0	68.7	62.3	6.3	27.5							
CH_3CN	32.5	99.5	66.0	33.5	−118.3							
$C_4H_8O_2$	17.0	80.7	48.8	31.8	−126.3							

Can. J. Chem. Downloaded from www.nrcresearchpress.com by 210.87.254.105 on 09/05/12
For personal use only.

TABLE 3

The wave numbers, half widths, shifts with respect to $C_2Cl_3F_3$ solution, and relative shifts of the fundamental, first and second overtones of γ-butyrolactam

Solvent	Concentration (moles/l)	Transitions	ν	$\Delta\nu_{\frac{1}{2}}$	$\nu_{C_2Cl_3F_3} - \nu$	$\frac{\Delta\nu}{\nu} \times 10^3$
$C_2Cl_3F_3$	0.12	01	3463	18		
		02	6788	35		
		03	9972	55		
CCl_4	0.12	01	3454	16	9	2.60
		02	6770	32	18	2.65
		03	9948	63	24	2.40
C_2Cl_4	0.05	01	3452	15	11	3.17
		02	6765	32	23	3.38
		03	9939	63	33	3.31
CS_2	0.13	01	3443	20	20	5.77
		02	6748	40	40	5.89
		03	9910	88	62	6.21
C_6H_6	0.2	01	3429	37	34	9.82
		02	6748	79	40	5.89
		03	9901	146	71	7.12
CH_3NO_2	0.06	01	3426	42	37	10.68
		02	6731	71	57	8.40
		03	9892	161	80	8.02
CH_3CN	1.0	01	3377	112	86	24.83
		02	6735	~200	53	7.80
		03	9886 / *9827*	~320	86 / 145	8.62 / 14.54
$C_4H_8O_2$		01	3325	85	138	39.85
		02	6745 / *6615*	~100 / ~300	173	25.49
		03	9904 / *9735*	~180 / ~400	237	23.77

[2] $$Y_{123} = \tfrac{1}{2}(\nu_{02} - \nu_{01} - \nu_{03}/3)$$

and

[3] $$X_{123} = \nu_{01} - \nu_{02}/2 - 4.5\,Y_{123}$$

The large values of Y_{123} again indicate the inapplicability of the second order approximation. The harmonic frequencies, ω_e, are also given where Y is small, as well as the isotopic ratios of the ν, the ω_e, and the X_{12}.

The isotopic ratios of the observed frequencies, and even more those of the harmonic frequencies, are close to the ratios of the square roots of the reduced masses. This shows that, on the one hand, anharmonicity plays a role in diminishing the isotopic ratios and, on the other, the diatomic approximation is justified at least in the case of simple solvent effects. The ratios of the anharmonicity constants are even closer to their "theoretical" values (the ratios of the reduced masses themselves). This was expected since it was recognized before (4), that anharmonicity constants should be less sensitive to solvent effects than the frequencies themselves.

TABLE 4

The anharmonicity constants and harmonic frequencies of γ-butyrolactam

Solvent	X_{12}	X_{23}	X_{13}	Y	X_{123}
$C_2Cl_3F_3$	69.0	70.0	69.5	0.5	66.8
CCl_4	69.0	69.0	69.0	0.0	69.0
C_2Cl_4	69.5	69.5	69.5	0.0	69.5
CS_2	69.0	70.7	69.8	0.8	65.3
C_6H_6	55.0	73.7	64.3	9.3	13.0
CH_3NO_2	60.5	68.2	64.3	3.8	43.3
CH_3CN	9.5	91.8	50.7	41.2	−175.8
$C_4H_8O_2$	17.5	62.5	40.0	22.5	−83.8

The results obtained with N-methylacetamide and N-methyl benzamide were similar.

γ-Butyrolactam (Tables 3 and 4) also falls in line. The 1:2:3 relation is obeyed for the three inert solvents; but discrepancies begin to appear for benzene and nitromethane, and the relationship breaks down completely for acetonitrile and

Can. J. Chem. Downloaded from www.nrcresearchpress.com by 210.87.254.105 on 09/05/12
For personal use only.

TABLE 5

The wave numbers, half widths, shifts with respect to $C_2Cl_3F_3$ solution, anharmonicity constants, and relative shifts of the fundamental, first and second overtones of acetanilide

Solvent	Concentration (moles/l)	Transition	ν	$\Delta\nu_{\frac{1}{2}}$	$\nu_{C_2Cl_3F_3}-\nu$	X_{12}	$\frac{\Delta\nu}{\nu}\times 10^3$
$C_2Cl_3F_3$	0.01	01	3452	14		66.0	
		02	6772	40			
CCl_4	0.02	01	3444	10	8	66.5	2.32
		02	6755	35	17		2.51
C_2Cl_4	0.02	01	3443	11	9	66.5	2.61
		02	6753	37	19		2.80
CS_2	0.02	01	3433	16	19	67.5	5.50
		02	6731	50	41		6.08
C_6H_6	0.05	01	3416	33	36	58.5	10.43
		02	6715	94	57		8.42
CH_3NO_3	0.05	01	3404	58	48	52.0	13.90
		02	6704	92	68		10.04
CH_3CN	0.12	01	3350	80	102	14.0	29.55
		02	6672	180	100		14.77
$C_4H_8O_2$	0.47	01	3333	70	119	28.0	34.47
		02	6610	220	162		23.92

TABLE 6

The wave numbers, half widths, shifts with respect to $C_2Cl_3F_3$ solution, and relative shifts of the fundamental, first and second overtones of pyrrole

			NH				ND			
Solvent	Concentration (moles/l)		ν	$\Delta\nu_{\frac{1}{2}}$	$\nu_{C_2Cl_3F_3}-\nu$	$\frac{\Delta\nu}{\nu}\times 10^3$	ν	$\Delta\nu_{\frac{1}{2}}$	$\nu_{C_2Cl_3F_3}-\nu$	$\frac{\Delta\nu}{\nu}\times 10^3$
$C_2Cl_3F_3$	0.05	01	3508	14			2595	14		
		02	6880	32			5131	22		
		03	10114	49			7590	33		
CCl_4	0.05	01	3497	12	11	3.13	2588	12	7	2.70
		02	6856	25	24	3.49	5117	22	14	2.72
		03	10076	43	38	3.76	7566	30	24	3.16
C_2Cl_4	0.05	01	3495	12	13	3.70	2587	12	8	3.08
		02	6853	28	27	3.92	5113	26	18	3.51
		03	10072	44	42	4.15	7563	32	27	3.55
CS_2	0.05	01	3483	18	25	7.12	2579	16	16	6.16
		02	6829	44	51	7.41	5098	36	33	6.43
		03	10034	85	80	7.91	7538	46	52	6.85
C_6H_6	0.05	01	3456	37	52	14.82	2566	20	29	11.17
		02	*6806* / 6785	107	74	10.75	5068	65	63	12.27
		03	9975	145	139	13.74	(7500)		(90)	(11.86)
CH_3NO_2	0.20	01	3456	53*	52	14.82				
		02	6797	112	83	12.06				
		03	9988	165	126	12.45				
CH_3CN	0.50	01	3410	100	98	27.93				
		02	6774	200	106	15.40				
		03	9924	~320	190	18.78				
$C_4H_8O_2$	0.45	01	3354	100	154	43.90				
		02	*6720* / 6653	250*	160	23.25				
		03	9938 / *9840*	~350*	274	27.09				

Can. J. Chem. Downloaded from www.nrcresearchpress.com by 210.87.254.105 on 09/05/12
For personal use only.

Can. J. Chem. Downloaded from www.nrcresearchpress.com by 210.87.254.105 on 09/05/12
For personal use only.

TABLE 7

The anharmonicity constants, harmonic frequencies, and isotopic ratios of pyrrole

	NH						ND										
Solvent	X_{12}	X_{23}	X_{13}	Y	X_{123}	ω_e	X_{12}	X_{23}	X_{13}	Y	X_{123}	ω_e	$\frac{\nu_{01}(NH)}{\nu_{01}(ND)}$	$\frac{\nu_{02}(NH)}{\nu_{02}(ND)}$	$\frac{\nu_{03}(NH)}{\nu_{03}(ND)}$	$\frac{\omega_e(NH)}{\omega_e(ND)}$	$\frac{X_{13}(NH)}{X_{13}(ND)}$
$C_2Cl_3F_3$	68.0	68.67	68.33	0.3	66.5	3644	29.5	35.5	32.5	3.0	16.0	2654	1.3518	1.3409	1.3325	1.3730	2.1026
CCl_4	69.0	69.3	69.2	0.2	68.2	3635	29.5	36.5	33.0	3.5	13.7	2647	1.3512	1.3398	1.3317	1.3733	2.0960
C_2Cl_4	68.5	69.2	68.8	0.3	67.0	3632	30.5	35.5	33.0	2.5	19.3	2648	1.3510	1.3403	1.3317	1.3716	2.0859
CS_2	68.5	69.8	69.2	0.7	65.5	3620	30.0	36.3	33.2	3.2	15.7	2639	1.3505	1.3395	1.3311	1.3717	2.0854
C_6H_6	53.0	78.0	65.5	12.5	−3.2	3562	32.0	34.0	33.0	1.0	27.5	2630	1.3468	1.3429	1.3300	1.3543	1.9848
CH_3NO_2	57.5	69.2	63.3	5.8	31.2												
CH_3CN	23.0	79.0	51.0	28.0	−103.0												
$C_4H_6O_2$	−6.0	70.0	32.0	38.0	−177.0												

Can. J. Chem. Downloaded from www.nrcresearchpress.com by 210.87.254.105 on 09/05/12
For personal use only.

dioxane. (Benzene appears to be more perturbing than nitromethane for these molecules.) The same can be said about the half widths and the constancy of the relative shifts. The X_{12} and X_{23} also show similar behavior to that of N-methylpropionamide, but undergo a lesser diminution in the hydrogen bonding solvents. δ-Valerolactam and ε-caprolactam gave similar results.

The results pertaining to acetanilide are given in Table 5. As to Buckingham's relations the results are as before. Unfortunately only X_{12} could be determined because of the ill-defined character of the second overtone. It behaves as in the case of the lactams. Salicylanilide and phenacetine behave similarly.

Indole, pyrrole, and imidazole still allow the same remarks concerning Buckingham's relations as well as the anharmonicity constants X_{12} and X_{23} (see Tables 6 and 7 relating to pyrrole). The ND vibration in indole shows anomalies in the shifts. This is probably due to the perturbation of the observed frequencies by Fermi resonance at the fundamental level (11).

In all three cases we find departures from the $(\Delta\nu/\nu)_{ND} = (\Delta\nu/\nu)_{NH}$ rule, similar to those found earlier by Leicknam, Lascombe, Fuson, and Josien (12) and by Huong, Lascombe, and Josien (13) at the fundamental level.

Thus, finally, the following generalization can be made: all hydrogen bonds formed by secondary N—H groups which have been studied show a decrease in anharmonicity at the level of the first overtone and increase again to the value of the free N—H group at the level of the second overtone. This might well indicate the existence of an inflexion or a second minimum in the potential curve relatively close to the first equilibrium position.

In general the shift of the band due to solute–solvent association follows approximately Buckingham's rules for inert solvents. The validity of these relations can be considered as a test both of the applicability of second order perturbation treatments and of the absence of hydrogen bond formation. In the case of hydrogen bonded N—H bonds, it is generally the first overtone that shifts less than it should (and is narrower than it should be), showing the role of anharmonicity in these phenomena. The large values of Y_{123} are another indication of hydrogen bond formation and the breakdown of second order approximations.

Conclusions

The results presented in this paper together with our earlier results on amines show that all secondary NH stretching vibrations have essentially the same anharmonic behavior. In inert solvents they follow Buckingham's relations.

We express our thanks to the National Research Council of Canada and the Quebec Department of Education for financial help.

1. C. Berthomieu and C. Sandorfy. J. Mol. Spectrosc. **15**, 15 (1965).
2. G. Durocher and C. Sandorfy. J. Mol. Spectrosc. **15**, 22 (1965).
3. A. Foldes and C. Sandorfy. J. Mol. Spectrosc. **20**, 262 (1966).
4. G. Durocher and C. Sandorfy. J. Mol. Spectrosc. **22**, 347 (1967).
5. M. Asselin, G. Bélanger, and C. Sandorfy. J. Mol. Spectrosc. **30**, 96 (1969).
6. J. L. Dunham. Phys. Rev. **41**, 721 (1932).
7. G. Herzberg. Molecular spectra and molecular structure. Vol. 1. Spectra of diatomic molecules. Van Nostrand, Princeton, New Jersey. 1950.
8. A. D. Buckingham. Proc. Roy. Soc. London, Ser. A, **248**, 169 (1958).
9. A. D. Buckingham. Proc. Roy. Soc. London, Ser. A, **255**, 32 (1960).
10. A. D. Buckingham. Trans. Faraday Soc. **56**, 753 (1960).
11. J. P. Leicknam. Thesis. Bordeaux, France. 1958.
12. J. P. Leicknam, J. Lascombe, N. Fuson, and M. L. Josien. Bull. Soc. Chim. Fr. 1516 (1959).
13. P. V. Huong, J. Lascombe, and M. L. Josien. J. Chim. Phys. **58**, 694 (1961).

Can. J. Chem. Downloaded from www.nrcresearchpress.com by 210.87.254.5 on 09/05/12
For personal use only.

Decomposition of some cyclic dithiocarbamates

RONALD R. VANDEBEEK, SERGE J. JORIS, KEIJO I. ASPILA, AND CHUNI L. CHAKRABARTI[1]
Department of Chemistry, Carleton University, Ottawa 1, Canada

Received February 12, 1970

The stability of some cyclic N,N-disubstituted dithiocarbamates has been studied by the analysis of the decomposition rates at different p*H* values. It is concluded that the most important factors which determine the relative stabilities of three cyclic dithiocarbamates (DTC) are the solvation of the DTC acid molecule and the ring strain associated with the substituents. This has been proven by a study of (*a*) the decomposition rates as a function of the dielectric constant of the medium, (*b*) order of the stability, and (*c*) activation energy.

The molar absorptivities and the apparent acid dissociation constants have been determined for pyrrolidine-, piperidine-, and hexamethylene-dithiocarbamates.

Canadian Journal of Chemistry, 48, 2204 (1970)

Introduction

The chelating properties of the dithiocarbamates have been of considerable importance in analytical chemistry (1). Ease of preparation and stability not only of the reagent but also of the chelate formed are important points to be considered in the study of these compounds.

The purpose of this paper is to describe some properties of two relatively unknown dithiocarbamates, viz., sodium hexamethylenedithiocarbamate (**1**) and sodium piperidinedithiocarbamate (**2**), and to compare them with sodium pyrrolidinedithiocarbamate (**3**), a widely used analytical reagent.

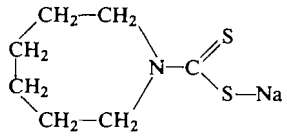

1, hexaDTCNa

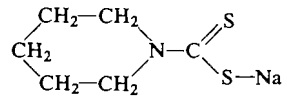

2, pipDTCNa

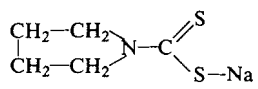

3, pyrDTCNa

Since the stability and the analytical selectivity of these complexing agents depend, often critically, on the p*H* of aqueous solutions, the behavior of these reagents at various p*H* values has been studied. Some other aspects, such as the influence of dielectric constant and of temperature on the decomposition of the DTC have also been described. These studies indicate that the ring size of the cyclic substituent influences the decomposition rate. Hence, it should be possible to make a comparison between the cyclic DTC and the dialkyl dithiocarbamates, the properties of which have already been extensively reviewed (2, 3).

Experimental

Reagents

All reagents used in this study were A.R. grade. The dithiocarbamates were prepared by the reaction between carbon disulfide and the particular cyclic imine in the presence of a base (4, 5). The product was recrystallized twice by dissolving it in a minimum of hot ethanol, allowing the solution to cool and then precipitating the reagent by the addition of diethyl ether. The percentage of dithiocarbamate in the recrystallized product was determined by amperometric titration and was found to be 81.7% for pyrDTCNa, 75.5% for pipDTCNa, and 86.3% for hexaDTCNA. The remaining 15 to 25% of the recrystallized product consists of water and ethanol (5).

Apparatus

A Polarecord E261 polarograph (Metrohm Herisau, Switzerland) with an Ag/AgCl reference electrode and saturated KCl salt bridge was used for the amperometric titrations. The polarographic cell was thermostatted at 25.0 ± 0.5 °C.

For the spectrophotometric determination, a Bausch & Lomb Spectronic 505 U.V. recording spectrophotometer was used. This instrument was modified in order to determine accurately the decomposition half-lives of the order of 3–20 s. A matched set of 10.0 mm quartz cells, thermostatted at 25.0 ± 0.1 °C was used in the study of the decomposition kinetics.

The p*H* of all solutions was measured with a Fisher Accumet p*H* meter, model 210.

[1]To whom correspondence should be addressed.

Can. J. Chem. Downloaded from www.nrcresearchpress.com by 210.87.254.5 on 09/05/12
For personal use only.

Procedure

Amperometric Titration

The amperometric titration of the dithiocarbamates (DTC) was done by adding accurately measured aliquots of a standard solution of 0.010 *M* $ZnCl_2$ to 50.0 ml of a deaerated solution consisting of approximately 5.0×10^{-5} *M* dithiocarbamate and 0.008% (v/v) of gelatin. The standard solution of $ZnCl_2$ was made slightly acidic (p*H* 4) to avoid any precipitation of $Zn(OH)_2$. The diffusion current corresponding to the reduction of the Zn^{2+} ions was measured at −1.20 V (vs. Ag/AgCl). This method gave results reproducible to within 1% (6).

Spectrophotometric and Kinetic Studies

For the study of the ultraviolet (u.v.) spectra and of the decomposition kinetics as a function of p*H*, buffers of ionic strength 0.010 were prepared (7) for the p*H* range 2.0–12.0. Solutions of p*H* less than 2.1 were dilute hydrochloric acid. For kinetic studies, buffered solutions of 10^{-3}–10^{-4} *M* DTC were prepared by adding DTC to the buffer in the quartz cells maintained at constant temperature, and mixing with a Teflon stirrer. The measurement of absorbance at fixed wavelength as a function of time was started within an average time of 6 s after mixing had been completed. For first-order half-lives greater than 30 min, absorbance measurements were made on samples withdrawn at various time intervals from buffered DTC solutions kept in a constant temperature bath (25.0 ± 0.1 °C). All absorbance measurements were made at about 275 nm as required by the choice of DTC and p*H*. A plot of log absorbance vs. time was found to be linear at all p*H* values, and gave reproducible half-life values (±2%) at any chosen p*H* value.

Water–methanol mixtures ranging from 0 to 98% methanol content were used for the study of the decomposition kinetics as a function of the bulk dielectric constant of the medium. The dielectric constants of the water–methanol mixtures were taken from the literature (8). Each solution was made 0.05 *N* in HCl to generate the DTC acid from the sodium salt. The presence of only the acid form was confirmed by u.v. spectrophotometry. It is realized that a small decrease occurs in the bulk dielectric constant (9) as a result of the presence of HCl but this correction has not been made since the change is small (<2%).

The activation energy and the pre-exponential factors have been determined from the Arrhenius plot of $\log_{10} k$ vs. $1/T$, in which the slope of the straight line is equal to $-E_a/2.303\ R$.

Results and Discussion

Ultraviolet Spectrophotometry

The cyclic dithiocarbamates show (as do the other dithiocarbamates), three absorption maxima in the u.v. region of the spectrum: (A) a band of low intensity at a maximum between 330 and 360 nm, (B) a band of intermediate intensity with maximum absorption between 275 and 296 nm and (C) a band of intermediate intensity with maximum absorption between 240 and 260 nm. Janssen (10, 11) assigned band A to an $n \rightarrow \pi^*$ transition, e.g. the transition of an electron of the lone pair on a sulfur atom to an anti-bonding orbital, and band B to a $\pi \rightarrow \pi^*$ transition in the N—C=S group. Band C was assigned (12) to a $\pi \rightarrow \pi^*$ transition in the S—C=S group.

Using Beer's Law, the molar absorptivity, ε, was determined by measuring the absorbance of a series of samples at low concentration of DTC in aqueous solutions. The results of duplicate analysis for the three absorption bands are given in Table 1.

TABLE 1

Molar absorptivity of the three absorption bands of some cyclic dithiocarbamates*

Reagent	Spectral band	Wavelength (nm ± 2)	Molar absorptivity, ε
pyrDTCNa	A	335	5.6×10
	B	277	14.9×10^3
	C	254	16.1×10^3
pipDTCNa	A	348	8.9×10
	B	281	16.4×10^3
	C	262	16.4×10^3
hexaDTCNa	A	350	5.8×10
	B	281	13.7×10^3
	C	258	13.7×10^3

*Temperature = 25 °C, p*H* = 12.

For all three cyclic dithiocarbamates considered, there was no shift in the spectra above p*H* 5. However, between p*H* 2.1 and 5, a significant change was observed. This is illustrated for pyrDTCNa in Fig. 1. The blue shift in the spectra of the dithiocarbamates has been explained (4) by the decrease of the resonance in the molecule as a result of protonation. In fact, it has been stated (13) that the anomalous acidic properties of the dithiocarbamates are due to a high degree of resonance in the DTC anion and that one of the sulfur atoms of the monobasic DTC protonates at about p*H* 3. The conjugation which extends in the DTC anion to the 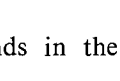 system is reduced in the acid form to essentially the 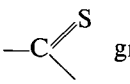 group by the formation of an intramolecular hydrogen bond between the sulfur and the nitrogen atoms after the protonation of the sulfur atom (13, 14). Hence a blue shift is expected and is observed.

Can. J. Chem. Downloaded from www.nrcresearchpress.com by 210.87.254.5 on 09/05/12
For personal use only.

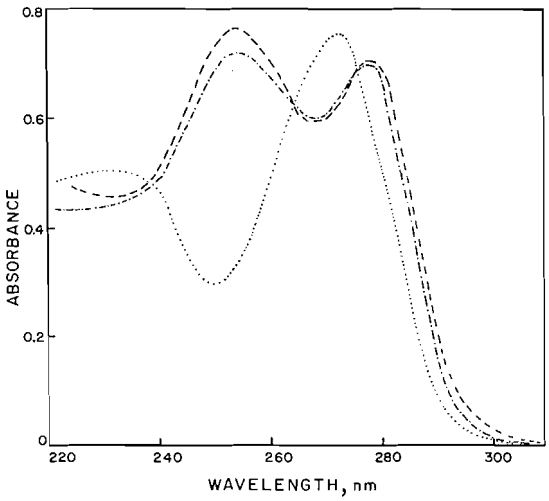

FIG. 1. Ultraviolet spectra of pyrDTCNa at different pH values: temperature = 25.0 °C, – – – pH = 5.80; -·-·- pH = 4.22; ... pH = 2.10.

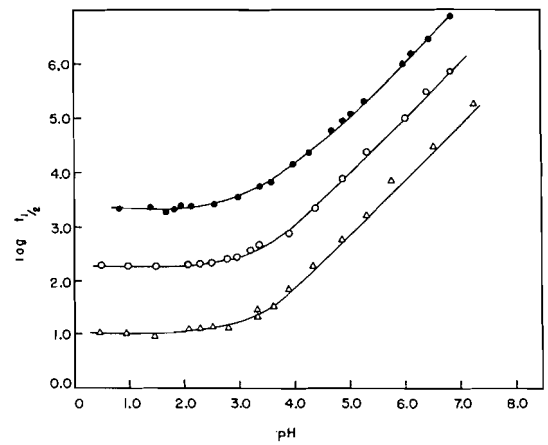

FIG. 2. log apparent half-life (s) for decomposition as a function of pH at 25.0 °C: △, pipDTCNa; ○, hexaDTCNa; ●, pyrDTCNa.

Kinetics of Decomposition

Figure 2 shows the apparent half-lives for decomposition as a function of pH for dithiocarbamates studied. At pH greater than 4, the results indicate a first order relationship between the log of the apparent half-life for decomposition, $t_{\frac{1}{2}\ app}$ and the pH. Below pH 2, the rate of decomposition is no longer pH dependent and assumes a limiting value ($t_{\frac{1}{2}\ lim}$). These results are similar to the results obtained for the decomposition of the dialkyl DTC (13–16), and indicate that only the acid form of the molecule, DTCH, decomposes. Therefore, the following rate equation can be written

$$[1] \qquad V = k_{lim}\,[DTCH]$$

For all pH values, the following relationships are satisfied

$$[2] \qquad [DTC]_{total} = [DTCH] + [DTC^-]$$

$$[3] \qquad K_S = [DTC^-][H^+]/[DTCH]$$

where K_S = DTC acid dissociation constant, $[DTC^-]$ = concentration of the anionic form, $[DTC]_{total}$ = total DTC concentration. Equation [1] can then be written in the following manner

$$[4] \qquad V = k_{app}\,[DTC]_{total}$$

where

$$[5] \qquad k_{app} = k_{lim}\,[H^+]/([H^+] + K_S)$$

Equation [5] indicates that $k_{app} = k_{lim}$ when $[H^+] \gg K_S$, and the rate of decomposition should be independent of pH. On the other hand, the apparent rate constant equals $k_{lim}\,[H^+]/K_S$ when $[H^+] \ll K_S$. In this case, the following relationship holds

$$[6] \qquad t_{\frac{1}{2}\ app} = t_{\frac{1}{2}\ lim}\,K_S/[H^+]$$

Therefore, the decomposition rate is expected to be first order with respect to the proton concentration, and this is, in fact, experimentally observed as can be seen from Fig. 2.

By replacing k_{app} and k_{lim} in eq. [5] by $0.6932/t_{\frac{1}{2}\ app}$ and $0.6932/t_{\frac{1}{2}\ lim}$, respectively, one can calculate the acid dissociation constant

$$[7] \qquad K_S = [H^+]\cdot(t_{\frac{1}{2}\ app}/t_{\frac{1}{2}\ lim} - 1)$$

The values of pK_S obtained from eq. [7] for the

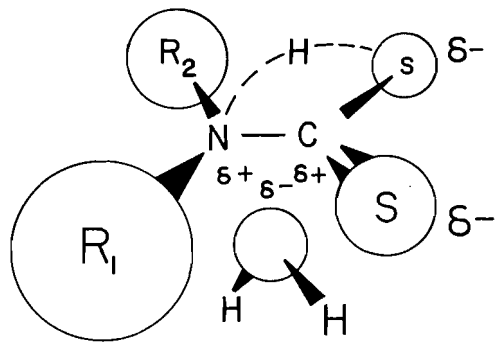

FIG. 3. Solvation of the DTC acid molecule.

three cyclic dithiocarbamates studied are presented in Table 2. These values have been obtained at an ionic strength equal to 0.010.

The following steps have been proposed (14) for the decomposition mechanism of the DTC: (*1*) protonation of one of the sulfur atoms of the DTC anion, (*2*) formation of an intramolecular hydrogen bond between this sulfur atom and the near nitrogen atom (Fig. 3), (*3*) cleavage of the N—C bond because of the repulsion between the fractional positive charges in the acid molecule, (*4*) protonation of the released amine.

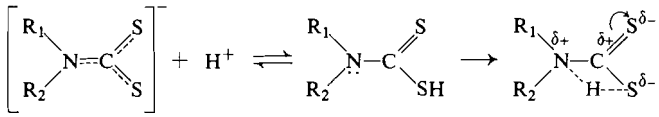

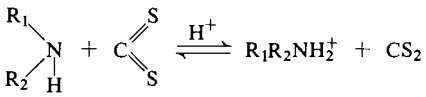

It has been concluded that in the case of the mono and the dialkyl DTC, the rate of decomposition is very dependent on the bulk of the substituents at the nitrogen atom. The size of the substituents determines the extent to which solvation reduces the fractional positive charges in the acid molecule. Bulky substituents would hinder a close approach of the negative pole of the solvent molecules to the fractional positive charges in the DTC acid (Fig. 3). As a result of this less efficient solvation, the activation energy for decomposition would be decreased, as is indicated by the low stability of the dialkyl DTC containing bulky substituents (14).

It appears from Fig. 4 that the effect of the dielectric constant on the limiting decomposition rate of the cyclic DTC is similar to the effect observed in the case of the monoalkyl and dialkyl DTC (14). As the dielectric constant of the solutions is decreased from 78 to 50, the stability of the DTC acid molecule initially decreases because of a decrease in the dipolar character and reduced ability of the solvent to diminish the repulsive forces between the like charges in the DTC molecule (14). Solutions of low dielectric constant (50–30) reduce the repulsion between the fractional positive charges in the acid molecule, and this results in decrease in the decomposition rate (see Fig. 3). However, this increase is not observed in all cases because the predominance of one or the other of these opposing effects (decrease or increase in stability) is determined by the size of the substituents on the nitrogen atom (14). The absence of an increased stability for pyrDTCH at very low values of the dielectric constant is similar to the same effect observed for the monomethyl DTC (14). This can be rationalized as due to the low steric hindrance that is expected (17) in the solvation of these molecules.

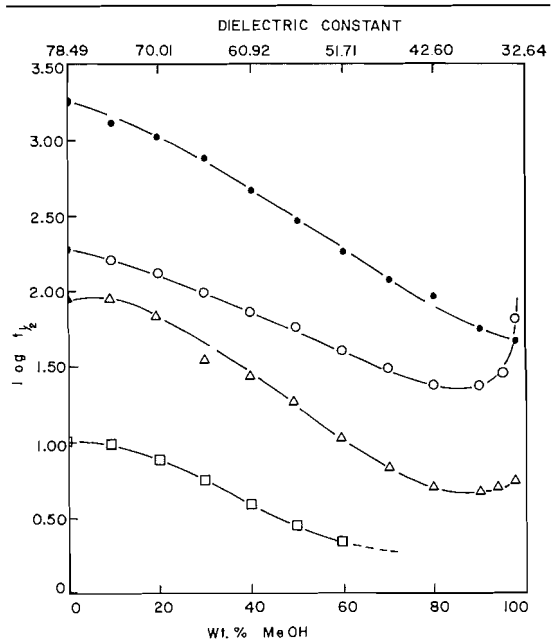

FIG. 4. Effect of dielectric constant on log apparent half-life (s) for decomposition: HCl = 0.05 *N*; ●, pyrDTCNa at 25.0 °C; ○, hexaDTCNa at 25.0 °C; □, pipDTCNa at 25.0 °C; △, pipDTCNa at 0.8 °C. The values for the dielectric constant do not apply to the solutions of PipDTCNa since the temperature is 0.8 °C.

If the conclusions drawn for the decomposition of the monoalkyl and the dialkyl DTC were to be entirely valid for the decomposition of the cyclic DTC, one would expect the following order of decreasing stability

pyrDTCH > pipDTCH > hexaDTCH

Can. J. Chem. Downloaded from www.nrcresearchpress.com by 210.87.254.5 on 09/05/12
For personal use only.

TABLE 2

Acid dissociation constant, limiting half-life, activation energy, and log$_e$ pre-exponential factor for the decomposition of some cyclic dithiocarbamates

Reagent	pK_S*	$t_{\frac{1}{2}\lim}$† (s)	E_a‡ (kcal/mole)	log A‡
pyrDTCNa	3.27±0.05	1920±60	20.3 ±0.3	11.5 ±0.2
hexaDTCNa	3.29±0.05	180±5	18.51±0.02	11.15±0.02
pipDTCNa	3.18±0.05	10±0.6	16.26±0.02	10.72±0.02

*μ = 0.010, temperature = 25 °C.
†Temperature = 25 °C.
‡At pH = 1.5.

in agreement with the order of increasing hindrance to the solvation of these cyclic DTC acids. Actually, the observed order of stability is (Table 2)

pyrDTCH > hexaDTCH > pipDTCH

Furthermore, the same order was found for the activation energies for the decomposition reaction, and for the pre-exponential factors of the Arrhenius equation (Table 2). Although it is indicated by Fig. 4 that the solvation of the cyclic DTC is the rate-determining step in the decomposition, it appears from the above order of stabilities that an additional factor also influences the rate of decomposition of these compounds. The following interpretation is proposed by the present authors. It is known (18, 19) that small differences in internal ring strain can have large effects upon the rates of reaction of five-, six-, and seven-membered ring compounds. If an analogy is drawn between the cyclic imines and the corresponding cycloalkanes (20), the order of increasing ring-strain would be

pyrrolidine > hexamethylenimine > piperidine

This order of internal strain would be present also in the DTC derivatives of these cyclic imines. The addition of a fourth substituent on the nitrogen atom (e.g. the proton of the intramolecular hydrogen bond in the DTC acid) results in crowding together of the three other groups on the nitrogen atom (21). If the conformation about the nitrogen atom is already strained, as in the case of pyrDTCNa, the addition of a fourth substituent would be unfavorable since the strain in the molecule would be increased even further. One would expect that a strained cyclic DTC would not favor a close approach of the proton of the intramolecular hydrogen bond to the nitrogen atom. Therefore, the fractional positive charge on the nitrogen atom would be lower and the stability of the acid would be increased. The stability of the cyclic DTC can thus be related partly to the strain in the ring, as is reflected in the order of the stabilities and the activation energies.

The steric factors (e.g. crowding) due to the alkyl substituents on the nitrogen atom when this atom attains the four-coordination state is probably reflected in the decomposition rates of the monoalkyl and the dialkyl DTC. For these compounds, the observed order of stabilities is (14)

monomethyl > dimethyl > di-*n*-butyl > di-*n*-propyl > diethyl > diisopropyl

The relative ease with which the nitrogen atom can attain a coordination number of four is an additional factor to be considered in the decomposition of the dithiocarbamic acids.

In conclusion, it should be remarked that the decomposition is perhaps more involved than that described above. In fact, definitive statements regarding the stability of dithiocarbamates cannot be made until further studies of thermodynamic parameters, now in progress, are completed. Furthermore, comprehensive studies of the pK values and inductive effects are required in order to explain more accurately the order of stability of the DTC acids. Such studies are also in progress and the results will be published when the studies are completed.

The authors are indebted to the National Research Council of Canada for financial support. Part of this study was submitted by R. R. Vandebeek in partial fulfilment of the requirements for the degree of Bachelor of Science with Honours.

1. A. HULANICKI. Talanta, **14**, 1371 (1967).
2. R. ZAHRADNIK. Chem. Tech., **11**, 546 (1959).
3. D. J. HALLS. Mikrochim. Acta, 62 (1969).
4. D. M. MILLER and R. A. LATIMER. Can. J. Chem. **40**, 246 (1962).
5. D. J. HALLS, A. TOWNSHEND, and P. ZUMAN. Anal. Chim. Acta, **40**, 459 (1968).

Can. J. Chem. Downloaded from www.nrcresearchpress.com by 210.87.254.5 on 09/05/12
For personal use only.

6. S. J. JORIS and C. L. CHAKRABARTI. Unpublished results.
7. D. D. PERRIN. Aust. J. Chem. **16**, 572 (1963).
8. P. S. ALBRIGHT and L. J. GOSTING. J. Amer. Chem. Soc. **68**, 1061 (1946).
9. G. KORTÜM. Treatise on electrochemistry. 2nd ed. Elsevier Publ. Co., New York. 1965. p. 144.
10. M. J. JANSSEN. Rec. Trav. Chim. **79**, 454 (1960).
11. M. J. JANSSEN. Rec. Trav. Chim. **79**, 1066 (1960).
12. M. L. SHANKARANARAYANA and C. C. PATEL. Acta Chem. Scand. **19**, 1113 (1965).
13. S. J. JORIS, K. I. ASPILA, and C. L. CHAKRABARTI. Anal. Chem. **41**, 1441 (1969).
14. S. J. JORIS, K. I. ASPILA, and C. L. CHAKRABARTI. J. Phys. Chem. **74**, 860 (1970).
15. R. ZAHRADNIK and P. ZUMAN. Coll. Czech. Chem. Commun. **24**, 1132 (1959).
16. P. ZUMAN and R. ZAHRADNIK. Z. phys. Chem. **208**, 135 (1958).
17. R. E. MARSH and J. DONOHUE. Advan. Protein Chem. **22**, 235 (1967).
18. H. C. BROWN, R. S. FLETCHER and R. B. JOHANNESEN. J. Amer. Chem. Soc. **73**, 212 (1951).
19. H. C. BROWN and M. GERSTEIN. J. Amer. Chem. Soc. **72**, 2926 (1950).
20. M. HANACK. Conformation theory. Academic Press Inc., New York, 1965. p. 20.
21. A. R. DAY and M. M. JOUILLIÉ. Organic chemistry. D. van Nostrand, Princeton, New Jersey. 1960. p. 569.

Can. J. Chem. Downloaded from www.nrcresearchpress.com by 210.87.254.5 on 09/05/12
For personal use only.

Can. J. Chem. Downloaded from www.nrcresearchpress.com by 210.87.254.5 on 09/05/12
For personal use only.

Studies of the pore structures of silica gels by electron microscopy and low-temperature nitrogen adsorption

E. ROBINSON[1]
Department of Chemistry, College of Technology, Belfast, Northern Ireland

AND

R. A. ROSS
Department of Chemistry, Lakehead University, Thunder Bay, Ontario

Received October 6, 1969

The pore structures of a number of silica gels have been examined by low-temperature (−196 °C) nitrogen adsorption isotherms and these data compared with information obtained from electron photomicrographs. Good general agreement was obtained in the comparison, although the electron photomicrographs reveal more details regarding pore arrangements and dimensional variations. Gel structures were modified by heating and also by treatments with superheated steam or nitric acid. The aggregation of ultimate particles is affected by the steam treatment and this phenomena is compared with the preliminary stages of accepted sintering mechanisms.

Canadian Journal of Chemistry, 48, 2210 (1970)

Introduction

Studies of the physical structure of silica gels aimed at deriving data on surface area and porosity are generally made by measurements of low-temperature gas adsorption/desorption isotherms (*1*, 2). Recently, detailed statistics of such isotherms (N_2: −196 °C) have been reported for silica gels modified by various degrees of heat treatment (3). However, the adsorption method can often lead to uncertainties in interpretation of measurements, for example, in decisions regarding pore shapes (1). Hence it seemed to be valuable to make a direct examination of pore structures by electron microscopy using thin slices of silica gels, and at the same time compare these results with those obtained by nitrogen adsorption.

Previous electron microscope studies have confirmed that silica gel has a corpuscular structure (4), while good agreement has been obtained in studies of particle size distributions by various classical methods when compared with results obtained from the electron microscope (5).

Experimental

Materials

Davison '923' chromatographic grade silica gel with a particle size range 75–150 μ was used. After activation at 240° in air for 15 h, the surface area (B.E.T.: N_2: −196°) was 660 m^2/g and the lump density (6) 1.20 g/cc. The other thermal treatments were carried out in air for 15 h at the temperatures specified in the text.

Modification of the gel by superheated steam was made by treatment in an autoclave for 2 h at 140° with a steam pressure of 38 $lb/in.^2$ followed by heating at 240° for 15 h in air. The nitric acid treatment was similar to that of Thorp and Woolf (7) using 50% v/v nitric acid at 80° for 24 h.

Apparatus

Nitrogen adsorption/desorption isotherms were measured at −196° in a standard apparatus (8) using purified cylinder nitrogen above 99.99% purity. Prior to the determination of isotherms, samples were outgassed carefully in the apparatus at 10^{-4} mm for 1 h.

The early electron photomicrographs were taken with an E.M.I. EM6G instrument using a carbon deposition method but this proved suitable only for observations of the edges of particles. Subsequently, gels were electron photomicrographed by Acon Laboratories, Egham, Surrey, England after applying the specialized technique of vacuum embedding and sectioning. The thickness of sections varied according to the strength and rigidity of samples. Davison '923' gave well-formed wedges of material varying from about 500 Å to less than 100 Å at the edges photomicrographed. The section thickness with superheated steam treated gel was more uniform at 200 ± 50 Å.

Results and Discussion

Electron Photomicrographs

An examination of the edges of a small fragment of '923' gel, 400 000 ×, showed that the gel globules varied in diameter between 300 and 1000 Å. The globules were deeply grown together, indicating that in the bulk material they could not be regarded as separate entities. Part of the sur-

[1]Address: Lambeg Research Institute, Lisburn, N. Ireland.

face was rough and pitted, suggesting that the large globules around the edges were not ultimate particles but were themselves composed of many smaller particles between 10 and 50 Å in diameter, similar to the size noted for ultimate particles earlier (9).

In Plate 1, the arrow indicates the direction in which the section was cut. The discontinuities at right angles are compression lines which are always obtained when hard materials, such as silica, are cut.

The marked effect of combined heat and steam treatment on the gel structure can be seen clearly by comparing Plate 2 with Plate 1. The pores circled C in the superheated steam gel range in size from approximately 40 to 100 Å and exist between discrete globules which vary in diameter between 150 and 500 Å.

After thermal modification of the superheated steam treated gel by heating for 15 h at 500°, the discrete nature of the gel globules is less obvious (Plate 3). The definition on this plate is excellent and a cross-section along the lengths of of many pores can be seen.

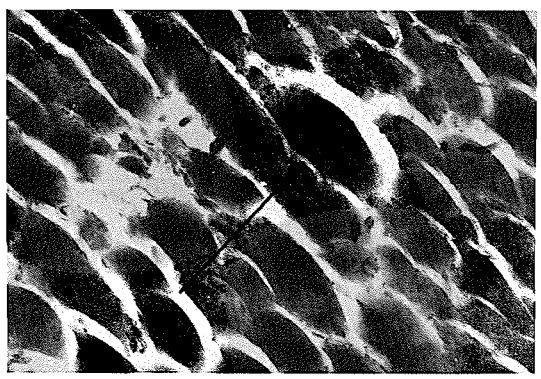

PLATE 1. Davison '923' silica gel, activated at 240°. Microscope magnification, 10 000 × ; total magnification, 20 000 × .

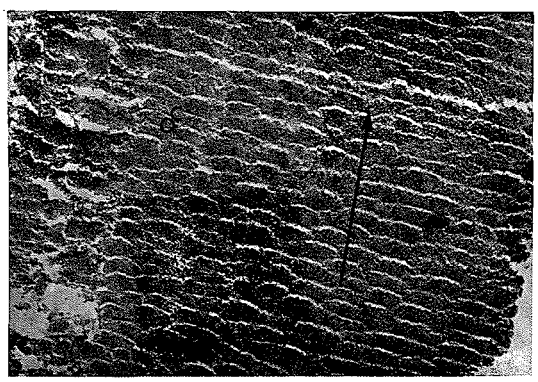

PLATE 2. Superheated steam treated gel. Microscope magnification, 10 000 × ; total magnification, 20 000 × .

PLATE 3. Superheated steam treated gel after heating to 500° for 15 h. Microscope magnification, 10 000 × ; total magnification, 20 000 × .

Nitrogen Adsorption

The hysteresis loop contained by the nitrogen adsorption–desorption isotherm determined on the 240° gel, (Fig. 1) has a sloping adsorption branch which closes almost vertically. This type of loop is generally accepted (10) as indicating a random distribution in the geometry of packing of the ultimate particles and a narrower distribution of pore openings. Such an explanation is consistent with the structure observed in the electron micrographs of this gel.

From similar nitrogen adsorption/desorption isotherms, B.E.T. plots (11) were drawn for all of the gels examined. These plots were all good straight lines over the range $p/p_0 = 0.05$ to 0.30 and from their slopes and intercepts, monolayer adsorbed amounts were computed in the usual way using 16.2 $Å^2$ as the cross-sectional area of a nitrogen molecule (11).

Pore size distribution charts were plotted from the adsorption branches by the Cranston and Inkley method (12) after data processing with an Elliott 803 computer. The chart for 240° gel showed that the range of pore diameters was from 100 to below 20 Å, with the majority of pores having diameters under 50 Å (Fig. 2). The most common pore diameter, given by the mode of the pore size distribution chart, was 25 Å. Treatment of gel with nitric acid appeared to reduce the number of pores below 25 Å. Steam treatment shifted the mode of the pore size dis-

Can. J. Chem. Downloaded from www.nrcresearchpress.com by 210.87.254.5 on 09/05/12
For personal use only.

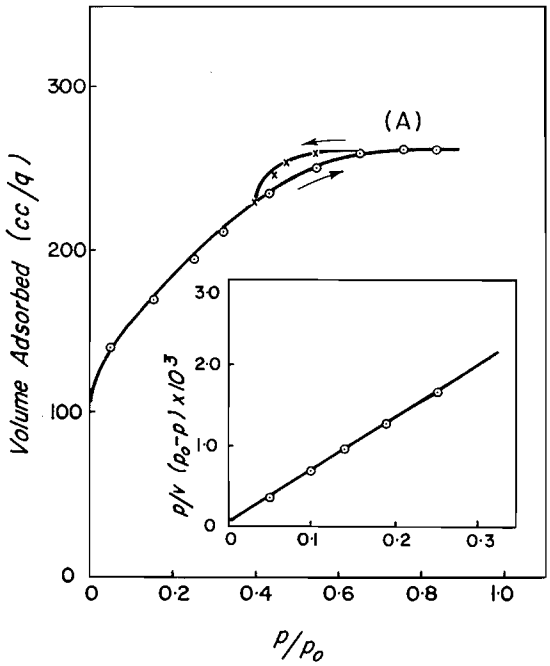

FIG. 1. Nitrogen adsorption/desorption isotherm on 240° gel at −196°. Inset, B.E.T. plot.

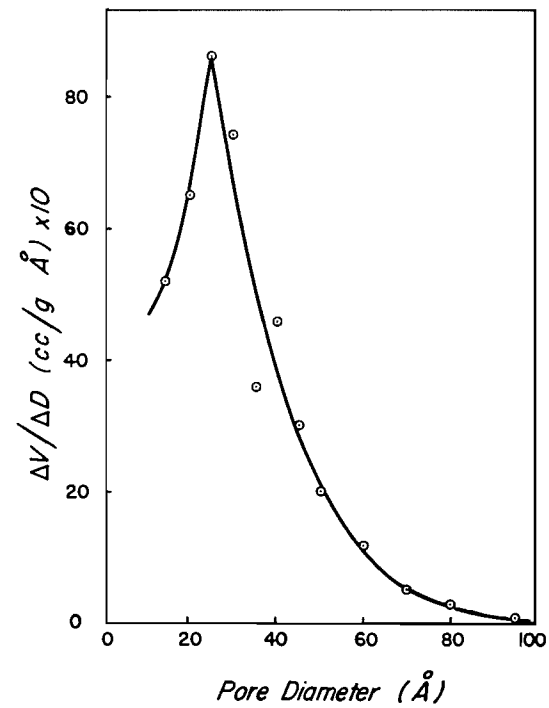

FIG. 2. Pore size distribution chart for 240° gel.

tribution to 40 Å with the majority of pores lying between 38 and 180 Å. Steam treatment followed by heating at 500° shifted the mode still further to 45 Å. Heat treatment (3) of normal '923' gel up to 900° causes little change in the pore size distribution, although the total pore volume diminishes rapidly above 500°.

The principal surface parameters of the gels examined by gas adsorption are shown in the Table 1.

TABLE 1

Surface parameters of gels determined from nitrogen adsorption/desorption isotherms at −196°

Treatment	Activation temperature (°C)	Surface area (m^2/g)	Mode of pore size distribution (Å)
None	240	660	25
None	500	600	—
Superheated steam	240	340	40
Superheated steam	500	335	45
Nitric Acid	240	600	30
10 tons/in.^{2}	240	495	25

The surface areas of two samples were also determined by the more recently introduced *t*-method (13), in which the volume of gas adsorbed/g of adsorbent at standard temperature and pressure, V_a, is plotted against the statistical thickness, *t*, of the adsorbed layer. So long as the multilayer forms unhindered, a straight line is obtained passing through the origin and its slope is a measure of the surface area, $S_t = 15.47\ V_a/t$. For many well-selected samples, Lippens and de Boer (14) found that the first parts of such curves were straight lines from which S_t could be calculated.

Surface areas determined from the *t*-plots in Fig. 3 were 620 and 325 m^2/g for 240° and superheated steam treated gels, respectively. When $t = 4.5$ Å the curve for 240° gel starts to bend downwards. At this value (13) some of the pores are completely filled by the adsorbed layers of nitrogen and the surface in them is no longer available for further adsorption which indicates a minimum pore diameter around 9 Å.

The separate effect of pressure on the surface parameters of '923' gel was determined after compression of the material at 10 tons/in.^{2} for 3 min. This treatment appeared to result in an increase in the number of pores < 20 Å diameter but it was apparent from photomicrographs,

Can. J. Chem. Downloaded from www.nrcresearchpress.com by 210.87.254.5 on 09/05/12
For personal use only.

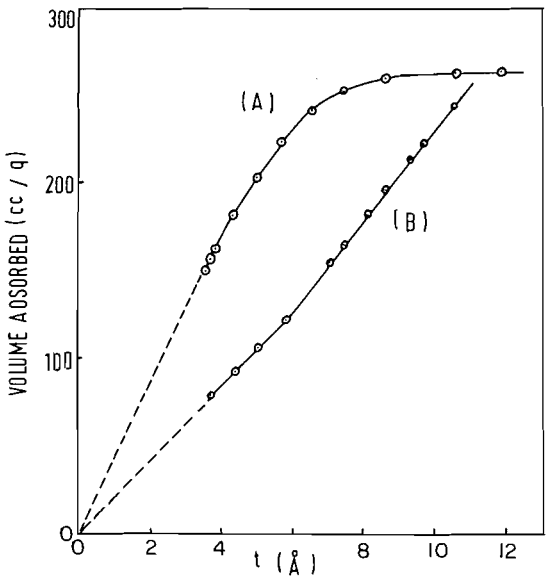

FIG. 3. V_a–t plot for (*A*) 240° and (*B*) superheated steam treated gel.

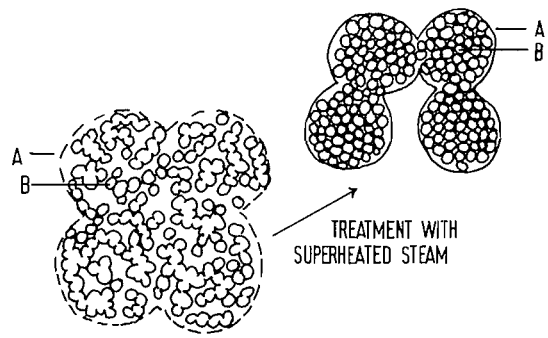

FIG. 4. Suggested effect of superheated steam treatment. (*A*) Silica gel globules, (*B*) ultimate particles.

50 ×, that compression had caused fragmentation of gel particles. The lump density measured by mercury displacement (6) was reduced to 0.99 g/cc, which indicates that the gel particles had been so reduced in size that the mercury was unable to penetrate the interstices between particles. Confirmation of this theory was obtained by reducing the particle size of the original gel to the same size range (< 5 μ) by light grinding. As a result the lump density was reduced to 0.76 from 1.20 g/cc.

General

Treatment of gel with superheated steam causes a severe loss in surface area, Table 1, while the pores increase in size to the 40 to 100 Å range. The electron micrographs indicate that treatment with superheated steam may cause the ultimate particles to aggregate and the globules to become denser and more discrete. The consequent loss of pore volume from the interior of the globules would explain the diminution in their size, the loss of surface area of the gel and the increase in its lump density to 1.48 g/cc.

It has been suggested (5, 9) that the increase in pore diameter and decrease in surface area is the result of a regular growth of the individual ultimate particles of the solid at the expense of others, large particles become larger and smaller ones disappear. Previous steam treatments have been more severe, e.g. up to 215° for 401 h (15), and it may be that the first step in the suggested mechanism is the aggregation of ultimate particles so that within the globules the mechanism is analogous to that of sintering (16) where adhesion of ultimate particles is involved as a preliminary stage. However, this process must be confined to the interior of the globules since treatment with superheated steam does not reduce the total pore volume (15). This suggested effect of superheated steam is shown in Fig. 4.

After consideration of 15 shape groups of pores, de Boer (1) analyzed the types of hysteresis loops which would result from capillary condensation in them. He proposed 5 main types of loops of which 2, Types *A* and *E*, are found here and in our previous studies on the adsorption of various gases on silica gels. For example, the type *A* loop is given by the isotherm for ethylene oxide at 283.7 °K on superheated steam treated gel (17). The adsorption/desorption branches of type *A* isotherms are steep, pores are cylindrical, radius r_n, and contain spherical cavities, r_ω, where $r_\omega \leq 2r_n$. The type E loop is found with cylindrical pores, r_n, which contain large cavities of variable radius, r_ω, while $r_\omega > 2r_n$. The adsorption branch has a sloping character and the desorption branch is steep. If there is a variation in r_n, the desorption branch will have a sloping character also, but the broadening of the loop still exists (13). This describes the loop shown by dimethyl ether isotherms (18) and indeed by most isotherms obtained on 240° '923' gel.

After treatment with superheated steam the hysteresis loops change, and satisfy the pressure relationship (1) shown by Type *A* loops which

Can. J. Chem. Downloaded from www.nrcresearchpress.com by 210.87.254.5 on 09/05/12
For personal use only.

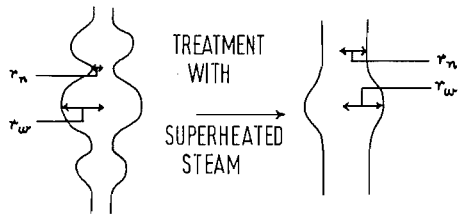

FIG. 5. Suggested effect of superheated steam on pore dimensions.

also persist on subsequent thermal treatment of the steam treated gel at 500° (19). This implies that the pore dimensions have changed, $r_\omega > 2r_n$ becoming $r_\omega \leq 2r_n$, which is consistent (1) with a widening of the constrictions between spheroidal cavities, Fig. 5. Comparison of the cross-sections of pores in the untreated gel, Plate 1, with those in the steam treated gel activated at 500°, Plate 3, shows that such a change probably occurs in the pore structure.

In addition to the pores in the 40 to 100 Å range, electron micrographs, 160 000 ×, indicate that pores < 10 Å may be present in the superheated steam treated gel. This bidisperse pore structure has been reported by Kiselev and co-workers (20) who proposed that the small pores were formed by water trapped as the gel structure changes under steam treatment. When driven out on drying the water molecules form the fine channels in the gel.

Conclusions

The deductions made from the adsorption isotherm analyses regarding the pore characteristics of these gels agree in general with the electron microscope observations, although the latter method is more discerning. Davison '923' silica gel has been examined, a highly pure, readily available, chromatographic-grade material, to provide the possible added advantage of links with earlier work on adsorbate/adsorbent and adsorbate/adsorbate interactions involving mainly reactive gases on hydrous oxides. All of these materials have been described (3) but past attention was largely focussed on '923' gel.

In computing the pore data of the normal and modified '923' gels from the nitrogen adsorption/desorption isotherms, extensive use was made of the Cranston and Inkley method of analysis (12) in which the critical pore radius is equated to the Kelvin radius. Now, when the molecular diameter of the adsorbed gas approaches a value of a few times the Kelvin radius and it is about three times here for the majority of pores in normal '923' gel, then the applicability of analytical schemes based on the classical Kelvin equation for macro-system capillaries remains unresolved (21). Clearly there is a need for additional theoretical study of this particular problem. However, in the present investigation the electron microscope observations have provided an independant model for the pore structures which is internally consistent with the other deductions.

We thank the British Petroleum Company for the award of a research scholarship (E.R.).

1. J. H. DE BOER. *In* Colston papers. Vol. 10. Butterworths, London. **68**, (1958).
2. H. A. BENESI, R. V. BONAR, and C. F. LEE. J. Phys. Chem. **58**, 95 (1954); R. A. BEEBE and D. M. YOUNG. Anal. Chem. **27**, 1963 (1955).
3. A. H. TAYLOR and R. A. ROSS. J. Chem. Eng. Data, **14**, (3), 347 (1969).
4. I. SUGAR and F. GUBA. Acta Chim. Acad. Sci. Hung. **7**, 233 (1955).
5. A. V. KISELEV. *In* Colston papers. Vol. 10, Butterworths, London. 195 (1958).
6. W. B. JEPSON. J. Sci. Inst. **36**, 319 (1959).
7. J. M. THORP and J. B. WOOLF. Trans. Faraday Soc. **63**, 2068 (1967).
8. A. S. JOY. Vacuum, **III**, No. 3, (1953).
9. C. R. ADAMS and H. H. VOGUE. J. Phys. Chem. **61**, 722 (1967).
10. R. VENABLE and W. H. WADE. J. Phys. Chem. **69**, 1395 (1965).
11. S. BRUNAUER, P. H. EMMETT, and E. TELLER. J. Amer. Chem. Soc. **60**, 309 (1938).
12. R. W. CRANSTON and F. A. INKLEY. Advan. Catal. **9**, 143 (1957).
13. B. G. LINSEN and A. VAN DER HEUVAL. The solid–gas interface. *Edited* by E. A. Flood. Edward Arnold London. **2**, 1025 (1967).
14. B. C. LIPPENS and J. H. DE BOER. J. Catal. **4**, 319 (1965).
15. V. M. CHERTOV, D. B. DZAMBAEVA, and I. E. NEIMARK. Kolloid. Zh. **27**, (2), 279 (1965).
16. G. F. HÜTTIG. Kolloid. Zh. **98**, 263 (1942).
17. E. ROBINSON and R. A. ROSS. J. Chem. Soc. (A), 2521 (1969).
18. E. ROBINSON and R. A. ROSS. Can. J. Chem., **48**, 13 (1970).
19. E. ROBINSON and R. A. ROSS. J. Chem. Soc. (A). In press.
20. V. YA DAVYDOV, A. V. KISLEV, and L. T. ZHURAVELEV. Trans. Faraday Soc. **60**, 2254 (1964).
21. D. H. EVERETT. The solid–gas interface. *Edited by* E. A. Flood. Edward Arnold, London. **2**, 1077 (1967).

Can. J. Chem. Downloaded from www.nrcresearchpress.com by 210.87.254.5 on 09/05/12
For personal use only.

Can. J. Chem. Downloaded from www.nrcresearchpress.com by 210.87.254.5 on 09/05/12
For personal use only.

Synthesis and cycloaddition reactions of 2-(2-thienyl)aziridines

J. W. Lown and K. Matsumoto[1]
Department of Chemistry, University of Alberta, Edmonton, Alberta
Received February 2, 1970

The synthesis of several new 2-(2-thienyl)aziridines and an examination of their cycloaddition with olefinic and acetylenic dipolarophiles is described.

Canadian Journal of Chemistry, **48**, 2215 (1970)

Addition reactions of substituted aziridines involving cleavage of the 2–3 bond to an azomethine ylide intermediate (both thermally and less frequently by photochemical means) and subsequent [2 + 3] cycloaddition to carbon–carbon and heteromultiple bonds have proven to be synthetically useful routes to pyrroles (1–4), pyrrolines (1, 4), pyrrolidines (3, 4), thiazolines (5), a thiazole (5), imidazolidines (6), imidazolines (7), oxazolines (8), oxazolidines (9, 10), and naphth[1,2-*d*]oxazoles (11).

We have employed 2-aryl-3-aroylaziridines mainly in our exploration of such reactions. However, 2-aryl-3-carboalkoxy and 2-aryl-3-cyanoaziridines underwent quite different reactions than 2-aryl-3-aroylaziridines with certain dipolarophiles (12). Also the nature of the *N*-substituent in 2-aryl-3-aroylaziridines had a profound effect on the course of the reaction with aryl isothiocyanates (5). These facts suggested a sensitivity of the course of the cycloaddition reactions and possibly the properties of the intermediate azomethine ylides to the type of substituent in the aziridine ring which required further investigation. Therefore we report the synthesis and examination of the cycloaddition reactions of the hitherto undescribed 2-(2-thienyl)-aziridines.

The Gabriel synthesis (13, 14) starting from 2-thiophene aldehyde **1** proved to be satisfactory in many cases as illustrated in Scheme 1. The yield of 3-benzoyl-1-cyclohexyl-2-thienylaziridine (**4**) (Ar = Ph) obtained as a *cis–trans* mixture from the corresponding dibromo compound was 89%. Sufficient representative examples of similar 2-(2-thienyl) aziridines were prepared to establish the scope of the method and to delineate its limitations. The analytical and spectral data are summarized in Tables 1 and 2.

The smooth and selective bromination of the conjugated double bond in the majority of the thienyl chalcones **1** is surprising in view of the known sensitivity of the thiophene nucleus to electrophilic substitution at the 4 and 5 positions, especially when the ring bears an electron-withdrawing substituent (15–17). However, attempted addition of bromine to **2** (Ar = pNO$_2$C$_6$H$_4$) probably led to preferential substitution in the thiophene nucleus as indicated by the mass and nuclear magnetic resonance (n.m.r.)

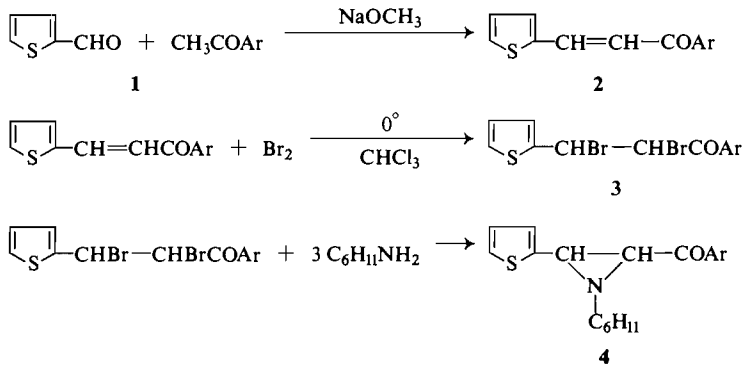

Scheme 1

[1]NRCC Postdoctorate Fellow, 1969 to present.

Can. J. Chem. Downloaded from www.nrcresearchpress.com by 210.87.254.5 on 09/05/12
For personal use only.

TABLE 1

1-Alkyl-2-(2-thienyl)-3-aroyl(or acyl)aziridines*

Number	R_1	R_2	Melting point (°C)	Yield (%)	*cis*: *trans*	Observed					Calculated				
						C	H	N	S	Molecular ion (mass spectrum)	C	H	N	S	Molecular ion (mass spectrum)
a	C_6H_{11}	C_6H_5	104–105 (*trans*)	89	0.4	73.25	6.76	4.58	10.39	311.1345	73.26	6.81	4.50	10.30	311.1344
			89–90 (*cis*)			73.37	6.71	4.47	10.36	311.1345	73.26	6.81	4.50	10.30	311.1344
b	C_6H_{11}	$mNO_2C_6H_4$	114–115 (*trans*)	91		63.98	5.71	7.78	9.00	356.1195	64.03	5.66	7.86	9.00	356.1195
c	C_6H_{11}	$pCH_3C_6H_4$	104–108†	79	1.4	73.79	7.15	4.28	9.85	325.1502	73.79	7.12	4.30	9.85	325.1500
d	C_6H_{11}	$pCH_3OC_6H_4$	87–93†	93	0.95	70.09	6.62	4.22	9.40	341.1447	70.34	6.79	4.10	9.37	341.1449
e	C_6H_{11}	$pC_6H_5C_6H_4$	110–115†	71	2.0	77.01	6.38	3.68	7.81	387.1661	77.49	6.50	3.62	8.27	387.1657
f	$(CH_3)_2CH$	$pC_6H_5C_6H_4$	42–46	82	0.61	76.10	6.10	4.03	9.23	347.1346	76.59	6.08	4.02	8.79	347.1344
g	C_6H_{11}	OCH_3	Oil†	62	1.2	—	—	—	—	265.1137	—	—	—	—	265.1136

*The compound has the following general structure: 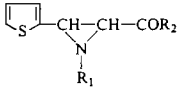

†*cis–trans* Mixture.

TABLE 2

Spectroscopic properties of 1-alkyl-2-(2-thienyl)-3-aroyl(or acyl)aziridines

Number	Infrared spectrum ($CHCl_3$) C=O	Nuclear magnetic resonance spectrum ($CDCl_3$) δ: Aryl and thienyl protons	Aziridine† ring protons	Aroyl methyl	*N*-Alkyl groups
a (*cis*)	1682	8.2–6.7(8H)m	3.35, 3.28(2H)ABq (J = 7 Hz)		2.2–0.9(11H)m C_6H_{11}
a (*trans*)	1666	8.2–6.7(8H)m	3.75(2H)s		2.2–0.5(10H)m, 3.0–2.2(1H)m C_6H_{11}
b (*trans*)	1676	8.5–6.8(7H)m	3.78, 3.62(2H)ABq (J = 1.5 Hz)		2.2–0.7(10H)m, 2.9–2.2(1H)m C_6H_{11}
*c**	1665, 1682	8.2–6.7(7H)m	(*i*) 3.27, 3.24(2H)ABq (J = 7 Hz *cis*)	2.37(3H)s	2.2–0.7(10H)m, 2.8–2.2(1H)m C_6H_{11}
			(*ii*) 3.72(2H)s *trans*	2.40(3H)s	
*d**	1656	8.3–6.7(7H)m	(*i*) 3.22, 3.17(2H)ABq (J = 7 Hz *cis*)	3.82(3H)s	2.2–0.7(10H)m, 2.9–2.2(1H)m C_6H_{11}
			(*ii*) 3.5–4.0(2H)m *trans*	3.85(3H)s	
*e**	1666(sh), 1682	8.3–6.7(12H)m	(*i*) 3.32, 3.28(2H)ABq (J = 7.5 Hz, *cis*)		3.0–0.7(11H)m
			(*ii*) 3.78(2H)s *trans*		
*f**	1663	8.3–6.7(12H)m	(*i*) 3.30(2H)s *cis*		0.95(6H)d (J = 6 Hz), 1.25(6H)d (J = 6 Hz), 3.2–2.6(1H)m
			(*ii*) 3.69(2H)s *trans*		
g	1726	7.8–6.8(3H)m	3.2–2.3(2H)m (—CH—N)	3.67 and 3.57 (3H)s ($—CO_2CH_3$)	2.2–0.5(10H)m

*cis–trans Mixture.
†*cis* and *trans* Isomers assigned following the work of Cromwell *et al.* (40).

spectra. Similar complications were encountered in attempted preparation of the 3-cyano and the 3-acetyl-2-(2-thienyl)aziridines.

The aziridines were normally prepared as *cis–trans* isomeric mixtures. Representative pairs of isomeric aziridines were separated (entries *a* and *d* in Table 1) and used for the stereochemistry experiments described below. The geometrical assignments were based on the spectroscopic methods due to Pohland *et al.* (18) and by Turner *et al.* (19).

2–3 Bond Cleavage and 1,3-Dipolar Additions of 2-(2-Thienyl)aziridines

(a) Olefinic Dipolarophiles

Reaction of 3-benzoyl-1-cyclohexyl-2-(2-thienyl)aziridine with maleic anhydride, *N*-phenylmaleimide, methyl fumarate, and methyl maleate in refluxing benzene for 16 h afforded the stereoisomerically pure pyrrolidines **5**, **6**, **7**, and **8** respectively in good yields. The isolation of these adducts shows that the reduced resonance energy of the thiophene ring (20 kcal $mole^{-1}$ (20) compared with benzene 36 kcal $mole^{-1}$) still allows facile 2–3 bond cleavage of the aziridine and subsequent 1,3-dipolar addition. Pyrrolidine **5** was obtained by reaction of maleic anhydride with either pure *cis* or pure *trans*-3-benzoyl-1-cyclohexyl-2-(2-thienyl)aziridine. Exactly similar results were obtained in the addition of *cis*- and

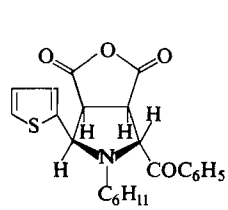

5

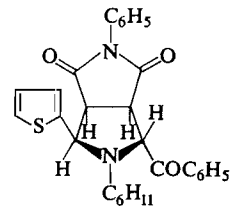

6

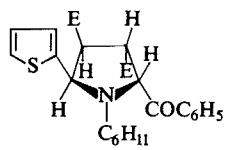

7

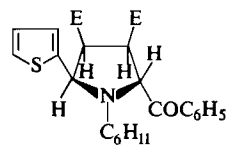

8

E = $COOCH_3$

Can. J. Chem. Downloaded from www.nrcresearchpress.com by 210.87.254.5 on 09/05/12
For personal use only.

Can. J. Chem. Downloaded from www.nrcresearchpress.com by 210.87.254.5 on 09/05/12
For personal use only.

trans-2-aryl-3-aroylaziridines (with *N*-alkyl substituents) to imines (6), sulfonylimines (6), and iminocyclopropenes (7) to give imidazolidines and to aryl aldehydes and chloral to give oxazolidines (10). We conclude that the prior equilibration of the *cis* and *trans* azomethine ylides (21) (from conrotatory thermal ring opening of the *trans* and *cis* aziridines respectively (22)) occurs and addition takes place exclusively via the more stable *trans* azomethine ylide.

The pyrrolidines **5**, **6**, **7**, and **8** were accordingly assigned the *trans* stereochemistry of the aziridine moiety shown on this basis.

Whether or not stereospecific addition to *cis* and *trans* azomethine ylides derived from aziridines is observed seems to depend only on the nature of the *N*-substituent. The only reported examples of such stereospecific additions have involved *N*-aryl substituents (21–23). This aspect of aziridine chemistry is currently under further investigation.

Both *cis* and *trans*-3-benzoyl-1-cyclohexyl-2-(2-thienyl)aziridine reacted with dimethyl acetylenedicarboxylate to form a 1:1 adduct, the spectral data of which are consistent with the *cis*-2-pyrroline structure **9**, together with some of

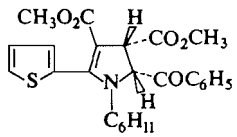

9

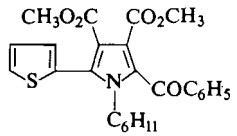

10

the pyrrole **10**. The n.m.r. absorption of the methine hydrogens of **9** showed an AB quartet at δ 4.34 and 5.52, J_{AB} = 12 Hz (1). The n.m.r. of a substituted 3-pyrroline would not have had as large a coupling constant as that observed (23–25). Heine *et al.* have shown that 3-pyrrolines are formed when 1,2,3-triphenylaziridine reacts with acetylenes (3) but Padwa and Hamilton isolated 2-pyrrolines like **9** when 2-aroylaziridines reacted with acetylenes (25). Padwa reports that *trans*-2-pyrrolines are surprisingly resistant to oxidation. The *cis*-2-pyrroline **9** however was easily dehydrogenated to the pyrrole **10** with tetrachloro-1,4-benzoquinone.

Unlike many of the adducts prepared from 1,2,3-triphenylaziridine with the above dipolarophiles by Heine *et al.* (3), the compounds **5**, **6**, **7**, and **8** lack a plane or center of symmetry. Elucidation of the complete stereochemistry of the adducts was however possible using specifically 3-deuterated-3-benzoyl-1-cyclohexyl-2-(2-thienyl)aziridine (**12**). Treatment of **2** with *tert*-butylamine allowed isolation of the monobromo-compound **11** from which **12** was prepared (with 86% deuterium in the 3-position) with cyclohexylamine-*N*-d_2 (7). Reaction of maleic anhydride with **12** afforded **5** deuterated at the 5

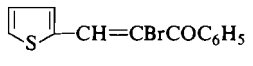

11

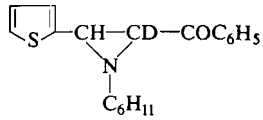

12

position of the pyrrolidine ring (56% *d*) and so allowed the unambiguous assignment of chemical shifts and coupling constants of the methine protons listed in Table 4 (see Fig. 1). The n.m.r. spectra of **5** and **6** are very closely similar and so analogous assignments were made for **6**. Heine has demonstrated the applicability of the Karplus relation (26) of vicinal coupling constants and dihedral angles in pyrrolidines (3). Pyrrolidines **5** and **6** show large $J_{2,3}$ = 10 Hz and zero values for $J_{4,5}$ in complete agreement with the assigned stereochemistry. Values for $J_{3,4}$ of 8.5 and 8.0 Hz respectively correspond to *cis* coupling also required by the structures.

Reaction of methyl fumarate and methyl maleate with **12** gave **7** and **8** with 54 and 60% deuterium incorporation at the 5 pyrrolidine positions. This labelling revealed that of the pair of 2 and 5 methine protons in **7** and **8**, the 5 proton resonates at lower field in contrast to the case in compounds **5** and **6** (see Figs. 1 and 2). The full stereochemistry of **7** depicted follows from the observation of $J_{2,3}$ = 9, $J_{4,5}$ = 8 Hz both characteristic of *cis* vicinal coupling (3). By similar reasoning the methyl maleate adduct **8** was assigned the stereochemistry shown, the smaller value of $J_{4,5}$ = 4.5 Hz, being assigned to *trans* coupled protons.

The isomeric pyrrolidine structures of **7** and **8** were confirmed by dehydrogenation with tetrachloro-1,4-benzoquinone to the pyrrole **10**, identical with that obtained from dimethyl acetylenedicarboxylate. In the addition of *cis* olefinic dipolarophiles to the thienyl aziridine, the addend in **6**, **7**, and **8** adopted positions remote from the 5-aroyl group. Methyl maleate retains its configuration in the addition of **4** in refluxing benzene

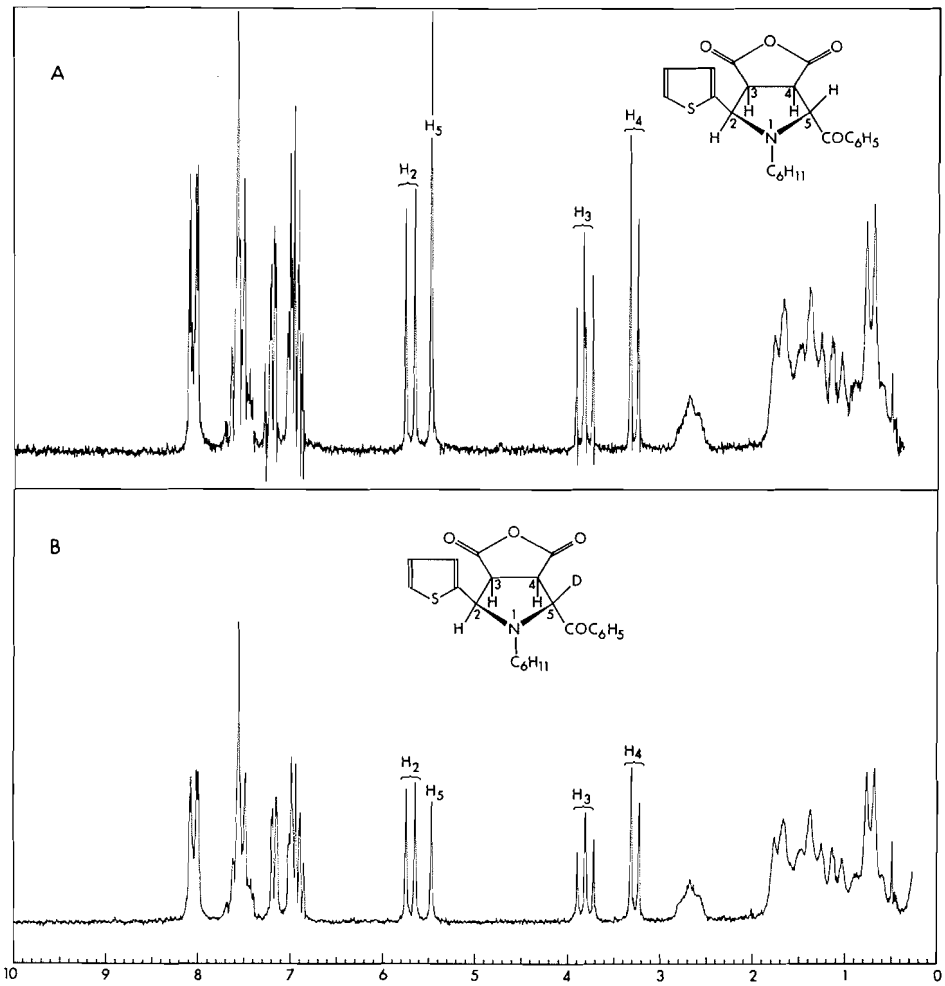

FIG. 1. (A) The n.m.r. spectrum at 100 MHz in $CDCl_3$ of maleic anhydride adduct of 3-benzoyl-1-cyclohexyl-2-(2-thienyl)aziridine. (B) The n.m.r. spectrum at 100 MHz in $CDCl_3$ of maleic anhydride adduct of 3-benzoyl-1-cyclohexyl-3-deutero-2-(2-thienyl)aziridine.

to give **8** in contrast to the addition of ethyl maleate to 1,2,3-triphenylaziridine in refluxing toluene to give **13** (3). The latter reaction probably involves thermal isomerization of ethyl maleate to ethyl fumarate at the higher reaction temperature. We have reported the partial isomerization of methyl maleate during the addition to 4-oxazolines to give 3-aroyl-4,5-dihydrofurans (27) and Huisgen *et al.* have observed complete thermal isomerization of methyl maleate in an attempt to observe stereospecific addition of a ketocarbene to maleate and fumarate (28).

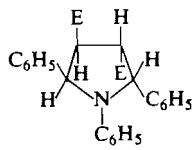

13

E = $COOC_2H_5$

Adducts **14**, **15**, and **16** prepared by reaction of 1-isopropyl-3-*p*-phenylbenzoyl-2-(2-thienyl)-aziridine to methyl fumarate, methyl maleate, and maleic anhydride respectively show a pronounced trend towards increasing difference in chemical shift of the non-equivalent *N*-isopropyl methyl groups (see Fig. 3). This would seem to be associated with increasing screening by ester and

Can. J. Chem. Downloaded from www.nrcresearchpress.com by 210.87.254.5 on 09/05/12
For personal use only.

Can. J. Chem. Downloaded from www.nrcresearchpress.com by 210.87.254.5 on 09/05/12
For personal use only.

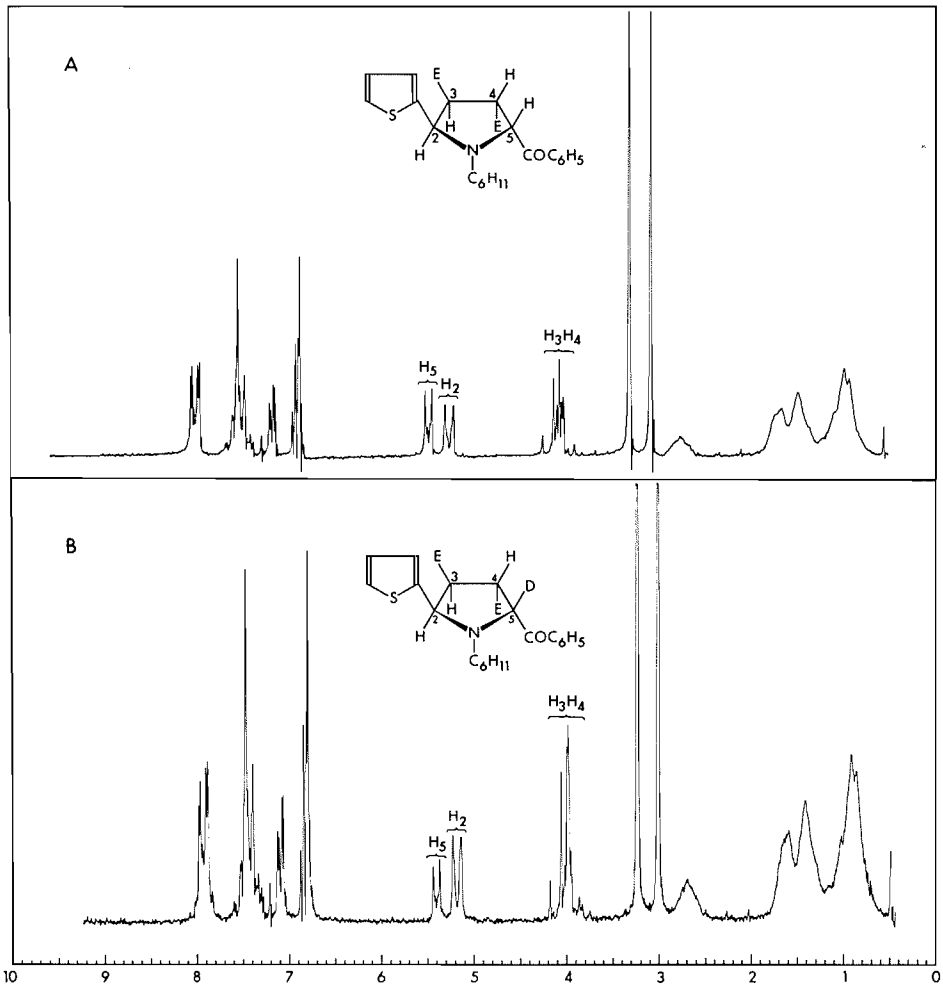

FIG. 2. (A) The n.m.r. spectrum at 100 MHz in $CDCl_3$ of methyl fumarate adduct of 3-benzoyl-1-cyclohexyl-2-(2-thienyl)aziridine (E = $COOCH_3$). (B) The n.m.r. spectrum at 100 MHz in $CDCl_3$ of methyl fumarate adduct of 3-benzoyl-1-cyclohexyl-3-deutero-2-(2-thienyl)aziridine.

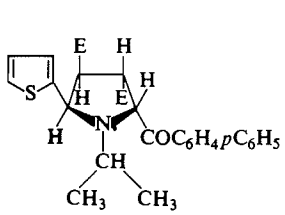

14

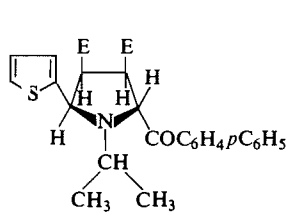

15

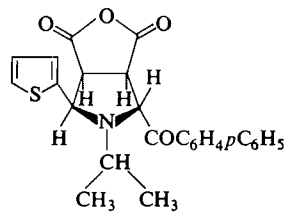

16

anhydride carbonyl groups on the rotating isopropyl methyl groups. Since anisotropic shielding due to the carbonyl group falls off rapidly with increasing distance (29) it seems likely the *N*-isopropyl groups in **14**, **15**, and **16** adopt average conformations *endo* to the addend.

Experimental

Melting points were determined on a Fisher–Johns apparatus and are uncorrected. Infrared (i.r.) spectra were recorded on a Perkin–Elmer model 421 spectrophotometer, and only the principal, sharply defined peaks are reported. The n.m.r. spectra were recorded on Varian A-60 and A-100 analytical spectrometers. The spectra

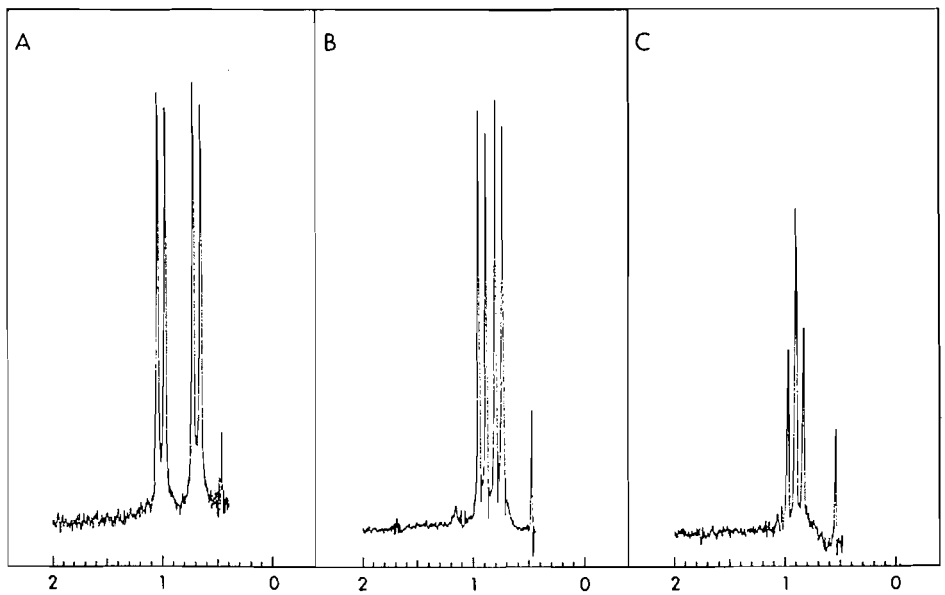

FIG. 3. The n.m.r. spectra at 100 MHz in $CDCl_3$ of isopropyl group resonances of the adducts of 1-isopropyl-3-(*p*-phenylbenzoyl)-2-(2-thienyl)aziridine with (A) maleic anhydride (B) methyl maleate, and (C) methyl fumarate.

were measured on approximately 10–15% (w/v) solutions in $CDCl_3$, with tetramethylsilane as a standard. Line positions are reported in parts per million from the reference. Absorption spectra were recorded in 'spectro'-grade solvents on a Beckman DB recording spectrophotometer. Mass spectra were determined on an Associated Electrical Industries MS-9 double focusing high resolution mass spectrometer. The ionization energy, in general, was 70 eV. Peak measurements were made by comparison with perfluorotributylamine at a resolving power of 15 000. Kieselgel DF-5 (Camag, Switzerland) and Eastman Kodak precoated sheets were used for thin-layer chromatography (t.l.c.). Microanalyses were carried out by Dr. C. Daesslé, Organic Microanalysis Ltd., Montreal, Quebec and by Mrs. D. Mahlow of this department.

General Preparation of 2-(2-Thienyl)aziridines

These compounds were prepared by established methods involving aldol type condensations to form the chalcones, then addition of bromine to form the dibromochalcone and treatment of the latter with amines to provide the 2-(2-thienyl)aziridines. Several new 2-(2-thienyl)aziridines have been prepared by this method exemplified as follows.

2,3-Dibromo-3-(2-thienyl)-propiophenone

The corresponding chalcone was prepared by a similar method described in ref. 38 in 95% yield, m.p. 58–59° (lit. m.p. 58.4–59.2°) (30). A solution of 16.0 g (0.10 mole) of bromine in 100 ml of chloroform was added dropwise to a stirred solution of 21.4 g (0.10 mole) of 1-phenyl-3-(2-thienyl)propenone in 400 ml chloroform at 0 °C during 30 min. The solution was stirred for 3 h, then the solvent removed *in vacuo* to give the dibromo compound as a pale yellow solid which was recrystallized from benzene: hexane as a white solid m.p. 125–126°, 29.6 g, (79.1% yield).

Anal. Calcd. for $C_{13}H_{10}OSBr_2$: C, 41.73; H, 2.70; S, 8.57; Br, 42.71. Found: C, 41.97; H, 2.52; S, 8.48; Br, 42.74.

The i.r. spectrum ν_{max} ($CHCl_3$): 1692 cm^{-1} (aryl C=O). The n.m.r. spectrum δ_{TMS} ($CDCl_3$): AB quartet centered at 5.79 and 6.01 (2H, J = 11 Hz, 2,3 protons); 6.85–8.3 (multiplet, 8H aryl protons).

3-Benzoyl-1-cyclohexyl-2-(2-thienyl)aziridine

A solution of 4.97 g (0.05 mole) cyclohexylamine in 15 ml dry benzene was added dropwise to a stirred solution of 3.74 g (0.01 mole) 2,3-dibromo-3-(2-thienyl)-propiophenone in 50 ml dry benzene at 0 °C during 20 min. The solution was stirred for 24 h at room temperature. The precipitated cyclohexylamine hydrobromide was filtered off. The filtrate was concentrated to ca. 5 ml, then chromatographed on alumina with benzene. Evaporation of the solvent gave an orange oil, which when triturated under hexane gave a pink solid 2.76 g (89% yield), m.p. 90–95 °C. This material was chromatographed on grade 1 alumina with initial elution by hexane followed by benzene. In this way two pure fractions were obtained, *trans*-aziridine m.p. 104–105° (from methanol), *cis*-aziridine m.p. 89–90° (from hexane). Full details on these compounds as well as the physical properties, analytical data and spectroscopic properties of the other 2-(2-thienyl)aziridines synthesized may be found in Tables 1 and 2.

2,3-Dibromo-3-(2-thienyl)-p-methoxypropiophenone

1-(*p*-Methoxyphenyl)-3-(2-thienyl)propenone (m.p. 103.5–104.5° (lit. m.p. 106–107°) (31–33)) was prepared in

Can. J. Chem. Downloaded from www.nrcresearchpress.com by 210.87.254.5 on 09/05/12
For personal use only.

Can. J. Chem. Downloaded from www.nrcresearchpress.com by 210.87.254.5 on 09/05/12
For personal use only.

88% yield by condensation of 2-thienyl aldehyde with 4-methoxyacetophenone using sodium methoxide as base. It was then brominated as described above to give 2,3-dibromo-3-(2-thienyl)-*p*-methoxypropiophenone in 75% yield, m.p. 104–105°.

Anal. Calcd. for $C_{14}H_{12}SBr_2O_2$: C, 41.61; H, 2.99; S, 7.75; Br, 39.56. Found: C, 41.77; H, 3.01; S, 7.71; Br, 39.43.

The i.r. spectrum ν_{max} ($CHCl_3$): 1680 cm^{-1} (aryl C=O). The n.m.r. spectrum ($CDCl_3$): AB quartet centered at 5.76 and 5.99 (2H, J = 11 Hz, 2,3 protons); 6.8–8.2 (7H, multiplet, thienyl and aryl protons); 3.88 (3H, singlet, methoxyl protons).

2,3-Dibromo-3-(2-thienyl)-m-nitropropiophenone

1-(*m*-Nitrophenyl)-3-(2-thienyl)propenone was prepared using sodium methoxide as base in 70% yield, m.p. 113–114° (lit. m.p. 114°) (34); then brominated to give 2,3-dibromo-3-(2-thienyl)-*m*-nitropropiophenone in 77% yield, m.p. 124–125°.

Anal. Calcd. for $C_{13}H_9NSBr_2O_3$: C, 37.25; H, 2.16; N, 3.34; S, 7.65; Br, 38.13. Found: C, 37.62; H, 1.99; N, 3.30; S, 7.75; Br, 38.21.

The i.r. spectrum ν_{max} ($CHCl_3$): 1703 cm^{-1} (aryl C=O).

The n.m.r. spectrum δ_{TMS} ($CDCl_3$): AB quartet centered at 5.99 and 5.79 (2H, J = 11 Hz, 2,3 protons); 6.8–9.0 (7H, multiplet, thienyl and aryl protons).

2,3-Dibromo-3-(2-thienyl)-p-methylpropiophenone

1-(*p*-Methylphenyl)-3-(2-thienyl)-propenone was prepared in 98% yield, m.p. 77–78° (lit. m.p. 79°) (32, 35) then brominated to give 2,3-dibromo-3-(2-thienyl)-*p*-methylpropiophenone in 92% yield, m.p. 133–134°.

Anal. Calcd. for $C_{14}H_{12}SBr_2O$: C, 43.33; H, 3.12; S, 8.26; Br, 41.19. Found: C, 43.22; H, 3.14; S, 7.98; Br, 41.09.

The i.r. spectrum ν_{max} ($CHCl_3$): 1690 cm^{-1} (aryl C=O). The n.m.r. spectrum δ_{TMS} ($CDCl_3$): 2.43 (3H, singlet methyl protons); AB quartet centered at 5.77 and 5.99 (2H, J = 11 Hz, 2, 3 protons); 6.8–8.1 (7H multiplet, thienyl and aryl protons).

1-Biphenyl-3-(2-thienyl)-propenone

This compound was prepared by condensation of 2-thienyl aldehyde with 4-phenylacetophenone using sodium methoxide as base in methanol, m.p. 155–156° (97%) (lit. m.p. 157°) (35, 36).

2,3-Dibromo-3-(2-thienyl)-p-phenylpropiophenone

This compound was prepared by bromination of 1-biphenyl-3-(2-thienyl)propenone in 89% yield, m.p. 146–147°.

Anal. Calcd. for $C_{19}H_{14}SBr_2O$: C, 50.69; H, 3.13; S, 7.12; Br, 35.50. Found: C, 50.31; H, 3.02; S, 7.13; Br, 36.05.

The i.r. spectrum ν_{max} ($CHCl_3$): 1684 cm^{-1} (aryl C=O). The n.m.r. spectrum δ_{TMS} (DMSO-d_6): AB quartet centered at 6.24 and 6.70 (2H, J = 12 Hz, 2, 3 protons); 7.0–8.9 (12H, multiplet, thienyl and aryl protons).

Attempted Preparation of 1-Cyclohexyl-3-p-nitrobenzoyl-(2-thienyl)aziridine

1-(*p*-Nitrophenyl)-3-(2-thienyl)-propenone (m.p. 173–174° (lit. m.p. 173°) (33, 34)) was prepared in 96% yield using sodium methoxide as base. It was then brominated in chloroform at 0 °C to give the dibromo compound in 93% yield, m.p. 145–146° (benzene–hexane). The n.m.r. spectra showed no AB quartet signal due to 2,3 protons.

Anal. Calcd. for $C_{13}H_9O_3NSBr_2$: C, 37.25; H, 2.16; N, 3.34; Br, 38.13; S, 7.65. Found: C, 38.59; H, 2.24; N, 3.29; Br, 38.62; S, 7.54.

The mass spectrum showed a molecular ion 419 ($C_{13}H_9O_3NSBr_2$) and a fragment ion 242 ($C_4H_3SBr_2$). These data suggest that in the bromination of the chalcone, bromination takes place mainly in the thiophene ring. Furthermore no aziridine could be obtained by treatment of this dibromo compound with an excess of cyclohexylamine.

3-Carbomethoxy-1-cyclohexyl-2-(2-thienyl)aziridine

(a) 1-Carbomethoxy-1,2-dibromo-2-(thienyl)ethane

Thienyl acrylic acid was obtained by a similar method as described in ref. 39 in 95% yield, m.p. 143–144° (lit. m.p. 143–144°) (37); then esterified in methanol – sulfuric acid to give thienyl acrylic acid methyl ester in 82% yield, m.p. 42–43°.

Anal. Calcd. for $C_8H_8SO_2$: C, 57.14; H, 4.79; S, 19.06. Found: C, 57.09; H, 4.71; S, 18.83.

The i.r. spectrum ν_{max} ($CHCl_3$): 1706 cm^{-1} (C=O). The n.m.r. spectrum δ_{TMS} ($CDCl_3$): 3.78 (3H, singlet, methyl protons); AB quartet centered at 6.23 and 7.78 (2H, J = 15.5 Hz, —CH=CH—); 6.9–7.5 (3H, multiplet, thienyl protons). Thienyl acrylic acid methyl ester was brominated to give the dibromo compound in 70% yield m.p. 74–75°.

Anal. Calcd. for $C_8H_8SO_2Br_2$: C, 29.29; H, 2.46; S, 9.77; Br, 48.73. Found: C, 29.16; H, 2.35; S, 9.78; Br, 48.88.

The i.r. spectrum: ν_{max} ($CHCl_3$), 1749 cm^{-1} (C=O). The n.m.r. spectrum δ_{TMS} ($CDCl_3$): 3.86 (3H, singlet, methyl protons); AB quartet centered at 4.80 and 5.67 (2H, J = 12 Hz, 1, 2, protons); 6.8–7.5 (3H, multiplet, thienyl protons).

(b) 3-Carbomethoxy-1-cyclohexyl-2-(2-thienyl)aziridine

This dibromo compound was treated with 11 equivalents of cyclohexylamine for 1 week and worked up as usual to give 3-carbomethoxy-1-cyclohexyl-2-(2-thienyl)-aziridine as a yellow oil.

Mol. Wt. Calcd. for $C_{14}H_{19}NSO_2$ (mass spectrum): 265.1136. Found: 265.1137.

The i.r. spectrum ν_{max} ($CHCl_3$): 1726 cm^{-1} (ester C=O). The n.m.r. spectrum δ_{TMS} ($CDCl_3$): 0.5–2.2 (10H, multiplet, cyclohexyl protons); 2.3–3.2 (2H, multiplet, aziridine protons), 3.57, 3.67 (3H, singlet, *cis* and *trans* $COOCH_3$); 6.8–7.8 (3H, ABX thienyl protons).

Reaction of 3-Benzoyl-1-cyclohexyl-2-(2-thienyl)aziridine with Dipolarophiles

(a) Maleic Anhydride

A solution of 0.933 g (0.003 mole) of 3-benzoyl-1-cyclohexyl-2-(2-thienyl)aziridine and 0.294 g (0.003 mole) of maleic anhydride in 50 ml dry benzene was heated under reflux for 5 h after which time no aziridine was detected by t.l.c. The solvent was evaporated and the residual oil treated with hexane and chilled when 1.192 g of the addition product, m.p. 156–159 °C (98% yield), precipitated, which was recrystallized from ether–hexane;

TABLE 3
Physical and analytical properties of the pyrrolidines

Compound	Melting point (°C)	Yield (%)	Observed C	H	N	S	Molecular ion (mass spectrum)	Calculated C	H	N	S	Molecular ion (mass spectrum)
5	159–160	98	67.41	5.63	3.48	7.55	409.1381	67.45	5.66	3.42	7.83	409.1382
6	85–86	87	71.22	5.91	5.65	6.19	484.1801	71.88	5.83	5.78	6.62	484.1801
7	131–132	55	66.36	6.42	3.08	7.07	455.1766	65.91	6.42	3.08	7.04	455.1767
8	Oil	47	—	—	—	—	455.1766	—	—	—	—	455.1767
14	133–134	57	68.28	5.73	2.83	6.70	491.1760	68.41	5.95	2.85	6.52	491.1767
15	113–114	35	68.07	5.92	2.88	6.55	491.1762	68.41	5.95	2.85	6.52	491.1767
16	193–194	92	70.07	5.07	3.35	7.04	445.1345	70.09	5.20	3.15	7.20	445.1348

m.p. 159–160°. Full details on this compound as well as the physical properties, analytical data, and spectroscopic properties of the other addition products prepared are summarized in Tables 3 and 4.

(b) N-Phenyl Maleimide

A similar reaction between 0.933 g (0.003 mole) of 3-benzoyl-1-cyclohexyl-2-(2-thienyl)aziridine and 0.52 g (0.003 mole) of *N*-phenylmaleimide in 50 ml of dry benzene, worked up in the same way afforded the adduct as a yellow solid 1.263 g (87% yield), m.p. 85–86° (ether–hexane).

(c) Methyl Fumarate

A solution of 0.933 g (0.003 mole) of 3-benzoyl-1-cyclohexyl-2-(2-thienyl)aziridine and 0.432 g (0.003 mole) of methyl fumarate in 50 ml of dry benzene was heated under reflux for 15 h. The solvent was evaporated and the residual yellow oil subjected to chromatography on grade 1 alumina (B.D.H.). Elution with benzene afforded one fraction. Evaporation of solvent and treatment with hexane gave a white solid 0.751 g (55% yield), m.p. 131–132° (from ether–hexane).

(d) Methyl Maleate

A solution of 0.933 g (0.003 mole) of 3-benzoyl-1-cyclohexyl-2-(2-thienyl)aziridine and 0.432 g (0.003 mole) of methyl maleate in 50 ml dry benzene was heated under reflux for 7 h. The reaction mixture was worked up as described for (*a*) above; yellow oil (0.647 g, 47% yield).

Reaction of Maleic Anhydride with Stereochemically Pure cis- and trans-3-Benzoyl-1-cyclohexyl-2-(2-thienyl)aziridine

(*a*) Reaction of 0.933 g (0.003 mole) of *trans*-3-benzoyl-1-cyclohexyl-2-(2-thienyl)aziridine and 0.294 g (0.003 mole) of maleic anhydride in 50 ml dry benzene in the manner described above gave 1.028 g (84% yield) of 5-benzoyl-1-cyclohexyl-2-(2-thienyl)pyrrolidine-3,4-dicarboxylic anhydride, m.p. 159–160°.

(*b*) A similar reaction of 0.311 g (0.001 mole) of *cis*-3-benzoyl-1-cyclohexyl-2-(2-thienyl)aziridine and 0.098 g (0.001 mole) of maleic anhydride gave the identical pyrrolidine 0.307 g (75% yield) m.p. 159–160°.

Preparation of 3-Benzoyl-1-cyclohexyl-3-deutero-2-(2-thienyl)aziridine

(a) 2-Bromo-2-benzoyl-1-(2-thienyl)ethylene

A solution of 8.77 g (0.12 mole) of *tert*-butylamine in 30 ml dry benzene was added dropwise to a slurry of 15.0 g (0.04 mole) of 2-benzoyl-1,2-dibromo-1-(2-thienyl)ethane in 100 ml dry benzene with stirring at 0 °C. Stirring was continued at room temperature for 12 h after addition. The solution was filtered to remove the precipitated *tert*-butylamine hydrobromide. The filtrate was concentrated to ca. 20 ml and subjected to chromatography on Alumina (B.D.H.) using benzene as eluent. Evaporation of benzene and treatment with hexanes gave mono bromide as a pale yellow solid 10.4 g (89% yield), m.p. 76–77°.

Anal. Calcd. for $C_{13}H_9OSBr$: C, 53.25; H, 3.10; Br, 27.26; S, 10.81. Found: C, 53.30; H, 2.89; Br, 27.05; S, 10.91.

The i.r. spectrum: ν_{max} ($CHCl_3$): 1658 cm^{-1} (aryl C=O). The n.m.r. δ_{TMS} ($CDCl_3$): 7.0–8.2 (9H, multiplet, =CH, thienyl and phenyl protons).

(b) Reaction of 2-Bromo-2-benzoyl-1-(2-thienyl)ethylene with Cyclohexylamine-ND_2

A solution of 15.0 g (0.15 mole) of cyclohexylamine-ND_2 (7) in 50 ml dry ether was added to a stirred solution of 8.80 g (0.03 mole) of 2-bromo-2-benzoyl-1-(2-thienyl)-ethylene in 100 ml ether at 0 °C. After addition, the stirring was continued for 12 h at room temperature. The mixture was filtered to remove the precipitated cyclohexylamine deuterobromide. The filtrate was concentrated *in vacuo* to ca. 20 ml then subjected to chromatography on Alumina (B.D.H.) using benzene as eluent. Evaporation of benzene gave a yellow oil which after trituration with hexane gave the solid aziridine 8.75 g (94% yield).

The integrals of the n.m.r. spectrum indicated 86% deuterium incorporation of the 3-position.

Reaction of 3-Benzoyl-1-cyclohexyl-3-deutero-2-(2-thienyl)aziridine with Maleic Anhydride

Reaction of 0.622 g (0.002 mole) of 3-benzoyl-1-cyclohexyl-3-deutero-2-(2-thienyl)aziridine (containing 86% deuterium incorporation) and 0.196 g (0.002 mole) of maleic anhydride in the manner described above gave 5-benzoyl-1-cyclohexyl-2-(2-thienyl)pyrrolidine-3,4-dicarboxylic anhydride in 75% yield, m.p. 159–160°. Examination of the n.m.r. spectrum showed the position and extent of deuterium incorporation. The product was identical in all other respects to the protium analogue listed in Table 4.

The n.m.r. spectrum δ_{TMS} ($CDCl_3$): 0.30–2.0 (10H, multiplet, cyclohexyl protons); 2.5–3.0 (1H, multiplet,

Can. J. Chem. Downloaded from www.nrcresearchpress.com by 210.87.254.5 on 09/05/12
For personal use only.

Can. J. Chem. Downloaded from www.nrcresearchpress.com by 210.87.254.5 on 09/05/12
For personal use only.

TABLE 4

Spectroscopic properties of pyrrolidines

Compound	Infrared spectrum $CHCl_3$ (C=O) cm^{-1}	Nuclear magnetic resonance spectrum δ TMS($CDCl_3$)						
		Aryl protons	Ring proton 2	Ring proton 5	Ring proton 3	Ring proton 4	Ester methyl protons	*N*-Substituents
5	1678 (aryl C=O) 1789, 1866 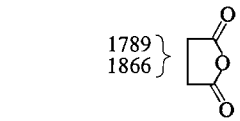	6.7–8.4(8H)m	5.71(1H)d $J_{2,3}$ = 10 Hz	5.48(1H)s (0.44H)*	3.83(1H)q $J_{3,4}$ = 8.5 Hz	3.29(1H)d $J_{4,5}$ = 0.0 Hz		0.3–2.1(10H)m 2.5–3.0(1H)m
6	1688 (aryl C=O) 1717, 1783 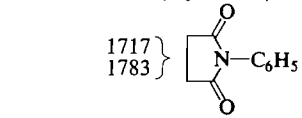	6.8–8.3(8H)m	5.74(1H)d $J_{2,3}$ = 10 Hz	5.59(1H)s (0.46H)*	3.72(1H)q $J_{3,4}$ = 8 Hz	3.16(1H)d $J_{4,5}$ = 0.0 Hz		0.3–2.1(10H)m 2.5–3.0(1H)m
7	1682 (aryl C=O) 1742 (ester C=O)	6.7–8.2(8H)m	5.27(1H)d $J_{2,3}$ = 9 Hz	5.49(1H)d $J_{4,5}$ = 8 Hz (0.4H)*	(3.9–4.26) (2H)m		3.06(3H)s 3.30(3H)s	0.3–2.1(10H)m 2.4–3.0(1H)m
8	1683 (aryl C=O) 1738 (ester C=O)	6.8–8.4(8H)m	5.40(1H)d $J_{2,3}$ = 9 Hz	5.55(1H)d $J_{4,5}$ = 4.5 Hz	(3.34–4.04) (2H)m		3.30(3H)s 3.60(3H)s	0.3–2.1(10H)m 2.4–3.0(1H)m
14	1675 (aryl C=O) 1711(sh), 1737 (ester C=O)	6.8–8.4(12H)m	5.24(1H)d $J_{2,3}$ = 9 Hz	5.47(1H)d (0.45H)* $J_{4,5}$ = 8 Hz	(3.9–4.37) (2H)m		3.17(3H)s 3.30(3H)s	0.96–(3H)d 1.04(3H)d J = 7 Hz 2.8–3.4(1H)m
15	1675 (aryl C=O) 1710(sh), 1735 (ester C=O)	6.8–8.4(12H)m	5.39(1H)d $J_{2,3}$ = 9 Hz	5.55(1H)d (0.43H)* $J_{4,5}$ = 4.5 Hz	(3.24–3.89) (2H)m		3.25(3H)s 3.54(3H)s	0.77(3H)d 1.02(3H)d J = 7 Hz 2.8–3.4(1H)m
16	1675 (aryl C=O) 1790, 1873 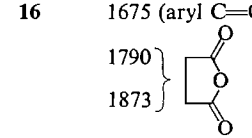	6.8–8.2(12H)m	5.61(1H)d $J_{2,3}$ = 10 Hz	5.49(1H)s (0.45H)*	3.87(1H)q $J_{3,4}$ = 8.8 Hz	3.29(1H)d $J_{4,5}$ = 0.0 Hz		0.69(3H)d 1.01(3H)d J = 7 Hz 2.8–3.4(1H)m

*Diminished in intensity upon selective deuteration at 3 position of aziridine.

Can. J. Chem. Downloaded from www.nrcresearchpress.com by 210.87.254.5 on 09/05/12
For personal use only.

cyclohexyl CH—N); 3.29 (1H, doublet, 4H ring proton); 3.83 (1H, quartet, 3 ring proton); 5.48 (0.44H, singlet, 5 ring proton); 5.71 (1H, doublet, 2 ring proton); 6.9–8.3 (8H, multiplet, thienyl and phenyl protons).

Averaging four integrals confirmed 56% deuterium incorporation at position 5.

Reactions of 3-benzoyl-1-cyclohexyl-3-deutero-2-(2-thienyl)aziridine with dimethyl fumarate or dimethyl maleate were carried out in the same manner.

Reaction of 3-Benzoyl-1-cyclohexyl-2-(2-thienyl)aziridine with Dimethyl Acetylenedicarboxylate

A solution of 0.933 g (0.003 mole) of 3-benzoyl-1-cyclohexyl-2-(2-thienyl)aziridine and 0.426 g (0.003 mole) of dimethyl acetylenedicarboxylate in 50 ml of dry benzene was heated under reflux for 12 h. The solution was concentrated to ca. 10 ml and subjected to chromatography using benzene as eluent. Two main fractions were obtained. (*1*) Pale yellow solid, 0.433 g (32% yield), m.p. 133–134° (petroleum ether). (*2*) Pale yellow solid 0.375 g (28% yield), m.p. 170–171° (ether – petroleum ether).

(*1*) Anal. Calcd. for $C_{25}H_{27}SNO_5$: C, 66.20; H, 6.01; N, 3.09; S, 7.05. Found: C, 66.48; H, 6.09; N, 3.16; S, 6.98.

The i.r. spectrum ν_{max} ($CHCl_3$): 1680 cm^{-1} (C=O, of aryl) 1736 cm^{-1} (C=O of ester). The n.m.r. spectrum δ_{TMS} ($CDCl_3$): 0.6–2.0 (10H, multiplet, cyclohexyl protons); 2.5–3.2 (1H, multiplet, CH—N); 3.36 and 3.40 (6H, singlets, methyl ester protons) 4.34 and 5.52 (2H, AB quartet, J = 12 Hz, 2, 3, protons), 6.9–8.4 (8H, thienyl and phenyl protons).

(*2*) Anal. Calcd. for $C_{25}H_{25}SNO_5$: C, 66.50; H, 5.58; N, 3.10; S, 7.10: Found: C, 66.36; H, 5.45; N, 3.36; S, 7.12.

The i.r. spectrum ν_{max} ($CHCl_3$): 1665 (aryl C=O), 1721 (ester C=O). The n.m.r. spectrum δ_{TMS} ($CDCl_3$): 0.6–2.4 (10H, multiplet, cyclohexyl protons); 3.28 and 3.65 (6H, singlets, methyl ester protons); 3.5–4.2 (1H, multiplet, CH—N); 7.0–8.1 (8H, multiplet, thienyl and phenyl protons).

From these data fractions *1* and *2* were identified as 5-benzoyl-1-cyclohexyl-3,4-dicarbomethoxy-2-(2-thienyl)-2-pyrroline and 5-benzoyl-1-cyclohexyl-3,4-dicarbomethoxy-2-(2-thienyl)pyrrole respectively.

The experiment was repeated with 10 equivalents of dimethyl acetylenedicarboxylate which gave only fraction *2*. The control experiment using *cis*-aziridine was carried out in the same way and the mixture of *1* and *2* was obtained in 53% yield.

Dehydrogenation of Pyrrolidines to Pyrroles

(*i*) A mixture of 0.455 g (0.001 mole) of 5-benzoyl-1-cyclohexyl-3,4-dicarbomethoxy-2-(2-thienyl)pyrrolidine H_2, H_3-*trans*, H_4, H_5-*cis* and 1.23 g (0.005 mole) of tetrachloro-1,4-benzoquinone in 25 ml dry chlorobenzene was heated under reflux for 3 days. The reaction mixture was cooled and 200 ml of ether was added. The solution was washed with 4% aqueous sodium hydroxide solution containing 1% sodium bisulfite and then washed with water and dried ($MgSO_4$). Evaporation of the solvent gave a pale yellow solid, which was recrystallized from ethyl ether – hexane m.p. 170–171°, (0.198 g, 44% yield).

(*ii*) Similarly, reaction of 0.455 g (0.001 mole) of 5-benzoyl-1-cyclohexyl-3,4-dicarbomethoxy-2-(2-thienyl) pyrrolidine H_2, H_3-*cis*, H_4, H_5-*trans* with 1.23 g (0.005 mole) of tetrachloro-1,4-benzoquinone afforded the identical pyrrole m.p. 170–171°, 0.183 g (40% yield).

Both of these products were identified from mixed m.p. and i.r. and n.m.r. spectra as 5-benzoyl-1-cyclohexyl-3,4-dicarbomethoxy-2-(2-thienyl)pyrrole.

(*iii*) A mixture of 0.906 g (0.002 mole) of 5-benzoyl-1-cyclohexyl-3,4-dicarbomethoxy-2-(2-thienyl)-2-pyrroline and 2.45 (0.01 mole of tetrachloro-1,4-benzoquinone was heated under reflux for 4 days and worked up in the same way as described above affording the pyrrole 0.483 g (54% yield) m.p. 169–170°. This compound was identified as 5-benzoyl-1-cyclohexyl-3,4-dicarbomethoxy-2-(2-thienyl)pyrrole from n.m.r. spectra.

1. A. PADWA and L. HAMILTON. Tetrahedron Lett. 4363 (1965).
2. H. W. HEINE, A. B. SMITH, and J. D. BOWER. J. Org. Chem. **33**, 1097 (1968).
3. H. W. HEINE, R. E. PEAVY, and A. J. DURBETAKI. J. Org. Chem. **31**, 3924 (1966).
4. R. HUISGEN, W. SCHEER, G. SZEIMIES, and H. HUBER. Tetrahedron Lett. 397 (1966).
5. J. W. LOWN, G. DALLAS, and T. W. MALONEY. Can. J. Chem. **47**, 3557 (1969).
6. J. W. LOWN, J. P. MOSER, and R. WESTWOOD. Can. J. Chem. **47**, 4335 (1969).
7. J. W. LOWN, R. WESTWOOD, and J. P. MOSER. Can. J. Chem. **48**, 1682 (1970).
8. J. W. LOWN, R. K. SMALLEY, and G. DALLAS. Chem. Commun. 1543 (1968).
9. H. W. HEINE and R. P. HENZEL. J. Org. Chem. **34**, 171 (1969).
10. G. DALLAS, J. W. LOWN, and J. P. MOSER. Chem. Commun. 278 (1970).
11. J. W. LOWN and J. P. MOSER. Chem. Commun. 247 (1970).
12. J. W. LOWN, T. W. MALONEY, and G. DALLAS. Can. J. Chem. **48**, 584 (1970).
13. S. GABRIEL. Chem. Ber. **21**, 1049 (1888).
14. S. GABRIEL and R. STELZNER. Chem. Ber. **28**, 2929 (1895).
15. L. A. PAQUETTE. Principles of modern heterocyclic chemistry. W. A. Benjamin Inc., New York, 1968. pp. 117, 125.
16. H. D. HARTOUGH. Thiophene and its derivatives. Interscience, New York, 1952.
17. S. GRONOWITZ. *In* Advances in heterocyclic chemistry. Vol. 1. *Edited by* A. R. Katritzky, Academic Press, New York, 1963. p. 46.
18. A. E. POHLAND, R. C. BADGER, and N. H. CROMWELL. Tetrahedron Lett. 4369 (1965).
19. A. B. TURNER, H. W. HEINE, J. IRVING, and J. B. BUSH. J. Amer. Chem. Soc. **87**, 1050 (1965).
20. S. SUNNER. Acta Chem. Scand. **9**, 847 (1955).
21. R. HUISGEN, W. SCHEER, H. MADER, and E. BRUNN. Angew. Chem. Int. Ed. **8**, 604 (1969).
22. R. HUISGEN, W. SCHEER, and H. HUBER. J. Amer. Chem. Soc. **89**, 1753 (1967).
23. J. A. DEYRUP. J. Org. Chem. **34**, 2724 (1969).
24. N. S. BHACCA and D. H. WILLIAMS. Application of n.m.r. spectroscopy in organic chemistry. Holden-Day, San Francisco, California, 1964. p. 115.
25. A. PADWA and L. HAMILTON. J. Heterocycl. Chem. **4**, 118 (1967).
26. M. KARPLUS. J. Chem. Phys. **30**, 11 (1959).
27. J. W. LOWN, R. K. SMALLEY, G. DALLAS, and T. W. MALONEY. Can. J. Chem. **48**, 89 (1970).

28. R. HUISGEN, H. KONIG, G. BINSCH, and H. J. STURM. Angew. Chem. **73**, 368 (1961).
29. L. M. JACKMAN and S. STERNHELL. Applications of nuclear magnetic resonance spectroscopy in organic chemistry. Second edition. Pergamon, New York, 1969. p. 89.
30. C. S. MARVEL, J. M. QUINN, and J. S. SHOWELL. J. Org. Chem. **18**, 1730 (1953).
31. W. S. EMERSON and T. M. PATRICK. J. Org. Chem. **14**, 790 (1969).
32. G. A. HANSON. Bull. Soc. Chim. Belg. **67**, 712 (1958).
33. V. F. LAVRUSHIN, S. V. TSUKERMAN, and V. M. NIKITCHENKO. Ukr. Khim. Zh. **27**, 379 (1961); Chem. Abstr., **56**, 3437 (1962).
34. N. P. BUU-HOI, N. DAT XUONG, and M. SY. Bull. Soc. Chim. France, 1646 (1956).
35. N. P. BUU-HOI and N. DAT XUONG. Bull. Soc. Chim. France, 758 (1958).
36. R. PALLAND and F. DELAVEAU. Bull. Soc. Chim. France, 1220 (1955).
37. W. F. KING and F. F. NORD. J. Org. Chem. **14**, 405 (1949).
38. Organic Synthesis. **1**, 78 (1944).
39. Organic Synthesis. **3**, 426 (1955).
40. A. E. POHLAND, R. C. BADGER, and N. H. CROMWELL. Tetrahedron Lett. 4369 (1965).

Can. J. Chem. Downloaded from www.nrcresearchpress.com by 210.87.254.5 on 09/05/12
For personal use only.

Can. J. Chem. Downloaded from www.nrcresearchpress.com by 210.87.254.105 on 09/05/12
For personal use only.

1,3-Dipolar cycloaddition of nitrosonaphthols to 3-aroylaziridines. Novel syntheses of substituted naphtho[1,2-*d*]oxazoles and naphtho[2,1-*d*]oxazoles

J. W. Lown and J. P. Moser
Department of Chemistry, University of Alberta, Edmonton, Alberta

Received February 23, 1970

A series of 3-aroyl-2-arylaziridines underwent 1,3-dipolar cycloadditions in both orientations to the nitrogen–oxygen bond of 1-nitroso-2-naphthol. Spontaneous 1,3-cleavage of the intermediate oxadiazolidines to nitrones and cyclodehydration of the latter afforded both 2-aryl- and 2-aroylnaphtho-[1,2-*d*]oxazoles in good yields. The interpretation of the reaction received confirmation by independent, unambiguous synthesis of several 2-aroylnaphtho[1,2-*d*]oxazoles.

Canadian Journal of Chemistry, **48**, 2227 (1970)

The thermal and photochemical cleavage of the carbon–carbon bond in aziridines to yield azomethine ylides and their subsequent [2 + 3] cycloaddition to reactive carbon–carbon multiple bonds, has been firmly established by several authors (1–14).

An interest in the general problem of synthesizing five and six membered ring heterocycles from the addition reactions of readily available small ring heterocycles led us to explore the analogous thermally induced additions of 3-aroylaziridines to heteromultiple bonds. We have reported the additions of 3-aroylaziridines and 3-carboalkoxyaziridines to the following heteromultiple bonds as dipolarophiles, (*i*) the C=S bond of aryl isothiocyanates with the formation of 4-aroyl-5-arylamino-4-thiazolines (15), (*ii*) the C=N bond of imines and sulfonylimines with the formation of imidazolidines (16), (*iii*) the C=O bond of diphenylcyclopropenone which ultimately affords 4-aroyl-4-oxazolines (17, 18), (*iv*) the C=O bond of aryl aldehydes and chloral to form oxazolidines (19), and (*v*) the C=N bond of cyclopropenimines to form imidazolines and imidazolidines (20).

We report full details of an examination of the 1,3-dipolar cycloaddition of 3-aroylaziridines to the N=O bond of isomeric nitrosonaphthols which produced substituted naphtho[1,2-*d*]-oxazoles and which in the case of 1-nitroso-2-naphthol provided compelling evidence for a concerted cycloaddition. These results have previously been published only in a preliminary form (21).

Treatment of 3-benzoyl-1-cyclohexyl-2-*p*-nitrophenylaziridine (22) with one equivalent of 1-nitroso-2-naphthol in refluxing benzene for 16 h resulted in the precipitation of 2-[4-nitrophenyl]-naphtho[1,2-*d*]oxazole (**1**), $C_{17}H_{10}N_2O_3$, m.p. 240° in 35.5% yield (R_1 = H; R_2 = NO_2). The infrared (i.r.) spectrum of **1** showed a 1532 cm^{-1} band characteristic of the nitro group.

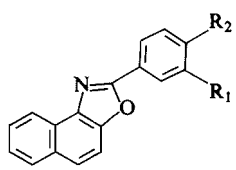

1

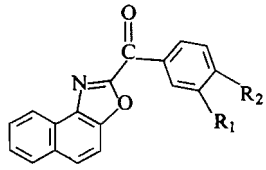

2

Concentration of the filtrate and chromatographic separation on alumina afforded the pale green solid 2-benzoylnaphtho[1,2-*d*]oxazole (**2**; R_1, R_2 = H), $C_{18}H_{11}NO_2$, m.p. 123° in 41.5% yield. The i.r. of **2** showed a strong band at 1660 cm^{-1} characteristic of a diaryl ketone (23). The absorption spectrum showed intense maxima at 264 and 356 mμ.

In view of the precedents for thermal carbon–carbon bond cleavage of aziridines quoted above, and the strong analogies for the subsequent concerted [2 + 3] cycloaddition to heteromultiple bonds also described, we interpret the reaction as proceeding by 1,3-dipolar addition of the intermediate azomethine ylide to the N=O bond in both possible orientations. Subsequent 1,3-cleavage of the intermediate oxadiazolidines **3** and **4** gives initially the nitrones **5** and **6** (Scheme 1).

The neighboring hydroxyl groups in **5** and **6** cyclize to the polarized azomethine bond with loss of water to produce **2** and **1** respectively. The secondary products of the 1,3-cleavage of the oxadiazolidines, which were expected to be the Schiff bases, could not be isolated. It has been our experience however that Schiff bases of

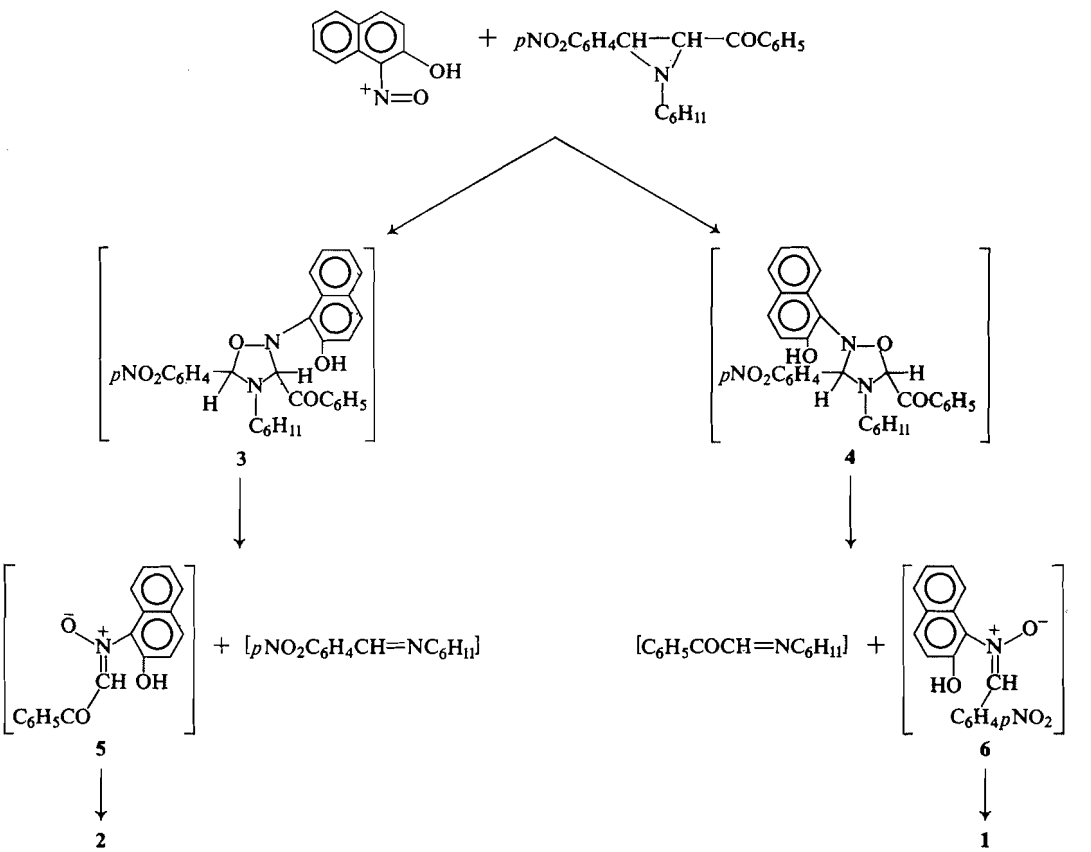

SCHEME 1

cyclohexylamine seldom survive elimination reactions of this type. For example in the 1,3-dipolar additions of 4-aroyl-4-oxazolines with olefinic and acetylenic dipolarophiles, the extruded cyclohexylamine Schiff base was isolated in only one case, but far more frequently was very easily hydrolyzed during the work-up procedure (24, 25). The oxadiazoline which results from the 1,3-dipolar addition of a nitrile ylide to nitrosobenzene similarly cannot be isolated and suffers a 1,3-cleavage to give a nitrone and benzonitrile (26). As far as we are aware the isolation of an oxadiazolidine has been reported only once in the literature by Agosta and that example was shown to be unstable (27).

Reactions between pyridinium or sulfonium ylides and aryl nitroso compounds to form nitrones have been reported previously (28–31) (e.g. eq. [1]). Accordingly, compound **2***a* was synthesized unambiguously by treating a mixture of 1-nitroso-2-naphthol and one equivalent of *N*-phenacylpyridinium bromide (32) with an equivalent of *N* aqueous sodium hydroxide at −20°. The yield of **2** was quantitative (see eq. [2]). The analytical and spectral data on several 2-aryl and 2-aroyl naphtho[1,2-*d*]oxazoles obtained by the 1,3-dipolar addition of 1-nitroso-2-naphthol with the appropriate 3-aroylaziridines are summarized in Tables 1 and 2. 2-Nitroso-1-naphthol reacted with 3-benzoyl-1-cyclohexyl-2-*p*-nitrophenylaziridine to give 2-*p*-nitrophenylnaphtho-[2,1-*d*]oxazole (**7**) in 8.0% yield. While the

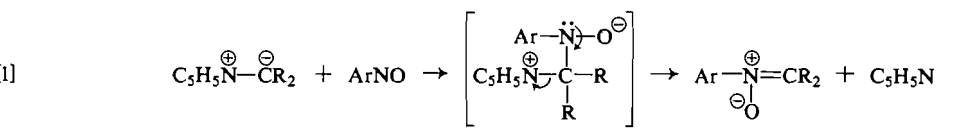

Can. J. Chem. Downloaded from www.nrcresearchpress.com by 210.87.254.105 on 09/05/12
For personal use only.

TABLE 1
2-Arylnaphtho[1,2-*d*]oxazoles*

No. 1	R_1	R_2	Melting point (°C)	Yield (%)	Observed C	H	N	Molecular ion (mass spectrum)	Calculated C	H	N	Molecular ion (mass spectrum)	Infrared spectrum Nujol (NO_2)
a	H	NO_2	240	35.5	70.18	3.64	9.66	290.0694	70.34	3.47	9.65	290.0691	1535 1350
b	NO_2	H	237–239	32	70.14	3.26	9.66	290.0694	70.34	3.47	9.65	290.0691	1529 1348
c	H	H	125–130	40	67.98	3.40	8.99	245.0840	67.94	3.17	8.86	245.0841	—

*Numbering of substituents refers to structure 1.

[2] 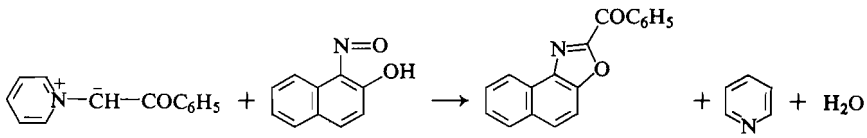

2

corresponding 2-aroylnaphtho[2,1-*d*]oxazole **8** was not obtained in this reaction, it was however prepared by the second procedure with *p*-bromophenacyl pyridinium bromide and sodium hydroxide (31) so that the two methods were quite complementary.

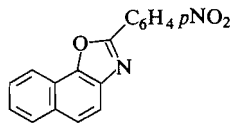

7

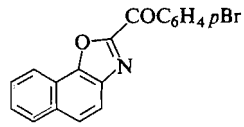

8

2-Nitroso-1-naphthol gave lower yields of the 2-arylnaphtho[2,1-*d*]oxazole in reaction with aziridines than did 1-nitroso-2-naphthol. This appears to be due to competing reactions including the formation of a product tentatively assigned as a naphtho[2,1-*f*]-1,3,5-oxadiazepine which is currently under further investigation.

The isolation of naphthoxazoles of both types **1** and **2** represents the first reported example of addition of a heteromultiple bond to an aziridine in both possible orientations and provides good evidence that the reaction involved is a 1,3-dipolar addition. Since **1** and **2** are obtained in approximately equal yields it is clear that the steric influence on orientation in the reactions with 1-nitroso-2-naphthol is negligible. A similar conclusion has very recently been reached by Kresze *et al.* in a study of the Diels–Alder additions of nitrosobenzene to substituted dienes (33).

In contrast, the 1,3-dipolar cycloadditions of 3-aroylaziridines to dipolarophiles containing heteromultiple bonds all took place exclusively in one orientation presumably due to more stringent steric control, for example in addition to the C=S bond in aryl isothiocyanates (15), the C=N bond in imines and sulfonylimines (16) and iminocyclopropenes (20), and the C=O bond in aryl aldehydes, chloral (19), and diphenylcyclopropenone (17, 18).

One isolated example of the addition of an aryl nitroso compound to an aziridine had previously been reported by Heine and his coworkers, involving the addition of nitrosobenzene to 1,1*a*-dihydro-1-(*p*-nitrophenyl)-2-phenylazirino-[1,2-*a*]quinoxaline (**9**) (14) (see eq. [3], Ar = *p*-$NO_2C_6H_4$—). The formation of the products, 2-phenylquinoxaline (**13**) and the nitrone **12** was interpreted either in terms of 1,3-dipolar addition via **10** or via the dipolar intermediate **11**. It seems likely that in this particular reaction, the orientation of the addition is dictated by the stability of the product quinoxaline **13** and the nitrone **12**.

Further studies of arylnitroso compounds with 3-aroylaziridines leading to imidazolidines and Schiff's bases will be reported subsequently.

Experimental

Melting points were determined on a Fisher–Johns apparatus and are uncorrected. The i.r. spectra were recorded on a Perkin–Elmer model 421 spectrophotometer, and only the principal, sharply defined peaks are reported. Nuclear magnetic resonance (n.m.r.) spectra

Can. J. Chem. Downloaded from www.nrcresearchpress.com by 210.87.254.105 on 09/05/12
For personal use only.

Can. J. Chem. Downloaded from www.nrcresearchpress.com by 210.87.254.105 on 09/05/12
For personal use only.

TABLE 2

2-Aroylnaphtho-[1,2-*d*]oxazoles*

No. **2**	R_1	R_2	Melting point (°C)	Yield (%)	Observed C	Observed H	Observed N	Observed Br	Observed Molecular ion (mass spectrum)	Calculated C	Calculated H	Calculated N	Calculated Br	Calculated Molecular ion (mass spectrum)	Infrared spectrum $CHCl_3$ (C=O)	Nuclear magnetic resonance spectrum ($CDCl_3$) δ Aryl protons	Nuclear magnetic resonance spectrum ($CDCl_3$) δ 2-*p*-Aroyl substituent
a	H	H	124	41.5† 100‡	78.90	3.97	5.17	—	273.0793	79.11	4.06	5.13	—	273.0790	1658	7.2–8.8 (11H) m	—
b	H	CH_3	114	32.3†	79.55	4.49	5.15	—	287.0946	79.41	4.56	4.88	—	287.0946	1652	7.2–8.3 (10H) m	2.46 (3H) s
c	H	OCH_3	124–125	41.5†	75.45	4.48	4.83	—	303.0893	75.25	4.32	4.62	—	303.0895	1651	6.9–8.5 (10H) m	3.98 (3H) s
d	H	NO_2	223–225	31.5† 76.5‡	67.68	3.23	9.26	—	318.0639	67.94	3.17	8.86	—	318.0641	1663	7.1–8.5 (10H) m	—
e	NO_2	H	167	50.5‡	67.92	3.14	8.89	—	318.0638	67.94	3.17	8.86	—	318.0641	1652	7.0–8.4 (10H) m	—
	H	Br	164	68.5‡	61.19	2.78	4.06	23.30	350.9893	61.41	2.86	3.98	22.70	350.9895	1655	6.9–8.3 (10H) m	—

*Numbering of substituents refers to structure **2**.
†Method *A*.
‡Method *B*.

[3] 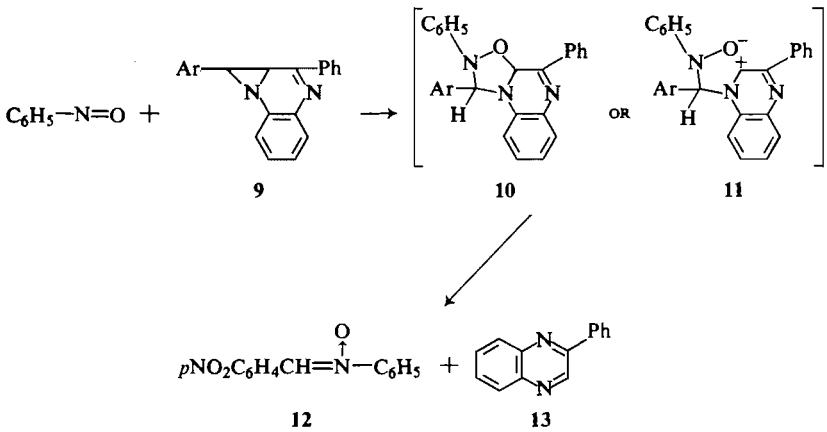

were recorded on Varian A-60 and A-100 analytical spectrometers. The spectra were measured on approximately 10–15% (w/v) solutions in $CDCl_3$, with tetramethylsilane as a standard. Line positions are reported in parts per million from the reference. Absorption spectra were recorded in 'spectro'-grade solvents on a Beckman DB recording spectrophotometer. Mass spectra were determined on an Associated Electrical Industries MS-9 double focusing high resolution mass spectrometer. The ionization energy, in general, was 70 eV. Peak measurements were made by comparison with perfluorotributylamine at a resolving power of 15 000. Kieselgel DF-5 (Camag, Switzerland) and Eastman Kodak precoated sheets were used for thin-layer chromatography. Microanalyses were carried out by Dr. D. Daesslé, Organic Microanalysis Ltd , Montreal, Quebec and by Mrs. D. Mahlow of this department.

Source of Nitrosonaphthols

1-Nitroso-2-naphthol and 2-nitroso-1-naphthol were obtained as practical grade chemicals from Eastman Organic Chemicals and were purified by recrystallization from petroleum ether.

General Preparation of 3-Aroylaziridines

The compounds used in this study were prepared by the Gabriel synthesis involving Claisen–Schmidt condensations to form chalcones, then addition of bromine to form the dibromochalcones and treatment of the dibromochalcones with a three molar proportion of a primary aliphatic amine to provide 3-aroylaziridines (15 and references therein).

Preparation of 2-Aryl- and 2-Aroylnaphtho[1,2-d]-oxazoles and 2-Aryl- and 2-Aroylnaphtho-[2,1-d]oxazoles

Representative examples of the preparation of naphthooxazoles of the four different types by the two methods, (*A*) reaction with a 3-aroylaziridine and (*B*) reaction with a phenacyl pyridinium halide and base, are described in detail.

The analytical and spectral data on further examples prepared in a similar fashion are summarized in Tables 1, 2, and 3.

TABLE 3

Absorption spectra of 2-aroylnaphtho[1,2-*d*]oxazoles in CH_2Cl_2

No. **2**	λ_{max}	log ε	λ_{max}	log ε
a	356	4.19	264	4.19
b	356	4.25	286	4.12
*c**	349	4.20	306	4.16
d	380	4.16	272	4.49
e	372	4.18	260	4.40
f	363	4.25	276	4.32

*Spectrum recorded in CH_3CN.

Method A

Reaction of 3-Benzoyl-1-cyclohexyl-2-p-nitrophenylaziridine with 1-Nitroso-2-naphthol

A solution of 1.75 g (0.005 mole) of 3-benzoyl-1-cyclohexyl-2-*p*-nitrophenylaziridine and 0.865 g (0.005 mole) of 1-nitroso-2-naphthol in 50 ml of dry benzene was stirred and heated under reflux for 24 h during which time the solution turned a dark brown. Upon cooling of the solution, a green–brown solid which had precipitated, 0.51 g (32% yield), was collected and purified by extraction of the impurities with hot ethyl acetate, m.p. 240°, representing 2-*p*-nitrophenylnaphtho[1,2-*d*]oxazole.

Anal. Calcd. for $C_{17}H_{10}N_2O_3$ (mol. wt. 290.0691): C, 70.34; H, 3.47; N, 9.65. Found (290.0694 (mass spectrum)): C, 70.18; H, 3.64; N, 9.66.

The i.r. spectrum ν_{max}(KBr disk): 1535, 1350 cm^{-1} (NO_2).

The filtrate was concentrated *in vacuo* and the residual oil was subjected to chromatography on alumina (B.D.H.) with benzene as eluant. Removal of the solvent and trituration of the resulting green oil with hexane gave 2-benzoylnaphtho[1,2-*d*]oxazole as a light yellow solid, 0.52 g (41.5% yield), m.p. 124° (benzene–hexanes).

Anal. Calcd. for $C_{18}H_{11}NO_2$ (mol. wt. 273.0790): C, 79.11; H, 4.06; N, 5.13. Found (273.0788 (mass spectrum)): C, 78.90; H, 3.97; N, 5.17.

The i.r. spectrum $\nu_{max}(CHCl_3)$: 1659 cm^{-1} (C=O); n.m.r. spectrum: $\delta_{TMS}(CDCl_3)$: 7.2–8.8 (11H, multiplet,

Can. J. Chem. Downloaded from www.nrcresearchpress.com by 210.87.254.105 on 09/05/12
For personal use only.

Can. J. Chem. Downloaded from www.nrcresearchpress.com by 210.87.254.105 on 09/05/12
For personal use only.

aromatic protons); absorption spectrum $\lambda_{max}(CH_2Cl_2)$: 264 (log ε 4.19); 356 mμ (log ε 4.19).

Reaction of 3-Benzoyl-1-cyclohexyl-2-p-nitrophenylaziridine with 2-Nitroso-1-naphthol

A solution of 1.75 g (0.005 mole) of 3-benzoyl-1-cyclohexyl-2-*p*-nitrophenylaziridine and 0.865 g (0.005 mole) of 2-nitroso-1-naphthol in 50 ml of dry benzene was stirred and heated under reflux for 24 h during which time the solution turned purple–black. The solution was concentrated *in vacuo* and the dark oil produced was subjected to chromatography on alumina (B.D.H.) Elution with benzene afforded as the first fraction (after removal of the solvent and trituration of the resulting red oil with a few drops of ethyl acetate and a greater amount of hexane) 2-*p*-nitrophenylnaphtho-[2,1-*d*]-oxazole as a red solid, 0.21 g (8.4% yield) m.p. 152–153° (ethyl acetate – hexanes).

Anal. Calcd. for $C_{17}H_{10}N_2O_3$ (mol. wt. 290.0691): C, 70.34; H, 3.47; N, 9.65. Found (290.0690 (mass spectrum)): C, 70.04; H, 3.13; N, 9.67.

The i.r. spectrum $\nu_{max}(CHCl_3)$: 1522, 1342 cm^{-1} (NO_2); n.m.r. spectrum: $\delta_{TMS}(CDCl_3)$: 7.3–8.6 (10H, multiplet, aromatic protons).

Further elution with 40:60 chloroform–benzene gave after removal of the solvent *in vacuo* a bright red solid, 0.21 g (8.4% yield), m.p. 220° (ethyl acetate).

Anal. Calcd. for $C_{31}H_{27}N_3O_4$ (mol. wt. 505.2002): C, 73.64; H, 5.38; N, 8.31. Found (505.1998 (mass spectrum)): C, 73.23; H, 5.13; N, 7.87.

Further elution with chloroform gave after removal of solvent a purple solid, 0.5 g m.p. 160° (ethylacetate–hexane).

Anal. Calcd. for $C_{20}H_{12}N_2O_2$ (mol. wt. 312.0899): C, 76.91; H, 3.88; N, 8.97. Found (312.0901 (mass spectrum)): C, 76.87; H, 4.04; N, 8.41.

These compounds are currently under further investigation.

Method B

2-Benzoylnaphtho-[1,2-d]oxazole

A solution of 1.73 g (0.01 mole) 1-nitroso-2-naphthol in 50 ml 95% ethanol was added to 2.78 g (0.01 mole) phenacyl pyridinium bromide in 5 ml of water. The solution was stirred at 0° to −10° during addition of 10 ml of 1 *N* sodium hydroxide over 1/2 h. After 5 min, the solution turned dark red and after 2 h of stirring, 20 ml of water was added and the dark red solid which had precipitated was collected and dried. The solid was dissolved in benzene and subjected to chromatography on alumina (B.D.H.) with benzene as eluant. Removal of the solvent and trituration of the resulting green oil with hexane gave 2-benzoylnaphtho-[1,2-*d*]oxazole as a light yellow solid, 2.70 g (100% yield), m.p. 124° (benzene–hexanes).

This compound was shown by mass, i.r., and n.m.r. spectroscopy to be identical in all respects to the compound prepared above by method *A*.

2-p-Bromobenzoylnaphtho-[2,1-d]oxazole

A solution of 1.73 g (0.01 mole) 2-nitroso-1-naphthol in 50 ml 95% ethanol was added to 3.23 g (0.01 mole) of *p*-bromophenacyl pyridinium bromide in 5 ml water. The solution was stirred at 0° to −10° during addition of 10 ml of 1 *N* sodium hydroxide over 1/2 h. After 5 min, the solution turned dark and after 2 h of stirring, 20 ml of water was added and the dark brown solid which had precipitated was collected and dried. The solid was chromatographed on alumina with benzene–chloroform (1:1) as eluant. Removal of the solvent and trituration of the resulting yellow oil with hexane gave 2-*p*-bromobenzoylnaphtho-[2,1-*d*]oxazole as a yellow solid, 0.13 g (2.6% yield), m.p. 191° (benzene–hexanes).

Anal. Calcd. for $C_{18}H_{10}BrNO_2$ (mol. wt. 350.9895): C, 61.41; H, 2.86; N, 3.98; Br, 22.70. Found (350.9895 (mass spectrum)): C, 61.53; H, 2.85; N, 4.17; Br, 22.72.

The i.r. spectrum $\nu_{max}(CHCl_3)$: 1658 cm^{-1} (C=O); n.m.r. spectrum: $\delta_{TMS}(CDCl_3)$: 7.2–8.8 (10H, multiplet, aromatic protons); absorption spectrum $\lambda_{max}(CH_2Cl_2)$: 278 (log ε 4.28), 316 (log ε 4.17), 365 mμ (log ε 4.09).

This research was supported by a National Research Council of Canada grant to J. W. Lown. We thank Mr. R. Swindlehurst and Dr. A. Hogg for the n.m.r. and mass spectra.

1. P. B. Woller and N. H. Cromwell. J. Heterocycl. Chem. **5**, 579 (1968).
2. H. W. Heine and R. Peavy. Tetrahedron Lett. 3123 (1965).
3. B. K. Campbell and K. N. Campbell. J. Org. Chem. **9**, 178 (1944).
4. R. Huisgen, W. Scheer, G. Szeimies, and H. Huber. Tetrahedron Lett. 397 (1966).
5. G. H. Coleman and G. P. Waugh. Proc. Iowa State Acad. Sci. **40**, 115 (1933). G. H. Coleman and G. P. Waugh. Proc. Iowa State Acad. Sci. **49**, 286 (1942).
6. A. Padwa and L. Hamilton. Tetrahedron Lett. 4363 (1965).
7. von R. V. Capeller, R. Griot, M. Haring, and T. Wagner–Jauregg. Helv. Chim. Acta, **40**, 1652 (1957).
8. H. W. Heine, A. B. Smith, and J. D. Bower. J. Org. Chem. **33**, 1097 (1968).
9. H. W. Heine, R. E. Peavy, and A. J. Durbetaki. J. Org. Chem. **31**, 3924 (1966).
10. A. Padwa and L. Hamilton. J. Heterocycl. Chem. **4**, 118 (1967).
11. A. Padwa and W. Eisenhardt. Chem. Commun. 380 (1968).
12. R. Huisgen, W. Scheer, and H. Huber. J. Amer. Chem. Soc. **89**, 1753 (1967).
13. S. Oida and E. Ohki. Chem. Pharm. Bull. (Tokyo), **16**, 764 (1968).
14. H. W. Heine and R. Henzel. J. Org. Chem. **34**, 171 (1969).
15. J. W. Lown, G. Dallas, and T. W. Maloney. Can. J. Chem. **47**, 3557 (1969).
16. J. W. Lown, J. P. Moser, and R. Westwood. Can. J. Chem. **47**, 4335 (1969).
17. J. W. Lown, R. K. Smalley, and G. Dallas. Chem. Commun. 1543 (1968).
18. J. W. Lown and R. K. Smalley. Tetrahedron Lett. 169 (1969).
19. G. Dallas, J. W. Lown, and J. P. Moser. Chem. Commun. 278 (1970).
20. J. W. Lown, R. Westwood, and J. P. Moser. Can. J. Chem. **48**, 1682 (1970).
21. J. W. Lown and J. P. Moser. Chem. Commun. 247 (1970).
22. P. L. Southwick and R. J. Schozda. J. Amer. Chem. Soc. **82**, 2888 (1960).

23. L. J. BELLAMY. The infrared spectra of complex molecules. Methuen, New York, 1958. p. 132.
24. J. W. LOWN, R. K. SMALLEY, G. DALLAS, and T. W. MALONEY. Can. J. Chem. **48**, 89 (1970).
25. J. W. LOWN, R. K. SMALLEY, G. DALLAS, and T. W. MALONEY. Can. J. Chem. **48**, 103 (1970).
26. R. HUISGEN, H. STANGL, H. J. STURM, and H. WAGENHOFER. Angew. Chem. Int. Ed. **1**, 50 (1962).
27. W. C. AGOSTA. J. Org. Chem. **26**, 1724 (1961).
28. F. KROHNKE and E. BORNER. Ber. **69**, 2006 (1936).
29. F. KROHNKE. Ber. **71**, 2583 (1938).
30. F. KROHNKE. Ber. **72**, 527 (1939).
31. A. W. JOHNSON. J. Org. Chem. **28**, 252 (1967).
32. F. KROHNKE. Angew. Chem. Int. Ed. **2**, 388 (1963).
33. G. KRESZE, L. FIRL, and H. BRAUN. Tetrahedron, **25**, 4481 (1969).

Can. J. Chem. Downloaded from www.nrcresearchpress.com by 210.87.254.105 on 09/05/12
For personal use only.

Can. J. Chem. Downloaded from www.nrcresearchpress.com by 210.87.254.5 on 09/05/12
For personal use only.

Stereoselective synthesis of α-bulnesene, 4-epi-α-bulnesene, and 5-epi-α-bulnesene

EDWARD PIERS AND KIN FAI CHENG
Department of Chemistry, University of British Columbia, Vancouver 8, British Columbia

Received March 2, 1970

Lithium–ammonia reduction of the hydroguaiazulene derivative **6**, followed by oxidation of the resulting diol **13**, gave, in a highly stereoselective manner, the keto alcohol **14**. The latter was converted into 5-epi-α-bulnesene (**2**). In a similar sequence of reactions, 4-epi-α-bulnesene (**3**) was obtained from compound **9**. Photochemical rearrangement of the previously obtained dienone **25** gave the hydroguaiazulene derivative **27**. Successive subjection of the latter to acetylation, hydrogenation, and sodium borohydride reduction gave a mixture of the epimeric diols **31** and **32**. When this mixture was treated with *p*-toluenesulfonic acid in pyridine, and the resulting olefinic diester **35** was sequentially subjected to hydrogenation [tris(triphenylphosphine)chlororhodium] and lithium aluminum hydride reduction, the crystalline diol **37** was obtained. The latter was converted into α-bulnesene (**1**) by standard reactions.

Canadian Journal of Chemistry, 48, 2234 (1970)

Structurally, one of the simplest of the rapidly expanding number of known guaiane-type sesquiterpenes (1–3) is α-bulnesene (formerly called δ-guaiene), a $C_{15}H_{24}$ hydrocarbon which has been isolated from a number of essential oils (3) and which has been shown (4, 5) to possess the structure and absolute stereochemistry depicted in **1**.[1] We report in this paper the stereoselective synthesis of natural α-bulnesene (**1**)[2] and of the two epimeric compounds 5-epi-α-bulnesene (**2**) and 4-epi-α-bulnesene (**3**).[3]

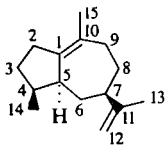

1

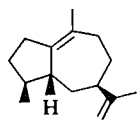

2

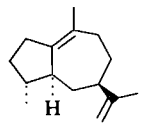

3

Previously, we had reported (13) the conversion of (+)-α-cyperone (**4**) (see ref. 14), of known absolute stereochemistry, into the corresponding hydroguaiazulene derivative **6**, via photochemical rearrangement of 1,2-dehydro-(+)-α-cyperone (**5**). Similarly, (−)-7-epi-α-cyperone (**7**) had been converted, via the dehydro derivative **8**, into the hydroguaiazulene **9**. Although the former conversion (**4** → **6**) (Scheme 1) could be realized in reasonable overall yield (55%), the latter sequence (**7** → **9**) (Scheme 2) was accomplished in only poor yield (15%). The chief reason for this inefficiency was the poor yield (25%) of the dehydrogenation reaction of (−)-7-epi-α-cyperone (**7**) with 2,3-dichloro-5,6-dicyanobenzoquinone. Attempts to improve the yield of this reaction by varying the reaction conditions were unsuccessful. Therefore, the first objective of the present work was to devise a more efficient conversion of **7** into **9**.

Condensation of (−)-7-epi-α-cyperone (**7**) with ethyl formate in the presence of sodium methoxide in benzene provided the 2-hydroxymethylene derivative **10** in good yield. Dehydrogenation of the latter with 2,3-dichloro-5,6-dicyanobenzoquinone (15) in dioxane for 10 min afforded the cross-conjugated dienone **11** in 79% yield. Conversion of compound **11** into the corresponding carboxylic acid **12** was accomplished by subjecting the former to silver oxide oxidation (see ref. 16). It had already been shown by Caine *et al.* (17) that photochemical rearrangement, in aqueous acidic medium, of cross-conjugated dienone carboxylic acids of the type **12** resulted in the formation of the corresponding decarboxylated hydroazulene. In keeping with this observation, we found that irradiation of **12** in 45% aqueous acetic acid gave a high yield of crude, non-acidic product. Purification of the latter by column chromatography gave the hydroguaiazulene **9**, identical (m.p., mixed m.p., infrared (i.r.) spectrum) with compound **9** prepared previously (13). The overall yield of the conversion of **7** into **9** via the route just described was 32%, obviously a considerable improvement over the previously described sequence (13).

[1]The numbering system shown in structure **1** is that normally used for guaiane-type sesquiterpenes.
[2]For a preliminary report, see ref. 6.
[3]For previous reports concerning the synthesis of guaiane-type sesquiterpenes, see refs. 7–12, inclusive.

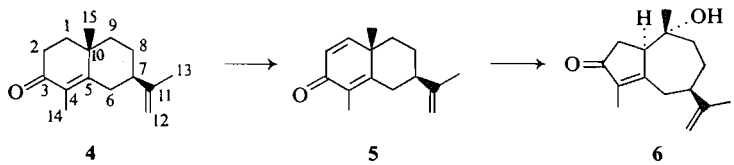

4 5 6

SCHEME 1

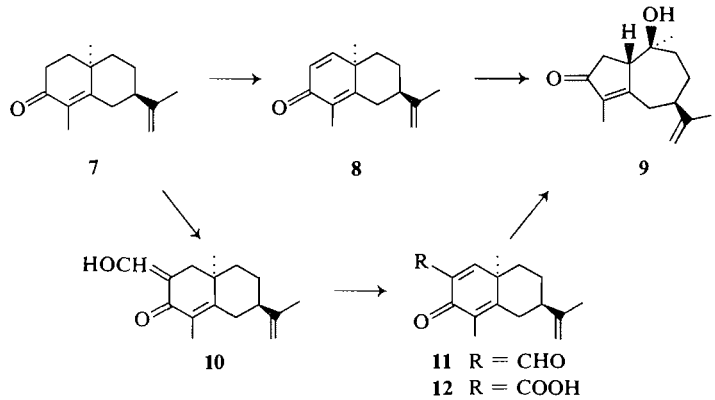

7 8 9

10 11 R = CHO 12 R = COOH

SCHEME 2

Stereoselective Synthesis of 5-epi-α-Bulnesene (2) and 4-epi-α-Bulnesene (3)

Having obtained the hydroguaiazulene derivatives **6** and **9**, it was decided to convert these materials into compounds structurally related to α-bulnesene (**1**). This would involve, in each case, removal of the C_4—C_5 double bond, removal of the carbonyl function at C-3, and the introduction of the C_1—C_{10} double bond. One obvious method for the removal of the C_4—C_5 double bond would involve Birch reduction of compounds **6** and **9**. It was felt, however, that insofar as the synthesis of α-bulnesene was concerned, this method would lead to stereochemical difficulties with respect to the C-4 and/or C-5 positions of the Birch reduction products (vide infra). Nevertheless, it was decided to carry out the lithium–ammonia reduction of compounds **6** and **9** (Scheme 3), since very little was known regarding the stereochemical outcome of the Birch reduction of systems of this type. Furthermore, subsequent modification of the products would, presumably, eventually lead to α-bulnesene-type molecules, and the synthetic reactions and intermediates involved would therefore provide models for subsequent projected work concerning the synthesis of α-bulnesene (**1**) itself.

Subjection of keto alcohol **6** to reduction with lithium in ammonia, followed by quenching of the reaction mixture with methanol, led to the formation of the crude, semicrystalline diol **13** in high yield. Direct oxidation of this crude material with chromium trioxide in pyridine gave the crystalline keto alcohol **14**.

The stereochemistry of **14** requires comment. Theoretically, four possible stereoisomeric keto alcohols could have been formed from compound **6** by the sequence just described. However, two of these, having the C-4 methyl group and the C-5 hydrogen in a *trans* arrangement could be eliminated from consideration as possible products, since compounds of this type are known to be thermodynamically unstable with respect to the corresponding C-4 epimers (10, 18, 19). Molecular models clearly show that when the C-4 methyl and the C-5 hydrogen are *trans*, the methyl group is nearly eclipsed with the C-6 methylene and the above-mentioned instability can, therefore, readily be attributed to the resulting steric and torsional strain. In view of this, it was necessary to distinguish only between the two remaining alternative structures, **14** and **15**. This was done by measuring the optical rotatory dispersion (o.r.d.) curve of the product (**14**).

The cyclopentanone ring of the *trans*-fused

Can. J. Chem. Downloaded from www.nrcresearchpress.com by 210.87.254.5 on 09/05/12
For personal use only.

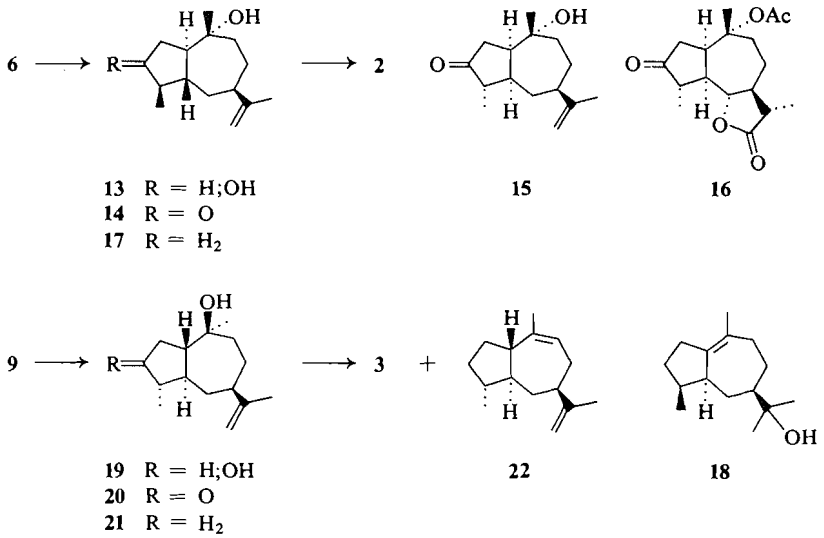

SCHEME 3

compound **14** is very rigid and application of the octant rule (20) readily allows the prediction that this compound should exhibit a strong negative Cotton effect curve,[4] since C-1, C-5, and the C-4 methyl group are all in negative octants. In contrast, the cyclopentanone ring of the alternative product (**15**) is relatively flexible and the sign and amplitude of the Cotton effect would depend upon the relative contribution of the various possible conformations (see ref. 22). However, with the help of molecular models, it could be clearly seen that compound **15** could not exhibit a strongly negative Cotton effect curve. Rather, depending upon the various conformational contributions, one would anticipate that the Cotton effect of **15** would be strongly or weakly positive, or weakly negative. It is pertinent to point out, in this connection, that the *cis*-fused hydroguaiazulene derivative **16** has been reported (22) to exhibit a weakly positive Cotton effect curve.

The o.r.d. curve of the product obtained from compound **6** by the Birch reduction – Sarett oxidation sequence showed a strong negative Cotton effect (see Table 1). Clearly this result was consistent only with the conclusion that the product possessed structure **14**. The lithium–ammonia reduction of the keto alcohol **6** was, therefore, highly stereoselective and produced the corresponding *trans*-fused hydroguaiazulene derivative.

Huang–Minlon reduction (24) of keto alcohol **14** gave the crystalline alcohol **17**. Dehydration of the latter with thionyl chloride in pyridine at 0° afforded a crude product which was shown by gas–liquid chromatographic (g.l.c.) analysis to be approximately 80% pure. The major component was isolated by preparative g.l.c. and, on the basis of analytical and spectral data, was assigned structure **2**. This compound, 5-epi-α-bulnesene (**2**) exhibited i.r. and nuclear magnetic resonance (n.m.r.) (see Table 2) spectra which were different from, although similar to, those of authentic α-bulnesene (**1**), obtained by dehydration (thionyl chloride–pyridine) of natural α-bulnesol (**18**).[5] Furthermore, the g.l.c. retention times of the two compounds (**1** and **2**) were clearly different.

In a sequence of reactions similar to that described above, keto alcohol **9** was converted into 4-epi-α-bulnesene (**3**). Thus, reduction of **9** with lithium–ammonia–methanol, followed by chromium trioxide – pyridine oxidation of the resulting crude diol **19**, afforded a crystalline keto alcohol with molecular formula $C_{15}H_{24}O_2$. The latter exhibited an o.r.d. curve with a strongly positive Cotton effect (see Table 1), and, in fact, this curve bore a nearly mirror image relationship

[4]For o.r.d. studies on compounds similar to those under discussion here, see refs. 21–23 inclusive.

[5]We are very grateful to Professor G. Chiurdoglu for a generous sample of authentic α-bulnesol.

Can. J. Chem. Downloaded from www.nrcresearchpress.com by 210.87.254.5 on 09/05/12
For personal use only.

TABLE 1

Optical rotatory dispersion data (pk = peak; tr = trough)*

Compound	Concentration (g/100 ml)	λ (mμ)	$[\phi] \times 10^{-2}$	Amplitude (A)
14	0.035	313(tr)	−60	−160
		300	0	
		276(pk)	+100	
20	0.036	312(pk)	+69	+147
		295	0	
		271(tr)	−78	
27	0.010	254(pk)	+163	+364
		240	0	
		212(tr)	−201	
29	0.026	310(tr)	−120	−232
		296	0	
		275(pk)	+112	

*The o.r.d. measurements were taken in methanol solution at 27 °C.

TABLE 2

Nuclear magnetic resonance data (d = doublet; m = multiplet; $w_{1/2}$ = width at half-height)*

Compound	$=C^{12}H_2$	$-C^{13}H_3$†	$-C^{14}H_3$	$-C^{15}H_3$†
α-Bulnesene(**1**)	5.37 (m, $w_{1/2}$ 3.5 Hz)	8.31 (m, $w_{1/2}$ 3 Hz)	9.11 (d, J 6.5 Hz)	8.34 (m, $w_{1/2}$ 4 Hz)
5-epi-α-Bulnesene(**2**)	5.34 (m, $w_{1/2}$ 10 Hz)	8.28 (m, $w_{1/2}$ 4.5 Hz)	9.05 (d, J 5.5 Hz)	8.33 (m, $w_{1/2}$ 6 Hz)
4-epi-α-Bulnesene(**3**)	5.38 (m, $w_{1/2}$ 3.5 Hz)	8.31(m)	8.99 (d, J 6.0 Hz)	8.34(m)

*The n.m.r. spectra were taken in deuteriochloroform and chemical shifts are given in the Tiers τ scale, with tetramethylsilane as internal standard.

†The chemical shifts assigned to the vinyl methyl groups were, in each case, confirmed by a frequency-swept decoupling experiment in which the protons at C12 were strongly irradiated, thus eliminating the allylic coupling between $-C^{13}H_3$ and $=C^{12}H_2$, and causing the signal due to $-C^{13}H_3$ to collapse to a sharp singlet.

to the o.r.d. curve obtained from compound **14**. Using arguments similar to those employed previously for compound **14**, this observation was consistent only with the conclusion that the keto alcohol possessed structure **20**. Therefore, as was the case with compound **6**, the Birch reduction of **18** was highly stereoselective and, again, the corresponding hydroguaiazulene system having *trans*-fused rings was produced.

Removal of the carbonyl group from **20** by means of Huang–Minlon reduction (24), followed by dehydration (thionyl chloride–pyridine) of the resulting alcohol **21**, gave a mixture of two dienes, in approximately equal amounts. These were separated and purified by means of preparative g.l.c. The component of shorter retention time exhibited spectral data consistent with structure **3**, 4-epi-α-bulnesene. Again, the i.r. and n.m.r. (see Table 2) spectra, as well as g.l.c. retention times, of this compound were different from those of authentic α-bulnesene (**1**). The second product isolated from the dehydration mixture exhibited spectral data consistent with structure **21**.

Stereoselective Synthesis of α-Bulnesene (1) (Scheme 4)

The synthetic work described above clearly revealed that the lithium–ammonia reduction of compounds **6** and **9** stereoselectively gave products possessing a *cis* configuration with respect to the C-4 methyl group and the C-5 hydrogen. Obviously, this was undesirable insofar as the synthesis of α-bulnesene (**1**) was concerned since, in the latter, the C-4 methyl group is *trans* to the C-5 hydrogen. One solution to this stereochemical problem would be to reduce the C_4—C_5 double bond by catalytic hydrogenation, and, indeed, it had already been shown, for example, that catalytic hydrogenation of isophotosantonic lactone (**23**) produced compound **24** as the only product (18). However, employing this reaction for the synthesis of α-bulnesene (**1**) would ne-

Can. J. Chem. Downloaded from www.nrcresearchpress.com by 210.87.254.5 on 09/05/12
For personal use only.

Can. J. Chem. Downloaded from www.nrcresearchpress.com by 210.87.254.5 on 09/05/12
For personal use only.

cessitate the use of a hydroguaiazulene intermediate different from **6**, since selective hydrogenation of the C_4—C_5 double bond in the latter would be impossible in the presence of the isopropenyl double bond. Therefore, it was planned to employ an intermediate with a C-7 side chain which would be stable to hydrogenation conditions and which contained the necessary functionality for (later) conversion to the isopropenyl moiety. The keto diester **28** was chosen as an appropriate intermediate for this purpose.

When the cross-conjugated cyclohexadienone **25** (14), of known absolute stereochemistry, was subjected to photolysis (25, 26) in 45% aqueous acetic acid, a crude product was obtained in high yield. The latter, upon purification by means of column chromatography on alumina, afforded, in addition to a small amount (10%) of the spiro compound **26**, the desired keto ester **27** in 79% yield. In each case, the spectral data fully supported the structural assignment. The keto ester **27** exhibited, in its o.r.d. curve, a strongly positive Cotton effect (see Table 1), an observation which was in full accord with this compound possessing absolute stereochemistry as shown (see ref. 13).

Acetylation of compound **27** with hot acetic anhydride in the presence of sodium acetate gave the keto diester **28**. Catalytic hydrogenation of the latter with 10% palladium-on-charcoal in ethanol at room temperature and atmospheric pressure afforded the keto diester **29**, in 85% yield. Since compound **29** was thermodynamically unstable with respect to its C-4 epimer (vide infra), it was subjected to the next reaction without rigorous purification. However, the spectral properties of this crude product were in complete accord with structure **29**. Of particular note was the o.r.d. curve, which exhibited a strongly negative Cotton effect (see Table 1). Furthermore, treatment of a small sample of the hydrogenation product **29** with 1% methanolic potassium hydroxide at room temperature, followed by purification of the crude product by column chromatography on alumina, gave a high yield of a clear oil which was shown by analytical data and by n.m.r. spectrum to consist largely of a compound **30** epimeric with starting material **29**. A small amount of the latter was also present. The o.r.d. curve of this material showed a weakly negative Cotton effect, A = −17. These o.r.d. measurements (see refs. 20–23), along with the epimerization, fully supported the idea that the structure and stereochemistry of the product obtained from the hydrogenation of **28** was correctly represented by **29**.

Reduction of the crude ketone **29** with sodium borohydride in methanol gave a mixture of epimeric alcohols, **31** and **32**. An analytical sample of this mixture, obtained by distillation of the crude material under reduced pressure, gave the expected spectral characteristics.

The epimeric mixture of **31** and **32**, upon treatment with *p*-toluenesulfonic acid in dry pyridine at room temperature, gave the tosylate **33** in 20% yield and the olefinic diester **35** in 55% yield. The tosylate **33**, which was isolated from the product mixture by means of column chromatography, was unstable and decomposed upon prolonged standing at room temperature. However, the spectral data obtained from the freshly isolated material was in full accord with structure **33**.

The olefin **35** could be thought to arise from the *trans* elimination of *p*-toluenesulfonic acid from the initially formed 3β-tosylate **34**. This would alleviate the steric interaction between the tosylate group and the C-4 methyl group. It should be noted that an observation similar to the one presently under discussion had been made by White *et al.* (10) in a different series of hydroguaiazulene derivatives. The formation of the olefin **35** as the major product from the tosylation of the epimeric mixture of alcohols **31** and **32**, presumably reflected the fact that compound **31** was the major compound in the epimeric mixture.

Hydrogenation of olefin **35** over Adams catalyst gave a product consisting of a mixture of epimers. Therefore, hydrogenation conditions which would result in increased stereoselectivity were sought and, indeed, it was found that hydrogenation of **35** in benzene in the presence of the homogeneous catalyst tris(triphenylphosphine)chlororhodium was highly stereoselective and afforded, in 85% yield, the diester **36**. Even though, from an inspection of molecular models, it was felt that the hydrogenation of olefin **35** would take place preferentially from the α-side of the molecule and thus be stereoselective in the desired sense, it should be noted that the configuration at C-4 of the product **36** was somewhat uncertain at this stage. This uncertainty was removed as follows. Reduction of the diester **36** with lithium aluminum hydride afforded, in high yield, the crystalline diol **37**. The same diol was also obtained, in approximately 60% yield,

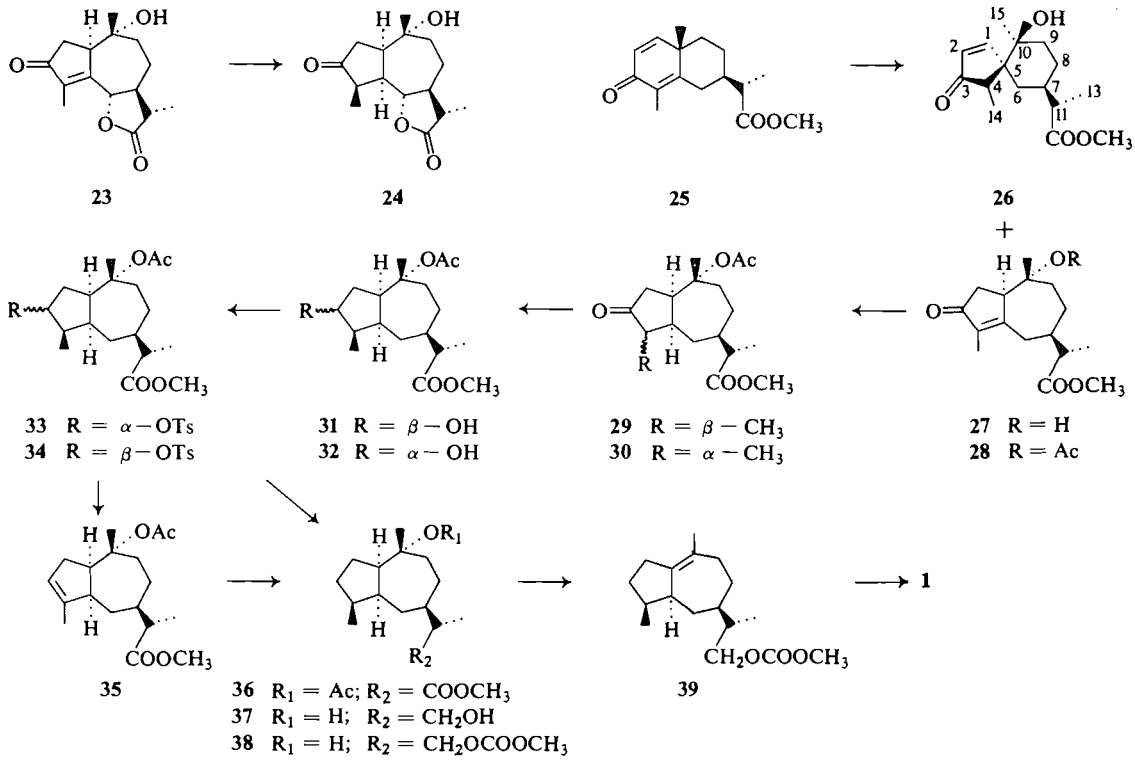

SCHEME 4

by lithium aluminum hydride reduction of the diester tosylate **33**. Since the stereochemistry at C-4 of the latter compound was known (vide supra) and would, of course, remain unchanged during the hydride reduction, this clearly established that the diester **36** possessed the desired stereochemistry with respect to the C-4 position.

Treatment of the diol **37** with methyl chloroformate in dry pyridine at room temperature gave the corresponding monocarbonate **38**, in 74% yield. Dehydration of the latter with thionyl chloride in pyridine afforded the olefinic carbonate **39**, which was contaminated by small amounts of two double-bond isomers. Pyrolysis of this crude material by passage through a heated (400°) helix-packed pyrex glass tube (14) effected elimination of methanol and carbon dioxide and gave a mixture of dienes, the major component of which exhibited a g.l.c. retention time identical with that of authentic α-bulnesene (**1**). Isolation of this component by preparative g.l.c. gave pure α-bulnesene (**1**), which exhibited i.r. and n.m.r. (see Table 2) spectra and g.l.c. retention times identical with those of natural α-bulnesene (**1**). It should be noted that synthetic and authentic α-bulnesene also gave identical negative plain o.r.d. curves. Since the absolute stereochemistry of all our synthetic intermediates was known, this observation corroborated the assigned absolute configuration of the latter compound.

Experimental

Melting points, which were determined on a Kofler block, and boiling points are uncorrected. The i.r. spectra were recorded on either a Perkin–Elmer Infracord model 137, –21, or –421 spectrophotometer. The latter instrument was employed for all comparison spectra. Ultraviolet (u.v.) spectra were measured in methanol solution on either a Cary 14 spectrophotometer or a Perkin–Elmer model 202 ultraviolet-visible spectrophotometer. The n.m.r. spectra were taken in deuteriochloroform solution on either a JEOLCO C-60H spectrometer, a Varian Associates model A-60 or HA-100 spectrometer, decoupling experiments being performed with the latter instrument. Signal positions are given in the Tiers τ scale, with tetramethylsilane as an internal standard; the multiplicity, integrated peak areas, and proton assignments are indicated in parentheses. The o.r.d. measurements were performed on a JASCO model ORD/UV-5

Can. J. Chem. Downloaded from www.nrcresearchpress.com by 210.87.254.5 on 09/05/12
For personal use only.

Can. J. Chem. Downloaded from www.nrcresearchpress.com by 210.87.254.5 on 09/05/12
For personal use only.

instrument. Mass spectra were recorded on an AEI, type MS-9, mass spectrometer. The g.l.c. was carried out on an Aerograph Autoprep, model 700. The following columns (10 ft × 1/4 in.) were employed, with the inert, supporting material being 60/80 mesh Chromosorb W in each case: column A, 20% Carbowax 20 M; column B, 20% SE 30; column C, 30% SE 30; column D, 20% Apiezon J; column E, 20% FFAP. The specific column used, along with the column temperature, are indicated in parentheses. The carrier gas (helium) flow-rate was 90–100 ml/min in each case.

Silica gel G and Woelm neutral alumina containing 2% by weight of a fluorescent indicator (electronic phosphor) were used for thin-layer chromatoplates. Aqueous potassium permanganate solution (10%) was used as a spray reagent. Column chromatography was performed using neutral Woelm silica gel or neutral Woelm alumina. The latter was deactivated as required by addition of the correct amount of water. In cases where basic Shawinigan alumina was used, 10% aqueous acetic acid was used for deactivation.

Microanalyses were performed by Mr. P. Borda, Microanalytical Laboratory, University of British Columbia, Vancouver, B.C.

2-Hydroxymethylene-(−)-7-epi-α-cyperone (10)

To a stirred slurry of sodium methoxide (23.5 g) n 60 ml of dry benzene was added a solution of ethyl formate (14.9 g) in 60 ml of dry benzene. The mixture was cooled to 0° and then a solution of (−)-7-epi-α-cyperone (7) (14.5 g) in 120 ml of dry benzene was added dropwise, over a period of 1 h in an atmosphere of nitrogen. The mixture was allowed to warm to room temperature and stirred for 48 h. Water was added, the mixture was thoroughly shaken, and the layers were separated. The organic layer was extracted with 500 ml of 7% aqueous sodium hydroxide. The combined aqueous layer and alkaline extract were cooled, acidified with 6 *N* hydrochloric acid, and thoroughly extracted with ethyl ether. The combined ether extracts were dried over anhydrous magnesium sulfate. Removal of solvent gave 14.5 g (86%) of the crude hydroxymethylene derivative **10** as a brown oil. Distillation under reduced pressure, of a small amount of this material gave an analytical sample as a clear, pale-yellow oil, b.p. 140–150° (bath temperature) at 0.015 mm; n_D^{20} 1.5589; $[\alpha]_D^{25}$ −50° (c, 0.5 in methanol); u.v., λ_{max} 263 mμ (ε = 8480), 310 mμ (ε = 5770), λ_{max}(MeOH + NaOH) 260 mμ (ε = 9800), 360 mμ (ε = 9970); i.r. (film), λ_{max} 3.48, 5.84, 6.13, 11.15 μ; n.m.r., τ 2.68 (broad signal, 1H, =C*H*OH), 5.20 and 5.38 (two broad signals, 2H, $=C^{12}H_2$), 8.14 (poorly resolved doublet, 3H, $-C^{14}H_3$, J = 1 Hz), 8.29 (unresolved multiplet, 3H, $-C^{13}H_3$), 8.94 (singlet, 3H, $-C^{15}H_3$).

Anal. Calcd. for $C_{16}H_{22}O_2$: C, 78.00; H, 9.00. Found: C, 78.09; H, 9.01.

1,2-Dehydro-2-formyl-(−)-7-epi-α-cyperone (11)

To a solution of the crude hydroxymethylene derivative **10** (21 g) in 200 ml of dry dioxane was added, in one portion, a solution of 21.6 g of 2,3-dichloro-5,6-dicyanobenzoquinone in dry dioxane (250 ml). The mixture was stirred, under an atmosphere of nitrogen, at room temperature for 10 min. The mixture was filtered and the filtrate was diluted with 1 l benzene. The resulting solution was filtered through a column of activity III Woelm neutral alumina (200 g). The column was washed with 2 l of benzene and 3 l of chloroform. Removal of the solvent from the combined eluant gave 16.5 g (79%) of the crude keto aldehyde **11**, as a brown oil. Purification of a small amount of the crude product by distillation under reduced pressure gave an analytical sample of aldehyde **11** as a clear yellow viscous oil, b.p. 150° (bath temperature) at 0.02 mm; n_D^{20} 1.5567; $[\alpha]_D^{23}$ +30° (*c*, 1.0 in methanol); u.v., λ_{max} 239 mμ (ε = 8850), 280 mμ (ε = 6200) (shoulder); i.r. (film), λ_{max} 3.51, 5.90, 6.10, 7.82, 7.98, 8.10, 11.13 μ; n.m.r., τ −0.27 (singlet, 1H, —CHO), 2.55 (singlet, 1H, C^1H), 5.25 and 5.43 (two broad signals, 2H, $=C^{12}H_2$), 8.02 (doublet, 3H, $-C^{14}H_3$, J = 1.3 Hz), 8.30 (unresolved multiplet, 3H, $-C^{13}H_3$), 8.68 (singlet, 3H, $-C^{15}H_3$). The chemical shifts assigned to $-C^{13}H_3$ and $-C^{14}H_3$ were confirmed by a frequency-swept decoupling experiment in which one of the protons of $=C^{12}H_2$ at τ 5.25 was strongly irradiated, thus eliminating part of the allylic coupling between $-C^{13}H_3$ and $=C^{12}H_2$, and causing the unresolved multiplet at τ 8.30 to sharpen to a broad singlet.

Anal. Calcd. for $C_{16}H_{20}O_2$: C, 78.65; H, 8.26. Found: C, 78.39; H, 8.49.

1,2-Dehydro-2-carboxy-(−)-7-epi-α-cyperone (12)

To a stirred solution of the aldehyde derivative **11** (16 g) in 18 ml of 95% aqueous ethanol was added a solution of silver nitrate (24.6 g) in 126 ml water, followed by the dropwise addition of a solution of sodium hydroxide (11.2 g) in 300 ml water. After the addition was complete (1.5 h), the mixture was stirred at room temperature for 4 h. The mixture was filtered and the residue was washed with 200 ml of saturated sodium bicarbonate solution. The combined filtrate and washings were acidified with 6 *N* hydrochloric acid and then made alkaline with sodium carbonate solution. The mixture was filtered and the filtrate was acidified with 4 *N* hydrochloric acid. The resulting mixture was extracted thoroughly with ether, and the combined ether extracts were evaporated. The residual material was dissolved in benzene and the resulting solution was dried over anhydrous sodium sulfate. Removal of the solvent gave 13.2 g (77%) of a light-yellow crystalline solid. Recrystallization of a small amount of this material from ether gave an analytical sample of the carboxylic acid derivative **12**, m.p. 102.5–104°; $[\alpha]_D^{23}$ +93.2° (*c*, 0.25 in methanol); u.v., λ_{max} 203 mμ (ε = 19 600), 246 mμ (ε = 7950); i.r. ($CHCl_3$), λ_{max} 5.77, 6.07, 6.33, 11.02 μ; n.m.r., τ 1.92 (singlet, 1H, C^1H), 5.28 and 5.52 (two broad signals, 2H, $=C^{12}H_2$), 8.01 (poorly resolved doublet, 3H, $-C^{14}H_3$, J = 1 Hz), 8.31 (broad singlet, 3H, $-C^{13}H_3$), 8.64 (singlet, 3H, $-C^{15}H_3$).

Anal. Calcd. for $C_{16}H_{20}O_3$: C, 73.79; H, 7.75. Found: C, 73.59; H, 7.92.

Preparation of Hydroguaiazulene Derivative 9

The irradiation of compound **12** was carried out with a Hanovia 450 W high-pressure mercury lamp, in an apparatus similar to that described by Kropp and Erman (27), except that the lamp was housed in a quartz water-jacketed immersion well.

A solution of the carboxylic acid **12** (2.0 g) in 400 ml of 45% aqueous acetic acid was irradiated, using a pyrex

Can. J. Chem. Downloaded from www.nrcresearchpress.com by 210.87.254.5 on 09/05/12
For personal use only.

filter, for 50 min. During the irradiation, the solution was vigorously stirred with a stream of nitrogen and the temperature was kept near 25° by adjusting the rate of flow of the cold water through the quartz water-jacket. After completion of the photolysis, the solvent was removed under reduced pressure, the temperature being kept below 50°. From a total of 12.5 g of **12**, there was obtained, in this manner, approximately 10 g of crude material which crystallized on standing. Recrystallization of this crude solid from chloroform – petroleum ether (b.p. 30–60°) afforded 7.5 g (60%) of the hydroguaiazulene derivative **9**, which was identical (i.r., n.m.r., m.p.) with the compound obtained previously by irradiation of compound **8** (see ref. 13).

*Preparation of Diol **13***

To a solution of lithium (1.5 g) in 1 l of liquid ammonia (which had been distilled from sodium metal), was added a solution of compound **6** (1.0 g) in 50 ml of ether. The mixture was stirred for 1.5 h and then the reaction was quenched by cautious addition of methanol. After the ammonia had evaporated, the residue was diluted with water. The resulting mixture was extracted with ether. The ether extract was washed with water and dried over anhydrous sodium sulfate. Removal of solvent yielded a white solid (0.9 g). This crude diol **13** was not purified further, but exhibited the following expected spectral properties: i.r. (nujol), λ_{max} 3.10, 6.10, 11.31 μ; n.m.r., τ 5.35 (unresolved multiplet, 2H, $=C^{12}H_2$), 6.49 (multiplet, 1H, C^3H), 8.33 (unresolved multiplet, 3H, $-C^{13}H_3$), 8.47 (broad singlet, —OH), 8.88 (singlet, 3H, $-C^{15}H_3$), 9.00 (doublet, 3H, $-C^{14}H_3$, J = 5 Hz).

*Preparation of Keto Alcohol **14***

To a slurry of chromium trioxide (7.2 g) in pyridine (120 ml) at 0° was added, in one portion, a solution of the diol **13** (3.6 g) in 60 ml of pyridine. The mixture was stirred at room temperature for 22 h, and then poured into 500 ml of cold water. The resulting mixture was extracted with ether (1.5 l) and the combined ether extracts were evaporated. The residual material was dissolved in benzene and the resulting solution was washed thoroughly with water and then dried over anhydrous sodium sulfate. Removal of solvent under reduced pressure gave 3.2 g of a viscous yellow oil. A small amount of this crude product was purified by column chromatography on activity III neutral Woelm alumina (70 g). Elution with 450 ml of 1:1 chloroform–benzene gave the keto alcohol **14** as a white solid. Recrystallization from ether – petroleum ether (b.p. 30–60°) afforded colorless needles, m.p. 58.5–59°; i.r. ($CHCl_3$), λ_{max} 2.81, 3.45, 5.81, 6.12, 11.15 μ; n.m.r., τ 5.33 (unresolved multiplet, $w_{1/2}$ = 4 Hz, 2H, $=C^{12}H_2$), 8.30 (poorly resolved doublet, 3H, $-C^{13}H_3$, J = 1 Hz), 8.82 (sharp singlet, 3H, $-C^{15}H_3$), 8.95 (doublet, 3H, $-C^{14}H_3$, J = 6.5 Hz). Pertinent o.r.d. data is given in Table 1.

Anal. Calcd. for $C_{15}H_{24}O_2$: C, 76.23; H, 10.24. Found: C, 76.11; H, 10.23.

*Preparation of Diol **19***

This compound was obtained from compound **9** by a procedure identical with that described above for the conversion of **6** into **13**. From 7.0 g of **9** there was obtained 7.9 g of **19** as a crude yellow solid. Two recrystallizations of a small sample of this material from 10:1 *n*-hexane – ether at 0° afforded colorless needles, m.p. 153–155°; i.r., (nujol), λ_{max} 3.00, 6.10, 11.30 μ; n.m.r., τ 5.32 (unresolved multiplet, 2H, $=C^{12}H_2$), 6.45 (multiplet, 1H, C^3H), 8.28 (unresolved multiplet, 3H, $-C^{13}H_3$), 8.88 (singlet, 3H, $-C^{15}H_3$), 9.02 (doublet, 3H, $-C^{14}H_3$, J = 5 Hz).

Anal. Calcd. for $C_{15}H_{26}O_2$: C, 75.57; H, 10.99. Found: C, 75.45; H, 11.07.

*Preparation of Keto Alcohol **20***

This compound was obtained from compound **19** by a procedure identical with that described above for the oxidation of compound **13**. From 7.9 g of crude diol **19** there was obtained 5.3 g of crude product as a light-brown oil. A small sample of the crude product, upon distillation under reduced pressure in a hot box, gave a pale-yellow oil which solidified on standing. Recrystallization from ether – petroleum ether (b.p. 30–60°) at 0° gave fine needles, m.p. 64.5–65°; $[\alpha]_D^{20}$ +38.2° (*c*, 0.2 in methanol); i.r. ($CHCl_3$), λ_{max} 2.96, 3.46, 5.82, 6.11, 11.15 μ; n.m.r., τ 5.32 (broad signal, $w_{1/2}$ = 6.5 Hz, 2H, $=C^{12}H_2$), 8.29 (poorly resolved doublet, 3H, $-C^{13}H_3$, J = 1 Hz), 8.85 (singlet, 3H, $-C^{15}H_3$), 8.95 (doublet, 3H, $-C^{14}H_3$, J = 6.5 Hz). Pertinent o.r.d. data is given in Table 1.

Anal. Calcd. for $C_{15}H_{24}O_2$: C, 76.23; H, 10.24. Found: C, 76.00; H, 10.31.

*Preparation of Alcohol **17***

To a solution of compound **14** (2.3 g) in 150 ml of purified diethylene glycol was added potassium hydroxide powder (3.1 g) and 85% hydrazine hydrate (70 ml). After the solution had refluxed at 155° for 2 h, hydrazine was distilled from the reaction mixture until the reaction temperature reached 205°. The reaction mixture was then refluxed at 205–210° for 5 h. The cooled reaction mixture was diluted with 300 ml of water and extracted several times with benzene. The combined extracts were washed several times with water, once with saturated brine, and then dried over anhydrous sodium sulfate. Removal of solvent afforded 1.93 g (89%) of a pale-yellow, viscous oil. A small amount of this crude product was purified further by means of preparative thin-layer chromatography (t.l.c.) (Woelm neutral alumina plates developed with 2:1 chloroform – ethyl acetate) whereby a pale yellow solid was obtained. Recrystallization from *n*-hexane at 0° gave colorless needles, m.p. 54.5–55°, $[\alpha]_D^{27}$ +34.7° (*c*, 0.35 in methanol); i.r. ($CHCl_3$), λ_{max} 3.47, 6.12, 11.3 μ; n.m.r., τ 5.35 (unresolved multiplet, $w_{1/2}$ = 5.5 Hz, 2H, $=C^{12}H_2$), 8.33 (poorly resolved doublet, 3H, $-C^{13}H_3$, J = 1 Hz), 8.88 (singlet, 3H, $-C^{15}H_3$), 9.05 (doublet, 3H, $-C^{14}H_3$, J = 6 Hz).

Anal. Calcd. for $C_{15}H_{26}O$: C, 81.01; H, 11.78. Found: C, 80.86; H, 11.76.

*Preparation of Alcohol **21***

This compound was obtained from keto alcohol **20** by a procedure identical with that described above for the preparation of **17**. From 3.0 g of keto alcohol **20** there was obtained 2.5 g (90%) of crude product as a viscous yellow oil which, upon distillation under reduced pressure, gave a clear, colorless oil, $[\alpha]_D^{22}$ −30.6° (*c*, 0.8 in methanol); n_D^{23} 1.6875; i.r. (film), λ_{max} 2.99, 3.43, 6.11,

Can. J. Chem. Downloaded from www.nrcresearchpress.com by 210.87.254.5 on 09/05/12
For personal use only.

11.14 μ; n.m.r., τ 5.37 (unresolved multiplet, $w_{1/2}$ = 8 Hz, 2H, $=C^{12}H_2$), 8.30 (poorly resolved doublet, 3H, $-C^{13}H_3$, J = 1 Hz), 8.88 (singlet, 3H, $-C^{15}H_3$), 9.05 (doublet, 3H, $-C^{14}H_3$, J = 6 Hz).

Anal. Calcd. for $C_{15}H_{26}O$: C, 81.01; H, 11.78. Found: C, 80.88; H, 12.09.

5-epi-α-Bulnesene (2)

To a solution of alcohol **17** (780 mg) in 40 ml of dry pyridine at 0° was added dropwise 1.5 ml of purified thionyl chloride. The mixture was stirred at 0° for 15 min, and then evaporated under reduced pressure at room temperature. Water was added to the residue and the resulting mixture was extracted thoroughly with benzene. The extract was washed thrice with water, once with brine, and then dried over anhydrous sodium sulfate. Removal of solvent afforded 600 mg of crude product as light-brown oil which was shown by g.l.c. analysis (column A, 167°) to be approximately 80% pure. An analytical sample of the major component, 5-epi-α-bulnesene (**2**) was collected by preparative g.l.c. (column A, 167°) and exhibited a positive plain o.r.d. curve. The i.r. (film), λ_{max} 3.42, 6.11, 6.88, 7.26, 11.00 μ. Pertinent n.m.r. data is given in Table 2. The i.r. and n.m.r. spectra of 5-epi-α-bulnesene (**2**) were clearly different from the corresponding spectra of α-bulnesene (**1**). Also, the g.l.c. retention times (column B, 180°) of the two compounds were different.

Mol. Wt. Calcd. for $C_{15}H_{24}$: 204.188. Found (high-resolution mass spectrometry): 204.187.

4-epi-α-Bulnesene (3)

This compound was obtained by dehydration (thionyl chloride in pyridine) of alcohol **21**, employing a procedure identical with that described above for the preparation of 5-epi-α-bulnesene (**2**). From 420 mg of compound **21** there was obtained 350 mg of crude product as a light-brown oil which was shown by g.l.c. analysis (column C, 170°) to consist of two components in approximately equal amounts. An analytical sample of each of these components was obtained by preparative g.l.c. (column C, 170°). The component of shorter retention time was 4-epi-α-bulnesene (**3**) and exhibited a negative plain o.r.d. curve. The i.r. (film), λ_{max} 3.46, 6.11, 6.94, 7.28, 11.32 μ. Pertinent n.m.r. data is given in Table 2. The i.r. and n.m.r. spectra of 4-epi-α-bulnesene (**3**) were clearly different from the corresponding spectra of α-bulnesene (**1**). Also, the g.l.c. retention times (column B, 175°) of the two compounds were different.

Mol. Wt. Calcd. for $C_{15}H_{24}$: 204.188. Found (high-resolution mass spectrometry): 204.187.

The second component isolated was compound **22** and exhibited the following spectral data: i.r. (film), λ_{max} 3.43, 6.11, 6.90, 7.27, 11.33 μ; n.m.r., τ 4.45 (poorly resolved triplet, 1H, C^9H, J = 7 Hz), 5.40 (unresolved multiplet, 2H, $=C^{12}H_2$), 8.32 (unresolved multiplet, 6H, two vinyl methyls), 9.06 (doublet, 3H, $-C^{14}H_3$, J = 6 Hz).

Preparation of α-Bulnesene (1) by Dehydration of Bulnesol (18)

The dehydration of bulnesol (**18**) was carried out under conditions identical with those described above for the dehydration of alcohol **17**. From 66 mg of bulnesol (**18**) there was obtained 50 mg of crude product as a brown oil. An analytical sample of α-bulnesene (**1**) was obtained from the crude product by means of preparative g.l.c. (column A, 175°), and exhibited a negative plain o.r.d. curve. The i.r. (film), λ_{max} 3.42, 6.10, 7.04, 7.39, 11.38 μ. Pertinent n.m.r. data is given in Table 2.

Photochemical Rearrangement of Compound 25

The irradiation of compound **25** was carried out under conditions very similar to those employed for compound **12** (vide supra). The crude gummy product obtained from the irradiation of 34 g of **25** in 4.5 l of 45% aqueous acetic acid was purified by column chromatography on activity III neutral Woelm alumina (1,100 g). Elution with 2 l of benzene gave 10.8 g (32%) of starting material **25**. Continued elution with 2 l of 1:1 benzene–chloroform gave 2.7 g (8.2%) of the spiro compound **26** which, upon distillation under reduced pressure, afforded a viscous pale-yellow oil, b.p. 170° (bath temperature) at 0.2 mm; i.r. (film), λ_{max} 2.95, 3.47, 5.94, 6.32 μ; n.m.r., τ 2.30 (doublet, 1H, C^1H), 3.87 (doublet, 1H, C^2H, $J_{1,2}$ = 6 Hz), 6.40 (singlet, 3H, $-COOCH_3$), 7.36 (quartet, 1H, C^4H, $J_{4,14}$ = 7.5 Hz), 8.87 (doublet, 3H, $-C^{13}H_3$, $J_{11,13}$ = 6.7 Hz), 8.90 (doublet, 3H, $-C^{14}H_3$, $J_{4,14}$ = 7.5 Hz), 8.96 (singlet, 3H, $-C^{15}H_3$).

Anal. Calcd. for $C_{16}H_{24}O_4$: C, 68.54; H, 8.63. Found: C, 68.34; H, 8.49.

Further elution with 2 l of 1:1 benzene–chloroform and 3 l of chloroform gave 18.3 g (79% based on unrecovered **25**) of hydroguaiazulene derivative **27** as a viscous yellow oil which, upon distillation under reduced pressure, afforded a clear, pale-yellow viscous oil, b.p. 175° (bath temperature) at 0.2 mm; $[\alpha]_D^{25}$ +88.5° (*c*, 0.1 in methanol); u.v., λ_{max} 243 mμ (ε = 13 760); i.r. (film), λ_{max} 2.93, 3.45, 5.82, 5.95, 6.16 μ; n.m.r., τ 6.37 (singlet, 3H, $-COOCH_3$), 6.83 (very broad signal, $w_{1/2}$ = 10 Hz, 1H, C^1H), 8.37 (poorly resolved doublet, 3H, $-C^{14}H_3$, J = 1 Hz), 8.83 (doublet, 3H, $-C^{13}H_3$, $J_{11,13}$ = 7 Hz), 9.13 (singlet, 3H, $-C^{15}H_3$). Pertinent o.r.d. data is given in Table 1.

Anal. Calcd. for $C_{16}H_{24}O_4$: C, 68.54; H, 8.63. Found: C, 68.42; H, 8.45.

Preparation of Keto Diester 28

A solution of the alcohol **27** (19 g) in 170 ml of acetic anhydride containing 11 g of sodium acetate was warmed at 90–95° for 60 h, under an atmosphere of dry nitrogen. The mixture was diluted with cold water (250 ml) and benzene (200 ml). The mixture was stirred at room temperature for 1 h, and the layers separated. The aqueous layer was extracted with benzene. The combined extracts were washed thoroughly with water and once with saturated brine and then dried over anhydrous sodium sulfate. Removal of solvent under reduced pressure gave a light-brown oil which was purified by column chromatography on activity III neutral Woelm alumina (400 g). Elution with 2.5 l of benzene and 1 l of 1:1 chloroform–benzene gave 15.5 g (70%) of the keto diester **28**. Removal of all traces of solvent by warming at 50–60° under vacuum for several days afforded an analytical sample of **28** as a clear, pale-yellow oil, $[\alpha]_D^{19}$ +27.5° (*c*, 1.0 in chloroform); u.v., λ_{max} 241 mμ (ε = 14 400); i.r. (film), λ_{max} 3.45, 5.87, 5.93, 6.15 μ; n.m.r., τ 5.93 (broad signal, $w_{1/2}$ = 10 Hz, 1H, C^1H), 7.61 (doublet, 2H, C^2H_2, $J_{1,2}$ = 4 Hz),

Can. J. Chem. Downloaded from www.nrcresearchpress.com by 210.87.254.5 on 09/05/12
For personal use only.

8.04 (singlet, 3H, —$COCH_3$), 8.34 (poorly resolved doublet, 3H, —$C^{14}H_3$, J = 1.5 Hz), 8.82 (doublet, 3H, —$C^{13}H_3$, $J_{11,13}$ = 7 Hz), 8.96 (singlet, 3H, —$C^{15}H_3$). The chemical shifts assigned to C^1H and C^2H_2 were confirmed by frequency-swept decoupling experiments. Firstly, the proton at C-1 was strongly irradiated, thus eliminating coupling between C^1H and C^2H_2, and causing the doublet at τ 7.61 to collapse to a singlet. Further when the protons at C-14 were strongly irradiated, thus eliminating the homoallylic coupling between C^1H and —$C^{14}H_3$, the broad signal at τ 5.93 sharpened to a poorly resolved triplet with $J_{1,2}$ = 4 Hz.

Anal. Calcd. for $C_{18}H_{26}O_5$: C, 67.06; H, 8.13. Found: C, 67.01; H, 8.14.

Preparation of Keto Diester ***29***

A solution of the unsaturated keto diester **28** (12.4 g) in 250 ml 95% aqueous ethanol was hydrogenated at room temperature and atmospheric pressure over 10% palladium-on-charcoal (4 g) for 40 h. Filtration and removal of solvent afforded 10.5 g (85%) of the saturated keto diester **29** as a clear, colorless oil. This crude product was not purified further, but exhibited the following expected spectra properties: i.r. (film), λ_{max} 5.80 μ; n.m.r., τ 6.44 (singlet, 3H, —$COOCH_3$), 8.00 (singlet, 3H, —$COCH_3$), 8.55 (singlet, 3H, —$C^{15}H_3$), 8.96 and 9.05 (doublets, 6H, secondary methyls, J = 7 Hz, 6 Hz, respectively). Pertinent o.r.d. data is given in Table 1.

Anal. Calcd. for $C_{18}H_{28}O_5$: C, 66.64; H, 8.70. Found: C, 66.87; H, 8.83.

Epimerization of Keto Diester ***29***

A small amount of compound **29** (0.8 g) was treated with 1% methanolic potassium hydroxide at room temperature for 2 h. The methanol was replaced by benzene and the benzene solution was washed twice with water, once with saturated brine and then dried over anhydrous sodium sulfate. The crude product was purified by column chromatography on activity III Woelm neutral alumina (85 g). Elution with 500 ml of benzene gave a clear oil which, upon removal of solvent by warming the oil at 40–50° under vacuum for 2 days, gave an analytical sample of an epimeric mixture of **29** and **30**, with the latter largely predominating. The i.r. (film), λ_{max} 5.81 μ; n.m.r., τ 6.34 (singlet, 3H, —$COOCH_3$), 7.93 and 8.00 (two singlets, 3H, —$COCH_3$ of **29** and **30**, respectively), 8.51 and 8.60 (two singlets, 3H, —$C^{15}H_3$ of **29** and **30**, respectively), 8.95 and 9.04 (overlapping doublets, 6H, secondary methyls of **29** and **30**); o.r.d., $[\phi]_{312}^{27}$ −1240 (trough), $[\phi]_{290}^{27}$ 0, $[\phi]_{272}^{27}$ +504 (peak), (*c*, 0.16 in methanol).

Anal. Calcd. for $C_{18}H_{28}O_5$: C, 66.64; H, 8.70. Found: C, 66.79; H, 8.63.

Sodium Borohydride Reduction of Keto Diester ***29***

To a solution of the crude keto diester **29** (10.5 g) in 400 ml of anhydrous methanol at 0° was added sodium borohydride (6 g). The resulting mixture was stirred at 0° for 2.5 h under an atmosphere of nitrogen. The reaction was quenched by cautious addition of water and the mixture was stirred for an additional 30 min. The methanol was evaporated under reduced pressure and the remaining aqueous layer was extracted with benzene. The benzene extract was washed with water and dried over anhydrous sodium sulfate. Removal of the solvent under reduced pressure gave 10.2 g (96%) of a mixture of the epimeric alcohols **31** and **32**, as a very viscous colorless oil. An analytical sample was obtained by distillation under reduced pressure, b.p. 130–140° (bath temperature) at 0.2 mm; i.r. (film), λ_{max} 2.96, 3.50, 5.87 μ; n.m.r.,[6] τ 6.32 (singlet, 3H, —$COOCH_3$), 7.47 (singlet, 1H, OH), 8.00 (singlet, 3H, —$COCH_3$), 8.54 (singlet, 3H, —$C^{15}H_3$), 8.94 and 9.04 (two doublets, 6H, secondary methyls, J = 6.5 Hz, 7 Hz, respectively).

Anal. Calcd. for $C_{18}H_{30}O_5$: C, 66.23; H, 9.26. Found: C, 66.24; H, 9.36.

Tosylation of the Mixture of Epimeric Alcohols ***31*** *and* ***32***

To a solution of the mixture of epimeric alcohols **31** and **32** (2 g) in 30 ml of dry pyridine was added 2 g of *p*-toluenesulfonyl chloride. The solution was stirred at room temperature under an atmosphere of nitrogen for 65 h. The solution was diluted with water (50 ml) and the resulting mixture was extracted with benzene. The benzene was washed twice with water, twice with sodium bicarbonate solution, and twice with saturated brine and then dried over anhydrous magnesium sulfate. Removal of solvent gave a light-brown oil which was subjected to column chromatography on activity III neutral Woelm alumina (100 g). Elution with 200 ml benzene afforded 1.04 g (55%) of the olefin **35**. Removal of the last traces of solvent from this material by warming the oil at 50° under vacuum for two days afforded a clear, pale-yellow oil, $[\alpha]_D^{23}$ +74.5° (*c*, 0.4 in methanol); i.r. (film), λ_{max} 3.47, 5.84 μ; n.m.r., τ 4.77 (broad signal, $w_{1/2}$ = 7 Hz, 1H, C^3H), 6.38 (singlet, 3H, —$COOCH_3$), 8.02 (singlet, 3H, —$COCH_3$), 8.37 (poorly resolved doublet, 3H, —$C^{14}H_3$, J = 1.5 Hz), 8.55 (singlet, 3H, —$C^{15}H_3$), 8.95 (doublet, 3H, —$C^{13}H_3$, $J_{11,13}$ = 7 Hz). The chemical shifts assigned to C^3H and —$C^{14}H_3$ were confirmed by frequency-swept decoupling experiments in which the proton at C-3 was strongly irradiated, thus eliminating the allylic coupling between C^3H and —$C^{14}H_3$, and causing the signals at τ 8.37 to sharpen.

Anal. Calcd. for $C_{18}H_{28}O_4$: C, 70.10; H, 9.15. Found: C, 70.39; H, 9.28.

Further elution with 300 ml of 1:4 chloroform–benzene gave 0.6 g (20%) of the tosylate **33** as a clear, colorless viscous oil which was unstable and decomposed upon standing at room temperature for a few days or upon warming to 35° under vacuum. However, the spectral data obtained were in complete accord with the structure **33**. The i.r. (film), λ_{max} 3.48, 5.85, 6.29, 6.92, 7.42, 8.07, 8.54, 15.05 μ; n.m.r., τ 2.24 (doublet, 2H, aromatic protons meta to the methyl group, J = 8 Hz), 2.70 (doublet, 2H, aromatic protons ortho to the methyl group, J = 8 Hz), 5.60 (multiplet, 1H, C^3H), 7.60 (singlet, 3H, Ar—CH_3), 8.05 (singlet, 3H, —$COCH_3$), 8.64 (singlet, 3H, —$C^{15}H_3$), 8.97 and 9.23 (two doublets, 6H, secondary methyls, J = 6.9 Hz, 6.8 Hz, respectively).

The instability of this compound precluded the acquisition of satisfactory analytical data.

---

[6]The n.m.r. signals of the epimeric mixture of alcohols **31** and **32** reported herein correspond to that of the major component **31**.

Can. J. Chem. Downloaded from www.nrcresearchpress.com by 210.87.254.5 on 09/05/12
For personal use only.

Preparation of Diester 36

To a solution of the olefin **35** (400 mg) in 40 ml of dry benzene was added a solution of 160 mg of tris(triphenylphosphine)chlororhodium in 20 ml of dry benzene. The resulting solution was subjected to hydrogenation at room temperature and atmospheric pressure for 10 h. The benzene was removed under reduced pressure and ether was added to the residue. The resulting mixture was filtered through a column of activity III Woelm neutral alumina (20 g), and the column was washed with 300 ml of ether. Evaporation of the combined filtrate and washings afforded a light-brown oil which, upon distillation under reduced pressure, gave 300 mg (84%) of diester **36** as a viscous, pale-yellow oil, b.p. 130° (bath temperature) at 0.2 mm; $[\alpha]_D^{23}$ −18.8° (*c*, 0.7 in methanol); i.r. (film), λ_{max} 3.47, 5.84, 6.88, 7.32, 8.02, 8.64, 9.17 μ; n.m.r., τ 6.37 (singlet, 3H, —$COOCH_3$), 8.01 (singlet, 3H, —$COCH_3$), 8.57 (singlet, 3H, —$C^{15}H_3$), 8.94 and 9.11 (two doublets, 6H, secondary methyls, J = 7 Hz, 6.4 Hz respectively).

Anal. Calcd. for $C_{18}H_{30}O_4$: C, 69.64; H, 9.74. Found: C, 69.39; H, 9.73.

Preparation of Diol 37

(a) From Diester 36

To a solution of diester **36** (600 mg) in 25 ml of anhydrous ether was added 200 mg of lithium aluminum hydride powder. The resulting mixture was refluxed under an atmosphere of nitrogen for 4 h, and then cooled to 0°. Excess lithium aluminum hydride was destroyed by dropwise addition of water. The resulting mixture was filtered and the filtrate was extracted with benzene. After the extract had been dried over anhydrous sodium sulfate, the solvent was removed under reduced pressure, giving 430 mg (92%) of a viscous oil which solidified upon standing at 0°. Recrystallization from ether at 0° gave colorless crystals, m.p. 100–102°; $[\alpha]_D^{22}$ −32.5° (*c*, 0.6 in methanol); i.r. ($CHCl_3$), λ_{max} 2.80, 2.90, 6.87, 7.28, 9.83 μ; n.m.r., τ 6.37–6.72 (septet, 2H, $C^{12}H_AH_B$ with H_A at τ 6.48 and H_B at τ 6.62, $J_{A,B}$ = 10.8 Hz, $J_{A,11}$ = 7.3 Hz and $J_{B,11}$ = 6.5 Hz), 7.86 (singlet, 2H, OH), 8.85 (singlet, 3H, —$C^{15}H_3$), 9.10 and 9.19 (two doublets, 6H, secondary methyls, J = 6.3 and 6.8 Hz, respectively).

Anal. Calcd. for $C_{15}H_{28}O_2$: C, 74.95; H, 11.74. Found: C, 75.14; H, 11.68.

(b) From Diester Tosylate 33

A solution of the diester tosylate **33** (150 mg) in 10 ml of a 1.3 *M* solution of lithium aluminum hydride in tetrahydrofuran was refluxed under an atmosphere of nitrogen for 20 h, and then cooled to 0°. The work-up procedure was similar to that described above and 50 mg (65%) of crude product was obtained. This crude material, upon recrystallization from ether at 0°, gave a colorless crystalline compound which was identical (i.r., n.m.r., m.p.) with the diol **37** obtained from lithium aluminum hydride reduction of compound **36**.

Preparation of Monocarbonate 38

A solution of the diol **37** (490 mg) in 10 ml of dry pyridine was cooled to 0°, and freshly distilled methyl chloroformate (4 ml) was added dropwise. The reactants were allowed to stand at room temperature, under an atmosphere of nitrogen, for 20 h. The reaction mixture was poured into cold (0°) 50% aqueous acetic acid (20 ml) and the resulting mixture was extracted thoroughly with ether. The combined ether extracts were washed several times with water and evaporated. The residual material was dissolved in benzene and the resulting solution was dried over anhydrous sodium sulfate. Removal of the solvent gave a clear oil which, upon distillation under reduced pressure gave 450 mg (74%) of the monocarbonate **38**, b.p. 135–140° (bath temperature) at 0.15 mm; $[\alpha]_D^{19}$ −20.7° (*c*, 0.5 in methanol); i.r. (film), λ_{max} 2.94, 3.48, 5.76 μ; n.m.r., τ 5.81–6.19 (octet, 2H, $C^{12}H_AH_B$ with H_A at τ 5.91 and H_B at τ 6.09, $J_{A,B}$ = 10.5 Hz, $J_{A,11}$ = 6.1 Hz, $J_{B,11}$ = 7.5 Hz), 6.25 (singlet, 3H, —OCH_3), 8.07 (singlet, 1H, —OH), 8.85 (singlet, 3H, —$C^{15}H_3$), 9.12 (two coincident doublets, 6H, secondary methyls, J = 6.5 Hz).

Anal. Calcd. for $C_{17}H_{30}O_3$: C, 68.42; H, 10.13. Found: C, 68.51; H, 10.09.

Synthetic α-Bulnesene (1)

Dehydration of compound **38** was carried out by a procedure very similar to that employed in the preparation of 5-epi-α-bulnesene (**2**) from alcohol **17** (vide supra). From 400 mg of **38**, there was obtained 300 mg (80%) of the unsaturated monocarbonate **39** as a clear, brownish oil. This crude material, which was not purified further, was shown (by n.m.r.) to be contaminated with small amounts of two double-bond isomers. However, this crude material exhibited the following expected spectral properties: i.r. (film), λ_{max} 3.50, 5.76 μ; n.m.r., τ 5.82–6.27 (octet, 2H, $C^{12}H_2$), 6.29 (singlet, 3H, —OCH_3), 8.39 (unresolved multiplet, 3H, —$C^{15}H_3$), 9.14 (two coincident doublets, 6H, secondary methyls, J = 7 Hz).

The crude olefinic carbonate **39** (300 mg) was introduced dropwise onto a vertical pyrex glass column (1.5 cm × 40 cm) packed with glass helices and heated to approximately 400° by a vertical furnace. During the pyrolysis, nitrogen was passed slowly through the column from top to bottom, and the pyrolysate was collected in a receiving tube cooled in an ice–water bath. The contact time of pyrolysis was about 2 min. The crude pyrolysate obtained in this manner was shown by g.l.c. analysis (column D, 170°) to contain, in addition to a number of minor unidentified components, one major component with retention time identical with that of α-bulnesene (**1**). The major product of the pyrolysis was collected by preparative g.l.c. (column D, 170°), and gave i.r. and n.m.r. spectra, and g.l.c. retention times (column B, 170°; column D, 170°; column E, 175°) identical with those of authentic α-bulnesene (**1**) obtained by dehydration of α-bulnesol (**18**) (vide supra). The synthetic α-bulnesene showed a plain negative o.r.d. curve, superimposable on that of authentic α-bulnesene.

We thank the National Research Council of Canada and the University of British Columbia Committee on Research for financial support, and the Canadian Commonwealth Scholarship and Fellowship Committee for a scholarship (to K.F.C.).

1. T. Nozoe and S. Itô. Progress in the chemistry of organic natural products. Vol. XIX. Springer-Verlag, Vienna, 1962. pp. 52–79.

2. F. ŠORM and L. DOLEJŠ. Guaianolides and germacranolides. Editions Scientifiques Hermann, Paris, and Holden–Day, Inc., San Francisco, 1966.
3. G. OURISSON, S. MUNAVALLI, and C. EHRET. International tables of selected constants. Vol. 15. Data relative to sesquiterpenoids. Pergamon, New York, 1966.
4. F. ŠORM, L. DOLEJŠ, and A. MIRONOV. Tetrahedron Lett. 18 (1960).
5. R. B. BATES and R. C. SLAGEL. J. Amer. Chem. Soc. **84**, 1307 (1962), and references therein.
6. E. PIERS and K. F. CHENG. Chem. Commun. 562 (1969).
7. G. BÜCHI, W. D. MACLEOD, JR., and J. PADILLA O. J. Amer. Chem. Soc. **86**, 4438 (1964).
8. G. BÜCHI, J. M. KAUFFMAN, and H. J. E. LOEWENTHAL. J. Amer. Chem. Soc. **88**, 3403 (1966).
9. G. BÜCHI, W. HOFHEINZ, and J. V. PAUKSTELIS. J. Amer. Chem. Soc. **88**, 4113 (1966); **91**, 6473 (1969).
10. E. H. WHITE and J. N. MARX. J. Amer. Chem. Soc. **89**, 5511 (1967); E. H. WHITE, S. EGUCHI, and J. N. MARX. Tetrahedron, **25**, 2099 (1969); J. N. MARX and E. H. WHITE. Tetrahedron, **25**, 2117 (1969).
11. H. HIKINO, K. ITO, K. AOTA, and T. TAKEMOTO. Chem. Pharm. Bull. Japan, **16**, 43 (1968).
12. J. A. MARSHALL and J. J. PARTRIDGE. J. Amer. Chem. Soc. **90**, 1090 (1968); Tetrahedron, **25**, 2159 (1969).
13. E. PIERS and K. F. CHENG. Can. J. Chem. **45**, 1591 (1967).
14. E. PIERS and K. F. CHENG. Can. J. Chem. **46**, 377 (1968).
15. D. WALKER and J. D. HIEBERT. Chem. Rev. **67**, 153 (1967).
16. K. J. CLARK, G. I. FRAY, R. H. JAEGER, and R. ROBINSON. Tetrahedron, **6**, 217 (1959).
17. D. CAINE, J. F. DEBARDELEKBEN, JR., and J. B. DAWSON. Tetrahedron Lett. 3627 (1966).
18. D. H. R. BARTON, J. E. D. LEVISALLES, and J. T. PINHEY. J. Chem. Soc. 3472 (1962).
19. D. H. R. BARTON, J. T. PINHEY, and R. J. WELLS. J. Chem. Soc. 2518 (1964).
20. W. MOFFITT, R. B. WOODWARD, A. MOSCOWITZ, W. KLYNE, and C. DJERASSI. J. Amer. Chem. Soc. **83**, 4013 (1961).
21. P. CRABBÉ. Optical rotatory dispersion and circular dichroism in organic chemistry. Holden-Day, Inc., San Francisco, 1965. pp. 90–94.
22. T. SASAKI and S. EGUCHI. Bull. Chem. Soc. Japan, **41**, 2453 (1968).
23. H. CHIKAMATSU, M. MAEDA, and M. NAKAZAKI. Tetrahedron, **25**, 4751 (1969).
24. HUANG–MINLON. J. Amer. Chem. Soc. **68**, 2487 (1946).
25. K. SCHAFFNER. Adv. Photochem. **4**, 81 (1966).
26. P. J. WAGNER. Adv. Photochem. **5**, 111 (1968).
27. P. J. KROPP and W. F. ERMAN. J. Amer. Chem. Soc. **85**, 2456 (1963).

Can. J. Chem. Downloaded from www.nrcresearchpress.com by 210.87.254.5 on 09/05/12
For personal use only.

Total synthesis of (±)γ_2-cadinene

R. B. KELLY AND J. EBER
Department of Chemistry, University of New Brunswick, Saint John, New Brunswick
Received December 30, 1969

A total synthesis of (±)γ_2-cadinene is described. The synthetic terpene was characterized by conversion to (±)-cadinene dihydrochloride.

Canadian Journal of Chemistry, **48**, 2246 (1970)

Can. J. Chem. Downloaded from www.nrcresearchpress.com by 210.87.254.42 on 09/05/12
For personal use only.

γ_2-Cadinene (**1**), isolated from Vetiver oil (*Vetiveria zizaniotles* linn.), is a relatively recently discovered member of the cadinane group of sesquiterpenoids. It has been assigned structure **1** (1). In connection with some other work, to be reported later, we took advantage of an opportunity to complete a total synthesis of **1** as a racemate which in turn was converted to (±)-cadinene dihydrochloride (**2**) (2). By so doing we were able to ascertain the stereochemical course of our synthetic work.

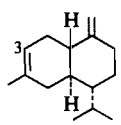

1

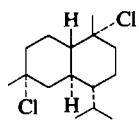

2

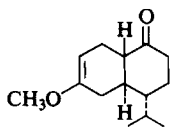

3

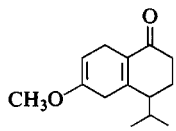

4

The ketoenol ether (**3**) (2) served as starting material. This was prepared, as previously reported (2), in eight steps from *p*-anisaldehyde and methylisobutyl ketone. It had previously been reported as an oil but we were fortunate in obtaining it as a crystalline compound. The stereochemistry assigned to **3** follows from the fact that it was obtained by reduction of **4** with lithium in liquid ammonia (3) and its eventual conversion to **1** thence to **2**. The absolute stereochemistry of the latter has been firmly established (4). The fact that it was unchanged after submission to equilibrating conditions (see Experimental) is further proof of the assigned *trans* ring fusion in **3**.

Reduction of **3** with lithium aluminum hydride afforded the alcohol **5** in 73% yield. The hydroxyl

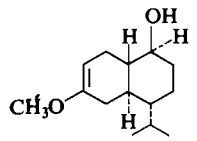

5

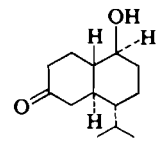

6

group in **5** is assigned the equatorial orientation on the basis of the nuclear magnetic resonance (n.m.r.) spectra of subsequent compounds (vide infra). Treatment of **5** with a dilute methanolic solution of oxalic acid converted it to the keto alcohol (**6**) in 95% yield. The broad signal with a half-width ($w_{1/2}$) of 20 Hz at δ 3.23 in the n.m.r. spectrum is indicative of an axial proton associated with a secondary alcohol (5), hence the assignment of the secondary hydroxyl group in **5**, **6**, **7**, and **8** to the equatorial orientation. In **5** this signal is partially obscured by the signal for the OCH_3 group at δ 3.51.

A Grignard reaction with methylmagnesium bromide converted **6** into a mixture of epimeric diols **7**, one of which was obtained in 40% yield as a crystalline compound. Selective dehydration of **7** under mild conditions afforded the olefin **8** in 80% yield. This olefin was also obtained by dehydration of the material from the mother liquors which had deposited crystalline **7**. The overall yield of **8** from **6** was 75%. Oxidation of **8** with the Sarett reagent (6) gave the enone **9** in 65% yield. The same enone was obtained by dehydration of the keto alcohol **10**, obtained by oxidation of the diol **7** with the Jones reagent (7). This ketone (**9**) was unchanged after submission to equilibrating conditions as in the case of **3** (see Experimental).

The enone **9** was subjected to a Wittig reaction and the product was purified by chromatography on silica gel impregnated with 20% of silver nitrate. Thereby, (±)γ_2-cadinene (**1**) was obtained in 90% yield. The synthetic terpene gave rise to a single peak on vapor phase chromatog-

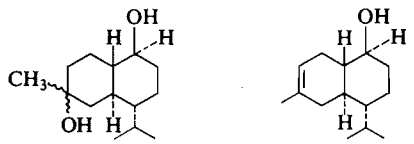

7

8

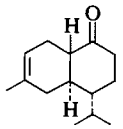

9

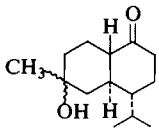

10

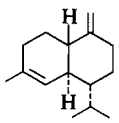

11

raphy (v.p.c.) under conditions whereby a mixture of cadinenes was separated into three components. The v.p.c., thin layer chromatography (t.l.c.) (silica gel – silver nitrate with various solvents), and n.m.r. spectrum all indicated that our synthetic compound (**1**) was uncontaminated.

Unfortunately, we have been unable to obtain a pure sample of naturally occurring γ_2-cadinene for direct comparison with our synthetic terpene. The infrared (i.r.) spectrum of **1** was similar to that of a published (1) spectrum of $(-)\gamma_2$-cadinene but there were differences in the detailed pattern of the fingerprint region. However, the i.r. spectrum of **1** was distinctly different from a spectrum of natural γ-cadinene (**11**). The possibility of our synthetic terpene being **11** is also excluded by the nature of the n.m.r. signal due to the vinylic proton at C_3. This signal appeared as a broad multiplet at δ 5.48 whereas the corresponding vinylic proton in **11** should resemble a singlet because the dihedral angle with the vicinal proton is approximately 90°.

Treatment of the synthetic terpene (**1**) with hydrogen chloride gas in ether, with rigorous exclusion of moisture afforded, in 60% yield, (±)-cadinene dihydrochloride (**2**) (2). The i.r. spectrum of the dihydrochloride was superimposable on the spectra of samples of cadinene dihydrochloride obtained from natural cadinenes. The conversion to cadinene dihydrochloride excludes the possibility of our compound (**1**) belonging to the bulgarene or amorphene series[1] (8). The remaining possibility, that our synthetic terpene might be "γ_2-muurolene"[2] (**1** with *cis* ring fusion) is excluded by the fact that the precursor ketones **3** and **9** have been shown, by equilibration, to possess *trans* ring fusions. The conversion of **1** to (±)-cadinene dihydrochloride under conditions whereby muurolene dihydrochloride could be expected in good yield from compounds of the muurolene (*cis* ring fusion) series (9, 10) provides further evidence against this possibility.

The synthetic route described above affords an opportunity to accomplish syntheses, through the various intermediates, of virtually all of the cadinenes. Moreover, since the appropriate optically active diketone corresponding to the starting material **3** has been prepared from cryptone (11), total syntheses of naturally occurring enantiomers of the cadinane series should now be possible.[3]

Experimental

General

The n.m.r. spectra were determined in deuteriochloroform ($CDCl_3$) solutions with a Varian T-60 instrument. Chemical shifts are expressed in parts per million (δ values) downfield from the tetramethylsilane signal as internal standard. Petroleum ether refers to the fraction with boiling point range 30–60°.

Reaction products were isolated by the following procedure. The product was extracted into the specified solvent and the extract was washed with appropriate aqueous solutions as indicated and finally with saturated brine. The aqueous washings were extracted three times with the solvent and the combined extracts were dried over anhydrous magnesium sulfate, filtered, and evaporated *in vacuo* on a rotary evaporator.

Ketoenol Ether (3)

The ketoenol ether (**3**) was prepared from *p*-anisaldehyde and methylisobutyl ketone in eight steps as previously described (2). The crude product was purified by column chromatography on silica gel. The column was rapidly developed with increasing proportions of ether in petroleum ether and the product was eluted with 10% of ether in petroleum ether. In a typical experiment when 13.0 g of crude product was chromatographed on 110 g of silica gel (column diameter 2.40 cm) there was obtained, after crystallization from pentane, 4.50 g of crystalline

[1]The isopropyl group is *trans* to the vicinal hydrogen atom at the ring junction in the bulgarene and amorphene series.

[2]To our knowledge this compound has never been isolated.

[3]After submission of this work for publication, a synthesis of (+)ε-cadinene along lines similar to those described in this paper was reported (ref. 12).

Can. J. Chem. Downloaded from www.nrcresearchpress.com by 210.87.254.42 on 09/05/12
For personal use only.

Can. J. Chem. Downloaded from www.nrcresearchpress.com by 210.87.254.42 on 09/05/12
For personal use only.

3, m.p. 47–48°; ν_{max} (Nujol) 1712 (ketone) and 1675 cm^{-1} (double bond); n.m.r., δ 0.77 and 0.97 (3H each, doublets, J = 7.0 Hz, isopropyl group[4]), 3.51 (3H, singlet, OCH_3), 4.63 (1H, multiplet, vinylic H); the overall yield of crystalline compound for the eight steps was ca. 10%.

A sample of **3** was unchanged after refluxing with a mixture (1:1) of ethanol – 10% aqueous sodium hydroxide for 1½ h.

Anal. Calcd. for $C_{14}H_{22}O_2$: C, 75.64; H, 9.97. Found: C, 75.52; H, 10.15.

Alcohol 5

A solution of 6.50 g of the ketoenol ether (**3**) in 160 ml of ether was added, over a period of 75 min, to a refluxing mixture of 1.50 g of lithium aluminum hydride in 160 ml of ether. After addition was completed the mixture was refluxed for 4 h, cooled, treated with 1.5 ml of concentrated brine and stirred for 18 h. Sodium sulfate was added to the mixture and the solids were removed by filtration and washed with ether. The combined filtrate and washes were evaporated *in vacuo*. The residue, on crystallization from methylcyclohexane, afforded 5.06 g (73%) of crystalline **5**, m.p. 103°; ν_{max}(Nujol) 3350 (OH) and 1675 cm^{-1} (double bond); n.m.r. δ 3.51 (3H, singlet, OCH_3), 4.65 (1H, broad multiplet, vinylic H), 3.25 (1H, very broad multiplet, H—C—OH).

Anal. Calcd. for $C_{14}H_{24}O_2$: C, 74.95; H, 10.78. Found: C, 75.12, H, 11.05.

Keto Alcohol (6)

A solution of 5.0 g of **5**, 33 ml of methanol and 7.5 ml of 0.6 *M* aqueous oxalic acid was left at room temperature for 75 min. The solvent was evaporated *in vacuo* and the residue dissolved in 50 ml of ether. The ethereal solution was worked up in the usual manner by washing with bicarbonate solution and brine. The residue, on crystallization from ether – petroleum ether afforded 4.47 g (95%) of crystalline **6**, m.p. 61–63°; ν_{max}(Nujol) 3290 (OH) and 1712 cm^{-1} (ketone); n.m.r., δ 3.23 (1H, broad multiplet, $w_{1/2}$ = 20 Hz, H—C—OH).

Anal. Calcd. for $C_{13}H_{22}O_2$: C, 74.25; H, 10.54. Found: C, 74.39; H, 10.67.

Diol 7

To a stirred solution of 100 ml of a 1 *M* ethereal solution of methylmagnesium bromide (freshly prepared) at −40 °C was added over a period of 45 min, a solution of 5.25 g of keto alcohol **6** in 150 ml of ether. After addition of the keto alcohol the reaction mixture was allowed to come to room temperature over a period of 1 h then stirred for a further 24 h. The solution was then treated with 52 ml of 2 *N* hydrochloric acid, washed with bicarbonate solution and thiosulfate solution, and worked up in the usual manner. The residue was crystallized from ethyl acetate – petroleum ether whereby 2.17 g (38%) of 7 was obtained as a crystalline compound, m.p. 149°; ν_{max}(Nujol) 3350 cm^{-1} (OH); n.m.r., δ 1.23 (3H, singlet, CH_3), 3.17 (1H, broad multiplet, $w_{1/2}$ = 20 Hz, *H*—C—OH).

Anal. Calcd. for $C_{14}H_{26}O_2$: C, 74.29; H, 11.58. Found: C, 74.19; H, 11.44.

[4]This pair of doublets appears in the n.m.r. spectra of all succeeding compounds.

Enol 8

A solution of 2.40 g of the diol 7 and 2.4 g of *p*-toluene sulfonic acid in 2400 ml of benzene was stirred at 52° for 2 h. The benzene solution was cooled, washed with bicarbonate solution and worked up in the usual manner. The residue, on crystallization from pentane, afforded 1.92 g (80%) of crystalline **8**, m.p. 79–80°; ν_{max}(Nujol) 3250 cm^{-1} (OH); n.m.r., δ 1.65 (3H, singlet, CH_3), 3.17 (1H, broad multiplet, $w_{1/2}$ = 20 Hz, *H*—C—OH), 5.40 (1H, broad multiplet, vinylic H).

Anal. Calcd. for $C_{14}H_{24}O$: C, 80.71; H, 11.61. Found: C, 80.43; H, 11.68.

This enol (**8**) was also obtained by dehydration of the material from the mother liquors from which the diol **7** had crystallized. Dehydration of 596 mg of such material afforded 428 mg (78%) of **8** identical with the compound described above. The overall yield of **8** from the keto alcohol **6** was 75%.

Ketone 9

To a mixture of 1.8 g of chromic anhydride in 20 ml of pyridine was added 832 mg of enol **8** in 20 ml of pyridine. The mixture was stirred at room temperature for 8 h. The solvent was removed *in vacuo* at room temperature and 150 ml of cold water was added to the residue. The aqueous mixture was worked up in the usual manner with ether. The crude product was chromatographed on a column (diameter 3.0 cm) of 35 g of silica gel impregnated with 20% of silver nitrate. Elution of the column with pentane–benzene (3:1) afforded 727 mg (87%) of crystalline **9**, m.p. 35°; ν_{max}(film) 1715 cm^{-1} (ketone); n.m.r., δ 1.67 (3H, singlet, CH_3), 5.47 (1H, multiplet, vinylic H).

A sample of this compound was unchanged after refluxing with a (50%) mixture of ethanol – 10% aqueous sodium hydroxide for 1½ h.

Anal. Calcd. for $C_{14}H_{22}O$: C, 81.49; H, 10.74. Found: C, 81.27; H, 10.52.

This compound was also obtained by dehydration of the keto alcohol **10** as follows. A solution of 330 mg of **10** and 16 mg of *p*-toluenesulfonic acid in 50 ml of benzene was refluxed for 5 h. Water was removed by means of a Dean–Stark trap. After cooling, the reaction solution was washed with 5% sodium carbonate solution and worked up in the usual manner. Distillation of the resulting oil *in vacuo* at 64° onto a cold finger afforded 304 mg of **9** identical with the enone obtained by oxidation of **8** (vide supra).

Keto Alcohol 10

A stirred solution of 258 mg of the diol **7** in 30 ml of acetone was cooled on an ice-bath and treated with 0.4 ml of 8 *N* Jones reagent (7). After 5 min, 6 ml of methanol was added and stirring was continued for 5 min then 18 ml of 5% sodium carbonate was added and the product was worked up with ether in the usual manner. Crystallization of the residue from ether – petroleum ether afforded 190 mg (67%) of **10**, m.p. 110°; ν_{max}(Nujol) 3400 cm^{-1} (OH); n.m.r., δ 1.23 (3H, singlet, CH_3).

Anal. Calcd. for $C_{14}H_{24}O_2$: C, 74.95; H, 10.78. Found: C, 74.51; H, 10.88.

(±)γ_2-Cadinene (1)

The Wittig reaction was carried out in an atmosphere

of dry oxygen-free nitrogen as follows. To a suspension of 1.35 g of methyltriphenylphosphonium bromide in 25 ml of ether was added 1.9 ml of a 2.3 *M* ethereal solution of *n*-butyllithium. The mixture was stirred at room temperature for 2 h. The resulting yellow suspension was treated with a solution of 250 mg of the enone **9** in 38 ml of tetrahydrofuran and stirring was continued at room temperature for 1 h. Ether was removed by distillation until the temperature reached 65° and the solution was refluxed at this temperature for 3 h. Water (2.5 ml) was added to the reaction solution and the organic solvent was removed *in vacuo*. The product was dissolved in 150 ml of pentane and the solution was washed with water. The residue obtained by evaporation of the extracts *in vacuo* was chromatographed on a column (diameter 2.0 cm) of 14.5 g of silica gel impregnated with 20% silver nitrate. After developing with 5% of benzene in cyclohexane the terpene was eluted with 10–25% benzene in cyclohexane. Thereby 226 mg (91%), of (±)γ_2-cadinene was obtained as a clear oil; n.m.r., δ 0.73 and 0.93 (3H each, doublets, $J = 7.0$ Hz, isopropyl group), 1.68 (3H, singlet, CH_3), 4.60 and 4.72 (1H each, broad overlapping singlets, exocyclic CH_2), 5.48 (1H, broad multiplet resembling a poorly developed triplet, vinylic H). The v.p.c. on a column (10′ × 3/8″) of 3% XE60 on Chromosorb W with the column temperature at 150° gave rise to a single peak with retention time of 4 min 10 s.

Anal. Calcd. for $C_{15}H_{24}$: C, 88.16; H, 11.89. Found: C, 87.91; H, 11.99.

Conversion of (±)γ_2-Cadinene to (±)-Cadinene Dihydrochloride (2)

The following manipulations were carried out with exclusion of moisture. A solution of 80 mg of synthetic (±)γ_2-cadinene in 5 ml of dry ether was saturated at −20° with dry hydrogen chloride gas. The solution was left at 5° for 18 h then the solvent was evaporated under a stream of dry nitrogen. The residue, after several crystallizations from petroleum ether, afforded 64 mg (60%) of crystalline **2**, m.p. 105° (lit. (2) m.p. 105–106°). The i.r. spectrum of the synthetic dihydrochloride was superimposable on the spectra of samples of optically active dihydrochloride obtained from natural cadinenes.

We are grateful to the National Research Council of Canada for a grant in aid of this work. Also, we thank Dr. M. Romanuk, Czechoslovakian Academy of Science, Dr. T. Norin, Swedish Institute of Forest Research, and Dr. R. Vlahov, Bulgarian Academy of Science, for samples of cadinene dihydrochloride and Dr. E. von Rudloff, Prairie Regional Laboratory, Saskatoon, Saskatchewan, for an i.r. spectrum of γ-cadinene.

1. C. C. KARTHA, P. S. KALSI, A. M. SHALIGRAM, K. K. CHAKRAVARTI, and S. C. BHATTACHARYYA. Tetrahedron, **19**, 241 (1963).
2. M. V. R. K. RAO, G. S. K. RAO, and S. DEV. Tetrahedron, **22**, 1977 (1966).
3. G. STORK and D. DARLING. J. Amer. Chem. Soc. **86**, 1761 (1964) and references there cited.
4. (*a*) F. HANIC. Chem. Listy. **52**, 165 (1958). (*b*) V. SYKORA, V. HEROUT, and F. SORM. Collect. Czech. Chem. Commun. **23**, 2181 (1958).
5. N. S. BHACCA and D. H. WILLIAMS. Applications of n.m.r. spectroscopy in organic chemistry. Holden–Day, Inc., San Francisco, 1964. pp. 77–83.
6. G. I. POOS, G. E. ARTH, R. E. BEYLER, and L. H. SARETT. J. Amer. Chem. Soc. **75**, 422 (1953).
7. K. BOWDEN, I. M. HEILBRON, E. R. H. JONES, and B. C. L. WEEDON. J. Chem. Soc. 39 (1946).
8. R. VLAHOV, M. HOLUB, and V. HEROUT. Collect. Czech. Chem. Commun. **32**, 822 (1967).
9. R. VLAHOV, M. HOLUB, I. OGNJANOV, and V. HEROUT. Collect. Czech. Chem. Commun. **32**, 808 (1967).
10. L. WESTFELT. Acta Chem. Scand. **20**, 2852 (1966).
11. M. D. SOFFER, G. E. GUNAY, C. KORMAN, and M. B. ADAMS. Tetrahedron Lett. **6**, 389 (1963).
12. M. D. SOFFER and L. A. BURK. Tetrahedron Lett. **3**, 211 (1970).

Can. J. Chem. Downloaded from www.nrcresearchpress.com by 210.87.254.42 on 09/05/12
For personal use only.

Can. J. Chem. Downloaded from www.nrcresearchpress.com by 210.87.254.40 on 09/05/12
For personal use only.

Preparation and acceptor power of the pentafluorogermanate ion

I. WHARF AND M. ONYSZCHUK
Department of Chemistry, McGill University, Montreal, Quebec

Received February 20, 1970

Preparations of $[(C_3H_7)_4N][GeF_5]$, $[(C_4H_9)_4N][GeF_5]$, $[(C_4H_9)_4N][GeF_5(H_2O)]$, and $[(C_6H_5)_4As][GeF_5]$ are described and their infrared spectra reported. The pentafluorogermanate ion forms a stable 1:1 adduct with ammonia, with $\Delta H = 17.5 \pm 1.0$ kcal mole^{-1} for the reaction: $[(C_3H_7)_4N][GeF_5(NH_3)]$ (s) $\rightarrow$ $[(C_3H_7)_4N][GeF_5]$ (s) + NH_3(g). The value for the corresponding pentafluorosilicate system is $\Delta H = 12.0 \pm 0.5$ kcal mole^{-1}.

Canadian Journal of Chemistry, 48, 2250 (1970)

Introduction

Many five coordinate complexes have been prepared but few are simple halogen derivatives of the type MX_5. Among Group IV metal complexes, the pentahalostannates, SnX_5^- (X = Cl, Br) have been studied extensively (1–3) while both $GeCl_5^-$ (2) and $TiCl_5^-$ (3) ions have been reported. Recently, the preparation and properties of salts of the pentafluorosilicate ion were described (4) and its ^{19}F nuclear magnetic resonance (n.m.r.) spectrum has been reported (5). In their preliminary communication (6) on the SiF_5^- ion, Clark and Dixon also reported a germanium compound which they postulated was a pentafluorogermanate salt. It is the purpose of this paper to describe the preparation of salts containing the GeF_5^- ion, and to compare the acceptor properties of these compounds with those of the analogous SiF_5^- salts.

Experimental

Microanalyses for carbon, hydrogen, nitrogen, and fluorine were performed by Schwarzkopf Microanalytical Laboratory, Woodside, N.Y. 11377, and melting points were measured using a capillary-tube apparatus. Germanium tetrafluoride (Ozark–Mahoning) was purified by the literature method (7); vapor pressure at −63.5°, 57.5 mm (lit. 57.4 mm). Ammonia (Matheson) was purified as described by Shriver (8). Methylene chloride was dried by distillation from calcium hydride, and hydrocarbon solvents were dried over sodium. Infrared (i.r.) spectra were obtained using Perkin–Elmer 521 and 337 instruments with samples examined as Nujol mulls. Since pentafluorogermanates react rapidly with water vapor, they were handled under anhydrous conditions in a conventional vacuum line system or in a nitrogen-filled dry-box (8).

Tetraphenylarsonium Pentafluorogermanate

Tetraphenylarsonium chloride (2.10 g, 5 mmoles) was placed in a 250 ml flask fitted with a magnetic stirrer and a sidearm closed by a serum cap, and the apparatus was then pumped for several hours under a high vacuum. With the flask isolated from the vacuum line, methylene chloride (30 ml) was injected through the serum cap and the mixture stirred to give a clear solution. Germanium tetrafluoride (9.4 mmoles) was condensed into the flask which was then closed to the vacuum system. On warming the flask in an ice-bath, a precipitate formed immediately but the mixture was stirred for 3 h at 0° to ensure complete reaction. Pentane (70 ml) was added through the serum cap and excess germanium tetrafluoride (with some solvent) removed by pumping for a few minutes. The white precipitate was filtered off under nitrogen, washed with pentane, and dried in a vacuum at 100°. Yield, 2.13 g, 78%.

Anal. Calcd. for $[(C_6H_5)_4As][GeF_5]$: C, 52.32; H, 3.66; F, 17.24. Found: C, 51.15; H, 3.78; F, 17.97.

Tetrabutylammonium Pentafluorogermanate

In a polythene beaker, tetrabutylammonium bromide (6.44 g, 20 mmoles) was stirred with silver carbonate (2.76 g, 10 mmoles) in concentrated hydrofluoric acid (10 ml) and water (40 ml) for 30 min and the mixture was then filtered. Germanium dioxide (2.09 g, 20 mmoles) and concentrated hydrofluoric acid were added to the filtrate to give a clear solution which was evaporated to an oil on a steam-bath. Methanol (50 ml) was added and the solution evaporated again. The process of evaporation and methanol addition was repeated about 10 times until the methanol solution was no longer acid. Finally the solution was evaporated to dryness under vacuum and the residue dissolved in methylene chloride (50 ml). The white aquo-complex which precipitated after hexane (400 ml) was added to the filtered solution was filtered off, washed with hexane, and dried in a vacuum at room temperature. Yield, 7.24 g, 86%.

Anal. Calcd. for $[(C_4H_9)_4N][GeF_5(H_2O)]$: C, 44.70; H, 8.88; N, 3.26. Found: C, 43.84; H, 8.55; N, 2.97.

The aquo-complex was heated in a vacuum at 100° for 2 h to give the anhydrous pentafluorogermanate salt. Yield, 6.56 g, 78%.

Anal. Calcd. for $[(C_4H_9N][GeF_5]$: C, 46.88; H, 8.82; N, 3.42. Found: C, 45.82; H, 8.60; N, 3.25.

Tetrapropylammonium Pentafluorogermanate

(*a*) Using the procedure described for the preparation of $[(C_6H_5)_4As][GeF_5]$, tetrapropylammonium bromide (2.66 g, 10 mmoles) was pumped for several hours and dissolved in methylene chloride (20 ml). Addition of

Can. J. Chem. Downloaded from www.nrcresearchpress.com by 210.87.254.40 on 09/05/12
For personal use only.

germanium tetrafluoride (17 mmoles) followed by stirring for several hours gave no solid product. Hexane (100 ml) was then added and the white precipitate filtered off under nitrogen, washed with hexane, and dried in a vacuum at 100°. Yield, 3.54 g, 80%.

Anal. Calcd. for $[(C_3H_7)_4N][GeF_5]$: C, 40.70; H, 7.97; N, 3.96; F, 26.84. Found: C, 39.85; H, 7.79; N, 3.92; F, 25.83.

(*b*) Following the procedure used for the preparation of $[(C_4H_9)_4N][GeF_5]$, tetrapropylammonium bromide (5.32 g, 20 mmoles) was stirred with silver carbonate (2.76 g, 10 mmoles) in dilute hydrofluoric acid. The resulting white precipitate was probably the aquo-complex $[(C_3H_7)_4N][GeF_5(H_2O)]$ but it was not analyzed, instead it was heated at 100° in a vacuum to give the anhydrous pentafluorogermanate salt. Yield, 5.10 g, 72%.

Anal. Calcd. for $[(C_3H_7)_4N][GeF_5]$: C, 40.70; H, 7.97; N, 3.96. Found: C, 39.97; H, 7.95; N, 3.70.

Tetraphenylarsonium Pentafluorosilicate and Tetrabutylammonium Pentafluorosilicate

These were prepared by the literature method (4) using polythene apparatus. Tetraphenylarsonium pentafluorosilicate was recrystallized from acetonitrile in 80% yield. The previously unreported tetrabutylammonium pentafluorosilicate was recrystallized from ethyl acetate – ether. Yield, 3.87 g, 55%.

Anal. Calcd. for $[(C_4H_9)_4N][SiF_5]$: C, 52.59; H, 9.89; N, 3.83; F, 26.00. Found: C, 52.92; H, 9.89; N, 3.50; F, 26.58.

Tetrapropylammonium Bromide Pentafluorosilicate

Silicon dioxide (1.20 g) and tetrapropylammonium bromide (5.33 g) were dissolved in a methanol (25 ml) and concentrated hydrofluoric acid (25 ml) mixture, and the clear solution evaporated to near dryness on a steam-bath. Methanol (25 ml) was added and the solution evaporated to an oil, which solidified on stirring with ether. The crude product was recrystallized from chloroform–ethyl acetate to give white crystals which were dried in a vacuum. Yield, 3.10 g, 54%; m.p. 206°.

Anal. Calcd. for $[(C_3H_7)_4N]_2[SiF_5]Br$: C, 50.07; H, 9.80; N, 4.86. Found: C, 51.14; H, 10.26; N, 4.74.

Tetrapropylammonium Pentafluorosilicate

Tetrapropylammonium bromide (5.33 g) was stirred with a solution of silver carbonate (2.75 g) in concentrated hydrofluoric acid (25 ml) and water (50 ml) for 30 min. The mixture was filtered, silicon dioxide (1.20 g) added to the filtrate, and the clear solution evaporated down on the steam-bath. The crude product was recrystallized from ethyl acetate to give white crystals. Yield, 1.54 g, 25%.

Anal. Calcd. for $[(C_3H_7)_4N][SiF_5]$: C, 46.57; H, 9.11; N, 4.52. Found: C, 46.34; H, 9.16; N, 4.37.

Tensimetric Titrations

Conventional procedures (8) were used. The pentafluorogermanate or pentafluorosilicate sample was dried by heating in a vacuum at 100° for several hours and then dissolved in methylene chloride. Aliquots of ammonia were added and the change in pressure of the reaction mixture at 0° followed. At the end of the titration, the reaction mixture was slowly evaporated to dryness at room temperature.

Vapor Pressures of the Ammonia Adducts

Excess ammonia was condensed onto a previously dried sample of $[(C_3H_7)_4N][GeF_5]$ or $[(C_3H_7)_4N][SiF_5]$ contained in a reaction tube attached to a tensimeter (9) and the system allowed to equilibrate at either 0 or −78° respectively, for 2 h. Unreacted ammonia was removed by pumping the sample at either 0 or −78° respectively. The variation in the ammonia pressure above the resulting adduct with temperature was then measured.

Results and Discussion

Preparations

Evaporation of a methanol – hydrofluoric acid mixture containing germanium dioxide and tetrabutylammonium bromide gave a product with the i.r. (750–500 cm^{-1}) shown in Fig. 1*a*, quite unlike the two peak pattern expected for the metal–halogen stretching region of a trigonal bipyramidal MX_5 species (4). A broad absorption at about 3300 cm^{-1}, indicative of coordinated water, was also observed and analysis of the material was consistent with the formula $[(C_4H_9)_4N][GeF_5(H_2O)]$. When this was heated for 2 h at 100 °C in a vacuum, a compound with no absorption at 3300 cm^{-1} and a two-band ν(Ge—F) spectrum in the range 750–500 cm^{-1}, Fig.1*b*, was obtained consistent with the presence of the GeF_5^- ion. Microanalysis confirmed that the anhydrous product was $[(C_4H_9)_4N][GeF_5]$. Similarly $[(C_3H_7)_4N][GeF_5]$ was obtained only after the crude product consisting of $[(C_3H_7)_4N][GeF_5(H_2O)]$ was dried for 2 h in a vacuum at 100°.

The i.r. spectra of all samples of $[(C_4H_9)_4N][GeF_5]$ and $[(C_3H_7)_4N][GeF_5]$ prepared by the "aqueous HF/methanol" procedure contained a weak absorption at about 570 cm^{-1}, in addition to the two major ν(Ge—F) bands. This weak absorption was much reduced but not eliminated by complete removal of bromide ion from the start-

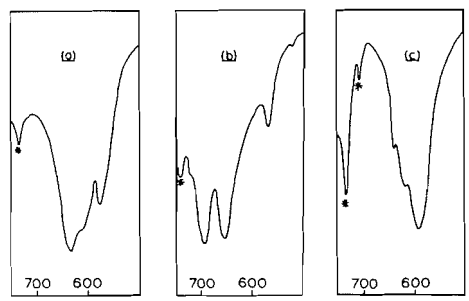

FIG. 1. Infrared spectra (750–500 cm^{-1}) of (*a*) $[(C_4H_9)_4N][GeF_5(H_2O)]$, (*b*) $[(C_4H_9)_4N][GeF_5]$, (*c*) $[(C_4H_9)_4N][GeF_5(NH_3)]$. Cation bands are shown by *.

Can. J. Chem. Downloaded from www.nrcresearchpress.com by 210.87.254.40 on 09/05/12
For personal use only.

ing material, $[(C_4H_9)_4N]Br$ or $[(C_3H_7)_4N]Br$, before adding germanium dioxide to the reaction mixture. Therefore, alternative preparative methods were investigated. Klanberg and Muetterties (5) prepared several SiF_5^- salts by the reaction of silicon tetrafluoride with tetraalkylammonium fluorides dissolved in methanol. Since the preparation of pure quaternary ammonium fluorides is difficult, the reaction of tetrabutylammonium chloride with germanium tetrafluoride was investigated instead. A tensimetric titration of $[(C_4H_9)_4N]Cl$ dissolved in methylene chloride with GeF_4 at 0°, shown in Fig. 2, reveals several equilibria but of particular significance is the distinct break at a GeF_4:Cl^- ratio of 1.25:1. The residue, after evaporating the titrated solution to dryness, contained no chloride ion and its i.r. spectrum in the 750 to 500 cm^{-1} region was almost the same as that obtained for $[(C_4H_9)_4N][GeF_5]$ prepared by the "aqueous HF/methanol" method. These results are consistent with the reaction as shown in eq. [1]. Analogous reactions

$$[1]\quad 4[(C_4H_9)_4N]Cl + 5GeF_4 \rightarrow 4[(C_4H_9)_4N][GeF_5] + GeCl_4$$

were used to prepare $[(C_6H_5)_4As][GeF_5]$ and $[(C_3H_7)_4N][GeF_5]$. The former precipitated when $[(C_6H_5)As]Cl$ and excess GeF_4 were mixed in methylene chloride but the latter was only obtained after addition of hexane to the solution produced by reacting excess GeF_4 with $[(C_3H_7)_4N]Br$ dissolved in CH_2Cl_2. The i.r. spectrum of this product was almost identical with that of $[(C_3H_7)_4N][GeF_5]$ prepared by the "aqueous HF/methanol" method. The absorption at about 570 cm^{-1} was absent, indicating that fewer impurities were introduced by preparation in methylene chloride. Ironically, tetrabutylammonium pentafluorogermanate could not be prepared on a large scale by this method since all procedures used gave intractable oils.

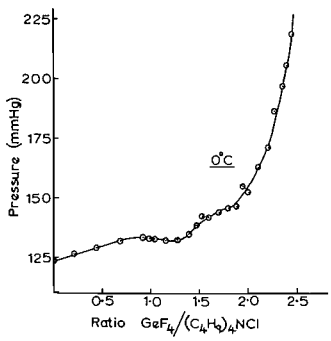

FIG. 2. Tensimetric titration of $[(C_4H_9)_4N]Cl$ (0.2105 g) in CH_2Cl_2 (0.6 ml) with GeF_4 at 0 °C.

No difficulty was found in preparing $[(C_6H_5)_4As][SiF_5]$ by the literature method (4) and this was also used to obtain solid $[(C_4H_9)_4N][SiF_5]$ for the first time. However, in this laboratory the published procedure (4) starting with tetrapropylammonium bromide always gave the double salt, $[(C_3H_7)_4N]_2[SiF_5]Br$, as evident from the elemental analysis, a positive test for the bromide ion, and an i.r. spectrum in the ν(Si—F) region very similar to that of $[(C_3H_7)_4N][SiF_5]$. Tetrapropylammonium pentafluorosilicate was only obtained after total removal of the bromide ion, as AgBr from the $[(C_3H_7)_4N]Br$ solution, before adding silicon dioxide.

Acceptor Power of the Pentafluorogermanate Ion

Germanium tetrahalides are usually significantly stronger Lewis acids than their silicon analogues (9). Since the pentafluorosilicate ion has been shown to be a weak Lewis acid (4), it might be expected that the GeF_5^- ion would be a similar or stronger electron acceptor. To determine this, the reactions of $[(C_3H_7)_4N][GeF_5]$ and $[(C_4H_9)_4N][GeF_5]$ with ammonia were investigated.

The result of a tensimetric titration of $[(C_4H_9)_4N][GeF_5]$, dissolved in methylene chloride, with ammonia, is shown in Fig. 3. Sharp breaks at NH_3/GeF_5^- ratios of 0.95–1.00, at −78, −63, and −23°, and even at 0° indicate the formation of a stable 1:1 adduct, $[GeF_5(NH_3)]^-$. The i.r. spectrum of the residue obtained by evaporating the reaction mixture to dryness, Fig. 1*c*, shows no absorptions of the GeF_5^- ion, and a strong peak at 578 cm^{-1} is consistent with the presence of the six-coordinate adduct. The residue also absorbed at 3150 cm^{-1}, typical for coordinated NH_3.

For comparison, plots of the tensimetric titration of $[(C_4H_9)_4N][SiF_5]$ in CH_2Cl_2 with NH_3 are shown in Fig. 4. At −78°, a break close to 1:1 is observed but at −63 and −23° the end-point is less well-defined. The residue obtained by evaporating the reaction mixture to dryness "effervesced", and its i.r. spectrum showed only $[(C_4H_9)_4N][SiF_5]$.

The variation of dissociation pressure (P) of the adduct $[(C_3H_7)_4N][GeF_5(NH_3)]$ with tem-

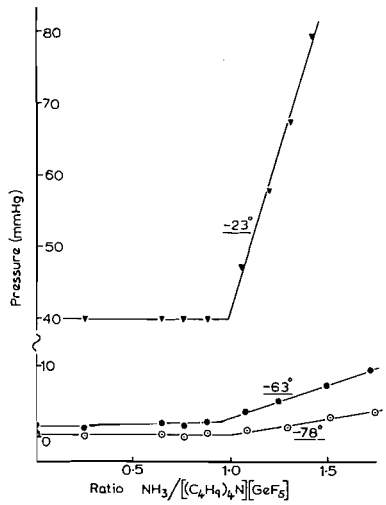

FIG. 3. Tensimetric titration of $[(C_4H_9)_4N][GeF_5]$ (0.1496 g) in CH_2Cl_2 (1.1 ml) with NH_3 at -23, -63, and $-78°$.

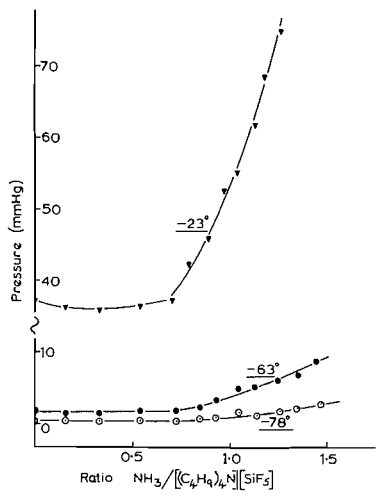

FIG. 4. Tensimetric titration of $[(C_4H_9)_4N][SiF_5]$ (0.1104 g) in CH_2Cl_2 (0.5 ml) with NH_3 at -23, -63, and $-78°$.

perature (T) is shown as a plot of $\log_{10}P$ against $1/T$ in Fig. 5, incorporating data from two completely separate experiments (A) and (B). Immediately noticeable are the relatively high vapor pressures at temperatures below 120°. The points from the first experiment (A) which are on a straight line probably correspond to a small heat of interaction between the gas and the solid. This would suggest that some of the ammonia condensed on to the solid pentafluorogermanate is simply adsorbed on the surface rather than

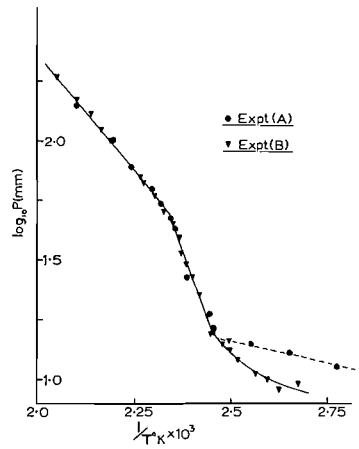

FIG. 5. Plot of $\log_{10}P$(mm) against $1/T$ °K for dissociation of $[(C_3H_7)_4N][GeF_5(NH_3)]$.

coordinated to individual GeF_5^- ions. Support for this hypothesis is given by the results of the second experiment (B). Vapor pressures below 120° did not follow those measured in the first experiment suggesting that the degree of subdivision of the sample is probably an important factor at low vapor pressures of ammonia. Any possibly adsorbed ammonia was removed by opening the tensimeter to the evacuated vacuum-line for a few seconds. The data shown for the second experiment in Fig. 5 were obtained after this had been done. The $\log_{10}P$ against $1/T$ plots obtained from the two experiments were identical above 130°. In the range 130–150°, the system, $[(C_3H_7)_4N][GeF_5] + NH_3$, is reversible and the points shown were obtained with both increasing and decreasing temperatures. The linear portion of the $\log_{10}P$ against $1/T$ plot (Fig. 5) in this temperature range corresponds to a heat of dissociation of 17.5 $\pm$ 1.0 kcal mole^{-1} for the conditions as shown in eq. [2]. At 150°, a further

[2] $[(C_3H_7)_4N][GeF_5(NH_3)]$ (s) $\rightarrow$

$[(C_3H_7)_4N][GeF_5]$ (s) + NH_3 (g)

change is seen in Fig. 5. During both experiments, the sample softened slowly above 150°, and, when cooled below this temperature, did not crystallize but remained as a glass. Above 150°, the system was irreversible, and points were obtained only with increasing temperatures. The heat of dissociation 9.4 $\pm$ 0.1 kcal mole^{-1} in the temperature range 150–210°, corresponds to the reaction shown in eq. [3]. The difference (8.1

Can. J. Chem. Downloaded from www.nrcresearchpress.com by 210.87.254.40 on 09/05/12
For personal use only.

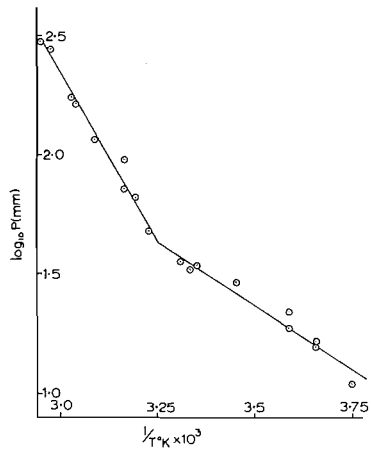

FIG. 6. Plot of $\log_{10}P$(mm) against $1/T$ °K for dissociation of $[(C_3H_7)_4N][SiF_5(NH_3)]$.

[3] $[(C_3H_7)_4N][GeF_5(NH_3)]$ (melt) →

$$[(C_3H_7)_4N][GeF_5] \text{ (melt)} + NH_3 \text{ (g)}$$

kcal mole^{-1}) between the two values includes the heat of fusion of $[(C_3H_7)_4N][GeF_5(NH_3)]$ and $[(C_3H_7)_4N][GeF_5]$.

Vapor pressure results for the $[(C_3H_7)_4N][SiF_5]$–NH_3 system were in substantial agreement with the published curve (4). However, a plot of $\log_{10}P$ against $1/T$ (Fig. 6) showed vapor pressures at lower temperatures to be greater than expected from the higher temperature data. From the line in the range -10 to $+30$ °C, the value $\Delta H = 4.9 \pm 0.4$ kcal mole^{-1} was obtained which is consistent with surface adsorption of ammonia. The second linear portion in the range 30 to 70° gives a $\Delta H = 12.0 \pm 0.5$ kcal mole^{-1} which corresponds to the dissociation shown in eq. [4]. Clark *et al.* (4) obtained a value of 7.9

[4] $[(C_3H_7)_4N][SiF_5(NH_3)]$ (s) →

$$[(C_3H_7)_4N][SiF_5] \text{ (s)} + NH_3 \text{ (g)}$$

kcal mole^{-1} using vapor pressure data in the wider range of -80 to 40°. Our results suggest that their value is an average of the two processes, adsorption and dissociation.

The difference of 5.5 kcal mole^{-1} in the condensed phase heats of formation (ΔH_1) of NH_3 adducts of $[(C_3H_7)_4N][SiF_5]$ and $[(C_3H_7)_4N][GeF_5]$ (Table 1) includes differences in the crystal lattice energies of the pentafluoro salts (ΔH_2) and the NH_3 adduct salts (ΔH_4) in addition to differences in the gas phase heats of complexation (ΔH_3), as evident from the enthalpy cycle shown in Scheme 1, in which M is Si or Ge. Values of ΔH_3 are necessary for an accurate comparison of the relative acceptor powers of SiF_5^- and GeF_5^-, but we are unable to measure them. Although experimental data is not yet available, it is likely that two salts as similar as $[(C_3H_7)_4N^+][SiF_5^-]$ and $[(C_3H_7)_4N^+][GeF_5^-]$ have similar crystal lattice energies because SiF_5^- and GeF_5^- probably differ only very slightly in size. The crystal lattice energies of $[(C_3H_7)_4N^+][SiF_5(NH_3)^-]$ and $[(C_3H_7)_4N^+][GeF_5(NH_3)^-]$ are also probably very similar. Accordingly, we think it is reasonable to attribute most of the 5.5 kcal mole^{-1} difference in the ΔH_1 values to differences in ΔH_3. This, in turn, suggests that GeF_5^- is a stronger Lewis acid than SiF_5^- toward NH_3. A comparison of the acceptor power of SiF_4 and GeF_4 toward NH_3 is not possible because the heat of formation of $GeF_4 \cdot 2NH_3$ has not yet been measured. However, the comparisons in Table 1 suggest that GeF_4 is a stronger acceptor than SiF_4 toward $(CH_3)_3N$ and pyridine. The difference is even greater toward a variety of oxygen electron-pair donors (13, 14). Ignoring differences in crystal lattice energies, the heat of formation of an Si—NH_3 bond in $SiF_4 \cdot 2NH_3$ is about twice that in $[(C_3H_7)_4N][SiF_5(NH_3)]$, suggesting that SiF_5^- is a weaker Lewis acid than SiF_4.

Infrared Spectra

Infrared spectra of GeF_5^- and SiF_5^- salts with the same cation are identical except for absorptions due to the anions which are reported in Table 2. The compounds $[R_4N][GeF_5]$, ($R = C_3H_7$; C_4H_9) gave only two absorptions in the germanium–fluorine stretching region, similar to spectra observed for the analogous pentafluorosilicates, PF_5, and AsF_5 (Table 2). This indicates that both tetrapropylammonium and tetrabutylammonium pentafluorogermanate contain a five coordinate anion with a trigonal bipyramidal structure. Tetraphenylarsonium pentafluorogermanate has three absorptions in the ν(Ge—F) region. Therefore, as with $[(C_6H_5)As][SiF_5]$ (4), the structure of the anions present in these salts must remain in doubt. The i.r. spectra of the adducts of $[(C_4H_9)_4N][GeF_5]$ with water and ammonia show the expected lowering of

Can. J. Chem. Downloaded from www.nrcresearchpress.com by 210.87.254.40 on 09/05/12
For personal use only.

$$\begin{array}{ccc} [R_4N^+][MF_5^-]\,(s) + NH_3\,(g) & \xrightarrow{\Delta H_1} & [R_4N^+][MF_5(NH_3)^-]\,(s) \\ \Delta H_2 \downarrow & & \uparrow \Delta H_4 \\ [R_4N^+]\,(g) + [MF_5^-]\,(g) + NH_3\,(g) & \xrightarrow{\Delta H_3} & [R_4N^+]\,(g) + [MF_5(NH_3)^-]\,(g) \end{array}$$

SCHEME 1

TABLE 1

Heats of formation of silicon and germanium fluoride compounds with nitrogen donors

Reaction	$-\Delta H$ kcal mole^{-1}	Reference
$[(C_3H_7)_4N][SiF_5]\,(s) + NH_3\,(g) \rightarrow [(C_3H_7)_4N][SiF_5(NH_3)]\,(s)$	12.0 ± 0.5	*
$[(C_3H_7)_4N][GeF_5]\,(s) + NH_3\,(g) \rightarrow [(C_3H_7)_4N][GeF_5(NH_3)]\,(s)$	17.5 ± 1.0	*
$[(C_3H_7)_4N][GeF_5]$ (melt) $+ NH_3\,(g) \rightarrow [(C_3H_7)_4N][GeF_5(NH_3)]$ (melt)	9.4 ± 0.1	*
$SiF_4\,(g) + 2NH_3\,(g) \rightarrow SiF_4{\cdot}2NH_3\,(s)$	54.6	10
$SiF_4\,(g) + (CH_3)_3N\,(g) \rightarrow SiF_4{\cdot}(CH_3)_3N\,(s)$	27.4	11
$GeF_4\,(g) + (CH_3)_3N\,(g) \rightarrow GeF_4{\cdot}(CH_3)_3N\,(s)$	38.4	11
$SiF_4\,(g) + 2py\,(g) \rightarrow SiF_4{\cdot}2py\,(s)$	50.1, 53.4	9, 12
$GeF_4\,(g) + 2py\,(g) \rightarrow GeF_4{\cdot}2py\,(s)$	70.6, 65.0	9, 12

*This work.

TABLE 2

Infrared spectra of pentafluorogermanate salts and related compounds

Compound	ν (M—F) cm^{-1}	δ (M—F) cm^{-1}
$[(C_3H_7)_4N][GeF_5]$*	690 vs, 652 vs	343 s, 317 vs
$[(C_3H_7)_4N][GeF_5(H_2O)]$*	647 s, 585 s, 567 m	
$[(C_4H_9)_4N][GeF_5]$*	690 vs, 654 s	343 m, 318 s
$[(C_4H_9)_4N][GeF_5(H_2O)]$*	644 vs, 613 sh, 582 s	
$[(C_4H_9)_4N][GeF_5(NH_3)]$*	628 sh, 607 sh, 578 vs	
$[(C_6H_5)_4As][GeF_5]$*	697 s, 660 m, 644 m	329 m, 319 m
$[(C_3H_7)_4N][SiF_5]$*	876 vs, 786 s	480 m, 447 m
$[(C_4H_9)_4N][SiF_5]$*	878 vs, 785 vs	479 s, 447 s
$[(C_6H_5)_4As][SiF_5]$*	883 vs, 796 m, 776 m	448 m
PF_5†	1026, 945	575, 533
AsF_5‡	819, 785	400, 372

*This work.
†Reference 15.
‡Reference 16.

germanium–fluorine stretching frequencies on increasing coordination from five to six. In addition, the three i.r. absorptions observed for both adducts are consistent with a square-pyramidal arrangement of fluorines in these anions. Clark and Dixon earlier reported (6) the preparation of a compound considered to be $[(C_6H_5)_4As][GeF_5]$, with absorptions at 650, 635, 575, and 560 cm^{-1}. These frequencies are more indicative of a six-coordinate fluorogermanate ion however, while later the material was shown to have O—H stretching frequency absorptions (17). From the results reported here, this evidence indicates that Clark and Dixon's product was probably the hydrated compound $[(C_6H_5)_4As][GeF_5(H_2O)]$.

The financial support of the National Research Council of Canada is gratefully acknowledged.

1. K. M. HARMON, L-L. HESSE, L. P. KLEMANN, C. W. KOCHER, S. V. MCKINLEY, and A. E. YOUNG. Inorg. Chem. **8**, 1054 (1969).
2. I. R. BEATTIE, T. GILSON, K. LIVINGSTON, V. FAWCETT, and G. A. OZIN. J. Chem. Soc. *A*, 712 (1967).
3. J. A. CREIGHTON and J. H. S. GREEN. J. Chem. Soc. *A*, 808, (1968).
4. H. C. CLARK, K. R. DIXON, and J. G. NICOLSON. Inorg. Chem. **8**, 450 (1969).
5. F. KLANBERG and E. L. MUETTERTIES. Inorg. Chem. 7, 155 (1968).

Can. J. Chem. Downloaded from www.nrcresearchpress.com by 210.87.254.40 on 09/05/12
For personal use only.

6. H. C. CLARK and K. R. DIXON. Chem. Commun. 717 (1967).
7. J. J. RUPP and D. F. SHRIVER. Inorg. Chem. **6**, 755 (1967).
8. D. F. SHRIVER. The manipulation of air-sensitive compounds. McGraw–Hill Book Co., New York, N.Y., 1969.
9. J. M. MILLER and M. ONYSZCHUK. J. Chem. Soc. *A*, 1132 (1967).
10. D. B. MILLER and H. H. SISLER. J. Amer. Chem. Soc. **77**, 4998 (1955); **78**, 6412 (1956).
11. J. E. FERGUSON, D. K. GRANT, R. H. HICKFORD, and C. J. WILKINS. J. Chem. Soc. 99 (1959).
12. G. VANDRISH and M. ONYSZCHUK. Private communication.
13. J. P. GUERTIN and M. ONYSZCHUK. Can. J. Chem. **47**, 1275 (1969).
14. R. C. AGGARWAL and M. ONYSZCHUK. J. Inorg. Nucl. Chem. **29**, 3351 (1968).
15. J. E. GRIFFITHS, R. P. CARTER, and R. R. HOLMES. J. Chem. Phys. **41**, 863 (1964).
16. L. C. HOSKINS and R. C. LORD. J. Chem. Phys. **46**, 2402 (1967).
17. H. C. CLARK. Private communication.

Can. J. Chem. Downloaded from www.nrcresearchpress.com by 210.87.254.40 on 09/05/12
For personal use only.

Can. J. Chem. Downloaded from www.nrcresearchpress.com by 210.87.254.105 on 09/05/12
For personal use only.

Pyoluteorin, a synthesis

K. BAILEY[1] AND A. H. REES[2]
Department of Chemistry, Trent University, Peterborough, Ontario

Received March 5, 1970

The synthesis of *Pyoluteorin*, an antibiotic from *Pseudomonas aeruginosa* is described. The method used produced in addition, an isomer 3,5-dichloro-2-(2′,6′-dihydroxybenzoyl)pyrrole, for which the name *isopyoluteorin* is proposed. The bromine analogue of pyoluteorin is also reported.

Canadian Journal of Chemistry, 48, 2257 (1970)

Pyoluteorin (**1**) (1, 2) is a powerful bactericide produced by certain strains of *Pseudomonas aeruginosa* (3). It is also a potent fungistat (4).

Attempts at its synthesis have devolved upon the benzoylation of a pyrrole or the pyrroylation of a benzenoid moiety.

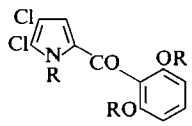

1 R = R′ = H
2 R = Me; R′ = H
3 R = R′ = Me
4 R = H; R′ = Me
5 R = H; R′ = $PhCH_2$

The former method (2) gave didechloro-*O*,*O*′-dimethylpyoluteorin (**6**) but not pyoluteorin. The latter (5) gave *N*,*O*,*O*′-trimethylpyoluteorin (**3**), *N*-methylpyoluteorin (**4**), and *N*-benzylpyoluteorin (**5**) but not pyoluteorin.

We reported briefly (6) that dimethylpyoluteorin (**2**) was obtained by heating 2,6-dimethoxybenzoyl chloride with sodium 4,5-dichloropyrrole-2-carboxylate and that the product could be demethylated to yield the synthetic antibiotic, 4,5-dichloro-2-(2′,6′-dihydroxybenzoyl)pyrrole, identical with the natural pyoluteorin originally reported by Takeda (1).

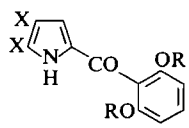

6 R = Me; X = H
7 R = Me; X = Br
8 R = H; X = Br

We now give full details of our synthesis. We chlorinated 2-carbomethoxypyrrole using chlorine in acetic acid or *t*-butyl hypochlorite in carbon tetrachloride, but were unable to reproduce the published results (7); in both cases a mixture of 4,5- and 3,5-dichloro derivatives was obtained which could not be completely resolved by column chromatography or fractional recrystallization. Rather than effect a tedious separation, we hydrolyzed the mixture to the corresponding acids and proceeded. By the method indicated above, we obtained a mixture of *O*,*O*′-dimethylpyoluteorin (**2**) and 3,5-dichloro-2-(2′,6′-dimethoxybenzoyl)pyrrole (*O*,*O*′-dimethylisopyoluteorin) (**9**).

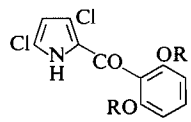

9 R = Me
10 R = H

Column and thin-layer chromatography (t.l.c.) were again not efficient methods of separation but fractional crystallization yielded pure isomer **9**. Demethylation of the mixture of ethers by boron trichloride followed by t.l.c. resulted in separation of **1** from isopyoluteorin (**10**). The nuclear magnetic resonance (n.m.r.) spectra of these compounds were in agreement with their structures and followed from those of the starting dichloropyrrole esters (7). Although a pure sample of **2** was not obtained here, its spectrum was easily determined from that of its mixture with the isomeric ether **9** and that of pure **9**. Subsequent confirmation has come from the spectrum of pure **2** synthesized by another route (8).

As noted by Birch *et al.* (2), the 3′- and 5′-protons of pyoluteorin are not equivalent in the n.m.r. spectrum for although they have almost

[1]Present address: Food and Drug Directorate, Tunney's Pasture, Ottawa 3, Canada.
[2]To whom enquiries should be directed.

TABLE 1*

The n.m.r. spectra of pyoluteorin analogues and derivatives

Compound solvent	CH_3 3′,5′	4′	3	4	OH	NH
1 DMSO-d_6	3.62 d	2.96 q [7.5,8.5]	3.57†		0.50	−3.08
2 $CDCl_3$	6.25 3.43 d	2.68 q [7.5,8.5]	3.54 d [3.0]			0.0
7 $CDCl_3$	6.24 3.42 d	2.66 q [7.5,9.0]	3.52 d [2.5]			−0.15
9 $CDCl_3$	6.25 3.42 d	2.66 q [7.5,8.5]		3.93 d [3.0]†		0.3
10 DMSO-d_6	3.66 d	2.99 q [7.2,8.5]		3.72†	0.60	−2.8

*T.M.S. internal standard; d = doublet, q = quartet; figures in brackets indicate splitting [Hz] observed: signals assigned to OH integrated for two protons and to NH (broad) for 1 proton, and disappeared on addition of D_2O.
†Sharpened or collapsed to singlet on adding D_2O.

indistinguishable chemical shifts, their coupling constants with the 4′-proton differ, J = 8.5 and 7.5 Hz. In compounds **1**, **2**, **6**, **9**, and **10** these protons give rise to more or less superimposed broad-branched doublets (Table 1). However, in certain related compounds (8) these protons have quite different chemical shifts. Although in **1** and isomer **10**, the pyrrole protons overlap with signals from the 3′- and 5′- benzenoid protons, on deuterium exchange the pyrrole proton fine doublets collapse to singlets and the signals show an obvious increase in height.

The infrared (i.r.) spectra (Nujol) of pyoluteorin and its dimethyl ether have carbonyl bands at 1633 cm^{-1} with a further characteristic band at 890 cm^{-1}. In the *iso*-series these appear at 1620 and about 915 cm^{-1} respectively while the bromine analogue **8** of pyoluteorin and its ether **7** have bands at 1635 and 895 cm^{-1}. The pyoluteorins and their ethers also show a band at about 1595 cm^{-1} but a further band at 1565 cm^{-1} which we assign to hydrogen-bonded carbonyl is only found in the free phenols.

The ultraviolet (u.v.) spectra of the pyoluteorins show a bathochromic shift from about 305 to 330 mμ on addition of alkali. However, if the analogues **1** or **10** in neutral ethanol ($\lambda_{max} \sim 305$ mμ) are made only faintly alkaline, the maximum shifts to about 365 mμ and more base must be added to bring this peak back to 330 mμ. Since the pyrrole NH is quite acidic, mesomeric mono-, di-, and trivalent anions are obviously involved.

A possible mechanism for the key reaction is indicated by formula **11**.

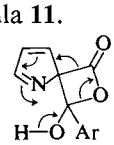

11

Experimental

Pyoluteorin and Isopyoluteorin Dimethyl Ethers

A mixture of dry sodium 3,5- and 4,5-dichloropyrrole-2-carboxylates (from 1.8 g acid mixture) was refluxed 75 min in 5 ml dry benzene with 2,6-dimethoxybenzoyl chloride (from 2 g acid). The solvent was then distilled off and the residue heated at 150° for 45 min and cooled. The products were exhaustively extracted with benzene and the concentrated extract adsorbed onto silica gel (120 g, containing 5% w/w water). Elution with light petroleum containing increasing amounts of ether gave the following fractions: (*i*) 410 mg oil using 15 × 100 ml eluate, 0–40% ether; (*ii*) 1.16 g mixture using 7 × 100 ml eluate, 40% ether. The third of fractions (*ii*) was evaporated giving 360 mg material. Crystallization from benzene/petrol gave *O*,*O*′-dimethylisopyoluteorin (90 mg) m.p. 204–205°, ν_{max} 3210, 1618, 1595, 1108, and 910 cm^{-1}.

Anal. Calcd. for $C_{13}H_{11}Cl_2NO_3$: C, 52.0; H, 3.7; Cl, 23.6; N, 4.7. Found: C, 52.1; H, 3.36; Cl, 23.5; N, 4.8.

The remainder of fraction (*ii*) (1.07 g) was purified by t.l.c. giving 200 mg material with λ_{max} 300 mμ, m.p. 155–185°, shown by n.m.r. spectroscopy to consist of comparable amounts of pyoluteorin and isopyoluteorin dimethyl ethers.

Fraction (*iii*) 825 mg using 50–100% ether. This was mainly 2,6-dimethoxybenzoic acid, also present as an impurity in (*ii*).

Isopyoluteorin

A solution of dimethylisopyoluteorin (40 mg) in methylene chloride (15 ml) at −70° was treated with boron trichloride (3 ml 40% w/w in methylene chloride). After 2 h the solution was allowed to warm up slowly, 20 h, when it became deep red. Excess reagent was destroyed by cautious addition of water and more solvent. The organic layer was washed with water, then with brine, dried ($MgSO_4$), and evaporated leaving isopyoluteorin (25 mg) m.p. 198–203° from benzene, ν_{max} 3350, 3240, 3130, 1620, 1565, 1017, 920 cm^{-1}.

Anal. Calcd. for $C_{11}H_{11}Cl_2NO_3$: C, 48.6; H, 2.6; Cl, 26.1; N, 5.15. Found: C, 48.6; H, 2.5; Cl, 26.2; N, 5.1.

Pyoluteorin

The mixture of the dimethyl ethers of pyoluteorin and isopyoluteorin (75 mg) was demethylated as above and the products separated by t.l.c. on silica plates using acetone/petrol (3:7). The lower band (23 mg) was the iso-compound **10** and the upper band was pyoluteorin

Can. J. Chem. Downloaded from www.nrcresearchpress.com by 210.87.254.105 on 09/05/12
For personal use only.

1 which crystallized as sulfur yellow needles (35 mg) from benzene/petrol with m.p. 177–186°, varying slightly with the rate of heating, undepressed in mixed melt with an authentic sample of m.p. 175–182°, ν_{max} 3470, 3370, 3160, 1633, 1599, 1023, 890 etc. cm^{-1}.

Anal. Calcd. for $C_{11}H_7Cl_2NO_3$: C, 48.6; H, 2.6; Cl, 26.0; N, 5.15. Found: C, 49.0; H, 2.5; Cl, 25.4; N, 5.15.

Pyoluteorin Bromine Analogue

4,5-Dibromopyrrole-2-carboxylic acid (4 g as the sodium salt) was refluxed in dry benzene (50 ml) with 2,6-dimethoxybenzoyl chloride (from 3 g acid) for 90 min. The solvent was then distilled off and the residue heated to 150° for 1 h, then extracted with three 150 ml portions of 1:1 benzene/ethyl acetate. The total extract was washed with sodium carbonate solution, then water, dried, and evaporated leaving 1 g residue. Preparative t.l.c. in 1:1 ether/petrol, three passes, gave a band at R_f 0.6 which was extracted to yield 300 mg crystalline product m.p. 200–205° from benzene/petrol.

Anal. Calcd. for $C_{13}H_{11}Br_2NO_3$: C, 40.1; H, 2.85; Br, 41.1; N, 3.6. Found: C, 40.3; H, 2.8; Br, 42.6; N, 3.9.

The n.m.r. spectrum (Table 1) confirmed the structure **7**. The mass spectrum revealed the presence of some 2-(2′,6′-dimethoxybenzoyl)-3,4,5-tribromopyrrole.

The above dimethyl ether (125 mg) in methylene chloride (10 ml), at −70° was treated with the methylene chloride solution of boron trichloride (6 ml) when a purple complex formed which rapidly turned deep red. The solution was allowed to warm up to room temperature (1 h) and left overnight then worked up as described to give 90 mg crystals which were further purified by t.l.c. in acetone/petrol 1:5. The major product, R_f 0.5, was crystallized from benzene/petrol to give yellow prisms m.p. 163–164°.

Anal. Calcd. for $C_{11}H_7Br_2NO_3$: C, 36.6; H, 1.95; Br, 44.3; N, 3.9. Found: C, 36.6; H, 2.25; Br, 44.2; N, 4.0.

The mass spectrum did not reveal any tribromoanalogue. Its cracking pattern resembled that of pyoluteorin.

We thank the National Research Council of Canada for financial support.

1. R. TAKEDA. J. Amer. Chem. Soc. **80**, 4749 (1958), Bull. Agr. Chem. Soc. Japan, **23**, 126, 165 (1959).
2. A. J. BIRCH, P. HODGE, R. W. RICKARDS, R. TAKEDA, and T. R. WATSON. J. Chem. Soc. 2641 (1964).
3. R. TAKEDA. J. Ferment. Technol. Osaka, **36**, 281 (1958).
4. (*a*) P. HODGE. Personal communication 1964. (*b*) R. J. O'CONNER, J. M. VAN DEREN, and W. A. DARLINGTON. U.S. Pat. 3 298 910 (1967).
5. J. A. ELIX and M. V. SARGENT. J. Chem. Soc. (C) 1718 (1967).
6. K. BAILEY and A. H. REES. J. Chem. Soc. (D) 1284 (1969).
7. P. HODGE and R. W. RICKARDS. J. Chem. Soc. 459 (1965).
8. G. R. BIRCHALL and A. H. REES. Unpublished observations.

Can. J. Chem. Downloaded from www.nrcresearchpress.com by 210.87.254.105 on 09/05/12
For personal use only.

Can. J. Chem. Downloaded from www.nrcresearchpress.com by 210.87.254.5 on 09/05/12
For personal use only.

220 MHz spectra of heparin, chondroitins, and other mucopolysaccharides[1]

A. S. PERLIN, B. CASU,[2] AND G. R. SANDERSON[3]
Department of Chemistry, McGill University, Montreal, Quebec

AND

L. F. JOHNSON
Varian Associates, Palo Alto, California

Received February 17, 1970

Characteristics of proton magnetic resonance spectra of heparins at 220 MHz, coupled with spectral data for model compounds and with information obtained chemically, indicate that heparins are composed principally of (1 → 4)-linked α-L-idopyranosyluronic acid residues (**3**) and 2-amino-2-deoxy-α-D-glucopyranosyl residues (**1**); also, that sulfate groups are located at position -2 and -6 of **1**, and -2 of **3**. D-Glucopyranosyluronic acid residues (**2**) appear to be minor constituents, which is at variance with all structures that have been proposed previously for heparin.

Spectra of chondroitins A, B, and C, which are readily distinguishable, are in close accord with formulae that have been proposed for these mucopolysaccharides; on the same basis, the spectrum of keratan sulfate is less consistent. Hyaluronic acid affords a poorly resolved though, nonetheless, distinctive spectrum. The general view that mucopolysaccharides are constituted basically of residues of hexosamine and uronic acid in equimolar proportion receives support from the current findings. However, heparitin appears to possess a more heterogeneous type of structure than do these other polymers.

Canadian Journal of Chemistry, **48**, 2260 (1970)

Major structural features of many mucopolysaccharides, heparin, the chondroitins, hyaluronic acid, etc., are well recognized (e.g. see ref. 1). It appears that common to each is a linear polymeric chain in which hexosaminyl and hexosyluronic acid residues alternate, although other types of sequences may occur. Differences among the mucopolysaccharides arise from variations in chain length, in the configuration of residues, their mode of glycosidic bonding, the number and location of *O*-sulfate groups, contents of other kinds of sugar residues and of acetamido and sulfamino groups, and in their association with amino acids and proteins. Structural studies on the mucopolysaccharides frequently are complicated by insufficiency of material, difficulty in assessing purity, and a general dearth of procedures that permit selective, high-yield, degradation of the polymers. Hence it is probably true at present to say that most mucopolysaccharides have only been partially characterized and that details of structure, perhaps even major features in some instances, remain to be determined.

In principle, proton magnetic resonance (p.m.r.) spectroscopy should be a highly useful physical method for examining such polymers, particularly because it can furnish excellent quantitative data. Hence, with suitable resolution, it should be feasible to estimate the relative proportions of the components of a mixed polymer from the relative intensities of resonance signals attributable to the different residues present. An attempt to estimate the compositions of various heparins by p.m.r. spectroscopy at 100 MHz has been described earlier (2). In the current study, possible advantages of measuring the spectra of heparins at a higher frequency, i.e., at 220 MHz are assessed, and the spectra of several other mucopolysaccharides are described as well.

Heparin

The 100 MHz spectra of heparins show notable variations among samples from different sources (2, 3), but all are characterized by three signals (*a*, *b*, and *c*) at 4.7–5.4 p.p.m., chemical shifts commonly associated with anomeric protons (Fig. 1A). Accordingly, each of these signals has been attributed to H-1 of the three main kinds of residues found in heparin, i.e., 2-deoxy-2-(sulfamino)-α-D-glucopyranosyl (**1**),α-D-glucopyranosyluronic acid (**2**), and L-idosyluronic acid (**3**), respectively and, based on the integrals, it has been suggested that heparins are comprised of approximately equimolar proportions of these residues (2). In addition, the total intensity of *a*, *b*,

[1]Presented in part at the 150th American Chemical Society meeting, New York, N.Y., September 8–12, 1969.
[2]Harold Hibbert Memorial Fellow (1968–1969); on leave of absence from Istituto G. Ronzoni, Milan, Italy.
[3]Postdoctoral Fellow, 1967–1969.

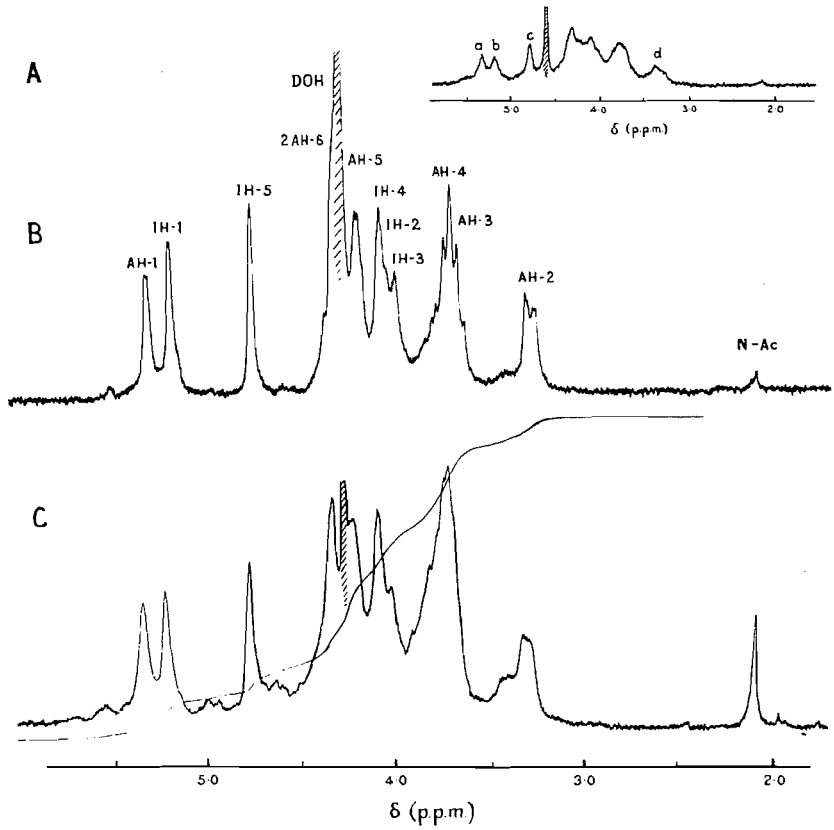

FIG. 1. Proton magnetic resonance spectrum of heparin in deuterium oxide of (A) type B heparin at 35 °C, 100 MHz; (B) type B heparin at 70 °C, 220 MHz; (C) type A heparin at 70 °C, 220 MHz. Peak designations are explained in the text.

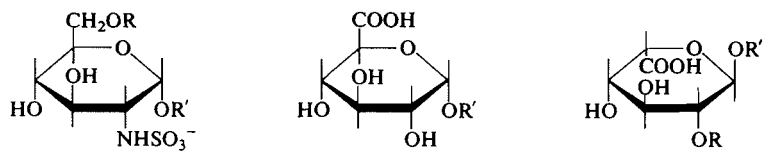

1 R = H
7 R = SO_3^-

2

3 R = H
15 R = SO_3^-

and *c* relative to that of the higher field signals (*d–h*) appeared to agree with the ratio expected. Thus, for a total of 17 protons in a trisaccharide basic unit, seven for each hexosaminyl residue, *plus* five for each of the two uronosyl residues, the expected ratio is 3:14, and the value found was about 3:15 (2).

In arriving at this latter value, an attempt was made to correct for overlap by the rather broad signals of the spectra (2). However, measurements at 220 MHz (Fig. 1B) substantially minimize the problem of overlap because they afford a better separation of signals. According to the integrals obtained under these more satisfactory conditions, the ratio of *a–c*:*d–h* is only about 3:10 (3:9.6–9.9 for four heparin samples). Thus, signals *a*, *b*, and *c* have a relatively higher intensity than had been deduced from the 100 MHz spectra, and therefore each can no longer be ascribed to the anomeric proton of a different residue. This finding contradicts our previous suggestion (2) that heparins contain approxi-

Can. J. Chem. Downloaded from www.nrcresearchpress.com by 210.87.254.5 on 09/05/12
For personal use only.

Can. J. Chem. Downloaded from www.nrcresearchpress.com by 210.87.254.5 on 09/05/12
For personal use only.

mately equimolar proportions of residues **1**, **2**, and **3**. Hence it is pertinent that a concurrent chemical examination of heparin (4) also does not support a 1:1:1 type of structure.[4] The chemical data in fact suggest a ratio of about 1:0.2:1, i.e., a relatively much lower proportion of residues of D-glucopyranosyluronic acid than would have been expected. In view of these results, it becomes necessary to reassess the p.m.r. spectra of heparins, and the following discussion deals with this question.

Signals *a* and *h* have previously been attributed to H-1 and H-2, respectively, of hexosaminyl residues by reference to chemical shifts and spacings in the spectra of model compounds, and particularly to the upfield displacement that these signals undergo upon hydrolysis of the sulfamino group (2). Since these similarities are even more clearly evident at 220 MHz, the earlier assignments are retained (AH-1 and AH-2, Fig. 1B).

As noted above, it appears no longer valid to assume that both *b* and *c* are produced by anomeric protons. However, an attractive alternative is to attribute signal *c* to H-5 of the L-idopyranosyluronic acid residues (**3**). This follows from an examination of the spectra of some methyl glycosiduronic acids both as salts and as free acids. Thus, H-5 of methyl α-D-idopyranosiduronic acid (**4**) or of its β-anomer (**5**) resonates in the region of signal *c* (see Fig. 1A) and, like the latter, these signals are characterized by a narrow spacing (Fig. 2).[5] Furthermore, all of these signals are shifted downfield by about 0.3 p.p.m. when the solution is acidified (Fig. 2). Although the H-5 signal for methyl α-D-glucopyranosiduronic acid (**6**) is displaced downward in the same way, its relatively low frequency and particularly its broad spacing (ca. 10 Hz) make it highly unlikely that *c* is produced by H-5 of the D-glucopyranosyluronic acid residues (**2**) in heparin. Therefore since H-5 of **3** most probably produces signal *c*, the anomeric proton (IH-1) of the same residue may now be regarded as the

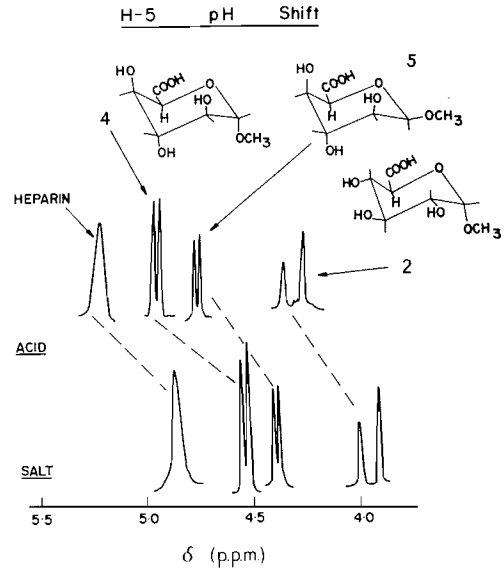

FIG. 2. The effect of p*H* (salt vs. free acid) on the chemical shift for H-5 of some uronosides in deuterium oxide (the acids were prepared by introducing excess of deuterium chloride); data obtained at 30 °C and at 100 MHz.

source of signal *b* rather than, as before (2), H-1 of residue **2**.

These revised assignments require that L-idosyluronic acid be a major constituent of heparin, in contrast to earlier views (1, 2, 6–8), and that it be present to about the same extent as the hexosamine constituent, which is consistent with our most recent chemical evidence (4). In addition, the total area of *a* and *b* relative to that of signals *c* to *h*, inclusive, agrees moderately well with expectation. The expected ratio is 1:5 (i.e., two anomeric protons as compared with six other protons of (**1**) *plus* four other protons of **3**, and the found value is 1:5.1–5.5[6] (for four samples of type B (3) represented in Fig. 1B).

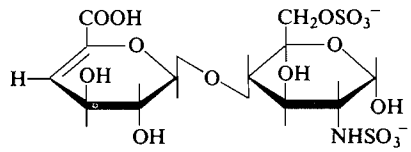

8

[4]Recent detailed analysis of various heparins also obviates this possibility and supports earlier indications that hexosamine accounts for about half of the carbohydrate portion of the heparin molecule (5).

[5]Representation of **4** and **5** in the conformations shown is based on unpublished p.m.r. data, and the preparation of these compounds (by catalytic oxidation of the corresponding D-idopyranosides) also has yet to be published (14).

[6]The limits of error of such measurements with solutions of polysaccharides in deuterium oxide are uncertain. That is, there are few fully characterized polysaccharides that give well resolved p.m.r. spectra to serve as standards.

Can. J. Chem. Downloaded from www.nrcresearchpress.com by 210.87.254.5 on 09/05/12
For personal use only.

Other signal assignments in Fig. 1B are suggested by reference to the spectra of various model compounds. The tall, narrow, signal at 4.4 p.p.m. (2AH-6) has about the same chemical shift (4.3 p.p.m.) as the two H-6 protons of 2-deoxy-2-(sulfamino)-α-D-glucopyranose-6-sulfate (**7**). Similarly, signals for the other protons of the hexosamine moiety (i.e. AH-3, -4, and -5) are designated on the basis of the spectra of **7** and of disaccharide **8** (Fig. 3A), both of which have been obtained by enzymolysis of heparin (9–11). That is, Fig. 3 illustrates the correspondence in chemical shift between signals (AH) for the hexosamine moiety of **8** and various signals of the heparin spectrum (Fig. 3C) (at 100 MHz). Shown also is the spectrum (Fig. 3B) of a higher oligosaccharide formed in the enzymolysis (9, 10) which, by clearly exhibiting characteristics of these two other spectra, emphasizes the similarities between them. Signals produced by protons -2, -3, and -4 of the L-idosyluronic acid residues are less easily designated because of the lack of suitable reference compounds. There is good evidence from periodate oxidation data (7, 12, 13) that an *O*-sulfate group generally is located at position-2 of the hexosyluronic acid residues in heparin, and this assignment is confirmed by structure **8**. Position-4 of the L-idopyranosyluronic acid residues is involved in glycosidic bonding (4, 11). Hence both H-2 and H-4 of **3** would be expected to resonate at perhaps 0.3–0.4 p.p.m. to low field of the corresponding signals for the related idopyranosyluronic acids (**4** and **5**) (14), i.e. at about 4.0 and 4.3 p.p.m., respectively, which is close to the assignments proposed for IH-2 and IH-4. The assignment for IH-3 is more tentative.

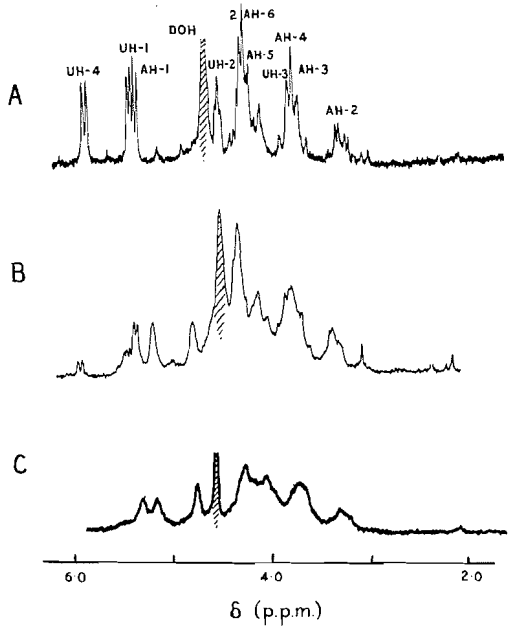

FIG. 3. Proton magnetic resonance spectrum at 100 MHz of (A) disaccharide **8** at 35 °C; (B) an oligosaccharide produced by enzymolysis of heparin (9), at 55 °C; (C) heparin, type B, at 35 °C. Solvent, deuterium oxide.

Missing from Fig. 1B are possible assignments for protons of the D-glucopyranosyluronic acid residues of heparin. Although such residues were formerly thought to account for a major proportion of the polymer, according to our current interpretation of the spectra they produce no easily recognizable signals. Nevertheless, there are some weak signals in the region of *a* and *b* and, probably, others underlying the latter signals. Surely some of these must be associated with type **2** residues, but in any event the proportion of such residues in heparin would have to be relatively low, in conformity with the recent chemical evidence (4), if the spectral assignments are to have general validity.

Relationships between the p.m.r. spectra of heparin and the glycosidic configuration of its component residues merits comment. It has been shown that the hexosaminyl residues **1** possess the α-D-linkage (1, 15, 16), and this designation receives support from the fact that AH-1 gives rise to a narrow signal and resonates at relatively low field (see ref. 17). Based on the structure of disaccharide **8**, the α-L-configuration is assigned for residues of L-idopyranosyluronic acid. Hence the narrow spacing of signal IH-1 and its relatively large chemical shift similarly indicate that IH-1 is equatorially oriented, which suggests further that these uronic acid residues of heparin possess the 1C conformation,[7] the mirror image of **4**.

Fig. 1C illustrates the spectrum of a representative of group A heparins (3). Several of the signals observed are not present, or are very weak, in Fig. 1B: in addition to the signal close to 2.0 p.p.m., attributed to protons of *N*-acetyl groups, there are others at about 3.4, 3.7, 4.6, and 5.0 p.p.m. This latter group of signals may represent residues that are not present in the group B

[7]In the alternate, C1 conformation, the diaxial arrangement of H-1 and H-2 should give rise to a much broader spacing (see ref. 17).

Can. J. Chem. Downloaded from www.nrcresearchpress.com by 210.87.254.5 on 09/05/12
For personal use only.

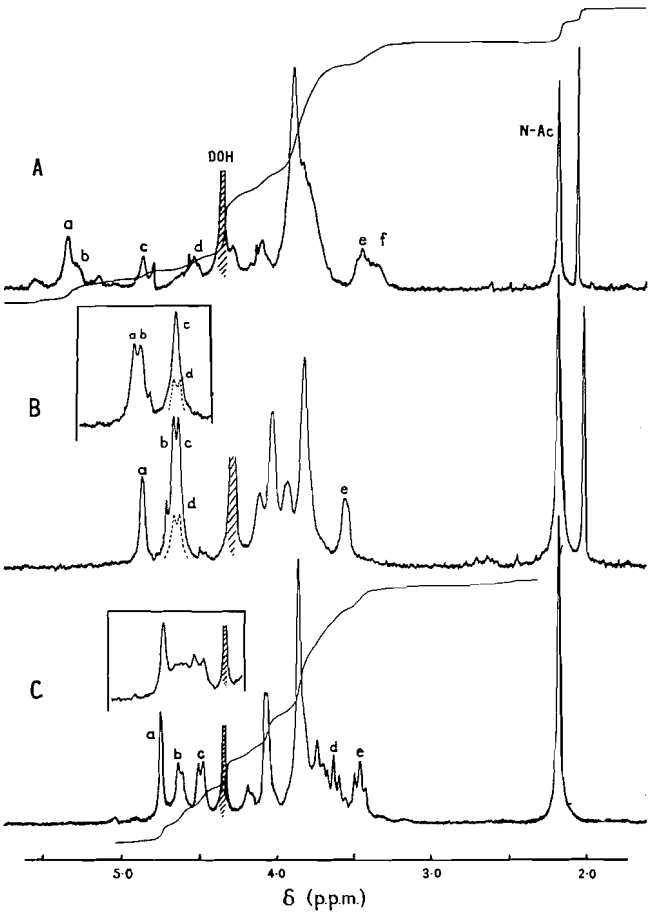

FIG. 4. Proton magnetic resonance spectrum at 220 MHz of (A) heparitin; (B) chondroitin B (inset: low field signals after acidification); (C) chondroitin A (inset: low field signals at 100 MHz). Solvent, deuterium oxide; 70 °C. The sharp singlet at about 2.0 p.p.m. in 4A or 4B is attributed to acetate anion.

heparins, but it is possible also that a small proportion of another polysaccharide is present (about 20% in this sample, based on the relative intensity of the *N*-acetyl signal, although the percentage is variable (Table 1, ref. 2)). Whatever the source of these "extra" signals in spectrum 1C, it is not eliminated by the currently best purification procedures, which favors the possibility that it is an integral part of the molecule, although another possibility is considered below.

Other Mucopolysaccharides

Other mucopolysaccharides afford p.m.r. spectra at 220 MHz that differ notably from those of heparins, and are themselves sufficiently distinctive to possibly serve for characterization purposes. Even at 60 MHz (18) substantial differences are apparent. However, since only one or two preparations of each polymer has as yet been examined, it is not known if variations occur from one source to another. Figs. 4 and 5 show the spectra of specimens that have been furnished by Dr. J. Cifonelli from the Reference Collection at the University of Chicago. Most of the better known mucopolysaccharides are represented, each having been the subject of substantial chemical and enzymic study (1), and the accompanying formulae (**9** to **14**) illustrate the basic structural sequences that are ascribed to them.

A general comment may be made concerning the region of lowest field signals in these spectra, which is associated most readily with anomeric protons. Aside from heparitin (Fig. 4A), these

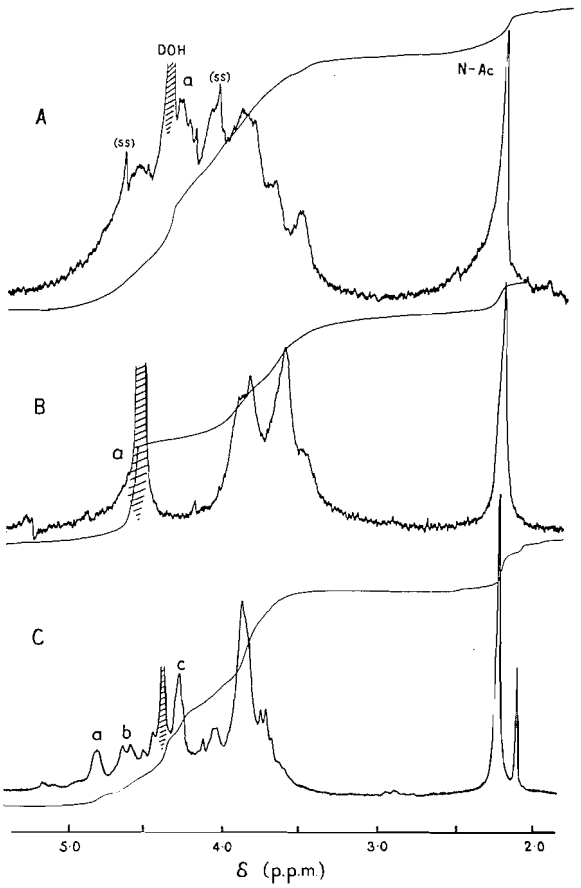

FIG. 5. Proton magnetic resonance spectrum at 220 MHz of (A) chondroitin C; (B) hyaluronic acid; (C) keratan sulfate. Solvent, deuterium oxide; 70 °C, (B) at 50 °C.

polymers do not produce signals comparable in chemical shift to AH-1 and IH-1 of Fig. 1 but, rather, at relatively higher field. In general this accords with the formulated structures in which the anomeric protons usually are axially oriented, and with the evidence that strongly-deshielding *N*- and *O*-sulfate groups usually are not found as 2-substituents of the glycosyl residues.

Heparitin

Heparitin shows several characteristics similar to heparin. Its lowest field signal (*a*, Fig. 4A) has the same chemical shift and shape as signal AH-1 of heparin which suggests that the 2-deoxy-2-sulfamino-D-glucosyl residues known to be present possess the α-D-configuration (as in **9**). Similarly, signal *b* (and an α-D-configuration) may be ascribed to the anomeric center of the

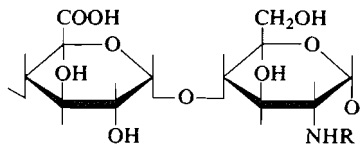

9 R = CH_3CO or SO_3^-
Heparitin

2 - acetamido - 2 - deoxy - D - glucosyl residues of heparitin. The combined intensity of *a* and *b* relative to the intensity of the upfield signal ascribed to *N*-acetyl protons, corresponds to an approximately equimolar ratio for the two types of hexosaminyl residues, in agreement with chemical analyses (1, 19, 20). There appear to be at least two signals at about 3.4 p.p.m.; signal *f* has the same chemical shift as AH-2 of the heparin spectrum and hence probably arises from the proton α to the sulfamino group, whereas *e* could account for H-2 of the 2-acetamido derivative. Signals *c* and *d* might well be associated with the D-glucosyluronic acid residues although, since the specific rotation of heparitin is very close to that of heparin, further examination of the uronoside composition should be pertinent.[8] In contrast to the situation with heparin, relatively few of the heparitin protons resonate in the region of the HOD signal, which is in accord with evidence that heparitin contains few, or no *O*-sulfate groups to cause deshielding of primary and secondary protons. Also, the fact that its spectrum contains a large number of signals of differing relative intensities, indicates that heparitin has a more heterogeneous type of structure than heparins appear to possess.

A comparison of the spectrum of heparitin with that of type A and B heparins (Fig. 1C and B) suggests the possibility that A heparins could contain some of heparitin. There is especially strong correspondence with respect to signal *e*, the *N*-acetyl signal, and the intense grouping of signals at about 3.7 p.p.m. (compare Figs. 1C and 4A), i.e., the signals that mainly differentiate between A and B heparins. Clearly this question merits further examination.

Chondroitin Sulfate B

The spectrum of dermatan (chondroitin sulfate B) (Fig. 4B) is better resolved, and suffers less

[8]Thus, for example, the chemical shift and shape of signal *c* suggest that it could be produced by H-5 of an iduronosyl residue, as for heparin.

Can. J. Chem. Downloaded from www.nrcresearchpress.com by 210.87.254.5 on 09/05/12
For personal use only.

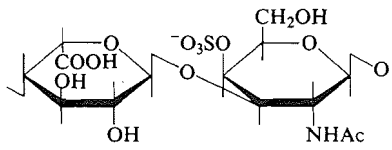

10
Chondroitin B

interference from the HOD signal, at 70 °C than at ambient temperature. Signal *a* and the group of signals *b*, *c*, and *d*, account for a total of about four protons. These protons likely are the anomeric ones of the two different residues (**10**), H-4 of the D-galactosaminyl residue, and H-5 of the L-idosyluronic acid residue. One of the *b*, *c*, *d* group of signals is shifted downfield on acidification by 0.3 p.p.m. and hence is most readily attributed to this H-5 proton (*b* in inset of Fig. 4B). Also, its chemical shift in both media is close to that of IH-5 of the heparin spectra and, like the latter signal, it is narrow. There is a relatively broad signal in this group (*d*). Because of its spacing and upfield position this signal is ascribed to H-1 of the hexosaminyl residue, which agrees with the assigned β-D-configuration for the latter (1, 21, 22). Proton H-1 of the L-idosyluronic acid residue probably produces signal *a*; as discussed for heparin, its narrow spacing is indicative of an α-L-configuration when the residue possesses the 1C chair conformation. The fact that its chemical shift is upfield relative to IH-1 of Fig. 1 is to be expected, in view of the absence of a 2-sulfate group in dermatan. By contrast, the presence of the 4-*O*-sulfate group, as well as its equatorial orientation, undoubtedly contributes to the downfield position of H-4 of the hexosaminyl residue (*c*), and the narrow spacing of this signal concurs with its gauche relationship to both H-3 and H-5.

From the relative intensities of these low field signals and the *N*-acetyl signal (Fig. 4B) (i.e. 4:27), the content of 2-acetamido-2-deoxy-hexosamine in the polymer is estimated to be about 45%, i.e., close to the expected value. However, the overall integral for this spectrum suggests that the largest group of signals (between 3.5 and 4.4 p.p.m.) account for a total of closer to nine protons rather than the value of eight required by formula **10**. Hence, as found with heparins, the relative intensities of the various signals do not furnish a simple numerical basis suitable for critically evaluating a given structural possibility. Whether this represents a problem of measurement[9] or one of structure has yet to be decided.

One further point merits comments. It is highly probable that a small proportion of the uronosyl residues in chondroitin B possess the D-*gluco* configuration (21–23). As found with heparin, the current spectral data are difficult to reconcile with a substantial content of a third type of residue. However, there is a relatively weak, broad, signal at about 4.5 p.p.m., which has not been commented on above, the chemical shift and spacing of which are close to those of H-1 signals in Fig. 4C (especially signal *c*) associated with the β-D-gluco configuration. Tentatively, then, this minor signal is attributed to H-1 of β-D-glucosyluronic acid residues in dermatan, its relative intensity showing that such residues could comprise perhaps 10% of the polymer.

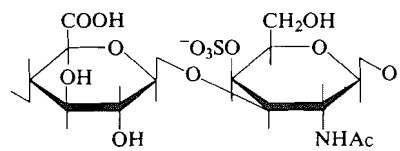

11
Chondroitin A

Chondroitin Sulfate A

Chondroitin sulfate A (**11**) differs from dermatan in possessing a β-D-glucuronosyl rather than α-L-iduronosyl residue (24, 25). Comparatively then, the presence of only three low field signals rather than four (Fig. 4C) is not unexpected in view of the relatively high field resonance for H-5 of D-glucosiduronic acids (Fig. 2). The chemical shifts and broad spacings of signals *b* and *c* appear to be consistent with the assigned β-D-anomeric configurations of the two different residues in **11**, and the much narrower signal (*a*) may reasonably be ascribed to H-4 of the sulfated hexosaminyl residue. As with dermatan, the total intensities of these low field signals relative to the intensity of the *N*-acetyl proton signal (3:2.7) corresponds to just under a 50% content of 2-acetamido-2-deoxy-hexose. Again also, the overall relative intensity of the other signals is slightly high, amounting to about ten, rather than nine, protons. Although the upfield

[9]Signals produced by *N*-acetyl groups have been observed, particularly in experiments at 100 MHz, to be relatively highly sensitive to saturation effects.

Can. J. Chem. Downloaded from www.nrcresearchpress.com by 210.87.254.5 on 09/05/12
For personal use only.

Can. J. Chem. Downloaded from www.nrcresearchpress.com by 210.87.254.5 on 09/05/12
For personal use only.

signals, *d* and *e*, have chemical shifts close to that of AH-2 of Fig. 1, H-2 of the 2-acetamido-2-deoxy-D-galactosaminyl residues would be expected to resonate further downfield because of deshielding by the axial C_4—O bond. In any event, attempts to relate these signals to the *b* and *c* doublets by spin-decoupling were unsuccessful. More probably, *d* and *e* are due to the 6-protons of the hexosaminyl residue; the tilt of signal *e* suggests that the shift of the adjacent H-5 is slightly downfield. Analogously, the upfield signal *e* of Fig. 4B also is probably produced by an H-6 of the hexosaminyl residue, but in this instance shifts for the second H-6 and for H-5 are likely to be almost coincident. Hence, the perturbed pattern observed for *e* could result from averaging of the negative geminal coupling and positive vicinal coupling. Although this type of hexosaminyl residue is common to **10** and **11** its environment is different in the two polymers, and therefore some spectral differences are to be expected.

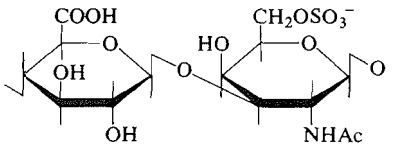

12
Chondroitin C

Chondroitin Sulfate C

Because the spectrum of chondroitin sulfate C (Fig. 5A) is not as well resolved as that of chondroitin A, a spectral comparison of these closely related polymers (compare **12** and **11**) is difficult. However, the fact that an *O*-sulfate group is located at C-6 of the hexosaminyl residue of the former mucopolysaccharide (26, 27) rather than at C-4, is reflected in the absence of a signal corresponding to *a* in Fig. 4C. Similarly, there are proportionately weaker signals at about 3.8 p.p.m. and stronger ones at 4.2–4.3 p.p.m. (signal *a*) in contrast with the situation in Fig. 3C, which corresponds to the expected downfield displacement of H-6 signals for protons α- to the 6-*O*-sulfate group (compare also with signal AH-6 of Fig. 1B).

Hyaluronic Acid and Keratan Sulfate

Hyaluronic acid, which forms highly viscous solutions, furnishes a poorly resolved spectrum (Fig. 5B). The anomeric proton signals (*a*) are almost obscured by their broadness and by the excessively broad HOD signals. However, in accord with the fact that this polymer contains no *O*-sulfate or other such strongly deshielding groups (**13**) (28, 29) the overall spectrum is produced at relatively high field. On the same basis, the spectrum of keratan sulfate (Fig. 5C) appears to detect the presence of several strongly deshielded protons (*a* and *b*) in addition to those (most probably signal *c*) that are located α- to the 6-*O*-sulfate group, as in **14** (30, 31).

In summary, the p.m.r. spectra of mucopolysaccharides at 220 MHz are sufficiently well resolved to permit more satisfactory assignments for many individual resonance signals than was possible with spectra obtained at lower frequency. The improved separation of signals also enhances quantitative evaluation of the spectra. This is of particular advantage because of difficulties inherent in the analysis of mucopolysaccharide composition. For heparin the current p.m.r. data, together with chemical and enzymic evidence, lead to the proposition that two types of residues (**7** and **15**), approximately equimolar, constitute most of the molecule. Accordingly also, they do not support the widely-accepted structure for heparin in which D-glucosyluronic acid (**2**) is depicted as the major uronosyl component. Differences between the two types of heparins are more clearly evident at 220 MHz, and the possibility is raised that these types may differ in having, or not having, heparitin as a contaminant.

Spectra of chondroitins A, B, and C appear to

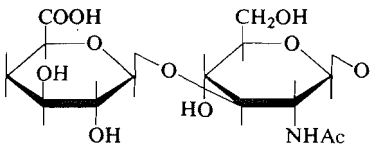

13
Hyaluronic acid

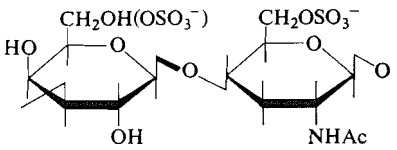

14
Keratan sulfate

be closely in accord with formulae (**11**, **10**, and **12**, respectively) that have been proposed for these mucopolysaccharides, and the samples examined give no indication that contaminating polymers are present in significant proportion. In terms of the ratio of constituent residues, heparitin probably has a more heterogeneous type of structure than do these other mucopolysaccharides, and it may have a substantial content of L-idosyluronic acid. The spectrum of keratan sulfate is not easily reconciled with formula **14**; the fact that this material has as yet received only relatively limited attention chemically allows for the possibility that there may yet be some revision of the formula.

In general, chemical and enzymic studies of the mucopolysaccharides have led to the view that these polymers are constituted basically of alternating residues of hexosamine and uronic acid. The current p.m.r. spectra serve to reinforce this view.

Experimental

The p.m.r. spectra were obtained with a Varian HR-220 MHz or HA-100 MHz spectrometer. Samples were given a preliminary deuterium-exchange by repeated treatments with deuterium oxide. Most spectra were recorded at about 70 °C because the higher temperature favored improved resolution, although lower temperatures were used also in minimizing the obscuring-effect of the DOH signal. Hyaluronic acid was recorded at a maximum of 50 °C, because it was precipitated from solution above this temperature. The 100 MHz spectra were obtained with the aid of an internal capillary containing tetramethylsilane which, however, caused a downward displacement of the signals by about 0.5 p.p.m.; accordingly, the actual spectra are corrected by −0.5 p.p.m. The 220 MHz spectra are not shift calibrated, although of precise width (i.e., 1000 Hz), and hence the chemical shifts in p.p.m. are given relative to the 100 MHz spectra.

The authors express their gratitude to Dr. J. A. Cifonelli, University of Chicago, who very generously provided samples of various mucopolysaccharides, and to Dr. E. L. Masson and the Upjohn Company, Don Mills, Ont., for kindly supplying heparin. The continuing interest and encouragement of Professor L. B. Jaques is deeply appreciated.

Figures 3A and B are presented through the kind cooperation of Dr. C. P. Dietrich.

The National Research Council of Canada and the Pulp and Paper Institute of Canada provided generous support.

1. (*a*) J. S. Brimacombe and J. M. Webber. Mucopolysaccharides. Elsevier Publishing Co., Amsterdam, 1964. (*b*) R. W. Jeanloz. Mucopolysaccharides. *In* Comprehensive biochemistry. Vol. 5. M. Florkin and E. H. Stotz (*editors*). Elsevier, Amsterdam, 1963. p. 262.
2. A. S. Perlin, M. Mazurek, L. B. Jaques, and L. W. Kavanagh. Carbohyd. Res. 7, 369 (1968).
3. L. B. Jaques, L. W. Kavanagh, M. Mazurek, and A. S. Perlin. Biochem. Biophys. Res. Comm. **24**, 447 (1966).
4. A. S. Perlin and G. R. Sanderson. Carbohyd. Res. **12**, 183 (1970).
5. L. B. Jaques and L. W. Kavanagh. Unpublished results. L. W. Kavanagh. Ph.D. Thesis. University of Saskatchewan, Saskatoon, Saskatchewan, 1969.
6. M. L. Wolfrom and F. A. H. Rice. J. Amer. Chem. Soc. **68**, 532 (1946).
7. A. B. Foster, A. H. Olavesen, M. Stacey, and J. M. Webber. Chem. Ind. (London), 143 (1961).
8. M. L. Wolfrom, J. R. Vercellotti, and G. H. S. Thomas. J. Org. Chem. **26**, 2160 (1961); **29**, 536 (1964).
9. C. P. Dietrich. Biochem. J. **108**, 647 (1968).
10. C. P. Dietrich. Biochem. **8**, 2089 (1969).
11. D. M. Mackie, C. P. Dietrich, and A. S. Perlin. Unpublished results.
12. G. J. Durant, H. Hendrickson, and R. Montgomery. Arch. Biochem. Biophys. 99, 418 (1962).
13. M. L. Wolfrom, H. Tomomatsu, and W. A. Szarek. J. Org. Chem. **31**, 1173 (1966).
14. B. Casu, A. S. Perlin, G. R. Sanderson, and J. Tse. Unpublished results.
15. M. L. Wolfrom, J. R. Vercellotti, and D. Horton. J. Org. Chem. **28**, 279 (1963); **29**, 540 (1964).
16. M. L. Wolfrom, R. Montgomery, J. V. Karabinos, and P. Rathgeb. J. Amer. Chem. Soc. **72**, 5796 (1950).
17. R. U. Lemieux, R. K. Kullnig, H. J. Bernstein, and W. G. Schneider. J. Amer. Chem. Soc. **80**, 6098 (1958).
18. S. Inoue and Y. Inoue. Biochem. Biophys. Res. Comm. **23**, 513 (1966).
19. A. Linker, P. Hoffman, P. Sampson, and K. Meyer. Biochem. Biophys. Acta, **29**, 443 (1958); **43**, 366 (1960).
20. J. A. Cifonelli. Carbohyd. Res. **8**, 233 (1968).
21. P. Hoffman, A. Linker, and K. Meyer. Sci. **124**, 1252 (1956).
22. J. A. Cifonelli, J. Ludowieg, and A. Dorfman. J. Biol. Chem. **233**, 541 (1958).
23. L. A. Fransson and L. Roden. J. Biol. Chem. **242**, 4161, 4170 (1967).
24. M. L. Wolfrom and B. O. Juliano. J. Amer. Chem. Soc. **82**, 1673 (1960).
25. E. A. Davidson and K. Meyer. J. Amer. Chem. Soc. **76**, 5686 (1954); 77, 4796 (1955).
26. A. Linker, P. Hoffman, K. Meyer, P. Sampson, and E. D. Korn. J. Biol. Chem. **235**, 3061 (1960).
27. S. Suzuki. J. Biol. Chem. **235**, 3580 (1960).
28. K. Meyer. Physiol. Rev. **27**, 335 (1947).
29. M. M. Rapport, B. Weissmann, A. Linker, and K. Meyer. Nature, **168**, 996 (1951).
30. S. Hirano, P. Hoffman, and K. Meyer. J. Org. Chem. **26**, 5064 (1961).
31. V. P. Bhavanandan and K. Meyer. J. Biol. Chem. **242**, 4352 (1967); **243**, 1052 (1968).

Can. J. Chem. Downloaded from www.nrcresearchpress.com by 210.87.254.5 on 09/05/12
For personal use only.

Photolysis of cyclopentanone[1]

A. T. BLADES
Research Council of Alberta, Edmonton, Alberta
Received February 10, 1970

The effect of wavelength and pressure on the distribution of products has been studied in the photolysis of cyclopentanone and cyclopentanone-2,2,5,5-d_4. At low pressures, C_2D_4 and C_2H_4 are formed in addition to the expected high pressure product $C_2H_2D_2$, confirming the intermediate formation of excited cyclobutane. The high pressure ratio of cyclobutane to ethylene is attributed to alternate reactions of the tetramethylene diradical which have equal energy sensitivity, and some evidence is presented for a further mechanism of ethylene formation at short wavelengths. Evidence is also presented for the formation of cyclobutane and ethylene following thermal re-excitation of the precursor of 4-pentenal.

Canadian Journal of Chemistry, **48**, 2269 (1970)

Can. J. Chem. Downloaded from www.nrcresearchpress.com by 210.87.254.42 on 09/05/12
For personal use only.

The vapor phase photolysis of cyclopentanone yields carbon monoxide, ethylene, cyclobutane (1), and 4-pentenal (2) and mechanisms, based on energetics (3), electronic states (4), and various diradical intermediates (1, 5), have been devised to explain these products. On the basis of quenching studies at 313 nm, Srinivasan (6) proposed a simple Stern–Volmer mechanism with unquenched species giving carbon monoxide (and ethylene and cyclobutane) and quenched species giving 4-pentenal. Recently, Mok (7) has elaborated this mechanism to include formation of 4-pentenal from both quenched and unquenched species. Srinivasan (3) also noted a temperature coefficient in the product yield, carbon monoxide being formed at the expense of 4-pentenal with increasing temperature. Since increased temperature has a marginal effect on the average energy of the absorbing molecules, this temperature effect must imply a re-excitation of that portion of the photo-excited species which had previously lost energy by collision. Carbon monoxide (and ethylene and cyclobutane) must therefore also have two origins, the original photo-excited and a thermally re-excited species.

Following the mechanisms of Srinivasan (6) and Mok (7), these species would be identified as different vibrational levels of the same electronic state. This would require collisional quenching and thermal excitation to occur simultaneously with the same molecule. Since this is clearly impossible it must be assumed that collisional quenching affects one species and thermal re-excitation another. The products of the photolysis may therefore be considered to arise from two separate precursors, one which bears the original photon energy and gives products according to the absorbed wavelength, and one which gives products according to the temperature. This doesn't imply that the former species is not transformed into the latter before product formation, but if it is, its lifetime precludes collision.

While positive identification of these two intermediates may be difficult, some evidence suggests that they may be the excited n,π^* singlet and triplet states. Rusbult and Lee (8) have estimated the non-radiative lifetime of the singlet to be 3×10^{-9} s and this species is, hence, an obvious choice for the collisionally quenchable species. The triplet, on the other hand, has been shown, by benzene triplet sensitization studies at room temperature, to give 4-pentenal (4) and is hence a possibility for the thermally excitable species. It is, however, reasonable to suppose that, by analogy with cyclohexanones (9–11), an acyl diradical, $\cdot CH_2CH_2CH_2CH_2CO\cdot$, may be the immediate precursor of stable products, and it is possible that this species has a sufficient lifetime for thermal excitation. The triplet might then be an alternate source, but not a necessary intermediate in the formation of the diradical. In solution, there is evidence for the intermediacy of the triplet in the diradical formation (12).

A further feature of the photolysis mechanism is the partitioning of the decomposition products between cyclobutane and ethylene. Above 5 Torr, this ratio is invariant with pressure, wavelength, and temperature (3), while below this pressure the ratio declines somewhat according to wavelength, presumably due to the decomposition of excited product cyclobutane to ethylene (13). The realization that cyclobutane arises from both a photo-excited and a thermally re-excited species

[1]Contribution No. 492 from the Research Council of Alberta, Edmonton, Alberta.

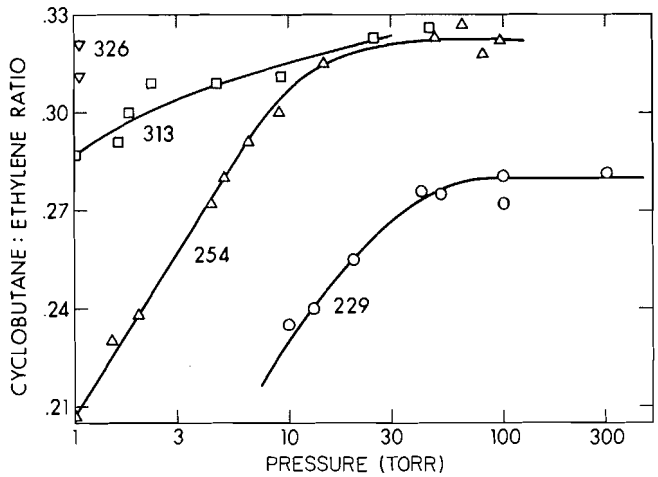

FIG. 1. Cyclobutane: ethylene ratio vs. pressure (Torr).

introduces the possibility that the constant high pressure ratio follows from the total formation of the products from the re-excited species under these conditions. To explore this mechanistic feature, the pressure effect has been examined in the photolysis of cyclopentanone-2,2,5,5-d_4 at 254 nm and in normal cyclopentanone from 326 to 229 nm, and the ratio of carbon monoxide to 4-pentenal has been examined from 326 to 254 nm.

Experimental

Commercial cyclopentanone was purified by preparative gas chromatography and was free of significant contaminants. Cyclopentanone-d_4 was prepared from this material by repeated exchange with D_2O (alkaline) and was shown by nuclear magnetic resonance spectroscopy to be better than 92% exchanged in the 2 and 5 positions. Heptane, used as an inert gas, was dried and distilled and was free of interfering contaminants.

Photolyses were carried out in a mercury-free metal–glass–teflon vacuum system. The photolysis cells were quartz, of volume 71 and 535 ml and were housed in aluminum block furnaces. The light sources were: (*a*) 229 nm: Osram low pressure cadmium with 1 cm Cl_2 filter; only absorbed impurities were 10% 227 nm and 0.5% 326 nm. (*b*) 254 nm: low pressure mercury arc with 1 cm Cl_2 and one 9-30 Corning filter, 0.5% other lines. (*c*) 307 nm: Osram low pressure zinc with one 0-53 Corning filter. (*d*) 313 nm: medium pressure mercury arc with one 0-54 filter, 2% at 302 nm. (*e*) 326 nm: Osram low pressure cadmium with four 0-54 filters, 0.2% at 313 nm. Photolysis times were several hours at both 229 and 326 nm due to very low extinction coefficients and were several minutes at the other wavelengths. Photolysis was carried to less than 2% conversion.

The products were separated at −80° into hydrocarbons (C_2H_4 and C_4H_8) and liquids (4-pentenal and cyclopentanone) and were then separately chromatographed on a 7 ft 1/4 in. diameter D.I.O.P. on Chromosorb *P* column, the hydrocarbons at room temperature and the liquids at 96°. In the photolysis of cyclopentanone-d_4, the product ethylenes were satisfactorily separated at −26° on a 75 ft 1/8 in. diameter nylon column packed with saturated $AgNO_3$ in ethylene glycol on Chromosorb *P*.

Results

Photolysis of cyclopentanone-2,2,5,5,-d_4 at 254 nm, 80°, and 11.2 Torr gave primarily $C_2H_2D_2$, with some C_2H_3D and C_2H_4 from less deuterated substrate. At 0.65 and 1.3 Torr, substantial yields of C_2D_4 and C_2H_4 in addition to $C_2H_2D_2$ were observed, suggesting approximately 14 and 10% cyclobutane decomposition at 0.65 and 1.3 Torr.

The effect of pressure on the ratio of the hydrocarbon products was investigated at 229, 254, 313, and 326 nm. This data, shown in Fig. 1, confirms the wavelength dependence previously noted (13) at 313 and 254 nm and shows the absence of the effect at 326 nm and the greater effect at 229 nm. Also, the constant high pressure ratio is confirmed in the range 326 to 254 nm, but a considerable decrease is noted at 229 nm at what is apparently the high pressure limit.

The relative yields of CO (i.e. C_4H_8 + 1/2 C_2H_4) and 4-pentenal were determined at 10 Torr and 25° and are listed in Table 1. The ratio at 313 nm is comparable to that reported by Srinivasan (3) and by Mok (7); the value at 254 nm is, however, considerably lower than their values, possibly because of a considerable contribution from longer wavelengths in their studies.

Can. J. Chem. Downloaded from www.nrcresearchpress.com by 210.87.254.42 on 09/05/12
For personal use only.

TABLE 1
Wavelength dependence of the product ratio

λ(nm)	4-Pentenal/CO
326	10.
313	1.4
307	1.0
254	0.02

Discussion

The observation of C_2D_4 and C_2H_4 in the photolysis of cyclopentanone-2,2,5,5-d_4 at 254 nm and at 0.65 and 1.3 Torr but not at 11.2 Torr confirms the partial decomposition of excited cyclobutane under conditions of low pressure and higher photon energy and hence qualitatively supports this reaction as the origin of the pressure effect in the cyclobutane–ethylene ratio. Quantitatively, the observed C_2D_4 would account for the ratio decrease at 1 Torr (see Fig. 1) if an isotope effect of 2 is assumed in the cyclobutane-d_4 decomposition.

The data in Fig. 1 confirm the wavelength dependence of the cyclobutane decomposition. At 326 nm and 1 Torr, the cyclobutane–ethylene ratio is at the high pressure value at longer wavelengths, suggesting no tendency for cyclobutane decomposition. This is in keeping with the exothermicity of the overall photo-reaction being just equal to the activation energy of the cyclobutane decomposition. The data at 313, 254, and 229 nm show a progressive trend to greater percentages of the cyclobutane decomposing at low pressures as the photon energy increases. At 229 nm, the high pressure limit is lower than observed with the longer wavelengths, and this suggests further complexity in the mechanism.

The effect of photon energy on the ratio of 4-pentenal to carbon monoxide (Table 1) fits the pattern that higher energy favors decomposition to carbon monoxide (3). The high ratio at 326 nm is reminiscent of the behavior of the benzene triplet sensitization system where the energy of the excited cyclopentanone is in the range of its triplet energy, 75 kcal/mole, and that of benzene, 85 kcal/mole. The small amount of carbon monoxide formed suggests that thermal re-excitation is not very important at room temperature. On the other hand, the almost trivial formation of 4-pentenal at 254 nm implies that the formation of that product directly from the photo-excited species, as observed by Mok (7) at 313 nm, is of little significance at shorter wavelengths. It also implies that at 10 Torr very little collisional deactivation of the excited singlet occurs and hence that the cyclobutane and ethylene arise from precursors bearing the full photon energy. Evidence from the cyclopentanone-d_4 and from Fig. 1 indicates that very little cyclobutane decomposition occurs under these conditions and hence it must be assumed that the cyclobutane to ethylene ratio in the products reflects the primary rates of formation from the highly excited species. At 313 nm, about the same ratio of cyclobutane to ethylene is obtained despite the 20 kcal/mole lower energy. It must therefore be assumed that cyclobutane and ethylene are formed in two parallel processes whose relative rates are insensitive to the energy of the precursor.

These aspects of the photolysis can be incorporated into a mechanism involving the several reactions of diradicals as is detailed in the approximate energy level diagram, Fig. 2.[2] The n,π^* excited singlet, as formed by photon absorption, presumably crosses over to a repulsive energy surface, potentially by way of the triplet, forming the acyl diradical $\cdot CH_2CH_2CH_2CH_2\dot{C}O$. Upon formation, this radical will bear excess energy characteristic of the absorbed energy, or of the thermally equilibrated excited state (n,π^*), minus the energy of the broken bond. Rearrangement of this biradical to 4-pentenal may then occur via a five-center cyclic transition state with a low Arrhenius A factor ($\sim 10^{11}$ s^{-1} due to loss of internal rotational degrees of freedom) and an activation energy determined primarily by the strain arising from formation of the five-member ring, >6 kcal/mole (15). Alternatively, the diradical may undergo a decarbonylation reaction, with an activation energy of 15 kcal/mole (by analogy with acetyl [16]) and a higher frequency factor, $\sim 10^{14}$ s^{-1}. This process would be expected to become increasingly significant with higher temperatures or decreasing wavelength of absorbed light, as is observed. The tetramethylene diradical so formed may then either decompose to ethylene or isomerize to cyclobutane; these processes occur with approximately equal activation energies (6.5 ± 1.5 kcal/mole) and frequency factors ($\sim 10^{12}$ s^{-1}) (14), in acceptable agreement with the observed

[2]The heats of formation have been estimated from the group additivity tables of refs. 14 and 15.

Can. J. Chem. Downloaded from www.nrcresearchpress.com by 210.87.254.42 on 09/05/12
For personal use only.

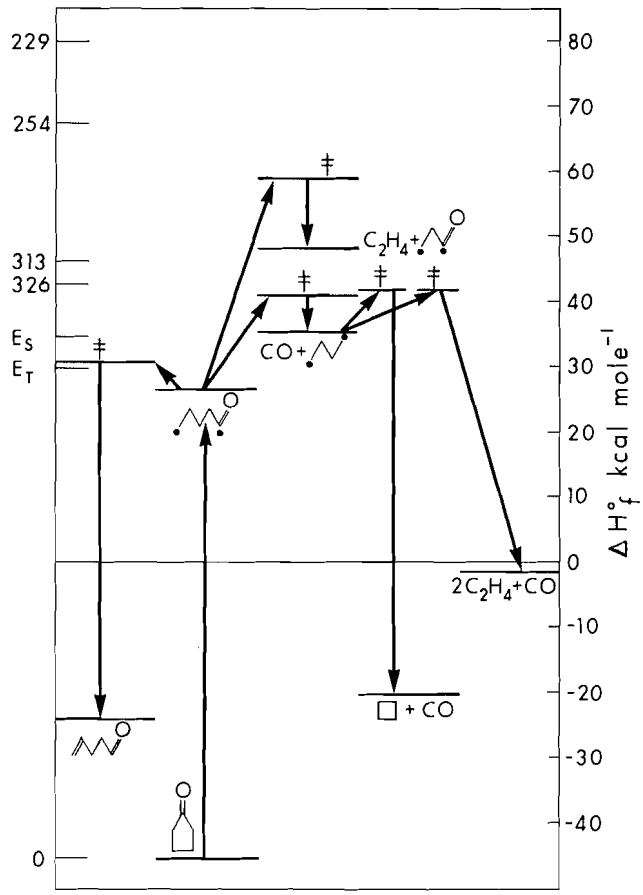

FIG. 2. The reaction mechanism (left-hand side: excited state energies and photon energies; right-hand side heats of formation).

high pressure ratio of cyclobutane: 1/2 ethylene of 0.64 (326 to 254 nm).

The increased yield of ethylene at 229 nm may be explained on the basis of a second decomposition reaction (eq. [1]) with an activation energy

$$[1] \quad \begin{aligned} \dot{C}H_2CH_2CH_2CH_2\dot{C}O &\rightarrow C_2H_4 + \dot{C}H_2CH_2\dot{C}O \\ \dot{C}H_2CH_2\dot{C}O &\rightarrow C_2H_4 + CO \end{aligned}$$

similar to that for the decomposition of *n*-butyl radical, ~30 kcal/mole (17). Simple R.R.K. theory estimates of the relative rates of the decarbonylation, and this decomposition suggests, however, that this latter process must have an Arrhenius *A* factor in excess of 10^{15}; the reaction is hence somewhat unreasonable. The onset of a second primary reaction, such as the formation of the alternate diradical $\dot{C}H_2CH_2COCH_2\dot{C}H_2$, is possibly a more reasonable explanation of this feature. Current studies on the photolysis at shorter wavelengths (18) may further elucidate this aspect of the mechanism.

The author wishes to acknowledge useful discussions with R. F. Klemm, W. A. Noyes, Jr., E. K. C. Lee, and A. A. Scala, and the technical assistance of D. N. Morrison.

1. S. W. BENSON and G. B. KISTIAKOWSKY. J. Amer. Chem. Soc. **64**, 80, (1942).
2. R. SRINIVASAN. J. Amer. Chem. Soc. **81**, 1546 (1959).
3. R. SRINIVASAN. J. Amer. Chem. Soc. **83**, 4344 (1961).
4. E. K. C. LEE. J. Phys. Chem. **71**, 2804 (1967).
5. F. E. BLACET and A. MILLER. J. Amer. Chem. Soc. **79**, 4327 (1957).
6. R. SRINIVASAN. J. Amer. Chem. Soc. **83**, 4348 (1961).

Can. J. Chem. Downloaded from www.nrcresearchpress.com by 210.87.254.42 on 09/05/12
For personal use only.

7. C. Y. MOK. J. Phys. Chem. **74**, 1432 (1970).
8. C. F. RUSBULT and E. K. C. LEE. J. Amer. Chem. Soc. In press.
9. C. C. BADCOCK, M. J. PERONA, G. O. PRITCHARD, and B. RICKBORN. J. Amer. Chem. Soc. **91**, 543 (1969).
10. R. G. SHORTRIDGE and E. K. C. LEE. J. Amer. Chem. Soc. **92**. 2228 (1970).
11. R. L. ALUMBAUGH, G. O. PRITCHARD, and B. RICKBORN. J. Phys. Chem. **69**, 3225 (1965).
12. P. J. WAGNER and R. W. SPOERKE. J. Amer. Chem. Soc. **91**, 4437 (1969).
13. R. F. KLEMM, D. N. MORRISON, P. GILDERSON, and A. T. BLADES. Can. J. Chem. **43**, 1934 (1965).
14. H. E. O'NEAL and S. W. BENSON. J. Phys. Chem. **72**, 1866 (1968).
15. S. W. BENSON. Thermochemical kinetics. J. Wiley and Sons, New York, 1968.
16. H. W. O'NEAL and S. W. BENSON. J. Chem. Phys. **36**, 2196 (1962).
17. J. A. KERR and A. F. TROTMAN–DICKENSON. Progress in reaction kinetics. G. Porter, *editor*. Pergamon Press, New York, 1961.
18. A. A. SCALA. Private communication.

Can. J. Chem. Downloaded from www.nrcresearchpress.com by 210.87.254.42 on 09/05/12
For personal use only.

Can. J. Chem. Downloaded from www.nrcresearchpress.com by 210.87.254.40 on 09/05/12
For personal use only.

Physicochemical properties of some new 1,5- and 5,5-alkyl-substituted barbituric acids

G. A. NEVILLE, H. W. AVDOVICH, AND A. W. BY
Research Laboratories, Food and Drug Directorate, Department of National Health and Welfare, Ottawa, Canada

Received January 28, 1970

The synthesis of six new barbituric acids **1***b*, **3***a*, **4***b*, **5**, and **6***b*, including the novel 5-hydroxy derivative **3***b*, is reported together with spectroscopic data (proton magnetic resonance, ultraviolet, and infrared) for these and for five related known barbiturates for which such data is lacking. An interesting occurrence of non-equivalence of the N-1 and N-3 CH_2(Et) protons in **3***b* is discussed.

Canadian Journal of Chemistry, 48, 2274 (1970)

Introduction

In the course of spectroscopic and fine structural studies of barbituric acid derivatives (1, 2), we have prepared several new barbiturates (**1***b*, **3***a*, **3***b*, **4***b*, **5**, and **6***b*) as model compounds. In addition to reporting the synthesis and various physical properties of these compounds, we also wish to report similar properties for several older related barbiturates for which such physicochemical data has not yet appeared in the literature. This set of barbiturates (**1–6**) affords an excellent basis for pharmacological studies by virtue of the progressive structural variation and isomeric character of the alkyl derivatives. These compounds may prove to be particularly useful in extending recently reported structure-activity relationships of barbiturates (3) and in the further elucidation of proposed mechanisms of barbiturate–ethanol interaction (4).

Discussion of Synthesis

The method most commonly used for the preparation of alkyl-substituted barbituric acids involves the condensation of monoalkyl or dialkyl malonic esters with urea or alkylated ureas in the presence of sodium ethoxide. Several procedures have been recorded (5, 6) which have culminated in a standard method for the preparation of barbituric acid (7) which uses molar proportions of the reactants in ethanol under reflux for 7 h. The merits of the method are its general applicability for the synthesis of 1,5-, 1,3,5-, 1,5,5-, or more simply alkyl-substituted barbiturates, the relative accessibility of substituted malonic esters, the generally high yields (70–98%) of barbiturates, and their purity, the latter merit being particularly important in pharmacological investigations (8).

The malonic ester condensations described in this paper were usually carried out using a slight molar excess of the urea. The sodium ethoxide reagent was prepared from absolute ethanol using a weight of freshly cut sodium equivalent to twice the number of moles of the urea to be used. Reaction mixtures that had been heated under reflux for 7 h or longer were left to stand overnight. Water was added to the solidified mixtures and heat was applied until dissolution of the salt-cake was complete. The warm solutions were then acidified to Congo red with concentrated hydrochloric acid and left to crystallize in a refrigerator.

The new alkyl-substituted barbiturates, 1-ethyl-5-methylbarbituric acid (**1***b*) and 1,3,5-triethylbarbituric acid (**3***a*), were prepared by methods similar to the standard malonic ester condensation (7). Although barbiturates having a single alkyl substituent at C-5 have been reported to be prone to air oxidation (9, 10), no difficulty with formation of oxidation by-products was experienced during the synthesis and purification of either **1***a* or *b*. In contrast, purification of the liquid barbiturate (**3***a*) was made very difficult by the presence of the 5-hydroxy derivative (**3***b*) in the distillate of **3***a*. Since little alteration of pure **3***a* occurs on long standing exposed to air under normal room conditions, it appears that oxidation of **3***a* may be favored by the ester condensation conditions of alkalinity and higher temperature.

Although the synthesis of 1,5-dimethylbarbituric acid (**1***a*) and of 1,5,5-trimethylbarbituric acid (**2***a*) has been reported in relatively recent years, no other physical data were reported for these compounds apart from melting range and the usual microanalyses. In addition to the barbiturates **1***a* and **2***a*, the long known barbitu-

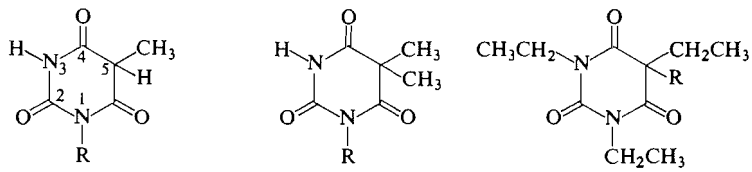

1

a R = CH_3
b R = CH_2CH_3

2

a R = CH_3
b R = CH_2CH_3

3

a R = H
b R = OH

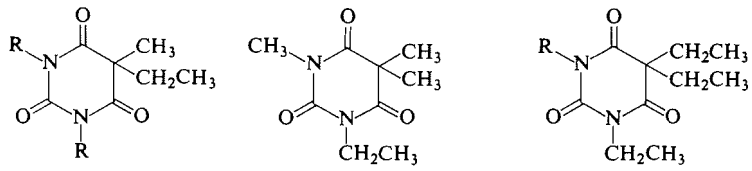

4

a R = H
b R = CH_3

5

6

a R = H
b R = CH_3

rates, 5 - ethyl - 5 - methylbarbituric acid (**4***a*), 1-ethyl-5,5-dimethylbarbituric acid (**2***b*), and 1,5,5-triethylbarbituric acid (**6***a*) were also prepared by the malonic ester condensation as precursors for 5-ethyl-1,3,5-trimethylbarbituric acid (**4***b*), 1-ethyl-1,5,5-trimethylbarbituric acid (**5**), and 1,5,5-triethyl-3-methylbarbituric acid (**6***b*) respectively, and their newly determined spectroscopic data are included in Tables 1 and 2 with those of the new compounds for comparison.

In spite of its general utility, the malonic ester condensation does possess some limitations for barbiturate synthesis. Fischer and Dilthey (11*a*) implied that *sym*-dialkylureas cannot be condensed with monoalkyl or dialkyl malonic esters while Cope *et al.* (12) demonstrated that monoalkyl malonic esters condense readily with *sym*-dimethylurea producing 1,3,5-trialkylbarbituric acids. The preparation of 1,3,5-triethylbarbituric acid (**3***a*) in this manner is interesting in that it constitutes an example of a more sterically hindered *sym*-dialkylurea condensing with a monoalkyl malonic ester. Like Cope *et al.* (12) who were unable to condense the dialkyl malonic ester, ethyl diethyl malonate, with *sym*-dimethylurea, we were also unable to prepare 5-ethyl-1,3,5-trimethylbarbituric acid (**4***b*) by condensing diethyl α-ethyl-α-methyl malonate with *sym*-dimethylurea. Whereas Bush and Butler (13) furnished evidence for ring cleavage when they obtained *N*-diethylacetyl-*N*,*N*′-dimethylurea from 1,3 - dimethyl - 5,5 - diethylbarbituric acid (dimethylbarbital) by the action of 2 *N* aqueous sodium hydroxide, we found no evidence for ring degradation products of **4***b* in the proton magnetic resonance (p.m.r.) spectra of material extracted with chloroform from the acidified reaction mixture. Apparently no cyclization of the dialkyl malonic ester occurs with the *sym*-dimethylurea to form **4***b* under the conditions of the malonic ester condensation.

Three new *N*-methylated barbiturates were prepared. 5-Ethyl-1,3,5-trimethylbarbituric acid (**4***b*) and 1-ethyl-3,5,5-trimethylbarbituric acid (**5**) were prepared by the action of diazomethane on 5-ethyl-5-methylbarbituric acid (**4***a*) and 1-ethyl-5,5-dimethylbarbituric acid (**2***b*) respectively. 1,5,5-Triethyl-3-methylbarbituric acid (**6***b*) was obtained by treating 1,5,5-triethylbarbituric acid (**6***a*) with dimethyl sulfate using the mild conditions of a procedure developed by Bush and Butler (13). Since the p.m.r. spectra from the three compounds **4***b*, **5**, and **6***b* show the same chemical shift for the *N*-methyl proton signal as **1***a*, **2***a*, and other *N*-methyl barbiturates prepared by the malonic ester condensation, *N*-methylation, as opposed to *O*-methylation, by diazomethane and by dimethyl sulfate is predominant with these 5,5-dialkyl barbiturates. This generalization has been substantiated further by p.m.r. spectroscopic studies of several 1,3-dimethylbarbiturates obtained by various methylation techniques (14).

Discussion of the Spectral Data

The spectral data in Tables 1 and 2 are given primarily as a means of further identification and characterization of these very similarly substi-

Can. J. Chem. Downloaded from www.nrcresearchpress.com by 210.87.254.40 on 09/05/12
For personal use only.

Can. J. Chem. Downloaded from www.nrcresearchpress.com by 210.87.254.40 on 09/05/12
For personal use only.

TABLE 1

Chemical shifts (p.p.m.) downfield from TMS (internal reference) for various alkyl-substituted barbiturates

	Barbiturate substitution					C-5 Substitution*				*N*-Substitution*			
Compound	C-5	C-5	N-1	N-3	Solvent	CH_3	CH_3(Et)	CH_2(Et)	H	CH_3	CH_3(Et)	CH_2(Et)	H
1*a*	Me	H	Me	H	DMSO-d_6	1.37bd	—	—	3.70bq	3.07s	—	—	11.2s
1*b*	Me	H	Et	H	$CDCl_3$	1.60d	—	—	3.48q	—	1.20t	3.90q	9.2bs
2*a*	Me	Me	Me	H	$CDCl_3$	1.57s	—	—	—	3.30s	—	—	9.0bs
2*b*	Me	Me	Et	H	$CDCl_3$	1.55s	—	—	—	—	1.20t	3.92q	9.2bs
3*a*	Et	H	Et	Et	$CDCl_3$	—	0.93t	2.18q	3.42t	—	1.20t	3.95q	—
3*b*	Et	OH	Et	Et	$CDCl_3$	—	0.96t	1.96q	—	—	1.23t	3.96 3.92	†
3*b*	Et	OH	Et	Et	DMSO-d_6	—	0.78t	1.83q	—	—	1.12t	3.96	†
4*a*	Me	Et	H	H	DMSO-d_6	1.37s	0.78t	1.83q	—	—	—	—	11.3s
4*b*	Me	Et	Me	Me	$CDCl_3$	1.52s	0.80t	2.02q	—	3.30s	—	—	—
5	Me	Me	Et	Me	$CDCl_3$	1.53s	—	—	—	3.28s	1.20t	3.93q	—
6*a*	Et	Et	Et	H	$CDCl_3$	—	0.83t	2.03q	—	—	1.22t	3.98q	8.6vbs
7*b*	Et	Et	Et	Me	$CDCl_3$	—	0.77t	2.02q	—	3.33s	1.22t	4.00q	—

*Key: d, doublet; q, quartet; s, singlet; t, triplet; b, broad; o, octet; vb, very broad.
†OH: 3.68 (bs, $CDCl_3$); 6.07 (s, DMSO-d_6).

TABLE 2

The u.v. and i.r. spectroscopic data for various alkyl-substituted barbiturates

Compound	Substitution C-5	C-5	N-1	N-3	λ_{max}(MeOH)(mμ (ε))	ν_{NH}(cm^{-1})‖	$\nu_{C=O}$(cm^{-1})‖
1*a*	Me	H	Me	H	263(1540); 218(7370)	3225b	1700, 1680sh, 1665sh
1*b*	Me	H	Et	H	266(2200); 218(7230)	3200b*	1700sh,* 1685, 1675sh
2*a*	Me	Me	Me	H	218(7950)	3190b	1715, 1685, 1675sh
2*b*	Me	Me	Et	H	218(7960)	3200b	1720sh, 1715, 1680
3*a*	Et	H	Et	Et	270(940); 226(7020)	—	1705sh,‡ 1700sh, 1690sh, 1680
3*b*	Et	OH	Et	Et	229(5870)	—	1708sh,§ 1685
4*a*	Me	Et	H	H	209†(10100)	3205	1755, 1740, 1720, 1695
4*b*	Me	Et	Me	Me	225(7350)	—	1687, 1670sh
5	Me	Me	Et	Me	225(7230)	—	1690
6*a*	Et	Et	Et	H	219(7500)	3205b	1705, 1685sh, 1675
6*b*	Et	Et	Et	Me	226(6960)	—	1680‡

*The i.r. data for the solid m.p. 148.2–149.0 (prec.).
†Shoulder, λ estimated for inflection point.
‡The i.r. spectra taken from liquid films.
§The i.r. spectra in CCl_4, γ_{OH} (free) 3530, and γ_{OH} (assoc.) 3450 and 3500 cm^{-1}.
‖Key: b, broad; sh, shoulder.

tuted barbiturates. The p.m.r. spectroscopy provides the best means of differentiating between these compounds, and the chemical shift values obtained for these derivatives are consistent with earlier published values (1, 2). It is noteworthy that the lone proton at C-5 in the C-5 monoalkylated barbiturates (**1***a*,*b*, and **3***a*) is seen as either a quartet (J = 7.5 Hz) or a triplet (J = 5.5 Hz) due to vicinal coupling with the adjacent methyl or methylene protons respectively.

The p.m.r. spectral features of 5-hydroxy-1,3,5-triethylbarbituric acid (**3***b*) are particularly interesting in that non-equivalence of the N-1 and N-3 protons is indicated by two sets of quartets centered at 3.96 and 3.92 p.p.m. ($CDCl_3$). This feature persists on addition of D_2O to the chloroform solution. An attractive model to account for this apparent non-equivalence is one in which the C-5 OH group is engaged in a weak σ–π hydrogen bond with one of the neighboring carbonyl oxygen atoms. The appearance of a single quartet for the four CH_2(Et) protons of **3***b* in DMSO-d_6 seems consistent with such a model in which the intramolecular hydrogen bonding could be disrupted by formation of an intermolecular hydrogen bond with DMSO. The situation appears to be more complex than suggested, however, since infrared (i.r.) spectra of **3***b* in CCl_4 solution, while showing both one free ν_{OH} band at 3530 cm^{-1} and associated ν_{OH} bands at 3450 and 3500 cm^{-1}, also show decreasing intensity of the associated ν_{OH} bands with retention of the free ν_{OH} band upon dilution.

The hydroxylated compound (**3***b*) also shows some fine structural features in further weak coupling ($J \lesssim 0.5$ Hz in both $CDCl_3$ and DMSO-d_6) in the signals for the C-5 CH_3(Et) and CH_2(Et) protons. Long-range coupling (^4J) of the CH_2(Et) protons with the hydroxyl protons is not responsible for these features since they persist with D_2O exchange.

Experimental

Apparatus

The p.m.r. spectra were obtained with a Varian A-60A spectrometer from solutions (solvents indicated in Table 1) 10–15% by weight in solute. No concentration effects were observed upon dilution, and chemical shifts, reported in p.p.m. downfield from tetramethylsilane (TMS) internal reference, are considered accurate to ± 0.02 p.p.m.

Ultraviolet (u.v.) spectra were obtained with a Beckman DK-2 recording spectrophotometer using 0.1 cm cells. Approximately 1 mg samples were weighed accurately on a Sartorius (MPR5) microgram balance and prepared as methanolic solutions in 10 ml volumetric flasks. Molecular extinction coefficients (ε) were calculated on the basis of absorption values corrected for blank absorption.

The i.r. spectra were obtained with a Perkin–Elmer model 621 grating spectrometer from fluorolube mulls except in two instances (Table 2) where films were used, and once where solutions were prepared.

Melting point determinations were made using different equipment indicated in abbreviated form as follows: (K) for Kofler hot stage with microscope attachment, (TH) for Thomas Unimelt capillary apparatus, and (prec.) for precision melting apparatus (15) containing Dow Corning 550 fluid and utilizing Anschutz immersion thermometers. All (K) and (TH) m.p. determinations are reported uncorrected.

Refractive indices were measured with a thermostated Abbe refractometer and were corrected on the basis of readings for distilled water.

Can. J. Chem. Downloaded from www.nrcresearchpress.com by 210.87.254.40 on 09/05/12
For personal use only.

Can. J. Chem. Downloaded from www.nrcresearchpress.com by 210.87.254.40 on 09/05/12
For personal use only.

Microanalyses were done either by Schwarzkopf Microanalytical Laboratory, Inc., 56-19 37th Ave., Woodside, New York 11377 or by Bernhardt Mikroanalytisches Laboratorium, 5251 Elbach uber Engelskirchen, Fritz-Pregl-Strasse 14-16, West-Germany.

Purity

All preparations were purified by crystallization or column chromatographic procedures until found free from starting materials and/or by-products by thin-layer chromatography (t.l.c.). The detailed t.l.c. procedures and development of new color detection methods particularly useful for tetra-substituted barbiturates will be reported later.

1,5-Dimethylbarbituric Acid (1a)

Diethyl methylmalonate (20.0 g, 0.115 mole, n_D^{20} 1.4134, Aldrich) was condensed with methylurea (8.6 g, 0.117 mole, m.p. 82–90° (TH), Aldrich) in absolute ethanol using sodium ethoxide. When a thick paste formed after the mixture had been heated under reflux for 4½ h, heating was stopped; the paste was dissolved by addition of water (150 ml), and the mixture was acidified and worked up in the usual way. The yield of product (m.p. 128–165° (K)) after a single recrystallization from water was 10.0 g (56%). Recrystallization from ethanol raised the m.p. to 138–152° (K) and three further recrystallizations from *iso*-propanol gave the constant m.p. 172.0–173.0° (prec.); lit. (16) m.p. 169–170°.

1-Ethyl-5-methylbarbituric Acid (1b)

Diethyl methylmalonate (20.0 g, 0.115 mole, n_D^{20} 1.4134, Aldrich) was condensed with ethylurea (10.3 g, 0.116 mole, m.p. 93–96° (TH), Aldrich) during 7 h heating under reflux in absolute ethanol with sodium ethoxide. The isolated dry solid (13 g, 66%; m.p. 144.2–146.2° (prec.)) was recrystallized from benzene to obtain the analytical sample, m.p. 146.8–147.5° (prec.).

Anal. Calcd. for $C_7H_{10}N_2O_3$: C, 49.41; H, 5.92; N, 16.46. Found: C, 49.67, 49.64; H, 6.16, 6.05; N, 16.30, 16.38.

1,5,5-Trimethylbarbituric Acid (2a)

Ethyl dimethylmalonate (10.0 g, 0.053 mole, $n_D^{25.0}$ 1.4105; lit. (17*a*) b.p. 88.7/21 mm, $n_D^{24.1}$ 1.41049) prepared by modification of the method for ethyl diethyl malonate (18*a*), was condensed with methylurea (4.0 g, 0.06 mole, m.p. 82–90° (TH), Aldrich) during 6½ h heating under reflux in absolute ethanol with sodium ethoxide. The crude product (9.0 g, 68%, m.p. 160–163° (K)) was recrystallized from chloroform–heptane (2:1) to give the analytical sample, m.p. 160.2–161.2° (prec.); lit. (19) m.p. 161–162°.

1-Ethyl-5,5-dimethylbarbituric Acid (2b)

Ethyl dimethylmalonate (10.0 g, 0.053 mole, $n_D^{25.0}$ 1.4110) was condensed with ethylurea (4.9 g, 0.06 mole, m.p. 92–94°, Aldrich) during 6 h heating under reflux in absolute ethanol with sodium ethoxide. The crude solid (m.p. 144–150° (K)) was recrystallized from chloroform–petroleum, ether (b.p. 30–60°) (1:1) to obtain solid (9.7 g, 51%) m.p. 148.2–149.0° (prec.). The t.l.c. analysis in three different solvent systems on silica gel indicated the compound to be pure. Seven months later, this material was found to melt 144–145° (K), and after two recrystallizations from absolute ethanol, the solid gave the constant m.p. 142.0–144.5° (TH).

Anal. Calcd. for $C_8H_{12}N_2O_3$: C, 52.17; H, 6.57; N, 15.21. Found: C, 52.80, 53.01; H, 6.71, 6.78; N, 15.16, 15.13 (Schwarzkopf).

Another portion of the low melting material was recrystallized from a dilute solution of absolute ethanol to obtain a fresh analytical sample for independent microanalysis. One recrystallization yielded cubic crystals m.p. 144.0° which appeared to undergo thermal transformation to give solid m.p. 157–159.5° (TH). A second recrystallization reproduced lower melting needles which showed slight softening at 142.6° followed by m.p. 147.8–149.2° (prec.). Again t.l.c. indicated the solid to be pure. Analysis of this material gave C, 52.35, 52.31; H, 6.36, 6.34; N, 14.65, 14.68 (Bernhardt).

Solid state i.r. spectra obtained on these needles were identical to similarly prepared spectra from the much earlier fraction, m.p. 148.2–149.0° (prec.). This compound appears to provide difficulties for microanalysis and appears to undergo relatively easy solid phase transformation. Unfortunately, succeeding attempts to obtain a higher melting form for i.r. characterization have failed.

1,3,5-Triethylbarbituric Acid (3a)

Diethyl ethylmalonate (20.0 g, 0.106 mole, n_D^{20} 1.4164, Aldrich) was condensed with *sym*-diethylurea (13.5 g, 0.117 mole, m.p. 108–111°, Aldrich) during 10 h heating under reflux in absolute ethanol with sodium ethoxide. Ethanol was then slowly distilled off at atmospheric pressure until a pasty residue formed. When water (100 ml) was added to the residue followed by addition of dilute sulfuric acid (7 ml concentrated H_2SO_4 in 100 ml H_2O), an oil layer formed. The mixture was extracted with chloroform and the combined extracts were dried overnight over $MgSO_4$. An oil (b.p. 90–102°/9 mm, $n_D^{25.0}$ 1.4867) was obtained by vacuum distillation of the combined extracts. On redistillation at high vacuum, the crude oil gave a fraction of 3*a* (b.p. 75–84°/0.2 mm, $n_D^{25.0}$ 1.4850) which was found to contain a small quantity of the by-product 3*b* present in larger quantity in the high boiling residue remaining from the first distillation of reaction products.

The impure oil (3*a*) was purified by column chromatography utilizing silica gel (Baker Analyzed Reagent) and benzene–acetone (40:1), purification being followed by t.l.c. (silica gel GF; benzene–acetone 20:1; detection by short wave u.v. light). All fractions were stripped of solvent at less than 30° by rotary evaporation; the concentrates so obtained were transferred to test tubes with the aid of benzene and further reduced in volume under a stream of dry nitrogen at room temperature after which residual solvent was removed under high vacuum. The oily fractions were stored under nitrogen at 3°. Combined fractions of the chromatographed oil (~3 ml) were slowly distilled in a Spath oven (80°/0.2 mm) to remove any traces of solvent. The freshly distilled oil, protected by nitrogen, was immediately examined by t.l.c. and found to be pure. Other physical parameters including $n_D^{25.0}$ 1.4855 were also immediately determined, and samples of the fresh material were sealed under nitrogen.

Anal. Calcd. for $C_{10}H_{16}N_2O_3$: C, 56.59; H, 7.60; N, 13.20. Found: C, 56.50, 56.56; H, 7.63, 7.52; N, 13.02, 13.05.

Can. J. Chem. Downloaded from www.nrcresearchpress.com by 210.87.254.40 on 09/05/12
For personal use only.

When left standing in air at room temperature, the pure colorless oil (**3***a*) was observed to develop a pale yellow color over a period of a few weeks and showed some formation of **3***b* by t.l.c.

5-Hydroxy-1,3,5-Triethylbarbituric Acid (3b)

The high boiling residue remaining from the initial distillation of **3***a* formed a sticky crystalline deposit on standing a few days. Three recrystallizations of this material from heptane gave the analytical sample, m.p. 63.2–64.5° (prec.).

Anal. Calcd. for $C_{10}H_{16}N_2O_4$: C, 52.62; H, 7.07; N, 12.27. Found: C, 52.61, 52.49; H, 6.91, 7.08; N, 12.43, 12.27.

N-Methylation by Diazomethane

Ethereal solutions of diazomethane were prepared from Diazald (Aldrich) according to the method of de Boer (20) and used immediately.

5-Ethyl-5-methylbarbituric Acid (4a)

Diethyl α-ethyl-α-methylmalonate (20.0 g, 0.099 mole, b.p. 52–58°/0.5 mm, $n_D^{25.0}$ 1.4172; lit. (17*b*) b.p. 102°/17 mm, $n_D^{18.2}$ 1.41896) prepared from diethyl ethylmalonate and methyl iodide by modification of the method for preparing ethyl diethylmalonate (18*a*), was condensed with urea (6.0 g, 0.10 mole) in ethanolic sodium ethoxide according to Vogel's directions for diethylbarbituric acid (18*b*). The product was isolated in the usual way and recrystallized from absolute ethanol to obtain solid, m.p. 212.2–213.4° (prec.); lit. (11*b*) m.p. 212°.

5-Ethyl-1,3,5-trimethylbarbituric Acid (4b)

5-Ethyl-5-methylbarbituric acid (**4***a*) (1.50 g, 0.0088 mole, m.p. 212.2–213.4° (prec.)) was treated in methanolic solution (25 ml) with excess ethereal diazomethane. The oil obtained on evaporation of the ethereal solution crystallized after standing at room temperature for a few days to give solid (1.74 g) m.p. 38–47° (TH). Two recrystallizations from heptane gave the constant m.p. 53.8–54.9° (prec.).

Anal. Calcd. for $C_9H_{14}N_2O_3$: C, 54.54; H, 7.11; N, 14.13. Found: C, 54.35, 54.27; H, 7.10, 7.04; N, 14.57, 14.32.

1-Ethyl-3,5,5-trimethylbarbituric Acid (5)

A solution of 1-ethyl-5,5-dimethylbarbituric acid (**2***b*) (3.0 g, 0.015 mole) in methanol (50 ml) was treated with excess ethereal diazomethane at 0°. On evaporation of the ethereal solution a yellow oil was obtained. High-vacuum distillation of the oil gave a fraction (b.p. 64–68°/0.4 mm) which crystallized immediately in the receiver. This solid (m.p. 34–39° (TH)) was recrystallized twice from heptane to obtain the analytical sample (1.75 g, m.p. 39.2–40.8° (prec.)).

Anal. Calcd. for $C_9H_{14}N_2O_3$: C, 54.54; H, 7.11; N, 14.13. Found: C, 54.81, 54.65; H, 7.21, 7.39; N, 14.19, 14.39.

1,5,5-Triethyl-3-methylbarbituric Acid (6b)

The mild conditions of the reaction developed by Bush and Butler (13) for the preparation of tetraalkylbarbituric acids were employed. 1,5,5-Triethylbarbituric acid (**6***a*) (5.0 g, 0.024 mole, m.p. 91.0–92.2° (prec.); lit. (21) m.p. 93°), prepared by condensation of ethyl diethylmalonate and ethylurea with sodium ethoxide in absolute ethanol, was suspended in aqueous sodium hydroxide (2 *N*, 14 ml, 0.024 mole). Dimethyl sulfate (2.4 ml, 0.024 mole, BDH 98% reagent) was added in portions to the reaction mixture followed by addition of chloroform (35 ml). The mixture was shaken mechanically for 2½ h after which the chloroform phase was separated. The chloroform phase was first shaken with aqueous sodium hydroxide (2 *N*, 15 ml) for 1 min, washed with water until neutral, and then dried over $MgSO_4$. Following vacuum distillation, **6***a* was obtained (b.p. 77–78°/0.45 mm, $n_D^{25.0}$ 1.4793).

Anal. Calcd. for $C_{11}H_{18}N_2O_3$: C, 58.39; H, 8.02; N, 12.38. Found: C, 58.44, 58.26; H, 8.33, 8.03; N, 12.62, 12.36.

We are grateful to Dr. O. E. Edwards of the National Research Council of Canada, Ottawa for the loan of a Spath oven.

1. G. A. Neville and D. Cook. Can. J. Chem. **47**, 743 (1969).
2. H. W. Avdovich and G. A. Neville. Can. J. Pharm. Sci. **4**, 51 (1969).
3. G. Hansch and S. M. Anderson. J. Med. Chem. **10**, 745 (1967); G. Hansch, A. R. Steward, S. M. Anderson, and D. Bentley. J. Med. Chem. **11**, 1 (1968).
4. G. S. Wiberg, B. B. Coldwell, and H. L. Trenholm. J. Pharm. Pharmacol. **21**, 232 (1969). G. S. Wiberg, H. L. Trenholm, and B. B. Coldwell. Toxicol. Appl. Pharmacol. **16**, 718 (1970). B. B. Coldwell, G. S. Wiberg, and H. L. Trenholm. Can. J. Physiol. Pharmacol. **48**, 254 (1970).
5. D. J. Brown. The chemistry of the pyrimidines. *Consulting editor* A. Weissberger. Interscience Publ. New York, 1962.
6. R. Ya. Levina and F. K. V. Velichko. Russ. Chem. Rev. **29**, 439 (1960), (in English).
7. J. B. Dickey and A. R. Gray. Organic syntheses. Coll. Vol. II. *Edited by* A. H. Blatt, 1943. p. 60.
8. H. Goldhahn. Pharm. **8**, 1016 (1953).
9. A. W. Dox. J. Amer. Chem. Soc. **53**, 1559 (1931).
10. T. Nishikawa. Mem. Ryojun Coll. Eng. **3**, 277 (1931); Chem. Abstr. **25**, 5390 (1931).
11. E. Fischer and A. Dilthey. (*a*) Ann. **335**, 334 (1904); (*b*) Ann. **335**, 343 (1904).
12. A. C. Cope, D. Heyl, D. Peck, E. Eide, and A. Arroyo. J. Amer. Chem. Soc. **63**, 356 (1941).
13. M. T. Bush and T. C. Butler. J. Pharmacol. **61**, 139 (1937).
14. G. A. Neville. Anal. Chem. **42**, 347 (1970).
15. E. B. Hershberg. Ind. Eng. Chem. Anal. Ed. **8**, 312 (1936).
16. H. Tsukamoto, H. Yoshimura, and S. Toki. Pharm. Bull. (Japan), **4**, 366 (1956).
17. K. V. Auwers. (*a*) Ber. **46**, 509 (1913); (*b*) Ber. **46**, 510 (1913).
18. A. I. Vogel. Practical organic chemistry. 3rd Ed. Longmans, Green & Co., 1956. (*a*) p. 1002; (*b*) p. 1003.
19. S. O. Ericksson and A. Holmgren. Acta Pharm. Suec. **2**, 293 (1965).
20. T. J. de Boer. Rec. Trav. Chim. **73**, 229 (1954).
21. A. W. Dox and A. M. Hjort. J. Pharmacol. **31**, 455 (1927).

Can. J. Chem. Downloaded from www.nrcresearchpress.com by 210.87.254.42 on 09/05/12
For personal use only.

The photolysis of azomethane in the presence of HN_3[1]

R. S. KONAR AND B. DEB. DARWENT
The Martin Maloney Chemistry Laboratory, The Catholic University of America, Washington, D.C. 20017

Received January 19, 1970

The photolysis of azomethane by 3660 Å light at 25 °C, has been used as the source of CH_3 to investigate their reactions with HN_3. CH_3 reacts rapidly with HN_3 to produce CH_4 with $k = 8.9 \times 10^4$ M^{-1} s^{-1}. The addition of CH_3 to the double bonds in HN_3 is much slower. The mechanism by which N_3 radicals disappear has been discussed.

Canadian Journal of Chemistry, 48, 2280 (1970)

Introduction

Some results obtained (1)[2] in a study of the photolysis of HN_3 and the fact that Woolley and Back (2) have shown that CH_3 reacted with HNCO extremely slowly, if at all, led us to investigate briefly the reactions of CH_3 with HN_3.

Experimental

The azomethane (Merck, Sharp & Dohme, Canada, Ltd.) contained traces of CH_4, C_2H_6, C_2H_4, and two unidentified high boiling hydrocarbons as shown gas chromatographically (18 ft 25% squalane column at 25 °C). The low boiling hydrocarbons were removed from the azomethane by degassing and fractionation. The hydrocarbons were Phillips research grade. Because of traces of impurities present in the reactants, it was necessary to analyze the reactants before and after photolysis for the quantitative estimation of products. Hydrogen azide was prepared by distilling a mixture of sodium azide and stearic acid (1:5 by weight) in vacuum at 100 °C, and finally dried by passing the HN_3 vapor through a tower packed with P_2O_5. Two columns: (*i*) 30 in. long silica gel (80–100 mesh) at 85 °C and (*ii*) 18 ft long squalane (25% squalane on 60–80 mesh chromosorb P) at 25 °C, were used for the analysis of the products. A flame ionization detector was used to estimate the hydrocarbons. Nitrogen was estimated mass spectrometrically after collecting the uncondensable gases at −192 °C.

The reaction was investigated in a conventional circulating system of total volume 826 ml. The photolysis occurred in a cylindrical Pyrex reaction vessel (200 ml) with an Osram Spectral Hg lamp as the source of radiation. The outer cover of the Hg lamp was Pyrex and transmits light above 2800 Å. The lamp was run off a Sola constant-voltage transformer, and was used without and with a Corning Pyrex 2 mm thick filter (0–52) which transmits above 3400 Å. To check the constancy of the intensity of light, a fixed amount of azomethane (20 mm Hg) was photolyzed from time to time, and the products (N_2, C_2H_6, and CH_4) were estimated quantitatively. The intensity was assumed not to alter significantly as long as the results were reproducible to within 5%.

Results and Discussion

The only products detected were N_2, CH_4, and C_2H_6; neither H_2 nor HCN were detected and, if present, amounted to less than 1% of N_2; neither NH_3 nor CH_3N_3 were detected and, if present, could have escaped detection due to the formation of CH_3N_4H or lost in the tail of the HN_3 peak.

The results are given in Table 1. It is evident that the addition of quite small quantities of HN_3 causes a considerable decrease in C_2H_6 and an increase in CH_4. Those effects are illustrated in Figs. 1 and 2. Figure 1 shows clearly that, although small quantities of HN_3 reduce C_2H_6 drastically, the rate of formation of C_2H_6 becomes independent of HN_3 at large concentrations, and does not approach zero as $[HN_3] \rightarrow \infty$.

The following reactions

[*a*] $CH_3N{=}NCH_3 + h\nu \rightarrow 2CH_3 + N_2$

[*b*] $\rightarrow C_2H_6 + N_2$

[1] $2CH_3 \rightarrow C_2H_6$

[2] $CH_3 + CH_3N{=}NCH_3 \rightarrow CH_4 + CH_3N{=}NCH_2$

are known to occur in the photolysis of azomethane. Since the quantity $\beta = N_2/(C_2H_6 + \frac{1}{2} CH_4)$ is invariably greater than unity, other reactions, e.g.

[2′] $CH_3 + CH_3N{=}NCH_3 \rightarrow (CH_3)_2N{-}NCH_3$

and

[2″] $CH_3 + R \rightarrow CH_3R$

where R is $CH_3N{=}NCH_2$ or $(CH_3)_2N{-}NCH_3$, have also been postulated to explain the "loss" of CH_3, i.e. that $\beta > 1.0$.

[1]This research was supported by the Petroleum Research Fund, administered by the American Chemical Society, under Grant No. PRF 2498-C.

[2]Presented at the American Society Meeting, Minneapolis, Minnesota, 1969.

TABLE 1

The photolysis of azomethane in the presence of HN_3 at 3660 Å and 28 ± 3 °C

Reactants (Torr)		Products (M min^{-1} × 10^7)					
$CH_3N{=}NCH_3$	HN_3	N_2	C_2H_6	CH_4	N_2^{corr}*	α†	β‡
20	0	2.86	2.53	0.057	2.86		1.11
0	10	0.18	—	—	—		—
0	20	0.26	—	—	—		—
0	52	0.28	—	—	—		—
20	3.5	3.51	0.96	2.47	3.48	0.53	1.30
20	5.5	—	0.61	3.02	—	—	—
20	5.5	3.96	0.63	3.13	3.91	0.52	1.31
20	10	6.52	0.28	3.67	6.43	0.77	1.35
20	20	6.90	0.11	4.58	6.77	0.69	1.19
20	51	7.01	0.07	4.90	6.87	0.65	1.13

*$N_2^{corr} = N_2 - \frac{1}{2}$ the N_2 produced in the photolysis of HN_3 alone.
†$\alpha = N_2/(N_2^0 + \frac{1}{2} CH_4)$.
‡$\beta = N_2^0/(C_2H_6 + \frac{1}{2} CH_4)$; $N_2^0 = N_2$ produced in the photolysis of $CH_3N = NCH_3$.

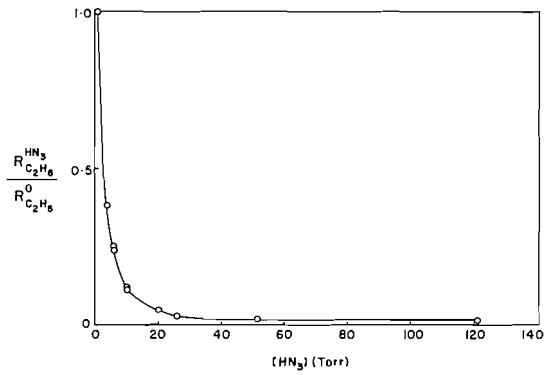

FIG. 1. The effect of $[HN_3]$ on the rate of formation of C_2H_6 at 3660 Å and 25 °C (rates in M s^{-1}). $R_{C_2H_6}^{HN_3}$ = the rate of formation of C_2H_6 in the presence of HN_3 alone. $R_{C_2H_6}^{0}$ = the rate of formation of C_2H_6 in the absence of HN_3.

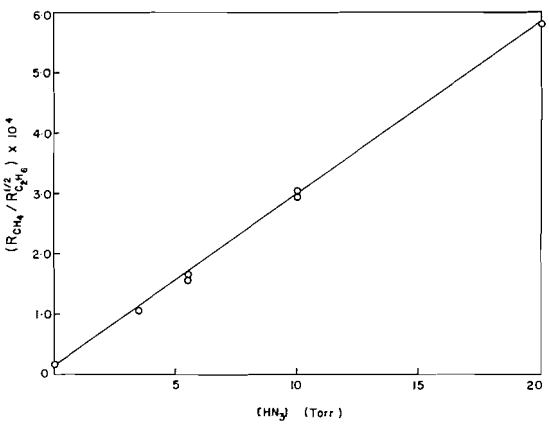

FIG. 2. The effect of $[HN_3]$ on the ratio of $R_{CH_4}/R_{C_2H_6}^{1/2}$ at 25 °C and 20 Torr of azomethane.

The results of the present investigation give $\phi_b = 0.013 \pm 0.01$, which is consistent with the value 0.01 ± 0.01 obtained by O_2 inhibition and other methods (3). Preliminary experiments showed $\beta = 1.10 \pm 0.03$ at 20 Torr of $CH_3N{=}NCH_3$ compared with 1.09 and 1.15 found (4, 5) previously under similar conditions. The ratio $k_2/k_1^{1/2}$ was 1.33×10^{-3} $M^{-1/2}$ s$^{-1/2}$, identical with that found previously (4), and, adopting Shepp's value (6) of 2.2×10^{10} M^{-1} s^{-1} for k_1, leads to $k_2 = 1.95 \times 10^2$, in excellent agreement with Gray and Thynne's value (7) of 1.74×10^2 M^{-1} s^{-1} extrapolated to 25 °C.

The marked effect of HN_3 on the rates of formation of C_2H_6 and CH_4 show that the reaction

[3] $$CH_3 + HN_3 \rightarrow CH_4 + N_3$$

is rapid at 25 °C. The linearity of the relationship between $CH_4/C_2H_6^{1/2}$ and $[HN_3]$ (Fig. 2), where the C_2H_6 has been corrected for that produced in reaction [*b*], shows that reactions [1], [2], and [3] account adequately for the formation of CH_4 and C_2H_6 from CH_3. The slope of the line in Fig. 2 gives $k_3 = 8.9 \times 10^4$ M^{-1} s^{-1}, based on $k_1 = 2.2 \times 10^{10}$ M^{-1} s^{-1}.

It was not feasible, because of the thermal instability of HN_3 and the vapor pressures of the reactants at low temperatures, to investigate the effect of a suitably wide range of temperature on k_3. However, the pre-exponential factors for reactions of CH_3 with NH_3, N_2H_4, and $CH_3N{=}NCH_3$ are all (7) close to 10^8 M^{-1} s^{-1}, and, if that is so for HN_3, we find $E_3 = 4.2$ kcal mole^{-1}. In view of the uncertainties inherent in this calculation, we suggest $E_3 = 4.2 \pm 0.5$ kcal mole^{-1}.

Can. J. Chem. Downloaded from www.nrcresearchpress.com by 210.87.254.42 on 09/05/12
For personal use only.

Can. J. Chem. Downloaded from www.nrcresearchpress.com by 210.87.254.42 on 09/05/12
For personal use only.

An unexpected observation (Table 1) is the increase of β on the addition of HN_3 up to 10 Torr. This is unexpected since the magnitude of k_3 is such that essentially none of the CH_3 should have reacted by [2] or [2′], so that β should have decreased from 1.10 to 1.00 instead of increasing up to 1.33 ± 0.03. The increasing loss of CH_3 requires that it react either with HN_3 to form products which do not include CH_4 or C_2H_6 or with the N_3 produced in reaction [3]. Those processes would be

$$[3'] \qquad CH_3 + HN_3 \rightarrow HN_3CH_3$$

in which CH_3 adds to one of the π bonds, and

$$[4] \qquad CH_3 + N_3 \rightarrow CH_3N_3$$

in which the product is "chemically activated" and may either decompose or be deactivated.

The first possibility, reaction [3′], may be discarded since β decreases with further increase of $[HN_3]$, to 1.07 at 50 Torr, and the results are not inconsistent with $\beta \rightarrow 1.00$ as $[HN_3] \rightarrow \infty$. Hence the only possible explanation for the effect of moderate $[HN_3]$ on β is reaction [4].

Information about the manner in which the N_3 disappears has been provided by flash-photolysis studies (8) with HN_3 which showed the process to be second order in $[N_3]$. Consequently the reaction

$$[5] \qquad 2N_3 \rightarrow 3N_2$$

is reasonably well established. That observation also suggests that N_3's do not disappear by reaction with HN_3. However, in the present experiments they may react with $CH_3N{=}NCH_3$ either to form HN_3 by abstracting H or to add to the N=N bond to form an unknown product which may well have escaped detection.

The suggestion that the N_3 disappears by reaction [4] or by reaction with $CH_3N{=}NCH_3$ in addition to reaction [5] receives support from the effect of $[HN_3]$ on the rate of formation of N_2. If all N_3 disappeared by reaction [5], then the rate of formation of N_2 should be $N_2{}^0 + \frac{3}{2} CH_4$, where $N_2{}^0$ is the rate of formation of N_2 in reactions [*a*] and [*b*]. The column $\alpha = N_2/(N_2{}^0 + \frac{3}{2} CH_4)$ in Table 1 shows that the N_2 recovered was between 23 and 48% less than expected and so the N_3 must disappear by reaction [4] or by reaction with $CH_3N{=}NCH_3$. At high $[HN_3]$ when $\beta \rightarrow 1.00$ and essentially all CH_3's disappear by reaction [3], we find that there is still a marked deficiency in N_2; indeed, the quantity α does not increase consistently with $[HN_3]$. Accordingly, a significant fraction (10–50%) of the N_3 must disappear by reacting with $CH_3N{=}NCH_3$ in a manner such that N_2 is not formed.

1. R. S. Konar, S. Matsumoto, and B. deB. Darwent. To be published.
2. W. D. Woolley and R. A. Back. Can. J. Chem. **46**, 295 (1968).
3. R. E. Rebbert and P. J. Ausloos. J. Phys. Chem. **66**, 2253 (1962). A. Good and J. C. J. Thynne. Trans. Faraday Soc. **63**, 2708 (1967). S. Toby and J. Nimoy. J. Phys. Chem. **70**, 867 (1970). L. Herk, M. Feld, and M. Szwarc. J. Amer. Chem. Soc. **83**, 2998 (1961). D. G. L. James and R. D. Suart. Trans. Faraday Soc. **65**, 175 (1969).
4. S. Toby and B. J. Weiss. J. Phys. Chem. **68**, 2492 (1964).
5. M. H. Jones and E. W. R. Steacie. J. Chem. Phys. **21**, 1018 (1953).
6. A. Shepp. J. Chem. Phys. **24**, 939 (1956). H. E. van den Berg, A. B. Callear, and R. J. Norstrom. Chem. Phys. Lett. **4**, 101 (1969).
7. P. Gray and J. C. J. Thynne. Trans. Faraday Soc. **60**, 1047 (1964).
8. B. A. Thrush. Proc. Roy. Soc. London. Ser. A. **235**, 143 (1956).

Can. J. Chem. Downloaded from www.nrcresearchpress.com by 210.87.254.6 on 09/05/12
For personal use only.

Broad-line nuclear magnetic resonance investigation of molecular motion in solid trimethylamine–halogen complexes

C. A. FYFE[1] AND J. RIPMEESTER[2]

Chemistry Department, University of British Columbia, Vancouver 8, British Columbia

Received February 18, 1970

Broad-line nuclear magnetic resonance studies of the charge-transfer complexes of trimethylamine (NMe_3) with iodine, bromine, and iodine monochloride indicate the presence of motion in the solid state. Trimethylamine itself was studied for purposes of comparison. The nature of the motional transitions for each species has been determined, and activation energies derived.

Canadian Journal of Chemistry, 48, 2283 (1970)

Introduction

Considerable interest has been shown, in recent years, in the structure and bonding of charge-transfer complexes in which the trimethylamine moiety acts as the electron donor. With halogen acceptors such as iodine, bromine, and iodine monochloride, the complexes formed are solids at room temperature. Single crystal X-ray measurements (1, 2) indicate that the nitrogen–halogen – halogen linkage is essentially linear and that the nitrogen–halogen and halogen–halogen bond lengths are slightly larger than their "normal" covalent values. Further implications of these studies, as well as additional experimental data, have been discussed and reviewed (3–5).

The purpose of the present work was to investigate possible molecular motions above 77 °K in the NMe_3–$(Halogen)_2$ complexes by the broad-line nuclear magnetic resonance (n.m.r.) method. For comparison, a study was made of NMe_3 itself between 77 °K and its melting point, as at the time the work was done no literature results were available.

Experimental

Materials

Consistent results were obtained from the following method of preparation of the complexes. An ice-cold solution of trimethylamine in absolute ethanol was added to an ethanolic solution of the appropriate halogen. Fine crystals of the complex separated from the solution immediately, and addition of the trimethylamine solution was continued until the characteristic halogen color disappeared. The product crystals were then filtered, washed with dry ether and air dried. Two samples of each complex were thus prepared; one sample was sealed in a 10 mm o.d. thin-walled glass tube under nitrogen. The second sample was recrystallized from methylene chloride at ~ -40 °C, dried and sealed in a similar tube. The samples were all kept under liquid nitrogen when not in use, since there was some tendency towards decomposition at room temperature. The thermal decomposition of the complexes has been studied (6) and the products characterized. One complex is also reported to be light sensitive (2).

Both samples of each complex gave analyses in satisfactory agreement with the proposed structure. Complete temperature runs were carried out on both samples of each complex, and both gave identical results.

Equipment and Procedure

The spectrometer used was a conventional crossed-coil type and has been previously described (7). The methods of data collection and treatment were also as in ref. 7. All calculations were carried out using Fortran IV programmes on an I.B.M. 360–67 computer.

Results and Discussion

Molecular Motion in Trimethylamine

The changes in linewidth and second moment of the proton resonance line of trimethylamine from 77 °K up to its melting point are shown in Fig. 1. It is evident from the temperature behavior of these parameters that a marked motional transition takes place, which is quite distinct from the melting transition. At 77 °K the spectrum showed the characteristic fine structure of a broadened, rigid, three-spin system (Fig. 1, inset). This fine structure disappeared at about 110 °K. The second moments change regularly from 30.5 G^2 at 77 °K to 2.7 G^2 at 140 °K. The general properties of the transition are similar to those reported recently by Haigh and co-workers (8). However, although there is good agreement in the reported linewidths, there is a significant difference in the limiting high-temperature second moment values (4.7 G^2 from ref. 8 c.f. 2.7 G^2 in the present study), which will be important in

[1]Present address: Department of Chemistry, University of Guelph, Guelph, Ontario, Canada.

[2]Present address: Department of Chemistry and Chemical Engineering, University of Illinois, Urbana, Illinois, U.S.A.

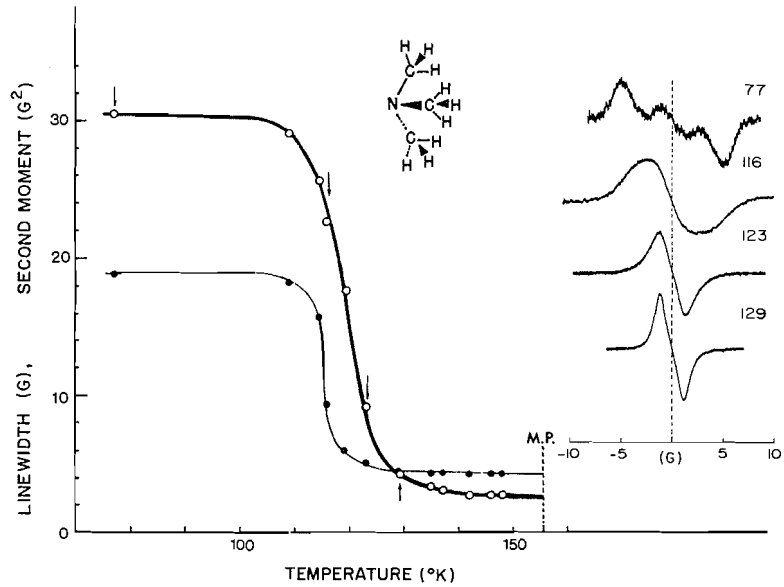

FIG. 1. The temperature dependence of the linewidth and second moment parameters of the proton resonance of solid trimethylamine with (inset) some representative spectra recorded at the positions on the second moment curve indicated by the vertical arrows.

determining the interpretation of the present results.

Molecular Motion in Trimethylamine–Bromine Complex ($NMe_3 \cdot Br_2$)

Changes of linewidth and second moments with temperature are shown together with some representative spectra in Fig. 2. As in the case of trimethylamine, the characteristic fine structure of the broadened three spin system observed at 77 °K disappears at about 130 °K near the linewidth transition. The second moment changes regularly from a value of 27.7 G^2 at 77 °K to 1.8 G^2 at 170 °K and remains constant from this temperature up to room temperature. The overall shape of the transition, and the limiting high and low temperature values of the linewidths and second moments, are very similar to those of trimethylamine itself.

Molecular Motion in Trimethylamine–Iodine (NMe_3–I_2) and Trimethylamine–Iodinemonochloride (NMe_3–ICl) Complexes

Figures 3 and 4 show the linewidth and second moment changes for $NMe_3 \cdot I_2$ and $NMe_3 \cdot ICl$, respectively. Again there are large spectral changes indicative of motional transitions, but these are quite different from those of NMe_3 itself and the $NMe_3 \cdot Br_2$ complex. The spectra at 77 °K both show fine structure characteristic of a rigid three-spin system, and this disappears during the linewidth transition. However, the linewidths and second moments do not decrease directly to their limiting high-temperature values, but show an intermediate step with a second moment value of 7–8 G^2. At higher temperatures, there is a second transition where the linewidths (l.w.) and second moments (s.m.) attain their limiting values (s.m. = 1.7 G^2, l.w. = 3.3 G for $NMe_3.I_2$ and s.m. = 1.9 G^2, l.w. = 3.3 G for $NMe_3 \cdot ICl$).

Calculated Second Moments

Complete theoretical second moments cannot be calculated a priori using Van Vleck's formula (9), because of the lack of structural data in the solid state for NMe_3 and $NMe_3 \cdot Br_2$ and the lack of data on the hydrogen co-ordinates of $NMe_3 \cdot I_2$ and $NMe_3 \cdot ICl$ whose structures are known. However, the data can be successfully interpreted by several more empirical approaches (Table 1). The relative hydrogen positions in the four complexes are similar enough for the four molecules to be considered together. It is convenient to divide the contributions to second moment into three: the contribution due to the interactions within a methyl group, $S1$; from interactions

Can. J. Chem. Downloaded from www.nrcresearchpress.com by 210.87.254.6 on 09/05/12
For personal use only.

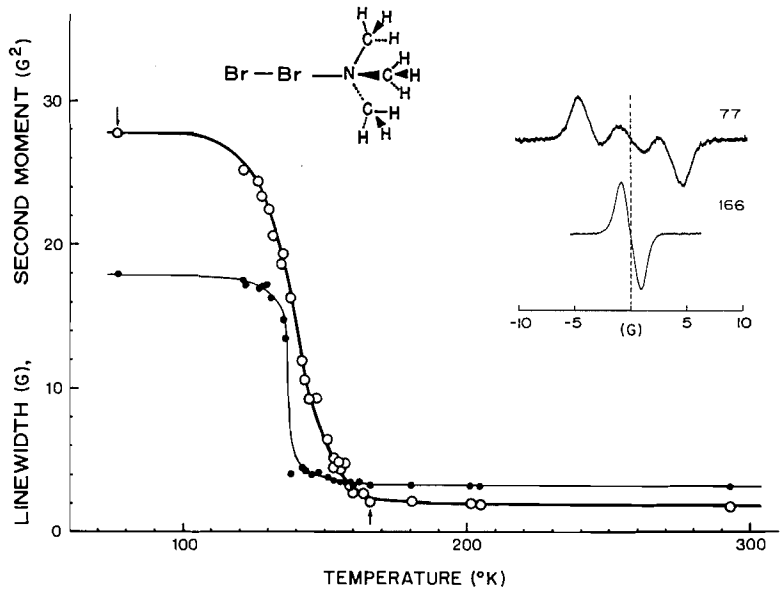

FIG. 2. The temperature dependence of the linewidth and second moment parameters of the proton resonance of the trimethylamine bromine complex with (inset) representative spectra recorded at the positions on the second moment curve indicated by the vertical arrows.

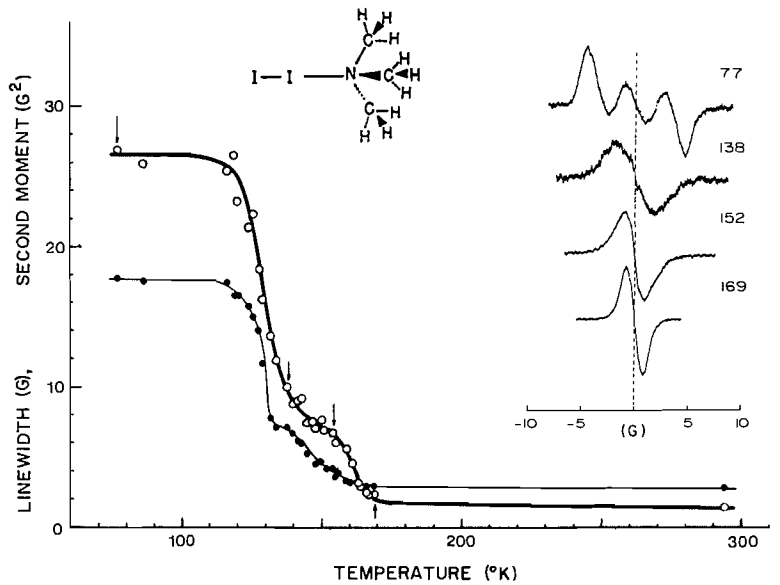

FIG. 3. The temperature dependence of the linewidth and second moment parameters of the proton resonance of the trimethylamine–iodine complex with (inset) representative spectra recorded at the positions on the second moment curve indicated by the vertical arrows.

between methyl groups on the same molecule, $S2$; and between methyl groups on different molecules, $S3$.

There are only two configurations of the hydrogens in an NMe_3 moiety which are consistent with C_{3v} symmetry; a form where three of the hydrogens are eclipsed with the C atoms and a form where they are staggered. The former involves hydrogen–hydrogen contacts less than the sum of the Van der Waals radii, and only the

Can. J. Chem. Downloaded from www.nrcresearchpress.com by 210.87.254.6 on 09/05/12
For personal use only.

Can. J. Chem. Downloaded from www.nrcresearchpress.com by 210.87.254.6 on 09/05/12
For personal use only.

TABLE 1

Observed second moment values (G^2) above and below motional transitions for NMe_3, $NMe_3 \cdot Br_2$, $NMe_3 \cdot I_2$, and $NMe_3 \cdot ICl$, and calculated values for different molecular motions

	NMe_3			$NMe_3 \cdot Br_2$			$NMe_3 \cdot I_2$			$NMe_3 \cdot ICl$		
	Second moment (G^2)		Temperature	Second moment (G^2)		Temperature	Second moment (G^2)		Temperature	Second moment (G^2)		Temperature
Motional type	Observed	Calculated*	(°K)	Observed	Calculated*	(°K)	Observed	Calculated*	(°K)	Observed	Calculated*	(°K)
Rigid lattice	30.5	31.9±2.0	77	27.7	28.0±2.0	77	27.1	28.18	77	28.0	29.29	77
Methyl rotation	—	—	—	—	—	—	7–8	7–8	148	7–8	7–8	195
Methyl rotation and rotation round NC_3 symmetry axis	2.7	2.7	143	1.8	2.1	170	1.7–1.9	2.1	295	1.7–1.9	2.1	295

*See text for details of the assumptions and approximations involved.

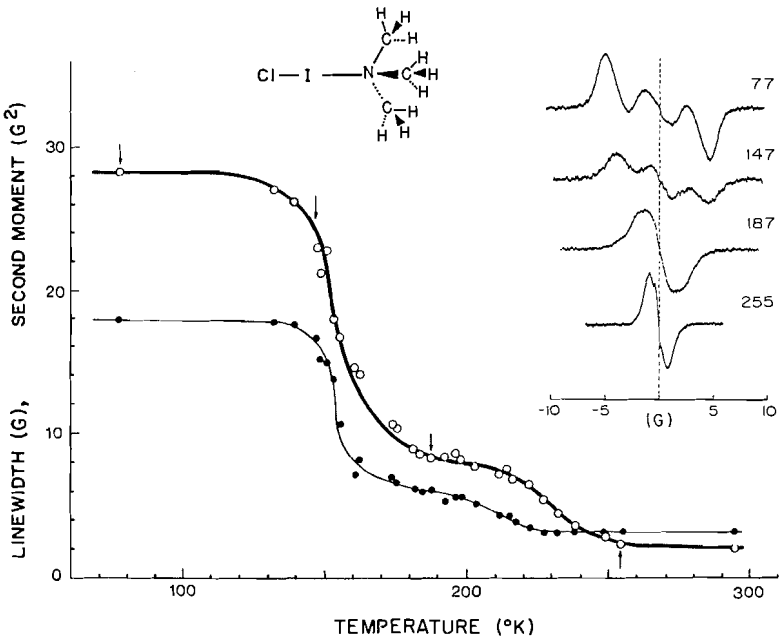

FIG. 4. The temperature dependence of the linewidth and second moment parameters of the proton resonance of the trimethylamine–iodinemonochloride complex with (inset) some representative spectra recorded at the positions on the second moment curve indicated by the vertical arrows.

latter is considered. Using this assumption and the microwave data for trimethylamine (10), the contributions $S1$ and $S2$ can be calculated exactly for this molecule ($S1 + S2 = 27.1$ G^2). The contribution $S3$ can, however, only be estimated. A value of 6.5 G^2 was found by Smith for the $S3$ contribution in $SiMe_4$ (11). Since there is one fewer methyl group in NMe_3, and nitrogen–methyl as well as methyl–methyl contacts, an approximate reduction by 25% may be reasonable, giving $S3 = 4.8 \pm 1$ G^2. Since $S3$ is a relatively small contribution to the total, the exact value will not be critical. The total second moment for NMe_3 will then be 31.9 ± 2 G^2, in good agreement with the experimental value of 30.5 ± 1 G^2 (Table 1).

It is also possible to obtain some information about the relative magnitudes of the intramethyl and intermethyl second moment contributions from the fine structure of the resonance line at 77 °K (12), although it is not known to what extent the approximations used hold in systems with a large intermethyl broadening. Assuming an intramethyl second moment of 22.5 ± 1.2 G^2 calculated from the microwave parameters, the best fit to the observed lineshape (Fig. 1, inset) is given by an intermethyl second moment contribution of 5.3–6.3 G^2, giving a total second moment value of 28.3 ± 2 G^2.

For the three halogen complexes, complete calculations can be performed for trimethylamine–iodine and trimethylamine – iodine monochloride, using the crystal structure data (1, 2), and assuming that the hydrogen atoms can be placed tetrahedrally around the carbons with a C—H bond length of 1.09 Å to give an overall C_{3v} symmetry. This procedure yields overall second moments of 28.18 and 29.29 G^2 for the iodine and iodine monochloride, respectively, in good agreement with the values found experimentally (Table 1). Consideration of the lineshapes at 77 °K as before (Figs. 2 and 3, inset), taking the intramethyl contribution as 22.5 G^2, gives total estimated second moments of 28 ± 1 G^2 for both complexes, in approximate agreement with the above values.

In the case of the trimethylamine–bromine complex, there are no structural data at all. However, it is expected to have a structure similar to the other two complexes, and its second moment could be approximated by using a value roughly equivalent to their values (~ 28 G^2).

Can. J. Chem. Downloaded from www.nrcresearchpress.com by 210.87.254.6 on 09/05/12
For personal use only.

Can. J. Chem. Downloaded from www.nrcresearchpress.com by 210.87.254.6 on 09/05/12
For personal use only.

There is some justification for this in the similarity of the second moments of the above two complexes both to each other, and also to trimethylamine, and in the fact that the experimental values are very similar for all the complexes (Table 1). The interpretation of the lineshape at 77 °K can, however, be made even though structural data are not available, assuming only that the intramethyl contribution is 22.5 G^2, giving a total second moment of ~ 28 G^2, similar to the other complexes.

Motional Effects

In the case of the motional transitions of trimethylamine itself and its bromine complex (Figs. 1, 2), the limiting high temperature second moments of 2.7 and 1.8 G^2, respectively, are too low to be explained simply by a rotation of the methyl groups around their threefold axes. The most satisfactory model would seem to be one where the methyl groups are rotating around their threefold axes, and the whole molecule is rotating about the molecular threefold symmetry axis. The intramethyl reduction factors may be calculated following Powles and Gutowsky (12). Assuming an angle of 71.3° between the N—C bonds and the molecular symmetry axis for trimethylamine (10), the reduced contribution is 0.7 G^2. The corresponding value for the bromine complex is also 0.7 G^2. The reduction in the remaining contributions for doubly rotating groups is more difficult to estimate. Koide (13) has calculated a reduction factor of $\frac{1}{4}$ for these interactions in hexamethylethane. Using this reduction factor yields intermethyl second moments of 2.0 and 1.4 G^2, and total reduced second moments of 2.7 and 2.1 G^2 for NMe_3 and $NMe_3 \cdot Br_2$, respectively. The satisfactory agreement between these values and those found experimentally (Table 1) is taken as evidence that the motional transition in these two species is in fact the onset of simultaneous rotation of the methyl groups about their threefold axes, and the whole molecule about its molecular symmetry axis. The recent investigation of trimethylamine by Haigh and co-workers (8), referred to in the introduction, gave a value of 4.6 G^2, and was interpreted as motion of the methyl groups with an additional contribution from oscillation about the molecular axis. However, it is felt that the experimental value quoted here is in accord both with the calculated reduced value and with the values found for the three halogen complexes (vide infra).

In the cases of the complexes with iodine and iodine monochloride (Figs. 3, 4), the first motional transition reduces the second moments to 7–8 G^2. This value is in accord with a reorientation of the methyl groups about their threefold axes, the rest of the molecule being stationary. Such a motion would reduce the intramethyl contribution by a factor of $\frac{1}{4}$, and the intermethyl contribution by a factor of 0.25–0.42 (13), giving a total reduced second moment of 7–8 G^2 for both complexes, in satisfactory agreement with the experimentally observed values. The second motional transition causes the second moments to drop to $\sim$ 1.8 G^2 in both cases, and can be interpreted as the onset of motion of the whole molecule around the molecular symmetry axis (Table 1) giving a reduced second moment of 1.7 G^2, as discussed above for the bromine complex.

Thus two distinct types of behavior are observed (Table 1). In NMe_3 and NMe_3–Br_2, the methyl group rotation and the rotation of the whole NMe_3 moiety seem to be very strongly coupled, and only one linewidth transition is observed. This type of motional transition is similar to that observed for Me_3CBr, Me_3CCl (12), and Me_3C—CMe_3 (13).

In the $NMe_3 \cdot I_2$ and $NMe_3 \cdot ICl$ complexes, however, the methyl group rotation and NMe_3 reorientation take place in two distinct steps. This type of behavior is observed for NMe_3—BF_3 (7), $Me_3S^+I^-$, $Me_3SO^+I^-$, Me_3NO (14) and has also been observed recently in several complexes of the type $NMe_3 \cdot BX_3$ (15). The reasons for this difference in behavior are difficult to determine. Unfortunately, in most cases, the crystal structures are not known, and no conclusions can be drawn about structural differences, which might account for these effects.

The X-ray investigations of these complexes show no evidence of motion which the n.m.r. indicates is taking place at room temperature. Thus, in these complexes, the motion must take place by a "jumping" mechanism between equivalent methyl sites. In view of the structural similarities between the compounds and the similarities in their spectra, this is probably true for all the compounds studied. In view of the molecular motions found, however, it would seem that the differences in bond lengths and angles to the different methyl groups found in the

TABLE 2

Motional types, limiting linewidths (G), and activation energies (kcal mole^{-1}) derived from the modified B.P.P. equation and activation energies (kcal mole^{-1}) estimated from Waugh's equation

Sample	Motional type	Linewidth		E_a	
		Low temperature	High temperature	Modified B.P.P.	Waugh equation
NMe_3	$CH_3 + NMe_3$	19.0	4.0–4.5	(6.6–8.4)±0.5*	4.25
$NMe_3 \cdot Br_2$	$CH_3 + NMe_3$	18.0	3.4	6.8±0.5	5.1
$NMe_3 \cdot I_2$	CH_3	17.8	7.2	6.9±0.4	4.4
	NMe_3	7.2	3.3	9.5±1.0	5.4
$NMe_3 \cdot ICl$	CH_3	17.9	6.6	6.2±0.5	5.6
	NMe_3	6.0	3.3	11.0±1.3	7.8

*Value is very dependent on the value of the limiting linewidth.

complexes (1, 2) are not real, but may be due to the errors inherent in the two dimensional analysis.

Activation energies

Activation energies were calculated for all the motional transitions observed by a least-square fitting of the linewidth transitions to the modified Bloembergen, Purcell, and Pound (B.P.P.) relationship (16). These are shown in Table 2 together with the description of the transitions derived above. Good fits were obtained in all cases, but the results must be approached with some degree of caution. Firstly, the relationship used is an empirical one, and the energies it gives have no absolute significance except for purposes of comparison within a series of related compounds. Furthermore, in the compounds studied here, there is a severe change in lineshape which accompanies the linewidth narrowing, and in some cases, different motional effects overlapped. For this reason, an even more empirical estimate of the energies using the Waugh estimate (17) of $V_0 = 37\,T$ (where T is the temperature of the transition) is also included in the table. The high values of the activation energies for methyl group rotation would tend to suggest that quantum mechanical tunneling through the potential barriers to rotation is relatively unimportant in the cases studied here.

The barrier to methyl group rotation in NMe_3 has been found by a number of methods (10, 18, 19). Thus a thermodynamic study, assuming a one dimensional potential energy barrier, yielded a value of 4.27 kcal mole^{-1} (18). A value of 4.4 kcal mole^{-1} was found from a study of the vibrational satellites in the microwave spectrum (10), and an infrared study of NMe_3 at 77 °K (19) yielded values of 4.13–5.19 kcal mole^{-1}, depending on the model chosen for the barrier.

The authors would like to thank the University of British Columbia for the award of a Killam Fellowship to C.A.F., the NRCC for the award of a studentship to J.R., and the Department of Chemistry, U.B.C. for the generous provision of facilities. They would also like to thank Professors C. A. McDowell and B. A. Dunell for their help and interest in this work and Dr. D. F. R. Gilson and Dr. C. T. Yim for the communication of results prior to their publication.

1. K. O. Strømme. Acta Chem. Scand. **13**, 268 (1959).
2. O. Hassel and H. Hope. Acta Chem. Scand. **14**, 391 (1960).
3. O. Hassel and Chr. Romming. Quart. Rev. **16**, 1 (1962).
4. C. K. Prout and J. D. Wright. Angew. Chem. Int. Ed. **7**, 659 (1968).
5. H. A. Bent. Chem. Rev. **68**, 587 (1968).
6. H. Bohme and W. Krausse. Ber. **84**, 170 (1950).
7. B. A. Dunell, C. A. Fyfe, C. A. McDowell, and J. Ripmeester. Trans. Faraday Soc. **65**, 1153 (1969).
8. P. J. Haigh, P. C. Canepa, G. A. Matzkanin, and T. A. Scott. J. Chem. Phys. **48**, 4234 (1968).
9. J. H. Van Vleck. Phys. Ref. **74**, 1168 (1948).
10. D. R. Lide and D. E. Mann. J. Chem. Phys., **28**, 572 (1958).
11. G. W. Smith. J. Chem. Phys. **42**, 4229 (1965).
12. J. G. Powles and H. S. Gutowsky. J. Chem. Phys. **21**, 1695 (1953).
13. T. Koide. Bull. Chem. Soc. Jap. **40**, 2026 (1967).
14. C. A. Fyfe and J. Ripmeester. Unpublished results.
15. D. F. R. Gilson and C. T. Yim. Private communication.
16. H. S. Gutowsky and G. E. Pake. J. Chem. Phys. **18**, 162 (1950).
17. J. S. Waugh and E. I. Fedin. Sov. Phys. Solid State, **4**, 1633 (1963).
18. J. G. Aston, M. R. Sagenkahn, G. J. Szasz, G. W. Moesser, and H. F. Zuhr. J. Amer. Chem. Soc. **66**, 1171 (1944).
19. T. D. Goldfarb and B. N. Kharl. J. Chem. Phys. **46**, 3379 (1967).

Can. J. Chem. Downloaded from www.nrcresearchpress.com by 210.87.254.6 on 09/05/12
For personal use only.

Can. J. Chem. Downloaded from www.nrcresearchpress.com by 210.87.254.5 on 09/05/12
For personal use only.

The use of Raman spectroscopy in the study of anion exchange of complex anions

P. DOBUD, D. SUTTON, AND D. G. TUCK
Department of Chemistry, Simon Fraser University, Burnaby 2, British Columbia

Received February 26, 1970

It is shown that Raman spectroscopy can be used to identify complex anions sorbed on an anion exchange resin. Results for $[AuCl_4]^-$ and $[AuBr_4]^-$, and for anionic halo-complexes of indium(III), are described.

Canadian Journal of Chemistry, **48**, 2290 (1970)

It is well established that the distribution coefficient for the exchange of anionic complexes between aqueous solution and an anion exchange resin is often critically dependent upon the aqueous phase conditions (1, and references therein). In the discussion of such effects, the nature of the sorbed species, and any changes in its chemical form, are therefore of prime importance. Identification of the sorbed species has normally depended mainly on the chemical analysis of changes in solution composition, although in a few cases visible absorption spectroscopy of the resin phase has been possible (2). This is in contrast to the associated problem of the identification of the organic phase extract species in solvent extraction, for which electronic (3), Raman (4), infrared (5), and Mössbauer (6) spectroscopy have all been successfully applied in various specific cases.

We now report on the use of Raman spectroscopy as a direct means of studying the anions sorbed onto anion exchange resins.[1] The results described refer to studies of anionic halo-complexes of indium(III) and gold(III). These particular elements were tested because of the availability of the vibrational spectroscopic data, and because of related interests in this Department in the chemistry of their complexes in solution. The technique is, however, of general applicability for other anionic complexes.

Experimental

Spectra

A Cary 81 Raman spectrometer, with He/Ne laser excitation, was used throughout this work.

Materials

The ion exchange resin was Dowex-1 (× 8), pretreated to convert it into the appropriate halide form. After equilibration with an acid solution of the element concerned, the resin was removed by filtration, quickly washed with water, vacuum dried, and then ground. This dried material was packed into the standard conical sample holder for coaxial viewing in the spectrometer.

Indium(III) solutions were prepared by dissolving the metal or the trihalide in an aqueous solution of hydrohalic acid.

Potassium tetrachloroaurate and tetrabromoaurate were prepared by standard methods (8).

Results and Discussion

Raman Emission of Pretreated Dowex-1 Resin

The pretreated resin in chloride, bromide, or iodide form was found not to exhibit any Raman emission lines of measurable intensity. Instead, a broad background of scattering was observed, which permitted recordings only at rather low spectrometer amplification; this probably accounts in part for the failure to record a Raman spectrum. With the resin in the iodide form, the background was lower than for the chloride form by a factor of 5–10. Sorbed ions which imparted an intense yellow color to the resin were generally found to emit with a much reduced background, and consequently yielded good Raman spectra.

The Sorption of Tetrahaloaurate(III) Anions

Kraus and Nelson (9) have shown that Au(III) species are strongly held on an anion exchange resin, with the distribution coefficient (K_d) $\sim 10^6$ for 2 *M* HCl, falling smoothly to $\sim 10^4$ at 10 *M* HCl. The predominant species in aqueous hydrochloric acid is $[AuCl_4]^-$ ($\log \beta_4 = 25$–30) (10), and spectroscopic studies show that the symmetry of this anion (D_{4h}) is the same in solution (11) as in the M^IAuCl_4 salts (12).

[1]After this work was completed, we learned that the spectrum of CrO_4^{2-} sorbed onto an anion exchange resin has been measured by Shriver (7).

Can. J. Chem. Downloaded from www.nrcresearchpress.com by 210.87.254.5 on 09/05/12
For personal use only.

We find that resin equilibrated with $KAuCl_4$ in aqueous or ethanolic 2 *M* HCl gives a good Raman spectrum, whose peaks can be readily assigned to $[AuCl_4]^-$, at 346(ν_1), 169(ν_3), and 325(ν_5) cm^{-1}. No other emission lines could be detected in this spectrum, which is shown in Fig. 1. Similarly for Au(III)/HBr, we find only lines at 195 and 212 cm^{-1}. No evidence was obtained in either of these two cases for the presence of $[AuX_5]^{2-}$ or $[AuX_6]^{3-}$ species in the resin phase (cf. ref. 13). Because of their higher charge, these anions would be more strongly hydrated than $[AuCl_4]^-$ and would therefore not exchange so well, but on the present spectroscopic evidence there seems no reason to invoke the formation of halo-complexes higher than $[AuX_4]^-$ to explain the decrease in K_d with increasing acid concentration. A more attractive theory, which will be discussed fully elsewhere, is that the decrease is due to a lowering of the dielectric constant of the aqueous phase consequent upon the addition of electrolyte (14).

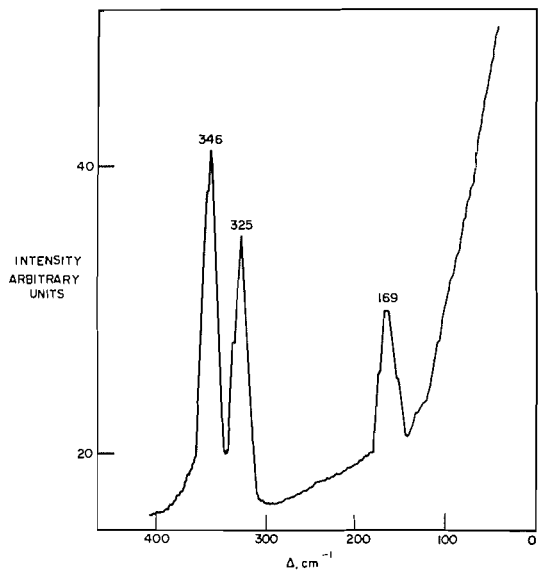

FIG. 1. The Raman spectrum of $[AuCl_4]^-$ sorbed onto Dowex-1 (× 8) from 2 *M* aqueous hydrochloric acid solution.

Indium(III) Halide Systems

The anion exchange of indium(III) from aqueous hydrochloric acid solution is relatively weak, with K_d reaching a maximum value of ~ 10 at 4 *M* hydrochloric acid (9). With hydrobromic and hydriodic acids, the maximum values of K_d are approximately 10^3 and 10^4, respectively (14).

We have examined the Raman spectrum of the resin phase resulting from equilibration with 3 *M* hydrohalic acid at indium(III) concentrations of ~ 0.5 *M*. Addition of ethanol was found to increase the uptake of indium by the resin (14). For In(III)/I^- and In(III)/Br^-, we find Raman spectra in agreement with earlier solution studies (4), and with the spectra of $[InX_4]^-$ salts (15): $[InBr_4]^-$, 198 s(ν_1); $[InI_4]^-$, 185 w,br (ν_3); 139 s(ν_1); 59 m(ν_4).

In the case of $[InI_4]^-$, we were not able to resolve ν_2, expected at approximately 42 cm^{-1}. In the case of $[InBr_4]^-$, only the strong, sharp line at 198 cm^{-1} could be observed without difficulty; the expected lines at 55 cm^{-1} (ν_2) and 79 cm^{-1} (ν_4) could not be resolved from background, nor could the weak and diffuse ν_3 at about 239 cm^{-1} be observed with certainty. As well as these characteristic $[InX_4]^-$ spectra, both samples showed weak additional lines, at 180 cm^{-1} (bromide) and 154 cm^{-1} (iodide). The extra line in the bromide spectrum has also been observed in the Raman spectrum of an aqueous solution of $InBr_3$ in hydrobromic acid, both by us and by Woodward and Bill (4). This may be due to $[InBr_5]^{2-}$, since extrapolation of the results of ν_1 of $SnBr_4$ and $[SnBr_5]^-$ (16) suggests that ν_1 for $[InBr_5]^{2-}$ should be at ~ 180 cm^{-1}. The extra peak in the iodide spectrum, however, does not correlate with expected frequencies of either $[InI_5]^{2-}$ or $[InI_6]^{3-}$. An alternative explanation is that we are observing emission from the X_3^- anion; Br_3^- has bands at 170 and 210 cm^{-1} (17) and I_3^- at 103 and 149 cm^{-1} (18, 19). These species would be readily sorbed by an anion exchange resin from solution; alternatively they might have been formed in situ as the result of photo-decomposition caused by the exciting radiation.

It is worth pointing out here that the anion exchange system parallels the solvent exchange with solvents such as ethers, in that one observes only $[InX_4]^-$ in the non-aqueous phase in both cases (4).

For In(III)/HCl, we observed no Raman bands, and this is certainly due in part to the inherently weak Raman scattering from In—Cl

bonds, relative to In—Br and In—I, as well as to the high background emission from the chloride form of the resin.

This work was supported in part by Operating Grants from the National Research Council of Canada.

1. F. HELFFERICH. Ion Exchange. McGraw-Hill Book Co. Inc., New York, 1962. p. 221.
2. J. L. RYAN. Inorg. Chem. **2**, 348 (1963).
3. N. H. NACHTRIEB and J. G. CONWAY. J. Amer. Chem. Soc. **70**, 3547 (1948).
4. L. A. WOODWARD and P. T. BILL. J. Chem. Soc. 1699 (1955); L. A. WOODWARD and G. H. SINGER. J. Chem. Soc. 716 (1958); L. A. WOODWARD and M. J. TAYLOR. J. Chem. Soc. 4473 (1960).
5. M. J. TAYLOR. J. Chem. Soc. A, 1780 (1968).
6. A. G. MADDOCK, L. O. MEDEIROS, and G. M. BANCROFT. Chem. Commun. 1067 (1967).
7. D. F. SHRIVER. Appl. Spectrosc. **23**, 552 (1969).
8. P. B. BLOCK. Inorg. Syn. **4**, 15 (1953).
9. K. A. KRAUS and F. NELSON. Proc. Int. Conf. Peaceful Uses At. Energy. Geneva. **7**, 113 (1956).
10. Stability constants. Chem. Soc. Spec. Publ. No. 17, London. 1964. p. 288.
11. H. STAMMREICH and R. FORNERIS. Spectrochim. Acta, **16**, 363 (1960).
12. A. SABATINI, L. SACCONI, and V. SCHETTINO. Inorg. Chem., **3**, 1775 (1964).
13. C. M. HARRIS and I. H. REECE. Nature, **182**, 1665 (1958).
14. P. DOBUD, H. M. LEE, and D. G. TUCK. Inorg. Chem. In press.
15. D. M. ADAMS, J. GISLASON, M. H. LLOYD, and D. G. TUCK. Unpublished results.
16. J. A. CREIGHTON and J. H. S. GREEN. J. Chem. Soc. A, 808 (1968).
17. J. C. EVANS and G. Y-S. LO. Inorg. Chem. **6**, 1483 (1967).
18. A. G. MAKI and R. FORNERIS. Spectrochim. Acta, **23A**, 867 (1967).
19. G. C. HAYWARD and P. J. HENDRA. Spectrochim. Acta, **23A**, 2309 (1967).

Can. J. Chem. Downloaded from www.nrcresearchpress.com by 210.87.254.5 on 09/05/12
For personal use only.

Can. J. Chem. Downloaded from www.nrcresearchpress.com by 210.87.254.40 on 09/05/12
For personal use only.

Fischer indole synthesis. The reaction of *N'*-methyl-2,6-dimethylphenylhydrazine hydrochloride with 2-methylcyclohexanone and 2,6-dimethylcyclohexanone

G. S. BAJWA[1] AND R. K. BROWN
Department of Chemistry, University of Alberta, Edmonton, Alberta

Received April 9, 1969[2]

When *N'*-methyl-2,6-dimethylphenylhydrazine hydrochloride (**1**) was heated with 2-methylcyclohexanone in refluxing dry benzene, the products isolated were ammonium chloride and methylammonium chloride (as a 1:1 mixture) as well as 1,8,9-trimethyl-1,2,3,4-tetrahydrocarbazole. The formation of these products was explained on the basis of the dienone-imine intermediate expected from the Fischer indole synthesis. The formation of methylamine hydrochloride indicated that at least one other route of reaction had occurred, in addition to that which provided the trimethyltetrahydrocarbazole and ammonium chloride.

The hydrazine, **1**, failed to react at all with 2,6-dimethylcyclohexanone under the reaction conditions employed.

Canadian Journal of Chemistry, **48**, 2293 (1970)

Introduction

In a series of investigations aimed at providing evidence for the dienone–imine postulated as an intermediate in the Fischer indole synthesis (1 and references therein), it was found (2) that *N'*-methyl-2,6-dimethylphenylhydrazine hydrochloride (**1**, Scheme 1), in refluxing benzene, reacts with cyclohexanone to produce 8,9-dimethyl-1,2,3,4-tetrahydrocarbazole (**3**, reaction *a*, Scheme 1). No evidence for a dienone-imine intermediate was found, although the formation of the product obtained could be explained only on the basis of such an intermediate. Subsequently (3) it was reported that **1** reacts readily with isobutyraldehyde, under similar conditions, to produce an isolable dienone–imine, **5** (reaction *b*, Scheme 1). This was an isomer of the dienone–imine **4** usually considered to be the intermediate (1). It was also found later (4) that when the hydrazine **1** was allowed to react with propionaldehyde (reaction *c*, Scheme 1) for a short period of time (10 min), a material could be isolated which had characteristics very much like those of the dienone–imine **5**, and accordingly a dienone–imine structure, **7**, was assigned to this material. When **7** was heated for an extended period of time (20 h) in refluxing benzene, the two compounds, 1,3,7-trimethylindole (**9**), and 3,7-dimethylindole (**10**) were formed, with the former as the predominant product. This constituted final proof that a dienone-imine was indeed an intermediate in the Fischer indole synthesis. The formation of **10** could take place by elimination of methylamine and a methyl group from **7**. But the formation of **9** could be explained only if it was accepted that **7** could be converted back to **6** (see Scheme 1) which would then form **8**, the compound which logically could provide the major product **9**. The formation of **9** as the predominant product requires the preferential loss of the nitrogen atom adjacent to the benzene ring rather than the nitrogen atom more remote from the ring, contrary to what is usually observed in the Fischer indole synthesis. This has been explained (4) as due to the strain developed in structure **8** by the amino group (as the hydrochloride) at position C-7*a*. When the substance is heated, the C-7*a* amino group of structure **8** is eliminated as ammonium chloride more rapidly than is the methylamine moiety from C-2 of compound **7**. The formation of a positive charge at C-7*a*, upon loss of the amino group, is stabilized by both the conjugated diene system as well as by participation of the electron pair of the adjacent nitrogen, and this might also favor nitrogen elimination from **8** over that from **7**.

In each of the above reactions of Scheme 1, the enamine, the first step of the reaction between **1** and the carbonyl compound, could not be obtained.

The present paper extends this study to the reaction of **1** with both 2-methylcyclohexanone and 2,6-dimethylcyclohexanone.

[1]Postdoctoral Fellow, 1968–1969.
[2]Revision received April 1, 1970.

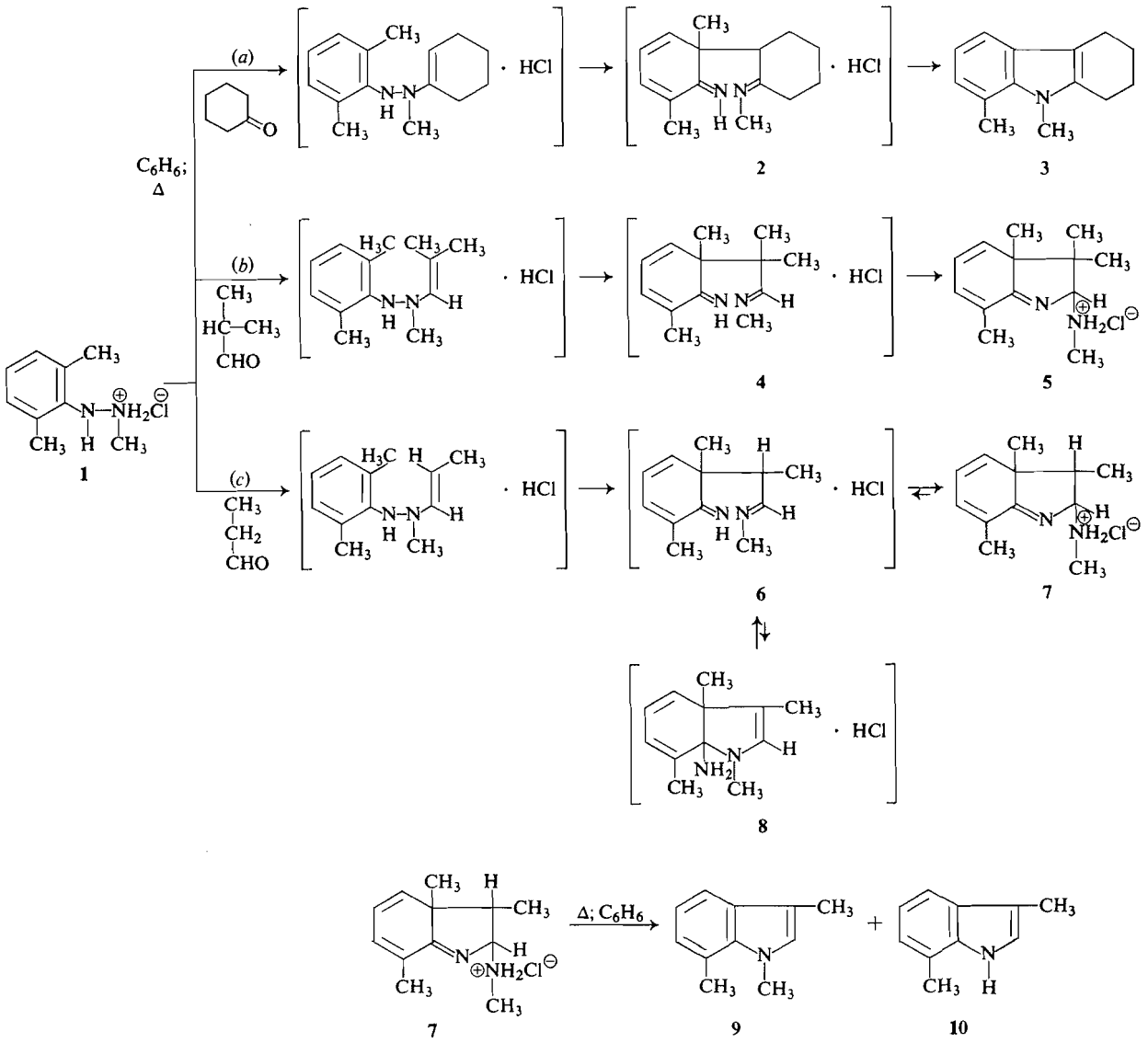

SCHEME 1

Results and Discussion

Two directions of reaction (*a* and *b*, Scheme 2) are possible when **1** reacts with 2-methylcyclohexanone. Route *a* would correspond to the reaction of **1** with propionaldehyde, while route *b* would be similar to the reaction of **1** with isobutyraldehyde.

Compound **1** was heated with 2-methylcyclohexanone in refluxing, dry, benzene for 20 h and water was removed by azeotropic distillation. This length of time appeared to be necessary since a 15 h reflux period provided a product which showed evidence of the presence of unreacted hydrazine **1**. A dark, solid material accumulated in the bottom of the reaction flask. This material was found to be nearly completely water soluble. The nuclear magnetic resonance (n.m.r.) spectrum of this solid in D_2O showed only two signals, one at τ 5.26 (broad singlet) and the other at τ 7.36 (narrow singlet). These are the signals expected respectively from the proton of deuterium hydroxide and the protons of the

Can. J. Chem. Downloaded from www.nrcresearchpress.com by 210.87.254.40 on 09/05/12
For personal use only.

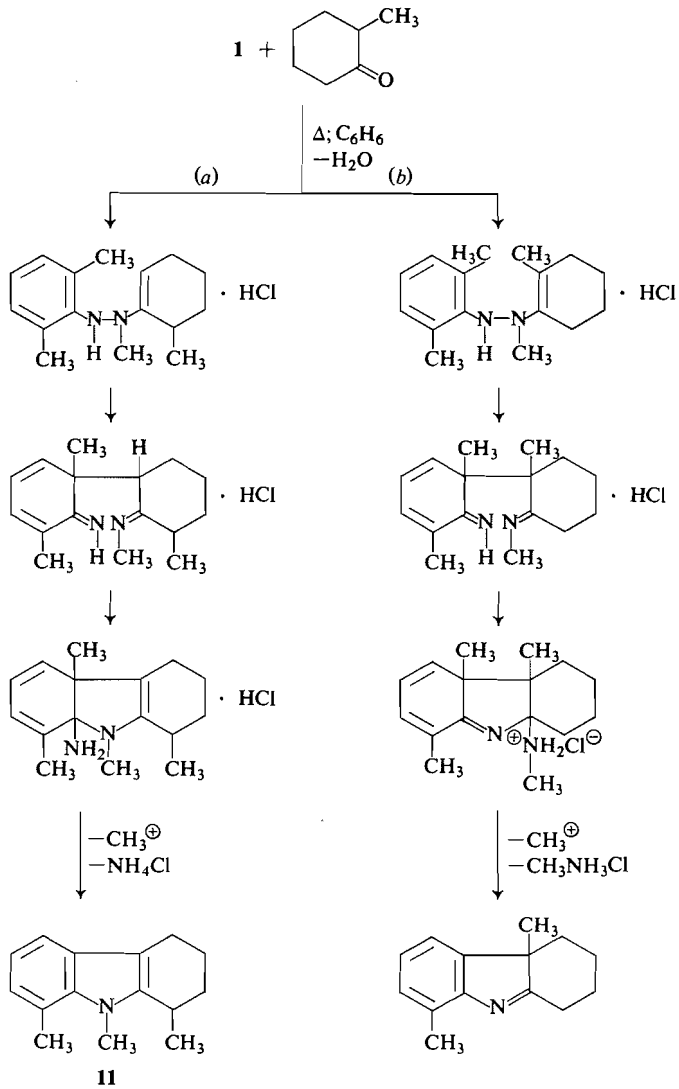

SCHEME 2

methyl group of methylamine. The area ratio of these two signals showed that the dark solid was nearly a 1:1 mixture of ammonium chloride and methylammonium chloride. Thus, both ammonium chloride and methylammonium chloride had been formed in the reaction, in about equal amounts. Two crystallizations of this solid from ethanol–ether gave a colorless solid melting at 187–230°. The n.m.r. spectrum of this crystallized material also showed that it was a mixture of ammonium chloride and methylammonium chloride but that some of the methylammonium chloride was lost in the crystallization process. A mixture of authentic methylammonium chloride and ammonium chloride gave the same n.m.r. spectrum and broad range of melting point.

The benzene filtrate obtained after removal of the dark solid, was freed from solvent. From the residual oily mixture it was possible to isolate only one substance, a solid in about 12% yield. This substance was considered to be 1,8,9-trimethyl-1,2,3,4-tetrahydrocarbazole (**11**). The assignment of structure **11** was supported by the elemental analysis, the infrared (i.r.) spectrum which showed no NH absorption in the region 3100 to 3500 cm^{-1}, the n.m.r. spectrum and the fact that

Can. J. Chem. Downloaded from www.nrcresearchpress.com by 210.87.254.40 on 09/05/12
For personal use only.

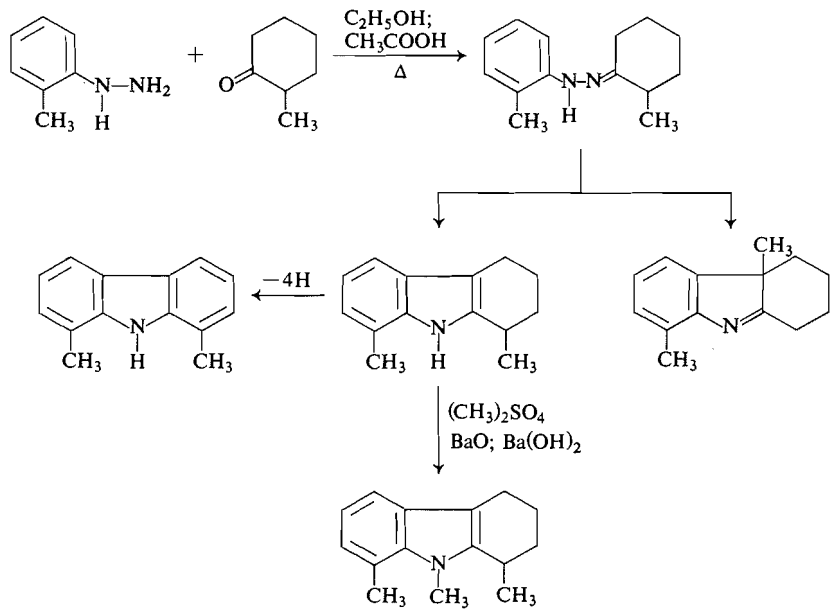

11

SCHEME 3

the ultraviolet (u.v.) spectrum was nearly the same as that of authentic 8,9-dimethyl-1,2,3,4-tetrahydrocarbazole (2) and of 1,8-dimethyl-1,2,3,4-tetrahydrocarbazole. The latter compound was prepared from the reaction of 2-methylcyclohexanone with *o*-tolylhydrazine. The cyclization of 2-methylcyclohexanone *o*-tolylhydrazone (5) furnished a mixture of 1,8-dimethyl-1,2,3,4-tetrahydrocarbazole and 8,11-dimethyl-1,2,3,4-tetrahydrocarbazolenine (Scheme 3). These could be separated readily since the carbazolenine is soluble in dilute hydrochloric acid while the tetrahydrocarbazole is not. Additional evidence for the assignment of structure **11** was the fact that it could be dehydrogenated to 1,8,9-trimethylcarbazole, whose n.m.r. spectrum clearly supports the assigned structure.

To provide an authentic sample of 1,8,9-trimethyl-1,2,3,4-tetrahydrocarbazole (**11**), *N*-methylation of 1,8-dimethyltetrahydrocarbazole was carried out using the procedure described for the *N*-methylation of 8-methyl-1,2,3,4-tetrahydrocarbazole (2). Much less satisfactory results were obtained when other methods of methylation were attempted. That *N*-methylation of the 1,8-dimethyl compound did occur but to a small extent was shown by the appearance of a weak signal in the n.m.r. spectrum of the crude methylated mixture at τ 6.13, where the signal of the *N*-methyl group is expected to appear. This was at the position identical to that found for the *N*-methyl signal in the n.m.r. spectrum of compound **11** obtained from the reaction of **1** with 2-methylcyclohexanone.

The area ratio of the signal at τ 6.13, in the n.m.r. spectrum of the crude material obtained from the methylation of 1,8-dimethyl-1,2,3,4-tetrahydrocarbazole, to one of the signals for the methyl protons was ~2:45. This indicated that the crude material was mainly unchanged 1,8-dimethyl-1,2,3,4-tetrahydrocarbazole containing the *N*-methylated material to the extent of 4 to 5%. A similar mixture of the two materials, the di- and trimethylated tetrahydrocarbazole, gave an n.m.r. spectrum identical to that found for the crude methylated material. The low yield of the *N*-methylated product was to be expected in view of the difficulty experienced in *N*-methylation of 8-methyl-1,2,3,4-tetrahydrocarbazole (2). Attempts to isolate a pure sample of 1,8,9-trimethyl-1,2,3,4-tetrahydrocarbazole from this mixture by fractional crystallization or chromatography were quite unsuccessful. Separation was hampered by the instability of the 1,8-dimethyl-1,2,3,4-tetrahydrocarbazole. Although our experience

Can. J. Chem. Downloaded from www.nrcresearchpress.com by 210.87.254.40 on 09/05/12
For personal use only.

Can. J. Chem. Downloaded from www.nrcresearchpress.com by 210.87.254.40 on 09/05/12
For personal use only.

has shown that the trimethyltetrahydrocarbazole crystallizes very easily from 95% ethanol, the swamping effect of the large amount of the 1,8-dimethyl-1,2,3,4-tetrahydrocarbazole no doubt was the cause of the failure to obtain the trimethyl compound by fractional crystallization.

Considerable effort was expended in attempts to isolate other products from the benzene filtrate obtained after removal of the ammonium chloride and methylammonium chloride, but no pure material other than the 1,8,9-trimethyltetrahydrocarbazole could be separated from the tarry residue. The formation of methylamine was clear evidence that at least one other course of reaction had been followed e.g. route *b*, Scheme 2. The n.m.r. spectrum of the dark oily material obtained after removal of the benzene, and before separation of the trimethyltetrahydrocarbazole, showed none of the significant signals between τ 3.0 and 4.2 indicative of the olefinic protons of the dienone–imine system (3, 4) such as is shown in **5** or **7** of Scheme 1.

An interesting and pertinent discovery is that an equimolar mixture of *N'*-methyl-2,6-dimethylphenylhydrazine hydrochloride, (**1**) and 2,6-dimethylcyclohexanone, when heated in refluxing dry benzene for as long as 41 h, failed to react at all since at least 90% of **1** was recovered unchanged and there was no evidence for the formation of water in the trap. Lack of reaction of the 2,6-dimethylcyclohexanone may be due to difficulty in forming the enamine by elimination of water. This is no doubt because of the presence of the methyl groups in each of the 2,6-positions of both rings. This does not constitute proof that route *b* of Scheme 2 will not be possible, but it could indicate that it is less favored.

The formation of 1,8,9-trimethyl-1,2,3,4-tetrahydrocarbazole is readily explained by the sequence of reactions shown in route *a* of Scheme 2. Here again the fate of the methyl group lost from the aromatic ring is not yet known (2–4). A similar route had been proposed to explain the formation of the products **3**, **9**, and **10** (Scheme 1) from the reaction of *N'*-methyl-2,6-dimethylphenylhydrazine hydrochloride with cyclohexanone (2) and propionaldehyde (4).

Experimental

Melting points and boiling points are uncorrected. Elemental analyses were made by Mrs. Darlene Mahlow of this Department.

The u.v. spectra of 8,11-dimethyl-1,2,3,4-tetrahydrocarbazolenine were obtained with a JASCO model ORD/UV-5 spectrometer. Those of the other compounds were obtained with a Perkin–Elmer model 202 ultraviolet-visible spectrometer.

The i.r. spectra were obtained with a Perkin–Elmer model 421 grating spectrometer.

The 60 MHz n.m.r. spectra were made by Mr. Robert Swindlehurst of this Department, using the 60 MHz Varian spectrometer.

Solvents were generally removed by a rotary evaporator under vacuum unless otherwise stated.

Condensation of N'-Methyl-2,6-dimethylphenylhydrazine Hydrochloride (1) with 2-Methylcyclohexanone

A mixture of 2 g (0.0108 mole) of *N'*-methyl-2,6-dimethylphenylhydrazine hydrochloride (2) and 1.5 g (0.0134 mole) of 2-methylcyclohexanone was heated in dry, refluxing benzene (40 ml) for 20 h. Water was collected in the trap. The reaction mixture became dark and deposited a dark gelatinous material (300 mg). This was separated by filtration and found to be water soluble. Its n.m.r. spectrum in D_2O showed only a broad singlet at τ 5.26 (DOH) and a narrow singlet at τ 7.36 (N—CH_3) due to ~1:1 mixture of ammonium chloride and methylammonium chloride. This solid was dissolved in 95% ethanol and to the solution was added ether until a faint turbidity occurred. There was deposited 160 mg of a colorless solid melting over a range of 187–230°. The n.m.r. spectrum of this solid in D_2O showed the same two signals at τ 5.26 and 7.36 but the proportion had changed indicating that some of the methylamine hydrochloride had been lost during the crystallization.

The benzene filtrate was freed from solvent. The dark tarry residue was suspended in 100 ml of water and the mixture was then extracted with ether (2 × 100 ml). The ether layer was washed with water (2 × 50 ml), then with 5% aqueous hydrochloric acid (2 × 100 ml), and finally with water (2 × 50 ml). The ether solution was dried over anhydrous magnesium sulfate for 2 h. The drying agent and solvent were removed leaving a solid (410 mg) melting at 80–92°. Two crystallizations from 95% ethyl alcohol gave 340 mg (12.3%) of pure *1,8,9-trimethyl-1,2,3,4-tetrahydrocarbazole* melting at 99–100°.

Anal. Calcd. for $C_{15}H_{19}N$: C, 84.50; H, 8.92; N, 6.57. Found: C, 84.34; H, 8.97; N, 6.77.

The u.v. spectrum in cyclohexane showed a narrow band at λ_{max} 236 mμ (ε, 29 800) and a broad band at λ_{max} 290 mμ (ε, 1300). The i.r. spectrum in CCl_4 showed a band at 3022 cm^{-1} (aromatic C—H stretching) and one at 1605 cm^{-1} (aromatic C=C), but no absorption above 3100 cm^{-1} (no NH).

The 60 MHz n.m.r. spectrum in $CDCl_3$ agreed completely with the structure assigned. It showed signals at τ 2.5–3.2 (3H multiplet, aromatic), 6.1 (3H singlet, N—CH_3), 7.25 (3H singlet, aromatic CH_3), 6.9–7.5 (3H multiplet, aliphatic), 8.0–8.3 (4H narrow multiplet, aliphatic), and 8.76 (3H doublet, aliphatic CH_3).

The acid washings and the aqueous solution left from the ether extractions were combined and basified with 5% aqueous sodium hydroxide. An ether extract (2 × 100 ml) was washed with water (2 × 50 ml) and dried ($MgSO_4$). The drying agent was separated and the solvent was removed, leaving a tarry mass (~1 g) from which

Can. J. Chem. Downloaded from www.nrcresearchpress.com by 210.87.254.40 on 09/05/12
For personal use only.

no pure compound could be isolated by chromatography or crystallization.

1,8,9-Trimethylcarbazole

The 1,8,9-trimethyl-1,2,3,4-tetrahydrocarbazole (100 mg) was heated for 2.5 h in refluxing mesitylene (2 ml) containing 40 mg of 5% palladium-on-charcoal. The hot solution was filtered and the solid was washed with methyl acetate (2 × 5 ml). The washings were filtered and combined with the mesitylene filtrate. Removal of the solvent gave a solid (52 mg) melting at 190–191°. One recrystallization from 95% ethyl alcohol raised the melting point to 193°. Yield, 40 mg (41%) of *1,8,9-trimethylcarbazole*.

Anal. Calcd. for $C_{15}H_{15}N$: C, 86.12; H, 7.18; N, 6.69. Found: C, 86.34; H, 7.39; N, 6.83.

The u.v. absorption spectrum in cyclohexane showed bands at λ_{max} 240 (ε, 354 000), 264 (ε, 9200), and 293 (ε, 9500).

The i.r. spectrum in CCl_4 showed a band at 3022 cm^{-1} (aromatic C—H stretching) and one at 1585 cm^{-1} (weak, aromatic C=C). No NH absorption was evident.

The 60 MHz n.m.r. spectrum in $CDCl_3$ was in complete agreement with the structure assigned. The signals were at τ 2.0–2.25 and 2.7–3.0 (6H multiplets, aromatic), 5.83 (3H singlet, N—CH_3), and 7.24 (6H singlet, aromatic CH_3).

2-Methylcyclohexanone o-tolylhydrazone

A solution of 50 g (0.41 mole) of *o*-tolylhydrazine and 46 g (0.41 mole) of 2-methylcyclohexanone in 130 ml of 95% ethanol containing a small amount (3–4 drops) of glacial acetic acid, was refluxed for 3 h. The reaction mixture was cooled, then placed in a refrigerator for 2 h. The solid (needles) which deposited weighed 60 g and melted at 45–46°. This hydrazone decomposed readily when left at room temperature, but could be preserved several days in a refrigerator No analysis was made because of its rapid decomposition.

The i.r. spectrum in CCl_4 showed bands at 3390 (NH), 3030 (aromatic C—H stretching), 1605, 1585 cm^{-1} (aromatic C=C, C=N).

The 60 MHz n.m.r. spectrum in $CDCl_3$ was consistent with the structure. It showed signals at τ 2.35–3.45 (4H, multiplet, aromatic), τ 3.03–3.45 (1H, broad, located by deuterium exchange, N—H), 7.86 (3H, singlet, aromatic CH_3), 8.8 (3H, doublet, J = 6.5 Hz, aliphatic CH_3), and broad absorption between 7.2–8.6 for the 9 protons of the cyclohexanone moiety.

Cyclization of 2-Methylcyclohexanone o-tolylhydrazone

A mixture of 15 g of 2-methylcyclohexanone *o*-tolylhydrazone in 200 ml of 3 *N* aqueous sulfuric acid was heated under reflux for 1.5 h. The mixture was cooled and extracted with ether (2 × 200 ml). The ether solution was washed with 5% hydrochloric acid (2× 100 ml) and then with water (3 × 100 ml) and then dried ($MgSO_4$) for 0.5 h. When the drying agent was separated and the solvent removed, a yellow oil (4.5 g) was obtained. This oil was dissolved in 10 ml of 95% ethyl alcohol, and water was added to faint turbidity. When kept in a refrigerator 5–6 h the solution deposited crystals (4 g) melting at 55–64°. One recrystallization from ethanol–water as above raised the melting point to 77–78°. Yield of pure *1,8-dimethyl-1,2,3,4-tetrahydrocarbazole* was 3.5 g (25%). Literature b.p. 145–148° at 1 mm (5).

Anal. Calcd. for $C_{14}H_{17}N$: C, 84.42; H, 8.54; N, 7.04. Found: C, 84.52; H, 8.65; N, 7.32.

This tetrahydrocarbazole had a tendency to decompose at room temperature.

The u.v. spectrum in cyclohexanone showed a broad band at λ_{max} 225 mμ (ε, 18 500).

The i.r. spectrum in CCl_4 showed bands at 3480 (NH), 3030 (aromatic C—H stretching), and at 1610 cm^{-1} (aromatic C=C).

The 60 MHz n.m.r. spectrum in $CDCl_3$ was consistent with the structure. The signals were at τ 2.28–3.11 (4H, multiplet for 3 aromatic protons and 1 NH), 7.59 (3H, singlet, aromatic methyl group), 8.72 (3H, doublet, J = 6.5 Hz, aliphatic methyl group), and at 6.85–7.5 (3H, multiplet) and 7.8–8.39 (4H, multiplet) for the 7 protons of the tetrahydro ring.

The acid washings were combined with the reaction mixture left after the ether extractions, and the whole was made basic with 5% aqueous sodium hydroxide. The basified solution was extracted with ether (2 × 200 ml). The ether extract was washed with water (2 × 100 ml) and dried ($MgSO_4$) for 1 h. Removal of the drying agent and solvent gave 6 g of yellow oil. This, when distilled, gave two fractions, the first boiling at 60–70° at 4 mm (1.5 g) and the second at 132–135° at 4 mm (4.5 g of yellow oil). The first fraction was identified as *o*-toluidine and the second fraction, redistilled again at 108° at 2 mm, gave 3.6 g (26%) of pure *8,11-dimethyl-1,2,3,4-tetrahydrocarbazolenine*. Literature b.p. 120–122° at 1.5 mm (5).

Anal. Calcd. for $C_{14}H_{17}N$: C, 84.42; H, 8.54; N, 7.04. Found: C, 84.04; H, 8.53; N, 7.28.

The u.v. spectrum in cyclohexanone showed bands at λ_{max} 205 mμ (ε, 63 300), 224 (ε, 29 200), and 252 (ε, 12 000).

The i.r. spectrum (film) showed bands at 3022 (aromatic C—H stretching), 1579 (C=N), 1610 cm^{-1} (aromatic C=C). A weak band appeared at 1660 cm^{-1} (unknown). No absorption was detected above 3100 cm^{-1} (no NH).

The 60 MHz n.m.r. spectrum in $CDCl_3$ was consistent with the structure. Signals appeared at τ 2.95 (3H, singlet, aromatic), 7.45 (3H, singlet, aromatic methyl), 8.75 (3H, singlet, aliphatic methyl), and between 6.92–9.08 (8H, multiplets of protons of the tetrahydro ring).

1,8-Dimethylcarbazole

A solution of 250 mg of 1,8-dimethyl-1,2,3,4-tetrahydrocarbazole in 3 ml of mesitylene containing 90 mg of 5% palladium-on-charcoal, was heated under reflux for 3 h. The hot solution was filtered, and the solid was washed with methyl acetate (2 × 2 ml). The washings were filtered and combined with the mesitylene solution and the whole freed from solvent, giving 180 mg of solid melting at 170–175°. Two crystallizations from 95% ethyl alcohol gave 140 mg of pure *1,8-dimethylcarbazole* melting at 176–177°. Literature m.p. 183–184° (6); 175–176° (5).

The i.r. spectrum in CCl_4 showed a band at 3480 cm^{-1} (NH).

The 60 MHz n.m.r. spectrum in $CDCl_3$ agreed completely with the structure. The signals were at τ 1.93–2.5

(6H, multiplet, aromatic) and 7.46 (6H, singlet for two aromatic CH_3).

Methylation of 1,8-Dimethyl-1,2,3,4-tetrahydrocarbazole

The methylation was carried out according to published directions (2). The n.m.r. spectrum of the crude product showed a small signal at τ 6.13 showing that 4–5% of the starting material had been methylated on the nitrogen atom.

The authors wish to thank the National Research Council of Canada for financial support for a part of this work.

1. B. ROBINSON. Chem. Rev. **63**, 373 (1963).
2. G. S. BAJWA and R. K. BROWN. Can. J. Chem. **46**, 1927 (1968).
3. G. S. BAJWA and R. K. BROWN. Can. J. Chem. **46**, 3105 (1968).
4. G. S. BAJWA and R. K. BROWN. Can. J. Chem. **47**, 785 (1969).
5. K. H. PAUSACKER and C. I. SCHUBERT. J. Chem. Soc. 1384 (1949).
6. H. SEYBERTH. Ber. **29**, 2594 (1896).

Can. J. Chem. Downloaded from www.nrcresearchpress.com by 210.87.254.40 on 09/05/12
For personal use only.

Can. J. Chem. Downloaded from www.nrcresearchpress.com by 210.87.254.5 on 09/05/12
For personal use only.

NOTES

The effect of electron scavengers on the γ-radiolysis of gaseous H_2S

D. W. HUYTON AND T. W. WOODWARD[1]

Department of Chemistry and Applied Chemistry, University of Salford, Salford M5 4WT, Lancashire, England

Received February 25, 1970

The effect of the electron scavengers SF_6 and N_2O on the γ-radiolysis of gaseous H_2S has been studied. Neither scavenger lowered the radiation yield of H_2, $G(H_2)$. With added N_2O, nitrogen was produced, though not in the amount G_c, the ion pair yield in H_2S. Possible explanations of the findings are discussed.

Canadian Journal of Chemistry, **48**, 2300 (1970)

Recent publications (1–4) have dealt with the effect of electron scavengers on the radiolysis of simple inorganic gaseous hydrides. We would like to present some results of a preliminary study on the radiolysis of gaseous H_2S that are, in general, quite different from those above (1–4).

Matheson C.P. grade H_2S (99.7%) was found to contain CO_2 (~0.2%) and CS_2 (<0.001%) as impurities when checked by gas chromatography. A 3 m Poropaq Q column maintained at 65 °C, helium carrier gas, and thermal conductivity detection were used (5). After several freeze–pump–thaw cycles at −130 °C, the concentration of CO_2 was reduced to ~0.005%. Some of this H_2S was irradiated to a dose of about 4×10^{22} eV g^{-1}. After degassing at −196 °C, this H_2S was found to contain ~0.005% CO_2 and no detectable amount of CS_2. Radiolysis experiments with the pre-irradiated H_2S gave identical results to the untreated H_2S, and so the latter was used for the bulk of the work presented here. SF_6 and N_2O (Matheson) were degassed several times by freeze–pump–thaw cycles at liquid nitrogen temperature and were used without further purification.

Dosimetry was effected by ion current measurements in vessels similar to those described by Back *et al.* (6), the extrapolation method of Scott and Greening (7) being used to obtain saturation ion currents. The same vessels were also used as irradiation vessels, as were ordinary Pyrex vessels of similar geometry. All vessels were baked out at 400 °C, to a pressure of less than 10^{-5} Torr prior to filling and irradiating.

The yield of hydrogen in the radiolysis of pure H_2S at 800 mm of Hg pressure was found to be 7.0 ± 0.2 molecules per 100 eV, taking $W(H_2S)$ as 25.3 ± 0.4 eV/ion pair (8). Figure 1 summarizes the results obtained in the scavenger experiments. Energy partition in the H_2S/scavenger mixtures was assumed to be proportional to the stopping power ratio of the gases concerned. The electron scavengers SF_6 and N_2O do not lower $G(H_2)$, which is in contrast to the effects observed in similar studies on HCl (1), HBr (2), NH_3 (4), and C_3H_8 (9). The H_2 yields in H_2S/N_2O mixtures and $(H_2S + 1\%\ SF_6)/N_2O$ mixtures are corrected for the production of H_2 with a $G(H_2) = 3.4$ produced in N_2O and $N_2O + 1\%$ SF_6 containing small amounts of H_2S (10). The H_2 yields in H_2S/SF_6 mixtures are not corrected for H_2 produced by species initially produced in SF_6. In SF_6 containing small amounts of H_2S, H_2 is produced but does not reach a limiting value as is the case in N_2O/H_2S and $(N_2O + 1\%$ $SF_6)/H_2S$ mixtures (10). It is, therefore, impossible to apply a correction in H_2S/SF_6 mixtures, and presumably this is why the H_2 yield increases with SF_6 concentration.

The N_2 yields shown in Fig. 1 also represent that produced from species initially produced in H_2S. N_2 yields in H_2S/N_2O mixtures are corrected for N_2 production with a $G(N_2) = 7.0$ by direct absorption in N_2O containing small amounts of H_2S. This correction gives an upper limit of about 1.6 for $G(N_2)$ in H_2S (800 Torr) containing up to 7.5% N_2O (see Fig. 1). N_2 yields in $(H_2S + 1\%\ SF_6)/N_2O$ mixtures are corrected for N_2 production with a $G(N_2) = 4.0$ from $(N_2O + 1\%\ SF_6)$ containing small amounts of H_2S, a correction that gives a zero yield of surplus N_2. These N_2 yields of $G(N_2) = 7.0$ and 4.0 were

[1]To whom correspondence should be addressed.

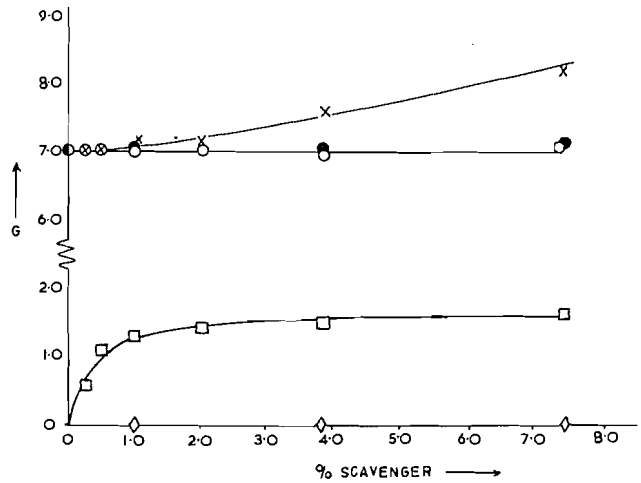

FIG. 1. Yields from the γ-radiolysis of H_2S at 800 Torr 23 ± 2 °C, calculated on the energy absorbed in H_2S. All yields are independent of dose from 10^{20}–10^{21} eV g^{-1} and of dose rate 7.5×10^{14}–2.5×10^{15} eV g^{-1} s^{-1}. Stopping powers for energy partition were calculated from the Bethe equation in a manner laid out elsewhere (23).

In gaseous mixtures the second named component is the one present in variable scavenger concentrations, e.g. H_2S/N_2O means scavenger concentrations of N_2O in H_2S, $(H_2S + 1\%\ SF_6)/N_2O$ means scavenger concentrations of N_2O in the constant composition mixture $(H_2S + 1\%\ SF_6)$. H_2 yields: ◐, Pure H_2S, mean of 10 experiments; ○, H_2S/N_2O; ×, H_2S/SF_6; ●, $(H_2S + 1\%\ SF_6)/N_2O$ (○ and ● are corrected for H_2 production with a $G(H_2) = 3.4$ from N_2O/H_2S and $(N_2O + 1\%\ SF_6)/H_2S$ mixtures (10)). N_2 yield: □, H_2S/N_2O (corrected for N_2 production directly from N_2O, using $G(N_2) = 7.0$ in N_2O/H_2S mixtures (10); ◇, $(H_2S + 1\%\ SF_6)/N_2O$ (corrected for N_2 production from $(N_2O + 1\%\ SF_6)/H_2S$ mixtures using $G(N_2) = 4.0$ (10)).

obtained experimentally and represent lower limits the N_2 yield reaches as the H_2S concentration is increased (10).

Previous work on H_2S (11) indicates that for gaseous H_2S at atmospheric pressure $G(H_2) = 9.3$ and that in liquid H_2S the electron scavengers CCl_4 and CS_2 both reduce the hydrogen yield. Although no mention was made in the above work of the dosimetry used, the discrepancy observed in $G(H_2)$ in the two cases may be partly due to a difference in approach to dosimetry. Recent work on the pulse radiolysis of H_2S produced the value $G(H_2) = 8.8$ (12) relative to $G(N_2) = 10.0$ in N_2O dosimetry. These workers also state that their hydrogen yield is lowered by SF_6 and organic chlorine containing compounds, all of which are electron scavengers. This is in sharp contrast to what we observe.

N_2O captures electrons near thermal energy by the 3 body reaction [1] (13, 14)

$$[1] \qquad e + N_2O + M \rightarrow X^- + M$$

The nature of the negative ion X^- is, as yet, unknown but in some systems apparently ultimately forms nitrogen (3, 9) by eq. [2]

$$[2] \qquad X^- \rightarrow N_2 + Y^-$$

The production of nitrogen in the H_2S/N_2O system suggests that reactions [1] and [2] are occurring. The fact that $G(N_2)$ does not approach G_e (3.95), the electron yield, must mean that reaction [2] is only occurring to a certain extent. Further evidence that reactions [1] and [2] may be occurring comes from the observation that the nitrogen yield is reduced to zero by the much more powerful electron scavenger SF_6 which captures thermal electrons according to reaction [3] (15, 16)

$$[3] \qquad SF_6 + e \rightarrow SF_6^-$$

This is in agreement with studies in other systems (3, 9).

The major positive ion formed in H_2S radiolysis should be H_3S^+ since reactions [4] and [5] have rate constants of the order of 10^{-10} cm^3 $particle^{-1}$ s^{-1} (17, 18)

$$[4] \qquad H_2S^+ + H_2S \rightarrow H_3S^+ + SH$$

$$[5] \qquad HS^+ + H_2S \rightarrow H_3S^+ + S$$

This ion would presumably become clustered at the pressures used in this work (19).

$$[6] \qquad H_3S^+ + mH_2S \rightarrow H_3S^+(mH_2S)$$

Possible modes of reactions of electrons formed

Can. J. Chem. Downloaded from www.nrcresearchpress.com by 210.87.254.5 on 09/05/12
For personal use only.

during radiolysis could be by reaction with the species $H_3S^+(mH_2S)$ (reaction [7]) and H_2S (reactions [8] and [9])

[7] $H_3S^+(mH_2S) + e \rightarrow (m + 1)H_2S + H$

[8] $H_2S + e \rightarrow H + SH^-$

[9] $H_2S + e \rightarrow H_2S^-$

A steady state kinetic treatment of the reactions possible in the H_2S/N_2O system indicates that at the dose rates and scavenger concentrations used in this investigation, reaction [7] is not fast enough to compete with reaction [1] if $k_7 \simeq 10^{-6}$ cm^3 particle^{-1} s^{-1} (20), and $k_1 \simeq 6 \times 10^{-33}$ cm^6 particle^{-2} s^{-1} (13, 14). However, the N_2 yields (see Fig. 1) indicate that competition occurs for electrons up to $\sim 1\%$ N_2O, and therefore reaction [7] is unlikely to be the fate of electrons in pure H_2S. Reaction [7] is far less likely to be capable of competing with reaction [3] in the H_2S/SF_6 system since $k_3 \simeq 3 \times 10^{-12}$ cm^3 particle^{-1} s^{-1} (20). The dissociative capture process (reaction [8]) has an appearance potential of $\sim$2 eV (21) and is therefore unlikely to occur to any great extent. Reaction [9] should have a threshold energy less than this and is more likely to occur, the resulting ion, H_2S^-, presumably becoming clustered at the pressure used here.

Addition of electron scavengers to H_2S should convert the electrons produced on radiolysis to negative ions characteristic of the scavengers, i.e. SF_6^-, X^-, and Y^-. The lack of decrease in $G(H_2)$ by the addition of SF_6 or N_2O indicates that the result of recombination of the ions H_2S^-, SF_6^-, X^-, and Y^- with H_3S^+ (all presumably clustered) results in H atom production by reactions [10], [11], and [12], and ultimately H_2 production by abstraction from H_2S.

[10] $H_3S^+ + H_2S^- \rightarrow H + 2H_2S$

[11] $H_3S^+ + SF_6^- \rightarrow H + H_2S + SF_6$

[12] $H_3S^+ + X^- \text{ or } Y^- \rightarrow H + H_2S + X \text{ or } Y$

Reactions of the type above are assumed not to produce H atoms or H_2 in other simple systems (1–3, 22) viz.

[13] $H_3O^+ + SF_6^- \rightarrow H_2O + HF + SF_5$

[14] $NH_4^+ + SF_6^- \rightarrow NH_3 + HF + SF_5$

[15] $H_2Cl^+ + SF_6^- \rightarrow HCl + HF + SF_5$

The key to the difference in behavior between H_2S and the other hydrides probably lies in the lower strength of the HS—H bond compared with the HO—H, H_2N—H, and H—Cl bonds, and the H atom abstraction reaction to produce H_2 being much faster for H_2S. It could be that ion-recombination reactions [13], [14], and [15] do produce H atoms but of insufficient energy to abstract efficiently from the hydride, while the H atoms produced in reactions [10], [11], and [12], while still of similar energy to those produced from H_2O, NH_3, and HCl are capable of producing H_2 by abstracting from the more reactive H_2S.

D.W.H. acknowledges the award of an S.R.C. studentship.

1. R. A. Lee, R. S. Davidow, and D. A. Armstrong. Can. J. Chem. **42**, 1906 (1964).
2. R. A. Lee and D. A. Armstrong. Int. J. App. Radiat. and Isotop. **19**, 585 (1968).
3. R. S. Dixon and M. G. Bailey. Can. J. Chem. **46**, 1181 (1968).
4. G. R. A. Johnson and M. Simic. Nature, **216**, 479 (1967).
5. O. L. Hollis and W. V. Hayes. Gas chromatography, 1966. *Edited by* A. B. Littlewood. Institute of Petroleum, London. 1967. p. 57.
6. R. A. Back, T. W. Woodward, and K. A. McLauchlan. Can. J. Chem. **40**, 1380 (1962).
7. P. B. Scott and J. R. Greening. Phys. Med. Biol. **8**, 51 (1963).
8. D. W. Huyton and T. W. Woodward. To be published.
9. G. R. A. Johnson and J. M. Warman. Trans. Faraday Soc. **61**, 1709 (1965).
10. D. W. Huyton and T. W. Woodward. To be published.
11. G. Meissner and A. Henglein. Z. Naturforsch. **20b**, 1005 (1965).
12. D. Perner and T. Franken. Ber. Bunsenges. Phys. Chem. **73**, 897 (1969).
13. A. V. Phelps and R. E. Voshall. J. Chem. Phys. **49**, 3246 (1968).
14. J. M. Warman and R. W. Fessenden. J. Chem. Phys. **49**, 4718 (1968).
15. I. S. Buchel'nikova. Sov. Phys. J.E.T.P. **35**, 783 (1959).
16. W. Hickam and R. Fox. J. Chem. Phys. **21**, 119 (1953).
17. F. H. Field and F. W. Lampe. J. Amer. Chem. Soc. **80**, 5583 (1958).
18. A. G. Harrison and J. C. Thynne. Trans. Faraday Soc. **62**, 3345 (1966).
19. P. Kebarle and A. M. Hogg. J. Chem. Phys. **42**, 798 (1965).
20. G. R. Freeman. Rad. Res. Rev. **1**, 17 (1968).
21. K. Jager and A. Henglein. Z. Naturforsch. **21a**, 1251 (1966).
22. G. R. A. Johnson and J. L. Redpath. J. Phys. Chem. **72**, 765 (1968).
23. D. W. Huyton and T. W. Woodward. Rad. Res. Rev. In press.

Can. J. Chem. Downloaded from www.nrcresearchpress.com by 210.87.254.5 on 09/05/12
For personal use only.

Nuclear magnetic resonance study of carbethoxypyrroles[1]

M. W. ROOMI[2] AND H. DUGAS[3]
Biochemistry Laboratory, National Research Council of Canada, Ottawa, Canada

Received December 22, 1969

The chemical shifts and the ring proton coupling constants of various substituted carbethoxypyrroles are reported.

The electron-withdrawing effect of the carbethoxy groups shifts the resonances of the ring substituents to low field while the inductive and mesomeric effects of the methyl groups shift the resonances to higher field. The deshielding effect is more pronounced with 2-carbethoxypyrroles than for 3-carbethoxypyrroles. The ring proton spin–spin coupling constants depend on the nature of substituents and increase with the electronegativity of the substituents. In some cases long-range coupling between the methyl side-chain protons and ring protons could be observed.

Canadian Journal of Chemistry, **48**, 2303 (1970)

Introduction

During the course of work on the Hantzsch synthesis and the alkylation of pyrroles, a large number of alkyl pyrroles and their carboxylic esters have been prepared (1, 2). Very little work has been reported on the nuclear magnetic resonance (n.m.r.) analysis of substituted pyrroles (4–9) and only few carbethoxypyrroles have been analyzed (7). It is the purpose of this paper to present a systematic analysis of the n.m.r. spectra of some substituted carbethoxypyrroles and also to investigate the effect of substitution on the chemical shifts and the magnitude of the spin–spin coupling constants between the ring protons in these molecules.

Experimental

The preparation of the pyrroles studied in the present investigation are reported elsewhere (1–3). The n.m.r. spectra were recorded with a Varian Associates A-60A instrument at a temperature of 38 °C. The samples were dissolved in deuterated chloroform to a concentration of 10% (w/v) and the chemical shifts are reported in parts per million (p.p.m.) from tetramethylsilane as internal reference, on the δ scale. The values of the coupling constants were rounded off to the nearest 0.1 Hz. All compounds were analyzed using a first order approximation except for **1***a* and *b* where second order treatment was found necessary. Only compound **1***a* was studied at 100 MHz with a Varian HA-100 high-resolution n.m.r. spectrometer. To exchange the N—H proton by deuterium, and thus simplify the spectra, the compounds were dissolved in deuterated chloroform containing a drop of deuterium oxide.

[1]Issued as NRCC No. 11326.
[2]NRCC Postdoctorate Fellow, 1968–1970.
[3]Guest worker (1968–1970). Present address: Département de Chimie, Faculté des Sciences, Université de Montréal, Montréal, Canada. To whom correspondence may be addressed.

Results and Discussion

The compounds under study are divided in three main groups: (*1*) monoalkyl-carbethoxypyrroles, (*2*) dialkyl-carbethoxypyrroles, and (*3*) trialkyl and trialkyl-carbethoxypyrroles. The substituents are numbered according to formula I and are listed as shown.

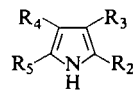

I

1

a $R_2 = CH_3$; $R_3 = CO_2C_2H_5$
b $R_2 = CH_3$; $R_3 = CO_2CH_2C_6H_5$
c $R_2 = CH_3$; $R_5 = CO_2C_2H_5$
d $R_3 = CH_3$; $R_4 = CO_2C_2H_5$
e $R_3 = CH_3$; $R_2 = CO_2C_2H_5$
f $R_3 = CH_3$; $R_2 = R_5 = CO_2C_2H_5$
g $R_2 = CH_3$; $R_3 = R_5 = CO_2C_2H_5$

2

a $R_2 = R_3 = CH_3$; $R_5 = CO_2C_2H_5$
b $R_2 = R_4 = CH_3$; $R_5 = CO_2C_2H_5$
c $R_3 = C_2H_5$; $R_4 = CH_3$; $R_5 = CO_2C_2H_5$
d $R_2 = R_4 = CH_3$; $R_3 = CO_2C_2H_5$
e $R_2 = R_5 = CH_3$; $R_3 = CO_2C_2H_5$

3

a $R_2 = R_3 = R_5 = CH_3$
b $R_2 = R_3 = R_5 = CH_3$; $R_4 = CO_2C_2H_5$
c $R_2 = R_3 = R_4 = CH_3$
d $R_2 = R_3 = R_4 = CH_3$; $R_5 = CO_2C_2H_5$

It should be mentioned that the resonances of the ring protons in analogous pyrroles (1, 2) with different alkyl groups are similar to those in the methyl derivatives, and therefore they are not reported here. In all the compounds under study the coupling constant, $J_{CH_2-CH_3}$, in the ethyl ester groups is 7.1 ± 0.1 Hz.

Can. J. Chem. Downloaded from www.nrcresearchpress.com by 210.87.254.5 on 09/05/12
For personal use only.

TABLE 1

Chemical shifts (p.p.m.) of carbethoxypyrroles in chloroform

Compound	Position of hydrogens and substituents on the pyrrole ring*				
	1†	2	3	4	5
1*a*	8.60	2.49(s)	4.25(q), 1.32(t)	6.54(m)	6.56(m)
b	9.10	2.47(s)	7.45(s), 5.37(s)	6.53(m)	6.65(m)
c	10.00	2.29(s)	5.89(m)	6.79(q)	4.39(q), 1.33(t)
d	9.32	6.57(m)	2.32(s)	4.30(q), 1.34(t)	7.43(q)
e	9.60	1.32(t), 4.38(q)	2.40(s)	6.17(t)	6.90(t)
f	9.94	4.33(q), 1.38(t)	2.32(s)	6.66(d)	4.35(q), 1.38(t)
g	10.76	2.63(s)	4.39(q), 1.39(t)	7.40(d)	4.43(q), 1.39(t)
2*a*	9.82	2.21(s)	2.01(s)	6.69(bd)	4.30(q), 1.32(t)
b	9.60	2.34(s)	5.81(bd)	2.29(s)	4.32(q), 1.38(t)
c	9.32	6.62(bd)	2.41(q), 1.15(t)	2.29(s)	4.30(q), 1.30(t)
d	9.16	2.50(s)	4.31(q), 1.37(t)	2.29(s)	6.40(m)
e	8.54	2.47(s)	4.25(q), 1.31(t)	6.20(m)	2.27(s)
3*a*	7.17	2.07(s)	1.96(s)	5.60(bd)	2.12(s)
b	8.08	2.15(s)	2.10(s)	4.27(q), 1.33(t)	2.44(s)
c	7.55	2.16(s)	1.99(s)	2.07(s)	6.51(bs)
d	9.26	2.24(s)	1.90(s)	2.16(s)	4.30(q), 1.32(t)

*bd = Broad doublet; bs = broad singlet; d = doublet; q = quartet; m = multiplet; and t = triplet.
†All N—H peaks are very broad.

TABLE 2

Spin–spin coupling constants (Hz) of carbethoxypyrroles

Compound	$J_{1,2}$	$J_{1,3}$	$J_{1,4}$	$J_{1,5}$	$J_{2,5}$	$J_{3,4}$	$J_{4,5}$	$J_{2\text{-}CH_3}$	$J_{3\text{-}CH_3}$	$J_{4\text{-}CH_3}$	$J_{5\text{-}CH_3}$
1*a*	—	—	2.2	2.8	—	—	3.2	—	—	—	—
b	—	—	2.4	3.1	—	—	3.2	—	—	—	—
c	—	2.8	2.8	—	—	3.5	—	—	0.8	0.8	—
d	2.3	—	—	3.2	2.3	—	—	1.1	—	—	—
e	—	—	2.8	2.8	—	—	2.8	—	—	*	—
f	—	—	2.9	—	—	—	—	—	—	0.7	—
g	—	—	2.8	—	—	—	—	—	—	—	—
2*a*	—	—	2.7	—	—	—	—	—	—	*	—
b	—	2.8	—	—	—	—	—	—	0.7	—	—
c	3.1	—	—	—	—	—	—	—	—	—	—
d	—	—	—	2.4	—	—	—	—	—	—	1.1
e	—	—	3.0	—	—	—	—	—	—	1.0	—
3*a*	—	—	2.4	—	—	—	—	—	—	*	—

*Peak too broad to measure the coupling constant.

The spectra of substituted pyrroles are complicated by the additional interaction of the N—H proton with the other ring protons. This coupling gives rise to multiplet splitting of ring proton resonances and adds considerably to the complexity of the spectra. Furthermore quadrupolar broadening by the nitrogen nucleus broadens the N—H absorption band.

In monoalkyl-carbethoxypyrroles the spectra of the ring protons are of the ABX type, but only the AB part can be analyzed since the X part (N—H proton) is broadened by the relaxation of the nitrogen nuclei. On the other hand the N—H proton of these molecules can be exchanged for a deuterium (4) and this simplifies the AB part of the spectrum. Additional interactions were found among the side-chain protons and the ring protons which further complicate the analysis.

The chemical shifts of the pyrrole ring protons and substituents are summarized in Table 1, and the spin–spin coupling constants of the ring protons in Table 2. The spectral data of com-

Can. J. Chem. Downloaded from www.nrcresearchpress.com by 210.87.254.5 on 09/05/12
For personal use only.

Can. J. Chem. Downloaded from www.nrcresearchpress.com by 210.87.254.5 on 09/05/12
For personal use only.

pounds **1***a,d* and **3***a,c* are known (5, 7, 8) but were nevertheless recorded and tabulated for comparison and clarity of discussion.

The important points to draw from these data are the following:

(*a*) According to current views on pyrroles (10) the 2-carbethoxy groups are more strongly conjugated with the pyrrole ring than the 3-carbethoxy groups. Hence, the resonance signals of the substituent R_5 would be expected to be at lower field for 2-carbethoxypyrroles than for the 3-carbethoxypyrroles, due to the electronegativity and mesomeric effects of the electron-withdrawing substituents. Such an effect is manifested throughout the present data; it was first observed in pyrrole systems by Abraham and Bernstein (6). For example, the experimental values in the series **1***a,c–e* and **2***a,b,d* show this very specific trend.

(*b*) The magnetic anisotropy of the ester groups is expected to deshield adjacent substituents. Hence, for 2-carbethoxypyrroles, R_3 should resonate at lower field than R_4; for 3-carbethoxypyrroles, R_2 should resonate to lower field than R_5. It is assumed that the ester group is freely rotating and the effects on adjacent substituents would be time averaged. The experimental data for compounds **1***d,e*, **2***a,d,e*, and **3***b,d* demonstrate this effect.

It is noteworthy that the replacement of the ethyl group by a benzyl group does not appear to have much effect on the chemical shifts of either ring or substituent protons. Comparison of **1***a* and *b* shows a small downfield shift of only 0.01 p.p.m. for the 4-proton and 0.02 p.p.m. for the 2-methyl protons. The deshielding of the 5-proton by the phenyl group to the extent of 0.09 p.p.m. is surprising in view of the very small effects on the other substituents.

(*c*) It is well known that methyl groups by their electron-donating effect, which is both inductive and mesomeric (hyperconjugative), increase the electron density in the pyrrole ring and also cause a redistribution of the electron densities at the different ring protons (6). This results in a general upfield shift of all resonances due to substituents attached to the ring relative to those in the unsubstituted compounds. This general effect is exemplified by comparing, for example, the ring protons of **1***a*, **2***d*, and **2***e*. The shifts are of the order of 0.2–0.4 p.p.m. A similar effect is evident on comparison of the data for other alkylpyrroles with pyrrole (5, 8).

(*d*) It is worthwhile to mention an interesting regularity observed among the ring proton coupling constants. It has been observed by Hoffman and Gronowitz (11) in substituted thiophenes, and also by Castellano andKostelnik (12) in benzene derivatives, that the ring proton spin–spin coupling constants depend on the nature of substituents and increase with the electronegativity of the substituents. Examination of the coupling constants of Table 2 yields a similar conclusion for carbethoxypyrroles.

Long-range coupling between protons is observed in some instances. Because of the perturbing effect of the nitrogen quadrupole relaxation (13) some peaks were too broad for measurement of the coupling constants.

In conclusion we can say that the chemical shifts and coupling constants of ring protons of substituted carbethoxypyrroles can be understood in terms of the current views on the effects of substituent electronegativity.

The authors wish to express their thanks to Dr. I. C. P. Smith for reading the manuscript before publication and to the National Research Council of Canada (M.W.R.) and to the North Atlantic Treaty Organisation (H.D.) for the financial support.

1. B. V. Gregorovich, K. S. Y. Liang, D. M. Clugston, and S. F. Macdonald. Can. J. Chem. **46**, 3291 (1968).
2. M. W. Roomi and S. F. Macdonald. Can. J. Chem. **48**, 139 (1970).
3. H. Fischer and H. Orth. Die Chemie des pyrroles. Vol. 1. Akademischer Verlag Leipzig, 1934.
4. R. J. Abraham and H. J. Bernstein. Can. J. Chem. **37**, 1056 (1959).
5. R. J. Abraham, E. Bullock, and S. S. Mitra. Can. J. Chem. **37**, 1859 (1959).
6. R. J. Abraham and H. J. Bernstein. Can. J. Chem. **39**, 905 (1961).
7. S. Gronowitz, A. B. Hörnfeldt, B. Gestblom, and R. A. Hoffman. Ark. Kem. **18**, 133 (1961).
8. R. L. Hinman and S. Theodoropulos. J. Org. Chem. **28**, 3052 (1963).
9. R. A. Jones, T. Mcl. Spotswood, and P. Cheuychit. Tetrahedron, **23**, 4469 (1967).
10. R. A. Jones. Adv. Heterocycl. Chem. **11**, 383 (1970).
11. R. A. Hoffman and S. Gronowitz. Ark. Kem. **16**, 563 (1960).
12. S. Castellano and R. Kostelnik. J. Amer. Chem. Soc. **90**, 141 (1968).
13. A. Taurins and W. G. Schneider. Can. J. Chem. **38**, 1237 (1960).

New chemical synthesis of 5′-phosphoribosyl-*N*-formylglycineamide[1]

SAMUEL Y. CHU[2] AND J. FRANK HENDERSON

University of Alberta Cancer Research Unit (McEachern Laboratory) and Department of Biochemistry, University of Alberta, Edmonton, Alberta

Received March 10, 1970

A new and convenient synthetic route to formylglycineamide ribonucleotide, an intermediate in the pathway of purine ribonucleotide biosynthesis de novo, is described. The method utilizes direct phosphorylation of the 5′-position of the linear riboside without protection of the 2′,3′-hydroxyl groups of the ribose, and gives a good yield of mixed α and β anomers. This route is suitable for synthesis of the natural product in quantities required for biological studies.

Canadian Journal of Chemistry, **48**, 2306 (1970)

Can. J. Chem. Downloaded from www.nrcresearchpress.com by 210.87.254.6 on 09/05/12
For personal use only.

Introduction

5′ - Phosphoribosyl - *N* - formylglycineamide (formylglycineamide ribonucleotide) (**5**) is one of the intermediates in the pathway of purine ribonucleotide biosynthesis de novo (1, 2). This pathway is of great importance in providing adenosine triphosphate and guanosine triphosphate, precursors of the nucleic acids. The enzyme which uses **5** as substrate is the site of action of the antitumor antibiotic azaserine, and the action of this compound and the binding of substrates to this enzyme have been studied in detail by Buchanan *et al.* (3–8). The enzymatic synthesis of this compound (9) requires the preparation of particular enzymes, and is not easily amenable to large-scale preparations. The chemical synthesis of **5** has been reported (10), but the yield was low, and the method used is not readily scaled up. We report here a new route (see Scheme 1) to this ribonucleotide in quantities which will permit more extensive studies of its metabolism. The overall yield is 20%.

Results and Discussion

Hydrogenation of 2,3,5-tri-*O*-benzoyl-β-D-ribofuranosyl azide (**1**) in acetone with Adam's catalyst at room temperature for 45 min resulted in complete loss of the azide infrared (i.r.) absorption maximum, 2120 cm^{-1}, and gave a compound which presumably was the 2,3,5-tri-*O*-benzoyl-β-D-ribofuranosyl amine (**2**). Baddiley *et al.* (11) have reported the isolation of the hydrochloride salt of **2** using ethyl acetate as solvent. The solvent used here has the advantage of requiring a smaller amount of catalyst, and of reducing the time of reaction; a longer time of hydrogenation in ethyl acetate can result in migration of the 2-benzoyl residue to the 1-position, forming 3,5-di-*O*-*N*-benzoyl-D-ribofuranosylamine (11). Furthermore, acetone is a better solvent for the formylglycine which is used in the subsequent reaction.

Freshly prepared **2** reacted readily with formylglycine at room temperature in the presence of *N*,*N*′-dicyclohexylcarbodiimide to give 2,3,5-tri-*O*-benzoyl-*N*-(*N*-formylglycyl)-α,β-D-ribofuranosylamine (**3**) in 67% yield.

Debenzoylation of **3** with sodium methoxide in anhydrous methanol gave *N*-(*N*-formylglycyl)-D-ribofuranosylamine (**4**) in good yield. The nuclear magnetic resonance (n.m.r.) spectrum of this compound in deuterated water with sodium 2,3-di-methyl-2 silapentane-5-sulfonate as reference standard showed peaks corresponding to 18 protons, with two proton singlets at 1.85 τ (formyl protons); doublets of 4.3 τ (anomeric proton of β-**4**) and 4.6 τ (anomeric proton of α-**4**); plus a series of multiplets from 5.61 to 6.4 τ corresponding to the 2, 3, 4, and 5 protons of ribose and two glycine protons. Either anomer, however, should exhibit but one formyl proton singlet and one anomeric proton doublet plus a simplified region for the remaining hydrogens to give a 9 proton spectrum. Thin-layer chromatography (t.l.c.) on silica gel showed only a single spot, and microanalysis indicated the empirical formula of **4** (α or β form). We conclude, therefore, that product **4** contains a mixture of α and β forms in approximately equal proportions. This conclusion was also based on the results of integration of proton signals. It has been noted by Baddiley *et al.* (11) that anomerization occurred immediately after hydrogenolysis of the azide to amine in the synthesis of *N*-(benzyloxy-

[1]Supported by the National Cancer Institute of Canada.
[2]Research Fellow of the National Cancer Institute of Canada 1969 – present.

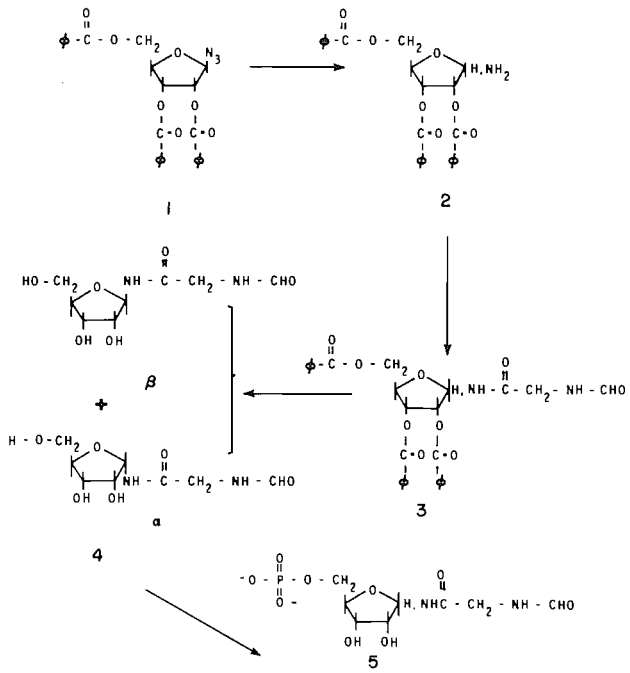

SCHEME 1

carbonylglycyl)-α,β-D-ribofuranosylamine, rather than in the subsequent steps.

Direct phosphorylation of **4** with phosphoryl chloride in triethylphosphate for 1½ h at 0 °C gave its 5′-phosphate (formylglycineamide ribonucleotide) (**5**). The direct phosphorylation of the linear ribonucleoside without protecting the 2′,3′-hydroxyl groups of the ribose extends the usefulness of the method of Yoshikawa *et al.* (12) of phosphorylation of unprotected nucleosides to 5′ nucleotides with phosphoryl chloride and trialkylphosphate. The direct phosphorylation of unprotected nucleosides to their 5′ nucleotides in different solvents has also been reported by Imai *et al.* (13).

This compound (**5**) gave the same R_f value (Table 1) as the authentic radioactive compound obtained from Ehrlich ascites tumor cells by the method of Henderson (14), and with values reported by others (15–17). On two chromatograms (solvents B and C) two zones were present, possibly due to the anomeric forms of compound **5** as noted by Westby and Gots (16) and Goldthwait *et al.* (15). The one with the higher R_f value had also been reported by Moore and LePage (17). Compound **5** also gave a negative ninhydrin test, but a positive test was obtained after acid hydrolysis to glycineamide ribonucleotide. The Schiff periodate test for *cis*-glycols was positive. Determination of the organic phosphate content using the method of Ames and Dubin (18), and ribose content by measuring spectrometrically the consumption of periodate (19), indicated their molar ratio to be 1.00:1.10 (Table 2). Phosphate analysis indicated this compound to be 92% pure, with impurities undoubtedly due to inorganic material. Compound **5**, 48.4%, can be converted to 5-amino-1-β-D-ribofuranosyl

TABLE 1

Paper chromatography of synthetic and authentic radioactive formylglycineamide ribonucleotide

	R_f of compounds*		
	Solvent A	Solvent B	Solvent C
Formylglycineamide ribonucleotide	0.26	0.31, 0.42	0.15, 0.35
Formylglycineamide ribonucleotide-^{14}C†	0.26	0.32, 0.43	0.15, 0.34
Ribose-5-PO_4	0.30	0.47	0.48

*Solvent systems are described in the Experimental section.
†Obtained from Ehrlich ascites tumor cells (14).

Can. J. Chem. Downloaded from www.nrcresearchpress.com by 210.87.254.6 on 09/05/12
For personal use only.

TABLE 2

Analysis of formylglycineamide ribonucleotide for organic phosphate and ribose content

	Experimental	Calculated
Organic phosphate	2.73 μmole/mg	2.97 μmole/mg
Ribose	2.76 μmole/mg	2.97 μmole/mg
Organic phosphate/ ribose	1.00/1.01	1.00/1.00

imidazole-5′-phosphate in the presence of adenosine triphosphate, L-glutamine, magnesium ion, and an enzyme preparation containing phosphoribosyl - formylglycine - amidine synthetase and phosphoribosyl-aminoimidazole synthetase. This result indicates that β and α anomers were synthesized in approximately equal amounts; although they have not been resolved, these and other studies have shown that the α anomer does not interfere with the enzymatic reaction of the naturally-occurring β form.

Experimental

Paper chromatography was carried out on Whatman No. 1 paper. The solvent systems used were: (*A*) 1-butanol:acetic acid:water (2:1:1), (*B*) 1-propanol:water (6:4), (*C*) 95% ethanol:water (77:23). Phosphate-containing compounds were detected with the ammonium molybdate reagent (20). The t.l.c. was done on silica gel, and compounds were detected by their ultraviolet (u.v.) absorption or with a sulfuric acid spray. The i.r. spectra were determined with a Perkin–Elmer 137B spectrophotometer. The n.m.r. measurements were performed by the Department of Chemistry and Faculty of Pharmacy, University of Alberta, with Varian A-60 instrument. Microanalyses were performed by George I. Robertson, Jr., 73 West End Avenue, Florham Park, New Jersey. Melting points were determined on a Kofler micro hot stage.

The enzymatic conversion of formylglycineamide ribonucleotide to 5-aminoimidazole ribonucleotide was carried out by incubation of the former with adenosine triphosphate, L-glutamine, KCl, $MgSO_4$, and phosphoribosyl - formylglycineamidine synthetase (5′ - phosphoribosyl - formylglycineamide : L - glutamine amidoligase [ADP], EC 6.3.5.3) (partially purified from Ehrlich ascites tumor cells); and phosphoribosyl-aminoimidazole synthetase (5′ - phosphoribosyl - formylglycineamidine cyclo-ligase [ADP], EC 6.3.3.1) (partially purified from chicken liver); the general procedure of Flaks and Lukens (21) was followed. The ribonucleotide product was determined by the Bratton–Marshall test for diazotizable amines (22).

2,3,5-Tri-O-benzoyl-N-(formylglycyl) α,β-D-ribofuranosylamine

2,3,5-Tri-*O*-benzoyl-β-ribofuranosyl azide (1 g) (10) was dissolved in 40 ml of anhydrous acetone, 50 mg of platinum oxide were added, and the mixture was hydrogenated with a Parr hydrogenation apparatus at room temperature at a pressure of 10 lb/sq in. for 45 min. Anhydrous magnesium sulfate was added and the solution filtered. The filtrate was added at once to a flask containing 400 mg of formylglycine (23) dissolved in 50 ml of acetone. To this solution, 600 mg of *N,N′*-dicyclohexylcarbodiimide were added and the mixture was allowed to stand at room temperature with occasional shaking for 2.5 h. The insoluble urea derivative was collected by filtration and the filtrate was concentrated to 20 ml and again filtered. The filtrate was kept at 0 °C overnight. After removing the residue, the filtrate was evaporated to a gum at room temperature. Ethyl acetate (5 ml) was added and the solution was applied to a column of silica gel (2 × 30 cm). The column was eluted with 2 ml fractions of ethyl acetate. A compound which absorbed u.v. light after t.l.c. (R_f 0.5) in ethyl acetate was collected (80 to 160 ml) and the solution was concentrated to 20 ml and set aside at 0° for 2–3 h. The residue was filtered and the filtrate was evaporated under high vacuum to a dry residue: 740 mg (67%), m.p. 58–63 °C, $[\alpha]_D^{20}$ + 42° (1% methanol). The t.l.c. gave a single spot detected by u.v. absorption (R_f 0.5; ethyl acetate), but a minor spot with R_f 0.42 also appeared when the H_2SO_4 spray was used. The i.r. spectroscopy of the product in chloroform gave absorption maxima at 3400, 1680, and 1520 cm^{-1} which were characteristic of the secondary amide group. Analysis showed this compound to be reasonably pure (90% based on N). Further purification of the compound was unsuccessful but this preparation was acceptable in the subsequent reaction.

Anal. Calcd. for $C_{29}H_{26}O_9N_2$: C, 63.4; H, 4.73; N, 5.10. Found: C, 62.51; H, 5.11; N, 5.70.

N-(N-Formylglycyl)-α,β-D-ribofuranosylamine

2,3,5-Tri-*O*-benzoyl-*N*-formylglycyl-α,β-D-ribofuranosylamine (550 mg, 1 mmole) was dissolved in 1 ml of dry methanol and sodium methoxide (from 0.01 g sodium in 5 ml methanol) added at room temperature. After 10 h the solution was evaporated to a small volume (about 1.5 ml) and filtered. Methanol (10 ml) was added to the filtrate and this was passed through a Dowex-50 column (1 × 1.5 cm, H^+ form, methanol washed), and the column was washed with 20 ml of methanol. The combined methanol fractions were evaporated to dryness, dissolved in 25 ml of water, and extracted once with 30 ml of ether. The water layer was lyophilized, giving 140 mg of product (66%): $[\alpha]_D^{20}$ + 18.6° (1% methanol). The compound is hydroscopic. The i.r. examination of the compound in a KBr disc showed no ester–carbonyl band at 1720 cm^{-1}, but a hydroxyl band at 3425 cm^{-1} was present. The t.l.c. showed only a single spot (R_f 0.71 in methanol) as detected by the sulfuric acid spray.

Anal. Calcd. for $C_{18}H_{14}N_2O_6$: C, 41.05; H, 5.90; N, 11.98. Found: C, 41.03; H, 6.20; N, 12.00.

Formylglycineamide Ribonucleotide

N-(*N*-Formylglycyl)-D-ribofuranosylamine (48 mg) was dissolved in 2 ml of triethylphosphate and the mixture was kept at 0 °C. Phosphorous oxychloride (0.2 ml) was added slowly with stirring. The reaction mixture was then kept at this temperature for 1.5 h with stirring. Ether (100 ml) was added to the reaction mixture to precipitate

Can. J. Chem. Downloaded from www.nrcresearchpress.com by 210.87.254.6 on 09/05/12
For personal use only.

the *N*-(*N*-formylglycyl)-D-ribose 5′-phosphordichloridate which was then collected by centrifugation. The product was washed once with 40 ml of ether and dissolved in 0.5 ml of cold water containing 0.1 ml of triethylamine. The aqueous solution was then adjusted to p*H* 8.5 with 1 *N* HCl. Barium bromide (1 *M*, 0.5 ml) was added and the barium salt was precipitated by addition of 5 volumes of cold 98% ethanol. The barium salt was centrifuged after 1 h at 0 °C to give 90 mg. Paper chromatography of the salt showed one major product together with other phosphorylated compounds. The barium salt was dissolved in 5 ml of water, passed through a 1 × 1.5 cm column of Dowex-50 (H^+ form) and the column was washed once with 10 ml of water. The combined effluents were adjusted with ammonium hydroxide to p*H* 8 and applied onto a column (1 × 12 cm) of Dowex-1-X8 in the formate form. The column was washed with 20 ml of water and eluted with 0.05 *M* ammonium formate, p*H* 5. Fractions from 110 to 250 ml were collected and neutralized to p*H* 8 with ammonium hydroxide (these were enzyme substrates and contained organic phosphate). Again this fraction was absorbed onto a column (1 × 4 cm) of Dowex-1-X8 in the chloride form. The column was washed with 150 ml of distilled water and the product was eluted with 0.24 *M* lithium chloride. Fractions from 2.0 ml to 20 ml were collected and lyophilized. The residue was washed twice with 4.5 ml of methanol:acetone (3:2) and dried under vacuum to give 28 mg of the lithium salt of *N*-(*N*-formylglycyl)-D-ribofuranosylamine-5′-phosphate (**5**) (yield 40%).

We wish to thank Profs. R. J. Crawford and M. Robins of the Chemistry Department, University of Alberta, and Dr. B. Paul, for their helpful discussions in the course of this work.

1. D. A. GOLDTHWAIT, R. A. PEABODY, and G. R. GREENBERG. J. Amer. Chem. Soc. **76**, 5258 (1954).
2. S. C. HARTMAN, B. LEVENBERG, and J. M. BUCHANAN. J. Amer. Chem. Soc. **77**, 501 (1955).
3. T. C. FRENCH, I. B. DAWID, R. A. DAY, and J. M. BUCHANAN. J. Biol. Chem. **238**, 2171 (1963).
4. I. B. DAWID, T. C. FRENCH, and J. M. BUCHANAN. J. Biol. Chem. **238**, 2178 (1963).
5. T. C. FRENCH, I. B. DAWID, and J. M. BUCHANAN. J. Biol. Chem. **238**, 2186 (1963).
6. K. MIZOBUCHI and J. M. BUCHANAN. J. Biol. Chem. **243**, 4842 (1968).
7. K. MIZOBUCHI and J. M. BUCHANAN. J. Biol. Chem. **243**, 4853 (1968).
8. K. MIZOBUCHI and J. M. BUCHANAN. J. Biol. Chem. **243**, 4863 (1968).
9. S. C. HARTMAN, G. LEVENBERG, and J. M. BUCHANAN. J. Biol. Chem. **221**, 1057 (1956).
10. R. CARRINGTON, G. SHAW, and D. V. WILSON. J. Chem. Soc. 6864 (1965).
11. J. BADDILEY, J. G. BUCHANAN, R. HODGES, and J. F. PRESCOTT. J. Chem. Soc. 4769 (1957).
12. M. YOSHIKAWA, T. KATO, and T. TAKENISHI. Tetrahedron Lett. **50**, 5065 (1967).
13. K. IMAI, S. FIJI, K. TAKANOHASHI, Y. FURUKAWA, T. MASUDA, and M. HONJO. J. Org. Chem. **34**, 1547 (1969).
14. J. F. HENDERSON. J. Biol. Chem. **237**, 2631 (1962).
15. D. A. GOLDTHWAIT, R. A. PEABODY, and G. R. GREENBERG. J. Biol. Chem. **221**, 555 (1956).
16. C. L. WESTBY and J. S. GOTS. J. Biol. Chem. **244**, 2095 (1969).
17. E. C. MOORE and G. A. LEPAGE. Cancer Res. **17**, 804 (1957).
18. B. N. AMES and O. T. DUBIN. J. Biol. Chem. **235**, 769 (1960).
19. J. S. DIXON and D. LIPKIN. Anal. Chem. **26**, 1092 (1952).
20. R. S. BANDURSKI and B. AXELROD. J. Biol. Chem. **193**, 405 (1951).
21. J. G. FLAKS and L. N. LUKENS. *In* Methods in enzymology. Vol. 6. S. P. Colowick and N. O. Kaplan (*editors*). Academic Press, New York, 1963. p. 52.
22. A. C. BRATTON and E. E. MARSHALL, JR. J. Biol. Chem. **128**, 539 (1939).
23. E. FISCHER and O. WARBURG. Ber. **38**, 3997 (1905).

Can. J. Chem. Downloaded from www.nrcresearchpress.com by 210.87.254.6 on 09/05/12
For personal use only.

Can. J. Chem. Downloaded from www.nrcresearchpress.com by 210.87.254.105 on 09/05/12
For personal use only.

Canadian Journal of Chemistry

Published by THE NATIONAL RESEARCH COUNCIL OF CANADA

VOLUME 48 AUGUST 1, 1970 NUMBER 15

The ethenoxy radical in the pyrolysis of acetaldehyde

H.-P. SCHUCHMANN AND K. J. LAIDLER

Department of Chemistry, University of Ottawa, Ottawa, Canada

Received March 5, 1970

In the pyrolysis of pure acetaldehyde at 450–525 °C it was found that ketene, although stable under these conditions, is not formed as a final reaction product. This result requires a modification of the mechanism of Liu and Laidler, according to whom the ethenoxy radical CH_2CHO splits into CH_2CO and H. It is concluded that instead of splitting unimolecularly, CH_2CHO disappears mainly through the reaction

$$CH_2CHO + CH_3CHO \rightarrow CH_3CHO + CH_3CO$$

and that it also undergoes the process

$$CH_2CHO + CH_3CHO \rightarrow CH_3\underset{\displaystyle O-}{\underset{|}{C}}HCH_2CHO \rightarrow CH_3COCH{=}CHOH + H$$

Canadian Journal of Chemistry, 48, 2315 (1970)

We have recently carried out a detailed investigation of the effect of added nitric oxide on the acetaldehyde pyrolysis and the results are in course of publication (1). These studies included further measurements of rates in the absence of nitric oxide. We have now found, contrary to the result of Liu and Laidler (2), that ketone does not decompose to a significant extent under the pyrolysis conditions. We confirm Liu and Laidler's result that ketene is not a product of the pyrolysis, but conclude that a modification is necessary to their reaction

[1] $$CH_2CHO \rightarrow CH_2CO + H$$

as an important one in removing the CH_2CHO radical.

The present paper reports rates of formation of a number of additional reaction products and suggests alternative fates for the CH_2CHO radical.

Experimental

The apparatus and procedures are described in detail in the paper on the effect of nitric oxide (1). The reaction vessel was Pyrex and had a volume of 209 cc.

The acetaldehyde was prepared from paraldehyde (British Drug Houses, Laboratory Grade) which was first purified by distillation and then converted into acetaldehyde by addition of concentrated H_2SO_4. It was purified by fractional distillation in an atmosphere of pure nitrogen, no air ever being allowed to come into contact with the acetaldehyde.

Products were determined by vapor-phase chromatography.

Results and Analysis

The following products were identified, and the rates of their formation were measured: H_2, CO, C_2H_6, C_2H_5CHO, CH_4, CO_2, C_3H_6, $CH_3COOC_2H_3$, C_2H_4, and CH_3COCH_3. A small amount was found of a compound which has a molecular weight of 70 when analyzed in the mass spectrometer, and which has the same retention time as crotonaldehyde $CH_3CH{=}CHCHO$. Other compounds which could be identified by chromatography but which were not obtained as pyrolysis products are CH_2O (10^{-14}), CH_2CO (10^{-13}), $CH_3OCH{=}CH_2$ (10^{-14}), $CH_3COCOCH_3$ (10^{-12}), CH_3OH (10^{-14}), C_2H_5OH (10^{-14}), $(CH_3)_2CHOH$ (10^{-13}), and H_2O (10^{-11}). The figures in parentheses indicate the detectability thresholds at 500 °C, in moles cc^{-1} s^{-1}; the high value for H_2O is due to strong tailing.

Small amounts of ketene were co-pyrolyzed with acetaldehyde, for reaction times from 10 to 400 s. There was no detectable disappearance of ketene.

Can. J. Chem. Downloaded from www.nrcresearchpress.com by 210.87.254.105 on 09/05/12
For personal use only.

In an effort to obtain an additional reaction that produced H atoms, to replace

$$CH_2CHO \rightarrow CH_2CO + H$$

the compound $CH_3COCH{=}CHOH$ (tautomeric with CH_3COCH_2CHO) was tested. Gas chromatograms of it could be obtained in the absence of acetaldehyde, but not in its presence. The pure compound is unstable and polymerizes (3).

Rates of product formation at 500 °C and an acetaldehyde pressure of 176 Torr are given in Table 1. Our rates for formation of $CH_4 + CO$, H_2, CH_3COCH_3, C_2H_6, and C_2H_5CHO are approximately of the same magnitude of those of Liu and Laidler (2, 4). The present investigation was not primarily concerned with measurements of activation energies, reliable values for which were given for the main products in the previous work. We did, however, measure rates at 450, 475, 500, and 525° and found for CO_2, C_2H_4, C_3H_6, and $CH_3COOC_2H_3$ an increase by about an order of magnitude over that range.

TABLE 1

Rates of pyrolysis product formation at 500 °C*

Product	Rate (mole cc^{-1} s^{-1})
CH_4	2.99×10^{-9}
CO	2.99×10^{-9}
H_2	4.79×10^{-12}
CH_3COCH_3	1.24×10^{-12}
CO_2	3.34×10^{-13}
C_2H_4	0.76×10^{-13}
C_2H_6	3.35×10^{-13}
C_3H_6	5.02×10^{-13}
C_2H_5CHO	1.44×10^{-13}
$CH_3COOC_2H_3$	1.5×10^{-13}

*Acetaldehyde pressure = 176.0 Torr.

Discussion

In order to reach a conclusion as to the reactions occurring, estimates have been made of free radical concentrations. The results are summarized in Table 2. In most cases the concentrations were calculated from the rate constant and the rate of formation of a product (in italics in the table). The CH_2CHO concentration has also been calculated on the basis of steady-state considerations, the important reactions involving CH_2CHO being

[2] $$CH_3 + CH_3CHO \rightarrow CH_4 + CH_2CHO$$

[3] $$CH_2CHO + CH_3CHO \rightarrow CH_3CHO + CH_3CO$$

The Arrhenius parameters of reaction [2] are not known, but comparison with a series of similar abstraction reactions $CH_3 + M \rightarrow CH_4 + CH_2R$ (cf. Table 3) suggests a rate constant of $\sim 10^9$ cc $mole^{-1}$ s^{-1}.

The rate constant for reaction [3] is estimated on the assumption that CH_2CHO behaves similarly to the allyl radical. Consider the reactions

[4] $$C_3H_5 + C_6H_5CH_3 \rightarrow C_3H_6 + C_6H_5CH_2$$

[5] $$CH_3 + C_6H_5CH_3 \rightarrow CH_4 + C_6H_5CH_2$$

[6] $$C_3H_5 + CH_3CHO \rightarrow C_3H_6 + CH_3CO$$

[7] $$CH_3 + CH_3CHO \rightarrow CH_4 + CH_3CO$$

The following rate constants are known (500 °C): $k_4 = 10^{6.4}$ cc $mole^{-1}$ s^{-1} (mean of values in refs. 5 and 6), $k_5 = 10^{8.9}$ cc $mole^{-1}$ s^{-1} (7), and $k_7 = 10^{9.9}$ cc $mole^{-1}$ s^{-1} (4). It is postulated that $k_4/k_5 = k_6/k_7$, whence $k_6 = 10^{7.4}$ cc $mole^{-1}$ s^{-1}, and this will be assumed to be the value of k_3. Substitution of these values into the steady-state equation leads to $[CH_2CHO] \approx 10^{-11.6}$ cc $mole^{-1}$. In this argument, the isomerization of CH_2CHO into CH_3CO has been assumed to be unimportant; this matter is discussed in Appendix 1. It is also assumed that reaction [1] is unimportant; this requires further discussion since it is at variance with the conclusion of Liu and Laidler (2, 4).

Liu and Laidler were led to postulate reaction [1] as important since the reactions

[8] $$CH_3 + CH_3CHO \rightarrow CH_3COCH_3 + H$$

and

[9] $$CHO \rightarrow CO + H$$

alone do not furnish enough H atoms to account for all of the H_2 formed. They considered that reaction [3] was less important than reaction [1], and this led them to a value of 7.5×10^6 cc $mole^{-1}$ s^{-1} for the rate constant of reaction [2] at 523 °C. This value is about two orders of magnitude lower than that obtained above on the basis of the comparison of the rate constants of the reactions listed in Table 3. Our present view is that the higher estimates are much more reliable, Liu and Laidler's lower value being due to their neglect of reaction [3].

This being so, it is no longer possible to maintain that reaction [1] is the main process by which CH_2CHO is removed, since this would lead to a rate of H_2 formation as high as one-tenth

TABLE 2

Estimates of free-radical concentrations
(T = 500 °C; [CH_3CHO] = $10^{-5.5}$ mole cc^{-1})

Radical	Reaction considered	Rate constant (s^{-1} or cc mole^{-1} s^{-1})	Estimated concentration (mole cc^{-1})
CH_3	$CH_3 + CH_3CHO \rightarrow CH_4 + CH_3CO$	$10^{9.9}$ (4)	$10^{-12.9}$
CH_3	$2\ CH_3 \rightarrow C_2H_6$	$10^{13.3}$ (11)	$10^{-12.9}$
CH_3CO	$CH_3CO \rightarrow CH_3 + CO$	$10^{6.4}$ (12)	$10^{-14.9}$
H	$H + CH_3CHO \rightarrow H_2 + CH_3CO$	$10^{11.3}$ (13)	$10^{-17.1}$
$(CH_3)_2CHO$	$(CH_3)_2CHO \rightarrow CH_3COCH_3 + H$	$10^{7.4}$ (4)	$10^{-19.3}$
C_2H_5O	$C_2H_5O + CH_3CHO \rightarrow C_2H_5OH + CH_3CO$	$10^{9.2}$*	$< 10^{-17.7}$
CH_3CHOCH_3	$CH_3CHOCH_3 \rightarrow CH_2{=}CHOCH_3 + H$	$\sim 10^{3}$†	$\leqslant 10^{-17}$
CH_3CHOH	$CH_3CHOH + CH_3CHO \rightarrow C_2H_5OH + CH_3CO$	$\sim 10^{7.7}$‡	$< 10^{-16.4}$
CHO	$CHO \rightarrow CO + H$	$10^{9.0}$ (14)	$< 10^{-20.3}$§
CH_2CHO	$CH_3 + CH_2CHO \rightarrow C_2H_5CHO$	10^{11}‖	$10^{-10.9}$
CH_2CHO	Steady-state; see text		$10^{-11.6}$

*This is the rate constant of the similar reaction $C_2H_5O + C_2H_5COOC_2H_5 \rightarrow C_4H_9COO$ (15).
†This estimate is based on a frequency factor of 10^{13} s^{-1} and an activation energy of 35 kcal mole^{-1}. The similar reaction $CH_3CHCH_3 \rightarrow C_3H_6 + H$ has a frequency factor of $10^{13.8}$ and an activation energy of 36.9 kcal mole^{-1} (14).
‡This estimate is based on a frequency factor of $10^{10.7}$ cc mole^{-1} s^{-1} and an activation energy of 10 kcal mole^{-1}. The latter value was chosen because CH_3CHOH is more stable than C_2H_5O; the reaction $C_2H_5O + C_2H_5COOC_2H_5 \rightarrow C_2H_5 + C_4H_9CO_2$ has an activation energy of 5.5 kcal mole^{-1} and a frequency factor of $10^{10.7}$ cc mole^{-1} s^{-1} (15).
§The rate of H_2 production is $10^{-11.3}$ mole cc^{-1} s^{-1}, but $CHO \rightarrow CO + H$ is not the only source of H atoms; thus $v_H > 10^{9.0}$ [CHO] s^{-1}.
‖This rate constant is assumed to be equal to that of $CH_3 + CH_2{-}CH{=}CH_2 \rightarrow C_2H_5CH{=}CH_2$, which has been given as 10^{11} cc mole^{-1} s^{-1} (16).

TABLE 3

Rate constants at 500 °C for reactions of the type
$CH_3 + M \rightarrow CH_4 + R{-}CH_2$

M	Rate constant (cc mole^{-1} s^{-1})	Reference
C_2H_6	$10^{8.6}$	17
CH_3COCH_3	$10^{9.1}$	17
C_3H_6	$10^{8.7}$	16
CH_3OCH_3	$10^{9.0}$	17
CH_3OH	$10^{8.5}$	18

of that of methane; experimentally $v_{H_2}/v_{CH_4} = 10^{-2.8}$. Moreover, ketene is not a product, and is stable under the experimental conditions. Reaction [1] must therefore be eliminated from the mechanism, and be replaced by another reaction which generates hydrogen atoms.

Further comments on the reactivity of the ethenoxy radical are given in Appendix 2.

Rate of Hydrogen Formation

Reactions [9] and [8] together do not generate H atoms at the desired rate. Thus at 500 °C the rate of acetone production is $10^{-11.9}$ mole cc^{-1} s^{-1}, and this can be equated to v_8. The steady-state equation for CHO is

$$k_{10}[CH_3CHO] = k_9[CHO]$$

where k_{10} refers to the reaction

[10] $CH_3CHO \rightarrow CH_3 + CHO$

Hence, since $k_{10} = 10^{-7.0}$ s^{-1} (4),

$$v_9 = k_9[CHO] = 10^{-12.5} \text{ moles cc}^{-1}\ s^{-1}$$

Thus

$$v_9 + v_8 = 10^{-12.5} + 10^{-11.9} = 10^{-11.8} \text{ moles cc}^{-1}\ s^{-1}$$

which is only 0.3 v_{H_2}.

The rest of the H_2 must be formed by a reaction which produces an H atom from either a CH_3 or a CH_2CHO radical; other radicals can be excluded since their concentrations are too low (cf. Table 2).[1] Possible reactions involving CH_3 and CH_2CHO are

[11] $CH_3 + CH_3CHO \rightarrow C_2H_6 + CHO$

[12] $CH_3 + CH_3CHO \rightarrow CH_3\underset{|}{C}HOCH_3 \rightarrow H + CH_2{=}CHOCH_3$

[13] $CH_2CHO + CH_3CHO \rightarrow CH_3\underset{|}{C}HCH_2CHO \rightarrow H + CH_3COCH_2CHO$ (O— on the C)

[14] $CH_2CHO + CH_3CHO \rightarrow CH_3\underset{|}{C}HOCH_2CHO \rightarrow H + CH_2{=}CHOCH_2CHO$

[15] $CH_2CHO + CH_3CHO \rightarrow CH_3\underset{|}{C}HOCH_2{=}CH_2 \rightarrow H + CH_3COOCH{=}CH_2$ (O— on the C)

[1]Even reaction [8] does not produce H atoms sufficiently rapidly to account for all of the H_2 produced, in spite of the high concentration of CH_3 radicals.

Can. J. Chem. Downloaded from www.nrcresearchpress.com by 210.87.254.105 on 09/05/12
For personal use only.

[16] $CH_2CHO + CH_3CHO \rightarrow CH_2{=}CHOCH_3 + HCO$

[17] $CH_2CHO + CH_3CHO \rightarrow C_2H_5CHO + CHO$

Of these, reactions [11], [15], and [17] can be excluded because of the very low rates of formation of C_2H_6, $CH_3COOCH{=}CH_2$, and C_2H_5CHO compared with H_2. Reactions [12] and [16] are excluded by the absence of methyl vinyl ether. Processes [13] and [14] cannot be excluded in any such way. We favor the conclusion that reaction [13] furnishes the H atoms required to explain the H_2 yield, possibly occurring as follows

[13] 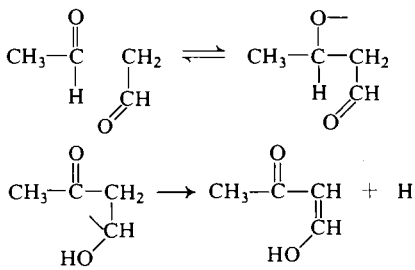

The tendency to form conjugated double bonds would aid the elimination of the H atom.

Our conclusion is that the Liu–Laidler scheme of reactions must be modified by the elimination of reaction [1] and the addition of the following reactions

[18] $H + CH_3CHO \rightarrow H_2 + CH_2CHO$

[13] $CH_2CHO + CH_3CHO \rightleftharpoons CH_3CH(O)CH_2CHO \rightarrow CH_3COCH{=}CHOH + H$

[15] $CH_2CHO + CH_3CHO \rightleftharpoons CH_3CH(O){-}OCH{=}CH_2 \rightarrow CH_3COOCH{=}CH_2 + H$

[19] $H + CH_2{=}CHOH \rightleftharpoons CH_2CH_2OH \rightarrow C_2H_4 + OH$

[20] $CH_3 + CH_2{=}CHOH \rightleftharpoons CH_2CH(CH_3)OH \rightarrow C_3H_6 + OH$

[21] $OH + CH_3CHO \rightarrow H_2O + CH_3CO$

[22] $CH_3CHO + CH_3CHO \xrightarrow{\text{wall?}} C_3H_6 + CO + H_2O$

[23] $CH_3CHO + CH_3CHO \xrightarrow{\text{wall?}} C_3H_6 + CO_2 + H_2$

[24] $CH_3CHO + CH_3CHO \xrightarrow{\text{wall?}} CH_3CH{=}CHCHO + H_2O$

These reactions also account for the formation of the products C_3H_6, C_2H_4, CO_2, and $CH_3COOC_2H_3$.

The authors are indebted to Dr. M. H. Back for valuable discussions and to Dr. R. J. Cvetanovic for a sample of pure ketene. H.-P.S. is grateful for the award of an Ontario Graduate Fellowship.

Appendix 1

Intramolecular Isomerization of CH_2CHO

The possibility that the unimolecular process

[25] $CH_2CHO \rightarrow CH_3CO$

is significant seems unlikely on the following grounds. The activated state would be a three-membered ring, and Benson (ref. 8, p. 65) has concluded that the ring strain in the activated state for a hydrogen 1,2-shift in an alkyl radical is the same as that in cyclopropane, viz. 27 kcal mole^{-1}. The strain in cyclopropene is about 56 kcal mole^{-1} (9). Since the bond order of the C—C bond in CH_2CHO may be about 1.5, because of mesomerism, the strain in the activated state may well be close to the average of 27 and 56, viz. $\sim$ 42 kcal mole^{-1}. (This agrees well with the value of 41 kcal mole^{-1} for the ring strain in methylene cyclopropane (10)). There will be an energy barrier of $\sim$ 5 kcal mole^{-1} for the H atom abstraction, so that the estimated activation energy for the isomerization is $\sim$ 47 kcal mole^{-1}. If the frequency factor is 10^{13} s^{-1}, one obtains at 500 °C, $k_{25} \approx 10^{0}$ s^{-1}, and $v_{25}/v_3 \approx 10^{-2}$.

Appendix 2

Further Comments on the Reactivity of CH_2CHO

The reactivity of CH_2CHO is obviously a matter of great importance for a complete understanding of the mechanism of the acetaldehyde pyrolysis. In the present work a value of $10^{7.4}$ cc mole^{-1} s^{-1} has been deduced for k_3, the rate constant of the reaction

$$CH_2CHO + CH_3CHO \rightarrow CH_3CHO + CH_3CO$$

on the assumption that the radical behaves similarly to the allyl radical. Benson, on the other hand, assumes the reactivity to be similar to that of CH_3 (ref. 8, p. 141). If CH_2CHO is in fact more reactive than the allyl radical, its concentration will be below that given in Table 2. This, however, would not materially affect the contention that CH_2CHO may play a considerable role in this pyrolysis; if its reactivity is low its steady-state concentration will be high, and vice versa, so that its net influence as a chain carrier will remain the same.

Can. J. Chem. Downloaded from www.nrcresearchpress.com by 210.87.254.105 on 09/05/12
For personal use only.

1. H.-P. SCHUCHMANN and K. J. LAIDLER. Int. J. Chem. Kinet. In press.
2. K. J. LAIDLER and M. T. H. LIU. Proc. Roy. Soc. London, Ser. A. **297**, 365 (1967).
3. L. CLAISEN and N. STYLOS. Ber. Dtsch. Chem. Ges. **21**, 1144 (1888).
4. M. T. H. LIU and K. J. LAIDLER. Can. J. Chem. **46**, 479 (1968).
5. M. SZWARC, B. N. GHOSH, and A. H. SEHON. J. Chem. Phys. **18**, 1142 (1950).
6. R. J. AKERS and J. J. THROSSELL. Chem. Commun. 432 (1966).
7. A. F. TROTMAN-DICKENSON and G. S. MILNE. Tables of bimolecular gas reactions. NSRDS–NBS Publication No. 9, Washington, D.C. 1967.
8. S. W. BENSON. Thermochemical kinetics. John Wiley and Sons, Inc., New York. 1968.
9. G. L. CLOSS. Advan. Alicyclic Chem. **1**, 67 (1966).
10. L. N. FERGUSON. J. Chem. Ed. **47**, 46 (1970).
11. A. J. SHEPP. J. Chem. Phys. **24**, 939 (1956).
12. J. G. CALVERT and J. T. GRUVER. J. Amer. Chem. Soc. **80**, 1313 (1958).
13. E. W. R. STEACIE. Atomic and free radical reactions. Reinhold, New York. 1954.
14. J. A. KERR and A. C. LLOYD. Quart. Rev. **22**, 549 (1968).
15. P. GRAY, R. SHAW, and J. C. J. THYNNE. Prog. React. Kinet. **4**, 106 (1964).
16. A. AMANO and M. UCHIYAMA. J. Phys. Chem. **68**, 1133 (1964).
17. S. W. BENSON. The foundations of chemical kinetics. McGraw-Hill, New York. 1960.
18. A. F. TROTMAN-DICKENSON. Advan. Free Radical Chem. **1**, 1 (1965).

Can. J. Chem. Downloaded from www.nrcresearchpress.com by 210.87.254.105 on 09/05/12
For personal use only.

Can. J. Chem. Downloaded from www.nrcresearchpress.com by 210.87.254.42 on 09/05/12
For personal use only.

Solid–liquid equilibrium in the system chlorine dioxide – chlorine

J. KEPINSKI AND K. KALUCKI
Department of Inorganic Chemical Technology, Technical University, Szczecin, Poland

Received[1] August 18, 1969

The method of preparation and analysis of liquid mixtures of chlorine dioxide and chlorine is described. The mixtures of chlorine dioxide and chlorine were found to be completely miscible. The freezing points were determined by using the dynamic method of measurement and the extrapolation procedure. An eutectic point was found to exist at -101.6 ± 0.1 °C. The eutectic solution contains 1.6 mole % of chlorine dioxide.

Canadian Journal of Chemistry, **48**, 2320 (1970)

Introduction

Because it is explosive in pure gaseous and liquid state (1, 2), chlorine dioxide must be prepared immediately prior to its use. This poses a severe limitation on all uses of chlorine dioxide other than bleaching of pulp, e.g. disinfection of water, treatment of phenolic waste waters, control of industrial odors, bleaching of flour, fats and waxes, and some other minor uses. Therefore, the transport of liquid mixtures of chlorine dioxide and chlorine has been the object of some patents (3). Since no information on this system could be found in the literature, its study was undertaken.

Experimental

Preparation of Chlorine Dioxide

Chlorine dioxide was prepared by oxidation of sodium chlorite with gaseous mixtures of chlorine and air (4). The apparatus used for this purpose is shown schematically in Fig. 1. The dry mixture of chlorine dioxide and air entered the glass trap in Fig. 2, inserted in a 1 l Dewar flask filled with Dry Ice. The temperature was measured with a thermocouple inside the trap. Before inserting the trap into the cooling medium, the air contained in it was displaced with the dry mixture containing chlorine dioxide. The chlorine dioxide condensed on the walls of the trap as a red liquid and solidified into a deep red solid. After filling one third of the trap with a measured quantity of chlorine dioxide, a suitable quantity of dry chlorine was taken from a cylinder. The ends of the capillary tubes were closed with small tubes containing phosphorus pentoxide, in order to avoid contamination with water vapor.

Safety Considerations

In order to prevent possible accidents, generation and condensation of chlorine dioxide was carried out under the laboratory hood secured with additional acrylic glass plates and steel net. The experimenter worked wearing leather gloves, behind a 10 mm thick acrylic glass plate.

No accident happened in the course of generating and liquefying chlorine dioxide. One serious explosion occurred while evaporating liquid chlorine dioxide when the trap was full of 100% gaseous chlorine dioxide. No one was hurt although all glassware was shattered to glass powder.

Analytical Procedure

The samples of mixtures of chlorine dioxide and chlorine were dissolved in dry c.p. carbon tetrachloride, cooled to -15 °C and analyzed by the method of Flis and Byniayeva (6) with some modifications.

An aliquot of the solution was transferred with a pipette to an Erlenmeyer flask fitted with a glass stopcock and containing a few grams of potassium iodide. The solution was acidified with aqueous 2 *N* sulfuric acid. The iodine produced was titrated with sodium thiosulfate.

Another aliquot of the carbon tetrachloride solution of chlorine dioxide and chlorine was added to a flask containing sodium hydroxide and a slight excess of hydrogen peroxide. After thorough mixing the excess hydrogen peroxide was destroyed by boiling for 5 min. The sodium chlorite formed by reduction of chlorine dioxide with hydrogen peroxide was determined iodimetrically by titration of iodine with thiosulfate in acid solution.

The amount of hydrogen peroxide required was established by analyzing the solution of chlorine dioxide and chlorine by the well-known Bray method (5).

Measurement of Freezing Points

The dynamic method of measuring the freezing temperature was used throughout the experiments. Taking into account the tendency of mixtures of chlorine dioxide and chlorine to super cooling, the procedure of Andrews, Kohman, and Johnston (7) was used. This method enables the establishment of freezing points by extrapolation. This could be carried out relatively easily in view of the fast rate of crystallization.

The temperature was measured using iron–constantan thermocouple shown in Fig. 3. This arrangement was checked for freezing points of pure mercury, -38.70 °C; and chlorine, -100.98 °C; and for the boiling point of oxygen and the sublimination point of carbon dioxide at atmospheric pressure.

The apparatus used for freezing point measurements is shown in Fig. 4. The trap containing the mixture of chlorine dioxide and chlorine was inserted into an aluminum block placed inside the 1 l Dewar flask with glass tube and stopcock. This flask was inserted in

[1]Revision received March 25, 1970.

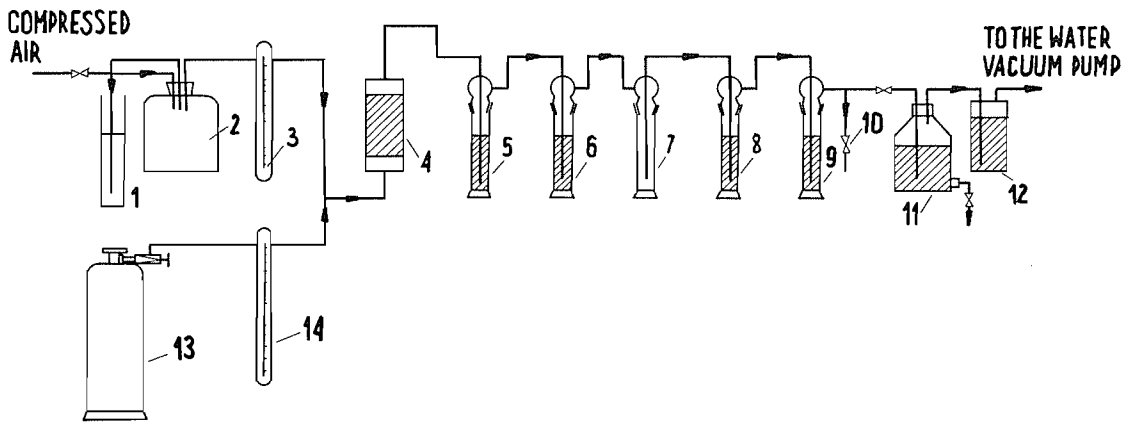

FIG. 1. Apparatus for generating chlorine dioxide. *1*, manostat; *2*, buffer vessel; *3*, flowmeter for air; *4*, mixing column; *5* and *6*, wash-bottles containing 20% sodium chlorite solution; *7*, safety trap; *8*, concentrated sulfuric acid; *9* phosphorus pentoxide on glass wool; *10*, line to the freezing trap; *11*, solution absorbing chlorine dioxide; *12*, pressure regulator; *13*, pressure cylinder with liquid chlorine; *14*, flowmeter for chlorine.

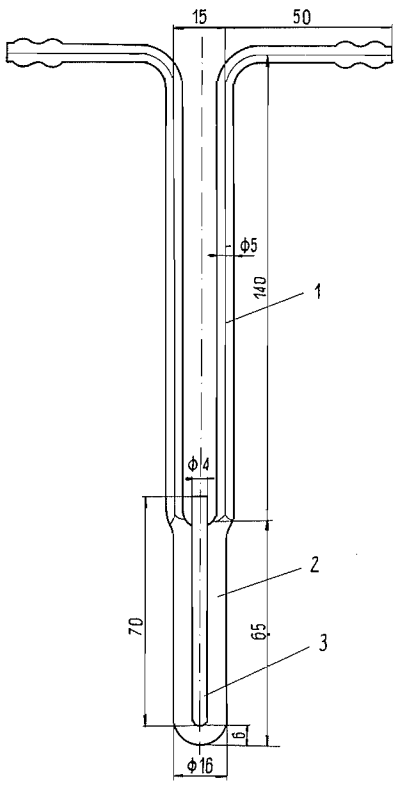

FIG. 2. Freezing trap for chlorine dioxide and chlorine. *1*, capillary tubing; *2*, container; *3*, sheath for thermocouple.

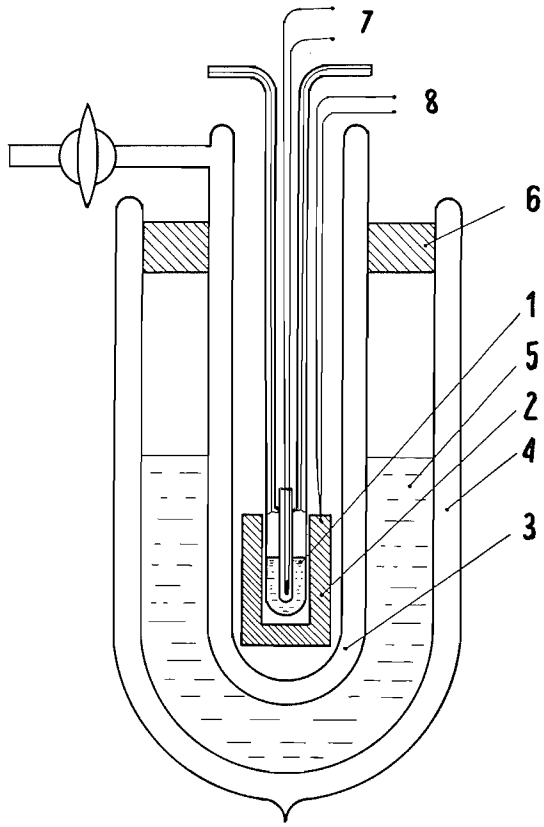

FIG. 3. Apparatus for measurement of temperature. *1*, iron–constantan thermocouple; *2*, thermostat for "cold" ends; *3*, Dewar flask; *4*, compensator; *5*, storage battery; *6*, mirror galvanometer; *7*, standard cell; *8*, thermostated container for standard cell (KO = constantan).

Can. J. Chem. Downloaded from www.nrcresearchpress.com by 210.87.254.42 on 09/05/12
For personal use only.

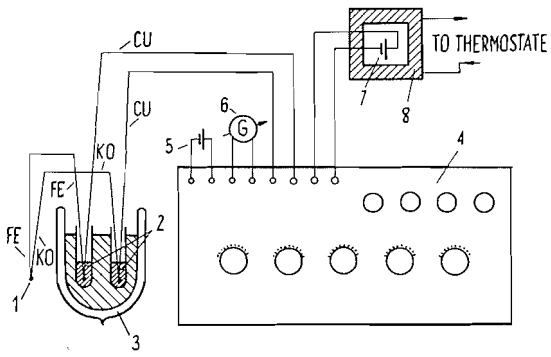

FIG. 4. Apparatus for freezing point measurements. *1*, trap with liquid mixture of ClO_2 and Cl_2; *2*, aluminum block; *3*, modified 0.25 l Dewar flask; *4*, 1 l Dewar flask; *5*, boiling pure oxygen; *6*, porous PCV plate; *7* and *8*, thermocouples.

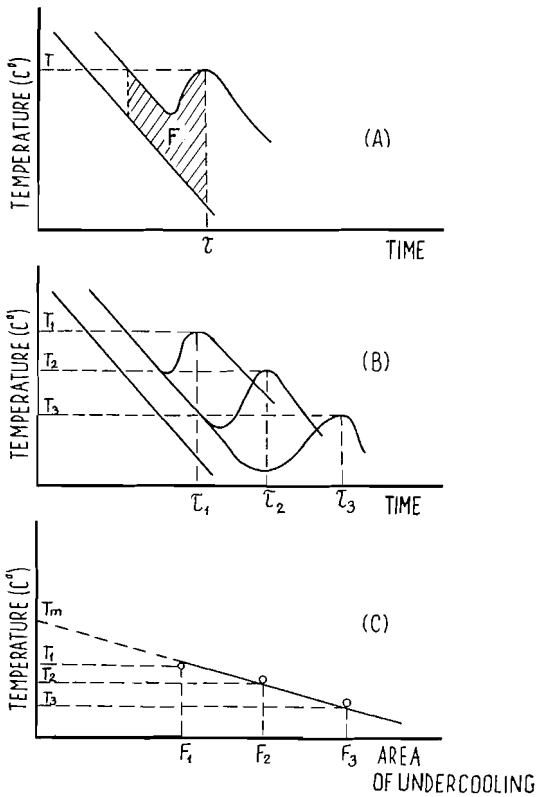

FIG. 5. *A* and *B* show a plot of dynamic measurements of freezing points at different degrees of undercooling; *C* shows graphic extrapolation.

another Dewar flask half filled with boiling pure oxygen and covered with a porous PCV plate. Each sample of the mixture of chlorine dioxide and chlorine was frozen several times at varying rates of cooling. The rate of cooling was regulated by suitable evacuation of the liquid oxygen in the Dewar flask. The temperature of the frozen

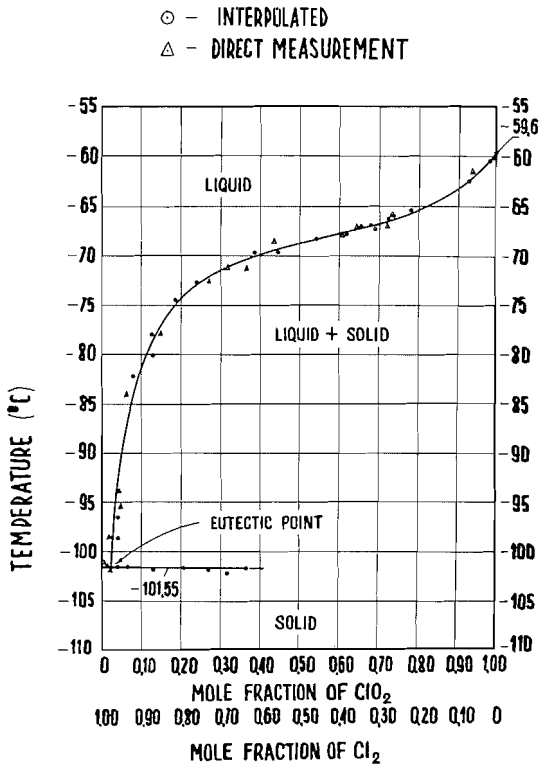

FIG. 6. The phase diagram for the system chlorine dioxide – chlorine.

mixture in the trap was measured every 30 s, the temperature of the aluminum block every few minutes. The measured temperatures of the sample were plotted against time, and the areas between the line of the block temperature and the sample temperature established by weighing. The freezing temperatures were then plotted against the area of undercooling, and the true freezing point was found by extrapolation as shown in Fig. 5*c*.

Results

The freezing temperatures of various samples are given in Table 1 and the extrapolated values in Table 2. Both sets of data are plotted in Fig. 6 giving the freezing point curve of the system chlorine dioxide – chlorine.

Conclusions

(*1*). The solutions of chlorine dioxide and chlorine may be prepared by dissolving liquid chlorine in chlorine dioxide or solid chlorine dioxide in liquid chlorine.

(*2*). Chlorine dioxide and chlorine in the liquid state are completely miscible above −59.6 °C.

Can. J. Chem. Downloaded from www.nrcresearchpress.com by 210.87.254.42 on 09/05/12
For personal use only.

TABLE 1

Freezing points of chlorine dioxide–chlorine mixtures by direct measurement

Mole fraction of ClO_2	Freezing point (°C)	Mole fraction of ClO_2	Freezing point (°C)
1.0000	−59.60	0.3885	−69.70
0.9887	−60.14	0.3872	−69.75
0.9855	−60.40	0.2396	−72.81
0.9267	−62.45	0.1876	−74.60
0.7830	−65.45	0.1303	−80.10
0.7369	−66.00	0.1283	−78.00
0.7248	−66.25	0.0802	−82.21
0.6801	−67.00	0.0390	−96.6
0.6577	−67.05	0.0275	−98.6
0.6207	−67.85	0.0178	−101.55
0.5435	−68.30	0.0166	−101.55
0.4474	−69.75	0.0023	−101.06
0.3984	−68.90	0.0000	−101.00

TABLE 2

Freezing points of chlorine dioxide–chlorine mixtures by extrapolation

Mole fraction of ClO_2	Freezing point (°C)	Mole fraction of ClO_2	Freezing point (°C)
0.9367	−61.25	0.3230	—
0.8496	−62.50	0.2703	−72.77
0.7354	−65.96	0.2073	—
0.7212	−66.88	0.1508	−77.89
0.6444	−67.24	0.1295	—
0.6067	−67.84	0.0638	−84.03
0.4364	−68.60	0.0463	−95.37
0.3677	−71.35	0.0204	—

(*3*). The liquidus curve of the solutions of chlorine in chlorine dioxide is S-shaped and has an inflection point at 0.6 mole fraction of ClO_2 (8, 9).

(*4*). The eutectic point at atmospheric pressure lies at -101.6 ± 0.1 °C, close to the freezing point of chlorine. The eutectic point composition is 1.6 mole% chlorine dioxide in chlorine.

(*5*). The freezing curves indicate that liquid chlorine dioxide and chlorine do not react with one another.

(*6*). The point of inflection of the liquidus curve together with the complete solubility in the liquid state may indicate the existence of mutual solid solubility.

(*7*). Contary to the existing literature, pure *liquid* chlorine dioxide and its solutions with chlorine do not tend to spontaneous decomposition. The one explosion which did occur during the present work happened while evaporating chlorine dioxide at 9 °C, when the gaseous phase was fairly pure chlorine dioxide, indicating that chlorine dioxide *gas* in high concentration is spontaneously explosive with detonation.

The help and advice of Dr. W. H. Rapson of the Department of Chemical Engineering of the University of Toronto is gratefully acknowledged.

1. Chem. Eng. News, **28**, 5030 (1950); **29**, 3196 (1951).
2. J. KEPINSKI. Chlorine dioxide and chlorites (in Polish). Szczecin, 1967. The Scientific Society.
3. J. F. HALLER. German Patent D.B.P. 838,239 (1952).
4. J. KEPINSKI and G. BLASZKIEWICZ. Chem. Stosow. Ser. A, **12**, 3 (1968).
5. W. BRAY. Z. Phys. Chem. **54**, 731 (1906).
6. I. E. FLIS and M. K. BYNIAYEVA. Zh. Anal. Chim. **12**, 740 (1957).
7. D. H. ANDREWS, G. T. KOHMAN, and J. JOHNSTON. J. Phys. Chem., **29**, 914 (1925).
8. J. E. RICCI. Phase rule and heterogeneous equilibrium. Van Nostrand, New York. 1951.
9. B. JA. ANOSOV and S. A. POGODIN. Principles of physicochemical analysis, Izd. Akad. Nauk. Moskva, Leningrad, 1947.

Can. J. Chem. Downloaded from www.nrcresearchpress.com by 210.87.254.42 on 09/05/12
For personal use only.

Can. J. Chem. Downloaded from www.nrcresearchpress.com by 210.87.254.40 on 09/05/12
For personal use only.

Spectrofluorometric studies. IX. Fluorescent and triplet yields of the tetrafluorobenzenes excited in the 2600 Å region

B. H. SCHOLZ AND I. UNGER

Department of Chemistry, University of New Brunswick, Fredericton, New Brunswick

Received March 5, 1970

The gas phase fluorescent and triplet yields of 1,2,4,5-, 1,2,3,4-, and 1,2,3,5-tetrafluorobenzene (TFB) excited in the 2600 Å region have been determined. For 1,2,4,5-TFB, the maximum fluorescent yield ($\Phi_f = 0.338$) occurs at $\lambda_{ex} = 2670$ Å and the triplet yield at this wavelength = 0.515. For 1,2,3,4-TFB, the maximum fluorescent yield is 0.186 and is obtained at $\lambda_{ex} = 2645$ Å; the triplet yield at this wavelength = 0.220. For 1,2,3,5-TFB the maximum fluorescent yield = 0.029 and the maximum triplet yield is 0.141, at an exciting wavelength of 2680 Å. The fluorescent and triplet yields of the three molecules, at any exciting wavelength studied, are not quenched by the addition of *cis*-butene-2 (*c*-B-2).

Canadian Journal of Chemistry, **48**, 2324 (1970)

Introduction

A number of techniques have been developed in recent years to determine the triplet yields of organic molecules which do not exhibit phosphorescence in the gas phase (1–5). Of these, two of the most frequently used are the sensitized emission of biacetyl (BiA) technique (4) and the isomerization of olefins technique (5). Although both of the above mentioned methods have certain disadvantages (6), the two should yield reliable results provided adequate precautions are taken (7). Also, in the case of certain molecules, the two techniques (8) may be combined; thus eliminating most of the undesirable features of both.

This paper presents the fluorescent and triplet yields as determined by the sensitized emission of BiA technique of the three isomers of TFB excited at various wavelengths. The effect of *c*-B-2 on the emission yield of BiA sensitized by the TFB isomers has also been examined.

Experimental

The three TFB isomers used in this study were obtained from the Aldrich Chemical Company and purified by preparative vapor phase chromatography. The BiA used was also obtained from the Aldrich Chemical Company. It was purified by bulb-to-bulb distillation in vacuo and stored in a blackened reservoir. Fluorometric grade benzene obtained from the Hartman–Ledden Company was used without further purification. Philips research grade *c*-B-2 containing less than 0.1% impurity was also used without further purification.

The vacuum system employed was a grease and mercury free high vacuum line, equipped with Hoke packless metal diaphragm valves. The pumping section of the high vacuum system was of conventional design.

Pressure measurements were carried out by means of a spiral gauge obtained from the National Research Council of Canada in Ottawa. The cell used was an Aminco flow-through cuvette type, 1 cm × 1 cm × 4.5 cm, polished on all four sides. Mixing was accomplished by an all-glass pump which circulated the vapors through the flow-through cell. Adequate mixing was indicated by constant absorption and emission. All emission measurements were performed on a modified Aminco–Bowman spectrofluorometer. Details concerning the modification and processing of raw data have been discussed in earlier publications (9, 10). The reported quantum yields are based on the singlet and triplet yields of benzene given by Noyes *et al.* (11, 12). Detailed tables of data complementing those reported here have been deposited in the Depository of Unpublished Data.[1]

Results and Discussion

The absorption spectra of the three isomers of TFB are given in Fig. 1.

1,2,3,4-TFB

The molecule was excited at 2520, 2600, and 2645 Å. The fluorescent yield at λ_{ex} 2520 Å = 0.056. At λ_{ex} 2600 Å, it is 0.157 and λ_{ex} 2645 Å, 0.186. The fluorescent yield was found to be independent of TFB pressure (range examined 2–35 Torr) at all exciting wavelengths, but quenched by BiA. Plots of $1/\Phi_f$ vs. [BiA] are linear. Equations of these lines are given in Table 1. The addition of *c*-B-2 had no effect on the fluorescent yield of 1,2,3,4-TFB at any exciting wavelength (Table 2). The triplet yield was found to increase with increasing BiA pressure and levelled off at about 20 Torr of BiA. The maximum triplet yield at each exciting wavelength is

[1]Photocopies of material on deposit may be obtained free of charge, upon request, from the Depository of Unpublished Data, National Science Library, National Research Council of Canada, Ottawa, Canada.

TABLE 1

Equations of lines of plots of $1/\Phi_f$ vs. [BiA] for the three isomers of TFB excited at various wavelengths

Molecule	λ_{ex} (Å)	Half band width (Å)	Equation of line	Pressure range (Torr) TFB	Pressure range (Torr) BiA	Triplet yield (maximum)
1,2,3,4-TFB	2520	~20	$1/\Phi_f = 17.8 + 3.73\times10^{-1}$ [BiA]	9.86	3 –28	0.12
	2600	~35	$1/\Phi_f = 7.7 + 1.20\times10^{-1}$ [BiA]	9.9	3 –18.5	0.08
	2645	~ 7	$1/\Phi_f = 6.0 + 7.68\times10^{-2}$ [BiA]	10	2.5–20.2	0.22
1,2,4,5-TFB	2520	~20	$1/\Phi_f = 6.7 + 7.82\times10^{-2}$ [BiA]	9.8	5.2–27.1	0.11
	2670	~10	$1/\Phi_f = 2.95 + 5.22\times10^{-1}$ [BiA]	10	2.8–28.4	0.51
1,2,3,5-TFB	2640	~10	$1/\Phi_f = 76 + 1.23$ [BiA]	9.6	2.5–17.9	0.12
	2680	~10	$1/\Phi_f = 29.15 + 3.4\times10^{-1}$ [BiA]	9.5	2.5–17.2	0.14

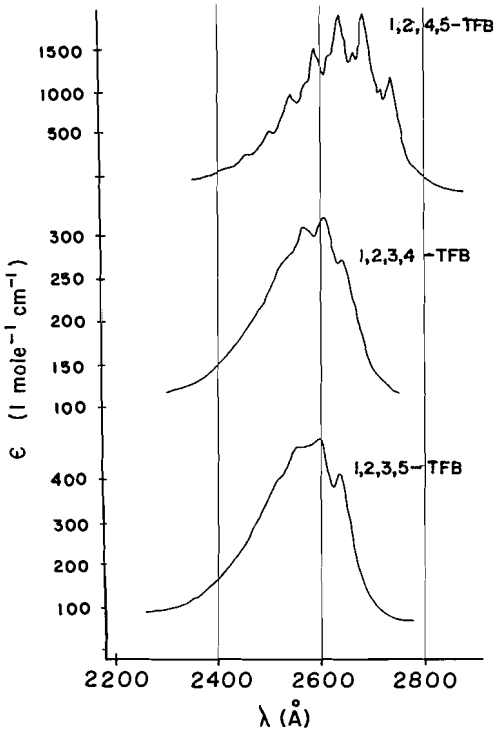

FIG. 1. The absorption spectra of the three isomers of TFB recorded on a Hitachi–Coleman Spectrophotometer, Model EPS-3T.

given in Table 1. The triplet yield was unaffected by the addition of *c*-B-2 (Table 2).

1,2,4,5-TFB

The excitation wavelengths used were 2520 and 2670 Å. The fluorescent yields at these wavelengths are 0.127 and 0.338, respectively. The experimental results indicate that self quenching does not occur at the two excitation wavelengths studied. However, BiA does quench the fluorescent emission and plots of $1/\Phi_f$ vs. [BiA] are linear (Table 1). *c*-B-2 had no effect on the fluorescent yield but appears to enhance somewhat the triplet yield (Table 2). The behavior of the triplet yield as a function of BiA pressure was very similar to that noted for 1,2,3,4-TFB. Maximum triplet yields for the two exciting wavelengths used are listed in Table 1.

1,2,3,5-TFB

Only two excitation wavelengths were used, 2640 and 2680 Å. At any wavelengths above 2680 Å or below 2640 Å, the fluorescent yields are negligible. The fluorescent yield at λ_{ex} 2640 = 0.013 while at λ_{ex} 2680 Å it is 0.029. The rest of the photochemical behavior is very similar to that observed for 1,2,3,4- and 1,2,4,5-TFB (Tables 1 and 2). Once again, neither the fluorescent yield nor the triplet yield is quenched by the addition of *c*-B-2 (Table 2).

The basic photochemistry of the three isomers of TFB appears to fit into the pattern of the photochemistry of the other fluorinated benzenes reported previously (10, 13–15) and thus the kinetic schemes given in the above references are likely valid for the isomers of TFB. The relatively low sum of the fluorescent yield plus the triplet yield for 1,2,3,4- and 1,2,3,5-TFB and hence the relatively large quantum deficit $[1 - (\Phi_f + \Phi_T)]$ at all the exciting wavelengths examined suggests that either intramolecular rearrangement (16) or radiationless transitions are important processes in these molecules. Further experimental work will be necessary before this point can be decided.

The "non-quenching" of the fluorescent and triplet yields of the three isomers of TFB on the addition of *c*-B-2 is not surprising. The singlets of the TFB isomers are expected to be at lower

Can. J. Chem. Downloaded from www.nrcresearchpress.com by 210.87.254.40 on 09/05/12
For personal use only.

TABLE 2

The effect of *c*-B-2 on the fluorescent and triplet yields of the isomers of TFB excited at various wavelengths*

Isomer	λ_{ex} (Å)	*c*-B-2 Pressure (Torr)	Φ_f	Φ_T
1,2,3,4-TFB	2520	0	0.043	0.048
		5	0.043	0.046
		10	0.044	0.053
		15	0.044	0.052
		20	0.053	0.053
		25	0.045	0.052
	2600	0	0.11	0.062
		10	0.11	0.079
		15	0.11	0.081
		20	0.13	0.087
		25	0.12	0.085
	2645	0	0.15	0.13
		5	0.14	0.14
		10	0.14	0.11
		15	0.14	0.12
		20	0.15	0.11
		25	0.15	0.10
1,2,4,5-TFB	2520	5	0.12	0.17
		10	0.12	0.19
		15	0.12	0.19
		20	0.12	0.18
		25	0.13	0.21
	2670	0	0.26	0.27
		5	0.26	0.28
		10	0.26	0.29
		15	0.26	0.29
		20	0.26	0.30
		25	0.26	0.31
1,2,3,5-TFB	2640	0	0.010	0.11
		5	0.010	0.11
		10	0.010	0.11
		15	0.010	0.12
		20	0.010	0.11
		25	0.010	0.11
		40	0.010	0.11
	2680	0	0.030	0.13
		5	0.030	0.13
		10	0.029	0.13
		15	0.030	0.13
		20	0.030	0.13
		25	0.029	0.13
		40	0.030	0.13

*TFB pressure = 10 Torr, BiA pressure = 15 Torr for all experiments.

energy levels than the singlet of benzene (9) and therefore, cannot transfer energy to *c*-B-2 (5). There is some speculation in the literature as to the exact location of the triplet of *c*-B-2, recent reports suggest that it lies at about 72 kcal (17, 18) although Fukano and Sato (19) claim to have observed sensitized *cis–trans* isomerization of *c*-B-2 with donors having only 65 kcal of energy. Theoretical considerations show that the triplet energy should decrease systematically as one progresses from benzene to hexafluorobenzene (9). Recent glassy matrix studies confirm these theoretical predictions (20). The triplet of 1,2,4-trifluorobenzene lies at approximately 73.5 kcal and it has been shown experimentally that it will not transfer energy to *c*-B-2 (14). Hence, one would not expect the isomers of TFB, all having energies lower than that of 1,2,4-trifluorobenzene, to be quenched by *c*-B-2 and this is confirmed by our experimental observations.

The authors wish to thank Dr. G. P. Semeluk and Dr. F. Grein for many stimulating discussions.

1. R. F. Borkman and D. R. Kearns. Chem. Commun. **14**, 446 (1966).
2. A. Kuppermaun and L. M. Raff. Discuss. Faraday Soc. **35**, 31 (1963).
3. R. G. W. Norrish and G. Porter. Nature, **164**, 658 (1949).
4. H. Ishikawa and W. A. Noyes, Jr. J. Chem. Phys. **37**, 583 (1962).
5. R. B. Cundall and T. F. Palmer. Trans. Faraday Soc. **56**, 1211 (1960).
6. W. A. Noyes, Jr. and I. Unger. Advan. in Photochem. **4**, 49 (1966).
7. M. E. MacBeath and I. Unger. Can. J. Chem. In Press.
8. I. Unger. J. Phys. Chem. **69**, 4284 (1965).
9. F. W. Ayer, F. Grein, G. P. Semeluk, and I. Unger. Ber. Bunsenges. Phys. Chem. **72**, 282 (1968).
10. M. E. MacBeath, G. P. Semeluk, and I. Unger. J. Phys. Chem. **73**, 995 (1969).
11. W. A. Noyes, Jr., W. A. Mulac, and D. A. Harter. J. Chem. Phys. **44**, 2100 (1966).
12. W. A. Noyes, Jr. and D. A. Harter. J. Chem. Phys. **46**, 674 (1967).
13. J. L. Durham, G. P. Semeluk, and I. Unger. Can. J. Chem. **46**, 3177 (1968).
14. G. P. Semeluk, R. D. S. Stevens, and I. Unger. Can. J. Chem. **47**, 597 (1969).
15. D. Phillips. J. Chem. Phys. **46**, 4679 (1967).
16. K. E. Wilzbach, J. S. Ritscher, and L. Kaplan. J. Amer. Chem. Soc. **89**, 1031 (1967) and references therein.
17. R. B. Cundall and A. S. Davies. J. Amer. Chem. Soc. **88**, 1329 (1966).
18. R. B. Cundall and A. S. Davies. Progr. React. Kinet. **4**, 149 (1967).
19. K. Fukano and S. Sato. Kogyo Kagaku Zasshi, **72**, 231 (1969). C.A. 48984s **71**, 294 (1969).
20. G. P. Semeluk and S. Lem. Private communication.

Can. J. Chem. Downloaded from www.nrcresearchpress.com by 210.87.254.40 on 09/05/12
For personal use only.

Studies of cobalt(III) complexes of thiosemicarbazide

KENNETH K. W. SUN AND ROLAND A. HAINES
Department of Chemistry, University of Western Ontario, London, Ontario
Received January 21, 1970

cis and *trans* geometric isomers of low spin octahedral cobalt(III) complexes containing either thiosemicarbazide (Htsc) or its anion (tsc) have been prepared and electronic spectra are presented and discussed. For the ionic form $[Co(Htsc)_3]^{3+}$ both isomers were resolved and absolute configurations were assigned on the basis of optical rotatory dispersion and circular dichroism measurements. The interconversion of these optically active complex ions in aqueous solution was studied and a bond rupture mechanism is proposed to account for the observed inversion and isomerization.

Canadian Journal of Chemistry, 48, 2327 (1970)

Can. J. Chem. Downloaded from www.nrcresearchpress.com by 210.87.254.42 on 09/05/12
For personal use only.

Tris-complexes of thiosemicarbazide (Htsc), $H_2N—CS—NH—NH_2$, were first reported by Jensen and Rancke-Madsen (1). Sadykova and co-workers (2) investigated the complex formation of thiosemicarbazide with various cobalt(II) salts in aqueous solutions and found that the cation was the species $[Co(Htsc)_3]^{3+}$. Further studies by Samus' and co-worker (3, 4) revealed *cis–trans* isomerism in these complexes and the kinetics of isomerization have been investigated using paper chromatography (5). However, in none of these studies have assignments of configuration been made.

In this paper we report investigations dealing with the structure and stereochemistry of these complexes, together with studies of the stereochemical path for the isomerization reactions.

Experimental

Starting chemicals were obtained from either Fisher Scientific Co. or Alfa Inorganics Inc. All cobalt analyses were carried out in this laboratory by standard methods and all microanalyses by Alfred Bernhardt, West Germany.

Magnetic moments were measured at room temperature on a Gouy balance and tubes were calibrated with $Hg[Co(SCN)_4]$. Infrared spectra were obtained using a Beckman IR-10 spectrophotometer using potassium bromide disks and Nujol mulls. Visible reflectance spectra were recorded on a Unicam SP 500 spectrophotometer with standard reflectance attachment while solution spectra were recorded on a Beckman DK-1 spectrophotometer. Optical rotatory dispersion and circular dichroism curves were obtained using a Durrum–Jasco ORD/UV/5 spectropolarimeter.

cis-Tris(thiosemicarbazide)cobalt(III) Chloride Trihydrate

The method of Samus' and Ablov (3) was followed. Solid thiosemicarbazide (0.03 mole or 2.73 g) was slowly added to a solution of cobalt(II) chloride hexahydrate (0.01 mole or 2.38 g) in water (100 ml). A strong current of air was passed through the solution for approximately 4 h. Then concentrated hydrochloric acid (33 ml) was added to precipitate the dark violet solid which was filtered off and washed with a 1:4 ethanol–ether mixture followed by ether. The product was recrystallized by dissolving in a minimum amount of water and precipitating with concentrated hydrochloric acid.

Anal. Calcd. for $[Co(SCN_3H_5)_3]Cl_3 \cdot 3H_2O$: Co, 11.96; C, 7.31; H, 3.07; N, 25.58; S, 19.52; Cl, 21.58; H_2O, 10.97. Found: Co, 11.95; C, 7.47; H, 3.13; N, 25.69; S, 19.56; Cl, 21.68. Loss of weight by drying at 70 °C in vacuum, 10.91.

cis-Tris(thiosemicarbazido)cobalt(III) Monohydrate

The method of Samus' and Ablov (3) was followed with slight modifications. Violet tris(thiosemicarbazide)cobalt(III) chloride trihydrate (5.0 g) was dissolved in water (500 ml) and 1.0 *M* ammonium hydroxide (50 ml) was added dropwise to precipitate pinkish lilac needles. The solid was filtered off and washed with small portions of water, ethanol, and ether.

Anal. Calcd. for $[Co(SCN_3H_4)_3] \cdot H_2O$: Co, 16.96; C, 10.37; H, 3.48; N, 36.29; S, 27.69; H_2O, 5.19. Found: Co, 17.37; C, 10.20; H, 3.44; N, 36.14; S, 27.53. Loss in weight by drying at 70 °C in vacuum, 5.12.

trans-Tris(thiosemicarbazido)cobalt(III)

The method of Samus' (4) was followed. Violet tris(thiosemicarbazido)cobalt(III), prepared above, was heated in its mother liquor to ~ 80 °C for 30 min. The greyish green product was filtered off and washed with small portions of water, ethanol, and ether.

Anal. Calcd. for $[Co(SCN_3H_4)_3]$: Co, 17.89; C, 10.94; H, 3.67; N, 38.28; S, 29.21. Found: Co, 18.09; C, 10.89; H, 3.75; N, 38.08; S, 29.08.

trans-Tris(thiosemicarbazide)cobalt(III) Chloride Tetrahydrate

This compound was also prepared by the method of Samus' (4). Green *trans*-tris(thiosemicarbazido)cobalt(III) (6.0 g), ground to fine powder, was suspended in 95% ethanol (500 ml). As hydrochloric acid (1:1, 50 ml) was added dropwise with vigorous stirring, the suspended greyish green solid gradually turned green. The solid was then filtered and washed with a 1:4 ethanol–ether mixture and finally ether. Although it was readily soluble in water, the purity of the compound actually deteriorated when attempts were made to recrystallize it.

Can. J. Chem. Downloaded from www.nrcresearchpress.com by 210.87.254.42 on 09/05/12
For personal use only.

Anal. Calcd. for $[Co(SCN_3H_5)_3]Cl_3 \cdot 4H_2O$: Co, 11.54; C, 7.05; H, 2.96; N, 24.68; S, 18.83; Cl, 20.82; H_2O, 14.11. Found: Co, 11.42; C, 7.17; H, 3.04; N, 24.80; S, 18.66; Cl, 20.96. Loss in weight by drying at 70 °C in vacuum, 14.14.

Sodium Antimonyl $(-)_{589}$-Tartrate

$(-)_{589}$-Tartaric acid (0.1 mole or 15.01 g) was half neutralized by treating with 1.0 *M* sodium hydroxide (100 ml) and brought into solution by an additional amount of water (500 ml). After heating to boiling, antimony trioxide (0.05 mole or 14.58 g) was slowly stirred into the boiling solution. An additional amount of hot water (300 ml) was added and the mixture was boiled for approximately 20 min until almost all the solid had been dissolved. The solution was filtered hot and then evaporated to ~ 40 ml on a steam bath in a stream of air. After the solution was cooled, 95% ethanol (12 ml) was added slowly, with stirring, to precipitate the product. Recrystallization was accomplished by dissolving the crude product in boiling water and reprecipitating with 95% ethanol after cooling in an ice bath.

Silver Antimonyl Tartrate

A solution of silver nitrate (0.1 mole or 16.99 g) in water (35 ml) was added slowly, with stirring, to a hot solution (~ 70 °C) of either potassium antimonyl $(+)_{589}$-tartrate hydrate or sodium antimonyl $(-)_{589}$-tartrate in water. The solution and suspended precipitate were stirred for 5 min and the white solid was filtered off and washed with water, ethanol, and ether.

Resolution of the cis-tris(thiosemicarbazide)cobalt(III) Ion

Solid silver antimonyl $(+)_{589}$-tartrate (0.03 mole or 11.81 g) was added slowly, within 5 min, to a mechanically stirred solution of violet *cis*-tris(thiosemicarbazide)-cobalt(III) chloride trihydrate (0.01 mole or 4.93 g) in water (100 ml). The mixture was stirred vigorously for another 15 min before the solution was filtered. A jet of air was then blown over the surface of the solution to accelerate evaporation. The diastereoisomer, $(-)_{589}$-$[Co(SCN_3H_5)_3](+)_{589}$-$[SbO(C_4H_4O_6)] \cdot 4H_2O$, separated from the solution on standing and was filtered and washed with ethanol and ether. Other fractions were obtained on further evaporation of the filtrate. The total yield was 0.20 g and the most pure fraction had a specific rotation of $[\alpha]_{589} = -1290°$. Recrystallization in water did not improve the optical purity of the diastereoisomer.

Following the same procedure as outlined above, the $(+)_{589}$-diastereoisomer was obtained using silver antimonyl $(-)_{589}$-tartrate as resolving agent. The product had a specific rotation of $[\alpha]_{589} = +1225°$.

All attempts to remove the resolving agent from the diastereoisomer were unsuccessful.

Anal. Calcd. for $(-)_{589}$-$[Co(SCN_3H_5)_3](+)_{589}$-$[SbO(C_4H_4O_6)]_3 \cdot 4H_2O$: C, 14.28; H, 2.16; N, 9.99; S, 7.62; Sb, 28.95; H_2O, 5.71. Found: C, 14.40; H, 2.29; N, 10.13; S, 7.53. Loss in weight by drying at 70 °C in vacuum, 5.71.

Anal. Calcd. for $(+)_{589}$-$[Co(SCN_3H_5)_3](-)_{589}$-$[SbO(C_4H_4O_6)]_3 \cdot 4H_2O$: as for the $(-)_{589}$-diastereoisomer above. Found: C, 14.44; H, 2.31; N, 10.12; Sb, 28.96. Loss in weight by drying at 70 °C in vacuum, 5.66.

Resolution of the trans-Tris(thiosemicarbazide)cobalt(III) Ion

This compound was resolved in a way similar to that for the violet isomer. Solid silver antimonyl $(+)_{589}$-tartrate (0.03 mole or 11.81 g) was added slowly, within 5 min, to a mechanically stirred solution of green *trans*-tris(thiosemicarbazide)cobalt(III) chloride tetrahydrate (0.01 mole or 5.11 g) in water (100 ml). The mixture was stirred vigorously for another 15 min before the solution was filtered. Ethanol (95%, 26 ml) was added slowly, with stirring, to precipitate the diastereoisomer, $(+)_{589}$-$[Co(SCN_3H_5)_3](+)_{589}$-$[SbO(C_4H_4O_6)]_3 \cdot 3H_2O$, which was filtered off and washed with ethanol and ether. Other fractions were obtained on further addition of 95% ethanol to the filtrate. The total yield was 0.34 g and the most pure fraction had a specific rotation of $[\alpha]_{589} = +375°$. Recrystallization in water also did not improve the optical purity of the diastereoisomer in this case.

Following the same procedure the $(-)_{589}$-diastereoisomer was obtained using silver antimonyl $(-)_{589}$-tartrate as resolving agent. The product had a specific rotation of $[\alpha]_{589} = -375°$.

All attempts to remove the resolving agent from the diastereoisomer were unsuccessful.

Anal. Calcd. for $(+)_{589}$-$[Co(SCN_3H_5)_3](+)_{589}$-$[SbO(C_4H_4O_6)]_3 \cdot 3H_2O$: C, 14.48; H, 2.19; N, 10.14; S, 7.73; Sb, 29.37; H_2O, 4.35. Found: C, 14.42; H, 2.35; N, 9.97; S, 7.87; Sb, 29.49. Loss in weight by drying at 70 °C in vacuum, 4.58.

Anal. Calcd. for $(-)_{589}$-$[Co(SCN_3H_5)_3](-)_{589}$[SbO-$(C_4H_4O_6)]_3 \cdot 3H_2O$: as for the $(+)_{589}$-diastereoisomer above. Found: C, 14.42; H, 2.34; N, 10.30; S, 7.51; Sb, 29.16. Loss in weight by drying at 70 °C in vacuum, 4.30.

Interconversion Studies

Solutions of the optically active *cis*- and *trans*-$[Co(Htsc)_3]^{3+}$ ions were prepared by dissolving the corresponding diastereoisomers in water in 100 ml volumetric flasks. The concentration of these solutions was approximately 10^{-3} *M*. The flasks were tightly stoppered and at various time intervals, aliquots of the solution were withdrawn and electronic and circular dichroism spectra were recorded.

Results and Discussion

Two geometric isomers were obtained for both the ionic and neutral complexes with the general formulae $[Co(Htsc)_3]^{3+}$ and $[Co(tsc)_3]$, respectively.[1] The synthetic route is outlined below and details are given in the experimental section.

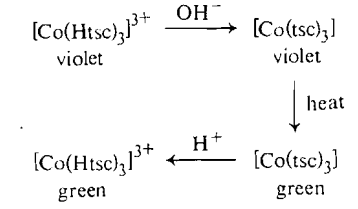

[1]Htsc represents the neutral ligand $H_2NNHCSNH_2$, and tsc is the uninegative ligand $H_2NNCSNH_2^-$.

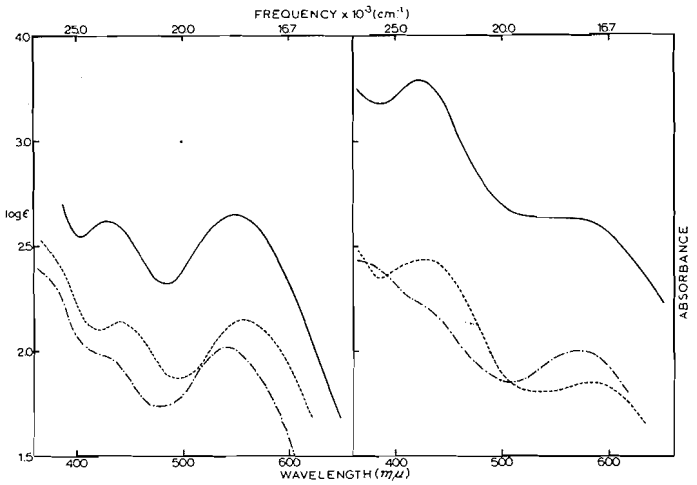

FIG. 1. Left, reflectance spectrum (– · – · –) of violet *cis*-$[Co(tsc)_3]\cdot H_2O$ and reflectance (----) and solution (—) spectrum of violet *cis*-$[Co(Htsc)_3]Cl_3 \cdot 3H_2O$; right, reflectance spectrum (– · – · –) of green *trans*-$[Co(tsc)_3]$ and reflectance (----) and solution (—) spectrum of green *trans*-$[Co(Htsc)_3]Cl_3 4\cdot H_2O$. (Reflectance spectra have arbitrary values of log ε.)

TABLE 1

Electronic spectra

Complex	Reflectance spectra (cm^{-1})*	Solution spectra (cm^{-1})*
cis-$[Co(Htsc)_3]Cl_3\cdot 3H_2O$ (violet)	22 700; 17 900	23 300 (414); 18 300 (447)† 23 200 (434); 18 200 (469)‡ 23 200 (370); 18 100 (427)§
cis-$[Co(tsc)_3]\cdot H_2O$ (violet)	23 600; 18 500	
trans-$[Co(Htsc)_3]Cl_3\cdot 4H_2O$ (green)	23 400; 17 100	23 800 (1900); 17 500 (sh)† 23 600 (2065); 17 800 (382)‡
trans-$[Co(tsc)_3]$ (green)	24 000 (sh); 17 400	

*Extinction coefficients are given in parentheses; sh signifies shoulder.
†In water.
‡In methanol.
§In 0.1 *M* HCL.

It should be pointed out that the green ionic compound could be prepared only by the indicated route and attempts at direct preparation from the ionic violet form failed. However, the ionic and neutral forms of either the violet or green compounds are interconvertible. All the cobalt(III) complexes were diamagnetic, as expected, and were very insoluble in common organic solvents.

Infrared spectra clearly indicate metal–sulfur bonding since the stretching ν(CS) bands for these complexes are shifted by $\sim 100\ cm^{-1}$ to lower energies compared to those for the free ligand. Such a shift is quite comparable to that observed in the spectra of square planar bis-complexes (6).

Electronic Spectra

The electronic absorption spectra for these complexes are shown in Fig. 1 and their characteristic data are given in Table 1. The lowest energy band may be assigned as $^1A_{1g} \rightarrow {}^1T_{1g}$ and the second band is the $^1A_{1g} \rightarrow {}^1T_{2g}$ transition.

The energies of the $^1A_{1g} \rightarrow {}^1T_{1g}$ transition are quite comparable to those for the model compounds $K_3[Co(cysteinate)_3]\cdot 3H_2O$ ($17\,200\ cm^{-1}$) and $[Co(2\text{-aminoethanethiolate})_3]$ ($17\,500\ cm^{-1}$) (7). In both of these cases coordination takes

Can. J. Chem. Downloaded from www.nrcresearchpress.com by 210.87.254.42 on 09/05/12
For personal use only.

Can. J. Chem. Downloaded from www.nrcresearchpress.com by 210.87.254.42 on 09/05/12
For personal use only.

place through sulfur and nitrogen as in thiosemicarbazide complexes.

The solution spectra of the ionic complexes in water bear very similar features to their solid reflectance spectra except that the bands in the former are shifted some 300–600 cm^{-1} towards higher energies. This may be attributed to solvent shifts since the spectra of these complexes in a less coordinating solvent methanol also show similar shifts in the same direction. Moreover, similar shifts are also observed when the complexes are dissolved in 0.1 *M* HCl in which they are stable for at least 12 days. Therefore, it is believed that the same species exist in the solid state and in solution.

It may be noted that the T_{1g} band of the violet isomers (Fig. 1, left) is symmetrical and sharp and is a little more intense than the T_{2g} band. The same features have been observed for *cis* and *trans* amino acid complexes such as $[Co(gly)_3]$, $[Co(DL\text{-}ala)_3]$, and $[Co(L\text{-}leu)_3]$ (8, 9).[2] Here the isomers with noticeable splittings in the T_{1g} bands were assigned as the *trans* (or meridional) isomers and those with symmetrical sharp T_{1g} bands as the *cis* (or facial) isomers. Semi-empirical molecular orbital calculations by Nakamoto *et al.* (10), and by Yamatera (11) and McClure (12) on complexes of the type CoA_3B_3 lead to the same conclusion. The assignments also agree with the spectra of the model compounds citratotriamminecobalt(III) which would prefer the *cis* arrangement of the ammonia ligands, and ammoniatriacetatoethylenediaminecobalt(III), which is most likely to have the *trans* arrangement of nitrogen donors (8). Hence, the violet isomers $[Co(Htsc)_3]Cl_3 \cdot 3H_2O$ and $[Co(tsc)_3] \cdot H_2O$ may similarly be assigned the *cis*, and the green isomers $[Co(Htsc)_3]Cl_3 \cdot 4H_2O$ and $[Co(tsc)_3]$, the *trans* configurations.

Optical Activity

Both the *cis*- and *trans*-$[Co(Htsc)_3]^{3+}$ ions have been resolved into their optically active forms. Unfortunately, all attempts to remove the resolving agent from the diastereoisomers were unsuccessful and hence studies in aqueous solutions had to be made on the diastereoisomers themselves. However, since the antimonyl tartrate ion does not exhibit circular dichroism (c.d.) in the visible region of interest, there is no contribution to the c.d. from the resolving agent.

The optical rotatory dispersion (o.r.d.), circular dichroism, and absorption spectra of the *cis*-(+)-isomer and *trans*-(−)-isomer in aqueous solution are shown in Figs. 2 and 3, respectively. Their enantiomers give mirror image o.r.d. and c.d. curves. In comparing the c.d. spectra of the *cis* and *trans* isomers it can be seen that the lowest energy c.d. band of the *cis* isomer is sharp and symmetrical while that of the *trans* compound is broader and non-symmetrical, indicating low symmetry splitting as predicted by the electronic absorption spectra discussed above. The high intensity of the c.d. bands in the region of the T_{1g} absorption may be attributed to cobalt–sulfur π bonding. Large c.d. values have previously been observed in dithiooxalato (13) and 2-aminoethanethiolo (14) complexes and π bonding has been used to explain the high rotational strength of tris(acetylacetonato)cobalt(III) (15). Further support derives from the fact that the

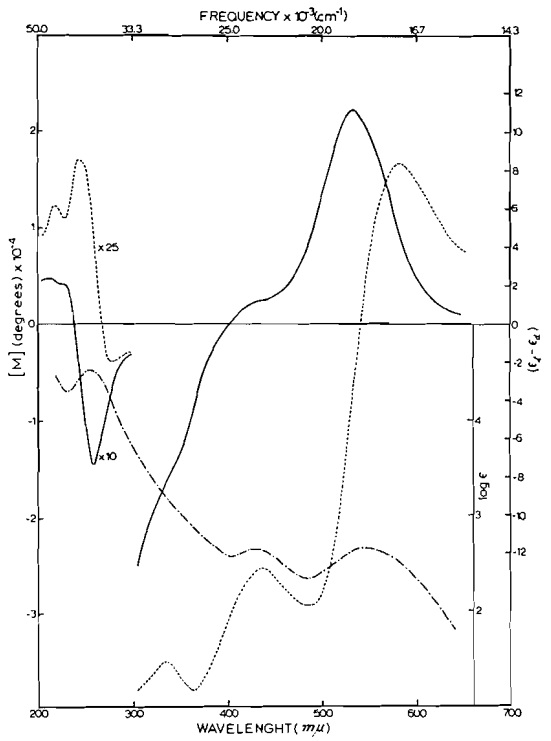

FIG. 2. Optical rotary dispersion (----), circular dichroism (—) and absorption spectra (- · - · -) of $\Lambda\text{-}(+)_{589}\text{-}cis[Co(Htsc)_3]^{3+}$ in aqueous solution.

[2]gly = glycinate anion; ala = alaninate anion; leu = leucinate anion.

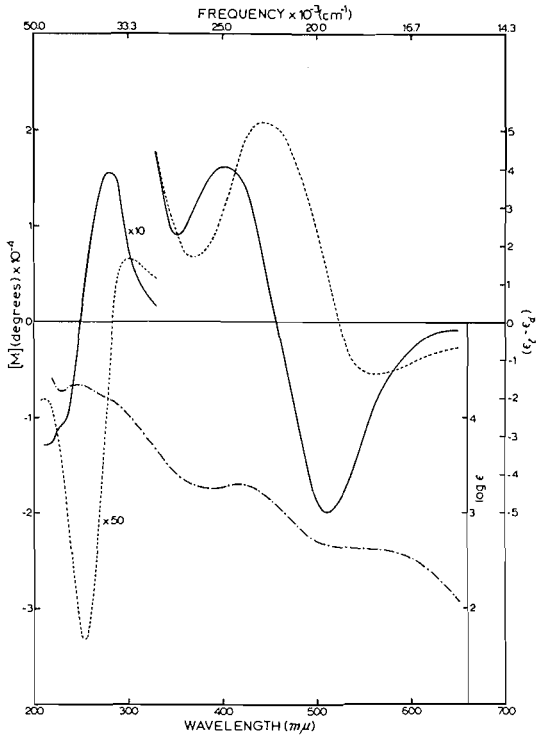

FIG. 3. Optical rotary dispersion (----), circular dichroism (—) and absorption spectra (-·-·-) of Δ-$(-)_{589}$-*trans*-$[Co(Htsc)_3]^{3+}$ in aqueous solution.

intensity of the c.d. band of the *cis* isomer is much greater than that of the *trans* compound. It is quite conceivable that π bonding should be more effective for the *cis* isomer, just as in the case of square planar complexes (16). In both cases the sulfur donor atoms of the ligand do not have to compete for the same d orbital of the metal ion.

The postulate that dihedral d^6 complexes have the Λ configuration (the configuration of the $(+)_{589}$-$[Co(en)_3]^{3+}$ ion[3]) if the E_a transition shows a positive Cotton effect has been most useful and reliable for determining absolute configurations (17, 18). It has been shown that in dihedral tris-diamine and tris-oxalato complexes of d^6 metal ions, the major c.d. band is due to the E_a transition (19). From studies of the c.d. spectra of *cis*-bisdiamine complexes, McCaffery *et al.* (20) concluded that in cobalt(III) complexes of lower symmetry the c.d. band with the larger area in the region of the octahedral T_{1g} absorption arises from a transition with predominant E_a dihedral parentage. Using such a criterion, Larsen and Mason (21) have assigned configurations to all four of the geometrical-optical isomers of $[Co(L\text{-}ala)_3]$. Their assignments are consistent with those obtained by Dunlop and Gillard (22) from studies of optical spectra and stereospecific considerations, and also with those obtained by Denning and Piper (23) from studies of $[Co(L\text{-}prolinate)_3]$ for which pronounced stereospecificity is expected. The X-ray analysis of *trans*-$(+)$-$[Co(L\text{-}ala)_3]$ (24) also confirmed the Λ configuration for this isomer.

By using arguments similar to those above, the single positive c.d. band in the region of octahedral T_{1g} absorption for *cis*-$(+)_{589}$-$[Co(Htsc)_3]^{3+}$ (Fig. 2) may be assigned to the transition with predominant E_a dihedral parentage, thus indicating that the complex has the Λ configuration. Although this spectrum is not exactly similar to that of Λ-*cis*-$(+)_{589}$-$[Co(L\text{-}ala)_3]$, closer examination reveals that the minor c.d. component in the region of T_{1g} absorption and both the A and E transitions in the region of T_{2g} absorption of *cis*-$(+)_{589}$-$[Co(Htsc)_3]^{3+}$ are greatly obscured by the huge negative charge-transfer band, thus producing a spectrum of different shape in that area. However, the o.r.d. curve of *cis*-$(-)_{589}$-$[Co(Htsc)_3]^{3+}$ is more similar to that of Δ-*cis*-$(-)$-$[Co[L\text{-}ala)_3]$, showing two inflection points both in the regions of T_{1g} and T_{2g} absorptions. The compound, therefore, can be tentatively assigned the Δ configuration.

The c.d. spectrum of *trans*-$(-)_{589}$-$[Co(Htsc)_3]^{3+}$ (Fig. 3) shows a negative and a positive band in the regions of T_{1g} and T_{2g} absorptions, respectively, and is quite similar to that of Δ-*trans*-$(-)$-$[Co(L\text{-}ala)_3]$. The o.r.d. curves of these two complexes also bear resemblance except in the near ultraviolet region where masking occurs by charge-transfer absorption. Hence, *trans*-$(-)_{589}$-$[Co(Htsc)_3]^{3+}$ may be tentatively assigned the Δ configuration, and its enantiomer, the Λ configuration.

Interconversion Studies

The interconversion of the optically active *cis*- and *trans*-$[Co(Htsc)_3]^{3+}$ ions has been studied in aqueous solution. Electronic spectra gave rather limited information but changes in c.d. spectra were very useful. It was observed that the *cis*

[3]en denotes ethylenediamine.

Can. J. Chem. Downloaded from www.nrcresearchpress.com by 210.87.254.42 on 09/05/12
For personal use only.

Can. J. Chem. Downloaded from www.nrcresearchpress.com by 210.87.254.42 on 09/05/12
For personal use only.

isomers slowly and gradually racemized until they completely lost their optical activity after about 5 months. During this period of time electronic spectra indicated that there was some conversion to the *trans* form but the amount converted was small. The *trans* isomers, however, behaved differently and the c.d. spectra showed that they underwent simultaneous inversion and isomerization. The Λ-*trans* isomer was converted to the Δ-*cis* form and the Δ-*trans* isomer to the Λ-*cis* form in approximately 15 days and then slow racemization followed. Changes in the c.d. spectra are shown in Fig. 4. During the course of the interconversion the color of the solution also gradually changed from green to reddish brown. It was necessary to carry out these interconversion studies in aqueous solution. In acidic media rapid racemization occurred while addition of base to an aqueous solution of any of the optically active complexes caused the neutral species to precipitate. This product was insoluble in all common media except acid where the racemic ionic species was obtained.

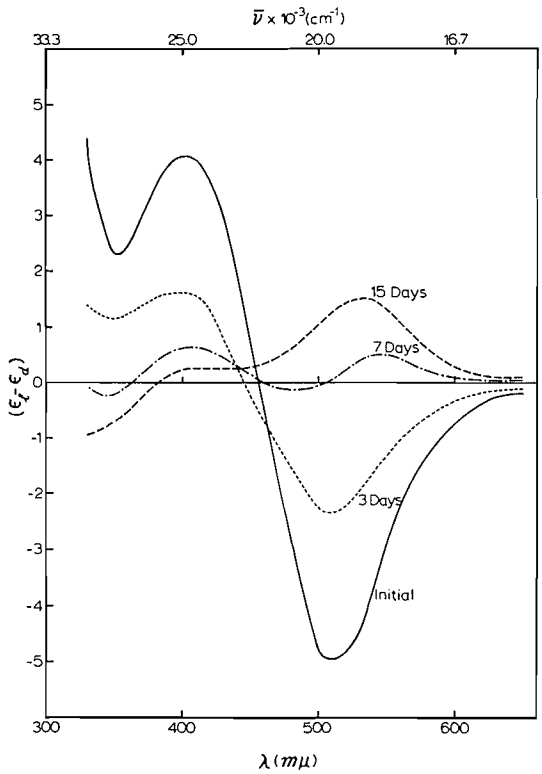

FIG. 4. Changes in c.d. spectrum of $\Delta(-)_{589}$-*trans*-$[Co(Htsc)_3]^{3+}$ in aqueous solution.

Inversions of configuration have been discussed previously in the equilibration of [Co(L-ala)$_3$] (22) and Denning and Piper (23) observed the inversion of *trans*-(−)-[Co(L-leu)$_3$] to the corresponding *trans*-(+)-compound as well as the isomerization of *cis*-(−)-[Co(prolinate)$_3$] to the corresponding *trans*-(−)-isomer. A bond rupture mechanism was proposed for the rearrangement reactions and the same mechanism was favored over the rhombic twist in the interconversion of trifluoroacetylacetonatocobalt(III) (25). More direct evidence for the possibility of bond rupture is shown by studies on the tris-(oxalato) complexes of rhodium(III) and cobalt-(III) (26, 19). In both cases, an ion of the type $[M(C_2O_4)_2(C_2O_4H)(OH)]^{3-}$ is indicated. The presence of an aquo species with monodentate thiosemicarbazide ligands for the tris complexes of nickel(II) in solution has been suggested (27). It is conceivable that the monodentate ligand bonds to the metal through the sulfur atom since M—S bonding was found in the compound Ag(Htsc)Cl (28) and analogous complexes of thiourea and related ligands (29). Hence an octahedral aquo intermediate in the proposed bond rupture mechanism (Fig. 5) seems likely

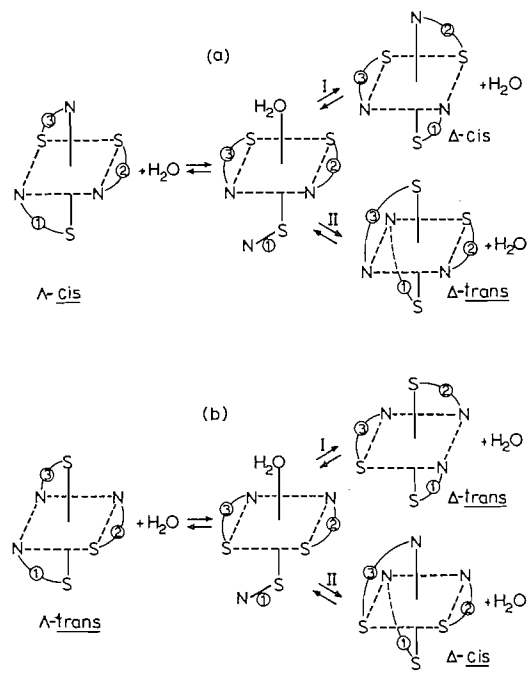

FIG. 5. Possible mechanisms for interconversion and racemization.

Can. J. Chem. Downloaded from www.nrcresearchpress.com by 210.87.254.42 on 09/05/12
For personal use only.

and can account for the simultaneous inversion and isomerization observed for the *trans*-$[Co(Htsc)_3]^{3+}$ ion. The Bailar twist mechanism can be ruled out because it cannot provide a path for *cis–trans* isomerization. Moreover, although the rhombic twist or a twist about a pseudo-C_3 axis can give simultaneous racemization and isomerization, it cannot account for the fact that both the *cis*- and *trans*-$[Co(Htsc)_3]^{3+}$ ions racemize exceedingly fast in acid media. Hence the bond rupture process involving a chelate ring opening and closing is favored.

This mechanism may take several different courses (Fig. 5) and in order to see which course the rearrangement reaction would most probably follow, the greater stability of the *cis* isomer over the *trans* must be re-emphasized. It has been pointed out that the neutral *trans* isomer is formed by heating the corresponding *cis* isomer while recrystallization of the ionic *trans* form from aqueous solutions actually produces a mixture of the *trans* with the corresponding *cis* isomer. In addition, even though both isomers are reasonably stable in 0.1 *M* HCl, the greater stability of the *cis* over the *trans* is quite evident by following their electronic spectra. This explains why path I in Fig. 5*a* is preferred and the conversion of Λ-*cis* (or Δ-*cis*) to Δ-*trans* (or Λ-*trans*) would be less favored. On the other hand, path II in Fig. 5*b* is more favorable because of the greater stability of *cis* isomer. The other possibilities (e.g. Λ-*trans* → Λ-*cis*) are excluded on grounds that such processes would involve a rotation of 180° in the Co—S bond (which presumably has some π character) and considerable energy would be needed.

We are grateful to the National Research Council of Canada for financial support of this work.

1. K. A. Jensen and E. Rancke-Madsen. Z. Anorg. Allg. Chem. **219**, 243 (1934).
2. M. K. Akhmedli and A. M. Sadyova. Russ. J. Inorg. Chem. **7**, 260 (1962).
3. N. M. Samus' and A. V. Ablov. Russ. J. Inorg. Chem. **6**, 1042 (1961).
4. N. M. Samus'. Russ. J. Inorg. Chem. **8**, 35 (1963).
5. Ts. B. Konunova, N. M. Samus', and V. N. Zubarev. Russ. J. Inorg. Chem. **8**, 589 (1963).
6. R. A. Haines and K. K. W. Sun. Can. J. Chem. **46**, 3241 (1968).
7. G. Gorin, J. E. Spessard, G. A. Wessler, and J. P. Oliver. J. Amer. Chem. Soc. **81**, 3193 (1959).
8. M. Mori, M. Shibata, E. Kyuno, and M. Kanaya. Bull. Chem. Soc. Japan, **34**, 1837 (1961).
9. Y. Shimura and R. Tsuchida. Bull. Chem. Soc. Jap. **29**, 311 (1956); Y. Shimura, Bull. Chem. Soc. Jap. **31**, 173 (1958); F. Basolo, C. J. Ballhausen, and J. Bjerrum. Acta Chem. Scand. **9**, 810 (1955).
10. K. Nakamoto, J. Fujita, M. Kobayashi, and R. Tsuchida. J. Chem. Phys. **27**, 439 (1957).
11. H. Yamatera. Bull. Chem. Soc. Jap. **31**, 95 (1958).
12. D. S. McClure. *In* Advances in the chemistry of the coordination compounds. *Edited by* S. Kirshner. MacMillan Co., New York. 1961.
13. J. Hidaka and B. E. Douglas. Inorg. Chem. **3**, 1724 (1964).
14. G. R. Brubaker and B. E. Douglas. Inorg. Chem. **6**, 1562 (1967).
15. T. Burer. Helv. Chim. Acta, **46**, 2388 (1963).
16. J. Chatt and R. G. Wilkins. J. Chem. Soc. 273 (1952).
17. R. D. Gillard. *In* Progress in inorganic chemistry. Vol. 7. *Edited by* F. A. Cotton. Interscience Publ. New York. 1966.
18. J. Fujita and Y. Shimura. *In* Spectroscopy and structure of metal chelate compounds. *Edited by* K. Nakamoto and P. J. McCarthy. John Wiley and Sons, Inc., New York. 1968.
19. A. J. McCaffery, S. F. Mason, and R. E. Ballard. J. Chem. Soc. 2883 (1965).
20. A. J. McCaffery, S. F. Mason, and B. J. Norman. J. Chem. Soc. 5094 (1965).
21. E. Larsen and S. F. Mason. J. Chem. Soc. **A**, 313 (1966).
22. J. H. Dunlop and R. D. Gillard. J. Chem. Soc. **A**, 6531 (1965).
23. R. G. Denning and T. S. Piper. Inorg. Chem. **5**, 1056 (1966).
24. M. G. B. Drew, J. H. Dunlop, R. D. Gillard, and D. Rogers. Chem. Commun. 42 (1966).
25. F. Basolo and R. G. Pearson. Mechanism of inorganic reactions. 2nd ed. John Wiley and Sons, Inc., New York, 1967.
26. A. L. Porte, H. S. Gutowsky, and G. M. Harris. J. Chem. Phys. **34**, 66 (196).
27. K. K. W. Sun. Ph.D. Thesis, University of Western Ontario, London, Ontario. 1969.
28. M. Nardelli, G. Fava Gasparri, G. G. Battistini, and A. Musatti. Chem. Commun. 187 (1965).
29. A. Lopez-Castro and M. R. Truter. J. Chem. Soc. 1309 (1963); G. Fava Gasparri, A. Musatti, and M. Nardelli. Chem. Commun. 602 (1966); W. T. Robinson, S. L. Holt, Jr., and G. B. Carpenter. Inorg. Chem. **6**, 605 (1967).

Can. J. Chem. Downloaded from www.nrcresearchpress.com by 210.87.254.40 on 09/05/12
For personal use only.

Preparation of *cis*- and *trans*-2,5-dimethoxytetrahydropyran and *cis*- and *trans*-2,5-dimethoxy-6-methyltetrahydropyran

R. M. SRIVASTAVA[1] AND R. K. BROWN
Department of Chemistry, University of Alberta, Edmonton, Alberta

Received January 2, 1970

Hydroboration and subsequent oxidation of 2-methoxy-3,4-dihydro-2*H*-pyran gave a 1:2 mixture of *cis*- and *trans*-5-hydroxy-2-methoxytetrahydropyran (**2**). From the methylated product **4**, *trans*-2,5-dimethoxytetrahydropyran could be obtained by gas–liquid chromatography. The *cis*-2,5-dimethoxytetrahydropyran (**8**) was obtained by conversion of **4** to 3-methoxy-3,4-dihydro-2*H*-pyran (**6**) which upon bromomethoxylation and subsequent reduction with palladium catalyst gave **8**.

Both *cis*- and *trans*-2,5-dimethoxy-6-methyltetrahydropyran (**11**) were obtained by hydroboration and oxidation of 2-methoxy-6-methyl-3,4-dihydro-2*H*-pyran (**9**) followed by methylation of the resulting product.

Canadian Journal of Chemistry, 48, 2334 (1970)

Introduction

A previous report from this laboratory (1) has described the preparation of *cis*- and *trans*-2,4-dimethoxytetrahydropyran as part of a long range program of total synthesis of DL-monosaccharides and DL-deoxymonosaccharides. These compounds were also of interest in the study of the influence of substituents and their location in the tetrahydropyran ring on the magnitude of the anomeric effect (2–5).

This paper describes the preparation of *cis*- and *trans*-2,5-dimethoxytetrahydropyran and the homologue *cis*- and *trans*-2,5-dimethoxy-6-methyltetrahydropyran.

Results and Discussion

Although neither 5-hydroxy-2-methoxytetrahydropyran nor 2,5-dimethoxytetrahydropyran have been reported,[2,3] the preparation of the *cis–trans* (unseparated) mixture of 5-hydroxy-2-*n*-butoxytetrahydropyran from the alkaline oxidation of hydroborated 2-*n*-butoxy-3,4-dihydro-2*H*-pyran has been described (6). The same procedure (6) was therefore used to convert 2-methoxy-3,4-dihydro-2*H*-pyran (**1**) to 5-hydroxy-2-methoxytetrahydropyran (**2**) in excellent yield (Scheme 1). The 100 MHz proton magnetic resonance (p.m.r.) spectrum in deuteriobenzene agreed with the structure, showing two overlapping triplets at τ 5.55 and 5.61 ($J_{H_2H_{3a}} + J_{H_2H_{3e}} \approx 6$ Hz in both cases) in the anomeric proton region indicative of the presence of two isomers, no doubt *trans* and *cis*, in the approximate ratio of 2:1. The small couplings for the anomeric proton signals of both showed that each of the isomers is very largely in the conformation in which the methoxy group on C-2 is axial. The 100 MHz p.m.r. spectrum of the acetate **3**, also showed two narrow triplets ($J_{H_2H_{3a}} + J_{H_2H_{3e}} \approx$ 6 Hz for both) at τ 5.52 and 5.69 in the area ratio of ~2:1 for the anomeric protons of the two isomers (*trans,cis*). Neither **2** nor **3** could be separated by gas–liquid chromatography (g.l.c.) since only one symmetrical peak was observed with the several column packings tried.

The methylated derivative **4** also was a 1:2 mixture of isomers according to the g.l.c. It was possible with a 50 ft column packed with *neo*-pentylglycol sebacate on Chrom W to separate some of the major component (retention time 32 min) but the minor component (retention time 29½ min) could not be obtained at all. The 100 MHz spectrum of the major isomer has defined the structure. Double irradiation has permitted the assignment of the signals to the protons and clearly shows that this substance is *trans*-2,5-dimethoxytetrahydropyran and this exists very largely in the conformation in which the methoxy group on the anomeric carbon C-2 is axial (see Experimental).

Equilibration of the 1:2 mixture of *cis*- and *trans*-2,5-dimethoxytetrahydropyran, as well as

---

[1]Postdoctoral Fellow, 1968–1970.

[2]After the manuscript had been submitted for publication, the synthesis of methyl 2,3-dideoxy-α-(and β-)-L-*glycero*-pentopyranosides and their *O*-acetyl derivatives has been described by R. U. Lemieux *et al.* (12).

[3]NOTE ADDED IN PROOF: After this manuscript was accepted for publication, a paper appeared (13) describing the conversion of 2-ethoxy-3,4-dihydro-2*H*-pyran to 2-ethoxy-5-hydroxytetrahydropyran by the hydroboration reaction.

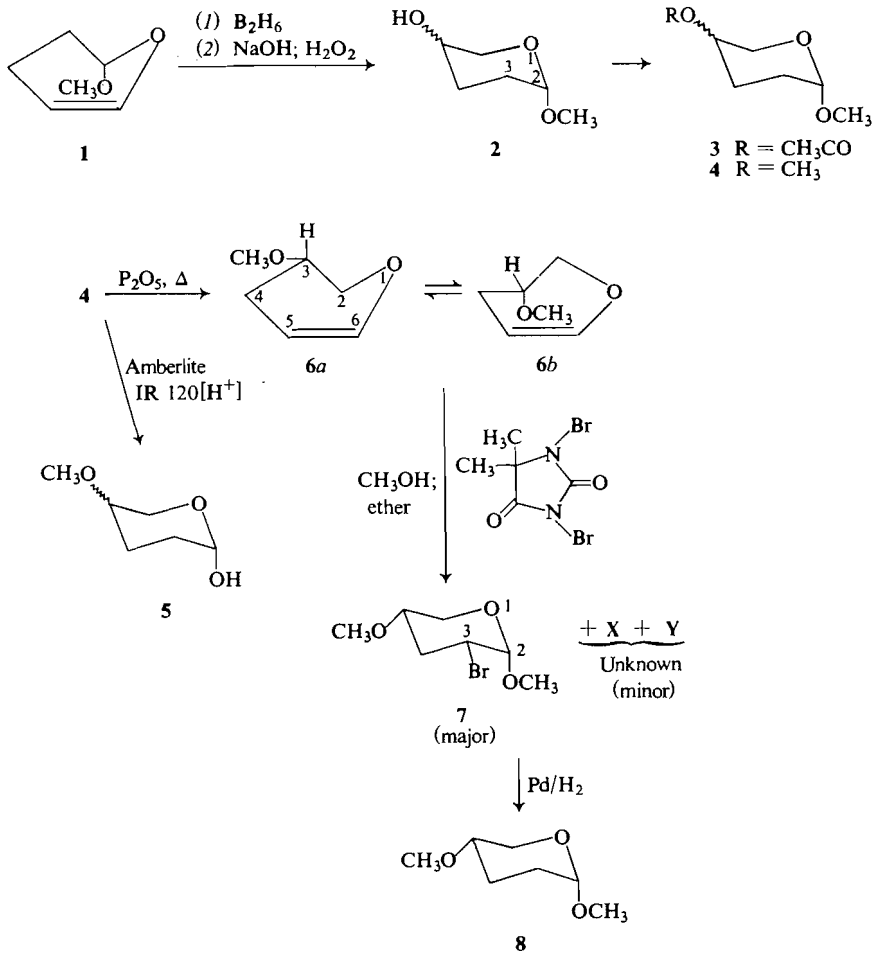

1 2 3 R = CH_3CO 4 R = CH_3 5 6a 6b 7 8

SCHEME 1

pure *cis*-2,5-dimethoxytetrahydropyran obtained later as described below, in the presence of a catalytic amount of *p*-toluenesulfonic acid provided an approximately 1:1 mixture of the *cis* and *trans* isomers which could not be separated by g.l.c. except by long and extremely tedious work. Hence the *cis* isomer was prepared by the following route.

Slow distillation of the 1:2 mixture of *cis*- and *trans*-2,5-dimethoxytetrahydropyran (**4**) over a *catalytic amount* of phosphorus pentoxide gave 3-methoxy-3,4-dihydro-2*H*-pyran (**6**) in 58% yield. Although the elemental analysis of this product was somewhat low in carbon (62.23, 62.62% found; 63.13% calculated) the fact that the molecular weight determination by mass spectrum analysis gave $m/e = 114$ (required, 114) and the 100 MHz p.m.r. spectrum agreed completely with the structure **6** leaves no doubt that the compound is indeed **6**. An estimation of the magnitude of the coupling constants between H-3 and H-4 (equatorial and axial) of about 5.0 and 6.1 Hz respectively, indicates that **6** exists as a mixture of the conformers **6***a* and **6***b*.

Bromomethoxylation of **6** with 1,3-dibromo-5,5-dimethylhydantoin in ether–methanol (7) gave a mixture of three isomers as shown by the elemental analysis of the mixture and the three g.l.c. peaks in the area ratio of about 7.3:2.0:1.0 (in order of increasing retention time) obtained with two different column packings. Only a partial separation of the three isomers could be attained by g.l.c. Column chromatography on neutral alumina still gave a mixture of material but when this was dissolved in pentane and the solution allowed to stand for several days a

Can. J. Chem. Downloaded from www.nrcresearchpress.com by 210.87.254.40 on 09/05/12
For personal use only.

Can. J. Chem. Downloaded from www.nrcresearchpress.com by 210.87.254.40 on 09/05/12
For personal use only.

crystalline deposit occurred (46% yield) which proved to be the major product. Spin decoupling experiments indicated its structure to be 3α-bromo-2α,5α-dimethoxytetrahydropyran (**7**).

The mixture left in the mother liquor was composed of **7**, **X**, and **Y** in the approximate proportion of 1.0:1.1:0.58 (g.l.c.). From this, only one of the isomers, that with the longest retention time (**Y**), could be separated by g.l.c. but it was still contaminated with a small amount of **7** and **X**. Its p.m.r. spectrum showed a doublet, $J \sim 7$ Hz, for the anomeric proton signal at τ 5.67. The large coupling of 7 Hz clearly shows that the H-2 and H-3 protons are *trans* diaxial, and thus the methoxy group at C-2 and the bromine atom at C-3 are *trans* diequatorial. No further work was done to identify the two minor products **X** and **Y**.

Since pure **7** did not isomerize when left 3 days at room temperature in methanol containing hydrogen bromide (cf. ref. 7), and also a mixture of **7**, **X**, and **Y** (area ratio on g.l.c. = 1.0:0.3:0.18 respectively in order of increasing retention time) under the same conditions showed a 50% decrease in the last component and a slight increase in the first component, it is clear that under our conditions of bromomethoxylation (−50°, short reaction time) the products **7**, **X**, and **Y** obtained can not be the result of isomerization, but must be the products stemming directly from the reaction of 1,3-dibromo-5,5-dimethylhydantoin and methanol on **6**. This is of interest from a theoretical standpoint (7). The reason why one isomer did isomerize slowly is no doubt due to the fact that the methoxy and bromo substituents are *trans* to each other and thus anchimeric assistance by the bromine atom could assist the anomeric methoxy group to leave. The isomer which accumulates would then be that in which both substituents on C-2 and C-3 are *cis*, i.e. **7**.

Hydrogenation of pure **7** with palladium-on-charcoal in the presence of sodium methoxide to avoid anomerization, gave a single product which was shown by 100 MHz p.m.r. decoupling experiments to be *cis*-2,5-dimethoxytetrahydropyran (**8**) (see Experimental). This compound has a retention time identical with that of the minor component obtained from the methylation of **2**.

Treatment of **4** with the cation exchange resin Amberlite IR-120 [$H^{\oplus}$] in a mixture of water and 1,2-dimethoxyethane gave 2-hydroxy-5-methoxytetrahydropyran (**5**) in 50% yield. The 100 MHz spectrum in deuteriobenzene showed a poorly resolved triplet at τ 5.04 ($w/2 \approx 7.5$ Hz) indicating that the C-2 hydroxyl group is *axial*. The presence of two OCH_3 signals of about equal intensity at τ 6.91 and 6.92 (expanded spectrum) indicated that there were present two isomers in about equal amounts.

Hydroboration and subsequent oxidation of 2-methoxy-6-methyl-3,4-dihydro-2*H*-pyran (**9**) (Scheme 2) gave the two expected isomeric products **10***a* and *b*, in each case with the hydroxyl group *trans* to the adjacent C-6 methyl group (8). Methylation (9) gave a mixture **11***a* and *b* whose 60 MHz p.m.r. spectrum showed the presence of two components in the ratio α:β = 1.0:2.6. However, g.l.c. of this mixture showed two peaks in the area ratio of 1.0:3.8 of retention time 10 and 14 min respectively. This change in composition is due to decomposition of some of the α isomer in the column. The major component could be obtained by g.l.c. in an amount sufficient for study whereas only a very small quantity of the minor component was obtained even after tedious g.l.c. separation.

The 100 MHz spectrum of the pure major component showed a quartet for the anomeric proton signal at τ 5.68 with observed couplings of 8.5 and 2.5 Hz. This along with the coupling of ~8 Hz observed for the C-6 proton doublet left on irradiation of the C-6 methyl proton nuclei, clearly shows that the major product has the structure and conformation shown by **11***b* (Scheme 2), 2α, 5β-dimethoxy-6α-methyltetrahydropyran.

When the mixture of **11***a* and *b* was heated in refluxing methanol containing a small amount of *p*-toluenesulfonic acid catalyst, an equilibrium mixture of **11***a* and *b* (7.2:2.8 respectively by g.l.c.) was obtained. From this, the isomer **11***a* could be readily isolated by g.l.c. The 100 MHz spectrum of **11***a* clearly supported the structure and conformation shown by **11***a*. The narrow multiplet $w/2 \approx 5.5$ Hz for the anomeric proton signal at τ 5.41 indicated that H-2 was equatorially disposed and gauche to both protons on C-3. The multiplet at τ 6.39 which collapsed to a doublet ($J \approx 9$ Hz) when the nuclei of the methyl protons were irradiated showed that the C-5 and C-6 protons are *trans* diaxially disposed.

The individual isomers **11***a* and *b*, separately

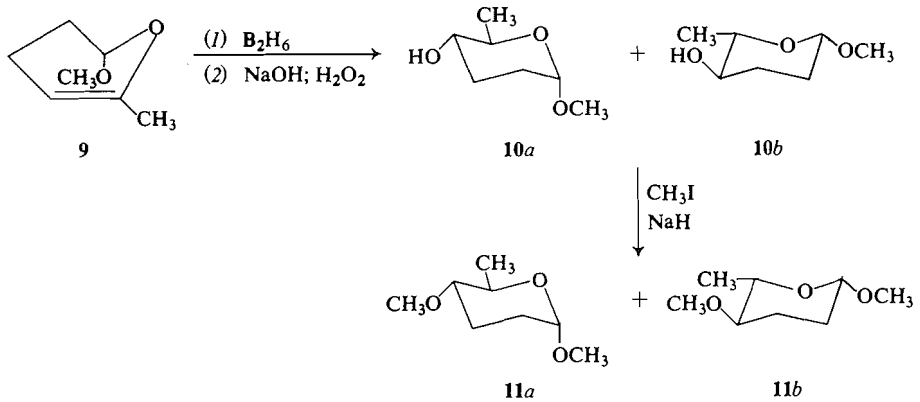

SCHEME 2

left for 7 days at room temperature in methanol containing *p*-toluenesulfonic acid, attained equilibrium in which the ratio of **11***a* and *b* was 7.4:2.6 (i.e. ~3:1) as determined by the g.l.c. and by the 60 MHz p.m.r. spectra.

Experimental

All the boiling points and melting points are uncorrected. The boiling points of the liquids obtained in small quantities, were determined in a two bulb apparatus, with the lower bulb dipped in the heating oil bath. The bath was slowly heated and when the liquid just started to distill, the temperature of the bath was recorded.

Solvents were removed by rotary evaporator unless otherwise stated. Anhydrous sodium sulfate was used to dry solutions.

Elemental analyses were done by Mrs. Darlene Mahlow, Department of Chemistry, University of Alberta, Edmonton.

Infrared (i.r.) spectra were obtained on a Perkin–Elmer model 421 spectrophotometer.

The 60 MHz p.m.r. spectra were taken by Mr. R. Swindlehurst of this Department on a Varian A-60 instrument. Mr. Glen Bigham and associates, all of this Department, took the 100 MHz p.m.r. spectra and carried out irradiation experiments, using a Varian HR-100 MHz instrument at 33° ± 1. Unless otherwise stated, deuteriochloroform was used as solvent to obtain the p.m.r. spectra with tetramethylsilane as internal standard. The *J* values reported have been estimated from the spacings and are therefore approximate values.

Gas–liquid chromatographic analyses were made with an F & M apparatus, model 700 or with an Aerograph Autoprep model A-700. Helium was the carrier gas. The following columns were used: (*a*) BDS. 20% butanediol succinate on Chrom P (60–80 mesh) in a column 1/8″ × 12′; (*b*) NPGS. 10% neopentylglycol sebacate on Chrom W (60–80 mesh) in a column 1/8″ × 24′; (*c*) CW. A column (1/8″ × 12′) containing 10% Carbowax 6000 on Chrom W (60–80 mesh); (*d*) CWP. 25% Carbowax 6000 on Chrom W (60–80 mesh) in a column 1/4″ × 12′.

The abbreviations used for solvents are as follows: DME = 1,2-dimethoxyethane; THF = tetrahydrofuran. The mass spectrum was obtained with an A.E.I., model MS2-H instrument.

*2-Methoxy-3,4-dihydro-2H-pyran (**1**)*

This compound was prepared by the published procedure (10) modified as follows: Acrolein (28.0g, 0.5 mole), and hydroquinone (100 mg) in 90–100 ml (large excess) of methyl vinyl ether was stirred constantly while heated at 180° for 9 h in an autoclave. The cooled mixture was transferred to a distillation flask with the help of some ether. Fractional distillation gave 50.5 g (88%) of colorless liquid. The b.p. 125° at 700 mm; η_D^{25}, 1.4385. The lit. b.p. 126–127° at 760 mm; η_D^{25}, 1.4397 (10).

*5-Hydroxy-2-methoxytetrahydropyran (**2**)*

Compound **2** was prepared by the method of Masamune and Castellucci (6). Since experimental details were not published, they are provided here.

A quantity (91.2 g, 0.8 mole) of 2-methoxy-3,4-dihydro-2*H*-pyran (**1**) in 400 ml of dry THF was put in a 1 l, three-neck flask. One neck was connected to a mercury bubbler while the other was attached to a generator in which diborane was produced by dropping a solution of 10.95 g (0.29 mole) of sodium borohydride in 280 ml of dry diglyme, over a period of 3 h, onto a stirred solution of 85.2 g (0.6 mole) of boron trifluoride etherate in 100 ml of diglyme. The generator was then heated to 70° and kept at this temperature for 1/2 h and then nitrogen was passed through to drive the remaining diborane over. During the latter process from the time that the generator was heated, the reaction flask containing **1** was kept cool in an ice bath. The reaction flask was then disconnected from the generator and cooled in an ice bath while the stirred solution was treated over 1/2 h period with 60 ml of water (dropwise). This was followed by the addition of 112 ml of 3 *N* aqueous sodium hydroxide over a 1 h period. The ice bath was then removed and 110 ml of 30% hydrogen peroxide added at such a rate as to maintain gentle reflux (1 1/4 h). The solution was stirred for an additional hour and then freed of most of the THF. The remaining aqueous solution was continuously extracted with methylene chloride for 2 days. The methylene

Can. J. Chem. Downloaded from www.nrcresearchpress.com by 210.87.254.40 on 09/05/12
For personal use only.

Can. J. Chem. Downloaded from www.nrcresearchpress.com by 210.87.254.40 on 09/05/12
For personal use only.

chloride extract was freed from solvent and the viscous liquid was dissolved in benzene and dried. The filtered solution was freed from solvent by fractional distillation, and the residue distilled under vacuum. Yield, 70–80%. The b.p., 100° at 10 mm; η_D^{23}, 1.4559.

Anal. Calcd. for $C_6H_{12}O_3$: C, 54.54; H, 9.15. Found: C, 54.51; H, 9.34.

The i.r. spectrum (neat) showed strong absorption at 3600–3100 cm^{-1} (OH). The 100 MHz p.m.r. spectrum in deuteriobenzene agreed with the structure and showed two overlapping triplets, each of total coupling ≈6 Hz.

5-Acetoxy-2-methoxytetrahydropyran (3)

A solution of 3.3 g (0.025 mole) of **2** and 2 ml of dry pyridine in 15.0 g (0.15 mole) of acetic anhydride was heated at 60° for 0.5 h and then left overnight at room temperature. More than half of the anhydride was then removed by fractional distillation at 24° at 4 mm. The residue was diluted with 50 ml of cold 4 *N* ammonium hydroxide, shaken for 10 min, and then extracted with chloroform (5 × 80 ml). The chloroform solution was washed with 50 ml of saturated aqueous sodium chloride solution, dried, and filtered. Removal of the solvent by fractional distillation, and subsequent distillation of the residue under vacuum gave 3.55 g (82%) of colorless liquid. The b.p. 61–66° at 1.9 mm; η_D^{27}, 1.4392.

Anal. Calcd. for $C_8H_{14}O_4$; C, 55.16; H, 8.10. Found: C, 55.05; H, 8.16.

The i.r. spectrum (neat) showed a strong band at 1735 cm^{-1} (—C(=O)—O—).

The 100 MHz p.m.r. spectrum (C_6D_6) agreed with the structure and showed two narrow triplets in the anomeric proton region at τ 5.52 and 5.69 indicative of two isomers.

Attempts to separate the two isomers by g.l.c. using the columns BDS, NPGS, or CW all failed since only one symmetrical peak was observed in each case.

2,5-Dimethoxytetrahydropyran (4)

The published directions (9) for methylation were modified advantageously as follows. A solution of **2** (19.0 g, 0.14 mole) in 100 ml of dry DME was added dropwise over a 2 h period to a well-stirred mixture of 5.16 g (0.22 mole) of sodium hydride and 30.5 g (0.22 mole) of methyl iodide in 100 ml of dry DME. The reaction flask was kept at ~20° in a water bath to avoid a rise in temperature. The mixture was stirred for several hours, then heated under reflux for an additional hour. Fractional distillation removed most of the solvent (~170 ml). To the cold residue was added 100 ml of ether to precipitate the sodium iodide. The solid was removed and the filtrate was freed from remaining solvent by fractional distillation. The residue was distilled under vacuum and afforded 18.85 g (89.7%) of colorless liquid boiling at 65° at 10 mm; η_D^{27}, 1.4317.

Anal. Calcd. for $C_7H_{14}O_3$; C, 57.51; H, 9.65. Found: C, 57.73; H, 9.95.

The g.l.c. on a NPGS column at 150° and at a flow rate of 40 ml/min showed two peaks of retention time 12 and 13 1/4 min in the area ratio of 1:2 respectively. Preparative g.l.c. on a NPGS column 1/4″ × 50′ at 145°, with a carrier gas flow rate of 75 ml/min, and with 10 μl injection quantities gave two peaks of retention time 29 1/2 and 32 min and of area ratio 1:2 respectively. A small amount (250 mg) of only the major isomer could be thus obtained. Reinjection gave only one peak of retention time 32 min.

Anal. Calcd. for $C_7H_{14}O_3$: C, 57.51; H, 9.65. Found: C, 57.77; H, 9.56.

The 100 MHz p.m.r. spectrum clearly supported the structural assignment as *trans-2,5-dimethoxytetrahydropyran*. Inspection, and spin decoupling by double irradiation gave the following signal assignments: H-2, triplet $J_{2,3e \text{ or } a} \approx 3.1$, $J_{2,3a \text{ or } e} \approx 2.5$ Hz. The small couplings showed that H-2 was equatorial; H-5, multiplet at τ 6.75; H-6_a, a doublet of doublets centered at τ 6.14, $J \approx 12$ and 2.5 Hz; H-6_e, a doublet of quartets centered at τ 6.46, $J \approx 12$, 3.5, and 1.5 Hz. Irradiation of H-5 at τ 6.75 eliminated the 2.5 Hz coupling at τ 6.14 and the 3.5 Hz coupling at τ 6.46. This loss of two small couplings showed that the H-5 proton was *equatorial*. H-3_a and H-4_a gave multiplets centered at τ 8.51 and 8.35 respectively. H-3_e and H-4_e, multiplets centered at τ 8.15 and 8.02 respectively.

Equilibration of the 1:2 Mixture of cis- and trans-2,5-Dimethoxytetrahydropyran (4)

The isomeric mixture **4** (0.5 g) in 50 ml of anhydrous methanol containing 50 mg of *p*-toluenesulfonic acid monohydrate was heated under reflux for 3 h. The cooled solution was treated with some sodium methoxide and the solution (p*H* ~ 9) was freed from most of the methanol by fractional distillation. The residue dissolved in 100 ml of ether was washed with water (5 × 5 ml) and dried. Removal of the solvent by fractional distillation gave a light yellow liquid. Distillation of this residue in a two-bulb apparatus gave 0.4 g of colorless liquid. The b.p. 64–65° at 9.2 mm; η_D^{26}, 1.4319.

Anal. Calcd. for $C_7H_{14}O_3$: C, 57.51; H, 9.65. Found: C, 57.70; H, 9.95.

The g.l.c. analysis on the NPGS column showed two peaks of approximately equal area and of retention time 11 1/2 and 12 1/2 min respectively.

The same results were obtained when pure *cis*-2,5-dimethoxytetrahydropyran was similarly equilibrated.

3-Methoxy-3,4-dihydro-2H-pyran (6)

The 1:2 mixture of *cis*- and *trans*-2,5-dimethoxytetrahydropyran (**4**) (20.0 g, 0.14 mole) was treated with a trace of phosphorus pentoxide and then heated slowly to an oil bath temperature of 165°. When kept at this temperature for 1 1/2 h, most of the methanol was removed through a fractionating column. The bath temperature was raised to 190° whereupon 11.8 g of liquid distilled within the boiling range 120–135°. This fraction stood over sodium metal overnight to destroy the methanol. Fractional distillation gave 9.1 g (58.3%) of colorless liquid boiling at 84° at 100 mm; η_D^{23}, 1.4459.

Anal. Calcd. for $C_6H_{10}O_2$: C, 63.13; H, 8.83. Found: C, 62.23, 62.62; H, 8.98, 8.76.

The i.r. spectrum (neat) showed a strong band at 1650 cm^{-1} (>C=C(—O—)—).

Can. J. Chem. Downloaded from www.nrcresearchpress.com by 210.87.254.40 on 09/05/12
For personal use only.

The molecular weight by mass spectrum was m/e = 114 (required 114).

The g.l.c. on an NPGS column at 100° showed a single symmetrical peak.

The 100 MHz p.m.r. spectrum agreed fully with the structure. Expansion of the high field portion of the spectrum where the two C-4 proton signals occur (τ 7.60 to 8.30) and irradiation of the nucleus of the C-5 proton at τ 5.50 gave a complicated multiplet from which it was possible to estimate the couplings between H-3, and the *cis* and *trans* C-4 protons to be about 5.0 and 6.1 Hz respectively.

3α-Bromo-2α,5α-dimethoxytetrahydropyran (7)

Compound **7** was prepared by the same method used to make 3-bromo-2,4-dimethoxytetrahydropyran (7). From 9.0 g (0.08 mole) of **6** and 11.4 g (0.04 mole) of 1,3-dibromo-5,5-dimethylhydantoin there was obtained 12.8 g (72%) of colorless liquid boiling at 65° at 0.7 mm; η_D^{26}, 1.4771.

Anal. Calcd. for $C_7H_{13}O_3Br$: C, 37.35; H, 5.82; Br, 35.50. Found: C, 37.51; H, 5.82; Br, 35.23.

The g.l.c. analysis on a BDS column at 165° with carrier gas flow rate of 30 ml/min showed three peaks with retention times of 12.0, 13.0, and 15.5 min in the area ratio of 7.3:2.0:1.0 respectively. The CW column gave three peaks of area ratio 5.7:1.26:1.0 at retention times 14.0, 15.0, and 16.0 min respectively.

The 60 MHz p.m.r. spectrum showed three signals in the anomeric proton region at τ 5.34, 5.47, and 5.65.

Chromatography over neutral alumina (Woelm, activity grade I) failed to separate the isomers. When the eluate containing the mixture was left at room temperature for several days, a precipitate appeared. This was crystallized twice from pentane and provided 8.2 g (46%) of material melting at 60–61°.

Anal. Calcd. for $C_7H_{13}O_3Br$: C, 37.35; H, 5.82; Br, 35.50. Found: C, 37.75, 37.28; H, 6.05, 5.87; Br, 35.44.

The g.l.c. of a benzene solution of this material on a BDS column as above showed one peak, of the same retention time as that of the major isomer.

The 100 MHz p.m.r. spectrum in deuteriobenzene agreed fully with the structure **7**. The anomeric proton H-2 gave a doublet at τ 5.58 ($J \approx 3.5$ Hz) indicating that H-2 was gauche to H-3. The splitting pattern of the signal for H-3, a multiplet, centered at τ 5.97 (total J = 14 Hz) can be accommodated only if H-3 is *trans* to one proton on C-4 and gauche to the second proton on C-4 and thus agrees with the conformation and structure shown by **7**. Irradiation of the nucleus of H-3 at τ 5.97 left a multiplet at τ 7.91 due to H-4$_e$ and H-4$_a$ showing geminal coupling of ~14 Hz and couplings of ~7.5 and ~3.0 Hz with H-5. These latter couplings can be accommodated only if H-5 is axial.

cis-2,5-Dimethoxytetrahydropyran (8)

A solution of 1.0 g (0.0044 mole) of **7** in 10 ml of methanol containing 0.33 g (0.006 mole) of sodium methoxide and 100 mg of 5% palladium-on-charcoal was shaken with hydrogen at 55 p.s.i. for 20 h at room temperature. Removal of the catalyst by filtration and then the methanol by fractional distillation left a residue which was dissolved in 100 ml of ether, washed with water (3 × 5 ml), and dried. The solvent was removed from the filtrate by fractional distillation and the residue distilled in a two-bulb apparatus to provide 0.24 g (38%) of colorless liquid, b.p. 84° (oil bath temperature) at 25–30 mm; η_D^{25}, 1.4312.

Anal. Calcd. for $C_7H_{14}O_3$: C, 57.51; H, 9.65. Found: C, 57.44; H, 9.59.

The g.l.c. with a NPGS column at 150° and a carrier gas flow rate of 30 ml/min gave a single peak of the same retention time as shown by the minor component of the mixture **4**.

The 100 MHz p.m.r. spectrum and spin decoupling experiments confirmed the structure to be *cis-2,5-dimethoxytetrahydropyran* (**8**). Irradiation of the four H-3 and H-4 protons (multiplet centered at τ 8.24) reduced the multiplet (two protons) between τ 6.25 and 6.57 to two overlapping quartets, one with couplings ~5 and ~11.5 Hz and the other of ~7.5 and ~11.5 Hz. This multiplet at τ 6.25 to 6.57 can be assigned to H-6$_e$ and H-6$_a$. The couplings observed can be accommodated only if H-5 is axial. The H-2 signal at τ 5.47 is a triplet of total coupling ~5.1 Hz, which can occur only if H-2 is gauche to *both* C-3 protons.

2-Hydroxy-5-methoxytetrahydropyran (5)

Method a

A solution of 7.0 g (0.048 mole) of **4** in 25 ml of DME containing 1.5 g of Amberlite IR-120[$H^{\oplus}$] was diluted with 75 ml of water. The mixture was stirred at room temperature for 24 h, then filtered and the resin washed with a 1:1 mixture of water and DME (2 × 5 ml). The combined washings and filtrate were extracted continuously with methylene chloride for 24 h. The methylene chloride extract was freed from solvent and the residual liquid dissolved in 25 ml of benzene and dried. The drying agent was separated by filtration and washed with benzene (5 × 5 ml). The combined filtrate and washings were freed from solvent and the residue was fractionally distilled to provide 0.95 g of recovered **4**, b.p. 61° at 9 mm; η_D^{25}, 1.4323; and 3.15 g (50%) of **5** boiling at 79–80° at 1.7–1.8 mm; η_D^{25}, 1.4567.

Anal. Calcd. for $C_6H_{12}O_3$: C, 54.53; H, 9.15. Found: C, 54.33; H, 9.29.

The i.r. spectrum of **5** showed a broad band at 3700–3100 cm^{-1} (OH).

The 100 MHz p.m.r. spectrum in deuteriobenzene at 40° showed two CH_3O signals of equal intensity and a poorly resolved triplet at τ 5.04, $w/2 \approx 7.5$ Hz. The structure of this triplet could be considered as due to two overlapping narrow triplets and thus suggests that in deuteriobenzene **5** occurs as two isomers each of which has the hydroxyl group in the axial position. In D_2O with tetramethylsilane as external standard the 100 MHz p.m.r. spectrum of **5** showed two quartets at τ 4.52 ($J \approx 5.0$ and 2.5 Hz) and 4.66 ($J \approx 6.0$ and 3.5 Hz) as well as two CH_3O signals of nearly equal intensity. This agrees with the existence of two isomers of **5**, both of which have the C-2 hydroxyl group equatorial.

Method b

A solution of 5 g (0.034 mole) of **4** in 7 ml of DME containing 7 ml of 1.5 *N* aqueous hydrochloric acid was stirred at room temperature for 45 h, then neutralized

Can. J. Chem. Downloaded from www.nrcresearchpress.com by 210.87.254.40 on 09/05/12
For personal use only.

with barium carbonate and filtered. The solid was washed successively with DME (3 × 5 ml) and methylene chloride (3 × 5 ml). The combined washings and filtrate were freed from solvent and the residual liquid was dissolved in methylene chloride and dried. This was filtered and the filtrate freed from solvent. The residue when distilled gave two fractions, one boiling at 64° at 10 mm (0.42 g) and the other boiling at 77° at 1.4 mm (1.85 g, 41%). The latter was compound **5**.

*2-Methoxy-6-methyl-3,4-dihydro-2H-pyran (**9**)*

A mixture of 35.05 g (0.5 mole) of methyl vinyl ketone (stabilized with hydroquinone) and 80 ml of methyl vinyl ether was heated in an autoclave at 180° for 5 1/2 h. Fractional distillation gave two fractions (*i*) 37.2 g (58%) boiling at 105° at 160 mm; $\eta_D^{26.5}$, 1.4396. The g.l.c. on the BDS column showed only one peak. Compare b.p. 81° at 100 mm; η_D^{23}, 1.4417 (11).

The i.r. spectrum and the 60 MHz p.m.r. spectrum agreed with the structure as 2-methoxy-6-methyl-3,4-dihydro-2*H*-pyran. Fraction (*ii*) gave 6.05 g (17%), b.p. 103° at 64 mm; η_D^{24}, 1.4568. Compare b.p. 67° at 24 mm (11). This material was 2-acetyl-6-methyl-3,4-dihydro-2*H*-pyran whose i.r. and p.m.r. spectra were identical with those obtained from an authentic sample prepared in this laboratory (11).

*5-Hydroxy-2-methoxy-6-methyltetrahydropyran (**10**)*

The mixture of the isomers of 2-methoxy-6-methyl-3,4-dihydro-2*H*-pyran (**9**) (35.0 g, 0.27 mole) was treated with diborane and then oxidized by the same procedure employed for the preparation of **2** above. The crude product was fractionally distilled and gave 23.0 g (58%) of colorless liquid, b.p. 75–77° at 2.1 mm; $\eta_D^{26.5}$, 1.4519.

Anal. Calcd. for $C_7H_{14}O_3$: C, 57.51; H, 9.65. Found: C, 57.73; H, 9.83.

The i.r. spectrum of the neat liquid showed two very weak bands at 1725 and 1640 cm^{-1} indicative of some impurity.

The 60 MHz p.m.r. spectrum showed two anomeric proton signals at τ 5.4 and 5.62 in the integrated area ratio of 1.0:2.4.

*2,5-Dimethoxy-6-methyltetrahydropyran (**11**)*

The isomeric mixture, **10**, was methylated by the same procedure as employed for the methylation of **2** above and provided an 81% yield of 2,5-dimethoxy-6-methyltetrahydropyran (**11**). The b.p. 59–60° at 7.5 mm; η_D^{25}, 1.4281.

The g.l.c. on the CWP column at 125° (carrier gas flow rate, 70 ml/min) showed two peaks in the area ratio 1.0:3.8 at retention times 10 and 14 min respectively. The major component was isolated by g.l.c. using injection quantities of 25 µl. No boiling point was obtained, η_D^{25}, 1.4288.

Anal. Calcd. for $C_8H_{16}O_3$: C, 59.98; H, 10.07. Found: C, 59.75; H, 10.03.

The 100 MHz p.m.r. spectrum and spin decoupling experiments showed the structure to be 2α,5β-dimethoxy-6α-methyltetrahydropyran (**11***b*) (see Discussion).

*Equilibration of the Isomeric Mixture of 2,5-Dimethoxy-6-methyltetrahydropyran (**11***a* and *b*). Isolation of **11***a*. Equilibration Separately of **11***a* and **11***b*

The mixture of **11***a* and *b* (2 g) was heated for 4 h in 50 ml of refluxing methanol containing 100 mg of *p*-toluenesulfonic acid monohydrate. The cooled solution was brought to p*H* ~ 9 with sodium methoxide and then freed from most of the solvent by fractional distillation. The residue, in 100 ml of ether, was washed with water (5 × 5 ml), dried, filtered and the filtrate freed from solvent. The crude liquid residue (1.8 g) on g.l.c. with a CWP column (25% Carbowax 6000 on Chrom W) at 125° and a carrier gas flow rate of 30 ml/min showed two peaks in the area ratio of 7.2:2.8. The latter peak was due to **11***b*.

Isomer **11***a* was isolated by g.l.c. using the column above. $\eta_D^{23.5}$, 1.4274.

Anal. Calcd. for $C_8H_{16}O_3$: C, 59.98; H, 10.07. Found: C, 59.98; H, 10.24.

The 100 MHz p.m.r. spectrum agreed fully with the structural assignment of **11***a* as 2α,5α-dimethoxy-6-β-methyltetrahydropyran (see Discussion).

Both **11***a* and *b* were left separately at room temperature in dry methanol containing a catalytic amount of *p*-toluenesulfonic acid monohydrate. Both reached equilibrium within 7 days. Both g.l.c. *and* the 60 MHz p.m.r. spectrum of each of the resulting mixtures contained **11***a* and *b* in the ratio of 7.4 to 2.6 respectively.

The authors wish to thank the National Research Council of Canada for financial assistance in this work.

1. F. Sweet and R. K. Brown. Can. J. Chem. **46**, 1543 (1968).
2. R. U. Lemieux. *In* Molecular rearrangements. *Edited by* P. de Mayo. John Wiley and Sons, Inc., New York, 1964. pp. 738–741.
3. E. L. Eliel, N. L. Allinger, S. J. Angyal, and G. A. Morrison. Conformational analysis. Interscience Publishers, New York, 1965. pp. 375–377.
4. G. O. Pierson and O. A. Runquist. J. Org. Chem. **33**, 2572 (1968).
5. C. B. Anderson and D. T. Sepp. Chem. Ind. (London), 2054 (1964); J. Org. Chem. **32**, 607 (1967).
6. S. Masamune and N. T. Castellucci. Chem. Ind. (London), 184 (1965). The experimental details were kindly supplied by Professor S. Masamune in a private communication.
7. M. J. Baldwin and R. K. Brown. Can. J. Chem. **47**, 3099 (1969).
8. H. C. Brown and G. Zweifel. J. Amer. Chem. Soc. **89**, 561 (1967).
9. U. E. Diner, F. Sweet, and R. K. Brown. Can. J. Chem. **44**, 1591 (1966).
10. R. I. Longley, Jr., and W. S. Emerson. J. Amer. Chem. Soc. **72**, 3079 (1950).
11. J. E. Roff and R. K. Brown. Unpublished results.
12. R. U. Lemieux, K. A. Watanabe, and A. A. Pavia. Can. J. Chem. **47**, 4413 (1969).
13. G. Zweifel and J. Plamondon. J. Org. Chem. **35**, 898 (1970).

Synthesis of methyl 4-*O*-methyl-α-DL-arabinopyranoside from 3-methoxy-3,4-dihydro-2*H*-pyran

R. M. SRIVASTAVA[1] AND R. K. BROWN
Department of Chemistry, University of Alberta, Edmonton, Alberta

Received January 12, 1970

3-Bromo-2,5-dimethoxytetrahydropyran (**2**), obtained by bromomethoxylation of 3-methoxy-3,4-dihydro-2*H*-pyran (**1**), was dehydrohalogenated to *cis*-2,5-dimethoxy-5,6-dihydro-2*H*-pyran (**3**). The epoxide **5**, derived from **3**, was converted to methyl 4-*O*-methyl-α-DL-arabinopyranoside (**7**) by treatment with aqueous potassium hydroxide. The structure and conformation of **7** and of its diacetate **8** were proven by analysis of their 100 MHz proton magnetic resonance spectra. Subsequent comparison with an authentic sample of methyl 4-*O*-methyl-α-L-arabinopyranoside corroborated the structural assignment.

Canadian Journal of Chemistry, **48**, 2341 (1970)

Can. J. Chem. Downloaded from www.nrcresearchpress.com by 210.87.254.105 on 09/05/12
For personal use only.

Introduction

In 1962 Siddiqui and Bishop (1) reported the preparation and isolation of both the α and β isomers of methyl 4-*O*-methyl-L-arabinopyranoside. In the same year Wolfrom and Lucke (2) published their preparation of methyl 4-*O*-methyl-D-arabinopyranoside. More recently, the synthesis of 4-*O*-methyl-β-D-arabinose (3, 4) and of methyl 4-*O*-methyl-β-D-arabinopyranoside (3, 4) had been described. In each of these cases, the starting material was a monosaccharide of known structure and configuration. To our knowledge no report has appeared describing the preparation of a 4-*O*-methylarabinopyranoside from non-carbohydrate precursors. This paper presents the synthesis of methyl 4-*O*-methyl-α-DL-arabinopyranoside (see Scheme 1) from 3-methoxy-3,4-dihydro-2*H*-pyran, which is in turn obtained from 2-methoxy-3,4-dihydro-2*H*-pyran, the condensation product of acrolein and methyl vinyl ether (5).

Results and Discussion

The starting material, **1**, was prepared and converted to 3α-bromo-2α,5α-dimethoxytetrahydropyran (**2**) according to methods already reported (5). Dehydrobromination of **2** with a boiling solution of potassium hydroxide in methanol gave a 78% yield of *cis*-2,5-dimethoxy-5,6-dihydro-2*H*-pyran (**3**) whose identity was established by its elemental analysis, its 100 MHz proton magnetic resonance (p.m.r.) spectrum, the absence of vinyl ether absorption usually present as a strong band in the infrared (i.r.) spectrum (6, 7), the absence of significant absorption in the i.r. spectrum between 1500 and 1800 cm^{-1} but the presence of a strong band at 1660 cm^{-1} in the Raman spectrum, and finally by its conversion by hydrogenation to *cis*-2,5-dimethoxytetrahydropyran **4** identical with an authentic specimen (5).

Treatment of **3** with *m*-chloroperoxybenzoic acid in methylene chloride for 5 1/2 days at room temperature gave the epoxide **5** in 67% yield. Gas–liquid chromatography (g.l.c.) showed that the epoxide **5** was contaminated with a very small amount (<2%) of substance, possibly the isomer **6**. This trace of impurity could not be discerned in the 60 MHz p.m.r. spectrum of **5**. The 100 MHz p.m.r. spectrum of **5** agreed with the structure **5** and showed a narrow singlet for the anomeric proton which clearly supported the view that epoxidation had occurred *trans* to the anomeric methoxy group (8). This selective direction of epoxidation was also expected on the basis of steric considerations (9–11).

When the epoxide **5** was heated in a refluxing solution of potassium hydroxide, water, and dioxane there was obtained a liquid which crystallized spontaneously. Two crystallizations and a subsequent sublimation provided a colorless material showing a single spot on a thin-layer chromatogram (t.l.c.). Its elemental analysis and the following evidence showed clearly that this material was methyl 4-*O*-methyl-α-DL-arabinopyranoside (**7**).

The i.r. spectrum in Nujol showed two broad overlapping bands at 3340 and 3220 cm^{-1} indicative of hydrogen bonded hydroxyl groups. At high dilution (0.005%) in carbon tetrachloride the i.r. spectrum showed two narrow overlapping bands at 3600 and 3560 cm^{-1}. This shift of the

[1]Postdoctoral Fellow, 1968–1970.

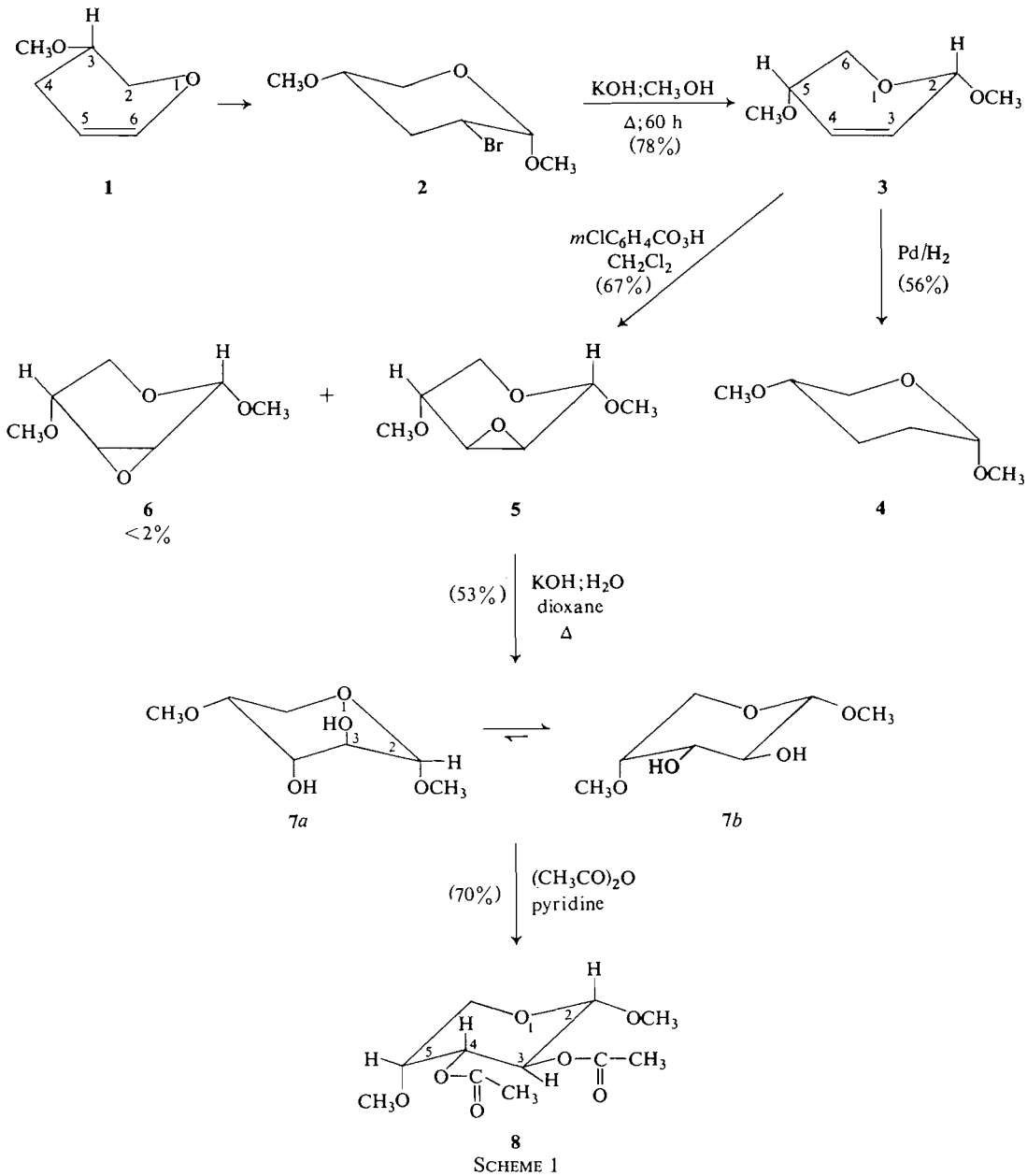

1 2 3 6 <2% 5 4 7a 7b 8

SCHEME 1

absorption bands to higher wave number in the non-polar solvent indicated the absence of *intra*molecular hydrogen bonding.

The 100 MHz p.m.r. spectrum in pyridine-d_5 showed a doublet at τ 5.6 ($J \approx 6$ Hz) for the anomeric proton signal. The magnitude of this coupling clearly requires the anomeric proton H-2 and the adjacent proton H-3 to be *trans* diaxially oriented, thus supporting the structure and conformation shown by **7***b*.

The di-*O*-acetyl derivative **8**, obtained in good yield, gave a 100 MHz p.m.r. spectrum which agreed with structure **8**. The signal for the anomeric proton H-2 appeared at τ 5.65 as a doublet $J \approx 5.5$ Hz. The magnitude of the coupling indicates that H-2 and H-3 are *trans* and the conformation of this product is primarily that in which H-2 and H-3 are both axial as in structure **8**. The signal for H-3 was a quartet centered at τ 4.85 ($J_{2a,3a} \approx 5.5, J_{3a,4a} \approx 8.0$ Hz) while that for

Can. J. Chem. Downloaded from www.nrcresearchpress.com by 210.87.254.105 on 09/05/12
For personal use only.

Can. J. Chem. Downloaded from www.nrcresearchpress.com by 210.87.254.105 on 09/05/12
For personal use only.

H-4 was also a quartet centered at τ 5.01 ($J_{3a,4a} \approx 8.0$, $J_{4a,5e} \approx 3.0$ Hz). Irradiation of the H-3 nucleus at τ 4.85 converted the anomeric proton (H-2) doublet at τ 5.65 to a singlet. Irradiation of the nucleus of H-4 at τ 5.01 reduced the multiplet for H-5 at τ 6.73 to a quartet, $J \approx 4.5$ and 2.5 Hz. The magnitude of these couplings indicates that H-5 is gauche to both protons on C-6. This information is in complete agreement with the structure and conformation shown by **8**.

The practically exclusive cleavage of the C—O bond of the oxirane ring of **5**, remote from the anomeric carbon C-2 is in agreement with similar preferential C—O bond cleavage of 1,6:2,3-dianhydro-4-deoxy-β-DL-*ribo*hexopyranose by aqueous potassium hydroxide to produce only 1,6-anhydro-4-deoxy-β-DL-*xylo*hexopyranose (12) and also with preferred direction of epoxide ring opening by lithium aluminum hydride of *cis*- and *trans*-2-alkoxy-3,4-epoxytetrahydropyran (13).

All of the signals in the 100 MHz p.m.r. spectrum and in the i.r. spectrum of the methyl 4-*O*-methyl-α-DL-arabinopyranoside (**7**) were found in the corresponding spectra of authentic methyl 4-*O*-methyl-α-L-arabinopyranoside. In addition, the mass spectrum of **7** was superimposable, with respect to the number and position of signals, with that of the authentic sample of the L-isomer.

Experimental

All boiling points and melting points are uncorrected. The boiling points of liquids obtained in very small quantities were determined in a two-bulb apparatus, with the lower bulb immersed in the heating bath. The bath was heated slowly, and when the liquid in the lower bulb just began to distill, the bath temperature was recorded as the boiling point.

Elemental analyses were made by Mrs. Darlene Mahlow and Miss Andrea Dunn of this Department.

The i.r. spectra were obtained on a Perkin–Elmer model 421 spectrophotometer by Mr. R. Swindlehurst. The instrument was calibrated in the 3600 cm^{-1} region with carbon dioxide.

The 60 MHz p.m.r. spectra were obtained by Mr. R. Swindlehurst using a Varian A-60 instrument. Mr. G. Bigham and associates of this Department made the 100 MHz p.m.r. spectra and carried out spin decoupling experiments using a Varian HR-100 MHz instrument at 33° ± 1. Deuteriochloroform was employed as solvent unless otherwise stated. Tetramethylsilane was the internal reference. The coupling constants reported have been estimated from the spacings and are therefore approximate values.

Gas–liquid chromatographic analyses were made with an F & M apparatus, model 700, or with an Aerograph Autoprep model A-700. Helium was the carrier gas. Unless otherwise stated, a column 1/8″ × 12′, filled with 20% butanediol succinate on Chrom P 60–80 mesh was used. This column is designated as BDS.

The t.l.c. was done using silica gel G (E. Merck and Co.). Iodine vapor was used to detect the spots.

Solvents were removed generally by rotary evaporator under vacuum unless otherwise mentioned. The drying agent was anhydrous magnesium sulfate.

The mass spectra were obtained with an A.E.I., MS-9 instrument.

cis-2,5-Dimethoxy-5,6-dihydro-2H-pyran (3)

A solution of 22.0 g (0.988 mole) of 3α-bromo-2α,5α-dimethoxytetrahydropyran (**2**) (5) and 12.5 g (0.22 mole) of potassium hydroxide in 200 ml of methanol was heated under reflux for 60 h. Most of the methanol was then removed by fractional distillation and the residual liquid, dissolved in 250 ml of ether, was washed with water (10 × 5 ml), dried, filtered, and freed from solvent by fractional distillation. The residue when distilled gave 11.0 g (78%) of colorless liquid. The b.p., 68° at 10 mm, $\eta_D^{23.5}$, 1.4474.

Anal. Calcd. for $C_7H_{12}O_3$: C, 58.32; H, 8.39. Found: C, 58.61; H, 8.15.

The g.l.c. on the BDS column at 170° gave a single peak.

The i.r. spectrum (neat) showed no absorption between 1700 and 1500 cm^{-1}. The Raman spectrum (neat) gave a strong band at 1660 cm^{-1} (>C=C<).

The 100 MHz p.m.r. spectrum agreed with the structure **3**. The anomeric proton signal appeared at τ 5.26 as a narrow multiplet, $w/2 \approx 6$ Hz.

cis-2,5-Dimethoxytetrahydropyran (4)

A quantity (0.7 g, 0.005 mole) of **3** in 5 ml of methanol containing 50 mg of sodium methoxide and 100 mg of 5% palladium-on-charcoal was hydrogenated at 1 atm pressure. After 3 1/2 h, the required amount of hydrogen was consumed and then the catalyst was removed by filtration and washed with ether (5 × 5 ml). The combined filtrate and washings were freed from solvent by fractional distillation to give a liquid which was distilled in a two-bulb apparatus to provide 0.4 g (56%) of colorless liquid. The b.p., 85° at 30 mm. The g.l.c. analysis with a column (1/8″ × 24′) of 10% neopentyl glycol sebacate on Chrom W (60–80 mesh) gave only one peak with the same retention time as that for authentic *cis*-2,5-dimethoxytetrahydropyran (5). The 100 MHz p.m.r. spectrum was also identical to that of authentic *cis*-2,5-dimethoxytetrahydropyran (5).

Methyl 2,3-Anhydro-4-O-methyl-α-DL-lyxopyranoside (5)

A solution of 7.0 g (0.049 mole) of **3** in 25 ml of methylene chloride was added dropwise over a period of 1 h to a stirred solution of 12.0 g (0.07 mole) of *m*-chloroperoxybenzoic acid in 100 ml of methylene chloride at 25°. The mixture was then stirred for 5 1/2 days at room temperature. The precipitate of *m*-chlorobenzoic acid was removed by filtration and washed with methylene chloride (2 × 25 ml). The combined filtrate and washings were washed with 10% aqueous sodium carbonate (5 × 25 ml), with water (5 × 15 ml), and then dried. The solid was separated and the filtrate freed from solvent. The residue was distilled to give 5.2 g (66.6%) of colorless liquid boiling at 62–64° at 1.3 mm; η_D^{25}, 1.4455.

Can. J. Chem. Downloaded from www.nrcresearchpress.com by 210.87.254.105 on 09/05/12
For personal use only.

Anal. Calcd. for $C_7H_{12}O_4$: C, 52.49; H, 7.55. Found: C, 52.36; H, 7.66.

The g.l.c. analysis on the BDS column at 160° with carrier gas flow rate of 30 ml/min gave two peaks in the area ratio of 9.8:0.2 in the order of increasing retention time.

The i.r. spectrum (neat) gave no absorption in the regions expected for C=O or OH.

The 100 MHz p.m.r. spectrum of the purified (g.l.c.) material agreed with structure **5** and showed a singlet at τ 5.23 for the anomeric proton.

Epoxidation of **3** at room temperature for a 50 h period gave a liquid whose 60 MHz p.m.r. spectrum showed that the product **5** was contaminated with unreacted **3** to the extent of ~20%.

Compound **5** was obtained free of the 2% of contaminating material (possibly **6**) by preparative g.l.c. using a BDS column (1/4″ × 6′) at 160° with a gas flow rate of 70 ml/min. The light yellow liquid so obtained was distilled (two-bulb) to provide a colorless liquid boiling at 80° at 2.5 mm; η_D^{25}, 1.4454.

*Methyl 4-O-Methyl-α-*DL*-arabinopyranoside (7)*

A solution of 2.5 g (0.016 mole) of **5** in a mixture of 5 ml of *p*-dioxane 5.0 g (0.09 mole) of potassium hydroxide and 45 ml of water was heated under reflux for 24 h. The resulting yellowish solution was cooled and to it was added, dropwise, a 7% solution of aqueous hydrochloric acid till the p*H* of the solution was ~9. This solution was continuously extracted with methylene chloride for 48 h. Removal of the methylene chloride from the extract gave a liquid which solidified immediately. The dried crude solid weighed 1.48 g (53%). With chloroform–methanol (9.0:1.0) as solvent, this crude material showed a single spot on the t.l.c. A repetition of this experiment, involving neutralization with acetic acid, saturation of the aqueous solution with sodium chloride followed by its continous extraction with methylene chloride for 5 1/2 days gave a 60% yield of crude product.

Two crystallizations from methylene chloride – hexane gave light fluffy crystals melting at 116°.[2] When sublimed at 80° (oil bath temperature) under vacuum (0.07 mm) there was no change of melting point.

Anal. Calcd. for $C_7H_{14}O_5$: C, 47.19; H, 7.92. Found: C, 47.33; H, 8.18.

The i.r. spectrum in a Nujol mull showed two broad bands at 3340 and 3220 cm^{-1} (OH, bonded). In carbon tetrachloride (0.005% solution) these bands were found at 3600 and 3560 cm^{-1}. Further dilution gave no further shift of the absorption bands.

The 100 MHz p.m.r. spectrum in deuteriochloroform did not allow identification of the anomeric proton signal. The 100 MHz p.m.r. spectrum in deuteriopyridine showed a doublet at τ 5.6 ($J \approx 6$ Hz).

The aqueous portion left after methylene chloride extraction was further extracted for 2 1/2 days with *n*-butyl alcohol. Removal of the solvent by fractional distillation at room temperature gave a minute quantity of unidentified material whose i.r. spectrum (neat) showed a band of medium strength at 1735 cm^{-1}. No further work was done on this material.

*Methyl 2,3-Di-O-acetyl-4-O-methyl-α-*DL*-arabinopyranoside (8)*

A solution of 0.15 g (0.00084 mole) of **7** in 1.5 ml of dry pyridine containing 1 ml of acetic anhydride was heated to 60° for 15 min and then stirred at room temperature overnight. Removal of the pyridine and excess acetic anhydride under vacuum (25° at 4–5 mm) gave a liquid to which 5 ml of water, then 10 ml of cold 3 *N* ammonium hydroxide was added. The aqueous layer was extracted with chloroform (5 × 25 ml) and the extract was washed once with 15 ml of saturated aqueous sodium chloride, then dried (Na_2SO_4). The solvent was removed from the filtered solution and to the residue was added some hexane. The oil, when rubbed with a spatula, crystallized (168 mg crude). Two further crystallizations from methylene chloride – hexane gave 155 mg (70%) of material melting at 94–95°. An analytical sample was dried under vacuum at 56° for 4 h and then at room temperature under vacuum for 4 h.

Anal. Calcd. for $C_{11}H_{18}O_7$: C, 50.38; H, 6.92. Found: C, 50.42; H, 6.95.

The i.r. spectrum in chloroform showed a very strong band at 1740 cm^{-1} (—C(=O)—O—).

The 100 MHz p.m.r. spectrum agreed fully with the structure shown by **8** (see Discussion).

The authors wish to thank the National Research Council of Canada for financial assistance throughout the course of this work.

The authors also thank Dr. Claude T. Bishop of the National Research Council of Canada for samples of authentic 4-*O*-methyl-L-arabinose and methyl 4-*O*-methyl-α-L-arabinopyranoside.

1. I. R. Siddiqui and C. T. Bishop. Can. J. Chem. **40**, 233 (1962).
2. M. L. Wolfrom and W. E. Lucke. NASA. Doc. N62-12090 (1962); Chem. Abstr. **60**, 8112 (1964).
3. H. G. Fletcher, Jr. and H. W. Diehl. J. Org. Chem. **30**, 2321 (1965).
4. S. C. Williams and J. K. N. Jones. Can. J. Chem. **45**, 275 (1967).
5. R. M. Srivastava and R. K. Brown. Can. J. Chem. This issue.
6. M. Sharma and R. K. Brown. Can. J. Chem. **44**, 2825 (1966).
7. R. J. Ferrier. J. Chem. Soc. 5443 (1964).
8. F. Sweet and R. K. Brown. Can. J. Chem. **46**, 1481 (1968).
9. H. B. Henbest and R. A. L. Wilson. J. Chem. Soc. 1958 (1957).
10. H. B. Henbest and B. Nicholls. J. Chem. Soc. 221 (1959).
11. F. Sweet and R. K. Brown. Can. J. Chem. **46**, 2283 (1968).
12. F. Sweet and R. K. Brown. Can. J. Chem. **46**, 2289 (1968).
13. F. Sweet and R. K. Brown. Can. J. Chem. **46**, 707 (1968).

[2]One of the referees has pointed out that since Siddiqui and Bishop (1) found a melting point of 83–84° for their methyl 4-*O*-methyl-α-L-arabinopyranoside, the melting point of 116° found for the methyl 4-*O*-methyl-α-DL-arabinopyranoside indicates that the latter is a racemic compound rather than a racemic mixture.

Can. J. Chem. Downloaded from www.nrcresearchpress.com by 210.87.254.105 on 09/05/12
For personal use only.

Spectrométrie de masse des peroxydes organiques. III.[1] Ozonides des styrènes substitués dans le noyau

J. CARLES, Y. ROUSSEAU, ET S. FLISZÁR
Département de Chimie, Université de Montréal, Montréal, Québec

Reçu le 14 novembre 1969

Les ozonides des styrènes comportant un substituant R dans le noyau aromatique ont été étudiés en spectrométrie de masse, avec R = *p*-CH_3O, *p*-CH_3, H, *p*-Cl, *m*-Cl, et *p*-NO_2. L'ion moléculaire est, en général, d'autant plus intense que R est plus attracteur d'électrons. Les abondances des fragments carbonylés $RC_6H_4CH{=}\dot{O}^+$ engendrés par la fragmentation de l'ion moléculaire suivent la relation de Hammett ($\rho = -0.44$), ainsi que la formation des ions $[RC_6H_4CH_2]^+$ à partir de $[M\text{-}32]^+$ ($\rho = -1.36$). L'abondance relative de $[M\text{-}32]^+$ par rapport à l'ion moléculaire est indépendante de R ($\rho \approx 0$). Les écarts observés lors de la fragmentation primaire de l'ozonide du *m*-chlorostyrène peuvent être interprétés par l'intervention possible d'états électroniquement excités de l'ion moléculaire de cet ozonide.

The mass spectrometry of the ozonides of ring substituted styrenes has been studied, with R = *p*-CH_3O, *p*-CH_3, H, *p*-Cl, *m*-Cl, and *p*-NO_2. Electron withdrawing substituents favor, in general, the appearance of molecular ions. The intensities of the carbonyl fragments $RC_6H_4CH{=}\dot{O}^+$ from the fragmentation of the molecular ions follow the Hammett relationship ($\rho = -0.44$), as does the formation of $[RC_6H_4CH_2]^+$ from $[M\text{-}32]^+$ ($\rho = -1.36$). The relative abundance of $[M\text{-}32]^+$ to that of the molecular ion is independent of R ($\rho \approx 0$). The possible participation of electronically excited states in the primary fragmentation process of the *m*-chlorostyrene ozonide has been invoked to explain its particular behavior.

Canadian Journal of Chemistry, **48**, 2345 (1970)

L'étude des voies de fragmentation caractéristiques des ozonides en spectrométrie de masse présente un intérêt non seulement en raison de son application à des fins d'identification, mais, encore, en vue d'une comparaison avec les processus de fragmentation propres à des hétérocycles voisins, tels que les peroxydes organiques cycliques; ces derniers ont fait l'objet d'une récente étude (1). De plus, la connaissance des fragments ioniques issus des ozonides, en spectrométrie de masse, permet la comparaison et la discussion, sur une base expérimentale, des divers mécanismes qui ont été proposés pour la formation des ozonides (2, 3). Ainsi, par exemple, il a été montré (2, 4) que l'ozonolyse, dans le tétrachlorure de carbone et le pentane, des stilbènes *cis* et *trans*, du β-méthylstyrène, du styrène, et du triphényléthylène, en présence de benzaldéhyde-^{18}O, conduit à une incorporation de l'oxygène aldéhydique uniquement en position éther des ozonides formés.

L'établissement, sur une base solide, des mécanismes de fragmentation des ozonides dans le spectromètre de masse et la compréhension de tous les facteurs intervenant lors de ces fragmentations motivent une étude systématique plus poussée. Le présent travail a pour but l'étude des ozonides d'une série de styrènes substitués dans le noyau aromatique en vue de déterminer l'influence des groupements fonctionnels (notamment par leur caractère donneur ou attracteur d'électrons) sur les différentes voies de fragmentation. Les ozonides suivants (**1**–**6**) ont fait l'objet de la présente étude.

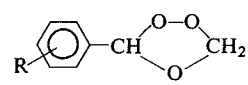

1 R = *p*-CH_3O **4** R = *p*-Cl
2 R = *p*-CH_3 **5** R = *m*-Cl
3 R = H **6** R = *p*-NO_2

Résultats et discussion

Les spectres de masse des composés **1** à **6** sont représentés par les figures 1 à 6.

Les modes de fragmentation des ozonides des styrènes substitués, déduits d'après l'analyse des résultats expérimentaux, sont représentés par le schéma 1. Ce schéma de fragmentation est en bon accord avec le mode général de fragmentation qui a été précédemment trouvé pour divers types d'ozonides (4). Une étude détaillée des modes de fragmentation a alors été présentée pour les ozonides du styrène, β-méthylstyrène, stilbène, triphényléthylène, octène-4, diphényl-1,4-

[1]Partie I: réf. 1; partie II: réf. 4.

Can. J. Chem. Downloaded from www.nrcresearchpress.com by 210.87.254.105 on 09/05/12
For personal use only.

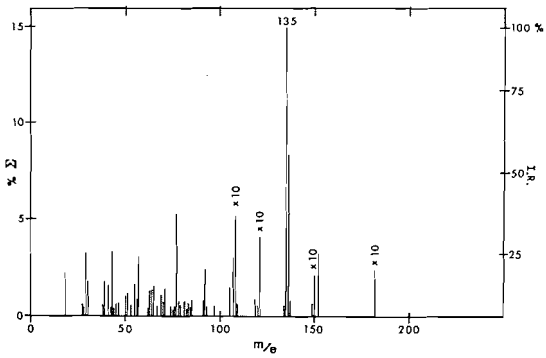

FIG. 1. Spectre de masse de l'ozonide du *p*-méthoxystyrène.

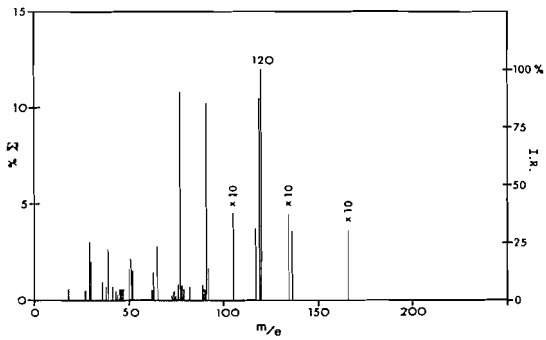

FIG. 2. Spectre de masse de l'ozonide du *p*-méthylstyrène.

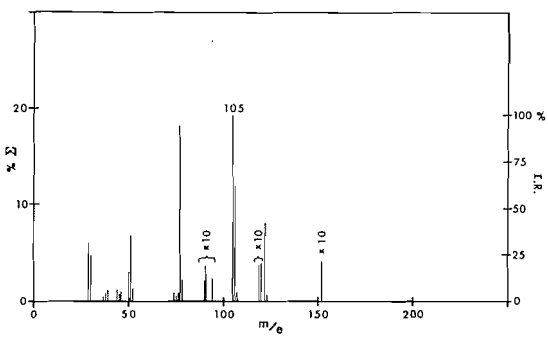

FIG. 3. Spectre de masse de l'ozonide du styrène.

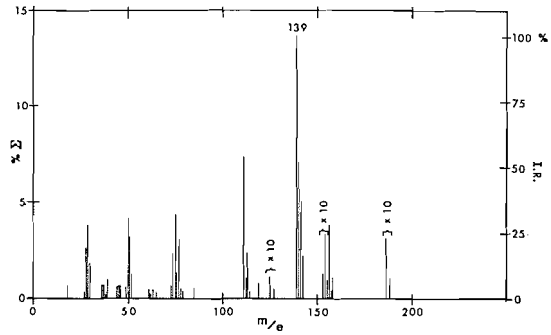

FIG. 4. Spectre de masse de l'ozonide du *p*-chlorostyrène.

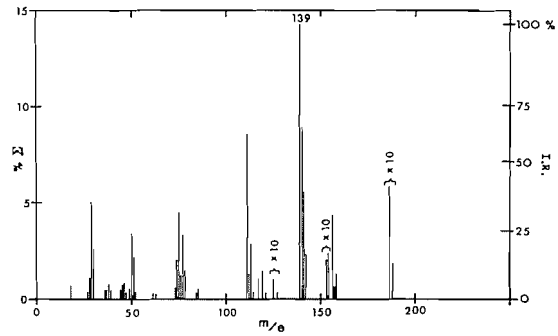

FIG. 5. Spectre de masse de l'ozonide du *m*-chlorostyrène.

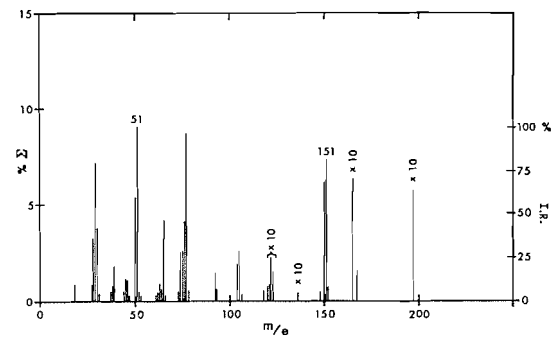

FIG. 6. Spectre de masse de l'ozonide du *p*-nitrostyrène.

butène-2, dichloro-1,4-butène-2, et du phényl-1-cyclopentène. Les résultats conduisant au schéma 1 de fragmentation ont été également corroborés par l'étude d'ozonides marqués à l'aide d'oxygène-18 (4).

Il apparaît, notamment, que la fragmentation de l'ion moléculaire (M^+) a lieu suivant deux voies distinctes. La première (voies *1* ou *1'*), se manifestant par l'apparition de l'ion M-32, implique la rupture de deux liaisons C—O, tandis que la seconde (voie *2*) se produit par suite de la rupture d'une liaison O—O et d'une liaison C—O. D'après les résultats obtenus antérieurement (4), notamment à l'aide d'ozonides marqués par ^{18}O en position éther, la voie *2* est nettement favorisée par rapport aux voies de fragmentation *1* et *1'*.

Dans le tableau 1, les abondances relatives des

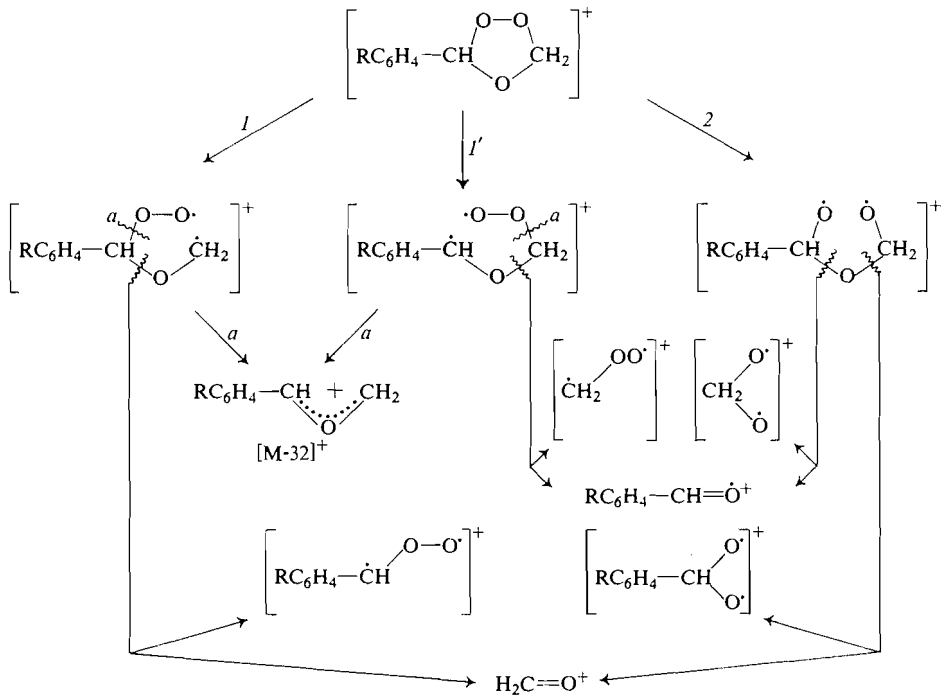

SCHÉMA 1. Fragmentation des ozonides dans le spectromètre de masse.

ions moléculaires et des différents ions formés lors de la fragmentation primaire des ozonides des styrènes substitués sont exprimés[2] en $\% \Sigma_{12}$.

Afin de mettre en évidence l'influence exercée par les substituants R sur le sens de la fragmentation, il est avantageux de rapporter les abondances relatives des différents ions formés à celles des ions moléculaires correspondants.[3] Le tableau 2 indique les logarithmes de ces rapports pour les fragments les plus significatifs. Les fragments à *m/e* 30 et 46 n'ont pas été considérés dans cette analyse. En effet, aucune conclusion certaine ne peut être déduite pour ces ions, en raison de leurs divers modes de formation probables, indiqués par le schéma 1.

L'influence des caractères donneur ou attracteur d'électrons des substituants R dans le noyau phényle est très nette dans le cas du fragment carbonylé $RC_6H_4CH{=}\dot{O}^+$. En effet, l'intensité de l'ion carbonylé diminue, relativement à l'ion moléculaire, d'autant plus que le caractère attracteur d'électrons du substituant R augmente. Cette observation est bien décrite par la relation linéaire d'énergie libre qui est obtenue en utilisant les constantes de substituant σ de Hammett (figure 7).

De semblables relations linéaires d'énergie libre ont été observées, lors d'études portant sur la spectrométrie de masse de benzophénones et d'acétophénones substitués, pour les intensités des fragments correspondant aux ions benzoyles et acétyles (5–7). Une interprétation de ces

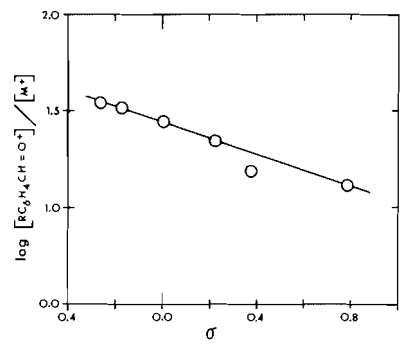

FIG. 7. Etude de la fragmentation primaire engendrant $RC_6H_4CH{=}O^+$: comparaison de log $[RC_6H_4CH{=}O^+]/[M^+]$ vs. les constantes de Hammett.

[2]Le $\% \Sigma_{12}$ = pourcentage rapporté à la somme des intensités de tous les ions de $m/e \geqslant 12$.

[3]Les intensités des pics considérés sont suffisamment importantes, même pour les ions d'intensité relativement faible, pour permettre des mesures à ±1% près.

Can. J. Chem. Downloaded from www.nrcresearchpress.com by 210.87.254.105 on 09/05/12
For personal use only.

Can. J. Chem. Downloaded from www.nrcresearchpress.com by 210.87.254.105 on 09/05/12
For personal use only.

TABLEAU 1

Spectres de masse des ozonides **1–6**: abondances relatives des ions moléculaires et des ions issus de la fragmentation primaire

	$RC_6H_4CH{=}\dot{O}^+$		$[R{-}C_6H_4{-}CH(O^{\cdot})O^{\cdot}]^+ + [RC_6H_4\dot{C}H{-}O{-}O^{\cdot}]^+$		$H_2C{=}\dot{O}^{+*}$		$[H_2\dot{C}{-}O{-}\dot{O}]^+ + [H_2C(O^{\cdot})O^{\cdot}]^{*+}$		$[M\text{-}32]^+$		$[M]^+$	
R	*m/e*	%Σ	*m/e*	%Σ	*m/e*	%Σ	*m/e*	%Σ	*m/e*	%Σ	*m/e*	%Σ
p-CH_3O	136	8.32	152	3.31	30	1.82	46	0.71	150	0.21	182	0.24
p-CH_3	120	12.01	136	3.59	30	2.00	46	0.60	134	0.44	166	0.36
H	106	12.07	122	8.23	30	4.77	46	1.11	120	0.39	152	0.43
p-Cl	140	7.01	156	3.74	30	1.93	46	0.88	154	0.34	186	0.32
m-Cl	140	8.97	156	4.35	30	2.68	46	0.94	154	0.24	186	0.58
p-NO_2	151	9.29	167	1.53	30	3.85	46†	1.16	165	0.58	197	0.64

*Les ions à *m/e* = 30 et *m/e* = 46 peuvent aussi provenir de la décomposition de certains fragments ioniques.
†Correspond également à l'ion NO_2^+.

TABLEAU 2

Logarithmes des abondances des ions $RC_6H_4CH{=}\dot{O}^+$, $RC_6H_4CHO_2{}^+$, et $[M\text{-}32]^+$ rapportées à l'abondance du pic moléculaire $[M^+]$

R	log $[RC_6H_4CH{=}\dot{O}^+]/[M^+]$	log $[RC_6H_4CHO_2{}^+]/[M^+]$	log $[M\text{-}32]^+/[M^+]$
p-CH_3O	1.54	1.14	−0.052
p-CH_3	1.52	1.00	+0.087
H	1.45	1.28	−0.042
p-Cl	1.34	1.06	+0.026
m-Cl	1.19	0.87	−0.38
p-NO_2	1.16	0.38	−0.042

relations linéaires d'énergie libre peut être donnée sur la base d'arguments cinétiques (7), pour autant que l'approximation de l'état stationnaire peut être appliquée aux ions dans la source.

Les résultats représentés par la figure 7 peuvent être interprétés en considérant que, dans l'ion moléculaire, la charge positive est distribuée à la fois sur le cycle ozonique et sur le cycle aromatique. Dans l'ion produit $[RC_6H_4CH{=}\dot{O}^+]$, par contre, la charge est plus localisée, si bien que dans l'état de transition le caractère positif ressenti par le substituant R est plus prononcé que dans l'ion moléculaire, ce qui se manifeste, finalement, par la valeur négative de ρ (−0.44) (8).

En ce qui touche les présentes observations, faites avec l'ozonide du *m*-chlorostyrène, il convient de rappeler qu'il a été relevé précédemment (9) que les effets des substituants méta dans l'état excité sont généralement altérés par l'augmentation du paramètre de résonance. Des observations semblables ont également été rapportées par Bursey et McLafferty (7) en ce qui a trait au comportement des substituants en position méta. La légère déviation qui est observée, par rapport à la droite de Hammett, pourrait, donc, également s'expliquer par une faible intervention des états excités de l'ion moléculaire dans la formation de l'ion carbonylé $[RC_6H_4\text{-}CH{=}\dot{O}^+]$. Une certitude quant à la participation éventuelle de tels états excités ne saurait, cependant, être gagnée qu'au moyen de recherches plus approfondies, présentement en cours.

L'analyse des rapports des abondances relatives des ions $[RC_6H_4CHO_2]^+$ aux ions moléculaires qui leur correspondent indique une tendance générale à défavoriser les ions comprenant les substituants attracteurs d'électrons. Cependant, ainsi que l'indiquent les valeurs rapportées au tableau 2, des écarts importants apparaissent par rapport à la relation de Hammett. Ce fait doit être relié aux observations précédantes (4) qui indiquent, de manière non ambiguë, que les ions $[RC_6H_4CHO_2]^+$ existent avec deux structures distinctes (**A** et **B**), démontrées par les spectres de masse d'ozonides marqués par ^{18}O en position éther. Par ailleurs, les processus donnant naissance à ces ions (**A** et **B**) sont entièrement différents, ainsi que l'indique le schéma 1, et requièrent donc des constantes ρ différentes (10).

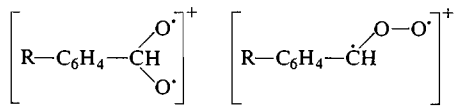

A **B**

Dans tous les spectres étudiés, il est possible de reconnaître le fragment ionique $[M\text{-}32]^+$ qui résulte de l'élimination d'une molécule d'oxygène à partir de l'ion moléculaire (schéma 1). L'influence du substituant R dans le noyau phényle n'apparaît que très faiblement sur cette élimination d'oxygène. Ceci est, en effet, indiqué par la valeur pratiquement constante (≈ 0) de la quantité log $[M\text{-}32]^+/[M]^+$ (tableau 2) pour tous les ozonides étudiés ici, ce qui signifie que le coefficient ρ de Hammett est voisin de 0 (figure 8). Seul le cas de l'ozonide du *m*-chlorostyrène diffère du comportement général, ce qui, avec les réserves

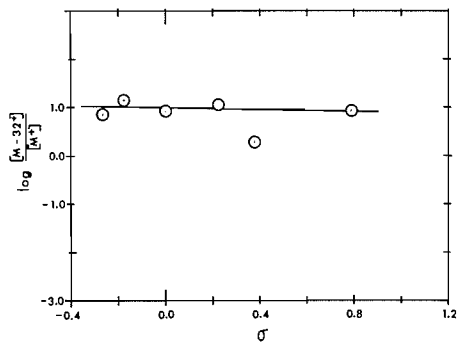

FIG. 8. Etude de la formation des ions $[M\text{-}32]^+$ à partir des ions moléculaires.

Can. J. Chem. Downloaded from www.nrcresearchpress.com by 210.87.254.105 on 09/05/12
For personal use only.

déjà exposées, peut être interpreté en termes d'une possible intervention d'états excités de l'ion moléculaire dans la formation de l'ion $[M-32]^+$.

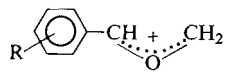

$[M-32]^+$

Les ions $[M-32]^+$ donnent lieu à des fragmentations secondaires, mais dont les probabilités sont souvent faibles. L'une de ces fragmentations correspond à une élimination d'hydrogène selon le processus probable (voir éq. [1])

[1] 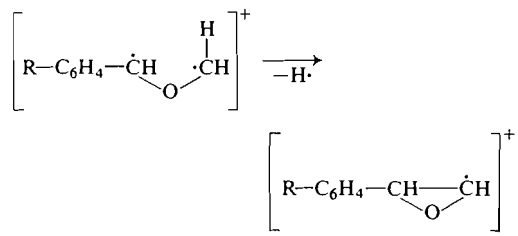

mis en évidence par les signaux de *m/e* 149, 133, 119, 153, 153, et 164 pour les composés **1** à **6**, respectivement. Ce processus est nettement favorisé par les substituants R donneurs d'électrons (log $[M-33]^+/[M-32]^+ = 0.55$ pour R = *p*-CH_3O) et nettement défavorisé par les groupements attracteurs d'électrons (log $[M-33]^+/[M-32]^+ = -1.06$ pour R = *p*-NO_2).

Cette élimination d'un atome d'hydrogène, probablement à partir de l'ion $[M-32]^+$, entre en compétition avec un mécanisme de clivage de la liaison C—O, suivi d'un transfert d'hydrogène (voir éq. [2]).

[2] 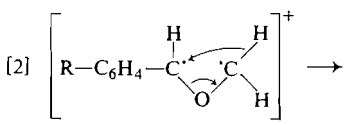

$[R-C_6H_4-CH_2]^+$ ou $[HC\equiv O]^+$

Ce dernier processus conduit aux ions dont les abondances relatives, aux valeurs de *m/e* spécifiées, sont indiquées au tableau 3.

Les valeurs rapportées aux tableau 3 font ressortir, d'une part, la faible probabilité de cette fragmentation secondaire et, d'autre part, la nette influence du substituant R. La figure 9 montre que la relation de Hammett est vérifiée de manière satisfaisante pour cette fragmentation. Lors de la formation de l'ion $[RC_6H_4CH_2]^+$ à partir de l'ion $[M-32]^+$ il y a une augmentation de la charge positive ressentie par le substituant, ce qui amène à expliquer la valeur fortement négative du coefficient ρ (-1.36). De plus, il n'y a pas, pour cette fragmentation, d'écart pour l'ozonide du *m*-chlorostyrène. Pour autant que l'on veuille admettre que les écarts précédemment observés avec les dérivés méta puissent être imputés à la participation d'états excités de l'ion moléculaire, l'observation que la fragmentation avec perte de HCO à partir de l'ion $[M-32]^+$ ne montre pas d'anomalie dans le cas de l'ozonide du *m*-chlorostyrène pourrait être interprétée en termes d'une non-participation d'états excités de l'ion $[M-32]^+$.

TABLEAU 3

Abondances relatives des ions $R-C_6H_4-\overset{+}{\underset{\cdot}{C}}H_2$

R	$RC_6H_4CH_2^+$ *m/e*	$RC_6H_4CH_2^+$ %Σ	log $[RC_6H_4CH_2]^+/[M-32]^+$
p-CH_3O	121	0.41	+0.29
p-CH_3	105	0.45	−0.01
H	91	0.39	0.00
p-Cl	125	0.11	−0.49
m-Cl	125	0.07	−0.54
p-NO_2	136	0.04	−1.16

Les ions $[M-32]^+$ conduisent encore à un autre type de fragmentation (voir éq. [3]).

Les ions $[RC_6H_4CH]^+$ ainsi formés se manifestent dans les spectres par des signaux de faible intensité qui correspondent à *m/e* 120, 104, 90, 124, 124, et 135, respectivement, pour les ozonides **1–6**.

D'autres processus de fragmentation secondaire engendrent des ions de fortes intensités. On observe, notamment, des ions ayant des abondances relatives importantes qui proviennent d'une décomposition des fragments carbonylés selon un mécanisme bien connu (11) (éq. [4]).

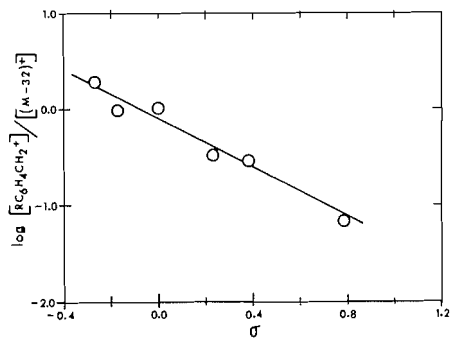

FIG. 9. Etude de la fragmentation des ions $[M-32]^+$ conduisant aux fragments $RC_6H_4CH_2^+$.

Can. J. Chem. Downloaded from www.nrcresearchpress.com by 210.87.254.105 on 09/05/12
For personal use only.

TABLEAU 4

Abondances relatives des ions issus de la décomposition des fragments carbonylés

	$RC_6H_4C{\equiv}O^+$		$[RC_6H_4]^+$		$[RC_6H_5]^+$	
R	*m/e*	%Σ	*m/e*	%Σ	*m/e*	%Σ
p-MeO	135	15.02	107	3.11	108	0.52
p-CH_3	119	10.54	91	10.25	92	1.66
H	105	19.49	77	18.40	78	2.34
p-Cl	139	13.65	111	7.48	112	1.19
m-Cl	139	14.30	111	8.56	112	1.38
p-NO_2	150	6.22	122	0.23	123	0.15

[3] 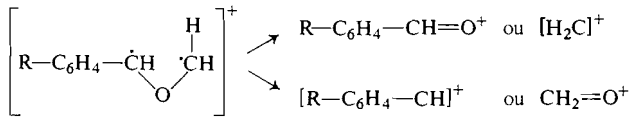

[4] 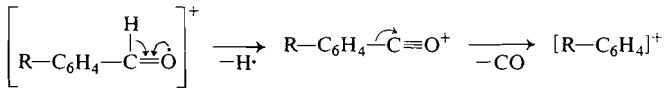

Les intensités relatives des ions engendrés par ce type de fragmentation sont indiquées dans le tableau 4.

Le tableau 4 indique également les abondances relatives des ions $[RC_6H_5]^+$ provenant de l'élimination d'une molécule de CO_2 des ions $[RC_6H_4CHO_2]^+$ (éq. [5]).

[5] $$[R{-}C_6H_4CHO_2]^+ \xrightarrow[-CO_2]{} [R{-}C_6H_5]^+$$

Les tentatives en vue de relier les valeurs du tableau 4 par la loi de Hammett ont échoué. Ceci peut être expliqué en considérant que lors de processus de fragmentation secondaire, se produisant avec une forte probabilité, il n'est plus possible d'appliquer l'approximation de l'état stationnaire aux concentrations des fragments ioniques intermédiaires. De plus, la cinétique de leur décomposition peut être également compliquée par l'intervention de plusieurs de leurs états électroniques excités.

Dans certains cas, enfin, le substituant R du noyau phényle donne lieu à un type de fragmentation qui lui est propre. Ainsi, pour l'ozonide du *p*-méthoxystyrène, le fragment $[CH_3OC_6H_4]^+$ subit une rupture de la liaison O—CH_3 et est responsable du pic à *m/e* = 92 (2.50% Σ_{12}). Le fragment primaire $CH_3O{-}C_6H_4{-}CH{=}\dot{O}^+$, d'autre part, donne naissance au pic *m/e* = 105 (1.49% Σ_{12}) par perte du radical OCH_3.

Dans le spectre de l'ozonide du *p*-nitrostyrène, les ions à *m/e* 92 (1.53% Σ_{12}) et à *m/e* 76 (3.22% Σ_{12}) ont été observés. Ces ions proviennent, respectivement, de l'élimination d'une molécule NO et d'une molécule NO_2. Le mécanisme bien connu d'élimination de NO_2 des composés aromatiques (12) se retrouve dans la fragmentation des ions de *m/e* 150 et 151 (voir éqs. [6*a*] et [6*b*]). L'élimination préliminaire de NO est mise en évidence par les pics de faible intensité à *m/e* 120 et 121.

Cette perte de NO_2 nécessite un réarrangement des ions de *m/e* 150 et 151 qui acquièrent ainsi des structures du type **C** ou **D** (13).

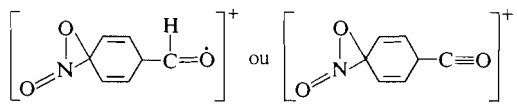

C **D**

[6*a*] $$[NO_2{-}C_6H_4{-}C{\equiv}O]^+ \xrightarrow[-NO]{} [O{-}C_6H_4{-}C{\equiv}O]^+ \longrightarrow [C_6H_4{-}C{\equiv}O]^+$$
m/e 150 *m/e* 120 (0.76% Σ) *m/e* 104 (1.99% Σ)

[6*b*] $$[NO_2{-}C_6H_4{-}CH{=}\dot{O}]^+ \xrightarrow[-NO]{} [O{-}C_6H_4{-}CH{=}\dot{O}]^+ \longrightarrow [C_6H_4{-}CH{=}\dot{O}]^+$$
m/e 151 *m/e* 121 (0.88% Σ) *m/e* 105 (2.63% Σ)

Can. J. Chem. Downloaded from www.nrcresearchpress.com by 210.87.254.105 on 09/05/12
For personal use only.

Can. J. Chem. Downloaded from www.nrcresearchpress.com by 210.87.254.105 on 09/05/12
For personal use only.

Conclusions

Contrairement aux peroxydes cycliques (1) et à certains ozonides ne comprenant pas de noyau aromatique fixé sur le cycle ozonique (4), tous les ozonides étudiés ici présentent un pic moléculaire dans leurs spectres de masse. D'une façon générale, ce pic est d'autant plus intense que le groupement R est plus attracteur d'électrons; ceci ne peut être considéré que comme une tendance générale, à l'intérieur de la série d'ozonides étudiés ici, qui est, cependant, mise en défaut par l'ozonide du *p*-chlorostyrène.

Les effets d'un substituant R dans le noyau aromatique apparaissent clairement dans la répartition du courant ionique et permettent de préciser les mécanismes de certaines fragmentations. Les abondances relatives des ions issus de certaines fragmentations sont reliées par la relation de Hammett, notamment en ce qui concerne la formation de fragments carbonylés ($\rho = -0.44$), ainsi que la formation des fragments $[RC_6H_4CH_2]^+$ à partir de $[M\text{-}32]^+$ ($\rho = -1.36$). Il est possible que les écarts, par rapport à l'équation de Hammett, observés lors de la fragmentation primaire de l'ozonide du *m*-chlorostyrène puissent être interpretés en termes de la participation d'états électroniquement excités, comme cela avait déjà été considéré dans d'autres cas, par Bursey et McLafferty (7). Des recherches plus approfondies sont actuellement en cours dans le but de vérifier la participation éventuelle d'états excités.

Partie expérimentale

Le mode de préparation et les caractéristiques physiques des ozonides étudiés ont été décrits précédemment (14).

Les spectres ont été enregistrés au moyen d'un spectromètre de masse à simple focalisation Hitachi RMU-6 D, muni du système d'introduction directe MG 150. Les pressions de vapeur des ozonides examinés sont suffisamment élevées, ce qui rend le chauffage externe inutile. Tous les spectres rapportés dans le présent travail ont été enregistrés dans des conditions identiques en ce qui a trait aux divers paramètres instrumentaux qui influencent les intensités ioniques relatives. La précision des mesures est satisfaisante car, même pour les ions d'intensité relativement faible qui ont été considérés, on observe des intensités suffisamment importantes pour permettre des mesures à $\pm 1\%$ près.

Il a été vérifié, avec l'ozonide du styrène, qu'une décomposition autre que par impact électronique ne contribue pas de manière significative aux spectres observés (4). Afin de s'assurer plus fermement que les spectres observés ne sont pas dus aux produits de décomposition thermique des ozonides, tous les produits ont été étudiés à différentes températures de la chambre d'injection: 110, 210, ou 250 °C. Même à 250°, il n'y a pratiquement pas de diminution de l'intensité des pics moléculaires, ni des pics provenant de la fragmentation primaire. Les spectres indiquent que les rapports $[A^+]/[M^+]$ sont, à toutes fins pratiques, indépendants de la température de la chambre d'injection. On observe, par conséquent, dans les cas indiqués dans le texte, une vérification de la loi de Hammett tout aussi bien à 250° qu'à 110°, avec les mêmes anomalies en ce qui a trait à l'ozonide du *m*-chlorostyrène. Les résultats exposés ont été obtenus en maintenant la température de la chambre d'ionisation à 110° et en accélérant les électrons ionisants par un potentiel de 70 V.

Nous tenons à remercier MM. J. C. Regenass et G. Sanchez de leur précieuse collaboration lors de la prise des spectres de masse. Nous remercions également le Conseil National de Recherches du Canada pour une subvention qui a permis la présente recherche.

1. M. Bertrand, S. Fliszár, et Y. Rousseau. J. Org. Chem. **33**, 1931 (1968).
2. S. Fliszár et J. Carles. J. Amer. Chem. Soc. **91**, 2637 (1969).
3. S. Fliszár et J. Carles. Can. J. Chem. **47**, 3921 (1969).
4. J. Castonguay, M. Bertrand, J. Carles, S. Fliszár, et Y. Rousseau. Can. J. Chem. **47**, 919 (1969).
5. F. W. McLafferty. Anal. Chem. **31**, 477 (1959).
6. A. Buchs, G. P. Rossetti, et B. P. Susz. Helv. Chim. Acta, **47**, 1563 (1964).
7. M. M. Bursey et F. W. McLafferty. J. Amer. Chem. Soc. **88**, 529 (1966).
8. J. M. S. Tait, T. W. Shannon, et A. G. Harrison. J. Amer. Chem. Soc. **84**, 4 (1962).
9. H. E. Zimmerman. Tetrahedron Suppl. **2**, 293 (1963).
10. F. Meyer et A. G. Harrison. Can. J. Chem. **42**, 1762, 2008 (1965).
11. K. Biemann. Mass spectrometry, organic chemical application. McGraw–Hill Book Co., Inc., New York, 1962. p. 101.
12. J. H. Beynon, R. A. Saunders, et A. E. Williams. Ind. Chim. Belge, **4**, 311 (1964).
13. J. H. Beynon, R. A. Saunders, et A. E. Williams. Z. Naturforsch. **20a**, 180 (1965).
14. J. Carles et S. Fliszár. Can. J. Chem. **48**, 1309 (1970).

Can. J. Chem. Downloaded from www.nrcresearchpress.com by 210.87.254.6 on 09/05/12
For personal use only.

Réactions dans le sulfolane. VI. Etude de solutions des acides perchlorique, fluorosulfurique, pyrosulfurique et hexachloroantimonique[1]

R. L. Benoit, C. Buisson et G. Choux
Département de Chimie, Université de Montréal, Case Postale 6128, Montréal, Québec

Reçu le 18 novembre 1969

Des mesures de résonance magnétique nucléaire et de conductivité ont été effectuées sur des solutions des acides perchlorique et fluorosulfurique dans le sulfolane. Des déterminations additionelles ont été faites sur des solutions des acides pyrosulfurique et hexachloroantimonique. L'acide complexe $HSbCl_6$ est un acide fort dans ce solvant polaire aprotique très peu basique. $HClO_4$, HSO_3F et $H_2S_2O_7$ sont incomplètement dissociés, avec respectivement $K = 10^{-2.7}$, $10^{-3.3}$, et $\sim 10^{-5}$. La force des acides en milieu dilué varie suivant $HClO_4 > HSO_3F > H_2S_2O_7$, c'est-à-dire un ordre différent de celui qui est observé dans H_2SO_4, un solvant polaire protique fortement associé.

Nuclear magnetic resonance and certain conductivity data are reported for solutions of perchloric and fluorosulfuric acids in sulfolane. Additional measurements were made on solutions of disulfuric and hexachloroantimony (V) acids. $HSbCl_6$ is a strong acid in this weakly basic dipolar aprotic solvent. $HClO_4$, HSO_3F, and $H_2S_2O_7$ are incompletely dissociated with $K = 10^{-2.7}$, $10^{-3.3}$, and $\sim 10^{-5}$, respectively. The acid strength in dilute solution in sulfolane follows the order $HClO_4 > HSO_3F > H_2S_2O_7$, which differs from that known in H_2SO_4 which is a strongly associated polar protic solvent.

Canadian Journal of Chemistry, **48**, 2353 (1970)

Introduction

Le sulfolane (tétraméthylènesulfone) est un solvant polaire aprotique qui, de part son groupe sulfone, possède des propriétés basiques très faibles. Hall et Robinson (1) et Gillespie et Robinson (2), à la suite de déterminations cryoscopiques et conductimétriques dans l'acide sulfurique ($H_0 = -12.2$), donnent pour le sulfolane (S) $pK_{SH^+} = -12.9$, ce qui permet de le classer parmi d'autres solvants polaires aprotiques suivant l'ordre de basicité croissante: nitrométhane (-13.0) $\sim$ sulfolane (-12.9) $>$ nitrobenzène (-12.4) $>$ acétonitrile (-11.2) $\gg$ diméthylformamide $>$ diméthylsulfoxyde. On devrait donc pouvoir atteindre des acidités très élevées dans le sulfolane. En admettant la validité des hypothèses de Hammett, à un acide fort à la concentration 1 *M* dans le sulfolane, correspondrait la valeur de la fonction d'acidité $H_0 = -11.9$ et l'acide perchlorique ($pK_{HClO_4} \sim -10.2$ dans H_2SO_4 (3)) devrait même s'y comporter en acide faible, comme cela semblerait être le cas dans le nitrométhane (4), mais non dans l'acétonitrile en présence d'acide acétique (5). On pourrait ainsi classer acides forts et bases faibles dans un milieu unique ce qui serait préférable à l'utilisation d'un milieu de composition variable, H_2SO_4–H_2O, ou de séries de solvants (6), pour lesquels des phénomènes de solvatation spécifique peuvent jouer.

On a examiné, comme première étape à l'établissement d'une échelle d'acidité, le comportement dans le sulfolane, de quatre acides susceptibles a priori d'être relativement forts, les acides simples, $HClO_4$, HSO_3F, $H_2S_2O_7$, et l'acide complexe formé a partir de HCl et du chlorure métallique $SbCl_5$ fortement accepteur de Cl^-. Les fonctions d'acidité H_0 de solutions dans le sulfolane de plusieurs acides ont été récemment mesurées et les résultats présentés succinctement (7) permettent d'évaluer pour des solutions 1 *M* les valeurs de H_0 : HPF_6 (-9.2), $HClO_4$ (-8.1), HSO_3F (-7.9), HBr (-6.1). Toutefois si l'on prenait pour la constante d'acidité de l'indicateur trinitroaniline, au lieu de $pK_{BH^+} = -8.2$ utilisé par ces auteurs, la valeur -10.1 déterminée dans H_2SO_4 aqueux (8), on obtiendrait pour les trois premiers acides respectivement -11.1 (?), -10.0 et -9.8, c'est-à-dire des valeurs proches de la valeur -11.9 calculée pour un acide fort à la concentration 1 *M*.

La résonance magnétique nucléaire (r.m.n.) du proton a été utilisée pour étudier la dissociation des acides forts dans l'eau. Dans le cas des solvants polaires aprotiques, la méthode ne semble pas avoir été employée. Nous avons com-

[1]Partiellement présenté au Congrès de l'Institut de Chimie du Canada, Montréal, 25–28 mai 1969.

Can. J. Chem. Downloaded from www.nrcresearchpress.com by 210.87.254.6 on 09/05/12
For personal use only.

plété les résultats de r.m.n. par des déterminations de conductivité. Des mesures de chaleur de solution et de pression de vapeur ont aussi été faites dans le cas de $HClO_4$.

Partie expérimentale

(1) Réactifs

Le sulfolane, fourni gracieusement par Shell Canada Ltd., a été purifié selon la méthode précédemment décrite (9). Des solutions de $HClO_4$ dans le sulfolane peuvent être préparées en faisant réagir des solutions de $AgClO_4$ avec HCl (10) comme cela l'a été fait dans le nitrométhane (4). On peut aussi obtenir $HClO_4$ anhydre à partir de solutions de $HClO_4$ dans H_2SO_4, soit par extraction par un solvant non-miscible (11) tel CH_2Cl_2, soit par distillation. Cette dernière méthode a été utilisée, des difficultés ayant été rencontrées dans l'élimination du solvant non-miscible. $HClO_4$ anhydre a été préparé par distillation à 50° sous pression réduite d'un mélange d'un volume d'acide à 70% et trois volumes de H_2SO_4 à 96%. La colonne était remplie d'hélices de 1/8 in. et les joints pour vide étaient lubrifiés à l'aide de graisse "fluorolube". Le liquide incolore obtenu par fractions de 10 ml environ révèle par dosage une pureté d'au moins 99%. HSO_3F, produit technique de "Allied Chemical", a été distillé à 163° dans un montage protégé par une colonne desséchante (12). $H_2S_2O_7$ a été préparé à partir d'anhydride sulfurique et d'oléum (13). Les acides méthanesulfonique et trifluoroacétique de qualité "Reagent" ont été utilisés sans purification ultérieure. Le pentachlorure d'antimoine, produit "Reagent" de "Fisher", a été distillé sous pression réduite avant utilisation. Le trichlorure d'antimoine, produit "Certified" de "Fisher" a été sublimé sous vide ; le trichlorure d'aluminium "Reagent" de B.D.H. a été également sublimé sous la pression atmosphérique. Les deux produits sont blancs et ont été dissous dans le sulfolane dès leur obtention. Les solutions des gaz chlorhydrique et bromhydrique ont été obtenues par barbotage dans le sulfolane de HCl et HBr anhydres de "Matheson".

(2) Mesures

(a) Résonance magnétique nucléaire

Les spectres de r.m.n. du proton de mélanges HSO_3F–sulfolane ont été déterminés à 25° sur un appareil JEOL, à la fréquence de 100 Mc, à l'aide d'un compteur. Les déplacements chimiques étaient repérés par rapport au tétraméthylsilane placé en référence externe dans le tube intérieur, scellé en suite, de la cellule commercialisée par "N.M.R. Specialties" selon la description de Frei et Bernstein (14). Dans ces conditions d'utilisation, les corrections de susceptibilité magnétique deviennent négligeables. L'appareil était réglé sur la position "internal lock". Les mélanges d'acide et de sulfolane, préparés par pesée, étaient introduits dans la cellule et le tube intérieur mis en place, l'étanchéité étant assurée à l'aide de graisse fluorolube.

Nous avons ainsi pu vérifier que la position du signal des protons β du sulfolane n'était que peu influencée par la présence d'acide et que ce signal pouvait donc constituer une référence interne convenable. Sa position repérée par rapport au tétraméthylsilane en référence externe est de 2.25 p.p.m., alors qu'en utilisant ce produit en référence interne dans le sulfolane la valeur trouvée est de 2.10 p.p.m., ce qui pourrait être attribué à un effet de solvant.

Les mélanges $HClO_4$–sulfolane ont été étudiés à 25° sur un appareil JEOL à la fréquence de 60 Mc, et la position du signal de $HClO_4$ était repérée par rapport au signal des protons β du sulfolane, dont la position a été supposée identique à ce qu'elle est dans une solution équivalente de HSO_3F, le tétraméthylsilane étant placé en référence externe. Il en a été de même pour les autres acides étudiés. Les cellules contenant le mélange préparé par pesée étaient scellées immédiatement après introduction de la solution. Les valeurs des déplacements chimiques sont données avec une incertitude maximale d'environ 0.1 p.p.m.

(b) Conductimétrie

Les mesures de conductivité des solutions d'acides dans le sulfolane ont été effectuées à 30.0° et pour la plupart à l'aide d'un conductimètre "Tacussel" à fréquence variable La concentration des solutions était modifiée en ajoutant au sulfolane des solutions concentrées d'acide dans ce solvant, ou même l'acide pur, à l'aide d'une microburette. Dans le cas des acides complexes on ajoutait à une solution de HCl dans le sulfolane, soit le chlorure métallique pur ($SbCl_5$), soit une solution concentrée de chlorure métallique.

(c) Pressions de vapeur

Les mesures de pressions de vapeur ont été effectuées à l'aide du tensimètre antérieurement décrit (9). On a dû en fait travailler à la limite des incertitudes expérimentales.

(d) Chaleurs de solution

Les chaleurs de solution ont été mesurées par microcalorimétrie, en utilisant les mêmes cellule et microcalorimètre que lors de l'étude du système eau–sulfolane (9).

Des essais au choc et à la flamme semblaient avoir démontré la non-réactivité de $HClO_4$ anhydre envers le sulfolane. Cependant une explosion s'est produite dans le tensimètre lors de la mesure de la pression de vapeur d'une solution de $HClO_4$, $X_{HA} \sim 0.4$. Une deuxième explosion, qui a résulté en accident grave, a eu lieu lors du bris, au moyen d'une lime, d'une ampoule scellée contenant une solution de $HClO_4$, $X_{HA} \sim 0.1$–0.2, gardée pendant 5 mois dans un congélateur. Il semble donc que la recommandation récente d'utilisation comme titrant, de $HClO_4$ anhydre dans le sulfolane (15) soit à déconseiller. Les solutions diluées de $HClO_4$ utilisées par ces auteurs paraissent d'ailleurs avoir contenu de l'eau (16). L'emploi de solutions de $HSbCl_6$ faciles à préparer serait préférable, et une étude des propriétés de ces solutions est en cours.

Résultats

(1) Résonance magnétique nucléaire

On a porté sur la Fig. 1 les valeurs des déplacements chimiques δ(p.p.m.) du proton des acides HA en solution dans le sulfolane, mesurés par

Can. J. Chem. Downloaded from www.nrcresearchpress.com by 210.87.254.6 on 09/05/12
For personal use only.

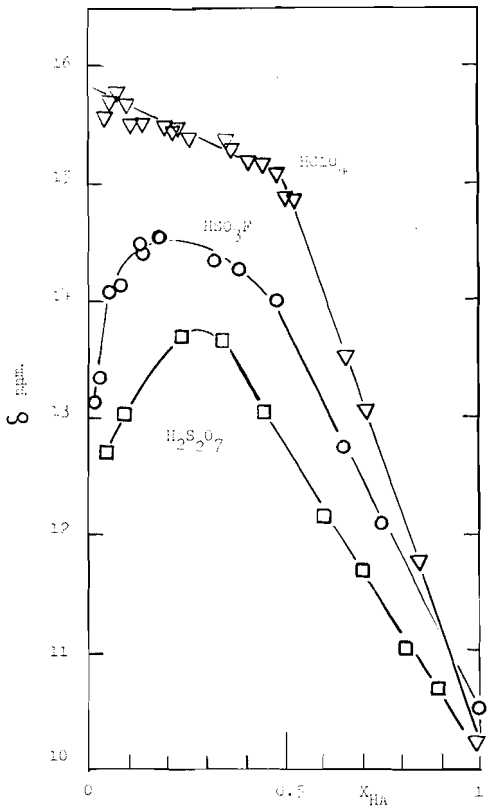

FIG. 1. Déplacement chimique du proton d'acides HA en fonction de la fraction molaire X_{HA}. $HClO_4$ (▽), HSO_3F (○), $H_2S_2O_7$ (□).

rapport au tétraméthylsilane, pour diverses fractions molaires X_{HA}. Les valeurs expérimentales de δ_{HA} et δ des protons α et β du sulfolane pour les solutions de HSO_3F sont aussi données dans le tableau 1.[2] Le premier acide étudié, $HClO_4$, a un déplacement chimique extrapolé de 15.7 p.p.m. en solution diluée dans le sulfolane, qui ne varie que peu jusqu'au mélange équimolaire (δ = 15.0 p.p.m.) pour décroître ensuite jusqu'à 10.2 p.p.m. pour l'acide pur (17) ; cette dernière valeur est d'ailleurs voisine de celle déterminée pour $X_{HA} \sim 0.10$ dans le solvant inerte CH_2Cl_2 (10.33 p.p.m., repéré par rapport au signal de CH_2Cl_2 à 5.47 p.p.m.). L'allure de la courbe obtenue (Fig. 1) est très semblable à celle des mélanges $HClO_4$–nitrométhane, où les

[2]Les autres résultats sont consignés au "Depository of Unpublished Data, National Science Library, National Research Council of Canada, Ottawa, Canada". Des copies en sont disponibles sur demande.

TABLEAU 1

Résonance magnétique nucléaire des solutions de HSO_3F dans le sulfolane*

X_{HA}	δ_{HA}	δ_α	δ_β
0.0167	13.14	3.09	2.25
0.0521	14.08	3.10	2.25
0.134	14.49	3.12	2.26
0.145	14.39	3.15	2.29
0.329	14.34	3.17	2.27
0.386	14.27	3.19	2.28
0.486	13·99	3.23	2.29
0.654	12.76	3.32	2.32
0.750	12.08	3.43	2.39
1.00	10.44	—	—
0.030	13.37†	—	—
0.080	14.13†	—	—
0.185	14.53†	—	—

*Mesures effectuées pour la plupart à 100 Mc avec le tétraméthylsilane en référence externe.
†Valeurs repérées par rapport aux protons β du sulfolane.

variations de δ sont cependant moins importantes (17), comme on l'a vérifié pour deux solutions (X_{HA} = 0.06, δ = 13.60 p.p.m. ; X_{HA} = 0.34, δ = 13.53 p.p.m.) en utilisant la position du signal des protons CH_3 située à 4.33 p.p.m. comme référence interne par rapport au tétraméthylsilane.

Les acides HSO_3F et $H_2S_2O_7$ ont un comportement quelque peu différent de celui de $HClO_4$ en ce que les valeurs de δ passent par un maximum pour $X_{HA} \sim 0.25$ pour décroître aux valeurs inférieures de X_{HA}. Des valeurs ont été accessoirement obtenues pour quelques acides ($X_{HA} \sim$ 0.05) : HCF_3CO_2, 11.5 p.p.m. ; H_2SO_4, 11.1 p.p.m. ; HCH_3SO_3, 10.5 p.p.m. ; HCl, 5.2 p.p.m. ; HBr, 2.0 p.p.m.

L'addition de composés accepteurs de chlorure MCl_n à une solution de HCl dans le sulfolane provoque un accroissement de δ qui dépend de la nature et de la concentration de MCl_n. En ajoutant, à 45 °C, $SbCl_5$ à une solution de HCl 1.0 *M*, δ augmente linéairement avec le rapport $SbCl_5$/HCl et la valeur extrapolée correspondant au rapport 1.0 est 16.0 p.p.m. Des valeurs obtenues avec différents chlorures, pour des concentrations supérieures à celle d'HCl, elle-même comprise entre 0.1 et 1.0 *M* sont données à titre d'indication : $SbCl_5$, 15.9 p.p.m. ; $AlCl_3$, 8.3 p.p.m. ; $SbCl_3$, 6.2 p.p.m. ; $GeCl_4$, 5.15 p.p.m.

(2) Mesures conductimétriques

Les résultats des mesures sont représentés sur la Fig. 2 pour $HClO_4$ anhydre, $HClO_4$ 72%, HSO_3F, $H_2S_2O_7$ et HCl–$SbCl_5$ (HCl = 0.29 *M*).

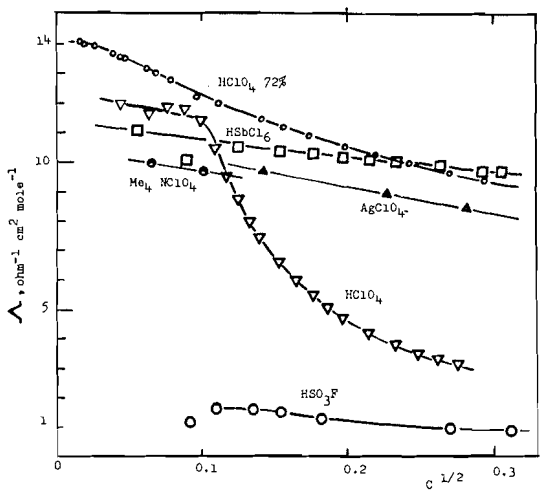

FIG. 2. Conductivité équivalente de solutions d'électrolytes en fonction de la racine carrée de la concentration C (mole $l^{-1})^{1/2}$. $HSbCl_6$ (□), $HClO_4$ (▽), $HClO_4$ 72% (○), HSO_3F (○), $AgClO_4$ (▲) (réf. 25), Me_4NClO_4 (◓) (réf. 25).

On a porté la conductivité équivalente Λ des solutions en fonction de la racine carrée de leur concentration molaire en acide, en supposant dans le cas de HCl–$SbCl_5$ la formation de $HSbCl_6$ quantitative. On donne aussi Fig. 2, aux fins de comparaison, les valeurs de Λ pour des perchlorates univalents, électrolytes forts. Dans le cas des autres chlorures MCl_n, les valeurs de Λ accessoirement obtenues avec une solution de HCl ~ 0.4 M sont : $AlCl_3$, 1–4 × 10^{-2} M, 5.0 Ω^{-1} cm^2 mole^{-1} ; $SbCl_3$, 5 × 10^{-3}–8 × 10^{-2} M, 0.47–0.35 Ω^{-1} cm^2 mole^{-1} ; $GeCl_4$, conductivité inchangée. La conductivité des solutions de $H_2S_2O_7$ et HSO_3F, bien que mesurée avec une cellule placée dans une boîte à gants, diminue avec le temps, particulièrement avec le premier acide. Les valeurs données Fig. 2 ont été obtenues après 15 min. Des difficultés du même ordre semblent avoir été rencontrées avec le système voisin HSO_3F–nitrobenzène (18).

(3) Pressions de vapeur

Les mesures de pression de vapeur de deux solutions de $HClO_4$ ont donné : X_{HA} = 0.07, p ~ 0.10 mm Hg ; X_{HA} = 0.29, p ~ 0.35 mm Hg. Une explosion avec une solution où X_{HA} ~ 0.4 nous a fait abandonner ces mesures.

(4) Enthalpie de solution

La chaleur de solution de $HClO_4$ dans le sulfolane a été déterminée pour plusieurs concentrations et les résultats sont donnés dans le tableau 2. Une valeur de $\Delta H_0 = -8.0$ kcal mole^{-1} a été obtenue par extrapolation à concentration nulle.

TABLEAU 2

Chaleurs de solution de $HClO_4$ dans le sulfolane

w (g)	Q (cal)	m (M kg^{-1})	$-\Delta H$(kcal mole^{-1})
0.1648	11.9	0.18	7.3
0.2133	15.3	0.24	7.2
0.1408	9.75	0.16	6.9
0.2915	20.1	0.39	6.9
0.5797	34.2	0.60	5.9
0.4136	21.5	0.82	5.2

Discussion

Si l'on considère la réaction entre un acide fort HA et le sulfolane S, $HA + S \rightleftarrows SH^+ + A^-$, le déplacement chimique δ observé en r.m.n. est relié aux valeurs des déplacements des espèces dont les protons peuvent s'échanger rapidement HA et SH^+, par l'intermédiaire du coefficient de dissociation α :

$$[1] \qquad \delta_{obs} = \alpha\delta_{SH^+} + (1 - \alpha)\delta_{HA}$$

On n'observe en effet qu'un seul signal dans les solutions de HA dans S, signal situé dans la région 2–16 p.p.m. et dépendant de la nature et de la concentration de HA. On pourrait donc penser calculer ainsi α en fonction de la concentration comme cela a été fait avec l'eau comme solvant (19).

Le fait que la valeur de δ de $HClO_4$ dilué dans le sulfolane, 15.7 p.p.m., soit nettement supérieure à celle de l'acide pur, 10.2 p.p.m., ou en solution dans CH_2Cl_2, et soit très voisine de celle d'une solution de $HSbCl_6$, 15.9 p.p.m., semblerait indiquer la protonation du solvant, α = 1 et $\delta_{obs} = \delta_{SH^+}$. Toutefois la forme de la courbe δ_{obs} en fonction de X_{HClO_4}, sensiblement deux droites se coupant à X_{HClO_4} = 0.5, montre qu'il n'est pas possible de calculer α suivant l'équation [1], la constante d'équilibre de la réaction entre $HClO_4$ et S étant trop grande.

Les mesures de conductivité permettent de différencier le comportement des acides $HClO_4$ et $HSbCl_6$. Toutefois la présence inévitable de traces d'eau dans le solvant complique l'interprétation des résultats. Si l'eau résiduelle (3–10 × 10^{-3} M) joue un rôle limité dans les mesures de r.m.n., effectuées à des concentrations relativement grandes des acides HA, il en va différemment dans les mesures de conductivité, qui devraient

Can. J. Chem. Downloaded from www.nrcresearchpress.com by 210.87.254.6 on 09/05/12
For personal use only.

Can. J. Chem. Downloaded from www.nrcresearchpress.com by 210.87.254.6 on 09/05/12
For personal use only.

être faites à des concentrations faibles de HA, pour obtenir en particulier Λ_0 la conductivité équivalente à dilution infinie. Des déterminations précises de la conductivité de sels dans le sulfolane (25, 26) indiquent que la présence de faibles quantités d'eau a peu d'influence. Par contre dans le cas des acides HA la conductivité sera affectée, suivant la position de l'équilibre $HA + H_2O \rightleftarrows H_3O^+ + A^-$, qui dépend des forces respectives des acides HA et H_3O^+ dans le sulfolane. Ainsi si l'acide, $HSbCl_6$, était fort dans le sulfolane, $HA + S \rightarrow HS^+ + A^-$, la courbe donnant Λ en fonction de la racine carée de la concentration de HA serait linéaire et pourrait, ou non, présenter une cassure lorsque l'on passe, dans la solution, de $H_3O^+SbCl_6^-$ provenant de l'eau résiduelle du solvent, à $SH^+SbCl_6^-$ aux plus fortes concentrations. Par contre si l'acide, $HClO_4$, était faible, mais plus fort que H_3O^+ dans le sulfolane, la courbe de Λ comporterait deux branches distinctes, la première rectiligne correspondant à la formation de $H_3O^+ClO_4^-$ électrolyte fort, la deuxième, une courbe classique correspondant à un acide faible. Dans le cas des acides HSO_3F et $H_2S_2O_7$ la présence d'eau résiduelle dans le sulfolane pourrait avoir un effet plus complexe dû à un équilibre supplémentaire, tel que $HSO_3F + H_2O \rightleftarrows H_2SO_4 + HF$, où H_2SO_4 et HF sont tous les deux des acides très faibles dans le solvant (7). De toute façon, on ne pourra obtenir, par extrapolation à dilution infinie, de valeur précise de Λ_0 (SH^+A^-). Dans un tout récent article (18) traitant du comportement de HSO_3F dans le nitrobenzène, solvant de basicité analogue au sulfolane, les auteurs n'ont pour cette raison, pu qu'estimer la valeur de la constante de dissociation de HSO_3F.

Pour les solutions de $HCl–SbCl_5$, les valeurs de Λ obtenues ainsi que la pente de la courbe $\Lambda = f(C^{1/2})$, comparées à celles d'autres perchlorates (Fig. 2), nous indique, que la réaction entre HCl et $SbCl_5$ est pratiquement complète, comme le laissaient prévoir les résultats de r.m.n., que $HSbCl_6$ est un électrolyte fort, et que les conductivités équivalentes de H_3O^+ et SH^+ sont voisines. Le mécanisme de conduction des protons solvatés SH^+ et H_3O^+ apparait ainsi normal, à l'encontre de ce qui est observé dans les solvants protiques. Dans le cas de $HClO_4$, la courbe $\Lambda = f(C^{1/2})$ comprend deux branches: la première linéaire, correspond à l'électrolyte fort $H_3O^+ClO_4^-$, la concentration de l'eau résiduelle dans le solvant étant environ 10^{-2} M, la deuxième est due à un électrolyte faible, soit $HClO_4$, soit la paire d'ions $[SH^+ClO_4^-]$. Bien que l'on ne puisse rejeter complètement cette dernière interprétation, elle paraît peu probable étant donné que les perchlorates étudiés jusqu'ici (25, 26), ainsi que le sel de pyridinium (16), sont des électrolytes forts. Il apparaît ainsi que $HClO_4$ est un acide faible dont on peut calculer la constante de dissociation, $K = 10^{-2.7}$, en prenant pour valeur approchée de Λ_0, 11.8 Ω^{-1} cm^2 mole^{-1}. La constante de dissociation de HSO_3F peut être estimée, en supposant aussi que l'acide est monomère aux concentrations étudiées (7, 18), on obtient $K = 10^{-3.3}$. Les solutions de $H_2S_2O_7$ sont très peu stables, une attaque du solvant est même possible, on a quand même calculé approximativement $K \sim 10^{-5}$. Il est intéressant de noter que si l'on suppose que HPF_6 est un acide fort, comme $HSbCl_6$, nos valeurs des constantes de dissociation de $HClO_4$, $K = 10^{-2.7}$ et HSO_3F, $K = 10^{-3.3}$, sont en accord satisfaisant avec les calculs faits à partir des mesures de la fonction H_0 de HPF_6, $HClO_4$ et HSO_3F de Alder *et al.* (7).

Le déplacement chimique observé, 15.7 p.p.m., pour les solutions les plus diluées de $HClO_4$ ($C \sim 0.5$ M), solutions où $HClO_4$ est très peu dissocié, indique donc seulement que les liaisons hydrogène sulfolane $HClO_4$ sont fortes comme le confirme la valeur de la chaleur de solution $\Delta H \sim -8.0$ kcal mole^{-1}. Cette valeur n'est qu'approximative vu la méthode d'extrapolation utilisée et le fait que $HClO_4$ est quelque peu dissocié ($\alpha \leqslant 0.10$) pour les solutions les plus diluées. On peut d'ailleurs comparer les chaleurs de solution pour le processus vapeur $\rightarrow$ solution dans le sulfolane, pour quelques solutés pouvant donner des liaisons hydrogène, on a: $HClO_4$, -17.2 kcal mole^{-1}; HSO_3F, -16.5 kcal mole^{-1}; HCl, -6.5 kcal mole^{-1}; HBr, -4.3 kcal mole^{-1} (16); H_2O, -8.9 kcal mole^{-1} (9); CH_3OH, -7.4 kcal mole^{-1} (20); et CH_2Cl_2, -11.9 kcal mole^{-1} (21). Les quelques résultats des mesures de pression de vapeur des solutions de $HClO_4$ dans le sulfolane confirment aussi l'existence de fortes intéractions soluté-solvant, ainsi pour $X_{HClO_4} = 0.29$, on calcule, en utilisant la pression de vapeur de $HClO_4$ pur (17), $a_{HClO_4} = 0.034$. D'après les travaux de Pavia (17) sur le système voisin $HClO_4$–nitrométhane, il ne semble pas qu'une étude en infra-rouge (i.r.), qui a essentiellement confirmé pour ce système la présence

Can. J. Chem. Downloaded from www.nrcresearchpress.com by 210.87.254.6 on 09/05/12
For personal use only.

de fortes liaisons hydrogène entre $HClO_4$ et le solvant, aurait apporté des éléments nouveaux sur le système $HClO_4$–sulfolane.

L'allure de la courbe de δ_{HSO_3F}, Fig. 1 diffère de celle de δ_{HClO_4} aux valeurs de $X_{HA} < 0.20$. Il est probable que cet effet est dû à ce que HSO_3F pur est fortement associé alors que $HClO_4$ ne l'est pas (17). Le maximum de δ_{HSO_3F} correspondrait à une forme polymérique pouvant impliquer le solvant, et à grande dilution on tendrait vers HSO_3F, fortement lié au solvant par des liaisons hydrogène, comme l'indique la valeur de la chaleur de solution. Des variations analogues de δ_{HA} ont déjà été observées pour des mélanges d'acide acétique avec des solvants de polarité variable (22), et des équilibres polymères–dimère–monomère ont été postulés. Le cas de l'acide $H_2S_2O_7$ est vraisemblablement voisin.

Une corrélation a été recherchée par Brownstein et Stillman (23) entre le déplacement chimique δ d'un acide HA dans un solvant ne contenant pas de proton échangeable, SO_2 liquide, et la constante d'acidité de HA dans l'eau. Nos résultats obtenus avec le sulfolane, joints à ceux de Whiting et coll. (7), indiquent l'absence de relation entre δ et la force de l'acide HA dans le même solvant. On a en effet: $HClO_4$ (15.7 p.p.m.) > HSO_3F(13.0) > HBr(2.0) > H_2SO_4(11.0) > HCl(5.2) et les acides de force vraisemblablement décroissante $H_2S_2O_7 > H_2SO_4 > HSO_3CH_3 > HCO_2CF_3$ ont des δ voisins. Un examen des résultats obtenus avec SO_2 (23) montre d'ailleurs que la corrélation invoquée repose surtout sur une valeur inattendue de δ_{HClO_4}, 2.0 p.p.m., et une valeur quelque peu arbitraire, de pK_{H_2O} pour HI, -10. Nos résultats fragmentaires indiquent aussi qu'il n'y a pas dans le sulfolane de corrélation entre les déplacements chimiques de composés HA et les chaleurs de solution ΔH des mêmes composés à l'état vapeur, particulièrement si l'on inclut dans la série, des composés aussi différents que HX, ROH et CH_2Cl_2.

En ajoutant aux solutions de HCl quelques chlorures métalliques accepteurs autres que $SbCl_5$, on avait pensé pouvoir mettre en évidence d'autres acides forts du type $HMCl_n$. Les résultats permettent seulement d'établir qualitativement l'ordre du pouvoir accepteur envers Cl^- : $SbCl_5 > AlCl_3 > SbCl_3 > GeCl_4$.

Un résultat important de ce travail est de mettre en évidence l'influence de la nature du solvant sur le classement des acides forts ; ainsi l'ordre $H_2S_2O_7 > HSO_3F > HClO_4$ (2, 3) obtenu dans le solvant protique fortement associé, H_2SO_4, devient $HClO_4 > HSO_3F > H_2S_2O_7$ en milieu dilué dans le sulfolane, un solvant polaire aprotique. Cet ordre est vraisemblablement commun aux solvants de cette dernière classe, si les énergies de transfert des gros anions A^- ne varient pas trop comme cela semble être le cas pour les enthalpies de transfert (24). L'utilisation d'une échelle unique d'acidité, ne tenant compte que de la basicité du solvant et non de la solvatation de l'anion A^-, risque donc de conduire à des prévisions erronées particulièrement pour des classes de solvants aussi différents que les solvants protiques et polaires aprotiques. L'effet de la solvatation de l'anion A^- sur la dissociation de l'acide HA apparaît même à l'intérieur de la classe polaire aprotique. Ainsi si l'on compare les solvants sulfolane et nitrobenzène, on note que HSO_3F est un acide nettement plus faible dans le nitrobenzène (18) en dépit de la basicité légèrement plus forte de ce solvant. Vraisemblablement l'ion SO_3F^- est moins solvaté dans le nitrobenzène que dans le sulfolane, comme le suggère déjà la dissociation incomplète de NMe_4SO_3F dans le nitrobenzène (18).

Nous sommes reconnaissants au Conseil National de Recherches du Canada pour son aide financière et au Conseil des Arts pour des bourses (G.C., C.B.). Nous remercions le Professeur Saint-Jacques et M. Williams de leurs conseils ainsi que le Docteur Pavia qui nous a aimablement prêté sa thèse.

1. S. K. Hall et E. A. Robinson. Can. J. Chem. **42**, 1113 (1964).
2. R. J. Gillespie et E. A. Robinson. *Dans* Non-aqueous solvent chemistry. *Edité par* T. C. Waddington, Academic Press, New York, 1965.
3. R. J. Gillespie. J. Chem. Soc. 2537 (1950).
4. C. P. Wright, D. M. Murray-Rost et H. Hartley. J. Chem. Soc. 199 (1931).
5. I. M. Kolthoff, S. Bruckenstein, et M. K. Chantooni, Jr. J. Amer. Chem. Soc. **83**, 3927 (1961).
6. G. Charlot et B. Trémillon. Les réactions chimiques dans les solvants et les sels fondus. Gauthier-Villars, *Editeurs*, Paris, 1963.
7. R. W. Alder, G. R. Chalkley et M. C. Whiting. Chem. Commun. 405 (1966).
8. M. J. Jorgenson et D. R. Hartter. J. Amer. Chem. Soc. **85**, 878 (1963).
9. R. L. Benoit et G. Choux. Can. J. Chem. **46**, 3125 (1968).
10. R. L. Benoit, A. L. Beauchamp et M. Deneux. J. Phys. Chem. **73**, 3268 (1969).
11. F. Klages et P. Hegenberg. Angew. Chem. **74**, 902 (1962).

12. J. BARR, R. J. GILLESPIE et R. C. THOMPSON. Inorg. Chem. **3**, 1149 (1964).
13. R. J. GILLESPIE et K. C. MALHOTRA. J. Chem. Soc. (A), 1194 (1967).
14. K. FREI et H. J. BERNSTEIN. J. Chem. Phys. **37**, 1891 (1962).
15. J. F. COETZEE et R. J. BERTOZZI. Anal. Chem. **41**, 860 (1969).
16. P. PICHET et J. CHARBONNEAU. Résultats non publiés.
17. A. C. PAVIA. Thèse de doctorat (CNRS., A.O.2664), Université, Montpellier, France. 1968.
18. W. REED, D. W. SECRET, R. C. THOMPSON, et P. A. YEATS. Can. J. Chem. **47**, 4275 (1969).
19. J. W. AKITT, A. K. COVINGTON, J. G. FREEMAN, et T. H. LILLEY. Chem. Commun. 349 (1965).
20. E. TOMMILA, E. LINDELL, M. L. VIRTALAINE, et R. LAAKSO. Suom. Kemistilehti, B42, 95 (1969).
21. R. L. BENOIT et J. CHARBONNEAU. Can. J. Chem. **47**, 4195 (1969).
22. L. W. REEVES et W. G. SCHNEIDER. Trans. Faraday Soc. **54**, 314 (1959).
23. S. BROWNSTEIN et A. E. STILLMAN. J. Phys. Chem. **63**, 2061 (1959).
24. G. CHOUX et R. L. BENOIT. J. Amer. Chem. Soc. **91**, 6221 (1969).
25. M. DELLA MONICA, U. LAMANNA, et L. SENATORE. J. Phys. Chem. **72**, 4329 (1968) et références citées des mêmes auteurs.
26. R. FERNANDEZ-PRINI et J. E. PRUE. Trans. Faraday Soc. **62**, 1257 (1966).

Can. J. Chem. Downloaded from www.nrcresearchpress.com by 210.87.254.6 on 09/05/12
For personal use only.

Can. J. Chem. Downloaded from www.nrcresearchpress.com by 210.87.254.6 on 09/05/12
For personal use only.

Reactions of the U(VI) complexes of oxine

A. CORSINI AND J. ABRAHAM[1]
Department of Chemistry, McMaster University, Hamilton, Ontario

Received March 4, 1970

The interaction of the oxine adduct, $UO_2(C_9H_6NO)_2 \cdot C_9H_6NOH$, and of the bis compound, $UO_2(C_9H_6NO)_2$, with several solvents has been studied. The oxine ligand in the adduct is displaced by DMSO but the adduct is stable in solvents of relatively low polarity. The bis compound is unstable and reacts to form both the adduct and solvates. Under appropriate conditions, the addition reaction between the bis compound and a solution of oxine is quantitative. Studies with [^{14}C]-oxine revealed that the addition is accompanied by two exchange reactions.

Canadian Journal of Chemistry, 48, 2360 (1970)

Introduction

The oxine (8-hydroxyquinoline) adduct, $UO_2(C_9H_6NO)_2 \cdot C_9H_6NOH$, long used in analysis for the determination of uranium, has been the subject of several investigations. Although these investigations have emphasized the compositional, structural, and thermal nature of the solid adduct (1–7), information about the solution reactions of the species is increasing (8–12).

In the present report, the interaction with various solvents of the adduct compound and of bis(8-hydroxyquinolinato)dioxouranium(VI), $UO_2(C_9H_6NO)_2$, which is derived thermally from the adduct, is described. Also presented are the results of studies on the interesting addition reaction which occurs when the bis compound is placed in contact with a solution of oxine. This reaction was first noted by Frere (12) but few details were provided in his report.

Experimental

Uranyl nitrate hexahydrate (ANALAR, British Drug Houses) was used without further purification. A stock solution (1.01×10^{-2} *M*) was prepared and standardized as outlined by Vogel (13). [^{14}C]-Oxine was synthesized as previously described (7). Unlabelled oxine (certified grade, Fisher Scientific Co.) was purified by sublimation. Ethanol (95%) and analytical grades of methanol, acetone, chloroform, and dimethylsulfoxide (DMSO) were used as supplied. Absolute ethanol and 1,2-dichloroethane were dried before use for 48 h over molecular sieves (Type A, Fisher Scientific Co.). Reagent-grade 1,4-dioxane was refluxed over sodium for at least 24 h and fractionally distilled (b.p. 100.5–101 °C) through a 1 m column packed with glass helices. All other chemicals were of suitable purity.

Infrared (i.r.) spectra were recorded with a Beckman IR-5 spectrophotometer. The samples were prepared as mulls in spectrally pure hexachloro-1,3-butadiene. Measurements of p*H* were made with a Radiometer PHM_4 meter equipped with Beckman saturated calomel and E-3 glass electrodes. The wet-oxidation of [^{14}C]-compounds and the measurement of [^{14}C]-radioactivity were carried out as noted previously (7). Sieves (U.S. Standard Sieve series, A.S.T.M. specifications) were used to control the initial particle size of the bis compound in the addition reaction with oxine. The pore diameter of the sieves was 74, 149, and 250 μ. Appropriate pairing of the sieves afforded initial particle-size ranges of < 74, 74–149, and 149–250 μ.

Microanalyses were by Alfred Bernhardt, Elbach über Engelskirchen, West Germany. Analysis of the oxine content of the U(VI) compounds was done bromometrically (14).

The red adduct and the greenish–black bis compound were prepared as described earlier (1).

The general procedure for the interaction of the adduct with 1,2-dichloroethane, 1,4-dioxane, absolute ethanol, and DMSO was as follows. A saturated solution of the adduct was prepared at the boiling point of the solvent. The excess solid was filtered off and the filtrate cooled to yield a crystalline solid. After filtration, the solid was dried at 105 °C for 3 h and its i.r. spectrum taken (Fig. 1).

The solubility of the adduct compound in DMSO was very high. Concentration of the solution to one-quarter of its original volume (10 ml) yielded no solid. After standing for 1 week at room temperature, the concentrated solution yielded a gum-like material which was filtered off and dried for 3 h at 105 °C (i.r. spectrum, B, Fig. 1). After an additional week, dark-red crystals appeared in the filtrate. These were removed and dried in the same manner. The i.r. spectrum of these crystals was identical to that of the gum-like material.

Anal. Calcd. for $UO_2(C_9H_6NO)_2 \cdot OS(CH_3)_2$: C, 37.71, H, 2.85; N, 4.40, S, 5.04. Found: C, 37.85; H, 2.99; N, 4.35; S, 4.85.

For the interaction of the bis compound with 95% ethanol, methanol, acetone, chloroform, and 1,2-dichloroethane, a mixture of 50 mg of the bis compound and 10 ml of the solvent was stirred continuously for 3 h at room temperature. With each solvent except dichloroethane, the solution and the surface of the undissolved compound became red in moments. The undissolved material was removed and a solid compound was isolated by evaporation of the filtrate. The compound was dried overnight in air and then at 105 °C for 1 h. The i.r. spectra

[1]Present address: Department of Chemistry, Kerala University, Trivandrum, Kerala, India.

Can. J. Chem. Downloaded from www.nrcresearchpress.com by 210.87.254.6 on 09/05/12
For personal use only.

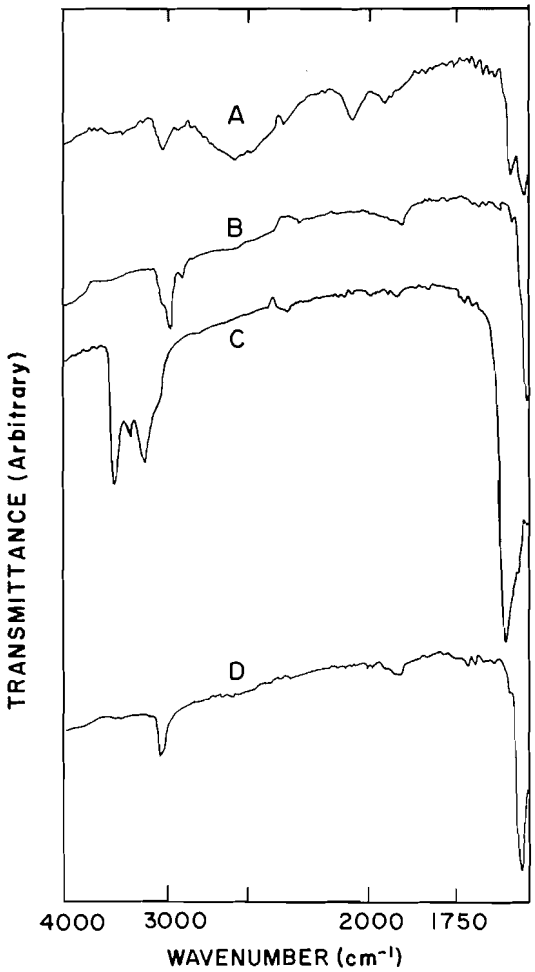

FIG. 1. Infrared spectra of $UO_2(C_9H_6NO)_2 \cdot C_9H_6NOH$ precipitated from aqueous solution (A), $UO_2(C_9H_6NO)_2 \cdot DMSO$ (B), $UO_2(C_9H_6NO)_2 \cdot OC(NH_2)_2$ precipitated from aqueous dioxane (C), $UO_2(C_9H_6NO)_2$ prepared thermally from adduct (D). The spectra of compounds obtained from the interaction of the adduct with dichloroethane, dioxane, and absolute ethanol were identical to (A).

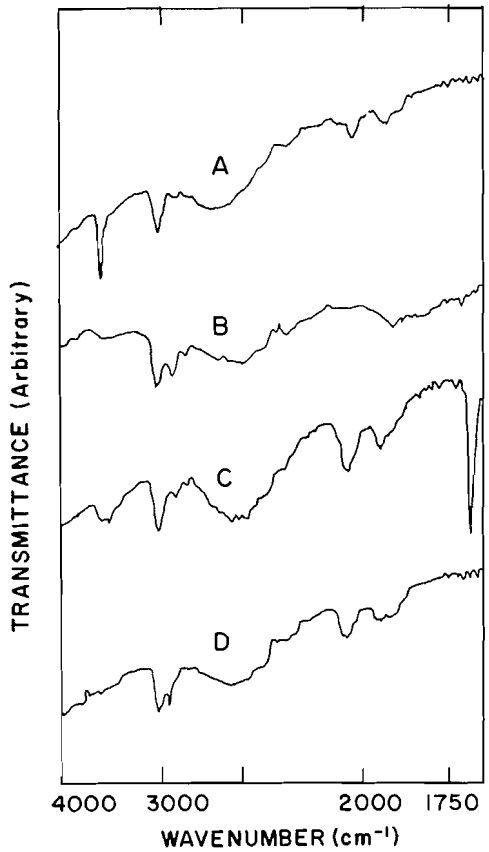

FIG. 2. Infrared spectra of compounds obtained from the interaction of $UO_2(C_9H_6NO)_2$ with 95% ethanol (A), methanol (B), acetone (C), chloroform (D).

of the solids are shown in Fig. 2. Microanalytical data did not correspond to simple formulae.

With dichloroethane, the supernatant liquid was yellow and the undissolved residue remained black. In dichloroethane saturated with water, however, the bis compound yielded a red solution, and the surface of the undissolved solid became red. After removal of this solid, concentration of the filtrate and subsequent cooling yielded red crystals, which were dried for 3 h at 105 °C (A, Fig. 1).

Anal. Calcd. for $UO_2(C_9H_6NO)_2 \cdot C_9H_6NOH$: C, 46.09; H, 2.72; N, 5.97. Found: C, 45.04; H, 2.74; N, 5.37.

The reaction between U(VI) and oxine in 50% v/v dioxane–water was studied. The potentiometric apparatus and procedure was essentially as described elsehwere (15). Solutions with U(VI):oxine ratios of 1:2 and 1:3 were titrated at 25 °C. The initial concentration of U(VI) in each solution was 4.7×10^{-4} *M*. The concentration of $HClO_4$ was 4.5×10^{-3} *M*. The ionic strength was adjusted to 0.1 with $NaClO_4$.

Precipitation of a solid compound from 50% v/v dioxane–water was effected as follows. $UO_2(NO_3)_2 \cdot 6H_2O$ (0.2 mmole) was dissolved in 50 ml of 50% aqueous dioxane containing 3 drops of concentrated nitric acid. Oxine (0.7 mmole) in 1 ml of dioxane was added, followed by urea (5 g). The solution was heated to boiling and placed on a steam bath for 3 h. The red needle-like crystals which formed were removed, washed with water, and dried at 105 °C for 3 h. The p*H* of the cooled filtrate was 7. The i.r. spectrum was taken (C, Fig. 1).

Anal. Calcd. for $UO_2(C_9H_6NO)_2 \cdot OC(NH_2)_2$: C, 37.25; H, 2.61; N, 9.06; U, 38.48. Found: C, 37.59; H, 3.05; N, 9.06; U, 38.80.

Bromometric analysis for the oxine anion content gave 46.39% (calculated, 46.63%).

For the reaction involving the addition of oxine to the bis compound, dry dichloroethane, in which the bis and adduct compounds are inert, was used as the solvent.

TABLE 1
Addition reaction with [^{14}C]-oxine*

Molar ratio taken (bis compound:oxine)	Extent addition (%)	Specific activity (mV/s mg)†		
		Reaction product	Bis compound	Sublimed oxine
1:1	67	1.39 ±0.01	1.23 ±0.02	1.69 ±0.02
1:2	92	2.03 ±0.03	1.88 ±0.03	2.20 ±0.02
	77‡	1.75 ±0.03	1.59 ±0.03	2.21 ±0.02
1:5	100	—	2.49 ±0.03	2.88 ±0.01

*Initial specific activity of oxine, 3.58 mV/s mg; bis compound taken, 100 mg (0.18 mmoles); initial particle size, < 74 μ; reaction time, 5 min. Each result is the average of three determinations. The precision measure is the standard error.
†See ref. 7 concerning the units mV/s mg.
‡Particle size of bis compound was 74–149 μ in this experiment.

Because of the limited solubility of the bis and adduct compounds in dichloroethane (2.3 and 2.1 mg/ml), the addition reaction was carried out heterogeneously and the percent addition was obtained by analysis of the filtered solid residue. The low and approximately equal solubilities of the compounds resulted in a minimal error in percent addition (< 2%). The reaction was quenched by rapid filtration. The general procedure was: 100 mg (0.18 mmole) of the bis compound of known particle size were added to a 15 ml reaction flask, followed by 5.0 ml of a dichloroethane solution of oxine. The mixture was kept at 25 °C and stirred magnetically at constant speed. At a specified time, the mixture was quickly filtered (~20 s) through a fritted-glass crucible (F porosity), washed with three 2 ml portions of dichloroethane, and dried at 85–90 °C (~5 mm Hg) for 3 h. The percent addition was obtained by bromometric determination of the relative amounts of the bis compound and oxine obtained by thermal conversion of the resultant adduct (1, 7). The effect of reaction time, oxine concentration and initial size of the bis compound was studied.

The addition reaction was also investigated by reacting [^{14}C]-oxine with unlabelled $UO_2(C_9H_6NO)_2$. A small portion of the reaction product was used to determine its specific activity (7). The remaining solid was thermally converted to the bis compound and oxine and the specific activity of each constituent determined. The data are given in Table 1.

Results and Discussion

Recent X-ray (3) and i.r. (4) studies have shown that the additional oxine molecule in the adduct compound is coordinated to the central uranium atom through the phenolate oxygen donor and that the proton is hydrogen-bonded between the nitrogen atom of this monodentate ligand and the oxygen donor of the neighboring bidentate ligand. In the i.r. spectrum, the bands at 2650 (broad) and 2050 cm^{-1} (weak) have been attributed to the $^{+}N—H\cdots O$ bonded system (4). These bands are also present in the spectra of the U(VI) adducts of several oxine derivatives (4) and in the Th(IV) and Sc(III) adducts of certain oxine derivatives (16, 17). Thus these bands, which are not present in the spectra of the normal complexes, are characteristic of the metal–oxine adducts and can be used to identify their formation.

In the i.r. spectra (Fig. 1) of the compounds isolated from the interaction of the adduct with dichloroethane, dioxane, and absolute ethanol, the 2650 and 2050 cm^{-1} bands show that the monodentate oxine ligand is still coordinated, and that no significant amount of solvolysis has occurred. This is contrary to the belief that in non-aqueous solution the adduct is dissociated to the normal complex and free oxine, and that the third molecule of bound oxine exists only in the solid state (8). The present work shows that in solvents of relatively low polarity, the integrity of the adduct is preserved. In polar solvents such as DMSO, however, the monodentate ligand is displaced by the solvent. In the i.r. spectrum (B, Fig. 1), the 2650 and 2050 cm^{-1} bands are absent and a new strong band at 1015 cm^{-1} (not shown), characteristic of the S=O stretching frequency, appears. The small shift in the S=O frequency from the free DMSO value of 1055 cm^{-1} suggests that the DMSO molecule is not as strongly coordinated as in $UO_2(NO_3)_2 \cdot 2DMSO$ (18), or as in the DMSO complexes of the actinide tetrachlorides (19). The formation of the DMSO solvate was confirmed by isolation and analysis of the solid. Baker and Sawyer (11) had previously

Can. J. Chem. Downloaded from www.nrcresearchpress.com by 210.87.254.6 on 09/05/12
For personal use only.

Can. J. Chem. Downloaded from www.nrcresearchpress.com by 210.87.254.6 on 09/05/12
For personal use only.

suggested the displacement of the oxine molecule by DMSO on the basis of nuclear magnetic resonance (n.m.r.) evidence. Recent observations by the present workers (17) suggest that displacement also occurs in dimethylformamide and pyridine.

The i.r. spectra of the compounds obtained from the interaction of the bis compound with 95% ethanol, methanol, acetone, and chloroform are shown in Fig. 2. The bands at 2650 and 2050 cm^{-1} provide strong evidence for the disproportionation of the bis compound to the adduct and other U(VI) species, as first suggested by Bullwinkel and Noble (9). Fleming and Lynton (20) have also reported the formation of the adduct by recrystallization of the bis compound from chloroform.

The analytical data for the compounds isolated from the above solvents did not correspond, however, to the adduct. This suggests that the adducts were contaminated, perhaps with solvates of the type $UO_2(C_9H_6NO)_2 \cdot H_2O$, $UO_2(C_9H_6NO)_2 \cdot CH_3OH$, and $UO_2(C_9H_6NO)_2 \cdot OC(CH_3)_2$. The presence of these solvates is indicated by bands at 3575 (OH), 2925 (aliphatic CH), and 1700 (C=O) cm^{-1} in spectra of the isolated compounds (Fig. 2). Similar solvates of the bis acetylacetone U(VI) complex have been reported (21). The C=O stretching frequency in the above acetone solvate is identical to that found in $UO_2(C_9H_4NOX_2)_2 \cdot OC(CH_3)_2$, where X = Cl or Br (17). The i.r. spectrum of the adduct formed in chloroform shows the presence of solvent of crystallization (bands at 2950 and 750 cm^{-1}), as described in the X-ray study by Hall *et al.* (3).

Further evidence for the formation of the solvate $UO_2(C_9H_6NO)_2 \cdot H_2O$ was obtained by potentiometric titration of the U(VI)-oxine system in 50% dioxane–water. The important features of the titration curves for 1:2 and 1:3 ratios of metal-to-ligand were identical. In each curve, two buffer regions in the p*H* ranges 4–6 and 7–10, were present. The lower buffer region corresponded to a release of two protons per U(VI), and the higher to a one-proton release. The two-proton release could only result from the formation of a 1:2 complex, and the single-proton release from the hydrolysis reaction shown in eq. [1]. The only difference noted between the

[1] $$UO_2(C_9H_6NO)_2 \cdot H_2O \rightleftharpoons [UO_2(C_9H_6NO)_2 \cdot OH]^- + H^+$$

two titration curves was the lack of coincidence in the p*H* range 10–12, due to the titration of *uncomplexed* oxine in the solution containing the 1:3 ratio of metal-to-ligand. Indeed, the oxine adduct compound could not be precipitated from 50% aqueous dioxane. The microanalytical data and i.r. spectrum (C, Fig. 1) show that the compound obtained was $UO_2(C_9H_6NO)_2 \cdot OC(NH_2)_2$. The source of the urea was the relatively large amount added to raise the p*H* through hydrolysis, as in the precipitation of the adduct from water. The urea ligand is likely bonded to the uranium atom through the carbonyl oxygen as in $UO_2(OH)_2\{OC(NH_2)_2\}_2$ (22), rather than through a terminal nitrogen as in $[Pt\{OC(NH_2)_2\}Cl_2]$ (23, 24). This is indicated by the C=O stretching frequency (1625 cm^{-1}), which is considerably shifted from that (1683 cm^{-1}) in free urea, and the N—H stretching frequencies (3300 and 3400 cm^{-1}), which are essentially as in free urea (22).

The interaction of the bis compound with dichloroethane is significant. In dry hot dichloroethane, the bis compound yielded a yellow solution and was recrystallized unchanged, giving an i.r. spectrum identical to that for the thermally-prepared bis compound (D, Fig. 1). In dichloroethane saturated with water, however, the bis compound decomposed to give a red solution and the adduct compound. The i.r. spectrum was identical to that of the adduct precipitated from aqueous solution (A, Fig. 1). The decomposition may occur according to eq. [2] where the role of water is to protonate an oxine anion in the formation of the adduct compound.

[2] $$3UO_2(C_9H_6NO)_2 + 2H_2O \rightleftharpoons 2UO_2(C_9H_6NO)_2 \cdot C_9H_6NOH + UO_2^{++} + 2OH^-$$

The above results provide evidence for the reactivity of the bis compound in several commonly available solvents and do not support Moeller and Ramaniah's conclusions (8), which were based on the reactivity (i.e., dissociation) of the adduct and the inertness of the bis compound. Recently, Baker and Sawyer (11) questioned the disproportionation reaction proposed by Bullwinkel and Noble since in DMSO, the bis compound was thought to form a solvate rather than the adduct. According to the present study, the interaction of the bis compound with solvents can yield the bis compound unchanged, the adduct, or a mixture of the adduct and solvate, depending on the polarity of the solvent.

The formation of the adduct by reaction of the bis compound with a solution of oxine was noted

Can. J. Chem. Downloaded from www.nrcresearchpress.com by 210.87.254.6 on 09/05/12
For personal use only.

several years ago (12) but the reaction conditions were not reported in detail. In the present study, it was found that the proper selection of reaction time, oxine concentration, and initial particle size of the bis compound yielded quantitative addition. For a particle size <75 μ and a reactant molar ratio (bis-compound:oxine) of 1:2 (0.36 mmole oxine), 92, and 100% addition was obtained for the reaction times of 5 and 10 min, respectively. For the same particle size and a reaction time of 5 min, 67, 92, and 100% addition was obtained for molar ratios of 1:1, 1:2, and 1:5, respectively. For a 5 min reaction time and a molar ratio of 1:2, 73, 77, and 92% addition was obtained for the particle size ranges 149–250, 74–149, and <74 μ, respectively. The inertness of both the bis and adduct compounds in dry dichloroethane demonstrated the suitability of this solvent for the addition reaction.

Because of the complicating heterogeneous-phase equilibria, no attempt was made to determine the rate-law for the addition reaction. The addition can be conceived, however, as occurring by one or both of the following processes.

(i) Addition in solution. On dissolution of a small amount of the bis compound, addition occurs and the adduct precipitates after saturation of the solution. Further dissolution of the bis compound and formation and precipitation of the adduct occur, until addition is essentially quantitative.

(ii) Heterogeneous addition. The oxine in solution interacts with the external and internal surfaces of the particles of the bis compound. The adduct molecules so formed dissociate from the solid matrix and pass into solution, ultimately to nucleate and precipitate. This mechanism implies that the initial particle size is important in determining the rate of addition. Indeed, the percent addition was found to increase with decreasing particle size, but this observation can also be explained readily by the first mechanism; i.e., as the particle size is decreased, the rate of dissolution of the bis compound, and therefore of the addition reaction, is increased.

It is fruitless to speculate on a more detailed mechanism of the addition reaction until the structure of the bis compound is known and the molecular weight of species arising from dissolution of the bis compound in dichloroethane is determined. Bullwinkel and Noble (9) have suggested that the bis compound is extensively polymerized. It would appear that the compound is at least dimeric with bridging donor oxygen atoms, as has been suggested (25) for bis(acetylacetonato)dioxouranium(VI).[2] Regardless of the degree of polymerization of the bis compound, the detailed mechanism must provide for the formation of the monomeric (3) adduct compound.

The driving force for the addition reaction is provided by the instability of the bis compound with respect to the adduct. This instability is demonstrated by the tendency of the bis compound to disproportionate and to form solvates. It is likely the result of the poorer donor properties of the (presumed) oxygen bridging atom in the bis compound compared to the oxygen donor of the monodentate ligand in the adduct, which is further stabilized by hydrogen bonding. Interestingly, the bis compound can be prepared only by thermal treatment of the adduct; all attempts to precipitate the bis compound from solution have been unsuccessful. Recently, however, the direct precipitation of the U(VI) bis complexes of α-picolinic acid (26) and of tropolone (27) has been reported. Since the adducts were also precipitated, it would be of interest to determine the structures and relative stabilities of the corresponding bis and adduct compounds.

Other bis complexes of U(VI) undergo addition. Indeed, several "mixed" ligand adducts have been formed from the bis compounds of α-picolinic acid (26) and acetylacetone (21). The formation of bis and adduct U(VI) complexes and their facile interconversion is not unique, apparently, to the ligand oxine.

Further information about the addition reaction was deduced from experiments with [^{14}C]-oxine. First, an exchange reaction involving the inactive ligands of the bis compound and the active oxine in solution occurs concurrently with the addition reaction, since there is more activity in the reaction product than is expected from the amount of active oxine added. For 67, 77, and 92% addition, the amount of oxine added to 100 mg of the bis compound is 17, 20, and 24 mg. From this data and the value 3.6 for the initial

[2]Several bis compounds of U(VI) have been reported (e.g., 25–27). From the molecular formula, the central U(VI) atom appears to be coordinately unsaturated. Higher coordination could be achieved, however, by molecular association into dimeric or larger units through bridging donor atoms.

specific activity of the oxine, calculation shows that in the absence of the exchange reaction, the activity expected in the reaction product is 0.90, 1.0, and 1.1 rather than 1.4, 1.8, and 2.0 mV/s mg, as observed (Table 1). The high values obtained could only result from the occurrence of exchange. Second, the exchange and addition reactions are independent and proceed with different rates. This conclusion is supported by the data for 100% addition (Table 1), which shows that the specific activity of the bis compound and sublimed oxine are significantly different. The same conclusion cannot be drawn from the data for additions of less than 100% since any unreacted bis compound would act as a diluent to the activity of the reaction products. Third, an intramolecular exchange equilibrium likely occurs. After sufficient time has elapsed (>15 min), the specific activity of the bis compound and oxine is essentially the same. An exchange as shown in eq. [3] would account for this observation.

[3] 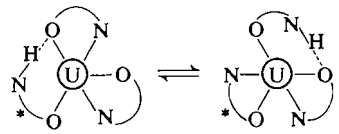

For the data in Table 1, the existence of radiobalance can easily be proved. For example, for 77% addition, the specific activity of the reaction product is $(2.00 \times 1.59 + 0.77 \times 2.21)/2.77 = 1.8$ mV/s mg, which is in accord with the experimental value.

Finally, the data are complicated by the occurrence of ligand exchange during the thermal conversion of the reaction products (7). The effect of the thermal exchange is to partially randomize the activity acquired by the adduct compound. This randomization reduces the difference in specific activity between the sublimed oxine and the bis compound and partially accounts for the uniform distribution of activity observed after 15 min. The difference is still finite, however, for reactions of shorter time.

We wish to thank the National Research Council of Canada for the financial support of this study.

1. A. CORSINI and J. ABRAHAM. Talanta, **15**, 562 (1968).
2. J. BORDNER, E. D. SALESIN, and L. GORDON. Talanta, **8**, 579 (1961).
3. D. HALL, A. D. RAE, and T. N. WATERS. Acta Cryst. **22**, 258 (1967).
4. A. CORSINI, J. ABRAHAM, and M. THOMPSON. Chem. Commun. 1101 (1967).
5. J. E. TACKETT and D. T. SAWYER. Inorg. Chem. **3**, 692 (1964).
6. R. J. MCGEE and L. GORDON. Talanta, **13**, 709 (1966).
7. A. CORSINI and J. ABRAHAM. Can. J. Chem. **47**, 1435 (1969), and references therein.
8. T. MOELLER and M. V. RAMANIAH. J. Amer. Chem. Soc. **76**, 5251 (1954).
9. E. P. BULLWINKEL and P. NOBLE, JR. J. Amer. Chem. Soc. **80**, 2955 (1958).
10. S. OKI. Anal. Chim. Acta, **44**, 315 (1969).
11. B. BAKER and D. T. SAWYER. Inorg. Chem. **8**, 1160 (1969).
12. F. FRERE. J. Amer. Chem. Soc. **55**, 4362 (1933).
13. A. I. VOGEL. A text-book of quantitative inorganic analysis. Third edition. John Wiley and Sons, Inc., New York, 1961. p. 539.
14. A. CORSINI and R. P. GRAHAM. Anal. Chim. Acta, **23**, 248 (1960).
15. A. CORSINI and E. J. BILLO. Can. J. Chem. **47**, 4655 (1969).
16. A. CORSINI and J. ABRAHAM. Chem. Commun. 856 (1968).
17. This laboratory. Unpublished work.
18. P. V. BALAKRISHNAN, S. K. PATIL, H. D. SHARMA, and H. V. VENKATASETTY. Can. J. Chem. **43**, 2052 (1965).
19. K. W. BAGNALL, D. BROWN, D. H. HOLAH, and F. LUX. J. Chem. Soc. (A), 465 (1968).
20. J. E. FLEMING and H. LYNTON. Can. J. Chem. **45**, 1637 (1967).
21. W. W. WENDLANDT, J. L. BEAR, and G. R. HORTON. J. Phys. Chem. **64**, 1289 (1960).
22. W. DEMBINSKI and A. DEPTUEA. J. Inorg. Nucl. Chem. **29**, 779 (1967).
23. K. NAKAMOTO. Infrared spectra of inorganic and coordination compounds. John Wiley and Sons, Inc., New York, 1958. p. 184–185.
24. R. B. PENLAND, S. MIZUSHIMA, C. CURRAN, and Y. V. QUAGLIANO. J. Amer. Chem. Soc. **79**, 1575 (1957).
25. A. E. COMYNS. Chem. Rev. **60**, 132 (1960).
26. S. H. EBERLE and W. ROBEL. Inorg. Nucl. Chem. Lett. **4**, 113 (1968).
27. D. L. PLYMALE and W. H. SMITH. J. Inorg. Nucl. Chem. **30**, 2267 (1968).

Can. J. Chem. Downloaded from www.nrcresearchpress.com by 210.87.254.6 on 09/05/12
For personal use only.

Can. J. Chem. Downloaded from www.nrcresearchpress.com by 210.87.254.105 on 09/05/12
For personal use only.

Reductions with sulfurated borohydrides. V. Reductions of ketones

J. M. Lalancette and A. Freche
Département de chimie, Faculté des Sciences, Université de Sherbrooke, Sherbrooke, Québec

Received February 17, 1970

Ketones can be reduced with sulfurated sodium borohydride. Very high yield (≈90%) of the corresponding alcohol is obtained with the appropriate ratio of ketone and hydride at room temperature. The reaction is much influenced by the steric environment around the carbonyl group. At high temperature (65°) disulfides and tetrasulfides are produced. In some cases the structure of those sulfides have been established. Conjugated ketones can be reduced to the corresponding alcohols with very high yields.

Canadian Journal of Chemistry, **48**, 2366 (1970)

We have reported the formation of sulfurated borohydrides of the general formula MBH_2S_3 (1) and the reduction of various groups with this new reducer, such as aldehydes (2) and oximes (3). This paper describes the reduction of typical ketones, conjugated ketones, and diketones.

Experimental

Nuclear magnetic resonance (n.m.r.) measurements were made with a Varian, A60 apparatus. Infrared (i.r.) measurements were made with a Perkin–Elmer, model 137 spectrophotometer. Vapor-phase chromatography (v.p.c.) measurements were made with a Microteck, model G.C. 2000R apparatus, using an Se30, 4 ft column. Mass spectrometry measurements were performed on a Hitachi Perkin–Elmer instrument, model RMU-6.

1) Reduction

The reduction of benzophenone can be taken as a typical experiment. To a suspension of 0.20 mole of $NaBH_2S_3$ obtained by the reaction of 0.20 mole (7.56 g) of $NaBH_4$ with 0.60 mole (19.2 g) of sulfur (rapid addition to the mixture of the two reactants of 150 ml of dry tetrahydrofuran without cooling and with stirring) was added 0.20 mole (36.5 g) of benzophenone in 50 ml of the same solvent. The reducer was used in situ, without isolation, being then partly dissolved and partly in suspension in THF and giving the quantitative amount of H_2 upon hydrolysis (1). The reaction mixture was stirred at 25 °C for 2 h. The mixture was then hydrolyzed by 100 ml of 10% HCl, (contact overnight at room temperature) and the alcohol extracted with chloroform, the yield (36 g) being quantitative.

The identification of the alcohol was made by comparison of i.r. and n.m.r. measurements with an authentic sample of diphenylcarbinol.

The reduction of typical ketones, under experimental conditions where time of contact temperature and ratio of reactants were varied, is reported in Table 1. The separation of the reaction mixtures from those experiments was made by preparative v.p.c. or by chromatography over Florisil and crystallization when the products were of low volatility.

2) Isolation of Intermediate Borates

It has been possible to isolate the intermediate borate in the reaction mixture, prior to hydrolysis. In the case of benzophenone for example, upon extraction of the crude reaction mixture with anhydrous petroleum ether (200 ml), after evaporation of THF at low temperature, a colorless oil was obtained. In the i.r., a strong B—O band was present at 1340 cm^{-1} (4). This borate was identical to the ester obtained by the reaction of diphenylcarbinol with boric acid, from i.r. and n.m.r. measurements. In the n.m.r., the usual shift of the proton attached to the 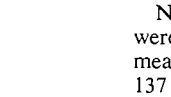 system was noted. Table 2 gives the various positions observed in n.m.r. for the proton of the , 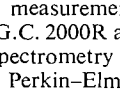 , and 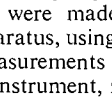 structures.

3) Hydrolysis

The hydrolysis of the boric ester can be done under acidic or basic conditions. With open chain or aromatic structures, this step is quantitative under either experimental conditions. With alicyclic derivatives, basic hydrolysis proved better. For example, after the reduction of cyclohexanone (0.20 mole, 19.6 g) by $NaBH_2S_3$ (0.2 mole, 26.4 g) in a fashion described in section *1*, the hydrolysis was done with 100 ml of 5% NaOH at 25°, for 2 h. There was then no trace of the borate left and the treatment of the reaction mixture was easy since most of the sulfur remained in the basic fraction.

4) Isolation and Identification of Polysulfides

With appropriate molecular ratios of reducer and carbonyl derivatives, polysulfides were formed along with the expected alcohols (Table 1). After reduction as described in section *1*, those polysulfides were isolated from the reaction mixtures by filtration after acid hydrolysis and purified by crystallization in ethanol. The characterization of the polysulfides is reported in Table 3.

With conjugated ketones the sulfurated products were much more complex and difficult to isolate in pure form. In the case of the *trans*-4-phenyl 3-butene 2-one, using a contact time of 15 min at 60°, a yield of 40% of sulfide was obtained, besides the unsaturated alcohol.

TABLE 1

Reduction of typical ketones with $NaBH_2S_3$

	Carbonyl/hydride molar ratio	Reaction temperature (°C)	Time of contact (h)	Conversion (%)	Yield of alcohol[‖‖]	Yield of polysulfide (%)[‖‖]
$C_6H_5COCH_3$	2/1	25	24	55	55	0
		65	3	95	45	55*
	1/1	20–25	2	100	94	0
$C_6H_5CH_2COCH_3$	2/1	25	24	95	90	—
	1/1	25	2	100	92	—
$C_6H_5COC_6H_5$	2/1	65	2.5	95	42	58*
	1/1	20	4	90	88	traces
	2/1	25	9	90	90	traces
		65	8	95	complex mixture	
	1/1	25	3	95	92	0
	2/1	25	72	70	70	traces
		65	3	95	60	≈40†
	1/1	25	20	95	92	0
	2/1	25	72	70	70	traces
		65	4	90	≈50	≈50†
	1/1	25	6	95	90	0
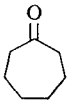	2/1	25	48	80	80	0
		65	4	65	complex mixture	
	1/1	25	4	95	90	0
$CH_3CH_2\overset{O}{\overset{\|}{C}}CH_2CH_3$	2/1	25	3	100	90	0
		65	3	100	45	55*
	1/1	25	1	100	90	0
$CH_3COCH_2CH_3$	2/1	0	1	100	90	0
	1/1	0	1	100	90	0
CH_3COCH_3	2/1	0	1	100	90	0
	1/1	0	1	100	90	0
$(CH_3)_3CCOCH_3$	2/1	25	6	100	90	0
	1/1	25	6	100	95	0
CH_3	1/1§	−50	1	100	95‡	0
$\diagdown$	2/1	65	0.25	50	trace	40[‖]
$C{=}CHCOCH_3$	2/1	65	1–3	90	variable amount	complex mixture
$\diagup$						
CH_3						
$C_6H_5CH{=}CH{-}CO{-}CH_3$	1/1§	−8	1	90	90	0
	2/1	65	0.25	100	60	40¶
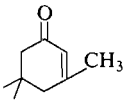	1/2	25	80	100	80	20 complex mixture
	1/1	65	20	100	present	complex mixture
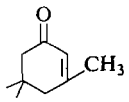	1/1	−20	1	100	100**	0
$C_6H_5\overset{O}{\overset{\|}{C}}-\overset{O}{\overset{\|}{C}}-C_6H_5$	1/1	25	12	100	100††	0

Can. J. Chem. Downloaded from www.nrcresearchpress.com by 210.87.254.105 on 09/05/12
For personal use only.

TABLE 1—(*Concluded*)

	Carbonyl/hydride molar ratio	Reaction temperature (°C)	Time of contact (h)	Conversion (%)	Yield of alcohol‖¶	Yield of polysulfide (%)‖¶
$CH_3COCH_2COCH_3$	1/1	−80	1	85	85‡‡	0
	1/1	20	1	95	95§§	0
	1/1	25	27	0	—	—
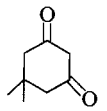	2/1	25	12	0	—	—
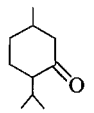	1/1	25	27	0	—	—

*Disulfide.
†Tetrasulfide.
‡Allylic alcohol.
§The reducer was added rapidly to the ketone.
‖Unsaturated disulfide.
¶Monosulfide.
**A mixture of cyclohexanol (33%) and cyclohexenol (66%).
††Diol, from n.m.r. and elementary analysis.
‡‡Diol (62%).
§§95% Diol.
‖‖Yield from v.p.c. analysis, ±3%.

TABLE 2

Position of proton in the n.m.r. of borates and disulfides obtained by reduction of various ketones

Ketone	δ values for H—C— 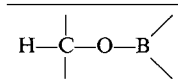	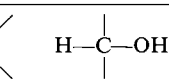	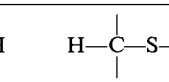
$C_6H_5COCH_3$	5.34	4.68	3.50*
$C_6H_5CH_2COCH_3$	4.36	3.87	—
$C_6H_5COC_6H_5$	6.30	5.55	4.81*
$C_6H_5CH_2COCH_2C_6H_5$	4.40	3.84	2.75*
Cyclopentanone	4.56	4.21	2.88†
Cyclohexanone	4.05	3.51	2.64†
Cycloheptanone	4.24	3.70	—
$C_2H_5COC_2H_5$	3.92	3.36	2.50*
$CH_3COC_2H_5$	4.10	3.62	—
CH_3COCH_3	4.32	3.91	—
$(CH_3)_3CCOCH_3$	3.89	3.38	—

*Disulfide.
†Tetrasulfide.

This sulfide, a solid, m.p. 190°, was recrystallized in CCl_4. The n.m.r.: 3 protons (singlet) at 1.25; 3 protons (singlet) 1.70; 2 protons (multiplet) at 2.18; 1 proton (doublet) at 3.22; 2 protons (multiplet) at 4.5–4.8; 1 proton (OH disappearing in presence of trifluoroacetic acid) at 4.10 δ. The i.r.: bands at 3500 (broad); 1695 cm^{-1} (very strong).

Anal. Calcd. for $C_{20}H_{22}O_2S$: C, 73.59; H, 6.79; S, 9.82; O, 9.80. Found: C, 73.87; H, 6.80; S, 10.09; O, 10.21.

Mass spectrometry *m/e* 326 (molecular ion), 309, 308, 266, 265.

With mesityl oxide, at 60°, with a 2/1 ratio of CO/reducer and with a 15 min contact, the main product was a sulfide eluted in hexane by chromatography on Florisil. The n.m.r.: 6 protons (singlet) at 1.50; 3 protons (doublet,

Can. J. Chem. Downloaded from www.nrcresearchpress.com by 210.87.254.105 on 09/05/12
For personal use only.

Can. J. Chem. Downloaded from www.nrcresearchpress.com by 210.87.254.105 on 09/05/12
For personal use only.

TABLE 3
Characterization of polysulfide

Ketone	Sulfide	Analysis C (%) Calcd.	C (%) Found	H (%) Calcd.	H (%) Found	S (%) Calcd.	S (%) Found	Melting point (°C)	Mass spectra *m/e*
$C_6H_5COC_6H_5$		78.34	78.19	5.56	5.49	16.09	15.85	152	167 $((C_6H_5)_2CH)$, 199 $((C_6H_5)_2CHS)$ ~395 (molecular ion)
$C_6H_5CH_2\overset{O}{\overset{\|}{C}}CH_2C_6H_5$	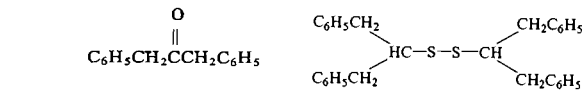	79.24	79.27	6.65	6.37	14.54	14.09	116–118	195 $(C_6H_5CH_2)_2CH$, 227 $(C_6H_5CH_2)_2CHS$ 454 (molecular ion)
	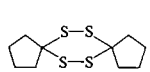	45.40	45.20	6.10	6.32	48.50	48.43	148	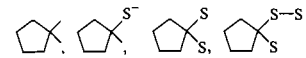 68 100 132 164 ~263 (molecular ion)
	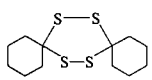	49.27	49.05	6.89	7.06	43.84	44.09	130	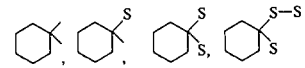 81 114 147 178 292 (molecular ion)

[1] 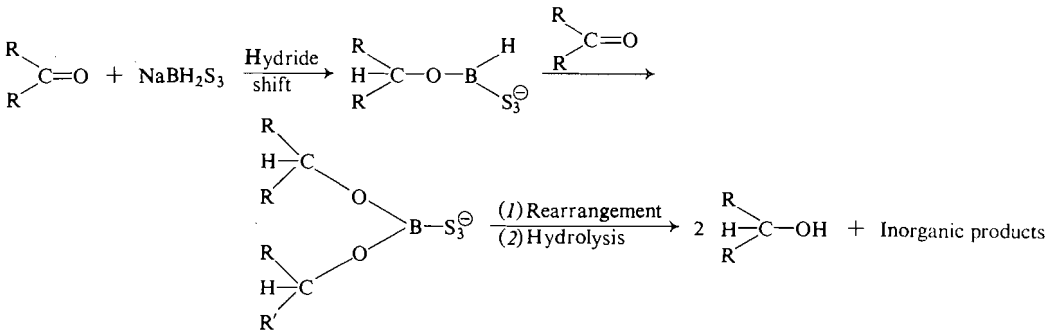

J = 1.3 c.p.s.) at 1.93; 1 proton (quadruplet, J = 1.3 c.p.s.) at 5.24 δ. The i.r.: band at 1640 cm^{-1}. Mass spectrometry: *m/e* 146 (molecular ion), 131.

5) Reduction with $NaBD_2S_3$

This reaction was performed on 1,3-diphenylacetone using the procedure described in section *1*. A quantitative yield of the corresponding alcohol was obtained with deuterium in the C-2 position. The i.r.: bands at 3550 (medium), 3400 (medium), 2150 cm^{-1} (very weak). No band in the 1700 cm^{-1} region. The n.m.r.: 1 proton at 2.18, 4 protons (singlet) at 2.60, 10 protons at 7.10 δ. Mass spectrum: *m/e* 213 (molecular ion), 122 (C_6H_5-CH_2CDOH).

Discussion

The reduction of aldehydic carbonyls with $NaBH_2S_3$ can be done by the two hydrogens on the sulfurated borohydride (2). When the steric hindrance around the ketone was not too pronounced, then both hydrogens became involved in the reduction as it was the case with aldehydes, if reaction time was long enough. But with sterically hindered ketones however, we have observed that generally the second hydrogen was rather difficult to involve in a reaction (Table 1). When 2/1 molar ratio of carbonyl over hydride was used, the yield of alcohol was always in the 50% range if steric hindrance was important. And when higher temperature was used, secondary products incorporating sulfur were obtained without increase in the yield of alcohol. The general reaction mechanism for the reduction when both hydrogen atoms on the reducer are involved, is described by eq. [1].

The first step in the course of the reaction must be a hydride shift, as shown by reduction with $NaBD_2S_3$. With this reagent, using 1,3-diphenylacetone as substrate, the corresponding alcohol incorporated deuterium in the C-2 position. The asymmetrical borate must be subject to a spontaneous disproportionation before hydrolysis, since we have been able to isolate the symmetrical ester very easily by petroleum ether extraction. Such a disproportionation is in accordance with the well known reactivity of unsymmetrical boric esters.

The reduction of ketones at room temperature led to very high yields of the corresponding alcohols, without any undesirable side reactions. Even in the case of sterically hindered ketones, the yield of alcohols remained high when equimolecular ratio of reducer and carbonyl was used. When high temperature (65°) was used, however, important yields of sulfurated products were noted. Presently, there is no simple explanation for the formation of a disulfide from open chain ketones and tetrasulfide from cyclic ketones (Table 1). The symmetrical tetrasulfides are reported in the literature (5) but their preparation from the ketone and ammonium polysulfide is very cumbersome. Except with acetone, the preparation of tetrasulfides from the corresponding ketones is reported as difficult and the yields described as low. Using sulfurated sodium borohydride, we observed that with cyclopentanone and cyclohexanone 40 to 50% of the starting ketone was transformed into the tetrasulfide, easily isolable by chromatography over Florisil. This new reaction is certainly an interesting alternate route to the tetrasulfides.

With unsaturated ketones we have been able to obtain very high yield of the corresponding allylic alcohols when the reaction was performed at low temperature (−30 to −50°). The yield of unsaturated alcohol was maximum for a 1/1 ratio of carbonyl and reducer. This reactivity was established with three ketones ($(CH_3)_2C{=}CH{-}CO{-}CH_3$, $C_6H_5CH{=}CH{-}CO{-}CH_3$, and cyclohexenone). A similar result can be obtained with $LiAlH_4$ (6) or $NaBH_4$ (7). When the reaction was performed at higher temperature and (or) with a 2/1 carbonyl/hydride ratio, the

Can. J. Chem. Downloaded from www.nrcresearchpress.com by 210.87.254.105 on 09/05/12
For personal use only.

yield of alcohol was lowered and sulfurated organic products were formed. The separation and purification of those secondary sulfurated products proved very difficult, because of their instability. It appears that the nature of those sulfurated derivatives depends very much on the structure of the starting ketone. In the case of *trans*-4-phenyl 3-butene 2-one, the sulfurated product proved to be the compound **1**, from the elementary analysis, n.m.r., and mass spectrometry. With mesityl oxide, a cyclic disulfide was obtained (compound **2**). Those structures illustrate the complexity of the sulfurated fraction, when the reduction is done at high temperature.

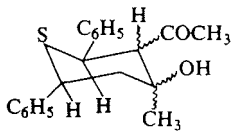

1

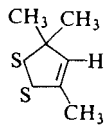

2

With β-diketones a mixture of ketol and diol was obtained and with one α-diketone, the diol only was observed. The results obtained with those reductions are reported in Table 1. With very hindered ketones such as camphor, no reduction was observed.

Those results illustrate the reactivity of sulfurated sodium borohydrides towards ketones. This reagent is more reactive than $NaBH_4$, without the overwhelming reducing capacity of $LiAlH_4$. We shall soon report the selective reducing capacity of $NaBH_2S_3$ in presence of nitro, nitrile, halogen, and ester groups. Under the mild conditions reported here for the reduction of ketone, those groups are not affected. And when the stereochemistry of the ketone is favorable, it is a stronger reducer than $NaBH_4$. Consequently, selective reductions different from those observed with $NaBH_4$ are possible. This will be shown in a study of selectivity of $NaBH_2S_3$ with steroids and other natural products. The reduction of conjugated ketone can be achieved at low temperature without 1,4-addition, giving a very good yield of the corresponding allylic alcohol. Finally, the secondary sulfurated products are of interest by themselves and easily accessible through this new reagent.

The authors thank the National Research Council of Canada and the Defence Research Board of Canada (grant 9530–30) for financial assistance.

1. J. M. LALANCETTE, A. FRECHE, and R. MONTEUX. Can. J. Chem. **46**, 2754 (1968).
2. J. M. LALANCETTE and A. FRECHE. Can. J. Chem. **47**, 739 (1969).
3. J. M. LALANCETTE and J. R. BRINDLE. Can. J. Chem. **48**, 735 (1970).
4. R. L. WERNER and K. G. O'BRIEN. Aust. J. Chem. **8**, 355 (1955).
5. (*a*) A. FREDGA. Acta Chem. Scand. **12**, 891 (1958). (*b*) B. MAGNUSSON. Acta. Chem. Scand. **13**, 1031 (1959).
6. N. G. GAYLORD. Reduction with complex metal hydrides. Interscience Publishers Ltd., New York, 1956. p. 170.
7. S. W. CHAIKIN and W. G. BROWN. J. Amer. Chem. Soc. **74**, 3022 (1952).

Can. J. Chem. Downloaded from www.nrcresearchpress.com by 210.87.254.105 on 09/05/12
For personal use only.

Can. J. Chem. Downloaded from www.nrcresearchpress.com by 210.87.254.42 on 09/05/12
For personal use only.

Stereochemical aspects of the synthesis of 4-benzoyl-1,3-dimethyl-4-phenylpiperidine from 1,3-dimethyl-4-piperidone

A. F. Casy, L. G. Chatten, and K. K. Khullar
Faculty of Pharmacy and Pharmaceutical Sciences, University of Alberta, Edmonton, Alberta

Received February 9, 1970

1,3-Dimethyl-4-piperidone reacts stereospecifically with potassium cyanide to give the *trans* (3-Me/4-OH) cyanohydrin. This was converted to 1,3-dimethyl-4-hydroxy-4-diphenylhydroxymethylpiperidine which rearranged with zinc chloride – acetic anhydride to *cis* (3-Me/4-Ph) 4-benzoyl-1,3-dimethyl-4-phenylpiperidine. The stereochemistry of all the products was established from proton magnetic resonance (p.m.r.) data and from the properties of diastereoisomeric 4-benzoyl-4-phenylpiperidines prepared from isomeric 4-cyano-1,3-dimethyl-4-phenylpiperidines of known configuration. Stable epimeric (+NH) hydrochlorides of 4-carboxylate and 4-carbethoxy analogues of the cyanohydrin of 1,3-dimethyl-4-piperidone were detected in DMSO-d_6 (p.m.r. evidence), and epimer formation in this series is discussed. The hot-plate activities in mice of some piperidine derivatives prepared during this work are reported.

Canadian Journal of Chemistry, 48, 2372 (1970)

1,3-Dimethyl-4-piperidone (**1**), the key intermediate for the synthesis of reversed esters of pethidine (**2**) (1) may be utilized for the preparation of 4-acyl analogues of pethidine by the sequence **1** → **3***a* through **3***d* → **4**. This synthesis has been reported by Unkovskii *et al.* (2) but the stereochemistry of the reactions was not established.

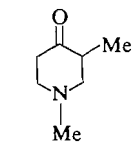

1

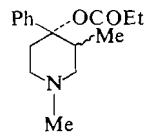

2

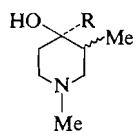

3

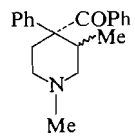

4

a R = CN
b R = CO_2H
c R = CO_2Et
d R = $C(OH)Ph_2$

We now report a proton magnetic resonance (p.m.r.) study of the same sequence and show how the results (*i*) aid the configurational assignment of the ketone **4** and all its intermediates, and (*ii*) provide information about factors governing the stability of protonated ($^+$NH) epimeric forms of substituted piperidines.

The reactions employed were essentially the same as those reported (2). Treatment of the piperidone **1** with potassium cyanide – hydrochloric acid or acetone cyanohydrin proceeded stereospecifically giving one of the two possible racemic diastereoisomeric cyanohydrins **3***a*. The isomeric purity of the product was supported by its p.m.r. spectrum which displayed a single set of sharply defined resonances. Two isomers form when 2-methylcyclohexanone is treated with acetone cyanohydrin and the major product (the result of preferred axial attack of cyanide upon the carbonyl group) has been shown to have a *trans* Me/OH configuration (3, 4). On these grounds the cyanohydrin **3***a* would be expected to have the configuration **5** (R = CN), an assignment which was subsequently confirmed. Hydrolysis of **3***a* by concentrated hydrochloric acid, and esterification of the product (**3***b*) with ethanol – sulfuric acid gave the isomerically pure ester **3***c*. This ester, with phenyl lithium, formed the diol **3***d* which rearranged under the influence of zinc chloride – acetic anhydride to give the phenyl ketone **4**. As there is no possibility of

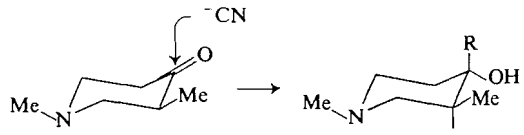

5

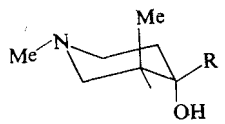

6

Can. J. Chem. Downloaded from www.nrcresearchpress.com by 210.87.254.42 on 09/05/12
For personal use only.

inversion of configuration at the C-4 asymmetric center during the reaction sequence outlined above, the configuration of the intermediates **3***b–d* must be identical with that of the starting cyanohydrin. The preferred conformation of the diol **3***d* is probably **6** rather than **5** (R = C(OH)-Ph_2) because of the bulk of the 4-diphenylhydroxymethyl substituent. The 3-methyl p.m.r. signal of the diol moved downfield when the basic center was protonated, and the magnitude of the shift (9 Hz at 60 MHz in DMSO-d_6) supports the axial environment of this group (5). Rearrangement of the diol **7** (shown in its preferred conformation) should yield the *cis* 3-Me/4-Ph phenyl ketone **8** since the same treatment of

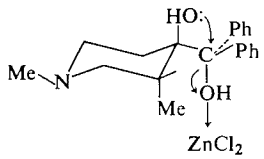

7

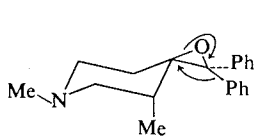

Intermediate epoxide

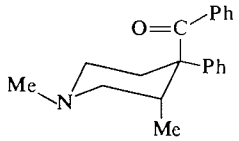

8

the tropane analogue **9** gives 3α-phenyl-3β-tropanyl phenyl ketone **10** (6), i.e. the phenyl substituent of the rearranged product has the same orientation as the diphenylhydroxymethyl group of the diol. These conclusions were confirmed by the identity of the ketone derived from the diol **3***d* and the authentic *cis* 3-Me/4-Ph ketone (see below); the sequence **7** through **8** depicts the probable steric course of the rearrangement. The large separation (69 Hz at 60

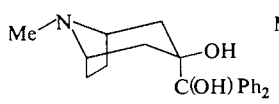

9

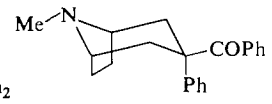

10

MHz) in chemical shift between the two OH resonances of the diol **3***d* hydrochloride in DMSO-d_6 shows that one of the groups is far more accessible to reagents (in this case to hydrogen bonding with the solvent) than the other.

The diastereoisomeric phenyl ketones **4** of known configuration were obtained by treating the *trans* and *cis* (3-Me/4-Ph) 4-cyano-4-phenylpiperidines (**11**) (5) with phenyl magnesium bromide and phenyl lithium respectively. Reaction of *trans*-**11** gave the ketone **4** directly, whereas *cis*-**11** yielded an intermediate ketimine

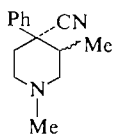

11

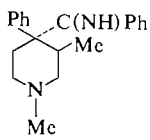

12

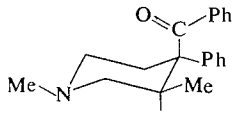

13

(**12**) which was converted to the corresponding ketone after hydrolysis with acid. The p.m.r. characteristics of the isomeric ketones **4** confirm their configuration and support **8** and **13** respectively as the preferred conformations of the *cis* and *trans* forms, as follows:

(*i*) In spectra of the free bases, the *trans* 3-methyl chemical shift is markedly lower field than the *cis* signal (chemical shifts differ by 18 Hz at 60 MHz in $CDCl_3$), in accord with the equatorial 3-methyl group of **13** being more subject to the magnetic anisotropic effects of the adjacent carbonyl function (7) than the axial group of **8**.

(*ii*) The chemical shift of the *cis* 3-methyl signal moves downfield by 18 Hz (at 60 MHz) upon base protonation in $CDCl_3$, whereas the corresponding *trans* signal is unaffected, in accord with axial 3-methyl in **8** being more deshielded by the $^+$NH function of the ring than is the more distant equatorial 3-methyl of **13** (8). The protonation shift of the *cis* 3-methyl signal was reduced to 9.5 Hz when DMSO-d_6 replaced $CDCl_3$ as solvent; this result is typical of piperidines carrying an axial 3-methyl substituent (5, 9).

An unusual feature of the p.m.r. spectra of the aminoacid **3***b* and aminoester **3***c* hydrochlorides in DMSO-d_6 was the appearance of a pair of 3-methyl doublets (Fig. 1) of similar intensities. This result demonstrates the separate existence of $^+$NH epimers which arise as a result of two modes (axial and equatorial) of proton uptake at the basic center. Normally, isomers of this nature are detected by the duplication of the N—R p.m.r. signal and/or nearby α-substituent signals, as in the case of pseudotropine (10) and 1,2-dimethylpyrrolidine (11). Epimer formation in salts of the tetrahydropyridines **14**, however, is manifested through the observation of duplicate *C*-methyl rather than N—R signals (12) as a result of the

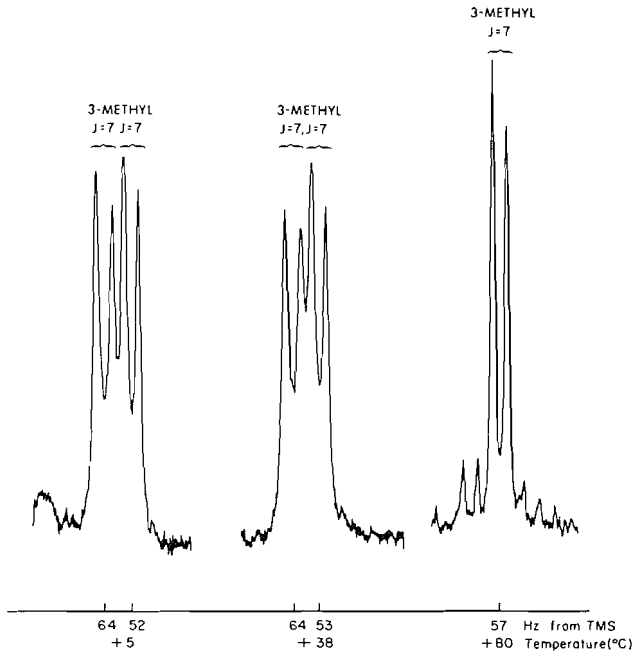

FIG. 1. Part of the 60 MHz p.m.r. spectra of *trans* (3-Me/4-OH) 1,3-dimethyl-4-hydroxypiperidine-4-carboxylate hydrochloride in DMSO-d_6 at various temperatures. At 38° the higher field 3-methyl doublet falls at τ 9.12 and that at lower field at τ 8.93. The authors thank Mr. J. Constantineau for these spectra which were recorded on a Jeolco spectrophotometer.

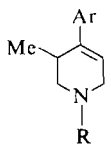

14

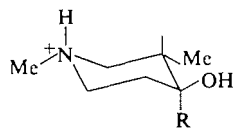

15

cis N-Me/3-Me

preferred conformations of the two epimers differing in 5-methyl rather than N—R orientation. The present cases must be further examples of this type.

The favored conformation of the *cis N*-Me/3-Me epimers is clearly **15** (R = CO_2H or CO_2Et). However, both conformers of the *trans* epimer **16** should be significantly populated because each entails two comparable 1,3-diaxial interactions involving ring substituents [note that the steric dimensions of OH and CO_2H or CO_2Et do not differ greatly (13)]. Axial 3-methyl in **16***b* is deshielded by the nearby charged nitrogen atom, hence the overall chemical shift of 3-methyl in the *trans* epimer will be lower field than that of 3-methyl in the *cis* epimer **15**, while chemical shift differences between the epimeric *N*-methyl signals are reduced to a point where separable signals are not observed. This interpretation is supported by

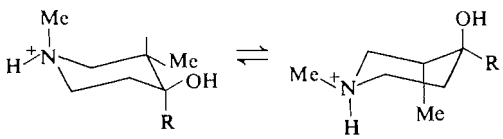

16*a* **16***b*

trans N-Me/3-Me

temperature studies. At higher temperatures (giving faster rates of proton exchange) the duplicate 3-methyl signals merge to a single doublet of an intermediate chemical shift, while at a lower temperature (slower rate of proton exchange) the duplicate signals move farther apart (Fig. 1). The 3-methyl signal is not duplicated in spectra of the hydrochlorides **3***a* and *d*. In the former, steric requirements of OH are substan-

Can. J. Chem. Downloaded from www.nrcresearchpress.com by 210.87.254.42 on 09/05/12
For personal use only.

Can. J. Chem. Downloaded from www.nrcresearchpress.com by 210.87.254.42 on 09/05/12
For personal use only.

tially greater than the cyano function (13) hence populations of the *trans* epimer **16***b* (R = CN) in which non-bonded interactions of this group are relieved while those of OH are increased, will be low. When R is much larger than OH, as in **3***d*, the *trans* epimer **16***b* is favored by a large factor and the p.m.r. spectrum of this salt provides no evidence of conjugate acid isomers. Evidence for the axial environment of 3-methyl in the diol **3***d* hydrochloride has already been mentioned.

Some of the compounds prepared during this work were screened for pharmacological activity in mice by the hot-plate test, a procedure which detects narcotic analgesics and other types of central nervous system (c.n.s.) depressant (14). The *cis*-3-Me/4-Ph propionyl ketone **17** (5) had an ED_{50} value of 4.0 mg/kg and is thus somewhat more potent than pethidine (ED_{50} 4.7 mg/kg);

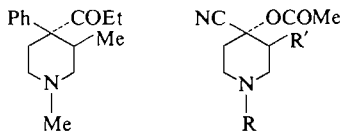

17 **18**

a R = $(CH_2)_2$Ph; R′ = H
b R = Me; R′ = H
c R = R′ = Me

the *cis* 4-benzoyl analogue (**8**) (ED_{50} 17.5 mg/kg) was much less active. 4-Acetoxy-4-cyano-1-phenethylpiperidine (**18***a*), derived from 1-phenethyl-4-piperidone, was significantly active in this test (ED_{50} 6.3 mg/kg), a result which confirms its reported c.n.s. depressant properties (15). The analogues **18***b* and *c* had ED_{50} values of 5.06 and 8.9 mg/kg respectively. Thus the usual rise in potency which follows replacement of *N*-methyl by *N*-phenethyl in pethidine and its congeners (16) does not occur in the 4-cyanopiperidines (**18**); it is likely, therefore, that their c.n.s. depressant effects are brought about in a different manner to those of narcotic analgesics.

Experimental

The p.m.r. spectra were recorded on a Varian A-60 spectrometer using $CDCl_3$ or DMSO-d_6 as solvent. Chemical shifts are expressed in τ units with TMS as standard. Infrared (i.r.) spectra of salts were recorded as Nujol mulls on a Beckman IR-10 spectrometer. Elemental analyses were by Drs. Weiler and Strauss, Oxford, England and by the Chemistry department, University of Alberta, Edmonton, Alberta.

1,3-Dimethyl-4-piperidone Cyanohydrin (3a)

1,3-Dimethyl-4-piperidone (17) (12.7 g) was added to a cold, stirred, solution of potassium cyanide (7.2 g) in water (15 ml) during 15 min. The mixture was made slightly acid with dilute hydrochloric acid, then treated with a large excess of potassium carbonate and extracted with ether. The ether was evaporated and the solid residue recrystallized from ethyl acetate to give the cyanohydrin **3***a* (10.3 g), m.p. 89–91°, lit. (2) 88–90°. It formed *hydrochloride*, m.p. 158–159° from ethanol.

Anal. Calcd. for $C_8H_{15}ClN_2O$: C, 50.4; H, 7.9. Found: C, 50.5; H, 7.7.

The total cyanohydrin was identical with the product obtained from the piperidone **1** and acetone cyanohydrin (2), and its p.m.r. spectrum in $CDCl_3$ displayed a sharply defined 3-methyl (doublet τ 8.9, *J* 6.0 Hz) and *N*-methyl (singlet τ 7.72) resonance. The 3-methyl resonance of **1** hydrochloride was a single doublet (τ 8.95, *J* 6.0 Hz) in DMSO-d_6.

cis(3-Me/4-Ph) 4-Benzoyl-1,3-dimethyl-4-phenylpiperidine (4)

The cyanohydrin **3***a* was converted to **4** by the reported procedure (2). 3-Methyl p.m.r. characteristics of the intermediate aminoacid **3***b* hydrochloride, m.p. 192–193°, lit. (2) 192–193°, are given in Fig. 1. The aminoester **3***c* hydrochloride, m.p. 157.5–158.8°, lit. (2) 148–150°, had a p.m.r. spectrum in DMSO-d_6 which displayed duplicate 3-methyl signals (doublets τ 8.97 and 9.15, *J* 7.0 Hz of similar intensities); the OCH_2Me (triplets centered at τ 8.78) and OCH_2Me (quartets centered at τ 5.99) signals were also in duplicate (separation ~2 Hz). No duplication of these signals was seen in the spectrum of this salt in DMSO-d_6–D_2O. The ester **3***c* (5.8 g) and phenyl lithium, prepared from bromobenzene (17.6 g) and lithium (1.6 g), gave the diol **3***d* hydrochloride (7.9 g), m.p. 258–259°, lit. (2) 259–259.5°; p.m.r. characteristics in DMSO-d_6: singlets τ 4.15 and 5.28 (OH) and 7.33 (*N*-Me), doublet τ 8.93, *J* 7.5 Hz (3-Me) (τ 9.08 in corresponding base). The diol **3***d* was rearranged with a mixture of zinc chloride and acetic anhydride to give an 82% yield of the *cis* phenyl ketone **4**, m.p. 115–117°, lit. (2) 118.5–120°. It formed a *hydrochloride*, m.p. 275–275.5° from ethanol, ν_{max} 1700 cm^{-1} (C=O).

Anal. Calcd. for $C_{20}H_{24}ClNO$: N, 4.25. Found: N, 4.25.

The p.m.r. characteristics of the product (base and hydrochloride) were identical with those of *cis* **4** prepared unambiguously (see below).

Conversion of the Diastereoisomeric 4-Cyanopiperidines (11) to cis and trans (3-Me/4-Ph) 4

Trans 4-cyano-1,3-dimethyl-4-phenylpiperidine (5) (5.4 g) in toluene (100 ml) was added to a Grignard reagent prepared from bromobenzene (10.9 g), magnesium (1.8 g) and ether (100 ml). The ether was removed by distillation and the toluene suspension heated under reflux for 10 h, then cooled and acidified with aqueous hydrochloric acid. The toluene was separated and extracted with the same acid, and the base (6.1 g), ν_{max} 1675 cm^{-1} (C=O), recovered from the combined aqueous fractions. This product was acidified with ethanolic hydrogen chloride to give the *trans (3-Me/4-Ph) phenyl ketone* **4** *hydro-*

chloride, m.p. 231–235° from acetone as a monohydrate, ν_{max} 3100–3600 (H_2O), 1695 cm^{-1} (C=O); p.m.r. characteristics in $CDCl_3$: singlets τ 2.62 and 2.5 (major and minor singlet features of aromatic multiplet), doublets τ 7.18, *J* 5.0 Hz (NH*Me*) and 8.97, *J* 7.5 Hz (3-Me).

Anal. Calcd. for $C_{20}H_{24}ClNO.H_2O$: C, 69.1; H, 7.5. Found: C, 69.3; H, 7.3.

Similar treatment of the *cis* 4-cyanopiperidine (**11**) (4.9 g), using phenyl lithium prepared from bromobenzene (9.4 g) and lithium (0.8 g) gave the *ketimine* **12** (6.3 g), m.p. 116–118° from ligroin, ν_{max} 3140 (HN) and 1620 cm^{-1} (C=N).

Anal. Calcd. for $C_{20}H_{24}N_2$: N, 9.6. Found: N, 9.8.

It formed a *dihydrochloride*, m.p. 262.5–264.5° from ethanol, ν_{max} 1665 cm^{-1} ($C=\overset{+}{N}H$) (18).

Anal. Calcd. for $C_{20}H_{26}Cl_2N_2$: N, 7.7. Found: N, 7.4.

The ketimine **12** was heated with excess of 10% aqueous hydrochloric acid for 12 h. The m.p. of the base (115–117° from ligroin) recovered after this treatment, and of the derived hydrochloride (274–275°) were undepressed when mixed with the appropriate form of the phenyl ketone **4** obtained from the diol **3***d*. The p.m.r. characteristics of the phenyl ketones obtained from *cis*-**11** and -**3***d* were identical, details being as follows: (*a*) base in $CDCl_3$: singlets τ 2.6 and 2.72 of similar intensity (main feature of aromatic signal) and 7.83 (NMe), doublet τ 9.27, *J* 7.5 Hz (3-Me); (*b*) hydrochloride in $CDCl_3$: closely placed singlets τ 2.58 and 2.62 (main feature of aromatic signal), and doublets τ 7.17, *J* 5.0 Hz ($H\overset{+}{N}Me$) and 8.97, *J* 7.5 Hz (3-Me).

*4-Acetoxy-4-cyano-1,3-dimethylpiperidine (**18***c*) and Related Esters*

A mixture of the cyanohydrin **3***a* (3.1 g), acetic anhydride (6 ml), and pyridine (3 ml) was heated at 120° for 3 h. Volatile materials were removed by evaporation under reduced pressure, and the residue dissolved in ether and filtered. The filtrate was evaporated to yield the ester **18***c* (4.1 g) which gave a *hydrochloride*, m.p. 234.5–235° from ethanol–ether, ν_{max} 1755 cm^{-1} (C=O).

Anal. Calcd. for $C_{10}H_{17}ClN_2O_2$: C, 51.5; H, 7.3. Found: C, 51.3; H, 7.3.

The analogues **18***a*, hydrochloride m.p. 257–258°, lit. (15) 258.5°, and **18***b* were prepared similarly from cyanohydrins derived from 1-phenethyl and 1-methyl-4-piperidone respectively. The ester **18***b* gave a *hydrochloride*, m.p. 191–192° from ethanol–ether, ν_{max} 1755 cm^{-1} (C=O).

Anal. Calcd. for $C_9H_{15}ClN_2O_2$: C, 49.4; H, 6.9. Found: C, 49.2; H, 7.2.

The authors thank the Medical Research Council of Canada for financial support and Dr. E. L. May, National Institute of Health, Bethesda, Maryland, for the pharmacological data.

1. R. A. Hardy, Jr. and M. G. Howell. *In* Analgetics. G. Destevens, *editor*. Academic Press, New York, 1965.
2. B. V. Unkovskii, G. S. Gusakova, and I. A. Mokhir. J. Gen. Chem. (U.S.S.R.), **30**, 3883 (1960).
3. I. N. Nazarov, A. V. Kamernitzky, and A. A. Akhrem. J. Gen. Chem. (U.S.S.R.), **28**, 1458 (1958).
4. A. V. Kamernitzky and A. A. Akhrem. Bull. Acad. Sci. U.S.S.R. 740 (1959); A. V. Kamernitzky and A. A. Akhrem. Tetrahedron, **18**, 705 (1962).
5. A. F. Casy, L. G. Chatten, and K. K. Khullar. J. Chem. Soc. (C), 2491 (1969).
6. M. R. Bell and S. Archer. J. Amer. Chem. Soc. **82**, 151, 4638 (1960).
7. G. J. Karabatsos, G. C. Sonnichsen, N. Hsi, and D. J. Fenoglio. J. Amer. Chem. Soc. **89**, 5067 (1967).
8. A. F. Casy. Tetrahedron, **22**, 2711 (1966).
9. M. A. Iorio and A. F. Casy. J. Chem. Soc. (C), 135 (1970).
10. G. L. Closs. J. Amer. Chem. Soc. **81**, 5456 (1959).
11. J. K. Becconsall, R. A. Y. Jones, and J. McKenna. J. Chem. Soc. 1726 (1965).
12. A. F. Casy, A. H. Beckett, M. A. Iorio, and H. Z. Youssef. Tetrahedron, **21**, 3387 (1965).
13. E. L. Eliel, N. L. Allinger, S. J. Angyal, and G. A. Morrison. Conformational analysis. John Wiley and Sons, Inc., New York, 1965.
14. A. H. Beckett and A. F. Casy. *In* Progress in medicinal chemistry. Vol. 2. G. P. Ellis and G. B. West, *editors*. Butterworths, London, 1962.
15. N. J. Harper and S. E. Fullerton. J. Med. Pharm. Chem. **4**, 297 (1961).
16. P. A. J. Janssen and N. B. Eddy. J. Med. Pharm. Chem. **2**, 31 (1960).
17. D. R. Howton. J. Org. Chem. **10**, 277 (1945).
18. A. F. Casy and M. M. A. Hassan. J. Chem. Soc. (B), 631 (1969).

Can. J. Chem. Downloaded from www.nrcresearchpress.com by 210.87.254.42 on 09/05/12
For personal use only.

Can. J. Chem. Downloaded from www.nrcresearchpress.com by 210.87.254.6 on 09/05/12
For personal use only.

Addition of nitromethane to L-idose. Stereochemistry of the Fischer–Sowden reaction

JAN KOVÁŘ[1] AND HANS H. BAER
Department of Chemistry, University of Ottawa, Ottawa, Canada

Received February 23, 1970

The addition of nitromethane to aldoses giving 1-deoxy-1-nitroalditols (the Fischer–Sowden reaction) was extended to L-idose. Both epimeric products, 1-deoxy-1-nitro-L-*glycero*-D-*ido*-heptitol (**1**) and 1-deoxy-1-nitro-L-*glycero*-D-*gulo*-heptitol (**2**), were isolated in crystalline form, and **2** was shown to preponderate. The stereoselectivity is evaluated by a comparison of literature data on the Fischer–Sowden reaction of other hexoses, and attention is drawn to the importance of the C-3 configuration in the hexose, which appears to be the main factor influencing the ratio of epimers produced. An explanation in conformational terms is offered.

Canadian Journal of Chemistry, **48**, 2377 (1970)

Introduction

In the Fischer–Sowden nitromethane synthesis, two 2-epimeric 1-deoxy-1-nitroheptitols arise from a given hexose (1, 2). The five hexoses from which either one or both of the expected nitroheptitols have been obtained in crystalline form are D-altrose (3), D-galactose (4, 5), D-glucose (6, 7), D-mannose (8, 9), and D-talose (10). A survey of the reported preparative yields of epimeric nitro alcohols (or products derived thereof) confirms the expectation that the nitromethane addition to hexoses proceeds with some degree of stereoselectivity. Although the observed values for these selectivities are not large and, moreover, may not lend themselves to meaningful quantitative comparisons because of varying reaction conditions to which they refer, it nevertheless is interesting to attempt at least a qualitative rationalization of the stereochemistry of the Fischer–Sowden reaction. To this end, the behavior of D-idose was felt to merit an investigation and comparison with that of the aforementioned sugars, the reason being pointed out in the Discussion.

Results

Although D-idose can be prepared (11), we decided for practical reasons to study the nitromethane synthesis with L-idose which appeared to be more conveniently available (12, 13). When a 10% solution of L-idose in methanol was allowed to react for 1 h at room temperature, with a 10 *M* excess of nitromethane in the presence of 1 equ. of sodium methoxide, two crystalline deoxynitroheptitols were produced. The less soluble epimer, m.p. 146.5–147°, which was levorotatory ($[\alpha]_D$ −6.7°, $[\alpha]_{365}$ −177°), was isolated in 23% yield; and the more soluble epimer, m.p. 123–124°, which was dextrorotatory ($[\alpha]_D$ +2.8°, $[\alpha]_{365}$ +149°), was isolated in 28% yield. Assignment of configurations could readily be made on the basis of the optical rotatory dispersions (o.r.d.) according to Satoh *et al.* (14). The former compound exhibited a negative Cotton effect, indicating the C-2 hydroxyl group to be on the left-hand side in the Fischer projection formula, and hence it was 1-deoxy-1-nitro-L-*glycero*-D-*ido*-heptitol (**1**), whereas the latter compound showed a positive Cotton effect and therefore was the L-*glycero*-D-*gulo* epimer (**2**).

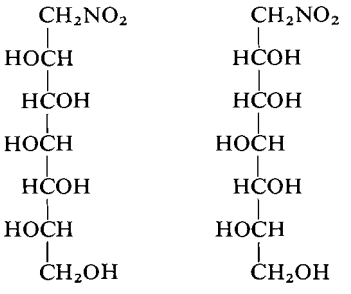

1 **2**

The main proportion (ca. 90%) of the isolable, crude mixture of **1** and **2** had been deposited directly from the reaction solution, predominantly as the sodium nitronates but partly also as the free nitro compounds. The remainder was obtained from the mother liquor following decationization. Spectroscopic and colorimetric analysis revealed that the noncrystallizable residue of the reaction contained 5–10% of hexose

[1]Visiting scientist on leave of absence (1968–1969) from the Laboratory of Monosaccharides, Institute of Chemical Technology, Prague, Czechoslovakia.

TABLE 1

Crude product mixtures isolated from 72.5 mg of L-idose

Time (min)	Weight (mg)	In water $[\alpha]_D^\circ$	In water $[\alpha]_{365}^\circ$	Nitro compounds (%)*
20	70	−12.5	−26.1	24–31
40	80	−9.2	−12.2	35–45
180	86	−2.7	+22.5	61–75

*Values calculated from optical densities at 270 nm (in water), the lower and upper limits being obtained with ε 63 (for **1**) and ε 50 (for **2**), respectively.

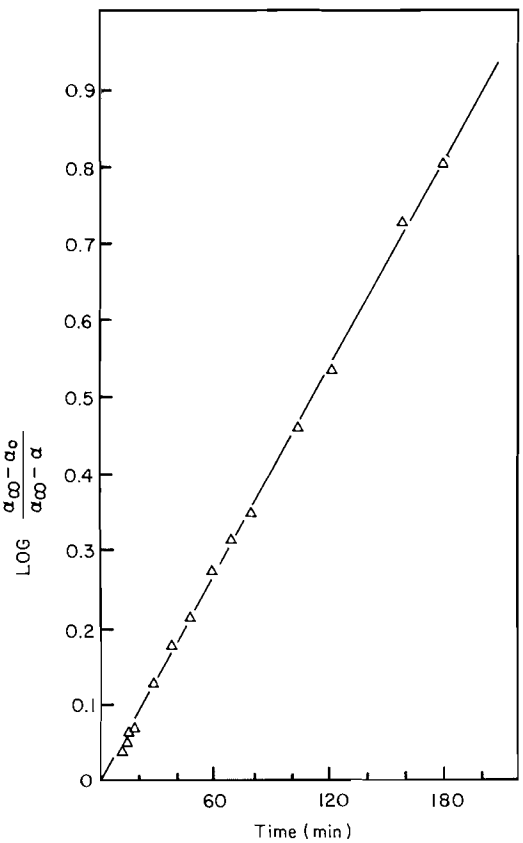

FIG. 1. First-order reaction rate of the addition of nitromethane to L-idose.

(presumably unreacted L-idose[2]) along with unidentified nitro carbohydrate material. No heptoses could be detected by means of the Dische test with cysteine – sulfuric acid (16), and this indicated that the work-up procedure employing deionization did not entail partial decomposition of heptitol nitronates by the Nef reaction.

The reaction half-time of the nitromethane addition under the conditions mentioned above was less than 10 min. In a series of experiments, the *crude* products crystallizing from the reaction solution were isolated after 10, 20, and 30 min, respectively, and amounted to 68, 70, and 85% of the theoretical yield (after conversion into mixtures of free **1** and **2**). Fractional crystallization then furnished pure **1** and **2** in the ratios 0.9 (10 min), 0.5 (20 min), and 0.6 (30 min). From the mother liquor of a run with a 2 h reaction time, **1** and **2** were also obtained in a ratio of 0.6.

When the reaction was performed at a lower initial concentration (0.04 *M*) in both L-idose and base but still with a large excess of nitromethane (1.5 *M*), the mixture stayed homogeneous throughout, and the reaction rate could be determined polarimetrically. The time-dependence of the rotational change obeyed the first-order law and revealed a reaction half-time of 67 min (Fig. 1).[3] Aliquots were worked-up at intervals (see Table 1). It is seen that after 20 and 40 min the $[\alpha]_D$-value of the isolated material was more negative than that of the pure levorotatory heptitol **1** (and therefore, more negative than that of any mixture consisting solely of **1** and **2**), which reflected the presence of starting L-idose ($[\alpha]_D$ −15.5°)[4] and was in accord with ultraviolet (u.v.) absorption data that gave a rough

[2]Only a trace of ketose was found. It is known (15) that idose is easily isomerized by base to sorbose, and we have convinced ourselves by experiment that this isomerization does take place in methanol – sodium methoxide at room temperature. However, the isomerization is slower than the nitromethane addition and moreover, it is probably retarded further by the buffer action of nitromethane present in excess.

[3]In the presence of a large excess of nitromethane, the concentration of one of the partners in the rate-determining, bimolecular addition step, namely the methanenitronate ion, can be regarded as constant, so that a pseudomonomolecular reaction rate is observed. However, the rate constant will be proportional to the methanenitronate concentration, and hence experiments differing in base concentration will show different half-times.

[4]Small amounts of L-sorbose ($[\alpha]_D$ − 43.4°), if present, would have influenced the rotation in the same direction; see also footnote 2.

Can. J. Chem. Downloaded from www.nrcresearchpress.com by 210.87.254.6 on 09/05/12
For personal use only.

TABLE 2
Deoxynitroheptitols from hexoses

Starting hexose	Configuration of deoxynitroheptitols: A (C-2 is D)	B (C-2 is L)	Ratio A:B	Reference
D-Glucose	D-*glycero*-D-*gulo*	D-*glycero*-D-*ido*	1.25*	(7)
D-Galactose	D-*glycero*-L-*manno*	D-*glycero*-L-*gluco*	3.3†	(5)
D-Mannose	D-*glycero*-D-*galacto*	D-*glycero*-D-*talo*	3.7†	(8)
D-Talose	D-*glycero*-L-*altro*	D-*glycero*-L-*allo*	1.5*†	(10)
D-Altrose	D-*glycero*-D-*gluco*	D-*glycero*-D-*manno*	0.25‡	(3)
D-Idose	D-*glycero*-L-*ido*	D-*glycero*-L-*gulo*	0.6§	This work

*Based on vapor-phase chromatography of derived products.
†Based on crystalline nitroheptitols isolated.
‡Based on derived products isolated.
§Based on nitroheptitols isolated in the enantiomeric L-*glycero* series.

indication of the extent of nitroheptitol formation. After 180 min, when 84% of the total change in rotation had occurred, the isolated crude product contained not more than 75% of nitroheptitols. An estimate of the ratio of epimers (**1**:**2**) existing at that point was obtained from the specific rotation at 365 nm (at which wavelength both epimers show large absolute values). Thus the rotation of the reaction mixture, $[\alpha]_{365}$ +22.5°, would indicate a ratio of 0.64 if the mixture consisted solely of **1** and **2** but, because of the presence of at least 25% of levorotatory non-nitro sugar, the actual ratio can be assumed to have an even smaller value.[5] Qualitatively, this result agrees quite well with the aforementioned, preparative experiments and it can therefore be stated, in summary, that 1-deoxy-1-nitro-L-*glycero*-D-*gulo*-heptitol (**2**) is the preponderant epimer arising from L-idose in the Fischer–Sowden reaction.

Discussion

Concerning the steric course of the Fischer–Sowden synthesis one may assume that, under the conditions usually employed, the epimeric product ratio is subject to kinetic control which has been found to be operative in several examples of the closely related nitromethane cyclization of sugar dialdehydes (2). Indeed, in the present case the preponderant product (**2**) is what appears to be the thermodynamically less stable epimer.[6] In trying to assess the main factors that determine the product distribution when the methanenitronate ion approaches C-1 of the aldose, one might well have thought of attaching special significance to the configuration at the neighboring C-2. However, the experimental results assembled in Table 2 do not bear this out. Thus, the configuration at C-2 in D-glucose and D-galactose is opposite to that in D-mannose and D-talose, yet the nitroheptitols produced in preponderance from these four sugars all have the same configuration (D) at the new asymmetric center. By contrast, D-altrose gives predominantly the nitroheptitol having the L-configuration at C-2. The same can now be said for D-idose, by translating our results with L-idose into the enantiometric series (Table 2). A feature shared by D-altrose and D-idose, and distinguishing them from the first four aldoses in Table 2, is the configuration at C-3, and this provides a clue to a qualitative understanding of the stereochemistry involved (see below). It remains to be seen whether D-allose and D-gulose when reacting with nitromethane follow the same pattern as their 2-epimers.[7] The results available to date show a parallel to the Kiliani cyanohydrin synthesis in which the nitriles having 2,4-*threo* hydroxyl groups predominate normally (18) even though they do not do so under all conditions (19). It is note-

[5]Fractional crystallization furnished **1** and **2** in yields of 6 and 35%, respectively, but these figures do not necessarily represent the true product ratio accurately.

[6]The opposite situation, which seems to occur in some of the other examples, does not in itself signify thermodynamic control.

[7]We have tried the reaction with D-allose but have not yet been able to isolate crystalline products. Efforts in this direction are continued. As far as we are aware, nitromethane has never been added to D-gulose; however, addition of nitroethanol followed by Nef reaction afforded (17) D-*glycero*-L-*galacto*-octulose in 9% yield, and the D-*glycero*-L-*talo* epimer in 4% yield. This agrees with assuming a preferential formation of the L-configuration at C-1 of D-gulose.

Can. J. Chem. Downloaded from www.nrcresearchpress.com by 210.87.254.6 on 09/05/12
For personal use only.

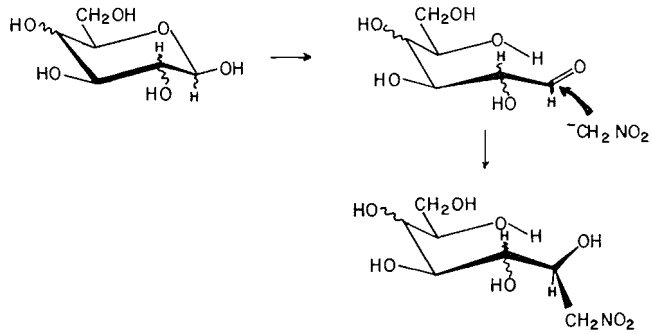

FIG. 2. Preferred pathway of the addition of nitromethane to D-glucose, D-galactose, D-mannose, and D-talose.

worthy in this connection that the rule does not hold in the Kuhn synthesis of α-aminonitriles (20).

With regard to the configuration at C-4 of the hexoses, Table 2 shows clearly that, in a given pair of 4-epimers, this configuration may influence the product ratio but not to the extent of inverting it. Thus the influence exerted by the orientation of the C-4 substituent is similar to that of the C-2 substituent, and both of these factors are surpassed in significance by the configuration at C-3.

The dominant role played by the C-3 configuration in directing the stereochemical course of the reaction suggests that this course is correlated with the conformational stability of the substrate. One may consider the favored conformation of the *aldehydo* form of the sugar in the transition state of the nitromethane addition (i.e. during the approach of the methanenitronate anion) to resemble a pyranose chair conformation (2). Assuming that the preferred rotational orientation of the carbonyl group is similar for each *aldehydo* hexose, and is as depicted in Fig. 2, attack by the nitronate anion from the less hindered, front side will generate the D-configuration in the aldehydic carbon atom of any aldose molecule adopting the *C1*(D) conformation in the transition state.[8] On the other hand, the L-configuration will arise when the molecule adopts the inverted chair conformation, *1C*(D) (Fig. 3). Since chair inversion is facile in D-idose and D-altrose due to the absence of nonbonded 3,5-diaxial substituent interaction in the *1C*(D) form, whereas it is hindered by such interaction in the other hexoses considered here, the stereochemical trend observed in the Fischer–Sowden reaction appears plausible.[9]

Experimental

Optical rotations were measured with a Perkin–Elmer 141 automatic polarimeter at about 25°. The o.r.d. curves were obtained with a Jasco ORD/UV-5 instrument. The u.v. and visible spectra were recorded on a Perkin–Elmer 202 spectrometer. Paper chromatography was performed by the descending technique using Whatman No. 1 paper, 1-butanol–ethanol–water (40:11:19, v/v) as irrigant, and ammoniacal silver nitrate solution as spray reagent; R_G is the mobility relative to D-glucose. Evaporations were carried out *in vacuo* at 35–40° (bath). Reagent grade methanol was dried with magnesium methoxide and redistilled before use in reactions. L-Idose was a chromatographically homogeneous, nearly colorless syrup, R_G 1.41–1.44, $[\alpha]_D$ − 15.5° (*c* 1.5, in water), obtained (13) from crystalline 1,2-*O*-isopropylidene-β-L-idofuranose; it was dried to constant weight (at 25° *in vacuo*) and stored in a refrigerator.

[8]Recently, Zanlungo *et al.* (21) also postulated a chair-like conformation, as a transient arrangement, for *aldehydo* hexoses and their ammonia adducts that arise as reaction intermediates when penta-*O*-acylhexopyranoses are subjected to ammonolysis. However, the authors (21) assume that the favored direction of attack (by the ammonia molecule) on the carbonyl carbon is from the rear, whereas we are contending that such an approach is impeded by the O-5, as is best seen by viewing a model from top:

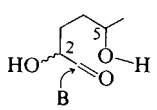

[9]It has been suggested (22) that the preferential formation of deoxynitroalditols with *threo* relationship of the 2,4-hydroxyl groups is due to freedom from eclipsing of these hydroxyls in the zig-zag conformation of the products. However, this explanation presupposes product stability as the decisive factor. It furthermore presupposes that the zig-zag conformation is indeed preferred by the acyclic products. Recent studies (23–25) have demonstrated that this concept is not valid for all acyclic carbohydrate derivatives, for the very reason of eclipsing of β-substituents in certain configurations. On the basis of these studies (23–25) one may predict that none of the deoxynitroheptitols produced from glucose, talose, altrose and idose prefer the zig-zag conformation. Among alternative conformations (e.g., twisted and "sickle" forms) there are some which, according to molecular models, appear more suitable to accommodate 2,4-*erythro* than 2,4-*threo* hydroxyl groups.

Can. J. Chem. Downloaded from www.nrcresearchpress.com by 210.87.254.6 on 09/05/12
For personal use only.

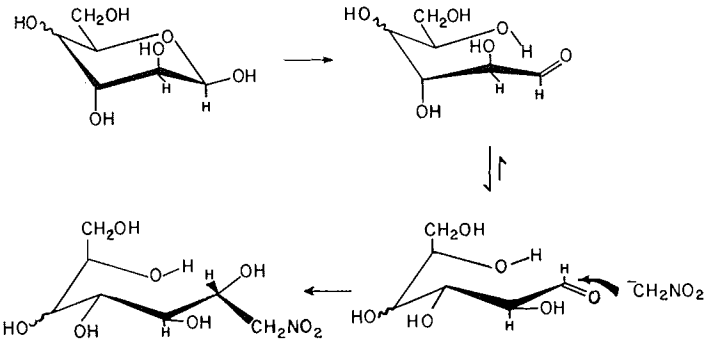

FIG. 3. Preferred pathway of the addition of nitromethane to D-altrose and D-idose.

TABLE 3

Specific rotations ([α]°) of **1** and **2**

Wavelength (nm)	589	578	546	436	365
Compound **1**					
(*c* 1, in H_2O)	−6.7	−7.2	−8.6	−30.4	−177
(*c* 1, in MeOH)	+9.2	+9.9	+9.4	−8.2	−170
(*c* 0.5, in 0.5 *N* NaOH*)	+22.3	+23.8	+28.4	+57	+116
Compound **2**					
(*c* 1, in H_2O)	+2.8	+3.4	+5.1	+24.2	+149
(*c* 1, in MeOH)	+11.9	+12.8	+15.6	+47.3	+215
(*c* 0.5, in 0.5 *N* NaOH*)	−7.9	−8.1	−8.8	−16.0	−32.3

*Rotations of alkaline solutions change with time, and the values given are extrapolated to zero time.

Reaction of L-*Idose with Nitromethane*

Preparation of 1-Deoxy-1-nitroheptitols ***1*** *and* ***2***

To a solution of L-idose (218 mg, 1.21 mmole) in methanol (1.0 ml) and nitromethane (0.65 ml, 12 mmole) was added 1.20 ml of 1.05 *N* methanolic sodium methoxide solution. A white precipitate began to form almost immediately. After 60 min, when the precipitate did not visually increase anymore, it was filtered off with exclusion of moisture, washed three times with 0.5 ml of cold methanol containing 9% nitromethane, and dissolved at once in 65 ml of the same solvent mixture. The solution was deionized by treatment with Amberlite IR-120 (H^+) (5 ml, methanol-washed). Evaporation furnished a crystalline product (218 mg) melting at 117–136° when washed with a small amount of ethanol. It consisted of approximately 40% nitroheptitol **1** and 60% nitroheptitol **2**; $[\alpha]_{365}$ + 15.9° (in water), λ_{max} 283 nm (ε 70, in water). An additional 30 mg of a similar, crystalline mixture was obtained from the mother liquor of the reaction after dilution with methanol and deionization; the total yield, therefore, was 85%. (Alkalimetric microtitration of a small aliquot of the mother liquor indicated that the nitronate precipitate which had been removed must have contained 10% less than the stoichiometric amount of sodium and hence, may have contained some free nitroheptitol.)

Fractional recrystallization of the heptitol mixture from ethanol yielded 66 mg (23%) of the less soluble L-*glycero*-D-*ido* epimer **1** and 83 mg (28%) of the more soluble L-*glycero*-D-*gulo* epimer **2**. There remained a noncrystallizable oil (128 mg) which according to its u.v. spectrum (λ_{max} 270 and 207 nm in H_2O, 244 nm in dilute NaOH) contained nitro carbohydrate material. Semiquantitative colorimetry with cysteine – sulfuric acid (16) revealed the presence of no more than 10% of aldohexose and a trace of ketohexose. No heptose was evident.

The *epimer* ***1*** showed m.p. 146.5–147°; R_G 1.48–1.52; λ_{max} 270 (ε 63) and 206 nm (ε 4000) in water; λ_{max} 244 nm (ε 8000) in 0.005 *N* NaOH. For specific rotations see Table 3. The o.r.d. in water, *c*, 0.2625: $[\phi]_{365}$ − 392, $[\phi]_{338}$ − 607 (first extremum), $[\phi]_{312}$ 0, $[\phi]_{290}$ + 910° (negative Cotton effect).

The *epimer* ***2*** showed m.p. 123–124°; R_G 1.66–1.70; λ_{max} 270 (ε 50) and 206 nm (ε 4000) in water; λ_{max} 244 nm (ε 8000) in 0.005 *N* NaOH. For specific rotations see Table 3. The o.r.d. in water, *c*, 0.2725: $[\phi]_{365}$ + 325, $[\phi]_{338}$ + 540 (first extremum), $[\phi]_{308}$ 0, $[\phi]_{290}$ − 585° (positive Cotton effect).

Anal. Calcd. for $C_7H_{15}NO_8$ (241.2): C, 34.85; H, 6.27; N, 5.81. Found for **1**: C, 35.10; H, 6.44; N, 5.95. Found for **2**: C, 34.94; H, 6.13; N, 5.94.

A nitromethane addition starting with 262 mg of L-idose and using the same proportions of solvent and reagents as the previous experiment was divided in three parts. The nitronate deposits were collected after 10, 20, and 30 min, respectively, and furnished, after work-up as described, crude mixtures of **1** and **2** in 68, 70, and 84% yield. Fractional recrystallization from ethanol gave 15, 16.5, and 13% of **1** plus 16.5, 30 and 23% of **2**, the ratios **1**:**2** being 0.90, 0.54, and 0.57 respectively. The com-

Can. J. Chem. Downloaded from www.nrcresearchpress.com by 210.87.254.6 on 09/05/12
For personal use only.

bined, alkaline mother liquors were allowed to stand for 2 h and thereafter afforded an additional 17% of crude product which gave pure **1** (2.5%) and **2** (4.5%) in the ratio 0.56. Thus the total yields were 91 (crude mixture), 17.5 (pure **1**), and 27.5% (pure **2**).

A solution of L-idose (226 mg, 1.25 mmole) in methanol (27.5 ml) and nitromethane (2.50 ml) was mixed with 1.20 ml of 1.05 *N* methanolic sodium methoxide. The solution stayed clear throughout the experiment. The optical rotation α_{436}^{26} was −0.003 (0 min, extrapolated) → −0.002 (4 min) → +0.222 (360 min) → +0.225° (end value, extrapolated). A logarithmic plot of the time-dependence of the rotation gave a straight line (Fig. 1).

The reaction mixture (30 ml, after the withdrawal of 1 ml for polarimetry) was divided in three equal parts, and the reaction was interrupted after 20, 40, and 180 min, respectively, by rapid cooling (Dry Ice) and deionization of the solutions with 2 ml of Amberlite IR-120 (H^+). The resin was filtered off and washed with methanol, and the filtrates were evaporated to dryness. The residues (72, 83, and 90 mg) were examined by polarimetry and u.v. spectroscopy (Table 1).

Support of this work by the National Research Council of Canada is gratefully acknowledged.

1. J. C. SOWDEN. Advan. Carbohyd. Chem. **6**, 291 (1951).
2. H. H. BAER. Advan. Carbohyd. Chem. **24**, 67 (1969).
3. R. K. HULYALKAR, J. K. N. JONES, and M. B. PERRY. Can. J. Chem. **41**, 1490 (1963).
4. J. C. SOWDEN and D. R. STROBACH. J. Amer. Chem. Soc. **82**, 954 (1960).
5. L. HOUGH and S. H. SHUTE. J. Chem. Soc. 4633 (1962).
6. J. YOSHIMURA and H. ANDO. Nippon Kagaku Zasshi, **85**, 138 (1964); Chem. Abstr. **61**, 16140 (1964).
7. D. T. WILLIAMS and M. B. PERRY. Can. J. Chem. **42**, 2763 (1969).
8. J. C. SOWDEN and R. SHAFFER. J. Amer. Chem. Soc. **73**, 4662 (1951).
9. J. C. SOWDEN and R. R. THOMPSON. J. Amer. Chem. Soc. **80**, 2236 (1958).
10. R. YOUNG and G. A. ADAMS. Can. J. Chem. **44**, 32 (1966).
11. L. F. WIGGINS. *In* Methods in carbohydrate chemistry. Vol. I. Academic Press, Inc., New York, N.Y., 1962. p. 140.
12. M. A. MILJKOVIC and E. A. DAVIDSON. Abstracts of papers, 155th National Meeting, American Chemical Society, C-7, 1968.
13. J. KOVÁŘ. Can. J. Chem. This issue.
14. C. SATOH, A. KIYOMOTO, and T. OKUDA. Carbohyd. Res. **5**, 140 (1967); C. SATOH and A. KIYOMOTO. Carbohyd. Res. **7**, 138 (1968).
15. L. VARGHA. Ber. **87**, 1351 (1954).
16. Z. DISCHE. J. Biol. Chem. **181**, 379 (1949); **204**, 983 (1953).
17. H. H. SEPHTON and N. K. RICHTMYER. J. Org. Chem. **28**, 1691 (1963), and personal communication.
18. J. G. MALTBY. J. Chem. Soc. 1404 (1923); 1629 (1926); 2769 (1929).
19. C. S. HUDSON. J. Amer. Chem. Soc. **73**, 4498 (1951). H. S. ISBELL, J. V. KARABINOS, H. L. FRUSH, N. B. HOLT, A. SCHWEBEL, and T. T. GALKOWSKI. J. Res. Nat. Bur. Stand. **48**, 163 (1952).
20. R. KUHN, W. BISTER, and H. FISCHER. Ann. **617**, 109 (1958).
21. A. B. ZANLUNGO, J. O. DEFERRARI, and R. A. CADENAS. Carbohyd. Res. **10**, 403 (1969).
22. L. HOUGH and A. C. RICHARDSON. *In* Rodd's chemistry of carbon compounds. Vol. 1F. Elsevier Publishing Company, Amsterdam, 1967. p. 62.
23. H. S. EL KHADEM, D. HORTON, and T. F. PAGE, JR. J. Org. Chem. **33**, 734 (1968).
24. D. HORTON and J. D. WANDER. Carbohyd. Res. **10**, 279 (1969).
25. J. M. WILLIAMS. Carbohyd. Res. **11**, 437 (1969).

Can. J. Chem. Downloaded from www.nrcresearchpress.com by 210.87.254.6 on 09/05/12
For personal use only.

Can. J. Chem. Downloaded from www.nrcresearchpress.com by 210.87.254.6 on 09/05/12
For personal use only.

Improvements for the preparation of L-idose from D-glucose

JAN KOVÁR[1]
Department of Chemistry, University of Ottawa, Ottawa, Canada

Received February 23, 1970

L-Idose (**10**) was prepared via its 1,2-*O*-isopropylidene derivative (**9**). The latter was prepared by means of the known principle of inverting the configuration of C-5 in sulfonic esters derived from 1,2-*O*-isopropylidene-α-D-glucofuranose, but a number of new intermediates and variations in procedure were studied in order to achieve practical improvements. Starting compounds were the 3,5-di-*p*-toluenesulfonate (**1**), the 3-methanesulfonate-5-*p*-toluenesulfonate (**4**), and the 5-*p*-toluenesulfonate (7) of 6-*O*-benzoyl-1,2-*O*-isopropylidene-α-D-glucofuranose, and intermediates were the 3-*p*-toluenesulfonate-5-acetate (**2**), the 3-methanesulfonate-5-acetate (**5**), and the 3,5-diacetate (**8**) of 6-*O*-benzoyl-1,2-*O*-isopropylidene-β-L-idofuranose. Compound **8** was converted into **9** directly, whereas **2** and **5** gave **9** by sodium reduction of their 5,6-deacylated derivatives **3** and **6**.

Canadian Journal of Chemistry, **48**, 2383 (1970)

L-Idose (**10**) was required for a study (1) of its reaction with nitromethane. It appeared that the most convenient and economical approach to this sugar, which does not occur in nature, was its synthesis by configurational inversion of C-5 in a suitable derivative of the readily available 1,2-*O*-isopropylidene-α-D-glucofuranose, followed by removal of the blocking groups. Several pathways based on this principle had already been published (2, 3) when Miljkovic and Davidson (4) announced a new modification that started from the known (5) 6-*O*-benzoyl-1,2-*O*-isopropylidene-3,5-di-*O*-*p*-tolylsulfonyl-α-D-glucofuranose (**1**) and involved selective replacement of its exocyclic tosyloxy group by an acetoxy group and subsequently, simultaneous cleavage of all the ester functions with lithium aluminum hydride or, better, with sodium in liquid ammonia. Displacements with Walden inversion in various blocked glucofuranose 5-tosylates have previously been achieved by use of potassium acetate in acetic anhydride (3) and sodium benzoate in *N*,*N*-dimethylformamide (6). However, employment of an anion-exchange resin in the acetate form appeared to hold promise as an improvement (4), and although no experimental details were recorded we were able to obtain readily by this method, not only 5-*O*-acetyl-6-*O*-benzoyl-1,2-*O*-isopropylidene-3-*O*-*p*-tolylsulfonyl-β-L-idofuranose (**2**) as stated (4), but also two analogous products (**5** and **8**) as outlined further below. Difficulties were encountered in the direct conversion of **2** into 1,2-*O*-isopropylidene-β-L-idofuranose (**9**) by the action of sodium in liquid ammonia, which we were unable to elaborate as a reliable procedure.[2] More successful, in our hands, was a stepwise conversion in which **2** was catalytically deacylated to 1,2-*O*-isopropylidene-3-*O*-*p*-tolylsulfonyl-β-L-idofuranose (**3**) prior to the detosylation, but even in this way a yield of only 59% of **9** was obtained.

An alternative approach to **9** started from 6-*O*-benzoyl-1,2-*O*-isopropylidene-3-*O*-methylsulfonyl-5-*O*-*p*-tolylsulfonyl-α-D-glucofuranose (**4**), a compound that is conveniently prepared (7) from 1,2:5,6-di-*O*-isopropylidene-3-*O*-methylsulfonyl-α-D-glucofuranose. Treatment of **4** with acetate ion-exchange resin in acetic anhydride furnished the mesyl analog (**5**) of **2** in 69% yield, and whereas the direct conversion of **5** into **9** with sodium in ammonia also proved unrewarding, the stepwise procedure involving prior catalytic deacylation to 1,2-*O*-isopropylidene-3-*O*-methylsulfonyl-β-L-idofuranose (**6**) gave excellent yields (89% in **5** → **6** and 95% in **6** → **9**).

The idose acetal (**9**) obtained from either 3-sulfonate (**3** or **6**) as just described always seemed to be slightly contaminated with sulfur-containing impurities. It was therefore considered that, for a practical synthesis of L-idose, the use of a precursor unsubstituted in position-3 would be preferable. Consequently, we decided to return to one of Vargha's reaction sequences (3) and to examine at the same time whether the ion-exchange method of inversion (4) is applicable to it and offers some advantage. It was found that 6-*O*-benzoyl-1,2-*O*-isopropylidene-5-*O*-*p*-tolylsulfonyl-α-D-glucofuranose (7) indeed reacted readily with Dowex-1 (acetate form) in refluxing acetic anhydride, giving 3,5-di-*O*-acetyl-

[1]Presently visiting scientist. Previous address: Laboratory of Monosaccharides, Institute of Chemical Technology, Prague, Czechoslovakia.

[2]Several attempts gave small yields of **9** or no pure product at all, although a 70% yield has been claimed (4) by Miljkovic and Davidson.

Can. J. Chem. Downloaded from www.nrcresearchpress.com by 210.87.254.6 on 09/05/12
For personal use only.

6-*O*-benzoyl-1,2-*O*-isopropylidene-β-L-idofuranose (**8**) in 73% yield. Subsequent base-catalyzed methanolysis of the ester groups quantitatively furnished **9** whose acid hydrolysis then gave L-idose (**10**), in 94% yield, as a chromatographically pure syrup. In spite of moderate difficulties associated with the preparation of the much-investigated (2, 3, 5, 8, 9) monotosylate 7 (see Experimental), we regard this procedure as the most convenient source of L-idose presently available (see Scheme 1).[3]

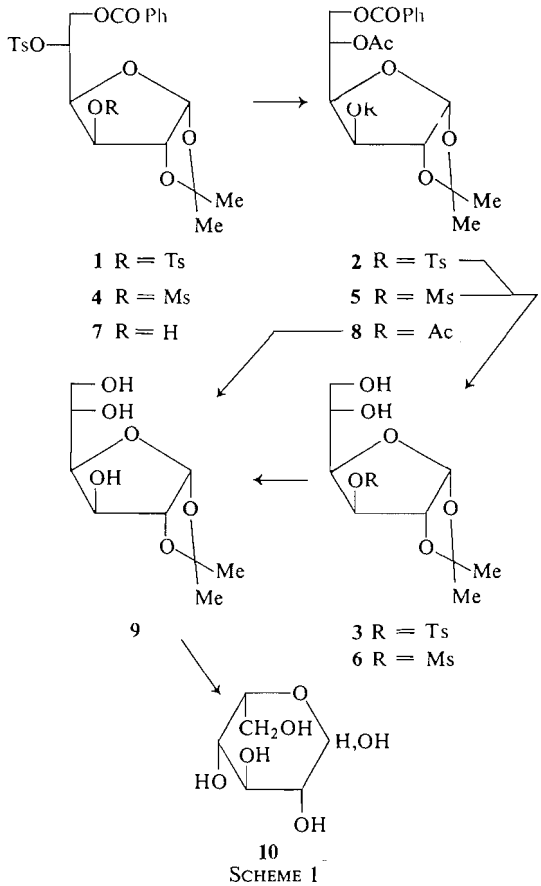

SCHEME 1

Experimental

6-O-Benzoyl-1,2-O-isopropylidene-3,5-di-O-p-tolylsulfonyl-α-D-glucofuranose (1)

1,2-*O*-Isopropylidene-α-D-glucofuranose (11) was monobenzoylated according to Ohle (12), to give its 6-benzoate (m.p. 196–197° or 203–204° depending on the mode of crystallization) in yields of 55–62%. The 6-benzoate was ditosylated essentially as directed by Ohle and Dickhäuser (5), although the product was found to require further purification. Thus, treatment of the 6-benzoate (5 g) with *p*-toluenesulfonyl chloride (7.5 g) in thoroughly dried pyridine (50 ml) at 38° for 11 h furnished a product which was then purified by column chromatography on silica gel (100 g). Elution with benzene (700 ml) yielded 8.3 g (85%) of the ditosylate **1**, m.p. 113–114°, $[\alpha]_D$ − 1.7° (*c* 1.3, chloroform), and further elution with benzene containing 1% ethanol gave 0.8 g of weakly dextrorotatory, incompletely tosylated material. Reported (5) for **1**: m.p. 113°, $[\alpha]_D$ + 1.6° (chloroform).

5-O-Acetyl-6-O-benzoyl-1,2-O-isopropylidene-3-O-p-tolylsulfonyl-β-L-idofuranose (2)

The ditosylate **1** (562 mg) and 4 ml of Dowex 1-X8 (acetate form) were heated with stirring in gently refluxing acetic anhydride (10 ml) for 24 h. Methanol (5 ml) was cautiously added to the cooled mixture which was then heated on a steam bath for 1 h in order to destroy excess anhydride. The resin was filtered off and the filtrate was poured over crushed ice. A crystalline product separated which was collected after 2 h, washed with water, and recrystallized from methanol to give **2** (408 mg, 88%) as colorless needles, m.p. 126–127°, $[\alpha]_D$ − 9.5° (*c* 1.1, chloroform). Reported (4), m.p. 125.5–126.5°.

1,2-O-Isopropylidene-3-O-p-tolylsulfonyl-β-L-idofuranose (3)

The compound **2** (752 mg) was suspended in dry methanol (8 ml) containing 0.2 mmole of sodium methoxide. After 2 h the clear solution was deionized with Amberlite IR-120 (H^+) (2 ml, prewashed with methanol) and evaporated. The residue, which failed to crystallize, was dried *in vacuo* to give a brittle foam in quantitative yield; $[\alpha]_D$ − 27.7° (*c* 0.62, chloroform).

Anal. Calcd. for $C_{16}H_{22}O_8S$ (mol. wt. 374.4): C, 51.33; H, 5.92; S, 8.56. Found: C, 51.33; H, 5.84; S, 8.45.

5-O-Acetyl-6-O-benzoyl-1,2-O-isopropylidene-3-O-methylsulfonyl-β-L-idofuranose (5)

The previously described (7) mixed ester **4** (6.32 g) and 25 ml of Dowex 1-X8 (acetate form) were stirred for 48 h in gently refluxing acetic anhydride, the volume of the reaction mixture being 60 ml. The mixture was then treated with methanol (30 ml) and worked-up as described for compound **2**. Crystallization from methanol yielded 3.40 g (69%) of **5** as long needles, m.p. 107–109°, $[\alpha]_D$ − 33.0° (*c* 1, chloroform).

Anal. Calcd. for $C_{19}H_{24}O_{10}S$ (mol. wt. 444.4): C, 51.34; H, 5.44; S, 7.21. Found: C, 51.41; H, 5.27; S, 7.06.

1,2-O-Isopropylidene-3-O-methylsulfonyl-β-L-idofuranose (6)

The compound **5** (1.0 g) was suspended in dry methanol (10 ml) containing 0.25 mmole of sodium methoxide. After 2 h the clear solution was deionized with methanol-washed Amberlite IR-120 (H^+) and evaporated. The residue was crystallized from ethanol to give 0.63 g (89%) of **6**, m.p. 129–129.5°.

[3]Vargha (3) reported a 50% yield in the displacement (**7** → **8**, using potassium acetate) and a 70% yield in the saponification (**8** → **9**, using NaOH in aqueous ethanol). The conversion (2) of **7** into **9** via a 5,6-anhydro derivative proceeded with 34% yield and involved purification by high-vacuum sublimation. An entirely different approach (10), also departing from 1,2-*O*-isopropylidene-α-D-glucofuranose, afforded **9** in low over-all yield after cumbersome separation of stereoisomers at one stage.

Can. J. Chem. Downloaded from www.nrcresearchpress.com by 210.87.254.6 on 09/05/12
For personal use only.

Anal. Calcd. for $C_{10}H_{18}O_8S$ (mol. wt. 298.3): C, 40.26; H, 6.08; S, 10.79. Found: C, 40.41; H, 6.18; S, 10.60.

6-O-Benzoyl-1,2-O-isopropylidene-5-O-p-tolylsulfonyl-α-D-glucofuranose (7)

Compound **7** has been obtained by monotosylation of 6-*O*-benzoyl-1,2-*O*-isopropylidene-α-D-glucofuranose in yields of 34 (5), 20 (2, 9), and 43% (8). In the present work the 6-benzoate (12) (1.09 g) was dissolved in dried pyridine (10 ml), and *p*-toluenesulfonyl chloride (0.71 g) was added to the ice-cooled solution which was then stored for 4 h at 24–26°. The mixture was treated with ice-water and the product extracted with chloroform. The washed (dilute H_2SO_4 and K_2CO_3) and dried ($MgSO_4$) extract was evaporated. Recrystallization of the residue from ethanol gave 508 mg (32%) of pure **7**, m.p. 144–144.5°, $[\alpha]_D$ + 16.9° (*c* 0.8, chloroform). Reported: m.p. 142 (5), 143–144 (9), 138–140° (8); $[\alpha]_D$ + 9.3 (5), +20.6° (8) (in chloroform).

The mother liquor of recrystallization yielded a second crop having a similar melting point but lower rotation (+5.6°); this material was not used for further work. In order to ascertain that the main product isolated was indeed the 5-tosylate **7**, a sample was treated with methanesulfonyl chloride in pyridine, whereby it was converted in 90% yield into compound **4**, m.p. 157–159°, $[\alpha]_D$ − 12.5° (*c* 0.9, chloroform). Reported (7): m.p. 153–154°, $[\alpha]_D$ − 12.3° (chloroform). Another sample was acetylated with acetic anhydride in pyridine to give in nearly quantitative yield the known 3-acetate of **7**, m.p. 155–156°, $[\alpha]_D$ − 3.7° (*c* 1.1, chloroform). Reported m.p. 151° (13); m.p. 152–153° and $[\alpha]_D$ − 3.75° (chloroform) (6).

3,5-Di-O-acetyl-6-O-benzoyl-1,2-O-isopropylidene-β-L-idofuranose (8)

The monotosylate **7** (500 mg) and 4 ml of Dowex 1-X8 (acetate form) were stirred for 26 h in gently refluxing acetic anhydride (volume of mixture, 7 ml). Upon cooling, the resin was filtered off and washed with methanol, and the filtrate was evaporated *in vacuo*. The resulting oil was diluted with methanol (1 ml) and introduced into ice-water (25 ml). After some standing at 0° the product crystallized and could be filtered off. Recrystallization from methanol furnished 308 mg (73%) of **8**, m.p. 120–121°, $[\alpha]_D$ − 22.5° (*c* 1.1, chloroform). The lit. (3): m.p. 121–122°, $[\alpha]_D$ − 19.6° (chloroform).

1,2-O-Isopropylidene-β-L-idofuranose (9)

a) From 8

To the triacyl derivative **8** (305 mg) in dry methanol (6.8 ml) was added 0.17 ml of 1 *N* sodium methoxide solution. After 2 h the reaction mixture was deionized with 1 ml of Amberlite IR-120 (H^+) and evaporated to give **9** (166 mg, 100%) which melted at 114–115° after recrystallization from ethyl acetate and showed $[\alpha]_D$ − 28.7° (*c* 0.50, water), in excellent agreement with the literature (2, 3, 10).

b) From 3

A solution of the tosylate **3** (523 mg) in liquid ammonia (40 ml) was kept at gentle refluxing, by intermittent removal from the Dry-Ice cooling bath, and sodium (0.15 g) was added in small chips through the condenser. After 30 min any remaining sodium was destroyed with ammonium chloride (0.5 g) which was rinsed down the condenser with methanol. The reaction mixture was then allowed to evaporate and the residue, after drying *in vacuo*, was extracted with hot ethyl acetate from which 183 mg (59%) of **9** crystallized on cooling and concentrating; m.p. 114–115° (after prior melting and resolidifying at 107–108°).

c) From 6

The mesylate **6** (400 mg) and sodium (0.20 g) in liquid ammonia (30 ml) were allowed to react essentially as described for **3** except that the reaction was performed, without reflux condenser, at a somewhat lower average temperature. After the addition of all the sodium a blue solution color persisted, and after 1 h, dry ammonium chloride was added and the mixture was worked up to give 280 mg (95%) of **9** (from ethyl acetate), m.p. 114–115°.

L-*Idose (10)*

The isopropylidene derivative **9** (774 mg) was hydrolyzed in 0.1 *N* sulfuric acid (15 ml) for 8 h at 40°. The cooled solution was treated with activated charcoal, and filtered successively through 5 ml of Dowex 1-X8 (HCO_3^- form) and 2 ml of Amberlite IR-120 (H^+) contained in small columns. Evaporation gave L-idose as a colorless syrup weighing 595 mg (94%; dried in a desiccator). It reduced Fehling solution, and showed $[\alpha]_D$ − 15.5° (*c* 2, water); reported for **10**, $[\alpha]_D$ − 17.4° (3); for the D-enantiomer, +15.8° (14). The syrup exhibited a single spot on a paper chromatogram sprayed with ammoniacal silver nitrate, $R_{glucose}$ 1.3 in 1-butanol–ethanol–water (40:11:19, v/v), and could be stored in a refrigerator for several weeks without deteriorating.

The author, who carried out this investigation during a leave-of-absence from the Institute of Chemical Technology, Prague, wishes to thank Professor Hans H. Baer sincerely for his interest and for giving the opportunity to work in his Laboratory at Ottawa. The technical assistance of Mrs. Siegrid Hancock is gratefully acknowledged.

1. J. Kovář and H. H. Baer. Can. J. Chem. This issue.
2. A. S. Meyer and T. Reichstein. Helv. Chim. Acta, **29**, 152 (1946).
3. L. Vargha. Ber. **87**, 1351 (1954).
4. M. A. Miljkovic and E. A. Davidson. Abstract of papers, 155th National Meeting of the American Chemical Society. C-7 (1968).
5. H. Ohle and E. Dickhäuser. Ber. **58**, 2593 (1925).
6. D. H. Buss, L. D. Hall, and L. Hough. J. Chem. Soc. 1616 (1965).
7. J. Kovář and J. Jarý. Coll. Czech. Chem. Commun. **33**, 549 (1968).
8. E. J. Reist, R. R. Spencer, and B. R. Baker. J. Org. Chem. **23**, 1757 (1958).
9. L. D. Hall, L. Hough, and R. A. Pritchard. J. Chem. Soc. 1537 (1961).
10. F. Shafizadeh and M. L. Wolfrom. J. Amer. Chem. Soc. **77**, 2568 (1955).
11. O. T. Schmidt. *In* Methods in carbohydrate chemistry. Vol. II, Academic Press, Inc., New York, N.Y., 1963. p. 318.
12. H. Ohle. Ber. **57**, 403 (1924).
13. H. Ohle, E. Euler, and R. Lichtenstein. Ber. **62**, 2885 (1929).
14. E. Sorkin and T. Reichstein. Helv. Chim. Acta, **28**, 1 (1945).

Can. J. Chem. Downloaded from www.nrcresearchpress.com by 210.87.254.40 on 09/05/12
For personal use only.

Conformational interconversion of 3,3,5,5-tetramethylmethylenecyclohexane and related compounds

MAURICE ST-JACQUES, MICHEL BERNARD, AND CAMBYSE VAZIRI
Department of Chemistry, University of Montreal, Montreal, Quebec

Received March 5, 1970

The proton magnetic resonance spectra of compounds **1** to **4** have been studied at various temperatures. The spectral changes observed for **2**, **3**, and **4** are interpreted in terms of interconverting chair conformations.

Canadian Journal of Chemistry, 48, 2386 (1970)

Introduction

Fascinating investigations have been concerned with the determination of the stable conformation of six-membered cyclic compounds (1, 2). In these endeavors numerous techniques, theoretical and experimental, have been used to approach conformational problems from different points of view. From such studies it has emerged that the chair form is highly favored for cyclohexane and that severe constraints, usually in the form of sp^2 hybridized carbon atoms (3), bulky axial substituents (4), and in some cases heteroatoms (5), must be present in the ring to make the twist-boat form more stable than the chair.

It has long been accepted that 3,3,5,5-tetramethylcyclohexanone (**1**) exists in a chair conformation (6) even though there are severe 1,3-*syn*-axial interactions between methyl groups estimated at about 3.7 kcal/mole (7) and comparable to the energy of the twist-boat form of cyclohexanone calculated to be about 3.5 kcal/mole (8).

Experimental evidence as a result of an X-ray analysis showed that 2,6-dibromo-3,3,5,5-tetramethylcyclohexanone and 2-bromo-3,3,5,5-tetramethylcyclohexanone existed as deformed chairs in the solid state (9). Recent calculations by Allinger (8) predict a greater stability (about 3.8 kcal/mole) for the chair.

In spite of these overwhelming results supporting a chair form, it has been suggested that the apparently structurally analogous molecule 3-phenyl-3,5,5-trimethylcyclohexanone appears to exist in a twist-boat conformation (8, 10).

Motivated by these apparently conflicting results, it seemed of interest to apply the dynamic nuclear magnetic resonance (d.n.m.r.) method (2) to increase our understanding of the conformational characteristics of **1**. A recent review (2) shows that this approach has met with considerable success in understanding such problems.

A close examination of the chair (c.) and twist-boat (t.b.) conformations suggests that the appearance of the proton magnetic resonance (p.m.r.) signal of the methylene group on carbon-4 (C-4) could supply information on the nature of the stable conformation of **1**. Other t.b. forms need not be considered because of excessive methyl repulsion.

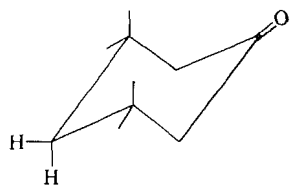

c.

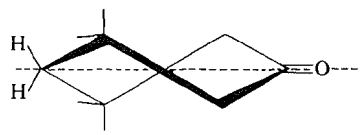

t.b.

In other words it was expected that if conformational interconversions for **1** could be slowed down on the n.m.r. time scale, the low temperature p.m.r. signal of the methylene group on C-4 would either be an AB quartet for c. because of the difference in chemical shifts of the axial (a) and equatorial (e) protons, or be an A_2 singlet for t.b. since the two-fold axis of symmetry through C-1 and C-4 make both methylene protons equivalent. The methyl and α-methylene protons would be of no evident use since the same appearance is expected for these signals for both conformations.

Can. J. Chem. Downloaded from www.nrcresearchpress.com by 210.87.254.40 on 09/05/12
For personal use only.

Unfortunately conformational interconversion for **1** like that for cyclohexanone (11) could not be slowed down sufficiently, even at −170 °C, to obtain the p.m.r. spectrum of the stable conformation of **1**. This molecule is therefore not amenable to a d.n.m.r. investigation. Fortunately, however, the recent observation (11) that the replacement of the carbonyl group in cyclohexanone by a methylene group markedly raises the energy barrier to ring inversion suggested that a similar modification of **1** might enable us to achieve our objective. We therefore prepared compounds **1** to **4** for our variable temperature p.m.r. investigation.

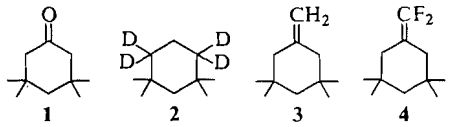

1 **2** **3** **4**

Compound **2** was prepared to serve as a model for the others as will be explained in detail later. Molecules **2**, **3**, and **4** showed temperature dependent p.m.r. spectra, the results of which will now be described.

Results and Discussion

(1) 1,1,3,3-Tetramethylcyclohexane-4,4,6,6-d_4 (2)

The starting material **1** was prepared as described by Chiurdoglu and Maquestiau (12). Refluxing **1** with a solution of 10% potassium carbonate in deuterium oxide gave 3,3,5,5-tetramethylcyclohexanone-d_4. Conversion to the tosylhydrazone and reduction with lithium aluminum hydride yielded **2** (13).

The 100 MHz p.m.r. spectra of **2** are shown in Fig. 1 at various temperatures with deuterium decoupling. At ambient temperature the decoupled spectrum consists of three singlets: 0.92 (methyl groups), 1.15 (methylene group on C-2), and 1.49 p.p.m. from internal TMS (methylene group on C-5). The assignment of the respective methylene peaks is based on the results of deuterium decoupling and the p.m.r. spectrum of the non-deuterated compound. As the temperature is lowered a spectral change takes place such that at −135 °C both methylene peaks have changed into AB quartets while the methyl groups now show a doublet of equally intense lines. The coalescence temperatures are estimated

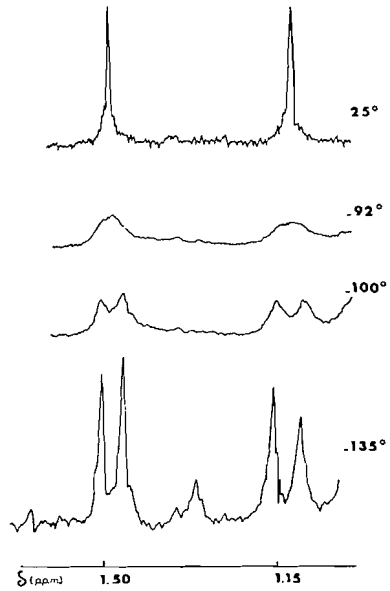

FIG. 1. The 100 MHz p.m.r. deuterium decoupled spectra of the ring protons of **2** at several temperatures. The scale is in p.p.m. relative to internal TMS.

at −94 °C for the C-5 methylene AB quartets and −97 °C for the methyl doublet.

From the spectrum at −135 °C it is possible to determine that the methyl peaks are separated by 10.8 ± 0.2 Hz while the chemical shift difference ($\Delta\nu$) for the protons on C-5 is 11.7 ± 0.5 Hz and the coupling constant is J = 13.7 ± 0.5 Hz. It is apparent that the upfield and downfield AB components of the C-5 and C-2 methylene groups are essentially superposed. Even though the upfield AB component of the C-2 methylene is not visible, it is nevertheless possible to determine that J = 14.0 ± 1.0 Hz and $\Delta\nu$ = 14.3 ± 1.0 Hz.

Using the equation given by Kurland and coworkers (14) one obtains the rate constant (k) for the process responsible for the coalescence of the AB quartets. Eyring's equation (15) then gives the free energy of activation ($\Delta F^{\ddagger}$ = 8.5 ± 0.3 kcal/mole) at −94 °C for the process. A transmission coefficient of ½ has been used; this value will be explained later. Analogically $\Delta F^{\ddagger}$ = 8.7 ± 0.3 kcal/mole was calculated using the rate constant equation given by Pople *et al.* (16) for the coalescence of the methyl doublet at −97 °C.

The presence of two AB quartets in the p.m.r. spectrum at −135 °C proves unambiguously that **2** exists in the chair form with axial and equatorial

TABLE 1

Summary of free energy barriers for cyclohexane and some *gem*-dimethylated cyclohexane derivatives

Compound	$\Delta F^{\ddagger a}$ (kcal/mole)	Reference
Cyclohexane	10.3	18
1,1-Dimethylcyclohexane	10.2	19
1,1,3,3-Tetramethylcyclohexane	8.7	This work
1,1,4,4-Tetramethylcyclohexane	11.1	20

[a]These values are for the chair-to-boat process.

protons of different chemical shifts at positions 2 and 5. This conclusion is in agreement with calculations by Allinger *et al.* (17) which predict c. to be more stable than t.b. by 4.78 kcal/mole.

Knowing that **2** exists in the c. form, immediately identifies the interconversion process as ring inversion, and assuming a mechanism analogous to cyclohexane, a transmission coefficient of $\frac{1}{2}$ was used in the calculation of $\Delta F^{\ddagger}$ above which therefore represents the free energy barrier for the chair-to-boat process (18).

Table 1 contains a summary of $\Delta F^{\ddagger}$ values for cyclohexane and some *gem*-dimethylated cyclohexane derivatives. It is interesting to note that one *gem*-dimethyl group has essentially no effect on the barrier and that two groups in a 1,4-relationship raise it by about 1 kcal/mole while two groups in a 1,3-relationship lower it by about 1 kcal/mole.

The value of $\Delta\nu = 14.3$ Hz for the methylene group on C-2 serves as a model for the next section where an analogous splitting would be expected for the methylene group on C-4 of **3** and **4** if these compounds exist as c. forms unless unusual effects associated with the presence of an sp^2 hybridized carbon are present.

(2) 3,3,5,5-Tetramethylcyclohexanone and Derivatives

Compound **3** was prepared from **1** by a Wittig reaction using the procedure of Greenwald and co-workers (21); **4** was also prepared from **1** by the method developed by Fuqua and co-workers (22).

The 100 MHz p.m.r. spectra of **3** at various temperatures are shown in Fig. 2. Above -100 °C the spectrum consists of three singlets: one at 0.93 (methyl groups), a second at 1.26 (methylene group on C-4), and the third at 1.87 p.p.m. (methylene groups on C-2 and -6). The vinyl methylene singlet is not shown. As the

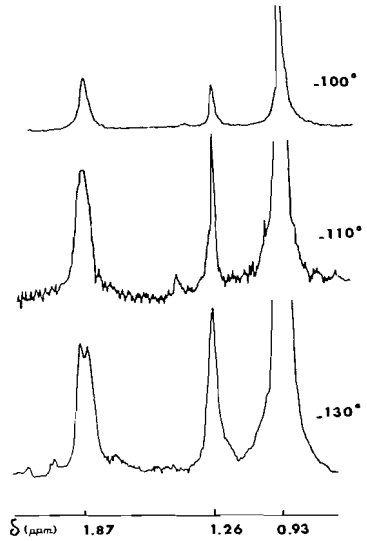

FIG. 2. Upfield portion of the 100 MHz p.m.r. spectra of **3** at several temperatures.

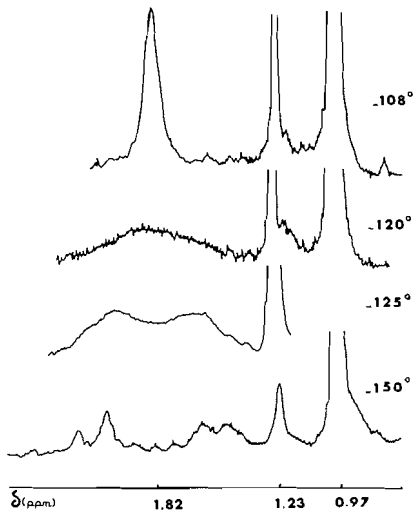

FIG. 3. The 100 MHz p.m.r. spectra of **4** at several temperatures.

temperature is lowered only the α-proton peak undergoes a spectral modification whereby the singlet becomes an AB quartet below -110 °C, the coalescence temperature. Spectra taken down to -165 °C showed a slight broadening of the other two singlets with respect to the TMS peak but no further splitting was observed. The vinyl proton peak also remained unchanged throughout this temperature interval.

The 100 MHz spectra of **4** as a function of temperature are shown in Fig. 3. The high tem-

Can. J. Chem. Downloaded from www.nrcresearchpress.com by 210.87.254.40 on 09/05/12
For personal use only.

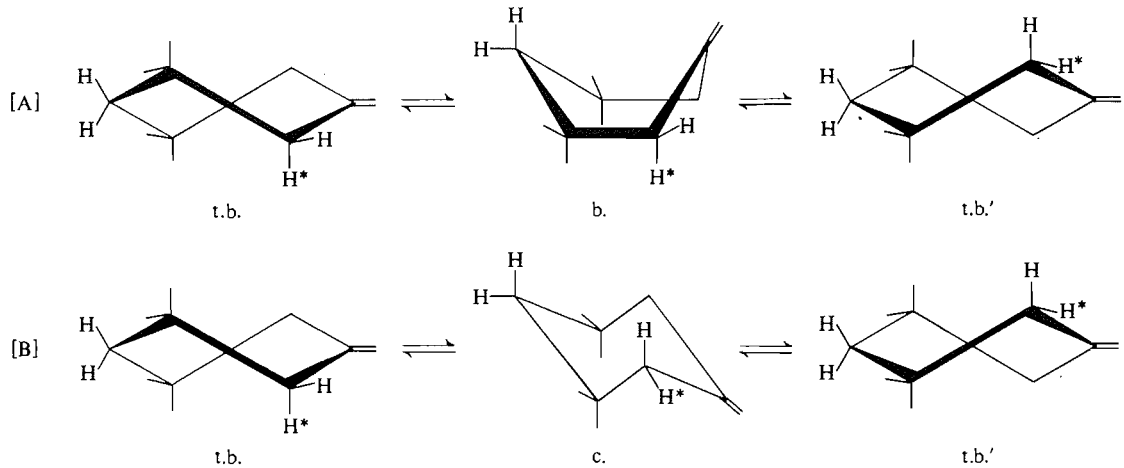

FIG. 4. Pseudorotation (A) and ring inversion (B) itineraries for the t.b. conformation of **1**, **3**, or **4**.

perature spectrum consists of three singlets: one at 0.97 (methyl groups), the second 1.23 (methylene group on C-4), and the third at 1.82 p.p.m. (methylene groups on C-2 and -6). At +25 °C, the last peak actually appears as a triplet (separation 2.2 Hz) because of coupling with the fluorine atoms. As for **3** only the α-proton peak undergoes a spectral change into an AB quartet below −120 °C, the coalescence temperature. The other peaks remained unsplit down to −165 °C. The upfield components of the AB quartet show a marked broadening with respect to the lower field components undoubtedly because of larger $^4J_{HF}$ values.

Spectral parameters for **3** were found to be $J = 13.0$ Hz and $\Delta\nu = 10.5$ Hz while those for **4** were $J = 12.5$ Hz and $\Delta\nu = 57.6$ Hz. The error in these parameters is about 0.5 Hz because of the broadness of the lines. From the equation given by Kurland and co-workers (14), k was obtained from each spectral change and the following $\Delta F^{\ddagger}$ values were calculated using a transmission coefficient of one: 7.9 ± 0.3 kcal/mole for **3** at −110 °C and 7.2 ± 0.3 kcal/mole at −120 °C for **4**.

It is immediately evident from the low temperature spectra of each of **3** and **4** that the multiplicity observed does not satisfy the symmetry requirement of either the c. or the t.b. forms. To be in agreement with c., the methyl singlet should be a doublet while the singlet due to protons on C-4 should be an AB quartet. On the other hand, agreement with the t.b. conformation would require a methyl doublet and a C-4 methylene singlet. There must therefore exist some accidental equivalence of chemical shifts of protons in different molecular environments. It is difficult *a priori* to say conclusively which conformation comes closer to satisfying the requirements of the low temperature spectra. It is possible to demonstrate, however, that the c. form best rationalizes the barriers to conformational interconversion determined from the spectral changes.

If we begin our argument by assuming that the conformational energies calculated (8) for the c. and t.b. forms of **1** are essentially correct, then c. is more stable than t.b. by about 3.8 kcal/mole. Calculations for methylenecyclohexane (23), cyclohexanone (8), cyclohexane and 1,1,3,3-tetramethylcyclohexane (17) indicate that 4 kcal/mole represents a reasonable estimate of the greater stability of the c. form of **3**. The process of conformational interconversion with $\Delta F^{\ddagger} = 7.9 \pm 0.3$ kcal/mole, responsible for the spectral change of **3**, would then be ring inversion analogous to cyclohexane (18) and involving a c. ⇄ t.b. ⇄ c.′ pathway (the prime represents an inverted conformation), where t.b. is a metastable intermediate. We may now deduce that the maximum barrier to pseudorotation (24) of the t.b. form should be no more than about 4 kcal/mole to be compatible with energy profiles constructed from the estimated energy difference between c. and t.b. and $\Delta F^{\ddagger}$ determined from the spectral change.

If, on the other hand, we assume as a working hypothesis that **3** exists in the t.b. form, then two

Can. J. Chem. Downloaded from www.nrcresearchpress.com by 210.87.254.40 on 09/05/12
For personal use only.

basic modes of interconversion are available, namely a ring inversion and a pseudorotation. Both processes, shown in Fig. 4, have the property of averaging the different types of protons of **3** such that the p.m.r. spectrum at high temperature be in agreement with that given in Fig. 2. If it can be shown that the barrier to pseudorotation should be less than the observed $\Delta F^{\ddagger}$, then it will follow that **3** cannot exist in the t.b. form, otherwise the spectral change depicted in Fig. 2 should be observed at much lower temperatures. Since the height of the pseudorotation energy profile is either of two possible boat forms, b., shown in Fig. 4 and **5**, their conformational energies relative to t.b. will now be estimated.

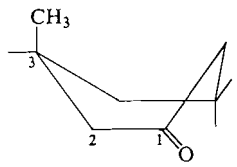

5

Strain energy minimization calculations not having been done for all conformations of **1** or **3**, maximum conformational energies relative to t.b. will be estimated by the simplest method. As a starting point we shall use results derived for the various boat forms of cyclohexanone (8) and then consider the effect of replacing hydrogen atoms by methyl groups on the basic skeleton. The energies for differently located methyl groups are taken as those calculated for cyclohexane by Hendrickson (25); these values will be used as such and modifications due to the presence of an sp^2 carbon on methyl repulsive interactions will be considered later.

The energy increment of the t.b. skeleton energy of cyclohexanone due to the presence of the four methyl groups arises essentially from two methyl interactions on C-3 and C-5, the sum estimated to be about 2 kcal/mole (25). The difference in conformational energies of the t.b. forms of cyclohexanone and **1** relative to their respective c. forms is calculated as about 0.5 kcal/mole (i.e. 3.78–3.26) (8), thus indicating that the effect of the methyl groups is greater in t.b. than in c. for **1** by about 0.5 kcal/mole. A fair estimate of the 1,3-*syn*-dimethyl interaction in the chair form of **1** is some 3.5 kcal/mole (8); it may therefore be concluded that 2 kcal/mole represents a minimum energy increment due to the presence of methyl groups. This value will be used since it will lead to maximum conformational energy values for b. and **5**, as desired.

The energy of the b. form is made up of 2.2 kcal/mole associated with the cyclohexanone skeleton and the energy of a 1,3-*syn*-dimethyl interaction, not estimated by Hendrickson, but expected to be some 3.5 kcal/mole or less. We may therefore say that 5.7 kcal/mole certainly represents the maximum energy possible for the b. form. Conformation **5** comprises essentially a skeleton contribution of 1.1 kcal/mole and a C-3 methyl interaction of about 3 kcal/mole leading to an energy of 4.1 kcal/mole. Since the replacement of a carbonyl group by an exo-methylene group is expected to lower the skeleton of b. relative to t.b., we can safely say that 3.5 kcal/mole represents a *maximum* value for the conformational energy of either b. or **5** for **3** *relative* to t.b. (taken as 0 kcal/mole), and therefore represents the *maximum* pseudorotation barrier. Even a more generous estimate of 6 kcal/mole would still mean that the spectral change observed for **3** should not occur at the observed temperatures, but at much lower temperatures. It therefore appears highly improbable that t.b. is the predominant conformation of **3** in solution, and, without specifying whether b. or **5** is the barrier height to pseudorotation, the maximum estimate made above is within the maximum limit deduced earlier from calculations and the observed $\Delta F^{\ddagger}$. Similar arguments are applicable to **4**.

The $\Delta F^{\ddagger}$ values determined for **3** and **4** are therefore most reconcilable with the c. form. The conformational process would then be ring inversion involving a c. $\rightleftarrows$ t.b. $\rightleftarrows$ c.′ itinerary. It is evident from Fig. 4 that this ring inversion averages the AB quartet of the α-protons to a singlet. It also appears more than likely that **1** should also exist in the c. form, although this cannot be demonstrated other than by analogy with **3** and **4**.

It is interesting to speculate as to the origin of the accidental equivalence of the axial and equatorial methyl groups and the protons on C-4. It appears that the anisotropy of the $=CH_2$ or $=CF_2$ groups is not responsible since it is very different for each substituent as reflected by the $\Delta\nu$ of the α-protons of **3** and **4**. It seems possible that the flattening of the ring caused by the introduction of an sp^2 carbon might account for

Can. J. Chem. Downloaded from www.nrcresearchpress.com by 210.87.254.40 on 09/05/12
For personal use only.

TABLE 2

Summary of free energy barriers for cyclohexanone, 3,3,5,5-tetramethylcyclohexanone, and their derivatives

Compound	$\Delta F^{\ddagger}$[a] (kcal/mole)	Reference
Cyclohexanone	< 5.0	11*a*
Methylenecyclohexane	8.4	11*b*
Difluoromethylenecyclohexane	6.8	27
1	< 5.0	This work
3	7.7	This work
4	7.0	This work

[a]These values are for the chair-to-boat process. That is, a transmission coefficient of $\frac{1}{2}$ is used in the calculation of $\Delta F^{\ddagger}$ instead of 1.

a large part of this phenomenon. Such a proposition finds precedence in the calculations (26) recently reported where similar effects are attributed in part to the flattening of the ring in t-butyl derivatives of cyclohexane.

Our results then suggest that the presence of the 3,3,5,5-tetramethyl moiety in **1**, **3**, and **4** does not lead to a change in basic conformation with respect to cyclohexanone and its corresponding derivatives. Moreover the free energy barriers are very similar for both classes of compounds as illustrated in Table 2.

The trends observed appear to reflect the trend found for the energy barriers to rotation about C_{sp^2}—C_{sp^3} bonds (28). As suggested for methylenecyclohexane (11), this behavior may be considered as indicative of an appreciable participation of the sp^2 carbon atom in the "flip" to reach the transition state for ring inversion.

Experimental

Infrared (i.r.) spectra were recorded on a Beckman IR-8 spectrophotometer, the sample being a thin film between sodium chloride plates. Mass spectra were obtained on a Hitachi-Perkin-Elmer mass spectrometer model RMU 6-D at 70 eV. Vapor phase chromatography (v.p.c.) analyses were carried out on an Aerograph A90-P3 instrument on 5 ft long, $\frac{1}{4}$ in. diameter columns described later. Carbon, hydrogen analyses were obtained by Midwest Microlab, Inc., Indianapolis, Indiana, U.S.A.

The p.m.r. spectra were recorded on a JEOL JNM-4 H-100 spectrometer operating at 100 MHz using solutions from 2 to 8% of the samples in a mixture of vinyl chloride and chlorodifluoromethane, m.p. −159.9 and −160 °C respectively. The freon was added for field-frequency locking purpose. Compound **1** was investigated as a 3% solution in chlorodifluoromethane alone, however. A small quantity of tetramethylsilane was added and the samples were degassed and sealed (18). Temperatures were monitored by means of a JEOL temperature control unit model JES-VT-3 and read off a calibration chart obtained with a thermocouple inside a dummy n.m.r. tube. Checks on the accuracy of the calibration curve were made repeatedly and are believed accurate to within ±2 °C. Deuterium decoupling was effected by means of the JEOL Hetero Spin Decoupler model JNM-SD-HC.

3,3,5,5-Tetramethylcyclohexanone-2,2,6,6-d_4

Compound **1** (34.0 g, 0.22 moles) (12) was refluxed with a solution of 10 g of potassium carbonate in 100 ml of deuterium oxide for 24 h. The product was then extracted with ether and dried with anhydrous magnesium sulfate. After evaporation of the ether, peak integration on the p.m.r. spectrum revealed essentially 50% deuteration. By repeating the above procedure three times it was possible to obtain 32 g (94%) of the ketone deuterated, essentially 99% as revealed by the complete absence of the peak due to the α-protons.

1,1,3,3-Tetramethylcyclohexane-4,4,6,6-d_4 (2)

Compound **2** was prepared following a sequence of known reactions (13). The deuterated ketone (0.990 g, 0.0062 moles) from the above exchange reaction and 1.20 g of tosylhydrazine were dissolved in 20 ml of hot absolute ethanol. The solution was left standing at room temperature for 24 h. The precipitated tosylhydrazone (1.75 g, 79%) was filtered and used in the next step. Uncorrected m.p. 162–164 °C.

The above tosylhydrazone (0.341 g, 0.00104 moles) was refluxed for 24 h with 0.575 g (0.15 moles) of lithium aluminum hydride in 25 ml of tetrahydrofuran. After hydrolysis of the mixture with 10% sulfuric acid, an extraction with petroleum ether was carried out. The organic solution was then washed with a 5% sodium hydroxide solution and several times with a saturated sodium chloride solution until neutral. Traces of water were removed with magnesium sulfate and the ether was distilled.

The v.p.c. analysis on a column of β,β′-oxydipropionitrile (13% on chromosorb P, HMDS, 60–80 mesh) gave two peaks corresponding to 72% of **2** at 10 min retention time and 28% of 3,3,5,5-tetramethylcyclohexene-2,6,6-d_3 at 11 min. These retention times were identical with those for nondeuterated products which are known substances (12).

Extraction of the concentrated petroleum ether solution with a saturated silver nitrate solution removed most of the olefin. Preparative v.p.c. gave a sample of **2** of purity greater than 98%. A sample of 8% of this compound in a mixture of vinyl chloride and chlorodifluoromethane (9:1, v:v) containing a little TMS was prepared for the low temperature p.m.r. study.

3,3,5,5-Tetramethylmethylenecyclohexane (3)

Following the method described by Greenwald (21), 4.92 g (0.033 moles) of **1** were reacted to yield **3**. Samples for analyses were purified by preparative v.p.c. on carbowax 20M (20% on chromosorb P, HMDS, 60–80 mesh). The i.r. and p.m.r. analytical date were in agreement with those reported in the literature (29). A 5% solution in a mixture of vinyl chloride and chlorodifluoromethane (9:1, v:v) containing a little TMS was prepared for the low temperature p.m.r. study.

3,3,5,5-Tetramethyldifluoromethylenecyclohexane (4)

Following the method described by Fuqua (22), 4.62 g

Can. J. Chem. Downloaded from www.nrcresearchpress.com by 210.87.254.40 on 09/05/12
For personal use only.

(0.030 moles) of **1** were reacted to yield **4**. Samples for analyses were purified by preparative v.p.c. on a carbowax 20M column. Mass spectrum, molecular ion at m/e = 188; i.r. 1758 ($C{=}CF_2$); p.m.r. (7% in a mixture of $CH_2{=}CHCl$: CHF_2Cl, 9:1, v:v), 0.97 (singlet, CH_3), 1.23 (singlet, CH_2), 1.82 p.p.m. (triplet, separation 2.2 Hz, α-CH_2).

Anal. Calcd. for $C_{11}H_{18}F_2$: C, 70.18; H, 9.64. Found: C, 70.18; H, 9.81.

A 2% solution of **4** in a mixture of vinyl chloride and chlorodifluoromethane (9:1, v:v) containing a little TMS was prepared for the low temperature p.m.r. study.

We are grateful for helpful discussions and encouragement from Professor H. Favre. We wish to thank D. F. Williams for recording the p.m.r. spectra, the National Research Council of Canada for financial support and a fellowship to M.B., and the Quebec Ministry of Education for a fellowship (France–Québec) to C.V. We are also very thankful to Dr. P. Laszlo for making available to us details of unpublished work presented at the American Society Meeting, Atlantic City, N.J., September, 1968, abstract ORGN-139.

1. (*a*) E. L. Eliel, N. L. Allinger, S. J. Angyal, and G. A. Morrison. Conformational analysis. Interscience Publishers, Inc., New York, N.Y., 1965. (*b*) H. Hanack. Conformation theory. Academic Press, New York, N.Y., 1965.
2. G. Binsch. Topics in stereochemistry. E. L. Eliel and N. L. Allinger *ed.* Vol. 3. Interscience Publishers, Inc., New York, N.Y., 1968. p. 97.
3. (*a*) P. Groth and O. Hassel. Acta Chem. Scand. **18**, 923 (1964). (*b*) A. Mossel and C. Romers. Acta Cryst. **17**, 1217 (1964). (*c*) C. Y. Chen and R. J. W. le Fevre. Aust. J. Chem. **16**, 917 (1963).
4. H. Kessler, V. Gusowski, and M. Hanack. Tetrahedron Lett. 4665 (1968).
5. C. H. Bushweller. J. Amer. Chem. Soc. **89**, 5978 (1967).
6. Ref. 1*a*, p. 126 and references cited therein.
7. N. L. Allinger and M. A. Miller. J. Amer. Chem. Soc. **83**, 2145 (1961).
8. N. L. Allinger, J. A. Hirsch, M. A. Miller, and I. J. Tyminski. J. Amer. Chem. Soc. **91**, 337 (1969).
9. L. C. G. Goaman and D. F. Grant. Tetrahedron, **19**, 1531 (1963).
10. M. Balasubramanian and A. D'Souza. Tetrahedron, **25**, 2973 (1969).
11. (*a*) F. R. Jensen and B. H. Beck. J. Amer. Chem. Soc. **90**, 1067 (1968). (*b*) J. T. Gerig and R. A. Rimerman. J. Amer. Chem. Soc. **92**, 1219 (1970).
12. G. Chiurdoglu and A. Maquestiau. Bull. Soc. Chim. Belgium, **63**, 357 (1964).
13. (*a*) M. Fisher and C. Djerassi. Ber. **98**, 3236 (1965). (*b*) P. Belanger. Ph.D. Thesis, University of Montreal, Montreal, Quebec, 1966.
14. R. J. Kurland, M. B. Rubin, and W. E. Wise. J. Chem. Phys. **40**, 2426 (1964).
15. K. J. Laidler. Chemical kinetics. McGraw-Hill, New York, N.Y., 1950, Chapt. 3.
16. J. A. Pople, W. G. Schneider, and H. J. Bernstein. High resolution nuclear magnetic resonance. McGraw-Hill, New York, N.Y., 1959. p. 233.
17. N. L. Allinger, J. A. Hirsch, M. A. Miller, I. J. Tyminski, and F. A. Van-Catledge. J. Amer. Chem. Soc. **90**, 1199 (1968).
18. F. A. L. Anet and A. J. R. Bourn. J. Amer. Chem. Soc. **89**, 760 (1967).
19. H. Friebolin, W. Faisst, H. G. Schmid, and S. Kabuss. Tetrahedron Lett. 1317 (1966).
20. R. W. Murray and M. L. Kaplan. Tetrahedron, **23**, 1575, (1967).
21. R. Greenwald, M. Chaykovsky, and E. J. Corey. J. Org. Chem. **28**, 1128 (1963).
22. S. A. Fuqua, W. F. Duncan, and R. M. Silverstein. J. Org. Chem. **30**, 2543 (1965).
23. N. L. Allinger, J. A. Hirsch, M. A. Miller, and I. Tyminski. J. Amer. Chem. Soc. **90**, 5773 (1968).
24. J. B. Hendrickson. J. Amer. Chem. Soc. **89**, 7047 (1967).
25. J. B. Hendrickson. J. Amer. Chem. Soc. **89**, 7043 (1967).
26. G. E. Hawkes and J. H. P. Utley. Chem. Commun. 1033 (1969).
27. M. Bernard. Master Thesis. University of Montreal, Montreal, Quebec, 1969.
28. J. Dale. Tetrahedron, **22**, 3373 (1966).
29. S. Marmor and J. G. Maroski. J. Org. Chem. **31**, 4278 (1966).

Can. J. Chem. Downloaded from www.nrcresearchpress.com by 210.87.254.40 on 09/05/12
For personal use only.

Quinoline *N*-oxides and hydroxamic acids with antibacterial properties

R. T. COUTTS, K. W. HINDMARSH, AND G. E. MYERS
Faculty of Pharmacy and Pharmaceutical Sciences, University of Alberta, Edmonton, Alberta

Received February 20, 1970

A number of quinoline *N*-oxides have been prepared and oxidized by means of lead tetraacetate to quinoline hydroxamic acids (i.e. derivatives of 1-hydroxy-2(1*H*)-quinolone). Contrary to the findings of other investigators, 1-hydroxy-4-nitro-2(1*H*)-quinolone (**2***e*) is obtained by treating 4-nitroquinoline 1-oxide with lead tetraacetate. Quinolines with a methyl group in the 8-position could not be oxidized to *N*-oxides with hydrogen peroxide.

The antibacterial properties of the hydroxamic acids and some of the *N*-oxides were evaluated against *S. aureus* and *E. coli*.

Canadian Journal of Chemistry, **48**, 2393(1970)

Can. J. Chem. Downloaded from www.nrcresearchpress.com by 210.87.254.42 on 09/05/12
For personal use only.

Some cyclic hydroxamic acids possess the ability to inhibit the growth of bacteria (1–7). 1-Hydroxy-2(1*H*)-quinolone (**2***a*) and its simple derivatives have been shown to be active compounds (1, 6, 7) and from the limited number of derivatives examined, it seemed that the nature of the substituents located at positions 3 and 4 on the quinoline nucleus influenced the magnitude of the antibacterial activity (6). Thus, the most active quinolone tested was 1-hydroxy-3-methyl-2(1*H*)-quinolone (**2***b*). In view of these results, it was desirable to prepare other quinoline derivatives and compare their antibacterial activities with those of **2***b*, and with aspergillic acid (**3**), a naturally-occurring antibacterial hydroxamic acid (8).

Most hydroxamic acids (**2**) were prepared in the manner illustrated in Scheme 1. The intermediate *N*-oxides were obtained using a variety of known methods, though most were prepared by oxidizing the appropriate quinoline with hydrogen peroxide. The *N*-oxides of 3,8-dimethylquinoline, 6,8-dimethylquinoline, and 7,8-dimethylquinoline did not form when these quinolines were treated with hydrogen peroxide in glacial acetic acid. The presence of an 8-methyl-substituent on the quinoline nucleus apparently hinders attack by the oxidizing agent on the nitrogen atom.

It has been established that stretching of the N—O group of various pyridine and pyrazine *N*-oxides results in a strong absorption band in the 1190 to 1350 cm^{-1} region of the spectrum (9). The infrared (i.r.) spectrum of each *N*-oxide prepared in this study was recorded for characterization purposes and compared with the spectrum of the parent quinoline. Listed in Table 1 are the positions of strong absorption bands observed in the 1220–1340 cm^{-1} region which were not present in the i.r. spectra of the corresponding quinolines.

TABLE 1
Infrared data on quinoline *N*-oxides*

Compound **1**	Infrared (cm^{-1})
a	1230, 1270 (KBr)
b	1220
c	1238, 1270 (KBr)
d	1222, 1320
e	1300, 1330
f	1270, 1295
g	1272, 1292
h	1260, 1340
i	1225, 1250, 1302
j	1310
k	1228, 1270
l	1230, 1270, 1310
m	1220, 1265, 1290

*Recorded as nujol mulls except where indicated.

Thirteen hydroxamic acids (**2***a–g*, *i*, *k–o*) were studied. The reported (10–12) antimicrobial activity of 4-nitroquinoline 1-oxide prompted the preparation of 1-hydroxy-4-nitro-2(1*H*)-quinolone (**2***e*). Ohta and Ochiai (13) concluded that this hydroxamic acid could not be obtained by treating 4-nitroquinoline 1-oxide with lead tetraacetate and rationalized why this was so. When their procedure was repeated in the present study it resulted in the formation of a brown solid which displayed properties characteristic of a hydroxamic acid. The product was soluble in sodium carbonate solution, gave a purple color with ferric chloride (14), and its i.r. spectrum was typical of a hydroxamic acid (15) having a broad hydroxyl band between 2100–3300 cm^{-1} and a carbonyl stretching band at 1660 cm^{-1}. Its mass spectrum was also consistent with a hydroxamic

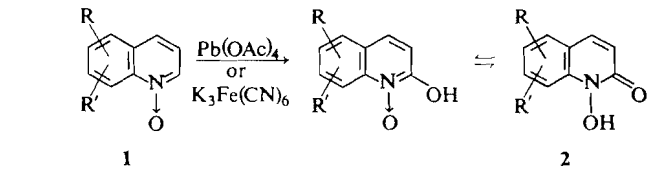

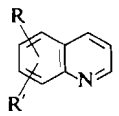

	R	R′		R	R′
a	H	H	*i*	4-Cl	H
b	3-Me	H	*j*	2-Cl	4-NO_2
c	4-Me	H	*k*	3-Me	6-Me
d	3-NO_2	H	*l*	3-Me	7-Me
e	4-NO_2	H	*m*	6-Me	7-Me
f	5-NO_2	H	*n*	3-CN	H
g	6-NO_2	H	*o*	3-NH_2	H
h	2-Cl	H			

SCHEME 1

acid structure. It exhibited peaks at *m/e* 206 and 190 for the molecular ion and the $(M-16)^+$ ion respectively (16).

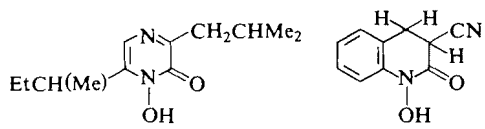

3 4

This conflict with the findings of Ohta and Ochiai made it imperative that the authenticity of the 4-nitroquinoline 1-oxide used in the lead tetraacetate reaction be established, especially as 5-nitroquinoline 1-oxide and 4-nitroquinoline 1-oxide have similar melting points and are both prepared (17) by nitration of quinoline 1-oxide with potassium nitrate and sulfuric acid. The authenticity of the 4-nitroquinoline 1-oxide was established by its facile conversion in excellent yield to 4-chloroquinoline 1-oxide when treated at 0° with acetyl chloride (18) or with hot concentrated hydrochloric acid (19). The 4-chloro-derivative was then oxidized with lead tetraacetate and the i.r. spectrum of the resulting hydroxamic acid was identical to that of 4-chloro-1-hydroxy-2(1*H*)-quinolone (**2***i*) prepared by an alternative route (20).

During the course of this study, an alternative method of synthesizing **2***e* was reported (20). The i.r. spectrum of the product obtained using this procedure was identical to that of the product isolated from the lead tetraacetate oxidation of 4-nitroquinoline 1-oxide. A commercial sample of 5-nitroquinoline was then successively oxidized with hydrogen peroxide and lead tetraacetate. The i.r. spectrum and the melting point of the product (**2***f*) differed significantly from those of **2***e*.

Antimicrobial Results

The five *N*-oxides which contained a nitro-group (**1***d*, *e*, *f*, *g*, *j*) and 13 cyclic hydroxamic acids (**2***a–g*, *i*, *k–o*) as well as aspergillic acid (**3**) and 3-cyano-3,4-dihydro-1-hydroxy-2(1*H*)-quinolone (**4**) (21) were tested for antibacterial activity and minimum inhibitory concentrations (m.i.c.) were determined. A tube dilution method using Kavanagh's method (22) for preparing the inoculum and performing the test, was employed. The antibacterial activities of the quinoline *N*-oxides and the hydroxamic acids are listed in Tables 2 and 3 respectively. Reference to Table 3 reveals that when a methyl group is located in the 3-position of the quinoline nucleus, the hydroxamic acid is active against both *S. aureus* and *E. coli*. The most active compound prepared and evaluated was 1-hydroxy-3,7-dimethyl-2(1*H*)-quinolone (**2***l*) but the antibacterial properties of other hydroxamic acids compared favorably with those of aspergillic acid. The hydroxamic acids containing a nitro-group, like the *N*-oxides,

Can. J. Chem. Downloaded from www.nrcresearchpress.com by 210.87.254.42 on 09/05/12
For personal use only.

Can. J. Chem. Downloaded from www.nrcresearchpress.com by 210.87.254.42 on 09/05/12
For personal use only.

TABLE 2

Antibacterial activities of some nitro-substituted quinoline *N*-oxides

Compound **1**	Minimum inhibitory concentration (mg %)	
	S. aureus	*E. coli*
d	7.8	4.0
e	0.25	0.1
f	>16	9.75
g	>16	>16
j	1.0	2.0

TABLE 3

Antibacterial activities of various 1-hydroxy-2(1*H*)-quinolones

Compound	Minimum inhibitory concentration (mg %)	
	S. aureus	*E. coli*
2*a*	>40	27.0
b	7.8	3.9
c	7.8	2.95
d	13.5	5.9
e	7.8	2.0
f	>16	>16
g	>16	>16
i	15.7	15.7
k	3.9	3.9
l	2.95	2.0
m	15.7	11.8
n	>16	>16
o	>16	11.8
3	7.8	3.9
4	5.9	15.7

exhibited greatest activity when the nitro-group was located in the 4-position of the quinoline nucleus. Subculturing showed that with one exception, all the compounds examined in this study and listed in Tables 2 and 3 were bacteriocidal agents. The exception was 4-chloro-1-hydroxy-2(1*H*)-quinolone (**2***i*) which was only bacteriostatic at 15.7 mg % against *S. aureus*.

It is of interest to compare the activities of 3-cyano-1-hydroxy-2(1*H*)-quinolone (**2***n*) and 3-cyano-3,4-dihydro-1-hydroxy-2(1*H*)-quinolone (**4**). The latter compound displayed much greater activity against *S. aureus*. This could mean that planarity of the molecule is not a necessary feature for antimicrobial activity. Further study on this topic is in progress.

As well as being treated for antibacterial properties as free acids, three compounds (**2***l*, **3**, **4**) were evaluated at p*H* 7 and found to be inactive at 15 mg % concentration. Changes in p*H* also affect the antibacterial activity of the chelating agent, oxine (23).

Experimental

Melting points are uncorrected. The i.r. spectra were recorded on a Beckman IR 10 spectrophotometer and mass spectra were measured with an A.E.I. MS 9 or MS 12 spectrometer using the direct insertion technique. Ethanolic solutions of all the hydroxamic acids prepared gave a purple color when treated with aqueous ferric chloride.

Most of the quinolines used in the preparation of *N*-oxides were purchased from commercial sources or were synthesized using literature methods; the dimethylquinolines used were provided by Dr. W. A. Ayer, Department of Chemistry, University of Alberta, Edmonton, Alberta.

General Method for the Preparation of N-Oxides

A procedure similar to that described by Kaslow and Buchner (24) was used in which 30% hydrogen peroxide (4 ml) was added to a solution of the quinoline (0.02 mole) in glacial acetic acid (20 ml). The reaction mixture was warmed to 65–70° for 3 h, then concentrated, basified with saturated sodium carbonate solution (70 ml), and extracted with chloroform. Removal of the chloroform yielded the *N*-oxide which was crystallized from acetone or ethanol. The known compounds **1***b*, *c*, *f*, and *g* were prepared in this way. Compounds **1***a* and *h* were prepared in a similar manner except that the reaction time was extended to 15 h. With the exception of **1***b*, these *N*-oxides had literature (25, 26, 28–30) melting points. Compound **1***b* melted at 81–83°, and not as previously reported (6). Oxides **1***i*, *j*, *d*, and *e* were prepared by alternative literature methods (18, 20, 27, 33).

Except for the nitro-quinoline *N*-oxides (**1***d*, *e*, *f*, *g*, *j*) which were yellow in color, all the *N*-oxides were colorless compounds.

3,6-Dimethylquinoline N-oxide (**1***k*), m.p. 69–71° (from ethanol), was prepared in 66% yield using the general method. Similarly, *3,7-dimethylquinoline N-oxide* (**1***l*), m.p. 131–132° (from ethanol) and *6,7-dimethylquinoline N-oxide* (**1***m*), m.p. 165–167° (from water) were obtained in 63 and 48% yields respectively. All were colorless compounds.

Anal. Calcd. for $C_{11}H_{11}NO$: C, 76.30; H, 6.36; N, 8.09. Found (**1***k*): C, 76.23; H, 6.72; N, 7.92. Found (**1***l*): C, 76.50; H, 6.70; N, 7.70. Found (**1***m*): C, 76.40; H, 6.59; N, 7.92.

General Method for the Preparation of Hydroxamic Acids

A procedure similar to that described by Ohta and Ochiai (13) was used. To a solution of the *N*-oxide (1 g) in benzene (ca. 50 ml) was added lead tetraacetate (5 g) and calcium carbonate (0.25 g). The mixture was boiled under reflux for 1.5 h then the precipitate was collected and washed with chloroform. The combined filtrate and washings were concentrated under reduced pressure. The residue was heated (95–98°) for 30 min in 10% hydrochloric acid to give the crude hydroxamic acid. It was collected by filtration and dissolved in 10% sodium

carbonate solution. This solution was extracted with ether and the ether extract was discarded. The aqueous layer was re-acidified (10% hydrochloric acid) and extracted with ether; evaporation of this ether extract yielded the hydroxamic acid which was crystallized from ethanol or benzene. All the hydroxamic acids were pale brown in color.

Hydroxamic acids (**2***a*, *b*, *c*, *i*, *n*, and *o*) were synthesized using literature methods (13, 21, 31, 32).

1-Hydroxy-4-nitro-2(1*H*)-quinolone (**2***e*), m.p. 198–200° (from ethanol) was obtained in 30% yield using the general method; lit. (20) m.p. 205–206°.

Anal. Calcd. for $C_9H_6N_2O_4$ (mol. wt. 206): C, 52.42; H, 2.91. Found (206 (mass spectroscopy)): C, 52.42; H, 3.32.

1-Hydroxy-3-nitro-2(1H)-quinolone (**2***d*), m.p. 214–216° (from ethanol), *1-hydroxy-5-nitro-2(1H)-quinolone* (**2***f*), m.p. 220–223° (from ethanol), and *1-hydroxy-6-nitro-2(1H)-quinolone* (**2***g*), m.p. 285–286° (from ethanol) were obtained in yields of 62, 23, and 47% respectively using the general method for the preparation of hydroxamic acids.

Anal. Calcd. for $C_9H_6N_2O_4$: C, 52.42; H, 2.91; N, 13.59. Found (**2***d*): C, 52.54; H, 3.31; N, 13.45. Found (**2***f*): C, 52.29; H, 3.04; N, 13.43. Found (**2***g*): C, 52.42; H, 2.74; N, 13.42.

1-Hydroxy-3,6-dimethyl-2(1H)-quinolone (**2***k*), m.p. 172–174° (from ethanol), *1-hydroxy-3,7-dimethyl-2(1H)-quinolone* (**2***l*), m.p. 169–170° (from ethanol), and *1-hydroxy-6,7-dimethyl-2(1H)-quinolone* (**2***m*), m.p. 228–230° (from benzene) were prepared in 46, 46, and 49% yields respectively using the above general method for hydroxamic acids.

Anal. Calcd. for $C_{11}H_{11}NO_2$: C, 69.84; H, 5.82; N, 7.41. Found (**2***k*): C, 69.64; H, 5.77; N, 7.06. Found (**2***l*): C, 69.45; H, 5.50; N, 7.24. Found (**2***m*): C, 69.65; H, 6.01; N, 7.54.

Antibacterial Testing

Six-hour cultures of *S. aureus* (strain F.D.A. 209 (A.T.C.C. 6538)) and *E. coli* (strain 402, Department of Microbiology, University of Alberta, Edmonton, Alberta) were separately diluted with nutrient broth using the method described by Kavanagh (22) to give two inoculated broths each containing 500–2000 bacteria per ml.

The general method of testing entailed the addition of serial dilutions of solutions of each *N*-oxide or hydroxamic acid (4 mg) in ethanol (0.5 ml) to tubes of nutrient broth (0.5 ml) followed by the addition of the inoculated broth (0.5 ml) to each serial tube. The tubes were then incubated at 37° and observed for growth at 16–18, 24, and 42 h intervals. Appropriate controls were performed also. Reproducible results were obtained.

Solution of compounds **2***j*, **3**, and **4** at p*H* 7 were prepared by dissolving the hydroxamic acid (10 mg) in excess 0.01 *N* sodium hydroxide solution and back-titrating with 0.01 *N* hydrochloric acid to p*H* 7. The solutions were diluted to 10 ml with water, then serial dilutions were made.

This study was supported financially by grants from Defence Research Board of Canada (No. 8875-05) and from Medical Research Council of Canada (No. MA 2993). The award of a Medical Research Council of Canada Studentship (to K.W.H.) is acknowledged. The authors thank Dr. W. A. Ayer for gifts of some quinolines.

1. G. T. Newbold and F. S. Spring. J. Chem. Soc. 1864 (1948).
2. W. A. Lott and E. Shaw. J. Amer. Chem. Soc. **71**, 70 (1949).
3. R. T. Coutts, M. Hooper, and D. G. Wibberley. J. Chem. Soc. 5058 (1961).
4. R. T. Coutts and D. G. Wibberley. J. Chem. Soc. 4610 (1963).
5. R. T. Coutts. Can. Pharm. J., Sci. Sect. **97** (6), 32 (1964).
6. R. T. Coutts, W. N. Pitkethly, and D. G. Wibberley. J. Pharm. Sci. **54**, 792, (1965).
7. R. T. Coutts, D. Noble, and D. G. Wibberley. J. Pharm. Pharmacol. **16**, 773 (1964).
8. F. Mathis. Bull. Soc. Chim. France, D9 (1953).
9. H. Shindo. Chem. Pharm. Bull. (Tokyo), **8**, 845 (1960).
10. I. Arai and I. Nakayama. J. Pharm. Soc. Japan, **72**, 167 (1952).
11. T. Okabayashi. J. Ferment. Technol. **31**, 416 (1953).
12. F. Leonard, F. A. Barkley, E. V. Brown, F. E. Anderson, and D. M. Green. Antibiot. Chemother. **6**, 261 (1956).
13. A. Ohta and E. Ochiai. Chem. Pharm. Bull. (Tokyo), **10**, 1260 (1962).
14. R. T. Coutts. Can. J. Pharm. Sci. **2**, 1 (1967).
15. R. T. Coutts, K. W. Hindmarsh, S. J. Powell, J. L. Pound, and E. M. Smith. Can. J. Pharm. Sci. **3**, 49 (1968).
16. R. T. Coutts and K. W. Hindmarsh. Org. Mass Spectrom. **2**, 681 (1969).
17. E. Ochiai and T. Okamoto. Yakugaku Zasshi, **70**, 384 (1950).
18. E. Ochiai. J. Org. Chem. **18**, 549 (1953).
19. T. Okamoto. J. Pharm. Soc. Japan, **71**, 297 (1951).
20. M. Yamazaki, K. Noda, J. Onoyama, and M. Hamana. Yakugaku Zasshi, **88**, 656 (1968).
21. R. T. Coutts. J. Chem. Soc. (C), 713 (1969).
22. F. Kavanagh. Analytical microbiology. Academic Press Inc., New York, 1963. p. 129, 131, 133.
23. A. Albert. Selective toxicity. Methuen and Co. Ltd., London, 1968. p. 331.
24. C. E. Kaslow and B. Buchner. J. Org. Chem. **23**, 271 (1958).
25. E. Ochiai. J. Org. Chem. **18**, 534 (1953).
26. E. Ochiai, M. Tshikawa, and S. Zai-Ren. J. Pharm. Soc. Japan, **64**, 72 (1944).
27. E. Ochiai and C. Kaneko. Chem. Pharm. Bull. (Tokyo), **7**, 267 (1959).
28. H. Tanida. Yakugaku Zasshi, **78**, 1079 (1958).
29. N. Kataoka, A. Imamura, Y. Kawazoe, G. Chichara, and C. Nagata. Chem. Pharm. Bull. (Tokyo), **14**, 177 (1966).
30. M. Yamazaki, N. Honjo, K. Noda, Y. Chono, and M. Hamana. Yakugaku Zasshi, **86**, 749 (1966).
31. M. Hamana, and M. Yamazaki. Chem. Pharm. Bull. (Tokyo), **10**, 51 (1962).
32. R. T. Coutts, G. Mukherjee, R. A. Abramovitch, and M. A. Brewster. J. Chem. Soc. (C), 2207 (1969).
33. M. Hamana and T. Nagayoshi. Chem. Pharm. Bull. (Tokyo), **14**, 319 (1966).

Can. J. Chem. Downloaded from www.nrcresearchpress.com by 210.87.254.42 on 09/05/12
For personal use only.

Can. J. Chem. Downloaded from www.nrcresearchpress.com by 210.87.254.6 on 09/05/12
For personal use only.

Surface studies by attenuated total reflection spectroscopy.[1] I. Corona treatment of polypropylene

D. J. CARLSSON AND D. M. WILES
Division of Chemistry, National Research Council of Canada, Ottawa, Canada

Received February 20, 1970

The chemical changes produced by brief corona treatments of polypropylene films have been studied by attenuated total reflection (a.t.r.) infrared spectroscopy. Surface layers of different thicknesses were investigated by varying the reflection conditions. Changes in the surface spectra were quantitatively compared by the use of an internal correction method which compensated for irreproducible experimental conditions. Corona treatment in a nitrogen atmosphere produced thin surface layers (less than 500 Å) of C—C unsaturation. Nitrogen derivatives were not detected in the surface. Corona treatment in oxygen caused surface changes which depended markedly on the corona conditions owing to the generation of ozone in the discharge zone. At low ozone concentrations, both unsaturation and oxidation were found in surface layers of under 500 Å thickness. At higher ozone concentrations, extensive oxidation occurred at appreciable depths into the polymer (several microns). An oxygen corona appears to result in essentially the same surface changes as does a nitrogen corona treatment, followed by exposure to ozone.

Canadian Journal of Chemistry, 48, 2397 (1970)

Introduction

The application of a high electric field to a gas can result in the partial ionization of the gas to give a plasma. Plasma treatment of polymers in general, and polyolefins in particular, offers a relatively cheap and effective method for the modification of the surface properties of films or fibers. For example, the printability of polyethylene film can be vastly improved by a brief air corona discharge treatment (i.e. exposure to a plasma at or near atmospheric pressure) (1). Some glow discharge treatments (i.e. plasma at about 2.0–0.2 Torr) improve the adhesive bonding properties of polyethylene surfaces (2, 3). The nature of the chemical and physical changes which occur during various types of plasma treatment of polyolefins has not yet been fully established, although the changes are reported to be confined to the surface layer of the substrates (2, 4). Because of this, many of the changes produced by plasmas are only detectable by conventional analytical techniques after extensive treatment. Surface changes in general can, however, be readily studied by an infrared (i.r.) technique known as attenuated total reflection (a.t.r.) spectroscopy. In the a.t.r. method, an i.r. beam is focussed into a suitable reflection element so that the beam undergoes total internal reflection at an interface between a substrate of relatively low refractive index, and the reflection element. If the surface of this substrate can absorb certain i.r. frequencies, the reflected beam is found to be accordingly attenuated. The reflected beam usually interacts strongly with a surface layer of the substrate which can vary from 0.1 to 4.0 μ (5). Attenuated total reflection spectroscopy has been employed to show qualitatively that surface changes have occurred during glow discharge treatment of polymers (2, 6). The quantitative use of a.t.r., however, has been limited by difficulties involved in the comparison of spectra recorded under various reflection conditions. In particular, it would be extremely useful to compare quantitatively the series of i.r. spectra which correspond to surface layers of increasing thickness for a given substrate. In this paper we describe a normalization procedure which allows a meaningful comparison of a.t.r. spectra. We have used a.t.r. spectroscopy to study the nature and location of the chemical changes which are produced by the corona discharge treatment of polypropylene in various atmospheres.

[1]NRCC No. 11 335.

Experimental

Materials

A 22 μ extruded film of predominantly isotactic polypropylene (Eastman) was used throughout. Prior to use, the film was Soxhlet extracted with acetone to remove additives and surface contaminants and then vacuum dried. Nitrogen (Linde 99.996%) and oxygen (Linde 99.5%) were used without further purification.

Corona Treatment

The demountable corona cell consisted of two concentric Pyrex tubes, separated by a 0.5 cm air gap. A cylindrical lead electrode was wrapped around the outer

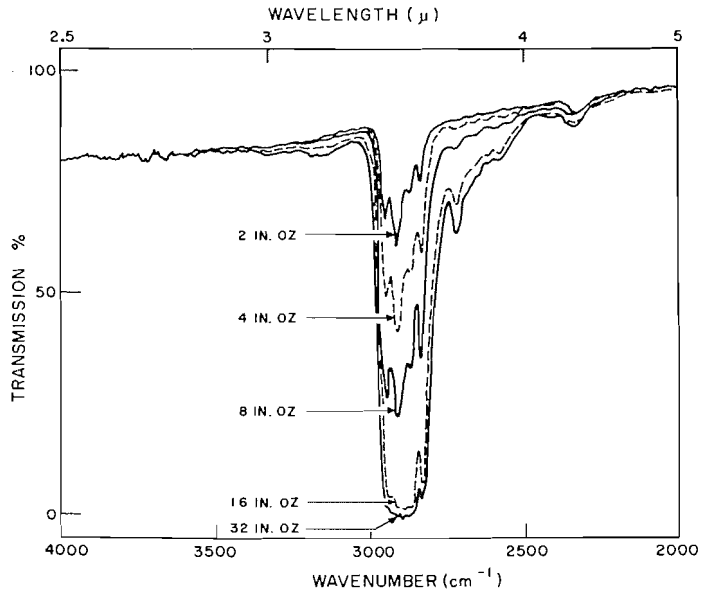

FIG. 1. Effect of film-reflection element contact on polypropylene a.t.r. spectra. Spectra recorded on KRS-5 at 45°. Values refer to torque wrench settings.

tube (i.d. 2.4 cm) and connected to ground. An aluminum rod fitted precisely inside the inner tube, and was connected to a small high frequency generator (Fisher Scientific Instruments, 120 V, 60 Hz, 0.28 A). The generator produces a potential of about 25 kV at a dominant frequency of 0.5 MHz, although overtones of this frequency are also present. The gap between the Pyrex tubes could be evacuated, or swept out by a gas. Polymer films (5 × 6 cm) were positioned centrally in the discharge zone, which extended over about 8 cm length. The films were attached to the inside wall of the outer tube by small pieces of adhesive tape, and the cells evacuated at 10^{-3} Torr for about 60 min before the required atmosphere was admitted. Gas was flowed through the cell at about 50 ml/min for 20 min, and then the flow rate was adjusted to the level required for the corona treatment. Immediately after the treatment, the cell was evacuated for at least 30 min before the sample was removed. Nitrogen coronas were accompanied by a uniform blue glow in the discharge zone, whereas the O_2 coronas did not emit visible light. Owing to decreases in the power output of the high frequency generator after prolonged use, comparison of data determined in different series of experiments was not possible. The reported quantitative experimental results are all comparable unless otherwise specified. Polypropylene film samples were also exposed to the gaseous effluent from corona discharges in a chamber attached to the corona cell. The volume separating these samples from the discharge zone was 15 ml.

Infrared Spectra

Infrared spectra were recorded on a Beckman IR-8 grating spectrometer coupled to a scale expansion unit and slave recorder. Surface spectra were recorded with the aid of a Wilks #9 a.t.r. attachment. Germanium or KRS-5 (TlBr–TlI mixed crystal) reflection elements (2 × 20 × 52.5 mm, 45° facets) were used at nominal angles of incidence of 30 or 45° (Ge) and 45 or 60° (KRS-5). Film samples were held against both faces of each reflection element with a Wilks MIR-29 sample holder. In order to improve the quality of the reflection spectra, the thumb screw provided with the MIR-29 was replaced with four 4-40 cap screws, as in the Wilks MIR-2 sample holder. The MIR-29 holder is more suitable than the MIR-2 holder for variable angle work, since the reflection element is always accurately located relative to the incident beam. Before use, each element was washed in benzene and acetone and vacuum dried. The a.t.r. spectra of each reflection element alone were frequently checked to guard against surface contamination with i.r.-absorbing impurities. To record an a.t.r. spectrum of a film, the film was cut into two pieces so as to cover most of each side of the reflection element. Each piece of film was backed by a resilient rubber pad (~1 mm thick) which was slightly smaller than the film sample. The steel pressure plates were assembled by sequentially tightening the four cap screws, by means of a small torque wrench, to the predetermined load. The rubber pads distributed the load provided by the pressure plates, and greatly improved the band intensity for a fixed torque setting (Fig. 1), especially for samples with slight surface irregularities. For quantitative work, reflection elements were selected which had transmissions in the range 35–40% (Ge) and 60–45% (KRS-5) at 2000 cm^{-1} on the IR8 spectrometer. All a.t.r. spectra were recorded with a scan speed of ~ 90 cm^{-1} min^{-1}; automatic slit control was used throughout.

The optical density (*O.D.*) values for corona-generated peaks were estimated from smooth base lines (curve *A*) as shown in Fig. 2. Each increase in normalized *O.D.*

Can. J. Chem. Downloaded from www.nrcresearchpress.com by 210.87.254.6 on 09/05/12
For personal use only.

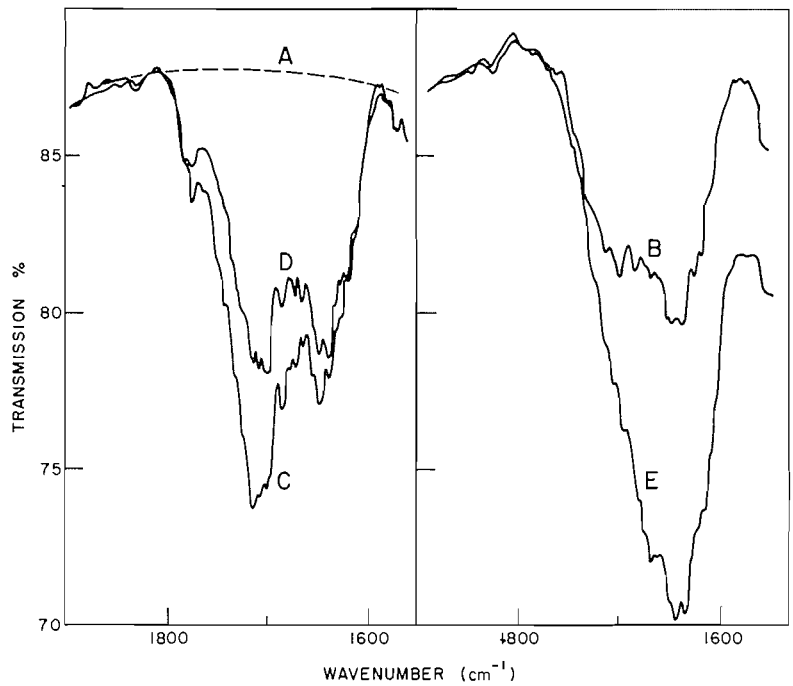

FIG. 2. Effect of corona treatment on polypropylene surfaces. *A*, artificial base line; *B*, spectrum due to untreated film and reflection element; *C*, surface exposed to 40 s O_2 corona, 20 ml/min O_2; *D*, surface exposed for 120 s to the effluent from an O_2 corona, 20 ml/min O_2; *E*, surface exposed to 100 s N_2 corona, 20 ml/min N_2. Attenuated total reflection spectra determined on KRS-5, 45°; each curve is an average of 3 or more scans. $O.D._{2840} \simeq 1.6$ in each case.

($\Delta O.D./O.D._{2840}$) due to corona treatment was calculated from the difference in normalized *O.D.* values between the treated sample and an untreated control sample (curve *B*). The control sample was always cut from an area adjacent to the film for corona treatment, and the two films marked so that the corresponding sides were always examined. Transmission spectra were recorded on double thicknesses of polymer film.

Results

Effect of Contact on a.t.r. Absorptions

Since the penetration of a reflected i.r. beam is quite low (roughly 0.1–4.0 μ, depending on wavelength) excellent contact between the sample and the face of the reflection element is required. This is shown in Fig. 1, which illustrates the variation in the intensity of the C—H absorptions in polypropylene with the torque used to tighten the sample holder screws. For practical purposes, loads of 24 in. oz. (KRS-5) and 40 in. oz. (Ge) were adopted. These values were chosen as the best compromise between the maximum attainable absorption and a reasonable working life for the reflection elements. Only slight frequency differences were observed between a given a.t.r. peak and the same peak recorded in the transmission mode. These differences were most noticeable on the KRS-5 element at 45°, when the a.t.r. frequencies were lower than the transmission values by less than 2 cm^{-1} for weak bands and about 5 cm^{-1} for intense bands ($O.D. \geqslant 0.7$). Consequently, the well-characterized transmission band assignments can easily be used to interpret a.t.r. spectra. The a.t.r. spectra of corona treated polypropylene films were usually recorded with the four reflection conditions listed in Table 1. The true angles of incidence listed in Table 1 were derived from the nominal values (30, 45, and 60°) by correcting for refraction at the 45° facets of the reflection elements.

Provided the absorbance is small, the absorbance ($O.D._1$) which results from a single internal reflection of the i.r. beam from a uniformly absorbing substrate is given by (5)

$$[1] \qquad O.D._1 = \varepsilon[C]E_0^2 \int_0^\infty e^{-\gamma z}\, dz$$

where ε is the molar extinction coefficient of the absorber, concentration [C], E_0 is the electric

Can. J. Chem. Downloaded from www.nrcresearchpress.com by 210.87.254.6 on 09/05/12
For personal use only.

TABLE 1

Attenuated total reflection conditions and calculated effective thicknesses

Reflection element	n_{31}*	θ† (degrees)	N‡	Infinite substrate§ $d_{e\perp}/\lambda_0$	Infinite substrate§ $d_{e\parallel}/\lambda_0$	Thin surface film¶ $d_{e\perp}/d$	Thin surface film¶ $d_{e\parallel}/d$
Ge	0.375	45	25	0.041	0.082	2.71	5.43
Ge	0.375	41	29	0.049	0.100	2.90	5.96
KRS-5	0.625	51	20	0.185	0.337	11.2	20.4
KRS-5	0.625	45	25	0.292	0.583	12.6	25.1

*Ratio of the refractive indices of polypropylene (medium 3, $n_3 = 1.50$) and the reflection element (medium 1).
†True angle of incidence, corrected for refraction at the 45° face.
‡Number of reflections from the full length of the element.
§Calculated from expressions [3*a*] and [3*b*].
¶Calculated from expressions [4*a*] and [4*b*].

field amplitude at the interface, z the depth of penetration into the sample, and γ is an experimental constant. Equation [1] is usually expressed in the form

$$[2] \qquad O.D._1 = \varepsilon[C]d_e$$

where d_e is known as the effective thickness. The effective thickness has been defined as the thickness of a film of the same material which would be required to give the same absorption for transmission at normal incidence (5). The d_e values depend on the polarization of the incident i.r. beam (polarization parallel, ||, or perpendicular, ⊥, to the plane of incidence), the incident wavelength in vacuum (λ_0), the refractive index (n_1) of the reflection element, and the angle of incidence θ. Harrick and du Pré (5) have published the following expressions for reflection from a uniformly absorbing, infinite substrate of refractive index n_3

$$[3a] \qquad d_{e\perp}/\lambda_0 = \frac{n_{31}\cos\theta}{\pi n_1(1 - n_{31}^2)(\sin^2\theta - n_{31}^2)^{\frac{1}{2}}}$$

$$[3b] \qquad \frac{d_{e\parallel}}{\lambda_0} = \frac{n_{31}\cos\theta(2\sin^2\theta - n_{31}^2)}{\pi n_1(1 - n_{31}^2)[(1 + n_{31}^2)\sin^2\theta - n_{31}^2](\sin^2\theta - n_{31}^2)^{\frac{1}{2}}}$$

For the special case of a very thin absorbing surface layer (thickness d, refractive index n_2) on an infinite substrate (5)

$$[4a] \qquad d_{e\perp}/d = 4n_{21}\cos\theta/(1 - n_{31}^2)$$

$$[4b] \qquad d_{e\parallel}/d = \frac{4n_{21}\cos\theta[(1 + n_{32}^4)\sin^2\theta - n_{31}^2]}{(1 - n_{31}^2)[(1 + n_{31}^2)\sin^2\theta - n_{31}^2]}$$

Various d_e values calculated from expressions [3] and [4] are shown in Table 1. In the calculation of the d_e/d values, n_2 and n_3 were taken to be equal. The d_e values increase with increasing depth of penetration (5) of the reflected beam. The beam penetration decreases in the sequence KRS-5 45° > KRS-5 60° > Ge 30° > Ge 45°. The polypropylene films can be regarded as being infinitely thick (at least up to $\lambda_0 = 10$ μ) for all reflection conditions.

For a given reflection element and substrate, the experimentally observed intensity of an a.t.r. absorption band depends on the sample area, the degree of contact of the sample with the element, the number of reflections from the interface, and the effective thickness. Consequently, it is difficult to make an absolute quantitative comparison of the a.t.r. intensities of a given i.r. absorption (band X), either for differently treated films, or for the same film under different reflection conditions. This problem can be overcome by using a polypropylene band as an internal standard. Ideally this band should not be affected by changes in long- and short-range order, or by extensive reaction. The polypropylene C—H stretching band at 2840 cm^{-1} (recorded during the same scan as band X) fulfilled these requirements. The normalized ratio of $O.D._X/O.D._{2840}$ is a convenient experimental parameter for comparing band absorbances. In most cases, the 2840 cm^{-1} polypropylene band was used directly for normalization. At high depths of penetration (KRS-5 at 45°) and in transmission spectra, the 2840 cm^{-1} band became too intense for accurate measurement (cf. Fig. 1). Under these conditions, the 2720 cm^{-1} band (possibly a C—H absorption) was used as a secondary standard and related to

Can. J. Chem. Downloaded from www.nrcresearchpress.com by 210.87.254.6 on 09/05/12
For personal use only.

Can. J. Chem. Downloaded from www.nrcresearchpress.com by 210.87.254.6 on 09/05/12
For personal use only.

the 2840 cm^{-1} normalization though the experimental ratio of $O.D._{2840}/O.D._{2720} = 10 \pm 1$ for the same film penetration. The validity of a normalization procedure can be illustrated by determining the normalized *O.D.* of the 1717 cm^{-1} $\rangle C{=}O$ absorption of a solution of 2,6-dimethyl-4-heptanone in isooctane (0.20 *M*) for the four reflection conditions listed in Table 1. The 2860 cm^{-1} band of isooctane was used as the reference absorption. The $O.D._{1717}/O.D._{2860}$ values were found to be constant to $\pm$ 8% despite the roughly 7-fold variation in $d_{e\perp}$. On the basis of a comparison of the theoretical *O.D.* values of several bands (calculated from $d_{e\perp}$, $d_{e\parallel}$ and the beam polarization) and the observed *O.D.* values, the contact between film samples and the reflection elements was estimated to be about 75% of the theoretical contact area (the total sample area).

Surface Changes During Corona Treatment

Polypropylene films were subjected to corona treatment in either oxygen or nitrogen at various flow rates for various periods of time. Corona treated surfaces were examined by transmission and a.t.r. spectroscopy. Attenuation total reflection spectra were recorded under the conditions listed in Table 1. Some changes in the a.t.r. spectra of corona treated surfaces are shown in Fig. 2. These spectra were recorded on the KRS-5 element at 45°. Other reflection conditions showed similar absorptions, although the band shapes were less well resolved due to the smaller absolute optical densities recorded for the lower depths of penetration. The corona-induced changes in the surfaces of polypropylene films (up to 150 s exposure) were not affected by physical processes such as evacuation or acetone extraction. Prolonged corona treatment, however, in both O_2 and N_2, produced surface oils and caused a decrease in the film thickness. A marked difference was always detected between the film surface which faced the air gap in the corona cell, and the surface which had been in contact with the Pyrex dielectric. For all types of corona, the latter surface showed only relatively slight changes in its a.t.r. spectrum, even on prolonged treatment. A similar effect has been observed previously during the O_2 corona treatment of polyethylene (4). All a.t.r. changes discussed in this paper refer to the surface facing the air gap.

(i) Nitrogen Corona

Changes in the i.r. spectra of polypropylene films after corona treatment in an N_2 atmosphere were only detected between 1750 and 1600 cm^{-1}. All a.t.r. spectra of corona treated films showed the fairly broad band centered at about 1650 cm^{-1} (Fig. 2). The absorption was extensively reduced after a few seconds exposure of the corona-treated film to ozone at room temperature, or after prolonged exposure (20 h or greater) to bromine water, and was not affected by prolonged exposure to concentrated aqueous HCl. A strong $\rangle C{=}O$ absorption ($\sim$ 1715 cm^{-1}) was detectable after O_3 treatment. The corona treatment of polypropylene in argon also resulted in a similar absorption at about 1650 cm^{-1}, which showed the same changes as the N_2 corona absorption under ozonolysis, bromination, and acid hydrolysis conditions. The 1650 cm^{-1} band is probably attributable to various types of C—C unsaturation (7), and not to the imine group ($\rangle C{=}N{-}$). The various polypropylene C—C unsaturation absorptions at about 900 cm^{-1} were difficult to determine due to overlap with the 900 and 974 cm^{-1} polypropylene bands (8). Shoulders at about 910 and 890 cm^{-1} indicated that some vinyl and vinylidene unsaturation was formed during corona treatment. A $\rangle C{=}O$ ($\sim$ 1715 cm^{-1}) absorption was not normally detected in the N_2 corona treated film samples, which were stored under vacuum for 30 min after treatment. However, immediate exposure of a treated surface to air, or the presence of trace amounts of O_2 in the cell during corona treatment, resulted in a small $\rangle C{=}O$ absorption as well as the dominant $\rangle C{=}C\langle$ band. This may indicate the presence of relatively long-lived macroradicals after corona treatment. Reaction of these radicals with air may contribute to some of the shoulders at $\sim$1700 cm^{-1} in curve *E* (Fig. 2). The observed normalized $\Delta O.D._{C=C}$ values for various corona conditions are listed in Table 2. The normalized $\Delta O.D._{C=C}$ values always decreased rapidly with increasing depth of penetration of the i.r. beam for the corona periods studied and appeared to be independent of the

TABLE 2

Normalized a.t.r. data for polypropylene corona treated at 23 °C*

Corona period (s)	Gas flow rate (ml/min)	$\Delta O.D._{C=C}/O.D._{2840}$† KRS-5 45°	KRS-5 60°	Ge 30°	Ge 45°	*Kd*
15	20	0.0025	0.0050	0.0076	0.0104	0.0043
40	0	0.0090	0.0126	0.0145	0.0211	0.0085
40	70	0.0060	0.0139	0.0153	0.0198	
100	0	0.0122	0.0178	0.0402	0.0528	0.0190
100	10	0.0159	0.0189	0.0349	0.0462	
15‡	70	0.0030	0.0050	0.0084	0.0092	
40‡	70	0.0009	−0.0141	−0.0206	−0.0242	

*N_2 corona unless otherwise specified. Normalized transmission $\Delta O.D._{C=C} < 0.0010$ in all cases.
†Depth of penetration increases in the sequence Ge 45° < Ge 30° < KRS-5 60° < KRS-5 45°.
‡O_2 corona.

TABLE 3

Normalized a.t.r. data for polypropylene, O_2 corona treated at 23 °C

Corona period (s)	Gas flow rate (ml/min)	$\Delta O.D._{C=O}/O.D._{2840}$† Trans-mission	KRS-5 45°	KRS-5 60°	Ge 30°	Ge 45°
15*	0	0.0020	0.0121	0.0118	0.0173	0.0111
30*	0	0.0041	0.0316	0.0324	0.0297	0.0308
60*	0	0.0063	0.0648	0.0960	0.0693	0.0790
15	0	0.0062	0.0291	0.0280	0.0314	0.0342
15	20	0.0048	0.0188	0.0224	0.0321	0.0342
15	70	<0.0010	0.0089	0.0114	0.0205	0.0238

*Generator power output much less than normal in these treatments.
†Depth of beam penetration increases in the sequence Ge 45° < Ge 30° < KRS-5 60° < KRS-5 45°.

N_2 flow rate during treatment. Corona treatment for periods greater than 200 s produced little further increase in the normalized $\Delta O.D._{C=C}$ values. This may indicate that surface ablation accompanies the chemical changes. Polypropylene films exposed to the gaseous effluent from N_2 corona discharges of up to 5 min duration showed no detectable changes in their a.t.r. spectra. The N_2 flow rate was 70 ml/min.

(ii) Oxygen Corona

A typical a.t.r. spectrum of a polypropylene film after corona treatment in an O_2 atmosphere is shown in Fig. 2. All corona treated films showed broad increases in the a.t.r. spectrum at about 1715 cm^{-1} and some also showed a 1650 cm^{-1} absorption. The former band is probably due to the presence of various types of carbonyl ($\rangle C{=}O$) substituents (7), and the latter is again due to various forms of C—C unsaturation. A broad absorption at about 3400 cm^{-1} which was probably attributable to —OH was detected, but only on prolonged corona treatment (of the order of minutes) at zero O_2 flow rate. After about 40 s of corona treatment a broad absorption also developed from about 1450 to 900 cm^{-1}. This absorption may be caused by the generation of backbone branch points in the sample surface. The observed $\rangle C{=}O$ and $\rangle C{=}C\langle$ a.t.r. absorptions were found to show a complicated dependence on the O_2 flow rate and the corona period. Examples of normalized $\Delta O.D.$ values recorded for these two absorptions under various corona conditions are shown in Tables 2 and 3. With zero gas flow through the cell, the normalized $\Delta O.D._{C=O}$ values were found to be independent of the depth of penetration of the i.r. beam for all lengths of corona treatment. This same effect was also observed for low flow rates ($\leqslant$ 20 ml/min) at the longer corona periods

Can. J. Chem. Downloaded from www.nrcresearchpress.com by 210.87.254.6 on 09/05/12
For personal use only.

Can. J. Chem. Downloaded from www.nrcresearchpress.com by 210.87.254.6 on 09/05/12
For personal use only.

($\geqslant$ 40 s). The small —OH absorption detected after prolonged corona treatment also appeared to be independent of the depth of penetration. Under all other corona conditions, the normalized $\Delta O.D._{C=O}$ absorbances decreased with increasing depth of penetration of the i.r. beam into the film sample. For relatively rapid O_2 flow rates ($\geqslant$ 20 ml/min) and short corona times ($\leqslant$ 30 s), the normalized $\Delta O.D._{C=C}$ values decreased with increasing depth of penetration of the i.r. beam. For longer corona periods, this ratio became negative and increased with depth of penetration (Table 2).

Polypropylene films were also exposed to the gaseous effluent from O_2 corona discharges. The a.t.r. spectra of these films usually showed a broad $\rangle C{=}O$ absorption centered at around 1715 cm^{-1}, but no increase in the C=C absorption. The normalized $\Delta O.D._{C=O}$ values were roughly constant for the four reflection conditions, but the $\rangle C{=}O$ band was not detectable in the transmission spectra of the samples. The $\rangle C{=}O$ bands produced in the film samples exposed to the O_2 corona effluent were always much weaker (5–10 times) than the corresponding bands produced in the surfaces of samples directly exposed to the corona, as shown in Fig. 1.

Discussion

A corona discharge contains a very low concentration of highly energetic electrons, which move under the applied voltage, and on collision with the gas, produce excited species (9). Consequently in a corona discharge, the gas is partially ionized and may contain electrons, ions, atoms, free radicals, and reactive molecules. From the a.t.r. changes observed as a result of the corona treatment of polypropylene, it is possible to draw some conclusions regarding the nature of the active species present in the discharge, together with the mode of interaction of these species with the polymer surface.

The a.t.r. changes observed during the N_2 corona treatment of polypropylene indicate that little nitrogen is incorporated into the surface. Absorptions at $\sim$ 3300 cm^{-1} (—NH), $\sim$ 2200 cm^{-1} (—C$\equiv$N), or $\sim$ 1420 cm^{-1} (—N=N—) were not detected, and the apparent resistance of the source of the 1650 cm^{-1} band to acid hydrolysis together with its ready ozonolysis and bromination precludes imine formation. The identification of C—C unsaturation as the major N_2 corona product is consistent with the observed generation of $\rangle C{=}C\langle$ during the low pressure He plasma treatment of polyethylene (2) and polypropylene (3). The reported absence of unsaturation after the low pressure N_2 plasma treatment of polypropylene (3) might possibly be due to the longer lifetime of reactive species at low pressure than that under our conditions. Since surface changes were not detected in polymer film samples exposed to the effluent from an N_2 corona for prolonged periods, long-lived gaseous reactive species (half-lives greater than about 2 s) are probably not produced during N_2 coronas. This is also indicated by the absence of an effect of N_2 flow rate on the surface spectra.

The theoretical treatment of attenuated reflection from a non-uniformly absorbing substrate is complex. However, attenuated reflection from a thin surface layer on an infinite substrate represents a simplified limiting case in a.t.r. theory, since the electrical field amplitude can be assumed to be constant across this thin layer (thickness d) (5). The $O.D._{C=C}$ value for a single reflection will then be given by substituting the values of d_e, for the thin layer case, expression [4], in expression [2]. The $O.D._{2840}$ value will, however, be given by substituting the values of d_e for an infinite substrate, expression [3], in expression [2]. The experimentally determined parameter, (the normalized $\Delta O.D.$) is then given by

$$[5] \quad \Delta O.D._{C=C}/O.D._{2840} = Kdn_1(\sin^2\theta - n_{21}^2)^{\frac{1}{2}}$$

where K is a constant for a given film.

$$K = 4\pi\varepsilon_{C=C}[\rangle C{=}C\langle]/(\lambda_{2840}\varepsilon_{2840}[C{-}H])$$

where λ_{2840} is the incident wavelength in vacuum, and $[\rangle C{=}C\langle]$ and [C—H] are, respectively, the concentrations of the unsaturation and the groups responsible for the 2840 cm^{-1} absorption. Expression [5] is independent of the polarization of the i.r. beam, but involves the assumption that the thin surface layer and the unreacted bulk of the substrate have similar refractive indices ($n_2 = n_3$). If $\varepsilon_{C=C}$ is assumed to be 20 M^{-1} cm^{-1} (7) and $\varepsilon_{2840}[C{-}H] = 6.6 \times 10^2$ cm^{-1} (calcu-

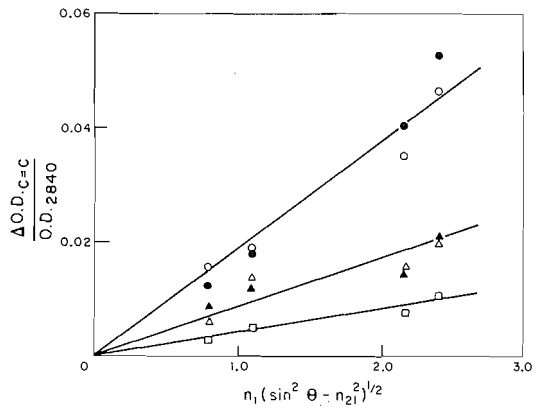

FIG. 3. Surface unsaturation produced during N_2 corona. Corona periods and N_2 flow rates were, respectively: □, 15 s, 20 ml/min; ▲, 40 s, 0 ml/min; △, 40 s, 70 ml/min; ●, 100 s, 0 ml/min; ○, 100 s, 10 ml/min.

lated from transmission spectra of films of known thickness), then $K = 0.11[C{=}C]\ \mu^{-1}$. Normalized transmission values approximate to the a.t.r. situation in which θ is equal to the critical angle, and $n_1(\sin^2\theta - n_{21}^2)^{\frac{1}{2}}$ is zero.

The N_2 corona data listed in Table 2 fit expression [5] quite closely. This is indicated by the linear plots through the origin of normalized $\Delta O.D.$ values against $n_1(\sin^2\theta - n_{21}^2)^{\frac{1}{2}}$ shown in Fig. 3. The slopes of these plots give the Kd values listed in Table 2. Unfortunately, the a.t.r. method does not allow the separation of the two parameters, the surface concentration [>C=C<] and the thickness of the reacted layer d. If [>C=C<] is arbitrarily assumed to be constant at 1.0 M, d values for N_2 corona periods of 15, 40, and 100 s are calculated to be about 40, 900, and 1900 Å, respectively. However, as the d values approach the smallest d_e values for an infinite substrate (~ 0.24 μ for Ge at 45°) the linear plots shown in Fig. 3 can be expected to level off at high $n_1(\sin^2\theta - n_{21}^2)^{\frac{1}{2}}$ values. Since curvature is not apparent, even after a 100 s N_2 corona (Fig. 3), d is probably less than 600 Å (certainly much less than 0.24 μ) in all cases, and prolonged corona must produce high concentrations of unsaturation in an extremely thin surface layer. Curvature was detected for data obtained from some O_2 corona treated films.

Soxhlet extraction with *p*-xylene at 138 °C under nitrogen showed that some gel was detectable after 100 s of N_2 corona treatment. If this gel is assumed to have a density of 1.0 g/ml and to be uniformly distributed over the treated surface, the thickness of the crosslinked layer was found to be about 400 Å (60 mg film sample). Based on the assumption that crosslinking and unsaturation are found together in the treated film, the gel value coupled with the a.t.r. Kd value leads to a [>C=C<] of 5 M after a 100 s corona. Based on the gel content, the surface film thickness produced by glow discharge treatment of polyethylene in inert gases (H_2, He, and Ne) has been estimated to range from 300 Å (1 s exposure) to 2000 Å (100 s exposure) and to be independent of the nature of the gas (2).

It may seem paradoxical that thin surface layers (possibly less than 100 Å) can be studied in the presence of surface irregularities, such as occasional calendering marks, which may be as great as 1000 Å in depth. The presence of ridges on the film surface will introduce the problem of frustrated attenuated total reflection (f.a.t.r.) due to the presence of gaps of varying thickness between the film and the element (10). This effect is responsible for the variation in intensity shown in Fig. 1. However, from expression [1], although the observed $O.D.$ is dependent on the field amplitude (E_0') at the film surface, the normalized $\Delta O.D.$ value is independent of E_0' and consequently is not influenced by variations in the degree of contact between the film and the reflection element. This conclusion was confirmed experimentally for a three-fold variation in degree of contact.

In some respects, O_2 corona treatment of polypropylene appears to be similar to the N_2 corona bombardment. The O_2 treatment, however, is complicated by the generation of ozone in the discharge. Ozone has been proposed to be mainly responsible for the oxidation products produced during the O_2 corona treatment of polyethylene (4). Ozone is known to combine rapidly with olefinic unsaturation to give ozonides, which at room temperature usually decompose rapidly to give carboxylic acids, aldehydes, ketones, and probably some peroxides (11). Some of these products have been detected after ozonolysis of polyethylene (12). For brief O_2 corona periods (15 s or less) at moderate flow rates, unsaturation appears to be formed in an

Can. J. Chem. Downloaded from www.nrcresearchpress.com by 210.87.254.6 on 09/05/12
For personal use only.

Can. J. Chem. Downloaded from www.nrcresearchpress.com by 210.87.254.6 on 09/05/12
For personal use only.

extremely thin surface layer, and in roughly the same total quantity as found in similar N_2 corona treatments (Table 2). Under static conditions, and for prolonged treatment in flow systems, O_3 reaction probably occurs with the surface unsaturation generated during the corona bombardment, and also with the unsaturation normally uniformly distributed across the polymer. This leads to a zero or negative change in unsaturation (Table 2). From Fig. 2 the main surface oxidation products appear to be $\sim C(=O)OH$ (~ 1710 cm^{-1}) and possibly $\sim CH_2—C(=O)—CH_2\sim$ (~ 1717 cm^{-1}) (7). The presence of O_3 in the discharge zone will also account for the oxidation of films placed in the effluent, since O_3 has a considerable half-life at 23 °C (11). The very low extent of oxidation observed in films exposed to the O_2 corona effluent as compared with the films placed directly in the discharge zone (Fig. 2) might indicate direct reaction in the discharge zone between short-lived activated oxygen species and the polymer surface or between radicals or ions generated in the polymer surface and O_2 (13). However, when a film was first corona treated in N_2 for 40 s and then exposed to an O_2 corona effluent for 40 s, the $\rangle C=O$ absorption of the corona treated surface was virtually identical (both in intensity and band contour) to the corresponding absorption of a film which had been O_2 corona treated for 40 s. Consequently, with respect to the polymer surface changes, the primary effect of an O_2 corona is equivalent to the effect of an N_2 corona bombardment followed by reactions with O_3, and the observed oxidation is due to O_3 attack.

The a.t.r. data in Table 3 for treatment under static conditions are consistent with extensive O_3 diffusion into the polymer (at least to depths greater than 2 μ), since the normalized $\Delta O.D._{C=O}$ is independent of the depth of penetration of the reflected i.r. beam. Oxidation had not proceeded throughout the sample, since the increase in the normalized transmission $\Delta O.D._{C=O}$ was usually very small. The dependence of the normalized $\Delta O.D._{C=O}$ values on $n_1(\sin^2\theta - n_{21}^2)^{\frac{1}{2}}$ is shown in Fig. 4 for samples exposed to 15 s corona treatments at various flow rates. As the flow rate is increased, the a.t.r. spectra indicate effects ranging from uniform oxidation (at least in a

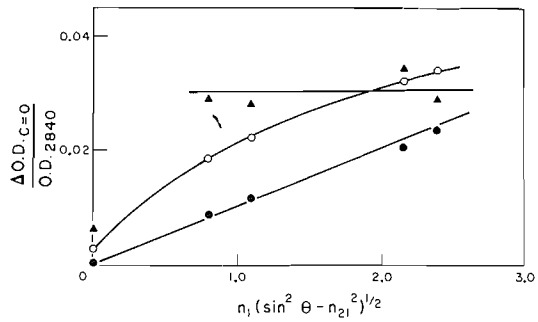

FIG. 4. Surface oxidation produced during O_2 corona. Corona period 15 s, O_2 flow rates: ▲, 0 ml/min; ○, 20 ml/min; ●, 70 ml/min.

surface layer of greater than ~ 2 μ in thickness) at zero flow, to the thin layer case at 70 ml/min (linear increase in normalized $\Delta O.D._{C=O}$). The plot for the intermediate flow rate (20 ml/min) appears to be curved, indicating oxidation close to the surface, but with some oxidation now extending into the sample (greater than ~ 0.2 μ) due to limited O_3 diffusion into the sample. If the average $[\rangle C=O]$ is assumed to be 1 *M*, the slope of the linear plot shown in Fig. 4 ($Kd = 0.0085$) leads to a value of about 400 Å for the average thickness of the corona induced layer. (The average $\varepsilon_{C=O}$ is assumed to be ~ 400 M^{-1} cm^{-1} (7).)

The surface products generated by O_2 and N_2 corona treatments of polypropylene must be explained in terms of the radicals, excited molecules, ions, and electrons which are generated in plasmas. Atomic nitrogen and excited molecules (N_2^*) are probably present in N_2 plasma (13), and oxygen plasma contains both atomic and singlet oxygen ($^1\Sigma_g$ and $^1\Delta_g$) (cf. ref. 3). However, the surface products from the N_2 corona discharge treatment contained no detectable N-products, and all of the surface oxidation which resulted from O_2 corona treatment was attributable to secondary reactions with O_3. In addition, both treatments appeared to lead to the same primary product, C—C unsaturation. This probably means that at atmospheric pressure, the maximum concentrations of species such as $N\cdot$, $O\cdot$, N_2^*, and O_2^* are too low to result in detectable chemical attack on the polymer. The effects of inert-gas glow discharges on polymers have been discussed in terms of energy transfer

from excited gas molecules to the polymer surface (2). This transfer was proposed to generate H atoms which diffused into the polymer and caused the observed penetration of the glow discharge effect (up to 10^4 Å). Alternatively, H· production has been attributed to trace amounts of H_2O in the glow discharge zone (14). However, extensive diffusion of any O_2 corona-generated H· into polypropylene would seem unlikely in the presence of O_2. Traces of moisture may result in H_2O ions being a major ionic product from O_2 and N_2 corona discharges (15). The penetration of ions into solids is very low (7×10^{-4} g/cm^2 for 1 MeV α particles) (16), and is probably much less than 10 Å for ions from a corona discharge. It has been suggested that electron bombardment was responsible for air corona effects observed on polyethylene surfaces (17). The observed primary corona products from polypropylene (unsaturation and gel) are similar to the products produced by electron bombardment of the polymer (8). However, Hougen has pointed out that only 4% of the electrons in a corona at 760 Torr can have energies $\geqslant$ 11 eV (18), and can thus have polypropylene penetrations $\geqslant$ 10 Å (16). Nevertheless, it may be possible that a small but significant fraction of the generated electrons do have energies of $\sim 10^3$ eV with sufficiently large penetrations ($\sim$ 400 Å) (16) to produce the observed O_2 and N_2 corona surface products. Obviously an extensive study of the reactive species and electron energy distribution is required to evaluate the possible reaction mechanisms which can occur in a solid subjected to corona discharge.

1. K. Rossmann. J. Polym. Sci. **19**, 141 (1956).
2. H. Schonhorn and R. H. Hansen. J. Appl. Polym. Sci. **11**, 1461 (1967).
3. J. R. Hall, C. A. L. Westerdahl, A. T. Devine, and M. J. Bodnar. J. Appl. Polym. Sci. **13**, 2085 (1969).
4. G. D. Cooper and M. Prober. J. Polym. Sci. **44**, 397 (1960).
5. N. J. Harrick and F. K. du Pré. Appl. Opt. **5**, 1739 (1966).
6. P. L. Kronick, K. E. Jesch, and J. E. Bloor. J. Polym. Sci. Part A1, 7, 767 (1969).
7. D. J. Carlsson and D. M. Wiles. Macromol. **2**, 587 (1969).
8. R. M. Black and B. J. Lyons. Proc. Roy. Soc. London, Ser. A, **253**, 322 (1959).
9. P. H. Dundas and M. L. Thorpe. Chem. Eng. **76**, 124 (1969).
10. N. J. Harrick. Internal reflection spectroscopy. Interscience Publishers, Inc., New York. 1967. p. 36 *et seq.*
11. J. S. Belew. In Oxidation. Vol. 1. *Edited by* R. L. Augustine. Marcel Dekker, Inc., New York. 1969. pp. 259–335.
12. H. C. Beachell and S. P. Nemphos. Advan. Chem. Ser. #21, 168 (1959).
13. (*a*) J. L. Weininger. J. Phys. Chem., **65**, 941 (1961). (*b*) P. M. Hay. Advan. Chem. Ser. #80, 350 (1969).
14. S. Schlick, T. Cole and H. C. Heller. J. Chem. Phys., **47**, 1874 (1967).
15. M. M. Shahin. Advan. Chem. Ser. #80, 48 (1969).
16. A. Charlesby. Atomic radiation and polymers. The Pergamon Press, Ltd., Oxford. 1960. Ch. 3.
17. R. F. Grossman and W. A. Beasley. J. Appl. Polym. Sci. **2**, 163 (1959).
18. L. R. Hougen. Nature, **188**, 577 (1960).

Can. J. Chem. Downloaded from www.nrcresearchpress.com by 210.87.254.6 on 09/05/12
For personal use only.

Can. J. Chem. Downloaded from www.nrcresearchpress.com by 210.87.254.5 on 09/05/12
For personal use only.

Effet des anions sur la vitesse d'oxydation de la cyclohexanedione-1,2 par l'ion thallique

R. FAVIER ET M. ZADOR
Département de chimie, Université de Montréal, Montréal, Québec

Reçu le 5 février 1970

The effect of acetate, chloride, bromide, nitrate, and sulfate anions on thallic ion oxidation of 1,2-cyclohexanedione has been studied. Reactivities of the different complexes Tl(III)–anions have been determined. Generally introduction of a ligand in the internal coordination sphere of thallic ion produces an increase in the rate constant.

L'influence des ions acétate, chlorure, bromure, nitrate, et sulfate sur la vitesse d'oxydation de la cyclohexanedione-1,2 par l'ion thallique a été étudiée. La réactivité des différents complexes de l'ion thallique avec les anions a été déterminée. En général l'introduction d'un ligand dans la sphère de coordination de l'ion thallique entraîne un accroissement de la constante de vitesse.

Canadian Journal of Chemistry, 48, 2407 (1970)

Introduction

La cyclohexanedione-1,2 a été oxydée en hydroxy-3, cyclohexanedione-1,2 par l'ion thallique. Dans ce travail précédent (1) nous avons effectué l'étude cinétique de la réaction et mis en évidence les espèces réactionnelles en milieu perchlorique. Dans l'étude présente nous avons analysé les effets des anions sur la cinétique de l'oxydation et étudié l'influence des anions, acétate, chlorure, bromure, sulfate, et nitrate.

Nous avons pensé qu'il serait intéressant de comparer nos résultats d'une part aux travaux sur l'oxydation des oléfines par l'ion Tl(III) en divers milieux (2–5) et d'autre part à l'oxydation de l'éthylène par les sels de palladium (6–9).

Les constantes de stabilité des complexes Tl(III)–anions ont été déterminées par diverses méthodes: calorimétrique, potentiométrique, spectrophotométrique (10–14).

Partie expérimentale

Les méthodes expérimentales ont été décrites auparavant (1).

Les divers anions ont été ajoutés sous forme de sels de pureté analytique. Les tampons acétiques ont été préparés par neutralisation partielle d'acide acétique au moyen d'une solution d'hydroxyde de sodium dosée au préalable.

La force ionique a été maintenue constante par une solution de perchlorate de sodium obtenue par neutralisation d'une solution d'acide perchlorique par l'hydroxyde de sodium ; ceci était rendu nécessaire parce que, comme nous l'avons vu auparavant (1), certains sels obtenus commercialement contiennent des traces suffisantes d'ions chlorure pour altérer d'une manière notable la vitesse de la réaction.

Résultats

L'oxydation de la cyclohexanedione-1,2 par l'ion thallique obéit à une équation de vitesse d'ordre deux (éq. [1]), où [E] est la concentration

$$[1] \qquad V = k_{exp}\,[Tl(III)]\,[E]$$

de la forme énolique de la cyclohexanedione-1,2 et le terme $k_{exp}\,[Tl(III)]$ comprend la contribution à la vitesse des complexes en solution du Tl(III) avec les ligands. Il est évident que dans ces conditions éq. [1] est valable pour autant que les rapports de concentration des différentes espèces réactives restent constants; pour cela on a travaillé en vitesse initiale (Br^-, Cl^-) ou bien on a maintenu un excès de ligand en solution (CH_3COO^-, SO_4^{2-}, NO_3^-).

La stabilité des complexes de l'ion thallique avec les anions étudiés a été rapportée dans la littérature (10–14). Ils se forment d'après l'équation globale [2]. Le tableau 1 résume les différentes valeurs des βmn obtenues ainsi que les $\beta' mn$ représentant les meilleures valeurs de ces constantes en vue de l'interprétation de nos résultats, valeurs qui sont très voisines de celles estimées en tenant compte de l'influence de la force ionique.

$$[2] \quad Tl^{3+} + nX^{p-} + mH_2O \overset{\beta mn}{\rightleftharpoons} [TlX_n(OH)_m]^{3-np-m} + mH^+$$

Influence de l'ion acétate

L'étude cinétique de l'influence de l'ion acétate a été effectuée dans une gamme très large de concentrations en acétate; dans ces conditions

Can. J. Chem. Downloaded from www.nrcresearchpress.com by 210.87.254.5 on 09/05/12
For personal use only.

TABLEAU 1

Composition et constantes de stabilité des complexes thallium(III)–anions*

Ion complexe	log βmn	log $\beta' mn$	Références
$TlOH^{2+}$	−1.18	−1.07	10
$TlOAc^{2+}$	6.17	5.60	11
$Tl(OAc)_2^{+}$	11.28	10.8	11
$Tl(OAc)_3$	15.10	15.10	11
$Tl(OAc)_4^{-}$	18.30	18.30	11
$Tl(OAc)_2OH$	8.91	8.91	11
$TlCl^{2+}$	6.25	6.25	12, 13
$TlCl_2^{+}$	11.41	11.41	12, 13
$TlCl_3$	14.50	14.50	12, 13
$TlCl_4^{-}$	17.00	17.00	12, 13
$TlBr^{2+}$	8.90	8.52	12, 13
$TlBr_2^{+}$	16.40	17.38	12, 13
$TlBr_3$	22.10	22.30	12, 13
$TlBr_4^{-}$	26.10	26.43	12, 13
$TlSO_4^{+}$	1.95	1.95	14
$Tl(SO_4)_2^{-}$	3.74	3.74	14
$H(TlSO_4)^{2+}$	0.27	0.27	14
$TlNO_3$	0.9	0.9	11
$Tl(NO_3)_2^{+}$	0.12	0.12	11

*$HOAc \rightleftarrows H^+ + OAc^-$; log $K_a = -4.53$ (5); $HSO_4^- \rightleftarrows H^+ + SO_4^{2-}$, log $K_a = -0.92$ (14).

l'éventuelle formation d'acétate d'énol peut être écartée.

Les conditions expérimentales sont données dans les trois premières colonnes du tableau 2 où $[OAc]_t$ est la concentration totale en acétate, $[H^+]$ la concentration en ion H^+ à l'équilibre, et $[OAc^-]$ la concentration en ion acétate à l'équilibre que nous avons faite varier de trois façons différentes: (*i*) de 1.0×10^{-8} à 3×10^{-5} *M* par addition de quantités croissantes d'acide acétique à une solution 0.5 *M* en acide perchlorique; (*ii*) de 5.9×10^{-5} à 3.2×10^{-4} *M* par diminution de la concentration d'acide perchlorique ajoutée à une solution 0.5 *M* en acide acétique. (Dans les deux cas ci-dessus (*i* et *ii*) la concentration en acétate à l'équilibre a été calculée à partir de la constante d'acidité.) (*iii*) de 2.0×10^{-3} à 6.0×10^{-2} *M* en utilisant divers tampons.

L'utilisation des valeurs des $\beta' mn$ du tableau 1 nous a permis de calculer à l'aide d'un ordinateur les concentrations des divers complexes à l'équilibre[1] (voir tableau 2). Dans nos conditions expérimentales éq. [1] est vérifiée dans toute la gamme de concentration d'ion acétate étudiée, en effet la concentration totale en ligand est toujours en grand excès par rapport au Tl(III) (sauf pour les premières expériences mais, même dans ces cas, la concentration en acétate peut être considérée comme constante compte tenu de la faible quantité d'acétate engagée dans les complexes).

A faible concentration en acétate nous obtenons une augmentation de la vitesse ce qui implique nécessairement une réactivité de l'espèce $Tl(OAc)^{2+}$ supérieure à l'espèce Tl^{3+}. Néanmoins l'ensemble des résultats nous impose de tenir compte de la contribution de certaines autres espèces à la vitesse. Nous avons interprété nos résultats à l'aide de éq. [3].

$$[3] \quad V = [E]\{k_{Tl}[Tl^{3+}] + k_{TlOH}[TlOH^{2+}] + k_{TlOAc}[TlOAc^{2+}] + k_{Tl(OAc)_2} \times [Tl(OAc)_2^{+}] + k_{Tl(OAc)_3}[Tl(OAc)_3] + k_{Tl(OAc)_2OH}[Tl(OAc)_2OH]\}$$

A des faibles concentrations en ion acétate le seul complexe en concentration appréciable est $TlOAc^{2+}$; sa constante de vitesse peut être calculée à partir de l'équation [3] en soustrayant de la vitesse expérimentale la contribution due aux espèces Tl^{3+} et $Tl(OH)^{2+}$, k_{Tl} et k_{TlOH} ayant été déterminées auparavant (1).

Par des itérations successives on a déterminé les autres constantes de vitesse de éq. [3]; les valeurs de ces constantes sont données dans le tableau 3.

Dans nos conditions il y a des espèces comme $Tl(OAc)OH^{+}$ dont nous ne pouvons déterminer la réactivité; sa concentration reste faible dans toute la gamme étudiée et sa contribution à la vitesse ne peut dépasser en aucun cas 5%. Dans la zone de fortes concentrations en acétate la réactivité est non négligeable; l'étude dans des mélanges tampon acide acétique – acétate de p*H* différents nous a porté à attribuer la réactivité à l'espèce $Tl(OAc)_2OH$.

Dans la fig. 1 nous avons porté la contribution à la vitesse totale de chaque espèce de éq. [3], contribution calculée avec les paramètres du tableau 3 et les concentrations des espèces du tableau 2.

La somme de ces contributions nous donne la vitesse totale calculée, courbe *a*. On constate un bon accord entre la courbe théorique et les points expérimentaux.

[1]On donne à l'entrée les concentrations totales des réactifs et la constante d'équilibre de chaque réaction et on calcule la concentration libre des espèces en utilisant le programme Potag 2 (15) que le Professeur A. L. Beauchamp du Département de Chimie (Université de Montréal) a bien voulu mettre à notre disposition dans une version adaptée à nos systèmes.

Can. J. Chem. Downloaded from www.nrcresearchpress.com by 210.87.254.5 on 09/05/12
For personal use only.

TABLEAU 2

Distributions des complexes Tl(III)–OAc*

$[OAc]_t$ $\times 10^2 M$	$[H^+]$ $\times 10^2 M$	$[OAc^-]$ $\times 10^5 M$	$[Tl^{3+}]$ $\times 10^5 M$	$[TlOH^{2+}]$ $\times 10^5 M$	$[TlOAc^{2+}]$ $\times 10^5 M$	$[Tl(OAc)_2^+]$ $\times 10^5 M$	$[Tl(OAc)_3]$ $\times 10^5 M$	$[Tl(OAc)_4^-]$ $\times 10^5 M$	$[Tl(OAc)_2OH]$ $\times 10^5 M$	$V_{exp}/[E]$ $\times 10^3 s^{-1}$	$V_{calc.}/[E]$ $\times 10^3 s^{-1}$
0.00	50.0	0.00	21.3	3.70	—	—	—	—	—	5.41	6.33
0.025	49.9	0.0014	21.1	3.59	0.123					5.78	6.35
0.10	49.9	0.0058	20.7	3.54	0.485					9.25	7.57
0.30	49.9	0.017	19.8	3.38	1.39					10.04	10.28
0.50	49.9	0.029	19.0	3.24	2.22	0.10				12.81	12.81
0.75	49.9	0.044	18.0	3.07	3.16	0.22				15.83	15.67
1.00	49.9	0.058	17.1	2.91	3.99	0.37				17.75	18.17
5.00	49.9	0.294	8.1	1.38	9.46	4.41	0.26		0.11	35.60	36.97
10.0	49.9	0.588	3.9	0.67	9.25	8.64	1.01		0.22	37.75	37.87
50.0	49.9	2.949	0.2	0.04	2.81	13.1	7.72	0.36	0.34	18.36	19.45
50.0	24.9	5.90			1.08	10.1	11.86	1.10	0.52	10.76	18.33
50.0	10.0	14.71			0.22	5.18	15.22	3.54	0.67	7.28	7.98
50.0	4.64	31.75			0.05	2.30	14.59	7.34	0.64	4.18	5.23
8.54	0.026	857.3					1.68	22.8	0.48	1.42	1.13
2.13	0.024	223.3					4.07	14.4	4.87	8.31	8.78
2.13	0.011	420.9					2.63	17.5	3.54	6.30	6.43
4.27	0.025	432.5					2.92	20.0	1.71	2.97	3.33
4.27	0.011	843.6					1.65	22.1	1.08	1.72	2.10
21.3	0.026	2135					0.72	24.2	0.08	0.17	0.17
58.0	0.026	5804					0.27	24.7	0.01	<0.17	<0.17

*$T = 25$ °C; $[E] = 1.0 \times 10^{-4} M$; $[Tl(III)] = 2.5 \times 10^{-4} M$; force ionique $\mu = 0.5$.

TABLEAU 3

Constantes de vitesse en milieu acétate*

k_{TlOAc} mole^{-1} l s^{-1}	$k_{Tl(OAc)_2}$ mole^{-1} l s^{-1}	$k_{Tl(OAc)_3}$ mole^{-1} l s^{-1}	$k_{Tl(OAc)_2OH}$ mole^{-1} l s^{-1}
3.3×10^2	0.67×10^2	0.18×10^2	1.67×10^2

*[E] = 1.0×10^{-4} M; [Tl^{3+}] = 2.5×10^{-4} M; force ionique $\mu = 0.5$; $T = 25$ °C; $k_{Tl} = 0.12 \times 10^2$ mole^{-1} l s^{-1}; $k_{TlOH} = 0.93 \times 10^2$ mole^{-1} l s^{-1}.

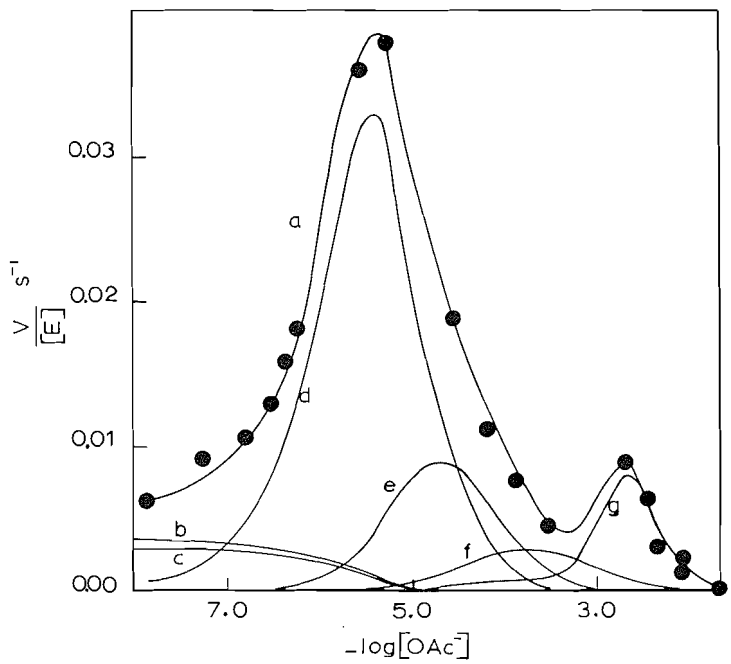

FIG. 1. Influence de l'ion acétate: courbes calculées et points expérimentaux; $T = 25$ °C; [Tl(III)] = 2.5×10^{-4} M; [Enol] = 1.0×10^{-4} M; force ionique $\mu = 0.5$; [H^+] = 0.5 M. Courbe *a* vitesse totale; contributions à la vitesse: Tl^{3+}, courbe *b*; $TlOH^{2+}$, courbe *c*; $TlOAc^{2+}$, courbe *d*; $Tl(OAc)_2^+$, courbe *e*; $Tl(OAc)_3$, courbe *f*; $Tl(OAc)_2OH$, courbe *g*.

En examinant la fig. 1 on constate que dans une gamme assez grande de concentration en acétate l'espèce $Tl(OAc)^{2+}$ a une contribution prépondérante, courbe *d*, ce qui nous permet de déterminer sa constante de vitesse sans ambiguité. Etant donné que dans la gamme où la contribution de $Tl(OAc)_2^+$, courbe *e*, serait la plus importante, celle de $Tl(OAc)^{2+}$ est loin d'être négligeable, la valeur de $k_{Tl(OAc)_2}$ obtenue est entachée d'erreur plus importante. Cet effet est encore plus important dans le cas de $Tl(OAc)_3$, courbe *f*. La courbe *g* représente la contribution à la vitesse de $Tl(OAc)_2OH$ obtenue dans des mélanges tampon de pH différents; dans ces conditions on a pu écarter l'intervention de toutes les autres espèces et l'incertitude sur la constante de vitesse est moins grande. L'incertitude sur les valeurs des constantes de stabilité β ne nous permet pas une détermination de l'erreur relative aux constantes de vitesse; dans ces conditions nous n'avons pas tenté de déterminer les paramètres d'activation.

Influence des ions chlorure et bromure

L'ion thallique forme des complexes du type TlX_n^{3-n} avec $X = Br^-$ ou Cl^-. Nous avons effectué d'une manière très approfondie l'étude de l'influence de ces ions; les résultats sont groupés dans les figs. 2 et 3.

(*i*) Dans le domaine de concentration en X^-

Can. J. Chem. Downloaded from www.nrcresearchpress.com by 210.87.254.5 on 09/05/12
For personal use only.

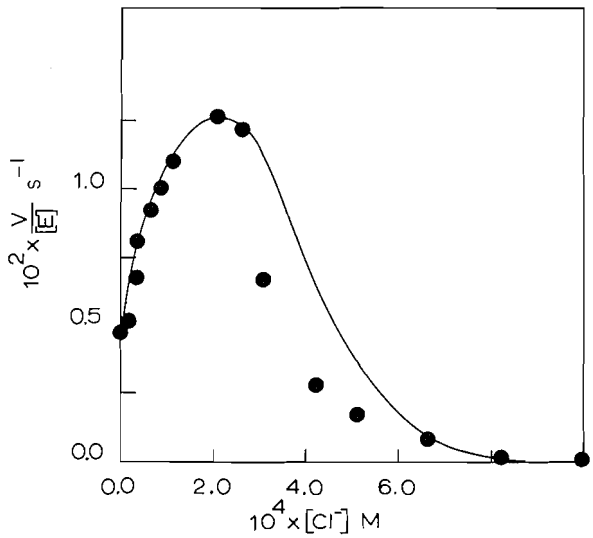

FIG. 2. Influence de l'ion chlorure: courbe calculée et points expérimentaux; $T = 25$ °C; [Tl(III)] = 2.5×10^{-4} M; [Enol] = 1.0×10^{-4} M; force ionique $\mu = 1.0$; $[H^+] = 0.5$ M.

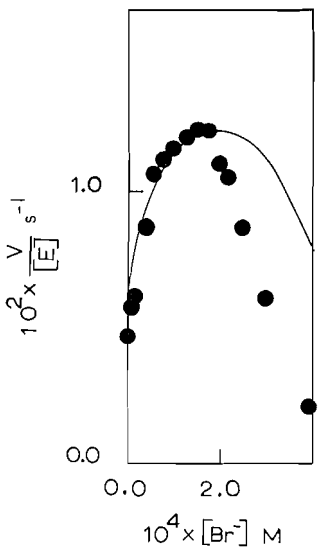

FIG. 3. Influence de l'ion bromure: courbe calculée et points expérimentaux; $T = 25$ °C; [Tl(III)] = 2.5×10^{-4} M; [Enol] = 1.0×10^{-4} M; force ionique $\mu = 1.0$; $[H^+] = 0.5$ M.

où l'espèce TlX^{2+} est prépondérante l'accord entre les résultats expérimentaux et calculés est bon.

$$[4] \quad V = [E]\{k_{Tl}[Tl^{3+}] + k_{TlOH}[TlOH^{2+}] + k_{TlX}[TlX^{2+}]\}$$

La vitesse est donnée par éq. [4]; la valeur k_{TlCl} a été déterminée auparavant dans diverses conditions (1). La constante k_{TlBr} a été obtenue à partir des données du tableau 4. Même à faible concentration en Br^- et malgré la très forte valeur de la constante de stabilité de $TlBr^{2+}$ l'approximation $TlBr^{2+} \sim Br^-$ n'est pas valable à cause de la très grande stabilité de $TlBr_2^+$ apparaissant déjà à faible concentration en Br^-. Les concentrations en $TlBr^{2+}$ ont été calculées à l'aide d'ordinateur en utilisant les constantes de stabilité et d'hydrolyse de la littérature ramenées à nos conditions expérimentales. Les valeurs ainsi obtenues ont été introduites dans éq. [4] pour déterminer k_{TlBr} et ceci pour différentes températures (voir tableau 5); de plus nous avons vérifié que l'acidité n'avait pas d'influence sur les valeurs obtenues.

(*ii*) Dans le domaine de concentrations en X^- supérieur à celle de l'ion Tl^{3+}, c'est-à-dire où les espèces TlX_n^{3-n} avec $n > 1$ sont prépondérantes, les vitesses calculées à l'aide de éq. [4] sont supérieures à celles obtenues expérimentalement (figs. 2 et 3).

L'étude approfondie des divers facteurs susceptibles d'être responsables de ces écarts tels que: l'acidité, l'ordre par rapport aux réactifs, l'influence des produits, a été effectuée à plusieurs concentrations en X^- et n'a pas donné des conclusions positives. Il faut toutefois noter que dans ce domaine de concentrations les incerti-

Can. J. Chem. Downloaded from www.nrcresearchpress.com by 210.87.254.5 on 09/05/12
For personal use only.

TABLEAU 4

Distributions des complexes Tl(III)–Br*

$[Br]_t$ $\times 10^4$ M	$[Tl^{3+}]$ $\times 10^4$ M	$[TlOH^{2+}]$ $\times 10^5$ M	$[TlBr^{2+}]$ $\times 10^5$ M	$[TlBr_2^{+}]$ $\times 10^5$ M	$V_{exp}/[E]$ $\times 10^3$ s^{-1}	$V_{calc.}/[E]$ $\times 10^3$ s^{-1}
0.00	2.13	0.37	0.00	0.00	4.7	5.7
0.10	2.04	3.48	0.81	0.07	5.7	7.2
0.20	1.97	3.36	1.45	0.23	6.2	8.0
0.40	1.84	3.14	2.44	0.71	8.7	9.3
0.60	1.72	2.93	3.20	1.30	10.7	10.2
0.80	1.61	2.74	3.82	1.98	11.2	10.9
1.00	1.50	2.56	4.32	2.71	11.3	11.5
1.25	1.37	2.34	4.82	3.69	12.0	11.9
1.50	1.25	2.13	5.20	4.74	12.2	12.2
1.75	1.13	1.93	5.49	5.84	12.2	12.4
2.00	1.02	1.73	5.70	6.98	11.0	12.4
2.25	0.91	1.54	5.81	8.17	10.5	12.3
2.50	0.80	1.36	5.85	9.39	8.7	12.0
3.00	0.59	1.00	5.70	11.90	6.0	11.1
4.00	0.23	0.39	4.32	17.70	2.0	7.8

*$[Br]_t$ = Concentration totale en Br^-; V_i = vitesse initiale; $T = 25\,°C$; $[E] = 1.0 \times 10^{-4}$ M; $[Tl(III)] = 2.5 \times 10^{-4}$ M; acidité totale $[H^+] = 0.5$ M; force ionique $\mu = 1$; $k_{Tl} = 0.12 \times 10^2$ $mole^{-1}\,l\,s^{-1}$; $k_{TlOH} = 0.93 \times 10^2$ $mole^{-1}\,l\,s^{-1}$; $k_{TlBr} = 1.67 \times 10^2$ $mole^{-1}\,l\,s^{-1}$.

TABLEAU 5

k_{TlBr} à différentes températures*

Température °C	k_{TlBr} $mole^{-1}\,l\,s^{-1} \times 10^{-2}$
25	1.67
16.4	1.17
11	1.07

*$[H^+] = 0.5$ M; $[E] = 1.0 \times 10^{-4}$ M; force ionique $\mu = 1$.

tudes sur les constantes de stabilité, incertitudes croissantes avec le nombre de X^- dans le complexe, contribuent certainement aux différences observées.

Influence de l'ion sulfate

L'influence de l'ion sulfate se manifeste seulement à des concentrations plus grandes que 1.0×10^{-3} M ce qui s'explique par le fait que les complexes Tl(III)–SO_4^{2-} ont des stabilités faibles. L'augmentation de la vitesse a été observée en fonction de la concentration en ion sulfate jusqu'à 0.2 M où elle est d'environ 50% par rapport à la vitesse sans sulfate; au delà de cette concentration la vitesse diminue. Cependant il nous a semblé assez hasardeux d'attribuer la réactivité à une espèce déterminée étant donné que dans nos conditions expérimentales les zones d'existence des divers complexes se recouvrent. On peut néanmoins tirer quelques conclusions intéressantes; en effet même à concentrations relativement faibles en sulfate les divers complexes représentent une partie importante du Tl(III) ce qui rend l'interprétation des résultats de Henry (3) sur les effets de sels en milieu sulfate discutables. De plus la constante de vitesse d'une ou plusieurs espèces telles que $TlSO_4^+$, $TlSO_4H^{2+}$ etc. est donc plus grande que celle du Tl^{3+}.

Influence de l'ion nitrate

Du point de vue cinétique le nitrate n'a pas d'influence significative jusqu'à une concentration de 0.1 M en nitrate ce qui correspond, compte tenu de la valeur de sa constante de stabilité, à la présence d'environ 40% de $TlNO_3^{2+}$ dans la solution laquelle, à part le nitrate, contient les mêmes quantités en réactifs que précédemment. Dans ces conditions les autres complexes contenant du nitrate ont des concentrations ne dépassant pas 2% du Tl^{3+}. Ceci implique que sa constante de vitesse, k_{TlNO_3}, a approximativement la même valeur que celle combinée de Tl^{3+} et $TlOH^{2+}$ dans les mêmes conditions (1) soit d'environ 0.25×10^2 $mole^{-1}\,l\,s^{-1}$.

Discussion

De nos résultats il ressort que toutes les espèces contenant un ligand (du type TlX) ont des constantes de vitesse plus grandes que l'ion Tl^{3+} ce qui confirmerait l'interprétation que nous avons proposée dans le travail précédent (1); l'ion thallique forme un édifice très stable avec les molécules de sa sphère de coordination le rendant moins réactionnel; le remplacement d'une molécule d'eau par un ligand chargé en

Can. J. Chem. Downloaded from www.nrcresearchpress.com by 210.87.254.5 on 09/05/12
For personal use only.

diminue la stabilité donc accroit la réactivité et ceci malgré la diminution de la charge du Tl(III). Cet effet électrostatique a apparemment un rôle moins important dans l'oxydation de la cyclohexanedione-1,2 que la perturbation de la sphère de coordination mais pourrait cependant être le facteur déterminant dans certains cas; ceci expliquerait l'ordre inverse des réactivités des espèces dans l'oxydation de l'éthylène où contrairement à nos résultats la réactivité de Tl^{3+} est supérieure à celle de $Tl(OAc)_2^+$.

Les résultats relatifs à l'ion acétate ont permis de mettre en évidence la réactivité de plusieurs complexes même ceux contenant plusieurs ligands. Nos résultats montrent qu'à des concentrations en ion acétate libre d'environ 1.0×10^{-5} *M* et plus, l'espèce $Tl(OAc)_2^+$ contribue d'une manière significative à la vitesse expérimentale (fig. 1); dans le cas de l'oxydation des oléfines par l'ion thallique (5) Henry avait proposé cette espèce comme réactionnelle ce qui est en accord avec nos résultats. Cependant, comme la gamme de concentrations que nous avons étudiée est beaucoup plus large que celle de Henry, nous avons pu déterminer les réactivités des autres espèces. En particulier le complexe $TlOAc^{2+}$ est plus réactif que $Tl(OAc)_2^+$ et prédomine dans la vitesse totale à des concentrations en acétate à l'équilibre plus faibles que 1.0×10^{-5} *M*. A hautes concentrations en acétate la vitesse n'est pas négligeable ce qui est en accord avec certains résultats expérimentaux de Henry; nous avons pu interprété ces résultats en utilisant des constantes de stabilité publiées récemment (tableau 1).

Dans le cas de l'influence du chlorure et du bromure on obtient des résultats très semblables entre eux; $\Delta H^{\neq}$ et $\Delta S^{\neq}$ pour $TlBr^{2+}$ sont respectivement de 5 ± 1 kcal et -30 ± 3 u.e. donc du même ordre que pour $TlCl^{2+}$ (1).

L'interprétation quantitative des résultats ne nous a pas été possible à hautes concentrations en chlorure et bromure. Expérimentalement on obtient une diminution de vitesse correspondant à l'inertie (ou à une faible réactivité) des complexes contenant plusieurs ligands. De ce point de vue les résultats sont semblables à ceux obtenus dans l'oxydation de l'éthylène par le Pd(II). Dans cette réaction on admet généralement l'intermédiaire réactionnel $[PdCl_2(H_2O)(C_2H_4)]$ dont la concentration diminue avec la concentration en ions Cl^- en faveur de $PdCl_4^{2-}$ (7–9). Il est intéressant de remarquer que l'oxydation de l'éthylène par le Pd(II) montre de plus une inhibition par H^+. Ce phénomène a été aussi observé dans l'oxydation thallique. Néanmoins dans ce cas nous avons proposé (1) que l'espèce $TlOH^{2+}$ contribuait, comme le font d'ailleurs d'autres complexes, à la vitesse d'oxydation, l'inhibition par H^+ correspondant à la diminution de la concentration de cette espèce réactionnelle, cependant que dans l'oxydation par le Pd(II) l'inhibition est due à une des étapes des mécanismes proposées.

Nous remercions le Conseil National de Recherches du Canada pour l'octroi grâce auquel ce travail a pu être réalisé ainsi que le Professeur A. L. Beauchamp pour la mise au point des programmes, et le Centre de Calcul de l'Université de Montréal pour l'utilisation de l'ordinateur.

1. R. Favier et M. Zador. Can. J. Chem. **47**, 3539 (1969).
2. R. R. Grinstead. J. Org. Chem. **26**, 238 (1961).
3. P. M. Henry. J. Amer. Chem. Soc. **87**, 990 (1965).
4. P. M. Henry. J. Amer. Chem. Soc. **87**, 4423 (1965).
5. P. M. Henry. J. Amer. Chem. Soc. **88**, 1597 (1966).
6. J. Smidt, W. Hafner, R. Jira, J. Sedlmeier, R. Sieber, R. Ruttinger, et H. Kojer. Angew. Chem. **71**, 176 (1959).
7. P. M. Henry. (*a*) J. Amer. Chem. Soc. **86**, 3246 (1964); (*b*) Advan. Chem. Ser. No. **70** 126–154 (1968).
8. P. François et Y. Trambouze. Bull. Soc. Chim. France, 51 (1969).
9. J. E. Germain. Catalytic conversion of hydrocarbons. Academic press, 1969.
10. F. Ya. Kul'ba, Yu. B. Yakovlev, et V. E. Mironov. Russ. J. Inorg. Chem. (Engl. Ed.), **9**, 1390 (1964).
11. F. Ya. Kul'ba, Yu. B. Yakovlev, et V. E. Mironov. Russ. J. Inorg. Chem. (Engl. Ed.), **10**, 886 (1965).
12. D. Peschanski et S. Valladas-Dubois. Bull. Soc. Chim. France, 1170, (1956).
13. S. Ahrland, L. Grenthe, L. Johansson, et B. Noren. Acta Chem. Scand., **17** (6) 1567 (1963).
14. F. Ya. Kul'ba, Yu. B. Yakovlev, et V. E. Mironov. Russ. J. Inorg. Chem. (Engl. Ed.), **10**, 1113 (1965).
15. R. L. Benoit, A. L. Beauchamp, et M. Deneux. J. Phys. Chem. **73**, 3268 (1969).

Can. J. Chem. Downloaded from www.nrcresearchpress.com by 210.87.254.5 on 09/05/12
For personal use only.

Can. J. Chem. Downloaded from www.nrcresearchpress.com by 210.87.254.6 on 09/05/12
For personal use only.

Kinetics of the oxidation of acetophenone by manganese(III) sulfate.

P. NATH AND K. K. BANERJI
Department of Chemistry, University of Jodhpur, Jodhpur, India

Received October 15, 1969

The oxidation of acetophenone with Mn(III) is first order with respect to each of the oxidant and the ketone. The rate is independent of acidity and solvent composition. The thermodynamic parameters have been evaluated. A mechanism consistent with the observed data is proposed.

Canadian Journal of Chemistry, **48**, 2414 (1970)

Introduction

Manganese(III) pyrophosphate oxidizes cyclohexanone at a rate equal to the rate of enolization. This supports the belief that ketones are oxidized via their enol form (1). Littler (2), however, observed that manganese(III) sulfate oxidizes cyclohexanone at a rate faster than its enolization and concluded that the keto form is being directly attacked. Oxidation of acetophenone has not received any attention; hence this investigation.

Experimental

Materials

Acetophenone (Bush) was purified by fractionation before use. Acetic acid (British Drug Houses, A.R.) was distilled over chromic oxide. All other chemicals used were of A.R. grade.

Manganese(III) sulfate was prepared by the method described by Vogel (3).

Kinetic Measurements

Reactions were carried out at 35 °C (± 0.05 °C) and in 20% acetic acid solvent unless mentioned otherwise. Reactions were followed by quenching aliquots withdrawn at known intervals of time in slight excess of Fe(II), and titrating the excess of Fe(II) against Ce(IV).

Results

Product Analysis

Reduction of 1 mole of manganese(III) by acetophenone produces 0.24 mole of formaldehyde as estimated colorimetrically by chromotropic acid method (4) (Table 1). The overall reaction may be written as

$$CH_3COC_6H_5 + 4Mn(III) + 2H_2O \rightarrow C_6H_5COOH + HCHO + 4Mn(II) + 4H^+$$

Rate Laws

When the ketone concentration is in excess, the rate at which Mn(III) disappears follows first order rate laws. Furthermore the first order rate constant is independent of the initial concentration of Mn(III). The oxidation rate varies linearly with the concentration of acetophenone (Table 2). Variation in the concentration of sulfuric acid (2.0–5.0 *M*) at constant ionic strength does not appreciably affect the rate of oxidation.

Addition of manganese(II) sulfate (0.05–0.51 *M*) has no effect on the oxidation rate. Similarly changes in the proportions of acetic acid (20–60%) in the solvent mixture have no effect on the oxidation rate.

Effect of Temperature

Data in Table 3 summarize the effect of temperature on the rate of oxidation. The specific rate constant, k, is obtained from the relation, $k = k_1/[\text{ketone}]$.

TABLE 1

Product analysis[a]

10^3[Mn(III)] (*M*)	10^3[HCHO] (*M*)	[HCHO]/[Mn(III)]
4.0	1.0	0.25
6.0	1.40	0.23
8.0	1.92	0.24
12.0	2.88	0.24
16.0	3.90	0.24
20.0	4.60	0.23

[a][Ketone], 0.12 *M*; [Mn(II)], 0.21 *M*; [H_2SO_4], 3.0 *M*.

TABLE 2

Variation of rate with concentration of acetophenone[a]

10^2[Ketone] *M*	$10^4\ k_1$ (s^{-1})	$10^3\ k_1$/[Ketone]
1.5	1.0	6.7
3.0	1.92	6.4
4.5	2.90	6.4
6.0	3.83	6.4
7.5	4.83	6.4
9.0	5.75	6.4

[a][Mn(III)], 4.0×10^{-3} *M*; [Mn(II)], 0.21 *M*; [H_2SO_4], 2.0 *M*.

TABLE 3

Effect of temperature on the oxidation rate[a]

Temperature (°K)	$10^3 k$ (l mole^{-1} s^{-1})
303	4.2
308	6.4
313	9.7
318	14.4

[a][Mn(III)], 4.0×10^{-3} *M*; [H_2SO_4], 2.0 *M*; [Mn(II)], 0.21 *M*; ΔH^*, 16.0 ± 1 kcal/mole; ΔS^*, −17.5 e.u.

A plot of log k against the inverse of temperature gave a straight line. Arrhenius equation is therefore valid for this reaction.

Rate of Enolization

The rate of enolization was measured by bromination method.

The rate of bromination of acetophenone is first order with respect to the ketone and hydrogen ions but zero order with respect to bromine. The rate of bromination increases with the proportion of acetic acid in solvent mixture. Table 4 records the rate constants of bromination (k_2) at different temperatures.

TABLE 4

Effects of temperature on enolization rate[a]

Temperature (°K)	$10^5 k_2$ (l mole^{-1} s^{-1})
303	8.5
308	15.0
313	25.2
318	44.7

[a]ΔH^*, 20.7 ± 1 kcal/mole; ΔS^*, −7.9 e.u.

Discussion

Manganese(III) solutions may contain some manganese(IV) species as well. If oxidation due to Mn(IV) is important, the addition of manganese(II) affects the rate because of the following equilibrium (5, 6)

$$Mn(IV) + Mn(II) \rightleftharpoons 2M(III)$$

Absence of any effect of manganese(II) on the rate of oxidation suggests that, in this case manganese(III) is the only oxidizing species.

The kinetics of the oxidation and enolization of acetophenone are quite different. Whereas the enolization is an acid-catalyzed reaction and is favored by increase in the proportion of acetic acid in the solvent mixture, the oxidation is independent of these variations. Hence both reactions cannot have the same mechanism.

Moreover, a comparison of the data in Tables 3 and 4 shows that activation energy of the oxidation of acetophenone by Mn(III) is much lower than that of its enolization. Therefore, the oxidation of acetophenone by manganese(III) sulfate involves a direct attack on the keto form.

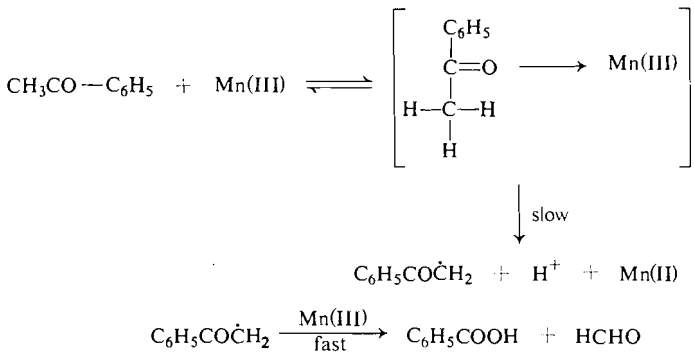

1. A. Y. Drummond and W. A. Waters. J. Chem. Soc. 497 (1955).
2. J. S. Littler. J. Chem. Soc. 832 (1962).
3. A. I. Vogel. A text book of quantitative inorganic analysis. Longmans Green and Co., London. 1964. p. 327.
4. J. Mitchell, Jr. Organic analysis. Vol. I. Interscience Publ. New York. 1953. p. 287.
5. T. J. Kemp and W. A. Waters. J. Chem. Soc. 339 (1964).
6. D. R. Rosseinsky. J. Chem. Soc. 1181 (1963).

Can. J. Chem. Downloaded from www.nrcresearchpress.com by 210.87.254.6 on 09/05/12
For personal use only.

Can. J. Chem. Downloaded from www.nrcresearchpress.com by 210.87.254.40 on 09/05/12
For personal use only.

Partial molal volume behavior of tetraalkylammonium chlorides in aqueous acetone and aqueous dimethylsulfoxide

DIGBY D. MACDONALD AND J. B. HYNE
Department of Chemistry, University of Calgary, Calgary, Alberta

Received February 2, 1970

The partial molal volumes of a series of tetraalkylammonium chlorides in aqueous acetone and aqueous dimethylsulfoxide at 25.000 °C are reported as a function of solvent composition. It is shown that for each solvent composition the partial molal volume data are better represented by a quadratic in solute molecular weight than by the linear expression previously employed in similar studies. Extrapolation of molecular partial molal volumes to zero cation molecular weight has permitted evaluation of the partial molal volumes of the ions R_4N^+ and Cl^-. The variation of molecular and ionic partial molal volume as a function of solvent composition is discussed.

Canadian Journal of Chemistry, **48**, 2416 (1970)

Introduction

In our continuing study of solvolysis reactions in aqueous organic solvent systems we have measured partial molal volumes of tetraalkylammonium chlorides in aqueous acetone and aqueous dimethylsulfoxide (DMSO) at 25.000 °C as a function of solvent composition. The purpose of this work was to obtain data on the variation of partial molal volume of stable solute species with solvent composition which should be of value as models in interpreting the volumetric behavior of initial and transition states of solvolysis reactions in the corresponding solvent systems.

The tetraalkylammonium chlorides (R_4N^+-Cl^-) were chosen for this study since the surface charge density of the cation can be conveniently varied by changing the nature of the alkyl group, R; in this case R ≡ Me, Et, *n*-Pr, and *n*-Bu. The two cosolvents, acetone and DMSO, were selected since, despite their close structural similarity, they have markedly different physical properties which might be expected to be reflected in the properties of dissolved ions.

Experimental

Materials

Eastman reagent grade tetraalkylammonium chlorides were purified by multiple recrystallization and dried in vacuo as described by Conway *et al.* (1). The purity of all salts, as determined by the modified Volhard method (2), was better than 99.8%.

Eastman practical grade DMSO was dried over freshly cut calcium hydride for a period of not less than 48 h. The decanted product was then distilled at reduced pressure (~ 10 mm Hg) and the middle 50% cut collected. The high purity of the distilled liquid was confirmed by melting point (18.52 °C, lit: 18.55 °C (3)) and refractive index (n_D^{20} = 1.3590, lit: $n_D^{19.4}$ = 1.35886 (3)).

Fisher spectral grade acetone was used without further purification. Doubly distilled water was used in preparation of all aqueous organic binary solvent systems.

Method

The aqueous binary solvent systems were prepared by volume to ± 0.0005 mole fraction. The solvents were degassed by refluxing beneath a Dry Ice/acetone condenser and their compositions checked by density measurements to ensure that the degassing procedure had not caused any change.

Salt solutions (0.0150 to 0.1500 *M*) were prepared to ± 0.0001 *M* units in calibrated 100 ml volumetric flasks and for each salt concentration three replicate density measurements were made using 25 ml Weld-type pycnometers. The pycnometers were thermostatted to 25.000 ± 0.005 °C for a period of not less than 1 h and weighed after 1½ h standing at room temperature. This standardization of procedure greatly improved reproducibility, which on average, was found to be ± 0.00002 g ml^{-1}.

Some difficulty was experienced in obtaining reproducible densities in aqueous acetone, no doubt due to the high volatility of the cosolvent acetone. This was particularly troublesome at acetone mole fractions greater than 0.20. It is for this reason that no data are reported for solutions of salts in solvent systems with greater than 0.20 mole fraction of acetone. No difficulties were experienced in accurately determining densities of solutions in aqueous DMSO. This was undoubtedly due to the much higher boiling point of DMSO (189 °C (3)) compared to that of acetone (56.5 °C (4)).

Results

Apparent molal volumes, ϕ, were calculated using the equation

$$[1] \qquad \phi = \frac{M}{d_0} - \frac{1000(d - d_0)}{d_0 c}$$

where M is the molecular weight of the salt, c is the concentration in moles l^{-1}, and d and d_0, the densities of solution and solvent, respectively. Partial molal volumes at infinite dilution, $\bar{V}^0$,

Can. J. Chem. Downloaded from www.nrcresearchpress.com by 210.87.254.40 on 09/05/12
For personal use only.

were then obtained by extrapolating ϕ to zero concentration using the relation

$$[2] \qquad \phi = \overline{V}^0 + Sc^{1/2}$$

where S is the limiting slope.

Uncertainties in apparent molal volumes were calculated using the equation of Redlich and Bigeleisen (5).

$$[3] \qquad \delta\phi = \frac{1000\delta d}{d_0 c} + \frac{1000(d - d_0)\delta c}{d_0 c^2}$$

δd and δc are uncertainties in density and concentration, respectively.

Illustrative plots of ϕ vs. $c^{1/2}$ for tetramethylammonium chloride in aqueous acetone at 25.000 °C are shown in Fig. 1. Partial molal volumes obtained by extrapolation to $c^{1/2} = 0$ are summarized in Table 1 and corresponding numerical values for S (eq. [2]) are listed in Table 2. Uncertainties in partial molal volume values, determined by inspection of the extrapolations, are considered not to exceed $\pm$ 1 ml mole^{-1}. Data contained in Table 1 reveal that where comparison is possible, the partial molal volumes measured in this study are in excellent agreement with those obtained by other workers.

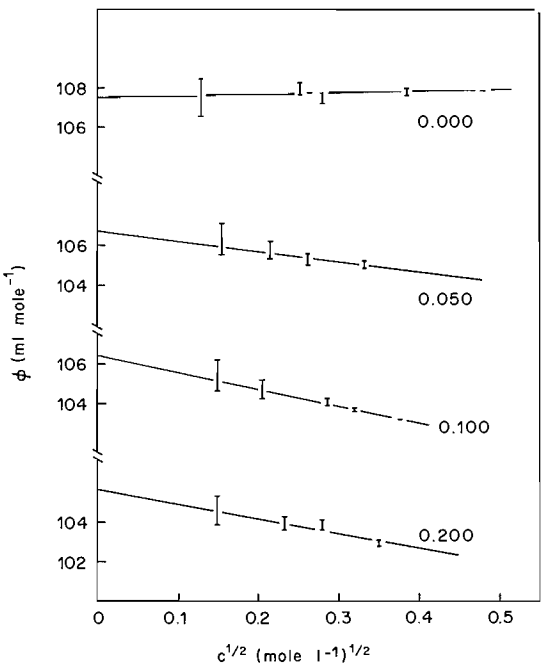

FIG. 1. Plots of ϕ vs. $c^{1/2}$ for tetramethylammonium chloride in aqueous acetone (numbers adjacent to each plot are mole fractions of acetone).

TABLE 1

Partial molal volumes of tetraalkylammonium chlorides in aqueous acetone and aqueous DMSO at 25.000 °C

Mole fraction cosolvent	Partial molal volume (ml mole^{-1}) when salt =			
	Me_4NCl	Et_4NCl	n-Pr_4NCl	n-Bu_4NCl
	Aqueous acetone			
0.000	107.5*	166.8†	232.9‡	294.3‡
0.050	106.7	163.3	229.0	288.7
0.100	106.4	166.0	231.2	297.8
0.200	105.6	161.8	228.4	296.7
	Aqueous DMSO			
0.100	106.1	162.2	223.0	283.6
0.200	103.3	157.9	220.0	284.7
0.300	103.0	158.9	223.8	291.5
0.400	103.1	159.0	224.8	292.4
0.500	102.0	158.4	227.3	294.9

*Value = 107.4 (ref. 1).
†Value = 167.0 (ref. 1).
‡Reference 1.

TABLE 2

Numerical values for S (eq. [2]) for tetraalkylammonium chlorides in aqueous acetone and aqueous DMSO at 25.000 °C

Mole fraction cosolvent	S* when salt =			
	Me_4NCl	Et_4NCl	n-Pr_4NCl	n-Bu_4NCl
	Aqueous acetone			
0.000	0.8	−0.6	—	—
0.050	−5.0	−2.8	−5.6	0
0.100	−8.4	−14.0	−14.6	−22.0
0.200	−6.6	−4.0	−2.0	−2.0
	Aqueous DMSO			
0.100	−8.0	−11.0	−2.0	−5.0
0.200	−2.0	1.6	7.0	1.6
0.300	−3.8	0	0.0	−9.2
0.400	−6.4	0	0.8	−3.0
0.500	−3.8	1.2	0	−4.0

*Units of ml mole^{-1} $M^{-1/2}$.

Since the solutes under investigation in this work certainly exist as ions at infinite dilution the molecular partial molal volume may be expressed as the sum of the partial molal volumes of the component ions.

$$[4] \qquad \overline{V}^0_{R_4NCl} = \overline{V}^0_{R_4N^+} + \overline{V}^0_{Cl^-}$$

A number of attempts have been made to calculate partial molal volumes of individual ions but the results obtained seem to differ according to the method used. For instance, a recent literature survey published by Lee and Hyne (6) reveals that estimates of the partial molal volume of chloride ion in water at 25 °C range from 18 to 37 ml mole^{-1}.

Can. J. Chem. Downloaded from www.nrcresearchpress.com by 210.87.254.40 on 09/05/12
For personal use only.

Conway *et al.* (1) recently proposed a new method for obtaining ionic partial molal volumes in water for tetraalkylammonium salts with a common anion. This type of analysis has been recently extended by Lee and Hyne (6) to solutions of tetraalkylammonium chlorides in aqueous ethanol binary solvent systems. In the Conway method anionic partial molal volumes are obtained by extrapolating $\bar{V}^0_{R_4NX}$ to zero cation weight in a linear plot of $\bar{V}^0_{R_4NX}$ vs. molecular weight.

$$[5] \qquad \bar{V}^0_{R_4NX} = A + BM_{R_4NX}$$

When $M_{R_4NX} = M_{X^-}$, i.e. at zero cation weight, the partial molal volume of the anion is given by eq. [6].

$$[6] \qquad \bar{V}^0_{X^-} = A + BM_{X^-}$$

and the partial molal volume of the cation can be calculated using eq. [4].

The use of a linear extrapolation (eq. [5]) in the present work requires discussion. Since $M_{R_4NCl} - M_{R_4'NCl}$, where R and R′ are adjacent homologues (e.g. Me, Et), is constant over the series of salts employed (i.e. $\Delta M = 56$), eq. [5] demands that $\bar{V}^0_{R_4NCl} - \bar{V}^0_{R_4'NCl}$ also be constant. An examination of data presented in Table 1 clearly shows that this condition is *not* satisfied, necessitating the conclusion that eq. [5] does not provide a good functional representation of the dependence of $\bar{V}^0_{R_4NCl}$ on molecular weight. In view of the demonstrated inadequacy of the linear expression (eq. [5]) the data presented in Table 1 were fitted to a quadratic (eq. [7]) by a least squares method using an IBM 360/50 computer.

$$[7] \qquad \bar{V}^0_{R_4NCl} = A + BM_{R_4NCl} + CM^2_{R_4NCl}$$

The same data were fitted to eq. [5] by the method of least squares so that the validity of using either the linear or the quadratic function could be assessed.

As a measure of the reliability of the functions chosen it is convenient to define a deviation function as follows

$$[8] \qquad d = \bar{V}^0_{R_4NCl}(\text{obsd}) - \bar{V}^0_{R_4NCl}(\text{calcd})$$

Plots of d vs. molecular weight are shown in Figs. 2 and 3. The dotted lines correspond to experimental error limits in $\bar{V}^0_{R_4NCl}$. It is clear from these plots that in both solvent systems the quadratic (eq. [7]) provides a better representation of the data than does the linear function

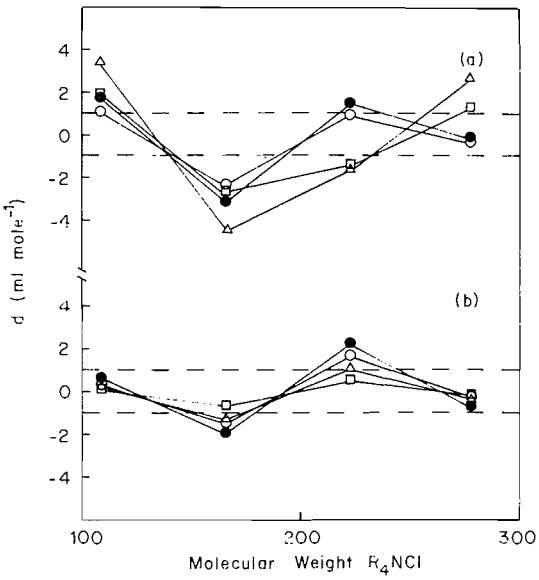

FIG. 2. Plot of d vs. molecular weight for tetraalkylammonium chlorides in aqueous acetone: (*a*) linear analysis; (*b*) quadratic analysis (○, 0.000; ●, 0.050; □, 0.100; △, 0.200 mole fraction acetone).

(eq. [5]). The lack of random distribution of d about $d = 0$ would appear to indicate, however, that even eq. [7] does not provide a "perfect" representation of the data. However, since d obtained using eq. [7] is comparable in magnitude to the experimental error in $\bar{V}^0_{R_4NCl}$ further refinement of the polynomial is not justified by the experimental data available here. Accordingly, eq. [7] was used to extrapolate $\bar{V}^0_{R_4NCl}$ to zero cation weight in order to determine $\bar{V}^0_{Cl^-}$. Cation partial molal volumes were then calculated using eq. [4]. The resulting numerical values for $\bar{V}^0_{Cl^-}$ and $\bar{V}^0_{R_4N^+}$ in aqueous acetone and aqueous DMSO are presented in Table 3.

Discussion

S Values

According to the Debye–Huckel theory for strong electrolytes (7) the dependence of apparent molal volume, ϕ, on the square root of concentration (eq. [2]) as $c \to 0$ can be expressed as follows

$$[9] \qquad S_{\text{lim}} = \omega^{3/2} N^2 \varepsilon^3 \left(\frac{8\pi}{1000 D^3 RT}\right)^{1/2} \left(\frac{\mathrm{d} \ln D}{\mathrm{d}p} - \frac{\beta}{3}\right)$$

where S_{lim} is the limiting slope, ω is the valence factor given by eq. [10]

TABLE 3

Partial molal volumes of various ions in aqueous acetone and aqueous DMSO at 25.000 °C

Mole fraction cosolvent	Partial molal volume* (ml mole^{-1})				
	Cl^-	Me_4N^+	Et_4N^+	n-Pr_4N^+	n-Bu_4N^+
		Aqueous Acetone			
0.000	27.3	80.2	139.5	205.6	267.0
0.050	29.7	77.0	133.6	199.3	259.0
0.100	31.8	74.6	134.2	199.4	266.6
0.200	37.9	67.7	123.9	190.5	258.8
		Aqueous DMSO			
0.100	34.0	72.1	128.2	189.0	249.6
0.200	37.4	65.9	120.5	182.6	247.3
0.300	36.3	66.7	122.6	187.5	255.2
0.400	35.8	67.3	123.2	189.0	256.6
0.500	31.8	70.2	126.6	195.5	263.1

*Calculated using eq. [7].

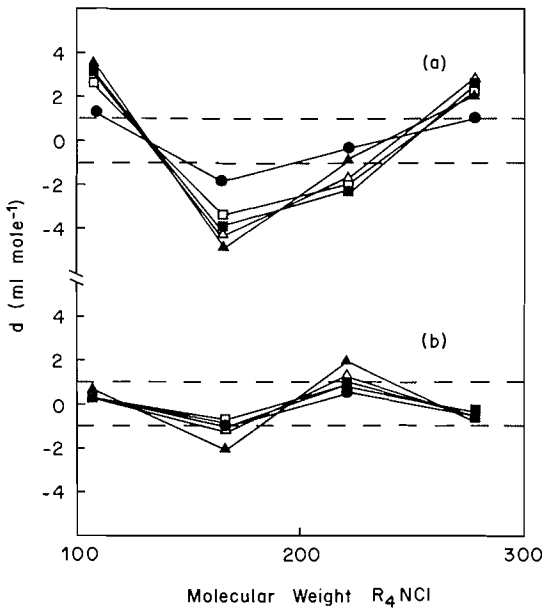

FIG. 3. Plot of d vs. molecular weight for tetraalkylammonium chlorides in aqueous DMSO: (*a*) linear analysis; (*b*) quadratic analysis (●, 0.100; □, 0.200; ■, 0.300; △, 0.400; ▲, 0.500 mole fraction DMSO).

$$[10] \qquad \omega = 0.5 \sum_i \nu_i Z_i^2$$

D is the dielectric constant of the medium, β, the isothermal compressibility, and ν_i is the number of ions of species i which have a valence Z_i. Clearly S_{lim} can be positive or negative depending on the relative magnitudes of β/3 and the pressure dependence of ln D. Equation [9] predicts a value of $S_{lim} = 1.86$ ml mole^{-1} $M^{-1/2}$ for 1:1 electrolytes in water at 25.000 °C. This prediction has been confirmed experimentally in studies using aqueous solutions of alkali halides (7).

Examination of the numerical values for S listed in Table 2 reveals two interesting features. First, many values are negative and second, the S values for any given solvent depend upon the nature of the salt. This latter observation is contrary to the predictions of the Debye–Huckel theory (see eq. [9]). Negative dependences of ϕ upon $c^{1/2}$ have been previously reported for solutions of alkylammonium salts in aqueous solution (8, 9) and this behavior appears to persist to much lower salt concentrations than that used in this work. Similar negative dependences have also been reported for solutions of other salts in both aqueous (10) and non-aqueous media (7). Possible origins of these negative dependences have been discussed in the literature (9). For solutions in water, where (d ln D/dp) is greater than β/3 and the Debye–Huckel limiting slope is positive (see eq. [9]), observed negative dependences of ϕ on $c^{1/2}$ have been attributed to ion pairing (11), hydrophobic bonding (12), micelle formation (13), salting-in effects (14), or solvent structural stabilization due to the effect of alkyl groups on the nature of hydrogen-bonding in water (9). Franks and Smith (9), however, show that in sufficiently dilute solutions (< 0.002 M) of tetraalkylammonium bromides in water the dependence of ϕ on $c^{1/2}$ does in fact approach the Debye–Huckel limiting value. The deviation of the S values obtained in the present work from the Debye–Huckel limiting value may result from the fact that the solutions were not sufficiently dilute so that the properties of the ions

Can. J. Chem. Downloaded from www.nrcresearchpress.com by 210.87.254.40 on 09/05/12
For personal use only.

Can. J. Chem. Downloaded from www.nrcresearchpress.com by 210.87.254.40 on 09/05/12
For personal use only.

are determined by electrostatic interactions alone. It should be noted, however, that in order to obtain apparent molal volumes to better than $\pm$ 0.5 ml mole^{-1} at concentrations less than 0.002 M, densities must be measured to better than $\pm$ 1 p.p.m. Few density measurements have been made with this precision (7, 9).

It is difficult to calculate the uncertainty introduced into the extrapolation of ϕ to $c^{1/2} = 0$ due to possible non-conformity of the observed S values with the Debye–Huckel theory since the data required to calculate S_{lim} are not available for the mixed solvents used in this study. In water the deviations of the observed S values from the theoretical limiting slope are negative. This probably results in the partial molal volumes listed in Table 1 being a little higher than the "correct" values. However, where comparison is possible, the partial molal volumes obtained in this study are in excellent agreement with those obtained by other workers, suggesting that the uncertainty is in fact small and well within the precision claimed in this work.

Partial Molal Volumes

Plots of partial molal volume vs. solvent composition for tetraalkylammonium chlorides in aqueous acetone and aqueous DMSO are shown in Fig. 4. In both solvent systems partial molal volume exhibits extremum behavior as a function of solvent composition. Similar behavior has been recently reported for these same salts in aqueous ethanol (6). The partial molal volume of a solute in solution can be divided into two contributions as expressed by eq. [11].

$$[11] \qquad \bar{V}^0 = \bar{V}_h^0 + \bar{V}_i^0$$

where $\bar{V}_h^0$ is the contribution due to formation of a hole in the medium of sufficient size to accommodate the solute and $\bar{V}_i^0$ is the volume change of the system due to interaction of the solute with the surrounding solvent. Clearly $\bar{V}_h^0$ can be zero or positive. The magnitude of this term will increase with the size of the solute, and decrease with increasing solvent-free volume available to the solute prior to hole formation. On the other hand, $\bar{V}_i^0$ can be positive or negative depending upon the nature of the interaction. For electrostrictive interaction, however, $\bar{V}_i^0$ should be negative. Numerous attempts have been made to calculate $\bar{V}_i^0$ using the first pressure derivative of the Born expression for the electrostatic free

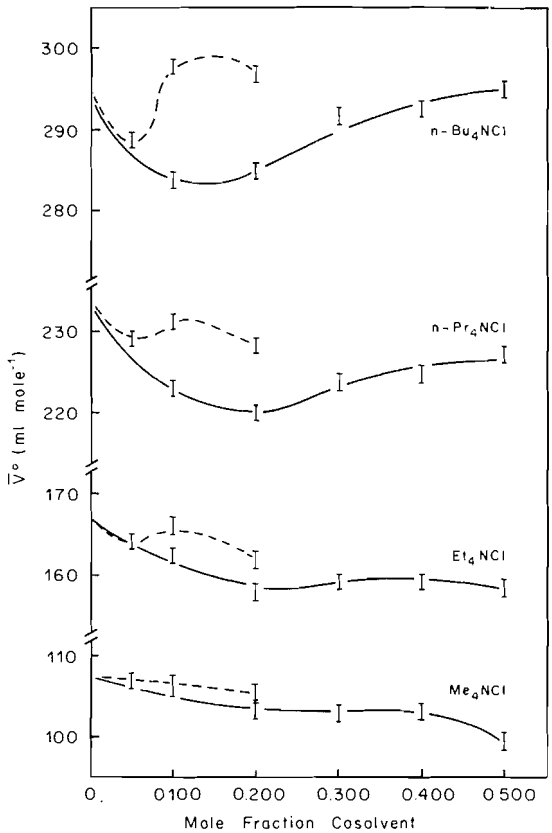

FIG. 4. Plot of partial molal volume vs. solvent composition for various salts in aqueous acetone (broken line) and aqueous DMSO (full line).

energy of solvation of ions in a dielectric continuum. However, these calculations have proved unreliable (15) and require knowledge of the pressure dependence of the solvent dielectric constant. As previously stated, this information is not available for the binary solvents used in this study and therefore the calulations cannot be attempted here.

In a recent study (16) concerning solvolysis reactions in mixed solvents, we measured the partial molal volume of benzyl chloride as a function of solvent composition in aqueous acetone and aqueous DMSO at 50.100 °C. In aqueous acetone the partial molal volume was found to pass through a large maximum at 0.1–0.2 mole fraction cosolvent whereas in aqueous DMSO, only a small maximum at $\sim$ 0.5 mole fraction cosolvent was evident. Since benzyl chloride is non-ionic, the solute–solvent interactions should be minimal and the partial

molal volume will reflect predominantly the behavior of the hole formation term $\overline{V}^0_h$. Accordingly, we expect $\overline{V}^0_h$ to pass through a maximum at 0.1–0.2 mole fraction acetone and at $\sim$ 0.5 mole fraction DMSO. When interpreting the behavior of the salts, however, the interaction term $\overline{V}^0_i$ is expected to make a large contribution to partial molal volume and therefore must be considered.

In light of the preceding discussion, an examination of the data illustrated in Fig. 4 reveals several important features. The initial decrease of $\overline{V}^0_{R_4NCl}$ as cosolvent is added to the system can be attributed to the influence of solute–solvent interaction (i.e. electrostriction), since the same behavior is not displayed by non-ionic benzyl chloride. In the case of Me_4NCl, where hole formation requirements are least but where the surface charge density is greatest, the partial molal volume shows no maximum in aqueous acetone and the least tendency to increase at compositions greater than 0.2–0.3 mole fraction DMSO. On the other hand, in the case of the larger salts, where hole formation requirements are greater but where the surface charge densities are less, the partial molar volumes exhibit maxima at 0.1–0.2 mole fraction acetone and show progressively greater tendencies to increase after passing through minima at 0.1–0.2 mole fraction DMSO. Clearly, in these latter cases the hole formation term, $\overline{V}^0_h$, makes an important contribution to the dependence of $\overline{V}^0_{R_4NCl}$ on solvent composition. In the case of Me_4NCl, however, the results are consistent with the hypothesis that solute–solvent interaction and not hole formation is the major factor determining the dependence of $\overline{V}^0$ on solvent composition.

The interpretation of electrolyte solution properties is subject to uncertainty as to whether the observed behavior arises from the cation, the anion, or both. Plots of ionic partial molal volume vs. solvent composition for the tetraalkylammonium cations and chloride anion in aqueous acetone and aqueous DMSO are shown in Fig. 5. In both solvent systems, $\overline{V}^0_{Cl^-}$ initially increases with solvent composition and in aqueous DMSO, it passes through a maximum at 0.2–0.3 mole fraction cosolvent. The fact that both $\overline{V}^0_{R_4NCl}$ and $\overline{V}^0_{R_4N^+}$ display similar variations with solvent composition reveals that the partial molal volume behavior of the salt is determined predominantly by the behavior of the cation. The

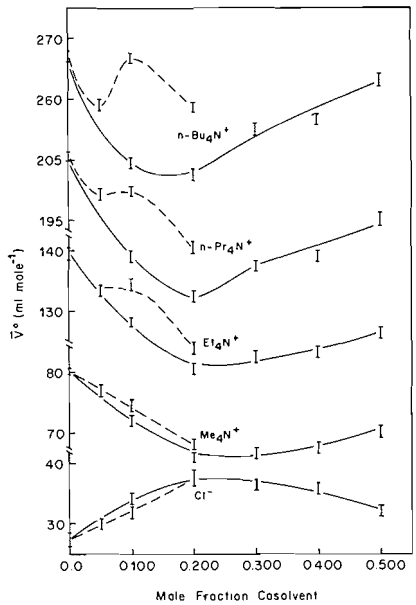

FIG. 5. Plot of partial molal volume vs. solvent composition for various ions in aqueous acetone (broken line) and aqueous DMSO (full line).

"mirror-like" dependences of the partial molal volumes of the two smallest ions, Me_4N^+ and Cl^-, on solvent composition in both systems deserves comment. Since these ions are small (compared to the other ions examined in this work) and possess high surface charge densities, it is reasonable to expect that the behavior of $\overline{V}^0_{Me_4N^+}$ and $\overline{V}^0_{Cl^-}$ will be greatly influenced by solute–solvent interaction. Thus the results obtained in this work suggest that the volume loss due to solute–solvent interaction is not only sensitive to changing solvent composition, as might be expected from changes in dielectric constant, but that it is also sensitive to charge type. This behavior is consistent with the existence of specific cation–solvent and anion–solvent interactions. Possible types of specific interaction include chloride anion–water hydrogen bonding and "hydrophobic hydration" of the hydrocarbon groups of the tetraalkylammonium cations.

In summary, the results presented in this paper have clearly demonstrated the importance of both solute–solvent interaction and hole formation factors in determining the properties of salts in aqueous acetone and aqueous DMSO. The results also show that the behavior of the cation determines the variation of $\overline{V}^0_{R_4NCl}$ with solvent composition in these solvent systems. Finally,

Can. J. Chem. Downloaded from www.nrcresearchpress.com by 210.87.254.40 on 09/05/12
For personal use only.

the existence of specific cation–solvent and anion–solvent interaction has been demonstrated for solutions of tetraalkylammonium chlorides in aqueous acetone and aqueous DMSO.

General financial assistance by the National Research Council of Canada as well as a studentship to D. D. Macdonald is gratefully acknowledged.

1. B. E. CONWAY, R. E. VERRALL, and J. E. DESNOYERS. Trans. Faraday Soc. **62**, 2738 (1966).
2. H. H. WILLARD, N. H. FURMAN, and C. E. BRICKER. Elements of quantitative analysis. 4th ed. D. Van Nostrand Co., Inc., New York. 1956.
3. D. MARTIN, A. WEISE, and H. J. NICLAS. Angew. Chem. Int. Ed. Cleveland, Ohio. **6**, 318 (1967).
4. Handbook of chemistry and physics. The Chemical Rubber Co., 46th ed. 1966.
5. O. REDLICH and H. BIGELEISEN. J. Amer. Chem. Soc. **64**, 758 (1942).
6. I. LEE and J. B. HYNE. Can. J. Chem., **46**, 2333 (1968).
7. O. REDLICH and D. M MEYER. Chem. Rev. **64**, 221 (1964).
8. R. E. VERRALL and B. E. CONWAY. J. Phys. Chem. **70**, 3961 (1966).
9. F. FRANKS and H. T. SMITH. Trans. Faraday Soc. **63**, 2586 (1967).
10. T. L. BROADWATER and D. F. EVANS. J. Phys. Chem. **73**, 164 (1969).
11. L. G. HEPLER, J. M. STOKES, and R. H. STOKES. Trans. Faraday Soc. **61**, 60 (1965).
12. F. FRANKS and H. T. SMITH. J. Phys. Chem. **68**, 3581 (1964).
13. S. LINDENBAUM and G. E. BOYD. J. Phys. Chem. **68**, 911 (1964).
14. J. E. DESNOYERS and M. AREL. Can. J. Chem. **45**, 359 (1967).
15. D. FEAKINS. Physico-chemical processes in mixed aqueous solvents. *Edited by* F. Franks, Heinemann Ltd., London. 1967. p. 71.
16. D. D. MACDONALD and J. B. HYNE. To be published.

Can. J. Chem. Downloaded from www.nrcresearchpress.com by 210.87.254.40 on 09/05/12
For personal use only.

Can. J. Chem. Downloaded from www.nrcresearchpress.com by 210.87.254.6 on 09/05/12
For personal use only.

The isothermal compressibility of dimethylsulfoxide–water mixtures at 35 °C

K. H. JUNG AND J. B. HYNE
Department of Chemistry, University of Calgary, Calgary, Alberta

Received February 4, 1970

The isothermal compressibility of a series of dimethylsulfoxide–water mixtures passes through a minimum near 0.4 mole fraction dimethylsulfoxide. This behavior is compared with that of other aqueous binaries and provides further evidence of specific hydrogen bonded complexes in the dimethylsulfoxide–water system.

Canadian Journal of Chemistry, 48, 2423 (1970)

Introduction

In connection with our continuing study of the effect of pressure on the rates of solvolytic reactions in aqueous binary solvent systems we have determined the isothermal compressibility, K_T, of dimethylsulfoxide–water mixtures from pure water to 0.7 mole fraction cosolvent. These results are presented here together with corresponding compressibility or compression data for other aqueous binary systems. The extremum behavior of K_T as a function of solvent composition is compared with the similar observed behavior of the excess heat of mixing of the aqueous binaries to illustrate the parallelism in the dependence of these thermodynamic parameters on solvent composition and structure.

Experimental

The compressibility determinations were made with a Ruska motor driven, semi-automatic volumetric pump (Ruska Instrument Corp., Houston, Texas) capable of being read to ± 0.001 ml. Mercury was used both to calibrate the apparatus and as the pressurizing fluid. The DMSO–water sample was contained in a 270 ml stainless steel compressibility cell mounted in a thermostatted jacket maintained at 35.00 ± 0.02 °C. The pressure range employed for the compressibility determinations was 34–680 atm and volumes were measured at approximately 100 atm intervals. The measured volume was corrected for both mercury and cell expansion as pressure was varied.

Triply distilled mercury was employed throughout the apparatus and was redistilled after each DMSO–water composition had been examined. Water was distilled in a Pyrex apparatus after passage through an ion exchange column. Conductivity was less than 1.7×10^{-6} mhos at 25 °C. Dimethylsulfoxide (Matheson, Coleman and Bell) was dried over calcium hydride and vacuum distilled at 10^{-3} mm Hg. Batches were stored over molecular sieve in air-tight bottles until required for use.

Results

The relative volumes, $V_{rel} = V_p/V_0$, where V_0 is the volume of liquid at 680 atm, as a function of pressure for the various dimethylsulfoxide–water compositions have been filed.[1] The pressure dependence of V_{rel} was found to be adequately represented by the quadratic expression

$$[1] \qquad \ln V_{rel} = A + Bp + Cp^2$$

within the limits of experimental error using a least mean square fit program and an IBM 360 computer. The values of the quadratic coefficients are given in Table 1. The need for a cubic expression was checked and the value for the D coefficient in a p^3 term was found to be insignificant, viz. 10^{-16} atm^{-3}.

Since the isothermal compressibility is given by

$$[2] \qquad K_T = -\frac{1}{V}\left(\frac{\partial V}{\partial p}\right)_T = -\left(\frac{\partial \ln V}{\partial p}\right)_T$$

By integration, rearrangement, and comparison of coefficients of eqs. [1] and [2] it can be shown that, at 1 atm

$$K_T \simeq -B$$

TABLE 1

Coefficients A, B, and C of the quadratic equation

Mole fraction DMSO	$A \times 10^2$	$B \times 10^5$ (atm^{-1})	$C \times 10^9$ (atm^{-2})
0.00	2.64±0.06	−4.19±0.06	4.68±0.87
0.10	2.04±0.01	−3.23±0.08	3.76±0.95
0.20	1.25±0.01	−2.89±0.02	11.2±0.33
0.30	7.27±0.18	−1.80±0.14	11.1±2.53
0.40	1.22±0.00	−1.77±0.00	−6.77±0.36
0.50	1.17±0.00	−2.30±0.01	8.40±0.07
0.60	1.36±0.19	−2.34±0.04	5.28±3.18
0.70	1.53±0.01	−2.52±0.05	4.15±0.50

[1]Photocopies of material may be obtained free of charge, upon request, from the Depository of Unpublished Data, National Science Library, National Research Council of Canada, Ottawa, Canada.

Can. J. Chem. Downloaded from www.nrcresearchpress.com by 210.87.254.6 on 09/05/12
For personal use only.

TABLE 2

Isothermal compressibility (K_T) of dimethylsulfoxide–water mixtures at 35 °C

Mole fraction DMSO	$K_T \times 10^6$ (atm^{-1})
0.00	41.9±0.6
0.10	32.3±0.8
0.20	25.9±0.2
0.30	18.0±1.4
0.40	17.7±0.0
0.50	23.0±0.1
0.60	23.4±0.4
0.70	25.2±0.5

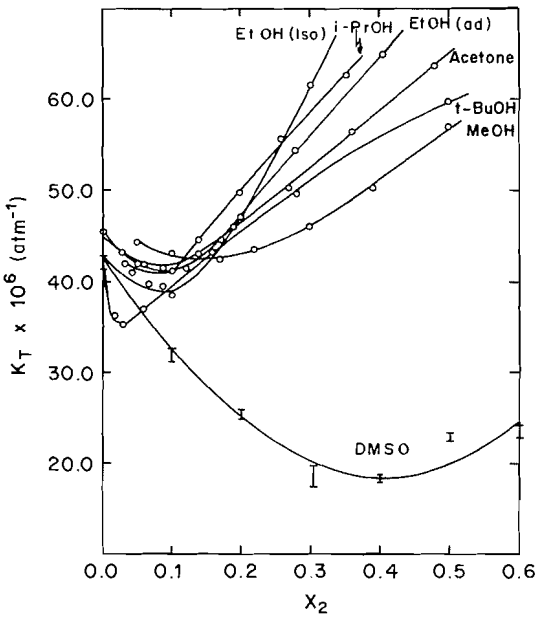

FIG. 1. Compressibilities of aqueous binary solvents vs. solvent compositions: data from EtOH (adiabatic, ref. 8; isothermal, ref. 5); acetone (ref. 7); *i*-PrOH (ref. 7); *t*-BuOH (ref. 6); and MeOH (ref. 7).

within the limits of the accuracy of the experimental data. The computed values of the isothermal compressibilities of aqueous dimethylsulfoxide mixtures are reported in Table 2.

It should be noted that the data for *t*-butylalcohol shown in Fig. 1 are compression viz. $\Delta V/V$ for a specific pressure interval and not compressibility as defined above.

Our value for the isothermal compressibility of water, 41.9 ± 0.6 × 10^{-6} atm^{-1} at 35 °C, is in reasonable agreement with the most recently reported determinations of Whalley, 44.8 × 10^{-6} atm^{-1} at 25 °C, and Stutchbury, 41.8 × 10^{-6} atm^{-1} at 30 °C. Values have been reported over the years varying from 30.9 × 10^{-6} to 48.7 × 10^{-6} atm^{-1}, although more recent determinations tend to have a narrower spread of values between 39.2 × 10^{-6} and 44.9 × 10^{-6} atm^{-1}.

Discussion

It is immediately obvious from the data plotted in Fig. 1 that the behavior of the compressibility of dimethylsulfoxide–water mixtures as a function of composition is significantly different from that of the other aqueous organic binary mixtures shown. Although it is true that the compressibility data for most of the alcohols are adiabatic and not isothermal, the difference between these two forms of compressibility measurement is not large enough to account for the large observed difference in DMSO–water behavior. The isothermal (6) and adiabatic (8) compressibility behavior for ethanol–water mixtures is shown in Fig. 1 to illustrate this point.

The much deeper minimum at considerably higher cosolvent mole fraction that characterizes the K_T behavior is also a pronounced feature of the excess heat of mixing behavior of the dimethylsulfoxide–water mixture as shown in Fig. 2. Indeed, if the binary compositions at which the

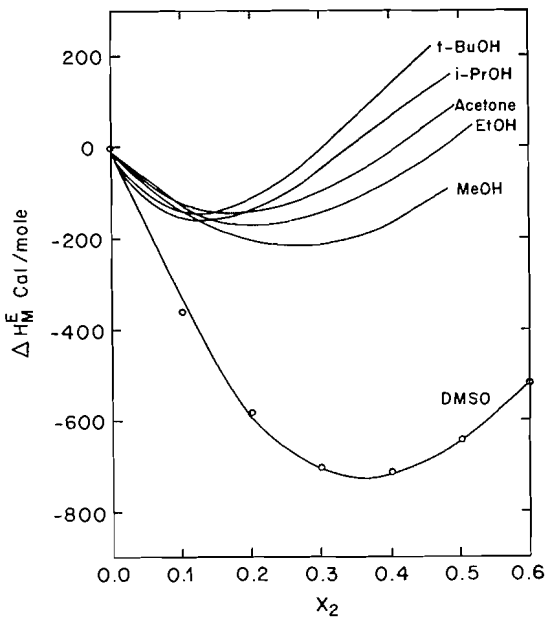

FIG. 2. Excess heats of mixing of aqueous binary solvents vs. solvent mole compositions: data from MeOH, EtOH, acetone, *i*-PrOH, *t*-BuOH (ref. 1); DMSO (ref. 3).

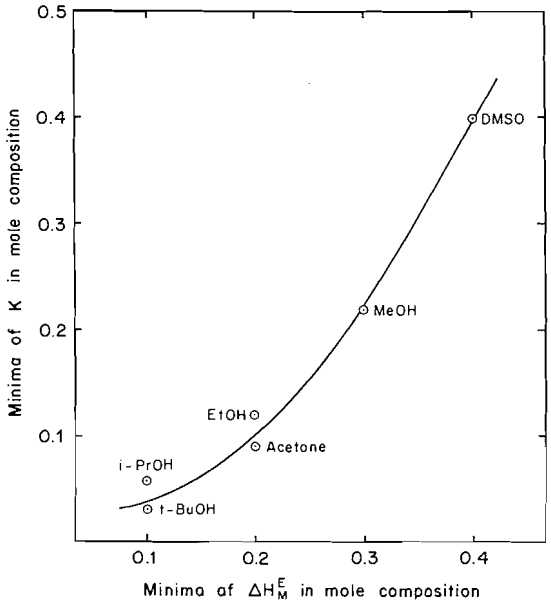

FIG. 3. Minima of compressibilities of aqueous binary mixtures vs. excess heats of mixing of the mixtures: data from (*i*) compressibilities: MeOH, EtOH, *i*-PrOH, and acetone (ref. 7); *t*-BuOH (ref. 6); DMSO (this work); (*ii*) excess heats of mixing: MeOH, EtOH, *i*-PrOH, *t*-BuOH, and acetone (ref. 1); DMSO (ref. 3).

minimum in the two parameters appears are plotted against each other, a smooth curve is obtained as shown in Fig. 3. There can be little doubt, therefore, that the extremum behavior manifest in the dependence of these parameters on solvent composition arises from the same source, most likely the intermolecular force and solvent structure variations as composition is changed.

Our main interest here, however, is in the particular behavior of the dimethylsulfoxide–water system. The extremum behavior observed for many of the other aqueous organic binary mixtures has been attributed to enhancement of water structure by initial additions of cosolvent (1) followed by destruction of this structure as the bulk composition increases in the organic component. In the case of dimethylsulfoxide, however, it is difficult to envisage "water structure" being maximized at such high cosolvent content.

Parker (2) and Lindberg and Kenttamaa (3) have suggested that a specific hydrogen bonded complex of composition $DMSO.2H_2O$ may be predominant between 0.3 and 0.4 mole fraction dimethylsulfoxide. The presence of a significant amount of this compact complex in the mixture would be expected to result in a reduction in the compressibility. Other workers (4) have cited specific dimethylsulfoxide–water complexes of the type suggested above as being responsible for the viscosity maximum in this binary system at 0.35 mole fraction dimethylsulfoxide.

The authors wish to acknowledge the helpful suggestions of, and discussions with, Dr. D. D. MacDonald and the financial support of the National Research Council of Canada.

1. F. FRANKS and D. J. G. IVES. Quart. Rev. XX, 1 (1966).
2. A. J. PARKER. Quart. Rev. XVI, 163 (1962).
3. J. J. LINDBERG and J. KENTTAMAA. Suomen Kemistilehti, **B33**, 104 (1960).
4. J. M. G. COWIE and P. M. TOPOROWSKI. Can. J. Chem., **39**, 2240 (1961).
5. K. H. JUNG. M.Sc. thesis. University of Calgary, Calgary, Alberta. 1969.
6. J. E. STUTCHBURY. Aust. J. Chem. **9**, 536 (1956).
7. B. JACOBSON. Ark. Kemi, **2**, 177 (1951).
8. J. KORPELA and J. KOSHEKALLIS, Suomen Kemistilehti, **B39**, 165 (1966).

Can. J. Chem. Downloaded from www.nrcresearchpress.com by 210.87.254.6 on 09/05/12
For personal use only.

Can. J. Chem. Downloaded from www.nrcresearchpress.com by 210.87.254.40 on 09/05/12
For personal use only.

Rate of addition of bromine atoms to ethylene

K. T. WONG[1] AND D. A. ARMSTRONG
Department of Chemistry, University of Calgary, Calgary, Alberta

Received[2] September 22, 1969

The rate of combination of bromine atoms in the photosensitized hydrobromination of ethylene has been determined by the rotating sector technique. From this and kinetic data reported previously the rate constant for the addition of bromine atoms to ethylene in the presence of 380 Torr of propane as deactivating gas has been calculated to be $1.5 \pm 0.3 \times 10^{-14}$ cm^3 molecule^{-1} s^{-1}, independent of temperature in the range 15 to 35 °C. This result is discussed and compared with rate constants for other addition reactions to ethylene.

Canadian Journal of Chemistry, 48, 2426 (1970)

Introduction

Rate constants for the addition of free radicals to olefin double bonds are of fundamental interest in chemical kinetics. Several photochemical determinations of these constants for chlorine atoms have been published (1, 2), but investigations of the analogous bromine atom additions are lacking. The object of this paper is to report a determination of the rate of reaction of bromine atoms with ethylene. The acetone-sensitized photo-addition of HBr to ethylene was used as a regenerative source of bromine atoms. In the presence of excess propane the main reactions are (3)

$$[1] \quad \mathrm{HBr}(+\ \mathrm{Acetone}) + h\nu \xrightarrow{I_a} \phi\mathrm{Br}$$

$$[2]/[-2] \quad \mathrm{Br} + \mathrm{C_2H_4} \underset{\mathrm{M}}{\overset{\mathrm{M}}{\rightleftharpoons}} \mathrm{BrC_2H_4}$$

$$[3] \quad \mathrm{BrC_2H_4} + \mathrm{HBr} \rightarrow \mathrm{BrC_2H_5} + \mathrm{Br}$$

$$[4] \quad \mathrm{Br} + \mathrm{Br} + \mathrm{M^1} \rightarrow \mathrm{Br_2} + \mathrm{M^1}$$

I_a is the absorbed light intensity and ϕ the quantum yield of bromine atoms ($= 1.7 \pm 0.3$ (3)) from acetone sensitization. [M^1] represents the overall effective concentration of third bodies for reaction [4], propane being the predominant one. Likewise [M] is the overall effective concentration of deactivating molecules for reactions [2] and [−2].

At propane pressures above 260 Torr, reactions [2] and [−2] are close to, if not within, their high pressure region and the following rate expression is obeyed (3)

$$[1] \quad \frac{\mathrm{d[C_2H_5Br]}}{\mathrm{d}t} = \left(\frac{\phi I_a}{2k_4[\mathrm{M^1}]}\right)^{1/2} \times \frac{k_2[\mathrm{C_2H_4}][\mathrm{HBr}]}{\{k_3[\mathrm{HBr}] + k_{-2}\}}$$

The magnitude of $k_2/(2k_4[\mathrm{M^1}])^{1/2}$ has been measured for 380 Torr of added propane and k_2 can be calculated if $(2k_4[\mathrm{M^1}])^{1/2}$ is determined for the same conditions. This was achieved by the rotating sector method as described below.

Experimental

Radical lifetimes were measured with a 12 in. diameter rotating sector constructed from an aluminum disk, which had been painted black. The two 60° cuts in it provided a dark-to-light ratio, r, of 2:1. On every revolution a small magnet attached to the sector triggered a magnetic switch fixed to the sector mounting and sent a pulse to a Nuclear Chicago model 186 counter, which served as a tachometer. This agreed to within ±1% with a stroboscope timer at high speeds and was taken as exact at low speeds.

The reaction rate for

$$\mathrm{C_2H_4} + \mathrm{HBr} \rightarrow \mathrm{C_2H_5Br}$$

was measured by following the decrease in pressure continuously with a Kern spiral gauge and optical lever. The experimental procedures and all other components of the apparatus were the same as those described in ref. 3.

Results

The reaction mixtures used in the radical lifetime determinations nominally contained 170

[1]Present address: Chemistry Department, Northern Alberta Institute of Technology, Edmonton, Alberta.

[2]Revision received April 6, 1970.

TABLE 1
Summary of experimental data for $2k_4[M]$ and k_2

Temperature (°C)	$2k_4[M^1]^a$ (cm^3 $molecule^{-1}$ s^{-1})	$(2k_4[M^1])^{1/2}/k_2{}^b$ ($cm^{-3/2}$ $molecule^{-1/2}$ $s^{1/2}$)	k_2 (cm^3 $molecule^{-1}$ s^{-1})
15.3	$7.6\pm1.7\times10^{-11}$	$5.2\pm0.5\times10^{8}$	$1.7\pm0.3\times10^{-14}$
25.0	$6.3\pm2.0\times10^{-11}$	$5.8\pm0.3\times10^{8}$	$1.4\pm0.2\times10^{-14}$
35.0	$5.5\pm1.9\times10^{-11}$	$5.4\pm0.4\times10^{8}$	$1.4\pm0.3\times10^{-14}$
		Mean	$1.5\pm0.3\times10^{-14}$

[a]This study.
[b]Reference 3.

Torr HBr, 60 Torr ethylene, and 380 Torr propane. Small variations in the initial propane and HBr concentrations are negligible; but reaction rates were corrected for differences in the ethylene concentration from one run to the next, since the rate is first order in this reactant (see eq. [1]).

In accordance with procedures normally employed in the analysis of sector experiments (4, 5), the length of the light period, t, was calculated from the speed of rotation and combined with ϕI_a to give $t(\phi I_a)^{1/2}$. Conventional plots of $(r+1)^{1/2}(\bar{R}/R)$ against $\log t(\phi I_a)^{1/2}$ are shown in Figs. 1*a*, *b*, and *c* for temperatures of 15.3, 25.0, and 35.0 °C, respectively. $\bar{R}$ is the average reaction rate for intermittent illumination at a given sector speed, and R the average rate for continuous illumination under the same conditions.

The best fit to the theoretical curves of $(r+1)^{1/2}(\bar{R}/R)$ vs. $\log m$, where $m = t/(2k_4 \times [M^1]\phi I_a)^{1/2}$, was obtained with the values of $2k_4[M^1]$ given in column 2 of Table 1. Column 3 contains $(2k_4[M^1])^{1/2}/k_2$ from the experimental results of ref. 3, and column 4 the magnitude of k_2 calculated from the two sets of data.

The quantity $2k_4[M^1]$ is actually composite and equal to $2\{k_{4(C_3H_8)}[C_3H_8] + k_{4(C_2H_4)}[C_2H_4] + k_{4(HBr)}[HBr]\}$. There is insufficient information to permit exact evaluation of the individual rate constants for each third body component. However, the data of ref. 3 show that the first term is the largest of the three, and it follows that $k_{4(C_3H_8)} \sim 1.6 \times 10^{-30}$ cm^6 $molecule^{-2}$ s^{-1}. Comparison of the rates of addition observed (3) in the presence of ~ 385 Torr of propane, sulfur hexafluoride, and ethyl chloride at 25.0 °C demonstrates that $k_{4(C_3H_8)}$ is about a factor of two larger than $k_{4(SF_6)}$ and $k_{4(C_2H_5Cl)}$. The temperature dependence of $2k_4[M^1]$ in Table 1 indicates that $E_{4(C_3H_8)} \simeq -3$ kcal $mole^{-1}$.

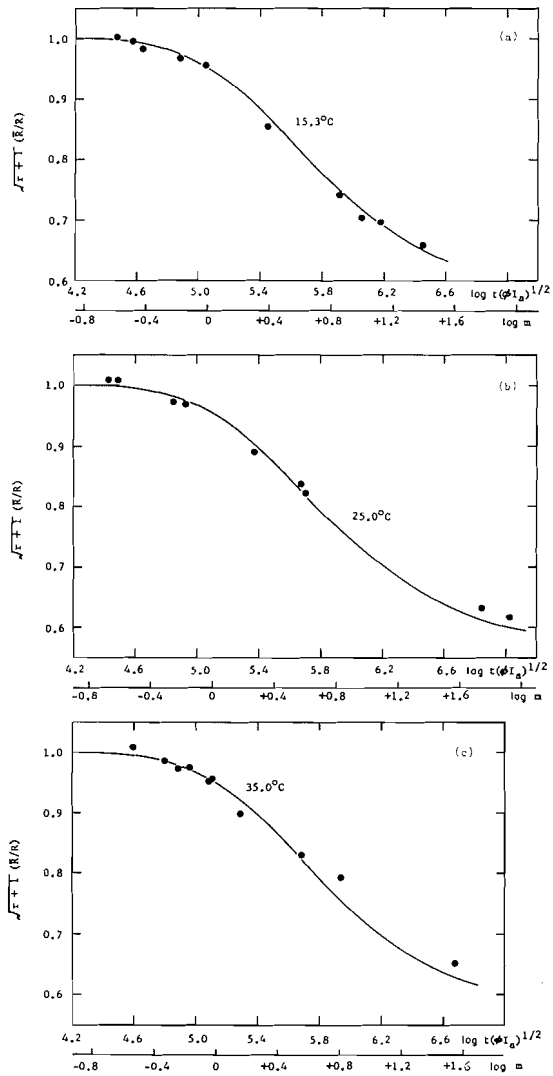

FIG. 1. The experimental points are plots of $(r+1)^{1/2}(\bar{R}/R)$ vs. $\log t(\phi I_a)^{1/2}$ and the lines are computed values of $(r+1)^{1/2}(\bar{R}/R)$ plotted against $m = t/(2k_4[M]\phi I_a)^{1/2}$; (*a*) 15.3 °C, (*b*) 25.0 °C, and (*c*) 35.0 °C.

Can. J. Chem. Downloaded from www.nrcresearchpress.com by 210.87.254.40 on 09/05/12
For personal use only.

TABLE 2

Comparison of rate constants for radical additions to ethylene

Radical (X)	Electron affinity (kcal mole^{-1})	$D_{C_2H_4-X}$ (kcal mole^{-1})	$k_{X+C_2H_4}$ 298 °K (cm^3 molecule^{-1} s^{-1})
Cl	83[a]	22.4[c]	2 to 7 × 10^{-11}[e]
Br	78[a]	8.2[c]	1.5 × 10^{-14}[f]
CH_3S	⩾ 74[b]	6.6[d]	8 × 10^{-16}[g]

[a]Reference 11.
[b]Reference 12.
[c]From ref. 8. All values of $D_{C_2H_4-X}$ are subject to an uncertainty of ±1 kcal mole^{-1}.
[d]Calculated from the data of ref. 13.
[e]References 1 and 2.
[f]This study.
[g]Reference 13.

Discussion

The present results show that the absolute magnitude of $k_{4(C_3H_8)}$ is surprisingly large, about 20 times greater than Russell and Simons' rate constant for the combination of iodine atoms on propane (6). Comparison with rate constants for bromine atom combination in the presence of other hydrocarbons as chaperon is impossible, because of the lack of data. However, it may be noted that the values of $E_{4(C_3H_8)}$ ($\simeq -3$ kcal mole^{-1}) and $k_{4(C_3H_8)}$ ($= 10^{-30}$ cm^6 molecule^{-2} s^{-1}) are self-consistent within the framework of the "complex" theory of atom recombination (7).

From the data of Table 1 it is evident that E_2 is close to zero.[3] This implies that A_2 must be $\simeq k_2$ and much smaller than the collision rate. If this is so then A_{-2} must also be small. Kerr and Lloyd (8) have reported $\Delta S_2 = -4.0$ cal deg^{-1} mole^{-1}, derived from thermodynamic data. From this and $A_2 = 1.5 \times 10^{-14}$ cm^3 molecule^{-1} s^{-1}, one finds $A_{-2} = 2.5 \times 10^{10}$ s^{-1}. In ref. 3 the magnitude of A_{-2}/A_3 was shown to be 1.3×10^{22} molecule cm^{-3}, and A_3 should not differ appreciably from A_5

[5] $\quad C_2H_5 + HBr \rightarrow C_2H_6 + Br$

Substituting $A_3 \simeq A_5 = 1.3 \times 10^{-12}$ cm^3 molecule^{-1} s^{-1} from ref. 9, one obtains $A_{-2} = 1.7 \times 10^{10}$ s^{-1} in good agreement with the result deduced above. Thus the low values of A_2 and A_{-2}, and $E_2 \simeq 0$ are consistent within the framework of available kinetic and thermodynamic data.

An important factor in radical addition reactions of olefins is the electrophilic character of the free radical addend. This has been established from studies with divalent atoms and other free radical addends (see, for example, ref. 10). Our value of k_2 is compared with the rate constants for two other monovalent addends of similar electron affinity in Table 2. The data are scant, but the following points are of particular interest. Since the relative differences between the electron affinities of the addends are small, the marked increase of $k_{X+C_2H_4}$ along the series X = CH_3S, X = Br and X = Cl seems to be associated with the changes in $D_{C_2H_4-X}$. The greatest difference occurs between X = Br and X = Cl. From the preceding paragraph it is evident that this cannot be ascribed to a larger activation energy for X = Br. Possibly the low value of $D_{C_2H_4-X}$ for X = Br (and CH_3S) requires that the addition proceed via a cross over between electronic states of different multiplicity. Such a process has already been suggested (14) for some types of radical additions to C=C bonds,[4] and could explain the low value of A_2 (and A_{-2}), since it would have a low transmission coefficient. In the case of X = Cl the much higher value of $D_{C_2H_4-X}$ may shift the system of potential energy curves for the initial and final states so that interaction between states of the same multiplicity can occur, thus giving a much higher A factor. These suggestions are obviously speculative, and a more complete explanation of the dependence of $k_{X+C_2H_4}$ on the

[3]When taken at face value the three results for k_2 actually give $E_2 = -1.7$ kcal mole^{-1}. However, we do not attach any significance to the negative value, since the possible error on E_2 is of the same magnitude and k_2 is pressure independent (3) in our pressure region. In fact E_2 is probably in the range -0.5 to $+0.5$ kcal mole^{-1}.

[4]Similar processes evidently must occur in the addition of CH_3 (15) and H (16) to the multiple bond of CO.

Can. J. Chem. Downloaded from www.nrcresearchpress.com by 210.87.254.40 on 09/05/12
For personal use only.

identity of X must await a better understanding of the potential energy surfaces for the reactions.

The authors are indebted to the University of Calgary and the National Research Council of Canada for financial support. They also wish to acknowledge helpful discussions with Dr. W. G. Laidlaw of this Department.

1. (*a*) G. CHILTZ, P. GOLDFINGER, G. HUYBRECHTS, G. MARTENS, and G. VERBEKE. Chem. Rev. **63**, 388 (1963); (*b*) J. A. FRANKLIN, P. GOLDFINGER, and G. HUYBRECHTS. Ber. Bunseng. **72**, 173 (1968).
2. P. B. AYSCOUGH, F. S. DAINTON, and B. E. FLEISCHFRESSER. Trans. Faraday Soc. **62**, 1 (1966).
3. K. T. WONG and D. A. ARMSTRONG. Can. J. Chem. **47**, 4183 (1969).
4. H. W. MELVILLE and G. M. BURNETT. Techniques of organic chemistry. Vol. VIII, *Edited by* A. Weissberger and S. L. Friess. Interscience Publ. Inc., New York. 1953.
5. A. SHEPP and K. O. KUTSCHKE. J. Chem. Phys. **26**, 1020 (1957).
6. K. E. RUSSELL and J. SIMONS. Proc. Roy. Soc. Ser. A. **217**, 271 (1953).
7. B. STEVENS. The international encyclopedia of physical chemistry and chemical physics, Topic 19. Vol. 3. *Edited by* A. F. Trotman-Dickenson. Pergamon Press, New York. (1967). p. 196.
8. J. A. KERR and A. C. LLOYD. Quart. Rev. **XXII**, 549 (1968).
9. G. C. FETTIS, J. H. KNOX, and A. F. TROTMAN-DICKENSON. J. Chem. Soc. 4177 (1960).
10. R. J. CVETANOVIC and R. S. IRWIN. J. Chem. Phys. **46**, 1694 (1967).
11. R. S. BERRY and C. W. REIMANN. J. Chem. Phys. **38**, 1540 (1963).
12. K. JÄGER and A. HENGLEIN. Z. Naturforsch. **21a**, 1251 (1966).
13. D. M. GRAHAM, R. L. MELVILLE, and C. SIVERTZ. Can. J. Chem., **42**, 2250 (1964); D. M. GRAHAM and J. F. SOLTYS. **47**, 2529 (1969).
14. V. N. KONDRAT'EV. Chemical kinetics of gas reactions. *Translated by* J. M. Crabtree and S. N. Carruthers. Pergamon Press, London. 1964.
15. E. O'NEAL and S. W. BENSON. J. Chem. Phys. **36**, 2196 (1962).
16. J. W. C. JOHNS, S. H. PRIDDLE and D. A. RAMSAY. Discuss. Faraday Soc. **35**, 90 (1963).

γ-Radiolysis of hydrocarbons using perfluorocyclohexane as an electron scavenger: determination of the free ion yields[1]

N. H. SAGERT[2] AND J. A. REID[3]

Physical Chemistry Branch, Chalk River Nuclear Laboratories, Atomic Energy of Canada Limited, Chalk River, Ontario

Received March 16, 1970

The room temperature, liquid phase radiolysis of *n*-hexane, 3-methylpentane, and 2,2,4-trimethylpentane has been examined using perfluorocyclohexane as an electron scavenger. Yields of $C_6F_{11}H$ and $C_6F_{11}CH_3$ were determined for scavenger concentrations below 5×10^{-3} *M*, and from these results free ion yields of 0.08, 0.17, and 0.37 G units were deduced for *n*-hexane, 3-methylpentane, and 2,2,4-trimethylpentane, respectively. These results are in good agreement with those obtained by other methods.

Canadian Journal of Chemistry, 48, 2429 (1970)

Introduction

It is now generally realized that the formation of ion pairs is important in the radiolysis of nonpolar liquids and several theoretical treatments of the formation of these ion pairs are available (1–3). A particularly important quantity is the yield of electrons which escape completely from the field of their parent positive ions and become uniformly distributed in the liquid. This free ion yield is commonly around 0.1 G units (0.1 ion pairs per 100 eV) for hydrocarbons of linear structure and increases as the hydrocarbon molecule becomes more spherical (4). The yield is usually determined by steady state conductivity (5) or by the clearing field technique (4). Recently Rzad and Warman have described a chemical scavenging method for determining free ion yields using $^{14}CH_3Br$ as a scavenger (6), and, more recently, we described a C_6F_{12} scavenging technique for determining the free ion yield in cyclohexane (7).

This work briefly describes the application of the C_6F_{12} electron scavenging technique to three

[1]AECL No. 3621.

[2]Present address: Materials Science Branch, Whiteshell Nuclear Research Establishment, Pinawa, Manitoba.

[3]AECL summer student, 1969. Present address: Department of Chemistry, University of Waterloo, Waterloo, Ontario.

Can. J. Chem. Downloaded from www.nrcresearchpress.com by 210.87.254.40 on 09/05/12
For personal use only.

identity of X must await a better understanding of the potential energy surfaces for the reactions.

The authors are indebted to the University of Calgary and the National Research Council of Canada for financial support. They also wish to acknowledge helpful discussions with Dr. W. G. Laidlaw of this Department.

1. (*a*) G. CHILTZ, P. GOLDFINGER, G. HUYBRECHTS, G. MARTENS, and G. VERBEKE. Chem. Rev. **63**, 388 (1963); (*b*) J. A. FRANKLIN, P. GOLDFINGER, and G. HUYBRECHTS. Ber. Bunseng. **72**, 173 (1968).
2. P. B. AYSCOUGH, F. S. DAINTON, and B. E. FLEISCHFRESSER. Trans. Faraday Soc. **62**, 1 (1966).
3. K. T. WONG and D. A. ARMSTRONG. Can. J. Chem. **47**, 4183 (1969).
4. H. W. MELVILLE and G. M. BURNETT. Techniques of organic chemistry. Vol. VIII, *Edited by* A. Weissberger and S. L. Friess. Interscience Publ. Inc., New York. 1953.
5. A. SHEPP and K. O. KUTSCHKE. J. Chem. Phys. **26**, 1020 (1957).
6. K. E. RUSSELL and J. SIMONS. Proc. Roy. Soc. Ser. A. **217**, 271 (1953).
7. B. STEVENS. The international encyclopedia of physical chemistry and chemical physics, Topic 19. Vol. 3. *Edited by* A. F. Trotman-Dickenson. Pergamon Press, New York. (1967). p. 196.
8. J. A. KERR and A. C. LLOYD. Quart. Rev. **XXII**, 549 (1968).
9. G. C. FETTIS, J. H. KNOX, and A. F. TROTMAN-DICKENSON. J. Chem. Soc. 4177 (1960).
10. R. J. CVETANOVIC and R. S. IRWIN. J. Chem. Phys. **46**, 1694 (1967).
11. R. S. BERRY and C. W. REIMANN. J. Chem. Phys. **38**, 1540 (1963).
12. K. JÄGER and A. HENGLEIN. Z. Naturforsch. **21a**, 1251 (1966).
13. D. M. GRAHAM, R. L. MELVILLE, and C. SIVERTZ. Can. J. Chem., **42**, 2250 (1964); D. M. GRAHAM and J. F. SOLTYS. **47**, 2529 (1969).
14. V. N. KONDRAT'EV. Chemical kinetics of gas reactions. *Translated by* J. M. Crabtree and S. N. Carruthers. Pergamon Press, London. 1964.
15. E. O'NEAL and S. W. BENSON. J. Chem. Phys. **36**, 2196 (1962).
16. J. W. C. JOHNS, S. H. PRIDDLE and D. A. RAMSAY. Discuss. Faraday Soc. **35**, 90 (1963).

γ-Radiolysis of hydrocarbons using perfluorocyclohexane as an electron scavenger: determination of the free ion yields[1]

N. H. SAGERT[2] AND J. A. REID[3]

Physical Chemistry Branch, Chalk River Nuclear Laboratories, Atomic Energy of Canada Limited, Chalk River, Ontario

Received March 16, 1970

The room temperature, liquid phase radiolysis of *n*-hexane, 3-methylpentane, and 2,2,4-trimethylpentane has been examined using perfluorocyclohexane as an electron scavenger. Yields of $C_6F_{11}H$ and $C_6F_{11}CH_3$ were determined for scavenger concentrations below 5×10^{-3} *M*, and from these results free ion yields of 0.08, 0.17, and 0.37 G units were deduced for *n*-hexane, 3-methylpentane, and 2,2,4-trimethylpentane, respectively. These results are in good agreement with those obtained by other methods.

Canadian Journal of Chemistry, 48, 2429 (1970)

Introduction

It is now generally realized that the formation of ion pairs is important in the radiolysis of nonpolar liquids and several theoretical treatments of the formation of these ion pairs are available (1–3). A particularly important quantity is the yield of electrons which escape completely from the field of their parent positive ions and become uniformly distributed in the liquid. This free ion yield is commonly around 0.1 G units (0.1 ion pairs per 100 eV) for hydrocarbons of linear structure and increases as the hydrocarbon molecule becomes more spherical (4). The yield is usually determined by steady state conductivity (5) or by the clearing field technique (4). Recently Rzad and Warman have described a chemical scavenging method for determining free ion yields using $^{14}CH_3Br$ as a scavenger (6), and, more recently, we described a C_6F_{12} scavenging technique for determining the free ion yield in cyclohexane (7).

This work briefly describes the application of the C_6F_{12} electron scavenging technique to three

[1]AECL No. 3621.

[2]Present address: Materials Science Branch, Whiteshell Nuclear Research Establishment, Pinawa, Manitoba.

[3]AECL summer student, 1969. Present address: Department of Chemistry, University of Waterloo, Waterloo, Ontario.

Can. J. Chem. Downloaded from www.nrcresearchpress.com by 210.87.254.40 on 09/05/12
For personal use only.

hydrocarbons of varying structure, to see if this technique could be used with hydrocarbons other than cyclohexane. The applicability of the technique to other systems would strengthen the contention that the chief effect of C_6F_{12} in the radiolysis of hydrocarbons is to capture electrons.

Experimental

The solvents, Fisher spectrograde 2,2,4-trimethylpentane, Phillips Research Grade *n*-hexane, and Phillips Pure Grade 3-methylpentane, were purified as described earlier for cyclohexane used with low concentrations of scavenger (7). Perfluorocyclohexane was obtained from Aldrich Chemical Co., and from K & K Laboratories and was vacuum sublimed between 25 and 0 °C before use. Undecafluorocyclohexane obtained from Aldrich Chemical Co. was used as received. Methylundecafluorocyclohexane was prepared from decafluorocyclohexene (Aldrich) according to the procedure of Sayers, Stephens, and Tatlow (8).

Sample preparation has been described previously (7). Samples were irradiated at 25 °C in a ^{60}Co γ-source at a mean dose rate (in cyclohexane) of 8.5×10^{15} eV/g s as determined by ferrous sulfate dosimetry, taking $G(Fe^{3+}) = 15.6$. Corrections were made to the absorbed dose for the varying electron densities of the solutions.

The liquid products of interest, $C_6F_{11}H$ and $C_6F_{11}CH_3$, were determined by gas chromatography, using a Varian 1800 gas chromatograph equipped with a ^{63}Ni electron capture detector and a Hewlett–Packard 700 equipped with a ^{3}H electron capture detector. The electron capture detector was sensitive to cyclic fluorocarbon groups, but was insensitive to hydrocarbon components (9). Because its dynamic range was limited, a curved calibration was generally obtained, and hence a complete set of calibration standards was run each day.

A column of 6 ft of 8% SE-30 on Porasil E plus 6 ft of 10% XE-60 on Aeropak 30 gave a useable separation of products and reactants at 70 °C. Mass spectra were obtained using a Varian CH7 spectrometer and a Consolidated 21–130 spectrometer.

Results

The only observed products containing C_6F_{11} groups were $C_6F_{11}H$ and $C_6F_{11}CH_3$. These products were identified by comparison of gas chromatographic retention times with those of authentic standards, and by mass spectrometry. Yields of these products were quite dose-dependent and G values were determined from the initial slopes of plots of concentration of product against dose. At low scavenger concentrations, these plots were linear only at doses below 3×10^{17} eV/g. The initial yield of C_6F_{11} radicals, defined as the sum of the yields of $C_6F_{11}H$ and $C_6F_{11}CH_3$, was then plotted in Figs. 1, 2, and 3, against the square root of the

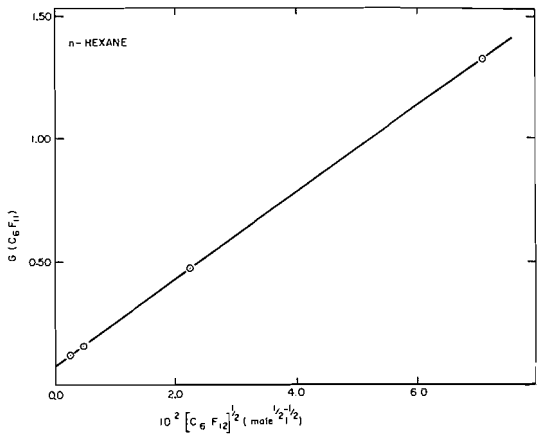

FIG. 1. Initial yields of C_6F_{11} from the radiolysis of C_6F_{12} in *n*-hexane.

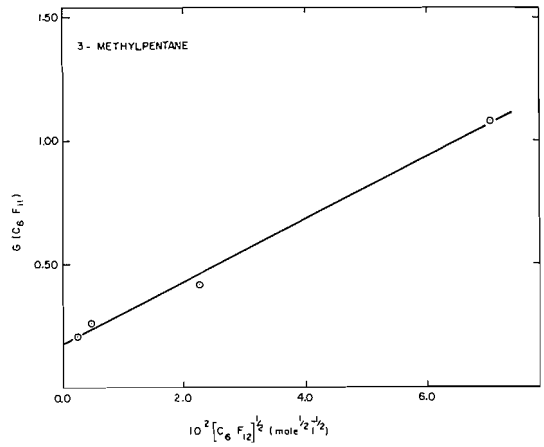

FIG. 2. Initial yields of C_6F_{11} from the radiolysis of C_6F_{12} in 3-methylpentane.

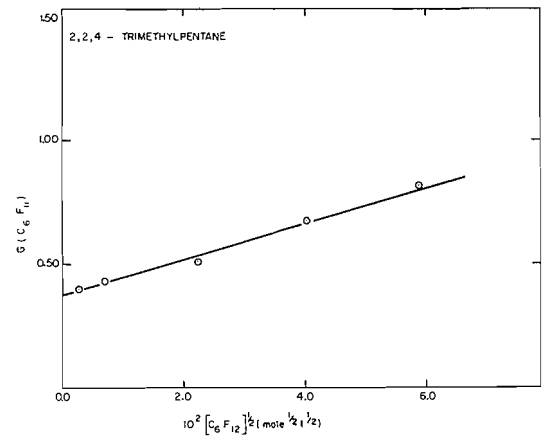

FIG. 3. Initial yields of C_6F_{11} from the radiolysis of C_6F_{12} in 2,2,4-trimethylpentane.

Can. J. Chem. Downloaded from www.nrcresearchpress.com by 210.87.254.40 on 09/05/12
For personal use only.

TABLE 1
Free ion yields in liquid hydrocarbons

Hydrocarbons	$G_{fi}(C_6F_{12})$	$G_{fi}(CH_3Br)$*	G_{ii}(Conductivity)†	G_{fi}(Clearing field)‡
Cyclohexane	0.14	0.12	0.11	0.16
n-Hexane	0.08	0.12	0.11	0.13
3-Methylpentane	0.17			0.15
2,2,4-Trimethylpentane	0.37	0.34		0.33

*Reference 6.
†Reference 5.
‡Reference 4.

solute concentration for each of the three solvents. The ratio of $C_6F_{11}CH_3$ to $C_6F_{11}H$ was somewhat variable, but in all cases the relative amount of $C_6F_{11}CH_3$ increased at lower concentrations of C_6F_{12}. At equal concentrations of C_6F_{12} the ratio of $C_6F_{11}CH_3$ to $C_6F_{11}H$ was highest for 2,2,4-trimethylpentane and lowest for *n*-hexane.

Discussion

Rajbenbach (10) has suggested that perfluorocycloalkanes affect the radiolysis of liquid hydrocarbons by capturing electrons, and more recent work supports this view (7, 11). We have shown (7, 12) that electron capture by C_6F_{12} in cyclohexane (reaction [1]) produces an anion, which, on neutralization, produces one C_6F_{11} radical, or $C_6F_{11}H$ molecule, for each electron scavenged.

$$[1] \qquad C_6F_{12} + e^- \rightarrow C_6F_{12}^-$$

$$[2a] \qquad C_6F_{12}^- + C_6H_{12}^+ \rightarrow C_6F_{11} + C_6H_{11} + HF$$

$$[2b] \qquad \rightarrow C_6F_{11}H + C_6H_{11} + F$$

Thus the yield of products containing C_6F_{11} can be equated with the yield of electrons. We have previously shown that the C_6F_{11} yield at low C_6F_{12} concentrations can be used to determine the yield of free ions in cyclohexane. In this work, the C_6F_{12} chemical scavenging technique has been extended to three other solvents to examine the general validity of the technique.

Results were fitted to the expression developed by Schuler and his co-workers (13, 14) and by Hummel (3)

$$[3] \qquad G(C_6F_{11}) = G_{fi} + \frac{G_{gi}\{\alpha_{C_6F_{12}}[C_6F_{12}]\}^{1/2}}{1 + \{\alpha_{C_6F_{12}}[C_6F_{12}]\}^{1/2}}$$

where $G(C_6F_{11})$ is the yield of $C_6F_{11}H$ plus $C_6F_{11}CH_3$, G_{fi} is the yield of electrons which escape from the field of their parent positive ion and G_{gi} is the yield of geminate electrons, or electrons which are eventually captured by their parent positive ion. The $\alpha_{C_6F_{12}}$ is a constant characterizing the reactivity of C_6F_{12} to electrons. This constant is given by k_1/λ, where k_1 is the rate constant for reaction [1] and λ is the ion recombination coefficient in the absence of scavengers (15, 16). At low scavenger concentrations, eq. [3] predicts a linear relationship between $G(C_6F_{11})$ and $[C_6F_{12}]^{1/2}$ with a slope given by $G_{gi}\cdot\alpha_{C_6F_{12}}{}^{1/2}$, and an intercept equal to G_{fi}. Such plots are shown in Figs. 1, 2, and 3.

Free ion yields determined from the intercepts of Figs. 1, 2, and 3, as well as that for cyclohexane, determined previously (7), are shown in Table 1. Results obtained by Rzad and Warman (6) using the methyl bromide scavenging technique, by Tewari and Freeman (5) using steady state conductivity, and by Schmidt and Allen using the clearing field technique (4), are given for comparison. In general, our results agree well with those obtained by other methods, although the value for *n*-hexane is somewhat low. Possibly for *n*-hexane either the purification was not adequate, or there are higher molecular weight products containing C_6F_{11} which were not detected on our column. The range of values for the hydrocarbons shown is noteworthy since it is larger than that expected on electron density considerations (4).

The good agreement with free ion yields determined by other methods indicates that the C_6F_{12} scavenging technique has a general applicability to the determination of free ion yields, and may be useful in polar media. It certainly supports the original contention that C_6F_{12} scavenges electrons of thermal energy to give one C_6F_{11} fragment per electron scavenged, and that

Can. J. Chem. Downloaded from www.nrcresearchpress.com by 210.87.254.40 on 09/05/12
For personal use only.

epithermal electrons are not necessary to produce these fragments.

The slopes of the lines in Figs. 1, 2, and 3 are given by $G_{gi}\alpha_{C_6F_{12}}{}^{1/2}$, for the range of $[C_6F_{12}]^{1/2} < 2.0 \times 10^{-2} M^{1/2}$. G_{gi} was not obtained separately in this work, but if it may be taken as 4.0 (7, 14), then estimates of $\alpha_{C_6F_{12}}$ may be made. These estimates are 24, 13, and 4 M^{-1} for *n*-hexane, 3-methylpentane, and 2,2,4-trimethylpentane, respectively. These values are only very rough estimates since small errors in slope caused by impurities or experimental difficulties will have a large effect on $\alpha_{C_6F_{12}}$. This may be especially true in the case of *n*-hexane where G_{fi} appears to be low.

Any discussion of the magnitude of $\alpha_{C_6F_{12}}$ in different solvents is inappropriate because of experimental difficulties. However, it should be noted that the value for 2,2,4-trimethylpentane is considerably lower than for the other solvents. A similar observation was made by Rzad and Warman (6) using $^{14}CH_3Br$ as a scavenger. Since $\alpha_{C_6F_{12}}$ is given by k_1/λ, changes in both k_1 and λ will have to be examined to determine how $\alpha_{C_6F_{12}}$ would be expected to vary on changing the solvent.

We would like to thank our colleagues at both the Chalk River Nuclear Laboratories and the Whiteshell Nuclear Research Establishment for aid and advice. We would also like to thank W. A. Boivin, D. Bell, and R. B. Stewart for assistance with gas chromatography and mass spectrometry, and R. W. Robinson for assistance in preparing the $C_6F_{11}CH_3$.

1. G. R. Freeman. J. Chem. Phys. **46**, 2822 (1967).
2. A. Mozumder. J. Chem. Phys. **48**, 1659 (1968).
3. A. Hummel. J. Chem. Phys. **48**, 3268 (1968).
4. W. F. Schmidt and A. O. Allen. J. Phys. Chem. **72**, 3730 (1968).
5. P. H. Tewari and G. R. Freeman. J. Chem. Phys. **49**, 4394 (1968).
6. S. J. Rzad and J. M. Warman. J. Chem. Phys. **49**, 2861 (1968).
7. N. H. Sagert, J. A. Reid, and R. W. Robinson. Can. J. Chem. **47**, 2655 (1969).
8. D. R. Sayers, R. Stephens, and J. C. Tatlow. J. Chem. Soc. 3035 (1964).
9. C. A. Clemons and A. P. Altshuller. Anal. Chem. **38**, 133 (1966).
10. L. A. Rajbenbach. J. Amer. Chem. Soc. **88**, 4275 (1966).
11. J. P. Mittal and W. F. Libby. Nature, **220**, 1027 (1968).
12. N. H. Sagert. Can. J. Chem. **46**, 95 (1968).
13. J. M. Warman, K–D. Asmus, and R. H. Schuler. Advan. Chem. Ser. **82**, 25 (1968).
14. J. M. Warman, K–D. Asmus, and R. H. Schuler. J. Phys. Chem. **73**, 931 (1969).
15. S. J. Rzad, R. H. Schuler, and A. H. Hummel. J. Chem. Phys. **51**, 1369 (1969).
16. S. J. Rzad, P. P. Infelta, J. M. Warman, and R. H. Schuler. J. Chem. Phys. **50**, 5034 (1969).

Anion exchange resin solvent selectivity and anion solvation: a nuclear magnetic resonance study

Lawrence S. Frankel

Rohm and Haas Co., Research Laboratory 13, 5000 Richmond St., Philadelphia, Pennsylvania 19137

Received March 4, 1970

Nuclear magnetic resonance has been utilized to study solvent selectivity of anion exchange resins in aqueous dimethyl sulfoxide and aqueous acetonitrile. Solvent selectivity data in the chloride ionic form is in qualitative agreement with independent preferential solvation studies of chloride ion. The importance of solvent activity coefficients is demonstrated for aqueous acetonitrile.

Canadian Journal of Chemistry, 48, 2432 (1970)

There have been few reports on solvent selectivity of anion exchange resins (1). In order to gain further insight into the dominant factors which determine solvent selectivity, we have studied aqueous dimethyl sulfoxide (DMSO) and aqueous acetonitrile mixtures. Results of a new method for studying chloride ion contact preferential solvation in these solvent mixtures (2) can be compared with anion exchange selectivity data and the importance of anion solvation (1, 3*a*) can be assessed.

The anion resins were commercial samples of polystyrene methylene trimethylammonium type (Amberlite IRA-400) of 8% cross-linking and 20–50 mesh size. The unprotonated weak base resin Amberlite IR-45 has similar physical characteristics. The F^-, Br^-, and I^- form of IRA-400 were prepared from the Cl^- form by

Can. J. Chem. Downloaded from www.nrcresearchpress.com by 210.87.254.40 on 09/05/12
For personal use only.

epithermal electrons are not necessary to produce these fragments.

The slopes of the lines in Figs. 1, 2, and 3 are given by $G_{gi}\alpha_{C_6F_{12}}{}^{1/2}$, for the range of $[C_6F_{12}]^{1/2} < 2.0 \times 10^{-2} M^{1/2}$. G_{gi} was not obtained separately in this work, but if it may be taken as 4.0 (7, 14), then estimates of $\alpha_{C_6F_{12}}$ may be made. These estimates are 24, 13, and 4 M^{-1} for *n*-hexane, 3-methylpentane, and 2,2,4-trimethylpentane, respectively. These values are only very rough estimates since small errors in slope caused by impurities or experimental difficulties will have a large effect on $\alpha_{C_6F_{12}}$. This may be especially true in the case of *n*-hexane where G_{fi} appears to be low.

Any discussion of the magnitude of $\alpha_{C_6F_{12}}$ in different solvents is inappropriate because of experimental difficulties. However, it should be noted that the value for 2,2,4-trimethylpentane is considerably lower than for the other solvents. A similar observation was made by Rzad and Warman (6) using $^{14}CH_3Br$ as a scavenger. Since $\alpha_{C_6F_{12}}$ is given by k_1/λ, changes in both k_1 and λ will have to be examined to determine how $\alpha_{C_6F_{12}}$ would be expected to vary on changing the solvent.

We would like to thank our colleagues at both the Chalk River Nuclear Laboratories and the Whiteshell Nuclear Research Establishment for aid and advice. We would also like to thank W. A. Boivin, D. Bell, and R. B. Stewart for assistance with gas chromatography and mass spectrometry, and R. W. Robinson for assistance in preparing the $C_6F_{11}CH_3$.

1. G. R. Freeman. J. Chem. Phys. **46**, 2822 (1967).
2. A. Mozumder. J. Chem. Phys. **48**, 1659 (1968).
3. A. Hummel. J. Chem. Phys. **48**, 3268 (1968).
4. W. F. Schmidt and A. O. Allen. J. Phys. Chem. **72**, 3730 (1968).
5. P. H. Tewari and G. R. Freeman. J. Chem. Phys. **49**, 4394 (1968).
6. S. J. Rzad and J. M. Warman. J. Chem. Phys. **49**, 2861 (1968).
7. N. H. Sagert, J. A. Reid, and R. W. Robinson. Can. J. Chem. **47**, 2655 (1969).
8. D. R. Sayers, R. Stephens, and J. C. Tatlow. J. Chem. Soc. 3035 (1964).
9. C. A. Clemons and A. P. Altshuller. Anal. Chem. **38**, 133 (1966).
10. L. A. Rajbenbach. J. Amer. Chem. Soc. **88**, 4275 (1966).
11. J. P. Mittal and W. F. Libby. Nature, **220**, 1027 (1968).
12. N. H. Sagert. Can. J. Chem. **46**, 95 (1968).
13. J. M. Warman, K–D. Asmus, and R. H. Schuler. Advan. Chem. Ser. **82**, 25 (1968).
14. J. M. Warman, K–D. Asmus, and R. H. Schuler. J. Phys. Chem. **73**, 931 (1969).
15. S. J. Rzad, R. H. Schuler, and A. H. Hummel. J. Chem. Phys. **51**, 1369 (1969).
16. S. J. Rzad, P. P. Infelta, J. M. Warman, and R. H. Schuler. J. Chem. Phys. **50**, 5034 (1969).

Anion exchange resin solvent selectivity and anion solvation: a nuclear magnetic resonance study

Lawrence S. Frankel

Rohm and Haas Co., Research Laboratory 13, 5000 Richmond St., Philadelphia, Pennsylvania 19137

Received March 4, 1970

Nuclear magnetic resonance has been utilized to study solvent selectivity of anion exchange resins in aqueous dimethyl sulfoxide and aqueous acetonitrile. Solvent selectivity data in the chloride ionic form is in qualitative agreement with independent preferential solvation studies of chloride ion. The importance of solvent activity coefficients is demonstrated for aqueous acetonitrile.

Canadian Journal of Chemistry, 48, 2432 (1970)

There have been few reports on solvent selectivity of anion exchange resins (1). In order to gain further insight into the dominant factors which determine solvent selectivity, we have studied aqueous dimethyl sulfoxide (DMSO) and aqueous acetonitrile mixtures. Results of a new method for studying chloride ion contact preferential solvation in these solvent mixtures (2) can be compared with anion exchange selectivity data and the importance of anion solvation (1, 3*a*) can be assessed.

The anion resins were commercial samples of polystyrene methylene trimethylammonium type (Amberlite IRA-400) of 8% cross-linking and 20–50 mesh size. The unprotonated weak base resin Amberlite IR-45 has similar physical characteristics. The F^-, Br^-, and I^- form of IRA-400 were prepared from the Cl^- form by

Can. J. Chem. Downloaded from www.nrcresearchpress.com by 210.87.254.6 on 09/05/12
For personal use only.

Can. J. Chem. Downloaded from www.nrcresearchpress.com by 210.87.254.6 on 09/05/12
For personal use only.

standard column procedures. To a 1.0 g sample of a resin of known water content was added 25 ml of a mixed solvent of known composition. The bulk mole fractions were in each case corrected for the water from the resin. The samples were equilibrated overnight (1) and centrifuged in the standard manner (3*b*) to remove excess surface solvent. The composition of the resin was determined by nuclear magnetic resonance (n.m.r.) technique (4). The resin was transferred to a standard high resolution n.m.r. tube and benzene placed in the tube to a level that just covered the resin. The use of an exterior solvent is desirable because it produces much narrower (approximately one third as broad) line widths from the solvent peaks inside the resin (approximately 10 c.p.s. broad). A Varian H.R. 60 spectrometer operating at 56.4 Mc was employed. The solvent peaks from the interior of the resin were integrated and the mole fraction of each component calculated.[1] A single point for the Cl^- form of a similar resin in water–acetonitrile mixed solvent has been analyzed by more classical techniques (1). At a bulk mole fraction water (X_W) of 0.50 the resin was reported to contain a mole fraction water ($\bar{X}_W$) of 0.84 while we observe $\bar{X}_W = 0.83$ (Fig. 3) in excellent agreement. Good integrals can only be obtained in the range $0.5 < \bar{X}_W < 1.0$. This limitation arises from an overlap of resonance peaks due to a net high field hydrogen bond dilution shift of water in the anion exchange resin.

The choice of aqueous DMSO and aqueous acetonitrile was made for the following reasons: (*a*) Solvent activity coefficient data is available (5, 6). (*b*) A new promising technique for studying contact chloride ion preferential solvation has recently been communicated for these solvents (2). (*c*) Activity coefficient data for anion transfer for these solvents may be calculated from available data (7). (*d*) Comparison with classical techniques is possible (1). (*e*) Ease of integration in the n.m.r. experiment. (*f*) General increasing interest in mixed solvents of this type, i.e., aqueous dipolar aprotic admixtures.

[1]Actually since both DMSO and acetonitrile are miscible with benzene a small peak for these solvents in the exterior solvent is observed at some mixed solvent compositions and must be taken into account in the integral. That the above explanation is indeed correct was confirmed by removing the exterior solvent, taking its spectra, and observing a cooperative alteration in the intensity as more dipolar aprotic solvent is added.

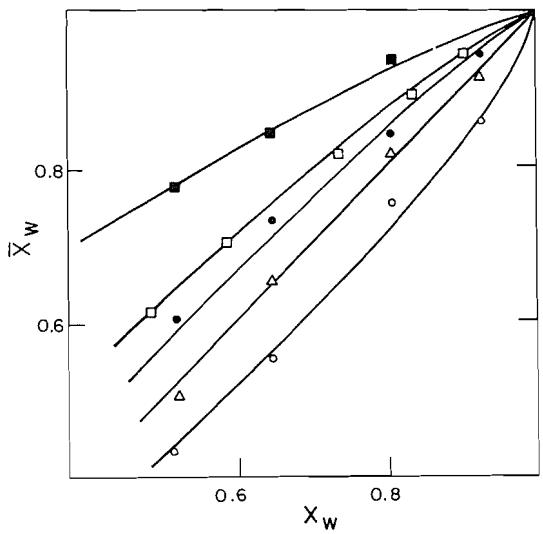

FIG. 1. Anion resin selectivity, water–DMSO; F^-, ■; Cl^-, □; Br^-, ●; I^-, △; weak base, ○. The mole fraction water in the bulk solution (X_W) vs. mole fraction in the resin ($\bar{X}_W$).

The data for aqueous DMSO mixtures is summarized in Fig. 1 as a plot of X_W vs. $\bar{X}_W$. As is apparent from the shape of these curves (8), a simple isotherm of the following form will fit the experimental data.

$$K = X_D\bar{X}_W/X_W\bar{X}_D$$

where K is the selectivity coefficient and the subscript D is for DMSO.[2] Values for K are summarized in Table 1. A value of $K > 1$ corresponds to a resin preference for water. Previous work suggests that the dominant effects are preferential anion solvation and solvent admixture structure rather than polymer matrix effects (fixed ionic group solvation or steric matrix requirements) (1). The variation in

TABLE 1

Summary of results for aqueous DMSO solvent mixtures

Resin functional group	K	$\log^W \gamma_{Y^-}{}^{D*}$
F^-	3.12±0.27	
Cl^-	1.60±0.06	8.0
Br^-	1.40±0.08	6.3
I^-	1.01±0.05	3.8
Free base	0.70±0.02	

*Data from ref. 12. $^W\gamma_{Y^-}{}^D$ is the anion (Y^-) activity change on transfer from water (W) to DMSO (D).

[2]More elaborate isotherms are needed to fit some experimental data of this type, see ref. 1.

Can. J. Chem. Downloaded from www.nrcresearchpress.com by 210.87.254.6 on 09/05/12
For personal use only.

selectivity coefficients is in agreement with these conclusions. The weak base resin prefers DMSO while the anion resins prefer water. The values of K in the anion resins vary in a systematic fashion. The smaller the charge density, the greater the preference for water.

The chloride ion preferential solvation experiment suggests that on a mole fraction basis, DMSO is slightly preferred to water in the chloride ion solvation shell (2), while we observe a slight preference for water in the resin. The weak base shows a slight preference for DMSO and tends to bring these experiments in closer agreement. We consider the two experiments to be in fair qualitative agreement in the sense that both conclude that there are no large preferential solvation effects. Activity coefficient data for anion solvent transfer summarized in Table 1 suggest a much greater anion preference (8). However, the general trend of anion activities is consistent with the resin selectivity results (log K vs. log ${}^{W}\gamma_{Y^-}{}^{D}$ gives a good straight line). An electrostatic model (Born equation) (9) predicts that the free energy of solvation is inversely proportional to the reciprocal of the anion radius (r). A plot of log K vs. $1/r$, Fig. 2, gives a reasonably linear plot.[3] Extrapolation of $1/r$ to zero gives $K_{r\to\infty} = 0.16$ (1.1 kcal). This implies that for very large anions, where the primary interactions are presumably dispersion forces, DMSO is strongly preferred; in agreement with predictions based on the known molar polarizations of these solvents.

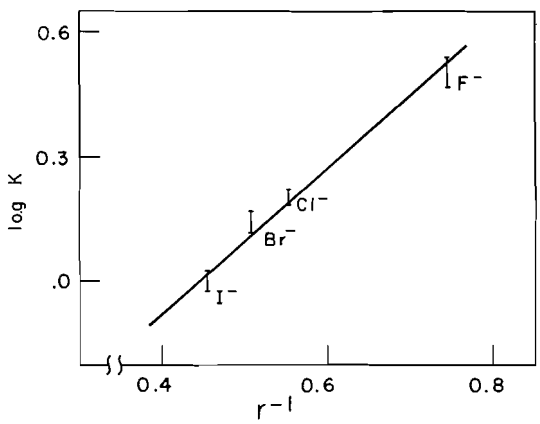

FIG. 2. Plot of log K vs. $1/r$ for anion exchange resins in water DMSO.

[3]Values for anion radii were obtained from ref. 10.

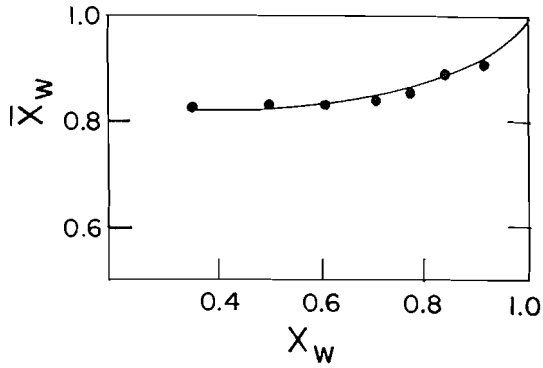

FIG. 3. Anion resin selectivity of IRA-400 Cl^-, water–acetonitrile, plot of mole fraction water in the bulk solution (X_W) vs. mole fraction water in the resin (X_W).

Data for the distribution of aqueous acetonitrile in IRA-400 in the chloride form is given in Fig. 3. The shape of this curve is very similar to that reported for the preferential solvation of chloride ion in this solvent mixture. The effect of solvent structure shows up very dynamically when comparing aqueous DMSO and aqueous acetonitrile mixtures. Water–DMSO solvent activity coefficients show relatively small variations (11)[4], in contrast to the extreme deviations for water–acetonitrile (2, 5). The activity coefficient of each component of the latter solvent system relatively independent of the solvent composition in the range $0.25 > X_W > 0.75$. Therefore the ratio of solvent activities shows an unusually small variation over this solvent range. We believe that this effect is the reason for the plateau region in Fig. 3 since virtually any isotherm used to fit these data will have this ratio as an important factor.

It is interesting to note that the ^{35}Cl chemical shift data in aqueous methanol mixtures suggest only small preferential solvation effects (12). Cl^- resin solvent selectivity has been reported to be small in this solvent system (1).

1. Ref. 5 of Y. MARCUS and J. NAVEH. J. Phys. Chem. **73**, 591 (1969).
2. C. H. LANGFORD and T. R. STENGLE. J. Amer. Chem. Soc. **91**, 4014 (1969).
3. F. HELFFERICH. Ion exchange. McGraw-Hill Book Co., Inc., New York. 1962. (*a*) Chap. 10. (*b*) p. 230.
4. J. E. GORDON. J. Phys. Chem. **66**, 1150 (1962).
5. V. DELANDSBERG. Bull. Soc. Chim. Belges. **49**, 59 (1940).

[4]Although this solvent system is known to interact, there are apparently compensating effects (11).

6. B. G. Cox and P. T. McTigue. Aust. J. Chem. **20**, 1815 (1967).
7. R. Alexander, E. C. F. Ko, A. J. Parker, and T. J. Broxton. J. Amer. Chem. Soc. **90**, 5049 (1968).
8. D. H. Everett. Trans. Faraday Soc. **60**, 1803 (1964).
9. M. Born. Z. Phys. **1**, 45 (1920).
10. L. Pauling. The nature of the chemical bond. Cornell University Press, Ithaca, New York. 1960. Table 13-9.
11. A. J. Parker. Chem. Rev. **69**, 1 (1969).
12. C. Hall, G. L. Haller, and R. E. Richards. Mol. Phys. **16**, 377 (1969).

Coordination compounds of olefins with anhydrous silver tetrafluoroborate V. Complexes with some cyclic di- and oligo-olefins[1]

H. W. Quinn and R. L. VanGilder
Exploratory Research Laboratory, Dow Chemical of Canada, Ltd., Sarnia, Ontario

Received January 13, 1970

The following complexes of di- and oligo-olefins have been prepared and characterized: $2AgBF_4$.3-cyclopentadiene, $AgBF_4$.cyclohexa-1,4-diene, $AgBF_4$.cyclohexene-1,3-diene, $2AgBF_4$.3cyclohexa-1,3-diene, $AgBF_4$.cycloheptа-1,3,5-triene hydrate, $AgBF_4$.2cycloheptа-1,3,5-triene, $AgBF_4$.2cycloocta-1,3,5-triene, $AgBF_4$.2cycloocta-1,5-diene, $AgBF_4$.cyclooctatetraene, and $AgBF_4$.dicyclopentadiene.

Canadian Journal of Chemistry, **48**, 2435 (1970)

Can. J. Chem. Downloaded from www.nrcresearchpress.com by 210.87.254.6 on 09/05/12
For personal use only.

Introduction

Earlier studies (1, 2) have shown that, in addition to 1:1 complexes like those produced with $AgNO_3$ (3), 1,3-butadiene, and norbornadiene in excess interact with silver tetrafluoroborate to yield the complex $2AgBF_4$.3olefin. In order to investigate the effect of olefin structure upon the complex stoichiometry the investigation of the $AgBF_4$ complexes now has been extended to include the olefins: cyclopentadiene, cyclohexa-1,3-diene, cyclohexa-1,4-diene, cycloheptа-1,3,5-triene, cycloocta-1,5-diene, cycloocta-1,3,5-triene, cyclooctatetraene, and dicyclopentadiene.

Experimental

Anhydrous $AgBF_4$ was obtained as previously described (4).

Cyclopentadiene was prepared by slow distillation of dicyclopentadiene (Eastman, technical grade) up a 2 ft column packed with glass halices, collected and stored at 0 °C.

Cycloocta-1,3,5-triene was prepared by reduction of cyclooctatetraene (Chemical Procurement Laboratories) using the method of ref. 5, example 1.

The remaining olefins were purchased from Aldrich Chemical and were used without further purification.

Preparation of Complexes

The complexes were prepared in 1–3 g quantities by addition of the olefin to a solution of $AgBF_4$ in toluene, 1,2-dichloroethane or nitromethane at 0 °C. The crystalline products were filtered, washed several times with petroleum ether and dried by evacuation at room temperature for 5 min. The olefin:salt ratio and the analytical data for the complexes are reported in Table 1.

Spectroscopic Data

The infrared data were obtained from fluorolube mulls of the complexes with a Beckman IR-9 spectrophotometer employing cells with KBr windows. The nuclear magnetic resonance (n.m.r.) spectra of 1,2-dichloroethane solutions of the complexes were recorded with a Varian A60 proton resonance spectrometer.

Results and Discussion

The stoichiometry and some of the physical data for the complexes are reported in Table 1.

The 2:3 complex was formed only by cyclopentadiene and cyclohexa-1,3-diene. The 1:1 $AgBF_4$ complex for each of these olefins has been reported previously (3). The infrared spectrum of the cyclopentadiene complex indicates that all of the double bonds are coordinated while that for the cyclohexa-1,3-diene complex does not yield any useful data in the C=C stretching region. Although an excess of cyclohexa-1,3-diene yields the 2:3 complex with toluene as solvent, from a nitromethane solution one obtains the solvated 1:1 complex, $AgBF_4.1.1\text{-}C_6H_8.0.7CH_3NO_2$. Some solvation of the complex was observed with tetrahydrofuran as well.

Regardless of the olefin:salt ratio employed, the 1:1 complex only is formed by cyclohexa-1,4-diene, cyclooctatetraene, and dicyclopentadiene. Both the absence of the 2:3 complex and

[1]Contribution No. 178.

6. B. G. Cox and P. T. McTigue. Aust. J. Chem. **20**, 1815 (1967).
7. R. Alexander, E. C. F. Ko, A. J. Parker, and T. J. Broxton. J. Amer. Chem. Soc. **90**, 5049 (1968).
8. D. H. Everett. Trans. Faraday Soc. **60**, 1803 (1964).
9. M. Born. Z. Phys. **1**, 45 (1920).
10. L. Pauling. The nature of the chemical bond. Cornell University Press, Ithaca, New York. 1960. Table 13-9.
11. A. J. Parker. Chem. Rev. **69**, 1 (1969).
12. C. Hall, G. L. Haller, and R. E. Richards. Mol. Phys. **16**, 377 (1969).

Coordination compounds of olefins with anhydrous silver tetrafluoroborate V. Complexes with some cyclic di- and oligo-olefins[1]

H. W. Quinn and R. L. VanGilder
Exploratory Research Laboratory, Dow Chemical of Canada, Ltd., Sarnia, Ontario

Received January 13, 1970

The following complexes of di- and oligo-olefins have been prepared and characterized: $2AgBF_4$.3-cyclopentadiene, $AgBF_4$.cyclohexa-1,4-diene, $AgBF_4$.cyclohexene-1,3-diene, $2AgBF_4$.3cyclohexa-1,3-diene, $AgBF_4$.cycloheptа-1,3,5-triene hydrate, $AgBF_4$.2cycloheptа-1,3,5-triene, $AgBF_4$.2cycloocta-1,3,5-triene, $AgBF_4$.2cycloocta-1,5-diene, $AgBF_4$.cyclooctatetraene, and $AgBF_4$.dicyclopentadiene.

Canadian Journal of Chemistry, **48**, 2435 (1970)

Introduction

Earlier studies (1, 2) have shown that, in addition to 1:1 complexes like those produced with $AgNO_3$ (3), 1,3-butadiene, and norbornadiene in excess interact with silver tetrafluoroborate to yield the complex $2AgBF_4$.3olefin. In order to investigate the effect of olefin structure upon the complex stoichiometry the investigation of the $AgBF_4$ complexes now has been extended to include the olefins: cyclopentadiene, cyclohexa-1,3-diene, cyclohexa-1,4-diene, cycloheptа-1,3,5-triene, cycloocta-1,5-diene, cycloocta-1,3,5-triene, cyclooctatetraene, and dicyclopentadiene.

Experimental

Anhydrous $AgBF_4$ was obtained as previously described (4).

Cyclopentadiene was prepared by slow distillation of dicyclopentadiene (Eastman, technical grade) up a 2 ft column packed with glass halices, collected and stored at 0 °C.

Cycloocta-1,3,5-triene was prepared by reduction of cyclooctatetraene (Chemical Procurement Laboratories) using the method of ref. 5, example 1.

The remaining olefins were purchased from Aldrich Chemical and were used without further purification.

Preparation of Complexes

The complexes were prepared in 1–3 g quantities by addition of the olefin to a solution of $AgBF_4$ in toluene, 1,2-dichloroethane or nitromethane at 0 °C. The crystalline products were filtered, washed several times with petroleum ether and dried by evacuation at room temperature for 5 min. The olefin:salt ratio and the analytical data for the complexes are reported in Table 1.

Spectroscopic Data

The infrared data were obtained from fluorolube mulls of the complexes with a Beckman IR-9 spectrophotometer employing cells with KBr windows. The nuclear magnetic resonance (n.m.r.) spectra of 1,2-dichloroethane solutions of the complexes were recorded with a Varian A60 proton resonance spectrometer.

Results and Discussion

The stoichiometry and some of the physical data for the complexes are reported in Table 1.

The 2:3 complex was formed only by cyclopentadiene and cyclohexa-1,3-diene. The 1:1 $AgBF_4$ complex for each of these olefins has been reported previously (3). The infrared spectrum of the cyclopentadiene complex indicates that all of the double bonds are coordinated while that for the cyclohexa-1,3-diene complex does not yield any useful data in the C=C stretching region. Although an excess of cyclohexa-1,3-diene yields the 2:3 complex with toluene as solvent, from a nitromethane solution one obtains the solvated 1:1 complex, $AgBF_4.1.1\text{-}C_6H_8.0.7CH_3NO_2$. Some solvation of the complex was observed with tetrahydrofuran as well.

Regardless of the olefin:salt ratio employed, the 1:1 complex only is formed by cyclohexa-1,4-diene, cyclooctatetraene, and dicyclopentadiene. Both the absence of the 2:3 complex and

[1]Contribution No. 178.

Can. J. Chem. Downloaded from www.nrcresearchpress.com by 210.87.254.40 on 09/05/12
For personal use only.

Can. J. Chem. Downloaded from www.nrcresearchpress.com by 210.87.254.40 on 09/05/12
For personal use only.

TABLE 1

$AgBF_4$ complexes of some di- and oligo-olefins

Olefin	Mole ratio Olefin:$AgBF_4$	Complex	Elemental analysis (wt. %) Observed Ag	Observed C	Calculated Ag	Calculated C	$\nu_{C=C}$* (cm^{-1}) Olefin	$\nu_{C=C}$* (cm^{-1}) Complex	Melting point (°C)
Cyclopentadiene	4.6:1†	$2AgBF_4.3C_5H_6$	35.5	31.3	36.7	30.6	1623,1588	1527	
Cyclohexa-1,4-diene	3.0:1†	$AgBF_4.C_6H_8$	39.0	26.6	39.3	26.2	1640	1575	
	2.0:1‡	,,	38.9	26.6					
Cyclohexa-1,3-diene	3.5:1†	$2AgBF_4.3C_6H_8$	35.5	32.1	34.3	34.3			
	0.9:1†	$AgBF_4.C_6H_8$	40.0	25.5	39.3	26.2			
	2.1:1‡		33.3	27.2§					
Cyclohepta-1,3,5-triene	2.0:1‖	$AgBF_4.2C_7H_8$	28.9	43.3	28.5	44.4	1611,1545	1540,1515	205(d)
	1.0:1‖	$AgBF_4.C_7H_8.H_2O$	35.2	26.6	35.4	27.6			117
Cycloocta-1,3,5-triene	2.1:1‖	$AgBF_4.2C_8H_{10}$		43.9		47.2			125(d)
Cycloocta-1,5-diene	1.0:1‖	$AgBF_4.2C_8H_{12}$	26.2	44.0	26.3	46.8			136
	2.0:1‖	,,		47.1			1656	1658,1603	
Cyclooctatetraene	1.0:1‖	$AgBF_4.C_8H_8$	35.3	31.3	36.1	32.1	1637	1583	210(d)
	2.1:1‖	,,	33.7	33.5					
Dicyclopentadiene	2.0:1†	$AgBF_4.C_{10}H_{12}$	32.0	37.7	33.0	36.7	1640,1612	1540,1502	110–115(d)

*Infrared frequency of double bond stretching vibration.
†Toluene solvent.
‡Nitromethane solvent.
§Corresponds to $AgBF_4.1.1C_6H_8.0.7CH_3NO_2$.
‖1,2-Dichloroethane solvent.

TABLE 2

Nuclear magnetic resonance data for $AgBF_4$ complexes* of cycloheptatriene and cyclooctatriene

Proton	Chemical Shift† (c.p.s.)				
	C_7H_8	$AgBF_4.C_7H_8$	$AgBF_4.2C_7H_8$	C_8H_{10}	$AgBF_4.2C_8H_{10}$
CH_2	132	123	122	145	147
α‡	318	370	361	343	365
β‡	369	399	393	353	385
γ‡	394	417	414	353	385

*In solution in 1,2-dichloroethane.
†Chemical shift with respect to tetramethylsilane.
‡Position of proton relative to that of methylene group(s).

the inability of nitromethane to solvate the 1:1 complex of cyclohexa-1,4-diene suggest an effect, perhaps of steric nature, which prevents formation of 3-coordinate silver(I) with that olefin. The tendency of the 2:3 complex to form more often with conjugated than with non-conjugated dienes suggests that the co-planarity of the double bonds may contribute to the complex stability. As was suggested for the buta-1,3-diene and the norbornadiene complexes (1, 2), the 2:3 and 1:1 complexes of these olefins are probably coordination polymers. Their infrared spectra show no evidence for uncoordinated double bonds.

Unique amongst the di- and oligo-olefins investigated in this laboratory is the tendency of cyclohepta-1,3,5-triene (6), cycloocta-1,3,5-triene, and cycloocta-1,5-diene to form 1:2 complexes with $AgBF_4$. This stoichiometry is analogous to that of the most stable $AgBF_4$ complexes of monoolefins (7). Although cycloocta-1,5-diene formed the 1:2 complex even when the salt:olefin ratio was 1:1, cyclohepta-1,3,5-triene produced the hydrated 1:1 complex $AgBF_4.C_7H_8.H_2O$. The hydration presumably resulted from adventitious water in the solvent or from exposure of the complex to atmospheric moisture. Similar behavior has been observed in the $AgBF_4$–bullvalene system (8).

Although the infrared data for cycloheptatriene do not indicate with certainty whether there are some uncoordinated double bonds in the 1:2 complex, the number of π electrons in the two coordinated molecules definitely exceeds the electron acceptance capability of the silver ion. The infrared spectrum of the cyclooctadiene complex definitely shows the presence of both free and coordinated double bonds.

In general, silver complexation of olefins results in an n.m.r. deshielding of all protons at or near the double bond (7). Cycloheptatriene experiences, however, a shielding of the methylene protons and a deshielding of the olefinic protons in the order $H_\alpha > H_\beta > H_\gamma$ (Table 2). Cyclooctatriene is not affected in the same way. The increased methylene proton shielding and small γ proton deshielding suggest the presence of a shielding effect which counteracts the deshielding resulting from a net shift of electron density toward the silver ion. It is possible that the bent cycloheptatriene molecule (9, 10), which at temperatures above about − 140 °C exists as a rapidly oscillating pair of nonplanar conformers (11, 12), assumes a somewhat different conformation when complexed which results in an increased shielding for the methylene and γ protons. If the change were in the shielding effect resulting from the diamagnetic anisotropy in the α,β-double bonds, one would suspect that the molecule is bent more when complexed than when free.

1. H. W. Quinn. Can. J. Chem. **45**, 1329 (1967).
2. H. W. Quinn. Can. J. Chem. **46**, 117 (1968).
3. E. O. Fischer and H. Werner. Metal π-complexes. Complexes with di- and oligo-olefinic ligands. Elsevier Publ. Inc., New York., 1966.
4. H. W. Quinn and R. L. VanGilder. Can. J. Chem. **47**, 4691 (1969).
5. W. O. Jones. British Patent 773,225 (1957).
6. H. Meerwein, V. Hederich, and K. Wunderlich. Arch. Pharm. **291**, 541 (1958).
7. H. W. Quinn, J. S. McIntyre, and D. J. Peterson. Can. J. Chem. **43**, 2896 (1965).
8. J. S. McKecknie and I. C. Paul. J. Chem. Soc. (B), 1445 (1968).
9. F. A. L. Anet. J. Amer. Chem. Soc. **86**, 458 (1964).
10. M. Traetteberg. J. Amer. Chem. Soc. **86**, 4265 (1964).
11. F. R. Jensen and L. A. Smith. J. Amer. Chem. Soc. **86**, 956 (1964).
12. J. B. Lambert, L. J. Durham, P. Lepoutere, and J. B. Roberts. J. Amer. Chem. Soc. **87**, 3896 (1965).

Can. J. Chem. Downloaded from www.nrcresearchpress.com by 210.87.254.40 on 09/05/12
For personal use only.

An inexpensive noise source for broad-band heteronuclear decoupling experiments

R. BURTON AND L. D. HALL

Department of Chemistry, The University of British Columbia, Vancouver 8, British Columbia

Received February 20, 1970

Experiments performed with trimethylphosphite demonstrate that music can be used as a source of "noise" for certain broad-band heteronuclear decoupling experiments.

Canadian Journal of Chemistry, 48, 2438(1970)

Can. J. Chem. Downloaded from www.nrcresearchpress.com by 210.87.254.6 on 09/05/12
For personal use only.

In a recent paper (1) we described an apparatus for effecting a variety of heteronuclear decoupling experiments. A key feature of that system is the use of a conventional "hi-fi" tape-recorder system as an inexpensive source of audio-frequency-noise for "noise-modulated" or "broad-band", (2) heteronuclear decoupling. In the present note we demonstrate that it is possible to use an even less sophisticated device, namely a portable record player, for this same purpose.

A portable record player was connected to one port of a Hewlett–Packard, double-balanced mixer (model 10514 A), via a pair of clip-leads attached to the loud-speaker terminals. The volume control of the record player was set so that the input limit of the mixer (40 mA) was not exceeded. The mixer was then connected to a frequency synthesizer and power amplifier in the usual fashion (1). By choosing a suitable record,[1] this simple system can be used for wide-band decoupling experiments.

An application of this approach is demonstrated in Fig. 1. The normal ^{1}H resonance of a solution of trimethylphosphite in deuterochloroform solution is shown in Fig. 1*A*. As we have previously demonstrated (1) it is a simple matter to effect complete decoupling of the phosphorus by continuous-wave irradiation at the ^{31}P resonance frequency (40.486, 570.0 MHz). However, offsetting the decoupling field by +1 kHz from

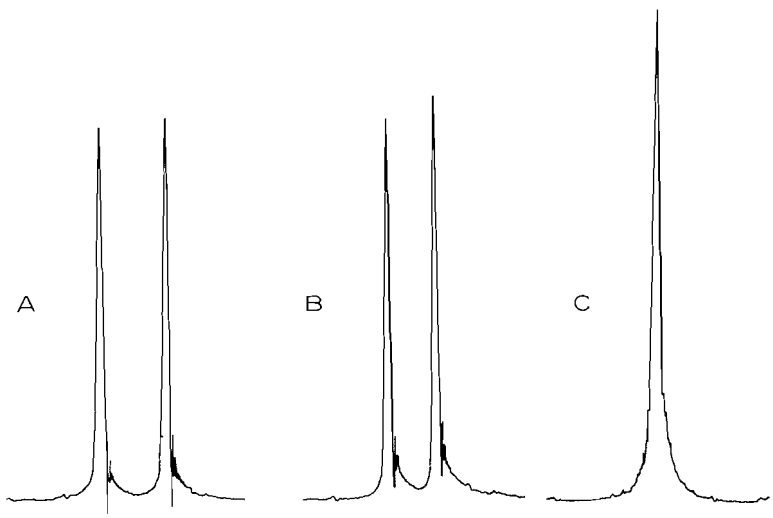

FIG. 1. The proton nuclear magnetic spectrum (100 MHz) of trimethylphosphite in deuterochloroform solution: *A*, normal spectrum; *B*, spectrum obtained with simultaneous irradiation at a point +1 kHz to high frequency of the ^{31}P resonance frequency (40.486, 570.0 MHz); *C*, as for *B* above, but with modulation of the frequency synthesizer using the track "Midnight in Moscow" by Kenny Ball and his Jazzmen.

[1]A referee commented that "improper selection of an LP record can potentially introduce serious distortions." This is indeed so, and some preliminary trials may be necessary before the "correct" record for a particular experiment is found.

this position virtually eliminates any effective spin-decoupling (Fig. 1*B*). Modulation of the ^{31}P decoupling field using the record player and the track "Midnight in Moscow" played by Kenny Ball and his Jazzmen (Kapp, KL 1276) resulted in complete recovery of the effectiveness of the decoupling, as is shown in Fig. 1*C*. This result compares very favorably with that previously (1) obtained with noise-modulation obtained from either a tape-recorder source, or from a pseudo-random sequence generator.

The main point of this note is to point out that for many heteronuclear decoupling experiments, the precise source of audio-frequency noise is almost irrelevant.

We thank the National Research Council of Canada for their generous financial support and Mr. R. B. Malcolm for the loan of his portable record player.

1. R. BURTON and L. D. HALL. Can. J. Chem. **48**, 59 (1970).
2. R. R. ERNST. J. Chem. Phys. **45**, 3845 (1966).

Studies of specifically fluorinated carbohydrates. Part VII. Furanosyl fluorides derived from the D-*xylo*-hexofuranose system

L. D. HALL AND P. R. STEINER[1]
Department of Chemistry, University of British Columbia, Vancouver 8, British Columbia

Received February 20, 1970

The ^1H and ^{19}F nuclear magnetic resonance spectra of several hexofuranosyl fluoride derivatives have been analyzed, using a combination of heteronuclear-decoupling and computer-analysis techniques. A long-range coupling of 4.8–6.3 Hz occurs between F_1 and H_4, whereas a very small coupling occurs between the similarly oriented F_1 and H_3 nuclei.

Canadian Journal of Chemistry, 48, 2439 (1970)

Introduction

We have previously (1) used the 3,6-anhydro ring of 3,6-anhydro-5-deoxy-5-fluoro-*L*-idofuranose as a model for systems containing fluorine attached to a secondary ring carbon atom. We have now prepared a series of furanosyl fluoride derivatives in order to investigate the properties of a fluorine substituent attached to the anomeric center of a furanose system.

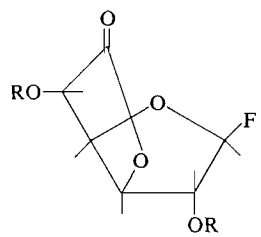

1 R = Bz
2 R = Ac

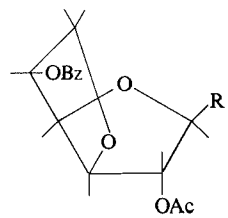

3 R = F
4 R = OAc

Discussion

The derivatives studied, **1–4**, were chosen with the anticipation that their ring conformations might be well defined and hence, that their ^{19}F nuclear magnetic resonance (n.m.r.) parameters might provide further information concerning the stereospecificity of ^{19}F—^1H coupling constants.

Compounds **1–3** were synthesized by reacting the corresponding tri-ester with anhydrous liquid hydrogen fluoride. In each case the major product had a very small coupling between H_1 and H_2, which implies (2) that these two protons are *trans* and hence, that the product is the β-anomer. For two of the products, **1** and **3**, this assignment was confirmed by independent syntheses; the sequence for the glucuronolactone system is shown in Scheme 1. The original tri-ester was converted to the corresponding furanosyl bromide by standard methods (3) and then the bromide was reacted with silver monofluoride. In both instances a single product was obtained, which was identical in all respects with that obtained via the *HF* route. In so far that it has previously been unequivocally established (3–5) that the AgF exchange reaction used in the sequence affords exclusively the

[1]Recipient of a NRCC Studentship, 1968–1970.

Can. J. Chem. Downloaded from www.nrcresearchpress.com by 210.87.254.6 on 09/05/12
For personal use only.

this position virtually eliminates any effective spin-decoupling (Fig. 1*B*). Modulation of the ^{31}P decoupling field using the record player and the track "Midnight in Moscow" played by Kenny Ball and his Jazzmen (Kapp, KL 1276) resulted in complete recovery of the effectiveness of the decoupling, as is shown in Fig. 1*C*. This result compares very favorably with that previously (1) obtained with noise-modulation obtained from either a tape-recorder source, or from a pseudo-random sequence generator.

The main point of this note is to point out that for many heteronuclear decoupling experiments, the precise source of audio-frequency noise is almost irrelevant.

We thank the National Research Council of Canada for their generous financial support and Mr. R. B. Malcolm for the loan of his portable record player.

1. R. BURTON and L. D. HALL. Can. J. Chem. **48**, 59 (1970).
2. R. R. ERNST. J. Chem. Phys. **45**, 3845 (1966).

Studies of specifically fluorinated carbohydrates. Part VII. Furanosyl fluorides derived from the D-*xylo*-hexofuranose system

L. D. HALL AND P. R. STEINER[1]
Department of Chemistry, University of British Columbia, Vancouver 8, British Columbia

Received February 20, 1970

The ^1H and ^{19}F nuclear magnetic resonance spectra of several hexofuranosyl fluoride derivatives have been analyzed, using a combination of heteronuclear-decoupling and computer-analysis techniques. A long-range coupling of 4.8–6.3 Hz occurs between F_1 and H_4, whereas a very small coupling occurs between the similarly oriented F_1 and H_3 nuclei.

Canadian Journal of Chemistry, 48, 2439 (1970)

Introduction

We have previously (1) used the 3,6-anhydro ring of 3,6-anhydro-5-deoxy-5-fluoro-*L*-idofuranose as a model for systems containing fluorine attached to a secondary ring carbon atom. We have now prepared a series of furanosyl fluoride derivatives in order to investigate the properties of a fluorine substituent attached to the anomeric center of a furanose system.

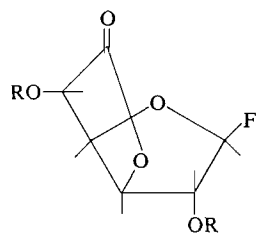

1 R = Bz
2 R = Ac

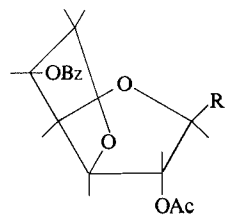

3 R = F
4 R = OAc

Discussion

The derivatives studied, **1–4**, were chosen with the anticipation that their ring conformations might be well defined and hence, that their ^{19}F nuclear magnetic resonance (n.m.r.) parameters might provide further information concerning the stereospecificity of ^{19}F—^1H coupling constants.

Compounds **1–3** were synthesized by reacting the corresponding tri-ester with anhydrous liquid hydrogen fluoride. In each case the major product had a very small coupling between H_1 and H_2, which implies (2) that these two protons are *trans* and hence, that the product is the β-anomer. For two of the products, **1** and **3**, this assignment was confirmed by independent syntheses; the sequence for the glucuronolactone system is shown in Scheme 1. The original tri-ester was converted to the corresponding furanosyl bromide by standard methods (3) and then the bromide was reacted with silver monofluoride. In both instances a single product was obtained, which was identical in all respects with that obtained via the *HF* route. In so far that it has previously been unequivocally established (3–5) that the AgF exchange reaction used in the sequence affords exclusively the

[1]Recipient of a NRCC Studentship, 1968–1970.

Can. J. Chem. Downloaded from www.nrcresearchpress.com by 210.87.254.6 on 09/05/12
For personal use only.

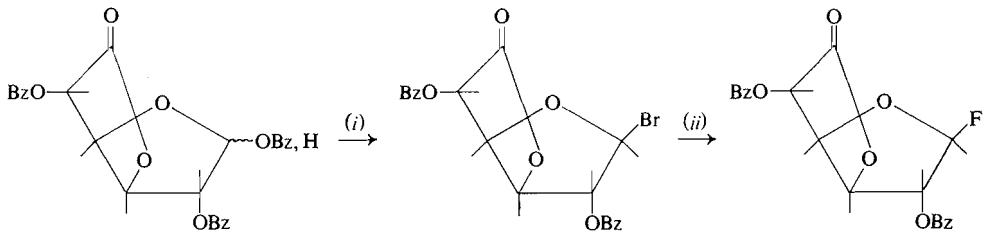

SCHEME 1

(*i*) Br_2–HOAc; (*ii*) AgF in CH_3CN.

product having the fluorine *trans* with respect to the participating group at C-2, this confirms that the fluorides **1** and **3** both have the β-configuration.

One preparation of **1** was quenched after half the usual reaction period, and the resultant material was examined by ^{19}F n.m.r. In addition to the resonance of **1**, a second quartet having splittings of 61 and 18 Hz was detected at ϕ_c + 138, and was assigned to the α-anomer.

The ^1H and ^{19}F n.m.r. spectra of compounds **1–3** were assigned and analyzed on the basis of techniques discussed in the Experimental section. The parameters obtained from these spectra are listed in Tables 1 and 2, together with those of a reference compound, **4**.

As mentioned earlier, the small magnitude of $J_{1,2}$ confirms that each of these derivatives has the β-configuration. The overall similarity between the *vicinal* ^1H—^1H coupling constants of **1–4** suggests that they favor conformations closely similar to those previously suggested (2) for derivatives of 3,6-anhydro-1,2-*O*-isopropylidene-α-L-idofuranose. Thus the furanose ring favors the $^3T_2$ conformation, **A**, while the 3,6-anhydro ring favors the V_4 conformation, **B**. The observation that the magnitude of $J_{3,4}$ is somewhat larger for these derivatives than for

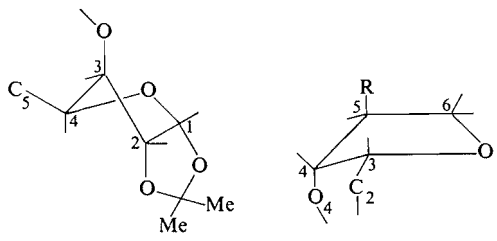

A B

the corresponding 1,2-*O*-isopropylidene derivatives (2) suggests that the furanose ring is now less-puckered; alternatively, the ^3V conformer may be favored.

It is of importance to note that a large (ca. 4.6 Hz) coupling occurs between F_1 and H_4 whereas the coupling between F_1 and H_3 is very small indeed. Since the coupled nuclei are *trans* disposed in both instances, this observation may imply that the ring-oxygen substituent has a significant influence on the magnitude of the $^4J_{F,4}$ coupling. Unfortunately, the spectra of the compounds were too complex for us to determine the signs of these couplings.

One of the H_6 protons of **3** shows a long range coupling with the fluorine substituent of 1.5 Hz; if this coupling is transmitted through the bonds of the system, it spans six bonds.

Experimental

Solutions were concentrated under reduced pressure. All m.p.'s were measured on a Fisher–Johns heating stage and are uncorrected. Optical rotations were measured with a Bendix ETL-NPL Automatic Polarimeter (model 143A) using either 4.0 or 0.5 cm cells; chloroform solutions were used throughout. Microanalyses were performed by Mr. P. Borda of this Department.

All n.m.r. spectra were measured with a modified (6) Varian HA-100 spectrometer operating in the "locked" mode. The ^{19}F shifts are quoted as "ϕ_c-values" and were obtained for chloroform solutions containing ca. 20% trichlorofluoromethane as reference.

The computer analyses of the n.m.r. spectra were performed with an I.B.M. 7044 computer in the Computer Center at U.B.C. The TWOSUM programme was used.[2]

The preparation of the furanosyl fluorides **1**, **2**, **3** was as follows: The appropriately *O*-acyl sugar (500 mg) was added slowly to a small volume (ca. 1 ml) of anhydrous, liquid hydrogen fluoride in a polyethylene flask, cooled by an acetone – solid CO_2 cold bath. The reaction mixture was agitated several times and allowed to warm to room temperature over a 20 min period. The solution was then poured into a mixture of saturated, aqueous sodium bicarbonate (100 ml) and ether (100 ml). After the neutralization was complete, the ether layer was separated, dried (Na_2SO_4), and concentrated. Purifica-

[2]Kindly provided by Dr. J. S. Martin, Chemistry Department, The University of Alberta, Edmonton, Alberta.

Can. J. Chem. Downloaded from www.nrcresearchpress.com by 210.87.254.6 on 09/05/12
For personal use only.

Can. J. Chem. Downloaded from www.nrcresearchpress.com by 210.87.254.6 on 09/05/12
For personal use only.

TABLE 1

First order coupling constants for two fused ring systems, (Hz)

Compound*	H_1F	H_1H_2	H_2F	H_2H_3	H_3F	H_3H_4	H_4F	H_4H_5	H_5F	$H_5H_{6_1}$	$H_5H_{6_2}$	$H_{6_1}H_{6_2}$
1 (*a*) 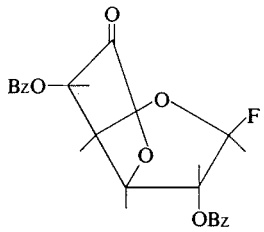	60.1	<0.5	4.0	<0.5	<0.5	4.6 H_3H_5 <0.5	4.6	6.3	0.3	—	—	—
2 (*a*) 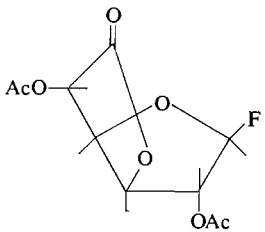	60.1	0.6	4.5	<0.5	<0.5	4.6 H_3H_5 0.5	4.4	6.3	<0.5	—	—	—
3 (*a*) 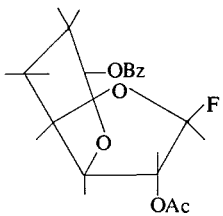	62.3	0.8	5.8	<0.5	<0.5	4.8	4.8	<1.0	—	4.0	1.5 $H_{6_2}F$ 1.5	−10.6†
4 (*c*) 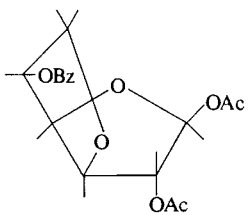	—	<0.5	—	<0.5	—	4.5	—	<0.5	—	4.1	1.0	−10.6†

*The compounds above were measured in (*a*) acetone-d_6 and (*c*) chloroform-*d* solutions.
†Assumed sign; see ref. 8.

TABLE 2

First order chemical shifts (τ values, ϕ_c values) for two fused ring systems

Compound*		F	H_1	H_2	H_3	H_4	H_5	H_{6_1}	H_{6_2}	OAc	OBz
1 (*a*)	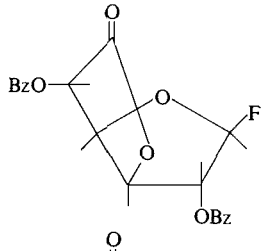	118.5	3.80	4.30	4.44	4.29	4.02	—	—	—	1.8–2.7
2 (*a*)	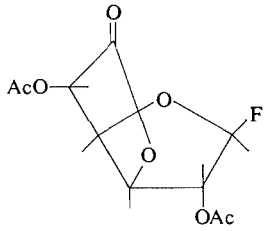	118.3	4.09	4.65	4.77	4.64	4.37	—	—	7.14	—
3 (*a*)	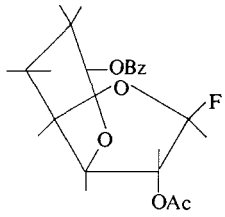	119.8	4.28	4.72	4.94	5.28	4.44	5.58	5.94	7.93	1.9–2.8
4 (*c*)	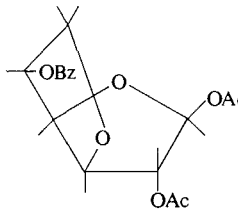	—	3.79	4:76	5.00	5.23	4.48	5.29	5.95	7.98 8.04	1.9–2.8

*The compounds above were measured in (*a*) acetone-d_6 and (*c*) chloroform-*d* solutions.

tion was achieved by column-chromatography on silica-gel (Mallinckrodt Silicar CC 7) using ethyl acetate:light petroleum 1:3 (v/v).

2,5-Di-O-benzoyl-β-D-glucuronyl-3 → 6-lactone Fluoride (1)

(*a*) 1,2,5-Tri-*O*-benzoyl-β-D-glucurono-3 → 6-lactone (7) (750 mg) was reacted with anhydrous hydrogen fluoride as described above. After 2 days at 0 °C in anhydrous ether – pentane solution, colorless crystals of **1** were obtained (290 mg. 46%), m.p. 132–134°, $[\alpha]_D^{22}$ + 70.8° (*c*, 1.28).

Anal. Calcd. for $C_{20}H_{15}O_7F$: C, 62.18; H, 3.89; F, 4.92. Found: C, 62.18; H, 4.13; F, 5.05.

The ^{19}F n.m.r. showed a "doubleted-triplet" at ϕ_c + 117.9 p.p.m.; the mother liquors remaining after isolation of **1** also showed only this resonance.

(*b*) 1,2,5-Tri-*O*-benzoyl-β-D-glucurono-3 → 6-lactone (1 g), was added to a saturated solution of bromine in glacial acetic acid. The mixture was stirred and the resultant solution was then kept at room temperature for 4 h. The reaction mixture was added slowly to a saturated solution of sodium hydrogen carbonate, (100 ml) and extracted, without delay, with chloroform. The dried (Na_2SO_4) chloroform solution was concentrated to an amber syrup, which was dissolved in dry acetonitrile (20 ml) and reacted immediately with silver fluoride (0.5 g). The mixture was stirred for 1 h, filtered, and concentrated. Pure product was not isolated from this reaction; however, the ^{19}F n.m.r. spectrum showed only one fluorine resonance, identical to that of the sample of **1** described above.

2,5-Di-O-acetyl-β-D-glucuronyl-3 → 6 lactone Fluoride (2)

A non-crystalline sample of this derivative was pre-

Can. J. Chem. Downloaded from www.nrcresearchpress.com by 210.87.254.6 on 09/05/12
For personal use only.

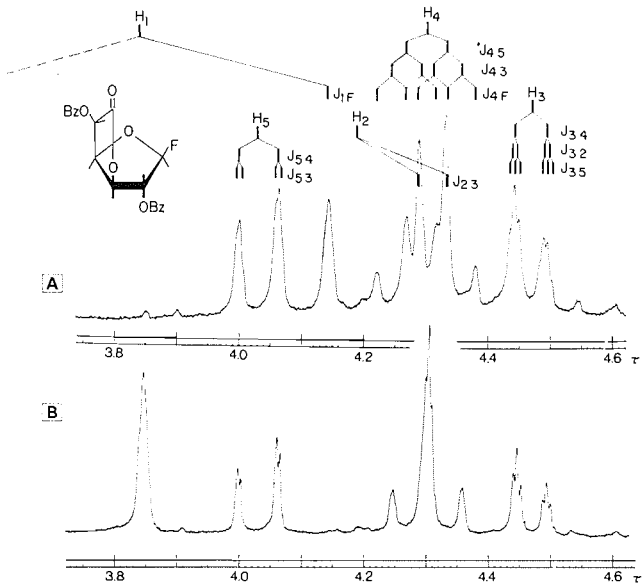

FIG. 1. Partial ^1H n.m.r. spectrum (100 MHz) of 2,5-di-*O*-benzoyl-β-D-glucuronyl-3 → 6-lactone fluoride (**1**) in acetone-d_6 solution. A, Normal spectrum and B, spectrum obtained with irradiation at the ^{19}F resonance frequency.

pared from 1,2,5-tri-*O*-acetyl-β-D-glucuro-3 → 6-lactone,[3] using the HF method described above for the corresponding dibenzoate. Since the ^1H and ^{19}F n.m.r. spectra of this derivative were so closely similar to those of **1**, no further characterization was attempted.

2-O-Acetyl-3,6-anhydro-5-O-benzoyl-β-L-idofuranosyl Fluoride (3)

(*a*) Following the general procedure outlined above, a sample of 1,2-di-*O*-acetyl-3,6-anhydro-5-*O*-benzoyl-β-L-idofuranose[3] (**4**) was converted to syrupy **3**, which was shown to be substantially pure by n.m.r. spectroscopy. The ^{19}F n.m.r. spectrum in chloroform solution gave a doubleted-sextet at ϕ_c + 120.6 p.p.m.

Examination by ^{19}F n.m.r. of a similar reaction mixture which had been quenched after 10 min showed the presence of 70% of **3** and 30% of a second furanosyl fluoride, whose resonance at ϕ_c + 138 p.p.m. was assigned to the α-anomer of **3**,

(*b*) Reaction of a sample of **4** with bromine in acetic acid, followed by fluorine exchange as outlined for **1** afforded a sample of **3** identical in all respects with the material discussed in (*a*) above. Neither sample has shown any tendency to crystallize during the past two years.

Spectral Assignments

The assignment of the ^1H n.m.r. spectrum of **1** typifies the approach we adopted for assignment of these spectra. The normal ^1H spectrum of **1**, Fig. 1A, cannot be assigned on a first-order basis. However, irradiation at the ^{19}F resonance frequency simplifies the spectrum, as is indicated in Fig. 1B. The H_1 resonance comes to lowest field, and irradiation at the ^{19}F resonance frequency causes it to collapse to a broadened singlet, indicating that $J_{1,2}$ is small. The broadened doublet at τ 4.30 collapsed on ^{19}F irradiation and was tentatively assigned to H_2. Of the remaining protons it was anticipated that the H_5 should have the lower-field shift; irradiation of the "doublet" at τ 4.02 caused the resonance centered around τ 4.29 to collapse, which identified it as arising from H_4.

The first-order parameters obtained from this assignment and from the ^{19}F spectrum were entered into the TWOSUM programme and a spectrum simulated which matched both the ^1H and ^{19}F spectra.

A similar sequence was applied to the other derivatives.

It is a pleasure to thank the National Research Council of Canada for their generous financial support and in particular for the equipment grant (E 1338) which provided the heteronuclear decoupling equipment.

[3]Sample donated by Dr. J. F. Manville.

1. P. R. STEINER. M.Sc. Thesis, University of British Columbia, Vancouver, B.C., 1969.
2. R. J. ABRAHAM, L. D. HALL, L. HOUGH, and K. A. MCLAUCHLAN. J. Chem. Soc. 3699 (1962).
3. J. F. MANVILLE. Ph.D. Thesis, University of British Columbia, Vancouver, B.C., 1967.
4. F. MICHEEL and A. KLEMER. Advan. Carbohyd. Chem. **16**, 85 (1961).
5. L. D. HALL and J. F. MANVILLE. Can. J. Chem. **47**, 1 (1969).
6. R. BURTON and L. D. HALL. Can. J. Chem. **48**, 59 (1970).
7. A. MOMOSE, K. KAMEI, and Y. NITTA. Chem. Pharm. Bull. **14**, 199 (1966).
8. L. D. HALL and J. F. MANVILLE. Carbohyd. Res. **8**, 295 (1968).

Can. J. Chem. Downloaded from www.nrcresearchpress.com by 210.87.254.6 on 09/05/12
For personal use only.

Oxidative addition of substituted benzenethiols to *trans*-chlorocarbonylbis(triphenyl phosphine)iridium(I)

C. V. SENOFF
Department of Chemistry, University of Guelph, Guelph, Ontario

Received March 4, 1970

A series of para-substituted benzenethiols have been shown to react with *trans*-$IrCl(CO)(Ph_3P)_2$ to form $IrHCl(SC_6H_4Y)(CO)(Ph_3P)_2$ where Y = NO_2, Br, Cl, F, H, CH_3, and CH_3O. A good correlation between the ν_{CO} vibration in the infrared spectra of these complexes and the Hammett substituent parameter, σ_p, was observed indicating that the ν_{CO} vibration may be used to provide a measure of the transmission of the para-substituent's electronic effect to the central iridium atom.

Canadian Journal of Chemistry, 48, 2444 (1970)

Oxidative addition reactions, particularly those involving Vaska's compound, *trans*-$IrCl(CO)(Ph_3P)_2$, have been well documented in recent review articles (1, 2). Toluenethiol has been recently shown to undergo an oxidative addition reaction with *trans*-$IrCl(CO)(Ph_3P)_2$ to form $IrHCl(SC_6H_4CH_3)(CO)(Ph_3P)_2$ (3). This note reports some spectroscopic results of an investigation into the oxidative addition of a series of para-substituted benzenethiols, YC_6H_4SH (Y = NO_2, Br, Cl, F, H, CH_3, and CH_3O) with Vaska's compound to form the corresponding oxidative addition adduct, $IrHCl(SAr)(CO)(Ph_3P)_2$.

Results and Discussion

Pertinent infrared (i.r.) and nuclear magnetic resonance (n.m.r.) spectral data are presented in Tables 1 and 2. These data, together with the analytical data given in Table 3 confirm the formulation of the complexes as $IrHCl(SAr)(CO)(Ph_3P)_2$.

Examination of the spectral data indicates that the ν_{CO} vibration in the i.r. is sensitive to the nature of the para-substituent associated with the $YC_6H_4S^-$ moiety in the complexes. On the other hand, both the high-field chemical shift of the hydride ligand bonded to iridium and the

TABLE 1

Infrared spectral data for the complexes, $IrHCl(SAr)(CO)(Ph_3P)_2$

Complex	Solvent	ν_{CO}* (cm^{-1})	ν_{Ir-H}* (cm^{-1})
$IrHCl(SC_6H_4NO_2)(CO)(Ph_3P)_2$	C_6H_6	2039 s	2250 w
	$CHCl_3$	2044 s	2252 w
	Nujol	2056 s	2249 w
$IrHCl(SC_6H_4Br)(CO)(Ph_3P)_2$	C_6H_6	2034 s	2236 w
	$CHCl_3$	2038 s	2245 w
	Nujol	2031 s	2260 w
$IrHCl(SC_6H_4Cl)(CO)(Ph_3P)_2$	C_6H_6	2033 s	2237 w
	$CHCl_3$	2038 s	2244 w
	Nujol	2033 s	2212 w
$IrHCl(SC_6H_4F)(CO)(Ph_3P)_2$	C_6H_6	2029 s	2234 w
	$CHCl_3$	2037 s	2244 w
	Nujol	2038 s	2260 w
$IrHCl(SC_6H_4H)(CO)(Ph_3P)_2 \cdot C_6H_6$	C_6H_6	2030 s	2236 w
	$CHCl_3$	2036 s	2245 w
	Nujol	2029 s	2263 w
$IrHCl(SC_6H_4CH_3)(CO)(Ph_3P)_2$	C_6H_6	2030 s	2239 w
	$CHCl_3$	2033 s	2253 w
	Nujol	2026 s	2265 w
$IrHCl(SC_6H_4OCH_3)(CO)(Ph_3P)_2$	C_6H_6	2028 s	2234 w
	$CHCl_3$	2034 s	2247 w
	Nujol	2023 s	2268 w

*s = Strong; w = weak.

Can. J. Chem. Downloaded from www.nrcresearchpress.com by 210.87.254.5 on 09/05/12
For personal use only.

TABLE 2

The n.m.r. data for the complexes, $IrHCl(SAr)(CO)(Ph_3P)_2$

Complex	^1H Chemical shift for Ir—H (p.p.m.)*	J_{P-H} (c.p.s.)
$IrHCl(SC_6H_4NO_2)(CO)(Ph_3P)_2$	16.5	12.4
$IrHCl(SC_6H_4Br)(CO)(Ph_3P)_2$	16.6	12.4
$IrHCl(SC_6H_4Cl)(CO)(Ph_3P)_2$	16.5	12.2
$IrHCl(SC_6H_4F)(CO)(Ph_3P)_2$	16.6	12.6
$IrHCl(SC_6H_4H)(CO)(Ph_3P)_2 \cdot C_6H_6$	16.6	12.6
$IrHCl(SC_6H_4CH_3)(CO)(Ph_3P)_2$	16.6	12.0
$IrHCl(SC_6H_4OCH_3)(CO)(Ph_3P)_2$	16.6	12.2

*Measured in $CHCl_3$ or $CDCl_3$ with TMS as internal reference.

TABLE 3

Analytical data for the complexes, $IrHCl(SAr)(CO)(Ph_3P)_2$

Complex	Calculated C	Calculated H	Found C	Found H	Melting point (°C)
$IrHCl(SC_6H_4NO_2)(CO)(Ph_3P)_2$	55.20	3.74	55.15	3.83	188
$IrHCl(SC_6H_4Br)(CO)(Ph_3P)_2$	53.27	3.61	53.35	3.57	244
$IrHCl(SC_6H_4Cl)(CO)(Ph_3P)_2$	55.83	3.79	55.89	3.79	246
$IrHCl(SC_6H_4F)(CO)(Ph_3P)_2$	56.84	3.86	56.01	3.75	235
$IrHCl(SC_6H_4H)(CO)(Ph_3P)_2 \cdot C_6H_6$	60.78	4.34	59.95	4.37	236
$IrHCl(SC_6H_4CH_3)(CO)(Ph_3P)_2$	58.43	4.21	58.60	4.33	260
$IrHCl(SC_6H_4OCH_3)(CO)(Ph_3P)_2$	57.43	4.13	56.92	4.30	227

phosphorus–hydrogen coupling constant are insensitive to the nature of the para-substituent. These observations support the suggestion that the CO stretching vibration may be used as a criterion for any change in electron density at the metal in the oxidative addition adduct as compared to the parent compound. Thus, an electron releasing substituent would be expected to increase the electron density at iridium resulting in an increase in the amount of "back-bonding" from the metal to the CO ligand; this would be reflected by a lowering of the energy of the ν_{CO} vibration and vice versa for an electron-withdrawing substituent. A plot of ν_{CO} (which should parallel the CO force constant) vs. the Hammett substituent parameter, σ_p, is shown in Fig. 1. The linearity of this plot indicates that there is a definite correlation between these two quantities. It may be pointed out that the position of the ν_{CO} absorption band is somewhat dependent on the solvent used (Table 1) and that the linear correlation holds for the ν_{CO} values obtained in benzene and chloroform but not for those obtained in Nujol. This suggests that the ν_{CO} vibration is significantly perturbed in the solid state and this is most apparent for the 4-nitro-

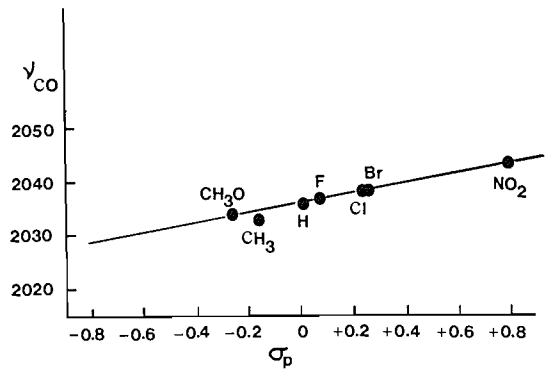

FIG. 1. Hammett plot for the ν_{CO} values observed in chloroform.

benzenethiolo derivative. This linear correlation between ν_{CO} and σ_p provides additional support for Singer and Wilkinson's claim that the stereochemistry of the oxidative addition product is that shown in Fig. 2 which would result from *cis*-addition (3). It may also be concluded that this stereochemistry is common to all the benzenethiolo adducts reported here by virtue of the fact that the high-field chemical shift of the hydrogen bonded to iridium is invariant to the nature of the para-substituent.

Can. J. Chem. Downloaded from www.nrcresearchpress.com by 210.87.254.5 on 09/05/12
For personal use only.

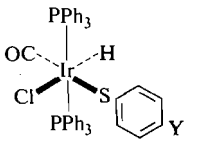

FIG. 2. Stereochemistry of the oxidative addition adduct.

Experimental

(1) Physical Measurements

The i.r. spectra were recorded on a Beckman IR-12 spectrophotometer which was calibrated with carbon monoxide; the ν_{CO} frequencies are reliable to ± 1 cm^{-1}. Proton n.m.r. spectra were recorded on a Varian T-60 spectrophotometer. Melting points were determined with a Fisher–Johns melting point apparatus and are uncorrected. Microanalyses were determined by A. B. Gygli, Toronto, Ontario.

(2) Preparation of the Complexes

(a) trans-Chlorocarbonylbis(triphenyl phosphine)-iridium(I), IrCl(CO)(Ph$_3$P)$_2$

This complex was prepared according to the method published in the literature (4).

Anal. Calcd. for $C_{37}H_{30}ClP_2OIr$: C, 56.92; H, 3.85. Found: C, 56.89; H, 3.95.

(b) Hydridochloro(arylthiolo)carbonylbis(triphenyl phosphine)iridium(III), IrHCl(SAr)(CO)(Ph$_3$P)$_2$

The following general procedure was used to prepare these complexes with exceptions as noted below. All manipulations with *trans*-IrCl(CO)(Ph$_3$P)$_2$ were carried out in an atmosphere of nitrogen or argon. To 0.50 g of *trans*-IrCl(CO)(Ph$_3$P)$_2$ suspended in oxygen-free benzene (20 ml) was added the appropriate benzenethiol (0.10 g or 0.10 ml). The resulting suspension was stirred at room temperature until a clear solution was observed (ca. 10–30 min) whereupon excess ligroin (b.p. 66–75°) ca. 100 ml) was added to precipitate the desired adduct. The adduct derived from 4-bromobenzenethiol was soluble in ligroin (b.p. 66–75°) and *n*-pentane was used as the precipitating reagent. The yields of these reactions were in the range, 45–85%. Each adduct was collected by filtration, washed with ligroin or *n*-pentane, ether, and dried *in vacuo* at 25°. Analytical data are given in Table 3.

The author wishes to thank the National Research Council of Canada and the Department of University Affairs for the Province of Ontario for their generous financial support. The author would also like to thank Dr. C. A. Fyfe of the Department of Chemistry, University of Guelph for carrying out the n.m.r. measurements and Dr. D. E. R. Gilson, Department of Chemistry, McGill University for the use of the n.m.r. spectrometer.

1. J. P. COLLMAN. Account. Chem. Res. **1**, 135 (1968).
2. L. VASKA. Account. Chem. Res. **1**, 335 (1968).
3. H. SINGER and G. WILKINSON. J. Chem. Soc. (A), 2516 (1968).
4. L. VASKA and J. W. DILUZIO. J. Amer. Chem. Soc. **84**, 679 (1962).

An abnormal reaction of a phosphonium ylide with diethyl ketomalonate[1]

WERNER H. PLODER AND DONALD F. TAVARES
Department of Chemistry, University of Calgary, Calgary 44, Alberta

Received February 5, 1970

An attempted Wittig reaction of *o*-xylylene-bistriphenylphosphorane with diethyl ketomalonate gave ethyl 3-ethoxy-2-naphthoate, representing formally, a Wittig reaction with an ester carbonyl.

Canadian Journal of Chemistry, 48, 2446 (1970)

As part of a study of the photochemistry of β-substituted *o*-divinylbenzenes (1), we have uncovered yet another example of a phosphorane–ester carbonyl condensation (2–4).

Phthalaldehyde condensed readily with carbethoxymethylenetriphenylphosphorane to give diethyl *o*-phenylenediacrylate in 58% yield (1). The related β,β,β′,β′-tetracarbethoxy-*o*-divinylbenzene derivative, **1**, could not be prepared by the same route since the nucleophilicity of the required phosphorane (dicarbethoxymethylene-triphenylphosphorane) is too low to be of any synthetic use in the Wittig reaction (5). The condensation of *o*-xylylenebistriphenylphosphorane (**2**) with diethyl ketomalonate (**3**) seemed promising, eq. [1].

A solution of **2** and **3** in absolute ethanol was treated with an excess of lithium ethoxide according to the procedure described by Griffin (6). The product, **4**, which melted at 59.5° after separation from triphenylphosphine oxide and chromatography on alumina, had a nuclear magnetic resonance (n.m.r.) spectrum which was much more complex than that expected for **1**.

[1]Taken in part from the Ph.D. Thesis of W. H. Ploder, University of Calgary, Calgary, Alberta, 1968.

Can. J. Chem. Downloaded from www.nrcresearchpress.com by 210.87.254.5 on 09/05/12
For personal use only.

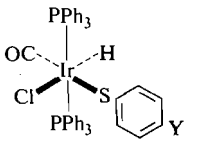

FIG. 2. Stereochemistry of the oxidative addition adduct.

Experimental

(1) Physical Measurements

The i.r. spectra were recorded on a Beckman IR-12 spectrophotometer which was calibrated with carbon monoxide; the ν_{CO} frequencies are reliable to ± 1 cm^{-1}. Proton n.m.r. spectra were recorded on a Varian T-60 spectrophotometer. Melting points were determined with a Fisher–Johns melting point apparatus and are uncorrected. Microanalyses were determined by A. B. Gygli, Toronto, Ontario.

(2) Preparation of the Complexes

(a) trans-Chlorocarbonylbis(triphenyl phosphine)-iridium(I), IrCl(CO)(Ph$_3$P)$_2$

This complex was prepared according to the method published in the literature (4).

Anal. Calcd. for $C_{37}H_{30}ClP_2OIr$: C, 56.92; H, 3.85. Found: C, 56.89; H, 3.95.

(b) Hydridochloro(arylthiolo)carbonylbis(triphenyl phosphine)iridium(III), IrHCl(SAr)(CO)(Ph$_3$P)$_2$

The following general procedure was used to prepare these complexes with exceptions as noted below. All manipulations with *trans*-IrCl(CO)(Ph$_3$P)$_2$ were carried out in an atmosphere of nitrogen or argon. To 0.50 g of *trans*-IrCl(CO)(Ph$_3$P)$_2$ suspended in oxygen-free benzene (20 ml) was added the appropriate benzenethiol (0.10 g or 0.10 ml). The resulting suspension was stirred at room temperature until a clear solution was observed (ca. 10–30 min) whereupon excess ligroin (b.p. 66–75°) ca. 100 ml) was added to precipitate the desired adduct. The adduct derived from 4-bromobenzenethiol was soluble in ligroin (b.p. 66–75°) and *n*-pentane was used as the precipitating reagent. The yields of these reactions were in the range, 45–85%. Each adduct was collected by filtration, washed with ligroin or *n*-pentane, ether, and dried *in vacuo* at 25°. Analytical data are given in Table 3.

The author wishes to thank the National Research Council of Canada and the Department of University Affairs for the Province of Ontario for their generous financial support. The author would also like to thank Dr. C. A. Fyfe of the Department of Chemistry, University of Guelph for carrying out the n.m.r. measurements and Dr. D. E. R. Gilson, Department of Chemistry, McGill University for the use of the n.m.r. spectrometer.

1. J. P. COLLMAN. Account. Chem. Res. **1**, 135 (1968).
2. L. VASKA. Account. Chem. Res. **1**, 335 (1968).
3. H. SINGER and G. WILKINSON. J. Chem. Soc. (A), 2516 (1968).
4. L. VASKA and J. W. DILUZIO. J. Amer. Chem. Soc. **84**, 679 (1962).

An abnormal reaction of a phosphonium ylide with diethyl ketomalonate[1]

WERNER H. PLODER AND DONALD F. TAVARES
Department of Chemistry, University of Calgary, Calgary 44, Alberta

Received February 5, 1970

An attempted Wittig reaction of *o*-xylylene-bistriphenylphosphorane with diethyl ketomalonate gave ethyl 3-ethoxy-2-naphthoate, representing formally, a Wittig reaction with an ester carbonyl.

Canadian Journal of Chemistry, 48, 2446 (1970)

As part of a study of the photochemistry of β-substituted *o*-divinylbenzenes (1), we have uncovered yet another example of a phosphorane–ester carbonyl condensation (2–4).

Phthalaldehyde condensed readily with carbethoxymethylenetriphenylphosphorane to give diethyl *o*-phenylenediacrylate in 58% yield (1). The related β,β,β′,β′-tetracarbethoxy-*o*-divinylbenzene derivative, **1**, could not be prepared by the same route since the nucleophilicity of the required phosphorane (dicarbethoxymethylene-triphenylphosphorane) is too low to be of any synthetic use in the Wittig reaction (5). The condensation of *o*-xylylenebistriphenylphosphorane (**2**) with diethyl ketomalonate (**3**) seemed promising, eq. [1].

A solution of **2** and **3** in absolute ethanol was treated with an excess of lithium ethoxide according to the procedure described by Griffin (6). The product, **4**, which melted at 59.5° after separation from triphenylphosphine oxide and chromatography on alumina, had a nuclear magnetic resonance (n.m.r.) spectrum which was much more complex than that expected for **1**.

[1]Taken in part from the Ph.D. Thesis of W. H. Ploder, University of Calgary, Calgary, Alberta, 1968.

Can. J. Chem. Downloaded from www.nrcresearchpress.com by 210.87.254.105 on 09/05/12
For personal use only.

[1] 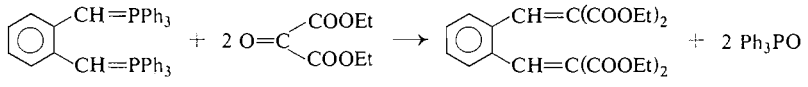

2 3 1

The n.m.r. spectrum showed peaks at τ 2.06 and 3.21, for one proton each, in addition to the aromatic multiplet centered at τ 2.8, and two ethyl groups. Saponification (equivalent found: 240) gave a product (m.p. 124°) which, by n.m.r. analysis, had lost only one ethyl group and showed an acidic proton at τ −0.21. The ultraviolet (u.v.) spectrum showed peaks at 340, 277, 268, and 232 mμ suggesting a substituted naphthalene ring system (7). That **4** was in fact ethyl 3-ethoxy-2-naphthoate was established by comparison with an authentic sample, with which it was found to be identical in every respect.

A possible mechanism for the formation of **4**, given in Scheme 1, can formally be described as a "normal" Wittig reaction of one phosphorane group of **2** with the keto group of **3** to give the intermediate **5**. This is followed by a second Wittig reaction with the ester carbonyl, as has been reported for "activated" esters such as diethyl oxalate and ethyl monofluoro- and trifluoroacetates (2–4). While diethyl ketomalonate, which forms a stable hydrate, should react readily at the oxo-carbonyl with a phosphorane, the present case is unique in that the use of a bisphosphorane affords the possibility for a subsequent cyclization to form the stable naphthalene system. It should be noted, however, that the more commonly observed displacement of alkoxyl (8) would likewise have given an aromatic compound, ethyl 3-hydroxy-2-naphthoate.

Experimental

Melting points were determined on a Kofler hotstage and are corrected; infrared (i.r) spectra were determined with a Perkin-Elmer spectrophotometer, model 337; u.v. spectra with a Perkin-Elmer model 220 spectrophotometer; and n.m.r. spectra were measured at 60 MHz in deuteriochloroform solution with tetramethylsilane as internal standard. Molecular weights were determined with a Mechrolab vapor pressure osmometer, model 301; microanalyses were performed by S. J. Swaddle, The University of Calgary, Calgary, Alberta.

Condensation of 2 with Diethyl Ketomalonate (3). Ethyl 3-Ethoxy-2-naphthoate (4)

The procedure of Griffin (6) was followed. *o*-Xylylenebis(triphenylphosphonium bromide), from Aldrich, was recrystallized from chloroform, m.p. 340°. Diethyl ketomalonate (diethyl mesoxalate) was dried with P_2O_5 according to Curtiss (9), to convert any diethyl dihydroxymalonate into the oxo compound, and redistilled under vacuum to give a yellow oil, b.p. 86°/9 mm (lit. (10) b.p. 103–105/15 mm), n_D^{20} = 1.4178 (lit. (10) n_D^{20} = 1.419).

A solution of 19.7 g (0.025 mole) of the bromide and 9.0 g (0.0517 mole) of diethyl ketomalonate (**3**) in 75 ml of absolute ethanol was treated with 250 ml of 0.4 *M* lithium ethoxide (0.69 g Li in 250 ml of ethanol). The solution was allowed to stand at room temperature for 30 min, and was then refluxed for 2 h, to yield a red–orange solution. The ethanolic solution was concentrated under reduced pressure to a volume of 50 ml. Addition of 150 ml of water gave a brown oil which soon solidified. The brown residue was washed with 500 ml hexane (in 100 ml portions) to leave brown crystalline triphenylphosphine oxide. The yellow oil, on evaporation of the hexane, was chromatographed on 300 g of alumina (Woelm). Elution with 2 l of hexane gave, on evaporation of the solvent, an oily fraction which slowly crystallized. Recrystallization from hexane yielded plates of ethyl 3-ethoxy-2-naphthoate (**4**), 0.92 g (15% yield), 59.5°, (lit. (11) m.p. 60°).

Anal. Calcd. for $C_{15}H_{16}O_3$ (mol. wt. 244 (for 1:1 reaction)): C, 73.55; H, 6.55. Found (242 (vapor pressure osmometer)): C, 73.45; H, 6.48.

The i.r. spectrum displays various bands in the range of 3100 to 2900 cm^{-1} and strong bands at 1720, 1630, 1210, 1070, and 745 cm^{-1}. The u.v. spectrum (hexane) showed strong absorptions at 232 (ε 58 000), 268 (ε 5200), 277 (ε 4800), and 340 mμ (ε 1850).

Saponification of **4** with ethanolic KOH afforded, on workup and recrystallization from ethanol, colorless needles of 3-ethoxy-2-naphthoic acid, m.p. 124° (lit. (12) m.p. 122, 128.5–9.5°). The n.m.r. spectrum showed two singlets at τ 1.35 (1H) and 2.83 (1H), a broad peak at τ −0.12 (1H), an aromatic multiplet centered at τ 2.4 (4H), and an ethyl group with peaks centered at τ 5.72 (2H) and 8.46 (3H).

An authentic sample of **4** was prepared from commercially available 3-hydroxy-2-naphthoic acid by

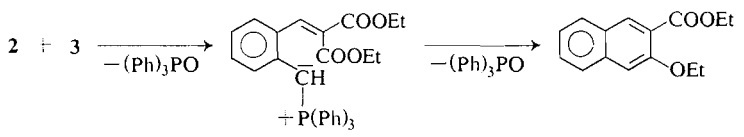

5 4

SCHEME 1

Can. J. Chem. Downloaded from www.nrcresearchpress.com by 210.87.254.105 on 09/05/12
For personal use only.

etherification and esterification; m.p. after several recrystallizations from hexane 59.5° (lit. (11) m.p. 60°). A mixed melting point determination with compound **4** was not depressed, and all spectroscopic data are identical to those determined for compound **4**.

We thank the National Research Council of Canada for financial support and The University of Calgary, Calgary, Alberta, for the award of a fellowship to one of us (W.H.P.).

1. D. F. TAVARES and W. H. PLODER. Tetrahedron Lett. 1567 (1970).
2. H. J. BESTMANN, K. ROSTOCK, and H. DORNAUER. Angew. Chemie Internat. Ed. **5**, 308 (1966).
3. H. MACHLEIDT and W. GRELL. Ann. Chem. **690**, 79 (1965).
4. W. GRELL and H. MACHLEIDT. Ann. Chem. **693**, 134 (1966).
5. A. W. JOHNSON. *Ylid chemistry*. Academic Press, New York, N.Y., 1966. p. 132.
6. C. E. GRIFFIN, K. R. MARTIN, and B. E. DOUGLAS. J. Org. Chem. **27**, 1627 (1962).
7. R. A. FRIEDEL and M. ORCHIN. *Ultraviolet spectra of aromatic compounds*. J. Wiley & Sons, Inc., New York, N.Y., 1951. Spectra 195, 239, and 258.
8. H. J. BESTMANN. Angew. Chemie Internat. Ed. **4**, 645 (1965); H. BEHRINGER and K. FALKENBERG. Chem. Ber. **96**, 1428 (1963).
9. R. S. CURTISS and E. K. STRACHAM. J. Amer. Chem. Soc. **33**, 396 (1911).
10. H. ADKINS, R. M. ELOFSON, A. G. ROSSOW, and C. C. ROBINSON. J. Amer. Chem. Soc. **71**, 3622 (1949).
11. Beilsteins Handbuch der Organischen Chemie. Vol. 10. Springer Verlag, Berlin, 1927. p. 335.
12. H. GILMAN, C. E. ARNTSEN, and F. WEBB. J. Org. Chem. **10**, 374 (1945); W. E. PARHAM and C. D. WRIGHT. J. Org. Chem. **22**, 1473 (1957).

Organic sulfur compounds. VI.[1] Reduction of three α-(*o*-nitrophenylthio)ketones with sodium borohydride

R. T. COUTTS[2] AND SHARON J. MATTHIAS
Faculty of Pharmacy and Pharmaceutical Sciences, University of Alberta, Edmonton, Alberta

AND

H. W. PEEL
College of Pharmacy, University of Saskatchewan, Saskatoon, Saskatchewan

Received March 19, 1970

Reduction of three α-(*o*-nitrophenylthio)ketones with sodium borohydride and palladium–charcoal gave mainly α-(*o*-nitrophenylthio)alcohols and, as minor products, α-(*o*-aminophenylthio)alcohols. Only two benzothiazines were formed. Bis[2-(3-phenyl-2*H*-1,4-benzothiazine)] was a minor product of the catalyzed reduction of ω-(*o*-nitrophenylthio)acetophenone whereas 1-(3,4-dihydro-4-hydroxy-3-oxo-2*H*-1,4-benzothiazin-2-yl)benzyl alcohol was the main product of the catalyzed reduction of α-benzoyl-α-(*o*-nitrophenylthio)acetate.

Canadian Journal of Chemistry, **48**, 2448 (1970)

Methyl α-(*o*-nitrophenylthio)acetate (**1***a*) and its simple derivatives are readily reduced by means of sodium borohydride and palladium–charcoal (1–3) to give 2*H*-1,4-benzothiazine hydroxamic acids (**2**). It was of interest to extend these studies to the reductive cyclization of α-(*o*-nitrophenylthio)ketones (**3**) to see if 2*H*-1,4-benzothiazine 4-oxides (**4**) could be obtained in this way. This proved not to be the case; however, some unexpected reactions were observed and they are now reported.

The ketones (**3***a–c*) were prepared in good yields by the interaction of *o*-nitrobenzenesulfenyl chloride with acetone, acetophenone, and ethyl benzoylacetate respectively, using acetonitrile as solvent (4, 5). Reduction of (*o*-nitrophenylthio)propan-2-one (**3***a*) with sodium borohydride in the presence of catalytic quantities of palladium-on-charcoal yielded mainly 1-(*o*-nitrophenylthio)propan-2-ol (**5***a*), characterized as its 3,5-dinitrobenzoate. The same nitroalcohol was also the product of the reduction of (**3***a*) using sodium borohydride without catalyst. An additional minor product of

[1]Part V, see ref. 3.
[2]To whom communications should be addressed.

Can. J. Chem. Downloaded from www.nrcresearchpress.com by 210.87.254.105 on 09/05/12
For personal use only.

etherification and esterification; m.p. after several recrystallizations from hexane 59.5° (lit. (11) m.p. 60°). A mixed melting point determination with compound **4** was not depressed, and all spectroscopic data are identical to those determined for compound **4**.

We thank the National Research Council of Canada for financial support and The University of Calgary, Calgary, Alberta, for the award of a fellowship to one of us (W.H.P.).

1. D. F. TAVARES and W. H. PLODER. Tetrahedron Lett. 1567 (1970).
2. H. J. BESTMANN, K. ROSTOCK, and H. DORNAUER. Angew. Chemie Internat. Ed. **5**, 308 (1966).
3. H. MACHLEIDT and W. GRELL. Ann. Chem. **690**, 79 (1965).
4. W. GRELL and H. MACHLEIDT. Ann. Chem. **693**, 134 (1966).
5. A. W. JOHNSON. *Ylid chemistry*. Academic Press, New York, N.Y., 1966. p. 132.
6. C. E. GRIFFIN, K. R. MARTIN, and B. E. DOUGLAS. J. Org. Chem. **27**, 1627 (1962).
7. R. A. FRIEDEL and M. ORCHIN. *Ultraviolet spectra of aromatic compounds*. J. Wiley & Sons, Inc., New York, N.Y., 1951. Spectra 195, 239, and 258.
8. H. J. BESTMANN. Angew. Chemie Internat. Ed. **4**, 645 (1965); H. BEHRINGER and K. FALKENBERG. Chem. Ber. **96**, 1428 (1963).
9. R. S. CURTISS and E. K. STRACHAM. J. Amer. Chem. Soc. **33**, 396 (1911).
10. H. ADKINS, R. M. ELOFSON, A. G. ROSSOW, and C. C. ROBINSON. J. Amer. Chem. Soc. **71**, 3622 (1949).
11. Beilsteins Handbuch der Organischen Chemie. Vol. 10. Springer Verlag, Berlin, 1927. p. 335.
12. H. GILMAN, C. E. ARNTSEN, and F. WEBB. J. Org. Chem. **10**, 374 (1945); W. E. PARHAM and C. D. WRIGHT. J. Org. Chem. **22**, 1473 (1957).

Organic sulfur compounds. VI.[1] Reduction of three α-(*o*-nitrophenylthio)ketones with sodium borohydride

R. T. COUTTS[2] AND SHARON J. MATTHIAS
Faculty of Pharmacy and Pharmaceutical Sciences, University of Alberta, Edmonton, Alberta

AND

H. W. PEEL
College of Pharmacy, University of Saskatchewan, Saskatoon, Saskatchewan

Received March 19, 1970

Reduction of three α-(*o*-nitrophenylthio)ketones with sodium borohydride and palladium–charcoal gave mainly α-(*o*-nitrophenylthio)alcohols and, as minor products, α-(*o*-aminophenylthio)alcohols. Only two benzothiazines were formed. Bis[2-(3-phenyl-2*H*-1,4-benzothiazine)] was a minor product of the catalyzed reduction of ω-(*o*-nitrophenylthio)acetophenone whereas 1-(3,4-dihydro-4-hydroxy-3-oxo-2*H*-1,4-benzothiazin-2-yl)benzyl alcohol was the main product of the catalyzed reduction of α-benzoyl-α-(*o*-nitrophenylthio)acetate.

Canadian Journal of Chemistry, **48**, 2448 (1970)

Methyl α-(*o*-nitrophenylthio)acetate (**1***a*) and its simple derivatives are readily reduced by means of sodium borohydride and palladium–charcoal (1–3) to give 2*H*-1,4-benzothiazine hydroxamic acids (**2**). It was of interest to extend these studies to the reductive cyclization of α-(*o*-nitrophenylthio)ketones (**3**) to see if 2*H*-1,4-benzothiazine 4-oxides (**4**) could be obtained in this way. This proved not to be the case; however, some unexpected reactions were observed and they are now reported.

The ketones (**3***a–c*) were prepared in good yields by the interaction of *o*-nitrobenzenesulfenyl chloride with acetone, acetophenone, and ethyl benzoylacetate respectively, using acetonitrile as solvent (4, 5). Reduction of (*o*-nitrophenylthio)propan-2-one (**3***a*) with sodium borohydride in the presence of catalytic quantities of palladium-on-charcoal yielded mainly 1-(*o*-nitrophenylthio)propan-2-ol (**5***a*), characterized as its 3,5-dinitrobenzoate. The same nitroalcohol was also the product of the reduction of (**3***a*) using sodium borohydride without catalyst. An additional minor product of

[1]Part V, see ref. 3.
[2]To whom communications should be addressed.

Can. J. Chem. Downloaded from www.nrcresearchpress.com by 210.87.254.40 on 09/05/12
For personal use only.

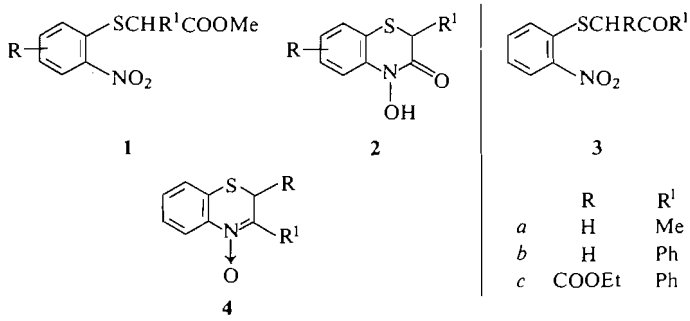

1 2 3

4

	R	R^1
a	H	Me
b	H	Ph
c	COOEt	Ph

the catalyzed reaction was deduced to be 1-(*o*-aminophenylthio)propan-2-ol (**5***b*) by comparing it with an authentic sample prepared from *o*-aminothiophenol and propylene glycol (6). Failure of the nitro-group in **5***a* to reduce readily in the catalyzed reaction was surprising in view of the ease with which this group was converted to the hydroxylamine when related esters were treated with the same reducing system (1, 3).

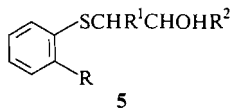

5

	R	R^1	R^2
a	NO_2	H	Me
b	NH_2	H	Me
c	NO_2	H	Ph
d	NH_2	H	Ph
e	NO_2	COOEt	Ph

In a similar manner, reduction of ω-(*o*-nitrophenylthio)acetophenone (**3***b*) with sodium borohydride in the presence or absence of palladium catalyst gave good yields 2-(*o*-nitrophenylthio)-1-phenylethanol (**5***c*), and 2-(*o*-aminophenylthio)-1-phenylethanol (**5***d*) was isolated from the catalyzed reduction only, in very low yield. Catalyst poisoning was apparently occurring and so the reduction of **3***b* was repeated using a much larger quantity of palladium–charcoal. Basic and neutral products were then formed. The neutral fraction was an oil from which one component was isolated, using column chromatography, as a bright orange solid, $C_{28}H_{20}N_2S_2$. Its mass spectrum showed a molecular ion of *m/e* 448, a strong $(M-2)^+$ ion at *m/e* 446 and a base peak of mass 224. The ions proposed in Scheme 1 are compatible with these observations and enable identification of this product as bis[2-(3-phenyl-2*H*-1,4-benzothiazine)] (**6**). The same compound was isolated by Fujii (7) when he attempted to prepare the picrate of 3-phenyl-4*H*-1,4-benzothiazine. The basic fraction again was 2-(*o*-aminophenylthio)-1-phenylethanol (**5***d*), the mass spectrum of which showed prominent ions of *m/e* 245, 139, 125 and 124. The formation of each fragment ion proposed in Scheme 2 was supported by the presence of a metastable ion of appropriate mass.

When ethyl α-benzoyl-α-(*o*-nitrophenylthio)-acetate (**3***c*) was reduced with sodium borohydride

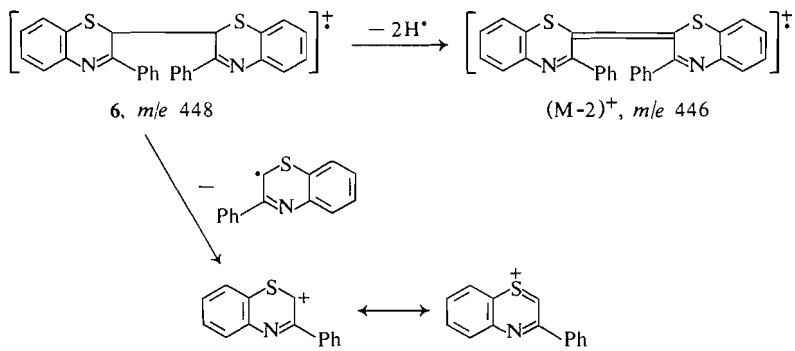

6, *m/e* 448 $(M-2)^+$, *m/e* 446

m/e 224

SCHEME 1

Can. J. Chem. Downloaded from www.nrcresearchpress.com by 210.87.254.40 on 09/05/12
For personal use only.

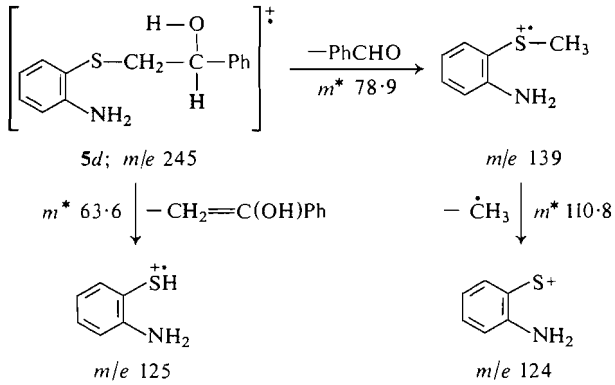

SCHEME 2

in the absence of catalyst, the product was not the expected nitro-alcohol (**5***e*). The ethoxycarbonyl group was lost during the reduction and 2-(*o*-nitrophenylthio)-1-phenylethanol (**5***c*) was obtained. When the reaction was repeated in the presence of catalyst, two identifiable products were isolated. The major one was an acidic viscous yellow oil which gave a violet color with ethanolic ferric chloride solution. Addition of water to this solution precipitated a purple ferric chelate. The infrared (i.r.) spectra of the oil and its ferric chelate were consistent (8) with the product being the cyclic hydroxamic acid 1-(3,4-dihydro-4-hydroxy-3-oxo-2*H*-1,4-benzothiazin-2-yl)benzyl alcohol (**7**). A purple ferrous chelate was also isolated which analyzed satisfactorily for $C_{30}H_{24}FeN_2O_6S_2$. It is of interest to contrast this result with the one obtained when another β-keto-ester, namely methyl *o*-nitrobenzoylacetoacetate (**8**), was reduced with sodium borohydride

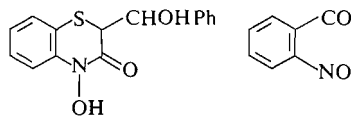

7

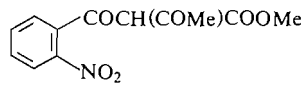

8

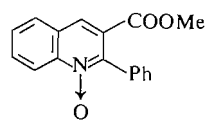

9

and palladium–charcoal (9). The product then was the *N*-oxide (**9**). The other product of the catalyzed sodium borohydride reduction of (**3***c*) was 1-(*o*-aminophenylthio)propan-2-ol (**5***b*). Once again, the ethoxycarbonyl group in **3***c* did not survive the reduction.

Experimental

Melting points and boiling points are uncorrected. The i.r. spectra were measured on KBr discs or thin films with a Beckman IR 10 spectrophotometer. Mass spectra were measured with an A.E.I. MS9 or MS12 spectrometer, using the direct insertion technique.

Preparation of α-(o-Nitrophenylthio)ketones (3)

General method: *o*-Nitrobenzenesulfenyl chloride (10 g) and an excess of the appropriate ketone (15 g) were dissolved in acetonitrile (100 ml) and the solution was heated under reflux for 2.5 to 4.5 h. Acetonitrile (80 ml) was then removed by distillation and the reaction mixture cooled to yield the product which was purified by crystallizing from methanol or ethanol.

(*o*-Nitrophenylthio)propan-2-one (**3***a*) was prepared from acetone in 97% yield as yellow crystals, m.p. 77–79° (from methanol); lit. (4) m.p. 81°.

ω-(*o*-Nitrophenylthio)acetophenone (**3***b*) was the product obtained in 93% yield when acetophenone was the ketone used in the reaction. It was a yellow solid, m.p. 143–145° (from methanol); lit. (4) m.p. 147°.

Ethyl α-benzoyl-α-(*o*-nitrophenylthio)acetate (**3***c*) was isolated in 95% yield as a yellow solid, m.p. 121–124° (from ethanol) when ethyl α-benzoylacetate was the ketone used. The i.r. spectrum: 1590, 1630 (β-ketoester C=O); 1510, 1335, 845 (NO_2) cm^{-1}.

Anal. Calcd. for $C_{17}H_{15}NO_5S$: C, 59.12; H, 4.38; N, 4.06; S, 9.28. Found: C, 59.25; H, 4.40; N, 4.00; S, 9.34.

Catalyzed Sodium Borohydride Reductions of α-(o-Nitrophenylthio)ketones (3)

General method: A solution of sodium borohydride (0.5 g) in water (5 ml) was added to a suspension of palladium (10%)-on-charcoal (0.1 g) in water (5 ml). Dioxane (10 ml) was added to the mixture and nitrogen gas was bubbled through it (1–2 min). The (*o*-nitrophenylthio)ketone (1.0 g), dissolved in a minimum of dioxane, was added to the reduction mixture over a period of 10 min. Nitrogen gas was bubbled through the reaction mixture during the addition of ketone and for an additional 30 min.

The reaction mixture was filtered and the filtrate extracted with ether (ether extract *i*). The aqueous layer

Can. J. Chem. Downloaded from www.nrcresearchpress.com by 210.87.254.40 on 09/05/12
For personal use only.

Can. J. Chem. Downloaded from www.nrcresearchpress.com by 210.87.254.40 on 09/05/12
For personal use only.

was acidified with concentrated hydrochloric acid, keeping the temperature below 30°, and then extracted with ether (ether extract *ii*). Ether extracts *i* and *ii* were then combined and extracted to completion with portions of 10% sodium hydroxide solution (extract A), washed with water, extracted to completion with portions of 10% hydrochloric acid solution (extract B), and washed with water. The ether layer was then dried (Na_2SO_4), and evaporated to yield the neutral product.

Basic extract A and its washings were acidified with concentrated hydrochloric acid and extracted with ether. The ether layer was washed with water, dried (Na_2SO_4), and evaporated to yield the acidic product.

Acidic extract B and its washings were basified with 10% sodium hydroxide solution and extracted with ether. The ether layer was washed with water, dried (Na_2SO_4), and evaporated to yield the basic product.

(*a*) Reduction of (*o*-nitrophenylthio)propan-2-one (**3***a*) (0.98 g), using the general method, gave a neutral product (0.65 g) and a basic product (0.03 g). No acidic product was isolated. The neutral product, 1-(*o*-nitrophenylthio)-2-propanol (**5***a*) was a yellow oil; i.r. spectrum: 3350 (broad, OH); 1510, 1335, 860 (NO_2) cm^{-1}.

The 3,5-dinitrobenzoate of **5***a* had a m.p. 144.5–146° (from ethanol); i.r. spectrum: 1723 (C=O); 1515, 1340, 860 (NO_2) cm^{-1}.

Anal. Calcd. for $C_{16}H_{13}N_3O_8S$: C, 47.17; H, 3.22; N, 10.36. Found: C, 47.53; H, 3.57; N, 10.36.

The basic fraction was a brown oil, mol. wt. (mass spectrum) 183 (calcd. for $C_9H_{13}NOS$: 183), which formed a hydrochloride, m.p. 166–167°; lit. (6) m.p. 159–160°. The i.r. spectra of the base and its hydrochloride were identical with authentic samples of **5***b* and **5***b*·HCl, prepared from propylene glycol and *o*-aminothiophenol using the reported (6) method.

(*b*) Reduction of ω-(*o*-nitrophenylthio)acetophenone (**3***b*) (0.94 g) using the general method gave a neutral fraction (0.86 g) and a basic fraction (0.01 g). No acidic fraction was isolated.

The neutral product, 2-(*o*-nitrophenylthio)-1-phenylethanol (**5***c*), was isolated as an orange oil which, on standing, slowly solidified to a yellow solid, m.p. 98–99°. The i.r. spectrum: 3300 (broad, OH); 1505, 1335, 840 (NO_2) cm^{-1}.

Anal. Calcd. for $C_{14}H_{13}NO_2S$: C, 61.07; H, 4.76; N, 5.09; S, 11.65. Found: C, 61.03; H, 4.60; N, 4.92; S, 11.52.

The *p*-nitrobenzoate of **5***c* had a m.p. 139–141° (from ethanol). The i.r. spectrum: 1732 (C=O); 1525, 1340, 850 (NO_2) cm^{-1}.

Anal. Calcd. for $C_{21}H_{16}N_2O_6S$: C, 59.42; H, 3.80; N, 6.60. Found: C, 59.58; H, 4.21; N, 6.67.

The basic product was a brown oil which had an i.r. spectrum identical with that of 2-(*o*-aminophenylthio)-1-phenylethanol (**5***d*) obtained as described below.

(*c*) Reduction of ω-(*o*-nitrophenylthio)acetophenone (**3***b*) using excess catalyst.

The title compound (10.03 g) was reduced using the general method on a 10-fold scale, except that the quantity of catalyst was increased to 2.64 g. A neutral fraction (3.83 g), a basic fraction (4.08 g), and an acidic fraction (0.74 g, starting material) were isolated.

The neutral product was an orange–red oil which was chromatographed on a neutral alumina column (1.1 × 15 cm) with petroleum ether as solvent. One bright orange component moved ahead of the remainder of the mixture and was collected. Subsequent elution with benzene and benzene/ethanol mixtures achieved some separation. Evaporation of the solvent in each instance gave a viscous orange oil and none of these oils were homogeneous as shown by mass spectrometry. Removal of the solvent from the bright orange solution described above gave 2,2′-*bis*(3-phenyl-2*H*-1,4-benzothiazine) (**6**, 0.31 g) as orange needles (from acetone), m.p. 243–244°; lit. (7) m.p. 234–236°. An i.r. spectrum confirmed the absence of C=O and NO_2 groups in **6**. Mass spectrum: 450(0.7), 449(3), 448(11), 447(29), 446(80), 445(13), 413(11), 369(10), 342(13), 325(12), 235(11), 225(32), 224(100), 223(28), 211(13), 121(23), 77(14), 76(10), 52(15), 51(14), 39(16), *m/e* (% relative abundance).

Anal. Calcd. for $C_{28}H_{20}N_2S_2$: C, 74.96; H, 4.49; N, 6.24. Found: C, 74.80; H, 4.94; N, 6.35.

The basic fraction was 2-(*o*-aminophenylthio)-1-phenylethanol (**5***d*) which was isolated as a brown oil. Its hydrochloride was a colorless solid, m.p. 180–181° (from acetone/*n*-hexane); lit. (6) m.p. 172°.

Anal. Calcd. for $C_{14}H_{16}ClNOS$: C, 59.67; H, 5.72; N, 4.97. Found: C, 60.08; H, 6.03; N, 5.12.

(*d*) Reduction of ethyl α-benzoyl-α-(*o*-nitrophenylthio)acetate (**3***c*) (1.93 g) using the general method gave a neutral product (0.32 g), an acidic product (0.91 g), and a basic product (0.18 g).

The acidic product, 1-(3,4-dihydro-4-hydroxy-3-oxo-2*H*-1,4-benzothiazin-2-yl)benzyl alcohol (**7**), was a viscous yellow oil which gave a violet color with ethanolic ferric chloride solution. The i.r. spectrum: 1690 (hydroxamate C=O), 2700–3600 (hydrogen-bonded OH) cm^{-1}. The ferric chelate was prepared as a purple–brown solid by dissolving the oil (100 mg) in the minimum of ethanol, adding excess ethanolic ferric chloride solution and flooding the mixture with water. The i.r. spectrum: 3450 (OH), 1528 (chelated C=O) (8) cm^{-1}. The ferrous chelate was prepared by dissolving the hydroxamic acid (50 mg) in glacial acetic acid (1 ml) and adding a solution of ferrous chloride (15 mg) in glacial acetic acid (1 ml) and then water (6 ml). The chelate was washed with 10% sodium hydroxide solution, then water, and dried to give a purple solid (38 mg), m.p. 140–145°.

Anal. Calcd. for $C_{30}H_{24}FeN_2O_6S_2$: C, 57.33; H, 3.85; Fe, 8.89. Found: C, 57.42; H, 3.61; Fe, 8.94.

The neutral fraction was a viscous oil which was not identified. Its i.r. spectrum differed from that of **5***c*.

The basic product was a viscous yellow oil with an i.r. spectrum which was superimposable upon that of 2-(*o*-aminophenylthio)-1-phenylethanol (**5***d*).

Reduction of α-(o-Nitrophenylthio)ketones (3) with Sodium Borohydride in the Absence of Catalyst

(*o*-Nitrophenylthio)propan-2-one (**3***a*) (0.95 g) was dissolved in dioxane (15 ml) and a solution of sodium borohydride (0.5 g) in water (10 ml) was added. After 1 h, the solution was acidified with dilute hydrochloric acid and extracted with ether. The ether solution was washed with 10% sodium hydroxide solution, then water, dried (Na_2SO_4), and evaporated to yield 1-(*o*-nitrophenylthio)propan-2-ol (**5***a*) (0.95 g) as a yellow oil,

which was characterized by its i.r. spectrum (identical to that of product obtained in the catalyzed reduction of **3***a*). The 3,5-dinitrobenzoate had m.p. 144–146°.

In the same way reduction of ω-(*o*-nitrophenylthio)-acetophenone (**3***b*) (0.62 g) gave 2-(*o*-nitrophenylthio)-1-phenylethanol (**5***c*) (0.58 g), m.p. 97–98°, and reduction of ethyl α-benzoyl-α-(*o*-nitrophenylthio)acetate (**3***c*) (0.52 g) yielded the same product (**5***c*) (0.39 g), m.p. 96–98°.

1. R. T. COUTTS, H. W. PEEL, and E. M. SMITH. Can. J. Chem. **43**, 3221 (1965).
2. R. T. COUTTS, D. L. BARTON, and E. M. SMITH. Can. J. Chem. **44**, 1733 (1966).
3. R. T. COUTTS and E. M. SMITH. Can. J. Chem. **45**, 975 (1967).
4. J. A. BALTROP and K. J. MORGAN. J. Chem. Soc. 4486 (1960).
5. N. KHARASCH. J. Chem. Educ. **33**, 585 (1956).
6. R. FUSCO and G. PALAZZO. Gazz. Chim. Ital. **81**, 735 (1951).
7. K. FUJII. Yakagaku Zasshi, **77**, 347 (1957).
8. R. T. COUTTS, K. W. HINDMARSH, S. J. POWELL, J. L. POUND, and E. M. SMITH. Can. J. Pharm. Sci. **3**, 49 (1968).
9. R. T. COUTTS and D. G. WIBBERLEY. J. Chem. Soc. 4610 (1963).

Can. J. Chem. Downloaded from www.nrcresearchpress.com by 210.87.254.40 on 09/05/12
For personal use only.

Can. J. Chem. Downloaded from www.nrcresearchpress.com by 210.87.254.42 on 09/05/12
For personal use only.

Conditions for the electrochemical formation of Ag_2O_3 on silver in aqueous KOH solutions

R. G. BARRADAS AND D. B. MCDONNELL[1]
Department of Chemistry, Carleton University, Ottawa 1, Canada

Received April 20, 1970

New evidence is presented to substantiate the electrochemical formation, at certain temperatures, of Ag_2O_3 as a reasonably stable species under galvanostatic conditions in aqueous KOH electrolytes saturated with Ag_2O and O_2. The experimental data offer a better understanding of the nature of the Ag_2O/AgO transition peak.

Canadian Journal of Chemistry, 48, 2453 (1970)

Many controversial papers regarding the possible existence of higher oxides of silver favor the electrochemical generation of Ag_2O_3. The best evidence is based on open circuit decay studies in eutectic KOH–H_2O at −40 °C and at current densities of the order of 100 μA cm^{-2} (1). We have re-examined this controversy by experiments using annealed and electro-polished silver electrodes. Anodic polarization under galvanostatic conditions in unstirred carbonate free KOH aqueous solutions presaturated with O_2 and Ag_2O was studied over a range of current densities and temperatures. At 60 and 50 °C, and at a current density of 0.5 mA cm^{-2} in 0.1 *N* KOH, standard polarization curves of the type first published by Luther and Pokorny (2) were observed. This was also true of the experiments at 40 °C (Fig. 1). At 30 °C an anomalous behavior, unlike any hitherto reported, was exhibited in the transition region from Ag_2O to AgO formation. At 20 °C the transition peak disappeared and in its place a distinct plateau occurred at a potential of about 0.85 V (vs. Hg/HgO reference electrode). The polarization profiles were reproducible to within 1% average deviation in the plateau lengths over a minimum of three similar runs. At higher current densities (1.0, 2.0, and 5.0 mA cm^{-2}) in 0.1 *N* KOH at 20 °C, as well as at 0 °C, and 3.5 and 5.0 mA cm^{-2} in 1.0 *N* KOH, the plateau at approximately 0.85 V and the disappearance of the peak

[1]Holder of a Province of Ontario Graduate Fellowship for 1969–1970.

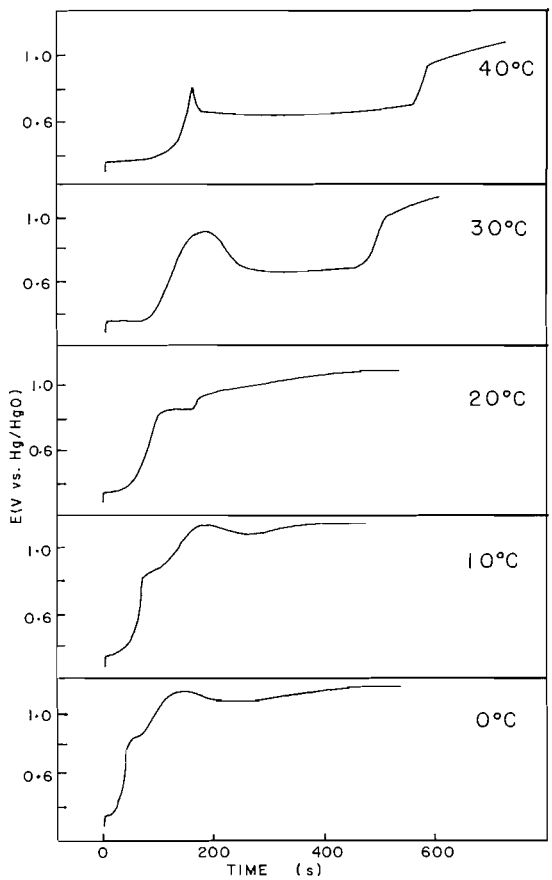

FIG. 1. Temperature dependent characteristics of anodic curves in a 0.1 *N* KOH aqueous solution presaturated with Ag_2O and O_2 at a current density of 0.5 mA/cm^2.

were again observed with good reproducibility in every run. The anodic behavior as shown by Fig. 1 at 20 °C can only be attributed to presaturation with Ag_2O. Apparently O_2 saturation is not a crucial factor in this case since comparable experiments at 20 °C without Ag_2O addition but in O_2 saturated solutions gave classical curves resembling Fig. 1 at 40 °C. At 10 and 0 °C, as depicted in the lower portions of Fig. 1, the new plateau was again recorded. In all cases, as the temperature is lowered, the lengths of the plateaus are shortened. The significant conclusion from inspection of Fig. 1 suggests that a new oxide of silver, with a moderate degree of stability, can be produced electrochemically. We are inclined to believe that the new oxide is likely to be $Ag_2O_3(Ag^{3+}, 4d^8)$ for the reasons following. Hickling and Taylor (3) proposed that the transition peak between Ag_2O and AgO plateaus in conventional polarization runs was due to Ag_2O_3 which, being thermodynamically unstable, rapidly decomposed to form AgO. Although this proposal had been refuted by numerous workers (see, e.g., ref. 4 and the literature cited therein), our results contained in Fig. 1 tend to support Hickling and Taylor's contention, because the peak at 40 °C gradually broadens and ultimately disappears with the formation of a new plateau. This indicates that at temperatures in excess of about 40–50 °C, Ag_2O_3 is unstable. Conversely, the anodic oxidation curves shown by Casey and Moroz (1) at −40 °C are morphologically similar to the one we obtained at 0 °C, which confirms that Ag_2O_3 formation is enhanced at lower temperatures. Further work in progress on the quantitative dependence of film thickness of the various oxides on current densities and temperatures, and related kinetic aspects will be reported later. Additional chemical reactions to form Ag^{3+} organic complexes with biguanides (5) are being re-investigated with a view to more conclusive establishment of Ag^{3+} compounds (6), thereby corroborating the existence of disilver trioxide (Ag_2O_3).

This project has been supported by a Defence Research Board Grant No. 5480-25.

1. E. J Casey and W. J. Moroz. Can. J. Chem. **43**, 1199 (1965).
2. R. Luther and F. Pokorny. Z. Anorg. Chem. **57**, 290 (1908).
3. A. Hickling and D. Taylor. Discuss. Faraday Soc. **1**, 277 (1947).
4. M. Fleischmann, D. J. Lax, and H. R. Thirsk. Trans. Faraday Soc. **64**, 3128 (1968).
5. D. Sen. J. Chem Soc. A, 1304 (1969).
6. F. A. Cotton and G. Wilkinson, Advanced inorganic chemistry. 2nd ed. Interscience Publishers Inc., New York. 1966. p. 1047.

Adsorption of water and ^{18}O exchange of surface hydroxyl groups on silica

B. A. Morrow[1] and A. Devi
Department of Chemistry, University of Ottawa, Ottawa 2, Canada

Received April 21, 1970

Infrared spectroscopy has been used to show that the surface hydroxyl groups on highly dehydrated silica will exchange with ^{18}O-labeled water. The degree of exchange depends on the sample temperature and is a maximum at about 400 °C, where approximately 65% of the silanol groups contain ^{18}O. The use of the ^{18}O exchange technique for assigning surface-adsorbate stretching modes is illustrated by considering the infrared spectra of BF_3 chemisorbed on silica.

Canadian Journal of Chemistry, **48**, 2454 (1970)

Infrared spectroscopic techniques have been used extensively to investigate the nature of the silica surface (1–7). In this communication we present some experimental results which demonstrate that the silanol groups on the surface of silica exchange with ^{18}O-labeled water under moderate reaction conditions and that such an exchange can aid in the assignment of infared absorption bands due to surface-adsorbate stretching modes. Although it is known that the bulk oxygen atoms of silica will exchange at high temperatures and pressures (8), this tech-

[1]To whom correspondence should be addressed.

Can. J. Chem. Downloaded from www.nrcresearchpress.com by 210.87.254.42 on 09/05/12
For personal use only.

were again observed with good reproducibility in every run. The anodic behavior as shown by Fig. 1 at 20 °C can only be attributed to presaturation with Ag_2O. Apparently O_2 saturation is not a crucial factor in this case since comparable experiments at 20 °C without Ag_2O addition but in O_2 saturated solutions gave classical curves resembling Fig. 1 at 40 °C. At 10 and 0 °C, as depicted in the lower portions of Fig. 1, the new plateau was again recorded. In all cases, as the temperature is lowered, the lengths of the plateaus are shortened. The significant conclusion from inspection of Fig. 1 suggests that a new oxide of silver, with a moderate degree of stability, can be produced electrochemically. We are inclined to believe that the new oxide is likely to be $Ag_2O_3(Ag^{3+}, 4d^8)$ for the reasons following. Hickling and Taylor (3) proposed that the transition peak between Ag_2O and AgO plateaus in conventional polarization runs was due to Ag_2O_3 which, being thermodynamically unstable, rapidly decomposed to form AgO. Although this proposal had been refuted by numerous workers (see, e.g., ref. 4 and the literature cited therein), our results contained in Fig. 1 tend to support Hickling and Taylor's contention, because the peak at 40 °C gradually broadens and ultimately disappears with the formation of a new plateau. This indicates that at temperatures in excess of about 40–50 °C, Ag_2O_3 is unstable. Conversely, the anodic oxidation curves shown by Casey and Moroz (1) at −40 °C are morphologically similar to the one we obtained at 0 °C, which confirms that Ag_2O_3 formation is enhanced at lower temperatures. Further work in progress on the quantitative dependence of film thickness of the various oxides on current densities and temperatures, and related kinetic aspects will be reported later. Additional chemical reactions to form Ag^{3+} organic complexes with biguanides (5) are being re-investigated with a view to more conclusive establishment of Ag^{3+} compounds (6), thereby corroborating the existence of disilver trioxide (Ag_2O_3).

This project has been supported by a Defence Research Board Grant No. 5480-25.

1. E. J Casey and W. J. Moroz. Can. J. Chem. **43**, 1199 (1965).
2. R. Luther and F. Pokorny. Z. Anorg. Chem. **57**, 290 (1908).
3. A. Hickling and D. Taylor. Discuss. Faraday Soc. **1**, 277 (1947).
4. M. Fleischmann, D. J. Lax, and H. R. Thirsk. Trans. Faraday Soc. **64**, 3128 (1968).
5. D. Sen. J. Chem Soc. A, 1304 (1969).
6. F. A. Cotton and G. Wilkinson, Advanced inorganic chemistry. 2nd ed. Interscience Publishers Inc., New York. 1966. p. 1047.

Adsorption of water and ^{18}O exchange of surface hydroxyl groups on silica

B. A. Morrow[1] and A. Devi
Department of Chemistry, University of Ottawa, Ottawa 2, Canada

Received April 21, 1970

Infrared spectroscopy has been used to show that the surface hydroxyl groups on highly dehydrated silica will exchange with ^{18}O-labeled water. The degree of exchange depends on the sample temperature and is a maximum at about 400 °C, where approximately 65% of the silanol groups contain ^{18}O. The use of the ^{18}O exchange technique for assigning surface-adsorbate stretching modes is illustrated by considering the infrared spectra of BF_3 chemisorbed on silica.

Canadian Journal of Chemistry, **48**, 2454 (1970)

Infrared spectroscopic techniques have been used extensively to investigate the nature of the silica surface (1–7). In this communication we present some experimental results which demonstrate that the silanol groups on the surface of silica exchange with ^{18}O-labeled water under moderate reaction conditions and that such an exchange can aid in the assignment of infared absorption bands due to surface-adsorbate stretching modes. Although it is known that the bulk oxygen atoms of silica will exchange at high temperatures and pressures (8), this tech-

[1]To whom correspondence should be addressed.

Can. J. Chem. Downloaded from www.nrcresearchpress.com by 210.87.254.40 on 09/05/12
For personal use only.

Can. J. Chem. Downloaded from www.nrcresearchpress.com by 210.87.254.40 on 09/05/12
For personal use only.

nique has not been used for studying the surface of silica.

Cab-O-Sil M-5 (Cabot Co., Boston) was pressed at 2000 lb/in.^{2} into a self-supporting disc containing 12 mg of silica per cm^2 and was mounted in an evacuable quartz cell equipped with NaCl windows. The sample could be heated to any temperature up to 1000 °C under vacuum and then be exposed repeatedly to $H_2{}^{18}O$ (98.8% ^{18}O, Oak Ridge National Laboratory) at a pressure of about 10 mm. The excess $H_2{}^{18}O$ was evacuated and infrared spectra of the room temperature sample was run on a Perkin–Elmer model 13G infrared spectrometer.

The spectrum in Fig. 1*A* was obtained after Cab-O-Sil had been heated at 800 °C under vacuum for 5 h and shows the well-known band at 3749 cm^{-1} due to non-hydrogen bonded surface silanol (SiOH) groups (3–7). The spectrum in Fig. 1*B* was obtained after four successive cycles of addition (for 10 min) and evacuation of $H_2{}^{18}O$ to the same sample at 400 °C and shows a new ^{18}O silanol band at 3738 cm^{-1}. No further changes occurred with further similar exposures

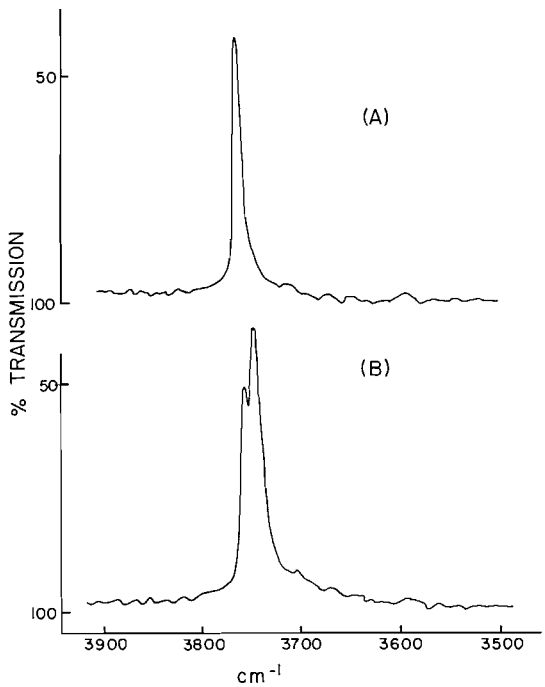

FIG. 1. Spectrum of Cab-O-Sil in the O—H stretching region: *A*, after evacuation at 800 °C for 5 h; *B*, after subsequent exchange (4 times) with $H_2{}^{18}O$ at 400 °C. Both spectra were recorded with samples at room temperature.

to $H_2{}^{18}O$ indicating that under these conditions a maximum of about 60–70% of the surface silanol groups can undergo exchange. The same result was obtained for a sample which had not been preheated to 800 °C prior to exchange, although in this case a weak shoulder remains at lower frequency which is due to hydrogen bonded silanols (3, 5, 7). On other silica samples which had also been preheated to 800 °C, no exchange takes place under similar adsorption conditions at room temperatures, only about 20% exchange occurs at 200 °C and above 500 °C, less than 50% exchange of silanol groups takes place.

On heating the sample up to 800 °C after exchange at 400 °C, an approximately 50% overall decrease in intensity occurs, with the ^{18}O silanol band decreasing more rapidly than the ^{16}O band, until at 800 °C, only about 40% of the remaining surface silanol groups contain ^{18}O. Therefore, as the temperature is raised dehydration processes are probably competing with the exchange reaction although the proportion of surface ^{18}O atoms at the higher temperature might still be quite large.

If the above sample is again saturated with $H_2{}^{18}O$ at 400 °C after evacuation at 800 °C, only the ^{18}O silanol band grows until it is about four times more intense than the ^{16}O silanol band. Therefore, it would appear that the readdition of $H_2{}^{18}O$ merely brings about the reformation of the ^{18}O silanols and that some of the silanol groups initially present do not exchange below a certain temperature. Since the dehydration of the silanol groups on silica depends mainly on the sample temperature and not on the time of evacuation (3), this temperature dependence for silanol exchange is probably to be expected.

The infrared spectra of boron trifluoride chemisorbed on silica will illustrate the usefulness of the ^{18}O exchange technique for assigning bands due to adsorbed species. Figure 2*A* shows the spectrum obtained after adsorption (and evacuation of excess gas phase) of 0.1 mm of $^{10}BF_3$ for 20 s on ordinary silica which had previously been dehydrated at about 900 °C. The spectrum is similar to that reported by Rhee and Basila (9) who used natural isotopic BF_3. From a comparison of the spectrum of free BF_3 with that of adsorbed BF_3, Rhee and Basila assigned the band at 1500 cm^{-1} (1450 cm^{-1} for $^{11}BF_3$) to the asymmetric stretching mode of physically adsorbed planar BF_3. This assignment

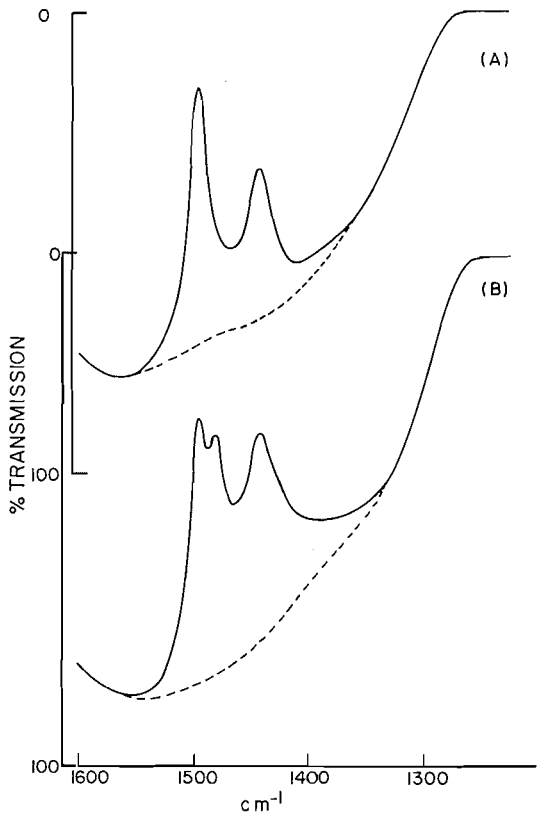

FIG. 2. Spectrum obtained after adsorption of $^{10}BF_3$ on dehydrated Cab-O-Sil: *A*, untreated silica; *B*, ^{18}O exchanged silica. The dotted line indicated the background spectrum of Cab-O-Sil before adsorption of BF_3.

is questionable as it is difficult to imagine why BF_3 should be so strongly physically adsorbed as a planar species on silica at room temperature. Moreover, boron–oxygen stretching modes occur in the same spectral region, and the lower frequency band at 1448 cm^{-1} (1394 cm^{-1} for $^{11}BF_3$) was assigned to the B—O stretching mode of a Si—O—BF_2 species (9).

Figure 2*B* shows the spectrum obtained after chemisorption of $^{10}BF_3$ on ^{18}O exchanged silica and it can be seen that the 1500 cm^{-1} band is split into a doublet with a new band at 1487 cm^{-1}. Therefore, this 1500 cm^{-1} absorption must be associated with a BO mode and cannot be a BF stretching mode. From a detailed study of the BF_3/SiO_2 system (which will be published later) both the 1448 and 1500 cm^{-1} bands are due to the same chemisorbed species, most probably a surface Si—O—BF_2 species. Accordingly, the 1500 cm^{-1} band is assigned to the B—O streching mode and the 1448 cm^{-1} band is assigned to the asymmetric BF_2 stretching mode of this species.

The authors wish to acknowledge the financial support of the National Research Council of Canada and the Ontario Department of University Affairs.

1. M. L. HAIR and W. HERTL. J. Phys. Chem. **73**, 4269 (1969).
2. M. L. HAIR and W. HERTL. J. Phys. Chem. **73**, 2372 (1969).
3. M. L. HAIR. Infrared spectroscopy in surface chemistry. Marcel Dekker Inc, New York. 1967.
4. C. G. ARMISTEAD, A. J. TYLER, F. H. HAMBLETON, S. A. MITCHELL, and J. A. HOCKEY. J. Phys. Chem. **73**, 3947 (1969).
5. A. J. TYLER, F. H. HAMBLETON, and J. A. HOCKEY. J. Catal. **13**, 35 (1969).
6. J. B. PERI. J. Phys. Chem. **70**, 2937 (1966).
7. F. H. HAMBLETON, J. A. HOCKEY, and J. A. TAYLOR. Trans. Faraday Soc. **62**, 801 (1966).
8. W. G. SPITZER and J. R. LIGENZA. J. Phys. Chem. Solids, **17**, 196 (1961).
9. K. H. RHEE and M. R. BASILA. J. Catal. **10**, 243 (1968).

Can. J. Chem. Downloaded from www.nrcresearchpress.com by 210.87.254.40 on 09/05/12
For personal use only.

Can. J. Chem. Downloaded from www.nrcresearchpress.com by 210.87.254.5 on 09/05/12
For personal use only.

Canadian Journal of Chemistry

Published by THE NATIONAL RESEARCH COUNCIL OF CANADA

VOLUME 48 AUGUST 15, 1970 NUMBER 16

Molar excess enthalpies, volumes, and Gibbs free energies of methanol – isomeric butanol systems at 25 °C[1]

JIŘÍ POLÁK,[2] SACHIO MURAKAMI,[3] V. T. LAM,[4] H. D. PFLUG,[5] AND G. C. BENSON

Division of Chemistry, National Research Council of Canada, Ottawa, Canada

Received March 16, 1970

The vapor–liquid equilibria of the 4 binary systems formed by mixing methanol with *n*-butanol, isobutanol, *sec*-butanol, and *tert*-butanol were investigated at 25 °C in a dynamic still with circulation. The results were used to calculate the molar excess Gibbs free energies. For the three systems containing isobutanol, *sec*-butanol, or *tert*-butanol, molar excess enthalpies and volumes were also determined (mainly at 25 °C) by direct calorimetric and dilatometric techniques. The behavior of the excess properties is discussed with reference to differences in the hydrogen bonding and in the shapes of the component molecules.

Canadian Journal of Chemistry, 48, 2457 (1970)

Previous publications from our laboratory have described measurements of the molar excess enthalpy (1) and volume (2) of methanol – *n*-butanol mixtures at 25 °C. These studies are continued and extended in the present paper by reporting the vapor–liquid equilibria of the system methanol – *n*-butanol (again at 25 °C) and also by reporting the results of similar investigations of the systems formed by mixing methanol with isobutanol (2-methyl-1-propanol), with *sec*-butanol (2-butanol) and with *tert*-butanol (2-methyl-2-propanol).

Experimental

Materials

The primary component liquids were obtained from several different commercial sources and were purified in an F&M preparative chromatograph (Model 775). The main features of these purifications are summarized in Table 1. The *sec*-butanol was a racemic form and no attempt was made to separate the enantiomorphs. In all cases, the final products failed to show any significant impurities when passed through a variety of column packings in an analytical chromatograph (Perkin–Elmer Model 154, equipped with a hot wire detector).

The purified liquids were characterized by densities (d^{25}, g cm^{-3}) measured at 25.00 °C, by refractive indices (n_D^{20}) measured at 20.00 °C and by vapor pressures (p_{25}^0, mm Hg) measured at 25.00 °C in a static vapor pressure apparatus (3). The results of these measurements are given in Table 2 along with values from the literature (4) for comparison. It should be noted that the values for *tert*-butanol refer to the supercooled liquid since this compound freezes at about 25.6 °C. However, freezing did not occur readily and, apart from one exception (noted later), no great difficulty was experienced in working with *tert*-butanol in the liquid state at temperatures as low as 20 °C.

Apparatus

Details of the equipment can be found in previous publications from our laboratory. A dynamic circulation still (5, 6) was used to study the vapor–liquid equilibria at 25 °C. Compositions of the equilibrium liquid and condensed vapor phases were determined by measuring their refractive indices at 20 °C. For each system, the variation of refractive index with concentration was established from measurements on a series of mixtures of known composition. The precision of the analyses was about ± 0.025 mole percent. In general, estimates of the errors of the results for the Gibbs free energy (derived from the vapor–liquid equilibria) are largest at low methanol mole fractions and decrease with increasing concentration. The estimated errors for equimolar mixtures are 13, 8, 6, and 3 J mole^{-1}, respectively, in the *n*-butanol, isobutanol, *sec*-butanol, and *tert*-butanol systems.

The mixing of methanol with isobutanol is endothermic

[1]NRCC No. 11 336.

[2]NRCC Postdoctorate Fellow 1968–1970.

[3]NRCC Postdoctorate Fellow 1967–1969. Present address: Department of Chemistry, Faculty of Science, Osaka City University, Sumiyoshi-ku, Osaka, Japan.

[4]NRCC Postdoctorate Fellow 1967–1969. Present address: Département de Chimie, Faculté des Sciences, Université de Sherbrooke, Sherbrooke, Québec.

[5]NRCC Postdoctorate Fellow 1965–1967. Present address: Metallgesellschaft-AG, Frankfurt/M, Germany.

TABLE 1

Purification of component liquids

Component	Primary material	Chromatograph operational conditions: Column: Overall length, ft	Column: Diameter, in.	Column: Substrate	Oven temperature °C
Methanol	British Drug Houses reagent grade	6	3/4	4.5 ft Poropak Q (40/60 mesh) 1.5 ft Poropak Q (80/100 mesh)	92
n-Butanol	Eastman Organic Chemicals Spectrograde	6	3/4	Chromosorb W (40/60 mesh) containing 10% PEG-400	130
Isobutanol	British Drug Houses analytical reagent	6	4	Chromosorb W (10/60 mesh) containing 20% Apiezon L	130
sec-Butanol	Matheson, Coleman & Bell Chromato-quality reagent shaken with mercury	Same as for isobutanol			130
tert-Butanol	Matheson, Coleman & Bell reagent grade	12	3/4	6 ft Chromosorb W (60/80) mesh containing 15% PEG-400 6 ft Chromosorb W (60/80 mesh) containing 15% di-isodecylphthalate	90

TABLE 2

Properties of pure component liquids

Property		Value: Methanol	*n*-Butanol	Isobutanol	*sec*-Butanol (racemic)	*tert*-Butanol (supercooled)
p_{25}^{0} mm Hg,	expt.	127.09	7.09	11.61	18.08	42.57
	lit. (4)	126.89	6.46	11.55	17.63	41.46
d^{25}, g cm^{-3},	expt.	0.78671	0.80604	0.79790	0.80246	0.78051
	lit. (4)	0.78652	0.8058	0.7981	0.8024	0.7808
n_D^{20}	expt.	1.32841	1.39924	1.39569	1.39716	1.38730
	lit. (4)	1.32857	1.3993	1.3958	1.3968	1.3879

(at 25 °C) and the excess enthalpies of this sytem were determined in the successive dilution calorimeter described by Pope *et al.* (1). The modified form of that calorimeter, containing a cooling module (7), was used to study the exothermic systems methanol – *sec*-butanol and methanol – *tert*-butanol. Measurements on the latter system were carried out at 26 °C since the *tert*-butanol tended to solidify in the hypodermic needle (L in Fig. 1 of ref. (7) and to upset the operation of the calorimeter in attempts to work at temperatures below the freezing point of *tert*-butanol. The error of the enthalpy measurements is believed to be less than 1% over nearly the entire concentration range.

A successive dilution technique (2) was also used to determine the excess volumes. In the present systems, the overall errors of the results for equimolar mixtures are estimated to lie in the range 1 to 2%.

Results

The results of the dynamic still studies are listed in Table 3 where x_1 and y_1 are the mole fractions of methanol in the equilibrium liquid and vapor phases at pressure p. Values of the molar excess enthalpy, H^E, and of the molar excess volume, V^E, determined from the calorimetric and dilatometric measurements are summarized in Tables 4 and 5, respectively. All of the results reported refer to 25.00 °C, except the excess enthalpies of methanol – *tert*-butanol, which were determined at 26.00 °C.

Table 3 also contains values of the molar excess Gibbs free energy

Can. J. Chem. Downloaded from www.nrcresearchpress.com by 210.87.254.5 on 09/05/12
For personal use only.

TABLE 3

Vapor–liquid equilibria of methanol (1) – butanol (2) systems at 25 °C

Methanol – *n*-butanol				Methanol – *tert*-butanol			
x_1	y_1	p mm Hg	G^E J mole^{-1}	x_1	y_1	p mm Hg	G^E J mole^{-1}
0.0871	0.6569	18.41	−37.5	0.0773	0.1535	45.88	−89.0
0.0953	0.6800	19.55	−35.6	0.1070	0.2045	47.18	−118.4
0.1200	0.7302	22.43	−47.2	0.1479	0.2744	49.13	−157.3
0.1295	0.7482	24.01	−18.5	0.1902	0.3455	51.40	−192.8
0.1690	0.8010	28.81	−28.6	0.2374	0.4206	54.24	−224.1
0.2340	0.8564	37.12	0.0	0.2891	0.5012	57.73	−256.8
0.2654	0.8751	41.21	19.0	0.3450	0.5802	61.95	−281.1
0.3072	0.8946	46.46	38.5	0.4029	0.6528	66.74	−296.3
0.3173	0.8993	47.80	36.9	0.4545	0.7096	71.34	−301.1
0.3557	0.9128	52.49	50.3	0.5104	0.7646	76.64	−302.1
0.3628	0.9150	53.55	62.3	0.5707	0.8147	82.77	−288.2
0.4172	0.9310	60.13	57.7	0.6361	0.8596	89.48	−266.4
0.4258	0.9329	61.26	66.9	0.7036	0.8967	96.48	−230.2
0.4569	0.9396	65.13	83.7	0.7573	0.9222	102.19	−196.6
0.5048	0.9487	70.76	93.1	0.8082	0.9430	107.61	−159.9
0.5845	0.9612	80.09	102.4	0.8515	0.9584	112.14	−126.2
0.6544	0.9702	88.10	99.6	0.8809	0.9677	115.12	−102.2
0.7237	0.9772	95.80	102.9	0.9211	0.9796	119.23	−68.2
0.8164	0.9855	106.17	90.9	0.9523	0.9880	121.96	−49.0
0.8660	0.9894	111.71	80.4				
0.9290	0.9943	118.82	52.7				

Methanol – *sec*-butanol				Methanol – isobutanol			
x_1	y_1	p mm Hg	G^E J mole^{-1}	x_1	y_1	p mm Hg	G^E J mole^{-1}
0.0837	0.3697	25.55	−89.2	0.0967	0.5620	23.59	−16.3
0.1058	0.4333	27.67	−98.1	0.1279	0.6370	27.46	−12.0
0.1337	0.5032	30.54	−102.1	0.1617	0.6964	31.55	−8.2
0.1705	0.5756	34.23	−106.3	0.2342	0.7816	40.25	8.2
0.2093	0.6399	38.32	−112.4	0.2981	0.8311	47.90	21.2
0.2734	0.7212	45.31	−113.3	0.3607	0.8666	55.42	32.2
0.3157	0.7629	50.02	−112.4	0.4279	0.8948	63.33	44.6
0.3453	0.7883	53.39	−112.3	0.5157	0.9229	73.69	56.3
0.4224	0.8403	62.07	−106.7	0.6028	0.9434	83.56	64.3
0.5256	0.8912	74.07	−90.9	0.6835	0.9585	92.51	66.3
0.6140	0.9223	84.33	−67.6	0.7561	0.9700	100.58	64.4
0.6977	0.9455	93.81	−51.6	0.8285	0.9795	108.31	60.0
0.7858	0.9647	103.65	−29.4	0.8967	0.9879	115.65	44.0
0.8654	0.9789	112.47	−7.4	0.9434	0.9935	120.74	25.4
0.9320	0.9897	119.64	−1.0				

[1] $$G^E = RT(x_1 \ln \gamma_1 + x_2 \ln \gamma_2)$$

where the activity coefficients γ_i were obtained from the results for the vapor–liquid equilibria using the equations

[2] $$\ln \gamma_i = \ln (y_i p / x_i p_i^0) + (B_{ii} - V_i^0) \times (p - p_i^0)/RT + (1 - y_i)^2 p\delta/RT$$

and

[3] $$\delta = 2B_{12} - B_{11} - B_{22}$$

In these equations, p_i^0, V_i^0, and B_{ii} are, respectively, the vapor pressure, molar volume, and second virial coefficient of pure component i, and B_{12} is the cross virial coefficient. Values of the virial coefficients employed in the calculations are summarized in Table 6. These were estimated from critical-point data (8) using the empirical correlation developed by O'Connell and Prausnitz (9); values of the parameters (ω_H, μ, η) required for polar components were taken from the table in ref. 9.

Graphical presentations of the experimental results for G^E, H^E, and V^E are provided in Figs.

Can. J. Chem. Downloaded from www.nrcresearchpress.com by 210.87.254.5 on 09/05/12
For personal use only.

TABLE 4

Experimental values of the molar excess enthalpy of some methanol (1) – butanol (2) systems

Methanol – isobutanol at 25 °C		Methanol – *sec*-butanol at 25 °C		Methanol – *tert*-butanol at 26 °C	
x_1	H^E J mole^{-1}	x_1	H^E J mole^{-1}	x_1	H^E J mole^{-1}
0.0491	20.0	0.0770	−63.3	0.0626	−235.7
0.1342	53.0	0.1820	−112.9	0.1346	−440.5
0.2408	90.9	0.2679	−130.0	0.2083	−584.0
0.3400	120.1	0.3494	−131.1	0.2133	−597.6
0.4375	142.0	0.4055	−125.5	0.2825	−669.4
0.5251	153.7	0.5374	−96.7	0.2927	−679.4
0.5973	156.9	0.6022	−78.1	0.3589	−708.5
0.6602	153.8	0.6214	−72.4	0.3668	−706.3
0.6852	152.3	0.6433	−66.7	0.4331	−703.6
0.7142	146.3	0.6607	−61.0	0.4406	−695.6
0.7338	144.0	0.6939	−52.1	0.5019	−662.9
0.7576	136.5	0.7060	−48.1	0.5071	−664.9
0.7834	130.5	0.7354	−40.6	0.5650	−616.6
0.8316	111.9	0.7515	−35.7	0.5823	−594.3
0.8724	90.9	0.8021	−23.5	0.6178	−561.3
0.9105	67.9	0.8526	−13.0	0.6667	−502.7
0.9418	45.1	0.9082	−4.6	0.7077	−448.9
				0.7191	−443.6
				0.7330	−427.1
				0.7565	−389.0
				0.7704	−371.2
				0.7914	−335.8
				0.8054	−318.2
				0.8262	−281.2
				0.8388	−266.4
				0.8593	−235.8
				0.8708	−215.2
				0.8898	−186.3
				0.9039	−161.4
				0.9175	−140.9
				0.9252	−126.4
				0.9371	−108.7
				0.9448	−94.0
				0.9675	−55.9
				0.9694	−53.3
				0.9852	−25.1
				0.9901	−18.6

1–3. The method of least squares was used to fit each set of results with a Redlich–Kister type of equation

$$[4] \qquad X^E = x_1(1 - x_1)\sum_{p=1}^{n} c_p(1 - 2x_1)^{p-1}$$

where X^E represents G^E, H^E, or V^E, and x_1 is the mole fraction of methanol. In treating the vapor–liquid equilibria, statistical weights, inversely proportional to the squares of their estimated errors, were assigned to the experimental quantities (x_1, y_1, p). Analyses of the results for the enthalpies and volumes assumed that the mole fractions were known accurately, and assigned equal weights to the excess quantities. The number, n, of coefficients, c_p, needed to represent the results adequately was determined for each set from an examination of the variation of the standard error of estimate defined by

$$[5] \qquad \sigma_X = [\sum(X_{obs}{}^E - X^E)^2/(n_{obs} - n)]^{1/2}$$

where the sum is taken over n_{obs} results. The least-squares values of the coefficients are summarized in Table 7, along with the value of the standard error of estimate associated with each representation. Also included in Table 7 are coefficients representing the smoothed results for the excess enthalpy and volume of the system methanol – *n*-butanol studied previously (1, 2). The continuous curves shown in Figs. 1–3 were

Can. J. Chem. Downloaded from www.nrcresearchpress.com by 210.87.254.5 on 09/05/12
For personal use only.

TABLE 5

Experimental values of the molar excess volumes of some methanol (1) – butanol (2) systems at 25 °C

Methanol – isobutanol		Methanol – *sec*-butanol		Methanol – *tert*-butanol	
x_1	V^E cm^3 mole^{-1}	x_1	V^E cm^3 mole^{-1}	x_1	V^E cm^3 mole^{-1}
0.0392	0.0110	0.0265	0.0067	0.0267	−0.0412
0.1040	0.0282	0.0783	0.0190	0.0809	−0.1014
0.1745	0.0455	0.1490	0.0353	0.1527	−0.1364
0.2679	0.0656	0.2288	0.0526	0.2340	−0.1381
0.3631	0.0823	0.3069	0.0670	0.3149	−0.1183
0.4483	0.0934	0.3828	0.0784	0.3905	−0.0912
0.5198	0.0995	0.4527	0.0857	0.4597	−0.0651
0.5787	0.1020	0.5164	0.0892	0.5231	−0.0432
0.6284	0.1017	0.5713	0.0900	0.5784	−0.0268
0.6699	0.0998	0.6188	0.0888	0.6260	−0.0156
0.7033	0.0970	0.6592	0.0864	0.6680	−0.0077
0.7316	0.0934	0.7025	0.0816	0.6882	−0.0054
0.7546	0.0877	0.7328	0.0779	0.7164	−0.0016
0.7916	0.0808	0.7656	0.0729	0.7475	0.0015
0.8287	0.0722	0.8025	0.0660	0.7815	0.0041
0.8659	0.0613	0.8403	0.0573	0.8184	0.0057
0.9020	0.0484	0.8775	0.0471	0.8575	0.0062
0.9362	0.0339	0.9122	0.0359	0.8959	0.0055
0.9636	0.0204	0.9409	0.0257	0.9320	0.0040
0.9813	0.0107	0.9641	0.0163	0.9624	0.0025
0.9931	0.0041	0.9814	0.0089	0.9833	0.0011
		0.9939	0.0027		

TABLE 6

Estimated second virial coefficients for methanol (1) – butanol (2) systems at 25 °C

System	Virial coefficients (cm^3 mole^{-1})		
	B_{11}	B_{22}	B_{12}
Methanol – *n*-butanol	−1834	−2557	−2254
Methanol – isobutanol	−1834	−2341	−2159
Methanol – *sec*-butanol	−1834	−2419	−2156
Methanol – *tert*-butanol	−1834	−1856	−1913

calculated from eq. [4] using the values of the coefficients given in Table 7.

The molar excess entropy S^E and the excess enthalpy and Gibbs free energy are related by the equation

$$[6] \qquad G^E = H^E - TS^E$$

The curves for TS^E at 25 °C, shown in Fig. 4, were calculated from this relation using the smoothed representations of the G^E and H^E results by eq. [4]. In the case of the system methanol – *tert*-butanol, this calculation neglects the deviation of the temperature for the enthalpy values from 25 °C.

Discussion

There are several theoretical formulations of the excess properties of mixtures containing associated liquids which might be considered in analysing our results. The quasi-lattice theory of Barker (10) has been used to correlate and interpret the excess properties of alcohol – carbon tetrachloride systems (11). However, application of this theory to methanol–butanol systems would require the introduction of a number of parameters (contact energies, geometric factors, etc.), and there appears to be no clear way of assigning their values. Another theoretical approach which has been used for alcohol – nonpolar solvent mixtures attributes the deviation from ideality primarily to the presence of association complexes (12–14), and expresses the excess free energy as a function of the constants describing the various equilibria. In applying this theory to methanol–butanol systems, equilibrium constants are needed not only for the self-association of each component, but also for the formation of mixed associates. The analysis is quite complicated and we were unable to reduce it to a tractable form by assuming reasonable

Can. J. Chem. Downloaded from www.nrcresearchpress.com by 210.87.254.5 on 09/05/12
For personal use only.

Can. J. Chem. Downloaded from www.nrcresearchpress.com by 210.87.254.5 on 09/05/12
For personal use only.

TABLE 7

Coefficients for least-squares fit of results by eq. [4]*

System	X^E	Coefficient c_1	c_2	c_3	c_4	c_5	σ_X
Methanol – *n*-butanol	G^E	395.0	−524.5	−464.4			12.1
	H^E†	569.66	−246.36	79.06	−35.52	17.11	0.31
	V^E‡	0.2952	−0.1700	0.0778	−0.0358		0.00030
Methanol – isobutanol	G^E	229.5	−316.4	−128.8			4.8
	H^E	605.84	−242.51	55.78			0.93
	V^E	0.3934	−0.1492	0.0451			0.00053
Methanol – *sec*-butanol	G^E	−349.1	−443.5	−285.9			10.0
	H^E	−425.11	−490.72	−53.79			0.39
	V^E	0.3535	−0.0912	0.00172	−0.0323		0.00028
Methanol – *tert*-butanol	G^E	−1204.9	−171.1	163.0			2.1
	H^E	−2669.49	−1294.21	−377.88			2.96
	V^E	−0.2017	−0.6750	−0.6265	−0.2419		0.00043

*Units: G^E and H^E, J mole^{-1}; V^E, cm^3 mole^{-1}.
†See ref. 1.
‡See ref. 2.

Can. J. Chem. Downloaded from www.nrcresearchpress.com by 210.87.254.5 on 09/05/12
For personal use only.

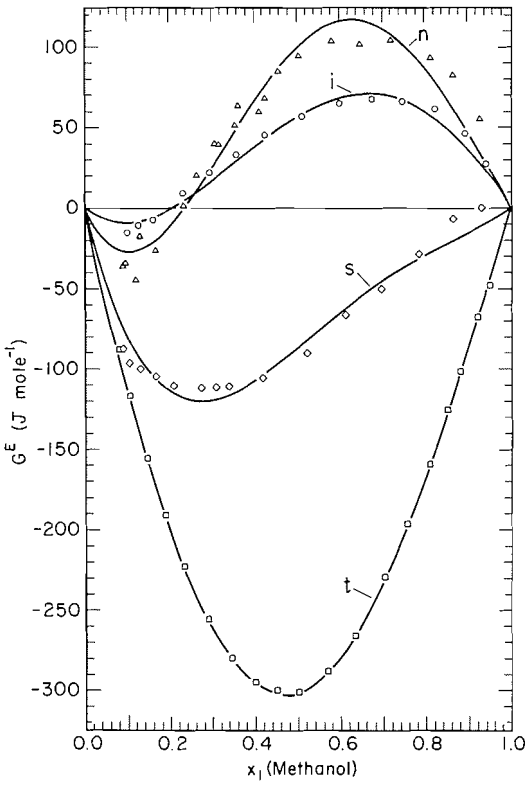

FIG. 1. Molar excess Gibbs free energies of methanol – isomeric butanol systems at 25 °C. Experimental results: △, *n*-butanol; ○, isobutanol; ◇ *sec*-butanol; □, *tert*-butanol. Curves are least-squares representations of results by eq. [4]. The labels *n*, *i*, *s*, and *t* indicate the 4 isomeric butanols.

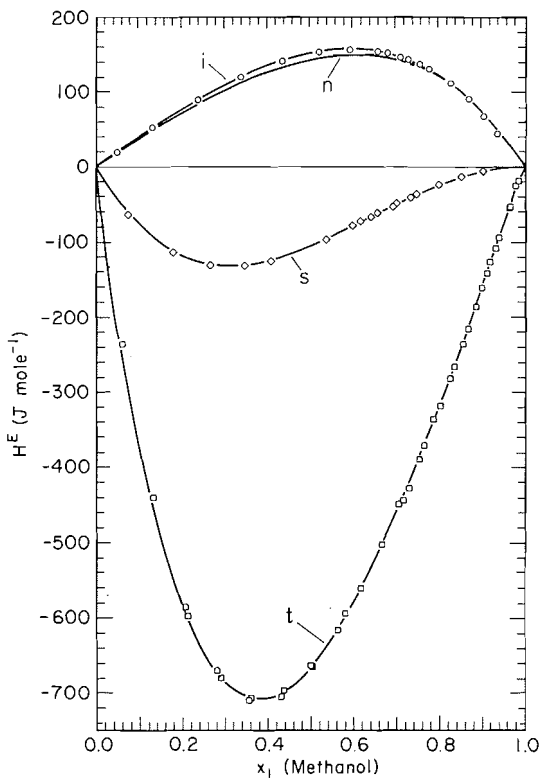

FIG. 2. Molar excess enthalpies of methanol – isomeric butanol systems. Experimental results: ○, isobutanol at 25 °C; ◇, *sec*-butanol at 25 °C; □, *tert*-butanol at 26 °C. *n*-Butanol curve from ref. 1; other curves are least-square representations of experimental results by eq. [4]. The labels *n*, *i*, *s*, and *t* indicate the 4 isomeric butanols.

relationships between the equilibrium constants. Since neither the Barker theory nor the model of an ideal associated solution proved to be adaptable to our results, only a qualitative interpretation, which of necessity is speculative in nature, can be offered at this time.

Differences in the relative behavior of the excess properties of methanol–butanol systems must reflect differences in the shapes of the component molecules and in the interactions between them. Dispersive forces in the four systems must be very similar, and we attribute the difference in the interaction mainly to differences in the strength and numbers of hydrogen bonds. Infrared spectroscopy indicates that the association of alcohols tends to decrease with increasing molecular weight and in the sequence primary > secondary > tertiary.

When an alcohol is diluted, there will be a positive contribution to H^E from the breaking of hydrogen bonds between the (like) alcohol molecules. This effect will be relatively more important at low methanol concentrations than at high where the dissociation of the (less associated) butanol polymers predominates. On the other hand, the formation of hydrogen bonds between unlike alcohol molecules will make a negative contribution to H^E. There is a variety of experimental evidence which indicates that the proton accepting facility of the oxygen atoms in the present components increases in the order *n*-butanol < isobutanol < *sec*-butanol < *tert*-butanol (15). On this basis, the formation of a mixed complex between methanol and *tert*-butanol is favored more than the one between methanol and *n*-butanol.

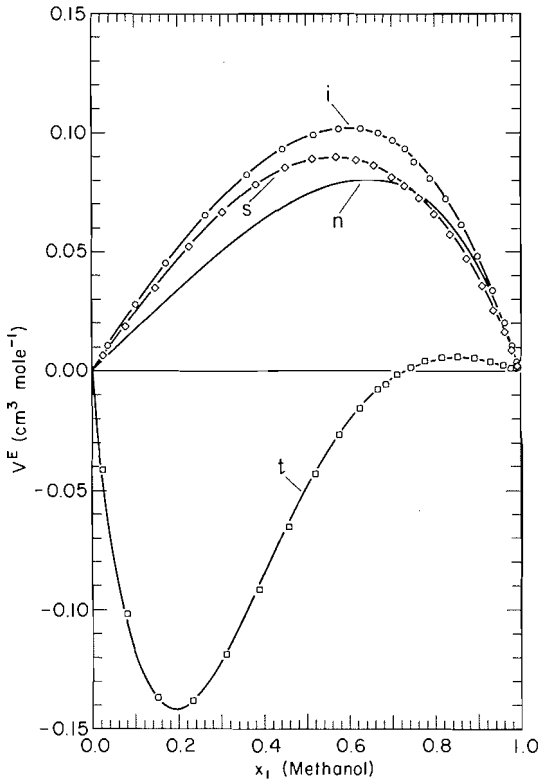

FIG. 3. Molar excess volumes of methanol – isomeric butanol systems at 25 °C. Experimental results: ○, isobutanol; ◇, *sec*-butanol; □, *tert*-butanol. *n*-Butanol curve from ref. 2; other curves are least-squares representations of experimental results by eq. [4]. The labels *n*, *i*, *s*, and *t* indicate the 4 isomeric butanols.

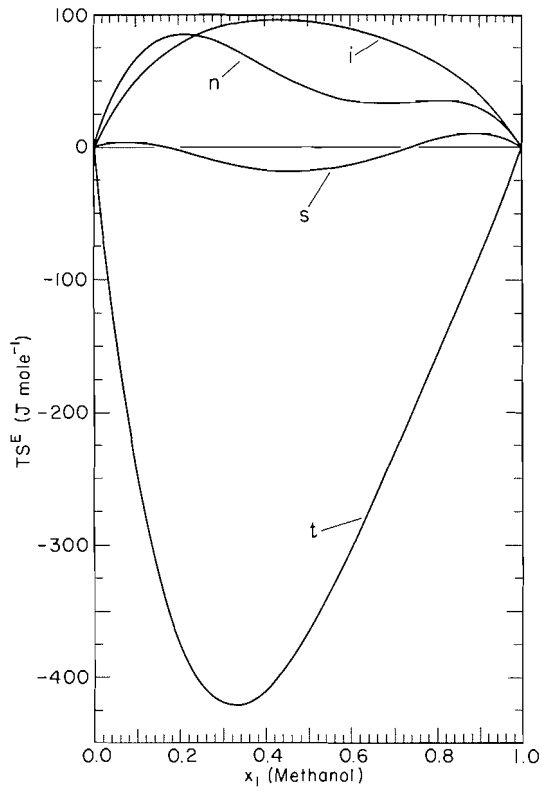

FIG. 4. Values of TS^E for methanol – isomeric butanol systems at 25 °C. The labels *n*, *i*, *s*, and *t* indicate the 4 isomeric butanols.

It appears from Fig. 2 that a fairly delicate balance exists between the breaking and forming of hydrogen bonds in our methanol–butanol systems. The breaking of bonds predominates for the *n*-butanol and isobutanol systems, which have very similar H^E curves; bond formation between unlike molecules is increasingly important in the *sec*-butanol and *tert*-butanol systems. In general, the breaking of hydrogen bonds increases the number of essentially independent particles in the mixture, and leads to a positive excess entropy. This is observed for the *n*-butanol and isobutanol systems (see Fig. 4). The entropy changes for methanol – *sec*-butanol are very small and the *tert*-butanol system shows a relatively large decrease in entropy, in line with the formation of a significant number of bonds between unlike molecules.

The sign of deviations from ideal behavior (as indicated by the curves for G^E in Fig. 1) is controlled almost completely by the energetic contribution H^E, which outweighs the entropy term in most cases. The only deviations from this pattern occur at low methanol mole fractions in the systems with *n*-butanol and isobutanol. The curves for these two systems are unusual in shape (16) since they indicate a change in sign of G^E. In the case of the system containing *n*-butanol, the negative values of G^E are fairly clearly established, since the magnitude of the minimum in G^E is larger by a factor of two than our estimate of the experimental uncertainty. Unfortunately, this is not true for the isobutanol system; at low mole fractions of methanol the errors estimated for this system are of the same magnitude as the experimental values of G^E.

The mixing of methanol with *n*-butanol, isobutanol, and *sec*-butanol leads to very similar positive values of V^E (See Fig. 3). The sign of this effect appears to be a fairly natural consequence

Can. J. Chem. Downloaded from www.nrcresearchpress.com by 210.87.254.5 on 09/05/12
For personal use only.

of the breakdown of linear alcohol polymers in the methanol – *n*-butanol and methanol – isobutanol systems. Similar considerations suggest that negative values of V^E should occur when there is appreciable bonding between unlike molecules, as in the *sec*-butanol and *tert*-butanol systems. The anomalous positive excess volumes observed for the *sec*-butanol system may be due to a steric effect which gives rise to a more bulky packing in these mixtures.

It is interesting to compare the excess function behavior of methanol–butanol systems with that of alcohol–water systems (e.g. ethanol–water, *tert*-butanol – water, etc.) reviewed recently by Franks and Ives (17). It appears that deviations from ideality in the latter systems are controlled by entropy effects, in contrast to those of the present systems for which the H^E term dominates. This difference is due to structural effects which are peculiar to aqueous solutions, and according to which, water molecules tend to form "icebergs" around the hydrophobic parts of other molecules.

We are indebted to Mr. C. J. Halpin for carrying out the chromatographic purification of the component alcohols and to Mr. P. J. D'Arcy for technical assistance during the calorimetric and dilatometric measurements.

1. A. E. Pope, H. D. Pflug, B. Dacre, and G. C. Benson. Can. J. Chem. **45**, 2665 (1967).
2. H. D. Pflug and G. C. Benson. Can. J. Chem. **46**, 287 (1968).
3. J. Singh and G. C. Benson. Can. J. Chem. **46**, 1249 (1968).
4. Amer. Petrol. Inst. Res. Proj. 44. Selected values of properties of hydrocarbons and related compounds. Texas A and M University, College Station, Texas.
5. T. Boublík and G. C. Benson. Can. J. Chem. **47**, 539 (1969).
6. J. Polák, S. Murakami, V. T. Lam, and G. C. Benson. J. Chem. Eng. Data, **15**, 323 (1970).
7. S. Murakami and G. C. Benson. J. Chem. Thermodyn. **1**, 559 (1969).
8. A. P. Kudchadker, G. H. Alani, and B. J. Zwolinski. Chem. Rev. **68**, 659 (1968).
9. J. P. O'Connell and J. M. Prausnitz. Ind. Eng. Chem. Process Des. Develop. **6**, 245 (1967).
10. J. A. Barker. J. Chem. Phys. **20**, 1526 (1952).
11. B. Dacre and G. C. Benson. Can. J. Chem. **41**, 278 (1963).
12. O. Redlich and A. T. Kister. J. Chem. Phys. **15**, 849 (1947).
13. C. B. Kretschmer and R. Wiebe. J. Chem. Phys. **22**, 1697 (1954).
14. H. Renon and J. M. Prausnitz. Chem. Eng. Sci. **22**, 299 (1967). Erratum, Chem. Eng. Sci. **22**, 1891 (1967).
15. W. Gerrard and E. D. Macklen. Chem. Rev. **59**, 1105 (1959).
16. M. L. McGlashan. J. Chem. Educ. **40**, 516 (1963).
17. F. Franks and D. J. G. Ives. Quart. Rev. London, **20**, 1 (1966).

Can. J. Chem. Downloaded from www.nrcresearchpress.com by 210.87.254.5 on 09/05/12
For personal use only.

Can. J. Chem. Downloaded from www.nrcresearchpress.com by 210.87.254.105 on 09/05/12
For personal use only.

Radiation-induced oxidation of alcohols by Tl(III) in acid aqueous solution

C. E. BURCHILL AND G. G. HICKLING
Department of Chemistry, University of Manitoba, Winnipeg 19, Manitoba

Received February 17, 1970

In deaerated aqueous perchloric acid solution Tl(III) is reduced and 2-propanol oxidized to acetone in essentially equivalent yields by a γ-ray induced chain reaction. The yields increase linearly with increasing alcohol concentration in the range (1–8) × 10^{-2} *M*, are independent of Tl(III) concentration in the range (1–4) × 10^{-3} *M* and vary inversely with the square root of the dose rate over the range 1.6 × 10^{17} to 1.8 × 10^{19} eV l^{-1} s^{-1}. A mechanism is proposed to account for the observed stoichiometry and kinetic parameters.

The same mechanism is found to apply to the reduction of Tl(III) by methanol and ethanol. *t*-Butyl alcohol gives a much lower yield of Tl(III) reduction and alcohol fragmentation products: acetone, methane, and ethane.

Canadian Journal of Chemistry, **48**, 2466 (1970)

Introduction

The radiation-induced reduction of Tl(III) in acid aqueous solution has been reported by Lefort and Tarrago (1). As reported by these authors, and confirmed in this study, $G(-Tl^{3+}) \sim 1.0$–1.2. It was also reported that in the presence of H_2O_2 or organic impurities the initial $G(-Tl^{3+}) > 10$ which implies the existence of a chain reaction. We now report an investigation of this chain reduction of Tl(III) by 2-propanol in deaerated aqueous perchloric acid solution. The results are compared with those obtained when ethanol, methanol, and *t*-butyl alcohol are the oxidizable substrates.

Experimental

Materials

Water was purified by double redistillation of laboratory distilled water, first from alkaline $KMnO_4$ solution and then from acid $K_2Cr_2O_7$ solution, in each case through 60 cm reflux columns packed with cut Pyrex tubing.

Tl_2O_3 (Fisher, purified), *$TlClO_4$* (City Chemical, purified), *ethanol* (Canadian Industrial Alcohols and Chemicals, absolute), *$HClO_4$* (Baker and Adamson, reagent, A.C.S., 70%) were used as received for the preparation of solutions for irradiation. The remaining starting materials (*2-propanol*, *methanol*, *t-butyl alcohol*) were Fisher Certified Reagent grade and were used as received.

Reagents used in all analytical procedures were Fisher Certified Reagent grade with the exception of *o*-phenylenediamine (Eastman, practical) which was dissolved in hot triply distilled water, filtered and recrystallized twice from aqueous solution.

Radiation Sources and Dosimetry

Gamma rays from ^{60}Co were used in all experiments with most of the experiments being carried out in a Gammacell 220 irradiation facility. In the sample position used the dose rate to the sample was approximately 1.8 × 10^{19} eV l^{-1} s^{-1}. A cylindrical lead attenuator was employed to reduce the dose rate to a nominal 30% of the normal value for studies of dose-rate effects. A few experiments at very low dose rates were carried out at the Manitoba Cancer Research Foundation using a radiation therapy source providing a dose rate of 1.6 × 10^{17} eV l^{-1} s^{-1}.

Dosimetry for all sources and sample positions was based on the measured oxidation of Fe^{2+} to Fe^{3+} in aerated 0.8 *N* H_2SO_4 solution. Fe^{3+} was measured as the change in absorbance at 304 nm assuming a molar absorbancy of 2200 M^{-1} cm^{-1}. The dose rate was calculated from the slope of linear yield vs. time plots having a minimum of five points and assuming $G(Fe^{3+}) = 15.6$ (2).

Absorbed doses were corrected for the time decay of the ^{60}Co source assuming a half-life of 5.27 yr (3) and for differences in electron density between the samples and the dosimeter solution on the assumption that all energy transfer to the absorber was by Compton scattering.

Sample Preparation

Tl_2O_3 was dissolved in hot $HClO_4$ solution and diluted with water to prepare a stock solution 2.0 × 10^{-2} *M* in Tl(III) and 3.7 *M* in $HClO_4$. Aliquots of this solution together with any other desired solutes were then quantitatively diluted with water to give solutions of a particular initial Tl(III) concentration. In a few cases solutions were prepared from $Tl(ClO_4)_3 \cdot 6H_2O$ (City Chemical, purified) with no significant change in the results.

Aliquots of 10 ml volume were placed in 25 ml sample bulbs (4 to 6 samples for each experiment) which were closed by demountable vacuum stop-cocks and degassed by the freeze–pump–thaw technique. No attempt was made to thermostat the Gammacell sample chamber during irradiation since it was felt that during the short times involved (< 1 min) the sample temperature would not vary significantly. Irradiation temperature was assumed to be 23 ± 2 °C.

Analytical Procedures

Tl(III) was determined spectrophotometrically by its oxidation of *o*-phenylenediamine as described by Papafil, Furnica, and Furnica (4). The p*H* of the solution was adjusted to 2.3 ± 0.1 with sodium acetate. The method was calibrated by oxidation of Tl_2SO_4 (British Drug

Can. J. Chem. Downloaded from www.nrcresearchpress.com by 210.87.254.105 on 09/05/12
For personal use only.

Houses, Analar) with Br_2 in hot $HClO_4$ solution followed by cooling, addition of excess Br_2 to ensure complete oxidation, and removal of excess Br_2 by bubbling with air for 1 h while the solution was maintained in an ice bath. The molar absorbancy determined at 460 nm was $(7.3 \pm 0.1) \times 10^3\ M^{-1}\ cm^{-1}$.

Acetone was determined by the salicylaldehyde method (5) using a slight modification of Berntsson's recommendations. The final volume after dilution was 25 ml, the quantity of salicylaldehyde was 0.25 ml and NaOH solution (106.25 g/250 ml) was added in two aliquots, one of 1.0 ml and one of 10.0 ml. Calibration using Fisher Certified Reagent acetone, with or without redistillation, gave a molar absorbancy at 474 nm of $(1.80 \pm 0.04) \times 10^4\ M^{-1}\ cm^{-1}$. The determination was unaffected by either $HClO_4$ or 2-propanol in amounts equivalent to those in the experimental solutions. In the analysis of acetone in the presence of unreduced Tl(III) a fine but stable suspension of thallic oxide formed and it was necessary to correct the apparent absorbance due to acetone for the light scattered by this suspension. The correction was based on the concentration of Tl(III) measured as previously described and an effective molar absorbancy of the oxide suspension of $1.4 \times 10^3\ M^{-1}\ cm^{-1}$ at 474 nm. The correction required was thus less than 10%.

Formaldehyde was qualitatively identified using a modified Schiff's reagent (6).

Acetaldehyde analysis was accomplished using nitroprusside and piperidine (7). Because of the rapid fading of the color the reaction was carried out directly in a spectrophotometer cell. To the cuvette were added, in turn, 0.25 ml of sodium nitroprusside solution, a 2.0 ml aliquot of the test solution and 0.25 ml of piperidine; the contents mixed rapidly and the absorbance measured within 10 s with reference to a water blank. The molar absorbancy measured was $(2.6 \pm 0.4) \times 10^3\ M^{-1}\ cm^{-1}$ at 575 nm.

All spectrophotometric measurements were made on a Zeiss PMQ-II spectrophotometer. In a few instances qualitative identification of gaseous products (volatile at Dry Ice/acetone temperature) was made using a Hitachi Perkin–Elmer RMU-6D mass spectrometer.

Results

Preliminary Experiments

In an air-saturated solution $2 \times 10^{-3}\ M$ in Tl(III) and $0.37\ M$ in $HClO_4$ the reduction of Tl(III) was linear with absorbed dose and corresponded to $G(-\ Tl^{3+}) = 1.08$. With the addition of $4 \times 10^{-3}\ M$ $TlClO_4$ the reduction remained linear with dose and $G(-\ Tl^{3+})$ was 0.93. Deaeration of the solutions before irradiation produced no significant change. These results are in good agreement with those of Lefort and Tarrago (1) whose mechanism predicts the stoichiometry of Tl(III) reduction to be $G(-\ Tl^{3+}) = \frac{1}{2}\ G_H + G_{H_2O_2} - \frac{1}{2}\ G_{OH}$.

Preliminary experiments employing deaerated solutions $2 \times 10^{-3}\ M$ in Tl(III), $0.3\ M$ in $HClO_4$, and containing $1 \times 10^{-2}\ M$ 2-propanol gave $G(-\ Tl^{3+})$ of the order of 30, clear indication of a chain reaction. In any particular experiment the reduction of Tl(III) was linear with absorbed dose to better than half the reduction of the thallium and there was very little scatter of the points from the best-fit straight line. However, lack of good reproducibility of the slopes of the yield–dose plots between different experiments suggested inhibition by some adventitious impurity.

An air-saturated solution of the same composition as those above gave $G(-\ Tl^{3+})$ of the order of 10 indicating that O_2 is an inhibitor of the chain reaction. However, more rigorous degassing of the samples failed to improve the reproducibility and it was considered improbable that the degassing procedure would leave identical O_2 concentrations in one set of six samples but a different concentration in another set. The addition of $10^{-4}\ M$ $FeSO_4$ was found to inhibit the chain reaction almost completely. Cr^{3+}, free Hg, and H_2SO_4 were found to have no inhibiting effect.

Eventually, through careful attention to the cleaning of glassware and handling of solutions a reasonable degree of reproducibility was obtained; whether by elimination of inhibiting impurities or by obtaining a reproducible impurity level may be argued. For a particular experiment the scatter of the points generally corresponded to an uncertainty in the slope of $< \pm 5\%$ but the reproducibility of this slope in replicate experiments corresponded to a standard deviation for a single slope determination of $\pm 20\%$. On the assumption that impurity effects had been largely eliminated the effects of concentration and dose rate on the chain yield were investigated.

Reduction of Tl(III) by 2-Propanol

With 2-propanol as the oxidizable substrate the only organic product identified was acetone. The results for a particular solution are shown in Fig. 1. Under continued irradiation the yield–dose plots became somewhat non-linear, $G(-\ Tl^{3+})$ decreasing after the concentration of Tl(III) was reduced below $5 \times 10^{-4}\ M$. The results of the remaining experiments are given in Table 1. The major conclusions are outlined below.

TABLE 1

G values for the radiation-induced reduction of Tl(III) by 2-propanol in deaerated aqueous solution

[Tl(III)] (10^{-3} *M*)	[2-Propanol] (10^{-2} *M*)	Other solutes	Dose rate (10^{18} eV l^{-1} s^{-1})	$G(-Tl^{3+})$*	*G*(Acetone)*
2	2.0	0.37 *M* $HClO_4$	17.5	41 ± 9†	—
2	4.0	"	"	81 ± 15†	78 ± 14
2	5.9	"	"	88 ± 18	93 ± 18
2	8.1	"	"	159 ± 32	169 ± 34
4	1.0	0.74 *M* $HClO_4$	17.5	25 ± 5	—
4	2.0	"	"	39 ± 8	—
4	4.0	"	"	71 ± 14	—
4	8.1	"	"	165 ± 33	196 ± 40
2	4.0	0.37 *M* $HClO_4$	4.59	162 ± 34	151 ± 30
2	4.1	0.37 *M* $HClO_4$	0.16	680 ± 130	—
2	4.1	0.37 *M* $HClO_4$ + 4 × 10^{-3} *M* Tl^+	18.1	76 ± 15	—
2	5.9	0.37 *M* $HClO_4$ + 2 × 10^{-3} *M* Tl^+	16.7	81 ± 16	94 ± 19

*All *G* values calculated from linear yield–dose plots having a minimum of four points.
†Standard deviation for a single trial based on four or more experiments. Remaining *G* values based on single experiments with relative uncertainty assumed to be the same.

(*1*). The initial value of $G(-Tl^{3+})$ was independent of the initial concentration of Tl(III) (2 or 4 × 10^{-3} *M*) and the reduction remained linear with absorbed dose to $[Tl^{3+}] \leqslant 1 \times 10^{-3}$ *M*.

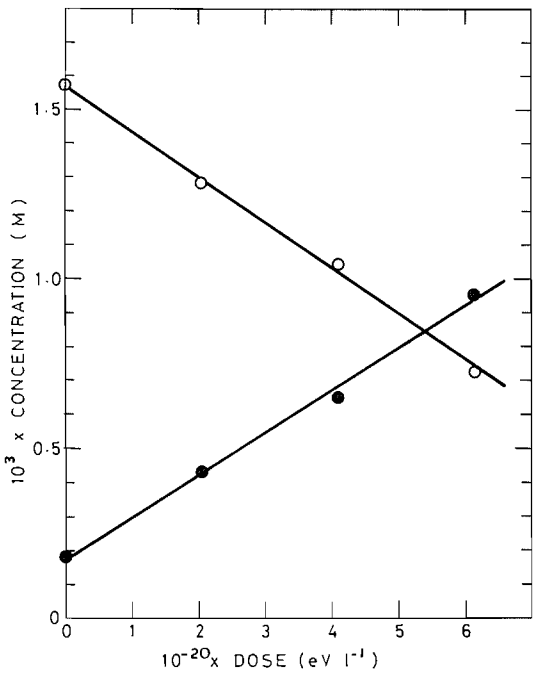

FIG. 1. Yield–dose plot for γ-irradiation of an aqueous perchloric acid solution of Tl(III) and 2-propanol ○, Tl(III); ●, acetone. [2-Propanol] = 4 × 10^{-2} *M*, dose rate = 1.71 × 10^{19} eV l^{-1} s^{-1}.

(*2*). $G(-Tl^{3+})$ increased with increasing concentration of 2-propanol and, as is demonstrated in Fig. 2, this increase is essentially linear over the range (1–8) × 10^{-2} *M*.

(*3*). The chain length increases with decreasing dose rate. For solutions containing 4.0 × 10^{-3} *M* Tl(III) and 4.0 × 10^{-2} *M* 2-propanol Fig. 3 demonstrates that $G(-Tl^{3+})$ varies inversely with the square root of the dose rate over a hundred-fold variation of the dose rate.

(*4*). In all cases where the formation of acetone was measured the yield of acetone was sensibly equal to that of Tl(III) reduction.

(*5*). The addition of Tl(I) to the solutions did not significantly alter the yields of Tl(III) reduction or acetone formation.

Reduction by Other Alcohols

1. Methanol and Ethanol

With methanol as the oxidizable substrate the results obtained were entirely analogous to those for 2-propanol. Although a quantitative analysis for formaldehyde was not attempted its presence was qualitatively established in the irradiated solutions. The yields for Tl(III) reduction are given in Table 2 and the salient features are the same as those for 2-propanol: $G(-Tl^{3+})$ is independent of the initial concentration of Tl(III), increases with increasing alcohol concentration and increases with a decrease in dose rate.

Only acetaldehyde was identified as an organic

Can. J. Chem. Downloaded from www.nrcresearchpress.com by 210.87.254.105 on 09/05/12
For personal use only.

TABLE 2

G values for the radiation-induced reduction of Tl(III) by methanol in deaerated aqueous solution

[Tl(III)] (10^{-3} *M*)	[Methanol] (10^{-2} *M*)	Other solutes	Dose rate (10^{18} eV l^{-1} s^{-1})	$G(-Tl^{3+})$*
2	2.0	0.37 *M* $HClO_4$	17.7	33.0±7.5†
2	4.0	"	"	67.8±11.7†
2	10.0	"	"	236±47
4	4.0	0.74 *M* $HClO_4$	17.7	68±14
2	4.0	0.37 *M* $HClO_4$	4.74	140±40
2	10.0	0.37 *M* $HClO_4$	4.74	364±73

*All *G* values calculated from linear yield–dose plots having a minimum of four points.
†Standard deviation for a single trial based on four or more experiments. Remaining *G* values based on single experiments with relative uncertainty assumed to be the same.

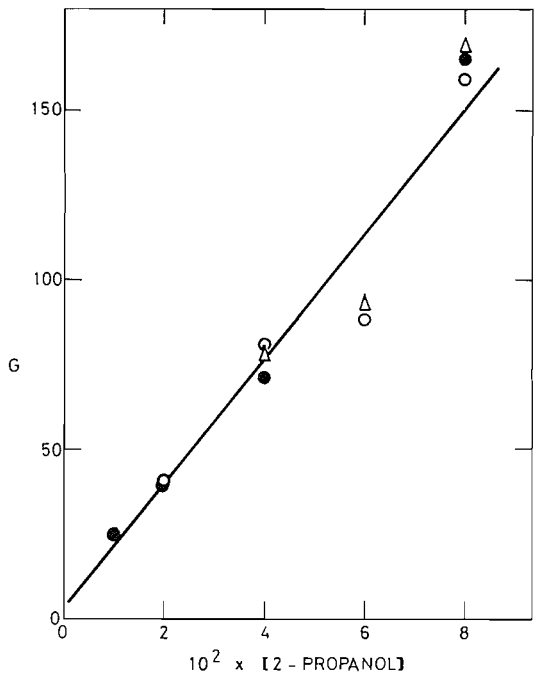

FIG. 2. Variation of yields with 2-propanol concentration: ○, $G(-Tl^{3+})$; △, *G*(acetone): $[Tl^{3+}]^\circ = 2 \times 10^{-3}$ *M*. ●, $G(-Tl^{3+})$: $[Tl^{3+}]^\circ = 4 \times 10^{-3}$ *M*.

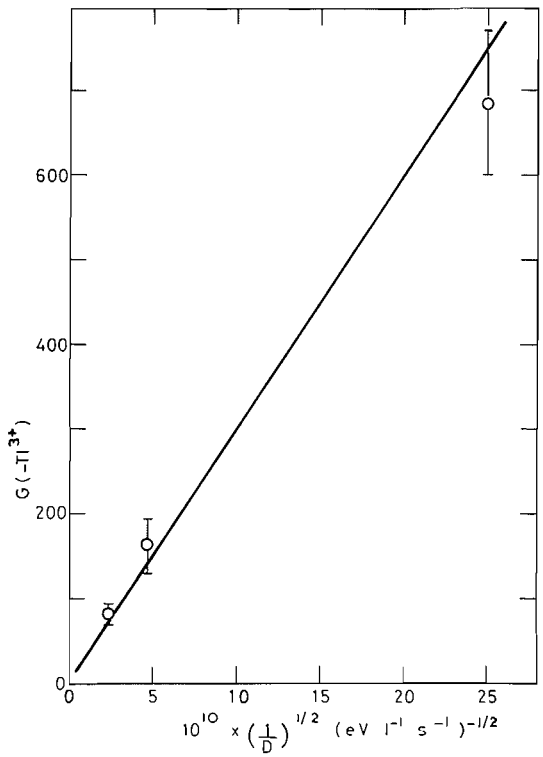

FIG. 3. Variation of yield with dose rate. [2-Propanol] = 4×10^{-2} *M*, $[Tl^{3+}]^\circ = 2 \times 10^{-3}$ *M*.

product in the reduction of Tl(III) by ethanol. The analysis for acetaldehyde is not considered to be fully quantitative and the failure to observe a good stoichiometric relationship between $G(-Tl^{3+})$ and $G(CH_3CHO)$ may, in part, be attributed to the uncertainty in the analysis rather than a real difference in the yields. The results for ethanol are outlined in Table 3. Considering $G(-Tl^{3+})$ as the most reliable data the parallelism with the results for 2-propanol and methanol in terms of concentration and dose-rate dependence is clear.

2. t-Butyl Alcohol

In solutions containing *t*-butyl alcohol the yields of Tl(III) reduction were an order of magnitude less than those for a corresponding

Can. J. Chem. Downloaded from www.nrcresearchpress.com by 210.87.254.105 on 09/05/12
For personal use only.

TABLE 3

G values for the radiation-induced reduction of Tl(III) by ethanol in deaerated aqueous solution

$[Tl^{3+}]$ $(10^{-3}\ M)$	[Ethanol] $(10^{-2}\ M)$	Other solutes	Dose rate (10^{18} eV l^{-1} s^{-1})	$G(-\ Tl^{3+})$*	*G*(Acetaldehyde)*
2	1.0	0.37 *M* $HClO_4$	16.9	39±8†	—
2	2.0	"	"	65±13	66
2	4.2	"	"	108±22	59
2	6.2	"	"	209±42	318
2	4.2	0.37 *M* $HClO_4$	4.52	206±42	—

*All *G* values calculated from linear yield–dose plots having a minimum of four points.
†Uncertainty assumed on the basis of replicate experiments using 2-propanol and methanol.

solution containing 2-propanol although still somewhat greater than those which could be attributed to a non-chain process. The effects of alcohol concentration and dose rate on $G(-\ Tl^{3+})$ are shown in Fig. 4. There is evidence for some dependence of the yield on alcohol concentration but the effect is much less than that for the other alcohols used and in this case there is no significant dependence on dose rate.

A carbonyl product was formed in these solutions as demonstrated by the formation of a yellow product with salicylaldehyde in alkaline solution. Although this test is not specific for acetone, other simple carbonyl compounds have significantly lower molar absorbancies (for methyl-ethyl ketone $\varepsilon_{460} = 1.05 \times 10^3\ M^{-1}\ cm^{-1}$). If this product is assumed to be acetone its yield, where measured, was very close to that of Tl(III) reduction. Other simple carbonyl compounds would require that the *G* value for their formation be many times greater to give the same absorbance. This latter suggestion was considered unlikely.

Mass spectrometric examination of gaseous products from the reaction yielded cracking patterns characteristic of both methane and ethane. Quantitative measurements of these products were not made.

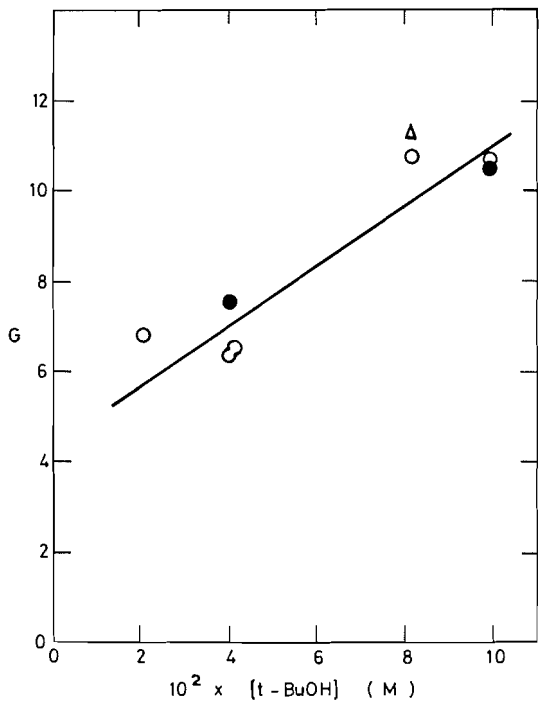

FIG. 4. Radiation-induced reduction of Tl^{3+} by *t*-butyl alcohol. ○, $G(-\ Tl^{3+})$; △, *G*(acetone): dose rate = 1.73×10^{19} eV l^{-1} s^{-1}. ●, $G(-\ Tl^{3+})$; dose rate = 4.67×10^{18} eV l^{-1} s^{-1}.

Discussion

Aside from the passing reference by Lefort and Tarrago (1), we have found no previously published study of the radiation-induced reduction of Tl(III) in the presence of organic materials. The homogeneous thermal reduction of Tl(III) by organic materials in acid aqueous solution has been studied only for the case of formic acid as the oxidizable substrate (8, 9).

The inorganic redox reactions of the Tl(III)/Tl(I) couple have been reported by a number of authors (10). It is generally concluded that, particularly for reactions with one-equivalent substrates, the oxidation of Tl(I) or reduction of Tl(III) proceeds via the formation of a Tl(II) intermediate. From studies of the electrolytic redox processes of Tl(I) and Tl(III) (11, 12), it has been concluded that the rate of the disproportionation reaction

[1] $$2\ Tl(II) \rightarrow Tl(I) + Tl(III)$$

is greater than the rates of the electron transfer processes represented by

Can. J. Chem. Downloaded from www.nrcresearchpress.com by 210.87.254.105 on 09/05/12
For personal use only.

Can. J. Chem. Downloaded from www.nrcresearchpress.com by 210.87.254.105 on 09/05/12
For personal use only.

[2] $Tl(III) + e^- \rightleftharpoons Tl(II)$

[3] $Tl(II) + e^- \rightleftharpoons Tl(I)$

It was also concluded that the standard electrode potential for reaction [3] is greater than that for the Tl(III)/Tl(I) couple; i.e. that Tl(II) is a stronger oxidant than Tl(III).

Radiation chemical reactions proposed for aqueous solutions containing Tl species also invoke the formation of a Tl(II) intermediate. Thus oxidation of Tl(I) by OH radicals is assumed to lead to the formation of Tl(II) (13, 14) as is the reduction of Tl(III) by H or HO_2 (1). In the pulse radiolysis of aqueous solutions of Tl_2SO_4 (15) a transient species with an absorption maximum in the region of 260 nm is observed which decays with second order kinetics. This transient is assigned to a Tl(II) species and, with certain assumptions as to the mechanism and yield of its formation, the bimolecular rate constant for its decay is estimated to be $2.3 \times 10^9\ M^{-1}\ s^{-1}$. This result is in accord with the suggestion by Catherino and Jordan (11) of a rapid disproportionation reaction.

The greater electrode potential for the reduction of Tl(II) compared to that for Tl(III) was also invoked by Lefort and Tarrago (1) to explain the radiation-induced chain reduction of Tl(III) by H_2O_2. They proposed that, although the thermal reduction of Tl(III) by H_2O_2 was slow, Tl(II) formed as an intermediate would initiate a chain reaction via the sequence

[4] $Tl(II) + H_2O_2 \rightarrow Tl(I) + H^+ + HO_2$

[5] $HO_2 + Tl(III) \rightarrow H^+ + O_2 + Tl(II)$

A mechanism is now proposed to account for the chain reduction of Tl(III) under γ-irradiation by primary and secondary alcohols. For convenience, and because the data are more complete for this system, the mechanism is outlined for the case of 2-propanol.

In the solutions employed the energy deposition from γ-rays is primarily in the water as the preponderant species. Thus the initial processes may be represented simply as the radiation decomposition of water.

[6] $H_2O \rightsquigarrow H, e_{aq}^-, OH, H_2, H_2O_2, H_3O^+$

In these strongly acidic solutions e^-_{aq} would be converted rapidly to H by the reaction

[7] $e_{aq}^- + H_3O^+ \rightarrow H_2O + H$

so that the significant primary free-radical products of this interaction may be represented as H and OH.

Both H and OH react with 2-propanol by H atom abstraction, primarily from the α position

[8] $H + (CH_3)_2CHOH \rightarrow H_2 + (CH_3)_2\dot{C}OH$

[9] $OH + (CH_3)_2CHOH \rightarrow H_2O + (CH_3)_2\dot{C}OH$

Radicals of this type are known to reduce oxidizing metal ions (16) and thus their subsequent reactions in this system would be expected to be

[10] $(CH_3)_2\dot{C}OH + Tl(III) \rightarrow (CH_3)_2CO + H^+ + Tl(II)$

Disproportionation of Tl(II) would yield a net reduction of Tl(III) but not a chain reaction. However, reaction of Tl(II) with the alcohol by H atom abstraction (analogous to the reaction with H_2O_2 proposed by Lefort and Tarrago) would lead to a chain reaction.

[11] $Tl(II) + (CH_3)_2CHOH \rightarrow Tl(I) + H^+ + (CH_3)_2\dot{C}OH$

Chain termination could occur in a number of ways, the most probable being

[1] $2\ Tl(II) \rightarrow Tl(I) + Tl(III)$

[12] $2\ (CH_3)_2\dot{C}OH \rightarrow (CH_3)_2CHOH + (CH_3)_2CO$

[13] $Tl(II) + (CH_3)_2\dot{C}OH \rightarrow Tl(I) + H^+ + (CH_3)_2CO$

However, termination by reaction [12] would result in a chain-length dependent upon [Tl(III)] and independent of $[(CH_3)_2CHOH]$, whereas in the concentration range investigated the converse was found. Termination by reaction [13] is similarly excluded on the basis of the observed concentration effects.

Attributing the over-all reaction to the sequence of reactions [6] through [11] with reaction [11] as the rate-determining step in the chain propagation in competition with reaction [1] as the chain terminating step, and applying the usual steady-state assumptions, the proposed mechanism gives

[14] $$G(-Tl^{3+}) = 1/2\,(G_H + G_{OH}) + k_{11}(G_H + G_{OH})^{1/2}\,(2k_1 D)^{-1/2} \times [(CH_3)_2CHOH]$$

Can. J. Chem. Downloaded from www.nrcresearchpress.com by 210.87.254.105 on 09/05/12
For personal use only.

[15] $$G(\text{acetone}) = G_H + G_{OH} + k_{11}(G_H + G_{OH})^{1/2}(2k_1 D)^{-1/2} \times [(CH_3)_2CHOH]$$

where D is the dose rate in units of 6.023×10^{25} eV l^{-1} s^{-1}. In both cases the yield expression consists of two parts: a chain term, $k_{11}(G_H + G_{OH})^{1/2}(2k_1 D)^{-1/2}[(CH_3)_2CHOH]$, which is common to both, and a non-chain term whose magnitude is determined by the stoichiometry of the initiation and termination reactions. For moderate chain lengths these latter are small in comparison with the chain term and their difference, $\frac{1}{2}(G_H + G_{OH}) = 3.4$, is less than the uncertainty in the experimental results. This mechanism thus accounts for the equivalence of acetone formation and thallium reduction, the linear dependence of the yields on alcohol concentration and the reciprocal square-root dose-rate dependence observed experimentally.

In the mechanism as outlined, all H atoms are assumed to react via reaction [8]. In view of the high rate of reaction of H with oxidizing metal ions (17), it is probable that a fraction of these would react directly with Tl(III).

[16] $$H + Tl(III) \rightarrow H^+ + Tl(II)$$

This reaction leads to formation of Tl(II) directly rather than indirectly through the intermediate organic radical, the chain term in the yield expressions is unaltered, but the non-chain term for the acetone yield would be reduced by an amount

$$G_H(1 + k_8[(CH_3)_2CHOH]/k_{16}[Tl(III)])^{-1}$$

which would not significantly alter the yields.

As Tl(III) is reduced to Tl(I), the product could begin to compete with the alcohol for OH radicals via the reaction

[17] $$OH + Tl(I) \rightarrow OH^- + Tl(II)$$

but such a reaction again leads to the formation of a Tl(II) intermediate and the yields are altered only in the non-chain term by an amount

$$G_{OH}(1 + k_9[(CH_3)_2CHOH]/k_{17}[Tl(I)])^{-1}$$

This is again in agreement with the experimental observation that the addition of Tl(I) in concentrations equal to or greater than that of Tl(III) did not significantly affect the yields.

One species whose reactions have not been considered in the over-all mechanism is H_2O_2. It was established in control experiments that the thermal reduction of Tl(III) by H_2O_2 is very slow. Lefort and Tarrago (1) postulated that the reaction

[4] $$Tl(II) + H_2O_2 \rightarrow Tl(I) + H^+ + HO_2$$

was rapid but, in the systems here employed, such a reaction would be in competition with reaction [11].

[11] $$Tl(II) + (CH_3)_2CHOH \rightarrow Tl(I) + H^+ + (CH_3)_2COH$$

It is probable that the H_2O_2 accumulates in the solution without reaction. In those solutions where a chain reaction was observed the maximum dose to a sample was $< 6 \times 10^{20}$ eV l^{-1} and the maximum concentration of H_2O_2 which could accumulate would be $< 7 \times 10^{-6}$ M. At this concentration the thermal reaction with Tl(III) would be vanishingly slow and the probability of its competition with $(2\text{–}8) \times 10^{-2}$ M alcohol for Tl(II) very small. It is possible that the curvature of the yield–dose plots at low Tl(III) concentration is a result of the reaction of accumulated H_2O_2 since the ultimate product of its oxidation is O_2, which was demonstrated to inhibit the chain reaction.

The radiation-induced reduction of Tl(III) by methanol and ethanol may be attributed to the same mechanism with the substitution of the corresponding H atom abstraction reactions to give the radicals $\dot{C}H_2OH$ and $CH_3\dot{C}HOH$, with the ultimate oxidized product being formaldehyde and acetaldehyde, respectively. Although the data are less complete for these systems, the same linear dependence of the reduction yield on alcohol concentration and reciprocal square-root dependence on dose rate are observed.

It is evident from the nature of the organic products formed and from the lack of dose-rate dependence that the radiation-induced reaction of Tl(III) with *t*-butyl alcohol proceeds by a mechanism which is significantly different from that with primary and secondary alcohols. We are unable to postulate a simple mechanism for these reactions at this time. The yield of Tl(III) reduction with *t*-butyl alcohol ($G \sim 10$) is, however, somewhat larger than might be anticipated for a non-chain process.

From the yield expressions derived for the oxidation of primary and secondary alcohols (eqs. [14] and [15]) the slope of the graph of

$G(-Tl^{3+})$ vs. [alcohol] is equal to $k_{11}(G_H + G_{OH})^{1/2}(2k_1D)^{-1/2}$. G_H and G_{OH} may be taken to be 3.7 and 3.0, respectively, for these acidic solutions (18) and it is thus possible to estimate a value for $k_{11}(2k_1)^{-1/2}$. From the data of Table 1 at a dose rate of 1.75×10^{19} eV l^{-1} s^{-1}, $k_{11}(2k_1)^{-1/2} = (4.2 \pm 0.3) \times 10^{-1}$ for 2-propanol. (Similarly for methanol and ethanol, the respective values are $(5.0 \pm 0.7) \times 10^{-1}$ for methanol and $(6.4 \pm 0.9) \times 10^{-1}$ for ethanol).

The most significant feature of these ratios is their similarity for the three alcohols. The values for 2-propanol and methanol are, within the estimated probable uncertainty, equal while that for ethanol is only marginally greater. Using the value of $k_1 = 2.3 \times 10^9$ M^{-1} s^{-1} obtained in the pulse radiolysis study (15) gives $k_{11} = (2.8 \pm 0.2) \times 10^4$ for 2-propanol.

The authors gratefully acknowledge financial support for this project from the University of Manitoba Graduate Research Fund and the National Research Council of Canada.

We also wish to express our thanks to Dr. A. F. Holloway of the Manitoba Cancer Treatment and Research Foundation for assistance in performing the low dose-rate experiments and to Dr. C. Reichert for obtaining mass spectra.

1. M. Lefort and X. Tarrago. J. Chim. Phys. **57**, 38 (1960).
2. A. O. Allen. Radiation chemistry of water and aqueous solutions. Van Nostrand, Princeton. 1958. pp. 21–22.
3. Decay correction from tables supplied by Atomic Energy of Canada, Ltd., Commercial Products Division.
4. M. Papafil, M. Furnica, and D. Furnica. Analele Stiint. Univ. "Al. I. Cuza," Iasi, Sect. Ic., Chim **11**, 133 (1965).
5. S. Berntsson. Anal. Chem. **28**, 1337 (1956).
6. J. F. Walker. Formaldehyde. 3rd. ed. Reinhold, New York. 1964. p. 468.
7. H. Haglund. Talanta, **11**, 1581 (1964).
8. H. N. Halvorson and J. Halpern. J. Amer. Chem. Soc. **78**, 5562 (1956).
9. J. Halpern and S. M. Taylor. Discuss. Faraday Soc. **29**, 174 (1960).
10. A. G. Sykes. *In* Advances in inorganic chemistry and radiochemistry. Vol. 10. *Edited by* H. J. Emeleus and A. G. Sharpe. Academic Press, Inc., New York. 1967. p. 153.
11. H. A. Catherino and J. Jordan. Talanta, **11**, 159 (1964).
12. J. Jortner and H. A. Catherino. J. Phys. Chem. **67**, 2241 (1963).
13. T. J. Sworski. Radiat. Res. **4**, 483 (1956).
14. E. Hayon. J. Phys. Chem. **65**, 1502 (1961).
15. B. Cercek, M. Ebert, and A. J. Swallow. J. Chem. Soc. A, 612 (1966).
16. R. O. C. Norman and P. R. West. J. Chem. Soc. B, 389 (1969).
17. M. Anbar and P. Neta. Int. J. Appl. Radiat. Isotop. **18**, 493 (1967).
18. E. Hayon. Trans. Faraday Soc. **61**, 734 (1964).

Can. J. Chem. Downloaded from www.nrcresearchpress.com by 210.87.254.105 on 09/05/12
For personal use only.

Can. J. Chem. Downloaded from www.nrcresearchpress.com by 210.87.254.6 on 09/05/12
For personal use only.

Analysis of periodate oxidation of carbohydrates by polarography

R. D. CORLETT, W. G. BRECK,[1] AND G. W. HAY[2]
Department of Chemistry, Queen's University, Kingston, Ontario
Received[3] August 14, 1969

Experimental conditions using a variety of p*H* buffers have been established to permit the rapid, accurate determination of periodate and formaldehyde by polarography. The application of these analyses to quantitative studies in the oxidation of carbohydrates was illustrated and the lower limit of detection presently available found to be equivalent to 0.04 μmole carbohydrate.

Canadian Journal of Chemistry, 48, 2474 (1970)

Introduction

During the last decade the improvements in methods for separating similar polysaccharides isolated from a single source, and the interest in the carbohydrate biopolymers of animal tissue, generally have resulted in the recovery of only small amounts of polysaccharide fractions of significantly diminished heterogeneity. This, in turn, has resulted in a need for techniques whereby the structural details of these compounds can be elucidated using micro-scale samples. Of major importance in such studies is the use of periodate oxidation and the detection and determination of the products of that oxidation with (1), or without (2), modification. The numerous applications of this selective reaction, first exploited by Malaprade (3), have been reviewed thoroughly (4–6). It is noteworthy that, whereas most reports deal with macro-scale oxidations, recently there has been an evident response to the need for microchemical analyses of the reactants and products (7–18). To this list electrochemical procedures now must be added.

In a recent communication (19), a polarographic technique for the analysis of the periodate oxidation of less than 1 μmole of some common sugars was outlined. This work was performed independently, and in ignorance, of the prior studies of Zuman (20) and Takiura (21), which involved the principle of periodate oxidation of certain alcohols and glycols as well as sugars, with polarographic determination of the uptake of periodate. These workers were also aware of the significance of the method for both structural and kinetic studies. Nevertheless the value of this technique seems to have escaped the attention of many organic chemists.

Polarography affords a rapid, essentially nondestructive, technique not only for following the course of the consumption of periodate, either as the acid or a salt, but also to extend the useful limits of substrate well below the milligram region while maintaining convenience, speed, and precision of analysis. This paper provides new experimental data to illustrate the great versatility and sensitivity of the method.

In the course of the oxidation the periodate ion is reduced in acid solution by a two-electron half reaction to iodate, which in turn is reducible to iodide in a second wave at a more negative potential.

$$[1] \qquad IO_4^- + 2H^+ + 2e = IO_3^- + H_2O$$

$$[2] \qquad IO_3^- + 6H^+ + 6e = I^- + 3H_2O$$

The height of the first polarographic wave is determined by the concentration of periodate ion while that of the second wave depends on the concentration of periodate as well as of iodate, both being reducible at the more negative potential. This fact can be advantageous in affording a check on the overall amount of iodate plus periodate.

Discussion

The data reported herein have established the adaptability of the polarographic method with respect to the latitude afforded in the selection of buffer, temperature, substrate, and oxidant concentration.

For the estimation of the half-wave potential ($E_{\frac{1}{2}}$) for periodate, a mercurous sulfate reference electrode has a sufficiently positive potential. Moreover, the electrode-active species (SO_4^{2-}) is not oxidized by periodate. For convenience, commercially available saturated calomel electrode

[1]On sabbatical leave, 1969–1970. Present address: Scripps Oceanographic Institution, La Jolla, California, U.S.A.
[2]To whom correspondence should be addressed.
[3]Revision received April 6, 1970.

TABLE 1

Accuracy and sensitivity of the polarographic analysis of potassium periodate reduction by simple carbohydrates[a]

Carbohydrate and buffer	Carbohydrate added (μmole)	KIO_4 consumed (μmole)	Ratio	
			Observed	Expected
Glucose[b]	0.2	0.98	4.9	5.0
	0.4	1.98	5.0	5.0
	1.0	4.90	5.0	5.0
Arabinose[b]	0.2	0.82	4.1	4.0
	0.4	1.63	4.1	4.0
	1.0	3.90	3.9	4.0
Glucose[c]	0.2	1.02	5.1	4.0
	0.4	1.98	5.0	5.0
	1.0	4.90	4.9	5.0
Arabinitol[d]	0.2	0.81[e]	4.0	4.0
Lower limits				
Glucose[b]	0.04	0.22	5.5	5.0
	0.02	0.03	1.5	5.0
Mannitol[b]	0.04	0.20	5.0	5.0
	0.02	0	0	5.0

[a]All analyses were made after 24 h reaction. See text for conditions.
[b]In buffer *c*.
[c]In buffer *d*.
[d]In buffer *g*.
[e]$NaIO_4$ consumed.

(s.c.e.) was used routinely and, providing that the analyses did not exceed 20 min, the amount of oxidation of Cl^- was limited to negligible proportions by the nature of the liquid junction.

Some masking of the periodate half-wave occurred because of the preceding anodic wave, and the absolute value of $E_{\frac{1}{2}}$ for the periodate wave therefore is doubtful. The detection of the residual current for the IO_4^- wave failed because the difficulties in switching from the low sensitivities needed for the anodic currents to the high sensitivities needed for the cathodic currents resulted in non-reproducible data. The i_d for the periodate ion in all buffers except *e* (see Experimental) was measured as the difference between the current at 0.0 V in the reaction mixture and that in the base electrolyte alone. This partial i_d was found to be quantitative and reproducible, and except in the case of buffer *e* (measured at −0.25 V), was found to have the expected ratio to the i_d for the iodate ion measured in the usual way. Nevertheless, values of the limiting diffusion current (i_d), obtained by difference of the sample wave height from that of the blank as residual current varied linearly with periodate concentration, so that the determination was quantitative and reliable in all buffers except 0.1 *M* KH phthalate. The most suitable buffers for use in carbohydrate oxidations appeared to be buffers *c*, *d*, or *g*. The particular selection will be governed chiefly by the choice of optimal p*H* for the substrate used.

The data of Table 1 established that the correlation of the observed with expected uptake of periodate was adequate at and above 0.04 μmole per 25 ml, there being no possibility of confusing a hexose with a pentose. The reliability could not be extended to 0.02 μmole without further refinements to cell design and calibration procedure; however, sample size could readily be reduced to 1 ml or less by the use of a suitable micro cell, and feasible refinements in the method, such as the use of a signal amplifier on the recorder, or the application of CAT (computer) methods, suggest that the technique may be capable of detecting 1 μg periodate.

The analyses of the periodate oxidations of maltose, fructose, and glucuronic acid (Table 2), showed measurable changes in uptake with time for all the sugars, as expected. There was a tendency for molar consumption ratios to show integer values even before complete uptake had been reached; these results suggested that the reactions may proceed in stages (22–24). Nisli and Townshend (8) used similar substrates at similar concentration ranges and found that there were

Can. J. Chem. Downloaded from www.nrcresearchpress.com by 210.87.254.6 on 09/05/12
For personal use only.

TABLE 2

Molar uptake of periodate for less rapidly oxidized sugars

Analysis after	Sugar	Sugar added (μmole)	KIO_4 consumed (μmole)	Ratio	
				Observed	Expected
1 h[a]	Maltose	0.2	0.48	2.4	5.0
		1.0	2.50	2.5	5.0
	Lactose	0.2	0.58	2.9	5.0
		1.0	3.94	3.9	5.0
	Fructose	0.2	0.64	3.2	5.0
		1.0	3.40	3.4	5.0
20 h[a] (repeated)	Maltose	0.2	0.78	3.9	5.0
		1.0	4.04	4.0	5.0
	Lactose	0.2	0.60	3.0	5.0
		1.0	3.00	3.0	5.0
	Fructose	0.2	0.76	3.8	5.0
		1.0	4.10	4.1	5.0
72 h[a]	Maltose	0.2	0.98	4.9	5.0
		1.0	5.75	5.7	5.0
	Lactose	0.2	1.06	5.3	5.0
		1.0	5.06	5.1	5.0
	Fructose	0.2	1.06	5.3	5.0
		1.0	4.81	4.8	5.0
20 h[b]	Maltose	0.1	0.80	4.0	5.0
		1.0	6.48	6.5	5.0
	Lactose	0.2	0.61	3.0	5.0
		1.0	4.20	4.2	5.0
	Glucuronic acid	0.2	0.95	4.7	5.0
		1.0	4.46	4.5	5.0

[a]In buffer *d*.
[b]In buffer *c*.

definite differences in the macro- and micro-scale oxidations with periodate. Their studies corroborated the sequential nature of the oxidation of aldohexoses,[4] the variation in rates of oxidations of different substrates, and the differences in tendencies to over-oxidation.

Large excesses of periodate tended to effect over-oxidation in the systems employed (Table 3) and occasionally gave rise to an undesired production of iodine. When molar ratios of periodate to carbohydrate exceeded by more than 100% the optimal two-fold stoichiometric excess of periodate used in these studies, the control of oxidation was diminished and the precision of the method often seriously affected.

[4]A more obvious example of the stages or "plateau-ing" effects occurring in the consumption of periodate by complex carbohydrates, and which are unequivocally evident from the data of Table 8 (and also Tables 5 and 6, especially when graphed), has been reported recently by Kochetkov and Bochkov (32). The present work has detected a greater number of plateaus which, like that of Kochetkov and Bochkov, correspond to integer values of periodate uptake.

The data of Tables 4 to 6 summarize the effects of temperature, p*H*, and buffer concentrations on the oxidation of some common carbohydrates. From Table 4 it was evident that an increase in temperature accelerated the rate of oxidation of 3-*O*-methyl-D-glucopyranose but did not affect the final stoichiometry. *myo*-Inositol was oxidized so rapidly that this temperature effect was not observable, even in samples assayed after only 1 h of oxidation. However, the typical over-oxidation (25) was not detected under the conditions used (8). The loss of formate ester from partially oxidized 3-*O*-methyl-D-glucose was not affected detectably by the removal of acetate during the oxidation (Table 4) (26). The hydrolysis of the ester was quantitative and occurred within the first 24 h of reaction. The slightly low value for the periodate consumption by *myo*-inositol may be due to impurities in the commercial product which was used without further purification.

The precision of the polarographic determinations of a range of concentrations of periodate by

Can. J. Chem. Downloaded from www.nrcresearchpress.com by 210.87.254.6 on 09/05/12
For personal use only.

TABLE 3

Molar uptake of potassium periodate with varying initial molar ratios of periodate to carbohydrate[a]

Sugar[b]	Sugar added (μmole)	KIO_4 added (μmole)	KIO_4 consumed (μmole)	Ratio	
				Observed	Expected
Glucose	0.2	4.0	1.00	5.0	5.0
	0.2	6.0	1.04	5.2	5.0
	0.2	10.0	1.00	5.0	5.0
	1.0	20	5.3	5.3	5.0
	1.0	30	4.0	4.0	5.0
	1.0	50	6.0	6.0	5.0
Lactose	0.2	4.0	0.8	4.0	5.0
	0.2	6.0	1.0	5.0	5.0
	0.2	10	1.0	5.0	5.0
	1.0	20	4.6	4.6	5.0
	1.0	30	4.0	4.0	5.0
	1.0	50	5.5	5.5	5.0
Maltose	0.2	4.0	0.6	3.0	5.0
	0.2	6.0	1.0	5.0	5.0
	1.0	20	4.6	4.6	5.0
	1.0	30	2.9	2.9	5.0
	1.0	50	6.0	6.0	5.0

[a]Analyses performed after 24 h reaction.
[b]In buffer *d*.

TABLE 4

Reduction of $NaIO_4$ by *myo*-inositol and 3-*O*-methyl-D-glucopyranose under a variety of conditions

Sample	Temperature (°C)	Hours of oxidation	Sample weight (μmole)	$NaIO_4$ reduced (μmole)	Ratio IO_4^-/Sample (μmole/μmole)	
					Observed	Theoretical
myo-Inositol in buffer *g*	5	48	0.04	0.246	6.1	6.0
	5	48	0.2	1.14	5.7	6.0
	5	96	0.2	1.12	5.6	6.0
	25	48	0.04	0.246	6.1	6.0
	25	48	0.2	1.14	5.7	6.0
	25	96	0.2	1.14	5.7	6.0
	35	24	0.2	1.14	5.7	6.0
	35	48	0.2	1.14	5.7	6.0
3-*O*-Methyl-D-glucose in buffer *g*	5	24	0.04	0.08	2.0	1.0 or 3.0
	5	96	0.04	0.116	2.9	1.0 3.0
	5	24	0.2	0.52	2.6	1.0 3.0
	5	96	0.2	0.61	3.1	1.0 3.0
	25	24	0.04	0.116	2.9	1.0 3.0
	25	96	0.04	1.122	3.1	1.0 3.0
	25	24	0.2	0.59	2.9	1.0 3.0
	25	96	0.2	0.61	3.1	1.0 3.0
3-*O*-Methyl-D-glucose without buffer	5	96	0.04	0.116	2.9	1.0 3.0
	5	96	0.2	0.56	2.8	1.0 3.0
	25	24	0.04	0.116	2.9	1.0 3.0
	25	96	0.04	0.116	2.9	1.0 3.0
	25	24	0.2	0.59	2.9	1.0 3.0
	25	96	0.2	0.59	2.9	1.0 3.0

itself in buffer solutions was determined at various times. The values of $\bar{x} \pm 2\sigma$ μmoles and of $2\sigma/\bar{x} \times 100\%$ are as follows: 6.645 ± 0.09 μmoles, 1.36%; 1.353 ± 0.026 μmole, 1.95%; 0.189 ± 0.002 μmole, 1.06%; 0.0192 ± 0.0004 μmole, 2.09%. Thus, the analyses provided a 95% confidence level that the concentrations of periodate stated were within ±2.1% of the true value.

In addition to the control afforded by selection of p*H*, or specific hydrogen ion, and reagent concentration, temperature can be used advan-

Can. J. Chem. Downloaded from www.nrcresearchpress.com by 210.87.254.6 on 09/05/12
For personal use only.

TABLE 5

Molar periodate uptake by glucose, maltose, and lactose in buffer *f*

Time		Periodate consumed							
		Weak, 4 °C[a]		Weak, 35 °C[a]		Strong, 4 °C[b]		Strong, 35 °C[b]	
h	min	μmole	Ratio	μmole	Ratio	μmole	Ratio	μmole	Ratio
Glucose									
3	0			0.43	3.2			2.70	4.1
3	30	0.25	1.8			2.30	2.5		
6	30			0.46	3.4			2.89	4.4
7	0	0.40	3.0			2.70	4.1		
24	0			0.63	4.8			3.51	5.2
24	30	0.51	3.8			2.88	4.4		
27	30			0.66	5.0			3.30	5.0
29	30	0.56	4.2			2.90	4.4		
47	30			0.72	5.4			3.32	5.0
48	0	0.60	4.5			3.12	4.5		
95	30			0.72	5.4			3.36	5.0
96	0	0.67	5.0			3.25	4.9		
Maltose									
3	0			0.27	2.0			1.80	2.7
3	30	0.25	1.9			0.65	1.0		
6	30			—	—			1.85	2.8
7	0	0.25	1.9			1.65	2.5		
24	0			0.49	3.7			2.76	4.1
24	30	0.23	1.7			1.95	3.0		
27	30			0.44	3.3			2.73	4.1
29	30	0.33	2.4			2.0	3.0		
47	30			0.98	7.4			3.86	5.8
48	0	0.42	3.2			2.40	3.6		
95	30			0.93	7.0			5.21	7.8
96	0	0.47	3.5			2.70	4.0		
Lactose									
3	0			0.19	1.4			2.10	3.1
3	30	0.16	1.2			2.05	3.1		
6	30			0.21	1.6			2.22	3.4
7	0	0.20	1.5			2.10	3.1		
24	0			0.48	3.6			2.70	4.0
24	30	0.32	2.4			2.31	3.4		
27	30			0.43	3.3			—	—
29	30	0.41	3.0			2.34	3.5		
47	30			0.70	5.2			3.04	4.5
48	0	0.47	3.5			2.50	3.8		
95	30			0.68	5.1			3.87	5.8
96	0	0.60	4.5			3.66	5.5		

[a]Weak = 0.2 μmole substrate in reaction solution.
[b]Strong = 2.0 μmole substrate in reaction solution.

tageously to promote stoichiometric oxidation within a suitable time period, or conversely, to decelerate the oxidation so that the intermediates formed in the process can be studied. The often used period of 24 h for oxidation at room temperature in many of these cases would be inadequate for presumption of complete uptake of periodate (Tables 2, 4–6), in contrast to the more facile oxidations of arabinose, arabinitol, *myo*-inositol, and mannitol which proceeded smoothly to completion within 24 h.

The kinetic experiments indicated that these systems provide a controllable rate of oxidation and may be a means of providing additional information concerning the structure–reactivity relationships operative during the course of the periodate oxidation of carbohydrates (8, 22–29).

The partial masking of the periodate reduction wave prompted an attempt to split the iodate and periodate waves by the addition of some substance which would alter the periodate to iodate reduction so as to give a means of distinguishing between them and to obtain a complete wave proportional to periodate concentration and with a clear half-wave value. One logical choice for such a substance was the iodide ion which, above p*H* 7, reacts specifically with periodate to give iodine and iodate according to

Can. J. Chem. Downloaded from www.nrcresearchpress.com by 210.87.254.6 on 09/05/12
For personal use only.

TABLE 6

Molar periodate uptake by glucose, maltose, and lactose in buffer *c*

Time		Periodate consumed							
		Weak, 4 °C[a]		Weak, 35 °C[a]		Strong, 4 °C[b]		Strong, 35 °C[b]	
h	min	μmole	Ratio	μmole	Ratio	μmole	Ratio	μmole	Ratio
Glucose									
3	0			0.37	2.6			2.90	4.4
3	30	0.35	2.6			2.70	4.05		
6	30			0.52	3.9			3.02	4.5
7	0	0.36	2.6			2.68	4.0		
24	0			0.76	5.7			3.49	5.2
24	30	0.55	4.1			2.85	4.3		
27	30			0.66	5.0			3.27	4.9
29	30	0.49	3.7			2.83	4.3		
47	30			0.80	6.0			3.59	5.4
48	0	0.66	5.0			3.10	4.4		
95	30			0.86	6.4			4.62	7.0
96	0	0.72	5.4			4.33	6.5		
Maltose									
3	0			0.28	2.1			2.02	3.0
3	30	0.27	2.0			2.02	3.0		
6	30			0.35	2.6			2.06	3.1
7	0	0.23	1.7			1.88	2.9		
24	0			0.49	3.7			2.86	4.3
24	30	0.35	2.6			2.20	3.3		
27	30			0.53	4.0			4.26	6.4
29	30	0.32	2.5			2.06	3.1		
47	30			0.95	7.1			5.60	8.4
48	0	0.42	3.2			2.61	3.9		
95	30			1.20	9.0			6.46	9.7
96	0	0.48	3.6			2.83	4.2		
Lactose									
3	0			0.25	1.9			2.62	4.0
3	30	0.24	1.8			2.33	3.5		
6	30			0.33	2.5			2.60	3.9
7	0	0.24	1.8			2.26	3.4		
24	0			0.59	4.5			4.17	6.2
24	30	0.39	3.0			2.65	4.0		
27	30			0.63	4.8			4.38	6.5
29	30	0.37	2.9			2.48	3.7		
47	30			0.75	5.6			5.60	8.4
48	0	0.48	3.6			2.90	4.3		
95	30			1.10	8.3			6.61	9.9
96	0	0.57	4.3			3.12	4.8		

[a]Weak = 0.2 μmole substrate, 2.00 μmole IO_4^-/15 ml reaction solutions; 0.133 μmole substrate, 1.33 μmole IO_4^-/25 ml analysis solutions.
[b]Strong = 2.0 μmole substrate, 20 μmole IO_4^-/15 ml reaction solutions; 0.76 μmole substrate, 6.67 μmole IO_4^-/25 ml analysis solutions.

[3] $IO_4^- + 2I^- + H_2O = IO_3^- + 2OH^- + I_2$

and, below p*H* 5, reacts with both periodate and iodate to produce iodine according to

[4] $IO_4^- + 8H^+ + 7I^- = 4I_2 + 4H_2O$

[5] $IO_3^- + 6H^+ + 5I^- = 3I_2 + 3H_2O$

In a buffer of a saturated solution of $NaHCO_3$, at p*H* above 8, periodate should be distinguished from iodate in being reduced to give iodine. Some doubt had been raised that within this system the periodate ion could exist for long, it being spontaneously reducible to iodate at voltages more positive than the range to be investigated. This question was answered presumptively by identifying iodine as a product upon addition of potassium iodide to the system (which contained 2 μmoles of periodate per 25 ml) on the basis of the deep blue color produced when starch indicator was added.

Attempts to calibrate the iodide and iodine were not completely successful. The iodide wave was non-stoichiometric, whereas the iodine wave was quantitative up to about 0.6 μA, but stopped there, possibly owing to the insolubility of the iodine in such dilute solutions of iodide. For

Can. J. Chem. Downloaded from www.nrcresearchpress.com by 210.87.254.6 on 09/05/12
For personal use only.

Can. J. Chem. Downloaded from www.nrcresearchpress.com by 210.87.254.6 on 09/05/12
For personal use only.

analytical purposes, the use of the iodide intermediate is disadvantageous, when compared to the reliable though less elegant routine polarographic analysis using only part of the periodate diffusion wave.

The pilot study of the applicability of Jahoda's (30) polarographic determination of formaldehyde, produced during periodate oxidation (31), to the conditions of the present investigation indicated that acceptable accuracy was obtainable. The IO_3^- and IO_4^- waves which preceded and interfered with that for formaldehyde, could not be eliminated electrically except at the expense of base line stability and the concomitant diminution of accuracy. This difficulty was surmounted by transfer of the reactants to 0.1 *M* LiOH buffer, p*H* 13. Lead(II) acetate was effective in precipitating iodate and periodate, thus stopping the oxidation, but introduced a new wave attributed to Pb(II). The use of $Ba(OAc)_2$ has been found to be an effective means of eliminating iodate and periodate in these systems.

The separation of formaldehyde by distillation (30) obviated the interference from lead but afforded no enhancement of formaldehyde wave, and resulted in lower accuracy unless the distillation was carefully controlled. The use of freeze drying to distil formaldehyde and of ion exchange to remove IO_3^- and IO_4^- are under study.

Experimental

Most of the polarograms were recorded on a Heathkit Polarograph Model EUW-19 but Metrohm E261 and Sargent Polarographs were also employed at times, along with their respective cells and H-cells of Lingane's design. Gelatin, but not Triton X100, was satisfactory as a maximum suppressor. All buffers were prepared to contain 0.008% (w/v) gelatin. The buffers used were: (*a*) 0.5 *M* H_2SO_4, 0.1 *M* K_2SO_4, p*H* 0; (*b*) 0.05 *M* H_2SO_4, 0.1 *M* K_2SO_4, p*H* 1; (*c*) 0.005 *M* H_2SO_4, 0.1 *M* K_2SO_4, p*H* 2; (*d*) 0.1 *M* HOAc, 0.02 *M* NaOAc, p*H* 3.6; (*e*) 0.1 *M* KH phthalate, p*H* 4.0; (*f*) 0.1 *M* HOAc, 0.1 *M* NaOAc, p*H* 4.6; (*g*) 0.1 *M* HOAc, 0.1 *M* LiOAc, p*H* 4.6; (*h*) 1 *M* KCl, p*H* 6.6; (*i*) saturated $NaHCO_3$, p*H* 8.1; (*j*) 0.1 *M* $NaHCO_3$, p*H* 8.4; (*k*) 0.1 *M* LiOH, 0.1 *M* LiCl, p*H* 13.

The substrates used were the highest purity grade available commercially and were used after drying without further purification. The 3-*O*-methyl-D-glucopyranose, m.p. 168 °C, was a gift from Professor J. K. N. Jones.

A typical polarogram showing the periodate and iodate waves is given in Fig. 1 (for KIO_4 in the buffer *d*). The first wave is due to the process of reaction [1] and the second corresponds to that of reaction [2].

1. The Investigation of Various Buffer/Supporting Electrolytes

The polarographic behavior of each buffer (18 ml) was recorded, and polarograms obtained upon the successive additions of each of 2 ml (1 μmole) of stock KIO_4 and KIO_3 solutions to the buffer solution. The half-wave potentials (vs. s.c.e.) and diffusion currents (μA per μmole) obtained for the periodate and iodate ions in each buffer are reported in Table 7.

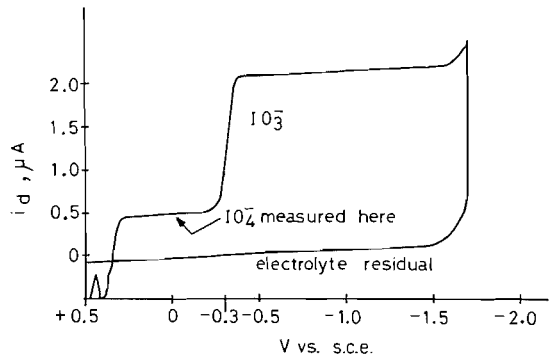

FIG. 1. Polarogram typical of KIO_4 in various buffer electrolytes (specifically buffer *d*), i_d for IO_4^- read at 0.0 V.

2. The Assessment of Current Precision in Carbohydrate Analysis

The precision of the determination of periodate and iodate alone in the buffer solutions was shown to be highly reproducible during calibrations. To assess the reliability of the actual uptake of periodate by any particular carbohydrate chosen for oxidation by this method, solutions of each of glucose and arabinose were prepared to give final concentrations of 0.2, 0.4, and 1.0 μmole in 25 ml of buffer *c*. The above solutions, with respectively 2, 4, and 10 μmoles KIO_4, together with the blanks and calibration solutions, were stored in the dark for 24 h. Polarograms were obtained from 0.20 to −0.20 V at a rate of 0.20 V per min. Similar solutions of glucose were made up in buffer *d*, and polarograms recorded. Similarly, solutions of glucose or mannitol containing 0.04 and 0.02 μmole and of L-arabinitol containing 0.2 μmole per 25 ml of buffer solution were oxidized with KIO_4 or (arabinitol only) $NaIO_4$ and polarograms obtained. The data obtained are reported in Table 1.

3. Trial of the Method with Less Readily Oxidized Sugars

Maltose, fructose, and glucuronic acid were prepared (1 ml = 0.2 μmole). Aliquots of each of these to contain 0.2 and 1.0 μmole, respectively, were pipetted into 25 ml flasks containing 10 ml buffer *d*. Aliquots of periodate solution containing 2 and 10 μmoles of KIO_4, respectively, were added, along with gelatin (0.008% final concentration) and the final volumes made up to 25 ml with buffer. Similarly blank solutions of KIO_4 were prepared. After 1 h the solutions were deaerated for 10 min and analyzed for excess periodate. Polarograms were recorded from 0.25 to −0.41 V at 0.20 V per min and a sensitivity of 1 μA full scale, and wave heights determined. The solutions were stored in the dark at room temperature and re-analyzed in the same manner after 20 and 72 h. A similar series of solutions were prepared in buffer *c* and analyzed after 20 h. The results of these analyses are summarized in Table 2.

TABLE 7

Half-wave potentials and diffusion currents of periodate and iodate[a] in various buffer electrolytes

	Buffer	Approximate p*H*	Sweep Range (V)	Sweep Rate (V/min)	$E_{\frac{1}{2}}$ (s.c.e.), V IO_4^-	$E_{\frac{1}{2}}$ (s.c.e.), V IO_3^-	i_d, μA IO_4^-	i_d, μA IO_3^-
a	0.5 *M* H_2SO_4, 0.1 *M* K_2SO_4	0	0.25 to −1.10	0.5	None	0.13	—	1.60
b	0.05 *M* H_2SO_4, 0.1 *M* K_2SO_4	1	0.25 to −1.20	0.5	0.20	−0.22	0.55	1.60
c	0.005 *M* H_2SO_4, 0.1 *M* K_2SO_4	2	0.40 to −1.40	0.5	0.20	−0.28	0.65	2.00
d	0.1 *M* HOAc, 0.02 *M* NaOAc	3.6	0.40 to −1.60	0.5	0.30	−0.30	0.50	1.60
e	0.1 *M* KH Phthalate	4.0	0.25 to −1.20	0.5	0.0	−0.50	0.28[b]	1.65
f	0.1 *M* HOAc, 0.1 *M* NaOAc	4.6	0.40 to −1.80	0.5	0.30	−0.30	0.50	1.60
g	0.1 *M* HOAc, 0.1 *M* LiOAc	4.6	0.40 to −1.60	0.5	0.30	−0.30	0.50	1.65
h	1 *M* KCl	6.6	0.25 to −1.2	2.0	0.0	−1.10	0.60	1.60
i	Saturated $NaHCO_3$	8.1	0.15 to −1.6	0.5	0.0	−1.00	0.40	1.25

[a]Electrode reaction product of IO_4^-.
[b]Measured at −0.25 V.

4. The Effect of Larger Excess of Periodate

Ratios of 20, 30, and 50 moles of periodate per mole of carbohydrate were reacted with glucose, lactose, and maltose, each at 0.2 and 1.0 μmole per 25 ml of final solution, and the excess determined, by obtaining polarograms from 0.20 to −0.20 V at 0.20 V per min with sensitivity 2 or 5 μA full scale, after each reaction had proceeded for 24 h. The results are given in Table 3.

5. The Effects of Temperature and Buffer

Solutions containing 0.04 and 0.2 μmole of each of *myo*-inositol and 3-*O*-methyl-D-glucopyranose in buffer *g* were prepared and oxidized with a 10-fold excess of $NaIO_4$ at 5, 25, and 35 °C. Samples were assayed in the usual manner after 1, 24, 48, 72, and 96 h of reaction. Control solutions were assayed concurrently. 3-*O*-Methyl-D-glucose also was oxidized at 5 and 25 °C without buffering. The solution p*H* was 5.6. The results are summarized in Table 4.

6. Rate Studies with Glucose, Lactose, and Maltose under a Variety of Conditions

Experiments were performed with glucose, lactose, and maltose at 4 and 35 °C, using each of buffers *c* and *f*, and sugar concentrations 0.2 and 2.0 μmoles in 25 ml of final solution. In all cases the mole ratio of periodate to sugar was 10:1. Solutions were divided in two parts, to be conditioned at the respective high and low temperatures. Reactions were carried out in 500 ml bottles, providing large samples for each of the 24 sets of experimental conditions (3 × 2 × 2 × 2). Aliquots were removed from each bottle at the required time and analyzed polarographically for periodate uptake. Reagent blanks were stored and analyzed similarly for each time interval; data were corrected for deviations in the blank which were not significant. Maximum deviations throughout the period were: weak + 0.02 to −0.04 μmole; strong + 0.01 to −0.12 μmole. Each final sample was purged with nitrogen for 5 min and the polarogram recorded between 0.20 and 0.0 V at a sweep rate of 0.20 V per min and at suitable sensitivity. The data are given in Tables 5 and 6.

In the case of maltose the unusual results were checked by a second series of experiments allowing for more frequent analysis of the reaction solution in the early stages. Bulk solutions were made up to give final concentrations in the reaction solution of 0.2 and 2.0 μmoles per 15 ml. Buffer *f* was used with an initial mole ratio of periodate to maltose of 10:1. Reactions were carried out at 4 and 35 °C in the dark with blanks treated similarly. After 30 min, 5 ml aliquots were taken every 15 min and made up to 15 ml to give a final concentration in the analysis solution of 0.008% gelatin and 6.67 μmoles of periodate minus the amount consumed in the reaction. After 4 h the sampling interval was increased to 30 min and after 14 h to 60 min. At 12 h duplicate reactions were started and these solutions used to obtain values between 12 and 24 h and between 36 and 48 h. The data from the offset series is presented consecutively with the original series but identified as offset. Polarograms were run from 0.20 to −0.10 V at a rate of 0.20 V per min and suitable sensitivity. Residual currents were obtained from analysis of the electrolyte solutions only. Data are reported in Table 8.

7. The Use of an Intermediate to Split the Periodate to Iodate Wave

Electrolyte blanks were clear of diffusion waves from 0.45 to −1.00 V. A solution having 1 μmole of periodate

Can. J. Chem. Downloaded from www.nrcresearchpress.com by 210.87.254.6 on 09/05/12
For personal use only.

TABLE 8

Molar periodate uptake ratio for maltose, varying with time[a]

	Periodate uptake					Periodate uptake			
	4 °C[b]		35 °C[b]			4 °C[c]		35 °C[c]	
Time (min)	μmole	Mole ratio	μmole	Mole ratio	Time (min)	μmole	Mole ratio	μmole	Mole ratio
30	0.48	0.7			Offset				
45	0.64	1.0	0.54	0.8	780	2.01	3.0	2.36	3.5
60	0.74	1.1	0.98	1.5	840	1.98	3.0	2.44	3.7
75	0.74	1.1	1.34	2.0	900	1.84	2.8	2.26	3.4
90	0.62	0.6	1.36	2.0	960	1.90	2.8	2.46	3.7
105	0.76	1.1	1.34	2.0	1020	1.96	2.8	2.36	3.5
120			1.56	2.3	1080	1.91	2.9	2.58	3.9
135			1.83	2.8	1140	1.86	2.8	2.71	4.2
150	1.30	2.0							
165	1.28	1.9			1440	2.01	3.0	3.04	4.6
180	1.12	1.7	2.01	3.0	1500	2.16	3.2	3.31	5.0
195	1.26	1.9	1.72	2.6	1560	2.26	3.4	3.26	4.9
210			1.78	2.7	1620	2.06	3.1	2.84	4.3
225			1.82	2.7	1680	2.26	3.4	3.16	4.7
240	1.26	1.9	1.91	2.9	1740	2.16	3.2	3.31	5.0
270			1.91	2.9	1800	2.46	3.7	3.16	4.7
300	1.26	1.9	1.91	2.9	Offset				
330	1.26	1.9	2.16	3.2	2220	2.26	3.4	3.94	5.8
360	1.31	2.0			2340	2.16	3.2	3.80	5.7
390	1.16	1.7	2.04	3.1					
420	1.53	2.3	2.16	3.2	2880	2.46	3.7		
450	1.48	2.2	2.11	3.2	3000	2.38	3.6		
510	1.46	2.2	2.06	3.1	3240	2.28	3.4		
540	1.46	2.2	2.21	3.3	3300	2.26	3.4		
570	1.53	2.3	2.31	3.5	4380	2.51	3.8		
600	1.66	2.5	2.28	3.4	4620	2.26	3.4		
630	1.71	2.6	2.36	3.5	8520	2.50	3.8		

[a]All reactions in buffer *g*.
[b]Reaction solution concentration 2 μmole maltose, 20 μmole IO_4^-/15 ml.
[c]Analysis solution concentration 0.67 μmole maltose, 6.67 μmole IO_4^-/15 ml.

per 20 ml of final solution was added and the polarogram from 0.20 to −1.30 V gave the two typical waves. Four μmoles of potassium iodide were added to the cell and the polarogram repeated. The cathodic periodate wave between 0.20 and 0.0 V was eliminated and replaced by an anodic wave due to excess iodide. The characteristic blue color with starch appeared and a new diffusion wave rose steeply from 0 μA at −0.25 V to a plateau at −0.60 V with i_d 0.40 μA/mole, before the usual iodate wave appeared, unchanged. The new wave was identified tentatively as being due to the process $I_2 + 2e = 2I^-$. The addition of 1 μmole of iodate did not affect the anodic wave or the new wave, but added quantitatively to the iodate wave as expected. These conclusions were corroborated by the addition of iodide and iodine to the system.

8. Polarographic Determination of Formaldehyde

(a) Quantitative Analysis

A stock solution containing 1 mg HCHO/ml was prepared (solution *A*) and an aliquot diluted to 1 μmole HCHO/ml (solution *B*).

One ml of solution *A* was added to 19 ml of each of buffers *c*, *g*, *j*, and *k*. Formaldehyde gave no diffusion wave in the range 0.0 to −1.4 and −1.8 V, respectively, in buffers *c* and *g*. Polarography from 0.0 to −1.7 V in buffer *j* afforded a diffusion wave for formaldehyde with $E_{\frac{1}{4}}$ −1.5 V and i_d 0.5 μA. Polarography from 0.0 to −1.8 V in buffer *k* gave a formaldehyde wave with $E_{\frac{1}{4}}$ −1.68 V and i_d 7 μA.

Solution *B*, 1 ml, was added to 19 ml buffer *k*. Polarography as before gave a diffusion wave with $E_{\frac{1}{4}}$ −1.68 V and i_d 0.20 μA. This calibration was repeated.

Solution *B*, 2 ml, was diluted to 10 ml with distilled water and distilled under reduced pressure. The condensor and receiver were water-cooled. A 5 ml distillate was collected, added to 15 ml buffer *k*, and polarographed. A diffusion wave at $E_{\frac{1}{4}}$ −1.68 indicated the presence of 1 μmole HCHO based on the above direct calibration. The experiment was repeated using a distillation (water bath) temperature of 40°, and cooling with ice-water. A 3 ml distillate was diluted to 20 ml with buffer *k* and was found, polarographically, to contain 0.3 μmole HCHO. The residual solution was diluted to 20 ml with buffer *k* and found to contain 1.2 μmole HCHO.

Solution *B*, 2 ml, was diluted to 10 ml as before and distilled at 100 °C under 1 atm, using an ice water-cooled condensor and receiver. A 5 ml distillate was collected, diluted to 20 ml with buffer *k*, and assayed polarographically. The diffusion wave at −1.68 V had i_d 0.29 μA which is equivalent to 1.45 μmole. Similar analysis of the residual solution revealed the presence of 0.5 μmole (i_d 0.1 μA) HCHO.

Can. J. Chem. Downloaded from www.nrcresearchpress.com by 210.87.254.6 on 09/05/12
For personal use only.

TABLE 9

Periodate consumed and formaldehyde formed during oxidation of glucose and maltose

Solution	Sugar added (μmole)	KIO_4 consumed (μmole)	Ratio mole IO_4^- / mole sugar	Formaldehyde: In distillate (μmole)	Formaldehyde: In residue (μmole)	Formaldehyde: Total (μmole)	Ratio mole HCHO / mole sugar
Glucose[a]	2.0	10.4	5.2	—	—	2.7	1.3
Glucose[b]	2.0	10.2	5.1	0.6	1.5	2.1	1.0
Maltose[a]	2.0	9.8	4.9	2.2	—	2.2	1.1
Maltose[b]	2.0	9.9	5.0	1.5	1.0	2.5	1.2

[a]In buffer *c*.
[b]In buffer *g*.

(b) Analysis of Formaldehyde Formed During the Periodate Oxidation of Carbohydrates

Solutions of each of glucose and maltose were prepared to contain 2 μmoles sugar and 20 μmoles periodate per 15 ml of each of buffers *c* and *g*. After 72 h reaction in the dark at room temperature periodate was assayed polarographically as described above.

A 5 ml aliquot of the solution of glucose in buffer *c* was diluted to 20 ml with buffer *k* and a polarogram obtained between 0.0 and −1.8 V. The IO_3^- and IO_4^- waves were cancelled out by the use of both charging and constant current compensators. Although uniform current compensation was difficult to establish, a measurable wave was obtained.

Aliquots (5 ml) of each of the solutions of glucose in buffer *g*, and maltose in buffers *c* and *g*, were treated with solid $Pb(OAc)_2$ and filtered. The filtrate was diluted to 10 ml by the washing of the flask and residue, and distilled at 1 atm until 7 ml distillate were collected. Each distillate and each residual solution was diluted to 20 ml with buffer *k* and subjected to polarographic analysis for formaldehyde in the usual manner. The results have been summarized in Table 9.

Solutions containing 0.002 *M* $NaIO_4$ and $NaIO_3$ were treated with an equivalent amount of $Ba(OAc)_2$, either prior to or after transfer to the polarographic cell. The solutions were polarographed over the range of 0.0 to −2.5 V. No periodate wave was detectable at highest instrument sensitivity. An iodate wave was detected in samples to which $Ba(OAc)_2$ was added in the polarographic cell; the wave was reduced in magnitude by approximately 30-fold. No iodate wave was detected in samples to which $Ba(OAc)_2$ was added prior to transfer to the polarographic cell.

This research was supported by operating grants (to W.G.B. and G.W.H.) from the National Research Council of Canada.

1. I. J. GOLDSTEIN, G. W. HAY, B. A. LEWIS, and F. SMITH. Abstr. 135th Nat. Meeting, Amer. Chem. Soc. 1959. p. 3D.
2. G. W. HAY, B. A. LEWIS, and F. SMITH. *In* Methods in carbohydrate chemistry. Vol. V. *Edited by* R. L. Whistler. Academic Press, Inc., New York. 1965. pp. 357–361.
3. L. MALAPRADE. Bull. Soc. Chim. France, 683 (1928).
4. B. SKLARZ. Quart. Rev. London, **21**, 3 (1967).
5. J. M. BOBBITT. Advan. Carbohyd. Chem. **11**, 1 (1956).
6. F. SMITH and R. MONTGOMERY. The chemistry of plant gums and mucilages. A.C.S. Monograph 141. Reinhold, New York. 1959.
7. J. A. SZIRMAI, E. VAN BOVEN-DE TYSSONSK, and S. GARDELL. Biochim. Biophys. Acta, **136**, 331 (1967).
8. G. NISLI and A. TOWNSHEND. Talanta, **15**, 1377 (1968).
9. R. BELCHER and A. TOWNSHEND. Anal. Chim. Acta, **41**, 395 (1968).
10. G. G. S. DUTTON and A. M. UNRAU. Can. J. Chem. **43**, 1738 (1965).
11. G. G. S. DUTTON, K. B. GIBNEY, G. D. JENSEN, and P. E. REID. J. Chromatog. **36**, 152 (1968).
12. LJ. JOSIMOVIĆ and O. GAL. Anal. Chim. Acta, **36**, 12 (1966).
13. S. A. BARKER and P. J. SOMERS. Carbohyd. Res. **3**, 220 (1966).
14. R. A. BAKER. J. Gas Chromatog. **4**, 418 (1966).
15. D. H. RAMMLER and J. C. RABINOWITZ. Anal. Biochem. **4**, 116 (1962).
16. R. BELCHER, G. DRYHURST, and A. M. G. MACDONALD. J. Chem. Soc. 3964 (1965).
17. V. E. VASKOVSK and S. V. ISAY. Anal. Biochem. **30**, 25 (1969).
18. K. BABOR, V. KALAC, and K. TIHLARIK. Czech. Patent, 122, 087 (1967); Chem. Abstr. **68**, 56455 (1968).
19. W. G. BRECK, R. D. CORLETT, and G. W. HAY. Chem. Commun. 604 (1967).
20. P. ZUMAN and J. KRUPICKA. Coll. Czech. Chem. Commun. **23**, 598 (1958).
21. K. TAKIURA and K. KOIZUMI. J. Pharm. Soc. Japan, **78**, 961 (1958).
22. S. A. WARSE and W. S. WHELAN. Chem. Ind. London, 71 (1958).
23. D. H. HUTSON and H. WEIGEL. J. Chem. Soc. 1546 (1961).
24. M. GUERNET, C. CIURO, and P. MALANGEAU. Bull. Soc. Chim. Biol. **47**, 1777 (1965).
25. S. J. ANGYAL and L. ANDERSON. Advan. Carbohyd. Chem. **15**, 150–152 (1959).
26. L. HOUGH, T. J. TAYLOR, G. H. S. THOMAS, and B. M. WOODS. J. Chem. Soc. 1212 (1958).
27. J. C. P. SCHWARTZ. J. Chem. Soc. 276 (1957).
28. F. S. H. HEAD. Chem. Ind. London, 360 (1958).
29. G. J. BUIST, C. A. BUNTON, and J. H. MILES. J. Chem. Soc. 743 (1959).
30. F. G. JAHODA. Coll. Czech. Chem. Commun. **7**, 415 (1935).
31. B. WARSHOWSKY and P. J. ELVING. Ind. Eng. Chem., Anal. ed. **18**, 253 (1946).
32. N. K. KOCHETKOV and A. F. BOCHKOV. Carbohyd. Res. **9**, 61 (1969).

Can. J. Chem. Downloaded from www.nrcresearchpress.com by 210.87.254.6 on 09/05/12
For personal use only.

Can. J. Chem. Downloaded from www.nrcresearchpress.com by 210.87.254.105 on 09/05/12
For personal use only.

Mass spectrometric study of the reaction of BF_3 with B_2O_3; the identification and heat of formation of B_2OF_4

D. R. BIDINOSTI AND L. L. COATSWORTH
Department of Chemistry, University of Western Ontario, London, Ontario

Received April 1, 1970

The reaction of BF_3 with B_2O_3 in a molecular flow reactor has been studied with a mass spectrometer. Over the temperature range 930–1300 °K the reaction has been found to produce B_2OF_4 with the stoichiometry

$$4\ BF_3(g) + B_2O_3(l) \rightleftarrows 3\ B_2OF_4(g)$$

From the temperature dependence of the equilibrium constant the enthalpy change for this reaction was determined to be 18.5 ± 3 kcal/mole and ΔH_f^0 (B_2OF_4) calculated to be −454 ± 2 kcal/mole at 1100 °K.

Canadian Journal of Chemistry, 48, 2484 (1970)

Introduction

Earlier mass spectrometric studies (1, 2) of equilibria in the B–O–F system at high temperatures have demonstrated the presence of BOF and $(BOF)_3$ for which thermodynamic data are now well documented (3). In addition to the ions BF_2^+ and BF_3^+ which are characteristic of BF_3, the mass spectra in these effusion studies contained the ions BOF^+, $(BOF)_3^+$, $B_3O_3F_2^+$, and $B_2OF_3^+$. The last ion was attributed to the fragmentive ionization of $(BOF)_3$ accompanied by a fluorine migration. By analogy with BF_2^+ from BF_3, $B_2OF_3^+$ is an expected ion in the mass spectrum of the unknown species B_2OF_4, and would probably be the principal ion from this compound. However, neither of these earlier works report the ion $B_2OF_4^+$ which would also be expected if B_2OF_4 were produced. More recently Brinckman and Gordon (4) have found the ion $B_2OF_4^+$ in the mass spectrum of the gaseous products produced from BF_3 vapor in a microwave discharge reactor made of quartz. They present an argument for the existence of the neutral parent molecule B_2OF_4 formed in the discharge. This has prompted our re-examination of the reaction of BF_3 with molten B_2O_3 in a molecular-flow reactor to show the existence of B_2OF_4, establish the stoichiometry of the reaction by pressure dependence studies, and determine the heat of the reaction from the temperature dependence of the equilibrium constant.

Experimental

The general features of the mass spectrometer have been described previously (5). This instrument has since been modified by the addition of an Edwards EM2 diffusion pump and liquid nitrogen trap to pump the ion source region. The plate P in Fig. 2 of ref. 5 has been extended to isolate the ion source region from the larger pumping port and so provide true differential pumping across the beam passage slit in P.

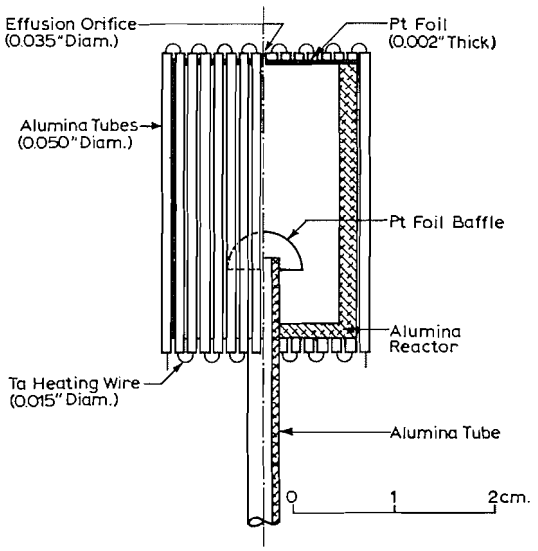

FIG. 1. Molecular-flow reactor.

The effusion cell shown in ref. 5 was replaced by the cylindrical molecular-flow reactor shown in Fig. 1. The reactor was made by drilling a 3.2 mm diameter hole in the center of the bottom of a Morganite cylindrical alumina crucible of 5 ml capacity. A snug fitting alumina tube was inserted until it penetrated 1/4 the interior length of the crucible, and then bonded to the exterior of the crucible base with Ceramabond 503 high temperature ceramic adhesive (Aremco Products Inc.). The top lip of the crucible was ground flat to accept a platinum foil cover containing the effusion orifice. This cover was held in place by a thin rim of ceramic adhesive applied after the foil was firmly pressed in place so that no adhesive was exposed to the reactants in the interior of the reactor. A platinum foil baffle was used to prevent line-of-sight transmission of the BF_3 reactant from the

Can. J. Chem. Downloaded from www.nrcresearchpress.com by 210.87.254.105 on 09/05/12
For personal use only.

inlet tube to the effusion orifice. Tantalum heating wire was threaded back and forth through 41 alumina tubes, 3 cm long × 1.25 mm o.d., which were cemented about the circumference of the reactor. The alumina gas inlet tube projected 8 cm from the bottom of the reactor and was held in a stainless steel Swagelok fitting using teflon ferrules. This fitting was in turn welded to the main source flange. The gas flow to this fitting, and hence to the reactor, was controlled by a Vacoa MV-25-XL precision gas metering valve located on the exterior of the main source flange. Reactor pressures were maintained below 10^{-2} Torr during all runs. The only materials with which the BF_3 reactant came into contact were: 304 stainless steel, Kel-F, teflon, and, at high temperatures, alumina and platinum.

A regulated constant-current power supply was used to heat the tantalum wire. With two radiation shields a cell temperature limit of 1350 °K was imposed by the rate of energy transfer from the small diameter tantalum wire. Temperatures were measured with a pair of chromel P/alumel thermocouples; one spot welded to the platinum top near its periphery and the second cemented to the base of the alumina reactor body. After full temperature equilibration the maximum temperature difference recorded by the two thermocouples was at the highest temperature, where the reactor base was approximately 3° hotter than the platinum top. During each run the temperature of each thermocouple remained constant to within 1°.

Matheson C.P. grade BF_3 was vacuum distilled and passed through Dry Ice – acetone traps several times to remove HF. All BF_3 samples were used within 18 h of purification. Samples of B_2O_3 were prepared by decomposing Fisher reagent-grade boric acid in a platinum dish over a Meker burner. The resulting oxide was fused at 650 °C for 72 h. After transfer to and assembly of the alumina reactor, the B_2O_3 glass was further dehydrated by fusing under high vacuum in the mass spectrometer. The molten boric oxide presented a surface area of approximately 2 cm^2 to the vapor phase in the reactor.

Appearance potentials were measured relative to xenon (ionization potential = 12.13 eV) (6) using Warren's extrapolated voltage difference method (7). Xenon was introduced into the ion source simultaneously with the effusion beam. All ion intensities were corrected for small contributions from background vapors by using the shutter S (5) to interrupt the molecular beam.

Results and Discussion

The appearance potentials for the ions observed in the mass spectrum of the effusing reaction mixture at a reactor temperature of 1100 °K are given in Table 1. For comparison the values reported by Hildenbrand *et al.* (2) are also presented together with the averaged electron impact values for BF_3 from the review by Svec (8) and the photoionization values for BF_3 by Dibeler and Liston (9). Ions of mass greater than $(BOF)_3^+$ were not observed.

Our values for BF_3^+ and BF_2^+ are in much closer accord with the existing data for BF_3 (8, 9) than those of Hildenbrand *et al.* With the exception of $B_3O_3F_2^+$, all of our appearance potentials are lower than theirs. The exceptional case is most interesting since Hildenbrand *et al.* report a value for $B_3O_3F_2^+$ which is lower than the ionization potential of $B_3O_3F_3$ from which $B_3O_3F_2^+$ arises by fragmentive ionization; a result which is most improbable. The low value for the $B_2OF_4^+$ potential confirms that it is due to a direct ionization rather than a fragmentation of some more complicated molecular species. In addition we have observed the metastable ion transition $B_3O_3F_3^+ \rightarrow B_2OF_3^+ + BO_2$ (observed, m/e = 64.55; calculated, m/e = 64.50) and have measured the appearance potential of the metastable as 15.3 eV, which substantiates the earlier (1, 2) assignment of $B_2OF_3^+$ as a fragment from $(BOF)_3$.

TABLE 1
Appearance potentials

Ion	Appearance potentials, eV			
	This work	Ref. 2	Ref. 8	Ref. 9
BF_3^+	15.87±0.1	16.4	15.7	15.55
BF_2^+	16.33±0.1	16.7	16.2	15.81
$(BOF)_3^+$	13.91±0.1	14.2		
$B_2OF_3^+$	15.35±0.2	16.6		
$B_2OF_4^+$	14.12±0.1			
$B_3O_3F_2^+$	16.15±0.2	13.4		
$B_2O_2F_2^+$	16.60±0.2	17.2		

With the reactor at 990 °K, the pressure dependence of B_2OF_4 on BF_3 was examined to establish the stoichiometry of the reaction producing this compound. In Fig. 2 we show logarithmic plots of the ion intensities of $B_2OF_4^+$, together with $(BOF)_3^+$, and $B_2OF_3^+$, vs. the ion intensity of BF_3^+ for 50 eV electrons. Unity slopes for $(BOF_3)_3^+$ and $B_2OF_3^+$ confirm the assignments by Porter *et al.* (1). The slope of 3/4 for $\log[BF_3^+]$ vs. $\log[B_2OF_4^+]$ confirms the stoichiometry to be

$$[1] \qquad 4BF_3(g) + B_2O_3(l) \rightleftarrows 3B_2OF_4(g)$$

As shown in Fig. 2, the ion intensities of $B_2OF_4^+$ are approximately 100 times smaller than those for $B_2OF_3^+$ and $(BOF)_3^+$. This is no doubt the reason why the two earlier studies did not observe it.

Under conditions of molecular flow, the partial pressure P_i of a gaseous species in an effusion

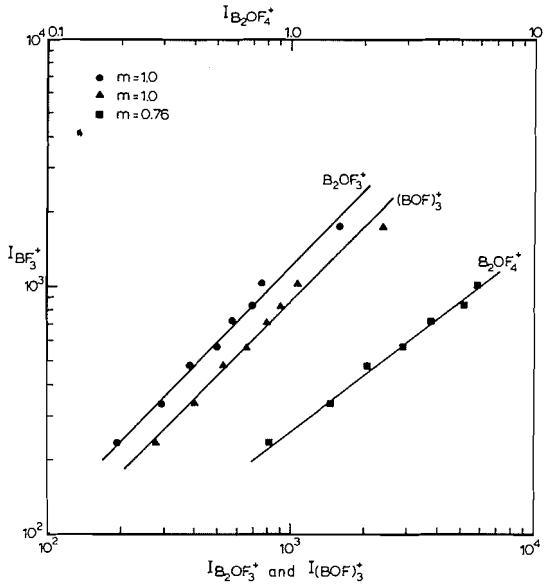

FIG. 2. Intensity dependence of ions from $(BOF)_3$ and B_2OF_4 on BF_3 pressure at a reactor temperature of 990 °K.

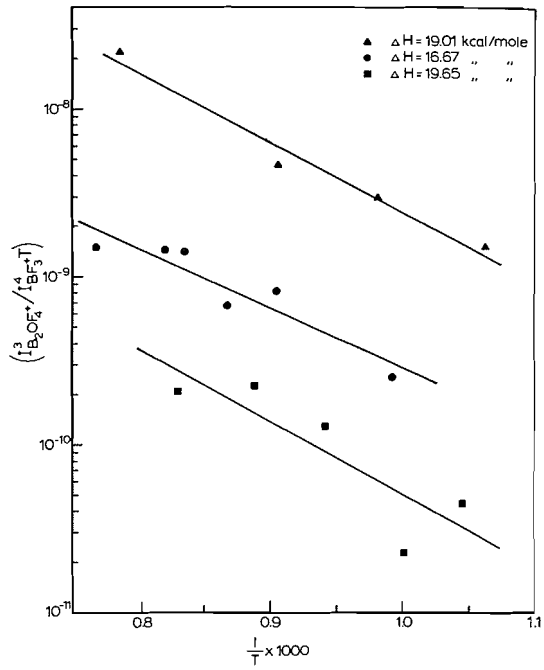

FIG. 3. Van't Hoff plots for the equilibrium $4\ BF_3(g) + B_2O_3(l) \rightleftarrows 3\ B_2OF_4(g)$.

reactor can be related to the observed ion current I_{i^+} by

$$[2] \qquad P_i = C_i\, I_{i^+} T$$

where T is the temperature of the gas in the reactor (10). The constant C_i contains a number of terms which depend on the geometry of both the reactor and ion source, the ion transmission characteristics of the mass spectrometer, the electron multiplier detection efficiency for the ion i^+, and the partial ionization cross section of the ith molecular species. All of these terms can be kept constant throughout each experiment except the last, which is assumed to be temperature independent. The Van't Hoff equation for reaction [1] can be written in terms of ion current intensities using eq. [2]

$$\log \frac{I_{B_2OF_4^+}{}^3}{I_{BF_3^+}{}^4 T} = \frac{-\Delta H^0}{2.303 RT} + C$$

where C is a temperature independent constant. Van't Hoff plots of ion currents taken at 50 eV for three different reactor pressures are shown in Fig. 3. At the start of the experiment the B_2O_3 surface area to effusion orifice area was approximately 300:1. To establish conclusively that equilibrium was attained, the effect of different values of this ratio on the Van't Hoff plots should be examined. It was observed that during the course of the temperature dependence studies, which were done over a 72 h period, chemical transport of B_2O_3 to the walls and inside of the top of the reactor was occurring. Hence the surface area ratio was continuously changing from a value of 300:1 to about 1500:1. In chronological sequence the ΔH values obtained were 19.01, 16.67, and 19.65 kcal/mole. Therefore it is concluded that equilibrium was attained over the full range of surface area ratios. The least-squares fitted slopes give an average $\Delta H = 18.5 \pm 3$ kcal/mole for reaction [1]. With the available data (3) for the heats of formation of BF_3 and B_2O_3, we calculate for B_2OF_4 a heat of formation at 1100 °K of -454 ± 2 kcal/mole.

This research was sponsored by the Air Force Office of Scientific Research, Office of Aerospace Research, United States Air Force, under AFOSR Grant No. 1356–68.

1. R. F. PORTER, D. R. BIDINOSTI, and K. F. WATTERSON. J. Chem. Phys. **36**, 2104 (1962).
2. D. L. HILDENBRAND, L. P. THEARD, and A. M. SAUL. J. Chem. Phys. **39**, 1973 (1963).
3. J. A. N. A. F. Thermochemical data. Thermal Laboratory, Dow Chemical Company, Midland, Michigan. 1965.
4. F. E. BRINCKMAN and G. GORDON. Proc. Int. Symp.

Can. J. Chem. Downloaded from www.nrcresearchpress.com by 210.87.254.105 on 09/05/12
For personal use only.

on Decompos. of Organometallic Comp. Dayton, Ohio. Nov. 1967; Univ. of Dayton Press. 1968. p. 29.
5. D. R. BIDINOSTI and N. S. MCINTYRE. Can. J. Chem. **45**, 641 (1967).
6. C. E. MOORE. Natl. Bur. Std. U.S. Circ. No. 467. 1958.
7. J. W. WARREN. Nature, **165**, 811 (1950).
8. H. J. SVEC. *In* Mass spectrometry. *Edited by* R. I. Reed. Academic Press, Inc., London. 1965. p. 235.
9. V. H. DIBELER and S. K. LISTON. Inorg. Chem. 7, 1742 (1968).
10. P. GOLDFINGER. *In* Mass spectrometry. *Edited by* R. I. Reed. Academic Press, Inc., London. 1965. p. 270.

Can. J. Chem. Downloaded from www.nrcresearchpress.com by 210.87.254.105 on 09/05/12
For personal use only.

Can. J. Chem. Downloaded from www.nrcresearchpress.com by 210.87.254.105 on 09/05/12
For personal use only.

Organobismuth compounds. I. Studies on triphenylbismuth(V) derivatives, Ph_3BiX_2

R. G. GOEL AND H. S. PRASAD

Department of Chemistry, University of Guelph, Guelph, Ontario

Received March 23, 1970

Triphenylbismuth(V) acid derivatives of the type, Ph_3BiX_2, where X = halide, nitrate, cyanate, acetate, haloacetate, or cyanoacetate have been prepared. Infrared spectra (4000 to 200 cm^{-1} region), electrical conductances, and molecular weights of these compounds have been studied to elucidate their structural features and chemical constitution. The molecular weight and conductance data show that these compounds behave as molecular species in benzene or nitromethane. The infrared spectroscopic results also indicate non-ionic five-coordinate structures. Bi—X stretching frequencies have been assigned for the difluoride, dichloride, dinitrate, dicyanate, and diacetate. These frequencies occur in the region 410–240 cm^{-1}.

Canadian Journal of Chemistry, **48**, 2488 (1970)

Introduction

Several organobismuth(V) compounds of the type R_3BiX_2 (R = aryl group, X = halide, acetate, nitrate etc.) are reported in literature (1). Although structural aspects of triphenylbismuth dihalides have been studied by several workers (2–5), very little is known about the structural features and chemical constitution of organobismuth(V) acid derivatives in general. On the basis of dipole moment studies, Jensen (2) proposed a trigonal bipyramidal structure for the dichloride. The proposed structure has been confirmed by X-ray crystallography (4). The molecular nature of triphenylbismuth dihalides has also been demonstrated by electrical conductance studies on some triphenylbismuth–halogen systems (3). The fluorine nuclear magnetic resonance (n.m.r.) spectrum (5) of triphenylbismuth difluoride is also consistent with a trigonal bipyramidal structure with axial fluorines. As part of our general study on the structural aspects of organometallic acid derivatives of the main group V elements, we have examined the infrared spectra, electrical conductances, and molecular weights of several triphenylbismuth(V) compounds, Ph_3BiX_2, where X = nitrate, cyanate, acetate, haloacetate, and cyanoacetate. Since the infrared spectra of triphenylbismuth dihalides have not been studied, we have also included the dihalides in our investigation. Several compounds included in this investigation have been synthesized for the first time.

Experimental

Reagents

Analytical grade solvents from Fisher, Baker, or Matheson, Coleman and Bell were used. Nitromethane was purified by treatment with calcium hydride and subsequent distillation under reduced pressure. Triphenylbismuth was recrystallized from benzene. Other chemicals were used without further purification.

Preparation

Triphenylbismuth dichloride and dibromide were prepared from triphenylbismuth and the halogen as described in the literature (1). Triphenylbismuth difluoride, dinitrate, and dicyanate were prepared by the metathetical reaction between triphenylbismuth dichloride and the appropriate silver salt in benzene. Triphenylbismuth diacetate, dihaloacetate, and dicyanoacetate were prepared by mixing a benzene solution of triphenylbismuth dichloride and an aqueous solution of silver acetate. The benzene layer was collected and was concentrated under reduced pressure. Addition of light petroleum ether to the concentrated benzene solution caused the desired compounds to precipitate. All of the compounds were recrystallized from a mixture of benzene and petroleum ether. The elemental analyses were performed by A. B. Gygli, Microanalytical Laboratory, Toronto.

Measurements

Infrared spectra were recorded on a Beckman Model IR-12 double beam spectrophotometer. Spectra were measured in the solid state in the 4000–200 cm^{-1} region and, in benzene solutions in the 500–200 cm^{-1} region. Solid samples were prepared as mulls in Nujol or Halocarbon oil, and the spectra were measured using demountable KRS-5 and polyethylene cells. Solution spectra were measured in sealed polyethylene cells.

The electrical conductances were measured at 25° with a Beckman Model RC-18A conductivity bridge using a glass cell with platinized platinum electrodes. The conductance of the solvent was measured in each case and corrections to the observed conductances were made. Molecular weights were determined in benzene solutions (concentration range: 10^{-2} to 10^{-3} mole/kg) with a Hitachi–Perkin–Elmer Model 115 vapor osmometer. Melting points were determined with a Fisher–Johns melting point apparatus as well as with a Gallenkamp melting point apparatus using glass melting point tubes.

Results and Discussion

The analytical and molecular weight data and melting points of the investigated compounds

TABLE 1
Analytical data

Compound	Analysis (%) Found C	Found H	Calculated C	Calculated H	Molecular weight* Found	Molecular weight* Calculated	Melting point (°C)
Ph_3BiBr_2	37.36	2.89	36.02	2.51	593	600	139
Ph_3BiCl_2	42.29	3.10	42.29	2.95	504	511	159–160
Ph_3BiF_2	44.79	3.06	45.19	3.16	483	478	127.5
$Ph_3Bi(NO_3)_2$	39.19	2.76	38.32	2.68	562	562	148†
$Ph_3Bi(OCN)_2$	46.65	2.79	45.82	2.88	524	524	125–126
$Ph_3Bi(CH_3COO)_2$	47.34	3.69	47.32	3.79	549	558	173
$Ph_3Bi(CCl_3COO)_2$	34.38	1.74	34.54	1.96	762	765	158
$Ph_3Bi(CHCl_2COO)_2$	37.61	2.24	37.95	2.46	687	696	118–119
$Ph_3Bi(CH_2ClCOO)_2$	42.07	2.95	42.12	3.05	614	627	166
$Ph_3Bi(CF_3COO)_2$	40.18	1.99	39.65	2.25	661	666	133
$Ph_3Bi(CHF_2COO)_2$	42.14	2.61	41.91	2.71	624	630	146
$Ph_3Bi(CH_2FCOO)_2$	45.14	3.07	44.45	3.22	580	594	165–166
$Ph_3Bi(CH_2BrCOO)_2$	36.56	2.35	36.90	2.67	711	716	171–172
$Ph_3Bi(CH_2CNCOO)_2$	47.06	3.03	47.37	3.14	608	608	123–124

*Solvent, benzene; concentration range, 10^{-2}–10^{-3} mole/kg.
†Explodes.

are recorded in Table 1. All the compounds are non-hygroscopic white crystalline solids and are soluble in common organic solvents like benzene, chloroform, and acetone. The molecular weight data show that all the compounds are molecular and monomeric in benzene. The equivalent conductances of these compounds in nitromethane at 25°, in the concentration range of 10^{-3} to 10^{-4} M, are recorded in Table 2. The conductivity data also show that all the compounds behave as molecular species in nitromethane. With the exception of the nitrate all the compounds show negligible conductivities. Moreover, the equivalent conductances do not change significantly on changing the X group. The observed conductances for the nitrate are also significantly lower than those reported (6) for 1:1 or 1:2 electrolytes. The conductances of triphenylbismuth dibromide and ditrifluoroacetate could not be determined due to decomposition of these compounds in nitromethane.

Infrared Spectra

Infrared spectra of all the compounds included in this investigation were examined in the solid state in the 4000–200 cm^{-1} region and, in benzene solutions in the 500–200 cm^{-1} region. The solution spectra were almost identical to those obtained in the solid state.

The infrared spectra of all the compounds in the region 4000–300 cm^{-1} show almost identical absorption bands due to the triphenylbismuth group. The absorption bands due to the anion group can, therefore, be assigned with confidence. In this region the spectrum due to the triphenylbismuth group is also very similar to that of triphenylantimony group in triphenylantimony dichloride and dibromide. Mackay and coworkers (7) have discussed the band assignments for triphenylantimony dichloride and dibromide. The infrared absorption frequencies for triphenylbismuth dibromide have also been reported (8) in the sodium chloride region. Infrared absorption bands due to the triphenylbismuth group in the 450–200 cm^{-1} region only are, therefore, included in our discussion.

The observed frequencies in 450 to 200 cm^{-1} region for triphenylbismuth dihalides, dinitrate, dicyanate, and diacetate are listed in Table 3. The spectrum of the difluoride in the 450 to 200 cm^{-1} region is shown in Fig. 1*c*. The spectra of the dichloride, dibromide, dinitrate, dicyanate, and the diacetate in the 300 to 200 cm^{-1} region are also shown in Fig. 1. A comparison of these spectra with the spectrum of triphenylbismuth-(III) (9) shows that the spectrum of the triphenylbismuth group in compounds of the type, Ph_3BiX_2, is almost identical to that of triphenylbismuth(III). Thus the absorption bands at ca. 450, 400, and 240–200 cm^{-1} can be attributed to the triphenylbismuth group.

In the spectrum of triphenylbismuth difluoride a very strong band is observed at 412 cm^{-1}. Since this band does not occur in any other Ph_3BiX_2 compounds, it can be assigned to Bi—F stretching vibration. The Bi—F stretching frequency in

Can. J. Chem. Downloaded from www.nrcresearchpress.com by 210.87.254.105 on 09/05/12
For personal use only.

TABLE 2

Conductance data of Ph_3BiX_2 compounds in nitromethane at 25 °C

Compound	Concentration (M)	Λ_e(ohm^{-1} cm^2 eq^{-1})	Compound	Concentration (M)	Λ_e(ohm^{-1} cm^2 eq^{-1})
Ph_3BiCl_2	2×10^{-3}	0.06	$Ph_3Bi(OCN)_2$	2×10^{-3}	0.11
	1×10^{-3}	0.13		5×10^{-4}	0.16
	5×10^{-4}	0.26		2×10^{-4}	0.40
	2×10^{-4}	0.65		1×10^{-4}	0.60
	1×10^{-4}	1.30	$Ph_3Bi(CH_3COO)_2$	2×10^{-3}	0.03
Ph_3BiF_2	2×10^{-3}	0.11		1×10^{-3}	0.12
	1×10^{-3}	0.13		5×10^{-4}	0.15
	5×10^{-4}	0.15		2.5×10^{-4}	0.20
	2.5×10^{-4}	0.26		1.25×10^{-4}	0.25
	1.25×10^{-4}	0.48	$Ph_3Bi(CCl_3COO)_2$	2×10^{-3}	1.13
$Ph_3Bi(NO_3)_2$	2×10^{-3}	2.42		1×10^{-3}	1.18
	1×10^{-3}	3.20		5×10^{-4}	1.26
	5×10^{-4}	4.40		2×10^{-4}	1.40
	2×10^{-4}	6.75		1×10^{-4}	1.80
	1.0×10^{-4}	9.00	$Ph_3Bi(CH_2FCOO)_2$	2×10^{-3}	0.12
$Ph_3Bi(CHCl_2COO)_2$*	2×10^{-3}	0.57		1×10^{-3}	0.11
	1×10^{-3}	0.44		5×10^{-4}	0.17
	5×10^{-4}	0.41		2.5×10^{-4}	0.28
	2.5×10^{-4}	0.32	$Ph_3Bi(CH_2BrCOO)_2$	2×10^{-3}	0.16
	1.25×10^{-4}	0.24		1×10^{-3}	0.23
$Ph_3Bi(CH_2ClCOO)_2$	2×10^{-3}	0.08		5×10^{-4}	0.36
	1×10^{-3}	0.07		2.5×10^{-4}	0.62
	5×10^{-4}	0.18		1.25×10^{-4}	1.08
	2×10^{-4}	0.30	$Ph_3Bi(CH_2CNCOO)_2$	2.0×10^{-3}	0.15
	1×10^{-4}	0.40		1×10^{-3}	0.20
$Ph_3Bi(CHF_2COO)_2$	2×10^{-3}	0.35		5×10^{-4}	0.23
	1×10^{-3}	0.49		2.5×10^{-4}	0.84
	5×10^{-4}	0.90			
	2.5×10^{-4}	1.64			
	1.25×10^{-4}	2.56			

*The compound decomposes slowly in nitromethane.

TABLE 3

Infrared absorption frequencies of Ph_3BiX_2 compounds (where X = Br, Cl, F, OAc, OCN, and NO_3) in the region 450–200 cm^{-1}*

Ph_3BiBr_2	Ph_3BiCl_2	Ph_3BiF_2	$Ph_3Bi(NO_3)_2$	$Ph_3Bi(OCN)_2$	$Ph_3Bi(OAc)_2$
445 s	444 s	448 s 412 vs	445 s	445 s	448 s
398 vw	405 vw		398 vw	400 w	396 vw
			320 vw		320 vw
			250 w	275 s	254 s
243 s	240 vs, b	244 s	236 sh	242 s	240 s, b
222 m	229 sh	228 sh	228 s	224 m	
	216 sh	214 s	212 sh		

*b = broad; m = medium; s = strong; sh = shoulder; vs = very strong; vw = very weak; w = weak.

triphenylbismuth difluoride compares very well with the Sb—F stretching frequency in triphenylantimony difluoride which occurs at 509 cm^{-1} (10). Since the spectrum of triphenylbismuth difluoride does not show any other band which can also be assigned to Bi—F stretching, the F—Bi—F group is indicated to be linear. The spectrum of triphenylbismuth dichloride shows a very strong broad band at 240 cm^{-1} with shoulders at 229 and 216 cm^{-1}. Considering the relative intensity, this band can be assigned to Bi—Cl stretching frequency. This again compares very well with Sb—Cl stretching frequency in triphenylantimony dichloride which is observed (10) at ca. 280–290 cm^{-1}. The Bi—Br stretching frequency is expected to occur below 200 cm^{-1} since in triphenylantimony dibromide the Sb—Br stretching frequency is observed in the region

Can. J. Chem. Downloaded from www.nrcresearchpress.com by 210.87.254.105 on 09/05/12
For personal use only.

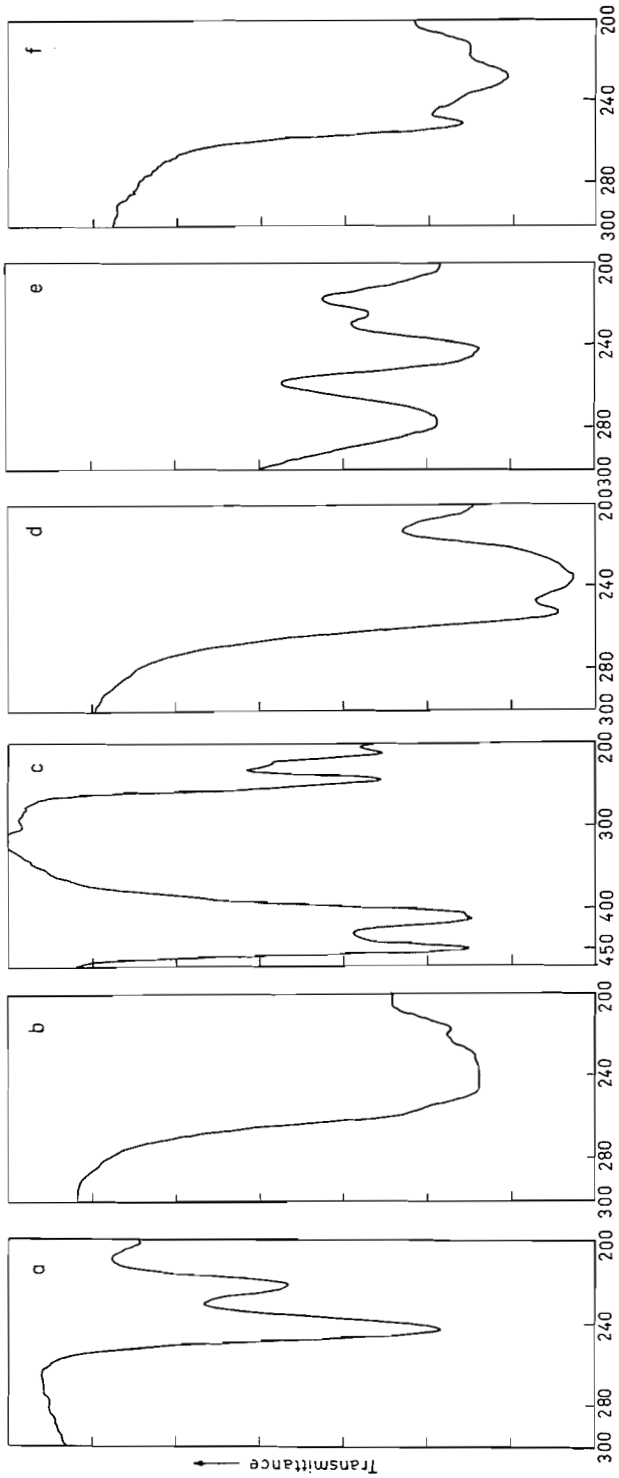

FIG. 1. Infrared spectra of *a*, Ph_3BiBr_2; *b*, Ph_3BiCl_2; *c*, Ph_3BiF_2; *d*, $Ph_3Bi(CH_3COO)_2$; *e*, $Ph_3Bi(OCN)_2$, and *f*, $Ph_3Bi(NO_3)_2$ in the low frequency region.

Can. J. Chem. Downloaded from www.nrcresearchpress.com by 210.87.254.105 on 09/05/12
For personal use only.

TABLE 4

Carboxylate frequencies (cm^{-1}) in triphenylbismuth carboxylates, $Ph_3Bi(OOCR)_2$

Compound	ν_{asym} (CO_2)	ν_{sym} (CO_2)	Δ ($\nu_{asym} - \nu_{sym}$)
$Ph_3Bi(CH_3COO)_2$	1592	1335	257
$Ph_3Bi(CCl_3COO)_2$	1660	1320	340
$Ph_3Bi(CHCl_2COO)_2$	1648	1364	284
	1620	1355	265
$Ph_3Bi(CH_2ClCOO)_2$	1635	1358	277
	1616		
$Ph_3Bi(CF_3COO)_2$	1685	1415	270
$Ph_3Bi(CHF_2COO)_2$	1660	1423	237
$Ph_3Bi(CH_2FCOO)_2$	1640	1425	215
$Ph_3Bi(CCH_2BrCOO)_2$	1638	1332	306
	1613		
$Ph_3Bi(CH_2CNCOO)_2$	1638	1365	273
	1625	1345	280

below 200 cm^{-1} (10). In the spectra of triphenylbismuth dinitrate, dicyanate, and diacetate, the bands at 250, 275, and 254 cm^{-1}, respectively, can be assigned to Bi—X stretching frequencies. Bi—X stretching frequencies in the dihaloacetates and dicyanoacetate cannot be identified due to the presence of anion bands in this region.

Regarding the absorption frequencies due to the anion groups, the following absorption bands are observed for the nitrate group: 1520–1510 (s) cm^{-1}; 1268–1255 (s) cm^{-1}; 985 (m) cm^{-1}; 800 (w), and 710 (w) cm^{-1}. Thus the observed absorption frequencies of the nitrate group are very similar to those observed for analogous antimony compound (11). In the spectrum of triphenylbismuth dicyanate, the O—C—N asymmetric stretching and O—C—N bending frequencies are observed at 2170 and 618 cm^{-1}, respectively. However the O—C—N symmetric stretching frequency cannot be assigned unambiguously. No band was observed in the 1400–1200 cm^{-1} region which could be assigned to this frequency. A triplet of medium intensity is observed at ca. 1170 cm^{-1} but since absorption bands due to phenyl groups also occur in this region, no conclusion can be reached about the O—C—N symmetric stretching frequency. Due to the uncertainty in the assignment of O—C—N symmetric stretching frequency, the mode of bonding of the cyanate group to the bismuth atom cannot be ascertained from infrared results.

The carboxylate stretching frequencies for triphenylbismuth diacetate dihaloacetates, and dicyanoacetate are given in Table 4. The assignments have been made by comparison with those for the acids (12, 13), sodium carboxylates (14), trimethyltin haloacetates (15, 16), trimethyl- and triphenyl-antimony haloacetates (17), and phenylmercuric carboxylates (18). The assignments for the monofluoroacetate require further comment. Deacon and Taylor (18) have assigned the CO_2 symmetric stretching frequency for pentafluorophenylmercuric monofluoroacetate at 1288 cm^{-1}. For monofluoroacetic acid (13) and its sodium salt (14), this frequency has been reported to occur at 1386 and 1488 cm^{-1}, respectively. Since the absorption corresponding to the CO_2 symmetric stretching frequency in metal–carboxylate complexes invariably occurs at a higher wave number than the corresponding frequency in the acid or organic esters, the assignment of the CO_2 symmetric frequency for pentafluorophenylmercuric monofluoroacetate is in error.

The carboxylate frequencies in triphenylbismuth dicarboxylates are indicative of the presence of unidentate carboxylate groups. The separation (Δ) between ν_{asym} (CO_2) and ν_{sym} (CO_2) is greater than that for the corresponding carboxylate ions (14). The presence of a doublet in the spectra of mono- and di-substituted acetates can be attributed to the presence of conformational isomers as discussed in the case of organotin haloacetates (15).

In summary, the molecular weight, conductance, and infrared data show that triphenylbismuth(V) acid derivatives such as dihalides, dinitrate, dicyanate, and dicarboxylates have non-ionic molecular constitution. The infrared spectroscopic data is consistent with five coordinate structures.

The financial assistance from the National Research Council of Canada is gratefully acknowledged.

Can. J. Chem. Downloaded from www.nrcresearchpress.com by 210.87.254.105 on 09/05/12
For personal use only.

1. Michael Dub (*Editor*). Organometallic compounds. Vol. 3. Springer–Verlag. New York. 1968.
2. K. A. JENSEN. Z. Anorg. Chem. **250**, 257 (1943).
3. A. D. BEVERIDGE, G. S. HARRIS, and F. INGLIS. J. Chem. Soc. (A), 520 (1966).
4. D. M. HAWLEY and G. FERGUSON. J. Chem. Soc. (A), 2539 (1968).
5. E. L. MUETTERTIES, W. MAHLER, K. J. PACKER, and R. SCHMUTZLER. Inorg. Chem. **3**, 1298 (1964).
6. R. S. DRAGO. *In* Non aqueous solvent systems. *Edited by* T. C. Waddington. Academic Press, Inc., New York. 1965. p. 235.
7. K. M. MACKAY, D. B. SOWERBY, and W. C. YOUNG. Spectrochim. Acta, **24A**, 611 (1968).
8. K. A. JENSEN and P. H. NELSON. Acta Chem. Scand. **17**, 4 (1963).
9. K. SHOBATAKE, C. POSTMUS, J. R. FERRARO, and K. NAKAMOTO. Appl. Spectrosc. **23**, 12 (1969).
10. R. G. GOEL, EDWARD MASLOWSKY, JR., and C. V. SENOFF. To be published.
11. G. O. DOAK, G. G. LONG, and L. D. FREEDMAN. J. Organometal. Chem. Amsterdam, **4**, 82 (1965).
12. J. BELLANATO and J. R. BARCELLO. Spectrochim. Acta, **16**, 1333 (1960).
13. J. R. BARCELLO and C. OTERO. Spectrochim. Acta, **18**, 1231 (1962).
14. E. SPINNER. J. Chem. Soc. 4217 (1964).
15. P. B. SIMONS and W. A. G. GRAHAM. J. Organometal. Chem. Amsterdam, **10**, 457 (1967).
16. E. V. VAN DEN BERGHE, G. P. VAN DER KELEN, and J. ALBRECHT. Inorg. Chim. Acta, **2**, 89 (1968).
17. R. G. GOEL and D. R. RIDLEY. To be published.
18. G. B. DEACON and F. B. TAYLOR. Aust. J. Chem. **21**, 2675 (1986).

Can. J. Chem. Downloaded from www.nrcresearchpress.com by 210.87.254.105 on 09/05/12
For personal use only.

Can. J. Chem. Downloaded from www.nrcresearchpress.com by 210.87.254.40 on 09/05/12
For personal use only.

The pressure dependence of benzyl chloride solvolysis in aqueous acetone and aqueous dimethylsulfoxide

DIGBY D. MACDONALD AND J. B. HYNE

Department of Chemistry, University of Calgary, Calgary, Alberta

Received April 6, 1970

First-order rate constants for the solvolysis of benzyl chloride in a series of aqueous acetone and aqueous dimethylsulfoxide (DMSO) mixtures at 50.100 °C and at various pressures in the range 1–4083 atm are reported. Volume of activation, calculated from the rate/pressure data, is found to exhibit extremum behavior with varying solvent composition in both solvent systems. The activation volumes are dissected into their initial state and transition state contributions by determining the "instantaneous" volumes of solution of benzyl chloride in the solvent systems. The contributions of both the initial state and the transition state to the behavior of the activation volume as a function of solvent composition are discussed.

Canadian Journal of Chemistry, 48, 2494 (1970)

Introduction

As part of our continuing program of study of solvolysis reactions in aqueous–organic binary solvent systems we have measured rates of solvolysis of benzyl chloride in aqueous acetone and aqueous dimethylsulfoxide (DMSO) as a function of pressure in the range 1–4083 atm and as a function of solvent composition at 50.100 °C. Acetone and DMSO were chosen as a cosolvent pair to permit examination of the effect of changing the polarity or hydrophilic character of the cosolvent while maintaining the hydrophobic nature, as conferred by the two methyl groups in each molecule, relatively constant. The dipole moments of the two cosolvents are 2.9 and 4.3 D, respectively, (1) and it might be reasonably expected that this significant change in polar group character would be reflected in the solvolytic behavior of a solute such as benzyl chloride. The pressure dependence of the reaction rate enables the volume of activation to be determined and used as a parameter for comparing the solvolytic behavior in the two solvent systems. Additionally, however, the volume of activation is dissected into initial and transition state contributions by using a recently developed technique (2) for determining the "instantaneous" volumes of solution of benzyl chloride in the solvent systems. The dependence of the volume of activation and the partial molal volumes of the initial and transition states on solvent composition in both solvent systems is discussed with reference to known properties of the binary solvent systems.

Experimental

Materials

Eastman practical grade DMSO was dried over freshly cut calcium hydride for a period of not less than 48 h. The decanted product was then distilled at reduced pressure (~ 10 mm Hg) and the middle 50% cut collected and stored in a tightly stoppered bottle. The purity of the distilled product was checked by melting point (found, 18.52 °C; lit., 18.55 °C (3)) and refractive index (found, $n_D^{20} = 1.3590$; lit., $n_D^{19.4} = 1.35886$ (3)).

Fisher spectral grade acetone was used without further purification.

Singly distilled water was passed through Illco-Way deionizing resin, redistilled, and stored in a tightly stoppered polyethylene container.

Eastman white label benzyl chloride was distilled at 23.5 mm Hg and the middle 50% cut collected at 78.5–80.0 °C. It was periodically distilled in small quantities (5 ml at 10^{-3} mm Hg) as needed. The purity was checked by refractive index (found, $n_D^{20} = 1.5385$; lit., $n_D^{20} = 1.5391$ (4)).

Kinetic Method

Aqueous–organic binary solvents were prepared by weight to ± 0.0002 mole fraction units.

The rate of production of hydrochloric acid resulting from hydrolysis of benzyl chloride was followed by an in situ conductimetric technique described previously (5). The high pressure vessel, pressure control, and conductance cell have been described in an earlier publication (5). Temperature control was maintained at ± 0.005 °C by oil bath thermostatting. Pseudo first-order rate constants were extracted from conductance/time data by the Guggenheim method (6).

Partial Molal Volumes

The aqueous–organic binary solvents used in the partial molal volume studies were prepared as described above. The solvents were degassed immediately before use by the conventional freeze–pump–thaw method.

The dilatometric technique used to measure the "instantaneous" volume of solution of reactive benzyl

Can. J. Chem. Downloaded from www.nrcresearchpress.com by 210.87.254.40 on 09/05/12
For personal use only.

chloride in the solvent systems has been described in detail (2). Briefly, the method involves determining the change in height of the solvent meniscus in the dilatometer capillary on rapid injection of a known number of moles of benzyl chloride. Efficient thermostatting to better than ± 0.005 °C at 50.100 °C was attained using a thermostat similar to that described in a previous publication (2). Thermal equilibration was indicated by time independence of the solvent meniscus in the capillary.

Results

Rates

Pseudo first-order rate constants for the solvolysis of benzyl chloride in aqueous acetone and aqueous DMSO as a function of pressure and solvent composition at 50.100 °C are presented in Table 1. Each rate constant represents the mean of at least four determinations and was normally reproducible to better than ± 1%.

Volumes of Activation

The volume of activation at a given temperature and pressure, ΔV^*, is related to the pressure dependence of rate constant by eq. [1].

$$[1] \qquad \Delta V^* = -RT\,(\partial \ln k/\partial p)_T$$

In order to evaluate ΔV^* it is necessary to ascertain the functional dependence of ln k upon p. A typical plot of ln k vs. p is shown in Fig. 1. The plot is clearly non-linear demanding at least a second-order function to describe the dependence of ln k upon p. The problem of deriving an analytical expression for this dependence has been discussed at length by various workers (7, 8). Golinkin, Laidlaw, and Hyne (7) concluded that the quadratic function

$$[2] \qquad \ln k = A + Bp + Cp^2$$

provided the best representation of the dependence of ln k upon p for benzyl chloride solvolysis in aqueous alcohols. Since the solvent systems used in this work are closely related to the aqueous alcohols, eq. [2] will be used here without further justification.

Differentiation of eq. [2] with respect to pressure and substitution into eq. [1] yields eq. [3] for the volume of activation at atmospheric pressure, ΔV_0^*.

$$[3] \qquad \Delta V_0^* = -RT\,(B + 2C)$$

The coefficients B and C in eq. [2] were obtained from a least-mean squares fit of the data listed in Table 1. Uncertainties in ΔV_0^* were calculated using eq. [4] where δB and δC are deviations in B and C obtained directly from the least-mean squares analysis.

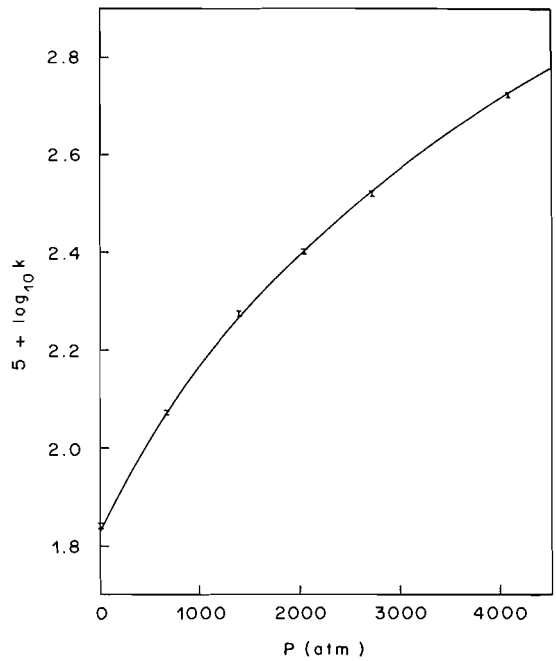

FIG. 1. Plot of log k vs. pressure for benzyl chloride solvolysis in 0.150 mole fraction acetone at 50.100 °C.

$$[4] \qquad \delta\Delta V_0^* = \pm\, RT\,(\delta B + 2\delta C)$$

The volumes of activation and corresponding uncertainties are listed in Table 2. It should be stressed at this point that the uncertainties listed in Table 2 are those obtained on the basis that eq. [2] represents the correct functional dependence of ln k upon p. Since this question is subject to considerable controversy (7, 8), the actual uncertainty in ΔV_0^* is probably greater than that calculated from the least-mean square fit of the rate/pressure data to eq. [2]. For benzyl chloride solvolysis in various aqueous ethanol solvents (7), the quadratic and incremental functions, the two most commonly used expressions for obtaining ΔV_0^* from rate/pressure data, yield values which show an average difference of less than 1 ml mole^{-1}. On this basis a reasonable estimate for the uncertainty in ΔV_0^* obtained in this work is ± 0.5 ml mole^{-1}.

Further differentiation of eqs. [1] and [2] with

Can. J. Chem. Downloaded from www.nrcresearchpress.com by 210.87.254.40 on 09/05/12
For personal use only.

TABLE 1

Rate constants as a function of pressure and solvent composition for benzyl chloride solvolysis in aqueous acetone and aqueous DMSO at 50.100 °C $10^7 \times k$ (s^{-1})

Mole fraction cosolvent	$10^7 \times k$ (s^{-1}) at pressure[a] (atm) =							
	1	340.2	680.5	1020.7	1360.9	2041.4	2721.8	4082.7
Aqueous Acetone								
0.050	647.5 ±5.8	772.5±2.5	911.1 ±5.6	1069.0±21.7	1180.8 ±0.4	1495.0 ±10	1809.0 ±21	
0.100	180.0 ±2.0	247.9±0.5	360.7 ±0.5	371.9± 3.0	430.8 ±1.7	589.5 ± 4.0	745.8 ± 3.0	1114.0 ±5.0
0.150	69.6 ±0.3		119.8 ±0.6		190.8 ±2.5	250.8 ± 0.1	329.4 ± 0.6	533.7 ±2.0
0.200	30.4 ±0.2	41.5±0.17	53.5 ±0.39	62.8± 1.5	78.5 ±1.0	109.3 ± 1.0	160.4 ±20	271.2 ±0.5
0.298	9.182±0.096		16.17 ±0.08		25.62 ±0.1	36.59± 0.41	53.0 ± 1	84.79±0.20
0.409	3.714±0.008		5.810±0.035		8.582±0.1	13.34± 0.04	17.54± 0.13	28.60±0.30
Aqueous DMSO								
0.075	1175 ±4	1314 ±2	1535 ±4	1714 ±7	1966 ±8	2386 ±50	2705 ±40	
0.150	673.2±4	798.3±0.8	938.9±3	1102 ±6	1237 ±1	1530 ±30	1906 ± 1	2541.7±10
0.225	424.4±0.1	515.0±0.8	616.6±3	709.6±3	833.3±3	1059 ± 2	1347.5±10	1916.6± 4.1
0.300	275.2±1	338.5±1	410.6±0.4	489.0±0.1	576.7±1.3	756.3± 1	981.7± 1.7	1414.6± 2.1
0.399	180.6±0.6		274.2±0.4		385.6±2	527.9± 1.7	695.0± 1.7	1067.1± 3.8
0.497	132.6±0.7		204.1±0.3		310.0±3	375.9± 0.9	492.6± 1.2	773.6± 1.5
0.600	63.6±1		103.5±1.2			221.9± 1.3	314.5± 0.3	557.5± 1.9

[a]Pressures greater than 1 atm are accurate to ±10 atm.

TABLE 2

Activation parameters for benzyl chloride solvolysis in aqueous acetone and aqueous DMSO at 50.100 °C

Solvent	Mole fraction of solvent	$-\Delta V_0^*$ (ml mole^{-1})	$10^3\,(\partial\Delta V^*/\partial p)_T$ (ml mole^{-1} atm^{-1})
Aqueous acetone	0.000	9.79±0.13[a]	0[a]
	0.050	13.91±0.16	2.94±0.13
	0.100	17.75±0.09	3.21±0.05
	0.150	20.22±0.05	3.59±0.02
	0.200	19.33±0.25	2.66±0.13
	0.298	20.37±0.30	3.15±0.13
	0.409	17.32±0.20	2.03±0.04
Aqueous DMSO	0.075	11.92±0.01	2.26±0.13
	0.150	13.10±0.06	2.23±0.13
	0.225	14.15±0.02	2.19±0.10
	0.300	15.87±0.10	2.60±0.05
	0.399	16.31±0.06	2.36±0.04
	0.497	16.30±0.08	2.51±0.03
	0.500	18.85±0.24	2.40±0.08

[a]Reference 24.

respect to pressure yields the pressure dependence of activation volume.

$$[5] \qquad (\partial\Delta V^*/\partial p)_T = -2RTC$$

While it is not our intention to discuss the significance of this second pressure differential of reaction rate in this paper, it is clear from the values and corresponding uncertainties recorded in Table 2 that the second derivative is not zero valued and that it also exhibits extremum behavior as a function of solvent composition. Uncertainties in $(\partial\Delta V^*/\partial p)_T$ were calculated from uncertainties in coefficient C yielded by the least-squares fit of the rate/pressure data to eq. [2].

Partial Molal Volumes

Since the solutions used in this study were very dilute ($\sim 5 \times 10^{-4}\ M$), it was assumed that the apparent molal volume could be taken as the partial molal volume of the solute at infinite dilution. The partial molal volume of benzyl chloride (initial state) at infinite dilution is therefore given by the following expression (2)

$$[6] \qquad \bar{V}_g^0 = \Delta V_{obs}/n$$

where ΔV_{obs} is the observed change in volume of the solvent on injection of n moles of benzyl chloride.

Numerical values for $\bar{V}_g^0$ as a function of aqueous acetone and aqueous DMSO solvent composition are given in Table 3. Each value represents the mean of four independent determinations and the errors quoted are average deviations from the means.

TABLE 3

Partial molal volumes of benzyl chloride at infinite dilution in aqueous acetone and aqueous DMSO at 50.100 °C

Solvent	Mole fraction of solvent	$\bar{V}_g^0$ (ml mole^{-1})
Aqueous acetone	0.000[a]	115.0±0.5
	0.050	116.5±0.3
	0.100	126.9±0.3
	0.150	128.5±0.3
	0.200	127.5±0.4
	0.298	124.0±0.3
	0.409	119.5±0.2
Aqueous DMSO	0.075	115.4±0.3
	0.150	115.6±0.4
	0.225	115.5±0.2
	0.300	116.2±0.4
	0.399	118.3±0.2
	0.497	119.0±0.2
	0.600	115.5±0.3

[a]Reference 2.

Discussion

The volumes of activation reported in this work for benzyl chloride solvolysis in aqueous acetone and aqueous DMSO are negative. Negative volumes of activation are also found for benzyl chloride solvolysis in aqueous alcohols (2, 5) and for a large number of alkyl ester solvolysis reactions in polar solvent systems (9–11). The negative sign for ΔV_0^* can be explained by the fact that where an S_N1 or S_N2 type mechanism is operative, as in benzyl chloride solvolysis, the transition state is normally a more

Can. J. Chem. Downloaded from www.nrcresearchpress.com by 210.87.254.40 on 09/05/12
For personal use only.

Can. J. Chem. Downloaded from www.nrcresearchpress.com by 210.87.254.40 on 09/05/12
For personal use only.

polar species than the initial state. Accordingly, volume reduction by greater electrostriction of solvent about the transition state than about the initial state will tend to outweigh any volume increase due to bond extension in the activation process (9–11).

The dependence of ΔV_0^* on solvent composition for benzyl chloride solvolysis in aqueous acetone (solid line) and aqueous DMSO (broken line) is shown in Fig. 2. In both solvent systems, ΔV_0^* is seen to exhibit extremum behavior as a function of solvent composition and it may be noted that the extremum behavior is more pronounced in aqueous acetone than in aqueous DMSO. Other pseudo thermodynamic activation parameters, namely ΔH^* and ΔS^*, also undergo extremum behavior with varying solvent composition for benzyl chloride solvolysis in aqueous acetone (12) and aqueous DMSO (13). Extremum behavior in the dependence of activation parameters on solvent composition is also well documented for various solvolysis reactions in aqueous–organic solvent systems (14, 15) including benzyl chloride solvolysis in aqueous alcohols (2, 5) and *p*-methylbenzyl chloride solvolysis in aqueous acetone (16). The appearance of extrema in the variation of ΔV_0^* with solvent composition for benzyl chloride solvolysis in the solvent systems of interest here is therefore not surprising, since this behavior appears to be the rule rather than the exception for solvolysis reactions in aqueous–organic binary solvent systems.

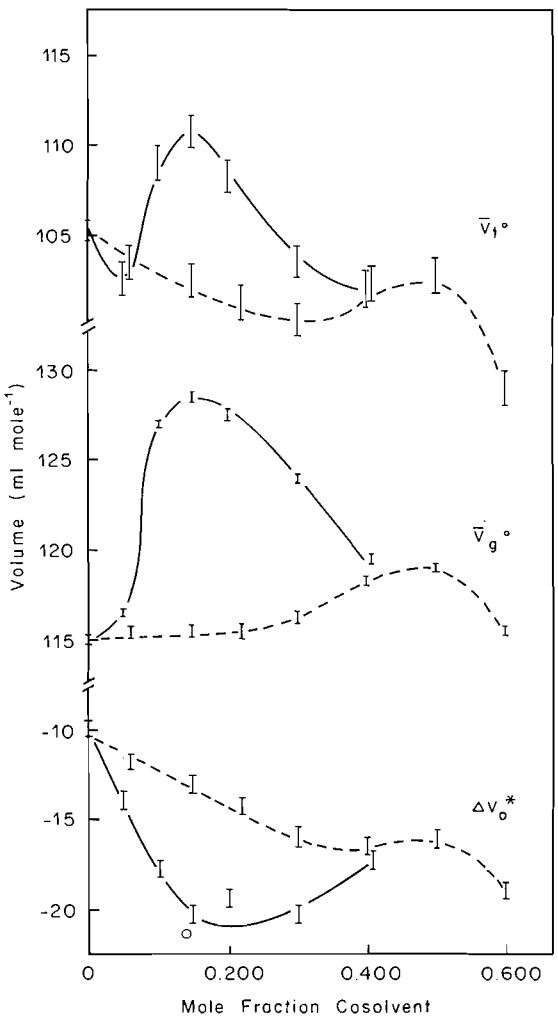

FIG. 2. Dependence of ΔV_0^*, $\bar{V}_g^0$, and $\bar{V}_t^0$ on solvent composition. Solid line, aqueous acetone; broken line, aqueous DMSO, ○, ΔV_0^* for benzyl chloride solvolysis in 0.1407 mole fraction acetone at 50 °C (14).

The volume of activation, ΔV_0^*, is defined as the difference between the partial molal volumes of the transition state ($\bar{V}_t^0$) and the initial state ($\bar{V}_g^0$).

$$[7] \qquad \Delta V_0^* = \bar{V}_t^0 - \bar{V}_g^0$$

Both ΔV_0^* and $\bar{V}_g^0$ have been determined experimentally in this work as a function of solvent composition for benzyl chloride solvolysis in aqueous acetone and aqueous DMSO. Consequently, the dependence of $\bar{V}_t^0$ on solvent composition can be easily determined using eq. [7]. Analyses of this type have been previously carried out for benzyl chloride solvolysis in aqueous alcohols (2) and for *p*-methylbenzyl chloride solvolysis in aqueous acetone (16).

The dependence of ΔV_0^*, $\bar{V}_g^0$, and $\bar{V}_t^0$ on solvent composition for the reactions under investigation is shown in Fig. 2. It is seen that in both solvent systems $\bar{V}_g^0$ passes through a maximum with varying solvent composition. In aqueous acetone the maximum in $\bar{V}_g^0$ occurs at the same solvent composition (0.15 mole fraction acetone) as the minimum in ΔV_0^*. Since no minimum occurs in $\bar{V}_t^0$ at 0.15 mole fraction acetone then the minimum in ΔV_0^* at this solvent composition arises principally from the maximum in $\bar{V}_g^0$. A similar conclusion was reached concerning the origin of the minima in ΔV_0^* for benzyl chloride solvolysis in aqueous alcohols (2) and *p*-methylbenzyl chloride solvolysis in aqueous acetone (16).

Can. J. Chem. Downloaded from www.nrcresearchpress.com by 210.87.254.40 on 09/05/12
For personal use only.

In aqueous DMSO, however, the situation is quite different. Although $\overline{V}_g^0$ does pass through a maximum it does not do so at the solvent composition where ΔV_0^* passes through a minimum, i.e. at 0.3–0.4 mole fraction DMSO. Instead, $\overline{V}_t^0$ is seen to pass through a minimum at this solvent composition and we must conclude that the minimum in ΔV_0^* at 0.3–0.4 mole fraction DMSO arises principally from the behavior of the *transition state* and not from the behavior of the initial state as was found to be the case in aqueous acetone.

The possible relationship between the solvolytic behavior of benzyl chloride and the properties of the aqueous organic binary solvent system deserves discussion. Aqueous acetone displays large positive deviations from Raoult's law (17) and in this respect the binary mixture behaves like the aqueous alcohols (18). It is not too surprising, therefore, to find that the minima in ΔV_0^* for benzyl chloride solvolysis in aqueous acetone and in the aqueous alcohols have common origins, viz. maxima in $\overline{V}_g^0$. Aqueous DMSO, however, displays large negative deviations from Raoult's law (19). Other binary mixtures that show large negative deviations from Raoult's law, e.g. chloroform–acetone, are characterized by strong intercomponent interaction (17, 18). Several workers (19–22) have suggested that strong intercomponent interaction determines the properties of aqueous DMSO and that these interactions are maximal at 0.33 mole fraction DMSO resulting in the formation of transient polymeric species of the type $(DMSO{\cdot}2H_2O)_n$. This is in the range of solvent composition where $\overline{V}_t^0$ passes through a minimum and it seems reasonable to conclude that the minimum in $\overline{V}_t^0$ reflects some solvent structural property such as the suggested transient co-polymer. The maxima in $\overline{V}_g^0$ and $\overline{V}_t^0$ in aqueous DMSO occur at nearly the same solvent composition as a negative minimum in the excess volume of mixing of the DMSO–H_2O system (23). This minimum very likely reflects a minimum in the free volume of the solvent system at this composition. Accordingly, the solute, be it either benzyl chloride or the solvolysis transition state, will require maximum expansion of the solvent mixture at this composition to accommodate it. Maxima in both $\overline{V}_g^0$ and $\overline{V}_t^0$ are therefore observed.

The results described in this paper provide further evidence of the very significant differences between aqueous acetone and aqueous DMSO as solvolytic media despite their similarity in both structure and hydrophobic character. The analysis also serves to illustrate the very considerable extent to which variations in solvent structural features are reflected in the kinetic behavior of reactions taking place in these media.

The authors would like to thank Dr. I. Lee for assistance in measuring partial molal volumes. General financial assistance, as well as a studentship to D. D. Macdonald, from the National Research Council of Canada, is gratefully acknowledged.

1. A. L. McClellan. Tables of experimental dipole moments. W. H. Freeman and Co., San Francisco. 1963.
2. H. S. Golinkin, I. Lee, and J. B. Hyne. J. Amer. Chem. Soc. **89**, 1307 (1967).
3. D. Martin, A. Weise, and H. J. Niclas. Angew. Chem. Int. Ed. **6**, 318 (1967).
4. Handbook of chemistry and physics. 46th. ed. The Chemical Rubber Co. 1966.
5. J. B. Hyne, H. S. Golinkin, and W. G. Laidlaw. J. Amer. Chem. Soc. **88**, 2104 (1966).
6. E. A. Guggenheim. Phil. Mag. **2**(7), 538 (1926).
7. H. S. Golinkin, W. G. Laidlaw, and J. B. Hyne. Can. J. Chem. **44**, 2193 (1966).
8. B. T. Baliga and E. Whalley. Can. J. Chem. **48**, 528 (1970).
9. E. Whalley. *In* advances in physical organic chemistry. Vol. 2. *Edited by* V. Gold. Academic Press Inc., New York. 1964.
10. W. J. le Noble. Prog. Phys. Org. Chem. **5**, 207 (1967).
11. S. D. Hamann. Physico-chemical effects of pressure. Butterworths Scientific Publ. London. 1957.
12. E. Tommila, E. Paakkala, U. K. Virtanen, A. Erva, and S. Varila. Ann. Acad. Sci. Fenn. **A11**(91), 1 (1959).
13. E. Tommila. Acta Chem. Scand. **20**, 923 (1966).
14. H. Heydtmann and H. Stieger. Ber. Bunsen. **70**, 1095 (1966).
15. B. T. Baliga, R. T. Withey, D. Poulton, and E. Whalley. Trans. Faraday Soc. **61**, 517 (1965).
16. K. J. Laidler and R. Martin. Int. J. Chem. Kinet. **1**, 113 (1969).
17. J. S. Rowlinson. Liquids and liquid mixtures. 2nd ed. Butterworth, London. 1969. p. 168.
18. F. Franks and D. J. G. Ives. Quart. Rev. **20**, 1 (1966).
19. J. Kenttamaa and J. J. Lindberg. Suomen Kem. **B33**, 98 (1960).
20. A. J. Parker. Quart. Rev. **16**, 163 (1962).
21. J. J. Lindberg and J. Kenttamaa. Suomen Kem. **B33**, 104 (1960).
22. J. M. G. Cowie and P. M. Toporowski. Can. J. Chem. **39**, 2240 (1961).
23. R. J. Fort and W. R. Moore. Trans. Faraday Soc. **61**, 2102 (1965).
24. S. J. Dickson. Ph.D. Thesis. University of Calgary, Calgary, Alberta. 1970.

Can. J. Chem. Downloaded from www.nrcresearchpress.com by 210.87.254.40 on 09/05/12
For personal use only.

Structural features of a lipopolysaccharide isolated from *Escherichia coli* 086:$K_{neg.}$[1]

PREM PAL SINGH[2] AND G. A. ADAMS
Biochemistry Laboratory, National Research Council of Canada, Ottawa, Canada

Received March 26, 1970

Lipopolysaccharide (LPS) prepared from *Escherichia coli* 086:$K_{neg.}$, in 5.5% yield contained D-galactose, D-glucose, L-fucose, L-*glycero*-D-*manno*-heptose, D-glucosamine, D-galactosamine, 2-keto-3-deoxy-octulosonic acid (KDO) and lipid A. The molecule appeared to be homogeneous as tested by free boundary electrophoresis, ultracentrifugation, and immunodiffusion against 'O' specific *E. coli* antiserum. Methylation studies of the LPS and also of the degraded polysaccharides obtained by partial acid hydrolysis showed that the molecule was highly branched. Sixty percent of the D-galactose units were non-reducing terminal groups, the remainder were linked (1 → 3) and (1 → 2) and 3-*O*-β-D-galactopyranosyl-D-galactose was identified as a product of mild acid hydrolysis of the parent LPS. Fucose occurred in the polysaccharide as (1 → 4) linked units. Methylation results showed that the D-glucose units were linked (1 → 3) and (1 → 4). Partial acid hydrolysis yielded cellobiose, cellotriose, and laminaribiose, showing that the glucose units formed a glucan chain within the polysaccharide and that the glucosidic linkages were in the β-D-configuration. Approximately one half of the L-*glycero*-D-*manno*-heptose units occurred as non-reducing end groups, the other half were linked at C-3 and either one of C-6 or C-7. One half of the D-galactosamine units was linked (1 → 3) with the remainder occurring as double branch points. D-Glucosamine residues occurred exclusively in the lipid A moiety in a (1 → 4) linked core structure.

Canadian Journal of Chemistry, **48**, 2500 (1970)

Introduction

Although the lipopolysaccharide composition of many chemotypes of *E. coli* has been determined, relatively little information is available on their chemical structure. Variability in composition with respect to the lesser sugar components has presented a very large number of chemically different lipopolysaccharides (LPS) within the *E. coli* species and their compositional and serological interrelationships, rather than their chemical structure, have been a primary consideration in most investigations (1, 2).

The present investigation of the chemical constitution of the LPS of *E. coli* 086:$K_{neg.}$ was of interest because it is a mutant free of K-antigen. It was thus possible to prepare the pure 'O'-somatic antigen (LPS) and to study its chemistry without the possibility of having K-antigen as an impurity. The other unusual feature of the LPS was its relatively high proportion of L-fucose which occurs rarely in the LPS of *E. coli*. The only other structural study on a fucose-containing LPS of *E. coli* was that on *E. coli* 086 by Springer *et al.* (3) who isolated an oligosaccharide to which was assigned the following structure: *O*-α-D-Gal*p*-(1 → 3)-*O*-β-D-Gal*p*-(1 → 3) or (1 → 4)-*O*-2-acetamido-2-deoxy-β-D-Gal with a fucopyranosyl residue attached α to the subterminal D-galactose unit.

Results and Discussion

E. coli cells on phenol extraction (4) afforded a crude lipopolysaccharide (LPS) from which nucleic acids were removed by 'Cetavlon' precipitation. The pure LPS had $[\alpha]_D^{22}$ + 37° (*c* 1, dimethyl sulfoxide) and was shown to be homogeneous by ultracentrifugation, free boundary electrophoresis, and immunodiffusion tests against an 'O' specific antiserum. The LPS was composed of D-galactose, D-glucose, L-fucose, L-*glycero*-D-*manno*-heptose, D-glucosamine, D-galactosamine in a molar ratio of 7.0:2.2:3.1:1.0:0.4:2.6 (Table 1). 2-Keto-3-deoxyoctulosonic acid (KDO) and lipid A were also identified as components of the LPS. Graded hydrolysis of the LPS with sulfuric acid yielded mainly monosaccharides. Galactose and fucose were readily removed by hydrolysis with 0.01 *N* acid and their removal was almost complete by additional heating in 0.1 *N* acid for 6 h. Glucose was not removed in significant amounts until 0.5 *N* acid hydrolysis was used. These results indicated that the galactose and fucose units were on the periphery of the molecule and also attached by weaker linkages than were the glucose residues. Identification of 3-*O*-β-D-galactopyranosyl-D-galactose showed that some D-galactose units were linked

[1]Issued as NRCC No. 11376.
[2]NRCC Postdoctorate fellow 1967–1969.

TABLE 1

Composition of lipopolysaccharides (LPS) and derived polysaccharides (PS **1**, PS **2**, and PS **3**) from *E. coli*

Compounds	$[\alpha]_D^\circ$		Sugars (molar ratio)					
	Original	Methylated	Galactose	Glucose	Fucose	Heptose	Glucos-amine	Galactos-amine
LPS	+37.0 (*c* 1, DMSO)	+47.0 (*c* 1, $CHCl_3$)	7.0	2.2	3.1	1.0	0.4	2.6
PS **1**	+77.0 (*c* 1, DMSO)	+91.0 (*c* 1, $CHCl_3$)	2.2	1.6	1.0	—	—	Trace
PS **2**	+84.0 (*c* 1, DMSO)	+92.0 (*c* 1, $CHCl_3$)	2.3	6.3	1.0	—	—	—
PS **3**	+96.0 (*c* 1, water)	+73.0 (*c* 1, $CHCl_3$)	—	+	—	—	—	—

$\beta(1 \rightarrow 3)$ to each other. The low yield of this disaccharide and the absence of higher oligosaccharides in the series suggested that there were few contiguous units linked in this way. No fucose oligosaccharides were found suggesting that the fucose residues were attached by relatively acid-labile linkages. The presence of cellotriose and cellobiose established the linkage between some glucose units as $\beta(1 \rightarrow 4)$; laminaribiose established the existence of $\beta(1 \rightarrow 3)$ linkages although the latter were present in the hydrolyzate in a relatively small proportion.

The methylated LPS, $[\alpha]_D$ + 47° (*c* 1, chloroform), on hydrolysis gave various methylated sugars which are recorded in Table 2. Results of the methylation studies showed that the LPS must contain the units shown in Chart 1 in the relative proportions indicated. From these data certain structural features become apparent. Since 60% of the galactose units occurred as terminal units (**2**) and the remaining 40% were branch points, it was clear that the molecule was highly branched. The relatively high proportion of component **8** showed that the branching occurred at C-2 and C-3. The occurrence of $(1 \rightarrow 3)$ linked galactose residues **6** was substantiated by the earlier identification of the disaccharide 3-*O*-β-D-galactopyranosyl-D-galactose. The relatively small amount of 3-*O*-β-D-galactopyranosyl-D-galactose found indicated that there were few continguous $\beta(1 \rightarrow 3)$ linked D-galactose residues.

The L-fucose units were all recovered as 2,3-di-*O*-methyl-L-fucose showing that they were joined exclusively by $(1 \rightarrow 4)$ linkages; this conclusion was supported by the oxidation of all L-fucose residues by periodate. These residues (**3**) could be in a main chain or in side chains, either position would yield 2,3-di-*O*-methyl-L-fucose on hydrolysis of the methylated polysaccharide and the present evidence does not specifically locate the L-fucose residues in the molecule.

The occurrence of **4** and **5** shows that the D-glucose units were linked $(1 \rightarrow 3)$ and $(1 \rightarrow 4)$; a conclusion that was confirmed by the identification of laminaribiose and cellobiose as products of partial hydrolysis. Almost one third of the D-glucose units were branched through both C-3 and C-6 giving rise to component **7**.

Partial acid hydrolysis of the LPS with 0.25 *N* sulfuric acid for 2.5 h followed by precipitation with ethanol yielded a polysaccharide (PS **3**) which contained only D-glucose residues. Also stepwise acid hydrolysis of LPS (Fig. 1) yielded polysaccharides PS **1** and PS **2**, both of which contained a higher proportion of D-glucose than the parent LPS (Table 1). These findings indicated that the D-glucose units were linked together in a block. Methylation of the glucan (PS **3**) yielded 2,3,6- and 2,4,6-tri-*O*-methyl-D-glucose in a molar ratio of 1:2 showing that the $(1 \rightarrow 3)$ linked glucose units were twice the number of $(1 \rightarrow 4)$ units. These conclusions were substantiated by the results of periodate degradation of the glucan (glucose:erythritol 1.66:1.0). Identification of the cellotriose, cellobiose, and laminaribiose established some of the linkage sequences and configurations. Methylation of the parent LPS yielded 2,3,6- and 2,4,6-tri-*O*-methyl-D-glucose and 2,4-di-*O*-methyl-D-glucose in approximately equimolar proportions while methylation of PS **1** and PS **2** gave 2,3,6- and 2,4,6-tri-*O*-methyl-D-glucose in a molar ratio of approximately 1:2. These data indicate that, in the parent LPS, one

Can. J. Chem. Downloaded from www.nrcresearchpress.com by 210.87.254.40 on 09/05/12
For personal use only.

Can. J. Chem. Downloaded from www.nrcresearchpress.com by 210.87.254.40 on 09/05/12
For personal use only.

TABLE 2

Methylated neutral sugars obtained on hydrolysis of methylated lipopolysaccharide and derived polysaccharides PS **1**, PS **2**, and PS **3** from *E. coli*

Sugars	R_F*	T_G†		Demethylation product	Molar ratio			
		Column *B*‡	Column *D*§		LPS	PS **1**	PS **2**	PS **3**
2,3,4,6,7-Penta-*O*-methyl-L-*glycero*-D-*manno*-heptose	0.85	4.0	3.1	Heptose	1.0	—	—	—
2,3,4,6-Tetra-*O*-methyl-D-galactose	0.68	1.23	1.22	Galactose	8.1	2.2	1.0	—
2,3-Di-*O*-methyl-L-fucose	0.67	0.42; 0.50; 0.69; 0.99	0.42; 0.48; 0.60; 0.66	Fucose	6.2	2.0	1.0	—
2,3,6-Tri-*O*-methyl-D-glucose	0.43	1.4; 2.34	1.34; 1.76	Glucose	1.0	1.0	1.0	1.0
2,4,6-Tri-*O*-methyl-D-glucose	0.43	2.58; 3.23	1.30; 1.80	Glucose	1.2	1.8	1.8	2.1
2,4,6-Tri-*O*-methyl-D-galactose	0.34	2.95; 3.4	1.60; 1.85	—	—	Trace	Trace	—
2,4-Di-*O*-methyl-D-glucose	0.26	3.92; 5.11	1.71; 2.47	Glucose	2.0	—	—	—
Tri-*O*-methyl-heptose	0.24			Heptose	1.0	—	—	—
4,6-Di-*O*-methyl-D-galactose	0.18	6.30; 11.9	2.07; 2.90	Galactose	6.3	2.2	1.0	—

*Solvent *c*: butanone saturated with water.
†T_G is the retention time relative to methyl-2,3,4,6-tetra-*O*-methyl-α-D-glucoside. When two values are given they represent retention times of the β and α anomers.
‡Ten percent butanediol succinate polyester on Chromosorb W at 150° (T_G = 1.00, 2 min).
§Fifteen per cent polyphenol on Chromosorb W at 190° (T_G = 1.00, 7 min).

Can. J. Chem. Downloaded from www.nrcresearchpress.com by 210.87.254.40 on 09/05/12
For personal use only.

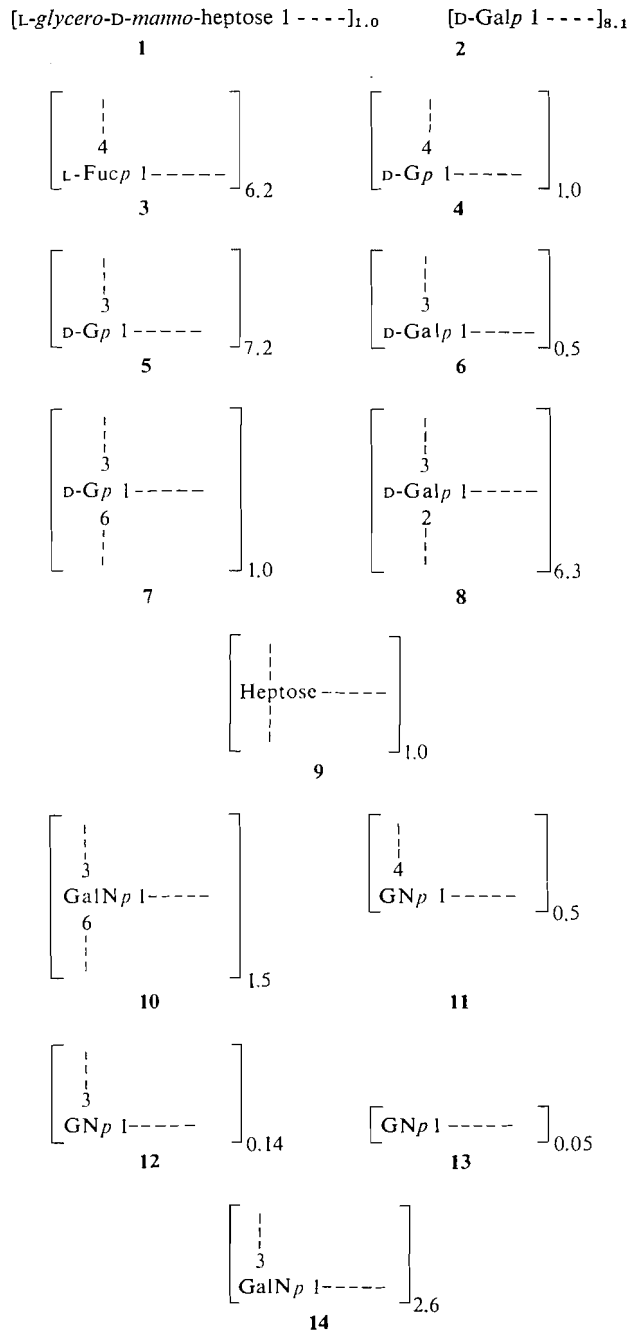

CHART 1

of every two (1 → 3) linked D-glucose units was branched at C-6 and on methylation gave rise to 2,4-di-*O*-methyl-D-glucose. Although the substituent on C-6 is not known, it may be speculated that it is D-galactose as it would account for the excess non-reducing terminal D-galactose units over the branched galactose units. The results of the periodate degradation experiments (Table 3) show that the 1 → 4 linked D-glucose residues were oxidized by periodate and on reduction yielded erythritol.

Hydrolysis of the methylated LPS yielded

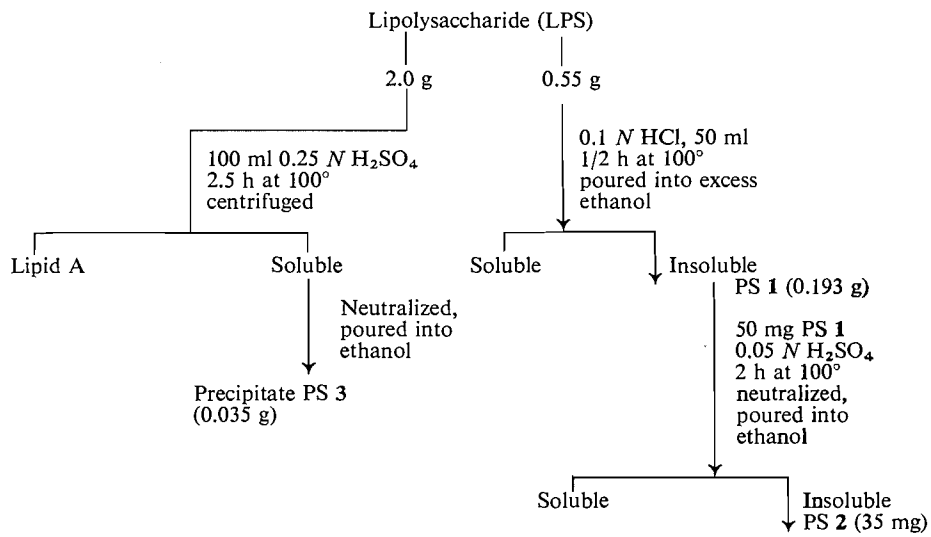

FIG. 1. Partial hydrolysis products of lipopolysaccharide of *E. coli* (polysaccharides PS **1**, PS **2**, and PS **3**).

TABLE 3

Results of periodate oxidation, reduction and hydrolysis of Lipopolysaccharide (LPS) and derived polysaccharides (PS **1**, PS **2**, and PS **3**) from *E. coli*

Polysaccharide material	Periodate oxidation*		Products (molar ratio)					
	IO_4 consumed	HCOOH liberated	Galactose	Glucose	Fucose	Glycerol	Erythritol	Heptose
LPS	0.63	0.13	6.5	2.0	—	7.5	2.2	0.5
PS **1**	0.76	0.25	2.2	2.3	—	2.0	1.0	+
PS **2**	—	—	+	+	—	+	+	+
PS **3**	—	—	—	1.66	—	—	1.0	—

*Moles/mole of anhydrohexose unit.

2,3,4,6,7-penta-*O*-methyl-L-*glycero*-D-*manno*-heptose (characterized by its rate of movement on paper chromatograms, by thin-layer chromatography (t.l.c.), and gas–liquid chromatography (g.l.c.), (column *A*), in comparison with authentic standards) and also an equal amount of an unidentified methyl ether of heptose whose rate of movement on paper suggested that it was a trimethyl ether. Since it did not react with triphenyl tetrazolium chloride it was apparent that the trimethyl heptose had a methoxyl group at C-2. In the parent LPS one half of the heptose units were oxidized by periodate corresponding to the penta-*O*-methyl-heptose found on methylation. The other half of the heptose units were not oxidized thus showing the absence of any contiguous hydroxyl groups. Since the trimethyl heptose from methylation contained a methoxyl at C-2, one of the linkage points in the intact LPS must have been at C-3 and the other at either C-6 or C-7. The substituents at either C-6 or C-7 could be sugars other than heptose although LPS structures containing heptoses have been shown to have all heptose residues in a homologous chain (5, 6). If that is true, then the present data indicate that heptose units are subtended as single branch units from C-6 or C-7 of a $1 \rightarrow 3$ linked heptose chain. The position of the heptose with respect to other constituents of the LPS has not been determined. Heptose units in LPS structures previously reported form a point of attachment between the main polysaccharide structure and KDO which in turn links the lipid A moiety to the remainder of the LPS molecule (7, 8). The KDO was identified in the present LPS but its structural attachment was not investigated. The composition and chemical structure of lipid A which comprised about 15% of the *E. coli* LPS

Can. J. Chem. Downloaded from www.nrcresearchpress.com by 210.87.254.40 on 09/05/12
For personal use only.

Can. J. Chem. Downloaded from www.nrcresearchpress.com by 210.87.254.40 on 09/05/12
For personal use only.

molecule and contained the D-glucosamine was the subject of a separate investigation and the results are reported elsewhere (9). D-Glucosamine and D-galactosamine were present in the LPS in a molar ratio of 1.0:6.6 and comprised 18.7% of the molecule. Analysis of the lipid A moiety of the LPS showed that all of the D-glucosamine was in that part of the molecule. Galactosamine was exclusively in the polysaccharide portion of the LPS. Methylated hexosamines were separated from the neutral sugars present in the hydrolyzate of the methylated LPS. The methyl ethers of D-glucosamine which comprised 13.7% of the total methylated hexosamines had the same composition as found in methylated lipid A (9) and showed that the D-glucosamine residues were linked (1 → 4). The methyl ethers of D-galactosamine were 4,6-di-*O*-methyl-D-galactosamine (53.5%) and a monomethyl-D-galactosamine (31.0%). The attachment of the main portion of the galactosamine was therefore 1 → 3 with a lesser amount forming a double branch point. Springer *et al.* identified D-galactosamine as part of an oligosaccharide isolated from *E. coli* 086 and containing two residues of D-galactose and one residue of L-fucose; D-galactosamine was attached to D-galactose either (1 → 3) or (1 → 4). The location of D-galactosamine in the LPS has not been determined in the present study.

While the present data do not permit formulation of a structure for the *E. coli* LPS, certain structural features become apparent. The molecule was highly branched with D-galactose units forming the non-reducing end groups. The galactose units were linked 1 → 3 with other substituents attached at C-2. L-Fucose units were exclusively joined 1 → 4 in the molecule. D-Glucose residues were linked β(1 → 3) and β(1 → 4) with some branching at C-6 in the 1 → 3 linked units. L-*glycero*-D-*manno* heptose residues constituted a branched chain linked (1 → 3) with half the heptose units as non-reducing terminal units. D-Galactosamine was part of the polysaccharide structure while D-glucosamine was the backbone of the lipid A part of the LPS molecule.

Experimental

General

All evaporations were carried out under reduced pressure under 40 °C. Melting points were determined on a Fisher–Johns hot stage and are corrected. Optical rotations were recorded at 25° on a Perkin–Elmer 141 polarimeter and are equilibrium values unless stated otherwise. Infrared (i.r.) spectra were recorded on a Perkin–Elmer Infracord. Sugars and their methyl glycosides were uncorrected for hydrolytic losses.

Chromatography

Paper chromatography was carried out on Whatman No. 1 paper using the following solvent systems (*a*) pyridine – ethyl acetate – water (2:5:5, v/v); (*b*) butanol–pyridine–water (6:4:3, v/v), (*c*) butanone saturated with water, and (*d*) butan-1-ol – ethanol – water (4:1:5, v/v). The R_G value is relative to the mobility of 2,3,4,6-tetra-*O*-methyl-D-glucose; R_g is relative to the mobility of D-glucose.

The g.l.c. was carried out using glass columns (120 × 0.5 cm) with the following packings: (*A*) A 50:50 mixture of 1.5% (w/w) ethylene glycol sebacate polyester and 1.5% GE-XF 1150 on Chromosorb W at 180°; (*B*) 10% butanediol succinate polyester on Chromosorb W at 150°; (*C*) 3% ECNSS-M on Gas Chrom Q (Applied Science Laboratories Inc., State College, Pa.) at 180°; (*D*) 15% polyphenyl ether on Chromosorb W at 190°.

The t.l.c. was carried out on plates coated with silica gel-G using a chloroform–methanol (9:1) solvent system.

Analytical Procedures

For neutral sugars, hydrolysis was carried out with *N* sulfuric acid in sealed tubes at 100° for 11 h. The hydrolyzate was neutralized with barium carbonate, filtered, and concentrated. Total sugar content was determined as glucose (10) and individual sugars were analyzed as their alditol acetates by g.l.c. on columns *B* and *C* (11). For amino sugars, hydrolysis was carried out with 5 *N* hydrochloric acid at 100° for 10 h. After removal of the acid, total hexosamine content was determined (12) and the relative proportion of the amino sugars in the hydrolyzate (D-glucosamine and D-galactosamine) was determined by g.l.c. of the aminoglycitol acetates on column *A* (13). The ratio of D-glucosamine to D-galactosamine was also determined by ion exchange chromatography on a Technicon amino acid analyzer. Lipid A was obtained by hydrolyzing the LPS with 0.25 *N* sulfuric acid for 2 h. The crude insoluble lipid A was recovered by centrifuging, washed with water, dried, dissolved in chloroform, and poured into excess acetone. The dry acetone-insoluble material (lipid A) was quantified by weighing. Fatty acid content of the LPS was determined as described by Adams *et al.* (6).

Preparation of Bacterial Cells

Escherichia coli 086:$K_{neg.}$[3] was grown on a medium consisting of the following ingredients (g/l): potassium dihydrogen phosphate, 4.7; disodium phosphate, 12.0; ammonium chloride, 5.0; heart infusion broth (Difco), 25; distilled water, 1000 ml. The p*H* was adjusted to 7.0–7.2. At the beginning of the growth period the following ingredients (g/l) which had been sterilized separately were added to the above medium: magnesium sulfate, 0.2; ferric chloride, 0.0006; and glucose, 5.0. Growth was carried out in shake flasks for 16–18 h at 37°.

[3] *E. coli* 086:$K_{neg.}$: Identified K antigen negative by National Enterics Reference Centre, Laboratory of Hygiene, Department of National Health and Welfare, Ottawa, Canada.

Can. J. Chem. Downloaded from www.nrcresearchpress.com by 210.87.254.40 on 09/05/12
For personal use only.

In large scale preparations the cells were grown in the same culture medium in a 100 l fermenter under continuous impeller agitation (200 r.p.m.) and aeration with oxygen-enriched air (30% oxygen), 2.5 c.f.m. at 37°. Additional glucose (500 g) was added to the fermentation at the end of 3 and 5 h respectively. Adequate growth was obtained in 7–8 h. The cells were killed by the addition of phenol (0.5% final concentration) and left to stand for 2 h. The sterile cells were then harvested on a Sharples supercentrifuge, washed once with 0.9% sodium chloride solution and twice with water, and freeze dried. Yield of cells (dry weight): 4.0 g/l of medium.

Preparation of Lipopolysaccharide (LPS) from Cells

The LPS was extracted from the dried cells by the phenol–water extraction procedure described by Westphal (4); 100 g of cells yielded 13 g of crude LPS.

Purification of LPS

Crude LPS (10 g) was dissolved in water (200 ml) and centrifuged to remove the insoluble material. To the supernatant, 'Cetavlon' (cetyltrimethylammonium bromide) solution, (5% in water) was added until no further precipitation took place. The precipitated material was removed by centrifugation and discarded. The supernatant was stirred for 4 h with sufficient sodium chloride to give a 0.5 *M* concentration and the solution was then poured into ethanol. The precipitated LPS was recovered by centrifugation, washed with 80% ethanol, and then freeze dried. Yield: 4.1 g, $[\alpha]_D$ + 37.0° (*c* 1, DMSO). Analysis: Total carbohydrate 49.0%;[4] total hexosamine 18.7% (D-glucosamine:D-galactosamine 1.0:6.6); fatty acids 9.2%;[5] lipid A, 14.0%; N, 1.5%; P, 2.2%; ash 8.0% and protein < 1.0%. Analysis showed D-galactose, D-glucose, L-fucose, L-*glycero*-D-*manno*-heptose, D-glucosamine, and D-galactosamine in a molar ratio of 7.0:2.2:3.1:1.0:0.4:2.6; (Table 1). On free boundary electrophoresis the LPS moved as a single peak with $\mu = 6.94 \times 10^{-5}$ cm^2 s^{-1} V^{-1}, strongly suggesting that the preparation was homogeneous. Ultracentrifugation in a Spinco model H at 57 000 r.p.m. for 2.5 h showed only a single peak providing further evidence of the homogeneity of the LPS. Examination of dilute aqueous solutions of the purified LPS by the Ouchterlony gel-diffusion technique (14) on agar plates against *E. coli* 'O' specific antiserum showed only a single precipitation band (Fig. 2). further proving the homogeneity of the LPS.

The LPS did not contain any chloroform soluble fraction (lipid B) when extracted by the Bligh and Dyer (15) lipid extraction procedure.

Methylation Procedures

LPS (2.40 g) was methylated once by the method of Srivastava *et al.* (16) using dimethyl sulfoxide (DMSO), solid sodium hydroxide, and dimethyl sulfate, followed by a series of two to four methylations by the Purdie procedure (17); the yield of methylated LPS was approximately 72%, methoxyl, 41.8%. Since repeated methylation did not increase the methoxyl content and there was an absence of —OH absorption in the i.r. spectrum, the LPS was considered to be fully methylated. The methylated LPS was methanolyzed with 3% methanolic hydrogen chloride in sealed tubes at 100° for 6 h. The methanolyzed mixture was then hydrolyzed by acid (*N* sulfuric acid at 100° for 8 h) to give the free methylated sugars (1.8 g).

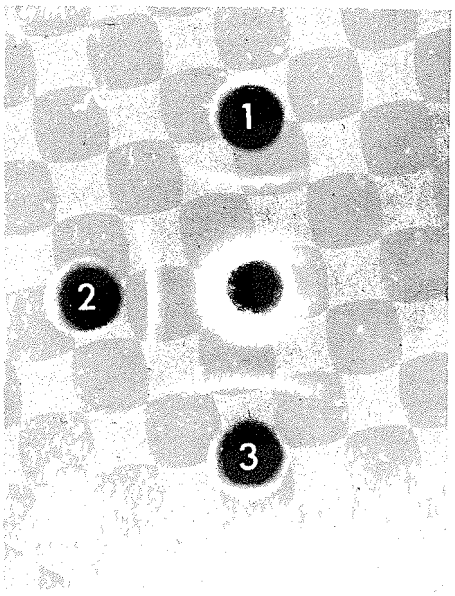

FIG. 2. Gel-diffusion patterns of *E. coli* lipopolysaccharide. *E. coli* 'O' specific antiserum in centre well. (1) lipopolysaccharide (250 μg/ml); (2) lipopolysaccharide (500 μg/ml); (3) lipopolysaccharide (1000 μg/ml).

Isolation and Identification of Methylated Sugars

Neutral Methylated Sugars

A portion (1 g) of the acid hydrolyzate containing the various methylated sugars was resolved on a cellulose column using a developing solvent of butanol one quarter saturated with water. Impure methylated sugars eluted from the column were further resolved by t.l.c. Chromatographically pure sugars were identified by specific optical rotation; rate of movement on paper chromatograms, g.l.c., and t.l.c.; demethylation to parent sugar (18); and wherever possible, as a crystalline derivative. The various sugars that were identified are listed in Table 2. The ratio of methylated sugars was estimated by a method described by Björndal *et al.* (19).

Methylated Amino Sugars

A portion (0.6 g) of the LPS methanolyzate was hydrolyzed with 5 *N* hydrochloric acid at 100° for 8 h. After removal of the acid from the hydrolyzate by azeotropic distillation with water under reduced pressure, the methylated sugars were dissolved in water and the solution was passed down a column of Rexyn 101 H^+ resin. Neutral sugars were removed by thorough washing with water. The methylated amino sugars were desorbed from the resin by *N* hydrochloric acid, the acid was removed as described above, and the sugars were re-

[4]Exclusive of hexosamines.

[5]Fatty acids are components of lipid A and are included in the lipid A value.

Can. J. Chem. Downloaded from www.nrcresearchpress.com by 210.87.254.40 on 09/05/12
For personal use only.

covered as a syrup (32 mg). Paper chromatography (solvent *a*) showed three spots (R_F, 0.09, 0.16, and 0.23; R_G, 0.41, 0.73, and 1.05) readily detectable by ninhydrin. No other spots were detectable by *p*-anisidine hydrochloride showing that neutral reducing sugars were absent. The sugar mixture was analyzed by (*1*) ion exchange chromatography (20), (*2*) g.l.c. of the reduced, acetylated products (21), and (*3*) ninhydrin degradation (22). Ion exchange chromatography and g.l.c. showed the presence of 3,6-di-*O*-methyl-D-glucosamine (10.5%); 4,6-di-*O*-methyl-D-glucosamine (2.7%); 3,4,6-tri-*O*-methyl-D-glucosamine (0.5%); and two unknown components, 53.5 and 30% respectively.

The major unknown component (R_F 0.23, solvent *a*) was isolated by paper chromatography. Ninhydrin degradation yielded a methylated sugar (R_F 0.63, solvent *a*) that gave a strongly positive test with triphenyl tetrazolium chloride. Demethylation of the sugar (18) yielded lyxose which showed that the original methylated hexosamine was a methyl ether of D-galactosamine. The movement of the methylated lyxose on paper chromatography indicated that it was a dimethyl sugar and the positive triphenyl tetrazolium chloride test showed that C-2 was unsubstituted. The possible di-*O*-methyl ethers of lyxose could be 3,5- or 3,4-di-*O*-methyl ether. The latter possibility was discounted because it would have to originate from 4,5-di-*O*-methyl-D-galactosamine which is unlikely. Hence it seemed likely that the lyxose derivative was 3,5-di-*O*-methyl-lyxose which established the original sugar as 4,6-di-*O*-methyl-D-galactosamine. The other component (30%) was not positively identified but its behavior on ion exchange chromatography and g.l.c. indicated that it was a monomethyl ether of D-galactosamine. The ratio of methylated D-glucosamine derivatives to methylated D-galactosamine derivatives was 1.0:6.2; the ratio of the unmethylated sugars was 1.0:6.6.

Periodate Oxidation

Polysaccharides were oxidized by 0.05 *M* periodate at 17–20° in the dark. Aliquots were removed at various time intervals for estimations of periodate consumed and formic acid liberated (23). The periodate oxidized polysaccharides were reduced and hydrolyzed (24). The results are given in Table 3.

Graded Hydrolyses

LPS (93 mg) was hydrolyzed with 0.01 *N* sulfuric acid (25 ml) at 100° for 4 h. Lipid A which separated as a white flocculent precipitate was removed by centrifugation. The solution was neutralized with barium carbonate, centrifuged and concentrated, and the unhydrolyzed polysaccharide was recovered by precipitation with 4 volumes of ethanol. The foregoing hydrolysis procedure was repeated successively on the unhydrolyzed portions with 0.02, 0.1, and 0.5 *N* sulfuric acid for 4, 6, and 8 h respectively. No further lipid A was produced. The following sugars were identified in the various acid hydrolyzates by paper chromatography in solvents *a* and *d* using authentic reference sugars: (0.01 *N* acid) galactose, fucose, and 3-*O*-β-D-galactopyranosyl-D-galactose (R_g, 0.34 (solvent *a*), 0.55 (solvent *d*)); (0.02 *N* acid) galactose, fucose, and 3-*O*-β-D-galactopyranosyl-D-galactose; (0.1 *N* acid) galactose, fucose, and glucose; (0.5 *N* acid) glucose, cellobiose (R_g, 0.50 (solvent *a*), 0.52 (solvent *d*)), cellotriose (R_g, 0.24 (solvent *d*)), and laminaribiose (R_g, 0.70 (solvent *a*), 0.69 (solvent *d*)). In the 0.01–0.1 *N* acid hydrolyzates, the monosaccharide content constituted over 95% of the released sugars; the 0.5 *N* acid hydrolyzate contained about 10% cellobiose and cellotriose but the laminaribiose yield was < 1%.

Composition and Structure of Degraded Polysaccharides

Quantities of degraded polysaccharides sufficient for compositional and structural studies were prepared from the LPS by partial acid hydrolysis.

*Polysaccharide **1** (PS **1**)*

LPS (0.55 g) was heated for 30 min in a boiling water bath with 0.1 *N* HCl (50 ml). The hydrolyzate was extracted with chloroform to remove lipid A and other lipid material. The aqueous solution was then poured into an excess of ethanol to precipitate the polysaccharide which was washed and freeze dried to give PS **1** (0.193 g); $[\alpha]_D^{22}$ + 77° (*c* 1, DMSO). The soluble portion was deionized and concentrated. Paper chromatographic examination in solvents *a* and *d* showed galactose, fucose, and 3-*O*-β-D-galactopyranosyl-D-galactose; no glucose could be detected. PS **1** on hydrolysis produced galactose, glucose, and fucose in a molar ratio of 2.2:1.6:1.0.

Fully methylated PS **1**, $[\alpha]_D$ + 91.0° (*c* 1, chloroform), on hydrolysis yielded several methylated sugars which were identified chromatographically and the results are listed in Table 2. PS **1** consumed 0.76 mole of periodate and liberated 0.25 mole of formic acid; and, followed by reduction and hydrolysis (24), yielded galactose, glucose, glycerol, and erythritol in a ratio of 2.2:2.3:2.0:1.0.

*Polysaccharide **2** (PS **2**)*

PS **1** (50 mg) was further hydrolyzed with 0.05 *N* sulfuric acid for 2 h in a boiling water bath. After neutralization with barium carbonate, the filtrate was poured into ethanol. The precipitate was collected and dried to give PS **2** (35 mg) $[\alpha]_D$ + 84.0° (*c* 1, DMSO) which on hydrolysis yielded glucose, galactose, and fucose in a molar ratio of 6.3:2.3:1.0.

Methylation and hydrolysis produced several methylated sugars which were identified and are listed in Table 2. PS **2** on periodate oxidation followed by reduction and hydrolysis produced galactose, glucose, erythritol, and glycerol.

*Polysaccharide **3** (PS **3**) and Lipid A*

LPS (2.0 g) was hydrolyzed with 0.25 *N* sulfuric acid (100 ml) for 2½ h in a boiling water bath. Lipid A appeared as a flocculent precipitate which was recovered by centrifugation, washed free of acid, and dried (yield 0.35 g). The supernatant was neutralized with $BaCO_3$ and filtered. The filtrate was poured into ethanol to precipitate PS **3** which was washed and dried (yield 35 mg). The soluble portion contained galactose, fucose, glucose, cellotriose, cellobiose, laminaribiose, and galactosamine. PS **3**, $[\alpha]_D$ + 96.0° (*c* 1, water) on hydrolysis yielded only glucose. Hydrolysis of methylated PS **3** $[\alpha]_D$ + 73.0° (*c* 1, chloroform) produced two tri-*O*-methyl ethers of glucose which are listed in Table 2. Periodate oxidation of PS **3** followed by reduction and hydrolysis yielded only glucose and erythritol in a ratio of 1.6:1.

The authors thank Dr. A. W. Jackson, Laboratory of Hygiene, Ottawa, Ontario, for providing the *E. coli* organism and supplies of 'O' specific antiserum; Dr. G. F. Springer, Northwestern University, Evanston, Ill., and Dr. P. A. J. Gorin, Prairie Regional Laboratory, Saskatoon, Saskatchewan, for generous gifts of *O*-methyl ethers of L-fucose.

1. O. LÜDERITZ, K. JANN, and R. WHEAT. Comprehensive biochemistry. *Edited by* M. Florkin and E. H. Stotz. Elsevier Publishing Co., Amsterdam. **26A**, 105 (1968).
2. O. LÜDERITZ, A. M. STAUB, and O. WESTPHAL. Bact. Rev. **30**, 192 (1966).
3. G. F. SPRINGER, E. T. WANG, J. H. NICHOLS, and J. M. SHEAR. Ann. N.Y. Acad. Sci. **133**, 566 (1966).
4. O. WESTPHAL, O. LÜDERITZ, and F. BISTER. Z. Naturforsch. **7B**, 148 (1952).
5. W. DRÖGE, O. LÜDERITZ, and O. WESTPHAL. Eur. J. Biochem. **4**, 126 (1968).
6. G. A. ADAMS, M. KATES, D. H. SHAW, and M. YAGUCHI. Can. J. Biochem. **4**, 1175 (1968).
7. R. D. EDSTROM and E. C. HEATH. Fed. Proc. **23**, 380 (1964).
8. M. J. OSBORN. Proc. Natl. Acad. Sci. (U.S.), **50**, 499 (1963).
9. G. A. ADAMS and P. P. SINGH. Biochim. Biophys. Acta (Lipid and Lipid Metabolism section). **202** 553 (1970).
10. M. DUBOIS, K. A. GILLIES, J. K. HAMILTON, P. A. REBERS, and F. SMITH. Anal. Chem. **28**, 350 (1956).
11. S. W. GUNNER, J. K. N. JONES, and M. B. PERRY. Can. J. Chem. **39**, 1892 (1961).
12. C. J. M. RONDLE and W. T. J. MORGAN. Biochem. J. **61**, 586 (1955).
13. M. B. PERRY and ANN C. WEBB. Can. J. Biochem. **46**, 1163 (1968).
14. O. OUCHTERLONY. Progress in allergy. S. Karger, Basel, Switzerland. **5**, 1 (1958).
15. E. G. BLIGH and W. J. DYER. Can. J. Biochem. Physiol. **37**, 911 (1959).
16. H. C. SRIVASTAVA, P. P. SINGH, S. N. HARSHE, and K. VIRK. Tetrahedron Lett. 493 (1964).
17. T. PURDIE and J. C. IRVINE. J. Chem. Soc. **83**, 1021 (1903).
18. T. G. BONNER, E. J. BOURNE, and S. MCNALLY. J. Chem. Soc. 2929 (1960).
19. H. BJÖRNDAL, B. LINDBERG, and S. SVENSSON. Acta Chem. Scand. **21**, 1801 (1967).
20. G. A. ADAMS, M. YAGUCHI, and M. B. PERRY. Carbohyd. Res. **12**, 267 (1970).
21. M. B. PERRY and ANN C. WEBB. Can. J. Chem. **47**, 4091 (1969).
22. P. J. STOFFYN and R. W. JEANLOZ. Arch. Biochem. Biophys. **52**, 373 (1954).
23. S. K. CHANDA, E. L. HIRST, J. K. N. JONES, and E. G. V. PERCIVAL. J. Chem. Soc. 1289 (1950).
24. M. ABDEL-AKER, J. K. HAMILTON, R. MONTGOMERY, and F. SMITH. J. Amer. Chem. Soc. **74**, 4970 (1952).

Can. J. Chem. Downloaded from www.nrcresearchpress.com by 210.87.254.40 on 09/05/12
For personal use only.

Can. J. Chem. Downloaded from www.nrcresearchpress.com by 210.87.254.5 on 09/05/12
For personal use only.

The 4-(methylthio)phenyl ester for the synthesis of polypeptides of a known repeating sequence of amino acids. Synthesis of poly-(L-lysylglycyl)glycine 1-C^{14} ethyl ester hydrobromide

BRIAN J. JOHNSON AND DONNA S. REA
Department of Chemistry, Tufts University, Medford, Massachusetts, 02155

Received March 20, 1970

The synthesis of the tetrapeptide, *N-t*-butoxycarbonyl-ε-*N*-carbobenzoxy-L-lysylglycyl-ε-*N*-carbobenzoxy-L-lysylglycine 4-(methylthio)phenyl ester is described. The utility of this protective ester is shown by its easy conversion to the protected tetrapeptide 4-(methylsulfonyl)phenyl activated ester without decomposition. Removal of the *N*-butoxycarbonyl protecting group afforded the polymerizing unit, ε-*N*-carbobenzoxy-L-lysylglycyl-ε-*N*-carbobenzoxy-L-lysylglycine 4-(methylsulfonyl)phenyl ester. Polymerization of this material on the partially blocked monomer glycine-1-C^{14} ethyl ester hydrochloride, at a relatively high dilution, gave poly-(ε-*N*-carbobenzoxyl-L-lysylglycyl)glycine-1-C^{14} ethyl ester. The carbobenzoxy protective groups were removed to give the title compound.

Canadian Journal of Chemistry, 48, 2509 (1970)

The amino acid carboxyl protecting group, the 4-(methylthio)phenyl ester (MTP), has been suggested for use in peptide synthesis by this laboratory (1). The attractive feature of this protective ester is its facile conversion, by oxidation (2, 3) and without racemization (4), to the activated 4-(methylsulfonyl)phenyl ester (MSO_2P). This method has been used successfully for peptide (2, 5) and *O*-depsipeptide synthesis (6).

We have now found that this method of protection, followed by activation, to be particularly useful for the synthesis of sequential polypeptides. In order to illustrate this we wish to report the synthesis of poly-(L-lysylglycyl)-glycine 1-C^{14} ethyl ester hydrobromide (**1**).

Glycine 4-(methylthio)phenyl ester hydrochloride (1), was coupled to *N-t*-butoxycarbonyl-ε-*N*-carbobenzoxy-L-lysine pentachlorophenyl ester (2) to give *N-t*-butoxycarbonyl-ε-*N*-carbobenzoxy-L-lysylglycine 4-(methylthio)phenyl ester (**2**). Treatment of **2** with HCl in glacial acetic acid yielded the dipeptide MTP ester hydrochloride **3** (eq. [1]).

The dipeptide *N-t*-butoxycarbonyl-ε-*N*-carbobenzoxy-L-lysylglycine methyl ester **4** was prepared from glycine methyl ester hydrochloride and *N-t*-butoxycarbonyl-ε-*N*-carbobenzoxy-L-lysine pentachlorophenyl ester. Saponification of **4** yielded the dipeptide free acid as an oil, which was then converted to the dipeptide pentachlorophenyl ester **5** (eq. [2]).

The tetrapeptide *N-t*-butoxycarbonyl-ε-*N*-carbobenzoxy-L-lysylglycyl-ε-*N*-carbobenzoxy-L-lysylglycine 4-(methylthio)phenyl ester (**6**) was prepared by the condensation of the two dipeptides **3** and **5**. Oxidation of **6** under the mild conditions, afforded by the use of *m*-chloroperoxybenzoic acid, gave the tetrapeptide 4-(methylsulfonyl)phenyl activated ester (**7**). Treatment of **7** with HCl in glacial acetic acid afforded the polymerizing unit **8** (eq. [3]).

It has been shown that polymerization at high dilution (7, 8) requires the use of a partially blocked monomer so that one end of the growing polypeptide chain is always protected. By this means the possibility of formation of large cyclic polypeptides is overcome. For this purpose, a solution of glycine-1-C^{14} ethyl ester hydrochloride in dimethylsulfoxide containing triethylamine was used. To this was added a solution of the polymerizing unit **8** such that the concentration of reactants was not more than 100 mmoles/l. The insoluble polypeptide, poly-(ε-*N*-carbobenzoxy-L-lysylglycyl)glycine-1-C^{14} ethyl ester (**9**) was obtained by centrifugation. Treatment of **9** with HBr in trifluoroacetic acid yielded the free polypeptide, poly-(L-lysylglycyl)glycine-1-C^{14} ethyl ester hydrobromide (**1**) (eq. [4]). The ultraviolet (u.v.) spectral measurements of this material (235–280 mμ) indicated that the *N*-carbobenzoxy groups had been removed. The molecular weight of the polymer was found to be 11 000 as shown by gel filtration through a calibrated column of sephadex (9).

Experimental

All melting points are uncorrected. The microanalyses were carried out by Dr. S. M. Nagy of Belmont, Mass., and the radioassays by the New England Nuclear Corp., Boston, Massachusetts.

N-t-Butoxycarbonyl-ε-N-carbobenzoxy-L-lysylglycine 4-(Methylthio)phenyl Ester (2)

To a solution of 11.9 g (0.019 mole) of *N-t*-butoxy-

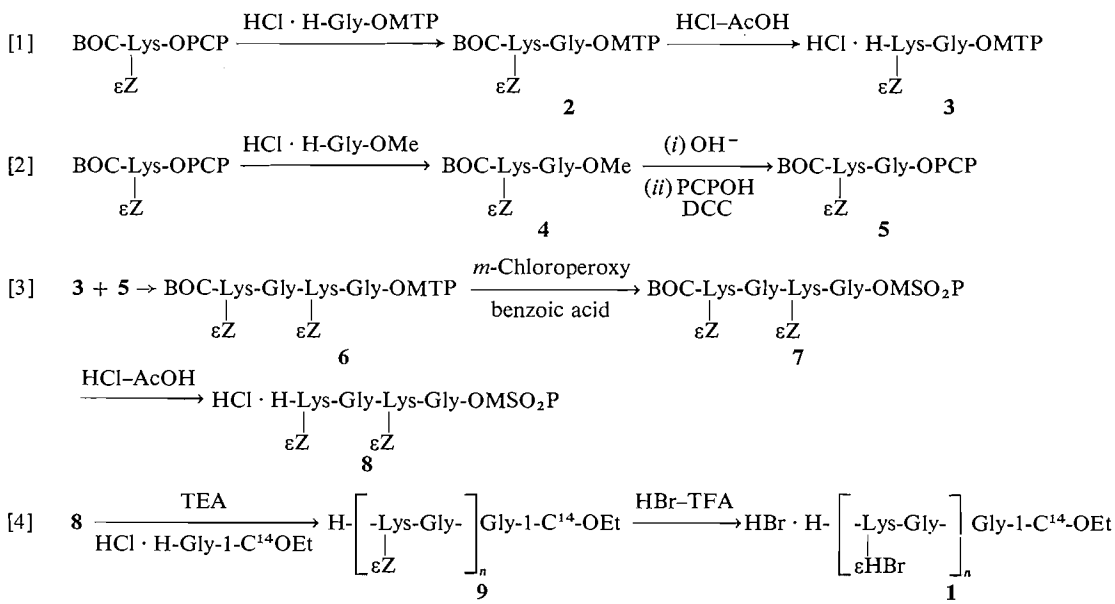

In eqs. [1]–[4]: PCP = pentachlorophenyl; MTP = 4-(methylthio)phenyl; MSO_2P = 4-(methylsulfonyl)phenyl.

carbonyl-ε-*N*-carbobenzoxy-L-lysine pentachlorophenyl ester (2) in 75 ml of methylene chloride was added 2.0 g (0.019 mole) of triethylamine and 4.5 g (0.019 mole) of glycine 4-(methylthio)phenyl ester hydrochloride. The solution was stirred for 12 h and then concentrated under reduced pressure. The solid residue was dissolved in ethyl acetate and washed quickly with 10% citric acid solution, water, and then dried (Na_2SO_4). The solvent was removed under reduced pressure to give an oil which was chromatographed on Silicar CC7, eluted with chloroform to give the dipeptide 4-(methylthio)phenyl ester 5.6 g (52.8%); m.p. 82–84° (from ethyl acetate – hexane); $[\alpha]_D^{26}$ −15.1° (*c*, 2.98, dimethylformamide).

Anal. Calcd. for $C_{28}H_{37}N_3O_7S$: C, 60.1; H, 6.7; N, 7.5. Found: C, 60.1; H, 6.7; N, 7.3.

ε-N-Carbobenzoxy-L-lysylglycine 4-(Methylthio)phenyl Ester Hydrochloride (3)

To a solution of 2.0 g (0.0036 mole) of *N-t*-butoxycarbonyl-ε-*N*-carbobenzoxy-L-lysylglycine 4-(methylthio)phenyl ester in glacial acetic acid was added 10 ml of *N*-hydrogen chloride in glacial acetic acid. The solution was left at room temperature for 35 min. The dipeptide hydrochloride which crystallized from this solution was collected by filtration and washed with ether to yield 1.7 g (94.4%); m.p. 168–169° (from methanol–ether); $[\alpha]_D^{26}$ −10.3 (*c*, 1.26, dimethylformamide).

Anal. Calcd. for $C_{23}H_{30}Cl\ N_3O_5S$: C, 55.7; H, 6.1; N, 8.5. Found: C, 56.0; H, 6.2; N, 8.4.

N-t-Butoxycarbonyl-ε-N-carbobenzoxy-L-lysylglycine Methyl Ester (4)

To a solution of 10.2 g (0.016 mole) of *N-t*-butoxycarbonyl-ε-*N*-carbobenzoxy-L-lysine pentachlorophenyl ester in 100 ml of methylene chloride was added 1.7 g (0.0165 mole) of triethylamine and 2.1 g (0.0165 mole) of glycine methyl ester hydrochloride. The mixture was stirred overnight at room temperature and then evaporated under reduced pressure to give an oil. The oil was dissolved in ethyl acetate and washed quickly with 10% citric acid solution, water and then dried (Na_2SO_4). The solvent was removed under reduced pressure to give an oil which was chromatographed on Silicar CC7; elution with chloroform gave the dipeptide methyl ester 4.9 g (67.1%); m.p. 82–83° (from ethyl acetate – hexane) $[\alpha]_D^{26}$ −4.1° (*c*, 7.12, dimethylformamide).

Anal. Calcd. for $C_{22}H_{33}N_3O_7$: C, 58.5; H, 7.4; N, 9.3. Found: C, 58.2; H, 7.3; N, 9.4.

N-t-Butoxycarbonyl-ε-N-carbobenzoxy-L-lysylglycine Pentachlorophenyl Ester (5)

To a solution of 28.0 g (0.062 mole) of *N-t*-butoxycarbonyl-ε-*N*-carbobenzoxy-L-lysylglycine methyl ester in 600 ml of methanol was added 68 ml of *N* NaOH. The mixture was stirred at room temperature for 1.5 h, evaporated under reduced pressure to a small volume, and then flooded with water. The alkaline solution was acidified with 10% citric acid solution and then extracted with ethyl acetate. The combined organic extracts were washed with water, dried (Na_2SO_4), and evaporated under reduced pressure to give the free acid as an oil 27.1 g (100%). To a cooled solution of 27.1 g (0.062 mole) of the dipeptide free acid in methylene chloride was added 12.8 g (0.062 mole) of dicyclohexylcarbodiimide and 16.5 g (0.062 mole) of pentachlorophenol. The mixture was stirred overnight at room temperature, and then evaporated under reduced pressure to dryness. The solid was dissolved in ethyl acetate, cooled, and the urea was removed by filtration. The dipeptide pentachlorophenyl ester was obtained by chilling the filtrate, 28.2 g (66.4%); m.p. 164–166 (from methanol); $[\alpha]_D^{27}$ −20.1° (*c*, 1.84, dimethylformamide).

Can. J. Chem. Downloaded from www.nrcresearchpress.com by 210.87.254.5 on 09/05/12
For personal use only.

Can. J. Chem. Downloaded from www.nrcresearchpress.com by 210.87.254.5 on 09/05/12
For personal use only.

Anal. Calcd. for $C_{27}H_{30}Cl_5N_3O_7$: C, 47.3; H, 4.4; N, 6.1. Found: C, 47.3; H, 4.6; N, 6.2.

N-t-Butoxycarbonyl-ε-N-carbobenzoxy-L-lysylglycyl-ε-N-carbobenzoxy-L-lysylglycine 4-(Methylthio)-phenyl Ester (6)

To a solution of 15.8 g (0.023 mole) *N-t*-butoxycarbonyl-ε-*N*-carbobenzoxy-L-lysylglycine pentachlorophenyl ester in 120 ml of dimethylsulfoxide was added 2.5 g (0.025 mole) of triethylamine and 12.5 g (0.025 mole) of ε-*N*-carbobenzoxy-L-lysylglycine 4-(methylthio)phenyl ester hydrochloride. The mixture was stirred overnight at room temperature, after which it was poured into water. The precipitate was filtered off and crystallized from ethyl acetate – hexane to yield the tetrapeptide 4-(methylthio)phenyl ester, 11.6 g (57.4%); m.p. 125–126° (from ethyl acetate – hexane); $[\alpha]_D^{26}$ −14.3° (*c*, 3.08, dimethylformamide).

Anal. Calcd. for $C_{44}H_{58}N_6O_{11}S$: C, 60.1; H, 6.7; N, 9.6. Found: C, 60.4; H, 6.5; N, 9.6.

N-t-Butoxycarbonyl-ε-N-carbobenzoxy-L-lysylglycyl-ε-N-carbobenzoxy-L-lysylglycine 4-(Methylsulfonyl)-phenyl Ester (7)

To 5.5 g (0.0062 mole) of *N-t*-butoxycarbonyl-L-lysylglycyl-ε-*N*-carbobenzoxy-L-lysylglycine 4-(methylthio)phenyl ester dissolved in 50 ml of dioxane was added 3.3 g (0.019 mole) of *m*-chloroperoxybenzoic acid. The mixture was stirred at room temperature for 4 h and then poured into water. The precipitate was collected, dried, and chromatographed on Silicar CC7. Elution with chloroform–methanol gave the tetrapeptide 4-(methylsulfonyl)phenyl ester 4.6 g (82.2%); m.p. 114° (from ethyl acetate – hexane) $[\alpha]_D^{26}$ −12.4° (*c*, 7.40, dimethylformamide).

Anal. Calcd. for $C_{44}H_{58}N_6O_{13}S$: C, 58.0; H, 6.4; N, 9.2. Found: C, 58.0; H, 6.4; N, 9.2.

ε-N-Carbobenzoxy-L-lysylglycyl-ε-N-carbobenzoxy-L-lysylglycine 4-(Methylsulfonyl)phenyl Ester Hydrochloride (8)

To a solution of 5.2 g (0.0057 mole) of *N-t*-butoxycarbonyl-ε-*N*-carbobenzoxy-L-lysylglycyl-ε-*N*-carbobenzoxy-L-lysylglycine 4-(methylsulfonyl)phenyl ester in 25 ml of glacial acetic acid was added 17 ml of *N*-hydrogen chloride in glacial acetic acid. The solution was left at room temperature for 1 h. The solvent was removed under reduced pressure to give an oil. This oil was triturated with ether to give the tetrapeptide hydrochloride, 2.6 g (54.3%); m.p. 155–156° (from methanol–ether); $[\alpha]_D^{26}$ +6.8° (*c*, 2.22, dimethylformamide).

Anal. Calcd. for $C_{39}H_{51}Cl\,N_6O_{11}S$: C, 55.3; H, 6.1; N, 9.9. Found: C, 55.2; H, 6.1; N, 9.9.

Poly-(ε-N-carbobenzoxy-L-lysylglycyl)glycine-1-C^{14} Ethyl Ester (9)

To a solution of glycine 1-C^{14} ethyl ester hydrochloride (specific activity 3.78 mc/mmole; 0.00093 g, 6.66×10^{-6} mole; 25.2 μc) in 2.0 ml dimethylsulfoxide containing 1.0 ml of triethylamine was added dropwise during 25 min a solution of 3.09 g (0.00365 mole) of ε-*N*-carbobenzoxy-L-lysylglycyl-ε-*N*-carbobenzoxy-L-lysylglycine 4-(methylsulfonyl)phenyl ester hydrochloride in 33.5 ml of dimethylsulfoxide, such that the concentration of the polymerizing species was never greater than 100 mmole/l. The mixture was stirred at room temperature for 6 days and then diluted with 40 ml of methanol. The insoluble material was collected by centrifugation and washed with 150 ml of water for 12 h, and then successively with 2 × 150 ml of water and 3 × 30 ml of ether. The precipitate was collected by filtration and dried to yield the protected polymer 2.147 g (92.3%). Radioassay of this polymer (7.6 nc/mg) indicated that 64% of the starting radioactive monomer was associated with it.

Anal. Calcd. for $C_{16}H_{21}N_3O_4$: C, 60.2; H, 6.6; N, 13.2. Found: C, 60.2; H, 6.7; N, 13.0.

Poly-(L-lysylglycyl)glycine-1-C^{14} Ethyl Ester Hydrobromide (1)

Through a mixture of 2.06 g (0.00322 mole) of poly-(ε-*N*-carbobenzoxy-L-lysylglycyl)glycine-1-C^{14} ethyl ester suspended in 100 ml of dry trifluoroacetic acid was bubbled dry hydrogen bromide for 45 min. The solvent was evaporated under reduced pressure and the residue was triturated with anhydrous ether. The polymer was collected by centrifugation, dissolved in water, and extensively dialyzed and then lyophilized. The solid was then dissolved in water and filtered through a column of Sephadex G-100 (100 × 2.5 cm) using distilled water as eluent (flow rate 10 ml/h). The first fractions containing the highest molecular weight were collected and lyophilized to give the free polypeptide hydrobromide 0.276 g, (16.1%); $[\alpha]_D^{29}$ −36.0° (*c*, 1.22, water); radioassay 13 nc/mg. The u.v. absorption spectrum (235–280 mμ) of this material taken in water, indicated negligible amounts of *N*-carbobenzoxy groups.

Anal. Calcd. for $C_8H_{16}Br\,N_3O_2$: C, 36.1; H, 6.0; N, 15.8. Found: C, 36.2; H, 5.9; N, 15.6.

Molecular Weight Determination

A column of Sephadex G-100 (50 × 2.5 cm) was calibrated by use of molecular weight markers by the method of Andrews (9). Passage of 5 mg of poly-(L-lysylglycyl)glycine-1-C^{14} ethyl ester hydrobromide through this column was eluted in a volume equivalent to that corresponding to a molecular weight of 11 000.

This work was supported by a grant from the National Science Foundation, and one of us (D.S.R.) also thanks this granting agency for a traineeship.

1. B. J. Johnson and P. M. Jacobs. Chem. Commun. 73 (1968).
2. B. J. Johnson and E. G. Trask. J. Org. Chem. **33**, 4521 (1968).
3. B. J. Johnson and T. A. Ruettinger. J. Org. Chem. **35**, 255 (1970).
4. B. J. Johnson and P. M. Jacobs. J. Org. Chem. **33**, 4524 (1968).
5. B. J. Johnson and D. E. Tracy. J. Pharm. Sci. **58**, 1299 (1969).
6. B. J. Johnson. J. Org. Chem. **34**, 1178 (1969).
7. B. J. Johnson. J. Chem. Soc. (C), 1412 (1969).
8. B. J. Johnson and E. G. Trask. J. Chem. Soc. (C), 2644 (1969).
9. P. Andrews. Biochem. J. **91**, 222 (1964).

Some pyrrolidone derivatives

K. BAILEY[1] AND A. H. REES
Department of Chemistry, Trent University, Peterborough, Ontario

Received January 12, 1970

4-Cyano-3-hydroxy-2-oxo-3-pyrrolines are strongly acidic and form salts rather than enamines with strongly basic amines. We have revised the structures proposed for some of their derivatives and report the first synthesis of the parent compound **1** (R = H) and other new related pyrrolines.

Canadian Journal of Chemistry, 48, 2512 (1970)

Pyrrolin-2-ones **1** have been obtained by the base-catalyzed condensation of ethyl oxalate with β-cyanoethylamines **2** (1, 2).

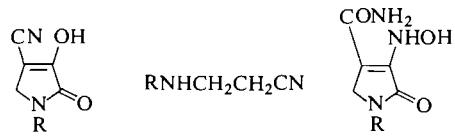

1 **2** **3**

However, the parent compound **1** (R = H) was not known. In the attempt to synthesize **1** (R = COOEt) from **2** (R = COOEt), hydrolysis and decarboxylation took place during work up, so we were able to obtain the parent **1** (R = H) directly.

We now report some reactions of compounds **1**. Our conclusions differ in part from those of other workers (4). When we prepared oximes of **1** (R = $PhCH_2$, H, or Me), the products analyzed as hydrates. The infrared (i.r.) spectra showed no nitrile bands and had increased carbonyl absorption as well as NH bands so we assigned to them the 4-carboxamido-3-hydroxylamino-2-oxo-3-pyrroline structures **3** (R = $PhCH_2$, H, or Me respectively). The spectra showed no saturated carbonyl bands indicating conjugation of the double bands in contrast to the ester-oxime **9** (see below).

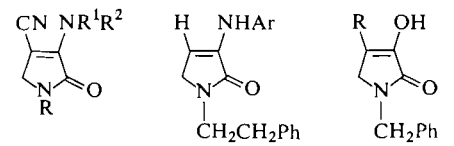

4 **5** **6**

The mass spectra showed the appropriate molecular ion peaks. Also present was *m/e* 44 ($CONH_2^+$ and CO_2^+) which was the base peak in the spectrum of **3** (R = H).

It was reported (4) that **1** (R = Me or *n*-Bu) formed products **4**, as hydrates with various amines. However, we regard these as salts of the strong acid **1** with strongly basic amines, by analogy with the products we obtained from **1** (R = $PhCH_2$) with piperidine and dimethylamine. Our products gave no ions in the mass spectra above *m/e* 214. The cracking pattern for the piperidine salt was identical to that of the starting acid, down to *m/e* 85 (piperidine) and the peak at *m/e* 214 from the dimethylamine salt was shown by high resolution to correspond with the correct formula $C_{12}H_{10}N_2O_2$.[2]

The nuclear magnetic resonance (n.m.r.) spectra of both salts had singlets at 6.18, 5.34, and 2.65 τ which integrated in the ratio 2:2:5 and are ascribed to the C-4, benzylic and aromatic protons respectively. A broad signal integrating for one to two protons at about −0.5 τ disappeared on addition of D_2O. The spectra had the correct peaks for the amine moieties. The compounds therefore cannot be enamines **4**, and since triethylamine gave a similar derivative, they must be salts. The ultraviolet (u.v.) spectra are summarized in Table 1 and the light absorption is clearly due to the mesomeric anion. The i.r. spectra of the salts are compared with that of compound **1** (R = $PhCH_2$) and other relevant derivatives in Table 2. In addition, the salts all showed two or three medium to weak bands in the region 2300–3000 cm^{-1}, appropriate for $\rangle\overset{+}{N}H$, whereas the acid **1** (R = $PhCH_2$) has a band at 2610 cm^{-1} and none between 3100–4000 cm^{-1}. Compounds **5** have bands at 3300 (NH), 1670 (C=O), and 1640 (C=C) cm^{-1} (5).

[1]Present address: Food and Drug Directorate, Tunney's Pasture, Ottawa 3, Canada.

[2]We thank Prof. A. G. Harrison of the Chemistry Department, University of Toronto, Toronto, Ontario, for this determination.

TABLE 1

The u.v. spectra (ethanol) of salts of amines with pyrrolin-2-ones **1***

1	Amine	λ_{max} mμ (ε)	λ_{max} mμ (ε)
R = $PhCH_2$	Piperidine	295 (9870)	231 (9650)
R = $PhCH_2$	Dimethylamine	294 (10050)	233 (9910)
R = $PhCH_2$	Triethylamine	294 (11510)	233 (12420)
R = Me	Piperidine	293 (9250)	232 (7100)

*Compound **1** (R = $PhCH_2$) in 0.01 *N* sodium hydroxide in aqueous ethanol has λ_{max} 293 (8390) and 234 (8730) mμ.

TABLE 2

The i.r. bands (cm^{-1}, nujol) of salts of amines and **1** (R = $PhCH_2$) and some related derivatives

Compound	C≡N	C=O	C=C
1 (R = $PhCH_2$)	2200	1695	1665
Salt of **1** (R = $PhCH_2$) with piperidine	2170	1690	1625
Dimethylamine	2160	1690	1610
Triethylamine	2170	1695	1610
Aniline	2170	1690	1618
1 (R = $PhCH_2$), OH replaced by NH_2	2200	1695	1665
OCH_2Ph	2200	1690	1635
NHNHPh	2180	1680	1660
N=NPh	2200	1675	1580
NHPh	2170	1695	1650

TABLE 3

The pK_a values* of pyrrolidones **1** and **6**

Pyrrolidone	R	pK_a
1	H	4.4
	Me	4.3
	NMe_2	4.25
	$CH_2CH_2CN_2$	4.45
	$PhCH_2$	4.4
6	CN	4.4
	$CONH_2$	5.4
	COOEt	5.7 ±0.1†

*Potentiometric titrations using 30 ml of 0.015 *M* solution of dione in 50% aqueous ethanol against 0.03 *N* solution of NaOH in 33% ethanol/water. A Beckmann 72 p*H* meter and glass electrode were used.
†Five determinations at varying concentrations of ethanol (10 → 50%) in water.

Enamines were obtained from aromatic amines by Nair and Malik (4) in the presence of acetic acid. We obtained the enamine **4** (R = $PhCH_2$, R^1 = H, R^2 = Ph) from **1** (R = $PhCH_2$) and aniline in alcoholic acetic acid. The anilinium salt which seemed to be the only product in the absence of acetic acid had no bands between 3600 and 3100 cm^{-1} whereas the "anil" had a band at 3300 cm^{-1}. We repeated the preparation (4) of a compound claimed to be **4** (R = Me, R^1R^2 = $[CH_2]_5$). Its spectra had ν_{max} 2706 weak (w), 2500 w, 2450 w, 2160, 1695, 1630, and 1595 cm^{-1}, λ_{max} (EtOH) 232 and 293 mμ (ε 7100 and 9250 respectively). From these data and our analysis, we consider this compound to be a salt.

The pK_a values of a number of pyrrolidones **1** are given in Table 3. The values are close to those of carboxylic acids. The effect of varying the group in position 4 of the pyrrolidone **6** is also shown. Our figure for the ester **6** (R = COOEt) is the average of our values, compare Southwick *et al.*, 4.25 (6). This ester gave enamines with amines, rather than salts, supporting our expectation that it would have a higher pK_a value than **1** (R = $PhCH_2$) since a 4-cyano group would enhance the acidity by its greater inductive effect.

We observed the easy hydrolysis of nitrile to amide, above, after we found that the alleged oxime (4) of **1** (R = Me) was a salt. When the amide **6** (R = $CONH_2$) was treated with hydroxylamine hydrochloride and aqueous sodium acetate, the oximeamide **3** (R = $PhCH_2$) was not formed. The only isolable product was 1-benzyl-3-hydroxylamino-2-oxo-3-pyrroline **7**, (ν_{max} 1680 (C=O), 1050 (C=C), 800, (>C=CH—)) identical with a sample prepared according to Southwick *et al.* (6). The nitrile hydrolysis may follow the same course as that outlined recently by Stephenson *et al.* (7).

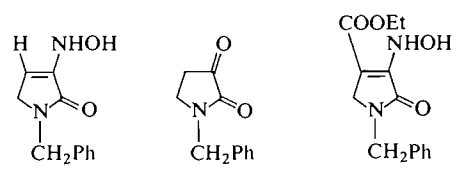

7 **8** **9**

Several investigators (4–6, 8) have reported on the keto–enol tautomerism of pyrrolidine-2,3-diones. The presence of a 4-substituent is stated to result in complete enolization as estimated from n.m.r. and i.r. spectra. Absence of a

4-substituent gives rise to the keto-form exclusively. The spectra of our compounds confirm these findings and reveal some additional points of interest.

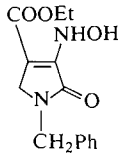

10

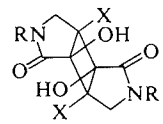

11

The i.r. spectrum of **1** (R = H), in which 1,4 interaction is low, indicates that it exists in the enol form, there being extended double bond conjugation. The n.m.r. spectrum of **8** confirms its structure, no enol being observed. However, the oxime **9** of the ester **6** (R = COOEt) had an n.m.r. spectrum showing one exchangeable proton at -0.4 τ and a complex ABC pattern for the protons at positions 4 and 5. The i.r. spectrum confirmed the double bond at position 3 to be exocyclic, structure **10** being contraindicated.

The u.v. irradiation of compounds **1** gave mainly dimers **11**. We obtained from **6** (R = COOEt) a solid which we conclude to be **11** (R = $PhCH_2$, X = COOEt). It had i.r. bands at 3320, 1730 (broad), and 1695 cm^{-1} and gave no ferric chloride color. A center of symmetry was indicated by the absence of any permanent dipole.[3]

The n.m.r. spectrum, along with two slowly exchangeable protons at 2.3, ten aromatic protons at 2.68 and two superimposed methyl group triplets at 8.9, had twelve lines in the region 5.0–6.5 τ. These were due to two superimposed methylene group quartets at 5.92 (splitting 7.3 Hz), a pair of doublets at 6.38 and 5.96 (splitting 12 Hz), assigned to ring methylene protons and a pair of doublets at 5.75 and 5.17 τ (splitting 15 Hz) assigned to the four benzylic protons of **11** (R = $PhCH_2$, X = COOEt) on the basis of their chemical shifts and J values which are in line with (negative) geminal coupling constants for methylene protons of each type (10).

Experimental

No attempt was made to optimize yields.

Melting points are uncorrected. The i.r. spectra are in nujol, u.v. spectra in ethanol, and n.m.r. spectra (Jeolco C-60HL) in $CDCl_3$. Mass spectra (A.E.I. M.S.12) were run on the probe at 70 eV, *m/e* (relative intensity) being quoted.

β-Aminopropionitriles, 2

Typically, (9), equimolar quantities of *N,N*-dimethylhydrazine and acrylonitrile were heated 24 h under reflux and fractionated to give β-cyanoethylaminodimethylamine, b.p. 50°/1 mm, yield 80%, characterized as the picrate, m.p. 74° from ethanol.

Anal. Calcd. for $C_{11}H_{14}N_6O_7$: C, 38.6; H, 4.1; N, 24.6. Found: C, 38.6; H, 4.0; N, 24.7.

Preparation of 4-Cyano-3-hydroxy-2-oxo-3-pyrrolines, 1

A β-aminopropionitrile and diethyl oxalate were reacted according to the literature (2).

Using β-(*N*-carbethoxyamino) propionitrile (3), hydrolysis took place during work up to give the hitherto unknown parent compound 4-cyano-3-hydroxy-2-oxo-3-pyrroline **1** (R = H), yield 41%, recrystallized from water, m.p. 215° (decomp.). Mass spectrum 167 (M^+, 75%), 43, (100%).

Anal. Calcd. for $C_5H_4N_2O_2$: C, 48.4; H, 3.2; N, 22.6. Found: C, 48.6; H, 3.2; N, 22.6.

From **2** (R = NMe_2) we obtained 4-cyano-1-dimethylamino-3-hydroxy-2-oxo-3-pyrroline **1** (R = NMe_2), m.p. 190° (decomp.) yield 1% after recrystallization from benzene. Mass spectrum 167 (M^+, 75%), 43 (100%).

Anal. Calcd. for $C_7H_9N_3O_2$: C, 50.3; H, 5.4; N, 25.1. Found: C, 50.5; H, 5.3; N, 25.0.

1-Benzyl-3-benzyloxy-4-cyano-2-oxo-3-pyrroline

The benzyl ether of **1** (R = $PhCH_2$) was obtained by treating a suspension of the silver salt in benzene (or methanol) with benzyl chloride at reflux overnight, yield 95%. It crystallized as prisms from ethanol, m.p. 210–214°, yield 50%. Mass spectrum 304 (M^+, 8%), 91 (100%).

Anal. Calcd. for $C_{19}H_{16}N_2O_2$: C, 75.1; H, 5.2; N, 9.1. Found: C, 75.0; H, 5.3; N, 9.1.

3-Benzyloxy-4-cyano-2-oxo-3-pyrroline

The benzyl ether of **1** (R = H) was prepared as above. It has m.p. 169°, crystallized from benzene, yield 7%. Mass spectrum 214 (M^+, 6%), 91 (100%).

Anal. Calcd. for $C_{12}H_{10}N_2O_2$: C, 67.3; H, 4.7; N, 13.1. Found: C, 67.6; H, 4.5; N, 13.2.

3-Amino-1-benzyl-4-cyano-2-oxo-3-pyrroline

The pyrroline **1** (R = $PhCH_2$), on treatment with urea (4), gave the amine, yield 90%, m.p. 189–191° crystallized from benzene/light petroleum. Mass spectrum 213 (M^+, 42%), 91 (100%).

Anal. Calcd. for $C_{12}H_{11}N_3O$: C, 67.6; H, 5.2; N, 19.7. Found: C, 67.6; H, 5.3; N, 19.9.

1-Benzyl-4-carboxamido-3-hydroxylamino-2-oxo-3-pyrroline (3, R = $PhCH_2$)

A mixture of the pyrroline **1** (R = $PhCH_2$) (5 g), hydroxylamine hydrochloride (6 g), sodium acetate (6 g) and water (40 ml) was kept at 96° for 3 h then cooled to 0°. The amide **3** (R = $PhCH_2$) was collected (4.5 g, 79%), m.p. 202° (decomp.). It was soluble in dilute alkali and could be precipitated unchanged by careful addition of dilute acid. It was sparingly soluble in all common organic solvents and an analytical sample was obtained

[3]We thank Prof. I. D. Chapman and Mr. A. R. Stevenson of this department for this result, using a General Radio Co. 1610 Capacitance assembly with 716-C bridge.

TABLE 4

Salts of **1** with amines, and their analyses

1	Melting point°	C		H		N	
		Calcd.	Found	Calcd.	Found	Calcd.	Found
R = $PhCH_2$							
Piperidine	134–137*	68.2	68.1	7.1	7.1	14.0	14.3
Dimethylamine	149–151*	64.8	65.0	6.6	6.6	16.2	16.3
Triethylamine	95–105†‡	68.5	68.3	8.0	8.0	13.3	13.2
Aniline	185–189†‡	70.3	70.1	5.6	5.4	13.7	13.6
R = Me							
Piperidine	138–143†§	59.2	59.2	7.7	7.7	18.8	19.0
Hydroxylamine	137–142†‖	42.1	42.4	5.3	5.4	24.5	24.2

*From benzene/light petroleum plus a little ethanol.
†With decomposition.
‡From benzene/light petroleum.
§From benzene/light petroleum, lit. m.p. 146–151° (4).
‖From ethanol, lit. m.p. 147–150° (4).

by thorough washing and drying. Mass spectrum 247 (M^+, 39%), 91 (100%). The i.r. bands 3400, 3100, 1685, 1630, 1605, 1570, 1260, and 950 cm^{-1}.

Anal. Calcd. for $C_{12}H_{13}N_3O_3$: C, 58.3; H, 5.3; N, 17.0. Found: C, 58.3; H, 5.3; N, 17.4.

4-Carboxamido-3-hydroxylamino-1-methyl-2-oxo-3-pyrroline (3, R = Me)

This was obtained as above, yield 14%, prisms decomposed 230°. Mass spectrum 171 (M^+, 100%).

Anal. Calcd. for $C_6H_9N_3O_3$: C, 42.1; H, 5.3; N, 24.5. Found: C, 42.2; H, 5.2; N, 24.0.

4-Carboxamido-3-hydroxylamino-2-oxo-3-pyrroline (3, R = H)

This compound was obtained by the above method, decomposed 210°. Mass spectrum 157 (M^+, 14%), 44 (100%). The latter peak was a doublet of CO_2 and $CONH_2^+$. Found 44.0132. Required 44.0136.

Anal. Calcd. for $C_5H_7N_3O_3$: C, 38.2; H, 4.5; N, 26.7. Found: C, 38.0; H, 5.1; N, 26.6.

1-Benzyl-4-carbethoxy-3-hydroxylimino-2-oxo-pyrrolidine (9)

1-Benzyl-4-carbethoxy-3-hydroxy-2-oxo-3-pyrroline (2 g), by the method described above, gave the oxime which was recrystallized from chloroform/light petroleum, needles (0.8 g), m.p. 87.5–90°. Mass spectrum 276 (M^+, 20%), 259 (M-17, 9%), 91 (100%).

Anal. Calcd. for $C_{14}H_{16}N_2O_4$: N, 10.15. Found: N, 10.2.

1-Benzyl-4-carboxamido-3-hydroxy-2-oxo-3-pyrroline (6, R = $CONH_2$)

The pyrroline **1** (R = $PhCH_2$) was left overnight at room temperature with five parts sulfuric acid and the solution poured onto ice. The product 91% yield, collected, dried, and recrystallized from ethanol, formed plates, m.p. 222–225° (decomp.). Mass spectrum 232 (M^+, 25%), 91 (100%).

Anal. Calcd. for $C_{12}H_{12}N_2O_3$: C, 62.1; H, 5.2; N, 12.1. Found: C, 62.1; H, 5.2; N, 12.0.

Reaction of 1-Benzyl-4-carboxamido-3-hydroxy-2-oxo-3-pyrroline with Hydroxylamine

The foregoing amide (0.2 g) was treated with hydroxylamine as described above. The product was extracted into ether, dried ($MgSO_4$), and concentrated giving 50 mg **7**, m.p. 213.5–215.5° twice recrystallized from water. Mixed m.p. with Southwick's material (6), having m.p. 213.5–215°, was 212–215°. The i.r. spectra of the two samples were identical. Mass spectrum 204 (M^+, 4%), 91 (100%).

Anal. Calcd. for $C_{11}H_{12}N_2O_2$: C, 64.7; H, 5.9; N, 13.7. Found: C, 64.5; H, 5.9; N, 13.8.

Preparation of Amine Salts of 4-Cyano-3-hydroxy-2-oxo-3-pyrrolines 1 (see Table 4)

The pyrroline **1** (0.2 g), a tenfold excess of amine, and enough benzene or ethanol for solution were left at room temperature or refluxed 2 h, then concentrated. Light petroleum was added to turbidity and the product crystallized as the mixture cooled. Catalytic amounts of *p*-toluenesulfonic acid did not affect the reactions using piperidine in benzene. Yields were nearly quantitative. The hydroxylamine salt of **1** (R = Me) was prepared according to the literature (4). The salts when washed with acid regenerated the pyrrolidones **1**.

1-Benzyl-4-cyano-2-oxo-3-(2'-phenylhydrazino)-3-pyrroline

The pyrroline **1** (R = $PhCH_2$) (1 g) and phenylhydrazine (1 g) in ethanol (50 ml) were refluxed for 6 h and concentrated to 25 ml. Addition of water precipitated the product which was recrystallized from benzene/light petroleum, needles (1.1 g), m.p. 158.5–160°. Mass spectrum 304 (M^+, 36%), 91 (100%); M-2 was also prominent.

Anal. Calcd. for $C_{18}H_{16}N_4O$: C, 71.0; H, 5.3; N, 18.4. Found: C, 71.1; H, 5.3; N, 18.3.

1-Benzyl-4-cyano-2-oxo-3-phenylazo-3-pyrroline

The above phenylhydrazone (0.3 g) was refluxed in xylene 1 week. Chromatography then gave the azo-compound (50 mg, 16%), yellow needles, m.p. 173–174.5° crystallized from benzene/light petroleum. Mass spectrum 302 (M^+, 52%), 91 (100%).

Anal. Calcd. for $C_{18}H_{14}N_4O$: C, 71.5; H, 4.7; N, 18.5. Found: C, 71.9; H, 4.7; N, 17.9.

3-Anilino-1-benzyl-4-cyano-2-oxo-3-pyrroline

Compound **1** (R = $PhCH_2$) (0.2 g), aniline (0.1 g),

ethanol (4 ml), and glacial acetic acid (6 drops) were heated together under reflux for 5 h then cooled to 0°. The deposit was recrystallized several times from ethanol/light petroleum to give the anil **4** (R = $PhCH_2$, R^1 = H, R^2 = Ph), 75 mg m.p. 148–151°, i.r. bands at 3300, 2170, 1695, 1650, 1600, and 1530 cm^{-1}. Mass spectrum 289 (M^+, 4%), 91 (100%).

Anal. Calcd. for $C_{18}H_{15}N_3O$: C, 74.7; H, 5.2; N, 14.5. Found: C, 74.5; H, 5.3; N, 14.4.

*1-Benzyl-4-carbethoxy-3-hydroxy-2-oxo-3-pyrroline Dimer (**11**)*

The monomer **6** (R = COOEt) (6) (9 g) in ethanol (500 ml) was irradiated using a 100 W medium pressure Hanovia mercury arc tube so that the solution refluxed gently overnight. Concentration gave the dimer, 3.3 g, m.p. 195–215° (decomp.) recrystallized from ethanol. Mass spectrum 522 (M^+, 1%), 91 (100%).

Anal. Calcd. for $C_{28}H_{30}N_2O_8$: C, 64.3; H, 5.8; N, 5.4. Found: C, 64.0; H, 5.5; N, 5.6.

The authors are grateful to the National Research Council of Canada for financial support.

1. R. ADAMS, S. MIYANO, and M. D. NAIR. J. Amer. Chem. Soc. **83**, 3323 (1961).
2. A. H. REES. J. Chem. Soc. 1749 (1965).
3. M. A. IORIO, M. MAROTTA, D. BOVET, and G. B. MARINI BETTOLO. Farm. (Pavia) Ed. Sci. **17**, 753 (1962). Chem. Abstr. **59**, 2642[f] (1963).
4. M. D. NAIR and P. A. MALIK. Indian J. Chem. **5**, 603 (1967).
5. A. H. BECKETT, C. M. LEE, and J. K. SUGDEN. J. Pharm. Pharmacol. **17**, 498 (1965).
6. P. L. SOUTHWICK, E. P. PREVIC, J. CASANOVA, and E. H. CARLSON. J. Org. Chem. **21**, 1087 (1956).
7. L. STEPHENSON, W. K. WARBURTON, and M. J. WILSON. J. Chem. Soc. (C) 861 (1969).
8. P. L. SOUTHWICK and R. T. CROUCH. J. Amer. Chem. Soc. **75**, 3414 (1953). P. L. SOUTHWICK and E. F. BARNES. J. Org. Chem. **27**, 98 (1962). W. R. VAUGHAN and I. S. COVEY. J. Amer. Chem. Soc. **80**, 2197 (1958). P. L. SOUTHWICK, J. A. FITZGERALD, R. MADHAV, and D. A. WELSH. J. Org. Chem. **34**, 3279 (1969).
9. H. A. BRUSON. Organic reactions. Vol. V. John Wiley & Sons Inc., New York, 1949. p. 79.
10. S. STERNHELL. Quart. Rev. **23**, 236 (1969).

Biosynthesis of dendrobine[1]

O. E. EDWARDS, J. L. DOUGLAS,[2] AND B. MOOTOO[3]
Biochemistry Laboratory, National Research Council of Canada, Ottawa, Canada

Received April 8, 1970

The incorporation of 4-^{14}C-mevalonate into dendrobine, the major alkaloid of *Dendrobium nobile* (Orchidaceae), is consistent with a biosynthesis involving successive intermediates with *trans–cis* farnesol, germacrane, and cadalane skeletons.

Canadian Journal of Chemistry, 48, 2517 (1970)

Can. J. Chem. Downloaded from www.nrcresearchpress.com by 210.87.254.6 on 09/05/12
For personal use only.

The biosynthesis of the picrotoxin family (1) of natural products, which includes picrotoxinin (**1**), tutin (2) and coriamyrtin (3) and the alkaloids of the orchid *Dendrobium nobile*[4] presents an interesting problem. The original speculation of Conroy (1) was that the skeleton was derived by oxidative removal of part of rings A and B of a 17-methylandrostane derivative (eq. [1]). The establishment of the absolute stereochemistry of picrotoxinin (5), tutin (6), and dendrobine (7) (**2**) discounted this possibility. The presence of fifteen carbons and the isopropyl group suggested that the skeleton was of sesquiterpene origin. However no unrearranged combination of three isoprene units would give it.

[1]

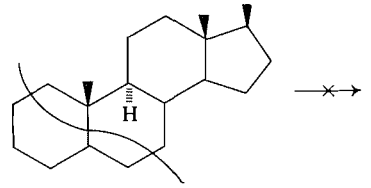

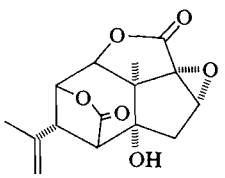

1

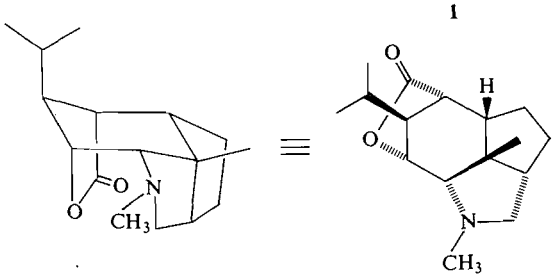

2

Three possible routes from mevalonic acid (**3**) via farnesol to the picrotoxinin skeleton have been proposed. One involves cyclization of *trans–cis* farnesol in an unprecedented manner, followed by synchronous methyl migrations (4) (eq. [2]). The second suggestion (8, 9) involved cyclization of farnesol to an intermediate with a cadalane skeleton followed by cleavage and cyclization (eq. [3*a*]) or cyclization to a tricyclic derivative (10, 16) and cleavage (eq. [3*b*]). The cyclization-cleavage sequence has a parallel in the postulated biosynthesis of helminthosporal (10, 16). The cadalane intermediate itself could arise in two ways, via the prior formation of a ten-membered ring (germacrane derivative) from *trans–cis* farnesol (eq. [4]), or via cyclization of *cis–cis*

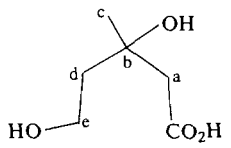

3

farnesol (eq. [5]) (by way of a bisabolane derivative).

We are grateful to a referee who suggested a third route from *trans–cis* farnesol (eq. [6]) to the tricyclic intermediate of eq. [3*b*].

We undertook to study these possibilities using ^{14}C-labelled mevalonic acid.

Our initial feeding of *D. nobile* was done using 2-^{14}C-mevalonate. A high level of incorporation into dendrobine was observed. However no degradation was attempted since the appearance of the communication by Yamazaki *et al.* (8) suggesting the cadalane route (eq. [3]) convinced us that feeding of 4-^{14}C-mevalonate would give

---

[1]Issued as NRCC No. 11398.
[2]NRCC Postdoctorate Fellow 1968–1970.
[3]NRCC Postdoctorate Fellow 1966–1968.
[4]For a review of work on these alkaloids see ref. 4*a*. We regret that at the time this biosynthetic proposal was made we were unaware of the comparable proposal by A. D. Cross (4*b*).

Can. J. Chem. Downloaded from www.nrcresearchpress.com by 210.87.254.6 on 09/05/12
For personal use only.

[2]

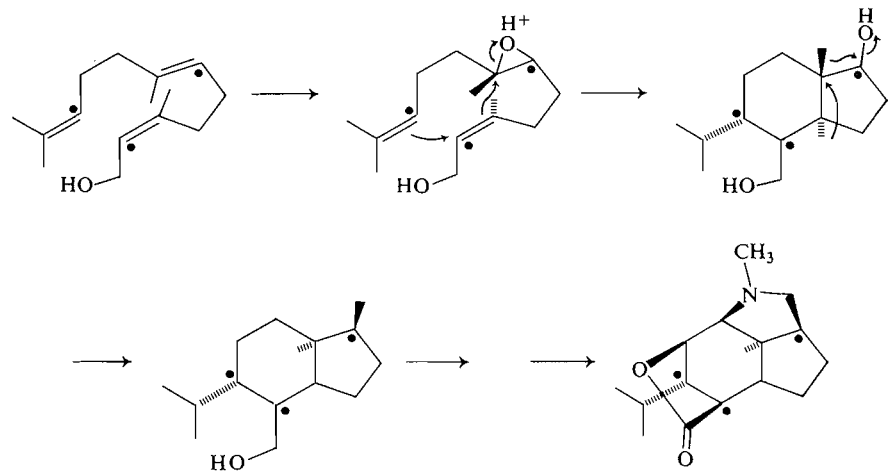

[3]

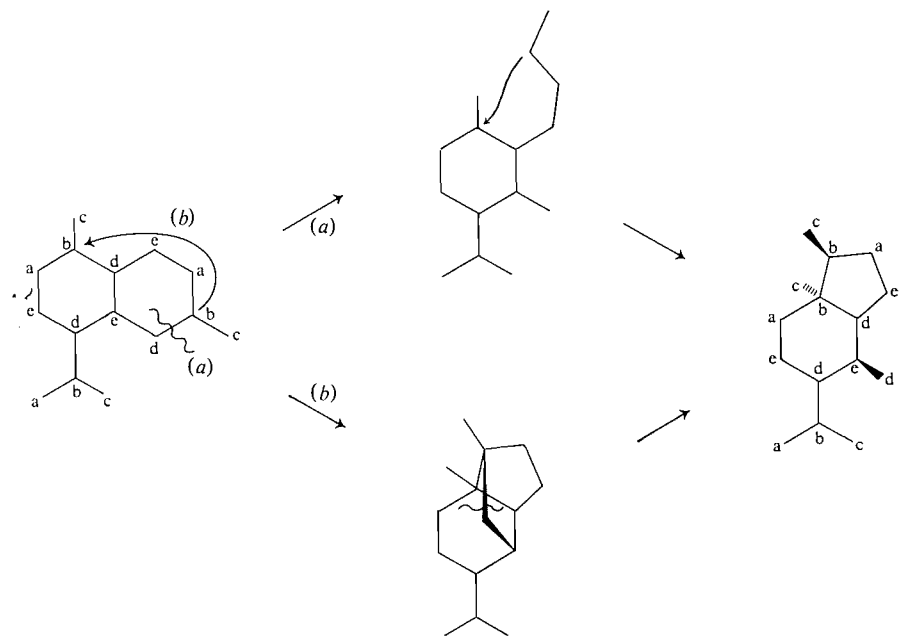

[4]

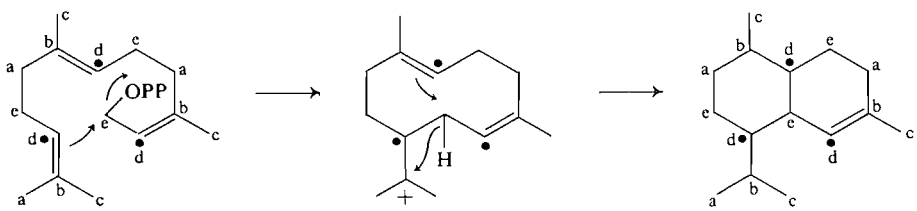

Can. J. Chem. Downloaded from www.nrcresearchpress.com by 210.87.254.6 on 09/05/12
For personal use only.

[5]

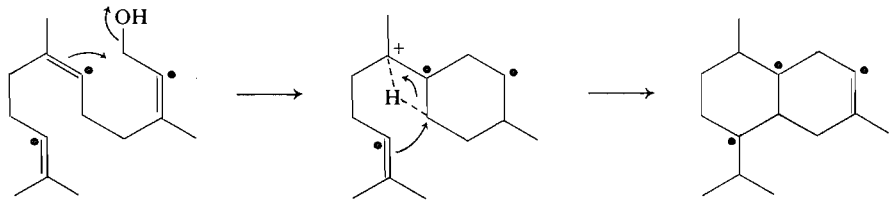

[6]

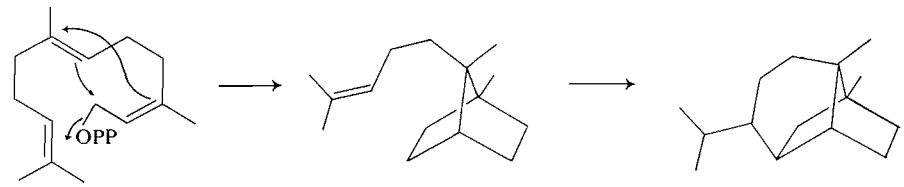

a more definitive answer relative to all three possibilities. (The isopropyl group would be labelled using 2-^{14}C-mevalonate for all of the biosynthetic routes.) The predicted position of the label for the 4-^{14}C-labelled mevalonate is indicated with dots in eqs. [2], [4], and [5] and the corresponding location in dendrobine indicated on formulae **4**, **5**, and **6**.

The required 4-^{14}C-mevalonolactone was prepared by the method of Cornforth *et al.* (11) and fed to *D. nobile* by the wick method. The dendrobine which was isolated showed a specific incorporation of 0.96% of the radioactivity. Labelled nobiline (**7**) was also obtained with a specific incorporation of 0.71%.

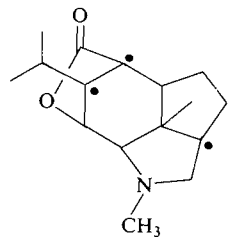

4

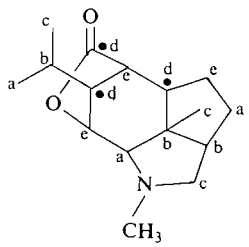

5

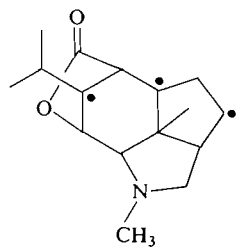

6

A variety of attempts were made to obtain a good yield of carbon dioxide or derivatives containing the carbonyl carbon of dendrobine. Under Schmidt reaction conditions (hydrazoic acid – chloroform – sulfuric acid), dendrobine hardly reacted at all (presumably the charge on the salt prevents protonation of the carbonyl). A Hunsdiecker reaction on the silver salt of oxodendrobinic acid (**8**) also gave very little carbon dioxide.

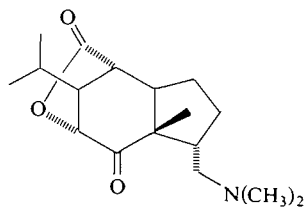

7

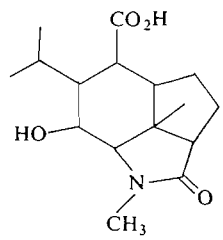

8

Three possible methods of obtaining the carbonyl group as benzoic acid or benzophenone were explored. One (eq. [7]) involved reduction of the lactone to a hemiacetal (**9**) and reaction of this with phenyl magnesium bromide. However the hemiacetal was difficult to purify and the phenyl derivative **10** could not be obtained pure on a small scale, hence this was abandoned. The second approach used direct phenyl magnesium bromide attack on dendrobine (eq. [8]). When a

[7]

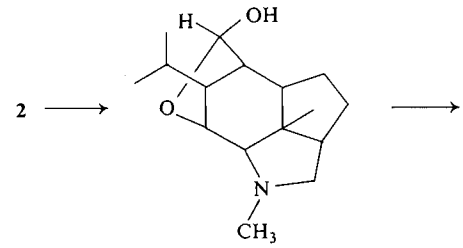

9

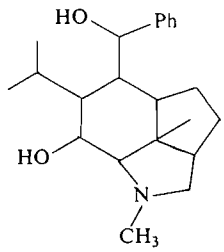

10

[8]

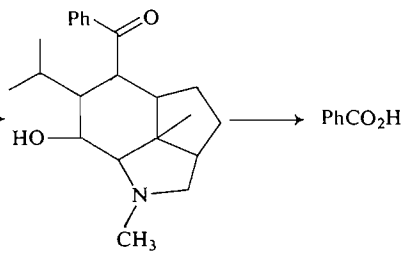

11

2 mole ratio of the Grignard reagent was used, a maximum 38% yield of the monophenyl derivative **11** was obtained, accompanied by unchanged dendrobine and diphenyl diol **12**. When this route was followed with radioactive dendrobine from the 4-^{14}C-mevalonolactone feeding, a 16% overall yield of radioactive benzoic acid was obtained by permanganate oxidation of **11**. Despite purification of the acid by sublimation and recrystallization, the specific activity of the benzoic acid was impossibly high (2.5 times that of the dendrobine being oxidized). Hence the dendrobine must have been contaminated with a highly radioactive impurity which efficiently gave benzoic acid. Since in addition the remainder of the molecule could not be recovered from this sequence, a third degradation was attempted.

The reaction of dendrobine with phenyl magnesium bromide was pushed to completion, giving an 84% yield of the diphenyl diol **12**. This was dehydrated to the known diphenyl olefin **13** (12) using modified conditions. This was converted to the lactam **14**. A variety of reagents (permanganate–periodate, ozone, and chromic acid) failed to yield benzophenone from **13** or **14**. Osmium tetroxide failed to oxidize **14**. However ruthenium tetroxide – periodate combination (13) cleaved **14** into benzophenone and the keto lactam **15**. The overall yield of benzophenone was 8.6%. Repetition of the sequence with dendrobine from plants which had been fed 4-^{14}C-mevalonate gave radioactive benzophenone and keto lactam. The specific activities are shown on Chart 1, with the labelling predicted for the cyclodecane route to cadalane (eq. [4]) followed by one of the steps in eq. [3]. Clearly, the observed labelling is in agreement with these predictions or those for the sequence outlined in (eq. [6]), and the alternate routes can be eliminated from consideration.

Although isolation of the labelled carbon atom adjacent to the isopropyl group of dendrobine would offer no distinction between the biosynthetic routes, it would provide a check on the method and show that the results of the benzophenone degradation route were not fortuitous. Accordingly, labelled dendrobine (specific activity 35 700 c.p.m./mmole) was subjected to a Kuhn–Roth oxidation (using the conditions employed by Money *et al.* (19) for oxidizing vindoline to propionic and acetic acids) and a mixture of acids containing one-third isobutyric acid:two-thirds acetic acid was obtained. The acids were separated, purified, and counted as their *p*-bromophenacyl esters. Thin-layer chromatography (t.l.c.) behavior, their melting points, and their nuclear magnetic resonance (n.m.r.) spectra showed that the products were indeed the desired acetate and isobutyrate esters. Due to the relatively mild conditions used in the oxidation to minimize oxidation of the isobutyric acid to acetic acid, a quantitative yield of acids was not obtained and it is doubtful if the tertiary methyl group contributed any acetic acid.

The *p*-bromophenacyl isobutyrate had a specific activity of 12 850 c.p.m./mmole, 36% of the activity of the dendrobine, and in good agreement with the theoretical requirement (33.3%). The low level of activity of the *p*-bromophenacyl acetate (330 c.p.m./mmole, 0.9% of the dendrobine activity), which could be due to a small amount of randomization of the label,

Can. J. Chem. Downloaded from www.nrcresearchpress.com by 210.87.254.6 on 09/05/12
For personal use only.

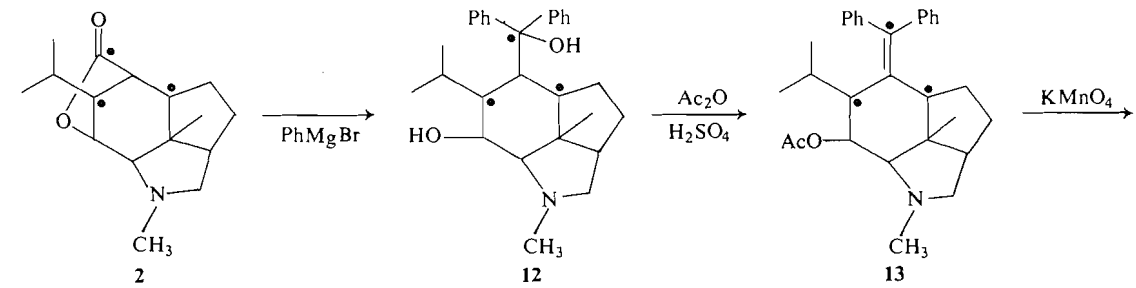

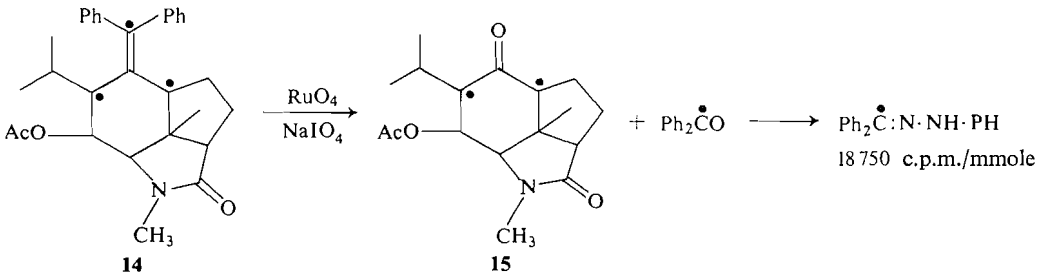

CHART 1

shows that the activity of the isobutyric acid was confined almost entirely to the carboxyl group.

The above results, those of Corbella *et al.* for coriamyrtin (15), and of Biollaz and Arigoni (14) for tutin all agree in requiring equal incorporation of radioactivity into the three mevalonate units giving rise to this class of sesquiterpenes. In contrast to this, the extensive work of Biollaz and Arigoni (14) on coriamyrtin requires unequal incorporation of label into the three mevalonate units.

These biosynthetic studies of the picrotoxin family of sesquiterpenes and the study of helminthosporal biosynthesis by de Mayo *et al.* (16) are consistent with a *trans–cis* farnesol → germacrane route to these polycyclic sesquiterpenes, but the route illustrated in eq. [6] is equally consistent with these labelling results.

Structure Proof and Spectra

The characteristic spectral feature which confirmed the structure of the hemiacetal **9** was a sharp n.m.r. signal at δ 5.47 corresponding to the hydrogen on the masked aldehyde carbon. The fact that it is unsplit is only consistent with the stereochemistry shown in **16**, in which H_A and H_B have a dihedral angle[5] of near 90°. An attempt to purify the hemiacetal by chromatography on alumina led to a mixture of dendrobine and dendrobidiol (Cannizzaro).

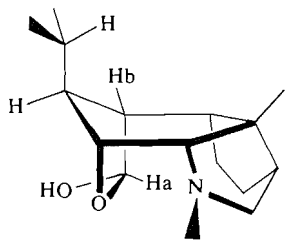

16

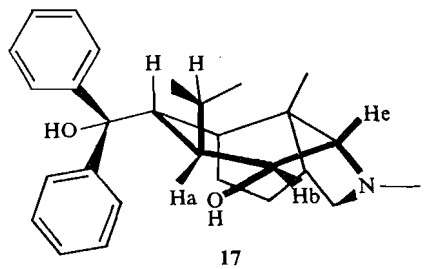

17

[5]All reported angles are for Dreiding stereo models.

Can. J. Chem. Downloaded from www.nrcresearchpress.com by 210.87.254.6 on 09/05/12
For personal use only.

Can. J. Chem. Downloaded from www.nrcresearchpress.com by 210.87.254.6 on 09/05/12
For personal use only.

The monophenyl derivative **11** exists largely in the open rather than hemiketal form, since the carbonyl stretching band is strong ($\nu_{max}(CHCl_3)$ 1685 cm^{-1}).

The n.m.r. spectrum of **11** required that the benzoyl and isopropyl groups be restricted in their rotation. For example the isopropyl signals appear as two sharp doublets at δ 1.09 and 0.92 (J = 6.5 c.p.s.).

The diphenyl diol **12** shows an even more dramatic effect, with both isopropyl methyl groups strongly shielded by one or both phenyl groups (pair of doublets centered at δ 0.87, J = 6 c.p.s., and at δ 0.32, J = 7 c.p.s.). The unusual difference between the two coupling constants suggests that the isopropyl group is distorted. A conformation close to that illustrated in **17** seems the likely one in solution in view of the above effect and the coupling of the hydrogens designated as H_a, H_b, and H_c on the structure (J_{ab} = 3 c.p.s. and J_{bc} = 6 c.p.s.). The measured dihedral angles for **17** are near 80 and 50° respectively. The diphenyl olefin **13** and the corresponding lactam **14** show similar effects (see Experimental).

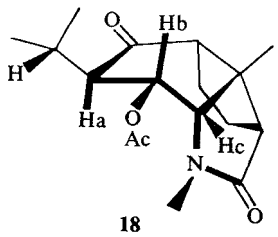

18

The structure of the keto lactam **15** follows from its empirical formula, infrared (i.r.) spectrum [ν_{max} 1740 (acetate), 1710 (cyclohexanone), 1685 cm^{-1} (γ-lactam)] and its n.m.r. spectrum (see Experimental). The isopropyl group still showed restricted rotation (pair of doublets with J = 7 c.p.s. centered at δ 0.97 and 1.09). The coupling constants J_{ab} = 11 c.p.s. (measured $\phi_{ab} \simeq 180°$) and J_{bc} = 2 c.p.s. (measured $\phi \simeq 70°$) are consistent with the stereochemistry illustrated in **18**.

Experimental

The i.r. spectra were determined using a Perkin–Elmer model 257 grating spectrometer with chloroform solutions, n.m.r. spectra using a Varian A-60-A spectrometer with deuteriochloroform solutions, and ultraviolet (u.v.) spectra using a Cary model 11 spectrometer with methanol solutions. The spectral data were obtained on non-radioactive compounds produced in preliminary experiments. Thin-layer chromatograms were done on silica plates. Counting of radioactive samples was done on a Beckman LS-250 liquid scintillation counter. Samples were dissolved in 15 ml of a counting solution consisting of 4 g PPO and 0.05 g POPOP per liter of toluene. The only sample to show significant quenching was the benzophenone phenylhydrazone (the count recorded is corrected for quenching). All samples were counted to a 2σ error of ±1.5%.

Preparation and Feeding of 4-^{14}C-Mevalonolactone

The 4-^{14}C-mevalonolactone was prepared by the method of Cornforth *et al.*, specific activity, 3.74 × 10^7 c.p.m./mmole. The mevalonolactone (218 mg in 176 ml water) was fed to 38 stems of intact plants of *Dendrobium nobile* by the wick method over a period of 14 days during August, 1968. After a further nine days, the plants were harvested.

Isolation of Alkaloids and Purification of Radioactive Dendrobine

The fresh aerial portion of the plant (1.2 kg) was macerated with ethanol in a Waring blender and the ethanol extract from three such treatments was evaporated to give a brown oil. The oil was dissolved in methylene chloride and extracted with 2 *N* sulfuric acid. The acid solution was made basic with sodium carbonate and the bases extracted with methylene chloride. The acid extraction was repeated and the resulting bases were triturated with ether. The ether soluble portion was sublimed twice at 90–110°, 5 × 10^{-2} mm to give 425 mg of crude alkaloids.

Careful crystallization of the alkaloids from ether gave first cubic crystals of dendrobine (**2**) and then filamentous crystals of nobiline (**7**). Repeated crystallization of the dendrobine from ether with recycling of the mother liquors gave pure dendrobine, (63 mg), m.p. 133–136° (lit. (17) m.p. 135–136°) and ν_{max} 1770 cm^{-1}. Its n.m.r. spectrum had signals at δ 0.99 (d, J = 6 c.p.s., 6H), 1.50 (s, 3H), 2.67 (s, 3H), and 4.89 (m, 1H). The specific activity of the dendrobine, which was unchanged on further recrystallization, was 3.60 × 10^5 c.p.m./mmole. The dendrobine was diluted six-fold to a specific activity of 55 200 c.p.m./mmole.

The nobiline was recrystallized from *n*-hexane to give material (54 mg) of m.p. 84–87° (lit. (17) m.p. 87–88°) and ν_{max} 1785 and 1710 cm^{-1}. Its n.m.r. spectrum had signals at δ 0.95, (d, J = 6.5 c.p.s., 3H), 0.98 (d, J = 6.5 c.p.s., 3H), 1.38 (s, 3H), 2.16 (s, 6H) and 4.58 (d, J = 5.5 c.p.s., 1H). The specific activity of the nobiline was 2.56 × 10^5 c.p.m./mmole.

Hemiacetal (9)

Dendrobine (263 mg) in ether (15 ml) was cooled to −20° and over a period of 15 min, 3 ml of a solution of di-*t*-butyl aluminum hydride in ether (about 0.6 *M*) (see reference 18) were added with stirring. After 30 min at room temperature, the clear solution was cooled to 0°, then Celite (0.5 g) and water (0.2 ml) were added. The mixture was stirred at 0° for 15 min, shaken at room temperature, filtered, dried (magnesium sulfate), and evaporated to a yellow oil (228 mg). The i.r. spectrum showed peaks at 3600 and 3400 cm^{-1} (hydroxyl), and a weak peak at 1715 cm^{-1} (carbonyl of an impurity). The

Can. J. Chem. Downloaded from www.nrcresearchpress.com by 210.87.254.6 on 09/05/12
For personal use only.

n.m.r. spectrum showed peaks at δ 1.0 (several overlapping signals, about 6H), 1.37 (s, 3H), 2.51 (s, 3H), 3.8 (removed by D_2O), 4.57 (doublet of doublets, J_1 = 5 c.p.s., J_2 = 2.5 c.p.s., 1H), 5.47 (s, 1H), plus other peaks in the *C*-methyl and *N*-methyl regions indicative of substantial amounts of impurities.

Attempted purification of the product led to degradation.

*Phenyl Ketone (**11**)*

To a solution of 263 mg of dendrobine in 15 ml of ether was added a solution of phenyl magnesium bromide (from 628 mg of bromobenzene) in 25 ml of ether. The mixture was stirred for 1 h at room temperature, then refluxed for 0.5 h. It was then poured onto 3 ml of 3 *N* sulfuric acid and crushed ice. A precipitate (largely the sulfate of diphenyl diol **12**) was removed by filtration, the filtrate made basic with ammonia and extracted with ethyl acetate. The 210 mg of product recovered from the ethyl acetate solution was adsorbed from benzene onto 5 g of neutral alumina, activity II. A 20% ethyl acetate – 80% benzene mixture rapidly eluted 200 mg of amorphous solid. After redissolving in 1.5 *N* sulfuric acid and recovery from solution, 172 mg of amorphous solid was obtained with the correct spectroscopic properties for **11**. It had λ_{max} 245 mμ and ν_{max} 1675 cm^{-1}. Its n.m.r. spectrum had signals at δ 7.2–8.2(5H), 3.5–4.1(1H mult.), 2.4(3H singlet), 1.30(3H singlet), and a pair of 3H doublets centered at 1.09 (J = 6.5) and 0.92(J = 6.5).

Attempts to oxidize **11** with trifluoroperacetic acid led (after reduction of amine oxide) to a mixture containing ketone (ν_{max} 1675 cm^{-1}), benzoic ester (ν_{max} 1717 cm^{-1}), and phenyl ester (ν_{max} 1775 cm^{-1}) so this was not pursued further.

*Diphenyl Diol (**12**)*

Dendrobine (**2**) (150 mg) in 11 ml ether was added to the Grignard reagent formed from 145 mg magnesium turnings and 0.94 g bromobenzene in 7 ml ether. The mixture was heated under reflux for 3 h, then cooled in ice and poured onto 4.5 ml of ice cold 2 *N* sulfuric acid. After the precipitate had coagulated, the ether was separated and extracted with small portions of 3 *N* sulfuric acid. The combined acid layers were washed several times with small portions of ether, care being taken to retain all of the precipitate. The acid layers and precipitate were made basic with 10% aqueous sodium carbonate and extracted with chloroform. The chloroform was evaporated to give the crude product. The crude product was dissolved in benzene:*n*-hexane (95:5) and placed on 10 g of silica gel. The column was eluted with benzene, then benzene:methanol (98:2) to give as a pale yellow oil, the diphenyl diol (**12**), 200 mg. The product showed ν_{max} 3300 (br), 1600 (w), 1490, and 700 cm^{-1} [lit. (12) ν_{max} (KBr) 3340, 1600, 1490, 746, and 704 cm^{-1}]. Its n.m.r. spectrum had signals at δ 0.33(d, J = 7 c.p.s., 3H), 0.87(d, J = 6 c.p.s., 3H), 1.27(s, 3H), 2.32(s, 3H), 4.09(doublet of doublets, J_1 = 6 c.p.s., J_2 = 3 c.p.s., 1H), 4.70(br, 1H), 5.63(br, 1H), and 7.5(m, 10H).

*Diphenyl Olefin (**13**)*

The diphenyl diol (**12**) (200 mg) was dissolved in acetic anhydride (1.5 ml) and two drops of concentrated sulfuric acid were added. The solution was heated at 100° for 12 h, then left at room temperature overnight. The resulting solution was mixed with 15 ml of ethyl acetate and extracted with 10% aqueous sodium carbonate until evolution of carbon dioxide ceased. The ethyl acetate was washed, dried, and evaporated to a brown oil. The oil was distilled at 125–135°, 7 × 10^{-5} mm, to give the diphenyl olefin (**13**) as a pale yellow glass (161 mg). This showed ν_{max} 1720, 1595(w), 1490, and 700 cm^{-1} (lit. (12) ν_{max} (CCl_4) 1750, 1600, 1490, and 710 cm^{-1}), and λ_{max} 248 mμ (ε 10 500). Its n.m.r. spectrum showed peaks at δ 0 83 (d, J = 7 c.p.s., 3H), 0.89(d, J = 6.5 c.p.s., 3H), 1.34(s, 3H), 2.25(s, 3H), 2.49(s, 3H), 5.77(t, J = 4.5 c.p.s., 1H), and 7.5(m, 10H).

*Diphenyl Olefin Lactam (**14**)*

Diphenyl olefin (**13**) (161 mg) was dissolved in a solution of 23 ml acetone and 7 ml water and a solution of potassium permanganate (120 mg) and hydrated magnesium sulfate (200 mg) in 8 ml acetone and 9 ml of water were added. The solution was kept at room temperature for 1 h, then cooled in ice and acidified with 3 *N* sulfuric acid. Ice cold acidic 5% hydrogen peroxide was added until all the potassium permanganate and manganese dioxide were reduced. The yellow solution was concentrated to one third volume, water added, and the resulting mixture extracted with chloroform. The chloroform was washed, dried, and evaporated to give a yellow oil. The oil was placed on a preparative t.l.c. plate and the plate was eluted with benzene:ethanol (9:1). Three overlapping bands resulted. The major band (central) was extracted to give an oil that was distilled at 140–145°/2 × 10^{-4} mm to give pure diphenyl olefin lactam (**14**) as a pale yellow glass (84 mg). The product showed ν_{max} 1735, 1670, 1595(w), 1570(w), 1490, and 700 cm^{-1} and λ_{max} 246 mμ (ε 10 000). Its n.m.r. spectrum showed signals at δ 0.93(d, J = 6.5 c.p.s., 3H), 0.95(d, J = 6 c.p.s., 3H), 1.48(s, 3H), 2.21(s, 3H), 2.79(s, 3H), 3.62(d, J = 5 c.p.s., 1H), 5.58(d of doublets, J_1 = 8 c.p.s., J_2 = 5 c.p.s., 1H), and 7.2(m, 10H). The mass spectrum showed peaks at *m/e* 457, 397, 355, and 354. The molecular ion had a mass of 457.2618 (Calcd. for $C_{30}H_{35}NO_3$: 457.26169). The specific activity was 56 500 c.p.m./mmole.

Preparation of Ruthenium Tetroxide Reagent

Polymeric ruthenium trichloride was dissolved in molten sodium hydroxide. After cooling, the mixture was dissolved in water and filtered through glass wool to give a clear orange solution. Either this solution, or the black suspension that formed on exposure to air over several days, could be used. Ruthenium tetroxide was formed as needed by acidifying a 1 ml portion of the basic ruthenium mixture with 3 *N* sulfuric acid, adding a small quantity of sodium *meta*-periodate, and extracting the resulting clear yellow solution with 1 ml of spectroscopic grade carbon tetrachloride.

*Oxidative Cleavage of the Diphenyl Olefin Lactam (**14**)*

The diphenyl olefin lactam (**14**) (80 mg) was dissolved in 1.5 ml of spectroscopic grade carbon tetrachloride and 1.5 ml water containing 100 mg of sodium *meta*-periodate was added. The mixture was stirred vigorously at room temperature and 10–12 1 ml portions of ruthenium tetroxide in carbon tetrachloride were added over a period of 1½ days. Water and chloroform were added to

Can. J. Chem. Downloaded from www.nrcresearchpress.com by 210.87.254.6 on 09/05/12
For personal use only.

the reaction mixture and the organic layer was separated, washed, dried, and evaporated to a black oil. The oil was placed on a preparative t.l.c. plate and the plate was eluted with *n*-pentane:ether (1:1). The high R_f band (same R_f as benzophenone) was extracted and combined with the product from re-cycling (see below). The resulting oil was distilled at 100°/2 mm to give benzophenone (8 mg) with an identical i.r. spectrum to authentic benzophenone. It gave a phenylhydrazone with m.p. 136.5–137.5°. The benzophenone phenylhydrazone had a specific activity of 18 750 c.p.m./mmole.

After removal of the benzophenone, the preparative t.l.c. plate was rerun twice in *n*-pentane:ether:chloroform:methanol (30:30:35:5) and the low R_f band extracted. The extract was placed on a preparative t.l.c. plate and the plate was eluted with benzene:ethanol (9:1). The two closely spaced bands at low R_f were extracted. The upper band (47 mg) was shown to be diphenyl olefin lactam (**14**) and was recycled. The lower band (and the lower band from the recycling) were distilled at 130°, 1.5×10^{-2} mm to give a crystalline product (15 mg). This was recrystallized from benzene to give the ketone (**15**), m.p. 187–190°, with ν_{max} 1740, 1710, and 1685 cm^{-1}. Its n.m.r. spectrum showed peaks at δ 0.97 (d, J = 7 c.p.s., 3H), 1.09 (d, J = 7 c.p.s., 3H), 1.45 (s, 3H), 2.14 (s, 3H), 2.82 (s, 3H), 3.62 (d, J = 2 c.p.s., 1H), and 5.57 (d of doublets, J_1 = 11, J_2 = 2 c.p.s., 1H). Its high resolution mass spectrum showed peaks at *m/e* 307.1774 (M^+, calcd. for $C_{17}H_{25}O_4N$: 307.17836), 248.1646 (M^+-CH_3CO_2, calcd. for $C_{15}H_{22}O_2N$: 248.16505), 222.1125 (M^+-[CH_3CO+CH_3CHCH_2], calcd. for $C_{12}H_{16}O_3N$: 222.11302), 204.1026 (M^+-[CH_3CO_2H+CH_3CHCH_3], calcd. for $C_{12}H_{14}O_2N$: 204.10245). It showed a specific activity of 39100 c.p.m./mmole.

Kuhn–Roth Oxidation of Dendrobine

Dendrobine (**2**) (124 mg, 0.473 mmole, specific activity 35 700 c.p.m./mmole) was mixed with 10 ml of 30% chromium trioxide in water. The mixture was distilled with addition of water to maintain constant volume until titration of fractions with *N*/10 sodium hydroxide showed negligible acid to be present (120 ml collected). Each fraction was boiled briefly before titration to remove carbon dioxide. The combined fractions were concentrated to 0.5 ml, 1 ml of 95% ethanol was added, and the solution was titrated to p*H* 6.6 by addition of *N* hydrochloric acid.

A 20% excess (88 mg) of *p*-bromophenacyl bromide was added and the solution heated under reflux for 2 h. The resulting solution was concentrated, water and chloroform added, and the chloroform separated and dried (sodium sulfate). The chloroform solution was concentrated, then placed on a 20 × 20 × 0.1 cm preparative plate (silica gel GF-254) which was developed twice in chloroform:benzene 75:25. Three major bands resulted (visualized under u.v. light): *p*-bromophenacyl acetate, R_f 0.08; *p*-bromophenacyl isobutyrate, R_f 0.16; and *p*-bromophenacyl bromide, R_f 0.38. Extraction of the two lower bands with ether gave the acetate ester (41 mg) and the isobutyrate ester (17 mg). The acetate was recrystallized from *n*-hexane and methanol:water to give platelets, m.p. 83–85° and the isobutyrate was recrystallized from *n*-hexane to give needles, m.p. 75–77°. The n.m.r. spectra of the acetate and isobutyrate (from unlabelled dendrobine) respectively showed peaks at δ 2.25 (s, 3H), 5.37 (s, 2H), 7.77 (d, J = 9 c.p.s., 2H), and 7.92 (d, J = 9 c.p.s., 2H) and peaks at 1.31 (d, J = 7 c.p.s., 6H), 2.82 (septet, J = 7 c.p.s., 1H), 5.39 (s, 2H), 7.80 (d, J = 9 c.p.s., 2H), and 7.92 (d, J = 9 c.p.s., 2H). The *p*-bromophenacyl acetate had a specific activity of 330 c.p.m./mmole and the *p*-bromophenacyl isobutyrate had a specific activity of 12 850 c.p.m./mmole.

We are grateful to Dr. W. D. Jamieson for high resolution mass spectra, Mr. H. Seguin for analyses, and Mr. A. Knoll and Mr. R. Kolt for technical assistance. We thank Prof. Y. Tsuda for a generous gift of dendrobine and Prof. Y. Hirata for an alkaloid mixture containing dendrobine and nobiline.

1. H. Conroy. J. Amer. Chem. Soc. **79**, 5551 (1957). Cyclopentanoid terpene derivatives. W. I. Taylor and A. R. Battersby, *editors*. Marcel Dekker Inc., New York, 1969. Chapt. 2.
2. B. M. Craven. Nature, **168**, 1193 (1963).
3. T. Okuda and T. Yoshida. Tetrahedron Lett. 439, 694 (1964).
4. (*a*) Cyclopentanoid terpene derivatives. W. I. Taylor and A. R. Battersby, *editors*. Marcel Dekker Inc., New York, 1969. Chapts. 2 and 6; (*b*) A. D. Cross. Quart. Rev. (London), **14**, 317 (1960).
5. B. M. Craven. Acta Cryst. **15**, 387 (1962).
6. M. T. MacKay and A. McL. Mathieson. Tetrahedron Lett. 1399 (1963).
7. Y. Sasaki, Y. Tsuda, B. Yasui, T. Konita, J. Matsumoto, E. Katarao, and J. Nakano. Tetrahedron, **20**, 2007 (1964).
8. M. Yamazaki, M. Matsuo, and K. Arai. Chem. Pharm. Bull. (Tokyo), **14**, 1058 (1966).
9. W. Parker, J. S. Roberts, and R. Ramage. Quart. Rev. (London), **21**, 331 (1967).
10. P. de Mayo and R. E. Williams. J. Amer. Chem. Soc. **87**, 3275 (1965).
11. J. W. Cornforth, R. H. Cornforth, A. Pelter, M. G. Horning, and G. Popjak. Tetrahedron, **5**, 311 (1959).
12. T. Onaka, S. Kamata, T. Maeda, Y. Kawazoe, M. Natsume, T. Okamoto, F. Uchimaru, and M. Shimizu. Chem. Pharm. Bull. (Tokyo), **12**, 506 (1964).
13. F. Sondheimer, R. Mechoulam, and M. Sprecher. Tetrahedron, **20**, 2473 (1964).
14. M. Biollaz and D. Arigoni. Chem. Commun. 633 (1969).
15. A. Corbella, P. Gariboldi, G. Jommi, and C. Scolastico. Chem. Commun. 634 (1969).
16. P. de Mayo, J. R. Robinson, E. Y. Spencer, and R. W. White. Exper. **18**, 359 (1962).
17. S. Yamamura and Y. Hirata. Tetrahedron Lett. 79 (1964).
18. J. Schmidlin and A. Wettstein. Helv. Chim. Acta, **46**, 2799 (1963).
19. T. Money, I. G. Wright, F. McCapra, E. S. Hall, and A. I. Scott. J. Amer. Chem. Soc. **90**, 4144 (1968).

Synthesis and properties of some α-D-alkyl glucosides and mannosides: apparent molal volumes and solubilization of nitrobenzene in water at 25 °C

G. M. BROWN, P. DUBREUIL, F. M. ICHHAPORIA, AND J. E. DESNOYERS
Chemistry Department, University of Sherbrooke, Sherbrooke, Quebec

Received April 1, 1970

Normal and cyclic α-D-alkyl glucosides and mannosides have been synthesized in a one-step procedure from the corresponding sugar. The apparent molal volume and the influence on the solubility of nitrobenzene of some of these glycosides have been measured in water at 25 °C. Evidence for micelle formation is presented for α-D-*n*-hexyl glucoside, -*n*-octyl glucoside, and -cyclohexyl mannoside. Comparison of the physical properties of the aqueous solutions shows that the stereochemistry of the sugar unit plays an important role in the hydrophobic hydration and hydrophobic interactions of the glycosides.

Canadian Journal of Chemistry, **48**, 2525 (1970)

Can. J. Chem. Downloaded from www.nrcresearchpress.com by 210.87.254.40 on 09/05/12
For personal use only.

Introduction

The investigation of thermodynamic and kinetic properties of aqueous solutions of homologous series such as the salts RNH_3Br (1–3) has proven to be very useful in the understanding of hydrophobic interactions between organic ions in the submicellar region. The general objective of the present work was to extend these studies to non-ionic systems. In this respect, solutes such as alkyl glycosides are of particular interest because, in addition to their potential biological and pharmaceutical applications, they furnish a means of investigating the influence of the polar group on the solute–solvent and solute–solute interactions.

Despite the very large number of possible isomers, the only work reported, to our knowledge, on the solution properties of such systems is on the surface tension of octyl, decyl, and dodecyl β-D-glucosides (4, 5). We have chosen to study the normal and cyclic alkyl α-D-glucosides and mannosides. Fewer α-D- than β-D-glycosides are known in the literature, and we felt that there was a possibility of preparing them using a one-step experimental procedure from the corresponding sugars, in spite of the fact that it is customary in the synthesis of α-D-glucosides to use a multistep process. A résumé of synthetic methods has been given by Wing and BeMiller (6).

The properties investigated were apparent molal volumes and solubilization of nitrobenzene. Apparent molal volumes are very informative since, in addition to defining the region over which a micelle is formed, this property is very sensitive to solute–solvent and solute–solute interactions. The choice of nitrobenzene as a nonelectrolyte for salting-in measurements was dictated because of the ease of analysis; it was shown recently (7) that the influence of the nitro group was to slightly decrease the salting-in effect when compared with a non-polar nonelectrolyte like toluene.

Surprisingly enough, the α-D-glucosides are significantly less soluble in water than the corresponding β-isomers. In addition, the crystallization of some of these compounds has proven to be a problem. Moreover, there is evidence that one sample (α-D-cyclohexyl glucoside) was contaminated with the β-isomer. Despite these drawbacks interesting conclusions can be drawn from these measurements on the influence of stereochemistry on hydrophobic hydration and interactions.

Experimental

Melting points were determined using the Fisher–Johns melting point apparatus and are uncorrected.

Nuclear magnetic resonance (n.m.r.) data were recorded using the Varian A-60 instrument.

Microanalyses were performed by the Schwarzkopf Microanalytical Laboratories at Woodside, New York.

Methyl α-D-glucoside is commercially available from Pfanstiehl Laboratories and was used as such.

cis–cis-2-Decalol (see Fig. 1 for formula) was obtained from the mixture of *cis*- and *trans*-decahydro-2-naphthols, supplied commercially by Aldrich, by filtering and recrystallization from ether. The product was identified by its melting point and n.m.r. spectrum (8).

Synthesis of Glycosides

The one-step preparations of α-D-gluco and α-D-mannopyranosides undertaken here are essentially based on a method employed by Gorin and Perlin (9) for the synthesis of benzyl-α-D-mannopyranoside. All compounds except the decalyl mannoside were prepared in the same manner. Essentially gaseous HCl is dissolved in an excess of the required alcohol until the desired weight concen-

TABLE 1

Preparations of α-D-alkyl glucosides and mannosides

R	Compound* abbreviation	Reaction time (h)	Temperature (°C)	Concentration HCl (% in alcohol)	Yield (%)	Analysis (%) Calculated C	Calculated H	Found C	Found H
Methyl	MG								
Ethyl	EG	48	60	5	22				
n-Hexyl	HG	24	60	15	21	54.53	9.15	54.77	9.19
n-Octyl	OG	24	60	20	24	57.51	9.65	57.13	9.61
n-Decyl	*n*DG	48	60	20	33	59.98	10.07	59.65	10.18
n-Dodecyl	DdG	48	60	20	54	62.04	10.41	61.53	10.50
Cyclohexyl‡	cHG	24	60	10	25	54.95	8.45	55.13	8.71
n-Decyl	DM	24	60	20	30	59.98	10.07	60.05	10.20
n-Dodecyl	dDM	24	60	20	72	62.04	10.41	62.08	10.56
Cyclohexyl	cHM	24	60	12	23	54.95	8.45	55.32	8.57
2-Decalyl	DcM	24	40	30†	11	60.74	8.92	60.24	8.88

*G = glucoside; M = mannoside.
†In $CHCl_3$ solution.
‡Mixture of anomers.

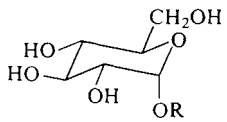

α-D-Glucopyranoside

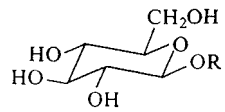

β-D-Glucopyranoside

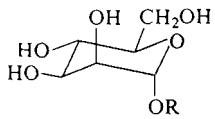

α-D-Mannopyranoside

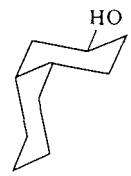

cis–cis-2-Decalol

FIG. 1. Organic compounds studied in the present investigation.

tration was reached. The sugar was added and the mixture stirred with heating at least 12 h. Specific experimental conditions are given in Table 1 and the physical constants of the purified pyranosides in Table 2. The detailed preparation and purification procedure of α-D-hexyl glucoside will serve as an example.

A 15% solution of HCl in 70 ml of hexanol is prepared; 10 g of D-glucose are added and the mixture is stirred for 24 h at 60 °C. Solid $NaHCO_3$ is added until a p*H* of 5 is reached. After filtering, the excess of alcohol is evaporated in vacuo. Water (50 ml) is added and the glucoside is extracted with ethyl acetate. After drying, the major portion of the solvent is removed; the glucoside crystallizes with some difficulty.

The octyl glucoside also takes some time to crystallize, the others are obtained quite readily.

This method is not useful for the preparation of galactosides, since too much degradation occurs.

The HCl concentration is somewhat lower in the cyclohexyl glycoside preparations; this is necessary to avoid charring. With one exception, the cyclohexyl glucoside, all the α-D-glycosides so prepared were uncontaminated with the β-isomer after purification; no peak of axial H_1 hydrogen is seen in the n.m.r. spectra of these compounds.

Two separate preparations of the cyclohexyl glucoside give products with quite similar melting points but vastly different specific rotations. An examination of the n.m.r. spectrum of the sample having the higher specific value leads one to believe that the β-isomer is present, peak integration suggests about 20% impurity. The chemical shift at $\tau = 5.69$, $J = 7.4$ c.p.s. agrees with published data for methyl β-D-glucopyranoside (10).

The preparation of the decalyl mannoside had to be modified since the starting alcohol was solid. Decalol (96 g) in 700 ml of dry $CHCl_3$ is treated with gaseous HCl to give a 30% solution of the acid. D-Mannose (20 g) is added and the mixture is stirred at 40 °C for 24 h. Solid $NaHCO_3$ is added until a p*H* of 5 is reached, the mixture is then filtered. Excess decalol is steam-distilled (a tedious process, the decalol is not too volatile) and most of the water evaporated. The aqueous portion is extracted with ethyl acetate; the mannoside crystallizes from a 1:1 mixture of ethyl acetate – isopropanol.

Density and Solubility Measurements

All sugar derivatives were dried in vacuo for at least 48 h, and the solutions were then prepared by volume using redistilled water.

Whenever sufficient material was available, the densities were measured with a previously described (2) densimeter which is capable of evaluating differences in densities to 2×10^{-6} g ml^{-1}. Otherwise a 25 ml pyknometer was used.

The solubilities of nitrobenzene in water and in the sugar solutions were obtained with a differential refractometer. The details of this technique for salting-in measurements have been given elsewhere (7).

Can. J. Chem. Downloaded from www.nrcresearchpress.com by 210.87.254.40 on 09/05/12
For personal use only.

TABLE 2

Physical constants of α-D-alkyl glucosides and mannosides

Compound	Transition point (°C)	Melting point* (°C)	$[\alpha]_D^{23}$ (MeOH)	R_F†	Chemical shift of H_1 doublet τ(DMSO-d_6)	J (c.p.s.)
EG	—	113–114.5‡	156.6§	0.36	5.35	3.5
HG	64–66	70	132.1	0.50	5.37	3.5
OG	71.5–72.5	124	117.9	0.53	5.37	3.3
DG	68–74	139	89.2	0.56	5.37	3.0
DdG	70–75	151–152	74.9	0.64	5.37	3.0
cHG‖	—	116.5–118–5	70.6	0.42		
		115.5–116.5	99.7	0.42	5.23	3.3
DM	65–67	158	58.0	0.56	5.37	1.5
DdM	73–75	164–165	55.9	0.62	5.38	1.0
cHM	—	113.5–114	95.0	0.46	5.15	1.0
DcM	—	160–162	89.6	0.62	5.22	0.5

*Recrystallized from EtOAc.
†Thin layer chromatography, silica gel G, MeOH/EtOAc = 1/4.
‡Solvent Me_2CO; literature value (6), 113–114 °C.
§Literature value (6), $[\alpha]_D^{20} = 153$ °C.
‖Literature values, m.p. = 125 °C (6), 126 °C (11, 12); $[\alpha]_D^{20} = 136$ (6), 137 (11, 12).

TABLE 3

Densities of aqueous solutions of α-D-alkyl glucosides and mannoside at 25 °C

Compound	c (moles l^{-1})	$(d - d_0)\,10^3$ (g ml^{-1})	Compound	c (moles l^{-1})	$(d - d_0)\,10^3$ (g ml^{-1})
MG	0.05	3.087	EG	0.05	2.957
	0.15	9.247		0.1	5.926
	0.25	15.422		0.15	8.912
	0.35	21.594			
	0.45	27.719	*n*HG	0.03	1.49*
				0.04	2.00*
cHG	0.02	1.302		0.06	3.02*
	0.04	2.621		0.15	7.81*
	0.05	3.27*		0.2	10.49*
	0.08	5.248		0.6	28.28*
	0.1	6.55*		0.8	37.26*
	0.2	13.12*			
	0.3	19.79*	*n*OG	0.002	0.094
				0.004	0.190
cHM	0.01	0.651		0.005	0.241
	0.03	1.962		0.007	0.343
	0.05	3.275		0.009	0.446
	0.07	4.588		0.01	0.496
	0.1	6.59*		0.011	0.542
	0.15	9.96*		0.012	0.590
	0.17	11.21*		0.013	0.638
	0.2	13.11*			
	0.25	16.36*			

*Values obtained with a 25 ml pyknometer.

Results

Because of solubility limitations, the densities were measured on the aqueous solutions of MG, EG, *n*HG, *n*OG, cHG, and cHM (see Table 1 for definition of abbreviations). For the same reasons, the salting-in measurements were made with the same glycosides with the exception of *n*OG.

Apparent molal volumes can be derived from the densities of the solutions using the well-known relation

$$[1] \qquad \phi_v = M/d_0 - 1000(d - d_0)/cd_0$$

where M is the molecular weight of solute, d_0 the density of water at 25 °C (0.997044 g ml^{-1}), and c the molarity. The densities of the α-D-glucosides and mannoside are given in Table 3, and the derived ϕ_v values were plotted vs. the concentra-

Can. J. Chem. Downloaded from www.nrcresearchpress.com by 210.87.254.40 on 09/05/12
For personal use only.

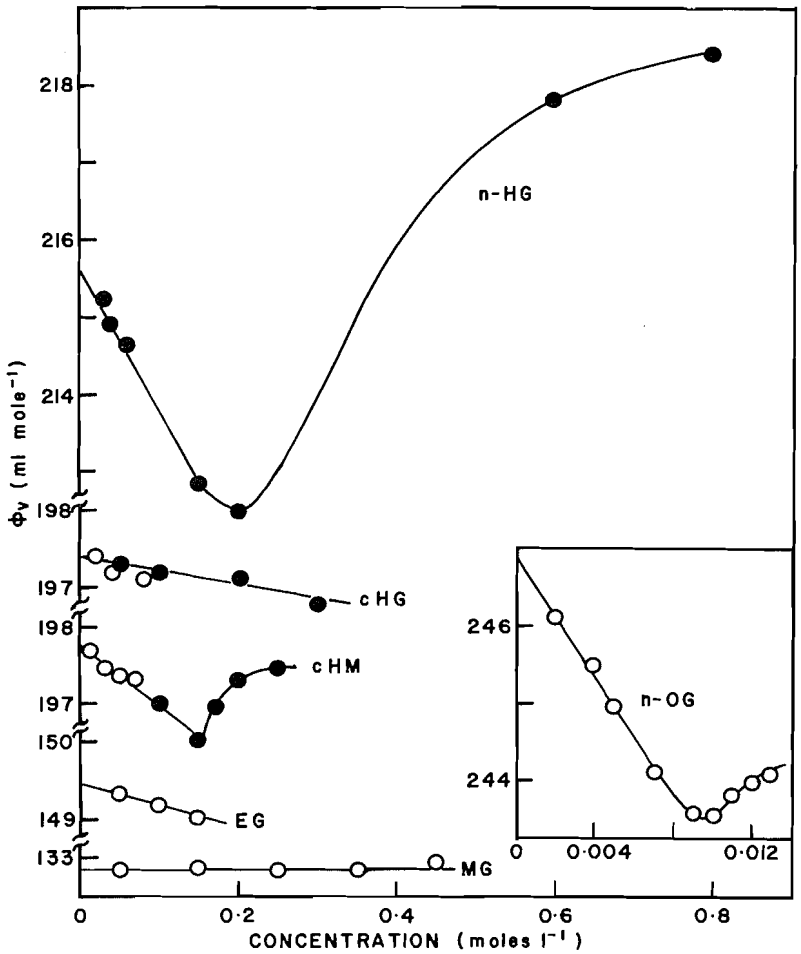

FIG. 2. Apparent molal volumes of α-D-alkyl glucosides and mannoside in water at 25 °C. Open circles obtained with a densimeter, filled circles with a 25 ml pyknometer.

tion in Fig. 2. As it can be seen from Fig. 2, these ϕ_v values are linear at low concentration; the parameters ϕ_v^0 and h are obtained from the relation

$$[2] \qquad \phi_v = \phi_v^0 + hc$$

and are given in Table 4. The ϕ_v values of cHG presented some difficulties since the first sample (see Table 2), obtained from the densimeter measurements, did not fall exactly on the same line as those of the second sample. As mentioned above, this may reflect the different proportion of β-isomer. However, even though this difference could be significant, the best line was drawn through both sets of data.

The differences between the ϕ_v^0 of MG, EG, *n*HG, and *n*OG are, respectively, 16.6, 66.1, and 31.2 ml mole^{-1} which can be compared with those of the corresponding *n*-alkylamine hydrobromides, 16.8, 64.4, and 31.8 ml mole^{-1}, obtained in the same laboratory (2). This comparison suggests that ϕ_v^0 of *n*HG and *n*OG may be in error by as much as 1 ml. Such an error is possible in these particular cases since the extrapolation depends entirely on the reliability of the points at low concentrations, and the uncertainty of ϕ_v obtained in this region increases very rapidly with dilution. Such an error would change to some extent the absolute value of the parameter h but would hardly affect the position of the minimum.

It has been shown (2) that a minimum in a ϕ_v

Can. J. Chem. Downloaded from www.nrcresearchpress.com by 210.87.254.40 on 09/05/12
For personal use only.

TABLE 4

Properties of aqueous solutions of α-D-alkyl glucosides and mannoside at 25 °C

Compound	ϕ_v^0 (ml mole^{-1})	h (ml l mole^{-2})	Critical micelle concentration (moles l^{-1})	k_s (l mole^{-1})
MG	132.85	0	—	0.190
EG	149.45	−2.7	—	0.214
*n*HG	215.6	−19	0.20	0.90
cHG	197.4	−1.8	0.3	0.63
cHM	197.7	−7.8	0.15	0.85
*n*OG	246.8	−400	0.010	

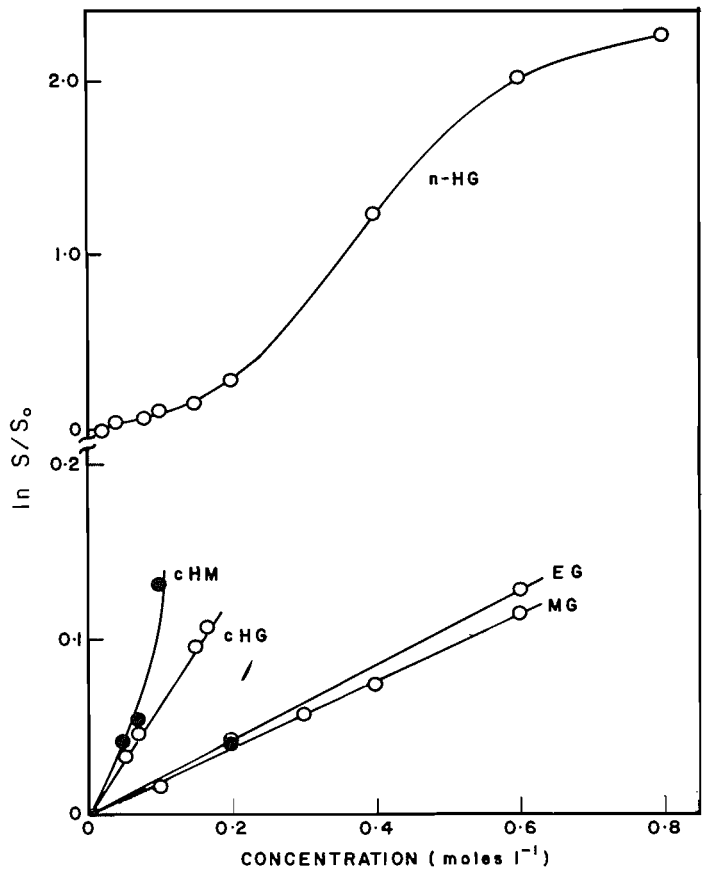

FIG. 3. Salting-in of nitrobenzene by α-D-alkyl glucosides and mannoside at 25 °C.

vs. c plot can usually be identified with association of hydrophobic solutes. Therefore, the critical micelle concentration (c.m.c.) of *n*HG, cHM, and *n*OG can be estimated from Fig. 2 and are given in Table 2.

The increase in solubility of a nonelectrolyte, caused by the presence of an hydrophobic salt, can usually be expressed (1) by the relation

$$[3] \qquad \ln S/S_0 = k_s c$$

where c is the salt concentration and k_s the salting-in constant. By analogy with this equation, the logarithms of the solubility ratio of nitrobenzene, were plotted vs. the concentration of

Can. J. Chem. Downloaded from www.nrcresearchpress.com by 210.87.254.40 on 09/05/12
For personal use only.

Can. J. Chem. Downloaded from www.nrcresearchpress.com by 210.87.254.40 on 09/05/12
For personal use only.

the glucosides and mannoside in Fig. 3. From the initial slopes the parameters k_s were estimated and are given in Table 4. In the case of *n*OG it was not possible to measure the solubilities of nitrobenzene below the c.m.c., and with cHM a stable emulsion was formed above 0.1 *M* concentration.

Discussion

Much information can be obtained from apparent molal volumes; ϕ_v^0 are related to solute–solvent interactions (13), h to solute–solute and changes in water–water interactions (14), and the sudden increase in ϕ_v with micelle formation (2). In the present series, the addition of alkyl groups on the glucose molecule increases the hydrophobic character; as such, their ϕ_v behave similarly to other aqueous solutions of organic solutes such as alcohols (15, 16), cyclic ethers (17), tetraalkylammonium salts (18, 19), and *n*-alkylammonium hydrobromides (2). The more hydrophobic the alkyl group the more negative is the concentration dependence. This arises since hydrophobic hydration causes a positive contribution to ϕ_v^0; as the concentration increases, the sharing of the hydrophobic co-spheres reduces the hydrophobic hydration per mole (2, 13) and ϕ_v decreases. However, when association occurs through hydrophobic bonds, the interior of the micelle regains the free space that the corresponding monomers, surrounded by a cage of hydrophobic hydration, have lost, and ϕ_v increases sharply.

While the behavior of *n*-alkyl glucosides is qualitatively identical with other homologous series, the cyclic derivatives present interesting features. Cyclohexane and *n*-hexane have fairly different molar volumes (108 and 130 ml mole^{-1}). It is, therefore, not unexpected that the ϕ_v^0 of cHG and *n*HG should differ by 18 ml. Similarly, the concentration dependences of ϕ_v of *n*HG and cHG are significantly different; cHG has a less negative h, and there is no evidence for micelle formation below 0.3 *M*. This is in agreement with the differences in ϕ_v^0. The cyclic group, being smaller, has less hydrophobic hydration, and consequently all the properties that depend on hydrophobic hydration are affected accordingly. The behavior of cHM is more difficult to account for. As expected the ϕ_v^0 of cHM and cHG are similar, but their concentration dependence suggests that the hydrophobic interactions with cHM are stronger than that with cHG; h is more negative and forms a micelle above 0.15 *M*. The slightly more positive value for ϕ_v^0 of cHM (0.3 ml mole^{-1}) also suggests that the water molecules around cHM are more ordered, despite the fact that these two isomers differ only by the position of one hydroxy group.

The difference in behavior of cHM and cHG suggests that other isomers should also show divergences. The only other comparison we can make presently is α-D-*n*OG with β-D-*n*OG. The densities of β-D-*n*OG are not available but the c.m.c. has been measured by the surface tension method (4). The β isomer forms a micelle at 0.025 mole l^{-1}, compared with 0.01 mole l^{-1} for the α isomer, and the solubility is about seven times larger.

These results would then suggest that the degree of hydrophobic hydration of isomeric glycosides should increase in the order β-D-glycopyranoside < α-D-glucopyranoside < α-D-mannopyranoside. Examination of Fig. 1 indicates that the hydrophobic group is probably closest to an OH group in the case of β-D-glucopyranoside and furthest with α-D-mannopyranoside. A comparison of models also confirms this. Presumably the interactions of the water molecules with the hydroxy group may affect the hydrophobic hydration of the alkyl group, but further proof would be required before pushing such an explanation too far. Still the present data strongly suggests that there is much specificity in the sugar–water interactions.

The nature of solubilization of nonelectrolytes by surfactants is still a controversial subject. Most authors (20) consider it different from hydrotropy or salting-in, and it is often said that the solubility of a nonelectrolyte is not affected by the surfactant below the c.m.c. The present measurements on the solubility of nitrobenzene support our previous suggestion (1) that there are no fundamental differences in the forces causing salting-in and solubilization. The earlier proposition (21) that van der Waals forces are responsible for salting-in has recently received support from the work of Masterton (22). However, the salting-in of polar nonelectrolytes by quaternary ammonium salts (7) has reinforced the hydrophobic interactions model for salting-in. In the presence of monomeric surfactants the solution is more ordered than pure water, and

the nonelectrolyte has less work to do against the structure of water to be dissolved. In other words, using a structural interaction model (14), the overlap of the co-spheres of the hydrophobic surfactant monomer and of the hydrophobic nonelectrolyte results in an attractive force. As the concentration of the surfactant increases, association suddenly arises between the surfactant and the nonelectrolyte (hydrophobic bonds), probably in the form of mixed micelles, and the solubility increases more sharply.

There is a general qualitative correspondence between the limiting k_s and h, the concentration dependence of ϕ_v. The more negative the h parameter, the larger is the salting-in (see Table 2). It seems, however, that not only the alkyl group is responsible for this salting-in since MG and EG increase the solubility of nitrobenzene, and they can hardly be considered overall hydrophobic molecules. Here again the interactions between the glucose ring and water probably play an important role in the solubilization of the nonelectrolyte.

In conclusion, we may say that the alkyl glucosides behave in water like any other homologous series. On the other hand a comparison of glucosides and mannosides and of α- and β-glucosides show that the hydration of these molecules is very sensitive to the stereo-orientation of the groups. It would not be surprising to find that much of the specificity in biochemical interactions (23, 24) could partly be related to these solvent effects.

We are grateful to the National Research Council of Canada for financial assistance. We would also like to thank Mr. Jean Léger for assisting in some aspects of the synthetic work.

1. J. E. Desnoyers, G. E. Pelletier, and C. Jolicoeur. Can. J. Chem. **43**, 3232 (1965).
2. J. E. Desnoyers and M. Arel. Can. J. Chem. **45**, 359 (1967).
3. J. E. Desnoyers, M. Arel, and P. A. Leduc. Can. J. Chem. **47**, 547 (1969).
4. K. Shinoda, T. Yamaguchi, and R. Hori. Bull. Chem. Soc. Japan, **34**, 237 (1961).
5. C. R. Bury and J. Browning. Trans. Faraday Soc. **49**, 209 (1953).
6. R. E. Wing and J. N. Bemiller. Carbohyd. Res. **10**, 441 (1969).
7. J. E. Desnoyers and F. M. Ichhaporia. Can. J. Chem. **47**, 4639 (1969).
8. H. Feltkamp, N. C. Franklin, W. Kraus, and W. Brugel. Ann. **683**, 75 (1965).
9. P. A. J. Gorin and A. S. Perlin. Can. J. Chem. **39**, 2474 (1961).
10. C. A. Glass. Can. J. Chem. **43**, 2652 (1965).
11. E. Pacsu. J. Amer. Chem. Soc. **52**, 2568 (1930).
12. R. E. Reeves and L. W. Mazzeno, Jr. J. Amer. Chem. Soc. **76**, 2219 (1954).
13. J. E. Desnoyers and C. Jolicoeur. Modern aspects of electrochemistry. Vol. 5. *Edited by*, J. O'M. Bockris and B. E. Conway. Plenum Press, New York. 1969. p. 1.
14. J. E. Desnoyers, M. Arel, G. Perron, and C. Jolicoeur. J. Phys. Chem. **73**, 3346 (1969).
15. F. Franks and D. J. G. Ives. Quart. Rev. London. **20**, 1 (1966).
16. F. Franks and H. T. Smith. Trans. Faraday Soc. **64**, 2962 (1968).
17. F. Franks and M. J. Quickenden. Chem. Commun. 388 (1968).
18. W.-Y. Wen and S. Saito. J. Phys. Chem. **68**, 2639 (1964).
19. B. E. Conway, R. G. Verrall, and J. E. Desnoyers. Trans. Faraday Soc. **62**, 2738 (1966).
20. P. H. Elworthy, A. T. Florence, and C. B. MacFarlane. Solubilization by surface-active agents. Chapman and Hall, London. (1968).
21. J. O'M. Bockris, J. Bowler-Reed, and J. A. Kitchener. Trans. Faraday Soc. **47**, 184 (1951).
22. W. L. Masterton and T. Bierly. J. Phys. Chem. **74**, 139 (1970).
23. B. Belleau and J. L. Lavoie. Can. J. Biochem. **46**, 1397 (1968).
24. D. T. Warner. Ann. New York Acad. Sci. **125**, 605 (1965).

Can. J. Chem. Downloaded from www.nrcresearchpress.com by 210.87.254.40 on 09/05/12
For personal use only.

Can. J. Chem. Downloaded from www.nrcresearchpress.com by 210.87.254.5 on 09/05/12
For personal use only.

The equilibration of ortho- and para-hydrogen on alumina at 77 °K and its influence on the determination of small amounts of excess para H_2, D_2, and HD in the presence of large amounts of normal H_2

K. A. QUICKERT AND D. J. LE ROY

Lash Miller Chemical Laboratories, University of Toronto, 80 St. George Street, Toronto 181, Ontario

Received March 24, 1970

When alumina is activated sufficiently to separate excess para H_2, D_2, and HD in a gas–solid chromatographic column at 77 °K using normal H_2 as the carrier gas, appreciable ortho–para equilibration takes place on the alumina. A kinetic study of the equilibration process was made, as the result of which procedures were established which made it possible to determine small concentrations of excess para H_2 in the presence of normal H_2. If D_2 and/or HD are also present in the sample, the observed peak area for excess para H_2 is subject to correction terms which are directly proportional to the concentrations of D_2 and/or HD.

Canadian Journal of Chemistry, **48**, 2532 (1970)

Introduction

In most cases the separation of the hydrogen isotopes, including the spin isomers, is readily accomplished by gas chromatographic methods using alumina columns at 77 °K and a rare gas carrier (1–4). Problems arise, however, when normal hydrogen[1] or normal deuterium is in large excess.

Such a situation arose in this laboratory in the course of kinetic studies on the relative rates of the reactions $H + H_2 = H_2 + H$ and $H + D_2 = HD + D$ (5). The rate of the first reaction was monitored by following the decrease in para hydrogen in systems containing D_2 and excess para H_2 in the presence of considerably larger amounts of normal H_2. A typical sample for analysis might contain 0.7% D_2, 0.1% HD, $p = 3.5\%$, and $n = 95\%$; helium was used as an internal reference and amounted to about 0.7%.

Even with columns containing pure alumina, some ortho–para equilibration of the hydrogen was expected to take place and this could have a serious effect on the determination of p in the original sample. Furthermore, the relatively large value of P in the normal hydrogen of the sample would make it difficult to measure p with the required accuracy if a rare gas carrier were used. The latter problem was overcome by using normal H_2 as the carrier gas, so that only the "excess" para H_2 appeared as a peak. However, we were still faced with the problem of partial para–ortho equilibration on the column. An additional problem was encountered in the form of "ghost" peak. The solution of these problems was the subject of the present investigation.

The ortho–para equilibration of hydrogen on alumina can be effected by the presence of paramagnetic impurities, principally iron (6). However, some equilibration occurs even on highly purified alumina. It has also been observed that the rate of equilibration increased with the temperature at which the alumina is activated and that even the H_2–HD–D_2 exchange can take place at temperatures as low as 147 °K if the alumina is sufficiently activated (7). This effect has been attributed to the highly strained surface left after dehydration (7). In studies on the adsorption of ortho hydrogen on highly activated alumina, it was found that a static monolayer of initially 100% O at 20 °K was converted to 50% O in 1 h (8), while a similar alumina, deactivated by the adsorption of xenon, did not give rise to any observed ortho–para conversion at either 27 or 55 °K (1). In the present work it was found that purified alumina, sufficiently activated to separate D_2, HD, and excess para H_2, as well as He, caused some ortho–para equilibration of the hydrogen.

Experimental

The alumina used was Fisher Scientific Chromatographic grade, 80–200 mesh, and was alleged to have a surface area of ca. 300 $m^2 g^{-1}$. It was calcined at 800 °C for 1 h to fully oxidize impurities and then leached in boiling 6 N HCl for 1 h to dissolve surface impurities. It was thoroughly washed and then activated by dry-

[1]The composition of a given sample of hydrogen can be given in two ways: in terms of ortho hydrogen, O, and para hydrogen, P; or in terms of "excess" para hydrogen, p, and normal hydrogen, n. Using percentages, the value of P for normal hydrogen is, by definition, 25%, and hence $p = (4/3)P - 33.3$ or $P = (3/4)p + 25$.

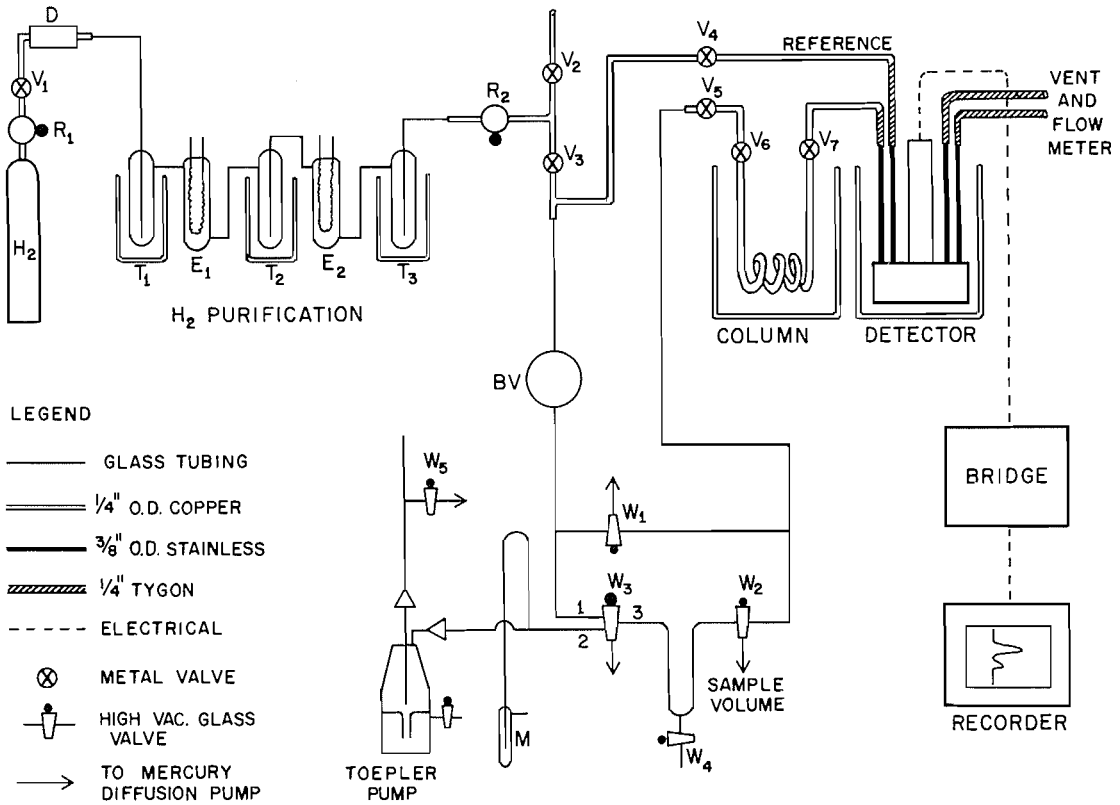

FIG. 1. System for analysis of excess para H_2, D_2, and HD in the presence of large amounts of normal H_2.

ing in air for 24 h at 170 °C. An iron analysis (9) on the acid and washings showed that the amount removed was approximately 0.01% by weight. No additional iron was removed by further leachings.[2]

The column was prepared using 52.5 g of the treated alumina in the range 100–150 mesh in a 10-ft length of 1/4 in. o.d. copper tubing wound in a 7-cm diameter spiral so that it could be completely immersed in liquid nitrogen.

The normal-H_2 carrier gas was Linde "99.95%". To remove any oxygen or water which could affect the catalytic behavior of the column, it was passed through a Deoxo unit, a trap at 77 °K, and then over two glowing tungsten filaments, each followed by a trap at 77 °K.

The analysis system, in the form used for routine analysis of excess para H_2, D_2, and HD, is shown in Fig. 1. (It was modified as described in a following section of the paper in order to study the kinetics of the ortho–para equilibration of H_2.) The regulating valves R_1 and R_2 reduced the gauge pressure of the H_2 supply to 16 and then to 12 p.s.i. A standardized carrier gas flow rate of 1.20 $cm^3\ s^{-1}$ was established in both the column and the reference sides of the detector by adjusting the Nupro metering valves V_4 and V_5. Because of the dependence of the extent of equilibration on the residence time in the column it was essential to maintain a constant and reproducible flow rate of carrier gas. This was achieved in that no detectable changes occurred over periods up to 18 h.

For the same reason it was necessary to avoid even temporary interruptions or surges in the flow of carrier gas by careful design and operation of the sampling system. The vacuum cups on the stopcocks W were pumped continuously. With the carrier gas by-passed through W_1, the sample volume was filled with the gas to be analyzed at a pressure of 1 atm, as indicated by the manometer M. Valve W_3 was then turned to connect lines 1 and 3 and 1 s later W_2 was opened; W_1 was then shut. During the first of these three operations there is a surge of gas into the sample volume to bring it up to 12 p.s.i. but the 2 l buffer volume BV prevents this from being reflected in the pressure or flow rate into the column.

When not in use the analysis system was kept under a positive pressure of purified hydrogen by closing V_3, V_4, V_6, and V_7; V_2 was connected to a mercury bubbler thus retaining a slight positive pressure in the purification system and allowing gas to escape as the traps warmed up. The column adsorbed about 0.5 l of hydrogen as it was cooled to the operating temperature of 77 °K

[2]The authors are grateful to Professor F. E. Beamish for his advice on the pre-treatment of the alumina.

Can. J. Chem. Downloaded from www.nrcresearchpress.com by 210.87.254.5 on 09/05/12
For personal use only.

initially, and during this cooling V_7 was closed to prevent air from being drawn into the column.

The detector was a dual channel thermal conductivity cell utilizing a matched pair of Veeco A33 2000 ohm thermistors which formed two arms of a resistance bridge. The bridge off-balance was followed on a L & N 0–1 mV Speedomax recorder. To take advantage of the greater sensitivity of the detector at low temperatures it was maintained at −78 °C in a Dry Ice – acetone slush. The para H_2 peak was negative relative to the others; ortho- and para-D_2 were only partially separated and were treated as a single peak. Peak areas were measured by a planimeter and were reproducible to 0.5% or better. Baseline drift and noise accounted for an additional uncertainty of about the same magnitude.

Kinetics of the Ortho–Para Equilibration on the Column

Following Bonhoeffer *et al.* (10), it was assumed that the measured rate of equilibration could be described by the simple first order processes

$$[1] \qquad \text{para } H_2 \underset{k_O}{\overset{k_P}{\rightleftharpoons}} \text{ortho } H_2$$

corresponding to the integrated rate equation

$$[2] \qquad P_e - P_\tau = (P_e - P_i) \exp(-k_c\tau)$$

where P_e is the equilibrium value of P at the temperature of the alumina column (approx. 50% at 77 °K), P_i is the value for the gas entering the column, and P_τ is the value for the gas leaving the column after a residence time τ; $k_c = k_P + k_O$. It is evident[1] that P in eq. [2] may be replaced by p, viz.

$$[3] \qquad p_e - p_\tau = (p_e - p_i) \exp(-k_c\tau)$$

The value used for τ was defined by

$$[4] \qquad \tau = V/f$$

where V is the dead volume of the column plus the volume of hydrogen desorbed on warming it from 77 °K to room temperature; this was dependent on the value of the flow rate f since there is a flow-dependent pressure drop across the column. With $f = 1.20$ cm^3 s^{-1}, $V = 590 \pm 8$ cm^3 and hence $\tau = 492$ s.[3]

Equation [3] was tested by analyzing the effluent from the alumina column by using a charcoal column 0 °C with normal H_2 as the carrier gas. By a modification of the system shown in Fig. 1, including the addition of a separate sampling system, it was possible to maintain a constant flow of normal H_2 carrier gas through the charcoal column and the two sides of the detector while analyzing a 25 cm^3 sample of the effluent from the alumina column which had been subjected to various residence times by varying the flow rate through the latter. In these particular experiments the gas entering the alumina column was always normal H_2, and hence $p_i = 0$.

The charcoal column had been used previously (11) and found to cause no appreciable equilibration. Actually Bonhoeffer *et al.* (10) found that eq. [3] was valid for charcoal and that the corresponding rate constant k_c' was 6.08×10^{-4} s^{-1} at 77 °K; the value at 0 °C would likely be somewhat less. Assuming this value of k_c' and using the residence time $\tau' = 60$ s for the charcoal column, $\exp(-k_c'\tau') = 0.996$. Thus the extent of equilibration on the charcoal column is very small. Nevertheless it can be taken into account as follows.

For the charcoal column analyses both the temperature and τ' were kept constant and hence for this column, eq. [3] may be written as

$$p_{e'} - p_{\tau'} = (p_{e'} - p_{i'}) \exp(-k_c'\tau')$$

or

$$[5] \qquad p_{\tau'} = p_{e'}(1 - C') + C'p_{i'}$$

where $C' = \exp(-k_c'\tau') =$ a constant. When only its carrier gas (normal H_2) is flowing into the charcoal column, eq. [5] may be written as

$$[6] \qquad p_{\tau'}^0 = p_{e'}(1 - C')$$

The integrated peak area A will be proportional to the difference, viz.

$$[7] \qquad A = a(p_{\tau'} - p_{\tau'}^0) = aC'p_{i'}$$

and hence directly proportional to the value of p (for fixed sample volume) in the gas leaving the alumina column.

Assuming that eq. [3] is valid for the alumina column, and noting that for the gas entering that column, $p_i = 0$, it follows that

$$[8] \qquad \ln[A_e/(A_e - A_\tau)] = k_c\tau$$

where $A_\tau = aC'p_{i'} = aC'p_\tau$ and $A_e = aC'p_e$.

The integrated peak area A_e was obtained

[3]An alternative measure of V is the retention volume for para H_2, which was found to be 545 ± 10 cm^3. This would be expected to be smaller than the value of V given above because para H_2 is less strongly adsorbed than ortho H_2.

Can. J. Chem. Downloaded from www.nrcresearchpress.com by 210.87.254.5 on 09/05/12
For personal use only.

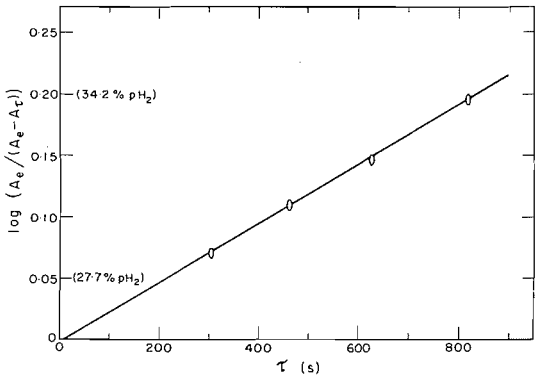

FIG. 2. Kinetics of the ortho–para conversion of H_2 on alumina at 77 °K.

using a sample left on the alumina column long enough (17 h or ca. 50 half lives) to be essentially completely equilibrated at the temperature of that column. The results shown in Fig. 2 substantiate the validity of eq. [8] and hence eq. [3] and give a value of $k_c = 5.5_3 \times 10^{-4}\ s^{-1}$ with a standard deviation of about 2%. This is somewhat larger than the value $1.90 \times 10^{-4}\ s^{-1}$ obtained by Cunningham and Johnston (6) for their alumina at 20 °K. For a flow rate of 1.20 $cm^3\ s^{-1}$ through the alumina column, normal H_2 ($p = 0$; $P = 25\%$) entering the column emerges with the composition $p = 7.8\%$ or $P = 30.8\%$.

Analysis of Mixtures of ortho- and para-H_2

In spite of the appreciable amount of conversion taking place on it, it is still possible to use the alumina column to determine small concentrations of excess para H_2 in an initial sample using normal H_2 as the carrier gas. Since eq. [3] is valid, then for constant column temperature and flow rate, $\exp(k_c\tau) = C$ = a constant. Equations analogous to [5], [6], and [7] will hold and the integrated peak area

$$[9] \qquad A = aCp_i$$

will be directly proportional to the value of p (for constant sample volume) in the initial sample.

Equation [9] was tested by analyzing different volumes of a gas mixture having a constant composition in terms of p, normal H_2, and He. The linearity of the detector response to He has been shown previously (12), and hence a plot of the peak area due to excess para H_2 against the peak area for He should give a straight line. That this is the case is shown in Fig. 3. In these particular experiments the sample size was varied over a

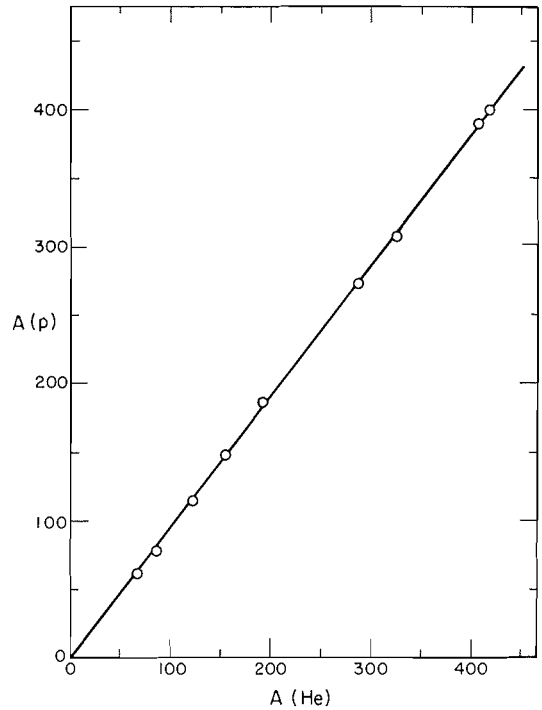

FIG. 3. Linearity of peak area due to excess para H_2 with amount of excess para H_2. The samples contained a constant ratio of excess para H_2 to He and the He area is directly proportional to the amount of He.

range of approximately a factor of 6. The mixture used contained known concentrations of pure para H_2, He, and normal H_2 and it was calculated that the range of proportionality covered by Fig. 1 was equivalent to a range of p in a constant sample size of 30 cm^3 from 0.80 to 3.73% or a range of P from 25.6 to 27.8%. The retention time for the excess para H_2 at the standard flow rate of 1.20 $cm^3\ s^{-1}$ was approximately 9 min.[4]

Analysis of D_2 and HD and their Influence on A(p)

The analysis for D_2 was not expected to lead to any complications when normal H_2 was used as the carrier gas. A 30 cm^3 sample containing 0.7% D_2 in normal H_2 gave a good peak with a retention time of about 12 min at the standard flow rate; the peak was slightly asymmetric as the result of a partial separation of ortho- and para-D_2. However, a small peak with a retention

[4]The constant aC must, of course, be determined experimentally with samples of known p if absolute values of p are to be determined. When only relative values of p are required (e.g. ref. 5), the value of aC is not required.

Can. J. Chem. Downloaded from www.nrcresearchpress.com by 210.87.254.5 on 09/05/12
For personal use only.

time of about 9 min always accompanied the D_2 peak. This "ghost" peak, which was given the symbol Gh, was coincident with the excess para H_2 peak but in the opposite direction. Thus if any excess para H_2 had been present in the sample the $A(p)$ peak would have been in error.

The Gh peak could not be accounted for by any impurity in the D_2 and was not caused by the method of sample introduction because it was absent when pure normal H_2 was used as a sample. It was absent when *highly* activated columns were used (which cause rapid equilibration of the para H_2/ortho H_2 ratio). It was therefore concluded that the presence of D_2 in a sample otherwise containing only normal H_2 must have given rise to a perturbation in the para H_2/ortho H_2 ratio in the column. In the case of highly activated columns this perturbation would be wiped out before the gas emerged, but in the columns developed for the present work it would persist.

The Gh peak had the same residence time as that of excess para H_2 although there was no excess para H_2 in the sample. In this sense it resembled the "reverse" peaks that are observed (13) when a plug of pure carrier gas is injected in a column that is being continuously fed with a mixture of carrier gas and one or more additional components. The situation is more complicated in the present situation, however. The ortho H_2/para H_2 ratio in the hydrogen in the 30 cm^3 sample is identical to that in the carrier gas entering the column.

Ortho H_2 is more strongly adsorbed than para H_2 (2), and so the adsorbed phase has a lower para H_2/ortho H_2 ratio than the gas phase. It was speculated that when D_2 enters the column and adsorbs on the alumina it displaces some of the adsorbed hydrogen and that this desorbed hydrogen has a lower para H_2/ortho H_2 ratio than that previously obtaining in the gas phase at that point. The effect would be similar to that of inserting a sample of H_2 with a lower para H_2/ortho H_2 ratio than that of the carrier gas. The result would be that eventually some of the hydrogen leaving the column would have a lower para H_2/ortho H_2 ratio than that of the regular effluent, and this will show up as a reversed excess para H_2 peak.

This theory led us to suppose that there should be a direct relationship between the area of the Gh peak and the amount of D_2 in the sample.

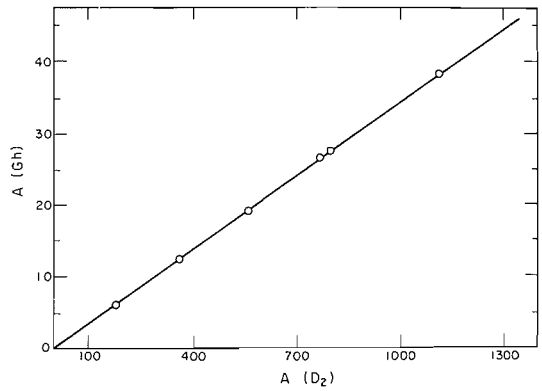

FIG. 4. Proportionality of area of ghost peak to amount of D_2 in the sample.

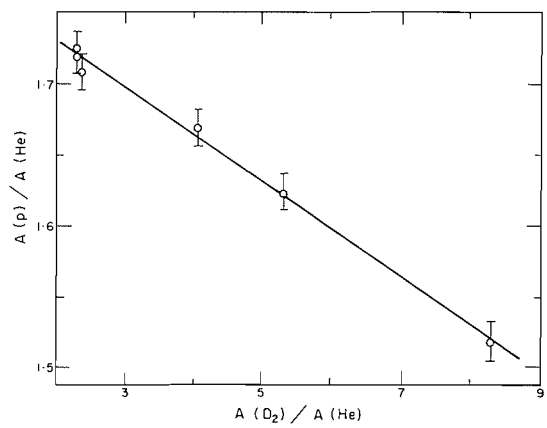

FIG. 5. Effect of D_2 concentration on the peak area for excess para H_2. The samples contained constant amounts of excess para H_2 and He and various amounts of D_2.

In Fig. 4 it is seen that A(Gh) is equal to $\alpha A(D_2)$, where $\alpha = 0.0341 \pm 0.0002$. This implies that if both excess para H_2 and D_2 are being determined the true value of $A(p)$ will be given by

$$[10] \qquad A(p) = A(p)_{obs} + \alpha A(D_2)$$

Equation [10] was tested by analyzing samples containing constant values of p and He and various values of D_2. The results are shown in Fig. 5 where the areas are normalized by dividing both $A(p)_{obs}$ and $A(D_2)$ by A(He). The slope of the linear curve is 0.0334 ± 0.0012, which is equal to the value of α determined above within the standard deviations. The "accepted" value was $\alpha = 0.034$.

By similar reasoning one would expect the Gh peak to be influenced by the presence of HD. Samples containing different amounts of HD

Can. J. Chem. Downloaded from www.nrcresearchpress.com by 210.87.254.5 on 09/05/12
For personal use only.

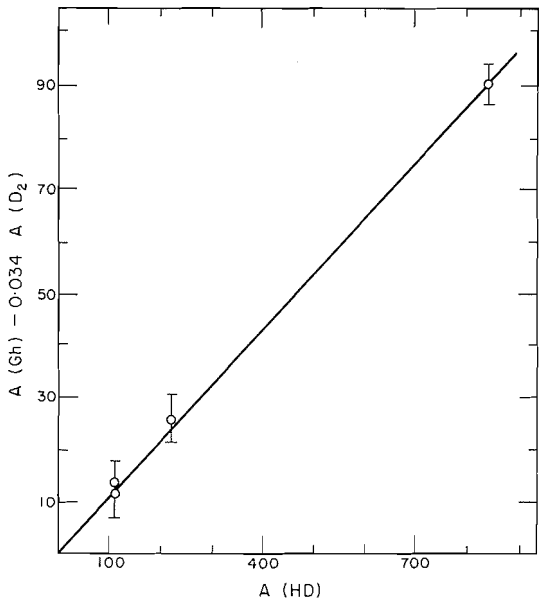

FIG. 6. Proportionality of ghost peak to amount of HD in the sample. The samples contained D_2 as well as HD (and normal H_2). The contribution of D_2 to A(Gh) is subtracted in the ordinate.

and D_2 were analyzed and the values of A(Gh) measured. Assuming that

$$[11] \qquad A(\mathrm{Gh}) = \alpha A(\mathrm{D_2}) + \beta A(\mathrm{HD})$$

and that $\alpha = 0.034$, $A(\mathrm{Gh}) - 0.034A(\mathrm{D_2})$ was plotted against A(HD), as shown in Fig. 6; β was found to be 0.107. It is not clear why β is larger than α.

Conclusion

Small concentrations of para H_2 in excess of that present in normal H_2 can be determined with good accuracy by g.s.c. methods using an alumina column at 77 °K and normal H_2 as the carrier gas.[5] Samples (30 cm^3) containing ca. 3.5% excess para H_2 gave peak areas which, allowing for the reproducibility in measuring the areas, could be determined to $\pm 1\%$. The accuracy is probably of the same order. This is equivalent to determining the absolute concentration of para H_2 in the sample, P, to ca. $\pm 0.1\%$. If small concentrations of D_2 and HD are also to be determined, the alumina must be activated to an extent which causes some equilibration of the H_2 passing through the column. Under proper operating conditions and in the absence of D_2 and HD, this equilibration causes no error in the analysis of excess para H_2. In the presence of D_2 and/or HD the apparent concentration of excess para H_2 is subject to correction terms which are directly proportional to the concentrations of D_2 and HD in the sample.

[5]Normal H_2 was used as the standard in the present instance. However, concentrations of para H_2 (or ortho H_2) in excess of that in any other standard could be determined equally well provided the standard is used as the carrier gas.

The authors are grateful to the National Research Council of Canada for financial support and for the award of a Scholarship to one of us (K.A.Q.).

1. W. J. HAUBACH, C. M. KNOBLER, A. KATORSKI, and D. WHITE. J. Phys. Chem. **71**, 1398 (1967).
2. W. MOORE and H. WARD. J. Amer. Chem. Soc. **80**, 2909 (1958).
3. M. MOHNKE and W. SAFFERT. Gas chromatography. *Edited by* M. Van Swaay. Butterworth Publishing Company, London. 1962. p. 216.
4. E. H. CARTER and H. A. SMITH. J. Phys. Chem. **67**, 1512 (1963).
5. K. A. QUICKERT and D. J. LE ROY. J. Chem. Phys. To be published.
6. C. M. CUNNINGHAM and H. L. JOHNSTON. J. Amer. Chem. Soc. **80**, 2377 (1958).
7. S. W. WELLER and S. G. HINDIN. J. Phys. Chem. **60**, 1506 (1956).
8. C. M. CUNNINGHAM, D. S. CHAPIN, and H. L. JOHNSTON. J. Amer. Chem. Soc. **80**, 2382 (1958).
9. A. I. VOGEL. A text-book of quantitative inorganic analysis. 3rd ed. Longmans, London. 1961. p. 786.
10. K. F. BONHOEFFER, A. FARKAS, and K. W. RUMMEL. Z. Phys. Chem. **B21**, 225 (1933).
11. W. R. SCHULZ and D. J. LE ROY. Can. J. Chem. **42**, 2480 (1964).
12. W. R. SCHULZ. M.A. Thesis, University of Toronto, Toronto, Ontario, 1963; Ph.D. Thesis, University of Toronto, Toronto, Ontario, 1965.
13. C. N. REILLEY, G. P. HILDEBRAND, and J. W. ASHLEY, JR. Anal. Chem. **34**, 1198 (1962).

Can. J. Chem. Downloaded from www.nrcresearchpress.com by 210.87.254.5 on 09/05/12
For personal use only.

Can. J. Chem. Downloaded from www.nrcresearchpress.com by 210.87.254.42 on 09/05/12
For personal use only.

Protonation of conjugated carbonyl groups in sulfuric acid solutions. III. α,β-Unsaturated ketosteroids[1]

R. I. Zalewski[2] and G. E. Dunn
Department of Chemistry, University of Manitoba, Winnipeg 19, Manitoba

Received February 25, 1970

Protonation of 20 α,β-unsaturated ketosteroids by sulfuric acid was studied by ultraviolet spectrophotometry. Plots of log [B]/[BH$^+$] from spectral data against the amide acidity function, H_A, gave straight lines with unit slope. The pK_{BH^+} values thus obtained show the same additive effects of substituents as that reported previously for simple α,β-unsaturated alicyclic ketones.

Canadian Journal of Chemistry, 48, 2538 (1970)

In the preceding paper of this series (1), it was shown that the protonation of α,β-unsaturated alicyclic ketones having 5- and 6-membered rings is better accommodated by the amide acidity function H_A than by the more familiar H_0 function. It was also shown that the electronic effects of substituents upon the basicity of α,β-unsaturated alicyclic ketones are constant and additive, so that the basicity of any such ketone can be expressed by the empirical equation

$$[1] \qquad pK_{BH^+} = \sum \Delta pK_{BH^+} - 3.57$$

in which ΔpK_{BH^+} represents the electronic effect of a single substituent upon basicity. It was the object of the present work to test the applicability of eq. [1] to more complicated molecules of biological interest.

Smoczkiewicz and Zalewski reported basicity data for 13 α,β-unsaturated ketosteroids (Δ^4-3-ones) in sulfuric and perchloric acids (2). Their data, used with the H_0 acidity function, indicated that the investigated steroids are stronger bases in perchloric than in sulfuric acid solutions. It was therefore of interest to reinvestigate the basicity of ketosteroids using the H_A acidity function. This paper presents pK_{BH^+} data for 20 α,β-unsaturated ketosteroids, 5 of which have been investigated previously (2).

Experimental

The steroids investigated are listed in Table 1. They are commercial materials, except for compounds **18** and **19**, which were synthesized from **1** and testosterone propionate, respectively, by dehydrogenation with chloranil in *t*-butyl alcohol (3). Compounds **18** and **19** melted at 168.5–169° and 135–136°, respectively, and their ultraviolet spectra in ethanol agreed with literature data (4, 5).

The method and apparatus used to determine pK_{BH^+} have been described previously (1). However, in the present work an additional complication is present. It is well known that the absorbance of most steroids in concentrated sulfuric acid increases with time and sometimes the maximum of the band shifts bathochromically (6). This is illustrated for our compounds by the data of Table 1. Consequently, it was sometimes necessary to extrapolate absorbance, A, in 70% or more sulfuric acid back to zero time. This was done from a plot of log ($A_\infty - A$) over a 2-hour interval. For acids with pK_{BH^+} less negative than −2.8 all measurements were made in less than 70% sulfuric acid so no extrapolation was necessary.

The organic materials were recovered from sulfuric acid solutions of some steroids, and ultraviolet and infrared spectra were taken. All the recovered substances show the

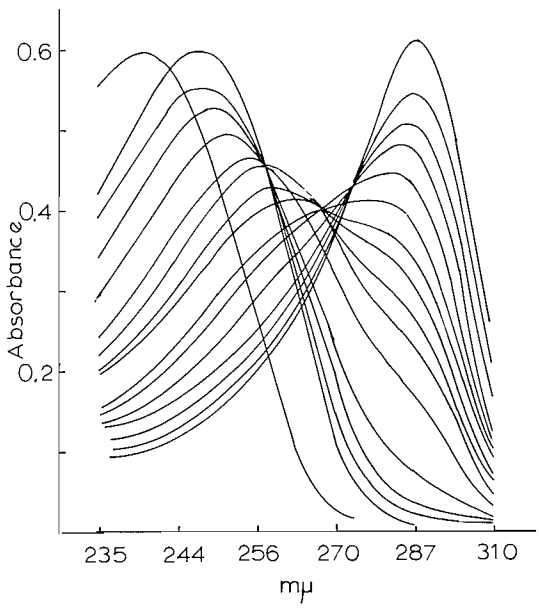

FIG. 1. Absorbance of 4-androsten-3,17-dione as a function of sulfuric acid concentration. Solvent (top to bottom at left-hand margin): methanol, water, sulfuric acid 21.0, 30.3, 40.1, 50.1, 52.5, 55.0, 57.5, 60.1, 62.4, 64.9, 69.9, 75.1, 80.2, and 96%.

[1]For Part II, see ref. 1.

[2]University of Manitoba Postdoctorate Fellow, 1967–1968. Present address: Katedra Chemii Ogólnej W.S.E., Poznań (Poland) ul. Marchlewskiego 146.

TABLE 1

Ultraviolet absorption of α,β-unsaturated ketosteroids in water, methanol, and concentrated sulfuric acid

Steroid		Methanol		Water		Concentrated sulfuric acid			
						Initial		After 2 h	
Number	Name	λ_{max}	ε_{max}	λ_{max}	ε_{max}	λ_{max}	ε_{max}	λ_{max}	ε_{max}
1	4-Androsten-3,17-dione	241	17.0	248	17.1	289	17.2	295	23.0
2	Testosterone	241	17.1	248	18.2	292	17.9	298	20.1
3	17α-Methyltestosterone	241	16.8	248	16.8	293	18.2	297	20.0
4	Progesterone	241	16.5	249	16.0	292	16.3	292	16.3
5	Cortisone acetate	238	16.8	245	15.0	287	14.8	287	17.0
6	2α-Methyltestosterone	241	13.0	249	13.0	294	12.0	296	12.7
7	2α-Methylprogesterone	240	15.5	249	14.5	296	15.5	296	15.5
8	2α,17α-Dimethyl-11β-hydroxytestosterone	241	15.5	247	15.3	292	16.0	305	21.0
9	2α-Methyl-11β-hydroxyprogesterone	236	14.0	245	14.5	285	15.4	285	15.4
10	4,17α-Dimethyltestosterone	256	17.1	259	16.8	306	14.1	306	19.0
11	4,17α-Dimethyl-11β-hydroxytestosterone	250	10.1	258	10.1	299	10.5	304	12.8
12	2α-Fluorotestosterone	242	13.6	250	14.0	298	12.6	298	13.7
13	2α-Fluorotestosterone propionate	242	12.3	251	12.0	295	14.3	296	20.1
14	4-Fluorotestosterone	249	14.0	256	—	305	13.3	306	15.5
15	6α-Fluoro-17α-methyltestosterone	235	15.7	242	15.5	292	15.3	293	17.0
16	6α-Fluoroprogesterone	236	16.0	243	15.0	290	13.4	290	13.6
17	1-Androsten-(5α)-3,11,17-trione	225	11.8	230	11.0	267	8.8	297	8.8
18	4,6-Androstadien-3,17-dione	282	23.7	289	22.8	345	28.2	345	28.6
19	17β-Hydroxy-4,6-androstadien-3-one propionate	283	27.5	291	26.0	351	32.0	351	33.0
20	6-Dehydro-6-methylcortisone acetate	283	22.2	293	21.8	351	26.0	351	26.4

characteristic absorption bands of α,β-unsaturated ketones in the ultraviolet and infrared. Infrared spectra of substances recovered from sulfuric acid solutions of 17β-hydroxy- and 17-keto-compounds showed the loss of these groups, but the Δ^4-3-one system was evidently not destroyed. It is noteworthy that the compounds whose ultraviolet spectra did not change with time (Table 1) are those which do not contain 17β-hydroxy or 17-keto groups. It therefore seems a reasonable hypothesis that compounds with time-dependent spectra are subject to chemical reactions of carbonyl or hydroxyl groups at the 17-position.

Results and Discussion

In Fig. 1 are shown spectra of **1** in methanol, water, and various concentrations of sulfuric acid. These are typical of the spectra obtained from all the α,β-unsaturated ketosteroids examined. In general they resemble very closely those of the simple α,β-unsaturated carbonyl compounds reported and discussed previously (1). The π–π^* band shifts bathochromically with increasing solvent polarity from 241 nm in methanol to 248 nm in water. Corresponding shifts for the other ketosteroids are shown in Table 1. The shift continues in increasing concentrations of sulfuric acid, so that the absorption curves do not pass through a single isosbestic point as the carbonyl compound, B, is protonated to BH^+. It is therefore very probable that the absorptivity ε_B of B at a fixed wavelength varies slightly over the range of acidities used. The same is probably true of ε_{BH^+}.

In order to calculate K_{BH^+}, the absorbance, A, was measured over a series of acidities, h, at a wavelength, λ_B, where B absorbs strongly, and at another wavelength, λ_{BH^+}, where BH^+ absorbs strongly. K_{BH^+} was then calculated at each of λ_B and λ_{BH^+} by fitting the data for that wavelength to eq. [2] as previously described (1).

$$[2] \qquad A = [C]\frac{\varepsilon_B K_{BH^+} + \varepsilon_{BH^+} h}{K_{BH^+} + h}$$

$[C]$ is the total concentration of steroid, protonated and unprotonated; h is an acidity function; and ε_B, ε_{BH^+}, pK_{BH^+} are disposable parameters evaluated from the least-squares fit of the data to eq. [2]. This procedure avoids the use of values of ε_B and ε_{BH^+} measured at acidities much above and below the equivalence point, and leads to calculated values of ε_B and ε_{BH^+} which are averages for the acidity range studied.

As in the case of the simple α,β-unsaturated carbonyl compounds reported previously (1), the amide acidity function, h_A (7), gives a better fit to eq. [2] than do any of the other acidity functions available. A more common criterion for the choice of acidity function is a plot of the data according to eq. [3]

Can. J. Chem. Downloaded from www.nrcresearchpress.com by 210.87.254.42 on 09/05/12
For personal use only.

TABLE 2

Absorbance and acidity data for 3.5×10^{-5} *M* 4-androsten-3,17-dione in sulfuric acid*

H_2SO_4 (%)	$-H_A$	λ_{max} (nm)	A_{max}	A_{287}		A_{248}		$-pK_{BH^+}$ eq. [3]
				Observed	Calculated	Observed	Calculated	
80.2	4.50	287.5	0.545	0.543	0.534	0.170	0.173	2.90
75.1	4.10	286.0	0.507	0.507	0.518	0.185	0.185	2.84
69.9	3.73	284.8	0.480	0.480	0.484	0.213	0.208	2.84
64.9	3.37	281.2	0.447	0.432	0.423	0.245	0.251	2.85
62.4	3.22	280.0	0.410	0.385	0.388	0.270	0.276	2.84
60.1	3.07	261.8	0.413	0.340	0.347	0.320	0.305	2.84
57.5	2.90	259.0	0.430	0.305	0.297	0.345	0.340	2.84
55.0	2.78	258.2	0.452	0.270	0.259	0.383	0.368	2.86
52.5	2.65	256.0	0.460	0.230	0.225	0.400	0.394	2.84
50.1	2.50	255.5	0.467	0.170	0.176	0.415	0.425	2.85
40.1	2.00	252.5	0.493	0.075	0.079	0.475	0.485	2.83
30.3	1.50	250.2	0.518	0.035	0.035	0.520	0.526	2.84
21.0	1.00	247.8	0.550	0.020	0.019	0.550	0.537	2.88

*From eq. [2], $[C]\varepsilon_B = 0.012 \pm 0.004$ ($\lambda = 287$), 0.542 ± 0.006 ($\lambda = 248$); $[C]\varepsilon_{BH^+} = 0.546 \pm 0.004$ ($\lambda = 287$), 0.165 ± 0.006 ($\lambda = 248$); $pK_{BH^+} = -2.85 \pm 0.02$ ($\lambda = 287$), -2.84 ± 0.04 ($\lambda = 248$).

TABLE 3

Absorbance and basicity data for α,β-unsaturated ketosteroids

Steroid number	λ_B (nm)	$10^{-3}\varepsilon_B$	λ_{BH^+} (nm)	$10^{-3}\varepsilon_{BH^+}$	$-pK_{BH^+}$	Slope log *Q* vs. H_A
1	248	15.5	287	15.6	2.85±0.02	1.00
2	249	15.7	288	16.3	2.86±0.04	0.99
3	249	15.1	287	14.7	2.84±0.04	0.99
4	250	15.6	288	16.0	2.87±0.03	0.98
5	250	14.3	280	13.0	2.98±0.03	0.98
6	256	10.5	287	13.0	2.80±0.03	1.01
7	255	13.8	290	14.6	2.92±0.04	0.97
8	248	15.2	286	14.6	3.11±0.02	1.00
9	248	15.0	285	14.8	3.20±0.04	0.98
10	261	16.3	306	18.0	2.59±0.03	0.99
11	257	11.3	296	11.8	2.81±0.03	1.03
12	—	—	299	14.0	4.66±0.05	0.99
13	258	13.0	298	13.1	4.71±0.03	1.00
14	265	14.4	305	17.0	4.59±0.03	1.02
15	248	15.0	288	14.3	3.56±0.04	1.02
16	248	14.3	288	13.4	3.44±0.05	0.98
17	232	11.0	267	8.6	3.60±0.03	0.99
18	293	22.7	344	29.5	2.46±0.02	1.01
19	292	26.0	346	32.2	2.31±0.03	0.98
20	297	20.2	351	25.2	2.49±0.02	0.98

$$[3] \quad H - pK_{BH^+} = \log \frac{[B]}{[BH^+]} = \log \frac{\varepsilon - \varepsilon_{BH^+}}{\varepsilon_B - \varepsilon} = \log Q$$

where $\varepsilon = A/[C]$. This should give a straight line of unit slope when log *Q* is plotted against an appropriate acidity function, *H*.

The results are illustrated by compound **1** for which Table 2 gives absorption and acidity data, values of ε_B, ε_{BH^+}, and pK_{BH^+} calculated from eq. [2], the absorbance at each acidity calculated from these values, and a value of pK_{BH^+} at each acidity calculated from eq. [3]. Data and results for all 20 steroids are summarized in Table 3, where the slopes of log *Q* vs. H_A plots are seen to be all near unity. The standard deviations in pK_{BH^+} calculated from eq. [2] are shown after the values of pK_{BH^+}. They average ± 0.03, which is about the same as the average for the simple α,β-unsaturated ketones (1) whose spectra do not show the time dependence characteristic of some steroids. It would appear, therefore, that the extrapolation of absorbance to zero time

Can. J. Chem. Downloaded from www.nrcresearchpress.com by 210.87.254.42 on 09/05/12
For personal use only.

Can. J. Chem. Downloaded from www.nrcresearchpress.com by 210.87.254.42 on 09/05/12
For personal use only.

which was required for those steroids with time-dependent spectra has not seriously increased the uncertainty in pK_{BH^+} values.

The most basic site in the compounds examined should be the 3-keto group, since in all 20 examples it is the only carbonyl group conjugated with a carbon–carbon double bond. On this basis, the remainder of the steroid molecule would be treated as substituents on the common α,β-unsaturated ketone structure of the *A* ring. Since methyl or methylene substituents on the γ and δ positions of α,β-unsaturated alicyclic ketones were found to have no effect on their basicities (1), compound **17** should have the same pK_{BH^+} as 2-cyclohexen-1-one (− 3.60), and Table 3 shows this to be the case.

In the remaining 19 ketosteroids carbons 4, 5, and 10 correspond to the α, β, and γ positions of an α,β-unsaturated ketone, and methyl or methylene groups at these positions were found to have ΔpK_{BH^+} values of + 0.30, + 0.75, and 0, respectively (1). On this basis eq. [1] predicts that compounds **1**–**4** should have $pK_{BH^+} = -2.83$, in excellent agreement with the experimental result. Since these compounds contain a variety of substituents at C_{17} and none elsewhere, it is evident that the unsubstituted *C* and *D* rings and substituents at C_{17} have no effect on pK_{BH^+}. Neither does the methyl group at C_2 in **6** and **7**.

The hydroxyl group at C_{11} in **8** and **9** decreases the basicity of these compounds by about 0.3 pK_{BH^+} units, and the carbonyl group at the same location in **5** decreases the basicity by about half as much. It is surprising that substituents so remote from the protonation site should have a detectable influence on the basicity of the 3-keto group, but the same effect of 11-hydroxyl is noted when **11** is compared with **10**.

Compounds **10** and **11** contain a methyl group at C_4. According to the 2-cyclohexen-1-one results (1), a 4-methyl group should increase the basicity by 0.3 units, and this is seen to be the case on comparing **10** with **3** and **11** with **8**.

A fluoro substituent is seen to be base-weakening by about 1.8 pK_{BH^+} units at C_2 in **12** and **13** and at C_4 in **14**. This is in the direction to be expected from the inductive effect of fluorine, but it is surprisingly large when it is compared with the very small effect of methyl at these positions. Fluorine at the more remote C_6 location in **15** and **16** is base-weakening by about 0.6 pK_{BH^+} unit.

TABLE 4

Substituent effects on the basicity of Δ^4-3-keto-steroids considered as derivatives of 2-cyclo-hexen-1-one

Substituent	ΔpK_{BH^+}	Number of examples
5-CH_2— (4-en-3-one)	+0.75	5
10-CH_2—	0.00	5
2α-CH_3	0.00	4
4-CH_3	+0.25	2
6-CH_3	0.00	1
2α-F	−1.85	2
4-F	−1.75	1
6α-F	−0.70	2
11β-OH	−0.30	4
11=O	−0.15	2
6,7 C=C	+0.45	3

In compounds **18** and **19**, a 6,7- double bond extends the conjugated system and consequently the stabilization of BH^+ by delocalization of its charge. As a result, these compounds are stronger bases than 2-cyclohexen-1-one by 0.4–0.5 pK_{BH^+} units. Compound **20** is a stronger base than **5** by 0.5 units, so the 6-methyl group has a negligible effect on basicity.

The substituent effects on basicity derived from this work are summarized in Table 4 in the form of ΔpK_{BH^+} increments to be used in eq. [1]. They permit the calculation of pK_{BH^+} within 0.1 unit for all the compounds examined. The number of examples of each substituent is small, but the fact that 20 steroids containing the α,β-unsaturated keto structure can be treated as extensions of the 2-cyclohexen-1-one system suggests that the relationship is probably valid.

The authors are grateful to the National Research Council of Canada for financial support and to Dr. J. T. Correll of Scientific Liaison Biochemical Research, The Upjohn Company, Kalamazoo, Michigan, for steroid samples **6**–**17** and **20**.

1. R. I. ZALEWSKI and G. E. DUNN. Can. J. Chem. **47**, 2263 (1969).
2. M. A. SMOCZKIEWICZ and R. I. ZALEWSKI. Steroids, **12**, 391 (1968).
3. E. J. ANGELLO and G. D. LAUBACH. J. Amer. Chem. Soc. **82**, 4293 (1960).
4. S. K. PRADHAN and H. J. RINGOLD. J. Org. Chem. **29**, 601 (1964).
5. M. B. RUBIN, G. E. HIPPS, and D. GLOVER. J. Org. Chem. **29**, 68 (1964).
6. L. L. SMITH and S. BERNSTEIN. *In* Physical properties of the steroid hormones. *Edited by* L. L. Engel. Pergamon Press, New York. 1963. p. 336.
7. K. YATES, J. B. STEVENS, and A. R. KATRITZKY. Can. J. Chem. **42**, 1951 (1964).

Can. J. Chem. Downloaded from www.nrcresearchpress.com by 210.87.254.6 on 09/05/12
For personal use only.

Radiolysis of aqueous 2,2,2-tribromoethanol solutions

V. G. SORENSEN,[1] V. M. BHALE,[2] K. J. MCCALLUM, AND R. J. WOODS
Department of Chemistry and Chemical Engineering, University of Saskatchewan, Saskatoon, Saskatchewan

Received February 25, 1970

Hydrogen bromide, glycolic acid, and carbon dioxide have been identified as products of the γ-radiolysis of aqueous 2,2,2-tribromoethanol solutions. The effect of oxygen, tribromoethanol concentration, and dose rate upon the yields of bromide ion and acid have been determined, and partial radiolysis mechanisms are proposed for reaction in the presence and absence of oxygen. Dibromoacetaldehyde, reported to be a product of the photochemical decomposition of tribromoethanol solutions, was not detected in the radiolysis experiments or in tribromoethanol solutions exposed to sunlight.

Canadian Journal of Chemistry, **48**, 2542 (1970)

Introduction

Organic chlorine compounds break down upon exposure to ionizing radiation to give acidic products (predominantly HCl) which are frequently formed in relatively high yield and which are readily detected and estimated. Such compounds have therefore found some use as chemical dosimeters for the detection and estimation of high-energy radiation (1). Organic bromine compounds have weaker carbon–halogen bonds than the corresponding chlorine compounds and are capable of giving larger yields of acid products upon irradiation (2, 3), so that they may also have potential use in dosimetry. However, high product yields from either chloro or bromo compounds are associated with the presence of chain reactions which lead to dependence of the product yield upon dose rate and, if the reaction is carried out in solution, solute concentration. In order to investigate the limitations imposed by such dose-rate and concentration dependence upon the use of 2,2,2-tribromoethanol in dosimetry, the effect of these variables upon the yield of acid radiolysis products has been studied. Preliminary investigation of the radiolysis of this compound in aqueous solution had shown the acid yield to be dose-rate and concentration dependent (3). It was also of interest to identify the radiolysis products since injection of mice with tribromoethanol prior to tumor irradiation has been shown to increase the number cured (4).

Solutions of tribromoethanol (Avertin) are used in medicine and veterinary medicine as anaesthetics and it has been widely reported (5–7) that such solutions readily decompose upon exposure to air and light, or upon heating above 35–40 °C, and that the decomposition of aqueous solutions produces dibromoacetaldehyde and hydrogen bromide. However, we find little decomposition when aqueous solutions are exposed to sunlight, although the addition of ethanol leads to greater decomposition and to the formation of acetaldehyde, and do not find dibromoacetaldehyde among the products of photochemical decomposition.

Experimental

Materials

2,2,2-Tribromoethanol was prepared by reduction of tribromoacetaldehyde (3) and crystallized from water to give material m.p. 78 °C, or obtained commercially (Brinckman, Montreal) and used as supplied. Solutions were made up in distilled water which had been redistilled from an alkaline permanganate and then an acid dichromate solution, and were stable for at least several weeks if stored out of direct sunlight.

Irradiation and Analytical Procedure

Irradiations were carried out with ^{60}Co sources containing approximately 1, 90, or 5000 C. The energy absorbed by the samples 10^{17}–2×10^{18} eV g^{-1} was estimated using the ferrous sulfate (Fricke) dosimeter (8) assuming $G(Fe^{3+})$ to be 15.5 and the Compton process to be the only significant mode of energy absorption. Aliquots (3 ml) of tribromoethanol solution were irradiated in the presence of air and also after purging with oxygen-free nitrogen as described previously (3). Bromide ion and acid were estimated by titration with silver nitrate (eosin) and sodium hydroxide (bromophenol blue) solutions, respectively (2).

Identification of Radiolysis Products

A solution of tribromoethanol (28.3 g; 0.1 mole) in water (1 l) was irradiated to a total dose of 2.0×10^{20} eV g^{-1} (1.3×10^{15} eV g^{-1} s^{-1}). During the irradiation, a slow stream of oxygen was passed through a sintered glass disc into the solution and the exit gases passed in succession through measured volumes of standard silver nitrate and standard sodium hydroxide solution. Aliquots

[1]Present address: Department of Chemistry, University of Calgary, Calgary, Alberta.
[2]Present address: Government Postgraduate College, Ratlam, M.P., India.

Can. J. Chem. Downloaded from www.nrcresearchpress.com by 210.87.254.6 on 09/05/12
For personal use only.

of the sodium hydroxide solution were removed at intervals during the irradiation and titrated with standard acid (phenolphthalein) to determine carbon dioxide; no significant precipitation occurred in the silver nitrate solution and the solution did not react with 2,4-dinitrophenylhydrazine reagent when tested following the irradiation.

After irradiation, aliquots of the solution were titrated with silver nitrate, sodium hydroxide (bromophenol blue), and after the addition of potassium iodide, sodium thiosulfate solution to determine the amount of bromide, total acid, and oxidizing products formed. Part of the oxidizing product estimated by thiosulfate titration was removed if a current of air was passed through the irradiated solution before adding potassium iodide; this was assumed to be bromine. The thiosulfate titre increased if the irradiated solution was allowed to stand several hours with potassium iodide before titration; the increase was attributed to the slow reaction of organic peroxides, RO_2R, while Br_2, H_2O_2, and organic hydroperoxides, RO_2H, were assumed to react rapidly with potassium iodide. A small portion of the irradiated solution treated with 2,7-dihydroxynaphthalene in sulfuric acid gave a deep violet-red coloration after warming, indicating the presence of glycolic acid (9).

The p*H* of the bulk of the irradiated solution was adjusted to 6.5–7 by the addition of barium carbonate and the solution extracted continuously with ether for 30 h (giving the "neutral" extract), acidified with hydrochloric acid, and extracted with ether for 180 h (the "acid" extract). Evaporation of the neutral extract and crystallization of the residue from benzene-light petroleum (Skelly F) gave white crystals (23.61 g), m.p. 74.5–76 °C, which did not depress the melting point of authentic tribromoethanol (m.p. 75.5–76.5 °C). The neutral extract and the material derived from it gave no reaction with 2,4-dinitrophenylhydrazine reagent. Evaporation of the acid extract gave a bromine-free oil which also gave no reaction with 2,4-dinitrophenylhydrazine reagent. When stored in a vacuum desiccator over phosphorous pentoxide, the oil dried to a glassy solid (0.772 g) which gave an equivalent weight of 77.3 ± 1.5 when dissolved in sodium hydroxide solution, allowed to stand between 1 and 21 h at room temperature, and back-titrated with hydrochloric acid (glycolic acid gave an equivalent weight of 76.05 under these conditions). The solid formed a *p*-bromophenacyl ester m.p. 135.5 °C which did not depress the melting point of an authentic specimen of the *p*-bromophenacyl ester of glycolic acid (m.p. 135.5 °C).

Photochemical Decomposition

Exposure of an aqueous solution of tribromoethanol (25 ml, 0.14 *M*), which absorbed strongly at wavelengths below 290 nm, in a sunny window for 21 days caused a fall in p*H* from 4.5 to 2.5 and the formation of a small quantity of Br^-; no carbonyl products could be detected by treatment of the solution with 2,4-dinitrophenylhydrazine reagent (dibromoacetaldehyde forms a 2,4-dinitrophenylhydrazone m.p. 146 °C or, if the reagent is in excess, the bis-2,4-dinitrophenylhydrazone of glyoxal m.p. 327 °C decomp. (2)) but the solution gave a positive reaction when tested with 2,7-dihydroxynaphthalene for glycolic acid (9). The p*H* of a solution of tribromoethanol (0.14 *M*) in aqueous ethanol (25 ml, 20% *v/v* ethanol) exposed in a similar manner fell from 4.5 to 1.5 in 7 days and to a p*H* less than 1 in 21 days. The solution smelt strongly of acetaldehyde and gave precipitates with both silver nitrate solution and 2,4-dinitrophenylhydrazine reagent after both 7 and 21 days. The 2,4-dinitrophenylhydrazone obtained after 21 days was chromatographed on acid-washed alumina and found to consist essentially of a single compound which, crystallized from aqueous ethanol, had m.p. 165 °C, undepressed upon admixture with authentic acetaldehyde 2,4-dinitrophenylhydrazone (m.p. 165 °C).

Results

Representative values of $G(Br^-)$ for air-saturated solutions are shown in Figs. 1 and 2 and for nitrogen-saturated (oxygen-free) solutions in Fig. 3. Individual *G* values were determined from linear plots of bromide produced against absorbed energy; with air-saturated solutions, the plots showed a change in slope (to a value corresponding to a lower *G* value) at a point associated with exhaustion of the oxygen originally present in solution (2). From the position of the break in a number of plots, the ratio (mole Br^- produced)/(mole O_2 consumed) was estimated to be about 3.6. The yield of

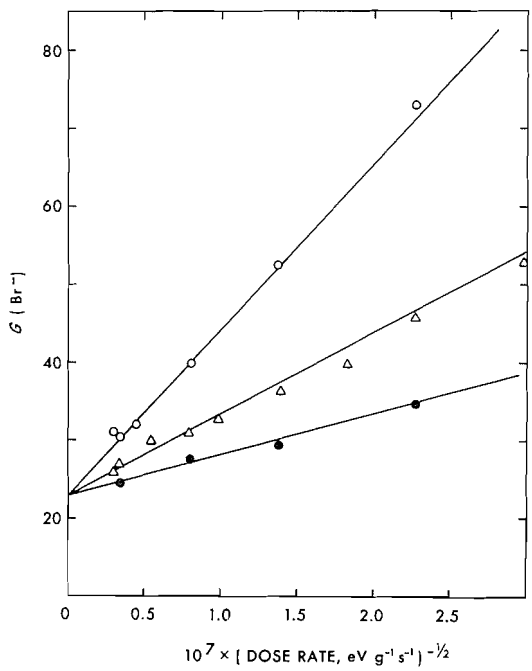

FIG. 1. Variation of $G(Br^-)$ with dose rate for air-saturated tribromoethanol solutions (22 ± 2 °C). The linear plots are described by eq. [4]. ○, 0.1 *M*; △, 0.05 *M*; ●, 0.025 *M*.

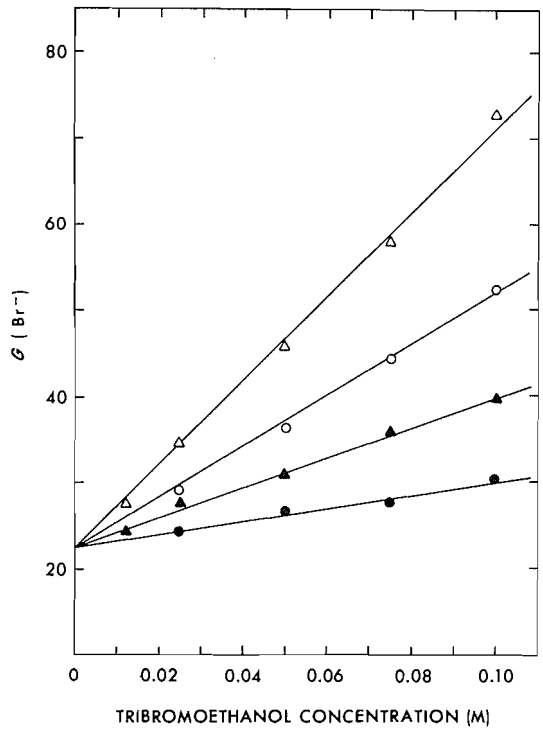

FIG. 2. Variation with tribromoethanol concentration of $G(Br^-)$ for air-saturated solutions (22 ± 2 °C). The linear plots are described by eq. [4]. ●, 84 × 10^{13} eV g^{-1} s^{-1}; ▲, 15.3 × 10^{13} eV g^{-1} s^{-1}; ○, 5.2 × 10^{13} eV g^{-1} s^{-1}; △, 1.9 × 10^{13} eV g^{-1} s^{-1}.

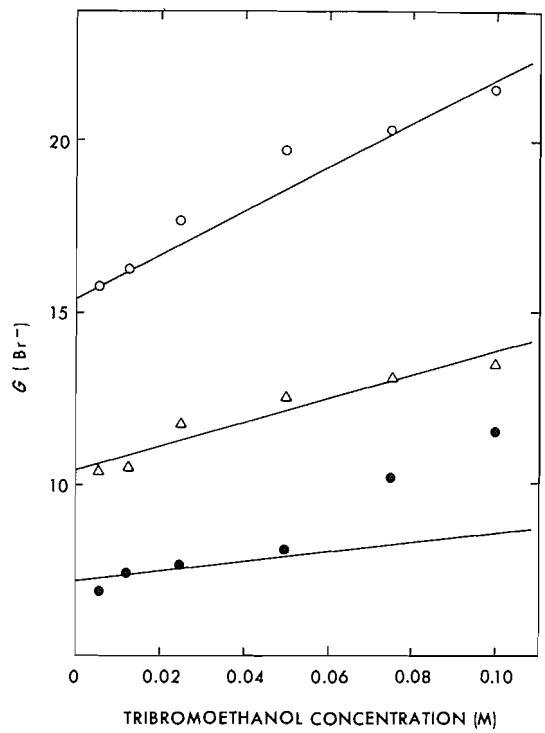

FIG. 3. Variation with tribromoethanol concentration of $G(Br^-)$ for nitrogen-saturated (oxygen-free) solutions (22 ± 2 °C). The linear plots are described by eq. [16]. ●, 84 × 10^{13} eV g^{-1} s^{-1}; △, 5.2 × 10^{13} eV g^{-1} s^{-1}; ○, 1.1 × 10^{13} eV g^{-1} s^{-1}.

bromide appeared to be independent of the reduction in oxygen concentration and of the build-up of bromide ion during radiolysis, although the addition of 0.05 M Br^- before irradiation reduced the radiolytic yield of bromide by about 30% (the highest concentration of bromide produced by irradiation of air-saturated solutions was about 2 × 10^{-3} M, and by irradiation of nitrogen-saturated solutions about 2 × 10^{-4} M). Irradiations were normally carried out at 22 ± 2 °C, but isolated experiments at 30 °C indicated an increase in $G(Br^-)$ of about 2.5% per °C between 22 and 30 °C. Solutions irradiated normally had an initial pH in the range 4–5 which fell during irradiation to 2.5–3; no significant change in $G(Br^-)$ occurred in isolated experiments in which the initial pH was adjusted to 2 or to 7.

Acid yields (determined by titration to the bromophenol blue end point at approximately pH 4.0) were 17.0 ± 1.5% higher than the corresponding bromide yields; the ratio of G(total monobasic acid) to $G(Br^-)$ was independent of dose rate and solute concentration and was the same in the presence or absence of oxygen. Qualitative experiments showed that the irradiated solution contained glycolic acid (K_a 1.475 × 10^{-4} at 25 °C) which would not be completely neutralized by titration to pH 4. Assuming this to be the only organic acid present, G(glycolic acid) = 1.68{G(total acid) − $G(Br^-)$} when allowance is made for the incomplete neutralization. Combined with the observed ratio of G(total acid) to $G(Br^-)$, this gives G(glycolic acid) = 0.285 $G(Br^-)$. Tribromoethanol is unstable in alkaline solution (3) but we found no evidence of decomposition during the titration procedure used here.

Figures 1 and 2 illustrate the effect of changing dose rate and tribromoethanol concentration, respectively, upon $G(Br^-)$ for air-saturated solutions, and Fig. 3 the effect of concentration (at three dose rates) upon $G(Br^-)$ from oxygen-free solutions.

Can. J. Chem. Downloaded from www.nrcresearchpress.com by 210.87.254.6 on 09/05/12
For personal use only.

Can. J. Chem. Downloaded from www.nrcresearchpress.com by 210.87.254.6 on 09/05/12
For personal use only.

Yields determined for the qualitative irradiation were: $G(-Br_3CCH_2OH) \approx 4.8$, $G(Br^-) = 12.0 \pm 0.15$, and G(total monobasic acid) $= 13.74 \pm 0.4$ (both by titration), G(glycolic acid) $= 2.95$ (based on the weight of solid acid recovered) or 2.90 (based on the difference between G(total acid) and $G(Br^-)$ as described above), $G(CO_2) = 1.88 \pm 0.05$, $G(Br_2) \approx 0.09$, $G(H_2O_2 + RO_2H) \approx 0.25$, $G(RO_2R) \approx 0.23$. The data presented in Figs. 1 and 3 predict $G(Br^-)$ to be 29 in the presence of oxygen and ~ 9 in the absence of oxygen at a dose rate of 1.3×10^{15} eV g^{-1} s^{-1}. The value observed is probably due in part to oxygen-depletion caused by inefficient stirring in the irradiation vessel and in part to the build-up of radiolysis products which, in the latter stages of the irradiation, react with some of the radicals produced by water radiolysis.

Discussion

Aqueous tribromoethanol solutions are generally described (5–7) as decomposing upon exposure to air and light or heat to dibromoacetaldehyde and hydrogen bromide, the process being attributed (10) to

[1] $Br_3CCH_2OH \rightarrow Br_2C{=}CHOH + HBr$

[2] $Br_2C{=}CHOH \rightarrow Br_2CH{-}CHO$

If these reactions are in fact induced by the absorption of light by aqueous tribromoethanol, they should also occur upon γ-irradiation to at least the extent of any excitation of the solute, and the absence of dibromoacetaldehyde among the radiolysis products would be evidence for the absence of such processes as solute excitation by fast secondary electrons, by sub-excitation electrons, and by energy transfer to the solute from excited water molecules. Dibromoacetaldehyde was not detected among the radiolysis products, although it was not detected either when aqueous tribromoethanol solutions were exposed to sunlight under conditions reported to produce appreciable decomposition. It appears probable, therefore, that reports of the instability of aqueous tribromoethanol solutions are exaggerated (the solutions appear to be stable for several weeks if stored out of direct sunlight and probably for longer periods if stored in the dark) and that dibromoacetaldehyde is not a product of photochemical decomposition in aqueous solution. Alcoholic solutions, however, may be more sensitive to photochemical decomposition since solutions in aqueous ethanol were found to decompose relatively rapidly when exposed to sunlight. The products included hydrogen bromide and acetaldehyde (but not dibromoacetaldehyde), suggesting a radical-initiated chain reaction of the type observed between carbon tetrachloride and alcohols (11), i.e.

[3] $Br_3CCH_2OH + CH_3CH_2OH \rightarrow Br_2CHCH_2OH + CH_3CHO + HBr$

Tertiary alcohols such as 2-methyl-2-butanol (amylene hydrate), which is frequently used as a solvent for tribromoethanol for medical use, would not take part in a chain reaction of the type shown. Relevant to the radiation-induced decomposition of aqueous solutions is the observation that the alcohol group of the ethanol is oxidized but that of the tribromoethanol is not.

Products formed when aqueous tribromoethanol solutions are irradiated in the presence of oxygen are hydrogen bromide, glycolic acid and, in smaller amounts, carbon dioxide. Small quantities of volatile (Br_2) and non-volatile (H_2O_2, RO_2H, and RO_2R) oxidizing products are also formed. Carbon dioxide was determined during a relatively long irradiation and the reported $G(CO_2)$ may be high due to oxidation of part of the glycolic acid formed in the early stages since the ratio G(glycolic acid)/$G(Br^-)$ was lower (0.242) in this experiment than in the titration experiments (0.284); the titrations indicated that the ratio had the same value whether oxygen was present or not, so that depletion of oxygen in the qualitative experiment should not affect this conclusion. Assuming the higher value of the ratio to be correct and the lower value to be due to oxidation of glycolic acid to carbon dioxide, $G(CO_2)$ becomes 0.90 and G(glycolic acid) 3.41 in the qualitative experiment. Whether this adjustment is made or not, $G(Br^-) = 3G$(glycolic acid) $+ 1.5G(CO_2)$ to within 4%, suggesting that no major radiolysis products have been missed. Particular efforts were made to detect carbonyl compounds among the products since acetaldehyde is a major product when aqueous solutions of ethanol are irradiated in the presence of oxygen (12), and dibromoacetaldehyde was believed to be produced by the photochemical decomposition of aqueous tribromoethanol solutions. However, no carbonyl products were found and it appears

TABLE 1

Propagation and termination rate constants for radiation-initiated chain reactions in air-saturated solutions of chloral hydrate, bromal hydrate, and tribromoethanol

Solute	Concentration (M)	Radiation	Dose rate (10^{13} eV g^{-1} s^{-1})	Propagation rate constant (M^{-1} s^{-1})	Termination rate constant (10^8 M^{-1} s^{-1})	Reference
$Cl_3CCH(OH)_2$	0.1	γ	11.0	220	2.5	14
	1.0	γ	11.0	170	8.8	14
	1.0	γ	3.4	110	6.9	14
	1.0	β	5.2	250	25	15
$Br_3CCH(OH)_2$	0.1	γ	11.0	270	1.4	14
	0.2	β	1.8	270	3.7	16
Br_3CCH_2OH	0.00625–0.1	γ	1.9–84	41	5*	This work

*Assumed value.

that substitution of the β-hydrogen atoms of ethanol by bromine causes the locus of the radiation-induced reaction to shift from the α-carbon with CH_3CH_2OH to the β-carbon with Br_3CCH_2OH. Products formed from tribromoethanol in the absence of oxygen were not identified.

The yield of bromide ion from air-saturated tribromoethanol solutions is given by the empirical equation,

$$[4] \qquad G(Br^-) = 22.5 + 2.13 \times 10^9[Br_3CCH_2OH]I^{\frac{1}{2}}$$

where the G value is in units of Br^-/100 eV, the concentration in moles l^{-1}, and the dose rate (I) in eV g^{-1} s^{-1}. Data plotted from this relationship are shown in Figs. 1 and 2 together with experimental points. The form of eq. [4] suggests that bromide is produced by a chain reaction that can be represented by

Initiation

$$[5] \qquad W \rightsquigarrow R \qquad cI'$$

Propagation

$$[6] \qquad R + A \rightarrow R + P \qquad k_p$$

Termination

$$[7] \qquad R + R \rightarrow P \qquad k_t$$

where W and A are water and tribromoethanol respectively, P is bromide ion, and R represents both radicals formed from water and those derived from the tribromoethanol; cI' is the rate of formation of initiating radicals, and k_p and k_t the rate constants for the propagation and termination steps, respectively. Application of steady state kinetics (13) gives

$$[8] \quad \text{Yield } Br^- \text{ (moles eV}^{-1}) = c \text{ (moles eV}^{-1}) + k_p(c/k_t)^{\frac{1}{2}} I'^{-\frac{1}{2}}$$

where I' is the dose rate in eV l^{-1} s^{-1} and the constant c is related to the yield of bromide in the absence of a chain reaction, i.e. from reactions [5] and [7] alone. Assuming k_t to be about 5×10^8 $M^{-1}s^{-1}$, a value comparable to experimental termination rate constants for similar systems (Table 1) and to rate constants for other radical–radical reactions in water (17), substitution in eq. [8] of the numerical values from eq. [4](in appropriate units) gives $k_p = 41$ M^{-1} s^{-1}. The assumed value for k_t and calculated value for k_p are consistent with the known radiation chemistry of chloral and bromal hydrates and tribromoethanol. Both aldehyde hydrates give higher yields of halogen acid upon irradiation than the alcohol and both have higher propagation rate constants (Table 1) that can be attributed to the presence of relatively weak C—H bonds which provide an additional point for radical attack (oxidation of the aldehyde group is a significant process in the radiolysis of bromal hydrate solutions (2)). Termination rate constants are expected to have approximately the same value for each of the three compounds since similar radicals are believed to be involved in the termination reactions in each case.

Reactive species formed in water by γ-irradiation are hydrated electrons, hydrogen atoms, and hydroxyl radicals; hydrogen and hydrogen peroxide are also formed but in the presence of much higher concentrations of tribromoethanol are not believed to play a major part in the radiolysis. Tabulated rate constants for reactions of the reactive species with organic solutes (17) indicate that in this system (0.05 M Br_3CCH_2OH, $\sim 2.5 \times 10^{-4}$ M O_2, $\sim 10^{-4}$ M H^+) the initial reactions will probably be

$$[9] \qquad e_{aq}^- + Br_3CCH_2OH \rightarrow Br^- + Br_2CCH_2OH$$

Can. J. Chem. Downloaded from www.nrcresearchpress.com by 210.87.254.6 on 09/05/12
For personal use only.

Can. J. Chem. Downloaded from www.nrcresearchpress.com by 210.87.254.6 on 09/05/12
For personal use only.

[10] $H + Br_3CCH_2OH \rightarrow HBr + Br_2CCH_2OH$

[11] $OH + Br_3CCH_2OH \rightarrow H_2O + Br_3CCHOH$

However, reaction [11] is not supported by the chemical evidence since subsequent reaction of the Br_3CCHOH radicals in the presence of oxygen would be expected to convert a large proportion of them to Br_3CCHO or Br_3CCOOH (cf. ref. 12); neither product was detected. The magnitude of the constant c in eq. [8](22.5 G units) suggests rather that hydroxyl radicals displace bromine from tribromoethanol since c, the bromide yield in the absence of a chain reaction, is approximately equal to $3(G_{e_{aq}^-} + G_H + G_{OH})$; the sum of the G values in parentheses is estimated to be 6.3 in the present system (18). Evidence of chlorine displacement from chloroacetic acid by hydroxyl radicals, in competition with hydrogen abstraction, has recently been described (19); displacement of bromine from tribromoethanol should occur more readily in view of the considerably weaker carbon–halogen bond. Organic radicals produced in the present system are expected to add oxygen and a possible chain reaction producing bromide and glycolic acid is summarized by the stoichiometric equations

[12] $Br_2CCH_2OH + O_2 + 2\,H_2O \rightarrow HO_2 + 2HBr + HOOCCH_2OH$

[13] $HO_2 + Br_3CCH_2OH \rightarrow Br_2CCH_2OH + HBr + O_2$

(HO_2, $pK_a = 4.5$ (20), will be appreciably ionized under our irradiation conditions and the active form may be O_2^-.) Reaction [12] can be broken down into a number of plausible steps initiated by the addition of oxygen to Br_2CCH_2OH. Yields of bromide ion appeared to be independent of the concentration of oxygen, suggesting that oxygen reacts rapidly with the intermediates in the radiolysis and that this step is not the rate-controlling step. The constant ratio of G(glycolic acid)/$G(Br^-)$ under a variety of conditions implies that $G(CO_2)/G(Br^-)$ must also be constant, since glycolic acid and carbon dioxide are the only carbon-containing products formed in significant amounts, and that carbon dioxide is produced by a side reaction of the main chain reaction producing glycolic acid and bromide. Chain termination will be by reaction of pairs of chain-propagating radicals, represented by such stoichiometric reactions as

[14] $OH + Br_2C(O_2)CH_2OH + H_2O \rightarrow HOOCCH_2OH + 2\,HBr + O_2$

[15] $HO_2 + Br_2C(O_2)CH_2OH + H_2O \rightarrow HO_3CCH_2OH + 2\,HBr + O_2$

In the absence of oxygen, $G(Br^-)$ is related to tribromoethanol concentration and dose rate by the empirical equation,

[16] $$G(Br^-) = 6.25(1 + [Br_3CCH_2OH]) + 10^7(3 + 20[Br_3CCH_2OH])I^{-\frac{1}{2}}$$

where I is the dose rate in eV g^{-1} s^{-1}. This relationship, which holds over the range of conditions studied except at the higher dose rate and highest concentrations (Fig. 3), indicates that bromide is formed by a chain reaction of the type represented by eqs. [5] to [7] with additional propagation, reaction [17], and termination, reaction [18], steps.

[17] $R \rightarrow R + P$

[18] $R + R + A \rightarrow P$

The coefficients in eq. [16] imply that in oxygen-free solutions each radical produced by the irradiation of water produces an average of about one bromide ion in the absence of a chain reaction (i.e. by reactions [5], [7], and [18] alone) and, assuming termination rate constants of about 5×10^8 M^{-1} s^{-1}, that the propagation rate constants for the chain reaction are one or two orders of magnitude lower than that (41 M^{-1} s^{-1}) calculated for the chain reaction in the presence of oxygen.

Grateful acknowledgment is made to the Atomic Energy Control Board and the National Research Council of Canada for financial support. One of us (V.G.S.) thanks the Saskatchewan Research Council for a scholarship.

1. H. Fricke and E. J. Hart. *In* Radiation dosimetry. Vol. 2. *Edited by* F. H. Attix and W. C. Roesch. 2nd ed. Academic Press, Inc., New York. 1966. p. 210.
2. R. J. Woods and J. W. T. Spinks. Can. J. Chem. **35**, 1475 (1957).
3. R. J. Woods and J. W. T. Spinks. Can. J. Chem. **38**, 77 (1960).
4. W. R. Franks, A. McGregor, G. A. Meek, M. M. Shaw, and J. Skublics. Proc. Can. Cancer Research Conf. Honey Harbour, Ontario, 1954. **1**, 394 (1955).
5. A. Osol and G. E. Farrar (*Editors*). Dispensatory of the United States of America. 1960 ed. J. B. Lippincott. Philadelphia. 1960. p. 1445.

6. Beilsteins Handbuch der Organischen Chemie, Zweites Erganzungswerk. Vol. 1. Julius Springer, Berlin. 1941. p. 338.
7. P. G. STECHER (*Editor*). The Merck index. 8th ed. Merck and Co., Inc., Rahway, New Jersey. 1968. p. 1066.
8. J. WEISS, A. O. ALLEN, and H. A. SCHWARZ. Proc. Int. Conf. Peaceful Uses At. Energ. United Nations. New York. **14**, 179 (1956).
9. F. FEIGL. *In* spot tests in organic analysis. *Translated by* R. E. OESPER. 6th Eng. ed. Elsevier Publ. Co., New York. 1960. p. 377.
10. F. B. PARSONS. Brit. Med. J. 709 (1929).
11. K. HANNERZ. Research, **9**, S1 (1956).
12. G. G JAYSON, G. SCHOLES, and J. WEISS. J. Chem. Soc. 1358 (1957).
13. J. W. T. SPINKS and R. J. WOODS. *In* An introduction to radiation chemistry. John Wiley and Sons, Inc., New York. 1964. p. 177.
14. R. G. MCINTOSH, R. L. EAGER, and J. W. T. SPINKS. Can. J. Chem. **43**, 3490 (1965).
15. R. F. PLATFORD and J. W. T. SPINKS. Can. J. Chem. **37**, 1022 (1959).
16. A. G. BRICKNELL. Ph.D. thesis, University of Saskatchewan, Saskatoon, Saskatchewan. 1959.
17. M. ANBAR and P. NETA. Int. J. Appl. Radiat. Isotop. **16**, 227 (1965).
18. E. HAYON. Trans. Faraday Soc. **61**, 734 (1965).
19. A. YOKOHATA, T. OHMURA, and S. TSUDA. J. Phys. Chem. **73**, 4013 (1969).
20. G. CZAPSKI and L. M. DORFMAN. J. Phys. Chem. **68**, 1169 (1964).

Can. J. Chem. Downloaded from www.nrcresearchpress.com by 210.87.254.6 on 09/05/12
For personal use only.

Can. J. Chem. Downloaded from www.nrcresearchpress.com by 210.87.254.40 on 09/05/12
For personal use only.

Free-energy relationships in coordination chemistry. I. Linear relationships among equilibrium constants[1]

E. NIEBOER[2] AND W. A. E. MCBRYDE
Department of Chemistry, University of Waterloo, Waterloo, Ontario

Received November 25, 1969

After a review of previous semi-empirical free-energy relationships applying to the formation of metal complexes, the following equations are derived within a framework of logical assumptions

$$\log K_{ML} = B \log K_{M_sL} + (\log K_{ML_0} - B \log K_{M_sL_0})$$
$$\log K_{ML} = C \log K_{ML_0} + (\log K_{M_sL} - C \log K_{M_sL_0})$$

These compare stability constants of complexes formed by a metal ion M and a ligand L with those formed by a reference metal M_s and a reference ligand L_0. The derivation of these equations reveals an inherent relationship between the constants B and C, which is formulated through an "exactness" test. The application of these relationships to stoichiometric equilibrium constants is discussed.

In the testing of the foregoing equations with data for various ligand families reacting with numerous metal ions, two principal modes of behavior were noted. In one, there was a mutual dependence of B on the particular metal ions compared and of C on the particular ligands compared. In the other, all values of B and C were found to equal unity irrespective of metal ion or ligand compared. The cause of this distinction is not yet understood.

Canadian Journal of Chemistry, **48**, 2549 (1970)

Introduction

The great interest shown by inorganic chemists during the past two decades in the thermodynamics of metal ion complex formation in solution has resulted in the compilation of a massive amount of equilibrium data (e.g., ref. 1). Analysis of such data has led to the recognition of certain linear free energy relationships (l.f.e.r.). These have been of two main types: (*i*) relationships among sets of equilibrium constants, and (*ii*) correlations of the magnitude of stability constants with properties of the metal ion. In addition, equilibrium data have been used as a criterion for the classification of ligands and metal ions.

In this paper equations are derived to rationalize the empirical relationships of the first type, and these are compared to the equations used in the past. In a subsequent paper[3] we plan to review relationships of the second kind, and to introduce a new, comprehensive index to metal ion complex stability. The related area of the classification of ligands and metals will also be examined.

[1]Presented in part at the 12th International Conference on Coordination Chemistry, Sydney, Australia. 1969.

[2]NRCC Postdoctorate Fellow; present address: Inorganic Chemistry Laboratory, Oxford University, Oxford, England.

[3]Part III, in preparation for publication in this journal.

Rationalizations of l.f.e.r. and the Empirical Evidence

The empirical linear correlation between proton dissociation constants of a series of related ligands and the stability constants of the corresponding metal ion complexes has received the most attention (2–9). Equations that describe the relationship have either been intuitively formulated (8, 10) or have been derived in a more rigorous fashion (4, 11). The pioneering work of Irving and Rossotti (4) has had the greatest impact. Their derivation of eq. [5] is based on the free-energy changes that accompany the displacement of a proton from a proton–ligand complex HL by a metal ion M, as in reaction [3].

[1] $$H + L = HL$$
$$^{T}K_{HL} = \{HL\}/\{H\}\{L\}$$

[2] $$M + L = ML$$
$$^{T}K_{ML} = \{ML\}/\{M\}\{L\}$$

[3] $$M + HL = ML + H$$
$$^{T}\kappa = \{ML\}\{H\}/\{M\}\{HL\}$$
$$= {}^{T}K_{ML}/{}^{T}K_{HL}$$

[4] $$\Delta G^0 = -2.303\, RT \log {}^{T}\kappa$$

[5][4] $$\log K_{ML} = pK + A + P$$

[4]Equation [5] is obtained by combining eqs. [3] and [4].

Can. J. Chem. Downloaded from www.nrcresearchpress.com by 210.87.254.40 on 09/05/12
For personal use only.

The quantities in braces are activities, and thus ${}^{T}K_x$ are thermodynamic stability constants, with the superscript T being dropped in the case of stoichiometric constants; ΔG^0 is the standard free-energy change for reaction [3]; $\log K_{HL}$ (association) = pK (dissociation); A is an expression in terms of the standard partial molar free energies and activity coefficients of species HL and ML; P is the analogous expression to A for species M and H; and charges are omitted for convenience and generality. It has been reasoned (4, 5) that if a plot of $\log K_{ML}$ vs. pK for a series of related ligands is found to be a straight line of unit slope, then the term A must be constant or perhaps negligible compared to pK. (The term P is independent of the nature of the ligand and remains constant in the comparison.) If a line of non-unit slope is obtained, then the term A must itself be a linear function of pK. In this latter instance eq. [5] should then assume the form of eq. [6].

$$[6] \qquad \log K_{ML} = a\,pK + b$$

where a and b are constants. Because a rigorous derivation of eq. [6] was lacking for some time, much emphasis has been placed on unit slopes. Consequently, the tendency has been to regard non-unit slopes from the viewpoint of deviations from some expected behavior (5, 11, 12). A more rigorous form (eq. [7]) of eq. [6] has now been reported (10, 11, 13). It was first derived (11) by application of the "extra-thermodynamic" treatment used by Leffler and Grunwald (14) in their enlightening analysis of rates and equilibria of organic reactions. Reference to this approach will be made in some detail in Part II of this series (15).

$$[7] \quad \log K_{ML} = B\,pK + [\log K_{ML_0} - B\,pK_0]$$

Thus B has replaced a in eq. [6], and the expression in square brackets on the right-hand side of eq. [7] has replaced the intercept b; the subscript 0 identifies L_0 as being the unsubstituted member of a ligand family.

In a derivation related to that described for eq. [5], Irving and Rossotti obtained eq. [8], which describes the relationship between the stabilities of two related ligands with a series of metal ions. (L_0 need not be the unsubstituted member of a ligand series, and A has the same significance as before.)

$$[8] \quad \log K_{ML} = \log K_{ML_0} + [\log K_{HL} - \log K_{HL_0}] + [A - A_0]$$

Equation [8] has been applied to only a limited extent and almost exclusively to comparisons that exhibit slopes of unity. It has been pointed out in a more detailed examination (16) of eq. [8] that the essence of a relationship with unit slope in this case is a constant value, irrespective of the metal ion, for the free-energy change accompanying the displacement reaction depicted in [9].

$$[9] \qquad ML_0 + L = ML + L_0$$

Hammett-type relationships (14, 17, 18) have also been used in comparisons of complex stabilities (10, 19–22). We have been able to show rigorously that such relationships are no different, intrinsically, from those already mentioned, and that contrary to previous interpretations (20, 23) no a priori evidence for the presence or absence of π bonding may be derived from the sign and magnitude of the observed slopes in these cases (13, 24).

Equation [6] (or eq. [7]) has been found to hold in numerous systems with slope a having values both equal to and different from unity. As explained, non-unit slopes have been rationalized on the basis of the non-constancy of the term A in eq. [5]. Explanations such as the presence of π bonding have also been proposed (5, 11, 12). The magnitude of the intercept on the vertical ($\log K_{ML}$) axis has similarly been associated with the degree of π bonding in a system (5, 12). In addition, the magnitudes of these slopes have been correlated with such properties of the metal ions as ionization potentials (7, 10, 25–27), reciprocal of ionic radius (10), charge-to-size ratio (5), electronegativities (10, 26, 27), and nuclear repulsion (28).

An analysis of the data reported in the references in the bibliography revealed the following general trends. In a great number of systems of related ligands, the magnitude of the rate of change of metal–ion complex stability with ligand basicity, although normally constant for a particular metal ion is dependent on that metal ion. Further, in such systems, the metal ion that forms the weakest complexes with a family of ligands also appears to exhibit the smallest value for the slope a. Although eq. [8] has found application only in comparisons yielding unit

Can. J. Chem. Downloaded from www.nrcresearchpress.com by 210.87.254.40 on 09/05/12
For personal use only.

slopes, the investigations of Van Uitert and Fernelius (28) provide evidence (as does other work on close examination) that in systems which have metal-dependent values for a, the slope associated with the comparison expressed in eq. [8] is ligand-dependent, and has a constant value for each ligand. More explicitly, these slopes are proportional to the inductive effect of a substituent placed on an unsubstituted parent ligand. In contrast, other ligand systems distinguish themselves by yielding unit values of a, independent of the metal ion considered. Such ligand families reveal another diagnostic characteristic: the value observed for the slopes of plots comparing the complex-ion constants for any two members of a series of selected ligands with a series of metal ions (cf. eq. [8]) is unity.

The theory introduced presently is not based on a rigorous model of complex formation and stability. Instead, the general observations outlined above are used as guidelines in the derivations and in support of any necessary assumptions. As we hope to show, the rational framework presented is consistent with the experimental evidence, provides the logic for a detailed examination of the conditions necessary for the existence of successful l.f.e.r., allows the introduction of new free energy relationships, ties together the existing rationalization of l.f.e.r., and finally, furnishes a solid basis for a wider and more meaningful application of such relationships.

Derivations

Suppose the standard free energy change of a reaction, ΔG^0, can be expressed as a function of a number of independent variables represented by $x, y, v, w, \cdots$ (17, 18). A change in ΔG^0 is then given by the differential eq. [10].

$$[10] \quad d\Delta G^0 = (\partial \Delta G^0/\partial x)_{y,v,w}\, dx + (\partial \Delta G^0/\partial y)_{x,v,w}\, dy + \cdots$$

If eq. [10] is a complete or total differential, then the value of its integral depends only on the initial and final values of the variables. Integration is uncomplicated in this case (29, 30). Expressions for comparing the standard free-energy changes accompanying two related reaction series have been derived from eq. [10] by considering $d\Delta G^0$ as a function of one independent variable only. Wells (17, 18) used this approach to place on a quantitative footing the empirical Hammett-type equations used to correlate chemical reactivity in organic chemistry.[5] The expressions involving the metal complex "stabilization factor" (13, 20) were also derived by considering the free energy of complex formation to be a function of a single variable.

The Parameter ϕ as a Function of Two Variables

In the present treatment, the standard free-energy change for metal complex formation in a reaction series is considered to be a function of two variables. We begin by defining the quantities ϕ, σ, and θ, as given in eqs. [11] to [13]; only 1:1 metal–ligand complexes are considered in this treatment.

$$[11] \quad M + L = ML$$
$$\phi = \log ({}^TK_{ML}/{}^TK_{M_sL_0})$$
$${}^TK_{M_sL_0} = \{M_sL_0\}/\{M_s\}\{L_0\}$$

The subscripts s and 0 identify a metal and a ligand, respectively, chosen as standards for comparison. The constant ${}^TK_{ML}$ is defined as before (eq. [2]), and the superscript T and the quantities in braces also have their previous significance.

$$[12] \quad M_s + L = M_sL$$
$$\sigma = \log ({}^TK_{M_sL}/{}^TK_{M_sL_0})$$

$$[13] \quad M + L_0 = ML_0$$
$$\theta = \log ({}^TK_{ML_0}/{}^TK_{M_sL_0})$$

It is evident that σ and θ are respectively the logarithms of the equilibrium constants for the following displacement reactions

$$M_sL_0 + L = M_sL + L_0$$
$$\sigma = \log {}^T\kappa_L$$
$$M_sL_0 + M = ML_0 + M_s$$
$$\theta = \log {}^T\kappa_M$$

We then postulate that ϕ may be expressed as a function of the dependent variables σ and θ. The reactions in [12] and [13] are chosen as reference reaction series. In reaction [12], a series of ligands are reacted with the standard or reference metal M_s. It is assumed, therefore, that the parameter σ depends on the ligand only, and

[5]The "extrathermodynamic" approach of Leffler and Grunwald (14) has provided a uniquely different framework for the rationalization of Hammett-type equations.

Can. J. Chem. Downloaded from www.nrcresearchpress.com by 210.87.254.40 on 09/05/12
For personal use only.

that it adequately accounts for the ligand-dependent contribution to ϕ. The reactions in [12] will hereafter be referred to as the "ligand-dependent" standard reaction series, and those in [13] as the "metal-dependent" standard reaction series. Thus, in reaction [13] the only variable is the metal ion M, with L_0 as the standard or reference ligand. It is assumed that the parameter θ depends on the metal ion only, and that it adequately accounts for the metal-dependent contribution to ϕ. These assumptions are examined critically below.

A change in ϕ caused by increments $d\sigma$ and $d\theta$ is given by the differential eq. [14], in analogy to eq. [10].

$$[14] \quad d\phi = (\partial\phi/\partial\sigma)_\theta \, d\sigma + (\partial\phi/\partial\theta)_\sigma \, d\theta$$

For the sake of simplicity let $B = (\partial\phi/\partial\sigma)_\theta$ and $C = (\partial\phi/\partial\theta)_\sigma$. Since ${}^TK_{M_sL_0}$ is invariant in any reaction series, $d \log {}^TK_{M_sL_0} = 0$. Consequently, $d\phi = d \log {}^TK_{ML}$, $d\sigma = d \log {}^TK_{M_sL}$, $d\theta = d \log {}^TK_{ML_0}$, and the gradients B and C may be written as in eqs. [15] and [16]

$$[15] \quad B = (\partial \log {}^TK_{ML}/\partial \log {}^TK_{M_sL})_\theta$$

$$[16] \quad C = (\partial \log {}^TK_{ML}/\partial \log {}^TK_{ML_0})_\sigma$$

Therefore B is the rate of change of stability in a series of complexes ML of the metal ion M with the stability of the related series of complexes M_sL of the reference metal ion M_s. Similarly C is the rate of change of stability in a series of complexes ML of the ligand L with the stability of the related series of complexes ML_0 of the reference ligand L_0.

Several assumptions are necessary before the evaluation of ϕ by integration of eq. [14] is possible. The restriction of linearity is one of these conditions. In support we recall from the previous section the observation that in many ligand systems the gradients B and C are invariant for a specific metal ion and ligand respectively. The experimental data suggest further that the magnitude of B varies with the choice of the metal ion and the magnitude of C with the choice of the ligand. In view of our postulation of σ as the ligand-dependent variable and of θ as the metal-dependent variable, we interpret these observations to mean that B is a function of θ but not of σ, and that C is a function of σ but not of θ. Finally we must assume that $d\phi$ is a complete or exact differential. If $d\phi$ were an *inexact* differential, then the value of the integral $\int[B(\theta)\, d\sigma + C(\sigma)\, d\theta]$ would depend on the path of integration (29, 30). (The terms $B(\theta)$ and $C(\sigma)$ emphasize that B and C are functions of θ and σ, respectively.) In this situation it is not possible to regard ϕ as a property of the system (31), and no explicit expression leading to the differential $d\phi$ exists (30). Conversely, the value of this integral is independent of the path and depends entirely on the initial and final values of σ and θ when $d\phi$ is *exact*. The assumption of exactness permits us to integrate along any path for which the value of B is specified for all σ, and the value of C for all θ. Two such possible routes are outlined in Fig. 1.

In this scheme ϕ_s is ϕ for reaction [11] with $M = M_s$, ϕ_0 with $L = L_0$, and $\phi_{0,s}$ with $M = M_s$ and $L = L_0$; σ_0 is σ for reaction [12] with with $L = L_0$; θ_s is θ for reaction [13] with $M = M_s$. The subscripts L and M identify the respective ligand and metal ion for which a variable is defined. It is clear that $\phi_s = \sigma_L$, $\phi_0 = \theta_M$, and $\phi_{0,s} = \sigma_0 = \theta_s = \log ({}^TK_{M_sL_0}/{}^TK_{M_sL_0}) = 0$.

We shall first evaluate the integral $\int[B(\theta)\, d\sigma + C(\sigma)\, d\theta]$ along the path XWZ, and then by integration along XYZ. Path XWZ may be considered to have two component parts XW and WZ. For component XW there is no change in σ and $d\sigma$ is equal to zero. The differential [14] for the change in ϕ from X to W assumes the form [17], where $(\partial\phi/\partial\theta)_{\sigma_0} = (\partial \log {}^TK_{ML_0}/\partial \log {}^TK_{ML_0}) = 1$.

$$[17] \quad d\phi_{xw} = (\partial\phi/\partial\theta)_{\sigma_0} \, d\theta = d\theta$$

Along WZ there is a change in σ but not in θ, and the differential eq. [18] applies.

$$[18] \quad d\phi_{wz} = (\partial\phi/\partial\sigma)_{\theta_M} \, d\sigma = B \, d\sigma$$

To evaluate $d\phi$ for the path XWZ we simply combine eqs. [17] and [18] as in eq. [19].

$$[19] \quad d\phi_{xwz} = B \, d\sigma + d\theta$$

Integration between the limits (σ_0, θ_s) and (σ, θ) yields eq. [20].

$$[20] \quad \phi - \phi_{0,s} = B(\sigma - \sigma_0) + (\theta - \theta_s)$$

But $\phi_{0,s} = \sigma_0 = \theta_s = 0$. Equation [20] may thus be simplified to give eq. [21].

$$[21] \quad \phi = B\sigma + \theta$$

By analogy, the differential $d\phi_{xyz}$ is the sum of

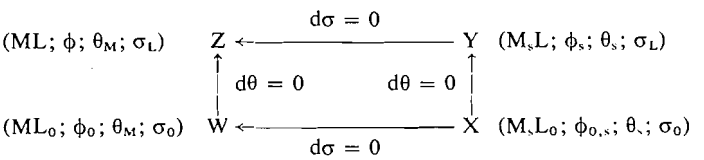

FIG. 1. Integration of dφ.

$d\phi_{xy}$ [22] and $d\phi_{yz}$ [23]. Integration along the path XYZ yields [24].

$$[22] \qquad d\phi_{xy} = (\partial\phi/\partial\sigma)_{\theta_s}\, d\sigma = d\sigma$$

$$[23] \qquad d\phi_{yz} = (\partial\phi/\partial\theta)_{\sigma_L}\, d\theta = C\, d\theta$$

$$[24] \qquad \phi = \sigma + C\theta$$

It is apparent that the expressions for φ in eqs. [21] and [24] must be equivalent if dφ is an exact differential.

φ as a Function of σ

For φ to be a function of σ alone, it must be independent of θ, or be dependent only on the ligand. Let us define a new variable φ′ which is restricted by definition, eq. [25], to a single test metal ion. The relationship between φ′ and φ as expressed in eq. [21] is self-evident.

$$[25] \qquad \phi' = \log ({}^{T}K_{ML}/{}^{T}K_{ML_0}) = \phi - \theta = B\sigma$$

When $M_s = H^+$, eq. [25] is a Hammett-type equation, although σ is not equal to the Hammett sigma factor.[6]

If φ, σ, and θ are expressed in terms of the appropriate equilibrium constants, then the following expression is derived from eq. [25].

$$[26] \qquad \log {}^{T}K_{ML} = B \log {}^{T}K_{M_sL} + [\log {}^{T}K_{ML_0} - B \log {}^{T}K_{M_sL_0}]$$

Equations [25] and [26] describe the *substituent* effect. They compare the stabilities of the complexes of two metal ions (M and M_s) with a series of related ligands L. The series of ligands L usually consist of a parent reagent (L_0; e.g., pyridine) and its substituted derivatives (e.g., 4-methylpyridine). Hence σ is a measure of the effect of ligand substitution on the "ligand-dependent" standard reaction series; similarly, φ′ is a measure of the same effect on the test reaction.

φ as a Function of θ

In order for φ to be dependent solely on the metal ion it must be redefined in such a manner that only one test ligand is involved in its definition, eq. [27]. The relationship between this new variable φ″ and φ as expressed in [24] is also summarized in eq. [27].

$$[27] \qquad \phi'' = \log ({}^{T}K_{ML}/{}^{T}K_{M_sL}) = \phi - \sigma = C\theta$$

Insertion of the appropriate logarithmic quantities in [27] generates the relationship in [28].

$$[28] \qquad \log {}^{T}K_{ML} = C \log {}^{T}K_{ML_0} + [\log {}^{T}K_{M_sL} - C \log {}^{T}K_{M_sL_0}]$$

Equations [27] and [28] compare the stabilities of the complexes of two related ligands (L and L_0) with a series of metal ions M, and may be said to describe the *quasi-substituent* effect. In analogy with the substituent effect we might invoke the notion that it is possible to construct the series of metal ions M by modification ("substitution") of the reference metal ion M_s. The parameters θ and φ″ are then measures of the effect of this quasi-substitution on the "metal-dependent" standard reaction series and the test reaction respectively.

Exactness Test

The condition expressed in eq. [29] is sufficient

[6]The Hammett equation is of the form $\log (k/k_0) = \rho\sigma_H$, where ρ is the slope and k and k_0 are rate or equilibrium constants for *m*- and *p*-substituted and unsubstituted benzene derivatives respectively; the Hammett sigma factor σ_H is defined at 25 °C: $\sigma_H = \log (K_{HL_0}/K_{HL})_{\text{benzoic acids}}$.

Thus in our terminology, σ_H is a "ligand-dependent" standard reaction series. For a family of reagents not directly derived from benzene, e.g., pyridines, σ_H is often replaced by $\bar{\sigma}$, the "effective" Hammett sigma factor (13, 32, 33). It is defined in terms of the pK's of the ligand family considered, $\bar{\sigma} = q(pK_0 - pK)$. The constant q relates $\bar{\sigma}$ to the σ_H scale. Consequently, σ in this paper is related to $\bar{\sigma}$; $\sigma = -\bar{\sigma}/q = pK - pK_0 = -\sigma'$. These ($\bar{\sigma}$ and σ′) and other Hammett sigma factors (14, 17, 18, 32, 34) have found application in the comparison of metal ion complex stability with ligand basicity (10, 13, 19–22, 35). However, the distinction between the various Hammett sigma factors is often overlooked in these applications.

Can. J. Chem. Downloaded from www.nrcresearchpress.com by 210.87.254.40 on 09/05/12
For personal use only.

Can. J. Chem. Downloaded from www.nrcresearchpress.com by 210.87.254.40 on 09/05/12
For personal use only.

to reveal whether $d\phi$ is an exact differential (29, 30, 36, 37).

$$[29] \qquad \partial B/\partial\theta = \partial^2\phi/\partial\sigma\partial\theta = \partial C/\partial\sigma$$

Evaluation of the second and third derivatives of ϕ[7] for a system which obeys the linear eqs. [25] and [27] reveals that verification of the exactness condition should be relatively simple in this case.[8] The results of the differentiation of ϕ' (eq. [25]) and ϕ'' (eq. [27]) are summarized in eqs. [30]–[33]. The subscripts M and L indicate the respective metal ion and ligand at which the variables are evaluated.

$$[30] \qquad (\partial B/\partial\theta)_L = (C_L - 1)/\sigma_L$$

$$[31] \qquad \partial[\partial B/\partial\theta]/\partial\sigma = [(\partial C/\partial\sigma) - (\partial B/\partial\theta)]/\sigma$$

$$[32] \qquad (\partial C/\partial\sigma)_M = (B_M - 1)/\theta_M$$

$$[33] \qquad \partial[\partial C/\partial\sigma]/\partial\theta = [(\partial B/\partial\theta) - (\partial C/\partial\sigma)]/\theta$$

It is illuminating to apply the exactness condition $\partial C/\partial\sigma = \partial B/\partial\theta$ to the expressions for these derivatives. The most obvious result of this equality is expressed in eq. [34].

$$[34] \qquad \sigma_L = \theta_M(C_L - 1)/(B_M - 1)$$

A more important consequence is that the third derivatives of ϕ in eqs. [31] and [33] are equal to zero. The significance of this is that $(C_L - 1)/\sigma_L$ is not a function of σ and $(B_M - 1)/\theta_M$ is not a function of θ. The third derivatives $\partial^2 B/\partial\theta^2$ and $\partial^2 C/\partial\sigma^2$ are also equal to zero.[9] Consequently the derivatives $\partial B/\partial\theta$ and $\partial C/\partial\sigma$ are invariant. Hence for systems that obey the linear eqs. [25] and [27], the exactness condition may be further qualified by the statement: $\partial B/\partial\theta = \partial C/\partial\sigma =$ constant. We conclude, therefore, that plots of slopes B *vs.* the appropriate θ values and of slopes C *vs.* the appropriate σ values should be linear and have slopes of equal magnitude.

We have stated previously that some ligand systems are distinguished by yielding values of unity for both B and C, irrespective of the metal ion and ligand. The second derivatives of ϕ are thus equal to zero by virtue of the fact that the derivative of a constant is zero. An examination of the expressions for the second derivatives in eqs. [30] and [32] reveals that $\partial B/\partial\theta$ and $\partial C/\partial\sigma$ can only assume a value of zero when $C_L = B_M = 1$, since σ_L and θ_M are finite quantities. Expressed differently, the exactness condition demands that the slopes B and C can only be independent of the metal ion and ligand when $B = C = 1$.

To conclude this section, let us evaluate ϕ by a Taylor's series (36) about the point (σ_0,θ_s) assuming that derivatives of higher order than two vanish. All derivatives are evaluated at the point (σ_0,θ_s).

$$[35] \qquad \phi = \phi_{0,s} + (\partial\phi/\partial\sigma)_{\theta_s}\sigma + (\partial\phi/\partial\theta)_{\sigma_0}\theta + (\partial^2\phi/\partial\sigma\partial\theta)\sigma\theta$$
$$= \sigma + \theta + (\partial^2\phi/\partial\sigma\partial\theta)\sigma\theta$$

Combination of eqs. [30] and [24] or [32] and [21] also generates the expression for ϕ in eq. [35].

In a subsequent section of this paper the various aspects of the exactness condition are shown to be consistent with the experimental evidence.

The Use of Stoichiometric Equilibrium Constants

The bulk of the equilibrium constants that have been compiled (1) are stoichiometric constants. It is of interest, therefore, to consider the validity of the equations just derived when applied to such constants, and to determine whether the slopes are affected.

One approach to this question is as follows. Equation [4] conveys a relationship between the equilibrium constant of a reaction, expressed as an activity quotient, and the difference in Gibbs' free energy content between reactants and products when each is in its standard state. The use of a concentration quotient for an equilibrium constant is tantamount to invoking a different definition of the standard state (7). For instance, one could adopt the convention that the reference state for metal ions, ligands and complexes was an aqueous solution containing 3 M sodium

[7] B and C are first derivatives of ϕ; $\partial B/\partial\theta$ and $\partial C/\partial\sigma$ are second derivatives; $\partial^2 B/\partial\sigma\partial\theta$ and $\partial^2 C/\partial\theta\partial\sigma$ are third derivatives.

[8] It should be stressed that the restriction of linearity is not essential to the success of the exactness test. The exactness condition will be equally satisfied in systems for which gradients B and C are themselves functions of both σ and θ, providing that $d\phi$ is exact. It is obvious that in such a case eq. [14] can only be integrated when these functions are known.

[9] Implicit in our integration of eq. [14] were several assumptions: that B and C are invariant for a specific metal ion and ligand respectively; and that σ is not a function of θ, or vice versa. Hence the derivative of $(C_L - 1)/\sigma_L$ with respect to θ and of $(B_M - 1)/\theta_M$ with respect to σ are both equal to zero.

Can. J. Chem. Downloaded from www.nrcresearchpress.com by 210.87.254.40 on 09/05/12
For personal use only.

perchlorate. We presently make use of the supposition that in this medium activity coefficients are constant; in fact, we might assign to all of these the value unity at all concentrations, and then activity coefficients in other media would require to be set to conform to this convention. Within such a group of 3 *M* perchlorate solutions all of the relationships developed above would apply to concentration quotients. Nothing in the derivation of these relationships is tied to any assumptions about a particular standard state. Hence one might expect that factors predisposing to linear relationships among thermodynamic constants would likewise lead to linear relationships within any corresponding set of concentration quotients, provided the latter were all based on a common ionic and solvent medium. We would not, however, expect that the numerical value of a slope such as *B* would be independent of the convention of defining reference states, although as the following considerations suggest, correspondence among the values of the slopes may be reasonably good.

A second approach to this matter is to examine how concentration quotients differ from conventional activity quotients; and this requires some consideration of activity coefficients. Briefly let us examine some of the factors that influence the magnitude of these (7, 38, 39). For ions in dilute solution (below 0.1 *M*), activity coefficients may often be predicted with reasonable accuracy on the basis of ionic strength and ionic charge. Such theoretical calculations are most successful for ions of charge ± 1. In more concentrated solutions activity coefficients show a dependence on the nature and concentration of each of the other kinds of species in the solution. Factors such as effective size and the degree of ion-pair formation also become extremely important. Measurement in mixed electrolytes indicates that the activity coefficient of a cation is determined primarily by the nature of the anion in the solution. Consequently, provided there is a high concentration of background electrolyte, the activity coefficient of a cation (anion) will be essentially the same as it would be in a solution of its salt with the anion (cation) of the bulk electrolyte. In summary, we would expect that in solutions of nearly identical composition, under conditions of constant temperature and ionic strength, the magnitude of an activity coefficient would be fixed.

The concentration quotient K_{ML} is converted to the thermodynamic constant ${}^{T}K_{ML}$ by multiplying it by the appropriate activity-coefficient ratio as in eq. [36]. In what follows, the activity coefficient y_x of the species x refers to the hypothetical 1 *M* state.

$$[36] \qquad {}^{T}K_{ML} = K_{ML}(y_{ML}/y_M y_L)$$

To express eq. [26] in terms of stoichiometric constants, we simply drop the superscript *T* and add the term $[BY_{M_s} - Y_M]$ to the right-hand side of this equation. *B* has the usual significance, and the terms in *Y* are defined as follows

$$Y_{M_s} = \log (y_{L_0}/y_L) + \log (y_{M_sL}/y_{M_sL_0})$$

$$Y_M = \log (y_{L_0}/y_L) + \log (y_{ML}/y_{ML_0})$$

Normally, L and L_0 are members of a structurally related group of ligands, and probably are of similar size and charge type. Under conditions of constant temperature, ionic strength, and solution composition for the determination of K_{ML} in a ligand family, $y_{L_0} \sim y_L$ and $y_{ML} \sim y_{ML_0}$ since M is a specific metal ion. We would expect Y_M to be approximately equal to zero. The same argument applies to Y_{M_s}. Consequently, the term $[BY_{M_s} - Y_M]$ should be relatively quite small along the series, and the slope *B* should not be affected. These comments also apply to eq. [25].

Equation [28] may be converted similarly; we drop the superscript *T* and add the term $[CY_{L_0} - Y_L]$ to the right-hand side.

$$Y_{L_0} = \log (y_{M_s}/y_{M_sL_0}) + \log (y_{ML_0}/y_M)$$

$$Y_L = \log (y_{M_s}/y_{M_sL}) + \log (y_{ML}/y_M)$$

As explained previously, eq. [28] compares the stabilities of the complexes of two related ligands (L and L_0) with a series of metal ions M. Thus y_{M_s}, $y_{M_sL_0}$, and y_{M_sL} are invariant along the series if conditions of constant temperature, ionic strength, and solution composition are met in the experimental determinations (L, L_0, and M_s are specific species). In addition, if the determinations are done in dilute solutions (low ionic strength), then the activity coefficients are fixed principally by the charge on a species and the ionic strength of the solution. Under these conditions two possibilities arise for which $[CY_{L_0} - Y_L]$ remains constant along a series: if L and L_0 are uncharged ligands, and if the metal ions M are of the same charge type. In the first case the *Y* terms should vanish, and in the second case they should

Can. J. Chem. Downloaded from www.nrcresearchpress.com by 210.87.254.40 on 09/05/12
For personal use only.

remain constant because the activity coefficients y_{ML_0}, y_{ML}, and y_M are now also invariant along the series. Normally, L and L_0 are related ligands, and $Y_{L_0} \sim Y_L$, so that $[C Y_{L_0} - Y_L] \sim Y_L(C - 1)$. This term should vanish when C has a value near or equal to unity, independently of the charge type of M. For the circumstances described, the slope C should not be affected by using concentration quotients. In the instance when the term $[C Y_{L_0} - Y_L]$ is variable along the series, it must be negligible relative to $\log K_{ML_0}$ in order for it not to affect the magnitude of the slope C, or in the extreme not to destroy the linear correlation. These arguments apply equally to eq. [27].

If the analysis of Irving and Rossotti (4) is correct, then the use of stoichiometric equilibrium constants determined in a mixed aqueous-organic solvent alters the definition of ${}^{T}K_{ML}$ in eq. [36] by making it the product of a stoichiometric constant and two activity-coefficient ratios. The new coefficients should behave similarly to y_x with respect to changes along the reaction series. The situations described are, therefore, not altered.

Regression Analysis of the Experimental Data

In this section equilibrium data for several metal–ligand systems are fitted by a weighted least-squares technique to the relationships derived earlier. The mathematical expressions required for the calculations are described in detail elsewhere (40, 41). Briefly, the best straight line through x and y coordinates is calculated by minimizing the weighted sum of the squares of the x and y residuals. The weighting is achieved by multiplying the square of each residual by its "weight". A measurement has its weight equal to 1/variance. If the weight of x is arbitrarily assigned a value of unity, then the weight of y is equal to λ, where λ = (weight of y)/(weight of x). The success of a linear correlation will be judged by the value of the correlation coefficient r and its associated confidence interval (40–42). The relationship between r and the Student's t-factor (42, 43) permits the evaluation of the associated confidence interval from tables of percentiles (44) of the t distribution for $(N - 2)$ degrees of freedom, with N equal to the number of (x,y) sets. The value of the correlation coefficient lies between -1 and $+1$. A value of -1 denotes perfect negative association, while a value of $+1$ denotes perfect positive association. Jaffé (17, 32) has suggested the following scheme as an arbitrary measure of the success of a correlation: $|r| > 0.99$ excellent, $|r| > 0.95$ satisfactory, and $|r| > 0.90$ fair fit. If a particular value of r has associated with it a 95% confidence interval, then the hypothesis that x and y are *independent* is rejected 5% of the time when it should not be. Alternatively, the hypothesis is rejected at the 5% level of significance.

A, The Exactness Condition

The data employed[10] in the regression analyses of the B and C slopes and the exactness test were selected with some care to include information obtained under the same experimental conditions, and preferably by one group of workers. The symbols used in the tabulation of the results of this statistical treatment are now defined: r is the correlation coefficient and *c.i.* the confidence interval associated with the evaluation of the various slopes, α and α' are intercepts for plots of $\log K_{ML}$ against $\log K_{M_sL}$ and of $\log K_{ML}$ against $\log K_{ML_0}$, respectively, μ is the ionic strength, and λ is the "weight" of the measurements plotted along the ordinate (y) relative to a value of unity for the measurements plotted along the abscissa (x). Unless stated to the contrary, λ is assigned a value of unity. The verification of the exactness condition is achieved by evaluating and comparing the reciprocals of $\partial B/\partial\theta$ and $\partial C/\partial\sigma$. This procedure was adopted for convenience.

TABLE 1

Values of B for the pyridine family[a, b]

Ion	B	r	*c.i.* (%)	α	$-\theta$[c]
H^+ (M_s)	1.000	1.000	100	0.000	0.00
Cu^{2+}	0.454	0.992	>99.9	0.085	2.84
Ag^+	0.285	0.991	>99.9	0.563	3.31
Ni^{2+}	0.268	0.979	>99.9	0.439	3.53

[a]The stability constants used were determined at 25.0 °C with $\mu = 0.61$ M (12). $x = pK$ and $y = \log K_{ML}$, except in the case of Ag^+ for ligands other than 3,5-lutidine and 4-pyridylcarbinol, where $y = \frac{1}{2}\log \beta_2$, $\beta_2 = [ML_2]/[M][L]^2$.

[b]The standard deviation for pK measurements is assumed to be ± 0.01 log units, which is equal to the average value reported for $\log K_{ML}$ (or $\log \beta_2$) measurements in the cases of Cu^{2+} and Ag^+. The average value for $\log K_{NIL}$ measurements is ± 0.02 log units, and consequently λ has a value of 0.250 in this instance.

[c]$\theta = \log K_{ML_0} - pK_0$: $M_s = H^+$ and L_0 = pyridine. For Ag^+ $\log K_{ML_0}$ is replaced by $\frac{1}{2}\log \beta_2$ in this definition.

[10]Photocopies of the actual data used are available in tabular form free of charge, upon request, from the Depository of Unpublished Data, National Science Library, National Research Council of Canada, Ottawa, Canada.

Can. J. Chem. Downloaded from www.nrcresearchpress.com by 210.87.254.40 on 09/05/12
For personal use only.

TABLE 2

Values of C for the pyridine family

Ligand	C^a	r	*c.i.* (%)	α'	σ^b
3,4-Lutidine	1.241	1.000	> 99.9	−0.114	1.20
3,5-Lutidine	1.187	1.000	> 99.9	−0.147	0.87
4-Picoline	1.174	1.000	> 99.9	−0.143	0.80
3-Picoline	1.109	1.000	> 99.9	−0.156	0.44
4-Pyridylcarbinol	1.053	1.000	> 99.9	−0.073	0.22
Pyridine (L_0)	1.000	1.000	100	0.000	0.00
3-Pyridylcarbinol	0.951	1.000	> 99.9	0.008	−0.25

[a] $x = \log K_{ML_0}$ and $y = \log K_{ML}$. In most instances the appropriate $\frac{1}{2} \log \beta_2$ values were used for Ag^+. See footnote *a*, Table 1.
[b] $\sigma = pK - pK_0$.

TABLE 3

Values of B for the salicylaldehyde family

Ion	B^a	r	*c.i.* (%)	α	$-\theta^b$
H^+ (M_s)	1.000	1.000	100	0.000	0.00
Cu^{2+}	0.643	0.987	>99.9	0.360	2.58
Y^{3+}	0.387	0.981	>99.9	1.192	3.80
La^{3+}	0.239	0.928	95.0–98.0	1.541	4.74
Ca^{2+}	0.065	0.461	60.0–80.0	0.492	7.04

[a] The experimental data were determined at 25.0 °C and $\mu = 0.10$ *M* (45). $y = \log K_{ML}$ and $x = pK$. Data for 3,5-dinitrosalicylaldehyde are not included in the least squares treatment because of the low r value associated with the evaluation of C (Table 4).
[b] $\theta = \log K_{ML_0} - pK_0$; $M_s = H^+$ and L_0 = salicylaldehyde.

TABLE 4

Values of C for the salicylaldehyde family

Ligand	C^a	r	*c.i.* (%)	α'	$-\sigma^b$
Salicyl-aldehyde (L_0)	1.000	1.000	100	0.000	0.00
5-Chloro-	0.894	0.999	>99.9	0.086	0.73
4-Chloro-	0.805	1.000	>99.9	0.624	0.96
3-Chloro-	0.734	1.000	>99.9	0.635	1.53
5-Nitro-	0.551	0.999	>99.9	0.808	2.82
3-Nitro-	0.530	0.988	90–95	0.841	2.93
3,5-Dinitro-	0.060	0.684	60–80	1.519	6.05

[a] $y = \log K_{ML}$ and $x = \log K_{ML_0}$. Data for Ca^{2+} are not included in the least squares treatment because of the low r value associated with the evaluation of B (Table 3).
[b] $\sigma = pK - pK_0$.

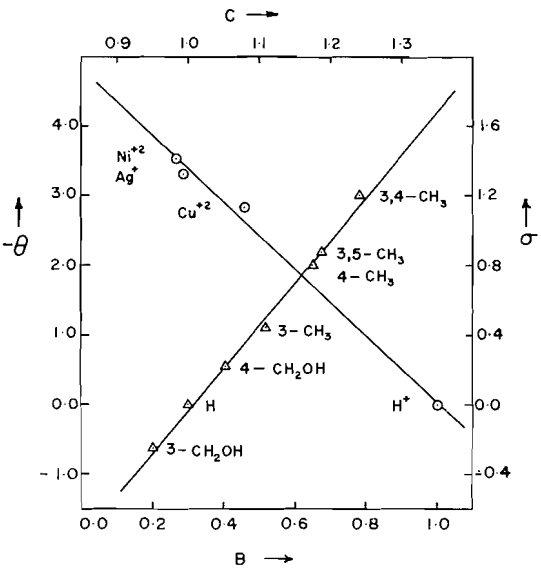

FIG. 2. Exactness test for the pyridine family: open circles, $-\theta$ vs. B, $(\partial\theta/\partial B) = 4.80$ with $r = 0.996$; open triangles, σ vs. C, $(\partial\sigma/\partial C) = 4.89$ with $r = 0.997$.

The Normal Substituent Effect

The appropriate statistical information for three metal–ligand systems that illustrate the mutual dependence of B on the metal ion and C on the ligand is compiled in Tables 1–8. Additional results are displayed in Figs. 2–4. Each system consists of a series of metal ions and a ligand family. The ligand families comprise a series of substituted pyridines (Tables 1, 2, Fig. 2), a series of derivatives of salicylaldehyde (Tables 3, 4, Fig. 3), and a set of aryl substituted (±)-α-di(carboxymethyl) amino-α-phenylacetic acids (Tables 5–8, Fig. 4).

We may infer from the high values of r and *c.i.* associated with the evaluations of B and C that eqs. [26] and [28] are adequate to describe the substituent and quasi-substituent effects in these systems. The goodness of fit for the nitrilotriacetic acids is forcibly demonstrated by comparing the observed intercepts on the vertical axes (α and α', Tables 5 and 6) with those calculated from eqs. [26] and [28] (α_{theo} and α'_{theo}). The near equality of the second derivatives of ϕ with corresponding values of r near unity demonstrates that the exactness condition [29] and its corollary of linearity are satisfied.

The information in Tables 7 and 8 has been collected to verify and illustrate various aspects

TABLE 5

Values of C for aryl derivatives of nitrilotriacetic acid[a]

Ligand[b]	C	r	$c.i.$ (%)	α'	$(\alpha'_{theo})^c$	σ^d
R = Cl—	0.967	1.000	> 99.9	0.07	0.07	−0.36
R = H— (L_0)	1.000	1.000	100	0.00	0.00	0.00
R = CH_3—	1.019	1.000	> 99.9	−0.05	−0.05	0.20
R = CH_3O—	1.031	1.000	> 99.9	−0.10	−0.09	0.32

[a]The experimental data were determined at 20 °C and μ = 0.1 M (10). y = log K_{ML} and x = log K_{ML_0}. The data for Mg^{2+} are omitted from the least squares treatment, explanation of which is given in the text.

[b] 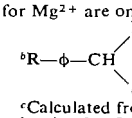

The substituent R is in the 4—position on the phenyl ring (ϕ). Three of the four functional groups have measurable acid dissociation constants.

[c]Calculated from the expression for the intercept in eq. [28], $(pK_T - C(pK_T)_0)$. $pK_T = pK_1 + pK_2 + pK_3$. The subscript 0 refers to the unsubstituted ligand.
[d]$\sigma = pK_T - (pK_T)_0$.

TABLE 6

Values of B for aryl derivatives of nitrilotriacetic acid

Ion	B^a	r	$c.i.$ (%)	α	$\alpha_{theo}{}^b$	$-\theta^c$
Ba^{2+}	0.166	0.992	99.0–99.8	2.10	2.11	8.82
Sr^{2+}	0.213	0.991	99.0–99.8	1.64	1.65	8.66
Ca^{2+}	0.285	0.994	99.0–99.8	2.42	2.44	6.93
Zn^{2+}	0.662	0.995	99.0–99.8	1.09	1.11	3.32
$H_T{}^+$ (M_s)	1.000	1.000	100	0.00	0.00	0.00
Mg^{2+}	0.467	0.989	98–99	−1.49	−1.48	8.46

[a]y = log K_{ML} and $x = pK_T = pK_1 + pK_2 + pK_3$. The average value for the standard deviation per measurement is ± 0.02 log units (10). Hence λ = 3.00 since the variance of pK_T is three times that of log K_{ML}. H_T indicates that more than one proton is involved in the standard reaction series.
[b]Calculated from (log $K_{ML_0} - B(pK_T)_0$), the expression for the intercept in eq. [26].
[c]θ = log $K_{ML_0} - (pK_T)_0$.

TABLE 7

Exactness tests for aryl derivatives of nitrilotriacetic acid

x	y	Slope[a,b]	r	$c.i.$ (%)	Metal ions considered
B	θ	9.69	1.000	99.0–99.8	Ca^{2+}, Zn^{2+}, and $H_T{}^+ = M_s$
C	σ	9.62	0.999	> 99.9	
B	θ	10.71	0.996	> 99.9	Ba^{2+}, Sr^{2+}, Ca^{2+}, Zn^{2+}, and $H_T{}^+ = M_s$
C	σ	10.66[c]	1.000	> 99.9	
B	θ	12.02	0.939	99.0–99.8	Mg^{2+}, Ba^{2+}, Sr^{2+}, Ca^{2+}, Zn^{2+}, and $H_T{}^+ = M_s$
C	σ	12.07	0.999	> 99.9	
B	θ	8.00[d]	0.915	95–98	Ba^{2+}, Sr^{2+}, Ca^{2+}, Zn^{2+}, and $H^+ = M_s$
C	σ	8.04[d]	1.000	> 99.9	

[a]The values of B employed were either evaluated from plots of log K_{ML} vs. pK_T ($M_s = H_T{}^+$) or from plots of log K_{ML} vs. pK_{NH} ($M_s = H^+$). pK_{NH} refers to the protonation of the nitrogen atom in the ligand molecule. Values of C were evaluated from plots of log K_{ML} vs. log K_{ML_0}, where M refers only to the metal ions indicated in the last column; they are all compiled elsewhere.[10] Unless stated otherwise B, θ, and σ are from Tables 5 and 6, and θ = log $K_{ML_0} - (pK_T)_0$ with $\sigma = pK_T - (pK_T)_0$.
[b]The choice λ = 1.000 is justified since the standard deviation of B or C is equal to (B/r) $[(1 - r^2)/n]^{\frac{1}{2}}$ (41), which is roughly equal in magnitude to the standard deviations of θ and σ. The number of points plotted is equal to n.
[c]Values of C are from Table 5.
[d]Values of B, C, σ, and θ are compiled elsewhere[10]; $\sigma = pK_{NH} - (pK_{NH})_0$ and θ = log $K_{ML_0} - (pK_{NH})_0$.

of the exactness condition. Figure 4 is also important in this respect. The experimental lines corresponding to the slopes B and the intercepts α reported in Table 6 are drawn in this figure. The line labelled L_0 is a perpendicular to the abscissa at $(pK_T)_0$. The experimental line for the metal ion M intersects this perpendicular at the point $[(pK_T)_0, \log K_{ML_0}]$. By definition $\theta = \log K_{ML_0} - (pK_T)_0$. The length of L_0 marked off by the lines for M and M_s ($H_T{}^+$) is equal to θ. Consequently θ can only be a good measure of B when all the experimental lines converge at a common point. By analogy, all plots of log K_{ML} against log K_{ML_0} must converge in order for σ to be a good measure of C.

The most obvious feature of Fig. 4 is the total

Can. J. Chem. Downloaded from www.nrcresearchpress.com by 210.87.254.40 on 09/05/12
For personal use only.

TABLE 8

Evaluation of ϕ and its second derivatives[a, b]

Ligand or ion	σ_L	ϕ_1	ϕ_2	ϕ_3	ϕ_4	$1/(\partial^2\phi/\partial\sigma\partial\theta)$ Calcd.[f]		Obsd.[i]
R = Cl—	−0.36[c]	−3.56	−3.57	−3.57	−3.59	10.91	10.62[g]	10.71[g]
R = CH_3O—	+0.32[c]	−3.11	−3.10	−3.10	−3.15	10.32		
Zn^{2+}	+0.30[d]					9.82	10.41[h]	10.66[h]
Sr^{2+}	−0.36[e]					11.00		

[a]For aryl derivatives of nitrilotriacetic acid. The B, C, θ, and σ values required for the calculations are taken from Tables 5 and 6.
[b]All ϕ values are evaluated for M = Zn^{2+}. ϕ_1 is calculated from eq. [21], ϕ_2 from eq. [24], and ϕ_3 from eq. [35] with $1/(\partial^2\phi/\partial\sigma\partial\theta)$ = 10.66; ϕ_4 is the observed value (eq. [11]).
[c]Observed value, from Table 5.
[d]Calculated value, from eq. [34] for ligand with R = CH_3O—.
[e]Calculated value, from eq. [34] for ligand with R = Cl—.
[f]Calculated from eq. [30] or eq. [32].
[g]$1/(\partial B/\partial\theta)$.
[h]$1/(\partial C/\partial\sigma)$.
[i]Observed values, from Table 7.

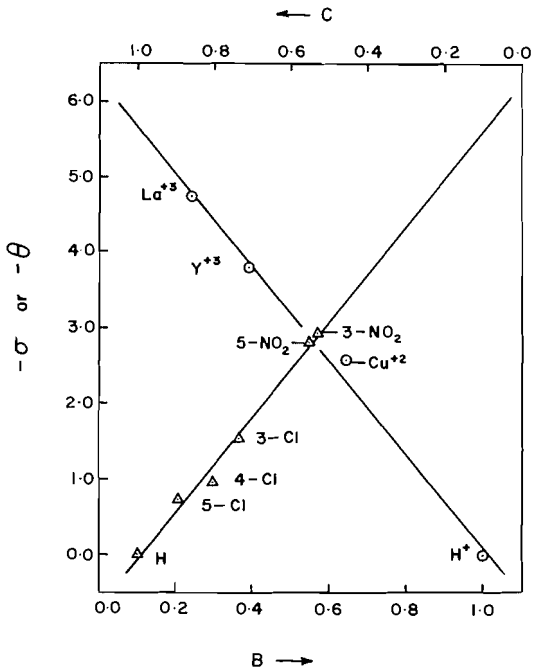

FIG. 3. Exactness test for the salicylaldehyde family: open circles, $-\theta$ vs. B, $(\partial\theta/\partial B) = 6.18$ with $r = 0.996$; open triangles, $-\sigma$ vs. C, $(\partial\sigma/\partial C) = 6.33$ with $r = 0.995$. Data for Ca^{2+} and 3,5-dinitrosalicylaldehyde are not included in the evaluation of the second derivatives of ϕ.

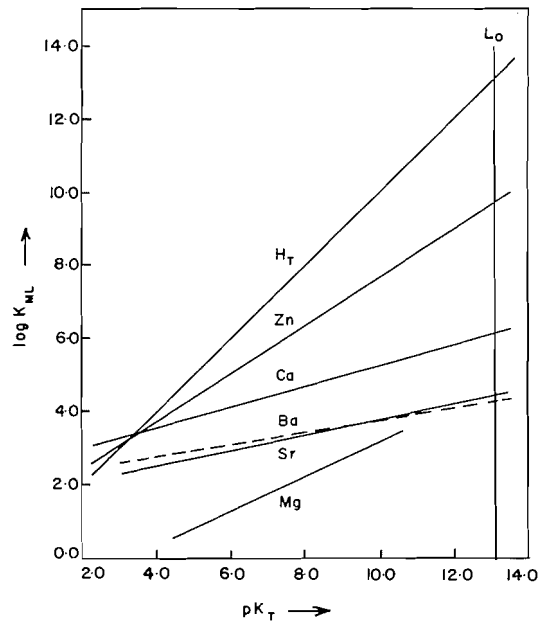

FIG. 4. Plots of log K_{ML} vs. pK_T for aryl derivatives of nitrilotriacetic acid.

lack of convergence of the Mg^{2+} line. The remaining lines converge roughly in the same region of the first quadrant. The results summarized in Table 7 illustrate that there is a relationship between the degree of convergence and the success of the exactness test. The near perfect convergence of the lines for H_T^+, Zn^{2+}, and Ca^{2+} is reflected in the excellent values of r and *c.i.* for the second derivatives of ϕ when the least squares treatment is limited to the data for these ions. Inclusion of the data for all metal ions in the regression analyses culminates in an exactness test of low significance. The value of r for $(\partial\theta/\partial B)$ has dropped from 1.000 for the previous set of ions to 0.939. In contrast, exclusion of the data for Mg^{2+} causes only a small drop in the statistical parameters ($r = 0.996$). This is in agreement with the approximate convergence in Fig. 4 for this set of ions. Hence, as the lack of convergence becomes more serious, the exactness

Can. J. Chem. Downloaded from www.nrcresearchpress.com by 210.87.254.40 on 09/05/12
For personal use only.

Can. J. Chem. Downloaded from www.nrcresearchpress.com by 210.87.254.40 on 09/05/12
For personal use only.

test becomes less meaningful since $(\partial\theta/\partial B)$ becomes less rigorously defined. We would expect a lack of convergence in comparisons of the other type to manifest itself in the significance of $(\partial\sigma/\partial C)$.

An interesting comment is now possible about the intercepts on the vertical axis of l.f.e.r. that obey eqs. [26] and [28]. If the exactness condition is fulfilled, then the location of the point of convergence will determine the magnitude of these intercepts. An inverse relationship between B and α (C and α') is expected if the point of intersection is located in the first or fourth quadrant, and a direct relationship when positioned in the second or third. The relationship is inverse for the comparisons reported in this section, although a direct correspondence has also been observed (24).

The various exactness tests summarized in Table 7 illustrate one other important principle. Users of eqs. [5] to [7] have been faced with the question of which pK value to select for correlations in a polyfunctional ligand series (e.g., refs. 4, 5, 7, 46). Two practices are in common use. Either the pK value for the protonation of the most basic center in the ligand molecule is selected (e.g., refs. 4, 10, 27, 47) or the sum corresponding to the total measurable basicity (e.g., ref. 5). Three of the four functional groups of the aryl derivatives of nitrilotriacetic acid (footnote *b*, Table 5) have measurable pK values. So far in our statistical analysis of this system we have chosen the total protonation reaction (pK_T) as the "ligand-dependent" standard reaction series. When the protonation of the most basic center (pK_{NH}) is selected, excellent correlation coefficients for the evaluation of slopes B and C are again observed.[10] In contrast, the value of r associated with $(\partial\theta/\partial B)$ has dropped from 0.996 to 0.915 and the significance of the exactness test is correspondingly lowered. The choice of the protonation of the nitrogen center as the "ligand-dependent" reaction series is thus inferior. In this way we are able to employ the exactness test as a criterion for selecting the proper standard reaction series.

The results of a numerical verification of several of the equations derived in an earlier section are reported in Table 8. The calculated values of σ and the second derivatives of ϕ compare well with the observed values. This agreement implies the exactness of $d\phi$ since eq. [34], which embodies the equivalence of eqs. [30] and [32], is a direct consequence of the exactness condition. We may conclude from the equivalence of ϕ_1 (eq. [21]), ϕ_2 (eq. [24]), and ϕ_4 (eq. [11]) that for this family of nitrilotriacetic acid derivatives the integration of $d\phi$ (eq. [14], Fig. 1) is indeed independent of the path. The Taylor's series evaluation of ϕ (eq. [35]) is also shown to be valid (ϕ_3).

Several other systems not discussed in this paper also conform to the regression analyses of the B and C slopes and the exactness test (24). These families are derived from 8-hydroxyquinoline, 8-hydroxyquinoline-5-sulfonic acid, iminodiacetic acid, 1-(*o*-hydroxyphenylazo)-2-naphthol, and dibenzoylmethane (furoyl- and thenoyl-substitutions). These systems offer no new evidence, although in some cases the correlations were somewhat poorer than those reported.

The mutual dependence of B on the particular metal ions compared and of C on the particular ligands compared is accepted as characteristic of a "normal" substituent effect.

The Structural Substituent Effect

The striking feature of the results reported in Tables 9 to 11 is that the free energy ($= \alpha'$ log units) of the displacement reaction $ML_0 + L = ML + L_0$ is independent of the metal ion ($C = 1$), and the free energy ($= \alpha$ log units) of the displacement reaction $M_sL + M = ML + M_s$ is independent of the ligand ($B = 1$). (The deviations of the B values from unity in these tables are small compared to values of $(1 - B)$ for the B values reported for the same ions in the previous

TABLE 9

Values of B and C for β-diketones[a]

Ligand or ion	C or B	r	*c.i.* (%)	α' or α
Acetylacetone (L_0)	1.000[b]	1.000	100	0.000[c]
Benzoylacetone	1.000[b]	1.000	>99.9	0.203[c]
Dibenzoylmethane	1.017[b]	1.000	>99.9	0.945[c]
H^+	0.942	0.999	95–98	1.523
Be^{2+}	1.113	1.000	99.0–99.8	−0.822
Cd^{2+}	0.923	1.000	98	−3.310
Ce^{3+}	0.990	1.000	98–99	−1.861
Co^{2+}	1.000	1.000	100	−2.630
Mg^{2+}	0.925	1.000	99.0–99.8	−3.459
Ni^{2+}	0.978	0.999	95–98	−2.228
Pb^{2+}	1.006	0.999	95–98	−3.304
Cu^{2+} (M_s)	1.000	1.000	100	0.000

[a]The stability constants employed were determined at 30 °C in 74.5 *v*% dioxane (1, 48, 49). $y = \log K_{ML}$ and $x = \log K_{CuL}$ except for evaluations of C.
[b]Values of C: $y = \log K_{ML}$ and $x = \log K_{ML_0}$.
[c]Values of α'.

TABLE 10

Values of B and C for alkanol-substituted ethylenediamines[a, b]

Ligand or ion	C or B	r	$c.i.$ (%)	α' or α
$R_1 = R_2 = R_3 = R_4 =$ EtOH	1.000[c]	1.000	100	0.000[d]
$R_1 =$ EtOH, $R_2 = R_3 = R_4 = i$PrOH	0.978[c]	1.000	> 99.9	1.052[d]
$R_1 = R_2 = R_3 = R_4 = i$PrOH	0.976[c]	1.000	> 99.9	1.459[d]
Cu^{2+}	0.910	1.000	99.0–99.8	4.206
Ni^{2+}	1.028	1.000	98–99	1.404
Co^{2+}	0.961	1.000	98–99	0.489
Zn^{2+} (M_s)	1.000	1.000	100	0.000

[a]The stability constants employed were determined at 25.0 °C with $\mu = 0.5$ (50). The data for Cd^{2+} do not conform to the treatment $y = \log K_{ML}$ and $x = \log K_{ZnL}$ except for evaluations of C.

[b] 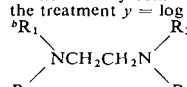

EtOH = $-C_2H_4OH$, iPrOH = $-CH_2CH(OH)CH_3$.

[c]Values of C. $y = \log K_{ML}$ and $x = \log K_{ML_0}$. L_0: $R_1 = R_2 = R_3 = R_4 =$ EtOH.

[d]Values of α'.

TABLE 11

Values of B and C for ligands related to gl ycine[a]

Ligand or ion	C or B	r	$c.i.$ (%)	α' or α
Glycine (L_0)	1.000[b, c]	1.000	100	0.000[e]
Pyridine-2-carboxylic acid	0.994[b, c]	0.986	>99.9	0.220[e]
8-Hydroxy-quinoline	1.023[b, d]	0.994	>99.9	3.401[e]
Cu^{2+}	1.082	0.999	95–98	4.834
Ni^{2+}	0.932	0.995	90–95	3.289
Zn^{2+}	0.964	0.995	90–95	2.042
Co^{2+}	1.026	0.998	95–98	1.937
Pb^{2+}	1.109	0.986	80–90	1.472
Fe^{2+}	1.020	0.997	90–95	1.087
Mn^{2+} (M_s)	1.000	1.000	100	0.000
Cd^{2+}	(0.882)	0.998	95–98	1.498

[a]The stability constants for glycine and 8-hydroxyquinoline complexes were determined at 20 or 25 °C and refer to a medium with $\mu = 0$ or 0.01; the data for pyridine-2-carboxylic acid complexes refer to 20 °C and $\mu = 0.1$ (1). The data for complexes of Ba^{2+} and Sr^{2+} with glycine are unexpectedly low (< one log unit) and are omitted from the least squares treatment. The data for the protonation of the ligands are also omitted (see footnote *d*). The data for Ba^{2+}, Sr^{2+}, Ca^{2+}, and Mg^{2+} (and perhaps Cd^{2+}) suggest that for these ions 8-hydroxyquinoline does not belong to the same family as the other two ligands. This observation finds support in our treatment of correlations of the second kind (footnote 3).

[b]C values.

[c]Regression also includes data for Ca^{2+}, Mg^{2+}, Cd^{2+}, and Ag^{+}.

[d]The data for the protonation reactions ($pK_1 + pK_2$) also fit this correlation (see text).

[e]Values of α'.

section.) The condition of exactness is satisfied in these systems since $(\partial B/\partial\theta) = (\partial C/\partial\sigma) = 0$. To distinguish this type of behavior from the "normal" substituent effect, we designate it as the "structural" substituent effect.

The term "structural" was adopted to emphasize that the dominant differences between the ligands in a series are geometric in nature. The series of β-diketones are generated by substitution of the methyl groups of acetylacetone by phenyl groups. The degree of unsaturation, therefore, increases along the series. In the alkanol-substituted ethylenediamines, primary alcohols are replaced by more bulky secondary alcohol groups. The series derived from glycine is created by incorporating the skeleton structure O—C—C—N into increasingly unsaturated molecules. It is noteworthy that in this system the point corresponding to the total basicity ($pK_{NH} + pK_{OH}$) nearly fits the regression line for 8-hydroxyquinoline ($(pK_T)_{calc} = 15.76$; $(pK_T)_{obs} = 15.02$) but does not for pyridine-2-carboxylic acid ($(pK_T)_{calc} = 12.23$; $(pK_T)_{obs} = 7.04$).[11]

The incorporation of the skeleton structure N—C—C—N into unsaturated molecular systems creates another ligand series for which the data suggest $B = C = 1$ (24).[12] In Fig. 5 the data for three members of this series are plotted.[13] Complexes of Cu^{2+}, Ag^{+} and H^{+} with 1,10-phenanthroline appear to be considerably destabilized relative to their ethylenediamine complexes. These deviations do not occur for the second plot in Fig. 5. Such destabilizations appear to be characteristic of the aromatic members of this ligand series and are of the same magnitude for 1,10-phenanthroline and 2,2′-bipyridyl.

Unit slopes have also been reported (4, 53) for plots of log K_{ML} against log K_{ML_0} for ligands re-

[11]The observed value is $(pK_T)_{obs}$ and that calculated from the "best" straight line (Table 11) is $(pK_T)_{calc}$.

[12]The series consists of 1,10-phenanthroline, 2,2′-bipyridyl, ethylenediamine, 2-picolylamine, and 2-pipecolylamine.

[13]The data for ethylenediamine are for $\mu = 1$ M (KCl) and 25 °C (1, 51). Data for 1,10-phenanthroline and 2,2′-bipyridyl are for 20 °C and $\mu = 0.1$ M, and are from ref. 1, except log K_{FeL} values which are from ref. 52. Irving and Rossotti (4) report a value of $C = 0.63$ for the plot of log K_{ML} (bipy) vs. log K_{ML_0} (phen).

Can. J. Chem. Downloaded from www.nrcresearchpress.com by 210.87.254.40 on 09/05/12
For personal use only.

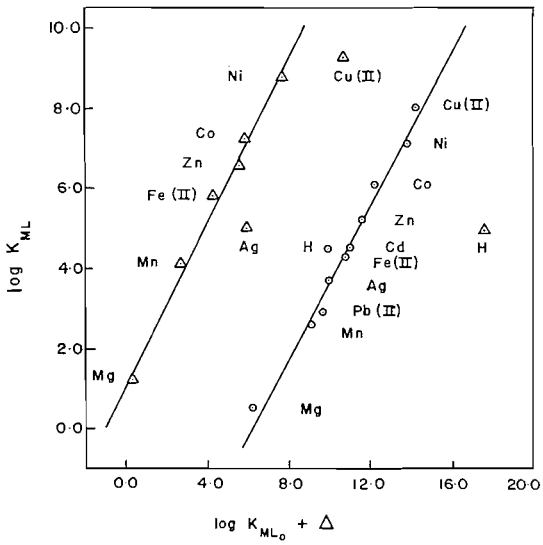

FIG. 5. Comparison of data for 1,10-phenanthroline, 2,2′-bipyridyl and ethylenediamine complexes: open triangles, log K_{ML} (phen) vs. log K_{ML_0} (en) with $C = 1.024$, $\alpha' = 1.075$, $r = 0.995$, and $\Delta = 0$; open circles, log K_{ML} (bipy) vs. log K_{ML_0} (phen) with $C = 0.953$, $\alpha' = -1.101$, $r = 0.993$, and $\Delta = 5.00$.

lated to ethylenediamine-N,N,N′,N′-tetra-acetic acid (EDTA). Complexes of the more rigid ligand *trans*-cyclohexane-1,2-diamine-N,N,N′,N′-tetra-acetic acid (4) and of propylenediamine-N,N,N′,N′-tetra-acetic acid (53) are each stabilized relative to EDTA complexes by a constant amount. Many metal ions are involved in these comparisons. Indeed, as an examination of the data revealed, $B = 1$ for many of the metal ions (e.g., the lanthanides).

Finally, the series of ligands XCO – CHR′ – NHR investigated by Leberman and Rabin (16) illustrates in a striking manner the difference between the two substituent effects. Changes in R (= CH_3, H) or R′ (= H, $(CH_3)_2CHCH_2$-) constitute a "structural" substituent effect, while changes in X (= OH, NH_2, $NHCH_2CO_2H$, etc.) constitute a "normal" substituent effect.[14] Changes in free energy of complex formation accompanying changes in R or R′ are independent of the nature of X.

B, General Remarks

In subsection *A* our examination of the experimental data was limited to systems for which l.f.e.r. were quite adequate. It is not our purpose in this paper to examine non-linear systems, nor to treat the vast subject of deviations from the observed relationships. We have, however, given in Part II of this series a detailed theoretical treatment of the requirements for successful free-energy relationships, and we feel that this provides a proper framework for consideration of non-regular systems.

Conclusions

The systems examined testify to the validity of eqs. [21] and [24]. These equations were derived from the assumption that the parameters σ and θ approximated the variables on which the free-energy changes accompanying reaction [11], M + L = ML, depended. As a result of the assumed exactness of the differential dϕ, the condition of exactness could be formulated. The exactness condition revealed the inherent relationship between the slopes *B* and *C*. When the condition of exactness is satisfied, then dϕ may be concluded to be exact for a particular reaction series. It further confirms that the "ligand-dependent" and "metal-dependent" reaction series were properly selected. The success of a particular choice may be judged from the equality or inequality and/or from the magnitude of the statistical parameters *r* and *c.i.*

In Part II of this series (15), it is shown that linear relationships are most probable when substituent changes are small. It is perhaps paradoxical that the "structural" substituent effect is often accompanied by drastic changes in the structure of the ligand. A possible clue as to what factors are operative in this case may come from the medium effect (14). The lack of dependence of the quasi-substituent effect on the ligand and of the substituent effect on the metal ion is reminiscent of the medium effect in the first approximation. The diagnostic feature of the latter is that the substituent effect is independent of the solvent: an l.f.e.r. of unit slope is obtained when log *K* for a series of compounds in one solvent is plotted against log *K* for the same series in a second solvent (14).[15] Attempts to explain the trend of increasing stability with increasing

[14]Some of the free-energy relationships in this system appear to be slightly curved.

[15]In principle it is possible to treat the relationship between the medium effect and either the substituent or quasi-substituent effect in a fashion analogous to that developed in this Paper for the relationship between the substituent and quasi-substituent effects. A study of this approach is in progress.

Can. J. Chem. Downloaded from www.nrcresearchpress.com by 210.87.254.40 on 09/05/12
For personal use only.

Can. J. Chem. Downloaded from www.nrcresearchpress.com by 210.87.254.40 on 09/05/12
For personal use only.

degree of unsaturation of the ligand in terms of π bonding are inadequate, since the "structural" substituent effect is the same for ions that can or cannot participate in such bonding.

Finally, let us compare the derived equations with those reported by other investigators. To facilitate this comparison we shall assume that it is possible to designate an appropriate standard state for which the activity coefficients of the reactants and products may be set equal to unity. Under such conditions eq. [26] with $M_s = H^+$ is equivalent to eq. [7]. The relationship between the Irving–Rossotti equations, [5] and [8], and [26] and [28] is self-evident. These authors (4) have also derived an equation equivalent to eq. [5] for comparing plots of log K_{ML} against log K_{M_sL}, where M and M_s are similar metal ions. M_s simply replaces H^+ in eq. [5]. We have shown that unit slopes describe a limiting condition. Strictly speaking, eqs. [5] and [8] are valid only for comparisons of the "structural" type, and in this case are equal to eqs. [26] and [28], respectively, with $M_s = H^+$. This becomes evident when eq. [5] is expressed in the alternative form $\log K_{ML} = pK + \log \kappa$. The term $A + P$ in eq. [5] must, therefore, be equal to $\log \kappa$ in eq. [4], and consequently unit slope in the plot of log K_{ML} vs. pK may be interpreted as evidence that $\log \kappa$ is independent of pK or of the ligand: $\log \kappa = A + P = A_0 + P_0 = \log \kappa_0 = \log K_{ML_0} - pK_0$. (The subscript 0 refers to the reference ligand.) In our discussion of eq. [5] we have pointed out that $P = P_0$, and it follows that the term $(A - A_0)$ in eq. [8] is equal to zero. When B and C have values other than unity, the partial molar free energy term A is a function of pK (eq. [5]), log K_{M_sL} (eq. [5]) or log K_{ML_0} (eq. [8]). This dependency was realized (4, 5) and finds expression in eq. [6]. However, it has not been sufficiently stressed (e.g., ref. 27) for eqs. [8] and [5] in the form with $H^+ = M_s$.

The distinction between "normal" and "structural" substituent effect permits us to see the Irving–Rossotti relationship in the proper perspective. Non-unit slopes are quite a natural occurrence, and it is incorrect to interpret them from the viewpoint of deviations from some expected behavior such as unit slope. Issues in the past have undoubtedly been aggravated by the almost universal choice of the hydrogen ion as the standard "metal" ion. Equation [26] places no restriction on the choice of the reference ion, nor eq. [28] on the choice of the reference ligand. In fact, in the systems discussed, any of the other ions could equally well have been selected as M_s or any other ligand as L_0. The magnitude of slope C is independent of the choice of M_s, but not of L_0; similarly the value of B is dependent on M_s but independent of L_0. Of course, the values of ϕ, σ, and θ depend by definition on the choice of M_s and L_0. The most suitable selection of M_s and L_0 may be judged from the equivalence of the second derivatives of and/or from the values of the statistical parameters.

This work was supported by a grant from the National Research Council of Canada for which grateful acknowledgment is made. One of the authors (E.N.) records his thanks for the award of a National Research Council of Canada Postgraduate Fellowship. We also thank Miss J. L. Rohr of this laboratory and members of the University of Waterloo Computer Centre for assistance with the statistical analyses.

1. L. G. SILLÉN and A. E. MARTELL. Stability constants of metal-ion complexes. Chem. Soc. Spec. Publ. No. 17, London. 1964.
2. J. BJERRUM. Chem. Rev. **46**, 381 (1950).
3. A. E. MARTELL and M. CALVIN. Chemistry of the metal chelate compounds. Prentice-Hall, New York. 1952. pp. 151–180.
4. H. IRVING and H. ROSSOTTI. Acta Chem. Scand. **10**, 72 (1956).
5. J. G. JONES, J. B. POOLE, J. C. TOMKINSON, and R. J. P. WILLIAMS. J. Chem. Soc. 2001 (1958).
6. S. CHABEREK and A. E. MARTELL. Organic sequestering agents. J. Wiley and Sons, Inc., New York. 1959. pp. 130–133.
7. F. J. C. ROSSOTTI. *In* Modern co-ordination chemistry. *Edited by* J. Lewis and R. G. Wilkins. Interscience Publishers, New York. 1960. pp. 1–77.
8. Y. T. CHEN. Zeit. Phys. Chem. **220**, 231 (1962).
9. M. M. JONES. Elementary co-ordination chemistry. Prentice-Hall, Englewood Cliffs, N.J. 1964. pp. 338–341.
10. H. M. N. H. IRVING and M. G. MILES. J. Chem. Soc. (A) 727 (1966).
11. Z. L. ERNST and F. G. HERRING. Trans. Faraday Soc. **61**, 454 (1965).
12. M. S. SUN and D. G. BREWER. Can. J. Chem. **45**, 2729 (1967).
13. E. NIEBOER and W. A. E. MCBRYDE. Inorg. Nucl. Chem. Letters, **3**, 569 (1967).
14. J. E. LEFFLER and E. GRUNWALD. Rates and equilibria of organic reactions. John Wiley and Sons, Inc., New York. 1963.
15. E. NIEBOER and W. A. E. MCBRYDE. Can. J. Chem. This issue.
16. R. LEBERMAN and B. R. RABIN. Trans. Faraday Soc. **57**, 785 (1961).
17. P. R. WELLS. Chem. Rev. **63**, 171 (1963).
18. P. R. WELLS. Linear free energy relationships. Academic Press, Inc., London. 1968.
19. W. R. MAY and M. M. JONES. J. Inorg. Nucl. Chem. **24**, 511 (1962).
20. J. J. R. F. DA SILVA and J. G. CALADO. J. Inorg. Nucl. Chem. **28**, 125 (1966).

21. L. D. PETTIT, A. ROYSTON, and R. J. WHEWELL. J. Chem. Soc. A 2009 (1968).
22. L. D. PETTIT, C. SHERRINGTON, and R. J. WHEWELL. J. Chem. Soc. A 2204 (1968).
23. H. IRVING and J. J. R. F. DA SILVA. Proc. Chem. Soc. 250 (1962).
24. E. NIEBOER. Ph.D. Thesis, University of Waterloo, Waterloo, Ontario. 1968.
25. G. SCHWARZENBACH, H. ACKERMANN, and P. RUCKSTUHL. Helv. Chim. Acta, **32**, 1175 (1949).
26. H. IRVING and J. J. R. F. DA SILVA. J. Chem. Soc. 3308 (1963).
27. H. M. N. H. IRVING and M. G. MILES. J. Chem. Soc. (A) 1268 (1966).
28. L. G. VAN UITERT and W. C. FERNELIUS. J. Amer. Chem. Soc. **76**, 379 (1954).
29. H. MARGENAU and G. M. MURPHY. The mathematics of physics and chemistry. 2nd ed. D. Van Nostrand Company, New York. 1956. pp. 1–11.
30. I. M. KLOTZ. Chemical thermodynamics. Revised ed. W. A. Benjamin Inc., New York. 1964. Chap. 2.
31. G. N. LEWIS and M. RANDALL. Thermodynamics. 2nd ed. McGraw-Hill Book Co., Inc., New York. 1961. Chap. 3.
32. H. H. JAFFÉ. Chem. Rev. **53**, 191 (1953).
33. A. FISCHER, W. J. GALLOWAY, and J. VAUGHAN. J. Chem. Soc. 3591 (1964).
34. G. B. BARLIN and D. D. PERRIN. Quart. Rev. **20**, 75 (1966).
35. L. D. PETTIT and C. SHERRINGTON. J. Chem. Soc. A 3078 (1968).
36. G. B. THOMAS, JR. Calculus and analytical geometry. 3rd ed. Addison–Wesley Publishing Co., Inc., Reading, Massachusetts. 1961.
37. M. M. NICOLSON. Fundamentals and techniques of mathematics for scientists. *Edited by* D. R. Hartree and D. G. Padfield. Longmans, Green and Co., Ltd., London. 1961.
38. J. N. BUTLER. Ionic equilibrium – a mathematical approach. Addison–Wesley Publ. Co., Inc., Reading, Massachusetts, 1964. Chap. 12.
39. L. E. STEINER. Introduction to chemical thermodynamics. 2nd ed. McGraw-Hill Book Co., Inc., New York. 1948. Chap. 21.
40. J. MANDEL. The statistical analysis of experimental data. Interscience Publ., New York. 1964. pp. 52–57, 114–121, and 288–292.
41. D. YORK. Can. J. Phys. **44**, 1079 (1966).
42. W. J. DIXON and F. J. MASSEY, JR. Introduction to statistical analysis. 2nd ed. McGraw-Hill Book Co., Inc., New York. 1957. pp. 112–138, 189–208, and 468.
43. G. W. SNEDECOR. Statistical methods. 4th ed. The Iowa State College Press, Ames, Iowa. 1946. Chap. 7.
44. A. HOLD. Statistical tables and formulas (supplement). John Wiley and Sons, Inc., New York. 1952.
45. C. POSTMUS, JR., L. B. MAGNUSSON, and C. A. CRAIG. Inorg. Chem. **5**, 1154 (1966).
46. H. FREISER, Q. FERNANDO, and G. E. CHENEY. J. Phys. Chem. **63**, 250 (1959).
47. H. IRVING and (MRS) H. S. ROSSOTTI. J. Chem. Soc. 2910 (1954).
48. L. G. VAN UITERT, W. C. FERNELIUS, and B. E. DOUGLAS. J. Amer. Chem. Soc. **75**, 455, 457, 2736, 2739 (1953).
49. L. G. VAN UITERT and W. C. FERNELIUS. J. Amer. Chem. Soc. **75**, 3862 (1953).
50. J. L. HALL, W. E. DEAN, and E. A. PACOFSKY. J. Amer. Chem. Soc. **82**, 3303 (1960).
51. C. S. G. PHILLIPS and R. J. P. WILLIAMS. Inorganic chemistry. Vol. 2. Oxford University Press, New York and Oxford. 1966. p. 247.
52. H. IRVING and D. H. MELLOR. J. Chem. Soc. 5222 (1962).
53. H. IRVING and J. P. CONESA. J. Inorg. Nucl. Chem. **26**, 1945 (1964).

Can. J. Chem. Downloaded from www.nrcresearchpress.com by 210.87.254.40 on 09/05/12
For personal use only.

Can. J. Chem. Downloaded from www.nrcresearchpress.com by 210.87.254.6 on 09/05/12
For personal use only.

Free-energy relationships in coordination chemistry. II. Requirements for linear relationships

E. NIEBOER[1] AND W. A. E. MCBRYDE
Department of Chemistry, University of Waterloo, Waterloo, Ontario

Received November 25, 1969

This paper discusses factors predisposing to linear free energy relationships among families of metal complexes. It is postulated that changes occurring at a reaction site in a test series of reactions and the corresponding changes in a reference series have their origins in the same independent variables. Linearity is seen to be favored when changes in the reaction site or in ligand substituents are small, and in the absence of strong interactions with the solvent. In addition to such considerations of a molecular sort, a number of relationships among the thermodynamic quantities ΔH^0, ΔS^0, and ΔG^0 which have been identified as having a significant influence on rate and equilibrium relationships in series of organic reactions are discussed in terms of their effect on metal–ligand systems.

Canadian Journal of Chemistry, 48, 2565 (1970)

Introduction

In Part I of this series (1) the authors offered a rational scheme for the derivation of equations that represent linear relationships among formation constants of metal–ion complexes or acids (proton complexes) formed within a set of metal ions and related ligands. The following are reproduced for discussion in this part.[2]

$$[1]\quad \text{(former [25])}\ \phi' = \log {}^{T}K_{ML} - \log {}^{T}K_{ML_0} = \phi - \theta = B\sigma$$

$$[2]\quad \text{(former [26])}\ \log {}^{T}K_{ML} = B \log {}^{T}K_{M_sL} + [\log {}^{T}K_{ML_0} - B \log {}^{T}K_{M_sL_0}]$$

$$[3]\quad \text{(former [27])}\ \phi'' = \log {}^{T}K_{ML} - \log {}^{T}K_{M_sL} = \phi - \sigma = C\theta$$

$$[4]\quad \text{(former [28])}\ \log {}^{T}K_{ML} = C \log {}^{T}K_{ML_0} + [\log {}^{T}K_{M_sL} - C \log {}^{T}K_{M_sL_0}]$$

Underlying these derivations was the notion that the change in free energy to which ϕ is proportional must depend on properties or variables ascribable to both the change in metal ion from M_s to M and the change in ligand from L_0 to L. Accordingly two standard reaction series were postulated: one (σ) dependent only on changes in the ligand, the other (θ) dependent only on changes in the metal ion. The dependence of ϕ on σ and θ was represented by an exact differential in which B and C appeared as partial differential quotients or gradients. From the behavior observed in a number of chemical systems a further inference was drawn, that B and C themselves were functionally dependent on θ and σ respectively. The restricted quantities ϕ' and ϕ'' were introduced as defined in eqs. [1] and [3] to apply respectively to the reactions of a single test metal ion with a series of related ligands (ϕ'), and to the reactions of a single test ligand with a series of metal ions (ϕ'').

Equations [2] and [4], derived simply from eqs. [1] and [3] respectively, denote the existence of linear free energy relationships (l.f.e.r.) among the reactions of a particular set of ligands or metal ions, provided the gradients B and C are invariant within the range of log K values encompassed. The evidence in Part I showed that numerous groups of metal ions and ligands exhibit such l.f.e.r. It is our purpose in this paper to examine critically what considerations must apply to permit the quantities B and C to remain constant within a set of reactants. These are discussed from two complementary points of view. We shall first consider how the quantities ϕ' and σ may be affected by changes in one or more molecular variables arising within a series of reactants; examples of such variables are

---

[1]NRCC Postdoctorate Fellow; present address: Inorganic Chemistry Laboratory, Oxford University, Oxford, England.

[2]For the derivation of these, see Part I. The symbols ϕ, σ, and θ were introduced to represent differences in logarithms of equilibrium constants.

$$\phi = \log {}^{T}K_{ML} - \log {}^{T}K_{M_sL_0}$$
$$\sigma = \log {}^{T}K_{M_sL} - \log {}^{T}K_{M_sL_0}$$
$$\theta = \log {}^{T}K_{ML_0} - \log {}^{T}K_{M_sL_0}$$

The subscripts s and 0 represent a standard or reference metal and ligand, respectively. The quantities B and C, are respectively, $(\partial \log {}^{T}K_{ML}/\partial \log {}^{T}K_{M_sL})_\theta$ and $(\partial \log {}^{T}K_{ML}/\partial \log {}^{T}K_{ML_0})_\sigma$.

Can. J. Chem. Downloaded from www.nrcresearchpress.com by 210.87.254.6 on 09/05/12
For personal use only.

given in the next section. Then we shall show how the variables ϕ', ϕ'', σ, and θ, and the relationships between pairs of them are dependent on certain relationships among changes in the thermodynamic quantities, free energy, enthalpy, and entropy, associated with the reaction series.

In Part I, eqs. [1] and [3] were derived without any reference to the microscopic mechanisms by which the substituent or quasi-substituent effect was transmitted to the reaction site. Yet it was recognized that σ and θ were themselves dependent on other unidentified variables of the sort mentioned below. The existence and demonstrated validity of l.f.e.r. among systems of metal complexes permit and support an analysis of the dependence of the functions ϕ', ϕ'', σ, and θ on such microscopic variables without the necessity of the latter being specifically identified. The same rational structure may be modified to incorporate the functional dependence of the free energy on the enthalpy, entropy, and temperature.

General Restrictions

We select eq. [1] for the following analysis, but point out that eq. [3] has the same form as eq. [1], differing only in the choice of variables, so that the substance of the argument would remain unaltered if eq. [3] were examined in the same way. It was previously asserted that σ adequately accounted for the ligand-dependent contribution to ϕ. Now we shall treat σ (and hence ϕ') as functionally dependent on certain properties of the ligand, which we might represent symbolically by x, v,$\cdots$, etc., that change systematically along a series of ligands. These properties cannot be specifically identified, but they are apt to include variables such as substituent polarizability, group electronegativity, charge, or bond dipole moment. This last property would be important for a substituent if the mechanism of interaction between it and the reaction site were of the charge–dipole type. Which of these properties are important in a specific reaction series will be determined by the mechanism(s) operating to transmit the effect of the substituent to the reaction center. Examples of these are dipole–dipole interactions, charge–dipole interactions, resonance, polarization, and steric interactions. Moreover, the independent variables and the interaction mechanisms named are not necessarily mutually exclusive.

In order for the gradient B of eq. [1] to be invariant, certain limitations must be placed on the independent variables x, v, $\cdots$.

ϕ' and σ as a Function of One Independent Variable

Given that B is a function of θ only we may simply write eq. [1] in differential form

$$[5] \qquad d\phi' = B\,d\sigma$$

Or we could refer back to Part I and note that by comparing eq. [18] or Fig. 1 there with eq. [1] of this paper, eq. [5] follows directly. If it is assumed that σ is a function of the independent variable x only, then $d\sigma = (\partial\sigma/\partial x)_v dx$. Equation [5] may be rewritten as in [6].

$$[6] \qquad d\phi' = B(\partial\sigma/\partial x)_v dx = (\partial\phi'/\partial x)_v dx$$

Consequently, both ϕ' and σ must be functions of x only if a free-energy relationship is to exist. But when do we expect such a relationship to be linear? The gradient B may be written as $B = (\partial\phi'/\partial x)_v/(\partial\sigma/\partial x)_v = g_x/f_x$. For B to be invariant, it is required that either g_x and f_x both remain constant throughout the range of variation of x, or both change proportionately. A complementary, but more informative, answer is obtained by the application of the "extra-thermodynamic" approach of Leffler and Grunwald (2) to the problem. A brief outline of this approach is now presented.

A molecule (e.g., L, ML, M_sL) is divided into two zones, one of which contains the substituent and the other the region of primary importance in the reaction. Each of these zones is regarded as contributing an additive term to the free energy, and also as interacting with the other zone. Let us represent the substituent zone by R in the case of a substituted ligand (as in L, M_sL, and ML) and R_0 for the unsubstituted ligand (as in L_0, M_sL_0, and ML_0); also the reaction zone by YM for ML and ML_0, YM_s for M_sL and M_sL_0, and Y for L and L_0. The standard free energy of the substance R–YM in the solvent S is then expressed as in eq. [7].

$$[7] \qquad \bar{G}_{RYM}{}^0 = G_R + G_{YM} + I_{R,YM} + I_{R,S} + I_{YM,S} + II_{R,YM,S}$$

The quantities G_R and G_{YM} are the independent additive terms (per mole) for the zones R and YM, respectively; $I_{R,YM}$ is the term resulting from the interaction between zones R and YM, $I_{R,S}$ that

Can. J. Chem. Downloaded from www.nrcresearchpress.com by 210.87.254.6 on 09/05/12
For personal use only.

from the interaction between the zone R and the solvent S, $I_{YM,S}$ that from the interaction between the zone YM and the solvent S; the term $II_{R,YM,S}$ arises from the failure of these interactions to be truly independent. The significance of the terms in eq. [7] can be better understood if it is pointed out that G_R, G_{YM}, and $I_{R,YM}$ are gas-phase quantities. The following relationships may thus be written

$$G_{R \text{ in } S} = G_R + I_{R,S}$$
$$G_{YM \text{ in } S} = G_{YM} + I_{YM,S}$$
$$I_{R,YM \text{ in } S} = I_{R,YM} + II_{R,YM,S}$$

In order to generate a linear free-energy relationship one must introduce a postulate of separability [8].

[8] $$I_{R,YM} = I_R \cdot I_{YM}$$

The interaction term $I_{R,YM}$ is assumed to be separable into two independent factors, one characteristic of the zone R (I_R) and the other characteristic of the zone YM (I_{YM}). Other interaction terms can be factored similarly

e.g., $$I_{R,YM_s} = I_R \cdot I_{YM_s}$$
$$I_{R_0,YM} = I_{R_0} \cdot I_{YM}$$
$$I_{R,Y} = I_R \cdot I_Y$$
$$I_{R_0,Y} = I_{R_0} \cdot I_Y$$

In the first approximation, the term $II_{R,YM,S}$ is assumed to be negligible. Applying the manipulations described by Leffler and Grunwald, ϕ' and σ may be expressed as in eqs. [9] and [10], respectively, and eq. [1] may be generated in the form [11].

[9] $$\phi' = (I_R - I_{R_0})(I_{YM} - I_Y)/(-2.303\,RT)$$

[10] $$\sigma = (I_R - I_{R_0})(I_{YM_s} - I_Y)/(-2.303\,RT)$$

[11] $$\phi' = [(I_{YM} - I_Y)/(I_{YM_s} - I_Y)]\sigma$$

A comparison of eqs. [1] and [11] shows that B is equal to the term in square brackets. All non-interaction terms and solvent-interaction terms have cancelled out in ϕ' and σ. If it is recalled that eq. [1] compares the stabilities of the complexes of a series of related ligands with the specific metal ion M against those formed with the standard metal ion M_s in the same series, then it is readily understood that the terms I_{YM}, I_{YM_s}, and I_Y are invariant along the series. Consequently, the gradient B is constant and is independent of the substituent and the solvent, provided the underlying assumption of separability is valid.

The separability postulate may be proven rigorously for the situation when the substituent and reaction zones interact through a single mechanism (2). By a single mechanism is meant that the free energy of interaction depends only on a single pair of independent variables, one characteristic of the substituent zone and one characteristic of the reaction zone. Consider the species R–YM, whose partial molar free energy $\bar{G}_{R-YM}{}^0$ may be expressed as a Taylor's series expansion about $\bar{G}_{R_0YM'}{}^0$, the corresponding quantity for a suitably chosen reference compound R_0–YM′.

$$\bar{G}_{RYM}{}^0 - \bar{G}_{R_0YM'}{}^0 = (\partial\bar{G}_{RYM}{}^0/\partial R)_{R_0YM'}(R - R_0) + (\partial\bar{G}_{RYM}{}^0/\partial YM)_{R_0YM'}(YM - YM') + (\partial^2\bar{G}_{RYM}{}^0/\partial R\partial YM)_{R_0YM'}(R - R_0) \times (YM - YM')$$

All partial derivatives are evaluated at (R_0,YM′) and are constants. For small changes in the variables R and YM other second order terms and higher order terms not shown may be assumed to vanish. We may now identify the quantities in this power series according to their independent variables and associate them with the appropriate quantities in the following expression derived from eq. [7] when only gas-phase quantities are considered.

$$\bar{G}_{RYM}{}^0 - \bar{G}_{R_0YM'}{}^0 = (G_R - G_{R_0}) + (G_{YM} - G_{YM'}) + (I_{R,YM} - I_{R_0,YM'})$$

Hence the quantity ($I_{R,YM} - I_{R_0,YM'}$) may be equated to the second order term in the Taylor's series. The interaction term $I_{R,YM}$ (since the constant $I_{R_0,YM'}$ may be conveniently set to zero) is thus indeed a product of two independent variables, one characteristic of the substituent zone and the other of the reaction zone. For large changes in YM and R the terms neglected become important, and no simple second-order term in which the variables are separated is possible. Separability is ruled out in this instance. In summary, we can expect the gradient B to be invariant when the interaction terms are separable into independent contributions, but this may fail in the event of changes in the R-variable being drastic (the value of the YM-variable is not altered in the comparison of eq. [1]).

If solvent interactions are important, then the term $II_{R,YM,S}$ must be considered. This is the second approximation. Only under special con-

Can. J. Chem. Downloaded from www.nrcresearchpress.com by 210.87.254.6 on 09/05/12
For personal use only.

ditions are we now able to factor the *I* and *II* terms simultaneously. Consequently, if the substituent zone and/or the reaction zone interact strongly with the solvent, a linear relationship is less likely. The first approximation with two mechanisms of interaction is discussed presently.

It ought to be possible, in principle, to identify the interaction terms with known or measurable properties of the individual members of a reaction series. A rigorous analysis of the substituent effect can only be achieved by the application of a molecular-orbital treatment (3). However, a simple electrostatic model has been applied with some success in the treatment of substituent effects in aliphatic carboxylic acids (3–5). The electric dipole field of a polar substituent is considered to be transferred across space, the "field effect". In order to illustrate that it would seem feasible to translate the interaction terms into a product of two independent physical properties, the following interpretation of $I_{R,Y}$ is rendered.

$$[12] \quad I_{R,Y} = [Z_Y e]\cdot[N(\mu_R \cos\theta)/r_{RY}{}^2 D] = I_Y \cdot I_R$$

The symbols signify as follows: Z_Y is the formal charge on the reaction site Y; e is the electronic charge; N is Avogadro's number; μ_R is the bond dipole moment of the substituent R; θ is the angle between the dipole axis and the line joining the center of the dipole and the site Y; r_{RY} is the dipole–charge separation; and D is the effective dielectric constant.

Other interaction terms may be evaluated in a similar manner. For example, in the evaluation of $I_{R,YM}$ the interaction of the substituent R with both the reaction site Y and the metal ion M at this site must be considered. Theoretical calculations of B should be relatively uncomplicated since the less accessible I_R quantities do not occur in the expression for B. However, suitable restrictions need to be placed on quantities like μ_R, θ, and r_{RY} to ensure that I_R is a scalar quantity. Preliminary calculations show promise.

ϕ' and σ as a Function of Two or More Independent Variables

It should be clear from our arguments thus far that the variables x, v, ⋯ may effectively denote independent microscopic variables or mechanisms. We have shown that a mechanism implies a single pair of independent variables, one of which is held constant in the comparisons of eqs. [1] and [3]. In this context the terms independent variable and interaction mechanism are synonymous.

A type of behavior that is indistinguishable from the case of a single independent variable arises when σ is a function of two variables, x and v, which are related or change in proportion. If dx and dv are related as in eq. [13], then eq. [14] follows.

$$[13] \quad dv = a_{x,v}\, dx$$

$$[14] \quad dx + dv = dx\,(1 + a_{x,v} + \cdots)$$

Expressed differently, two apparent interaction mechanisms may indeed reduce to one. It is not unlikely that the field, π-inductive, and mesomeric effects (6) are related in some reaction series.

Another possibility arises for which eq. [5] holds: σ and ϕ' are functions of x and v, which are independent of each other, with $d\sigma$ and $d\phi'$ as exact differentials (eq. [15]).

$$[15] \quad \begin{aligned} d\phi' &= g_x dx + g_v dv + \cdots \\ &= B\, d\sigma \\ &= B[f_x dx + f_v dv + \cdots] \end{aligned}$$

where

$$g_x = (\partial\phi'/\partial x)_v \qquad g_v = (\partial\phi'/\partial v)_x$$
$$f_x = (\partial\sigma/\partial x)_v \qquad f_v = (\partial\sigma/\partial v)_x$$

An examination of the coefficients of dx and dv shows that the value of B is severely restricted: $B = g_x/f_x = g_v/f_v$. The significance of this restriction is that there can only be an association between ϕ' and σ when $g_x f_v = f_x g_v$, or when the Jacobian

$$\begin{vmatrix} g_x & f_x \\ g_v & f_v \end{vmatrix}$$

vanishes. The simultaneous separation into independent contributions of the interaction terms corresponding to two mechanisms (i.e., g_x, g_v, f_x, and f_v are all constant) can only lead to eq. [1] when the two mechanisms are in constant ratio for any given substituent in both the test and reference reactions ($g_x/g_v = f_x/f_v$). This limitation may not be as drastic as it would appear. The relative contributions of the inductive and resonance effects appear to satisfy this condition for many Hammett relationships (2).

Can. J. Chem. Downloaded from www.nrcresearchpress.com by 210.87.254.6 on 09/05/12
For personal use only.

Implicit in the discussion of eqs. [14] and [15] has been the possibility of more than two independent variables.

General Restrictions and the Exactness Test

In Part I a simple means was suggested by which to test whether the expression for $d\phi$ (eq. [16]) is an exact differential; this was called the exactness test.

$$[16] \qquad d\phi = (\partial\phi/\partial\sigma)_\theta d\sigma + (\partial\phi/\partial\theta)_\sigma d\theta = B d\sigma + C d\theta$$

It consisted of checking, where possible, the equality or otherwise of the observed second derivatives $\partial B/\partial\theta$ and $\partial C/\partial\sigma$.

The evaluation of this condition is greatly facilitated when both gradients B and C in eq. [16] are invariant. Since in many systems B and C are indeed constant, we shall limit the present discussion to linear free energy relationships. In our discussion of general restrictions it was shown that a free-energy relationship will occur when both the test and standard reaction series show a functional dependence on the same independent variables. Linearity is most favored when the substituent changes are small. (In the case of eq. [3], the metal ion may be considered as the "substituent", and the substituent group R as the "reactant".[3]) Consider the hypothetical situation of the reaction of two metal ions, M and M_s, with a series of related ligands L. For simplicity, let us assume that the only mechanism important in the transmission of the effect of the substituent to the reaction site Y of the ligand L is the "field effect". It is further postulated that the interaction of the metal M with the reaction site Y is largely ionic, while that of M_s is largely covalent. The covalent interaction of M_s with Y should greatly reduce the charge on both these groups. On this basis, we would expect the "field effect" to be small in M_sL complexes, but large in ML complexes. By definition (see footnote 2) ϕ'' depends on the stability constants of the complexes M_sL and ML, and θ on those of M_sL_0 and ML_0. Separability of the interaction terms would likely fail for the wide range of values of the independent variable determining the "field effect" that must be spanned in going from complexes of M_s to complexes of M. Linearity, and thus eq. [3], would probably break down. Turning to eq. [1], we see that by definition ϕ' depends on the stability constants of the complexes ML and ML_0, and σ on those of M_sL and M_sL_0. We would expect the "field effect" to contribute significantly to ϕ', although the opposite is true for σ. The choice of M_s as the reference metal ion for the "ligand-dependent" standard reaction series (i.e., σ) should in all probability cause the failure of eq. [1]. A metal ion more closely resembling M would be a more suitable choice.

It is clear that if the exactness test is to be successfully applied to systems where B and C are invariant, then the system must consist of a series of structurally similar ligands and a series of similar metal ions. The successful application of Hammett-type equations to rates and equilibria of organic reactions has done much to elucidate the substituent effect. Substituent groups, in relation to various parent molecules, have been classified as to their ability to transmit their influence to the reaction site. Various modes of transmission have been identified, such as the electromeric, mesomeric, inductive field, and steric effects (2–4, 6). Any of these effects, when contributing to the substituent effect in an abnormal degree, could be responsible for the breakdown of l.f.e.r. Much stands to be learned about these various contributions in studies of reaction series in which the metal ion is the substrate or substituent. Metal ions have also been classified (7) on the basis of their reactions with ligands. It would appear that class (*a*) ions characteristically participate in ionic interactions, and class (*b*) in covalent interactions, while borderline ions exhibit an intermediate behavior (8).[4] Breakdown of l.f.e.r. and the failure of the exactness test are to be expected if a series of metal ions includes members of each of the extreme classes.

Thermodynamic Restrictions

In our treatment thus far we have purposely considered changes in free energy under isothermal conditions. Thus we considered σ to be a function of several independent variables $x, v, \cdots$.

[3]For ϕ'' we may write $M_lY + R = M_lYR$ (for θ, $R = R_0$), and for ϕ', $R_lY + M = R_lYM$ (for σ, $M = M_s$). The inherent relationship between the comparisons of eqs. [1] and [3] as revealed by the exactness test, is a result of the equivalence of these two reaction schemes.

[4]This concept will be discussed in full in Part III of this series, in preparation.

Can. J. Chem. Downloaded from www.nrcresearchpress.com by 210.87.254.6 on 09/05/12
For personal use only.

For small changes in these variables we may write eq. [17].

$$[17] \qquad \Delta G_\sigma^0 = f_x{}^G \Delta x + f_v{}^G \Delta v + \cdots$$

where $\Delta G_\sigma^0 = -2.303\ RT\sigma$; $d\Delta G_\sigma^0 = -2.303\ RTd\sigma$, with $f_x{}^G = (\partial \Delta G_\sigma^0/\partial x)_{T,v,\ldots} =$ constant, and $\Delta x = x - x_0$; $f_v{}^G$ and Δv are similarly defined.

But at constant temperature, ΔG_σ^0 may also be defined by eq. [18]

$$[18] \qquad \Delta G_\sigma^0 = \Delta H_\sigma^0 - T\Delta S_\sigma^0$$

Both expressions for ΔG_σ^0 are dependent on the substituent and the temperature. We must now ask what restrictions must be imposed for these two expressions to remain equal for a broad range of temperature and substituent changes. Leffler and Grunwald (2) approach the problem by considering the temperature variations of ΔH_σ^0 (eq. [19]) and ΔS_σ^0 (eq. [20]).

$$[19] \qquad (\partial \Delta H_\sigma^0/\partial T)_p = \Delta C_p^0$$

$$[20] \qquad (\partial \Delta S_\sigma^0/\partial T)_p = \Delta C_p^0/T$$

They show in the first approximation, when $\Delta C_p^0 = 0$, that the equivalence of eqs. [17] and [18] is satisfied when such variables as $x, v, \cdots$ are each separable into two variables, one characteristic of the substituent $(x', v', \cdots)$ and one characteristic of the temperature. In addition, ΔH_σ^0 must be proportional to ΔS_σ^0 [21], with β a temperature-independent constant.

$$[21] \qquad \Delta H_\sigma^0 = \beta \Delta S_\sigma^0$$

In the second approximation, $\Delta C_p^0 =$ constant, with $(d\Delta C_p^0/dT) = 0$; β is expected to be temperature dependent. Because the variables $x, v, \cdots$ are separable, the following series of relationships may be written.

$$[22] \qquad \Delta G_\sigma^0 = f_{x'}{}^G \Delta x' + f_{v'}{}^G \Delta v' + \cdots$$

$$[23] \qquad \Delta H_\sigma^0 = f_{x'}{}^H \Delta x' + f_{v'}{}^H \Delta v' + \cdots$$

$$[24] \qquad \Delta S_\sigma^0 = f_{x'}{}^S \Delta x' + f_{v'}{}^S \Delta v' + \cdots$$

Several situations may now be distinguished. In an isoentropic series $\Delta S_\sigma^0 = 0$, and $\Delta G_\sigma^0 = \Delta H_\sigma^0$. In an isoenthalpic series $\Delta H_\sigma^0 = 0$, and $\Delta G_\sigma^0 = -T\Delta S_\sigma^0$. Another situation arises when eq. [21] applies, i.e., an isokinetic series (2, 3, 9). The free energy in this case may be expressed as in eq. [25].

$$[25] \qquad \Delta G_\sigma^0 = (1 - T/\beta_{x'}) f_{x'}{}^H \Delta x' + (1 - T/\beta_{v'}) f_{v'}{}^H \Delta v' + \cdots$$

The isokinetic relationship in eq. [21] demonstrates the principle referred to as the Compensation Law.[5] Ives and Marsden (10) have given a novel interpretation to the slope β for reactions that are accompanied by a considerable change in the degree of solvation. In all reactions considered in this paper, the part played by the solvent has been omitted. It would be more accurate to write the reaction M + L = ML as in eq. [26] when water is the reaction medium.

$$[26] \qquad M(H_2O)_k + L(H_2O)_l = ML(H_2O)_m + (k + l - m)\,H_2O$$

The standard free energy, enthalpy, and entropy of a reaction like [26] are divided into a "reaction part" and a "hydration part". The "reaction part" is that part of a reaction, according to Ives and Marsden (10), in which water is not directly involved; in the "hydration part" water is solely involved.[6] Consequently, the standard free-energy change for reaction [26] may be written as a sum of the contributions shown in eq. [27].

$$[27] \qquad \Delta G^0 = \Delta G^r + \Delta G^h = \Delta H^r + \Delta H^h - T(\Delta S^r + \Delta S^h)$$

Arguments are presented that call for the conclusion that $\Delta G^h = 0$. If eq. [18] is applied to the hydrational part alone, then it follows that $\Delta H^h = T\Delta S^h$.

In contrast to ΔG^h, ΔH^h and ΔS^h may contribute significantly to ΔH^0 and ΔS^0. Such contributions are expected to be major in water and like polar solvents. This is suggested as one of the principal reasons for observing a linear relationship between ΔH^0 and ΔS^0 in polar solvents. Thus the slope β (eq. [21]) should have a value close to the experimental temperature for a set of allied reactions. This is indeed observed frequently (e.g., refs. 2, 10, 17, 18). In addition to the solvation effects, there appears to be a natural tendency for ΔH^0 and $T\Delta S^0$ terms to contain contributions of the same sign. Attractive forces impose con-

[5]Simply a linear enthalpy–entropy effect.

[6]The distinction "internal" and "external" has also found use in designating the "reaction part" and the "hydration part", respectively (11–16).

straint (ΔH^0 and ΔS^0 both negative), and the release of such forces confers greater freedom (ΔH^0 and ΔS^0 both positive). This is often referred to as the normal compensation, and may be expressed as in eq. [28], in analogy with eq. [21].

$$[28] \qquad \Delta H_\sigma{}^r = \alpha \Delta S_\sigma{}^r$$

Ives and Marsden stress that a simple picture, such as that presented, will always be inadequate to describe the complexity of interactions in solution, especially in polar solvents. It can only serve to explain general trends. It will always be difficult to determine what effects are due to solvent influencing solute, or vice versa. All measurable thermodynamic quantities attributable to a solute will inevitably contain some solvent contribution.

Continuing our discussion of eq. [25], we see that if eq. [21] applies to a system, then

$$\beta = \beta_{x'} = f_{x'}{}^H/f_{x'}{}^S = f_{v'}{}^H/f_{v'}{}^S = \beta_{v'}$$

This may be confirmed by combining eqs. [21] and [24] and comparing the coefficients of the resultant equation with those of [23]. Equation [29] then follows from the combination of eqs. [25] and [23].

$$[29] \qquad \Delta G_\sigma{}^0 = (1 - T/\beta)\Delta H_\sigma{}^0$$

β has the dimensions of temperature, and is often called the isokinetic temperature. It is evident from eq. [25] that if one or other of $\beta_{x'}$ or $\beta_{v'}$ is equal to the experimental temperature T, then changes in the variable x' or v' would fail to contribute to $\Delta G_\sigma{}^0$. In consequence, the free energy depends on one less variable than the enthalpy or entropy.[7] We have already reported the suggestion that for solvational changes β should tend toward T. Consider the hypothetical reaction series for which $\Delta G_\sigma{}^0$ is a measure of the inductive effect over a wide range of temperatures, but with no such relationship being apparent for the enthalpy and entropy[7] changes. Neither is a linear enthalpy–entropy relationship detectable. Each member in such a reaction series may be thought of as having its enthalpy and entropy[7] determined by a different number of mechanisms, most of which are likely to be solvent effects. However, if $\Delta H^h = T\Delta S^h$ for nearly all of the hydrational processes, it is eq. [30] that determines the relationship between $\Delta G_\sigma{}^0$ and the inductive effect. This equation is derived from eqs. [18] and [23] applied to the "reaction part" alone, and eq. [28].

$$[30] \quad \Delta G_\sigma{}^0 = (1 - T/\alpha) f_{x'}{}^{H^r} \Delta x' + (1 - T/\alpha) f_{v'}{}^{H^r} \Delta v' + \cdots$$

When one major mechanism operates in a reaction series, then the interpretation of all three standard thermodynamic quantities should be relatively simple. Equation [29] implies that for this situation all three quantities should be well-behaved, in the sense that they are all linear functions of, let us say, the variable x. Differentiation of eq. [29] yields eq. [31].

$$[31] \quad (d\Delta G_\sigma{}^0/dx)_T = (1 - T/\beta)(d\Delta H_\sigma{}^0/dx)_T$$

However, what may appear to be a dependency of $\Delta G_\sigma{}^0$ on a single variable may indeed be a dependency of $\Delta H_\sigma{}^0$ and $\Delta S_\sigma{}^0$ on two: one continuous variable (x) and one discontinuous variable which may only exhibit certain discrete values. In such a system $\Delta G_\sigma{}^0$ is a continuous function of x, and eq. [31] implies that $\Delta H_\sigma{}^0$ and $\Delta S_\sigma{}^0$ are as well. However, all that is required is that the derivatives of $\Delta H_\sigma{}^0$ and $\Delta S_\sigma{}^0$ with respect to x be invariant. For this system, plots of $\Delta G_\sigma{}^0$ vs. $\Delta H_\sigma{}^0$ and of $\Delta H_\sigma{}^0$ vs. $\Delta S_\sigma{}^0$ should produce a series of parallel lines with slope $(1 - T/\beta)$ or β, respectively, the number of lines depending on the number of discrete values the other variable may assume. Such a series of parallel lines has not infrequently been reported (2, 19, 20). Again, in this situation $\Delta G_\sigma{}^0$ will be a measure of polar inductive or other effects due to the substituent, while $\Delta H_\sigma{}^0$ and $\Delta S_\sigma{}^0$ are not. It may be concluded that the operation of compensation laws often helps to protect standard free energies of reactions from extreme complexities. This is especially so for reactions in polar solvents. Hence ΔG^0 is often a better measure of the enthalpy changes at absolute zero, which arise for example from polar substituent effects, than ΔH^0.[8] Changes in enthalpy at absolute zero can be related to molecular models (10, 21).

[7]These are standard quantities.

[8]Hepler (13) and Milburn (15) have arrived at the same conclusion in a manner not unlike that used to obtain eq. [30] in this work.

Can. J. Chem. Downloaded from www.nrcresearchpress.com by 210.87.254.6 on 09/05/12
For personal use only.

Can. J. Chem. Downloaded from www.nrcresearchpress.com by 210.87.254.6 on 09/05/12
For personal use only.

A word of caution must be sounded, however (2). Even in systems that exhibit excellent correlations of ΔH_σ^0 with ΔS_σ^0, a certain amount of scatter or "noise" is to be expected due to contributions of minor variables to these quantities. This has the following consequence for the standard free energies: ΔG_σ^0 values measured at temperatures near the isokinetic temperature will only exhibit the random "noise". Unless all ΔG_σ^0 values are equal to zero within the experimental error, such quantities will be difficult to interpret. It is important to evaluate free energies or equilibrium constants over a range of temperatures if an isokinetic system is suspected. The reverse of the situation just described is also possible: only at the isokinetic temperature does σ correlate with expected substituent effects. Other complications are to be expected. It is possible for the derivative of ΔG_σ^0 with respect to x (eq. [31]) to change sign by virtue of the relative magnitudes of T and β, without a corresponding change in $(\partial \Delta H_\sigma^0/\partial x)$. Changes in the sign of the slope for linear free energy relationships could thus occur (see below, eq. [32]).

It should be possible to evaluate the slope B in eq. [1] in the light of these thermodynamic restrictions. Slope C may be similarly discussed. By analogy with ΔG_σ^0, $\Delta G_{\phi'}^0$ may be expressed as in eqs. [18], [22], [25], and [30]; similarly $\Delta H_{\phi'}^0$ and $\Delta S_{\phi'}^0$ may be expressed in forms similar to eqs. [23] and [24], respectively. To illustrate one of the various situations that may arise when the test reaction (ϕ') and the standard reaction (σ) fall into different categories as discussed above, let us develop an expression for B applying to a comparison between an isokinetic test reaction series and an isoenthalpic reference reaction series. Since in the previous section of this paper we demonstrated that the same variables must operate in both reaction series, we may determine B by combining the modified form of eq. [1], $\Delta G_{\phi'}^0 = -BT\Delta S_\sigma^0$, with eq. [24], and comparing the coefficients of the resulting equation with those in the expression for $\Delta G_{\phi'}^0$ in eq. [25].

$$[32] \qquad B = \frac{(1 - T/\beta_{\phi'})f_{x'}^H}{-Tf_{x'}^S} = \frac{(1 - T/\beta_{\phi'})f_{v'}^H}{-Tf_{v'}^S}$$

Thus, as mentioned previously, B may change sign simply as a result of the relative values for T and $\beta_{\phi'}$. It is obvious that extreme care must accompany any interpretation of the magnitude and sign of slopes (2, 9, 17). In a like manner, B may be evaluated for comparisons of other reaction series of different thermodynamic types.

Concluding Remarks

In our discussion of General Restrictions it was shown that a free energy relationship should occur when both the test and standard reaction series show a functional dependence on the same independent variables. Linearity is most favored when the substituent and quasi-substituent changes are small, and when the substituent and reaction site do not interact strongly with the solvent. The requirement of common variables finds full support in the observation that a ligand family must comprise a series of closely related reagents in order to fix factors such as the number and type of donor atoms, and the number and size of chelate rings along the series (22). It may be relevant to the comments on linearity that in Tables 3 and 4 of Part I (1) the correlation coefficients are comparatively low for the least electronegative metal ion and the most acidic ligand. It is tempting to assign this phenomenon, also observed in other cases (23), to too drastic changes in the variables. However, changes in the number of independent variables may not be excluded. Curvature has also been observed for drastic substituent changes (22, 24–26).

A detailed regression analysis of the available thermodynamic data (ΔH^0, ΔS^0, and ΔG^0) should prove to be extremely profitable. The classification of metal-complex systems into isoenthalpic, isoentropic, and isokinetic series is essential in establishing the dependence of B and C on β and T as outlined, for example in eq. [32]. Such studies are a prerequisite to any theoretical calculations of B and C based on models of the substituent effect (e.g., eq. [12]). The problem of the significance of the magnitude of the intercept on the vertical axis also has no easy answers. It is probably more fundamental to investigate what factors determine the location of the point of convergence of a set of l.f.e.r. (1).

This work was supported by a grant from the National Research Council of Canada for which grateful acknowledgment is made. One of the authors (E.N.) records his thanks for the award of a National Research Council Postgraduate Fellowship.

1. E. NIEBOER and W. A. E. McBRYDE. Can. J. Chem. This issue.
2. J. E. LEFFLER and E. GRUNWALD. Rates and equilibria of organic reactions. John Wiley and Sons, Inc., New York. 1963.
3. P. R. WELLS. Linear free energy relationships. Academic Press, Inc., London. 1968.
4. C. F. WILCOX and C. LEUNG. J. Amer. Chem. Soc. **90**, 336 (1968).
5. G. W. WHELAND. Advanced organic chemistry. 3rd. ed. John Wiley and Sons, Inc., New York. 1960. pp. 521–531.
6. (*a*) M. J. S. DEWAR and P. J. GRISDALE. J. Amer. Chem. Soc. **84**, 3539 (1962); **84**, 3541 (1962); **84**, 3546 (1962); **84**, 3548 (1962); (*b*) M. J. S. DEWAR and A. P. MARCHAND. J. Amer. Chem. Soc. **88**, 354 (1966); **88**, 3318 (1966); (*c*) W. ADCOCK and M. J. S. DEWAR. J. Amer. Chem. Soc. **89**, 379 (1967); **89**, 386 (1967); (*d*) M. J. S. DEWAR and Y. TAKEUCHI. J. Amer. Chem. Soc. **89**, 390 (1967); (*e*) M. J. S. DEWAR and T. G. SQUIRES. J. Amer. Chem. Soc. **90**, 210 (1968).
7. (*a*) S. AHRLAND, J. CHATT, and N. R. DAVIES. Quart. Rev. London, **12**, 265 (1958); (*b*) S. AHRLAND. Struct. Bonding, Berlin, **1**, 207 (1966).
8. R. J. P. WILLIAMS and J. D. HALE. Struct. Bonding, Berlin, **1**, 249 (1966).
9. P. R. WELLS. Chem. Rev. **63**, 171 (1963).
10. D. J. G. IVES and P. D. MARSDEN. J. Chem. Soc. 649 (1965).
11. L. G. HEPLER and W. F. O'HARA. J. Phys. Chem. **65**, 811 (1961).
12. W. F. O'HARA and L. G. HEPLER. J. Phys. Chem. **65**, 2107 (1961).
13. L. G. HEPLER. J. Amer. Chem. Soc. **85**, 3089 (1963).
14. K. E. JABALPURWALA and R. M. MILBURN. J. Amer. Chem. Soc. **88**, 3224 (1966).
15. R. M. MILBURN. J. Amer. Chem. Soc. **89**, 54 (1967).
16. A. G. DESAI and R. M. MILBURN. J. Amer. Chem. Soc. **91**, 1958 (1969).
17. E. NIEBOER and W. A. E. McBRYDE. Inorg. Nucl. Chem. Lett. **3**, 569 (1967).
18. K. J. LAIDLER *et al.* Trans. Faraday Soc. **55**, 1725 (1959); **55**, 1731 (1959); **55**, 1734 (1959); **55**, 1738 (1959); **55**, 1743 (1959).
19. R. F. BROWN. J. Org. Chem. **27**, 3015 (1962).
20. R. F. BROWN and H. C. NEWSOM. J. Org. Chem. **27**, 3010 (1962).
21. C. S. G. PHILLIPS and R. J. P. WILLIAMS. Inorganic chemistry. Vol. 1. Oxford University Press, New York and Oxford. 1965. p. 252.
22. F. J. C. ROSSOTTI. In modern co-ordination chemistry. *Edited by* J. Lewis and R. G. Wilkins. Interscience Publ., Inc., New York. 1960. pp. 1–77.
23. E. NIEBOER. Ph.D. Thesis. University of Waterloo, Waterloo, Ontario. 1968.
24. J. G. JONES, J. B. POOLE, J. C. TOMKINSON, and R. J. P. WILLIAMS. J. Chem. Soc. 2001 (1958).
25. C. POSTMUS, JR., L. B. MAGNUSSON, and C. A. CRAIG. Inorg. Chem. **5**, 1154 (1966).
26. K. CLARKE, R. A. COWEN, G. W. GRAY, and E. H. OSBORNE. J. Chem. Soc. 245 (1963).

Can. J. Chem. Downloaded from www.nrcresearchpress.com by 210.87.254.6 on 09/05/12
For personal use only.

Can. J. Chem. Downloaded from www.nrcresearchpress.com by 210.87.254.40 on 09/05/12
For personal use only.

Stability constants of three iron(III) salicylates[1]

W. A. E. McBryde, Janet L. Rohr, J. S. Penciner,[2] and J. A. Page[3]
Department of Chemistry, University of Waterloo, Waterloo, Ontario

Received February 20, 1970

Stability constants of the iron(III) complexes of salicylic acid, sulfosalicylic acid, and 4-aminosalicylic acid, together with several of the acidity constants of these, have been determined at 25 °C and in solutions with 0.5 *M* background electrolyte. For the spectrophotometric measurement of the stability constants improved methods for determining the extinction coefficients of the first and second complexes are described. Protonated species appear only with the aminosalicylate complexes, and the site of this protonation is discussed. Previous values of these equilibrium constants have been collected and critically assessed.

Canadian Journal of Chemistry, 48, 2574 (1970)

Introduction

A spectrophotometric procedure for the estimation of formation constants of metal complexes initially suggested by Vareille (1) has been extended (2, 3), particularly by increasing the number of independent estimates that could be extracted from measurements on a suitable group of solutions. In this paper are communicated some additional refinements to the experimental procedure and to the treatment of the experimental data, together with the results of studies on complexes formed by iron(III) with salicylates.

These particular complexes were selected for study for several reasons. The substantially different magnitudes of the successive stability constants make it possible to study spectrophotometrically the individual steps in the formation of these complexes. One of the advantages of the procedure is its ability to test the dependence of the measured values of formation constants on hydrogen-ion concentration. Thus the method had been used (3) to confirm the formation of a protonated complex MHL in the reaction between iron(III) and Tiron (disulfonated catechol) (4). It was of interest to see whether, under comparable conditions of low p*H*, a similar reaction occurred with sulfosalicylic acid. The iron(III) complexes of this reagent have already been investigated by several workers (5–10), and apart from some early observations (5), no dependence of the formation constants on the acidity of the solution had been reported. However, the experimental methods or conditions applying to these previous investigations may not have been chosen with the objective of proving or disproving the formation of a protonated species. Mattoo (7) specifically commented on the absence of a protonated 1:1 complex when subjecting Vareille's experimental results to his own method of calculation. Salicylic acid and some other salicylates have been reported in one study to form protonated iron(III) complexes (11), though other workers (9, 10, 12–14) have not reported on such a species. Three previous investigations of the reaction of 4-aminosalicylic acid with iron(III) appear to have demonstrated the formation of protonated species, though these authors do not agree on the number or range of existence of these complexes (9, 13, 15). We hoped to be able to bring additional evidence to bear on the nature of these reactions at low p*H*.

Although these reactions have, as indicated, been examined already by a number of investigators, concordance among the different published stability constants is not very good. Some of the inconsistencies are due to the use of different ionic media by various workers, but some can be traced to the use of inappropriate acidity constants for the ligands, and to other causes which are discussed in the last section of this paper. Clearly, if these colored complexes are to be applied in a quantitative manner for the spectrophotometric determination of stability constants of other iron(III) complexes or other metal salicylates (e.g. refs. 16, 17), much more accurate values of their formation constants will be required.

[1]This work was begun in the Department of Chemistry, University of Toronto, and completed and prepared for publication in the Department of Medical Chemistry, Australian National University, Canberra.

[2]Present address: Department of Chemistry, Tel-Aviv University, Tel-Aviv, Israel.

[3]Present address: Department of Chemistry, Queen's University, Kingston, Ontario.

Can. J. Chem. Downloaded from www.nrcresearchpress.com by 210.87.254.40 on 09/05/12
For personal use only.

Précis of the Method

For the reaction

$$ML_{n-1} + H_jL = ML_n + jH$$

an equilibrium concentration quotient can be formulated

$$[1] \qquad \kappa_n = a_n[H]^j/[H_jL] \qquad (n = 1, 2, 3)$$

in which

$$[2] \qquad a_n = (\varepsilon_{n-1} - \varepsilon)/(\varepsilon - \varepsilon_n) = [ML_n]/[ML_{n-1}]$$

$$[3] \qquad [H_jL] = (C_L - \bar{n}C_M)(1 + K_{a2}/[H] + K_{a1}K_{a2}/[H]^2 + \cdots)^{-1}$$

$$[4] \qquad \bar{n} = (n - 1) + a_n/(a_n + 1)$$

C_L and C_M represent the total analytical concentrations of ligand and metal ion, respectively. The other symbols have their usual meanings. Species participating in the reactions are shown with charges omitted. Also ε = Absorbance (1 cm)/C_M.

The key to the method lies in the ability to assign values to the extinction coefficients ε_n and ε_{n-1}. Given the chemical suitability of the system of complexes, which implies a wide spacing of the κ_n already referred to, this can be accomplished by inferences about the species present at various values of pL (or of pH at constant C_L) drawn from the appearance of isobestic points in networks of absorption curves, $\varepsilon = f(\lambda, pH)$.

In the system of complexes here under consideration, ε_0, the extinction coefficient of uncomplexed metal can be put equal to zero at the wavelengths where absorbances are measured. The value of ε_1 at any particular wavelength can be assigned with some confidence as follows. An isobestic point appearing over a range of pH (at fixed C_M and C_L) can be identified with the condition $\varepsilon_1 = \varepsilon_2$ at some wavelength λ'; from this ε_1' can be determined. Below some pH value the spectra fail to pass through the isobestic point, and it may be inferred that in such solutions ML is the sole absorbing species.[4] For these solutions the absorbance at a particular wavelength λ compared to that at the isobestic wavelength λ' permits evaluation of the ratio ε/ε'. Then for the wavelength in question one can calculate $\varepsilon_1 = \varepsilon_1'\varepsilon/\varepsilon'$. It is also simple to assign values to ε_3 at any wavelength by measuring absorbances in solutions of pH high enough to convert all metal to the highest complex.

In a previous paper (3) it was noted that "the weakest feature in the method is the selection of appropriate ε_n values for the individual complexes." We have now evolved the procedure just described for setting values of ε_1, and have obtained values of ε_2 in this work by calculation rather than by direct observation from spectra. A number of solutions were prepared containing known amounts of metal ion and ligand and suitable buffers; for each solution the pH and the absorbances at several wavelengths were measured. For any such solution the quantity $[ML_2]/[ML]$ or $[ML_3]/[ML_2]$ is fixed, and accordingly there will be several supposedly equal values of $(\varepsilon_1 - \varepsilon)/(\varepsilon - \varepsilon_2)$ or $(\varepsilon_2 - \varepsilon)/(\varepsilon - \varepsilon_3)$ for different wavelengths, eq. [2]. Provided that values can be assigned to ε_1 and ε_3 for these wavelengths and that ε is obtained by direct observation, it becomes a question of finding a value of ε_2 at each wavelength which results in the minimum scatter in values of a_2 or a_3 at each pH. Insofar as possible the value of ε_2 sought was required to meet the condition of minimum variance in both a_2 and a_3. This was quite easily accomplished by a computer program prepared for this purpose. The optimized values of a_2 or a_3 were then used in eq. [1].

Systems Investigated

Sulfosalicylic Acid

No evidence, spectroscopic or from hydrogen-ion balance, suggested the binding of hydrogen ions to the sulfonate group in the region of pH investigated. The equilibrium constant for ionization of the carboxyl hydrogen was determined by titration in solutions maintained at essentially constant ionic strength by addition of the specified background electrolyte (0.5 M). The acidity constant was calculated as a concentration quotient from the following relationship[5]

$$[5] \qquad K_{a2} = \frac{[H]\{C_B - C_A + [H]\}}{2C_A - C_B - [H]}$$

[4]Or possibly a mixture of ML and MHL; see the case of 4-aminosalicylic acid.

[5]Throughout this paper acidity constants are numbered to correspond to the number of dissociable hydrogens in the "molecule" of the more acidic species participating in the equilibrium. Although this is the reverse of the usual practice (except for pK_a values of bases) it offers the advantage of being unambiguous and compatible with the numbering of metal complex stability constants.

Can. J. Chem. Downloaded from www.nrcresearchpress.com by 210.87.254.40 on 09/05/12
For personal use only.

In this, C_A and C_B are, respectively, the concentrations at each stage of the titration of acid taken and base added (i.e. with allowance being made for the change in volume during titration). The value of [H], the hydrogen-ion concentration, was measured with a pH meter employed as a hydrogen-ion concentration probe (18); a relationship between H (= antilog (− pH)) and [H] was established by direct measurement for the salt background in which the titration was carried out.

In a similar way the ionization constant for the dissociation of the phenolic hydrogen was obtained from titration data applied to the following relationship

$$[6] \qquad K_{a1} = \frac{[H]\{C_B - 2C_A - [OH]\}}{3C_A - C_B + [OH]}$$

In this case an empirical relationship was established between [OH] in solutions with 0.5 M background electrolyte and H^{-1}. The two relationships involving H when combined provided an estimate of K_{cw}, the ion-concentration product for water, in the medium in which it was measured. In this way a value of [H] in alkaline solutions could be assigned. A similar, but independent evaluation of K_{cw} by the method of Liberti and Light (19) yielded an almost identical result.

For determination of κ_1 sets of solutions were prepared within the range of pH ca. 1 to 2. Within each set solutions contained fixed concentrations of metal ion, sulfosalicylic acid, and either perchloric acid and sodium perchlorate or nitric acid and potassium nitrate for a total background electrolyte concentration of 0.5 M. Different sets of solutions contained different ratios of reagent to metal. The absorption spectra of these solutions showed only differences in intensity which could be attributed to changes in concentration of a single species, assumed to be ML. The pH of every solution was measured, and absorbance measurements were made at three wavelengths, 470, 510, and 550 nm, of which the last corresponds to an isobestic point where $\varepsilon_1 = \varepsilon_2$.

To evaluate κ_1 through eq. [1], j was put equal to 2, and an additional factor included to allow for the hydrolysis of the uncomplexed iron(III). The right-hand side of eq. [1] was multiplied by $(1 + K_h/[H])$, in which K_h is a first-stage hydrolysis constant for iron(III). The value of K_h used was that of Wilson and Taube (20) for 0.5 M $NaClO_4$ background. For practical purposes, at the level of free iron concentration in these solutions, first-stage hydrolysis only need be considered.

For the measurement of κ_2 and κ_3 solutions were prepared in the same way, but at higher pH it was found necessary to add buffers to maintain constant pH and spectra. Presumably hydrolysis of uncomplexed iron(III) causes a shift in the equilibria under consideration, although this effect had not been observed in the case of iron(III)–Tiron solutions (3). Buffering agents were chosen that had small affinity for iron(III), namely, for buffer bases hexamethylenetetraamine, α-picoline, ammonia; the pH ranges are 4–6, 5–7.8, and 8–10, respectively. They were all used with their nitrate salts at molarities of 0.05 and with compensating reductions in the amount of potassium nitrate taken for the background electrolyte. Suitable values for determination of κ_2 lay between 2.7 and 4.1, and for κ_3 between 5.8 and 7.1. Absorbance measurements were made at 400, 420, 460, and 500 nm, although values at 460 nm proved unsuitable for evaluation of κ_3 by eqs. [1] and [2] since this wavelength corresponds to the isobestic point where $\varepsilon_2 = \varepsilon_3$.

Values of the stability constants K_n are related to the foregoing equilibrium constants by the equation

$$[7] \qquad K_n = \kappa_n / K_{a1} K_{a2}$$

Additional estimates of K_1 were made from measurements on solutions prepared for Job analysis (21) of the composition of the first complex. Solutions were prepared containing xC molar iron(III) and $(1 - x)C$ molar sulfosalicylic acid, with the pH within each set maintained constant and with potassium nitrate added to give a total background electrolyte concentration of 0.5 M. Four such sets of solutions were prepared, each differing in pH but falling within the range 1.6 to 2.5. The absorbances A at 505 nm ($\varepsilon_1 = 1880$) were measured, and the equilibrium constant calculated by means of eq. [8].

$$[8] \qquad K_1 = \frac{A/\varepsilon_1}{\dfrac{xC - A/\varepsilon_1}{1 + K_h/[H]} \cdot \dfrac{(1-x)C - A/\varepsilon_1}{1 + [H]/K_{a1} + [H]^2/K_{a1}K_{a2}}}$$

Salicylic Acid

Measurements with this compound were con-

Can. J. Chem. Downloaded from www.nrcresearchpress.com by 210.87.254.40 on 09/05/12
For personal use only.

fined to determination of the dissociation constant for the carboxyl hydrogen and of κ_1 for the first iron(III) complex. The data were obtained and treated in the same fashion as for sulfosalicylic acid. Absorbance measurements were made at 500, 530, and 560 nm, of which wavelengths the second is λ_{max} ($\varepsilon_1 = 1530$) and the third is that of the isobestic point where $\varepsilon_1 = \varepsilon_2$.

4-Aminosalicylic Acid

Quantitative studies with this compound are complicated by the fact that it undergoes decarboxylation to form *m*-aminophenol (22) with the product of this reaction also capable of forming a colored complex with iron(III). In our studies we worked quickly with fresh solutions in the hope of avoiding this side reaction, but we were frequently conscious of some instability of our solutions, and cannot claim for our equilibrium constants the same accuracy or precision as were obtained with the preceding two compounds.

This acid possesses an extra ionization constant K_{a3} for proton transfer at the amino group. There appears to be some confusion about the assignment of acidity constants for this acid. Thus Colleter (9) employed an ionization scheme comparable to that for an amino acid such as tyrosine, viz. $pK_{COOH} < pK_{NH_2} < pK_{OH}$, and Agren (13) appears to have done the same. Others (15, 22–25) have considered that $pK_{NH_2} < pK_{COOH}$, or at least that of the two ionization pathways for H_3L^+ forming neutral amino acid is strongly favored over that producing zwitterion. The latter view is also supported by simple calculations with the Hammett equation. By appropriate substitution of σ-factors in the following relationships (26)

$$pK\,(\text{anilines}) = 4.57 - 2.81\sum\sigma$$

$$pK\,(\text{benzoic acids}) = 4.20 - \sum\sigma$$

the pK values predicted for 4-aminosalicylic acid are $pK_{NH_2} = 2.19$ and $pK_{COOH} = 3.64$. Since values about 2 and 3.7 have been reported for this acid (see Table 2) there seems little reason to question their correct assignment.

The two acidity constants in question were determined as concentration quotients for a background of 0.5 *M* perchlorate. This necessitated special care in the evaluation of [H] by the glass electrode. As a calibration known amounts of 0.5 *M* perchloric acid were added to a known volume of 0.5 *M* sodium perchlorate solution, and the pH measured (to 0.001 unit) with a glass and calomel electrode. The latter was protected from the perchlorate solution by a sleeve-type salt bridge (18) to avoid formation of potassium perchlorate at the orifice of the calomel half-cell. The values observed with the apparatus used could be fitted down to pH 1.3 to a relationship[6] $[H] = aH + bH^2$ with $a = 0.971$ and $b = 4.3$.

Solutions of the sodium salt of 4-aminosalicylic acid were prepared from weighed samples and immediately titrated with 0.5 *M* perchloric acid under the same conditions; the total time required did not exceed 45 min. The data from the titrations, in the form $\bar{n}_H$ and [H], were processed by a computer program which selected values of the acidity constants giving best fit to the experimental results on a least squares basis. Some spectrophotometric measurements in the ultraviolet were also made, but yielded K_{a3} values of poorer precision.

The spectra of the iron(III) complexes with this reagent showed the typical shift to lower values of λ_{max} and higher values of ε_{max} with increasing pH. We have interpreted peaks at 500, 465, and 420 nm to denote absorbing species which, by analogy with the other salicylates, Tiron, etc., we assume to be ML, ML_2, and ML_3, respectively. Below p$H \sim 1.5$ the band with $\lambda_{max} = 500$ nm diminishes in intensity but does not change in contour. Isobestic points were less clearly defined, but were identified and assigned as follows: $\varepsilon_1 = \varepsilon_2$ at 587 nm and $\varepsilon_2 = \varepsilon_3$ at 460 nm (cf. ref. 15).

To evaluate κ_1 for the first metal complex, eq. [3] was expressed in the form

$$[3a] \quad [H_2L] = (C_L - \bar{n}C_M)(1 + [H]/K_{a3} + K_{a2}/[H])^{-1}$$

the term $K_{a1}K_{a2}/[H]^2$ being negligible in acidic solutions. The quantity $a_1[H]^2/[H_2L]$ on the right-hand side of eq. [1], after applying the correction for hydrolysis of iron(III), showed a dependence on hydrogen-ion concentration, in contrast to corresponding values for the other two salicylates. As did Agren (13) and Tsin-jao *et al.* (15) we interpreted this observation in terms of a protonated complex.

The formation of this has been represented

[6]On the basis of accumulated experience with this kind of calibration (e.g. ref. 18) we are only prepared at this time to treat *a* and *b* as systematic empirical parameters.

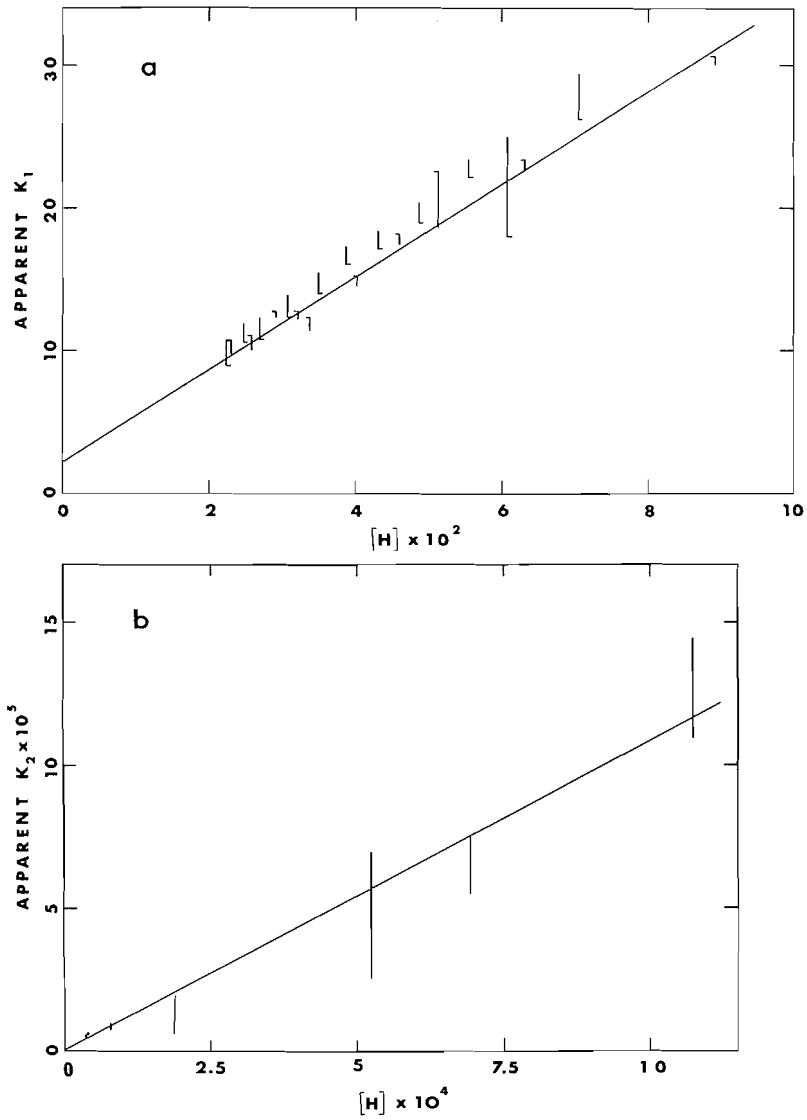

FIG. 1. (*a*) Variation of apparent κ_1 for Fe-4-aminosalicylate with hydrogen-ion concentration. The vertical lines show the range of values for four different wavelengths; left hook for $C_L/C_M = 10$; right hook for $C_L/C_M = 5$. The regression line was fitted by least squares. Intercept = 2.52 ± 0.40 (estimated); slope = 336 (± 30); slope calculated for zero intercept = 386 (± 38). (*b*) Variation of apparent κ_2 for Fe-4-aminosalicylate with hydrogen-ion concentration. The vertical lines show the range of values for six different wavelengths. The correlation line was fitted by least squares. Slope = 0.107 (± 0.031).

by ML + H = MHL for which an equilibrium constant κ_H has been introduced

$$[9] \qquad \kappa_H = [MHL]/[ML][H]$$

In applying the spectrophotometric procedure eq. [2] must be reinterpreted to provide for the possible existence of a protonated species. Since no detectable shift was observed in the spectra of solutions within the p*H* range 0.9 to 2.5 apart from increase or decrease in intensity of the whole band, it was inferred that MHL, if present, either has the same absorption spectrum as ML in the visible region or is non-absorbing. Since absorption at ca. 500 nm is undoubtedly associated with the iron–phenol link, it seems more reasonable to accept the former assumption. In

Can. J. Chem. Downloaded from www.nrcresearchpress.com by 210.87.254.40 on 09/05/12
For personal use only.

TABLE 1

Acidity constants for salicylic acids*

Acid	Medium (0.5 *M*)	$K_{a1} \times 10^{12}$ Value	σ	No.	$K_{a2} \times 10^{3}$ Value	σ	No.	$K_{a3} \times 10^{3}$ Value	σ	No.
Salicylic acid	$(Na)ClO_4$				1.53	0.11	26			
Sulfosalicylic acid	$(Na)ClO_4$	3.91	0.06	37	5.05	0.23	26			
	$(K)NO_3$	2.66	0.07	51	4.96	0.02	68			
4-Aminosalicylic acid	$(Na)ClO_4$				0.220	0.001	42	8.8	0.6	32

*T = 25 °C; No. refers to the number of independently calculated values of K_a.

this case

$$[2a] \quad a_1 = \frac{\varepsilon}{\varepsilon - \varepsilon_1} = \frac{[ML] + [MHL]}{[M]} = \frac{[ML]}{[M]}(1 + \kappa_H[H])$$

Consequently eq. [1] now represents

$$[1a] \quad a_1[H]^2/[H_2L] = \text{"apparent } \kappa_1\text{"} = \kappa_1(1 + \kappa_H[H])$$

with an added term to compensate for hydrolysis. By plotting "apparent κ_1" against [H] values were obtained for κ_1 and κ_H from the intercept and slope of a straight line (15); this is shown in Fig. 1. Solutions were prepared as described for sulfosalicylic acid, and absorbance measurements made at 470, 500 (max. ε_1 = 1630), 520, and 550 nm.

The existence of a protonated complex must be taken into account in evaluating κ_2. The observed quantity $(\varepsilon_1 - \varepsilon)/(\varepsilon - \varepsilon_2)$ must now be interpreted as equivalent to $[ML_2]/([ML] + [MHL]) = ([ML_2]/[ML])(1 + \kappa_H[H])^{-1}$. Consequently the right-hand side of eq. [1] must be multiplied by $(1 + \kappa_H[H])$ to get satisfactory values of κ_2. In this case we are assuming that the only *bis* complex formed is ML_2 (see below).

In stabilizing the pH of solutions for measurement of κ_3, α-picoline, or 2,4-lutidine with appropriate quantities of acid provided suitable buffering. Hexamethylenetetraamine could not be used because of a rapid reaction in which a gelatinous solid was formed.

Results and Discussion

Values of the acidity constants measured in this study are given in Table 1. Comparison of these with results already in the literature are difficult because of the great variety of conditions under which these quantities have been measured. In Table 2 we have gathered together most of the published pK values for these acids, indicating as far as possible whether these refer to thermodynamic, mixed or concentration constants, and the conditions under which they are applicable.

The relationship between mixed constants and thermodynamic constants involves the activity coefficients of the ions generated by the acid. As a crude test of internal consistency we might invoke Davies' equation (46) to estimate such activity coefficients at some value of ionic strength, say 0.1 M. The variation of these coefficients for higher ionic strengths, up to 1 or 1.5 M is not particularly great. The following approximate relationships are thus predicted: (*a*) for salicylic and 4-aminosalicylic acids $(pK_2)_m = (pK_2)_t - 0.11$ and $(pK_1)_m = (pK_1)_t - 0.34$; (*b*) for 4-aminosalicylic acid $(pK_3)_m = (pK_3)_t + 0.11$; (*c*) for sulfosalicylic acid $(pK_2)_m = (pK_2)_t - 0.34$ and $(pK_1)_m = (pK_1)_t - 0.56$. The relationship between mixed constants and concentration quotients could be estimated by an extension of these equations to include an estimate of the hydrogen-ion activity coefficient. This estimation is complicated, however, by the fact that the hydrogen-ion function H which is incorporated in most mixed constants is based on the pH scale, and is not really a proper measure of hydrogen-ion activity since its measurement usually involves a liquid junction potential which is unknown. The relationship between H and [H] has been shown to depend on the background salt in the measured solution (18).

In general then, for backgrounds of moderate ionic strength, say up to 1 M, we would expect $(pK)_c < (pK)_m < (pK)_t$ save for pK_3 for 4-aminosalicylic acid for which we would predict $(pK)_c \sim (pK)_m > (pK)_t$. We must except from any such

Can. J. Chem. Downloaded from www.nrcresearchpress.com by 210.87.254.40 on 09/05/12
For personal use only.

Can. J. Chem. Downloaded from www.nrcresearchpress.com by 210.87.254.40 on 09/05/12
For personal use only.

TABLE 2

pK values* for salicylic acids collected from the literature

Acid	Nature of variable	pK_3	pK_2	pK_1	Temperature (°C)	Medium	Reference number
Salicylic acid	Thermodynamic		2.995[e]		25		27
			2.98[s]		25		28
			2.97[p]		25		29
			2.97[s]	13.59[s]	25		30
			2.93[s]	13.65[s]	25		31
				13.40[s]	Room		32
				13.40	18		33
	Mixed		2.88[p]		30	0.1 M KCl	34
			2.98[p]	13.61[s]	25	0.1–0.15 M KCl	10
			2.9[s]		26–28	Dilute salt	35
			2.95[p]		25	Quite dilute salt	36
			2.85[s]		25	Quite dilute salt	36
			3.14	13.4	18	0.1 M	37
	Concentration		2.69[p]	12.3[p]	20	0.1 M KCl	38
			2.82[p]		25	0.1 M $NaClO_4$	11
			2.82[p]		25	0.1 M $NaClO_4$	39
			2.82[p]		25	0.5 M $NaClO_4$	This work
			3.14[p]†	13.12[s]	25	3.0 M $NaClO_4$	13, 45
Sulfosalicylic acid	Thermodynamic		2.86		25		40
			2.84[p]		25		41
				11.4–11.57[s]	25		42
				11.6–11.81[p]	25		42
	Mixed		2.49[p]	12.00[s]	25	0.1 M $NaClO_4$	43
			2.62[p]	11.95[s]	25	0.1–0.15 M KCl	10
	Concentration		2.27[p]	11.40[p]	25	0.1 M KNO_3	44
			2.33[p]	11.32[p]	25	1.0 M KNO_3	44
			2.23–2.31[p]		25	1 M salts	18
			2.30[p]	11.41[p]	25	0.5 M $NaClO_4$	This work
			2.30[p]	11.58[p]	25	0.5 M KNO_3	This work
			2.67[p]	11.74[p]	25	3.0 M $NaClO_4$	8
4-Aminosalicylic acid	Thermodynamic	1.99[s]	3.92[s]				24
	Mixed	1.7[p]	3.9[p]			Dilute salt	23
		2.02[p]	3.73[p]			0.1 M NaCl or $NaClO_4$	15
		1.80[s]	3.66[s]	14[s]	18	0.25 M	9
	Concentration	1.78[p]	3.635[p]		20	0.1 M KCl	22
		1.79[s]			20	0.1 M KCl	22
		1.684[p]	3.625[p]		50	0.1 M KCl	25
		2.05[p]	3.66[p]		25	0.5 M $NaClO_4$	This work
		2.08[p]	4.08[p]	13.74[s]	25	3.0 M $NaClO_4$	13, 45

*Superscript e stands for electrical conductance; s for spectrophotometric; and p for potentiometric measurements.
†This value was given incorrectly as 3.86 in the original paper, and the wrong value reproduced elsewhere.

Can. J. Chem. Downloaded from www.nrcresearchpress.com by 210.87.254.40 on 09/05/12
For personal use only.

comparisons all of the constants measured in 3 *M* sodium perchlorate (8, 13, 45).

With one or two doubtful exceptions the values in Table 2 for pK_2 for all three acids conform with the relationships just given. With respect to values of pK_1 the situation is acceptable only for sulfosalicylic acid, but even here the thermodynamic values of Nair (42) seem incompatible with the remainder. For salicylic acid the values of pK_1 are not interrelated as expected, and the present authors have not been able to make a critical assessment of several of the original values to select preferred values. For 4-aminosalicylic acid the situation is even worse; only Agren's value (45) can be regarded as established with sufficient precision, yet obviously this cannot be used in conjunction with data secured in solutions of lower ionic strength.

Concerning pK_3 for 4-aminosalicylic acid, the one thermodynamic value does not appear to be correctly related to the remainder, and the variance among the mixed and concentration constants is appreciably higher than for the values of pK_2. The instability of the acidic solutions, the problems of working at such low p*H* values especially in perchlorate solutions, and of separating out two constants differing by less than two orders of magnitude all contribute to making this measurement difficult. Attention is drawn to the poorer precision of our K_{a3} values compared to those for K_{a2} even though the results were calculated from the same titrations. These difficult determinations were done with maximum care.

We have assembled the results of our determinations of metal complex equilibrium constants together with measures of dispersion in Table 3. Our results are not given in the form of stability constants by the application of eq. [7], owing to the unsatisfactory situation regarding K_{a1} values for salicylic acid and 4-aminosalicylic acid, but it would be easy to do so in the case of sulfosalicylic acid complexes. The different values of κ_1 for the sulfosalicylate complexes in potassium nitrate and sodium perchlorate media appear to be significant, though one cannot, on the basis of these experiments, identify a cause; a similar sort of difference was found with the Tiron complex (3). It seems worth noting, however, that the variation in κ_1 between perchlorate and nitrate is paralleled by that in K_{a1} in the same media. Thus values of K_1 calculated by eq. [7] are nearly equal: 2.48×10^{14} for perchlorate and 2.32×10^{14} for nitrate.

In Table 4 are shown the results of most of the studies known to us on the iron(III) salicylates. Because these have been reported in a variety of ways we have reduced them, and our own, to a common basis; namely, values of $\kappa_n' = [ML_n][H]/[ML_{n-1}][HL]$. This has necessitated applying in a few cases values of acidity constants; where given, we used the values in the original papers, otherwise we employed values shown in footnotes to the table.

From this compilation we have omitted some early spectrophotometric measurements of κ_1 for the sulfosalicylate complex (5, 17) on the grounds that these (*a*) did not take into account hydrolysis of the metal ion, (*b*) did not take into account ionization of the carboxyl group of the ligand, and (*c*) employed limiting slopes on Job curves (47) to determine ε_1 and so to calculate [ML]. This last procedure is known to be valid only for relatively stable complexes (48); for the sulfosalicylate complex the effect of low p*H* is to limit the degree of conversion to ML to such an extent that the procedure fails. In our measurements on solutions prepared for continuous variations analysis it was observed that the apparent values of ε_1 deduced from limiting slopes (as $x \rightarrow 0$ or $x \rightarrow 1$) varied according to the p*H* of each set of solutions. We have also omitted a value of β_3 for the sulfosalicylate complexes based on polarographic measurements (43*a*); this early work entailed a number of estimates and assumptions, and led to a value of β_3 at variance with all subsequent determinations.

The results collected in Table 4 display considerable variance, some of which undoubtedly can be assigned to the different conditions under which the various experiments were conducted. Small temperature differences do not seem to affect these equilibria much; but medium effects are bound to be significant, and will be reflected in the values of these stability constants which, with one or two exceptions, are concentration quotients within which are embodied activity coefficients of some ions of appreciable charge.

There are, however, some other sources of errors in the data of Table 4 which are revealed by careful reading of the original papers. It is significant that the quite disparate results of Mattoo (7) and Vareille (6) for the sulfosalicylates were obtained from the same experimental data

Can. J. Chem. Downloaded from www.nrcresearchpress.com by 210.87.254.40 on 09/05/12
For personal use only.

TABLE 3

Formation constants of iron(III) salicylates*

Acid	Medium (0.5 *M*)	κ_1			κ_2			κ_3		
		Value	σ	No.	Value	σ	No.	Value	σ	No.
Salicylic acid	$(Na)ClO_4$	1.08	0.14	30						
Sulfosalicylic acid	$(Na)ClO_4$	4.92	0.65	102						
	$(K)NO_3$	3.06	0.35	33	5.66×10^4	1.10×10^4	40	3.67×10^7	0.52×10^7	57
		2.62	0.42	18†						
4-Aminosalicylic acid	$(Na)ClO_4$	2.52	0.40‡	84	0.107×10^4§	0.301×10^4	38	4.51×10^{10}	1.45×10^{10}	45

*$\kappa_n = [ML_n][H]^2/[ML_{n-1}][H_2L]$. No. refers to the number of independently calculated values of κ_n; each set includes measurements at least at three wavelengths.
†Mean of determinations from four sets of solutions prepared by Job analysis.
‡Estimated.
§For this ligand only, κ_2 is of the form [complex][H]/[ML][H_2L].

TABLE 4

Formation constants of iron(III) salicylates

Acid	κ_1'	κ_2'	κ_3'	Reference: Authors	Year	Ref. No.
Salicylic acid	1000‡	1.15×10^{-2}‡	2×10^{-8}‡	Babko	1945	14
	900	—	—	Bertin-Batsch	1952	52
	500	3.6×10^{-2}	4.4×10^{-5}	Agren	1954	13
	470	3.2×10^{-2}	1×10^{-5}			
	320	1.2×10^{-3}	4×10^{-6}	Vareille	1955	12
	550	1.95×10^{-2}	—	Perrin	1958	10
	1200	4.4×10^{-2}	10^{-6}	Colleter	1960	9
	1000‡	1.6×10^{-2}‡	—	Shchigol	1961	53
	1010	—	—	Tsin-jao *et al.*	1961	37
	7000*	—	—	Ernst and Menashi	1963	54
	170§	5.1×10^{-2}§	9.5×10^{-5}§	Ogawa and Tobe	1966	55
	820	2.1×10^{-2}	—	Park	1966	11
	710	—	—	This work		
Sulfosalicylic acid	480	11×10^{-2}	2×10^{-5}	Agren	1954	8
	800	4.4×10^{-2}	2×10^{-5}	Vareille	1954	6
	2200	15×10^{-2}	1.6×10^{-5}	Mattoo	1957	7
	450	4×10^{-2}	—	Perrin	1958	10
	1900	10×10^{-2}	1.3×10^{-5}	Colleter	1960	9
	1250	5.5×10^{-2}	10^{-3}	Tsin-jao *et al.*	1961	37
	200§	3.4×10^{-2}§	10^{-3}§	Ogawa and Tobe	1966	56
	970	—	—	This work (ClO_4^-)		
	615	11.4×10^{-2}	7.4×10^{-5}	(NO_3^-)		
4-Aminosalicylic acid	1500	2.3×10^{-2}	1×10^{-5}	Agren	1954	13
	$\kappa_1'\kappa_H = 1.6\times10^6$					
	—	10^{-1}†	1.6×10^{-6}†	Colleter	1960	9
	$\kappa_1'\kappa_H = 1.15\times10^6$					
	5200*	—	—	Das and Aditya	1960	57
	4400	—	—			
	$\kappa_1'\kappa_H = 1\times10^6$			Tsin-jao *et al.*	1962	15
	11 500	1.07×10^{-1}	2.0×10^{-6}	This work		
	$\kappa_1'\kappa_H = 1.53\times10^6$					

*Thermodynamic constant.
†For constants respectively defined as $[MH_2L_2][H]/[MHL][H_2L]$ and $[MH_2L_3][H]/[MH_2L_2][HL]$.
‡Calculated with $pK_1 = 13.4$.
§Calculated with Agren's values of pK_1.

by different manipulation of the figures. It is not unknown for different mathematical procedures to yield different values of equilibrium constants from the same observations (49). In at least two sets of results cited the authors appear to have made no allowance for hydrolysis of the uncomplexed iron(III) in their evaluation of κ_1; this omission significantly affects the value of the equilibrium constant. In two cases acetate buffers have been used to stabilize pH in solutions prepared for spectral measurements, but acetate and chloracetate have been shown to compete with similar ligands (2) for reaction with iron(III). In evaluation of κ_1 the values of K_{a2} and K_h put into eqs. [1] and [3] affect the answers, since measurements are made in a region of pH near pK_{a2} and pK_h. But instances can be found of the use of inappropriate values of these constants in arriving at the values of κ_n' in Table 4. Some authors have used thermodynamic values of K_{a2} to obtain κ_1, but as the data of Table 2 show, this factor could cause a value of κ_1, expressed as a mixed or concentration quotient, to be in error by as much as a factor of two. Finally, in respect of the measurement of reactions at low pH, such as the study of the protonated complex of 4-aminosalicylate, it is evident that close attention must be paid to the relationship between hydrogen-ion concentration and that property measured by a glass and reference electrode. Although this was not a consideration in Colleter's choice of complex compositions (9), it undoubtedly has contributed to the difficulty in securing good agreement among the different studies of this reaction.

Our conclusions regarding the 4-aminosalicylate complexes differ in some respects from those of Agren (13) and Colleter (9). The former based

Can. J. Chem. Downloaded from www.nrcresearchpress.com by 210.87.254.40 on 09/05/12
For personal use only.

Can. J. Chem. Downloaded from www.nrcresearchpress.com by 210.87.254.40 on 09/05/12
For personal use only.

a spectrophotometric estimate of κ_1 and κ_H on the assumption that the species ML and MHL had different absorption spectra. He assigned a band with λ_{max} = 510 nm (identifiable with our 500 nm band) to MHL (ε_{max} = 1330), and maxima at 460 and 470 nm, respectively, to ML (ε_{max} = 2800) and ML_2 (ε_{max} = 3400). By analogy with other iron(III)—phenolic chelates, it is improbable that the absorption maximum for ML occurs at a lower wavelength than that for ML_2; we observed no absorption curves that would support such an assignment. Our observations are consistent with the assignment of spectra for individual species shown in Fig. 2. Agren's suppositions about the species present in certain p*H* ranges have naturally led him to assign somewhat different stability constants.

Colleter, on the other hand, found his observed data fitted an expression for κ_1 having the form [complex][H]/[Fe][H_2L], and so concluded that his first complex was solely MHL. Tsin-jao *et al.* (15) deduced, like Agren, the existence of two separate complexes ML and MHL. The results of these authors and our own with respect to the mono complexes are in reasonable agreement.

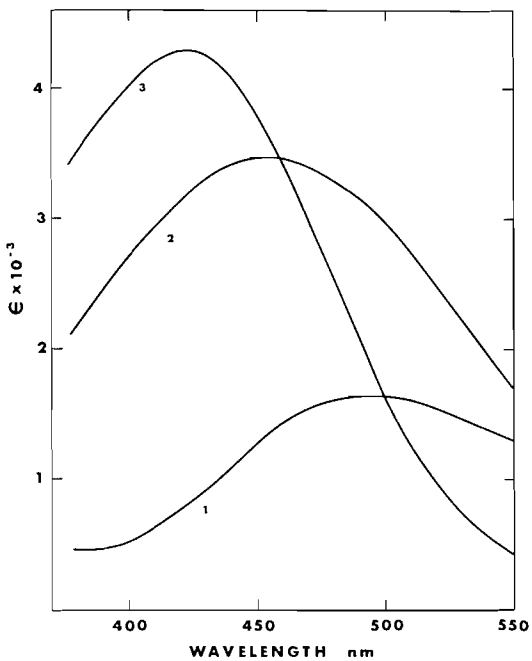

FIG. 2. Absorption spectra of Fe-4-aminosalicylate complexes. **1** = ML or MHL; **2** = MHL_2 or ML_2; **3** = MHL_3 or ML_3. For calculation of ε_2 see text.

Although the several values of κ_1' for the 4-aminosalicylate complex shown in Table 4 vary considerably, it is noteworthy that the values of $\kappa_1'\kappa_H$ = [MHL]/[M][HL] are in good agreement. This seems to signify that, if one were to consider mixing iron(III) and this reagent in acidic solution and then gradually raising the p*H*, the various studies are essentially unanimous concerning the onset of formation of MHL, but differ in their estimates of the region of p*H* in which this dissociates to ML. This is apparent from a comparison of values of p*K* for deprotonation of MHL^{2+}, i.e. log κ_H, viz.,

Author	log κ_H	pK_{a3}
Agren (13)	3.02	2.08
Colleter (9)	Very large	1.80
Tsin-jao *et al.* (15)	2.36	2.02
This work	2.12	2.05

To our surprise the values of κ_2 calculated as described above proved not to be constant; instead they were proportional to [H] as shown in Fig. 1. It appears that a protonated *bis* complex MHL_2 is indicated, so that our equilibrium constant "κ_2" in this case is of the form [MHL_2]-[H]/[ML][H_2L]. This observation and the value of κ_2 are in agreement with Colleter's results. The same applies to our data for the third complex which fitted an expression for the stability constant having the form [MHL_3][H]^2/[MHL_2]-[H_2L].

Agren quite plausibly attributed protonation of the 4-aminosalicylate complex to the uptake of a hydrogen ion by the *para* amino group. There appear to be grounds for questioning this notion, although it is clear that equilibrium studies such as are discussed in this paper cannot alone provide a satisfactory explanation. One would expect that substitution of a tervalent metal ion for two hydrogen ions (if ML is a chelate complex) would considerably deter the addition of a proton at the amino group. Instances are known (50) where bivalent metal complexes of amino acids with a remote acidic functional group (e.g. tyrosine, ornithine) show a p*K* for the latter lower than the corresponding value in the free ligand. A more striking, though not strictly comparable, instance of the same effect is seen in the work of Freiser and co-workers (51). Hence one would expect that log κ_H should be smaller than pK_3 here; the reverse is seen to be the case. An

Can. J. Chem. Downloaded from www.nrcresearchpress.com by 210.87.254.40 on 09/05/12
For personal use only.

alternative explanation is that protonation occurs at the carboxyl group, so that the complex MHL no longer has the chelate structure but retains the chromophoric iron(III)–phenol link. The occurrence of this would account for log κ_H being greater than pK_3, and to some extent for the appearance of a protonated species at higher p*H*. However, since the κ_2 values were determined in the p*H* range 3 to 4.5 and κ_3 between 6 and 7.5, it is difficult to believe that the carboxyl group continues to bind a proton throughout this range of p*H*. If the higher complexes are, as might be expected, ML_3 and ML_2, then the formation of the latter must, to fit our data, have been from MLOH; but the existence of such a species is not indicated by our results. By forcing the correlation line of Fig. 1*a* through the origin, one can at small sacrifice in precision infer that MHL is the sole mono species. In this case we would be in complete agreement with Colleter's conclusions; however, we regard these as questionable at higher p*H*.

The addition of a proton to the ML complexes could not be detected within the ranges of p*H* examined with salicylic acid or sulfosalicylic acid. We are, therefore, unable to support the suggestion tentatively advanced by Park (11) that a protonated iron(III) salicylate is formed under these conditions.

Experimental

The data reported here have been accumulated in different laboratories and over a long period of time so that there has been some evolution of procedures and instrumentation throughout; consequently what follows is only a general outline. The three reagents studied were purchased in Laboratory Reagent grade, assayed by acid–base titration, and as their purity was in each case found to be close to 100% they were used without further purification. The iron(III) solution was prepared from the appropriate salt dissolved in the dilute acid of that salt; the solution was analyzed for content of iron and of hydrogen ion. All chemicals were of AnalaR or similar grade, and Class A volumetric glassware was used throughout. Temperatures of solutions were maintained at 25 ± 0.1 °C.

The hydrogen-ion concentrations were determined from p*H* measurements (18) with glass and calomel electrodes. The equipment was standardized with fresh NBS buffers (phthalate, phosphate, or borax) and the interval in p*H* between a suitable pair of buffers fitted if necessary by adjustments of the temperature-compensating control on the meter. The consistency of performance of the electrodes was checked frequently with these buffers, since ultimately all hydrogen-ion values related back to this standardization.

Absorption spectra were measured with recording spectrophotometers, mainly Cary Model 14, but all absorbance measurements to be incorporated in equilibrium constant calculations were obtained on a null-type instrument, mainly Beckman Model DU. Experience has shown that only individually measured absorbance values are accurate enough to be applied in calculations of the sort made here.

Most of the repetitive calculations were handled by computer, with programs developed on an *ad hoc* basis. The experimental results are on file with the Depository of Unpublished Data.[7]

The authors thank the National Research Council of Canada for grants-in-aid in support of this work, and members of the staff of the Computing Centers, University of Waterloo and Australian National University for guidance in the computer programming. One author (McB) is grateful for the tenure of a Visiting Fellowship at the Australian National University and for helpful discussions with Dr. D. D. Perrin.

1. L. Vareille. Bull. Soc. Chim. France, 870 (1955).
2. W. A. E. McBryde and G. F. Atkinson. Can. J. Chem. **39**, 510 (1961).
3. W. A. E. McBryde. Can. J. Chem. **42**, 1917 (1964).
4. G. Schwarzenbach and A. V. Willi. Helv. Chim. Acta, **34**, 528 (1951).
5. R. T. Foley and R. C. Anderson. J. Amer. Chem. Soc. **70**, 1195 (1948).
6. L. Vareille. Bull. Soc. Chim. France, 872 (1955).
7. B. N. Mattoo. Z. Phys. Chem. Frankfurt, **13**, 316 (1957).
8. A. Agren. Acta Chem. Scand. **8**, 266 (1954).
9. J. C. Colleter. Ann. Chim. Paris, **5**, 415 (1960).
10. D. D. Perrin. Nature, **182**, 741 (1958).
11. M. V. Park. Nature, **197**, 283 (1963); J. Chem. Soc. A, 816 (1966).
12. L. Vareille. Bull. Soc. Chim. France, 1493 (1955).
13. A. Agren. Acta Chem. Scand. **8**, 1059 (1954).
14. A. K. Babko. J. Gen. Chem. U.S.S.R. **15**, 745 (1945).
15. J. Tsin-jao, L. Sommer, and A. Okáč. Coll. Czech. Chem. Commun. **27**, 1150 (1962).
16. A. K. Babko and T. N. Rychkova. J. Gen. Chem. U.S.S.R. **18**, 1617 (1948). *cf.* Chem. Abstr. **43**, 2536d (1949).
17. R. K. Nanda and S. Aditya. J. Indian Chem. Soc. **34**, 577 (1957).
18. W. A. E. McBryde. Anal. **94**, 337 (1969).
19. A. Liberti and T. S. Light. J. Chem. Educ. **39**, 236 (1962).
20. A. S. Wilson and H. Taube. J. Amer. Chem. Soc. **74**, 3509 (1952).
21. P. Job. Ann. Chim. Phys. **9**, 113 (1928); W. C. Vosburgh and G. R. Cooper. J. Amer. Chem. Soc. **63**, 437 (1941).
22. A. V. Willi and J. F. Stocker. Helv. Chim. Acta, **37**, 1113 (1954).
23. S. Fallab, W. Vogtli, M. Blumer, and H. Erlenmeyer. Helv. Chim. Acta, **34**, 26 (1951).
24. A. M. Liquori and A. Ripamonti. Gazz. Chim. Ital. **85**, 578 (1955).

[7]Photocopies may be obtained free of charge, upon request, from: Depository of Unpublished Data, National Science Library, National Research Council of Canada, Ottawa, Canada.

25. J. M. Los, R. F. Rekker and C. H. T. Tonsbeek. Rec. Trav. Chim. **86**, 609 (1967).
26. G. B. Barlin and D. D. Perrin. Quart. Rev. **20**, 75 (1966); J. Clark and D. D. Perrin. Quart. Rev. **18**, 295 (1964).
27. L. J. Bray, J. F. J. Dippy, S. R. C. Hughes, and L. W. Laxton. J. Chem. Soc. 2405 (1957).
28. L. J. Minnick and M. Kilpatrick. J. Phys. Chem. **43**, 259 (1939).
29. R. Kuhn and A. Wasserman. Helv. Chim. Acta, **11**, 1 (1928).
30. Z. L. Ernst and J. Menashi. Trans. Faraday Soc. **59**, 230 (1963).
31. V. P. Vasil'ev, L. S. Mukhina and A. F. Belyakova. Izv. Vyssh. Ucheb. Zaved. Khim. Tekhnol. **9**, 879 (1966); *cf.* Chem. Abstr. **66**, 15669*m* (1967).
32. N. Konopik and O. Leberl. Monatsh. **80**, 655 (1949).
33. E. Larsson. Z. Anorg. Allgem. Chem. **183**, 30 (1929).
34. M. Cefola, A. S. Tompa, A. V. Celiano, and P. S. Gentile. Inorg. Chem. **1**, 290 (1962).
35. R. C. Das and S. Aditya. J. Indian Chem. Soc. **36**, 473 (1959).
36. J. M. Vandenbelt, C. Henrich, and S. G. Vanden Berg. Anal. Chem. **26**, 726 (1954).
37. J. Tsin-jao, L. Sommer, and A. Okáč. Spisy Prirodovedeké Fakulty, Universität J. E. Purkyne, Brno, 1961, No. 420, 93; *cf.* Chem. Abstr. **56**, 1118*li* (1962).
38. A. V. Willi and J. F. Stocker. Helv. Chim. Acta, **38**, 1279 (1955).
39. B. Hok. Svensk. Kem. Tidskr. **65**, 182 (1953).
40. R. G. Bates, cited by R. T. Foley and R. C. Anderson. J. Amer. Chem. Soc. **71**, 909 (1949).
41. R. Nasänen and P. Merilainen. Suomen Kem. **35B**, 74 (1962).
42. V. S. K. Nair. Trans. Faraday Soc. **57**, 1988 (1961).
43. *a* C. V. Banks and J. H. Patterson. J. Amer. Chem. Soc. **73**, 3062 (1951); *b* C. V. Banks and R. S. Singh. J. Amer. Chem. Soc. **81**, 6159 (1960); J. Inorg. Nucl. Chem. **15**, 125 (1960).
44. K. S. Rajan and A. E. Martell. J. Inorg. Nucl. Chem. **26**, 789 (1964).
45. A. Agren. Acta Chem. Scand. **9**, 49 (1955).
46. C. W. Davies. J. Chem. Soc. 2093 (1938).
47. Y. Schaeppi and W. D. Treadwell. Helv. Chim. Acta, **31**, 577 (1948).
48. G. Schwarzenbach. Helv. Chim. Acta, **32**, 839 (1949).
49. W. A. E. McBryde. Can. J. Chem. **45**, 2093 (1967).
50. D. D. Perrin and associates. Unpublished work.
51. S. P. Bag, Q. Fernando, and H. Freiser. Inorg. Chem. **1**, 887 (1962); **3**, 93 (1964).
52. C. Bertin-Batsch. Ann. Chim. Paris, **7**, 481 (1952).
53. M. B. Shchigol. J. Inorg. Chem. U.S.S.R. **6**, 664 (1961).
54. Z. L. Ernst and J. Menashi. Trans. Faraday Soc. **59**, 1794 (1963).
55. K. Ogawa and N. Tobe. Bull. Chem. Soc. Japan, **39**, 227 (1966).
56. K. Ogawa and N. Tobe. Bull. Chem. Soc. Japan, **39**, 223 (1966).
57. R. C. Das and S. Aditya. J. Indian Chem. Soc. **37**, 557 (1960).

Can. J. Chem. Downloaded from www.nrcresearchpress.com by 210.87.254.40 on 09/05/12
For personal use only.

Can. J. Chem. Downloaded from www.nrcresearchpress.com by 210.87.254.105 on 09/05/12
For personal use only.

Etude de la cycloalcoylation des (thiényl-2)-5 pentènes-1 [1]

J. GOURIER ET P. CANONNE

Département de chimie, Université Laval, Québec 10, Québec

Reçu le 24 mars 1970

La cyclisation des (thiényl-2)-5 pentènes-1 substitués en β de la double liaison par des groupements fonctionnels variés (COOH, $COOCH_3$, CH_2OH, CH_3) à l'aide des acides protoniques et de Lewis, démontre que le rendement en produits cyclisés dépend du groupement fonctionnel, du catalyseur, et de la durée de la réaction.

Cyclizations of 5(2-thienyl)pent-1-enes substituted at carbon-4 (COOH, $COOCH_3$, CH_2OH, or CH_3) by the action of mineral and Lewis acids are reported. The yield of cyclized product varies with the nature of the substituent, the acid catalyst employed, and the reaction time.

Canadian Journal of Chemistry, 48, 2587 (1970)

Introduction

Les hétérocycles sulfurés à noyaux aromatiques condensés présentent un intérêt certain en pharmacologie. Leur synthèse s'effectue par deux voies principales : la formation de l'hétérocycle en partant d'un thiol ou la formation des carbocycles en partant du thiophène. La première cycloacylation du thiophène a été réalisée en 1936 avec la cyclisation du chlorure de l'acide γ (thiényl-2)-butyrique (1). Ces travaux ont été ensuite repris et développés largement par Cagniant et Cagniant et ont abouti à la synthèse de thiénocyclènones et benzothiénocyclenones variées (2–5). Cependant la cycloacylation, vu la nature des produits que l'on y utilise, ne permet de conserver dans le carbocycle d'autres groupements fonctionnels que le carbonyle. Dans le but de pallier cette faiblesse de la méthode, il était utile d'étendre au thiophène les travaux sur la cycloalcoylation que l'un d'entre nous a consacrés aux benzène et naphtalène (6–8). Le thiophène, par rapport aux carbocycles aromatiques, offre l'avantage, en raison de la présence de l'hétéroatome, de ne donner qu'un seul dérivé cyclisé (9 et 10). Dans une note préliminaire (10) et pour la première fois, nous avons mentionné la cycloalcoylation, avec d'excellents rendements, des oléfines **11** en tétrahydrobenzothiophènes et octahydrodibenzothiophènes par les acides de Lewis.

Dans le présent article nous rapportons une étude systématique de la cycloalcoylation de thiényloléfines, substituées en β de la double liaison, par divers groupements fonctionnels (Schéma 1). Leur préparation repose essentiellement sur la condensation d'halogénoalcoylthiophènes **1** avec l'allylmalonate d'éthyle sodé. Cette méthode permet un contrôle efficace de la position de la chaîne sur le substrat aromatique, avantage que n'offre ni l'acylation ni l'alcoylation. La condensation simultanée de deux molécules d'allylmalonate d'éthyle conduit, en une seule étape, à des composés possédant deux chaînes oléfiniques. Enfin, le groupement dicarbéthoxyle installé en β de la double liaison, permet le passage aux oléfines, objet de cette étude (Schéma 2).

Etudes des cycloalcoylations

Monocycloalcoylation

Cycloalcoylation des oléfines 11

La cycloalcoylation des oléfines **11** en tétrahydrobenzothiophènes **12** se produit sans difficultés, au moyen soit des acides de Lewis à température ambiante, $AlCl_3$ dans le dichlométhane ou BF_3 dans l'éthérate de trifluorure de bore, soit des acides protoniques, mélange d'acides acétique et sulfurique concentrés 95:5 à température de reflux. Pour cycliser de faibles quantités, nous retenons la facilité de manipulation de BF_3 dissous dans l'éthérate de trifluorure de bore. Au contraire, pour des quantités plus importantes les deux autres catalyseurs seront préférés pour leur manipulation plus aisée et leur coût moindre (Schéma 3).

Cycloalcoylation des alcools 9

Les alcools **9** se cyclisent aisément par le mélange H_2SO_4–AcOH dans les mêmes conditions que **11** et donnent les acétates **10** avec de très bons rendements (Schéma 6).

[1]Ce travail a fait l'objet d'une communication au 38e Congrès international de chimie industrielle (Istanbul, Turquie, septembre 1969).

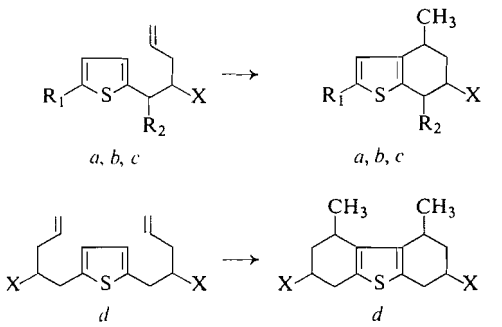

a, *b*, *c* *a*, *b*, *c*

d *d*

a: $R_1 = R_2 = H$; *b*: $R_1 = H$, $R_2 = CH_3$; *c*: $R_1 = R_2 = CH_3$
$X = CH_3$; CH_2OH; $COOCH_3$; COOH ($\neq d$)

SCHÉMA 1

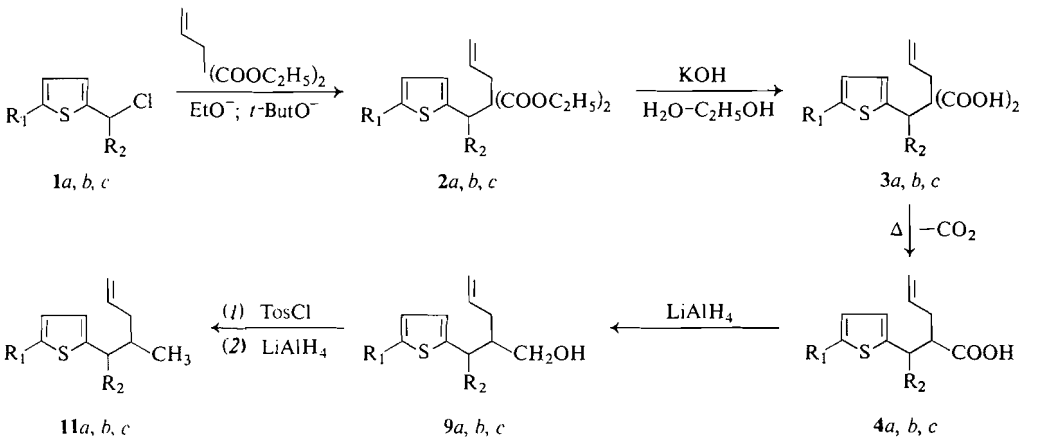

1*a*, *b*, *c* **2***a*, *b*, *c* **3***a*, *b*, *c*

11*a*, *b*, *c* **9***a*, *b*, *c* **4***a*, *b*, *c*

a: $R_1 = R_2 = H$; *b*: $R_1 = H$, $R_2 = CH_3$; *c*: $R_1 = R_2 = CH_3$

SCHÉMA 2

Cycloalcoylation des esters 7

Les esters **7** préparés par action du diazométhane sur les acides **4** sont cyclisés au moyen du chlorure d'aluminium et conduisent aux esters correspondants **8**. Toutefois le contrôle de cette cyclisation est plus difficile que dans les réactions précédemment décrites et les rendements ne sont que de l'ordre de 70% (Schéma 3).

Cycloalcoylation des acides 4

Le rendement de cette cyclisation ne dépasse guère 15% alors qu'il lui arriva d'être quantitatif en série benzénique et de 60% en série naphtalénique.

Ce médiocre résultat provient de la réaction concurrente de lactonisation qu'en dépit de nos multiples efforts en vue de favoriser l'acide cyclisé aux dépens de la lactone, par un choix approprié et des quantités différentes de catalyseurs, il n'a pas été possible d'éliminer (Schéma 4).

Double cycloalcoylation

Cycloalcoylation de l'oléfine 11d

Alors que l'oléfine **11***d* se transforme très aisément et avec des bons rendements en octahydrodibenzothiophènes par le chlorure d'aluminium ou le mélange H_2SO_4–AcOH, elle reste au contraire, inchangée en présence de BF_3 quelles que soient les conditions opératoires. L'inefficacité de ce catalyseur n'entraîne aucun inconvénient dans la réussite de la double cyclisation car les catalyseurs premiers cités profitent d'une manipulation facile et d'un coût peu élevé (Schéma 5).

Cycloalcoylation du diol 9d

Effectuée dans les mêmes conditions que la

Can. J. Chem. Downloaded from www.nrcresearchpress.com by 210.87.254.105 on 09/05/12
For personal use only.

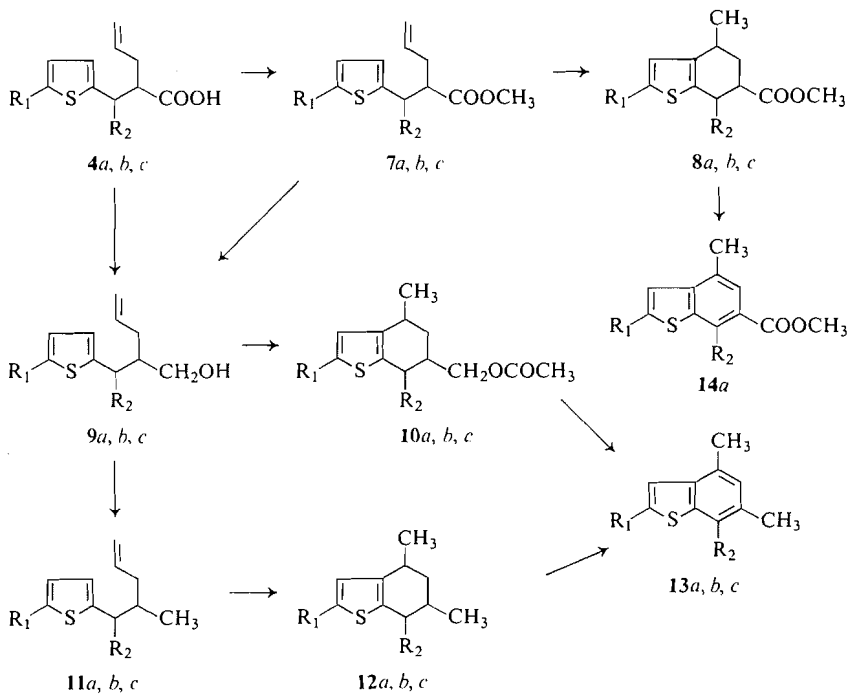

a: $R_1 = R_2 = H$; *b*: $R_2 = CH_3$, $R_1 = H$; *c*: $R_1 = R_2 = CH_3$

SCHÉMA 3

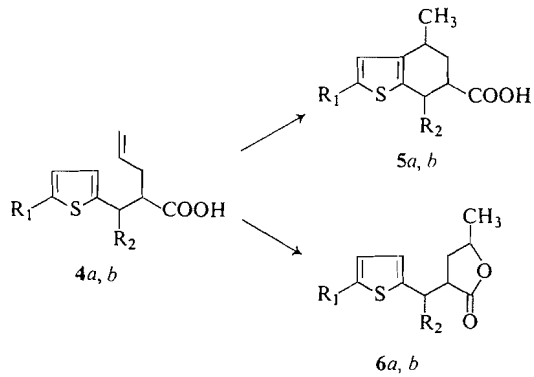

a: $R_1 = R_2 = H$; *b*: $R_1 = H$, $R_2 = CH_3$

SCHÉMA 4

simple, la double cyclisation du diol **9***d* conduit, avec d'excellents résultats, au diacétate **10***d* (Schémas 5 et 6).

Cycloalcoylation du diester 7d

Cette cyclisation, à cause de la quantité importante de catalyseur ($AlCl_3$) mise en jeu, est d'un contrôle difficile. Toute prolongation de la durée de réaction, toute élévation de température favorise les réactions secondaires; le rendement ne dépasse pas 50% (Schéma 5).

Remarque

Nous avons renoncé à la double cycloalcoylation du diacide **4***d* après avoir constaté la baisse corrélative du rendement en passant de la mono

Can. J. Chem. Downloaded from www.nrcresearchpress.com by 210.87.254.105 on 09/05/12
For personal use only.

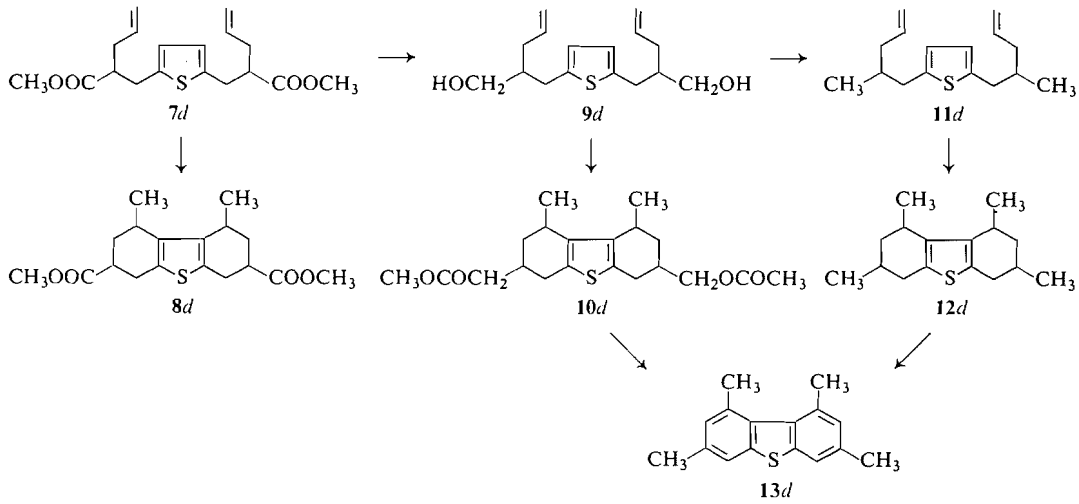

SCHÉMA 5

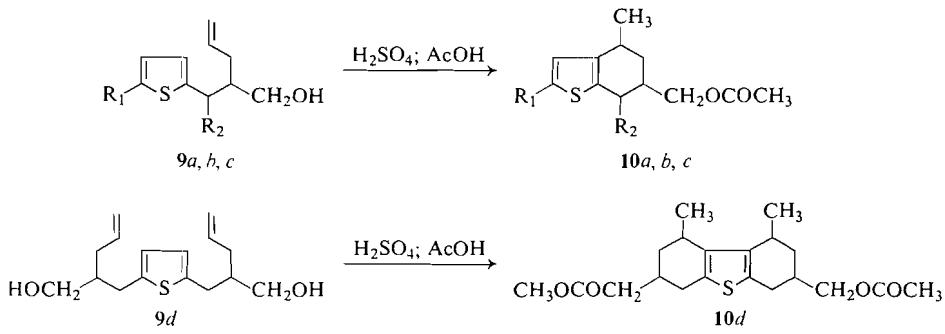

a: $R_1 = R_2 = H$; *b*: $R_1 = H$, $R_2 = CH_3$; *c*: $R_1 = R_2 = CH_3$

SCHÉMA 6

à la double cycloalcoylation et noté la difficulté de la séparation en raison de la présence de l'acide-lactone (8).

Stéréochimie

Comme l'on pouvait s'y attendre toutes les cyclisations conduisent à des mélanges d'isomères *cis* et *trans* traduits par la présence de deux doublets ($J = 7$ Hz) d'égale intensité dans la région des méthyles cyclaniques, et par la modification du motif aromatique.

La chromatographie de **8***a* sur gel de silice en éluant au pentane à 0.25% d'acétate d'éthyle permet la séparation des deux isomères. On observe la présence de cinq signaux dans la région des protons aromatiques dus à la superposition de deux doublets de doublets (système AB), l'un étant décalé de 0.10 p.p.m. Dans le cas de l'isomère *trans* (méthyle en 4 axial) ces signaux se manifestent ainsi : δ CH_3 (3H) 1.10 ($J = 7$ Hz) ; H_2 (1H) 6.98 (d, $J = 5$ Hz) ; H_3 (1H) 6.81 p.p.m. (d, $J = 5$ Hz) ; et pour l'isomère *cis* : (méthyle en 4 équatorial) : δ CH_3 (3H) 1.12 (d, $J = 7$ Hz) ; H_2 (1H) 6.98 (d, $J = 5$ Hz) ; H_3 (1H) 6.71 p.p.m. (d, $J = 5$ Hz). Cette distinction devient très difficile lorsque le nombre des méthyles cyclaniques augmente.

Les cyclisations envisagées sont réalisables quels que soient les catalyseurs, les groupements fonctionnels portés par les chaînes latérales ou le nombre de celles-ci, mais les rendements sont fortement affectés par la nature du groupement fonctionnel ou la durée de la réaction et par le choix du catalyseur. Si l'on désire conserver un

Can. J. Chem. Downloaded from www.nrcresearchpress.com by 210.87.254.105 on 09/05/12
For personal use only.

Can. J. Chem. Downloaded from www.nrcresearchpress.com by 210.87.254.105 on 09/05/12
For personal use only.

groupement fonctionnel il est préférable de réaliser la cyclisation au niveau de l'ester **7** et de l'alcool **9**. Si au contraire on souhaite la préparation des hydrocarbures polyméthylés la cyclisation au niveau d'oléfines **11** est plus facile et de loin la plus rentable.

Partie expérimentale

Les points de fusion sont repérés sur un appareil Thomas–Hoover et ne sont pas corrigés. Les spectres de masse sont enregistrés sur un spectromètre Varian M-66. Les spectres infrarouges (i.r.) ont été pris sur un spectrophotomètre Perkin–Elmer 457, soit en film pour les liquides (fenêtres de NaCl) soit en pastilles de KBr pour les solides.

Etant donné la grande similitude entre les différents composés décrits nous aurons toujours les absorptions suivantes : C=O (esters méthyliques) $\simeq$ 1740; C=O (esters maloniques) $\simeq$ 1735; C=O (acides **3** et **4**) $\simeq$ 1710; C=O (lactone) $\simeq$ 1770 et 1190; OH (alcool) $\simeq$ 3350 et 1060; CH_2—OSO_2—(tosylate) $\simeq$ 1360 et 1178; CH=CH_2—(allyle) $\simeq$ 3080 et 1640 cm^{-1}.

Les spectres de résonance magnétique nucléaire (r.m.n.) sont enregistrés sur un spectromètre Varian A-60 et sont pris en solution dans CCl_4 à 1% de TMS. Ils nous permettent de suivre avec précision les réactions de cyclisation (disparition du multiplet —CH=CH_2 entre 4.80 et 6.00 p.p.m.), et d'aromatisation (disparition des méthyles cyclaniques vers 1.1 p.p.m., et apparition de méthyles aromatiques vers 2.3 p.p.m.).

Halogénoalcoylthiophènes ***1***

*Chlorométhyl-2 thiophène (**1a**) selon (11)*

On sature à 0 °C par 78 g de chlorure d'hydrogène, un mélange de 81 g d'une solution aqueuse de formol à 37% et 1 mole d'acide chlorhydrique concentré. Sous forte agitation, on l'additionne goutte à goutte, en 35 min à 1 mole de thiophène (84 g) refroidie entre −10 et 0 °C. Après introduction on ajoute 150 cm^3 d'eau, extrait à l'éther de pétrole, lave à l'eau, au bicarbonate de sodium et encore à l'eau. On sèche la phase aqueuse sur $MgSO_4$ anhydre, évapore le solvant, distille sous pression réduite. Rendement : 50%; p.é. 82–83 °C sous 20 mm Hg.

*(Chloro-1 éthyl)-1 thiophène-2 (**1b**)*

A une suspension de 0.15 mole (5.7 g) de $LiAlH_4$ dans 250 cm^3 d'éther éthylique anhydre, on ajoute goutte à goutte, en refroidissant, une solution de 0.5 mole (63 g) d'acétyl-2 thiophène dans 150 cm^3 d'éther éthylique anhydre. Après introduction on porte à reflux 1 h, puis refroidit et détruit l'excès de $LiAlH_4$ par l'acétate d'éthyle et l'eau. On filtre les hydroxydes, sèche la phase organique sur $MgSO_4$ anhydre, évapore le solvant et distille sous pression réduite.

On obtient 62 g d'(hydroxy-1 éthyl)-1 thiophène-2. Rendement : 98%; p.é. 48 °C sous 0.05 mm Hg.

On dissout l'alcool obtenu dans 200 cm^3 d'éther de pétrole, refroidit à 0 °C et introduit sous agitation magnétique 250 cm^3 d'HCl concentré. Après 10 min, on ajoute 500 cm^3 d'eau glacée, décante, lave la phase organique à l'eau, au bicarbonate et encore à l'eau. On sèche sur $MgSO_4$ anhydre, évapore le solvant, distille sous pression réduite. On obtient 65 g de (chloro-1 éthyl)-1 thiophène-2. Rendement : 90%; p.é. 75 °C sous 15 mm Hg.

*Méthyl-5, (chloro-1 éthyl)-1 thiophène-2 (**1c**)*

On traite comme précédemment 0.5 mole d'acétyl-2, méthyl-5 thiophène. Rendement (2 étapes) : 70% en **1c**; p.é. 85 °C sous 15 mm Hg.

*Bischlorométhyl-2,5 thiophène (**1d**) selon (12)*

On sature par HCl gazeux, une solution de 245 cm^3 de formol à 37% et 60 cm^3 d'HCl concentré. On refroidit à 30 °C et introduit goutte à goutte, en agitant, 1 mole (84 g) de thiophène. L'introduction terminée on maintient sous agitation 20 min, puis laisse décanter. On récupère la couche huileuse inférieure, lave à l'eau froide jusqu'à neutralité. L'huile est laissée une nuit à 0 °C puis filtrée sur verre fritté afin d'éliminer la paraformaldéhyde. On refroidit ensuite dans un mélange réfrigérant, l'huile se solidifie. On filtre, et recristallise dans le pentane. On obtient 75 g de bischlorométhyl-2,5 thiophène. Rendement : 50%; p.f. 36 °C [litt. 36–37 °C (12)].

Esters maloniques ***2***

Mode opératoire A

On introduit 0.12 atome-gramme de Na dans 100 cm^3 d'éthanol absolu. Après attaque complète du sodium on ajoute 0.13 mole d'allylmalonate d'éthyle, puis en maintenant la température vers 35 °C on introduit goutte à goutte 0.1 mole de **1** dissoute dans 100 cm^3 d'éthanol absolu. Après introduction complète on porte à reflux 1 nuit. On distille le solvant, verse dans l'eau glacée, extrait à l'éther, sèche la phase organique sur $MgSO_4$ anhydre, évapore le solvant, distille sous pression réduite. Pour une double condensation, on introduit 50% d'allylmalonate en excès.

Mode opératoire B

On remplace l'éthanol absolu par le *tert*-butanol distillé sur sodium pour la préparation de **2***b* et **2***c*.

Mode opératoire C

On introduit 0.10 atome-gramme de Na dans 200 cm^3 de benzène anhydre, puis 0.10 mole d'allylmalonate d'éthyle, et porte à reflux. Après attaque complète du sodium, on ajoute goutte à goutte à 35 °C une solution de 0.1 mole de **1** dans 50 cm^3 de benzène anhydre. Après introduction, on porte à reflux 1 nuit, verse dans l'eau glacée, décante, extrait la phase aqueuse à l'éther, sèche la phase organique sur $MgSO_4$ anhydre, évapore le solvant et distille sous pression réduite.

Les constantes physiques et les rendements sont rassemblés dans le tableau 2, les signaux de r.m.n. des protons aromatiques dans le tableau 1.

Spectre de r.m.n. du motif allylique : δ CH_2=CH—CH_2— (2H), 4.85 (m) et 5.06 (m) ; CH_2=CH—CH_2— (1H) 5.75 (m) ; CH_2=CH—CH_2— (2H) 2.60 p.p.m. (d, J = 6.5 Hz).

Anal. Calc. pour $C_{15}H_{20}O_4S$ (**2***a*) : C, 60.78 ; H, 6.80. Trouvé : C, 61.00 ; H, 6.70.

Anal. Calc. pour $C_{16}H_{22}O_4S$ (**2***b*) : C, 61.90 ; H, 7.14. Trouvé : C, 62.03 ; H, 7.08.

Anal. Calc. pour $C_{17}H_{24}O_4S$ (**2***c*) : C, 62.93 ; H, 7.45. Trouvé : C, 63.01 ; H, 7.36.

TABLEAU 1

Les δ en p.p.m. des protons aromatiques des esters maloniques **2**

Esters **2**	H_3	H_4	H_5	$J_{3,4}$ (c.p.s.)	$J_{4,5}$ (c.p.s.)	$\Delta_{3,4}$	$\Delta_{4,5}$	$CH_3(5)$
a	6.78	6.85	7.05	5	2	0.07	0.20	—
b	6.80	6.85	7.05	5	2.5	0.05	0.20	—
c	6.50	6.50	—	—	—	—	—	2.40
d	6.55	6.55	—	—	—	—	—	—

TABLEAU 2

Caractéristiques physiques des composés préparés

Composé	Point d'ébullition (°C/0.05 mm)	Point de fusion (°C)	*m/e*	Mode opératoire	Rendement (%)
2*a*	124	—	296	A ou C	80
b	128	—	310	B	60
c	132	—	324	B	50
d	>200	48	508	A	55
4*a*	108	—	196	A ou B	95
b	110	—	210	B	90
c	126	—	224	A	90
d	>200	—	—	B	95
5*a*	—	62–67	196	A, B, ou C	10–15
b	—	96–102	210	A, B, ou C	10–15
7*a*	69	—	210	—	95
b	73	—	224	—	95
d	147	—	336	—	90
8*a*	81	—	210	—	60
b	87	—	224	—	60
d	—	102–105	336	—	50
9*a*	75	—	182	—	95
b	78	—	196	—	95
d	160	—	280	—	90
10*a*	97	—	224	—	85
b	101	—	238	—	82
c	108	—	242	—	80
d	—	—	364	—	80

Anal. Calc. pour $C_{26}H_{36}O_8S$ (**2***d*) : C, 61.39 ; H, 7.13. Trouvé : C, 62.50 ; H, 7.06.

Hydrolyse des esters maloniques **2**

On introduit 0.6 mole (33.6 g) de KOH dans 100 cm^3 d'eau, puis 0.1 mole d'ester **2** dissoute dans 100 cm^3 d'éthanol à 99%. On porte à reflux 1 nuit puis distille l'alcool. On refroidit le résidu de distillation, extrait une fois à l'éther. La phase aqueuse est alors acidifiée jusqu'à p*H* 1. On extrait à l'éther, lave la phase éthérée jusqu'à p*H* 3–4, sèche sur $MgSO_4$ anhydre, évapore le solvant. Rendement : 95% à 99%. Pour **2***d* on double les quantités de KOH et de solvant. On recristallise dans le méthanol aqueux ou dans l'eau (**2***d*); p.f. **3***a* : 90 °C; p.f. **3***d* : 180 °C. Les acides, **3***b* et *c*, sont des liquides très visqueux difficilement cristallisables.

Anal. Calc. pour $C_{11}H_{12}O_4S$ (**3***a*) : C, 54.98 ; H, 5.03. Trouvé : C, 55.01 ; H, 5.25.

Anal. Calc. pour $C_{12}H_{14}O_4S$ (**3***b*) : C, 56.67 ; H, 5.54. Trouvé : C, 56.52 ; H, 5.69.

Anal. Calc. pour $C_{13}H_{16}O_4S$ (**3***c*) : C, 58.18 ; H, 6.01. Trouvé : C, 57.95; H, 6.22.

Anal. Calc. pour $C_{18}H_{20}O_8S$ (**3***d*) : C, 54.53 ; H, 5.08. Trouvé : C, 54.68 ; H, 5.19.

Décarboxylation des acides maloniques **3**

Mode opératoire A

Décarboxylation thermique : Les acides maloniques **3** sont chauffés sous vide à 170 °C pendant 1 h et distillés ensuite sous pression réduite. Rendement : 90–95%.

Mode opératoire B

Décarboxylation dans la pyridine : On dissout 0.1 mole d'acide **3** dans 90 cm^3 de pyridine et ajoute 10 cm^3 de pipéridine. On porte à reflux jusqu'à cessation du dégagement de CO_2. On verse alors dans l'acide chlorhydrique glacé dilué 2 fois. On amène à p*H* 1. On extrait à l'éther, lave à l'eau jusqu'à p*H* 4, sèche la phase organique sur $MgSO_4$ anhydre, évapore le solvant, distille sous pression réduite. Rendement : 90–95%; p.é. cf. tableau 2; **4***a* :

Can. J. Chem. Downloaded from www.nrcresearchpress.com by 210.87.254.105 on 09/05/12
For personal use only.

Can. J. Chem. Downloaded from www.nrcresearchpress.com by 210.87.254.105 on 09/05/12
For personal use only.

$n_D^{25} = 1.5278$; **4***b* : $n_D^{20} = 1.5248$; **4***c* : $n_D^{25} = 1.5230$; **4***d* : $n_D^{27} = 1.5185$.

Anal. Calc. pour $C_{10}H_{12}O_2S$ (**4***a*) : C, 61.19 ; H, 6.16. Trouvé : C, 61.40 ; H, 6.02.

Anal. Calc. pour $C_{11}H_{14}O_2S$ (**4***b*) : C, 62.82 ; H, 6.71. Trouvé : C, 62.60 ; H, 6.82.

Anal. Calc. pour $C_{12}H_{16}O_2S$ (**4***c*) : C, 64.25 ; H, 7.18. Trouvé : C, 64.02 ; H, 7.25.

Anal. Calc. pour $C_{16}H_{20}O_4S$ (**4***d*) : C, 62.31 ; H, 6.53. Trouvé : C, 62.12 ; H, 6.66.

Cyclisation des acides éthyléniques **4**

Mode opératoire A

On dissout 1 g d'acide **4** dans 100 cm³ de dichlorométhane et refroidit à 10 °C. On ajoute 2 eq/g de trichlorure d'aluminium anhydre et laisse réagir sous agitation magnétique pendant 10 min. On refroidit à 0 °C et ajoute avec précaution quelques cm³ d'eau jusqu'à hydrolyse complète du complexe. On décante, extrait une fois la phase aqueuse avec 20 cm³ d'éther éthylique. La phase organique (dichlorométhane et éther éthylique) est alors traitée jusqu'à p*H* 11–12 par NaOH à 10%. On décante la phase organique, sèche sur $MgSO_4$ anhydre, filtre, évapore le solvant. On récupère environ 500 mg de γ-valérolactone **6**. On acidifie la phase aqueuse avec HCl dilué; extrait à l'éther de pétrole 30–60, lave à l'eau jusqu'à p*H* 3–4, sèche sur $MgSO_4$, filtre et évapore le solvant. On recristallise dans l'éther de pétrole 30–60. Rendement : 10–15% en acide **5**.

Mode opératoire B

On dissout 1 g d'acide **4** dans 20 cm³ de réactif de Bradsher et porte à reflux 1 h. On verse ensuite dans l'eau glacée saturée en NaCl, et extrait au benzène. La phase organique est alors traitée comme dans le mode opératoire A. Rendement : 50–60% en lactone **6** et 10–15% en acide **5**.

Mode opératoire C

On dissout 1 g d'acide **4** dans un mélange de 19 cm³ d'acide acétique glacial et 1 cm³ d'acide sulfurique concentré. On porte à reflux 10 min, puis verse dans une solution saturée de NaCl glacée. On extrait au benzène. La phase organique est traitée comme le mode opératoire A. Rendement : 50–60% en lactone **6** et 10–15% d'acide **5** ; p.f. des acides **5** : cf. tableau 2 ; **6***a* : p.é. : 95 °C sous 0.05 mm Hg. $n_D^{26} = 1.5308$.

Anal. Calc. pour $C_{10}H_{12}O_2S$ (**5***a*) : C, 61.19 ; H, 6.16. Trouvé : C, 61.05 ; H, 6.35.

Anal. Calc. pour $C_{11}H_{14}O_2S$ (**5***b*) : C, 62.82 ; H, 6.71. Trouvé : C, 62.97 ; H, 6.61.

Anal. Calc. pour $C_{10}H_{12}O_2S$ (**6***a*) : C, 61.19 ; H, 6.16. Trouvé : C, 61.33 ; H, 6.09.

Esters méthyliques **7**

On dissout 5 g d'acide **4** dans 50 cm³ d'éther éthylique, puis on ajoute une solution éthérée de CH_2N_2 jusqu'à cessation du dégagement de N_2. L'excès de CH_2N_2 est détruit par quelques gouttes d'acide acétique. On lave à l'eau, sèche la solution éthérée sur $MgSO_4$ anhydre, filtre, évapore le solvant, et distille sous pression réduite. Rendement : 95% ; p.é. : cf. tableau 2 ; **7***a* : $n_D^{24} = 1.5112$, **7***b* : $n_D^{24} = 1.5066$, **7***c* : $n_D^{25} = 1.5079$; **7***d* : $n_D^{25} = 1.5099$.

Spectres de r.m.n. : les protons aromatiques présentent les mêmes signaux que ceux donnés dans le tableau 1. Le massif allylique ne subit pas de changement par rapport à celui des esters maloniques **2**, en ce qui concerne les δ CH_2=CH— et CH_2=C*H*—, alors que le signal de CH_2—CH=CH_2 se trouve blindé de 0.20 p.p.m. ; δ $COOCH_3$ (3H) = 3.55 p.p.m. (s).

Anal. Calc. pour $C_{11}H_{14}O_2S$ (**7***a*) : C, 62.82 ; H, 6.71. Trouvé : C, 63.02 ; H, 6.95.

Anal. Calc. pour $C_{12}H_{16}O_2S$ (**7***b*) : C, 64.24 ; H, 7.18. Trouvé : C, 64.01 ; H, 7.23.

Anal. Calc. pour $C_{13}H_{18}O_2S$ (**7***c*) : C, 65.50 ; H, 7.61. Trouvé : C, 65.29 ; H, 7.44.

Anal. Calc. pour $C_{18}H_{24}O_4S$ (**7***d*) : C, 66.24 ; H, 7.41. Trouvé : C, 66.01 ; H, 7.60.

Cyclisation des esters méthyliques **7**

On dissout 1 g d'ester **7** dans 100 cm³ de dichlorométhane, refroidit à 10 °C et ajoute 2 eq/g de trichlorure d'aluminium anhydre. On laisse réagir 10 min, puis refroidit à 0 °C et ajoute quelques cm³ d'eau. On décante, extrait la phase aqueuse 1 fois au dichlorométhane. On lave la phase organique jusqu'à neutralité, sèche sur $MgSO_4$ anhydre, filtre, évapore le solvant et reprend par l'éther de pétrole 30–60. On chromatographie sur Alumine Woëlm grade III en éluant avec du pentane à 0.5% d'acétate d'éthyle. Rendement : 60%; p.é. et p.f. : cf. tableau 2 ; **8***a* : $n_D^{25} = 1.5230$; **8***b* : $n_D^{25} = 1.5225$.

Les spectres de r.m.n. confirment les structures proposées : CH_3 doublets vers 1.20 p.p.m. $J = 7$ Hz, H aromatiques doublet de doublet pour **8***a* et *b*, et disparition des protons allyliques et des protons aromatiques pour **8***d*.

Anal. Calc. pour $C_{11}H_{14}O_2S$ (**8***a*) : C, 62.82 ; H, 6.71. Trouvé : C, 62.61 ; H, 6.53.

Anal. Calc. pour $C_{12}H_{16}O_2S$ (**8***b*) : C, 64.24 ; H, 7.18. Trouvé : C, 64.48 ; H, 6.99.

Anal. Calc. pour $C_{18}H_{24}O_4S$ (**8***d*) : C, 66.24 ; H, 7.41. Trouvé : C, 65.98 ; H, 7.36.

Préparation des alcools **9**

Dans une suspension de 1.2 eq/g de $LiAlH_4$ dans 150 cm³ d'éther éthylique anhydre, refroidie à 0 °C, on introduit goutte à goutte, avec précaution, et sous agitation magnétique, 0.1 mole de **4** ou **7** dissoute dans 100 cm³ d'éther éthylique anhydre (13). L'introduction terminée on porte à reflux 1 nuit, détruit l'excès de $LiAlH_4$ par quelques cm³ d'acétate d'éthyle, la même quantité de soude à 15% puis le même volume d'eau (14). On filtre le précipité, lave la phase organique à l'eau, sèche sur $MgSO_4$ anhydre, filtre, évapore le solvant, distille sous pression réduite. Rendement : 95% ; p.é. : cf. tableau 2 ; **9***a* : $n_D^{25} = 1.5283$; **9***b* : $n_D^{25} = 1.5315$; **9***c* : $n_D^{25} = 1.5298$; **9***d* : $n_D^{25} = 1.5320$.

Les spectres de r.m.n. confirment la structure attendue ; δ CH_2OH 3.50 p.p.m. (d, $J = 6$ Hz).

Anal. Calc. pour $C_{10}H_{14}OS$ (**9***a*) : C, 65.89 ; H, 7.74. Trouvé : C, 65.72 ; H, 7.90.

Anal. Calc. pour $C_{11}H_{16}OS$ (**9***b*) : C, 67.30 ; H, 8.21. Trouvé : C, 67.23 ; H, 8.02.

Anal. Calc. pour $C_{12}H_{18}OS$ (**9***c*) : C, 68.52 ; H, 8.62. Trouvé : C, 68.39 ; H, 8.83.

Anal. Calc. pour $C_{16}H_{26}O_2S$ (**9***d*) : C, 68.03 ; H, 9.27. Trouvé : C, 67.85 ; H, 9.45.

Cyclisation des alcools **9**

On porte 10 min à reflux un mélange de 1 g d'alcool **9**,

Can. J. Chem. Downloaded from www.nrcresearchpress.com by 210.87.254.105 on 09/05/12
For personal use only.

19 cm³ d'acide acétique glacial et 1 cm³ d'acide sulfurique concentré. On verse ensuite dans une solution saturée glacée de NaCl, extrait à l'éther de pétrole, lave la phase organique jusqu'à neutralité, sèche sur $MgSO_4$ anhydre, filtre, évapore le solvant. On chromatographie sur alumine Woëlm grade I en éluant au pentane à 0.5% d'acétate d'éthyle. Rendement : 85% ; p.é. : cf. tableau 2.

Spectres i.r. 1245 et 1740 cm^{-1} (acétate). Spectres de r.m.n. : δ CH_3 cyclaniques, doublets vers 1.2 J = 7 Hz, δ

$$CH_3—\overset{O}{\overset{\|}{C}}—O \quad (3H)\ 2.0\ (s)\ ;\ CH_2—O—\overset{O}{\overset{\|}{C}}— \quad (2H)\ 4.05$$

p.p.m. (d, J = 6 Hz).

Anal. Calc. pour $C_{12}H_{16}O_2S$ (**10***a*) : C, 64.24 ; H, 7.18. Trouvé : C, 64.50 ; H, 7.02.

Anal. Calc. pour $C_{13}H_{18}O_2S$ (**10***b*) : C, 65.50 ; H, 7.61. Trouvé : C, 65.32 ; H, 7.50.

Anal. Calc. pour $C_{14}H_{20}O_2S$ (**10***c*) : C, 66.62 ; H, 7.98. Trouvé : C, 66.81 ; H, 8.13.

Anal. Calc. pour $C_{20}H_{28}O_4S$ (**10***d*) : C, 65.80 ; H, 7.68.. Trouvé : C, 65.50 ; H, 7.92.

Préparation des oléfines ***11***

On dissout 0.1 mole d'alcool **9** dans 50 cm³ de pyridine (distillée et conservée sur potasse). On refroidit à − 10 °C, et introduit lentement, sous agitation magnétique, une solution à 0 °C de 1.1 eq/g de chlorure de *p*-toluène sulfonyle (fraîchement distillé et conservé dans un dessicateur à potasse) dans la pyridine.

Après introduction on laisse une nuit au réfrigérateur. On verse ensuite dans une solution glacée d'HCl dilué. On amène à pH < 2, extrait à l'éther, lave avec 50 cm³ d'HCl dilué une fois, lave à l'eau saturée de NaCl jusqu'à neutralité, sèche la phase organique sur $MgSO_4$ anhydre, filtre, évapore le solvant. Rendement : 98%.

On réduit ensuite le tosylate, en procédant comme pour la réduction des acides **4** ou des esters 7, en utilisant 2.5 eq/g de $LiAlH_4$. Rendement : 98% après chromatographie sur gel de silice en éluant à l'éther de pétrole 30–60 °C à 0.25% d'acétate d'éthyle. Les oléfines **11**, sont des liquides, p.é. sous 8 mm Hg ; **11***a* = 112 ; *b* = 117 ; *d* = 150 °C.

L'examen des spectres de r.m.n. permet de confirmer leur structure : δ CH_3 0.9 (d, J = 6.5 Hz) ; δ CH_2=CH— 4.85 (m) et 5.06 (m) ; CH_2=CH— 5.75 p.p.m. (m).

Anal. Calc. pour $C_{10}H_4S$ (**11***a*) : C, 72.27 ; H, 8.43. Trouvé : C, 77.01 ; H, 8.15.

Anal. Calc. pour $C_{11}H_{16}S$ (**11***b*) : C, 73.27 ; H, 8.94. Trouvé : C, 73.11 ; H, 9.06.

Anal. Calc. pour $C_{12}H_{18}S$ (**11***c*) : C, 74.16 ; H, 9.33. Trouvé : C, 74.35 ; H, 9.45.

Anal. Calc. pour $C_{16}H_{24}S$ (**11***d*) : C, 77.40 ; H, 9.67. Trouvé : C, 77.65 ; H, 9.90.

Cyclisation des oléfines ***11***

Mode opératoire A

On dissout 1 g d'oléfine **11** dans 100 cm³ de dichlorométhane et refroidit à 10 °C. On ajoute 1.5 eq/g de trichlorure d'aluminium anhydre. On laisse réagir 5 min sous agitation magnétique. On hydrolyse ensuite avec précaution, décante, extrait une fois la phase aqueuse par quelques cm³ de dichlorométhane, lave à l'eau la phase organique, sèche sur $MgSO_4$ anhydre, filtre, évapore le solvant et reprend par l'éther de pétrole 30–60. On chromatographie sur alumine Woëlm grade III avec de l'éther de pétrole. Rendement : 80–90%.

Mode opératoire B

On dissout 1 g d'oléfine **11** dans 25 cm³ d'éthérate de trifluorure de bore fraîchement distillé. On y ajoute 1 goutte d'eau, et sature en trifluorure de bore gazeux. On abandonne 1 h à température ordinaire. On verse ensuite dans l'eau glacée, extrait à l'éther de pétrole, lave une fois à l'eau, sèche sur $MgSO_4$ anhydre, filtre, évapore le solvant, et chromatographie comme le mode opératoire A. Rendement : 90–95%.

Mode opératoire C

On dissout 1 g d'oléfine **11** dans 19 cm³ d'acide acétique glacial et 1 cm³ d'acide sulfurique concentré. On porte à reflux 5 min. On verse dans l'eau glacée saturée en NaCl, extrait à l'éther de pétrole et traite ensuite comme le mode opératoire B, après lavage à l'eau de la phase organique jusqu'à neutralité. Rendement : ≃90% en composés **12**.

Les spectres i.r. montrent la disparition des bandes dues à CH_2=CH—, les spectres de r.m.n. montrent la disparition des multiplets dus à CH_2=CH— et CH_2=CH—, ainsi que l'apparition de méthyles cyclaniques. cf. **5**, **8** et **10**.

Anal. Calc. pour $C_{10}H_{14}S$ (**12***a*) : C, 72.27 ; H, 8.43. Trouvé : C, 72.14 ; H, 8.20.

Anal. Calc. pour $C_{11}H_{16}S$ (**12***b*) : C, 73.27 ; H, 8.94. Trouvé : C, 73.01 ; H, 8.99.

Anal. Calc. pour $C_{12}H_{18}S$ (**12***c*) : C, 74.16 ; H, 9.33. Trouvé : C, 73.95 ; H, 9.27.

Anal. Calc. pour $C_{16}H_{14}S$ (**12***d*) : C, 77.40 ; H, 9.67. Trouvé : C, 77.22 ; H, 9.40.

Préparation des benzo(b)thiophènes et dibenzothiophènes, ***13***

Mode opératoire A

On introduit 500 mg de **12** dans un ballon de 5 ml muni d'un réfrigérant. On fait passer un courant d'azote, puis on ajoute 100 mg de catalyseur (Pd/C à 5%) et porte 2 h à 250 °C pour un benzothiophène et 3 h à 280 °C pour un dibenzothiophène. On dissout ensuite le contenu du ballon dans le dichlorométhane, filtre le catalyseur, évapore le solvant et reprend par le pentane. On chromatographie sur gel de silice en éluant au pentane à 0.25% d'acétate d'éthyle. On recristallise ensuite dans l'éthanol à 99% (**13***d*) ou sublime sous vide (**13***b* et *c*), **13***a* est liquide. Le p.f. : **13***b* = 55, *c* = 76, *d* = 109 °C ; T.N.B., p.f. **13***a* = 125, *b* = 123, *c* = 142 °C ; picrates : p.f. **13***a* = 109, *d* = 115 °C.

Anal. Calc. pour $C_{10}H_{10}S$ (**13***a*) : C, 74.02 ; H, 6.21. Trouvé : C, 73.89 ; H, 6.33.

Anal. Calc. pour $C_{11}H_{12}S$ (**13***b*) : C, 74.94 ; H, 6.86. Trouvé : C, 75.08 ; H, 6.82.

Anal. Calc. pour $C_{12}H_{14}S$ (**13***c*) : C, 75.73 ; H, 7.41. Trouvé : C, 75.58 ; H, 7.42.

Anal Calc. pour $C_{16}H_{16}S$ (**13***d*) : C, 79.95 ; H, 6.70. Trouvé : C, 79.70 ; H, 6.85.

Préparation des esters ***14***

L'aromatisation des esters **8** s'effectue de la même façon que celle des composés **12**. On utilise 50% en poids de Pd/C à 5%, la durée est de 4 h. On opère à 310–320 °C. On aboutit à un équilibre entre composé aromatisé et non aromatisé. On chromatographie sur alumine Woëlm

grade I en éluant au pentane à 0.5% d'acétate d'éthyle. On recristallise dans l'éthanol à 99% ; **14***a* p.f. 66 °C, $m/e = 206$.

Spectres de r.m.n. : δ H_7 (1H) 8.37 (s, large) ; H_5 (1H) 7.75 (s, large) ; δH_2 (1H) 7.50 (d, $J_{2,3} = 5$ Hz) ; H_3 (1H) 7.30 (d, $J_{2,3} = 5$ Hz) ; CH_3 (4) (3H) 2.53 (s) ; —C(=O)—O—CH_3 (3H) 3.84 p.p.m. (s).

Les auteurs expriment leur gratitude au Conseil National de Recherches du Canada pour l'aide financière apportée sous forme de subvention.

1. L. F. Fieser et R. G. Kennely. J. Amer. Chem. Soc. **57**, 1611 (1935).
2. P. Cagniant et D. Cagniant. Bull. Soc. Chim. Fr. 713 (1953).
3. P. Cagniant et D. Cagniant. Bull. Soc. Chim. Fr. 681 (1955).
4. P. Cagniant et D. Cagniant. Bull. Soc. Chim. Fr. 1252 (1955).
5. P. Cagniant et D. Cagniant. Bull. Soc. Chim. Fr. 1152 (1956).
6. P. Canonne, A. Regnault, et L. C. Leitch. Tetrahedron Lett. **3**, 355 (1968).
7. P. Canonne et A. Regnault. Can. J. Chem. **47**, 2837 (1969).
8. P. Canonne et A. Regnault. Tetrahedron, **25**, 2349 (1969).
9. P. Cagniant, G. Merle, et D. Cagniant. Bull. Soc. Chim. Fr. 322 (1970).
10. P. Canonne et J. Gourier. C.R. Acad. Sci. Paris, **268**, 2319 (1969).
11. L. P. Kyrides et D. G. Sheets. Chem. Abstr. **45**, 1166b (1951) U.S. Patent 2 527 680 (1950).
12. J. Griffin et L. Salisbury. J. Amer. Chem. Soc. **70**, 3416 (1948).
13. L. F. Fieser et M. Fieser. Reagents for organic synthesis. John Wiley and Sons, 1967. p. 589.
14. M. Micovic et M. Mihailovic. J. Org. **18**, 1190 (1953).

Can. J. Chem. Downloaded from www.nrcresearchpress.com by 210.87.254.105 on 09/05/12
For personal use only.

Can. J. Chem. Downloaded from www.nrcresearchpress.com by 210.87.254.6 on 09/05/12
For personal use only.

Configurational and conformational influences on the carbon-13 chemical shifts of some carbohydrates

A. S. PERLIN, B. CASU,[1] AND H. J. KOCH[2]
Department of Chemistry, McGill University, Montreal, P.Q.

Received February 20, 1970

Carbon-13 chemical shifts for sugars and methyl glycosides are reported. The following general effects have been observed: (*a*) a comparison of chemical shifts with expected electron densities suggests that ^{13}C-2 and -4 experience relatively stronger shielding than do ^{13}C-1, -3, and -5, possibly because they oppose the ring O; (*b*) inversion of an equatorial O to axial O is associated with increased shielding of the ^{13}C nucleus to which it is bonded, of adjacent ^{13}C nuclei, and of those in the β-position (i.e., having an opposing axial H or O); (*c*) removal of a gauche O,O interaction is associated with ^{13}C deshielding. It appears that since these same steric relationships affect stability, the overall shielding states of ^{13}C nuclei of the different isomers reflect variations in the magnitude of repulsive interactions in the molecules; on this basis, the anomeric effect does not arise through instability of the equatorial anomeric C—O bond. A destabilizing interaction appears to cause polarization of most C—H bonds in a molecule, ^{13}C becoming more shielded, and ^{1}H less shielded, suggestive of a concerted means for delocalizing the instability. In comparing anomers or epimers, this polarization is evident as a reordering of the shielding state of different nuclei, e.g., for several sugars and their glycosides increased shielding of ^{13}C-1 is accompanied by deshielding of the bonded H and increased shielding of the appended O—*H* or methoxyl ^{13}C nucleus.

Canadian Journal of Chemistry, **48**, 2596 (1970)

In a recent communication (1) we report carbon-13 (^{13}C) chemical shifts for α- and β-D-glucose in water. Some of those signal assignments were made tentatively, but they have now been confirmed by more complete data presented here.[3] As shown in Table 1 (and in Fig. 2 of ref. 1), C-3 and -5 of β-D-glucose have the same chemical shift, C-4 and -6 of both anomers also have congruent chemical shifts whereas signals corresponding to the remaining six C atoms of the two anomers are detectable independently. The spectra of the anomeric methyl D-glucopyranosides are close counterparts of those of the parent sugars (Table 1), except for the C-1 signals. Hence, although those of the latter appear downfield by about 7 p.p.m., which helps to confirm the C-1 assignments, there is relatively little impact on the chemical shifts of the other ^{13}C nuclei (C-2 is deshielded by 0.4 p.p.m.). This closely confined effect of an added *O*-methyl is consistently large and has permitted a check on the assignments for C-2, -3, and -4; for example, with 3-*O*-methyl-D-glucose the resultant downfield shift relative to D-glucose for C-3 is about 10 p.p.m. for each anomer, whereas the position of other signals is barely affected. The fact that deuteration has a marked impact on the signal of the adjacent ^{13}C nucleus (2, 3),[4] has been utilized to confirm chemical shifts for C-3, -5, and -6 through examination of the appropriately deuterated D-glucoses. Measurements with other derivatives and with structurally related compounds also contribute to an overall self-con-

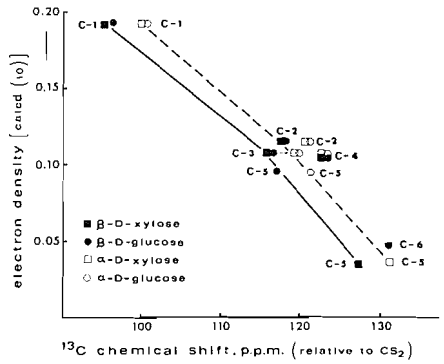

FIG. 1. A plot of calculated values of carbon electron density (10) vs. ^{13}C chemical shift (p.p.m.) for anomers of D-xylose and D-glucose; ■, β-D-xylose; ●, β-D-glucose; □, α-D-xylose; ○, α-D-glucose.

[1]Harold Hibbert Memorial Fellow (1968–1969); on leave of absence from Istituto G. Ronzoni, Milan, Italy.
[2]Postdoctoral Fellow, 1969–1970.
[3]An extensive ^{13}C spectral study of aldoses by Dorman and Roberts (31) has appeared since this paper was submitted. Since it deals with many of the same compounds, it is especially noteworthy that the interpretations of spectra in these two studies agree closely, differing in only a few minor respects.
[4]These literature reports and our own unpublished findings show that the deuteration gives highly variable results: in some instances the ^{13}C resonance is not detectable, or barely so, whereas in others the signal is readily observed.

TABLE 1

Carbon-13 chemical shifts for hexoses and their methyl glycopyranosides*

Compound	Carbon 1	2	3	4	5	6	CH_3
α-D-Glucose	100.4	120.9	119.5	122.8	121.2	131.4	—
-Glycoside	92.9	120.6	118.9	122.4	120.9	131.3	137.2
β-D-Glucose	96.5	118.2	116.6	122.8	116.6	131.4	—
-Glycoside	89.1	119.1	117.3	122.5	117.3	131.1	135.0
α-D-Galactose	100.0	123.5	123.5	123.8	122.0	131.2	—
-Glycoside	93.0	122.9	122.6	123.9	121.6	131.0	137.2
β-D-Galactose	95.8	120.2	119.5	123.1	117.3	131.4	—
-Glycoside	88.7	121.6	119.5	123.7	117.5	131.4	135.4
α-D-Mannose	97.6	121.0	121.5	124.9	119.8	130.7	—
-Glycoside	91.8	122.0	122.7	125.8	120.1	131.6	137.5
β-D-Mannose	98.2	120.8	118.7	125.2	115.9	130.7	—
-Glycoside	91.5	122.2	119.5	125.7	116.2	131.4	135.9
β-D-Allose	99.0	121.2	121.4	125.6	119.0	131.2	—
Methyl α-D-altroside	91.7	122.8	122.8	128.0	122.8	131.5	137.4
Methyl α-D-idoside	91.3	121.9	121.0	122.5	122.0	132.6	137.0

*In p.p.m. from carbon disulfide.

TABLE 2

Carbon-13 chemical shifts for pentoses and their methyl glycopyranosides*

Compound	Carbon 1	2	3	4	5	CH_3
α-D-Xylose	100.0	120.6	119.2	123.1	131.1	—
-Glycoside	94.2	121.3	119.3	123.2	131.8	137.9
β-D-Xylose	95.5	118.0	116.1	122.8	127.2	—
-Glycoside	88.7	119.8	116.8	123.2	127.8	135.9
β-L-Arabinose	99.4	123.6	123.6	123.8	129.9	
α-L-Arabinose	95.3	120.1	119.7	123.8	126.1	
α-D-Lyxose	98.2	122.1	121.6	124.7	129.4	
β-D-Lyxose	98.2	122.1	119.6	125.5	128.3	
α-D-Ribose	98.9	123.6	122.0	124.7	129.4	
β-D-Ribose	98.4	121.1	121.1	123.7	129.4	

*In p.p.m. from carbon disulfide.

sistent group of data that support the assignments proposed.

The ^{13}C spectra of α- and β-D-xylose, which have been described recently by Hall and Johnson (4), closely resemble those of the D-glucoses, aside from the relative upfield position of C-5 signals (and absence of C-6) in the pentose spectra. On most of the assigned resonances there is concurrence between their data and ours but, based on the spectrum for D-glucose and those of some D-xylose derivatives, we favor the listings in Table 2.

The electron density at a given carbon nucleus is a major factor in determining the chemical shift of that atom (5–9). Hence it is pertinent to compare the observed chemical shifts for D-glucose and D-xylose with molecular orbital data for sugars. Recent information on the pentose molecule (10) is utilized for this purpose (Fig. 1); calculated electron densities for C-4 and -5 of the pentofuranose (10) are taken as being approximately those for C-5 and -6 of the hexopyranose. As shown, there is a generally good correspondence between the two sets of parameters: the anomeric nuclei and those of C-5 (pentose) or C-6 (hexose) represent the two extremes, whereas the secondary ^{13}C nuclei constitute an intermediate group. When the anomers are considered separately, close to a direct relationship between chemical shift and electron density is found for C-1, -3, and -5 of each of the four sugars, whereas the values for C-2 and -4 deviate substantially upfield relative to the plotted lines. The effect is especially large for C-4, which is more shielded than C-3 and -5 by +6.2 p.p.m.; e.g., this is greater than the effect induced by an axial methyl

Can. J. Chem. Downloaded from www.nrcresearchpress.com by 210.87.254.6 on 09/05/12
For personal use only.

Can. J. Chem. Downloaded from www.nrcresearchpress.com by 210.87.254.6 on 09/05/12
For personal use only.

group on a β-carbon (+5.4 p.p.m.) (11, 12). Overall data for other sugars (Tables 1 and 2) show that this difference is a common feature, and that C-2 and -4 are almost always more shielded relative to these electron density data than are the other ring carbons.

Because of the approximate nature of these charge density calculations (10) conclusions derived from Fig. 1 are necessarily tentative. It appears, however, that C-1, -3, and -5, which may be regarded as in one plane of the chair conformation, are affected differently than C-2 and -4 which, by analogy, lie in a second plane that includes the ring oxygen atom. This "excess" shielding observed for C-2 and -4 may arise from a transannular interaction between the two nuclei and the bonds involving C-1, -5, and the ring oxygen, or between H-2 or -4 and the p orbitals of the ring oxygen atom. Presumably also, the chemical shift differences between the anomers, and between other sugars to be considered later, result from interactions that are superimposed on this "ground state" of the pyranose ring.

Additivity effects, such as that due to the second oxygen atom at C-1, or the replacement of a carbinol group with a second H (glucose to xylose) are clearly reflected in the chemical shift as well as electron density data. Consistent also are the observed upfield shifts, relative to D-glucose, of C-1 in 1,5-anhydro-D-sorbitol (by about 25 p.p.m.), of C-2 in 2-deoxy-D-glucose (by about 35 p.p.m.), and of C-6 in 6-deoxy-D-glucose (by about 40 p.p.m.); these shifts are all accompanied by a slight deshielding of the adjacent ^{13}C nuclei.

In ascribing chemical shift differences between anomers of D-glucose and D-xylose to differences in orientation at C-1, as has been achieved with respect to proton chemical shifts (13, 14), it appears relevant to examine orientational influences in cyclohexane (11, 12, 15). These show that an axial substituent is associated with greater shielding of the ^{13}C nucleus to which it is bonded, than is an equatorial one. In addition, the axial substituent favors greater shielding of other ^{13}C nuclei in the molecule. Examples of these relationships are given in Chart 1. Not only is the ^{13}C nucleus bearing the axial substituent affected, as are those nuclei that bear opposing axial protons, but also the nuclei adjacent to the substituted carbon. The latter effect may be evidence of an overall compensatory mechanism tending to dissipate the destabilizing action of the axial group over several carbon atoms and their appended protons (16). Only nuclei in the 4-position are unaffected materially by the configurational change.

A comparison of α-D-glucose with β-D-glucose, or α-D-xylose with its β-anomer (Chart 1), indicates that similar relationships apply for these compounds also; they are expressed by the following generalizations and, in greater detail, in Chart 2: (*a*) An axial oxygen atom (*ax. O*) is associated with increased shielding (+) of the ^{13}C nucleus to which it is bonded. (*b*) A ^{13}C nucleus adjacent (*adj*) to the axial C—O bond experiences increased shielding (+). (*c*) An axial hydrogen atom in 1,3 relationship to an axial oxygen atom (H//*O*)[5] is associated with increased shielding (+) of the ^{13}C nucleus to which it is bonded.

These empirical relationships imply that the introduction of a destabilizing factor promotes an increase in shielding of ^{13}C, a possibility that we have discussed recently in conjunction with the cyclohexane derivatives (16). In this context it may be noted that in the β-anomers of the sugar molecules the equatorial C_1—O bond should introduce an additional destabilizing factor associated with the neighboring ring oxygen atom (anomeric effect (18–20)). However, the results show no obvious requirement that this latter factor be invoked as well in accounting for the chemical shift differences between the anomers. Thus, the C-1 difference (Δ) is about 4 p.p.m. for both sugars, which is approximately the same (or smaller) as the corresponding Δ values for the cyclohexane derivatives (Chart 1, underlined values). Because the *a,e* isomer of 1,4 cyclohexanediol undergoes ring inversion, the corresponding Δ value is 4 p.p.m.; on the same basis the 1,2 and 1,3 diols give Δ values of 8.6 and 4.2 p.p.m., respectively (16), and the dimethylcyclohexanes (12) slightly larger values.

Substantial variations in ^{13}C chemical shift are found also among other compounds examined (Tables 1 and 2). Most of these signal assignments have been derived, as for D-glucose, by comparison with spectra of derivatives, *O*-methyl,

[5]This method of notation is described by Lemieux (17).

CHART 1

Effect of an axial substituent on ^{13}C chemical shifts (δ) (p.p.m. relative to benzene for cyclohexanes, to CS_2 for sugars)

C	δ	δ	Δ	δ	δ	Δ
	1,2,4-Trimethylcyclohexane			*1,3,5-Trimethylcyclohexane*		
	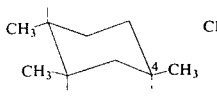			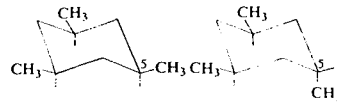		
1	89.3	89.7	0.4	95.8	102.1	6.3
2	89.6	94.9	5.3	84.3	83.5	−0.8
3	83.4	87.8	4.4	95.8	102.1	6.3
4	95.6	100.5	4.9	84.3	87.6	3.3
5	92.6	96.7	4.1	95.8	99.9	4.1
6	92.8	99.0	6.2	84.3	87.6	3.3
	4-t-Butylcyclohexanol			*1,4-Cyclohexanediol*		
	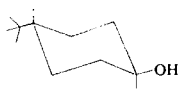			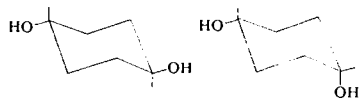		
1	56.3	61.8	5.5	57.6	59.6	2.0
2	91.0	93.5	2.5	94.8	97.4	2.6
3	101.0	105.9	4.9	94.8	97.4	2.6
4	79.5	78.7	−0.8	57.6	59.6	2.0
5	101.0	105.9	4.9	94.8	97.4	2.6
6	91.0	93.5	2.5	94.8	97.4	2.6
	D-*Glucose*			D-*Xylose*		
	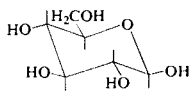			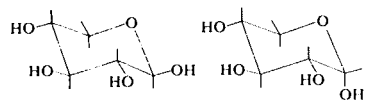		
1	96.5	100.4	3.9	95.5	100.0	4.5
2	118.2	120.9	2.7	118.0	120.6	2.5
3	116.6	119.5	2.9	116.1	119.2	3.1
4	122.8	122.8	0	122.8	123.1	0.3
5	116.6	121.2	4.6	127.2	131.1	3.9
6	131.4	131.4	0	—	—	—

O-acetyl, deoxy, or deuterated specimens. Some have been deduced by analogy, however, taking into account the chemical shift interaction relationships considered in this paper. Assignments for α-D-arabinose, methyl α-D-altropyranoside and methyl α-D-idopyranoside (which produce groups of closely spaced signals), and for α-D-ribose, probably are the least reliable.

As shown in Chart 2, differences between the anomers of D-galactose, L-arabinose, D-mannose, and D-lyxose also are qualitatively in accord with those anticipated by invoking appropriate interactions, and assuming that there is essentially no difference in conformation between anomeric pairs. A vicinal gauche interaction (*O*/*O*) is added to those listed above and, as in the cyclohexane series (12), is treated as a shielding factor (+); e.g., inversion of β- to α-D-mannose removes the 1,2-gauche arrangement and appears to promote deshielding (−). We see no ready basis for a rigorous quantitative treatment of these data, and hence would expect to discern only relatively large stereochemical changes from them. A value of about 3.5 p.p.m. is representative of most of the shielding changes associated with these configurational inversions. Substantial deviation then is observed only for C-2 and -3 of the methyl D-glucosides, C-2 of the methyl D-galactosides, and C-3 and -5 of D-lyxose; but whether these arise because of conformational aberrations or, simply, unrecognized shielding influences is not known. Noteworthy is the fact

Can. J. Chem. Downloaded from www.nrcresearchpress.com by 210.87.254.6 on 09/05/12
For personal use only.

CHART 2

Carbon-13 shielding differences between anomers

Inversion*	Carbon	Interaction	Expected shielding	$\delta_b-\delta_\alpha$ (p.p.m.)†		
				1	2	3
A	1	*ax. O*	+	4.5	3.9	3.8
	2	*adj.* 1	+	2.6	2.7	1.5
	3	H//*O*-1	+	3.1	2.9	1.6
	4	0	0	0.3	0	−0.1
	5	H//*O*-1	+	3.9	4.6	3.6
	6	0	0	—	0	0.2
B	1	*ax. O*	+	4.1	4.2	4.3
	2	*adj.* 1	+	3.5	3.3	1.3
	3	H//*O*-1	+	3.9	4.1	3.1
	4	0	0	0	0.7	0.2
	5	H//*O*-1	+	3.8	4.6	4.1
	6	0	0	—	−0.2	−0.4
C	1	*ax. O*, −*O*//*O*-2	+, −	0	−0.6	0.3
	2	*adj.* 1, −*O*//*O*-1	+, −	0	0.2	−0.2
	3	H//*O*-1	+	2.0	2.8	3.2
	4	0	0	−0.8	0	0.1
	5	H//*O*-1	+	1.1	3.9	3.9
	6	0	0	—	0	0

*Inversions are as follows:

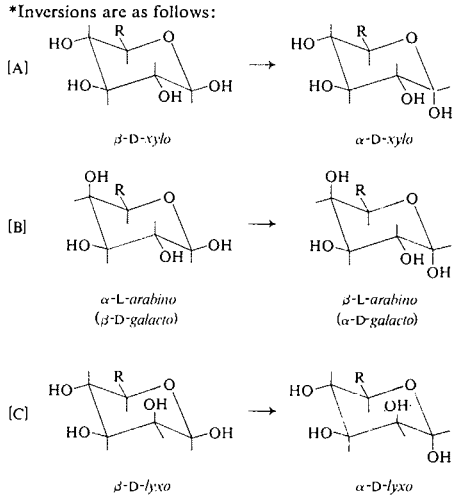

†Obtained from data of Tables 1 and 2. 1-Pentose (R = H); 2-hexose (R = CH_2OH); 3-methyl hexoside (R = CH_2OH).

that the close agreement between data for arabinose and galactose involves the assumption, now well founded (21), that the arabinopyranoses favor the inverted chair conformation (Cl(L), 1C(D)).

Epimeric forms of the sugars are compared in Charts 3 and 4; e.g., α- or β-D-glucose with α- or β-D-mannose (2-epimer), etc. As above, these comparisons entail no allowance for possible conformational change on inversion. Although a generally self-consistent pattern of chemical shift differences is again observed in these instances variations are wider than those of Chart 2, and several large deviations are evident. In particular, the axial O-4 of isomers possessing the L-*arabino* configuration makes little impact on shielding of C-4 and -5, relative to the D-*xylo* series, and comparisons of the D-*xylo* and D-*lyxo* series lead to an erratic pattern for C-5 chemical shift differences. An instance involving 1,3-diaxially disposed oxygen atoms (*O*//*O*) is encountered in Chart 4. Comparison of methyl α-D-mannopyranoside with methyl α-D-altropyranoside (C-1), indicates that this type of relationship has a shielding

Can. J. Chem. Downloaded from www.nrcresearchpress.com by 210.87.254.6 on 09/05/12
For personal use only.

CHART 3

Carbon-13 shielding differences between epimers (β-anomers)

Inversion*	Carbon	Interaction	Expected shielding	$\delta_b-\delta_a$ (p.p.m.)†		
				1	2	3
A	1	*adj.* 2	+	2.7	1.7	2.6
	2	*ax. O*	+	4.1	2.6	3.1
	3	*adj.* 2	+	3.5	2.1	2.2
	4	H//*O*-2	+	2.7	2.4	3.2
	5	0	0	1.1	−0.7	−0.9
	6	0	0	—	0.7	0.3
B	1	H//*O*-3	+	2.9	2.5	—
	2	*adj.* 3	+	3.1	3.0	—
	3	*ax. O*	+	5.0	4.8	—
	4	*adj.* 3	+	0.9	2.8	—
	5	H//*O*-3	+	2.2	2.4	—
	6	0	0	—	−0.2	—
C	1	0	0	−0.2	−0.7	−0.4
	2	H//*O*-4	+	2.1	2.0	2.5
	3	*adj.* 4	+	3.6	2.9	2.2
	4	*ax. O*	+	1.0	1.2	0.3
	5	*adj.* 4	+	−1.1	0.7	0.2
	6	0	0	—	0	0.3

*Inversions are as follows:

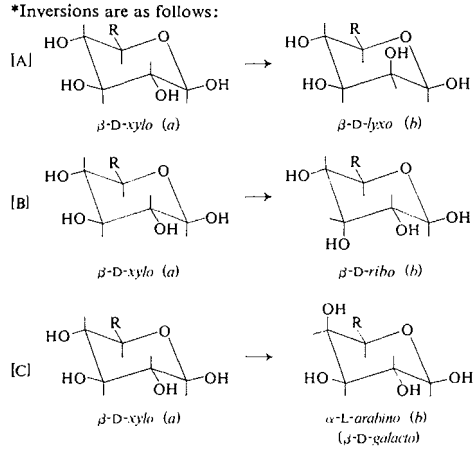

†Obtained from data of Tables 1 and 2. 1-Pentose (R = H); 2-hexose (R = CH_2OH); 3-methyl hexoside (R = CH_2OH).

effect (+) on the ^{13}C nuclei involved, although its impact is taken to be about the same as an *O*//H interaction, or smaller. Thus, a similar comparison of chemical shifts for C-2 of methyl α-D-altropyranoside and methyl α-D-idopyranoside (Table 1), gives a value of −0.4 p.p.m.; and for C-1 of α-D-xylose and α-D-ribose (Table 2), a value of −1.1 p.p.m.[6] The data have been examined also for possible evidence that the strong shielding described above for C-2 and -4 of D-*xylo* isomers is modified by inversion. In this context, no consistent effect of axial O-2 or -4 has been detected although, as just noted, C-4 of L-*arabino* isomers (axial O-4) appears to behave atypically.

These various steric relationships considered as possible sources of differences in ^{13}C chemical shift, include most of those that are customarily evaluated in assessing conformational stability. As noted elsewhere (16), ^{13}C chemical shift variations can be correlated satisfactorily with the presence of destabilizing interactions in cyclohexane derivatives: ^{13}C nuclei affected by such

[6]A larger net deshielding effect associated with an *O*//*O* interaction has recently been described in the inositol series (*myo-* → *epi*-inositol (22)).

Can. J. Chem. Downloaded from www.nrcresearchpress.com by 210.87.254.6 on 09/05/12
For personal use only.

CHART 4

Carbon-13 shielding differences between epimers (α-anomers)

Inversion	Carbon	Interaction	Expected shielding	$\delta_b-\delta_a$ (p.p.m.)† 1	2	3
A	1	*adj.* 2, −*O*//*O*-2	+, −	−1.8	−2.8	−1.1
	2	*ax.* *O*, −*O*//*O*-1	+, −	−1.5	−0.1	−1.4
	3	*adj.*	+	2.4	2.0	3.8
	4	H//*O*-2	+	1.6	2.1	3.4
	5	0	0	−1.7	−1.4	−0.8
	6	0	0	—	−0.7	0.3
B	1	0	0	−0.6	−0.4	0.1
	2	H//*O*-4	+	3.0	2.6	2.0
	3	*adj.* 4	+	4.4	4.0	4.0
	4	*ax.* *O*	+	0.7	1.0	1.5
	5	*adj.* 4	+	−1.2	0.8	0.7
	6	0	0	—	−0.2	−0.3
C	1	*O*//*O*-3, −*O*//H-3	+, −		−0.1	
	2	*adj.* 3, −*O*//*O*-3	+, −		0.8	
	3	*ax.* *O*, *O*//*O*-1,	++			
		O//H-5,	+		0.1	
		−*O*//*O*-2, −*H*//*O*-1	−−			
	4	*adj.* 3	+		2.2	
	5	H//*O*-3	+		2.7	
	6	0	0		−0.1	

*Inversions are as follows:

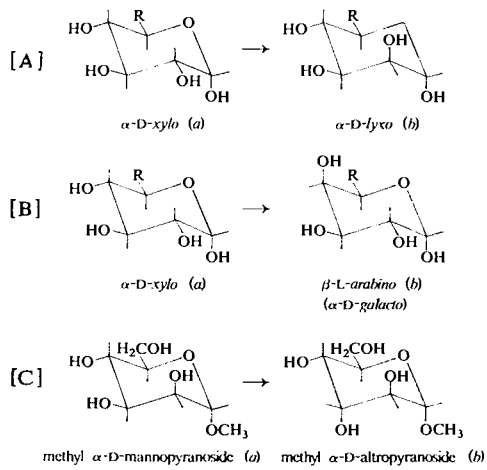

†Obtained from data of Tables 1 and 2. 1-Pentose (R = H); 2-hexose (R = CH_2OH); 3-methyl hexoside (R = CH_2OH).

interactions exhibit increased shielding. Analogously, the current data reflect differences in stability between the isomeric sugars. Thus, if the overall shielding experienced by the ^{13}C nuclei of each sugar is evaluated (in Table 3 this value is expressed as the sum total (16) of the observed chemical shifts for a given sugar[7]), it is found that total shielding increases as the energy (21) (see next paragraph) of the molecule increases. For example, the ^{13}C nuclei of β-D-xylose and β-D-glucose may be classed as the least shielded, and also as components of the most stable isomers, within the series. Similarly, sugars that are regarded as highly unstable, α-altrose, α-ribose, α-galactose, also are those that contain the most shielded group of ^{13}C nuclei. In the intermediate range there are relatively small differences in

[7]An average value may be taken equally well or, a much more complex task, individual nuclei may be considered.

Can. J. Chem. Downloaded from www.nrcresearchpress.com by 210.87.254.6 on 09/05/12
For personal use only.

TABLE 3

Comparison of ^{13}C shielding and stability

Hexoses (methyl glycopyranosides)			Pentoses		
	Σ ^{13}C Chemical shifts*	Free energy†		Σ ^{13}C Chemical shifts*	Free energy†
β-D-Glucose	702.1 (696.4)‡	2.05	β-D-Xylose	579.6	1.6
β-D-Galactose	707.3 (702.4)	2.5	α-L-Arabinose	583.3	1.95
β-D-Mannose	709.5 (706.5)	2.95	β-D-Lyxose	593.7	2.4
α-D-Glucose	716.2 (707.0)	2.4	α-D-Xylose	594.0	1.9
α-D-Mannose	715.5 (714.0)	2.5	β-D-Ribose	594.7	2.3
β-D-Allose	717.4 —	2.95	α-D-Lyxose	596.0	1.85
α-D-Galactose	724.0 (715.0)	2.85	β-L-Arabinose	598.4	2.2
α-D-Idose	— (711.3)	3.65	α-D-Ribose	598.6	3.1
α-D-Altrose	— (719.6)	3.35			

*Sum of chemical shifts (p.p.m.) in Table 1; *values are relative to downfield* CS_2.
†Data from ref. 21 (kcal/mole).
‡Sum of chemical shifts (p.p.m.) in Table 1, not including that of methyl ^{13}C.

chemical shift, as well as in stability, although the sequences of values are not always mutually consistent. Perhaps most noticeable is the low value relative to that expected for methyl α-D-idopyranoside,[8] and the fact that the order of shielding for the anomers of D-mannose and D-lyxose, as well as for some glycosides, compared with their parent sugars is the reverse of that anticipated (see below). Hence, these variations in ^{13}C chemical shift broadly reflect differences in stability, but furnish only a partial assessment of the situation.

The comparisons presented in Table 3 use calculated free energy values (21). The latter are pertinent for this purpose because they are computed almost entirely with non-bonding interaction energy terms (entropy contributions are minimal) (21), and also they furnish the most comprehensive energy data currently available for the sugars. One of these energy terms accounts for the anomeric effect. As discussed above, however, the anomeric effect makes no obvious contribution to shielding and hence differs in this respect from repulsive interactions (vicinal, *syn*-diaxial) that lead to destabilization. This difference is particularly noticeable in comparing the sugars and their glycosides. For example, the relative stabilities of anomers of D-glucose or D-xylose are reversed in going from the sugar to the methyl glycoside, the α- rather than β-glycosides being the more stable (18, 19). Yet the ^{13}C chemical shift patterns are virtually unchanged by methylation (aside from the inductive deshielding effect evident at ^{13}C-1). Hence, if steric interactions do indeed contribute to the various changes in charge density cited above, this reversal in stability should be attributed to selectively enhanced *stabilization*, rather than to an increase in repulsive interactions. On this basis, the chemical shift data appear to be in accord with recent theoretical considerations (20) which show that the anomeric effect represents a balance between attractive- and repulsive-dominant interactions (24), to which the attractive term makes the greater contribution (see also ref. 19).

Another aspect of these data merits comment. Increased shielding of a ^{13}C nucleus has been found in several instances (16, 25–27) to be accompanied by a decrease in the shielding of the appended proton, i.e., ^{13}C and ^{1}H shifts are affected inversely. Therefore, it appears that a change in bond polarization[9] occurs as a result of the impact of a destabilizing interaction. The data of Table 4 show that this kind of relationship applies also in the sugar series. Additional examples are cited in Table 5 for several individual

[8]Although conformational analysis leads to the expectation that α- and β-idopyranose are highly unstable in either chair conformation and that both of the latter are important in representing these sugar molecules (e.g., 21), recent proton magnetic resonance evidence indicates that the α-D-pentaacetate assumes virtually only the C1 conformation (23).

[9]If the change were basically in the state of hybridization of carbon, parallel changes in chemical shift for ^{13}C and ^{1}H would be expected; i.e. both ^{13}C nuclei and protons of alkanes are more shielded than those of alkenes, arenes, or alkynes.

Can. J. Chem. Downloaded from www.nrcresearchpress.com by 210.87.254.6 on 09/05/12
For personal use only.

TABLE 4
Comparison of ^{13}C and ^{1}H shielding

	$\Sigma\,^{13}C$ Chemical shift*	α–β†	$\Sigma\,^{1}H$ Chemical shift*	α–β§
α-D-Glucose	716.2 (594.0)	+14.1 (+14.4)	34.5	−1.0
β-D-Glucose	702.1 (579.6)		33.5	
α-D-Galactose	724.0 (598.4)	+16.7 (+15.1)	35.2	−1.1
β-D-Galactose	707.3 (583.3)		34.1	
α-D-Mannose	715.5 (596.0)	+6.0 (+2.3)	34.1	+0.3
β-D-Mannose	709.5 (593.7)		34.4	

*Data from Table 3; values in brackets are those for corresponding pentose.
†Plus sign indicates increased shielding, since values are relative to *downfield* CS_2.
‡Data from ref. 13 for pentaacetates in chloroform.
§Minus sign indicates decreased shielding, since values are relative to *upfield* TMS.

TABLE 5
Comparison of ^{13}C and ^{1}H shielding

Nucleus	Compound	^{13}C*	Δ	^{1}H†	Δ
1	α-D-Glucose	100.4	+4.5	5.32	−0.58
	β-D-Glucose	96.5		4.74	
2	α-D-Glucose	120.9	+2.6	3.60	−0.28
	β-D-Glucose	118.2		3.32	
1	α-D-Xylose	100.0	+4.5	5.26	−0.61
	β-D-Xylose	95.5		4.65	
2	α-D-Xylose	120.6	+2.6	3.63	−0.37
	β-D-Xylose	118.0		3.26	
1	α-D-Galactose	100.0	+4.2	5.34	−0.66
	β-D-Galactose	95.8		4.68	
2	α-D-Galactose	123.5	+3.3	3.87	−0.32
	β-D-Galactose	120.2		3.55	
1	β-L-Arabinose	99.4	+4.1	5.34	−0.74
	α-L-Arabinose	95.3		4.60	
2	β-L-Arabinose	123.6	+3.5	3.93	−0.35
	α-L-Arabinose	120.1		3.58	

*Data from Tables 1 and 2.
†Data obtained from ref. 14.

C—H bonds; in all instances the $\Delta^{13}C$ for an anomeric pair is in one direction whereas the $\Delta^{1}H$ value[10] is in the reverse direction. Anisotropy effects have an important bearing on proton chemical shifts (although much less so on those for ^{13}C (5, 9)), and have for long been invoked to account for the observation that an axial proton usually is more shielded than is an equatorial one (28). The current findings illustrate that this difference also is intimately associated with the shielding state of the carbon to which it is bonded.

It may be pertinent to what has been mentioned above, that the difference in ^{13}C shielding be-

[10]In Table 4, these values are derived from proton chemical shifts for the peracetates in chloroform (13), and hence may not be strictly comparable with the other data obtained with aqueous solutions.

Can. J. Chem. Downloaded from www.nrcresearchpress.com by 210.87.254.6 on 09/05/12
For personal use only.

Can. J. Chem. Downloaded from www.nrcresearchpress.com by 210.87.254.6 on 09/05/12
For personal use only.

tween anomers of mannose or lyxose is much smaller than between anomers of glucose, galactose, xylose, or arabinose (Table 4). Moreover for protons, the data (Table 4) imply, if anything, that α-mannose is slightly more stable than β-mannose. Hence the ^{13}C chemical shifts alone may not adequately reflect interactions within the molecules, and a better assessment of stability may yet be obtainable by also considering proton chemical shifts, i.e., evidence of bond polarization (and conceivably ^{17}O chemical shifts as well).

According to these considerations then, ^{13}C and proton chemical shift differences are attributable at least partly to interactions within the molecule that cause destabilization, or else that remove stabilizing influences. Expressed, for example, in terms of the anomeric center (Fig. 2, similar results are given by several sugars for which the data are available), inversion of the equatorial to the axial anomer causes the introduction of a destabilizing interaction. This may lead to widespread alterations of bond angles and dimensions, state of hybridization, etc., over the molecule. At the anomeric center itself, the event is evidenced by an increase in the shielding of C-1 and a decrease in shielding of H-1. The C_1—O_1 bond also must be affected by the changes and, in turn, the O—H bond. Possibly, the axial C—O bond becomes less polarized, because the carbon nucleus is less positive, and contributes to the fact that the difference in hydroxyl proton shifts (at least in methylsulfoxide (29, 30)) is such that the axial C—O bond bears the more shielded (less positive) proton.[11] For the corresponding methyl glycosides the same qualitative relationships apply. In this instance the ^{13}C nucleus of the methyl group, like the hydroxyl proton, is more shielded when bonded to the axial O atom

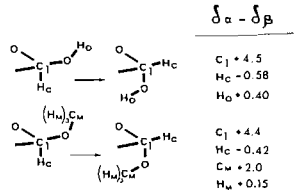

FIG. 2. Comparison of ^{13}C and ^{1}H shieldings at the anomeric center of α- and β-D-xylose; +, increased shielding; −, decreased shielding.

[11]However, the relative importance of electron density in determining hydroxyl proton chemical shifts, and of factors such as hydrogen bonding and solvation, remains to be evaluated.

(Tables 1 and 2). However, the protons of the methyl group also become more shielded, in contrast to the effect on protons attached to carbons of the ring. Nevertheless, this is in accord with what should be expected of carbon-bonded protons,[9] and may indicate that the methyl C—H bonds are too remote from the focal point of the destabilizing interaction to be affected like the C—H bonds of the ring.

Experimental

Carbon-13 magnetic resonance spectra were measured at a frequency of 25.15 MHz by means of a Varian HA-100 spectrometer. The nuclear magnetic resonance system included a probe doubly-tuned to 25.15 and 100 MHz, a voltage controlled generator, a V2513-1 heteronuclear decoupler, and a time averaging computer, which permitted the recording (in frequency sweep mode) of proton-decoupled ^{13}C resonance signals in natural abundance. Methyl iodide-^{13}C (about 90% enriched; Merck, Sharpe and Dohme, Montreal, Quebec), contained in a coaxial capillary, furnished the internal reference "lock" signal. Chemical shifts are reported relative to carbon disulfide, which produces its resonance signal 213.1 p.p.m. (5730 Hz) downfield from the methyl iodide reference signal. Resolution was 0.1 p.p.m. or better. The sample temperature was 55° ± 5° C.

In preliminary experiments chemical shift variations due to a change in solute concentration were no greater than the resolution attainable. Therefore, the concentration of the aqueous sugar and glycoside solutions used varied directly with the quantity of sample available and its solubility; hence, commonly, the concentration was 0.5–0.6 g/ml H_2O, but in some instances was one-fifth of this figure. An aqueous solution of uniformly labelled D-glucose-^{13}C (about 50% enriched; Merck, Sharpe and Dohme, Montreal, Quebec) was utilized to facilitate the selection of optimal spectrometer settings (homogeneity, phasing, etc.).

Representative spectra are illustrated in Fig. 2 of ref. 1.

Generous support by the Pulp and Paper Research Institute of Canada and the National Research Council of Canada is gratefully acknowledged. Mr. R. Simoneau kindly provided very helpful technical assistance.

1. A. S. PERLIN and B. CASU. Tetrahedron Lett. 2921 (1969).
2. H. SPIESECKE and W. G. SCHNEIDER. J. Chem. Phys. **35**, 722 (1961).
3. F. J. WEIGERT and J. D. ROBERTS. J. Amer. Chem. Soc. **89**, 2967 (1967).
4. L. D. HALL and L. F. JOHNSON. Chem. Commun. 509 (1969).
5. P. C. LAUTERBUR. J. Amer. Chem. Soc. **83**, 1838–1846 (1961).
6. J. M. SICHEL and M. A. WHITEHEAD. Theor. Chim. Acta, **5**, 35 (1966).
7. T. YONEZAWA, I. MORISHIMA, and H. KATO. Bull. Chem. Soc. Japan, **39**, 1398 (1966).
8. V. CHENEY and D. M. GRANT. J. Amer. Chem. Soc. **89**, 5319 (1967).

9. J. B. STOTHERS. Quart. Rev. **19**, 144 (1965).
10. Y. A. ZHDANOV, V. I. MINKIN, Y. A. OSTROUMOV, and G. A. DOROFEENKO. Carbohyd. Res. **7**, 156 (1968).
11. D. M. GRANT and E. G. PAUL. J. Amer. Chem. Soc. **86**, 2984 (1964).
12. D. K. DALLING and D. M. GRANT. J. Amer. Chem. Soc. **89**, 6612 (1967).
13. R. U. LEMIEUX and J. D. STEVENS. Can. J. Chem. **43**, 2509 (1965).
14. R. U. LEMIEUX and J. D. STEVENS. Can. J. Chem. **44**, 249 (1966).
15. G. W. BUCHANAN, D. A. ROSS, and J. B. STOTHERS. J. Amer. Chem. Soc. **88**, 4301 (1966).
16. A. S. PERLIN and H. J. KOCH. This issue..
17. R. U. LEMIEUX. *In* Molecular rearrangements. Part II. *Edited by* P. de Mayo, Interscience, 1964. p. 736.
18. J. T. EDWARD. Chem. Ind. 1102 (1955).
19. R. U. LEMIEUX. *In* Molecular rearrangements. Part II. *Edited by* P. de Mayo, Interscience, 1964. p. 739.
20. S. WOLFE, A. RAUK, L. M. TEL, and I. G. CSIZMADIA. J. Chem. Soc. In press.
21. S. J. ANGYAL. Angew. Chem. Int. Ed. **8**, 157 (1969).
22. D. E. DORMAN, S. J. ANGYAL, and J. D. ROBERTS. Proc. Nat. Acad. Sci. **63**, 612 (1969).
23. N. S. BHACCA, D. HORTON, and H. PAULSEN. J. Org. Chem. **33**, 2484 (1968).
24. L. C. ALLEN. Chem. Phys. Lett. **2**, 597 (1968).
25. D. M. GRANT and B. V. CHENEY. J. Amer. Chem. Soc. **89**, 5315 (1967).
26. B. V. CHENEY. J. Amer. Chem. Soc. **90**, 5386 (1968).
27. G. W. BUCHANAN, J. B. STOTHERS, and S. WU. Can. J. Chem. **47**, 3113 (1969).
28. R. U. LEMIEUX, R. K. KULLNIG, H. J. BERNSTEIN, and W. G. SCHNEIDER. J. Amer. Chem. Soc. **79**, 1005 (1957).
29. B. CASU, M. REGGIANI, G. G. GALLO, and A. VIGEVANI. Tetrahedron Lett. 39–40, 2839 (1964).
30. A. S. PERLIN. Can. J. Chem. **44**, 539 (1966).
31. D. E. DORMAN and J. D. ROBERTS. J. Amer. Chem. Soc. **92**, 1355 (1970).

Can. J. Chem. Downloaded from www.nrcresearchpress.com by 210.87.254.6 on 09/05/12
For personal use only.

Can. J. Chem. Downloaded from www.nrcresearchpress.com by 210.87.254.40 on 09/05/12
For personal use only.

Some problems affecting the determination by gas–liquid chromatography of vanillin[1] and syringaldehyde[2] in oxidized neutral sulfite pulping liquors

K. J. Harrington and Janet Hamilton
Division of Forest Products, CSIRO, South Melbourne, Victoria, Australia
Received March 21, 1969[3]

Gas–liquid chromatographic parameters for the quantitative evaluation of syringaldehyde and vanillin in oxidized neutral sulfite pulping liquors are discussed.

Canadian Journal of Chemistry, **48**, 2607 (1970)

Introduction

The phenolic aldehydes, vanillin and syringaldehyde, are of importance in the fields of lignin and flavor chemistry. Historically, these materials have been isolated and quantitatively evaluated by means of paper chromatography (1, 2) and by photometric techniques (3, 4). More recently, Underwood and Fillipic (5, 6) have described the use of gas–liquid chromatography (g.l.c.) in the estimation of vanillin and syringaldehyde in maple syrup, and Martin *et al.* (7) have determined vanillin in vanilla samples by g.l.c. using an internal standard. In the field of lignin chemistry, g.l.c. techniques have been used for the study of lignin degradation products by Pepper *et al.* (8), Hrutfiord (9), Brand (10), and Shaw and Waldock (11).

Work in this laboratory concerning a study of the neutral sulfite semi-chemical (NSSC) method of producing wood pulp for papermaking has included g.l.c. methods for determination of vanillin and syringaldehyde. The present note discusses some of the important aspects of this technique and its associated problems.

Experimental

The instrument used in these investigations was a Beckman GC-4 gas chromatograph equipped with a hydrogen flame ionization detector using nitrogen as carrier gas. The vanillin was analytical reagent grade and was obtained commercially.[4] Syringaldehyde was synthesized in this laboratory from vanillin (12).

Liquors were taken from the NSSC cooking of *Eucalyptus regnans*. From the lignin present in these liquors, nitrobenzene oxidation (1) yielded vanillin and syringaldehyde, which after acidification were extracted with chloroform. The chloroform extracts were evaporated to dryness and the residues re-dissolved in ethanol. These ethanolic solutions were used directly for chromatographic analysis.

Discussion

Column Construction Material

Columns constructed from copper, glass, aluminum, and stainless steel were evaluated for this determination. Each was 2 m in length with an internal diameter of 2 mm. Columns were filled with the selected packing and a solution containing 1% each of vanillin and syringaldehyde in ethanol was injected. Typical chromatograms (Fig. 1) show significant differences in peak tailing and the appearance of an additional peak where an aluminum column was used. The latter observation suggests a catalytic action of the metal or its oxide in the degradation of either or both of the parent materials. For quantitative evaluation, the peaks obtained when using copper columns were the only ones acceptable.

Solid Support

Of the three types of solid support tried, namely glass beads, acid-washed Chromosorb W[5], and granulated teflon, the last-named proved to be the most inert. Column packing was made easier when both the empty column and the coated support were chilled beforehand.

Stationary Phase

Several different stationary phases have been used with varying degrees of success. Hrutfiord (9) has listed many of these, but for the present work Apiezon N was found to produce the most

[1]4-Hydroxy-3-methoxy benzaldehyde.
[2]4-Hydroxy-3,5-dimethoxy benzaldehyde.
[3]Revision received May 1, 1970.
[4]By-Products & Chemicals Pty. Ltd., Sydney, Australia.
[5]60/80 Mesh from Varian Autograph, Palo Alto, California, U.S.A.

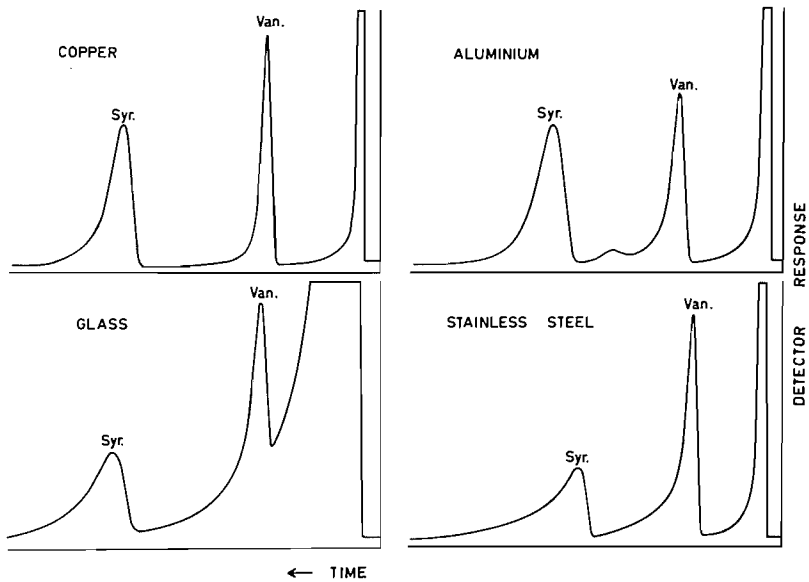

FIG. 1. Effect of column construction material on chromatogram characteristics.

satisfactory results. An optimum loading of 15% (by weight) was obtained using the evaporation technique.

Temperature of Chromatograph Components

With due regard for desirable peak shapes, convenient retention times, prevention of condensation, or thermal degradation of the sample, the following temperatures were found to be suitable: injection port, 300 °C; inlet line, detector line, and detector oven, 250 °C; column oven, 220 °C.

Gas Flow Rates

The hydrogen flame ionization detector is well known for its high sensitivity, but variability in its response to eluting components can be encountered unless considerable care is taken to establish and control the flow rates of hydrogen, carrier gas, and to a lesser extent, air. These adjustments, of critical importance in quantitative g.l.c., have been discussed fully by McWilliam (13).

Sample Introduction

In the absence of an internal standard, quantitative g.l.c. is obviously very dependent upon achieving an accurate and reproducible sample introduction technique. Evaporation from the tip of the needle as it approaches the heated injection block can be minimized by slightly withdrawing the plunger of the syringe before injection. There was some evidence in the present work that the first one or two samples injected after the placement of a new septum gave rise to peaks smaller than expected. This effect has been noted by Tamsma *et al.* (14) and is possibly due to adsorption of the solute on the underside of the septum.

For calibration purposes, a series of injections was made over the range from 5 to 50 μg of each aldehyde. The relationship between peak area and sample concentration was shown to be nonlinear with a positive intercept on the concentration axis. Since precautions had been taken to prevent premature evaporation from the needle tip and corrections for syringe dead-volume had been made, it appeared that adsorption of solute had taken place in the column; a phenomenon previously observed by Shaw and Waldock (11). Repeated injections of vanillin and

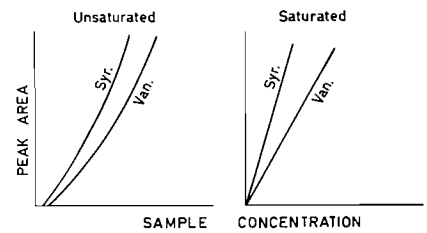

FIG. 2. Effect of in-column solute adsorption on column behavior.

Can. J. Chem. Downloaded from www.nrcresearchpress.com by 210.87.254.40 on 09/05/12
For personal use only.

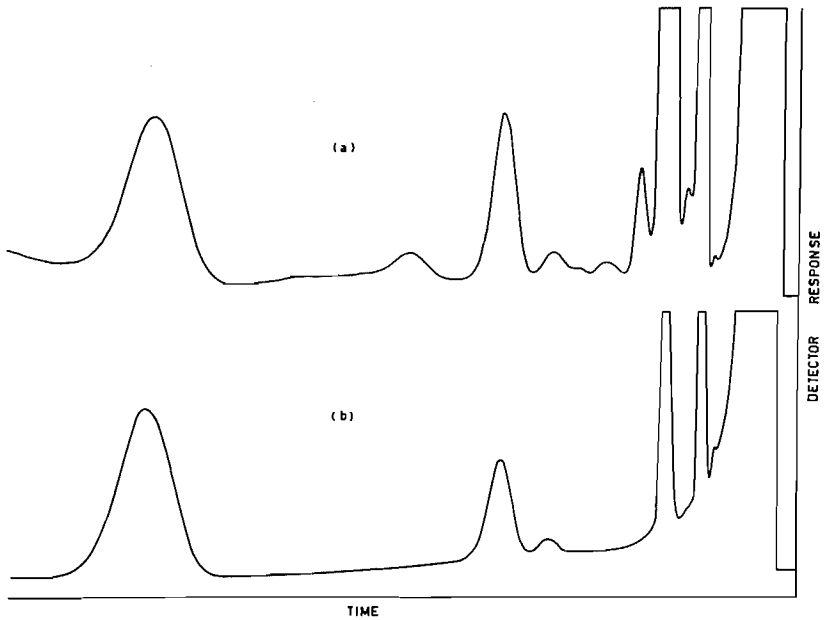

FIG. 3. Chromatograms of nitrobenzene oxidation products of NSSC liquor. (*a*) No alkaline pre-extraction. (*b*) Alkaline pre-extraction.

syringaldehyde were made and the calibration was again carried out. Peak area was then shown to be proportional to solute concentration (Fig. 2).

Fig. 3*a* shows a chromatogram of the alkaline nitrobenzene oxidation products of an NSSC liquor. Several of the larger peaks can be attributed to excess nitrobenzene and its reduction products. To simplify the chromatographic separation, Pepper *et al.* (8) extracted the oxidized liquor with diethyl ether before acidification, and found that this removed much of the unwanted material (Fig. 3*b*). It can be demonstrated, however, that both vanillin and syringaldehyde are significantly soluble (up to 10%) in both ether and chloroform when in alkaline solution. Thus, the use of such a "cleaning-up" extraction results in the loss of wanted aldehydes.

This means that quantitative evaluation must be carried out in the presence of extraneous materials some of whose chromatogram peaks are difficult to resolve completely from those of the aldehydes under consideration. Quantitative measurement of overlapping peaks is subject to considerable difficulty. Solute matrix effects have been discussed by several workers, e.g., Weinstein (15) and Juvet and Chiu (16). Dal Nogare and Juvet (17) have described a method of standard addition by means of which the effects of matrix interactions are greatly reduced or eliminated. For overlapping peaks, however, the difficulty in deciding in the first instance which is in fact the true area to measure would make the application of this addition method of more limited value. Figure 4 demonstrates an example of matrix interaction.

Varying amounts of iso-vanillin (3-hydroxy-4-methoxy-benzaldehyde) were added to a constant amount of vanillin and the peak areas of vanillin were measured by means of a planimeter. To eliminate the necessity of estimating the trailing half of the vanillin peak, the areas of the leading half only were measured (shaded). The results are shown in Table 1. In the presence of an unknown degree of matrix interaction, it is not possible to evaluate the total area of an overlapping peak.

TABLE 1

Magnitude of matrix interaction between vanillin and iso-vanillin

Weight ratio iso-vanillin/vanillin	Vanillin shaded area (cm^2)
0.7	2.6
3.0	2.1
8.0	1.7

Can. J. Chem. Downloaded from www.nrcresearchpress.com by 210.87.254.40 on 09/05/12
For personal use only.

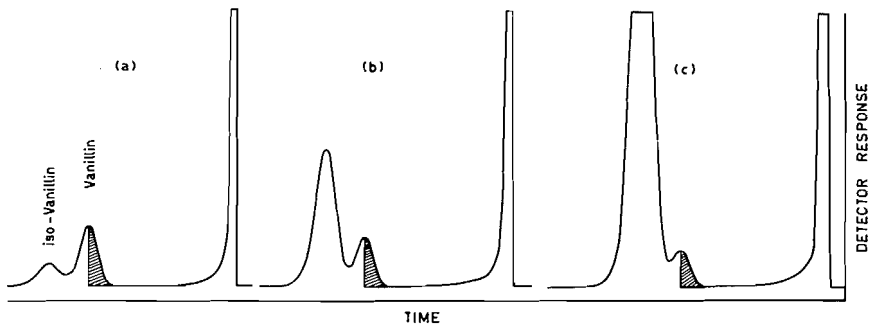

FIG. 4. Matrix interaction between vanillin and iso-vanillin. Weight ratio iso-vanillin/vanillin: (*a*) 0.7; (*b*) 3.0; (*c*) 8.0.

Juvet and Chiu (16) attempted to overcome this problem by using synthetic blends similar in composition to that of the solutions being studied. It would not be practicable, however, to apply this technique to the present study of NSSC liquor oxidation products.

Summary

The quantitative separation and evaluation of vanillin and syringaldehyde by g.l.c. present certain problems which markedly affect the accuracy of the determination. For complex solution systems, such as nitrobenzene-oxidized NSSC pulp liquors, the presence of solute matrix interactions disturbs the relationship between the concentration of a component and its chromatogram peak area.

As it has been shown that a "cleaning-up" extraction of the oxidized liquors results in a loss of syringaldehyde and vanillin, it is necessary to employ chromatographic conditions which provide the maximum amount of peak resolution.

Adsorption of vanillin and syringaldehyde occurs on the column packing and an equilibrium state is reached only when the column has been conditioned by repeated injections of the two aldehydes.

The authors wish to thank Miss N. Ditchburne of the Division of Mathematical Statistics, CSIRO, for her assistance in the statistical planning of certain parts of the experimental work, and Mr. M. Menshun for making available a pure sample of syringaldehyde.

1. D. E. BLAND and CLARE STAMP. Aust. J. Appl. Sci. **6**, 353 (1955).
2. J. E. STONE and M. J. BLUNDELL. Anal. Chem. **23**, 771 (1951).
3. L. G. ENSMINGER. J. Ass. Offic. Anal. Chem. **36**, 679 (1953).
4. F. J. FEENY. J. Ass. Offic. Anal. Chem. **47**, 555 (1964).
5. J. C. UNDERWOOD and V. J. FILLIPIC. J. Ass. Offic. Anal. Chem. **48**, 689 (1965).
6. J. C. UNDERWOOD and V. J. FILLIPIC. J. Ass. Offic. Anal. Chem. **46**, 334 (1963).
7. G. E. MARTIN, F. J. FEENEY, and F. P. SCARINGELLI. J. Ass. Offic. Anal. Chem. **47**, 561 (1964).
8. J. M. PEPPER, M. MANOLOPOULO, and R. BURTON. Can. J. Chem. **40**, 1976 (1962).
9. B. F. HRUTFIORD. Tappi, **48**, 48 (1965).
10. J. M. BRAND. J. Chromatogr. **26**, 373 (1967).
11. A. C. SHAW and K. T. WALDOCK. Pulp Pap. Mag. Can. **68**, T118 (1967).
12. I. A. PEARL and D. L. BEYER. J. Amer. Chem. Soc. **74**, 4262 (1952).
13. I. G. MCWILLIAM. J. Chromatogr. **6**, 110 (1961).
14. A. TAMSMA, F. E. KURTZ, N. RAINEY, and M. J. PALLANSCH. J. Gas. Chromatogr. **5**, 271 (1967).
15. A. WEINSTEIN. Anal. Chem. **32**, 288 (1960).
16. R. S. JUVET, JR. and J. CHIU. J. Amer. Chem. Soc. **82**, 1560 (1961).
17. S. DAL NOGARE and R. S. JUVET, JR. Gas-liquid chromatography. Interscience Publishers, 1960.

Can. J. Chem. Downloaded from www.nrcresearchpress.com by 210.87.254.40 on 09/05/12
For personal use only.

Can. J. Chem. Downloaded from www.nrcresearchpress.com by 210.87.254.40 on 09/05/12
For personal use only.

Fluorescence of chloropentafluoroacetone

H. S. SAMANT AND A. J. YARWOOD
Department of Chemistry, McMaster University, Hamilton, Ontario

Received March 6, 1970

The fluorescence of chloropentafluoroacetone in the gaseous state at room temperature is reported. The fluorescence extends from 337 nm to greater than 560 nm with a maximum intensity at 420 nm and is unaffected by low pressures of oxygen. The energy of the first excited singlet state is estimated as about 83 kcal and the fluorescence data for 313 and "290" nm excitation indicate that fluorescence enhancement occurs as the pressure increases. The fluorescent yield at high pressures ($\phi_f^{\infty} = 0.02_3$) is independent of the nature of the gas used to attain the high pressure. The lifetime of the fluorescent state is 35.1 ± 0.3 ns.

A simple mechanism correlates the experimental observations and the values of the rate constants are considered. The reciprocal of the natural radiative lifetime is calculated to be $6.6 \times 10^5\ s^{-1}$ and the rate constant assigned to intersystem crossing to the triplet is $2.8 \times 10^7\ s^{-1}$. A comparison with the data in the literature for hexafluoroacetone shows the effect of substitution by a heavy atom in the fluorinated ketone. It about doubles the value of the rate constant associated with intersystem crossing from the first excited singlet state in the gas phase.

Canadian Journal of Chemistry, **48**, 2611 (1970)

Luminescence studies have been indispensable in clarifying the primary processes in the photochemistry of ketones in the gas phase. The fluorescence and phosphorescence of acetone (1), hexafluoroacetone (2), and biacetyl (3) have been investigated extensively and have been correlated with the photodecomposition processes. However, the photochemistry of chlorinated ketones in the gas phase has been concerned mainly with photodecomposition studies and the investigation of radical reactions, e.g. chloroacetone (4), chlorobutanone (5), hexachloroacetone (6), 1,3-dichlorotetrafluoroacetone (7), 1,1,3-trichlorotrifluoroacetone (8), 1,1,3,3- and tetrachlorodifluoroacetone (9). While this study of the luminescence of chloropentafluoroacetone was in progress the photodecomposition was reported (10). Carbon monoxide and substituted methyl radicals were the major primary products but an alternative decomposition to an acetonyl radical and a chlorine atom became significant at the shorter excitation wavelengths.

Experimental

Chloropentafluoroacetone (Allied Chemical Co.) was purified by trap-to-trap distillation at temperatures of −78, −95, and −112°. The −95° fraction was retained after large head and tail fractions were discarded. This technique removed small traces of an unidentified impurity which was detected in the initial ketone by gas chromatographic separation on DC-703, Porapak-P, and Porapak-Q columns. The samples purified by distillation had properties similar to small quantities of the ketone purified by gas chromatography. The ketone was stored at −196 °C in the dark and thoroughly degassed each time before use.

Sulfur hexafluoride, oxygen, and carbon dioxide were supplied by Matheson and, after appropriate distillation and degassing, the purities were checked gas chromatographically. The quinine sulfate (Fisher) was N.F. grade.

The vacuum system was grease free and the purification section was saturated with mercury vapor. Contamination of the storage and cell sections was prevented by maintaining two U traps in series at −78 or −196°. The pure quartz cells were attached to the vacuum system via a metal valve (Nupro) and the pressures were measured on a glass spoon gauge.

Preliminary measurements on the luminescence of the ketone were made on an Aminco–Bowman spectrofluorometer (with phosphoroscope attachment). Detailed measurements on the luminescence of the ketone in the gas phase at room temperature were made using a different apparatus. The excitation source, either a 1000 W Hg/Xe lamp or 450 W Xe lamp, was used in conjunction with a small Bausch and Lomb monochromator (with a 1200 grooves/mm grating blazed at 400 nm). The vacuum tight Suprasil cell (Hellma) was polished on all four sides and was 1 cm square in cross-section. The light emitted perpendicular to the incident beam was analyzed using a 0.5 m Ebert Jarrell–Ash monochromator (with a 1180 lines/mm grating blazed at 400 nm) fitted with a cooled RCA 8575 photomultiplier. The output was measured with a Keithley electrometer.

Fluorescence lifetimes were measured using a TRW nanosecond spectral source system. The 316 nm line from the pulsed nitrogen lamp was isolated by a third order 313 nm interference filter (Baird Atomic). The emitted light passed through a glass filter (Corning 3-75) and was detected by a 1P28 photomultiplier.

The total ketone luminescence, without wavelength resolution, was also measured. The excitation source was a medium pressure mercury lamp (Hanovia #673A). The light was collimated and the excitation wavelength selected by filters. The 334 nm radiation was isolated

Can. J. Chem. Downloaded from www.nrcresearchpress.com by 210.87.254.40 on 09/05/12
For personal use only.

using filter solutions (11). The 313 nm line was selected using a third order interference filter (Baird Atomic).The radiation classed as the "290" nm group consisted mainly of 289 and 297 nm radiation isolated by an interference filter (Optics Technology #2700). The quartz cell used for experiments at the higher pressures was 1 cm long. A 10 cm long T-shaped quartz cell was used for the lower pressure experiments. The light passed through the cell as a parallel beam and was condensed by a quartz lens onto a photocell (RCA 935). The emitted light was observed at right angles to the incident beam. The light was collimated by a tube (0.8 cm diameter and 12.8 cm long), passed through a glass filter (Corning 0-52), detected by a photomultiplier (1P28), and measured on an electrometer (Keithley type 610B). The lamp, filters, and cell were housed in separate compartments of a light-tight box and the scattered light plus dark current signal was approximately 3×10^{-9} A. The relative fluorescence yield Q is defined (12) as $(I_f - I_f^0)/g(I_t^0 - I_t)$. I_f and I_f^0 are the emission intensities when the ketone is present and absent; I_t and I_t^0 are the intensities of light transmitted through the cell in the presence and absence of ketone; g is a factor which takes into account that the emission is observed at a distance from the entrance window of the cell. For the 1 cm long cell g is assumed to be unity and for the 10 cm cell equal to $\sinh(\varepsilon c\delta/2)/\sinh \varepsilon cl/2)$. ($\varepsilon = 2.303\ \alpha$, where α is decadic molar extinction coefficient, c is the concentration, l is the length of the cell, and δ is the length of the cell observed by the photomultiplier.) No corrections were made for reflections.

The experimentally observed Q vs. wavelength curve for the fluorescence of the ketone was corrected using a sensitivity factor derived from measurements on quinine sulfate. The quantum yield of fluorescence at 313 nm was obtained by comparing areas under the corrected Q vs. λ curves for the ketone and quinine sulfate and assuming the fluorescence yield of quinine sulfate to be 0.55 (13). Provided the emission profile does not change with variation of the pressure, and provided the experimental system is not altered, the relative fluorescence yields using 313 nm radiation, Q^f, can be related to the quantum yields ϕ^f at 313 nm by $Q^f = \beta\phi^f$ where β is a proportionality factor. The Q values at other excitation wavelengths are corrected using the manufacturers' specifications to allow for the different sensitivities of the photocells.

Results

The ultraviolet absorption spectrum of chloropentafluoroacetone at room temperature extends from below 250 to greater than 356 nm with a maximum at 303 nm ($\varepsilon = 48$). The spectrum is quite asymmetric with structure evident, especially at the longer wavelengths. There are at least five bands (339, 325, 314, 303, 293, 283 ? nm) with a spacing of about 1200 cm^{-1}.

When chloropentafluoroacetone in the gas phase at room temperature is excited in the region 280 to 334 nm, luminescence is observed. Figure 1 shows that the luminescence of chloropentafluoroacetone (109 Torr) excited at 313 nm extends from about 337 to greater than 560 nm (the emission is corrected for monochromator and detector sensitivity). The emission spectrum is asymmetric, has a maximum at 420 nm but is devoid of structure. The emission spectrum is unaffected by the presence of mercury vapor in the cell. The addition of 24 Torr of oxygen to 109 Torr of ketone does not decrease the intensity of the emission spectrum, nor does it alter the emission profile as a function of wavelength. No emission can be detected when the pure ketone is studied in the spectrophosphorometer with the rotating shutter operating.

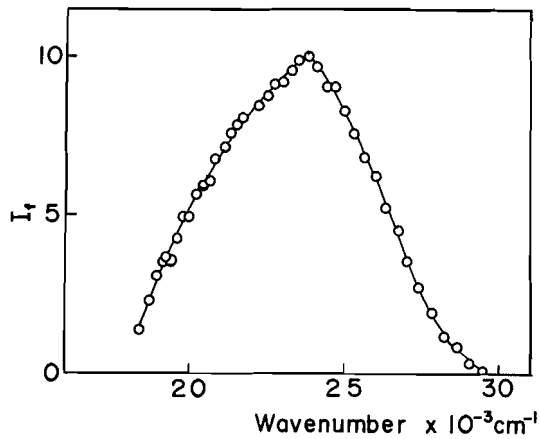

FIG. 1. Variation of the fluorescence intensity, I_f, of chloropentafluoroacetone (109 Torr) with wavenumber. $\lambda_{Ex} = 313$ nm.

The lifetime of the excited ketone molecule is independent of the pressure of the ketone in the range 9 to 600 Torr. In particular there is no systematic variation in the lifetime at pressures below 100 Torr (five experiments). The decay of the light intensity appears to be exponential, although it would be difficult to detect non-exponential decay using this nanosecond technique. The average lifetime of the fluorescence at 25 °C is 35.1 $\pm$ 0.3 ns.

Many experiments were performed to investigate the emission profile as a function of wavelength. As indicated earlier, using 313 nm excitation and a chloroketone pressure of 109 Torr the onset of the fluorescence is at 337 nm, the maximum at 420 nm, and the long wavelength limit at greater than 560 nm. Identical wavelengths were observed at the following ketone pressures: 3, 11, 34, 96, and 209 Torr. However, the sensitivity of the photomultiplier decreases rapidly at wavelengths longer than 560 nm and it is likely that

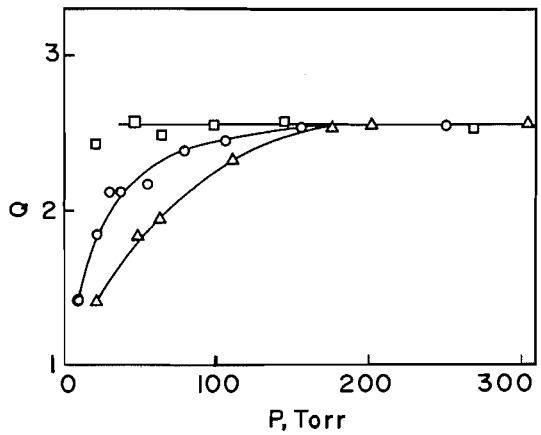

FIG. 2. Variation of the relative fluorescence yield Q with pressure of chloroketone. □, λ_{Ex} = 334 nm; ○, λ_{Ex} = 313 nm; △, λ_{Ex} = "290" nm.

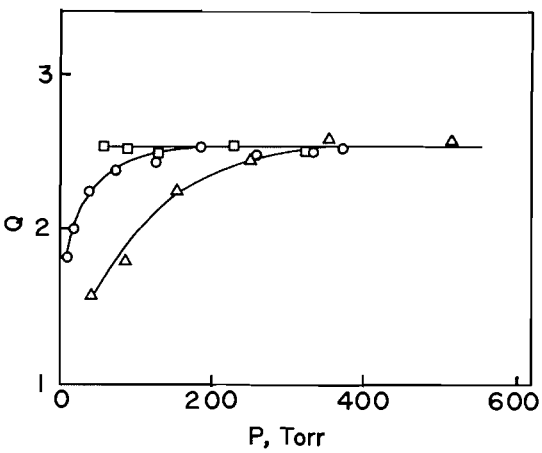

FIG. 3. Variation of the relative fluorescence yield Q of chloroketone with pressure of added carbon dioxide. □, λ_{Ex} = 334 nm; P_{ketone} = 38.1 Torr. ○, λ_{Ex} = 313 nm; P_{ketone} = 20.4 Torr. △, λ_{Ex} = "290" nm; P_{ketone} = 22.0 Torr.

the tail of the luminescence extends further to the red. Experiments at 209 Torr ketone show that the emission profile also does not depend on the excitation wavelength in the range 334, 313, and "290" nm. Further, there is no change in the profile when 30 Torr of ketone are illuminated with 313 and "290" nm radiation.

Measurements in the steady-state apparatus show that there is fluorescence enhancement at the higher pressures. Figure 2 shows Q values plotted vs. ketone pressure for the 334, 313, and "290" nm excitation wavelengths. The fluorescence yields are low at the lower pressures and

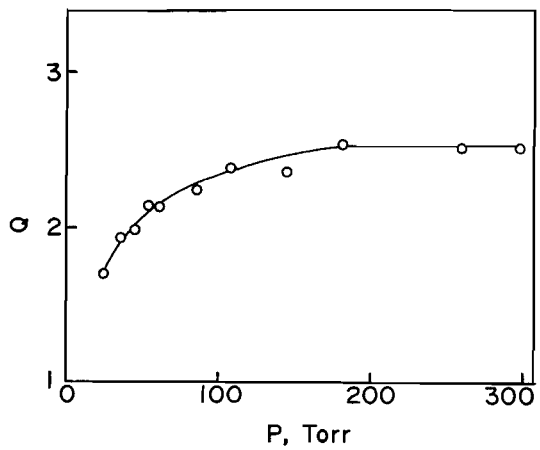

FIG. 4. Relative fluorescence yield Q of chloroketone (12.3 Torr) with pressure of sulfur hexafluoride. λ_{Ex} = 313 nm.

increase to a plateau value at high pressures at all wavelengths. Since the radiation classed as "290" nm contains both 289 and 297 nm radiation no quantitative significance should be attached to the data obtained. However, qualitatively, it is clear that at the shorter wavelengths a higher pressure is required to attain the maximum enhancement and that the approach to the plateau region is slower at the shorter wavelengths. A similar effect is observed when the pressure is increased by adding various pressures of inert gas to a fixed low pressure of ketone. Figure 3 shows the results for carbon dioxide addition at the different excitation wavelengths. Figure 4 is a similar plot for sulfur hexafluoride addition to ketone excited at 313 nm.

The quantum yield of fluorescence of chloropentafluoroacetone excited at 313 nm was determined for ketone pressures of 113, 221, and 168 Torr as 0.024, 0.025, and 0.021 and the mean value is 0.023.

Discussion

The electronic spectra of aliphatic carbonyl compounds have been considered recently by Csizmadia and co-workers (14). In an experimental and theoretical study they point out that the largest effects on the π^*–n transition energies of RCOX systems arise principally from the nature of the first atom in the group X. When X is a halomethyl substituent they find that there are only very small shifts in π^*–n bands relative to the standard methyl derivatives. The absorption spectrum of chloropentafluoroacetone in

Can. J. Chem. Downloaded from www.nrcresearchpress.com by 210.87.254.40 on 09/05/12
For personal use only.

Can. J. Chem. Downloaded from www.nrcresearchpress.com by 210.87.254.40 on 09/05/12
For personal use only.

the gas phase has a maximum at 303 nm and its intensity ($f \simeq 10^{-3}$) is thus consistent with excitation of the π^*–n transition of the ketone. The structure in the absorption spectrum could be a vibrational progression in the excited state C—O stretching frequency. (The 1200 cm^{-1} frequency of the chloroketone might then be the analogue of the 1182.6 cm^{-1} stretching vibration in $^1A''$ state of formaldehyde (15) and the 1460 cm^{-1} progression in the ^1A_u state of oxalyl chloride (16)).

From the absorption spectrum the natural radiative lifetime, τ_0, of the singlet state populated on absorption in the π^*–n band can be estimated using $1/\tau_0 = 2.88 \times 10^{-9}\,\bar{\nu}^2 \int \varepsilon d\bar{\nu}$. The value of $1/\tau_0$ derived for chloropentafluoroacetone is $8.8 \times 10^5\ s^{-1}$. This is probably a valid estimate of the natural radiative lifetime of the excited singlet state, although there are assumptions made in applying the formula to large molecules. The value may be compared to the estimate of $4 \times 10^6\ s^{-1}$ for acetone (17) and $1.8 \times 10^5\ s^{-1}$ for hexafluoroacetone (18).

The luminescence spectrum of chloropentafluoroacetone shown in Fig. 1 is the first report of luminescence from a chlorinated carbonyl compound in the gas phase. The long wavelength limit appears to be at greater than 560 nm. It is usually assumed that low pressures of oxygen quench only the triplet states of carbonyl compounds in the gas phase and the emission observed in the presence of a few Torr of oxygen is assigned as fluorescence from the excited singlet state. There is evidence for hexafluoroacetone that much higher pressures of oxygen (1 atm) also quench the singlet states (18). Since low pressures of oxygen do not decrease the luminescence intensity and do not alter the emission profile the luminescence is considered to be fluorescence. This assignment is consistent with the observation that no long-lived emission is detected when the pure chloroketone is investigated using a rotating shutter with a time resolution of about 10^{-3} s. The lack of phosphorescence of the ketone does not imply that triplet state molecules are absent from the system. The internal heavy atom effect of the chlorine could modify the rates of processes competitive with phosphorescence, e.g. radiationless conversion to the ground state. (Unpublished work indicates that triplet molecules are an important feature of the system.)

The overlap of the absorption and fluorescence spectra is at about 345 nm and the energy of the 0–0 band of the singlet–singlet transition is about 83 kcal. If one accepts the suggestion that the structure in the absorption spectrum is due to a vibrational frequency of about 1200 cm^{-1} then the excitation of chloroketone using 313 nm radiation would result in excited singlet molecules with about three quanta of vibrational energy.

Excited singlet state chloroketone molecules that are also vibrationally excited should be capable of deactivation and fluorescence enhancement might result. The data of Fig. 2 show that enhancement does occur in this system.

Since the fluorescence as a function of wavelength is, within experimental error, independent of excitation energy and concentration of chloroketone the fluorescence yields Q^f can be related to the quantum yields of fluorescence by $Q^f = \beta\phi^f$. The constant emission profile also suggests that the majority of the fluorescence is from the zeroth vibrational level of the singlet state since a large contribution by emission from vibrationally excited states might alter the emission profile, especially at the shorter wavelengths.

The following mechanism is adequate to correlate all the experiments reported on the chloropentafluoroacetone

[1]	$A \rightarrow {}^1A^n$	I_a
[2]	${}^1A^n + A \rightarrow {}^1A^\circ + A$	k_2
[3]	${}^1A^n \rightarrow$ Removal	k_3
[4]	${}^1A^\circ \rightarrow A + h\nu_f$	k_4
[5]	${}^1A^\circ \rightarrow$ Removal	k_5

The collisional deactivation of vibrationally excited singlet state ketone molecules has a rate constant k_2. k_3 is the rate constant for all other processes that remove $^1A^n$, e.g. intersystem crossing or decomposition. $^1A^0$ is the excited singlet ketone molecule in its zeroth vibrational level and it is removed by fluorescence (rate constant k_4) or by processes such as decomposition or intersystem crossing to the ground triplet state (combined rate constant k_5). The mechanism implies that vibrational deactivation is by strong collisions and a steady state analysis yields

$$[6] \qquad \frac{1}{\phi_f} = \frac{k_4 + k_5}{k_4} + \frac{k_3(k_4 + k_5)}{k_2 \quad k_4} \frac{1}{[A]}$$

Thus a plot of $1/\phi_f$ or $1/Q_f$ vs. $1/[A]$ would be linear. When the 313 nm data for the pure ketone

Can. J. Chem. Downloaded from www.nrcresearchpress.com by 210.87.254.40 on 09/05/12
For personal use only.

are plotted in this way they do lie on a line within experimental error. The value of the slope-to-intercept ratio is 4.5×10^{-4} mole/l and is a measure of k_3/k_2 according to the above mechanism. If one assumes that k_2 is 2×10^{11} l mole^{-1} s^{-1} at room temperature then k_3 becomes 9×10^7 s^{-1}. As expected, the efficiency of carbon dioxide and sulfur hexafluoride in deactivating the vibrationally excited singlet state is less than that of the ketone itself. However, for the case of hexafluoroacetone, Kutschke and Gandini (2) have evidence that vibrational deactivation is via weak collisions (i.e. involves a cascade through vibrational levels). In that situation there is no simple interpretation of the $1/\phi_f$ vs. $1/[A]$ plot. The type of vibrational deactivation in the chloroketone can be decided only when more precise data are available (experiments using a more sensitive photomultiplier in a cooled housing are planned).

The role of vibrationally excited states is further displayed in Fig. 2. The Q value at the high pressure limit is independent of the excitation wavelength, as required by the mechanism. However, the limiting value is reached at progressively greater pressures as the excitation wavelength is decreased; at below 50 Torr ketone pressure at 334 nm, about 140 Torr at 313 nm, and about 170 Torr at "290" nm. This is again consistent with formation of excited singlet states in higher vibrational levels at the shorter wavelengths. If the mechanism is extended to include deactivation by added gas M, then the mechanism is in agreement with the observation that the same value of Q is obtained when the high pressure limit is attained by increasing the pressure of added gas.

Regardless of the type of vibrational deactivation assumed for the system the quantum yield of fluorescence in the high pressure limit, ϕ_f^∞ is equal to $k_4/(k_4 + k_5)$. The reciprocal of $(k_4 + k_5)$ is the actual singlet state lifetime (3.51×10^{-8} s) and since $\phi_f^\infty = 0.023$ then k_4 is 6.6×10^5 and k_5 is 2.8×10^7 s^{-1}. This value for k_4 can be compared with that obtained from the integrated area under the absorption curve, 8.8×10^5 s^{-1}. This is excellent agreement considering the approximations inherent in the use of the $1/\tau_0$ formula. If one assumes that the excited singlet state in the ground vibrational level does not decompose and that internal conversion to the ground singlet state is negligible, then the rate constant k_5 corresponds to that for intersystem crossing to a triplet state.

A comparison of k_4 and k_5 for chloropentafluoroacetone and hexafluoroacetone is of interest, since it might show the effect of the chlorine atom as an intramolecular heavy atom on the excited singlet state of a $\pi^* \leftarrow$ n carbonyl compound. The actual lifetime of singlet hexafluoroacetone was determined to be 7.8×10^{-8} s by Ware and co-workers (18) and they used a value of ϕ_f^∞ to calculate rate constants that are the equivalent of k_4 and k_5. Kutschke and Gandini (2) have redetermined ϕ_f^∞ for hexafluoroacetone as 0.018_5 and obtained $k_4 = 2.4 \times 10^5$ and $k_5 = 1.2 \times 10^7$ s^{-1}. In chloropentafluoroacetone $k_4 = 6.6 \times 10^5$ and $k_5 = 2.8 \times 10^7$ s^{-1}, so the presence of the chlorine atom has increased the rate constants of both the radiative and radiationless processes from the singlet state in the gas phase by a factor of only about two. Since Franck–Condon factors etc. could also alter the rate constants this suggests that the spin–orbit coupling effect of chlorine as an internal heavy atom on the π^*–n singlet state is small.

In aliphatic carbonyl compounds the intermolecular and intramolecular heavy atom effects reported in the literature are concerned mainly with the radiative and radiationless processes involving the triplet state. Thus McGlynn and co-workers (19) have calculated the intramolecular effect of a chlorine atom on the natural radiative lifetime of the formaldehyde triplet state. Shimada and Kanda (20) have considered the intramolecular effects on the forbidden singlet to triplet absorption in glyoxal, oxalyl chloride, and oxalyl bromide. Apart from specific chemical interactions of triplet states of aliphatic ketones with halogenated compounds (e.g., acetone and hydrogen bromide (21), acetone and dichlorobutane (22),and hexafluoroacetone and bromine (23)), there are also intermolecular effects of a physical nature. Thus the effect of xenon as a heavy atom on the triplet state of biacetyl in the gas phase has been proposed recently (24), and the triplet state of hexafluoroacetone is quenched (25) by mercury vapor.

The intermolecular heavy atom effect on the first excited singlet state has been investigated by Wagner (26). He concluded that there was no effect of propyl bromide on the intersystem crossing from the singlet to the triplet in 2-hexanone,

2-heptanone, and 2-octanone. It has also been suggested that the excited singlet state of hexafluoroacetone can transfer energy to bromine (23).

The chlorine atom in chloropentafluoroacetone is not attached directly to the carbonyl group and the size of the intramolecular effect on the singlet to triplet intersystem crossing rate constant is understandable. The small heavy atom effect in chloropentafluoroacetone suggests other chlorinated aliphatic carbonyl compounds may luminesce and this could be a useful tool in elucidating the photochemistry of halogenated compounds.

We thank the National Research Council of Canada for financial support. We are grateful to Dr. J. D. Laposa for the use of the scanning monochromator.

1. H. E. O'Neal and C. W. Larson. J. Phys. Chem. **73**, 1011 (1969).
2. A. Gandini and K. O. Kutschke. Proc. Roy. Soc. A **306**, 511 (1968).
3. W. A. Noyes, Jr., G. B. Porter, and J. E. Jolley. Chem. Rev. **56**, 49 (1956).
4. A. N. Strachan and F. E. Blacet. J. Amer. Chem. Soc. **77**, 5254 (1955).
5. R. P. Taylor and F. E. Blacet. J. Amer. Chem. Soc. **78**, 706 (1956).
6. S. Hautecloque. Compt. Rend. **250**, 3992 (1960); **254**, 3671 (1962).
7. R. Bowles, J. R. Majer, and J. C. Robb. Trans. Faraday Soc. **58**, 1541 (1962).
8. R. Bowles, J. R. Majer, and J. C. Robb. Trans. Faraday Soc. **58**, 2394 (1962).
9. J. R. Majer and J. P. Simons. Advan. Photochem. **2**, 177 (1964).
10. J. R. Majer, C. Olavesen, and J. C. Robb. J. Chem. Soc. (A), 893 (1969).
11. J. G. Calvert and J. N. Pitts. Photochemistry. J. Wiley, New York. 1966. p. 733.
12. R. K. Boyd, G. B. Carter, and K. O. Kutschke. Can. J. Chem. **46**, 175 (1968).
13. W. H. Melhuish. J. Phys. Chem. **64**, 762 (1960).
14. K. Yates, S. L. Klemenko, and I. G. Csizmadia. Spectrochim. Acta, **25A**, 765 (1969).
15. G. Herzberg. Electronic spectra of polyatomic molecules. Van Nostrand. New York. 1966. p. 612.
16. W. J. Balfour and G. W. King. J. Mol. Spectry. **26**, 384 (1968).
17. R. F. Borkman and D. R. Kearns. J. Chem. Phys. **44**, 945 (1966).
18. W. R. Ware and M. L. Dutton. J. Chem. Phys. **47**, 4670 (1967). W. R. Ware and S. K. Lee. J. Chem. Phys. **49**, 217 (1968).
19. D. G. Carroll, L. Vanquickenborne, and S. P. McGlynn. J. Chem. Phys. **45**, 2777 (1966).
20. H. Shimada and Y. Kanda. Bull. Chem. Soc. Jap. **40**, 2742 (1967).
21. C. W. Larson and H. E. O'Neal. J. Phys. Chem. **70**, 2475 (1966).
22. M. A. Golub. J. Amer. Chem. Soc. **91**, 4925 (1969).
23. J. S. E. McIntosh and G. B. Porter. Trans. Faraday Soc. **64**, 119 (1968).
24. A. Cook, G. P. Semeluk, and I. Unger. Can. J. Chem. **47**, 4527 (1969).
25. A. Gandini, D. A. Whytock, and K. O. Kutschke. Ber. der Bunsen. **72**, 296 (1968).
26. P. Wagner. J. Chem. Phys. **45**, 2335 (1966).

Can. J. Chem. Downloaded from www.nrcresearchpress.com by 210.87.254.40 on 09/05/12
For personal use only.

Can. J. Chem. Downloaded from www.nrcresearchpress.com by 210.87.254.105 on 09/05/12
For personal use only.

Studies on metal hydroxy compounds. X. Thermal analyses, decomposition kinetics, and infrared spectra of lead halide (Cl, Br, I) derivatives

P. RAMAMURTHY, E. A. SECCO, AND M. BADRI[1]

Chemistry Department, St. Francis Xavier University, Antigonish, Nova Scotia

Received January 5, 1970

The thermal analyses, thermogravimetry (TG), and differential thermal analysis (DTA) of PbOHCl, PbOHBr, and PbOHI reveal that the initial mode of decomposition is via dehydroxylation. Calorimetric measurements along with related enthalpy values for the decomposition reaction are given.

The infrared spectra of these compounds are interpreted in terms of folded bands of $(PbOH^+)_n$ tied together by halide ions consistent with their crystal structures.

The kinetics of thermal decomposition of lead hydroxyhalides follow a diffusion-type rate equation which is in contrast to the simple first-order rate equation observed for most Cd, Zn, and Cu compounds. These two distinct rates are interpreted in terms of mobile OH or H species in the dehydroxylation step.

Canadian Journal of Chemistry, 48, 2617 (1970)

Introduction

Lead hydroxyhalides have been known for some time, but no study on the physico-chemical aspects and modes of decomposition of these compounds has appeared in the literature to date.

As part of a program of research on metal hydroxy compounds (1–3), this paper reports on the thermal analyses including calorimetric measurements, isothermal kinetics of thermal decomposition, and the infrared spectra of the hydroxyhalides of lead.

Experimental

All compounds used in this study were prepared in this laboratory by following known methods with slight modification of the procedures to obtain compounds of the highest purity. Brief descriptions of the procedures are given below; all chemicals were of reagent grade.

All efforts to prepare $Pb(OH)_2$ of high purity in our laboratory have failed; all preparations resulted in a mixed product, $Pb(OH)_2$ intermixed with a basic salt. Attempts to secure high purity $Pb(OH)_2$ commercially also failed; our analyses of $Pb(OH)_2$ furnished by two suppliers indicated an impurity greater than that in our preparations. As a result, this paper cannot assess the physico-chemical properties of the hydroxyhalides relative to the parent hydroxide but only contrast the hydroxyhalides of lead with the hydroxyhalides already reported.

(i) PbOHCl

This compound was prepared by two different procedures. The first procedure (4) is by incomplete precipitation of aqueous $PbCl_2$ solution with lime water. The second procedure is a modified version of that used for the preparation of PbOHBr (5), 5.6 g of KCl dissolved in 200 ml of distilled H_2O was slowly added, while stirring, to aqueous solution containing 6.7 g of lead acetate in 150 ml of H_2O.

[1]In partial fulfillment for a B.Sc. Honors degree.

The white precipitate obtained from each procedure was filtered, thoroughly washed with distilled H_2O, and oven-dried overnight at 100 °C. Both preparations displayed identical physico-chemical behavior.

(ii) PbOHBr

The procedure is due to Knowles (5). A solution containing 9.0 g of KBr dissolved in 200 ml of distilled H_2O was slowly added, while stirring, to an aqueous lead acetate solution paralleling the second procedure for PbOHCl detailed above.

(iii) PbOHI

The method of de Schulten (6) was used. A hot solution of 20 g of KI in 100 ml of distilled H_2O was added to a liter of distilled H_2O containing 400 g of lead acetate and 30–40 ml of glacial acetic acid. The filtered solution was heated on a water bath for 5–8 h. The yellow crystals formed on cooling were separated, washed with distilled H_2O and oven-dried overnight at 100 °C.

The identities of the compounds were confirmed by the available X-ray diffraction patterns (7, 8).

The thermograms, calorimetric measurements, and isothermal kinetic traces were recorded on a duPont thermal Analyzer, DTA-900 and TGA-950 with the appropriate accessories and programming adjustments, as previously described (1, 9, 10).

The heating rate used for most thermograms was 20 °C/min; slower heating rates of 5 °C/min or 10 °C/min were used in an attempt to resolve overlapping processes. An ambient atmosphere of dry N_2 (Matheson Prepurified Grade with stated impurity of 0.003% oxygen) was maintained during all the experiments.

The infrared spectra of the compounds were obtained by using the standard KCl or KBr disc technique in a Perkin–Elmer 521 spectrophotometer; the spectra were independent of the matrix material.

Results and Discussion

Thermogravimetry

The results of thermogravimetry are presented in Table 1 and each compound is discussed in sequence. The proposed decomposition reactions

TABLE 1

Thermogravimetric analyses

Compound	Reaction	Temperature range* (°C)	% of total weight lost	
			Observed	Calculated
PbOHCl	[1]	177–246	3.44	3.47
PbOHBr	[2]	200–320	3.04	3.06
PbOHI	[3]	220–350	2.55	2.56

*Onset and terminal temperatures.

TABLE 2

Differential thermal analyses

Compound	Peak number*	Peak temperature (°C)	Process
PbOHCl	1	216	Dehydroxylation
	2	300	$PbO–PbCl_2$ interaction
	3	530	
PbOHBr	1	250	Dehydroxylation
	2	340	$PbO–PbBr_2$ solid phase transition
	3	500	$PbO·PbBr_2$ peritectic
PbOHI	1	280	Dehydroxylation
	2	390	$PbO–PbI_2$ interaction
	3	490	

*All endotherms.

for each compound, represented by the equation with its onset and terminal temperatures, are those which best fit the observed weight loss; the products of decomposition were confirmed by X-ray diffraction and correlated with DTA curves.

(i) PbOHCl

This compound decomposes via dehydroxylation yielding a residue of the oxide and chloride according to

$$[1]\quad 2PbOHCl_{(s)} \xrightarrow{177\text{–}246\ ^\circ C} PbO_{(s)} + PbCl_{2(s)} + H_2O_{(g)}$$

Slow volatilization of $PbCl_2$ begins at 650 °C and continues above 900 °C.

(ii) PbOHBr

Dehydroxylation is the mode of decomposition for this compound yielding lead oxy-bromide as residue according to

$$[2]\quad 2PbOHBr_{(s)} \xrightarrow{200\text{–}300\ ^\circ C} PbO·PbBr_{2(s)} + H_2O_{(g)}$$

At 550 °C further weight loss occurs, attributed to sublimation of $PbBr_2$ resulting from dissociation of $PbO·PbBr_2$, and continues above 800 °C.

(iii) PbOHI

This compound breaks down via dehydroxylation leaving an oxide–iodide residue as follows

$$[3]\quad 2PbOHI_{(s)} \xrightarrow{220\text{–}350\ ^\circ C} PbO_{(s)} + PbI_{2(s)} + H_2O_{(g)}$$

PbI_2 begins to sublime at 550 °C and continues above 800 °C.

Differential Thermal Analysis

The DTA results are presented in Table 2 and each compound is discussed in sequence to accompany the TG results.

(i) PbOHCl

Three endotherms are observed on heating to 700 °C. The first endotherm at 216 °C is due to dehydroxylation whereas the remaining two thermal effects arise from $PbO–PbCl_2$ interaction which were confirmed by the heating curve of 1:1 mixture. These latter two thermal effects cannot be fitted, however, to the reported phase diagram (11); the $PbO–PbCl_2$ system is now the subject of a study in this laboratory.

(ii) PbOHBr

The heating curve up to 650 °C revealed three endotherms. The first endotherm, due to dehydroxylation and occurring at 250 °C, is followed by endotherms at 340 and 500 °C associated with a phase transition of the compound

Can. J. Chem. Downloaded from www.nrcresearchpress.com by 210.87.254.105 on 09/05/12
For personal use only.

TABLE 3
Heat of decomposition*

Compound	Reaction	ΔH per mole of H_2O formed (kcal/mole)	ΔH per mole of compound decomposed (kcal/mole)	ΔH_f°‡ (kcal/mole)
$Pb(OH)_2$	$\rightarrow PbO_{(s)} + H_2O_{(g)}$	13.15†	13.15	−123.00†
PbOHCl	[1]	5.04±0.04	2.52±0.02	−100.4
PbOHBr	[2]	11.14±0.08	5.57±0.04	−95.8
	$\rightarrow PbO_{(s)} + PbBr_{2(s)} + H_2O_{(g)}$	—	—	−93.6
PbOHI	[3]	14.58±0.08	7.29±0.04	−83.2

*All determinations done in duplicate; ΔH values include average deviations.
†Literature values.
‡ΔH_f° values of compounds used in our calculation are from Natl. Bur. Stand. Circular No. 500 (1951). The above ΔH_f° values were calculated using Kopp's rule approximation (9).

TABLE 4
Infrared absorption band frequencies of Pb hydroxyhalides*

Assignment	Frequency (cm^{-1}) PbOHCl	PbODCl	PbOHBr	PbODBr	PbOHI
ν(OH)	3515 (m)	2593 (m)	3505 (m)	2590 (m)	3493 (m)
δ(OH)	588 (s br)	440 (s br)	592 (s br)	443 (s br)	600 (s br)
ν(PbO)	—	509 (w)	—	500 (w)	—
δ(OPbO)	430 (w)	—	425 (w)	—	428 (w)
ν(XPb)†	330 (s)	330 (s)	—	—	—

*s = strong, m = medium, w = weak, and br = broad.
†X = Cl, Br, I.

$PbO{\cdot}PbBr_2$ (12) and the peritectic of this compound (13), respectively.

(iii) PbOHI

The first of the three endotherms evident on heating to 700 °C is identified as dehydroxylation with the remaining two attributed to reactions of the PbO–PbI_2 system as confirmed by a physical mixture of 1:1 mole ratio of PbO–PbI_2. The PbO–PbI_2 phase diagram is not reported in the literature and is now the subject of study in this laboratory.

Calorimetric Measurements

The calorimetric results along with the related enthalpy values for the decomposition of the lead hydroxy compounds are presented in Table 3 according to reactions [1]–[3] cited for each compound under thermogravimetry.

The column of values for ΔH per mole of H_2O formed indicates an increasing trend, PbOHCl → PbOHBr → PbOHI, where ΔH for PbOHI is the only one greater than the respective parent $Pb(OH)_2$ value. These data suggest that the substitution of I in $Pb(OH)_2$ strengthens the Pb—OH bond whereas the presence of Br and Cl in both PbOHBr and PbOHCl, respectively weakens the Pb—OH bond.

Infrared Spectra

The absorption bands of the three compounds along with the deuterated analogues, PbODCl and PbODBr are tabulated in Table 4. The bands of all compounds occurring in the 3515–3493 cm^{-1} interval are assigned to the fundamental OH stretching mode, ν_{OH}, whereas the bands in the 600–588 cm^{-1} region are attributed to the OH bending mode, δ_{OH}. The shift of all bands in these two regions to lower frequencies on deuteration was observed with the ν_H/ν_D ratio falling in the range 1.33–1.35.

The bands in the 430–425 cm^{-1} region are present in all hydroxy compounds and these are unaffected on deuteration. Absorption bands in the 510–500 cm^{-1} region, not observed in the hydroxy compounds because of masking by the strong δ_{OH} band, become evident in the deuterated analogues as shown in Fig. 1 due to the isotopic shift of δ_{OD} to 440 cm^{-1}. The spectra in Fig. 1 also illustrate the masking of the normal 430–425 cm^{-1} bands by the strong δ_{OD} at 440 cm^{-1}.

Can. J. Chem. Downloaded from www.nrcresearchpress.com by 210.87.254.105 on 09/05/12
For personal use only.

Can. J. Chem. Downloaded from www.nrcresearchpress.com by 210.87.254.105 on 09/05/12
For personal use only.

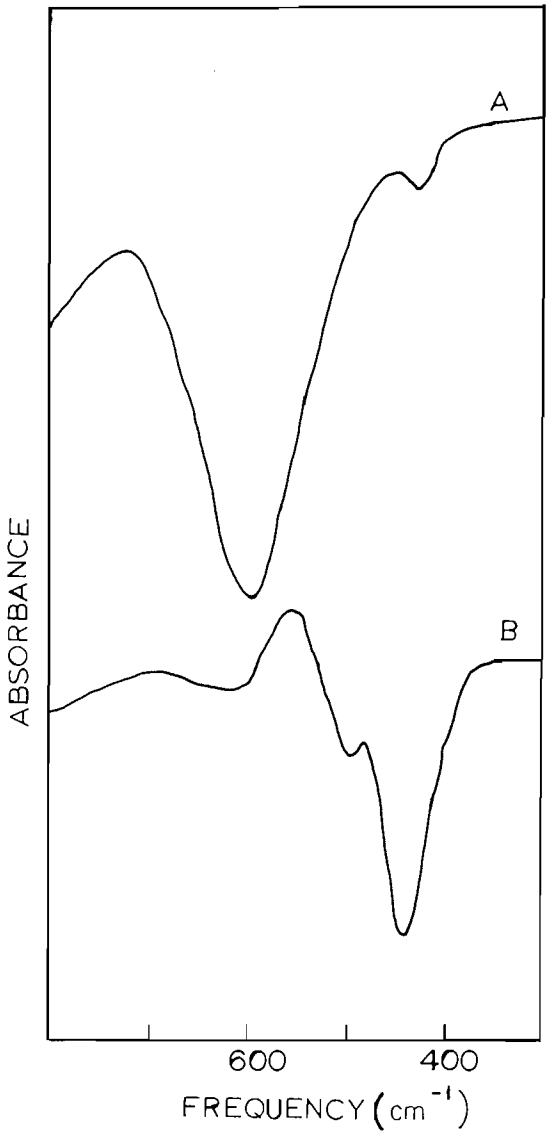

FIG. 1. Infrared spectra: *A*, PbOHBr; *B*, PbODBr.

The 330 cm^{-1} band occurs in PbOHCl and PbODCl only. This frequency value agrees very well with the Pb—Cl stretching mode in $PbCl_4$, viz. 327 cm^{-1} (14). On the basis of simple mass considerations the analogous Pb—Br and Pb—I stretching frequencies were calculated to be at 245 and 170 cm^{-1}, respectively, which were not observed because of the limitations in the infrared instrument available to us.

Crystallographic studies of PbOHI and PbOHCl reveal crystal structures that are very closely related (15). In the case of PbOHI, each Pb is surrounded by four I and two OH in the corners of a triangular prism and one I and two OH outside the rectangular faces of the prism. The structure consists of infinite folded bands of $(PbOH^+)_n$ extending along a direction parallel to the *b*-axis and tied together by iodide ions, i.e.

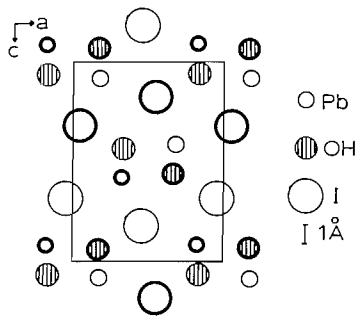

The structure of PbOHI projected on (010). Atoms at heights $b/4$ and $3b/4$ are differentiated by light and heavy circles, respectively.

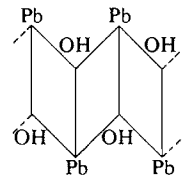

Arrangement of Pb and OH in PbOHI as infinite, folded bands.

The presence of $(PbOH^+)_n$ bands prompts us to assign the absorption bands in the 510–500 cm^{-1} range to the Pb—O stretching mode and the normal 430–425 cm^{-1} absorption bands to O—Pb—O bending. These assignments are supported by (*i*) the essentially constant frequency in the compounds and (*ii*) the occurrence of an absorption band at 500 cm^{-1} in PbO and 445 cm^{-1} in Pb_3O_4 (16). The absorption band frequencies with the appropriate assignments are given in Table 5.

Reaction Kinetic Data

The experimental α, t data for the decomposition reactions were processed through a large number of kinetic rate equations. The best fits between the experimental data and the known rate expressions over the maximum reaction fraction $\alpha \geqslant 0.8$ and over the temperature ranges studied are given in Table 5. In all cases, the data were fitted to three or more diffusion-type rate expressions with PbOHBr also fitting the first-

TABLE 5

Compound	Temperature range (°C)	Number of temperatures	Rate expression	Activation energy E_a (kcal)	A
PbOHCl	150–200	5	$[1-(1-\alpha)^{1/3}]^2 = (D/r^2)t$*	19.6±1.8	1.0×10^8
			$[1-2/3\alpha-(1-\alpha)^{2/3}] = (D/r^2)t$†	20.7±2.4	2.9×10^8
			$(1-\alpha)\ln(1-\alpha)+\alpha = (D/r^2)t$‡	18.2±1.5	7.8×10^7
PbOHBr	230–280	5	$-\ln(1-\alpha) = kt$§	17.6±1.5	5.9×10^6
			$[1-(1-\alpha)1/3]^2 = (D/r^2)t$	19.5±1.2	4.6×10^6
			$[1-2/3\alpha-(1-\alpha)^{2/3}] = (D/r^2)t$	17.6±2.1	5.0×10^5
			$(1-\alpha)\ln(1-\alpha)+\alpha = (D/r^2)t$	21.5±1.8	6.9×10^7
PbOHI	220–280	6	$[1-(1-\alpha)^{1/3}]^2 = (D/r^2)t$	30.1±1.9	6.0×10^{10}
			$[1-2/3\alpha-(1-\alpha)^{2/3}] = (D/r^2)t$	26.5±2.3	1.3×10^9
			$(1-\alpha)\ln(1-\alpha)+\alpha = (D/r^2)t$	24.2±1.8	6.8×10^8
			$\alpha^2 = kt$‖	24.7±1.8	1.4×10^9

*Jander's equation for sphere.
†Ginstling–Brounshtein (G–B) equation for sphere.
‡Two-dimensional diffusion equation for cylinder.
§First-order rate equation.
‖Parabolic rate law.

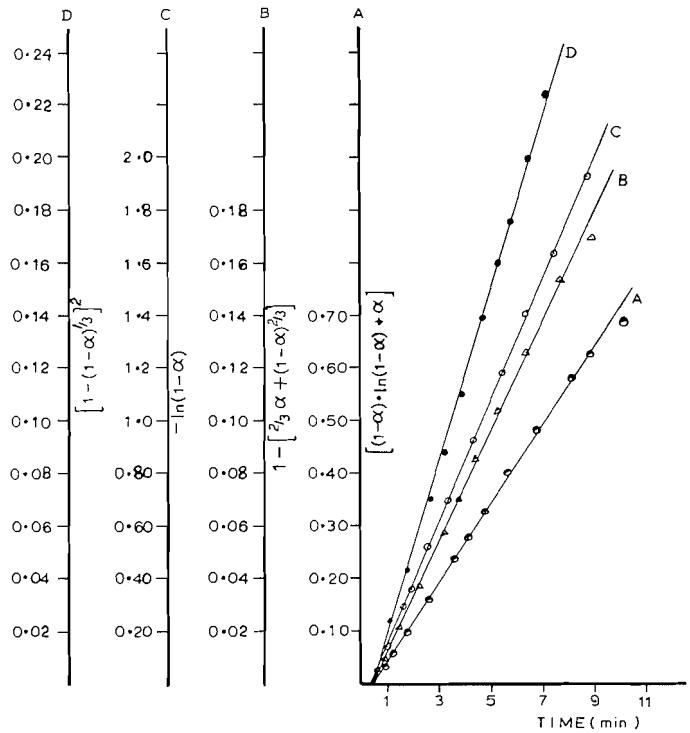

FIG. 2. Plots of $f(\alpha)$ vs. time of PbOHBr at 250 °C for different rate expressions. *A*, two-dimensional diffusion equation for cylinder; *B*, Ginstling–Brounshtein equation for sphere; *C*, First-order rate equation; *D*, Jander's equation for sphere.

order rate expression and the modified *P–T* equation. The diffusion equations satisfied, in the order of listing in Table 5, are (*i*) Jander and (*ii*) Ginstling–Brounshtein (G–B) equations for reaction into a sphere, (*iii*) two-dimensional diffusion reaction into a cylinder, and (*iv*) one-dimensional diffusion governed by the parabolic rate law. Typical $f(\alpha)$ vs. t plots for the different rate expressions obeyed by PbOHBr at 250 °C are presented in Fig. 2 to illustrate the linearity or quality of fit.

The E_a values of PbOHCl and PbOHBr

Can. J. Chem. Downloaded from www.nrcresearchpress.com by 210.87.254.105 on 09/05/12
For personal use only.

evaluated from the various rate expressions, excluding the modified *P–T* equation, are effectively constant within the error limits, viz. 19.5 ± 2.0 kcal/mole. The analogous E_a values of PbOHI are higher, displaying a greater spread, and fall within the range 25–30 kcal/mole.

A striking feature of lead hydroxyhalide decomposition kinetics is the predominance of diffusion-controlled equations relative to the hydroxyhalides of cadmium, zinc, and copper where a simple first-order rate prevailed in the majority of compounds with no evidence whatever for a diffusion-type rate.

We visualize dehydroxylation in the decompositon reaction of a hydroxy compound to involve as its fundamental step an abstraction process. This is, dehydroxylation can occur by (*i*) OH abstraction by a mobile H or (*ii*) H abstraction by a mobile OH. In each abstraction process the rate of decomposition would be determined by (*a*) the nature of the Me—O—H bonds, i.e. acidic or basic character, (*b*) the concentration of the mobile species, (*c*) the mobility of the particular species in the solid, and (*d*) the solid particle size. The nature of the Me—O—H bonds determines the concentration of the mobile species, H or OH, in the solid. With the particle size of all hydroxy compounds expected to be essentially constant, radius of 10^{-3} cm as determined for PbOHCl by nitrogen adsorption measurements, we envisage the rate of abstraction of OH by H to be governed by a straight-forward first-order rate in view of the high mobility of H. On the other hand, the rate of abstraction of H by the OH of lower mobility might be expected to lead to a diffusion-controlled process. On the basis of the above interpretation, we speculate that the predominant activated species in the Cd, Zn, Cu hydroxyhalides is a loosely bonded H to the XMeO group with a net acidic character, i.e. [X—Me—O...H]‡, whereas in the Pb compounds reported here the predominant species is the loosely bonded OH with a net basic character, i.e. [X—Pb...OH]‡.

A referee has suggested the likelihood of diffusion of molecular water as the rate controlling process. A critical test of this process was made by passing water vapor, instead of dry N_2 gas, over the solid during the decomposition reaction. Using N_2 as the carrier gas passing over water at room temperature during a run at 270 °C on PbOHBr, the rate data were precisely identical to that from the experiments with pure N_2 gas. It is concluded then that water vapor in contact with the decomposing solid does not affect the rate of reaction and the rate controlling process is not likely to be due to the diffusion of molecular water.

The authors are grateful to the National Research Council of Canada for financial support and to Dr. Michael Falk, Atlantic Regional Laboratory, Halifax, for providing infrared facilities.

1. O. K. Srivastava and E. A. Secco. Can. J. Chem. **45**, 579 (1967); **45**, 585 (1967).
2. O. K. Srivastava and E. A. Secco. Can. J. Chem. **45**, 1375 (1967); **45**, 3199 (1967).
3. P. Ramamurthy and E. A. Secco. Can. J. Chem. **47**, 2185 (1969); **47**, 2303 (1969).
4. J. N. Mellor. Comprehensive treatise on inorganic and theoretical chemistry. Vol. VII. Longmans, Green and Co. Ltd., London. 1923. p. 738.
5. L. M. Knowles. J. Chem. Phys. **19**, 1128 (1951).
6. J. N. Mellor. Comprehensive treatise on inorganic and theoretical chemistry. Vol. VII. Longmans, Green and Co. Ltd., London. 1923. p. 767.
7. Amer. Soc. Testing Materials. Diffraction pattern No. 6-0268, 0-0257.
8. R. Nasanen, P. Merilainen, R. Uggla, and M. Hyle. Suomen Kem. Pt. B. **27(4)**, 45 (1964); Chem. Abstr. **61**, 6481*g*.
9. P. Ramamurthy and E. A. Secco. Can. J. Chem. **46**, 3605 (1968).
10. P. Ramamurthy and E. A. Secco. Can. J. Chem. **47**, 2181 (1969).
11. E. M. Levin, C. R. Robbins, and H. F. McMurdie. Phase diagrams for ceramists. Amer. Ceramic Soc. U.S.A. 1964. p. 502.
12. F. W. Lamb and L. M. Niebylski. Anal. Chem. **23**, 1388 (1951).
13. F. W. Lamb and L. M. Niebylski. J. Amer. Chem. Soc. **75**, 511 (1953).
14. J. T. Neu and W. D. Gwinn. J. Amer. Chem. Soc. **70**, 3463 (1948).
15. R. Nasanen. Suomen Kem. Pt. **B 39**, 105 (1966).
16. N. T. McDevitt and W. L. Baun. Spectrochim. Acta, **20**, 799 (1964).

Can. J. Chem. Downloaded from www.nrcresearchpress.com by 210.87.254.105 on 09/05/12
For personal use only.

Can. J. Chem. Downloaded from www.nrcresearchpress.com by 210.87.254.105 on 09/05/12
For personal use only.

NOTES

The $^3A_2$ state of thiocarbonyl difluoride

D. C. MOULE
Department of Chemistry, Brock University, St. Catharines, Ontario

Received March 16, 1970

The 4500 Å band system of thiocarbonyl difluoride F_2CS has been photographed under conditions of moderately high resolution and has been assigned to the activity of the ν_1, ν_2, ν_3, and ν_4 modes arising from the $^3A_2 \leftarrow {}^1A_1$ electronic transition. The out-of-plane wagging levels were found to be strongly anharmonic, the observed inversion doubling indicating that the maximum in the potential function was greater than 3100 cm^{-1}.

Canadian Journal of Chemistry, **48**, 2623 (1970)

The thiocarbonyl chromophore of Cl_2CS exhibits an $n \rightarrow \pi^*$ transition which lies in the visible region of the spectrum and gives the liquid a deep red color. An analysis of the band spectrum (1, 2) of vapor Cl_2CS has revealed that the origins of the $^1A_2 \leftarrow {}^1A_1$ and $^3A_2 \leftarrow {}^1A_1$ transitions lie at 18 716.3 and 17 492.0 cm^{-1}, respectively, and that the geometrical changes which accompany the transitions are similar to those observed in H_2CO (3). Thiocarbonyl difluoride, F_2CS, the fluorine analogue to Cl_2CS has been known for 10 years (4). It is a colorless gas which condenses to a light yellow liquid at − 54 °C. In view of the similarities in the spectra of H_2CO and Cl_2CS, it seemed of interest to us to investigate the electronic spectra of F_2CS and observe the influence of the more electronegative fluorine on the spectroscopic properties of the thiocarbonyl group. The infrared spectrum of F_2CS has been recorded by Downs (5) who was able to assign all six ground state frequencies. A confirmation of his work has been obtained through two independent force constant treatments, one employing a Urey–Bradley force field (6), the other, a valence force field (7). We have recently reported (8) an analysis of the near ultraviolet $^1A_2 \leftarrow {}^1A_1$ band spectrum of F_2CS in which we were able to assign 4 out of the 6 fundamental frequencies in the upper state and establish that the structure was pyramidal. The vibrational assignments of this analysis, along with the work of Downs, are given in the first two columns of Table 1.

The ultraviolet spectrum of F_2CS was photographed under conditions of low resolution at Dry Ice temperature and in the second order of a 20 ft concave grating spectrograph at room temperature. Pressure – path lengths for the experiments varied from 1 m – atm at − 77 °C to 20 m – atm. at room temperature. Thiocarbonyl difluoride was prepared by the pyrolysis of the dimer 2,2,4,4-tetrafluorodithietene following the method of Middleton (9).

In the analysis of the singlet–singlet transition in F_2CS a number of bands were observed in the low frequency end of the spectrum which could not be fitted into the band pattern. By an analogy to the spectrum of Cl_2CS these bands were assigned to the spin forbidden $^3A_2 \leftarrow {}^1A_1$ transition. All of the bands assigned to this system displayed a peculiar intensity doubling which gave the spectrum the appearance of two independent systems superimposed on each other. The separation between the doublets varied from 20 cm^{-1} for the origin band to 15 cm^{-1} for the higher members of the ν_4' mode.

A prominent set of bands was located in the spectrum and was fitted into a progression in a frequency of 565 cm^{-1}. From the analysis of the singlet–singlet transition given in Table 1 this progression was assigned to ν_4'. A somewhat weaker progression in a frequency of 729 cm^{-1} was observed in the spectrum which from Table 1 was taken to be ν_2'. The progressions in ν_4' and ν_2' converged on a common band at 22 191.1 cm^{-1} which was assigned to the origin. This gave a singlet–triplet split $^1A_2$–$^3A_2$ of 1286 cm^{-1} which is close to the value of 1224 cm^{-1} obtained for Cl_2CS. Weak bands in the room temperature spectrum which strengthened at − 77 °C were observed at 22 582 and 23 377 cm^{-1}. These were assigned to single

TABLE 1

Vibrational frequencies of thiocarbonyl difluoride

Vibrational mode	Vibrational level	Frequency (cm^{-1}) $^1A_1$ (ground state)*	$^1A_2$ (excited state)†	$^3A_2$ (excited state)
$\nu_1(a_1)$		1368	1100.6	1186
$\nu_2(a_1)$		787	736.5	729
$\nu_3(a_1)$		526	385.8	391
$\nu_4(b_1)$	1	623.4	0.0	0.0
	2	1245.7	557.9	565.9
	3	1867.3	557.9	565.9
	4	2488.2	1112.8	1126.4
	5		1113.1	1126.4
	6		1650.8	
	7		1657.1	
$\nu_5(b_2)$		1189		
$\nu_6(b_2)$		417		

*Data taken from refs. 5 and 8.
†From ref. 8.

quantum additions of ν_3' and ν_1'. The assignments along with their frequencies are given in the third column of Table 1. Transitions to the even levels of the ν_4' manifold were observed directly in the spectrum as a cold band progression in ν_4'. On the other hand, transitions to the odd members of ν_4' ($\Delta\nu_4$ odd) arise from terms in the expression for the electric dipole transition moment involving the first derivative in the nuclear displacement, i.e. vibrationally induced spin–orbit coupling, and would be expected to be relatively very weak. They appeared therefore only in combination with odd quanta of ν_4''.

Table 2 lists the frequency differences isolating quanta of ν_4' and ν_4''. The third column of this Table tabulates the differences for the components of the triplet bands lying to higher frequencies and the fourth column the components at lower frequencies. The wave members of the ν_4' manifold of levels relative to the origin band are given in Table 1. They display the small–large–small intervals characteristic of an oscillator undergoing inversion motion. Because of the distortion of the doubling band pattern at high quanta of ν_4', the levels $v' = 6$ and $v' = 7$ remain unassigned. From the small splitting between the $v' = 4$ and $v' = 5$ levels it may be concluded that the barrier is equal to, or greater than, 3100 cm^{-1}, the value calculated for the $^1A_2$ state (8).

In terms of the 3000 cm^{-1} singlet–triplet splitting of H_2CO (10), the 1286 cm^{-1} value observed here is unusually small. To a first approximation the difference in energy between the singlet and triplet states is twice the exchange integral $K\pi^*n$. If it is assumed that the $n\pi^*$ orbital charge densities in the thiocarbonyl group are not dissimilar to those of the carbonyl group, the ratio of the singlet–triplet splits for Cl_2CS/H_2CO is given by the ratios of the atomic exchange integrals $\Delta(S)/\Delta(0) \simeq K3px3py(S)/K2px2py(0)$. A value of $\Delta(S) = 1688$ cm^{-1} was obtained from the 4421 and 7854 cm^{-1} exchange integrals of $3s^23p^4$ sulfur and $2s^22p^4$ oxygen (11) which is reasonable in light of the approximation employed.

TABLE 2

Frequency differences isolating ν_4' and ν_4''

	Vibrational level	Difference	Frequency (cm^{-1}) Upper component	Lower component
$\Delta\nu_4''$	0–1	4_0^2–4_1^3	623.8	622.8
		4_0^4–4_1^5	622.8	623.3
		4_0^6–4_1^7	625.6	623.6
	1–2	4_1^5–4_2^4	622.5	622.4
		4_1^7–4_2^6	622.1	622.1
$\Delta\nu_4'$	1–0	4_0^2–4_0^0	565.9	
	2–1	4_0^4–4_0^2	560.5	559.6
		4_1^5–4_1^3	561.5	559.1
	3–2	4_0^6–4_0^4	557.2	558.2
		4_1^7–4_1^5	554.3	557.9
		4_2^6–4_2^4	554.7	558.2

At the present time the mechanism responsible for the doubling of the bands is not understood. It is believed that the observed features are due to different spin multiplets of the triplet system and are not the result of widely separated heads in a single vibronic band. It may not be unreason-

Can. J. Chem. Downloaded from www.nrcresearchpress.com by 210.87.254.105 on 09/05/12
For personal use only.

able to consider a splitting of 20 cm^{-1} between a pair of components of $^3A_2$ F_2CS, since it is known (12) that the spin splitting of the A_1 and B_2 spin–orbit states of $^3A_2$ carbon disulfide is about 20 cm^{-1}.

The author would like to thank Dr. W. H. Sharkey, Central Research Department, E. I. Dupont Co., Wilmington, Delaware, for a sample of tetrafluorodithietene, Dr. A. E. Douglas for use of the concave grating spectrograph, and the National Research Council of Canada for financial support.

1. J. C. D. Brand, J. H. Callomon, D. C. Moule, J. Tyrrell, and T. H. Goodwin. Trans. Faraday Soc. **61**, 2365 (1965).
2. D. C. Moule and C. R. Subramaniam. Chem. Commun. 1341 (1969).
3. V. A. Job, V. Sethuraman, and K. K. Innes. J. Mol. Spectry, **30**, 365 (1969).
4. A. J. Downs and E. A. V. Ebsworth. J. Chem. Soc. 3516 (1960).
5. A. J. Downs. Spectrochim. Acta, **19**, 1165 (1963).
6. D. C. Moule and C. R. Subramaniam. Can. J. Chem. **47**, 1011 (1969).
7. M. G. K. Pillai and A. Ramaswamy. J. Annanalai Univ. Pt. B **25**, 115 (1964).
8. D. C. Moule and A. K. Mehra. J. Mol. Spectry. To be published.
9. W. H. Middleton, E. J. Howard, and W. H. Sharkey. J. Org. Chem. **30**, 1375 (1965).
10. V. T. Jones and J. B. Coon. J. Mol. Spectry, **31**, 137 (1969).
11. C. E. Moore. Atomic energy levels. Vol. I. Natl. Bur. Stand. No. 467.
12. A. E. Douglas and E. R. V. Milton. J. Chem. Phys. **41**, 357 (1964).

A wide line nuclear magnetic resonance study of molecular motion in pyridinium salts

C. H. Matthews and D. F. R. Gilson
Department of Chemistry, McGill University, Montreal 110, Quebec

Received March 26, 1970

Wide line nuclear magnetic resonance studies of pyridinium hexafluorophosphate, chloride, and nitrate show line width and second moment transitions which are attributed to reorientational motions of the pyridinium ring. The differences in transition temperatures are due to the different hydrogen bonded structures in the three salts.

Canadian Journal of Chemistry, 48, 2625 (1970)

Introduction

The room temperature crystal structures of several pyridinium salts have been determined by X-ray methods (1–3). It is typical of these structures that large anisotropic temperature factors are observed and, in some cases, a disordering of the ring positions or difficulties in distinguishing directly between carbon and nitrogen atoms have been reported. These observations suggest that the pyridinium ions may be reorienting in the solid phase and this paper presents the results of a wide line nuclear magnetic resonance investigation of molecular motion in three representative pyridinium salts; (*i*) pyridinium nitrate in which the ring nitrogen atom was distinguishable in the X-ray investigation (1) and a relatively short distance between this atom and an oxygen atom of the nitrate ion indicated a moderately strong hydrogen bond, (*ii*) pyridinium chloride in which the nitrogen atom was placed by symmetry arguments and the existence of a closer distance of approach between one particular ring position and the chloride ion (2), and (*iii*) pyridinium hexafluorophosphate in which the ring atoms were disordered, no hydrogen bonding occurred and, furthermore, either a cylindrical or spherical rotation of the anion was required to explain the high anisotropic temperature factors for the fluorine atoms (3).

It is relevant to note that Daycock *et al.* (4) have reported a low frequency reorientation of imidazole molecules in the solid state and suggested that this provides evidence for a protonic conduction mechanism in biological materials.

Experimental

Pyridinium nitrate and hexafluorophosphate were prepared by adding pyridine to the aqueous acid followed by recrystallization from aqueous solution. The nitrate was sublimed, m.p. 116 °C, and the hexafluorophosphate dried in vacuo at 100 °C, m.p. 230 °C (decomp.). Pyridinium chloride was prepared by passing dry hydrogen

Can. J. Chem. Downloaded from www.nrcresearchpress.com by 210.87.254.105 on 09/05/12
For personal use only.

able to consider a splitting of 20 cm^{-1} between a pair of components of $^3A_2$ F_2CS, since it is known (12) that the spin splitting of the A_1 and B_2 spin–orbit states of $^3A_2$ carbon disulfide is about 20 cm^{-1}.

The author would like to thank Dr. W. H. Sharkey, Central Research Department, E. I. Dupont Co., Wilmington, Delaware, for a sample of tetrafluorodithietene, Dr. A. E. Douglas for use of the concave grating spectrograph, and the National Research Council of Canada for financial support.

1. J. C. D. Brand, J. H. Callomon, D. C. Moule, J. Tyrrell, and T. H. Goodwin. Trans. Faraday Soc. **61**, 2365 (1965).
2. D. C. Moule and C. R. Subramaniam. Chem. Commun. 1341 (1969).
3. V. A. Job, V. Sethuraman, and K. K. Innes. J. Mol. Spectry, **30**, 365 (1969).
4. A. J. Downs and E. A. V. Ebsworth. J. Chem. Soc. 3516 (1960).
5. A. J. Downs. Spectrochim. Acta, **19**, 1165 (1963).
6. D. C. Moule and C. R. Subramaniam. Can. J. Chem. **47**, 1011 (1969).
7. M. G. K. Pillai and A. Ramaswamy. J. Annanalai Univ. Pt. B **25**, 115 (1964).
8. D. C. Moule and A. K. Mehra. J. Mol. Spectry. To be published.
9. W. H. Middleton, E. J. Howard, and W. H. Sharkey. J. Org. Chem. **30**, 1375 (1965).
10. V. T. Jones and J. B. Coon. J. Mol. Spectry, **31**, 137 (1969).
11. C. E. Moore. Atomic energy levels. Vol. I. Natl. Bur. Stand. No. 467.
12. A. E. Douglas and E. R. V. Milton. J. Chem. Phys. **41**, 357 (1964).

A wide line nuclear magnetic resonance study of molecular motion in pyridinium salts

C. H. Matthews and D. F. R. Gilson
Department of Chemistry, McGill University, Montreal 110, Quebec

Received March 26, 1970

Wide line nuclear magnetic resonance studies of pyridinium hexafluorophosphate, chloride, and nitrate show line width and second moment transitions which are attributed to reorientational motions of the pyridinium ring. The differences in transition temperatures are due to the different hydrogen bonded structures in the three salts.

Canadian Journal of Chemistry, 48, 2625 (1970)

Introduction

The room temperature crystal structures of several pyridinium salts have been determined by X-ray methods (1–3). It is typical of these structures that large anisotropic temperature factors are observed and, in some cases, a disordering of the ring positions or difficulties in distinguishing directly between carbon and nitrogen atoms have been reported. These observations suggest that the pyridinium ions may be reorienting in the solid phase and this paper presents the results of a wide line nuclear magnetic resonance investigation of molecular motion in three representative pyridinium salts; (*i*) pyridinium nitrate in which the ring nitrogen atom was distinguishable in the X-ray investigation (1) and a relatively short distance between this atom and an oxygen atom of the nitrate ion indicated a moderately strong hydrogen bond, (*ii*) pyridinium chloride in which the nitrogen atom was placed by symmetry arguments and the existence of a closer distance of approach between one particular ring position and the chloride ion (2), and (*iii*) pyridinium hexafluorophosphate in which the ring atoms were disordered, no hydrogen bonding occurred and, furthermore, either a cylindrical or spherical rotation of the anion was required to explain the high anisotropic temperature factors for the fluorine atoms (3).

It is relevant to note that Daycock *et al.* (4) have reported a low frequency reorientation of imidazole molecules in the solid state and suggested that this provides evidence for a protonic conduction mechanism in biological materials.

Experimental

Pyridinium nitrate and hexafluorophosphate were prepared by adding pyridine to the aqueous acid followed by recrystallization from aqueous solution. The nitrate was sublimed, m.p. 116 °C, and the hexafluorophosphate dried in vacuo at 100 °C, m.p. 230 °C (decomp.). Pyridinium chloride was prepared by passing dry hydrogen

Can. J. Chem. Downloaded from www.nrcresearchpress.com by 210.87.254.105 on 09/05/12
For personal use only.

chloride gas into pyridine solution in ether followed by sublimation, m.p. 144 °C (lit. 145 °C).

Nuclear magnetic resonance spectra were recorded at 60 MHz using a spectrometer built essentially from Varian units with a V3400 9 in. high field magnet and Fieldial Mk II regulator. The sample temperature was controlled by a cooled, or heated, flow of nitrogen gas through a Dewar system, and measured with copper–constantan thermocouple and Rubicon potentiometer. Second moments were calculated from the experimental derivative curves using a computer program written in this laboratory, and corrected for finite modulation.

Results and Discussion

Proton second moments and line widths for the three pyridinium salts are given in Figs. 1–3 as a function of temperature. All three compounds exhibit transitions but the nature of the transitions is different in each case. The hexafluorophosphate shows a relatively sharp transition to limiting values of second moment and line width which are maintained over a wide temperature range. In contrast, the transition in pyridinium nitrate is extremely broad, consisting of decreasing second moment and line width values from 130 to about 300 °K when a more rapid decrease occurs. No plateau values of line width and second moment are reached prior to melting. The behavior of the line width and second moments of pyridinium chloride is intermediate between the hexafluorophosphate and nitrate salts in that the transition is broad but limiting

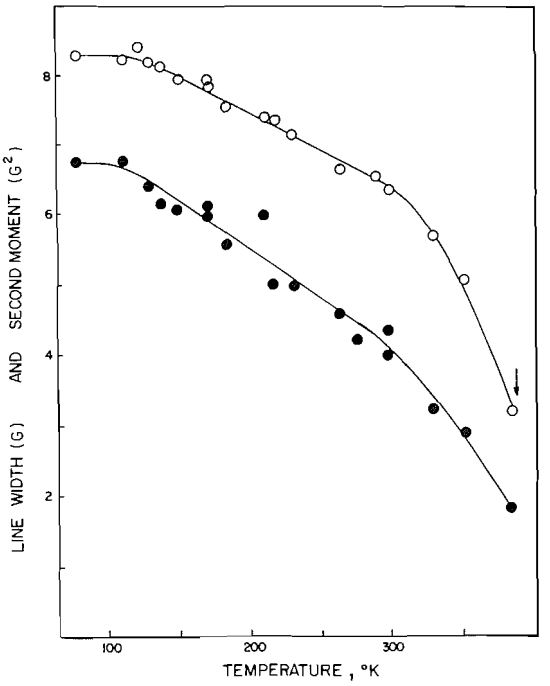

FIG. 2. Temperature dependence of the line width (open symbols) and second moment (filled symbols) in pyridinium nitrate.

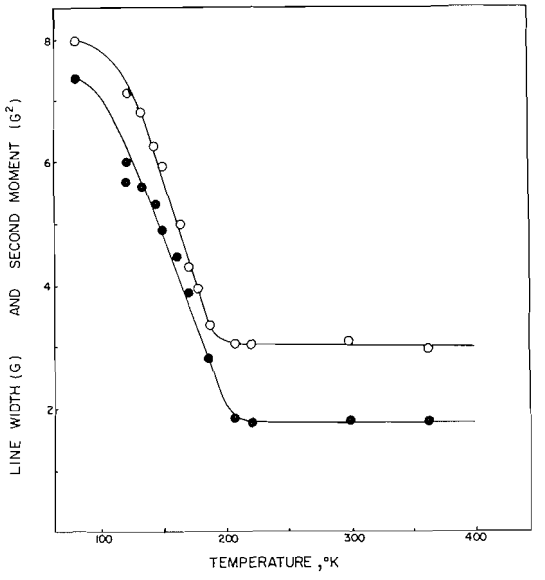

FIG. 1. Temperature dependence of the proton line width (open symbols) and second moment (filled symbols) in pyridinium hexafluorophosphate.

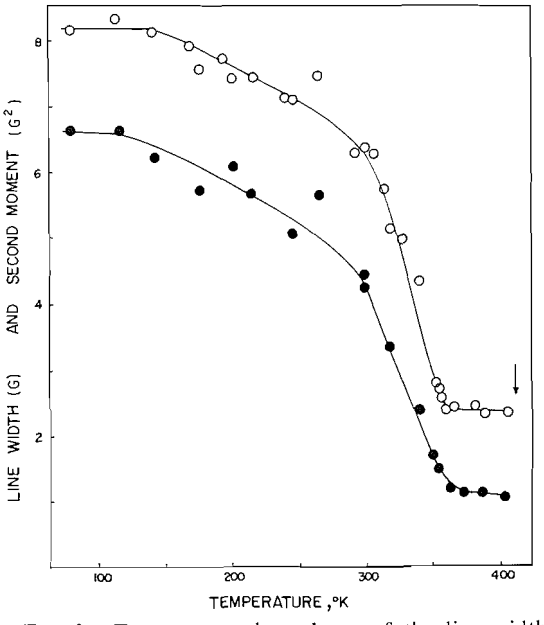

FIG. 3. Temperature dependence of the line width (open symbols) and second moment (filled symbols) in pyridinium chloride.

Can. J. Chem. Downloaded from www.nrcresearchpress.com by 210.87.254.105 on 09/05/12
For personal use only.

TABLE 1
Second moments of pyridinium salts (G^2)

	Calculated second moment			Experimental second moment
	Intramolecular	Intermolecular	Total	
Pyridinium chloride				
Rigid lattice	3.64	3.30	6.94	6.6 (77 °K)
Ring reorientation	0.91	0.35	1.26	1.1 (390 °K)
Pyridinium nitrate				
Rigid lattice	4.52	2.87	7.39	6.6 (77 °K)
Ring reorientation	1.13	0.39	1.52	1.8 (385 °K)
Pyridinium hexafluorophosphate				
^1H Resonance				
Rigid lattice	4.12	3.43	7.55	7.4 (77 °K)
PF_6^- Reorientation (isotropic)	4.12	2.95	7.07	
Ring and PF_6 reorientation	1.03	0.80	1.83	1.8 (210 °K)
^{19}F Resonance				
Rigid lattice	12.24	3.13	15.37	2.75 (77 °K)
PF_6^- Reorientation (isotropic)	0.0	1.82	1.82	
Ring and PF_6^- reorientation	0.0	0.56	0.56	0.95 (170 °K)

values are reached about 50° below the melting point.

Theoretical second moments were calculated, based on the reported crystal structures, for the rigid lattice case and for reorientation about an axis through the center of the pyridinium ion and perpendicular to the molecular plane. Proton positions were not determined in the X-ray structural studies and were assumed, for the purposes of second moment calculations, to be situated at positions given by C—H and N—H bond distances of 1.08 Å with bond angles 120°. The calculated and experimental values are compared in Table 1. In each compound the pyridinium ring is rigid at 77 °K and in the chloride and hexafluorophosphate salts the transition is due to reorientation of the ring about the axis normal to the plane. The decrease in second moment between 120 and 300 °K for the chloride salt is probably due to torsional oscillation of the pyridinium ring. It must be emphasized that the rate of reorientation which causes line narrowing in the nuclear magnetic resonance spectra is of the order of the line width expressed as a frequency, i.e. 10^4–10^5 Hz. In pyridinium nitrate the results can be rationalized as a torsional oscillation of increasing amplitude with increasing temperature. The torsional motion may be about more than one axis. Melting of the nitrate salt occurs at the temperature at which a rotational motion is approached, i.e. when sufficient energy is available for reorientation, the lattice forces are also overcome. This different behavior for pyridinium nitrate can be attributed to the stronger hydrogen bond to the anion oxygen atom. The calculated value of the second moment for a structure in which the proton is attached to the nitrate ion is about 6.8 G^2, a value which falls within the experimental error.

The ^{19}F second moment values of the hexafluorophosphate salt remain essentially constant at about 1.0 G^2 down to 175 °K below which the second moment increases with decreasing temperature. The value at 77 °K is well below the calculated rigid lattice second moment. The intramolecular second moments for reorientation about the C_2, C_3, and C_4 symmetry axes of the octahedral PF_6^- ion are 2.4, 2.5, and 2.2 G^2, respectively. Isotropic rotation reduces the intramolecular second moment to zero, leaving only intermolecular interactions responsible for the second moment. That the hexafluorophosphate ion is undergoing extensive molecular reorientation at room temperature confirms the results of the X-ray structural study (3). Similar dynamic behavior has been observed by Miller and Gutowsky (5) for alkali hexafluorophosphate salts.

Financial support from the National Research Council of Canada is gratefully acknowledged.

1. A. J. Serewicz, B. K. Robertson, and E. A. Meyers. J. Phys. Chem. **69**, 1915 (1965).
2. C. Rérat. Acta Cryst. **15**, 427 (1962).
3. R. F. Copeland, S. H. Conner, and E. A. Meyers. J. Phys. Chem. **70**, 1288 (1968).
4. J. T. Daycock, G. P. Jones, J. R. N. Evans, and J. M. Thomas. Nature, **218**, 672 (1968).
5. G. R. Miller and H. S Gutowsky. J. Chem. Phys. **39**, 1983 (1963).

Can. J. Chem. Downloaded from www.nrcresearchpress.com by 210.87.254.105 on 09/05/12
For personal use only.

The radiation-induced oxidation of ethanol and methanol by hydrogen peroxide in aqueous solution[1]

C. E. BURCHILL AND I. S. GINNS
Department of Chemistry, University of Manitoba, Winnipeg 19, Manitoba

Received March 2, 1970

The radiation-induced chain oxidation of ethanol and methanol by hydrogen peroxide in deaerated aqueous solutions has been investigated. In each case the alcohol is oxidized to the corresponding aldehyde and hydrogen peroxide is reduced in equivalent yield. With ethanol as the oxidizable substrate the yields are independent of peroxide concentration in the range 5×10^{-2} to 5×10^{-3} *M* and linearly dependent on ethanol concentration in the range 0.085 to 0.85 *M*. In contrast, the oxidation of methanol is first order in hydrogen peroxide, independent of methanol concentration up to 2.0 *M* and shows a simple square root dependence on dose rate. The differences are explained by consideration of the participation of two different radicals derived from ethanol, $CH_3\dot{C}HOH$ and $\dot{C}H_2CH_2OH$, whereas only one radical, $\dot{C}H_2OH$, is formed from methanol.

Canadian Journal of Chemistry, 48, 2628 (1970)

Introduction

In a preceding publication (1) we have described the radiation-induced oxidation of 2-propanol by hydrogen peroxide in neutral aqueous solution. In order to explain the unexpected dependence of the yields of this chain reaction on the concentrations of the alcohol and hydrogen peroxide, it was concluded that the abstraction of hydrogen atoms from 2-propanol by the OH radical was not specifically from the α- position but that both the radical species $(CH_3)_2\dot{C}OH$ (**1**) and $CH_3CHOH\ \dot{C}H_2$ (**2**) were formed. It was suggested that only radical **1** would undergo the propagating reaction with H_2O_2 but that radical **2** could be converted to **1** by a hydrogen atom transfer reaction with the parent alcohol. To test the generality of this proposal we have carried out a study of the oxidation of ethanol, which may form both α and β radicals by loss of a hydrogen atom from a C—H bond, and methanol which can form only the α radical, $\dot{C}H_2OH$.

Experimental

Ethanol (Canadian Industrial Alcohols, absolute), *methanol* (Fisher Certified Reagent) and *hydrogen peroxide* (Fisher Reagent, 30%, unstabilized) were used without further purification. All other materials were of reagent grade and were used as received. The general techniques for sample preparation and irradiation have been previously described (1).

Product analysis was carried out immediately after irradiation. Hydrogen peroxide was determined by the iodide method (2). Acetaldehyde, from ethanol, was determined quantitatively by vapor-phase chromatography using a 6 ft column of Chromosorb 102 at 120°C and flame-ionization detection. Formaldehyde, from methanol, was estimated spectrophotometrically using chromotropic acid (3) while the presence of ethylene glycol was confirmed by vapor-phase chromatography.

Results

In neutral deaerated aqueous solutions of ethanol (0.085 to 0.85 *M*), H_2O_2 at concentrations less than 0.02 *M* is reduced in a yield which is independent of its concentration. Acetaldehyde is formed in an equivalent yield and both yields increase linearly with alcohol concentration as shown in Fig. 1. Extrapolation to zero alcohol concentration gives an intercept of $G(-H_2O_2) = 45.4 \pm 2.0$. In this concentration range there is a significant dose rate effect which is shown in Fig. 2. As the ethanol concentration is increased to values > 1.0 *M*, the peroxide reduction yield increases non-linearly to a maximum value of $G(-H_2O_2) \simeq 75$ at 7 mole% ethanol and then decreases to 18 ± 2 in pure ethanol. This variation is shown in Fig. 3.

With methanol as the oxidizable substrate the reduction of hydrogen peroxide is dependent upon its concentration at all peroxide and methanol concentrations examined. Formaldehyde is formed in an amount equivalent to H_2O_2 reduced. When $\log [H_2O_2]$ is plotted as a function of irradiation time, a straight line results indicating a first-order dependence on peroxide concentration. This is demonstrated in Fig. 4. Apparent first-order rate constants for peroxide

[1]This work was supported in part by Atomic Energy of Canada, Limited, Commercial Products Division and, in part, by the Defence Research Board of Canada, Grant No. 9530-78.

Can. J. Chem. Downloaded from www.nrcresearchpress.com by 210.87.254.40 on 09/05/12
For personal use only.

Can. J. Chem. Downloaded from www.nrcresearchpress.com by 210.87.254.40 on 09/05/12
For personal use only.

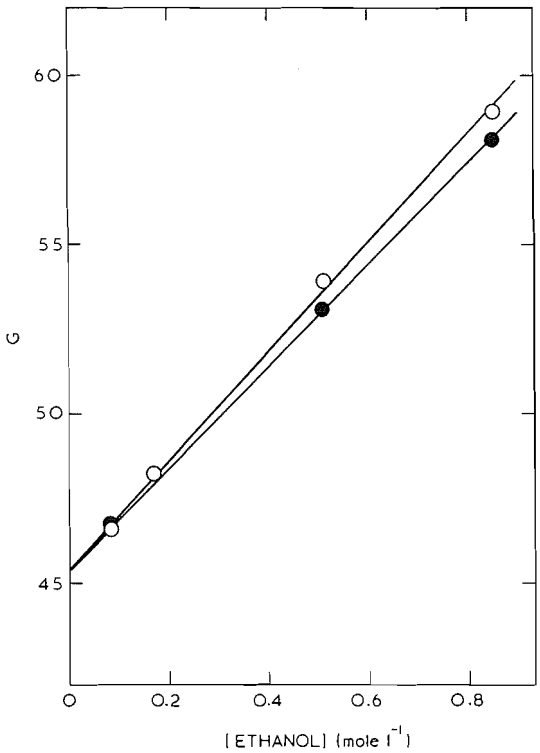

FIG. 1. Variation of yields with ethanol concentration in γ-irradiated aqueous solutions of H_2O_2. $[H_2O_2]^0$ = 0.02 *M*; dose rate = 1.50×10^{19} eV l^{-1} s^{-1}; ○, $G(-H_2O_2)$; ●, G(acetaldehyde).

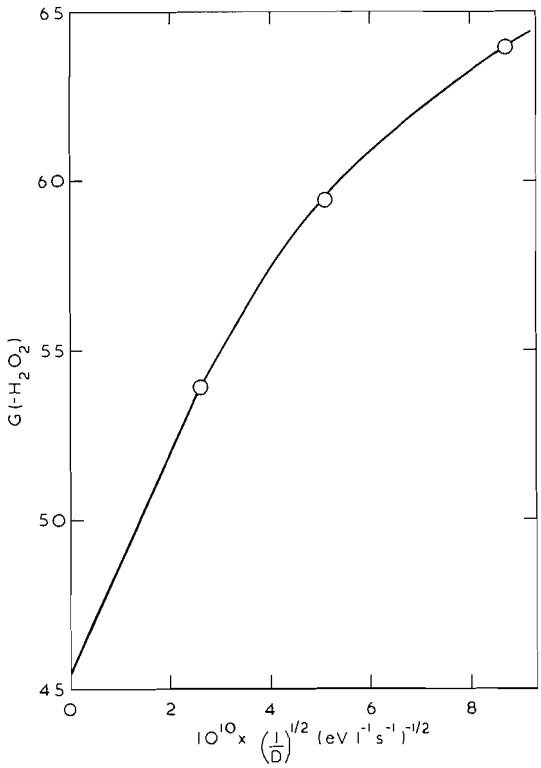

FIG. 2. Variation of peroxide removal yields with dose rate in γ-irradiated aqueous solutions of ethanol: [ethanol] = 0.51 *M*; $[H_2O_2]^0$ = 0.02 *M*.

removal at several different methanol concentrations are given in Table 1 and show no significant dependence on alcohol concentration. Figure 4 and Table 1 also indicate the effect of altering the dose rate. A square root dependence on dose rate is observed. At a constant initial concentration of H_2O_2 (0.01 *M*) *initial* $G(-H_2O_2)$ values are independent of methanol concentration in the range 0.2 to 2.0 *M* and then decrease as the methanol concentration is further increased (Fig. 3).

TABLE 1

Apparent first-order rate constant for H_2O_2 removal in irradiated aqueous solutions of methanol and H_2O_2*

$[CH_3OH]$ (*M*)	$10^{-19} \times$ Dose rate (eV l^{-1} s^{-1})	$10^4 \times k$ (s^{-1})
0.13	1.60	8.87
0.49	1.60	9.58
0.99	1.60	9.95
0.99	0.43	4.54
1.98	1.60	9.53

*$[H_2O_2]^0$ = 0.01 *M*.

Discussion

The results for the radiation-induced oxidation of ethanol by hydrogen peroxide are very similar to those previously observed for 2-propanol (1). As with ethanol, this latter system showed a linear dependence on alcohol concentration below 1.0 *M* extrapolating to a large positive intercept at zero alcohol concentration. A similar lack of dependence on H_2O_2 concentration was also observed. This suggests that the reaction mechanism is essentially the same in both cases. We therefore propose, by analogy, the following reaction scheme for low concentrations of the alcohol.

[1] $H_2O \rightsquigarrow e_{aq}^-$, H, OH, H_2O_2, H_2, H_3O^+

[2] $e_{aq}^- + H_2O_2 \rightarrow OH^- + OH$

[3] $H + CH_3CH_2OH \rightarrow H_2 + CH_3\dot{C}HOH$

[4] $H + CH_3CH_2OH \rightarrow H_2 + \dot{C}H_2CH_2OH$

[5] $OH + CH_3CH_2OH \rightarrow H_2O + CH_3\dot{C}HOH$

[6] $OH + CH_3CH_2OH \rightarrow H_2O + \dot{C}H_2CH_2OH$

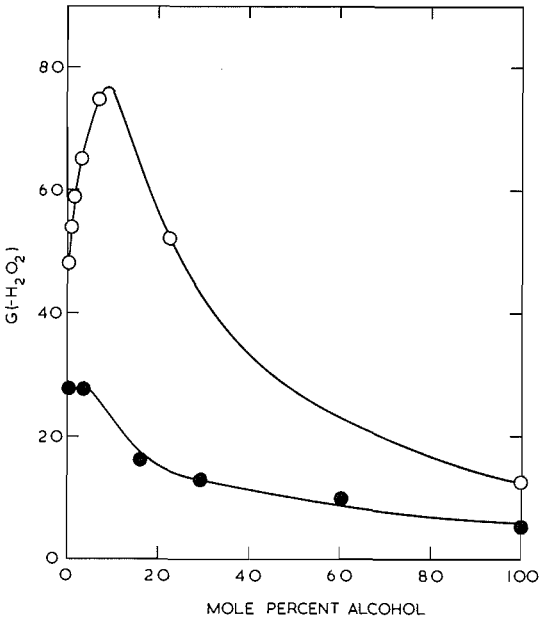

FIG. 3. Variation of peroxide reduction yields with composition in mixed water alcohol solvent. Dose rate = 1.6×10^{19} eV l^{-1} s^{-1}; ○, ethanol, $[H_2O_2]^0 = 0.02$ *M*; ●, methanol, $[H_2O_2]^0 = 0.01$ *M*.

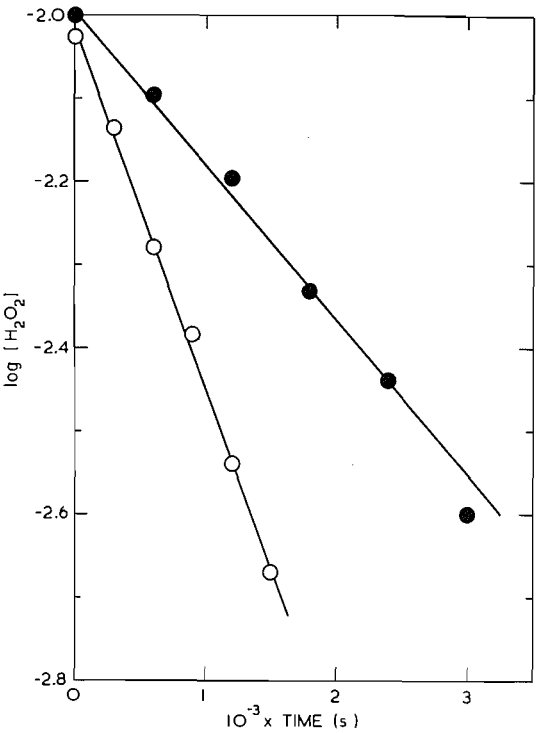

FIG. 4. First order plots for peroxide reduction in γ-irradiated aqueous solutions of methanol: [methanol] = 0.99 *M*; ○, dose rate = 1.60×10^{19} eV l^{-1} s^{-1}; ●, dose rate = 0.43×10^{19} eV l^{-1} s^{-1}.

[7] $CH_3\dot{C}HOH + H_2O_2 \rightarrow CH_3CHO + H_2O + OH$

[8] $\dot{C}H_2CH_2OH + CH_3CH_2OH \rightarrow CH_3CH_2OH + CH_3\dot{C}HOH$

[9] $2\,\dot{C}H_2CH_2OH \rightarrow$ 1,4-butanediol or $CH_3CHO + CH_3CH_2OH$

Although abstraction of H atoms from alcohols by H or OH is often assumed to be specific to the α site (4, 5), it has been demonstrated that this is not the case for abstraction by H atoms (6) and there is considerable evidence that abstraction by OH occurs also from other C—H positions (1, 7, 8). Thus reactions [4] and [6] must be included in the overall mechanism. The hydrogen atom transfer reaction [8], or its analogue for other alcohol radicals, has been previously proposed (1, 9). The exclusion of a reaction of the β radical, $\dot{C}H_2CH_2OH$, with H_2O_2 is in part supported by the observation that the β radical is much less reactive as a reductant than the α radical (8). 1,4-Butanediol was tentatively identified as a reaction product using vapor-phase chromatography.

On the basis of the proposed mechanism an expression for the yield of H_2O_2 reduction may be derived.

$$[10]\quad G(-H_2O_2) = \left[G_{e_{aq}^-} - G_{H_2O_2} + G_H\left\{\frac{k_3}{k_6}\left(\frac{k_6 + k_5}{k_3 + k_4}\right)\right\} + \frac{k_5}{k_6}(G_{e_{aq}^-} + G_{OH})\right] + \left(1 + \frac{k_5}{k_6}\right)k_8\left(\frac{G_{e_{aq}^-} + G_H + G_{OH}}{2k_9D}\right)^{1/2} \times [CH_3CH_2OH]$$

where D is the dose rate in units of 6.03×10^{25} eV l^{-1} s^{-1}.

The form of this yield expression is in excellent agreement with the experimental results. The first term in the equation (in square brackets) represents the intercept obtained on extrapolation of Fig. 1 to zero alcohol concentration. Assuming the following values, $G_{e_{aq}} = 2.28$ (10), $G_H = 0.57$, $G_{OH} = 2.25$, $G_{H_2O_2} = 0.77$, $k_3 = 1.6 \times 10^7$ M^{-1} s^{-1} (11), $k_4 = 1.7 \times 10^6$ M^{-1} s^{-1}, the ratio k_5/k_6, the relative probability of

Can. J. Chem. Downloaded from www.nrcresearchpress.com by 210.87.254.40 on 09/05/12
For personal use only.

TABLE 2

Principal numerical results of oxidation of alcohols

Alcohol	Percentage of α attack by OH	Rate constant (M^{-1} s^{-1}) β + alcohol → α	Rate constant (M^{-1} s^{-1}) α + H_2O_2
Methanol	100		4.0×10^4
Ethanol	90	16 ± 3	
2-Propanol*	86	53 ± 10	

*From ref. 1.

abstraction by OH from the α and β positions in the alcohol, may be estimated from the intercept as 8.6. This may be compared to our estimate of 6.2 for the analogous ratio when 2-propanol is the substrate (1). Adams and Willson (8) have estimated that 97 and 95% of the radicals formed by OH attack on ethanol and 2-propanol, respectively, are the result of attack at the α position whereas our ratios correspond to 90 and 86% α attack. These percentages are similar but those derived from this work are significantly lower. The percentages quoted by Adams and Willson were estimated from the fraction of the total reduction of ferricyanide which was accomplished by the faster-reacting α radical relative to that when methanol was used (100% α attack).

Using an average value for the absolute rate of OH + ethanol of 1.1×10^9 M^{-1} s^{-1} (11) this may be equated with $k_5 + k_6$ and gives values of

$$k_5 = 1.0 \times 10^9 \ M^{-1} \ s^{-1}$$

$$k_6 = 1.1 \times 10^8 \ M^{-1} \ s^{-1}$$

These may be compared with the values of the corresponding rate constants for 2-propanol (1).

$$k_\alpha = 1.2 \times 10^9 \ M^{-1} \ s^{-1}$$

$$k_\beta = 2 \times 10^8 \ M^{-1} \ s^{-1}$$

The second part of the yield expression [10] predicts, as observed experimentally, a linear dependence of the yield on alcohol concentration and the coefficient of the alcohol concentration term includes a reciprocal square-root dose-rate dependence. As shown in Fig. 2 the system displays a significant dose-rate dependence although not a simple square-root relationship. The observed curvature suggests that, in addition to a bimolecular termination, there is a first-order termination which becomes significant at low dose rates. This was also observed with 2-propanol (1) but, as in that case, the curve is readily extrapolated to the same intercept as that observed for zero ethanol concentration. If, at the highest dose rate employed, the termination occurs primarily by the bimolecular reaction [9], it is possible to estimate a lower limit for k_8, the hydrogen atom transfer reaction, from the slope of Fig. 1. Using $k_5/k_6 = 8.6$, the value of the primary yields previously assumed, and $2k_9 = 2 \times 10^9$ M^{-1} s^{-1}, we obtain $k_8 = 16 \pm 3$ M^{-1} s^{-1}. This may be compared with the value 53 ± 10 for the comparable reaction of the β radical from 2-propanol.

The similarity in the results for the radiation-induced chain oxidation of 2-propanol and ethanol confirms that the mechanism is the same in both cases and the contrast in the results when methanol is the oxidizable material may be attributed to the fact that only one radical, $\dot{C}H_2OH$, may be formed by abstraction from a C—H bond in methanol. In the case of methanol the results conform to the simple mechanistic scheme

[1] $H_2O \rightsquigarrow e_{aq}^-$, H, OH, H_2O_2, H_2, → H_3O^+

[2] $e_{aq}^- + H_2O_2 \rightarrow OH^- + OH$

[11] $H + CH_3OH \rightarrow \dot{C}H_2OH$

[12] $OH + CH_3OH \rightarrow H_2O + \dot{C}H_2OH$

[13] $\dot{C}H_2OH + H_2O_2 \rightarrow H_2CO + H_2O + OH$

[14] $2\ \dot{C}H_2OH \rightarrow$ ethylene glycol or $H_2CO + CH_3OH$

$$[15] \quad \frac{-d[H_2O_2]}{dt} = (G_{e_{aq}^-} - G_{H_2O_2})D + k_{13} \times \left(\frac{(G_{e_{aq}^-} + G_H + G_{OH})D}{2k_{k_4}}\right)^{1/2} [H_2O_2]$$

Equation [15] predicts that the rate of peroxide reduction will be independent of methanol concentration and, for moderate to

Can. J. Chem. Downloaded from www.nrcresearchpress.com by 210.87.254.40 on 09/05/12
For personal use only.

large chain lengths, first order in H_2O_2. Table 1 and Fig. 4 demonstrate that these are experimentally realized. The apparent first-order rate constant includes a square-root dependence on dose rate which is again in agreement with the experimental results. Assuming a value of $2k_{14} = 2.4 \times 10^9$ (12) for the bimolecular termination reaction, a rate constant for the chain propagating reaction may be estimated as $k_{13} = (4.0 \pm 0.4) \times 10^4\ M^{-1}\ s^{-1}$. This is somewhat less than the rate constant found by Seddon and Allen (4) for the propagating reaction in the ethanol/H_2O_2 chain reaction. It may be noted that the rate constant for reduction of ferricyanide by $\dot{C}H_2OH$ is slightly less than that for reduction by $CH_3\dot{C}HOH$ (8).

The small yield of ethylene glycol found (G(glycol) ~ 0.5) represents approximately 20% of the termination reaction. In the photolysis of methanol–water solutions (13), the major product of radical combination was said to be ethylene glycol.

At high concentrations of either alcohol the yield of the chain reaction is decreased. This phenomenon has previously been reported for the photo-induced reaction in mixed water–alcohol systems (5) and in the radiation-induced oxidation of 2-propanol (1). In the latter case the decreased yield was attributed to a decrease in the rate of reaction [7], as a result of the decreasing dielectric constant of the medium at alcohol concentrations sufficiently high to make reaction [7] rather than reaction [8] the rate-determining propagation step.

Summary

The principal numerical results are summarized in Table 2. We have demonstrated that the two-radical model for the chain oxidation of alcohols by H_2O_2, as developed for 2-propanol, is applicable also to ethanol but that a one-radical model accounts satisfactorily for the features of the oxidation of methanol.

1. C. E. Burchill and I. S. Ginns. Can. J. Chem. In press.
2. A. O. Allen, C. J. Hochanadel, J. A. Ghormley, and T. W. Davis. J. Phys. Chem. **56**, 575 (1952).
3. C. E. Bricker and H. R. Johnson. Ind. and Eng. Chem. (Anal. Ed.) **17**, 400 (1945).
4. W. A. Seddon and A. O. Allen. J. Phys. Chem. **71**, 1914 (1967).
5. J. Barrett, A. L. Mansell, and R. J. M. Ratcliffe. Chem. Commun. 48 (1968).
6. (*a*) M. Anbar and D. Meyerstein. J. Phys. Chem. **68**, 3184 (1964); (*b*) C. Lifshitz and G. Stein. J. Chem. Soc. 3706 (1962).
7. R. Livingston and H. Zeldes. J. Amer. Chem. Soc. **88**, 4333 (1966).
8. G. E. Adams and R. L. Willson. Trans. Faraday Soc. **63**, 2981 (1969).
9. R. O. C. Norman and P. R. West. J. Chem. Soc. Ser. B, 389 (1969).
10. G. V. Buxton. Radiat. Res. Rev. **1**, 209 (1968).
11. M. Anbar and P. Neta. Int. J. Appl. Radiat. Isotop. **18**, 493 (1967).
12. M. Simic, P. Neta, and E. Hayon. J. Phys. Chem. **73**, 3794 (1969).
13. J. Barrett and J. H. Baxendale. Trans. Faraday Soc. **54**, 37 (1960).

Structure of a product obtained on treatment of 1-thioacetoacetanilide with sulfuryl chloride

M. Curcumelli-Rodostamo and W. A. Harrison
Uniroyal Limited, Research Laboratories, Guelph, Ontario

Received April 3, 1970

Treatment of 1-thioacetoacetanilide with sulfuryl chloride or thionyl chloride produced a crystalline compound identified as 3,5-diacetonylidene-4-phenyl-1,2,4-dithiazolidine. The absence of carbonyl absorption in the infrared spectrum of the compound indicated that it should be represented by a resonance structure (**2**) involving non-carbonyl components.

Canadian Journal of Chemistry, **48**, 2632 (1970)

In connection with our synthetic work on pesticides, the preparation of 2-chloro-1-thioacetoacetanilide was required. Accordingly 1-thioacetoacetanilide (**1**) was treated at room temperature with an equimolar quantity of sulfuryl chloride. Reaction occurred readily; but instead of the desired product, a chlorine-free crystalline compound (m.p. 195–195.5°) was obtained.

In the present publication we provide evidence establishing the structure of this compound.

The molecular formula $C_{14}H_{13}NO_2S_2$, estab-

Can. J. Chem. Downloaded from www.nrcresearchpress.com by 210.87.254.40 on 09/05/12
For personal use only.

large chain lengths, first order in H_2O_2. Table 1 and Fig. 4 demonstrate that these are experimentally realized. The apparent first-order rate constant includes a square-root dependence on dose rate which is again in agreement with the experimental results. Assuming a value of $2k_{14} = 2.4 \times 10^9$ (12) for the bimolecular termination reaction, a rate constant for the chain propagating reaction may be estimated as $k_{13} = (4.0 \pm 0.4) \times 10^4\ M^{-1}\ s^{-1}$. This is somewhat less than the rate constant found by Seddon and Allen (4) for the propagating reaction in the ethanol/H_2O_2 chain reaction. It may be noted that the rate constant for reduction of ferricyanide by $\dot{C}H_2OH$ is slightly less than that for reduction by $CH_3\dot{C}HOH$ (8).

The small yield of ethylene glycol found (G(glycol) ~ 0.5) represents approximately 20% of the termination reaction. In the photolysis of methanol–water solutions (13), the major product of radical combination was said to be ethylene glycol.

At high concentrations of either alcohol the yield of the chain reaction is decreased. This phenomenon has previously been reported for the photo-induced reaction in mixed water–alcohol systems (5) and in the radiation-induced oxidation of 2-propanol (1). In the latter case the decreased yield was attributed to a decrease in the rate of reaction [7], as a result of the decreasing dielectric constant of the medium at alcohol concentrations sufficiently high to make reaction [7] rather than reaction [8] the rate-determining propagation step.

Summary

The principal numerical results are summarized in Table 2. We have demonstrated that the two-radical model for the chain oxidation of alcohols by H_2O_2, as developed for 2-propanol, is applicable also to ethanol but that a one-radical model accounts satisfactorily for the features of the oxidation of methanol.

1. C. E. Burchill and I. S. Ginns. Can. J. Chem. In press.
2. A. O. Allen, C. J. Hochanadel, J. A. Ghormley, and T. W. Davis. J. Phys. Chem. **56**, 575 (1952).
3. C. E. Bricker and H. R. Johnson. Ind. and Eng. Chem. (Anal. Ed.) **17**, 400 (1945).
4. W. A. Seddon and A. O. Allen. J. Phys. Chem. **71**, 1914 (1967).
5. J. Barrett, A. L. Mansell, and R. J. M. Ratcliffe. Chem. Commun. 48 (1968).
6. (*a*) M. Anbar and D. Meyerstein. J. Phys. Chem. **68**, 3184 (1964); (*b*) C. Lifshitz and G. Stein. J. Chem. Soc. 3706 (1962).
7. R. Livingston and H. Zeldes. J. Amer. Chem. Soc. **88**, 4333 (1966).
8. G. E. Adams and R. L. Willson. Trans. Faraday Soc. **63**, 2981 (1969).
9. R. O. C. Norman and P. R. West. J. Chem. Soc. Ser. B, 389 (1969).
10. G. V. Buxton. Radiat. Res. Rev. **1**, 209 (1968).
11. M. Anbar and P. Neta. Int. J. Appl. Radiat. Isotop. **18**, 493 (1967).
12. M. Simic, P. Neta, and E. Hayon. J. Phys. Chem. **73**, 3794 (1969).
13. J. Barrett and J. H. Baxendale. Trans. Faraday Soc. **54**, 37 (1960).

Structure of a product obtained on treatment of 1-thioacetoacetanilide with sulfuryl chloride

M. Curcumelli-Rodostamo and W. A. Harrison
Uniroyal Limited, Research Laboratories, Guelph, Ontario

Received April 3, 1970

Treatment of 1-thioacetoacetanilide with sulfuryl chloride or thionyl chloride produced a crystalline compound identified as 3,5-diacetonylidene-4-phenyl-1,2,4-dithiazolidine. The absence of carbonyl absorption in the infrared spectrum of the compound indicated that it should be represented by a resonance structure (**2**) involving non-carbonyl components.

Canadian Journal of Chemistry, **48**, 2632 (1970)

In connection with our synthetic work on pesticides, the preparation of 2-chloro-1-thioacetoacetanilide was required. Accordingly 1-thioacetoacetanilide (**1**) was treated at room temperature with an equimolar quantity of sulfuryl chloride. Reaction occurred readily; but instead of the desired product, a chlorine-free crystalline compound (m.p. 195–195.5°) was obtained.

In the present publication we provide evidence establishing the structure of this compound.

The molecular formula $C_{14}H_{13}NO_2S_2$, estab-

Can. J. Chem. Downloaded from www.nrcresearchpress.com by 210.87.254.105 on 09/05/12
For personal use only.

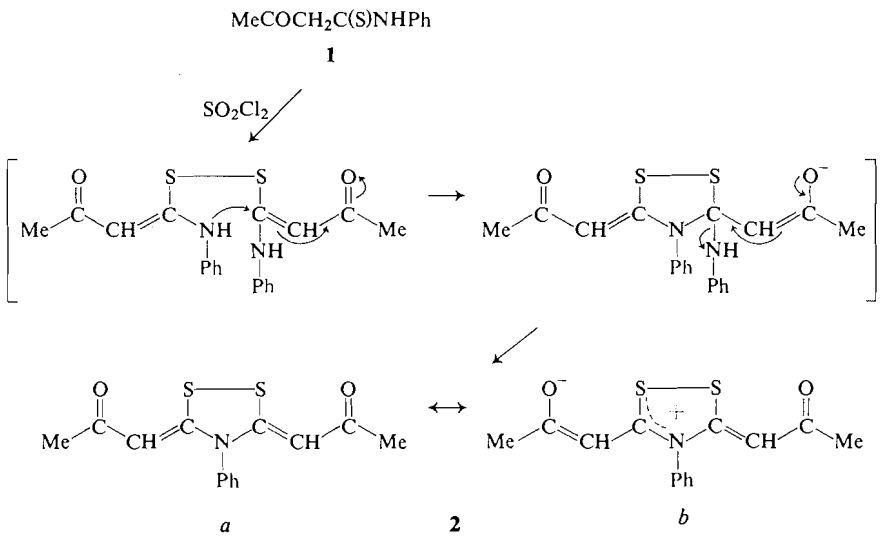

SCHEME 1

lished by elemental analysis and high-resolution mass spectrometry, indicated that the product was formed from two reactant molecules with loss of two hydrogen atoms and the elements of aniline.

The nuclear magnetic resonance (n.m.r.) spectrum shows aromatic absorption centered at 2.5 τ and singlets at 4.59 and 7.94 τ. The intensities of the peaks are in the ratios 5:2:6, respectively.

Consideration of the foregoing data indicated structure **2***a* (3,5-diacetonylidene-4-phenyl-1,2,4-dithiazolidine) for the compound under study.

The mechanism postulated for the conversion of 1-thioacetoacetanilide (**1**) to **2***a* is indicated in Scheme 1. The initial oxidative step, involving a thiol form of **1**, is consistent with early work on the action of sulfuryl chloride on mercaptans (1, 2). The latter were found convertible to the corresponding disulfides according to eq. [1].

[1] $2RSH + SO_2Cl_2 \rightarrow RSSR + 2HCl + SO_2$

Interestingly, when 1-thioacetoacetanilide and sulfuryl chloride were used in the proportions indicated by this equation, the yield of product was increased from 60 to 96%.

The conversion of mercaptans to disulfides and analogous oxidations of thioureas to 1,1′-dithiodiformamidine derivatives on treatment with thionyl chloride have also been reported (2, 3). Oxidation of 1-thioacetoacetanilide (**1**) by this method led to an almost quantitative yield of the same dithiazolidine derivative.

Although the data presented above appear entirely consistent with structure **2***a*, the infrared (i.r.) spectrum of the product indicated a modification of this structure to be necessary. The i.r. spectrum shows no absorption attributable to a normal conjugated carbonyl group; within the 1700–1600 cm^{-1} range there is only one broad peak at 1610 cm^{-1}.

The necessary modification was suggested by earlier work on the structure of the related (5-methyl-1,2-dithiol-3-ylidene)-2-propanone (**3**) (4). The i.r. spectrum of this compound also lacks bands in the carbonyl region and thus indicated that formula **3***a* is an inadequate representation of the molecule. X-ray crystallographic studies (5, 6) supported this conclusion and appear consistent with a resonance hybrid **3** including non-carbonyl components **3***b* (7).

Similarly it can be concluded that structure **2***a* should be replaced by a resonance hybrid involving, besides **2***a*, ionic structures such as **2***b*.

Confirmatory evidence was obtained from a study of (3,4-diphenyl-4-thiazolin-2-ylidene)-2-propanone (8) and (4-methyl-3-phenyl-4-thiazolin-2-ylidene)-2-propanone, prepared by reaction of 1-thioacetoacetanilide (**1**) with 2-bromoacetophenone and chloroacetone, respectively. As expected of structures **4***a* and *b* the i.r. spectra of these compounds showed no absorption in the usual conjugated carbonyl region.

Experimental

The i.r. spectra were recorded on a Perkin–Elmer 521 i.r. spectrophotometer. Accurate mass measurement of

Can. J. Chem. Downloaded from www.nrcresearchpress.com by 210.87.254.105 on 09/05/12
For personal use only.

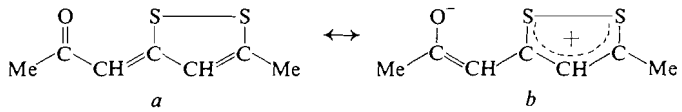

a *b*

3

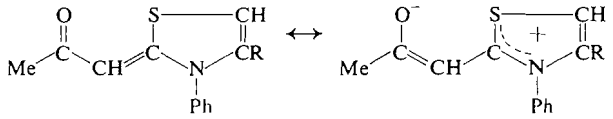

4

a R = Ph
b R = Me

the molecular ion was carried out on a CEC 110B double-focusing mass spectrometer by reference to appropriate peaks in the spectrum of perfluorokerosene, through the courtesy of Professor D. B. MacLean of McMaster University, Hamilton, Ontario.

1-Thioacetoacetanilide (1)

This compound was prepared by the method of Worrall (9): reaction of phenylisothiocyanate with the sodio derivative of acetylacetone and deacetylation of the 2-acetyl-1-thioacetoacetanilide produced with alkali. The sodio derivative of acetylacetone was conveniently prepared by use of sodium hydride in place of the sodium employed in the original method.

3,5-Diacetonylidene-4-phenyl-1,2,4-dithiazolidine (2)

(*1*) To a stirred solution of 1-thioacetoacetanilide (19.3 g, 0.10 mole) in benzene (150 ml) was added dropwise sulfuryl chloride (6.8 g, 0.05 mole) over 0.5 h. The reaction mixture was stirred for a further 3 h and then cooled. The precipitate was collected, washed with cold benzene, and then treated with boiling benzene. The insoluble material (aniline hydrochloride) was removed by filtration. Crystallization from the concentrated filtrate afforded material melting at 185–187°. Recrystallization from benzene gave crystals (14 g, 96%) of m.p. 190–191°. Two more recrystallizations from acetonitrile gave an analytical sample, m.p. 195–195.5°. The i.r.: ν_{max} (KBr and $CHCl_3$) 1610 (broad), no other absorption in the 1700–1600 cm^{-1} region; n.m.r.: 2.5 (5H, multiplet), 4.59 (2H, singlet), 7.94 τ (6H, singlet).

Anal. Calcd. for $C_{14}H_{13}NO_2S_2$ (291.0388): C, 57.73; H, 4.50; N, 4.82; S, 21.97. Found (mass spectroscopy 291.0395): C, 57.65; H, 4.29; N, 4.87; S, 21.81.

When equimolar quantities of the two reagents were used, the product was obtained in 60% yield.

(*2*) To a stirred solution of 1-thioacetoacetanilide (9.6 g) in benzene (100 ml) was added dropwise thionyl chloride (3.0 g) over 15 min. The temperature of the reaction mixture during the addition and for a further hour was kept at 10–15°. Then it was allowed to rise to 25° within 20 min. The crystalline product was collected and washed with cool benzene. Then it was treated with boiling benzene and the insoluble material removed by filtration. Crystallization from the concentrated filtrate afforded material (7.2 g, 99%) of m.p. 194–195°. The identity of this product with that obtained by the sulfuryl chloride method was established by comparison of i.r. spectra and determination of the m.p. of a mixture of the two specimens.

(3,4-Diphenyl-4-thiazolin-2-ylidene)-2-propanone (4a)

This compound was prepared by the reaction of 1-thioacetoacetanilide and 2-bromoacetophenone, according to the procedure of Borisevich *et al.* (8). The i.r.: ν_{max} ($CHCl_3$) 1595 and 1585, no absorption in the 1700–1600 cm^{-1} region; n.m.r.: 2.8 (10H, multiplet), 3.61 (1H, singlet), 4.47 (1H, singlet), 7.99 τ (3H, singlet).

(4-Methyl-3-phenyl-4-thiazolin-2-ylidene)-2-propanone (4b)

1-Thioacetoacetanilide (3.1 g) and chloroacetone (2.1 g) were dissolved in ethanol (30 ml); the resulting solution was heated under reflux for 3 h and then left to stand at room temperature for 42 h. The hydrochloride obtained after removal of the ethanol was recrystallized from acetonitrile to give material (1.3 g) of m.p. 250–255° decomposition. From the mother liquors an additional amount (0.3 g) of product was crystallized.

The hydrochloride was chromatographed on neutral alumina with ethanol as eluent. The free base was thus obtained (1.1 g, 37%), m.p. 155–157°. Two recrystallizations from ethanol–water yielded an analytical sample of m.p. 157–158.5°. The i.r.: ν_{max} ($CHCl_3$) 1592 and 1577, no absorption in the 1700–1600 cm^{-1} region; n.m.r.: 2.6 (5H, multiplet), 3.88 (1H, singlet), 4.73 (1H, singlet), 8.01 (3H, singlet), 8.10 τ (3H, singlet).

Anal. Calcd. for $C_{13}H_{13}NOS$: C, 67.52; H, 5.67; N, 6.06. Found: C, 67.46; H, 5.70; N, 5.81.

1. E. Courant and V. v. Richter. Chem. Ber. **18**, 3178 (1885).
2. B. Holmberg. Ann. **359**, 81 (1908).
3. P. K. Srivastava. Indian J. Chem. **1** (8), 354 (1963).
4. G. Guillouzo. Bull. Soc. Chim. France, 1316 (1958).
5. M. Mammi, R. Bardi, G. Traverso, and S. Bezzi. Nature, **192**, 1282 (1961).
6. J. A. Kapecki and J. E. Baldwin. J. Amer. Chem. Soc. **91**, 1120 (1969).
7. E. Klingsberg. J. Amer. Chem. Soc. **85**, 3244 (1963).
8. A. N. Borisevich, S. A. Shulezhko, and P. Pelkis. Khim. Geterotsikl. Soedin., Akad. Nauk Latv. S.S.R. (3), 368 (1966).
9. D. E. Worrall. J. Amer. Chem. Soc. **42**, 1055 (1920).

Can. J. Chem. Downloaded from www.nrcresearchpress.com by 210.87.254.105 on 09/05/12
For personal use only.

Hydrogenolysis of steroid 3β-acetoxy-5-ene systems[1]

GEORGE R. PETTIT AND BRIAN GREEN
Department of Chemistry, Arizona State University, Tempe, Arizona 85281
AND
Department of Chemistry, University of Maine, Orono, Maine 04473

Received January 15, 1970

Palladium catalyzed hydrogenation of 3β-acetoxy (or hydroxy)-5-ene-type steroids was shown to afford small amounts (5–10%) of the corresponding 3-deoxy derivatives. The hydrogenolysis reaction appeared general in scope and offers a one-step method for converting, e.g., cholesteryl acetate to 5α-cholestane.

Canadian Journal of Chemistry, 48, 2635 (1970)

Can. J. Chem. Downloaded from www.nrcresearchpress.com by 210.87.254.6 on 09/05/12
For personal use only.

Catalytic hydrogenation of 3β-acetoxy- or 3β-hydroxy-5-ene substituted steroids is one of the most commonly encountered reactions in steroid chemistry. The small amount of side product generally accompanying hydrogenation had been known to us for some time and with adoption of thin-layer chromatography (t.l.c.) in our laboratory (1959), it became apparent that such reactions were generally accompanied by approximately 5% of a relatively nonpolar component readily identified as the 3-deoxy hydrogenolysis product.[2] In a typical hydrogenation, pregnenolone acetate (**1**) was treated with hydrogen under a slight positive pressure for three days in the presence of 10% palladium-on-carbon to yield primarily 3β-acetoxy-20-oxo-5α-pregnane (**2***a*) accompanied by 20-oxa-5α-pregnane (**2***b*) (eq. [1]). Using small amounts of 70% perchloric acid, reduction was complete in 4 h and led to a 10% yield of hydrogenolysis product **2***b*. In each instance, evidence for any significant formation of the 5β-isomers was not detected. Similarly, 5α-cholestane (**3***a*) was obtained from cholesteryl acetate. Repeating the reduction reaction with saturated 3β-acetates **2***a*, **3***b*, or **4** gave only quantitative recovery of starting material.

[1] 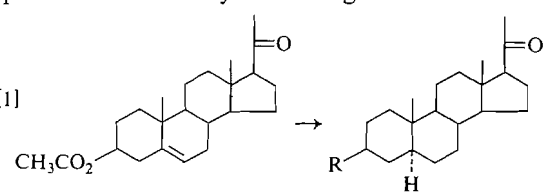

1 **2**
a, R = $OCOCH_3$
b, R = H

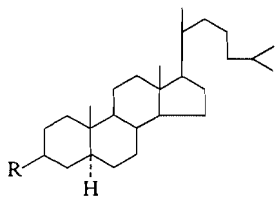

3
a, R = H
b, R = $OCOCH_3$

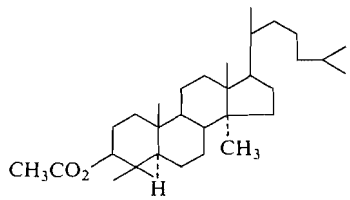

4

Resistance of the 3β-acetoxy-5α-steroids implicated a partial isomerization of the Δ^5-olefin to the Δ^4-position.[3] In order to explore this possibility (**5** → **6**), reduction of cholesteryl acetate was repeated employing deuterium gas (eq. [2]). As previously observed (4) during

[2] 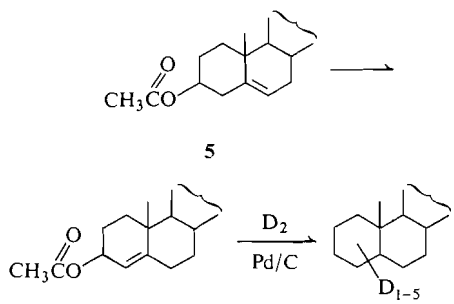

5 **6** **7**

[1]Steroids and Related Natural Products. 61. For Part 60, see ref. 1.

[2]We earlier reported (2) reduction of 3β-hydroxy-17-oxo-androst-5-ene to 17-oxo-5α-androstane (ca. 6% yields) by this means.

[3]Hydrogenolysis of allylic acetates readily occurs: see, e.g., ref. 3.

Can. J. Chem. Downloaded from www.nrcresearchpress.com by 210.87.254.6 on 09/05/12
For personal use only.

analogous reduction of cholesterol, excessive introduction of deuterium occurred. Extensive scrambling (see **7**) was illustrated by a mass spectrum of the product which exhibited molecular ions of gradually decreasing relative abundance from M^+ to M + 5. Doubtlessly, future efforts concerned with the mechanism of such hydrogenolysis reactions will profit from employing one of the recently introduced homogeneous solution catalysts which are referred to in an important review (5) of selective deuteration in steroid chemistry.

In summary, palladium catalyzed reductive removal of 3β-acetoxy or 3β-hydroxyl groups from Δ^5-steroids appears general in scope and offers a one-step, albeit low yield, procedure for obtaining certain saturated A/B ring steroids.

Experimental

Silica gel (0.05–0.20 mm) used for column chromatography and silica gel G employed for t.l.c. were obtained from E. Merck, Darmstadt. The thin-layer chromatograms were developed with concentrated sulfuric acid. Melting points were determined using a Kofler apparatus.

*Hydrogenation of 3β-Acetoxy-20-oxo-5-pregnane (**1**)*

Method A

An ethyl acetate (50 ml) solution of pregnenolone acetate (1.0 g) was shaken under a slightly positive pressure of hydrogen (72 h) with 10% palladium-on-carbon (0.20 g). Following filtration and concentration, the residue in 3:1 hexane–benzene was chromatographed on silica gel (30 g). Elution with 1:1 hexane–benzene gave 54 mg of 20-oxo-5α-pregnane (**2***b*). Recrystallization from methanol gave 40 mg of platelets (**2***b*) melting at 133–134° (lit., ref. 6, m.p. 133–135°); ν 1700 (20-ketone) cm^{-1}; proton magnetic resonance δ 0.6 (18-methyl), 0.77 (19-methyl), and 2.06 ($COCH_3$). Continued elution with benzene and benzene-chloroform mixtures gave 0.91 g of 3β-acetoxy-20-oxo-5α-pregnane (**2***a*).[4]

A solution of 3β-acetate **2***b* (0.63 g) in ethyl acetate (40 ml) was subjected to hydrogenation in the presence of 10% palladium-on-carbon (0.12 g) during 120 h as described above. A t.l.c. examination of the product indicated presence of only starting material (**2***b*).

Method B

The hydrogenation experiment described above in method *A* was repeated using ethyl acetate (100 ml), pregnenolone acetate (2.0 g), 10% palladium-on-carbon (0.4 g) and 2 ml of 70% perchloric acid. After 4 h the solution was passed through a bed of filter aid and washed with saturated aqueous sodium bicarbonate and water. Removal of solvent gave a residue which was chromatographed on silica gel (60 g) as noted above. By this means, 0.20 g of 20-oxo-5α-pregnane (10% yield, pure by t.l.c.) was isolated. Two recrystallizations from methanol gave a specimen melting at 137–138.5°.

Hydrogenation of 3β-acetoxy-5-Cholestene

The hydrogenation reaction described in method *A*, above, was repeated employing ethyl acetate (100 ml), cholesteryl acetate (2.0 g), and 10% palladium-on-carbon (0.4 g). Reaction was followed by t.l.c. and seemed complete after 6 h. A solution of the product in hexane was chromatographed on silica gel (50 g) and elution with the same solvent gave 0.11 g of 5α-cholestane (**11***a*).The hydrocarbon was shown to be pure by t.l.c. and recrystallization from isopropyl ether – methanol gave plates melting at 77–80°.[4] Elution with benzene gave 1.6 g of 3β-acetoxy-5α-cholestane[4] which recrystallized from chloroform–methanol as needles melting at 108°.

Reduction of cholesteryl acetate (4.0 g) in ethyl acetate (200 ml) was repeated in the presence of 10% palladium-on-carbon (0.8 g) as summarized in the preceding paragraph except that deuterium was substituted for hydrogen and catalyst was removed by filtering the solution through a layer of activated alumina. Following chromatography on silica gel (75 g) a hexane fraction provided 0.27 g of extensively deuterated 5α-cholestane. Three recrystallizations from isopropyl ether – methanol gave plates melting at 78–80°. The benzene fractions provided 3.7 g of deuterated 3β-acetoxy-5α-cholestane.

Repeating the hydrogenation experiment over a 20 h period with 3β-acetoxy-5α-cholestane or with 3β-acetoxy-5α-lanostane (**4**) over 48 h gave, in each case, only starting material. Examination of both products by t.l.c. revealed no trace of 3-deoxy derivatives.

[4]Identification was confirmed by mixture melting point determination and infrared spectral comparison with an authentic sample.

This investigation was supported by Public Health Service Research Grants CY-4074 (C3) to CA-04074-06 from the National Cancer Institute. We also wish to thank John Occolowitz for providing the mass data.

1. G. R. Pettit and J. R. Dias. Chem. Commun. In press.
2. G. R. Pettit, A. K. Das Gupta, and R. L. Smith. Can. J. Chem. **44**, 2023 (1966).
3. M. E. Wall, T. Perlstein, and S. G. Levine. J. Org. Chem. **26**, 159 (1961).
4. D. K. Fukushima and T. F. Gallagher. J. Amer. Chem. Soc. **77**, 139 (1955).
5. C. Djerassi. Proceedings of the Second International Congress on Hormonal Steroids. Milan, Italy, May, 1966, p. 261.
6. J. Romo, G. Rosenkranz, and C. Djerassi. J. Org. Chem. **17**, 1413 (1952).

Vibrational spectra and proposed crystal structure of some tetraphenylarsonium compounds

L. K. WALFORD AND RICHARD J. BLATTNER
Faculty of Physics, Southern Illinois University, Edwardsville, Illinois 62025

AND

STEPHEN FELDMAN AND R. L. BAIN
Faculty of Chemistry, Southern Illinois University, Edwardsville, Illinois 62025

Received April 1, 1970

The crystal structures of $(C_6H_5)_4AsBF_4$, $(C_6H_5)_4AsPF_6$, $(C_6H_5)_4AsAsF_6$, and $(C_6H_5)_4AsSbF_6$ have been studied by X-ray diffraction. The unit cells are all tetragonal. The fluoroborate compound is probably isostructural with $(C_6H_5)_4AsFeCl_4$. The other three compounds are almost isostructural with $(C_6H_5)_4AsFeCl_4$, the only change being the accommodation of the dipyramidal PF_6^- ion in the space group $I\bar{4}$ (No. 82). Infrared absorption spectra are in general agreement with previous work on tetraphenylarsonium halides and compounds with hexafluoro Group VA ions. It is concluded that crystal field effects for this series of salts do not markedly affect the vibrational spectra.

Canadian Journal of Chemistry, 48, 2637 (1970)

Can. J. Chem. Downloaded from www.nrcresearchpress.com by 210.87.254.6 on 09/05/12
For personal use only.

Introduction

X-Ray diffraction and vibrational studies of several ionic tetraphenylarsonium compounds have been recently reported and the results suggest that a variation in crystal class may depend upon the anion. The present study was undertaken to investigate the structural relationships between various tetraphenylarsonium compounds and to examine possible crystal field effects on the vibrational spectrum by highly symmetric fluoro-anions. The anions chosen for study were tetrafluoroborate, hexafluorophosphate, hexafluoroarsenate, and hexafluoroantimonate.

Experimental Methods

Approximately 1.0 g of tetraphenylarsonium chloride (K and K Laboratories) was dissolved in a minimum of absolute methanol. To this solution, a filtered solution of the appropriate silver salt of hexafluoroborate, hexafluorophosphate, hexafluoroarsenate, or hexafluoroantimonate (K and K Laboratories) was added dropwise until precipitation was completed. The solids formed were filtered, then washed with ammonia water until the wash water showed no evidence for the presence of chloride ion. The remaining solid, the tetraphenylarsonium salt, was washed with cold methanol once and dissolved in dimethylsulfoxide. The resulting solution was placed in a vacuum oven at ca. 80 °C and crystallization allowed to occur at reduced pressure. After 3 to 5 days, the resulting crystals were transferred to a watch glass and dried at ca. 70 °C under reduced pressure for at least 3 days.

The crystals isolated were colorless, tetragonal needles elongated along "*c*" and stable in air. The infrared spectrum of each compound gave no indication of water of hydration nor of dimethylsulfoxide present in the crystals. The infrared spectra of the crystals from 4000 to 400 cm^{-1} were recorded in a KBr disc with a Perkin–Elmer Model 621 double-beam grating spectrophotometer. Low frequency studies (400 to 200 cm^{-1}) were made with the compounds in a Nujol mull using cesium iodide windows.

The crystal class, Laue groups, and cell parameters were determined from $\{hk0\}$, $\{hk1\}$, $\{h0l\}$ data recorded on Weissenberg and oscillation photographs. A powder pattern was obtained using a diffractometer. Both techniques used β filtered Cu Kα radiation.

The densities of the crystals were measured by displacement in dimethylsulfoxide at 20 °C. The solubility and rate of dissolution are very low at this temperature.

Results

The results of X-ray studies of some tetraphenylarsonium salts have been reported (1–7). The symmetry of the structures seems to depend on the complexity of the anion. In the present compounds, the anions have tetrahedral or octahedral symmetry. The unit cells of the compounds studied are tetragonal and the Laue group is $4/m$. Systematic absences in the reflections as determined from Weissenberg photographs indicated the space group possibilities to be $I\bar{4}$, $I4_1$, $I4$, and $I4/m$. However, the fourfold inversion axis at the arsenic atom in the cation $[(C_6H_5)_4As]^+$ is sufficient to fix the space group as $I\bar{4}$. This is the same as the tetrachloroferrate(III) (6) and the iodide (7) compounds.

The approximate lattice parameters measured from the Weissenberg and oscillation photographs were used to index the powder pattern, from which more accurate parameters were deter-

TABLE 1
Lattice parameters and densities for $(C_6H_5)_4As$ compounds

Compound	a_0 (Å)	c_0 (Å)	d (g cm^{-3}) Observed	d (g cm^{-3}) Calculated
$(C_6H_5)_4AsFeCl_4$	13.160±0.005	7.15±0.02	1.56±0.02	1.55
$(C_6H_5)_4AsBF_4$	12.49±0.02	6.99±0.02	1.38±0.02	1.43
$(C_6H_5)_4AsPF_6$	12.77±0.02	7.03±0.02	1.51±0.02	1.53
$(C_6H_5)_4AsAsF_6$	12.46±0.01	7.18±0.01	1.70±0.02	1.71
$(C_6H_5)_4AsSbF_6$	12.59±0.02	7.213±0.005	1.84±0.02	1.80

mined using the highest angle reflections possible. These lattice parameters and the measured densities of the compounds are presented in Table 1, together with densities calculated assuming two formula units per unit cell. The standard deviations of the lattice parameters were estimated from five measurements of several orders of reflection.

Low frequency absorption bands were observed for all the compounds and are presented in Table 2. The infrared spectrum of tetraphenylarsonium chloride was also obtained for comparison purposes.

TABLE 2
Low frequency vibrations of some tetraphenylarsonium compounds

Compound	Observed vibrational frequencies (cm^{-1})
$(C_6H_5)_4AsCl$*	405, 348, 375, 364, 351, 345
$(C_6H_5)_4AsCl$†	383, 373, 361, 348, 333, 321, 299
$(C_6H_5)_4AsBF_4$	383, 372, 368, 347, 333, 320, 313
$(C_6H_5)_4AsPF_6$	382, 373, 368, 347
$(C_6H_5)_4AsAsF_6$	392, 348, 317
$(C_6H_5)_4AsSbF_6$	382, 372, 367, 348, 332, 320, 300

*Values listed are taken from ref. 9.
†This work.

Discussion

The space group and chemical structure suggest that the structure of the tetrafluoroborate salt is probably isostructural with the tetrachloroferrate(III), $[(C_6H_5)_4AsFeCl_4]$ (6). In the space group $I\bar{4}$ (No. 82) (8) the atomic sites would be: 2 As in 2*a*, 2 B in 2*c*, 8 F in 8*g*, and 48 C in 8*g*.

The anion in the other three compounds has six fluorine atoms so the structures cannot be identical to tetrafluoroborate. From chemical evidence we know that the six fluorine atoms must be in octahedral coordination about the central atom (P, As, or Sb) and this arrangement may be accommodated in the space group $I\bar{4}$ as follows: 2 As in 2*a*, 2 P, As, or Sb in 2*c*, 8 F in 8*g* (with $z = 1/4$), 4 F in 4*f*, and 48 C in 8*g*.

Setting $z = 1/4$ for the 8*g* sites causes the tetrahedron of fluorine atoms in the tetrafluoroborate to collapse to form a square (the base of the bipyramid of fluorine atoms). The fluorine atoms in 4*f* sites provide the apices of the bipyramid.

The 8*g* sites have two unknown parameters (x and y) and the 4*f* sites have one (z). These parameters fix the orientation of the hexafluoride ions. The position of the center of these ions is, however, fixed by symmetry.

Although final confirmation of these three structures rests on a full crystal structure refinement, there is no doubt that the space group is the same for each compound and the known geometry of the hexafluoride ions PF_6^-, AsF_6^-, and SbF_6^- then leads to the structure proposed above.

The unit cell parameters show no systematic variation with the size of the anion and suggest that the packing mechanism is dominated by the size and shape of the cation. The holes for the anion are large enough even for the SbF_6^- ions so that no large expansion occurs for increasing anion sizes.

The general features of the infrared spectra from 1600 to 400 cm^{-1} are in agreement with those assignments suggested by Mackay *et al.* (9) for the tetraphenylarsonium halides and those assignments suggested by Begun and Rutenberg (10) for hexafluoro Group VA ions.

The two infrared-active vibrations ν_3 and ν_4 associated with MF_6^- ions are reported (10) to be triply degenerate. The ν_4 frequencies reported and those observed in this study are in good agreement: PF_6^-, 556 cm^{-1} (observed), 558 cm^{-1} (reported); AsF_6^-, 392 cm^{-1} (observed),

Can. J. Chem. Downloaded from www.nrcresearchpress.com by 210.87.254.6 on 09/05/12
For personal use only.

392 cm^{-1} (reported); SbF_6^-, 348 cm^{-1} (observed), 350 cm^{-1} (reported).

The ν_3 frequencies are reported as strong singlets. However, the observed spectra suggest some splitting: PF_6^-, 835 cm^{-1} (observed), 830 cm^{-1} (reported); AsF_6^-, 704, 686 cm^{-1} (observed), 699 cm^{-1} (reported); SbF_6^-, 689, 661, 649 cm^{-1} (observed), 669 cm^{-1} (reported).

Judging from the relative constancy of the tetraphenylarsonium infrared bands and the X-ray work, these new bands are attributed to the hexafluoro-anion species.

The low frequency bands reported for the tetrafluoroborate salt are in general agreement with those of the other tetraphenylarsonium compounds. The features of the spectra from 1600 to 400 cm^{-1} may be interpreted for the most part in terms of the tetraphenylarsonium spectra coupled with the tetrafluoroborate ion spectra as reported by Greenwood (11).

Crystal field effects for this series of tetraphenylarsonium salts do not appear to have marked effects on the vibrational spectrum.

We are indebted to the Office of Research and Projects, Southern Illinois University for continued financial support.

1. F. A. COTTON and S. J. LIPPARD. Inorg. Chem. **5**, 416 (1966).
2. F. A. COTTON and C. B. HARRIS. Inorg. Chem. **7**, 2140 (1968).
3. G. H. PALENIK. Acta Cryst. **20**, 471 (1966).
4. R. C. SLATER. Acta Cryst. **12**, 187 (1959).
5. R. P. TAYLOR, D. H. TEMPLETON, A. ZALKIN, and W. D. HORROCKS, JR. Inorg. Chem. **7**, 2629 (1968).
6. B. ZASLOW and R. E. RUNDLE. J. Phys. Chem. **61**, 490 (1957).
7. R. C. L. MOONEY. J. Amer. Chem. Soc. **62**, 2955 (1940).
8. International tables for X-ray crystallography. Kynoch Press, Birmingham. 1965.
9. K. M. MACKAY, D. B. SOWERBY, and W. C. YOUNG. Spectrochim. Acta, **24A**, 611 (1968).
10. G. M. BEGUN and A. C. RUTENBERG. Inorg. Chem. **6**, 2212 (1967).
11. N. N. GREENWOOD. J. Chem. Soc. 3811 (1959).

Carbon-13 and proton chemical shifts of cyclohexanes in relation to interaction energy

A. S. PERLIN AND H. J. KOCH[1]
Department of Chemistry, McGill University, Montreal, Quebec

Received February 23, 1970

A comparison of nuclear magnetic resonance spectra for isomeric cyclohexane derivatives (methyl, hydroxyl, halogen) shows that net shielding of carbon-13 nuclei of these compounds increases additively with an increase in repulsive non-bonding interactions, and thus with decreasing enthalpy in the series. By contrast, an inverse shielding pattern is found for the appended protons. Hence, a destabilizing interaction in these compounds alters polarization of the C—H bond, placing greater electron density on carbon, and its impact appears to be delocalized over many C—H bonds of the molecule.

Canadian Journal of Chemistry, **48**, 2639 (1970)

Carbon-13 chemical shifts in the cyclohexane series are influenced strongly by conformational and geometrical factors (1–3). The methylcyclohexanes, for which extensive data are available (3), provide a particularly clear illustration of the kinds of effects that occur. In general, individual ^{13}C nuclei of a compound may experience either deshielding or increased shielding, the direction and magnitude of which is determined by the position and orientation of the methyl substituents. Enhanced shielding is attributed mainly to steric hindrance associated with gauche interactions of the methyl groups, and deshielding to relief of these interactions (3–6). For example, several ^{13}C nuclei of an isomer containing an axial methyl group come into resonance at higher field than when the group is equatorial; similarly, vicinal methyl groups are associated with greater shielding than are 1,3 or 1,4 arrangements (3).

Because these destabilizing interactions influence ^{13}C chemical shifts, it is to be expected that the spectroscopic data, in turn, should bear some relationship to conformational stability of the methylcyclohexanes. The current note pro-

[1]Postdoctoral Fellow, 1969–1970.

Can. J. Chem. Downloaded from www.nrcresearchpress.com by 210.87.254.6 on 09/05/12
For personal use only.

392 cm^{-1} (reported); SbF_6^-, 348 cm^{-1} (observed), 350 cm^{-1} (reported).

The ν_3 frequencies are reported as strong singlets. However, the observed spectra suggest some splitting: PF_6^-, 835 cm^{-1} (observed), 830 cm^{-1} (reported); AsF_6^-, 704, 686 cm^{-1} (observed), 699 cm^{-1} (reported); SbF_6^-, 689, 661, 649 cm^{-1} (observed), 669 cm^{-1} (reported).

Judging from the relative constancy of the tetraphenylarsonium infrared bands and the X-ray work, these new bands are attributed to the hexafluoro-anion species.

The low frequency bands reported for the tetrafluoroborate salt are in general agreement with those of the other tetraphenylarsonium compounds. The features of the spectra from 1600 to 400 cm^{-1} may be interpreted for the most part in terms of the tetraphenylarsonium spectra coupled with the tetrafluoroborate ion spectra as reported by Greenwood (11).

Crystal field effects for this series of tetraphenylarsonium salts do not appear to have marked effects on the vibrational spectrum.

We are indebted to the Office of Research and Projects, Southern Illinois University for continued financial support.

1. F. A. COTTON and S. J. LIPPARD. Inorg. Chem. **5**, 416 (1966).
2. F. A. COTTON and C. B. HARRIS. Inorg. Chem. **7**, 2140 (1968).
3. G. H. PALENIK. Acta Cryst. **20**, 471 (1966).
4. R. C. SLATER. Acta Cryst. **12**, 187 (1959).
5. R. P. TAYLOR, D. H. TEMPLETON, A. ZALKIN, and W. D. HORROCKS, JR. Inorg. Chem. **7**, 2629 (1968).
6. B. ZASLOW and R. E. RUNDLE. J. Phys. Chem. **61**, 490 (1957).
7. R. C. L. MOONEY. J. Amer. Chem. Soc. **62**, 2955 (1940).
8. International tables for X-ray crystallography. Kynoch Press, Birmingham. 1965.
9. K. M. MACKAY, D. B. SOWERBY, and W. C. YOUNG. Spectrochim. Acta, **24A**, 611 (1968).
10. G. M. BEGUN and A. C. RUTENBERG. Inorg. Chem. **6**, 2212 (1967).
11. N. N. GREENWOOD. J. Chem. Soc. 3811 (1959).

Carbon-13 and proton chemical shifts of cyclohexanes in relation to interaction energy

A. S. PERLIN AND H. J. KOCH[1]
Department of Chemistry, McGill University, Montreal, Quebec

Received February 23, 1970

A comparison of nuclear magnetic resonance spectra for isomeric cyclohexane derivatives (methyl, hydroxyl, halogen) shows that net shielding of carbon-13 nuclei of these compounds increases additively with an increase in repulsive non-bonding interactions, and thus with decreasing enthalpy in the series. By contrast, an inverse shielding pattern is found for the appended protons. Hence, a destabilizing interaction in these compounds alters polarization of the C—H bond, placing greater electron density on carbon, and its impact appears to be delocalized over many C—H bonds of the molecule.

Canadian Journal of Chemistry, **48**, 2639 (1970)

Carbon-13 chemical shifts in the cyclohexane series are influenced strongly by conformational and geometrical factors (1–3). The methylcyclohexanes, for which extensive data are available (3), provide a particularly clear illustration of the kinds of effects that occur. In general, individual ^{13}C nuclei of a compound may experience either deshielding or increased shielding, the direction and magnitude of which is determined by the position and orientation of the methyl substituents. Enhanced shielding is attributed mainly to steric hindrance associated with gauche interactions of the methyl groups, and deshielding to relief of these interactions (3–6). For example, several ^{13}C nuclei of an isomer containing an axial methyl group come into resonance at higher field than when the group is equatorial; similarly, vicinal methyl groups are associated with greater shielding than are 1,3 or 1,4 arrangements (3).

Because these destabilizing interactions influence ^{13}C chemical shifts, it is to be expected that the spectroscopic data, in turn, should bear some relationship to conformational stability of the methylcyclohexanes. The current note pro-

[1]Postdoctoral Fellow, 1969–1970.

Can. J. Chem. Downloaded from www.nrcresearchpress.com by 210.87.254.42 on 09/05/12
For personal use only.

TABLE 1

Summed values for ^{13}C and ^{1}H chemical shifts for some methylcyclohexanes (in p.p.m.)

Compound*	$\Sigma\delta^{13}C$†	$\Sigma\delta^{1}H$†	Compound*	$\Sigma\delta^{13}C$†	$\Sigma\delta^{1}H$†
Dimethyl			*Trimethyl*		
1,3 (*e,e*)	774.9	17.9	1,3,5 (*e,e,e*)	857.4	18.5
1,4 (*e,e*)	774.9	19.7	1,2,4 (*e,e,e*)	865.7	18.7
1,2 (*e,e*)	782.7	18.1	1,1,3 (*e,a,e*)	868.6	20.4
1,1 (*e,a*)	788.8	18.8	1,2,3 (*e,e,e*)	874.6	19.4
1,3 (*e,a*)	803.0	20.1	1,3,5 (*e,e,a*)	883.2	20.1
1,4 (*e,a*)	804.1	19.9	1,1,2 (*e,a,e*)	893.8	19.4
1,2 (*e,a*)	817.3	19.8	1,2,4 (*e,e,a*)	894.7	21.2

*In descending order of stability, considering only the more important conformers. Detailed evaluations of the interaction energies are given in refs. 3 and 7.

†The sum of the chemical shifts (p.p.m.) reported for each compound in ref. 3. The ^{13}C shifts are relative to *downfield* benzene, ^{1}H shifts are relative to *upfield* tetramethylsilane.

poses that this indeed is the case, and that such a relationship may apply also for proton data, as well as for other series of compounds.

In evaluating the data in these terms, it has been more convenient to consider *overall* shielding states of the molecules rather than to focus attention on the chemical shifts of individual nuclei. Hence a comparison has been made of *sum totals*[2] of ^{13}C chemical shifts for the various methylcyclohexanes from the data provided by ref. 3. This comparison (Tables 1 and 2) shows that there is a systematic additivity of effects and thus a progressive increase in total shielding as the number of repulsive interactions increases (Table 1): e.g., overall shielding and also the number of gauche interactions (7) increase in the sequence 1,4 *e,e* (no interactions) < 1,2 *e,e* (one) < 1,3 *e,a* (two) < 1,2 *e,a* (three). Since the same interactions are the major ones evaluated in conformational analysis of the methylcyclohexanes (7), the ^{13}C chemical shifts understandably reflect the relative order of stability of compounds within the series. A direct comparison of *cis–trans* isomers (Table 2) emphasizes these differences as well as the fact that there is a moderately good correspondence with interaction energies and enthalpy data cited (7) for several of the isomeric pairs. Thus, a positive total chemical shift difference (Δ) of about 30 p.p.m. (± 5 p.p.m.) is observed throughout for a ΔH of 1.8–2.0 kcal/mole.

Carbon-13 chemical shifts appear to be determined principally by the electron density of the atoms (5, 8–11). Hence these chemical shift variations are regarded as an indication of differences in electron density that are mainly of conformational origin. It may be pertinent, therefore, that in contrast to the dimethylcyclohexanes, the dimethylbenzenes differ relatively little in total $\delta^{13}C$ values (*o*-xylene, 722.0; *m*-, 721.2; *p*-, 718.2) whereas individual chemical shifts vary widely (8).[3]

The effect of steric hindrance on the chemical shift of a proton appears to be opposite (i.e., deshielding) to that of the ^{13}C nucleus to which it is bonded (3–6, 12). Accordingly, summed values for the methylcyclohexanes generally exhibit the inverse of this presumed relationship between chemical shift and interaction energy (Tables 1 and 2). Thus, whereas ^{13}C nuclei of isomers containing only equatorial or non-vicinal methyl groups are more strongly deshielded on the average than those of isomers containing an axial methyl group or vicinal ones, the pattern is clearly reversed for protons (footnote†, Table 1).

Perhaps these opposite shielding effects for ^{13}C and the protons attached thereto result from compensatory changes in electronic configuration of C—H and C—C bonds that permit the molecule to attain an overall minimum energy level. It appears, in any event, that the nature of a destabilizing interaction in these compounds is such as to generate an overall increase in the shielding of ^{13}C and decreased shielding of ^{1}H. That is, the less favorable energy state is associated with a net change in the "charge polarization" (4–6) of C—H bonds, placing greater electron density on carbon. Most of the C—H bonds in a molecule are affected in this manner,

[2]Summed values also eliminate the considerable difficulty of unambiguously establishing assignments for all of the individual signals.

[3]Similarly, the dimethoxybenzenes show a wide range of ^{13}C chemical shifts (8), but relatively uniform total $\delta^{13}C$ values: *o*-, 664.6; *m*-, 667.6; *p*-, 664.0.

Can. J. Chem. Downloaded from www.nrcresearchpress.com by 210.87.254.42 on 09/05/12
For personal use only.

TABLE 2
Comparison of some *cis–trans* methylcyclohexanes (in p.p.m.)

Methylcyclohexane	$\Sigma\delta^{13}C$*	Δ†	$\Sigma\delta^{1}H$*	Δ†	*E*‡
1,2-*cis*(*e,a*)	817.3	34.6(+)	19.9	1.8(−)	1.8
-*trans*(*e,e*)	782.7		18.1		
1,3-*trans*(*e,a*)	803.0	28.1(+)	20.1	2.1(−)	1.8
-*cis*(*e,e*)	774.9		17.9		
1,4-*cis*(*e,a*)	804.0	29.1(+)	19.9	1.2(−)	1.8
-*trans*(*e,e*)	774.9		18.7		
1,2,4-*trans,trans*(*e,e,a*)	894.7	29.0(+)	21.1	2.4(−)	1.8
-*trans,cis*(*e,e,e*)	865.7		18.7		
1,3,5-*cis,trans*(*e,e,a*)	883.2	25.8(+)	20.1	1.6(−)	1.8
-*cis,cis*(*e,e,e*)	857.4		18.5		

*Values from Table 1.
†Values for *e,a* (or *e,e,a*) isomer *minus* value for *e,e* (or *e,e,e*) isomer; (+) indicates increased shielding, (−) decreased shielding.
‡Interaction energy for *e,a* isomer *minus* value for *e,e* isomer (kcal/mole) (7).

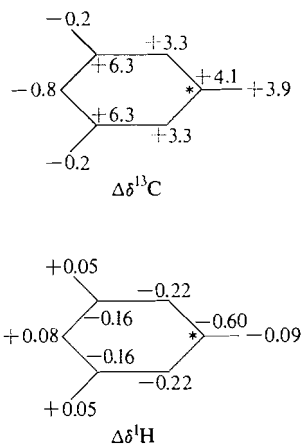

FIG. 1. The ^{13}C and ^{1}H chemical shift differences (Δδ) between the *e,e,e* and *e,e,a* isomer of 1,3,5-trimethylcyclohexane. The Δδ values (p.p.m.) (derived from data of ref. 3, Table IV) correspond to the changes observed when the orientation of the methyl group attached to the starred (*) carbon is altered from *e* to *a*; +, increased shielding; −, decreased shielding.

although those that are relatively remote from the orientational (equatorial → axial) rearrangement show little change or even a slight polarization in the opposite direction. This widespread alteration of shielding effects, illustrated typically for the group of compounds by Fig. 1, provides a graphic demonstration of the impact of a non-bonding interaction. Its translation into numerous electron density readjustments over the molecule as a whole, presumably is a form of delocalization commensurate with optimum stabilization. Although an increase in ^{13}C shielding is suggestive of a contraction of C—C—C bond angles (decrease in s character) and/or lengthening of C—H bonds, the simultaneous decrease in shielding of the attached proton is not consistent with this direction of hybridization change; thus, a proton on sp^3 carbon is normally expected to be *more* shielded than a proton on sp^2 carbon. Most pertinent to the current findings would be a bonding model (cf. 4, 6) that permits for a simultaneous decrease in excitation energy for ^{13}C, and an increase for ^{1}H, as the C—H bond becomes affected by a destabilizing interaction.

The ^{13}C spectra of cyclohexane derivatives that contain more polar types of bonds, i.e., *cis–trans* isomers of the cyclohexanediols, 4-*t*-butylcyclohexanol, and 1,2-dichlorocyclohexane (Table 3), suggest that a relationship of this kind applies in a broader context. Thus, total ^{13}C values, and most individual ^{13}C chemical shifts, for these compounds also reflect greater deshielding effects in the more stable isomer. It is noteworthy that cholestane-3-α- and β-yl acetates afford results (13) closely similar to those for the monocyclic compounds. Hence, the isomeric difference in total ^{13}C chemical shifts (derived from Table II of ref. 13) is + 17.5 p.p.m., compared with a value of + 15.0 for the acetates of *cis*- and *trans*-4-*t*-butylcyclohexanol (from

Can. J. Chem. Downloaded from www.nrcresearchpress.com by 210.87.254.42 on 09/05/12
For personal use only.

TABLE 3

Comparison of *cis–trans* isomers of some cyclohexane derivatives (in p.p.m.)**

	C	$\delta^{13}C$*	$\Sigma\delta^{13}C$	Δ†	*E*‡		C	$\delta^{13}C$*	$\Sigma\delta^{13}C$	Δ†	*E*‡
Diol§						*Dichloro*‖					
1,2-*cis* (*e,a*)	1,2	56.2				1,2-*cis* (*e,a*)	1,2	64.1			
	3,6	97.4	518.2				3,6	94.3	526.0		
	4,5	105.5		21.4(+)	0.9		4,5	104.6		6.4(+)	~0.5
1,2-*trans* (*e,e*)	1,2	51.9				1,2-*trans* (*e,e*)	1,2	63.5			
	3,6	94.0	496.8				3,6	92.9	519.6		
	4,5	102.5					4,5	103.4			
1,3-*trans* (*e,a*)	1,3	60.3				*4-t-Butylcyclohexanol*¶					
	2	85.4	500.5			*cis* (*e,a*)	1	61.8			
	4,6	93.4					4	78.7			
	5	107.7		10.3(+)	0.9		2,6	93.5	931.1		
1,3-*cis* (*e,e*)	1,3	58.2					3,5	105.9			
	2	82.7	490.2				C	94.5			
	4,6	92.5					CH_3	99.1		19.2(+)	0.9
	5	106.1				*trans* (*e,e*)	1	56.3			
							4	79.5			
1,4-*cis* (*e,e*)	1,4	59.6	508.8				2,6	91.0	911.9		
	2,3 5,6	97.4					3,5	101.0			
				14.4(+)	0.9		C	94.8			
1,4-*trans* (*e,e*)	1,4	57.6	494.4				CH_3	99.1			
	2,3 5,6	94.8									

*Relative to downfield benzene.
†As for Table 2.
‡As for Table 2.
§In water.
‖Neat liquid.
¶In chloroform-*d*.
**Although not recorded here the δ^1H data available show differences similar to those noted for the methylcyclohexanes.

Table 1 of ref. 13). Differences between the isomeric steroids are confined mainly to the A-ring. However, minor ones extend over a substantial distance, thus, the α isomer exhibits a small increased shielding of the angular methyl ^{13}C (C-19), as well as of C-6 and -11 the C—H bonds of which are oriented 1,3-diaxially relative to this methyl group.

In general, the current data resemble those pertaining to bulk molecular properties such as expressed in the von Auwer's rule (14). However, since solutions as well as neat liquids are represented here, possible intermolecular effects do not appear to be of major importance.

The ^{13}C nuclear magnetic resonance (n.m.r.) data for the aldopyranose sugars (15–18) show relationships similar to those described above, although the results are not as straightforward and accordingly are treated in detail elsewhere (18).

Experimental

Carbon-13 magnetic resonance spectra were measured at a frequency of 25.15 MHz by means of a Varian HA 100 spectrometer. The n.m.r. system included a probe doubly-tuned to 25.15 and 100 MHz, a voltage controlled generator, a V3512-1 heteronuclear decoupler, and a time averaging computer, which permitted the recording (in frequency sweep mode) of proton-decoupled ^{13}C resonance signals in natural abundance. Methyl iodide-^{13}C

Can. J. Chem. Downloaded from www.nrcresearchpress.com by 210.87.254.42 on 09/05/12
For personal use only.

(about 90% enriched; Merck, Sharpe and Dohme, Montreal, Quebec), contained in a coaxial capillary, furnished the internal reference "lock" signal. Chemical shifts are reported relative to benzene, which produces its resonance signal 147.9 p.p.m. (3720 Hz) downfield from the methyl iodide reference signal. (Since ^{13}C chemical shifts frequently are reported relative to carbon disulfide, it may be noted that the corresponding value for the latter relative to methyl iodide is 213.1 p.p.m. (5370 Hz).) Resolution was 0.1 p.p.m. or better. The probe temperature was $55° \pm 5$ °C, the operating temperature of the instrument.

The authors are grateful to Dr. P. G. Farrell and D. M. Mackie for helpful discussions, and to the Pulp and Paper Research Institute of Canada and the National Research Council of Canada for generous support. R. Simoneau kindly assisted in the recording of spectra.

1. D. M. Grant and E. G. Paul. J. Amer. Chem. Soc. **86**, 2984 (1964).
2. G. W. Buchanan, D. A. Ross, and J. B. Stothers. J. Amer. Chem. Soc. **88**, 4301 (1966).
3. D. K. Dalling and D. M. Grant. J. Amer. Chem. Soc. **89**, 6612 (1967).
4. D. M. Grant and B. V. Cheney. J. Amer. Chem. Soc. **89**, 5315 (1967).
5. B. V. Cheney and D. M. Grant. J. Amer. Chem. Soc. **89**, 5319 (1967).
6. B. V. Cheney. J. Amer. Chem. Soc. **90**, 5386 (1968).
7. E. L. Eliel, N. L. Allinger, S. J. Angyal, and G. A. Morrison. *In* Conformational Analysis. Interscience, 1967. p. 53–62, and p. 356.
8. P. C. Lauterbur. J. Amer. Chem. Soc. **83**, 1838, 1846 (1961).
9. J. B. Stothers. Quart. Rev. **19**, 144 (1965).
10. J. M. Sichel and M. A. Whitehead. Theor. Chim. Acta, **5**, 35 (1966).
11. T. Yonezawa, I. Morishima, and H. Kato. Bull. Chem. Soc. Japan, **39**, 1398 (1966).
12. G. W. Buchanan, J. B. Stothers, and S. Wu. Can. J. Chem. **47**, 3113 (1969).
13. H. J. Reich, M. Jautelat, M. T. Messe, F. J. Weigert, and J. D. Roberts. J. Amer. Chem. Soc. **91**, 7445 (1969).
14. K. von Auwers. Ann. 84, 420 (1920); N. L. Allinger. Exper. **10**, 328 (1954).
15. L. D. Hall and L. F. Johnson. Chem. Commun. 509 (1969).
16. A. S. Perlin and B. Casu. Tetrahedron Lett. 2921 (1969).
17. D. E. Dorman and J. D. Roberts. J. Amer. Chem. Soc. **92**, 1355 (1970).
18. A. S. Perlin, B. Casu, and H. J. Koch. Can. J. Chem. This issue.

Erratum: New nitrochalcones. IX

T. Széll and I. Sohár
Department of Applied Chemistry, University of Szeged, Szeged, Hungary

Received May 19, 1970

(Ref.: Can. J. Chem. **47**, 1254 (1969))

Canadian Journal of Chemistry, **48**, 2643 (1970)

On page 1254, in the left-hand column, the order of effectiveness of reactants with substituents should read 4-Cl > H and not H > 4-Cl.

In Table II on p. 1256, for compound 12 the yield should read 73 and not 39%, and the melting point 184–185 and not 215–216°.

Can. J. Chem. Downloaded from www.nrcresearchpress.com by 210.87.254.42 on 09/05/12
For personal use only.

Can. J. Chem. Downloaded from www.nrcresearchpress.com by 210.87.254.6 on 09/05/12
For personal use only.

Canadian Journal of Chemistry

Published by THE NATIONAL RESEARCH COUNCIL OF CANADA

VOLUME 48 SEPTEMBER 1, 1970 NUMBER 17

Pyrone studies.[1] Photochemistry of triacetic acid lactone[2]

C. T. BEDFORD, J. M. FORRESTER, AND T. MONEY

Chemistry Department, University of British Columbia, Vancouver 8, B.C.

Received February 27, 1970

The irradiation of triacetic acid lactone in various solvents results in novel rearrangement to β-methylglutaconic acid derivatives. In benzene solution an efficient conversion to β-methylglutaconic acid anhydride occurs while in methanol solution a mixture of products is obtained whose structures represent retention and rearrangement of the original carbon skeleton. Results obtained from irradiation of the corresponding methyl ether of triacetic acid lactone in methanol solution are also described.

Canadian Journal of Chemistry, **48**, 2645 (1970)

In connection with our studies of ring cleavage-aromatization reactions of pyrones and polypyrones (2) we have recently investigated the photolysis of some suitable 2-pyrone systems. 4-Hydroxy-6-methyl-2-pyrone (**3**) (triacetic acid lactone, TAL) and its methyl ether, **12**, were chosen as simple analogs of a series of compounds we wished to study and this paper describes the photochemistry of these compounds in different solvents. Pertinent to this study were the previous results of de Mayo and his colleagues (3) who demonstrated that irradiation of 4,6-dimethyl-2-pyrone (**1**) in methanol solution affords methyl β-acetonylcrotonate (**2**) (see Scheme 1). A keten intermediate, **1***a*, was invoked to explain the formation of **2** although an alternative explanation involving the bicyclic β-lactone **1***b* as intermediate was suggested by Corey and Streith (4). Recent studies by Pirkle and McKendry (5) and by de Mayo and his coworkers (6) support the original view (3) that keten (**1***a*) is an intermediate in this reaction.

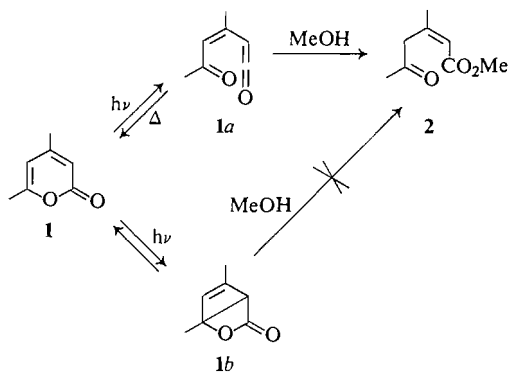

SCHEME 1

At the outset of our investigations we considered that a similar photochemical process would efficiently convert triacetic acid lactone **3** into methyl 3,5-dioxohexanoate (**4***b*), and, by extension, other 2-pyrone systems into poly-β-keto esters of varying chain length (Scheme 2). In our initial experiment irradiation of a 0.1% methanolic solution of TAL for 3 h at room temperature and examination of the reaction mixture by thin-layer chromatography (t.l.c.) showed that complete conversion to a mixture of products had occurred.[3] Careful removal of solvent and steam distillation of an aqueous solution (p*H* 6.3) of the residue afforded a distillate from which methyl 3,5-dioxohexanoate (**4***b*) was isolated as a colorless oil. The nuclear magnetic resonance (n.m.r.) spectrum of this product showed that it existed as a tautomeric mixture of keto **4***b* and enol **4***a* forms. In an alternative work-up of the evaporated reaction mixture crystallization from ether–petroleum ether yielded *cis*-β-methoxycarbonylmethylcrotonic

[1]For earlier parts in this series see ref. 2.

[2]Much of this work has been described in a preliminary communication (1) and presented, in part, at the C.I.C. Conference, Vancouver, B.C., May 1968.

[3]Similar treatment of triacetic acid lactone in the dark gave a quantitative recovery of starting material.

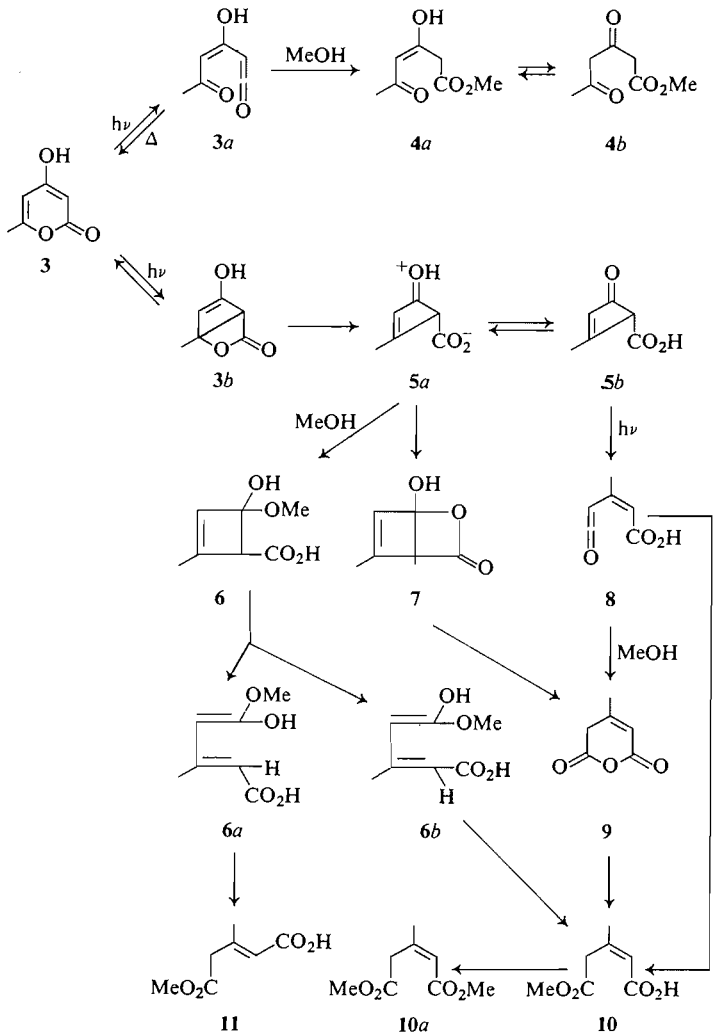

SCHEME 2

acid (**10**) which, on treatment with diazomethane, was converted to the known dimethyl ester, **10***a* (11). A third compound isolated from the crude reaction product was β-methylglutaconic anhydride (**9**) (12) and the yield of photoproducts **9**, **4***a*, *b*, and **10**, based on ultraviolet (u.v.) and n.m.r. spectroscopic analysis, were 27, 13, and 42% respectively.[4] The formation of β-methyl glutaconic anhydride **9** and the corresponding unsaturated acid ester **10** was contrary to our expectations.[5] To explain their formation we have invoked (1) the intermediacy of the bicyclic β-lactone **3***b* since we considered that only an intermediate of this type could adequately explain the skeletal rearrangement which had taken place during the formation of **9** and **10**. Thus initial photoisomerization to the bicyclic-β-lactone **3***b* could occur followed by either of

[4]Other compounds of the crude reaction mixture have proved difficult to isolate in pure form but n.m.r. spectroscopic evidence seems to indicate the presence of *trans*-unsaturated acid ester **11** and β-methylglutaconic acids.

[5]The possibility that anhydride was acting as the precursor of the unsaturated acid ester **10** was investigated by a series of blank experiments. The anhydride was photochemically inert in ether or benzene while in methanol a 15% conversion of anhydride to **10** was noted after 3 h. However, the same conversion was noted in the dark and total conversion was accomplished in 48 h.

Can. J. Chem. Downloaded from www.nrcresearchpress.com by 210.87.254.6 on 09/05/12
For personal use only.

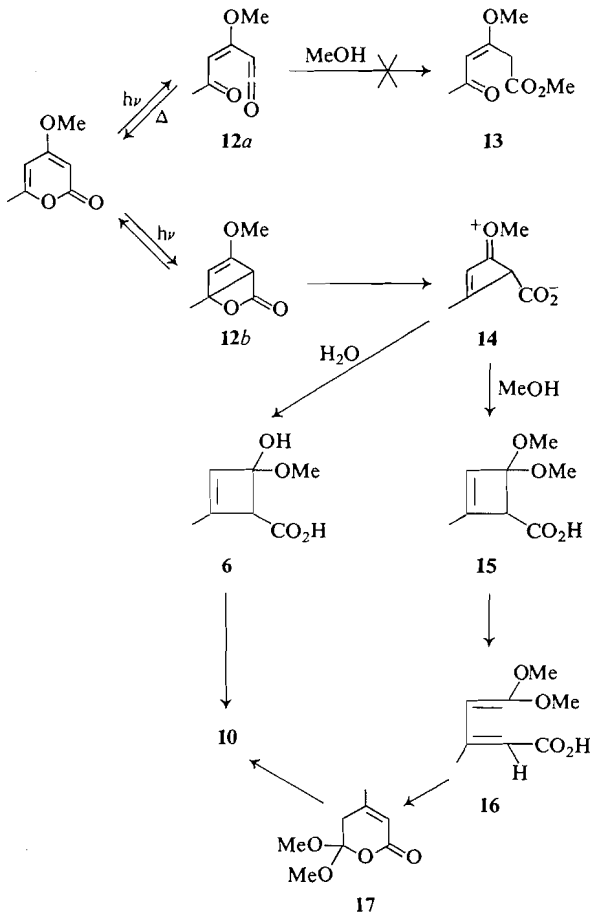

SCHEME 3

two speculative routes to the photoproducts **9** and **10**. In one pathway rearrangement to the cyclobutenone **5***b* could occur followed by photoisomerization to the cisoid keten **8** (7). Intramolecular cyclization or methanol addition would then complete the sequence to **9** and **10** respectively. In the route described above we have assumed that cyclization of the keten **8** to anhydride **9** competes favorably with addition of methanol. Other examples where intramolecular cyclization of ketens has competed favorably with methanol addition have been reported (8). An alternative non-photochemical route from the bicyclic β-lactone **3***b* to **9** and **10** could involve the protonated carboxylcyclobutenone, **5***a*. Intramolecular cyclization to the lactol **7** followed by dealdolization would lead to the anhydride **9**. The formation of the *cis*-unsaturated acid ester **10** could be explained by intermediate formation of the hemiketal **6**. Thermal conrotatory ring opening of **6** (5) could lead to a mixture of *cis*- and *trans*-acid esters, **10** and **11**.[4] An examination of the photochemical behavior of TAL in *dry* benzene or *dry* ether supported the intermediacy of the bicyclic β-lactone. Under these conditions TAL was efficiently converted to β-methylglutaconic anhydride in 85–90% yield (estimated by u.v. and n.m.r. spectra). Intramolecular cyclization of the keten **8** or rearrangement of the lactol **7** can again be cited as reasonable mechanistic routes to the anhydride **9**.

Our photochemical studies were then extended to 4-methoxy-6-methyl-2-pyrone (**12**) (10) in an attempt to increase the yield of straight chain product (see Scheme 3). When a 0.2% solution of **12** in methanol was irradiated for 6 h an almost quantitative conversion to a single photo-

Can. J. Chem. Downloaded from www.nrcresearchpress.com by 210.87.254.6 on 09/05/12
For personal use only.

product occurred. The product was isolated as a colorless oil whose spectroscopic and analytical properties were in agreement with the assigned structure **17**.[6] Chemical support for this structure was obtained when treatment with wet ether resulted in quantitative conversion to the *cis*-acid ester, **10**. The efficient photochemical conversion of methoxypyrone, **12**, to dimethoxypyrone, **17**, in methanol solution differs markedly from the behavior of the corresponding hydroxypyrone, **3**, under identical conditions. In particular there was a notable absence of straight chain ester **13** arising from a keten intermediate. The preferred pathway, therefore, seems to involve the intermediacy of bicyclic β-lactone, **12**,[7] which could be converted to **15** by methanol addition to the zwitterionic intermediate **14**.[8,9] Thermal conrotatory ring opening of **15** followed by intermolecular cyclization would complete the sequence to the photoproduct **17**.

In summary the photochemical behavior of 4-oxygenated 2-pyrone systems (1, 6) differs markedly from the corresponding 4-alkyl (3) or unsubstituted systems (4, 5, and 9). In the latter cases the major reaction products in methanol solution were esters, **2** and **20**, derived by methanol addition to intermediate ketens **1***a* and **19**. No products are formed under these conditions which require the intervention of an intermediate bicyclic β-lactone. The latter compounds (e.g. **1***b*, **21**) can be detected as photoproducts at low reaction temperatures (5, 6) and **21** has been isolated from ether solution (4). Pirkle and McKendry (5) have shown that treatment of the bicyclic lactone **21** with methanol results in the formation of the *cis* and *trans*-acids, **26** and **25**, and have proposed a zwitterionic intermediate, **22**, for this reaction (see Scheme 4). Methanol addition to **22** followed by thermal conrotatory

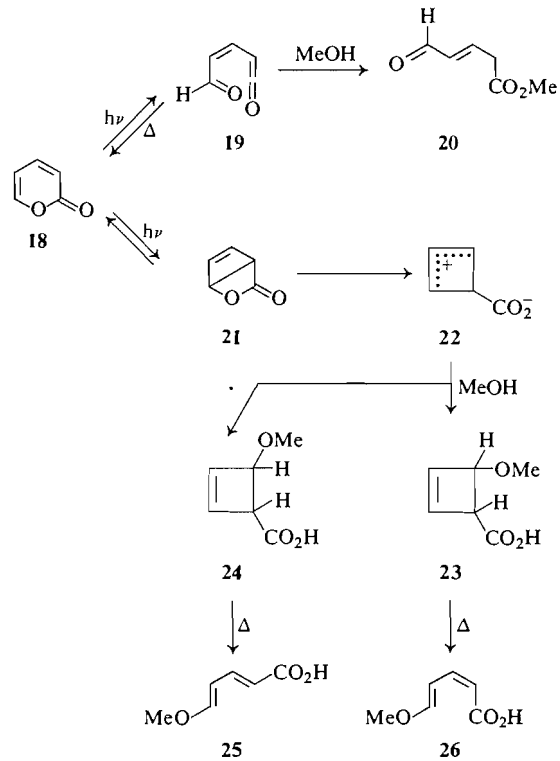

SCHEME 4

ring opening of the *cis* and *trans* cyclobutene acids, **23** and **24**, would yield the products **26** and **25**. In the case of the 4-hydroxy- and 4-methoxy-2-pyrones, **3** and **12**, the presence of the electron-donating oxygen substituent induces irreversible rearrangement of the intermediate bicyclic β-lactone to cyclobutene derivatives which can be converted to branched-chain compounds.[10] Also in these cases this is the major reaction pathway and products formed from the ketens, **3***a* and **12***a*, are either formed in comparatively low yield or not at all.

Experimental

Irradiation experiments were conducted at room temperature under dry nitrogen using an internal water-cooled mercury arc lamp (Hanovia, 450 W) equipped with

[6]At this point in our investigations a private communication from Professor de Mayo described his recent studies on the photochemical behavior of 4-methoxy-6-methyl-2-pyrone (**12**) in water and benzene. We thank Professor de Mayo for informing us of his results prior to publication (6).

[7]Evidence for the formation of bicyclic β-lactone (**12***b*) during low temperature irradiation of pyrone (**12**) has been obtained by de Mayo and his colleagues (6).

[8]Addition of water to the zwitterionic intermediate **14** was also postulated by Professor de Mayo and his colleagues (6) to explain the formation of the *cis*-acid ester **10** from **12** after irradiation in water.

[9]The formation of zwitterionic intermediates during rearrangement of bicyclic β-lactones was first suggested by Corey and Pirkle (9).

[10]Triacetic acid lactone is a naturally occurring pyrone (14) derived by linear condensation of three acetate units. The efficient conversion of this compound to a branched six-carbon unit of the glutaconic acid type may have significance in polyprenoid biosynthesis since it provides an alternative explanation for the derivation of mevalonic acid from three acetate units. We are presently investigating this possibility.

Can. J. Chem. Downloaded from www.nrcresearchpress.com by 210.87.254.6 on 09/05/12
For personal use only.

Can. J. Chem. Downloaded from www.nrcresearchpress.com by 210.87.254.6 on 09/05/12
For personal use only.

a Pyrex filter. Infrared (i.r.) spectra were obtained in $CHCl_3$ or CCl_4 with a Perkin Elmer model 137B spectrometer and u.v. spectra in AR methanol with a Unicam SP 820. The n.m.r. spectra were determined with a Varian A-60 or a Varian HA-100 spectrometer using tetramethylsilane as internal standard (values in τ units, s = singlet, d = doublet, t = triplet, m = multiplet) and the mass spectra with an MS 9 spectrometer. Melting points were determined on a Kofler heating stage and are uncorrected. The t.l.c. results were obtained using silica gel $G^{256+366}$ of 0.25 mm thickness. Solvent A was chloroform – acetic acid (9:1). Petroleum ether had b.p. 60–80°.

Irradiation of Triacetic Acid Lactone (3)

(i) In Methanol

The progress of the irradiation experiments of triacetic acid lactone in dilute (ca. 0.1–0.4%) dry methanol solution was monitored by the disappearance of the light absorption band at λ_{max} 285 nm, and the appearance of three new bands at λ_{max} 217, 276, and 342 nm. In the course of several pilot runs it was found that virtually no triacetic acid lactone remained after 3 to 4 h irradiation and that at least three new compounds had been formed (t.l.c.). The volatility in steam of one of them permitted its isolation and identification. Thus steam distillation of an aqueous solution of the crude photoproduct (5.75 g; from 4.56 g of triacetic acid lactone) yielded a distillate from which a pale yellow oil (525 mg; 9%) was isolated by extraction with ether. Distillation afforded methyl 3,5-dioxohexanoate (**4***b*) as a colorless oil (325 mg); b.p. 65°/11 mm; M^+ *m/e* 158.

Anal. Calcd. for $C_7H_{10}O_4$: C, 53.16; H, 6.33. Found: C, 52.92; H, 6.17.

Spectroscopic data: λ_{max} (MeOH) 276 nm (7650), λ_{max} (0.1 *N* NaOMe/MeOH) 296 nm (19 700); ν_{max} (film) 1740, 1621, 1610 cm^{-1}; $FeCl_3$: wine red. The n.m.r. spectrum (12% in CCl_4) showed that the compound existed as a tautomeric mixture of enol (**4***a*) [τ 7.97 (3H, s), 6.78 (2H, s), 6.35 (3H, s), 4.48 (1H, s), −4.70 (1H, broad s)] and keto (**4***b*) [τ 7.83 (3H, s), 6.57 (2H, s), 6.36 (2H, s), 6.35 (3H, s)] forms.

Repeated fractional crystallization from ether – petroleum ether of the crude photoproduct yielded *cis*-β-carbomethoxymethylcrotonic acid (**10**), m.p. 77–78° (petroleum ether); λ_{max} (MeOH) 213 nm (11 840), λ_{max} (MeOH) (NaOH), 204 nm (11 500); ν_{max} (CCl_4) 1740, 1695, 1650, 1268, 1169 cm^{-1}; τ (CCl_4) 8.00 (3H, d, *J* 1.4 Hz); 6.34 (3H, s), 6.30 (2H, broad d), 4.16 (1H, m), 2–.00 (1H, s).

The third component of the crude photoproduct appeared to be β-methylglutaconic anhydride (**9**) (see below) on the basis of t.l.c. and u.v. (λ_{max} 342 nm) of the reaction solution and this was confirmed by n.m.r. assay of the crude photoproduct, which, as a result of the characteristic and distinguishable chemical shifts of each of the three products, also permitted a direct estimate of the yield of each. The anhydride is solvolyzed slowly by methanol to one of the other photoproducts, β-carbomethoxymethylcrotonic acid (**10**) and thus in order to obtain an optimum value of the yield of anhydride a sample of the irradiated reaction mixture (containing some unreacted triacetic acid lactone) was removed after 2 h and carefully evaporated (25°/12 mm). Since triacetic acid lactone is virtually insoluble in chloroform, an n.m.r. spectrum ($CDCl_3$) of the mixture of photoproducts was readily obtained after treatment of the evaporated reaction mixture with deuteriochloroform. In two runs the figures shown in Table 1 were obtained by n.m.r. assay. If the irradiated solution was set aside for 2 days prior to evaporation of the methanol no anhydride could be detected by n.m.r. or t.l.c. and an increased yield of β-carbomethoxymethylcrotonic acid (70 ± 3%) was observed; the yield (13 ± 3%) of methyl 3,5-dioxo hexanoate was unaffected.

TABLE 1

Yield of photoproducts

Compound	Yield
β-Methylglutaconic anhydride (**9**)	27 ± 3%
β-Carbomethoxymethylcrotonic acid (**10**)	40 ± 3%
Methyl 3,5-diketohexanoate (**4***b*)	13 ± 3%

No reaction was observed when triacetic acid lactone was subjected to similar treatment in the dark.

(ii) In Benzene or Diethyl Ether

Triacetic acid lactone (1 g) was irradiated under nitrogen for 24 h as a stirred suspension in dry benzene (500 ml). Some unreacted starting material (400 mg) was isolated by filtration. The filtrate was evaporated at 30° *in vacuo* to give a pale yellow solid (549 mg), which showed virtually only one spot (R_f = 0.50) by t.l.c. (solvent A), and contained no triacetic acid lactone (R_f = 0.15). Recrystallization of a portion (515 mg) of this crude photoproduct, first from dry ether (20 ml) at −20°, and then from 5% benzene – petroleum ether (200 ml) at 0° gave colorless crystals (394 mg) of β-methylglutaconic anhydride (**9**), m.p. 89–90° (lit. m.p. 90° (13), 86° (12)); M^+ *m/e* 126.

Anal. Calcd. for $C_6H_6O_3$: C, 57.20; H, 4.80. Found: C, 57.35; H, 4.89.

Spectroscopic data: λ_{max} (ether) 218 nm (9850), λ_{max} (MeOH) 222 (10 700), and 340 nm (520), λ_{max} (MeOH) (NaOH) 236.5 (7500) and 342 nm (15 600); ν_{max} ($CHCl_3$) 1800, 1740, and 1660 cm^{-1}; τ ($CDCl_3$) 7.93 (3H, double triplet, *J* = 1.5 Hz, 1.0 Hz), 6.57 (2H, double quartet, *J* = 1.5 Hz, 1.0 Hz), 3.97 (1H, sextet, *J* = 1.5 Hz). The yield of anhydride based on u.v. and n.m.r. spectra of the reaction solution was 85–90%. Essentially identical results were obtained using diethyl ether as solvent.

Methyl β-Carbomethoxymethylcrotonate (10a)

β-Carbomethoxymethylcrotonic acid (21 mg) was treated with ethereal diazomethane to yield methyl β-carbomethoxymethylcrotonate as an oil, the n.m.r., i.r., and u.v. spectra of which were identical with those described by Jackman and Wiley (11).

Methanolysis of β-Methylglutaconic Anhydride (9)

(*i*) β-Methylglutaconic anhydride (50 mg) in dry methanol (50 ml) was set aside at room temperature in the dark for 48 h, and then evaporated at 30° *in vacuo* to yield, as sole product (t.l.c. and n.m.r.), *cis*-β-carbomethoxymethylcrotonic acid (**10**), m.p. 78–80°.

(*ii*) β-Methylglutaconic anhydride (48 mg) in dry methanol (50 ml) was set aside in the dark at room temperature for 3 h. Evaporation at 20° *in vacuo* gave a white

solid, m.p. 63–86°, which, by n.m.r. assay, was a mixture of *cis*-β-carbomethoxymethylcrotonic acid (13 ± 3%) and unchanged β-methylglutaconic anhydride (87 ± 3%). Essentially identical results were obtained by irradiating a solution of β-methylglutaconic anhydride in dry methanol for 3 h.

*Irradiation of 4-Methoxy-6-methyl-2-pyrone (**12**) (**10**) in Methanol*

The progress of the reaction was monitored by the disappearance of the light absorption band at 281 nm and the appearance of a new band at 220 nm. It was found that no triacetic acid lactone methyl ether remained after about 6 h irradiation, and t.l.c. analysis of the product indicated that one photoproduct had been formed. When triacetic acid lactone methyl ether (1.00 g, 7.16 mmole) was irradiated for 6 h, evaporation of the methanol gave a pale yellow oil (1.07 g, 96.5%) which on distillation yielded a colorless oil with spectral properties consistent with the assigned structure (**17**), b.p. 80°/9 mm; M^+ *m/e* 172.

Anal. Calcd. for $C_8H_{12}O_4$: C, 55.82; H, 6.98. Found: C, 55.62; H, 6.88.

Spectroscopic data: λ_{max} (MeOH) 220 nm (9540); ν_{max} (CCl_4) 1730, 1380, 1360, 850 cm^{-1}; τ (CCl_4) 8.02 (3H, s), 7.45 (2H, s), 6.68 (6H, s), 4.33 (1H, s).

*Conversion of Photoproduct **17** to cis-β-Carbomethoxymethylcrotonic Acid (**10**)*

(a) Photoproduct (87.6 mg) was dissolved in wet ether (20 ml) and allowed to stand at room temperature for 24 h. Evaporation to dryness followed by crystallization of the solid residue from petroleum ether yielded *cis*-β-carbomethoxymethylcrotonic acid (**10**).

(b) To a solution used to measure the n.m.r. of photoproduct (~30 mg in 0.4 ml CCl_4) was added water (2 drops). Periodic n.m.r. assay showed gradual disappearance of peaks corresponding to photoproduct **17** and the appearance of peaks attributed to the acid ester **10**. After 3 days reaction was complete and after evaporation to dryness the solid product exhibited an n.m.r. spectrum identical to that of pure acid ester (**10**).

We are grateful to the National Research Council of Canada for generous financial support (NRC A 2267).

1. C. T. Bedford and T. Money. Chem. Commun. 685 (1969).
2. T. Money. Chem. Rev. In press (1970) and references cited.
3. P. de Mayo. Adv. Org. Chem. **2**, 394 (1960).
4. E. J. Corey and J. Streith. J. Amer. Chem. Soc. **86**, 950 (1964).
5. W. H. Pirkle and L. H. McKendry. J. Amer. Chem. Soc. **91**, 1179 (1969).
6. J. P. Guthrie, C. L. McIntosh, and P. de Mayo. Can. J. Chem. **48**, 237 (1970).
7. cf. J. E. Baldwin and M. C. McDaniel. J. Amer. Chem. Soc. **90**, 6118 (1968); O. L. Chapman and J. D. Lassila. J. Amer. Chem. Soc. **90**, 2449 (1968); G. B. Gill. Quart. Rev. **22**, 344 (1968); D. H. R. Barton. Helv. Chim. Acta, **42**, 2604 (1959).
8. R. H. Young and H. Hart. Chem. Commun. 828 (1967); J. Griffiths and H. Hart. J. Amer. Chem. Soc. **90**, 3297 (1968); W. F. Erman. J. Amer. Chem. Soc. **89**, 3828 (1968); L. Barber, O. L. Chapman, and J. D. Lassila. J. Amer. Chem. Soc. **90**, 5933 (1968).
9. E. J. Corey and W. H. Pirkle. Tetrahedron Lett. 5255 (1967).
10. J. D. Bu'Lock and H. G. Smith. J. Chem. Soc. 502 (1960).
11. L. M. Jackman and R. H. Wiley. J. Chem. Soc. 2884 (1960).
12. R. H. Wiley and N. R. Smith. J. Amer. Chem. Soc. **74**, 3893 (1952).
13. N. Bland and J. F. Thorpe. J. Chem. Soc. **101**, 856 (1912).
14. T. M. Harris, C. M. Harris, and R. J. Light. Biochim. Biophys. Acta, **121**, 420 (1966).

Can. J. Chem. Downloaded from www.nrcresearchpress.com by 210.87.254.6 on 09/05/12
For personal use only.

Can. J. Chem. Downloaded from www.nrcresearchpress.com by 210.87.254.40 on 09/05/12
For personal use only.

Interferometric investigation of the polarographic maxima

R. N. O'Brien and F. P. Dieken
Department of Chemistry, University of Victoria, Victoria, British Columbia

Received[1] July 16, 1969

The flow patterns around the mercury drop at the positive and negative polarographic maxima have been investigated by suspensions of activated carbon particles and laser interferometry. The accepted patterns due to Antweiler have been shown to require modification. Specifically the positive maximum flow is a downflowing annulus with a gently upwelling interior below the equator of the drop and the negative maximum flow is a torroidal whorl surrounding the drop. Speeds of particles were recorded by motion picture photography and concentration changes by interferograms.

Canadian Journal of Chemistry, 48, 2651 (1970)

The polarographic maxima have been investigated by many authors. A summary of the phenomena and the postulated explanation for the maxima are reviewed by Heyrovský and Kůta (ref. 1, pp. 440–450). Most of the experimental data on which the explanations for the occurrence of the maxima are based were obtained by conventional methods except the work of Antweiler (2, 3), who used a Schlieren-interferometric system in conjunction with oscilloscopic traces to examine a number of positive and negative maxima. The Schlieren method allowed Antweiler to establish streaming directions and relative areas near the electrode where refractive index changes occur during the maximum.

This work was accomplished by laser interferometry in which concentration changes from the bulk value are observed as perturbations to multiple beam interference fringes which were recorded on 16 mm motion picture film. Quantitative evaluation of the depletion effect around the mercury drop has not yet been accomplished. Qualitative evaluation of the concentration depletion is clearly indicated as a shift or bending of the interference fringes. The direction and velocity of stirring were measured by observing the movement of the solid particles.

Experimental

The experimental apparatus was similar to that described by O'Brien (4). A cylindrical cell was used with a 3 electrode system: a dropping mercury electrode, a silver wire in saturated KCl medium as the counter electrode, and a saturated calomel electrode (s.c.e.) as a reference electrode. The light source was a Spectra-Physics He–Ne gas laser equipped with a spatial filter and beam expanding telescope.

A 0.010 *M* solution of $CuSO_4$ and a 0.032 *M* solution of $CoSO_4$ were used for the positive and negative maximum, respectively. The supporting electrolyte for all experiments was 0.100 *M* $NaClO_4$. No surface active agents were added. All solutions were purged with nitrogen before electrolysis. Bakelite particles were used in the positive maximum studies; however, activated charcoal particles were found to enhance the maximum and were used in all subsequent experiments.

Results

The $CuSO_4$ solution exhibits a typical positive maximum polarogram having a maximum current of 1000 μA compared with a limiting current of 74 μA.

A positive maximum for a reduction process is associated with a downward streaming of the electrolyte; flow from the neck to the base of the drop where it is continued downward from the base of the drop. The general pattern of particle movement shown in Fig. 1 is similar to that reported by Antweiler (5). Each line represents the movement of a single particle with some lines indicating particle position at 1/8 s intervals.

In contrast to the work of Antweiler, our results indicate that the electrolyte does not stream downward from all parts of the drop. The electrolyte streams downward in an annular type structure with an inner diameter formed by the equator of the drop. The outer diameter extends to about 2 mm.

The absence of particles entering the central portion of the annulus is easily seen in Fig. 1. Particle motion in the electrolyte directly beneath the drop indicates an area of weak upward flow, which rapidly decreases in velocity with increasing distance from the base of the drop. Although fewer particles are available for measurement in this smaller volume, a sufficient number were present to establish the upward movement of

[1]Revision received February 26, 1970.

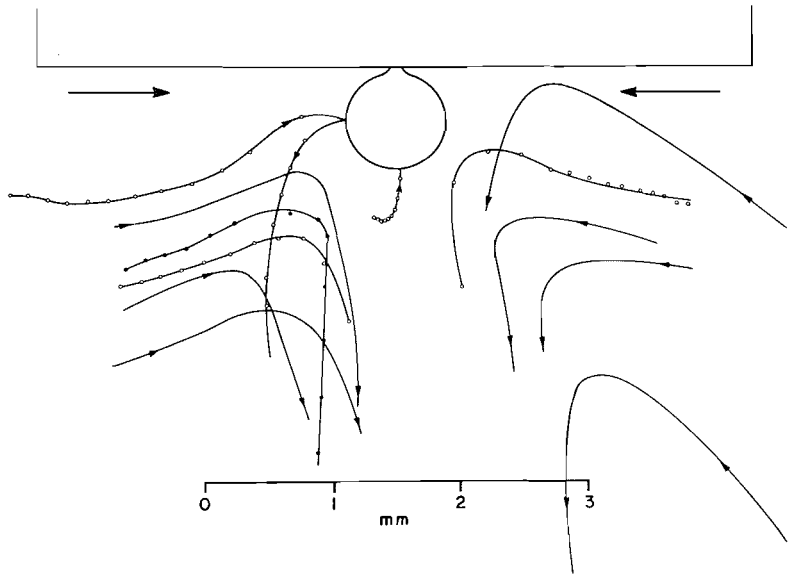

FIG. 1. Typical particle paths during a positive maximum.

TABLE 1
Particle velocity study

Positive maxima			Negative maxima		
Distance from center of electrode (mm)	Particle direction*	Particle velocity (mm/s)	Distance from center of drop (mm)	Particle direction*	Particle velocity (mm/s)
	Particle 1			*Particle 1*	
2.0	+	—	2.1	+	—
1.7	+	0.9	1.9	+	2.0
1.3	+	1.6	1.6	+	2.1
0.9	+	3.2	1.3	+	2.2
1.5	−	8.0	1.0	+	2.2
2.2	−	12.8	0.8	+	2.2
3.1	−	14.7	0.5	+	2.1
	Particle 2			*Particle 2*	
1.9	+	—	1.8	+	—
1.7	+	0.9	1.7	+	0.6
1.4	+	1.1	1.6	+	0.6
1.2	+	1.3	1.5	+	0.9
1.0	+	1.6	1.4	+	1.4
0.9	+	2.2	1.1	+	2.2
0.9	−	2.3	0.9	−	1.9
1.3	−	6.8			

*+ denotes particle moving toward drop, − denotes particle moving away from drop.

electrolyte. Particles located 1 to 2 mm below the center of the drop exhibit a random type motion until they are drawn into the downward flowing annulus.

The existence of particles within this upward flowing region is verified by the limited depth of field 0.1 mm, which would not permit continuous observation of particles moving perpendicular to the picture plane. These particles attain a maximum velocity of 0.8 mm/s at a distance of 0.7 mm from the center of the drop, which is significantly less than the corresponding particles advancing to the drop from the bulk solution (see Table 1).

Can. J. Chem. Downloaded from www.nrcresearchpress.com by 210.87.254.40 on 09/05/12
For personal use only.

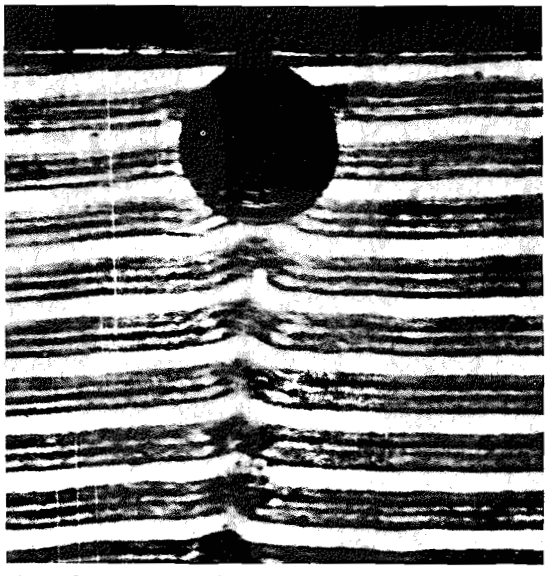

FIG. 2. Concentration gradients around the dropping mercury electrode during the positive maximum.

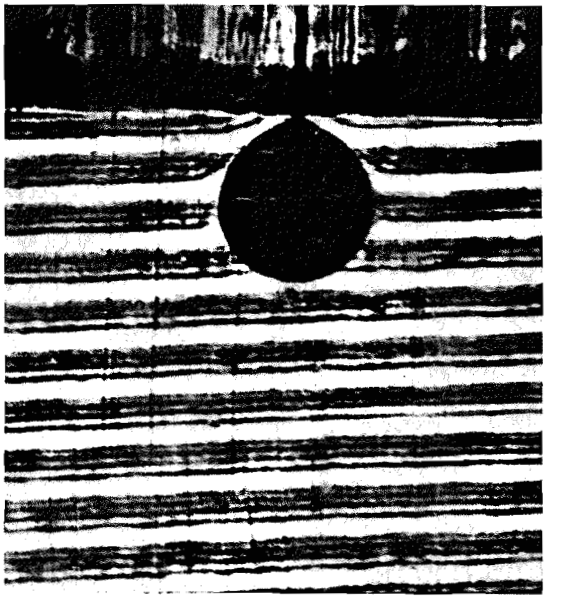

FIG. 3. Concentration gradients around the dropping mercury electrode during limiting current conditions.

Particle velocities shown in Table 1 are calculated from large scale plots of particle movements as a function of distance from the center of the drop. The velocities are not constant and without exception accelerate up to and away from the drop. Only maximum values approach those reported by other authors (ref. 1, p. 442.).

The interference pattern in Fig. 2 shows many of the expected features of the positive maximum. The fringes nearest the capillary remain parallel up to the neck region of the drop. The diffusion layer is destroyed by electrolyte flow. The fringes intersecting the drop below its equator are shifted upward indicating a decrease in refractive

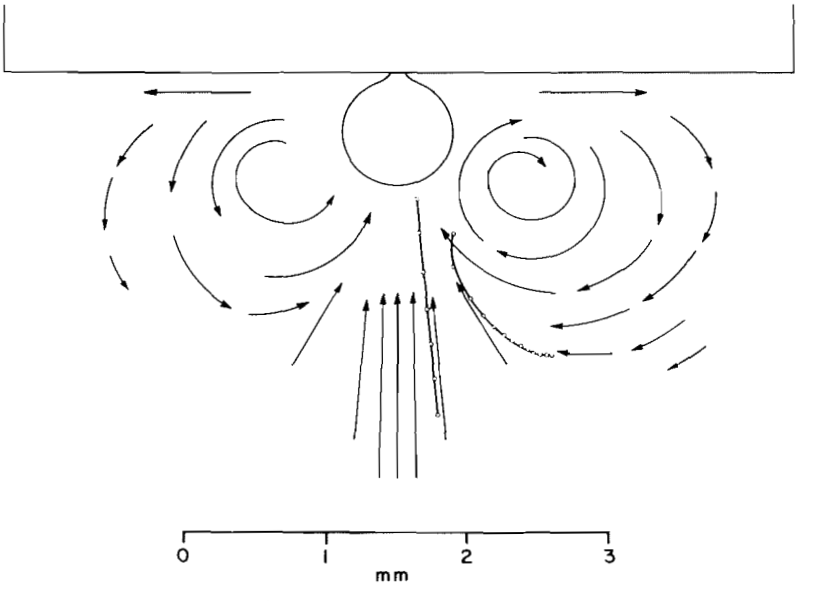

FIG. 4. Typical particle paths during a negative maximum.

Can. J. Chem. Downloaded from www.nrcresearchpress.com by 210.87.254.40 on 09/05/12
For personal use only.

Can. J. Chem. Downloaded from www.nrcresearchpress.com by 210.87.254.40 on 09/05/12
For personal use only.

index and in concentration of depolarizer. The split fringes between the 3rd and 4th bright fringe show progressively larger fringe shifts extending to the shear boundary formed by the equator of the drop. The 4th bright fringe outlines the concentration distribution at the base of the drop. The extension of the depleted region on either side of the drop does not agree with a spherically concentric laminar flow of electrolyte from the neck to the base of the drop at velocities mentioned in Table 1. The fringes below the drop indicate the volume of depleted solution which appears to be trapped within the annulus.

Figure 3 shows a limiting current condition. No maximum is occurring and normal concentration gradients near the neck are apparent from the upward fringe shift.

The 0.032 M solution of $CoSO_4$ shows a normal negative maximum which terminates at about -1.5 V vs. s.c.e. A maximum current – limiting current ratio of 5 was obtained in solutions of suspended charcoal.

A negative maximum for a reduction process is associated with an upward movement of electrolyte towards the bottom of the drop, past the surface to the neck and sideways under the capillary (ref. 1, p. 440). Levich (6) indicates that the streaming takes the form of a horizontal torroid. The flow pattern of particles (Fig. 4) is obtained from the mass movement of finely dispersed activated charcoal particles. The relative lengths of the arrows in the torroid region give a relative velocity of stirring. The center of the vortex moves outward as the drop increases in size. Large particles often become trapped within this vortex and clearly demonstrate a circular type stirring.

Particle velocities measured during the negative

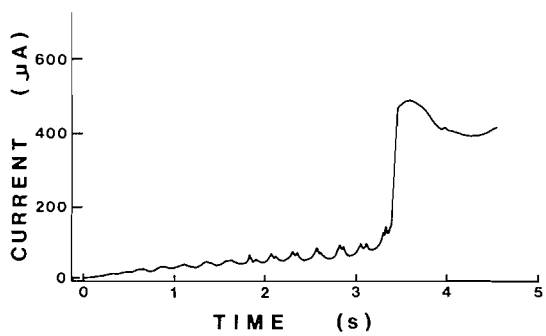

FIG. 5. Current–time curve of a drop experiencing a delayed maximum.

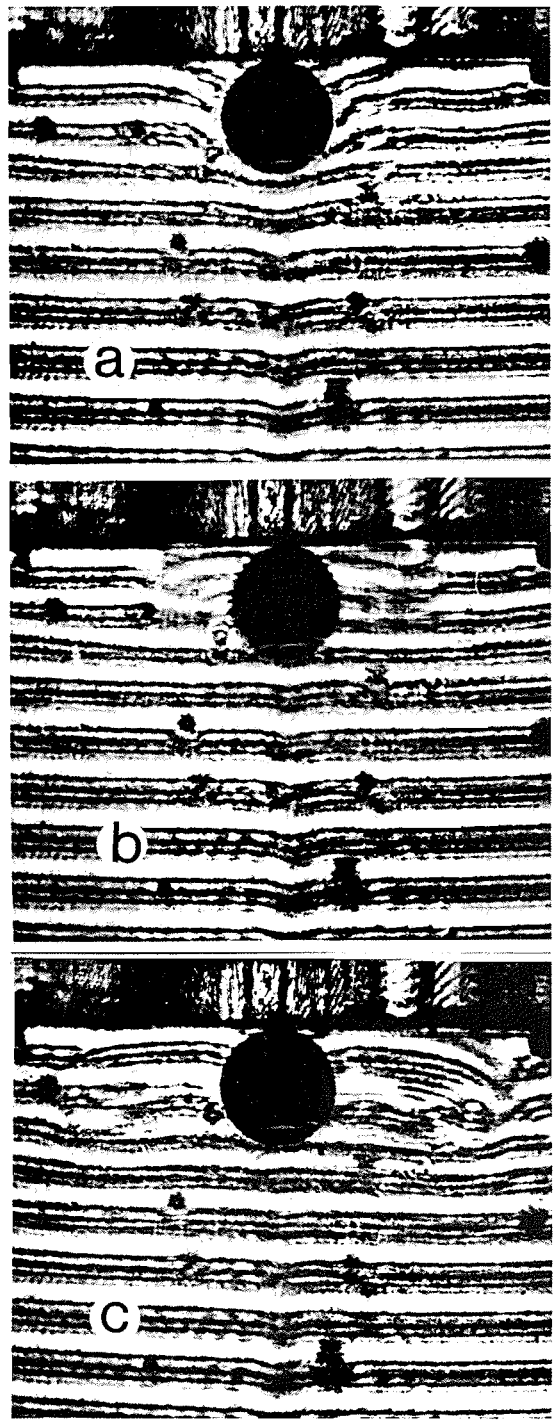

FIG. 6 Events surrounding a negative maximum current rise: (*a*) 3.3 s from fall of previous drop; (*b*) upward movement of solution during vertical current rise; (*c*) fully developed negative maximum.

maximum are reported in Table 1. Particles moving to the base of the drop show a uniform velocity while those trapped in the vortex accelerate upon approaching the drop.

As voltages approach the fall of the negative maximum of Co, the onset of the streaming is irreproducibly delayed. The current–time curve for one such drop is shown in Fig. 5. The events surrounding the initiation of streaming are recorded on film.

Figure 6*a* shows the polarized electrode (drop diameter 0.7 mm) at 3.3 s from the fall of the previous drop. Large concentration gradients are indicated by the prominent downward fringe shift near the surface of the drop. Figure 6*b* shows the streaming associated with the vertical current rise (see Fig. 5). The volume of solution that is moved during the initiation of the maximum is indicated by the fringes that are blurred by the rapid refractive index change which occurs over a diameter of 1.8 mm. The maximum is fully developed in Fig. 6*c*. The horizontal boundary of the torroidal stirring is indicated by the fringe reversal at a diameter of 2.5 mm.

Discussion

The streaming of electrolyte during a positive maximum is not a smooth laminal flow from the neck to the base of the drop. Particle movement indicates that the electrolyte moves downward in the form of an annular ring with an inner diameter created by the equator of the drop. In the region directly below the drop, a weak upward movement of the electrolyte has been observed.

Initiation of the negative maximum during the growth of a polarized drop causes an immediate and distinct streaming of the surrounding electrolyte. The stirring and concentration depletion of solution during a fully developed negative maximum occurs in a volume equal to 25 times the volume of the drop.

The authors suggest that this evidence conflicts with the theory that streaming of the electrolyte during the maxima event is caused by simple streaming of the mercury surface.

The National Research Council of Canada is thanked for generous financial assistance and the award of a scholarship (to F.P.D.).

Interesting and useful conversations with J. Leja are also acknowledged.

1. J. Heyrovský and J. Kůta. Principle of polarography. Academic Press, Inc., New York. 1966.
2. H. J. Antweiler. Z. Electrochem. **43**, 596 (1937).
3. H. J. Antweiler. Z. Electrochem. **44**, 719, 831, 888 (1938).
4. R. N. O'Brien. Rev. Sci. Instrum. **35**, 803 (1964).
5. H. J. Antweiler. Z. Electrochem. **44**, 893 (1938).
6. V. G. Levich. Physicochemical hydrodynamics. Prentice-Hall. New Jersey. 579 (1962).

Can. J. Chem. Downloaded from www.nrcresearchpress.com by 210.87.254.40 on 09/05/12
For personal use only.

Can. J. Chem. Downloaded from www.nrcresearchpress.com by 210.87.254.40 on 09/05/12
For personal use only.

Studies on metal hydroxy compounds. XI. Thermal analyses, decomposition kinetics, and infrared spectra of cadmium and zinc halide derivatives

P. RAMAMURTHY AND E. A. SECCO
Chemistry Department, St. Francis Xavier University, Antigonish, Nova Scotia

Received January 30, 1970

The thermal analyses of $Cd_2(OH)_3X$ type of basic halides reveal that the decomposition occurs via a two-step dehydroxylation pattern, yielding CdOHX as an intermediate product after the initial mode. These results suggest that $Cd_2(OH)_3X$ is an addition compound of the hydroxide and the 1:1 hydroxyhalide, i.e. $Cd(OH)_2 \cdot CdOHX$. Calorimetric measurements along with related enthalpy values for the decomposition reaction are given.

The kinetics of thermal decomposition of the compounds are classified into two main groups: (*i*) two-dimensional contracting plate model equation and (*ii*) first-order rate law.

The infrared spectral data of thirteen Cd and Zn basic halides in the frequency region 4000–250 cm^{-1} are presented with their assignments.

Canadian Journal of Chemistry, 48, 2656 (1970)

Introduction

This study extends our earlier studies on zinc and cadmium compounds (1, 2). While it was in progress Walter–Levy and Groult reported on the preparation and X-ray data of cadmium basic bromides and iodides (3, 4) as well as the thermal analysis of cadmium basic iodides (5).

This paper represents a more comprehensive physico-chemical study which includes differential thermal analysis (DTA), thermogravimetry (TG), calorimetric measurements, decomposition kinetics, and infrared spectra of basic halides represented by the formulas CdOHX, $Cd_2(OH)_3X$, where X = Br, I, Cl along with $Zn_5(OH)_8Br_2$.

Experimental

All the compounds used in this study were prepared in this laboratory by following known methods with slight modification of the procedures to obtain compounds of the highest purity. Brief descriptions are given below; all chemicals used were of reagent grade. Unless otherwise specified, the solid product was filtered and washed thoroughly with distilled H_2O followed by drying overnight at 110 °C.

(*i*) CdOHBr was prepared by digesting CdO with aqueous $CdBr_2$ solution at 80 °C until all the brown oxide disappeared. A two-fold excess of bromide over oxide ensured complete consumption of the oxide (6).

(*ii*) $Cd_2(OH)_3Br$ was prepared by precipitation from 0.25 *M* aqueous $CdBr_2$ solution with NaOH in 2:3 mole ratio (7).

(*iii*) CdOHI was prepared in analogous manner as CdOHBr, using CdI_2 solution (8, 9).

(*iv*) $Cd_2(OH)_3I$ was obtained by precipitation from 0.02 *M* CdI_2 solution with NaOH at p*H* 8.6 (10, 11).

(*v*) $Cd_2(OH)_3Cl$ was prepared in analogous manner as $Cd_2(OH)_3Br$, using $CdCl_2$ solution (12).

(*vi*) $Zn_5(OH)_8Br_2$ was obtained from digestion of ZnO with 60% aqueous $ZnBr_2$ solution. The compound was obtained from the filtrate by adding acetone (13). The precipitate was settled, filtered, washed thoroughly with acetone, and dried overnight at 110 °C.

The identities of the compounds were confirmed by the available X-ray diffraction patterns (3, 4).

The heating curves, calorimetric measurements, and isothermal kinetic traces were recorded on a duPont Thermal Analyzer, d.t.a.-900 and t.g.a.-950 with the appropriate accessories and programming adjustments, as previously described (1, 2, 14, 15).

The heating rate used for most curves was 20 °C/min; slower heating rates of 2 or 4 °C/min were also used in an attempt to resolve overlapping processes. An ambient atmosphere of dry N_2 (Matheson Prepurified Grade with stated impurity of 0.003% oxygen) was maintained during all the experiments.

The infrared spectra of the compounds were obtained by using the standard KBr disc technique in a Perkin–Elmer 521 spectrophotometer.

Results and Discussion

Thermogravimetry

The results of TG are presented in Table 1; the proposed reactions for each compound are those which best fit the observed weight loss. The intermediate and final products were further identified by X-ray diffraction and correlated with DTA curves.

The first step in the decomposition reaction via dehydroxylation for the two types of basic halides can be represented by the following two general equations

$$[1] \quad 2MeOHX_{(s)} \rightarrow MeO_{(s)} + MeX_{2(s)} + H_2O_{(g)}$$

$$[2] \quad 2Me_2(OH)_3X_{(s)} \rightarrow 3MeO_{(s)} + MeX_{2(s)} + 3H_2O_{(g)}$$

The second process in the heating curve of all

TABLE 1
Thermogravimetric analyses

Compound	Step No.*	Temperature range† (°C)	% of total weight loss	
			Observed	Calculated
CdOHBr	1	300–370	4.27	4.30
	2	450–800	69.16	69.31
$Cd_2(OH)_3Br$	1	250–360	7.56	7.59
	2	450–800	45.47	45.83
CdOHI	1	250–320	3.49	3.51
	2	350–700	74.92	74.54
$Cd_2(OH)_3I$	1	200–300	6.68	6.70
	2	350–700	51.88	52.17
$Cd_2(OH)_3Cl$	1	300–400	8.60	8.67
	2	570–750	38.00	38.00
$Zn_5(OH)_8Br_2$	1	180–250	11.49	11.55
	2	280–700	47.03	47.64

*In all cases, first step is due to dehydroxylation and second step is associated with the volatilization of metal halide.
†Onset and terminal temperatures.

TABLE 2
Differential thermal analyses

Compound	Peak No.*	Peak temperature (°C)	Process
CdOHBr	1	380	Dehydroxylation
	2	550	$CdBr_2$ fusion
$Cd_2(OH)_3Br$	1 (doublet)	310, 370	Dehydroxylation via [2*a*] and [2*b*]
	2	550	$CdBr_2$ fusion
CdOHI	1	325	Dehydroxylation
	2	390	CdI_2 fusion
$Cd_2(OH)_3I$	1 (doublet)	280, 320	Dehydroxylation parallel to [2*a*] and [2*b*]
	2	390	CdI_2 fusion
$Cd_2(OH)_3Cl$	1 (doublet)	305, 390	Dehydroxylation parallel to [2*a*] and [2*b*]
	2	680	$CdCl_2 \cdot 2CdO$ decomposition
$Zn_5(OH)_8Br_2$	1	200	Dehydroxylation
	2	390	$ZnBr_2$ fusion

*All endotherms.

compounds involved the volatilization of the appropriate halide resulting from the first step.

Differential Thermal Analysis

The DTA results are given in Table 2 and each compound is discussed in sequence to accompany the TG results.

(i) CdOHBr

Heating up to 650 °C revealed two endotherms corresponding to dehydroxylation and melting of $CdBr_2$. On cooling, the exotherm for the solidification of $CdBr_2$ was observed.

(ii) $Cd_2(OH)_3Br$

Three endotherms were observed with the first two always appearing as a doublet. The doublet consists of a two-step dehydroxylation while the remaining endotherm was due to $CdBr_2$ melting.

The two-step dehydroxylation process described by the reactions

[2*a*] $Cd_2(OH)_3Br_{(s)} \rightarrow CdO_{(s)} + CdOHBr_{(s)} + H_2O_{(g)}$

and

[2*b*] $2CdOHBr_{(s)} \rightarrow CdO_{(s)} + CdBr_{2(s)} + H_2O_{(g)}$

Can. J. Chem. Downloaded from www.nrcresearchpress.com by 210.87.254.40 on 09/05/12
For personal use only.

TABLE 3
Calorimetric results

Compound	Heat of decomposition* (kcal/mole) ΔH of H_2O formed	ΔH of compound decomposed	$-\Delta H_f^0$† (kcal/mole) This work	Literature
CdOHBr	16.90±0.16	8.45±0.08	102.73	108.00
$Cd_2(OH)_3Br$	8.46±0.13	12.70±0.20	220.40	—
			220.39‡	—
CdOHI	17.28±0.16	8.64±0.08	89.40	89.50
$Cd_2(OH)_3I$	10.35±0.03	15.52±0.05	209.64	—
			209.79‡	—
$Cd_2(OH)_3Cl$	10.84±0.13	16.23±0.20	233.13	—
			233.59‡	—
$Zn_5(OH)_8Br_2$	8.72±0.08	34.90±0.32	677.57	—

*All determinations done in duplicate; ΔH values indicate average deviations.
†ΔH_f^0 values of compounds used in our calculations and given in literature column are from Natl. Bur. Stand. Circular No. 500 (1951). The above ΔH_f^0 values were calculated using Kopp's Rule approximation (14).
‡ΔH_f^0 values calculated using indirect approach (Hess' heat of summation rule).

represents a contrast to the analogous copper series compounds (14). The intermediate CdOHBr, along with CdO, was identified by X-ray diffraction after arresting the decomposition at the first part of the doublet.

(iii) CdOHI

Two endotherms observed when heated to 650 °C correspond to dehydroxylation and CdI_2 melting. The exotherm due to CdI_2 freezing was observed on cooling.

(iv) $Cd_2(OH)_3I$

The heating curve was analogous to that for $Cd_2(OH)_3Br$; it consisted of a doublet due to the two-step dehydroxylation with CdOHI as intermediate and the final endotherm due to CdI_2 melting.

(v) $Cd_2(OH)_3Cl$

The decomposition process parallels the two-step dehydroxylation observed for (*ii*) and (*iv*) as is evident by the endotherm doublet and X-ray confirmation. The endotherm at 680 °C arises from the decomposition of the compound $CdCl_2 \cdot 2CdO$ (16).

(vi) $Zn_5(OH)_8Br_2$

The two endotherms are due to dehydroxylation and melting of $ZnBr_2$; the exotherm for $ZnBr_2$ freezing was observed on cooling.

The two-step dehydroxylation pattern observed in the $Cd_2(OH)_3X$ type compounds yielding CdOHX as an intermediate strongly suggests that these compounds be represented by the formula $Cd(OH)_2 \cdot CdOHX$, i.e., an addition type compound of the hydroxide and the 1:1 hydroxyhalide.

Calorimetric Measurements

The calorimetric results along with the related enthalpy values for the decomposition of the above hydroxy-compounds are presented in Table 3 according to the following equations showing the onset and terminal temperatures

$$[3] \quad 2CdOHBr_{(s)} \xrightarrow{350\text{–}410\ ^\circ C} CdO_{(s)} + CdBr_{2(s)} + H_2O_{(g)}$$

$$[4] \quad 2Cd_2(OH)_3Br_{(s)} \xrightarrow{265\text{–}400\ ^\circ C} 3CdO_{(s)} + CdBr_{2(s)} + 3H_2O_{(g)}$$

$$[5] \quad 2CdOHI_{(s)} \xrightarrow{250\text{–}330\ ^\circ C} CdO_{(s)} + CdI_{2(s)} + H_2O_{(g)}$$

$$[6] \quad 2Cd_2(OH)_3I_{(s)} \xrightarrow{230\text{–}328\ ^\circ C} 3CdO_{(s)} + CdI_{2(s)} + 3H_2O_{(g)}$$

$$[7] \quad 2Cd_2(OH)_3Cl_{(s)} \xrightarrow{280\text{–}425\ ^\circ C} 3CdO_{(s)} + CdCl_{2(s)} + 3H_2O_{(g)}$$

$$[8] \quad Zn_5(OH)_8Br_{2(s)} \xrightarrow{155\text{–}220\ ^\circ C} 4ZnO_{(s)} + ZnBr_{2(s)} + 4H_2O_{(g)}$$

Our ΔH_f^0 value for CdOHI is in excellent agreement with the literature whereas a noticeable disparity is evident in the ΔH_f^0 values for CdOHBr.

The ΔH_f^0 values for $Cd_2(OH)_3X$ type compounds were calculated using a direct approach, i.e. reactions [4], [6], and [7], and an indirect approach taking advantage of the intermediate

Can. J. Chem. Downloaded from www.nrcresearchpress.com by 210.87.254.40 on 09/05/12
For personal use only.

TABLE 4
Reaction rate results

Compound	Temperature range (°C)	Number of temperatures	Rate expression	Activation energy E_a (kcal/mole)	log A
CdOHBr	300–350	5	$1-(1-\alpha)^{\frac{1}{2}} = kt$	25.3±2.0	12.5
$Cd_2(OH)_3Br$	250–300	5	$\alpha = kt^n$ [$\alpha<0.4$] $-\ln(1-\alpha) = kt$ [$\alpha>0.4$]	31.5±2.5 18.1±1.5	10.2 6.4
CdOHI	230–280	5	$1-(1-\alpha)^{\frac{1}{2}} = kt$	26.7±2.1	9.9
$Cd_2(OH)_3I$	200–250	5	$-\ln(1-\alpha) = kt$	22.5±2.0	9.7
$Cd_2(OH)_3Cl$	310–350	5	$-\ln(1-\alpha) = kt$	38.5±2.5	14.0

CdOHX. By the latter approach the following relationships were used

[*a*] $2Cd_2(OH)_3X_{(s)} \rightarrow 3CdO_{(s)} + CdX_{2(s)} + 3H_2O_{(g)}$ (ΔH_a)

[*b*] $2CdOHX_{(s)} \rightarrow CdO_{(s)} + CdX_{2(s)} + H_2O_{(g)}$ (ΔH_b)

Subtracting [*b*] from [*a*] and dividing the difference by 2, we obtain

[*c*] $Cd_2(OH)_3X_{(s)} \rightarrow CdO_{(s)} + CdOHX_{(s)} + H_2O_{(g)}$ ($\Delta H_c = (\Delta H_a - \Delta H_b)/2$)

Hence, ΔH_f^0 of $Cd_2(OH)_3X$ is easily evaluated; these values are designated in Table 3 by the symbol ‡. The excellent agreement of the ΔH_f^0 values obtained by both methods confirms the internal consistency of the calorimetric data.

The column of values for ΔH per mole of H_2O formed for the CdOHX series indicates a decreasing trend, CdOHCl → CdOHF → CdOHI → CdOHBr. This trend suggests that the substitution of Cl in $Cd(OH)_2$ strengthens the Cd—OH bond to a greater degree than does either of the substituents F, I, or Br. Furthermore, this column also reveals that the higher hydroxyhalide compounds possess lower values than their 1:1 analogues, i.e. MeOHX.

Reaction Kinetics Data

The experimental α, t data for the decomposition reactions were processed through a large number of kinetic rate equations. The best linear relations between the experimental data and the known rate expressions over the maximum reaction fraction $\alpha \geqslant 0.8$ for all compounds (except $Cd_2(OH)_3Br$) and over the temperature ranges studied are given in Table 4.

The decomposition rate data of $Zn_5(OH)_8Br_2$ could not be fitted to any known rate expression.

The compounds studied can be classified on the basis of their reaction kinetics into two groups.

(*i*) Phase-boundary control with the kinetic data fitting the two-dimensional contracting plate model equation, viz.

$$1 - (1 - \alpha)^{1/2} = kt$$

where $k = (u/r)$; u, the velocity of movement of an interface and r, the distance or length of particle interface. CdOHBr and CdOHI obey this rate expression.

(*ii*) First-order rate kinetics. The remaining compounds follow this rate expression throughout except $Cd_2(OH)_3Br$, where initial accelerator process obeys a power relationship up to $\alpha = 0.4$,

$$\alpha = kt^n$$

The basis of the power expression has been described by Jacobs and Tompkins (17). The range of values for n is usually 2–6 and in this case n was found to be 2.02–2.36. The non-integral and temperature-dependent nature of n has been interpreted by Thomas and Tompkins (18) in terms of nuclei growth rates dependent on nucleus size.

No dependence of E_a on ΔH is revealed in Tables 3 and 4 nor is there any relationship discernible between the pre-exponential factor A of the Arrhenius equation and E_a.

The pre-exponential A values for first-order rate decomposition kinetics in the solid state have been examined and interpreted by Shannon (19), Cordes (20), and the authors (15).

Infrared Spectral Data

The infrared spectral data of the compounds prepared above along with previously reported derivatives are presented in Table 5.

Can. J. Chem. Downloaded from www.nrcresearchpress.com by 210.87.254.40 on 09/05/12
For personal use only.

Can. J. Chem. Downloaded from www.nrcresearchpress.com by 210.87.254.40 on 09/05/12
For personal use only.

TABLE 5

Infrared absorption band frequencies of Cd and Zn hydroxyhalides*

	Frequency (cm^{-1})												
Assignment	$Cd(OH)_2$	CdOHF	CdOHCl	CdOHBr	CdOHI	$Cd_2(OH)_3Cl$	$Cd_2(OH)_3Br$	$Cd_2(OH)_3I$	$Zn(OH)_2$	ZnOHF	ZnOHCl	$Zn_5(OH)_8Cl_2$‡	$Zn_5(OH)_8Br_2$
ν_{OH}†	3620 (vs) 3500 (mbr)	3400 (vs) 3200 (sh)	3540 (vs)	3500 (vs)	3490 (vs)	3570 (vsbr) 3490 (w) 3400 (w)	3570 (vsbr) 3440 (w)	3560 (vs) 3500 (w) 3400 (sh)	3260 (vs)	3590 (vs) 3400 (vs)	3480 (vs)	3600 (vs) 3590 (vs) 3540 (vs) 3480 (vs)	3570 (vs) 3555 (vs) 3460 (vs) 3440 (vs)
δ_{OH}†	430 (sbr)	975 (s) 940 (s) 845 (s)	770 (w) 735 (s) 715 (w)	753 (s) 706 (s) 683 (s)	738 (s) 680 (s) 665 (s)	750 (w) 675 (s) 600 (w)	700 (w) 620 (s) 600 (w)	700 (sh) 650 (w) 600 (s)	1080 (s) 1025 (s)	1015 (vs) 885 (m) 780 (vs)	850 (vs) 830 (w) 790 (vs) 755 (vs)	1030 (m) 990 (m) 870 (vs) 815 (s) 695 (vs) 620 (m)	980 (m) 870 (m) 810 (m) 690 (vs) 620 (s)
Combination									550 (sh)	515 (mbr)	575 (w) 530 (w)	565 (w) 530 (w)	510 (w)
$\nu_{(MeO)}$ and $\delta_{(XMeO)}$	330 (mbr)	345 (s) 295 (sbr)	335 (s) 285 (sbr)	330 (s) 280 (m)	305 (s) 265 (m)	330 (sbr)	325 (w) 285 (m)	300 (s)	440 (s)	450 (sbr)	430 (m) 380 (mbr)	465 (s) 430 (w) 380 (m)	455 (s) 430 (s) 360 (br) 310 (s)
ν_{Cd-F}		400 (m)											
ν_{Zn-Cl}											325 (mbr)	275 (sbr)	

*vs = very strong; s = strong; m = medium; w = weak; br = broad; sh = shoulder.
†Affected by isotopic (D) substitution.
‡Three very weak bands in the 2930–2330 cm^{-1} frequency region previously reported in ref. 27 have been confirmed to arise from organic impurities acquired during prolonged storage.

The bands assigned to ν_{OH} and δ_{OH} are shifted to lower frequencies on deuteration with the ν_H/ν_D ratio falling in the range 1.33–1.35. The multiple bands assigned to ν_{OH} and δ_{OH} can originate from a variety of Me—O—H bond distances present in the lattice as pointed out by Hartert and Glemser (21). However, the identification of strong bands in the 800–600 cm^{-1} range with librational modes of the OH groups (22) is a distinct possibility especially for the Zn derivatives.

The bands for the Cd derivatives below 400 cm^{-1} and for Zn derivatives below 575 cm^{-1} are unaffected by deuterium substitution. For Cd derivatives, the band in the region 345–300 cm^{-1} is attributed to ν_{Cd-O}, which is concordant with 330 cm^{-1} observed in both $Cd(OH)_2$ and $Cd(OD)_2$ and with 345 cm^{-1} in cadmium metastannate (23). The parallel ν_{Zn-O} assignment is made for the band in the 465–430 cm^{-1} region of the Zn compounds which is in good agreement with ν_{Zn-O} in $Zn(OH)_2$ and ZnO (24).

The band for the Cd derivative located in the 295–265 cm^{-1} frequency range is attributed to O—Cd—X bending which appears consistent with an expected decreasing frequency, from mass considerations, in going from F to I derivatives. The parallel O—Zn—X assignment is made for the 380, 360, and 310 cm^{-1} bands of the Zn derivatives.

On the basis that Coates and Ridley (25) have assigned the Zn—Cl stretching of a number of zinc chloride complexes to the frequency range 330–270 cm^{-1}, we identify the 325 and 275 cm^{-1} bands for the Zn derivatives to the Zn—Cl stretching modes. There is no evidence in our view for the analogous Cd—X stretching modes except for Cd—F at 400 cm^{-1}, occurring in both CdOHF and CdODF. The missing Cd—X stretching frequencies have been observed to occur (26) at 212, 122, and 88 cm^{-1} for X = Cl, Br, and I, respectively; this frequency range is beyond the limits of the infrared facilities available to us.

The bands in the 510–550 cm^{-1} range for the Zn compounds cannot be identified with known similar vibrational modes in comparable Zn compounds. We are compelled, therefore, to speculate that these observed bands may originate from lattice vibrations, librational overtone modes, or combinations of vibrational modes.

The authors are indebted to the National Research Council of Canada for financial support and to Dr. M. Falk, Atlantic Regional Laboratory, Halifax, for providing the infrared facilities.

1. O. K. Srivastava and E. A. Secco. Can. J. Chem. **45**, 579 (1967).
2. O. K. Srivastava and E. A. Secco. Can. J. Chem. **45**, 1375 (1967).
3. L. Walter-Levy and D. Groult. Compt. Rend. **263**, 220 (1966).
4. L. Walter-Levy and D. Groult. Compt. Rend. **265**, 715 (1967).
5. L. Walter-Levy and D. Groult. Compt. Rend. **267**, 310 (1968).
6. W. Feitknecht. Kolloid Z. **92**, 257 (1940).
7. W. Feitknecht. Helv. Chim. Acta, **29**, 1807 (1949).
8. W. Feitknecht. Fortschr. Chem. Forsch. **2**, 670 (1953).
9. W. Feitknecht. Experimentia, **1**, 230 (1945).
10. S. A. Levina and N. F. Ermolenko. Kolloid Zh. **19**, 673 (1957). Chem. Abstr. **52**, 5082*g* (1958).
11. T. Moeller and P. W. Rhymer. J. Phys. Chem. **46**, 477 (1942).
12. A. K. Kirakosyan. Russ. J. Inorg. Chem. 1372 (1962).
13. W. Feitknecht and H. Widemann. Helv. Chim. Acta, **13**, 22 (1930); **26**, 1564 (1943); **26**, 1911 (1943).
14. P. Ramamurthy and E. A. Secco. Can. J. Chem. **46**, 3605 (1968); **47**, 2185 (1969).
15. P. Ramamurthy and E. A. Secco. Can. J. Chem. **47**, 2181 (1969).
16. P. Ramamurthy and E. A. Secco. Can. J. Chem. **47**, 1045 (1969).
17. P. W. M. Jacobs and F. C. Tompkins. Chemistry of the solid state. *Edited by* W. E. Garner. Butterworths Sci. Publ. London. 1955. Chap. 7.
18. J. G. N. Thomas and F. C. Tompkins. Proc. Roy. Soc. London. **A209**, 550 (1951); **A210**, 111 (1951).
19. R. D. Shannon. Trans. Faraday Soc. **60**, 1902 (1964).
20. H. F. Cordes. J. Phys. Chem. **72**, 2185 (1968).
21. E. Hartert and O. Glemser. Z. Elektrochem. **60**, 746 (1956).
22. R. G. Snyder, J. Kumamoto, and J. A. Ibers. J. Chem. Phys. **33**, 1171 (1960).
23. T. Dupuis. Chim. Anal. **50**, 302 (1968).
24. N. T. McDevitt and W. L. Baun. Spectrochim. Acta, **20**, 799 (1964).
25. G. E. Coates and D. Ridley. J. Chem. Soc. 166 (1964).
26. G. Randi. Atti Accad. Naz. Lincei. Rend. Cl. Sci. Fis. Mat. Nat. **41** (3–4), 197–199 (1966); Chem. Abstr. **66**, 120323*s*.
27. O. K. Srivastava and E. A. Secco. Can. J. Chem. **45**, 585 (1967).

Can. J. Chem. Downloaded from www.nrcresearchpress.com by 210.87.254.40 on 09/05/12
For personal use only.

Can. J. Chem. Downloaded from www.nrcresearchpress.com by 210.87.254.42 on 09/05/12
For personal use only.

Titration curves of fulvic acid: the analytical chemistry of a weak acid polyelectrolyte[1]

DONALD S. GAMBLE
Analytical Chemistry Research Service, Research Branch, Department of Agriculture, Ottawa, Canada

Received March 11, 1970

The fulvic acid molecular weight fraction studied has two general types of carboxyl groups, one of which is ortho to phenolic —OH groups. The number of each type per gram of fulvic acid has been measured. The acid ionization equilibrium of each type has been calculated as a function of its degree of ionization in 0.1 *m* KCl at 25.0 °C. In both cases the acid strength decreases with increasing degree of ionization. The sample used shows the potentiometric titration behavior expected of a low molecular weight polyelectrolyte.

Canadian Journal of Chemistry, **48**, 2662 (1970)

Introduction

Fulvic acid is a typical humic material occurring widely in nature (1). It is a low molecular weight, poorly condensed aromatic polymer. Because it is highly substituted with carboxyl groups, an aqueous solution of it constitutes a typical weak acid type of polyelectrolyte. A study of the weak acid behavior of fulvic acid is prerequisite to the calculation of metal ion – fulvic acid complexing equilibria. Because of electrostatic effects on polyvalent molecules and the possibility of configurational changes in polymers, it should not be assumed that acid equivalence point methods developed for monomeric acids are valid for polyelectrolytes. Accordingly, the objectives of the present work are: (*a*) to correlate two or more independent methods of measuring the acid equivalence points of fulvic acid so that dependable, accurate values may be obtained; (*b*) to measure acid ionization equilibria as functions of the degrees of ionization in 0.1 *m* KCl at 25.0 °C; (*c*) to learn the extent to which fulvic acid shows the potentiometric titration properties of a polyelectrolyte.

Schnitzer and co-workers (2–6) used a number of experimental methods to determine the types of functional groups present in fulvic acid. Their techniques included functional group analysis, conductivity, and back titrations, and the selective blocking of functional groups followed by metal ion retention measurements. It is concluded from their evidence that fulvic acid has two general types of carboxyl groups: (*a*) Type I carboxyl groups; these are on the aromatic rings, ortho to phenolic —OH groups and are quite acidic; together with the phenolic functional groups they form bidentate chelating sites for metal ions, (*b*) Type II carboxyl groups; these simply consist of the more weakly acidic carboxyl groups, which are not ortho to phenolic —OH groups.

The following points are pertinent to the polyelectrolyte chemistry of fulvic acid: (*a*) Because of the very irregular polymer structure which contains no identifiable monomer units (1), one must assume, as the most general case, that no two carboxyl groups are inherently chemically identical. (*b*) Since fulvic acid is a low molecular weight polymer fraction, the properties of the carboxyl groups will, in the most general case, depend on molecular weight. (*c*) As neutralization advances to more weakly acidic carboxyl groups, the electrostatic charge accumulating on the polymer molecules will make the carboxyl groups even more weakly acidic. (*d*) Only two acid titration end points can be found experimentally for fulvic acid. (*e*) Each fulvic acid sample taken from a given geographical location will be a unique mixture of the same molecular weight components.

A practical conceptual framework for this system is obtained by adapting the "titration constant" defined originally by Simms (7). This was used for titrations of polyvalent acids having only one end point. Simms described it as being calculated in the same way as would the acid dissociation constant of a monovalent, monomeric weak acid. As an approximation, Simms neglected activity coefficients. Because activity coefficients can deviate from unity by 20 to 25% in 0.1 *m* electrolyte, mass action quotients are

[1]Analytical Chemistry Research Service. Contribution No. 124.

Can. J. Chem. Downloaded from www.nrcresearchpress.com by 210.87.254.42 on 09/05/12
For personal use only.

being evaluated here to avoid this approximation.

Assume that a polymer has a number of carboxyl groups, Type A, which are chemically non-identical but whose acid strengths are so similar as to prevent the appearance of separate titration end points. Following Simms, eqs. [1] and [2] are written for all Type A carboxyl groups

$$[1] \qquad AH \overset{\bar{K}}{\rightleftharpoons} A^- + H^+$$

$$[2] \qquad \bar{K}(\alpha) = \frac{m_A m_H}{m_{AH}} = \bar{\kappa}\left(\frac{\gamma_{AH}}{\gamma_A \gamma_H}\right)$$

where m_H, m_A, m_{AH} and γ_H, γ_A, γ_{AH} are the molality and molal activity coefficient of H^+, all Type A carboxyl groups that are ionized, and all Type A carboxyl groups that are unionized, respectively; $\bar{\kappa}$ is the thermodynamic equilibrium constant, $\bar{K}$ is the mass action quotient corresponding to $\bar{\kappa}$, and α is the mole fraction of Type A carboxyl groups, including mole fraction ionized ($m_A/(m_A + m_{AH})$ = degree of ionization). This must now be related to the components of the mixture. Consider the ith infinitesimal increment of carboxyl groups at a given value of α

$$c_i = m_{A_i} + m_{A_iH}$$

which is equilibrated between the ionized and unionized forms

$$[3] \qquad A_iH \rightleftharpoons A_i^- + H^+$$

$$[4] \qquad K_i(\alpha) = \frac{m_{A_i} m_H}{m_{A_iH}} = \kappa_i\left(\frac{\gamma_{A_iH}}{\gamma_{A_i}\gamma_H}\right)$$

The mass action quotient, K_i corresponds roughly to the dissociation constant which Katchalsky and Spitnik (9) have used for the carboxyl groups of the vth stage of ionization of polymethacrylic acid. Following the practice of Katchalsky and Gillis (10) and of Arnold and Overbeek (18), Bjerrum's electrostatic field effect is here assumed to apply to the ith infinitesimal increment of Type A carboxyl groups. Equation [5] gives this.

$$[5] \qquad \kappa_i = K_i^0\left(\frac{\gamma_{A_i}{}^0\gamma_H}{\gamma_{A_iH}{}^0}\right) e^{-\Delta G_i^e/RT}$$

where ΔG^e is the electrostatic free energy and the superscript "0" refers to the uncharged state of the polymer. In terms of mass action quotients, eq. [5] becomes

$$[6] \qquad K_i(\alpha) = K_i{}^0\Gamma_i e^{-\Delta G_i^e/RT}$$

$$\Gamma_i = (\gamma_{A_i}{}^0\gamma_{A_iH}/\gamma_{A_i}\gamma_{A_iH}{}^0)$$

The total numbers of ionized and unionized carboxyl groups A are given respectively by

$$[7] \qquad m_A = \sum_{i=0}^{k} m_{A_i}$$

$$[8] \qquad m_{AH} = \sum_{i=0}^{k} m_{A_iH}$$

where k = total number of c_i increments. The experimental $\bar{K}$ may now be related to the mass action quotients, K_i, by combining eqs. [2], [4], [7], and [8]. The result is eq. [9].

$$[9] \qquad \bar{K}(\alpha) = \sum_{i=0}^{k} m_{A_iH}K_i \Big/ \sum_{i=0}^{k} m_{A_iH}$$

According to eq. [9], the experimentally observed $\bar{K}(\alpha)$ is an average of the K_i's for all of the k infinitesimal increments, c_i, of Type A carboxyl groups. Fulvic acid samples obtained from the same source should have the same K_i values at a given degree of ionization. They will generally differ, however, in their relative values of the m_{A_iH} factors. Different $\bar{K}$ vs. α curves will therefore be observed experimentally.

The ith infinitesimal mole fraction increment of unionized Type A carboxyl groups is $[\Delta(1-\alpha)]_i = m_{A_iH}/c$ where $c = m_A + m_{AH}$. Dividing the numerator and denominator of eq. [9] by c and substituting from eq. [6]

$$[10] \qquad \bar{K}(\alpha) = \frac{1}{(1-\alpha)} \sum_{i=0}^{k} K_i{}^0\Gamma_i(\alpha)\, e^{-\Delta G_i^e/RT} \times [\Delta(1-\alpha)]^i$$

It is postulated, on the basis of titration results, that the $(K_i^0 - K_{i+1}{}^0)$ intervals are small. The multitude of mass action quotients, K_i, may therefore be replaced by a continuous function

$$[11] \qquad K(\alpha) = K^0\Gamma e^{-\Delta G^e/RT} = \delta m_A m_H/\delta m_{AH}$$

δm_A and δm_{AH} are the infinitesimal concentration increments of carboxyl groups Type A which occur at mole fraction $(1-\alpha)$. The summation of eq. [10] can now be replaced by an integration

$$[12] \qquad \bar{K}(\alpha) = \frac{1}{(1-\alpha)} \times \int_0^{(1-\alpha)} K^0(\alpha)\Gamma(\alpha)\, e^{-\Delta G^e/RT}\, d(1-\alpha)$$

This is finally differentiated.

$$[13] \qquad K(\alpha) = K^0(\alpha)\,\Gamma(\alpha)e^{-\Delta G^e/RT} = -\mathrm{d}[(1-\alpha)\bar{K}]/\mathrm{d}\alpha$$

The K which characterizes any particular infinitesimal increment of Type A carboxyl groups can therefore be calculated from experimental $\bar{K}$ vs. α data by using eq. [13]. This conceptual framework applies separately to the Type I and Type II carboxyl groups, for which $\bar{K}$ becomes $\bar{K}_1$ and $\bar{K}_2$, respectively.

If C_1, C_2, C_H denote the total molality of Type I, Type II carboxyl groups and the molality of the total titratable acid remaining, the material balance equations for C_1, C_2, C_H, and the definitions of $\bar{K}_1$ and $\bar{K}_2$ then combine to give eq. [14]. This is used for calculating $\bar{K}_1$ and $\bar{K}_2$ from the titration data.

$$[14] \qquad C_H = m_a + \frac{C_1 m_H}{(\bar{K}_1 + m_H)} + \frac{C_2 m_H}{(\bar{K}_2 + m_H)}$$

where m_a is the molality of ionized, unneutralized acid, corrected for H_2O ionization equilibrium.

Experimental

(a) Chemicals

Fulvic acid Batch No. 4 was received from Dr. M. Schnitzer's laboratory, in which it was prepared as previously described (2, 3). The ash content was 1.6%. Drying to constant weight at ambient temperature under a stream of cylinder N_2 gave a moisture content of 8.53%. Analyis showed an iron content of 0.337 ± 0.03 mmole g^{-1}. Hansen and Schnitzer (11) have reported that fulvic acid prepared as described has a number-average molecular weight of 951 ± 2%, with narrower fractions of it ranging in weight from 275 to 2110.

H_2O used for the preparation of sample solutions and standards was redistilled under N_2 and found to have a resistance of about 20 megohms.

KCl (Fisher Certified A.C.S. grade crystals) was used as received.

HCl standard solution (0.1 *N*) from Fisher, was of density 3.646 mg/ml at 25 °C.

NaOH 0.01 *N*, NaOH 0.1 *N*, and $Ca(OH)_2$ 0.01 *N* were standardized British Drug Houses volumetric solutions.

KOH (0.1 *N*), Fisher certified reagent, was standardized at 25 °C.

(b) Apparatus

The apparatus consisted of the following: (*i*) Koch 5 ml microburette with "Teflon" stopcock plug. (*ii*) Beckman Research Model p*H* meter; used with Metrohm combination glass/AgCl micro electrode, p*H* range 0 to 11, temperature range 10 to 100 °C. (*iii*) Haake model F-J circulating thermostat, used with a magnetic stirrer. Adjusted to 25.0 °C. (*iv*) Sargent thermometer; Hg-in-glass, total immersion, range 0 to 50 °C; graduations 0.1 °C; − 0.015 correction at 25 °C. Serial No. 580210A. Calibrated by Division of Applied Physics, National Research Council of Canada. (*v*) Impedance Bridge model 290A with a.c. generator and detector model 860A, operating frequency 1 kHz (Electro Scientific Industries of Portland, Oregon) and (*vi*) Leeds and Northrup platinum electrode No. 1072582.

(c) Conductivity Titration Procedure

The conductivity titrations were carried out at ambient temperature with the microburette. The burette error was ± 0.003 ml, and the conductivity error was ± 0.2%.

(d) Acid Standards for Potentiometric Titration Curve

Thirty five acid standard solutions having 0.1 *m* KCl were prepared by weight, under N_2. The H^+ molalities ranged from 4×10^{-3} down to 1×10^{-6} *m*. Activity coefficient data from the literature (12) were used to correct the H^+ concentrations for H_2O ionization.

(e) Potentiometric Titration Procedure

A sample solution of 0.1 g of fulvic acid in 100 g of 0.1 *m* KCl was prepared by weight under N_2. This solution and the acid standards were thermostated overnight at 25.00 ± 0.02 °C. Voltage measurements were made on the standard solutions before the titration, and rechecked afterward. The stirrer was turned off during voltage measurements. All potentiometric measurements were made under N_2 at 25.0 ± 0.1 °C. Burette readings were reproducible to ± 0.003 ml, and the potentiometric measurements from ± 0.5 to ± 1 mV.

Results and Calculations

(a) Conductivity Titrations

The minima seen in Fig. 1 verify the existence of the anticipated first end point corresponding to the Type I carboxyl groups. The other significant features noted in the conductivity curves are

(*1*) The minimum obtained by titration with NaOH is evidently concentration-dependent, and extrapolation to zero fulvic acid concentration indicates an equivalence point value of 3.12 milliequivalents/g ± > 1%. This result is accepted here merely as supporting evidence, since the numerical value obtained in this way is not sufficiently reliable to be used for calculations.

(*2*) The second end point corresponding to total carboxyl groups is given unambiguously by the 0.1 *N* titration curve in Fig. 1, but is scarcely discernible for the more dilute case.

(*3*) The shape of the $Ca(OH)_2$ titration curve precludes the calculation of reliable numerical values for the equivalence points, since speculation about the exact nature of the binding of Ca^{2+} by the polyelectrolyte would be required.

Can. J. Chem. Downloaded from www.nrcresearchpress.com by 210.87.254.42 on 09/05/12
For personal use only.

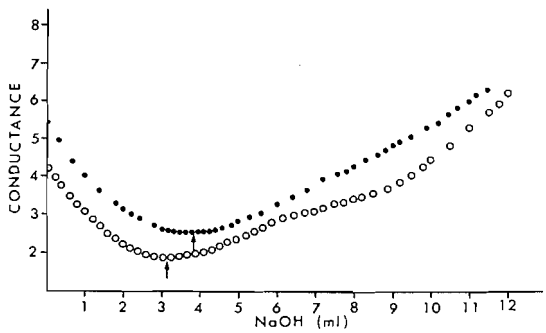

FIG. 1. Conductivity titration of fulvic acid Batch No. 4. ●, 0.01 g/100 g H_2O; mhos × 10^4 vs. ml 0.01 *N* standard NaOH; ○, 0.10 g/100 g H_2O; mhos × 10^3 vs. ml 0.1 *N* standard NaOH.

(b) Potentiometric Titration[2]

Only the second end point corresponding to total carboxyl groups is visible in the potentiometric titration curve, Fig. 2. By using Gran's equivalence point calculation method (13, 14) for the particular case of a weak acid having two end points, however, excellent agreement was obtained with the conductivity values for both end points. Since in Gran's method the calculated value of each equivalence point depends on the other, an iterative calculation was required. This converged after two iterations. The equivalence point data from both titration methods are summarized in Table 1.

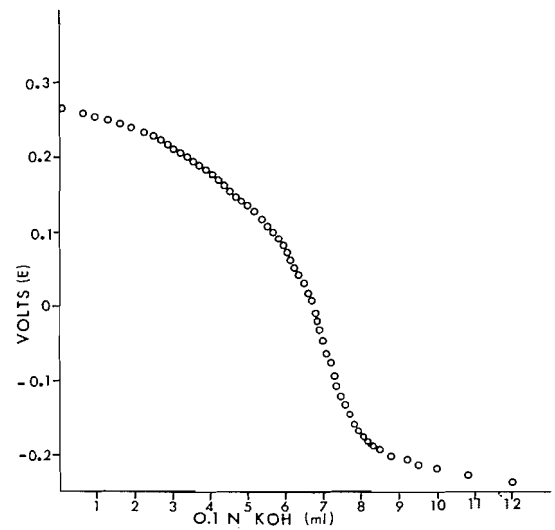

FIG. 2. Potentiometric titration of fulvic acid Batch No. 4. 0.1 g/(100 g 0.1 *M* KCl); 0.1 *N* standard KOH at 25.0 °C.

The acid standards were divided into groups, each of which covered a H^+ molality range of about 10. The concentration vs. voltage data for each group were fitted to a suitable function by the method of least squares. These regression equations were then used to convert the titration voltages into H^+ molalities. This assumes that γ_H is determined primarily by the KCl, and that the KCl concentration is constant. A 100 g of the sample solution contained about 10 milliequivalents of KCl but less than 0.8 milliequivalent of total fulvic acid carboxyl groups. The KCl was diluted less than 6% over the range of the H^+ molality measurements. Using Henderson's equation to estimate the liquid junction potentials of a calomel reference electrode filled with saturated KCl solution, Cannan found that for $0.01 \leqslant M_{KCl} \leqslant 2$, the liquid junction potential ranged up to 4 mV (15). The two assumptions used here are therefore considered to be justified.

(c) The Calculation of $\bar{K}_1$ and $\bar{K}_2$

The method of calculating $\bar{K}_1$ and $\bar{K}_2$ was dictated by two facts: first, they are not constants but instead are decreasing functions of the electrostatic charge on the polyelectrolyte; secondly, the numerical value of each is only moderately dependent on the value of the other. An iterative calculation based on eq. [14] was therefore both necessary and possible. The zero order approximations were obtained by treating several pairs of eq. [14] as simultaneous equations. About five iterations were required to obtain the final values of $\bar{K}_1$ and $\bar{K}_2$. α_1 and α_2 were calculated in the usual way from $\bar{K}_1$ and $\bar{K}_2$, respectively. Tables 2 and 3 show the dependence of $\bar{K}_1$ and $\bar{K}_2$ on their respective degrees of ionization.

(d) The Calculation of K_1 and K_2

K_1 and K_2 were readily calculated according to eq. [13], by fitting $(1 - \alpha)\bar{K}$ vs. α data to a polynomial by the method of least squares. The Fortran IV computer program used for this produced a print-out of the first derivative, that is, $d[(1 - \alpha)\bar{K}]/d\alpha$. Figures 3 and 4 show, as expected, that the acid strengths of both types

[2]Additional data for the potentiometric titration curve of fulvic acid have been deposited. Photo copies may be obtained free of charge upon request, from the Depository of Unpublished Data, National Science Library, National Research Council of Canada, Ottawa, Canada.

Can. J. Chem. Downloaded from www.nrcresearchpress.com by 210.87.254.42 on 09/05/12
For personal use only.

TABLE 1

Titration end point data

End point	$\frac{\text{equivalents acid}}{\text{g. fulvic acid}} \times 10^3$	Titration method	Comment
First	3.159±0.7%	Potentiometric	Value used for subsequent calculations
	3.12 ±|>1%|	Conductimetric	Supporting evidence only; not used for calculations
Second	7.734±0.2%	Conductimetric	
	7.701±0.4%	Potentiometric	
	7.723±0.28%	Weighted average of two values above	Value used for subsequent calculations

TABLE 2

Ionization of Type I carboxyl groups in 0.1 *m* KCl

H^+ molality $\times 10^3$	$\bar{K}_1 \times 10^3$	α_1
2.21 ±1%	4.7 ±10%	0.680±3.1%
2.05 ±1%	4.6	0.691
1.69 ±1%	4.3	0.718
1.46 ±1%	4.1 ±8.5%	0.737±2.1%
1.20 ±1%	3.8	0.761
1.01 ±1%	3.6 ±5.7%	0.782±1.1%
0.805±1%	3.4	0.810
0.624±1%	3.24±2.0%	0.838±0.18
0.508±2%	3.13	0.860
0.427±2%	3.04	0.877
0.351±2%	2.85	0.890
0.271±2%	2.75±2.6%	0.910±0.42
0.222±2%	2.64	0.922
0.197±2%	2.6	0.930
0.170±2%	2.5	0.937
0.141±2%	2.5 ±10%	0.947±0.49%

TABLE 3

Ionization of Type II carboxyl groups in 0.1 *m* KCl

H^+ molality $\times 10^4$	$\bar{K}_2 \times 10^5$	α_2
2.71 ±2%	3.2 ±20%	0.11±17%
2.22 ±2%	3.1	0.12
1.97 ±2%	3.0	0.13
1.70 ±2%	2.9	0.15
1.41 ±2%	2.7 ±18%	0.16±11%
1.15 ±2%	2.6	0.18
0.94	2.4	0.20
0.78 ±2%	2.2	0.22
0.62 ±3.6%	2.1 ±18%	0.25±11%
0.52 ±3.6%	1.9	0.27
0.43 ±3.6%	1.8	0.29
0.37 ±3.6%	1.6	0.31
0.30 ±3.5%	1.5 ±9.1%	0.33± 3.6%
0.25 ±3.6%	1.4	0.36
0.18 ±3.6%	1.2	0.39
0.13 ±3.6%	0.92	0.42
0.084±6%	0.69±9.9%	0.45± 2.5%
0.056	0.52	0.48
0.042±12%	0.43	0.50
0.030	0.33	0.53
0.020	0.25	0.55
0.014±20%	0.19±22%	0.57± 1.1%

TABLE 4

Henderson–Hasselbalch plot for Type II carboxyl groups in 0.1 *m* KCl

α_2	n_2	α_2	n_2
0.11	1.2	0.45	3.2
0.12	1.3	0.48	3.5
0.13	1.3	0.50	3.8
0.15	1.4	0.53	4.0
0.16	1.4	0.55	4.1
0.18	1.5	0.57	4.1
0.20	1.5		
0.22	1.6		
0.25	1.6		
0.27	1.7		
0.29	1.7		
0.31	1.8		
0.33	2.0		
0.36	2.1		
0.39	2.4		
0.42	2.8		

of carboxyl groups decrease with increasing electrostatic charge on the polymer.

(e) Henderson–Hasselbalch Plots

Because polyelectrolytes are generally characterized by Henderson–Hasselbalch plots having slopes greater than unity, such plots were prepared by the least squares procedure for Type I and Type II carboxyl groups. The Type I carboxyl group plot (Fig. 5) is linear as expected but has a rather low slope. Figure 6 and Table 4 show two interesting features for the Type II carboxyl groups. Not only is the Henderson–Hasselbalch plot strongly non-linear, but also the slope increases from rather low values at low α_2 up to the unusually high value of 4.1 at $\alpha_2 = 0.57$.

(f) Experimental Errors

The experimental errors in the equivalence point values of Table 1 were estimated from the reproducibilities of the p*H* meter, burette, and conductivity apparatus. The potentiometric

Can. J. Chem. Downloaded from www.nrcresearchpress.com by 210.87.254.42 on 09/05/12
For personal use only.

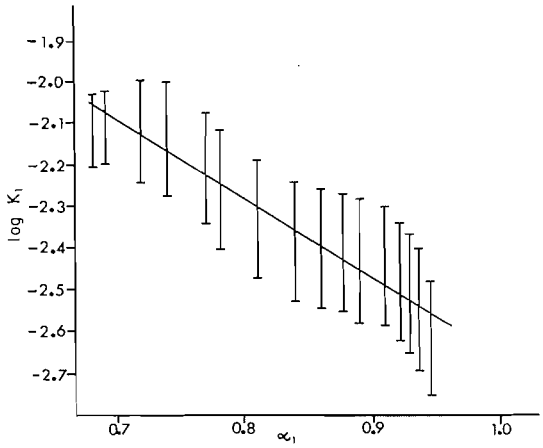

FIG. 3. Ionization of Type I carboxyl groups in 0.1 *m* KCl at 25.0 °C.

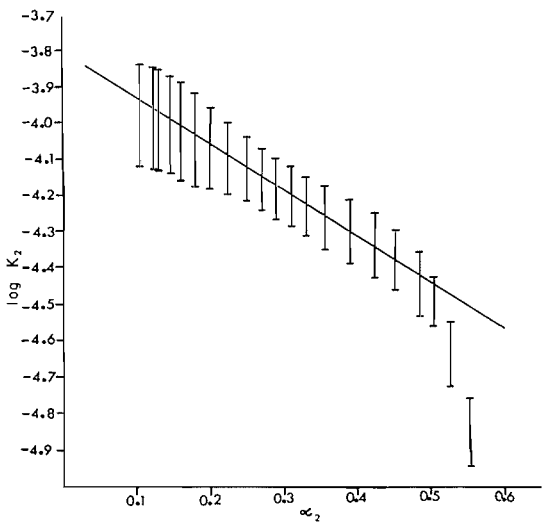

FIG. 4. Ionization of Type II carboxyl groups in 0.1 *m* KCl at 25.0 °C.

errors were also used for estimating the errors in H^+ molality. The errors in the two equivalence points and in H^+ molality were then used with eq. [14] to estimate the errors in $\overline{K}_1$, α_1, $\overline{K}_2$, and α_2. Because K_1 and K_2 were calculated by differentiation, their errors were estimated from the effects of the equivalence point and H^+ molality errors on the slopes of $[1 - \alpha_1]\,\overline{K}_1$ and $[1 - \alpha_2]\,\overline{K}_2$ plots, respectively. Speiser *et al.* (16), Gregor and Frederick (17), and Arnold and Overbeek (18) have all reported experimental errors for titration data that were comparable or greater.

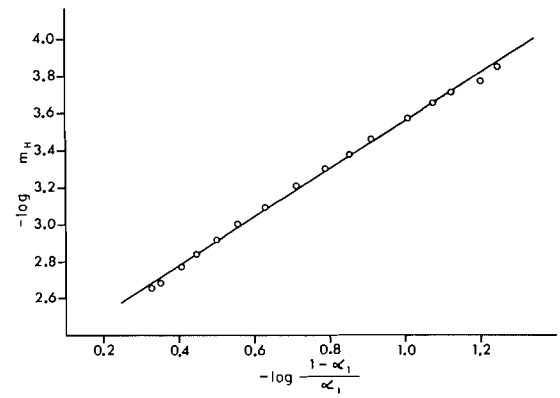

FIG. 5. Henderson–Hasselbalch plot for Type I carboxyl groups in 0 1 *m* KCl at 25.0 °C. $n_1 = 1.29$ $\sigma = \pm 0.02$.

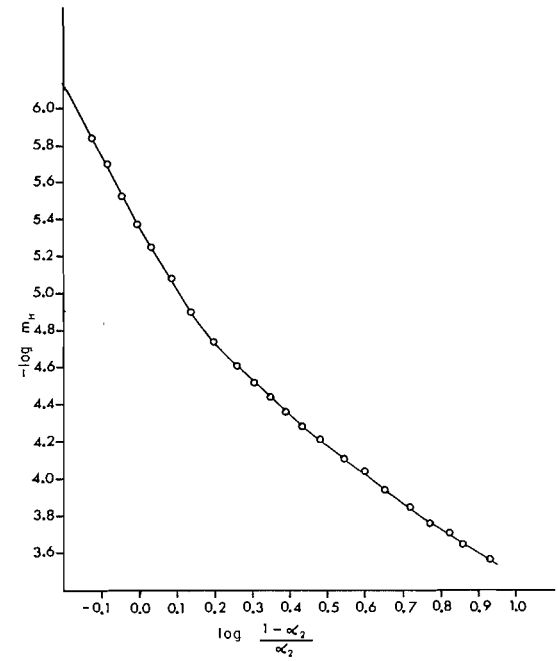

FIG. 6. Henderson–Hasselbalch plot for Type II carboxyl groups in 0.1 *m* KCl at 25.0 °C. $\sigma = \pm 0.008$.

Discussion

Although the conductivity measurements made in the absence of background electrolyte, and potentiometric measurements made in the presence of 0.1 *m* KCl are quite different both in operating principle and in solution conditions, they give equivalence point values in excellent agreement. These results and methods can therefore be accepted with confidence for the case of

Can. J. Chem. Downloaded from www.nrcresearchpress.com by 210.87.254.42 on 09/05/12
For personal use only.

Can. J. Chem. Downloaded from www.nrcresearchpress.com by 210.87.254.42 on 09/05/12
For personal use only.

fulvic acid. The application of Gran's calculation method to the potentiometric titration curve of fulvic acid is also seen to be justified.

Qualitatively, the two ends of the flat Ca^{2+}-binding region correspond to the two equivalence points. Unfortunately, the shape of the curve does not permit unambiguous calculation of their locations.

The Handbook of Chemistry and Physics (19) gives the following dissociation constants for hydroxybenzoic acids and benzoic acid: ortho-hydroxybenzoic acid, $K_a = 1.07 \times 10^{-3}$; metahydroxybenzoic acid, $K_a = 9.7 \times 10^{-5}$; parahydroxybenzoic acid, $K_a = 3.3 \times 10^{-5}$; benzoic acid, $K_a = 6.46 \times 10^{-5}$. A comparison of these with the fulvic acid data supports the conclusion that the Type I carboxyl groups are ortho to phenolic —OH groups.

The chemical and physical properties of low molecular weight polymers, unlike those of high polymers, may depend on molecular weight. The unexpected shape of the Henderson–Hasselbalch plot for the Type II carboxyl groups (Fig. 6, Table 4) therefore raises the question of whether increasingly higher molecular weight fractions of fulvic acid were being ionized as the titration proceeded. This might be answered by titrating a series of narrower molecular weight fractions of fulvic acid.

The experimental errors in $\overline{K}_1$ and $\overline{K}_2$ partly cancel during the calculation of α_1 and α_2. This minimizes the errors that are introduced into the calculation of metal ion complexing equilibria, with the use of these acid dissociation data. On the other hand, Figs. 3 and 4 show the extent to which the calculation of K_1 and K_2 magnifies the experimental errors. This must be explicitly taken into account in any attempt to test a theoretical polyelectrolyte model against the experimentally based K_1 and K_2. For a case in which $\overline{K}$ reduces to K, as for example for idealized polyacrylic acid lacking end group effects, this problem is less severe.

A variety of acid dissociation functions is found in the polyelectrolyte literature. These functions include the polyvalent stepwise constants described by von Muralt (8), and the equilibrium constant described by Katchalsky and Spitnik (9) for the equilibrium of polymer molecules between the $(\nu - 1)$-times ionized and the ν-times ionized states. The function corresponding to the Henderson–Hasselbalch plot, $\beta = [\alpha/(1 - \alpha)]^n m_H$, is also frequently found. The requirements that acid dissociation functions for polyelectrolytes should meet are

(*1*) An experimental acid dissociation function is needed, with which titration data can be tabulated in a simple, direct way. It must be useful for practical applications, such as the calculation of metal ion complexing stability constants.

(*2*) A second acid dissociation function is required for describing individual types of acid functional groups. Its importance is that it has more direct theoretical relevance. For example, it would be the vehicle for comparing a Poisson–Boltzmann calculation for a physical model with the experimental results.

(*3*) A rigorous but tractable relationship between the above two types of acid dissociation functions should be found. The simpler and more useful it is, the better.

Stepwise and other polymer molecule acid dissociation functions are clumsy to use, and of limited relevance. The Henderson–Hasselbalch equation, as frequently used, does not clearly reflect the dependence of polyelectrolyte acid strength on electrostatic charge. The slope of the Henderson–Hasselbalch plot is, however, of considerable value for gaining insight into the nature of the polyelectrolyte. The mass action quotient corresponding to Simms' titration constant fulfills the first requirement almost ideally, and has been adopted here. The $K = K(\alpha)$ developed here for eq. [13] most nearly meets the second requirement. The K_i upon which it is based resembles closely the "K" which Katchalsky and Spitnik[3] defined for the carboxyl groups of $(\nu - 1)$-times ionized and ν-times ionized polymer molecules. Unlike the Katchalsky–Spitnik function, however, its definition is not tied to particular polymer molecules. The relationship between $\overline{K}$ and K expressed in eq. [13] follows directly from their definitions and from the chemical assumptions made for the most general case of an irregular polymer. The feasibility of this relationship for fulvic acid has been demonstrated with both Type I and Type II carboxyl groups. The third requirement has therefore been largely met.

[3]The Katchalsky–Spitnik K should not be confused with their K_ν defined for polymer molecules.

The careful conduct of experiments by Mr. K. A. Wilson has made an important contribution to this work. Mr. D. Hindle has rendered valuable assistance with the experimental work and with preparation of figures.

1. H. KODAMA and M. SCHNITZER. Fuel, **46**, 87 (1967).
2. M. SCHNITZER and J. G. DESJARDINS. Soil Sci. Soc. Amer. Proc. **26**, 362 (1962).
3. M. SCHNITZER and S. I. M. SKINNER. Soil Sci. **96**, 86 (1963).
4. M. SCHNITZER and S. I. M. SKINNER. Soil Sci. **99**, 278 (1965).
5. M. SCHNITZER and J. R. WRIGHT. Trans. 7th Intern. Congr. Soil Sci. II, 112 (1960).
6. M. SCHNITZER and I. HOFFMAN. Geochim. Cosmochim. Acta, **29**, 859 (1965).
7. HENRY S. SIMMS. J. Amer. Chem. Soc. **48**, 1239 (1926).
8. ALEXANDER L. VON MURALT. J. Amer. Chem. Soc. **52**, 3518 (1930).
9. AHARAON KATCHALSKY and PNINA SPITNIK. J. Polymer Sci. **2**, 432 (1947).
10. A. KATCHALSKY and J. GILLIS. Rec. Trav. Chim. **68**, 879 (1949).
11. E. H. HANSEN and M. SCHNITZER. Anal. Chim. Acta, **46**, 247 (1969).
12. HERBERT S. HARNED and WALTER J. HAMER. J. Amer. Chem. Soc. **55**, 2194 (1933).
13. GUNNAR GRAN. Analyst. **77**, 661 (1952).
14. GUNNAR GRAN. Acta Chem. Scand. **4**, 559 (1950).
15. R. KEITH CANNAN. Cold Spring Harbor Symp. Quant. Biol. **6**, 1 (1938).
16. R. SPEISER, C. H. HILLS, and C. R. EDDY. J. Phys. Chem. **49**, 328 (1945).
17. HARRY P. GREGOR and MICHAEL FREDERICK. J. Polymer Sci. **23**, 451 (1957).
18. R. ARNOLD and J. TH. G. OVERBEEK. Rec. Trav. Chim. **69**, 192 (1950).
19. Handbook of chemistry and physics. 44th ed. 1962–1963. Chemical Rubber Publ. Co., Cleveland, Ohio. pp. 1753–1755.

Can. J. Chem. Downloaded from www.nrcresearchpress.com by 210.87.254.42 on 09/05/12
For personal use only.

Can. J. Chem. Downloaded from www.nrcresearchpress.com by 210.87.254.40 on 09/05/12
For personal use only.

π-Bonding between C=C bonds and tin in alkenyltin compounds

H. C. CLARK AND R. C. POLLER
Department of Chemistry, University of Western Ontario, London, Ontario

Received April 6, 1970

The infrared and nuclear magnetic resonance spectra of a number of allyl-, but-3-enyl-, crotyl-, and vinyl-tin compounds in dimethylsulfoxide have been examined and compared with measurements made on solutions in methylene chloride and carbon tetrachloride. It is concluded from the changes which occur in the positions of the ν(C=C) bands and in the chemical shifts of the olefinic protons that there are no significant π-interactions between the d orbitals on tin and the olefinic π-systems.

Canadian Journal of Chemistry, 48, 2670 (1970)

Introduction

In a number of recent publications (1–4) it has been suggested that interactions between the π-electrons of olefinic systems and empty metal d orbitals in organotin(IV) compounds may occur. Such interactions have been postulated intermolecularly, for example between 1,1-diphenylethylene and organotin chlorides (3, 4), or intramolecularly in alkenyltin compounds (1, 2). Since π-complexes of this nature are normally associated with transition metals, unequivocal demonstration of this phenomenon for tin, a main-group metal, is of fundamental importance.

It is known (5) that when an olefin forms a π-complex with a metal such as silver the ν(C=C) band in the free olefin is shifted by ~55 to ~70 cm^{-1} to lower frequencies. Similarly the nuclear magnetic resonance (n.m.r.) signal of an olefinic proton is moved downfield on conversion of an olefin to its silver complex (5). In the present investigation a number of allyl-, but-3-enyl-, crotyl-, and (for comparison) vinyl-tin compounds have been prepared and their infrared (i.r.) and n.m.r. spectra in dimethylsulfoxide solutions compared with the spectra obtained using methylene chloride and carbon tetrachloride solutions. Since sulfoxides interact strongly with organotin compounds, giving solid complexes with organotin halides (6), any π-interactions of the type shown in **1** which are present when the compounds are in the chlorinated solvents should be markedly reduced on dissolution in dimethylsulfoxide when the tin d orbitals become utilized to bond the donor solvent molecules (**2**). Thus changes would be expected to occur in the positions of the ν(C=C) bands and in the chemical shifts of the olefinic protons, the changes being most marked in the organotin dihalides, decreasing in the monohalides and being least in the tetraorganotin compounds as the acceptor strength of tin declines.

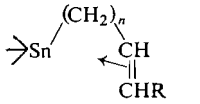

1

in CH_2Cl_2 or CCl_4

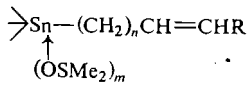

2

in Me_2SO

Experimental

The i.r. measurements were carried out using a Beckman IR 10 spectrophotometer; 20% w/v solutions were used in 0.2 mm cells having KBr windows; solids were measured as Nujol mulls using KBr supports. A Varian A-60 instrument was used for the n.m.r. measurements. Details of the Mössbauer spectrometer have been published elsewhere (7).

Tetraallyltin and divinyltin dichloride were commercial samples. Triphenylallyltin, m.p. 75–76° (lit. (8) m.p. 73.5–74.5°), and trimethylallyltin, b.p. 126–128° (lit. (9) b.p. 128–129°), were made by the Grignard method. Diallyltin dibromide, b.p. 112–116°/4.5 mm (lit. (10) b.p. 77–79°/2 mm), and dicrotyltin dibromide, b.p. 108–112°/0.3 mm (lit. (11) b.p. 104–106°/0.2 mm), were made by the direct method (11) using, respectively, allyl bromide and crotyl bromide together with powdered tin.

But-3-enyltriphenyltin

To a solution of a Grignard reagent made from but-3-enyl bromide (10.0 g) and magnesium (3.6 g) in ether (65 ml) which had been decanted from excess magnesium, was added triphenyltin chloride (14.3 g) in benzene (75 ml). The mixture was heated under reflux for 3 h and excess Grignard reagent was decomposed with saturated ammonium chloride solution. The organic layer was separated, dried over sodium sulfate, the solvent removed, and the resulting solid crystallized from alcohol to give colorless crystals (8.43 g) m.p. 97–102°. The analytical specimen was crystallized from methanol when it had m.p. 98–100°.

Anal. Calcd. for $C_{22}H_{22}Sn$: C, 65.2; H, 5.5. Found: C, 65.3; H, 5.25.

TABLE 1

Infrared spectra of alkenyltin compounds

Compound	ν(C=C) (cm^{-1})*		
	CH_2Cl_2 solution	$(CH_3)_2SO$ solution	Nujol mull
$(CH_2{=}CHCH_2)_4Sn$	1620s	1614s	—
$CH_2{=}CHCH_2SnMe_3$	1622s	1616s	—
$CH_2{=}CHCH_2SnPh_3$	1624s	1620m	—
$(CH_2{=}CHCH_2)_2SnBr_2$	1627s	1625m	—
$(CH_2{=}CHCH_2)_2SnBr_2 \cdot$ 2,2′-bipyridyl	—	—	1621m
$(CH_3CH{=}CHCH_2)_2SnBr_2$	1642m	1638m	—
$(CH_3CH{=}CHCH_2)_2SnBr_2 \cdot$ 2,2′-bipyridyl	—	—	1644w†
$CH_2{=}CHCH_2CH_2SnPh_3$	1638s	1637w	—
$CH_2{=}CHCH_2CH_2Sn(Ph)_2I$	1638s	1635m	—
$CH_2{=}CHCH_2CH_2Sn(Ph)_2Mn(CO)_5$	1637s	1635m	—
$(CH_2{=}CH)_2SnCl_2$	1602m	1588m	—
$(CH_2{=}CH)_2SnCl_2 \cdot 2(CH_3)_2SO$	—	—	1588w

*These measurements are estimated to be accurate to ±3 cm^{-1}.
†This band was broad, and of unexpectedly weak intensity.

But-3-enyldiphenyltin Iodide

To a refluxing solution of but-3-enyltriphenyltin (8.43 g) in chloroform (50 ml) was added, during 3 h, iodine (5.28 g) dissolved in chloroform (150 ml). The resulting pale yellow solution was heated for a further 15 min and then left at room temperature overnight. The solvent was removed under reduced pressure and the remaining oil fractionally distilled under reduced pressure; the main fraction had b.p. 162–168°/0.5 mm (5.65 g).

Anal. Calcd. for $C_{16}H_{17}ISn$: C, 42.2; H, 3.8. Found: C, 42.3; H, 4.0.

But-3-enyldiphenyl(pentacarbonylmanganese)tin

A solution of sodium pentacarbonylmanganese, made by the reduction of dimanganese decacarbonyl (1.128 g) in tetrahydrofuran (25 ml) using excess sodium amalgam and decanted from mercury, was added to a solution of but-3-enyldiphenyltin iodide (2.50 g) in tetrahydrofuran (25 ml). The solution was allowed to stand for 45 min; all operations up to this point were carried out in an atmosphere of nitrogen. The solvent was removed under reduced pressure and the resulting material partitioned between benzene and water. After drying with sodium sulfate, the benzene was evaporated to give an oil (2.92 g). The material was placed in a vacuum sublimation apparatus and heated at 110–120°/0.001 mm when a pale yellow solid (1.9 g), m.p. 26–32°, was collected.

Anal. Calcd. for $C_{21}H_{17}O_5MnSn$: C, 48.2; H, 3.3. Found: C, 48.4; H, 3.4.

Bis(dimethylsulfoxide)divinyltin Dichloride

Divinyltin dichloride (0.488 g) was treated with dimethylsulfoxide (0.34 g, 2.2 equ), the mixture rapidly solidified, and was crystallized from benzene to give the adduct as colorless crystals, (0.56 g) m.p. 86–88°.

Anal. Calcd. for $C_8H_{18}Cl_2O_2S_2Sn$: C, 24.0; H, 4.5; S, 16.1. Found: C, 23.8; H, 4.45; S, 15.9.

Diallyl(2,2′-bipyridyl)tin Dibromide

Diallyltin dibromide (1.00 g) in benzene (5 ml) was treated with a solution of 2,2′-bipyridyl (0.49 g, 1.1 equ) in benzene (5 ml) to give pale yellow crystals, (1.37 g) m.p. 181–182° with decomposition, unchanged on recrystallization from ethanol.

Anal. Calcd. for $C_{16}H_{18}Br_2N_2Sn$: C, 37.2; H, 3.5; N, 5.4. Found: C, 37.3; H, 3.6; N, 5.4.

Dicrotyl(2,2′-bipyridyl)tin Dibromide

Dicrotyltin dibromide (1.00 g) in ethanol (10 ml) was treated with a solution of 2,2′-bipyridyl (0.44 g, 1.1 equ) in ethanol (5 ml) to give the adduct as pale yellow crystals, (1.05 g) m.p. 149–154° with decomposition, raised to 156–160° with decomposition on crystallization from ethanol.

Anal. Calcd. for $C_{18}H_{22}Br_2N_2Sn$: C, 39.7; H, 4.1; N, 5.1. Found: C, 39.3; H, 4.3; N, 5.1.

Results and Discussion

It has been suggested (2) that intramolecular π-interactions are particularly important for allyltin compounds and four examples of this class of compound were examined. Dicrotyltin dibromide was included because the presence of the additional methyl groups should enhance the donor properties of the olefinic bond. Three mono(but-3-enyl)tin compounds were prepared in which the electron acceptor properties of the tin atom were varied by the presence of $SnPh_3$, $Sn(Ph)_2I$, and $SnMn(CO)_5$ groups. (Examination of models of but-3-enyldiphenyl(pentacarbonylmanganese)tin suggested that intramolecular coordination of the butenyl group to manganese, with displacement of carbon monoxide, could occur, but careful heating of the compound, under a variety of conditions, failed to effect this reaction.)

The i.r. results are given in Table 1. If π-bonding of the type shown in **1** occurs then the figures given in the first column should be lower

Can. J. Chem. Downloaded from www.nrcresearchpress.com by 210.87.254.40 on 09/05/12
For personal use only.

Can. J. Chem. Downloaded from www.nrcresearchpress.com by 210.87.254.40 on 09/05/12
For personal use only.

TABLE 2

Chemical shift values (in p.p.m. downfield from Me_4Si) for alkenyltin compounds§

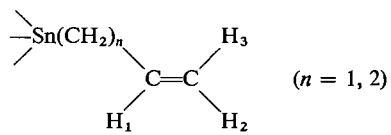

(n = 1, 2)

Compound	δ_1			δ_2			δ_3		
	CCl_4	$(CH_3)_2SO$	Δ_1*	CCl_4	$(CH_3)_2SO$	Δ_2*	CCl_4	$(CH_3)_2SO$	Δ_3*
$(CH_2{=}CHCH_2)_4Sn$	5.87	5.91	−0.04	4.69	4.68	0.01	4.77	4.77	0
$CH_2{=}CHCH_2SnMe_3$	5.86	5.93	−0.07	4.63	4.65	−0.02	4.71	4.73	−0.02
$CH_2{=}CHCH_2SnPh_3$	6.00	6.13	−0.13	4.74	4.78	−0.04	4.89	4.99	−0.10
$(CH_2{=}CHCH_2)_2SnBr_2$	5.98	6.04	−0.06	5.14	4.93	0.21	5.18	4.96	0.22
$(CH_3CH{=}CHCH_2)_2SnBr_2$†	~5.60	~5.50	~0.1	—	—	—	~5.60	~5.50	~0.1
$CH_2{=}CHCH_2CH_2SnPh_3$	5.82	—‡	—	4.88	4.86	0.02	4.94	4.92	0.02
$CH_2{=}CHCH_2CH_2Sn(Ph)_2I$	5.72	5.82	−0.10	4.80	4.94	−0.14	4.86	5.04	−0.18
$CH_2{=}CHCH_2CH_2Sn(Ph)_2Mn(CO)_5$	5.74	—	—	4.81	—	—	4.87	—	—

*$\Delta = \delta[CCl_4] - \delta[(CH_3)_2SO]$.
†In this compound $H_2 = CH_3$; $\delta_{CH_3} = 1.716$.
‡The compound was too insoluble for accurate measurement of the chemical shift for this proton.
§These measurements are estimated to be accurate to ± 0.03 p.p.m.

Can. J. Chem. Downloaded from www.nrcresearchpress.com by 210.87.254.40 on 09/05/12
For personal use only.

than those given in the second column of Table 1. In no case is this observed and the agreement between the two sets of figures is good for all the allyl-, crotyl-, and but-3-enyl-tin compounds. The positions of the ν(C=C) bands in the solid state spectra of the two 2,2′-bipyridyl derivatives (which dissociate in solution) are close to those of the corresponding bands recorded for dimethylsulfoxide solutions of the parent compounds. It was of interest to include divinyltin dichloride in these studies where, although π-interactions of the type shown in **1** are not possible, dπ–pπ character in the Sn—C bonds may be present (12). The i.r. results do not support this view and the lower frequency of the ν(C=C) band for divinyltin dichloride in dimethylsulfoxide may reflect increased importance of resonance structures of the type $Sn—\overset{+}{C}H—\overset{-}{C}H_2$ when the electron density at tin is increased by solvent coordination. The crystalline bis(dimethylsulfoxide) adduct was isolated and shown to have a ν(C=C) band, in the solid-state spectrum, at the same frequency as for the parent dichloride dissolved in dimethylsulfoxide.

The results of the n.m.r. measurements are given in Table 2. But-3-enyldiphenyl(pentacarbonylmanganese)tin reacted with dimethylsulfoxide to form a deep yellow solution; the reaction was slow and i.r. measurements were possible but the n.m.r. spectra in this solvent were not sufficiently well resolved for reliable interpretation. The chemical shift data must be regarded as approximate since they were obtained by a first order treatment of the spectra. However, these results are considered acceptable since changes in chemical shifts are significant rather than absolute values and also, in the case of tetraallyltin, there is good agreement with previous measurements (lit. (12) values: δ_1 5.88, δ_2 4.72, δ_3 4.83 p.p.m.). For π-interactions of the type shown in **1** it is anticipated (5) that the chemical shift of H_1 (see Table 2) would show the greatest downfield displacement on changing the solvent from carbon tetrachloride to dimethylsulfoxide. (The mean downfield change in chemical shift for the H_1 proton of 11 olefins on conversion to their silver complexes was 0.88 p.p.m. (5)). Hence significant positive values of Δ_1 in Table 2 would be indicative of the presence of π-bonding. In fact, the values are all small and are negative in all but one case. Although the chemical shifts of the H_2 and H_3 protons are somewhat less sensitive, they also move downfield when an olefin becomes complexed to a metal (5). However, examination of Table 2 shows that small and negative values are obtained for Δ_2 and Δ_3 for all the compounds except diallyltin dibromide. For this compound $\Delta_2 = 0.21$ and $\Delta_3 = 0.22$; we cannot account satisfactorily for these figures. They do not, however, indicate π-bonding of the C=C group to tin since (*a*) Δ_1 should also be positive, with a value $> \Delta_2$, whereas it is negative and (*b*) the i.r. spectra indicate no interaction.

As a further test the Mössbauer spectrum of allyltriphenyltin was measured at 78 °K where interaction between the d orbitals on tin and the olefinic π-electrons would probably be expected to give quadrupole splitting. A singlet spectrum was observed; the isomer shift was 1.30 mm s^{-1} relative to tin(IV) oxide and the bandwidth was 0.80 mm s^{-1}.

From all these measurements it is concluded that there are no significant π-interactions of the type shown in **1** in any of the alkenyltin compounds examined. These results refer, of course, to the ground-state and do not rule out excited-state π-interactions of the type postulated by Roberts (2).

We thank the National Research Council of Canada for financial support of this work, and Mr. J. N. R. Ruddick of Queen Elizabeth College, University of London, for the Mössbauer measurement.

1. R. M. G. Roberts and F. El Kaissi. J. Organometal. Chem. **12**, 79 (1968).
2. R. M. G. Roberts. J. Organometal. Chem. **18**, 307 (1969).
3. I. P. Gol'dshtein, E. M. Gur'yanova, and K. A. Kocheshkov. Sin. i Svoistva Mononomerov, Akad. Nauk. S.S.S.R., Inst. Neftekhim. Sin., Sb. Rab. 12-oi [Dvenadtsatoi] Konf. po Vysokomol. Soedin. 109 (1962), [Chem. Abstr. **62**, 6501*b*, (1965)].
4. I. P. Gol'dshtein, N. Kh. Faizi, N. A. Slovokhotova, E. M. Gur'yanova, I. M. Viktorova, and K. A. Kocheshkov. Dokl. Akad. Nauk. S.S.S.R., **138**, 839 (1961).
5. H. W. Quinn, J. S. McIntyre, and D. J. Peterson. Can. J. Chem. **43**, 2896 (1965).
6. H. G. Langer and A. H. Blut. J. Organometal. Chem. **5**, 288 (1966).
7. R. C. Poller and J. N. R. Ruddick. J. Chem. Soc. A, 2273 (1969).
8. H. Gilman and J. J. Eisch. J. Org. Chem. **20**, 763 (1955).
9. D. Seyferth and F. G. A. Stone. J. Amer. Chem. Soc. **79**, 515 (1957).
10. K. V. Vijayaraghavan. J. Indian Chem. Soc. **22**, 135 (1945).
11. K. Sisido and Y. Takeda. J. Org. Chem. **26**, 2301 (1961).
12. D. J. Blears, S. S. Danyluk, and S. Cawley. J. Organometal. Chem. **6**, 284 (1966).

Can. J. Chem. Downloaded from www.nrcresearchpress.com by 210.87.254.42 on 09/05/12
For personal use only.

Oxidation of hydrocarbons. II. Kinetics of the oxidation of *p*-toluenesulfonic acid by potassium permanganate[1]

DONALD G. LEE AND BRIAN E. SINGER[2]
Department of Chemistry, University of Saskatchewan Regina Campus, Regina, Saskatchewan

Received January 19, 1970

The kinetics of the oxidation of *p*-toluenesulfonic acid by aqueous potassium permanganate have been studied in perchloric acid solutions ranging from 0.296 to 3.16 *M* $HClO_4$. Below 1 *M* $HClO_4$ the rate law is found to be, $v = k_3[\text{Arene}][Mn^{VII}]h_0$ while above 2 *M* $HClO_4$ it is $v = k_2[\text{Arene}]h_0$. The values obtained for k_3 and k_2 are $8.09 \pm 0.25 \times 10^{-4}$ and $1.19 \pm 0.13 \times 10^{-7}$ M^{-1} s^{-1} respectively.

Canadian Journal of Chemistry, **48**, 2674 (1970)

Introduction

Although permanganate ion is an extremely useful oxidant for the degradation of alkyl side chains attached to aromatic systems comparatively little work has been directed toward the elucidation of the reaction mechanism (1*a*, 2). The reasons for this probably stem from difficulties involved with the insolubility of most arenes in aqueous solutions which requires that the reaction be studied either in a two phase system or in one to which a cosolvent has been added. In the most thorough investigation reported to date, Cullis and Ladbury employed the latter technique to follow the oxidation of substituted toluenes (3). Using a 54% aqueous acetic acid solution these authors observed that no simple integral kinetic rate law was obeyed throughout the reaction and consequently they were restricted to using initial reaction rates. Their results indicated that the reaction was first order with respect to toluene and with respect to oxidant; however, second order kinetics were not maintained throughout the reaction thus suggesting the probability that the mechanism consisted of a complex sequence of steps.

Although variations in the concentration of acetic acid were found to cause marked changes in the rate of oxidation it was concluded that the principal influence of the solvent was as a source of hydrogen ions. Only a small difference was found in the rate when sulfuric acid and acetic acid were used in various ratios to produce the same p*H*.

The primary isolable products were those which would be obtained from oxidation of the methyl side chain, benzaldehyde and benzoic acid. Formation of these products was accompanied by some ring degradation which the authors attributed to oxidation by manganese species of intermediate 3, 4, 5, or 6 oxidation states.

In a slightly different approach to the study of the mechanism of this reaction we have chosen to investigate the oxidation of a water soluble arene, *p*-toluenesulfonic acid, in aqueous solutions. Use of a water soluble substrate greatly simplifies the kinetic system and allows for a more direct interpretation of the data obtained.

Experimental

Reagents

The water used in making up the following standard solutions was doubly distilled from basic permanganate to insure the removal of organic contamination.

Baker reagent grade potassium permanganate was dissolved in a known volume of purified water and standardized with a sodium oxalate solution of known concentration (4).

Analar analytical reagent grade perchloric acid (>60%) was mixed with the appropriate volumes of doubly distilled water and standardized against a sodium hydroxide solution of known concentration.

Fisher certified reagent grade *p*-toluenesulfonic acid was dissolved in a known volume of purified water and titrated against a standard sodium hydroxide solution.

Kinetic Method

In a typical kinetic experiment stock solutions of *p*-toluenesulfonic acid, perchloric acid, and permanganate ion were first placed in a constant temperature bath at 25.0 ± 0.1°. Then given volumes of perchloric acid and permanganate stock solutions were mixed and allowed to thermostat for an additional 15 min, followed by addition of a definite excess (~ ten-fold) of *p*-toluenesulfonic acid solution. A timer was started and the reaction vessel swirled to insure complete mixing. Three millilitres of this solution were transferred to a glass cuvette and the reaction was followed by observing the

[1]For part I of this series see ref. 15.
[2]NRCC Scholarship holder 1969–1970.

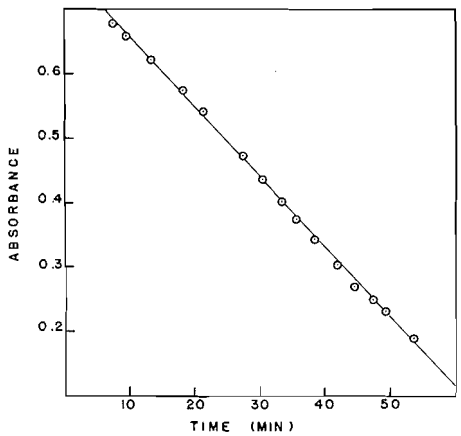

FIG. 1. Zero order plot for the oxidation of 0.0521 *M* *p*-toluenesulfonic acid by 3.03×10^{-4} *M* $KMnO_4$ in 2.53 *M* $HClO_4$.

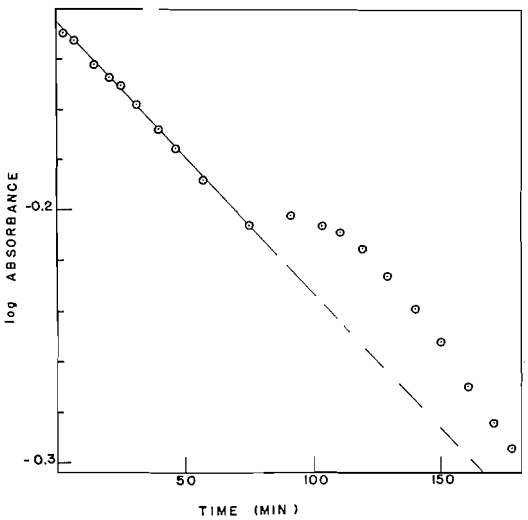

FIG. 2. First order plot for the oxidation of 0.0521 *M* *p*-toluenesulfonic acid by 3.03×10^{-4}*M* $KMnO_4$ in 0.463 *M* $HClO_4$.

disappearance of permanganate ion with time at 529 mμ using a Unicam model SP500 Series 2 Spectrophotometer fitted with a constant temperature cell compartment. The extinction coefficient of permanganate was found at the point of maximum absorbance to be 2435.

Under highly acidic conditions (2 *M* $HClO_4$ or greater) straight lines were obtained from a plot of absorbance against time indicating that the order with respect to permanganate is zero. As Fig. 1 indicates good plots were obtained up to 80% of the reaction. It was also found possible to duplicate these rates with good precision using an iodometric method to titrate unreacted oxidant (1*b*).

Under less acidic conditions the kinetic rate plots were complicated by the insolubility of one of the products, MnO_2 (1*c*). The deposition of MnO_2 interferes with both the spectrophotometric and titrimetric methods of determining the concentration of $KMnO_4$. A typical plot is shown in Fig. 2. The initial deviation from a straight line corresponds to the visible appearance of MnO_2 in the solutions. Obviously such plots cannot be used to establish the kinetics of the system and we were thus forced to resort to the use of initial reaction rates.

Wherever appropriate the data were analyzed by a least squares technique with the aid of an IBM 1130 computer.

Results

The results of this investigation clearly indicate that the rate law for the oxidation of *p*-toluenesulfonic acid by $KMnO_4$ is dependent on acidity. It is convenient to discuss the establishment of the rate law under conditions of "low" acidity (1 *M* $HClO_4$ or less) and "high" acidity (2 *M* $HClO_4$ or greater) separately.

The Rate Law under Conditions of "Low" Acidity ($HClO_4$ < 1 M)

As Fig. 2 clearly indicates it is not possible to establish the order of the reaction with respect to permanganate from an analysis of the integral rate plots. Consequently, the initial reaction rates were determined under conditions of constant acidity and concentration of *p*-toluenesulfonic acid but with variable concentrations of $KMnO_4$ (5). As Fig. 3 indicates a plot of log (initial rate) against log [$KMnO_4$] gave a straight line of approximately unit slope indicating that the reaction is first order in permanganate. In subsequent reactions the assumption was then made that the order with respect to $KMnO_4$ under conditions of low acidity was unity and the

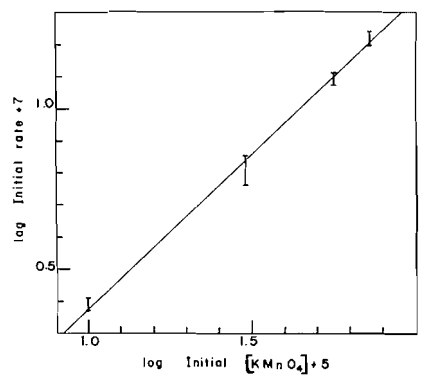

FIG. 3. Plot of log (initial rate) against log (initial permanganate concentration) for the oxidation of 0.0521 *M* *p*-toluenesulfonic acid in 0.517 *M* $HClO_4$.

Can. J. Chem. Downloaded from www.nrcresearchpress.com by 210.87.254.42 on 09/05/12
For personal use only.

Can. J. Chem. Downloaded from www.nrcresearchpress.com by 210.87.254.42 on 09/05/12
For personal use only.

pseudo first order rate constants were obtained by plotting log absorbance against time over the first 25% of reaction. Reasonably reproducible results (usually within ±6%) were obtained in this way. Apparently MnO_2 remains in solution (and thus does not interfere with the spectroscopic measurements) until a certain minimum concentration has been attained.

In a second series of experiments the acidity of the solution was varied from 0.292 to 1.04 M $HClO_4$ while the initial concentrations of $KMnO_4$ and *p*-toluenesulfonic acid were maintained at 3.03×10^{-4} and 5.21×10^{-2} M respectively. A plot of the logarithm of the pseudo first order rate constants against H_0 (6) gave a straight line of near unit slope thus indicating that the reaction is subject to acid catalysis. This fact is also indicated by the constancy of the values for $\log k_1 + H_0$ given in the last column of Table 1.

Finally, the pseudo first order rate constants were measured under conditions of constant acidity but variable *p*-toluenesulfonic acid concentration to determine the order with respect to the reductant. The results are presented in Table 2. The approximate constancy of the k_2 values obtained through division of the pseudo first order rate constants by reductant concentration indicates that the reaction is also first order in *p*-toluenesulfonic acid.

Hence the rate law for this reaction in solutions of low acidity is, $v = k_3[MnO_4^-]\,[\text{Arene}]h_0$, with the value of k_3 being $8.09 \pm 0.25 \times 10^{-4}$ $M^{-2}\,s^{-1}$.

The Rate Law under Conditions of "High" Acidity ($HClO_4 > 2$ M)

The good straight lines obtained when absorbance is plotted against time clearly indicate that the reaction is zeroth order with respect to oxidant under these conditions (Fig. 1). Attempts to plot the data in other forms such as log absorbance against time resulted in lines with a definite curvature.

The effect of varying the acidity of the reaction medium is apparent from the data reported in Table 3. The fact that this reaction, under conditions of both low and high acidity, appears to be first order with respect to the Hammett acidity function, h_0, may be fortuitous. There is evidence that the protonation of arenes does not follow this function (7), and while little is known about the protonation behavior of oxy anions there is no reason to suspect that such a reaction would follow a simple Hammett acidity relationship (1*d*). In fact it has been discovered that this function is completely satisfactory only for reactions which involve protonation of primary amines; even the protonation of tertiary amines does not conform exactly (8). Hence as far as the oxidation of arenes is concerned, it may well be that the apparent first order dependence is the result of several compensating factors. However, it is obvious that the over-all reaction is subject to acid catalysis.

For determination of the order with respect to

TABLE 1

Variation of k_1 with perchloric acid concentration under conditions of low acidity*

$[HClO_4]$ (M)	H_0	$k_1(s^{-1}) \times 10^5$†	$\log k_1 + H_0$
0.296	0.15	2.57 ± 0.02	−4.44
0.463	0.04	3.88 ± 0.09	−4.37
0.517	0.00	4.12 ± 0.05	−4.39
0.693	−0.12	4.79 ± 0.08	−4.44
1.042	−0.33	8.65 ± 0.04	−4.39

*p-Toluenesulfonic acid concentration = 0.0521 M; temperature = 25.0 ± 0.1°.
†The errors quoted are the probable deviation of the mean for three to six runs (14).

TABLE 2

Variation of k_1 with concentration of *p*-toluenesulfonic acid under conditions of low acidity*

[Arene] (M)	$k_1(s^{-1}) \times 10^5$†	$k_2 = k_1/[\text{Arene}]$ ($M^{-1}\,s^{-1}$)
0.0260	2.08 ± 0.03	8.00×10^{-4}
0.0383	3.22 ± 0.06	8.41×10^{-4}
0.0521	4.12 ± 0.05	7.92×10^{-4}
0.0765	6.52 ± 0.14	8.52×10^{-4}
0.0979	8.40 ± 0.13	8.59×10^{-4}

*$HClO_4$ = 0.517 M; temperature = 25.0 ± 0.1°.
†The errors quoted are the probable deviation of the mean for three to eight runs (14).

TABLE 3

Variation of k_0 with perchloric acid concentration under conditions of high acidity*

$[HClO_4]$ (M)	H_0	$k_0(M\,s^{-1}) \times 10^8$†	$\log k_0 + H_0$
2.00	−0.87	4.54 ± 0.01	−8.21
2.47	−1.08	6.80 ± 0.05	−8.25
2.53	−1.12	7.36 ± 0.04	−8.25
3.16	−1.40	13.5 ± 0.2	−8.27

*p-Toluenesulfonic acid concentration = 0.0521 M; temperature = 25.0 ± 0.1°.
†The errors quoted are the probable deviation of the mean for three to six runs (14).

TABLE 4

Variation of k_0 with *p*-toluenesulfonic acid concentration under conditions of high acidity*

[Arene] (M)	$k_0(M\,s^{-1}) \times 10^8$†	$k_1 = k_0/$ [Arene] (s^{-1})
0.0260	4.32 ± 0.02	1.66×10^{-6}
0.0383	6.70 ± 0.11	1.75×10^{-6}
0.0521	7.36 ± 0.04	1.41×10^{-6}
0.0765	11.7 ± 0.1	1.53×10^{-6}
0.0979	14.8 ± 0.1	1.51×10^{-6}

*$HClO_4$ = 2.53 M; temperature 25.0 ± 0.1°.
†The errors quoted are the probable deviation of the mean for three to five runs (14).

reductant the reaction was studied under conditions of constant $KMnO_4$ and $HClO_4$ concentrations but with variable concentrations of *p*-toluenesulfonic acid. All runs give a first order rate constant of $1.58 \pm 0.17 \times 10^{-6}\ s^{-1}$ when k_0 is divided by the concentration of *p*-toluenesulfonic acid indicating that the reaction is first order in reductant (see Table 4).

Hence the rate law under conditions of "high" acidity appears to be, $v = k_2[\text{Arene}]h_0$, with the value of k_2 being $1.19 \pm 0.13 \times 10^{-7}\ M^{-1}\ s^{-1}$.

While introduction of the sulfonate group into the structure of the arene greatly simplifies the kinetic procedure it has the converse effect on the ease with which the products of the reaction can be separated. To date we have been unable to identify the products because they all seem to have physical properties very similar to each other and to unreacted starting material. However in a related study it was observed that when an excess of toluene was oxidized under conditions of both low and high acidity (0.5 and 3.0 M $HClO_4$) the mixtures obtained from both experiments were nearly the same with benzaldehyde being the major product (9).

Discussion

All of the results presented in the preceding section can be incorporated reasonably well into reaction Scheme 1.

$$\text{Arene} + H^+ \underset{k_{-1}}{\overset{k_1}{\rightleftharpoons}} \text{Arene—}H^{\oplus} \xrightarrow[k_2]{Mn^{VII}} \text{Products}$$

SCHEME 1

Assuming that Arene—H^+ is a reactive intermediate and applying steady state assumptions the rate law for this system is expressed by eq. [1].

$$[1] \qquad \frac{-\,d[KMnO_4]}{dt} = \frac{k_1k_2[\text{Arene}][Mn^{VII}]h_0}{k_{-1} + k_2[Mn^{VII}]}$$

If we assume at "low" acidity that $k_{-1} \gg k_2[Mn^{VII}]$ then eq. [1] can be approximated by eq. [2] and the rate is first order in $KMnO_4$ as

$$[2] \qquad \frac{-\,d[KMnO_4]}{dt} = \frac{k_1k_2[\text{Arene}][Mn^{VII}]h_0}{k_{-1}}$$

required by the experimental results. Conversely if under conditions of "high" acidity we assume that $k_{-1} \ll k_2[Mn^{VII}]$ eq. [1] is then best approximated by eq. [3] and the reaction is zeroth order with respect to Mn^{VII} as is observed.

$$[3] \qquad \frac{-\,d[KMnO_4]}{dt} = k_1[\text{Arene}]h_0$$

The inversion in the relative magnitude of k_1 and $k_2[Mn^{VII}]$ on going from low to high acidity may be associated with the development of a more active form of the oxidant, permanganic acid ($HMnO_4$), at high acidities. Permanganic acid is known to be a more vigorous oxidant than permanganate ion and its formation would increase k_2. It should be noted however, that the pK_a of $HMnO_4$ is about -2.25 indicating that the bulk of the oxidant is still in the form of MnO_4^- at 2 M $HClO_4$ ($H_0 = -0.78$) (10). However, if $HMnO_4$ is a much more vigorous oxidant a large concentration need not be generated to increase k_2 markedly.[3]

Banoo and Stewart have recently reported similar results for the acid catalyzed oxidation of benzhydrol with permanganate (11). They also found that the rate of reaction was zeroth order in permanganate at high acidities and first order in oxidant at low acidities. As an explanation for these observations they suggested that the reaction at high acidities involved a slow step in which the diarylcarbonium ion was formed followed by a rapid oxidation step. Conclusive evidence for this mechanism was supplied by the

[3]A referee has suggested that the active oxidant under highly acidic conditions might be MnO_3^+ which could form via $MnO_4^- + 2H^+ \rightarrow MnO_3^+ + H_2O$. Alternatively the active oxidant could be a manganese species of intermediate 3, 4, 5, or 6 oxidation state. The evidence to distinguish between these possibilities is scarce, but most of the available data suggests that $HMnO_4$ and *not* MnO_3^+ is the species formed when permanganate protonates (see ref. 1*e*).

Can. J. Chem. Downloaded from www.nrcresearchpress.com by 210.87.254.42 on 09/05/12
For personal use only.

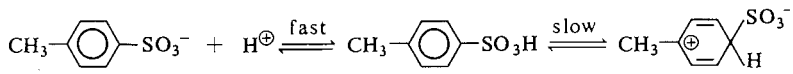

SCHEME 2

observation that the rate of oxidation was equal to the rate of carbonium ion formation.

Similarly it follows, if our suggestions regarding the mechanism of this reaction are correct, that the rate of oxidation under conditions of high acidity should be equal to the rate of protonation of *p*-toluenesulfonic acid. While no direct measurement of this reaction has yet been made a good prototype should be the detritiation of isotopically labelled aromatic systems and it is of interest to note that our k_1 values (Table 3) are of the same order of magnitude as the corresponding rate constants reported for the detritiation of a number of azulene derivatives under similar conditions (12).

It must be recognized that the rate data do not provide any information concerning the identity of the reactant arene or the protonated intermediate which we have designated as Arene—$H^{\oplus}$. However it is instructive (but at the same time highly speculative) to attempt to anticipate the nature of the reaction and its intermediates in greater detail. Since *p*-toluenesulfonic acid is a strong acid it probably exists under the conditions of these experiments as a highly dissociated ion-pair (13). Consequently the substrate is most likely the *p*-toluenesulfonate anion and the protonated arene (Arene—$H^{\oplus}$) would then be neutral *p*-tolüenesulfonic acid. However proton transfers to oxygen are very fast and if protonation is to be the rate determining step it must involve transfer of a proton to carbon. An attractive possibility which is consistent with the available data has been suggested by a referee; the rate determining step could occur intramolecularly via tautomerization of neutral *p*-toluenesulfonic acid (Scheme 2).

In conclusion, it is apparent that the use of *p*-toluenesulfonic acid as a substrate to investigate the oxidation of arenes results in the generation of kinetic data which can be used to define the rate laws for the reaction precisely. However, it leaves unanswered several questions as to the significance of these rate laws with respect to the mechanism of the reaction. Experiments designed to expose certain features of the reaction mechanism are now under way in our laboratories.

The authors are grateful to the National Research Council of Canada for the award of an operating grant (D.G.L.) and a Scholarship (B.E.S.) which supported this work.

1. R. STEWART. *In* Oxidation in organic chemistry, Part A. K. B. Wiberg, *editor*. Academic Press, New York, 1965. (*a*) p. 39, (*b*) p. 15, (*c*) p. 9, (*d*) p. 22, (*e*) p. 22–23.
2. D. G. LEE. *In* Oxidation techniques and applications in organic synthesis. Volume 1. R. L. Augustine, *editor*. Dekker, 1969. p. 36.
3. C. F. CULLIS and J. W. LADBURY. J. Chem. Soc. 555, 1407, 2850 (1955).
4. G. H. AYRES. Quantitative chemical analysis. Harper and Rowe, New York, 1958. p. 397.
5. K. J. LAIDLER. Chemical kinetics. Second edition. McGraw-Hill, New York, 1965. p. 15.
6. K. YATES and H. WAI. J. Amer. Chem. Soc. **86**, 5408 (1964).
7. M. T. REAGAN. J. Amer. Chem. Soc. **91**, 5506 (1969).
8. E. M. ARNETT and G. W. MACH. J. Amer. Chem. Soc. **86**, 2671 (1964).
9. R. J. SCHAFFER. Honors Thesis, University of Saskatchewan, Regina, Saskatchewan, 1970.
10. U. KLANING and M. C. R. SYMONS. J. Chem. Soc. 3269 (1959).
11. F. BANOO and R. STEWART. Can. J. Chem. **47**, 3199 (1969).
12. J. SCHULZE and F. A. LONG. J. Amer. Chem. Soc. **86**, 331 (1964).
13. O. D. BONNER and A. L. TORRES. Chem. Abstr. **63**, 12399*d* (1965). B. J. BERKOWITZ and E. GRUNWALD. J. Amer. Chem. Soc. **83**, 2956 (1961).
14. I. M. KOLTHOFF and E. B. SANDELL. Textbook of quantitative inorganic analysis. Macmillan, Toronto, 1952. p. 271.
15. D. G. LEE and U. A. SPITZER. J. Org. Chem. **34**, 1493 (1969).

Can. J. Chem. Downloaded from www.nrcresearchpress.com by 210.87.254.42 on 09/05/12
For personal use only.

Studies of carbohydrate derivatives by nuclear magnetic double resonance. Part V. Some ^1H–$\{^1H\}$ INDOR experiments[1]

R. BURTON, L. D. HALL, AND P. R. STEINER[2]
Department of Chemistry, The University of British Columbia, Vancouver 8, British Columbia
Received March 16, 1970

A simple modification is described which enables a Varian HA-100 spectrometer to be used routinely for ^1H–$\{^1H\}$ internuclear double resonance experiments. Several examples are given to illustrate the results which may be obtained via this technique, with particular emphasis on carbohydrate derivatives.

Canadian Journal of Chemistry, **48**, 2679 (1970)

Can. J. Chem. Downloaded from www.nrcresearchpress.com by 210.87.254.6 on 09/05/12
For personal use only.

Introduction

For organic substances of low molecular weight it is generally a simple matter to identify and evaluate the spin coupling constants of individual resonances, and thereby obtain evidence concerning the structure of the compound being investigated. Unfortunately, for substances of higher molecular weight it often happens that the proton resonances of particular interest are obscured by the fortuitous overlap of other resonances. This seriously diminishes the effectiveness of the proton nuclear magnetic resonance (^1H n.m.r.) technique as a structural probe.

Although it is often possible to estimate the chemical shift of the "hidden" resonance by a spin-decoupling experiment, this gives no indication of the magnitudes of other couplings in that resonance. In principle it is possible to obtain both the shift and coupling data by a series of spin-tickling experiments, but in practice the amount of time required for these experiments is usually prohibitive. A preferable alternative to either of the above methods is based on the ^1H–$\{^1H\}$ InterNuclear DOuble Resonance (INDOR) technique (4).

In the present paper we describe a trivial modification which enables a Varian HA-100 spectrometer to be used for the measurement of ^1H–$\{^1H\}$ INDOR spectra on a routine basis. Since the many possible applications of the method are best discussed in relation to specific chemical problems, we shall only discuss here a minimum of illustrative examples.

In a conventional frequency-swept double resonance experiment, the magnetic field (H_0) is held constant, while a "decoupling" (ω_2) radiofrequency field is applied within the vicinity of one resonance and its effect is detected by means of a weak "observing" field (ω_1) which is scanned through the rest of the spectrum.

In the INDOR mode of operation, the functions of these two radiofrequencies are effectively interchanged. Again H_0 is held constant, but now "ω_1" is used to monitor a particular transition in the spectrum. Then "ω_2" is scanned through the spectrum; whenever its frequency coincides with a transition which has a connective relationship[3] (5) with the one being monitored, the recorder (ω_1) will show a response.

There are several "mechanisms" whereby INDOR responses can occur and for detailed discussions of these the reader is referred to two review articles (6, 7) and several original papers (4, 8, 9). Suffice for the present discussion to point out that for most systems the observed INDOR responses will either arise predominantly as a result of changes in the populations of various energy levels, or predominantly to changes in the actual energy levels, which are similar to those changes encountered in "spin-tickling" experiments (6, 7). When the strength of "ω_2" is set at a sufficiently low power level, rearrangements of the populations of individual energy levels are detected by "ω_1" as a series of both positive and negative responses; the experiments described later in this paper correspond to this class. Somewhat higher power levels of "ω_2" give responses which correspond primarily to spin-tickling effects, and in this case the recorder shows a series of negative-going peaks only. In practice both of these "mechanisms" may operate simultaneously; fortunately the positions of INDOR responses do not depend on the particular "mechanism" operative.

[1]For previous papers in this series, see refs. 1–3.
[2]Recipient of an NRCC Studentship, 1969–1970.
[3]That is, having an energy level in common.

Can. J. Chem. Downloaded from www.nrcresearchpress.com by 210.87.254.6 on 09/05/12
For personal use only.

Experimental

The basic spectrometer system used for these experiments is a Varian HA-100 instrument, equipped with a high impedance, 12″ magnet.

Conversion to the INDOR mode of operation requires only one minor modification of the V-4354A "lock-box". The "Shim–Normal" switch (S-1309) of this unit is replaced by a 3 position rotary switch, which is wired up according to Fig. 1. When this switch is in the INDOR

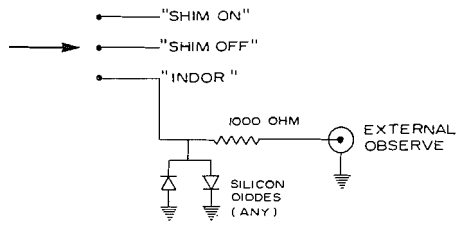

FIG. 1. Modification of switch (S 1309) of the Varian V-4354A unit for INDOR mode of operation.

position the phase detector of the analytical channel receives its reference voltage (ca. 1 V peak to peak) from the external oscillator, via the jack labelled "external observe".

The system interconnections required for the INDOR mode of operation are given in Fig. 2. The amplitude control and phase-shift network we use is a modified version of the unit developed by A. W. Douglas (10).

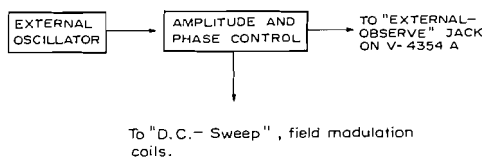

FIG. 2. Block-diagram of the system-interconnections used for the INDOR mode of operation.

INDOR Experiments on 2-Deoxy-D-arabino-hexopyranose in D_2O Solution

Although it should be emphasized that spectrometer calibrations are seldom absolute and that the settings quoted below are unlikely to be optimal ones for other HA-100 spectrometers, these settings should ensure at least a marginal response on a first-run basis, which then can be optimized.

A sample of 2-deoxy-D-arabino-hexopyranose[4] was lyophilized several times with D_2O and then a ca. 30% (w/v) solution was made. A capillary tube containing tetramethylsilane was used to provide the lock signal.

With the spectrometer operating in the frequency-sweep mode the spectrum was recorded and the transition frequencies of the anomeric resonances were measured (±0.1 Hz).

The spectrometer functions were now adjusted as shown in Table 1. The output-frequency of the external oscillator was then set to monitor transition 1 (see Fig. 3).

[4]From Pfanstiehl Laboratories, Waukegan, Illinois.

TABLE 1

Function selection and approximate control settings required for the INDOR mode of operation

Function	Adjustment
V-4311	Attenuator: 26 dB
V-4354A	Switch S-1309: INDOR
	Amplitude of sweep oscillator: 0.6 to 0.8 (as indicated by the dial)
	Sweep-width: 500 Hz
	Frequency response: 0.5
	Spectrum amplitude: maximum
Recorder	Sweep time: 500 s
V-4391	Spin decoupler
External oscillator	10–20 mV (as indicated on scope)

The first scan of the spectrum produced a series of rather broad transitions; small variations in the power output of the "external" and "sweep-oscillators" resulted in a marked increase in the "resolution" of these transitions and in the effective disappearance of several "ghost" transitions (vide infra).

Sucrose octaacetate (2)

A sample of sucrose octaacetate was kindly provided by Dr. J. F. Manville and was used as a ca. 20% (w/v) solution in acetone-d_6.

D-Ribose (3)

The D-ribose[4] was lyophilized several times with D_2O and then made to a ca. 30% (w/v) solution in D_2O, with ca. 30 mg of sodium dimethylsilapentanesulfonate as internal reference.

Results and Discussion

A simple illustration of the effectiveness of the INDOR technique in the carbohydrate area is afforded by the spectra shown in Fig. 3. The normal, H-1 and H-2 resonances of a fully mutarotated solution of 2-deoxy-D-arabino-hexopyranose (**1**) in D_2O solution is given across the center of the figure. The problem is to identify which of the many transitions in the higher-field region correspond to which of the two H_2 resonances. The assignment shown for the H-1 resonances is trivial.

The group of spectra in the upper set of inserts [Fig. 3*A*, *B*, *C*, and *D*] show the effect of monitoring respectively transitions 1, 2, 3, and 4 and then scanning the decoupling field through the region shown. The pair of spectra shown in Fig. 3*A*, *D* serve to identify the positions of all sixteen of the $\beta[H_2]$ transitions. The same data is contained in Fig. 3*B*, *C*. It is interesting to note that some "ghost" responses from the alternate subspectra occur in each of the spectra *A*, *B*, *C*, *D*. This is

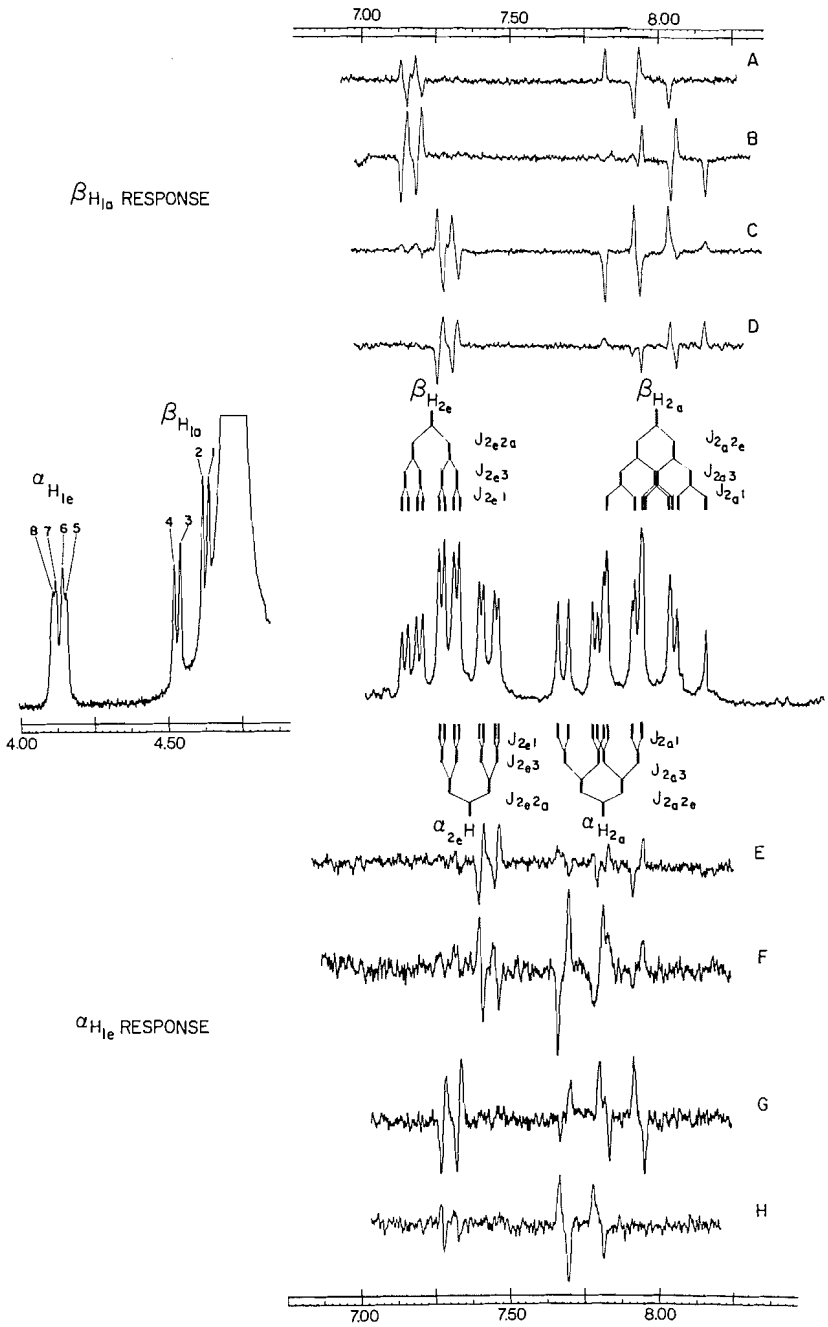

FIG. 3. Partial ^1H n.m.r. spectra for a fully mutarotated solution of 2-deoxy-α-D-*arabino*-hexopyranose (**1**) in D_2O. The normal H-1 and H-2 resonances are shown across the center of the figure. The upper set of spectra {*A*, *B*, *C*, and *D*} show the effect of monitoring the four $\beta\{H_{1a}\}$ transition $1 \rightarrow 4$, in that order. The lower set of spectra {*E*, *F*, *G*, and *H*} result from monitoring the four $\alpha\{H_{1e}\}$ transitions 8, 7, 6, and 5 respectively. The resultant first-order assignments for the H-2 resonances are indicated.

Can. J. Chem. Downloaded from www.nrcresearchpress.com by 210.87.254.6 on 09/05/12
For personal use only.

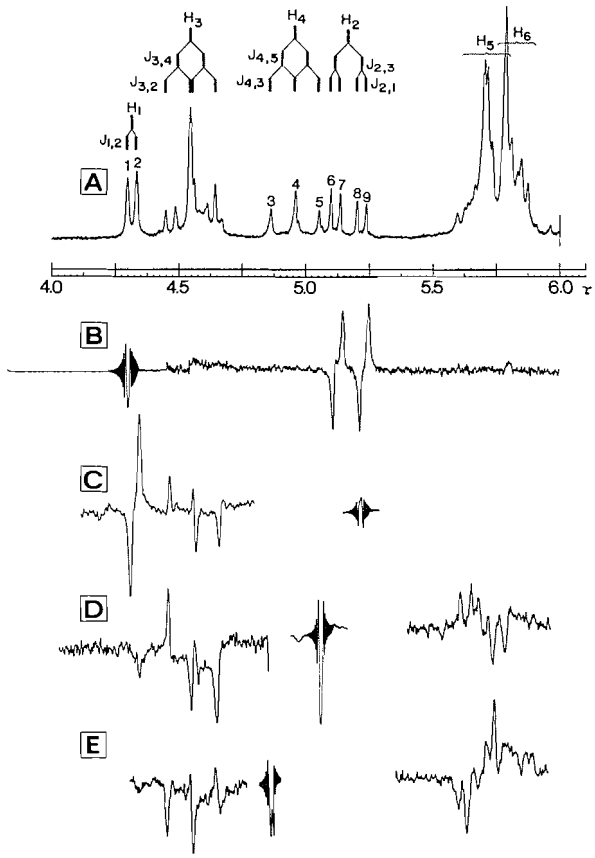

FIG. 4. (*A*), Partial ^{1}H n.m.r. spectrum of sucrose octaacetate (**2**) in acetone-d_6 with assignment of pyranose protons obtained from INDOR spectra. (*B*, *C*, *D*, and *E*), Responses obtained from monitoring transitions 1, 8, 3, and 5 respectively (see text).

due[5] to the fact that $[\gamma \mathbf{H}_2]/2\pi$ was set rather too high in relationship to $J_{2e,1}$. This behavior is even more clearly discernible in the series of spectra shown in Fig. 3*E*, *F*, *G*, and *H* which correspond to the monitoring of four transitions 8, 7, 6, 5 of $\alpha[H_{1e}]$. In this case $J_{2e,1}$ is rather small (0.7 Hz) and it is necessary to significantly decrease the strength of the decoupling field in order to prevent too many ambiguous responses. It is evident from these spectra that even when a serious decrease in signal-noise ratio is accepted, it is difficult to avoid "ghosting" when another transition is close to one being monitored. Nevertheless, the complete spectra of the $\alpha[H_{2e}]$ and $\alpha[H_{2a}]$ resonances can be readily assembled from the spectra shown in Fig. 3*F*, *G*.

It is also noteworthy that the pattern of the responses obtained via such INDOR experiments define the relative signs of the appropriate spin-couplings. For a discussion of this point the reader is referred to an excellent paper by Anet *et al.* (11).

The ^{1}H n.m.r. spectra of oligo- and polysaccharide derivatives are generally rather complex and, even at the higher fields available via superconducting solenoids, spectral assignments are difficult (12). That the ^{1}H–{^{1}H} INDOR method would appear to have some potential in this area is indicated by the spectra of sucrose octaacetate (**2**) shown in Fig. 4. A reasonable, partial assignment of some of the resonances can be made by inspection of the normal spectrum (Fig. 4*A*). The resonance of the anomeric proton

[5]To obtain the sharpest responses, ω_1 should be set to $\leqslant \pm 0.1$ Hz; deviation by more than this amount causes broadening of the observed responses together with the formation of "spikes" on either side of the major responses.

Can. J. Chem. Downloaded from www.nrcresearchpress.com by 210.87.254.6 on 09/05/12
For personal use only.

Can. J. Chem. Downloaded from www.nrcresearchpress.com by 210.87.254.6 on 09/05/12
For personal use only.

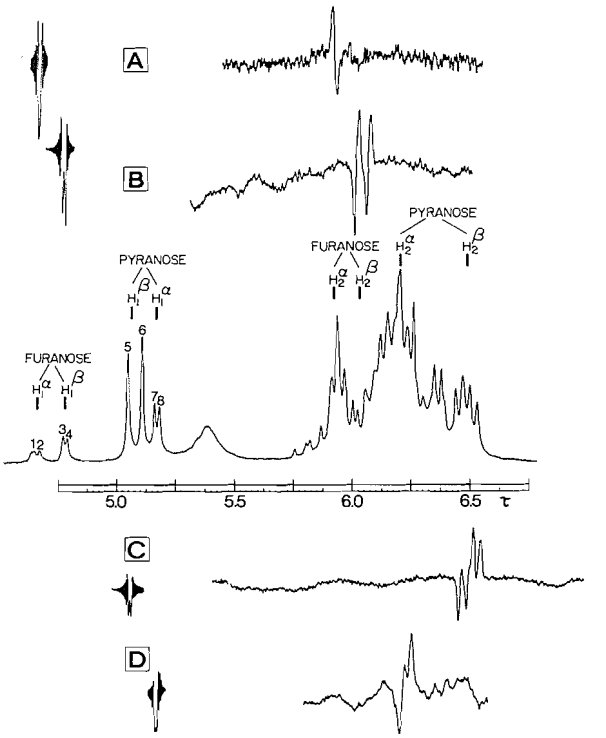

FIG. 5. ^1H spectra for a full mutarotated solution of D-ribose (3) in D_2O using the methyl groups of sodium dimethylsilapentane sulfonate for an internal lock signal. The normal spectrum is shown across the top of the figure with some of the intensity between τ 6.0 and 6.5 due to the methylene protons of the lock standard. The H-2 responses obtained from monitoring lines 2, 3, 5, and 7 are shown in *A*, *B*, *C*, and *D* respectively.

of the glucopyranose ring can be readily assigned to the doublet at τ 4.32. The INDOR responses obtained by monitoring line 1 of the normal spectrum are shown in Fig. 4*B*. These responses correspond to lines 6, 7, 8, and 9 and represent the H-2 resonance of the glucopyranose ring. Monitoring line 2 produced responses in the same positions but with the peaks inverted. A continuation of this procedure made possible the assignment of the resonances of the other pyranose ring protons. Figure 4*C* shows the responses corresponding to the H-1 and H-3 pyranose resonance, obtained by monitoring line 8 of the H-2 resonance. Sequential monitoring of lines 3 and 5 (Fig. 4*D* and *E* respectively) produced responses which designate the H-3 and H-5 transitions and confirm that the triplet comprising lines 3, 4, and 5 is the resonance of H-4. The complex responses for H-5 in these last two spectra reflect the highly coupled relationship of the H-5 and H-6 resonances, and are not assignable on a first-order basis. It is noteworthy that the H-3 pyranose resonance is essentially hidden in the normal spectrum, but can be assigned using the INDOR mode. Furthermore, the "resolution" of the INDOR response is sufficient to distinguish the ca. 1 Hz difference between $J_{2,3}$ and $J_{3,4}$.

D-Ribose (**3**) exists in aqueous solution as a mixture of four anomers. Lemieux and Stevens (13) had previously made some progress with the assignment of the secondary, ring-proton resonances by using field-sweep, spin-coupling experiments. We have now confirmed their assignment for the H-2 resonances. The normal spectrum of **3** in D_2O solution, shown in Fig. 5, indicates that four anomers are present at equilibrium. The anomeric resonances of the α- and β-pyranose and the α- and β-furanose forms have previously been assigned (13, 14). The spectra in Fig. 5*A*, *B*, *C*, and *D* show the responses obtained by monitoring lines 2, 3, 5, and 7 respectively and serve to identify the individual H-2 resonances of each of the anomeric forms. The resolution of the spectrometer was somewhat unstable at the time these experiments were performed, and the broad

Can. J. Chem. Downloaded from www.nrcresearchpress.com by 210.87.254.6 on 09/05/12
For personal use only.

responses in Fig. 5*B*, *C*, *D* indicate the effect of this instability.

Most previous applications of the ^1H–$\{^1H\}$ INDOR technique have been concerned with comparatively simple molecules. However, it is obvious from the three examples discussed above that the technique can be readily extended to more complex molecules, the only requirement being that some transitions be clearly removed from all others. We anticipate that many useful applications will be found in the area of natural product chemistry; for example, steroidal derivatives and many simple biopolymers give spectra which should respond well in an INDOR study.

Some limitations of the INDOR technique which may be commonly encountered during studies of more complex systems are as follows.

(a) When a degenerate transition is monitored. This will produce more responses than if a single, non-degenerate transition is being monitored, and it may be difficult to determine the multiplicity of the INDOR spectrum. Similarly, INDOR experiments performed on a strongly coupled system will produce responses which cannot be assigned on a first-order basis.

(b) When a transition is irradiated at a power-level such that both of the response "mechanisms" can operate simultaneously. It is possible under this condition for a positive and negative-going response to effectively cancel each other out and hence for the INDOR spectrum to contain too few responses.

(c) When a transition having an unusually long relaxation time is monitored. This condition may produce responses which are unduly broadened and may be alleviated, albeit with a loss of resolution, by increasing the scan-rate. Fortunately, this does not seem to be a serious problem in ^1H–$\{^1H\}$ experiments, although we have encountered several examples during heteronuclear INDOR measurements.

(d) When the spectrum to be studied contains one or more intense resonances. A spurious response is often observed whenever "ω_2" is scanned through an intense resonance, such as a methoxyl resonance, even when that particular resonance has no direct involvement in the experiment being performed. This response arises as the result of overloading of certain amplifier circuits in the HA-100 spectrometer, which can be readily observed on the spectrometer oscilloscope as a distorted sign wave (receiver lock monitor). This condition can be readily avoided by operating at low signal levels, either by dilution of the sample, or by reduction of the "receiver gain" setting of the V-4311 unit.

It is a pleasure to thank the National Research Council of Canada for their generous financial support of this work, and Dr. R. Freeman and LeRoy Johnson of Varian Associates for helpful discussions. Dr. Freeman, in particular, provided us with much useful insight concerning the INDOR technique.

1. L. D. HALL and J. F. MANVILLE. Advan. Chem. Ser. **74**, 228 (1968).
2. L. D. HALL and J. F. MANVILLE. Carbohyd. Res. **8**, 295 (1968); **9**, 11 (1969).
3. R. BURTON and L. D. HALL. Can. J. Chem. **48**, 59 (1970).
4. E. B. BAKER. J. Chem. Phys. **37**, 911 (1962).
5. R. FREEMAN and W. A. ANDERSON. J. Chem. Phys. **37**, 2053 (1962).
6. R. HOFFMAN and S. FORSEN. *In* Progress in n.m.r. spectroscopy. *Editor* J. W. Emsley, J. Feeney, and L. H. Sutcliffe. Pergamon Press, 1966. p. 1–204.
7. W. MCFARLANE. *In* Annual reviews of n.m.r. spectroscopy. Vol. 1. *Editor* E. F. Mooney. Academic Press, 1968. p. 135–163.
8. R. KAISER. J. Chem. Phys. **39**, 2435 (1962); E. B. BAKER. J. Chem. Phys. **45**, 609 (1966).
9. V. J. KOWALEWSKI. J. Mol. Spectry. **30**, 531 (1969); **31**, 256 (1969).
10. A. W. DOUGLAS. Private communication.
11. F. A. L. ANET, H. H. LEE, and J. L. SUDMEIR. J. Amer. Chem. Soc. **89**, 4431 (1967).
12. W. W. BINKLEY, D. HORTON, and N. S. BHACCA. Carbohyd. Res. **10**, 245 (1969).
13. R. U. LEMIEUX and J. D. STEVENS. Can. J. Chem. **44**, 249 (1966).
14. S. A. ANGYAL. Angew. Chem. Int. Ed., **8**, 157 (1969).

Can. J. Chem. Downloaded from www.nrcresearchpress.com by 210.87.254.105 on 09/05/12
For personal use only.

Electron spin resonance studies of methyl radicals stabilized on porous VYCOR glass: various surface interactions, second-order splitting, and a linewidth temperature study

G. B. GARBUTT[1] AND H. D. GESSER
Department of Chemistry, University of Manitoba, Winnipeg, Manitoba

Received[2] April 9, 1969

Electron spin resonance studies have been performed on methyl radicals stabilized on the surface of porous VYCOR glass. As previously reported, two very different methyl radicals, denoted Me and Me′, were seen. Results indicate that the radical Me′ is most probably weakly bound to the boroxane group (=B—O—B=) which is prominent on the surface of high temperature (700–900 °C) pretreated porous VYCOR glass. Four satellite lines about each Me line, denoted previously as radical X, were observed when the surface was pretreated at lower temperatures (400–500 °C). In an earlier publication radical X was attributed to the interaction between methyl radicals and the isotopic surface species ^{11}B. In this study two additional satellite lines about each Me line are reported as well as a reassignment of the origin of all satellite lines. Four of the six satellite lines have been assigned to forbidden "spin–flip" transitions while the other two have been assigned to direct interaction between methyl radicals and the surface hydroxyl protons. Support for the irreversibility of high temperature dehydroxylation of porous VYCOR glass is also presented.

A partial resolution of the second-order splitting of each of the central pair of lines was achieved for the normal methyl radical. The value of the second-order splitting was between 220 and 230 mG. The linewidths of the two central lines were measured at 77 °K. The samples were then allowed to warm up to various temperatures and then recooled to 77 °K. The linewidths were smaller after completing this cycle. Storage of the sample at 77 °K allowed the linewidths to return to their original values. These linewidths effects are explained by postulating the existence of two different types of potential wells on the surface.

Canadian Journal of Chemistry, **48**, 2685 (1970)

Introduction

Turkevitch and Fujita were the first to report methyl radical stabilization on porous VYCOR glass (PVG, Corning Code No. 7930) (1). This laboratory has also been involved in the study of this system (2–4). In both laboratories the methyl radicals were produced by low temperature ultraviolet (u.v.) photolysis of adsorbed methyl iodide. Turkevitch and Fujita also reported spectra due to deuterium and ^{13}C enriched methyl radicals (1). We have recently reported on a detailed temperature-dependence study on this system (4). Pretreatment of the PVG at one temperature leads to observable side bands while pretreatment at another temperature yields a second type of methyl radical (2, 3). Further information regarding the sidebands and the various types of methyl radicals is reported here. Certain reassignments have been necessary in order to account for the results.

Second-order splitting of alkyl radicals in solution has been treated theoretically by Fessenden (5). Fessenden and Schuler achieved partial resolution of the second-order splitting (0.23 G) of each of the central pair of lines while studying methyl radicals in liquid methane (6). Partial resolution of the second-order splitting has been observed in this study for the methyl radical stabilized at low temperatures on PVG. The asymmetry of the methyl radical spectrum allowed better resolution of the second-order splitting of the high field *3* intensity line (designated as line *3a*) because the linewidth of line *3a* is smaller than the linewidth of the low field *3* intensity line (designated as line *3*). A typical methyl radical spectrum for this system may be seen in Fig. 1. The peak-to-peak linewidths and the second-order splittings of lines *3* and *3a* have been studied on warming and recooling the sample.

Experimental

Methyl radicals were produced on the surface of PVG by the u.v. photolysis at liquid nitrogen temperatures of adsorbed methyl iodide. The methyl iodide was reagent grade obtained from Matheson, Coleman, and Bell. The deuterated methyl iodide (minimum isotopic purity of 99 atom % D) was obtained from Merck, Sharpe, and Dohme, Ltd., of Canada (Montreal). Having undergone normal degassing procedures these compounds were used

[1]Canadian Industries Limited Research Fellow, 1966–1968. Present address: Chemical Technology, Red River Community College, Winnipeg, Manitoba.

[2]Revision received April 20, 1970.

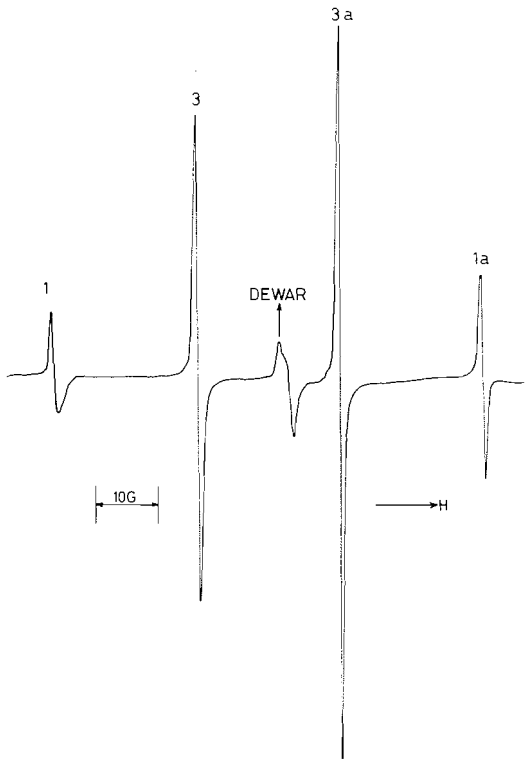

FIG. 1. Spectrum of methyl radical at 77 °K (low surface coverage). The four lines are designated *1*, *3*, *3a*, and *1a* on increasing *H*.

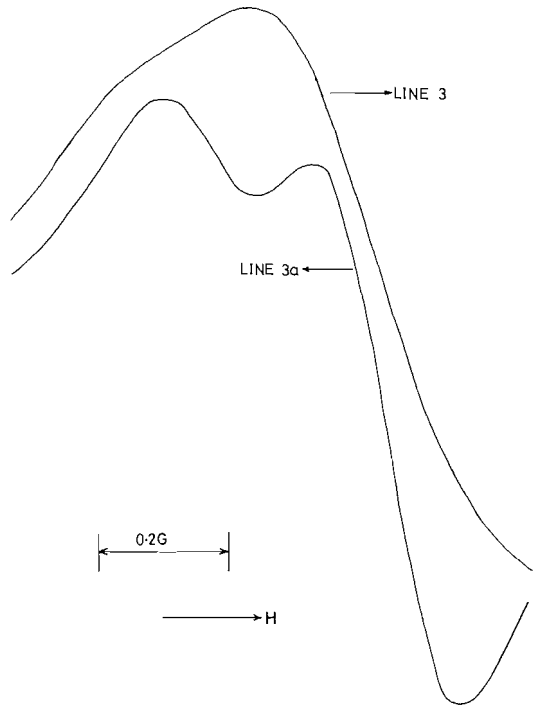

FIG. 2. Spectra of partially resolved second-order splittings of lines *3* and *3a* (recorded at 77 °K).

without any further purification. Each sample of PVG (Corning Code No. 7930) was preheated in oxygen to remove organic impurities and then heated in vacuum to dehydrate the surface. The specific values of the temperatures employed and the duration of these pretreatments are noted at the appropriate places. The methyl iodide was adsorbed at room temperature giving predetermined surface concentrations. The resulting samples were immersed in liquid nitrogen and photolyzed using the full focused arc of a Hanovia S-100 Alpine burner. The electron spin resonance (e.s.r.) spectra were then recorded. The previous published work (2, 3) was performed on a homemade X-band e.s.r. spectrometer.[3] The work reported here was done with a Varian E-3 e.s.r. spectrometer employing 100 kHz modulation. The measurements were made with the aid of the Fieldial field control included in the spectrometer. A large number of measurements were made in order to compensate for any instabilities in the e.s.r. spectrometer when linewidths were determined.

The second-order splittings were observed on decreasing the modulation amplitude. The best resolution of the second-order splittings was recorded at modulation amplitudes of 5 to 10 mG and is shown in Fig. 2. Lines *1* and *1a* showed no detectable splitting under the experimental conditions.

The second-order splittings and the linewidths of lines *3* and *3a* were measured at 77 °K. The sample was then warmed up and recooled. The second-order splittings and the linewidths were then measured once again at 77 °K. This process was repeated several times on warming the sample to various temperatures and then recooling to 77 °K.

Results

The four methyl radical lines are designated as lines *1*, *3*, *3a*, and *1a* on increasing field (see Fig. 1).

(A) A Second Kind of Methyl Radical (denoted Me′)

Under certain conditions a second kind of methyl radical was observed on photolysis of adsorbed methyl iodide at 77 °K (Fig. 3). Radical Me′ increases in concentration more rapidly than radical Me, the normal methyl radical, but decays at liquid nitrogen temperatures with a maximum half-life of about 12 h. The half-life decreases as the surface coverage of methyl iodide increases. It was believed that Me′ decayed at 77 °K into another radical (radical X) (2). It has now been shown, however, that Me′ does not

[3]This spectrometer was built by Dr. M. Fujimoto.

Can. J. Chem. Downloaded from www.nrcresearchpress.com by 210.87.254.105 on 09/05/12
For personal use only.

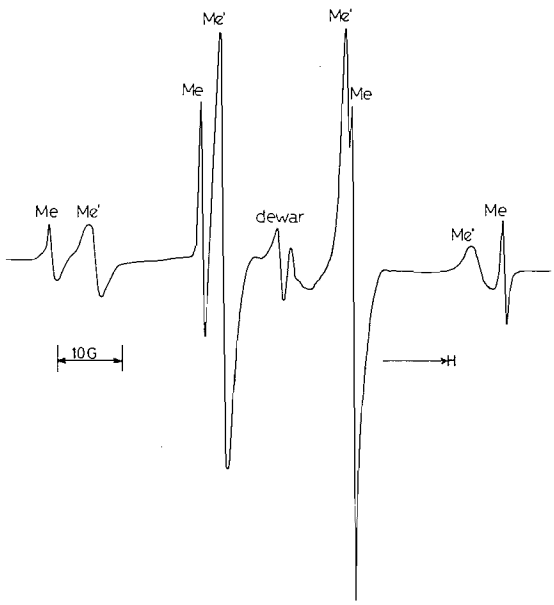

FIG. 3. Spectrum of Me and Me′ at 77 °K. Note that in this case the concentration of Me′ is larger than the concentration of Me.

decay into radical X or any other noticeable radical. It is important to note that Me′ only occurs when the preliminary heat treatment of the PVG sample is at 700–850 °C under high vacuum for long periods (i.e. 14 h or more). Also, Me′ may appear on many reirradiations of the same sample. The largest concentration of Me′ occurred when studying a sample which had been pretreated at very high temperatures and which had less than 1% of a monolayer of methyl iodide adsorbed on it. Another sample, similarly heat treated, but with twice the methyl iodide surface coverage, yielded Me′ but not nearly to the same extent. The hyperfine splitting in Me′ was 19.3 ± 0.05 G which is smaller than the value (20.2 ± 0.4 G) reported previously (2). The linewidths (peak-to-peak) in Me′ spectra are larger than those in Me spectra. For example, a comparison is made between the Me and Me′ low field lines: l.w._{p-p} (Me) = 0.83 G and l.w._{p-p} (Me′) = 1.48 G at 77 °K. Both Me′ and Me have similar saturation properties.

On irradiation of a deuteromethyl iodide sample, a broad seven-line spectrum was observable in addition to the normally obtained deuteromethyl radical spectrum. This spectrum was assigned to a deutero-Me′ species, but, because of the smaller splittings and broad lines, no measurements could be made on this radical.

An interesting and significant experiment was

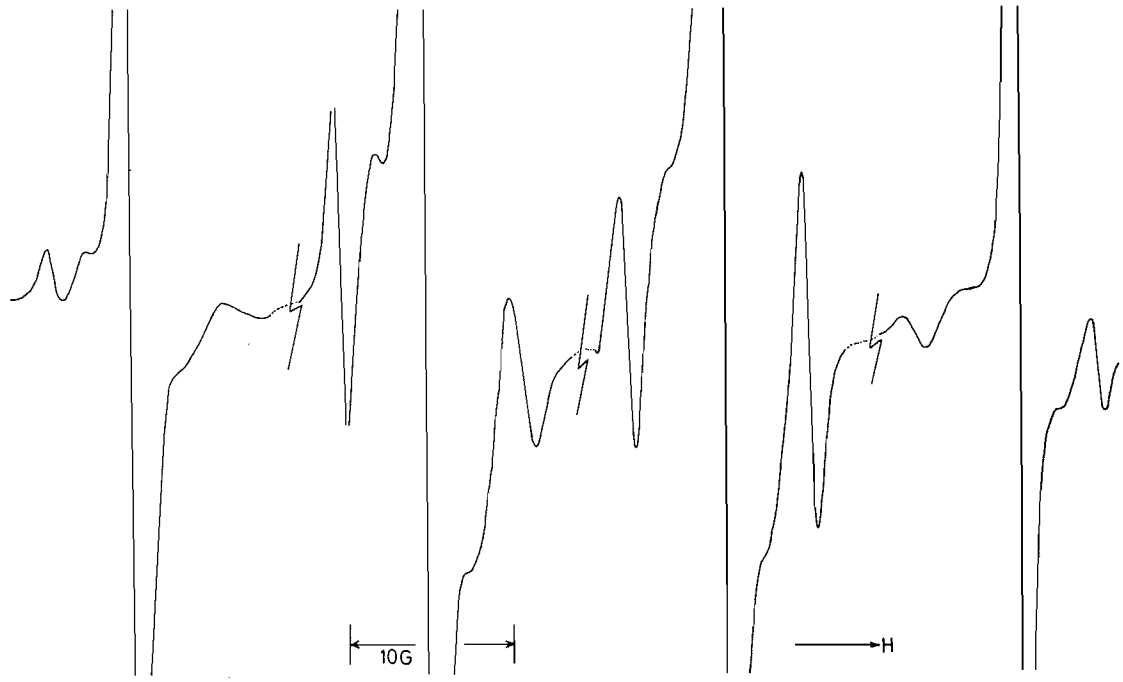

FIG. 4. Spectrum showing radical X.

Can. J. Chem. Downloaded from www.nrcresearchpress.com by 210.87.254.105 on 09/05/12
For personal use only.

performed on a sample which had yielded large quantities of Me'. A small quantity of water vapor was added at room temperature and the sample was reirradiated at 77 °K. The Me radical was the only product under these conditions.

(B) Satellite Lines about the Four Main Lines of the Methyl Radical Spectrum

In previous publications (2, 3) these satellites were reported and were referred to as radical X. A more recent spectrum of radical X is shown in Fig. 4. Radical X is prominent on PVG samples pretreated at approximately 450 °C prior to adsorption of methyl iodide. Samples pretreated at 700 °C or higher for about 4 h or more under vacuum did not yield radical X. Radical X was interpreted initially as being formed due to the interaction of some methyl radicals with the isotopic impurity ^{11}B which has a nuclear spin of 3/2 (3).

A "stick" diagram of the satellites about each proton line in the methyl radical spectrum is shown in Fig. 5. Satellites *A*, *A'*, *B*, and *B'* are those belonging to the radical X spectrum. In addition, two other satellite lines (*C* and *C'*) have been noticed (Fig. 6).

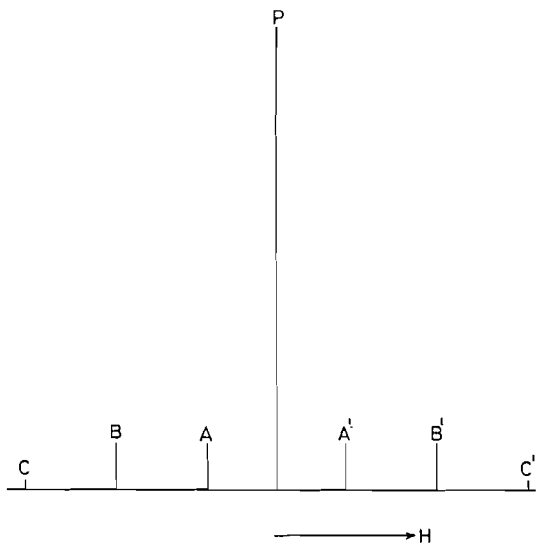

FIG. 5. "Stick" diagram of the satellites around one of the four proton lines P.

After considering the results of the following experiment, it is apparent that none of the satellites shown in Fig. 5 is in fact due to interaction between methyl radicals and ^{11}B nuclei.

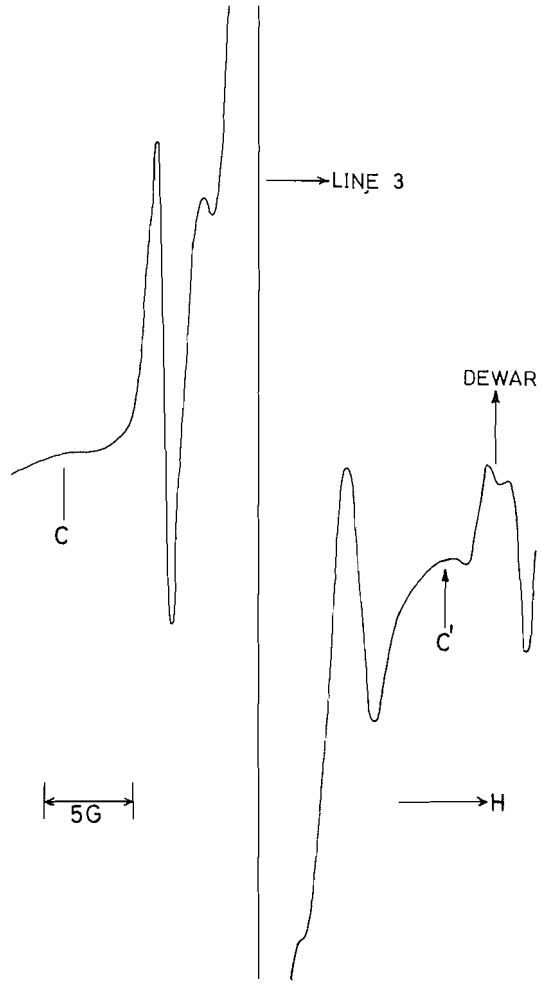

FIG. 6. Spectrum exhibiting the satellites *C* and *C'* about proton line *3*.

Two samples of PVG were heated in oxygen at 550 °C for 17½ h and then evacuated at room temperature for 24 h. One sample was dosed with heavy water vapor (99.7 atom % D) several times at 164 °C while the other was dosed with water vapor several times at 164 °C. Both samples were then heated in vacuum at 425 °C for 6 h. Methyl iodide was then adsorbed on both surfaces to a concentration of 5% of a monolayer. Both samples were then photolyzed for 1 h at 77 °K. The sample which had been treated with water vapor exhibited large satellite lines while the sample which had been treated with heavy water vapor showed hardly any satellite structure at all (Fig. 7). A similar experiment was performed

Can. J. Chem. Downloaded from www.nrcresearchpress.com by 210.87.254.105 on 09/05/12
For personal use only.

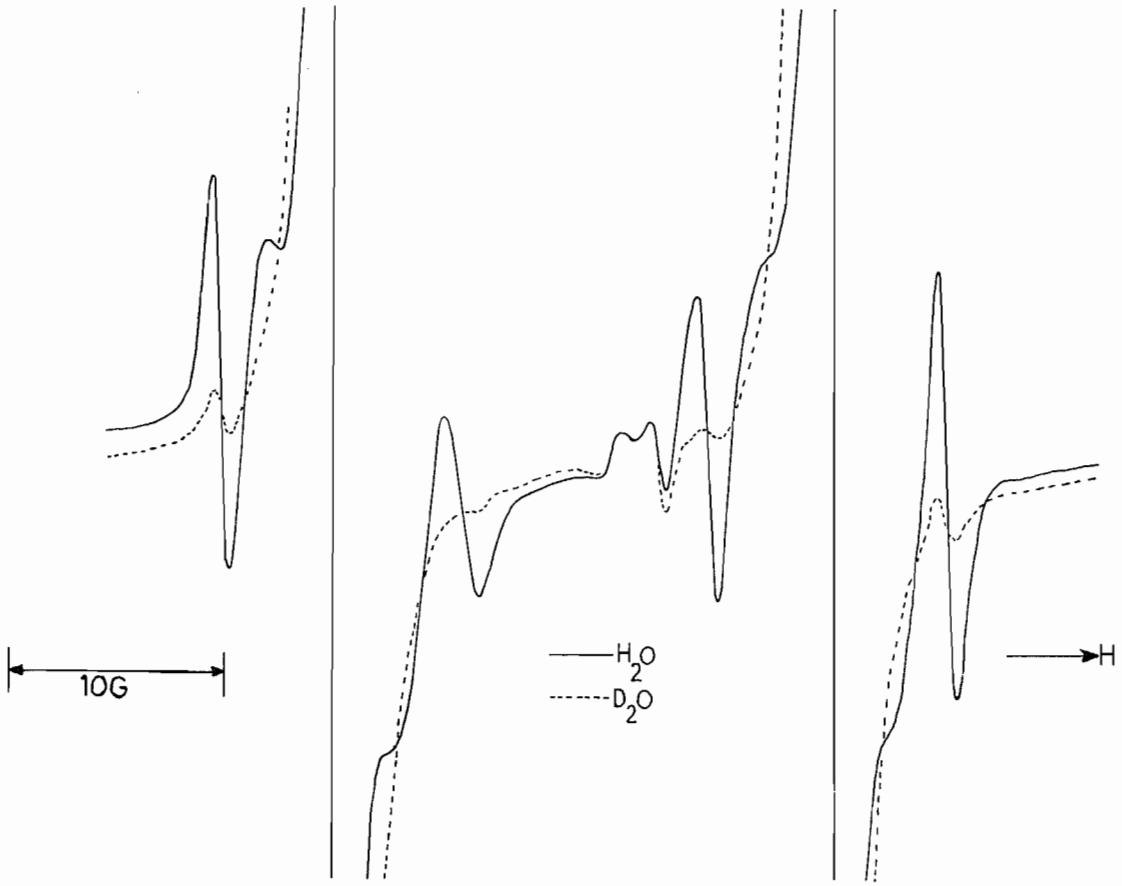

FIG. 7. Comparison of satellites observed about proton lines *3* and *3a* when studying samples treated with H_2O and D_2O.

on two other samples except that they were oxidized at 750 to 800 °C for 17 h and then heated in vacuum at the same temperature for 22 h. The samples which had been treated with water vapor showed very weak satellite lines while the sample which had been treated with heavy water vapor exhibited no satellite structure at all.

Certain properties of the six satellite lines should be mentioned. Satellites *C* and *C'*, which are broader than *B* and *B'*, are seen only under very high gain. Satellites *B* and *A* about proton lines *1* and *3* have larger amplitudes than satellites *A'* and *B'* about the same proton lines. The reverse is true for the satellites about proton lines *1a* and *3a*. Satellites *A* and *A'* are never completely resolved from the proton lines. The magnitude of the splittings between *C* and *C'* and the proton lines are about twice the magnitude of the splittings between *B* and *B'* and the proton lines. The linewidth of satellite *B* increases with increase in field of the line it is associated with whereas the linewidth of satellite *B'* decreases with increase in field of the line it is associated with. Both the satellites and the main proton lines seem to have similar saturation properties. All e.s.r. lines increased in amplitude on increasing the power to 8.0 mW and then decreased in amplitude on increasing the power above 8.0 mW. Complete saturation did not occur. Average values of the measurable splittings (at 77 °K) of the satellites from the main proton lines are shown in Table 1. The linewidths (peak-to-peak) of satellites *B* and *B'* as well as the amplitudes of *B* and *B'* compared to the main proton lines (relative amplitudes) are shown in Table 2. The relative amplitude of satellite *B* to proton line *3* has been measured for the samples that were dosed with heavy water vapor instead of water

Can. J. Chem. Downloaded from www.nrcresearchpress.com by 210.87.254.105 on 09/05/12
For personal use only.

TABLE 1

Average splittings of satellites from main proton lines at 77 °K

Proton line	Field (G)	Splittings* (G)						
		C	*B*	*A*	*A'*	*B'*	*C'*	*B* + *B'*
1	3234	—	4.6	2.1	—	6.2	—	10.8
3	3257	10.7	5.1	2.6	—	5.8	11.6	10.9
3a	3280	—	5.8	—	—	5.3	—	11.1
1a	3303	—	6.5	—	—	4.8	—	11.3

*Error = ±0.2 G.

TABLE 2

Average linewidths and relative amplitudes of *B* and *B'* at 77 °K

Proton line	Field (G)	Linewidth* (G)		Relative amplitude	
		B	*B'*	*B*	*B'*
1	3234	0.93	2.13	0.036	0.015
3	3257	0.82	1.68	0.038	0.019
3a	3280	0.98	0.90	0.018	0.025
1a	3303	1.40	0.84	0.013	0.027

*Error = ±0.03 G.

vapor. The result was 0.003 as compared to 0.038 for the corresponding samples dosed with water vapor. Therefore, the sample dosed with heavy water vapor yielded satellites which are at least a factor of ten smaller in amplitude than the corresponding samples treated with water vapor.

The splittings of satellites *B* and *B'* from proton lines *3* and *3a* and the linewidths of *B* and *B'* have been studied as a function of temperature. No large change was observed in the linewidths on going from 77 to 201 °K. The splittings as a function of temperature have been tabulated (Table 3). Satellites *B* and *B'* were still observable at 233 °K. On increasing the temperature satellites *A* and *A'* seemed to disappear or at least become unresolvable.

(C) Second-Order Splittings

The average value of the second-order splitting of line *3a* was found to be 225 ± 20 mG. The second-order splitting of line *3* is much less precise because of poor resolution due to its increased linewidth. The average value of the second-order splitting of line *3* was found to be 221 ± 30 mG.

(D) Warming and Recooling Cycles

The second-order splitting and linewidth results for line *3a* are shown in Table 4. The measurements were made using 100 mG modulation and small scan ranges. The results for line *3* are given in Table 5 (only linewidth measurements were made because of the poor resolution of the second-order splitting).

Discussion

(A) The Radical Me'

Several possible assignments for Me' can be made

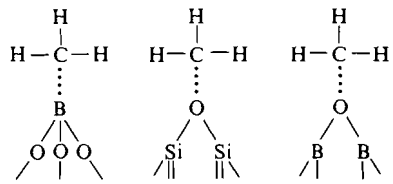

1 **2** **3**

TABLE 3

Splittings of satellites *B* and *B'* as a function of temperature

Temperature (°K)	Splittings about proton line *3** (G)			Splittings about proton line *3a** (G)		
	B	*B'*	*B* + *B'*	*B*	*B'*	*B* + *B'*
77	5.1	5.8	10.9	5.8	5.3	11.1
113	5.1	5.8	10.9	5.7	5.3	11.0
151	5.0	5.6	10.6	5.6	5.2	10.8
178	5.1	5.6	10.7	5.5	5.3	10.8
201	—	—	—	5.3	5.3	10.6

*Error = ±0.2 G.

Can. J. Chem. Downloaded from www.nrcresearchpress.com by 210.87.254.105 on 09/05/12
For personal use only.

TABLE 4

Second-order splitting and linewidth of line *3a* on warming and recooling

Measurement number	Measurement temperature (°K)	Temperature sample warmed to (°K)	Measured second-order splitting (G)	Measured linewidth (G)‡
1*	77	—	0.206	0.457
2	77	132	0.211	0.450
3	125	125	Poor resolution	0.456
4	160	160	Poor resolution	0.461
5	77	160	0.219	0.443
	Sample stored overnight at 77 °K			
6†	77	—	0.227	0.461
7	77	193	0.220	0.445
8	77	193	0.227	—

*Values recorded before warming and cooling cycle on sample (reference values).
†Values recorded after overnight storage at 77 °K.
‡Error = ±0.010 G.

TABLE 5

Linewidth of line 3 on warming and recooling

Measurement number	Measurement temperature (°K)	Temperature sample warmed to (°K)	Measured linewidth (G)*
1†	77	—	0.569
2	77	132	0.542
3	125	125	0.524
4	77	160	0.507
	Sample stored overnight at 77 °K		
5‡	77	—	0.558
6	77	193	0.495
7	77	193	0.511
8	77	300	0.519
	Single results for proton line *1*		
9§	77	160	0.770
	Single results for proton line *1a*		
10‖	77	160	0.409

*Error = ±0.010 G.
†Value recorded before warming and cooling cycles (reference value).
‡Value recorded after overnight storage at 77 °K.
§Original linewidth measured at 77 °K was 0.825 G.
‖Original linewidth measured at 77 °K was 0.478 G.

Me′ is known to occur only after high temperature pretreatment. The diffusion of boron to the surface of PVG occurs at 600 °C and above (7). Siloxane groups are known to be present at much lower temperatures. Ramasubramanian and Low (8) studied the sorption of water on dry PVG. They concluded that water adsorbs primarily on the surface boron atoms with the formation of $=BOH$ and $\equiv BOH_2$ structures. The silica network was found to be hydrophobic. From the experiment where water vapor was added at room temperature to a sample which had yielded large quantities of Me′ and which on reirradiation only Me appeared, one could postulate no change to have occurred in the siloxane network while the $\equiv B$ sites have reacted to form $=BOH$ and $\equiv BOH_2$ structures. Therefore, the fact that Me′ did not form on reirradiation supports assignment *1* or *3*.

Most infrared surface studies (9, 10) tend to agree that the main adsorption sites on PVG are the surface silanol groups (Brønsted sites) and the $\equiv B$ groups (Lewis acid sites). The siloxane bridges are active only when they are strained or when higher temperature adsorption studies are carried out. Normally, however, annealing of strained siloxane groups occurs on high temperature treatment. Also, adsorption studies at elevated temperatures are of the "chemisorption followed by decomposition" variety. Me′ is thought to be more highly oriented than Me because the linewidths of the Me′ lines are larger than those of the Me lines, because $|a_{Me'}{}^{H}| < |a_{Me}{}^{H}|$, and because the first sites populated on irradiation are of the Me′ variety. The fact that $|a_{Me'}{}^{H}| < |a_{Me}{}^{H}|$ indicates unpaired spin density transfer to the surface site. The boron Lewis acid site is a known electron acceptor while the siloxane and boroxane groups are not known as electron acceptors except under strained or high temperature conditions. Also, in agreement with assignment *1* or *3*, Me′ was not detected while studying methyl radicals adsorbed on pure (boron-free) silica aerogels (11). The mechanism of Me′ decay at 77 °K is not understood but is consistent with a weak surface interaction or a slow surface rearrangement. The above arguments support assignment *1* or *3* and not assign-

Can. J. Chem. Downloaded from www.nrcresearchpress.com by 210.87.254.105 on 09/05/12
For personal use only.

Can. J. Chem. Downloaded from www.nrcresearchpress.com by 210.87.254.105 on 09/05/12
For personal use only.

ment *2* which was first suggested (2). A 1% spin delocalization to boron should cause the four CH_3 lines to split into 4 components with a splitting of about 6 G (12). The absence of such an effect would seem to eliminate assignment *1* in favor of assignment *3*.[4] However, infrared studies support assignment *1* more than assignment *3*.

(B) Satellites about the Four Main Proton Lines of the Methyl Radical Spectrum

The present evidence suggests that the satellites are due to interaction between methyl radicals and the protons of the surface silanol groups. These satellites were previously assigned to interaction between methyl radicals and ^{11}B nuclei (3). Low and Ramasubramanian (7), studying the dehydroxylation of PVG, have pointed out that pretreatment above 300 °C removes geminal hydroxyl groups; pretreatment below 600 °C leaves a fully hydroxylated surface; pretreatment above 600 °C removes adjacent (or vicinal) hydroxyl groups and free hydroxyl groups become prominent; pretreatment above 600 °C allows boron to migrate to the sample surface. The above work (7) plus the fact that the satellites are only prominent after pretreatment at lower temperatures (approximately 450 °C), tends to support the assignment of these satellites to interaction between methyl radicals and the surface protons. This assignment was confirmed by the heavy water experiments. The fact that the satellites appeared at all on the heavy water treated samples could be due to incompleted deuteration. Some unresolved satellites were detected about the methyl radical lines on the deuterated samples, particularly about the narrower lines *3a* and *1a*. These could be due to a mechanism similar to that responsible for the satellites depicted in Fig. 5. They are not resolved, however, because $a^H/a^D = 6.514$. Also, samples dehydroxylated at high temperatures before addition of water vapor yielded smaller satellites than samples dehydroxylated at room temperature before the addition of water vapor. This supports the idea that high temperature dehydroxylation is almost irreversible. It also supports the belief that water vapor adsorption occurs mainly at adjacent hydroxyl groups.

The temperature dependence studies suggest that A and A' are not related to B and B'. A and A' may be reasonably attributed to a small amount of spin delocalization from the π orbital of the methyl radical to the hydrogen atom upon which this radical is stabilized. The assignment of A and A' to this type of interaction

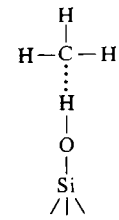

is due mainly to the fact that on increasing the temperature these satellites become unresolvable. This is consistent with a decrease in the strength of this interaction on increasing the temperature.

The total spectrum indicates that only a small fraction of the radicals are interacting with the silanol proton.

The satellites B and B' could be reasonably assigned to a weak magnetic dipole–dipole interaction coupling the electron spin to a neighboring nuclear spin. B and B' would then correspond to a change in the spin state of neighboring nucleus concurrent with the change in the spin state of the electron (forbidden spin–flip transitions) (13). In this case, B and B' would be interpreted as the occasional concurrent spin–flip of the electron and a nearby proton. Since the satellite intensity is proportional to $1/r^6$, it is relatively insensitive to all but the nearest protons. A second set of satellites (with a $1/r^{12}$ intensity dependence) may be observed when two neighboring protons concurrently change state. Calculated values of the satellite separation from the main lines, for magnetic field strengths of 3030 and 3390 G, are 4.6 and 5.2 G, respectively. One, two, and three neighboring protons concurrently changing state have been observed (14–16). Rogers and Kispert (17), while studying the methyl radical in irradiated single crystals of sodium acetate trihydrate, noticed two satellites spaced 5.6 ± 0.2 G on either side of the main methyl radical lines. The low field satellite lines had larger amplitudes than the corresponding high field satellite lines. This trend had been noticed previously in other systems (14–16). Rogers and Kispert also noticed, at high gains, a second set of satellites spaced 11.2 ± 0.2 G from the main lines. These satellites were attributed to spin–flip transitions due to

[4]We wish to thank one of the referees for bringing this to our attention.

Can. J. Chem. Downloaded from www.nrcresearchpress.com by 210.87.254.105 on 09/05/12
For personal use only.

dipole–dipole coupling with the protons of the water of crystallization. In accordance with the above discussion, satellites *C* and *C'* have been assigned to spin–flip transitions due to two neighboring protons concurrently changing state. A comparison of many of the spin–flip spectral characteristics is difficult because the systems studied are so very different.

The question may be asked: Why are *A* and *A'* not visible when employing high temperature pretreated glass? Relative amplitude and linewidth studies (18) indicate that the methyl radical is more strongly bound to the surface of low temperature pretreated PVG (or wet glass). Therefore *A* and *A'* are not visible on dry PVG probably because the interaction between the π orbital of the methyl radical and the surface hydroxyl group is not as strong as for wet PVG.

(C) Second-Order Splittings

It is noteworthy that the measured value of the second-order splitting is very nearly the value theoretically predicted (5). The narrowness of the lines, which allowed partial resolution of the second-order splitting, indicates that only weak interaction exists between the radical and the surface. Linewidth studies indicate that the higher the temperature used to oxidize and dehydroxylate the surface, the smaller is the resulting interaction between the methyl radicals and the surface. In this case high temperatures were employed.

(D) Warming and Recooling Cycles

Table 4 will be discussed first. Measurements No. 1 were performed at 77 °K immediately after the formation of the radicals. The sample was then warmed to 132 °K and then recooled to 77 °K (measurements No. 2). Measurements 3 and 4 were made at higher temperatures, 125 and 160 °K, respectively. The sample was then cooled to 77 °K (measurements No. 5), then stored overnight at 77 °K. Measurements No. 6 were made the next morning while the sample was still at 77 °K. Measurements Nos. 7 and 8 were made at 77 °K after warming the sample to 193 °K. Significantly, the linewidths are seen to decrease on warming and recooling and the second-order splitting becomes unresolvable at higher temperatures. The linewidth approaches its original value on sample storage at 77 °K during which no radical decay occurs. This trend was reproducible for several samples.

Some of the above observations are more clearly seen in Table 5. The increased clarity is due to the fact that line *3* is broader than line *3a*. Single results for methyl radical lines *1* and *1a* are also included in Table 5.

The above observations may be explained in the following manner. The radicals stabilized on the surface are found in a variety of potential wells (Type I) having various depths. In order for radical decay to take place the radical must leave these potential wells. This requires various activation energies and accounts for the cascade effect observed previously (2). It has been repeatedly observed in this laboratory that the normal methyl radical does not decay at 77 °K. Therefore, the linewidth effects reported above must be due to radical migration to differing sites located within the potential wells of Type I. This leads to the postulation of other potential wells (Type II) or sites within Type I wells. Free radical migration between Type II wells accounts for the observed linewidth effects.

After an initial decay at elevated temperatures the radicals on the surface are distributed so that Type I wells are singly occupied. The smaller linewidths at the higher temperatures are due to a narrower distribution of the radicals among the various Type II sites. A slow redistribution of the radicals among the Type II sites can occur at 77 °K resulting in a broadening of the linewidth without free radical decay.

Conclusions

The radical Me' is seen as an interaction between a methyl radical and a boroxane group. The satellites *A* and *A'* have been attributed to an interaction such as $\equiv SiOH \cdots CH_3$. The satellites *B* and *B'* are probably due to the simultaneous change in spin state of the electron and a nearby proton. Satellites *C* and *C'* are probably due to the simultaneous change in spin state of the electron and two nearby protons. Support for the virtual irreversibility of high temperature dehydroxylation of PVG has also been presented.

The second-order splitting of the methyl radical has been observed and measured. Evidence for radical diffusion at liquid nitrogen temperatures has been presented even though there is no measurable radical decay. Two types of potential wells, or energy sites, one within the other, have been postulated in order to explain the observed linewidth effects. It is anticipated that surface

heterogeneity may be examined by this process and a linewidth–temperature study is planned for homotactic surfaces.

The authors wish to thank Dr. M. Fujimoto for his helpful discussions. This work was supported by the Directorate of Chemical Sciences, Air Force Office of Scientific Research Grant No. AF-AFOSR 642-66, and by the National Research Council of Canada.

1. J. TURKEVITCH and Y. FUJITA. Science **152**, 1619 (1966).
2. M. FUJIMOTO, H. D. GESSER, B. GARBUTT, and A. COHEN. Science, **154**, 381 (1966).
3. M. FUJIMOTO, H. D. GESSER, B. GARBUTT, and M. SHIMIZU. Science, **156**, 1105 (1967).
4. G. B. GARBUTT, H. D. GESSER, and M. FUJIMOTO. J. Chem. Phys. **48**, 4605 (1968).
5. R. W. FESSENDEN. J. Chem. Phys. **37**, 747 (1962).
6. R. W. FESSENDEN and R. H. SCHULER. J. Chem. Phys. **39**, 2147 (1963).
7. M. J. D. LOW and N. RAMASUBRAMANIAN. J. Phys. Chem. **71**, 730 (1967).
8. N. RAMASUBRAMANIAN and M. J. D. LOW. J. Phys. Chem. **71**, 3077 (1967).
9. M. L. HAIR. Infrared spectroscopy in surface chemistry. M. Dekker, Inc., New York. 1967.
10. L. R. LITTLE. Infrared spectra of adsorbed species. Academic Press, Inc., London. 1966.
11. M. ZAMMITT. Private communication.
12. J. R. MORTON. Chem. Rev. **64**, 453 (1964).
13. G. T. TRAMMELL, H. ZELDES, and R. LIVINGSTON. Phys. Rev. **110**, 630 (1958).
14. H. ZELDES and R. LINGINSTON. Phys. Rev. **96**, 1702 (1954).
15. W. SNIPES and W. BERNHARD. J. Chem. Phys. **43**, 2921 (1965).
16. W. KOHNLEIN and J. H. VENABLE, JR. Nature, **215**, 618 (1967).
17. M. T. ROGERS and L. D. KISPERT. J. Chem. Phys. **46**, 221 (1967).
18. G. B. GARBUTT and H. D. GESSER. To be published.

Can. J. Chem. Downloaded from www.nrcresearchpress.com by 210.87.254.105 on 09/05/12
For personal use only.

Can. J. Chem. Downloaded from www.nrcresearchpress.com by 210.87.254.40 on 09/05/12
For personal use only.

d Orbitals in the noble-gas dihalides

R. C. CATTON AND K. A. R. MITCHELL
Department of Chemistry, University of British Columbia, Vancouver 8, British Columbia

Received[1] October 6, 1969

Model calculations are reported for ArF_2, KrF_2, XeF_2, $ArCl_2$, $KrCl_2$, and $XeCl_2$. The approach is to compare the energies of a number of valence-bond structures for each molecule. The calculations use Slater-type radial functions and simplify the electron repulsion integrals with the Mulliken approximation. Energies are optimized by varying the d orbital exponent and a parameter which governs the ionic character of the covalent bonds. For all the molecules it is found that the structures such as ($X—M^+X^- + X^-M^+—X$) and $X^-M^{2+}X^-$, which maintain the octet rule and exclude the use of d orbitals, are less stable than the structure X—M—X which implies localized electron-pair bonds based on pd hybrids at the noble-gas atom M.

Approximate molecular wave functions are obtained from a configuration interaction calculation, and the general conclusion is that the valence-bond structures incorporating d orbitals become more important as the atomic number of the central atom increases. A preliminary study of the role of the $4f_{z^3}$ orbital is also presented, but it seems this orbital contributes mainly as a polarization effect.

Canadian Journal of Chemistry, 48, 2695 (1970)

Introduction

The bonding in the noble-gas dihalides has recently attracted much attention (1–4). In 1964 Coulson (3) showed that the observed trends in stability,[2] namely that stability increases with increasing atomic number of the noble gas atom and with decreasing atomic number of the halogen, could be rationalized with a simple valence-bond model involving resonance of structures which maintain the octet at the central atom. A more recent investigation of XeF_2 and $XeCl_2$, however, indicates that the halogens may perturb the atomic potential at xenon sufficiently to expand the octet and allow the use of 5d orbitals in bonding models (4). Additionally, there has been a suggestion (5) that 4f orbitals also may contribute to the electronic structures of the xenon fluorides. The purpose of the present paper is to present some new calculations for the linear difluorides and dichlorides of argon, krypton, and xenon, with the view of providing a basis for more quantitative discussions of the bonding in these molecules.

The approach is first to compare the energies of some valence-bond structures of each molecule (designated in general by MX_2) including those structures represented schematically by X—M—X, $X—M^+X^-$, and $X^-M^{2+}X^-$. The first implies a shared localized pair of electrons in each inter-nuclear region and the use of pd hybridization at the central atom M. The other two structures maintain the octet at M; bond equivalence being maintained in the second by resonance between the two ionic–covalent structures. The valence-bond structures which seem likely to contribute most to the total wave function are then mixed in a configuration interaction calculation. Throughout, the calculations assume a fixed core defined by $X^+M^{2+}X^+$, the valence shell configurations being $s^2p_\pi^4$ for both X^+ and M^{2+}. In this approximation the various valence-bond structures considered here differ only in the locations of two electron pairs. The σ atomic orbitals accommodating these four electrons are orthogonalized to the core orbitals.

Calculations

The model calculations which are reported in this paper are based on four types of wave functions which are designated in unnormalized forms in eqs. [1]–[4].

$$[1]\quad \Psi_I = |l_1\bar{h}_1l_2\bar{h}_2| + |h_1\bar{l}_1l_2\bar{h}_2| + |l_1\bar{h}_1h_2\bar{l}_2| + |h_1\bar{l}_1h_2\bar{l}_2|$$

$$[2]\quad \Psi_{II} = |l_1\bar{l}_1l_2\bar{h}_2| + |l_1\bar{l}_1h_2\bar{l}_2| + |h_1\bar{l}_1l_2\bar{l}_2| + |l_1\bar{h}_1l_2\bar{l}_2|$$

$$[3]\quad \Psi_{III} = |l_1\bar{l}_1l_2\bar{l}_2|$$

$$[4]\quad \Psi_{IV} = |p\bar{l}_1l_2\bar{l}_2| + |l_1\bar{p}l_2\bar{l}_2| - |l_1\bar{l}_1p\bar{l}_2| - |l_1\bar{l}_1l_2\bar{p}|$$

The two X atoms in MX_2 are subscripted 1

[1]Revision received May 22, 1970.

[2]No halides of argon are known at present; the discrete halides of xenon and krypton are XeF_2, XeF_4, XeF_6, $XeCl_2$, and KrF_2.

Can. J. Chem. Downloaded from www.nrcresearchpress.com by 210.87.254.40 on 09/05/12
For personal use only.

TABLE 1

Representative values of the coefficients in eq. [8] for the noble gas difluorides*

		C_{ij}								
Molecule	Orbital	ns	np_z	nd_{z^2}	$1s(F_1)$	$2s(F_1)$	$2p_z(F_1)$	$1s(F_2)$	$2s(F_2)$	$2p_z(F_2)$
ArF_2	l_1	−0.1610	0	0	0.0013	0.0216	1.0123	0.0013	0.0216	0.0124
	h_1	0.0733	0.7502	0.8012	−0.0527	−0.4471	−0.0001	−0.0202	−0.0829	−0.0116
	p	0	1.0653	0	−0.0231	−0.2586	0	0.0231	0.2586	0
KrF_2	l_1	−0.1365	0	0	0.0009	0.0159	1.0090	0.0009	0.0159	0.0090
	h_1	0.0712	0.7443	0.8226	−0.0541	−0.4666	−0.0002	−0.0238	−0.1189	−0.0208
	p	0	1.0599	0	−0.0216	−0.2475	0	0.0216	0.2475	0
XeF_2	l_1	−0.1290	0	0	0.0010	0.0153	1.0080	0.0010	0.0153	0.0080
	h_1	0.0729	0.7483	0.8227	−0.0541	−0.4752	−0.0002	−0.0208	−0.1118	−0.0209
	p	0	1.0653	0	−0.0237	−0.2587	0	0.0237	0.2587	0

*In this Table the exponents for the ns, np_z, and nd_{z^2} orbitals are 2.59, 2.25, and 1.84, respectively, for ArF_2; 2.83, 2.44, and 1.93 for KrF_2; and 2.84, 2.48, and 2.07 for XeF_2.

TABLE 2

Representative values of the coefficients in eq. [8] for the noble gas dichlorides*

		C_{ij}											
Molecule	Orbital	ns	np_z	nd_{z^2}	$1s(Cl_1)$	$2s(Cl_1)$	$2p_z(Cl_1)$	$3s(Cl_1)$	$3p_z(Cl_1)$	$1s(Cl_2)$	$2s(Cl_2)$	$2p_z(Cl_2)$	$3s(Cl_2)$	$3p_z(Cl_2)$
$ArCl_2$	l_1	−0.2385	0	0	0.0002	0.0021	0.0011	0.0287	1.0269	0.0002	0.0021	0.0011	0.0287	0.0269
	h_1	0.0849	0.7383	0.8681	−0.0157	−0.1324	−0.0342	−0.4912	0.0000	−0.0116	−0.0916	−0.0158	−0.1923	−0.0014
	p	0	1.0447	0	−0.0029	−0.0288	−0.0131	−0.2115	0	0.0029	0.0288	0.0131	0.2115	0
$KrCl_2$	l_1	−0.2000	0	0	0.0001	0.0014	0.0007	0.0202	1.0192	0.0001	0.0014	0.0007	0.0202	0.0192
	h_1	0.0723	0.7252	0.8558	−0.0130	−0.1115	−0.0306	−0.4590	−0.0006	−0.0094	−0.0759	−0.0146	−0.1792	−0.0332
	p	0	1.0402	0	−0.0026	−0.0256	−0.0115	−0.2006	0	0.0026	0.0256	0.0115	0.2006	0
$XeCl_2$	l_1	−0.1883	0	0	0.0001	0.0015	0.0007	0.0189	1.0171	0.0001	0.0015	0.0007	0.0189	0.0171
	h_1	0.0716	0.7246	0.8512	−0.0121	−0.1044	−0.0286	−0.4570	−0.0007	−0.0081	−0.0652	−0.0123	−0.1670	−0.0417
	p	0	1.0436	0	−0.0029	−0.0282	−0.0118	−0.2088	0	0.0029	0.0282	0.0118	0.2088	0

*In this table the exponents for the ns, np_z, and nd_{z^2} orbitals are 2.59, 2.25, and 1.34, respectively, for $ArCl_2$; 2.83, 2.44, and 1.61 for $KrCl_2$; and 2.84, 2.48, and 1.78 for $XeCl_2$.

Can. J. Chem. Downloaded from www.nrcresearchpress.com by 210.87.254.40 on 09/05/12
For personal use only.

and 2 and the z axis at M points towards X_1; local z axes at X_1 and X_2 point towards M. In eqs. [1]–[4], h_1 and h_2 are hybrids directed at l_1 and l_2, respectively the bonding orbitals at X_1 and X_2, and p is the p_z orbital at M.

In eqs. [1]–[4], Ψ_I corresponds to the structure X—M—X, Ψ_{II} accounts for resonance between the structures X—M^+X^- and X^-M^+—X where the covalent bonds involve one of the diagonal hybrids h_1 and h_2, Ψ_{III} is the completely ionic structure $X^-M^{2+}X^-$, and Ψ_{IV} describes the resonance between the two ionic–covalent structures where the covalent bonding components are due to the overlap of the valence-shell p_z orbital at M.

For discussing the localized electron-pair model it is convenient to introduce Ψ_{loc} expressed in unnormalized form in eq. [5] and defined in

$$[5] \qquad \Psi_{loc} = \Psi_I + 2k\Psi_{II} + 4k^2\Psi_{III}$$

terms of a parameter k ($0 \leqslant k \leqslant \infty$) which governs the ionic character of the localized electron-pair bonds.

The Hamiltonian used in these calculations is in eq. [6],

$$[6] \qquad H = \sum_{i=1}^{4}\left(-\frac{1}{2}\nabla_i^2 + V_i^{core}\right) + \sum_{i<j}\frac{1}{r_{ij}}$$

where V_i^{core} refers to the interaction of electron i with the $X^+M^{2+}X^+$ core. The Hamiltonian and overlap matrix elements for the wave functions in eqs. [1]–[4] are obtained by standard techniques (6). The complete numerical evaluation of the Hamiltonian matrix elements would, however, be a complex calculation for the molecules treated here, and in consequence the matrix elements of $1/r_{ij}$ in eq. [6] are simplified with the Mulliken approximation (7) which is expressed in eq. [7] for a two orbital overlap distribution.

$$[7] \qquad q_iq_j = 0.5\,S_{ij}\,(q_iq_i + q_jq_j)$$

In eq. [7], S_{ij} is the overlap integral for q_i and q_j.

A number of different combinations of atomic orbitals are needed for investigating the various valence-bond structures of MX_2. The atomic orbitals at X are unhybridized, mutually orthogonal, and are indicated by the notation $1s(X_1)$, $2s(X_1)$, etc. The orbitals l_1, l_2, h_1, h_2, and p in eqs. [1] to [4] are covered by the notation $\{\phi_i\}$ and are conveniently expressed as in eq. [8]

$$[8] \qquad \phi_i = \sum_j C_{ij}\chi_j$$

where the valence-shell orbitals at M and the σ-type atomic orbitals at the halogens are denoted by $\{\chi_j\}$. The coefficients in eq. [8] are chosen so that the ϕ_i are orthogonal to the halogen core orbitals and so that the ϕ_i satisfy the orthogonality conditions in eqs. [9]–[11] and are normalized.

$$[9] \qquad \langle h_1|h_2\rangle = 0$$

$$[10] \qquad \langle h_1|l_2\rangle = \langle h_2|l_1\rangle = 0$$

$$[11] \qquad \langle l_1|l_2\rangle = 0$$

Typical values of the coefficients in eq. [8] for MF_2 and MCl_2 are given in Tables 1 and 2 for the basis functions specified below.

The calculations used Slater-type orbitals with exponents reported by Clementi, Raimondi, and Reinhardt (8, 9) from minimum-basis self-consistent-field calculations for the atoms in their ground states. The Schmidt method (10) was used to orthogonalize the valence-shell orbitals at M and all orbitals at X to inner orbitals with the same spherical harmonics. Some instances of non-orthogonality between orbitals of the halogens and inner-orbitals at M were neglected since the overlap integrals never exceeded 0.01. The bond lengths used were Ar—F, 3.00 a.u. (1 a.u. ≡ 0.529 Å); Kr—F, 3.30; Xe—F, 3.60; Ar—Cl, 3.65; Kr—Cl, 4.00; and Xe—Cl, 4.35. The one-electron integrals in the Hamiltonian matrix elements were evaluated numerically following the method of Roothaan (11) for the kinetic energy terms, and the procedures described by Magnusson and Zauli (12, 13) were used for deriving analytical expressions for the potentials of the $X^+M^{2+}X^+$ cores. The electron repulsion integrals were approximated by using the Mulliken approximation eq. [7] for the cross terms in the potential derived from the squares of the orbital combinations in eq. [8]. The numerical integrations were made by two-dimensional Gaussian quadrature (14) over a net of 1536 points.

Results and Discussion

The energies of the wave functions Ψ_I, Ψ_{III}, Ψ_{IV}, and Ψ_{loc} are given in Table 3 for the difluorides and dichlorides of argon, krypton, and xenon. For all these structures, the ns and np_z orbitals have exponents fixed at the values found for the ground state configurations (8, 9), but the nd_{z^2} orbital exponents and the ionic character

TABLE 3

Values of energy, orbital exponents, and ionic character parameter k for some valence-bond structures of ArF_2, KrF_2, XeF_2, $ArCl_2$, $KrCl_2$, and $XeCl_2$

Molecule	Wave function	Energy‡	Orbital exponents α_d	Orbital exponents α_f	k
ArF_2	ψ_I	−2.69	1.68	—	—
	ψ_{loc}	−2.94	1.84	—	0.41
	ψ_{III}	−2.11	—	—	—
	ψ_{IV}	−2.74	—	—	—
	ψ_{loc}*	−2.24	1.84†	2.40†	2.0
	ψ_{IV}*	−0.61	—	2.40†	—
KrF_2	ψ_I	−2.35	1.85	—	—
	ψ_{loc}	−2.61	1.93	—	0.43
	ψ_{III}	−1.84	—	—	—
	ψ_{IV}	−2.33	—	—	—
	ψ_{loc}*	−2.06	1.93†	1.90†	1.39
	ψ_{IV}*	−0.98	—	1.90†	—
XeF_2	ψ_I	−1.99	1.98	—	—
	ψ_{loc}	−2.31	2.07	—	0.52
	ψ_{III}	−1.66	—	—	—
	ψ_{IV}	−1.92	—	—	—
	ψ_{loc}*	−1.98	2.07†	1.70	1.00
	ψ_{IV}*	−1.15	—	1.70†	—
$ArCl_2$	ψ_I	−2.65	1.36	—	—
	ψ_{loc}	−2.79	1.34	—	0.40
	ψ_{III}	−2.25	—	—	—
	ψ_{IV}	−2.77	—	—	—
	ψ_{loc}*	−2.28	1.34†	2.40†	3.7
	ψ_{IV}*	−0.69	—	2.40†	—
$KrCl_2$	ψ_I	−2.28	1.60	—	—
	ψ_{loc}	−2.47	1.61	—	0.47
	ψ_{III}	−1.96	—	—	—
	ψ_{IV}	−2.27	—	—	—
	ψ_{loc}*	−2.05	1.61†	1.90†	2.43
	ψ_{IV}*	−1.06	—	1.90†	—
$XeCl_2$	ψ_I	−2.10	1.75	—	—
	ψ_{loc}	−2.28	1.78	—	0.49
	ψ_{III}	−1.83	—	—	—
	ψ_{IV}	−2.05	—	—	—
	ψ_{loc}*	−1.96	1.78†	1.70†	1.69
	ψ_{IV}*	−1.25	—	1.70†	—

*In these wave functions the valence-shell p_z orbital at M is replaced by the $4f_{z^3}$ orbital.
†These values have not been optimized.
‡In atomic units (1 a.u. ≡ 27.205 eV). Values are relative to the energy of the appropriate $X^+M^{2+}X^+$ core.

parameters[3] k are varied for minimum energy. Additionally, results are given in Table 3 for the wave functions Ψ_{loc} and Ψ_{IV} where the p_z valence shell orbital at M is replaced by the $4f_{z^3}$ orbital.[4] With this substitution, Ψ_{loc} covers the model of localized electron-pair bonds based on fd diagonal hybridization at M. The optimization of the 4f orbital exponents showed very low values (less than 0.5) for the wave functions of type Ψ_{IV}, which describe the resonance of the ionic–covalent structures, and likewise very small 4f exponent values, corresponding to diffuse and weakly bound orbitals, were found for Ψ_I. For Ψ_{loc}, however, the variation of the 4f exponent and k for XeF_2 showed the optimum 4f exponent to be 1.70. With this exponent, the distance of maximum radial probability for the $4f_{z^3}$ orbital is close to that for the $5d_{z^2}$ orbital. Correspondingly, for the other molecules, 4f exponents were fixed, at the values given in Table 3, such that the radial maxima occur close to those of the valence-shell d_{z^2} orbitals.

The calculations reported in Table 3 differ in three respects from the related calculations

[3]k does not completely specify the ionic character since the valence orbitals at M are contaminated by halogen orbitals from the orthogonalization procedure.

[4]The notation for f orbitals is that in ref. 15.

Can. J. Chem. Downloaded from www.nrcresearchpress.com by 210.87.254.40 on 09/05/12
For personal use only.

Can. J. Chem. Downloaded from www.nrcresearchpress.com by 210.87.254.40 on 09/05/12
For personal use only.

presented earlier (4) for XeF_2 and $XeCl_2$. The first difference is that here the halogen bonding orbitals have been orthogonalized to the nonbonding valence-shell orbitals of the central atom. As expected this raises energies relative to those quoted in the earlier work. This effect increases with increased occupancy of the halogen bonding orbitals, and therefore is greatest for the structures of the type $X^-M^{2+}X^-$ and least for the structure covered by X—M—X. The second difference is the introduction of the parameter k which governs the variation in ionic character of the covalent bonds; in the earlier work the calculations were made for fixed values of k. Thirdly, resonance between structures of the types $X—M^+X^-$ and $X^-M^+—X$ is now included. However, the main conclusion reached previously (4) for XeF_2 and $XeCl_2$ is reconfirmed here, and this is that the most favorable valence-bond structures are those including the $5d_{z^2}$ orbital at xenon.

Within the series of fluorides and within the series of chlorides, the trends found for the ionic-character parameter k are consistent with the electronegativities of the noble-gas atoms decreasing with increasing atomic number, and this agrees with the usual trends in electronegativities (16). By contrast, the optimized value of k for each difluoride is very close to the value for the corresponding dichloride, and substantial increases may have been expected for the difluorides considering that fluorine is one unit more electronegative than chlorine on the Pauling scale (16). An explanation is that the valence-shell orbitals of the noble-gas atoms are stabilized more by the fluorines than by the chlorines, and this is presumably due to the smaller size of the fluorine atoms, and therefore to their ability to get an effective nuclear charge closer to the valence shell of the noble-gas atom. This rationalization accounts for another conclusion from Table 3, namely, that the energy gain from including outer-d orbitals in localized bonds is greater for the fluorides than for the chlorides. This suggests, moreover, that the d-orbital bonding model can account qualitatively for the empirical observation that the stabilities of the noble-gas fluorides are greater than those of the corresponding chlorides.

Further indications of the comparative abilities of fluorine and chlorine to modify the electronic structure of the noble-gas atoms in the difluorides and dichlorides are provided by the optimized d exponents and by the results for Ψ_{loc} when the $4f_{z^3}$ orbital is included. The optimized d exponents are always less than the valence-shell p orbital exponents[5] used for the noble-gas atoms in these calculations, and the interpretation is that the d orbitals are less compact than the p orbitals in these molecules, although it is possible that this difference in size is in part exaggerated by the use of fixed exponents for the p orbitals. The exponent values in Table 3 indicate that the d orbitals are less compact in the chlorides than in the corresponding fluorides. To some extent this is determined by the longer bonds to chlorine, but another effect is due to the effective nuclear potential of the chlorines being less than that of the fluorines, and consequently that the chlorines are less able than the fluorines to contract and stabilize the outer-d orbitals. It is assumed here that the d orbitals in the valence-shell configurations $s^2p^5d^1$ are diffuse for both argon and krypton. This is likely both because the energies of these orbitals are known to be high (17), and because 3d orbitals in $(3d)^1$ configurations of aluminum (18), phosphorus (19), and sulfur (20) are diffuse, and so are 5d orbitals in $(5d)^1$ configurations of the xenon atom (4).

As expected the results in Table 3 indicate that hybrids formed from the nd_{z^2} and $4f_{z^3}$ orbitals have higher energies in the molecules than do the corresponding hybrids formed from np_z and nd_{z^2} orbitals, and this is reflected in part by the optimized values of the parameter k, which, for the structures including the $4f_{z^3}$ orbital, are always larger for the chlorides than for the fluorides. This is strongly against the trend expected with the simplest electronegativity considerations, and again suggests that chlorine is much less efficient than fluorine at stabilizing excited orbitals for bonding purposes. In this context, the value of k is least for XeF_2 and suggests that 4f involvement may be greater for this molecule than for the other noble-gas dihalides, but the involvement is probably always small. That there is a stabilization of the $4f_{z^3}$ orbital operating in XeF_2 is suggested by the optimized exponent (1.70) which is much larger than the value of 0.25 found for the $(5s)^1(5p)^6(4f)^1$ and $(5s)^2(5p)^5(4f)^1$ configurations of the

[5]The exponents of the valence-shell p orbitals used are 2.48, 2.44, and 2.25 for xenon, krypton, and argon, respectively.

TABLE 4

Results of the configuration interaction calculation for ArF_2, KrF_2, XeF_2, $ArCl_2$, $KrCl_2$, and $XeCl_2$

Molecule	Energy*	Coefficients in eq. [12]				Coefficients in eq. [13]			
		C_I	C_{II}	C_{III}	C_{IV}	D_1	D_2	D_3	k†
ArF_2	−3.02	0.4923	0.1512	0.1470	0.4393	0.8956	−0.2702	0.4393	0.41
KrF_2	−2.66	0.5121	0.2041	0.1759	0.3561	0.9638	−0.2630	0.3561	0.44
XeF_2	−2.33	0.4807	0.3288	0.2456	0.2090	1.0304	−0.2026	0.2090	0.53
$ArCl_2$	−2.88	0.4144	0.0711	0.1324	0.5579	0.8093	−0.3086	0.5579	0.44
$KrCl_2$	−2.50	0.4622	0.2301	0.1856	0.3056	0.9853	−0.2479	0.3056	0.49
$XeCl_2$	−2.30	0.4665	0.2682	0.2045	0.2391	1.0337	−0.2383	0.2391	0.51

*In atomic units (1 a.u. ≡ 27.205 eV). Values are relative to the energy of the appropriate $X^+M^{2+}X^+$ core.
†Value of k for Ψ_{loc} in eq. [13].

free xenon atom (4), although to a considerable extent the increased f-orbital exponent must be put down to the increased positive charge at the noble-gas atom.

The Configuration Interaction Calculation

The configuration interaction was restricted to mixing, as in eq. [12], the normalized forms of the wave functions Ψ_I, Ψ_{II}, Ψ_{III}, and Ψ_{IV}

$$[12] \quad \Psi = C_I\Psi_I + C_{II}\Psi_{II} + C_{III}\Psi_{III} + C_{IV}\Psi_{IV}$$

in eqs. [1]–[4]. The results from solving the secular equation, using a standard computer program (21), are given in Table 4 for each molecule. The energy values can usefully be compared with those for the function Ψ_{loc} in Table 3, and it may be noted that the energy gain from the free mixing of the functions in eq. [12] is least for the dihalides of xenon (0.02 a.u.) and is larger in the compounds of krypton (0.05 a.u.) and argon (0.09 a.u.). These calculations suggest, therefore, that the localized electron-pair bonding model should be helpful especially for the xenon compounds.

The large contribution of Ψ_{loc} to Ψ can also be seen when eq. [12] is re-expressed as in eq. [13], where the value of k for Ψ_{loc} is chosen such

$$[13] \quad \Psi = D_1\Psi_{loc} + D_2\Psi_{II} + D_3\Psi_{IV}$$

that Ψ_{loc} takes up the contributions of Ψ_I and Ψ_{III} in eq. [12]. For all molecules, the values of k found in this way are within 0.02 of the appropriate values in Table 3 for Ψ_{loc} based on pd hybrids at M. The values of D_1, D_2, and D_3 in eq. [13] are included in Table 4.

The coefficients in Table 4 indicate that the contributions of the structures which include d orbitals increase with the atomic number of the central atom. It is interesting to note that the wave function Ψ_{IV}, corresponding to the resonance of the ionic-covalent structures, has a smaller coefficient than the other contributing wave functions for XeF_2, and this result contrasts with a commonly-held view of the bonding in this molecule (2, 3). The contribution of Ψ_{IV} is greatest for the non-existent molecule $ArCl_2$; indeed it is only for this single molecule that the coefficient of Ψ_{IV} is greater than the coefficient of Ψ_I.

Although this study suggests that there may be an empirical relation between the calculated contributions of valence-bond structures to the total electronic wave function and the relative stabilities of the noble gas halides, other factors are also expected to be important to this stability problem. Thus bonding by d_π orbitals of the noble-gas atom must occur to some extent, but alternatively there is the destabilization arising from the overlapping of the doubly-filled π-type atomic orbitals in the $X^+M^{2+}X^+$ core. The latter is neglected in the present work, but this effect is likely to be greatest for the molecules of argon with the shorter bond lengths. This may, therefore, be one reason why ArF_2 is less stable than KrF_2.

Conclusions

The model calculations reported in this paper suggest that the ground-state molecular wave functions for the noble-gas dihalides are likely to include important contributions by the valence-bond structures which incorporate outer-d_{z^2} orbitals in localized electron-pair bonds. In a full treatment, however, the valence-shell p_z orbitals will probably make larger contributions to the electronic wave functions than do the valence-shell d_{z^2} orbitals, but the calculations reported here suggest that the d orbitals are

Can. J. Chem. Downloaded from www.nrcresearchpress.com by 210.87.254.40 on 09/05/12
For personal use only.

involved to a degree which is chemically significant. By contrast, the participation of the $4f_{z^3}$ orbitals is probably best seen as a polarization effect (22).

Finally, the results of this work should be relevant to more general discussions of bonding in hypervalent molecules. It seems likely that a clarification of the degree of involvement of outer-d orbitals in the bonding of molecules like SF_6, Cl_3PO, and the polyhalides will come especially from analyses of molecular wave functions of the individual molecules rather than from correlations between theoretical quantities and experimental measurements for a series of molecules, and this mainly because of the present recognition that stereochemical details, and a number of other properties, can be discussed *in principle* both with those models of bonding which emphasize the role of outer-d orbitals and with the alternative models which neglect contributions by the outer-d orbitals altogether (23). The results in the present paper suggest that for many uncharged hypervalent molecules, the model of d-orbital involvement in σ bonds is likely to be useful for considering stability and other features of chemical interest. In a future publication we propose to discuss further some aspects of d_π bonding.

We are grateful for support by the National Research Council of Canada.

1. H. H. HYMAN (*Editor*). Noble gas compounds. Univ. of Chicago Press, Chicago. 1963. Part IX.
2. J. G. MALM, H. SELIG, J. JORTNER, and S. A. RICE. Chem. Rev. **65**, 199 (1965).
3. C. A. COULSON. J. Chem. Soc. 1442 (1964).
4. K. A. R. MITCHELL. J. Chem. Soc. A, 1637 (1969).
5. K. A. R. MITCHELL. Chem. Commun. 368 (1969).
6. J. C. SLATER. Quantum theory of molecules and solids. Vol 1. McGraw-Hill Book Co., Inc., New York. 1963. Append. 9.
7. R. S. MULLIKEN. J. Chim. Phys. **46**, 497 (1949); K. RUEDENBERG. J. Chem. Phys. **19**, 1433 (1951).
8. E. CLEMENTI and D. L. RAIMONDI. J. Chem. Phys. **38**, 2686 (1963).
9. E. CLEMENTI, D. L. RAIMONDI, and W. P. REINHARDT. J. Chem. Phys. **47**, 1300 (1967).
10. J. O. JACKSON. Mathematics for quantum mechanics. W. A. Benjamin, Inc., New York. 1962 p. 33.
11. C. C. J. ROOTHAAN. J. Chem. Phys. **19**, 1445 (1951).
12. E. A. MAGNUSSON and C. ZAULI. Proc. Phys. Soc. London. **78**, 53 (1961).
13. K. A. R. MITCHELL. Mol. Phys. **16**, 633 (1969).
14. A. N. LOWAN, N. DAVIDS, and A. LEVENSON. Bull. Amer. Math. Soc. **48**, 739 (1942).
15. H. G. FRIEDMAN, G. R. CHOPPIN, and D. G. FEUERBACHER. J. Chem. Educ. **41**, 354 (1964).
16. L. PAULING. The nature of the chemical bond. Cornell Univ. Press, Ithaca. 1960. p. 93.
17. C. E. MOORE. Atomic energy levels. Vols. 1–3. Nat. Bur. Stand. Circ. 467, U.S. Government Printing Office, Washington. 1949–1958.
18. M. SYNEK. Phys. Rev. **131**, 1572 (1963).
19. G. S. CHANDLER and T. THIRUNAMACHANDRAN. J. Chem. Phys. **47**, 1192 (1967).
20. D. W. J. CRUICKSHANK, B. C. WEBSTER, and D. F. MAYERS. J. Chem. Phys. **40**, 3733 (1964).
21. F. PROSSER. Program 62.1. Quantum Chemistry Program Exchange, Chemistry Department, Indiana University, Bloomington, Indiana 47401.
22. C. A. COULSON. Nature, **221**, 1107 (1969).
23. K. A. R. MITCHELL. Chem. Rev. **69**, 157 (1969).

Can. J. Chem. Downloaded from www.nrcresearchpress.com by 210.87.254.40 on 09/05/12
For personal use only.

Structure of sepedonin, a tropolone metabolite of *Sepedonium chrysospermum* Fries[1]

J. L. C. WRIGHT,[2] A. G. MCINNES, D. G. SMITH, AND L. C. VINING
Atlantic Regional Laboratory, National Research Council of Canada, Halifax, Nova Scotia

Received December 15, 1969

The structures of sepedonin, 3,6,9-trihydroxy-3-methyl-1,3,4,7-tetrahydrocyclohepta[*c*]pyran-7-one, and its two dimethyl ether derivatives, as well as anhydrosepedonin and its three dimethyl ether derivatives, are unequivocally established from proton magnetic resonance and nuclear Overhauser enhancement parameters.

Canadian Journal of Chemistry, 48, 2702 (1970)

Can. J. Chem. Downloaded from www.nrcresearchpress.com by 210.87.254.42 on 09/05/12
For personal use only.

Introduction

Chemical, ultraviolet (u.v.), infrared (i.r.), and proton magnetic resonance (p.m.r.) evidence obtained during an earlier investigation (1) of sepedonin, a metabolite of *Sepedonium chrysospermum* Fries, did not allow an unequivocal choice between structures **1** and **2** but **1** was assigned on biogenetic grounds.

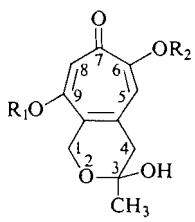

1 $R_1 = R_2 = H$
1*a* $R_1 = R_2 = OCH_3$

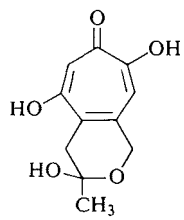

2

Before investigating the biosynthesis of sepedonin, unambiguous proof of structure was required. An account of the biosynthetic study, in which we employed ^{13}C as the isotopic tracer and p.m.r. to determine the positions of the labeled atoms, has already been reported (2). In this communication we report new evidence which independently establishes structure **1** for sepedonin, and allows structures to be derived for the methyl ethers of sepedonin and anhydrosepedonin.

Discussion

Structure

The structure of sepedonin can be fully and unequivocally defined from the following observations.

(*1*) Sepedonin ($C_{11}H_{12}O_5$) is easily converted to anhydrosepedonin ($C_{11}H_{10}O_4$) by loss of one molecule of water (1).

(*2*) The p.m.r. spectra (all p.m.r. data are reported in Table 1) of sepedonin and anhydrosepedonin each contained signals for two hydrogens (singlets) in the aromatic region. In the presence of D_2O these hydrogens were gradually replaced with deuterium, the hydrogen at lowest field (**1**, τ 2.81; **4**, τ 2.73) exchanging at least an order of magnitude faster than the one at higher field (**1**, τ 3.08; **4**, τ 3.10). Both compounds also contained an allylic methylene group (**1**, average τ 4.85; **4**, τ 4.67) bearing an oxygen substituent. The spectra of the compounds differed, however, in that sepedonin gave signals for three hydroxyl groups (replaceable by deuterium; temperature dependent) whereas anhydrosepedonin gave only two. In addition sepedonin contained a tertiary methyl (singlet, τ 8.28) and an allylic methylene (average τ 7.02) group. No signal for the latter was observed in the spectrum of anhydrosepedonin. Instead there was an olefinic hydrogen (τ 4.40) which was allylic coupled (J = 0.6 Hz) to a methyl (τ 8.11) group. It can be concluded that sepedonin contains the group $-CH_2-C(OH)(CH_3)-$ which readily dehydrates to give the group $-CH=C(CH_3)-$ found in anhydrosepedonin. Moreover, the paramagnetic shift of the methyl group (τ 8.28) in sepedonin requires that it be part of a $-OC(OH)(CH_3)-$ system since the alternative, an allylic methyl, is excluded. The methylene group attached to the carbon bearing these three substituents must also be the allylic one which appears at τ 7.02 in the spectrum of sepedonin. In all other respects the structures of sepedonin

[1]Issued as NRCC No. 11409.
[2]NRCC Postdoctorate Fellow 1967–1968. Present address: Dyson Perrins Laboratory, Oxford University, England.

TABLE 1

Proton magnetic resonance data for sepedonin and derivatives*

Compound†	τ						J_{pq}(Hz)¶	
	H_1‡	H_4‡	H_5	H_8	$OR_{1,2}$	CH_3		
1	4.85	7.02	3.08	2.81	0.3§	8.28	$J_{1,1}$ $J_{4,4}$	17.1 17.2
4	4.67	4.40	3.10	2.73	−1.4	8.11	J_{4,CH_3}	0.6
4a	4.91	4.50	3.33	3.22	6.13(R_1)	8.03	J_{4,CH_3} J_{8,OR_1}	0.9 0.6
4b	4.95	4.50	3.84	3.38	6.18(R_1);6.10(R_2)	8.02	J_{4,CH_3} $J_{4,5}$ J_{8,OR_1} J_{5,OR_2}	0.8 0.4 0.5 0.5
5	4.97	4.58	3.40	3.51	6.08;6.10‖	8.07	J_{4,CH_3} J_{8,OR_1} J_{8,CH_2}	0.7 0.6 or <0.4
6	4.88	4.68	4.10	3.44	6.15(R_1);6.17(R_2)	8.05	J_{4,CH_3} J_{5,OR_1} J_{8,OR_2}	0.8 0.6 0.5

*Spectra (100 MHz) for compounds 1 and 4 were recorded in pyridine-d_5, for compounds 4*a* to 6 in chloroform-d_1.
†Compounds 4*b*, 5, and 6 were previously referred to as anhydrosepedonin dimethyl ethers A, B, and A_1 (1).
‡Methylene protons H_1 and H_4 in compound 1 formed AB systems where $\Delta\nu_{1,1} = 8.2$ and $\Delta\nu_{4,4} = 11.4$ Hz. τ-Values are for centers of the AB quartets. In the remaining compounds, protons H_1 were chemically equivalent.
§Hydroxyl proton on C-3 also occurs at τ 0.3.
‖Methoxyl resonances could not be assigned.
¶In addition to measured couplings, long range couplings were detected (decrease in line width at half height on double irradiation) between H_5 and H_4 and H_5 and H_1 in all compounds. H_1 and H_4 were also coupled in compound 1 ($J \simeq 1.4$ Hz). The intensities of the H_5 and H_8 protons were integrated during decoupling experiments with some compounds. An increase of 16–22% in the intensity (intramolecular n.O.e.) of the H_5 signal was observed on irradiation of H_4 in 1, 4, 4*a*, and 4*b*. The intensity of H_5 also increased (23%) on irradiation of the adjoining methoxyl protons OR_2 in 4*b*. Similarly the intensity of H_8 increased (20 and 34%) on irradiation of OR_1 in 4*a* and *b*.

and anhydrosepedonin should be identical.

(*3*) The signals for both methylene groups in sepedonin were uncomplicated by vicinal coupling, and decoupling experiments indicated that they were in a homoallylic relationship ($J \simeq 1.4$ Hz; estimated from decrease in line width at half height on double irradiation). Chemical non-equivalence of the hydrogens in each methylene group (both gave characteristic broadened AB quartets, $J_{AB} \simeq 17$ Hz) also indicated that they were either part of a ring system, in which no averaging of the environment occurred due to conformer interconversion, or in an otherwise asymmetric environment. Previous work (1) had also shown that anhydrosepedonin contained two phenolic-type hydroxyl groups (p$K \simeq 6$ and 9) and a masked carbonyl group. These functional groups are also present in sepedonin since they were not involved in its dehydration. The presence of secondary or primary alcohol groups was also excluded by recording the spectra of sepedonin and anhydrosepedonin in DMSO-d_6 (3).

It can be concluded that the oxygen attached to the allylic methylene group appearing at τ 4.85 in the spectrum of sepedonin is also attached to the carbon atom bearing the hydroxyl, methyl, and methylene (τ 7.02) groups. The combined evidence so far is consistent only with the presence in sepedonin of a 6-methyl-6-hydroxy-5,6-dihydro-2-pyran ring carrying carbon substituents on the double bond. By analogy anhydrosepedonin possesses a 6-methyl-2-pyran ring bearing carbon substituents at the 3- and 4-positions. This is consistent with lack of vicinal coupling to the methylene group and olefinic hydrogen (τ 4.40), and with all other evidence presented above.

(*4*) The remaining fragment of sepedonin and anhydrosepedonin, namely $C_5H_4O_3$, must now contain two phenolic-type hydroxyl groups, a carbonyl group and two =CH groups which are part of a system capable of keto–enol tautomerism (since they are replaceable by deuterium). Further decoupling experiments established that both methylene groups in sepedonin were long-range coupled to the hydrogen at τ 3.08 but not to the one at τ 2.81. Irradiation of one methylene group (τ 7.02) resulted in an enhancement (relative intensity 122 ± 2) of the integrated intensity of the signal at τ 3.08, whereas no increase was observed when the other methylene

Can. J. Chem. Downloaded from www.nrcresearchpress.com by 210.87.254.42 on 09/05/12
For personal use only.

Can. J. Chem. Downloaded from www.nrcresearchpress.com by 210.87.254.42 on 09/05/12
For personal use only.

group (τ 4.85) was irradiated. Such increases in intensity are due to the nuclear Overhauser effect (n.O.e.) (4). The methylene hydrogens (τ 7.02) must contribute appreciably to the relaxation of the hydrogen appearing at τ 3.08, and since this effect operates only over small interatomic distances, its presence establishes that this methylene group and aromatic hydrogen have a close steric relationship. Conversely its absence when the other methylene (τ 4.85) was irradiated means that this group is not sterically close to the hydrogen at τ 3.08. It follows that the methylene group (τ 7.02) and aromatic hydrogen (τ 3.08) must be in the relationship shown in structure **1** and not **2**.

Similar decoupling experiments on anhydrosepedonin showed that both the methylene group and olefinic hydrogen (τ 4.40) were long-range coupled to the aromatic hydrogen appearing at τ 3.10. The intensity of the latter was increased (relative intensity 116 ± 2; n.O.e.) when the olefinic hydrogen was irradiated whereas no similar enhancement occurred on irradiating the methylene group. It can be concluded, therefore, that the aromatic (τ 3.10) and olefinic (τ 4.40) hydrogens have the steric relationship shown in **4**. This independently establishes that structure **1** correctly depicts the steric relationship of the methylene group (τ 7.02) and aromatic hydrogen (τ 3.08) in sepedonin, since we have already proven that the olefinic hydrogen (τ 4.40) in anhydrosepedonin is derived from the methylene group at τ 7.02.

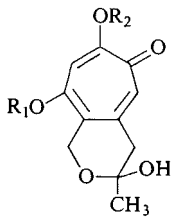

3 $R_1 = R_2 = CH_3$

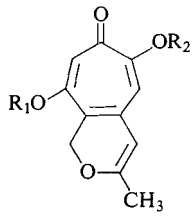

4 $R_1 = R_2 = H$
4*a* $R_1 = CH_3$, $R_2 = H$
4*b* $R_1 = R_2 = CH_3$

The methylene group in anhydrosepedonin was also long-range coupled to the other aromatic-type hydrogen (τ 2.73). However, no n.O.e. was seen when the methylene group was irradiated, so the second aromatic hydrogen (τ 2.73) in anhydrosepedonin cannot be at position 9 in structure **4**. This and a lack of coupling between the τ 4.85 methylene and τ 2.81 aromatic hydrogens in sepedonin prove that the second aromatic hydrogen is not at position 9 of structure **1**. Decoupling experiments also showed that the two aromatic hydrogens in sepedonin (τ 2.81 and 3.08) and anhydrosepedonin (τ 2.73 and 3.10) were not coupled. These observations are consistent only with structure **1** for sepedonin and structure **4** for anhydrosepedonin. Any other positioning of the hydroxyl or carbonyl functional groups would produce steric relationships resulting in the two tropolone hydrogens being coupled.

The facile dehydration and the difference in the rates of exchange of the two aromatic-type hydrogens in sepedonin are explained by **1**. Protonation of the hemi-ketal hydroxyl group followed by loss of a molecule of water would produce a tertiary carbonium ion which would be further stabilized by delocalization of the lone pair of electrons on the other oxygen substituent, thereby facilitating the dehydration process. Moreover, the hydrogen at C-8 in sepedonin (or anhydrosepedonin) should exchange more rapidly than the one at C-5 if it is located between two oxygen functions as shown in **1** and **4**. Finally, the chemical shifts of the two tropolone ring hydrogens in sepedonin and anhydrosepedonin are consistent with those found in similar environments in other tropolones (5).

Conformation of the Dihydropyran Ring

Although sepedonin (**1**) contains an asymmetric center at C-3 it is not optically active. The 5,6-dihydro-2-pyran ring can exist in two conformations and, although each conformer and its mirror image are equally populated, the populations of the conformers could differ. It is therefore necessary to explain why p.m.r. signals are not observed for each. It is known that the energy barriers between the two minimum conformations of cyclohexene (6) and 4-bromocyclohexene (7) are lower than for cyclohexane (8). The number of unfavorable torsional interactions in the transition state between the two conformations of the 5,6-dihydro-2-pyran ring of sepedonin, or in the conformers themselves, suggests that energy differences and energy barriers between the two conformations are unlikely to greatly exceed those found in 4-bromocyclohexene.

There are two averaging processes responsible for the methyl hydrogens appearing as a singlet. The methyl group possesses a three-fold axis

Can. J. Chem. Downloaded from www.nrcresearchpress.com by 210.87.254.42 on 09/05/12
For personal use only.

of symmetry coincident with the bond attaching it to the asymmetric center and consequently rapid internal rotation about this bond will average the magnetic environment of the methyl hydrogens. In addition, rapid interconversion of the ring conformers will simultaneously average the chemical shifts of the methyl groups in these conformers. The presence of an asymmetric center precludes any type of averaging of the chemical shifts of the hydrogens in each methylene group. In principle each methylene group will give two AB systems, one for each ring conformer, but these will be averaged by rapid conformer interconversion. When an attempt was made to observe the two conformers of sepedonin by recording the p.m.r. spectrum in pyridine–methanol (1:4) at $-90°$ the only change observed was a broadening of the signal envelopes. Solubility problems in the above and other solvents prevented studies at lower temperatures. At $-164°$ separate signals for axial and equatorial hydrogens at C-4 and -5 of cyclohexene have been observed at 60 MHz (6). Since at $-90°$ and 100 MHz only an averaged spectrum was observed for the two conformers of sepedonin, it seems reasonable to conclude that the activation barrier for interconversion of the dihydropyran ring in this compound must be of similar magnitude, or perhaps even lower, than that for cyclohexene.

Methyl Ethers

Controlled addition of diazomethane to anhydrosepedonin was reported to give a monomethyl ether, whereas a mixture of three isomeric dimethyl ethers, A, A_1, and B were obtained with excess reagent (1). Anhydrosepedonin dimethyl ether A was believed to be unstable, rearranging slowly to dimethyl ether A_1. We have checked and found that the latter belief was unfounded; all three dimethyl ethers are stable and are not interconvertible. The only dimethyl ethers obtained when anhydrosepedonin was treated with base and dimethyl sulfate in acetone, or alternatively with silver oxide and methyl iodide in benzene, were A and B. Sepedonin gave dimethyl ethers A and B when reacted with diazomethane, and these were dehydrated to anhydrosepedonin dimethyl ethers A and B, respectively (1). The structures of all of these derivatives were not determined.

The methyl ethers of anhydrosepedonin gave p.m.r. spectra containing characteristic signals for all types of hydrogens present in anhydrosepedonin except the hydroxyl hydrogens, one or both of which was replaced by the corresponding methoxyl signal. With this additional data, structures can now be assigned, and they offer additional confirmation of the structures assigned to anhydrosepedonin and sepedonin.

Anhydrosepedonin Monomethyl Ether (4a)

The spin–spin couplings observed in **4***a* were the same as for anhydrosepedonin except that the tropolone hydrogen (τ 3.22) was also long-range coupled to the methoxyl hydrogens. Irradiation of the methoxyl group caused an enhancement (relative intensity 120 ± 2) of the signal for the tropolone hydrogen (τ 3.22), and irradiation of the olefinic hydrogen (τ 4.50) caused a similar increase (117 ± 2) in intensity of the other tropolone hydrogen (τ 3.33; n.O.e.). If anhydrosepedonin contains the 4-hydroxytropolone ring system shown in **4** the hydroxyl group at position 9 is the most acidic (9) and should therefore be preferentially methylated. The above evidence is consistent only with methylation having occurred at this position and consequently the monomethyl ether must have structure **4***a*.

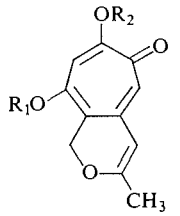

5 $R_1 = R_2 = CH_3$

Anhydrosepedonin Dimethyl Ether B (5)

The hydrogens of both methoxyl groups in anhydrosepedonin dimethyl ether B were long-range coupled to the high field (τ 3.51), but not to the low field (τ 3.40) tropone hydrogen. Thus one hydrogen (τ 3.51) is vicinal to both methoxyl groups and the other (τ 3.40) is not vicinal to either. In addition the methyl group was allylic coupled to the olefinic hydrogen (τ 4.58) and the latter, together with the methylene hydrogens (τ 4.97), were long-range coupled to the low field tropone hydrogen (τ 3.40). No other couplings were observed. These data are consistent only with anhydrosepedonin dimethyl ether B having structure **5**.

It follows that sepedonin dimethyl ether B has

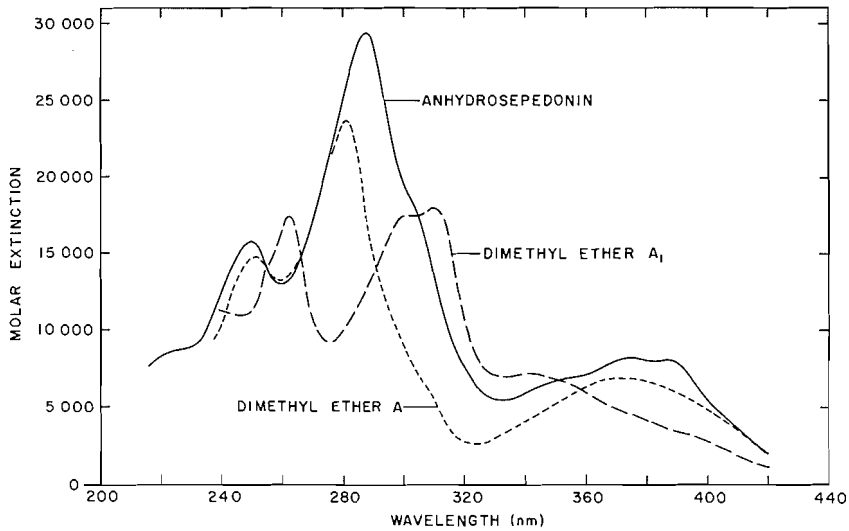

FIG. 1. Ultraviolet absorption spectra in 0.1 *M* ethanolic hydrogen chloride of anhydrosepedonin (——), anhydrosepedonin dimethyl ether A_1 (- - - -), and anhydrosepedonin dimethyl ether A (· · · · · ·).

structure **3** since **5** is obtained on dehydration (1).

Anhydrosepedonin Dimethyl Ether A (4b)

The methyl group was allylic coupled to the olefinic hydrogen (τ 4.50) and the high field tropone hydrogen was long-range coupled to the methylene hydrogens (τ 4.95), the olefinic hydrogen, and the hydrogens of one methoxyl group (τ 6.10). Only one other coupling was observed, namely that between the second methoxyl group (τ 6.18) and the low field tropone hydrogen (τ 3.38). Irradiation of the appropriate methoxyl signal increased the intensities (relative values 123 ± 2; 134 ± 2) of the tropone hydrogens (τ 3.84, 3.38; n.O.e.). Moreover, the u.v. spectrum of dimethyl ether A was similar to that of anhydrosepedonin whereas that of dimethyl ether A_1 was different (Fig. 1). The combined evidence therefore establishes anhydrosepedonin dimethyl ether A as **4***b* and the corresponding derivative of sepedonin as **1***a*.

Anhydrosepedonin Dimethyl Ether A_1 (6)

The low field tropone hydrogen (τ 3.44) was long-range coupled to the methoxyl group at τ 6.17 whereas the high field one (τ 4.10) was similarly coupled to the methoxyl group at τ 6.15. One tropone hydrogen (τ 4.10) was also long-range coupled to the methylene (τ 4.88) and olefinic (τ 4.68) hydrogens and the latter was once again allylic coupled to the methyl group. No other hydrogens were vicinal or long-range coupled. The only remaining structure compatible with this evidence and the u.v. spectrum of A_1 is **6**.

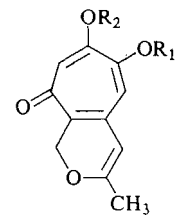

6 $R_1 = R_2 = CH_3$

Aromatic solvent induced shifts observed when the anhydrosepedonin dimethyl ethers were examined in a benzene-d_6 – chloroform-d_1 (ca. 1:1) mixture instead of chloroform-d_1 were consistent with the foregoing structural assignments (10). In dimethyl ether A_1 the methylene group was deshielded by 0.11 p.p.m., whereas in A and B it was shifted upfield by 0.10 and 0.11 p.p.m. respectively. Only in **6** would the steric relationship of the methylene and carbonyl groups be expected to result in a substantial deshielding effect by benzene (11). With dimethyl ether B a weak (0.03 p.p.m.) deshielding effect was observed on the vicinal low field tropone proton (τ 3.40), whereas with A and A_1 the corresponding proton signals showed large upfield shifts (0.24 and 0.28 p.p.m., respectively).

Can. J. Chem. Downloaded from www.nrcresearchpress.com by 210.87.254.42 on 09/05/12
For personal use only.

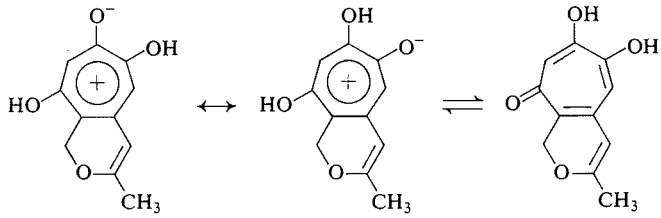

FIG. 2. Resonance and tautomeric forms of anhydrosepedonin.

It is now possible to account for the methylation products of anhydrosepedonin and sepedonin. Ionization followed by methylation at position 9 of anhydrosepedonin occurs when methyl iodide, or dimethyl sulfate, is used in the presence of a base (Ag_2O or K_2CO_3). This result would be expected from the relative magnitudes of the ionization constants (pK 6 and 9) of the two hydroxyl groups in the 4-hydroxytropolone ring of anhydrosepedonin which has contributions from two resonance forms (see Fig. 2). Subsequent methylation of the initial product (**4***a*) at positions 6 or 7 would then produce only A (**4***b*) or B (**5**) in agreement with experiment. Similarly sepedonin must exist only as **1** in ethanol since reaction with diazomethane only produces **1***a* and **3** indicating that methylation at positions 6 and 7 are subsequent to methylation at position 9.

Since anhydrosepedonin reacts with diazomethane in neutral solvents to give the three isomeric dimethyl ethers **4***b*, **5**, and **6**, the equilibrium shown in Fig. 2 must exist. This equilibrium is also necessary to explain exchange of the tropolone ring hydrogens of anhydrosepedonin with deuterium (pyridine/D_2O). The concentration of the tropone form, however, is too small to be observed in our p.m.r. studies. A similar equilibrium between the tropone and tropolone forms of sepedonin is required to account for the replacement of the tropolone ring hydrogens with deuterium.

After this paper was submitted Takenaka and Seto (12) reported independent studies on the anhydrosepedonin dimethyl ethers. We agreed with their structural assignments, but the relative yield of dimethyl ether B which we obtained upon reacting anhydrosepedonin in acetone with excess ethereal diazomethane was higher than they described for a similar reaction in methanol/ether. Since only isolated yields of methyl ethers have hitherto been reported we have remeasured the true yields more accurately, and confirmed our earlier results.

While it is clearly inadmissible to deduce the reactivities of the three potential hydroxyl functions from the amounts of dimethyl ethers formed, the presence of all three isomers in fairly similar proportions indicates that the initial reaction does not yield one monomethyl ether exclusively.

Experimental

Proton Magnetic Resonance

Spectra were recorded with a Varian HA-100 nuclear magnetic resonance spectrometer. Samples (20 to 30 mg) were dissolved in 0.4 ml of solvent containing a small amount of tetramethylsilane to provide the reference and field/frequency locking signal. Solutions were degassed prior to determining n.O.e. by double irradiation in the frequency sweep mode (4). To observe deuterium exchange, 20 μl of D_2O were added to the solution of the compound in pyridine-d_5 or dimethylformamide-d_7.

Ultraviolet Absorption

Spectra were recorded with a Beckman model DK-2 spectrophotometer.

Optical Rotation

Sepedonin (2 μg/ml in ethanol) had no measurable optical activity at 365, 436, 546, 578, or 589 mμ when examined with a Perkin–Elmer model 141 polarimeter.

Sepedonin

Samples were isolated from cultures of *Sepedonium chrysospermum* Fries and purified as described previously (1). Anhydrosepedonin was obtained from sepedonin by heating under reflux for 1 h in glacial acetic acid and purified as described (1).

Methylation of Sepedonin

Sepedonin (200 mg) in chloroform (10 ml) and dry ethanol (10 ml) was treated with excess ethereal diazomethane for 24 h at ambient temperature. Concentration *in vacuo* yielded a waxy solid (208 mg), shown by thin-layer chromatography (t.l.c.) on silica gel HF_{254} (E. Merck & Co., Darmstadt) with methanol–chloroform (1:20) to be a mixture of two main products (R_F 0.20 and 0.31) which quenched fluorescence and stained orange–brown with ferric chloride.

Preparative t.l.c. (500 × 20 × 0.8 cm layers of silica gel HF_{254} irrigated with methanol–chloroform, 7:93) of

Can. J. Chem. Downloaded from www.nrcresearchpress.com by 210.87.254.42 on 09/05/12
For personal use only.

part (100 mg) of this product and elution of the zone at R_F 0.31 with ethyl acetate afforded sepedonin dimethyl ether A (34 mg), crystallizing from ethyl acetate as almost colorless needles m.p. 170–178°. The zone at R_F 0.20 gave sepedonin dimethyl ether B (28 mg), crystallizing from ethyl acetate as pale cream prisms m.p. 140–146°.

Methylation of Anhydrosepedonin

(*a*) Anhydrosepedonin (500 mg) in acetone (8 ml) was treated with excess ethereal diazomethane for 24 h at ambient temperature. Concentration *in vacuo* afforded a brown oil (510 mg), shown by t.l.c. (silica gel HF_{254}; methanol–chloroform, 1:20) to be a mixture of three products (R_F 0.75, 0.64, and 0.50) which quenched fluorescence and stained with ferric chloride. A portion (400 mg) of the product was separated by preparative t.l.c. (four plates spread with 500 × 20 × 0.8 cm layers of silica gel HF_{254} and irrigated with methanol–chloroform, 7:93). Quenching zones were scraped from the plates and eluted with ethyl acetate to give (*a*) dimethyl ether A_1 (111 mg, R_F 0.75) crystallized from benzene–petroleum ether (60–80°) as yellow needles m.p. 157–159°; (*b*) dimethyl ether A (120 mg, R_F 0.64) crystallized from benzene as yellow needles m.p. 153–154°; (*c*) dimethyl ether B (90 mg, R_F 0.50), crystallized from water as pale yellow needles m.p. 145°.

(*b*) A suspension of anhydrosepedonin (32 mg, 0.15 mmole) in methanol (1.6 ml) was agitated at 4° with an ethereal solution (14.4 ml) of diazomethane prepared from *N*-methyl-*N'*-nitro-*N*-nitrosoguanidine (0.22 g, 1.5 mmole). After the sample had dissolved completely (10 min) the solution was evaporated and the residue, in chloroform, extracted successively with aqueous 1% sodium carbonate and 0.1 *N* sodium hydroxide solutions. The product remaining after extraction was separated by t.l.c. and the three dimethyl ethers eluted with ethanol. The amounts of unreacted anhydrosepedonin (sodium carbonate extract; 0.32 mg), its monomethyl ethers (sodium hydroxide extract; as **4***a*, 0.76 mg), and dimethyl ethers A_1 (10 mg), A (13 mg), and B (7 mg) were measured spectrophotometrically (1).

1. P. V. Divekar, H. Raistrick, T. A. Dobson, and L. C. Vining. Can. J. Chem. **43**, 1835 (1965).
2. J. Wright, D. G. Smith, A. G. McInnes, L. C. Vining, and D. W. S. Westlake. Can. J. Biochem. **47**, 945 (1969).
3. O. L. Chapman and R. W. King. J. Amer. Chem. Soc. **86**, 1256 (1964).
4. F. A. L. Anet and A. J. R. Bourn. J. Amer. Chem. Soc. **87**, 5250 (1965).
5. W. C. Wildman and B. A. Pursey. *In* The alkaloids, chemistry and physiology. Vol. XI. *Edited by* R. H. F. Manske. Academic Press Inc., New York, 1968. p. 420.
6. F. A. L. Anet and M. Z. Hag. J. Amer. Chem. Soc **87**, 3147 (1965).
7. F. R. Jensen and C. H. Bushweller. J. Amer. Chem. Soc. **87**, 3285 (1965).
8. F. A. L. Anet, M. Ahmad, and L. D. Hall. Proc. Chem. Soc. 145 (1964).
9. N. Yui. Sci. Rep. Tohoku Univ. First Ser. **40**, 114 (1956).
10. Y. Fujise and S. Ito. Chem. Pharm. Bull. **14**, 797 (1966).
11. J. D. Connolly and R. McCrindle. Chem. Ind. 379 (1965).
12. S. Takenaka and S. Seto. Sci. Rep. Tohoku Univ. **A21**, 106 (1969).

Can. J. Chem. Downloaded from www.nrcresearchpress.com by 210.87.254.42 on 09/05/12
For personal use only.

Can. J. Chem. Downloaded from www.nrcresearchpress.com by 210.87.254.42 on 09/05/12
For personal use only.

β-Ketoalkylthioacrylic acid derivatives as precursors of thiophenes, thiazolines, and thienopyrimidines[1]

RÉAL LALIBERTÉ AND GEORGES MÉDAWAR
Department of Chemistry, Ayerst Research Laboratories, Montreal, Quebec

Received April 3, 1970

Nous avons poursuivi l'étude de la réaction de certains sels sodés de dérivés de l'acide amino-3-cyano-2-thioacrylique avec des dérivés halogénés. L'action de méthylcétones α-halogénées a permis d'obtenir dans certaines conditions soit des dérivés d'acide acyl-5-diamino-2,4-thiophène-3-carboxylique soit des dérivés d'acide thiazoline-$\Delta^{2\alpha}$-acétique. L'acétylation de certains thiophènes a conduit à la formation de thiènopyrimidines.

Reactions of sodium salts of substituted 3-amino-2-cyano-3-thioacrylic esters and amides with α-halomethylketones were studied. Conditions were found which led to the synthesis of either 5-acyl-2,4-diaminothiophene-3-carboxylic esters and amides or thiazoline-$\Delta^{2\alpha}$-acetic esters and amides. Some thiophene-3-carboxamides were also transformed into thienopyrimidines upon acetylation.

Canadian Journal of Chemistry, **48**, 2709 (1970)

Introduction

Some thioamides with a carbonyl group in β position (i.e. **13**) exist mainly as enols **12** and form sodium salts **3** which may be reacted further to produce substituted heterocycles by mechanisms involving additions, eliminations or displacements. The first example of this type of reaction goes as far back as 1908 (1), but it is only since 1965 that these β-thioamides **13** were used as starting materials versatile enough to yield heterocycles as diverse as 3,4-diarylthiazole-2-acetic esters (2), benzothiazoline-2-acetic esters (3, 5), 5-amino-3-hydroxythiophenedicarboxylic esters (6), 3-amino-5-hydroxypyrazoles (7, 8), 3-amino-5-hydroxypyrazole-4-carboxylic acid derivatives (6), 3-anilino-5-hydroxyisoxazoles (8, 9), 3-aminoisothiazoles (10), and tetrahydrobenzothiazoline-2-acetic esters (4).

The presence of a nitrile group in some of these β-thioamides **13** allows an easy synthesis of the hitherto unreported 5-acyl-2,4-diaminothiophene-3-carboxylic acid derivatives **8**, herein described as thiophene-3-carboxylic esters and amides. This paper will elaborate on the use of those β-thioamides **13** and will show how they yielded selectively derivatives of thiophene-3-carboxylic esters and amides **8** or derivatives of thiazoline-2-acetic esters and amides **11**. We will also show how some of these thiophene-3-carboxamides **8** have been transformed into fused thienopyrimidines **15**.

[1]This work has been supported by the Industrial Research Assistance Program of the National Research Council of Canada.

Synthesis

The sodium salts **3** of the enol form of β-thioamides **13**, herein described as sodium salts of 3-substituted amino-2-cyano-3-thioacrylic esters and amides **3** have provided versatile starting materials for this synthesis. They were obtained "in situ" by reaction of isothiocyanates **1** to derivatives of cyanoacetic acid (**2** where Z is O or N) (see Scheme 1). Originally described (1, 11) as an addition of cyanoacetic ethyl ester (**2** where ZR^2 is OC_2H_5) to an aryl isothiocyanate this reaction has been extended to include alkyl isothiocyanates such as methyl (4), allyl, *tert*-butyl, cyclohexyl, and benzyl isothiocyanates. We have also used cyanoacetamides in addition to the cyanoacetic ethyl ester. Accordingly we were able to prepare as starting materials a variety of sodium salts of 3-arylamino and 3-alkylamino-2-cyano-3-thio-acrylic esters as well as amides (**3** where ZR^2 is OC_2H_5, $NH{-}CH_3$, NHC_6H_5, $NH{-}N\langle\rangle$, $NHN(CH_3)_2$).

The sodium salts **3** were reacted "in situ" with halocompounds. This addition of α-halomethylketones was carried out at temperatures ranging from 0 °C to the boiling point of ethanol. In most cases, the use of either low or high temperature resulted in a selective preparation of thiophene-3-carboxylic esters or amides **8** or of thiazoline-2-acetic esters, **11**, respectively. For example, the reaction of an α-halomethylarylketone (**4** where R^3 is aryl) with the sodium salt of a 3-arylamino-2-cyano-3-thioacrylic ester (**3** where ZR^2 is OC_2H_5 and R^1 is aryl) in *boiling* ethanol resulted in the formation of a 3-arylthiazoline-2-acetic

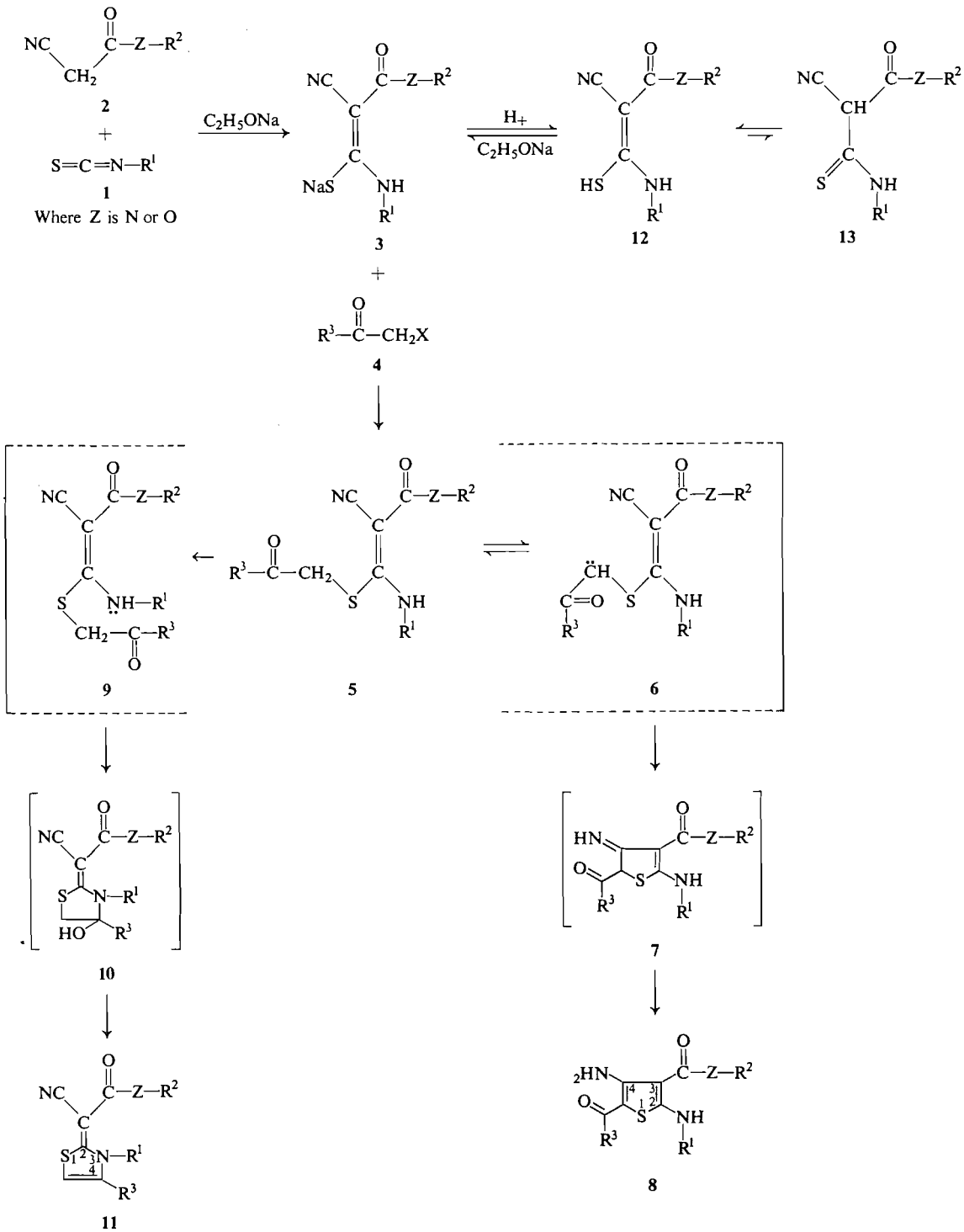

SCHEME 1
Synthesis of thiophenes and thiazolines

Can. J. Chem. Downloaded from www.nrcresearchpress.com by 210.87.254.42 on 09/05/12
For personal use only.

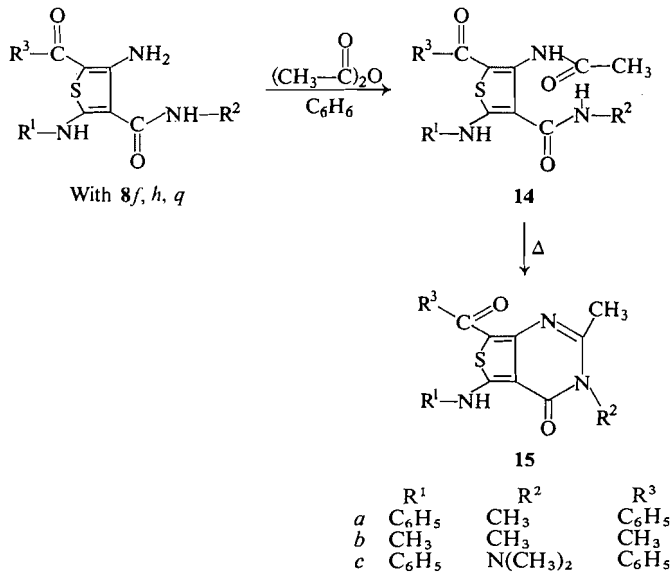

	R^1	R^2	R^3
a	C_6H_5	CH_3	C_6H_5
b	CH_3	CH_3	CH_3
c	C_6H_5	$N(CH_3)_2$	C_6H_5

SCHEME 2

ester, **11**, as published earlier (2). When the same reaction was effected in the same solvent in the *cold*, a 5-acyl-4-amino-2-arylamino-thiophene-3-carboxylic ester **8***a*, was the only product isolated.

We have applied this modification of a known reaction (2) to a variety of new 3-amino-2-cyano-3-thioacrylamides (**3** where Z is N) and observed similarly the formation of 12 substituted thiophene-3-carboxamides (Table 1, **8***e*, *g*–*q* where Z is N), in yields ranging from 30 to 80%. This procedure has allowed the use of 3-arylamino as well as 3-alkylamino-2-cyano-3-thioacrylamides and has worked nicely with the 3 α-halomethyl-*aryl*ketones investigated (**4** where R^3 is phenyl, *p*-chlorophenyl, and biphenylyl).

Difficulties were encountered when an α-halomethyl*alkyl*ketone (**4** where R^3 is alkyl) such as chloroacetone was used. Reaction with a sodium salt of a 3-arylamino-2-cyano-3-thioacrylamide (**3** where R^1 is aryl) was found to give the expected 5-acetyl-2-arylamino-4-aminothiophene-3-carboxamide, **8***o*, while the same reaction with a 3-alkylamino-2-cyano-3-thioacrylamide (**3** where R^1 is alkyl) yielded a 3-alkylthiazoline-2-acetamide, **11**. This difficulty was overcome by changing the reaction conditions, by adding chloroacetone slowly at a higher temperature. A 5-acetyl-4-amino-2-methylaminothiophene-3-carboxamide, **8***f*, was obtained.

The above showed that certain combinations of substituents R^1 and R^3 have a pronounced influence on the course of the reaction. In addition, the ZR^2 group was also quite important. As mentioned above, amides yielded easily thiophene-3-carboxamides but the esters of 3-thioacrylic acid **3** were more sensitive to substituent influences. For example, when R^1 and R^3 were phenyls, reaction in the cold gave the expected thiophene-3-carboxylic ester **8***a*, in good yield. When R^1 was a large aliphatic group such as *tert*-butyl, cyclohexyl, or even benzyl, the addition of chloropropanone (R^3 is CH_3) had to be done slowly in warm ethanol, to result in the preparation of thiophene-3-carboxylic esters, **8***b*, *c*, *d*, and the yields were poor. When R^1 was a small alkyl group such as a methyl or an ethyl the slow addition of chloropropanone (R^3 is CH_3) in warm ethanol yielded thiazoline-2-acetic esters, **11**. We were unable to isolate the corresponding thiophene-3-carboxylic esters, **8**.

We also observed the reaction of 2,4-diaminothiophene-3-carboxamides (**8** where Z = N) with acetic anhydride to yield a monoacetamide, **14**, the primary amine being the only one to react. Heating a solution of a thiophene-3-carboxamide in benzene containing some pyridine for 1 h to reflux has not acylated the secondary amine in position 2, no difference being seen between arylamine and alkylamine. A prolonged heating period has rather effected ring closure between amides in positions 3 and 4 to generate thieno-[3,4-*d*]pyrimidines, **15**, described in Scheme 2.

Can. J. Chem. Downloaded from www.nrcresearchpress.com by 210.87.254.42 on 09/05/12
For personal use only.

Can. J. Chem. Downloaded from www.nrcresearchpress.com by 210.87.254.42 on 09/05/12
For personal use only.

TABLE 1

Derivatives of 5-acyl-2-alkylamino-4-aminothiophene carboxylic acid*

8	R^1	ZR^2	R^3	Method	Solvent of crystallization	Yield**	Melting point (°C)	Anal. Found (Calcd.) (%) C	H	N	S	Formula
a	C_6H_5	OC_2H_5	C_6H_5	*a*	Acetone†	60	138–139	65.51 (65.56)	5.24 (4.95)	7.89 (7.65)	8.80 (8.73)	$C_{20}H_{18}N_2O_3S$
b	CH_2—C_6H_5	OC_2H_5	CH_3	*b*	Acetone, toluene	20	130	60.30 (60.37)	5.80 (5.70)	8.62 (8.80)	9.84 (10.02)	$C_{16}H_{18}N_2O_3S$
c	$C(CH_3)_3$	OC_2H_5	CH_3	*b*	Acetone,‡ methylcyclohexane	40	88–90	54.75 (54.92)	7.04 (7.09)	9.97 (9.85)	11.37 (11.25)	$C_{13}H_{20}N_2O_3S$
d	C_6H_{11}	OC_2H_5	CH_3	*b*	Acetone§ + hexane, methylcyclohexane	40	80–82	57.79 (58.05)	7.00 (7.15)	8.93 (9.03)	10.48 (10.31)	$C_{15}H_{22}N_2O_3S$
e	CH_3	NH—CH_3	C_6H_5	*a*	Acetonitrile‖	40	220–222 d	58.53 (58.12)	5.27 (5.23)	14.25 (14.53)	11.27 (11.06)	$C_{14}H_{15}N_3O_2S$
f	CH_3	NH—CH_3	CH_3	*b*	Acetonitrile	30	221–223 d	47.76 (47.57)	5.85 (5.77)	18.30 (18.49)	14.16 (14.07)	$C_9H_{13}N_3O_2S$
g	C_3H_5¶	NH—CH_3	C_6H_5	*a*	Propanol	30	127–128 d	61.25 (60.94)	5.63 (5.43)	13.08 (13.33)	10.02 (10.15)	$C_{16}H_{17}N_3O_2S$
h	C_6H_5	NH—CH_3	C_6H_5	*a*	Isopropanol	75	207–209 d	64.95 (64.95)	4.89 (4.88)	11.91 (11.96)	9.35 (9.11)	$C_{19}H_{17}N_3O_2S$
i	C_6H_5	NH—CH_3	*p*-C_6H_4Cl	*a*	Acetonitrile	30	233–235 d	59.17 (59.13)	4.31 (4.17)	10.70 (10.88)	8.26 (8.31)	$C_{19}H_{16}ClN_3O_2S$
j	C_6H_5	NH—CH_3	C_6H_4–C_6H_5	*a*	Ethoxyethanol	60	251–253 d	70.33 (70.24)	4.87 (4.95)	9.84 (9.83)	7.69 (7.48)	$C_{25}H_{21}N_3O_2S$
k	*m*-$C_6N_4NO_2$	NH—CH_3	C_6H_5	*a*	Ethoxyethanol	45	259–260 d	57.85 (57.57)	4.30 (4.07)	13.94 (14.14)	8.25 (8.07)	$C_{19}H_{16}N_4O_4S$
l	C_6H_5	NH—C_6H_5	C_6H_5	*a*	Methoxyethanol	70	228–230 d	69.63 (69.72)	4.61 (4.63)	10.40 (10.61)	7.83 (7.74)	$C_{24}H_{19}N_3O_2S$
m	C_6H_5	NH—C_6H_5	C_6H_4–C_6H_5	*a*	Methoxyethanol	70	256–258 d	73.41 (73.60)	4.60 (4.74)	8.48 (8.58)	6.48 (6.53)	$C_{30}H_{23}N_3O_2S$
n	*m*-$C_6H_4NO_2$	NH—C_6H_5	C_6H_5	*a*	Ethoxyethanol	60	213–215 d	63.11 (62.88)	4.25 (3.96)	12.46 (12.22)	6.98 (6.98)	$C_{24}H_{18}N_4O_4S$
o	C_6H_5	NH—C_6H_5	CH_3	*a*	Acetonitrile	30	223–225 d	64.73 (64.95)	4.73 (4.88)	11.92 (11.96)	9.20 (9.11)	$C_{19}H_{17}N_3O_2S$
p	C_6H_5	NH—N⟨⟩	C_6H_5	*a*	Methoxyethanol	80	243–245 d	65.66 (65.70)	5.93 (5.75)	13.42 (13.33)	7.65 (7.61)	$C_{23}H_{24}N_4O_2S$
q	C_6H_5	NH—$N(CH_3)_2$	C_6H_5	*a*	Acetonitrile	60	232–234 d	63.51 (63.15)	5.50 (5.30)	14.70 (14.73)	8.47 (8.41)	$C_{20}H_{20}N_4O_2S$

*The compound has the following general structure:

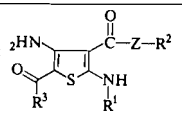

8

†Chromatographed on Merck silica gel with 2% ethyl acetate in benzene.
‡Chromatographed on alumina of activity I with 20% ethyl acetate in benzene.
§After chromatography on alumina activity I with 10% ethyl acetate in benzene.
‖This substance crystallized partly from the reaction mixture.
¶Allyl.
**In most cases, as obtained after a single assay, calculated from quantity of cyanoacetamide used.

Can. J. Chem. Downloaded from www.nrcresearchpress.com by 210.87.254.42 on 09/05/12
For personal use only.

This has afforded an easy synthesis of a new group of substituted thieno-pyrimidines.

Discussion

The reaction which led to derivatives of thiophene-3-carboxylic acids, **8**, or of thiazoline-2-acetic acids, **11**, could be explained as shown in Scheme 1. Reaction of a sodium salt of a 3-amino-2-cyano-3-thioacrylic ester or amide **3** with a α-halomethylketone resulted in a hypothetical 3-(β-ketomethylthio)-3-amino-2-cyanoacrylic ester or amide **5**. This unstable substance **5** having a methylene adjacent to a carbonyl and a sulfur could have formed a carbanion **6** in the presence of unreacted sodium salt **3**. This could have added to the nitrile to form a 4-iminothiophene-3-carboxylic ester or amide[2] **7** that stabilized itself by rearranging into a 4-aminothiophene-3-carboxylic ester or amide **8**. Obviously a key step in this reaction would have been the formation of a carbanion, **6**, originating by interaction of a 3-(β-ketomethylthio) acrylic acid derivative, **5**, and some unreacted sodium salt **3**, indicating that some kind of equilibrium must exist between **3**, **5**, and **6**. Ring closure of the carbanion **6** to a 4-iminothiophene-3-carboxamide regenerated the sodium salt **3** and the reaction proceeded further as long as some sodium salt was present. This reaction mechanism is supported by the fact that thiophenes were obtained only when the reaction conditions favored such an equilibrium, namely when the reaction was carried out in the cold as in "method *a*", or when the addition of the α-halomethylketone to a warm solution was effected slowly as in "method *b*".

The dehydrative cyclization route (sequences **5** to **9** to **10** and **11**) ensued if the reaction was carried out under conditions enhancing the formation of the 3-(β-ketomethylthio) acrylic acid derivatives, namely when the haloketone was added at once in warm ethanol. The simultaneous presence in the molecule of a nucleophile and of an available carbonyl should lead to addition products. 4-Hydroxythiazolidine-2-acetic esters, **10**,[3] were indeed formed which, on loss of water, yielded thiazoline-2-acetic esters, **11**. This addition was also influenced by the bulkiness of the groups R^1 on the nitrogen; a small alkyl or an aryl giving a faster addition than large alkyl groups such as *tert*-butyl or cyclohexyl.

We previously assigned the *cis* configuration to the sodium salt of 3-amino-2-cyano-3-thioacrylic acid, esters and amides **3** and their *S*-alkyl derivatives **5** (4). This choice was based mainly on infrared (i.r.), and ultraviolet (u.v.) data. The easy addition of the carbanion **6** to the adjacent nitrile provides an additional argument for the *cis* configuration. The reverse configuration would have made this addition impossible, the nitrile being too far from the active methylene. We isolated, in many cases, the free thio compound **12**. Theoretically **12** could have been transformed via **13** into the *trans* isomer to give a mixture of isomers. This was not the case and addition of C_2H_5ONa regenerated the same sodium salt **3**. This can be explained by the increased stability due to hydrogen bonding between —NH— and —C(=O)—.

All i.r. and u.v. data of thiophene-3-carboxylic esters and amides **8** are summarized in Table 2. The u.v. maxima were more influenced by R^1 than by R^3. Carbonyls of esters at 1655 ± 5 cm^{-1} in $CHCl_3$ and of amides at 1625 ± 15 cm^{-1} in Nujol were normal for this type of compound (5). In some cases, more than one crystalline structure were detected in Nujol. Similarity of isomers was then proven by comparison of u.v. and nuclear magnetic resonance (n.m.r.) data. All n.m.r. spectra were recorded and found to agree with the proposed structure. The absence of any proton on the thiophene ring has given n.m.r. spectra showing the substituents only, rendering their description unnecessary. However, they have consistently shown a broad NH_2 and a sharp NH, plus an additional NH for amides. In one case, namely for **8***h*, a mass spectrum of a thiophene-3-carboxamide was recorded. As expected, the correct molecular ion was detected together with a strong peak at 294 resulting from the loss of —C(=O)—NH—CH_3.

The presence in the i.r. of a strong conjugated nitrile at 2190 cm^{-1} ± 10 for thiazoline-2-acetic esters, **11**, made it possible to differentiate **11** from thiophene **8** or to detect **11** in mixtures. The i.r., u.v., and n.m.r. data for thiazoline-2-acetic esters, **11**, and thienopyrimidines, **15**, are included in the Experimental.

[2]The stability of those iminothiophenes is influenced to a great extent by the substituents on the ring. Examples of stable 4-iminothiophene-3-carboxamides will be given in another paper.

[3]Stable 4-hydroxythiazoline-2-acetic esters were described in a previous paper (4).

Can. J. Chem. Downloaded from www.nrcresearchpress.com by 210.87.254.42 on 09/05/12
For personal use only.

TABLE 2

The u.v. and i.r. of 5-acyl-2-alkylamino-4-aminothiophene-3-carboxylic acids

				Ultraviolet			Infrared				
								ν (cm^{-1})			
8	R^1	ZR^2	R^3	λ_{max} (ε) (mμ)	λ_{max} (ε) (mμ)	λ_{max} (ε) (mμ)	Solvent	NH	C=O	O ‖ C	C=C strong
a	C_6H_5	OC_2H_5	C_6H_5	262 (15 500)	297 (20 500)	369 (23 900)	$CHCl_3$	3490, 3460, 3360, 3280	1660	1580	1550
b	$CH_2—C_6H_5$	OC_2H_5	CH_3	258 (17 600)	277 (26 100)	340 (22 100)	$CHCl_3$	3490, 3390, 3300	1655	1580	1550
c	$C(CH_3)_3$	OC_2H_5	CH_3	260 (22 500)	278 (26 600)	345 (23 700)	$CHCl_3$	3490, 3370, 3255, 3200	1650	1580	1545
d	C_6H_{11}	OC_2H_5	CH_3	260 (19 200)	277 (27 400)	343 (25 400)	$CHCl_3$	3490, 3380, 3295	1655	1575	1545
e	CH_3	NH—CH_3	C_6H_5	254 (16 040)	285 (12 210)	357 (23 700)	Mull	3420, 3300, 3260	1625	1595	1570
f	CH_3	NH—CH_3	CH_3	253 (6 500)	278 (6 740)	347 (10 900)	Mull	3410, 3320, 3275	1635	1598	1550
g	C_3H_5	NH—CH_3	C_6H_5	253 (17 250)	285 (13 250)	350 (25 200)	Mull	3410, 3270	1618	1580	1540
h	C_6H_5	NH—CH_3	C_6H_5	258 (15 700)	308 (18 500)	375 (27 800)	Mull	3400, 3330, 3300	1610	1590	1550
i	C_6H_5	NH—CH_3	*p*-C_6H_4Cl	260 (18 000)	305 (17 250)	376 (26 200)	Mull	3400, 3320	1616	1585 1570	1550
j	C_6H_5	NH—CH_3	$C_6H_4—C_6H_5$	272 (27 500)	300 (21 250)	380 (27 600)	Mull	3400, 3300	1615	1580 1560	1550
k	*m*-$C_6H_4NO_2$	NH—CH_3	C_6H_5	Insoluble			Mull	3435, 3350, 3280	1640	1585 1565	1550
l	C_6H_5	NH—C_6H_5	C_6H_5	Insoluble			Mull	3400, 3300	1620	1580	1550
m	C_6H_5	NH—C_6H_5	$C_6H_4—C_6H_5$	Insoluble			Mull	3390, 3280	1620	1580 1565	1550
n	*m*-$C_6H_4NO_2$	NH—C_6H_5	C_6H_5	282 (24 800)	305 (23 500)	378 (24 000)	Mull	3420, 3340, 3275	1638	1590	1550
o	C_6H_5	NH—C_6H_5	CH_3		300 (25 100)	360 (21 500)	Mull	3430, 3300, 3265	1640	1590	1550
p	C_6H_5	NH—N⟨ ⟩	C_6H_5	258 (16 650)	307 (18 750)	375 (29 100)	Mull*	3425, 3310, 3225	1620	1585	1565
q	C_6H_5	NH—$N(CH_3)_2$	C_6H_5	258 (16 500)	305 (18 500)	375 (29 500)	Mull	3435, 3325		1585	1565

*Two crystalline structures were found—the other one has shown C=O at 1580.

Can. J. Chem. Downloaded from www.nrcresearchpress.com by 210.87.254.42 on 09/05/12
For personal use only.

Experimental

The melting points were determined with a Reichert melting point apparatus and are uncorrected. The i.r. spectra were recorded on a Perkin–Elmer model 225 spectrometer as a solution in $CHCl_3$ or as dispersion in Nujol. All u.v. spectra were obtained on a Perkin–Elmer 350 spectrophotometer in ethanol solution. The n.m.r. spectra were obtained with a Varian A-60-A apparatus and were recorded in deuterated chloroform, trifluoroacetic acid, or dimethylsulfoxide by Mrs. J. Jachner. Exchanges with D_2O were performed to detect NH and NH_2. Microanalyses were performed in our laboratories by Mr. W. Turnbull.

Preparation of Substituted Cyanoacetamides 2

2a, N-Methylcyanoacetamide (2 where ZR^2 is $NHCH_3$)

To 24 g of ethyl cyanoacetate in 50 ml of ethanol, 30 ml of 30% CH_3NH_2 in water were added. The solution was kept at 50° for 3 h and the solvents were evaporated to leave a residue which was crystallized twice from isopropanol to give the title compound in 30% yield. It melted at 98–99° (lit. (12*a*) m.p. 101°).

2b, Cyanoacetanilide (2 where ZR^2 is $NH—C_6H_5$)

A solution of 45 g of aniline in 37 g of ethyl cyanoacetate was kept at 150–160° for 6 h. It was left at room temperature overnight and the crystals were filtered off and washed with some ethanol. The solid (30 g) crystallized from acetone on addition of water. It melted at 199–200° (lit. (12*b*) m.p. 199–200°).

2c, N-(1-Piperidinyl)cyanoacetamide

(2 where ZR^2 is NH—N⬡)

A mixture of 0.2 mole of ethyl cyanoacetate and of *N*-aminopiperidine was left at room temperature for 4 days. A solid resulted that was filtered off and crystallized from isopropanol. It was obtained in 65% yield and melted at 131–132°.

Anal. Calcd. for $C_8H_{13}N_3O$: C, 57.46; H, 7.84; N, 25.13. Found: C, 57.48; H, 7.88; N, 25.25.

2d, Cyanoacetic Acid, N,N-Dimethylhydrazide (2 where ZR^2 is $NH—N(CH_3)_2$)

Prepared as described by E. G. Howard in ref. (13).

Sodium Salts of Substituted 3-Amino-2-cyano-3-thioacrylic Esters and Amides, 3

3a, Sodium Salt of 3-Anilino-2-cyano-3-thioacrylic Acid, Ethyl Ester

To a cold solution of sodium ethoxide (0.05 mole of sodium in 50 ml of ethanol), 0.05 mole of cyanoacetic acid ethyl ester was added. The solution was cooled and 0.05 mole of phenyl isothiocyanate was added. It was left on ice for 3 min and at room temperature for 1 h. The yellow solution was used as such.

3b, Sodium Salt of 2-Cyano-3-methylamino-3-thioacrylic Acid, Ethyl Ester

Prepared as for **3***a* using methyl isothiocyanate instead of phenyl isothiocyanate and refluxing for 1 h.

3c, Sodium Salt of 2-Cyano-3-ethylamino-3-thioacrylic Acid, Ethyl Ester

Prepared as for **3***b* but using ethyl isothiocyanate.

3d, Sodium Salt of 3-Allylamino-2-cyano-3-thioacrylic Acid, Ethyl Ester

Prepared as for **3***a* but using allyl isothiocyanate and refluxing for 30 min.

3e, Sodium Salt of 2-Cyano-3-methylamino-3-thioacrylic Acid, Methyl Ester

To a cold solution of sodium methoxide (0.05 mole of sodium in 75 ml of dry methanol) cyanoacetic acid, methyl ester was added. The solution was cooled and 0.05 mole of methyl isothiocyanate was added. The solution was heated under reflux for 1 h.

3f, Sodium Salt of 3-Benzylamino-2-cyano-3-thioacrylic Ethyl Ester

A solution of this salt in ethanol was obtained by the same procedure as described for **3***a* but using benzyl isothiocyanate instead of phenyl isothiocyanate.

3g, Sodium Salt of 3-tert-Butylamino-2-cyano-3-thioacrylic Acid, Ethyl Ester

Prepared as **3***a* using *tert*-butyl isothiocyanate instead of phenyl isothiocyanate. The solution was heated for 90 min to complete the reaction.

3h, Sodium Salt of 3-Cyclohexylamino-2-cyano-3-thioacrylic Ethyl Ester

Prepared as **3***a* using cyclohexyl isothiocyanate. The solution was heated for 60 min.

3i, Sodium Salt of 2-Cyano-3-methylamino-N-methyl-3-thioacrylamide

To a solution of sodium ethoxide (0.05 mole) in 150 ml of dry ethanol, 0.05 mole of *N*-methylcyanoacetamide, **2***a*, followed after 2 min by 0.05 mole of methyl isothiocyanate were added. The mixture was heated on a steam-bath for 2 h, some solid was filtered off, and the solution was used as such.

3j, Sodium Salt of 3-Allylamino-2-cyano-N-methyl-3-thioacrylamide

It was prepared as **3***i* using allyl isothiocyanate.

3k, Sodium Salt of 3-Anilino-2-cyano-N-methyl-3-thioacrylamide

It was prepared as **3***i* using phenyl isothiocyanate.

3l, Sodium Salt of 2-Cyano-N-methyl-3-m-nitroanilino-3-thioacrylamide

It was prepared as **3***i* using *m*-nitrophenyl isothiocyanate

3m, Sodium Salt of 3-Anilino-2-cyano-3-thioacrylanilide

It was prepared as **3***i* using cyanoacrylanilide **2***b* as starting material and replacing methyl isothiocyanate by phenyl isothiocyanate.

3n, Sodium Salt of 2-Cyano-3-m-nitroanilino-3-thioacrylanilide

It was prepared as **3***i* using *m*-nitrophenyl isothiocyanate.

3o, Sodium Salt of 3-Anilino-2-cyano-N-piperidino-3-thioacrylamide

It was prepared as **3***i* using *N*-(1-piperidinyl)cyanoacetamide **2***c* as starting material and replacing methyl isothiocyanate by phenyl isothiocyanate.

3p, Sodium Salt of 3-Anilino-2-cyano-3-thioacrylic Acid, N,N-Dimethyl Hydrazide

It was prepared as **3***i* using cyanoacetic acid, *N,N*-dimethyl hydrazide **2***d* as starting material and replacing methyl isothiocyanate by phenyl isothiocyanate.

Preparation of 5-Acyl-2,4-diaminothiophene-3-carboxylic Esters and Amides

They are described in Table 1. Two methods were used to prepare them. All the thiophenes were yellow solids.

Can. J. Chem. Downloaded from www.nrcresearchpress.com by 210.87.254.42 on 09/05/12
For personal use only.

Method a for **8***a, e, g–q*

The solution in ethanol of a convenient sodium salt of a substituted 3-amino-2-cyano-3-thioacrylic ester or amide (0.05 mole) prepared as described above was cooled to 5°. A solution in ethanol of an equivalent of an α-chloromethylketone such as chloropropanone, 2-chloroacetophenone, or an α-bromomethylketone such as 4′-phenyl-2-bromoacetophenone was added to it slowly with stirring and keeping the temperature between 5–10°. The solution was left at 10° for 2 h. In some cases, as for **8***j, l, m,* and *p*, the thiophene crystallized out of the reaction mixture. It was then filtered off and recrystallized twice from the solvent given in Table 1. If no yellow solid appeared, the ethanol was evaporated under vacuum and the residue was dissolved in $CHCl_3$ and washed. Evaporation of the $CHCl_3$ left a residue that was crystallized from the given solvent as for **8***e, g, h, i, k, n, o, q* or chromatographed as for **8***a*.

Method b for **8***b, c, d, f*

In most cases the addition of 0.05 mole of chloroacetone was effected slowly on a warm solution in ethanol of 0.05 mole of an appropriate sodium salt of a 3-amino-2-cyano-3-thioacrylic ester **3***f–h*; or amine **3***i*. The mixture was heated for 1 h. The solvent was then evaporated, the residue was taken into $CHCl_3$ and washed. The residue after evaporation was crystallized as shown for **8***b* and *f* or chromatographed and crystallized as for **8***c* and *d*.

Preparation of α-*Cyanothiazoline-*$\Delta^{2\alpha}$*-acetic Acid, Ethyl Ester,* **11**

11a, *α-Cyano-3,4-dimethylthiazoline-*$\Delta^{2\alpha}$*-acetic Acid, Ethyl Ester*

Chloropropanone 0.06 mole was added slowly to a warm solution in ethanol of 0.05 mole of the sodium salt of 2-cyano-3-methylamino-3-thioacrylic acid, ethyl ester **3***b*. The mixture was refluxed for 2 h and the solvent evaporated. The residue was dissolved in $CHCl_3$, washed with diluted HCl and with water. Evaporation left an oil that was crystallized from isopropanol and from ethyl acetate. This substance was obtained as a white solid (75%) melting at 176°; ν_{max} ($CHCl_3$) CN 2195, C=O 1650 cm^{-1}. In n.m.r. ($CDCl_3$) H_5 was at 388 Hz, u.v. ν_{max} 335 (ε 19 500).

Anal. Calcd. for $C_{10}H_{12}N_2O_2S$: C, 53.57; H, 5.39; N, 12.50; S, 14.27. Found: C, 53.50; H, 5.39; N, 12.76; S, 14.03.

11b, *α-Cyano-3-ethyl-4-methylthiazoline-*$\Delta^{2\alpha}$*-acetic Acid, Ethyl Ester*

This substance was prepared as described for **11***a* using the sodium salt of 2-cyano-3-ethylamino-3-thioacrylic acid ethyl ester **3***c* as starting material. It was crystallized from isopropanol and was obtained as a white solid (65%) melting at 112°; ν_{max} ($CHCl_3$) CN 2190, C=O 1650 cm^{-1}. In n.m.r. ($CDCl_3$) H_5 was a singlet at 385 Hz.

Anal. Calcd. for $C_{11}H_{14}N_2O_2S$: C, 55.45; H, 5.92; N, 11.76; S, 13.43. Found: C, 55.35; H, 6.18; N, 12.01; S, 13.46.

11c, *3-Allyl-α-cyano-4-methylthiazoline-*$\Delta^{2\alpha}$*-acetic Acid, Ethyl Ester*

This substance was prepared as described for **11***a* using as starting material the sodium salt of 3-allylamino-2-cyano-3-thioacrylic acid ethyl ester **3***d*. Hexane was added to a concentrated solution of it in $CHCl_3$. The white solid obtained (40%) was crystallized from isopropanol and from ethyl acetate. It melted at 99°; ν_{max} ($CHCl_3$) CN 2200, C=O 1652 cm^{-1}. In n.m.r. ($CDCl_3$) H_5 was a singlet at 389.

Anal. Calcd. for $C_{12}H_{14}N_2O_2S$: C, 57.29; H, 5.64; N, 11.20; S, 12.79. Found: C, 57.66; H, 5.89; N, 11.37; S, 12.65.

11d, *α-Cyano-3,4-dimethylthiazoline-*$\Delta^{2\alpha}$*-acetic Acid, Methyl Ester*

This substance was prepared as described for **11***a* using as starting material the sodium salt 2-cyano-3-methylamino-3-thioacrylic acid methyl ester **3***e*. Evaporation of the methanol left a dark solid which was filtered out, washed with isopropanol, and crystallized from acetonitrile. This methyl ester was much less soluble than the ethyl ester **11***a*. It was obtained in 55% yield as a white solid melting at 222–224°; ν_{max} (Nujol) CN 2195, C=O 1645 cm^{-1}. In n.m.r. (TFA) H_5 was at 420 Hz, u.v. ν_{max} at 333 (ε 22 600).

Anal. Calcd. for $C_9H_{10}N_2O_2S$: C, 51.42; H, 4.80; N, 13.33; S, 15.22. Found: C, 51.40; H, 4.84; N, 13.52; S, 15.30.

11e, *α-Cyano-N,3,4-trimethylthiazoline-*$\Delta^{2\alpha}$*-acetamide*

To a cold solution (5°) of the sodium salt of 2-cyano-3-methylamino-*N*-methyl-3-thioacrylamide, **3***i* (0.05 mole), 0.055 mole of chloropropanone was added slowly with constant stirring while keeping the temperature at 5°. After 1 h the ethanol was evaporated, the residue was dissolved in $CHCl_3$, and washed with diluted HCl and with water. Evaporation of the solvent left a solid that was washed with hexane and crystallized from CH_3CN or 2-heptanone. The pale yellow solid obtained in 35% yield melted at 257–259°; ν_{max} (Nujol) NH 3380, CN 2160, C=O 1610 cm^{-1}; n.m.r. (TFA) has shown H_5 to be at 445 Hz; u.v.$_{max}$ at 336 (ε 41 800).

Anal. Calcd. for $C_9H_{11}N_3OS$: C, 51.67; H, 5.30; N, 20.09; S, 15.29. Found: C, 51.70; H, 5.33; N, 20.38; S, 15.44.

14, *4-Acetamido-2-anilino-5-benzoyl-N-methylthiophene-2-carboxamide*

To 0.017 mole of 4-amino-2-anilino-*N*-methyl-5-benzoylthiophene-3-carboxamide, **8***h*, in 100 ml of benzene, 0.10 mole of acetic anhydride and 15 drops of pyridine were added. The mixture was refluxed for 1 h. On cooling, a yellow solid precipitated. It was filtered off, washed with isopropanol, and crystallized from acetonitrile. The yellow solid (55%) melted at 182–184°: ν_{max} (Nujol) NH 3330, C=O 1690 and 1620 cm^{-1}; u.v. ν_{max} at 290 (ε 12 810).

Anal. Calcd. for $C_{21}H_{19}N_3O_3S$: C, 64.11; H, 4.87; N, 10.68; S, 8.13. Found: C, 64.39; H, 4.99; N, 10.60; S, 8.04.

15a, *5-Anilino-7-benzoyl-2,3-dimethylthieno[3,4-d]-pyrimidin-4(3H)-one*

To 0.04 mole of 4-amino-2-anilino-*N*-methyl-5-benzoylthiophene-3-carboxamide, **8***h*, in 150 ml of benzene, 0.24 mole of acetic anhydride and 5 drops of pyridine were added. The mixture was kept under reflux overnight. On cooling a solid precipitated out. It was filtered off, washed with isopropanol, and crystallized from methoxyethanol. The yellow solid (55%) melted at 232–234°; ν_{max} (Nujol)

NH 3170, C=O 1655 and 1590 cm^{-1}; in u.v. maxima at 247 (ε 13 900), 288 (ε 22 600) and 420 (ε 23 600).

Anal. Calcd. for $C_{21}H_{17}N_3O_2S$: C, 67.19; H, 4.57; N, 11.20; S, 8.52. Found: C, 67.38; H, 4.67; N, 11.58; S, 8.40.

15b, 7-Acetyl-2,3-dimethyl-5-methylaminothieno[3,4-d]-pyrimidin-4(3H)-one

To 0.09 mole of 5-acetyl-4-amino-*N*-methyl-2-methylaminothiophene-3-carboxamide, **8***f*, in 300 ml of benzene, 0.4 mole of acetic anhydride and 8 drops of pyridine were added. The solution was kept under reflux overnight. On cooling a solid was obtained. It was filtered off, washed with isopropanol, and crystallized from methoxyethanol. The yellow solid obtained (75%) melted at 276–278°; ν_{max} (Nujol) NH 3300, C=O 1650 and 1605 cm^{-1}; in u.v. maxima at 282 (ε 27 700), 321 (ε 6460) and 380 (ε 19 250).

Anal. Calcd. for $C_{11}H_{13}N_3O_2S$: C, 52.58; H, 5.22; N, 16.73; S, 12.73. Found: C, 52.67; H, 5.37; N, 16.44; S, 12.76.

15c, 5-Anilino-7-benzoyl-3-dimethylamino-2-methylthieno[3,4-d]pyrimidin-4(3H)-one

To 0.033 mole of 4-amino-2-anilino-5-benzoylthiophene-3-carboxylic acid, *N,N*-dimethyl hydrazide, **8***q*, in 250 ml of benzene, 0.165 mole of acetic anhydride and 7 drops of pyridine were added. The mixture was refluxed overnight, cooled, and the solid formed was filtered off. It was washed with isopropanol and crystallized from 2-methoxyethanol. This yellow solid (90%) melted at 223–224°; ν_{max} (Nujol) NH 3220, C=O 1650 and 1580 cm^{-1}; in u.v. maxima at 248 (ε 16 100) and 286 (ε 24 300).

Anal. Calcd. for $C_{22}H_{20}N_4O_2S$: C, 65.33; H, 4.99; N, 3.86; S, 7.91. Found: C, 65.46; H, 5.27; N, 4.04; S, 8.04.

1. S. RUHEMANN. Chem. Soc. **93**, 621 (1908).
2. A. D. GRABENKO, L. N. KULAEVA, and P. PELKIS. Khim. Geterotsikl. Soedin. **3**, 364–367 (1966) cf Chem. Abstr. **65**, 12190*c* (1966).
3. G. BARNIKOW and H. KUNZEK. J. Prakt. Chem. **30**, 13 (1965).
4. R. LALIBERTE, H. WARWICK, and G. MEDAWAR. Can. J. Chem. **46**, 3643 (1968).
5. H. KUNZEK and G. BARNIKOW. Chem. Ber. **102**, 351 (1969).
6. G. BARNIKOW. J. Prakt. Chem. **34**, 251 (1966).
7. G. BARNIKOW, H. KUNZEK, and D. RICHTER. Ann. Chem. **695**, 49 (1966).
8. D. E. WORRALL. J. Amer. Chem. Soc. **44**, 1551 (1922); **46**, 2832 (1924).
9. A. DORNOW and K. DEHMER. Chem. Ber. **100**, 2577 (1967).
10. K. HARTKE and L. PESHKAR. Arch. Pharm. **301**, 611 (1968).
11. A. D. GRABENKO, L. N. KULAEVA, and P. S. PELKIS. Khim. Geterotsikl. Soedin. **5**, 698–703 (1965) cf Chem. Abstr. **64**, 9702*d* (1966).
12. BEILSTEIN. Springer-Verlag. (*a*) 4, II, 565. (*b*) Vol. 12, p. 294.
13. E. G. HOWARD. J. Amer. Chem. Soc. **81**, 4357 (1959).

Can. J. Chem. Downloaded from www.nrcresearchpress.com by 210.87.254.42 on 09/05/12
For personal use only.

Can. J. Chem. Downloaded from www.nrcresearchpress.com by 210.87.254.42 on 09/05/12
For personal use only.

Relative reactivities of dihydrophenazine and dihydrophenazonium radicals in electron-transfer to an azobenzene

RICHARD L. REEVES
Research Laboratories, Eastman Kodak Company, Rochester, New York 14650

Received February 26, 1970

A kinetic study of the electron-transfer reaction between a model azobenzene and dihydrophenazonium ion-radical and dihydrophenazine was carried out in 0.2 *N* sulfuric acid in 50 v/v aqueous acetonitrile. The second-order rate constant for the dihydrophenazine is greater than that of the ion-radical by a factor of 10^4. It is shown that in solutions in which the ion-radical is the predominant species, the principal electron-transfer agent is the dihydrophenazine formed by dismutation of the radical.

Canadian Journal of Chemistry, 48, 2718 (1970)

Introduction

Phenazine is reduced in acid solutions in one-electron steps to give first a green radical or "semiquinone" and then the nearly colorless 5,10-dihydrophenazine. The reduced forms of phenazine are oxidized by azobenzenes in acid solutions. In this paper we report the results of a kinetic study of the reduction of a model azobenzene which establishes the roles and relative effectiveness of the radical and the dihydrophenazine as electron-transfer agents toward these substrates. Throughout the paper we adopt the Michaelis notation shown beneath the structures in eq. [1].

[1] 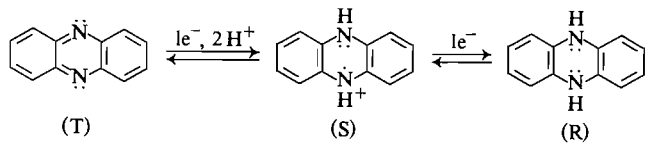

(T) (S) (R)

The existence of reversible one-electron steps in acid solution has been established by potentiometric redox titration (1). The intermediate radical (S) was shown to exist in acid solution as the 5,10-dihydrophenazonium ion-radical by its electron spin resonance (e.s.r.) spectrum (2).

The stability of the radical is expressed by its formation constant, eq. [3], for equilibrium,

$$[2] \qquad 2H^+ + T + R \overset{K_s}{\rightleftarrows} 2S$$

$$[3] \qquad K_s' = K_s\,[H^+]^2 = [S]^2/[T][R]$$

$$[4] \qquad E_2^0 - E_1^0 = -0.06 \log K_s'$$

eq. [2]. The value of K_s' can be determined from the difference in standard potentials for the two reduction steps (eq. [4] for 25°) (3). The spread in the potentials, and hence the radical stability, increases with increasing acidity. A solution containing S as the predominant species will always contain a low concentration of R in equilibrium with S. The equilibrium concentration of R is determined by the acidity and the magnitude of K_s'. The problem to be solved by kinetic analysis is whether, in solutions containing predominantly S, the active electron-transfer agent is S or the R in equilibrium with it.

We chose as a typical substrate 4-trimethylammonium-4′-azobenzene sulfonate (**1**). Our earlier work (4) indicated that the presence of two strong electron-withdrawing substituents would ensure high reactivity, as well as the necessary potential differences between **1** and S and R so that both phenazine species should be oxidizable.

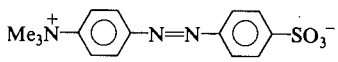

1

Experimental

Materials

Phenazine, m.p. 174.7–175.7° (lit. 174.9–175.6° (5)) was purchased from Aldrich Chemical Co. and was used without further purification. The azobenzene (**1**) was the sample described previously (6).

Preliminary studies showed that the solubility of

Can. J. Chem. Downloaded from www.nrcresearchpress.com by 210.87.254.42 on 09/05/12
For personal use only.

dihydrophenazine in dilute aqueous acid was less than 2×10^{-4} *M*, and that an aqueous medium was unsatisfactory for polarographic analysis of the redox species of phenazine. A 50% (v/v) acetonitrile–water mixture containing 0.2 *N* sulfuric acid was a satisfactory solvent for kinetic studies and polarography. Polarograms of the acid solvents prepared from commercially available acetonitrile gave small anodic waves at potentials close to the reduction potential of the azobenzene. These solvent samples also decolorized dilute solutions of potassium permanganate. Distillation of the acetonitrile from solid potassium permanganate removed these reducing impurities. Dihydrophenazine was prepared *in situ* by reduction of weighed samples of phenazine in either acetic acid or 0.2 *N* sulfuric acid in 50% acetonitrile–water with Mallinckrodt Analytical Reagent zinc dust.

Polarographic Analysis

Polarograms were obtained with a Metrohm Polarecord Type E 261R, using a two-electrode cell equipped with a drop-controlling device. More satisfactory polarograms were obtained if the potential range was scanned slowly while the mercury drops were rapidly knocked from the capillary. Charging current compensation was necessary with this procedure. The Ag/AgCl reference electrode was used for the measurements, but all potentials cited are referred to the standard calomel electrode. The European sign convention is used whereby the reducing power of a series of substances increases as the oxidation potentials become more negative.

The shapes of the polarograms of phenazine and dihydrophenazine were concentration-dependent. At concentrations greater than 0.001 *M*, both species gave two well-defined waves of nearly equal height. As the concentrations were decreased, the second wave became more poorly defined until at 1×10^{-4} *M* a single wave was obtained. The total limiting cathodic currents for phenazine and the total limiting anodic currents for dihydrophenazine were proportional to the concentrations of the respective species at low concentrations. The current–concentration calibration for phenazine was obtained from polarograms of a dilution series of a phenazine solution prepared by weight. The calibration was linear up to a concentration of 2×10^{-4} *M*. A calibration curve was used for higher concentrations. The linearity of the current–concentration relationship for dihydrophenazine was established in the following way: 0.36 g of phenazine in 50 ml glacial acetic acid was completely reduced with zinc in a nitrogen atmosphere. A 0.2 ml aliquot was withdrawn in a syringe which had been flushed with nitrogen and was added through a rubber diaphragm to 20 ml of deaerated 0.2 *N* sulfuric acid in 50% acetonitrile, contained in the polarographic cell. After obtaining the polarogram of the solution containing approximately 4×10^{-4} *M* dihydrophenazine, half the solution was withdrawn with a hypodermic syringe, and the same volume of solvent added. The procedure was repeated through four dilutions. The current–concentration plot was linear up to 4×10^{-4} *M*. To obtain the calibration constant for the dihydrophenazine analysis, a second solution containing approximately 4×10^{-4} *M* dihydrophenazine was prepared in the polarographic cell, and the polarogram was obtained. The solution was then titrated in the cell with a solution of potassium permanganate in 50% acetonitrile to a very faintly pink endpoint. The concentration of phenazine by polarographic analysis was 4.13×10^{-4} *M* after correction for dilution. This not only provided the calibration constant for the dihydrophenazine solutions, but it showed that zinc reduction of phenazine and reoxidation of the dihydrophenazine by permanganate was quantitative.

Kinetics

All runs were made at 25° in 0.2 *N* sulfuric acid in 50% acetonitrile. Solutions containing the phenazonium radical and phenazine as the predominant species were prepared by mixing solutions containing varying known concentrations of dihydrophenazine with a constant excess of phenazine. Since we show that K_s' is approximately 10^4 in 0.2 *N* acid, the added dihydrophenazine is converted to the radical in the presence of excess phenazine. The equilibrium concentrations of S and T are then: $[S]_e = 2\,[R]_t$, and $[T]_e = [T]_t - [R]_t$, where $[R]_t$ and $[T]_t$ are the total analytical concentrations. The concentrations of R ranged from 1.52×10^{-4} to 4.76×10^{-4} *M* before mixing with equal volumes of solutions containing 0.001 *M* T. The mixed solutions containing S and T were then mixed with an equal volume of an 8.8×10^{-5} *M* solution of **1** by forcing the two solutions from motor-driven syringes through a Y-tube and into a quartz flow cell. The reaction was monitored by following the disappearance of absorbance of **1** at 310 nm. The rate was sufficiently slow and the flow rate fast enough that no reaction occurred during the establishment of the steady state. The zero time was taken with a stopwatch at the time the flow was stopped. Under the conditions where S and T are the predominant species present, initial rates were obtained by monitoring the reaction for 80 to 210 s. The same solutions were mixed in a Durrum–Gibson stopped-flow spectrophotometer, which allowed us to show that no rapid reactions preceded the slow reaction.

The rates of reaction of **1** in solutions containing only dihydrophenazine were fast and were mixed and monitored in the stopped-flow spectrophotometer. The second-order rate constant, k_R, was calculated by eq. [5]

$$[5] \qquad k_R t = \frac{2.3}{na - b} \log \frac{b(a - x)}{a(b - x)} = \frac{2.3}{na - b} \times \log \frac{(b/a)(A_t - A_\infty)}{(b/a)(A_0 - A_\infty) - n(A_0 - A_t)}$$

where a = initial molarity of **1**, b = initial molarity of R, A_0, A_∞, and A_t are the initial, final, and intermediate absorbances, respectively, and n is the molar stoichiometric factor.

Results and Discussion

The half-wave potentials for the two steps in the reduction of phenazine shown in eq. [1] are +0.069 and −0.195 V, respectively, in 0.2 *N* acid. The value of K_s' in eq. [3] is estimated to be 2×10^4 from eq. [4].

Can. J. Chem. Downloaded from www.nrcresearchpress.com by 210.87.254.42 on 09/05/12
For personal use only.

Here we assume that the difference between the measured half-wave potentials is approximately equal to the difference in standard potentials.

Earlier work showed that **1** is reduced reversibly to the hydrazobenzene stage, **2**, in acid solution (4). The hydrazobenzene undergoes a slow benzidine rearrangement but is not reduced further. The half-wave potential for reduction of **1** is +0.105 V in 0.2 *N* acid. Either R or S should be capable of reducing **1**. We showed that a solution containing S as the predominant species would reduce **1** quantitatively by a two-equivalent process.

Semiquantitative experiments showed that solutions containing S as the predominant phenazine species reduced **1** much more slowly than solutions containing only R. The overall reaction between R and **1** can be described by either Scheme 1 or 2.

[6] $R + \mathbf{1} \xrightarrow{k_R} T + Me_3\overset{+}{N}\text{-}C_6H_4\text{-}NHNH\text{-}C_6H_4\text{-}SO_3^-$ (rate-determining)

2

[2] $2H^+ + T + R \overset{K_s}{\rightleftarrows} 2S$ (fast)

[7] $2S + \mathbf{1} \rightarrow 2T + \mathbf{2}$ (slow or nil)

SCHEME 1

A single two-electron transfer

[8] $R + \mathbf{1} + 2H^+ \overset{k_R}{\rightleftarrows} S + \left[\begin{matrix} ArN\text{-}N\text{-}Ar \\ \dot{H}\ \dot{H} \end{matrix}\right]^+$ (rate-determining)

3

[9] $\mathbf{3} + R \rightarrow \mathbf{2} + S$ (fast)

SCHEME 2

Consecutive one-electron transfers

Two moles of R are consumed per mole of azobenzene reduced because of the high stability of S and its slow rate of oxidation by **1**. Therefore, $n = 2$ in eq. [5]. Using this value, we obtained with eq. [5] good second-order plots through 85% reaction, under conditions where only R and **1** were present initially. The value of k_R in 0.2 *N* acid is $8.2 \times 10^4\ M^{-1}\ s^{-1}$.

To determine whether the slow reduction of **1** obtained in solutions containing S and T as the predominant species was due to two one-electron transfers by S, we measured the dependence of the initial rate, v_0, on $[S]_0$ and $[T]_0$. In these solutions the only R present was that formed through the equilibrium as shown in eq. [2]. If the active reducing agent is the radical, then, at constant initial concentration of azobenzene,

$$[10] \qquad v_0/[\mathbf{1}]_0 = k_s\,[S]_0$$

and a plot of v_0 against $[S]_0$ should be linear. If R is the only active electron-transfer agent,

$$[11] \qquad \frac{v_0}{[\mathbf{1}]_0} = k_R[R]_0 = \frac{k_R}{K_s'}\frac{[S]_0^2}{[T]_0}$$

and a plot of v_0 against $[S]_0^2/[T]_0$ should be linear.

The results are given in Table 1 and Fig. 1. It is clear that v_0 is not proportional to $[S]_0$ but is nearly proportional to $[S]_0^2/[T]$ and hence to $[R]_0$. The linear plot (solid line) in Fig. 1 does not extrapolate to the origin, as it should if R is the only electron-transfer agent contributing to the rate. This suggests that there is a small contribution to the rate from the radical and that the appropriate rate expression is as shown in eq. [12].

$$[12] \qquad \frac{v_0}{[\mathbf{1}]_0} = \frac{k_R}{K_s'}\frac{[S]_0^2}{[T]_0} + k_s[S]_0$$

TABLE 1

Variation of initial reduction rate at 25° with initial concentrations of S and T; $[\mathbf{1}]_0 = 4.4 \times 10^{-5}\ M$

$[S]_0 \times 10^4$ (M)	$[T]_0 \times 10^4$ (M)	$[S]_0^2/[T]_0 \times 10^4$ (M)	$v_0 \times 10^7$ ($M\ s^{-1}$)
0.76	2.12	0.27	0.24
1.18	1.91	0.73	0.50
1.58	1.71	1.46	0.91
2.08	1.46	2.96	1.51
2.38	1.31	4.32	2.16

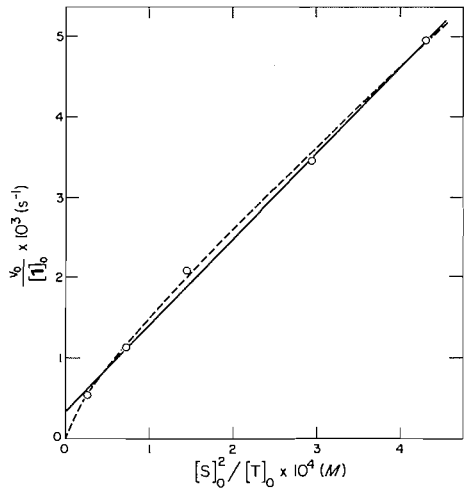

FIG. 1. Variation of initial rate at 25° with the initial concentrations of S and T.

The two parameters in eq. [12] were evaluated by least-squares fit to the data, in which v_0 was constrained to pass through the origin. The calculated values of $v_0/[\mathbf{1}]_0$ obtained from eq. [12] are shown as a function of $[S]_0^2/[T]_0$ by the dashed line in Fig. 1. The fit obtained by using eq. [12] is significantly better than that given by eq. [11] if the linear plot is also constrained to pass through the origin. The value of k_R/K_s' is 4.28 M^{-1} s^{-1} and that of k_s is 9.0 M^{-1} s^{-1}. Using the value of $k_R = 8.2 \times 10^4$ M^{-1} s^{-1} measured independently, we calculate $K_s' = 1.9 \times 10^4$ in 0.2 N acid, in excellent agreement with the value of 2×10^4 obtained from polarographic measurement. The value of K_s', as defined in eq. [3], will depend on the acidity since protons are involved in the formation of S from R and T. The value of K_s is 4.8×10^5 M^{-2}.

Our finding that the dihydrophenazine is a more effective electron-transfer agent toward azobenzenes than the ion-radical by 10^4 contradicts the statement of Mason (7) wherein the dihydro species of diazines such as phenazine are declared to be inactive as reducing agents for azo dyes. It seems reasonable that the radicals would react slowly with protonated azobenzenes (4) because single encounters should result in one-electron transfers to give the azo cation radical, **3**. The position of equilibrium of eq. [8] undoubtedly lies far to the left. The dihydrophenazine can transfer two electrons on each encounter and give stable products directly. There is evidence that hydroquinones reduce some azobenzenes by a hydride-transfer mechanism (4).

The author thanks Dr. L. K. J. Tong for helpful suggestions on this work.

1. L. MICHAELIS and E. S. HILL. J. Amer. Chem. Soc. **55**, 1481 (1933).
2. (*a*) B. L. BARTON and G. K. FRAENKEL. J. Chem. Phys. **41**, 1455 (1964). (*b*) J. R. BOLTON, A. CARRINGTON, and J. DOS SANTOS-VEIGA. Mol. Phys. **5**, 465 (1962).
3. W. M. CLARK. Oxidation-reduction potentials of organic systems. The Williams and Wilkins Co., Baltimore, 1960. p. 186.
4. R. L. REEVES and R. W. ANDRUS. J. Amer. Chem. Soc. **89**, 1715 (1967).
5. D. N. BAILEY, D. K. ROE, and D. M. HERCULES. J. Amer. Chem. Soc. **90**, 6291 (1968).
6. R. L. REEVES. J. Amer. Chem. Soc. **88**, 2240 (1966).
7. L. F. A. MASON. Photographic processing chemistry. The Focal Press, London, 1966. p. 279.

Can. J. Chem. Downloaded from www.nrcresearchpress.com by 210.87.254.42 on 09/05/12
For personal use only.

Can. J. Chem. Downloaded from www.nrcresearchpress.com by 210.87.254.5 on 09/05/12
For personal use only.

Cusp constraints for atomic wavefunctions

J. A. CHAPMAN[1] AND D. P. CHONG
Department of Chemistry, University of British Columbia, Vancouver 8, British Columbia

Received April 1, 1970

A hierarchy of cusp constraints, from necessary to sufficient, is examined. A flexible approach of cusp-satisfying orbitals is proposed. This is tested on some simple wavefunctions for the ground state of lithium. It is found that cusp-satisfying wavefunctions give good values for the spin as well as electron densities at the nucleus.

Canadian Journal of Chemistry, 48, 2722 (1970)

Introduction

In this work, we are interested in the calculation of the electron and spin densities at the nucleus of an atom. These densities, $Q^e(0)$ and $Q^s(0)$, play important roles in Mössbauer spectroscopy and hyperfine interactions, respectively.

In general, $Q^s(0)$ is difficult to calculate reliably,[2] as demonstrated by the tabulations of various workers (2–7) for the ground state of Li. Moreover, approximate wavefunctions with better energies do not necessarily give better values of $Q^s(0)$.

On the other hand, it has been inferred (8–10) that, to give good values for electronic properties near the nucleus, an approximate wavefunction should satisfy the cusp condition fairly well. Partial support for this reasoning has been found in the ground state of He: a strong statistical correlation was discovered (11) between the error in $Q^e(0)$ and the error in the cusp value for a variety of approximate wavefunctions; and better values of $Q^e(0)$ were obtained (12) when configuration-interaction (c.i.) wavefunctions were constrained to satisfy the necessary, but not sufficient, integral cusp condition (10).

The aim of this work is to impose the cusp condition on relatively simple approximate wavefunctions for the ground state of Li, in order to calculate good values for $Q^s(0)$ as well as $Q^e(0)$.

Cusp Conditions

Since the derivation by Kato (13) in 1957, cusp conditions have been studied by many authors (8–12, 14–18). In particular, Pack and Byers Brown (8) presented the most general coalescence conditions.

In this work, we are primarily concerned with the special case of cusp behavior of atomic wavefunctions at the nucleus. Mass-corrected atomic units are used, and λ and γ of Pack and Byers Brown (8) become 0 and $-Z$, respectively. In order to simplify some of the equations below, we define a cusp remainder operator for the coalescence of the ith electron with the nucleus as

$$[1] \qquad R(i) = \lim_{r_i \to 0} p(i)(4\pi)^{-1} \int d\Omega_i$$

where

$$[2] \qquad p(i) = Z + \partial/\partial r_i$$

For spatial eigenfunctions of the usual non-relativistic Hamiltonian, we can make use of the result of Pack and Byers Brown (8) and obtain the cusp condition $R(i)\Phi = 0$. For exact wavefunctions containing spins, we follow their arguments on the inclusion of spin and get

$$[3] \qquad R(i)\Psi = 0$$

Since Ψ is antisymmetric with respect to electron exchange, one can take $i = 1$. Similarly, (exact) eigenfunctions ϕ of a Hartree–Fock (H.F.) Hamiltonian with electron-nucleus singularity satisfying $R\phi_k = 0$.

Let us now turn to approximate wave functions constructed from one-electron orbital basis $\{\varphi\}$. When the cusp condition in eq. [3] is imposed, it becomes a constraint. Such a constraint leads to a hierarchy of conditions ranging from necessary (but not sufficient) to sufficient (but not necessary).[3]

[1]Present address: Mathematical Institute, 24–29 St. Giles, Oxford, England.

[2]We disagree with Vetchinkin and Kristenko (1), who described 10–40% discrepancy between calculated and experimental $Q^s(0)$ as "entirely satisfactory."

[3]In this and subsequent contexts, sufficiency and necessity refer to conditions after the type of wavefunction is specified.

Can. J. Chem. Downloaded from www.nrcresearchpress.com by 210.87.254.5 on 09/05/12
For personal use only.

On one hand, one can derive the necessary integral cusp condition (10)

$$[4] \qquad \langle \Psi | \sum_i (4\pi r_i^2)^{-1} \delta(r_i) p(i) | \Psi \rangle = 0$$

or even weighted non-diagonal integral cusp conditions (40)

$$[5] \qquad \langle W | \sum_i (4\pi r_i^2)^{-1} \delta(r_i) p(i) | \Psi \rangle = 0$$

However, these constraints were found to be of little use in our preliminary attempts (40) to improve the calculated values of $Q^e(0)$ and $Q^s(0)$ for Li. We are inclined to conclude that such conditions are probably too weak.

At the other extreme, a Slater-type orbital (S.t.o.) basis $\{\chi\}$ can be chosen so that

$$[6] \qquad R\chi_k = 0$$

for each member of the set. Since this guarantees that eq. [3] is automatically satisfied, we regard eq. [6] as a set of sufficient cusp constraints. Such cusp-satisfying S.t.o. basis sets have been described by Roothaan and Kelly (19) and others (20, 21). However, these basis sets have been used (19, 22–24) primarily for the calculation of analytical H.F. wavefunctions for atomic systems. To satisfy eq. [6], $\{\chi\}$ is restricted to a single 1s orbital with orbital exponent Z and no 2s orbitals. Consequently, such sets may need many 3s and higher orbitals to give wavefunctions of reasonable accuracy.[4] Hence, we tend to regard eq. [6] as too strong a condition, especially for calculations with relatively small basis sets.

In a more flexible approach, the one-electron basis orbitals can be chosen as linear combinations of normal (that is, not all cusp-satisfying) S.t.o.'s.

$$[7] \qquad \varphi_j = \sum_k a_{jk} \chi_k$$

Then, the coefficients can be constrained so that

$$[8] \qquad R\varphi_j = 0$$

for each member of $\{\varphi\}$. This also guarantees the satisfaction of eq. [3] and therefore forms a set of sufficient cusp constraints; but in some instances (see Discussion section) eq. [8] also represents necessary conditions. Recently, Weber, Handy, and Parr[5] obtained such cusp-satisfying functions as analytical H.F. orbitals for atoms, utilizing the elegant constraint procedure of Weber and Handy (27). An alternative method of imposing the constraint can be derived[6] by combining eqs. [7] and [8]

$$[9] \qquad \varphi_j = \sum_{k \neq l} a_{jk} \xi_k$$

$$[10] \qquad \xi_k = \chi_k - (R\chi_k)(R\chi_l)^{-1} \chi_l$$

where χ_l is any S.t.o. which does not satisfy eq. [6]. Then, eq. [8] is satisfied for any set of a_{jk} in eq. [9]. Hence, they can be varied freely. It should be noted that while each φ_j may contain linear coefficients to be optimized, the linear combination in each ξ_k is fixed by the S.t.o. basis $\{\chi\}$. Such basis sets are admirably suited to H.F. computations and various extended Hartree–Fock (e.H.F.) schemes. However, to use them in a c.i. calculation would, in general, lead to a multiconfigurational self-consistent field formalism, in the sense that two sets of linear coefficients must be optimized. A compromise is to limit the expansion length in eq. [9] to a single term, leaving only one set of coefficients. Then, $\varphi_k = \xi_k$, and $\{\xi\}$ takes on the role of a cusp-satisfying basis set. This approach, although sacrificing flexibility, is adopted in the present study.

^{2}S Ground State of Li

For several obvious reasons, we have chosen the ^{2}S ground state of the lithium atom as an example.[7] Technical limitations have led us to test cusp-satisfying orbitals with relatively simple wavefunctions.

The basis orbitals are listed in Table 1 and three simple functions are presented in Table 2. The entries B and C represent the sets of coefficients $(B_2, B_3, B_4; C_5, C_6)$ in the wavefunctions Ψ_i. The first one, Ψ_1, is a crude approximation to the spin-optimized extended Hartree–Fock (s.o.e.H.F.)

[4]Synek and Grossgut (25) recently discarded the condition [6] in order to save computer time. However, Goddard (26) noted that cusp-satisfying S.t.o. basis sets converge faster with respect to basis size for the calculation of $Q^s(0)$.

[5]T. A. Weber, N. C. Handy, and R. G. Parr, private communication. These authors, however, were not trying to improve $Q^s(0)$. Within the independent-particle approximation, one can bypass the cusp-satisfying basis orbitals φ and obtains cusp-satisfying H.F. orbitals ϕ directly, as these authors did. In the present study, we are trying to generalize their work to c.i. wavefunctions.

[6]This is done by (*a*) substituting eq. [7] into eq. [8], (*b*) solving for a_{jl}, and (*c*) putting a_{jl} back into eq. [7].

[7]The ^{2}S state of Li has become almost a classic for the calculation of $Q^s(0)$.

TABLE 1

One-electron cusp-satisfying basis orbitals used in constructing Ψ_1 to Ψ_3 (eq. [10])

ξ_k	χ_k	ζ_k[a]	χ_l	ζ_l[a]
ξ_1	1s	[b]	δ[c]	[b]
ξ_2	1s′	[b]	δ'	[b]
ξ_3	2s″	3.0	δ	20
ξ_4	2s‴	2.5	δ'	15
ξ_5	2p	5.0η[d]	—	—
ξ_6	3p	5.0η	—	—
ξ_7	2s	[b]	2s′	[b]

[a]Orbital exponent.
[b]See Table 2.
[c]"Spike" function: 1s orbital with unusually large ζ.
[d]See Table 3.

TABLE 2

Three simple wavefunctions Ψ_1 to Ψ_3[a]

Ψ_l	B	C	ζ_{1s}	ζ_δ	$\zeta_{1s''}$	$\zeta_{\delta'}$	ζ_{2s}	$\zeta_{2s'}$
Ψ_1	0	0	3.3η[c]	20η	2.065η	13η	0.7η	1.8η
Ψ_2	[b]	0	3.5	20	2.2	15	0.7	1.82
Ψ_3	0	[b]	3.3η[c]	24η	2.065η	14η	0.7η	1.8η

[a]Wavefunctions Ψ_1 to Ψ_3 can be collected into the form

$$\Psi_l = \mathcal{A}\{[\xi_1(1)\xi_2(2) + B_2\xi_1(1)\xi_4(2) + B_3\xi_3(1)\xi_2(2) + B_4\xi_3(1)\xi_4(2) + C_5\xi_5(1)\xi_5(2) + C_6\xi_6(1)\xi_6(2)]\xi_7(3)[\theta_1 + k\theta_2]\}$$

where $\mathcal{A}$ is the antisymmetrizer

$$\theta_1 = \alpha\beta\alpha - \beta\alpha\alpha$$
$$\theta_2 = 2\alpha\alpha\beta - \alpha\beta\alpha - \beta\alpha\alpha$$

and k is optimized.
[b]Optimized.
[c]See Table 3.

wavefunction of Ladner and Goddard (28) or Kaldor and Harris (29) The simplest split-core wavefunction, Ψ_H, obtained by Hurst *et al.* (30), is

$$[11] \quad \Psi_H = \det|1s\ \overline{1s'}\ 2s| + \det|1s'\ \overline{1s}\ 2s|$$

in the usual notations. The function Ψ_B, due to Brigman and Matsen (31) is the spin optimized version of Ψ_H. Our Ψ_1 is only a simple extension of Ψ_B. The other two wavefunctions Ψ_2 and Ψ_3 contain, respectively, some s-type and p-type correlations in the core.

Linear parameters in Ψ_1 to Ψ_3 are easy to optimize. On the other hand, optimization of orbital exponents ζ requires more computer time. This was done in two steps. Firstly, each cusp-satisfying orbital ξ_k was fitted into Ψ_H one at a time, to get a set of roughly optimum ζ values. Then, the wavefunctions were formed and each set of ζ values was reoptimized. For Ψ_1 and Ψ_3, the reoptimized orbital exponents were further scaled with a uniform scale factor, η, to minimize the energy. All computations were performed in double precision on an IBM 360/67 computer.

The results are shown in Table 3, together with a few selected wavefunctions for comparison. It is gratifying to obtain such excellent values for $Q^s(0)$ as well as $Q^e(0)$ from all of our simple wavefunctions.

The importance of triplet core terms is well known, as indicated by a comparison of Ψ_H with Ψ_B or $\Psi_{e.H.F.}$ with $\Psi_{s.o.e.H.F.}$. It is interesting to note that, if the parameter k in Table 2 is set to zero, the spin densities from Ψ_1 ($\eta = 1$) and Ψ_2 ($\eta = 1$) become 0.2265 and 0.2298 respectively (40).

The first entry, Ψ_N, is a c.i. wavefunction constructed by Nesbet (32) with 1s orbitals having orbital exponents of 1.75, 3.5, and 7.0. The usually high value of 7.0 has been criticized by Breggren and Wood (38). In the present study, these "spike" functions[8] are a direct consequence of energy minimization subject to cusp constraints embodied in eq. [10]. Closer examination of our basis orbitals reveals that ξ_1 for Ψ_1 is essentially the 1s orbital of Brigman and Matsen (31) with a very small contribution from a "spike" function to correct for the cusp behavior at the nucleus

$$[12] \quad \xi_1 = 1s - 0.00115\delta$$

A similar conclusion applies to ξ_2.

The present results may be considered fortuitous because of the reasonably good value of $Q^s(0)$ from Ψ_B, but two pieces of evidence should be examined. Firstly, the energy is not particularly sensitive to ζ_δ and $Q^s(0)$ from Ψ_1 and similar functions (40) varies less than 0.5% for a 5% variation in ζ_δ. Secondly, a free-variational c.i. wavefunction using the same S.t.o. basis as the scaled Ψ_1 exhibits the following properties: $E = -7.4457$, slightly better than Ψ_1; $Q^s(0) = 0.2232$, 3.5% error; and $Q^e(0) = 13.8459$, 0.1% error. In other words, the presence of the "spike" functions reduces the % error in $Q^s(0)$ from 4.5 to 3.5%, but the satisfaction of the cusp condition decreases the % error further to only 0.6%.

The obvious shortcoming of this work is the limited sizes of our basis sets. The results of Goddard (26) and Shaefer, Klemm, and Harris (39) indicate that $Q^s(0)$ is strongly dependent on basis size. Therefore, we hope that other workers, especially those doing s.o.e.H.F. calculations,

[8]A 1s orbital with unusually large ζ, compared to Z, is called a "spike" function here, and denoted by δ, as it resembles a Dirac δ-function, loosely speaking.

Can. J. Chem. Downloaded from www.nrcresearchpress.com by 210.87.254.5 on 09/05/12
For personal use only.

TABLE 3

Properties of selected wavefunctions for the ^2S ground state of Li[a]

Ψ	η	$-E$	$Q^s(0)$	% error[b]	$Q^e(0)$	% error[c]
Ψ_N		7.431849[d]	0.2284[d]	−1.3		
Ψ_H		7.4436[e]	0.3002[f]	+29.8		
Ψ_B		7.4436[g]	0.2417[h]	+4.5	13.5240[i]	−2.2
Ψ_1	1.0	7.445329[i]	0.2341[i]	+1.2	13.9552[i]	+0.9
Ψ_1	0.996592	7.445411[i]	0.2298[i]	−0.6	13.8333[i]	−0.01
Ψ_2	1.0	7.446279[i]	0.2299[i]	−0.6	13.8094[i]	−0.2
$\Psi_{e.H.F.}$		7.447560[j]	0.2095[j]	−9.4	13.864[j]	+0.2
$\Psi_{s.o.c.H.F.}$		7.447565[k,l]	0.2265[k,l]	−2.1	13.8646[k]	+0.2
Ψ_2	1.0	7.467491[l]	0.2296[l]	−0.7	13.9203[l]	+0.6
Ψ_3	0.997727	7.467528[l]	0.2277[l]	−1.6	13.8372[l]	+0.02
Ψ_L		7.478025[m]	0.2313[m]	0.0	13.8341[n]	
Experimental		7.478069[o]	0.2313[p]			

[a]Quantities are in atomic units. Entries are arranged in the order of decreasing energy. More extensive tables of previous studies can be found in refs. 2–7.
[b]% error in $Q^s(0)$, = 100% × (calculated − experimental)/(experimental).
[c]% error in $Q^e(0)$ = 100% × (calculated − Larsson)/(Larsson).
[d]Nesbet (32).
[e]Hurst *et al.* (30).
[f]Kerwin and Burke (33).
[g]Brigman and Matsen (31).
[h]Martin and Weiss (2); calculated in the course of this work to be 0.2425.
[i]This work.
[j]Goddard (34).
[k]Ladner and Goddard (28).
[l]Kaldor and Harris (29).
[m]Larsson (35).
[n]S. Larsson, private communication.
[o]Scherr *et al.* (36).
[p]Kusch and Taub (37).

will be encouraged by our results to test cusp-satisfying orbitals in their studies.

Discussion

In this discussion, we wish to answer four questions: (*a*) what about molecules? (*b*) what about wavefunctions with nodes at the coalescence? (*c*) under what circumstance are the sufficient conditions in eq. [8] also necessary? and (*d*) what are the necessary and sufficient cusp conditions when eq. [8] is not necessary?

To answer (*a*), we only need to retrace our steps to find out where we have limited ourselves to atoms. Thus, for molecules, we simply have to change $\gamma = -Z$ to $\gamma = -\mu Z$ (8), where μ is the reduced mass of the electron in absolute atomic units.

Question (*b*) is also easy to answer. It is obvious from the results of Pack and Byers Brown (8) that eq. [1] should be generalized to

$$[13]\quad R_\lambda(i) = \lim_{r_i \to 0} p(i)(4\pi)^{-1/2} r_i^{-\lambda} \sum_{m=-\lambda}^{\lambda} \int d\Omega_i Y_{\lambda m}^*$$

The cusp remainder operator of eq. [1] is then just $R_0(i)$.

To answer both of the remaining questions with respect to any wavefunction not containing interelectronic coordinates, we can expand such a wavefunction

$$[14]\quad \Psi = \sum_i d_i \psi_i = \sum_i d_i \sum_j \varphi_j{}^i(1)\sigma_j{}^i(1) D_{1j}{}^i(2, \ldots, N)$$

where $\varphi_j{}^i(1)$ and $\sigma_j{}^i(1)$ are the spatial and spin functions for the first row and jth column of the ith determinant ψ_i, and $D_{1j}{}^i$ $(2, \ldots, N)$ is the corresponding cofactor. Then

$$[15]\quad R(1)\Psi = \sum_i \sum_j [d_i R(1)\varphi_j{}^i(1)] \times [\sigma_j{}^i(1) D_{1j}{}^i(2, \ldots, N)]$$

It should be noted that each $d_i R(1)\varphi_j{}^i(1)$ is a number and each $\sigma_j{}^i(1)D_{1j}{}^i(2, \ldots, N)$ represents a function. Therefore, if these functions are all different for a particular Ψ, then $R\varphi_j = 0$ becomes both necessary and sufficient.[3] Finally, when several $\sigma_j{}^i(1)D_{1j}{}^i$ $(2, \ldots, N)$ are the same to within a constant multiplier, we must sum over the corresponding numerical factors. In other

Can. J. Chem. Downloaded from www.nrcresearchpress.com by 210.87.254.5 on 09/05/12
For personal use only.

words, the necessary and sufficient cusp condition becomes

$$[16] \qquad \sum_i \sum_j d_i R(1)\varphi_j{}^i(1) = 0$$

where the summations run over all identical $\sigma_j{}^i(1)D_{1j}{}^i(2, ..., N)$.

The authors are grateful to the National Research Council of Canada for financial support.

1. S. I. VETCHINKIN and S. V. KRISTENKO. Theor. Exp. Chem. **3**, 79 (1969) (Teor. i Eksp. Khim. **3**, 143 (1967)).
2. J. B. MARTIN and A. W. WEISS. J. Chem. Phys. **39**, 1618 (1963).
3. E. A. BURKE. Phys. Rev. **135**, A621 (1964).
4. W. A. GODDARD III. Phys. Rev. **157**, 93 (1967).
5. F. A. MATSEN and A. A. CANTU. J. Phys. Chem. **72**, 21 (1968).
6. D. L. HARDCASTLE, J. L. GAMMEL, and R. KEOWN. J. Chem. Phys. **49**, 1358 (1968).
7. S. LUNNELL. Phys. Rev. **173**, 85 (1968).
8. R. T. PACK and W. BYERS BROWN. J. Chem. Phys. **45**, 556 (1966).
9. D. P. CHONG. J. Chem. Phys. **47**, 4907 (1967).
10. D. P. CHONG. Mol. Phys. **13**, 577 (1967).
11. D. P. CHONG and D. M. SCHRADER. Mol. Phys. **16**, 137 (1969).
12. C. P. YUE and D. P. CHONG. Theor. Chim. Acta, Berlin, **12**, 431 (1968).
13. T. KATO. Commun. Pure Appl. Math. **10**, 151 (1957).
14. C. C. J. ROOTHAAN and A. W. WEISS. Rev. Mod. Phys. **32**, 194 (1960).
15. W. KOLOS and C. C. J. ROOTHAAN. Rev. Mod. Phys. **32**, 205 (1960).
16. E. STEINER. J. Chem. Phys. **39**, 2365 (1963).
17. W. A. BINGEL. Z. Naturforsch. **18a**, 1249 (1963).
18. W. A. BINGEL. Theor. Chim. Acta, Berlin, **8**, 54 (1967).
19. C. C. J. ROOTHAAN and P. S. KELLY. Phys. Rev. **131**, 1177 (1963); **133**, 11 (1964).
20. G. MALLI and S. FRAGA. Can. J. Phys. **44**, 3131 (1966).
21. S. FRAGA and G. MALLI. Many-electron systems. Properties and interactions. Saunders, Philadelphia. 1968. p. 70.
22. M. SYNEK. Phys. Rev. **131**, 1572 (1963).
23. C. C. J. ROOTHAAN and M. SYNEK. Phys. Rev. A **133**, 1263 (1964).
24. M. SYNEK, A. E. RAINIS, and C. C. J. ROOTHAAN. Phys. Rev. **141**, 174 (1966).
25. M. SYNEK and P. GROSSGUT. Phys. Rev. **A1**, 1 (1970).
26. W. A. GODDARD III. Phys. Rev. **182**, 48 (1969).
27. T. A. WEBER and N. C. HANDY. J. Chem. Phys. **50**, 2214 (1969).
28. R. C. LADNER and W. A. GODDARD III. J. Chem. Phys. **51**, 1073 (1969).
29. U. KALDOR and F. E. HARRIS. Phys. Rev. **183**, 1 (1969).
30. R. P. HURST, J. D. GRAY, G. H. BRIGMAN, and F. A. MATSEN. Mol. Phys. **1**, 189 (1958).
31. G. H. BRIGMAN and F. A. MATSEN. J. Chem. Phys. **27**, 829 (1957).
32. R. K. NESBET. Phys. Rev. **118**, 681 (1960).
33. J. KERWIN and E. A. BURKE. J. Chem. Phys. **36**, 2987 (1962).
34. W. A. GODDARD III. Phys. Rev. **169**, 120 (1968).
35. S. LARSSON. Phys. Rev. **169**, 49 (1968).
36. C. W. SCHERR, J. N. SILVERMAN, and F. A. MATSEN. Phys. Rev. **127**, 830 (1962).
37. P. KUSCH and H. TAUB. Phys. Rev. **75**, 1477 (1949).
38. K. F. BREGGREN and B. F. WOOD. Phys. Rev. **130**, 198 (1963).
39. H. F. SHAEFER III, R. A. KLEMM, and F. E. HARRIS. Phys. Rev. **176**, 49 (1968).
40. J. A. CHAPMAN. Ph.D. Thesis, University of British Columbia, Vancouver, British Columbia. 1970.

Can. J. Chem. Downloaded from www.nrcresearchpress.com by 210.87.254.5 on 09/05/12
For personal use only.

Can. J. Chem. Downloaded from www.nrcresearchpress.com by 210.87.254.105 on 09/05/12
For personal use only.

Photolysis of 4,6,6-trimethyl-5,6-dihydro-2(1*H*)-pyridone. Intermediates and mechanism

E. CAVALIERI[1] AND D. GRAVEL
Department of Chemistry, University of Montreal, Montreal, Quebec

Received March 11, 1970

Irradiation of dihydropyridone **1***a* in water yields mainly the unsaturated amides **3** (73%), **4** (8%), and acetone. A 1.3% yield of photohydration product **5***a* is also obtained. Irradiation of **1***a* in anhydrous methanol yields carbinolamidoether **8** (57%), whereas in *t*-butyl alcohol enamide 7 is the reaction product. Irradiation of the *N*-methyl derivative of **1***a* (**1***b*) yields 90% of starting material and 5% of a photohydrate **5***b*. The mechanistic path of the reaction is shown to involve the cleavage of compound **1***a* to the enolic form **9** of the acylimine **6** which reacts differently depending on the solvent used.

Canadian Journal of Chemistry, **48**, 2727 (1970)

Introduction

To date, the photochemical transformations of conjugated cyclohexenones in solution have led to a great number of investigations and have been observed to undergo mainly rearrangement, dimerization, and addition reactions (1). Work pioneered by Chapman, Jeger, and Zimmerman has led to our present understanding of these reactions.

On the other hand, it is also well known that saturated amides can react photochemically to give cleavage products of the Norrish type I and type II (2). Although no systematic work had been reported on the photochemistry of δ-valerolactams in solution it nevertheless seemed interesting to undertake a study of the photochemical behavior of molecules combining both these types of functional groups i.e. α,β-unsaturated lactams. The first compound chosen for study was the readily available 4,6,6-trimethyl-5,6-dihydro-2(1*H*)-pyridone (**1***a*) because of its relation to isophorone (**2**), the corresponding α,β-unsaturated ketone, which upon irradiation in polar solvents yields dimeric products only (3).

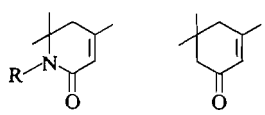

1 **2**

a R = H
b R = CH_3

Preliminary results in this study have been reported in a short communication elsewhere (4).

[1]Present address: University of California, Lawrence Radiation Laboratory, Berkeley, California 94720, U.S.A.

In the present paper we wish to report the full experimental details of our findings and also to discuss recently accumulated evidence towards elucidation of the mechanism of the observed transformation (see Chart 1).

Photolysis of Dihydropyridone 1a in Water

As previously reported (4), dihydropyridone **1***a* (6.0 g) was irradiated for 7 h in water (600 ml) using 2537 Å light. A stream of nitrogen was bubbled through the solution during the irradiation. The reaction mixture thus obtained was separated to yield three products: amide **3**, m.p. 117°, 3.12 g (73%); amide **4**, m.p. 108–109°, 0.35 g (8%), and hydroxylactam **5***a*, m.p. 189–190°, 0.085 g (1.3%). No starting material was recovered from the reaction. In an alternate run where the bubbling of nitrogen was omitted, the distillation of part of the solvent permitted the isolation of acetone as its 2,4-dinitrophenylhydrazone derivative.

Structure of Photoproducts

The structure of compound **3** was established by the mass spectrum, the elemental analysis, the infrared (i.r.) spectrum, the nuclear magnetic resonance (n.m.r.) spectrum, and conversion to known isovaleramide by catalytic hydrogenation. The mass spectrum and the elemental analysis established a molecular weight of 99 and a molecular formula of C_5H_9NO. The i.r. spectrum showed characteristic bands at 3540 and 3420 (N—H), 1680 (C=O), 1650 (C=C), 1585 (N—H), and 900 cm^{-1} (C—H, terminal methylene). The n.m.r. spectrum showed singlets at δ 1.82 (3H, methyl protons) and 2.95 (2H, methylene protons), a multiplet at 4.93 (2H, terminal methylene protons), and a broad band

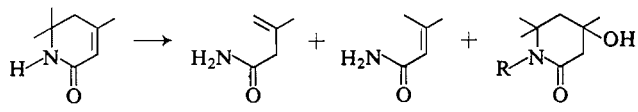

1*a* 3 4 5

a R = H
b R = CH_3

CHART 1

Photolysis of 4,6,6-trimethyl-5,6-dihydro-2(1*H*)-pyridone (**1***a*)

at 5.8 (amide protons on nitrogen, exchangeable with D_2O). Hydrogenation over palladium on charcoal (5%) gave an almost quantitative yield of isovaleramide identical in all respects with an authentic sample prepared from isovaleric acid.

The structure of compound **4** was also established by spectroscopic and chemical means. The molecular weight as determined by mass spectrometry indicated that compounds **3** and **4** were isomers. The i.r. spectrum showed characteristic bands at 3550 and 3430 (N—H), 1675 (C=O), 1640 (C=C), and 1590 cm^{-1} (N—H). The absence of an absorption band at 900 cm^{-1} suggested that compound **4** was the conjugated isomer of amide **3**. This hypothesis was confirmed by the n.m.r. spectrum which showed singlets at δ 1.85 (3H, methyl protons, *trans* to $-CONH_2$) and 2.13 (3H, methyl protons *cis* to $-CONH_2$), a multiplet at 5.6 (1H, vinyl proton), and a broad singlet at 6.0 (2H, amide protons, exchangeable with D_2O). The proposed structure was then verified by comparison with an authentic sample prepared from 3,3-dimethylacrylic acid. That photoamides **3** and **4** were not photochemically interconvertible under the present conditions was shown by irradiating aqueous solutions of both photoamides for 7 h and recovering starting material exclusively in each case. It was also ascertained that photoamides **3** and **4** are not interconvertible under the conditions of chromatography.

Evidence for the structure of compound **5***a* was again obtained by spectroscopic and chemical means. The molecular ion in the mass spectrum was found at *m/e* 157, which corresponds to the addition of a water molecule (18 mass units (m.u.)) to the starting material. The i.r. spectrum showed characteristic bands at 3345, 3270, and 3190 (O—H and N—H), and at 1640 cm^{-1} (C=O). The n.m.r. spectrum in dimethyl-d_6 sulfoxide showed singlets at δ 1.15 (6H, *gem*-dimethyl protons), 1.30 (3H, methyl protons), an AB system centered at 1.63 (2H, methylene protons), 2.10 (2H, methylene protons α to CO), 4.47 (1H, hydroxyl proton, exchangeable with D_2O), and 7.35 (1H, amide proton, exchangeable with D_2O). Further evidence in favor of the proposed structure was obtained by treating compound **5***a* with a 1:1 mixture of sulfuric acid and water at 80° for 1 h and showing by n.m.r. that the mixture of products obtained was composed of 56% of dihydropyridone **1***a* and 44% of its deconjugated isomer (5)[2].

Photolysis in Anhydrous t-Butyl Alcohol and Methanol

The results summarized in Chart 1 strongly suggest that an unstable intermediate formed in this reaction is hydrolyzed in a non-photochemical step to lead to products **3**, **4**, and acetone. A logical structure for this intermediate would be either the acylimines (**6***a* and *b*) or the corresponding enamides (**7***a* and *b*). However, it

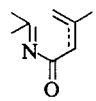

6
a Conjugated
b Unconjugated

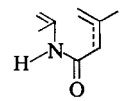

7
a Conjugated
b Unconjugated

is well known (6) that acylimines tautomerize rapidly to the corresponding enamide and that the reverse reaction generally does not take place under neutral conditions. In the isolated case (7*a*), where an enamide was found to tautomerize to the corresponding acylimine on treatment with acid, the transformation was ascribed (7*b*) to conformational factors.

The photolysis of dihydropyridone **1***a* in dry

[2]The pure deconjugated isomer of **1***a* has been prepared by J. Hébert of this laboratory and its n.m.r. spectrum shown to correspond exactly to the 44% component in the mixture.

Can. J. Chem. Downloaded from www.nrcresearchpress.com by 210.87.254.105 on 09/05/12
For personal use only.

Can. J. Chem. Downloaded from www.nrcresearchpress.com by 210.87.254.105 on 09/05/12
For personal use only.

t-butyl alcohol yielded a product mixture consisting for the greater part of starting material as shown by the i.r. spectrum. Nevertheless, separation of the mixture by chromatography gave a small amount of a new compound[3] shown to be the unconjugated enamide **7***b* and having the following spectral characteristics. The mass spectrum established the molecular weight at 139 indicating that the compound isolated was an isomer of the starting material **1***a*. The i.r. spectrum showed characteristic bands at 3420 (N—H), 1680 (C=O), 1648 (C=C), 1505 (N—H), and 910 cm^{-1} (C—H, terminal methylene). The n.m.r. spectrum showed singlets at δ 1.92 (3H, methyl protons on the enamide side), 3.02 (2H, methylene protons α to CO), an AX system with the high field component at 4.45 and the low field component at 5.43 (2H, terminal methylene protons of the enamide moiety (8), a doublet at 1.82 (3H, methyl protons on the olefin, $J = 1$ c.p.s.), and a multiplet at 4.91 (2H, terminal methylene protons of the olefin moiety). Finally, acid hydrolysis of chromatographic fractions containing either pure enamide **7***a* or a mixture of enamides **7***a* and *b* gave the corresponding photoamides **3** and **4** thus confirming the proposed structure. The isolation and characterization of enamide **7** is significant in that it confirms our hypothesis concerning the intervention of a water labile intermediate. One important problem however is to determine whether or not the acylimine intermediate **6** plays a role in this reaction. *A priori*, as will be shown later, one would expect initial formation of acylimine **6** followed by an irreversible tautomerization (6) to intermediate **7** (**6***a* → **7***a* and **6***b* → **7***b*).

Since it is known that enamides do not react with pure alcohols (9) and that acylimines add primary, secondary, and in certain cases tertiary alcohols (6, 9–11) an attempt was made to trap the acylimine intermediate by carrying out the irradiation of dihydropyridone **1***a* in anhydrous methanol. The latter should have a better chance to add to the acylimine than the bulky *t*-butyl alcohol. The reaction afforded a very good yield of an adduct which was shown after chromatographic purification to be the corresponding carbinolamidoether **8**.

The i.r. spectrum of this product showed characteristic bands at 3420 (N—H), 1672 (C=O), 1645 (C=C), 1503 (N—H), and 907 cm^{-1} (C—H, terminal methylene). The n.m.r. spectrum showed singlets at δ 1.56 (6H, *gem*-dimethyl protons), 1.80 (3H, methyl protons), 2.98 (2H, methylene protons), and 3.20 (3H, methyl protons), a multiplet at 4.86 (2H, terminal methylene protons), and a broad band at 7.52 (1H, amide proton). The mass spectrum did not show the molecular ion peak at *m/e* 171 as expected of structure **8**, but showed a strong

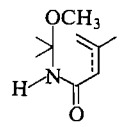

8
a Conjugated
b Unconjugated

M-32 peak at *m/e* 139 corresponding to a loss of methanol. A molecular weight determination using a Mechrolab Vapor Pressure Osmometer gave a value of 167 ± 2%.

Finally, chromatographic fractions containing either pure carbinolamidoether **8***a* or a mixture of carbinolamidoether **8***a* and *b* were hydrolyzed in dilute acid to the corresponding photoamides **3** and **4** thus confirming the proposed structure.

Photolysis of N-Methyl Dihydropyridone 1b in Water

In an effort to gain further insight into the mechanism of this transformation, *N*-methyl dihydropyridone **1***b* was prepared and irradiated in water (300 mg/30 ml) for 7 h using 2537 Å light. The reaction mixture thus obtained was composed almost entirely of starting material, as evidenced by thin-layer chromatography (t.l.c.). A chromatographic separation yielded unreacted starting material (270 mg, 90%) and another product (15 mg, 5%) to which the hydroxylactam structure **5***b* was assigned. The mass spectrum of this product indicated a molecular weight of 171 which differs from that of the starting material by 18 m.u. indicating an addition of a molecule of water. The i.r. spectrum showed characteristic bands at 3620 and 3380 (O—H) and 1615 cm^{-1} (C=O). The n.m.r. spectrum which is quite similar to that of **5***a* showed singlets at δ 1.30 (6H, *gem*-dimethyl protons), 1.46 (3H, methyl protons), an AB system centered at 1.85 (2H, methylene protons), 2.44 (2H, methylene protons α to CO), 2.89 (3H, methyl

[3]No attempt was made to isolate any pure conjugated isomer **7***a* present.

protons), and 3.14 (1H, hydroxyl proton, exchangeable with D_2O).

Multiplicity of the Cleavage Reaction

Evidence for the multiplicity of the excited intermediate in this reaction was obtained by one of us (12). It was shown (12) that acetophenone sensitization of the reaction led only to dimer formation and none of the cleavage products **3** and **4**.

These results clearly demonstrated that the unsensitized irradiation of dihydropyridone **1***a* in water to yield photoamides **3** and **4** does not proceed via the lowest triplet state. It is also interesting to note that the reactivity of compound **1***a* seems to differ depending on the multiplicity of the excited intermediate produced in the reaction. Thus, while the direct photolysis of lactam **1***a* in water leads, via what is possibly a singlet state,[4] to cleavage products **3** and **4**, the triplet sensitized reaction leads primarily to a photodimer of the starting material and none of the cleavage products **3** and **4** (12).

Discussion

From the above results it appears reasonable to suggest that the irradiation of dihydropyridone **1***a* leads to an excited singlet which could react according to two competing pathways (*a* and *b*) prior to crossing over to the corresponding triplet state. (*a*) The excited molecule (or a strained ground-state derived from it) may add the elements of water to form the 4-hydroxypiperidone **5***a*. Similar photoinduced additions of protic solvents have been reported for various α,β-unsaturated carbonyl compounds such as uracil (13), 4a-methyl-4,4a,9,10-2(3*H*)-phenanthrone (14), Pummerer's ketone (15), 1-acetylcyclohexene (16), and 2-cycloheptenone (17). It is interesting to note that Lamola and Mittal (13) have stated that "the photohydration of uracil probably does not involve the triplet state". Our results would also seem to eliminate the lowest triplet state as the excited intermediate leading to hydroxypiperidone **5***a*; however, the small amount of the compound isolated from the reaction mixture renders this conclusion very tenuous. (*b*) In an alternate reaction pathway, the excited molecule may undergo cleavage of the 5–6 bond concerted with the migration of the proton from nitrogen to oxygen.[5] Evidence in favor of this hypothesis rests on the fact that the presence of hydrogen on nitrogen is necessary for the reaction to take place. Thus, when *N*-methyl dihydropyridone **1***b* was irradiated in water, no appreciable reaction had taken place after 7 h as shown by t.l.c. Chromatographic analysis indicated that 90% of the starting material had remained unchanged and that 5% was converted to hydroxylactam **5***b*. Such a cleavage of the 5–6 bond in **1***a*, accompanied by proton migration, would then lead to intermediate **9**, which is the enolic form of the proposed acylimine **6** (vide supra).

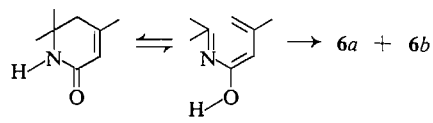

1*a* **9**

CHART 2

This labile intermediate might then be expected to undergo two competing transformations (see Chart 2) namely: recyclization to the starting dihydropyridone (**1***a*) or tautomerization to the corresponding acylimines **6***a* and *b* or, in the case of *t*-butyl alcohol, to the corresponding enamides **7***a* and *b*. The predominance of the unconjugated isomer **6***a* or **7***a* would seem to indicate that protonation of **9** is a kinetically controlled process favoring protonation at the α-carbon in accordance with the Hughes–Ingold rule (18).

In an effort to test the possible recyclization of **9**, dihydropyridone **1***a* was irradiated in *t*-butyl alcohol containing 1% of water. Thus, after 15 h of irradiation, under conditions otherwise identical to those used in the experiment with anhydrous *t*-butyl alcohol where low conversion to enamide **7** was observed, an i.r. spectrum of the crude material showed that all of the starting dihydropyridone **1***a* had disappeared and that only the photoamides **3** and **4** were present. It can be concluded therefore that intermediate **9**, which does not seem to react appreciably with *t*-butyl alcohol, can recyclize to the starting lactam **1***a* and that this reaction can be prevented

[4]The possibility of reaction from an upper triplet state cannot be ruled out at this point.

[5]The all importance of the double bond in this reaction was illustrated by irradiating an aqueous solution of the corresponding piperidone and showing that no reaction takes place.

Can. J. Chem. Downloaded from www.nrcresearchpress.com by 210.87.254.105 on 09/05/12
For personal use only.

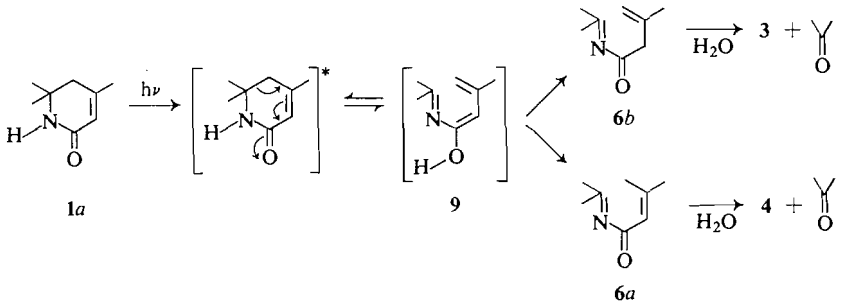

CHART 3

if a small amount of water is present in the mixture to trap the intermediate.

On the other hand, as previously stated, (vide supra) the tautomeric equilibrium between acylimines and enamides has been shown to lie completely on the enamide side in acyclic systems (6). In the present photochemical reaction, direct evidence for the possible formation of enamide **7** was obtained from the irradiation of dihydropyridone **1***a* in anhydrous *t*-butyl alcohol which permitted the isolation and characterization of pure enamide **7***a* and a mixture of **7***a* and *b*. (Chart 2).

The intervention of enamide **7** as a reaction intermediate could raise the question as to which of the intermediates, **6**, **7**, or **9** is responsible for the observed hydrolysis and methanol addition reactions. It seems quite evident from the preceding discussion that acylimine **6** (or perhaps the corresponding enolic form **9**) undergoes nucleophilic attack by solvent rather than enamide **7**.

Finally, in an attempt to gain evidence for the intervention of a diradical-like intermediate (**10**) in this reaction, the photolysis of dihydropyridone **1***a* was investigated in isopropyl alcohol which is known to be a good photoreducing agent. Unfortunately, as in the case of methanol, the reaction led to the addition of solvent to give **11** as the sole product.

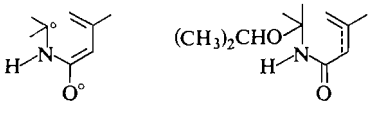

10 **11**

Following the above discussion, the reaction could be represented as a polar cleavage of **1***a* (see Chart 3). This mechanism is similar to that already proposed (4) by us and is somewhat analogous to that operative in the photochemistry of 4,4-dialkyl substituted cyclohexene-2 ones (14, 19). In addition however, a proton migration must take place from nitrogen to oxygen in a manner concomitant with ring opening.

On the other hand, this very migration of hydrogen to oxygen and the formation of an intermediate of structure **9** suggests a much more reasonable fragmentation path of the electrocyclic type as was envisaged in our previous communication (4). Indeed, the reaction could proceed through the lactim **12** which is liable to undergo electrocyclic ring opening (20) to intermediate **9** as shown in Chart 4.

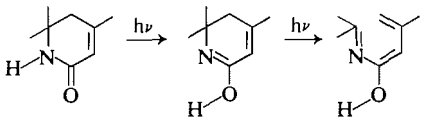

1*a* **12** **9**

CHART 4

This hypothesis, however, could not be substantiated experimentally. It had been anticipated that the photolysis of dihydroazepinone **13** could yield information on the cleavage path

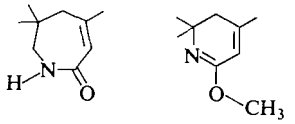

13 **14**

operative in this reaction. Indeed, a cleavage such as that described in Chart 4 could not have taken place in this seven-membered ring model. There remained two possibilities, namely, dimerization or cyclization to a bicyclic β-lactam (21).

Can. J. Chem. Downloaded from www.nrcresearchpress.com by 210.87.254.105 on 09/05/12
For personal use only.

Can. J. Chem. Downloaded from www.nrcresearchpress.com by 210.87.254.105 on 09/05/12
For personal use only.

Unfortunately, upon photolysis at room temperature, dihydroazepinone **13** yielded only a mixture of two dimers (12).

Finally, in a second attempt to substantiate the fragmentation path described in Chart 4, the corresponding lactim ether[6] (**14**) of dihydropyridone **1***a* was irradiated in *t*-butyl alcohol and to date we have been unable to obtain conclusive evidence for an electrocyclic cleavage of this molecule. Further investigation of the mechanism and scope of this reaction is in progress.

Experimental

Irradiations were carried out in quartz vessels, using a Rayonet Photochemical Reactor (16 low pressure Hg lamps, 2537 Å). A stream of oxygen-free nitrogen was bubbled through the solutions before and during irradiations. The alumina used for column chromatography was obtained from Woelm and the activity described is in accordance with the prescriptions of the Company. The t.l.c. was done on Eastman Chromagram sheets coated with alumina containing a fluorescent indicator. Melting points were taken on a Büchi apparatus and are uncorrected. The i.r. spectra were recorded in chloroform (unless otherwise stated) on a Beckman IR-8 spectrophotometer and n.m.r. spectra were obtained partly on a Varian A-60 instrument and partly on a Jeolco JNM-C-60H instrument using deuteriochloroform as solvent and tetramethylsilane as internal standard. Ultraviolet (u.v.) spectra were recorded on a Bausch & Lomb Spectronic 505 and mass spectra were measured on a Hitachi–Perkin–Elmer RMU 6-D spectrometer. A molecular weight determination was made on a Mechrolab Vapor Pressure Osmometer. Elemental analyses were carried out by Dr. C. Daesslé, Montreal.

4,6,6-Trimethyl-5,6-dihydro-2(1H)-pyridone (1a)

The procedure of Hall (22) was followed with a slight modification. Mesityl oxide (50 g, 0.51 mole) was stirred overnight with an equal volume of 28% aqueous ammonium hydroxide, at room temperature. The excess ammonia was removed by evaporation *in vacuo* or by bubbling nitrogen for 2 h. The solution was then chilled in ice and ethyl cyanoacetate (50 g, 0.442 mole) added with stirring. The reaction product which precipitated over a period of 2 h was filtered, washed with ether, and dried *in vacuo* to give 3-cyano-4,6,6-trimethyl-5,6-dihydro-2(1*H*)-pyridone (52 g, 62%), m.p. 196–197° (lit. (22) m.p. 194–196°).

The dihydrocyanopyridone thus obtained (20 g, 0.122 mole) was heated to reflux for 48 h in 18 *N* sulfuric acid (75 ml). The solution was then neutralized at 0° to p*H* 6 using a potassium hydroxide solution. After extraction of the mixture with chloroform, drying over sodium sulfate, and removing the solvent, a good yield (12.5 g, 74%) of crude dihydropyridone **1***a* was obtained. Recrystallization from dichloromethane–hexane gave the pure product (10.4 g), m.p. 116–118°. Further purification by sublimation (0.05 mm, 110°) brought the m.p. to 118° (lit. (22) 116.5–118°). The u.v. spectrum (95% EtOH) showed λ_{max} 213 nm (ε 15 600).

Photolysis of 4,6,6-Trimethyl-5,6-dihydro-2(1H)-pyridone (1a) in Water

A 1% solution (6 g/600 ml) of dihydropyridone **1***a* in distilled water was irradiated for 7 h after which time no more starting material could be observed by t.l.c. Distillation of part (~ 50 ml) of the solvent permitted the isolation of acetone as its 2,4-dinitrophenylhydrazone derivative. The remaining solution was saturated with ammonium sulfate, extracted with chloroform, and the organic layer dried over sodium sulfate. After evaporation of the solvent, the residue was taken up in ether and hydroxylactam **5***a* (85 mg, 1.3%), m.p. 189–190°, remained insoluble. The m.p. remained unchanged after recrystallization from chloroform–ether. The i.r. spectrum (nujol) showed absorption in the 3620 to 3200 region and at 1640 cm^{-1} while the n.m.r. spectrum (dimethyl-d_6 sulfoxide) had δ 1.15 (6H, singlet), 1.30 (3H, singlet), 1.61 (2H, quadruplet), 2.10 (2H, singlet), 4.47 (1H, singlet, exchanged with D_2O), and 7.35 (1H, broad singlet, exchanged with D_2O). The mass spectrum revealed a weak molecular ion at *m/e* 157.

Anal. Calcd. for $C_8H_{15}NO_2$: C, 61.11; H, 9.61; N, 8.91. Found: C, 61.50; H, 9.72; N, 8.92.

Further evidence for the structure of **5***a* was obtained by treating the above compound (50 mg) with a 1:1 mixture of sulfuric acid – water at 80° for 1 h. Extraction with chloroform in the usual manner yielded a mixture of two products (t.l.c.), the n.m.r. spectrum of which indicated 56% of dihydropyridone **1***a* and 44% of its deconjugated isomer.

Evaporation of the remaining ethereal solution containing the photolysis mixture gave a solid residue which upon recrystallization from acetone–hexane yielded a first crop of the unconjugated amide **3**. Evaporation of the mother liquors and chromatography on neutral alumina, activity IV yielded after elution with chloroform the conjugated amide **4** (351 mg, 8%). Further elution with chloroform gave more of the unconjugated isomer **3** for a total yield of 3.12 g (73%).

Amide **3** had m.p. 117° after recrystallization from acetone–hexane. The i.r. spectrum showed characteristic absorptions at 3540, 3420, 1680, 1650, 1585, and 900 cm^{-1}. The n.m.r. spectrum had δ 1.82 (3H, singlet), 2.95 (2H, singlet), 4.93 (2H, multiplet), and 5.8 (1H, flat band) while the u.v. spectrum (95% EtOH) indicated an end-absorption only. The mass spectrum showed a molecular ion peak at *m/e* 99.

Anal. Calcd. for C_5H_9NO: C, 60.57; H, 9.04; N, 14.14. Found: C, 60.72; H, 9.23; N, 14.38.

The proposed structure **3** was confirmed by carrying out a catalytic hydrogenation over palladium on charcoal (5%) in methanol. The isovaleramide obtained, m.p. 138–139° (acetone–hexane), was identical in all respects (mixed m.p. and i.r. spectra) with an authentic sample prepared from isovaleric acid by the standard procedure.

Conjugated amide **4** had m.p. 108–109° after recrystallization from acetone–hexane. The i.r. spectrum showed characteristic absorptions at 3550, 3430, 1675, 1640, and 1590 cm^{-1}. The n.m.r. spectrum had δ 1.85

[6]This compound was prepared by J. Hébert of this laboratory.

Can. J. Chem. Downloaded from www.nrcresearchpress.com by 210.87.254.105 on 09/05/12
For personal use only.

(3H, singlet), 2.13 (3H, singlet), 5.6 (1H, multiplet), and 6.0 (2H, broad band). The u.v. spectrum (95% EtOH) indicated λ_{max} 217 nm (ε 12 600) and the mass spectrum showed a molecular ion peak at *m/e* 99. The assignment of structure **4** was verified by comparison (mixed m.p., n.m.r. spectra, and i.r. spectra) with an authentic sample prepared from 3,3-dimethyl acrylic acid.

Photolysis of 4,6,6-Trimethyl-5,6-dihydro-2(1H)-pyridone (1a) in t-Butyl Alcohol

A 1% solution (6 g/600 ml) of dihydropyridone **1***a* in dry *t*-butyl alcohol (distilled over sodium *t*-butoxide and kept on Molecular Sieves, Linde type 4A) was photolyzed for 12 h. A stream of dry and oxygen-free nitrogen was bubbled through the solution for 20 min prior to and during the entire irradiation. An i.r. spectrum of the crude product obtained after evaporation of the solvent showed a great amount of unreacted starting material; however, a new characteristic band appeared at 1505 cm^{-1} and a new spot, of lower R_f than the starting material, was revealed by t.l.c. analysis.

The crude material was therefore washed with 30 ml of hexane, which dissolved the new product, plus a small amount of the starting material **1***a*. A simple filtration through alumina activity II, using hexane-dichloromethane (2:1) as eluent, yielded the pure enamide **7***b* as a pale yellow oil in the first fraction. The second and third fractions contained a mixture of **7***b* and its conjugated isomer **7***a*, as shown by dilute acid hydrolysis to a mixture of the known amides **3** and **4**. Further fractions eluted with methylene chloride – ether (1:1) contained dihydropyridone **1***a* and the primary amides **3** and **4**, which were separated in a subsequent chromatography on alumina activity IV. No yields are reported in this experiment as the enamides sought are partially hydrolyzed on the column.

The i.r. spectrum of the pure enamide **7***b* showed characteristic absorptions at 3420, 1680, 1648, 1505, and 910 cm^{-1}. The n.m.r. spectrum had δ 1.82 (3H, doublet, J = 1 c.p.s.), 1.92 (3H, singlet), 3.02 (2H, singlet), 4.91 (2H, multiplet, J = 1 c.p.s.), 4.45 and 5.43 (2H, AX system). The mass spectrum revealed a molecular ion peak at *m/e* 139.

Photolysis of 4,6,6-Trimethyl-5,6-dihydro-2(1H)-pyridone (1a) in t-Butyl Alcohol Containing 1% of Water

A 1% solution (6 g/600 ml) of dihydropyridone **1***a* in *t*-butyl alcohol, containing 1% of distilled water (6 g/600 ml), was photolyzed for 15 h under the same conditions as stated above. An i.r. spectrum of the crude product clearly showed the primary amides. No starting material **1***a* and no enamide **7** were observed.

Irradiation of Photoamides 3 and 4 in Water

When a 1% solution (300 mg/30 ml) of either photoamide **3** or photoamide **4** in water was irradiated for 18.5 h, no photochemical interconversion could be observed as shown by melting points, thin-layer chromatograms, and u.v. and i.r. spectra. Also, it is of importance to note that no interconversion was observed when the pure amides were chromatographed on alumina.

Photolysis of 4,6,6-Trimethyl-2-piperidone

The above piperidone (22), m.p. 119–121°, was prepared by catalytic hydrogenation of dihydropyridone **1***a* in acetic acid, using palladium (5%) on powdered charcoal as catalyst.

No photoreaction could be observed when an aqueous solution of the piperidone (300 mg/30 ml) was photolyzed during 7 h.

Photolysis of 4,6,6-Trimethyl-5,6-dihydro-2(1H)-pyridone (1a) in Methanol

A 1% solution (4 g/400 ml) of dihydropyridone **1***a* in dry methanol (distilled over sodium methoxide) was irradiated during 7 h. The solution was then evaporated to dryness and the i.r. spectrum of the crude product revealed a new characteristic band at 1505 cm^{-1}. Purification by filtration through a short column of alumina activity I, using dichloromethane–hexane, (1:1) as eluent gave the following results. The first few fractions gave the carbinolamidoethers, **8***a* and *b* (2.8 g, 57%, containing mostly the unconjugated isomer in a ratio of about 6:1). Elution with dichloromethane and dichloromethane–ether gave some unreacted starting material (1.3 g, 32%) and mixtures of the photoamides **3** and **4** which probably arose via partial hydrolysis of the labile amidoethers **8***a* and *b* on the column.

One fraction containing almost pure unconjugated amidoether **8***b* was further purified by distillation at 50° and 0.5 mm. The solid obtained melted at room temperature and was shown to contain a very small percentage of the conjugated amidoether **8***a* by n.m.r. and t.l.c. The i.r. spectrum showed characteristic absorptions at 3420, 1672, 1645, 1503, and 907 cm^{-1}. The n.m.r. spectrum had δ 1.56 (6H, singlet), 1.80 (3H, singlet), 2.98 (2H, singlet), 3.20 (3H, singlet), 4.86 (2H, multiplet), 7.52 (1H. broad band).

The mass spectrum did not reveal a molecular ion but showed an intense peak at *m/e* 139 corresponding to a loss of methanol. A molecular weight determination was however obtained by means of a "Mechrolab" Vapor Pressure Osmometer. Calcd.: 171. Found: 167.

Anal. Calcd. for $C_9H_{17}NO_2$: C, 63.20; H, 9.94; N, 8.19. Found: C, 63.16; H, 9.93; N, 8.23.

N-Methyl-3-cyano-4,6,6-trimethyl-5,6-dihydro-2-pyridone

The general procedure of Hall (22) (vide supra) was followed with the exception that aqueous methylamine was used instead of aqueous ammonia. The compound obtained in a low yield (16%) had m.p. 139–140° (methanol–water). The i.r. spectrum showed characteristic absorptions at 2240, 1655, 1620, and 1575 cm^{-1}. The n.m.r. spectrum had δ 1.32 (6H, singlet), 2.27 (3H, singlet), 2.52 (2H, singlet), and 2.97 (3H, singlet). The mass spectrum revealed a molecular ion peak at *m/e* 178.

N-Methyl-4,6,6-trimethyl-5,6-dihydro-2-pyridone (1b)

Hydrolysis and decarboxylation of the above cyanopyridone was carried out according to the procedure of Hall (22) (vide supra). The *N*-methyl lactam **1***b* obtained in a good yield (67%) had m.p. 43–44° (pentane–ether). The i.r. spectrum showed characteristic absorptions at 1675 and 1615 cm^{-1}. The n.m.r. had δ 1.25 (6H, singlet), 1.87 (3H, singlet), 2.23 (2H, singlet), 2.90 (3H, singlet), and 5.75 (1H, singlet). The mass spectrum revealed a molecular ion peak at *m/e* 153.

Photolysis of N-Methyl-4,6,6-trimethyl-5,6-dihydro-2-pyridone (1b)

A 1% solution (300 mg/30 ml) of *N*-methyl dihydropyridone **1b** in distilled water was irradiated during 7 h. The solution was then saturated with ammonium sulfate and extracted with chloroform. After drying and evaporating the solvent, a t.l.c. of the crude product revealed the presence of a large amount of starting material along with a new compound of lower R_f.

Chromatography of the mixture on silica gel using acetone–ether 1:4 as eluent gave unreacted starting material (270 mg, 90%) in the first fractions. Further elution using the same solvent system afforded a solid, m.p. 125° (15 mg, 5%). The i.r. spectrum of the compound showed characteristic bands at 3620, 3380, and 1615 cm^{-1}. The n.m.r. spectrum had δ 1.30 (6H, singlet), 1.45 (3H, singlet), 1.85 (2H, AB system with low field component showing additional splitting), 2.45 (2H, broad singlet), 2.89 (3H, singlet), and 3.14 (1H, singlet, exchangeable with D_2O). The mass spectrum revealed a molecular ion peak at *m/e* 171.

The authors are indebted to the National Research Council of Canada for support of this research through Grant A-2034 to D.G. Valuable technical assistance from Messrs. J. Hébert and B. Jodoin is also gratefully acknowledged.

1. (*a*) K. SCHAFFNER. *In* Advances in photochemistry. Vol. 4. Interscience Publishers, New York, 1966. p. 81; (*b*) P. J. KROPP. *In* Organic photochemistry. Vol. 1. Marcel Dekker, Inc., New York, 1967. p. 1.
2. J. G. CALVERT and J. N. PITTS, JR. Photochemistry. John Wiley and Sons, Inc., New York, 1966. p. 460.
3. O. L. CHAPMAN, P. J. NELSON, R. W. KING, D. J. TRECKER, and A. A. GRISWOLD. Rec. Chem. Progr. **28**, 167 (1967).
4. E. CAVALIERI and D. GRAVEL. Tetrahedron Lett. 3973 (1967).
5. H. K. REIMSCHUESSEL, J. P. SIBILIA, and J. V. PASCALE. J. Org. Chem. **34**, 959 (1969).
6. Y. HENG SUEN and H. B. KAGAN. Bull. Soc. Chim. France, 1460 (1965).
7. (*a*) K. TSUDA and R. HAYATSU. J. Amer. Chem. Soc. **78**, 4107 (1956); (*b*) N. J. DOORENBOS, C. LI HUANG, C. R. TAMORRIA, and M. T. WU. J. Org. Chem. **26**, 2546 (1961).
8. D. BEN-ISHAI and R. GIGER. Tetrahedron Lett. 4523 (1965).
9. J. E. BANFIELD, G. M. BROWN, F. H. DAVEY, W. DAVIES, and T. H. RAMSAY. Aust. J. Sci. Res. AI, 330 (1948).
10. S. W. BREUER, T. BERNATH, and D. BEN-ISHAI. Tetrahedron, **23**, 2869 (1967).
11. Y. HENG SUEN, A. HOREAU, and H. B. KAGAN. Bull. Soc. Chim. France, 1454, 1457 (1965).
12. E. CAVALIERI and S. HOROUPIAN. Can. J. Chem. **47**, 2781 (1969).
13. A. A. LAMOLA and J. P. MITTAL. Sci. **154**, 1560 (1966); see also J. G. BURR. *In* Advances in photochemistry. Vol. 6. Interscience Publishers, New York, 1968. p. 193.
14. O. L. CHAPMAN, J. B. SIEJA, and W. J. WELSTEAD, JR. J. Amer. Chem. Soc. **88**, 161 (1966).
15. T. MATSUURA and K. OGURA. Bull. Chem. Soc. Japan, **40**, 945 (1967).
16. B. J. RAMEY and P. D. GARDNER. J. Amer. Chem. Soc. **89**, 3949 (1967).
17. H. NOZAKI, M. KURITA, and R. NOYORI. Tetrahedron Lett. 2025 (1968).
18. (*a*) C. K. INGOLD. Structure and mechanism in organic chemistry. Cornell University Press, Ithaca, N.Y. 1953. p. 565; (*b*) see also J. F. WOLFE, G. B. TRIMITSIS, and D. R. MORRIS. J. Org. Chem. **34**, 3263 (1969) and C. D. BROADDUS. Accounts Chem. Res., **1**, 231 (1968).
19. H. E. ZIMMERMAN, R. G. LEWIS, J. J. MCCULLOUGH, A. PADWA, S. STALEY, and M. SEMMELHACK. J. Amer. Chem. Soc. **88**, 159 (1966).
20. R. HOFFMANN and R. B. WOODWARD. Accounts Chem. Res. **1**, 17 (1968).
21. O. L. CHAPMAN and W. R. ADAMS. J. Amer. Chem. Soc. **90**, 2333 (1968).
22. H. K. HALL, JR. J. Amer. Chem. Soc. **79**, 5444 (1957).

Can. J. Chem. Downloaded from www.nrcresearchpress.com by 210.87.254.105 on 09/05/12
For personal use only.

Can. J. Chem. Downloaded from www.nrcresearchpress.com by 84.22.46.98 on 09/08/12
For personal use only.

Methoxy group migrations in the reaction of some methyl-pyranoside chlorosulfate ester derivatives with aluminum chloride[1]

C. F. GIBBS[2] AND H. J. JENNINGS
Biochemistry Laboratory, National Research Council of Canada, Ottawa, Canada

Received March 25, 1970

The treatment of methyl β-D-xylopyranoside 2,3,4-tri(chlorosulfate) with aluminum chloride yielded a mixture of two major components identified as methyl α-D-xylopyranoside 2,3,4-tri(chlorosulfate) and 4-*O*-methyl-α-L-arabinopyranosyl chloride 2,3-di(chlorosulfate). The latter compound constituted about 25% of the mixture and was formed as a result of the preferential migration of the anomeric methoxy group to C-4 of the pyran ring. Similar treatment of methyl α-D-glucopyranoside 2,3,4,6-tetra(chlorosulfate) with aluminum chloride yielded crystalline 6-*O*-methyl-α-D-glucopyranosyl chloride 2,3,4-tri(chlorosulfate) as the only major methoxy migration product. This methoxy migration occurred to the extent of 66% and in contrast to the results obtained with methyl pentapyranoside derivative the anomeric methoxy group migrated preferentially to C-6 in this case. The factors controlling these highly selective methoxy migrations are discussed.

Canadian Journal of Chemistry, **48**, 2735 (1970)

Introduction

The ability of the methoxy group to participate in solvolytic displacement reactions was first established by Winstein and Henderson (1), and significant participation has been observed in reactions where the methoxy group participates through the formation of a three-membered (MeO-3 participation), five-membered (MeO-5 participation), and a six-membered (MeO-6 participation) oxonium ion (2). In the carbohydrate field a number of examples of methoxy group participation have also been established. The solvolysis of both methyl 5-*O*-*p*-bromobenzenesulfonyl-6-deoxy-2,3-*O*-isopropylidene-β-L-allofuranoside (3) and methyl 4-*O*-nitrobenzene-*p*-sulfonyl-β-D-xylopyranoside (4) resulted in MeO-5 participation with the subsequent migration of the glycosidic methoxy group. Similarly the benzoate displacement of 2,3,5-tri-*O*-benzyl-4-*O*-toluene-*p*-sulfonyl-D-ribose dimethyl acetal resulted in MeO-5 participation with the subsequent migration of one of the acetal methoxy groups (5). Evidence for the MeO-5 participation of a methoxy group not situated at the hemi-acetal position has also been obtained when the solvolysis of methyl 2,3-di-*O*-benzyl-6-*O*-methanesulfonyl-β-D-galactopyranoside yielded 3,6-anhydro-2-*O*-methyl-β-D-galactopyranoside as one of the products (6). One incidence of MeO-3 participation has been reported where the brominolysis of methyl 3,4,6-tri-*O*-acetyl-2-deoxy-2-iodo-α-D-mannopyranoside in acetic acid yielded as one of the products 1,3,4,6-tetra-*O*-acetyl-2-*O*-methyl-D-glucopyranose (7).

In all the above reactions, competitive methoxy participation involving the possibility of the simultaneous formation of oxonium ions of differing ring sizes was avoided by the introduction of only one leaving group in each molecule. We would now like to report a series of methoxy group migrations carried out by treating fully chlorosulfated methylglycopyranosides with aluminum chloride. These migrations occurred almost exclusively as a result of MeO-5 participation despite the possibility of MeO-3 and MeO-4 participation. This work was prompted by a previous observation that the treatment of β-D-xylopyranosyl chloride 2,3,4-tri(chlorosulfate) and its α-D-lyxopyranosyl analogue with aluminum chloride resulted in predominant Cl-3 participation (8) and it was hoped to determine some of the factors responsible for this selective migration by varying the nature of the migrating group.

Discussion

Methyl β-D-xylopyranoside 2,3,4-tri(chlorosulfate) when treated with aluminum chloride yielded a syrupy mixture containing two major components, subsequently identified as methyl α-D-xylopyranoside 2,3,4-tri(chlorosulfate) (anomerization product) and methyl 4-*O*-methyl-α-L-arabinopyranosyl chloride 2,3-di(chlorosulfate) (**4**) (methoxy migration product). The

[1]NRCC No. 11412.
[2]NRCC Postdoctorate Fellow, 1967–1969.

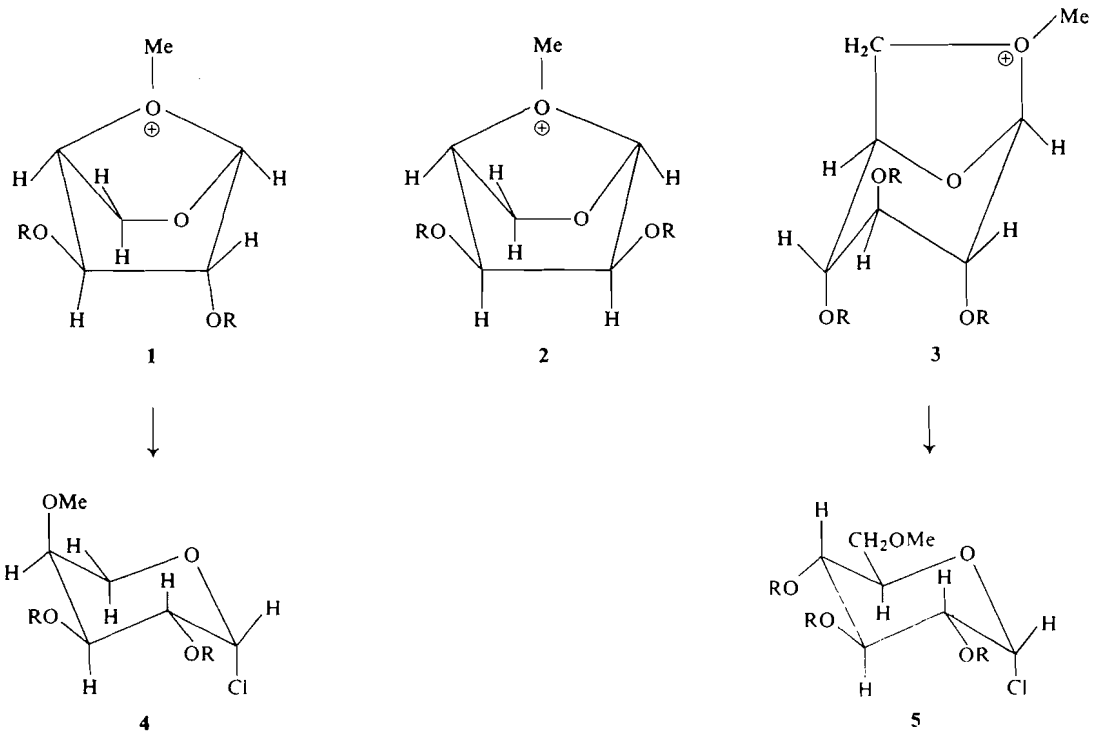

migration was easily followed using proton magnetic resonance (p.m.r.) spectroscopy by the distinguishable methoxy signals of the compounds above in the crude reaction product and also, in the case of **4**, by the appearance of a characteristic low-field anomeric doublet, due to the introduction of the more electronegative chloro-group at the anomeric position. The extent of migration was estimated as 25% by comparison of the integrated areas of the above p.m.r. signals and this was confirmed by the subsequent isolation of the dechlorosulfated products of the reaction. Dechlorosulfation of the syrupy mixture above yielded two major components (paper chromatography) which were separated by cellulose column chromatography. The individual components were identified as syrupy 4-*O*-methyl-L-arabinopyranose and crystalline methyl α-D-xylopyranoside, the former component constituting 28% of the mixture. The isolation of only one major monomethylpentose from the reaction mixture indicates a distinct preference for the anomeric methoxy group of methyl β-D-xylopyranoside 2,3,4-tri(chlorosulfate) to migrate to C-4 rather than to C-2 or -3 of the pyran ring. This preferential methoxy migration probably involves the formation of the intermediate bicyclic oxonium ion (1), despite the high energy requirement of this ion (1) due to the unfavorable non-bonded steric interactions which would occur in its boat conformation. Related ions in the boat conformation have been encountered in the acetolysis of *trans* 4-methoxycyclohexyl tosylate (9) and more recently in the hydrolysis of methyl 4-*O*-nitrobenzene-*p*-sulfonyl-β-D-xylopyranoside (4).

Methyl α-D-lyxopyranoside 2,3,4-tri(chlorosulfate) when treated with aluminum chloride yielded no detectable quantity of methoxy migration product even after an extended period of reaction. This was determined by the absence of any new methoxy singlet or the appearance of any low-field anomeric signal in the p.m.r. spectrum of the reaction product. The failure of the anomeric methoxy group to migrate to C-4 in the lyxopyranoside derivative can probably be attributed to the higher energy required to form the oxonium ion **2** compared with that necessary to form **1** because of the greater non-bonded interactions. Oxonium ion **2** has an

Can. J. Chem. Downloaded from www.nrcresearchpress.com by 84.22.46.98 on 09/08/12
For personal use only.

Can. J. Chem. Downloaded from www.nrcresearchpress.com by 84.22.46.98 on 09/08/12
For personal use only.

unfavorable eclipsed (*cis*) orientation of the C-2 and -3 chlorosulfate groups whereas **1** has the more favorable *trans*-orientation of these groups.

Methyl α-D-glucopyranoside 2,3,4,6-tetra-(chlorosulfate) when treated with aluminum chloride gave a good yield of methoxy migration product (**5**). This was determined by the appearance in the p.m.r. spectrum of the syrupy reaction product of an additional methoxy signal (τ 6.58) to the methoxy signal of the original reactant (τ 6.42), plus a low-field anomeric doublet (τ 3.53), characteristic of a methoxy migration product. The amount of **5** present in the mixture was estimated at approximately 66% by the integration of these signals in the p.m.r. spectrum of the syrupy reaction product. The migration product (**5**) was isolated crystalline from the syrupy mixture and the p.m.r. spectrum of crystalline **5** confirmed the assignments made previously on the p.m.r. spectrum of the syrupy reaction product. The elemental analysis of **5** was consistent with the structure assigned to it and this structure was confirmed when the dechlorosulfation of **5** yielded crystalline 6-*O*-methyl-D-glucose. That only one major methoxy migration product was formed in the reaction was determined by dechlorosulfation, and acid hydrolysis of the product of the mother liquors obtained from the recrystallization of **5**. This yielded two reducing components which were identified as D-glucose and a faster running monomethyl-glycopyranose derivative (paper chromatography). The faster running component was isolated by cellulose column chromatography and was characterized as crystalline 6-*O*-methyl-D-glucose. Methoxy migration in this case probably occurs via oxonium ion **3** which requires for its formation that the glycosidic methoxy group have the β-D-configuration. This is obviously readily achieved by the continual equilibration of the methoxy group of the original reactant (α-D-anomer) in the presence of aluminum chloride. Once more the preference for MeO-5 participation is established but this time the anomeric methoxy group migrates to the exocyclic C-6 position, a route not available in the pentopyranoside derivatives. This is readily explained by the lower energy requirement of the chair conformation of **3** in comparison with the ion in the boat conformation that would be required for the alternative MeO-5 participation. The lower energy requirement of the ion in the chair conformation is also reflected in the higher yield of methoxy migration product resulting from **4** in comparison with that resulting from **1**. A related ion in the same chair conformation has been encountered in the solvolysis of methyl 1-thio-6-*O*-toluene-*p*-sulfonyl-β-D-glucopyranoside (10).

Although energy factors do exert an influence on the route of methoxy migration in these pyranoside derivatives (c.f. **1** and **3**) they do not seem to affect the overall preference for MeO-5 participation. This preference is in accord with the results of kinetic studies carried out by Winstein *et al.* on the solvolysis of the acyclic ω-methoxyalkyl *p*-bromobenzenesulfonates, where methoxy participation was the most favorable when it occurred via a monocyclic five-membered oxonium ion (11). Also this preference for MeO-5 participation is in direct contrast to the results obtained using the analogous pentapyranosyl chloride derivatives, as these exhibited a distinct preference for Cl-3 participation using identical conditions (8). Thus the nature of the participating group is a dominant factor in determining the ring-size of the intermediate ion even to the extent of overcoming the substantial energy-requirements involved in the formation of **1**. To our knowledge, no kinetic data is available to establish a preference for Cl-3 participation but the results obtained using the pentapyranosyl chloride derivatives would seem to indicate that this would prove to be the case.

It is interesting to note that in all the reactions carried out no significant MeO-3 participation was observed, whereas MeO-3 participations have been reported by Winstein and Henderson (1) and Lemieux and Fraser–Reid (7). The latter example is particularly relevant to our work as it does involve MeO-3 participation of the anomeric methoxy group in a pyranose ring structure. Although the factors controlling migration are complex, nevertheless, for neighboring group participation the electronic effects (inductive) of the participating group and the leaving group on each other are of some consequence (2). Thus the more electronegative chlorosulfate group might tend to inhibit MeO-3 participation to a greater extent than the less electronegative iodo group used by Lemieux and Fraser–Reid (7) as a leaving group. Certainly, the chlorosulfate group is more electronegative than iodine as it is also more electronegative than chlorine. This can be

ascertained from chemical shift data obtained from the p.m.r. spectra of configurational analogues, where the substitution of a chlorosulfate group by chlorine caused a considerable upfield shift ($\simeq 1.0$ p.p.m.) in the α-proton signal (8). It has been established that a qualitative comparison of the degree of electronegativity of substituent groups can be obtained from the relative positions of the resonance frequencies of their α-protons (12).

Experimental

Melting points were determined on a Kofler hot stage and are uncorrected, and optical rotations were measured at 21 ± 3°. Paper chromatograms were run by the descending method using butan-1-ol – ethanol – water (3:1:1) (v/v) as the solvent. Sugars were located on paper chromatograms by *p*-anisidine hydrochloride (13) or by periodate–permanganate (14) spray reagents. Column chromatography was performed using Whatman cellulose powder (CF11) with butan-1-ol half saturated with water as the eluant. The p.m.r. spectra were obtained from a Varian A60A spectrometer using deuteriochloroform as the solvent and tetramethylsilane ($\tau = 10.0$) as the internal standard.

Methyl α- and β-D-Xylopyranoside 2,3,4-Tri(chlorosulfate)

Crystalline methyl α-D-xylopyranoside 2,3,4-tri(chlorosulfate) was prepared by the methanolysis of β-D-xylopyranosyl chloride 2,3,4-tri(chlorosulfate) as previously described (15) and the p.m.r. spectrum of the crystalline product indicated one methoxy singlet at τ 6.46. Crystalline methyl β-D-xylopyranoside 2,3,4-tri(chlorosulfate) was also prepared as previously described by treating methyl β-D-xylopyranoside with sulfuryl chloride and the p.m.r. spectrum of the crystalline product indicated one methoxy-singlet at τ 6.38.

Reaction of Aluminum Chloride with Methyl β-D-Xylopyranoside 2,3,4-Tri(chlorosulfate)

Methyl β-D-xylopyranoside 2,3,4-tri(chlorosulfate) (10 g, 0.022 mole) was dissolved in absolute chloroform (750 ml) and the solution was heated to 60°. The large volume of chloroform was found to be advantageous in reducing decomposition in these reactions. Finely divided aluminum chloride (4.3 g, 0.032 mole) was added to the solution with vigorous stirring and the stirring was maintained for 3 h. The optimum time of reaction which yielded the maximum amount of methoxy migration product was determined by examination of the methoxy signals of the p.m.r. spectra of a number of preliminary reactions carried out using a time variable. The chloroform solution was then washed with water, saturated sodium bicarbonate solution, and dried over anhydrous sodium sulfate. Following clarification with charcoal, the solution was filtered and concentrated to a syrup (7 g). Examination of the p.m.r. spectrum of the syrup indicated two major methoxy signals at τ 5.89 (assigned to compound **4**) and τ 6.46 (assigned to the methyl α-D-anomer of the original reactant) in the ratio of 1:3. A small methoxy signal at τ 6.38 (assigned to the original reactant) was also detected. The spectrum also indicated a low field doublet at τ 3.56 ($J_{1,2}$ 3.1 Hz) which was assigned to the anomeric proton of **4**.

4-O-Methyl-L-arabinose

The syrup above was dechlorosulfated with sodium iodide in aqueous-acetone in the presence of barium carbonate (16). The solution was filtered free of insoluble salts and deionized by passage through Amberlite 1R120 and Duolite A4 ion-exchange resins. Concentration of the solution gave a syrup (2.6 g) which was shown by paper chromatography to contain two major components; one reducing component and a faster running non-reducing component. The two components were separated by cellulose column chromatography and the non-reducing component was obtained as a syrup (1.8 g, 50%) which on crystallization from ethyl acetate gave crystals of m.p. 85–87°, undepressed on admixture with an authentic sample of methyl α-D-xylopyranoside. The chromatographically pure reducing component was obtained as a syrup (0.5 g, 14%) which resisted crystallization and had $[\alpha]_D$ + 130° (*c*, 1.0 in water); literature reports $[\alpha]_D$ + 132 ± 2° for 4-*O*-methyl-L-arabinose (17). The syrup gave a crystalline phenylosazone derivative of m.p. 174–176° undepressed on admixture with an authentic sample of the phenylosazone of 4-*O*-methyl-L-arabinose (17) and methanolysis of the syrup with methanolic hydrogen chloride (17) yielded a crystalline methyl glycoside of $[\alpha]_D$ + 240° (*c*, 0.15 in methanol) of m.p. 112–114° undepressed on admixture with authentic methyl 4-*O*-methyl-α-L-arabinopyranoside (17).

Methyl α-D-Lyxopyranoside 2,3,4-Tri(chlorosulfate)

Methyl α-D-lyxopyranoside (5 g) (18) was treated with sulfuryl chloride (13 ml) and pyridine (20 ml) in chloroform solution using identical conditions to those used in the synthesis of methyl β-D-xylopyranoside 2,3,4-tri(chlorosulfate) (13). The chloroform soluble product was crystallized from chloroform – light petroleum (b.p. 30–60°) and gave crystals (4.2 g, 30%) of m.p. 135–137° and $[\alpha]_D$ −9° (*c*, 1.0 in chloroform).

Anal. Calcd. for $C_6H_9Cl_3S_3O_{11}$: C, 15.68; H, 1.97; Cl, 23.15; S, 20.92. Found: C, 15.90; H, 2.30; Cl, 23.24; S, 20.34.

The p.m.r. spectrum of the above crystals indicated one methoxy singlet at τ 6.47.

Reaction of Aluminum Chloride with Methyl α-D-Lyxopyranoside 2,3,4-Tri(chlorosulfate)

The tri-chlorosulfate derivative above (4 g) was treated with aluminum chloride and the chloroform soluble product was obtained using identical procedures to those described previously for methyl β-D-xylopyranoside 2,3,4-tri(chlorosulfate). The chloroform soluble product (2.5 g) gave an almost identical p.m.r. spectrum to that of the starting material. No significant quantity of methoxy migration product could be detected in the p.m.r. spectrum of the product by either the appearance of any other methoxy signal or a low-field anomeric signal. This latter signal has been shown to be a characteristic feature of the migration of an anomeric methoxy group in this type of reaction. Prolongation of the reaction for a further 2 h also produced negligible changes in the p.m.r. spectrum of the product.

Can. J. Chem. Downloaded from www.nrcresearchpress.com by 84.22.46.98 on 09/08/12
For personal use only.

6-O-Methyl α-D-Glucopyranosyl Chloride 2,3,4-Tri(chlorosulfate)

Crystalline methyl α-D-glucopyranoside 2,3,4,6-tetra-(chlorosulfate) (6.5 g) (14) was treated with aluminum chloride in absolute chloroform (450 ml) using identical conditions to those previously described for methyl β-D-xylopyranoside 2,3,4-tri(chlorosulfate). The chloroform solution was also washed, dried, and clarified as described previously. Concentration of the chloroform solution yielded a syrup (4.0 g), the p.m.r. spectrum of which indicated two major methoxy singlets at τ 6.42 (identical chemical shift to that of the methoxy signal of the original reactant) and at τ 6.58 (assigned to **5**), in the ratio of 1:2 respectively. The spectrum also gave a low-field doublet at τ 3.53 ($J_{1,2}$ 3.8 Hz) which was assigned to the anomeric proton of **5**. The syrup slowly crystallized and recrystallization from propan-2-ol gave crystals (0.9 g, 16%) of m.p. 143–145° and $[\alpha]_D$ + 130° (*c*, 1.0 in chloroform).

Anal. Calcd. for $C_7H_{10}O_{11}S_3Cl_4$: C, 16.54; H, 1.98; Cl, 27.90; S, 18.92. Found: C, 16.63; H, 2.14; Cl, 28.20; S, 18.64. An examination of the p.m.r. spectrum of crystalline **5** confirmed the assignments made previously for **5** in the crude reaction product above.

6-O-Methyl-D-glucose

Crystalline **5** (0.4 g) was dechlorosulfated with sodium iodide in aqueous acetone in the presence of barium carbonate (16). The solution was filtered free of insoluble salts and deionized by passage through Amberlite IR120 (H^+) and Duolite A4 (OH^-) ion exchange resins. Concentration of the solution gave a syrup (0.17 g) which was shown to be homogeneous by paper chromatographic analysis. The syrup slowly crystallized and recrystallization from benzene–ethanol gave crystals (0.032 g, 20%) of m.p. 143–144° and $[\alpha]_D$ + 104° → + 55° (equilibrium) (*c*, 0.8 in water); literature reports m.p. 142–143° and $[\alpha]_D$ + 56° (equilibrium in water) for 6-*O*-methyl-D-glucose (19). The syrupy product obtained by concentrating the mother liquors of the recrystallization above gave a crystalline phenylosazone derivative which when recrystallized from methanol had m.p. 186–188° and $[\alpha]_D$ −72° → −47° (equilibrium) (*c*, 0.4 in ethanol). These physical constants are consistent with those reported in the literature for the phenylosazone of 6-*O*-methyl-D-glucose (20).

The mother liquors obtained from the crystallization of **5** were concentrated to a syrup which was dechlorosulfated and deionized by the same procedure used for the dechlorosulfation of **5**. The syrupy dechlorosulfated product was then hydrolyzed with normal sulfuric acid and the neutralized hydrolyzate was concentrated to a syrup which was shown to contain only two major components (paper chromatography). These components had identical R_F values to those of D-glucose and 6-*O*-methyl-D-glucose and the latter component was isolated by cellulose column chromatography. The crystalline product thus obtained had m.p. 143–144° undepressed on admixture with authentic 6-*O*-methyl-D-glucose isolated previously from **5**.

We wish to thank Mrs. A. Martin for technical assistance and Mr. A. E. Castagne for determination of the microanalyses and the 60 MHz p.m.r. spectra. The authentic crystalline 4-*O*-methyl-L-arabinose derivatives were kindly provided by Dr. C. T. Bishop.

1. S. Winstein and R. B. Henderson. J. Amer. Chem. Soc. **65**, 2196 (1943).
2. B. Capon. Quart. Rev. London, **18**, 45 (1964).
3. C. L. Stevens, R. P. Glinski, K. G. Taylor, P. Blumbergs, and F. Sirokman. J. Amer. Chem. Soc. **88**, 2073 (1966).
4. J. G. Buchanan, A. R. Edgar, and D. G. Large. Chem. Commun. 558 (1969).
5. N. A. Hughes and P. R. H. Speakman. J. Chem. Soc. (C), 1182 (1967).
6. J. S. Brimacombe and O. A. Ching. Carbohyd. Res. **9**, 287 (1969).
7. R. U. Lemieux and B. Fraser-Reid. Can. J. Chem. **42**, 539 (1964).
8. H. J. Jennings. Can. J. Chem. **48**, 1834 (1970).
9. D. S. Noyce, B. R. Thomas, and B. N. Bastian. J. Amer. Chem. Soc. **82**, 885 (1960).
10. E. V. E. Roberts, J. C. P. Schwarz, and C. A. McNab. Carbohyd. Res. 7, 311 (1968).
11. S. Winstein, E. Allred, R. Heck, and R. Glick. Tetrahedron, **3**, 1 (1958).
12. L. M. Jackman. Nuclear magnetic resonance spectroscopy. The Pergamon Press Ltd., New York, 1958.
13. L. Hough, J. K. N. Jones, and W. H. Wadman. J. Chem. Soc. 1702 (1950).
14. R. U. Lemieux and H. F. Bauer. Anal. Chem. **26**, 920 (1954).
15. H. J. Jennings. Can. J. Chem. **46**, 2799 (1968).
16. H. J. Jennings and J. K. N. Jones. Can. J. Chem. **43**, 2372 (1965).
17. I. R. Siddiqui and C. T. Bishop. Can. J. Chem. **40**, 233 (1962).
18. F. P. Phelps and C. S. Hudson. J. Amer. Chem. Soc. **48**, 503 (1926).
19. H. B. Wood, H. W. Diehl, and H. G. Fletcher. J. Amer. Chem. Soc. **79**, 3862 (1957).
20. D. J. Bell. J. Chem. Soc. 859 (1936).

Can. J. Chem. Downloaded from www.nrcresearchpress.com by 84.22.46.98 on 09/08/12
For personal use only.

Can. J. Chem. Downloaded from www.nrcresearchpress.com by 210.87.254.105 on 09/05/12
For personal use only.

Magnetic resonance studies of metal–olefin complexes. I. Electron spin resonance spectra of γ-irradiated silver perchlorate cycloalkene complexes

D. R. GEE, K. E. RUSSELL, AND J. K. S. WAN
Department of Chemistry, Queen's University, Kingston, Ontario

Received April 10, 1970

Paramagnetic species have been detected in γ-irradiated polycrystalline silver perchlorate – cycloalkene complexes at room temperature and identified as Ag^+cycloalkenyl radicals, with spin density on Ag decreasing from 4.6 to 1.5% with increasing size of the cycloalkenyl ring. The extent of the spin density on Ag increases with the stability of the parent complexes.

Canadian Journal of Chemistry, 48, 2740 (1970)

Introduction

Complex formation between Ag(I) and olefins is well known (1–3) and Dewar (4) has proposed that the complexes are formed by the σ overlap between the bonding olefin π orbital with a vacant s or sp hybrid orbital on the Ag(I) together with π overlap of an occupied silver d orbital with an antibonding olefin π orbital. In recent years proton magnetic resonance (p.m.r.) studies (5) of these complexes in solution have suggested that σ-bonding is more important than π bonding. However, many problems concerning the interpretation of the changes of the chemical shifts of the vinyl protons in the complexes still remain as have been very recently pointed out by Parker and Roberts (6).

Studies of the relative stability of silver–olefin complexes (7, 8) reveal the order of increasing stability to be: bicycloolefins > *endo*cyclo-monoolefins > aliphatic olefins. Traynham and Olechowski (8) attribute this to the effect of ring strain upon the π basicity of the olefins and thus upon the strength of the coordinate bond.

Crystalline complexes with a 2:1 cycloalkene:Ag ratio have been obtained with silver nitrate (9, 10), silver perchlorate (9, 11), and silver tetrafluoroborate (12). With a series of cyclomonoolefins, infrared (i.r.) and solution p.m.r. studies (11, 12) indicate the order of relative stability of the complexes to be: cyclopentene > cyclohexene > cycloheptene ⩾ *cis*-cyclooctene. This order was found to be virtually independent of the anions used.

The present investigation describes a new approach to the understanding of the nature of bonding in silver–cycloalkene complexes by electron spin resonance (e.s.r.) studies. Although the solid silver – cycloalkene complexes are diamagnetic, paramagnetic species such as Ag^+cycloalkenyl radicals can be produced by γ-irradiation. Analysis of the e.s.r. spectra of these radicals leads to direct evidence for the importance of the σ overlap between the cycloalkenyl π orbital with the vacant 5s orbital on the Ag ion.

Experimental

The solid complexes were prepared from anhydrous silver perchlorate (Alfa Inorganic) and redistilled pure cycloalkenes (Aldrich) using the method of Comyns and Lucas (9). Cyclohexene-3,3,6,6-d_4 was prepared by the method of Wolfe and Campbell (13) and the cyclohexene-3,3,4,4,5,5,6,6,-d_8 was generously supplied by Professor S. Wolfe of this Department. Characterization data for these complexes are presented in Table 1.

TABLE 1
Characterization data for $AgClO_4$–cycloalkene

Olefin	Silver analysis (%) Calculated for $Ag(cycloalkene)_2$	Silver analysis (%) Found	Melting point (°C)
Cyclopentene	31.38	31.05	102
Cyclohexene	29.02	28.86	110
Cycloheptene	26.99	27.05	129
cis-Cyclooctene	25.22	25.01	172

Polycrystalline samples of the complexes were each irradiated at room temperature in a 19 500 Ci source of 1.3 MeV ^{60}Co γ-rays. The dose rate was approximately 1 Mrad/h and the total dose was 0.1 to 0.2 Mrad. The e.s.r. spectra were obtained with a Varian V4502 spectrometer and auxiliary equipment. A Fabri-Tek 1074 instrument computer was used for signal enhancement and for integration and differentiation of the recorded spectra.

The radiation G value for radical formation was determined from a measurement of the absolute number of spins in a given irradiated sample. Absolute spin determinations can be carried out using various methods of calibration (14). We have developed a simpler and

Can. J. Chem. Downloaded from www.nrcresearchpress.com by 210.87.254.105 on 09/05/12
For personal use only.

reliable technique employing only a single cavity and a reference Mn^{++} sample. A standard polycrystalline sample of CaO containing about 0.01% $MnSO_4$ was prepared by directly heating the mixed salts with a strong gas-oxygen flame for 15 min. This firing process ensures an even distribution of Mn^{++} ions in the host lattice (15). The e.s.r. spectrum of this standard sample was entirely due to Mn^{++} ions and consisted of an equally spaced sextet with splittings about 90 G. The absolute number of spins in a given prepared Mn^{++} standard, contained in a sealed capillary, was calibrated by comparison of the integrated spectrum of this sample with that of a known amount of DPPH. Calibration of only one of the six Mn^{++} lines was necessary, since they are equal. This sealed standard sample was found to be very stable and insensitive to temperature changes and exposure to room light. Thus it was used to estimate the absolute number of spins in known weights of the four irradiated silver–olefin complexes. The problem of spectral overlap was resolved by scanning a range of magnetic field sufficiently wide as to record an outer Mn^{++} line with which no overlap occurred.

Simulation of spectra was done on an IBM 360/50 computer using a modified program made available by Bell Telephone Laboratory.

The experimental e.s.r. spectra of four $AgClO_4$(cycloalkene)$_2$ complexes irradiated and recorded at room temperature are shown in Figs. 1*a* to 4*a*. Inspection of these spectra reveals some asymmetric line-width broadening whose origin is not known for certain at the present time. It is, however, possible that the small variation is due to dipolar and *g*-tensor interactions with the silver nucleus which has a negative magnetogyric ratio. Another possible explanation of the line-width effect is the superposition of the main spectrum on a single broad line having a *g* value slightly different from that of the main spectrum. A considerably stronger underlying broad line, assigned to trapped electrons, has been observed (16) following the γ-irradiation of the silver perchlorate cycloheptatriene complex.

The available spectral parameters of Ag^0, Ag^{++} (17), and the chlorine oxyradicals (18, 19) eliminate them as possible species responsible for the observed spectra. Since cycloolefins and some of their adducts yield cycloalkenyl radicals when subjected to ionizing radiation (20, 21), it is probable that the corresponding Ag^+cycloalkenyl radicals are produced upon γ-irradiation of the silver–cycloalkene complexes (eq. [1]).

[1] $Ag^+(cycloalkene)_2 \longrightarrow$ 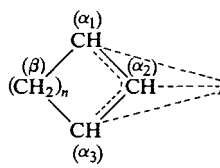 $+ Ag^+ + H +$ Alkene

Analysis of the experimental spectra on the basis of these Ag^+cycloalkenyl radicals yields the spectral parameters presented in Table 2. Despite the small line-width variation in the experimental spectra, the computed spectra constructed using the assignments in Table 2 fit reasonably well with the experimental spectra (Figs. 1*b* to 4*b*). As a further confirmation of the assignments quoted in Table 2, the silver perchlorate complexes of two specifically deuterated cyclohexenes were prepared and irradiated. Their e.s.r. spectra are compared with those computed using an a_D/a_H ratio of 0.1535 and the hyperfine coupling constants of the cyclohexene complex in Table 2. The agreement observed is thought to confirm the silver–cycloalkenyl postulate.

The experimental proton coupling constants show many similarities with those reported for the cycloalkenyl radicals (20, 21). This appears to support the other observations based on i.r. and p.m.r. data (11, 12) that little ring distortion occurs when the metal–olefin bond is formed. The observed near-equivalence of the four β protons of the cyclopentene, cycloheptene, and *cis*-cyclooctene complexes, suggests a planar structure for the Ag^+cyclopentenyl radical and some mechanism rendering rapid interchange of the β protons in the other two larger rings. In the cyclohexenyl–silver radical, however, the β protons appear to be locked in a particular orientation with respect to the remainder of the molecule. Spectra of this radical recorded at 373 °K indicate no change in β proton orientation, suggesting that the restraint may be imposed by the crystal lattice.

Although the hyperfine splitting for separate ^{107}Ag and ^{109}Ag isotopes are not resolved in the experimental spectra, it is possible to derive the spin density on the Ag^+ of the silver–cycloalkenyl radicals by comparing the experimental average

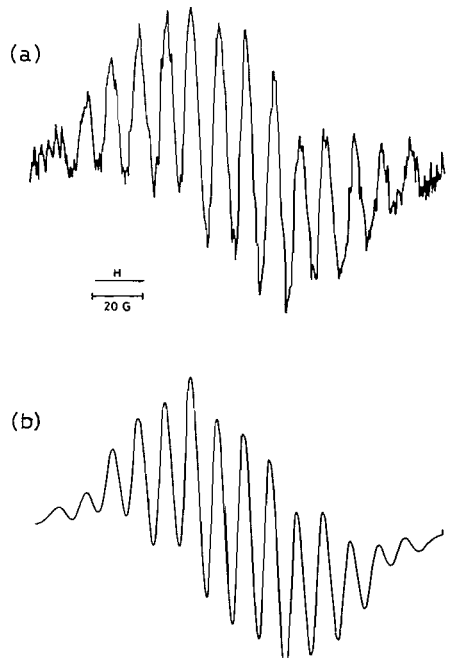

FIG. 1. The e.s.r. spectra of γ-irradiated $AgClO_4$–cyclopentene: (*a*) experimental spectrum, (*b*) computer-simulated spectrum of Ag^+cyclopentenyl radical.

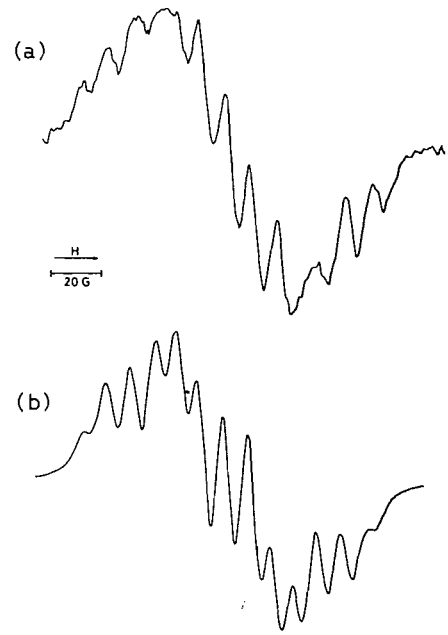

FIG. 2. The e.s.r. spectra of γ-irradiated $AgClO_4$–cyclohexene: (*a*) experimental spectrum, (*b*) computer-simulated spectrum of Ag^+cyclohexenyl radical.

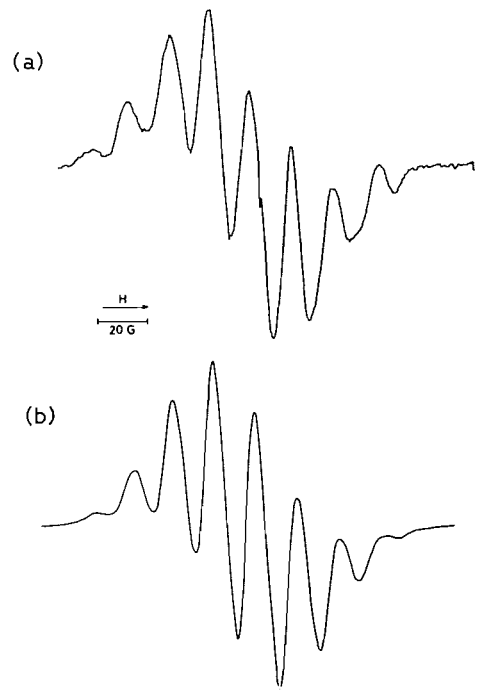

FIG. 3. The e.s.r. spectra of γ-irradiated $AgClO_4$–cycloheptene: (*a*) experimental spectrum, (*b*) computer-simulated spectrum of Ag^+cycloheptenyl radical.

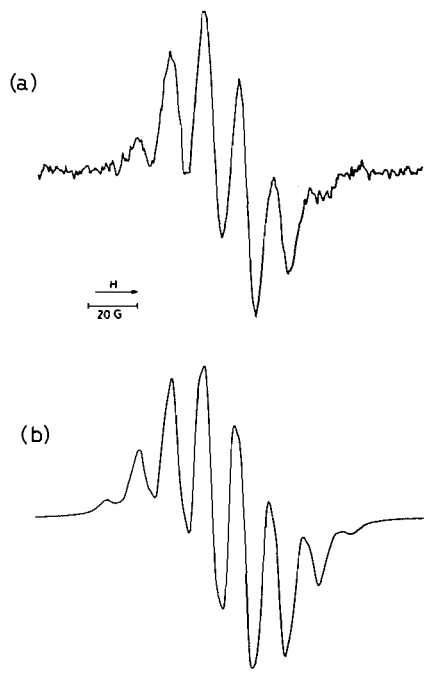

FIG. 4. The e.s.r. spectra of γ-irradiated $AgClO_4$–*cis*-cyclooctene: (*a*) experimental spectrum, (*b*) computer-simulated spectrum of Ag^+cyclooctenyl radical.

Can. J. Chem. Downloaded from www.nrcresearchpress.com by 210.87.254.105 on 09/05/12
For personal use only.

TABLE 2

Spectral parameters for Ag^+cycloalkenyl radicals

	Ag^+Cyclopentenyl	Ag^+Cyclohexenyl	Ag^+Cycloheptenyl	Ag^+Cyclooctenyl
g Factor splitting constants (Gauss)	2.0016 ± 0.0002	2.0017	2.0019	2.0020
a_{Ag}	30.5 ± 0.4	22.5	17.5	10.0
a_H (α_1)	10.9	11.0	14.0	14.0
a_H (α_2)	3.0	3.8	4.6	4.0
a_H (α_3)	10.9	11.0	14.0	14.0
a_H (β)	22.0	28.5 (β_1) 8.5 (β_2)	17.6	15.0
Spin density on Ag %	4.6	3.4	2.7	1.5

silver splitting with the atomic silver value (17). These derived spin densities, listed in Table 2, probably arise from a spin polarization of the σ overlap. Based on the generally accepted Dewar theory (4) of the metal–olefin bonding, many authors (8, 22, 23) have suggested that the σ component of the coordinate bond may predominate in silver or indeed in Group IB metal–olefin complexes, while the π bonding probably is more important in others. Studies of Quinn *et al.* (24, 25) on the relative stability of the aliphatic olefin–$AgBF_4$ complexes appear to confirm such a conclusion. Our results of the spin densities of the Ag ion and the proton splittings in the silver-cycloalkenyl radicals give independent and direct evidence of the importance of the σ overlap and may in turn give a relative measure of the strength of the metal–cycloalkenyl bond. Thus a decrease in the spin density on silver accompanies an increase in the size of the cycloalkenyl ring. This parallels the results of the stability of the parent complexes obtained by other methods (8, 12). Work in progress includes wide-line nuclear magnetic resonance (n.m.r.) studies of solid silver – deuterated cycloalkenes complexes and pulsed electrolysis studies by e.s.r. of silver and other metal–olefin complexes in solution. It is hoped that this series of investigations may lead to further insight into the nature of metal–olefin bond.

In view of the stability and ease of formation of these silver–cycloalkenyl radicals in the solid complexes, an attempt was made to estimate their radiation *G* values. The *G* values for the four silver-cycloalkenyl radicals were found to lie within the range 3.5 to 4.5 radicals per 100 eV. Similar radiation yields are reported for the radicals formed when hexadexene-1 (26) and substituted acetylene (27) are irradiated at 77 °K.

The authors are indebted to Mr. L. Fabes, Drs. L. Desilva, A. Rudge, and Professor J. A. Stone for helpful discussions and some technical assistance, and to Dr. H. W. Quinn of the Exploratory Research Laboratory, Dow Chemical of Canada, Sarnia, Ontario, for sending some preprints of his work. Financial support by the National Research Council of Canada, the Defence Research Board, and the Public Health Department, is gratefully acknowledged.

1. S. Winstein and H. J. Lucas. J. Amer. Chem. Soc. **60**, 836 (1938).
2. M. A. Bennett. Chem. Rev. **62**, 611 (1962).
3. H. W. Quinn and J. H. Tsai. Olefin complexes of the transition metals. Adv. Inorg. Radiochem. **12**, 217 (1969).
4. M. J. S. Dewar. Bull. Soc. Chim. Fr. **18**, C79 (1951).
5. D. B. Powell and N. Sheppard. J. Chem. Soc. 2519 (1960); J. Schug and R. J. Martin. J. Phys. Chem. **66**, 1554 (1962).
6. R. G. Parker and J. D. Roberts. J. Amer. Chem. Soc. **92**, 743 (1970).
7. M. A. Muhs and F. T. Weiss. J. Amer. Chem. Soc. **84**, 4697 (1962).
8. J. G. Traynham and J. R. Olechowski. J. Amer. Chem. Soc. **81**, 571 (1959).
9. A. E. Comyns and H. J. Lucas. J. Amer. Chem. Soc. **79**, 4339 (1957).
10. A. C. Cope, D. C. McLean, and N. A. Nelson. J. Amer. Chem. Soc. **77**, 1628 (1955).
11. H. Hosoya and S. Nagakwa. Bull. Chem. Soc. Japan, **37**, 249 (1964).
12. H. W. Quinn and R. L. Van Gilder. Can. J. Chem. **47**, 4691 (1969).
13. S. Wolfe and P. G. C. Campbell. Can. J. Chem. **43**, 1184 (1965).
14. R. S. Alger. Electron paramagnetic resonance techniques and applications. Interscience, N.Y., 1968. Chapter 5.
15. P. H. Kasai. J. Phys. Chem. **66**, 674 (1962).
16. D. R. Gee, K. E. Russell, and J. K. S. Wan. J. Chem. Phys. In press.
17. L. Shields. Trans. Faraday Soc. **62**, 1042 (1965).
18. T. Cole. J. Chem. Phys. **35**, 1169 (1961).
19. P. W. Atkins, J. A. Brivatai, N. Keen, M. C. R. Symons, and P. A. Trevalion. J. Chem. Soc. 4785 (1962); J. R. Morton. J. Chem. Phys. **45**, 1800 (1966).
20. T. Ohmae, S. Ohnishi, K. Kuwata, H. Sakwai, and I. Nitta. Bull. Chem. Soc. Japan, **40**, 226 (1967).

Can. J. Chem. Downloaded from www.nrcresearchpress.com by 210.87.254.105 on 09/05/12
For personal use only.

21. G. A. HELCKE and R. FANTECHI. Mol. Phys. **18**, 1 (1970).
22. H. P. FRITZ and P. SELLMAN. J. Organometal. Chem. **6**, 558 (1966).
23. R. CRAMER. J. Amer. Chem. Soc. **89**, 4621 (1967).
24. H. W. QUINN and G. N. GLEW. Can. J. Chem. **40**, 1103 (1962).
25. H. W. QUINN, J. S. MCINTYRE, and D. J. PETERSON. Can. J. Chem. **43**, 2896 (1965).
26. P. B. AYSCOUGH, A. P. MCCANN, C. THOMSON, and D. C. WALKER. Trans. Faraday Soc. **57**, 1487 (1961).
27. P. B. AYSCOUGH. Electron spin resonance in chemistry. Methuen, London, 1967. p. 343.

Can. J. Chem. Downloaded from www.nrcresearchpress.com by 210.87.254.105 on 09/05/12
For personal use only.

Can. J. Chem. Downloaded from www.nrcresearchpress.com by 210.87.254.40 on 09/05/12
For personal use only.

Allyl radicals from 3,3′-azo-1-propene

BASIL H. AL-SADER AND ROBERT J. CRAWFORD
Department of Chemistry, University of Alberta, Edmonton, Alberta

Received March 12, 1970

3,3′-Azo-1-propene (**4**), 3,3′-azo-1-propene-*3,3-d*$_2$ (**5**) and 3,3′-azo-1-propene-*3,3,3′3′-d*$_4$ (**6**) have been synthesized and characterized. Thermolysis of **4**, at 40–300 Torr, and in the region 150–170°, followed first order kinetics ($E_a = 36.1 \pm 0.2$ kcal mole^{-1}, log $A = 15.54 \pm 0.10$) the major product, >99.9%, being 1,5-hexadiene (**9**). The presence of less than 0.1% propene suggests that the allyl radical is unable to abstract hydrogen from **4** or **9**. Statistical scrambling of deuterium, in the products of thermolysis of **5** and **6**, was observed. These results are interpreted in terms of a mechanism wherein allyl radicals are generated. Comparison of the activation energies for azoalkanes and **4** with the bond dissociation energies of hydrocarbons suggest that a good Polanyi plot is possible.

Canadian Journal of Chemistry, 48,2745 (1970)

Introduction

In a previous paper (1) we used secondary deuterium kinetic isotope effects to assist us in assessing whether one or two carbon–nitrogen bonds are cleaving in the rate determining step of pyrazoline thermolysis. We decided, on the basis of the magnitude of the isotope effect

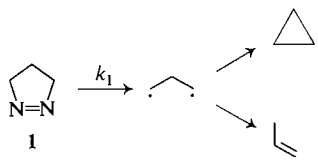

1

SCHEME 1

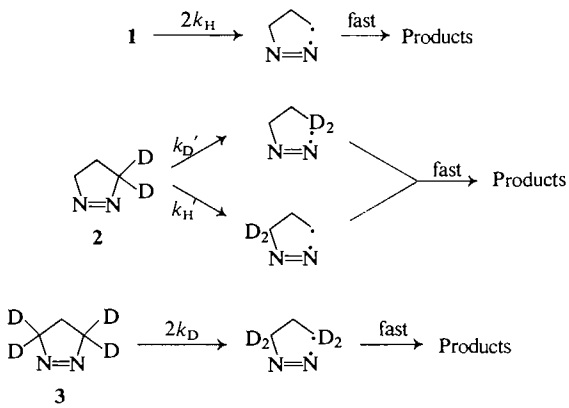

SCHEME 2

observed, that both carbon–nitrogen bonds are breaking. This decision, i.e., the choice between Scheme 1 and Scheme 2, could be placed upon a firmer basis if the magnitude of the k_H/k_D values were larger. This may be illustrated by re-examining the data of our earlier work.

TABLE 1

Calculated and observed value for secondary deuterium kinetic isotope effects at 229.5 °C

Scheme number	Ratio of rate constants		
	k_1/k_2	k_1/k_3	k_2/k_3
I[a]	1.19	1.43	1.19
II[a]	1.09	1.19	1.10
III[b]	1.17	1.43	1.22
Observed	1.19±0.02	1.40±0.02	1.17±0.02

[a]Calculated using $\Delta\Delta G^{\ddagger}$ of 89 cal mole^{-1} for eq. [1].
[b]Calculated using $\Delta\Delta G^{\ddagger}$ of 178 cal mole^{-1} for eq. [1].

[1] $$\log k_H/k_D = n\Delta\Delta G^{\ddagger}/2.303RT$$

Table 1 shows the values predicted, from eq. [1], by using a model wherein $\Delta\Delta G^{\ddagger}$ per deuterium corresponds to the frequently observed value of 90 cal mole^{-1} (2, 3). However, if we use a value of 180 cal mole^{-1}, then the values obtained for the ratio of the observed rates are those of the third column, and it is obvious that within the experimental precision of the kinetic techniques that we cannot distinguish between predicted values of columns 1 and 3 with the observed results. It is also necessary in calculating the isotope effects by Scheme 2 to make the assumption that $k_D' = k_D$ and that $k_H' = k_H$, i.e., to essentially assume that deuterium substitution in the γ-position does not give rise to any change in rate. While the value of $\Delta\Delta G^{\ddagger}$ used for the third column of Table 1 is larger than any observed (3), it is not greater than a theoretical maximum (4). The possibility exists that if the magnitude of the observed k_H/k_D

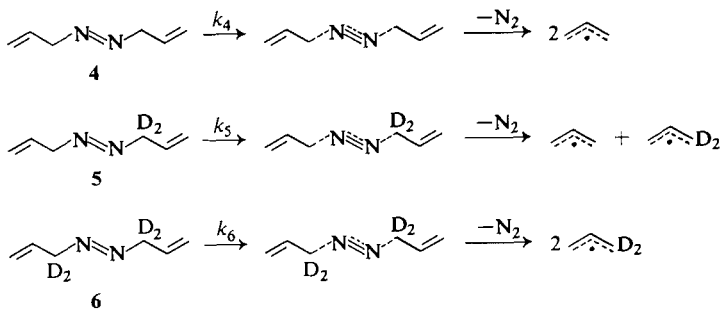

Scheme 3

TABLE 2

Comparison of the predicted values of observed rate constant ratios for Scheme 3 and 4 at 100 °C

Scheme number	Ratio of rate constants		
	k_4/k_5	k_4/k_6	k_5/k_6
3[a]	1.31	1.72	1.31
4[b]	1.26	1.72	1.36

[a]This row was calculated using a value of 100 cal mole^{-1} per deuterium for $\Delta\Delta G^{\ddagger}$.

[b]This row was calculated algebraically using the k_4/k_6 ratio from the first row (which is effectively a $\Delta\Delta G^{\ddagger}$ value of 200 cal mole^{-1} per deuterium).

ratio could be enhanced significantly, and experimental precision maintained, then an algebraic test, such as that shown in Table 2, is available that will distinguish between step-wise one carbon–nitrogen bond cleavage in the rate determining step and a concerted two carbon–nitrogen bond cleavage process. Such a test requires that n, in eq. [1], the number of α-deuteriums be kept large and that the temperature at which the rates are measured be kept as low as possible. In the hope that the thermolysis of 3,3′-azo-1-propene would proceed with an average value for the secondary deuterium kinetic isotope effect, i.e., $\Delta\Delta G^{\ddagger}$ of 100 cal

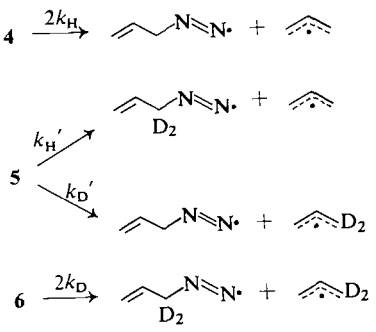

SCHEME 4

mole^{-1}, at a temperature in the order of 100 °C, then the values for Scheme 3 and Scheme 4 may be calculated. The 3,3′-azo-1-propene system has the added advantage that the γ-deuterium isotope effect is no longer significant in the sense of the cyclic system.

If $k_H' = k_H$ and $k_D' = k_D$ then we may solve for k_H/k_D per α-deuterium by comparing k_4 with k_5, k_4 with k_6, and k_5 with k_6 in the following ways

$$k_H/k_D = (k_4/k_6)^{1/2}$$

$$k_H/k_D = [k_4/(2k_5 - k_4)]^{1/2}$$

and

$$k_H/k_D = (2k_5/k_6 - 1)^{1/2}$$

Synthesis

The synthesis of **4** was achieved by the mercuric oxide oxidation of the corresponding hydrazine, which in turn was obtained by the hydrolysis of diethyl-N,N′-diallylbicarbamate (**8**). The bicarbamate was prepared by the stepwise allylation of diethyl hydrazodicarboxylate in dimethoxyethane (DME) using allyl benzenesulfonate. The monoallyl compound, **7**, was carefully purified by distillation on a spinning band column so as to remove any trace of **8**. This was particularly important to the synthesis of the dideuterio compound **5**. The synthesis of **5** was achieved by the allylation of **7** using allyl-*1,1-d*$_2$ benzenesulfonate. The reaction mixture was kept at 10° so as not to allow any allylic rearrangement of the allyl-*1,1-d*$_2$ benzenesulfonate. Integration of the nuclear magnetic resonance (n.m.r.) spectrum of **5** produced by this method indicated that all of the deterium was in the allylic position. The synthesis of **6** however, was complicated by scrambling of the deuterium labelling. The evidence suggests that this scrambling occurs during the first allylation step.

Can. J. Chem. Downloaded from www.nrcresearchpress.com by 210.87.254.40 on 09/05/12
For personal use only.

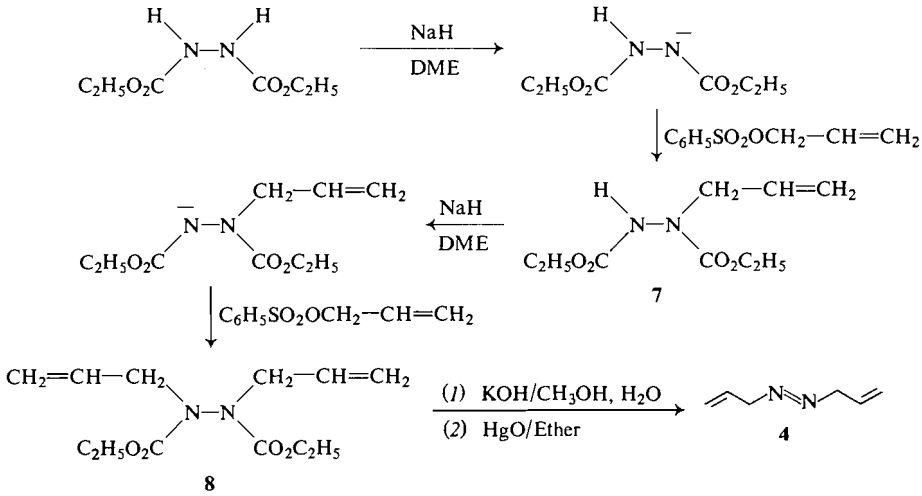

7 8 4

SCHEME 5

The monoallyl compound **7** produced by using allyl-*1,1-d*$_2$ benzenesulfonate gave an n.m.r. spectrum wherein the integration of the vinylidene, methine, and allyl signals[1] indicated that some scrambling had occurred. The final product, **6**, produced a V:M:A ratio of 1.73:1.00:0.275. This ratio indicates that 13.9% of the deuterium labelling is at the vinylidene position. On the basis of no scrambling of label in the synthesis of **5**, and n.m.r. evidence for scrambling of the deuterium in the first allylation step, it was assumed that the major contaminant of **6** was **9**, and that little, if any, of **10** was present.

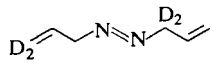

9

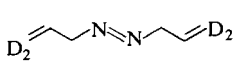

10

[1]Throughout this paper the protons of the terminal methylene group will be referred to as the vinylidine protons (V) that proton on C_2 will be referred to as the methine proton (M) and the tetrahedral set as the allylic protons (A). The n.m.r. integral of each will be expressed as a ratio V:M:A. e.g.

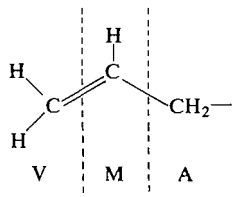

V:M:A of 2:1:2

Experimental

The deuterated and natural azo compounds were purified by gas–liquid chromatography (g.l.c.) using a Wilkens Aerograph Autoprep Model A-700 with a 20 ft column of 10% Ucon-insoluble on Fluoropak support. Product analyses were carried out on a gas chromatograph consisting of a Gow–Mac Model TR-2-B,W thermal conductivity cell with a Gow–Mac Model 40–50 power supply in conjunction with a Sargent Model SR recorder.

Deuterium analyses were carried out on a Metropolitan-Vickers MS-2, single focusing mass spectrometer. The infrared spectra were obtained on a Perkin–Elmer Model 421 spectrophotometer. The ultraviolet spectra were derived from a Carey Model 14M Spectrophotometer. The nuclear magnetic resonance spectra were obtained using a Varian A-60 and an HR-100 spectrometer.

Diethyl N,N'-Diallylbicarbamate (8)

Diethyl hydrazodicarboxylate (15.8 g, 0.09 mole) was added in portions to a well stirred slurry of 57.2% sodium hydride (4.32 g, 0.17 mole) in dry 1,2-dimethoxyethane (DME) (160 ml) under an atmosphere of nitrogen. After completion of addition the slurry was stirred an additional 3 h, cooled to 10° and a solution of allyl benzenesulfonate (35.6 g, 0.18 mole) in dry DME was added dropwise. The reaction mixture was stirred overnight, and it was then cautiously heated with excess water. The diallyl compound was extracted with benzene and purified by distillation to give 19.2 g (83%) b.p. 92–93° (0.5 Torr) (5).

N,N'-Diallylhydrazine

A solution of diethyl N,N'-diallylbicarbamate (16.6 g, 0.065 mole) and potassium hydroxide (14.6 g, 0.26 mole) in methanol (60 ml) and water (15 ml) was refluxed under a nitrogen atmosphere for 3 h. Upon cooling the precipitated potassium carbonate was filtered off, the residue was extracted with ether, dried over anhydrous sodium sulfate and purified by distillation through a 10 cm.

Can. J. Chem. Downloaded from www.nrcresearchpress.com by 210.87.254.40 on 09/05/12
For personal use only.

Can. J. Chem. Downloaded from www.nrcresearchpress.com by 210.87.254.40 on 09/05/12
For personal use only.

Vigreaux column. The N,N′-diallylhydrazine distilled at 75–76° (42 Torr) (3.0 g, 41%). The product was sufficiently susceptible to oxygen that a good microanalysis could not be obtained, however, an appropriate n.m.r. spectrum was obtained.

3,3′-Azo-1-propene (4)

To a well stirred slurry of red mercuric oxide (25 g, 0.115 mole) and sodium sulfate (25 g) in dry ether (140 ml) at 0 °C, was added dropwise a solution of N,N′-diallylhydrazine (3.0 g, 0.265 mole) in ether (30 ml). The mixture was stirred for 8 h, the ether solution was then filtered off, concentrated, and the azo compound separated by preparative gas chromatography using a column temperature of 90 °C and 60 ml per min carrier gas flow rate. The yield was 1.5 g (51%) n_D^{20} 1.5794. The ultraviolet spectrum has a λ_{max} at 358 nm (ε 24 in methanol).

Anal. Calcd. for $C_6H_{10}N_2$: C, 65.40; H, 9.17; N, 25.43. Found C, 65.43; H, 9.17; N, 25.26.

Allyl-1,1-d_2 Alcohol

The procedure of Schultz *et al.* (6) wherein acrylyl chloride was reduced with lithium aluminum deuteride was used. The n.m.r. peak at 4.13 p.p.m. in allyl alcohol was absent indicating that the compound was greater than 99% deuterated in the desired position.

Allyl-1,1-d_2 Benzenesulfonate

Allyl-1,1-d_2 alcohol was allowed to react, using the procedure of Bergstrom and Siegel (7), with benzenesulfonyl chloride and 2,4,6-collidine at −4 °C.

N-Allyl-N,N′-dicarbethoxyhydrazine (7)

This compound was prepared in the same manner as the aforementioned diallyl compound **8** except that 57% sodium hydride (2.77 g, 0.115 mole) was added to a solution of diethyl hydrazodicarboxylate (20.33 g, 0.115 mole + 10% in excess) in 1,2-dimethoxyethane (160 ml), allyl benzenesulfonate (22.77 g, 0.115 mole) was then added to the mono-anion solution. Purification and separation by distillation were carried out using a spinning band fractionating column, the yield was 16.5 g (59%), b.p. 99–101° (0.5 Torr). The n.mr. spectrum in carbon tetrachloride with tetramethylsilane displayed a singlet at 7.76 p.p.m. (N–H), multiplet at 5.86 p.p.m. (methine), multiplet at 5.12 p.p.m. (vinylidine), overlapping doublet and quartet at 4.12 p.p.m. (allyl and methylenes), and a triplet at 1.25 p.p.m. (methyls) in the ratio of 0.91:1.00:2.03:6.05:6.06, calculated 1:1:2:6:6.

Diethyl N-allyl-N′-allyl-1,1-d_2-bicarbamate

This analog was prepared in the same manner as for the aforementioned undeuterated diallyl compound **8**, except that a solution of the monoallyl compound **7** (14.0 g, 0.0648 mole) in dry 1,2-dimethoxyethane (30 ml) was added to 57% sodium hydride (1.6 g, 0.065 mole) in 1,2-dimethoxyethane (150 ml). The dideuterio allyl benzenesulfonate (13.5 g, 0.675 mole) in 1,2-dimethoxyethane (20 ml) was then added to the solution. Distillation gave 15.1 g (90% yield) b.p. 92–93° (0.5 Torr).

3,3′-Azo-1-propene-3,3-d_2 (5)

The preparation of **5** was accomplished from the hydrolytic decarboxylation of the aforementioned diallyl compound, (15.1 g, 0.0585 mole) then subsequent oxidation, using the same procedure used for the preparation of the natural azo compound **4**. The yield was 1.4 g (51%). The n.m.r. spectrum corresponded to that having over 98% deuteration in the allylic position of one of the allyl groups, mass spectral analysis (10 eV) showed a molecular ion which has a mass of 112.

Diethyl N,N′-bis(allyl-1,1-d_2)-bicarbamate

This was initially synthesized in the same manner as the undeuterated diallyl compound except that dideuterio allyl benzenesulfonate was used. The n.m.r. analysis revealed that about 16–17% of the total deuteriums were scrambled to the vinylidine positions of the molecule. Thus, a second method was used. The tetradeuterio diallylbicarbamate was then prepared using the same method described for the preparation of the dideuterio diallyl compound, except that dideuterio allyl benzenesulfonate was used in both steps. Starting with diethyl hydrazodicarboxylate (20.3 g, 0.115 mole) there was collected 15.2 g (51% yield) of the diallyl compound, b.p. 92–93 °C (0.5 Torr). The n.m.r. analysis indicated that 13.9% of the total deuterium was at the vinylidine position.

3,3′-Azo-1-propene-3,3,3′,3′-d_4 (6)

The preparation of **6** was achieved by the hydrolysis and the subsequent oxidation of the tetradeuterio diallyl compound (15.2 g, 0.0584 mole) using the same procedure as described for the preparation of the undeuterated azo compound **4**. The yield was 1.42 g (51%). The n.m.r. spectrum shows that the deuterium content at the vinylidine position is 13.9 ± 0.8% of the total deuterium present in the molecule, mass spectral analysis (10 eV) showed a molecular ion which has a mass of 114.

Nuclear Magnetic Resonance Measurements

Many of the experiments described in this work are dependent upon sound analytical results using the n.m.r. spectrometer's integrator. In all of those cases where a V:M:A ratio is quoted an appropriate reference sample was first used and its spectrum obtained, the integration checked using six sweeps, the deuterated sample was then placed in the spectrometer and its spectrum and integration (four to six sweeps) obtained. The reference was again placed in the spectrometer and used to check upon any possible drift in the spectrometer. The spectrometer's integrator gave values better than ± 2% (standard deviation).

Kinetic Measurements

The rates of thermolysis of the azo compounds **4**, **5**, and **6** were measured in a well conditioned stainless steel reactor and the increase in pressure was measured by a null-point system described previously (8). In a typical run a sample of 65 μl was injected into the reactor by means of a Hamilton hypodermic syringe using a 6 in. needle. This corresponds to an initial pressure of 90 Torr. The thermolysis was carried to greater than nine half-lives, the product inside the reactor was then pumped out and those materials trapped on the vacuum line were taken for further identification and analysis. The rate constant was obtained by taking 20 points at regular intervals and between 20 and 80% completion and by plotting log $(P_\infty - P_t)$ vs. t.

Can. J. Chem. Downloaded from www.nrcresearchpress.com by 210.87.254.40 on 09/05/12
For personal use only.

Control Experiments

(*a*) 3,3'-Azo-1-propene-*3,3,3',3'-d*$_4$ (**6**) (70 mg), having 13.9 ± 0.8% of its deuterium label in the vinylidene position, was heated in the reactor at 142 °C to 40% decomposition. The reactor was then pumped out and those materials which trapped on the vacuum line were separated on an Autoprep using 20% Ucon-insoluble on Fluoropak column at 80° and 60 ml per min carrier gas flow rate. The deuterated azo compound was then transferred to an n.m.r. tube containing carbon tetrachloride and tetramethylsilane for analysis. The analysis indicated that 17.1 ± 0.8% of the total deuterium was at the vinylidene position.

(*b*) 3,3'Azo-1-propene-*3,3-d*$_2$ (**5**) (50 mg) was distilled under vacuum into a break seal of approximately 12 ml. The tube was then removed from the vacuum rack and heated in an oil bath to 142 ± 0.5° for 32 min (calculated 40% reaction). The content was then transferred into a vacuum line connected directly to the ionization chamber of a mass spectrometer for analysis. The analyses were carried out at 70, 10, 9 eV. No fragmentation was observed at 9 eV and only the molecular ions were detected. The initial sample showed only a peak at 112 (and a smaller ^{13}C, ^{15}N natural abundance peak at mass 113, 7.5% of the intensity of the 112 peak). After being subjected to the thermolysis conditions the azo compound displayed a peak at mass 114 of approximately 2% of the intensity of the 112 peak. This is interpreted as indicating the formation of $C_6H_6D_4N_2$ ($m = 114$) during the reaction.

Product Analysis

(*i*) Product analysis studies were carried out on samples trapped directly from the reaction at the end of each kinetic run. Each sample was then analyzed on a gas chromatograph for product compositions.

(*ii*) Exact product compositions were obtained using the bulb crusher method as described earlier (8).

(*iii*) Identification of the product was achieved by the comparison of retention times with those of an authentic sample on the following columns; 19 ft dimethylsulfolane on chromsorb W, 20 ft mineral oil on firebrick in tandem with a 20 ft, 10% *n*-butylmaleate columns. The product of the thermolysis of **4**, **5**, and **6** were trapped at the end of a kinetic run, and then distilled under vacuum into n.m.r. tubes containing carbon tetrachloride and tetramethylsilane, the tubes were then removed from the vacuum rack and their n.m.r. spectra obtained.

Results and Discussion

Products

The thermolysis of **4** produced 1,5-hexadiene (**11**) with only a trace (< 0.1%) of propene present. That the 1,5-hexadiene is produced by the dimerization of allyl radicals is supported by an examination of the products of thermolysis of **5**. Although the mixture of deuterated 1,5-hexadienes produced from **5** is not readily amenable to mass spectrometry (the peak intensities are very susceptible to small changes in ionization potential, and the parent peaks are small relative to the other peaks), we were able to observe a molecular ion peak corresponding to $C_6H_6D_4$ at mass 86 and evidence for peaks at mass 84 and 82 suggestive of a 1:2:1 mixture of C_6H_{10}, $C_6H_8D_2$, and $C_6H_6D_4$. The n.m.r. spectrum of the 1,5-hexadiene (**11**), derived from **4** gave a V:M:A ratio of 2.00:1.00:2.01. The 1,5-hexadiene produced from **5** gave a V:M:A ratio of 3.02:2.00:3.03 consistent with a mixture having the statistical distribution 4:4:4:2:1:1 of 1,5-hexadienes **11**, **12**, **13**, **14**, **15**, and **16**, respectively. Similarly thermolysis of **6**, if it

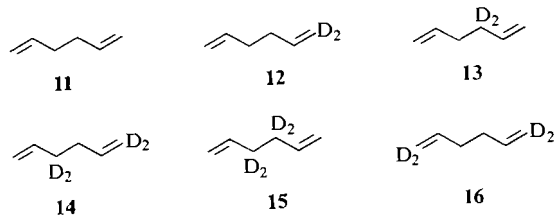

11 **12** **13** **14** **15** **16**

proceeds through allyl radicals should give a 2:1:1 mixture of **14**, **15**, and **16**. The n.m.r. spectrum of the 1,5-hexadienes produced from **6** gave a V:M:A ratio of 1.00:2.00:1.02 consistent with such a mixture. A Cope rearrangement of **15** to **16** could, at equilibrium,[2] bring about the same statistical ratio as that observed for the product. Doering and Toscanno (9) have observed such a rearrangement and from their kinetic data we can conclude that less than 1% of the initially formed product will have rearranged under the reaction conditions.

The control runs, wherein the stability of the starting material was examined, indicate that a small, but detectable amount of scrambling is occurring during the reaction. Examination of the recovered starting material, after the thermolysis of **6** to 40% completion, showed that the deuterium labelling in the vinylidene position increased from 13.9 ± 0.8% to 17.1 ± 0.8%.[3] This is confirmed by the observation that **5** under the same reaction conditions generates approximately 2% of **6**, at 40% completion, as detected by mass spectrometry. The scrambling then arises by an intermolecular process, either by the reversible addition of an allyl radical to the azo

[2]Assuming that $K = 1$ for the equilibrium **15** $\rightleftharpoons$ **16**, i.e., that the isotope effect is small.

[3]Assuming no kinetic isotope effect for the vinylidene deuteriums and using the values observed in the kinetic section we calculate that the percentage of vinylidene deuterium at 40% completion should have decreased to 13.4% if no scrambling occurred.

starting material, or by the trapping of allyl radicals by the nitrogen radical (**17**).

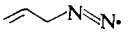

17

This scrambling process is, however, considerably slower than the thermolysis reaction. The addition process is supported by the formation of tetraalkylhydrazines in the photolysis of azoalkanes (10).

The absence of any significant amount of propene implies that there is little or no chain induced decomposition via a scheme analogous to that observed in azomethane thermolysis (11, 12). Similarly the possibility of an induced decomposition occurring via the addition of allyl radicals to the olefinic double bonds may be ruled out since such a process would not give the statistical deuterium scrambling observed for the products of **5** and **6**.

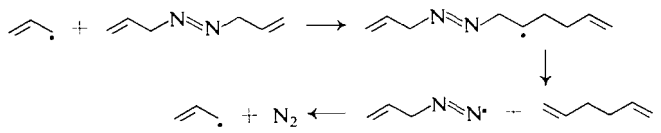

Kinetic Studies

The thermolysis of **4** was carried out at the pressures and temperatures described in Tables 3 and 4, each rate constant was reproducible to within 1%. Each rate constant was calculated by taking 20 points between 20 and 80% completion. In the case of **4** excellent first order rate plots were obtained when the rates were measured out to 95% completion.

The observed rate constants in Table 5 require corrections for (*a*) the scrambling of the label during the synthesis of **6**, and (*b*) the scrambling of the label during the thermolysis process. The observed rate constants are measured from points taken between 20 and 80% completion wherein an estimated maximum 10 to 12% of the scrambling process occurs. Thus for **5** there will be the compounds **4**, **6**, **9**, **10**, and **18** present in mole fractions f_4, f_6, f_9, f_{10}, and f_{18}, respectively.

$$[2] \quad k_{obs}{}^5 = f_4k_4 + f_5k_5 + f_6k_6 + f_9k_9 + f_{10}k_{10} + f_{18}k_{18}$$

If we attempt the correction using [2] then we will require several assumptions[4] since many of the mole fractions and rate constants cannot be observed directly. If we assume that deuteriums in the γ position, as in **9**, **10**, and **18**, give rise to no decrease rate relative to the protio compound,[5]

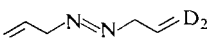

18

then eq. [2] becomes

$$k_{obs}{}^5 = (f_{10} + f_{18} + f_4)k_4 + (f_5 + f_9)k_5 + f_6k_6$$

Judging by the control runs (see Experimental section) the amount of scrambled material will be approximately 10 to 12%, of which the amount of **10** formed will be less than 1% since it requires two events. If the scrambling process is random then **4**, **6**, **9**, and **18** will be produced in the ratio 2:1:1:1. This allows a further simplification of the original equation to give

$$[3] \quad k_{obs}{}^5 = 0.08k_4 + 0.90k_5 + 0.12k_6$$

If we now divide each component of eq. [3] by k_4 we obtain

$$k_{obs}{}^5/k_4 = 0.08 + 0.90k_5/k_4 + 0.02k_6/k_4$$

TABLE 3

Rates of thermolysis of **4** at different initial pressures and 158.81 ± 0.05 °C

Sample volume (μl)	Pressure (Torr)	$k \times 10^4$ (s^{-1})
30	41	19.4
60	82	19.9
90	123	19.3

[4]The method of correction used herein is not exact since it assumes that the contaminating isomers are present initially rather than being formed during the reaction. As may be seen from Table 6 the final isotope effect is not very sensitive to the size of this correction.

[5]Bélanić-Lipovac, Borčić, and Sunko have observed a k_H/k_D value of 1.00 for the ethanolysis of 1,1-dimethylallyl chloride and 1,1-dimethylallyl-3,3-d_2 chloride (13).

Can. J. Chem. Downloaded from www.nrcresearchpress.com by 210.87.254.40 on 09/05/12
For personal use only.

TABLE 4

Rate constants and activation parameters for the thermolysis of **4** at an initial pressure of 80 Torr

Run number	T (°C)	$k \times 10^4$ (s^{-1})	Activation parameters
1	142.65±0.05	3.88±0.04	E_a = 36.1 kcal mole^{-1}
2	152.68	11.0±0.01	
3	158.81	19.9±0.3	$\Delta S_{150°}^{*}$ = +9.8±0.5 e.u.
4	161.65	25.9±0.3	log A = 15.54 ±0.08
5	167.12	44.5±0.4	

The values of k_5/k_4 and k_6/k_4 are related to one another (see Introduction section) in the following manner

$$k_4/k_6 = (k_4/k_5)^2$$

By using the value for k_{obs}^5 and k_4 in Table 5 and letting $k_5/k_4 = x$ we get the quadratic equation $0.02x^2 + 0.90x - 0.794 = 0$ for eq. [3]. The values $x = 0.87$ and $x = -45.9$ are solutions. The former value corresponds to a kinetic isotope effect for **5** of $(k_H/k_D)^2 = 1.15$, the latter is negative and unrealistic. If the amount of scrambling was as high as 18% then eq. [3] becomes

$$k_{obs}^5 = 0.12k_4 + 0.85k_5 + 0.03k_6$$

and the k_4/k_5 value obtained is 1.16.

Similarly correcting the observed rate constant in Table 5 for the amount of **9** produced during the synthesis of **6** is simplified by the assumption that the initial reaction mixture consists of only **6** and **9** with no **10** present.[6] This corresponds to 72% of **6** and 28% of **9**, with 10–12% scrambling during the reaction some **10** is likely to be produced. If the allyl groups are again considered to scramble in a statistical fashion then the average values of mole fractions of **6**, **9**, and **10** present are 0.66, 0.32, and 0.02, respectively. Carrying out the same treatment for **6** as used for the correction of rate constants on **5**, we obtain the equation

$$k_{obs}^6 = 0.02k_4 + 0.32k_5 + 0.66k_6$$

and similarly dividing k_4 and substituting the value k_5/k_4 obtained earlier we obtain the k_4/k_6 ratio of 1.33. If an extreme value of 18% scrambling is used the above calculations render the value 1.36. Thus we can see from Table 6

[6]This assumption can be justified on the basis that no deuterium scrambling was observed in the second allylation step during the synthesis of **5**.

TABLE 5

Rate constants and secondary kinetic isotope effects for α-deuterated 3,3-azo-1-propenes

Compound	T (°C)	$k \times 10^4$ (s^{-1})	k_H/k_D[a]
4	161.65	25.94	
	161.65	25.86	
		Ave. 25.90±0.05	
	161.75	26.23	
	161.75	26.17	
		Ave. 26.20±0.04	
5	161.65	22.69	
	161.65	22.78	
		Ave. 22.76±0.06[a]	1.14±0.004
6	161.75	20.77	
	161.75	20.65	
	161.75	20.69	
		Ave. 20.70±0.06	1.26±0.004

[a]Uncorrected for deuterium scrambling (see Discussion).

TABLE 6

Corrected rate ratios for 12 and 18% deuterium scrambling

Percentage scrambling	Ratio of rate constants (±0.03)		
	k_4/k_5	k_5/k_6	k_4/k_6
12	1.15	1.16	1.33
18	1.16	1.17	1.36

that even using values that overestimate the amount of rearrangement we get values for the secondary kinetic isotope for **5** and **6** that are smaller than those expected on the basis of Seltzer's work (2). Whereas Seltzer has observed values for k_H/k_D of 1.12–1.16 per α-deuterium atom, at 105°, **5**, and **6** give values of 1.08, unusually small for such reactions (3). These small values for α-deuteration do not allow a test of the one-bond-cleavage vs. the two-bond cleavage mechanism as set out in the Introduction section. It seems possible that upon placing the vinyl group into the structure we

Can. J. Chem. Downloaded from www.nrcresearchpress.com by 210.87.254.40 on 09/05/12
For personal use only.

TABLE 7

Values for kinetic isotope effects for concerted and stepwise cleavage mechanism, 161.7°

Percentage D scrambling	Kinetic isotope effects			$\Delta\Delta G^{\ddagger}$ (cal mole^{-1})
	k_4/k_5	k_5/k_6	k_4/k_6	
Concerted Scheme 4				
12	1.07±0.03	1.07	1.07	60±10
18	1.08±0.03	1.08	1.08	66±10
Stepwise Scheme 5				
12	1.15±0.03	1.15	1.15	120±15
18	1.17±0.03	1.17	1.17	135±15

have shifted the transition state towards that wherein the carbon–nitrogen bond cleavage has progressed to only a small extent in the transition state (as per Hammond's postulate (14)), and consequently there is not as great a change in the C—H and C—D force constants on going from the ground state to the transition state. However, this does not appear to be the case with many of Seltzer's examples which are benzylic and consequently expected to be similar to allylic systems (2). Most of the previous secondary isotope effects have been carried out in solution whereas **5** and **6** were studied in the gas phase. It would, however, be unreasonable to ascribe such a significant difference to only a change in phase for homolytic processes such as these. We are left to conclude that something more fundamental is happening.

It is of particular interest to compare the activation energy for the 3,3′-azo-1-propene (**4**) thermolysis (36.1 ± 0.2 kcal mole^{-1}) with that of azoethane (48.5 ± 0.5 kcal mole^{-1}) (15) and assuming that the activation energy for azo-*n*-propane is similar (as evidenced by the fact that the bond dissociation energy values for *n*Pr—H and Et—H are both 98.0 kcal mole^{-1} (16)). The decrease in activation energy, 12.4 ± 0.9 kcal mole^{-1}, is attributed to a contribution from the allylic resonance energy to the rate-determining transition state. There is some doubt as to the correct value for the resonance energy of the allyl radical since early experimental results predict a value of 15–18 kcal mole^{-1} (17). More recently Benson *et al.* (18) and Ellis and Frey (19) have suggested smaller values of 13 ± 1 and 12 ± 1 kcal mole^{-1}. In a recent communication Golden, Gac, and Benson (20) have provided evidence for a value of the allylic resonance energy of 9.6 kcal mole^{-1}, and have stated that their study of the dissociation and recombination of the 2 allyl ⇄ 1,5-hexadiene system

19

E_a = 41.0 ± 0.3 kcal E_a = 32.2 ± 0.2 kcal

"must surely lay to rest any thought that the allyl resonance energy is much greater than 12 kcal mole^{-1}". In an earlier study on the thermolysis of 3-vinyl-1-pyrazoline (**19**),Cameron and coworkers (21) found a decrease in activation energy of 8.8 kcal mole^{-1}, upon replacing a 3-methyl group by a vinyl group. The decrease of activation energy, 12.4 kcal mole^{-1}, observed on going from azoethane to 3,3-azo-1-propene then is essentially 2 × 6.2 and implies that if both carbon–nitrogen bonds are undergoing cleavage then only a fraction of the allylic resonance energy is being utilized to decrease the activation energy. It may equally be suggested that only one carbon–nitrogen bond is cleaving and that the full significance of its allylic resonance energy is being felt i.e., approximately 12 kcal mole^{-1}.

Table 7 shows the values of the secondary kinetic isotope effect per deuterium for both the concerted two-bond cleavage mechanism (Scheme 4) and that obtained per deuterium for the stepwise process (Scheme 5) wherein only one C—N bond is breaking in the rate determining step. There are two alternatives: (*a*) that both carbon–nitrogen bonds are breaking in the rate determining step involving only a fraction of the allylic resonance energy of each, and that the C—H force constants of all of the α-hydrogens have undergone a fractional change from sp^3 to sp^2 in the transition state or (*b*), that only one carbon–nitrogen bond is cleaving in the rate determining step giving a maximum measure of the allylic resonance energy and a maximum measure of the secondary isotope effect. No real choice can be made, however; the former

Can. J. Chem. Downloaded from www.nrcresearchpress.com by 210.87.254.40 on 09/05/12
For personal use only.

TABLE 8
Radical α-deuterium isotope effects

No.	Reaction	Solvent	T (°C)	k_H/k_D[a]	$\Delta\Delta G^{\ddagger}/n$ (cal)	Reference
1	Thermolysis of 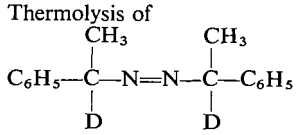	Ethylbenzene	105	1.27	89±6	2*a*
2	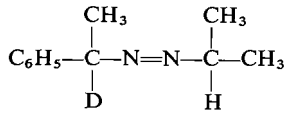	Diphenylether–benzoquinone solution	143.2	1.148	114±10	2*b*
3	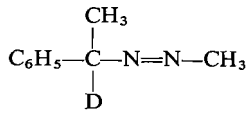	Diphenylether–benzoquinone solution	161.0	1.13	105±8	2*c*
4	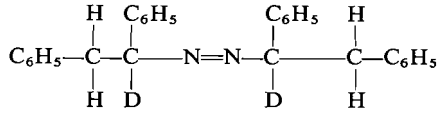					
	meso	Ethylbenzene	106.47	1.221	75±10	22
	dl	Ethylbenzene	106.47	1.202	69±10	22
5	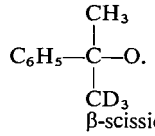 β-scission	Carbontetrachloride -cyclohexane	75	1.12	78±10	23
6	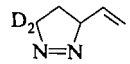	Gas phase	134.5	1.21	77±7	21
7	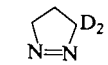	Gas phase	229.4	1.19	86±6	1
8	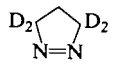	Gas phase	229.4	1.40	84±6	1
9	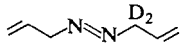	Gas phase	161.7	1.15	60[b]±10 120[c]±10	This work This work
10	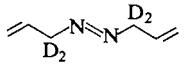	Gas phase	161.7	1.33	60[b]±10 120[c]±10	This work This work

[a]Rate ratio observed for deuterated and non deuterated compound, not corrected for number of deuteriums.
[b]Assuming Scheme 4.
[c]Assuming Scheme 5.

introduces the complication that if the allylic azo compounds in the gas phase are undergoing the same mechanism as that observed by Seltzer (2) for the azo-bis-α-phenylethane system (see Table 8), then the magnitude of the secondary isotope effect is unusually low. For compounds **4**, **5**, and **6** to be undergoing thermolysis by Scheme **5**, we then would obtain values of the secondary isotope effect on the high side.

The possibility of observing a good Polanyi plot (24, 16) for the thermolysis of azoalkanes is enhanced by the observation that the thermolysis of 3,3'-azo-1-propene (**4**) is such that induced decomposition is insignificant. When the activation energy of well-studied azo compounds (25, 26) (Table 9) are plotted against bond dissociation energy of the corresponding R—H bond, then a fit as shown in Fig. 1 is obtained.

Can. J. Chem. Downloaded from www.nrcresearchpress.com by 210.87.254.40 on 09/05/12
For personal use only.

TABLE 9

Activation energies of some azoalkanes and bond dissociation energies of the corresponding R—H bonds

Compound	E_a (kcal mole^{-1})	D(R—H)[a] (kcal)
CH_3—N=N—CH_3	55.5 (11)	$D(CH_3$—H) = 104 ±1
CH_3—CH_2—N=N—CH_2CH_3	48.5 (15)	$D(C_2H_5$—H) = 98 ±1
CH_2=CH—CH_2—N=N—CH_2—CH=CH_2[b]	36.1	$D(C_3H_5$—H) = 85 ±1
$(CH_3)_3$C—N=N—$C(CH_3)_3$	42.8 (25)	$D(t$-C_4H_9—H) = 91 ±1
$(CH_3)_2$CH—N=N—$CH(CH_3)_2$	40.9 (26)	$D(i$-C_3H_7—H) = 94.5±1

[a]Taken from ref. 16, p. 496.
[b]This work.

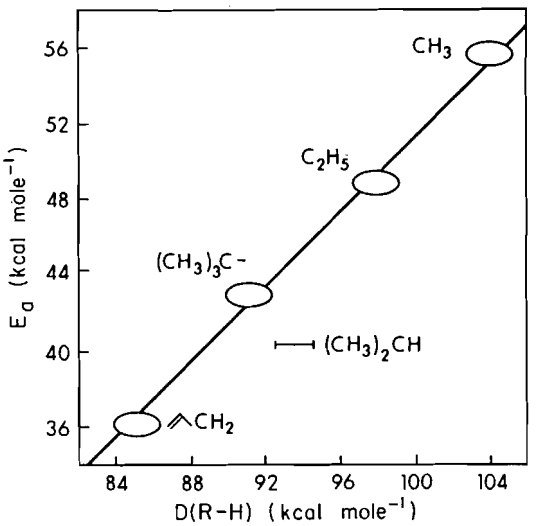

FIG. 1. Polanyi plot for the thermolysis of azo compounds.

A least-squares analysis using the data in Table 9 gives a best fit straight line of eq. [5] where D stands for bond dissociation energy.

[5] $E_a = 0.996\ D(\text{R—H}) - 48.4\,(\text{kcal mole}^{-1})$

The data gives a correlation coefficient of 0.998. Consequently there appears the possibility that the activation energy obtained from the thermolysis of azo compounds, wherein chain induced decomposition is suppressed, can be correlated with the bond dissociation energy of the corresponding R—H bond. This matter is under further study by K. Takagi of this laboratory.

The authors acknowledge support from the National Research Council of Canada and from the Petroleum Research Fund of the American Chemical Society. The carefully executed n.m.r. integrations carried out by Mr. Glen Bigam are gratefully acknowledged.

1. B. H. AL-SADER and R. J. CRAWFORD. Can. J. Chem. **46**, 3301 (1968).
2. *a*. S. SELTZER. J. Amer. Chem. Soc. **83**, 2625 (1961); *b*. **85**, 14 (1963); *c*. S. SELTZER and F. T. DUNNE. J. Amer. Chem. Soc. **87**, 2628 (1965).
3. E. A. HALEVI *In* Progress in physical organic chemistry. Vol. 1. Interscience Publ. Inc., New York. 1963.
4. M. WOLFSBERG and M. J. STERN. Pure Appl. Chem. **8**, 225, 325 (1964).
5. A. ZWEIG and A. H. HOFFMANN. J. Amer. Chem. Soc. **85**, 2736 (1963).
6. R. D. SCHULTZ and F. W. MILLARD. J. Org. Chem. **24**, 297 (1959).
7. G. G. BERGSTROM and S. SIEGEL. J. Amer. Chem. Soc. **74**, 254 (1962).
8. R. J. CRAWFORD and A. MISHRA. J. Amer. Chem. Soc. **88**, 3963 (1966).
9. W. VON E. DOERING and V. TOSCANNO. Unpublished results cited in Table 4, H. E. O'NEAL and S. W. BENSON. J. Phys. Chem. **71**, 2903 (1967).
10. H. CERFONTAIN and K. O. KUTSCHKE. Can. J. Chem. **36**, 344 (1958); O. P. STRAUSZ, R. E. BERKLEY, and H. E. GUNNING. Can. J. Chem. **47**, 3470 (1969).
11. W. FORST and O. K. RICE. Can. J. Chem. **41**, 562 (1963).
12. C. STEEL and A. F. TROTMAN-DICKENSON. J. Chem. Soc. 975 (1959).
13. V. BĚLANIĆ-LIPOVAC, S. BORČIĆ, and D. E. SUNKO. Croat. Chem. Acta, **37**, 2895 (1965).
14. G. S. HAMMOND. J. Amer. Chem. Soc. **77**, 334 (1955).
15. H. S. SANDHU. J. Phys. Chem. **72**, 1857 (1968).
16. J. A. KERR. Chem. Rev. **66**, 465 (1966).
17. J. L. FRANKLIN and F. H. FIELD. J. Amer. Chem. Soc. **75**, 2819 (1953).
18. S. W. BENSON, A. N. BOSE, and P. NANGIA. J. Amer. Chem. Soc. **85**, 1388 (1963).
19. R. J. ELLIS and H. M. FREY. J. Chem. Soc. 5578 (1964).
20. D. M. GOLDER, N. A. GAC, and S. W. BENSON. J. Amer. Chem. Soc. **91**, 2136 (1969).
21. R. J. CRAWFORD and D. M. CAMERON. Can. J. Chem. **45**, 691 (1967).
22. S. E. SCHEPPELE and S. SELTZER. J. Amer. Chem. Soc. **90**, 358 (1968).
23. T. W. KOENIG and W. D. BREWER. Tetrahedron Lett. 2773 (1965).
24. M. G. EVANS and M. POLANYI. Trans. Faraday Soc. **34**, 11 (1938).
25. J. B. COPELAND and B. K. W. LEVY. J. Amer. Chem. Soc. **82**, 5314 (1960).
26. H. C. RAMSPERGER. J. Amer. Chem. Soc. **49**, 1617 (1927).

Can. J. Chem. Downloaded from www.nrcresearchpress.com by 210.87.254.40 on 09/05/12
For personal use only.

Can. J. Chem. Downloaded from www.nrcresearchpress.com by 210.87.254.6 on 09/05/12
For personal use only.

Surface tension of some non-aqueous salt solutions[1]

R. A. STAIRS[2] AND W. T. RISPIN[3]
Department of Chemistry, Queen's University, Kingston, Ontario
AND (IN PART)
R. C. MAKHIJA
Department of Chemistry, Trent University, Peterborough, Ontario

Received April 21, 1970

The surface tensions of methanol, acetone, dimethylformamide, dimethylsulfoxide, and methylamine over limited temperature ranges, and of solutions of alkali halides in the first three of these liquids at 25 °C have been measured by the method of maximum bubble pressure, with precautions against moisture. The data for the pure liquids are compared with literature data where these exist. The results for the solutions are discussed in the light of various existing theories.

On a déterminé la tension superficielle du méthanol, de l'acétone, de la diméthylformamide, du diméthylsulfoxyde et de la méthylamine dans des intervalles limités de température, ainsi que des solutions dans les trois premiers liquides à 25 °C, par la méthode de Sugden, à l'abri de l'humidité. Les valeurs obtenues pour les liquides purs ont été comparées aux valeurs reconnues, là où ces valeurs existent. Les résultats pour les solutions ont été considérés dans le contexte des théories diverses déjà avancées.

Canadian Journal of Chemistry, **48**, 2755 (1970)

A number of theories have been proposed for the surface tension of salt solutions. They agree in predicting that dissolved salts should raise the surface tension of molecular solvents, and they agree roughly with one another and with experiment in the magnitude of the effect. Only one of them (1) predicts substantial differences among salts of the same charge-type in a given solvent, though such differences are readily apparent in the data (2).

The simplest of these theories, in the form of the dependence of the surface-tension increment, $\Delta\sigma = \sigma(c) - \sigma(0)$, on the concentration of salt in the bulk solution, c, is that of Oka (3). He makes a direct calculation of the work required, against the additional forces arising from the presence of dissolved ions, to divide a solution into two portions, thereby creating new surfaces. His result is of the form

$$[1] \qquad \Delta\sigma = A\alpha c$$

where the constant $A = Ne^2/1000\varepsilon$, N being Avogadro's number, e the electronic charge, and ε the dielectric constant of the solvent, and α is the "apparent degree of dissociation" of the salt. For strong electrolytes at low concentration this reduces to a linear dependence on concentration.

The theory of Wagner (4) is based on the calculation, first, of the degree to which ions are excluded from the surface by interaction of their fields with the change in dielectric constant at the surface. The change in the surface tension is then calculated using the Gibbs adsorption isotherm. It was not expressed in analytical form, but the approximation of Onsager and Samaras (5), while also not in analytical form at higher concentrations, yielded a limiting law at low concentrations of the form

$$[2] \qquad \Delta\sigma = \frac{79.5c}{\varepsilon}\log_{10}\left(\frac{1.14 \times 10^{-13}(\varepsilon T)^3}{c}\right)$$

This expression is expected to be valid only at concentrations much smaller than the numerator of the argument of the logarithm. It is effectively of the form: $-Kc \log c$, which approaches the origin with infinite slope, but with such a sharp curvature that it is doubtful if this will ever be experimentally testable. (The problem of obtaining a sufficiently pure solvent gives one pause.) Wagner's numerical calculation agrees closely with the limiting law below 0.01 mole/l in aqueous solution at 25 °C and with the extended

[1]Taken in part from the M.A. Thesis of W. T. Rispin, Queen's University, 1959.
[2]Present address: Department of Chemistry, Trent University, Peterborough, Ontario.
[3]Present address: Department of Pharmaceutics, Sunderland Polytechnic, Chester Road, Sunderland, Co. Durham, England.

Can. J. Chem. Downloaded from www.nrcresearchpress.com by 210.87.254.6 on 09/05/12
For personal use only.

version of the Onsager and Samaras treatment to several times this concentration, so it may be presumed to approach the origin in the same manner.

Pérez Masiá approached the problem by using perturbation of the solvation sphere of the ion by the presence of the surface of the solution. It seems clear that this and the method used by Wagner and Onsager and Samaras must be closely related, though the relationship is not easy to demonstrate. In spite of this, this theory, in contrast to the theories based on Wagner's approach, predicts differences among salts of the same charge type, the predicted surface-tension increment decreasing as the size of the ions is increased. Because of the differential (negative) adsorption of the two ions of a salt if these differ in size, an electrical double layer at the surface is predicted, and the effect of this on the surface tension was taken into account in the theory, which thus predicts a dependence of $\Delta\sigma$ both on the sum and on the difference of the sizes of the two ions. This theory, too, is not expressed in analytical form, nor has a "limiting law" been derived from it for low concentrations.

Stairs and Sienko (6) refer obliquely to a theory of the differences between salts of similar type, involving the polarizabilities of the solvated ions. Rough calculation has shown that modification of the Onsager–Samaras approach by the inclusion of higher order terms in the "image force" between the ions and the surface should yield a smaller increment of surface tension as the polarizability of the ions is increased. What the proper value of the polarizability for a solvated ion should be is a puzzle, as the papers by Sack (7) and by Hasted *et al.* (8) imply, but it would be expected to increase with increasing ionic size, as the size of the region of dielectric saturation of the solvent is decreased. Thus an effect of ionic size similar to that predicted by Pérez Masiá is to be expected. Stairs and Sienko found that a graph of the coefficient of c in $\Delta\sigma = Ac + Bc^2$ for alkali halides in water and in ammonia vs. the sum of the polarizabilities of the unhydrated ions according to Böttcher (9) gave a rough straight line with the expected negative slope, greater in the solvent of lower dielectric constant.

The form of the expression for $\Delta\sigma$ used by Stairs and Sienko was chosen as being the simplest that gave a reasonable fit to the data, with some slight justification from Oka's theory.

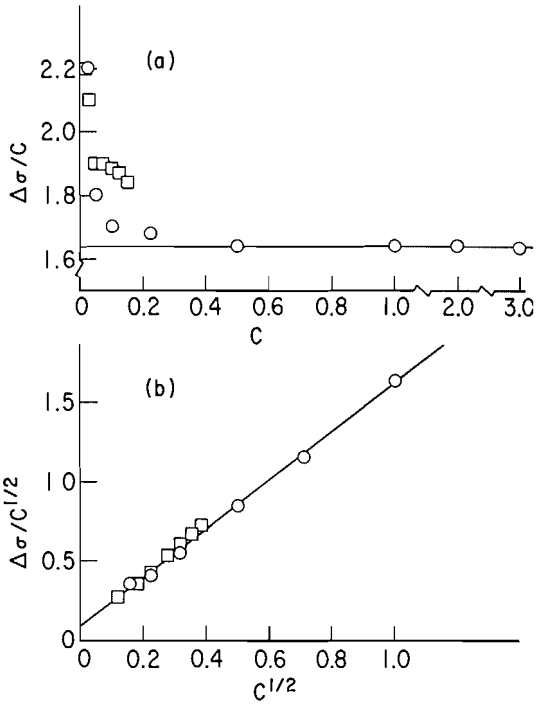

FIG. 1. Surface tension functions for aqueous sodium chloride solutions. (*a*) $\Delta\sigma/c$ vs. c. (*b*) $\Delta\sigma/c^{1/2}$ vs. $c^{1/2}$. Data from International critical tables (2*a*) and Schwenker (10).

Various empirical expressions have been used in the past, usually power series in c, with and without the addition of a constant term. There is of course no theoretical justification for a constant term, and its appearance is merely a signal that a power series in c is a poor form to use. This is apparent in Fig. 1*a*, showing the quantity $\Delta\sigma/c$ plotted against c for aqueous NaCl solutions (2, 10), in which the experimental points rise above an otherwise straight line at the lowest concentrations. In the present work, a term in $c^{1/2}$ was added to the expression used by Stairs and Sienko, suggested by a naive analogy with the theoretically-based Jones and Dole expression for viscosity (11*a*, for theory of Falkenhagen, see ref. 11*b*), giving

$$[3] \qquad \Delta\sigma = A_0c^{1/2} + Ac + Bc^2$$

If B is not large, data at low concentrations should yield a straight line if $\Delta\sigma c^{-1/2}$ is plotted against $c^{1/2}$. This has been done for the same aqueous solution data in Fig. 1*b*. No theoretical significance is attached to the $c^{1/2}$ term, except that such terms arise naturally from the Debye–Hückel theory and are therefore not unexpected

Can. J. Chem. Downloaded from www.nrcresearchpress.com by 210.87.254.6 on 09/05/12
For personal use only.

in any physical property of electrolyte solutions. The purpose of the measurements here described was further to test the relationships between the coefficient A and the polarizability of the ions discussed by Stairs and Sienko, and also to study the effect of the dielectric constant of the solvent, which occurs in one way or another in all the theories.

Adequate values of the surface tension of some of the solvents used were not available, so they were measured over limited ranges of temperature before proceeding with the solution measurements. The method of maximum bubble pressures was used as described by Sugden (12, see also ref. 14) as modified for use in a closed system by Stairs and Sienko (6). Measurements of the surface tension of solutions of alkali halides in dimethylformamide (DMF), acetone, and methanol were carried out, as well as of the pure solvents. Pure dimethylsulfoxide (DMSO) and methylamine were also studied, but no data on solutions in these solvents were obtained.

Experimental

Materials

Dimethylformamide (British Drug Houses) was pre-dried with Drierite and fractionated off-line, b.p. 148.2–148.6 °C (755.7 Torr), then dried overnight on the vacuum line with fresh Drierite, prior to two bulb-to-bulb fractional distillations, and then distilled into the bubble cell. Methanol (Mallinckrodt, A.R.) was dried with magnesium, fractionated off-line, b.p. 64.3 to 64.4 °C (757.1 Torr, uncorrected), then re-dried with magnesium on the line, degassed by repeated freezing and evacuation, and distilled as with DMF. Dimethylsulfoxide (Stepan) was dried with CaO and distilled off-line, b.p. ca. 85.0 °C (17 Torr). One of the three distillations in vacuo was omitted as the time required was long. Acetone (Fisher, A.C.S. and Baker, A.R.) was shaken with silver oxide, roughly fractionated to remove gross quantities of water, then dried with Drierite on and off the vacuum line, and subjected to several vacuum fractionations. Attempts to use Molecular Sieve 5A caused darkening of the acetone, so its use was discontinued. The acetone, purified as described, had density 0.7842 ± 0.0001 at 24.96 °C (cf. Howard and Pike (13) 0.78424 ± 0.00003 at 25 °C) and refractive index $n_D^{20} = 1.3585$ (cf. Handbook (2c, pC-505) 1.3588). Methylamine (Matheson) was distilled from the cylinder onto lithium on the vacuum line, and let stand at −78 °C for 24 h. It was then degassed, and subjected to several bulb-to-bulb fractional distillations. Benzene, used to calibrate the surface-tension apparatus, was Baker and Adamson (R) dried over sodium and fractionated off-line, b.p. 79.9 to 80.0 °C (756.5 Torr), then redried and redistilled on line as were the solvents.

The salts; NaBr, KCl, KI, NaCl (Baker and Adamson, R or A.C.S.), KBr (B.D.H. AnalaR), CsCl (Fisher Purified), and NaI (Merck), were used as purchased after drying at 110 °C, except KI and NaI which were recrystallized from aqueous methanol to improve crystal size and to effect some purification. All salts were stored over anhydrous $CaCl_2$.

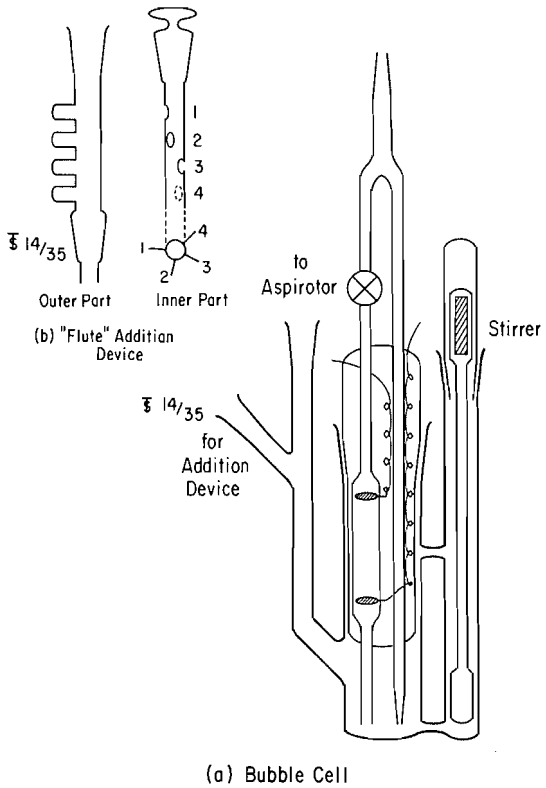

FIG. 2. Surface tension apparatus. (*a*) Bubble cell, with magnetic stirrer. (*b*) "Flute" addition device.

The gas used to form the bubbles was air drawn over Anhydrone and Ascarite, except where hydrogen was used, as noted. The manometer fluid was Amoil S(di-isoamyl sebacate) Distillation Products, Inc., degassed by evacuation on-line. It had a density of 0.9230 at 25 °C.

Apparatus and Method

The apparatus was essentially that of Stairs and Sienko (6) with two minor additions. In order to permit measurement of the surface tension at more than one concentration without opening the apparatus to moist air, the "flute" addition device shown in Fig. 2 was used. A weighed crystal of the solute was placed in each pocket, and when the device was rotated to a position with the pockets inverted, rotation of the key with the spirally-placed openings allowed the crystals to be dropped one at a time into the liquid. In each experiment the surface tension of the pure solvent was first measured, then after each addition of solute, the solution was stirred and its surface tension measured. When all four additions had been made, the apparatus was opened and the solution analyzed. The concentrations of the first three solutions were obtained from the weights of solute in each compared to the final weight.

The other addition was the pair of platinum electrodes

TABLE 1

Surface tension of pure liquids, against air (except as noted)

Liquid	t (°C)	σ (dyn cm^{-1})	t (°C)	σ (dyn cm^{-1})	σ_0*	a*
DMF	6.7	38.36	22.1	36.46	39.27	0.1241
	13.0	37.58	22.4	36.50		
	14.5	37.43	24.3	36.22		
	18.5	37.06	26.0	36.06		
DMSO	22.7	43.29	31.1	42.29	45.90	0.1165
	22.9	43.23	32.9	42.09		
	25.0	43.01	35.0	41.83		
	25.0	42.98	36.9	41.60		
	29.1	42.53	39.0	41.35		
Acetone	20.2	23.35	24.9	22.76	25.93	0.1275
	22.2	23.09	25.0	22.68		
	24.6	22.78	26.8	22.51		
Methanol	15.4	22.97	24.8	22.19	24.21	0.0810
	20.0	22.58	24.9	22.21		
	20.5	22.57				
Methylamine†	−69.0	31.90	−40.0	28.30	22.62	0.1376
	−65.0	31.26	−30.0	26.63		
	−60.0	30.69	−25.0	26.20		
	−55.0	30.21	−20.0	25.64		
	−50.0	29.71	−15.0	25.02		
	−45.0	29.04	−10.0	24.02		

*Constants in the equation $\sigma = \sigma_0 - at$, valid to 0.05 dyn cm^{-1} over the range of temperatures covered by the tabulated data, except for methylamine, where the equation is valid to 0.15 dyn cm^{-1} from −69 to + 35 °C, and includes the data of Swift and Calkins (24).
†Against hydrogen.

in the larger of the two dipping tubes of the surface tension cell. By their aid the conductance of each solution could be measured. The electrodes were platinized, but the rigorous cleaning and drying of the apparatus before each filling rendered the coating relatively ineffective. This and the simple circuitry employed reduced the significance of the conductance measurements but when calibrated, they provided a convenient secondary method of analysis (used mostly with the solutions in methanol).

The apparatus was cleaned by washing with chloroform and alcohol, then treating with chromic acid cleaning solution. Some authors advise avoidance of this step (14), but we found that there was so great a chance of contamination by grease from the many joints and taps that it was better to use it. The apparatus was then washed with several changes of tap water and distilled water, then steamed out, and dried at 140 °C.

The procedure of calibration and measurement was essentially as described before (6) except as noted above. Analysis of the solutions was carried out by argentimetric titration using dichlorofluorescein as adsorption indicator for titrations where the amount of precipitate was expected to be sufficient, and the Mohr method when it was not. When sufficient data were obtained with each solute and solvent to establish a conductance calibration curve, the conductance alone was used for concentration measurement.

Results and Discussion

Pure Solvents

The values of surface tension for the five liquids are listed in Table 1 together with the constants in the equation

$$\sigma = \sigma_0 - at \qquad [4]$$

which was found to express the data within the expected precision of the measurements, ±0.05 dyn cm^{-1}, over the ranges of temperatures in the table.

Our data for acetone are about 0.3 dyn cm^{-1} lower than those cited in the Handbook (2c, pF-28). Literature values show considerable variation (15–18) which in some measure is due to the difficulty of drying this liquid. When the data of Morgan and Scarlett (18) are recalculated using more recent correction factors for the drop-weight method (14), their results are less than 0.2 dyn cm^{-1} above the values reported here. If their acetone contained water as the sole impurity their given density represents 0.6% water (13, 19), which, according to their own figures for the effect of water on the surface tension of acetone, should increase it by 0.12 dyn cm^{-1}. With these corrections, the measurements of Morgan and Scarlett are within 0.05 dyn cm^{-1} of our figures. We calculate the parachor to be 162.1, cf. 162.0 from Glasstone's table of additive parachor equivalents (20).

Our results for methanol are consistent with

Can. J. Chem. Downloaded from www.nrcresearchpress.com by 210.87.254.6 on 09/05/12
For personal use only.

TABLE 2

Salt solutions. Surface tension increments at 25 °C. Against air except where noted

c (mole l^{-1})	$\Delta\sigma$ (dyn cm^{-1})	c (mole l^{-1})	$\Delta\sigma$ (dyn cm^{-1})	c (mole l^{-1})	$\Delta\sigma$ (dyn cm^{-1})
LiCl in DMF		NaBr in DMF		KI in DMF	
0.0798	0.150	0.0408	0.082	0.0640	0.107
0.1595	0.228	0.0628	0.130	0.1243	0.335
0.2810	0.451	0.0980	0.211	0.1526	0.397
0.2840	0.472	0.1537	0.314	0.327	0.763
0.459	0.763	0.2004	0.412	0.396	0.928
0.611	0.997	0.192	0.420		
		0.232	0.499		
LiCl in acetone		NaI in acetone*		LiCl in methanol	
0.0139	0.0325	0.0110	0.046	0.0166	0.063
0.0297	0.0525	0.0329	0.139	0.0462	0.149
0.0337	0.0585	0.0598	0.203	0.0698	0.173
0.0555	0.0650	0.1223	0.349	0.1334	0.304
0.0794	0.1065	0.1328	0.399	0.2208	0.473
0.0909	0.121	0.1815	0.490	0.2990	0.559
0.1035	0.144	0.1926	0.528	0.3966	0.712
				0.456	0.866
				0.736	1.240
NaBr in methanol		NaI in methanol		NaCl in methanol	
0.0175	0.048	0.0050	0.026	0.0033	0.023
0.0314	0.076	0.0133	0.060	0.0034	0.018
0.0469	0.127	0.0164	0.076	0.0069	0.046
0.0640	0.147	0.0222	0.094	0.0098	0.046
0.0864	0.198	0.0319	0.122	0.0127	0.064
0.1043	0.241	0.0550	0.179	0.0153	0.062
0.1252	0.299	0.0660	0.212	0.0229	0.094
0.293	0.616	0.0987	0.300	0.0327	0.120
0.386	0.779	0.1278	0.368	0.0379	0.145
0.443	0.898	0.1645	0.446	0.0384	0.135
		0.2668	0.666	0.0472	0.146
KBr in methanol		KI in methanol		CsCl in methanol	
0.0050	0.030	0.0282	0.085	0.030	0.0056
0.0132	0.059	0.0495	0.167	0.063	0.0158
0.0156	0.059	0.0527	0.144	0.076	0.0211
0.0282	0.089	0.0547	0.200	0.111	0.0353
0.0475	0.141	0.1013	0.255	0.152	0.0487
0.0511	0.163	0.1610	0.388	0.185	0.0625
0.0600	0.174	0.3075	0.718	0.273	0.1063
0.0829	0.215	0.520	1.117		
0.0900	0.232	0.705	1.457		
0.1136	0.271	0.771	1.530		

*Against hydrogen.

those in the literature (21–23). Dimethylformamide and dimethylsulfoxide do not appear to have been measured before. We obtained the following values for parachor at 25 °C (Glasstone's additive values in parentheses): methanol, 88.2 (91.0, difference characteristic of hydrogen-bonded liquids); DMF, 36.17 (36.8); DMSO, 182.5 (180.1).

For methylamine we obtained data that appear to be consistent with those reported for higher temperatures by Swift and Calkins (24). The only other available data are those of Jaeger (25) which lie 2 to 2.5 dyn cm^{-1} lower. His results are known to be low by nearly the same amount for ethanol (6). With surface-tension data from this work and Swift and Calkins, and densities from Felsing and Thomas (26), we calculate the parachor to be 97.8 at −40 °C, 99.8 at 25 °C (Glasstone 102.8). This low and temperature-dependent parachor is again characteristic of hydrogen-bonded liquids.

Salt Solutions

Table 2 contains the surface tension increments $\Delta\sigma$ for the various salts in the three solvents DMF, methanol, and acetone, all at 25.0 °C. The

Can. J. Chem. Downloaded from www.nrcresearchpress.com by 210.87.254.6 on 09/05/12
For personal use only.

TABLE 3

Surface-tension increment of salt solutions as a function of molar concentration

Solvent	Temperature (°C)	σ (0)	Salt	A_0*	A*
DMF	25	36.17	LiCl	0.02 (0.10)	1.62 (0.10)
			NaBr	−0.04 (0.05)	2.22 (0.10)
			KI	0.0 (0.3)	2.3 (0.3)
Acetone	25	22.76	LiCl	0.13 (0.10)	0.9 (0.3)
			NaI	0.27 (0.07)	2.08 (0.30)
Methanol	25	22.18	LiCl	0.36 (0.10)	1.30 (0.20)
			NaBr	0.12 (0.05)	1.90 (0.15)
			NaI	0.36 (0.06)	1.83 (0.10)
			KCl	0.24 (0.10)	2.4 (1.0)
			KBr	0.36 (0.08)	1.44 (0.40)
			KI	0.20 (0.10)	1.90 (0.20)
			CsCl	0.27 (0.03)	1.84 (0.20)
Ammonia (6)	−40	35.46	NaCl	0.25 (0.25)	1.5 (1.0)
			NaBr	0.6 (0.3)	0.75 (0.60)
			KBr	0.35 (0.15)	1.15 (0.45)
			KI	−0.10 (0.10)	1.73 (0.20)
Water (2)	20	72.75	LiCl	−0.04 (0.02)	1.66 (0.02)
			NaCl	0.08 (0.06)	1.56 (0.10)
			NaBr	−0.04 (0.02)	1.34 (0.04)
			KCl	0.06 (0.04)	1.34 (0.04)
			KBr	0.04 (0.02)	1.30 (0.04)
			NH_4Cl	0.08 (0.03)	1.30 (0.04)

*A and A_0 are the constants in the equation $\Delta\sigma = A_0c^{\frac{1}{2}} + Ac$. Numbers in parentheses are standard deviations.

three salts in DMF all yielded data that appeared to lie on a straight line through the origin, that is to say, with no term in $c^{1/2}$ needed, nor any apparent departure of the factor α of Oka's theory from unity. This implies that no ion pairing occurs in the region of the measurements. According to Bjerrum's theory (27) this means that DMF strongly solvates at least one ion (presumably positive) in each of LiCl, NaBr, and KI, for these should all be somewhat weak in DMF if the distance of closest approach of the ions is calculated from the crystal radii. The solutions in acetone and in methanol all showed some curvature at low concentrations, but tended to become more nearly linear at higher concentractions. Accordingly, no term in c^2 was used in the empirical equation, which was fitted in the form

$$[5] \qquad \Delta\sigma/c^{1/2} = A_0 + Ac^{1/2}$$

graphically by plotting $\Delta\sigma/c^{1/2}$ against $c^{1/2}$ Table 3 contains the constants in eq. [5] for the data from this work plus data from Stairs and Sienko for ammonia and some data from aqueous solutions (2*a*, 10). (We considered including the data of Kosakewitsch (28, 29), but as they were obtained in open vessels with solvents of uncertain dryness, and added mainly to the scatter, they were omitted.) The fit of the data for ammonia, and for KI in DMF, is poor, but it is moderately good for the remainder.

The values of A_0 for the various salts in methanol appear to be the same within experimental error, and no trends are obvious. If the origin of this term lies in the effect of interionic forces on the activity coefficient, as expressed in the Debye–Hückel theory, which in its simplest form, valid at the lowest concentrations, yields

$$\ln \gamma_{\pm} = - \text{constant } c^{1/2} (\varepsilon T)^{-3/2}$$

independent of the size of the ions for a given charge type, then one might expect that A_0 would be a constant for each solvent, and would be a function of εT to some negative power. In Fig. 3 we have plotted A_0 vs. $(\varepsilon T)^{-1}$ for the three solvents examined in this work, plus ammonia (6) and water (2*a*, 10). The bars represent one standard deviation in each direction from the plotted points. (The standard deviations of the values of A_0 for each solvent were consistent with the errors in A_0 estimated from their graphical determination.) There appears to be a trend in

Can. J. Chem. Downloaded from www.nrcresearchpress.com by 210.87.254.6 on 09/05/12
For personal use only.

Can. J. Chem. Downloaded from www.nrcresearchpress.com by 210.87.254.6 on 09/05/12
For personal use only.

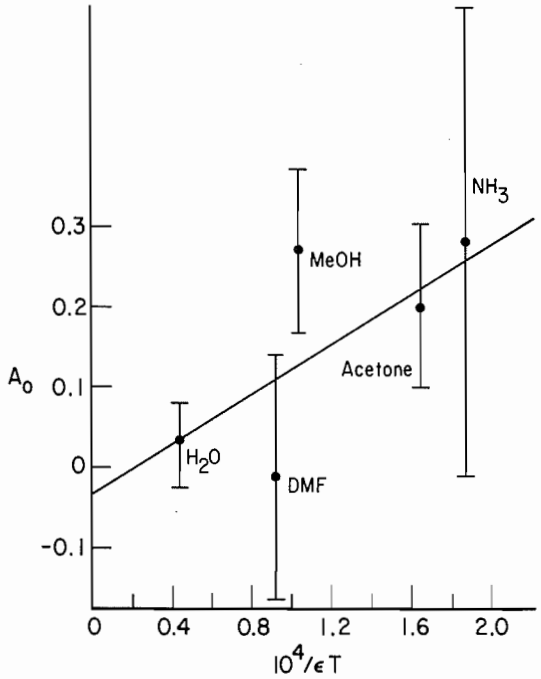

FIG. 3. Surface tension of salt solutions. The constant A_0 for five liquids vs. $(\varepsilon T)^{-1}$.

the direction expected, but it is impossible to decide what power of εT to use on the basis of presently available data.

The second parameter, A, is expected from the theories of Oka and of Pérez Masiá to depend upon ε^{-1}, and from the Wagner theory and its variant to show the same or a weaker inverse dependence on ε. From the theory of Pérez Masiá and our approximate calculations (see above) it was expected that A would show a tendency to decrease as the size of the ions increased. Table 3 shows the expected decrease in water, scatter in ammonia, virtual constancy in methanol, and actually an increase in acetone and in DMF.

It appears that the situation might be improved by retaining the third term, in $c^{3/2}$, in eq. [5], but the data are not of sufficient precision to justify a three-parameter expression. The conductance data for these methanol solutions (see also ref. 2*a*) gave a better straight line when plotted as Λ vs. $c^{1/2}$ than as Λc vs. Λ^{-1} (30), suggesting that these salts are strong electrolytes in this solvent, so the third term should be small. The data were examined for any regularity in the magnitude of A as a function of sums or differences of single-ion constants. None was found.

It does not appear at present that any of the theories predict the dependence of the surface tension of salt solutions on the nature of the salt or of the solvent. More data are needed for a variety of salts in a number of solvents, with attention to purity, particularly dryness. It does appear, however, that the form of the dependence of the surface tension of all the solutions on concentration is represented by eq. [3] at moderate concentrations.

We acknowledge with thanks support from the National Research Council of Canada.

1. *a.* A. PÉREZ MASIÁ. An. real soc. espan. fis. y quim. (Madrid). **50A**, 5 (1954); *b.* K. SCHÄFER, A. PÉREZ MASIÁ, and H. JÜNGTEN. Z. Electrochem. **59**, 425 (1955).
2. *a.* C. J. WEST and C. HULL (*Editors*). International Critical Tables. McGraw-Hill Book Co., Inc., New York. 1933; *b.* W. A. ROTH and K. SCHEEL (*Editors*). Landolt-Börnstein Tabellen. 5 ed. Springer, Berlin. 1936; *c.* Handbook of chemistry and physics. 46th ed. The Chemical Rubber Co. (1965–6) p. F–25.
3. S. OKA. Proc. Phys. Math. Soc. Jap. **14**, 233, 649 (1932).
4. C. WAGNER. Phys. Zeits. **25**, 474 (1924).
5. L. ONSAGER and N. N. T. SAMARAS. J. Chem. Phys. **2**, 46 (1934).
6. R. A. STAIRS and M. J. SIENKO. J. Amer. Chem. Soc. **78**, 920 (1956).
7. H. SACK. Phys. Zeits. **27**, 206 (1926).
8. J. B. HASTED, D. M. RITSON, and C. H. COLLIE. J. Chem. Phys. **16**, 1 (1948); D. M. RITSON and J. B. HASTED. J. Chem. Phys. **16**, 11 (1948).
9. C. J. F. BÖTTCHER. Rec. trav. chim. **65**, 19 (1946).
10. G. SCHWENKER. Ann. der Phys. **11** (5), 525 (1931).
11. *a.* G. JONES and M. DOLE. J. Amer. Chem. Soc. **51**, 2950 (1929); *b.* H. S. HARNED and B. B. OWEN. Physical chemistry of electrolytic solutions. 3rd ed. Reinhold, New York. 1958. pp. 97–105.
12. S. SUGDEN. The parachor and valency. Geo. Routledge and Sons, Ltd., London. 1930. p. 208 ff, p. 220.
13. KATHERINE S. HOWARD and F. P. PIKE. J. Phys. Chem. **63**, 2 (1959).
14. W. D. HARKINS and A. E. ALEXANDER. *In* A. Weissberger Technique of organic chemistry. Vol. 1. 3rd ed. Interscience, Publ. New York. 1960. p. 757 ff.
15. J. R. PARTINGTON. Advanced physical chemistry. Vol. II. Longmans, Green, London, New York. 1949–54, p. 194.
16. J. J. BIKERMAN. Surface chemistry, Academic Press, Inc., New York. 1948. p. 46.
17. A. I. VOGEL. J. Chem. Soc. 174 (1940).
18. J. L. R. MORGAN and A. J. SCARLETT, JR. J. Amer. Chem. Soc. **39**, 2275 (1917).
19. R. THIRION and E. C. CRAVEN. J. Appl. Chem. **2**, 210 (1952).
20. S. GLASSTONE. Textbook of physical chemistry. 2 ed. Van Nostrand. Princeton, New Jersey. 1946. p. 526.
21. T. W. RICHARDS and L. B. COOMBS. J. Amer. Chem. Soc. **37**, 1656 (1915).
22. A. I. VOGEL. J. Chem. Soc. 1815 (1948).
23. J. L. R. MORGAN and M. NEIDLE. J. Amer. Chem. Soc. **35**, 1856 (1913).

24. E. SWIFT, JR. and C. R. CALKINS. J. Amer. Chem. Soc. **65**, 2415 (1943).
25. F. M. JAEGER. Z. Anorg. Allgem. Chem. **101**, 1 (1917).
26. W. A. FELSING and A. R. THOMAS. Ind. Eng. Chem. **21**, 1269 (1929).
27. N. BJERRUM. Kgl. Danske Vidensk. Selskab. **7**, No. 9 (1926). See, e.g., H. S. HARNED and B. B. OWEN. Physical chemistry of electrolytic solutions. 3rd ed. Reinhold, New York. 1958. pp. 70–73.
28. P. P. KOSAKEWITSCH. Z. Phys. Chem. **133**, 1 (1928).
29. P. P. and N. S. KOSAKEWITSCH. Z. Phys. Chem. **150** (A), 370 (1930).
30. H. S. HARNED and B. B. OWEN. Physical chemistry of electrolytic solutions. 3rd ed. Reinhold, New York. 1958. p. 156.

Can. J. Chem. Downloaded from www.nrcresearchpress.com by 210.87.254.6 on 09/05/12
For personal use only.

Can. J. Chem. Downloaded from www.nrcresearchpress.com by 210.87.254.5 on 09/05/12
For personal use only.

ortho-Diquaternary aromatic compounds. III. Syntheses and reactions of polyalkyltetralones and derivatives

L. R. C. BARCLAY, K. L. ADAMS,[1] H. M. FOOTE,[2] E. C. SANFORD, AND R. H. YOUNG[2]
Department of Chemistry, Mount Allison University, Sackville, New Brunswick

Received November 3, 1970

A new synthesis is reported of polyalkyltetralones based on reactions of α,α-dialkylarylacyl chlorides with branched alkenes in the presence of stannic chloride. The following were synthesized by this method: 1,1,4,4-tetramethyl-2-tetralone (*7a*), 1,1,3,4,4-pentamethyl-2-tetralone (*7b*), 1,1,4,4,6-pentamethyl-2-tetralone (*7c*), 1,1-diethyl-4,4-dimethyl-2-tetralone (*7d*), and 3-keto-1,1,4,4-tetramethyl-1,2,3,4-tetrahydrophenanthrene (*7e*). Cyclialkylation of toluene with 2,2,5,5-tetramethyltetrahydrofuranone yielded 1,1,4,4,7-pentamethyl-2-tetralone. Monobromoderivatives were prepared from ketones *7a*, *b*, and *e* and dibromoderivatives from ketones *7a* and *e*. The polyalkyltetralones are used as intermediates in the synthesis of ortho-diquaternary aromatic compounds by various oxidative procedures.

Canadian Journal of Chemistry, **48**, 2763 (1970)

Introduction

Polyalkyltetralones such as 1,1,4,4-tetramethyltetralone are useful precursors for the synthesis of crowded aromatics (1, 2). 1,1,4,4-Tetramethyl-2-tetralone is usually synthesized by Friedel–Crafts cyclialkylation using 2,2,5,5-tetramethyltetrahydrofuranone (**2**) (3). Extensive rearrangements take place using this method and these will be the subject of a separate publication (4). It was very desirable to have a more general method applicable to the synthesis of polyalkyltetralones. In this investigation, a new method for the synthesis of such ketones was developed. The synthesis is based upon acylation of appropriately branched alkenes by α,α-dialkylarylacyl chlorides followed by Friedel–Crafts cyclization of the resulting unsaturated ketones to polyalkyltetralones. Some reactions analogous to these have been reviewed by Nenitzescu and Balaban (5). Synthesis of five polyalkyltetralones by this method are discussed and the limitation of the reaction was tested. A number of mono- and dibromo derivatives of the polyalkyltetralones were prepared and the *gem* dimethyl resonances in their nuclear magnetic resonance (n.m.r.) spectra are discussed in terms of nonbonded interactions. A simple three-step synthesis of the new aromatic hydrocarbon, 1,1,4,4-tetramethyl-1,4-dihydronaphthalene, from 1,1,4,4-tetramethyl-2-tetralone is described. A new strained aromatic compound 2-ethyl-2-*o*-(1-methyl-1-carboxyethyl)-phenylbutanoic acid was synthesized by oxidation reactions on 1,1-diethyl-4,4-dimethyl-2-tetralone. The photochemistry of nonenolizable α-diketones is of interest. We now report an exploratory photooxidation of 2,3-dioxo-1,1,4,4-tetramethyltetralin to *o*-phenylenediisobutyric anhydride as an alternative route to strained aromatic systems.

Results and Discussion

Syntheses of Polyalkyltetralones

Cyclialkylations of aromatic hydrocarbons with 2,2,5,5-tetramethyltetrahydrofuranone (**2**) are outlined in Table 1. 1,1,4,4-Tetramethyltetralone is usually readily prepared in this way (no. *1*), although longer contact times at elevated temperatures result in rearrangement products (4). Toluene can be converted into 1,1,4,4,7-pentamethyl-2-tetralone (**4**) using a much shorter contact time (no. *2*) and cyclialkylation of naphthalene at lower temperature (no. *3*) yielded 2-keto-1,1,4,4-tetramethyl-1,2,3,4-tetrahydroanthracene as reported earlier (2).

Cyclialkylation of toluene with **2** could possibly give a mixture of isomeric ketones **4** and **7***c* (Schemes 1 and 2). The reaction yielded only **4** and not **7***c* as was determined by comparison with **7***c* which was synthesized by an alternative unambiguous method (see Scheme 2, and Table 1, no. *6*). The formation of **4** can be explained by cleavage *a* of **2**, remote from the carbonyl, and para alkylation to yield intermediate **3**. Cleavage *b* of **2** is apparently inhibited because the incipient carbonium ion would be adjacent to the electropositive carbonyl carbon.

[1]On leave of absence from Prince of Wales College, Charlottetown, P.E.I.
[2]Recipients of NRCC Scholarships.

Can. J. Chem. Downloaded from www.nrcresearchpress.com by 210.87.254.5 on 09/05/12
For personal use only.

TABLE 1

Syntheses of polyalkyltetralones

No.	Aromatic compound (mole)	Alkylating* agent (mole)	Catalyst (mole)	Conditions (solvent, temperature, time)	Products (%)†
1	Benzene (5.65)	TMTHF (0.895)	$AlCl_3$ (1.69)	C_6H_6; 80°; 4 h	1,1,4,4-Tetramethyl-2-tetralone (*7a*) (54); rearrangement products (46)‡
2	Toluene (0.211)	TMTHF (0.035)	$AlCl_3$ (0.070)	$C_6H_5CH_3$; 74°; 10 min	1,1,4,4,7-Pentamethyl-2-tetralone (**4**) (70); rearrangement products (24)‡
3	Naphthalene (0.035)	TMTHF (0.035)	$AlCl_3$ (0.071)	CS_2; 25°; 8 h	2-Keto-1,1,4,4-tetramethyl-1,2,3,4-tetrahydroanthracene (29)§
4	(*a*) α-Phenylisobutanoyl chloride (**5***a*) (0.025)	$(CH_3)_2C{=}CH_2$ (excess)	$SnCl_4$ (0.002)	CS_2; −10–25°; 18 h	2,5-Dimethyl-5-phenyl-4-oxo-2-hexene (*6a*) (46); *7a* (15)
	(*b*) **6** (0.230)		$BF_3{:}O(C_2H_5)_2$ (1.13)	CH_2Cl_2; reflux; 48 h	*7a* (50)
5	**5***a* (0.027)	$(CH_3)_2C{=}CHCH_3$	$SnCl_4$ (0.004)	CS_2; 25°; 30 h	1,1,3,4,4-Pentamethyl-2-tetralone (*7b*) (71)
6	α-*p*-Tolylisobutanoyl chloride (**5***c*) (0.023)	$(CH_3)_2C{=}CH_2$ (0.115)	$SnCl_4$ (0.003)	CS_2, −10°; 28 h	1,1,4,4,6-Pentamethyl-2-tetralone (*7c*) (61)
7	2-Ethyl-2-phenylbutanoyl chloride (**5***d*) (0.028)	$(CH_3)_2C{=}CH_2$ (0.080)	$SnCl_4$ (0.018)	CS_2; −10°; 96 h	1,1-Diethyl-4,4-dimethyl-2-tetralone (*7d*) (70)
8	(*a*) α-(1-Naphthyl)-isobutanoyl chloride (**5***e*) (0.069)	$(CH_3)_2C{=}CH_2$ (excess)	$SnCl_4$ (0.0068)	CS_2; −10°; 16 h	2,5-Dimethyl-5-(1-naphthyl)-4-oxo-2-hexene (**6***e*) (77)
	(*b*) **6***e* (0.02)		P.P.A.	none; 95°; 3 h	1-Acetyl-1,3,3-trimethylbenz(*e*)-indane (**8**) (33)
	(*c*) **6***e* (0.032)		$BF_3{:}O(C_2H_5)_2$ (0.822)	CH_2Cl_2; 25°; 7 days	3-Keto-1,1,4,4-tetramethyl-1,2,3,4-tetrahydrophenanthrene (*7e*) (55); **8** (14)
9	**5***a* (0.014)	$(C_6H_5)_2C{=}CH_2$ (0.011)	$SnCl_4$ (0.023)	$CHCl_2CHCl_2$; 0°; 48 h	1,1,3-Triphenyl-3-methylindane (**9**); 1,1,3-trimethyl-3-phenylindane (**10**)
10	**5***a* (0.011)		$SnCl_4$ (0.002)	CS_2; reflux; 23 h	**10**

*TMTHF refers to 2,2,5,5-tetramethyltetrahydrofuranone.

†The percentages of products from nos. *1* and *2* are relative amounts by gas chromatographic analyses. Other percentages are actual yields. Numbers *9* and *10* yielded mainly polymeric material and yields of **9** and **10** were not estimated.

‡The structures for these rearrangement products will be discussed later (**4**).

§Reference 2.

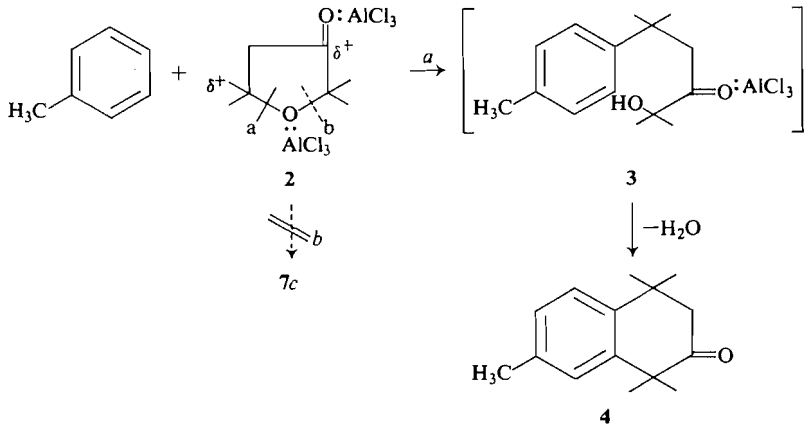

SCHEME 1

Cyclodehydration of **3** would produce the product **4**. We did not isolate the intermediate **3**, but its use in Scheme 1 is consistent with the reported isolation of an α-ketol during cyclialkylation of benzene (3).

The new route for syntheses of polyalkyltetralones is outlined in Scheme 2. The reaction scheme involves acylation of an alkene by an appropriate α,α-dialkylarylacyl chloride (**5**) in the presence of stannic chloride in the cold. The intermediate unsaturated ketone (**6**) is usually not characterized as such. Actually a mixture usually results which contains **6**, the corresponding tertiary chloride, and frequently the desired final product **7**. Prolonged treatment of the mixture (**6**) with $SnCl_4$ can be used to convert it directly to the required ketone (**7**). Alternatively the compound **6** can be isolated and cyclized with boron fluoride-etherate. The procedure has the advantage of producing **7** without using aluminum chloride which causes extensive rearrangements.

Some examples of the utilization of this synthetic procedure are summarized in Table 1 and Scheme 2. The two step procedure using α-phenylisobutanoyl chloride (**5***a*) and isobutylene with stannic chloride catalyst (no. *4a*) followed by boron fluoride etherate (no. *4b*) yielded tetramethyltetralone (*7a*). 1,1,3,4,4-Pentamethyl-2-tetralone (*7b*) was prepared in one step from **5***a* and 2-methyl-2-butene (no. *5*). The isomeric ketone, 1,1,4,4,6-pentamethyl-2-tetralone (*7c*) was prepared from α-(*p*)tolylisobutanoyl chloride (**5***c*) and isobutylene (no. *6*). By using 2-ethyl-2-phenylbutanoyl chloride (**5***d*) and isobutylene (no. *7*), a polyalkyltetralone 1,1-diethyl-4,4-dimethyl-2-tetralone (*7d*) bearing *gem* diethyls and dimethyls was synthesized.

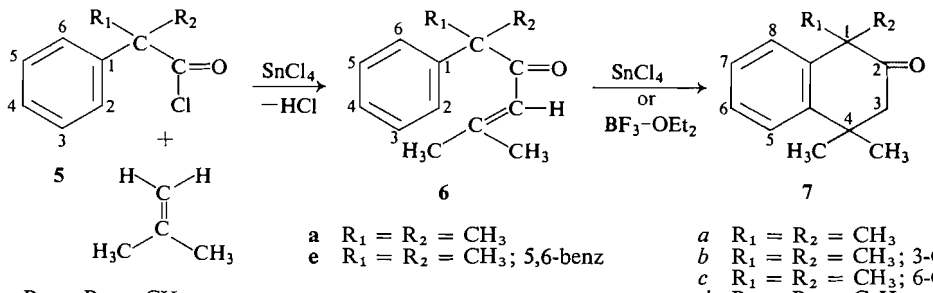

a $R_1 = R_2 = CH_3$
b **5***a* + $CH_3CH = C(CH_3)_2$
c $R_1 = R_2 = CH_3$; 4-CH_3
d $R_1 = R_2 = C_2H_5$
e $R_1 = R_2 = CH_3$; 5,6-benz

a $R_1 = R_2 = CH_3$
e $R_1 = R_2 = CH_3$; 5,6-benz

a $R_1 = R_2 = CH_3$
b $R_1 = R_2 = CH_3$; 3-CH_3
c $R_1 = R_2 = CH_3$; 6-CH_3
d $R_1 = R_2 = C_2H_5$
e $R_1 = R_2 = CH_3$; 7,8-benz

SCHEME 2

Can. J. Chem. Downloaded from www.nrcresearchpress.com by 210.87.254.5 on 09/05/12
For personal use only.

Can. J. Chem. Downloaded from www.nrcresearchpress.com by 210.87.254.5 on 09/05/12
For personal use only.

TABLE 2

Nuclear magnetic resonance spectral data

No.	Compound	Chemical shift (τ)	Multiplicity	Relative* areas	Assignment
1	1,1,4,4-Tetramethyl-2-tetralone (7*a*)	8.69	Singlet	6.1	$>C_4(CH_3)_2$
		8.56	Singlet	6.0	$>C_1(CH_3)_2$
		7.36	Singlet	2.1	$—CH_2—$
		2.74	Multiplet	4.0	Aromatic H's
2	1,1,4,4,6-Pentamethyl-2-tetralone (7*c*)	8.69	Singlet	11.4	$>C_4(CH_3)_2$
		8.60	Singlet		$>C_1(CH_3)_2$
		7.62	Singlet	3.0	$Ar—CH_3$
		7.39	Singlet	2.2	$—CH_2—$
		2.72	Multiplet	3.0	Aromatic H's
3	1,1,4,4,7-Pentamethyl-2-tetralone (**4**)	8.72	Singlet	5.8	$>C_4(CH_3)_2$
		8.59	Singlet	6.0	$C_1(CH_3)_2$
		7.62	Singlet	2.9	$Ar—CH_3$
		7.40	Singlet	2.1	$—CH_2—$
		2.69	Multiplet	3.0	Aromatic H's
4	1,1,3,4,4-Pentamethyl-2-tetralone (7*b*)	8.98	Singlet	6.2	$>C_4—CH_3$ and
		8.80	Doublet (7 c.p.s.)		$>C_3—CH_3$
		8.60	Singlet	8.7	$>C_1(CH_3)_2$ and $>C_4—CH_3$
		7.19	Quartet (7 c.p.s.)	0.9	$>C_3—H$
		2.82	Multiplet	4.0	Aromatic H's
5	1,1-Diethyl-4,4-dimethyl-2-tetralone (7*d*)	9.38	Triplet (8 c.p.s.)	6.2	$>C_1(—C(—)—CH_3)_2$
		8.72	Singlet	6.0	$>C_4(CH_3)_2$
		8.11	Multiplets	4.1	$>C_1(—CH_2—C<)_2$
		7.52	Singlet	2.1	$—CH_3—$
		2.71	Multiplet	4.0	Aromatic H's
6	1-Acetyl-1,3,3-trimethylbenz(*e*)indane (**8**)	8.63	Singlet	2.9	$>C_3(CH_3)_2$
		8.57	Singlet	3.0	
		8.40	Singlet	3.1	$>C_1—CH_3$
		8.19	Singlet	3.0	$—C(=O)—CH_3$
		7.87	Quartet	2.0	$—CH_2—$
		2.47	Multiplet	6.0	Aromatic H's

TABLE 2 (*concluded*)

No.	Compound	Chemical shift (τ)	Multiplicity	Relative* areas	Assignment
7	3-Keto-1,1,4,4-tetramethyl-1,2,3,4-tetrahydrophenanthrene (*7e*)	8.65	Singlet	6.0	$\overset{}{\underset{1}{C}}(CH_3)_2$
		8.19	Singlet	6.2	$\overset{}{\underset{4}{C}}(CH_3)_2$
		7.31	Singlet	1.8	$-CH_2-$
		2.32	Multiplet	5.1	Aromatic H's 6–10
		1.51	Multiplet	1.0	Aromatic H 5
8	3-Bromo-1,1,4,4-tetramethyl-2-tetralone (**11**)	8.61	Singlet	8.9	$\overset{}{\underset{4}{C}}(CH_3)_2$
		8.58	Singlet		$-\underset{1}{C}-CH_3$
		8.34	Singlet	3.1	$-\underset{1}{C}-CH_3$
		5.53	Singlet	1.3	Br—CH—
		2.78	Multiplet	4.0	Aromatic H's
9	1,1,3,4,4-Pentamethyl-3-bromo-2-tetralone	8.78	Singlet	3.2	$-CH_3$
		8.52	Singlet	3.1	$-CH_3$
		8.29	Singlet	3.1	$-CH_3$
		8.13	Singlet	6.3	$2 \times CH_3$
		8.08	Singlet		
		2.73	Multiplet	4.0	Aromatic H's
10†	3,3-Dibromo-1,1,4,4-tetramethyl-2-tetralone (**12**)	8.67	Singlet	2.8	$\overset{}{\underset{4}{C}}(CH_3)_2$
		8.43	Singlet	3.5	
		8.06	Singlet	5.4	$\overset{}{\underset{1}{C}}(CH_3)_2$
		8.01	Singlet		
		2.66	Multiplet	4.0	Aromatic H's
11	2-Bromo-3-keto-1,1,4,4-tetramethyl-1,2,3,4-tetrahydrophenanthrene (**13**)	8.67	Singlet	3.1	$\underset{1}{C}-CH_3$
		8.49	Singlet	2.9	$\underset{1}{C}-CH_3$
		8.18	Singlet	3.0	$\underset{4}{C}-CH_3$
		8.06	Singlet	3.1	$\underset{4}{C}-CH_3$
		5.17	Singlet	0.9	$Br-\underset{2}{C}-H$
		2.48	Multiplet	5.1	Aromatic H's 6–10
		1.71	Multiplet	1.0	Aromatic H 5
12	2,2-Dibromo-3-keto-1,1,4,4-tetramethyl-1,2,3,4-tetrahydrophenanthrene (**14**)	8.70	Singlet	2.9	$\underset{1}{C}-CH_3$
		8.03	Singlet	2.9	$\underset{1}{C}-CH_3$
		7.90	Singlet	2.9	$\underset{4}{C}-CH_3$
		7.70	Singlet	2.9	$\underset{4}{C}-CH_3$
		2.31	Multiplet	5.0	Aromatic H's 6–10
		1.56	Multiplet	1.0	Aromatic H 5

*Integrations of peaks were calculated relative to the aromatic hydrogens.
†The spectrum of 12 was determined at 0°.

The method was also applied to α-(1-naphthyl)-isobutanoyl chloride (**5***e*) and isobutylene. When polyphosphoric acid was used as the cyclization reagent (no. *8b*), rearrangement ensued resulting in the formation of 1-acetyl-1,3,3-trimethyl-benz(*e*)indane (**8**) (4). Boron fluoride etherate (no. *8c*) effected cyclization without rearrangement to yield 3-keto-1,1,4,4-tetramethyl-1,2,3,4-tetrahydrophenanthrene (**7***e*).

A limitation was found in the applicability of

Can. J. Chem. Downloaded from www.nrcresearchpress.com by 210.87.254.5 on 09/05/12
For personal use only.

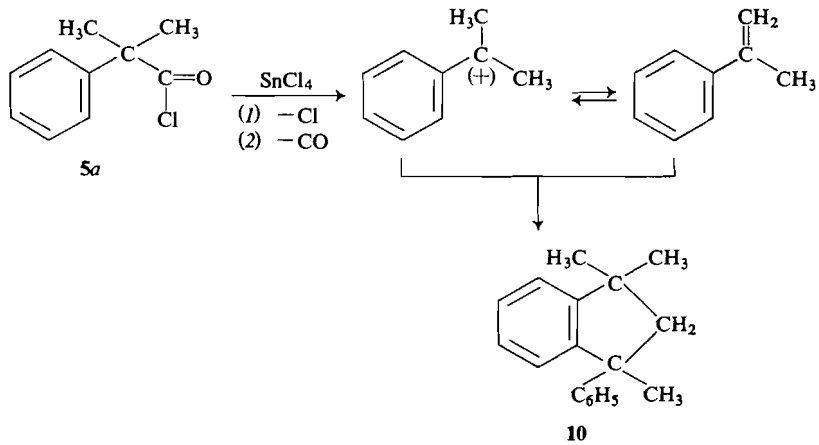

5*a*

10

SCHEME 3

this polyalkyltetralone synthesis. When attempts were made to use 1,1-diphenylethylene in the synthesis (no. *9*), the only products identified were the hydrocarbons 1,1,3-triphenyl-3-methylindane (**9**) and 1,1,3-trimethyl-3-phenylindane (**10**). Apparently 1,1-diphenylethylene undergoes the known (6) cyclic dimerization to form **9** rather than entering into reaction with the acyl chloride (**5***a*). The hydrocarbon **10** would result from decarbonylation of **5***a* followed by the well-known formation (7) of **10**, the cyclic dimer of α-methylstyrene, according to Scheme 3. Treatment of **5***a* with stannic chloride also yielded **10** (no. *10*) as expected.

The various ketones discussed above were characterized by their n.m.r. spectra which are summarized in Table 2 (see spectra nos. *1* to *7*).

Derivatives of Polyalkyltetralones

(a) Bromo Derivatives

Non Bonded Interactions and Nuclear Magnetic Resonance Spectra

The bromo derivatives of the tetralones provided a useful means of further characterization of these compounds. The n.m.r. spectra of the bromocompounds (Table 2, nos. *8* to *12*) exhibited separation of the methyl resonances. These can be viewed from the standpoint of the probable conformations involved. The ketones can be considered in quasi-chair conformers (illustrated in Scheme 4) which are normally rapidly interconverting so that the two methyls of a *gem* dimethyl have the same average shielding. In the ketones **7***a*, **4**, and **7***c*, the absorption near 8.7 τ is assigned to the *gem* dimethyls on C-4 while the peak at lower field (near 8.6 τ) is assigned to the *gem* dimethyls on C-1. In the latter case the carbonyl group would be responsible for the paramagnetic shift of the methyl resonances. A bromine at position 3 could be in the axial or equatorial position. The fact that the carbonyl stretching frequency occurs at the same position in the monobromo derivative **11** as in **7***a* (Experimental, Table 3) indicates a preference for the axial position (8) at least in the solid state. In the monobromo compound (**11**), the methyls at C-1 are assigned to the bands at 8.58 and 8.34 τ. The splitting may be due to 1:3 methyl:bromine diaxial interactions. The dibromoderivative (**12**) exhibited three (partially resolved) methyl resonances at 40°. However, at lower temperature (no. *10*) there were four bands (for assignments see Table 2). The interconversion of conformers is presumably slowed so that the shielding of the methyls is no longer averaged.

3-Keto-1,1,4,4-tetramethyl-1,2,3,4-tetrahydrophenanthrene (**7***e*) also showed two sets of methyl resonances (Table 2, no. *7*). In the monobromoderivative (**13**), and dibromoderivative (**14**), the methyl resonances occurred in four distinct peaks (nos. *11* and *12*). This is expected if the conformational interconversion discussed above is slowed at ordinary temperatures. This could result from additional nonbonded interactions in ketones such as **7***e*, **13**, and **14** due to the compression effects (2) in both conformers (Scheme 4) between the *gem* dimethyls on C-4 and position 5 of the adjacent aromatic ring. Evidence for this nonbonded interaction in **7***e*,

Can. J. Chem. Downloaded from www.nrcresearchpress.com by 210.87.254.5 on 09/05/12
For personal use only.

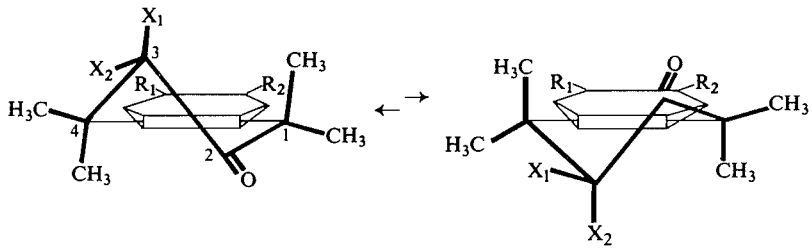

7a $R_1 = R_2 = H$; $X_1 = X_2 = H$
4 $R_1 = H$; $R_2 = CH_3$; $X_1 = X_2 = H$
7c $R_1 = CH_3$; $R_2 = H$; $X_1 = X_2 = H$
11 $R_1 = R_2 = H$; $X_1 = Br$; $X_2 = H$
12 $R_1 = R_2 = H$; $X_1 = X_2 = Br$

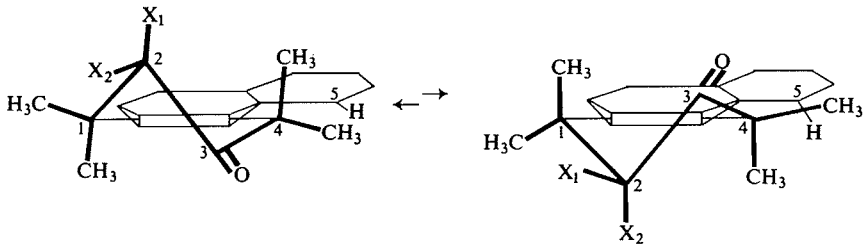

7e $X_1 = X_2 = H$
13 $X_1 = Br$; $X_2 = H$
14 $X_1 = X_2 = Br$

SCHEME 4

13, and **14** shows up in the compression shift (downfield) of the aromatic hydrogen at position 5. The infrared (i.r.) spectrum of the monobromo compound (**13**) showed a shift of 15 cm^{-1} to higher frequency from the parent ketone (*7e*) which is indicative of an equatorial α-bromine. The second α-bromine in the dibromo compound (**14**) does not shift the carbonyl frequency further (Table 3).

This interpretation of the chemical shifts is obviously empirical and the assignments of the methyl resonances somewhat arbitrary. Nevertheless, the argument is a useful one in making assignments of the methyl resonances for the substituted tetralones outlined in Table 2.

(b) 1,1,4,4-Tetramethyl-1,4-dihydronaphthalene (16)

The hydrocarbon 1,1,4,4-tetramethyl-1,4-dihydronaphthalene (**16**) was required for our studies on molecular rearrangements (4). Arnett (9) earlier reported an unsuccessful attempt to synthesize this hydrocarbon as a route for the synthesis of *o*-di-*t*-butylbenzene. Ketone *7a* proved to be a convenient starting material for a simple synthesis of **16** according to the sequence shown in Scheme 5.

(c) 2-Ethyl-2-o-(1-methyl-1-carboxyethyl)-phenylbutanoic Acid (18)

A New Crowded Aromatic Compound

The polyalkyltetralone synthesis outlined in Scheme 2 provides a starting point for the synthesis of new crowded aromatic compounds. For example, 1,1-diethyl-4,4-dimethyl-2-tetralone (*7d*) was converted into the α-diketone (**17**) and the latter on oxidation yielded the crowded aromatic system (**18**) (Scheme 6). The dicarboxylic acid **18** showed evidence of intramolecular crowding in its ultraviolet (u.v.) spectrum. The crowded acid **18** (λ_{max} 262 mμ, ε = 318) like *o*-phenylenediisobutyric acid (λ_{max} 261–264 mμ, ε = 233) showed only a very broad band in its spectrum. The new acid **18** can therefore be classed among the several well-known strained *o*-di-quaternary aromatic compounds (10).

The yield of **18** from periodate oxidation was only 33%. The major product was a neutral compound which was not completely charac-

Can. J. Chem. Downloaded from www.nrcresearchpress.com by 210.87.254.5 on 09/05/12
For personal use only.

TABLE 3

Elemental and spectral (i.r.) data for polyalkyltetralones and bromo derivatives

Compound	Melting point (°C)	Analyses						$\nu_{C=O}(cm^{-1})$
		Calculated			Found			
		C	H	Br	C	H	Br	
1,1,4,4-Tetramethyl-2-tetralone (*7a*)	78–79	—	—	—	—	—	—	1715
3-Bromo-1,1,4,4-tetramethyl-2-tetralone (**11**)	45–46	59.79	6.05	28.47	59.57	6.21	28.53	1715
3,3-Dibromo-1,1,4,4-tetramethyl-2-tetralone (**12**)	100–102	46.67	4.44	44.44	46.54	4.47	44.40	1725
1,1,4,4,7-Pentamethyl-2-tetralone (**4**)	59–61	83.29	9.32	—	83.50	9.41	—	1710
1,1,4,4,6-Pentamethyl-2-tetralone (*7c*)	81–82	83.29	9.32	—	82.91	9.39	—	1710
1,1,3,4,4-Pentamethyl-2-tetralone (*7b*)	(b.p. 130°/ 1.1 mm)	83.29	9.32	—	82.88	9.34	—	1700
3-Bromo-1,1,3,4,4-pentamethyl-2-tetralone	68–69	61.03	6.55	27.07	61.06	6.58	26.80	1700
1,1-Diethyl-4,4-dimethyl-2-tetralone (*7d*)	55–56.5	82.80	9.50	—	82.77	9.12	—	1710
1-Acetyl-1,3,3-trimethylbenz(*e*)indane		85.65	7.99	—	85.74	8.13	—	1715
3-Keto-1,1,4,4-tetramethyl-1,2,3,4-tetrahydrophenanthrene (*7e*)	113–114	85.71	7.94	—	85.80	8.15	—	1715
2-Bromo-3-keto-1,1,4,4-tetramethyl-1,2,3,4-tetrahydrophenanthrene (**13**)	117–118	65.26	5.74	24.17	64.79	5.85	24.84	1730
2,2-Dibromo-3-keto-1,1,4,4-tetramethyl-1,2,3,4-tetrahydrophenanthrene (**14**)		(Failed to crystallize for analysis)						1730

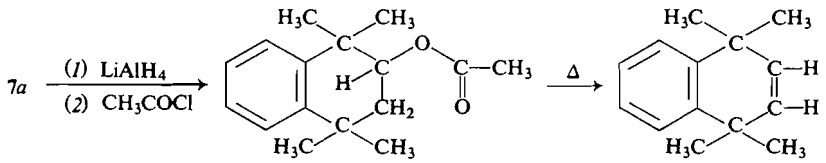

SCHEME 5

terized. The spectral evidence (see Experimental) supported the lactone structure **19**. An analogous lactone was reported to form in a similar synthesis of *o*-phenylenediisobutyric acid (1).

(d) Photochemistry of 2,3-Dioxo-1,1,4,4-tetramethyl-tetralin (20)

Cyclic non-enolizable α-diketones are known to form cyclic anhydrides on photooxidation. For example, Meinwald and Klingele (11) carried out a photooxidation of camphorquinone to camphoric anhydride and Rigaudy and Paillous (12) obtained diphenylhomophthalic anhydride by photooxidation of 3,3-diphenyl-1,2-indanedione. 2,3-Dioxo-1,1,4,4-tetramethyltetralin (**20**) was selected as a model compound for some exploratory photooxidation studies. In particular, it was desirable to determine if photooxidation would convert the diketone (**20**) into the corresponding anhydride, *o*-phenylenediisobutyric anhydride (**23**). This would provide for a convenient alternate route to crowded *o*-diquaternary aromatic compounds.

The products from photolysis of **20** in benzene were 1,1,3,3-tetramethylindanone (**21**), 3-hydroxyl-1,1,4,4-tetramethyl-2-tetralone (**22**), and *o*-phenylenediisobutyric anhydride (**23**) in varying amounts depending on whether a nitrogen or an oxygen atmosphere was maintained in the reaction, (see Experimental). While this work was in progress, Gream *et al.* (13) reported the

Can. J. Chem. Downloaded from www.nrcresearchpress.com by 210.87.254.5 on 09/05/12
For personal use only.

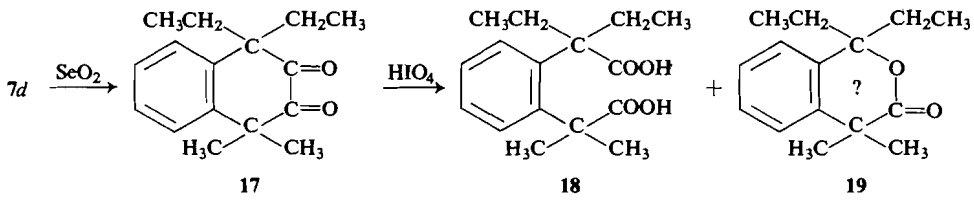

SCHEME 6

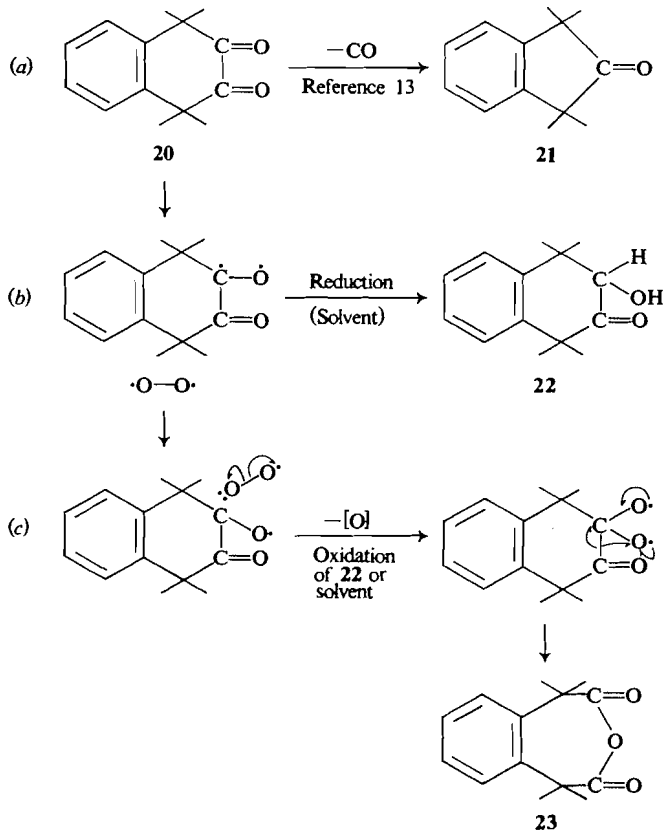

SCHEME 7

photolysis of **20** in a nitrogen atmosphere to yield **22**, as the predominant product, along with **21** and a few percent of **23**. The latter was attributed to diffusion of oxygen into the reaction mixture. Because the objective of our photooxidation was different from the studies of others (13), some speculation on the mechanism of the photooxidation process leading to the formation of **23** is desirable. The formation of **21** occurs in an oxygen atmosphere as well as (or better than) in the presence of nitrogen and this suggests an independent route to **21**, (Scheme 7*a*). On the other hand, oxygen obviously decreases the formation of the reduction product **22** (Scheme 7*b*), since the yield of **22** is reduced from 81% to 48% in the presence of oxygen. The anhydride could possibly form from addition of oxygen to a biradical excited state followed by reduction of the biradical adduct and rearrangement (Scheme 7*c*).

Experimental

The n.m.r. spectra were recorded on a Varian A-60 NMR Spectrometer equipped with a variable temperature probe. (The solvent was carbon tetrachloride containing tetramethylsilane, unless indicated otherwise.) The i.r. spectra were recorded on a Perkin–Elmer model 137

Can. J. Chem. Downloaded from www.nrcresearchpress.com by 210.87.254.5 on 09/05/12
For personal use only.

Can. J. Chem. Downloaded from www.nrcresearchpress.com by 210.87.254.5 on 09/05/12
For personal use only.

Infracord or on a Perkin–Elmer model 337 Grating Spectrophotometer using potassium bromide pellets for solids and films for liquids. The i.r. spectra of polyalkyltetralones and corresponding mono- and dibromoderivatives (Table 3) were determined on the same (model 337) instrument. Ultraviolet (u.v.) spectra were recorded on a Beckmann DK-2 Spectrophotometer using spectro-grade cyclohexane as solvent. Gas–liquid chromatographic (g.l.c.) analyses were determined by means of an F&M model 500 programmed temperature gas chromatograph equipped with a dual column attachment. Columns were ¼ in., packed with Apiezon grease (30%) on Chromosorb W. Melting points were determined on a Thomas Hoover capillary melting point apparatus and are uncorrected. Elemental analyses were determined by Dr. E. Thommen, Basel, Switzerland and by Dr. C. Daesslé, Montreal.

Friedel–Crafts Cyclialkylations with 2,2,5,5-Tetramethyltetrahydrofuranone

The procedure for cyclialkylation was similar to that reported by Bruson *et al.* (3). We found it essential, especially for activated aromatics (toluene and naphthalene) to monitor the reactions by taking aliquots and determining the composition by gas chromatography. Information on three typical runs is summarized in Table 1 (nos. *1*, *2*, and *3*),

Preparation of α,α-Dialkylarylacetic Acids

(1) α-Phenylisobutyric Acid

α-Phenylisobutyric acid was prepared by alkylation of benzene with methylacrylic acid using a procedure similar to that of Prijs (14). Little or no alkylation of benzene by methacrylic acid resulted unless relatively large amounts of aluminum chloride catalyst were used. In a typical run, 1.4 moles of methacrylic acid in 50 ml of benzene was added to a mixture of 8.4 moles of benzene and 3.8 moles of anhydrous aluminum chloride. The mixture was stirred for 12 h, after which time gas chromatography showed essentially complete conversion of methacrylic acid into α-phenylisobutyric acid. The acid was recrystallized from benzene and gave a m.p. = 78–79°; i.r. band at 1700 cm^{-1} (carbonyl); n.m.r. bands at 8.45 (singlet), 2.68 (multiplet), and −2.50 τ (singlet) in the ratio 6:5:1 and assigned to the $(CH_3)_2C$ group, aromatic protons, and —COOH protons respectively.

(2) α-p-Tolylisobutyric Acid

α-*p*-Tolylisobutyric acid was prepared from α-*p*-tolylisobutyronitrile by the procedure of Lambert *et al.* (15). The acid, m.p. 82–84° (lit. (15) 82°), showed n.m.r. bands at 8.44 (singlet), 7.70 (singlet), 2.80 (symmetrical quartet), and −2.15 τ (singlet) in the ratio 6:3:4:1, assigned to the $(CH_3)_2C$ group, aryl-CH_3, aromatic protons, and —COOH proton respectively.

(3) 2-Ethyl-2-phenylbutanoic Acid

2-Ethyl-2-phenylbutyronitrile (Aldrich) was converted into 2-methyl-2-phenylbutyramide by the procedure of Sperber *et al.* (16). 2-Ethyl-2-phenylbutyramide (19.5 g, 0.012 mole) was dissolved in 140 ml of dioxane and anhydrous hydrogen chloride was passed into the solution for 15 min. Butylnitrite (23 g, 0.223 mole) was added to the solution over 30 min. The reaction mixture was stirred for 2 h and heated on a steam cone for 3 h. The solvent was distilled under reduced pressure and the residue partitioned between ether and 10% potassium hydroxide. The alkaline layer was acidified and the precipitated acid extracted with ether. Distillation of the ether yielded the crystalline acid (13.9 g, 71%). Recrystallization from petroleum ether gave colorless crystals, m.p. 91–93° (lit. (17) m.p. 95°); i.r. band at 1700 cm^{-1} (carbonyl); n.m.r. bands at 9.26 (triplet), 7.96 (quartet), 2.77 (multiplet), and −1.20 τ (singlet) in the ratio 6:4:5:1 assigned to the 2 × CH_3, 2 × CH_2, aromatic protons, and COOH group respectively.

(4) α-1-Naphthylpropionic Acid and α-1-Naphthylisobutyric Acid

α-1-Naphthylpropionic acid and α-1-naphthylisobutyric acid were synthesized by a modification of the Birch procedure (18). Liquid ammonia (200 ml) was condensed in a thermos and ferric nitrate (0.05 g) and a piece of potassium (0.2 g) were added. The mixture was stirred until the blue color disappeared. The remainder of the potassium (3.8 g, 0.095 mole) was added in small pieces and the mixture allowed to stand again. 1-Naphthaleneacetic acid (Aldrich) (2.5 g, 0.013 mole) was added. The deep red solution was titrated to the disappearance of the red color with methyl iodide (14.0 g, 0.099 mole). Water (50 ml) was cautiously added to the reaction mixture which was then poured into a large beaker to allow the ammonia to evaporate. The residue was acidified with 50% hydrochloric acid and partitioned between ether and 10% sodium hydroxide. The alkaline layer was acidified and there was obtained 2.44 g (91%) of crystalline α-1-naphthylpropionic acid. After recrystallization from petroleum ether and sublimation, it melted at 149–149.5° (lit. (19) m.p. 148–149°); i.r. band at 1690 cm^{-1} (carbonyl); u.v. peaks at λ_{max} 292 (ε = 5340), 281.5 (ε = 7940), 271 (ε = 6590), 262 mμ (shoulder) (ε = 4030); n.m.r. bands ($CHCl_2CHCl_2$) at 8.41 (doublet), 5.04 (quartet) and 2.53 τ (multiplet) in the ratio 3:1:7 assigned to CH_3—C(α), (α)C—H, and aromatic protons respectively.

The α-1-naphthylpropionic acid described above was treated with potassium in liquid ammonia and methylated with methyl iodide again as described above. There was obtained in 81% yield α-1-naphthylisobutyric acid, m.p. 121.5–123.5° (lit. (18) m.p. 120–121°); i.r. band at 1690 cm^{-1} (carbonyl); u.v. peaks at λ_{max} 291.5 (ε = 6840), 288 (ε = 6700). 280.5 (ε = 11 700), 270.5 (ε = 8600), and 261 mμ (ε = 6920); n.m.r. bands ($CHCl_2$-$CHCl_2$) at 8.22 (singlet), 2.30 (multiplet), and −1.47 τ (singlet) the ratio 6:7:1 assigned to $(CH_3)_2C$, aromatic protons, and COOH group respectively.

In subsequent syntheses it was convenient to make three treatments of naphthaleneacetic acid with potassium and methyl iodide to prepare α-1-naphthylisobutyric acid directly.

Preparations of α,α-Dialkylarylacetyl Chlorides

The α,α-dialkylarylacetic acids were converted into the corresponding acyl chlorides by treatment with thionyl chloride. In each case the acid was added to an excess of thionyl chloride. After the initial vigorous reaction, the mixture was refluxed until i.r. analysis showed that the —COOH carbonyl was completely converted into —COCl carbonyl. The acyl chlorides were distilled *in vacuo* as outlined in Table 4.

Can. J. Chem. Downloaded from www.nrcresearchpress.com by 210.87.254.5 on 09/05/12
For personal use only.

TABLE 4

Boiling points and i.r. data for acyl chlorides

Compound	Boiling point (°C/mm)	Infrared (—CO—Cl) (cm^{-1})
α-Phenylisobutanoyl chloride	83/3	1760
α-*p*-Tolylisobutanoyl chloride	141/24	1790
2-Ethyl-2-phenylbutanoyl chloride	115–120/2	1790
α-1-Naphthylisobutanoyl chloride	Melting point 56–58	1750
		1775
		1800

Reactions of α,α-Dialkylarylacetyl Chlorides with Alkenes

The following general procedure was used in the reactions of α,α-dialkylarylacetyl chlorides with alkenes. A three-necked flask equipped with a magnetic stirrer, thermometer, and porous glass gas inlet tube was charged with the acyl chloride and carbon disulfide solvent. The mixture was cooled just below −10° in an acetone – Dry Ice bath and the anhydrous stannic chloride catalyst added. When isobutylene was the alkene used, it was condensed in a pre-calibrated cold trap and a measured amount slowly passed into the stirred reaction mixture through the gas inlet tube. Liquid alkenes were added dropwise from a dropping funnel. The progress of the reaction was followed by removing aliquots periodically and determining the i.r. absorption in the carbonyl region. The reaction was terminated when the acyl chloride carbonyl absorption in the 1760–1800 cm^{-1} region was replaced by carbonyl absorption in the 1675–1700 cm^{-1} region. The reaction mixture was then added to ice-water. The mixture was extracted with ethyl ether and the extract washed with 10% sodium hydroxide, then with water, and dried with anhydrous sodium sulfate. The solvent was distilled, the residue dissolved in petroleum ether (b.p. 30–60°) and chromatographed on alumina. The latter procedure proved a convenient method to separate small amounts of hydrocarbon by-products such as diisobutylene which collected in the first fractions on elution with benzene. The major fraction containing the ketonic components was collected and analyzed by g.l.c. The results are given in Table 1. Spectral and analytical data on the new ketones are outlined in Tables 2 and 3.

In runs nos. *4* and *8* the intermediate unsaturated ketones were formed. These were not unequivocally identified because they were mixtures containing cyclization products (tetralones). In run *4* the initial product showed carbonyl absorption at 1675 cm^{-1} (conjugated) as well as a band at 1715 cm^{-1}. The product from run *8* was almost entirely the unsaturated ketone according to spectral evidence. The i.r. spectrum showed bands at 1675 and 1630 cm^{-1} attributed to the α,β-unsaturated carbonyl chromophore. The n.m.r. spectrum had bands at 8.44–8.41 (singlets), 7.88 (singlet), 4.46 (multiplet), and 2.55 τ (multiplet, in the ratio 9:3:1:7 assigned to $(CH_3)_2\underset{5}{C}\!\!<$ plus $CH_3-\underset{2}{\overset{|}{C}}=$, $-\underset{2}{\overset{CH_3}{\overset{|}{C}}}=$, olefinic proton, and aromatic protons respectively.

The unsaturated ketones of runs *4* and *8* were cyclized to the corresponding tetralones with boron fluoride-etherate. The boron fluoride-etherate was either used directly or dissolved in methylene chloride. The ketone was added to the solution and the mixture stirred at room temperature until aliquots showed that the carbonyl absorption in the i.r. changed to a single strong band near 1700 cm^{-1}. Then the reaction mixture was poured into ice-water, made basic with ammonium hydroxide, and extracted with ether. The ether was distilled and the residue dissolved in petroleum ether and chromatographed on alumina by elution with benzene. An attempt was made to use polyphosphoric acid in the cyclization step (run *8*). The reaction mixture was worked up as before. However, the only identifiable product from the reaction was a rearrangement product. This was tentatively characterized to be 1-acetyl-1,3,3-trimethylbenz(*e*)-indane from the n.m.r. spectrum (Table 2, no. *6*) and elemental analysis (Table 3).

As noted in the Discussion and Table 1, no. *9*, attempts to use diphenylethylene in the reaction resulted in side reactions producing hydrocarbons. The 1,1,3-triphenyl-3-methylindane gave a m.p. of 143° (lit. (6) m.p. 143°).

Mol. Wt. Calcd: 360. Found (mass spectrum): 360.

The 1,1,3-trimethyl-3-phenylindane was identified by comparing its u.v. and i.r. spectra with those of an authentic sample prepared earlier (20).

Preparation of Bromo Derivatives of Polyalkyltetralones

The monobromoderivatives were prepared by treating a solution of the polyalkyltetralone in carbon tetrachloride at room temperature with an equimolar amount of bromine in carbon tetrachloride. The progress of the reactions were followed by direct n.m.r. measurements. The methylene absorption adjacent to the carbonyl group (near 7.4 τ) was replaced by methine absorption further downfield (5.5 to 5.2 τ). The dibromoderivatives were prepared in a similar manner using 2.5 moles of bromine per mole of ketone. In each case the carbon tetrachloride was distilled and the residue recrystallized from petroleum ether. The yields were 90% or better. The n.m.r. spectra of the mono- and dibromo compounds are summarized in Table 2 (nos. *8* to *12*). Analytical data are given in Table 3.

1,1,4,4-Tetramethyl-1,4-dihydronaphthalene

1,1,4,4-Tetramethyl-2-tetralone was reduced by lithium aluminum hydride to yield 1,1,4,4-tetramethyl-2-tetralol, m.p. 85–87.5° (lit. (3) m.p. 86–87°).

The above 1,1,4,4-tetramethyl-2-tetralol (2.0 g, 0.01

Can. J. Chem. Downloaded from www.nrcresearchpress.com by 210.87.254.5 on 09/05/12
For personal use only.

mole) and freshly distilled *N,N*-dimethylaniline (2.4 g, 0.02 mole) were dissolved in anhydrous ethyl ether. Freshly distilled acetyl chloride (1.5 g, 0.02 mole) was added and the mixture was heated under reflux for 6 h. Water was added and the ether layer was washed with dilute hydrochloric acid, dilute sodium bicarbonate, and dried over anhydrous sodium sulfate. The ether was distilled and the residue recrystallized from petroleum ether to give colorless crystals of 1,1,4,4-tetramethyl-2-acetoxytetralin in 71% yield, m.p. 65–66°; i.r. bands at 1700 (carbonyl), 1240 cm^{-1} (acetoxy).

Anal. Calcd. for $C_{16}H_{22}O_2$: C, 78.05; H, 8.94. Found: C, 77.58, 77.56; H, 9.12, 9.04.

The above acetate was distilled in a nitrogen atmosphere at 300° without decomposition. The acetate was decomposed by heating in a thick-walled Carius tube at 345–350° for 3.5 h. The reaction product was dissolved in ether, washed with aqueous sodium carbonate, water, and dried over anhydrous sodium sulfate. The ether was distilled and the liquid product showed one component by vapor phase chromatography (v.p.c.); $n_D^{25} = 1.5207$; i.r. lacked carbonyl; n.m.r. bands at 9.06 (singlet), 4.97 (singlet) and 3.17 τ (A_2B_2 symmetrical multiplet) in the ratio 12:2:4 assigned to the four CH_3's, the —CH=CH group, and the four aromatic hydrogens respectively.

Mol. Wt. Calcd. for $C_{14}H_{18}$: 186. Found (mass spectrum): 186.

2-Ethyl-2-o-(1-methyl-1-carboxyethyl)-phenylbutanoic Acid

1,1-Diethyl-4,4-dimethyl-2-tetralone (*7d*) (1.0 g, 0.004 mole) and selenium dioxide (0.56 g, 0.005 mole) were dissolved in 10 ml of dioxane and the mixture was heated under reflux for 28 h. The dioxane was distilled under reduced pressure and the residue recrystallized from petroleum ether to give a 93% yield of yellow crystals of 2,3-dioxo-1,1-diethyl-4,4-dimethyltetralin, m.p. 57–58°; i.r. band at 1720 cm^{-1} (carbonyl); n.m.r. bands at 9.31 (triplet), 8.56 (singlet), 7.95 (quartet) and 2.70 τ (multiplet) in the ratio 6:6:4:4 and assigned to the two CH_3's of the C_2H_5 groups, the $(CH_3)_2C$ group, the two —CH_2's of the C_2H_5 groups, and the aromatic protons respectively.

Anal. Calcd. for $C_{16}H_{20}O_2$: C, 78.75; H, 8.27. Found: C, 78.33; H, 8.27.

2,3-Dioxo-1,1-diethyl-4,4-dimethyltetralin (2.3 g, 0.009 mole) and periodic acid (2.95 g, 0.013 mole) were dissolved in a mixture of 22 ml of dioxane and 15 ml of water. The reaction mixture was heated in a constant temperature oil bath at 62 ± 0.5° for 42 h. The solvent was distilled under reduced pressure and the residue partitioned between ether and dilute sodium hydroxide.

The above sodium hydroxide extract was acidified with concentrated hydrochloric acid and the precipitate taken up into ethyl ether. Distillation of the ether yielded 0.86 g (33%) of solid. Two recrystallizations from ethyl acetate gave colorless crystals, m.p. 161.5–163°; i.r. band at 1690 cm^{-1} (carbonyl); u.v. band 262 mμ (ε = 318); n.m.r. bands ($CDCl_3$) at 9.27 (triplet), 8.32 (singlet), 7.91 (quartet), 2.26 (multiplet), and −1.23 τ (singlet) in the ratio 6:6:4:4:2 and assigned to the two CH_3's of the C_2H_5 groups, the $(CH_3)_2C$ group, the two —CH_2—'s of the C_2H_5 groups, the aromatic protons, and the two COOH protons respectively.

Anal. Calcd. for $C_{16}H_{22}O_4$: C, 68.98; H, 7.98. Found: C, 68.81, 68.63; H, 8.02, 8.08.

The neutral ether soluble fraction above (1.15 g) showed three components by gas chromatography analysis. An attempt was made to identify the major component which was collected from the chromatography for analysis. It showed i.r. band at 1720 cm^{-1} (carbonyl); u.v. bands at 270 (ε = 318), 263 mμ (ε = 355); n.m.r. bands at 9.37 (triplet), 8.46 (doublet), 7.97 (quartet), and 2.75 τ (multiplet) in the ratio 6:6:4:4 attributed to the two CH_3's of the C_2H_5 groups, the $(CH_3)_2C$ group, the two —CH_2—'s of the C_2H_5 groups, and the aromatic protons respectively.

Photolysis of 2,3-Dioxo-1,1,4,4-tetramethyltetralin

The photochemical experiments were carried out in a Rayonet Photochemical Reactor using RPR-3500 Å lamps which supply approximately 24 W of irradiation, about 90% of which is in the 3500 Å region. The reaction vessel was pyrex and a cooling fan maintained a temperature of approximately 35°.

(1) In the Presence of Oxygen

2,3-Dioxo-1,1,4,4-tetramethyltetralin (1) (1.00 g, 0.0046 mole) was dissolved in 17 ml of benzene. The system was evacuated, filled with oxygen, and irradiated for 97 h. The solvent was distilled under reduced pressure. Gas chromatography of the residue showed three components *A*, 21, *B*, 48, and *C*, 30% which were collected from the chromatograph for analyses. Component *A* was found to be 1,1,3,3-tetramethylindanone. It was a colorless solid, m.p. 75–77° (lit. (21) m.p. 75–76.5°); i.r. band at 1745 cm^{-1} (carbonyl); u.v. bands at 272.7 (ε = 1194), 265.8 (ε = 1363), 259.6 (ε = 699), and 254 mμ (ε = 391); n.m.r. bands at 8.71 (singlet) and 2.80 τ (singlet) in the ratio 12:4 assigned to the two $(CH_3)_2C$ groups and the aromatic protons respectively.

Component *B* was identified as 3-hydroxyl-1,1,4,4-tetramethyl-2-tetralone, m.p. 41–43° (lit. (13) m.p. = 40–42°); i.r. bands at 1715 (carbonyl) and 3500 cm^{-1} (hydroxyl); n.m.r. bands at 9.11 (singlet), 8.58, 8.52, 8.47 (singlets), 6.36 (singlet), 5.70 (singlet), and 2.80 τ (multiplet) in the ratio 3:9(3 singlets):1:1:4. The four bands between 9.11–8.47 τ were attributed to the four methyls. The three bands at 6.36, 5.70, and 2.80 were assigned to hydroxyl, methine, and aromatic hydrogens respectively.

Component *C*, a colorless solid, had a melting point of 96–98° and was identified as *o*-phenylenediisobutyric anhydride (1) by mixed melting point and i.r. spectrum.

(2) In a Nitrogen Atmosphere

A sample of 2,3-dioxo-1,1,4,4-tetramethyltetralin was dissolved in benzene as above. The system was alternately evacuated and flushed with purified nitrogen five times. It was then filled with nitrogen and irradiated as before for 97 h. The solvent was distilled under reduced pressure. Gas chromatographic analysis on the product showed component *A* (1,1,3,3-tetramethyltetralone), 14%, component *B* (3-hydroxy-1,1,4,4-tetramethyl-2-tetralone), 81%, and component *C* (*o*-phenylenediisobutyric anhydride), 4%.

The financial support of this research provided by the National Research Council of Canada is gratefully acknowledged.

1. L. R. C. BARCLAY, C. E. MILLIGAN, and N. D. HALL. Can. J. Chem. **40**, 1664 (1962).
2. L. R. C. BARCLAY, G. R. NIXON, H. M. FOOTE, and S. L. BARCLAY. Can. J. Chem. **47**, 4313 (1969).
3. H. A. BRUSON, F. W. GRANT, and E. BOBKO. J. Amer. Chem. Soc. **80**, 3633 (1958).
4. L. R. C. BARCLAY, K. L. ADAMS, R. H. YOUNG, and H. M. FOOTE. In preparation.
5. C. D. NENITZESCU and A. T. BALABAN. Friedel–Crafts and related reactions. Vol. III. *Editor* G. A. Olah, Interscience Publishers, Inc., New York, 1964. p. 1033.
6. E. BERGMANN and H. WEISS. Ann. **480**, 49 (1930).
7. L. R. C. BARCLAY. Friedel–Crafts and related reactions. Vol. II. *Editor* G. A. Olah, Interscience Publishers, Inc., New York, 1964. p. 946.
8. R. N. JONES, D. A. RAMSAY, F. HERLING, and K. DOBRINER. J. Amer. Chem. Soc. **74**, 2828 (1952).
9. E. M. ARNETT. J. Org. Chem. **25**, 324 (1960).
10. E. M. ARNETT, J. C. SANDA, J. M. BOLLINGER, and M. BARBER. J. Amer. Chem. Soc. **89**, 5389 (1967).
11. J. MEINWALD and H. O. KLINGELE. J. Amer. Chem. Soc. **88**, 2071 (1966).
12. J. RIGAUDY and N. PAILLOUS. Tetrahedron Lett. No. 40, 4825 (1966).
13. G. E. GREAM, J. C. PAICE, and C. C. R. RAMSAY. Aust. J. Chem. **20**, 1671 (1967).
14. B. PRIJS. Helv. Chim. Acta, **35**, 780 (1952).
15. A. LAMBERT, J. D. ROSE, and B. C. L. WEEDON. J. Chem. Soc. **42** (1949).
16. N. SPERBER, D. PAPA, and E. SCHWENK. J. Amer. Chem. Soc. **70**, 3091 (1948).
17. H. CHRISTOL, A. LAURENT, and M. MOUSSERON. Bull. Soc. Chim. France, 2319 (1961).
18. A. J. BIRCH. J. Chem. Soc. 1551 (1950).
19. F. F. BLICKE and R. F. FELDKAMP. J. Amer. Chem. Soc. **66**, 1087 (1944).
20. L. R. C. BARCLAY and R. A. CHAPMAN. Can. J. Chem. **42**, 25 (1964).
21. J. E. STARR and R. H. EASTMAN. J. Org. Chem. **31**, 1393 (1966).

Can. J. Chem. Downloaded from www.nrcresearchpress.com by 210.87.254.5 on 09/05/12
For personal use only.

Can. J. Chem. Downloaded from www.nrcresearchpress.com by 210.87.254.40 on 09/05/12
For personal use only.

Kinetic study of addition of nitrogen and phosphorus donors bis(maleonitriledithiolate)cobalt(III)[1]

HON GEE TSIANG AND C. H. LANGFORD[2]
Department of Chemistry, Carleton University, Ottawa 1, Canada

Received[3] October 9, 1969

Kinetics of adduct formation of the dimeric form of bis(maleonitriledithiolate)cobalt(III) with pyridine, triphenylphosphine, triphenylarsine, and 1,10-phenanthroline are reported. Rates are first order in ligand and half order in complex dimer in acetone. This suggests addition of the fifth ligand to an uncoordinated axial position of the square planar species as rate controlling. A (presumably) five coordinate intermediate can be detected kinetically on the way to six coordination in the reaction with 1,10-phenanthrioline and its rearrangement to an octahedral six coordinate chelate is slow. All these results may be interpreted in terms of the significant delocalized π bonding in the square planar dithiolene complexes.

Canadian Journal of Chemistry, **48**, 2776 (1970)

Introduction

The recent literature is full of accounts of syntheses, physical properties, and electronic structure of square planar metal complexes containing sulfur donor ligands in which the sulfur atoms are part of unsaturated organic systems (1). However, kinetic and mechanistic aspects have received little attention. It has been reported that $Co(MNT)_2^-$ ($MNT = C_4N_2S_2^{2-}$ or maleonitriledithiolate) forms adducts with ligands such as pyridine, triphenylphosphine, and triphenylarsine which are five coordinate and adducts with ligands such as 1,10-phenanthroline which are six coordinate (2). This note reports the kinetics of such adduct formation and discusses the mechanism. It should be noted here that the studies were carried out in the essentially non-coordinating solvent acetone where the species $Co(MNT)_2^-$ has been shown to be dimeric (1).

Experimental

The rates were measured using a Durrum–Gibson stopped flow spectrometer. Equilibrium quotients were evaluated spectrophotometrically using a Cary 14 instrument. The complex $Bu_4NCo(MNT)_2$ was prepared after the recipe in ref. 3. Other chemicals were of reagent grade and were used without additional purification.

Results and Discussion

The dimer-to-adduct reactions were followed from small spectral changes which correspond to "relaxation conditions" and are effectively linearized. Therefore, the order of reaction with respect to complex could not be determined from these experiments at fixed metal complex concentration. Table 1 collects, therefore, reaction half times as a function of ligand concentration when ligand is in excess. The rate constants in Table 2 where initial complex concentration was varied show that the reaction is in fact *half order* with respect to complex.

The rate law may be written as shown in eq. [1]

$$[1] \quad d[Co(MNT)_2L]/dt = k_s[(Co(MNT)_2)_2^{2-}]^{\frac{1}{2}}[L]$$

where k_s is the specific rate constant in $M^{-\frac{1}{2}}\,s^{-1}$. This is consistent with the mechanism shown in eq. [2].

$$[2] \quad (Co(MNT)_2)_2^{2-} \overset{k_d}{\rightleftharpoons} 2Co(MNT)_2^- \quad \text{(fast, equilibrium)}$$

$$Co(MNT)_2^- \overset{k}{\rightarrow} Co(MNT)_2L^- \quad \text{(slow)}$$

At fixed excess ligand concentration, the pseudo half order rate constants calculable from the half times in Table 1 are equal to $k_d^{\frac{1}{2}}k[L]$. The specific rate constants are these values divided by the ligand concentrations.

The reaction with *o*-phenanthroline is unique. In addition to the fast reaction described in Table 1, there was a slower process observable in the

[1]We thank the National Research Council of Canada for financial support
[2]Alfred P. Sloan Foundation Research Fellow, 1968–1970. Author to whom correspondence should be addressed.
[3]Revision received May 19, 1970.

TABLE 1

Half times for the formation of various adducts of $Co(MNT)_2^-$ at 25° in acetone solvent*

Ligands (L)	Wavelength (mμ)	Concentration (M)	$t_{\frac{1}{2}}$ (s)
Triphenylphosphine	382	0.0081	0.104
		0.023	0.045
		0.033	0.030
		0.0507	0.025
		0.087	0.015
		0.118	0.010
Pyridine	375	0.02	17
		0.10	3.3
		0.15	1.9
		0.25	1.5
Triphenylarsine	360	0.0137	78
		0.077	17
		0.134	9.0
		0.229	5.3
o-Phenanthroline†	440	0.0077	0.182
		0.0153	0.103
		0.0202	0.062
		0.0306	0.048

*Concentration of $Co(MNT)_2^- = 0.206\ M$.

†There are two resolvable steps in the stopped flow records for this reaction. The faster one is assumed to refer to the formation of a five-coordinate species which precedes formation of the final octahedral complex. Data on the fast process appear here for comparison with systems going only to five coordinate species. Data on the slower process appear in Fig. 1.

TABLE 2

Specific rate constants of the adduct formation of $Co(MNT)_2^-$ at 25 °C in acetone solvent

$[Co(MNT)_2]_2^-$ ($M \times 10^4$)	[Pyridine] ($M \times 10^4$)	Specific rate constants ($M^{-1/2}\ s^{-1} \times 10^2$)
1.1	2.5	1.09
1.1	5.0	1.05
2.5	5.0	0.98

stopped flow traces. The final product corresponds to the $(Co(MNT)_2$*o*-phen$)^-$ six coordinate species shown to be octahedral by crystallography (4). We suggest that the slow step be assigned to conversion of a square pyramidal five coordinate intermediate (analogous to the adducts formed with $(C_6H_5)_3P$, $(C_6H_5)_3As$, and pyridine) into the octahedral species. At high concentration of *o*-phenanthroline, the formation of the five coordinate species becomes fast and a limiting process is observed in which formation of the six coordination species becomes observably first order, since it is no more than isomerization of the five coordinate complex to the six coordinate one of the same stoichiometry. Pseduo first order rate constants (calculated from the slow step in the traces) are plotted as a function of the (excess) *o*-phenanthroline concentration in Fig. 1. The expected limiting behavior is clear.

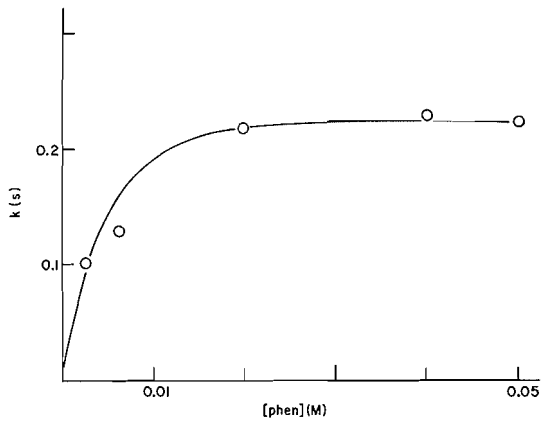

FIG. 1. The rate constant (pseudo first order) for adduct formation with k in s^{-1} as a function of the molar concentration of phen. $T = 25°$. These data apply to the slower process described in the text.

A remark is warranted by the relationship between rate and equilibrium constants for five coordinate adduct formation collected in Table 3. As the attacking ligand is varied, the formation rate parallels the formation constant. This suggests that the transition state is similar to

Can. J. Chem. Downloaded from www.nrcresearchpress.com by 210.87.254.40 on 09/05/12
For personal use only.

product with respect to the role of the attacking ligand. This is a little surprising since the ligand is attacking an "uncoordinated" position. The only obvious explanation for strong product like binding in the transition state is that the transition state lies well along the reaction coordinate because the square planar four coordinate complex is resistant to alteration. Such resistance is consistent with the often suggested (1) π delocalization over the planar metal ligand system.

TABLE 3

Specific rate constants and equilibrium quotients of adduct formation

Ligand	Equilibrium quotient	Specific rate constant ($M^{-1/2}$ s^{-1} $\times 10^3$)
Triphenylarsine	6.3×10^2	2.3
Pyridine	3.2×10^3	8.8
Triphenylphosphine	1.25×10^6	2600

1. J. H. McCleverty. Prog. Inorg. Chem. **10**, 49 (1968).
2. C. H. Langford, E. Billig S. I. Shupack, and H. B. Gray. J. Amer. Chem. Soc. **86**, 2958 (1964).
3. A. Davison and R. H. Holm. Inorg. Synth. **10**, 15 (1967).
4. G. P. Khare, C. G. Pierpont, and R. Eisenberg. Chem. Commun. 1692 (1968).

The decomposition of aqueous dithionite III. Stabilization of dithionite by cations

W. J. Lem[1] and M. Wayman

Department of Chemical Engineering and Applied Chemistry, University of Toronto, Toronto

Received February 10, 1970

At the same conditions of pH (3.5 to 5.0), temperature (23 °C), and concentration (1 to 10 $\times$ 10^{-3} M), ZnS_2O_4 is more stable in aqueous solution than $Na_2S_2O_4$, and the rate of decomposition is much less sensitive to $[H^+]$. At pH 4.5 and 5.0, the decomposition of the Zn salt is essentially linear, whereas the $Na_2S_2O_4$ decomposes slowly at first, during an induction period, and then rapidly by an autocatalytic reaction. The rate of decomposition of dilute aqueous $Na_2S_2O_4$ at pH about 4 is slowed greatly by the addition of small quantities of In^{3+}, Cd^{2+}, or Zn^{2+}. The effect of the stabilizing ions is attributed to anti-catalytic action.

Canadian Journal of Chemistry, **48**, 2778 (1970)

Introduction

ZnS_2O_4 is used industrially as a reducing agent or for bleaching, especially by the pulp and paper industry. It is unstable in aqueous solution, especially under acidic conditions, but the kinetics and mechanism of its decomposition have not been investigated. Qualitatively it is known to be more stable than $Na_2S_2O_4$ under similar conditions of pH (1). Following our studies of the kinetics and mechanism of the decomposition of $Na_2S_2O_4$ (2, 3), aqueous ZnS_2O_4 was studied in the same manner. The dependence of its rate of decomposition on pH was determined. Methods of stabilizing dithionite by cations such as Zn^{2+} were tried since, if successful, they could be of commercial significance.

[1]Present address: Imperial Oil Enterprises Ltd., Sarnia, Ontario.

Experiments and Results

(a) Decomposition of ZnS_2O_4

Several concentrations of ZnS_2O_4 from 0.8 to 8.0 $\times$ 10^{-3} M were studied, some at fixed pH values in the same way as aqueous buffered $Na_2S_2O_4$ described in Part 1 (2), and some in unbuffered solution, with pH measurement (3). The continuous polarographic method previously described (4) was used to determine the concentration of ZnS_2O_4 against time continuously; the experimental arrangements are shown in Fig. 2 of ref. 2 and Fig. 1 of ref. 3. The ZnS_2O_4 used was the best commercial grade obtainable, but was only 80% pure, the impurities being mainly the sulfate and sulfite, with about 0.3% of each of thiosulfate and sulfide. Sodium acetate – acetic acid buffers were used, where indicated, to provide constant pH values of 3.5 to 5.0. The work was carried out at 23 °C.

The decomposition of $Na_2S_2O_4$ in aqueous

Can. J. Chem. Downloaded from www.nrcresearchpress.com by 210.87.254.40 on 09/05/12
For personal use only.

product with respect to the role of the attacking ligand. This is a little surprising since the ligand is attacking an "uncoordinated" position. The only obvious explanation for strong product like binding in the transition state is that the transition state lies well along the reaction coordinate because the square planar four coordinate complex is resistant to alteration. Such resistance is consistent with the often suggested (1) π delocalization over the planar metal ligand system.

TABLE 3

Specific rate constants and equilibrium quotients of adduct formation

Ligand	Equilibrium quotient	Specific rate constant ($M^{-1/2}$ s^{-1} $\times 10^3$)
Triphenylarsine	6.3×10^2	2.3
Pyridine	3.2×10^3	8.8
Triphenylphosphine	1.25×10^6	2600

1. J. H. McCleverty. Prog. Inorg. Chem. **10**, 49 (1968).
2. C. H. Langford, E. Billig S. I. Shupack, and H. B. Gray. J. Amer. Chem. Soc. **86**, 2958 (1964).
3. A. Davison and R. H. Holm. Inorg. Synth. **10**, 15 (1967).
4. G. P. Khare, C. G. Pierpont, and R. Eisenberg. Chem. Commun. 1692 (1968).

The decomposition of aqueous dithionite III. Stabilization of dithionite by cations

W. J. Lem[1] and M. Wayman

Department of Chemical Engineering and Applied Chemistry, University of Toronto, Toronto

Received February 10, 1970

At the same conditions of pH (3.5 to 5.0), temperature (23 °C), and concentration (1 to 10 $\times$ 10^{-3} M), ZnS_2O_4 is more stable in aqueous solution than $Na_2S_2O_4$, and the rate of decomposition is much less sensitive to [H^+]. At pH 4.5 and 5.0, the decomposition of the Zn salt is essentially linear, whereas the $Na_2S_2O_4$ decomposes slowly at first, during an induction period, and then rapidly by an autocatalytic reaction. The rate of decomposition of dilute aqueous $Na_2S_2O_4$ at pH about 4 is slowed greatly by the addition of small quantities of In^{3+}, Cd^{2+}, or Zn^{2+}. The effect of the stabilizing ions is attributed to anti-catalytic action.

Canadian Journal of Chemistry, **48**, 2778 (1970)

Introduction

ZnS_2O_4 is used industrially as a reducing agent or for bleaching, especially by the pulp and paper industry. It is unstable in aqueous solution, especially under acidic conditions, but the kinetics and mechanism of its decomposition have not been investigated. Qualitatively it is known to be more stable than $Na_2S_2O_4$ under similar conditions of pH (1). Following our studies of the kinetics and mechanism of the decomposition of $Na_2S_2O_4$ (2, 3), aqueous ZnS_2O_4 was studied in the same manner. The dependence of its rate of decomposition on pH was determined. Methods of stabilizing dithionite by cations such as Zn^{2+} were tried since, if successful, they could be of commercial significance.

[1]Present address: Imperial Oil Enterprises Ltd., Sarnia, Ontario.

Experiments and Results

(a) Decomposition of ZnS_2O_4

Several concentrations of ZnS_2O_4 from 0.8 to 8.0 $\times$ 10^{-3} M were studied, some at fixed pH values in the same way as aqueous buffered $Na_2S_2O_4$ described in Part 1 (2), and some in unbuffered solution, with pH measurement (3). The continuous polarographic method previously described (4) was used to determine the concentration of ZnS_2O_4 against time continuously; the experimental arrangements are shown in Fig. 2 of ref. 2 and Fig. 1 of ref. 3. The ZnS_2O_4 used was the best commercial grade obtainable, but was only 80% pure, the impurities being mainly the sulfate and sulfite, with about 0.3% of each of thiosulfate and sulfide. Sodium acetate – acetic acid buffers were used, where indicated, to provide constant pH values of 3.5 to 5.0. The work was carried out at 23 °C.

The decomposition of $Na_2S_2O_4$ in aqueous

Can. J. Chem. Downloaded from www.nrcresearchpress.com by 210.87.254.105 on 09/05/12
For personal use only.

Can. J. Chem. Downloaded from www.nrcresearchpress.com by 210.87.254.105 on 09/05/12
For personal use only.

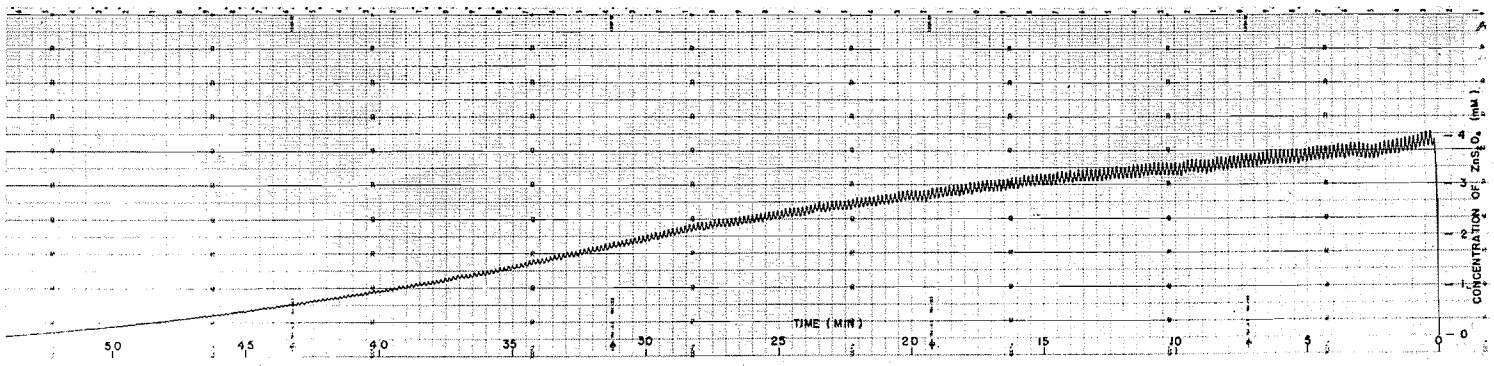

FIG. 1. Decomposition of 4×10^{-3} *M* ZnS_2O_4 at p*H* 4.0.

Can. J. Chem. Downloaded from www.nrcresearchpress.com by 210.87.254.105 on 09/05/12
For personal use only.

solution in this range of pH is characterized by a slow "induction" period followed by a much more rapid autocatalytic reaction. The decomposition of ZnS_2O_4 in the same pH region does not follow the same course. Figure 1 shows the decomposition of 4×10^{-3} M ZnS_2O_4 at pH 4.0. It is seen that there is a gradual increase in the rate of decomposition, but the division into an induction period and an autocatalytic period is by no means obvious. This figure may be compared with Fig. 5 of ref. 2 showing the decomposition of 5×10^{-3} M $Na_2S_2O_4$ at pH 4.0. In the case of the sodium salt the curve is sharply S-shaped: an induction period of about 10 min is followed by a sharp decrease in concentration, decomposition is half complete at 14 min and essentially complete at 17 min. The initial rate of decomposition of the zinc salt is in fact somewhat more rapid, but the change in slope is less sharp, although there appears to be a distinct change at about 25 min, and decomposition, which is half complete at 30 min, is essentially complete at 60 min. At higher pH the rate of decomposition is slower and nearly linear; decomposition is half complete at 40 min at pH 4.5 and at 60 min at pH 5.0. The rates of decomposition in terms of the slopes of the concentration–time curves initially, S_0, and when half the dithionite is decomposed, $S_{\frac{1}{2}}$, are compared for these two salts in Table 1.

While the data are not strictly comparable since they are affected by initial concentration, it is evident that there is a large difference in behavior between the two salts. The rate of decomposition $S_{\frac{1}{2}}$ is the same as S_0 for the zinc salt at the two higher pH's, decomposition being linear through nearly all of its course, and at the two lower pH's $S_{\frac{1}{2}}$ is about twice S_0, whereas for the sodium salt $S_{\frac{1}{2}}$ is about 10 to 20 times S_0.

TABLE 1

Decomposition of aqueous zinc and sodium dithionites at constant pH*

	ZnS_2O_4 4×10^{-3} M		$Na_2S_2O_4$ 5×10^{-3} M	
pH	S_0	$S_{\frac{1}{2}}$	S_0	$S_{\frac{1}{2}}$
3.5	0.97	1.75	1.85	22.17
4.0	0.80	1.67	0.70	13.88
4.5	0.60	0.60	0.28	4.57
5.0	0.45	0.45	0.12	1.17

*S_0 and $S_{\frac{1}{2}}$ in mole l^{-1} s^{-1} $\times 10^6$.

Thus the evidence for the rapid autocatalytic reaction characteristic of aqueous sodium dithionite is absent with the zinc salt in this range of pH. Also S_0 is much less sensitive to pH for aqueous zinc dithionite, being about twice as great at pH 3.5 as at pH 5.0, whereas S_0 for sodium dithionite solutions is about 15 times greater for the same difference in pH. It is also noteworthy that S_0 is smaller for aqueous sodium dithionite than for the zinc salts at pH 4 to 5.

The form of the rate law for the decomposition of $Na_2S_2O_4$ was shown (2) to be as in eq. [1]

$$[1] \qquad -dC/dt = k_1[H^+]^m C^n + k_2[H^+]^p C^q (C_0 - C)^r$$

where C is the concentration of dithionite at time t, in mole l^{-1}; C_0 is the initial concentration of dithionite, in mole l^{-1}; $[H^+]$ is hydrogen ion concentration, in mole l^{-1}; k_1 and k_2 are rate constants, and m, n, p, q, and r are orders of reaction.

The slopes S_0, $S_{\frac{1}{2}}$, and $\Delta S = S_{\frac{1}{2}} - S_0/2$ were measured and their logarithms plotted against log C_0 and log $[H^+]$ to obtain the reaction orders (2), listed in Table 2. The average value of reaction order n was 0.905, which is close to 1, as was the case with $Na_2S_2O_4$. The average value of reaction order m was 0.27, compared to 1 for $Na_2S_2O_4$, reflecting the reduced dependence on acidity of the initial rate of decomposition of aqueous ZnS_2O_4 compared to the sodium salt in this pH range.

In the plots of log ΔS against log $[H^+]$ to obtain reaction order p, the slopes varied greatly from 0.15 to 0.80 at C_0 of 8 to 0.8×10^{-3} M. When log ΔS was plotted against log C_0 to obtain reaction order $(q + r)$, the curves were not linear. The non-linearity and variable slopes were thought to be caused by the impurities in the ZnS_2O_4 used. To test this, very pure (99.999%) Zn^{2+} was added to the purest $Na_2S_2O_4$ obtainable (98%); in equimolar proportions at 1 and 10×10^{-3} M, at pH 4.0 and 4.5. The average value of n was 0.856 (compared to 0.905) and of m was 0.31 (compared to 0.27), both of which may be considered to be in reasonable agreement with the results obtained with aqueous ZnS_2O_4. In the plots of log ΔS against log $[H^+]$, the slopes, reaction order p, varied from 0.03 to 0.380 at C_0 of 10 and

Can. J. Chem. Downloaded from www.nrcresearchpress.com by 210.87.254.105 on 09/05/12
For personal use only.

TABLE 2

Determination of the orders of reaction for the decomposition of aqueous ZnS_2O_4

(*a*) From the plot of log S_0 vs. log C_0

p*H*	Slope, *n*
3.5	0.95
4.0	0.95
4.5	0.87
5.0	0.85

(*b*) From the plot of log S_0 vs. log $[H^+]$

C_0, $M \times 10^3$	Slope, *m*
8	0.30
4	0.25
0.8	0.25

(*c*) From the plot of log ΔS vs. log $[H^+]$

C_0, $M \times 10^3$	Slope, *p*
8	0.15
4	0.50
0.8	0.80

(*d*) From the plot of log ΔS vs. log C_0

p*H*	Slope, $(q + r)$
3.5	0.15
4.0	0.56
4.5	—
5.0	—

1×10^{-3} *M*. It was apparent that the decomposition of aqueous dithionite followed a similar path when Zn^{2+} was added to $Na_2S_2O_4$, or when the solution was made by dissolving ZnS_2O_4.

(b) Stabilization of Dithionite Solutions

The stabilization effect of various cations on dithionite solutions was studied. Preliminary studies (5) showed that certain cations, Pb^{2+}, Co^{2+}, Bi^{3+}, Sb^{3+}, Al^{3+}, reacted with dithionite to form sulfides or other products which rendered them unsuitable as stabilizers, while a few others were effective in stabilizing aqueous $Na_2S_2O_4$. This last group consisted of In^{3+}, Cd^{2+}, and Zn^{2+}. Their effect on the rate of decomposition was studied extensively both at constant p*H* and in unbuffered solution. The same methods, polarographic concentration vs. time, were employed. Concentrations of $Na_2S_2O_4$ were 1, 5, and 10×10^{-3} *M*, added cations were at 0.01, 0.1, 1.0, and 10×10^{-3} *M* and p*H*, when controlled, was at 4.0 or 4.5. Only very pure cations were used.

Figures 2 and 3 show the decomposition of 5×10^{-3} *M* $Na_2S_2O_4$ in unbuffered solution with 0.01 and 0.1×10^{-3} *M* Zn^{2+}, the figures showing the concentration of dithionite against time and the changes in p*H*. As the Zn^{2+} concentration was raised from 0.01×10^{-3} to 0.1×10^{-3} *M*, the initial rates of decomposition S_0 decreased from 1.28×10^{-6} to 0.56×10^{-6} mole l^{-1} s^{-1}, and $S_{\frac{1}{2}}$ from 6.95×10^{-6} to 3.29×10^{-6} mole l^{-1} s^{-1}, the induction period of about 7 min was increased to about 20 min, and the time for $\frac{1}{2}$ decomposition increased from 12 to 32 min. These are rather large effects considering that the higher Zn^{2+} concentration is only 2% of the dithionite concentration.

The p*H* changes were similar to those reported previously for $Na_2S_2O_4$ (3), that is, the p*H* initially about 4.5 in these experiments fell during the induction period, rose during the period of rapid decomposition, and then fell again during the last part of the decomposition. The p*H* changes of $\pm$ 1 unit must be considered very large in terms of production and consumption of H^+ since these are very dilute dithionite solutions.

The data obtained in buffered solutions at p*H* 4.0 and 4.5 are summarized in Table 3, where S_0 and $S_{\frac{1}{2}}$ are shown for 3 concentrations of added cation, Zn^{2+}, In^{3+} or Cd^{2+}, at 3 concentrations of dithionite. When these cations were added the decomposition pattern was in most cases altered in favor of stabilizing the $Na_2S_2O_4$. The concentration limits for stabilization were wider at p*H* 4.5 than at p*H* 4.0. The pattern of decomposition at p*H* 4.5 was as follows:

(*i*) In 10×10^{-3} *M* $Na_2S_2O_4$, In^{3+}, Cd^{2+}, or Zn^{2+} at 10×10^{-3} *M* or 1×10^{-3} *M* gave linear or nearly linear decomposition curves, $S_{\frac{1}{2}}/S_0$ being 1 to 3 instead of about 20 in pure $Na_2S_2O_4$ solution. At 0.1×10^{-3} *M*, the added cations had very little stabilizing effect.

(*ii*) In 5×10^{-3} *M* $Na_2S_2O_4$, the three ions had a considerable stabilizing effect, although the lowest concentration of Cd^{2+} appears to be anomalous.

(*iii*) The rate of decomposition of 1×10^{-3} *M* $Na_2S_2O_4$ is quite low, and the effects of the added cations were very small.

The stabilizing effects of the three cations at

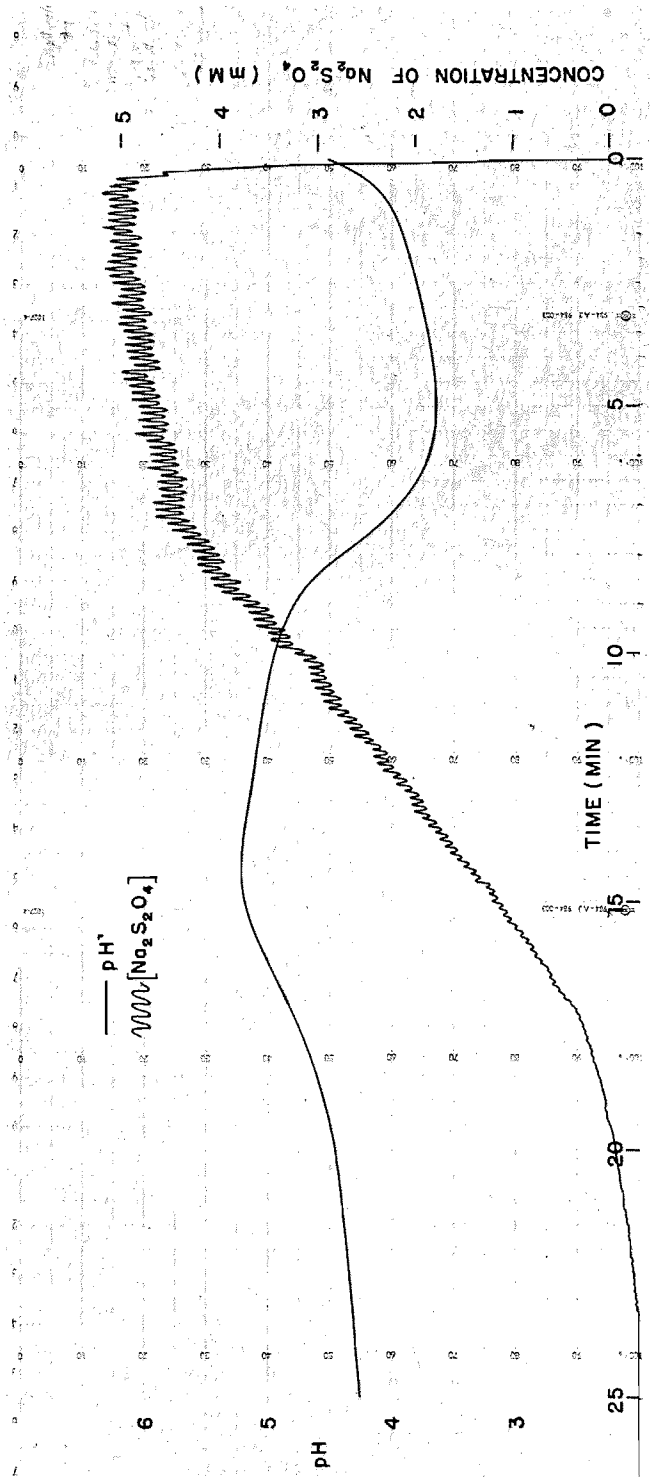

FIG. 2. Decomposition of 5×10^{-3} *M* $Na_2S_2O_4$ + 0.01×10^{-3} *M* Zn^{2+}.

Can. J. Chem. Downloaded from www.nrcresearchpress.com by 210.87.254.105 on 09/05/12
For personal use only.

Can. J. Chem. Downloaded from www.nrcresearchpress.com by 210.87.254.105 on 09/05/12
For personal use only.

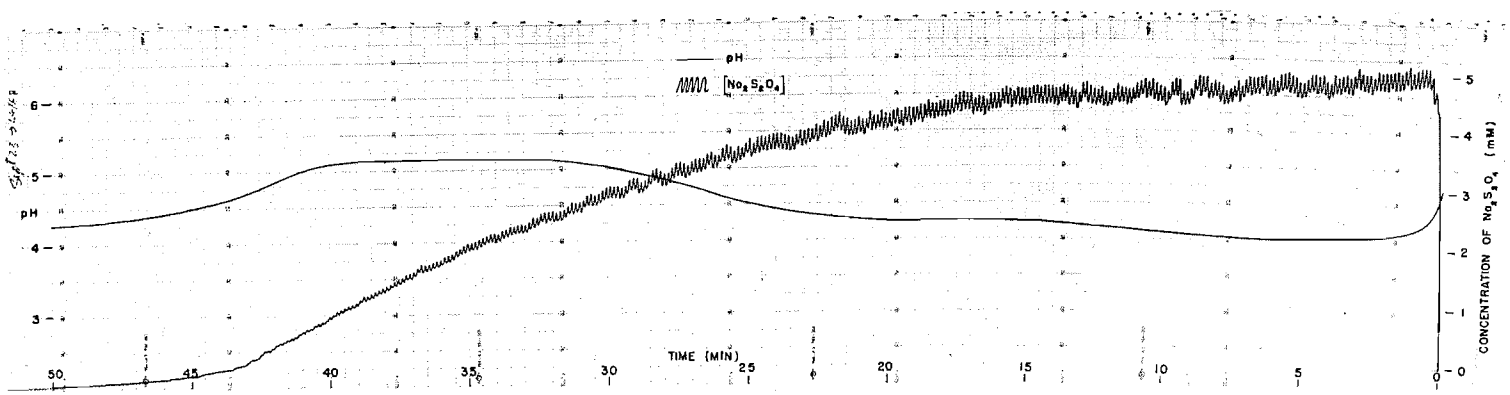

FIG. 3. Decomposition of 5×10^{-3} *M* $Na_2S_2O_4$ + 0.1×10^{-3} *M* Zn^{2+}.

TABLE 3

Rates of decomposition of aqueous $Na_2S_2O_4$ with added cations*

$[Na_2S_2O_4]$ $M \times 10^{-3}$	No cation added		Added cation, $M \times 10^{-3}$	In^{3+}		Cd^{2+}		Zn^{2+}	
	S_0	$S_{\frac{1}{2}}$		S_0	$S_{\frac{1}{2}}$	S_0	$S_{\frac{1}{2}}$	S_0	$S_{\frac{1}{2}}$
$pH = 4.0$									
10	2.44	36.6	10	0.99	0.99	1.17	1.93	1.72	3.05
			1	1.40	1.40	1.46	3.25	1.97	20.9
			0.1	1.20	37.5	1.02	33.0	1.97	18.7
5	0.70	13.9	10	0.44	0.44	0.99	0.99	0.74	1.33
			1	1.23	1.23	0.63	1.94	0.75	13.3
			0.1	0.87	13.4	0.43	11.0	0.67	11.7
1	0.20	0.81	10	0.073	0.089	0.18	0.18	0.27	0.37
			1	0.13	0.13	0.18	0.18	0.26	0.35
			0.1	0.13	0.28	0.21	0.70	0.18	0.32
$pH = 4.5$									
10	0.87	19.2	10	1.58	1.58	1.09	1.11	1.17	2.68
			1	0.67	2.08	0.96	2.78	0.85	3.00
			0.1	0.52	22.5	0.58	19.5	1.34	14.3
5	0.28	4.6	10	0.43	0.43	0.40	0.90	0.50	1.74
			1	0.47	0.47	0.62	0.89	0.47	2.00
			0.1	0.43	0.83	0.64	8.10	0.60	2.18
1	0.087	0.39	10	0.17	0.17	0.12	0.16	0.18	0.34
			1	0.076	0.19	0.21	0.21	0.12	0.40
			0.1	0.090	0.18	0.10	0.20	0.10	0.41

*S_0 and $S_{\frac{1}{2}}$ in mole l^{-1} $s^{-1} \times 10^6$.

pH 4.0 were similar to those at pH 4.5 except that at 10×10^{-3} M $Na_2S_2O_4$, 1×10^{-3} M Zn^{2+} had little or no stabilizing effect; at 5×10^{-3} M $Na_2S_2O_4$ Zn^{2+} was ineffective at 1×10^{-3} M and all three ions were ineffective at 0.1×10^{-3} M. Thus In^{3+} and Cd^{2+} had a broader range of effective concentrations than Zn^{2+} at pH 4.0.

Discussion

The slow decomposition reaction in the induction period has been described (3) as the hydrolysis of $HS_2O_4^-$

[2] $$S_2O_4^{2-} + H^+ \rightleftharpoons HS_2O_4^-$$

[3] $$HS_2O_4^- + H_2O \rightarrow HSO_2^- + HSO_3^- + H^+$$

The more rapid reaction, represented as

[4] $$HS_2O_4^- + HSO_2^- \rightarrow S_2O_3^{2-} + HSO_3^- + H^+$$

is catalyzed by election acceptors such as sulfide or sulfur which result in free radical formation (3, 6)

[5] $$HS_2O_4^- + HSO_2 \rightarrow S_2O_3^{2-} + HSO_3 + H^+$$

The shapes of the decomposition curves and the data, such as those of Table 3, suggest that the function of the stabilizing cations is anti-catalytic. The sulfides of these three cations have extremely low solubility, and the ions may function by removing the catalytic sulfides from solution.

Conclusions

(1). The rate of decomposition of dilute aqueous ZnS_2O_4 in the pH range 3.5 to 5.0 is slower than that of aqueous $Na_2S_2O_4$ at 23 °C, and is much less sensitive to $[H^+]$. At pH 4.5 and 5.0 the decomposition of the Zn salt is essentially linear, whereas $Na_2S_2O_4$ decomposes slowly at first during an induction period, and then rapidly by an autocatalytic reaction.

(2). The rate of decomposition of dilute aqueous $Na_2S_2O_4$ at pH about 4 is slowed greatly by the addition of small quantities of In^{3+}, Cd^{2+}, or Zn^{2+}.

(3). The effect of the stabilizing ions is attributed to anti-catalytic action.

This work was carried out at the University of Toronto, assisted by grants from the National Research Council of Canada and the Department of University Affairs of the Province of Ontario. One of us (W.J.L.) is grateful for an NRCC Scholarship held during 1967–1969.

1. O. V. INGRUBER and J. KOPANDIS. Pulp and Paper Mag. of Can. **68**, 258 (June, 1967).

Can. J. Chem. Downloaded from www.nrcresearchpress.com by 210.87.254.105 on 09/05/12
For personal use only.

2. W. J. LEM and M. WAYMAN. Can. J. Chem. **48**, 776 (1970).
3. M. WAYMAN and W. J. LEM. Can. J. Chem. **48**, 782 (1970).
4. W. J. LEM and M. WAYMAN. J. Soc. Dyers and Colourists, **83**, 277 (1967).
5. W. J. LEM. Ph.D. Thesis. University of Toronto. 1969; see also O. BRUNCK. Annalen, **327**, 240 (1903) and **327**, 281 (1903); M. WAYMAN, C. B. ANDERSON, W. J. LEM, and W. H. RAPSON. Tappi, **52**, 89 (No. 1 Jan. 1969).
6. R. G. RINKER and S. LYNN. Industrial & Engineering Chemistry Product Research and Development. **8**, 338 (1969).

Spin–lattice relaxation in liquid ethylene chloride

E. BOCK AND G. WOLLNER
Parker Chemistry Laboratory, University of Manitoba, Winnipeg, Manitoba

AND

E. TOMCHUK
Department of Physics, University of Winnipeg, Winnipeg, Manitoba

Received March 24, 1970

The proton spin – lattice relaxation time of ethylene chloride in deuterated ethylene chloride was determined as a function of concentration and temperature over the temperature range 230 to 390 °K. It was found that the activation energy for the total spin–lattice relaxation as well as for the *intra*-molecular contribution to the total spin–lattice relaxation was 2.0 kcal/mole and was nearly equal to the activation energy for viscous flow, viz. 2.3 kcal/mole.

Canadian Journal of Chemistry, **48**, 2785 (1970)

Introduction

Linder (1) found that the activation energy for the proton spin – lattice relaxation in pure solid ethylene chloride was 1.5 kcal/mole and in pure liquid ethylene chloride 0.6 kcal/mole. He attributed the spin–lattice relaxation in the solid state to a rocking motion of the molecule and in the liquid state to an end-over-end tumbling motion of the molecule. Now the activation energy for viscous flow for pure liquid ethylene chloride i.e. the value of the parameter E in the equation $\eta = \eta_0 \exp(-E/RT)$ is 2.3 kcal/mole (2) and one would expect that the activation energy for molecular tumbling should be of the same order as the activation energy for viscous flow, unless of course the main or significant contribution to the total spin–lattice relaxation comes from some internal molecular motion or from spin–rotation interaction. To clarify this point we repeated and extended the earlier measurements of Linder on the spin–lattice relaxation time of ethylene chloride in pure liquid ethylene chloride. In addition we also determined the spin–lattice relaxation of ethylene chloride in solution of deuterated ethylene chloride as a function of concentration and temperature.

Experimental

Solvent

The deuterated ethylene chloride, 99.5 atom % D was obtained from Merck, Sharp, and Dohme of Canada, Ltd., and was used without further purification.

Solute

The ethylene chloride was obtained from Eastman Organic Chemicals. It was redistilled once under reduced pressure and stored in a dark bottle.

Apparatus and Procedure

The apparatus used and procedure followed have been described elsewhere (3). The temperature of the samples was maintained constant within ± 0.2 °C by means of a gas (nitrogen) flow thermostat.

Results and Discussion

The experimental results are summarized in Table 1. If log T_1 (T_1 is the relaxation time) for each concentration is plotted vs. the reciprocal of the absolute temperature, $1/T$, there results a family of straight lines of nearly equal slope. From the slope of the line for pure ethylene chloride (shown in Fig. 1), there results an activation energy of 2.0 kcal/mole. The activation energy values derived from the temperature dependence of the spin–lattice relaxation of the other four solutions varied from 1.95 to 2.10

Can. J. Chem. Downloaded from www.nrcresearchpress.com by 210.87.254.105 on 09/05/12
For personal use only.

2. W. J. LEM and M. WAYMAN. Can. J. Chem. **48**, 776 (1970).
3. M. WAYMAN and W. J. LEM. Can. J. Chem. **48**, 782 (1970).
4. W. J. LEM and M. WAYMAN. J. Soc. Dyers and Colourists, **83**, 277 (1967).
5. W. J. LEM. Ph.D. Thesis. University of Toronto. 1969; see also O. BRUNCK. Annalen, **327**, 240 (1903) and **327**, 281 (1903); M. WAYMAN, C. B. ANDERSON, W. J. LEM, and W. H. RAPSON. Tappi, **52**, 89 (No. 1 Jan. 1969).
6. R. G. RINKER and S. LYNN. Industrial & Engineering Chemistry Product Research and Development. **8**, 338 (1969).

Spin–lattice relaxation in liquid ethylene chloride

E. BOCK AND G. WOLLNER
Parker Chemistry Laboratory, University of Manitoba, Winnipeg, Manitoba

AND

E. TOMCHUK
Department of Physics, University of Winnipeg, Winnipeg, Manitoba

Received March 24, 1970

The proton spin – lattice relaxation time of ethylene chloride in deuterated ethylene chloride was determined as a function of concentration and temperature over the temperature range 230 to 390 °K. It was found that the activation energy for the total spin–lattice relaxation as well as for the *intra*-molecular contribution to the total spin–lattice relaxation was 2.0 kcal/mole and was nearly equal to the activation energy for viscous flow, viz. 2.3 kcal/mole.

Canadian Journal of Chemistry, **48**, 2785 (1970)

Can. J. Chem. Downloaded from www.nrcresearchpress.com by 210.87.254.5 on 09/05/12
For personal use only.

Introduction

Linder (1) found that the activation energy for the proton spin – lattice relaxation in pure solid ethylene chloride was 1.5 kcal/mole and in pure liquid ethylene chloride 0.6 kcal/mole. He attributed the spin–lattice relaxation in the solid state to a rocking motion of the molecule and in the liquid state to an end-over-end tumbling motion of the molecule. Now the activation energy for viscous flow for pure liquid ethylene chloride i.e. the value of the parameter E in the equation $\eta = \eta_0 \exp(-E/RT)$ is 2.3 kcal/mole (2) and one would expect that the activation energy for molecular tumbling should be of the same order as the activation energy for viscous flow, unless of course the main or significant contribution to the total spin–lattice relaxation comes from some internal molecular motion or from spin–rotation interaction. To clarify this point we repeated and extended the earlier measurements of Linder on the spin–lattice relaxation time of ethylene chloride in pure liquid ethylene chloride. In addition we also determined the spin–lattice relaxation of ethylene chloride in solution of deuterated ethylene chloride as a function of concentration and temperature.

Experimental

Solvent

The deuterated ethylene chloride, 99.5 atom % D was obtained from Merck, Sharp, and Dohme of Canada, Ltd., and was used without further purification.

Solute

The ethylene chloride was obtained from Eastman Organic Chemicals. It was redistilled once under reduced pressure and stored in a dark bottle.

Apparatus and Procedure

The apparatus used and procedure followed have been described elsewhere (3). The temperature of the samples was maintained constant within ± 0.2 °C by means of a gas (nitrogen) flow thermostat.

Results and Discussion

The experimental results are summarized in Table 1. If log T_1 (T_1 is the relaxation time) for each concentration is plotted vs. the reciprocal of the absolute temperature, $1/T$, there results a family of straight lines of nearly equal slope. From the slope of the line for pure ethylene chloride (shown in Fig. 1), there results an activation energy of 2.0 kcal/mole. The activation energy values derived from the temperature dependence of the spin–lattice relaxation of the other four solutions varied from 1.95 to 2.10

TABLE 1

Proton spin – lattice relaxation time of $C_2H_4Cl_2$ in $C_2D_4Cl_2$ as a function of temperature and concentration*

Temperature (°K)	T_1, for concentration of $C_2H_4Cl_2$ in $C_2D_4Cl_2$ (mole %) =				
	18.05	38.90	63.80	76.20	100.00
242.1	4.76*	4.40	4.33	4.04	3.90
255.8	6.28	5.99	5.77	5.27	4.83
302.1	12.12	11.69	10.68	10.25	9.09
316.5	14.72	14.00	13.42	12.12	9.67
327.9	15.44	15.01	14.72	13.56	10.53
339.0	16.74	16.45	16.31	15.44	12.55
349.7	18.18	17.60	17.32	16.16	13.28
362.3	18.33	19.05	18.33	17.89	15.15
375.9	19.04	18.47	19.34	19.34	14.86
393.7	22.51	21.65	21.36	21.07	16.16

*T_1 in seconds.

kcal/mole. Finally the activation energy derived from the temperature dependence of the extrapolated value of the spin–lattice relaxation time, i.e. the *intra*-molecular contribution to the overall relaxation rate, was also found to be 2.0 kcal/mole. As has already been mentioned in the Introduction, the activation energy for viscous flow is 2.3 kcal/mole. From the close agreement between the activation energy values for viscous flow and that for the spin–lattice relaxation mechanism, it would seem that the chief contribution to the latter is indeed the end-over-end tumbling motion of the molecule as first suggested by Linder. This conclusion is further corroborated by the fact that the *intra*-molecular spin–lattice relaxation rate, at all temperatures studied, is about three times larger than the *inter*-molecular relaxation rate. Now if it is assumed that the nuclear magnetic relaxation is due mainly to the dipole–dipole interaction between neighboring spins then the *intra*-molecular contribution arises from the rotational motion of the molecule and the *inter*-molecular contribution from the translational motion of the molecule. Moreover, it is possible, following Powles (4) and Torrey (5), to obtain from the measured values of the *inter*- and *intra*-molecular contributions to the overall spin–lattice relaxation rate an estimate for the molecular rotational reorientation time, τ_r, and for the molecular jump time, τ_t, for the molecule in the liquid state. The result for 20 °C is: $\tau_r = 8.6 \times 10^{-12}$ s, and $\tau_t = 54 \times 10^{-12}$ s. The relative magnitudes of these values suggest that the molecular motion in the liquid state is dominated by rotational diffusion. The fact that the energy of activation for viscosity is equal to the energy of activation for the *intra*-molecular spin–lattice relaxation is in agreement with the above suggestion.

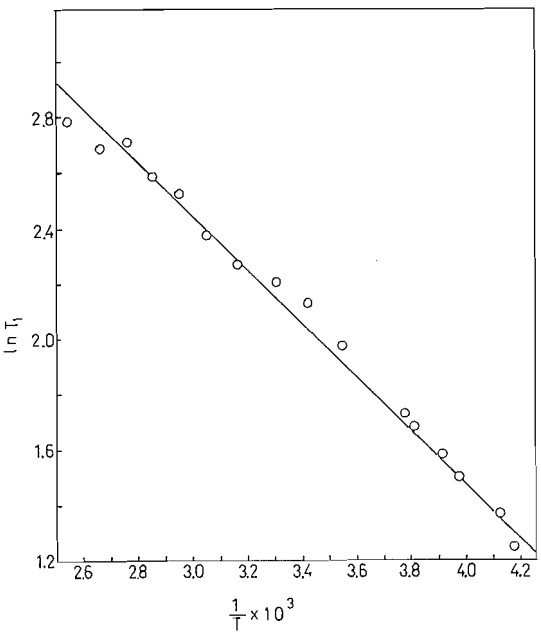

FIG. 1. Plot of ln T_1 vs. $1/T$ for pure ethylene chloride.

We thank Dr. J. Czubryt for his help in the analysis of the numerical data. The financial assistance of the National Research Council of Canada is gratefully acknowledged.

1. S. LINDER. J. Chem. Phys. **26**, 900 (1957).
2. International critical tables. Vol. VII. McGraw–Hill Book Co., Inc., New York and London. 1930. p. 213.
3. E. BOCK and E. TOMCHUK. Can. J. Chem. **47**, 2301 (1969).
4. J. G. POWLES. Ber. Bunsenges. Phys. Chem. **67**, 328 (1963).
5. H. C. TORREY. Phys. Rev. **92**, 962 (1953).

Can. J. Chem. Downloaded from www.nrcresearchpress.com by 210.87.254.5 on 09/05/12
For personal use only.

The preparation and vibrational spectra of some phenylchlorostannates

I. WHARF, J. Z. LOBOS, AND M. ONYSZCHUK
Department of Chemistry, McGill University, Montreal, Quebec

Received January 9, 1970

The preparations of tetra-alkylammonium salts of the $[(C_6H_5)_2SnCl_3]^-$, $[(C_6H_5)_2SnCl_4]^{2-}$, and $[(C_6H_5)_3SnCl_2]^-$ ions are described. Infrared spectra (1300–100 cm^{-1}) and Raman (400–100 cm^{-1}) spectra are reported and an assignment of the bands is made.

Canadian Journal of Chemistry, 48, 2787 '(1970)

Can. J. Chem. Downloaded from www.nrcresearchpress.com by 210.87.254.105 on 09/05/12
For personal use only.

Infrared spectra have been reported for adducts of alkyltin halides with neutral ligands (1), dimethylhalostannate salts (2), and neutral complexes of diphenyltin dihalides (3), but little is known about the corresponding anionic complexes. Several phenylhalostannates, possibly six-coordinate, were prepared sixty years ago (4), while recently some probable five-coordinate species have been identified in solution (5) and precipitated with the tetraphenylarsonium ion (6). A brief note has appeared on the preparation and far-infrared spectrum of $[(CH_3)_4N][(C_6H_5)_3SnCl_2]$ (7), but the interpretation has already been questioned by the original author (8). In this article we report the preparation and vibrational spectra of some phenylchlorostannate salts and provide tentative assignments which are consistent with those reported in the literature for related compounds.

The phenylchlorostannate salts reported in Table 1 were prepared by the addition of a hot (~90°) solution of the tetra-alkylammonium chloride in *n*-propanol (50 ml) to a solution of the phenyltin chloride in *n*-propanol (30 ml), following Srivastava's method (7). The salts precipitated after the mixtures were cooled to 0° or evaporated to half-bulk before cooling. They were filtered off, washed with ice-cold propanol and ether, and dried in a vacuum at 65°. In the preparation of $[(CH_3)_4N]_2[(C_6H_5)_2SnCl_4]$, it was necessary to saturate the hot propanol solution of $[(CH_3)_4N]Cl$ with HCl before the diphenyltin dichloride solution was added to it.

Infrared spectra in the range 1300 to 400 cm^{-1} are given in Table 2 for completeness; the modes described by Whiffen (9) for the C_6H_5X system account for practically all the observed bands. Of the three "X"-sensitive vibrations that occur in this range two are easily recognized as the bands of medium to strong intensity near 1060 (*q*) and 450 (*y*) cm^{-1}. These lie between the values of the respective modes for bromobenzene and iodobenzene. The assignment of the weak absorption near 650 cm^{-1} to the third "X"-sensitive mode is consistent with this trend.

Raman and infrared spectra in the 400 to 100

TABLE 1
Preparations and analyses of the phenylchlorostannate salts

Reactants	Product (yield)	Melting point*	Analysis (%)†			
			C	H	N	Cl
$[(CH_3)_4N]Cl + (C_6H_5)_2SnCl_2$	$[(CH_3)_4N][(C_6H_5)_2SnCl_3]$	205°	42.38	4.89	3.08	23.45
0.95 g 3.00 g	(3.57 g, 90%)		41.98	5.13	3.07	22.89
$[(C_2H_5)_4N]Cl + (C_6H_5)_2SnCl_2$	$[(C_2H_5)_4N][(C_6H_5)_2SnCl_3]$	136°	47.14	5.93	2.47	20.87
1.44 g 3.00 g	(3.62 g, 82%)		46.94	5.96	2.62	20.69
$[(C_4H_9)_4N]Cl + (C_6H_5)_2SnCl_2$	$[(C_4H_9)_4N][(C_6H_5)_2SnCl_3]$	101°	54.09	7.45	2.25	17.10
2.41 g 3.00 g	(1.20 g, 67%)		52.81	7.31	1.89	16.83
$[(CH_3)_4N]Cl + (C_6H_5)_2SnCl_2$	$[(CH_3)_4N]_2[(C_6H_5)_2SnCl_4]$	> 300°	42.62	6.08	4.97	25.18
0.66 g 1.00 g	(1.17 g, 70%)		42.14	6.08	4.40	25.16
$[(CH_3)_4N]Cl + (C_6H_5)_3SnCl$	$[(CH_3)_4N][(C_6H_5)_3SnCl_2]$	300°	53.37	5.49	2.82	14.32
1.10 g 3.86 g	(3.90 g, 80%)		52.89	5.26	2.69	13.31
$[(C_2H_5)_4N]Cl + (C_6H_5)_3SnCl$	$[(C_2H_5)_4N][(C_6H_5)_3SnCl_2]$	139°	56.65	6.40	2.54	12.86
1.29 g 3.86 g	(3.15 g, 74%)		55.97	6.28	2.38	12.18

*Melting points were measured with a Kofler block.
†Microanalyses were by Schwarzkopf Microanalytical Laboratory, Woodside, New York. Chloride was determined by Volhard's method. Experimental results are shown directly underneath corresponding calculated values.

TABLE 2

Infrared spectra* (1300–400 cm^{-1}) of some tetraalkylammonium phenylchlorostannates

Assignment	Mode†	$[(CH_3)_4N][(C_6H_5)_2SnCl_3]$	$[(C_2H_5)_4N][(C_6H_5)_2SnCl_3]$	$[(CH_3)_4N]_2[(C_6H_5)_2SnCl_4]$	$[(CH_3)_4N][(C_6H_5)_3SnCl_2]$	$[(C_2H_5)_4N][(C_6H_5)_3SnCl_2]$
β(C—H)	(*e*)	1262 vw	1265 vw		1262 vw	1259 vw
β(C—H)	(*a*)	1194 w 1180 w 1172 vw	(1181) wm 1172 m	1184 w 1169 1167 w	1185 w	(1180) m
β(C—H)	(*c*)	1154 vw	1156 w	1155 w	1160 w	1154 w
β(C—H)	(*d*)	1069 m	1070 w	1068 wm	1070 m	1071 m
X-sensitive	(*q*)	1061 m	1065 wm 1053 w	1060 sh	1065 m	1066 m 1060 m
			(1029) vw			(1029) wm
β(C—H)	(*b*)	(1023) vw (1018) m	1021 w 1018 w	(1023) m (1015) wsh	(1019) m (1017) m	1020 m
Ring	(*p*)	995 m	995 m	998 wm	996 m	996 m
γ(C—H)	(*j*)	982 vw			984 vw	984 vw
γ(C—H)	(*h*)	971 w (949) s (943) s		970 vw (952) sh (943) vs	(948) s	966 vw
γ(C—H)	(*i*)	912 w	916 vw	915 vw 910 vw	926 w	917 vw
γ(C—H)	(*g*)	851 vw	853 vw (789) sh (784) m			(794) w (789)
γ(C—H)	(*f*)	732 s 729 s	740 s 722 sh	734 vs 732 vs	755 s 748 vs 744 vs	743 s 738 sh
ϕ(C—C)	(*v*)	702 sh 695 vs 689 s	696 s	694 vs	704 s 699 s	699 s
X-sensitive	(*r*)	672 vw 661 vw 653 vw	672 vw 660 vw	658 vw	653 w	656 w 652 w
α(C—C—C)	(*s*)				620 vw	621 vw
X-sensitive	(*y*)	(461) m 454 s 446 s	452 s 448 s	(462) vs	457 s	454 s 443 m

*Infrared spectra were recorded on a Perkin–Elmer 521 spectrometer using samples in Nujol mulls.
†Whiffen's notation, ref. 9. Frequencies in parentheses are in part or totally due to cation vibrations.

cm^{-1} range are given in Table 3 together with data for $(C_6H_5)_2SnCl_2$ (11), $(C_6H_5)_3SnCl$ (11), and $(C_6H_5)_2SnCl_2 \cdot dipy$ (3). Complete analysis of these spectra cannot be made because the structures of the anions reported here are not known, although they are undoubtedly related to the well-known octahedral $SnCl_6^{2-}$ and the trigonal bipyramidal $SnCl_5^-$ (10). Nevertheless, reasonable empirical assignments for the phenyl group "X"-sensitive vibrations (*t*), (*u*), and (*x*), and the Sn—Cl stretching and bending modes can be made by comparing these spectra with those of tetracovalent phenyltin chlorides (11) and six-coordinate diphenyltin dihalide complexes with neutral ligands (3). The assignments for $[(C_6H_5)_2SnCl_4]^{2-}$ follow logically from a comparison of its spectrum with that of $(C_6H_5)_2SnCl_2 \cdot dipy$. Since the frequencies near 280 and 235 cm^{-1} (*t*) and (*t'*), respectively, corresponding to mainly tin–phenyl stretching modes, alter little on going from $(C_6H_5)_2SnCl_2$ (11) to $[(C_6H_5)_2SnCl_4]^{2-}$, the same assignments were made for the bands at 285 and 235 cm^{-1} in the spectrum of the intermediate $[(C_6H_5)_2SnCl_3]^-$ ion. This leaves bands near 330 and 250 cm^{-1} to be assigned to Sn—Cl stretching vibrations.

Similarly, a comparison of the spectra of $(C_6H_5)_3SnCl$ and $[(C_6H_5)_3SnCl_2]^-$ strongly indicates that in the latter asymmetric and symmetric Sn—C stretching modes occur near 275 and 235

Can. J. Chem. Downloaded from www.nrcresearchpress.com by 210.87.254.105 on 09/05/12
For personal use only.

Can. J. Chem. Downloaded from www.nrcresearchpress.com by 210.87.254.105 on 09/05/12
For personal use only.

TABLE 3

Far-infrared and Raman spectra (400–100 cm^{-1}) of tetra-alkylammonium phenyl chlorostannates and related compounds*

$(C_6H_5)_2SnCl_2$	$[(CH_3)_4N][(C_6H_5)_2SnCl_3]$		$[(C_2H_5)_4N][(C_6H_5)_2SnCl_3]$		$[(CH_3)_4N]_2[(C_6H_5)_2SnCl_4]$		$(C_6H_5)_2SnCl_2dipy$‡	
Infrared	Infrared	Raman	Infrared	Raman	Infrared	Raman	Infrared	Assignment
360 s								ν(Sn—Cl)
	326 vs	332 m	332 vs, sp	328 s, sp				
273 s	285 vs		285 m		292 m		286 s	ν_{as}(Sn—C)(*t*)
	252 s	249 vs	246 s	247 vs	267 vw		252 s	ν(Sn—Cl)
					254 m		246 s	
						237 vs		
235 s	235 vs	233 sh	231 vs	234 sh	233 m	231 vs	234 s	ν_s(Sn—C)(*t'*)
213 m	217 vs	215 m	219 vs	223 wm		217 w		(*u*)
	204 vs			206 wm	201 vs	201 w	207 s	
180 s	182 vs		188 m			181 wbr		(*x*)
					174 vs, br			
	152 s	151 m	152 m	153 wm				
						141 s, sp		δ($SnCl_n$)
	132 sh				128 s	133 s, br		
	123 sh		123 sh			124 vs		
115 s			116 m	115				
		108 vs		109 vs				

$(C_6H_5)_3SnCl$†	$[(CH_3)_4N][(C_6H_5)_3SnCl_2]$		$[(C_2H_5)_4N][(C_6H_5)_3SnCl_2]$		
Infrared	Infrared	Raman	Infrared	Raman	Assignment
344 m					ν(Sn—Cl)
268 w	276 s	276 wm	273 vs	274 wm	ν_{as}(Sn—C)(*t*)
	240 sh		244 sh		ν(Sn—Cl)
233 s		230 vs		238 vs	ν_s(Sn—C)(*t'*)
217 w	219 vs	221 w	220 vs	223 sh	(*u*)
210 s	208 vs, br	211 w	210 vs	208 w	
182 s			202 vs		(*x*)
176 w		194 m		194 m	
150 m	157 m		155 m		
	145 m				δ($SnCl_n$)
	134 m	134 w, sp	139 br, sh	138 sh	

*Far-infrared spectra were recorded on a Beckman IR-11 spectrometer using samples in Nujol mulls. Raman spectra of powdered samples were measured on a Jarrell–Ash 25-300 instrument equipped with a Krypton-ion laser. The salts were not sufficiently soluble in suitable solvent to allow observation of solution spectra.

†Reference 12.

‡Reference 3, data not available below 200 cm^{-1}.

cm^{-1}, respectively, leaving a band near 240 cm^{-1} to be assigned to a Sn—Cl stretching mode. The second Sn—Cl stretching mode in $[(C_6H_5)_3SnCl_2]^-$ expected to be Raman and infrared active may overlap with the asymmetric Sn—C stretching vibration at 275 cm^{-1}.

The assignment of bands in the 220 to 150 cm^{-1} region to phenyl group "X"-sensitive modes (*u*) and (*x*) follows that made for $(C_6H_5)_2SnCl_2$ and $(C_6H_5)_3SnCl$ (11). Bands below 150 cm^{-1} are tentatively attributed to Sn—Cl deformation vibrations. Unfortunately the spectra of corresponding bomide complex ions are not available to test the empirical assignments made in Table 3.

Evidently there is a marked decrease in Sn—Cl stretching frequencies with increasing coordination number (Table 3), an effect which agrees with a mainly ionic character for the Sn—Cl bond (12). The tin–phenyl stretching frequencies are little changed with higher degrees of coordination, indicating that the strength of the tin–phenyl bond is virtually unchanged under these circumstances. A similar effect has been noted for alkyltin halide adducts, both neutral and anionic (1, 2). This suggests that the Sn—C bonds in these compounds are primarily covalent and relatively unaffected by changes in the coordination number of the central tin atom.

The financial support of the National Research Council of Canada is gratefully acknowledged. We thank Professor D. F. Shriver for permission to use the Beckmann IR-11 spectrometer at Northwestern University, Evanston, Illinois.

1. R. J. H. Clark, A. G. Davies, and R. J. Puddephatt. J. Chem. Soc. A, 1828 (1968).
2. J. P. Clark and C. J. Wilkins. J. Chem. Soc. A, 871 (1966).
3. R. C. Poller, J. N. R. Ruddick, M. Theverasa, and W. R. McWhinnie. J. Chem. Soc. A, 2327 (1969).
4. P. Pfeiffer. Annal. **376**, 337 (1910).
5. G. Tagliavini and P. Zanella. Anal. Chim. Acta, **46**, 33 (1968).
6. G. Tagliavini and P. Zanella. J. Organometal. Chem. Amsterdam, **12**, 355 (1968).
7. T. S. Srivastava. J. Organometal. Chem. Amsterdam, **10**, 375 (1967).
8. T. S. Srivastava. J. Organometal. Chem. Amsterdam, **16**, 53 (1969).
9. D. H. Whiffen. J. Chem. Soc. 1350 (1956).
10. K. M. Harmon, L-L. Hesse, L. P. Klemann, C. W. Kocher, S. V. McKinley, and A. E. Young. Inorg. Chem. **8**, 1052 (1969).
11. A. L. Smith. Spectrochim. Acta, **24A**, 695 (1967).
12. I. Wharf and D. F. Shriver. Inorg. Chem. **8**, 914 (1969).

Erratum: Electron spin resonance studies of radiation damage. Part III. Gamma irradiated acetonitrile

F. P. Sargent
Department of Chemistry and Chemical Engineering, The University of Saskatchewan, Saskatoon, Saskatchewan

Received June 25, 1970

(Ref. Can. J. Chem. **48**, 1780 (1970))

Canadian Journal of Chemistry, 48, 2790 (1970)

The legend to Fig. 1 on p. 1781 should read as follows: "Fig. 1. The e.s.r. spectra of gamma irradiated acetonitrile at 77 °K: (*a*) 5 min after removal from the gamma source, in the dark, gain setting 160, (*b*) immediately after photobleaching, gain setting 32."

Can. J. Chem. Downloaded from www.nrcresearchpress.com by 210.87.254.105 on 09/05/12
For personal use only.

Can. J. Chem. Downloaded from www.nrcresearchpress.com by 210.87.254.105 on 09/05/12
For personal use only.

Canadian Journal of Chemistry

Published by THE NATIONAL RESEARCH COUNCIL OF CANADA

VOLUME 48 SEPTEMBER 15, 1970 NUMBER 18

The mass spectrum of exo-2-norbornyl chloride; the elucidation of the fragmentation mechanism and ion structures by metastable ion analysis

J. L. HOLMES AND D. MCGILLIVRAY
Chemistry Department, University of Ottawa, Ottawa, Canada

AND

N. S. ISAACS
Chemistry Department, The University, Whiteknights Park, Reading, Berkshire, England

Received April 29, 1970

The mass spectra of exo-2-norbornyl chloride and several deuterated analogues have been examined in detail with particular regard to metastable peaks involving the molecular ions and norbornyl cations. The molecular ion does not undergo Wagner–Meerwein isomerization prior to fragmentation; in the norbornyl cation the hydrogen atoms have lost their identity as shown by random H and D loss when the ion ejects an ethylene molecule. Metastable ion analysis is proposed as a method for studying the participation of norbornyl carbonium ions in the preparation of 2-norbornyl chloride.

Canadian Journal of Chemistry, 48, 2791 (1970)

Introduction

Bunton and Del Pesco (1) have described the mass spectra of exo-2-norbornyl chloride and 12 of its methyl derivatives. They had difficulty in interpreting some of the spectra owing to the possibility of thermally induced decompositions and Wagner–Meerwein isomerizations. The latter effect made it uncertain as to whether the molecular ions themselves underwent such a rearrangement prior to fragmentation.

We report here a detailed investigation of the mass spectra of exo-2-norbornyl chloride and some of its deuterated derivatives. We found the spectra of these compounds to be rich in metastables, in contrast with the earlier work (1) where few were observed. We have made considerable interpretative use of metastable peaks and their relative intensities in the labeled compounds.

Results and Discussion

The mass spectrum of exo-2-norbornyl chloride (**1**) is shown as Fig. 1; it agrees well with the previously tabulated data (1). Table 1 lists the twelve most prominent metastable peaks observed, their relative abundances and the fragmentations responsible for their genesis. Although even the most intense metastable (*m/e* 34.6) is of low abundance, $\sim 0.05\%$ relative to the base peak, C_5H_8 *m/e* 68, little difficulty was experienced in identifying some 25 metastable peaks. It is noteworthy that there is no metastable peak arising from the formation of the base peak, C_5H_8 *m/e* 68; the metastable at *m/e* 35.3 (131 → 68) corresponds to the natural ^{13}C content of *m/e* 67 which arises in part from the molecular ion by elimination of a C_2H_4Cl radical. There are two likely sources of the base peak, namely the molecular ion and the norbornyl cation *m/e* 95. In order to elucidate this and other features of the fragmentation mechanism a number of deuterium labeled compounds were prepared; 3,3-d_2-exo-2-norbornyl chloride (**2**), and 3,3,2-d_3-exo-2-norbornyl chloride (**3**), were prepared by treating 3,3-d_2-endo-2-norborneol, and 3,3,2-d_3-endo-2-norborneol with triphenyl phosphine in CCl_4 (2); 6-d_1-exo-2-norbornyl chloride (**4**), was prepared by the addition of DCl to nortricyclene at -78 °C (3). The mass spectra of these labeled compounds were closely similar to that of **1**; the major differences lay in the relative intensities of the peaks *m/e* 67, 68, 69, and 70. These are listed in

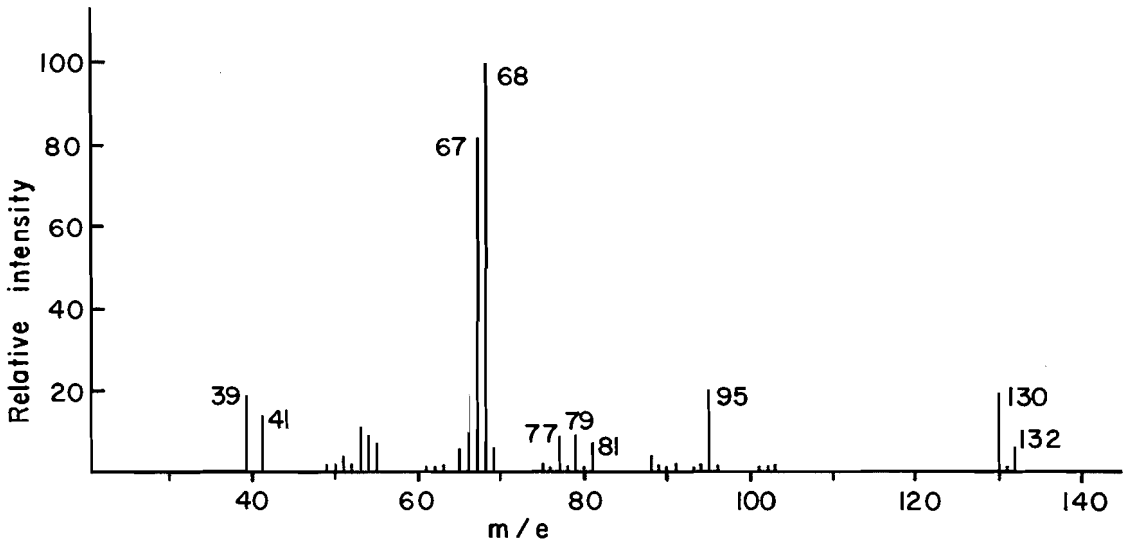

FIG. 1. The mass spectrum of exo-2-norbornyl chloride.

TABLE 1

Metastable (m*) peaks observed in the mass spectrum of exo-2-norbornyl chloride

m/e of m*		Relative intensity	Generating fragmentation
Observed	Calculated	%	
91.2	91.1	21	95 → 93
77.0	77.1	11	81 → 79
75.0	75.0	18	79 → 77
63.1	63.1	20	67 → 65
47.3	47.3	25	95 → 67
37.15	37.1	11	41 → 39
35.3	35.3	~9	131 → 68
34.6	34.55	100	130 → 67
34.0	34.0	32	132 → 67
33.6	33.6	11	90 → 55
25.15	25.15	10	67 → 41
15.3	15.3	~5	55 → 29

Table 2 together with the norbornyl and molecular ions. The changes of relative intensity in this group of peaks did not permit conclusive identification of the fragmentation mechanism leading to their production and so the metastables corresponding to the loss of C_2H_4 and its labeled analogues from the norbornyl cation and to C_2H_4Cl (and deuterated chloroethyl radicals) lost from the molecular ion were carefully examined. These metastables are shown in Figs. 2 and 3, respectively. It was found that the relative heights of the metastables were not a function of electron energy (provided that both parent and daughter ion remained in the spectrum). In order to facilitate their measurement the metastables illustrated in Figs. 2 and 3 were obtained at electron energies of ~20 eV, a voltage at which the integral-mass peaks in the same region as the metastables were of low abundance. The relative intensities of these metastables are given in Table 3, the peak heights having been averaged from a series of scans. On the assumption that the heights of metastable peaks are directly proportional to the abundances of their precursor ions (for which there is precedent (4)), we have drawn the following conclusions.

The results obtained from compounds **2** and **3** reveal three important features of the fragmentation mechanism.

(*i*) The molecular ion does not undergo a Wagner–Meerwein rearrangement prior to fragmentation by elimination of a chloroethyl radical, because it loses only carbons 2 and 3, together with the deuterium, hydrogen, and chlorine atoms attached thereto. This is illustrated by the metastables shown in Fig. 3 and listed in Table 3. The origin of the fourth hydrogen atom can be inferred from the behavior of compound **4** (see below).

(*ii*) When the norbornyl cation, *m/e* 97 (**2**), *m/e* 98 (**3**), *m/e* 96 (**4**) dissociates by ejecting ethylene, hydrogen and deuterium are lost in a completely random manner; the random-loss ratios for hydrogen and deuterium in the labeled ethylenes are shown in Table 3 together with the

Can. J. Chem. Downloaded from www.nrcresearchpress.com by 210.87.254.105 on 09/05/12
For personal use only.

Can. J. Chem. Downloaded from www.nrcresearchpress.com by 210.87.254.105 on 09/05/12
For personal use only.

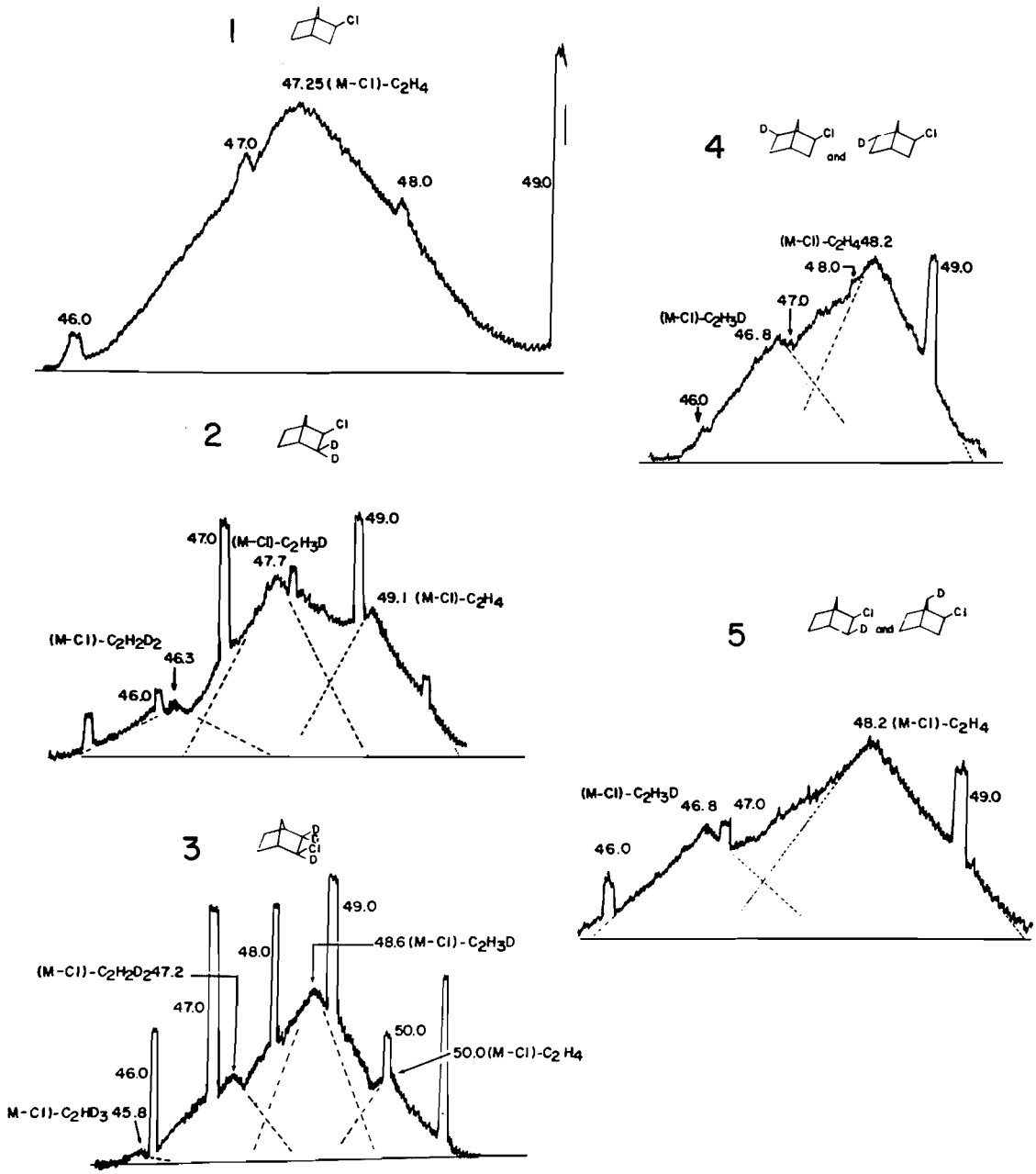

FIG. 2. Metastables arising from the process (norbornyl cation–ethylene) → $C_5(H, D)_7$.

observed intensity ratios for the corresponding metastable peaks, which are illustrated in Fig. 2. This does not allow conclusions to be drawn concerning the arrangement of the carbon atoms in this ion; we can, however, infer from the behavior of the molecular ions of norbornene and nortricyclene[1] that the bicyclic structure is probably no longer present. These results also eliminate such organized structures as the protonated nortricyclenium ion observed by Olah *et al.* (5)

[1]Results to be published.

Can. J. Chem. Downloaded from www.nrcresearchpress.com by 210.87.254.105 on 09/05/12
For personal use only.

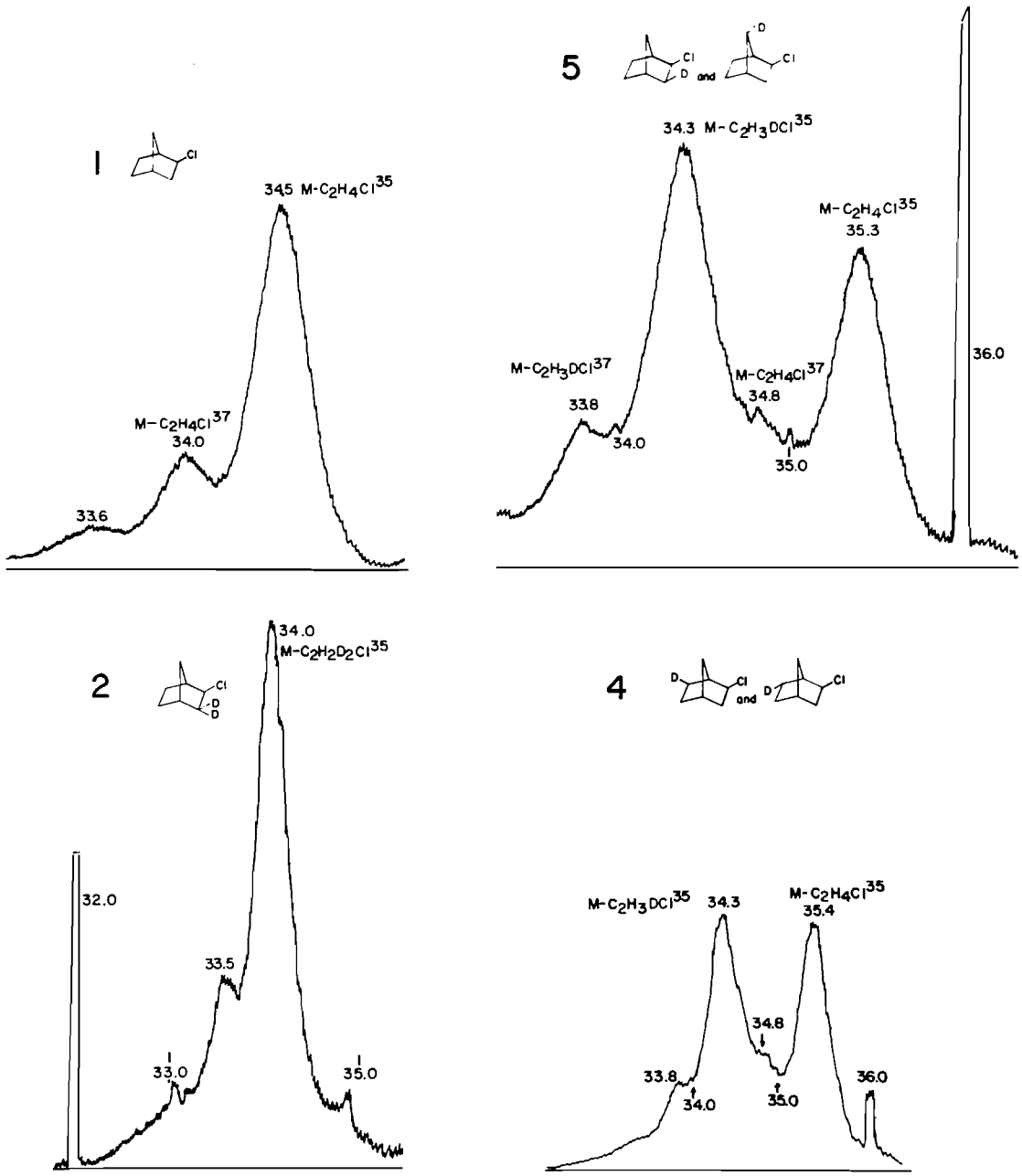

FIG. 3. Metastables arising from the process (molecular ion–chloroethyl radical) → $C_5(H, D)_7$.

in solution and inferred as existing in the gas phase by Spencer and Mo (6). Determination of the symmetry of the carbon skeleton is attendant upon a ^{13}C labeling experiment.

(*iii*) The base peak remains at *m/e* 68 in **2** and **3** and is shifted to *m/e* 69 in **4**. Since hydrogen atoms are randomly lost in fragmentation of the norbornyl cation it is therefore unlikely to be the precursor of the base peak. The latter almost certainly proceeds from the molecular ion directly by loss of C_2H_3Cl, i.e. by loss of carbon atoms 2 and 3 together with the atoms originally attached thereto.

The origin of the fourth hydrogen atom elim-

TABLE 2

Relative intensities of the peaks *m/e* 67–70, the norbornyl cation and molecular ion (^{35}Cl)

Compound	Relative intensity (corrected for ^{13}C contributions)					
	m/e = 67	*m/e* = 68	*m/e* = 69	*m/e* = 70	Norbornyl cation	$M^{+\cdot}$
1	82	95	0	0	20	19
2	68	96	10	0	22	19
3	72	96	18	8	31	23
4	40	59	97	0	21	18
5	53	97	44	0	20	20

TABLE 3

Relative intensities of metastables in labeled compounds
Loss of ethylene from the norbornyl cation*

Compound	$(M-Cl)-C_2H_4$		$(M-Cl)-C_2H_3D$		$(M-Cl)-C_2H_2D_2$		$(M-Cl)-C_2HD_3$	
	m/e	Relative intensity	*m/e*	Relative intensity	*m/e*	Relative intensity	*m/e*	Relative intensity
2	49.1	40 ± 2 38 (calcd.)	47.7	48 ± 2 51 (calcd.)	46.3	12 ± 2 11 (calcd.)	—	—
3	50.0	22 ± 2 21 (calcd.)	48.6	50 ± 2 51 (calcd.)	47.2	25 ± 2 25.5 (calcd.)	45.8	3 ± 2 2.5 (calcd.)
4	48.2	64 ± 2 64 (calcd.)	46.8	36 ± 2 36 (calcd.)	—	—	—	—

Loss of chloroethyl radical from the molecular ion

Compound	$M-C_2H_4Cl$		$M-C_2H_3DCl$		$M-C_2H_2D_2Cl$		$M-C_2HD_3Cl$	
	m/e	Relative intensity	*m/e*	Relative intensity	*m/e*	Relative intensity	*m/e*	Relative intensity
2	—	—	—	—	34.0	100	—	—
3	—	—	—	—	—	—	33.8	100
4	35.3	49 ± 1	34.3	51 ± 1	—	—	—	—

*The calculated figures are for random hydrogen and deuterium loss.

inated in C_2D_3HCl in **3** (and $C_2D_2H_2Cl$ in **2** etc.) can be ascertained from the behavior of compound **4**. Brown and McIvor (3) showed (by means of nuclear magnetic resonance spectra obtained using a 220 MHz instrument) that the addition of DCl to nortricyclene in $CHCl_3$ solution at −78 °C, yields pure exo-2-norbornyl chloride with the D atom 50 ± 3% at the 6-endo-position and 43 ± 3% at 6-exo; the remainder, 6%, was believed to be at the 7-anti-position. We observe that **4** eliminates both C_2H_4Cl (49%) and C_2H_3DCl (51%) from the molecular ion, see metastables in Fig. 3. This result is compatible with the fourth H atom originating from the 6-position; either the endo- and exo-hydrogen atoms are equivalent (in which case 46.5 ± 3% of the 6-hydrogen contained in the chloroethyl radical lost from **4** would be deuterium) or the loss is specifically the 6-exo- or 6-endo-hydrogen atom. Both possibilities are within the experimental errors.

Brown and McIvor (3) also reported on the position of deuterium in exo-2-norbornyl chloride prepared by the addition of DCl to norbornylene, also in $CHCl_3$ solution at −78 °C. They showed that the reaction produced pure exo-2-norbornyl chloride with all the deuterium at the 3-exo- or 7-syn-positions in the ratio 55:45 ± 3%, respectively. In order to test the possible use of relative metastable intensities as an analytical tool in these or similar labeled systems we prepared the compound **5** as described above and examined the metastables for C_2H_4Cl and C_2H_3DCl loss from the molecular ion. The result is shown in Fig. 3; we find the ratio of the metastable intensities to be 56:44 ± 1%, respectively, and therefore con-

Can. J. Chem. Downloaded from www.nrcresearchpress.com by 210.87.254.105 on 09/05/12
For personal use only.

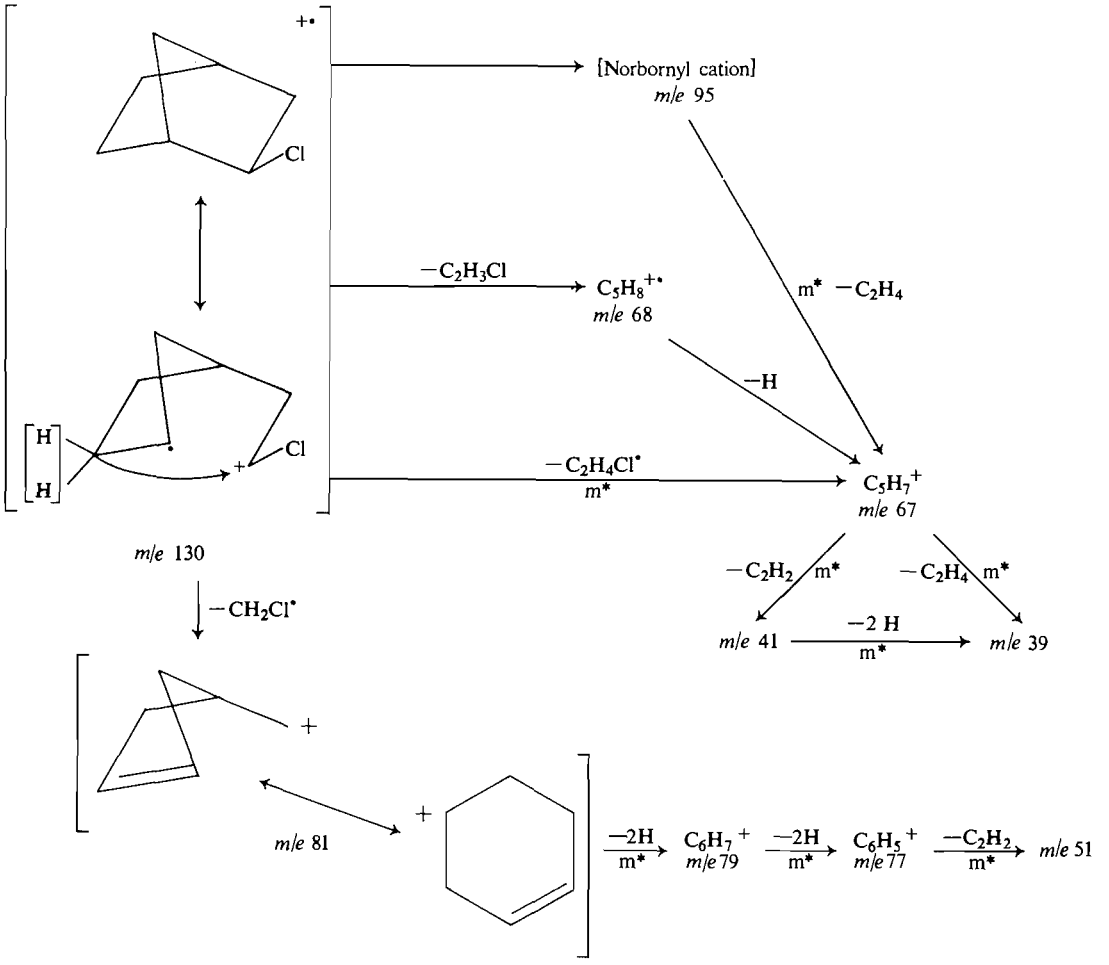

SCHEME 1. Fragmentation mechanism of exo-2-norbornyl chloride.

clude that 56% of the deuterium is in the 3-position, in excellent agreement with the observations of Brown and McIvor. Certainly, such mass spectral analyses are not as specific as those obtained by the use of n.m.r. spectra but in this work they yield useful quantitative values for the proportions of deuterium substituted in the 2-, 3-, and 6-positions in norbornyl chloride. Labeled endo-3d_1-exo-2-norbornyl chloride was also prepared from the endo-3d_1-endo-2-alcohol by the $SOCl_2$–pyridine method (7). Analysis of the M—C_2H_4Cl, M—C_2H_3DCl metastable peaks indicated that 45% of the deuterium was on the 3-carbon atom (adjacent to that bearing chlorine). Both this and the previous result indicate participation of the 2-norbornyl carbonium ion in the method of preparation; this ion can yield isomeric products via a Wagner–Meerwein rearrangement (considering the ion to be classical) i.e.

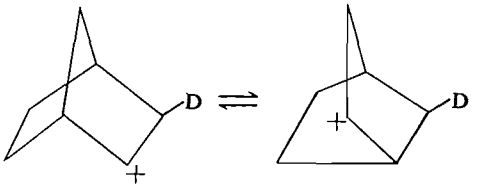

We also conclude that the triphenylphosphine–CCl_4 method of preparing the chloride does not involve a norbornyl carbonium ion since there was no evidence of halogen substitution other than in the exo-2-position. These results were confirmed by n.m.r. spectra.

The proposed fragmentation mechanism for exo-2-norbornyl chloride is shown in Scheme 1

Can. J. Chem. Downloaded from www.nrcresearchpress.com by 210.87.254.105 on 09/05/12
For personal use only.

in which the major and some minor fragmentation routes are depicted. The major difference between Scheme 1 and that previously proposed (1) lies in the origin of *m/e* 67 which was shown as arising only from *m/e* 68 by H loss and from the norbornyl cation by ethylene loss.

From the relative intensities of the metastables corresponding to ethylene loss from the norbornyl cation in the labeled compounds, one may calculate the contributions of the daughter peaks to the series of ions *m/e* 67–70. By difference, the proportions of *m/e* 67 and *m/e* 68 which arise from chloroethyl radical and C_2H_3Cl loss, respectively, from the molecular ion, can be evaluated. Comparing the spectra of the labeled and unlabeled compounds one can then readily show that at most 15% of the $C_5H_8^{+\cdot}$ ion in **1** dissociates by H loss. This result makes the structure of this ion questionable because molecular ions of this formula mostly lose H to yield an intense or base peak at *m/e* 67 or display a major fragment ion at *m/e* 53 (8).

Experimental

The mass spectra were obtained using a Hitachi RMU-6D instrument. Unless otherwise stated all spectra were obtained at 70 eV. Samples were introduced via the liquid inlet system and this and the ion source were maintained at temperatures below 50 °C to avoid thermal decomposition.

The 3,3-d_2-endo-2-norbornyl alcohol was prepared from norcamphor which was dideuterated by exchange with alkaline D_2O. The labeled norcamphor was reduced with $LiAlH_4$. The 3,3-exo-2-d_3-endo-2-alcohol was prepared similarly using $LiAlD_4$ as reducing agent.

The authors are indebted to Mr. A. Philpot for assistance in obtaining the mass spectra. J.H. and D.M. thank the National Research Council of Canada for financial support.

1. C. A. BUNTON and T. W. DEL PESCO. Org. Mass Spectrom. **2**, 81 (1969).
2. I. M. DOWNIE and J. B. LEE. Tetrahedron, **23**, 359 (1967).
3. J. M. BROWN and M. C. MCIVOR. Chem. Commun. 238 (1969).
4. J. H. BEYNON, B. E. JOB, and A. E. WILLIAMS. Z. Naturforsch. **20A**, 883 (1965).
5. G. A. OLAH and A. M. WHITE. J. Amer. Chem. Soc. **91**, 3956 (1969).
6. H. SPENCER and Y. K. MO. Can. J. Chem. **48**, 384 (1970).
7. J. K. STILLE and F. M. SONNENBERG. J. Amer. Chem. Soc. **88**, 4915 (1966).
8. A. CORNU and R. MASSOT, Compilation of mass spectral data. Heyden and Son, Spectrum House, Alderton Crescent, London, England. 1966. p. 21c.

Can. J. Chem. Downloaded from www.nrcresearchpress.com by 210.87.254.105 on 09/05/12
For personal use only.

Can. J. Chem. Downloaded from www.nrcresearchpress.com by 210.87.254.5 on 09/05/12
For personal use only.

Electron spin resonance spectra of the triple ions $[Na_2\text{-pyrazine}]^+$ and $[Na_2\text{-tetramethylpyrazine}]^+$

S. A. Al-Baldawi and T. E. Gough[1]

Department of Chemistry, University of Waterloo, Waterloo, Ontario

Received May 13, 1970

Reduction of pyrazine (P) and tetramethylpyrazine (TMP) by sodium in the presence of sodium tetraphenylboride produces Na_2P^+ and Na_2TMP^+, respectively. The electron spin resonance spectra of these species are presented and compared with those of the corresponding ion pairs. From line-broadening effects within the sodium hyperfine multiplets of the triple ion spectra, it is deduced that the sodium ions occupy positions close to the N–N axes of the ring systems.

Canadian Journal of Chemistry, **48**, 2798 (1970)

Introduction

The detection, by electron spin resonance spectroscopy, of triple ions of the formula Na_2Q^+ has been reported (1, 2) for Q equals *p*-benzoquinone, 2,3-, 2,5-, 2,6-dimethyl-*p*-benzoquinone, and duroquinone. The proton hyperfine splitting constants of the triple ion indicate that one sodium associates with each oxygen of the semiquinone. Molecular tumbling does not completely average the anisotropies within the hyperfine and **g** tensors of the triple ion with the result that asymmetric broadening of the sodium hyperfine septets was observable. From this broadening it was deduced (2) that the sodium ions occupy positions close to the O–O axis of the semiquinone. It is of interest to determine whether these effects are limited to semiquinones, or whether the experiment has more general application to the structure of other ionic associates.

A number of papers (3–10) have concerned themselves with the structure of ion pairs formed between pyrazine anions and alkali metal cations. The observation of line-width alternation for sodium-pyrazine in tetrahydrofuran (4) and 1,2-dimethoxyethane and of two non-equivalent nitrogen nuclei for lithium-pyrazine in tetrahydrofuran (5) makes it clear that these cations associate with one of the nitrogens of pyrazine, rendering the anion asymmetric. Calculations on the structure of these ion pairs (5, 8, 10) indicate that at realistic interionic distances the most stable position for the cation is above the center of the pyrazine ring, which obviously does not agree with the experimental results. Calculations on the structure of the protonated pyrazine anion (9) predict an asymmetric structure with the proton lying on the N–N axis. However, protonation is very different from ionic association and extrapolation of this result to ion pairs is not satisfactory.

Since the observation of anisotropic broadening within the sodium multiplets of Na_2Q^+ enabled the position of the cations within the triple ion to be determined, we attempted to prepare triple ions of pyrazine and tetramethylpyrazine with two aims in mind; to show that triple ion formation is not limited to semiquinones, and to investigate the stereochemistry of the sodium pyrazine interaction.

Experimental

Pyrazine (Aldrich) and tetramethylpyrazine (Alfred Bader) were used without purification. Ion-pairs and triple ions were generated as described previously (2, 11). Spectra were recorded on a Varian E-3 spectrometer equipped with a Varian E4540 variable temperature unit: the latter was calibrated using a copper–constantan thermocouple in conjunction with a Hewlett–Packard 3420A voltmeter.

Results

Reduction of pyrazine and tetramethylpyrazine by sodium in tetrahydrofuran produced the expected ion pairs, with electron spin resonance spectra in good agreement with previous reports. Proton and nitrogen hyperfine splitting constants, given in Table 1, were found to be independent of temperature within the accuracy of measurement. Sodium hyperfine splitting constants, plotted as functions of temperature, are given in Fig. 1. The signs used for the isotropic hyperfine splitting constant of sodium are discussed below. At lower temperatures, for both ion pairs, line-width alternation within the nitrogen and proton hyperfine splitting patterns was observed; however, broad-

[1]To whom correspondence should be addressed.

TABLE 1

Proton and nitrogen hyperfine splitting constants (±0.02 G) for ion pairs and triple ions of pyrazine and tetramethylpyrazine. All values are for sample temperatures of 20 °C, counter ion = sodium

Anion	Solvent	Species	a_N (G)	a_H (G)
Pyrazine	Tetrahydrofuran	Ion pair	7.17	2.69
Pyrazine	Tetrahydrofuran	Triple ion	7.12	2.70
Pyrazine	2-Methyltetrahydrofuran	Triple ion	7.13	2.69
Tetramethylpyrazine	Tetrahydrofuran	Ion pair	6.18	1.75
Tetramethylpyrazine	Tetrahydrofuran	Triple ion	6.19	1.77
Tetramethylpyrazine	2-Methyltetrahydrofuran	Triple ion	6.10	1.80

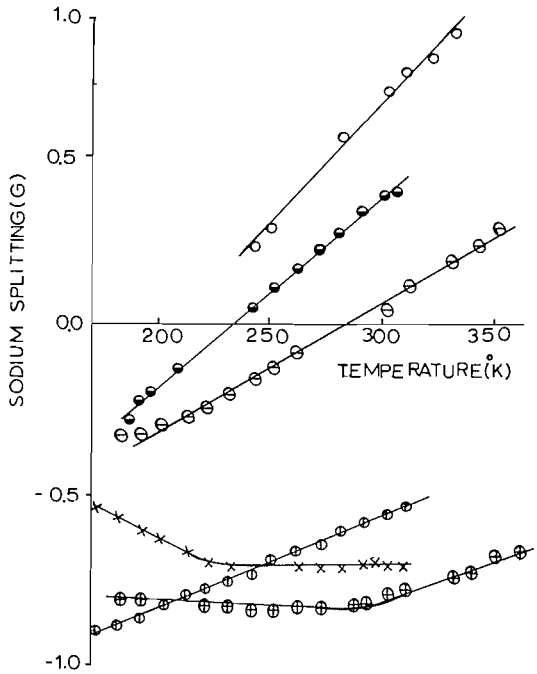

FIG. 1. Sodium hyperfine splitting constants, in gauss, plotted as functions of temperature for the systems: ○, NaTMP in tetrahydrofuran; ⊖, Na_2TMP^+ in tetrahydrofuran; ◒, Na_2TMP^+ in 2-methyltetrahydrofuran; ⊙, NaP in tetrahydrofuran; ×, Na_2P^+ in tetrahydrofuran; ⊕, Na_2P^+ in 2-methyltetrahydrofuran.

ening of the spectrum caused by incomplete averaging of the anisotropic components of the nitrogen hyperfine tensor precluded satisfactory analysis of spectra recorded at low temperatures in terms of "locked-in" configurations for the ion-pairs (cf. ref. 4). When the reductions were attempted in 2-methyltetrahydrofuran, the pyrazine ion pair was not formed in detectable concentrations, and only a weak signal was obtained for the tetramethylpyrazine ion pair.

Reduction of pyrazine and of tetramethylpyrazine in the presence of approximately equimolar quantities of sodium tetraphenylboride produced solutions containing the triple ions Na_2P^+ and Na_2TMP^+, respectively. The reductions were rapid in both tetrahydrofuran and 2-methyltetrahydrofuran, and in each case intense signals were obtained. Hyperfine splitting constants for these systems are included in Table 1 and Fig. 1. It should be remembered that the splitting constants in Fig. 1 for the triple ions are for two equivalent ^{23}Na nuclei. Typical spectra are shown in Fig. 2.

The electron spin resonance spectra of the triple ions did not show line-width alternation, but did show large variations in line-width due to incomplete averaging of hyperfine and **g** tensors. In Fig. 3 relative widths, determined from reduced intensity ratios, of the principal nitrogen lines are plotted as functions of the spectral index $\tilde{M}_N$ of these lines. Similar plots are given in Fig. 4 for the central sodium septet of the triple ion of tetramethylpyrazine in tetrahydrofuran and in 2-methyltetrahydrofuran. In Figs. 3 and 4 the line-width data are for principal lines: $\tilde{M}$ for all nuclei other than the one of interest are zero, thereby eliminating cross-terms in the spectral indices. The sodium hyperfine splitting patterns of Na_2P^+ were always asymmetrically broadened to high field; however, the $\tilde{M}_{Na} = \pm 3$ lines were overlapped by more intense lines and so the results for this species are not presented in graphical form.

Discussion

The hyperfine splitting constants determined for the ion-pair sodium-pyrazine in tetrahydrofuran are in good agreement with previous reports. The temperature coefficient of the sodium hyperfine splitting constant, da_{Na}/dT, has been reported as 0.0025 G/°K (4); our results give a value of 0.0027 G/°K, to which we have assigned a positive value, thereby making a_{Na} negative.

Can. J. Chem. Downloaded from www.nrcresearchpress.com by 210.87.254.5 on 09/05/12
For personal use only.

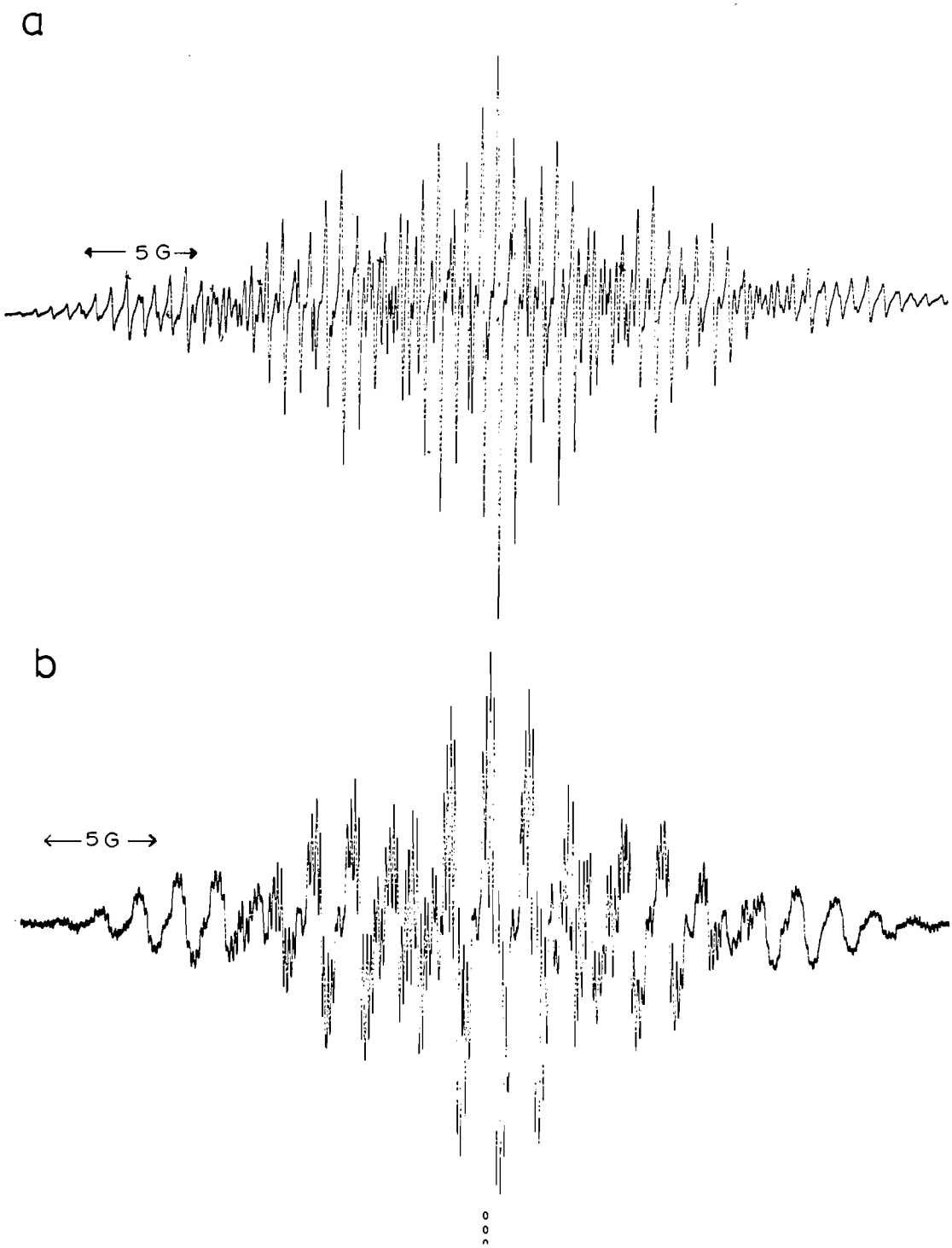

FIG. 2. Electron spin resonance spectra of (*a*) Na_2P^+ in tetrahydrofuran at 25 °C; (*b*) Na_2TMP^+ in tetrahydrofuran at 35 °C.

Can. J. Chem. Downloaded from www.nrcresearchpress.com by 210.87.254.5 on 09/05/12
For personal use only.

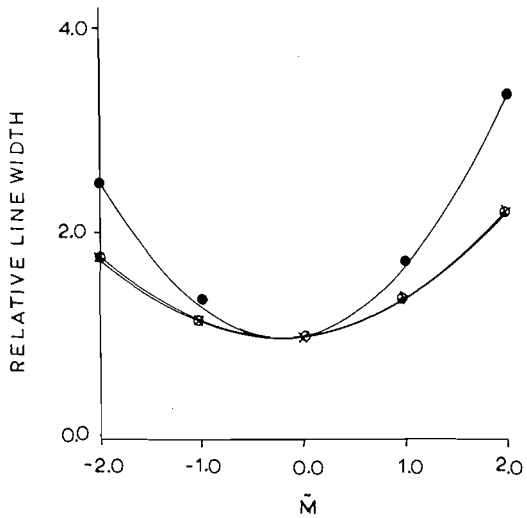

FIG. 3. Experimental relative widths of the principal nitrogen lines of triple-ion spectra at 10 °C, and the least-squares fit of the data to the expression $1 + A\tilde{M}_N + B\tilde{M}_N^2$: ●, Na_2TMP^+ in tetrahydrofuran $A = 0.210$, $B = 0.480$; ○, Na_2P^+ in tetrahydrofuran $A = 0.122$, $B = 0.250$; ×, Na_2P^+ in 2-methyltetrahydrofuran $A = 0.109$, $B = 0.248$.

Positive values for the temperature coefficient of metal hyperfine splitting constants have generally been assumed (12–14), and in two cases (15, 16) demonstrated by measurements of nuclear magnetic resonance contact shifts of ^{23}Na counter ions. The electron spin resonance spectrum of the sodium-tetramethylpyrazine ion-pair in tetrahydrofuran has been reported for a sample temperature of 296 °K (8), and once again our findings are in good agreement. However, if the temperature coefficient of a_{Na} is taken as positive, then clearly a_{Na} is positive; comparisons between the sodium hyperfine splitting constants of the two ion-pairs (8) should only be made after the difference in sign of a_{Na} has been recognized.

Addition of sodium tetraphenylboride to the ion-pairs produced triple ions, characterized by the presence of hyperfine interaction with two equivalent ^{23}Na nuclei. The signs of a_{Na} for the triple ions, given in Fig. 1, follow from comparisons with the ion pairs. Except for the species Na_2P^+ in tetrahydrofuran at low temperatures, da_{Na}/dT is thereby found to be zero or positive. It is possible that, for this exception, the solvent is becoming sufficiently polar at the lower temperatures to begin disrupting the structure of the triple ion. Over large ranges of temperature a_{Na} for Na_2P^+ is essentially constant, indicating that

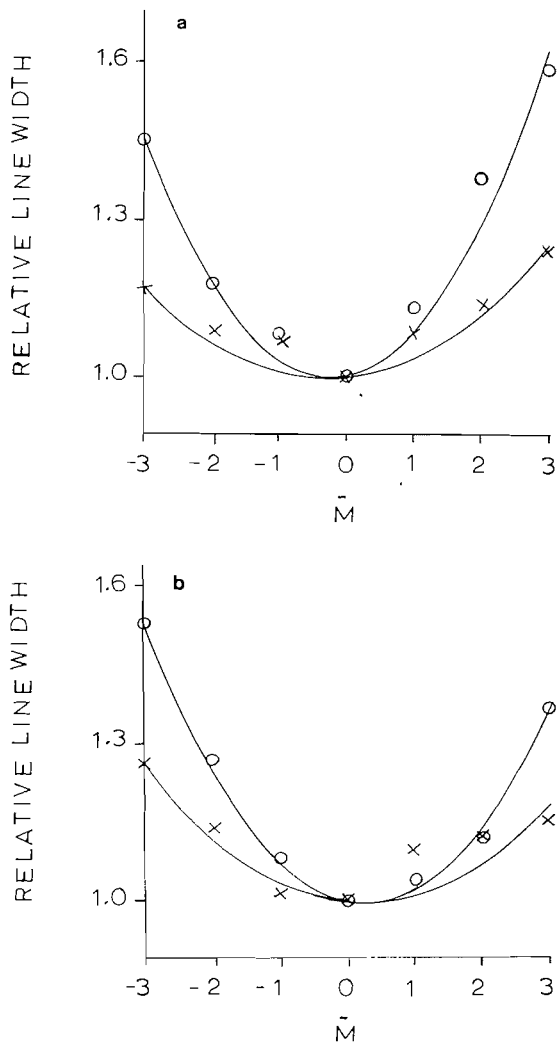

FIG. 4. Experimental relative widths of the principal sodium lines of Na_2TMP^+, and the least squares fit of the data to the expression $1 + A\tilde{M}_{Na} + B\tilde{M}_{Na}^2$: (*a*) ○, in 2-methyltetrahydrofuran at −70 °C $A = 0.028$, $B = 0.056$; ×, in tetrahydrofuran at −40 °C $A = 0.013$, $B = 0.023$; (*b*) ○, in 2-methyltetrahydrofuran at −20 °C $A = -0.026$, $B = 0.046$; ×, in tetrahydrofuran at +30 °C $A = -0.013$, $B = 0.023$.

within these limits this unit has a static configuration between its constituent ions.

Remembering that the sodium septets of Na_2P^+ always show asymmetric broadening to high field, a comparison between Figs. 1 and 4 shows that assigned positive values of a_{Na} are always accompanied by low field broadening of the hyperfine septets, while assigned negative values of a_{Na} are accompanied by high field

Can. J. Chem. Downloaded from www.nrcresearchpress.com by 210.87.254.5 on 09/05/12
For personal use only.

Can. J. Chem. Downloaded from www.nrcresearchpress.com by 210.87.254.5 on 09/05/12
For personal use only.

broadening of the septets. Identical correlations were found for triple ions formed between sodium and a series of semiquinones (2), though for these semiquinone systems the amount of broadening is much larger. In order to use these broadening effects to deduce the positions of the sodium ions within the pyrazine triple ions, it is necessary to know the form of the **g** tensor of the radical.

Following previous notation (17) we label the principal components of the **g** tensor as g_1, g_2, and g_3, taking g_3 perpendicular to the plane of the molecule and g_1 along the N–N axis. Theoretically (18) $g_3 = 2.00232$, the "free-spin" value, while g_1 and g_2 are expected to be somewhat greater. For the dihydropyrazine cation g_1 has been reported as the largest component (17); for pyrazine anions, the presence of the non-bonding lone pairs will further enhance the value of g_1. Therefore, the **g** tensor of a pyrazine anion must be similar in form to that of *p*-benzosemiquinone (19), for in each case the tensors will be dominated by contributions from the lone pairs.

Given this similarity, and the similar broadening trends of the sodium hyperfine septets of the pyrazine and semiquinone triple ions, it is obvious that one may apply the arguments used to deduce the structure of Na_2Q^+ units (2) to the pyrazine and tetramethylpyrazine triple ions. Hence, we deduce that the sodium ions of the pyrazine and tetramethylpyrazine triple ions occupy positions analogous to those occupied by sodium in the *p*-benzosemiquinone and durosemiquinone triple ions, respectively. Thus for Na_2P^+ the sodium ions must be along the N–N axis where they are able to interact with the spin-polarized lone-pair electrons of nitrogen, causing a_{Na} to be negative. For Na_2TMP^+, the flanking methyl groups cause the sodium ions to move away from the N–N axis, allowing direct overlap between the $2p_z$ orbital on nitrogen and the 3s orbital on sodium. This overlap generates a positive contribution to a_{Na}, so that the net value of a_{Na} will be a sensitive function of the position of the sodium ion. Increases in temperature cause the sodium ions to vibrate further from the plane of the molecule, causing da_{Na}/dT to be positive, as assumed when constructing Fig. 1. Recently the ^{23}Na nuclear resonance of sodium-2,2′-bipyridyl ion-pairs has been reported (20), and interpreted in terms of the sodium ion occupying an "in-plane" position where it is able to interact with lone-pairs from both nitrogens. The nuclear magnetic resonance contact shift shows conclusively that a_{Na} is negative, supporting the general format of the above discussion.

As noted above, the extent of the broadening linear in $\tilde{M}_{Na}$ is greater for the semiquinone triple ions than for the pyrazine triple ions. The ratio of the relevant spin orbit coupling constant to $n \rightarrow \pi^*$ transition energy is roughly three times larger for benzoquinone than for pyrazine, and so the **g** tensor for the semiquinone is expected to be more anisotropic than that of the pyrazine anion. Since g_3 must equal 2.00232 for both species, it is expected that g_{iso} for the semiquinone should be greater than g_{iso} for the pyrazine anion. Experimentally, for *p*-benzosemiquinone $g_{iso} = 2.0046$ (9), while for the Na_2TMP^+ we find $g_{iso} = 2.0035$. Thus the greater amount of broadening linear in $\tilde{M}_{Na}$ observed for the semiquinone triple ions may be understood in terms of the more anisotropic **g** tensor of this species.

Because of overlapping lines it was not possible to obtain, at one temperature, relative widths of the principal nitrogen lines for both triple ions in both solvents. However, from comparisons of diagrams similar to Fig. 3, obtained at several temperatures, the following conclusions emerge. For a given solvent the spectrum of Na_2TMP^+ showed greater differential broadening of the principal nitrogen lines than did the spectrum of Na_2P^+; this result is in keeping with the larger size of the tetramethylpyrazine species causing it to have a slower tumbling rate. For a particular triple ion, the relative width of each principal nitrogen line is, within experimental error the same in tetrahydrofuran and in 2-methyltetrahydrofuran, indicating that molecular tumbling rates in these solvents are comparable.

From Fig. 4 it is evident that the sodium hyperfine septets of Na_2TMP^+ show considerable broadening proportional to $\tilde{M}_{Na}^2$, and furthermore that this broadening is greater in 2-methyltetrahydrofuran than in tetrahydrofuran. Broadening proportional to $\tilde{M}_{Na}^2$ could be due to random modulation of the hyperfine splitting constant of each sodium (21) caused, for example by exchange reactions between definite solvates of the triple ion (cf. ref. 14). However, this mechanism is unlikely to cause broadening over such a wide range of experimental conditions. Incomplete averaging of the anisotropic hyperfine

tensor of sodium would seem to be a more likely cause of the broadening, though more quantitative studies are required to prove this point. This interpretation affords an explanation of the greater effect observed in the less polar solvent 2-methyltetrahydrofuran: in this solvent tighter ionic association and hence a larger dipole–dipole interaction between the sodium nucleus and $2p_z$ electron density on nitrogen is expected. Hence a greater amount of $\tilde{M}_{Na}{}^2$ broadening is anticipated.

This work was supported by an operating grant from the National Research Council of Canada, and by a scholarship to S.A.Al-B from the Gulbenkian Foundation.

1. T. E. Gough and P. R. Hindle. Can. J. Chem. **47**, 1698 (1969).
2. T. E. Gough and P. R. Hindle. Can. J. Chem. **47**, 3393 (1969).
3. N. M. Atherton and A. E. Goggins. Mol. Phys. **8**, 99 (1964).
4. N. M. Atherton and A. E. Goggins. Trans. Faraday Soc. **61**, 1399 (1965).
5. N. M. Atherton and A. E. Goggins. Trans. Faraday Soc. **62**, 1702 (1966).
6. N. M. Atherton. Trans. Faraday Soc. **62**, 1707 (1966).
7. J. Santos-Veiga and A. F. Neiva-Correia. Mol. Phys. **10**, 395 (1965).
8. C. A. McDowell and K. F. G. Paulus. Can. J. Chem. **43**, 224 (1965).
9. T. A. Claxton. Trans. Faraday Soc. **65**, 2289 (1969).
10. T. A. Claxton and D. McWilliams. Trans. Faraday Soc. **65**, 3129 (1969).
11. P. S. Gill and T. E. Gough. Trans. Faraday Soc. **64**, 1997 (1968).
12. E. deBoer. Rec. Trav. Chim. **84**, 609 (1965).
13. N. Hirota. J. Amer. Chem. Soc. **89**, 32 (1967).
14. N. Hirota. J. Phys. Chem. **71**, 127 (1967).
15. G. W. Canters, E. deBoer, B. M. P. Hendriks, and A. Van Willigen. Chem. Phys. Lett. **1**, 627 (1968).
16. G. W. Canters, E. deBoer, B. M. P. Hendriks, and A. A. K. Klassen. Proc. Collogue Ampère, **15**, 242 (1968).
17. B. L. Barton and G. K. Fraenkel. J. Chem. Phys. **41**, 695 (1964).
18. A. J. Stone. Mol. Phys. **6**, 509 (1963).
19. J. W. H. Schreurs and G. K. Fraenkel. J. Chem. Phys. **34**, 756 (1961).
20. T. Takeshita and N. Hirota. Chem. Phys. Lett. **4**, 369 (1969).
21. G. K. Fraenkel. J. Phys. Chem. **71**, 139 (1967).

Can. J. Chem. Downloaded from www.nrcresearchpress.com by 210.87.254.5 on 09/05/12
For personal use only.

Can. J. Chem. Downloaded from www.nrcresearchpress.com by 210.87.254.105 on 09/05/12
For personal use only.

Free radicals in γ-irradiated disodium succinate. Part 1. Monoclinic crystals[1]

H. M. VYAS,[2] J. JANECKA, AND M. FUJIMOTO
Department of Physics, University of Guelph, Guelph, Ontario

Received January 19, 1970

Crystals of disodium succinate have two distinct modifications, monoclinic and triclinic. These were recognized by electron spin resonance (e.s.r.) studies of the free radicals produced by γ-irradiation. In the monoclinic crystals, e.s.r. spectra and radiation processes appear similar to those observed in γ- (or x-) irradiated succinic acid. The situation in triclinic crystals is more complex (see Part 2). In monoclinic crystals irradiated at 77 °K, two types of radical coexist. They were identified as $^{-}O_2CCH_2$-$CH_2\dot{C}O_2^{2-}$, **1**, together with a distorted conformation of the radical $^{-}O_2C(\dot{C}HCH_2)^*CO_2^{-}$, **2**. On warming to room temperature the former species disappears while the latter changes irreversibly to a stable conformation $^{-}O_2C\dot{C}HCH_2CO_2^{-}$, **3**.

Canadian Journal of Chemistry, 48, 2804 (1970)

Introduction

Free radicals in γ- (or x-) irradiated succinic acid crystals have been studied by many investigators (1–6). It is well known that the radicals $HO_2C\dot{C}HCH_2CO_2H$ are the major stable species at room temperature (1, 2) and that $HO_2C\dot{C}HCH_3$ and CO_2^{-} radicals occur to a minor extent (4–6). Ionic radicals HO_2CCH_2-$CH_2\dot{C}O_2H^{-}$ are believed to be stabilized at 77 °K (3), although their relation to the subsequent stable radicals is not clear. Bales, Schwartz, and Hanna (7) have recently reported results on x-irradiated disodium succinate in which the room temperature stable species was shown to be $^{-}O_2C\dot{C}HCH_3$. They attributed the differences between succinic acid and the disodium salt to difference in molecular configuration within the crystal lattice.

We have also studied this system independently (14), but the overall results were complex and confusing. This confusion arose from the existence of two crystal modifications, the form of which was not clearly defined in the literature. In Groth's Chemische Krystallographie (8), the crystal symmetry of disodium succinate was described as either monoclinic or triclinic. In our studies, both symmetries were found to exist when the crystals were prepared from saturated aqueous solutions at room temperature. Furthermore, the e.s.r. spectra and irradiation processes were different in both types of crystal.

For the purpose of comparison some of the experiments reported in refs. 3 and 5 were repeated in our laboratory. In spite of poor resolution the e.s.r. spectrum observed in γ-irradiated succinic acid crystals at 77 °K bore a striking resemblance to that obtained from the monoclinic disodium salt at 77 °K. In partially deuterated disodium succinate, $Na_2(CH_2CO_2)_2 \cdot 6D_2O$, the resolution was greatly improved, and we believe that some important aspects in the post-radiation processes are now understood.

The results obtained from triclinic crystals are presented in the following paper (Part 2).

Experimental

Monoclinic crystals grown from saturated aqueous solution at room temperature have a typical form as sketched in Fig. 1. The form is rarely obtained and is similar to that of triclinic symmetry. It was therefore difficult to distinguish the two modifications just by inspection. In both types, the crystals form elongated plates, on which the rectangular coordinate axes *x*, *y*, and *z* are set for determining the tensor components. Single crystals were grown by repeated recrystallization from 99.9% D_2O solution to obtain better resolution of the e.s.r. spectra at 77 °K. The crystal habit was identical with the undeuterated salt. Samples were oriented in "spectrosil" tubing and irradiated at liquid nitrogen temperature in a Gammacell 220 ^{60}Co source to a dose of 1–2 Mrads. Over this range, e.s.r. spectra appeared independent of dose. Irradiation at room temperature gave spectra identical to those obtained from samples irradiated at 77 °K and then warmed to room temperature.

The radicals only stable at 77 °K appeared to have a longer spin–lattice relaxation time than those stabilized in the lattice at room temperature. At 77 °K, the spectrometer was operated at about 1 mW microwave power level to avoid distortion due to fast-passage effects. At room temperature a higher power level ($\sim$ 100 mW) was used.

The e.s.r. spectrometer was a simple microwave bridge operated at X-band frequencies with a cylindrical cavity

[1]Supported by a grant from the National Research Council of Canada.

[2]Based in part on M.Sc. thesis (H.M.V.) submitted to the Department of Physics, University of Guelph.

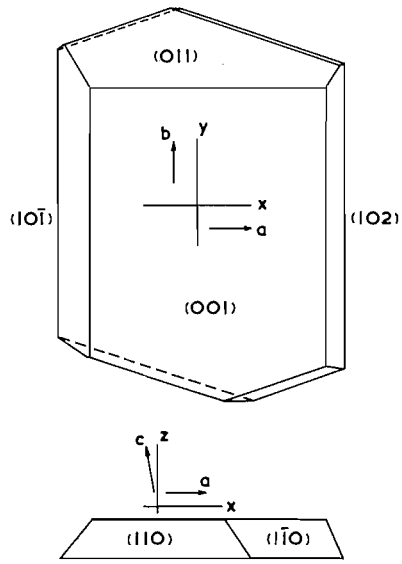

FIG. 1. Crystal habit of monoclinic single crystals of disodium succinate·6D_2O ($\beta = 103°$). The axes *a*, *b*, and *c* are notations used in Groth's book (8), while *x*, *y*, and *z* are the reference axes for tensor determination.

of TE_{011} mode. A Varian 4 in. magnet was used throughout. The magnetic field was modulated at 65 kHz and the sweep-rate calibrated by a proton resonance magnetometer.

Results and Discussion

The hyperfine structure in the observed e.s.r. spectra results from proton interactions in the radicals. The first-order eigenvalues of the hyperfine energy $\sum_i \boldsymbol{S}\cdot \mathbf{A}_i \cdot \boldsymbol{I}_i$ are expressed by $\sum_i K_i M m_i$, where $K_i = |\boldsymbol{u}_H \cdot \mathbf{A}_i|$ and $\boldsymbol{u}_H$ is the unit vector along the static field $\boldsymbol{H}$. It should be noted that $M = \pm \frac{1}{2}$ represents the electron spin magnetic quantum number along $\boldsymbol{H}$, whereas $m_i = \pm \frac{1}{2}$ is for the *i*th proton spin $\boldsymbol{I}_i$, quantized along the effective field consisting of $\boldsymbol{H}$ and the field due to the electron spin. From the observed angular dependence of K_i^2, the elements of the tensor $\mathbf{A}\dagger\mathbf{A}$ were computed, which were then diagonalized to obtain the principal values of the tensor $\mathbf{A}$ and their direction cosines.

The spectra at 77 °K

Electron spin resonance spectra obtained at 77 °K were complex and composed of two overlapping spectra. One spectrum consisted of four lines of equal intensity, and the second of eight component groups also of equal intensity. With the static field applied in the *xy* and *xz* planes, both spectra indicated the presence of two magnetically inequivalent sites in the unit cell, giving rise to an additional splitting in each spectrum. In the *yz* plane, no site-splittings were observed. Figure 2 shows a representative spectrum for $\boldsymbol{u}_H = (0, \cos 60°, \cos 30°)$, in which the best resolution (other than site-splittings) was observed.

The spectrum showing four lines in the *yz* plane indicates that the unpaired spin is interacting with two inequivalent protons. The angular variations of the two splitting constants K_1 and K_2 are clearly observed with H applied in the *y*–*z* plane. As shown in Fig. 3 both protons show fairly large anisotropies, but a complete determination of the tensors was hindered by poor spectral resolution in the *xz* and *xy* planes. The species responsible for this spectrum can be interpreted as the one corresponding to the anionic radicals identified by Box *et al.* (3) in

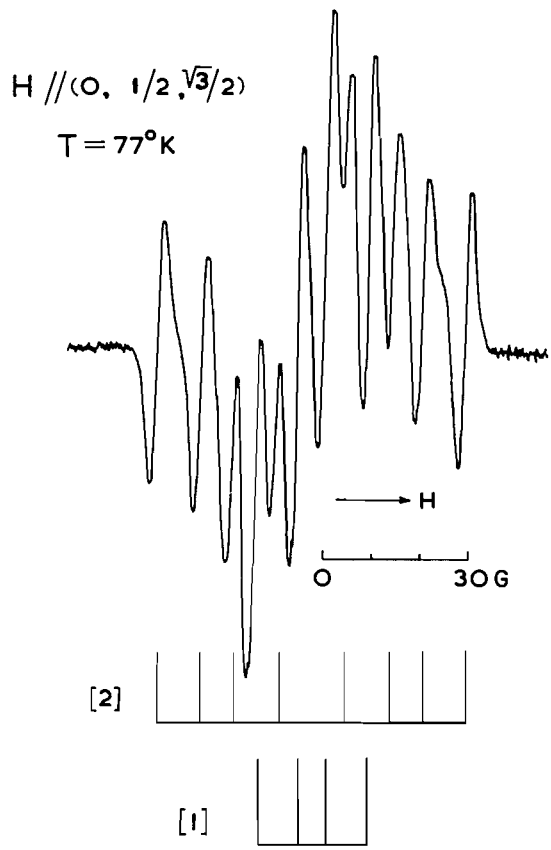

FIG. 2. Electron spin resonance spectrum from a monoclinic single crystal of disodium succinate·6D_2O γ-irradiated and observed at 77 °K. $H\|(0, \cos 60°, \cos 30°)$. The stick diagrams indicate the spectra of the identified radicals **1** and **2**.

Can. J. Chem. Downloaded from www.nrcresearchpress.com by 210.87.254.105 on 09/05/12
For personal use only.

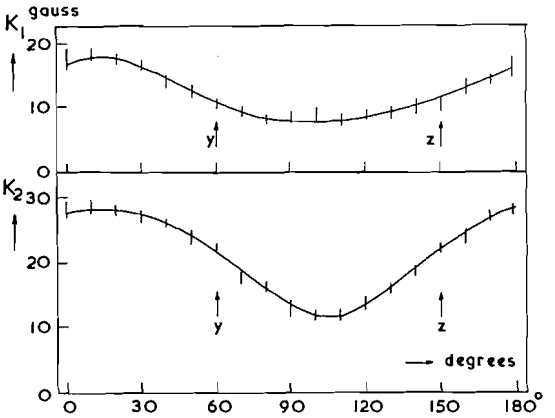

FIG. 3. Angular variations of the proton coupling constants K_1 and K_2 in radicals **1** at 77 °K. H is yz plane.

x-irradiated succinic acid. In the disodium salt such anionic radicals can be

$$^{-}O_2CCH_2CH_2\dot{C}O_2^{2-}$$

1

which are formed by electron capture at one of the carboxyl groups of the parent molecule. Bennett and Gale (9) have also shown the occurrence of such electron capture at 77 °K with a variety of carboxylic acids. The unpaired spin density in such a case is known to be highly localized at the carbon atom, ($\rho_c \sim 1.0$), as was demonstrated by Sinclair and Hanna (10) in the similar case of *l*-alanine-1 ^{13}C irradiated at 77 °K.

The observed hyperfine anisotropies appear to be too large for the proposed radical **1**, although the results may suggest the possibility of a substantially different conformation from the planar structure. The justification of the magnitude of the anisotropies is however difficult, because of the lack of knowledge about the structure.

The possibility for radicals $^{-}O_2CCH_2CH_2\text{-}C\dot{O}_2$, formed by loss of electrons in the parent molecules, can be ruled out by a simple MO-argument for 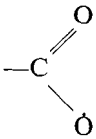 . In this case the spin density at the center carbon atom is too small to account for the observed hyperfine splittings.

The eight component groups in the second spectrum are interpreted as hyperfine structure due to three inequivalent protons. A complete analysis of this spectrum was not possible because the center part was obscured by the spectrum of the species **1**. From a well defined angular variation of the outer peaks, one of the hyperfine tensors, say $\mathbf{A}_1$, was determined, but the other two, $\mathbf{A}_2$ and $\mathbf{A}_3$ could not be measured for all orientations of the crystal. However, a reasonable estimate of $\mathbf{A}_2$ and $\mathbf{A}_3$ could be made from the observed overall spacing, $K_1 + K_2 + K_3$, and K_1. K_3 was then computed, assuming K_2 is isotropic and equal to 16.6 G. This value of K_2 was obtained in some orientations of the crystal, in which this second splitting was measurable in the spectrum. The computed tensor $\mathbf{A}_3$ is much less anisotropic than $\mathbf{A}_1$. It is therefore reasonable to assign the tensor $\mathbf{A}_1$ to an α-proton and $\mathbf{A}_2$ and $\mathbf{A}_3$ to two β-protons. The radical may thus be identified as

$$^{-}O_2C(\dot{C}HCH_2)^{*}CO_2^{-}$$

2

where ( )* indicates the presence of an unusual conformation in this part of the molecule. The results of the analysis are summarized in Table 1.

This isotropic component, 36 G, of the α-proton coupling is much larger than those commonly observed in planar π radicals. This unusual value can, however, be justified by Karplus' calculation which will be discussed in a later section.

Comparing with the spectra obtained from the triclinic salt, the radical **2** is believed to be the most likely species responsible for the eight-line spectrum observed at 77 °K. However, other possible alternatives should not be ignored at this stage. For example, radicals of the type $^{-}O_2CCH_2\dot{C}H_2$ may be formed by dissociation after ionization of the parent molecule (see Part 2). It is necessary in this case to assume that one of the β-proton couplings is negligible. However, this assumption is not easily accepted for the two different crystal modifications, both of which showed the radical **2** eight-line spectra.

Spectra at Room Temperature

On warming to room temperature, the spectrum changed irreversibly to a simple one, as shown in Fig. 4, which was obtained with the static field $\boldsymbol{H}$ parallel to the x-axis. It was noted that in all orientations sets of lines with an intensity ratio 1:2:1 were observed, implying that two protons within the radical are identical. As in the low temperature spectra, angle-

Can. J. Chem. Downloaded from www.nrcresearchpress.com by 210.87.254.105 on 09/05/12
For personal use only.

TABLE 1

Hyperfine tensors in the free radical $^{-}O_2C(\dot{C}HCH_2)^*CO_2^{-}$, **2**, in γ-irradiated monoclinic crystals of disodium succinate·$6D_2O$ at 77 °K[a]

Tensors	Principal value	Isotropic values	Anisotropy	Direction cosines
$\mathbf{A}_1$	52.2		(−) 16.2	(0.847 ∓0.369 ∓0.382)
	(−) 20.8	(−) 36.0	(+) 15.2	(±0.498 0.803 0.328)
	35.1		(+) 0.9	(±0.185 −0.468 0.800)
$\mathbf{A}_2$	Assumed isotropic	(+) 16.6	—	—
$\mathbf{A}_3$	7.8		(−) 2.0	(0.832 ±0.499 ∓0.244)
	(+) 7.2	(+) 9.8	(−) 2.6	(∓0.199 0.677 0.709)
	14.4		(+) 4.6	(±0.519 −0.541 0.662)

[a]Unit: gauss, error ± 1.0 G, theoretical signs are indicated for the tensor components.

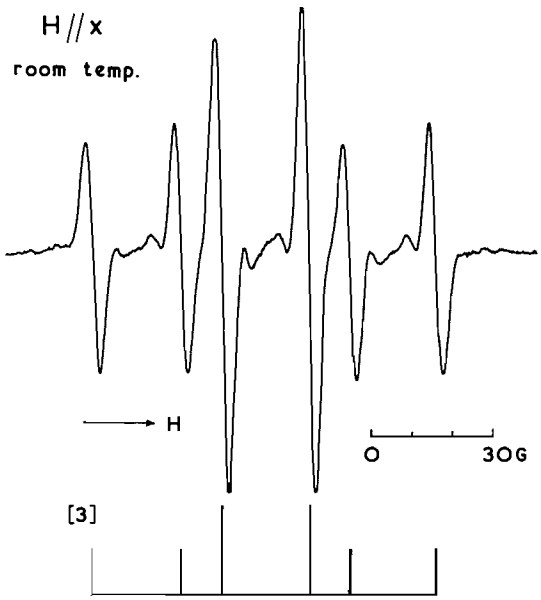

FIG. 4. Electron spin resonance spectrum observed at room temperature from a monoclinic single crystal of disodium succinate $6D_2O$ γ-irradiated at 77 °K. $H||x$. The stick diagram indicates the spectrum of radicals **3**.

dependent site-splittings were only observed in the *zx* and *xy* planes. The results of analysis are shown in Table 2. These values are all acceptable quantities for a stable π radical

$$^{-}O_2C\dot{C}HCH_2CO_2^{-}$$
3

The agreement with previously reported constants for this type of radical in various host crystals is very good (11). The fact that $\mathbf{A}_2 = \mathbf{A}_3$ and both are almost isotropic indicates that the radical **3** does not have a twisted structure in the methylene group, in contrast with a twisted form of the corresponding radical in many cases (11).

Structure of the Radicals $^{-}O_2C(\dot{C}HCH_2)^*CO_2^{-}$ and $^{-}O_2C\dot{C}HCH_2CO_2^{-}$

The radical **3** is undoubtedly a planar π radical, in which the unpaired electron is on the 2pπ orbital of the carbon atom, being normal to the plane of the three $sp^2\sigma$ bonds. The observed α-proton tensor $\mathbf{A}_1$ has a typical isotropic value, 21.1 ± 0.5 G, of a σ–π interaction.[3]

The radical **2** has not been reported previously, but it is believed to have a different conformation from that of **3**. The observed isotropic constant of the α-proton interaction, 36 G, is much larger than 21 G observed in the radical **3**. It is interesting to compare these values with a theory of methyl radicals, CH_3, published by Karplus (12).

The basic molecular skeleton of an undamaged molecule is believed to have a tetrahedral structure formed by four sp^3 orbitals of the carbon atom. The theory dealt with the proton hyperfine constant for a pyramidal CH_3 as a function of the angle between the three-fold symmetry axis and one of the three CH bonds. The observed value for the radical **2**, 36 G, agrees reasonably with the calculated values, 34–42 G for the tetrahedral CH_3. It is therefore legitimate to assume that the conformation of the radical **2** is nearly tetrahedral. This implies that the radical **2** may retain its original tetrahedral structure even after removal of a hydrogen atom from the parent molecule at 77 °K. It may be a general occurrence that free radicals formed in

[3]The spin density at the carbon atom is expected to be slightly less than 1. In this case $\rho_c = 0.91$ can account for the small difference from the ideal σ–π coupling constant, 23 G.

Can. J. Chem. Downloaded from www.nrcresearchpress.com by 210.87.254.105 on 09/05/12
For personal use only.

TABLE 2

Hyperfine tensors in the free radicals $^{-}O_2C\dot{C}HCH_2CO_2^{-}$, **3**, in γ-irradiated monoclinic crystals of sodium succinate·$6D_2O$ at 300 °K[a]

Tensors	Principal values	Isotropic value	Anisotropy	Direction cosines
A_1	19.7		(+) 1.4	(0.913 ±0.317 ∓0.258)
	(−) 12.4	(−) 21.1	(+) 8.7	(∓0.226 0.917 0.328)
	31.1		(−) 10.0	(±0.340 −0.241 0.909)
$A_2 = A_3$	32.0		(−) 0.4	(1.000 0.000 0.000)
	(+) 30.9	(+) 32.4	(−) 1.5	(0.000 0.843 0.538)
	34.5		(+) 2.1	(0.000 −0.538 0.843)

[a]Unit: gauss, error ±0.5 G, theoretical signs are indicated for the tensor components.

solids at low temperature retain the original undamaged molecular structure. A similar finding was reported in some amino acid crystals irradiated at 77 °K (13).

Radiolysis Mechanism

An accurate intensity comparison of the e.s.r. spectra observed at 77 °K and room temperature was very difficult, because of the difference in relaxation time, T_1, in addition to differences in temperature, microwave power, and Q-factor of the cavity. Qualitatively, however, the conformation change in the radical $^{-}O_2C(\dot{C}H—CH_2)^*CO_2^{-}$ is believed to be established. The radical **1** simply decayed on warming. The decay of such radicals could be understood as a thermal electron releasing process, but such an interpretation is not obvious from e.s.r. data alone.

As mentioned in the Introduction, comparison with the results of irradiated succinic acid suggests that the dominant radiation processes observed by e.s.r. are very similar in the acid and monoclinic salt. The overall processes are, however, not as simple as the e.s.r. spectra imply. Irradiated salt crystals differ from acid crystals in that the former showed a dark brown color at 77 °K, whereas the latter was virtually colorless. This color of the salt crystals could be bleached by illumination with visible light at 77 °K or warming to about − 20 °C. Photo-bleaching at 77 °K also removed the e.s.r. spectra entirely in marked contrast to the thermal process where the formation of different radicals was observed.

This work was carried out as a continuation of the experiments performed by one of us (M.F.), while working as visiting scientist at Chalk River Nuclear Laboratories in the summer of 1968. Special thanks are due to Dr. W. A. Seddon for his valuable comments.

1. C. Heller and H. M. McConnell. J. Chem. Phys. **32**, 1535 (1960).
2. D. Pooley and D. H. Whiffen. Mol. Phys. **4**, 81 (1961).
3. H. C. Box, H. G. Freund, and K. T. Lilga. J. Chem. Phys. **42**, 1471 (1965).
4. S. F. J. Reed and D. H. Whiffen. Mol. Phys. **12**, 159 (1967).
5. R. E. Klinck. J. Chem. Phys. **49**, 4722 (1968).
6. R. N. Schwartz, M. W. Hanna, and B. L. Bales. J. Chem. Phys. **51**, 4336 (1969).
7. B. L. Bales, R. N. Schwartz, and M. W. Hanna. J. Chem. Phys. **51**, 1974 (1969).
8. P. Groth. Chemische Krystallographie, 3 Teil. Wilhelm Engelmann, Leipzig. 1910. p. 266.
9. J. E. Bennett and L. H. Gale. Trans. Faraday Soc. **64**, 1174 (1968).
10. J. Sinclair and M. W. Hanna. J. Chem. Phys. **50**, 2125 (1969).
11. H. Fischer. Magnetic properties of free radicals. (Landolt–Börnstein, New Series), Group II, Vol. 1. Springer Verlag, Berlin. 1965.
12. M. Karplus. J. Chem. Phys. **30**, 15 (1959).
13. M. Fujimoto, W. A. Seddon, and D. R. Smith. J. Chem. Phys. **48**, 3345 (1968).
14. M. Fujimoto and W. A. Seddon. Unpublished results.

Can. J. Chem. Downloaded from www.nrcresearchpress.com by 210.87.254.105 on 09/05/12
For personal use only.

Can. J. Chem. Downloaded from www.nrcresearchpress.com by 210.87.254.5 on 09/05/12
For personal use only.

Free radicals in γ-irradiated disodium succinate. Part 2. Triclinic crystals[1]

M. FUJIMOTO[2] AND W. A. SEDDON

Physical Chemistry Branch, Chalk River Nuclear Laboratories, Atomic Energy of Canada Limited, Chalk River, Ontario

Received January 19, 1970

Electron spin resonance (e.s.r.) spectra and radiation processes in γ-irradiated triclinic crystals of disodium succinate are more complex than those observed in monoclinic crystals. At 77 °K, three species coexist, $^{-}O_2CCH_2CH_2\dot{C}O_2^{2-}$ (**1**), a distorted conformation of the radical $^{-}O_2C(\dot{C}HCH_2)^*CO_2^{-}$ (**2**), and an unidentified radical X. On warming to room temperature, **1** and X disappear, while **2** changes to a more stable conformation $^{-}O_2C\dot{C}HCH_2CO_2^{-}$ (**3**). In addition the species $\dot{C}O_2^{-}$ (**4**), and $^{-}O_2C\dot{C}HCH_3$ (**5**) are produced. On further warming to 40 °C, species **4** disappears while at the same time species **3** increases in intensity. Radical **5** remains unaffected. Possible mechanism and comparisons with monoclinic crystals are discussed.

Canadian Journal of Chemistry, 48, 2809 (1970)

Introduction

Crystals of disodium succinate grown from aqueous solution at room temperature have either a monoclinic or a triclinic symmetry (1). The triclinic form is the more common. On standing these crystals gradually become opaque and brittle, although some remain stable for months. This deterioration is enhanced by γ-irradiation at room temperature and depends presumably on the number of imperfections in the crystal. No such deterioration occurred on irradiation at 77 °K.

Bales, Schwartz, and Hanna (2) recently reported that the stable species observed at room temperature in X-irradiated disodium succinate (of unspecified crystal symmetry) is $^{-}O_2C\dot{C}HCH_3$ with no indication of the radical $^{-}O_2C\dot{C}HCH_2$-CO_2^{-}. We have found that the radical $^{-}O_2$-$C\dot{C}HCH_2CO_2^{-}$ exists in both types of disodium succinate single crystals. It was also noted that in irradiations at room temperature the spectrum of $^{-}O_2C\dot{C}HCH_3$ predominated in triclinic crystals that had to some extent deteriorated.

This paper presents the results of e.s.r. studies on γ-irradiated triclinic crystals of disodium succinate $6D_2O$ at 77 °K followed by warming to room temperature. The post-radiation mechanism is briefly discussed.

Experimental

Most of the procedures have been described in the preceding paper (Part 1). A Varian X-band V4502 spectrometer with 100 kHz magnetic field modulation was used to record the e.s.r. spectra and a variable temperature accessory to observe the change in spectra with increasing temperature.

Results and Discussion

Triclinic crystals have a very similar crystal habit to that of monoclinic crystals (1). Figure 1 shows a sketch of a general habit of triclinic crystals. The reference coordinate axes *x*, *y*, and *z* are set on the crystals as indicated.

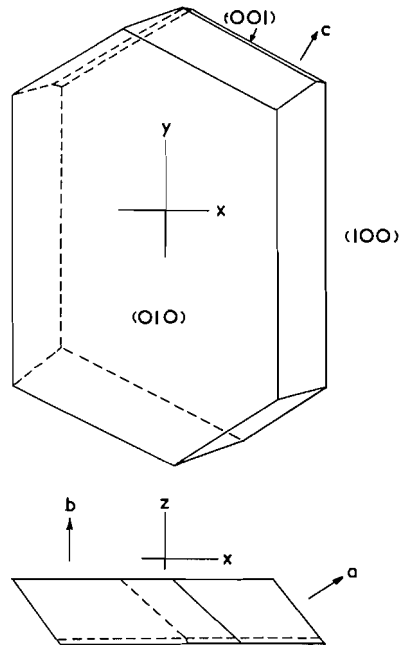

FIG. 1. Typical habit form of triclinic disodium succinate $6D_2O$ crystals. Angles $a{:}b = 63°$, $b{:}c = 80°$, and $c{:}a = 74°$ (8).

[1]AECL No. 3649.

[2]Visiting Scientist (Summer 1968). Present address: Department of Physics, University of Guelph, Guelph, Ontario.

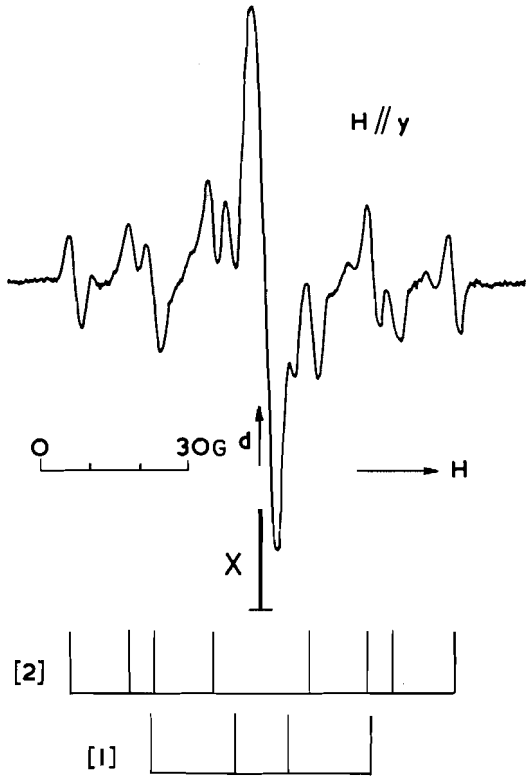

FIG. 2. Electron spin resonance spectrum from triclinic $Na_2(CH_2CO_2)_2.6D_2O$ γ-irradiated and observed at 77 °K. The d.c. field H was applied parallel to the y axis. The vertical arrow d indicates the position for DPPH ($g = 2.0036$). The stick diagrams show the spectra of the component radicals, X, **1**, and **2**.

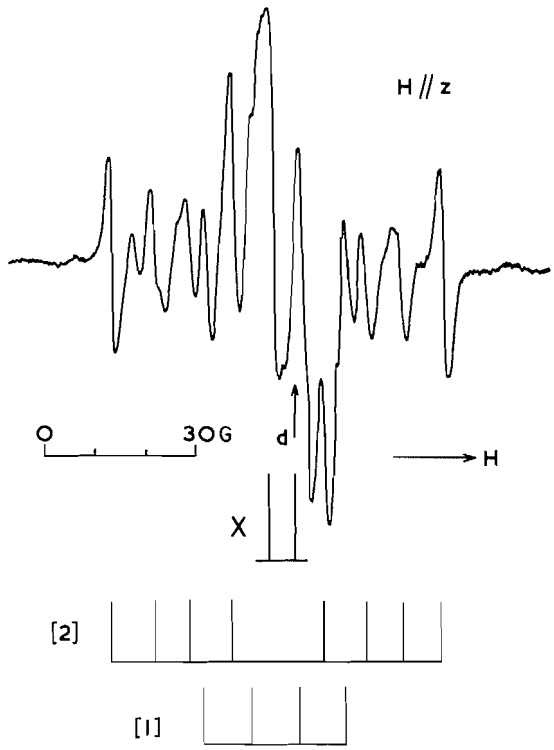

FIG. 3. Electron spin resonance spectrum from triclinic $Na_2(CH_2CO_2)_2.6D_2O$, γ-irradiated and observed at 77 °K. The d.c. field H was parallel to the z axis. The vertical arrow d indicates the position for DPPH ($g = 2.0036$). The stick diagrams show the spectra of the component radicals, X, **1** and **2**.

Spectra at 77 °K

Representative spectra at 77 °K observed from γ-irradiated deuterated triclinic crystals of disodium succinate, $Na_2(CH_2CO_2)_2$ $6D_2O$, are shown in Figs. 2 and 3. The complex pattern can be resolved into three components consisting of a quartet, an octet, and a doublet.

The former spectrum contains four lines of equal intensity, corresponding to two inequivalent proton interactions, but unlike the monoclinic crystals shows no evidence of site splitting with change in crystal orientation. One proton hyperfine coupling is anisotropic but the other is nearly isotropic. The anisotropic tensor has the principal values along the x, y, and z axes of 19.0, 25.6, and 15.7 ± 1.0 G, respectively, while the isotropic tensor has the value 10 ± 1 G. The isotropic components of these tensors, i.e. 20 and 10 G, respectively, are consistent with those for the corresponding radical in the monoclinic crystal (1). The radical responsible for this quartet spectrum is therefore identified as

$$^{-}O_2CCH_2\dot{C}H_2CO_2^{2-}$$

1

The observed hyperfine tensors in the disodium salts are different from those reported for irradiated succinic acid crystals (3). This may be attributed to the difference in electron spin density distribution in $—CO_2^{2-}$ compared with $—CO_2H^{-}$.

The second spectrum, showing eight component lines, is considered identical to the corresponding radical in the monoclinic crystals (1), i.e.

$$^{-}O_2C(\dot{C}HCH_2)^{*}CO_2^{-}$$

2

The bracket ( )* indicates, as in Part 1, the presence of a distorted structure in this part of the molecule. Again, contrary to the monoclinic crystals, no site-splitting was recognized for this

Can. J. Chem. Downloaded from www.nrcresearchpress.com by 210.87.254.5 on 09/05/12
For personal use only.

TABLE 1

Hyperfine coupling tensors in the free radical **2**, in triclinic crystals of disodium succinate $6D_2O$ at 77 °K*

Tensors	Principal values	Isotropic values	Anisotropy	Direction cosines		
$\mathbf{A}_1$	24.9		(+)17.9	(0.642	−0.681	−0.352)
	(−)61.3	(−)42.8	(−)18.5	(0.661	0.724	−0.196)
	42.1		(+) 0.7	(0.389	−0.106	0.915)
$\mathbf{A}_2$	8.3		(−) 1.4	(0.926	−0.378	0.000)
	(+)13.0	(+) 9.7	(+) 3.3	(0.378	0.926	0.000)
	7.9		(−) 1.8	(0.000	0.000	1.000)
$\mathbf{A}_3$	19.3		(+) 2.9	(0.883	0.354	0.309)
	(+)14.1	(+)16.4	(−) 2.3	(−0.470	0.666	0.580)
	15.8		(−) 0.6	(−0.000	−0.657	0.754)

*Unit: gauss; error ±0.5 G. Theoretical signs are indicated for comparison with known α- and β-couplings.

radical. Table 1 summarizes the analysis for this species. Tensors $\mathbf{A}_1$, $\mathbf{A}_2$, and $\mathbf{A}_3$ were determined independently from the observed spectra. $\mathbf{A}_1$ is found anisotropic compared with $\mathbf{A}_2$ and $\mathbf{A}_3$, and these tensors are therefore assigned to one α and two β protons, respectively. It should be noted that the isotropic components of these tensors are all consistent with the values found in the monoclinic crystals (1). The small difference between the α-proton couplings in the two types of crystal may be due to a different degree of distortion. Nevertheless, they are both consistent with the values calculated for a tetrahedral form of CH_3 (34–42 G, see Part 1).

The third spectrum is a simple angle-dependent doublet, showing appreciable **g**-variation compared with the other species. This species has not been identified and is designated by X. Table 2 summarizes the parameters for X.

TABLE 2

Observed hyperfine and **g**-tensors in the radicals X, in γ-irradiated triclinic $Na_2(CH_2CO_2)_2$ $6D_2O$ at 77 °K

Hyperfine tensor			Isotropic value
3.3	—	0	
—	1.7	0	3.9
0	0	6.6	(Unit: gauss, error ± 0.5 G)

g-Tensor

Principal values	Direction cosines		
2.0041	(0.569	−0.594	0.569)
2.0014	(0.420	0.805	0.420)
2.0032	(−0.727	0.000	0.727)

Spectra at Room Temperature

On warming to room temperature (approximately 20 °C), the spectra described above changed irreversibly to another three component spectrum. The following radicals were identified at room temperature.

$^-O_2C\dot{C}HCH_2CO_2^-$

3

CO_2^-

4

$^-O_2C\dot{C}HCH_3$

5

A representative spectrum is shown in Fig. 4*a*.

The radical **3** is identical to the corresponding radical observed in monoclinic crystals, but the spectra are different in two respects. In the triclinic crystals the radical **3** has only one site in the unit cell and the two β-couplings are not equal, implying a twisted structure in the adjacent CH_2 group. Table 3 summarizes the results on the stable conformation of the radical **3**.

The CO_2^- radical **4** is known to show a relatively large **g**-variation in the range of 2.000–2.015. The agreement of the observed **g**-tensor for the radical **4** (Table 4), with known values for CO_2^- (4), can be accepted as a reasonable evidence for this identification.

The identification of radical **5** was based on the presence of sets of four lines with an intensity ratio 1:3:3:1 in all orientations of the static field. This signifies the presence of a rotating $-CH_3$ group. A complete determination of the tensors was not possible because of spectral overlap. The α-proton tensor was determined from the measured angular variation of the overall spacings of the spectra, assuming that the proton couplings

Can. J. Chem. Downloaded from www.nrcresearchpress.com by 210.87.254.5 on 09/05/12
For personal use only.

TABLE 3

Hyperfine tensors in the free radical **3** in triclinic crystals of disodium succinate $6D_2O$ at 298 °K

Tensors	Principal values	Isotropic values	Anisotropy	Direction cosines		
A_1	30.6		(−) 9.7	(−0.196	−0.505	0.841)
	(−)20.7	(−)20.9	(+) 0.2	(0.735	−0.492	0.467)
	11.5		(+) 9.4	(0.649	0.709	0.275)
A_2	39.4		(+) 3.5	(0.493	0.839	0.231)
	(+)35.3	(+)35.9	(−) 0.6	(0.331	−0.064	−0.941)
	33.0		(−) 2.9	(0.804	0.541	0.246)
A_3	Isotropic	(+)24.5	0			

*Unit: gauss, error: ±0.4 G. Theoretical signs are indicated for comparison with known α- and β-couplings.

in $-CH_3$ are isotropic and equal to 26.0 G. Table 5 gives the results on the radical **5**. Unlike radicals **1**, **2**, **3**, and **4**, the radical **5** has two inequivalent sites in the unit cell which is in agreement with the observation of Bales *et al.* (2).

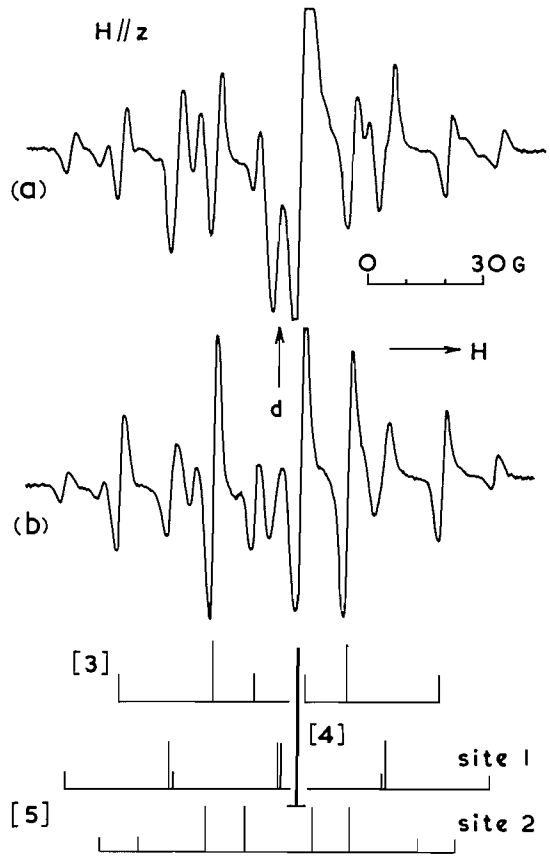

FIG. 4. Electron spin resonance spectra observed at room temperature from triclinic $Na_2(CH_2CO_2)_2.6D_2O$ γ-irradiated at 77 °K. The static field *H* was applied parallel to the *z* axis. A comparison is shown between the spectra (*a*) before and (*b*) after annealing. The stick diagrams show the spectra of the component radicals **3**, **4**, and **5**.

The presence of the two sites for the radical **5** may be attributed to the two possible locations for the unpaired electron following cleavage of the parent molecule. This may in turn give rise to two sterically different α-proton tensors in the unit cell of the triclinic salt. The presence of a CH_3 group in **5** was further confirmed by observing the change in hindered rotation of CH_3. A reversible change in the e.s.r. spectrum of **5** in which the rotational motion of $-CH_3$ ceases at 77 °K was observed to be similar to that noted for $H_3C\dot{C}HCO_2H$ in irradiated *l*-α alanine (5).

Annealing the sample at 40 °C changed the relative proportions of the above component spectra. Figures 4*a* and *b* show a comparison of the spectra before and after annealing for 30 min with the static field *H* parallel to the *z*-axis. It was noted that the intensity of the spectrum **3** increased as **4** decreased, whereas the intensity of the spectrum **5** remained unchanged.

Electron spin resonance spectra from triclinic salts irradiated at room temperature were different to those observed at room temperature from salts irradiated at 77 °K. After prolonged irradiation at room temperature, the e.s.r. spectra were dominated by radical **5** as reported by Bales *et al.* (2). The factors responsible for this effect are not understood.

Radiolysis Mechanism

The results obtained from both monoclinic and triclinic salts can be qualitatively summarized in terms of the following steps.

(*a*) Primary ionization and subsequent electron capture processes produce the carboxylate radical anion, **1**, stable at 77 °K in both crystals.

[1] $^-O_2CCH_2CH_2CO_2^- \rightsquigarrow {}^-O_2CCH_2CH_2C\dot{O}_2 + e^-$

[2] $^-O_2CCH_2CH_2CO_2^- + e^- \rightarrow {}^-O_2CCH_2CH_2CO_2^{2-}$

Can. J. Chem. Downloaded from www.nrcresearchpress.com by 210.87.254.5 on 09/05/12
For personal use only.

TABLE 4

g-Tensor components of the free radical CO_2^-, **4**, in irradiated triclinic crystals of disodium succinate $6D_2O$ at 298 °K*

g Tensor			Principal values	Direction cosines		
2.0000	0.0046	0.0073	2.0145	(0.507	0.566	0.650)
0.0046	2.0012	0.0080	1.9960	(−0.750	0.661	−0.001)
0.0073	0.0083	2.0016	1.9923	(−0.457	−0.454	0.766)

*Error = ±0.0002 G.

TABLE 5

Components of the α-proton hyperfine interaction of the radical **5** in triclinic crystals of sodium succinate $6D_2O$ at 298 °K*

Site	Tensors			Isotropic values
1	24.9	0.6	−0.8	21.4
	0.6	21.6	—	
	−0.8	—	17.7	
2	11.8	—	0.0	21.0
	—	18.4	0.6	
	0.0	0.6	32.8	

*Unit: gauss, experimental error: ±0.5 G. Hyperfine coupling constants for rotating CH_3 in the radical 5 are isotropic and equal 26.0 G. The missing matrix elements could not be determined in our experiments.

Bennet and Gale (6), have demonstrated the occurrence of reaction 2 at 77 °K with a variety of carboxylic acids. The parent radical ion, $^-O_2CCH_2CH_2C\dot{O}_2$, may be responsible for the spectrum assigned to radical X in the triclinic crystals, but its absence in monoclinic salts is then difficult to understand. The electron spin density at the carbon atom in 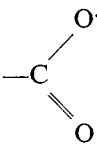 should be very small (see Part 1), and could therefore account for the small doublet structure of the spectrum of X, assuming that one of the methylene proton couplings is larger than the other.[3]

(*b*) With increasing temperature species **1** disappears while the conformation change, **2** to **3**, is characteristic of both crystals.

[3] $^-O_2C(\dot{C}HCH_2)^*CO_2^- \rightarrow {}^-O_2C\dot{C}HCH_2CO_2^-$
2 **3**

[3]Recently, Box *et al.* (7) have reported that radicals formed by oxidation of parent organic molecules are characterized by a large positive g-shift ($\Delta g \sim 0.05$) with no hyperfine structure. Our interpretation of the radical X is inconsistent with their assignment. Further investigation is necessary to clarify this view.

(*c*) The presence of radical X in the triclinic crystals seems to be responsible for the difference in the post-irradiation annealing process observed in these two modifications. If X is a positive hole, then the decay of radical **1** may be a charge neutralization process resulting in the formation of species **4** and **5**.

[4] $^-O_2CCH_2CH_2CO_2 + (\mathbf{1}) \rightarrow (^-O_2CCH_2CH_2CO_2^-)^* + {}^-O_2CCH_2CH_2CO_2^-$

[5] $(^-O_2CCH_2CH_2CO_2^-)^* \rightarrow CO_2^- + {}^-O_2CCH_2\dot{C}H_2$
4

[6] $^-O_2CCH_2\dot{C}H_2 \rightarrow {}^-O_2C\dot{C}HCH_3$
5

The rearrangement process [6] was discussed by Bales *et al.* (2). Finally, on further warming to 40 °C the subsequent disappearance of CO_2^- and concomitant appearance of species **3** suggests that CO_2^- may abstract hydrogen atoms from neighboring parent molecules during the annealing process.

[7] $CO_2^- + {}^-O_2CCH_2CH_2CO_2^- \rightarrow {}^-O_2C\dot{C}HCH_2CO_2^- + HCO_2^-$
4 **3**

1. H. M. Vyas, J. Janecka, and M. Fujimoto. Can. J. Chem. This issue.
2. B. L. Bales, R. N. Schwartz, and M. W. Hanna. J. Chem. Phys. **51**, 1974 (1969).
3. H. C. Box, H. G. Freund, and K. T. Lilga. J. Chem. Phys. **42**, 1471 (1965).
4. D. W. Ovenall and D. H. Whiffen. Mol. Phys. **4**, 135 (1961); J. E. Bennett, B. Mile, and A. Thomas. Trans. Faraday Soc. **61**, 2357 (1965); P. W. Atkins and M. C. R. Symons. The structure of inorganic radicals. Elsevier Publ. Co., Inc., New York, 1967. p. 132.
5. I. Miyagawa and W. Gordy. J. Chem. Phys. **32**, 255 (1960); A. Horsfield, J. R. Morton, and D. H. Whiffen. Mol. Phys. **4**, 425 (1961); **5**, 115 (1961).
6. J. E. Bennett and L. H. Gale. Trans. Faraday Soc. **64**, 1174 (1968).
7. H. C. Box, H. G. Freund, K. T. Lilga, and E. E. Budzinski. J. Phys. Chem. **74**, 40 (1970).
8. P. Groth. Chemische Kristallographie, Teil 3. Wilhelm Engelmann, Leipzig. 1910. p. 266.

Can. J. Chem. Downloaded from www.nrcresearchpress.com by 210.87.254.5 on 09/05/12
For personal use only.

Can. J. Chem. Downloaded from www.nrcresearchpress.com by 210.87.254.40 on 09/05/12
For personal use only.

Proton spin–lattice relaxation time of aniline-d_2 in deuterated benzene and deuterated aniline solution

E. Bock and J. Czubryt[1]
Parker Chemistry Laboratory, University of Manitoba, Winnipeg, Manitoba

and

E. Tomchuk
Department of Physics, University of Winnipeg, Winnipeg, Manitoba

Received February 11, 1970

The proton spin – lattice relaxation time of aniline-d_2 in deuterated aniline solution was determined as a function of concentration and temperature over the temperature interval 260–360 °K using a pulsed nuclear magnetic resonance technique. In addition the proton spin – lattice relaxation time of aniline-d_2 in deuterated benzene solution at 20 °C was also determined. It was found that the activation energies of the *intra-* and *inter*-molecular relaxation rates were of similar magnitude, viz. 4.5 and 4.4 kcal/mole, respectively. It was also found that at 20 °C the rotational correlation time, τ_r, of the $C_6H_5NH_2$ molecule in infinitely dilute perdeutero benzene solution was approximately half that of the partially deuterated aniline molecule, viz. 3.0×10^{-12} and 6.3×10^{-12} s, respectively, and that τ_r of $C_6H_5ND_2$ in infinitely dilute perdeutero aniline solution is much larger than in infinitely dilute perdeutero benzene solution and is equal to 19×10^{-12} s.

Canadian Journal of Chemistry, 48, 2814 (1970)

Introduction

In a recent Note published in this Journal we reported on the molecular rotational relaxation time, τ_r, of the aniline molecule in infinitely dilute deuterated benzene solution (1). We noted there that our experimental results at that time were not sufficient to warrant a meaningful comment on whether or not the motion of the amino group did contribute to the overall spin–lattice relaxation rate of the molecule. Since the publication of that Note we have extended our investigations of this problem to the point where we are now in a position to make more definite comments on the contribution of the various molecular motions of the aniline molecule to its spin–lattice relaxation rate in dilute benzene solution as well as in pure liquid aniline.

Experimental

Solvents

The solvents used, benzene-d_6, 99.5 atom% D and aniline-d_7, 98.0 atom% D were obtained from Merck, Sharp, and Dohme Co. of Canada Ltd., and were used without further purification.

Solutes

Aniline-d_2, 98.0 atom% D was also obtained from Merck, Sharp, and Dohme Co. of Canada Ltd., and it too was used without further purification.

The ordinary aniline, obtained from Eastman Organic Chemicals was further purified by redistillation from anhydrous KOH.

Apparatus and Procedure

The experimental procedure followed and apparatus used have been described elsewhere (1).

The temperature of the samples was maintained constant within ± 0.2 °C by means of a gas (nitrogen) flow thermostat.

Results and Discussion

Typical experimental results for 20 °C are shown graphically in Fig. 1 in a form of a graph of T_1^{-1} vs. x, the mole fraction of the proton-containing solute in solution. Figure 2 shows the temperature dependence of the proton spin – lattice relaxation time of the $C_6H_5ND_2$ molecule in perdeutero aniline solution as a function of concentration and temperature. From Fig. 1 it is immediately apparent that the *intra-* and the *inter*-molecular contribution to the overall relaxation rate, i.e. the rotational or tumbling motion of the aniline molecule and its translational motion both depend on the hydrodynamic properties of their immediate surroundings. Thus when the relaxation time is measured in benzene solution the graph of T_1^{-1} vs. x exhibits a definite curvature. But when the relaxation time is determined in aniline-d_7 solution, the resulting plot is a straight line with an average deviation from the straight line of 0.005 T_1^{-1} units. The linearity of the graph suggests that

[1]NRCC Postdoctorate Fellow, 1969–1970.

Can. J. Chem. Downloaded from www.nrcresearchpress.com by 210.87.254.40 on 09/05/12
For personal use only.

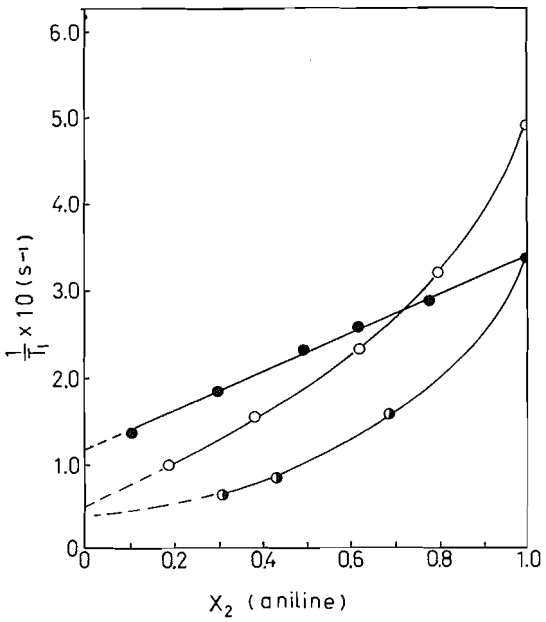

FIG. 1. Plot of T_1^{-1} vs. mole fraction of aniline ○, ordinary aniline in C_6D_6; ●, aniline-d_2 in aniline-d_7; ◑, aniline-d_2 in C_6D_6.

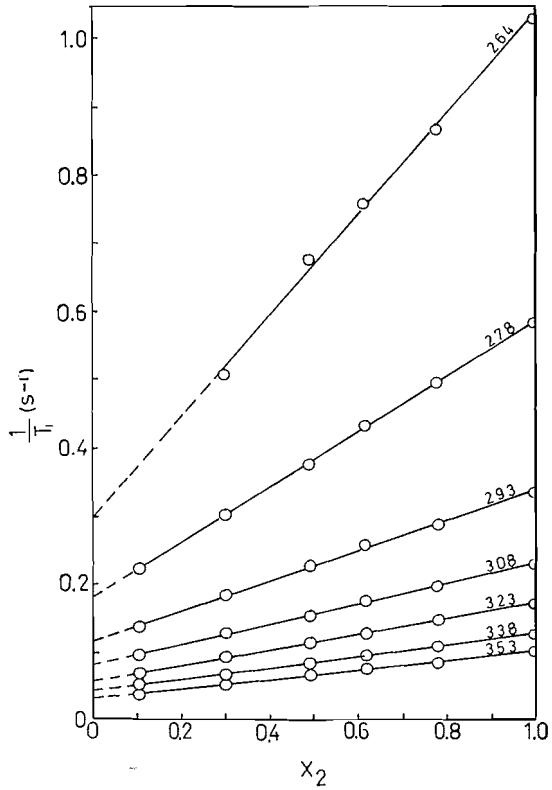

FIG. 2. Plot of T_1^{-1} vs. mole fraction of aniline at different temperatures.

only two mechanisms contribute to the spin–lattice relaxation of the aniline-d_2 molecule when dissolved in aniline-d_7, viz. an intramolecular mechanism which arises from the interaction of protons in the same molecule and an intermolecular mechanism due to the interaction between protons on neighboring molecules. It should be noted here that the aniline-d_2 molecule was deuterated in the amino group which essentially eliminated any interaction between this group and the ring protons. If it is assumed that only two mechanisms contribute to the overall relaxation i.e.

$$[1] \qquad 1/T_1 = 1/T_{1\text{intra}} + 1/T_{1\text{inter}}$$

then it is possible, following Powles (2) and Torrey (3), to derive from the experimentally determined values of $T_{1\text{intra}}$ and $T_{1\text{inter}}$ the correlation times for the tumbling motion of the molecule, τ_r, and for the translational motion, τ_t. The results for aniline-d_2 in aniline-d_7 are: $\tau_r = 19 \times 10^{-12}$ and $\tau_t = 200 \times 10^{-12}$ s. In evaluating τ_r it was assumed, following Goldammer and Zeidler (4), that all protons in aniline-d_2 were chemically equivalent and in evaluating τ_t, the translational diffusion coefficient, D_t, was approximated by the expression

$$[2] \qquad D_t = kT/6\,\pi\eta r f_t$$

Here k is Boltzmann's constant; T, the absolute temperature; η, the viscosity; r, the molecular radius; and f_t, a microviscosity coefficient. The value of r in eq. [2] was estimated from the density of the liquid and assuming a close packing of spheres in the liquid. The value of the microviscosity coefficient was estimated from the work of Kessler, Weiss, and Witte (6) and was taken to be 0.7. It should be noted here that in evaluating τ_t the effect of the rotational molecular motion on the intermolecular relaxation rate was neglected. Zeidler (5) has shown that for molecules which have structures similar to that of aniline, e.g. benzene cyclohexane, pyridine, etc., the rotational motion enhances the intermolecular relaxation rate by $\sim$ 0–12%, depending on the particular structure of the molecule. Since the "true" value of f_t in eq. [2] is rather uncertain and since we estimate our experimental error to be $\pm$ 5%, we felt justified in neglecting this effect in our calculation of τ_t. Now the

Can. J. Chem. Downloaded from www.nrcresearchpress.com by 210.87.254.40 on 09/05/12
For personal use only.

correlation times may be roughly interpreted as the time taken by the molecule to turn through a unit angle, in the case of τ_r, and as the time taken by the molecule to move laterally away from a neighboring molecule by a distance equal to a molecular diameter, in the case of τ_t. The calculated values of τ_r suggest that an aniline molecule executes 10 twisting or turning motions before it executes a lateral or translational jump to a different site in the liquid. This conclusion is in agreement with the generally held notion that aniline in the liquid state is strongly hydrogen-bonded and also with the fact that the viscosity of aniline, a molecule of roughly the same size as chlorobenzene, is approximately 6 times that of chlorobenzene. Our value of τ_r for aniline-d_2 in aniline-d_7 is in qualitative agreement with the dielectric relaxation time determined for the aniline molecule in pure liquid aniline. Thus Smyth (7) reported a value for τ_r, the molecular reorientation time in pure liquid aniline at 20 °C as 22×10^{-12} s, whereas our value for τ_r is 19×10^{-12} s. According to Powles (8) one would expect the ratio $\tau_{diel}/\tau_{n.m.r.} \sim 3$ if the molecule reorients itself by small jumps ($< 15°$), whereas for jumps larger than about 60° the ratio is ~ 1. Since our value for τ_r is closer to being equal to τ_{diel} rather than to $\frac{1}{3}\tau_{diel}$, it would appear that the rotational diffusion of the aniline molecule in pure liquid aniline proceeds by large angular displacements of the molecule. This conclusion is corroborated by our measurements of τ_r for the aniline molecule in deuterated benzene solution. The benzene molecule is in many respects structurally similar to the aniline molecule and one would therefore expect that particularly the angular reorientation of the aniline molecule in benzene solution should be similar in nature to the angular reorientation of the molecule in liquid aniline. The dielectric relaxation time of the aniline molecule in dilute benzene solution has been measured by several workers (9, 10). The most recent determination of this quantity by Tucker and Walker (10) in dilute cyclohexane and *p*-xylene solution yields a value of 8.5×10^{-12} and 8.1×10^{-12} s, respectively for the reorientational relaxation time of the molecule and a value of 2.1×10^{-12} – 3.3×10^{-12} s for a second relaxation time presumably associated with some inter-molecular motion taking place withing the molecule. The value 8.1–8.5 $\times 10^{-12}$ s may be compared with the value determined by us for the aniline-d_2 molecule in dilute deuterated benzene solution, viz. 6.3×10^{-12} s. Now the only molecular motion that could conceivably contribute significantly to the proton spin – lattice relaxation of the aniline-d_2 molecule is the reorientation of the whole molecule since any contribution from the internal rotation of the $—ND_2$ group or from the deuteron exchange between neighboring groups may be neglected because the deuteron contribution to the proton relaxation rate is only 1/24 that of the proton contribution. Again it will be noted that the dielectric relaxation time is approximately equal to the n.m.r. relaxation time. This suggests that the rotational diffusion mechanism of the aniline molecule in dilute benzene solution is similar to the mechanism in pure liquid aniline; viz. the molecule reorients by large angular jumps ($> 60°$).

Our earlier reported measurements on ordinary aniline in dilute deuterated benzene solution are in general agreement with the above conclusions. In our earlier paper we reported a value of 3.2×10^{-12} s for τ_r for aniline in dilute benzene solution. In arriving at the above value we distinguished in our calculations between chemically shifted protons in the aniline molecule. However, in the light of the investigations of Goldammer and Zeidler (4) such distinction was unwarranted in our calculations since our instrument does not distinguish between chemically shifted protons but records an average signal from all the protons in the molecule. If all the protons in ordinary aniline are considered as chemically equivalent then the value of τ_r derived from $T_1^{-1}{}_{intra}$ results as 3.0×10^{-12} rather than 3.2×10^{-12} s, as reported earlier. According to Woessner (11) any internal molecular motion will decrease the overall spin–lattice relaxation rate and hence also decrease the calculated relaxation time τ_r. The effect of the internal rotation on the spin–lattice relaxation rate, T_1^{-1}, is given approximately by

$$[3] \qquad T_1^{-1} = \alpha A \tau_r$$

Here α is a parameter which depends on the magnitude of the two relaxation times, i.e. the relaxation time associated with the internal molecular motion and the tumbling motion of the molecule. A is a geometric parameter and depends on the molecular structure of the molecule, and τ_r is the relaxation time associated with

Can. J. Chem. Downloaded from www.nrcresearchpress.com by 210.87.254.40 on 09/05/12
For personal use only.

the tumbling motion of the molecule. Woessner has shown that in the case of a rotating methyl group α is 0.63 when the frequencies of the two motions are equal, and α is 0.25 when the frequency of the internal motion is very much larger than the frequency of the tumbling motion of the molecule. Now it is well known that the dielectric relaxation of the aniline molecule in dilute solution of nonpolar solvents is best explained in terms of two relaxation times; one of the order of 8–10 $\times$ 10^{-12} s and one of the order of 1–3 $\times$ 10^{-12} s. There is no doubt that the longer relaxation time is associated with the tumbling motion of the molecule, i.e. with the reorientation of the whole molecule, and the shorter relaxation time with the internal motion of the $-NH_2$ group (12). If in eq [3] we use the value of τ_r = 6.3 $\times$ 10^{-12} s determined for aniline-d_2 in deuterated benzene solution and the value of $T_1^{-1}{}_{intra} = 5.5 \times 10^{-2}$ s determined for ordinary aniline in the same solvent, and the appropriate value for the constant $A = 1.83 \times 10^{10}$ there results a value of 0.48 for the parameter α; a value which is in agreement with the generally held view that the internal motion of the $-NH_2$ group takes place with a greater but not very much greater frequency than the tumbling motion of the molecule.

The temperature dependence of the *intra-* and *inter*-molecular relaxation time is shown in Fig. 3 in a form of a log T_1 vs. $1/T$ graph. Both plots are linear and yield an activation energy of 4.5 and 4.4 kcal for the *intra-* and *inter*-molecular relaxation, respectively. A similar plot of the logarithm of the viscosity of ordinary aniline vs. $1/T$ yields a curved line shown in Fig. 4. The data for the construction of this graph were taken from the literature (13). Since the temperature dependence of the viscosity does not exhibit the simple Arrhenius-type behavior it is not possible to derive an unequivocal value for the activation energy for viscous flow in aniline. However, one can obtain albeit a very rough value for this parameter from the average slope of the two dashed lines shown in Fig. 4. The result is $\sim$ 5.2

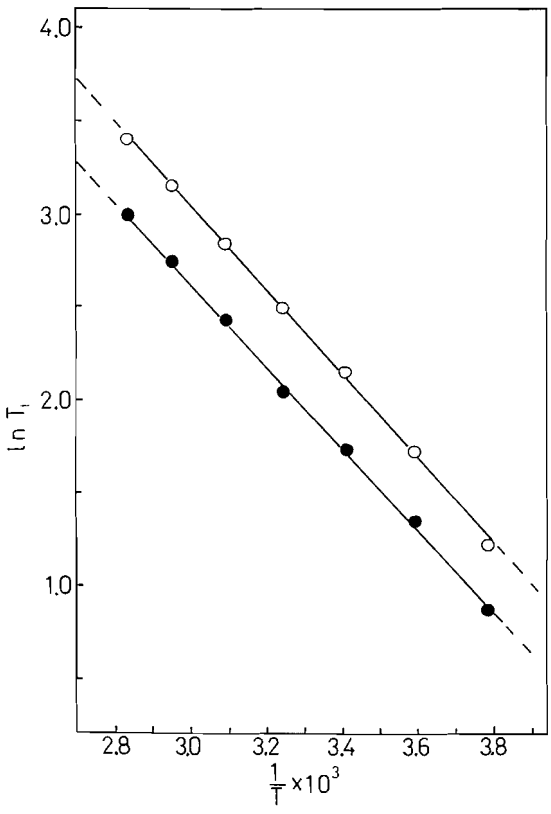

FIG. 3. Plot of ln T_{1intra} (○) and of ln T_{1inter} (●) vs. $1/T$.

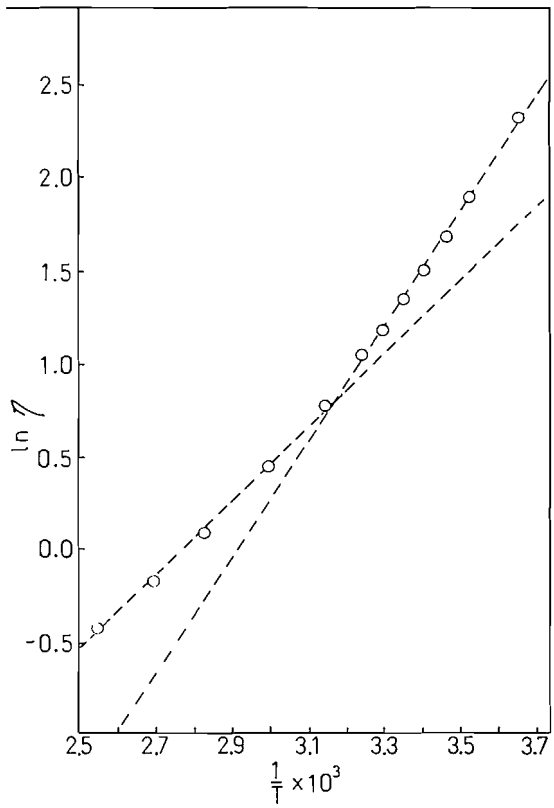

FIG. 4. Plot of ln η for ordinary aniline vs. $1/T$.

kcal/mole. Although this value is somewhat higher than the activation energy for either the *intra-* or *inter*-molecular relaxation time, it is nevertheless of the same order of magnitude as the activation energy for the latter two processes. This agreement in turn supports the interpretation of the proton spin – lattice relaxation mechanism for liquid aniline presented in this paper, viz. that the relaxation mechanism is dominated by the dipole–dipole interactions, i.e. by the Brownian motion of the molecules in the liquid state.

The financial assistance of the National Research Council of Canada is gratefully acknowledged.

1. E. BOCK and E. TOMCHUK. Can. J. Chem. **47**, 2301 (1969).
2. J. G. POWLES. Ber. Bunsenges. Phys. Chem. **67**, 328 (1963).
3. H. C. TORREY. Phys. Rev. **92**, 962 (1953).
4. E. V. GOLDAMMER and M. D. ZEIDLER. Ber. Bunsenges. Phys. Chem. **73**, 4 (1969).
5. M. D. ZEIDLER. Ber. Bunsenges. Phys. Chem. **69**, 659 (1965).
6. D. KESSLER, A. WEISS, and H. WITTE. Ber. Bunsenges. Phys. Chem. **71**, 3 (1967).
7. C. P. SMYTH. *In* Molecular relaxation processes. Chemical Soc. Spec. Publ. No. 20. Academic Press, London and New York. 1966. p. 8.
8. J. G. POWLES. *In* Molecular relaxation processes. Chem. Soc. Spec. Publ. No. 20. Academic Press, London and New York. 1966. p. 132.
9. E. L. GRUBB and C. P. SMYTH. J. Amer. Chem. Soc. **83**, 4879 (1961).
10. S. W. TUCKER and S. WALKER. Can. J. Chem. **47**, 681 (1969).
11. D. E. WOESSNER. J. Chem. Phys. **36**, 1 (1962) and **42**, 1855 (1965).
12. G. WILLIAMS. Trans. Faraday Soc. **64**, 1219 (1968).
13. INTERNATIONAL CRITICAL TABLES. Vol. VII. McGraw-Hill Book Co., Inc., New York and London. 1930. p. 213.

Can. J. Chem. Downloaded from www.nrcresearchpress.com by 210.87.254.40 on 09/05/12
For personal use only.

Can. J. Chem. Downloaded from www.nrcresearchpress.com by 210.87.254.6 on 09/05/12
For personal use only.

Cyanoethylations and Michael additions. II.[1] The synthesis of allylic cyclohexenols by γ-cyanoethylation of α,β-unsaturated aldehydes and ketones. Part II[2,3]

CH. R. ENGEL AND J. LESSARD
Department of Chemistry, Laval University, Quebec, Quebec

Received April 1, 1970

The detailed report of the first cyclo-γ-cyanoethylation of an α,β-unsaturated carbonyl system, 3β-acetoxy-5α-pregn-17-en-21-al, is given. This reaction, which proceeds in high yields, gives rise, in a single operation, to products with an additional functionalized six-membered ring, primarily to allylic α′-cyanohexenols.

Canadian Journal of Chemistry, 48, 2819 (1970)

In the majority of Michael additions reported in the literature, in which the carbanion is derived from α,β-unsaturated polar systems, such as α,β-unsaturated carbonyl compounds, the electrophile is added to the carbon atom α to the polar function of the product from which the anion is derived (cf., inter alia, ref. 5). According to the literature, cyanoethylations of such systems make no exception (6); even in the absence of a hydrogen substituent in position α to the polar function, the addition occurs in that location, with migration of the original double bond. Numerous examples (cf., for instance, ref. 7) exist also for α-alkylations of α,β-unsaturated carbonyl compounds, which bear a certain mechanistic resemblance to such Michael additions.

That the α-position of conjugated polar products should be the preferred site of reaction with electrophiles, seems plausible since it corresponds to the most negative carbon atom of the derived mesomeric anion (8). However, the greater negativity of the α-position should not totally exclude a reaction in the γ-position, which represents also a negative center of the anion (cf. 8*c*). As a matter of fact, the literature contains a few examples of γ-alkylations of α,β-unsaturated ketones, for instance the dimethylation of 3-methyl-2-cyclohexenone (9), in which the second methyl group enters, in part, at the γ-position. One also knows of some cases of base-catalyzed dimerizations of α,β-unsaturated carbonyl compounds in which the reaction products may be considered to originate from an addition in position γ, followed by cyclization (10). However, with the exception of such dimerizations, no authentic Michael additions to carbanions derived from α,β-unsaturated polar systems were known until the appearance of our preliminary reports (1, 3), and Fleury *et al.* (11) stated in 1963 that "one can note that one has never been able to show that there occurred a cyanoethylation on the γ-carbon atom" (of an α,β-unsaturated polar system). In this article, and in the following papers of this series, we endeavor to show that such γ-cyanoethylations of α,β-unsaturated aldehydes and ketones are not only possible but may be performed in very attractive yields, and that, therefore, such reactions may be regarded as valuable tools in the synthesis of polycyclic systems.[4]

We report here in detail the γ-cyanoethylation of an α,β-unsaturated aldehyde, 3β-acetoxy-5α-pregn-17-en-21-al (**4**). The addition products presented themselves as cyclized derivatives so that the reaction led directly to a system with an additional functionalized ring.

Aldehyde **4** was prepared from 3β-acetoxy-5α-androstan-17-one (**1**) in an overall yield of 75%, by the method described by Heusser *et al.* (13*a*, cf. also 13*b–d*) for the preparation of an analogous

[1]For paper I of this series see ref. 1.

[2]This publication represents part XXXI in the series on Steroids and related products. For paper XXX see ref. 2.

[3]Abbreviated in part from the doctoral thesis of J. Lessard, submitted to the School of Graduate Studies of Laval University, Quebec, 1964, and from the "thèse de doctorat d'Etat ès-sciences," University of Paris, registered at the C.N.R.S. under the number A.O. 1987. For preliminary reports on the results described in this paper see refs. 1, 3, and 4.

[4]After the first publications of our results (1, 3), Chabalier *et al.* (12*a*) reported that the cyanoethylation of mesityl oxide, catalyzed by metallic sodium in benzene, occurs in part on the α-carbon atom, as observed earlier by Bruson and Riener (6*a*), in part on the γ-carbon atom. In the presence of metallic lithium in dry ether, mesityl oxide adds to 4-phenyl-3-buten-2-one and 4-furanyl-3-buten-2-one again in the γ-position (12*b*). The French authors studied also the base-catalyzed dimerization of mesityl oxide and found that the two main isoxylitones obtained had not the structures proposed by Naves and Conia (5*e*), but structures consistent with products arising from Michael additions in position γ, followed by aldol cyclizations.

Can. J. Chem. Downloaded from www.nrcresearchpress.com by 210.87.254.6 on 09/05/12
For personal use only.

5-unsaturated aldehyde. Addition of ethoxyacetylene magnesium bromide, prepared according to the method of Nazarov *et al.* (14), to ketone **1** gave 17α-ethoxyethynyl-5α-androstane-3β,17β-diol (**2**) and its 3-acetate, **2***a*. Hydrogenation of the latter over 2.5% palladium-on-calcium carbonate led to the 17α-ethoxyvinyl derivative **3** which gave with hydrochloric acid in aqueous dioxane 3β-acetoxy-5α-pregn-17-en-21-al (**4**).

The cyanoethylation of this conjugated aldehyde (**4**) was carried out with catalytic amounts of sodium *t*-amylate in benzene at 55°, using a slight excess of acrylonitrile. Chromatography of the reaction product afforded in 74% yield a 2:1 mixture of acetoxy hydroxy nitriles (**5***a* and **6***a*), in 7% yield a mixture of dihydroxy nitriles (**5** and **6**), and in 5% yield a 7:3 mixture of the acetoxy dienonitriles **7***a* and **8***a*. The elemental analyses of the products indicate the addition of one only acrylonitrile molecule. The spectra of the isomeric acetoxy hydroxy nitriles **5***a* and **6***a* (cf. Experimental) show the presence of a non-conjugated nitrile function, of a hydroxyl group, and of a trisubstituted double bond (1 vinylic proton, at 5.33 δ for compound **5***a*, at 5.27 δ for compound **6***a*). Both acetoxy hydroxy nitriles (**5***a* and **6***a*) are readily converted to the corresponding diacetates **5***b* and **6***b*. These findings are compatible with the assumption of a cyanoethylation, followed by an aldol cyclization. They also suggest that the cyanoethylation had occurred in the γ-position (cf. structure **i**) and not in the α-position (cf. structure **ii**), since the infrared (i.r.) absorption of the double bond of

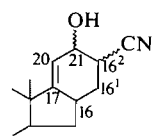

i

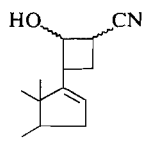

ii

compounds **5***a* and **6***a* [ν_{max} ($CHCl_3$) 1676 cm^{-1}] corresponds well to that of a double bond exocyclic to a five-membered ring[5] and not to a double bond of a compound of type **ii** which should absorb at much lower frequencies (1621–1613 cm^{-1}) (16).

The correctness of partial structure **i** for the acetoxy hydroxy nitriles **5***a* and **6***a* was established by their oxidation with Jones' reagent to the α,β-unsaturated ketones **9** and **10**; the latter is transformed very readily into its isomer (**9**), either by fusion or by treatment with a protic solvent. The nuclear magnetic resonance (n.m.r.) spectra of the unsaturated ketones **9** and **10** show a single olefinic proton, which confirms that their double bond is trisubstituted. The relatively high i.r. frequencies of these double bonds [ν_{max} ($CHCl_3$) 1640 and 1638 cm^{-1}, respectively for ketones **9** and **10**] is again in accord with the fact that these double bonds are exocyclic to a five-membered ring.[5] In both ketones the carbonyl absorption in the i.r. showed a hypsochromic shift from normal positions of α,β-unsaturated cyclohexenones (16*b*), which can be rationalized by the presence of the polar nitrile function in position α′.

Catalytic hydrogenation of both unsaturated ketones **9** and **10** afforded the same saturated cyano ketone **11***b* (under the reaction conditions, ketone **10** is isomerized to ketone **9**). Treatment of the saturated cyano ketone **11***b* with hydrochloric acid in acetic acid at reflux temperature, followed by acetylation, led to the α′-unsubstituted cyclohexanone **11***a*. It shows in the i.r. a normal carbonyl absorption, in contradistinction to ketone **11***b*; this confirms the hypsochromic effect of the nitrile group. The spectral characteristics of the unsaturated ketones **9** and **10**, and of the saturated derivatives **11***a* and *b*, exclude the possibility of cyclic derivatives which would have arisen from an α-cyanoethylation product (compare structures **iii** and **iv**).[6]

A classical proof of structure came from the ozonolysis of the unsaturated ketones **9** and **10** which gave the same cyano acid **12** (the unsaturated ketone **10** is transformed into its isomer **9** under the reaction conditions). Evidence for structure **12** is derived from the i.r. spectra of the free acid, of the corresponding hydroxy methyl ester **12***a*, and the acetoxy methyl ester **12***b*, and from the elemental analysis of the latter.

[5]Since the frequency of vibration of an exocyclic double bond increases with the tension in the ring (15), the slight hypsochromic shift of the absorption of the double bond of compounds **5***a* and **6***a* from the frequencies of vibration of unstrained double bonds, such as Δ^5- and Δ^7-double bonds, is plausible.

[6]The carbonyl absorption of α,β-unsaturated ketones of type **iii** should lie beyond 1720 cm^{-1}, that of saturated cyclobutanones (cf. **iv**) far above those observed for ketones **11***a* and *b* [ν_{max} ($CHCl_3$) 1710 and 1728 cm^{-1}, respectively].[7]

[7]Structure **iii** with a tetrasubstituted double bond between positions 17 and 20 is also excluded on the grounds of n.m.r. (see above) and ultraviolet (u.v.) evidence: the ketones **9** and **10** absorb at 238 nm.

Can. J. Chem. Downloaded from www.nrcresearchpress.com by 210.87.254.6 on 09/05/12
For personal use only.

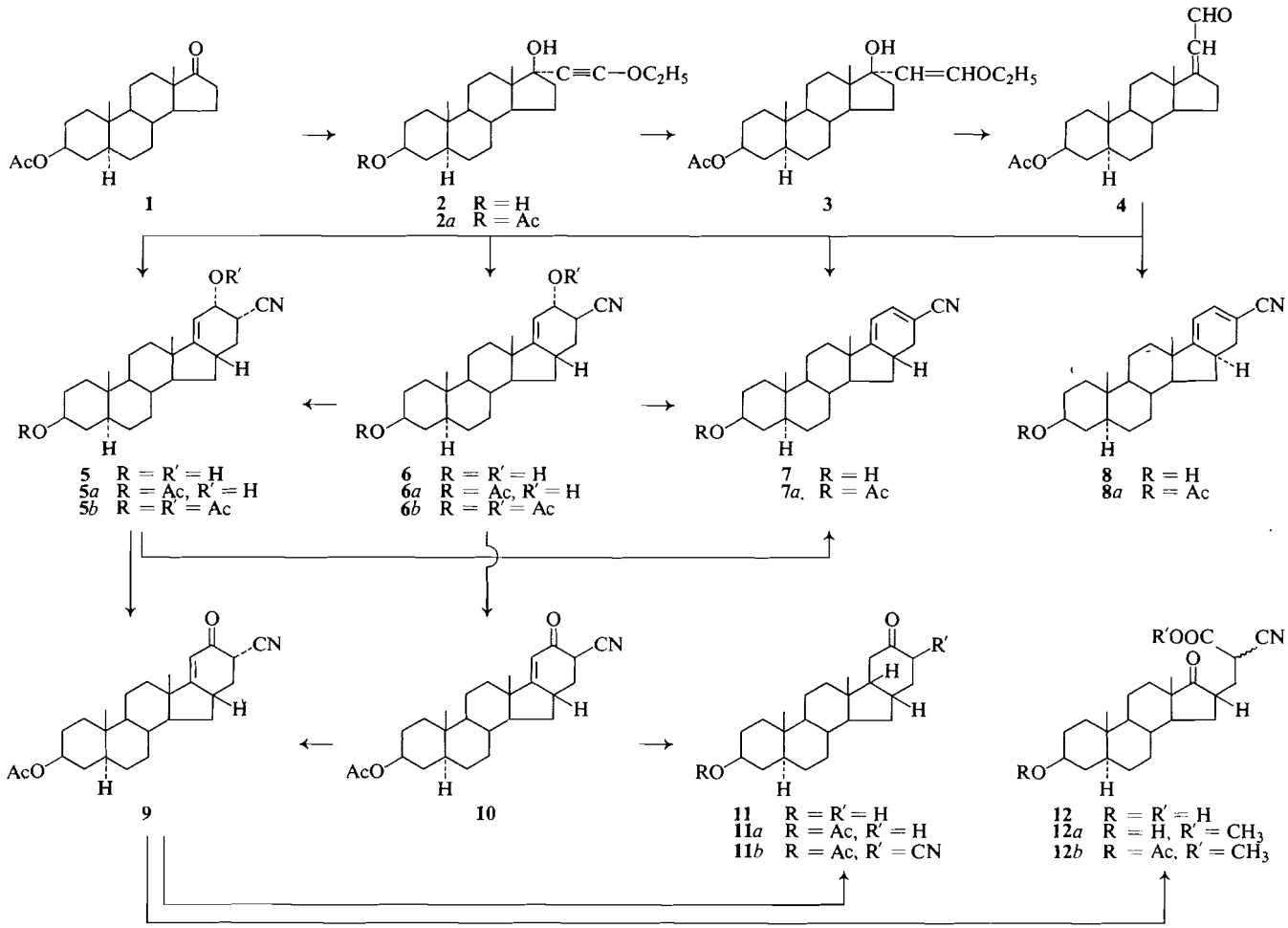

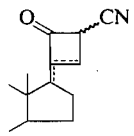
iii

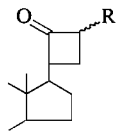
iv

R = H, CN

The elemental composition and the spectral characteristics of the isomeric dienonitriles **7***a* and **8***a* agree with structures arising from dehydration of allylic cyclohexenols of type **5***a* and **6***a*. The spectra (cf. Experimental) show the presence of a nitrile function conjugated with a homodiene. In the n.m.r. there appear two olefinic protons on vicinal carbon atoms, each of them coupled further with an axial or quasi-axial allylic proton.

The structure of dienonitrile **7***a* was confirmed by its formation from the two acetoxy hydroxy nitriles **5***a* and **6***a*, by the action of *p*-toluenesulfonyl chloride in pyridine, and by dehydroacetylation of the corresponding diacetates **5***b* and **6***b*, with potassium carbonate in methanol, to the hydroxy dienonitrile **7**. The acetoxy hydroxy nitrile **5***a* is dehydrated with considerably greater ease than its epimer **6***a*. Similarly, the diacetoxy nitrile **5***b* is dehydroacetylated in much better yields than its epimer **6***b*. The acetoxy hydroxy nitriles **5***a* and **6***a* are also dehydrated with methanolic potassium carbonate, both to the same dienonitrile **7**; both of them give, in this reaction, the same side-product: the dihydroxy nitrile **5**, which is also obtained as side-product in the dehydroacetylations of the isomeric diacetoxy nitriles **5***b* and **6***b*. These epimerizations in position 16[2] parallel the already mentioned very facile epimerization of ketone **10** to ketone **9**.

The cyanoethylation of the α,β-unsaturated aldehyde **4** was also carried out in *t*-butanol with catalytic amounts of potassium hydroxide. In that case, chromatography of the acetylated product led, in 13% yield, to a mixture of the dienonitriles **7***a* and **8***a* (in a relative proportion of 9:1) and in 54% yield to a mixture of the diacetoxy nitriles **5***b* and **6***b*, isomer **6***b* representing the main constituent of that mixture.

Stereochemistry

Stereochemistry in Position 16

The fact that the dehydration of both acetoxy alcohols **5***a* and **6***a* led exclusively to the same dienonitrile **7***a*, and the dehydroacetylation of the corresponding diacetates **5***b* and **6***b* to the same nitrile **7**, seems to indicate the identity of configuration of the main reaction products (**5**, **6**, and **7**, and their ester derivatives) in position 16. This assumption is confirmed by the fact that under the dehydroacetylation conditions dienonitrile **8** is not significantly epimerized to dienonitrile **7**.[8]

If the cyanoethylation were to proceed under kinetic control, one would have to assume a 16β-hydrogen configuration of the main reaction products, the α-side of the molecule being less hindered. However, since equilibration through an enol form is possible, a proof of configuration becomes necessary. According to Moscowitz *et al.* (17), a non-planar cyclohexadiene, such as either dienonitrile **7** or **8**, should exhibit a strongly positive Cotton effect in the case of a right-handed helicity of the chromophore, a strongly negative Cotton effect in the case of a left-handed helicity of this moiety. According to models, the dienonitriles **7** and **8** would present a right-handed helicity in the case of a 16β-hydrogen configuration, a left-handed helicity in the case of a 16α-hydrogen configuration. Since the observed Cotton effect of dienonitrile **7***a* is strongly negative, that of its epimer **8***a* strongly positive, one would have to conclude that the configuration of the main reaction products **5**, **6**, and **7** be 16α-hydrogen. We suggest, however, that the configuration of these reaction products be 16β-hydrogen, *which is in opposition to Moscowitz rule*, but which is in accord with all other observations at our disposal. At first, a Diels–Alder addition of acrylonitrile to the enol acetate of aldehyde **4**, under conditions under which a reverse reaction and therefore an equilibration are most improbable, leads exclusively to the diacetate **5***b* (4, 18), which cannot be reconciled with a 16α-hydrogen configuration since this would suggest an exclusive attack from the more hindered side. Also, a 16β-hydrogen configuration of products arising from Diels–Alder and Michael additions to 16-unsaturated 20-ketones has been rigorously established (19, 20). Furthermore, the n.m.r. spectra of the

[8]The identity of configuration in position 16 of the hydroxy acetoxy nitriles **5***a* and **6***a* and their derivatives is further confirmed by the ready epimerization of the hydroxy nitriles **6** and **6***a* to their stereo-isomers **5** and **5***a*, and the extremely facile epimerization of ketone **10** to ketone **9**; an abstraction of a proton in the 16-position under the reaction conditions is improbable (especially in the case of the hydroxy nitriles **5** and **6**), whereas an enolization towards the nitrile function is perfectly plausible.

Can. J. Chem. Downloaded from www.nrcresearchpress.com by 210.87.254.6 on 09/05/12
For personal use only.

TABLE 1

Chemical shifts of the 18-methyl groups of the cyano alcohols **5***a*, **6***a*, **13***a*, and **14***a*, and of the cyano ketones **9***a* and **10***a*

Compound	Conformation of nitrile group	δ (p.p.m.)	$\Delta\delta_{\text{axial CN}-\text{equatorial CN}}$ (p.p.m.)
5*a*	equatorial	0.84	0.04
6*a*	axial	0.88	
14*a*	equatorial	0.84	0.04
13*a*	axial	0.88	
9*a*	equatorial	0.96	0.04
10*a*	axial	1.00	

acetoxy hydroxy nitriles **5***a* and **6***a*, of their isomers **13***a* and **14***a* (see below), and of the ketones **9** and **10**, the *relative* stereochemistry of which, with respect to the configuration in position 16, is clearly established (see below), militate in favor of a 16β-hydrogen configuration. The 18-methyl group of the products with an axial nitrile substituent in position 16^2 is more deshielded than the 18-methyl group of the products with an equatorial 16^2-nitrile group (cf. Table 1), and this is only plausible if one assumes that in each case the axial nitrile group is *cis* to the 18-methyl group; since in these nitriles the axial cyano group is *cis* to the hydrogen in position 16 (see below), this hydrogen must be *cis* to the 18-methyl group and therefore β. Analogous and confirmatory results were obtained in the case of the cyanoethylations of a 21-methyl 21-ketone, homologous to aldehyde **4**, and in that of the D-homo analog of aldehyde **4** (4, 21, 22).[9]

Configuration of Ketones 9 and 10

Since no isomerization in position 16 occurs during the oxidation of 21-alcohols of type **5***a*, **6***a*, **13***a*, and **14***a* (cf. below), the ketones **9** and **10** must have the same configuration in position 16 as dienonitrile **7**; they must, therefore, differ in stereochemistry in position 16^2. The ready epimerization of ketone **10** to ketone **9** suggests that the conformation of the nitrile group of the former be axial, that of the latter equatorial. This agrees (23) with the u.v. spectra, the maximum corresponding to the $n \rightarrow \pi^*$ transition of ketone **10** appearing at 325 nm ($CHCl_3$), that of ketone **9** at 305 nm. In the n.m.r. spectrum of ketone **10**, the 16^2-proton appears at 3.48 δ as a doublet of doublets with *J* values of 2.5 and 5.0 Hz, which corresponds to an equatorial conformation of the 16^2-hydrogen, and therefore an axial conformation of the nitrile group. The 16^2-proton of ketone **9** is seen at 3.56 δ, as a doublet of doublets, with *J* values of 14 and 4 Hz, which confirms the axial conformation of this proton and therefore the equatorial conformation of the nitrile substituent.[10] Ring E of ketones **9** and **10** must present itself in the half-chair conformation,[10] since one can calculate only in that instance acceptable constants for the Karplus equation (25) from the *J* values of the 16^2-protons and the corresponding dihedral angles. Furthermore, the optical rotatory dispersion (o.r.d.) curves of both ketones **9** and **10** show a positive Cotton effect in the region corresponding to the $n \rightarrow \pi^*$ transition, from which a half-chair conformation of their E-rings may be inferred (cf. 26). Interestingly, both the equatorial and the axial nitrile groups of ketones **9** and **10** exert a hypsochromic effect on the i.r. maximum corresponding to the stretching frequencies of the carbonyl function, this effect being, however, greater for the equatorial substituent of ketone **9**; thus, the nitrile group behaves in this respect not like a bromine, chlorine, or acetoxy substituent, but rather like a fluorine substituent (23*e*, 27).[11]

[9]An X-ray investigation of the 3-bromoacetate of compound **5** is in progress.

[10]The axial 16^2-proton of ketone **9** is more deshielded than the equatorial 16^2-proton of ketone **10**, which corresponds well to the situation in the case of α-halogenated cyclohexanones (24). We have already discussed the deshielding by the axial nitrile function of the 18-methyl group of ketone **10**. The axial β-cyano group also causes a deshielding of the axial proton in position 16, which appears as a multiplet at 3.2 δ for ketone **10**, whereas it appears as a multiplet at 2.9 δ in the case of ketone **9** in which the 16^2-cyano group is equatorial. This not only confirms the 1,3-diaxial relationship of the nitrile function and the 16-hydrogen in ketone **10**, but indicates also a half-chair conformation of ring E.

[11]We therefore have to rectify the preliminary proposal of conformation and configuration of the nitrile group of compound **10** (1), which had been based on the assumption that an α-cyano substituent would have an effect on the i.r. carbonyl absorption similar to that of a bromine or acetoxy group.

Can. J. Chem. Downloaded from www.nrcresearchpress.com by 210.87.254.6 on 09/05/12
For personal use only.

Can. J. Chem. Downloaded from www.nrcresearchpress.com by 210.87.254.6 on 09/05/12
For personal use only.

Stereochemistry in Position 16^2 and E-Ring Conformation of the Acetoxy Hydroxy Nitriles 5a and 6a

As the oxidation of the acetoxy hydroxy nitrile **6***a* leads to the thermodynamically unstable ketone **10**, no epimerization in position 16^2 occurs in that reaction. Hence, the nitrile group of the hydroxy nitrile **5***a* must be α (assuming a 16β-hydrogen configuration), that of the hydroxy nitrile **6***a*, β. Since, according to models, the preferred conformation of ring E for both compounds **5***a* and **6***a* should be a half-chair, the nitrile group of hydroxy nitrile **5***a* should be equatorial, that of isomer **6***a*, axial. This is confirmed by the n.m.r. spectra at 100 MHz.[12] The 16^2β-proton of the hydroxy nitrile **5***a* appears as a doublet of triplets at 2.798 δ which, upon irradiation at the absorption frequency of the 21-proton, collapses to a doublet of doublets with coupling constants of 12.0 and 2.6 Hz (corresponding to the coupling with the two protons in position 16^1); this indicates an axial conformation of the 16^2-hydrogen, and therefore an equatorial conformation of the nitrile group. The 16^2α-proton of isomer **6***a* gives rise to a multiplet at 3.02 δ which, upon simultaneous irradiation at the frequencies of the 21-proton and of the olefinic proton in position 20, is simplified to a triplet with J values of approximately 3 Hz, which confirms the equatorial conformation of the 16^2-hydrogen and the axial conformation of the nitrile group.[13]

Configuration of the Alcohols 5a and 6a in Position 21

The facile dehydration of the hydroxy nitrile **5***a* and the ready dehydroacetylation of its acetate **5***b* (see above) suggests a *trans*-diaxial arrangement of the 21-oxygen substituent and the 16^2-hydrogen, thus an α-configuration of the 21-oxygen groups of compounds **5**, **5***a*, and *b*. The relatively difficult dehydration and dehydroacetylation of isomers **6***a* and *b* could either suggest a *trans*-diequatorial relationship of the 21-oxygen functions and the 16^2-hydrogen, or a *cis* relationship of these groups. The latter seemed more probable in view of the isomerization with base of the dihydroxy nitrile **6** to the dihydroxy nitrile **5** (see above), an epimerization of the axial 16^2-nitrile function being more likely than an isomerization involving a retroaldol–aldol sequence. These tentative conclusions are confirmed by n.m.r. spectroscopy at 100 MHz.[12] The study was facilitated by the availability of the other pair of epimeric acetoxy hydroxy nitriles **13***a* and **14***a*. They were obtained, in high yield, by sodium borohydride reduction of the isomeric ketones **9** and **10**. Careful oxidation of the major reduction product, hydroxy nitrile **13***a* (representing 66% of the mixture of the two epimers), led to the α,β-unsaturated ketone **10**, oxidation of isomer **14***a* to ketone **9**. The nitrile function of hydroxy nitrile **13***a* must therefore be β and axial, that of hydroxy nitrile **14***a*, α and equatorial. This is again confirmed by the fact that the 16β-proton and the protons of the 18-methyl group of isomer **13***a* are more deshielded than those of isomer **14***a*. The equatorial conformation of the 16^2-proton of compound **13***a* is further evident from its coupling with the two 16^1-protons (3.5 and 3.0 Hz). Conversely, the coupling constants of the 16^2-proton of isomer **14***a* (12.5 and 2.9 Hz) indicate an axial conformation of the 16^2-proton. Thus, the hydroxy nitriles **13***a* and **14***a* are 16^2-epimers, as are the hydroxy nitriles **5***a* and **6***a*, from which they must differ in their configuration in position 21.

The significant data (concerning ring E) from the n.m.r. analyses at 100 MHz, with multiple spin decoupling, of the four isomeric acetoxy hydroxy nitriles **5***a*, **6***a*, **13***a*, and **14***a* are summarized in Table 2.[12]

The relatively small (3 Hz) coupling constant arising from the coupling between the axial 16^2β-proton of isomer **5***a* with the 21-proton is indicative of the quasi-equatorial conformation of the 21-hydrogen and therefore of an axial conformation and α-configuration of the 21-hydroxy group, which is in accord with the

[12]The n.m.r. spectra at 100 MHz were very kindly performed by Prof. R. U. Lemieux and Mr. J. Bigam, the University of Alberta, Edmonton, Alberta, to whom we express our very sincere appreciation for their important help. The spectra were recorded on a Varian H 100 instrument, in deuteriochloroform, tetramethylsilane being used as internal standard.

[13]The exact value of $J_{16^1\alpha,16^2\alpha}$ (3.5 Hz) was measured from the doublet obtained by triple decoupling, by irradiating simultaneously protons 20, 21, and 16^1β; the exact value of $J_{16^1\beta,16^2\alpha}$ (2.7 Hz) was determined from the doublet obtained by simultaneous irradiation at the frequencies of the protons 20, 21, and 16^1α. One again observes in the case of the hydroxy nitriles **5***a* and **6***a* that the axial 16-hydrogen is more deshielded in the case of the isomer with the axial β-nitrile function; we have already mentioned that the 18-methyl group is more deshielded in the case of isomer **6***a* than in the case of isomer **5***a*.

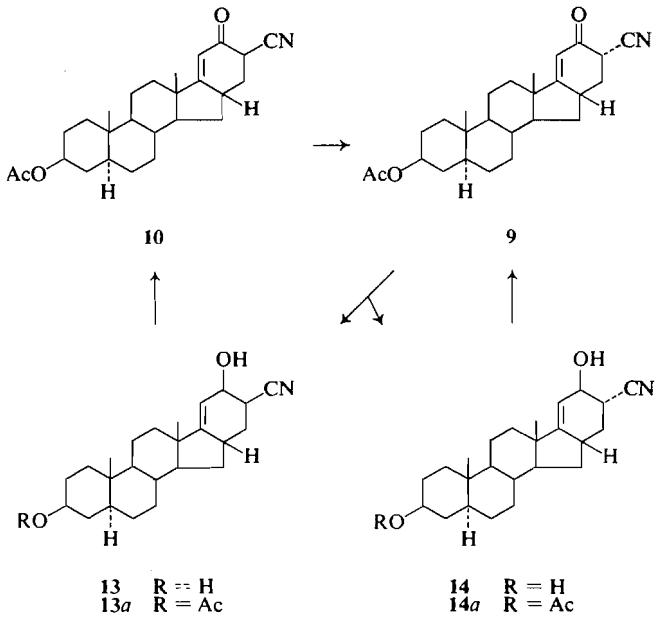

above-mentioned chemical evidence. The coupling between the axial 16^2β-proton of isomer **14***a* and the 21-proton (~9.5 Hz) suggests an axial conformation of the 21-proton and therefore an equatorial β-stereochemistry of the 21-hydroxy substituent. The difference in the couplings of the olefinic 20-proton and the 21-proton in isomers **5***a* and **14***a* agrees with the difference in dihedral angles. The quasi-axial conformation of the 21-proton of isomer **14***a* is further confirmed by its homo-allylic coupling (~2.8 Hz) with the axial 16β-proton (cf. 28).

In the case of isomer **6***a*, the coupling between the olefinic 20-proton and the proton in position 21 (3.5 Hz) is larger than the coupling (2.3 Hz) of the 20- and 21-protons of epimer **13***a*, which corresponds again to the difference in dihedral angles, when a quasi-axial α-stereochemistry of the hydroxyl function of isomer **6***a* and a quasi-equatorial β-stereochemistry of the 21-hydroxyl group of isomer **13***a* are assumed. These stereochemical assignments are borne out by the difference of the couplings between the quasi-equatorial 21-proton and the quasi-equatorial 16^2-proton of isomer **6***a* on one hand, and between the quasi-axial 21-proton and the quasi-equatorial 16^2-proton of isomer **13***a* on the other hand. Finally, the 21-proton of isomer **13***a* shows homo-allylic coupling (in contradistinction to isomer **6***a*) with the axial 16β-proton, which further confirms the quasi-axial conformation of the 21-proton of compound **13***a*.[14]

Stereochemistry of the Saturated Ketones 11a and b

The strong negative Cotton effects of both these ketones suggest a 17β-hydrogen configuration if one assumes that during the reduction of the 17,20-double bond and in the course of the removal of the nitrile function no isomerization in position 16 occurs. The fact that the unsubstituted saturated ketone **11***a* shows the same u.v. absorption maximum as the saturated cyano ketone **11***b*, agrees with an equatorial conformation of the nitrile substituent of the latter.

[14]The major sodium borohydride reduction product of ketone **9**, hydroxy nitrile **13***a*, has a β-configuration and axial conformation of the nitrile substituent. An epimerization prior to the reduction of the stable ketone **9** to the unstable ketone **10** can, of course, be excluded. Epimerization after the reduction has to be excluded also since none of the four isomeric hydroxy nitriles **5***a*, **6***a*, **13***a*, and **14***a*, is isomerized under the reduction conditions (see Experimental). The epimerization *during* reduction can be rationalized if one assumes an equilibrium between an enolic and a ketonic form in the intermediate complex of the 21-oxygen function with the metal and if one considers that this complex is attacked primarily from the less hindered α-side, an assumption borne out by the fact that the reduction products are 21β-alcohols. If one thus considers the steric crowding on the α-face, produced by the reducing agent, it becomes plausible that the nitrile group will have the tendency to assume the β-configuration upon the return of the 16^2-carbon atom to a tetrahedral geometry.

Can. J. Chem. Downloaded from www.nrcresearchpress.com by 210.87.254.6 on 09/05/12
For personal use only.

Can. J. Chem. Downloaded from www.nrcresearchpress.com by 210.87.254.6 on 09/05/12
For personal use only.

TABLE 2

Summary of n.m.r. data of the protons of ring E of the acetoxy hydroxy nitriles **5***a*, **6***a*, **13***a*, and **14***a*, from the spectra at 100 MHz[12]

Compound	Proton	Conformation	δ (p.p.m.)	Signal	Approximative *J* values (Hz)	Spin decoupling: [H] Irradiated	Spin decoupling: Signal	Spin decoupling: *J* Values (Hz)	Assignment	Approximative dihedral angles measured* (°)
5*a*	20		5.298	d of d	4.0	[16β]	d	4.0	20,21β	55
					2.2				16β,20 (allylic)	85
	21β	equatorial	4.334	t	3.8				20,21β	55
					3.8				16^2β,21β	50
	16^2β	axial	2.798	d of t		[21β]	d of d	12.0	16^1α,16^2β	180
								2.6	16^1β,16^2β	60
						[21,16^1β]	d	12.0	16^1α,16^2β	180
						[16^1β]	d of d	12.0	16^1α,16^2β	180
								3.8	16^2β,21β	50
	16β	axial	2.466	m						
	16^1β	equatorial	2.04†							
14*a*	20		5.175	t	2.6	[16β]	d	3.0	20,21α	65
					2.6				16β,20 (allylic)	85
	21α	axial	4.498	d of t	10				16^2β,21α	170
					2.8				20,21α	65
					2.8				16β,21α (homo-allylic)	155
	16^2β	axial	2.690	7 lines	12.5				16^1α,16^2β	180
					9.5				16^2β,21α	170
					2.9				16^1β,16^2β	60
	16β	axial	2.66†							
	16^1β		2.265	d of d of d	12.2				16^1α,16^1β (geminal)	110
					4.6				16β,16^1β	55
					3.0				16^1β,16^2β	60

Can. J. Chem. Downloaded from www.nrcresearchpress.com by 210.87.254.6 on 09/05/12
For personal use only.

TABLE 2 *(Concluded)*

Compound	Proton	Conformation	δ (p.p.m.)	Signal	Approximative *J* values (Hz)	[H] Irradiated	Spin decoupling: Signal	Spin decoupling: *J* values (Hz)	Assignment	Approximative dihedral angles measured* (°)
	20		5.244	t		[16β]	d	3.5	20,21β	55
						[21]	d	2.3	16β,20 (allylic)	85
						[16β,21]	s/w½	2.4		
						[16β,16²α,21]	s/w½	1.8		
							Δw½	0.6	16²α,20	W arrang.
	21β	equatorial	4.354	m		[16²α,OH]	d	3.5	20,21β	55
6a						[20,OH]	d	1.0	16²α,21β	70
						[16²α,20,OH]	s/w½	2.0		
	16²α	equatorial	3.016	t (ill-defined)		[20,21β]	t	~3.0		
						[20,16¹α,21β]	d	2.7	16¹β,16²α	60
						[20,16¹β,21β]	d	3.5	16¹α,16²α	60
	16β	axial	2.848	m						
	16¹β	equatorial	2.02†							
	16¹α	axial	1.52†							
	20		5.140	t	2.3	[16β,16²α]	d	2.3	20,21α	65
					2.3				20,16β (allylic)	85
	21α	axial	4.451	quint.	6.0				16²α,21α	50
					2.5				20,21α	65
					2.5				16β,21α (homo-allylic)	155
13*a*	16²α	equatorial	3.370	sext.	6.0				16²α,21α	50
					3.5				16¹α,16²α	60
					3.0				16¹β,16²α	60
	16β	axial	2.96†							
	16¹β	equatorial	2.216	d of t	13				16¹β,16¹α (geminal)	110
					3.5				16¹β,16²α	60
					3.5				16¹β,16β	55

*From Barton models.
†Determined by spin decoupling.

Can. J. Chem. Downloaded from www.nrcresearchpress.com by 210.87.254.6 on 09/05/12
For personal use only.

We reserve the discussion of the mechanism of the cyclo-γ-cyanoethylation for subsequent papers of this series (18, 22), since for this discussion the results obtained with an α,β-unsaturated ketone, analogous to aldehyde **4**, and those obtained in the Diels–Alder addition of acrylonitrile and methyl vinyl ketone to the enol acetate of aldehyde **4**, are essential.

Experimental[15]

3β-Acetoxy-17α-ethoxyethynyl-5α-androstan-17β-ol (2a) and 17α-Ethoxyethynyl-5α-androstane-3β,17β-diol (2)

(*a*) To an ethereal solution of ethyl magnesium bromide prepared from 1.3 g of magnesium, 5 ml of ethyl bromide, and 50 ml of anhydrous ether, there was added, dropwise and with stirring over a period of 30 min, a solution of 3.9 g of ethoxyacetylene in 30 ml of anhydrous ether. The addition was controlled so as to maintain the reaction mixture refluxing. The ethoxyacetylene magnesium bromide complex separated as a dark oil. After stirring at room temperature for one additional hour, a solution of 1.56 g of 3β-acetoxy-5α-androstan-17-one (**1**), m.p. 114–116°, in 30 ml of anhydrous ether was added, dropwise and with stirring, over a period of 30 min. The reaction mixture was refluxed for 1 h, then cooled in an ice bath, and 100 ml of a cold 20% ammonium chloride solution was added slowly. The organic phase was decanted and the aqueous phase was extracted with ether. The ethereal solution was washed with a cold 10% aqueous ammonium chloride solution and with water, dried over sodium sulfate, and the solvent was removed. The residue (2.24 g) was adsorbed on 67 g of aluminum oxide. Elutions with petroleum ether – benzene (1:1) afforded 860 mg (45%) of *3β-acetoxy-17α-ethoxyethynyl-5α-androstan-17β-ol (2a)*, m.p. (dec.) 126–129°. A sample was recrystallized three times from ether–hexane for analysis; colorless plates, m.p. (dec.) 130.5–131.5°; $[\alpha]_D^{23}$ −46° (*c*, 1.00 in $CHCl_3$); ν_{max} (KBr) 3560 (hydroxyl), 2280 (triple bond), 1722 and 1260 (acetate), and 1038 cm^{-1} (broad band: acetate, ether, and alcohol).

Anal. Calcd. for $C_{25}H_{38}O_4$: C, 74.59; H, 9.51. Found: C, 74.61; H, 9.47.

Elutions in the above chromatogram with benzene gave 410 mg (24% yield) of *17α-ethoxyethynyl-5α-androstane-3β,17β-diol (2)*, m.p. (dec.) 121–122°. A sample was recrystallized twice from ether–hexane for analysis; colorless needles, m.p. (dec.) 122.5–123°; $[\alpha]_D^{23}$ −40° (*c*, 1.00 in $CHCl_3$); ν_{max} (KBr) 3440 (hydroxyls), 2280 (triple bond), and 1045 cm^{-1} (broad band: alcohols and ether).

Anal. Calcd. for $C_{23}H_{36}O_3$: C, 76.62; H, 10.06. Found: C, 76.48; H, 10.11.

Acetylation of Diol 2

The 17α-ethoxyethynyl diol **2** (200 mg) in 3 ml of pyridine was treated with 1.5 ml of acetic anhydride at room temperature for 16 h. The usual work-up gave 220 mg of acetylated product representing crude *3β-acetoxy-17α-ethoxyethynyl-5α-androstan-17β-ol (2a)*, m.p. (dec.) 114–122°; one recrystallization from ether–hexane gave 170 mg (67% yield) of a product melting with decomposition at 127–129°.

(*b*) In another run, the ethoxyacetylenation of two portions of 13 g of the 17-ketone **1** was carried out as described above. The crude products were acetylated in the usual fashion. Chromatography of the combined residues (43 g) on 1 kg of aluminum oxide afforded 30 g of crude *3β-acetoxy-17α-ethoxyethynyl-5α-androstan-17β-ol (2a)*, m.p. (dec.) 119–123°, eluted with petroleum ether – benzene mixtures (9:1, 4:1, and 1:1). Further purification by chromatography and recrystallization from ether–hexane gave two crops of crystals: 18.8 g, m.p. (dec.) 129–130°; and 5.2 g, m.p. (dec.) 127–129°; (total yield: 76%).

3β-Acetoxy-17α-ethoxyvinyl-5α-androstan-17β-ol (3)

A solution of 12 g of 3β-acetoxy-17α-ethoxyethynyl-5α-androstan-17β-ol (**2a**), m.p. (dec.) 126–128°, in 280 ml of pyridine was hydrogenated over 3.6 g of 2.5% palladium-on-calcium carbonate at atmospheric pressure. The hydrogenation was stopped after the absorption of 1 molecular equivalent of hydrogen. The catalyst was filtered, washed with benzene, and the organic solution was taken to dryness *in vacuo*, leaving 12.2 g (quantitative yield) of 3β-acetoxy-17α-ethoxyvinyl-5α-androstan-17β-ol (**3**), m.p. 126–128°. A sample was recrystallized twice from ether–hexane for analysis; short, colorless prisms, m.p. 130.5–132°; $[\alpha]_D^{23}$ +19° (*c*, 0.696 in $CHCl_3$); λ_{max} (cyclohexane) 201 nm (ε 13 700); ν_{max} (KBr) 3560 (hydroxyl), 1735 and 1242 (acetate), 1664 (double bond), 1100 (ether), and 1042 and 1032 cm^{-1} (acetate and alcohol).

Anal. Calcd. for $C_{25}H_{40}O_4$: C, 74.21; H, 9.97. Found: C, 74.55; H, 9.82.

3β-Acetoxy-5α-pregn-17-en-21-al (4)

A solution of 12.2 g of 3β-acetoxy-17α-ethoxyvinyl-5α-androstan-17β-ol (**3**), m.p. 126–128°, in 600 ml of dioxane was treated with 165 ml of 2 *N* aqueous hydrochloric acid. The mixture was shaken at room temperature for 25 min, diluted with 700 ml of cold water, and extracted with ether. The organic layer was washed with cold aqueous sodium bicarbonate and with water, and was dried over sodium sulfate. Evaporation of the solvent left 10.7 g (99% yield) of 3β-acetoxy-5α-pregn-17-en-21-al (**4**), m.p. 150–154°. Recrystallization from ether–hexane gave 8.4 g (78%) of crystals melting at 157–158°. A sample was recrystallized twice for analysis; colorless needles, m.p. 160–161°; $[\alpha]_D^{23}$ +36° (*c*, 1.00 in $CHCl_3$); ν_{max} ($CHCl_3$) 2760 (aldehyde), 1728 (acetate), 1672 (aldehyde), 1610 (double bond), 1252 and 1040 cm^{-1} (acetate).

[15]All melting points were taken in evacuated capillaries and the temperatures were corrected. The microanalyses were performed by the late Mr. A. Bernhardt, Max Planck Institute, Mülheim, Germany, and by Dr. C. Daesslé, Montreal, Quebec, to whom we are much obliged. For chromatography, non-alkaline Woelm's aluminum oxide, activity III, and Davison's silica gel No. 923 were used, if not otherwise stated. The i.r. spectra were determined on a Beckman model IR-4 spectrophotometer and u.v. spectra on a Beckman model DK-1A spectrophotometer.

Can. J. Chem. Downloaded from www.nrcresearchpress.com by 210.87.254.6 on 09/05/12
For personal use only.

Anal. Calcd. for $C_{23}H_{34}O_3$: C, 77.05; H, 9.56. Found: C, 76.99; H, 9.52.

Cyanoethylation of 3β-Acetoxy-5α-pregn-17-en-21-al (4)

(a) In Dry Benzene in Presence of Sodium t-Amylate[16]

A stream of nitrogen was passed through a stirred solution of 8 g of 3β-acetoxy-5α-pregn-17-en-21-al (**4**), m.p. 158–160°, in 70 ml of dry benzene, and 0.8 ml of a 2 *N* solution of sodium *t*-amylate in benzene was added dropwise. Subsequently there was added, dropwise, over a period of 10 min, 21 ml of a 0.83 *M* solution of acrylonitrile in benzene. The reaction mixture was stirred at room temperature for another 3 h and at 55° for 5 h. After the addition of another 10 ml of 0.83 *M* acrylonitrile solution in benzene, the mixture was left at room temperature for 12 h, then poured into ice water. The precipitate was extracted with ether; the ethereal layer was washed with water, dried over sodium sulfate, and the solvents were removed *in vacuo*. The residue (9.4 g) was adsorbed on 700 g of silica gel. Elutions with benzene – ethyl acetate mixtures gave six main groups of fractions.

(*1*) A (97:3) mixture of benzene – ethyl acetate eluted 384 mg of a mixture of the *dienonitriles 7a and* **8***a*, m.p. 168–184°; $[\alpha]_D^{28}$ −121° (*c*, 1.15 in $CHCl_3$). Ten recrystallizations from hexane gave 24 mg of pure *3β-acetoxy-16β-ethyl-16²-cyano-16²,21-cyclo-5α-pregna-17,21-diene (**8a**)*; m.p. 224.5–226.5°; $[\alpha]_D^{27}$ +271° (*c*, 0.94 in $CHCl_3$); o.r.d.[17] in dioxane (*c* = 0.1 from 700 to 345 nm, 0.02 from 345 to 335 nm, 0.004 from 335 to 330 nm): $[\alpha]_{700}$ +70, $[\alpha]_{589}$ +118, $[\alpha]_{400}$ +912, $[\alpha]_{370}$ +1556, $[\alpha]_{350}$ +2275, $[\alpha]_{340}$ +3060, $[\alpha]_{330}$ +3250° (positive Cotton effect); λ_{max} (EtOH) 299 (ε 11 170) and 238 nm (ε 1430); ν_{max} (KBr) 3040 (vinylic hydrogens), 2180 (conjugated nitrile), 1736 (acetate), 1651 and 1564 (conjugated double bonds), 1255 and 1030 (acetate), 844, 836, and 829 cm^{-1} (bands which allow a distinction between the two isomeric dienonitriles).

Anal. Calcd. for $C_{26}H_{35}O_2N$: C, 79.34; H, 8.96; N, 3.56. Found: C, 79.08; H, 8.82; N, 3.77.

Recrystallizations of the mother liquors did not allow the isolation of the pure dienonitrile **7***a*. It was obtained from the dehydroacetylation of the diacetoxy nitriles **5***b* and **6***b* (see below).

(*2*) In the main chromatogram of the cyanoethylation, a (97:3) mixture of benzene – ethyl acetate eluted 178 mg of a partly crystalline material which was purified further by chromatography on 16 g of silica gel. Elutions with benzene – ethyl acetate (98:2) gave 45 mg of *dienonitriles* **7***a and* **8***a*, m.p. 170–185°, $[\alpha]_D^{27}$ −59° (*c*, 1.05 in $CHCl_3$); and 42 mg of a crystalline product, m.p. 133–142°, ν_{max} (KBr) 1730, 1685, 1250, and 1035 cm^{-1}. This product does not contain a nitrile function and was not further investigated.

(*3*) Always in the main chromatogram, benzene – ethyl acetate (95:5) eluted 660 mg of starting material, *3β-acetoxy-5α-pregn-17-en-21-al (4)*, m.p. 135–144°, identified by its i.r. spectrum, u.v. absorption, and the determination of a mixture melting point with an authentic sample.

(*4*) Benzene – ethyl acetate (95:5) eluted 1.06 g of an amorphous material which was purified further by chromatography on 100 g of silica gel. Elutions with benzene – ethyl acetate (95:5) gave 320 mg of a crystalline substance, m.p. 310–315°, which does not contain a nitrile group and which represents a *dimer*. Its constitution will be discussed elsewhere. In this secondary chromatogram, elutions with benzene – ethyl acetate mixtures (93:7 and 91:9) afforded 600 mg of a partly crystalline material, the i.r. spectrum of which was characteristic of *acetoxy hydroxy nitriles* of type *5a* and *6a* (vide infra); ν_{max} (KBr) 3460 (hydroxyl), 2240 (nonconjugated nitrile), 1740 (acetate), 1685 (double bond), 1245 (acetate), and 1035 cm^{-1} (acetate and alcohol).

(*5*) In the main chromatogram, benzene – ethyl acetate (93:7) eluted 6.1 g of a crystalline mixture of isomeric acetoxy hydroxy nitriles. The head fractions (2.64 g m.p. 189–192°) were recrystallized from ether–hexane to yield 1.36 g of *3β-acetoxy-16α-ethyl-16²α-cyano-16²,21-cyclo-5α-pregn-17-en-21α-ol (5a)*, m.p. (dec.) 216–219°. A sample was recrystallized twice from ether for analysis; colorless, clustered, broad needles, m.p. (dec.) 219–220°; $[\alpha]_D^{23}$ +22° (*c*, 0.96 in $CHCl_3$); λ_{max} (cyclohexane) 188–191 nm; ν_{max} (KBr) 3510 (hydroxyl), 2240 (nitrile), 1732 (acetate), 1688 (double bond), 1245 (acetate), 1034 and 1022 cm^{-1} (acetate and alcohol); ν_{max} ($CHCl_3$) 3582 and 3427; 2245, 1724, 1676, 1260, and 1028 cm^{-1}; weak positive reaction with tetranitromethane; n.m.r.[18] δ 0.84 (18- and 19-CH_3), 2.02 (acetate), 4.37 (21β-H), 4.67 (3α-H), 5.33 (20-H; doublet of doublets, J = 2.2 and 3.9 Hz).

Anal. Calcd. for $C_{26}H_{37}O_3N$: C, 75.87; H, 9.07; N, 3.40. Found: C, 76.00; H, 8.92; N, 3.60.

The tail fractions of the above-mentioned series of fractions (940 mg, m.p. 190–195°) were recrystallized from ether–hexane to give 780 mg of *3β-acetoxy-16α-ethyl-16²β-cyano-16²,21-cyclo-5α-pregn-17-en-21α-ol (6a)*, m.p. (dec.) 208–210°. A sample was recrystallized twice from ether for analysis; very short, broad needles, m.p. (dec.) 210–211°; $[\alpha]_D^{22}$ −17° (*c*, 0.71 in $CHCl_3$); λ_{max} (cyclohexane) 185–191 nm (ε 12 000); ν_{max} (KBr) 3505 (hydroxyl), 2240 (nitrile), 1738 (acetate), 1688 (double bond), 1248 (acetate), 1042 and 1018 cm^{-1} (acetate and alcohol); ν_{max} ($CHCl_3$) 3587 and 3442; 2245, 1724, 1676, 1260, and 1028 cm^{-1}; weak positive reaction with tetranitromethane; n.m.r.[18] δ 0.86 (19-CH_3), 0.88 (18-CH_3), 2.02 (acetate), 4.38 (21β-H), 4.63 (3α-H), 5.27 (20-H).

Anal. Calcd. for $C_{26}H_{37}O_3N$: C, 75.87; H, 9.07; N, 3.40. Found: C, 75.99; H, 8.81; N, 3.36.

The intermediate fractions of the mixture of isomeric acetoxy hydroxy nitriles and the material isolated from the mother liquors of the previous crystallizations were

[16]According to the procedure described for the cyanoethylation of isophorone by S. Julia (*6d*).

[17]We are indebted to Dr. A. Cross and Dr. P. Crabbé, Syntex S.A., Mexico, for the determination of this measurement.

[18]The n.m.r. spectrum was recorded on a Varian A-60 spectrometer in deuteriochloroform, using tetramethylsilane as internal standard. We are indebted to Dr. A. D. Cross, Syntex, S.A., Mexico, and Dr. P. W. Landis, E. Lilly & Co., Indianapolis, for their valuable help in determining and interpreting this spectrum.

Can. J. Chem. Downloaded from www.nrcresearchpress.com by 210.87.254.6 on 09/05/12
For personal use only.

combined (total: 3.95 g) and purified by repeated chromatography on silica gel and recrystallizations from ether – hexane to yield 1.06 g [0.62 g, m.p. (dec.) 217–219°; 440 mg, m.p. (dec.) 213–218°] of *acetoxy hydroxy nitrile* **5***a* and 495 mg of *acetoxy hydroxy nitrile* **6***a*, m.p. (dec.) 206–208°. The i.r. spectrum of the amorphous product (1.95 g) isolated from the mother liquors was characteristic of acetoxy hydroxy nitriles of type **5***a* and **6***a*.

(*6*) In the main chromatogram, ethyl acetate eluted 560 mg of the *dihydroxy nitrile mixture*, m.p. 240–260°. Recrystallization from methanol gave 190 mg of *16α-ethyl-16²α-cyano-16²,21-cyclo-5α-pregn-17-en-3β,21α-diol (5)*, m.p. 282–286°. A sample was recrystallized twice for analysis; colorless needles; m.p. 291–294°; $[\alpha]_D^{27}$ +64° (*c*, 1.02 in pyridine); ν_{max} (KBr) 3320 and 3150 (hydroxyls), 2240 (nitrile), 1685 (double bond), 1048 and 1038 cm^{-1} (alcohols).

Anal. Calcd. for $C_{24}H_{35}O_2N$: C, 78.00; H, 9.55; N, 3.79. Found: C, 77.85; H, 9.30; N, 3.83.

In summary, there were obtained 2.42 g (29%) of acetoxy hydroxy nitrile **5***a*, 1.28 g (15%) of acetoxy hydroxy nitrile **6***a*, 2.55 g (30%) of a mixture of acetoxy hydroxy nitriles, 190 mg (2%) of dihydroxy nitrile **5**, 370 mg (5%) of a mixture of dihydroxy nitriles, and 430 mg (5%) of dienonitriles **7** and **8**. For the calculation of these yields the recovery of 660 mg of starting material, aldehyde **4**, was taken into consideration. The total yield in products arisen from a γ-cyanoethylation amounted to 86%.

(b) In t-Butanol with Potassium Hydroxide

A solution of 1.1 g of 3β-acetoxy-5α-pregn-17-en-21-al (**4**), m.p. 156–158°, in 25 ml of *t*-butanol was heated to 45° under a nitrogen stream and treated, with stirring, first with 1 ml of a 10% aqueous solution of potassium hydroxide, then with 2 ml of a 1.65 *M* solution of acrylonitrile in *t*-butanol. The mixture was stirred at 55° for 4.5 h, then kept at room temperature for 18 h. A precipitate formed. After the addition of 3 ml of an aqueous 0.8 *M* acetic acid solution, the solvents were removed *in vacuo*. The residue was taken up in methylene chloride. An insoluble material was filtered off, washed with water, and dried to afford 57 mg of a mixture of *dihydroxy nitriles* (mainly dihydroxy nitrile **5**), m.p. 244–252°; ν_{max} (KBr) 3400 and 3200 (hydroxyls), 2240 (nitrile), 1685 (double bond), and 1035 cm^{-1} (alcohols). The methylene chloride filtrate was washed with aqueous saturated sodium bicarbonate and with water, then dried over sodium sulfate and the solvent was evaporated *in vacuo*. The residue (1.07 g) was dissolved in 5 ml of pyridine and treated with 2.5 ml of acetic anhydride for 16 h at room temperature. The usual work-up gave 1.26 g of a crude product which was purified by chromatography on 32 g of aluminum oxide.

(*1*) Elutions with a (4:1) mixture of petroleum ether – benzene gave 126 mg of *dienonitriles* **7***a and* **8***a*, m.p. 152–159°, which was recrystallized five times from hexane to yield 22 mg of crystals melting at 185–187°; $[\alpha]_D^{23}$ −108° (*c*, 0.85 in $CHCl_3$); λ_{max} (EtOH) 298 (ε 9000) and 238 nm (ε 2500); ν_{max} (KBr) 3030 (vinylic hydrogens), 2180 (conjugated nitrile), 1735 (acetate), 1652 and 1574 (conjugated double bonds), 1250 and 1030 (acetate), 851 and 834 cm^{-1} (bands which allow a distinction between the two dienonitriles).

Anal. Calcd. for $C_{26}H_{35}O_2N$: C, 79.34; H, 8.96; N, 3.56. Found: C, 79.59; H, 8.95; N, 3.63.

(*2*) A (1:1) mixture of petroleum ether – benzene eluted 633 mg of crystalline material which was purified further by chromatography on 19 g of aluminum oxide to afford: 18 mg of *dienonitriles* 7*a* and **8***a*, m.p. 169–172°, eluted with petroleum ether – benzene mixtures (9:1 and 4:1); 178 mg of *3β-acetoxy-5α-pregn-17-en-21-al (4)*, m.p. 145–150°, identified by its i.r. spectrum and the determination of a mixture m.p. with an authentic sample; 347 mg (266 mg melting between 182–200°; 81 mg of amorphous material) of a mixture of *diacetoxy nitriles* **5***b and* **6***b* (vide infra), eluted with petroleum ether – benzene (1:1), benzene, and benzene–ether (4:1).

(*3*) In the main chromatogram, a (1:1) mixture of petroleum ether – benzene eluted 154 mg of a crystalline mixture of the diacetoxy nitriles **5***b* and **6***b*, m.p. 190–205°. This material was combined with the crystalline material of analogous composition obtained above (total: 420 mg). Recrystallization from ether–hexane afforded 220 mg of *3β,21α-diacetoxy-16α-ethyl-16²β-cyano-16²,21-cyclo-5α-pregn-17-ene (6b)*, m.p. 211–216°. A sample was recrystallized three times for analysis; colorless needles, m.p. (dec.) 219.5–220.5°; $[\alpha]_D^{23}$ +68° (*c*, 0.96 in $CHCl_3$); the product was identified also by its i.r. spectrum and by the determination of a mixture m.p. with an authentic sample obtained by acetylation of the acetoxy hydroxy nitrile **6***a* (see below).

Anal. Calcd. for $C_{28}H_{39}O_4N$: C, 74.14; H, 8.66; N, 3.09. Found: C, 74.54; H, 8.30; N, 2.93.

(*4*) Elutions with petroleum ether – benzene (1:4) and benzene afforded 100 mg of an amorphous mixture of diacetoxy nitriles; ν_{max} (KBr) 2240 (nitrile), 1740 (acetates), 1685 (shoulder: double bond), 1245 and 1030 cm^{-1} (acetates).

(*5*) Benzene and a (4:1) mixture of benzene–ether eluted 90 mg of *3β,21α-diacetoxy-16α-ethyl-16²α-cyano-16²,21-cyclo-5α-pregn-17-ene (5b)*, m.p. 159–163°, identified by comparison of its i.r. spectrum with that of an authentic sample obtained by acetylation of the acetoxy hydroxy nitrile **5***a* (see below).

In summary, there were obtained 144 mg (13%) of dienonitriles **7***a* and **8***a*, 90 mg (7%) of diacetoxy nitrile **5***b*, 220 mg (17%) of diacetoxy nitrile **6***b*, 390 mg (30%) of a mixture of diacetoxy nitriles. For the calculation of these yields, the recovery of 176 mg of starting material, aldehyde **4**, was taken into consideration. The total yield of products arisen from a γ-cyanoethylation amounted to 73%.

3β,21α-Diacetoxy-16α-ethyl-16²α-cyano-16²,21-cyclo-5α-pregn-17-ene (5b)

(a) By Acetylation of the Acetoxy Hydroxy Nitrile 5a

A solution of 105 mg of acetoxy hydroxy nitrile **5***a*, m.p. (dec.) 217–219°, in 1 ml of pyridine was treated with 0.5 ml of acetic anhydride at room temperature for 16 h. The usual work-up gave 123 mg of partly crystalline material. Washing with methanol removed the oils and left 98 mg (85% yield) of 3β,21α-diacetoxy-16α-ethyl-16²α-cyano-16²,21-cyclo-5α-pregn-17-ene (**5***b*), m.p. (dec.) 165–167°. A sample was recrystallized twice from ether–hexane for analysis; colorless prisms, m.p. (dec.) 169–170°; $[\alpha]_D^{27}$ +134° (*c*, 0.94 in $CHCl_3$); ν_{max} (KBr) 2240

Can. J. Chem. Downloaded from www.nrcresearchpress.com by 210.87.254.6 on 09/05/12
For personal use only.

(nitrile), 1748 and 1745 (acetates), 1685 (double bond), 1240, 1218, 1034, and 1018 cm^{-1} (acetates).

Anal. Calcd. for $C_{28}H_{39}O_4N$: C, 74.14; H, 8.66; N, 3.09. Found: C, 74.01; H, 8.68; N, 3.06.

(b) By Acetylation of the Dihydroxy Nitrile **5**

The dihydroxy nitrile **5** (50 mg, m.p. 291–294°) was acetylated as described above (1 ml of pyridine and 0.5 ml of acetic anhydride) to give 63 mg of partly crystalline material. Washing with cold ether removed the oils and left 39 mg (63%) of diacetoxy nitrile **5***b*, m.p. (dec.) 163–165°. One recrystallization from ether–hexane raised the m.p. to 166–167°; $[\alpha]_D^{27}$ +131° (*c*, 1.05 in $CHCl_3$); the product was also identified by its i.r. spectrum and the determination of a mixture m.p. with the sample obtained above.

*3β,21α-Diacetoxy-16α-ethyl-16²β-cyano-16²,21-cyclo-5α-pregn-17-ene (**6b**)*

A solution of 63 mg of acetoxy hydroxy nitrile **6***a*, m.p. 208–210°, in 1 ml of pyridine was treated with 0.5 ml of acetic anhydride at room temperature for 14 h. The usual work-up gave 70 mg (quantitative yield) of 3β,21α-diacetoxy-16α-ethyl-16²β-cyano-16²,21-cyclo-5α-pregn-17-ene (**6***b*), m.p. (dec.) 216–218°. Two recrystallizations from ether–hexane gave an analytical sample; colorless needles, m.p. (dec.) 220–221°; $[\alpha]_D^{25}$ +62° (*c*, 0.99 in $CHCl_3$); ν_{max} (KBr) 2240 (nitrile), 1738 (broad band: acetates), 1688 (double bond), 1245, 1225, and 1025 cm^{-1} (acetates).

Anal. Calcd. for $C_{28}H_{39}O_4N$: C, 74.14; H, 8.66; N, 3.09. Found: C, 74.25; H, 8.70; N, 3.20.

*3β-Acetoxy-16α-ethyl-16²α-cyano-16²,21-cyclo-5α-pregn-17-en-21-one (**9**)*

A stirred solution of 836 mg of acetoxy hydroxy nitrile **5***a*, m.p. (dec.) 217–219°, in 60 ml of absolute acetone was cooled in an ice bath and 0.75 ml of Jones' reagent (29) was added dropwise. The mixture was stirred at 0° for 2.5 min, then poured into 800 ml of ice water. The precipitate was filtered, washed with water, and dried in a vacuum desiccator over phosphorous pentoxide to afford 823 mg (98% yield) of 3β-acetoxy-16α-ethyl-16²α-cyano-16²,21-cyclo-5α-pregn-17-en-21-one (**9**), m.p. 250–252°. A sample was recrystallized twice from methylene chloride – ether for analysis; small, colorless prisms, m.p. 252–253°; $[\alpha]_D^{25}$ −18° (*c*, 0.82 in $CHCl_3$); o.r.d.[19] (*c*, 0.11, dioxane); $[\alpha]_{589}$ −19, $[\alpha]_{358}$ +764 (max), $[\alpha]_{349}$ +649 (min), $[\alpha]_{342}$ +691 (max), $[\alpha]_{330}$ 0, $[\alpha]_{250}$ −2445° (min) (positive Cotton effect); λ_{max} (EtOH) 239 nm (ε 14 700); λ_{max} (cyclohexane) 230 nm; λ_{max} ($CHCl_3$) 306 nm (ε 83); ν_{max} ($CHCl_3$) 2240 (nitrile), 1725 (acetate), 1683 and 1640 (α,β-unsaturated ketone), 1255 and 1025 cm^{-1} (acetate); n.m.r.[20] δ 0.87 (19-CH_3), 0.96 (18-CH_3), 2.03 (acetate), 2.53 (16¹β-H), 3.12 (16β-H), 3.56 (16²β-H; quartet: J = 4.1 and 14.1 Hz), 4.69 (3α-H), 5.75 (doublet: J = 1.8 Hz) (20-H).

Anal. Calcd. for $C_{26}H_{35}O_3N$: C, 76.25; H, 8.62; N, 3.42. Found: C, 76.50; H, 8.64; N, 3.59.

*3β-Acetoxy-16α-ethyl-16²β-cyano-16²,21-cyclo-5α-pregn-17-en-21-one (**10**)*

A stirred solution of 710 mg of acetoxy hydroxy nitrile **6***a*, m.p. 209–210°, in 73 ml of absolute acetone was treated, at 0°, with 0.7 ml of Jones' reagent (29), as described above. The usual work-up gave 707 mg (99% yield) of 3β-acetoxy-16α-ethyl-16²β-cyano-16²,21-cyclo-5α-pregn-17-en-21-one (**10**), m.p. 200–202°; the melting at 200° was followed by recrystallization and the new crystals melted at 253–254°; the fusion transforms the α,β-unsaturated ketone **10** into its isomer **9** (vide infra). Ketone **10** was recrystallized three times from ether for analysis; colorless, prismatic needles, m.p. 200–202°; $[\alpha]_D^{25}$ −48° (*c*, 1.05 in $CHCl_3$); o.r.d.[19] in dioxane (*c* = 0.10 from 610 to 330 nm, 0.05 from 320 to 256 nm); $[\alpha]_{610}$ −19.6, $[\alpha]_{589}$ −19.6, $[\alpha]_{365}$ +1100 (max), $[\alpha]_{358}$ +784 (min), $[\alpha]_{352}$ +901 (max), $[\alpha]_{344}$ 0, $[\alpha]_{315}$ −3330, $[\alpha]_{270}$ −5150, $[\alpha]_{256}$ −7950° (positive Cotton effect); λ_{max} (EtOH) 238 nm (ε 16 000); λ_{max} ($CHCl_3$) 325 (ε 90) and 318 nm (shoulder, ε 87); ν_{max} ($CHCl_3$) 2240 (nitrile), 1725 (acetate), 1678 and 1638 (α,β-unsaturated ketone), 1255 and 1030 cm^{-1} (acetate); n.m.r.[20] δ 0.87 (19-CH_3), 1.00 (18-CH_3), 2.03 (acetate), 2.45 (16¹β-H; octet: J = 2.3, 4.8, and 12.5 Hz), 3.20 (16β-H), 3.48 (quartet: J = 2.5 and 5.0 Hz) (16²α-H), 4.67 (3α-H), 5.75 (doublet: J = 1.18 Hz) (20-H).

Anal. Calcd. for $C_{26}H_{35}O_3N$: C, 76.25; H, 8.62; N, 3.42. Found: C, 75.72; H 9.01; N, 3.59.

It was not possible to obtain better analytical figures for this compound.

*Isomerization of the α,β-Unsaturated Ketone **10** to the α,β-Unsaturated Ketone **9***

(a) Upon Fusion

A quantity of 35 mg of 3β-acetoxy-16α-ethyl-16²β-cyano-16²,21-cyclo-5α-pregn-17-en-21-one (**10**), m.p. 199–200°, was heated at 220° for 15 min under reduced pressure to give 35 mg of 3β-acetoxy-16α-ethyl-16²α-cyano-16²,21-cyclo-5α-pregn-17-en-21-one (**9**), m.p. 248–250°. Two recrystallizations from methylene chloride – ether gave 18 mg of crystals melting at 252.5–253.5°; $[\alpha]_D^{25}$ −17° (*c*, 1.03 in $CHCl_3$); the product was further identified by its i.r. spectrum and the determination of a mixture m.p. with an authentic sample.

(b) In a Protic Solvent

(i) In a Mixture of Glacial Acetic Acid and Ethyl Acetate

A solution of 49 mg of α,β-unsaturated ketone **10**, m.p. 198–200°, in 0.8 ml of glacial acetic acid and 1.2 ml of ethyl acetate was kept at room temperature for 16 h. The product was poured into ice water and the mixture was extracted with methylene chloride. The organic layer was washed with a cold sodium bicarbonate solution and with water, and was dried over sodium sulfate. Removal of the solvent left 50 mg of the α,β-unsaturated ketone **9**, m.p. 249.5–251°, identified by its i.r. spectrum and the determination of a mixture melting point with an authentic sample. After one recrystallization from methylene chloride – ether, the product melted at 251–252°; $[\alpha]_D^{25}$ −16° (*c*, 1.00 in $CHCl_3$).

---

[19]We are indebted for this measurement and its discussion to Prof. C. Djerassi, Stanford University, Stanford, California.

[20]The n.m.r. spectrum was recorded at 60 MHz on a Varian 4300 spectrometer in deuteriochloroform, using tetramethylsilane as internal standard. We are indebted to Dr. S. Rakhit and Mr. T. A. Wittstruck, Worcester Foundation for Experimental Biology, Shrewsbury, Mass., for their valuable help in determining and discussing this spectrum.

Can. J. Chem. Downloaded from www.nrcresearchpress.com by 210.87.254.6 on 09/05/12
For personal use only.

(ii) In a Mixture of Dioxane and Ethanol in Presence of Palladium-on-calcium Carbonate

A solution of 9 mg of α,β-unsaturated ketone **10**, m.p. 198–200°, in 1 ml of absolute dioxane and 5 ml of ethanol was shaken at room temperature for 16 h in presence of 10 mg of 5% palladium-on-calcium carbonate. The solid was filtered and the filtrate was evaporated to dryness, leaving 9 mg of α,β-unsaturated ketone **9**, m.p. 245–249°. Recrystallization from methylene chloride – ether gave 6 mg of crystals melting at 251–253°; $[\alpha]_D^{27}$ −17° (*c*, 0.78 in $CHCl_3$).

*3β-Acetoxy-16α-ethyl-16²α-cyano-16²,21-cyclo-5α,17β-pregnan-21-one (**11b**)*

*(a) By Hydrogenation of the α,β-Unsaturated Ketone **9***

A solution of 625 mg of the α,β-unsaturated ketone **9** in 30 ml of dioxane and 200 ml of ethanol was hydrogenated at atmospheric pressure in presence of 600 mg of 5% palladium-on-calcium carbonate. Two other portions of catalyst were added: 500 mg after 4 h and 400 mg after 6 h. The hydrogenation was complete after 8.5 h. The catalyst was filtered, washed with ethanol, and the filtrate and washings were taken to dryness. The residue (700 mg, m.p. 190–200°) was recrystallized from ether to give 390 mg of 3β-acetoxy-16α-ethyl-16²α-cyano-16²,21-cyclo-5α,17β-pregnan-21-one (**11b**), m.p. 205–209°. Chromatography of the amorphous material (310 mg), isolated from the mother liquors, on 30 g of silica gel, and elutions with benzene – ethyl acetate (97:3) afforded an additional 165 mg of saturated cyano ketone **11b**, m.p. 204–208° (total yield: 84%). A sample was sublimed at 185° under high vacuum; m.p. 212.5–213°; $[\alpha]_D^{23}$ −94° (*c*, 1.02 in $CHCl_3$); o.r.d.[21] (*c* = 0.1, in dioxane): $[\alpha]_{700}$ −110, $[\alpha]_{589}$ −144, $[\alpha]_{317.5}$ −1870, $[\alpha]_{315}$ −1870, $[\alpha]_{310}$ −1954 (min), $[\alpha]_{297.5}$ −792° (negative Cotton effect); ν_{max} (KBr) 2240 (nitrile), 1735–1730 (broad band: acetate and 21-ketone), 1242 and 1030 cm^{-1} (acetate); ν_{max} ($CHCl_3$) 2250, 1733, 1728, 1260 (broad), 1030 cm^{-1}.

Anal. Calcd. for $C_{26}H_{37}O_3N$: C, 75.87; H, 9.06; N, 3.41. Found: C, 75.85; H, 8.99; N, 3.49.

*(b) By Hydrogenation of the α,β-Unsaturated Ketone **10***

A solution of 339 mg of α,β-unsaturated ketone **10**, m.p. 198–200°, in 20 ml of dioxane and 110 ml of ethanol was hydrogenated in presence of 880 mg of 5% palladium-on-calcium carbonate (added in three portions as described above). The usual work-up gave 400 mg of a crystalline residue melting between 163 and 183°, which was recrystallized twice from ether to afford 70 mg of 3β-acetoxy-16α-ethyl-16²α-cyano-16²,21-cyclo-5α,17β-pregnan-21-one (**11b**), m.p. 206–209°. Chromatography of the material isolated from the mother liquors on 30 g of silica gel and elutions with benzene – ethyl acetate (97:3) gave an additional 135 mg of the saturated cyano ketone **11b**, m.p. 204–208° (total yield: 60%). A sample was recrystallized from ether; m.p. 209–211°; it was identified by its i.r. spectrum and the determination of a mixture melting point with an authentic sample.

[21]We are indebted to Dr. P. Crabbé, Syntex S.A., Mexico, for the determination of this measurement.

*3β-Acetoxy-16α-ethyl-16²,21-cyclo-5α,17β-pregnan-21-one (**11a**)*

A solution of 560 mg of the saturated cyano ketone **11b**, m.p. 206–209°, in 12 ml of glacial acetic acid and 19 ml of concentrated hydrochloric acid was heated at reflux temperature for 20 h (a precipitate formed after 2.5 h and was then gradually replaced by a dark oil floating on the solution). The mixture was cooled and poured into 125 ml of ice water. The precipitate was extracted with ether, the ethereal layer was washed with water, with aqueous 2 *N* sodium hydroxide and again with water, and was dried over sodium sulfate. Evaporation of the solvent left 440 mg of an amorphous product. Acidification of the alkaline extracts, followed by extraction with ether, and the usual work-up, led to the isolation of 25 mg of an amorphous material, which was not investigated. The neutral fraction, representing, in part, crude *3β-hydroxy-16α-ethyl-16²,21-cyclo-5α,17β-pregnan-21-one (**11**)*, was acetylated under the usual conditions (3 ml of pyridine and 1.5 ml of acetic anhydride). The residue (460 mg) was adsorbed on 50 g of silica gel. Elutions with a (97:3) mixture of benzene – ethyl acetate gave 240 mg of an amorphous material; ν_{max} (KBr) 1718 and 755 cm^{-1}. Chromatography on 8 g of aluminum oxide and elutions with mixtures of petroleum ether – benzene (9:1, 4:1, 1:1) afforded 131 mg of a partly crystalline material melting between 110 and 125°. It was recrystallized from methanol to give 25 mg of crystals melting at 155–164°; the i.r. spectrum was similar to that of the amorphous material: ν_{max} (KBr) 1718 and 756 cm^{-1}; the Beilstein test was strongly positive. This product was not investigated further. In the main chromatogram, a (97:3) mixture of benzene – ethyl acetate eluted 63 mg of a partly crystalline product; λ_{max} (EtOH) 241 nm; ν_{max} (KBr) 3450, 1670, 1242, and 1198 cm^{-1}. The product was not investigated further. Elutions with benzene – ethyl acetate (90:10) gave 60 mg of *3β-acetoxy-16α-ethyl-16²,21-cyclo-5α,17β-pregnan-21-one (**11a**)*, m.p. 150–156°. Recrystallization from ether–hexane afforded 35 mg of crystals melting at 162–165°. The product was recrystallized three times for analysis; slightly yellowish crystals, m.p. 166–168°; $[\alpha]_D^{25}$ −102° (*c*, 1.04 in $CHCl_3$); o.r.d.[21] (*c* = 1.09 in dioxane): $[\alpha]_{700}$ −22, $[\alpha]_{589}$ −115, $[\alpha]_{350}$ −894, $[\alpha]_{317.5}$ −2685 (min), $[\alpha]_{315}$ −2456, $[\alpha]_{310}$ −2585 (min), $[\alpha]_{295}$ −190° (negative Cotton effect); ν_{max} (KBr) 1731 (acetate), 1718 (21-ketone), 1242 and 1030 cm^{-1} (acetate); ν_{max} ($CHCl_3$) 1730, 1710, 1255 (broad), 1220, 1029 cm^{-1}.

Anal. Calcd. for $C_{25}H_{38}O_3$: C, 77.67; H, 9.91. Found: C, 77.87; H, 10.03.

*2ξ-Cyano-3-(3β-hydroxy-17-oxo-5α-androstan-16ξ-yl)-propanoic Acid (**12**), Methyl 2ξ-Cyano-3-(3β-hydroxy-17-oxo-5α-androstan-16ξ-yl)-propanoate (**12a**), and Methyl 2ξ-Cyano-3-(3β-acetoxy-17-oxo-5α-androstan-16ξ-yl)-propanoate (**12b**)*

*(a) By Ozonolysis of the α,β-Unsaturated Ketone **9***

A stream of oxygen containing 4.8% of ozone (230 ml/min) was passed through a solution of 520 mg of the α,β-unsaturated ketone **9**, m.p. 250–252°, in 11 ml of ethyl acetate and 10 ml of acetic acid, at −10° for 3 h. Subsequently, 0.7 ml of water and 0.4 ml of 30%

Can. J. Chem. Downloaded from www.nrcresearchpress.com by 210.87.254.6 on 09/05/12
For personal use only.

hydrogen peroxide solution were added. The mixture was left for 14 h at room temperature and was then poured into 100 ml of ice water. The precipitate was extracted with ether, the ethereal layer was washed with water, with a 2 *N* sodium hydroxide solution, and again with water, and was dried over sodium sulfate. No neutral material was obtained after evaporation of the ether. The combined alkaline extracts were acidified to the *Congo-blue* reaction with 5 *N* sulfuric acid. The precipitate was extracted with methylene chloride. The organic layer was washed with water and dried over sodium sulfate. Removal of the solvent left 466 mg of *2ξ-cyano-3-(3β-hydroxy-17-oxo-5α-androstan-16ξ-yl)-propanoic acid (**12**)*, m.p. 183–189°; ν_{max} (KBr) 3450 (3-hydroxyl), 3260–2600 (acid hydroxyl), 2245 (nitrile), 1750–1730 (broad band: 17-ketone and acid), 1240 (broad band: acid), 1035 cm^{-1} (alcohol).

Methylation

The crude acid **12** (460 mg) in 5 ml of absolute methanol and 1 ml of dry ether was treated, at 0°, with 20 ml of a 1.3% solution of diazomethane in ether. The mixture was kept for 18 h at room temperature. The excess diazomethane was destroyed with a few drops of acetic acid and the solvents were evaporated under reduced pressure to give 500 mg of an amorphous product consisting mainly of *methyl 2ξ-cyano-3-(3β-hydroxy-17-oxo-5α-androstan-16ξ-yl)-propanoate (**12a**)*; ν_{max} (KBr) 3460 (hydroxyl), 2240 (nitrile), 1748 (broad band: 17-ketone and ester), 1260 (ester), 1040 cm^{-1} (alcohol).

Acetylation

The crude ester **12***a* (496 mg) in 3 ml of pyridine was treated with 1.5 ml of acetic anhydride at room temperature for 14 h. The residue (530 mg), isolated by the usual work-up, was adsorbed on 50 g of silica gel. Elutions with benzene – ethyl acetate (95:5) gave 210 mg of partly crystalline material. Washing with hexane removed the oils and left 120 mg of *methyl 2ξ-cyano-3-(3β-acetoxy-17-oxo-5α-androstan-16ξ-yl)-propanoate (**12b**)*, m.p. 122–133°. Recrystallization from ether–hexane gave 45 mg of crystals melting at 153–156°. The product was recrystallized three times for analysis; long, fine, colorless needles, m.p. 162.5–163.5°, $[\alpha]_D^{25}$ +65° (*c*, 1.02 in $CHCl_3$); ν_{max} (KBr) 2240 (nitrile), 1758 (17-ketone), 1738–1728 (acetate and methyl ester), 1248 (acetate), 1028 cm^{-1} (acetate).

Anal. Calcd. for $C_{26}H_{37}O_5N$: C, 70.40; H, 8.41; N, 3.16. Found: C, 70.14; H, 8.51; N, 3.36.

The amorphous material isolated from the hexane washings and from the mother liquors of the first recrystallization (total: 162 mg) was adsorbed on 16 g of silica gel. Elutions with benzene – ethyl acetate (95:5) afforded another 100 mg of *acetoxy methyl ester **12b***, m.p. 137–140° [over-all yield from the α,β-unsaturated ketone **9**: 145 mg (26%)].

*(b) By Ozonolysis of the α,β-Unsaturated Ketone **10***

A stream of oxygen containing 4.5% of ozone was passed for 2 h (250 ml/min) through a solution of 448 mg of the α,β-unsaturated ketone **10**, m.p. 199–200°, in 12 ml of ethyl acetate and 8 ml of acetic acid, at −10°. Subsequently, 0.6 ml of water and 0.4 ml of a 30% hydrogen peroxide solution were added. The mixture was left at room temperature for 14 h. The work-up, as described above, afforded 400 mg of crude *2ξ-cyano-3-(3β-hydroxy-17-oxo-5α-androstan-16ξ-yl)-propanoic acid (**12**)*, identified by its i.r. spectrum. The crude acid was methylated as described under (*a*) (4 ml of absolute methanol, 2 ml of dry ether, and 25 ml of a 1% solution of diazomethane in ether) to give 390 mg of crude *methyl 2ξ-cyano-3-(3β-hydroxy-17-oxo-5α-androstan-16ξ-yl)-propanoate (**12a**)*, identified by its i.r. spectrum. The crude ester was acetylated in the usual fashion (3 ml of pyridine and 1.5 ml of acetic anhydride). The crude reaction product was adsorbed on 40 g of silica gel. Elutions with benzene – ethyl acetate (95:5) gave 244 mg of *methyl 2ξ-cyano-3-(3β-acetoxy-17-oxo-5α-androstan-16ξ-yl)-propanoate (**12b**)* [90 mg, melting between 118 and 128°; 130 mg, melting at 130–135°]. The latter sample was recrystallized four times from ether–hexane to give crystals melting at 160–161°; $[\alpha]_D^{25}$ +60° (*c*, 0.93 in $CHCl_3$); the identification was completed by the determination of the i.r. spectrum and that of a mixture m.p. with an authentic sample. The amorphous material isolated from the mother liquors from the first recrystallization and some amorphous material from the chromatogram (total: 210 mg) were purified by chromatography on 30 g of silica gel to afford another 180 mg of *acetoxy ester **12b***, m.p. 139–144°, eluted with benzene – ethyl acetate (95:5) [over-all yield from the α,β-unsaturated ketone **10**: 215 mg (44%)].

*Dehydroacetylation of 3β,21α-Acetoxy-16α-ethyl-16²α-cyano-16²,21-cyclo-5α-pregn-17-ene (**5b**)*

A solution of 114 mg of diacetoxy nitrile **5***b*, m.p. 163–164°, in 15 ml of methanol was treated with 7.5 ml of a 10% aqueous potassium carbonate solution. The mixture was heated to reflux temperature for 3 h and was then cooled and poured into 100 ml of ice water. The precipitate was filtered, washed with water, and dried in a vacuum desiccator over phosphorous pentoxide. The dried material (92 mg) was adsorbed on 3.5 g of silica gel. Elutions with benzene – ethyl acetate (97:3) gave 70 mg (79% yield) of *3β-hydroxy-16α-ethyl-16²-cyano-16²,21-cyclo-5α-pregna-17,21-diene (**7**)*, m.p. 193–197°. For analysis a sample was recrystallized twice from ether–hexane; colorless, prismatic needles, m.p. 199–200°; $[\alpha]_D^{25}$ −352° (*c*, 0.68 in $CHCl_3$); λ_{max} (EtOH) 298 nm (ε 11 500); ν_{max} (KBr) 3480 (hydroxyl), 3030 (vinylic hydrogens), 2180 (conjugated nitrile), 1653 and 1574 (conjugated double bonds), 1042 (alcohol), 844 and 838 cm^{-1}; n.m.r.[22]: δ 0.80 (18-CH_3 and 19-CH_3), 1.87 (OH), 2.3 (16^1-H), 2.65 (16β-H), 3.43 (3α-H), 5.40 (doublet of doublets; J = 2.2 and 5.3 Hz) (20-H), 6.49 (doublet of doublets; J = 2.4 and 5.3 Hz) (21-H).

Anal. Calcd. for $C_{24}H_{33}ON$: C, 81.99; H, 9.47; N, 3.99. Found: C, 81.99; H, 9.35; N, 4.04.

Elutions with benzene–methanol (9:1) gave 20 mg (21% yield) of *16α-ethyl-16²α-cyano-16²,21-cyclo-5α-pregn-17-ene-3β,21α-diol (**5**)*; m.p. 270–280°, identified by its i.r. spectrum.

[22]The spectrum, for which we are indebted to Prof. G. Just and Mr. G. Stammer, McGill University, Montreal, was recorded on a Varian HR-60 spectrometer in deuteriochloroform, with tetramethylsilane as internal standard.

Can. J. Chem. Downloaded from www.nrcresearchpress.com by 210.87.254.6 on 09/05/12
For personal use only.

Acetylation of the Hydroxy Dienonitrile 7

The product isolated from the mother liquors from the recrystallizations for analysis of the hydroxy dienonitrile **7** (40 mg) was acetylated under the usual conditions (1 ml of pyridine and 0.5 ml of acetic anhydride; 9 h at room temperature). Removal of the solvents left 41 mg of *3β-acetoxy-16α-ethyl-16²-cyano-16²,21-cyclo-5α-pregna-17,21-diene (7a)*, m.p. 162–164°. Two recrystallizations from hexane afforded the analytical sample; colorless prismatic needles, m.p. 166–167°; $[\alpha]_D^{25}$ −325° (*c*, 0.91 in $CHCl_3$); o.r.d.[17] in dioxane (*c* = 0.1 from 700 to 350 nm, 0.02 from 350 to 335 nm) $[\alpha]_{700}$ −138, $[\alpha]_{589}$ −253, $[\alpha]_{400}$ −921, $[\alpha]_{375}$ −1276, $[\alpha]_{350}$ −2288, $[\alpha]_{335}$ −2970° (negative Cotton effect); λ_{max} (EtOH) 298 nm (ε 10 000); ν_{max} (KBr) 3040 (vinylic hydrogens), 2180 (conjugated nitrile), 1653 and 1574 (conjugated double bonds), 1250 and 1030 (acetate), 848 and 836 cm^{-1} (bands allowing a distinction between the two isomeric dienonitriles).

Anal. Calcd. for $C_{26}H_{35}O_2N$: C, 79.34; H, 8.96; N, 3.56. Found: C, 79.21; H, 8.89; N, 3.78.

Treatment of 3β,21α-Diacetoxy-16α-ethyl-16²α-cyano-16²,21-cyclo-5α-pregn-17-ene (5b) with Potassium Hydroxide

A solution of 70 mg of diacetoxy nitrile **5b**, m.p. 163–164°, in 9 ml of methanol was left with 3 ml of a 12% methanolic potassium hydroxide solution for 18 h at room temperature in a nitrogen atmosphere. The product was poured into 200 ml of ice water and the precipitate was extracted with ether. The ethereal layer was washed with water and dried over sodium sulfate. Evaporation of the solvent gave 57 mg of a crystalline residue which was chromatographed on 3 g of silica gel. Benzene – ethyl acetate (90:10) eluted 5 mg (9%) of *3β-hydroxy-16α-ethyl-16²-cyano-16²,21-cyclo-5α-pregna-17,21-diene (7)*, m.p. 194–196°. Acetylation under the usual conditions (0.2 ml of acetic anhydride and 0.4 ml of pyridine) gave *3β-acetoxy-16α-ethyl-16²-cyano-16²,21-cyclo-5α-pregna-17,21-diene (7a)*, m.p. 164–168°, identified by its i.r. spectrum and the mixture m.p. with an authentic sample.

Further elutions in the chromatogram, with benzene – ethyl acetate (80:20), gave 52 mg (91%) of *16α-ethyl-16²α-cyano-16²,21-cyclo-5α-pregn-17-ene-3β,21α-diol (5)*, m.p. 281–285°, identified by its i.r. spectrum and the mixture m.p. with a sample originating from the cyanoethylation reaction.

Dehydroacetylation of 3β,21α-diacetoxy-16α-ethyl-16²β-cyano-16²,21-cyclo 5α-pregn-17-ene (6b)

A mixture of 75 mg of diacetoxy nitrile **6b**, m.p. 207–209°, 10 ml of methanol, and 5 ml of a 10% aqueous potassium carbonate solution, was heated to reflux temperature for 3 h. The mixture was cooled and poured into ice water (100 ml). The precipitate was filtered, washed with water, and dried in a vacuum desiccator over phosphorous pentoxide. The product (55 mg) was adsorbed on 5 g of silica gel. Elutions with benzene – ethyl acetate (95:5 and 93:7) afforded 21 mg (35% yield) of *3β-hydroxy-16α-ethyl-16²-cyano-16²,21-cyclo-5α-pregna-17,21-diene (7)*, m.p. 192–194°; λ_{max} (EtOH) 298 nm (ε 8400), identified by its i.r. spectrum. Acetylation in the usual way (1 ml of pyridine and 0.5 ml of acetic anhydride) gave 22 mg of *3β-acetoxy-16α-ethyl-16²-cyano-16²,21-cyclo-5α-pregna-17,21-diene (7a)*, m.p. 155–160°. Recrystallization from methanol–water afforded 8 mg of crystals melting at 167–168°; $[\alpha]_D^{28}$ −302° (*c*, 0.66 in $CHCl_3$); the i.r. spectrum was identical with that of an authentic sample.

In the chromatogram mentioned above, elutions with benzene – ethyl acetate (80:20 and 70:30) gave 26 mg (42%) of *16α-ethyl-16²α-cyano-16²,21-cyclo-5α-pregn-17-ene-3β,21α-diol (5)*, m.p. 263–269°. The sample (8 mg) obtained after recrystallization from aqueous methanol melted at 284–286°; its i.r. spectrum was identical with that of an authentic product. A 5 mg sample was acetylated under the usual conditions (0.15 ml of acetican hydride and 0.3 ml of pyridine). Filtration of the residue (7 mg) through a column of 2 g of silica gel, with benzene – ethyl acetate (97:3), afforded 3 mg of *3β,21α-diacetoxy-16α-ethyl-16²α-cyano-16²,21-cyclo-5α-pregn-17-ene (5b)*, m.p. 164–165°, identified by its i.r. spectrum and the determination of a mixture m.p. with an authentic sample.

Dehydration of 3β-acetoxy-16α-ethyl-16²α-cyano-16²,21-cyclo-5α-pregn-17-en-21α-ol (5a)

(a) With p-Toluenesulfonyl Chloride in Pyridine

(*i*) A mixture of 81 mg of acetoxy hydroxy nitrile **5a**, m.p. 216–219°, 1.2 ml of pyridine, and 112 mg of *p*-toluenesulfonyl chloride, was kept at room temperature for 4 days under a nitrogen atmosphere. It was then poured into 33 ml of a cold, saturated, aqueous sodium bicarbonate solution and the precipitate was extracted with methylene chloride. The organic layer was washed with water, with cold 2 *N* hydrochloric acid, with cold aqueous sodium bicarbonate solution, and again with water, and was dried over sodium sulfate. Evaporation of the solvent left 76 mg of a partly crystalline residue which was adsorbed on 7.6 g of silica gel. Elutions with benzene – ethyl acetate (99:1) gave 37 mg (40%) of a crystalline material, consisting mainly of *3β-acetoxy-16α-ethyl-16²-cyano-16²,21-cyclo-5α-pregna-17,21-diene (7a)*, m.p. 170–174°. The sample obtained after three recrystallizations from methanol melted at 174–177°; $[\alpha]_D^{20}$ −214° (*c*, 0.55 in $CHCl_3$); λ_{max} (EtOH) 298 (ε 10 050) and 238 nm (ε 2900); ν_{max} (KBr) 3040 (vinylic hydrogens), 2220 (weak band: α,β-unsaturated nitrile), 2180 (α,β,γ,δ-unsaturated nitrile), 1735 (acetate), 1655 and 1574 (conjugated double bonds), 1253 and 1030 (acetate), 851 and 839 cm^{-1}. According to the u.v. absorption at 238 nm and the i.r. absorption at 2220 cm^{-1}, the dienonitrile **7a** was contaminated with a product possessing an α,β-unsaturated nitrile group, presumably *3β-acetoxy-16-ethyl-16²-cyano-16²,21-cyclo-5α-pregna-16,21-diene*. This sample and the material isolated from the mother liquors were combined. A portion of 30 mg was dissolved in 5 ml of methanol and treated with 2.5 ml of a 12% methanolic solution of potassium hydroxide at room temperature for 2 days. The mixture was then poured into cold water. The precipitate was filtered, washed with water, and dried to afford 38 mg of *hydroxy dienonitrile 7*, m.p. 189–193°; $[\alpha]_D^{28}$ −282° (*c*, 0.96 in $CHCl_3$). Acetylation in the usual way (1.4 ml of pyridine and 0.7 ml of acetic anhydride) gave the *dienonitrile 7a*, m.p. 170–172°; $[\alpha]_D^{28}$ −274° (*c*, 0.96 in $CHCl_3$). There was no absorption at 238 nm in the u.v. spectrum and no absorption at 2220 cm^{-1} in the i.r.

Can. J. Chem. Downloaded from www.nrcresearchpress.com by 210.87.254.6 on 09/05/12
For personal use only.

spectrum. This indicated that the contamination product (presumably the 16,21-dienonitrile) was isomerized to the fully conjugated 17,21-dienonitrile *7a* upon treatment with base.

In the chromatogram mentioned above, methanol eluted 15 mg of an amorphous product; ν_{max} (KBr) 3400, 2240, 1740, 1635, 1255, and 1030 cm^{-1}. This substance was not investigated further.

(*ii*) In another run, 470 mg of acetoxy hydroxy nitrile **5***a* in 7.5 ml of pyridine was treated with 670 mg of *p*-toluenesulfonyl chloride under the same conditions. Chromatography of the residue on silica gel and elutions with benzene – ethyl acetate (99:1) gave 144 mg (32%) of dienonitrile *7a*: 65 mg, melting between 160 and 170°, $[\alpha]_D^{28}$ −262° (*c*, 0.77 in $CHCl_3$); 79 mg, m.p. 170–176°, $[\alpha]_D^{28}$ −262° (*c*, 0.95 in $CHCl_3$). The yield of dehydration in this run was smaller than in the previous run but the dienonitrile *7a* was not contaminated with the 16,21-dienonitrile according to the i.r. spectrum which showed no trace of an absorption at 2220 cm^{-1}: ν_{max} (KBr) 3030 (vinylic hydrogens), 2180 (α,β,γ,δ-unsaturated nitrile), 1735 (acetate), 1655 and 1574 (conjugated double bonds), 1255 and 1030 (acetate), 850 and 836 cm^{-1}. Elutions with methanol gave 153 mg of the amorphous product isolated in the previous run.

(b) With Potassium Carbonate in Aqueous Methanol

A mixture of 75 mg of acetoxy hydroxy nitrile **5***a*, 6.6 ml of methanol, and 3.3 ml of a 10% aqueous solution of potassium carbonate, was refluxed for 3.5 h, cooled, and poured into cold water. The organic products were extracted with methylene chloride. Some material was not soluble and was collected by filtration to give 5 mg of *dihydroxy nitrile 5*, m.p. 285–288° (vide infra). The organic layer was washed with water, dried over sodium sulfate, and the solvent was evaporated. The crystalline residue (60 mg) was adsorbed on 5 g of silica gel. Elutions with benzene – ethyl acetate (93:7) gave 22 mg (33%) of *3β-hydroxy-16α-ethyl-16²-cyano-16²,21-cyclo-5α-pregna-17,21-diene (7)*, m.p. 193–197°; $[\alpha]_D^{28}$ −278° (*c*, 1.01 in $CHCl_3$); its i.r. spectrum was identical with that of an authentic sample.

Elutions with benzene – ethyl acetate (1:1) gave 42 mg (total yield: 62%) of *16α-ethyl-16²α-cyano-16²,21-cyclo-5α-pregn-17-ene-3β,21α-diol (5)*, m.p. 188–191°, identified by its i.r. spectrum and the determination of a mixture m.p. with an authentic sample.

Dehydration of 3β-Acetoxy-16α-ethyl-16²β-cyano-16²,21-cyclo-5α-pregn-17-en-21α-ol (6a)

(a) With p-Toluenesulfonyl Chloride in Pyridine

In one run, 82 mg of acetoxy hydroxy nitrile **6***a* in 1.3 ml of pyridine was treated with 112 mg of *p*-toluenesulfonyl chloride, as described in the preceding section under (*a*). The crude product (70 mg) was adsorbed on 7.8 g of silica gel. Benzene – ethyl acetate (99:1) eluted 6 mg of amorphous material containing some *dienonitrile*, according to the u.v. absorption at 298 nm (ε 6000). Benzene – ethyl acetate (93:7) eluted 44 mg of starting material, the *acetoxy hydroxy nitrile 6a*, m.p. 206–209°. Methanol eluted 10 mg of an amorphous product, analogous to the one obtained from the acetoxy hydroxy nitrile **5***a* (see above).

In another run, the reaction mixture, consisting of 81 mg of acetoxy hydroxy nitrile **6***a*, 112 mg of *p*-toluenesulfonyl chloride, and 1.3 ml of pyridine, was heated to 53° for 5 days in a nitrogen atmosphere. The usual work-up gave 84 mg of an amorphous residue which was adsorbed on 9 g of silica gel. Elutions with benzene – ethyl acetate (99:1) afforded 11 mg of a crystalline material, m.p. 157–158°, $[\alpha]_D^{19}$ −158° (*c*, 0.63 in $CHCl_3$), containing 53% (6.5% yield) of *3β-acetoxy-16α-ethyl-16²-cyano-16²,21-cyclo-5α-pregna-17,21-diene (7a)*, according to the u.v. absorption at 297 nm (ε 5300). The u.v. spectrum showed an additional absorption at 238 nm (ε 3600). The i.r. spectrum was very similar to that of an authentic sample of dienonitrile *7a*, except for a weak band at 2220 cm^{-1} (α,β-unsaturated nitrile). Assuming that the product giving rise to these additional absorptions was a 16,21-dienonitrile (see above), the total yield in dehydration products amounted approximately to 12%.

Methanol eluted 40 mg of an amorphous product having an i.r. spectrum similar to that of the analogous fraction obtained from the dehydration of acetoxy hydroxy nitrile **5***a*. The intermediate fractions (25 mg) eluted with benzene – ethyl acetate (95:5 and 92:8) were not investigated.

(b) With Potassium Carbonate in Aqueous Methanol

A mixture of 48 mg of acetoxy hydroxy nitrile **6***a*, 5 ml of methanol, and 2 ml of a 10% aqueous solution of potassium carbonate, was refluxed for 3.5 h. The usual work-up (see above) gave 39 mg of crystalline material which was adsorbed on 6 g of silica gel. Benzene – ethyl acetate (97:3) eluted 15 mg (33% yield) of *3β-hydroxy-16α-ethyl-16²-cyano-16²,21-cyclo-5α-pregna-17,21-diene (7)*, m.p 190–192°; $[\alpha]_D^{27}$ −287° (*c*, 0.91 in $CHCl_3$); λ_{max} (EtOH) 297 nm (ε 8700). Acetylation of 9 mg in the usual way (0.4 ml of pyridine and 0.2 ml of acetic anhydride) gave 11 mg of *3β-acetoxy-16α-ethyl-16²-cyano-16²,21-cyclo-5α-pregna-17,21-diene (7a)*, m.p. 154–165°; $[\alpha]_D^{27}$ −255° (*c*, 0.93 in $CHCl_3$). Recrystallization from aqueous methanol raised the m.p. to 170–174°; $[\alpha]_D^{27}$ −286° (*c*, 0.67 in $CHCl_3$); the i.r. spectrum was identical with that of an authentic sample.

Elutions with benzene – ethyl acetate (80:20 and 70:30) gave 20 mg (47%) of *16α-ethyl-16²α-cyano-16²,21-cyclo-5α-pregn-17-ene-3β,21α-diol (5)*, m.p. 267–277°. Recrystallization from aqueous methanol gave 8 mg of crystals melting at 289–291°; the i.r. spectrum was identical with that of authentic dihydroxy nitrile **5**. Acetylation of 5 mg under the usual conditions (0.3 ml of pyridine and 0.15 ml of acetic anhydride) and filtration of the residue (6 mg) through a 1 g column of silica gel, with benzene – ethyl acetate (97:3), afforded 3 mg of *3β,21α-diacetoxy-16α-ethyl-16²α-cyano-16²,21-cyclo-5α-pregn-17-ene (5b)*, m.p. 160–162°.

Treatment of a Mixture of 3β-Acetoxy-16α-ethyl-16²-cyano-16²,21-cyclo-5α-pregna-17,21-diene (7a) and 3β-Acetoxy-16β-ethyl-16²-cyano-16²,21-cyclo-5α-pregna-17,21-diene (8a) with Potassium Carbonate in Aqueous Methanol and with Methanolic Potassium Hydroxide

A mixture of dienonitriles *7a* and *8a* [47 mg, m.p. 210–216°, $[\alpha]_D^{27}$ +190° (*c*, 0.85 in $CHCl_3$)], containing 85% of dienonitrile *8a* (according to the rotation of the mixture) was dissolved in 10 ml of methanol and was

Can. J. Chem. Downloaded from www.nrcresearchpress.com by 210.87.254.6 on 09/05/12
For personal use only.

refluxed for 4 h with 5 ml of a 10% aqueous potassium carbonate solution. The reaction mixture was then poured into ice water and the precipitate was filtered and dried to give 44 mg of a mixture of the *hydroxy dienonitriles 7 and 8*. Acetylation under the usual conditions (1 ml of pyridine and 0.5 ml of acetic anhydride) afforded 42 mg of a mixture of the *dienonitriles 7a and 8a*, m.p. 192–204°, $[\alpha]_D^{27}$ +117° (*c*, 0.82 in $CHCl_3$), containing about 72% of dienonitrile **8***a*, according to the rotation. This mixture (40 mg) was dissolved in 8 ml of methanol and treated with 3 ml of a 12% methanolic potassium hydroxide solution at room temperature for 2 days. The reaction mixture was then poured into ice water. The precipitate was filtered and dried to yield 30 mg of a mixture of the *hydroxy dienonitriles 7 and 8*, m.p. 191–206°; $[\alpha]_D^{27}$ +85° (*c*, 0.89 in $CHCl_3$). It was acetylated (0.8 ml of pyridine and 0.4 ml of acetic anhydride) to give 32 mg of a mixture of the *dienonitriles 7a and 8a*, containing about 68% of dienonitrile **8***a*; m.p. 190–200°; $[\alpha]_D^{27}$ +85° (*c*, 0.88 in $CHCl_3$). Filtration through 3 g of silica gel with benzene – ethyl acetate (99:1) did not result in a change in the relative proportions of the dienonitriles 7*a* and **8***a*: 24 mg, m.p. 196–202°, $[\alpha]_D^{28}$ +88° (*c*, 0.76 in $CHCl_3$). Heating this mixture for several hours in solvents used for crystallization of the dienonitriles (methanol–water and hexane) did not cause any change in the rotation.

Reduction of 3β-Acetoxy-16α-ethyl-16²α-cyano-16²,21-cyclo-5α-pregn-17-en-21-one (9) with Sodium Borohydride

To a solution of 205 mg of sodium borohydride in 24 ml of methanol, 894 mg of ketone **9** in 23 ml of dioxane and 14 ml of methanol was added. The mixture was stirred at room temperature for 17 h and poured into 400 ml of ice water. After acidification to p*H* 3 with 2 *N* sulfuric acid the precipitate was extracted with ether. The ethereal layer was washed with water and dried over sodium sulfate. Removal of the solvent gave a crystalline residue which was chromatographed on 80 g of silica gel. Benzene – ethyl acetate (93:7) eluted 118 mg of *3β-acetoxy-16α-ethyl-16²α-cyano-16²,21-cyclo-5α-pregn-17-en-21β-ol (14)*, m.p. 239–245°. A sample was recrystallized three times for analysis from acetone–hexane; m.p. 242–246°; $[\alpha]_D^{25}$ −52° (*c*, 1.08 in $CHCl_3$); ν_{max} (KBr) 3520 (hydroxyl), 2240 (non-conjugated nitrile), 1735 (acetate), 1683 (double bond), 1248 and 1022 (acetate), 990 cm^{-1} (alcohol); n.m.r.[18] δ 0.84 (18- and 19-CH_3), 2.02 (acetate), 4.68 (3α-H), 4.50 (21α-H), 5.20 (20-H; triplet: 309.4, 312.0, and 314.6 Hz).

Anal. Calcd. for $C_{26}H_{37}O_3N$: C, 75.87; H, 9.07; N, 3.40. Found: C, 75.78; H, 9.01; N, 3.35.

Further elutions with benzene – ethyl acetate (97:3) gave mixtures of the hydroxy nitriles **13***a* and **14***a* (214 mg, m.p. 222–236°; 149 mg, m.p. 180–200°; 151 mg, m.p. 201–211°).

Further elutions with the same solvent mixture gave 139 mg of *3β-acetoxy-16α-ethyl-16²β-cyano-16²,21-cyclo-5α-pregn-17-en-21β-ol (13a)*, m.p. 213–218°. A sample was recrystallized three times from ether–hexane for analysis; m.p. 219.5–220.5°, depressed upon admixture of hydroxy alcohol **5***a*; $[\alpha]_D^{27}$ −57° (*c*, 1.09 in $CHCl_3$); ν_{max} (KBr) 3450 (hydroxyl), 2240 (non-conjugated nitrile), 1728 (acetate), 1688 (double bond), 1240 (acetate), 1024 cm^{-1} (acetate and alcohol); n.m.r.[18] δ 0.85 (19-CH_3), 0.88 (18-CH_3), 2.02 (acetate), 4.44 (21α-H), 4.68 (3α-H), 5.15 (20-H).

Anal. Calcd. for $C_{26}H_{37}O_3N$: C, 75.87; H, 9.07; N, 3.40. Found: C, 75.73; H, 8.80; C, 3.53.

By repeated crystallizations and chromatographies of the fractions containing mixtures of hydroxy nitriles **13***a* and **14***a*, and by purification of the mother liquors, an additional 105 mg of hydroxy nitrile **14***a*, m.p. 235–244°, and 102 mg of hydroxy nitrile **13***a*, m.p. 216–218°, were obtained. There remained 289 mg of mixtures of hydroxy nitriles **13***a* and **14***a*.

In the original chromatogram, benzene – ethyl acetate (60:40) eluted 128 mg of a mixture of the *dihydroxy nitriles 13 and 14*, m.p. 260–273°; ν_{max} (KBr) 3400 (large hydroxyl band), 2240 (non-conjugated nitrile), 1685 (double bond), 1040 cm^{-1} (alcohols).

In toto, 241 mg (27%) of pure hydroxy nitrile **13***a*, 223 mg (25%) of pure hydroxy nitrile **14***a*, 283 mg (32%) of a mixture of these hydroxy acetoxy nitriles in which isomer **13***a* predominated according to the i.r. spectrum, and 128 mg (16%) of a mixture of the dihydroxy nitriles **13** and **14**, were obtained.

Reduction of 3β-Acetoxy-16α-ethyl-16²β-cyano-16²,21-cyclo-5α-pregn-17-en-21-one (10) with Sodium Borohydride

To a solution of 29 mg of sodium borohydride in 2 ml of methanol, 110 mg of the unsaturated ketone **10** in 2 ml of methanol and 3.5 ml of dioxane was added. The mixture was stirred for 16 h at room temperature and the product was worked up as described for the reduction of isomer **9**. The crude reaction product (115 mg) was chromatographed on 9 g of silica gel. Elutions with benzene – ethyl acetate (93:7) gave 12 mg of crude *3β-acetoxy-16α-ethyl-16²α-cyano-16²,21-cyclo-5α-pregn-17-en-21β-ol (14a)*, m.p. 225–235°. After recrystallization the product melted at 239–244°, m.p. not depressed upon admixture of an authentic sample; $[\alpha]_D^{27}$ −49° (*c*, 0.51 in $CHCl_3$); the i.r. spectrum of the product was identical to that of an authentic sample.

Benzene – ethyl acetate (97:3) further eluted mixtures of alcohols **13***a* and **14***a* (24 mg, m.p. 195–200°, and 63 mg, m.p. 185–195°). The second fraction was recrystallized from ether–hexane and gave 20 mg of *3β-acetoxy-16α-ethyl-16²β-cyano-16²,21-cyclo-5β-pregn-17-en-21β-ol (13a)*, m.p. 222–223°, identified by its i.r. spectrum and the mixture m.p. with an authentic sample; $[\alpha]_D^{27}$ −55° (*c*, 0.73 in $CHCl_3$).

Benzene – ethyl acetate (60:40) eluted 10 mg of a mixture of the *dihydroxy nitriles 13 and 14*, m.p. 249–253°.

Oxidation of 3β-Acetoxy-16α-ethyl-16²β-cyano-16²,21-cyclo-5α-pregn-17-en-21β-ol (13a)

To a stirred solution of 11 mg of hydroxy nitrile **13***a*, m.p. 220–222°, in 2 ml of absolute acetone there were added, at 0°, two drops of Jones' chromic acid reagent (29). The mixture was stirred for 2 min and poured into ice water. The precipitate was filtered, washed, and dried. Thus, 10 mg of *3β-acetoxy-16α-ethyl-16²β-cyano-16²,21-cyclo-5α-pregn-17-en-21-one (10)*, m.p. 199–200°, was

Can. J. Chem. Downloaded from www.nrcresearchpress.com by 210.87.254.6 on 09/05/12
For personal use only.

obtained; $[\alpha]_D^{25}$ −38° (*c*, 1.09 in $CHCl_3$); λ_{max} (EtOH) 238 nm (ε 15 300); the i.r. spectrum was identical with that of an authentic sample.

*Oxidation of 3β-Acetoxy-16α-ethyl-16²α-cyano-16²,21-cyclo-5α-pregn-17-en-21β-ol (**14a**)*

A quantity of 44 mg of the hydroxy nitrile **14***a*, m.p. 238–244°, in 5 ml of absolute acetone was oxidized with 0.08 ml of Jones' reagent (29), as described above, to give 43 mg of *3β-acetoxy-16α-ethyl-16²α-cyano-16²,21-cyclo-5α-pregn-17-en-21-one (**9**)*, m.p. 249–252°. After purification by recrystallization from dichloromethane–ether, the product melted at 253–254°; $[\alpha]_D^{27}$ −18.5° (*c*, 0.975 in $CHCl_3$); the i.r. spectrum was identical with that of an authentic sample.

Treatment of the Hydroxy Nitrile 5a with Sodium Borohydride

To a solution of 12 mg of sodium borohydride in 1.5 ml of methanol, 56 mg of hydroxy nitrile **5***a*, m.p. 216–219°, in 1 ml of dioxane and 1.5 ml of methanol was added. After 18 h at room temperature the mixture was poured into ice water and the precipitate was filtered, washed, and dried. The crude reaction product (60 mg, m.p. 207–214°), was treated with dichloromethane. The non-soluble material (10 mg) was identified as *16α-ethyl-16²α-cyano-16²,21-cyclo-5α-pregn-17-ene-3β,21α-diol (**5**)*, m.p. 283–286°, by its i.r. spectrum. A portion of 7 mg was acetylated with 0.3 ml of acetic anhydride in 0.6 ml of pyridine; the crude product (10 mg) was filtered through 200 mg of silica gel and thus gave 6 mg of *3β,21α-diacetoxy-16α-ethyl-16²α-cyano-16²,21-cyclo-5α-pregn-17-ene (**5b**)*, m.p. 164–165°, not depressed upon admixture of an authentic sample. From the dichloromethane-soluble fraction, 50 mg of *hydroxy nitrile **5a***, m.p. 213–217°, was recuperated; the product was identified by its i.r. spectrum, thin-layer analysis, and a mixture m.p. with an authentic sample.

Treatment of Hydroxy Nitrile 6a with Sodium Borohydride

A quantity of 76 mg of hydroxy nitrile **6***a*, m.p. 206–209°, was treated as described above for hydroxy nitrile **5***a* with 16 mg of sodium borohydride in 3.5 ml of methanol and 1.5 ml of dioxane for 16 h. The reaction product was chromatographed on 3 g of silica gel. Elutions with benzene – ethyl acetate (93:7) gave 57 mg of starting material, *hydroxy nitrile **6a***, m.p. 208–211°, identified by a mixture m.p. with an authentic sample and by i.r. and thin-layer analyses. Benzene – ethyl acetate (50:50) eluted 15 mg of *16α-ethyl-16²β-cyano-16²,21-cyclo-5α-pregn-17-ene-3β,21α-diol (**6**)*, m.p. 262–263°; the m.p. was depressed upon admixture of dihydroxy nitrile **5**; ν_{max} (KBr) 3300–3200 (large hydroxyl band), 2240 (non-conjugated nitrile), 1688 (double bond), 1032 and 1008 cm^{-1} (alcohols).

Treatment of Hydroxy Nitrile 13a with Sodium Borohydride

As described above, 71 mg of hydroxy nitrile **13***a*, m.p. 219–221°, was treated with 15 mg of sodium borohydride in 3.6 ml of methanol and 1.5 ml of dioxane. The crude reaction product (68 mg) was filtered through a column of 3 g of silica gel. Elutions with benzene – ethyl acetate (97:3) gave 59 mg of starting material, *hydroxy nitrile **13a***, m.p. 220–222°, identified by a mixture m.p. with an authentic sample, by i.r. and thin-layer analyses. Benzene – ethyl acetate (50:50) eluted 6 mg of *16α-ethyl-16²β-cyano-16²,21-cyclo-5α-pregn-17-ene-3β,21β-diol (**13**)*, m.p. 253–258°; ν_{max} (KBr) 3510 and 3450 (hydroxyls), 2240 (non-conjugated nitrile), 1690 (double bond), 1042 cm^{-1} (alcohols).

Treatment of Hydroxy Nitrile 14a with Sodium Borohydride

As described above, 55 mg of hydroxy nitrile **14***a*, m.p. 238–244°, was treated with 12 mg of sodium borohydride in 3.5 ml of methanol and 1 ml of dioxane in the course of 20 h. The reaction product (58 mg) was chromatographed on 3 g of silica gel. Elutions with benzene – ethyl acetate (93:7) gave 40 mg of starting material, *hydroxy nitrile **14a***, m.p. 240–247°, identified by a mixture m.p. with an authentic sample, by i.r. and thin-layer analyses. Benzene – ethyl acetate (50:50) eluted 12 mg of *dihydroxy nitrile **14***, m.p. 304–306°; ν_{max} (KBr) 3460 and 3400 (hydroxyls), 2240 (non-conjugated nitrile), 1688 (double bond), 1040 cm^{-1} (alcohols).

We express sincerest thanks to Prof. R. L. Lemieux and Mr. J. Bigam for the n.m.r. studies, with multiple spin decouplings, at 100 MHz, and for the very helpful discussion of the results. We also acknowledge with gratitude the help of Dr. A. D. Cross, Syntex S.A., Mexico, and Dr. P. W. Landis, Ely Lilly & Co., Minneapolis, Minnesota; of Dr. S. Rakhit and Mr. T. A. Wittstruck, the Worcester Foundation for Experimental Biology, Shrewsbury, Massachusetts; of Prof. G. Just and Mr. C. Stammer, McGill University, Montreal, Quebec, in the determination and discussion of n.m.r. spectra at 60 MHz. Sincere thanks are due to Prof. C. Djerassi, Stanford University, Stanford, California, and to Dr. A. D. Cross and Dr. P. Crabbé, Syntex S.A., Mexico, for their much appreciated help with rotatory dispersion measurements and for their valuable comments. We are greatly indebted to Mrs. J. Capitaine and Mr. H. Martel for their excellent cooperation in some of the experiments, and to Mr. D. Capitaine and Mrs. G. Pelletier for devoted technical assistance. Financial support from the National Research Council of Canada and from Ayerst Laboratories, Montreal, Quebec, is gratefully acknowledged. One of us (J.L.) sincerely thanks the National Research Council of Canada for the award of N.R.C.C. scholarships.

1. Ch. R. Engel and J. Lessard. J. Amer. Chem. Soc. **85**, 638 (1963).
2. Ch. R. Engel, R. Bouchard, A. F. de Krassny, L. Ruest, and J. Lessard. Steroids, **14**, 637 (1969).
3. Ch. R. Engel and J. Lessard. Abstracts of Communications 2nd Int. Symp. Chem. Nat. Products, Prague, 1962. p. 34.
4. Ch. R. Engel, J. Lessard, L. Ruest, and S. Bory. Abstracts of Communications, 5th Int. Symp. Chem. Nat. Products, London, 1968. p. 359.
5. (*a*) A. L. Wilds, J. W. Ralls, D. A. Tyner, R. Daniels, S. Kraychy, and M. Harnik. J. Amer. Chem. Soc. **75**, 4878 (1953); (*b*) P. Wieland, H. Ueberwasser, G. Anner, and K. Miescher.

Helv. Chim. Acta, **36**, 1231 (1953); (*c*) W. S. JOHNSON, J. SZMUSZKOWICZ, E. R. ROGIER, H. I. HADLER, and H. WYNBERG. J. Amer. Chem. Soc. **78**, 6285 (1956); (*d*) E. D. BERGMANN and P. BRACHA. J. Org. Chem. **24**, 994 (1959); **26**, 4685 (1961); (*e*) Y. R. NAVES and J. M. CONIA. Bull. Soc. Chim. France, 378 (1960); C. R. Acad. Sci. **251**, 1130 (1960); (*f*) J. J. BEEREBOOM. J. Org. Chem. **31**, 2026 (1966).

6. (*a*) H. A. BRUSON and T. W. RIENER. J. Amer. Chem. Soc. **65**, 18 (1943); (*b*) H. A. BRUSON and T. W. RIENER. J. Amer. Chem. Soc. **66**, 56 (1944); (*c*) R. B. WOODWARD, F. SONDHEIMER, D. TAUB, K. HEUSLER, and W. M. MCLAMORE. J. Amer. Chem. Soc. **74**, 4223 (1952); (*d*) S. JULIA. C. R. Acad. Sci. **237**, 913 (1953); Bull. Soc. Chim. France, 780 (1954).
7. (*a*) J. M. CONIA. Bull. Soc. Chim. France, 24 (1956); (*b*) R. B. WOODWARD, A. A. PATCHETT, D. H. R. BARTON, D. A. J. YVES, and R. B. KELLY. J. Amer. Chem. Soc. **76**, 2852 (1954).
8. (*a*) W. E. HUGH and G. A. R. KON. J. Chem. Soc. 775 (1930); (*b*) C. K. INGOLD, E. DE SALAS, and C. L. WILSON. J. Chem. Soc. 1328 (1936); (*c*) J. WARKENTIN and L. K. M. LAM. Can. J. Chem. **42**, 1676 (1964).
9. J. M. CONIA and A. SANDRE-LE CRAZ. Bull. Soc. Chim. France, 904 (1962); Tetrahedron Lett. 505 (1962).
10. (*a*) F. G. FISCHER and K. LÖWENBERG. Ann. **494**, 263 (1932); (*b*) C. GRUNDMANN. Ber. **81**, 513 (1948); (*c*) W. I. TAYLOR. Chem. Ind. (London), 252 (1954); (*d*) L. H. BRIGGS and L. D. COLEBROOK. Chem. Ind. (London), 200 (1955); (*e*) W. A. AYER and W. I. TAYLOR. J. Chem. Soc. 2227 (1955); (*f*) A. T. NIELSEN. J. Amer. Chem. Soc. **79**, 2524 (1957).
11. J. P. FLEURY, A. LANTZ, and J. LICHTENBERGER. Bull. Soc. Chim. France, 391 (1963).
12. (*a*) J. CHABALIER, O. CONVERT, M. L. BOUGUERRA, and J. WIEMANN. C. R. Acad. Sci. **264**, 1186 (1967); (*b*) B. FURTH and J. WIEMANN. Bull. Soc. Chim. France, 1819 (1965).
13. (*a*) H. HEUSSER, K. EICHENBERGER, and PL. A. PLATTNER. Helv. Chim. Acta, **33**, 370 (1950); (*b*) N. A. PREOBRAZHENSKII and V. V. SHOKINA. J. Gen. Chem. U.S.S.R. **15**, 65 (1945); (*c*) D. A. VAN DORP and J. F. ARENS. Nature **160**, 189 (1947); (*d*) D. A. VAN DORP and J. F. ARENS. Rec. Trav. Chim. Pays-Bas, **67**, 973 (1948); **68**, 604, 609 (1949).
14. I. N. NAZAROV, A. A. KRASNAIA, and V. P. VINOGRADOV. J. Gen. Chem. U.S.S.R. **28**, 451 (1958).
15. L. J. BELLAMY. The infrared spectra of organic molecules. Methuen and Co., London, 1958. pp. 35–38.
16. (*a*) R. N. JONES, P. HUMPHRIES, E. PACKARD, and K. DOBRINER. J. Amer. Chem. Soc. **72**, 86 (1950); (*b*) R. N. JONES and F. HERLING. J. Org. Chem. **19**, 1252 (1954).
17. A. MOSCOWITZ, E. CHARNEY, U. WEISS, and H. ZIFFER. J. Amer. Chem. Soc. **83**, 4661 (1961).
18. S. BORY and CH. R. ENGEL. Bull. Soc. Chim. France, (1970). In press.
19. (*a*) J. E. PIKE, M. A. REBENSTORF, G. SLOMP, and F. A. MACKELLAR. J. Org. Chem. **28**, 2499 (1963); (*b*) J. E. PIKE, G. SLOMP, and F. A. MACKELLAR. J. Org. Chem. **28**, 2502 (1963).
20. (*a*) M. E. WALL, S. SEROTA, H. E. KENNEY, and G. S. ABERNETHY. J. Amer. Chem. Soc. **85**, 1844 (1963); (*b*) M. E. WALL, F. I. CARROLL, and G. S. ABERNETHY, JR. J. Org. Chem. **29**, 604 (1964).
21. CH. R. ENGEL and L. RUEST. Can. J. Chem. In press.
22. CH. R. ENGEL, V. S. SALVI, and L. RUEST. Can. J. Chem. In press.
23. (*a*) R. C. COOKSON. J. Chem. Soc. 282 (1954); (*b*) R. C. COOKSON and S. H. DANDEGAONKER. J. Chem. Soc. 352 (1955); (*c*) C. DJERASSI. Optical rotatory dispersion. McGraw-Hill Book Company, New York, 1960. p. 115; (*d*) E. L. ELIEL. Stereochemistry of carbon compounds. McGraw-Hill Book Company, New York, 1962. p. 241; (*e*) P. D. KLIMSTRA and R. E. COUNSELL. J. Med. Pharm. Chem. **5**, 1216 (1962).
24. A. NICKON, M. A. CASTLE, R. HARADA, C. E. BERKOFF, and R. O. WILLIAMS. J. Amer. Chem. Soc. **85**, 2185 (1963).
25. M. KARPLUS. J. Chem. Phys. **30**, 11 (1959).
26. (*a*) C. DJERASSI, R. RECORDS, E. BUNNENBERG, K. MISLOW, and A. MOSCOWITZ. J. Amer. Chem. Soc. **84**, 870 (1962); (*b*) U. B. WHALLEY. Chem. Ind. (London), 1024 (1962).
27. N. L. ALLINGER and H. M. BLATTER. J. Org. Chem. **27**, 1523 (1962).
28. D. W. CAMERON, D. G. I. KINGSTON, N. SHEPPARD, and LORD TODD. J. Chem. Soc. 98 (1964).
29. (*a*) K. BOWDEN, J. M. HEILBRON, E. R. H. JONES, and B. C. L. WEEDON. J. Chem. Soc. 39 (1946); (*b*) A. BOWERS, T. G. HALSALL, E. R. H. JONES, and A. J. LEMIN. J. Chem. Soc. 2548 (1953).

Can. J. Chem. Downloaded from www.nrcresearchpress.com by 210.87.254.6 on 09/05/12
For personal use only.

Application of proton magnetic resonance to rotational isomerism in halotoluene derivatives. III. α,α-Dichloro-2,4,6-tribromotoluene

J. PEELING, T. SCHAEFER, AND C. M. WONG
Department of Chemistry, University of Manitoba, Winnipeg, Manitoba

Received April 20, 1970

At room temperature the proton magnetic resonance spectrum of α,α-dichloro-2,4,6-tribromotoluene is ABX where the methine proton in the sidechain is X and is lying in the plane of the aromatic ring. At higher temperatures the ring proton spectrum, AB, broadens and eventually collapses to yield an A_2X spectrum. From an analysis of the ring proton line shapes the barrier to rotation of the dichloromethyl group about the sp^2–sp^3 carbon–carbon bond is obtained; $\Delta G^* = 17.5 \pm 0.1$ kcal/mole at 304 °K, $\Delta H^* = 15.67 \pm 0.08$ kcal/mole, $\Delta S^* = -7$ e.u., $E_a = 16.38 \pm 0.08$ kcal/mole, $\log A = 11.78 \pm 0.23$ where the least squares errors given should probably be multiplied by a factor of from 3 to 5 to take possible systematic errors into account. The barrier is about 2 kcal/mole higher than in α,α,2,4,6-pentachlorotoluene. The barrier to rotation arises from the conformation in which chlorine and bromine atoms are eclipsed.

Canadian Journal of Chemistry, 48, 2839 (1970)

Can. J. Chem. Downloaded from www.nrcresearchpress.com by 210.87.254.42 on 09/05/12
For personal use only.

Introduction

The previous paper (1) in this series presented a detailed description of a proton magnetic resonance (p.m.r.) study of hindered rotation of the dichloromethyl group in α,α,2,4,6-pentachlorotoluene (PCT). A computer program based on a density matrix treatment of intramolecular proton exchange was developed and applied in the extraction of preexchange lifetimes from the temperature dependent ring proton spectrum of PCT. The present paper gives the results of a similar application to the ring proton spectrum of α,α-dichloro-2,4,6-tribromotoluene (DCTBT).

Experimental

(1) Preparation of DCTBT

A mixture of 2,4,6-tribromotoluene (20 g) and phosphorous pentachloride (0.2 g) in a 50 ml flask (pyrex) was heated with a small flame into a melt. The mixture was then irradiated with ultraviolet (u.v.) light while a stream of chlorine gas was bubbling into the mixture through a gas dispersing tube. The progress of chlorination was followed by observing the disappearance of the proton resonance peaks at 7.5 τ and 5.7 τ corresponding to the methyl and the monochloromethyl groups, respectively. The product was then distilled under reduced pressure to give PCT (14.5 g), identified by analysis and by comparing the p.m.r. and infrared (i.r.) spectra with those of an authentic sample prepared by chlorination of 2,4,6-trichlorotoluene. The residue (3 g) was transferred to a microdistillation flask and another portion of the PCT (1.8 g) was distilled out. The residue was then purified by extensive thin-layer chromatography (t.l.c.) on silica and DCTBT was isolated, slightly contaminated with PCT.

(2) Proton Magnetic Resonance Spectra

The available amount of DCTBT was insufficient to produce a reasonable signal to noise ratio on a DA60I spectrometer. Its solubility was also very low in methylcyclohexane, hexamethyldisiloxane, and other solvents of low dielectric constant. In perchlorobutadiene the 100 MHz proton spectrum consisted of a tightly coupled ABC spectrum at 30 °C. However, in toluene-d_8 the 100 MHz proton spectrum is ABX, very similar to the spectrum for PCT at −40 °C (1). It was previously shown that the intrinsic temperature dependence of the internal ring proton shift of PCT in toluene-d_8 can and must be found in order to obtain reliable exchange rates from fitted spectra. A similar procedure was followed with DCTBT.

The p.m.r. spectrum of an approximately 4 mole % solution of DCTBT in degassed toluene-d_8 was recorded at 2° intervals between 40 and 74 °C on an HA-100-D spectrometer under conditions of a signal to noise ratio of about 80:1. The residual proton resonance of the solvent (Merck) interfered with the low-field ring proton resonance (H_A) so that only the line shapes of the high-field ring proton peaks (H_B) could be reliably measured (a very small amount of PCT did not overlap with signals of interest between 40 and 74 °C). The spectra were repeatedly calibrated by reading oscillator frequencies in the frequency sweep mode. The homogeneity of the external magnetic field was monitored by the appearance of the methine proton peaks (H_X), whose widths are independent of exchange times (1). Over the temperature range used here, the homogeneity could be accurately controlled to give an effective $T_2 = 1.72 \pm 0.12$ s. The internal ring proton shift was measured as a function of temperature in the region of slow exchange (10–35 °C).

The temperature settings on the dial of the 6040 proportional controller were calibrated against an ethylene glycol sample. The dial settings were then checked with a thermocouple immersed in a sample of toluene. Temperature gradients near the receiver coil were apparently very small between 30 and 70 °C. The thermocouple had been calibrated at a few set points. It is fairly certain that the temperature data are accurate to ±1 °C and precise to ±0.5 °C.

(3) Extraction of Rate Constants

The computer program for an ABX spectrum in which A and B exchange under conservation of spin states (1) was used to fit calculated to observed spectra as exten-

TABLE 1

The chemical shifts and proton–proton coupling constants of DCTBT in toluene-d_8 solution between 10 and 35 °C

Temperature (°C)	Chemical shift*			Coupling constants (Hz)†		
	H_X	H_A	H_B	J_{AB}	J_{AX}	J_{BX}
10	7.267	6.872	6.658	2.16_5	0.52_1	-0.00_1
15	7.271	6.883	6.672	2.16_7	0.53_6	-0.00_1
20	7.276	6.895	6.886	2.15_1	0.54_4	-0.00_1
25	7.281	6.909	6.702	2.19_7	0.55_3	-0.00_2
28	7.283	6.915	6.711	2.17_3	0.55_6	-0.00_1
35	7.290	6.933	6.731	2.17_1	0.53_9	-0.00_1

*In p.p.m. to low field from internal tetramethylsilane.

†The coupling constants are given as obtained from the computer analysis and we feel their accuracy lies near 0.03 Hz. J_{BX}, of course, is unmeasurably small and of unknown sign.

sively described previously (1). The intrinsic temperature dependence of the internal ring proton shift is fitted by the least squares equation: shift in Hz = 21.81 − 0.0456 T(°C). These shifts were used as input parameters in the computer program. A constant T_2 of 1.72 s was assumed throughout (see above).

Results and Discussion

(1) Spectral Parameters at Low Exchange Rates

The program LAOCOON 3 (2) was used to extract the chemical shifts and coupling constants from the 3-spin p.m.r. spectra between 10 and 35 °C. At these temperatures the mean lifetime before exchange in conformation **1** or its mirror image is relatively long. The spectra themselves

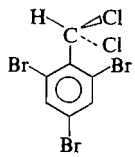

1

are very similar to those of PCT presented in ref. 1. Table 1 gives the spectral parameters in the region of slow exchange. Figure 1 displays the plot of the internal shift of H_A and H_B vs. temperature in this region. The least squares equations representing this dependence are:

$$\text{shift of } H_A = 0.2489T\,(°C) + 684.61 \text{ Hz}$$

$$\text{shift of } H_B = 0.2945T\,(°C) + 662.80 \text{ Hz}$$

where shifts are in Hz to low field of internal tetramethylsilane. These equations were used to calculate the internal ring proton shift in the presence of exchange at each of 18 temperatures between 40 and 74 °C. As was shown in ref. 1, this procedure is necessary if large errors in activation parameters are to be avoided.

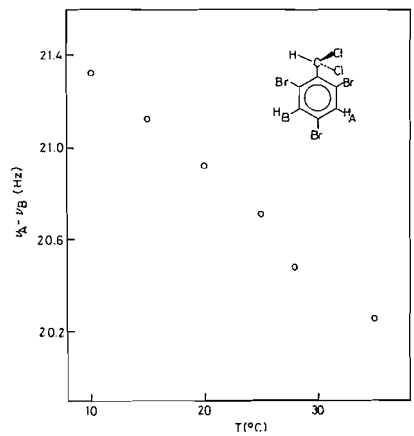

FIG. 1. The internal chemical shift, in Hz, of protons H_A and H_B of α,α-dichloro-2,4,6-tribromotoluene, as a dilute solution in toluene-d_8, is plotted vs. temperature between 10 and 35 °C.

(2) Proton Resonance Spectra under Conditions of Exchange

Coalescence of the spectral peaks from H_A and H_B occurs at about 80 °C. The line-shape fitting procedure (1) was applied at 2° intervals between 40 and 74 °C to the H_B resonance for reasons mentioned earlier. The preexchange lifetimes, τ, are listed in Table 2. For most temperatures, two values of τ are given. These represent the limits of τ which gave a reasonable fit of calculated to experimental line shapes. Because of the experimental difficulties mentioned above, τ varies only between 0.50 and 0.036 s, a factor of 14.

(3) Activation Parameters for the Hindered Rotation

Plots of log k and of log (k/T) vs. $1/T$ were prepared ($k = 1/\tau$) and were used to extract E_a, ΔH^*, and ΔS^* in the usual way (3). Further-

Can. J. Chem. Downloaded from www.nrcresearchpress.com by 210.87.254.42 on 09/05/12
For personal use only.

TABLE 2

Preexchange lifetimes, τ, for DCTBT at various temperatures

Temperature (°C)	τ (s)	Temperature (°C)	τ (s)
40	0.4825–0.5225	58	0.110–0.1125
42	0.4050–0.4125	60	0.08375–0.0839
44	0.305–0.280	62	0.079–0.080
46	0.265–0.295	64	0.067
48	0.1900–0.2025	66	0.056
50	0.1725–0.1950	68	0.048–0.049
52	0.170–0.175	70	0.048–0.049
54	0.1275–0.1500	72	0.0375–0.0400
56	0.1125–0.1175	74	0.0350–0.0375

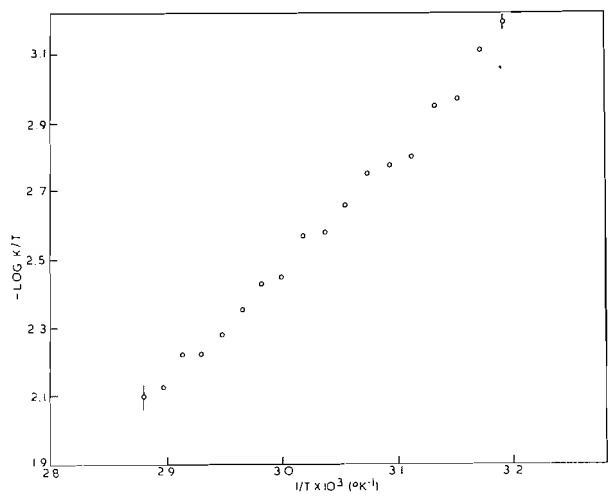

FIG. 2. A plot of log (k/T) vs. $1/T$ for α,α-dichloro-2,4,6-tribromotoluene in toluene-d_8 solution between 40 and 74 °C; $k = 1/\tau$ where τ is the mean lifetime before effective exchange of the ring protons. The error bars in log (k/T) indicated for the lowest and highest temperatures are typical but many are smaller. The correlation coefficient, $r = 0.995$ for the least squares straight line and the derived parameters are given in the text.

more, ΔG^* was calculated from log k at each temperature using the equation from transition state theory and assuming a transmission coefficient of 1/2 (1). Plots of ΔG^* vs. T were also prepared. In Fig. 2 a plot of log (k/T) vs. $1/T$ is displayed as an example (correlation coefficient, $r = 0.995$, 18 values).

The results of the least squares analyses with statistical errors given are as follows: $E_A = 16.38 \pm 0.08$ kcal/mole, log A $= 11.78 \pm 0.23$; $\Delta H^* = 15.69 \pm 0.08$ kcal/mole from log (k/T) vs. $1/T$; $\Delta H^* = 15.65 \pm 0.40$ kcal/mole from ΔF^* vs. T; $\Delta S^* = -10 \pm 1$ e.u. from log (k/T) vs. $1/T$; $\Delta S^* = -5.6 \pm 0.3$ e.u. from ΔG^* vs. T; $\Delta S^* = -5 \pm 1$ e.u. from $A = e(kT/2h)\exp(\Delta S^*/R)$; $\Delta G^* = 17.5 \pm 0.1$ kcal/mole at 304 °K. In view of the possible systematic errors in these parameters, a more reasonable estimate of the errors in E_A and ΔH^* is probably nearer 0.4 kcal/mole. The three different estimates of ΔS^* can be arbitrarily averaged to give $\Delta S^* = -7.2$ e.u. implying that ΔS^* is very probably negative but small in magnitude.

(4) Comparison with Activation Parameters for PCT

Perhaps the best comparison of the present results for DCTBT with those for PCT (1) involves the composite treatment of the rate data for the latter in the two solvents, methylcyclohexane and toluene-d_8. In ref. 1 the rate data were treated separately for the two solvents, in particular because of the problem of the internal ring proton shift. However, there exists a satisfactory least squares fit of the data for PCT if log (k/T) is plotted vs. $1/T$ without reference to

Can. J. Chem. Downloaded from www.nrcresearchpress.com by 210.87.254.42 on 09/05/12
For personal use only.

the solvent. One finds $\Delta H^* = 13.9 \pm 0.2$ kcal/mole and $\Delta S^* = -3.7 \pm 0.6$ e.u. where the correlation coefficient, $r = 0.991$ for 19 values.

Apparently the potential energy barrier to rotation about the sp^2–sp^3 carbon–carbon bond is 10% or nearly 2 kcal/mole higher in DCTBT than in PCT; reasonably indicating that an eclipsed Cl...Br interaction is sterically less favorable than an eclipsed Cl...Cl interaction. As with PCT the conformation **2** is of highest energy and represents the activated state during the rotation of the dichloromethyl group. Conformation **1** and its mirror image are the ground state of the molecule. From the arguments in ref. 1 it follows that conformation **3** is of intermediate stability, but at least 10 kcal/mole less stable than **1**. Hence **3** is not appreciably populated at any of the temperatures under consideration.

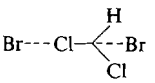

2

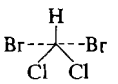

3

We thank Mr. K. C. Tam for help with the synthesis of DCTBT and are grateful to the National Research Council of Canada for monetary support.

1. B. J. Fuhr, B. W. Goodwin, H. M. Hutton, and T. Schaefer. Can. J. Chem. **48**, 1558 (1970).
2. S. Castellano and A. A. Bothner-By. J. Chem. Phys. **41**, 3863 (1964).
3. G. Binsch. *In* Topics in stereochemistry. Volume 3. *Edited by* E. L. Eliel and N. L. Allinger. Interscience Publishers, New York, 1968.

Can. J. Chem. Downloaded from www.nrcresearchpress.com by 210.87.254.42 on 09/05/12
For personal use only.

Can. J. Chem. Downloaded from www.nrcresearchpress.com by 210.87.254.5 on 09/05/12
For personal use only.

Solubility of alkali metal and ammonium thiocyanates and iodides in tri-*n*-butyl phosphate

J. HÁLA AND D. G. TUCK[1]

Department of Chemistry, Simon Fraser University, Burnaby 413, British Columbia

Received March 24, 1970

The solubilities of lithium, sodium, potassium, caesium, and ammonium thiocyanates and iodides, and of rubidium thiocyanate, in tri-*n*-butyl phosphate (TBP), have been measured. In general, the solubilities decrease with increasing cation size, but the values for the ammonium salts are anomalously high. This is shown to be due to hydrogen-bonding between NH_4^+ and the phosphoryl oxygen of the solvent. The results are compared with those reported for other alkali metal salts in TBP.

Canadian Journal of Chemistry, **48**, 2843 (1970)

Introduction

Tri-*n*-butyl phosphate (TBP) has been the subject of a large number of physico-chemical studies by reason of its wide application in solvent extraction, and the solubilities of a number of inorganic nitrates in the anhydrous solvent have been reported (1, 2). During preliminary studies of the TBP – liquid ammonia system, we investigated the solubility of a series of alkali metal and ammonium salts in TBP, and found relatively high solubilities for iodides and thiocyanates. Chlorides and bromides of these elements are almost insoluble in the solvent at room temperature. We now report solubility measurements for lithium, sodium, potassium, caesium, and ammonium thiocyanate and iodide, and rubidium thiocyanate, in TBP, together with the results of spectroscopic investigations of the properties of such solutions.

Experimental

Materials

Sodium, potassium, and ammonium salts were supplied by Fisher Scientific Co. Rubidium and caesium salts were prepared by neutralizing the corresponding hydroxides (Alfa Inorganics) with hydriodic or thiocyanic acid solution, obtained by ion-exchange of the sodium salts on a column of Dowex 50W-X8 (H-form). Anhydrous lithium iodide was prepared from the trihydrate (Alfa Inorganics) by heating in a stream of dry nitrogen (3). A solution of lithium thiocyanate, obtained by neutralization of lithium carbonate, was evaporated to dryness, and the residue then heated at 70–80° in a stream of dry nitrogen (4); the final product was approximately 85% LiCNS, but it was not possible to remove the remainder of the water since the substance decomposes above about 80°. All salts were stored in a desiccator over phosphorus pentoxide.

The TBP (Fisher Scientific Co.) was purified by refluxing with 0.5% caustic soda solution, followed by steam distillation, dried with anhydrous magnesium sulfate, and finally dried *in vacuo* at ~50° with a bleed of dry nitrogen (5, 6).

Solubility Measurements

An excess of salt was shaken overnight with 5 ml of dry TBP in a stoppered vessel; preliminary experiments showed that this period was sufficient for equilibrium to be reached. Samples of solution were removed through a sinter, and analyzed for iodide or thiocyanate by titration against silver nitrate after dilution with acetone. Blank titrations showed that a small corrrection was required because of the presence of TBP. Each result in Table 1 is the average of between three and five experiments.

Spectra

Infrared (i.r.) spectra were obtained with a Beckman IR-12 instrument. The H^1 nuclear magnetic resonance (n.m.r.) spectra were run on a Varian A56-60 instrument, and P^{31} spectra on a Varian HA-100 spectrometer with P_4O_6 as a reference substance; we are grateful to Prof. L. D. Hall (University of British Columbia, Vancouver, B.C.) for these latter measurements.

Measurements of Heats of Solution

The heats of solution of sodium, potassium, and ammonium thiocyanate were measured, using a simple calorimeter (7). In each experiment, three weighed samples of salt (approximately 1 g) were successively dissolved in a weighed quantity of TBP (approximately 600 ml). Dissolution was usually complete within 10 min. The final molality of dissolved salt was always less than 0.07, and the measured heat evolution did not show any change with concentration within the experimental error. The mean of these three measurements was therefore taken as giving the integral heat of dissolution at infinite dilution. Three sets of measurements were carried out for each salt.

Results and Discussion

Solubilities

The measured solubilities are given in Table 1, together with the ionic radii of the cations and the lattice energies of the salts, taken from the papers of Morris (8) (alkali metal iodides), Ladd and Lee (9) (ammonium iodide), and Yatsimirskii (10)

[1]Correspondence to Prof. D. G. Tuck, Department of Chemistry, Simon Fraser University, Burnaby 413, B.C.

TABLE 1

Solubilities of alkali metal and ammonium thiocyanates and iodides in TBP at 22 °C

		Thiocyanates			Iodides		
Cation	r_+ (A°)*	Solubility (g/100 g TBP)	TBP:MNCS at saturation	Lattice energy (kcal mole^{-1})	Solubility (g/100 g TBP)	TBP:MI at saturation	Lattice energy (kcal mole^{-1})
Li	0.60	12.0 ±0.1	2.03	†	6.8–7.8‡	6.5–7.5‡	180
Na	0.95	12.5 ±0.4	2.44	178	18.07±0.13	3.12	167
K	1.33	6.96±0.10	5.25	162	0.84±0.1	74	156
Rb	1.48	3.4 ±0.05	15.7	155	—	—	149
Cs	1.69	0.57±0.02	125	149	<0.4	>240	143
NH_4	1.48	11.6 ±0.1	2.46	158	12.7 ±0.2	4.28	142

*Values from A. F. Wells (23).
†No value available.
‡These results are for the gel formed by LiI in TBP.

(thiocyanates). No value was found in the literature for the lattice energy of lithium thiocyanate.

For the thiocyanates, the molar solubilities are in the order Li > Na ≈ NH_4 > K > Rb > Cs, although it should be noted that the value for the lithium salt may be high because of the presence of residual water. The same order is found with the iodides (although in this case the lithium salt gave a gel), and in previous studies of the solubility of alkali metal nitrates in TBP (1, 2). Similar orders are seen in the solubilities of the halides of these elements in a variety of basic organic solvents (11).

Saturated solutions of LiSCN in TBP have very high viscosities, as do solutions of lithium chloride extracted into TBP from concentrated aqueous solution (12). This appears to be a common property of solutions of lithium salts in aprotic solvents such as acetone and dimethyl sulfoxide (13), and is equally pronounced with lithium iodide and TBP, which, as noted above, yielded a solid gel on equilibration. In the latter case, the high viscosity of the solution before solidification may hamper good contact of the solute with the solvent, so that the true equilibrium state is probably very difficult to reach. There is therefore considerable variation in the values for the solubility of lithium iodide reported in Table 1.

A number of authors have used solvent extraction techniques to show that lithium and sodium salts extracted by solutions of TBP in non-polar diluents form complexes with TBP in the organic phase. The solvates $LiNO_3$.2TBP and $NaNO_3$.3TBP (1, 2), LiCl.2TBP (12), and LiI.3TBP (14) have been identified in this way. It has been argued that the limiting solubility of lithium nitrate in TBP (TBP:$LiNO_3$ ratio 2.61) confirms the existence of the di-solvate, believed to exist in the saturated solution with excess TBP and some water (1). On this basis, some of the results in Table 1 (columns 4 and 7) suggest that such solvates may be important for iodides and thiocyanates. The formation of a (possibly hydrated) LiSCN.2TBP complex is strongly indicated, and it also seems likely that NaSCN and NH_4SCN are present as di-solvates, with some free TBP present at saturation. Sodium iodide may be forming either di- or tri-solvates; a di-solvate was found in the extraction of NaI from aqueous solutions into both TBP (15) and di-*iso*pentyl-methyl phosphonate (14).

Solute–Solvent Interactions

In view of the above evidence of solvate formation, the nature of the solute–solvent interaction in these solutions has been investigated. Unfortunately the whole range of salts of the six cations is not available; lithium salts give either a gel or a very viscous solution, while the solubilities of rubidium and caesium salts are too low for study.

We first note that the solubilities of the alkali metal salts decrease smoothly with cation ionic radius (Table 1) and, for a given anion, increase with lattice energy (which itself is a function of the ionic radii of the component ions). Lattice energies are obviously an important factor in the total energy picture, but the relationship is far from simple, as can be demonstrated by comparing a series of ammonium salts (see Table 2).

For both ammonium thiocyanate and iodide, however, the solubilities are anomalously high

Can. J. Chem. Downloaded from www.nrcresearchpress.com by 210.87.254.5 on 09/05/12
For personal use only.

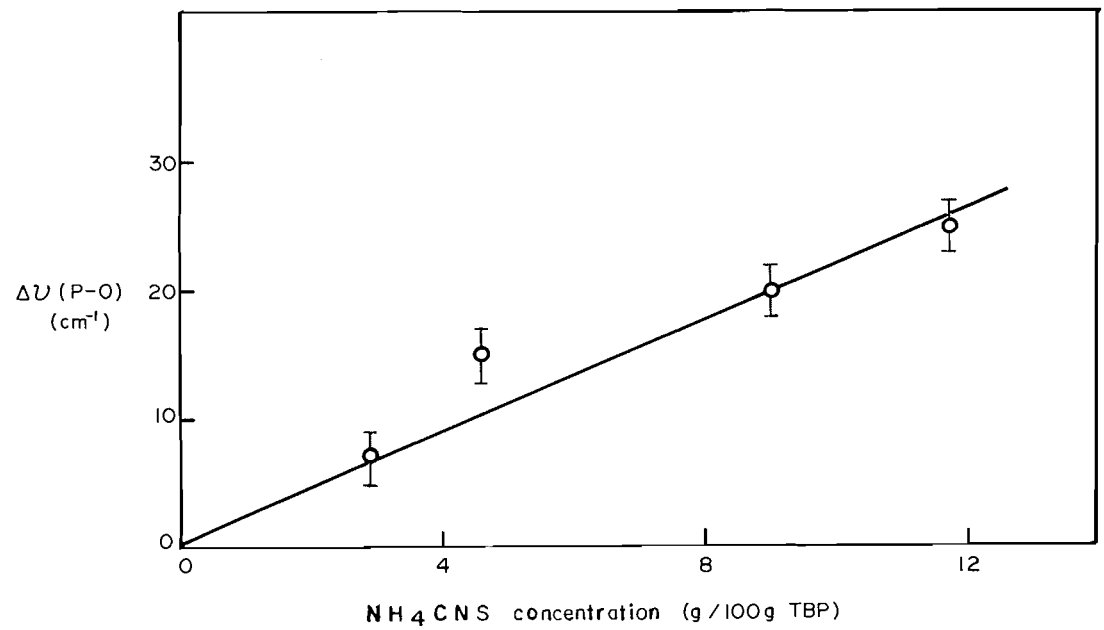

FIG. 1. Change in ν(P—O) in TBP as a function of ammonium thiocyanate concentration.

TABLE 2

Relationship between solubility and lattice energy for a series of ammonium salts

	NH_4NCS	NH_4I	NH_4Br	NH_4Cl
Solubility (g/100 g TBP)	11.6	12.7	~0.07	insol.
Lattice energy (kcal mole^{-1} (16))	158	142	151	156

relative to the alkali metal salts, judged against either ionic radius or lattice energy. The integral enthalpies of solution in TBP also show an unexpectedly high value for ammonium thiocyanate relative to the sodium and potassium salts (see Table 3). High accuracy was not sought in these measurements, and the errors are fairly large. The most important conclusion is that ΔH_{int} for NH_4NCS is higher than one would predict from the ionic radius argument, which generally holds in comparing the heats of solution of alkali metal salts in organic solvents (e.g. ref. 17).

The high solubility and enthalpy of solution of ammonium salts can be ascribed to hydrogen-bonding between the hydrogen atoms of NH_4^+ and the basic phosphoryl oxygen of TBP. The i.r. spectra confirm this. The ν(P—O) mode in TBP

TABLE 3

Integral enthalpies of solution for various salts

	NaCNS	KNCS	NH_4NCS
$-\Delta H_{int}$ (kcal mole^{-1})	5.9±0.1	1.5±0.2	4.6±0.1

is at 1275 cm^{-1}, but in concentrated solutions of ammonium thiocyanate or iodide, this shifts to lower frequencies, as found in other cases of hydrogen-bonding with this solvent (18); ν(P—O) in saturated solutions of ammonium thiocyanate and iodide is at 1250 and 1255 cm^{-1} respectively. For ammonium thiocyanate, the ν(P—O) shift is linearly dependent on the salt concentration (Fig. 1). The magnitude of the shift indicates slightly stronger hydrogen bonding than in the case of the 1:1 TBP–H_2O complex, for which Δν(P—O) of 12–16 cm^{-1} has been reported (19, 20). In the case of a concentrated solution of ammonium thiocyanate in water-saturated TBP, the shift in the P—O stretching frequency is only about 10 cm^{-1}, although the solubility of the salt is higher (15.3 ± 0.1 g NH_4SCN per 100 g wet TBP), suggesting that in such solutions there is some competition between water and NH_4^+ for the basic oxygen of TBP.

The ν(P—O) frequency in a saturated solution

Can. J. Chem. Downloaded from www.nrcresearchpress.com by 210.87.254.5 on 09/05/12
For personal use only.

Can. J. Chem. Downloaded from www.nrcresearchpress.com by 210.87.254.5 on 09/05/12
For personal use only.

of lithium thiocyanate was shifted to 1255 cm^{-1}, which agrees well with the shift of 21 cm^{-1} in $LiNO_3$ solution (20). The solid gel of lithium iodide showed a P—O stretch at 1268–1270 cm^{-1}. No significant shifts were observed in saturated solutions of sodium iodide, sodium thiocyanate or potassium thiocyanate.

A more direct proof of a hydrogen bonding interaction between NH_4^+ and TBP comes from the i.r. spectrum in the 2500–2700 cm^{-1} region, where the broad band of the P—O—H stretching mode occurs (21). The ν(C—H) absorption in TBP is a strong sharp line at 2800 cm^{-1}, but there is an additional broad absorption starting from 2400 cm^{-1} in the spectrum of a saturated solution of NH_4SCN in TBP. This is obviously due to the P—O—H absorption, overlapped by the C—H absorption on the high frequency side. Similar absorptions were also found in saturated solutions of ammonium iodide and perchlorate in TBP.

We also investigated the H^1 and P^{31} n.m.r spectra of solutions of sodium, potassium, and ammonium salts in TBP. The P^{31} spectrum of TBP is a septet, due to coupling with the protons of the α-CH_2 group; we find $J_{P-H} = 7.54$ c.p.s. (cf. 7.65 c.p.s. reported by Axtmann *et al.* (22)). The P^{31} spectra of solutions of ammonium or sodium thiocyanate show some broadening, but the P—H coupling constant does not change significantly. The P^{31} septet moves to high field relative to TBP, as shown in Table 4. With ammonium thiocyanate, δ has a monotonic dependence on the NH_4CNS:TBP ratio; with the sodium salt, the nature of the dependence of δ on salt concentration is not clear from the present results. The high-field shift of the signal indicates an increasing shielding of the phosphorus atom in TBP as the solvent interacts with NH_4^+, which is not in agreement with the usual interpretation of the i.r. shifts of ν(P—O) to lower frequency on hydrogen-bonding. The H^1 spectrum of TBP shows an almost overlapping pair of triplets for the α-CH_2 resonance, and changes in this part of the spectrum occur as the concentration of salt is increased, when the two triplets appear to coalesce. It is planned to investigate these phenomena further.

TABLE 4

The P^{31} n.m.r. spectra of solutions of ammonium and sodium thiocyanate in TBP

TBP:NH_4CNS (mole ratio)	δ (c.p.s.)	TBP:NaCNS (mole ratio)	δ (c.p.s.)
12.0	10	10.4	6
5.25	20	6.56	10
2.46*	34	2.44*	7

*Saturated solution.

This work was supported in part by an Operating Grant from the National Research Council of Canada.

1. T. V. Healy and H. A. C. McKay. Rec. Trav. Chim. **75**, 730 (1956).
2. T. V. Healy and H. A. C. McKay. Trans. Faraday Soc. **52**, 633 (1956).
3. A. B. Hart and J. R. Partington. J. Chem. Soc. 104 (1943).
4. J. E. Coates and E. J. Taylor. J. Chem. Soc. 1245 (1936).
5. D. G. Tuck. J. Chem. Soc. 2783 (1958).
6. C. J. Hardy, D. Fairhurst, H. A. C. McKay, and A. M. Willson. Trans. Faraday Soc. **60**, 1626 (1964).
7. See, for example, D. P. Shoemaker and C. W. Garland. Experiments in physical chemistry. McGraw-Hill, New York, 1962. p. 119.
8. D. F. C. Morris. Acta Cryst. **9**, 197 (1956).
9. M. F. C. Ladd and W. H. Lee. J. Inorg. Nucl. Chem. **13**, 218 (1960).
10. K. B. Yatsimirskii. Russ. J. Gen. Chem. **26**, 2655 (1956).
11. Y. Marcus and A. S. Kertes. Ion exchange and solvent extraction of metal complexes. Wiley, New York, 1969. p. 137.
12. D. F. C. Morris and E. L. Short. J. Inorg. Nucl. Chem. **25**, 291 (1963).
13. A. J. Parker. Quart. Rev. **16**, 163 (1962).
14. A. M. Rozen and A. I. Mikhailichenko. Russ. J. Inorg. Chem. **12**, 387 (1967).
15. E. V. Lapitskaya, E. D. Kukhkina, and F. P. Gorbenko. Russ. J. Inorg. Chem. **13**, 1427 (1968).
16. M. F. C. Ladd and W. H. Lee. Prog. Solid State Chem. **1**, 37 (1964).
17. G. Somsen and J. Coops. Rec. Trav. Chim. **84**, 985 (1965). L. Weeda and G. Somsen. Rec. Trav. Chim. **85**, 159 (1966); **86**, 263 (1967).
18. K. B. Yatsimirskii. Russ. J. Gen. Chem. **26**, 528 (1956).
19. S. S. Grimley, T. V. Healy, J. Kennedy, and H. A. C. McKay. Trans. Faraday Soc. **52**, 39 (1956).
20. L. I. Katzin. J. Inorg. Nucl. Chem. **20**, 300 (1961).
21. J. R. Ferraro. Prog. Infrared Spectrosc. **2**, 127 (1964).
22. R. C. Axtmann, W. E. Shuler, and J. H. Eberly. J. Chem. Phys. **31**, 850 (1959).
23. A. F. Wells. Structural inorganic chemistry. 3rd Edition. Oxford University Press, 1962. p. 71.

Dissolution of bismuth metal by tri-iodide ion in acidified potassium iodide solution

DIGBY D. MACDONALD
Department of Chemistry, University of Calgary, Calgary, Alberta

AND

G. A. WRIGHT
Department of Chemistry, University of Auckland, Auckland, New Zealand

Received March 10, 1970

Dissolution of bismuth metal by tri-iodide ion in acidified potassium iodide medium has been studied using a rotating disc technique. The rate constant for the dissolution process, k_T, in solutions 0.5 *M* in potassium iodide at 25.0 °C has been shown to be related to the square root of the disc angular velocity, ω, by the following expression

$$k_T = 0.75 \times 10^{-3}\ \omega^{1/2}\ \text{cm s}^{-1}$$

The activation energy for this reaction was found to be 4.7 kcal mole^{-1}. These data clearly establish that the rate of dissolution is determined by the rate at which tri-iodide ion is transported to the metal surface. In solutions of [KI] = 0.10 *M*, however, the rate determining step appears to involve diffusion of tri-iodide ion through a layer of BiI_3 which forms on the bismuth metal surface as the reaction proceeds.

Canadian Journal of Chemistry, 48, 2847 (1970)

Can. J. Chem. Downloaded from www.nrcresearchpress.com by 210.87.254.42 on 09/05/12
For personal use only.

Introduction

Dissolution reactions of the type represented by eq. [1] have been described in terms of five

[1] $\text{M(surface)} + \text{Ox}(m) \rightarrow \text{M}^{n+}\text{(solution)} + \text{Red}(m - n)$

basic processes (1, 2): (*i*) diffusion of the oxidizing agent to the metal surface, (*ii*) adsorption of the oxidizer on to the surface, (*iii*) electron exchange, (*iv*) desorption of products, and (*v*) diffusion of the products from the metal surface. Steps (*i*) and (*v*) are commonly referred to as "diffusion" processes and steps (*ii*), (*iii*), and (*iv*) as "chemical activation" processes. In theory, any one of steps (*i*) to (*v*) can be rate determining for a given dissolution reaction and many examples have been documented in the literature (1, 2).

In this paper we report a study performed to determine which of the above steps ((*i*) to (*v*)) controls the rate of dissolution of bismuth metal by tri-iodide ion in an acidified potassium iodide medium. The rotating disc technique was employed since the dependence of reaction rate on disc angular velocity and temperature provides a means of distinguishing between diffusion controlled and chemically controlled processes (1, 3). Hedvall, Hedin, and Anderson (4) have observed the oxidation of bismuth by iodine, but their conditions were not well defined and no kinetic study was attempted.

Experimental

Materials

Water: All solutions were prepared with water distilled from dilute potassium permanganate solution to remove oxidizable impurities.

Potassium Iodide: British Drug Houses analytical reagent grade potassium iodide was used throughout this work. The chloride and bromide content was stated not to exceed 0.01%

Sulfuric Acid: Acidified solutions were prepared by diluting 96% analytical reagent grade sulfuric acid.

Bismuth: British Drug Houses bismuth having a minimum purity of 99% was used without further purification.

Apparatus

The rotating disc apparatus was similar in design to that described by Gregory and Riddiford (5) and is shown in Fig. 1. The bismuth inset was prepared as follows. Bismuth was melted in a small beaker and poured into the depression on the underside of the brass disc. The inset was allowed to cool and a good fit ensured by expansion of solidifying bismuth (6) and contraction of cooling brass. The bismuth surface was filed down to within 0.5 mm of the surrounding brass. A protective coating of "Apiezon" wax was applied to the brass surface by the method described in the literature (7). Final treatment of the bismuth surface involved grinding with 240 × A carborundum cloth until the bismuth surface was level with the surrounding wax. The bismuth surface was cleansed before use with carbon tetrachloride and 5 *M* nitric acid. Care was taken to ensure that no holes existed in the wax coating. This was tested by immersing the disc in 5 *M* nitric acid. Any holes appeared as bright "brassy" specks and were covered with wax (7).

The area of plane bismuth surface was determined by measuring the diameter of the inset with a travelling microscope. The area (7.06 cm^2) was reproducible to better than ± 1% after each renewal of the bismuth metal.

The disc was joined to a steel shaft by a screw thread which passed through a bearing in the top of an enclosed reaction vessel (500 ml) and was connected to a Citenco type KQPS/21 variable speed electric motor. The bearing could be adjusted to ensure minimum eccentricity of the disc.

Measurement of rotation speed was performed with a

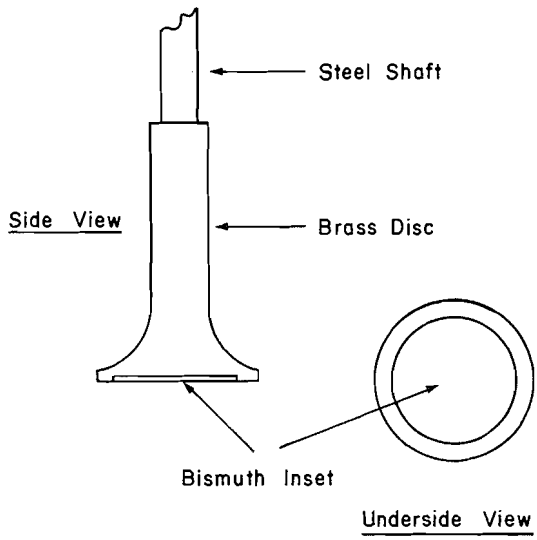

FIG. 1. Rotating disc.

Dukes and Briggs model M.P.S. flashing light stroboscope. The flashing light was aimed at a vertical white line painted on the shaft. The stroboscope was set at the desired frequency and the motor speed adjusted until the white line appeared stationary. Rotation speeds could be varied between 15.68 and 48.50 rad s^{-1} (150 and 463 r.p.m., respectively), well within the limits for non-turbulent flow (1, 3)[1] and are accurate to better than $\pm$ 1%. The reaction vessel was thermostatted in a water bath controlled by a mercury–toluene regulator connected to two 150 W heaters. At 25 °C the bath temperature could be controlled to better than $\pm$ 0.1 °C.

Kinetic Method

Reaction solutions 0.01 *M* in iodine, 0.10, 0.50, and 1.00 *M* in potassium iodide and 0.5 *M* in sulfuric acid were prepared by weighing out the solid components and dissolving them (KI first, I_2 second) in the required volume of sulfuric acid. The reaction solutions were deoxygenated by a stream of dry nitrogen in order to prevent oxidation of iodide ion to iodine in acid media according to the following equation (8).

$$4\,I^- + 4\,H^+ + O_2 = 2\,I_2 + 2\,H_2O$$

Twenty minutes of deoxygenation was sufficient as shown by the time-independence of the iodine concentration of a sample of reaction solution. All iodine determinations were performed by titration with standard 0.005 *M* sodium thiosulfate solution which was prepared and standardized by well documented methods (9, 10). The same sodium thiosulfate solutions were used in the kinetic determinations. The end points were determined using sodium starch glycollate indicator.

The apparatus was assembled and placed in the thermostat. The reaction solution (400 ml) was pipetted into the reaction vessel and allowed to reach thermal equilibrium. After equilibrium had been achieved the disc was checked to ensure that no gas bubbles were trapped under the bismuth surface. The motor was started and adjusted to the desired rotation speed. When the motor speed had been adjusted satisfactorily an aliquot (5 ml) of reaction solution was removed by pipette for analysis of iodine by titration against the standard sodium thiosulfate solution. Further aliquots were removed and analyzed at regular known time intervals.

Results

Rates

The rate constant, k_T, was determined by plotting eq. [2] for first order surface kinetics (11)

$$[2] \qquad \sum V\Delta \log_{10} c = k_T A t/2.303$$

where t is time in minutes from the start of the run, A is the area of the bismuth surface, and $\Delta \log_{10} c$ denotes the difference in the logarithm of the concentration of tri-iodide ion at the beginning and end of an interval for which the volume of solution is V ml. A typical plot of eq. [2] is shown in Fig. 2. Excellent linearity was obtained in all cases except those performed in solutions 0.10 *M* in potassium iodide. Possible causes for the breakdown of first order kinetics in this latter case are discussed in detail in the Discussion section.

Rate constants are listed in Table 1 as a function of disc rotation velocity, temperature, and potassium iodide concentration and are considered accurate to better than $\pm$ 5%.

Activation Energy

The activation energy, E_a, was found by plotting $\log_{10} k_T$ vs. reciprocal absolute temperature in accordance with eq. [3]

$$[3] \qquad \log_{10} k_T = \log_{10} A - E_a/2.303RT$$

where A is the Arrhenius pre-exponential frequency factor. A plot of eq. [3] for data obtained in this work is shown in Fig. 3. The activation energy obtained is 4.7 $\pm$ 0.7 kcal $mole^{-1}$.

Discussion

The Reaction

The stoichiometry of the reaction was established by comparing the weight loss of bismuth pellets with the amount of tri-iodide ion con-

[1]The Reynold number, Re, is defined as $r^2\omega/\nu$, where ν is the kinematic viscosity of the medium and r is the radius. Above the numerical value of Re $\sim 2 \times 10^5$, turbulent flow becomes important in the case of a rotating disc. In the present work the maximum Reynold number occurs when $r = 1.50$ cm (the radius of the bismuth inset) and $\omega = 48.50$ rad s^{-1} and has a value of $\sim 1.23 \times 10^4$. This is considerably less than the maximum value allowed for non-turbulent flow.

Can. J. Chem. Downloaded from www.nrcresearchpress.com by 210.87.254.42 on 09/05/12
For personal use only.

Can. J. Chem. Downloaded from www.nrcresearchpress.com by 210.87.254.42 on 09/05/12
For personal use only.

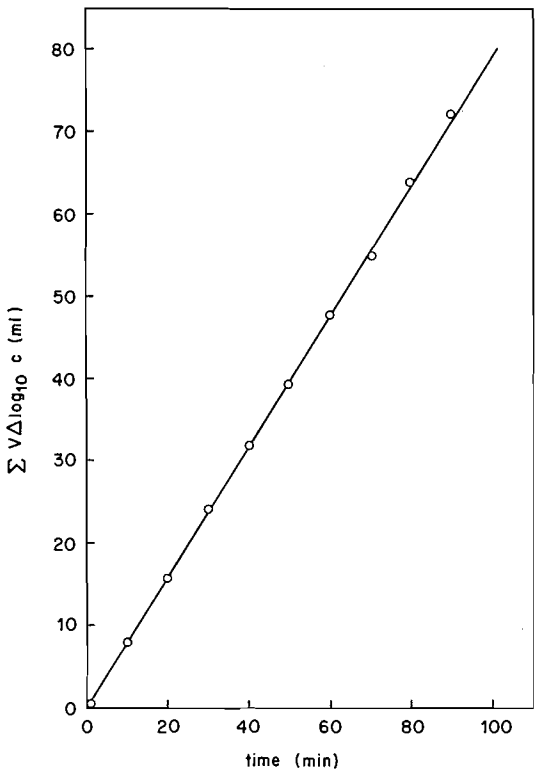

FIG. 2. Rate plot for dissolution of bismuth metal by tri-iodide ion in acidified potassium iodide (0.50 *M*) solution. $T = 25.0$ °C; $\omega = 31.42$ rad s^{-1}.

sumed. A mole ratio $Bi:I_3^- = 0.66$ was obtained. In the presence of sufficient KI [> 0.4 *M* (12)] such that Bi(III) exists predominantly as the complex BiI_6^{3-} and with sufficient H^+ [1 *M* (13)] to suppress hydrolysis of Bi(III), the reaction may be written as eq. [4]

$$[4] \qquad Bi + \frac{3}{2} I_3^- + \frac{3}{2} I^- = BiI_6^{3-}$$

Using the standard potentials for Bi^{3+}/Bi (14) and I_3^-/I^- and the stability constant of BiI_6^{3-} (15), it was estimated that for reaction [4], $\log_{10} K = 31.4$. Experimentally it was observed that in time all the tri-iodide ion was consumed showing that the equilibrium lies far to the right-hand side.

Dependence of Rate on Rotation Velocity

According to the Nernst theory for diffusion controlled reactions (1, 2) the rate constant k_T can be expressed by eq. [5]

$$[5] \qquad k_T = D/\delta$$

TABLE 1

(*a*) Rate constants as a function of disc rotation velocity*

ω (rad s^{-1})	$k_T \times 10^3$ (cm s^{-1})
15.68	2.92
20.95	3.44
26.10	3.76
31.42	4.30
41.90	4.69
48.50	5.22

*$T = 25.0 \pm 0.1$ °C, [KI] = 0.50 *M*.

(*b*) Rate constants as a function of temperature*

T (°C)	$k_T \times 10^3$ (cm s^{-1})
0.6	2.12
10.5	2.51
19.2	3.44
20.0	3.88
25.0	4.30
33.0	4.52
42.0	4.95

*$\omega = 31.42$ rad s^{-1}, [KI] = 0.50 *M*.

(*c*) Rate constants as a function of [KI]*

[KI] (M)	$k_T \times 10^3$ (cm s^{-1})
0.10	—
0.50	4.30
1.0	4.40

*$\omega = 31.42$ rad s^{-1}, $T = 25.0 \pm 0.1$ °C.

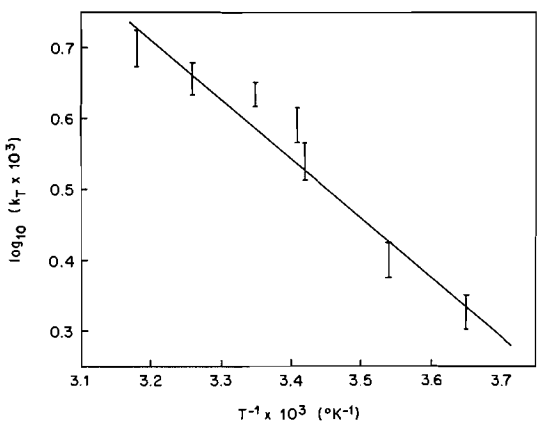

FIG. 3. Arrhenius plot. [KI] = 0.50 *M*; $\omega = 31.42$ rad s^{-1}.

Can. J. Chem. Downloaded from www.nrcresearchpress.com by 210.87.254.42 on 09/05/12
For personal use only.

where D is the diffusion coefficient for the oxidant and δ is the thickness of the "ideal" Nernst diffusion layer. Levich (16) and Gregory and Riddiford (5) solved the hydrodynamical equations for non-turbulent mass transport of a solute species to the surface of a disc rotating about an axis to the disc plane. The mathematical details of their solutions have been reviewed recently (1, 3) and will not be presented in detail here. Levich (16) derived an expression for the distance (δ') over which the concentration of the oxidant differs significantly from the bulk concentration in terms of D, the kinematic viscosity (ν) of the medium, and the rotation velocity (ω) of the disc.

$$[6] \qquad \delta' = 1.805 D^{1/3} \nu^{1/6} \omega^{-1/2}$$

This "effective" diffusion layer thickness, δ', is related to the "ideal" Nernst layer thickness, δ, by eq. [7] (1, 16)

$$[7] \qquad \delta = 0.8934 \delta'$$

A more exact expression has been derived by Gregory and Riddiford (5) and is given by eq. [8]

$$[8] \quad \delta = 1.805 D^{1/3} \nu^{1/6} \omega^{-1/2} [0.8934 + 0.316 (D/\nu)^{0.36}]$$

In aqueous solutions D/ν is about 10^{-3} and results in a difference of about 3% between eqs. [7] and [8] (5). Since rate data obtained in this work are accurate to only $\pm$ 5% the correction to δ contained in eq. [8] will be neglected.

Combining eqs. [5], [6], and [7] results in eq. [9] for the rate constant for a diffusion controlled dissolution reaction.

$$[9] \qquad k_T = 0.620 D^{2/3} \nu^{-1/6} \omega^{1/2}$$

The above expression predicts that a plot of k_T vs. $\omega^{1/2}$ should be linear. Such a plot for data obtained in this work is shown in Fig. 4. The solid line represents eq. [9] using $D = 1.25 \times 10^{-5}$ cm^2 s^{-1} and $\nu = 8.90 \times 10^{-3}$ cm^2 s^{-1} (17). The agreement between the experimental dependence of k_T on $\omega^{1/2}$ and the calculated value is excellent, clearly establishing that the rate of dissolution of bismuth by tri-iodide ion in acidified potassium iodide medium (> 0.5 M in KI) is controlled by the rate of transport of tri-iodide ion to the metal surface.

Activation Energy

The dependence of diffusion coefficient, D, and kinematic viscosity, ν, on temperature may be expressed as (18)

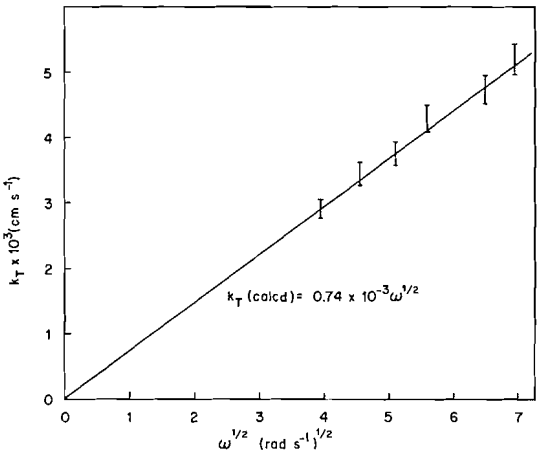

FIG. 4. Plot of k_T vs. $\omega^{1/2}$. T = 25.0 °C; [KI] = 0.50 M.

$$[10] \qquad D = Z_D \exp(-E_D/RT)$$

$$[11] \qquad \nu = Z_\nu \exp(E_\nu/RT)$$

where E_D and E_ν are activation energies for diffusion and kinematic viscosity, respectively. Substitution of eqs. [10] and [11] into eq. [9] results in eq. [12] for the temperature dependence of k_T for a diffusion controlled reaction (18).

$$[12] \quad k_T = 0.620 Z_D^{2/3} Z_\nu^{-1/6} \omega^{1/2} \exp[-(4E_D + E_\nu)/6RT]$$

Data required to calculate E_D and E_ν from eqs. [10] and [11], respectively, for the solutions used in this work are unavailable. However, for aqueous solutions of most electrolytes E_D and E_ν lie in the range 2 to 7 kcal mole^{-1}, thus restricting the activation energy for diffusion controlled reactions in aqueous electrolyte solution to 1.7 to 6 kcal mole^{-1}. The experimental value of $E_a = 4.7 \pm 0.7$ kcal mole^{-1} obtained in this work agrees well with this theoretical value for diffusion controlled reactions, and therefore lends further support to the conclusion reached in the previous section that the reaction under study in this work is in fact diffusion controlled.

Dependence of Rate on Potassium Iodide Concentration

In the Results section it was stated that breakdown of first order kinetics was observed for reactions in solutions 0.10 M in potassium iodide.

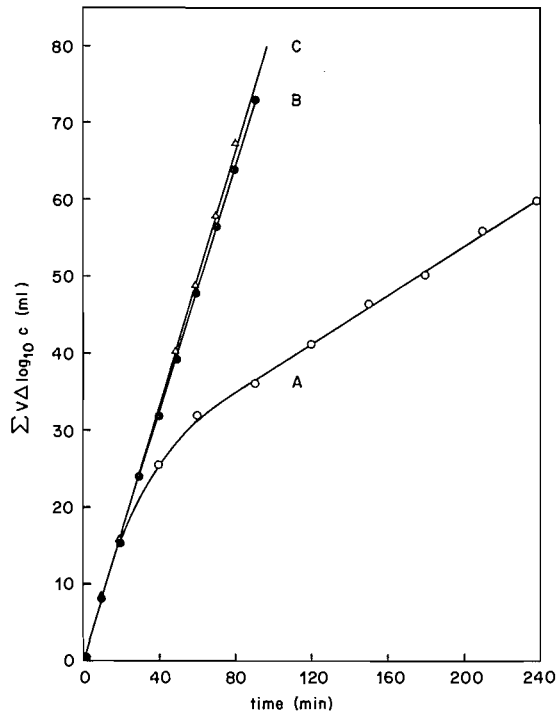

FIG. 5. Rate plots at different potassium iodide concentrations. (*A*) [KI] = 0.10 *M*; (*B*) [KI] = 0.50 *M*; (*C*) [KI] = 1.00 *M*; T = 25.0 °C; ω = 31.42 rad s^{-1}.

This is well illustrated in Fig. 5 where first-order rate plots (eq. [2]) for dissolution of bismuth in solutions 0.10, 0.50, and 1.0 *M* in potassium iodide are shown. The two linear plots reveal little, if any, dependence of k_T on iodide concentration. Such behavior is predicted by eq. [9] for diffusion controlled reactions of the type under investigation in this work (5). In 0.10 *M* potassium iodide solution, however, k_T falls off rapidly as a function of time from a limiting value close to those for the 0.5 and 1.0 *M* potassium iodide solutions at zero time. Examination of the bismuth surface of the disc after a run with a potassium iodide concentration of 0.10 *M* revealed the existence of a layer of black bismuth tri-iodide (BiI_3). This layer apparently takes some time to form since k_T shows a gradual decrease from the "clean surface" value at zero time until a constant value is obtained after a period of about 60 min from initial contact of the bismuth metal with the reaction solution. In this case the rate determining step of the reaction is probably diffusion of tri-iodide ion through the surface layer of BiI_3. A similar process has been proposed by Bircumshaw and Everdell (19, 20) for dissolution of copper by tri-iodide ion in acidified potassium iodide solution. The time-independent rate constant obtained after 60 min can be explained by the thickness of the BiI_3 layer reaching a steady state value, i.e. δ_{BiI_3} in eq. [13] is independent of time.

$$k_T = D'/\delta_{BiI_3} \qquad [13]$$

D' is the coefficient of diffusion for I_3^- in the BiI_3 layer. Since both quantities on the right hand side of eq. [13] are independent of time, then so is k_T.

Reaction Mechanism

It has been established above that the rate determining step in the oxidation of bismuth by tri-iodide ion is the transport of tri-iodide ion to the metal surface by a process of combined convection and diffusion at the rotating disc. Other oxidizing agents of lower standard potentials may be expected to react at a chemically controlled rate, and it was found qualitatively that vanadyl and uranyl ions attacked bismuth much more slowly than tri-iodide ion.

At sufficiently high iodide concentrations (i.e. 0.5 and 1.0 *M* KI) the surface reaction between bismuth and tri-iodide ion is undoubtedly an electrochemical process composed of the following anodic [14] and cathodic [15] reactions

$$\begin{aligned} &Bi + 6\,I^- \rightarrow BiI_6^{3-} + 3e^- \\ &\tfrac{3}{2}\,I_3^- + 3e^- \rightarrow \tfrac{9}{2}\,I^- \end{aligned} \qquad [14]$$

The standard potential of reaction [14] can be estimated as − 0.08 V from the standard potential of Bi^{3+}/Bi (+ 0.29 *V* (14)) and the stability constant of BiI_6^{3-} (15). The standard potential of reaction [15] is 0.54 V (21). During the dissolution of bismuth in tri-iodide ion solution it was found that the metal adopted a mixed potential of + 0.12 V decaying to 0.09 V as the tri-iodide ion was depleted. The mixed potential lies closer to the standard potential of the anodic reaction, and the reaction can be described by class 4 of Hoar's (22) classification. For this case the reaction rate is controlled by the limiting current of the cathodic reaction [15] and the mixed potential will be given by the overpotential of the anodic process [14] when its current exactly opposes the cathodic reaction.

Can. J. Chem. Downloaded from www.nrcresearchpress.com by 210.87.254.42 on 09/05/12
For personal use only.

At low iodide concentrations (i.e. [KI] = 0.1 *M*) the kinetic scheme is complicated by the fact that BiI_6^{3-} is no longer the dominant Bi(III) species in the system. Instead, the solution now contains significant amounts of both BiI_3 and BiI_4^- as well as BiI_6^{3-} (12). This contention is fully supported by the observation of a layer of BiI_3 on the bismuth surface during runs carried out in 0.1 *M* KI solutions. It is evident, therefore, that in this case the anodic reaction cannot be adequately described by a single process of the type represented in eq. [14]. A more realistic mechanism would involve a "mixed" anodic process consisting of as many elementary reactions as necessary to account for all Bi(III) species in the system.

The authors thank the New Zealand University Grants Committee for a research grant and the National Research Council of Canada for financial support for D. D. Macdonald.

1. L. L. BIRCUMSHAW and A. C. RIDDIFORD. Quart. Rev. **6**, 157 (1952).
2. C. V. KING. The surface chemistry of metals and semiconductors. *Edited by* H. C, Gates. John Wiley and Sons Inc., New York. 1960. p. 357.
3. A. C. RIDDIFORD. Advances in electrochemistry and electrochemical engineering. *Edited by* P. Delahay. Interscience Publ. Inc., New York. **4**, 47 (1966).
4. J. A. HEDVALL, R. HEDIN, and E. ANDERSON. Zeit. Anorg. Allg. Chem. **212**, 84 (1933).
5. D. P. GREGORY and A. C. RIDDIFORD. J. Chem. Soc. 3756 (1956).
6. J. W. MELLOR. A comprehensive treatise on inorganic and theoretical chemistry. Longmans, Green and Co., Inc., London. **9**, 604 (1929).
7. J. D. NEWSON and A. C. RIDDIFORD. J. Electrochem. Soc. **108**, 697 (1961).
8. R. B. HESLOP and P. L. ROBINSON. Inorganic chemistry. 2nd ed. Elsevier Publ. Inc., Amsterdam. 1963. p. 397.
9. A. I. VOGEL. Quantitative inorganic analysis. 3rd ed. Longmans, Green and Co., Inc., London. 1961. p. 348.
10. A. I. VOGEL. Qualitative inorganic analysis. 3rd ed. Longmans, Green and Co., Inc., London. p. 349.
11. R. S. BRADLEY. Trans. Faraday Soc. **34**, 278 (1938).
12. A. J. EVE and D. N. HUME. Inorg. Chem. **6**, 331 (1967).
13. A. OLIN. Svensk Kem. Tidskr. **73**, 482 (1961).
14. A. F. M. BARTON and G. A. WRIGHT. *In* Electrochemistry. Pergamon Press. Oxford. 1964. p. 124.
15. A. AHRLAND and I. GRENTHE. Acta Chem. Scand. **11**, 1111 (1957).
16. V. G. LEVICH. Physicochemical hydrodynamics. Prentice-Hall, Inc., Englewood Cliffs, New Jersey. 1962.
17. International critical tables. *Edited by* E. W. Washburn. McGraw-Hill Co., Inc., New York. **5**, 64 (1929).
18. A. C. RIDDIFORD. J. Phys. Chem. **56**, 745 (1952).
19. L. L. BIRCUMSHAW and M. H. EVERDELL. J. Chem. Soc. 598 (1942).
20. L. L. BIRCUMSHAW and M. H. EVERDELL. J. Chem. Soc. 119 (1947).
21. W. M. LATIMER. Oxidation potentials. 2nd ed. Prentice-Hall, Inc., New York. 1952.
22. T. P. HOAR. *In* Modern aspects of electrochemistry. *Edited by* J. O'M. Bockris. Butterworths Publ. Inc., London **2**, 234 (1959).

Can. J. Chem. Downloaded from www.nrcresearchpress.com by 210.87.254.42 on 09/05/12
For personal use only.

Can. J. Chem. Downloaded from www.nrcresearchpress.com by 210.87.254.42 on 09/05/12
For personal use only.

Vibrational and Mössbauer spectra of some hexachloro- and hexafluorostannate complexes

H. A. CARTER, A. M. QURESHI, J. R. SAMS, AND F. AUBKE[1]

Department of Chemistry, University of British Columbia, Vancouver 8, British Columbia

Received April 24, 1970

^{119}Sn Mössbauer and vibrational spectra for a number of SnF_6^{2-} and $SnCl_6^{2-}$ complexes have been obtained. One fundamental for the SnF_6^{2-} ion has been reassigned. Strong evidence for anion–cation interaction for $(ClO_2)_2SnF_6$ is obtained both from the vibrational spectra and from the Mössbauer spectra where a non-zero quadrupole splitting is found.

Canadian Journal of Chemistry, **48**, 2853 (1970)

During a general study of hexafluorometallate complexes with heterocations (1–3) in view of a possible anion–cation interaction in those complexes, we became interested in $SnCl_6^{2-}$ and SnF_6^{2-} complexes for the following reasons: (*a*) Application of infrared and laser Raman spectroscopy should indicate whether anion distortion and subsequently symmetry lowering in these complexes exists. Whereas the $SnCl_6^{2-}$ complexes are expected to absorb in the far infrared region, out of the range of most instruments, a complete vibrational analysis should be possible for the hexafluorostannate ion. Previous reports on the vibrational spectrum of SnF_6^{2-} (4–7) are often incomplete and not internally consistent, so that the simple compounds K_2SnF_6 and Na_2SnF_6 had to be included in this study to provide a good basis for comparisons. (*b*) Application of ^{119}Sn Mössbauer spectroscopy should indicate whether the distortion expected for heterocation complexes and found in corresponding SbF_6^- complexes (2, 3) is large enough to produce an electric field gradient and subsequently a quadrupole splitting and whether such distortion is due to electronic interaction rather than site symmetry effects. Any electronic charge transfer should result in a change in the isomer shift.

In spite of earlier attempts (4) to explain the quadrupole splitting in hexacoordinated tin as a π-bonding effect, it is now generally believed (9, 10) that σ-bonding effects, that is, differences in bond polarities, are sufficient to produce a quadrupole splitting. It has been shown quite recently (11) for adducts of the type $SnCl_4 \cdot 2R_2SO$ that molecular distortion caused by bulky ligand groups can give rise to small quadrupole splittings. Quadrupole splitting for SnF_6^{2-} complexes with heterocations has been found recently (12) for the compounds $(BrF_2)_2SnF_6$, $(BrF_4)_2SnF_6$, $(ClF_2)_2SnF_6$, $(IF_4)_2SnF_6$, $(NO_2)_2SnF_6$, and $(NO)_2SnF_6$.

The ^{119}Sn isomer shift is commonly used as a measure of the 5s electron density around tin. Previous reports (13) indicate a very low isomer shift for SnF_6^{2-}. The reported value for K_2SnF_6 and Cs_2SnF_6 of -0.44 mm/s from SnO_2 is even lower than the calculated value for an Sn^{4+} ion (14). The SnF_6^{2-} should therefore provide a good sensor for electronic interactions between the anion and heterocations.

Experimental

Hexafluorostannate compounds containing oxycations were prepared using a monel metal vacuum line. The reaction vessel consisted of a $\sim$ 100 ml monel can with removable lid and Teflon gaskets, equipped with Hoke and Whitey valves. Transfer and handling of these moisture sensitive compounds was achieved in a dry box containing a highly purified nitrogen atmosphere.

Materials

Chloryl fluoride $FClO_2$ was prepared according to Woolf (15) by reaction of $KClO_3$ with BrF_3 in a monel metal reactor. For the preparation of $(ClO_2)_2SnF_6$ the method of Schmeisser and Fink (16) was adopted with alterations and without the use of $CFCl_3$ as a solvent. The preparation is described in detail. To minimize the hazard involved in handling ClO_2, 89.1 mmoles of $FClO_2$ were introduced in small portions into a reaction vessel containing 8.43 mmoles of purified $SnCl_4$ by vacuum distillation. The reactor was warmed to room temperature and the volatile by-products ClO_2 and Cl_2 were removed by pumping. This procedure was repeated several times until all the $FClO_2$ was added. The volatile by-products were removed again by pumping and the involatile solid, indicated by the weight increase, corresponded to $(ClO_2)_2SnF_6$. Potassium hexafluorostannate (Alpha Inorganic Chemicals) was purified by recrystallization from anhydrous HF in a polyethylene reactor.

Sodium hexafluorostannate was prepared from Na_2SnO_3 (Fisher Scientific Co.) in 49% HF (Fisher Scientific Co.).

[1]To whom correspondence should be addressed.

TABLE 1

Vibrational frequencies for SnF_6^{2-} compounds*

Na_2SnF_6		K_2SnF_6		$(NO_2)_2SnF_6$		$(NO)_2SnF_6$		$(ClO_2)_2SnF_6$	
Infrared	Raman	Infrared	Raman	Infrared	Raman	Infrared	Raman	Infrared	Raman
			628 vw, sh	2392 m		2322 m	2325 s	1302 vs	1309 m
590 sh	594 vs	582 w, sh	598 vs	602 s	1390 s	585 m, sh	593 s	1290 vs	1293 m
					627 vw, sh				
560 vs		557 vs		590 w, sh	592 vs	555 vs		1076 s	1080 vs
	480 m	480 vw	478 vs	565 vs	478 m, sh	481 m, sh	480 m	1072 s	
475 vw, sh				480 m, sh		400 vw		634 s, sh	628 m, s
								624 s, sh	
	416 w	420 vw	423 w		421 vw	420 vw		606 s	613 s
								561 vs	563 vw, sh
	367 vw	367 vw	368 w		370 w	365 vw, sh		541 s, sh	549 s
								522 s, sh	519 m
	255 ms	257 s	258 s			258 s	256 ms	470 m, s	482 m
			254 s, sh						465 w, sh
	162 m		163 m		161 m, sh				423 w
								314 w	367 w

*vw = very weak; s = strong; w = weak; vs = very strong; m = medium; sh = shoulder. All frequencies in cm^{-1}.

Both $(NO)_2SnF_6$ and $(NO_2)_2SnF_6$ were prepared from SnF_4 (Research Inorganic Chemicals) and the halides ClNO and $ClNO_2$ in anhydrous HF (Matheson of Canada Co.) according to Kuhn (17). Nitrosyl- (18) and nitryl chloride (19) were prepared as described. $(NO)_2SnCl_6$ was formed by the interaction of ClNO and $SnCl_4$ (20) with the former in excess in a Pyrex reactor.

Potassium, ammonium, and cesium hexachlorostannates were prepared by the reaction of saturated solutions of the alkali chlorides with stannic chloride in aqueous solution (21).

Infrared Spectra

Infrared spectra were recorded on a Perkin–Elmer 457 Grating Spectrophotometer, covering the region 4000–250 cm^{-1}. Silver chloride and KSR-5 windows (Harshaw Chemicals) were used. For the highly reactive heterocation complexes no mulling agents were used; for the rest, Nujol was employed.

The infrared spectrum of K_2SnF_6 was recorded on a Perkin–Elmer 301 High Resolution Grating Spectrophotometer for the range 666–166 cm^{-1}. Nujol as mulling agent and cesium iodide windows (Harshaw Chemicals) were used.

Raman Spectra

A Cary 81 spectrophotometer equipped with a Spectra Physics Model 125 laser as source for exciting light was used. The samples were contained in flat bottom Pyrex tubes (5 mm o.d.).

Mössbauer Spectra

Mössbauer spectra were obtained on a constant acceleration type spectrometer, the electromechanical velocity transducer being phase-locked to a 400 channel analyzer operating in time mode. The transmitted radiation was detected by a Reuter–Stokes RSG-60 proportional counter with 2 atm Xe–CH_4 as fill gas. A narrow line 5 mC $Ba^{119m}SnO_3$ source was employed and the velocity scale calibrated with an N.S.B. standard sodium nitroprusside absorber. The powdered absorbers (approximately 0.5 mm in thickness) were contained in brass cells with Mylar windows and Teflon spacers. The samples were run at 295 and 80 °K. The isomer shifts are reported relative to SnO_2 at 80 °K.

Results

The infrared and Raman data for the compounds Na_2SnF_6, K_2SnF_6, $(NO)_2SnF_6$, $(NO_2)_2SnF_6$, and $(ClO_2)_2SnF_6$ are listed in Table 1. Table 2 contains the Raman frequencies for $(NO)_2SnCl_6$ and K_2SnCl_6. The vibrational frequencies for the SnF_6^{2-} in K_2SnF_6 and $(ClO_2)_2SnF_6$ are tabulated in Table 3, and compared to previously reported values. The vibrational frequencies assigned to the chloronium-cation ClO_2^+ are listed in Table 4 and compared to the previous values. The high resolution infrared (i.r.) spectrum of K_2SnF_6 and the Raman spectrum of $(ClO_2)_2SnF_6$ are shown in Figs. 1 and 2.

The Mössbauer data for all SnX_6^{2-} complexes studied are listed in Table 6 for 80 and 298 °K. The accuracy limit for the Mössbauer data is judged to be $\pm$ 0.03 mm/s for both the isomer shift and the quadrupole splitting. The spectrum of $(ClO_2)_2SnF_6$ at 298 °K is shown in Fig. 3. Also listed in Table 6 are the linewidth values and the room temperature effect R (36) where R is defined as $\varepsilon_{298°}/\varepsilon_{80°}$, ε being the magnitude of the Mössbauer effect.

Discussion

(a) Vibrational Spectra

Of the alkali metal compounds, K_2SnF_6 and Cs_2SnF_6 appear to have the trigonal K_2GeF_6

Can. J. Chem. Downloaded from www.nrcresearchpress.com by 210.87.254.42 on 09/05/12
For personal use only.

TABLE 2

Vibrational frequencies of $SnCl_6^{2-}$ compounds*

K_2SnCl_6		$(NO)_2SnCl_6$		$SnCl_6^{2-}$	
Infrared	Raman	Infrared	Raman	Raman (22)	Assignment
		2202 m	2207 s		ν_{NO}
341 w, sh		325 w, sh			
	317 vs	317 vs			ν_3
322 s			315 s	311	ν_1
	218 w, sh		215 w, sh	229	ν_2
	167 vs		175 vs	158	ν_5

*Footnote to Table 1 applies here.

TABLE 3

Vibrational frequencies for the SnF_6^{2-} ion

Compound	$\nu_1(A_{1g})$	$\nu_2(E_g)$	$\nu_3(F_{1u})$	$\nu_4(F_{1u})$	$\nu_5(F_{2g})$	Reference
K_2SnF_6(s)	598	478*	582, 557	257, 254	257	This work
Na_2SnF_6(s)	594	480*	590, 560		255	This work
$(NO)_2SnF_6$(s)	593	481*	585, 555	258	256	This work
$(NO_2)_2SnF_6$(s)	590	478	590, 565	—	—	
Cs_2SnF_6(s)	572	460	577, 555	256, 249	247	7
K_2SnF_6(s)	593	620	564		342	6
Na_2SnF_6(s)	592	477	559	300	252	8
$(NH_4)_2SnF_6$ Aqueous solution	585	470			241	7

*Denotes i.r. and Raman active.

TABLE 4

Vibrational modes of the ClO_2-group (cm^{-1})

Compound	Method	ν_1	ν_2	ν_3	Average $\nu_3 + \nu_1$	Reference
$NaClO_2$(s)	Raman	804	432	832	818	1
$NaClO_2$ (Aqueous solution)	Raman	790	400	840	815	23
$FClO_2$(s)	Raman	1097	533	1253	1175	24
ClO_2BF_4(s)	Infrared	?	518	1308, 1294	—	25
ClO_2AsF_6(s)	Infrared	1045	515	1293, 1280	1166	1
ClO_2AsF_6(s)	Raman	1045	518	1296, 1281	1168	1
ClO_2SbF_6(s)	Infrared	1050	510	1304, 1291	1174	1
ClO_2SbF_6(s)	Raman	1053	518	1314, 1293	1178	2
$(ClO_2)_2SnF_6$	Infrared	1076, 1072	522	1302, 1290	1185	This work
$(ClO_2)_2SnF_6$	Raman	1080	519	1309, 1293	1190	This work
SO_2	Infrared	1147	521	1330, 1308	1233	26

TABLE 5

Vibrational frequencies for NO_2^+ and NO^+

Compound	ν_1	ν_2	ν_3	Reference
NO_2AsF_6	1404	598	2385	3
NO_2SbF_6	1411	601	2368	3
$(NO_2)_2SnF_6$	1390	602	2392	This work
$NOAsF_6$	2341			3
$NOSbF_6$	2343			3
$(NO)_2SnF_6$	2325			This work

structure (27) with the anion having D_{3d} site symmetry. Whereas for Na_2SnF_6 an orthorhombic structure with D_{2h} symmetry site for the anion is found (27*a*). As a consequence (28) the infrared active vibrations $\nu_3[F_{1u}]$ and $\nu_4[F_{1u}]$ for K_2SnF_6 should both be split into the two components a_{2u} and e_u. A similar splitting is expected for $\nu_5[F_{2g}]$ resulting in the components a_{1g} and e_g.

As can be seen from the spectral data presented in Table 1, these expectations are only partially

Can. J. Chem. Downloaded from www.nrcresearchpress.com by 210.87.254.42 on 09/05/12
For personal use only.

TABLE 6

Mössbauer data for SnX_6^{2-} compounds

Compound	Temperature (°K)	Isomer-shift* δ (mm/s)	Quadrupole splitting Δ (mm/s)	Linewidth Γ(mm/s)		R
SnF_6^{2-} compounds						
Na_2SnF_6	80	−0.480	—	1.77		0.71
	298	−0.528	—	1.35		
K_2SnF_6	80	−0.432	—	1.59		0.61
	298	−0.468	—	1.11		
$(NO)_2SnF_6$	80	−0.421	—	1.45		
	298	−0.456	—	1.10		
$(NO_2)_2SnF_6$	80	−0.431	0.769	1.46	1.57	0.58
	298	−0.504	0.680	1.11	1.75	
$(ClO_2)_2SnF_6$	80	−0.403	1.008	1.46	1.46	0.71
	298	−0.433	0.956	1.16	1.11	
Chlorides						
K_2SnCl_6	80	0.476	—	1.35		0.377
	298	0.463	—	0.99		
Cs_2SnCl_6	80	0.421	—	1.41		0.252
	298	0.423		0.87		
$(NH_4)_2SnCl_6$	80	0.474	—	1.31		0.62
	298	0.431	—	1.00		
$(NO)_2SnCl_6$	80	0.522	—	1.36		0.20
	298	0.484		0.96		

*SnO_2 as reference.

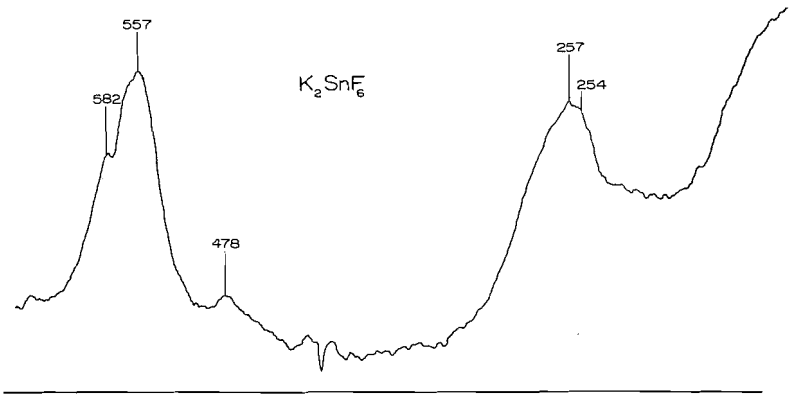

FIG. 1. Infrared spectrum of K_2SnF_6.

fulfilled and recognized best for K_2SnF_6, where a high resolution infrared spectrum was recorded. Both ν_3 and ν_4 have shoulders as shown in Fig. 1. The Raman active vibration ν_5 is found as a single line, in agreement with previous work (7).

When comparing the obtained spectra with previous reports, agreement seems to be best with the spectrum of Na_2SnF_6 reported by Begun and Rutenberg (8) except for the assignment of ν_4 at 300 cm^{-1} which is not confirmed, and their failure to report splittings for ν_3 and ν_4. In addition $\nu_2[E_g]$ is found to be weakly i.r. active, appearing as a shoulder in all SnF_6^{2-} spectra, best recognizable in the high resolution spectrum.

Of all heterocation complexes, $(NO)_2SnF_6$ shows the greatest similarity with the alkali metal

Can. J. Chem. Downloaded from www.nrcresearchpress.com by 210.87.254.42 on 09/05/12
For personal use only.

Can. J. Chem. Downloaded from www.nrcresearchpress.com by 210.87.254.42 on 09/05/12
For personal use only.

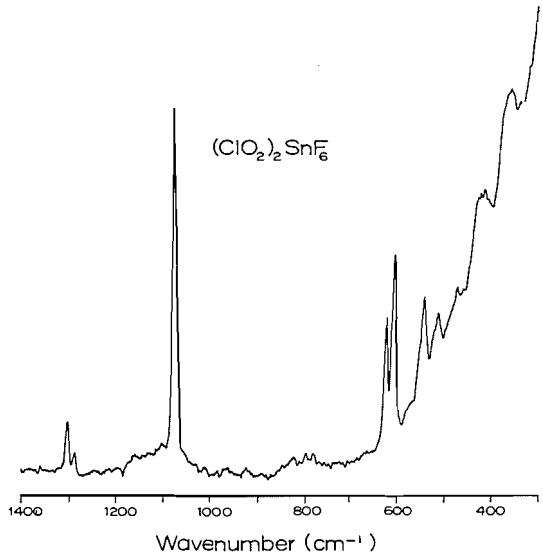

FIG. 2. Raman spectrum of $(ClO_2)_2SnF_6$.

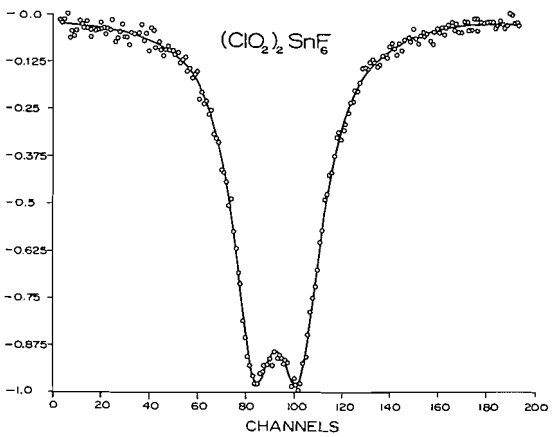

FIG. 3. Spectrum of $(ClO_2)_2SnF_6$ at 298 °K.

hexafluorostannates in the vibrational spectrum. The band positions, the observed splittings, and the relaxation of the mutual exclusion rule for ν_2 indicate D_{3d} site symmetry as well for this compound. The NO stretch is in agreement with a previous report (29).

In all cases a more or less intense shoulder in the Raman spectrum at $\sim$ 625 cm^{-1} can best be explained by solid state splitting of ν_1 as remarked by Dean and Evans. An interpretation of this band as ν_2 as proposed by Kriegsmann and Kessler (6) appears to be very unlikely (for a detailed discussion see ref. 7). All SnF_6^{2-} Raman spectra showed two very weak and diffuse background bands, produced in the Pyrex tubes at $\sim$ 420 and $\sim$ 367 cm^{-1}, and a moderately strong band at $\sim$ 165 cm^{-1}.

The spectrum $(NO_2)_2SnF_6$ could not be obtained over the whole range. Where the positions of the fundamentals could be established, good agreement with the nitrosyl hexafluorostannate spectrum is found. The cation frequencies are listed in Table 5 and compared to the ones for related molecules. No general trend appears to be recognizable; only the cation symmetric stretching frequency ν_1 appears to be slightly lower for $(NO_2)_2SnF_6$.

No simple explanation based on an ionic compound with an anion site of lower symmetry than O_h appears to be possible for $(ClO_2)_2SnF_6$. The high reactivity of these compounds has prevented high resolution infrared spectroscopy. All attempts to observe low frequency Raman bands failed. Our interpretation, therefore, has to be restricted to the range down to 300 cm^{-1} and the anion fundamentals ν_1, ν_2, and ν_3. The Raman spectrum of $(ClO_2)_2SnF_6$ for the range of 800–300 cm^{-1} is shown in Fig. 2.

The following features are noteworthy. ν_1 is split into two strong components and noticeably shifted to higher frequencies relative to the position of ν_1 in the Raman spectrum of K_2SnF_6. The strong band at 628 cm^{-1} had been found previously as a weak shoulder. The observed splitting is quite likely a solid state splitting as suggested before. A strong vibration at 549 and a weak shoulder at 563 are possibly due to the normally Raman inactive ν_3, indicating a breakdown of the mutual exclusion rule. ν_2 appears to be split into two components.

The infrared spectrum has a very broad, barely resolved band in the region from 630–520 cm^{-1}. The listed peaks appear partially as shoulders and indicate a complete removal of the degeneracy of ν_3 resulting in the components at 624, 561, and 541 cm^{-1}. However, assignment becomes very difficult for two reasons: (*a*) resolution is rather poor, and (*b*) it becomes difficult to distinguish between a true splitting or additional peaks caused by a breakdown of the exclusion rules. Such a breakdown occurs again for ν_1 at 606 and 634 cm^{-1} and ν_2 at 470 cm^{-1} where a medium strong band is observed. A weak band at 314 cm^{-1} remains unexplained and could possibly be an impurity band.

The strong departure from expected behavior for $(ClO_2)_2SnF_6$ is difficult to explain as a site

Can. J. Chem. Downloaded from www.nrcresearchpress.com by 210.87.254.42 on 09/05/12
For personal use only.

symmetry effect and suggests strong anion–cation interaction. This is quite in keeping with the spectra reported for ClO_2AsF_6 (1) and ClO_2SbF_6 (2), where the spectrum of the SbF_6^- group shows a remarkable similarity (1). Such interaction should logically affect the vibrational modes of the cation as well. Since ClO_2^+ is isoelectronic with SO_2, it is reasonable to expect C_{2v} symmetry, in agreement also with Walsh's diagram (30). This would make all three vibrations non-degenerate and infrared as well as Raman active. A possible interaction should therefore affect only the band positions. This is shown in Table 4 where the reported ClO_2^+ frequencies are compared. The average stretching frequencies are raised by 5–10 cm^{-1} when going from ClO_2AsF_6 over ClO_2SbF_6 to $(ClO_2)_2SnF_6$. In particular, the symmetric vibration ν_1 for the hexafluorostannate anion is shifted upwards by $\sim$ 30 wave numbers compared to ClO_2AsF_6 and ClO_2SbF_6.

Interaction between anion and cation will likely occur over fluorine bridges. A plausible model is provided by BrF_2SbF_6, where an X-ray diffraction study is reported (31). The noted increase in the average stretching frequencies of the ClO_2^+ cation and of some of the anion stretching frequencies can be explained by electron transfer involving the antibonding molecular orbitals b_1'' and possibly a_1' on ClO_2^+ and bridging fluorines, where electron withdrawal from the cation results in an increased electron density in the tin–fluorine bonding region.

Involvement of the supposedly empty b_1'' molecular orbital in bonding in ClO_2AsF_6 and $FClO_2$ had been invoked previously to explain the absence of color for ClO_2^+. In solution of HSO_3F, this species is red (32) and the lowest energy electronic transition would have to involve the b_1'' orbital as found also for ClO_2 (30). If this idea is correct and provided an electron transfer stabilizes certain SnF bonds over others, the effect on the Mössbauer spectrum should be noticeable.

The vibrational spectra obtained on $SnCl_6^{2-}$ compounds, as listed in Table 2, allow an assignment of ν_1, ν_2, ν_3, and ν_5. No abnormal features for $(NO)_2SnCl_6$ are observed, even though the NO stretching frequency is found to be fairly low. More detailed infrared work is needed in order to come to definite conclusions for this group of compounds.

(b) Mössbauer Spectra

The Mössbauer data for the SnF_6^{2-} anions are listed in Table 6. Agreement with previous reports is generally satisfactory for K_2SnF_6 (13) and the $SnCl_6^{2-}$ (33–35) compounds. Only the room temperature effect for potassium hexafluorostannate is found to be higher than previously reported (13) and an unusually low isomer shift for $(NO)_2SnCl_6$ as reported by Greenwood and Ruddick (4) is not confirmed. The found isomer shift appears to be higher than for the other $SnCl_6^{2-}$ compounds. Agreement with the previous studies (12*a*, *b*) on heterocation hexafluorostannates is satisfactory except for some minor discrepancies for the isomer shift values. We were also able to resolve a small quadrupole splitting for $(NO_2)_2SnF_6$.

All compounds studied (including the hexachlorostannates) gave well-resolved spectra at room temperature, a feature normally associated with intermolecular association (36–38) and polymeric structures.

As indicated by the vibrational spectra, the exceptional position of $(ClO_2)_2SnF_6$ is also found for the Mössbauer spectrum. The isomer shift is the highest reported in this series, indicating an increase in s-electron density around tin. A well resolved quadrupole splitting of about 1.00 mm/s (as shown in Fig. 3) is observed. The Δ value is comparable to the previously (12*a*) reported values for $(BrF_2)_2SnF_6$ and $(BrF_4)_2SnF_6$ of 0.80 and 1.15 mm/s, respectively. For both compounds an upward shift from K_2SnF_6 is reported for the isomer shift indicating a similar structural type. Unfortunately no vibrational spectra for the bromine fluoride derivatives are reported. The occurrence of quadrupole splitting in these compounds indicates considerable departure from octahedral symmetry for the SnF_6^{2-} which is best explained by anion–cation interaction.

All compounds do show unusually broad lines, possibly due to small, unresolved quadrupole splittings as can be produced by the low site symmetry. The observable quadrupole splitting for $(NO_2)_2SnF_6$ may indicate some weak anion–cation interaction for this compound, but unfortunately no complete vibrational spectrum could be obtained to confirm this conclusion.

In agreement with the results from the vibrational spectra, it seems impossible to interpret the dichloryl-hexafluorostannate as a simple ionic compound without making allowance for

substantial anion–cation interaction. The high first ionization potential of 11.1 eV for ClO_2 (39) already gave first indications that some covalent character for ClO_2^+ might be expected. Such interaction resulting in slight electron transfer is illustrated by the vibrational spectra of the anion and the cation as well as by the Mössbauer spectrum. It appears, however, not possible to discriminate between D_{4h} and C_{2v} site symmetry for the tin atom, as the two most obvious possibilities for a distorted octahedral anion, mainly because no satisfactory vibrational spectra in the region of ν_4 and ν_5 could be obtained. For the $SnCl_6^{2-}$, no quadrupole splitting could be resolved but the number of heterocation complexes known is very limited and does not allow a good comparative study. Similar conclusions as we have reached for $(ClO_2)_2SnF_6$ were made previously by Sukhovrekhov and Dzevitskii (12*b*) for $(ClF_2)_2SnF_6$, $(BrF_2)_2SnF_6$, $(BrF_4)_2SnF_6$, and $(IF_4)_2SnF_6$ on the basis of Mössbauer spectroscopy. It is of course dangerous to extrapolate to other fluoroanion complexes but our previous work (1, 2) had shown that anion–cation interaction in these complexes is the rule rather than the exception.

Financial support from the National Research Council of Canada is gratefully acknowledged. We are indebted to Mr. R. Green for his help in obtaining the high resolution i.r. spectra and Mrs. L. Sallos and Dr. J. Thompson for their technical assistance in obtaining the Mössbauer spectra. We also thank Mr. E. Matter for his help in building the metal vacuum system employed in this research.

1. H. A. CARTER, W. M. JOHNSON, and F. AUBKE. Can. J. Chem. **47**, 4619 (1969).
2. H. A. CARTER and F. AUBKE. Can. J. Chem. To be published.
3. A. M. QURESHI and F. AUBKE. Can. J. Chem. To be published.
4. N. N. GREENWOOD and J. N. R. RUDDICK. J. Chem. Soc. A, 1679 (1967).
5. R. D. PEACOCK and D. W. A. SHARP. J. Chem. Soc. 2762 (1959).
6. H. KRIEGSMANN and G. KESSLER. Nahmoissenschaften, **47**, 393 (1969).
7. P. A. W. DEAN and D. F. EVANS. J. Chem. Soc. A, 698 (1967).
8. G. M. BEGUN and A. RUTENBERG. Inorg. Chem. **6**, 2213 (1967).
9. R. V. PARISH and R. H. PLATT. J. Chem. Soc. A, 2145 (1969).
10. T. CHIVERS and J. R. SAMS. Chem. Commun. 249 (1969).
11. P. A. YEATS, J. R. SAMS, and F. AUBKE. Inorg. Chem. **9**, 740 (1970).
12. (*a*) V. F. SUKHOVREKHOV and B. E. DZEVITSKII. Dokl. Akad. Nauk. SSSR. **170** (5), 1089 (1966); Chem. Abstr. **67**, 59300j (1967); (*b*) V. F. SUKHOVREKHOV and B. E. DZEVITSKII. Dokl. Akad. Nauk. SSSR. **177**, 611 (1967).
13. V. I. GOL'DANSKII, E. F. MAKAROV, R. A. STUKAN, T. N. SUMAROKOVA, V. A. TRUKHTANOV, and V. V. KHRAPOV. Dokl. Akad. Nauk. SSSR, **156**, 400 (1964).
14. J. K. LEES and P. A. FLINN. J. Chem. Phys. **48**, 882 (1968).
15. A. A. WOOLF. J. Chem. Soc. 4113 (1954).
16. M. SCHMEISSER and W. FINK. Angew. Chem. **69**, 780 (1957).
17. S. J. KUHN. Can. J. Chem. **45**, 3207 (1967).
18. G. BRAUER. Handbook of preparative inorganic chemistry. 2nd ed. Academic Press Inc., New York. 1963. p. 511.
19. G. BRAUER. Handbook of preparative inorganic chemistry. 2nd ed. Academic Press Inc., New York. 1963. p. 513.
20. H. RHEINBOLDT and R. WASSERFUHR. Chem. Ber. **60**, 732 (1927).
21. J. C. BAILAR. Inorganic synthesis. IV. McGraw–Hill Book Co., Inc., New York.
22. L. A. WOODWARD and L. E. ANDERSON. J. Chem. Soc. 1284 (1957).
23. J. P. MATHIEU. Compt. Rend. **234**, 2272 (1952).
24. D. F. SMITH, G. M. BEGUN, and W. H. FLETCHER. Spectrochim. Acta, **20**, 1763 (1964).
25. K. O. CHRISTE, C. J. SCHACK, D. PILIPOVICH, and W. SAWODNY. Inorg. Chem. **8**, 2489 (1969).
26. R. N. WIENER and E. R. NIXON. J. Chem. Phys. **25**. 175 (1956).
27. (*a*) W. KLEMM, J. KRAUSE, K. WAHL, E. HUSS, R. HOPPE, E. WEISE, and W. BRANDT. Forschungsber. Wirtschafts u. Verkehrsministerium Nordrhein–Westfalen, **160**, 38 (1955); (*b*) D. H. BROWN, K. R. DIXON, R. D. W. KEMMILL, and D. W. A. SHARP. J. Chem. Soc. 1559 (1965).
28. R. S. HALFORD. J. Chem. Phys. **14**, 8 (1946).
29. D. W. A. SHARP and J. THORLEY. J. Chem. Soc. 3557 (1963).
30. A. D. WALSH. J. Chem. Soc. 2266 (1953).
31. A. J. EDWARDS and G. R. JONES. J. Chem. Soc. A, 1467 (1969).
32. H. A. CARTER, A. M. QURESHI, and F. AUBKE. Chem. Commun. 1461 (1968).
33. M. CORDEY-HAYES. J. Inorg. Nucl. Chem. **26**, 915 (1964).
34. J. PHILIP, M. A. MULLINS, and C. CURRAN. Inorg. Chem. **7**, 1895 (1968).
35. R. H. HERBER and H. S. CHENG. Inorg. Chem. **8**, 2145 (1969), and references therein.
36. R. H. HERBER and H. A. STÖCKLER. Application of the Mössbauer effect in chemistry and solid state physics. Tech. Rept. Ser. Intern. At. Energy Agency, **50**, 110 (1966).
37. H. A. STÖCKLER, H. SANO, and R. H. HERBER. J. Chem. Phys. **47**, 1567 (1967).
38. P. A. YEATS, B. F. E. FORD, J. R. SAMS, and F. AUBKE Chem. Commun. 791 (1969).
39. V. H. DIBELER, R. M. REESE, and D. E. MANN. J. Chem. Phys. **27**, 176 (1957).

Can. J. Chem. Downloaded from www.nrcresearchpress.com by 210.87.254.42 on 09/05/12
For personal use only.

Can. J. Chem. Downloaded from www.nrcresearchpress.com by 210.87.254.40 on 09/05/12
For personal use only.

Computer study of Br_2 shock wave dissociation[1]

J. K. K. Ip and George Burns
Lash Miller Chemical Laboratories, University of Toronto, Toronto 181, Ontario

Received March 12, 1970

Computational studies of Br_2 shock wave dissociation in argon were conducted, and the possibility of vibrational relaxation–dissociation coupling, stronger than previously suspected (2), was investigated. In order for such a coupling to occur, the vibrational temperature in the lower vibrational levels of Br_2 must be lower than that in the higher vibrational levels. The approximate shapes of vibrational distribution functions were obtained, and corresponding shock wave profiles were computed. The calculations predict an appreciable difference between the translational and vibrational temperatures of the dissociating Br_2. In order to check this conclusion, the Br_2 absorption coefficients at 440 mμ, measured at equilibrium by heating Br_2 in a furnace from 300 to 1250 °K, were compared to the absorption coefficients measured in shock waves.

Canadian Journal of Chemistry, 48, 2860 (1970)

Introduction

Recently (1) it was found that the Br_2 dissociation rate constants, k_d's, obtained by three different methods (flash photolysis, shock waves-absorption spectroscopy, and shock waves-emission spectroscopy) differ from each other; in particular, at 1300 °K, $k_{d,shock,abs} \approx 3k_{d,flash} \approx 3k_{d,shock,em}$. The discrepancy appears to be outside experimental error (1, 2) and has been explained (1, 2) in terms of a model in which the Br_2 shock dissociation is coupled to its vibrational relaxation (d–v coupling). Using this model it was possible to compute reaction profiles for Br_2 dissociation in shock waves, and to compare these profiles to the experimental (1, 2). In agreement with all previous work, the d–v coupling was found to be weak; the vibrational relaxation is almost, but not quite, complete at the onset of dissociation. Because of the weak coupling, the computed reaction profiles yielded sharp peaks ("spikes") when the Br_2 optical absorption was calculated as a function of reaction time. The peaks associated with the vibrational relaxation were approximately 0.5 μs long and appeared immediately behind the shock front. An inclusion of corrections for finite resolution time (2) lowered and broadened these peaks, which, nonetheless, remained well separated from the rest of the reaction profile.

In order to explain the differences between rate constants at 1300 °K it had been necessary to assume (2) that the judgement of experimenters who measured $k_{d,shock,abs}$ was influenced by the existence of the "spikes". Below, we investigate conditions which would broaden the "spikes": a broader peak would blend better with the rest of the reaction profile and would yield the $k_{d,shock,abs} > k_{d,shock,em}$ in agreement with the experiment.

For this purpose, the possibility of stronger d–v coupling is considered. The alternative coupling (dissociation to electronic relaxation in Br_2) has been briefly considered previously (1), and is not studied further here.

Shock Wave Profile Calculations

The starting point in the present calculations is the model used previously (1, 2). However, the form of the previous model does not provide a feasible way by which the d–v coupling could be further increased. The model contains two parameters: τ_v, the vibrational relaxation time, and D, the average energy of the dissociating molecules. These parameters cannot be adjusted in such a way as to significantly increase the d–v coupling because τ_v was already chosen at its reasonable maximum (1), and D was already taken (1) to be equal to the dissociation energy. However, stronger d–v coupling should occur if there is an appropriate structure in the vibrational distribution function, previously (1, 2) completely defined by one time-dependent vibrational temperature, T_v.

Underlying Assumptions

We approached this problem in the simplest possible manner by suggesting that the vibrational distribution function of dissociating Br_2 might be better described by two vibrational temperatures. Thus, molecules in the lower vibrational energy

[1]This work was supported, in part, by the Directorate of Chemical Sciences, Air Force Office of Scientific Research, Grants No. 506-64, 66, and 69.

Can. J. Chem. Downloaded from www.nrcresearchpress.com by 210.87.254.40 on 09/05/12
For personal use only.

states (from 0th to nth level) are in the region A and have time-dependent vibrational temperature T_v^A. On the other hand, molecules in the higher vibrational energy states (from $(n + 1)$th to the dissociation limit) are in the region B, defined by the time-dependent vibrational temperature T_v^B. Even such a relatively small modification of the model (1, 2) introduces new parameters, which must be determined or approximated in order to generate on a computer the shock wave reaction profiles. In order to do this, we first retain the assumption, used previously (1, 2), that diatomic molecules dissociate from the uppermost vibrational level. The vibrational relaxation time, used previously (1), is assumed here to be a good approximation for the A region only. In order to define the profile, however, it is also necessary to know (*1*) the rate coefficient for A → B process, k_{AB}, (*2*) the rate coefficient for the reverse B → A process, k_{BA}, (*3*) the vibrational relaxation time in B region, τ_v^B, and (*4*) the value of n, the highest vibrational level in the region A. An estimate of k_{AB} is perhaps the most difficult one. It might be argued that, at least for the lowest vibrational levels, the most probable transitions involve $\Delta v = \pm 1$, where v is the vibrational quantum number. On this somewhat weak ground, we assumed that the accumulation of vibrational energy in the A region proceeds by a random walk process with $\Delta v = \pm 1$ transitions only. Under this approximation, the k_{AB} may be expressed in a closed form as a reciprocal of the mean first passage time for a random walker with 0th vibrational level as the reflecting barrier and the $(n + 1)$th vibrational level as the absorbing barrier (3) for region A. The latter assumption implies that the rate from B to A region is zero, which might be a satisfactory approximation only at the beginning of the shock wave reaction before a significant concentration of atoms is produced. Use of such a random walker approximation permits calculation of an appropriate vibrational distribution function for the A region (3); however, for the sake of simplicity, the assumption that the vibrational distribution function for A region is defined by T_v^A is retained in the present calculations.

In order to explain the experimentally observed (1, 2) difference between the $k_{d,shock,abs}$ and the $k_{d,shock,em}$ at 1300 °K, it was necessary to assume (1, 2) that the perturbation due to reaction extends to the lowest vibrational levels of Br_2. In order to increase further the coupling between the dissociation and relaxation of Br_2 in its lowest vibrational levels, it is necessary to assume that the upper vibrational levels are in the state close to the local equilibrium, while the disequilibrium occurs primarily in the lowest vibrational levels. This condition is described by the inequality $T_v^A < T_v^B$.

Another variable of importance for the present calculations is the average vibrational relaxation time in the region B, τ_v^B, a quantity which is difficult to determine. Fortunately, we found that the computed reaction profiles do not agree with the experimental shock wave data unless $\tau_v^B \ll \tau_v^A$. For this reason, it was decided to assume that after an unobservably short transient period of time, T_v^B becomes equal to the translational temperature T. Use of this extreme assumption is justified only because we are interested in finding the conditions for maximum plausible d–v coupling. We also disregard the possibility of molecules in A region dissociating directly (in a single collision) without passing through region B. In other details, these calculations are similar to those described elsewhere (2), so that the assumptions used previously (1, 2) were retained whenever possible. As a result, it became possible to determine plausible values of n and $\Delta T_v^A = T - T_v^A$ at various T and to generate shock wave profiles. Here T is the translational temperature of the gas.

"Steady State" Calculations

Just as previously (2), two types of calculations were made. In the first group of calculations, an infinitely dilute solution of Br_2 in argon was assumed, and the values of T_v^A and $G = k_{r,noneq}/k_{r,eq}$ in a "steady state" condition, defined elsewhere (2), were determined for reasonable values of n. The results are shown in Table 1. Here, G_{exp} is the ratio of the recombination rate constant obtained in the "emission" shock wave experiments (4), $k_{r,shock,cm}$, to the extrapolated value of the recombination rate constant obtained in the high temperature flash photolysis experiments (2). It is interesting to note that if the calculations are made according to the model used previously (1), the agreement between the experimental and calculated results is very good. Thus, the agreement between G_{exp} and G (1) (Table 1) is satisfactory throughout the whole temperature range, 1300–2300 °K.

Can. J. Chem. Downloaded from www.nrcresearchpress.com by 210.87.254.40 on 09/05/12
For personal use only.

TABLE 1

Steady state values of ΔT_v^A and G as a function of vibrational level n and temperature

T (°K)	G_{exp}	Reference 1		$n = 14$		$n = 15$		$n = 16$		$n = 17$		$n = 18$		$n = 19$		$n = 20$	
		ΔT_v	G	ΔT_v^A	G	ΔT_v^A	G	ΔT_v^A	G	ΔT_v^A	G	ΔT_v^A	G	ΔT_v^A	G	ΔT_v^A	G
1300	0.96	3	0.96	100	0.72	80	0.76	60	0.80	49	0.83	37	0.86	29	0.88	20	0.91
1500	0.89	14	0.86	194	0.61	157	0.66	127	0.70	104	0.74	84	0.77	67	0.81	54	0.83
1700	0.85	45	0.70	317	0.52	264	0.57	220	0.61	184	0.65	150	0.70	127	0.73	104	0.76
1900	0.69	96	0.55	474	0.44	404	0.48	344	0.53	290	0.57	249	0.61	210	0.65	179	0.68
2100	0.44	167	0.43	660	0.36	574	0.41	494	0.46	429	0.50	370	0.54	319	0.58	274	0.61
2300	0.34	250	0.33	877	0.29	770	0.34	674	0.39	590	0.43	517	0.47	450	0.51	394	0.55

Can. J. Chem. Downloaded from www.nrcresearchpress.com by 210.87.254.40 on 09/05/12
For personal use only.

Table 1 is internally self-consistent. Thus, for a given n, ΔT_v^A increases smoothly with T. This is because the model used prescribes larger deviation from the equilibrium if the translational temperature is increased. Moreover ΔT_v^A decreases smoothly with increasing n. This is also to be expected because larger n implies smaller deviation from the equilibrium in the region A. For a given value of n, the G values decrease monotonically with the increasing temperature, reflecting, again, the fact that the system is farthest from the equilibrium at highest temperatures. We have not attempted to make calculations below $n = 14$, because at 1300 °K the value of G is already as small as 0.72. The experimental results (2) suggest that it is not likely to be smaller than this number. Since the calculations involved random walker (3) approximation, the value of k_{AB} increases very rapidly with n; for this reason, at the lower temperatures, calculations for n much larger than ~ 20 should not be made because the value of G cannot exceed unity. At higher temperatures, calculations for $n > 20$ can be made, but in this case the value of G will be much larger than G_{exp}; in fact at $T = 2300$ °K, $G_{exp} = G\ (n = 14)$. For this reason calculations for $n > 20$ were also not attempted.

Generation of Profiles

In the second group of calculations, the initial stages of three shock wave profiles (optical absorption vs. time) were computed at 1310, 1380, and 1520 °K. In these calculations, as previously (2), the experimental raw data reported by Palmer and Hornig (5) were used. A representative profile is shown in Fig. 1. The choice of assumptions described above was made in such a way as to insure that the profiles are "physically significant", i.e. all of the physically meaningful parameters exhibited physically reasonable behavior. In particular, the rate of vibrational energy accumulation in the A region, $\dot{\varepsilon}_A$, is initially positive, becomes zero at the "steady state", and is negative thereafter. On the other hand, $\Delta \dot{T}_v^A$ is negative throughout the entire reaction time. In computations of these profiles, $n = 17$ was arbitrarily used; it was found that the profiles are not very sensitive to the value of n. Furthermore, it was assumed that the rise time of the electronics is infinitely fast; the removal of this assumption would produce somewhat smoother profiles, but otherwise would not greatly affect their shape.

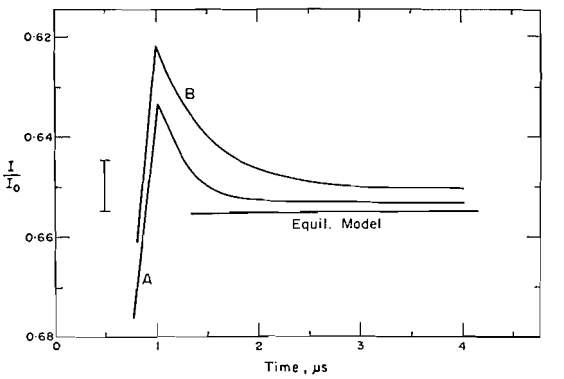

FIG. 1. Simulated optical absorption against time profiles for shock dissociation experiments. Br_2 in Ar. The shock temperature in this experiment was calculated by Palmer and Hornig (5) to be 1310 °K. Curve *A*, calculated using assumptions of the previous model (1, 2). Curve *B*, present work. Equilibrium model profile was generated using Palmer and Hornig's assumption that $T_v = T$ at all times. Error bar in noise level based on signal-to-noise ratio of 100.

Discussion

There are several interesting conclusions that follow from these calculations (Table 1, Fig. 1). In the first place, the introduction of the assumption that $T_v^A < T_v^B$ does not alter coupling drastically: the "spikes" (1, 2) now decay somewhat more slowly and are broader, but still remain well separated from the rest of the reaction profile. Therefore, an investigation of shock wave dissociation under conditions which make observation of the peaks feasible, is an attractive route for testing the reality of the present d–v coupling model as applied to Br_2–Ar system. Although classical optical absorption techniques (5–8) appear to be unsuitable for such experiments because of inadequate signal-to-noise ratio (2) (Fig. 1), newer methods (9), presently attempted in our laboratory, shall settle this question.

Furthermore the "break" in the vibrational distribution function, as defined by the value of n, occurs relatively low on the vibrational ladder of Br_2: $n = 14$ corresponds to the excitation of about 13 kcal/mole and $n = 20$ to about 19 kcal/mole while the dissociation energy of Br_2 is 45 kcal/mole.

Another conclusion to be drawn from these calculations is that, if the d–v coupling is as strong as the present work suggests, then the value of ΔT_v^A might indeed be observed; in the previous calculations (1, 2), at 1300 °K, ΔT was only 3 °K. In fact, large ΔT and ΔT_v^A produce some additional absorption, and it is for this

Can. J. Chem. Downloaded from www.nrcresearchpress.com by 210.87.254.40 on 09/05/12
For personal use only.

reason that curves *B* were found to be above curves *A* as shown in the representative Fig. 1. In principle, a large ΔT_v^A value might be detected by comparison of the equilibrium absorption coefficients, obtained by measuring the absorption of Br_2 heated in a furnace (2, 10, 11), with the absorption coefficients obtained in a "steady state" in shock wave (5, 6, 8). Such a comparison is made in Fig. 2. Both equilibrium and shock wave absorption coefficients are in fair agreement with the theoretical predictions of Sulzer and Wieland (12). A better agreement with theory could hardly be expected in view of the number of approximations employed in their theoretical analysis. At 440 mμ the absorption coefficients obtained in shock waves appear uniformly higher than those obtained at equilibrium (Fig. 2), so that at 1300 °K, the difference between the vibrational and translational temperature (ΔT_v^A) is of the order of 200 °K with the possible uncertainty of the order of 200 °K. Thus, and only to that extent, the experimental data favor the idea of stronger d–v coupling as suggested in this work.

Another interesting conclusion arises from a comparison of the G_{exp} with the calculated G values (Table 1). For best agreement with the experiment, the value of n increases from 15 at 2300 °K to > 20 at 1300 °K. This implies that, within a "steady state" approximation, T_v^A is approximately independent of the translational temperature T and is equal to about 1500 °K if $T > 1500$ °K. It must be pointed out that this conclusion is not supported by the experiment: it can be seen (Fig. 2) that in all shock wave experiments the absorption coefficient is decreasing with temperature. This implies, in the language of the present model, that T_v^A decreases with T. The discrepancy illustrates the approximate nature of our model, which, just as its earlier version (1), is most accurate at lowest temperatures.

It might be of interest to point out some unusual aspects of the present calculations. In the transition state theory, as well as in unimolecular reaction rate theory (high pressure limit), the vibrational distribution function is defined by the assumption $T_v = T$. At the low pressure limit, unimolecular reaction rate theory assumes that $T = T_v^A > T_v^B$ in the present terminology, provided the temperature of the activated molecules is definable. On the other hand, the present calculations suggest that $T_v^B > T_v^A$, i.e. the plot of the ln N_v vs. energy, where N_v is the population

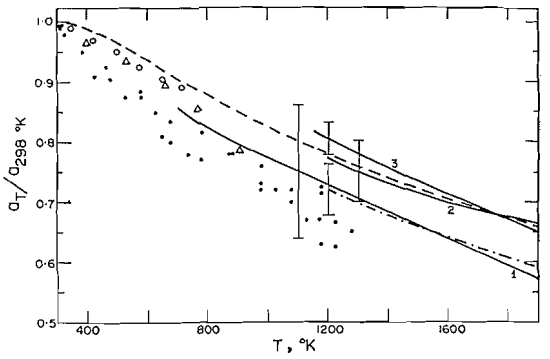

FIG. 2. Reduced optical absorption coefficients of Br_2 at 443 mμ against absolute temperature. ●, Ip and Burns (2); ○, Passchier, Christian, and Gregory (10); △, Acton, Aickin, and Bayliss (11); solid curve *1*, Britton and Davidson (6) at 436 mμ; curve *2*, Palmer and Hornig (5) at 439 mμ; curve *3*, Warshay (8) at 440 mμ; ---, theory of Sutzer and Wieland (12); flags are the standard deviations.

in the vth level, has a positive second derivative. Such a distribution might arise if there is a low lying electronic level in Br_2, but it might also arise by accumulation of vibrational energy within a single electronic state; the latter possibility is not very likely, however.

The results of these and previous (1, 2) calculations show that various d–v coupling schemes do not affect greatly the shape of the shock wave reaction profile. This conclusion is not unexpected: it is generally accepted that the absolute value of the first nonzero eigenvalue for the reaction transport matrix, λ_1, is equal to the dissociation rate constant, while the second eigenvalue is of the order of τ_v^{-1}. If $\lambda_1 \ll \lambda_2$, as in the case of Br_2 at 1300 °K, the coupling is weak. Therefore, disregarding of d–v coupling should not introduce a major error in τ_v, if the latter is extracted from the experimental data using the Bethe–Teller law. If τ_v is measured at such high temperatures that dissociation is not negligible, and if the $d^2 \ln N_v/dE^2$ is positive, then the present work suggests that the value of τ_v^A, calculated using the Bethe–Teller law, would be larger than the true vibrational relaxation time.

The present work deals with the problem of Br_2 dissociation in Ar. However, it is felt that the conclusions are important for other systems, in which d–v coupling may be important.

Conclusions

The difference among $k_{r,fl}$, $k_{sh,abs}$, and $k_{sh,em}$ at 1300 °K is so well substantiated in the works of different investigators (2) that further effort to

resolve the discrepancy experimentally seemed at this time unwarranted. For this reason, a computational "experiment" was presently designed to provide further insight into the problem. To date the only plausible explanation of the discrepancy involves the assumption of d–v coupling. In the present work, we established what may be a reasonable upper limit for such a coupling. The calculations confirm that if the d–v coupling contributes to the discrepancy, the shock wave optical absorption reaction profiles should be preceded by well separated absorption "spikes" which should be observable under proper experimental conditions. Thus, the present work firmly binds the d–v coupling explanation to the existence of "spikes". The model considered here, being a reasonable upper limit, provides a d–v coupling which is considerably stronger than usually expected. However, it does not seem possible to disprove the model on experimental grounds; if anything, the experiments provide some qualified support for the model.

This work was supported in part by the Air Force Office of Scientific Research, National Research Council of Canada, and the Defence Research Board of Canada, Grant No. 9530-54. Acknowledgement is also made to the donors of the Petroleum Research Fund, administered by the American Chemical Society, for partial support of this research. One of us (J. K. K. Ip) was a holder of the Bursary Award from the National Research Council of Canada and a Province of Ontario Graduate Fellowship.

1. J. K. K. Ip and George Burns. Discuss. Faraday Soc. **44**, 241 (1967).
2. J. K. K. Ip and George Burns. J. Chem. Phys. **51**, 3425 (1969).
3. S. K. Kim. J. Chem. Phys. **28**, 1058 (1958).
4. R. K. Boyd, George Burns, T. R. Lawrence, and J. H. Lippiatt. J. Chem. Phys. **49**, 3822 (1968).
5. H. B. Palmer and D. F. Hornig. J. Chem. Phys. **26**, 98 (1957).
6. D. Britton and N. Davidson. J. Chem. Phys. **25**, 810 (1956).
7. D. Britton. J. Phys. Chem. **64**, 742 (1960).
8. M. Warshay. 5th Int. Shock Tube Symp. White Oak, Maryland. 1965. U.S. Naval Ordnance Lab., A.D. 484600. 1966.
9. J. H. Kiefer and R. W. Lutz. J. Chem. Phys. **44**, 658 (1966).
10. A. A. Passchier, J. D. Christian, and N. W. Gregory. J. Phys. Chem. **71**, 937 (1967).
11. A. P. Acton, R. G. Aickin, and N. S. Bayliss. J. Chem. Phys. **4**, 474 (1936).
12. P. Sulzer and K. Wieland. Helv. Phys. Acta, **25**, 653 (1952).

Can. J. Chem. Downloaded from www.nrcresearchpress.com by 210.87.254.40 on 09/05/12
For personal use only.

Can. J. Chem. Downloaded from www.nrcresearchpress.com by 210.87.254.6 on 09/05/12
For personal use only.

Determination of the molecular conformation of uridine in aqueous solution by proton magnetic resonance spectroscopy. Comparison with β-pseudouridine[1]

BARRY J. BLACKBURN,[2] ARTHUR A. GREY,[2,3] AND IAN C. P. SMITH
Biochemistry Laboratory, National Research Council of Canada, Ottawa 7, Ontario

AND

FRANK E. HRUSKA
Department of Chemistry, University of Winnipeg, Winnipeg 2, Manitoba

Received April 29, 1970

A complete analysis of the 220 MHz proton magnetic resonance spectrum of aqueous uridine is reported. From the data a model for the molecular conformation is presented and compared with that of β-pseudouridine. It is concluded that in both compounds the ribose rings are in rapid equilibrium between classical puckered structures. The temperature-independence of the ribose proton coupling constants and chemical shifts suggests that all the conformers involved in this equilibrium have very similar energies. Both compounds exhibit a preference for the *gauche–gauche* rotamer about the exocyclic 4′—5′ bond; this conclusion is shown to be independent of the parameters in the Karplus equation or the energy minima chosen for the rotamers. The *anti* conformation of the uracil base is shown to exist in both compounds. It is proposed that the special structural significance of β-pseudouridine in transfer RNA must be due to the potential hydrogen bond that may be formed by the nitrogen atom at position one in uracil.

Canadian Journal of Chemistry, 48, 2866 (1970)

Introduction

We have recently reported an analysis of the 100 MHz proton magnetic resonance (p.m.r.) spectrum of β-pseudouridine (5-β-D-ribofuranosyluracil) in aqueous solution, and the resultant model for its molecular conformation (1, 2). Our ultimate objective was to compare the conformation of uridine and β-pseudouridine (Fig. 1) under identical conditions and thus gain insight into the role of the latter in the structure of transfer RNA. At the time a thorough analysis of the p.m.r. data for uridine was lacking and the partial results of Fujiwara and Uetsuki (3) were used. We report here a complete analysis of the 220 MHz p.m.r. spectrum of aqueous uridine (U), a model for its conformation, and a comparison with the previous model proposed for β-pseudouridine (β–ψ).

Experimental

The p.m.r. spectra were obtained on a Varian HA100 spectrometer and a Varian 220 MHz instrument (Canadian 220 MHz Center, Ontario Research Foundation, Sheridan Park, Ontario). Assignment of the spectral regions to the protons was carried out by double-irradiation experiments on the 100 MHz instrument. Because of the complexity of the 100 MHz spectra, analysis for chemical shifts and coupling constants was carried out on the 220 MHz spectra. A modified version of the computer program LAOCOON II (4) was used as an aid in this respect. Samples were prepared by adjusting acidity in D_2O and freeze-drying three times from 99.8% D_2O (Merck, Sharpe and Dohme, Canada, Ltd.). Chemical shifts were measured versus internal DSS (2-trimethylsilyl-propanesulfonic acid, sodium salt), a product of E. Merck, Darmstadt, Germany.

Results and Discussion

The 220 MHz p.m.r. spectrum of aqueous uridine is shown in Fig. 2. Above the second order part of the spectrum (2′ to 5′ region) is shown the simulated spectrum generated by LAOCOON II for the chemical shifts and coupling constants of Table 1. Also included in Table 1 are the corresponding data for β–ψ taken from (1), and the incomplete data of Fujiwara and Uetsuki (3). Differences between the results of our analysis and those of (3) are attributable in part to our inclusion of the 5′ hydrogens (which are significantly coupled to the 4′ hydrogen) in the full analysis. Our values are therefore more reliable. The spectra of U at 28 and 78 °C are essentially superimposable, and therefore no detailed analysis of the 78 °C spectrum was performed. The maximum variation in the nuclear magnetic resonance (n.m.r.) parameters over this temperature range is 0.03 p.p.m. for the chemical shifts, and 0.5 Hz for the coupling constants.

A close similarity exists between the data for uridine and β-pseudouridine. The difference in

[1]Issued as NRCC No. 11439.
[2]NRCC Postdoctorate Fellow.
[3]Permanent address: Ontario Research Foundation, Sheridan Park, Ontario.

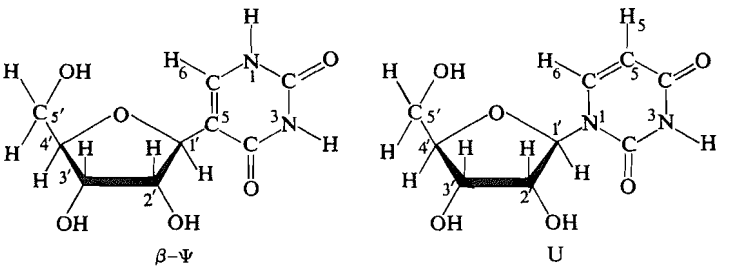

FIG. 1. Structural formulae for uridine (U) and β-pseudouridine (β–ψ).

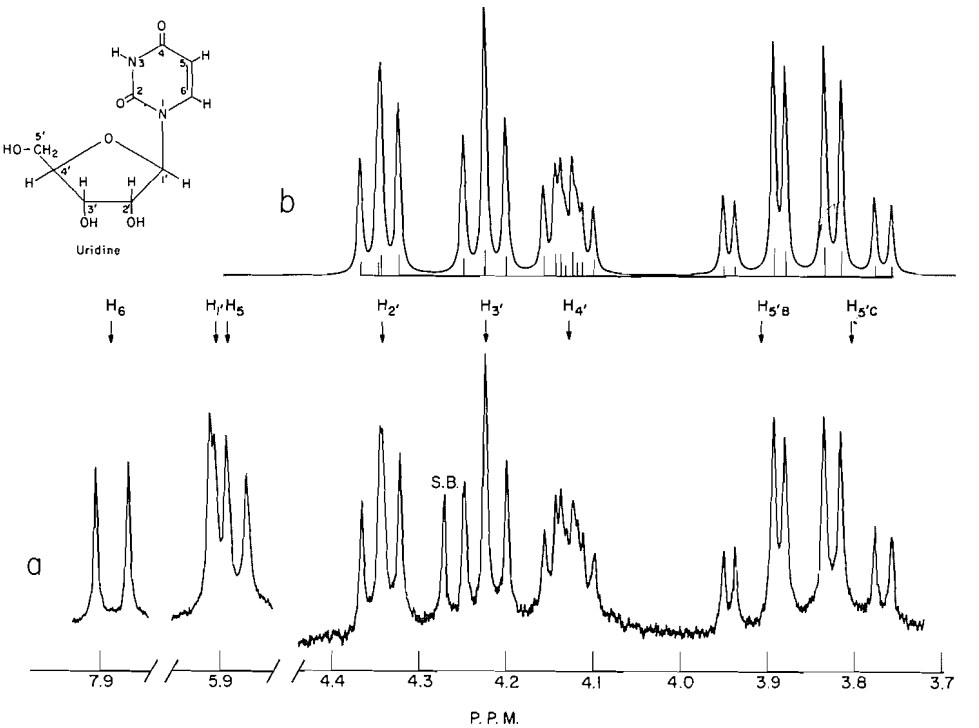

FIG. 2. (*a*) The p.m.r. spectrum at 220 MHz of uridine in D_2O (pD = 6.6, 0.1 M, 28 °C). Chemical shifts are relative to internal 3-(trimethylsilyl)propanesulfonic acid. (*b*) Computer-simulated 220 MHz spectrum of the region due to ribose protons 2′ to 5′.

Note that the structural formula of uridine given in this figure is in the *syn* conformation (as is commonly given in textbooks) whereas the structural formulae in Fig. 1 are in the *anti* conformation. The peak marked S.B. is a spinning side band of water.

chemical shifts 6 and 1′ may be rationalized in terms of the different points of attachment of the respective ribose and uracil moieties (2). Corresponding chemical shifts of the 2′ to 5′ hydrogens differ by not more than 0.10 p.p.m., and the furanose ring coupling constants by not more than 0.6 Hz.

The Ribose Ring Conformation

From the coupling constants between the hydrogens of the ribose ring it is possible to gain insight into the conformation of the ring via the Karplus relationship (1, 2). We have shown that the data for β-pseudouridine preclude the existence of the ring in any of the classical puckered forms (2′-*endo*, 2′-*exo*, 3′-*endo*, 3′-*exo*); only a rapid equilibrium between these forms is consistent with the data (1, 2). Similar conclusions must be reached for the ribose ring of uridine; its conformation is a rapid time average of the classical static forms. This is in accord with the conclusions of Prestegard and Chan, based upon measurement of the coupling constant between hydrogens at positions 1′ and 2′ only (5). Further-

Can. J. Chem. Downloaded from www.nrcresearchpress.com by 210.87.254.6 on 09/05/12
For personal use only.

TABLE 1

Chemical shifts and coupling constants of uridine and β-pseudouridine

	Chemical shifts (p.p.m.)			Coupling constants (Hz)			
	β–ψ*	U†	U‡		β–ψ*	U†	U‡
H_6	7.660		7.862	J_{56}			8.0
H_5			5.887	$J_{61'}$	0.8		
$H_{1'}$	4.674	5.820	5.901	$J_{1'2'}$	5.0	4.4	4.4
$H_{2'}$	4.279	4.260	4.341	$J_{2'3'}$	5.0	4.6	5.3
$H_{3'}$	4.141	4.150	4.222	$J_{3'4'}$	5.2	4.9	5.5
$H_{4'}$	4.009	4.060	4.128	$J_{4'5'B}$	3.2		3.0
$H_{5'B}$	3.840	3.825	3.907	$J_{4'5'C}$	4.6		4.4
$H_{5'C}$	3.726	3.735	3.803	$J_{5'B5'C}$	−12.7		−12.7

*References 1 and 2, 30 °C.
†Reference 3, 28 °C.
‡The chemical shifts and coupling constants are estimated to be accurate to within 0.01 and 0.2 Hz, respectively. The high error limit on the coupling constants is due to the somewhat larger line width obtained with the 220 MHz instrument. The sample temperature was 28 °C.

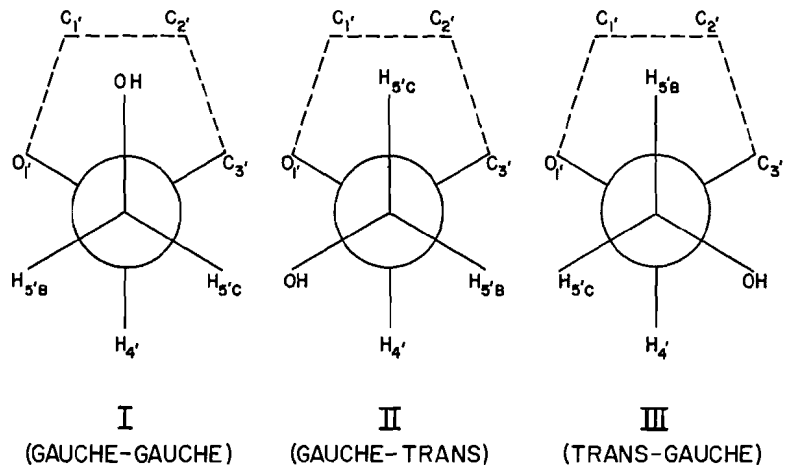

FIG. 3. Schematic representation of the three possible rotational isomers around the $C_{4'}$—$C_{5'}$ bond of uridine.

more, the similarity in coupling constants of β–ψ and U suggests that the relative populations of the various puckered forms in equilibrium are not very different in the two compounds. The temperature-independence of the coupling constants suggests that the energies of the various forms in equilibrium are essentially equal (2, 18).

Conformation about the Exocyclic $C_{4'}$—$C_{5'}$ Bond

From the coupling between the hydrogen at position 4′ and those at 5′, it is possible to estimate the relative populations of rotational isomers corresponding to the energy minima which occur upon rotation about the 4′–5′ bond. Implicit is the assumption that the lifetime of a molecule in any of the three energy minima is long compared to the time spent rotating between energy minima. For a rapid interconversion the 4′—5′ coupling constants will be a weighted average (weighted according to the relative populations) of the coupling constants in the three rotamers.

Algebraically this can be expressed as eqs. [1] and [2], where P_I, P_{II}, and P_{III} are the mole

$$[1] \quad J_{4'5'_B} = P_I J_{IB} + P_{II} J_{IIB} + P_{III} J_{IIIB}$$

$$[2] \quad J_{4'5'_C} = P_I J_{IC} + P_{II} J_{IIC} + P_{III} J_{IIIC}$$

fractions of each rotamer. Figure 3 is a schematic representation of the three rotamers. The coupling constant between the protons 4′ and $5'_B$ is J_{IB} if the molecule existed completely as rotamer I. Coupling constants J_{IIB}, J_{IIIB}, etc. are defined similarly. Values $J_{4'5'_B}$ and $J_{4'5'_C}$ are obtained from the n.m.r. spectrum. Thus we can determine the relative rotamer populations if we can

Can. J. Chem. Downloaded from www.nrcresearchpress.com by 210.87.254.6 on 09/05/12
For personal use only.

TABLE 2

Limits for the relative populations of rotational isomers around the $C_{4'}$—$C_{5'}$ bond of uridine

	Classical staggered rotamers				Rotamers with 15° 0–0 repulsion			
J_0 for $0 \leq \phi \leq 90°$	9.27	9.27	9.27	9.27	9.27	9.27	9.27	9.27
J_0 for $90 \leq \phi \leq 180°$	10.36	10.36	12.00	12.00	10.36	10.36	12.00	12.00
$J_{4'5'_B}$	3.0	4.4	3.0	4.4	3.0	4.4	3.0	4.4
$J_{4'5'_C}$	4.4	3.0	4.4	3.0	4.4	3.0	4.4	3.0
P_I	0.58	0.58	0.65	0.65	0.46	0.46	0.58	0.58
P_{II}	0.30	0.12	0.25	0.10	0.24	0.08	0.16	0.02
P_{III}	0.12	0.30	0.10	0.25	0.29	0.45	0.25	0.39

estimate the angles of rotation corresponding to the three energy minima, and if the coupling constants of the rotamers representing these energy minima can be accounted for by the Karplus relation (6).

Lemieux, basing his argument on optical rotation data for hexoses, has suggested that the classical 60° staggered conformers are not likely to be energy minima and that conformers in which oxygen–oxygen repulsions have been taken into consideration would be more reasonable (7). One cannot know precisely the angles of rotation corresponding to energy minima, but it is possible to choose limits between which energy minima will occur. As one limit we have taken the classical rotamer in each case; as the other limit we have taken angles enlarged by 15° from the classical values due to oxygen–oxygen repulsion for all rotamers, which represents an extreme value observed in X-ray studies of crystalline nucleosides (8–10).

The Karplus equation (6) is given by eq. [3]

$$[3] \qquad J_{HH'} = J_0 \cos^2 \phi - 0.28 \text{ Hz}$$

where $J_{HH'}$ is the vicinal coupling constant, ϕ is the dihedral angle between the H—C—C′ and C—C′—H′ planes in the fragment H—C—C′—H′. The general form of this expression is thought to be correct, but values of the constant J_0 from 8 to 16 Hz have been applied (11). Consequently we decided to take both an upper and a lower limit for the values of J_0. For the lower limit we have selected the values suggested by Abraham *et al.* (12) for a number of carbohydrate ring systems: $J_0 = 9.27$ Hz for $0° \leqslant \phi \leqslant 90°$ and $J_0 = 10.36$ Hz for $90° \leqslant \phi \leqslant 180°$. Lemieux has suggested that for this type of system the coupling constants under discussion should be substantially greater for $\phi = 180°$ than is normally encountered in a ring system where both carbons are secondary, perhaps as high as 12 Hz (7). Accordingly we have selected for the upper limit, $J_0 = 9.27$ Hz for $0° \leqslant \phi \leqslant 90°$ and $J_0 = 12.0$ Hz for $90° \leqslant \phi \leqslant 180°$.

The only problem remaining is assignment of the two experimental 4′—5′ coupling constants. Some workers have attempted this assignment (13, 14) but it suited our purposes to do the calculations for both possible assignments. Taking into account limits between which the energy minima will occur, upper and lower limits for J_0 values, and two possible ways of assigning the coupling constants we obtain eight sets of values for the relative populations (Table 2). All the calculations indicate that the *gauche–gauche* rotamer (I), in which the 5′-hydroxyl group comes very near the 6 position of the uracil base, is preferred. This interaction could be responsible for the very different response to increasing temperature of the resonances due to the hydrogens at positions 5 and 6 in the uracil base of uridine (15, 17). The *gauche–gauche* rotamer is apparently also preferred in aqueous solution for β-pseudouridine (1, 2). This conformation has been found to occur frequently in single crystals of nucleosides (8, 10). The close similarity of the values at 28 and 78 °C for $J_{4'5'_B}$ and $J_{4'5'_C}$, and for the chemical shifts of the two 5′ protons, suggests that although the populations of the various rotamers are unequal, the energy differences between them are not large (18).

The Sugar–base Torsion Angle

Previous consideration of the chemical shift of the hydrogen at position 6 in uridine and uridine-5′-monophosphate has suggested that the uracil base exists in the *anti* conformation about the *N*-glycosidic bond, in which the 2-keto group points away from the 5′-CH_2OH moiety (15–17). It has been proposed that the presence of the *syn*

Can. J. Chem. Downloaded from www.nrcresearchpress.com by 210.87.254.6 on 09/05/12
For personal use only.

conformation in pyrimidine nucleosides should be detectable by large changes in the ribose proton chemical shifts due to the diamagnetic anisotropy of the keto group on the base (2). Recently Dugas *et al.* have analyzed the p.m.r. spectrum of β-cyanuric acid riboside [α-*N*-(β-cyanuric acid)-D-ribofuranoside], in which a keto group must lie over the ribose ring (19).

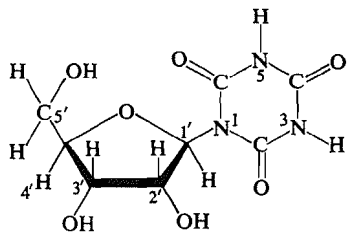

β-cyanuric acid riboside

The protons at positions 1′, 2′, and 3′ were appreciably deshielded relative to those in uridine, whereas those at positions 4′ and 5′ were slightly shielded. The earlier assertion is thus confirmed. Comparison of the ribose hydrogen chemical shifts for U and β–ψ indicates that the sugar–base torsion angles are similar in these compounds. The lack of any significant temperature dependence of the ribose chemical shifts suggests that no change in the sugar–base torsion angle of uridine takes place over the range 28–78 °C.

Conclusions

The ribose ring of uridine in aqueous solution exists in a rapid equilibrium between various puckered conformations. The *gauche–gauche* rotamer is preferred for the 5′-CH_2OH group, and the uracil base is present in the *anti* orientation relative to the 5′-CH_2OH. The molecular conformation is independent of temperature over the range 28–78 °C. The conformations of uridine and β-pseudouridine are very similar, and therefore the specific structural role of β–ψ in transfer RNA must be attributable to the availability for hydrogen-bonding of an extra nitrogen atom in the uracil base.

We are grateful to Dr. R. R. Fraser for the use of the HA-100 spectrometer at the University of Ottawa, Ottawa, Canada and for helpful discussions.

1. F. E. Hruska, A. A. Grey, and I. C. P. Smith. J. Amer. Chem. Soc. **92**, 214 (1970).
2. F. E. Hruska, A. A. Grey, and I. C. P. Smith. J. Amer. Chem. Soc. **92**, 4088 (1970).
3. S. Fujiwara and M. Uetsuki. *In* Recent developments of magnetic resonance in biological systems. *Edited by* S. Fujiwara and L. H. Piette, Hirokawa Publishing Company, Tokyo, 1968. p. 1.
4. S. Castellano and A. A. Bothner-By. J. Chem. Phys. **41**, 3868 (1964).
5. J. H. Prestegard and S. I. Chan. J. Amer. Chem. Soc. **91**, 2843 (1969).
6. M. Karplus. J. Chem. Phys. **30**, 11 (1959).
7. R. U. Lemieux. Personal communication.
8. M. Sundaralingam and L. H. Jensen. J. Mol. Biol. **13**, 914 (1965).
9. R. D. Harris and W. M. Macintyre. Biophys. J. 203 (1964).
10. M. Sundaralingam. J. Amer. Chem. Soc. **87**, 599 (1965).
11. S. Sternhell. Quart. Rev. **23**, 86 (1969).
12. R. J. Abraham, L. D. Hall, L. Hough, and K. A. McLauchlan. J. Chem. Soc. 3699 (1962).
13. R. U. Lemieux and J. D. Stevens. Can. J. Chem. **43**, 2059 (1965).
14. L. D. Hall, J. F. Manville, and N. S. Bhacca. Can. J. Chem. **47**, 1 (1969).
15. I. C. P. Smith, B. J. Blackburn, and T. Yamane. Can. J. Chem. **47**, 513 (1969).
16. M. P. Schweizer, A. D. Broom, P. O. P. Ts'O, and D. P. Hollis. J. Amer. Chem. Soc. **90**, 1042 (1968).
17. P. O. P. Ts'O, N. S. Kondo, M. P. Schweizer, and D. P. Hollis. Biochem. **8**, 997 (1969).
18. J. A. Pople, W. G. Schneider, and H. J. Bernstein. High-Resolution nuclear magnetic resonance. McGraw-Hill Book Co., Inc., New York, N.Y., 1959. p. 381.
19. H. Dugas, B. J. Blackburn, R. K. Robins, and I. C. P. Smith. In preparation.

Can. J. Chem. Downloaded from www.nrcresearchpress.com by 210.87.254.6 on 09/05/12
For personal use only.

Enthalpies of reaction of zirconium and molybdenum tetrachlorides with pyridine, tetrahydrofuran, and tetrahydrothiophene

A. D. WESTLAND AND V. UZELAC
Department of Chemistry, University of Ottawa, Ottawa 2, Canada

Received January 15, 1970

Enthalpies of addition were determined calorimetrically for the crystalline complexes $MCl_4.2L$ where M = Zr and L = pyridine or M = Mo and L = pyridine, tetrahydrofuran, or tetrahydrothiophene. Molybdenum(IV) is a significantly better acceptor than zirconium(IV) toward pyridine and tetrahydrofuran but not toward tetrahydrothiophene. A possible explanation for this is discussed.

Canadian Journal of Chemistry, 48, 2871 (1970)

Can. J. Chem. Downloaded from www.nrcresearchpress.com by 210.87.254.5 on 09/05/12
For personal use only.

In a continuing study of the comparative physical chemistry of second and third row transition elements, we have compared heats of adduct formation with zirconium and hafnium tetrahalides as acceptors (1). We now report a comparison between two elements chosen from the same periodic row viz., zirconium and molybdenum. In these studies we are able to compare bonding in pairs of compounds in which molecular dimensions and charges are very nearly the same for both members of the pair.

In a previous publication (1), we examined essentially the influence of an inner shell of 4f-electrons upon the acceptor behavior of a quadrivalent atom. We have now examined the change in acceptor strength which accompanies the addition of two positive charges to the nucleus of the acceptor atom and two electrons to its outermost d-shell. A related study of the relative heat of formation for the complexes MCl_4^{2-}, where M = Mn, Fe, Co, Ni, Cu, and Zn has been carried out by Blake and Cotton (2). We were particularly interested to see whether there would be a significant change in the degree of "softness" (3) of the acceptor with a different choice of acceptor atom. To this end, complexing with a soft base, tetrahydrothiophene (THT), was compared with that of a hard base, tetrahydrofuran (THF).

In order to provide a supply of $MoCl_4$, we found that a pure product could be prepared most conveniently by the method of Shchukarev and co-workers (4). Subsequent to our work, a very convenient procedure was reported by Kepert and Mandyczewsky (5). In following Shchukarev's procedure, we found that it was essential to operate at the lowest temperature possible at which the reaction would proceed at a reasonable rate. Otherwise, the disproportionation $2MoCl_4(g) \rightarrow MoCl_3(c) + MoCl_5(g)$ (6) led to contamination with $MoCl_3$. We have established by differential thermal analysis that this process occurs in a sealed capsule at 288°. Our investigation of the physical properties of $MoCl_4$ prepared by Shchukarev's procedure will be the subject of a future publication.

Properties of the Complexes

The preparation and physical properties of $ZrCl_4.2py$, $MoCl_4.2py$, and $MoCl_4.2THF$ have been described previously (7–9). The infrared spectra of $ZrCl_4.2py$ and $MoCl_4.2THF$ suggest that these compounds have the *cis* configuration. $ZrCl_4.2py$ has bands at 339, 332, and 300 cm^{-1} which were attributed to metal–chlorine stretching (8). There is almost exact agreement with the bands exhibited by $ZrCl_4.dipy$. We have now obtained infrared spectra for $ZrCl_4.2THF$, $ZrCl_4.2THT$, $MoCl_4.2py$, and $MoCl_4.2THT$ as well. The frequencies of the absorption maxima are listed in Table 1.

The assignment of the *cis* configuration for $MoCl_4.2py$ is supported by the appearance of three bands at approximately 363, 340, and 312 cm^{-1}, respectively. The last band is broad and is possibly composed of two components. These bands are assigned as Mo—Cl stretching modes of which four should be infrared active. Only one band is permitted for the perfectly regular *trans* structure. However, Beattie *et al.* have shown that such arguments should be treated with caution for in *trans*-$SiCl_4.2py$, the $\nu(SiCl_4)$ band is split by mixing with pyridine ring vibrations and this would account for one additional band (10). Moreover, $\delta(SiCl_4)$ mixed with $\nu(SiN)$ appears in the Si—Cl stretching region. Heavier central atoms such as those we are dealing with are likely to inhibit mixing of modes. This is

TABLE 1

Infrared absorption maxima of complexes of $ZrCl_4$ and $MoCl_4$ with pyridine, tetrahydrofuran, and tetrahydrothiophene as Nujol mulls

Compound	Frequency (cm^{-1})*
$ZrCl_4$.2THF	280–325 broad absorption, 650 sh, 679 s, 730 sh, 800 s, br, 850 sh, 919 m, 950 sh, 990 s, 1044 s, 1102 w, 1140 sh, 1172 m, 1234 sh, 1250 s, 1300 w, 1320 w, 1349 s, 1367 w, 1382 m, 1428 sh, 1450 s, 1468 s, 1480 sh, 2300 w, 2600 w.
$ZrCl_4$.2THT	285–395 broad absorption, 460 br, 666 s, 724 w, 740 w, 807 m, 880 s, 956 s, 1017 m, 1070 m, 1127 s, 1196 w, 1210 m, 1253 s, 1268 sh, 1308 s, 1330 w, 1369 sh, 1377 s, 1440 s, 1460 s, 1475 sh.
$MoCl_4$.2py	260 s, 312 m, br, 340 sh, 363 w, 437 sh, 445 s, 550 w, 640 s, 668 sh, 681 vs, 720 sh, 733 m, 753 vs, 856 w, 888 w, 923 sh, 947 w, 1009 s, 1040 m, 1059 vs, 1082 w, 1150 w, 1207 s, 1230 w, 1347 sh, 1371 vs, 1440 vs, 1455 sh, 1476 s, 1520 m, 1598 vs, 1622 w, 1650 w, 1891 w, 1960 w, 2330 w, 2600 br, 2920 br.
$MoCl_4$.2THF	284 m, 343 s, 700 sh, 730 w, 746 sh, 822 vs, 850 sh, 925 m, 955 m, 1000 s, 1025 w, 1050 m, 1135 sh, 1173 m, 1225 w, 1250 m, 1303 w, 1349 s, 1382 s, 1464 vs, 1590 w, 2660 w, br, 2880 s, 2920 s, 2970 sh.
$MoCl_4$.2THT	332–393 broad absorption, ~ 450 m, ~ 465 m, ~ 520 m, br, 665 s, 724 w, 740 sh, 807 s, 880 s, 956 s, 1016 m, 1070 m, 1127 m, 1195 w, 1210 m, 1254 s, 1260 sh, 1308 s, 1360 sh, 1372 s, 1420 sh, 1440 s, 1460 s, 1475 sh.

*vs = very strong, s = strong, m = medium, w = weak, br = broad, sh = shoulder.

supported by work with pyridine complexes of nickel, cobalt, and zinc (11). Thus the close correspondence of the spectra of $MoCl_4$.2py and $ZrCl_4$.2py can be taken as reasonably good evidence of *cis* structure in the molybdenum compound.

In the case of $ZrCl_4$.2THT and $MoCl_4$.2THT, the spectra below 400 cm^{-1} were poorly resolved. The broad absorptions referred to in Table 2 probably included both M—Cl and M—S stretching bands. The broadness suggests that there are many bands in this region and this constitutes slight evidence for a *cis* configuration.

If our assignment is correct, the slightly higher values of the Mo—Cl stretching frequencies compared to the corresponding Zr—Cl frequencies indicate a stronger bonding in the former. The pyridine ring vibration at 405 cm^{-1} is raised to 424 cm^{-1} in $ZrCl_4$.2py and 437 cm^{-1} in $MoCl_4$.2py. This may also be taken to be indicative of a greater electrical field about the molybdenum atom (11).

The spectra of the THF complexes differ from the spectrum of uncomplexed THF principally in the region 700–1000 cm^{-1}. The strong THF bands at 920 and 1080 cm^{-1} are shifted to ~ 800 and ~ 1000 cm^{-1}. These bands are apparently associated with C—O—C stretching.

There is comparatively little change in the spectrum of THT upon complexing. There is a slight reduction in frequency of the C—S—C stretching bands at 687 and ~ 740 cm^{-1} to 665 (or 666) and 724 cm^{-1}, respectively. These modes are not sensitive to any possible differences in the acceptor power of zirconium and molybdenum tetrachlorides.

We have determined the magnetic susceptibility of $MoCl_4$.2THT at several temperatures. The results are given in Table 2. The data are consistent with a distorted octahedral field geometry. The slight decrease in μ_{eff} toward lower temperatures is expected for an ion with a $^3T_{1g}$ ground state (12). The magnetic susceptibilities of $MoCl_4$.2py and $MoCl_4$.2THF have been previously reported (7, 9).

TABLE 2

Results of magnetic susceptibility measurements on $MoCl_4.2(C_4H_8S)$

T (°K)	χ_g (c.g.s.)	χ_M(Corrected) (c.g.s.)	μ_{eff} (B.M.)
297	6.37	2883	2.62
227	8.58	3793	2.62
173	11.30	4923	2.61
108	17.09	7303	2.51

Thermal Measurements

Because the donor compounds were liquids, it was possible to determine directly the heats of adduct formation by solution calorimetry. The acceptors MCl_4 and the adducts were solids so that we have the following

$$MCl_4(c) + xL(l) = MCl_4.2L \text{ (dissolved in } (x-2) \text{ moles of L)} \quad \Delta H_1$$

$$MCl_4.2L(c) + xL(l) = MCl_4.2L \text{ (dissolved in } x \text{ moles of L)} \quad \Delta H_2$$

Can. J. Chem. Downloaded from www.nrcresearchpress.com by 210.87.254.5 on 09/05/12
For personal use only.

TABLE 3

Molar heats of solution, ΔH_1 and ΔH_2, for the process $MCl_4(c)$ + excess ligand → complex in solution and complex(c) + excess ligand → complex in solution†

Solute compound	Solvent	Weight of solute (g)	$-\Delta H_1$ (kcal/mole)	$-\Delta H_2$ (kcal/mole)
$ZrCl_4$	Pyridine	0.2375	58.3	
		0.2873	58.2	
$ZrCl_4$.2py	Pyridine	0.1790		17.1
		0.3125		16.9
$MoCl_4$	Pyridine	0.1931	53.6*	
		0.2253	54.2*	
$MoCl_4$.2py	Pyridine	0.175		17.2
$MoCl_4$	THF	0.2953	40.8	
		0.3305	42.0	
$MoCl_4$.2THF	THF	Insoluble		0.0
$MoCl_4$	THT	0.695	39.6	
		0.1060	38.8	
		0.1720	39.6	
$MoCl_4$.2THT	THT	0.1274		8.6
		0.2109		7.4

*These values are $-\Delta H$ which were calculated by taking into account the partial solubility of the complex. The enthalpy required to saturate a known quantity of pyridine by the addition of $MoCl_4$.2py was subtracted from the enthalpy measured when an excess of $MoCl_4$ was added to the same quantity of pyridine.

†A referee has drawn our attention to experience elsewhere which has shown that the heats of solution may be considerably in error owing to hydrolysis. However, the results reported herein rely upon the difference of two measurements both of which will depend in nearly the same way upon the concentration of moisture in the solvent; thus ideally, errors due to moisture should be compensated to the degree that the measurements are done on nearly equimolar amounts in both cases. The reproducibility of heat measurements is an indication that errors due to impurity in the solvent are not too great.

The solutions in both of the above processes are nearly alike provided that x is large, say of the order of 5000. In that case, subtraction gives us

$$MCl_4(c) + 2L(l) = MCl_4.2L(c)$$

$$-\Delta H = -\Delta H_1 + \Delta H_2$$

It is of no concern whether the dissolved species has recognizable stereochemistry or whether it is ionized.

The thermochemical results are summarized in Table 3. The temperature rise at the calorimeter thermopile produced changes in potential of the order of 200 μV for the dissolving of the tetrachlorides. The calibration gave a calorimeter constant of about 0.250 cal per μV. The calorie was taken to be 4.1840 J. All results refer to 25 °C.

Zirconium Tetrachloride–Pyridine

The reaction in the calorimeter was rapid, requiring about 1 min for completion. The reaction proceeded without a step in the ΔT vs. time plots. Such steps or discontinuities in the uniform progression of the ΔT vs. time plots were observed by Greenwood *et al.* in the complexing of pyridine with triphenylboron (13). This was attributed to the initial very rapid formation of solid complex which subsequently dissolved with absorption of heat. In our systems, formation of the complex and its dissolution apparently took place at comparable rates.

There is reason to believe that at least three pyridine molecules are associated with the zirconium in solution as we have isolated crystalline $ZrCl_4$.3py from solution (8). The heat of solution of 17 kcal/mole is thus associated with a further complexing in addition to the simple dissolving process.

The heat of formation of crystalline *cis*-$ZrCl_4$.2py is given by

$$ZrCl_4(c) + 2C_5H_5N(l) = ZrCl_4.2(C_5H_5N)(c)$$

$$-\Delta H = 41.3 \pm 0.2 \text{ kcal/mole}$$

Molybdenum Tetrachloride–Pyridine

As in all cases reported here, the reaction was complete in about 1 min. The adduct formed in this case was only partially dissolved in the calorimetric liquid. For this reason it was necessary to assume that when $MoCl_4$ was dissolved in pyridine, a saturated solution of the adduct was formed during the time that potential readings were recorded (about 0.5 h). Further, it was assumed that when $MoCl_4$.2py was added to the calorimeter liquid, a saturated solution was again formed in the same time. Different weights

Can. J. Chem. Downloaded from www.nrcresearchpress.com by 210.87.254.5 on 09/05/12
For personal use only.

Can. J. Chem. Downloaded from www.nrcresearchpress.com by 210.87.254.5 on 09/05/12
For personal use only.

of the adduct added to the same volume of liquid gave temperature changes which agreed to within 1.2%.

The heat of solution of the adduct was found to be $-\Delta H_2 = 17.2$ kcal/mole. This was found by means of a determination in which the solution in the calorimeter did not quite reach saturation. In calculating $-\Delta H$ for the complexing of $MoCl_4$, the heat involved in saturating a known weight of pyridine with the adduct was subtracted from the heat found for the dissolving of $MoCl_4$ in the same weight of solvent.

The heat of adduct formation for crystalline $MoCl_4.2py$ is given by

$$MoCl_4(c) + 2C_5H_5N(l) = MoCl_4.2(C_5H_5N)(c)$$
$$-\Delta H = 53.9 \pm 0.4 \text{ kcal/mole}$$

Molybdenum Tetrachloride–Tetrahydrofuran

The complex $MoCl_4.2THF$ is practically insoluble in THF so that the heat of complexing was simply the heat involved when $MoCl_4$ was added to the calorimeter liquid. Reaction occurred quite readily and the precision suggests that the reactions went to completion even though the final system was heterogeneous. Addition of $MoCl_4.2THF$ to the THF in the calorimeter gave no temperature change.

The heat of adduct formation for crystalline $MoCl_4.2THF$ is given by

$$MoCl_4(c) + 2(C_4H_8O)(l) = MoCl_4.2(C_4H_8O)(c)$$
$$-\Delta H = 40.4 \pm 0.6 \text{ kcal/mole}$$

Molybdenum Tetrachloride–Tetrahydrothiophene

Unlike the preceding system, $MoCl_4.2THT$ was completely soluble in the calorimeter liquid. The heat of solution of the complex in THT was small. The exothermic nature of this solution process suggests that a higher complex, e.g. $MoCl_4.3THT$ may be formed; however, this would be relatively unstable compared with the 1:2 adduct. The heat of adduct formation of crystalline $MoCl_4.2THT$ is given by

$$MoCl_4(c) + 2(C_4H_8S)(l) = MoCl_4.2(C_4H_8S)(c)$$
$$-\Delta H = 31.3 \pm 0.8 \text{ kcal/mole}$$

The data reported here should be compared with that found by Chung and Westland (1). Ideally, one should compare enthalpies for the gas phase reaction

$$MCl_4(g) + 2L(g) = MCl_4.2L(g)$$

These would be obtained from the calorimetric data by means of a thermal cycle. It is impossible to obtain heats of sublimation for the complexes by direct vapor pressure measurements as decomposition precedes sublimation even in vacuum when the adducts are heated. A more serious difficulty is the lack of data on the vapor pressure of $MoCl_4$. Work is in progress in this laboratory to obtain these and other physical data for $MoCl_4$.

In view of the lack of sublimation data we are forced to compare the heats of reaction of the crystalline metal chlorides to produce crystalline adducts. We see that $MoCl_4(c)$ is a much better acceptor than $ZrCl_4(c)$ toward pyridine. Qualitatively, one should expect the acceptor ability of the halides MCl_4 to increase in proceeding toward the right within a transition period. There would be fluctuations owing to changing crystal field stabilization similar to those which are found in the stability of complexes in aqueous solution (14).

The desirability of obtaining data for other members of the series of MCl_4 compounds is apparent. We tried to obtain heats of reaction for $NbCl_4$ in pyridine but the reaction was so slow that it was impossible to obtain meaningful results. The heats of formation of $NbCl_4.2py$ and $RuCl_4.2py$ will have to be obtained in other ways.

The addition of $MoCl_4$ to THF is likewise more exothermic than the corresponding reaction between $ZrCl_4$ and THF (1). The difference, 6.8 kcal/mole, is not as great as that observed when pyridine is the donor. One should expect pyridine to be more strongly polarized by the Mo(IV) atom with its greater effective nuclear charge so that on the basis of an ion-dipole model of the adduct, stronger bonding should result. Moreover, pyridine generates a stronger ligand field than ethers so that the pyridine complex should have stronger ligand field stabilization.

The result for $MoCl_4.2THT$ is surprising. The heat of adduct formation in this case is only slightly greater than that for the zirconium analogue for which 29.8 ± 0.9 kcal/mole was found (1). On the basis of the polarizability of the sulfur atom and the position of thioethers in the spectrochemical series, one should have expected a much greater difference between $ZrCl_4.2THT$ and $MoCl_4.2THT$. The complex of THT with $MoCl_4$ is formed with markedly less heat evolution than is $MoCl_4.2THF$. This is still true if we consider the enthalpy of the gas phase process and

Can. J. Chem. Downloaded from www.nrcresearchpress.com by 210.87.254.5 on 09/05/12
For personal use only.

account is taken of the heats of vaporization of the ligands in the manner described previously (1).[1] Mo(IV) therefore appears to be an ion of definite class *a* character (16) while Zr(IV) has possibly some slight degree of class *b* character.

There is a plausible explanation for this difference. We assume that d_π–p_π bonding is very important in the Zr—S bond. The fact that the THT complex is formed more exothermically than the THF complex would be difficult to understand otherwise. We have noted the stability of similar complexes with $TiCl_4$ (17). In Mo(IV) two of the three d-orbitals which are designated t_{2g} in a regular octahedral complex are half occupied. The resulting antibonding may well be sufficient to offset the advantage that sulfur would have if the d-orbitals were all vacant.

Sulfur bonds more readily than does oxygen with transition metal ions like Pt(II) and Au(I). In such cases, there is certainly no d_π–p_π bonding of the type discussed above but with the lower-valent ions d_π–d_π bonding with donation by the metal ion to the sulfur atom is a possibility. There should be a type of transition metal ion between the two extremes which has neither strong π-accepting nor π-donating ability. As it is not possible to determine whether the Mo—S bond owes some of its strength to π-bonding or to induced polarization of the type postulated in ion-dipole complexes, it is premature to say whether Mo(IV) is a representative of that type of ion which is more or less exactly intermediate between the extremes of π-accepting and π-donating ions.

We were interested to discover how W(IV) compares with Mo(IV) in this regard. However, WCl_4 prepared by the method of McCarley and Brown (18) failed to react with our donors. Like $NbCl_4$ and $TaCl_4$, WCl_4 appears to contain a much stronger metal–metal bond (5).

Experimental

Preparations

$MoCl_4$

Molybdenum dioxide (Research Organic/Inorganic Chemical Co., 99.9%) mixed with activated charcoal (Norit-A) in the ratio of five parts of the former to one part of the latter was heated at 280–290° in a stream of nitrogen saturated at room temperature with carbon tetrachloride vapor (4). A vertical spiral tube at the outlet end replaced the condenser recommended by Shchukarev *et al.*, for it was found to be more effective in collecting the fine powdered product. The powder descended the spiral into a receiver when the former was tapped gently. The temperatures cited above are recommended if contamination with trichloride is to be avoided. Oxychloride was formed along with the tetrachloride but it was sublimed away from the desired product by heating the mixture to 100° in one end of a sealed tube. All handling operations were performed in dry nitrogen atmosphere. The purified $MoCl_4$ was soluble in water, ethanol, acetone, and other strong donor solvents and insoluble in benzene, ether, and carbon tetrachloride.

Anal. Calcd. for $MoCl_4$: Mo, 40.35; Cl, 59.65. Found: Mo, 40.41; Cl, 59.70.

$ZrCl_4$

Commercial zirconium tetrachloride (Alpha Inorganics) was sublimed in a sealed tube containing 1 atm of dry nitrogen.

Tetrahydrofuran (Fisher Certified Reagent) was freshly distilled from $LiAlH_4$. Tetrahydrothiophene (Aldrich) was freshly distilled through an efficient fractionating column. Pyridine (Baker Analyzed) was dried over sodium hydroxide pellets and freshly distilled. Benzene (Spectrophotometric grade) was dried with sodium benzophenone ketyl and distilled directly into a Schlenk type reaction vessel.

Adducts

$MoCl_4$ or $ZrCl_4$ (2–3 g) was stirred for several hours in benzene (100 ml) with a 50% excess of the donor substance. The volume of solvent was reduced by distillation and *n*-hexane added to promote precipitation. The adduct was removed by filtration in an apparatus described by Fritz *et al.* (19), washed with *n*-hexane, and dried *in vacuo*.

Anal. Calcd. for $C_{10}H_{10}Cl_4N_2Zr$: C, 30.7; H, 2.58; N, 7.16. Found: C, 31.2; H, 2.63; N, 7.13, white powder.

Anal. Calcd. for $C_{10}H_{10}Cl_4MoN_2$: Mo, 24.2; Cl, 35.8; C, 30.3; H, 2.6; N, 7.07. Found: Mo, 23.7; Cl, 35.0; C, 32.1; H, 2.7; N, 7.45, orange powder.

Anal. Calcd. for $C_8H_{16}Cl_4MoO_2$: Mo, 25.1; Cl, 36.9; C, 25.3; H, 4.7. Found: Mo, 25.2; Cl, 37.0; C, 24.9; H, 4.3, orange crystals.

Anal. Calcd. for $C_8H_{16}Cl_4MoS_2$: Mo, 23.1; Cl, 34.3; C, 23.2; H, 3.89; S, 15.49. Found: Mo, 22.9; Cl, 34.2; C, 23.3; H, 3.94; S, 15.44, red crystals.

Molybdenum was determined gravimetrically as lead molybdate and zirconium as the oxide. Chloride was determined volumetrically with $AgNO_3$ using a silver electrode. The samples were prepared for these determinations by fusion with Na_2O_2 in a Parr bomb. Determinations of carbon, hydrogen, nitrogen, and sulfur were performed by Schwarzkopf Microanalytical Laboratory, Woodside, New York, using glove box techniques.

Magnetic Susceptibility Measurements

Susceptibilities were measured using a Guoy apparatus employing field strengths up to 5200 Oe. The sample tube was suspended inside a copper jacket the temperature of which was maintained within ± 1 °C by a stream of cold nitrogen. A thermocouple in the stream of nitrogen controlled by negative feedback the rate at which liquid nitrogen was vaporized in a reservoir connected to the cryostat.

Diamagnetic corrections were applied to the measured

[1]The heat of vaporization of tetrahydrothiophene is 9.4 kcal/mole (15). The value for tetrahydrofuran (7.1 kcal/mole) was estimated from Trouton's rule.

susceptibility values using the values tabulated by Selwood (20).

Infrared Spectra

Spectra were obtained using Beckman IR-8 and IR-20 spectrometers. Spectra in the range 600–250 cm^{-1} were obtained as Nujol mulls between polyethylene plates. Resolution in this region was poor owing to the low energy.

Calorimetric Measurements

A solution calorimeter similar to that described by Greenwood and Perkins (21) was used. The thermocouple had eight junctions of No. 30 copper–constantan wire. The temperature–time curves in the linear period before mixing the reagents were extrapolated forward to the point in time when the temperature had risen half way to its maximum value. The post-mixing curves were extrapolated back to that time. The difference in level of the two curves gave the temperature jump. The calibration of the associated equipment was checked by determining the heat of hydrolysis of $POCl_3$ in the calorimeter. Three determinations gave 79.7, 80.3, and 80.7 kcal/mole in reasonable agreement with the published value of 79.9 ± 0.3 kcal/mole (22).

The volume of liquid employed in the calorimeter was normally 150 cc. The temperature of the calorimeter was within about 2° of the temperature of the thermostat which was maintained at 25 °C.

The authors wish to express their appreciation to the National Research Council of Canada for financial assistance.

1. F. M. Chung and A. D. Westland. Can. J. Chem. **47**, 195 (1969).
2. A. B. Blake and F. A. Cotton. Inorg. Chem. **3**, 5 (1964).
3. R. G. Pearson. J. Amer. Chem. Soc. **85**, 3533 (1963).
4. S. A. Shchukarev, I. V. Vasil'kova, and B. N. Sharupin. Vestnik Leningrad. Univ. **14**, Ser. Fiz. i Khim. 72 (1959).
5. D. L. Kepert and R. M. Mandyczewsky. Inorg. Chem. 7, 2092 (1968).
6. W. Biltz and C. Fendius. Z. Anorg. Allgem. Chem. **172**, 385 (1928).
7. M. L. Larson and F. W. Moore. Inorg. Chem. **3**, 285 (1964).
8. T. C. Ray and A. D. Westland. Inorg. Chem. **4**, 1501 (1965).
9. E. A. Allen, K. Feenan, and G. W. A. Fowles. J. Chem. Soc. 1636 (1965).
10. I. R. Beattie, T. R. Gilson, and G. A. Ozin. J. Chem. Soc. A, 2772 (1968).
11. R. J. H. Clark and C. S. Williams. Inorg. Chem. **3**, 350 (1965).
12. B. N. Figgis. Introduction to ligand fields. Interscience Publ. Inc., New York. 1966. p. 273.
13. N. N. Greenwood, P. G. Perkins, and M. E. Twentyman. J. Chem. Soc. A, 249 (1969).
14. P. George and D. S. McClure. Prog. Inorg. Chem. **1**, 381 (1959).
15. J. V. Davies and S. Sunner. Acta Chem. Scand. **16**, 1870 (1962).
16. S. Ahrland, J. Chatt, and N. R. Davies. Quart. Rev. **12**, 265 (1958).
17. A. D. Westland and L. Westland. Can. J. Chem. **43**, 426 (1965).
18. R. E. McCarley and T. M. Brown. Inorg. Chem. **3**, 1232 (1964).
19. G. Fritz, D. Havel, D. Kummer, and G. Teichman. Z. Anorg. Allgem. Chem. **302**, 60 (1959).
20. P. W. Selwood. Magnetochemistry. Interscience Publ. Inc., New York. 1956. p. 78.
21. N. N. Greenwood and P. G. Perkins. J. Inorg. Nucl. Chem. **4**, 291 (1957).
22. E. Neale and L. T. D. Williams. J. Chem. Soc. 4535 (1952).

Can. J. Chem. Downloaded from www.nrcresearchpress.com by 210.87.254.5 on 09/05/12
For personal use only.

Can. J. Chem. Downloaded from www.nrcresearchpress.com by 210.87.254.105 on 09/05/12
For personal use only.

Pyranosiduloses. II. The synthesis and properties of some alkyl 2,3-dideoxy-2-enopyranosid-4-uloses[1]

BERT FRASER-REID, ANGUS MCLEAN,[2] E. W. USHERWOOD,[3] AND MARK YUNKER[4]
Department of Chemistry, University of Waterloo, Waterloo, Ontario

Received October 10, 1969[5]

Ethyl 2,3-dideoxy-α-D-*erythro*-hex-2-enopyranoside (**9***a*) an accessible and highly crystalline substance is selectively oxidized at the allylic position to ethyl 2,3-dideoxy-α-D-*glycero*-hex-2-enopyranosid-4-ulose (**10***a*) in 80% yield. This hydroxyketone can be benzoylated, acetylated, and tosylated, and the resulting esters are all highly crystalline, as is the parent ketone. 3,4-Di-*O*-acetyl-D-xylal reacts with ethanol under boron trifluoride catalysis to give the anomeric mixture of ethyl 4-*O*-acetyl 2,3-dideoxy-D-*glycero*-pent-2-enopyranosides which may be separated after deacetylation. The deacetylated α-D anomer (**14**α) is readily oxidized by manganese dioxide to give an ethyl 2,3-dideoxy pent-2-enopyranosid-4-ulose (6-ethoxy-2,6-dihydropyran-3-one) (**12**); however, the corresponding β-D (**14**β) anomer resists oxidation. All of these ketones display a diagnostic nuclear magnetic resonance pattern consisting of clean doublets for H-1 and -3, and a doublet of doublets for H-2. Reduction of **10***a* with lithium aluminum hydride gives back the parent D-*erythro* alcohol exclusively, and catalytic hydrogenation saturates the olefinic double bond. These α,β-unsaturated ketones (**10**) in the hexose series are all *levo*rotatory although their parent D-*erythro* alcohols (**9**) are strongly *dextro*rotatory; the saturated ketones derived from them are also strongly *dextro*rotatory. The epimeric D-*threo* alcohols which should also be oxidizable to **10** are however strongly *levo*rotatory.

Canadian Journal of Chemistry, 48, 2877 (1970)

Carbohydrate molecules possessing ketonic (2) and olefinic (3, 4) unsaturation are favorite precursors for synthesis of branched-chain and amino (5) sugars, two classes of compounds of considerable interest because of their occurrence in many major antibiotics (6, 7). Molecules possessing both types of unsaturation in conjugation are of interest in view of the array of synthetic techniques available to them (8). The α,β-unsaturated carbonyl residue occurs in two carbohydrate molecules of considerable physiological importance, namely kojic acid (9) and ascorbic acid (10). However, neither is a "pure" α,β-unsaturated ketone, one being a substituted γ-pyrone, and the other an unsaturated furanolactone, and in both the olefinic portion is hydroxylated. It is interesting, although probably not significant, that two structurally related systems have been encountered in the laboratory. In one case (11), Sarret oxidation of methyl 4,6-*O*-benzylidene-2-deoxy-α-D-*lyxo*-hexopyranoside gave a dihydro γ-pyrone, namely methyl 4,6-*O*-benzylidene-2-deoxy-α-D-*threo*-hexopyranosid-3-ulose (**1**) instead of the expected (12) α-methylene ketone. In the other case, attempts to purify methyl 3,4,6-tri-*O*-benzoyl-α-D-*arabino*-hexopyranosidulose by silica gel chromatography led to elimination of benzoic acid and formation of the benzoylated diosphenol 2-D-*glycero*-benzoyloxymethyl-4-benzoyloxy-6-D-*glycero*-methoxy-5,6-dihydro-α-pyran-5-one (**2**) (11).

Hexopyranoses containing "pure" α,β-unsaturated ketone groupings have also been obtained. 3,4-Dideoxy-D-*glycero*-hex-3-ene-2-ulopyranose (**3**) is formed in low yield by hydrolysis of difructose glycine (13), and syrupy methyl glycosides of **3** (**4** and **5**) and has been prepared by acid-catalyzed elimination from enolic precursors having the appropriate anomeric configuration (14). An alternative route to **4** and **5** via the anomeric fluorides has been recently described (15). These unsaturated monosaccharides, **1** to **5**, are of synthetic interest, but their potential as precursors is restricted because of their instability, their inaccessibility, or the low yields in which they are obtainable. We wish to report the preparation of some alkyl 2,3-dideoxy-hex-2-enopyranosid-4-uloses, all of which are produced simply and in high yield as stable, crystalline compounds. An alkyl 2,3-dideoxy-pent-2-enopyranosid-4-ulose (**12**) is also described.

It was recently reported from this laboratory (3) that elimination of the vicinal sulfonyloxy

[1]This work has been presented in preliminary form in Part 1 of the series (1).
[2]Taken in part from the M.Sc. thesis of A. McLean, University of Waterloo, Waterloo, Ontario, 1969.
[3]Undergraduate Summer Research participant, 1968.
[4]Undergraduate Summer Research participant, 1969.
[5]Revision received May 21, 1970.

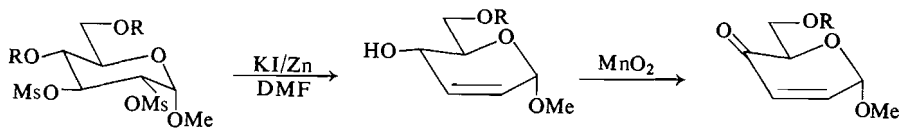

6 7 8

SCHEME 1

groups from di-*O*-acyl compounds such as **6** (R = Ac or PhCO) was accompanied by deacylation at C-4 to give **7** (R = Ac or PhCO) (Scheme 1). Since it was found (3) that the primary ester **7** (R = PhCO) could also be prepared efficiently by selective benzoylation of the corresponding olefinic diol (**7**; R = H) we were prompted to investigate the synthetic possibilities of these monoesters. Oxidation of the allylic alcohol to the ketone (16) was one of the obvious possibilities to explore. Accordingly, compound **7** (R = PhCO) was oxidized with manganese dioxide (16*c*) (Scheme 1) and ketone **8** (R = PhCO) was produced in 53% yield. Attempts to debenzoylate the primary alcohol of **8** caused destruction of the molecule and hence another route to hydroxyketones (such as **8**; R = H) was desirable.

Ethyl 2,3-dideoxy-α-D-*erythro*-hex-2-enopyranoside (**9***a*) (17) seemed a likely precursor since it is a stable crystalline substance which can be prepared in high yield by Ferrier's excellent new method (4*f*). Some reservations about the

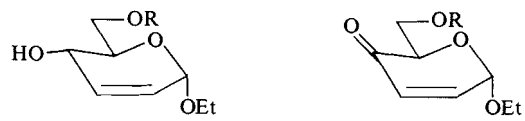

9 10

a R = H
b R = PhCO
c R = Ts
d R = CH_3CO

specificity of manganese dioxide oxidations have been expressed (18), but it was found that diol **9***a* could be oxidized to the crystalline hydroxyketone **10***a* in 82% yield without any evidence for aldehyde formation from the primary alcohol being obtained (c.f. 18*a*). The hydroxyketone (**10***a*) was exceedingly labile to triethylamine (vide infra), however, it could be benzoylated in very cold pyridine – methylene chloride mixture. The yield of the keto-ester **10***b* by the latter route is 81% and is therefore to be preferred over the above described sequence involving selective benzoylation of the olefinic diol prior to the oxidation, whereby the same product is obtained in 40% yield based on **9***a*. In a similar way ketone **10***a* could be esterified with the usual reagents to give the tosylate (**10***c*) and the acetate (**10***d*). The latter two reactions gain in significance because lack of selectivity in acetylation and tosylation of diol **9***a* (19), makes the latter route the only feasible one. Unfortunately, attempts to tritylate the compound (**10***a*) have so far been unsuccessful.

These 2,3-dideoxy-hex-2-enopyranosiduloses (**10**) (Table 1) all show the expected absorptions in the ultraviolet (u.v.) and infrared (i.r.). The nuclear magnetic resonance (n.m.r.) spectrum of the hydroxyketone (**10***a*) presented in Fig. 1, is typical. The first order patterns for H-1, -2, and -3 are diagnostic as may be deduced from Table 2. Hydrogen-1 always shows up as a doublet completely devoid of any secondary splitting. The projected angle between the pseudoequatorial anomeric proton (H-1) and the vinyl hydrogens is approximately 40° and the coupling constant is therefore expected to be small (20). In the present case, J_{13} is apparently as small as zero (cf. 20*c*). The patterns and chemical shifts for H-5, -6, and H′-6 are of course subject to wider variation and these are discussed for the individual cases in the Experimental.

It had been hoped that the primary alcohol ethyl 2,3-dideoxy-α-D-*erythro*-hex-2-enopyranosid-4-ulose (**9***a*) would provide convenient access to the *pent*-2-enopyranosid-4-ulose, **12**, via base-induced retro-aldol liberation of formaldehyde. However, although 83 mole percent of formaldehyde was liberated when **9***a* was treated with base (Scheme 2), the product isolated gave no evidence for an α,β-unsaturated ketone. Apparently **12** (or the initially formed dienolate **11**) was not able to survive in base; hence another route to **12** was developed.

The product from reaction of 3,4-di-*O*-acetyl-D-xylal (**13**) (21) with ethanol using boron trifluoride as catalyst (4*f*) gave only one spot on thin-layer chromatography (t.l.c.); however,

Can. J. Chem. Downloaded from www.nrcresearchpress.com by 210.87.254.105 on 09/05/12
For personal use only.

TABLE 1

Physical constants of some alkyl 2-enopyranosid-4-uloses

Compound	Melting point °C	$[\alpha]_D$* (*c*, in $CHCl_3$)	λ_{max} mμ (ε)	μ_{max}† (cm^{-1})	R_f‡
8	70	−38.85§ (1.02)	226‖ (14 620)	1722, 1702 1633	0.77
10*a*	85–86	−14.50 (2.06)	214¶ (9 025)	3600, 1700 1640	0.52
DNP** of **10***a*	178.5–179.5	−37.60 (0.99)	296†† (25 090)	1618	—
10*b*	50–51	−41.77 (2.60)	213‖ (21 000) 231‖ (13 200)	1721, 1701 1633	0.76
DNP** of **10***b*	156.6–157.5	−12.81 (1.72)	363‖ (27 690)	1721, 1618	—
10*c*	84–85	−29.61 (2.04)	225‖ (17 960)	1701, 1640	0.76
10*d*	41–52.5	−24.14 (2.24)	210‖ (7 800)	1735, 1701 1640	0.73
DNP** of **10***d*	206–208.5	−33.69 (1.40)	362‖ (29 030)	1735, 1618	—
SC‡‡ of **12**	183–184	+4.55 (0.22)	269‖ (9 954)	1553, 1690	—

*23 ± 2 °C.
†In $CHCl_3$.
‡In EtOAc.
§This value was reported incorrectly in the preliminary communication (1).
‖In EtOH.
¶In H_2O.
**DNP = 2,4-dinitrophenylhydrazone.
††In MeOH.
‡‡SC = semicarbazone.

TABLE 2

Nuclear magnetic resonance parameters for H-1, -2, and -3 of some alkyl 2,3-dideoxy-2-enopyranosid-4-uloses in $CDCl_3$*

Compound	Chemical shift† (τ) H-1§	H-2‖	H-3§	Coupling constants‡§ J_{12}	J_{23}
8	4.92	3.20	3.98	3.5	10.0
10*a*	4.82	3.24	4.04	4.0	10.0
10*b*	4.52	2.78	3.60	3.3	10.4
10*c*	4.64	3.00	3.82	3.3	10.4
10*d*	4.82	3.15	3.60	3.0	10.5
12	4.90	3.22	4.02	3.0	10.0

*Spectra were run on a JEOLCO C-60-H or a Varian T-60 spectrometer.
†From internal TMS.
‡Coupling constants measured directly and quoted in Hz.
§In all cases this signal was a doublet completely devoid of any additional splitting, i.e. $J_{13} = 0$.
‖In all cases this signal was a doublet of doublets.

upon deacetylation, two components were detected and the compounds responsible for these were isolated by preparative layer chromatography. The faster-running substance (*A*) was oxidized to the α,β-unsaturated ketone (**12**) in 9 h. However, under the same conditions the slower-running substance (*B*) was surprisingly resistant to oxidation. After treatment with manganese dioxide for 14 days, the bulk of the alcohol was still present as judged by t.l.c., and at no time during this period was there any transient u.v. evidence that an α,β-unsaturated ketone had formed.

In view of these surprising results it was necessary to confirm that *A* and *B* were in fact anomeric compounds. Characterization as the 3,5-dinitrobenzoate esters established that they were isomeric; and since they charred immediately on spraying with sulfuric acid they were indeed the anomeric pent-2-enopyranosides **14**α and **14**β. Substance *A* is tentatively assigned the α-D configuration[6] by examination of the ketone **12** obtained from it, on the assumption that the ketone will preferentially exist in the H1 (≡C1) conformation. Its n.m.r. spectrum (Fig. 2) shows that the three-bond vinyl–allylic coupling J_{12} = 3.0 Hz, is in line with the other values reported in Table 2. A much smaller value (< 1.0 Hz) would have been expected had H-1 been pseudoaxial (20) i.e. if the ketone had the 1H conformation. Again the four-bond vinyl–allylic coupling constant (J_{13}) is 0 Hz, also in line with values reported in Table 2 (see footnote §). Had H-1 been pseudoaxial, J_{13} would be ~ 1.0 Hz (20). The doublets at τ 5.60 and 6.06 with a coupling constant of 16.0 Hz are assigned to H-5*a* and -5*e* respectively in accordance with a recent report from Birkbeck College (22).

[6]These assignments are being examined and will be considered more fully in future publications.

Can. J. Chem. Downloaded from www.nrcresearchpress.com by 210.87.254.105 on 09/05/12
For personal use only.

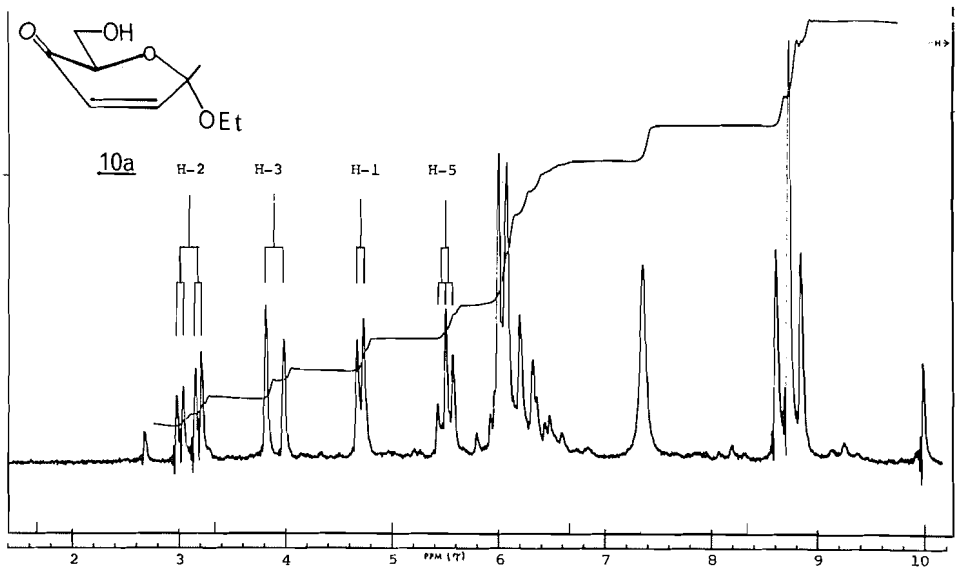

FIG. 1. Nuclear magnetic resonance spectrum (60 MHz) of ethyl 2,3-dideoxy-α-D-*erythro*-hex-2-enopyranosid-4-ulose (**10***a*) in $CDCl_3$ (TMS).

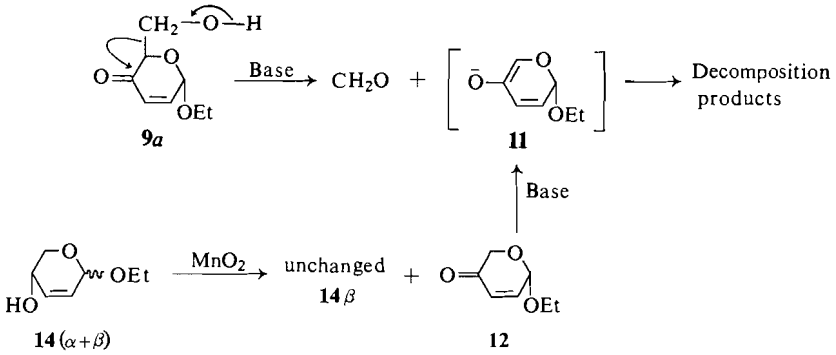

SCHEME 2

The difference in oxidizability of **14**α and **14**β proved fortuitous since it meant that there was no need to separate them prior to oxidation. Thus the mixture was oxidized for 12 h, and ethyl 2,3-dideoxy-pent-2-enopyranosid-4-ulose (**12**) was readily separated from unchanged **14**β by extraction from aqueous solution with petroleum ether. The purity of the ketone (**12**) available by the latter route may be judged by the n.m.r. spectrum it gives (Fig. 2). The ketone (12) was destroyed instantly by treatment with triethylamine to give a number of degradation products which have so far not been characterized. It is not surprising therefore that the attempt to convert **10***a* to **12** with base was unsuccessful.

All of these unsaturated ketones excepting **12** prepared so far are *levo*rotatory (Table 1), in spite of the fact that the parent D-*erythro* compounds (e.g. 7) are all strongly *dextro*rotatory. It is interesting to note that the D-*threo* alcohols (i.e. the 4-epimers of 7) which should be oxidizable to the same ketones (16*b*) are all strongly *levo*rotatory. Furthermore, the saturated ketones, such as **15** are strongly *dextro*rotatory! Experiments to determine what, if any, significance is attached to these observations are currently underway.

A point of some analytical value centers around the behavior of these compounds on t.l.c. plates. Because of the chromophore, the ketones (**10**) are detected readily by exposure to u.v. light, and their behavior on spraying with sulfuric acid is equally instructive. Unlike the parent allylic alcohols which char immediately (4*c*), the ketones are sluggish and frequently require heating to

Can. J. Chem. Downloaded from www.nrcresearchpress.com by 210.87.254.105 on 09/05/12
For personal use only.

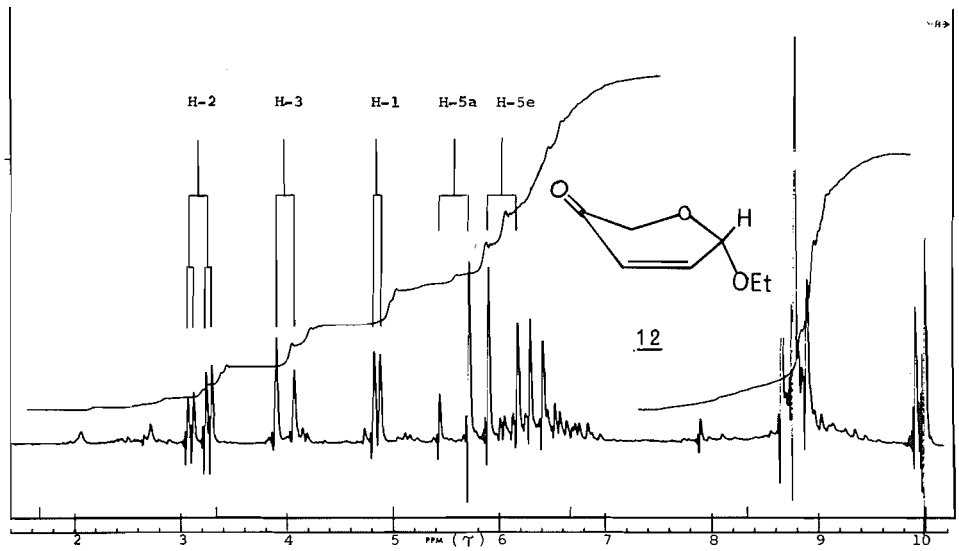

FIG. 2. Nuclear magnetic resonance spectrum (60 MHz) of ethyl 2,3-dideoxy-pent-2-enopyranosid-4-ulose (6-ethoxy-2,6-dihydropyran-3-one) (**12**) in $CDCl_3$ (TMS).

hasten visualization. Consistent with this observation, the ketones are found to be quite stable to acid whereas they are exceedingly labile to base. Thus the u.v. chromophore of **10***a* disappears immediately upon treatment with base, but it persists in acid. If, as has been suggested (*4c*), the acid-lability of the 2-alkenes such as **7** results from the ease with which the allylic carbonium ion forms at C-1, then the behavior of the ketones would indicate that the molecules are polarized away from C-1, and presumably toward C-4. It should be noted, however, that acidification of an aqueous solution of **10***a* caused no enhancement (nor diminution) in the extinction coefficient of the n–π^* or π–π^* chromophore nor was there any shift of the maxima to new wavelengths.

The olefinic double bond of these pyranosiduloses can be hydrogenated to give the saturated ketone (e.g. 15) using 5% palladized charcoal; the carbonyl group remains unaffected even over prolonged periods. Lithium aluminum hydride reduction gives the D-*erythro* compounds (e.g. **9**) exclusively.

The chemistry of these molecules is being studied at the ground as well as the excited state levels. In this way it is hoped to gather information which will define precisely the full synthetic potential of these alkyl 2,3-dideoxy-hex-2-enopyranosid-4-uloses. The failure of **14**β to be oxidized raises a question about the presumed generality of allylic hydroxyl oxidation by manganese dioxide (*16b*). Experiments are underway to determine whether the failure of the reaction is due only to the orientation of the hydroxyl group.

Experimental

Melting points were determined on a Fischer–Johns heating stage and are uncorrected. The n.m.r. spectra were recorded using either a JEOLCO C-60-H, a Varian T-60 or a Varian HA 100 spectrometer, and unless otherwise specified, the solvent was deuteriochloroform containing 1% tetramethylsilane as internal standard. The i.r. spectra were recorded on a Beckman IR-5 spectrometer using chloroform solutions. The u.v. spectra were recorded on a Beckman DBG grating spectrometer. For analytical t.l.c., Merck Silica Gel HF_{254} was used, and for preparative work, the GF_{254} variety was used. The manganese dioxide used for the oxidations was the neutral hydrated form precipitated in alkaline solution as

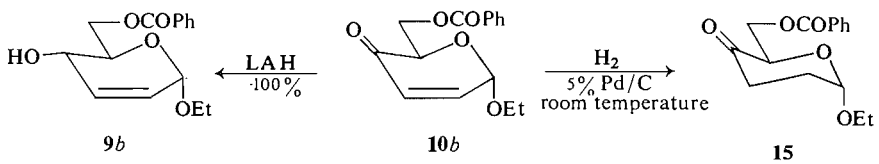

9b **10***b* **15**

SCHEME 3

Can. J. Chem. Downloaded from www.nrcresearchpress.com by 210.87.254.105 on 09/05/12
For personal use only.

Can. J. Chem. Downloaded from www.nrcresearchpress.com by 210.87.254.105 on 09/05/12
For personal use only.

described by Henbest *et al.* (23). After the oxidation the chloroform used as solvent can be collected in a rotary evaporator and used for several subsequent oxidations without prior fractional distillation. Specific rotations were measured using a 0.1 dm tube. Microanalyses were performed by Chemalytics Inc., Tempe, Arizona.

Methyl 6-O-Benzoyl-2,3-dideoxy-α-D-glycero-hex-2-enopyranosid-4-ulose, 8 (R = PhCO)

Methyl 6-*O*-benzoyl-2,3-dideoxy-α-D-*erythro*-hex-2-enopyranoside (**7**; R = PhCO) was prepared by selective benzoylation of the corresponding diol (**7**; R = H) as described previously (3). The benzoate (1.0 g) was dissolved in chloroform (500 ml) and stirred with manganese dioxide (10.4 g) at room temperature. After a reaction period of 6 h, t.l.c. plates developed in petroleum ether (b.p. 35–60°) : ethyl acetate mixture (1:1) and observed under u.v. light showed the disappearance of the starting material and a new faster-running component. The manganese dioxide was removed by filtration through celite and the filtrate was evaporated under reduced pressure. A brown semi-solid residue remained and the crystalline portion (0.11 g) was collected by filtration of the slurry formed by addition of ice-cold ethanol. The ethanolic mother liquors were concentrated, and upon prolonged cooling a further 0.42 g of crystalline material was precipitated, raising the yield of **8** (R = PhCO) to 53%. After two recrystallizations from ethanol the substance had an m.p. of 70°. Its physical properties are listed in Table 1, and n.m.r. parameters for H-1, -2, and -3 are given in Table 2. Hydrogens-5, -6, and H′-6 give overlapping signals in the narrow range τ 5.30–5.40.

Anal. Calcd. for $C_{14}H_{14}O_5$: C, 64.12; H, 5.34. Found: C, 64.03; H, 5.42.

Ethyl 2,3-Dideoxy-α-D-glycero-hex-2-enopyranoside (9a)

Tri-*O*-acetyl-D-glucal was converted to ethyl 4,6-di-*O*-acetyl 2,3-dideoxy-α-D-*erythro*-hex-2-enopyranoside by the method of Ferrier and Prasad (4*f*). A 2% solution of the product in methanol–water–triethylamine mixture (5:4:1) required 2.5 h at room temperature for deacetylation as determined by t.l.c. The solution, after evaporation under reduced pressure, gave the diol **9***a* in quantitative yield from the diacetate. One crystallization from ethyl acetate gave material m.p. 94–96° suitable for use without further purification (c.f. lit. value 99–100° (4*f*)).

Ethyl 2,3-Dideoxy-α-D-glycero-hex-2-enopyranosid-4-ulose (10a)

The olefinic diol **9***a* (5.43 g; 0.03 mole) was dissolved in chloroform (2.5 l) and activated manganese dioxide (54.3 g) was added. Efficient mechanical stirring was maintained, and the progress of the reaction was followed by t.l.c. using ethyl acetate as irrigant. The starting material (R_f = 0.38) had disappeared after 5 h and a new, faster-running spot (R_f = 0.52), detectable by exposure to u.v. light, was produced. After removal of the solids by filtration, the chloroform was evaporated to yield **10***a*, 4.40 g (82% yield) which was analytically pure after one recrystallization from ethanol. Physical constants of **10***a* are recorded in Table 1 and n.m.r. parameters for H-1, -2, and -3 are listed in Table 2. The entire spectrum is shown in Fig. 1; H-5 appears as a triplet at τ 5.60 with J_{56} = 4.5 Hz. Hydrogen-6 and H′-6 are not chemically shifted, and appear as a doublet at τ 6.01 superimposed upon the signal for the methylene protons of the ethoxy aglycon.

Anal. Calcd. for $C_8H_{12}O_4$: C, 55.81; H, 7.02. Found: C, 55.70; H, 6.88.

The hydroxyketone (**10***a*) was also characterized as its 2,4-dinitrophenylhydrazone, physical constants for which are also listed in Table 1.

Anal. Calcd. for $C_{14}H_{16}O_7N_4$: C, 47.73; H, 4.55; N, 15.92. Found: C, 47.97; H, 4.74; N, 15.78.

Ethyl 6-O-Benzoyl-2,3-dideoxy-α-D-glycero-hex-2-enopyranosid-4-ulose (10b)

(*a*) In a manner similar to that described above for the analogous methyl glucoside **7** (R = PhCO), ethyl 2,3-dideoxy-α-D-*glycero*-hex-2-enopyranoside (**9***a*) was benzoylated selectively at the primary position. The syrupy monoester was oxidized directly in the manner described above and the ketone (**10***b*) crystallized on prolonged cooling (40% yield).

(*b*) Ketone **10***a* (0.50 g, 0.003 mole) was dissolved in methylene chloride (6 ml) and cooled to −30° with Dry-Ice acetone before adding dry pyridine (3 ml). Benzoyl chloride (0.61 ml, 0.73 g, 0.005 mole) was added dropwise during 0.5 h and the mixture was maintained for an additional 0.5 h at −30°. It was then placed in the refrigerator (ca. 8°) for 10 h at which time t.l.c. indicated that the reaction was complete. The mixture was poured into ice–water mixture (ca. 50 ml) and the ester was extracted with methylene chloride. After drying with calcium chloride the methylene chloride was evaporated on a rotary evaporator and traces of pyridine were removed by co-distillation with toluene. On standing in the refrigerator the syrupy residue deposited 0.61 g (81% yield) of the benzoate **10***b*.

Its physical constants are recorded in Table 1 and n.m.r. parameters in Table 2.

The substance was characterized as its 2,4-dinitrophenylhydrazone, physical constants for which are also shown in Table 1.

Anal. Calcd. for $C_{21}H_{20}O_8N_4$: C, 55.26; H, 4.39; N, 12.28. Found: C, 55.15; H, 4.28; N, 11.36.

Ethyl-6-O-p-toluenesulfonyl 2,3-Dideoxy-α-D-glycero-hex-2-enopyranosid-4-ulose (10c)

Ketone **10***a* (0.50 g, 0.003 mole) was esterified with *p*-toluenesulfonyl chloride (1.11 g, 0.005 mole) in a manner similar to that described above for benzoylation except that the reaction period was 14 h. The residue from the usual work up was crystallized from petroleum ether – diethyl ether mixture (3:1) affording a 0.71 g, 75% yield. A second crystallization gave material (**10***c*) whose physical properties are recorded in Table 1 and n.m.r. parameters for H-1, -2, and -3 in Table 2. Hydrogen-6*e* shows up as a four-line pattern (c.f. 24) centered at τ 5.34; the signals for H-6*a* and -5 overlap around τ 5.5.

Anal. Calcd. for $C_{15}H_{18}O_6S$: C, 55.20; H, 5.56. Found: C, 55.24; H, 5.50.

Ethyl 6-O-Acetyl-2,3-dideoxy-α-D-glycero-hex-2-enopyranosid-4-ulose (10d)

Ketone **10***a* (0.50 g, 0.003 mole) was added to pyridine which had been cooled in an ice–salt bath. Acetic anhydride (1.3 ml) was added with good stirring and the cooling was maintained until the reaction was complete (t.l.c., 3 h). Methanol (5 ml) was added to utilize the

Can. J. Chem. Downloaded from www.nrcresearchpress.com by 210.87.254.105 on 09/05/12
For personal use only.

excess acetic anhydride and then the solution was evaporated under reduced pressure at 40°. Toluene was evaporated from the residue three times to remove the pyridine. The residue was crystallized from ethanol to give 0.283 g of **10***d* (46% yield). Physical constants for the keto-acetate are recorded in Table 1 and n.m.r. parameters for H-1, -2, and -3 are recorded in Table 2. Hydrogen-6*a* occurs as four lines between τ 5.19 and 5.36; H-5 and -6*e* give overlapping signals between τ 5.40 and 5.57 (c.f. 27).

The keto-acetate (**10***d*) was characterized as its 2,4-dinitrophenyldrazone, physical constants for which are shown in Table 1.

Anal. Calcd. for $C_{16}H_{18}O_8N_4$: C, 48.73; H, 4.57; N, 14.2. Found: C, 48.72; H, 4.34; N, 13.17.

*Ethyl 2,3-Dideoxy-α-*D*-glycero-hexopyranosid-4-ulose and its 6-O-Benzoyl Derivative* ***15***

The benzoylated ketone (**10***b*) (0.1 g) was dissolved in ethyl acetate and 5% palladized charcoal (0.01 g) was added. Hydrogenation at atmospheric pressure and ambient temperature was continued until the uptake of hydrogen ceased (usually within 1 h). Prolonged exposure to hydrogen caused no further reaction. The catalyst was removed by filtration through celite. The residue after evaporation showed the absence of olefinic protons in the n.m.r., and the i.r. absorption for the α,β-unsaturated ketone at 1701 cm^{-1} had disappeared. The material (**15**) was a syrup; $[\alpha]_D^{23} = +128.4$ (*c*, 2.16 in chloroform), which was characterized as its 2,4-dinitrophenylhydrazone; m.p. 156.5–157.5; $[\alpha]_D^{23} = +184.0$ (*c*, 0.82 in chloroform).

Anal. Calcd. for $C_{21}H_{22}O_8N_4$: C, 55.01; H, 4.80; N, 12.23. Found: C, 54.72; H, 4.66; N, 11.58.

The hydroxyketone **10***a* could similarly be hydrogenated to a dihydroketone; $[\alpha]_D^{23} = +29.5$ (*c*, 1.26 in chloroform).

Ethyl 2,3-Dideoxy-α- and β-D-*Glycero-pent-2-enopyranosides (****14****α and* ***14****β)*

3,4-Di-*O*-acetyl-D-xylal (**13**) (21) (16 g) was treated with ethanol (6.4 ml) and boron trifluoride etherate (3.2 ml) for 1 h. The residue (12.3 g) from the usual work up (4*f*) showed on t.l.c. an intense new spot, but the starting diacetyl xylal, which is readily recognized by the rose color it forms when sprayed with sulfuric acid, was completely absent. The material was allowed to stand in 350 ml of triethylamine–water–methanol mixture (1:4:5) for 2.5 h and the resulting deacetylated substance (11.3 g) showed two discrete spots, R_f 0.58 and 0.46, *A* and *B* respectively, on t.l.c. in petroleum ether – ethyl acetate mixture (1:1). The mixture (300 mg) was separated on a preparative layer chromatogram made from 60 g of silica gel. The plate was developed three times successively in the irrigant used for the analytical run; the plate was allowed to dry completely between developments. The spots were visualized by spraying at the edges with sulfuric acid, and an overlapping zone was discarded.

A pure sample of *A* (64 mg) obtained from the preparative chromatogram $[\alpha]_D^{23} = +22.2$ (*c*, 0.2 in chloroform) showed the following n.m.r. spectral parameters: H-1: τ 4.99, $J_{12} = 2.5$, $J_{13} = 1.1$ Hz; H-2: τ 4.26, $J_{23} = 10.0$ Hz; H-3: τ 3.70.

The compound was characterized as the 3,5-dinitrobenzoate ester; m.p. 148–148.5°.

Anal. Calcd. for $C_{14}H_{14}O_8N_2$: C, 49.71; H, 4.14; N, 8.28. Found: C, 49.41; H, 3.96; N, 7.57.

Compound *B* obtained from the preparative chromatogram (48 mg) $[\alpha]_D^{23} = +44.3$ (*c*, 5.8 in chloroform) showed the following n.m.r. parameters: H-1: τ 5.12, $J_{12} = 3.0$, $J_{13} = 0$ Hz; H-2: τ 4.19, $J_{12} = 3.0$, $J_{23} = 10.5$ Hz; H-3: τ 3.91, $J_{13} = 0$, $J_{23} = 10.5$ Hz; H-5*e*: τ 5.88, $J_{5a5e} = 13.0$, $J_{4,5e} = 3.0$ Hz.

The substance was characterized as its 3,4-dinitrobenzoate ester: m.p. 165–165.5°.

Anal. Calcd. for $C_{14}H_{14}O_8N_2$: C, 49.71; H, 4.14; N, 8.28. Found: C, 49.62; H, 4.00; N, 7.57.

*Ethyl 2,3-Dideoxy-pent-2-enopyranosid-4-ulose (6-Ethoxy-2,6-dihydropyran-3-one) (****12****)*

(*a*) A portion of **14**α (*A*) obtained above (0.050 g) was dissolved in 37 ml of chloroform and stirred with manganese dioxide (0.55 g) for 7 h, at which time t.l.c. showed the complete disappearance of the alcohol. The product isolated in the usual way weighed 35 mg, 70% yield. It was identified as ketone **12** (vide infra).

(*b*) The crude mixture of alcohols obtained from the methylene chloride layer (see above experiment) (5.0 g) was dissolved in 2.5 l of chloroform and oxidized with manganese dioxide (53 g) for 14 h. The solid was removed by filtration and the chloroform by evaporation under reduced pressure. The residue was dissolved in methylene chloride and washed well with water. The organic phase after drying with calcium chloride and evaporation afforded 0.923 g of substance. This was dissolved in water and poured into a separatory funnel. Petroleum ether (60–80°) was swirled *very gently* with the aqueous phase. The dried organic layer afforded 0.118 g of ketone **12**. The substance obtained in this way gave the n.m.r. spectrum shown in Fig. 2; H-1: τ 4.90, $J_{12} = 3.0$, $J_{13} = 0$ Hz; H-2: τ 3.22, $J_{12} = 3.0$, $J_{23} = 10.0$ Hz; H-3: τ 4.02, $J_{13} = 0$, $J_{23} = 10.0$ Hz; H-5*a*: τ 5.60, $J_{5a5e} = 16.0$ Hz; H-5*e*: τ 6.06, $J_{5a5e} = 16.0$ Hz. The ketone was a syrup which was characterized as its semicarbazone, m.p. 183–184°; $[\alpha]_D^{23} = +4.55$ (*c*, 0.22 in chloroform); $\lambda_{max} =$ 269 (ε, 9954) in ethanol; $\mu_{max} = 1553$ and 1690 cm^{-1} in chloroform.

Anal. Calcd. for $C_8H_{13}O_3N_3$: C, 48.23; H, 6.52; N, 21.12. Found: C, 48.41; H, 6.21; N, 21.41.

We are grateful to the National Research Council of Canada and the Department of University Affairs of Ontario for generous financial support. We are deeply indebted to Varian Associates of Toronto for lending the Varian T-60 n.m.r. spectrometer to the Chemistry Department. Some technical assistance by Mrs. S. Subramanian is acknowledged.

1. B. Fraser-Reid, A. McLean, and E. W. Usherwood. J. Amer. Chem. Soc. **91**, 5392 (1969).
2. J. M. Sugihara and G. U. Yuen. J. Amer. Chem. Soc. **79**, 5780 (1957); W. G. Overend. Chem. Ind. (London), 342 (1963) and references cited therein; V. M. Parikh and J. K. N. Jones. Can. J. Chem. **43**, 3452 (1965); P. T. Benyon, P. M. Collins, D. Gardiner, and W. G. Overend. Carbohyd. Res. **6**, 431 (1968); D. Horton, M. Nakadate, and J. M. J. Trochet. Carbohyd. Res. **7**, 56 (1968); K. G. A. Jackson and J. K. N. Jones. Can. J. Chem. **47**, 2498 (1969).
3. B. Fraser-Reid and B. Boctor. Can. J. Chem. **47**, 393 (1969).

4. (*a*) R. J. FERRIER. J. Chem. Soc. 5443 (1964); (*b*) R. S. TIPSON and A. COHEN. Carbohyd. Res. **1**, 338 (1965); (*c*) E. ALBANO, D. HORTON, and T. TSUCHIYA. Carbohyd. Res. **2**, 349 (1966); (*d*) R. U. LEMIEUX, E. FRAGA, and K. A. WATANABE. Can. J. Chem. **46**, 61 (1968); (*e*) A. ROSENTHAL and J. N. C. WHYTE. Can. J. Chem. **46**, 2245 (1968); (*f*) R. J. FERRIER and N. PRASAD. J. Chem. Soc. C. 570 (1969); (*g*) R. D. GUTHRIE, R. D. WELLS, and G. J. WILLIAMS. Carbohyd. Res. **10**, 172 (1969).
5. R. J. FERRIER. Chem. Brit. **5**, 15 (1969); L. HOUGH, R. KHAN and B. A. OTTER. *In* Deoxy Sugars. *Edited by* S. Hanessian. American Chemical Society Publications, 1966; J. S. BRIMACOMBE. Chem. Brit. **2**, 9 (1966); A. ROSENTHAL and L. B. NGUYEN. Tetrahedron Lett. 2393 (1968); A. ROSENTHAL and H. J. KOCH. J. Amer. Chem. Soc. **90**, 2182 (1968); D. HORTON, J. B. HUGHES, and J. K. THOMPSON. J. Org. Chem. **33**, 728 (1968); R. U. LEMIEUX and S. W. GUNNER. Can. J. Chem. **46**, 397 (1968); R. U. LEMIEUX and T. L. NAGABUSHAN. Can. J. Chem. **46**, 401 (1968).
6. F. SHAFIZADEH. Advan. Carbohyd. Chem. **11**, 263 (1956).
7. R. U. LEMIEUX and M. L. WOLFROM. Advan. Carbohyd. Chem. **3**, 337 (1948).
8. E. D. BERGMANN, D. GINSBURG, and R. PAPPO. *In* Organic reactions. R. Adams, *Editor*. John Wiley and Sons, Inc., New York, **10**, 179 (1959); J. A. MARSHALL and W. S. JOHNSON. J. Org. Chem. **28**, 421 (1963); E. J. COREY and D. CROUSE. J. Org. Chem. **33**, 298 (1968); D. H. R. BARTON, E. F. LIER, and J. F. MCGHIE. J. Chem. Soc. 1031 (1968).
9. A. BEELIK. Advan. Carbohyd. Chem. **11**, 145 (1956).
10. F. SMITH. Advan. Carbohyd. Chem. **2**, 79 (1946).
11. P. J. BENYON, P. M. COLLINS, P. T. DOGANGES, and W. G. OVEREND. J. Chem. Soc. C, 1131 (1966).
12. B. FLAHERTY, W. G. OVEREND, and N. R. WILLIAMS. J. Chem. Soc. C, 398 (1966).
13. E. F. L. J. ANET. Austr. J. Chem. **15**, 503 (1962).
14. E. F. L. J. ANET. Carbohyd. Res. **1**, 348 (1966).
15. K. BOCK and C. PEDERSEN. Tetrahedron Lett. 2983 (1969).
16. (*a*) O. MANCERA, G. ROSENKRANZ, and F. SONDHEIMER. J. Chem. Soc. 2189 (1953); (*b*) F. SONDHEIMER, C. AMENDOLLA, and G. ROSENKRANZ. J. Amer. Chem. Soc. **75**, 5930 (1953); (*c*) E. J. COREY and D. CROUSE. J. Org. Chem. **33**, 298 (1968).
17. M. BERGMANN. Ann. **443**, 223 (1925).
18. (*a*) H. BRUDERER, D. ARIGONI, and O. JEGER. Helv. Chim. Acta, **39**, 858 (1956); (*b*) M. Z. BARAKAT, M. F. ABDEL-WAHAB and M. M. EL-SADR. J. Chem. Soc. 4685 (1956).
19. See for example S. LALAND, W. G. OVEREND, and M. STACEY. J. Chem. Soc. 738 (1950).
20. (*a*) E. W. GARBISCH. J. Amer. Chem. Soc. **86**, 5562 (1962); (*b*) R. J. FERRIER and N. PRASAD. J. Chem. Soc. C, 581 (1969); M. SHARMA and R. K. BROWN. Can. J. Chem. **44**, 2825 (1966).
21. F. WEYGAND. Methods Carbohyd. Chem. **1**, 182 (1962).
22. R. F. BUTTERWORTH, P. M. COLLINS, and W. G. OVEREND. Chem. Commun. 378 (1969).
23. H. B. HENBEST, E. R. H. JONES, and T. C. OWEN. J. Chem. Soc. 4909 (1957).
24. L. D. HALL and L. F. JOHNSON. Tetrahedron, **20**, 883 (1964).

Can. J. Chem. Downloaded from www.nrcresearchpress.com by 210.87.254.105 on 09/05/12
For personal use only.

Benzene solvent induced shifts of the proton magnetic resonance spectra of some benzene derivatives. Importance of charge effects

R. WASYLISHEN, T. SCHAEFER, AND R. SCHWENK
Chemistry Department, University of Manitoba, Winnipeg, Manitoba
Received April 27, 1970

The benzene solvent shifts of the proton magnetic resonance spectra of numerous polysubstituted benzene derivatives are measured with respect to cyclohexane as reference solvent. For many of these compounds, an additive scheme can be devised in which the effect of a substituent, X, on the solvent shift, Δ, of a proton is given by Δ_i^X so that $\Delta = \Sigma_x \Sigma_i \Delta_i^X$ where i = ortho, meta, or para. There is a linear correlation of Δ_m^X or Δ_p^X with Taft's substituent constants σ_m^0 and σ_p^0. It is suggested that charge effects are much more important than steric effects in determining both the magnitude and sign of Δ.

Canadian Journal of Chemistry, 48, 2885 (1970)

Introduction

Aromatic solvent induced shifts (a.s.i.s.) of proton magnetic resonance (p.m.r.) spectra have been studied intensively (1–4). Apart from their utility in the simplification of complex spectra and in the structural and stereochemical elucidations of organic molecules, a.s.i.s. have been investigated with a view to specifying the physical nature of the interaction between a solute molecule and the aromatic solvent: its geometry, its stoichiometry, and its energy (1, 2, 5). The interaction has been widely assumed to involve a 1:1 complex with a heat of formation near kT (6, 7) and rather precise geometries have often been proposed for this complex (8, 9).

Reasonable and sometimes severe doubt exists as to the general and continuing usefulness of this model (1, 10–13). Thus, the existence of a 1:1 complex in the solid state at a certain relative concentration of the two components as indicated, say, by the phase diagram, does not prove its existence in the liquid unless, of course, the heat of formation of the complex is of sufficient magnitude: never the case in the systems under discussion. Nor does the absence of a charge-transfer band in the optical spectrum of a solution (14) disprove the existence of the complex of one aromatic molecule with another: symmetry may forbid such a band and the interaction energy may be a dispersion or a polarization energy (15). The problem is complex. Precise and consistent descriptions in terms of thermodynamic parameters are not likely in the near future.

However, the available results suggest that in many instances a.s.i.s. arise from nonrandom orientations of the benzene solvent molecules in the vicinity of the solute molecule, a probable consequence of weak specific solute–solvent interactions. The a.s.i.s. often depend additively on the various substituents in a solute molecule and the solvent molecules tend to avoid electron-rich relative to electron-deficient regions of the solute molecule (16).

In the absence of a sophisticated and generally useful model, there is predictive value in correlating a.s.i.s. with well-defined parameters of the solute molecules (these parameters, e.g., dipole moments or sigma constants, can sometimes be derived most simply by a.s.i.s. measurements on a single peak in a nuclear magnetic resonance (n.m.r.) spectrum). This paper takes such an empirical approach to the discussion and systematization of the a.s.i.s. values for about 200 protons in many benzene derivatives.

Experimental

The benzene derivatives, obtained from the usual commercial sources, were used without further purification. Peaks due to impurities would have been easily recognized. 1-Bromo-3-chloro-5-iodobenzene was prepared by the method of Ault and Kraig (17). The compounds were prepared as 3 mole % solutions in benzene-d_6 and cyclohexane and were degassed by the freeze–pump–thaw technique.

Proton resonance spectra were measured at 28.5 ± 1 °C and calibrated by period averaging in the frequency sweep mode of a Varian DA-60-I spectrometer locked to internal tetramethylsilane (TMS). Peak positions were normally obtained with a precision of better than 0.05 Hz.

Nontrivial spectra were analyzed with the aid of LAOCOON 3 (18), total root mean square errors lying between 0.004 and 0.025 Hz. Matched experimental and computed spectral curves were often compared. In some cases three-spin systems were also analyzed by the method of Castellano and Waugh (19) and Cavanaugh (20).

Can. J. Chem. Downloaded from www.nrcresearchpress.com by 210.87.254.5 on 09/05/12
For personal use only.

Can. J. Chem. Downloaded from www.nrcresearchpress.com by 210.87.254.5 on 09/05/12
For personal use only.

The spectrum of 2,3-dichloronitrobenzene in benzene-d_6 was ABC, approaching AB_2, and an iteration to a consistent set of parameters was not possible using LAOCOON 3. The chemical shifts, however, could be extracted with sufficient accuracy by analyzing the spectrum as AB_2.

The shifts are not those at infinite dilution. The a.s.i.s. values (Δ) in the present study are: shift relative to internal TMS in a 3 mole % solution in benzene minus the shift relative to internal TMS in a 3 mole % solution in cyclohexane. A few dilution experiments with representative solutes indicated that the measured Δ values at 3 mole % could differ from their infinite dilution values by as much as 10%. However, such differences are systematic in the following sense. Consider two observed Δ values which deviate from their infinite dilution values by 7 and 10%. Because the observed Δ values are *always* smaller than the ones at infinite dilution, the errors tend to cancel in a comparison of the two Δ values and are not near 17%. The quoted deviation above includes the effect of dilution by TMS in the benzene solutions.

Our use of 3 mole % solutions, although not ideal, follows the general practice in this field of using dilute solutions without extrapolating to infinite dilution. The ideal practice would use an external reference (21) but, in the absence of the field configuration of a solenoid magnet (22), the uncertainties in the bulk susceptibilities also lead to considerable errors. The recent work of Becconsall *et al.* (22) with two field configurations implies that an approximate conversion to their newly defined reference–independent solvent shift, $\bar{\Delta}$, can be made for our data by adding 25 Hz to the Δ values in Table 1.

Results and Discussion

In Table 1 the proton chemical shifts of polysubstituted benzenes as 3 mole % solutions in cyclohexane and benzene-d_6 are given. The shifts are reported in Hz in the fashion adopted by at least some other workers (23–25) when reporting the results of the precise analyses of a series of molecules. The number of significant figures is consistent with the precision of our analyses (the reader may convert these primary data to other scales, giving due consideration to the uncertainties mentioned in the Experimental section).

For purposes of discussion, the first 48 compounds in Table 1 are trisubstituted (except for 1,3-dichlorobenzene, no. **13**) and contain no more than two adjacent substituents. The next 51 compounds are 1,2,3-tri-, tetra-, or penta-substituted derivatives.

(1) Additivity of Substituent Effects on the Solvent Shifts, Δ

In early work Diehl (26, 27) demonstrated that in disubstituted benzenes, the Δ value of a given proton is a linear superposition of contributions from the individual substituents, X. If Δ_i^X represents the contribution of substituent X to the total Δ of a proton in position i (i = ortho, meta, or para) relative to X then $\Delta = \sum_i \sum_X \Delta_i^X$. Agreement between observed and calculated Δ values was reasonably good (deviation of up to 10% of the observed Δ or more generally up to 2 to 3 Hz at 60 Mz) but became markedly worse when substituents were placed ortho to one another. Diehl derived mainly Δ_o^X and Δ_m^X values and used an external reference for 5 mole % solutions.

In Table 2 are given $\Delta_{o,m,p}^X$ values for nine substituents (a sizeable series of compounds having X = OCH_3 was also analyzed but a "reasonable" set of Δ^X values for OCH_3 evaded our analysis). These Δ^X values were derived by writing numerous equations in Δ and Δ_i^X, followed by judicious minimization of the deviations between observed and calculated Δ values. A simple systematic minimization procedure was not applicable because of the varied nature of the combinations of substituents in our compounds. The Δ_i^X values in Table 2 were derived from those trisubstituted compounds containing no more than two adjacent substituents. This was done to avoid as far as possible the compounding of the difficulty pointed out by Diehl. Nomura and Takeuchi (28) recently measured values under our conditions for a series of xylene derivatives and their data were also used in finding Δ^{CH_3} and Δ^{OH} values.

The Δ_i^X values in Table 2 are not a unique set. They are derived for cyclohexane as the reference solvent and for 3 mole % solutions. Thus, if carbon tetrachloride (a better solvent in general and therefore less "inert") were used as the reference solvent the Δ_i^X values would be a little larger because proton shifts in this solvent are normally somewhat to low field of those in cyclohexane (29). Nevertheless, as long as an internal reference is used, the Δ_i^X values in Table 2 can probably be applied with some confidence to other polysubstituted benzenes when carbon tetrachloride or chloroform are the reference solvents, but deviations of observed from calculated Δ values will likely be larger than those discussed next.

(a) Δ Values for the First 48 Compounds in Table 1

In Table 1 the deviations between 108 observed and calculated Δ values average to 1.6 Hz

TABLE 1

Observed and calculated solvent shifts of the ring protons in some benzene derivatives

Compound	Proton	In C_6H_{12}†	In C_6D_6†	$\Delta_{C_6D_6}^{C_6H_{12}}$	Δ (calcd.)‡	Deviation
2,4-Dichloronitrobenzene (**1**)	H_3	446.603	404.064	42.54	41.61	0.93
	H_5	434.837	382.760	52.08	53.88	−1.80
	H_6	463.205	411.998	51.20	47.39	3.81
2,5-Dichloronitrobenzene (**2**)	H_3	440.33	386.64	53.69	53.13	0.56
	H_4	439.77	387.72	52.05	52.05	0.00
	H_6	464.56	424.75	39.81	35.87	3.94
3,4-Dichloronitrobenzene (**3**)	H_2	495.247	462.678	32.57	35.87	−3.30
	H_5	449.364	395.922	53.44	53.13	0.31
	H_6	478.083	434.379	43.70	48.14	−4.44
1,2,4-Trimethoxybenzene (**4**)	H_3	382.82	390.21	−7.39	—	—
	H_5	374.08	377.57	−3.49	—	—
	H_6	398.25	398.55	−0.30	—	—
2,5-Dimethoxychlorobenzene (**5**)	H_3	400.819	384.157	16.66	—	—
	H_4	395.885	393.088	2.79	—	—
	H_6	410.258	416.408	−6.15	—	—
3-Chloro-4-fluoronitrobenzene (**6**)	H_2	495.57	461.182	34.39	34.70	−0.31
	H_5	428.44	369.364	59.08	55.62	3.46
	H_6	483.91	437.530	46.38	46.97	−0.59
3,5-Dichloroaniline (7)	H_2, H_6	382.116	358.31	23.81	23.93	−0.12
	H_4	398.22	398.52	−0.30	−0.98	0.68
2,5-Dichloroaniline (5 mole % in both C_6D_6 and C_6H_{12}) (**8**)	H_3	419.83	405.681	14.15	12.80	1.35
	H_4	391.61	381.765	9.85	10.72	−0.87
	H_6	393.95	369.880	24.07	23.18	0.89
3,5-Dichlorobenzaldehyde (**9**)	H_2, H_6	457.43	428.84	28.59	—	—
	H_4	448.72	421.18	27.54	—	—
3-Chloro-4-bromonitrobenzene (**10**)	H_2	493.166	461.172	32.00	35.24	−3.24
	H_5	460.991	407.694	53.30	52.13	1.17
	H_6	472.228	428.618	43.61	47.51	−3.90
2,4-Dichloroaniline (**11**)	H_3	428.020	424.307	3.71	1.10	2.61
	H_5	413.320	404.088	9.23	13.37	−4.14
	H_6	387.817	353.883	33.94	34.70	−0.76
3,5-Dichlorobenzonitrile (**12**)	H_2, H_6	444.35	396.44	47.91	44.86	3.05
	H_4	447.97	409.33	38.64	38.07	0.57
1,3-Dichlorobenzene (**13**)	H_2	436.68	425.82	10.86	7.22	3.64
	H_4, H_6	426.59	407.21	19.38	19.49	−0.11
	H_5	423.74	391.15	32.59	31.76	0.83
3,5-Dichloronitrobenzene (**14**)	H_2, H_6	482.56	449.38	33.18	36.62	−3.44
	H_4	453.44	410.74	42.70	40.53	2.23
3,5-Dichlorophenol (**15**)	H_2, H_6	397.25	373.66	23.59	26.79	−3.20
	H_4	411.72	404.44	7.28	8.29	−1.01
3,5-Dimethylaniline (**16**)	H_2, H_6	366.50	362.57	3.93	2.26	1.67
	H_4	376.10	381.34	−5.24	−9.08	3.84
1,3,5-Trimethoxybenzene (**17**)	H_2, H_4, H_6	357.65	372.22	−14.57	—	—
1,3,5-Trifluorobenzene (**18**)	H_2, H_4, H_6	389.95	368.42	21.53	24.93	−3.40
1,3,5-Trichlorobenzene (**19**)	H_2, H_4, H_6	429.78	406.68	23.10	23.10	0.00
1,3,5-Tribromobenzene (**20**)	H_2, H_4, H_6	451.26	429.54	21.72	22.95	−1.23
3,5-Dichlorobromobenzene (**21**)	H_2, H_6	439.50	416.94	22.56	22.10	0.46
	H_4	432.18	408.60	23.58	24.95	−1.37
1-Bromo-3-chloro-5-iodobenzene (**22**)	H_2, H_4	442.02	419.22	22.80	20.30	2.50
	H_6	449.04	427.68	21.36	19.63	1.73
1,2,4-Trichlorobenzene (**23**)	H_3	441.30	418.44	22.86	22.35	0.51
	H_5	422.52	387.90	34.62	34.62	0.00
	H_6	433.38	400.02	33.36	33.87	−0.51
1,2,4-Tribromobenzene (**24**)	H_3	460.92	440.76	20.16	19.72	0.44
	H_5	428.94	392.70	36.24	34.84	1.40
	H_6	439.86	408.48	31.38	31.61	−0.23
1-Bromo-2,5-dichlorobenzene (**25**)	H_3	433.62	402.66	30.96	33.24	−2.28
	H_4	425.16	388.14	37.02	36.47	0.55
	H_6	451.98	430.80	21.18	21.35	−0.17
1-Bromo-3,4-dichlorobenzene (**26**)	H_2	450.78	428.22	22.56	21.35	1.21
	H_5	429.84	394.32	35.52	33.24	2.28
	H_6	431.22	398.40	32.82	33.62	−0.80
1-Iodo-2,4-dichlorobenzene (**27**)	H_3	466.26	447.66	18.60	21.62	−3.02
	H_5	423.00	390.48	32.52	33.89	−1.37
	H_6	436.98	404.16	32.82	31.40	1.42

Can. J. Chem. Downloaded from www.nrcresearchpress.com by 210.87.254.5 on 09/05/12
For personal use only.

TABLE 1 *(Continued)*

Compound	Proton	In C_6H_{12}†	In C_6D_6†	$\Delta_{C_6D_6}^{C_6H_{12}}$	Δ(calcd.)‡	Deviati
1-Iodo-2,5-dichlorobenzene (**28**)	H_3	432.78	398.76	34.02	33.14	0.8
	H_4	427.14	394.32	32.82	32.82	0.0
	H_6	466.32	447.36	18.96	19.88	−0.9
1-Iodo-3,4-dichlorobenzene (**29**)	H_2	461.88	440.88	21.00	19.88	1.1
	H_5	420.60	383.76	36.84	33.14	3.7
	H_6	442.80	413.34	29.46	32.15	−2.6
1-Fluoro-3,4-dichlorobenzene (**30**)	H_2	425.04	400.50	24.54	24.84	−0.3
	H_5	436.08	402.48	33.60	32.78	0.8
	H_6	406.92	372.90	34.02	37.11	−3.0
1-Fluoro-2,4-dibromobenzene (**31**)	H_3	456.72	435.54	21.18	19.18	2.0
	H_5	435.72	402.30	33.42	34.30	−0.8
	H_6	409.62	372.12	37.50	35.10	2.4
3,5-Difluoroiodobenzene (**32**)	H_2, H_6	429.90	408.72	21.18	19.97	1.2
	H_4	398.88	373.56	25.32	26.28	−0.9
3,5-Dichlorotoluene (**33**)	H_2, H_6	416.82	399.06	17.76	19.05	−1.2
	H_4	424.92	420.18	4.74	5.48	−0.7
3,5-Dimethylaniline* (**34**)	H_2, H_6	366.6	363.6	3.0	2.26	0.7
	H_4	375.6	382.8	−7.2	−9.08	1.8
3,5-Dimethylphenol* (**35**)	H_2, H_6	382.20	375.60	6.6	5.12	1.4
	H_4	387.0	385.8	1.2	0.19	1.0
3,5-Dimethylchlorobenzene* (**36**)	H_2, H_6	412.2	410.4	1.8	1.43	0.3
	H_4	403.8	390.0	13.8	15.0	−1.2
3,5-Dimethylbromobenzene* (**37**)	H_2, H_6	422.4	420.0	2.4	0.43	1.9
	H_4	406.8	391.2	15.6	16.85	−1.2
3,5-Dimethyliodobenzene* (**38**)	H_2, H_6	436.2	433.2	3.0	−1.04	4.0
	H_4	409.2	392.4	16.8	13.20	3.6
3,5-Dimethylbenzonitrile* (**39**)	H_2, H_6	426.6	402.6	24.0	23.19	0.8
	H_4	424.2	394.8	29.4	29.97	−0.5
3,5-Dimethylnitrobenzene* (**40**)	H_2, H_6	466.2	454.8	11.4	14.95	−3.5
	H_4	430.2	396.6	33.6	32.43	1.1
2,4-Dimethylaniline* (**41**)	H_3	402.0	406.8	−4.8	−7.00	2.2
	H_5	400.8	409.2	−8.4	−8.30	−0.1
	H_6	379.8	381.0	−1.2	−0.98	−0.2
2,4-Dimethylphenol* (**42**)	H_3	403.2	406.2	−3.0	−2.65	−0.3
	H_5	401.4	405.0	−3.6	−3.95	0.3
	H_6	387.0	383.4	3.6	1.88	1.7
2,4-Dimethylchlorobenzene* (**43**)	H_3	414.0	400.2	13.8	14.25	−0.4
	H_5	407.4	396.6	10.8	12.95	−2.1
	H_6	424.8	427.2	−2.4	−1.81	−0.5
2,4-Dimethylbromobenzene* (**44**)	H_3	414.6	400.2	14.4	13.62	0.7
	H_5	402.0	390.6	11.4	12.32	−0.9
	H_6	436.8	441.0	−4.2	—	—
2,4-Dimethyliodobenzene* (**45**)	H_3	417.6	400.8	16.8	13.52	3.2
	H_5	394.8	381.0	13.8	12.22	1.5
	H_6	453.6	454.8	−1.2	−4.28	3.0
2,4-Dimethylbenzonitrile* (**46**)	H_3	420.0	389.4	30.6	30.65	−0.0
	H_5	417.0	387.6	29.4	29.35	0.0
	H_6	438.0	421.2	16.8	19.95	−3.1
2,4-Dimethylnitrobenzene* (**47**)	H_3	420.0	387.6	32.4	33.51	−1.1
	H_5	418.2	390.0	28.2	32.21	−4.0
	H_6	465.0	457.2	7.8	11.71	−3.9
Mesitylene (**48**)	ring	400.32	402.54	−2.22	−2.62	0.4
2,3-Dichloronitrobenzene (**49**)	H_4	451.15	402.397	48.75	52.05	−3.3
	H_5	431.04	370.131	60.91	65.40	−4.4
	H_6	451.15	405.730	45.42	48.14	−2.7
1,2,3-Trimethoxybenzene (**50**)	H_4, H_6	385.96	382.94	3.02	—	—
	H_5	406.56	409.85	−3.29	—	—
2,6-Dimethoxytoluene (**51**)	H_3, H_5	382.22	381.83	0.39	—	—
3 mole % in C_6D_6; 5 mole % in C_6H_{12}	H_4	146.42	422.29	−5.87	—	—
2,6-Dichloroaniline (**52**)	H_3, H_5	422.08	411.08	11.00	13.37	−2.3
	H_4	387.12	367.52	19.60	22.06	−2.4
2,6-Dibromoaniline (**53**)	H_3, H_5	434.00	422.315	11.68	14.22	−2.5
	H_4	379.06	359.38	19.68	20.80	−1.1
2,6-Dichlorobenzaldehyde (**54**)	H_3, H_5	434.72	403.02	31.70	—	—
	H_4	431.58	386.14	45.44	—	—

Can. J. Chem. Downloaded from www.nrcresearchpress.com by 210.87.254.5 on 09/05/12
For personal use only.

TABLE 1 *(Concluded)*

Compound	Proton	In C_6H_{12}†	In C_6D_6†	$\Delta_{C_6D_6}^{C_6H_{12}}$	Δ(calcd.)‡	Deviation
1,2,3-Trichlorobenzene (**55**)	H_4, H_6	433.50	404.88	28.62	34.62	−6.00
	H_5	416.70	375.48	41.22	46.14	−4.92
1-Iodo-2,3-dichlorobenzene (**56**)	H_4	437.82	409.56	28.26	32.82	−4.56
	H_5	402.42	362.76	39.66	45.41	−5.75
	H_6	459.48	432.30	27.18	32.15	−4.97
1-Fluoro-2,4,5-trichlorobenzene (**57**)	H_3	443.44	409.51	33.93	36.31	−2.38
	H_6	427.91	389.48	38.43	39.97	−1.54
1-Bromo-2,4,5-trichlorobenzene (**58**)	H_3	445.87	412.77	33.10	36.85	−3.75
	H_6	456.33	424.71	31.62	36.48	−4.86
1-Iodo-2,4,5-trichlorobenzene (**59**)	H_3	444.32	412.77	31.55	36.75	−5.20
	H_6	469.23	440.90	28.33	35.01	−6.68
2,6-Dichloro-3-nitrotoluene (**60**)	H_4	444.37	400.69	43.68	45.65	−1.97
	H_5	436.31	392.53	43.78	51.17	−7.39
2,3,6-Trichlorotoluene (**61**)	H_4	425.57	399.98	25.59	32.13	−6.54
	H_5	425.57	399.98	25.59	31.91	−6.32
2,4,5-Trichloronitrobenzene (**62**)	H_3	452.43	400.02	52.41	56.74	−4.33
	H_6	474.07	424.96	49.11	51.00	−1.89
2-Ethyl-4,5-dimethylphenol (**63**)	H_3	404.72	408.17	−3.45	—	—
	H_6	380.36	369.55	10.81	—	—
2,4,5-Trimethylbromobenzene (**64**)	H_3	411.30	400.50	10.80	10.91	−0.11
	H_6	431.03	433.47	−2.44	−3.25	0.81
2,4,5-Trichlorotoluene (**65**)	H_3	439.87	424.20	15.67	19.64	−3.97
	H_6	431.25	403.26	27.99	33.43	−5.44
2,4,6-Trimethoxytoluene (**66**)	H_3, H_5	359.76	368.39	−8.63	—	—
2,4,6-Trimethylaniline (**67**)	H_3, H_5	395.94	402.84	−6.90	−8.74	1.84
1,2,4,5-Tetramethylbenzene (**68**)	H_3, H_6	405.43	410.67	−5.24	−6.30	1.06
1,2,3,4-Tetramethylbenzene (**69**)	H_5, H_6	405.07	412.95	−7.88	−7.60	−0.28
1,2,3,5-Tetramethylbenzene (**70**)	H_4, H_6	401.13	405.39	−4.26	−5.33	1.07
2,4,6-Trichlorotoluene (**71**)	H_3, H_5	432.00	416.19	15.81	20.39	−4.58
2,4,6-Trichloroaniline (**72**)	H_3, H_5	424.68	411.35	13.33	16.98	−3.65
1,2,3,4-Tetramethoxybenzene§ (**73**)	H_5, H_6	385.2	382.02	3.2	—	—
1,2,4,5-Tetramethoxybenzene§ (**74**)	H_3, H_6	385.8	389.77	−4.0	—	—
1,2,3,4-Tetrafluorobenzene (**75**)	H_5, H_6	405.66	360.96	44.70	46.75	−2.05
1,2,3,5-Tetrafluorobenzene (**76**)	H_4, H_6	395.58	363.30	32.28	38.89	−6.61
1,2,4,5-Tetrafluorobenzene (**77**)	H_3, H_6	413.22	371.52	41.70	40.12	1.58
1,2,3,4-Tetrachlorobenzene (**78**)	H_5, H_6	429.72	388.32	41.40	49.75	−8.35
1,2,4,5-Tetrachlorobenzene (**79**)	H_3, H_6	445.92	410.88	35.04	37.48	−2.44
1,2,4,5-Tetrabromobenzene (**80**)	H_3, H_6	466.08	434.34	31.74	34.22	−2.48
2,4,6-Tribromoiodobenzene (**81**)	H_3, H_5	456.30	429.30	27.00	37.35	−10.35
1,4-Difluoro-2,5-dibromobenzene (**82**)	H_3, H_6	432.36	393.48	38.88	37.17	1.71
2,4,6-Trichlorophenol (**83**)	H_3, H_5	429.18	406.32	22.86	21.33	1.53
2,4,6-Triiodophenol (**84**)	H_3, H_5	471.90	454.14	17.76	14.59	3.17
2,6-Dinitro-4-chlorophenol (**85**)	H_3, H_5	487.26	435.00	52.26	52.28	−0.02
2,4-Dichloro-5-ethyl-3-methylphenol (**86**)	H_6	403.01	396.46	6.55	—	—
	methyl	145.19	135.27	9.22	—	—
2,4-Dichloro-3-ethyl-5-methylphenol (**87**)	H_6	401.92	392.52	9.40	—	—
	methyl	135.68	121.42	14.26	—	—
2,4-Dibromo-3,6-dichloroaniline (**88**)	H_5	444.15	422.87	21.28	32.96	−11.68
2,3,5,6-Tetrafluoroanisole (**89**)	H_4	394.59	360.41	34.18	—	—
Pentamethylbenzene (**90**)	H_6	400.35	407.24	−6.89	−8.04	1.15
2,3,5,6-Tetrafluorotoluene (**91**)	H_4	403.63	374.12	29.51	38.38	−8.87
4-Chloro-2,3,5-trimethylphenol (**92**) 1.5 mole % in C_6H_{12}; 3 mole % in C_6D_6	H_6	380.03	354.44	25.59	17.54	8.05
2,3,5,6-Tetrafluoroaniline (**93**)	H_4	374.29	352.02	22.27	31.92	−9.65
2,3,5,6-Tetrafluorophenol (**94**)	H_4	387.67	357.38	30.29	—	—
2,3,5,6-Tetrafluorothiophenol (**95**)	H_4	402.09	360.61	41.48	—	—
Pentamethoxybenzene§ (**96**)	H_6	370.2	368.82	1.4	—	—
Pentafluorobenzene (**97**)	H_6	403.14	351.24	51.90	52.85	−0.95
Pentachlorobenzene (**98**)	H_6	444.42	403.62	40.80	53.36	−12.56
2,3,5,6-Tetrachloronitrobenzene (**99**)	H_4	454.32	392.34	61.98	70.79	−8.81

*Taken from ref. 28.
†In Hz at 60 MHz to low field from internal TMS for 3 mole% solutions unless otherwise stated.
‡Calculated from Δ values in Table 2.
§Inert solvent was carbon tetrachloride.

Can. J. Chem. Downloaded from www.nrcresearchpress.com by 210.87.254.5 on 09/05/12
For personal use only.

TABLE 2

Substituent constants, Δ_i^X, in Hz at 60 MHz, and Taft σ^0 parameters (40)

Substituent X	Δ_o^X	Δ_m^X	Δ_p^X	σ_p^0	σ_m^0
NH_2	4.44	−6.12	−8.20	−0.38	−0.14
CH_3	−0.44	−2.71	−1.74	−0.15	−0.07
OH	7.30	−1.77	1.07	−0.13	0.04
F	6.10	13.96	12.73	0.21	0.35
Cl	3.61	15.13	15.88	0.27	0.37
Br	2.61	14.50	17.73	0.26	0.38
I	1.14	14.40	14.08	0.27	0.35
CN	25.37	31.53	30.85	0.69	0.62
NO_2	17.13	34.39	33.31	0.82	0.70
OCH_3	—	—	—	−0.12	0.13
CHO	—	—	—	0.43	—

for an observed range of 74 Hz in Δ, a mean deviation of 2.2%. If we arbitrarily take 3.7 Hz (5% of the observed range) as a reasonable upper limit to inaccuracy of a calculated Δ value, then eight values of the 108 fall outside this limit. Note, however, that only four of these are just greater than 4 Hz (some deviations can be reduced by a physically reasonable procedure as shown below, see section *3a*). The additivity scheme is roughly as satisfactory for these trisubstituted benzenes as the scheme devised by Diehl for disubstituted benzenes.

(b) The Δ Values for Compounds 49 to 99 in Table 1

The calculated Δ values for these compounds are expected to deviate more from the observed values than for the first 48 compounds in Table 1. The expectation is based on the nonlinear effect of substituents accumulated in adjacent positions, as noted first by Diehl; and is borne out by an average deviation of 3.5 Hz in a range of 69.5 Hz for the 71 observed Δ values, or 5.0% of the range. Twenty-three of these deviations are larger than 4 Hz and may be as large as 12.6 Hz. With ten exceptions, the magnitude of the calculated Δ values is larger than the observed values. Such consistent behavior is not noted for the first 48 compounds and one is tempted to ascribe this to steric effects. On the other hand, those compounds (**64**, **67–70**, **90**) containing three or more methyl groups show very small deviations of calculated from observed Δ values (average deviation = 0.9 Hz). There is no obvious relationship between size of substituent and size of deviation among compounds **49–99** in Table 1.

(2) Dependence of Δ Values on Charge Effects

Benzene solvent molecules prefer positive to negative regions of the solute molecule. An attempt to describe this preference quantitatively must involve a molecular parameter which measures relative charge densities at various sites in the solute molecule. Theoretical calculations of charge densities in aromatic molecules have, until recently, considered only the π electrons and it is hardly expected that a solvent molecule can differentiate between a fictitious division of σ and π charge densities. Nevertheless, we have measured the ring proton shifts in many polymethoxybenzenes in both cyclohexane and benzene-d_6. Zweig *et al.* (30) measured these shifts in carbon tetrachloride and calculated the π electron densities at the carbons attached to hydrogen by Hückel methods. They found a satisfactory linear dependence of the ring proton shift on the π charge density at the bonded carbon: shift = 9.95 p.p.m./electron. In cyclohexane solution we find a similar linear relationship (correlation coefficient, $r = 0.9472$) with the shift = 8.5 ± 0.9 p.p.m./electron. But the Δ values do not correlate with the calculated π densities ($r = 0.36$). This is not unexpected but note also that we did not find consistent Δ^X values for the methoxy group. Both negative results may be a consequence of the various orientations, two planar and also nonplanar ones with respect to the ring, which the methoxy group may display: depending on whether or not it is crowded by adjacent substituents (see a similar situation for the nitro group, discussed below). Therefore, it may be that satisfactory correlations of Δ with π charge

Can. J. Chem. Downloaded from www.nrcresearchpress.com by 210.87.254.5 on 09/05/12
For personal use only.

densities can be found for other series of benzene derivatives.

(a) Correlation of Δ with Taft's Sigma Constants

Many workers have satisfactorily correlated chemical shifts of protons, fluorine, and carbon nuclei in benzene derivatives dissolved in inert solvents with various types, or linear combinations, of sigma constants (31–39) of substituents placed para or meta to the nuclei. Apparently the sigma parameters are a measure of the charge density near the nuclei, as determined by a resonance and/or an inductive (field) effect from the substituent.

Diehl (26) first plotted Δ values vs. $\sigma_I + 1/2\sigma_R$ where σ_I and σ_R are, respectively, the inductive and resonance constants of X. In correlations of this sort it is probably wise to restrict as much as possible the number of adjustable parameters. Consequently we use one sigma parameter only: the Taft constants, σ_p^0 and σ_m^0, which apparently include the polar and resonance effects of the substituent. They are taken mainly from a compilation by Ritchie and Sager (40). The σ_p^0 value for fluorine was taken from Niwa (41*a*), while for the formyl group, σ_p^0 was assumed to be equal to its Hammett σ_p value (41*b*).

There exist many sets of sigma constants (42). We do not find a good correlation between the Δ^x values in Table 2 and the individual resonance or field parameters given by Swain and Lupton (42) and in terms of which any other defined sigma constants can be written.

Figure 1 gives the least squares straight line relating the Δ values of H_4 in some 1-X-3,5-dichlorobenzenes to σ_p^0. The plot includes the Δ values for *m*-dichlorobenzene (measured in this laboratory) and is represented by eq. [1].

[1] $\Delta(H_4) = (37.50 \pm 1.17)\sigma_p^0 + (12.25 \pm 0.50)$ Hz (correlation coefficient, $r = 0.9966$ for nine values)[1]

Using the data of Nomura and Takeuchi (28) for the 1-X-3,5-dimethylbenzenes we find eq. [2]. Comparing solvent shifts of H_4 in these two series yields eq. [3]. These correlations imply a similar dependence of the Δ values of H_4 on X in the two series and indicate that this dependence is not strongly influenced by the steric or electronic nature of the methyl and chlorine substituents adjacent to H_4.

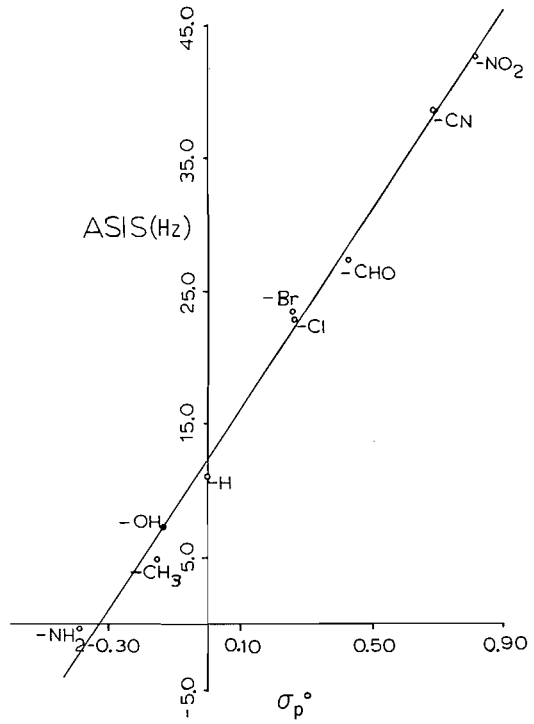

FIG. 1. The aromatic solvent induced shift, Δ, of proton 4 in a series of 1-X-3,5-dichlorobenzenes is plotted vs. the Taft sigma parameter, σ_p^0 of X. The least squares straight line is that defined by eq. [1] in the text. Shifts are given in Hz at 60 MHz.

[2] $\Delta(H_4) = (35.21 \pm 2.13)\sigma_p^0 + (3.92 \pm 0.86)$ Hz ($r = 0.9821$ for 12 values)

[3] $\Delta(H_4$ in 3,5-diCl$) = (1.07 \pm 0.02)\ \Delta(H_4$ in 3,5-di$CH_3) + (7.09 \pm 0.38)$ Hz ($r = 0.9991$ for seven values)

There also exists a correlation between the Δ value of H_4 and σ_p^0 of X in some 1-X-2,3,5,6-tetrafluorobenzenes, eq. [4].

[4] $\Delta(H_4) = (53.38 \pm 5.75)\sigma_p^0 + (40.46 \pm 1.07)$ Hz ($r = 0.9722$, 6 values)

The $\Delta_{p,m}^x$ parameters in Table 2 correlate with σ_p^0 and σ_m^0. The plot of Δ_p^x vs. σ_p^0 in Fig. 2 is described by the least squares eq. [5]. The

[1]When employing these equations under somewhat different solvent or concentration conditions, it would be wise to round the numbers off to two significant figures.

Can. J. Chem. Downloaded from www.nrcresearchpress.com by 210.87.254.5 on 09/05/12
For personal use only.

correlation between Δ_m^x and σ_m^0 is given by eq. [6].

[5] $\Delta_p^x = (35.83 \pm 1.30)\sigma_p^0 + (5.39 \pm 0.55)$ Hz ($r = 0.9948$, 10 values)

[6] $\Delta_m^x = (48.69 \pm 2.83)\sigma_m^0 + (-1.48 \pm 1.13)$ Hz ($r = 0.9884$, nine values)

The Δ_o^x values do not correlate with σ_p^0 ($r = 0.703$). It appears (43–45) that ortho and para substituents should have comparable electrical effects. The σ_o^- values of Tribble and Traynham (44*b*) apparently describe the electrical effects of ortho substituents. We find no correlation between σ_o^- and Δ_o^x ($r = 0.642$). Of course, the Δ_o^x values will also depend on the charge on the substituent itself.

We prefer to take the existence of the good correlations above to imply the importance of charge effects in determining the packing of solvent molecules about these solute species.[2] Relatively small extensions of the list in Table 1 would provide correlations for other series of molecules.

(b) Correlation of Δ *with Dipole Moments*

Schneider (46), Diehl (27), and Brown and Stark (47) have correlated dipole moments of solute molecules of various types with solvent shifts. The correlation equation of Δ for H_4 in the 1-X-3,5-dichlorobenzenes with the dipole moments (48) of the corresponding 1-X-benzenes is eq. [7]. The direction of the dipole

[7] $\Delta(H_4) = (7.08 \pm 0.52)\,\mu D + (11.23 \pm 1.22)$ Hz ($r = 0.9814$, nine values)

moment for X = NH_2, OH, and CH_3 is taken opposite to that of the halogens, NO_2 and CN. The NH_2 group, for example, is a good π electron donor to the para position and itself becomes a center of positive charge. Hence the "solvation cloud" of benzene molecules is shifted nearer to the NH_2 group, leading to a negative Δ value for the para proton.

The correlation implies a dipole-induced dipole or dipole–quadrupole interaction (the quadrupole moment of benzene is -5.6 ± 2.82 esu cm^2 (49)) between solute and solvent molecules. In this connection, the heats of mixing (50) of pyridine derivatives with benzene have been interpreted in terms of an association whose heat of formation lies near 1 kcal/mole. However, thermodynamic data (51) for pyridine and carbon tetrachloride mixtures can be interpreted in a similar way (50). As we have pointed out before (52), the p.m.r. measurements employ the large magnetic anisotropy of aromatic molecules as an amplified indicator of weak interactions. Yet 1:1 complexes between solute molecules and carbon tetrachloride are never suggested even though the low-field shifts of protons in benzene derivatives in this solvent are roughly proportional to, but much smaller in magnitude than, the high-field shifts observed in benzene as a solvent (the mean polarizabilities of carbon tetrachloride and benzene are nearly equal).

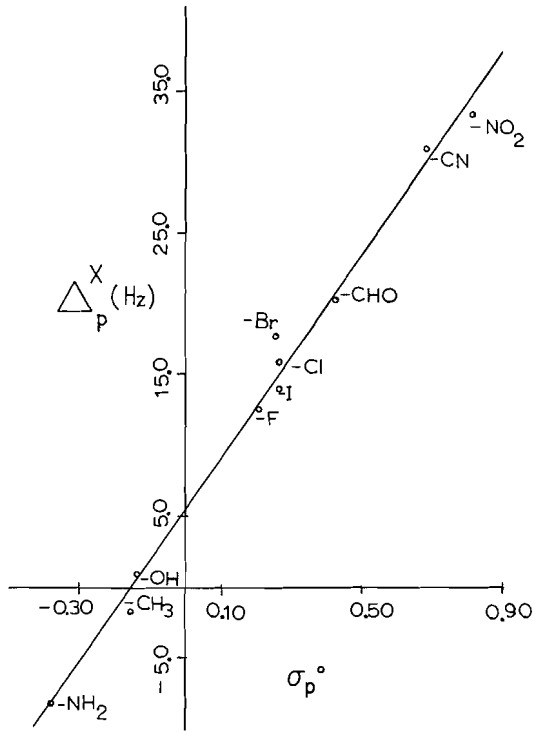

FIG. 2. The substituent constant Δ_p^x in Hz from Table 2 is plotted vs. the Taft sigma parameter, σ_p^0 of X. The least squares straight line is defined by eq. [5] in the text.

(3) The Question of Steric Effects on Δ *Values*

Steric, in the sense of bulk, effects are widely assumed to play an important role in determining Δ values (1, 26, 28, 53, 54). Some workers,

[2]The ease of measuring σ_p^0 for a given substituent is obvious: the position of one peak (antisymmetric transition) in the AB_2 spectrum of a 1-X-3,5-dichlorobenzene gives the shift of proton 4.

Can. J. Chem. Downloaded from www.nrcresearchpress.com by 210.87.254.5 on 09/05/12
For personal use only.

TABLE 3

The Δ value in 1-X-2,4-dichlorobenzenes and 1-X-2,4-dimethylbenzenes

Compound	X	$\Delta(H_3)$	$\Delta(H_5)$	$\Delta(H_5)/\Delta(H_3)$
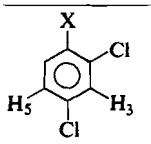	NH_2	3.71	9.23	2.49
	H	10.86	19.38	1.79
	I	18.60	32.52	1.75
	Cl	22.86	34.62	1.51
	NO_2	42.54	52.08	1.22
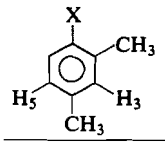	NH_2	−4.8	−8.5	
	Cl	13.8	10.8	
	I	16.8	13.8	
	NO_2	32.4	28.2	

Laszlo (1) in particular, argue against such an interpretation of observed Δ values. The steric interpretation typically (9, 28) involves an argument about the precise orientation, or modification thereof by a steric effect, of one solvent molecule near the proton whose Δ value is of interest. In this section we discuss a few examples from Table 1: the first suggests that steric effects can arise when a bulky substituent forces a change in the conformation of another substituent with respect to the ring; the others indicate the ambiguity which arises when more general steric effects are adduced from the Δ values.

(a) A Steric Effect on $\Delta_o^{NO_2}$

An apparently straightforward steric effect occurs when a bulky substituent is placed ortho to a nitro group. If, in the presence of an ortho chlorine atom, $\Delta_o^{NO_2} = 21.01$ and if, in the absence of an ortho chlorine atom, $\Delta_o^{NO_2} = 13.59$ Hz, the large deviations of the calculated from the observed Δ values of protons ortho to the nitro group decrease to near zero (compounds **1**, **2**, **3**, **10**, **14** but not **6** in Table 1). That an ortho chlorine atom can twist the nitro group out of the plane of the ring by a substantial angle is confirmed by crystallographic (55) and chemical shift (56) data. The oxygen atoms in the nitro group are centers of relative negative charge. As they move out of the plane of the ring the benzene solvent molecules can approach the ortho proton more closely, leading to the larger, observed $\Delta_o^{NO_2}$.

The insensitivity of $\Delta_{m,p}^{NO_2}$ to an ortho chlorine substituent can be understood in terms of the very large field constant, *F*, of the nitro group as compared to its resonance constant, *R* (42). Consequently, a rotation out of the ring plane by a substantial angle need not decrease the overall σ_m^0 or σ_p^0 constant by very much.

A correlation may exist between the size of the ortho substituent and $\Delta_o^{NO_2}$ (the "steric" Δ values above do *not* work for 2,4-dimethylnitrobenzene but do work for 3,5-dimethylnitrobenzene). At present it is not certain that groups other than chlorine will show such a steric effect.

The amino group does not appear to display effects similar to nitro. However, its Δ_o value is much smaller than that of nitro and an actual effect may be lost in the experimental error.

(b) Cases Where an Apparent Steric Effect is Hard to Substantiate

Consider the Δ values in the 1-X-2,4-dichlorobenzenes (Table 3). Spatial crowding of H_3 suggests $\Delta(H_5) > \Delta(H_3)$, as found. However, as the electron-withdrawing power of X increases, the ratio $\Delta(H_5)/\Delta(H_3)$ decreases. If a simple steric effect were the only factor in causing $\Delta(H_5) > \Delta(H_3)$ the ratio should be approximately constant.

In this connection consider the Δ values in 1-X-2,4-dimethylbenzenes in Table 3. Spatial crowding again implies $\Delta(H_5) > \Delta(H_3)$, contrary to observation. Nomura and Takeuchi (28) explain this by a detailed description of the rearrangement of the plane of the solvent molecules relative to that of the solute. However, the sizes of the chlorine atom and the methyl group cannot greatly differ, so that the opposite trends in the above two series are hard to understand on a steric basis. On the other hand, chlorine atoms behave as negative centers relative to methyl groups and hence the benzene solvent molecules tend more to solvate the

Can. J. Chem. Downloaded from www.nrcresearchpress.com by 210.87.254.5 on 09/05/12
For personal use only.

"positive" methyl groups near H_3, leading to $\Delta(H_3) > \Delta(H_5)$.

The decrease of the ratio $\Delta(H_5)/\Delta(H_3)$ in the 2,4-dichlorobenzene series above may be rationalized by noting that, for example, when X = NO_2, the electron density at the chlorine atoms is reduced relative to the molecule in which X = NH_2. Hence, when X = NO_2, the solvent molecules will solvate H_3 and H_5 more equally than when X = NH_2. Hence a charge effect only is needed to rationalize the observed trends in Δ. Other examples from Table 1 can be discussed in a similar way. Arguments based on charge effects are often sufficient to rationalize trends which, at first sight, may be taken as evidence for steric effects.

Finally, the Δ values of the ring protons of a series of polyalkylbenzenes (11) decrease in the order $H > CH_3 > CH(CH_3)_2 > C(CH_3)_3$, suggesting a steric effect. Yet the electron-releasing capacities increase in the order $C(CH_3)_3 > CH(CH_3)_2 > CH_3 > H$, implying at least the presence of a charge effect. Similar remarks apply to the Δ values of H_6 of compounds **86** and **87** in Table 1. Some time ago (57) it was shown that the Δ values of the ring protons of para-*t*-butyltoluene are equal, again pointing to the importance of a charge effect.

We thank Dr. A. Zweig for a generous gift of some polymethoxybenzenes and are grateful to the National Research Council of Canada for financial assistance in the form of grants and of a bursary to R. S.

1. P. LASZLO. *In* Progress in nuclear magnetic resonance spectroscopy. Volume 3. *Edited by* J. W. Emsley, J. Feeney, and L. H. Sutcliffe. Pergamon Press Ltd. Oxford, 1967.
2. J. RONAYNE and D. H. WILLIAMS. *In* Annual review of nuclear magnetic resonance spectroscopy. Volume 2. *Edited by* E. F. Mooney. Academic Press, New York, 1969.
3. A. A. BOTHNER-BY and R. E. GLICK. J. Chem. Phys. **26**, 1651 (1957).
4. A. D. BUCKINGHAM, T. SCHAEFER, and W. G. SCHNEIDER. J. Chem. Phys. **32**, 1227 (1960).
5. R. J. ABRAHAM. Mol. Phys. **4**, 369 (1961).
6. R. E. KLINCK and J. B. STOTHERS. Can. J. Chem. **40**, 1071 (1962).
7. P. H. EMSLIE, R. FOSTER, I. HORMAN, J. W. MORRIS, and D. R. TWISELTON. J. Chem. Soc. B, 1161 (1969).
8. T. LEDAAL. Tetrahedron Lett. 1683 (1968).
9. J. HOMER and M. C. COOKE. J. Chem. Soc. A, 773, 777 (1969).
10. J. E. BALDWIN. J. Org. Chem. **30**, 2423 (1965).
11. R. G. WILSON and D. H. WILLIAMS. J. Chem. Soc. B, 1163 (1968).
12. M. I. FOREMAN, R. FOSTER, and D. R. TWISELTON. Chem. Commun. 1318 (1969).
13. C. L. WATKINS and W. S. BREY, JR. J. Phys. Chem. **74**, 235 (1970).
14. T. G. BEAUMONT and K. M. C. DAVIS. J. Chem. Soc. A, 145 (1968).
15. W. J. GAW and F. L. SWINTON. Trans. Faraday Soc. **64**, 2023 (1968).
16. T. SCHAEFER. Can. J. Chem. **39**, 1864 (1961).
17. A. AULT and R. KRAIG. J. Chem. Educ. **43**, 213 (1966).
18. S. CASTELLANO and A. A. BOTHNER-BY. J. Chem. Phys. **41**, 3863 (1964).
19. S. CASTELLANO and J. S. WAUGH. J. Chem. Phys. **34**, 295 (1961).
20. J. R. CAVANAUGH. J. Chem. Phys. **39**, 2378 (1963).
21. C. LUSSAN. J. Chim. Phys. **61**, 462 (1964).
22. J. K. BECCONSALL, G. DOYLE DAVES, JR., and W. R. ANDERSON, JR. J. Amer. Chem. Soc. **92**, 430 (1970).
23. S. CASTELLANO, C. SUN, and R. KOSTELNIK. Tetrahedron Lett. **50**, 5205 (1967).
24. M. P. WILLIAMSON, R. J. KOSTELNIK, and S. CASTELLANO. J. Chem. Phys. **49**, 2218 (1968).
25. R. J. KOSTELNIK, M. P. WILLIAMSON, D. E. WISNOSKY, and S. M. CASTELLANO. Can. J. Chem. **47**, 3313 (1969).
26. P. DIEHL. Helv. Chim. Acta, **45**, 568 (1962).
27. P. DIEHL. J. Chim. Phys. **61**, 199 (1964).
28. Y. NOMURA and Y. TAKEUCHI. Tetrahedron, **25**, 3825 (1969).
29. T. SCHAEFER, B. RICHARDSON, and R. SCHWENK. Can. J. Chem. **46**, 2775 (1968).
30. A. ZWEIG, J. E. LEHNSEN, J. E. LANCASTER, and M. T. MEGLIA. J. Amer. Chem. Soc. **85**, 3940 (1963).
31. R. W. TAFT. J. Amer. Chem. Soc. **79**, 1045 (1957).
32. P. C. LAUTERBUR. J. Amer. Chem. Soc. **83**, 1846 (1961).
33. H. SPIESECKE and W. G. SCHNEIDER. J. Chem. Phys. (1961).
34. P. DIEHL. Helv. Chim. Acta, **49**, 829 (1961).
35. G. W. SMITH. J. Mol. Spectry. **12**, 146 (1964).
36. I. D. RAE and L. K. DYALL. Aust. J. Chem. **19**, 835 (1966).
37. S. H. MARCUS, W. F. REYNOLDS, and S. I. MILLER. J. Org. Chem. **31**, 1872 (1966).
38. J. G. TRAYNHAM and G. A. KNESEL. J. Org. Chem. **31**, 3350 (1966).
39. K. HAYAMIZU and O. YAMAMOTO. J. Mol. Spectry. **29**, 183 (1969).
40. C. D. RITCHIE and W. F. SAGER. *In* Progress in physical organic chemistry. Volume 2. *Edited by* S. G. Cohen, A. Streitwieser, and R. W. Taft. Interscience, New York, 1964.
41. (*a*) J. NIWA. Bull. Chem. Soc. (Japan), **42**, 1926 (1969). (*b*) A. A. HUMFFRAY, J. J. RYAN, J. P. WARREN, and Y. H. YUNG. Chem. Commun. 610 (1965).
42. C. G. SWAIN and E. G. LUPTON. J. Amer. Chem. Soc. **90**, 4328 (1968).
43. H. H. JAFFÉ, L. D. FREEDMAN, and G. O. DOAK. J. Amer. Chem. Soc. **76**, 1548 (1954).
44. (*a*) M. CHARTON. J. Amer. Chem. Soc. **86**, 2033 (1964). (*b*) M. T. TRIBBLE and J. G. TRAYNHAM. J. Amer. Chem. Soc. **91**, 379 (1969).
45. G. P. SCHIEMENZ. Angew. Chem. **80**, 559 (1968).
46. W. G. SCHNEIDER. J. Phys. Chem. **66**, 2653 (1962).
47. T. L. BROWN and K. STARK. J. Phys. Chem. **69**, 2679 (1965).
48. J. W. SMITH. Electric dipole moments. Butterworths, London, 1955; A. L. MCCLELLAN. Table of experimental dipole moments. Freeman and Co., San Francisco, California, 1963.

Can. J. Chem. Downloaded from www.nrcresearchpress.com by 210.87.254.5 on 09/05/12
For personal use only.

49. R. L. SHOEMAKER and W. H. FLYGARE. J. Chem. Phys. **51**, 2988 (1969).
50. T. MURAKAMI, S. MURAKAMI, and R. FUJISHIRO. Bull. Chem. Soc. (Japan), **42**, 35 (1969).
51. K. W. MORCOM and D. N. TRAVERS. Trans. Faraday Soc. **62**, 2063 (1966).
52. G. KOTOWYCZ and T. SCHAEFER. Can. J. Chem. **46**, 3110 (1968).
53. D. H. WILLIAMS, J. RONAYNE, and R. G. WILSON. Chem. Commun. 1089 (1967).
54. K. D. BARTLE, D. W. JONES, and R. S. MATTHEWS. J. Chem. Soc. A, 876 (1969).
55. J. R. HOLDEN and D. DICKINSON. J. Phys. Chem. **73**, 1199 (1969).
56. W. B. SMITH, A. M. IHRIG, and J. L. ROARK. J. Phys. Chem. **74**, 812 (1970).
57. T. SCHAEFER and W. G. SCHNEIDER. J. Chem. Phys. **32**, 1218 (1960).

Can. J. Chem. Downloaded from www.nrcresearchpress.com by 210.87.254.5 on 09/05/12
For personal use only.

Can. J. Chem. Downloaded from www.nrcresearchpress.com by 210.87.254.40 on 09/05/12
For personal use only.

Studies on nucleation from solution of some soluble inorganic salts

J. A. VELAZQUEZ[1] AND O. E. HILEMAN, JR.[2]
Department of Chemistry, McMaster University, Hamilton, Ontario

Received February 12, 1970

Vonnegut's droplet technique in combination with selective extraction of solvent is reported as a new method for the study of nucleation from solution of soluble substances at constant temperature. The method is applied to studies on NH_4Cl, NH_4NO_3, NH_4SCN, $(NH_4)_2Cr_2O_7$, and $K_2Cr_2O_7$. The results are reported and various nucleation parameters are calculated and discussed in terms of the limitations of the Becker–Doring model of nucleation when it is applied to crystal nucleation from solutions of electrolytes.

Canadian Journal of Chemistry, **48**, 2896 (1970)

Introduction

Vonnegut's droplet technique (1) has been used with considerable success in studies on the nucleation process (2–6). Usually, in studies on nucleation from solution, supersaturation within the droplets has been generated by cooling a saturated solution, a limitation which, if overcome, would represent a "major technical advance" (7) in nucleation studies. In 1967 Thompson and Gordon (8) and Hileman (9) simultaneously reported the results of preliminary experiments employing precipitation from homogeneous solution (p.f.h.s.) as a means of generating the supersaturation required to initiate crystallization within each droplet. Further work (10, 11) has shown that the combination of p.f.h.s. and the droplet technique is readily applicable to nucleation studies of sparingly soluble substances but is somewhat limited in its application to similar studies on soluble substances.

This paper describes a new technique of producing supersaturated solutions within the droplets and reports the results of studies on nucleation from aqueous solution of some soluble salts.

Experimental

The supersaturation required to initiate crystallization was generated in droplets of aqueous salt solutions dispersed in a suitable silicone oil. Photomicrographs of the results of the nucleation events were taken at appropriate times.

Apparatus

The dispersions were prepared with the aid of a Virtis microhomogenizer, then placed in cups (diameter 32 mm, height 25 mm) made from Nessler tubes and centrifuged by means of an International Clinical centrifuge.

The droplets were examined with an MPS Lumex polarizing microscope (40 × magnification) which was provided with high intensity illumination by adapting an AO Spencer Ortho-illuminator with a 600 W projector lamp.

The photographs were taken with an Olympus PM-6 microscope camera using Anscochrome 500 film and a shutter speed of 1/50 s. The 35 mm slides were projected (Leitz projector) on a calibrated screen so that accurate drop diameter measurements could be made.

Reagents and Solutions

All saturated salt solutions were prepared from "Analytical Reagent" grade chemicals and were kept in contact with the solid salt at room temperature. Each was filtered just prior to use.

Silicone Fluids No. 200, 200 centistokes viscosity, and No. 210, 1 000 000 centistokes viscosity (Dow Corning Silicones Ltd., Toronto), and the mineral oil, 21 centistokes viscosity (The British Drug Houses (Canada) Ltd., Toronto) were used as supplied.

Procedure

One drop of a freshly filtered, saturated salt solution was added to 5 ml of light mineral oil and stirred at 10 000 r.p.m. for 10–15 s with the microhomogenizer. The dispersion was transferred to a Nessler cup which was coated inside with a thin layer of heavy silicone oil, and centrifuged for a few seconds. Then nearly all of the dispersion was decanted from the Nessler cup and 1 ml of light silicone oil was added. The dispersion was again centrifuged until a layer of droplets was situated at the interface between the two silicone oils. The first photomicrograph was taken and then the Nessler cup and contents were placed in a vacuum desiccator over P_2O_5. Subsequent photomicrographs were taken at suitable intervals until crystallization had occurred in all of the droplets.

Results and Discussion

Results from preliminary experiments showed that the average diameter of water droplets dispersed in certain silicone oils decreased with time. Further, it was noted that solutes which

[1]Present address: Chemistry Department, College of Agriculture and Mechanic Arts, Mayaguez, Puerto Rico.
[2]Author to whom all correspondence should be addressed.

Can. J. Chem. Downloaded from www.nrcresearchpress.com by 210.87.254.40 on 09/05/12
For personal use only.

were sparingly soluble in the same silicone oils and readily soluble in water were not extracted from their aqueous droplets. Consequently, selective extraction of the solvent from the droplets into the surrounding oil appeared to circumvent a major difficulty encountered when applying Vonnegut's droplet technique to studies of nucleation from solution; namely, generation of the requisite supersaturation in the droplets. In addition, the supersaturation could be generated isothermally. Thus, the combination of Vonnegut's droplet technique and selective extraction of the solvent from the droplets was applied to studies on nucleation from aqueous solution of soluble salts.

Figure 1 shows that, in the size range studied, the onset of crystallization within a droplet was independent of its initial size. (Data for $K_2Cr_2O_7$ are shown for illustration.) Thus, the relative frequency of crystallization as a function of the ratio d_2/d_1, the diameter of the droplet when crystallization was first detected divided by the initial diameter of the droplet, was calculated without regard to droplet size. The results of these calculations are shown in Fig. 2. From the data of Fig. 2, the probability of crystallization as a function of d_2/d_1 was determined. The results are shown in Fig. 3.

The probability, P, that a droplet of a certain volume, V, will contain a crystal at a given time, t, is expressed by eq. [1] (12).

$$[1] \qquad -\ln (1 - P) = V \int_0^t J \, dt$$

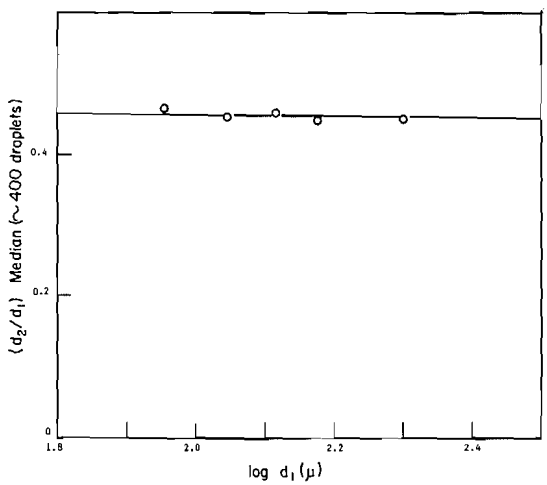

FIG. 1. Median d_2/d_1 vs. log d_1 for $K_2Cr_2O_7$.

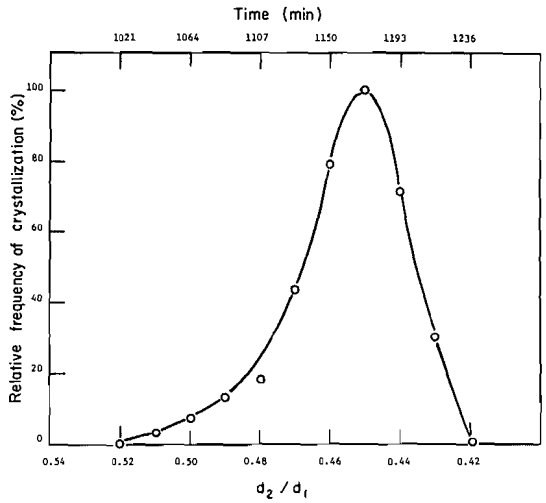

FIG. 2. Relative frequency of crystallization vs. d_2/d_1 for $K_2Cr_2O_7$.

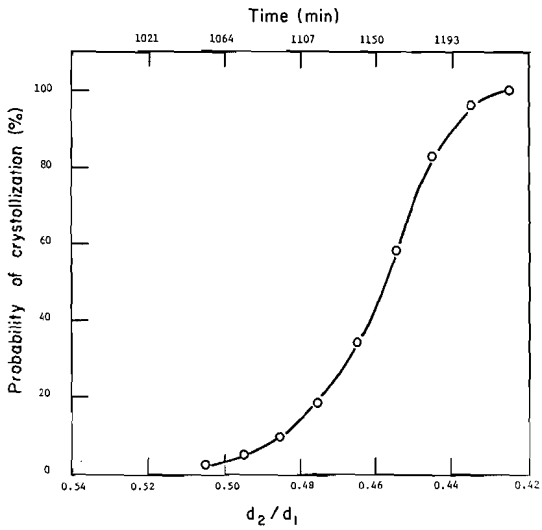

FIG. 3. Probability of crystallization vs. d_2/d_1 for $K_2Cr_2O_7$.

Consequently, the rate of nucleation, J, was calculated from the slope of Fig. 3 at various values of P after transforming from d_2/d_1 to time dependence. Figure 4 shows the form of the transformation for droplets with an initial diameter of 135 μ, the drop size used for the calculation.

The Becker–Doring model of the nucleation process (13*a*) described by eq. [2] (13*b*) predicts a linear relationship between log J and $(\log S)^{-2}$.

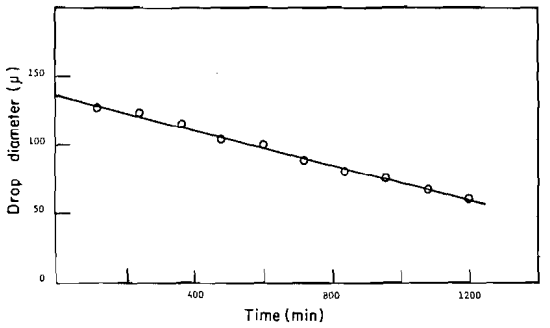

FIG. 4. Drop diameter vs. time for $K_2Cr_2O_7$.

$$[2] \qquad J = A \exp\left[\frac{-16\pi\sigma^3 v^2}{3(kT)^3(\ln S)^2}\right]$$

where A = kinetic factor = (D/d^5n^*) $(4\Delta G^*/3\pi kT)^{1/2}$, σ = surface energy, v = molecular volume of the solid state, k = Boltzman's constant, T = absolute temperature, D = diffusion coefficient, d = mean ionic diameter, n^* = critical number of ions, and ΔG^* = critical free energy change. To evaluate the applicability of the model to the nucleation of the salts studied, plots of this functional relationship were prepared. The data for $K_2Cr_2O_7$ are shown in Fig. 5. The super saturation was calculated using eq. [3].

$$[3] \quad S = \frac{d_s\left[\frac{W_s}{M_s} + \frac{W_w}{M_w}\right]}{d_s\left[\frac{W_s}{M_s} + \frac{W_w}{M_w}\right] - \frac{d_w}{M_w}\left[1 - \left(\frac{d_2}{d_1}\right)^3\right]}$$

where d_s = density of the saturated solution, d_w = density of water, W_s = weight of solute/gram of saturated solution, W_w = weight of water/gram of saturated solution, M_s = molecular weight of solute, and M_w = molecular weight of water. Similar calculations were carried out on the other salt systems and subsequently, values of the various nucleation parameters appearing in the Becker–Doring model were calculated. These are collected in Table 1 along with n^* and r^*, the critical radius, calculated from σ by use of the Gibbs–Thompson equation. Also shown for comparison are data taken from the literature for NH_4Cl and $K_2Cr_2O_7$ (14).

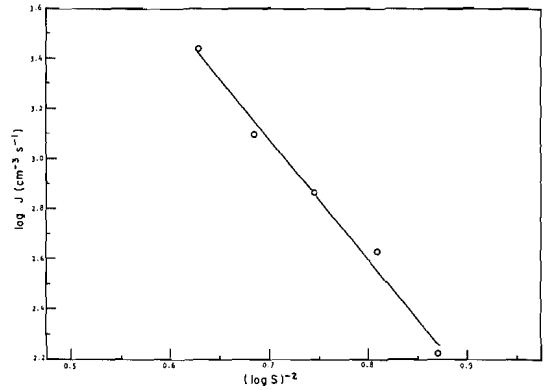

FIG. 5. Log J vs. $(\log S)^{-2}$ for $K_2Cr_2O_7$.

TABLE 1

Results of the calculation of nucleation parameters

Substance	d_2/d_1	S	σ (ergs cm^{-2})	n^*	r^* (Å)
NH_4SCN	0.89	2.07	37	151	12
NH_4NO_3	0.86	2.33	47	141	10
NH_4Cl	0.76	2.82	66(35)[a]	107	9.0
$(NH_4)_2Cr_2O_7$	0.63	6.85	58	58	9.6
$K_2Cr_2O_7$	0.46	18.3	82(72)[a]	43	8.6

[a] Reference 14.

The value of the kinetic constant computed from the data of Fig. 5 is many orders of magnitude lower than the calculated value of 10^{32} cm^{-3} s^{-1}. An explanation for this discrepancy between the experimental and calculated values of the kinetic constant may reside in the classical theory. Presently, the validity of the functional relationships predicted by the Becker–Doring model when applied to nucleation of liquid drops from the vapor is being debated (15). Further, Dunning (16, 17) has pointed out that entropy changes which accompany phase transformations are neglected in the model. With the additional complications of the ionic nature of the species present in solutions and solvation and entropy effects which are known to accompany nucleation from solution, it is doubtful if agreement between calculated and experimental values of A should be expected.

The authors acknowledge the financial assistance provided by the National Research Council of Canada and the Department of University Affairs, Province of Ontario, Canada.

1. B. VONNEGUT. J. Colloid Sci. **3**, 563 (1948).
2. G. M. POUND and V. K. LAMER. J. Amer. Chem. Soc. **74**, 2323 (1952).
3. D. TURNBULL. Solid state physics. Academic Press, Inc., New York. 1956.
4. E. K. BIGG. Proc. Phys. Soc. **66B**, 688 (1953).
5. T. P. MELIA and W. P. MOFFITT. J. Colloid Sci. **19**, 433 (1964).

Can. J. Chem. Downloaded from www.nrcresearchpress.com by 210.87.254.40 on 09/05/12
For personal use only.

6. J. B. NEWKIRK and D. TURNBULL. J. Appl. Phys. **26**, 579 (1952).
7. T. P. MELIA. J. Appl. Chem. **15**, 345 (1965).
8. S. THOMPSON and L. GORDON. Talanta, **14**, 137 (1967).
9. O. E. HILEMAN, JR. Talanta, **14**, 139 (1967).
10. J. A. VELAZQUEZ and O. E. HILEMAN, JR. Talanta, **15**, 1060 (1968).
11. J. A. VELAZQUEZ and O. E. HILEMAN, JR. Talanta. In Press.
12. I. E. KUHNS and B. J. MASON. Proc. Roy. Soc. Ser. A. **302**, 437 (1968); A. E. CARTE. Proc. Phys. Soc. London, **73**, 324 (1959); D. TURNBULL. J. Chem. Phys. **18**, 768 (1950).
13. (*a*) R. BECKER and W. DORING. Ann. Phys. **24**, 719 (1935); (*b*) A. E. NIELSEN. Kinetics of precipitation. The Macmillan Co., New York. 1964. p. 15.
14. G. CLEGG and T. P. MELIA. Talanta, **14**, 989 (1967).
15. F. F. ABRAHAM. J. Chem. Phys. **50**, 3977 (1969).
16. W. J. DUNNING and N. T. NOTLEY. Z. Electrochem. **61**, 55 (1957).
17. W. J. DUNNING and A. J. SHIPMAN. Proc. Agr. Ind. Tenth Int. Congr. Madrid. 1954.

Can. J. Chem. Downloaded from www.nrcresearchpress.com by 210.87.254.40 on 09/05/12
For personal use only.

Can. J. Chem. Downloaded from www.nrcresearchpress.com by 210.87.254.5 on 09/05/12
For personal use only.

Unsaturated derivatives of the 1,2;5,6-di-*O*-isopropylidene-D-hexofuran-3-uloses

K. N. SLESSOR AND A. S. TRACEY
Department of Chemistry, Simon Fraser University, Burnaby 2, British Columbia

Received April 1, 1970

The formation of the two 3-*O*-acetyl-1,2;5,6-di-*O*-isopropylidene-D-hex-3-enoses from the four 1,2;5,6-di-*O*-isopropylidene-D-hexofuran-3-uloses is reported. Treatment of the two enol acetates with hydrogen or deuterium in the presence of palladium or platinum leads to rearrangement as well as reduction and reductive hydrogenolysis of the acetoxy group. This rearrangement makes the enol acetates unsuitable as intermediates in the stereospecific synthesis of deuterated sugars of high isotopic purity.

Canadian Journal of Chemistry, 48, 2900 (1970)

During our investigation of the reactions and syntheses of the 1,2;5,6-di-*O*-isopropylidene-D-hexofuranoses (1) it was observed that reduction of the enol acetate of 1,2;5,6-di-*O*-isopropylidene-α-D-*ribo*hexofuranos-3-ulose prepared by the method of Meyer zu Reckendorf (2) did not proceed through a simple *cis* addition of hydrogen. In an attempt to clarify the mechanism by which the reduction proceeds, we have studied the reduction of the enol acetates derived from diacetone 3-keto-D-*ribo*hexose and 3-keto-D-*lyxo*hexose under a variety of conditions.

In the formation of the two enol acetates from their parent ketones a marked difference in the rate of formation of the final products was observed. Treatment of the four ketones; 1,2;5,6-di-*O*-isopropylidene-α-D-*ribo*hexofuranos-3-ulose (**1**), 1,2;5,6-di-*O*-isopropylidene-α-D-*xylo*hexofuranos-3-ulose (**2**), 1,2;5,6-di-*O*-isopropylidene-β-D-*lyxo*hexofuranos-3-ulose (**3**), and 1,2;5,6-di-*O*-isopropylidene-β-D-*arabino*hexofuranos-3-ulose (**4**) as 1% solutions of the sugar in 30% acetic anhydride in pyridine at 36° yielded the enolic sugars (**5** and **6**) (see Scheme 1). A qualitative comparison of reaction rates was provided by following the reactions by thin layer chromatography (t.l.c.) until complete. The results are given in Table 1.

TABLE 1

Times for the formation of enol acetates from 1,2;5,6-di-*O*-isopropylidene-D-hexofuranos-3-uloses in acetic anhydride – pyridine (3:7) at 36°

Ketone	Time* (days)
1	3.8–4.3
2	1.5–1.8
3	22–24†
4	1.1–1.3

*The times given are estimated from a series of t.l.c. plates which were run on the reaction mixtures.
†This time may be longer than given. After this length of time breakdown products begin appearing on the t.l.c. plates.

An attempt to form **5** by treating the 3-keto-diacetone-D-*ribo*hexose with isopropenyl acetate resulted in the formation of 1,2-*O*-isopropylidene-3,5-di-*O*-acetyl-α-D-*ribo*hexofuranos-3-ulose (**13**) in good yield. The identity of this compound was deduced from nuclear magnetic resonance (n.m.r.), infrared (i.r.), ultraviolet (u.v.), and mass spectroscopy. The n.m.r. spectroscopy indicated the presence of two isopropylidene methyls (8.43 and 8.59 τ), two acetate methyls (7.79 τ), and six non-equivalent protons which were assigned as shown in Table 2. The presence of acetate was also confirmed by the presence of an i.r. absorbance at 1750 cm^{-1}. The absence of an OH absorbance above 3000 cm^{-1} in the i.r. and the absence of any carbonyl absorption in the 260–340 mμ region ruled out the presence of a free or hydrated ketone in **13**. The mass spectrum gave a large $(M-15)^+$ peak at *m/e* 287. Identification of this compound was confirmed by acetylating the known 1,2-*O*-isopropylidene-α-D-*ribo*hexofuranos-3-ulose prepared from 1,2;5,6-di-*O*-isopropylidene-α-D-*ribo*hexofuranos-3-ulose by the method of Theander (3).

Reduction of **5** in ethanol over palladium black provides an almost quantitative yield of 3-*O*-acetyl-1,2;5,6-di-*O*-isopropylidene-α-D-gulohexofuranose (**9**) while reduction of **6** provides the corresponding 3-*O*-acetyl-1,2;5,6-di-*O*-isopropylidene-β-D-mannofuranose (**10**) in comparable yield. This identification was verified by deacetylation to the known 1,2;5,6-di-*O*-isopropylidene-β-D-mannofuranose (1, 4).

Reduction of **5** with deuterium over palladium

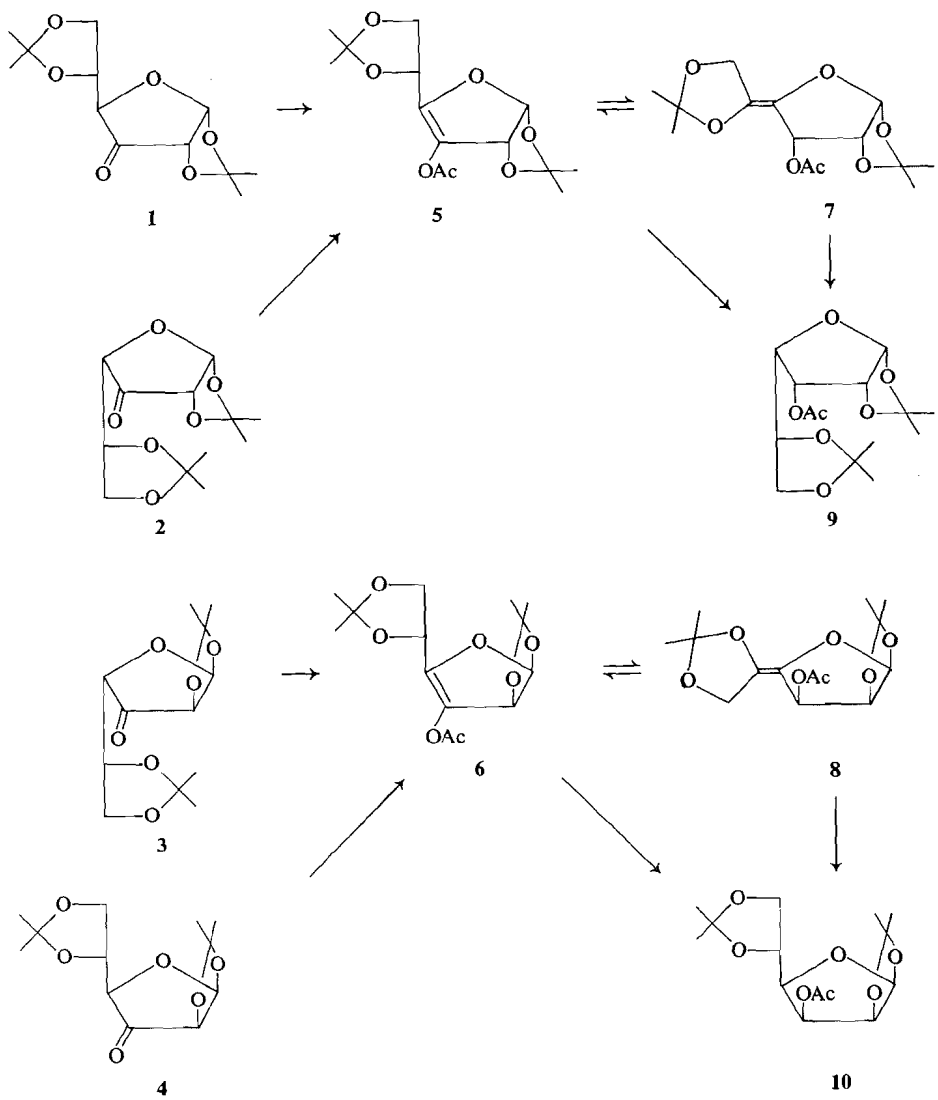

SCHEME 1

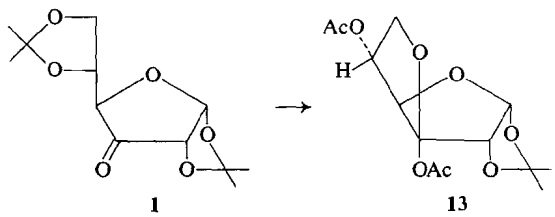

black in ethanol resulted in scrambling of deuterium and hydrogen throughout the 3, 4, and 5 positions as judged by n.m.r. spectroscopy. On changing the solvent to ether, an identical scrambling pattern was observed. This indicated that either some sort of exchange reaction was occurring on the catalytic surface, or the double bond was migrating to the exocyclic position as shown in compound 7. The latter is of considerable interest since it has been found that methylene and ethylene cycloalkanes rearrange on catalytic surfaces to give a very high percentage of the alkyl cycloalkene; that is, 97.6% of 1-methylcyclopentene and 94.2% of 1-ethylcyclopentene (5). After various unsuccessful attempts to observe catalytic exchange in these products, an attempt was made to identify and isolate a rearranged product if it did in fact exist.

Can. J. Chem. Downloaded from www.nrcresearchpress.com by 210.87.254.5 on 09/05/12
For personal use only.

TABLE 2

The n.m.r. data for 1,2;5,6-di-*O*-isopropylidene-D-hexose derivatives

Compound	Chemical shift*													Coupling
	H-1	H-2	H-3_1	H-3_2	H-4	H-5	H-6_1	H-6_2	*O*-Ac	*O*-Isopropylidene				$J_{1,2}$
5	3.94	4.66	—	—	—	5.26	5.95	6.06	7.83	8.49	8.57	8.57	8.65	5.4
6	3.96	4.61	—	—	—	5.31	5.88	6.01	7.82	8.57	8.57	8.57	8.67	5.5
7	4.09	5.12	4.35	—	—	—	5.47	5.50	7.90	8.51	8.58	8.58	8.58	4.1
8	4.03	5.10	4.58	—	—	—	5.48	5.48	7.88		8.6			4.0
9	4.20	5.19	4.92	—	5.93	5.38	5.91	6.46	7.89	8.43	8.62	8.62	8.62	4.1
10	4.29	5.25	4.83	—	5.95	5.49	5.93	6.01	7.90	8.47	8.68	8.68	8.68	4.0
11	4.22	5.27	7.78	8.16	5.90	5.58	5.97	6.39	—	8.46	8.60	8.67	8.70	3.8
12	4.28	5.29	7.68	7.81	6.02	5.71	5.91	6.13	—	8.48	8.62	8.67	8.71	3.8
13	4.08	5.02	—	—	5.26	4.71	5.64	6.01	7.79	—	—	8.43	8.59	3.7
14	4.17	5.32	5.22	—	—	—	5.45	5.45	—	8.48	8.51	8.51	8.53	3.5

*The chemical shifts are given in tau values and are for a chloroform solution. The coupling is in Hz.

To this end **5** was partly reduced in ethanol and the fully reduced 3-*O*-acetyl-1,2;5,6-di-*O*-isopropylidene-D-gulofuranose (**9**) was crystallized out. The t.l.c. of the mother liquor gave a spot corresponding to the complete reduction product, a minor second spot, and a spot with an R_f corresponding to the starting material but which on development (10% H_2SO_4 and heat) came up initially a different color from starting material (**5**). The n.m.r. spectroscopy showed that this compound (**7**) was substantially different from the starting material. Partial reduction of (**5**) in ether gave a much higher yield of **7**, which finally, under optimal conditions (method A) was formed in an approximately 65% yield of crystalline product.

The n.m.r. spectrum in chloroform gave a low field doublet with a chemical shift of 4.09 τ and a coupling of 4.1 Hz consistent with an assignment of H_1 for this proton (6). On the basis of this assignment H_2 is found at 5.12 τ with an H_2 to H_3 coupling of 6.2 Hz. Such a value of 6.2 Hz indicates that H_2 and H_3 are *cis*, as the related *cis* H_2–H_3 compounds **9**, **10**, **11**, and **12** all have $J_{2,3}$ couplings of 5.5–6.5 Hz.[1] Specifically 3,4-dideuterated **11** proved that the proper proton assignments had been made for **11**. The *trans* H_2–H_3 compounds 1,2;5,6-di-*O*-isopropylidene-D-glucofuranose and -L-idofuranose derivatives have small couplings of less than 0.5 Hz (6). With H_2 and H_3 *cis* in **7**, the acetate group (7.9 τ) must be *cis* to the oxygen at C-2, the expected arrangement since catalytic reduction gives only the D-gulo compound (**9**). The C-3 hydrogen is at 4.35 τ occurring as a tripleted doublet being coupled to the two C-6 hydrogens at 5.5 τ. The four isopropylidene methyls are found at 8.6 τ. The assignment of the ring protons was verified by the formation of **7***a* containing deuterium in the three position by rearranging **5** in the presence of deuterium rather than hydrogen. The n.m.r. showed the loss of the signal at 4.35 τ and the collapse of the signal at 5.5 τ to a single peak and the collapse of the quartet at 5.12 τ to a doublet. The mass spectrum of **7** gave a molecular ion at *m/e* 300 corresponding to a compound isomeric with **5**. No significant peak at *m/e* 101 was observed. This is an important

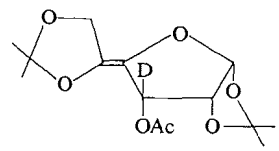

7a

peak from 5,6-*O*-isopropylidene hexofuranose derivatives as it has been shown by DeJongh and Biemann (7) to be the peak resulting from the loss of the 5,6-carbons complete with their isopropylidene group. The i.r. spectrum showed an absorbance at 1740 cm^{-1} indicating the presence of an ester carbonyl. The presence of the double bond, although not clearly discernible in the i.r., was confirmed by reduction over palladium to 3-*O*-acetyl-1,2;5,6-di-*O*-isopropylidene-α-D-gulofuranose (**9**). Reduction of **7** with deuterium gave a scrambling pattern identical to that obtained from reduction of **5** with deuterium. It thus seems that equilibrium between **5** and **7** is set up on the catalyst surface prior to reduction. Such allylic rearrangements have been observed on catalytic surfaces in several systems (5, 8).

[1]Unpublished results.

Can. J. Chem. Downloaded from www.nrcresearchpress.com by 210.87.254.5 on 09/05/12
For personal use only.

Can. J. Chem. Downloaded from www.nrcresearchpress.com by 210.87.254.5 on 09/05/12
For personal use only.

Treatment of **7** with 0.01 *N* NaOMe in methanol gave a product **14** whose n.m.r. spectrum had no peak in the acetate region, but had four isopropylidene methyl groups and a D_2O exchangeable hydrogen. The mass spectrum of this compound gave a molecular ion at *m/e* 258, confirming the loss of acetate on treatment with base, and no significant peak at *m/e* 101 indicated that no ordinary 5,6-isopropylidene group was present.

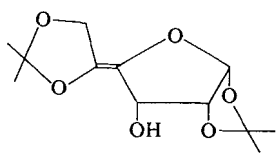

14

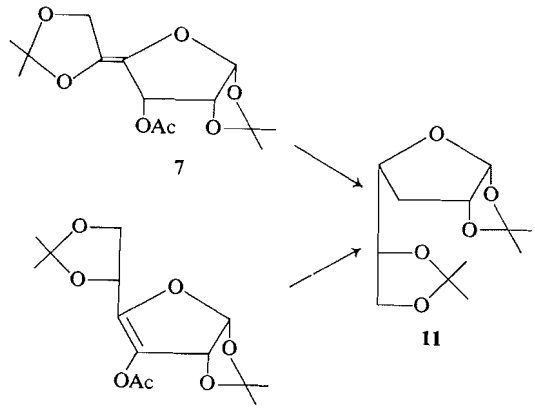

7 **11** **5**

SCHEME 2

The configuration about C-5 in **7** is difficult to establish but can be inferred from the stereochemistry of the reduction product. *cis*-Reduction must occur *trans* to the 1,2-*O*-isopropylidene group and results in the known D-gulo product (**9**). In the hope that n.m.r. could be useful in resolving stereochemical problems of this nature through use of the observed long range coupling, it was decided to attempt the synthesis of the isomer which should be preparable from 3-ketodiacetone D-*lyxo*hexose or D-*arabino*hexose. That **6** was the product obtained on treating the *lyxo*hexose or *arabino*hexose derivatives (**3** and **4**) with acetic anhydride – pyridine was confirmed by n.m.r. and mass spectroscopy. The mass spectrum of **6** was very similar to that of **5** with a molecular ion at *m/e* 300 and a large peak at *m/e* 101. Reduction of this compound yielded 3-*O*-acetyl-1,2;5,6-di-*O*-isopropylidene-β-D-mannofuranose (**10**), which was identified by n.m.r. and mass spectrometry. Deacetylation afforded 1,2;5,6-di-*O*-isopropylidene-β-D-mannofuranose, in high yield, identical to that obtained by borohydride reduction of 1,2;5,6-di-*O*-isopropylidene-β-D-*arabino*hexofuranose-3-ulose (**4**) (1, 4).

Under the rearrangement conditions of method A, **6** was converted into the desired **8** in approximately 65% yield as judged by n.m.r. Compound **8** did not crystallize and attempts to purify it in other ways failed or resulted in decomposition. The n.m.r. parameters determined from the impure product are given in Table 2.

Reduction of **5** or **7** (Scheme 2) over platinum in anhydrous ether proceeded quite slowly compared with the reduction over palladium, requiring at least 24 h compared with about 7 h for the palladium reduction. The t.l.c. indicated the formation of two major compounds, one having an R_f corresponding to 3-*O*-acetyl-1,2;5,6-di-*O*-isopropylidene-α-D-gulofuranose (**9**) and the n.m.r. spectrum of the reaction mixture supported this assignment. The second spot had an R_f different from that of the starting material and n.m.r. indicated that this compound was 3-deoxy-1,2;5,6-di-*O*-isopropylidene-α-D-*xylo*hexofuranose (**11**). The product was purified and was found identical by n.m.r., i.r., mass spectroscopy, melting point, and optical rotation to **11** prepared by the reduction of 1,2;5,6-di-*O*-isopropylidene-α-D-*erythro*hex-3-enose (9).

Hydrogenolysis of **6** occurs under conditions identical to that of the hydrogenolysis of **5** and in similar yield. The n.m.r. spectrum was consistent with the expected products, 3-deoxy-1,2;5,6-di-*O*-isopropylidene-β-D-*arabino*hexofuranose (**12**). The mass spectrum gave a large peak $(M-15)^+$ at *m/e* 229 and a large peak at *m/e* 101. High resolution mass spectroscopy showed this to be 101.0620 which is in good agreement with the calculated value of 101.0602 and our observed value of 101.0610 for the tail fragment of diacetone D-glucose.

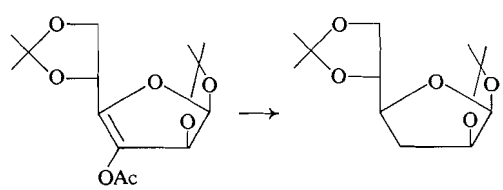

6 **12**

Can. J. Chem. Downloaded from www.nrcresearchpress.com by 210.87.254.5 on 09/05/12
For personal use only.

3-Deoxy-D-mannose (10) was acetonated directly and the product was found identical by i.r., n.m.r., and mass spectroscopy, melting point and optical rotation to the product of hydrogenolysis of **6**. This work adds conclusive evidence, therefore, that the 3-deoxy-di-*O*-isopropylidene-β-D-*arabino*hexofuranose (**12**) prepared by Rembarz (11) from 3-deoxy-D-mannose is in fact the 1,2;5,6-diketal as postulated by Prokop and Murray (12) and not the 1,2;4,6-diketal originally proposed.

This work has shown that enolization of the 1,2;5,6-di-*O*-isopropylidene-hexofuranos-3-ulose systems occurs between C-3 and -4. No evidence of 2,3 double bond formation was encountered in agreement with Bredt's rule. The rearrangement of the enol acetate to an exocyclic double bond system was surprising since the reaction was reversible, indicating the exo form to be more stable, the opposite of that of the 1-alkylcyclopentenes. An effort to eliminate this rearrangement by substituting platinum for palladium failed in that a major pathway of this reaction was the hydrogenolytic cleavage of the acetoxy group. Since both the enol acetate **5** and the rearranged **7** gave the same products on platinum reduction, it seems likely that the double bond rearrangement occurs on the platinum surface as well.

Experimental

Melting points were determined on a Fisher–Johns melting point apparatus and are uncorrected. Evaporations were carried out under reduced pressure on Buchi rotatory evaporators at bath temperatures not exceeding 50°. Optical rotations were measured on a Perkin Elmer P22 Spectropolarimeter. Infrared studies were performed on a Beckman IR 12, the samples being prepared as KBr discs. The n.m.r. spectra were obtained from a Varian A56-60 Spectrometer with TMS as internal reference. All proton assignments have been checked using the n.m.r. program LACOON III of Bothner-By and Castellano (13) on an IBM 360/50 computer. The t.l.c. was carried out on silica gel G in ethylether:toluene (2:1). Ten percent sulfuric acid and heat were used for development.

3-O-Acetyl-1,2;5,6-di-O-isopropylidene-α-D-erythrohex-3-enose (5)

Method A

Prepared according to the method of Meyer zu Reckendorf (2) with the following minor changes. 1,2;5,6-Di-*O*-isopropylidene-α-D-*ribo*hexofuranos-3-ulose (**1**) (hydrate) (1) (10 g) was dissolved in 30% acetic anhydride in pyridine (45 ml). The solution was kept at 35° until the reaction was complete by t.l.c. (4 days). Ice water (500 ml) was seeded with several crystals of the product and the reaction mixture was slowly added to the vigorously stirred solution. The solution was kept at 0° until crystallization was complete. The mixture was filtered, and the product washed thoroughly with water, then recrystallized from ethanol–water. A further small amount of product was obtained by extracting the aqueous solution once with chloroform (50 ml). Crystalline product (10 g of long needles) was obtained melting at 58–59°, $[\alpha]_D^{22}$ −32° (*c*, 0.95 $CHCl_3$); literature (2) m.p. 62–63°, $[\alpha]_D^{20}$ −33° (*c*, 1 $CHCl_3$).

Method B

1,2;5,6-Di-*O*-isopropylidene-α-D-*xylo*hexofuranos-3-ulose (**2**) (150 mg) was dissolved in an acetic anhydride (1 ml) – pyridine (2 ml) mixture and the solution was kept at 35° for 30 h. The solution was evaporated several times with toluene until no further pyridine was present. The resulting sirup was dissolved in $CHCl_3$ (25 ml) and washed with dilute (2%) aqueous sodium bicarbonate. The chloroform fraction was dried over magnesium sulfate, filtered, and evaporated. The residue was crystallized from an ethanol–water solvent then recrystallized to give material (95 mg) melting at 57.5–58.5°. The mixed m.p. with material prepared from method A was 58–59°, $[\alpha]_D$ −31.4 (*c*, 0.94 $CHCl_3$).

3-O-Acetyl-1,2;5,6-di-O-isopropylidene-β-D-threohex-3-enose (6)

Method A

1,2;5,6-Di-*O*-isopropylidene-β-D-*arabino*hexofuranos-3-ulose (**4**) (2.5 g) was dissolved in 30% acetic anhydride in pyridine (30 ml) and was kept at 35° until the reaction was judged complete by t.l.c. (2 days). The solution was poured into ice water (300 ml) and extracted into chloroform (3 × 75 ml). The solution was evaporated and then distilled, $b.p._{0.05}$ 118°. The distillate crystallized and was recrystallized from ethanol–water to give crystals (1.5 g) melting at 57–58°, $[\alpha]_D^{20}$ 43.4° (*c*, 0.87 $CHCl_3$).

Anal. Calcd. for $C_{14}H_{20}O_7$: C, 56.0; H, 6.67. Found: C, 55.95; H, 6.57.

Method B

1,2;5,6-Di-*O*-isopropylidene-β-D-*lyxo*hexofuranos-3-ulose (**3**) (2 g) was dissolved in 30% acetic anhydride in triethylamine (45 ml). The solution was kept at room temperature until the reaction was complete by t.l.c. (1½–2 days). The solution was evaporated down several times with toluene and then ethanol, care being taken to prevent the sirup from becoming too thick since de-*O*-acetylation appeared to occur quite readily. The product was taken up in ethanol, water was added, and the solution seeded. The short, chunky needles (1.5 g) of the recrystallized product were identical to the material produced in method A (above).

3-O-Acetyl-1,2;5,6-di-O-isopropylidene-α-D-erythrohex-trans-4-enose (7)

Method A

3-*O*-Acetyl-1,2;5,6-di-*O*-isopropylidene-α-D-*erythro*hex-3-enose (**5**) (1 g) was dissolved in anhydrous ether (75 ml). This solution was added to a reduction vessel containing palladium black (300 mg) in anhydrous ether (30 ml) which had been prereduced for 1 h at atmospheric pressure. The reaction vessel was flushed with hydrogen at atmospheric pressure, then stirred for 4 min. The solution was filtered and the catalyst washed with several small

Can. J. Chem. Downloaded from www.nrcresearchpress.com by 210.87.254.5 on 09/05/12
For personal use only.

portions of ether. The ether solution was evaporated and the resulting product crystallized. Recrystallization from hot ethanol gave the product (650 mg) as cubes. The m.p. 106–107°, $[\alpha]_D^{22}$ 67.8° (*c*, 0.814 $CHCl_3$).

Anal. Calcd. for $C_{14}H_{20}O_7$: C, 56.00; H, 6.67. Found: C, 55.80; H, 6.61.

Method B

Compound **5** (0.5 g) was dissolved in anhydrous ether (50 ml) and added to a reduction flask containing palladium black (75 mg). The system was flushed with deuterium gas several times and then reduced at atmospheric pressure for 22 min. The product was worked up as in method A to yield a product (300 mg) virtually identical to **7**. Spectroscopy indicated that the 3-deuterio **7***a* had ~80% isotopic purity.

*1,2;5,6-Di-O-isopropylidene-α-D-erythrohex-trans-4-enose (**14**)*

3-*O*-Acetyl-1,2;5,6-di-*O*-isopropylidene-α-D-*erythro*hex-*trans*-4-enose (**7**) (1 g) was dissolved in anhydrous methanol (100 ml) and 0.1 *N* NaOMe in methanol (5 ml) was added. The reaction was followed by t.l.c. until it was complete (approximately 4 h). The solution was neutralized with solid CO_2 and evaporated. On evaporation the product crystallized and was recrystallized from petroleum ether (65–110°). Extremely fine needles of the recrystallized product (750 mg) were obtained. The m.p. 89–90°, $[\alpha]_D^{22}$ −19.0°, (*c*, 0.918 $CHCl_3$).

Anal. Calcd. for $C_{12}H_{18}O_6$: C, 55.81; H, 6.98. Found: C, 55.93; H, 6.91.

*3-O-Acetyl-1,2;5,6-di-O-isopropylidene-α-L-erythrohex-cis-4-enose (**8**)*

3-*O*-Acetyl-1,2;5,6-di-*O*-isopropylidene-β-D-*threo*hex-3-enose (**6**) (500 mg) was dissolved in anhydrous ether (50 ml) and reacted for 4 min with prereduced palladium catalyst as described for the formation of 3-*O*-acetyl-1,2;5,6-di-*O*-isopropylidene-α-D-*erythro*hex-3-enose (**8**, method A). The mixture was filtered and the catalyst washed with several small portions of ether. The filtrate and washings were combined and evaporated to a sirup which contained about 65% of the rearranged product as judged by n.m.r. and t.l.c. All attempts to purify this compound by crystallization, distillation, and chromatography have been unsuccessful.

*3-O-Acetyl-1,2;5,6-di-O-isopropylidene-α-D-gulofuranose (**9**)*

3-*O*-Acetyl-1,2;5,6-di-*O*-isopropylidene-α-D-*erythro*hex-3-enose (**5**) was reduced as previously reported (1) to yield long needles melting at 76–77°, $[\alpha]_D^{22}$ 68.3 (*c*, 0.832 $CHCl_3$), literature (1), m.p. 73–74°, $[\alpha]_D^{20}$ 66.0 (*c*, 0.36 $CHCl_3$).

*3-O-Acetyl-1,2;5,6-di-O-isopropylidene-β-D-mannofuranose (**10**)*

3-*O*-Acetyl-1,2;5,6-di-*O*-isopropylidene-β-D-*threo*hex-3-enose (**6**) (300 mg) was dissolved in ethanol (50 ml) and reduced over palladium black (100 mg) for 8 h at atmospheric pressure. The t.l.c. showed one major component with a trace of a minor component. The solution was filtered and evaporated to a sirup. The sirup was kept in the freezing compartment of a refrigerator (~ −20°) until crystallization started. The product was taken up in warm petroleum ether (65–110°), the solution cooled, and seeded. The product crystallized out in flat cubes (200 mg). The m.p. 45–46°, $[\alpha]_D^{22}$ −22.6° (*c*, 0.866 $CHCl_3$).

Anal. Calcd. for $C_{14}H_{22}O_7$: C, 55.63; H, 7.28. Found: C, 55.43; H, 7.13.

1,2;5,6-Di-O-isopropylidene-β-D-mannofuranose

3-*O*-Acetyl-1,2;5,6-di-*O*-isopropylidene-β-D-mannofuranose (**10**) (180 mg) was dissolved in methanol (15 ml) and 0.1 *N* NaOMe in methanol was added until the solution stayed slightly basic to p*H* paper. When deacetylation was complete as indicated by t.l.c., solid CO_2 was added to neutralize the solution. Evaporation and recrystallization from petroleum ether (65–110°) gave material (130 mg) identical in every way to 1,2;5,6-di-*O*-isopropylidene-β-D-mannofuranose. The m.p. and mixed m.p. 52–53°, $[\alpha]_D$ 12.3° (*c*, 0.83 water).

*3-Deoxy-1,2;5,6-di-O-isopropylidene-α-D-xylohexofuranose (**11**)*

3-*O*-Acetyl-1,2;5,6-di-*O*-isopropylidene-α-D-*erythro*hex-3-enose (**5**) (1.1 g) was dissolved in anhydrous ether (75 ml) and reduced over platinum (100 mg) for 24 h. The mixture was filtered, evaporated to a thin sirup, taken up in chloroform (100 ml), and washed with dilute sodium bicarbonate solution. The chloroform fraction was dried over magnesium sulfate, filtered, and evaporated. The resulting sirup was dissolved in methanol (25 ml) and 0.01 *N* sodium methoxide in methanol was added until the solution stayed basic to p*H* paper. When de-*O*-acetylation of the 3-*O*-acetyl-1,2;5,6-di-*O*-isopropylidene-α-D-gulofuranose was complete as indicated by t.l.c., the base was neutralized with solid CO_2 and evaporated. Water (20 ml) was added and the product was extracted into petroleum ether (65–110°) (10 × 100 ml). The combined extracts were dried over magnesium sulfate, filtered, and evaporated. The product was recrystallized from petroleum ether to give the crystalline product (0.6 g) as long needles. The m.p. and mixed m.p. with authentic material (9) 79–80°, $[\alpha]_D^{22}$ −27.4°, (*c*, 0.972 $CHCl_3$); literature (9), m.p. 81°, $[\alpha]_D$ −38.1, (*c*, 4.11 ethanol).

*3-Deoxy-1,2;5,6-di-O-isopropylidene-β-D-arabinohexofuranose (**12**)*

Method A

3-*O*-Acetyl-1,2;5,6-di-*O*-isopropylidene-β-D-*threo*hex-3-enose (**6**) (250 mg) was dissolved in anhydrous ether (50 ml) and reduced with hydrogen over platinum for 24 h at atmospheric pressure. The solution was filtered, the catalyst washed with ether, the filtrate and washings combined and evaporated to a sirup. The product was dissolved in anhydrous methanol (40 ml) and deacetylated as described in the preparation of **11** to remove the acetyl from the side product 3-*O*-acetyl-1,2;5,6-di-*O*-isopropylidene-β-D-mannofuranose (**10**). The deacetylated sirup was dissolved in water (15 ml) and extracted with petroleum ether (65–110°) (6 × 100 ml). The extracts were combined, dried over magnesium sulfate, filtered, and evaporated. The product was distilled under high vacuum, $b.p._{0.01}$ 68°, to give a sirup (80 mg) which crystallized on standing in the refrigerator. The m.p. 21–22°, $[\alpha]_D^{22}$ 24.1°, (*c*, 1.17 $CHCl_3$).

Method B

3-Deoxy-D-mannose (10) (2 g) was dissolved in acetone (60 ml) containing zinc chloride (4 g) and phosphoric acid (0.2 ml) and the solution stirred for 24 h. The solution was then neutralized with 50% sodium hydroxide and the mixture filtered. The filtrate was evaporated to about 5 ml, dissolved in chloroform, and washed with dilute sodium bicarbonate solution. The chloroform solution was dried over magnesium sulfate, evaporated, and distilled under high vacuum, b.p.$_{0.01}$ 68°. The redistilled product (2.1 g) crystallized on standing in the refrigerator. Careful recrystallization from 30–60° petroleum ether gave material melting at 22–23°, $[\alpha]_D^{22}$ 27.5, (*c*, 0.40 $CHCl_3$); literature (11) sirup, $[\alpha]_D^{20}$ 21.1, (*c*, 1.5 $CHCl_3$).

Anal. Calcd. for $C_{12}H_{20}O_5$: C, 59.02; H, 8.16. Found: C, 58.91; H, 8.07.

3,5-Di-O-acetyl-1,2-O-isopropylidene-α-D-ribohexofuranos-3-ulose (13)

Method A

1,2;5,6-Di-*O*-isopropylidene-α-D-*ribo*hexofuranos-3-ulose (2.5 g) was dissolved in isopropenyl acetate (50 ml). *p*-Toluenesulfonic acid (50 mg) was added and the solution was heated on a steam bath for 8 h. Water (100 ml) was added and the mixture extracted with chloroform (6 × 75 ml). The combined extracts were washed with water (2 × 150 ml), dried over calcium chloride, filtered, and evaporated to a sirup. The sirup was dissolved in ethanol. The crystalline material (950 mg) obtained could be recrystallized from ethanol or sublimed under reduced pressure at 100°. The m.p. 124–126°, $[\alpha]_D^{22}$ 74.8° (*c*, 0.334 methanol).

Anal. Calcd. for $C_{13}H_{18}O_8$: C, 51.66; H, 5.96. Found: C, 51.63; H, 6.06.

Method B

1,2-*O*-Isopropylidene-α-D-*ribo*hexofuranos-3-ulose was prepared from the 1,2;5,6-diketal (1 g) by the method of Theander (3). This material was acetylated directly without prior purification by dissolving it in a mixture of acetic anhydride (5 ml) and pyridine (10 ml). The solution was kept overnight at room temperature, then evaporated repeatedly with toluene until no further pyridine was present. The sirup was dissolved in hot ethanol, cooled, and the resulting crystalline material (310 mg) was recrystallized from ethanol. This material had a m.p. and mixed m.p. with the product of method A of 124–126°, and an identical n.m.r. and mass spectrum and optical rotation.

We are pleased to acknowledge the financial support of the National Research Council of Canada. We wish to thank M. M. Tracey for the i.r. studies, G. Owen for the mass spectral work and Professor L. D. Hall of the University of British Columbia, Vancouver, B.C., for a LACOON III deck and very helpful suggestions regarding the n.m.r. work.

1. K. N. Slessor and A. S. Tracey. Can. J. Chem. **47**, 3989 (1969).
2. W. Meyer zu Reckendorf. Angew. Chem. Int. Ed. **6**, 177 (1967).
3. O. Theander. Acta Chem. Scand. **17**, 1751 (1963).
4. J. S. Brimacombe and P. A. Gent. Carbohyd. Res. **12**, 1 (1970).
5. J. Herling, J. Shabtai, and E. Gil-Av. J. Amer. Chem. Soc. **87**, 4107 (1965).
6. R. J. Abraham, L. D. Hall, L. Hough, and K. A. McLauchlin. J. Chem. Soc. 3699 (1962).
7. D. C. DeJongh and K. Biemann. J. Amer. Chem. Soc. **86**, 67 (1964).
8. P. N. Rylander. Catalytic hydrogenation over platinum metals. Academic Press, 1967. p. 96.
9. F. Weygand and H. Wolz. Chem. Ber. **85**, 256 (1952).
10. G. Rembarz. Chem. Ber. **93**, 622 (1960).
11. G. Rembarz. J. Prakt. Chem. **19**, 315 (1963).
12. J. Prokop and D. H. Murray. J. Pharm. Sci. **57**, 1697 (1968).
13. A. A. Bothner-By and S. M. Castellano. Computer Programs for Chemistry. Vol. 1. *Editor* D. F. DeTar, W. A. Benjamin Inc., New York, 1968. p. 10.

Can. J. Chem. Downloaded from www.nrcresearchpress.com by 210.87.254.5 on 09/05/12
For personal use only.

Can. J. Chem. Downloaded from www.nrcresearchpress.com by 210.87.254.105 on 09/05/12
For personal use only.

Aryl complexes of platinum(II). A study of the bonding between platinum and tertiary phosphine, arsine, and stibine

A. D. WESTLAND AND M. NORTHCOTT
Department of Chemistry, University of Ottawa, Ottawa, Canada

Received March 25, 1970

Phenyl and fluorophenyl complexes but not alkyl complexes of platinum may be prepared from $(Et_3Sb)_2PtCl_2$ by Grignard reactions. Dipole moment and ^{19}F nuclear magnetic resonance studies indicate a slight gradation in electronic properties which correlates with previous equilibrium studies.

Canadian Journal of Chemistry, 48, 2907 (1970)

Despite the existence of numerous complexes of platinum group metals containing tertiary phosphines, arsines, and stibines, little information is available as yet concerning the relative bond characters of the metal–ligand coordinate links. Previous work in this laboratory on equilibria involving the formation of five-coordinate complexes of platinum and palladium has suggested that the positive charge on the metal atom increases in the order of ligands: phosphine → arsine → stibine (1, 2). The argument presented which was based on variations in d_π–d_π bonding is at variance with the ideas of previous workers who believed that phosphorus encourages the strongest component of π-bonding amongst the Group V donor atoms (3). More recently, Venanzi has argued that d_π–d_π bonding has been much overemphasized and that most data may equally well be interpreted by a proper recognition of σ-inductive effects (4).

Parshall has developed a technique based upon an examination of the ^{19}F nuclear magnetic resonance (n.m.r.) chemical shift in meta and para positions of a phenyl group bonded to a platinum atom (5). This group is placed in a coordination position *trans* to the ligand whose π-bonding potential is being investigated. Bruce has examined ^{19}F resonance in pentafluorophenyl complexes (6). However, Church and Mays have questioned Parshall's conclusions concerning π-bonding, for when they applied the ^{19}F n.m.r. technique to a series of cationic platinum complexes, the results seemed to indicate that a σ-inductive mechanism was more strongly operative than a π mechanism (7).

The present state of confusion about interpreting the more indirect physical phenomena in chemical terms suggests that further work is much needed. The present paper examines the comparison of dipole moment data and ^{19}F resonance spectra obtained for complexes of the type *cis*-$(Et_3M)_2Pt(C_6H_4F)_2$ where M = P, As, or Sb.

Experimental

Reagents

The compounds PtL_2Cl_2 where L = Et_3P, Et_3As, and Et_3Sb were prepared by established procedures (8) from commercial grade platinum sponge. The ligands were prepared in the manner described by Adams and Raynor (9). Bromofluorobenzenes supplied by Aldrich Chemical Company were distilled prior to use. Grignard reagents were prepared in diethylether which had been freshly distilled from an ethyl Grignard solution containing excess magnesium.

Preparation of Aryl Complexes

The *cis*-diaryl complexes were prepared by a method of which the following is a typical example.

cis-(Et₃Sb)₂PtPh₂

Solid *cis*-$(Et_3Sb)_2PtCl_2$ (1 g) was added slowly to a cooled (−60 °C) solution of phenylmagnesium bromide in ether (50 cc). After the addition was complete, the sample was allowed to warm to room temperature at which point it was stirred for 1 h. The solution was then cooled to 0 °C and hydrolyzed with water (50 cc).[1] The ether layer was dried over $MgSO_4$ and the solvent removed by evaporation. The residue was placed on a 100 g alumina column and eluted with a 5% solution of diethylether in light petroleum. A pure fraction was located by thin layer chromatography (t.l.c.) and this solution was evaporated to dryness. The product, which consisted of white needles, was recrystallized from methanol in 29% yield.

cis and trans-(Et₃As)₂Pt(m-FC₆H₄)₂

cis-$(Et_3As)_2PtCl_2$ (0.5 g) was added to *m*-FC_6H_4MgBr (1.16 g) in ether (50 cc) which had been cooled to −60 °C. The solution was allowed to warm to room temperature and it was stirred for 2 h. After hydrolysis with NH_4Cl solution, the dried ether layer was evaporated to an oil which was purified chromatographically on an alumina column. Elution with petroleum ether (30–60°) gave white *trans*-$(Et_3As)_2Pt(m\text{-}FC_6H_4)_2$ which was recrystallized from methanol. Further elution with 5% ether – petro-

[1]Dilute HCl acid was used to prepare the complexes containing triethylphosphine or triethylarsine.

TABLE 1
Analytical data for aryl complexes of platinum(II)

Compound	Melting point (°C)	Yield	Anal. Calcd. (%) C	H	F	Anal. Found (%) C	H	F
cis-$[(C_2H_5)_3P]_2Pt(m\text{-}FC_6H_4)_2$	159–160	47	46.38	6.16	6.11	46.23	6.22	5.96
cis-$[(C_2H_5)_3P]_2Pt(p\text{-}FC_6H_4)_2$	158–159	38	46.38	6.16	6.11	46.54	6.14	6.02
cis-$[(C_2H_5)_3As]_2Pt(m\text{-}FC_6H_4)_2$	123–124	40	40.63	5.40	5.36	40.56	5.51	5.41
trans-$[(C_2H_5)_3As]_2Pt(m\text{-}FC_6H_4)_2$	144–145	13	40.63	5.40	5.36	40.47	5.39	5.47
cis-$[(C_2H_5)_3As]_2Pt(p\text{-}FC_6H_4)_2$	125–126	38	40.63	5.40	5.36	40.64	5.49	5.28
cis-$[(C_2H_5)_3Sb]_2Pt(m\text{-}FC_6H_4)_2$	78–79	22	35.89	4.77	4.73	35.75	4.89	3.44
cis-$[(C_2H_5)_3Sb]_2Pt(p\text{-}FC_6H_4)_2$	92–93	35	35.89	4.77	4.73	35.21	4.71	4.66
trans-$[(C_2H_5)_3Sb]_2PtCl(p\text{-}FC_6H_4)$	106–107	28	29.08	4.61	2.55	28.66	4.60	2.23
cis-$[(C_2H_5)_3Sb]_2Pt(C_6H_5)_2$	68–69	29	37.57	5.25		37.50	5.52	
$[(C_6H_5)_3P]Au(m\text{-}FC_6H_4)$	146–147 (dec.)	64	52.04	3.45	3.42	52.19	3.43	3.33

leum ether gave white *cis*-$(Et_3As)_2Pt(m\text{-}FC_6H_4)_2$ which was recrystallized from methanol.

trans-$(Et_3Sb)_2PtCl(p\text{-}FC_6H_4)$

A solution of *cis*-$(Et_3Sb)_2PtCl_2$ which had been treated with $p\text{-}FC_6H_4MgBr$ as described above, was hydrolyzed with 4 *N* HCl. A t.l.c. of this solution gave a spot with an R_f value of about one half that for $(Et_3Sb)_2Pt(p\text{-}FC_6H_4)_2$. Purification by chromatography using 10% ether – petroleum ether gave white *trans*-$(Et_3Sb)_2PtCl(p\text{-}FC_6H_4)$ which was recrystallized from methanol.

Prolonged treatment with HCl solution resulted in complete conversion back to $(Et_3Sb)_2PtCl_2$. Hydrolysis with NH_4Cl solution also resulted in replacement of one of the aryl groups of the diaryl complex although not so rapidly as when HCl was used.

Nuclear Magnetic Resonance Spectra

Proton n.m.r. spectra were obtained with a Varian Associates model T-60 spectrometer. Fluorine spectra were obtained with a Varian Associates model HR-100 spectrometer using side-band modulation for calibration. Spectra were run using chloroform or deuterochloroform as a solvent and with external reference substances.

Dipole Moments

A Wissenschaftlich–Technische Werkstatten Dipolmeter model DM-01 was employed for dielectric constant determination at 25 °C. Samples were dissolved in benzene.

Smith's method was used for evaluating the dipole moment values (10). The results were consequently corrected for electronic polarization but not atomic polarization.

Analyses

Analyses were performed by the firm of A. Bernhardt Mikroanalytisches Laboratorium, Elbach, West Germany.

Results and Discussion

At the commencement of our work no organometallic compounds of platinum stabilized by a tertiary stibine had been reported. Recently, however, triphenylstibine complexes were described by Kistner *et al.* (11). These were made by a method which differed fundamentally from that which employs Grignard reactions (12). Although we were successful in making aryl complexes, *cis*-dichloro*bis*-(triethylstibine)platinum(II) gave dark decomposition products when it was added to strongly cooled ethylmagnesium bromide. We conclude that alkyl compounds of this type are too unstable to be prepared by the Grignard method and that tertiary stibine is less effective than tertiary arsine or phosphine in stabilizing organometallic derivatives of platinum. The meta-fluorophenyl complex containing Ph_3Sb was least stable of the platinum complexes and it decomposed readily during evaporations and chromatographic treatment. The para-fluorophenyl complex was more stable owing possibly to an enhancement of the π-bonding from platinum to carbon.

Still less stable was $(Ph_3P)Au(m\text{-}C_6H_4F)$. Repeated attempts to prepare the para-fluorophenyl analogue failed as the solutions were found to be so unstable at room temperature, they could not be worked up. In striking contrast to our experience, Vaughan succeeded in preparing this compound in a Grignard reaction which involved refluxing at 60° (13). It may be that the quality of the reagents is of crucial significance here.

Melting points and analyses of the compounds prepared are given in Table 1.

The location of the fluoro group in the phenyl rings was verified in all cases by proton magnetic resonance spectra. The stereochemistry of the isomers was established by dipole moment measurements. The data associated with these measurements is presented in Table 2. Refractive indices were measured for one isomer in each case. Solutions of the other isomer were assumed to have the same molar refractive index.

As expected, the para-fluorophenyl isomers

Can. J. Chem. Downloaded from www.nrcresearchpress.com by 210.87.254.105 on 09/05/12
For personal use only.

TABLE 2

Dipole moment measurements on aryl complexes of platinum(II)

Compound	Weight fraction, w ($\times 10^4$)	$\Delta\varepsilon/w$	$\Delta(n^2)/w$	μ (D)
cis-$[(C_2H_5)_3P]_2Pt(m\text{-}FC_6H_4)_2$	4.235	14.36		9.0
cis-$[(C_2H_5)_3P]_2Pt(p\text{-}FC_6H_4)_2$	4.940	16.15		9.4
	9.180	15.58		
	5.859	15.98		
	219.8		0.17	
cis-$[(C_2H_5)_3As]_2Pt(m\text{-}FC_6H_4)_2$	11.854	11.729		8.7
	7.333	11.916		
	5.105	12.013		
trans-$[(C_2H_5)_3As]_2Pt(m\text{-}FC_6H_4)_2$	10.566	0.449		1.2
cis-$[(C_2H_5)_3As]_2Pt(p\text{-}FC_6H_4)_2$	14.759	13.920		9.4
	11.720	13.720		
	9.489	14.028		
	6.547	13.700		
	238		0.214	
cis-$[(C_2H_5)_3Sb]_2Pt(m\text{-}FC_6H_4)_2$	3.697	10.47		8.7
cis-$[(C_2H_5)_3Sb]_2Pt(p\text{-}FC_6H_4)_2$	8.824	11.90		9.1
	2.453	11.11		
trans-$[(C_2H_5)_3Sb]_2PtCl(p\text{-}FC_6H_4)$	13.533	0.4670		1.3
	271.6		0.2062	
cis-$[(C_2H_5)_3Sb]_2Pt(C_6H_5)_2$	9.118	5.978		6.3
	5.575	5.952		
	4.478	5.998		
	220		0.232	
$[(C_6H_5)_3P]Au(m\text{-}FC_6H_4)$	15.469	10.08		7·0
	9.044	9.91		
	5.916	10.08		
	229.6		0.339	

have a somewhat higher dipole moment in each case than the meta-fluorophenyl analogues. The trend in moment exhibited by the phosphorus, arsenic, and antimony analogues is interesting although one must be careful not to place too much reliance upon any given interpretation. We have obtained for both $(Et_3P)_2PtPh_2$ and $(Et_3As)_2PtPh_2$ dipole moment values of 7.2 D. These agree well with the values obtained by Chatt and Shaw (12). The value obtained for $(Et_3Sb)_2PtPh_2$ was 6.3 D. The generally lower value for the antimony analogue is observed in the chloro compounds $(Et_3M)_2PtCl_2$ (13) and the meta- and para-fluorophenyl series of compounds as well. One might assume that the Sb—Pt—Sb bond angle is larger than the As—Pt—As and P—Pt—P angles which would have the effect of diminishing the observed resultant of the bond moments. Molecular models fail to indicate categorically whether steric crowding must occur. However, we have previously shown a similar trend in the moments of the compounds $(Ph_3M)AuBr$ where the steric factor does not arise (2). It is conceivable that solvation effects are responsible or that indeed, as previously suggested (1, 2), the π electron drift from platinum to antimony is greater than that toward either arsenic or phosphorus. In any case, the dipole moment data appear to reflect the same influences as do the equilibrium data of our previous studies.

When interpreted in the manner proposed by Parshall (5), the ^{19}F n.m.r. spectra indicate a marginally greater π-bonding ability on the part of triethylstibine relative to triethylphosphine. The last column in Table 3 labelled "π-bonding index" contains the differences between values in the preceding two columns. These differences, according to Parshall's argument, are a measure of the extent to which the aromatic ring draws electron density from the platinum atom by a mesomeric mechanism. This should bear an inverse relationship to the degree of π-bonding to the ligand in the *trans* position.

Parshall observed only a small variation in the π-bonding index as do we. This represents an uncertain result. Furthermore, Dewar has pointed

Can. J. Chem. Downloaded from www.nrcresearchpress.com by 210.87.254.105 on 09/05/12
For personal use only.

TABLE 3

The ^{19}F chemical shift data for fluorophenyl derivatives of platinum(II) and gold(I)

Compound	Chemical shift* (p.p.m.) meta-Fluoro	Chemical shift* (p.p.m.) para-Fluoro	π-Bonding index (p.p.m.)
cis-$(Et_3P)_2Pt(FC_6H_4)_2$	2.75	10.40	7.65
cis-$(Et_3As)_2Pt(FC_6H_4)_2$	2.75	10.20	7.45
cis-$(Et_3Sb)_2Pt(FC_6H_4)_2$	2.30	9.70	7.40
trans-$(Et_3As)_2Pt(FC_6H_4)_2$	3.25	—	—
$(Ph_3P)_2Au(FC_6H_4)$	0.90	—	—

*Relative to fluorobenzene. Values are rounded off to the nearest 0.05 p.p.m.

out that the influence of remote groups on ^{19}F n.m.r. chemical shifts is a vector quantity while chemical equilibria and reactivity depend upon a scalar quantity (14). Since the exact geometry of these molecules is not known and hence the orientation of the meta C—F bond may differ somewhat from one compound to another, it may be that the "π-bonding index" is a more complex quantity than Parshall or Church and Mays (7) suggested.

The chemical shift of the para fluorine atom alone may be a simpler quantity for the orientation if the para C—F bond is fixed. Indeed, Hogben *et al.* (15) concluded that it is determined largely by σ_R, the Hammett–Taft resonance parameter (16), and so to a first approximation it is a measure of π interaction between the phenyl ring and its substituent. The series of values for the para fluorine chemical shift given in Table 3 agree qualitatively with the trend in dipole moments. The same trend was observed in the chemical shift for the para hydrogen atoms in the pyridine complexes *trans*-$(Pr_3M)PtCl_2py$, although in these the "π-bonding index" difference values did not correlate with any obvious chemical facts (17). While we cannot account for these various observations with any certainty, we suggest that their consistency may be significant.

In *trans*-$(Et_3As)_2Pt(m\text{-}FC_6H_4)_2$ the chemical shift of the meta fluorine atom is slightly higher than that of the *cis* isomer. The value is similar to that reported for *trans*-$(Et_3P)_2Pt(m\text{-}FC_6H_4)_2$ (5). We have also included in Table 3 the ^{19}F chemical shift for $(Ph_3P)Au(m\text{-}FC_6H_4)$ which is seen to be lower than comparable values for the platinum complexes. Vaughan obtained a higher value for this compound but he worked in a different solvent (13). Although this low value for the chemical shift in the gold compound would seem to indicate that there is less electronic charge build-up in the phenyl ring, the dipole moment of $(Ph_3P)AuC_6H_5$ (6.2 D) is large relative to 5.1 D estimated for the linear $(Et_3P)PtC_6H_5$ grouping[2] (18). Vaughan has commented on the low degree of electron delocalization onto the phenyl ring in $(Ph_3P)Au(p\text{-}FC_6H_4)$ as estimated using Parshall's technique. Further work on gold(I) is being hampered by the generally low stability of its complexes.

This work was supported by a grant from the National Research Council of Canada.

1. A. D. WESTLAND. J. Chem. Soc. 3060 (1965).
2. A. D. WESTLAND. Can. J. Chem. **47**, 4135 (1969).
3. J. CHATT, L. A. DUNCANSON, B. L. SHAW, and L. M. VENANZI. Discuss. Faraday Soc. **26**, 131 (1958).
4. A. PIDCOCK, R. E. RICHARDS, and L. M. VENANZI. Proc. Chem. Soc. 184 (1962).
5. G. W. PARSHALL. J. Amer. Chem. Soc. **88**, 704 (1966).
6. M. I. BRUCE. J. Chem. Soc. (A), 1459 (1968).
7. M. J. CHURCH and M. J. MAYS. J. Chem. Soc. (A), 3074 (1968).
8. GMELIN'S Handbuch der anorganischen Chemie. Platin. Teil D, System Nummer 68. Verlag Chemie, 1957.
9. D. M. ADAMS and J. B. RAYNOR. Advanced practical inorganic chemistry. Wiley, 1965. p. 117.
10. J. W. SMITH. Trans. Faraday Soc. **46**, 394 (1950).
11. C. R. KISTNER, J. D. BLACKMAN, and W. C. HARRIS. Inorg. Chem. **8**, 2165 (1969).
12. J. CHATT and B. L. SHAW. J. Chem. Soc. 4020 (1959).
13. J. CHATT and R. G. WILKINS. J. Chem. Soc. 4300 (1952).
14. M. J. S. DEWAR and T. G. SQUIRES. J. Amer. Chem. Soc. **90**, 210 (1968). W. ADCOCK and M. J. S. DEWAR. J. Amer. Chem. Soc. **89**, 379 (1967).
15. M. G. HOGBEN, R. G. GAY, and W. A. G. GRAHAM. J. Amer. Chem. Soc. **88**, 3457 (1966).
16. R. W. TAFT and J. W. RAKSHYS, JR. J. Amer. Chem. Soc. **87**, 4387 (1965) and references cited therein.
17. J. CHATT and A. D. WESTLAND. J. Chem. Soc. (A), 88 (1968).
18. G. CALVIN, G. E. COATES, and P. S. DIXON. Chem. Ind. 1628 (1959).

[2]This is $1/\sqrt{2}$ (μ_D) where μ_D is the observed moment for *cis*-$(Et_3P)_2Pt(C_6H_5)_2$ (7). The negative end of the dipole lies between the phenyl rings.

Can. J. Chem. Downloaded from www.nrcresearchpress.com by 210.87.254.105 on 09/05/12
For personal use only.

Can. J. Chem. Downloaded from www.nrcresearchpress.com by 210.87.254.42 on 09/05/12
For personal use only.

Biosynthesis of lycopodine. Incorporation of Δ^1-piperideine and of pelletierine[1]

M. CASTILLO, R. N. GUPTA, Y. K. HO, D. B. MACLEAN, AND IAN D. SPENSER
Department of Chemistry, McMaster University, Hamilton, Ontario

Received April 16, 1970

The biogenetic hypothesis that the Lycopodium alkaloids are modified dimers of pelletierine (2, 3) was tested experimentally in *Lycopodium tristachyum*. Pelletierine is indeed incorporated into lycopodine, but only one pelletierine unit entered the alkaloid, rather than two units, as predicted. The hypothesis thus requires modification.

Δ^1-Piperideine serves as a specific precursor of lycopodine. Two Δ^1-piperideine moieties are incorporated in such a way that the identity of C-2 and -6 of each of the precursor units is maintained.

Canadian Journal of Chemistry, 48, 2911 (1970)

Lysine and acetate supply the atoms of the entire ring skeleton of lycopodine (**2**) (2, 3). The mode of incorporation of these precursors into the alkaloid, inferred from tracer experiments with 2-^{14}C- and 6-^{14}C-lysine (**1**) (2, 3) and with 1-^{14}C- and 2-^{14}C-acetate (3), is shown in Schemes 1 and 2.

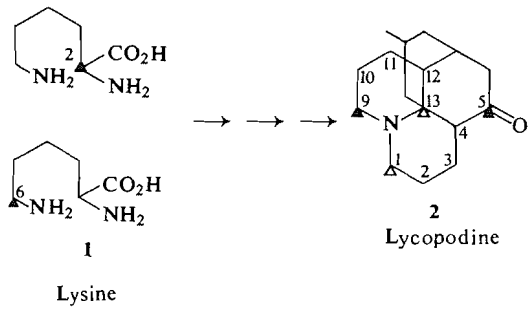

1
Lysine

2
Lycopodine

SCHEME 1

Incorporation of lysine into lycopodine. Sites of activity derived from 2-^{14}C-lysine and 6-^{14}C-lysine, established by degradation (▲) (~25% of total activity, from either radiomer) or inferred (△).

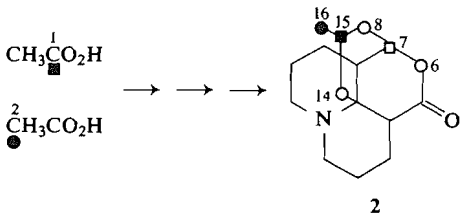

2

SCHEME 2

Incorporation of acetate into lycopodine. Sites of activity derived from 1-^{14}C-acetate (squares) (~50% of total activity) and 2-^{14}C-acetate (circles) (~25%), established by degradation (●, ■) or inferred (○, □).

The distribution of label from 2-^{14}C- and 6-^{14}C-lysine (approximately one quarter of the activity of the intact alkaloid at each of C-5 and -9, in either case) is consistent with the view, fully discussed in an earlier paper (3), that two identical C_5 units, derived from lysine via a symmetrical intermediate, are incorporated, yielding the C_5 units, C-1 to -5 and C-9 to -13, of the alkaloid. The mode of incorporation of activity from 1-^{14}C-acetate (approximately one half of the activity of lycopodine within the fragment C-15,16, presumably at C-15) and from 2-^{14}C-acetate (approximately one quarter of the activity within the fragment C-15,16, presumably at C-16), supports the inference that two identical C_3 units, generated by decarboxylation of acetoacetate,[2] supply the C_3 units, C-6 to -8 and C-14 to -16, of lycopodine.

These results support the view that the lycopodine molecule consists of two "halves", both of which originate from a common eight-carbon intermediate, and that this intermediate is in turn derived from lysine and acetate.

We made the suggestion (2, 3) that pelletierine (**5**) might be the common eight-carbon intermediate in question and proposed (2) a hypothetical sequence from lysine and acetate to lycopodine (Scheme 3) which is consistent with the incorporation data. The sequence predicts that cadaverine (**3**), a symmetrical molecule formed from lysine by decarboxylation (4), was a stage on the route of biosynthesis. Cadaverine does indeed enter lycopodine in the predicted manner (approximately one quarter of the activity at C-5 and approximately one quarter at C-9) (Scheme 4) (3).

[1]A preliminary report of part of this work has been published (1).

[2]Direct incorporation of an intact C_3 unit derived from acetoacetate could not be demonstrated, however (3).

Can. J. Chem. Downloaded from www.nrcresearchpress.com by 210.87.254.42 on 09/05/12
For personal use only.

TABLE 1

Incorporation of pelletierine and Δ^1-piperideine into lycopodine. Chemical and radiochemical yields

Experiment no.	Compound administered (see Experimental)	Nominal total activity (mCi)	Nominal specific activity (mCi/mmole)	Mode of administration	Date	Weight of dry plant (g)	Lycopodine	
							Yield (mg)	Specific activity (counts min^{-1} $mmole^{-1}$) $\times 10^{-4}$
7	2-^{14}C-Pelletierine	0.07	1.0	Wick	June 1968	55	180	4.14 ± 0.08 (^{14}C)
	4,5-$^{3}H_2$-Pelletierine	0.6	10					
10	2,3′-$^{14}C_2$-Pelletierine	0.07	0.7	Wick	August 1968	55	165	18.0 ± 0.25
12	6-^{14}C-Pelletierine	0.04	1.0	Cuttings	June 1969	46	133	13.1 ± 0.27
13	2-^{14}C-Δ^1-Piperideine	0.1	0.4	Cuttings	June 1969	35	88	104.4 ± 1.6
14	6-^{14}C-Δ^1-Piperideine	0.1	0.8	Cuttings	June 1969	38	104	190.4 ± 4.1

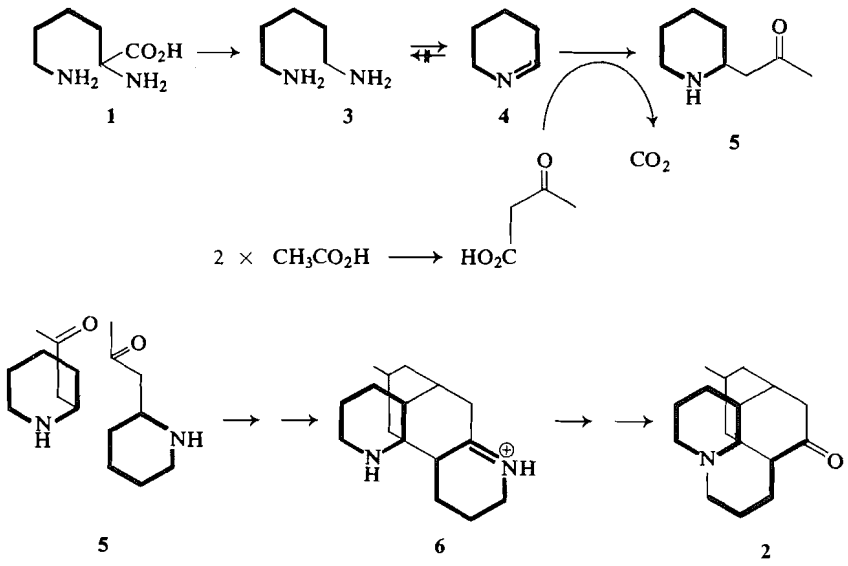

SCHEME 3

Incorporation of lysine and acetate into lycopodine. Postulated intermediates.

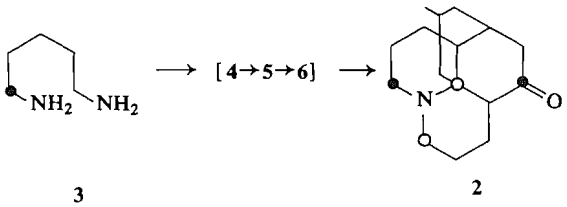

SCHEME 4

Incorporation of cadaverine into lycopodine. Sites of activity derived from 1-^{14}C-cadaverine, established by degradation (●) (~25%) or inferred (○).

In the present investigation we have examined the status in the biosynthesis of lycopodine of two further intermediates of the hypothetical sequence, Δ^1-piperideine (**4**) and pelletierine (**5**).

Labelled Δ^1-piperideine was prepared by oxidation of lysine (5), labelled pelletierine was synthesized by condensation of Δ^1-piperideine with acetoacetate (5). The radiomers of Δ^1-piperideine and of pelletierine which were administered to *Lycopodium tristachyum* Pursh are listed in Table 1, which summarizes the details of the feeding experiments that were carried out.

Each of the experiments yielded radioactive lycopodine. To locate the sites of labelling the lycopodine samples were partially degraded by reactions, which are fully described in an earlier paper (3) and are summarized in Scheme 5. The results of these degradations are presented in Tables 2, 3, and 4.

As anticipated, Δ^1-piperideine (**4**) serves as a specific precursor of lycopodine. Consistent with the established evidence (5, 6) that the position of the double bond in Δ^1-piperideine is fixed, the patterns of distribution in lycopodine of activity from 2-^{14}C- and from 6-^{14}C-Δ^1-piperideine differ (Table 2). Half of the radioactivity of the lycopodine, derived from 2-^{14}C-Δ^1-piperideine, was recovered from C-5 (benzoic acid), whereas C-9 (formic acid) was devoid of activity. Conversely, half the activity of the alkaloid derived from 6-^{14}C-Δ^1-piperideine was present at C-9 (formic acid), while C-5 (benzoic acid) was essentially inactive.

The observed mode of incorporation into lycopodine of activity from the two radiomers of Δ^1-piperideine (Scheme 6) corresponds exactly to that predicted by the hypothesis (Scheme 3), that two intact units of this substrate are incorporated in a non-symmetrical manner, supplying the piperidine nuclei of the $C_{16}N_2$ intermediate **6**, modification of which accounts for the formation of lycopodine, $C_{16}N$ (**2**).

Δ^1-Piperideine is the third substrate, the others being lysine and cadaverine, whose specific incorporation into the two C_5 units, C-1 to -5 and C-9 to -13, of lycopodine can be inferred from tracer data. But whereas the individuality of C-2 and -6 of labelled Δ^1-piperideine is maintained within the product, the corresponding carbon atoms, C-2 and -6, of labelled lysine become

Can. J. Chem. Downloaded from www.nrcresearchpress.com by 210.87.254.42 on 09/05/12
For personal use only.

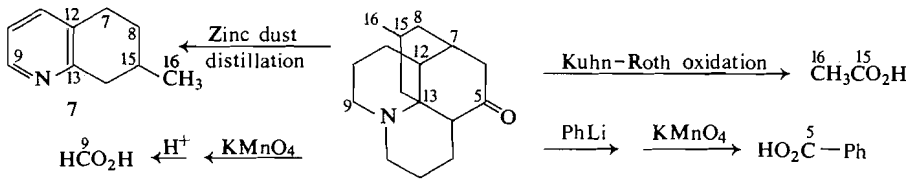

7 2

SCHEME 5
Degradation of lycopodine.

TABLE 2
Incorporation of Δ^1-piperideine into lycopodine

Precursor Experiment no.	2-^{14}C-Δ^1-Piperideine 13		6-^{14}C-Δ^1-Piperideine 14			
Product	SA*	RSA†	SA	RSA	SA	RSA
Lycopodine	3.14±0.05‡	100±2	13.82±0.30§	100±2	2.42±0.06§	100±3
Benzoic acid (C-5)	1.62±0.05	52±2	0.14±0.03	1±0.2	—	
Formic acid (C-9) (as α-naphthylamide)	0.03±0.01	1±0.2	—		1.26±0.02	52±2

*Specific activity (counts min^{-1} mmole^{-1}) × 10^{-4}.
†Relative specific activity: percent (lycopodine = 100).
‡Obtained from the original lycopodine (specific activity (104.4 ± 1.6) × 10^4 counts min^{-1} mmole^{-1}) of experiment 13 by dilution with inactive lycopodine.
§Obtained from the original lycopodine (specific activity (190.4 ± 4.1) × 10^4 counts min^{-1} mmole^{-1}) of experiment 14 by dilution with inactive lycopodine.

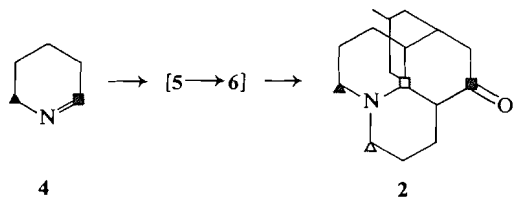

4 2

SCHEME 6

Incorporation of Δ^1-piperideine into lycopodine. Sites of activity from 2-^{14}C-Δ^1-piperideine (squares) and from 6-^{14}C-Δ^1-piperideine (triangles), established by degradation (▲, ■) (~50%) or inferred (△, □).

identical on route to the product. If Δ^1-piperideine is an obligatory intermediate of the pathway to lycopodine, as seems likely in view of the comparatively high radiochemical yield (Table 1), and lysine is the primary precursor, randomization of C-2 and -6 of lysine must take place at a stage of the metabolic route prior to the formation of Δ^1-piperideine, since, once the latter is formed, equilibration of these centers does not occur. The incorporation data suggest that a symmetrical intermediate lies between lysine and Δ^1-piperideine. Cadaverine has the attributes of the intermediate in question. It is a symmetrical molecule. It is incorporated into lycopodine in the expected manner (3). It is formed from lysine by decarboxylation (4) and is directly convertible to Δ^1-piperideine (7), in well documented enzymic reactions which are essentially irreversible. Both of these enzymic reactions have been detected in higher plants (8, 9). The evidence is clearly compatible with the view that the sequence lysine → cadaverine → Δ^1-piperideine constitutes part of the biosynthetic route to lycopodine.

The quantitative distribution within lycopodine, of label from all the tracers which have been tested as precursors,[3] presents a consistent pattern. In every case it can be inferred that each of the two C_8 units, C-1 to -8 and C-9 to -16, which constitute lycopodine, contains one half of the activity of the intact alkaloid. Equal incorporation of radioactivity into the two segments of a "dimeric" product is obligatory only if two identical units of "monomeric" precursor combine to yield a true dimer as a biosynthetic intermediate (10). Such a distribution of label, found in every one of eleven separate experiments with six different precursors,[3] is unlikely to be coincidental.

[3]Lysine (4 experiments) (3); cadaverine (3); Δ^1-piperideine (2 experiments) (this paper); sodium acetate (2 experiments) (3); sodium acetoacetate (3); sodium β-hydroxybutyrate (3).

Can. J. Chem. Downloaded from www.nrcresearchpress.com by 210.87.254.42 on 09/05/12
For personal use only.

TABLE 3

Incorporation of pelletierine into lycopodine

Experiment no.	Precursor	Product	SA*	RSA†	$^3H/^{14}C$ Ratio In precursor	$^3H/^{14}C$ Ratio In lycopodine
7	2-^{14}C-Pelletierine	Lycopodine Benzoic acid (C-5)	4.14±0.08 0.05±0.01	100±2 1±0.1		
7	2-^{14}C-Pelletierine	Lycopodine 7-Methyltetrahydroquinoline hydrochloride (C-7 to -16)	0.63±0.02‡ 0.59±0.02	100±2 94±4		
7	4,5-3H_2,2-^{14}C-Pelletierine				9.5±0.1	9.6±0.1
12	6-^{14}C-Pelletierine	Lycopodine Formic acid (C-9) (as α-naphthylamide)	0.87±0.02§ 0.90±0.02	100±2 104±3		
10	2,3′-$^{14}C_2$-Pelletierine	Lycopodine Acetic acid (C-15,16) (as α-naphthylamide)	2.60±0.05‖ 0.47±0.01	100±2 18±2		
10	2,3′-$^{14}C_2$-Pelletierine	Lycopodine 7-Methyltetrahydroquinoline hydrochloride (C-7 to -16)	0.72±0.01‖ 0.69±0.02	100±1 96±3		

*Specific activity (counts min^{-1} $mmole^{-1}$) × 10^{-4}.
†Relative specific activity: percent (lycopodine = 100).
‡Obtained by recrystallizing a mixture of 35 mg lycopodine, specific activity (4.14 ± 0.08) × 10^4 counts min^{-1} $mmole^{-1}$, and 190 mg carrier lycopodine.
§Obtained from the original lycopodine (specific activity (13.1 ± 0.27) × 10^4 counts min^{-1} $mmole^{-1}$) of experiment 12 by dilution with carrier lycopodine.
‖Obtained from the original lycopodine (specific activity (18.0 ± 0.25) × 10^4 counts min^{-1} $mmole^{-1}$) of experiment 10 by dilution with carrier lycopodine.

Indications are thus strong that lycopodine is generated by modification of a true dimer, $C_{16}N_2$ (e.g., **6**), formed from a C_8N monomer which is in turn derived from lysine and acetate. On the basis of the observed pattern of incorporation of these substrates into lycopodine (2, 3) and into *N*-methylpelletierine (11) we advanced the idea (2, 3) that pelletierine (**5**) might serve as the required C_8N monomer. Radioactivity from labelled pelletierine is indeed incorporated into lycopodine (Table 1).

Recovery, from the experiment with 4,5-$^3H_2$,2-^{14}C-pelletierine, of lycopodine whose ^3H:^{14}C ratio matched that of the precursor (experiment 7, Table 3), was consistent with the hypothesis that lycopodine is a modified dimer of pelletierine. The absence of activity derived from 2-^{14}C-pelletierine (experiment 7, Table 3) at C-5 of lycopodine (benzoic acid) was not, however. The hypothesis demands 50% of activity at this site. It is evident that the C_8 unit of the lycopodine molecule which includes C-5 (i.e. C-1 to -8) is not derived from pelletierine in the predicted manner. Since all activity derived from 2-^{14}C-pelletierine (experiment 7, Table 3) was confined to the portion of the molecule represented by 7-methyl-5,6,7,8-tetrahydroquinoline (C-7 to -16), it seemed likely that whereas the C_8 unit, C-1 to -8, was not derived from pelletierine at all, a pelletierine unit did indeed serve as the precursor of the other C_8 unit of the lycopodine molecule, C-9 to -16. This conclusion is supported by the recovery from C-9 (formic acid) of all activity derived from 6-^{14}C-pelletierine (experiment 12, Table 3). Intact incorporation of a pelletierine moiety into the C_8 unit, C-9 to -16, is clearly established by the results of the experiment with 2,3′-$^{14}C_2$-pelletierine(experiment 10). Not only was all activity from this precursor present in the quinoline derivative (C-7 to -16) (experiment 10, Table 3), but the fraction of this activity, recovered in the Kuhn–Roth acetate (C-15,16), was identical with the fraction of activity at the C-methyl group of the precursor (Table 4).

It is thus demonstrated that an intact pelletierine unit serves as a specific precursor of the C_8 unit, C-9 to -16, of lycopodine, as predicted

Can. J. Chem. Downloaded from www.nrcresearchpress.com by 210.87.254.42 on 09/05/12
For personal use only.

TABLE 4

Incorporation of 2,3′-$^{14}C_2$-pelletierine into lycopodine (experiment 10)

Distribution of label in					
2,3′-$^{14}C_2$-Pelletierine			Lycopodine		
	SA*	RSA†		SA*	RSA†
Pelletierine	5.98±0.10‡	100±2	Lycopodine	2.60±0.05	100±2
Acetic acid (C-2′,3′) (as α-naphthylamide)	1.09±0.01	18±0.3	Acetic acid (C-15,16) (as α-naphthylamide)	0.47±0.01	18±0.4
Pipecolic acid (nucleus, C-1′)	4.72±0.08	79±2			

*Specific activity (counts min^{-1} $mmole^{-1}$) × 10^{-4}.
†Relative specific activity: percent.
‡Obtained by mixing a small sample (total activity ~0.2 μCi) of the original 2,3′-$^{14}C_2$-pelletierine hydrochloride, used in experiment 10, with inactive pelletierine hydrochloride (350 mg), and recrystallizing the mixture to constant activity.

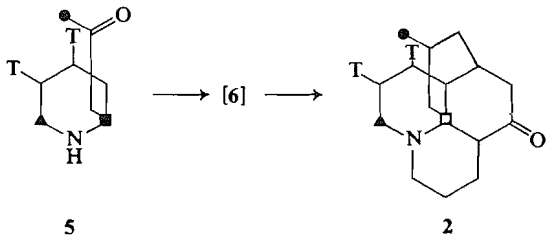

5 2

SCHEME 7

Incorporation of pelletierine into lycopodine. Sites of activity established by degradation (▲, ●) or inferred (□ ,T).

(Scheme 7). Contrary to prediction, however, the C_8 unit, C-1 to -8, is not derived from this precursor. It follows that lycopodine is not a modified dimer of pelletierine.

Incorporation of pelletierine into one of the two C_8N units of the Lycopodium base cernuine has recently been shown to take place in an analogous manner (12).

One of two conclusions is thus inescapable: Either (*i*), pelletierine is an obligatory precursor of lycopodine, in which case the alkaloid cannot be derived from a dimeric intermediate, $C_{16}N_2$. This inference is inconsistent with the finding, discussed earlier, that in 11 experiments with other tracers the two "halves" of lycopodine were equally labelled. Or (*ii*), lycopodine is indeed generated by modification of a dimeric intermediate, $C_{16}N_2$, in which case pelletierine cannot be a normal precursor. This conclusion gives rise to the apparent paradox that pelletierine can replace one but not the other of two identical C_8N moieties, serving as precursors of the dimeric intermediate.

Each one of these apparent contradictions can be rationalized. The model, shown in Scheme 8, can, in principle, account for equal incorporation of early precursors into the pelletierine-derived as well as the non-pelletierine-derived "half" of lycopodine, as demanded by alternative (*i*), provided the steady-state concentration of **5** is small compared to that of **8**, and the conversion of **8** to **5** is irreversible.

A hypothetical sequence, consistent with alternative (*ii*) is shown in Scheme 9. It is suggested that 2-allylpiperidine (**11**) rather than pelletierine serves as the C_8N unit, from which the dimeric precursor **6** of lycopodine is ultimately derived. Dimerization of an oxidized derivative (**12**) of 2-allylpiperidine is initiated by protonation at the terminal carbon atom of the side chain. In the dimerization step the protonated species **13** may be replaced by pelletierine, if the latter is available, whereas the non-protonated species **12** cannot be so replaced.

Investigations to test these and other hypotheses are in progress.

Experimental

Synthesis of Labelled Compounds

^{14}C-Δ^1-Piperideine

The samples of 2-^{14}C-Δ^1-piperideine (experiment 13) and 6-^{14}C-Δ^1-piperideine (experiment 14) were obtained from 2-^{14}C-DL-lysine monohydrochloride (New England Nuclear) and from 6-^{14}C-DL-lysine dihydrochloride (Commissariat à l'Energie Atomique, France), respectively.

2-^{14}C-Δ^1-Piperideine was prepared as follows (c.f. ref. 5): 2-^{14}C-DL-Lysine monohydrochloride (0.1 mCi), together with unlabelled DL-lysine monohydrochloride to make a total of 0.25 mmole, was dissolved in water (10 ml). *N*-Bromosuccinimide (0.52 mmole) was added and the solution was kept at 40–50° for a few minutes. Light suction was applied to remove bromine vapors. Dilute hydrochloric acid (0.25 *M*, 1 ml) was added to the clear solution which contained Δ^1-piperideine

Can. J. Chem. Downloaded from www.nrcresearchpress.com by 210.87.254.42 on 09/05/12
For personal use only.

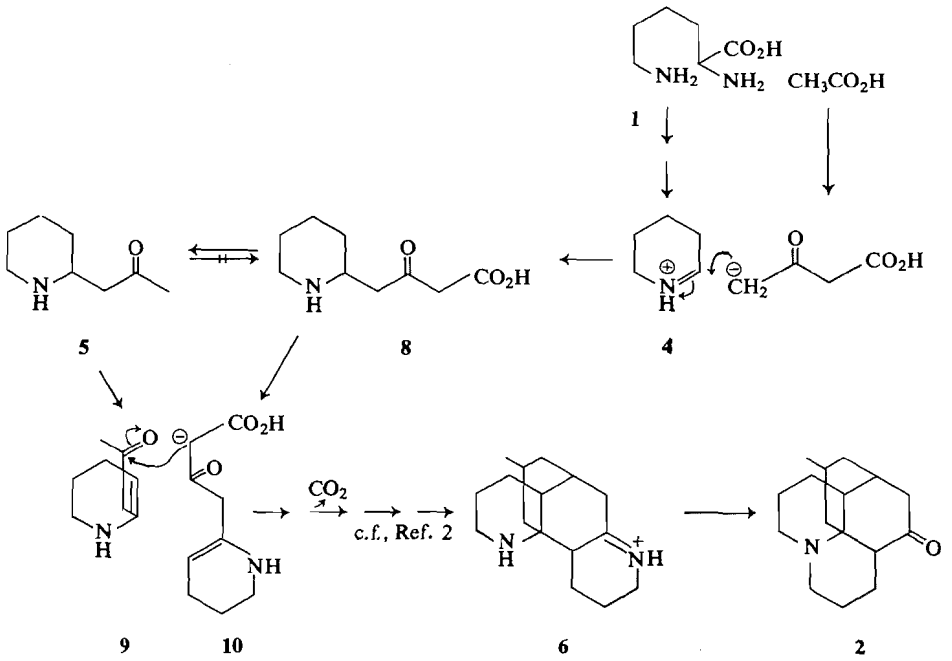

SCHEME 8

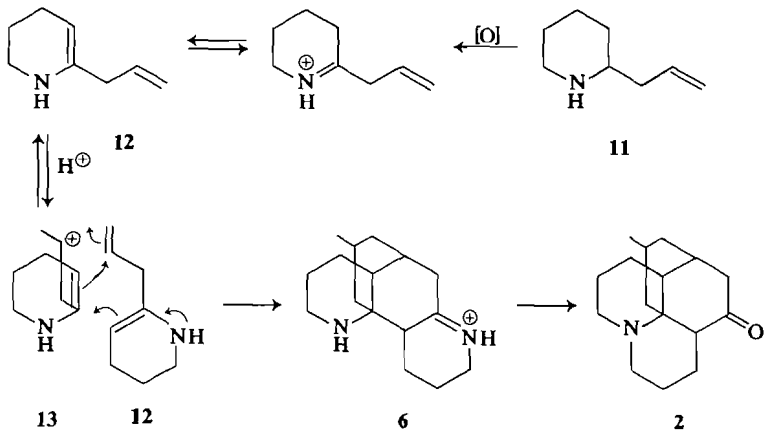

SCHEME 9

hydrochloride as the major radioactive component and was administered to *L. tristachyum* without further manipulation. For radiochemical analysis a drop of the solution was applied to a thin-layer plate coated with silica gel (MN-Polygram SILS-HR). The chromatogram was developed in 1-butanol – acetic acid – water, 2:1:1, and scanned (Packard Radiochromatogram scanner, model 7201), to reveal Δ^1-piperideine, R_f 0.55, as the major radioactive component (85–95%) together with some unchanged lysine, R_f 0.25 (5–15%).

A solution of 6-^{14}C-Δ^1-piperideine hydrochloride was prepared in an analogous manner, from 6-^{14}C-DL-lysine dihydrochloride (0.1 mCi).

^{14}C-Pelletierine

The samples of 2-^{14}C-pelletierine hydrochloride (experiments 7 and 10), 6-^{14}C-pelletierine hydrochloride (experiment 12), and 4,5-$^3H_2$-pelletierine hydrochloride (experiment 7) were prepared from 2-^{14}C-DL-lysine monohydrochloride (New England Nuclear), from 6-^{14}C-DL-lysine dihydrochloride (Commissariat à l'Energie Atomique, France), and from 4,5-$^3H_2$-L-lysine monohydrochloride (Radiochemical Centre), respectively (5).

The sample of 3′-^{14}C-pelletierine hydrochloride (experiment 10) was prepared as follows: a mixture of ethyl 4-^{14}C-acetoacetate (nominal total activity 0.5 mCi,

Can. J. Chem. Downloaded from www.nrcresearchpress.com by 210.87.254.42 on 09/05/12
For personal use only.

Can. J. Chem. Downloaded from www.nrcresearchpress.com by 210.87.254.42 on 09/05/12
For personal use only.

nominal specific activity 0.25 mCi per mmole) (Radiochemical Centre) and of sodium hydroxide solution (4.1 ml, 0.5 *M*) was kept at room temperature overnight, and citrate buffer, p*H* 6.9 (5 ml) was then added. A solution of Δ^1-piperideine hydrochloride, prepared from inactive DL-lysine monohydrochloride (0.5 mmole) (5) was then added dropwise, over 24 h, and (±)-pelletierine hydrochloride, total activity 0.034 mCi (7% yield), was isolated and purified by the method reported previously (5). Final purification was achieved by sublimation at 140° and 3×10^{-3} mm.

The site of label within this product was confirmed by degradation to pipecolic acid and acetic acid (c.f. ref. 11) as follows: a small sample (total activity approximately 0.6 μCi) of this pelletierine hydrochloride was mixed with unlabelled (±)-pelletierine hydrochloride (500 mg) in methanol. The solution was concentrated, ether was added, and the (±)-pelletierine hydrochloride which crystallized was purified to constant activity by repeated sublimation. This pelletierine hydrochloride (350 mg, specific activity $(14.2 \pm 0.3) \times 10^4$ counts min^{-1} $mmole^{-1}$) was dissolved in sulfuric acid (10 *M*, 3 ml). Chromic acid (120 mg) in water (3 ml) was added and the mixture was kept at 90° for 4 h. Steam was passed through the reaction mixture until 50 ml distillate had been collected. The distillate was neutralized with sodium hydroxide (0.1 *M*, 5 ml) and the solution evaporated to dryness. The sodium acetate so obtained was converted to acetyl-α-naphthylamide (53% yield) (13). Pipecolic acid, isolated from the residual aqueous solution as described previously (14), was purified by sublimation. The pipecolic acid (specific activity $(0.022 \pm 0.003) \times 10^4$ counts min^{-1} $mmole^{-1}$) contained less than 0.2% of the activity of the starting material. The acetic acid derivative (specific activity $(13.4 \pm 0.3) \times 10^4$ counts min^{-1} $mmole^{-1}$) contained essentially all the activity of the original pelletierine. Condensation of 4-^{14}C-acetoacetate with Δ^1-piperideine had thus taken place entirely in the expected manner, the product being 3′-^{14}C-pelletierine, uncontaminated by 1′-^{14}C-pelletierine.

The doubly labelled pelletierine, used in experiment 10, was a mixture of 2-^{14}C-pelletierine and 3′-^{14}C-pelletierine. The total activity of the intermolecularly labelled *2,3′-$^{14}C_2$-pelletierine hydrochloride* used in experiment 10 was 0.072 mCi. A small sample (total activity approximately 0.2 μCi) of this 2,3′-$^{14}C_2$-pelletierine was mixed with unlabelled carrier pelletierine (350 mg), and the resulting product was purified to constant activity and oxidized to a mixture of pipecolic and acetic acid (see above). The distribution of label in 2,3′-$^{14}C_2$-pelletierine, deduced from the specific activity of these degradation products, is shown in Table 4.

The doubly labelled pelletierine, used in experiment 7, was a mixture of 2-^{14}C-pelletierine (0.07 mCi) and 4,5-$^3H_2$-pelletierine (0.6 mCi). The ^{3}H:^{14}C ratio of the mixed sample, determined by liquid scintillation counting, was found to be 9.5 ± 0.1.

Tracer Experiments

The labelled samples of Δ^1-piperideine and pelletierine were administered to *Lycopodium tristachyum* Pursh. The labelled lycopodine, isolated from each of the five experiments, was purified to constant activity and partially degraded. Carbon-5 of lycopodine was obtained as benzoic acid, C-9 as formic acid, C-15 and -16 as acetic acid, and C-7 to -16 as 7-methyl-5,6,7,8-tetrahydroquinoline (Scheme 5). The experimental methods used in the administration of tracers to the plants, in the isolation and degradation of the labelled samples of lycopodine and in the determination of radioactivity were those described in our earlier publication (3).

This investigation was supported by the National Research Council of Canada.

1. M. CASTILLO, R. N. GUPTA, Y. K. HO, D. B. MACLEAN, and I. D. SPENSER. J. Amer. Chem. Soc. **92**, 1074 (1970).
2. R. N. GUPTA, M. CASTILLO, D. B. MACLEAN, I. D. SPENSER, and J. T. WROBEL. J. Amer. Chem. Soc. **90**, 1360 (1968).
3. M. CASTILLO, R. N. GUPTA, D. B. MACLEAN, and I. D. SPENSER. Can. J. Chem. **48**, 1893 (1970).
4. M. F. UTTER. *In* The enzymes. *Edited by* P. D. Boyer, H. Lardy, and K. Myrbäck. Vol. 5. 2nd Ed. Academic Press, Inc., New York, 1961. p. 319.
5. R. N. GUPTA and I. D. SPENSER. Can. J. Chem. **47**, 445 (1969).
6. E. LEETE. J. Amer. Chem. Soc. **91**, 1697 (1969).
7. E. A. ZELLER. *In* The enzymes. *Edited by* P. D. Boyer, H. Lardy, and K. Myrbäck. Vol. 8. 2nd Ed. Academic Press, Inc., New York, 1963. p. 313.
8. K. HASSE, O. T. RATYCH, and J. SALNIKOW. Z. Physiol. Chem. **348**, 843 (1967).
9. J. M. HILL and P. J. G. MANN. *In* Aspects of nitrogen metabolism in plants. *Edited by* E. J. Hewitt and C. V. Cutting. Academic Press, Inc., New York, 1968. p. 149.
10. J. R. GEAR and I. D. SPENSER. Nature, **191**, 1393 (1961).
11. R. N. GUPTA and I. D. SPENSER. Phytochem. **8**, 1937 (1969).
12. R. N. GUPTA, Y. K. HO, D. B. MACLEAN, and I. D. SPENSER. Chem. Commun. 409 (1970).
13. E. LEETE, H. GREGORY, and E. G. GROS. J. Amer. Chem. Soc. **87**, 3475 (1965).
14. R. N. GUPTA and I. D. SPENSER. Can. J. Chem. **45**, 1275 (1967).

Vibrational energy distribution in HF formed by elimination from activated CH_3CF_3 and CH_2CF_2

P. N. CLOUGH,[1] J. C. POLANYI, AND R. T. TAGUCHI
Department of Chemistry, University of Toronto, Toronto, Ontario
Received[2] December 2, 1969

The combination–elimination reaction $CH_3 + CF_3 \rightarrow CH_3CF_3\dagger \rightarrow CH_2CF_2 + HF$ has been studied in a fast-flow system. Infrared chemiluminescence arising from the HF product has been observed from vibrational levels $v = 1$–4, and relative rate constants, $k(v)$, have been obtained for HF formation in these levels. A study has also been made of the reaction $CH_2CF_2 + Hg^*(6^3P_1) \rightarrow CHCF + HF + Hg(6^1S_0)$, which has been found to produce vibrationally-excited HF. Relative rate constants $k(v)$ for vibrational levels $v = 1$–4 have been obtained. It appears that channelling of the potential energy into HF vibration, in the course of the elimination step, is more efficient in the first than in the second of these reactions. In the second reaction HF is eliminated with considerable rotational excitation.

Canadian Journal of Chemistry, **48**, **2919** (1970)

Introduction

The type of reaction in which halogenated methyl radicals combine and eliminate hydrogen halide was discovered by Pritchard, Venugopalan, and Graham (1), who found CH_2CHF and HF in the photolysis products of $(CH_2F)_2CO$. The combining radicals in this case were $2CH_2F$. Giles and Whittle (2) demonstrated that such a process also occurs in the combination of methyl and trifluoromethyl radicals, and showed that the combination occurs with zero activation energy to give an activated trifluoroethane molecule ($CH_3CF_3\dagger$) which may decompose to give difluoroethylene and HF or may be stabilized by collision

[1] $CH_3 + CF_3 \longrightarrow CH_3CF_3^\dagger \longrightarrow CH_2CF_2 + HF$

[2] $CH_3CF_3^\dagger + [M] \longrightarrow CH_3CF_3 + [M]$

The activated molecule is formed with some 99 kcal mole^{-1} of energy above its zero point (see Discussion).

Berry and Pimentel were first to show that reaction [1] produces vibrationally excited HF which can give rise to laser emission (3). From an examination of the laser characteristics, they obtained limits for the ratio of reaction rates into the lowest and first excited vibrational levels of HF, $k(v = 1)/k(v = 0)$.

In the present work, reaction [1] has been investigated under quite different experimental conditions from those in the elimination laser. CF_3 and CH_3 radicals were generated by $Hg^*(6^3P_1)$ sensitized photolysis of $(CF_3)_2CO$ and $(CH_3)_2Hg$, respectively, in a fast-flow system. Observations have been extended to higher vibrational levels of HF than in the laser measurements (3), and values of the relative rate constants for the levels $v = 1$–4 obtained. It has also been possible to gain some qualitative information on the extent of rotational excitation of the HF.

An elimination process analogous to that for haloethanes occurs in the case of activated haloethylenes, and as a complementary study, the reaction

[3] $CH_2CF_2 + Hg^*(6^3P_1) \longrightarrow CH_2CF_2^* + Hg(6^1S_0)$

$CH_2CF_2^* \longrightarrow HCCF + HF$

which is closely related to reaction [1], has been examined. Mercury-sensitized elimination of this type has previously been reported by Trobridge and Jennings, who found that for CH_2CHF it was the only photolytic process occurring (4). The present work shows that reaction [3] yields HF molecules with considerable vibrational excitation, and thus resembles direct photoelimination in a number of haloethylenes which has recently been found by Berry and Pimentel to give vibrationally excited hydrogen halide molecules (5). Relative rate constants for formation of HF in vibrational levels 1 to 4 in reaction [3] are reported, for the first time, in the present work.

[1]Present address: Department of Chemistry, University of Reading, Reading, England.
[2]Revision received June 22, 1970.

Can. J. Chem. Downloaded from www.nrcresearchpress.com by 210.87.254.40 on 09/05/12
For personal use only.

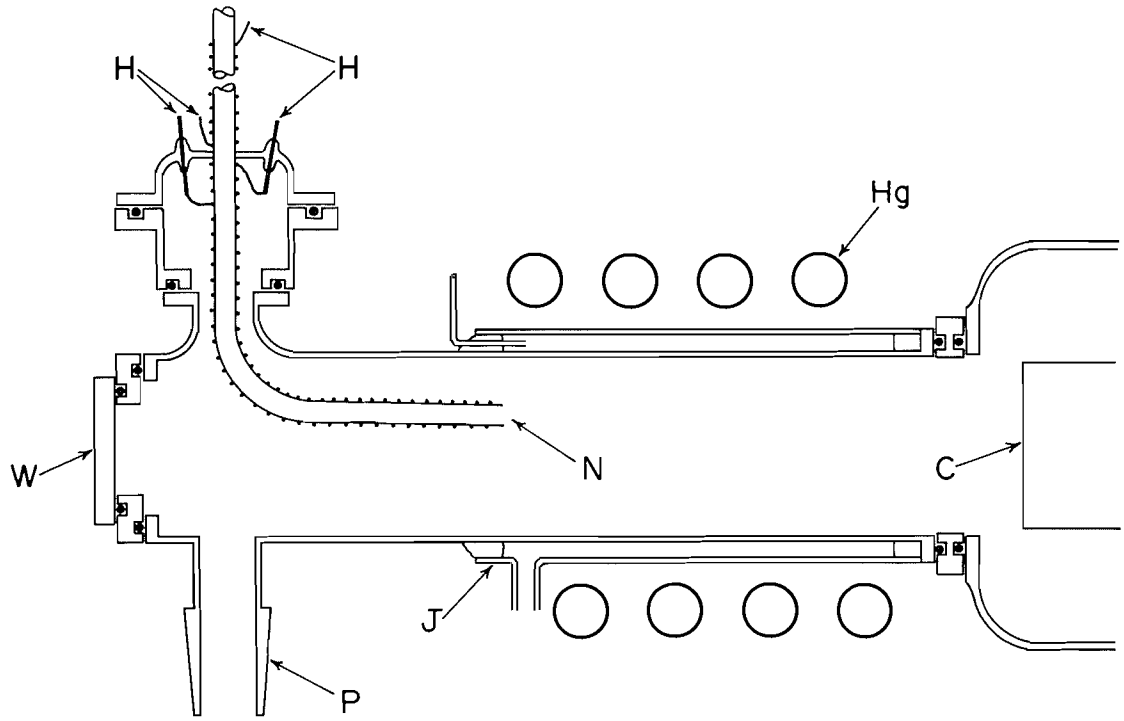

FIG. 1. Reaction vessel and mercury lamp: C, cold wall; H, lead to heating wire; Hg, mercury lamp; J, water jacket; N, nozzle; P, sidearm to pressure gauges; W, CaF_2 window.

Experimental

Apparatus

The reactions were investigated under two sets of experimental conditions. For both, the reaction vessel was a fused quartz tube of 65 mm internal diameter, jacketed in a larger quartz tube. Distilled water was circulated through the 5 mm annular space between the tubes; this served to filter out infrared lines from the mercury lamp, which might otherwise have been scattered into the spectrometer, and also to eliminate the 1849 Å Hg resonance line.

Figure 1 shows the arrangement of the reaction vessel and mercury lamp. The lamp was a quartz spiral Toronto arc, providing intense Hg 2537 Å resonance radiation, and the reaction vessel, placed inside the spiral, had an illuminated zone 14 cm long. Infrared emission was observed through a calcium fluoride end-window using a Perkin–Elmer 12-G monochromator, equipped with a liquid-nitrogen-cooled lead sulfide detector. Only emission from a central cone, well clear of the reaction vessel walls, could enter the spectrometer.

The first set of experimental conditions was designed for reaction at low pressure and short residence time, approaching the conditions of Method II described by Anlauf *et al.* (6). The reagents, saturated with mercury vapor, were introduced into the vessel through a heated 6 mm i.d. nozzle, and condensed out on a cold wall 3 cm beyond the end of the illuminated zone. This cold wall, which formed part of a Pyrex cold-trap, was cooled by liquid nitrogen (77 °K) or liquid helium (4 °K). The system could be pumped out to an ultimate pressure of 10^{-5} Torr with a 2 in. NRC oil diffusion pump. In most experiments, with the reagents flowing, the pressure measured by a Mcleod gauge at the point indicated in Fig. 1 was in the range (2–5) $\times$ 10^{-3} Torr.

The second conditions were similar to those described by Karl, Kruus, and Polanyi in investigating electronic-to-vibrational energy transfer (7). The reagents flowed through the vessel at high velocity in a large excess of argon carrier, at total pressures of 0.35 to 0.55 Torr. A Stokes 412H rotary pump was used to achieve high pumping speed. Blackened metal vanes set at 30° to the flow direction cut off the spectrometer cone-of-sight immediately at the end of the illuminated zone.

Reagents

Hexafluoroacetone (HFA) supplied in cylinders by Matheson Ltd., was passed through a trap at −20 °C to remove any hydrate. Dimethyl mercury (DMM), from Strem Chemicals Inc., was vacuum distilled before use, and was stored in the dark. 1,1-Difluoroethylene (Matheson) was dried by passage through a trap at − 78 °C, but not otherwise purified.

All gas flow-rates were measured with Fisher–Porter triflat floating-ball meters.

Results

Reaction Conditions

Details of the optimum reaction conditions for which adequate emission intensities could be

Can. J. Chem. Downloaded from www.nrcresearchpress.com by 210.87.254.40 on 09/05/12
For personal use only.

TABLE 1
Reaction conditions

Experiment	Pressure (Torr) HFA	DMM	CH_2CF_2	Ar	τ_c (s)
1	2.2×10^{-3}	3.0×10^{-4}	—	—	2.5×10^{-3}
2	8.5×10^{-4}	1.5×10^{-4}	—	0.37	6.0×10^{-3}
3	—	—	2.2×10^{-3}	—	1.9×10^{-3}
4	—	—	2.0×10^{-4}	0.37	6.0×10^{-3}

obtained, with and without argon carrier gas, are given for both reactions in Table 1. Information on mercury concentrations is not included in the table since these were not accurately known. However, from the measured temperatures and gas pressures in the saturator, the Hg vapor pressure in the reaction vessel can be estimated as close to 5×10^{-4} Torr in the low pressure experiments, and approaching the 20 °C saturation vapor pressure of 10^{-3} Torr in the Ar carrier runs. Liquid helium cooling was necessary in the low pressure experiments on $CH_3 + CF_3$ combination, to trap CO released in the photolysis of HFA, but liquid nitrogen cooling was adequate for the $Hg^* + CH_2CF_2$ observations.

The contact time, τ_c, given in Table 1 is the mean residence time of the reagents in the illuminated zone. This quantity cannot be determined accurately for the low pressure experiments, since pressures were in the region between viscous and molecular flow. However, values calculated assuming viscous flow and assuming diffusion from the nozzle to the cold surface agree within 25%; the average value is given in the table. Pressure "mapping" measurements in the reaction vessel showed that the pressure was almost uniform across the vessel 5 cm downstream from the inlet nozzle. Contact times for the argon carrier experiments are better-defined, and the values given in Table 1 were calculated assuming Poiseuille flow and taking an average within the cone-of-acceptance of the spectrometer.

$CH_3 + CF_3$ Recombination

A spectral trace of the HF fundamental emission from the recombination–elimination reaction [1] is reproduced in Fig. 2, and corresponds to the reaction conditions of experiment 2. At the resolution of about 8 cm^{-1} employed, the rotational structure was clearly resolved. Emission intensity in experiments without argon carrier was somewhat lower than in those with it, but the same resolution could still be used. In both cases, the highest vibrational level which could be detected was $v = 4$.

Evidence that the HF emission was in fact due to reaction [1] was obtained by examining variation of the emission intensity with incident Hg light intensity. Reaction conditions were close to those for experiment 2, and the incident intensity was changed by introducing perforated cylinders of calculated transmission between the mercury lamp and the reaction vessel. The results of these measurements are given in Fig. 3, which shows an accurate dependence of the emission intensity on the square of the incident intensity.

To explain this simple square-law dependence, some consideration of the extent of photolysis in these experiments is required. From the $Hg^*(^3P_1)$ concentration measured by Karl *et al.* (7) under closely similar conditions, an estimated maximum value of $[Hg^*(^3P_1)] = 2 \times 10^{-14}$ g-atom cm^{-3} can be arrived at for experiment 2. The reactive quenching cross-section of HFA is probably smaller than that of acetone, due to the absence of C—H sites. As a maximum, the value of 32 $Å^2$ corresponding to acetone (8) will be taken, giving a quenching rate constant $k_Q = 1.5 \times 10^{14}$ cm^3 $mole^{-1}$ s^{-1}. The HFA concentration in the experiment was 5×10^{-11} mole cm^{-3}, so that the product $k_Q[HFA] = 7.5 \times 10^3$ s^{-1}. Since the radiative rate constant of $Hg(^3P_1)$ is $>10^7$ s^{-1}, it is clear that the concentration of excited mercury was determined by radiative processes and not by quenching, so that it was independent of [HFA]. Thus, the decomposition of HFA along the reaction vessel was first order, with maximum effective rate constant $k_Q[Hg^*] = 3.0$ s^{-1}. The maximum extent of HFA decomposition in the residence time then comes to 1.8%, giving a CF_3 radical concentration of about 10^{-12} mole cm^{-3}. Similarly, for DMM, taking the quenching rate constant as

Can. J. Chem. Downloaded from www.nrcresearchpress.com by 210.87.254.40 on 09/05/12
For personal use only.

Can. J. Chem. Downloaded from www.nrcresearchpress.com by 210.87.254.40 on 09/05/12
For personal use only.

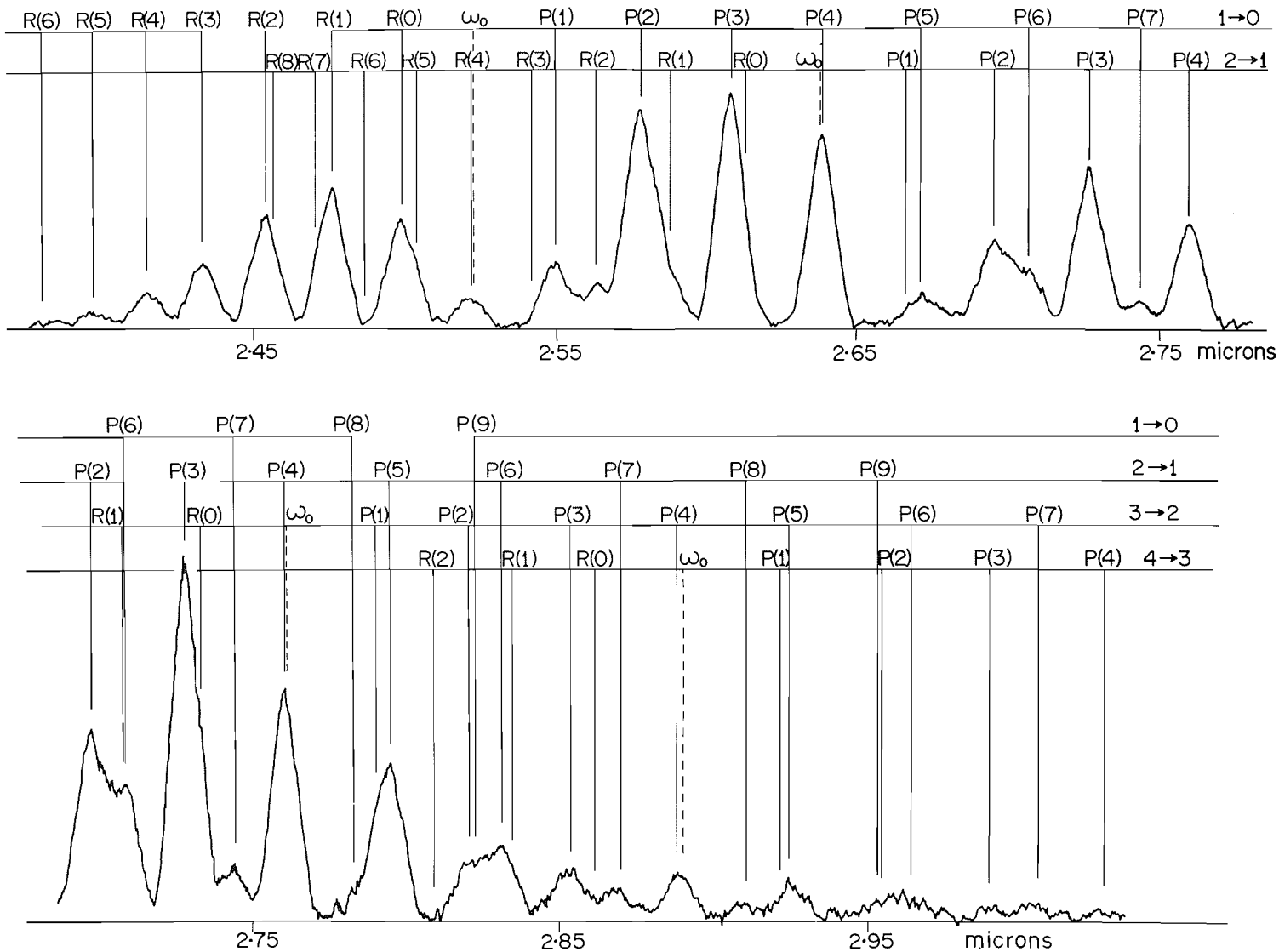

FIG. 2. Spectral trace of HF fundamental ($\Delta v = -1$) emission. Experiment 2 of Table 1. Grating 300 grooves/mm blazed at 3μ, used in first order. Grating monochromater slit width 0.800 mm. The lines are labelled P(J) and R(J) for P- and R-branches, where J is the rotational quantum number of the lower vibrational state.

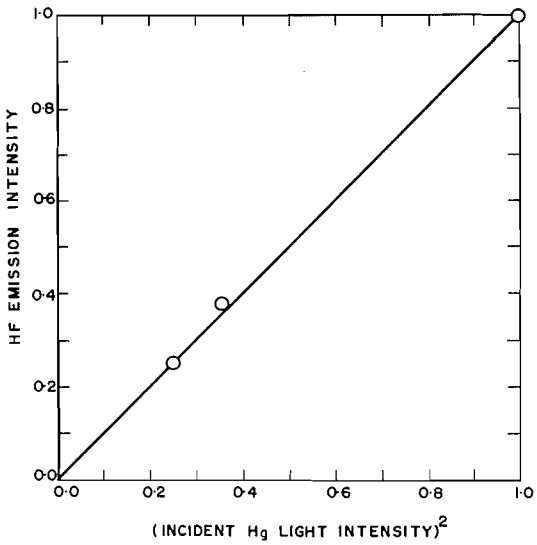

FIG. 3. HF emission intensity vs. (incident mercury light intensity)^2, for $CH_3 + CF_3$.

3×10^{14} cm^3 mole^{-1} s^{-1} (8), the percentage decomposition calculated is 3.7%, giving a maximum CH_3 radical concentration of about 5×10^{-13} mole cm^{-3}. With a $CH_3 + CF_3$ recombination rate constant of 5×10^{13} cm^3 mole^{-1} s^{-1} (9), it is calculated that, for these low radical concentrations, gas phase recombination made a much smaller contribution (<10%) to radical removal than did pumping from the vessel or loss at the walls.

The steady-state concentration of CF_3 radicals can be expressed as $k_Q[HFA][Hg^*]/(k_1 + R_1)$, where k_1 is a first order rate constant for radical removal by pumping and at the wall, and R_1 the combined rate of all second-order gas phase processes for radical loss. Since it has just been concluded that k_1 was much greater than R_1, this expression reduces to $[CF_3] = k_Q[HFA][Hg^*]/k_1$, and an analogous expression holds for $[CH_3]$. It therefore follows that if reaction [1] was the only process contributing to HF emission, the emission intensity should have been proportional to $[HFA][DMM][Hg^*]^2$, and hence depended on the square of the incident intensity, as observed.

Additional evidence was obtained confirming the absence of contributions to excited HF formation by reactions other than [1]. It is shown below that reaction [3], which was a possible secondary process in the system, gives rise to HF emission, but separate experiments demonstrated that this emission was insignificant for the CH_2CF_2 concentrations which could have resulted from reaction [1]. Investigations were also made of direct electronic-to-vibrational energy transfer from $Hg^*(^3P_1)$ to HF, but HF emission was only detected for concentrations of the gas several orders of magnitude higher than could have been present in these experiments.

The observed rotation–vibration lines of HF were identified using the spectroscopic data of Mann *et al.* (10), and the steady-state vibrational distribution determined by the rotational population sum method described by Charters and Polanyi (11). Only the fundamental region of HF was examined. The Einstein coefficients for spontaneous emission were calculated according to the quadratic expression of Heaps and Herzberg (12), employing the known absolute value of the probability for the $1 \rightarrow 0$ transition (13). Rotational line areas were measured by planimeter, and corrected for wavelength variation of the spectrometer transmission before conversion to relative populations. There was always a slow build-up of brownish deposit inside the reaction vessel during experiments, but the emission intensity (as checked by repeated scanning of the same group of lines) never fell by more than 10% over a complete trace, and a correction was made for this fall with time.

The results of these measurements, expressed as steady-state vibrational populations of HF, $N(v)$, relative to a value of $N(1) = 1.0$, are given for both sets of experimental conditions in Table 2*a*. These results are in fact averaged over a number of measurements in the two cases. The maximum uncertainty in $N(2)$ and $N(3)$ is ± 5%, but for $N(4)$ a much larger uncertainty of ± 20% exists, due to the low emission intensities from this level. No change in the distributions was found on varying the incident light intensity or the mercury concentration. This provides further evidence that the emission resulted from reaction [1] with no other contributions.

In the low-pressure experiments, plots of the quantity $\ln I_J/\omega_J{}^4S_JF_J$ vs. $J(J+1)$, where I_J is the intensity of the line originating from rotational level J of a given vibrational level, always yielded straight lines corresponding to Boltzmann rotational temperatures of 450–500 °K. The difference between these temperatures and the ambient temperature can be adequately accounted for as the combined result of introducing

Can. J. Chem. Downloaded from www.nrcresearchpress.com by 210.87.254.40 on 09/05/12
For personal use only.

TABLE 2

Relative rate constants, $k(v)$, and mean steady-state vibrational distributions, $N(v)$, along the length of the cone-of-sight

v	$k(v)$	$N(v)$ Experimental	$N(v)$ Computed*	τ_c ($s \times 10^3$)
		(*a*) $CH_3 + CF_3$		
1	1.0	1.0	1.0	
2	0.43	0.39	0.390	2.5
3	0.13	0.11	0.108	
4	0.033	0.027	0.0242	
1	1.0	1.0	1.0	
2	0.43	0.34	0.350	6.0
3	0.13	0.081	0.0895	
4	0.033	0.018	0.0184	
		(*b*) $Hg^* + CH_2CF_2$		
1	1.0	1.0	1.0	
2	0.40	0.36	0.380	2.0
3	0.21	0.16	0.173	
4	0.072	0.046	0.050	
1	1.0	1.0	1.0	
2	0.40	0.34	0.335	6.0
3	0.21	0.13	0.126	
4	0.072	0.029	0.0314	

*Using the stated $k(v)$.

the reagents through a nozzle heated to about 450 °K, and of heating due to reaction. As the following section shows, any significant extent of rotational excitation of the HF formed in reaction [1] should have been evident under the low pressure conditions as curvature of the rotational plots, and the straight-line nature of the plots indicates that HF is eliminated from activated CH_3CF_3 without large rotational excitation.

$Hg^* + CH_2CF_2$

The intensities of HF emission in the Hg sensitized elimination from CH_2CF_2 were considerably higher both with and without argon carrier than in the recombination–elimination reaction. Nonetheless, it was not possible to detect emission from vibrational levels above $v = 4$.

By comparison with $CHFCH_2$ (4), reaction [3] is expected to be the only process in the $Hg^* + CH_2CF_2$ system forming HF (see, however, Discussion, part (b)). Evidence that the excited HF detected in this work resulted directly from reaction [3] was obtained by investigating the variation of infrared emission intensity with incident Hg light intensity, as for the recombination reaction. The results of these measurements, carried out under the conditions of experiment 4,

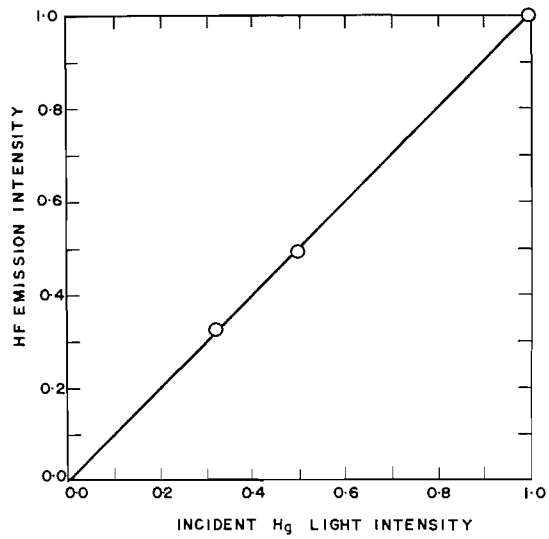

FIG. 4. HF emission intensity vs. mercury light intensity, for $Hg^* + CH_2CF_2$.

Table 1, are given in Fig. 4, which shows a linear relationship between the intensities. The $Hg(^3P_1)$ quenching cross-section of CH_2CF_2 has been measured as 27.2 Å^2 (14), and performing a similar calculation to that given above for HFA, a maximum extent of CH_2CF_2 decomposition of 2.3% is arrived at. Thus, the rate of HF formation along the reaction vessel was essentially constant, and this resulted in the linear intensity relationship. Such linearity would not be expected if any secondary processes had contributed appreciably to the formation of excited HF.

Determinations of the steady-state vibrational population distribution of HF under the conditions of experiments 3 and 4 were made as for the recombination reaction. The results are given in Table 2*b*. The uncertainty limits in the values for $v = 2$ and 3 are $\pm$ 5%. Although intensities from the level $v = 4$ were much higher in this case than for the recombination reaction, a corresponding increase in the accuracy of measurement was not possible because of uncertainties about the background level in the spectral region concerned. A weak, apparently continuous emission underlay much of the P branch of the $4 \rightarrow 3$ HF transition, from 3400 to 3200 cm^{-1}. It seems most likely that this was emission from vibrationally excited HCCF, the ν_1 C—H stretching mode of which has its origin at 3360 cm^{-1} (15). Because of these difficulties, an uncertainty

Can. J. Chem. Downloaded from www.nrcresearchpress.com by 210.87.254.40 on 09/05/12
For personal use only.

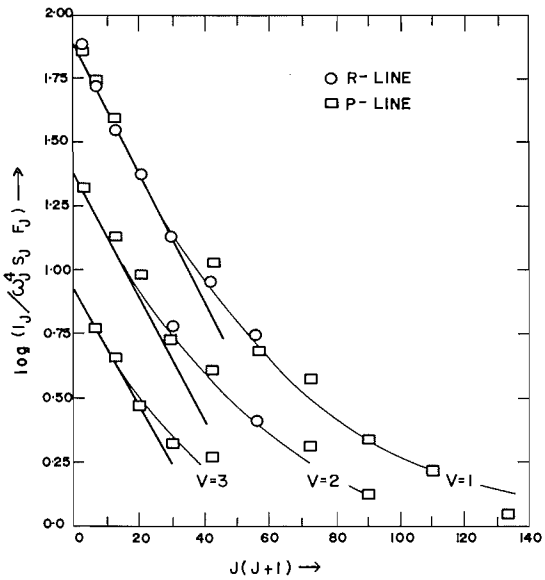

FIG. 5. Rotational plot for Hg* + CH_2CF_2. Straight lines represent 500 °K.

limit of ± 15% exists for the relative population of the $v = 4$ level. The population distribution was independent of incident Hg light intensity, further evidence for a single formation process for vibrationally excited HF.

For the low pressure conditions of experiment 3, rotational plots of $\ln I_J/\omega_J^4 S_J F_J$ vs. $J(J+1)$ exhibited marked curvature, as shown in Fig. 5. Such curvature is characteristic of a non-Boltzmann initial rotational distribution which has undergone partial collisional relaxation, and comparison with the results of Anlauf *et al.* (6) and Pacey (16) for the H + Cl_2 reaction leads to the conclusion that HF is eliminated in reaction [3] with considerable rotational excitation. The work on H + Cl_2 also shows that unrelaxed vibrational population distributions can be observed even when extensive rotational relaxation has occurred, a point of importance in the present measurements.

Relative Rates of Formation, k(v), from Steady-state Populations, N(v)

In order to obtain relative rates of formation into different vibrational levels from observed steady-state distributions, it is necessary to consider the possible vibrational relaxation processes. Since these processes are similar for both cases, the two reactions will be discussed together in the following sections.

(a) Gas Phase Relaxation

Vibration-to-translation (V–T) collisional relaxation will be considered first. Under the conditions of experiments 1 and 3, assuming diameters of 10 and 8 Å, respectively, for collisions of HF with HFA and CH_2CF_2, the mean numbers of collisions undergone by HF in the residence times for the two cases are calculated as approximately 90 and 50. For such small collision-numbers, V–T relaxation would be negligible. In the argon-carrier experiments 2 and 4, the calculated mean number of HF–Ar collisions in τ_c for a 5 Å diameter is close to 10^4. There are no experimental data on the vibrational relaxation rate of HF in Ar, but it can be estimated from two approaches. Although HF is a highly polar molecule, the S.S.H. theory (17) should not be seriously in error in treating its relaxation in a noble gas. Calculations using the theory (with $\varepsilon/k = 500$ °K, $\sigma = 2.8$ Å for HF) yield a value 2.7×10^{11} as the number of collisions needed to bring about a $1 \rightarrow 0$ transition. Recent measurements on the relaxation of HCl in noble gases show that in this case $\sim 10^7$ collisions are required for V–T relaxation at room temperature (18). It seems unlikely that HF relaxes faster than HCl in view of its higher vibration frequency. Thus, it can be concluded that in the experiments with argon carrier, V–T relaxation was entirely negligible.

Consideration of the importance of vibration-to-vibration (V–V) energy transfer presents more difficulties. The possibility of vibrational exchange between HF molecules can be eliminated, since for the low concentrations present in these experiments the calculated number of HF–HF collisions per molecule in the residence time is less than unity. No theoretical calculations can be made of the probable rates of vibrational transfer from HF to the organic molecules present, but the available data on this type of process (19) suggest that for a molecule with such a high vibration frequency as HF, considerably larger numbers of collisions than the $\sim 10^2$ quoted at the beginning of this section would be needed even for near-resonant transfer.

Direct experimental evidence for the unimportance of V–V relaxation under the conditions employed was also obtained by varying the reagent concentrations. The HF population distribution from reaction [1] showed no change under the conditions of experiment 2, Table 1,

Can. J. Chem. Downloaded from www.nrcresearchpress.com by 210.87.254.40 on 09/05/12
For personal use only.

Can. J. Chem. Downloaded from www.nrcresearchpress.com by 210.87.254.40 on 09/05/12
For personal use only.

on reducing the HFA pressure from 8.5×10^{-4} to 3×10^{-4} Torr. With this latter pressure, an HF molecule underwent only ~ 20 collisions with HFA in the residence time, so that V–V transfer was completely negligible. As shown below, the observed steady-state vibrational populations in these Ar carrier experiments and in the experiments with higher HFA pressures but without carrier, such as experiment 1, can be well explained in terms of a single set of rate constants for HF formation. This could only be so if V–V transfer at the higher HFA concentrations were also negligibly small. Similar conclusions can be reached in the case of reaction [3] from the fact that a single set of $k(v)$ values fits the observed $N(v)$ distributions in experiments 3 and 4, in which the CH_2CF_2 concentrations differed by a factor of ten.

(b) Wall Relaxation

Since HF reacts readily with silica, it seems reasonable to assume that vibrationally excited HF molecules which diffused to the wall in the low pressure experiments were removed there by reaction, or at least completely deactivated, so that the observed steady-state distribution was not distorted by wall relaxation. Part of the purpose of the argon carrier experiments was to confirm this supposition. In the presence of 0.4 Torr of argon a negligible fraction of excited HF molecules which had undergone collision with the wall could diffuse back into the observation zone before radiating. The fact that the vibrational distributions observed with and without argon can be accounted for in terms of single sets of relative reaction rate constants for each of the reactions therefore supports the assumption that in the low pressure experiments there was no contribution to the emission from molecules which had undergone partial wall deactivation.

(c) Radiative Relaxation

The mean radiative lifetimes of the relevant vibrational levels of HF are in the range $(2\text{–}5) \times 10^{-3}$ s, so that appreciable radiative distortion of the initially-formed vibrational distribution occurred in the contact times quoted in Table 1. In order to correct for this, a computer program was employed which, for given relative formation rates, simulated the build-up and loss by radiation of HF in each vibrational level along the illuminated zone, taking into account the flow velocity. The calculations given earlier show that in both reactions the concentrations of primary photolysis products increased linearly with distance along the reaction vessel, so that for the $CH_3 + CF_3$ recombination the HF formation rate was taken to increase as the square of the distance into the illuminated zone, while for elimination from CH_2CF_2 a constant formation rate was assumed. Having calculated the steady-state vibrational distribution at each point, the computer program integrated along the reaction vessel to give the average distribution observed by the spectrometer.

The rate constants $k(v)$ for HF formation in the levels $v = 1$ to 4 giving a best fit to the observations, are presented in Table 2. The table also compares the steady-state distributions computed from these $k(v)$ values with the observed distributions at the two contact times, for both reactions. The agreement in both cases is sufficiently good to justify the conclusions reached earlier about the unimportance of relaxation processes other than radiation. Uncertainty limits in the $k(v)$ ratios, arrived at by considering the extremes which could still be consistent with the observations, are $\pm$ 8% for $v = 2$ and $v = 3$, and $\pm$ 15% for $v = 4$.

Discussion

(a) $CH_3 + CF_3$

The thermochemistry of the $CH_3 + CF_3$ combination–elimination reaction involves several uncertain quantities. Results concerning the value of $\Delta H_f(CF_3)$ are in conflict, but the figure of -112.6 kcal mole^{-1} obtained by Coomber and Whittle (20) from thermal and kinetic data appears more reliable than results based on electron impact methods, and is adopted here. The value of $\Delta H_f(CH_3) = 34.0$ kcal mole^{-1} quoted by Coomber and Whittle (20) will also be employed.

A second uncertainty arises regarding the value of $\Delta H_f(CH_3CF_3)$. Lacher and Skinner (21), in a recent compilation of adjusted thermochemical data of fluorinated hydrocarbons give $\Delta H_f(CH_3CF_3) = -178.2$ kcal mole^{-1} based on the combustion measurements of Kolesov *et al.* (22). This figure, together with those quoted above, would require $D(CH_3—CF_3) = 99.6$ kcal mole^{-1}, which is higher than both $D(CF_3—CF_3)$ ($= 96.5$ kcal mole^{-1}) and $D(CH_3—CH_3)$ ($= 88$ kcal mole^{-1}) (20). It seems more likely

Can. J. Chem. Downloaded from www.nrcresearchpress.com by 210.87.254.40 on 09/05/12
For personal use only.

that $D(CH_3—CF_3)$ lies between these latter two figures. However, in the absence of alternative experimental data the value of 99 kcal mole^{-1} has been used. A preferred value for $\Delta H_f(CH_2CF_2)$ of $-$ 82.5 kcal mole^{-1} is given by Lacher and Skinner (21), and this is employed here, together with $\Delta H_f(HF)_g = -$ 64.9 kcal mole^{-1}. All of these values refer to 298 °K; in view of the uncertainties correction to 0 °K is unnecessary.

Finally the critical energy for HF elimination from CH_3CF_3 is required. A recent shock-tube measurement of the activation energy for this elimination (23) has yielded a value of 71 kcal mole^{-1}, corresponding to a critical energy of 69 kcal mole^{-1}. This is in good agreement with the value $\varepsilon_0 = 68$ kcal mole^{-1} arrived at by Chang and Setser in an R.R.K.M. treatment of the decomposition rate of chemically activated CH_3CF_3 (24), based on $D(CH_3—CF_3) = 98$ kcal mole^{-1}; we have therefore used $\varepsilon_0 = 69$ kcal mole^{-1}. The thermochemistry of reaction [1], incorporating all of these data, is summarized in Fig. 6.

From Fig. 6 it can be seen that the activated CH_3CF_3 molecule formed on radical combination has some 30 kcal mole^{-1} of energy in excess of the minimum needed for HF elimination. The lifetime of the activated molecule with respect to elimination has been shown by Giles and Whittle (2) to be in the range 10^{-8}–10^{-9} s. It follows that in both the low pressure and argon carrier experiments reported here, the probability of gas-phase collision during the lifetime of the activated molecule was very much less than unity. Thus, the relative rate constants, $k(v)$, measured, correspond to dissociation of $CH_3CF_3\dagger$ in a narrowly-defined energy range.

The $k(v)$ values, given in Table 2*a*, correspond to an initial vibrational distribution of HF which is non-Boltzmann. Successive population ratios from $v = 1$ to 4 define "vibrational temperatures" of 6500, 4300, and 3600 °K. Thus a trend of decreasing vibrational temperature with increasing v exists. It is interesting to note that Berry and Pimentel's results (3) for the lowest v levels are in qualitative accord with this trend, their lowest limit for the $N(1)/N(0)$ ratio corresponding to a temperature of 10 600 °K. If $N(1)/N(0)$ is taken as 0.75, in the middle of the range they quote, then combining this result with those of the present work, the average amount of energy entering vibration of HF in reaction [1] is calculated to be 9.1 kcal mole^{-1}, representing 13% of the total available energy in the products. No definite conclusion can be drawn about the extent of rotational excitation in the reaction, but the present observations suggest that it is not large.

The kinetics of unimolecular elimination from chemically activated halo-ethanes have been treated in terms of the R.R.K.M. theory with considerable success (25–28). This theory is essentially concerned with the transition from the "energized" to the "activated" state of the decomposing molecules, and cannot predict product energy distributions when the activated molecules break up.

However, in terms of the theory, a distinction can be made between the "critical energy" of the activated molecule, that is, the minimum energy needed for elimination, and the "excess energy" possessed above this minimum. In the present case, the "excess energy" is 30 kcal mole^{-1}, all of which is available to the products, and the "critical energy" is 69 kcal mole^{-1}, of which only 42 kcal mole^{-1} is available to the products (Fig. 6).

It is clear that the "excess energy", which on an R.R.K.M. basis would be randomly distributed between the products, cannot alone account for the observed HF excitation, since it is lower than the energies of the $v = 3$ and $v = 4$ levels of HF, viz. 32.5 and 42.4 kcal mole^{-1}, respectively. Thus the 42 kcal mole^{-1} of "critical energy", about which the R.R.K.M. theory can make no prediction, must be contributing to the

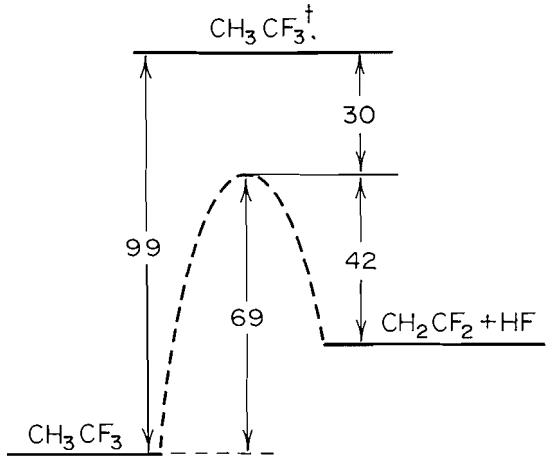

FIG. 6. Thermochemistry of $CH_3 + CF_3$. All values in kcal mole^{-1}.

Can. J. Chem. Downloaded from www.nrcresearchpress.com by 210.87.254.40 on 09/05/12
For personal use only.

vibrational excitation in the HF. An indication of the maximum possible extent to which random distribution of energy could be responsible for the excitation can be made by assuming that this second contribution is also random in nature, as has been done in the following calculation. A completely statistical distribution of the 72 kcal mole^{-1} total available energy amongst the vibrational modes of the products was assumed, and the vibrational energy level sum for CH_2CF_2 was calculated according to the formula of Whitten and Rabinovitch (29) at energies corresponding to the total available energy minus 0, 1, 2, ... quanta of HF. The result was taken to be proportional to the probability of that number of HF quanta being vibrationally excited. Since energy could also flow into HF translation and rotation, these calculated values represent upper limits. The probabilities obtained were, in order (relative to $N(1) = 1$) 5.1, 1.0, 0.163, 0.021, 0.0019; indicating a much more rapid fall with increasing v than the measured values. This discrepancy grows larger as the amount of energy which is assumed to be randomly distributed is reduced.

Although the calculation is oversimplified, it strongly indicates that excitation of HF in the elimination process does not result to a significant extent from that part of the available energy which is statistically distributed in the activated precursor (namely, the 30 kcal which we termed the "excess energy"). The excitation therefore derives from forces which are released as HF splits off from CH_2CF_2, with the release of the residual 42 kcal. The forces operating during this process are the slopes on the potential energy hypersurface on which the elimination can be pictured as taking place. It is interesting to note that the energy of the highest HF level observed, 42.4 kcal mole^{-1}, is close in value to the 42 kcal mole^{-1} released in the course of elimination.

The rearrangement energy (approx. 42 kcal) is observed to be inefficiently channelled into HF vibration. If it becomes, instead, translational energy of the products, this would suggest that the energy-release occurs along the coordinate of separation of HF from CH_2CF_2, rather than during the approach of H to within normal bonding distance from F. This is analogous to the "*repulsive*" type of energy-release in exchange reactions, A + BC → AB + C. The energy-release is termed "repulsive" if it occurs as the products, in this case HF + CH_2CF_2, separate. It is termed "attractive" if it occurs as a new bond, in this case H—F, is forming. Repulsive energy-release tends to be less efficient in channeling reaction-energy into product vibration in reactions A + BC → AB + C (30). This is understandable since the release of AB · C repulsion resembles the second half of an AB + C collision. Such collisions have a low probability of producing AB vibration. The probability is low because the forces on A and B are not sufficiently different to produce internal motion in AB. This is especially likely to be true if AB recoils laterally from BC, as in the present case.

Alternatively, the energy of reaction might be deposited in vibration of CH_2CF_2. This would suggest a type of *attractive* energy-release, in which the change in CC bond-length (in the course of forming a double bond) corresponded to the coordinate of descent on the potential-energy hypersurface. In the absence of information concerning the ultimate fate of the missing energy, it is not possible to choose between these alternatives. However, the failure to observe a high degree of rotational excitation in the HF (cf. (*b*) below) argues against predominantly repulsive energy release, and in favor of the mechanism leading to vibrational excitation in the CH_2CF_2. This conclusion is at variance with the models of the activated complex which best fit the observed kinetics of unimolecular eliminations in R.R.K.M. treatments (25–27). In these models the formation of the CC double bond is taken to be almost complete, whilst the HX bond order is only 0.1–0.2 of a single bond.

(b) CH_2CF_2 + $Hg^*(6^3P_1)$

The 6^3P_1 state of mercury lies at an energy of 112 kcal mole^{-1} above the 6^1S_0 ground state, and presumably all of this energy is transferred to electronic plus vibrational energy of CH_2CF_2 on collision. The process

$$CH_2CF_2 \rightarrow CHCF + HF$$

is 43 kcal mole^{-1} endothermic if the JANAF value for ΔH_f(CHCF) of 30 kcal mole^{-1} is taken, though this value has a large probable error of ± 15 kcal mole^{-1}. Thus, the total energy-release in reaction [3] is approximately 70 kcal mole^{-1}.

The excited electronic states of CH_2CF_2 have not been investigated, but by comparison with ethylene (31) it should have a triplet state lying

Can. J. Chem. Downloaded from www.nrcresearchpress.com by 210.87.254.40 on 09/05/12
For personal use only.

at an energy well below that of $Hg^*(6^3P_1)$, while the lowest excited singlet state probably lies above this energy. If spin is conserved on collision between $Hg(6^3P_1)$ and CH_2CF_2, the initially-formed excited CH_2CF_2 molecule must be in a triplet state, and must possess considerable energy of vibrational excitation. In the Hg-sensitized decomposition of CH_2CF_2, Trobridge and Jennings (4) arrived at a lifetime of the excited state with respect to elimination of $(2\text{–}3) \times 10^{-10}$ s. They suggested that the triplet molecules underwent a rapid crossing to high vibrational levels of the ground electronic state, with elimination occurring from the singlet molecules so formed. This mechanism could also apply in reaction [3]. The alternative route of direct decomposition of the initially-formed triplet into HF and triplet acetylene appears impossible on energetic grounds, since the present results show HF to be formed with up to 4 vibrational quanta ($= 42.4$ kcal mole^{-1}), which would require the lowest triplet state of monofluoroacetylene to lie only 30–40 kcal above the ground state. However, if spin is not conserved in the quenching collision, as is possible for a heavy atom such as Hg*, direct formation of vibrationally excited ground state CH_2CF_2 could occur, or a singlet ethylidene species might be formed which could give rise to 1,1-elimination of HF.

The initial vibrational distribution resulting from reaction [3], which corresponds to the relative $k(v)$ values in Table 2*b*, differs significantly from that for elimination from activated CH_3CF_3. Not only are the relative rates into higher vibrational levels greater, but the "vibrational temperatures" defined by successive population ratios go through a maximum. These temperatures are 5900, 7700, and 4600 °K for the ratios from $v = 1$ to $v = 4$. For the pressures used in these experiments, an activated CH_2CF_2 molecule would not undergo any collisions in its lifetime, provided that the latter is $\sim 10^{-9}$–10^{-10} s as for CH_2CHF. A statistical calculation, similar to that described above, was performed for CH_2CF_2† assuming elimination occurred from molecules in the ground electronic state with some 112 kcal mole^{-1} of vibrational excitation. Then, taking all of the 70 kcal mole^{-1} available to the products to be statistically distributed between them, relative rate constants of 1.0, 0.31, 0.084, and 0.018 were obtained for HF formation in the levels $v = 1$ to 4. These values do not differ as greatly from the observed distribution as in the case of reaction [1], but the discrepancy is still large. It appears that here again vibrational excitation is due predominantly to energy release associated with specific forces arising in the course of HF excision. This is easiest to understand if there exists a significant activation energy for the elimination; then the energy released on the far side of the barrier could be channelled to some extent into product vibration. However, it is also possible that the type of motion required for the system to climb the endothermic hill is such as to channel a portion of the excess energy into HF vibration (cf. ref. 32).

The observation that HF formed in reaction [3] must have considerable rotational excitation is of some interest. Substantial rotational excitation has been found in the H-atom transfer reactions $A + HC \rightarrow AH + C$ studied in this laboratory (6). This is attributed to $AH \cdot C$ repulsion (the dot represents the location of the repulsion) in a bent configuration. In the present case the requirement is that the repulsive forces resulting in the separation of HF should be greater at one end of the incipient HF than at the other. If the repulsion is to result in a significant torque on the HF it must be greater at the H-atom end, at a distance from the center-of-mass. The location of the repulsion can be symbolized

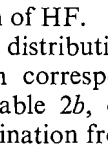

The. $C \cdot HF$ axis is sharply bent.

We are grateful to Dr. Horst Heydtmann for a helpful discussion, and to Dr. D. W. Setser for useful comments and for communicating some of his results prior to publication. P.N.C. thanks the University of Toronto for the award of a postdoctoral fellowship, 1968–1969, and R.T.T. thanks the National Research Council of Canada for a research scholarship. This work was supported by grants from the National Research Council of Canada and the Petroleum Research Fund administered by the American Chemical Society.

1. G. O. Pritchard, N. Venugopalan, and T. F. Graham. J. Phys. Chem. **68**, 1786 (1964).
2. R. D. Giles and E. Whittle. Trans. Faraday Soc. **61**, 1425 (1965).
3. M. J. Berry and G. C. Pimentel. J. Chem. Phys. **49**, 5190 (1968).
4. A. R. Trobridge and K. R. Jennings. Trans. Faraday Soc. **61**, 2168 (1965).
5. M. J. Berry and G. C. Pimentel. J. Chem. Phys. **51**, 2274 (1969).

6. K. G. ANLAUF, P. J. KUNTZ, D. H. MAYLOTTE, P. D. PACEY, and J. C. POLANYI. Discuss. Faraday Soc. **44**, 183 (1967).
7. G. KARL, P. KRUUS, and J. C. POLANYI. J. Chem. Phys. **46**, 224 (1967).
8. R. J. CVETANOVIĆ. Prog. Reaction Kinetics. Vol. 2. *Edited by* G. Porter. 1964. p. 39.
9. J. A. KERR and A. F. TROTMAN-DICKENSON. Prog. Reaction Kinetics. Vol. 1, *Edited by* G. Porter. 1961. p. 105.
10. D. E. MANN, B. A. THRUSH, D. R. LIDE, J. J. BALL, and N. ACQUISTA. J. Chem. Phys. **34**, 420 (1961).
11. P. E. CHARTERS and J. C. POLANYI. Discuss. Faraday Soc. **33**, 107 (1962).
12. H. S. HEAPS and G. HERZBERG. Z. Phys. **133**, 48 (1952).
13. G. A. KUIPERS. J. Mol. Spectros. **2**, 75 (1958).
14. A. R. TROBRIDGE and K. R. JENNINGS. Proc. Chem. Soc. 335 (1964).
15. G. R. HUNT and M. K. WILSON. J. Chem. Phys. **34**, 1301 (1961).
16. P. D. PACEY. Ph.D. Thesis, Univ. of Toronto, Toronto, Ontario. 1967.
17. K. F. HERZFELD and T. A. LITOVITZ. Absorption and dispersion of ultrasonic waves. Academic Press. 1959.
18. HAO-LIN CHEN and C. B. MOORE. 2nd Conference on Chemical and Molecular Lasers, St. Louis, Mo. 1969; J. Quant. Electron. To be published.
19. J. D. LAMBERT. Quart. Rev. Chem. Soc. **21**. 67 (1967).
20. J. W. COOMBER and E. WHITTLE. Trans. Faraday Soc. **63**, 1394 (1967).
21. J. R. LACHER and H. A. SKINNER. J. Chem. Soc. **A**, 1034 (1968).
22. V. P. KOLESOV, A. M. MARTYNOV, and S. M. SHURATOV. Zh. Fiz. Khim. **39**, 435 (1965).
23. P. CADMAN, M. DAY, A. W. KIRK, and A. F. TROTMAN-DICKENSON. Chem. Commun. 203 (1970).
24. D. W. SETSER. Private communication.
25. J. C. HASSLER and D. W. SETSER. J. Chem. Phys. **45**, 3246 (1966).
26. K. DEES and D. W. SETSER. J. Chem. Phys. **49**, 1193 (1968).
27. H. W. CHANG and D. W. SETSER. J. Amer. Chem. Soc. **91**, 7648 (1969).
28. J. A. KERR, B. V. O'GRADY, and A. F. TROTMAN-DICKENSON. J. Chem. Soc. **A**, 275 (1969).
29. G. Z. WHITTEN and B. S. RABINOVITCH. J. Chem. Phys. **38**, 2466 (1963).
30. P. J. KUNTZ, E. M. NEMETH, J. C. POLANYI, S. D. ROSNER, and C. E. YOUNG. J. Chem. Phys. **44**, 1168 (1966).
31. G. HERZBERG. Electronic spectra of polyatomic molecules. Van Nostrand, Princeton, New Jersey. 1966.
32. J. C. POLANYI and W. H. WONG. J. Chem. Phys. **51**, 1439 (1969).

Can. J. Chem. Downloaded from www.nrcresearchpress.com by 210.87.254.40 on 09/05/12
For personal use only.

Can. J. Chem. Downloaded from www.nrcresearchpress.com by 210.87.254.42 on 09/05/12
For personal use only.

The single crystal Raman spectrum of orthorhombic $PbCl_2$

G. A. OZIN

Lash Miller Chemical Laboratories and Erindale College, University of Toronto, Toronto 181, Ontario

Received May 22, 1970

The frequencies and symmetries of the even parity lattice vibrations of orthorhombic lead dichloride are determined by means of polarized Raman scattering from an oriented single crystal. The frequencies of the vibrations are interpreted in terms of symmetry co-ordinates and by comparison with the modes of the isomorphous lead dibromide.

Canadian Journal of Chemistry, 48, 2931 (1970)

The previously reported Raman data for $PbCl_2$ was for the powdered solid (1) where it was assumed that the six observed lines belonged to the totally symmetrical A_{1g} class, on the basis that these modes would be expected to be the most intense in the Raman spectrum. While it is true that the four highest frequency observed lines can be assigned to vibrations involving motion chiefly of the chlorine atoms (undergoing shifts to lower frequency in $PbBr_2$), the single crystal Raman polarization data of the present study proves quite unambiguously that many of the observed lines are not of A_{1g} class and allows a more detailed assignment of the vibrational spectrum to be made.

One of the advantages of single crystal Raman measurements compared to powder measurements is that weak lines in the close proximity of strong lines and lines obscured because of accidental coincidence can often be resolved in different polarization measurements. This is certainly true in the case of lead dichloride where it is found that the 18 expected Raman active optical phonon transitions occur below 180 cm^{-1} and accidental or near coincidences are to be expected. Let us formalize the single crystal Raman data for lead dichloride.

Lead dichloride crystallizes in the orthorhombic system with space group *Pnam* (D_{2h}^{16}) with four $PbCl_2$ molecules in the primitive unit cell (2). The lead and chlorine atoms are each situated (3) at the equipoint 4(*c*), that is, on the *xy* mirror planes with $z = 1/4$ and 3/4.

The lead atoms have nine chlorine atoms as nearest neighbors where the co-ordination of the lead atoms may be approximately described as trigonal prismatic with the remaining three chlorine atoms lying in a plane (*xy*) and occupying central positions of the rectangular faces of the prism.

A factor group analysis of the primitive unit cell predicts 18 Raman active and 15 infrared active optical phonons ($k = 0$) as follows

D_{2h}	E	$C_2(x)$	$C_2(y)$	$C_2(z)$	i	$\sigma(xy)$	$\sigma(xz)$	$\sigma(yz)$
D_{2h}^{16}	E	2_1	2_1	2_1	i	m	a	n
χ_J	3	−1	−1	−1	−3	1	1	1
ω_R	12	0	0	0	0	12	0	0
$\omega_R\chi_J$	36	0	0	0	0	12	0	0

divided into modes of the following symmetry

$$\Gamma_{vib} = 6A_g + 6B_{1g} + 3B_{2g} + 3B_{3g} + 3A_u + 2B_{1u} + 5B_{2u} + 5B_{3u}$$

where the three rigid translations of the whole unit cell have been removed. The g modes are Raman active and the corresponding derived polarizability components under D_{2h}^{16} are as follows: A_g: α_{xx}', α_{yy}', α_{zz}'; B_{1g}: α_{xy}'; B_{2g}: α_{xz}'; B_{3g}: α_{yz}'.

While the assignment of normal modes is more difficult for ionic lattices than for molecular crystals some assignment is possible in the present case. In $PbCl_2$ the internal binding in the nine co-ordinate lead–chlorine polyhedron may not be significantly different from other ionic forces in the crystal, so it is not very helpful to examine the vibrational spectra from the point of view of internal and external vibrations. However, the symmetries of the crystal and its normal vibrations allow us to exclude certain types of motion, because each mode must transform in a definite way under the operations of the point group of the crystal. As $PbCl_2$ and $PbBr_2$ have been shown to be isomorphous (4), then to a first

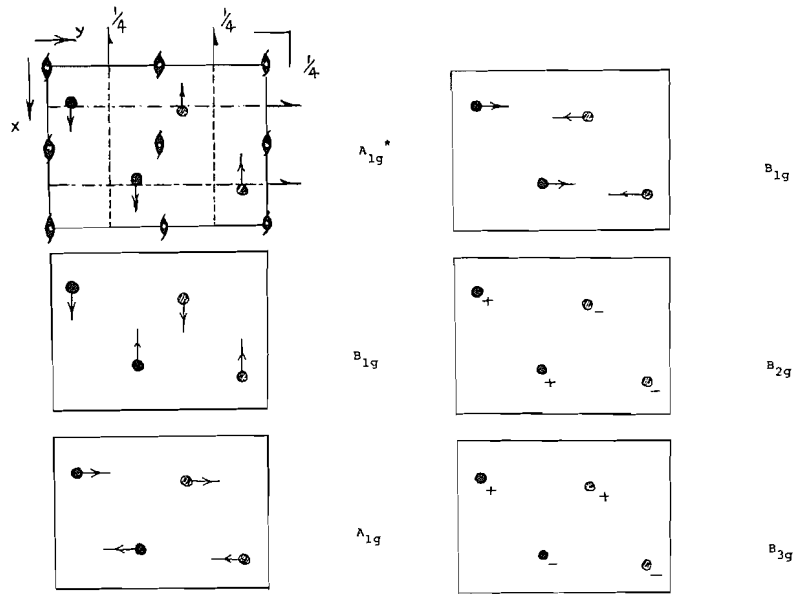

FIG. 1. A diagrammatic representation of the symmetry co-ordinates of the six predicted Raman allowed modes involving motion of the lead atoms in the primitive unit cell*. Conventional crystallographic symbols are used here to designate the unit cell symmetry elements.

approximation it would be expected that (*a*) modes involving motion mainly of the lead atoms should occur at very similar frequencies and (*b*) modes involving motion mainly of the chlorine atoms would be expected to occur at frequencies greater than 100 cm^{-1} and to be shifted by a factor of approximately 1.5, that is, the ratio (mass of Cl/mass of Br)$^{1/2}$, in $PbBr_2$.

Figure 1 shows a diagrammatic representation of the symmetry co-ordinates of the six predicted Raman allowed modes involving motion of the four lead atoms in the primitive unit cell. It must be emphasized that these are not normal modes; a normal mode of a given symmetry will, in general, be a mixture of all the co-ordinates of that symmetry.

Thus we expect Raman active modes of symmetry type

$$\Gamma_{vib}^{Pb} = 2A_g + 2B_{1g} + B_{2g} + B_{3g}$$

which involve mainly lead atom movement to occur (*a*) at very low frequencies ($< 100\ cm^{-1}$) and (*b*) to be approximately invariant on passing from $PbCl_2$ to $PbBr_2$.

Inspection of the Raman data for $PbCl_2$ and $PbBr_2$ shows this to be the case for the lines observed at 86, 58, and 35 cm^{-1} and 88, 54, and 34 cm^{-1} for $PbCl_2$ and $PbBr_2$, respectively. The single crystal Raman polarization data for these three lines in $PbCl_2$ show that at least two of them have intensity contributions arising from more than one polarizability component of the Raman tensor, of which the corresponding symmetry species agree reasonably well with those predicted for the lead atom modes. Regarding the high frequency modes at 178, 158, 134, and 126 cm^{-1} in $PbCl_2$, if these modes are

TABLE 1

The single crystal Raman polarization data for $PbCl_2$*

Symmetry	Frequency†
B_{1g}	178
$A_{1g} + B_{2g} + (B_{3g}?)$	156§
B_{2g}	134
B_{1g}	126
$(B_{1g}?)$	100‡
$B_{2g} + B_{3g}$	86
B_{1g}	58
$A_{1g} + (B_{2g}?)$	35
B_{1g}	26
A_{1g}	18

*Frequencies in cm^{-1}, uncertainties ±2 cm^{-1}.

†The powder Raman data for $PbBr_2$ (1) shows lines at 118, 108, 88, 74, 54, and 34 cm^{-1}.

‡Very weak shoulder observed only in B_{1g} measurements.

§Very broad and strong in parallel measurements and could possibly conceal the presence of weaker A_{1g} modes.

Can. J. Chem. Downloaded from www.nrcresearchpress.com by 210.87.254.42 on 09/05/12
For personal use only.

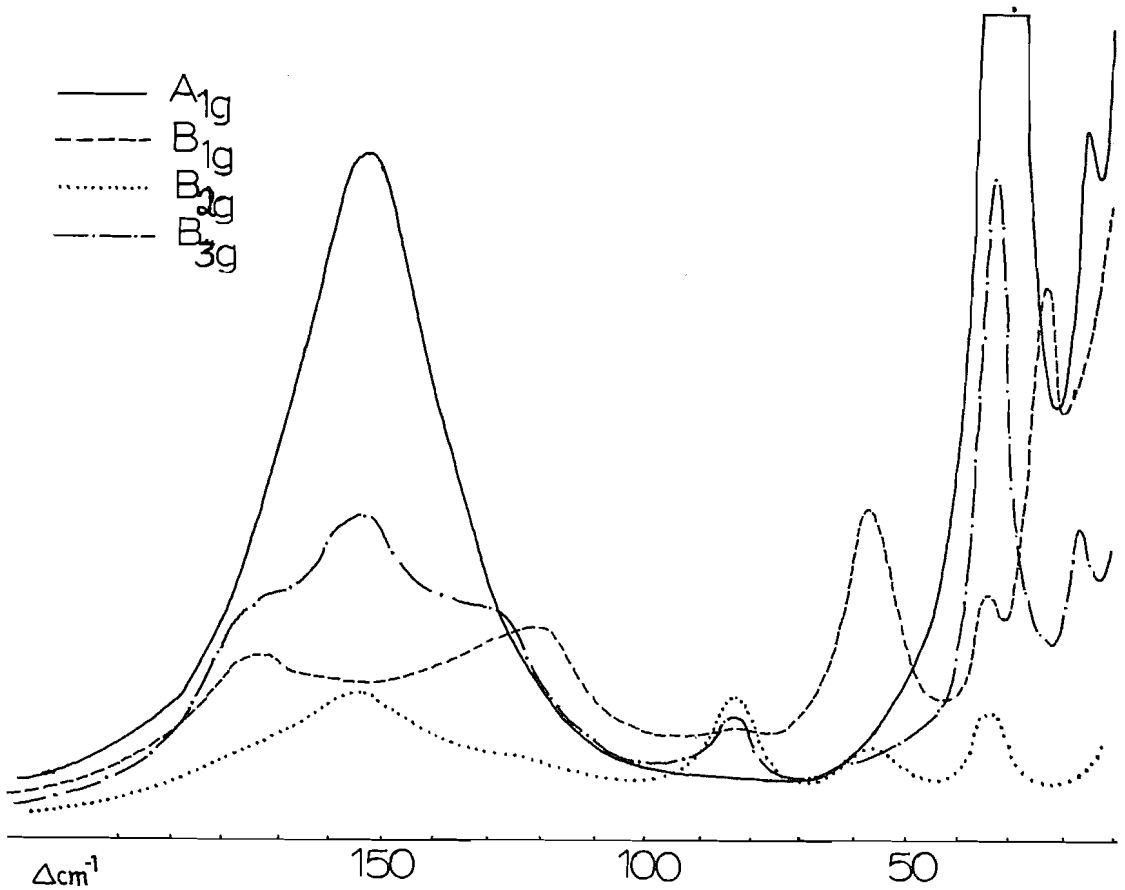

FIG. 2. The single crystal Raman polarization data for orthorhombic $PbCl_2$.

mainly associated with chlorine atom motion, then on the basis of the previous discussion they would be expected to shift to approximately 121, 106, 97, and 67 cm^{-1}, respectively in $PbBr_2$. This could then account for the bands observed at 118, 108, 88, and 74 cm^{-1} in the spectrum of $PbBr_2$ (1).

Table 1 and Fig. 2 list the frequencies and polarization behavior of the 10 observed lines where many are found to have intensity contributions arising from more than one tensor component.

Experimental

The Raman data were obtained at room temperature with the use of a Carson argon ion laser emitting 1–2 W at 4880 and 5145 Å coupled to a Spex Model 1401 Raman Spectrometer. Both lines were used to record Stokes and anti-Stokes lines and to check for low frequency argon spontaneous emission lines. Spectral slit widths were typically 2–3 cm^{-1}.

The lead dichloride crystals were grown from the melt in a sealed evacuated silica tube, allowing the sample to cool slowly for several days. Raman polarization measurements were recorded on many different crystals in order to obtain the best data and to check for incomplete polarization discrimination which arises from crystal imperfections and birefringence depolarization effects (5).

I would like to thank the National Research Council of Canada for generous financial support.

1. L. A. ISUPOVA and E. V. SOBOLEV. Zh. Struct. Khim. **9**, 324 (1968).
2. H. BRAEKKEN. Z. Krist. **83**, 222 (1932).
3. International tables for X-ray crystallography. Kynoch Press, Birmingham. 1962.
4. R. W. G. WYCKOFF. Crystal structures. 2nd ed. Vol. 1. John Wiley and Sons, Inc., New York, 1963. p. 298.
5. I. R. BEATTIE and T. R. GILSON. Proc. Roy. Soc. **307**, 407 (1960).

Can. J. Chem. Downloaded from www.nrcresearchpress.com by 210.87.254.42 on 09/05/12
For personal use only.

Group vibrations

J. M. FREEMAN AND T. HENSHALL
Department of Chemistry and Applied Chemistry, University of Salford, Salford M5 4WT, England

Received February 5, 1970

The procedure introduced by King and Crawford (1) for the factorization of group frequencies from the vibrational secular determinant is extended to cover more than two group frequencies in any symmetry species. The case in which the frequencies are not sequential is included.

Canadian Journal of Chemistry, 48, 2934 (1970)

Can. J. Chem. Downloaded from www.nrcresearchpress.com by 210.87.254.6 on 09/05/12
For personal use only.

When a molecule exhibits vibrational frequencies that are characteristic of a substituent group (e.g. CH_3, CH_2, NH_2), a reduction in the order of the vibrational secular determinant is possible using a procedure developed by King and Crawford (1). This involves the construction of an orthogonal matrix **A** from an $\mathbf{L}^{-1}$ matrix of a "standard molecule", R—X, wherein R is the substituent group under consideration, and X an "anchor atom" of "infinite" mass.

Under the matrix **A**, itself a product of orthogonal transformations, the matrix $\mathbf{H} = \mathbf{GF}$ in each symmetry species is reduced to the Jacobian canonical form

$$\left(\begin{array}{cccc:c} \lambda_1 & & & & \\ \gamma_{12} & \lambda_2 & & 0 & \\ \gamma_{13} & \gamma_{23} & \lambda_3 & & 0 \\ \cdot & & \cdot & & \\ \cdot & & & \cdot & \\ \cdot & & & & \cdot \\ \gamma_{1g} & \cdots & \cdots & \cdots & \lambda_g \\ \hdashline & & & & \\ \multicolumn{4}{c:}{\bar{\mathbf{H}}_{gf}} & \bar{\mathbf{H}}_{ff} \end{array}\right) \quad (\gamma_{ij} = 0, j > i)$$

wherein $\lambda_1, \cdots, \lambda_g$ are the group frequency parameters ($\lambda_i = 4\pi^2 c^2 \nu_i^2$), and the submatrix $\bar{\mathbf{H}}_{ff}$ leads to a reduced secular determinant $|\mathbf{G}^+_{ff}\mathbf{F}^+_{ff} - \lambda\mathbf{E}_{ff}| = 0$ for the framework vibrations. Perturbations arising from the factorization procedure are accountable in $\mathbf{G}^+_{ff}$ through an effective inverse mass matrix $(\mathbf{M}^{-1})^+$, and in $\mathbf{F}^+_{ff}$ by a matrix $\mathbf{\Phi}_{ff}$ of corrections which should be small for satisfactory application of the factorization method. Solution of this reduced secular determinant leads either to the frequencies of the framework modes $Q_{g+1} \rightarrow Q_{3N-6}$, or to $\mathbf{F}^+_{ff}$ if the former are known.

The construction of the matrix **A** is based on repeated application of a theorem on canonical transformations due to Schur, described in detail in ref. 2. Under appropriate substitutions, the orthogonal matrix **R** of eq. [13] on p. 104 of ref. 2 leads to the notation of King and Crawford (1), viz.

$$[1] \quad \mathbf{R} \rightarrow \mathbf{J}(i) = [a_i\{(\mathrm{L}^{-1})_1{}^i + a_i\}]^{-1} \times [(\tilde{\mathrm{L}}^{-1})^i + \tilde{\mathrm{Z}}_i][(\mathrm{L}^{-1})^i + \mathrm{Z}_i] - \mathbf{E}$$

whereby a group frequency parameter λ_i can be factorized from **H** knowing the ith row of the $\mathbf{L}^{-1}$ matrix of the standard molecule.

King and Crawford (1), however, sketch the development and construction of **A** only for the case of two group frequencies in any one symmetry species. It is the purpose of this note to extend their development, and to include the case in which, as in the vinylidene group (3), the group frequencies are not sequential.

We first consider briefly the development in ref. 1. If $i = 1$ in eq. [1], then $(\mathrm{L}^{-1})^1\mathbf{H} = \lambda_1(\mathrm{L}^{-1})^1$; and since $(\mathrm{L}^{-1})^1 = \mathrm{Z}_1\tilde{\mathbf{J}}(1)$ by ref. 2, then also $\mathrm{Z}_1\tilde{\mathbf{J}}(1)\mathbf{H} = \lambda_1\mathrm{Z}_1\tilde{\mathbf{J}}(1)$. Hence $\mathrm{Z}_1\tilde{\mathbf{J}}(1)\mathbf{H}\mathbf{J}(1) = \lambda_1\mathrm{Z}_1$, or $\mathrm{Z}_1\bar{\mathbf{H}}(1) = \lambda_1\mathrm{Z}_1$. But Z_1 is of the form $\{a_1, 0, 0, \cdots, 0\}$, with $a_1 = [(\mathrm{L}^{-1})^1(\mathrm{L}^{-1})^1]^{\frac{1}{2}}$ by ref. 2; hence the transformed matrix $\bar{\mathbf{H}}(1)$ has the required canonical form

$$\bar{\mathbf{H}}(1) = \left(\begin{array}{c:c} 1 & 0 \\ \hdashline \mathbf{M}(1) & \mathbf{N}(1) \end{array}\right)$$

Consider now the second row of $\mathbf{L}^{-1}$. Then $(\mathrm{L}^{-1})^2\mathbf{H} = \lambda_2(\mathrm{L}^{-1})^2$, and therefore

$$(\mathrm{L}^{-1})^2\mathbf{J}(1)\bar{\mathbf{H}}(1)\mathbf{J}(1) = \lambda_2(\mathrm{L}^{-1})^2,$$

or

$$(\mathrm{L}^{-1})^2\mathbf{J}(1)\bar{\mathbf{H}}(1) = \lambda_2(\mathrm{L}^{-1})^2\mathbf{J}(1)$$

Evidently $(\mathrm{L}^{-1})^2\mathbf{J}(1)$ is an eigenvector of $\bar{\mathbf{H}}(1)$ corresponding to the eigenvalue λ_2; and the vector obtained from $(\mathrm{L}^{-1})^2\mathbf{J}(1)$ by omitting the first element is clearly an eigenvector of $\mathbf{M}(1)$ corresponding to λ_2.

Hence the second orthogonal matrix, $\mathbf{J}(2)$, by which λ_2 is factorized from **H**, is obtained from

Can. J. Chem. Downloaded from www.nrcresearchpress.com by 210.87.254.6 on 09/05/12
For personal use only.

eq. [1] on substitution of $(L^{-1})^2J(1)$ for $(L^{-1})^i$, having first suppressed the first element in the former. The matrix $J(2)$ is of order one less than $J(1)$; and hence a new matrix $\bar{J}(2)$ is defined by

$$\bar{J}(2) = \begin{pmatrix} 1 & 0 \\ 0 & J(2) \end{pmatrix},$$

so that $\bar{H}(2) = \tilde{\bar{J}}(2)\bar{H}(1)\bar{J}(2)$, with $\bar{H}(2)$ now of the form

$$\left(\begin{array}{cc|c} \lambda_1 & 0 & \\ * & \lambda_2 & 0 \\ \hline M(2) & & N(2) \end{array}\right)$$

Extension of this procedure to the g-rows of the L^{-1} matrix which involve group frequencies leads to a modified H matrix of the form

$$\bar{H}(g) = \tilde{A}HA = \left(\begin{array}{cccc|c} \lambda_1 & & & & \\ x & \lambda_2 & & 0 & \\ x & x & \lambda_3 & & 0 \\ \cdot & \cdot & \cdot & \cdot & \\ x & x & x & \lambda_g & \\ \hline M(g) & & & & N(g) \end{array}\right)$$

$$= \left(\begin{array}{c|c} \bar{H}_{gg} & 0 \\ \hline \bar{H}_{gf} & H_{ff} \end{array}\right)$$

Now

[2] $\bar{H}(g) = \tilde{\bar{J}}(g)\bar{H}(g-1)\bar{J}(g)$

[3] $= \tilde{\bar{J}}(g)\tilde{\bar{J}}(g-1)\bar{H}(g-2) \times \bar{J}(g-1)\bar{J}(g)$ etc.

and by comparison of eqs. [2] and [3], evidently the matrix $A = \prod_{i=1}^{g}\bar{J}(i)$. Since each $\bar{J}(i)$ is orthogonal, so also is A.

The problem remains of how to construct the eigenvectors of H for $g = 3, 4, \cdots$. The following further development covers not only this situation, but also the case for which the group frequencies are not sequential (e.g. in the A_1 vibrational species of the vinylidene halides ν(C—H) and δ(HĈH), the first and third frequencies, respectively, are group frequencies).

It is convenient to introduce a slight change of notation. Let the eigenvector of $\bar{H}(n)$ corresponding to the frequency parameter λ_i be denoted by $(L_n^{-1})^i$, wherein the suffix n denotes the number of eigenvalues already factorized from H, and $i = (n+1)$ when the group frequencies are sequential.

Then

[3] $\bar{H}(n) = \tilde{\bar{J}}(n)\bar{H}(n-1)\bar{J}(n)$

[4] $(L_{n-1}^{-1})^i\bar{J}(n)\bar{H}(n)$
$= (L_{n-1}^{-1})^i\bar{J}(n)\tilde{\bar{J}}(n)\bar{H}(n-1)\bar{J}(n)$
$= (L_{n-1}^{-1})^i\bar{H}(n-1)\bar{J}(n)$
$= \lambda_i(L_{n-1}^{-1})^i\bar{J}(n)$

[5] $(L_n^{-1})^i\bar{H}(n) = \lambda_i(L_n^{-1})^i$

and hence by eqs. [4] and [5]

$$(L_n^{-1})^i = (L_{n-1}^{-1})^i\bar{J}(n)$$

But

$$(L_1^{-1})^2 = (L_0^{-1})^2\bar{J}(1)$$

and hence by induction

$$(L_2^{-1})^3 = (L_1^{-1})^3\bar{J}(2) = (L_0^{-1})^3\bar{J}(1)\bar{J}(2)$$

or generally

$$(L_n^{-1})^i = (L_0^{-1})^i\prod_{k=1}^{n}\bar{J}(k)$$

To illustrate the procedure, we continue with the example of the A_1 vibrational species of the vinylidene group. The analysis of the "standard molecule" is described in ref. 3, and the corresponding normal coordinate matrix (L^{-1}) is given in Table 1 (the computer outputs have, in all Tables, been rounded to four decimal places).

The frequencies calculated for the "standard molecule" are 3020, 1602, 1398, 537, 0 (cm^{-1}), of which the first and third satisfy the requirements (1) of group frequencies.

Then to factorize the frequency parameter λ_1 from H: (*1*) Consider the leading element in L^{-1}, and calculate

$$a_1 = [(L^{-1})^1(L^{-1})^1]^{\frac{1}{2}} = 0.9809$$

(*2*) Construct the row vector

$$\{(L_0^{-1})^1 + Z_1\} = \{(L_0^{-1})^1 + a_1\} = \{0.0054, 0.0094, 0.1020, -0.0074, 0.0031\}$$

and from it, the normalization factor

$$[a_1\{(L_0^{-1})_1{}^1 + a_1\}]^{-1} = [0.9809 \times 0.0054]^{-1} = 1.889 \times 10^2$$

TABLE 1

The $\mathbf{L}^{-1}$ matrix of the A_1 species of the standard molecule CH_2X_2

$$\mathbf{L}^{-1} = \begin{pmatrix} -0.9755 & 0.0094 & 0.1020 & -0.0074 & 0.0031 \\ -0.1686 & -0.1392 & -1.8455 & 0.6228 & -0.2623 \\ -0.0287 & -0.5747 & 0.7451 & -0.3829 & 0.1612 \\ -0.1648 & 0.1868 & -3.1710 & -3.8485 & 1.6205 \\ -0.0003 & 0.0004 & -0.0067 & 866.0 & 433.0 \end{pmatrix}$$

TABLE 2

The J(1) matrix

$$\mathbf{J}(1) = \begin{pmatrix} -0.9945 & 0.0096 & 0.1040 & -0.0075 & 0.0032 \\ & -0.9833 & 0.1810 & -0.0131 & 0.0055 \\ & & 0.9658 & -0.1419 & 0.0598 \\ & \text{(Symmetric)} & & -0.9898 & -0.0043 \\ & & & & -0.9982 \end{pmatrix}$$

TABLE 3

The $\bar{\mathbf{J}}(2)$ matrix

$$\bar{\mathbf{J}}(2) = \begin{pmatrix} 0.6893 & 0.6608 & 0.2738 & -0.1153 \\ & -0.7415 & 0.1071 & -0.0451 \\ & & -0.9556 & -0.0187 \\ & \text{(Symmetric)} & & -0.9921 \end{pmatrix}$$

TABLE 4

The A matrix

$$\mathbf{A} = \begin{pmatrix} -0.9945 & 0.0729 & -0.0717 & 0.0209 & -0.0088 \\ 0.0096 & -0.5624 & -0.7857 & -0.2374 & 0.1000 \\ 0.1040 & 0.7172 & -0.6144 & 0.2875 & -0.1210 \\ -0.0075 & -0.3732 & -0.0092 & 0.9272 & 0.0307 \\ 0.0032 & 0.1572 & 0.0039 & 0.0310 & 0.9871 \end{pmatrix}$$

TABLE 5

The $\bar{\mathbf{H}}$ matrix, Jacobian canonical form

$$\bar{\mathbf{H}} = \begin{pmatrix} 5.3713 & 0.0000 & 0.0000 & 0.0000 & 0.0000 \\ -0.4281 & 1.1513 & 0.0000 & 0.0000 & 0.0000 \\ -0.4150 & -0.4241 & 1.4821 & 0.0719 & -0.0303 \\ -0.1903 & -0.0337 & 0.3144 & 0.1137 & -0.0479 \\ 0.1564 & 0.7018 & -0.5447 & -0.2035 & 0.0857 \end{pmatrix}$$

(*3*) Now form $\mathbf{J}(1)$ according to

$$\mathbf{J}(1) = [a_1\{(\mathrm{L_0}^{-1})_1{}^1 + a_1\}]^{-1}\,[(\widetilde{\mathrm{L}_0}^{-1})^1 + \widetilde{\mathrm{Z}}_1] \times [(\mathrm{L_0}^{-1})^1 + \mathrm{Z}_1] - \mathbf{E}$$

The result is the 5 × 5 matrix of Table 2; and by definition, this is also $\bar{\mathbf{J}}(1)$.

We now proceed to the factorization from $\mathbf{H}$ of the second group frequency λ_3, and to this end we consider the third row of $\mathbf{L}^{-1}$. The corresponding results are

(*1*) $a_3 = 1.0237$.

(*2*) $(\mathrm{L_1}^{-1})^3 = (\mathrm{L_0}^{-1})^3\bar{\mathbf{J}}(1) = \{(0.1040)^*, 0.7057, 0.6765, 0.2803, -0.1180\}$.

Suppress the leading element (0.1040)* before proceeding to the calculation of

(*i*) $\{(\mathrm{L_1}^{-1})^3 + \mathrm{Z}_3\} = \{(\mathrm{L_0}^{-1})^3\bar{\mathbf{J}}(1) + \mathrm{Z}_3\}$

$= \{(\mathrm{L_0}^{-1})^3\bar{\mathbf{J}}(1) + a_3\}$

$= \{1.7294, 0.6765, 0.2803, -0.1180\}$

(*ii*) The normalization factor

$[a_3\{(\mathrm{L_1}^{-1})_1{}^3 + a_3\}]^{-1}$

$= 1.0237 \times 1.7294 = 0.5648.$

(*3*) Now construct the 4 × 4 matrix $\mathbf{J}(2)$ according to

$$\mathbf{J}(2) = [a_3\{(\mathrm{L_1}^{-1})_1{}^3 + a_3\}]^{-1}[(\widetilde{\mathrm{L}_1}^{-1})^3 + \widetilde{\mathrm{Z}}_3] \times [(\mathrm{L_1}^{-1})^3 + \mathrm{Z}_3] - \mathbf{E}$$

The result is given in Table 3, and the corresponding "bordered" matrix

Can. J. Chem. Downloaded from www.nrcresearchpress.com by 210.87.254.6 on 09/05/12
For personal use only.

$$\bar{\mathbf{J}}(2) = \begin{pmatrix} 1 & 0 \\ 0 & \mathbf{J}(2) \end{pmatrix}$$

Finally, the orthogonal matrix, **A**, by which **H** is reduced to Jacobian canonical form, and from which the $\bar{\mathbf{G}}$, $\bar{\mathbf{F}}$, $\mathbf{W}_{gg}$, $(\mathbf{M}^{-1})^{+}$, and $\mathbf{\Phi}_{ff}$ matrices (1) are derived, is obtained from the product

$$\mathbf{A} = \prod_{k=1}^{g} \mathbf{J}(k)$$

and is presented in Table 4. The matrix $\bar{\mathbf{H}}$ in canonical form is given in Table 5.

The procedure has been programmed in English-Electric KDF-9 Algol, and copies are available on request.

1. W. T. KING and B. L. CRAWFORD, JR. J. Mol. Spectrosc. **5**, 421 (1960).
2. H. W. TURNBULL and A. C. AITKEN. An introduction to the theory of canonical matrices. Blackie and Son, Ltd., London. 1952.
3. J. M. FREEMAN and T. HENSHALL. Can. J. Chem. **47**, 935 (1969).

Phosphorescence of chloropentafluoroacetone at 77 °K

H. S. SAMANT AND A. J. YARWOOD
Department of Chemistry, McMaster University, Hamilton, Ontario

Received April 14, 1970

The phosphorescence of chloropentafluoroacetone at 77 °K is reported and the energy of the triplet state is estimated to be 74 kcal. The phosphorescence lifetimes and the relative phosphorescence yields of chloropentafluoroacetone and hexafluoroacetone at 77 °K were measured. The results show that substitution of a chlorine atom in the fluorinated aliphatic ketone changes the radiative and non-radiative rate constants from the triplet state at 77 °K by factors of about 1.7 and 2.3, respectively.

Canadian Journal of Chemistry, **48**, 2937 (1970)

In a recent gas phase study (17) the first excited singlet state of chloropentafluoroacetone (chloroketone) was populated by absorption in the π^*–n band. The effect of chlorine substitution in hexafluoroacetone on the radiative and non-radiative processes from the singlet state was investigated. Only fluorescence was observed in the gas phase. However, studies of energy transfer to biacetyl (unpublished work) showed that triplet state molecules are a major feature of the gaseous photochemical system. The quantum yield of phosphorescence would be given by $\phi_p = k_r\phi_{i.s.c.}/(k_r + k_{nr})$, where $\phi_{i.s.c.}$ is the efficiency of intersystem crossing from the first excited singlet state to the triplet state, k_r is the rate constant for the radiative triplet to singlet process, and k_{nr} is the sum of the rate constants for the non-radiative processes from the triplet state. The internal heavy atom effect on k_r and k_{nr} for the triplet state of fluorinated ketones is an important feature of the system and the experimental data can be compared with the theoretical calculations (1–3) on aliphatic carbonyl compounds.

In principle, k_r may be estimated from $f = 1.500\, g_u k_r/g_l\, \bar{\nu}^2$ where f is the oscillator strength, $\bar{\nu}$ the wavenumber of the forbidden transition, and g the degeneracy of the upper (u) and lower (l) states. However, for aliphatic ketones the singlet–triplet absorption is usually hidden under the long wavelength tail of the singlet–singlet π^*–n transition (4). Experimentally, k_r can be determined from $k_r = \phi_p/\phi_{i.s.c.}.\tau_p$, where τ_p is the actual phosphorescent lifetime.

This study of the phosphorescence of chloropentafluoroacetone at 77 °K was undertaken to explore the effect of chlorine substitution in hexafluoroacetone on the rate constants associated with the radiative and radiationless transitions from the triplet state. A further advantage of such studies is that the energy of the triplet state can be estimated.

Experimental

The chloropentafluoroacetone (Allied Chemical) and hexafluoroacetone (Pierce Chemical Co.) were purified by low temperature distillation and stored in the dark at 77 °K. The 3-methyl pentane (Philips pure grade) was

Can. J. Chem. Downloaded from www.nrcresearchpress.com by 210.87.254.6 on 09/05/12
For personal use only.

$$\bar{\mathbf{J}}(2) = \begin{pmatrix} 1 & 0 \\ 0 & \mathbf{J}(2) \end{pmatrix}$$

Finally, the orthogonal matrix, **A**, by which **H** is reduced to Jacobian canonical form, and from which the $\bar{\mathbf{G}}$, $\bar{\mathbf{F}}$, $\mathbf{W}_{gg}$, $(\mathbf{M}^{-1})^{+}$, and $\mathbf{\Phi}_{ff}$ matrices (1) are derived, is obtained from the product

$$\mathbf{A} = \prod_{k=1}^{g} \mathbf{J}(k)$$

and is presented in Table 4. The matrix $\bar{\mathbf{H}}$ in canonical form is given in Table 5.

The procedure has been programmed in English-Electric KDF-9 Algol, and copies are available on request.

1. W. T. KING and B. L. CRAWFORD, JR. J. Mol. Spectrosc. **5**, 421 (1960).
2. H. W. TURNBULL and A. C. AITKEN. An introduction to the theory of canonical matrices. Blackie and Son, Ltd., London. 1952.
3. J. M. FREEMAN and T. HENSHALL. Can. J. Chem. **47**, 935 (1969).

Phosphorescence of chloropentafluoroacetone at 77 °K

H. S. SAMANT AND A. J. YARWOOD
Department of Chemistry, McMaster University, Hamilton, Ontario

Received April 14, 1970

The phosphorescence of chloropentafluoroacetone at 77 °K is reported and the energy of the triplet state is estimated to be 74 kcal. The phosphorescence lifetimes and the relative phosphorescence yields of chloropentafluoroacetone and hexafluoroacetone at 77 °K were measured. The results show that substitution of a chlorine atom in the fluorinated aliphatic ketone changes the radiative and non-radiative rate constants from the triplet state at 77 °K by factors of about 1.7 and 2.3, respectively.

Canadian Journal of Chemistry, **48**, 2937 (1970)

In a recent gas phase study (17) the first excited singlet state of chloropentafluoroacetone (chloroketone) was populated by absorption in the π^*–n band. The effect of chlorine substitution in hexafluoroacetone on the radiative and non-radiative processes from the singlet state was investigated. Only fluorescence was observed in the gas phase. However, studies of energy transfer to biacetyl (unpublished work) showed that triplet state molecules are a major feature of the gaseous photochemical system. The quantum yield of phosphorescence would be given by $\phi_p = k_r\phi_{i.s.c.}/(k_r + k_{nr})$, where $\phi_{i.s.c.}$ is the efficiency of intersystem crossing from the first excited singlet state to the triplet state, k_r is the rate constant for the radiative triplet to singlet process, and k_{nr} is the sum of the rate constants for the non-radiative processes from the triplet state. The internal heavy atom effect on k_r and k_{nr} for the triplet state of fluorinated ketones is an important feature of the system and the experimental data can be compared with the theoretical calculations (1–3) on aliphatic carbonyl compounds.

In principle, k_r may be estimated from $f = 1.500\, g_u k_r/g_l \bar{\nu}^2$ where f is the oscillator strength, $\bar{\nu}$ the wavenumber of the forbidden transition, and g the degeneracy of the upper (u) and lower (l) states. However, for aliphatic ketones the singlet–triplet absorption is usually hidden under the long wavelength tail of the singlet–singlet π^*–n transition (4). Experimentally, k_r can be determined from $k_r = \phi_p/\phi_{i.s.c.}.\tau_p$, where τ_p is the actual phosphorescent lifetime.

This study of the phosphorescence of chloropentafluoroacetone at 77 °K was undertaken to explore the effect of chlorine substitution in hexafluoroacetone on the rate constants associated with the radiative and radiationless transitions from the triplet state. A further advantage of such studies is that the energy of the triplet state can be estimated.

Experimental

The chloropentafluoroacetone (Allied Chemical) and hexafluoroacetone (Pierce Chemical Co.) were purified by low temperature distillation and stored in the dark at 77 °K. The 3-methyl pentane (Philips pure grade) was

Can. J. Chem. Downloaded from www.nrcresearchpress.com by 210.87.254.40 on 09/05/12
For personal use only.

Can. J. Chem. Downloaded from www.nrcresearchpress.com by 210.87.254.40 on 09/05/12
For personal use only.

stored over molecular sieves and distilled. The ether–pentane–alcohol was supplied by Matheson, Coleman and Bell. The samples were degassed by the freeze–pump–thaw technique and sealed in quartz tubes (2 mm internal diameter). The phosphorescence spectra and relative quantum yields were measured using an Aminco Bowman spectrofluorometer with rotating can phosphorometer attachment. The lifetimes of the chloroketone at 77 °K were determined using a Xenon flash (25J with 1/e lifetime of 6×10^{-6} s). The phosphorescence was analyzed by a 0.5 Ebert grating monochromator and the wavelengths in the 460 nm region were detected by a RCA 8575 photomultiplier, displayed on an oscilloscope, and photographed. The lifetimes were calculated from log intensity vs. time plots.

Results and Discussion

The phosphorescence of chloropentafluoroacetone (0.02 *M*) in 3-methyl pentane at 77 °K extends from about 380 to a maximum at about 460 nm and has a long wavelength limit of about 610 nm (the actual long wavelength limit probably lies at longer wavelengths since the sensitivity of the detection system decreases very rapidly at these wavelengths). Similar emission behavior was observed for ketone solutions in EPA and for the pure solid at 77 °K. The only other simple chlorinated aliphatic ketone reported to phosphoresce is oxalyl chloride (5) and the triplet state energy is given by Kanda as 69 kcal.

The difference in energy between the first excited singlet state and the lowest triplet state of chloropentafluoroacetone can be estimated from a comparison of the onset of the phosphorescence (380 nm) and the fluorescence (337 nm) (17) as about 9 kcal. A further estimate of 8 kcal for the singlet–triplet splitting may be made from the comparison of the maximum in the phosphorescence and the fluorescence (460 and 408 nm, respectively, in the uncorrected spectra). Since the energy of the first excited singlet state of chloropentafluoroacetone is about 83 kcal, this places the energy of the triplet at about 74 kcal.

The singlet and triplet energies of chloropentafluoroacetone can be compared to those of hexafluoroacetone and contrasted to those of acetone. The energy of the singlet state of acetone was estimated (4) as about 80 $\pm$ 4 kcal from the absorption and fluorescence spectra which do not overlap in the gas phase. The triplet state of acetone is estimated (6) at 77 kcal from phosphorescence studies and at 80 kcal from kinetic data (7). The energies of the singlet and triplet states of hexafluoroacetone are about 83 and 74 kcal, respectively (8). Thus the triplet states of chloropentafluoroacetone and hexafluoroacetone are about 9 kcal lower than the singlet states whereas the triplet–singlet splitting in acetone is probably smaller. The photochemistry of chloropentafluoroacetone is expected to be similar to that of hexafluoroacetone. For example, electronically excited hexafluoroacetone reacts with fluorinated olefins in the gas phase to form oxetanes (9, 10) and the chloroketone might be expected to form oxetanes under similar conditions.

In the determination of the phosphorescence lifetimes of chloroketone and hexafluoroacetone, good exponential decays were observed at the times when the scattered light from the flash was negligible. Table 1 collects the data for chloroketone and hexafluoroacetone and the literature data for acetone for experiments at 77 °K. The lifetime of the chloroketone depends on the environment, as expected, (e.g. the lifetimes in the pure solids are about 1.7 times as long as those in the polar EPA solvent).

The emission spectra as a function of wavelength for chloropentafluoroacetone and hexafluoroacetone at 77 °K are almost identical, so the relative quantum yields of phosphorescence can be simply determined from the relative intensities of the emissions. The concentrations were such that the amount of light absorbed by both ketones was the same. The spectra were recorded while the phosphoroscope was operating so that only the long-lived emission was detected. (The triplet lifetimes of the ketones at 77 °K were different, and the apparent relative yields were corrected for the phosphoroscope factor). The

TABLE 1

Triplet state lifetimes at 77 °K

Ketone	Solvent	Lifetime (ms)
0.02 *M* Chloropentafluoroacetone	3-Methyl pentane	3.1
0.02 *M* Chloropentafluoroacetone	EPA	4.7
Chloropentafluoroacetone crystals	—	7.8
0.06 *M* Hexafluoroacetone	3-Methyl pentane	6.6
Acetone	EPA	0.6*
Acetone	EPA	0.33†
0.2 *M* Acetone	Ether–isopropanol	0.4‡
0.2 *M* Acetone	Glycerine	0.3‡
Acetone crystals	—	1.0‡

*Reference 11.
†Reference 12.
‡Reference 4.

ratio of the phosphorescence quantum yield of chloropentafluoroacetone, ϕ_p^C, to that of hexafluoroacetone, ϕ_p^H, is 0.82 in 3-methyl pentane at 77 °K. The ratio k_r^C/k_r^H ($= \phi_p^C\phi_{i.s.c.}^H\tau_p^H/\phi_p^H\phi_{i.s.c.}^C\tau_p^C$) can be estimated if $\phi_{i.s.c.}^C/\phi_{i.s.c.}^H$ is assumed to be unity. This is reasonable since $\phi_{i.s.c.}$ in acetone is 1.0 ± 0.1 (4). The effect of substituting a chlorine atom in hexafluoroacetone is to alter the radiative rate from the triplet state by a factor of about 1.7. This effect on the radiative rate constant from the triplet state of the fluorinated ketone can be compared with that on the singlet state where the radiative rate constant is increased (17) by about 2.7.

The calculations of Carroll, Vanquickenborne, and McGlynn (1) concern the radiative rate constants for aliphatic carbonyl compounds in which the heavy atom is substituted directly on the carbonyl group. For the dihalogenated formaldehydes they show that the radiative rate constants from the triplet state should be greater for Br_2CO and I_2CO than for H_2CO, F_2CO, and Cl_2CO. Shimada and Kanda (5) calculated the matrix elements of the spin orbit interaction in glyoxal and its halogenated derivatives to interpret the experimental behavior of the forbidden singlet to triplet absorption in oxalyl chloride ($f = 2.7 \times 10^{-7}$) and oxalyl bromide ($f = 3 \times 10^{-6}$). The experimental data presented above on the fluorinated ketones support the proposal of El-Sayed (3) that the internal heavy atom effect on the radiative rate constant from the triplet state of aliphatic ketones is small when the substitution is not directly on the carbonyl group.

The value of k_r^H has been determined as 37 s^{-1} from gas phase measurements at room temperature (13). If there is a negligible effect of temperature and phase on k_r^H then k_r^C is 65 s^{-1}. These values for the fluorinated acetones can be compared to the data obtained recently by O'Sullivan and Testa (12) on alkyl substituted acetones in EPA at 77 °K. They showed that the radiative rate constant from the triplet state only varied between about 70 and 120 s^{-1} in the ketones studied.

From the actual phosphorescent lifetimes the non-radiative rate constants from the triplet state in 3-methyl pentane at 77 °K can be obtained; $k_{nr}^H = 115$ s^{-1} and $k_{nr}^C = 260$ s^{-1}. The substitution of a chlorine atom in the fluorinated ketone has increased the non-radiative rate constant by a factor of about 2.3. In contrast, when bromine and iodine atoms are substituted in acetone the triplet lifetime at 77 °K is too small to measure (11).

O'Sullivan and Testa (12) found that replacing the α-hydrogens in acetone by alkyl substituents decreased the radiationless rate constant from the triplet state. They tentatively proposed that a major feature governing the radiationless rate constant is the energy of the C—H stretching vibration. That is consistent with the data on hexafluoroacetone and chloropentafluoroacetone since the energies of the C—F vibration (1100 cm^{-1}) and the C—Cl vibration (650 cm^{-1}) are much lower than the energy of the C—H vibration (2900 cm^{-1}) (14).

Although phosphorescence of chloropentafluoroacetone is prominent at 77 °K in 3-methyl pentane no phosphorescence was observed in the gas phase at room temperature (17). Similar behavior is exhibited by many other molecules e.g. cyclopentanone (15) and benzene (11, 16) and indicates that there is a large increase in the non-radiative processes with the change in environment and temperature.

We thank the National Research Council of Canada for financial support and Dr. J. D. Laposa and Dr. J. J. McCullough for the use of the spectrometers.

1. D. G. Carroll, L. Vanquickenborne, and S. P. McGlynn. J. Chem. Phys. **45**, 2777 (1966).
2. H. Shimada and Y. Kanda. Bull. Chem. Soc. Japan. **40**, 2742 (1967).
3. M. F. A. El-Sayed. J. Chem. Phys. **41**, 2462 (1964).
4. R. F. Borkman and D. R. Kearns. J. Chem. Phys. **44**, 945 (1966).
5. H. S. Shimada, R. S. Shimada, and Y. Kanda. Spectrochim. Acta, **23A**, 2821 (1967).
6. W. A. Noyes, Jr., G. B. Porter, and J. E. Jolley. Chem. Rev. **56**, 49 (1956).
7. H. E. O'Neal and C. W. Larson. J. Phys. Chem. **73**, 1011 (1969).
8. A. Gandini and K. O. Kutschke. Proc. Roy. Soc. Ser. A, **306**, 511 (1968).
9. E. W. Cook and B. F. Landrum. J. Heterocyclic Chem. **2**, 327 (1965).
10. R. H. Knipe, A. S. Gordon, and W. R. Ware. J. Chem. Phys. **51**, 840 (1969).
11. D. S. McClure. J. Chem. Phys. **17**, 905 (1949).
12. M. O'Sullivan and A. C. Testa. J. Amer. Chem. Soc. **92**, 258 (1970).
13. A. Gandini, D. A. Whytock, and K. O. Kutschke. Proc. Roy. Soc. Ser. A, **306**, 541 (1968).
14. G. Herzberg. Infrared and Raman spectra. D. Van Nostrand, New York. (1945).
15. S. R. Lapaglia and B. C. Rocquitte. Can. J. Chem. **41**, 287 (1963).
16. G. B. Kistiakowsky and C. S. Parmenter. J. Chem. Phys. **42**, 2942 (1965).
17. H. S. Samant and A. J. Yarwood. Can. J. Chem. **48**, 2611 (1970).

Can. J. Chem. Downloaded from www.nrcresearchpress.com by 210.87.254.40 on 09/05/12
For personal use only.

Structure of an artifact formed during isolation of *Penicillium gladioli* metabolites[1]

A. N. STARRATT

Research Institute, Canada Department of Agriculture, University Sub Post Office, London 72, Ontario

Received April 6, 1970

A new compound obtained from extracts of *Penicillium gladioli* has been shown to be 3-ethoxy-4-hydroxymethyl-7-methoxy-6-methyl phthalide, an artifact formed from dihydrogladiolic acid during isolation.

Canadian Journal of Chemistry, 48, 2940 (1970)

Can. J. Chem. Downloaded from www.nrcresearchpress.com by 210.87.254.42 on 09/05/12
For personal use only.

An alteration in the usual method (1) employed for the isolation of gladiolic acid (**1**) and dihydrogladiolic acid (**2**) (2, 3), required for biochemical studies, from *Penicillium gladioli* McCull. and Thom, led to the formation of a new substance. The charcoal used to adsorb the metabolites in the culture filtrate was treated with boiling ether and a neutral compound, $C_{13}H_{16}O_5$, was obtained for which structure **3** is proposed. It yielded a monoacetyl (**4**) and a monobenzoyl (**5**) derivative. The close relationship of this substance to dihydrogladiolic acid was apparent from the nuclear magnetic resonance (n.m.r.) spectrum (see Experimental), which had bands attributable to methyl, methoxyl, and hydroxymethyl groups as well as a proton on an aromatic nucleus. Upon acetylation or benzoylation, the signal, a singlet at δ 4.70, assigned to the methylene protons of the benzylic alcohol grouping, showed the expected downfield shift; however, it appeared as a quartet indicating non-equivalence of the two protons due to restricted rotation. The neutral compound upon heat or acid treatment rearranged (2) with loss of ethanol to deoxygladiolic acid (dihydrogladiolide, **6**) under conditions analogous to those used by Raistrick and Ross (4) to obtain the same product from dihydrogladiolic acid. Also, the neutral compound was hydrolyzed easily by hot water giving dihydrogladiolic acid.

The presence of an ethoxyl group was indicated by the occurrence in the n.m.r. spectrum of a triplet (3H) at δ 1.33 and a complex multiplet (2H) at δ 3.95, partly obscured by the methoxyl band, with a pattern typical of methylene protons of an ethoxyl group attached to an asymmetric center (5). Oxidation of the neutral compound with chromium trioxide – pyridine complex (6) yielded an aldehyde identified by melting point and spectra as 3-ethoxy-4-formyl-7-methoxy-6-methyl phthalide (gladiolic acid pseudo-ethyl ester, **7**) (1, 7).

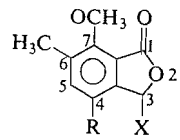

1 R = CHO; X = OH
2 R = CH_2OH; X = OH
3 R = CH_2OH; X = OC_2H_5
4 R = CH_2OAc; X = OC_2H_5
5 R = CH_2OBz; X = OC_2H_5
6 R = CHO; X = H
7 R = CHO; X = OC_2H_5

On the basis of these results the neutral compound is proposed to be 3-ethoxy-4-hydroxymethyl-7-methoxy-6-methyl phthalide (**3**). It can be obtained from dihydrogladiolic acid under the conditions of the original isolation but was not observed when the metabolites were eluted, under milder conditions, from the charcoal in a Soxhlet apparatus. This indicates that **3** is an artifact apparently formed during lengthy contact of dihydrogladiolic acid with the charcoal in boiling ether. As expected, dihydrogladiolic acid was unchanged by treatment with boiling ether in the absence of charcoal.

Experimental

Melting points are uncorrected and were determined on a Kofler hot stage or Büchi melting point apparatus. Infrared (i.r.) spectra were obtained on a Perkin–Elmer model 21 spectrometer and n.m.r. spectra were obtained, in $CDCl_3$ unless otherwise stated, with a Varian A-60A spectrometer using TMS as internal standard. The molecular weight was determined with a Varian M-66 mass spectrometer. Kieselgel (Camag) containing fluorescent indicator was used for thin-layer chromatography (t.l.c.). Microanalyses were performed by Dr. C. Daesslé, Montreal, Quebec.

[1]Contribution No. 446.

Can. J. Chem. Downloaded from www.nrcresearchpress.com by 210.87.254.42 on 09/05/12
For personal use only.

Isolation of the Neutral Compound (3)

The conditions used to culture *Penicillium gladioli* McCull. and Thom were those described by Grove (1). The culture filtrate (15 l) was adjusted to p*H* 4.0 and treated with activated charcoal (British Drug Houses; 5 g/l). The charcoal was removed by filtration, dried, and treated with boiling ether for 15 h. After removal of the charcoal, the ether extract was shaken with 5% sodium bicarbonate solution to remove gladiolic and dihydrogladiolic acids and with 5% sodium hydroxide solution to remove phenols. The ether was evaporated and the residue (5.25 g) recrystallized from ether – isopropyl ether to yield as needles a substance identified as 3-ethoxy-4-hydroxymethyl-7-methoxy-6-methyl phthalide (**3**), m.p. 80–81°; ν_{max} (KBr) 3475, 1762, 1602 cm^{-1}; δ 1.33 (triplet, J = 7 Hz, 3H, $-OCH_2CH_3$), 2.32 (singlet, 3H, $ArCH_3$), 2.66 (broad band, 1H, hydroxyl proton), 3.95 (multiplet, 2H, $-OCH_2CH_3$), 4.05 (singlet, 3H, $-OCH_3$), 4.70 (singlet, 2H, $ArCH_2O$), 6.36 (singlet, 1H, $ArCH(=O)$), 7.48 (singlet, 1H, Ar*H*); mass spectrum: M^+, 252.

Anal. Calcd. for $C_{13}H_{16}O_5$: C, 61.89; H, 6.39. Found: C, 62.23; H, 6.47.

Dihydrogladiolic acid was isolated in good yield and neutral compound **3** was not obtained when the charcoal was eluted in a Soxhlet apparatus.

Acetate 4

The neutral compound (112 mg) was treated with acetic anhydride – pyridine (1:2) for 3 h at room temperature. After addition of water the product was extracted into chloroform. Recrystallization of the product from isopropyl ether gave the acetate (**4**), m.p. 46–48°; ν_{max} (CCl_4) 1773, 1744 cm^{-1}; δ (CCl_4) 1.31 (triplet, J = 7 Hz, 3H, $-OCH_2CH_3$), 2.03 (singlet, 3H, —OAc), 2.29 (singlet, 3H, $ArCH_3$), 3.88 (multiplet, 2H, $-OCH_2CH_3$), 4.13 (singlet, 3H, $-OCH_3$), 5.07 (quartet, 12.5 Hz, 2H, $ArCH_2O$), 6.27 (singlet, 1H, $ArCH(=O)$), 7.37 (singlet, 1H, Ar*H*).

Anal. Calcd. for $C_{15}H_{18}O_6$: C, 61.21; H, 6.17. Found: C, 61.64; H, 6.17.

Benzoate 5

The neutral compound (34 mg) in pyridine was treated with benzoyl chloride for 75 min at room temperature. The product, isolated in the manner described for the acetate, was filtered through Woelm alumina (Grade I; 3 g) and crystallized from an acetone – aqueous ethanol mixture to give the benzoate (**5**) as plates, m.p. 68–70°; ν_{max} (KBr) 1774, 1722 cm^{-1}; δ 1.29 (triplet, J = 7 Hz, 3H, $-OCH_2CH_3$), 2.33 (singlet, 3H, $ArCH_3$), 3.92 (multiplet, 2H, $-OCH_2CH_3$), 4.11 (singlet, 3H, $-OCH_3$), 5.41 (quartet, 12.5 Hz, 2H, $ArCH_2O$), 6.43 (singlet, 1H, $ArCH(=O)$), 7.55 (singlet, 1H, Ar*H*), 7.41–8.16 (multiplet, 5H, —OBz).

Anal. Calcd. for $C_{20}H_{20}O_6$: C, 67.40; H, 5.66. Found: C, 67.50; H, 5.50.

Deoxygladiolic Acid (6) from Neutral Compound 3

(*a*) The neutral compound (52 mg) was heated *in vacuo* (25 mm Hg) at 155° for 22 h yielding a sublimate (27 mg) which was recrystallized from chloroform–methanol giving needles identified as deoxygladiolic acid (**6**), m.p. (capillary) 174–175°; ν_{max} (KBr) 1755, 1694, 1592 cm^{-1}; δ 2.41 (singlet, 3H, $ArCH_3$), 4.28 (singlet, 3H, $-OCH_3$), 5.56 (singlet, 2H, $ArCH_2O$), 7.92 (singlet, 1H, Ar*H*), 10.03 (singlet, 1H, —CHO). Raistrick and Ross (4) report m.p. 172.5–173° for deoxygladiolic acid (dihydrogladiolide).

(*b*) The neutral compound (22 mg) was dissolved in dioxane (3 ml) containing 2% (v/v) sulfuric acid and the mixture allowed to stand (nitrogen atmosphere) at room temperature for 1.5 h. After dilution with water the product was extracted into ether. Separation by preparative t.l.c. (chloroform–methanol, 49:1 v/v) gave deoxygladiolic acid (7 mg) identical with that described above. A small amount of deoxygladiolic acid was formed when the neutral compound (34 mg) was heated on the steam bath in acetic acid (3 ml) and water (3 ml).

Hydrolysis of the Neutral Compound 3

The neutral compound (39 mg) was converted quantitatively to a single substance (t.l.c. evidence) by heating in water (10 ml) for 15 min on the steam bath. Removal *in vacuo* of part of the water yielded needles of dihydrogladiolic acid (**2**), m.p. 135–137° (dec.), ν_{max} (KBr) 3340, 1717 cm^{-1}, which was identical with that obtained from the culture filtrate. The n.m.r. spectrum of this compound in acetic acid-d_4 showed signals at δ 2.32 (singlet, 3H, $ArCH_3$), 4.02 (singlet, 3H, $-OCH_3$), 4.82 (singlet, 2H, $ArCH_2O$), 6.68 (singlet, 1H, $ArCH(=O)$), 7.59 (singlet, 1H, Ar*H*).

Oxidation of Neutral Compound 3

The neutral compound (45 mg) in pyridine (1 ml) was added to chromium trioxide (55 mg) in pyridine (1 ml). After 18 h at room temperature, water was added and the product extracted into ether. Recrystallization of the product from chloroform – isopropyl ether and then from chloroform–ethanol gave the aldehyde (**7**), needles, m.p. 109–110°; ν_{max} (KBr) 1774, 1701, 1610 cm^{-1}; δ 1.32 (triplet, J = 7 Hz, 3H, $-OCH_2CH_3$), 2.38 (singlet, 3H, $ArCH_3$), 4.04 (multiplet, 2H, $-OCH_2CH_3$), 4.28 (singlet, 3H, $-OCH_3$), 6.62 (singlet, 1H, $ArCH(=O)$), 7.96 (singlet, 1H, Ar*H*), 10.12 (singlet, 1H, —CHO). Grove (1, 7) reports m.p. 105° and ν_{max} (nujol) 1770, 1705 cm^{-1} for the pseudo-ethyl ester of gladiolic acid.

Preparation of 3 from Dihydrogladiolic Acid (2)

Dihydrogladiolic acid (47 mg) was dissolved in water (10 ml) and treated with activated charcoal (B.D.H.; 213 mg). The charcoal was removed by filtration, dried, and extracted twice with boiling ether (40 ml) for periods of 16 and 20 h. The materials contained in the first (22 mg) and second (11 mg) extracts were combined in ether and acidic components removed by washing with 3% sodium bicarbonate solution. After removal of the ether, the neutral fraction (21 mg) was crystallized from ether – isopropyl ether to give pure **3** (6 mg), identical (t.l.c.,

m.p., mixture m.p.) with that described above. Neutral compound **3** was not produced (t.l.c. evidence) when dihydrogladiolic acid (8 mg) was treated with boiling ether (15 ml) for 21 h in the absence of charcoal.

The author wishes to thank Dr. G. A. White for kindly providing the crude culture extracts, the technical staff of the Chemistry Department, University of Western Ontario, London, Ontario, for obtaining the mass spectrum, and Mrs. M. E. Stevens for technical assistance.

1. J. F. GROVE. Biochem. J. **50**, 648 (1952).
2. L. A. DUNCANSON, J. F. GROVE, and J. ZEALLEY. J. Chem. Soc. 3637 (1953).
3. J. J. BROWN and G. T. NEWBOLD. J. Chem. Soc. 3648 (1953).
4. H. RAISTRICK and D. J. ROSS. Biochem. J. **50**, 635 (1952).
5. P. DE MAYO, R. E. WILLIAMS, and E. Y. SPENCER. Can. J. Chem. **43**, 1357 (1965).
6. J. R. HOLUM. J. Org. Chem. **26**, 4814 (1961).
7. J. F. GROVE. J. Chem. Soc. 3345 (1952).

Can. J. Chem. Downloaded from www.nrcresearchpress.com by 210.87.254.42 on 09/05/12
For personal use only.

The limiting high-pressure rate constant for the thermal isomerization of methyl isocyanide

C. K. YIP AND H. O. PRITCHARD
Centre for Research in Experimental Space Science, York University, Downsview, Ontario

Received April 20, 1970

The rate of the thermal isomerization of methyl isocyanide is reduced by about 20% when the system is pressurized with 100 atm of propane, but is unaffected when the system is pressurized with carbon dioxide. It is suggested that these observations can be explained by the presence of a concurrent free-radical catalyzed isomerization.

Canadian Journal of Chemistry, **48**, **2942** (1970)

Introduction

Traces of methane and hydrogen cyanide are formed during the thermal isomerization of methyl isocyanide at 200 °C. Both substances are formed in similar amounts, to the extent of 0.1–0.5% of the methyl cyanide produced. These by-products were identified by their gas-chromatographic retention times together with high-resolution mass-spectrographic analysis of the corresponding portions of the chromatographic effluent.

If the formation of methane involves the presence of methyl radicals, then the thermal decomposition of the isocyanide

[1] $$CH_3NC \rightarrow CH_3CN$$

must have a substantial chain component, since the reaction

[2] $$CH_3NC + CH_3 \rightarrow CH_3 + CH_3CN$$

is known to have a long chain-length at high isocyanide concentrations (1). In this note, we describe the effect of adding large quantities of a radical trapping agent, propane, to the reacting isocyanide.

Materials and Experimental Technique

The preparation and/or purification of methyl isocyanide (1), ethyl isocyanide (1), propane (2), and carbon dioxide (3) have been described previously.

Experiments were carried out in a manner which we have already described (2, 3) using a pair of stainless-steel cylindrical pressure vessels (volume 12 cc, approximately 10 cm long). All runs were carried out at 200 °C, the lowest of the three temperatures used by Schneider and Rabinovitch (4), since the apparatus, which was not designed for this experiment, could not be used above 210 °C. A quantity of about 4×10^{-5} mole of isocyanide was used in each experiment, either alone, or pressurized with propane or carbon dioxide up to pressures of about 100 atm; all reactions were of 30 min duration, and at no time in the whole series of experiments was air or moisture admitted to the reaction vessels.

The analytical procedure was as follows. The contents of the reaction vessel were condensed out at liquid nitrogen temperature, any methane escaping being trapped in silica gel, also held at −195 °C: the reaction products were then raised to −160 °C to complete the collection of methane in the silica-gel trap; the methane was desorbed by warming, and measured chromatographically using a silica-gel column. The bulk of the propane (or carbon dioxide) was then removed at −130 °C using two LeRoy stills as described previously (2, 3): the remaining mixture was analyzed using a 12 ft silicone oil/chromosorb chromatographic column, the residual propane being eluted at 0 °C, the hydrogen cyanide at 35 °C, and the isocyanide–cyanide mixture at 90 °C.

m.p., mixture m.p.) with that described above. Neutral compound **3** was not produced (t.l.c. evidence) when dihydrogladiolic acid (8 mg) was treated with boiling ether (15 ml) for 21 h in the absence of charcoal.

The author wishes to thank Dr. G. A. White for kindly providing the crude culture extracts, the technical staff of the Chemistry Department, University of Western Ontario, London, Ontario, for obtaining the mass spectrum, and Mrs. M. E. Stevens for technical assistance.

1. J. F. GROVE. Biochem. J. **50**, 648 (1952).
2. L. A. DUNCANSON, J. F. GROVE, and J. ZEALLEY. J. Chem. Soc. 3637 (1953).
3. J. J. BROWN and G. T. NEWBOLD. J. Chem. Soc. 3648 (1953).
4. H. RAISTRICK and D. J. ROSS. Biochem. J. **50**, 635 (1952).
5. P. DE MAYO, R. E. WILLIAMS, and E. Y. SPENCER. Can. J. Chem. **43**, 1357 (1965).
6. J. R. HOLUM. J. Org. Chem. **26**, 4814 (1961).
7. J. F. GROVE. J. Chem. Soc. 3345 (1952).

Can. J. Chem. Downloaded from www.nrcresearchpress.com by 210.87.254.105 on 09/05/12
For personal use only.

The limiting high-pressure rate constant for the thermal isomerization of methyl isocyanide

C. K. YIP AND H. O. PRITCHARD
Centre for Research in Experimental Space Science, York University, Downsview, Ontario

Received April 20, 1970

The rate of the thermal isomerization of methyl isocyanide is reduced by about 20% when the system is pressurized with 100 atm of propane, but is unaffected when the system is pressurized with carbon dioxide. It is suggested that these observations can be explained by the presence of a concurrent free-radical catalyzed isomerization.

Canadian Journal of Chemistry, **48**, **2942** (1970)

Introduction

Traces of methane and hydrogen cyanide are formed during the thermal isomerization of methyl isocyanide at 200 °C. Both substances are formed in similar amounts, to the extent of 0.1–0.5% of the methyl cyanide produced. These by-products were identified by their gas-chromatographic retention times together with high-resolution mass-spectrographic analysis of the corresponding portions of the chromatographic effluent.

If the formation of methane involves the presence of methyl radicals, then the thermal decomposition of the isocyanide

[1] $$CH_3NC \rightarrow CH_3CN$$

must have a substantial chain component, since the reaction

[2] $$CH_3NC + CH_3 \rightarrow CH_3 + CH_3CN$$

is known to have a long chain-length at high isocyanide concentrations (1). In this note, we describe the effect of adding large quantities of a radical trapping agent, propane, to the reacting isocyanide.

Materials and Experimental Technique

The preparation and/or purification of methyl isocyanide (1), ethyl isocyanide (1), propane (2), and carbon dioxide (3) have been described previously.

Experiments were carried out in a manner which we have already described (2, 3) using a pair of stainless-steel cylindrical pressure vessels (volume 12 cc, approximately 10 cm long). All runs were carried out at 200 °C, the lowest of the three temperatures used by Schneider and Rabinovitch (4), since the apparatus, which was not designed for this experiment, could not be used above 210 °C. A quantity of about 4×10^{-5} mole of isocyanide was used in each experiment, either alone, or pressurized with propane or carbon dioxide up to pressures of about 100 atm; all reactions were of 30 min duration, and at no time in the whole series of experiments was air or moisture admitted to the reaction vessels.

The analytical procedure was as follows. The contents of the reaction vessel were condensed out at liquid nitrogen temperature, any methane escaping being trapped in silica gel, also held at −195 °C: the reaction products were then raised to −160 °C to complete the collection of methane in the silica-gel trap; the methane was desorbed by warming, and measured chromatographically using a silica-gel column. The bulk of the propane (or carbon dioxide) was then removed at −130 °C using two LeRoy stills as described previously (2, 3): the remaining mixture was analyzed using a 12 ft silicone oil/chromosorb chromatographic column, the residual propane being eluted at 0 °C, the hydrogen cyanide at 35 °C, and the isocyanide–cyanide mixture at 90 °C.

Can. J. Chem. Downloaded from www.nrcresearchpress.com by 210.87.254.105 on 09/05/12
For personal use only.

Results

First, a comparison was made between unpressurized experiments in metal and in glass vessels at (a nominal) 200 °C. The mean of six experiments in glass vessels gave $k_1 = (6.35 \pm 0.15) \times 10^{-5}$ s^{-1}, whilst four experiments in metal vessels gave $k_1 = (6.50 \pm 0.15) \times 10^{-5}$ s^{-1}; Schneider and Rabinovitch (4) found $k_1 \approx 7.0 \times 10^{-5}$ s^{-1} at about the same temperature and pressure.

In the presence of high pressures of propane, the rate constant was significantly reduced, and the following is a summary of the observed rate constants expressed as a fraction of that observed in the unpressurized reactions: 1 atm C_3H_8, 1.04; 25 atm C_3H_8, 0.89, 0.91; 75 atm C_3H_8, 0.80, 0.81; 100 atm C_3H_8, 0.80, 0.75, 0.75, 0.83, 0.80. This decrease in apparent rate constant could have been due to preferential losses of methyl cyanide in the analytical procedure, but tests on synthetic cyanide/isocyanide mixtures showed that even in the presence of 100 atm of propane, the cyanide and isocyanide were recoverable with an accuracy of ±5% in their ratio.[1] This conclusion is reinforced by a parallel set of experiments using carbon dioxide instead of propane, when the rate constants relative to unpressurized runs were: 10 atm CO_2, 1.00; 30 atm CO_2, 1.01, 1.05; 100 atm CO_2, 0.97, 1.03, 0.97. Thus, the rate constant is unchanged by the addition of 100 atm of carbon dioxide. The formation of traces of methane and hydrogen cyanide persisted through both sets of high-pressure experiments. No ethane (detection limit ~10% of the methane formed) was found in any experiment, and it should also be noted that in the propane experiments, we did not positively identify any of the possible secondary radical products i.e. butanes, hexanes, or isopropyl cyanide.

A similar reduction in the rate of isomerization of ethyl isocyanide was observed when the reaction was carried out at 200 °C in the presence of 100 atm of propane; however, further study of this reaction was not undertaken.

[1]One needs only two quantities, the time and the cyanide/isocyanide ratio to determine k_1. Since every run was of the same duration, warm-up time uncertainties (3) are eliminated, hence the accuracy of values of k_1 obtained in pressurized experiments may be put conservatively at ±5% for purposes of comparison with each other.

Discussion

The difference in behavior of propane and carbon dioxide as pressurizing gases is clearly consistent with the supposition that the thermal isomerization of methyl isocyanide occurs by two parallel reaction paths [1] and [2]. So is the persistence of methane formation at high propane pressures, since reaction [2] neither consumes nor generates methyl radicals: thus, all that happens is that in the presence of propane, the methyl radicals are converted to methane before they have had a chance to catalyze the isomerization via reaction [2]. An analysis of the effect of propane on this reaction requires (at least) the following unknown information: (*i*) the rate of abstraction of hydrogen from methyl isocyanide by methyl radicals; (*ii*) some characterization of how methyl (and presumably also CN) radicals appear in the system; (*iii*) a knowledge as to whether there is an analogous CN-catalyzed isomerization route[2]

[3] $$CN + CH_3NC \rightarrow CH_3CN + CN$$

or

[3*a*] $$CH_3NC + CN \rightarrow CH_3 + C_2N_2$$

(*iv*) the rate of propyl-radical analogue of reaction [2].

A steady-state treatment of the reaction scheme [1] and [2], even excluding [3] and [3*a*], shows that there are many plausible combinations of the known and the unknown parameters for which the apparent rate constant k_1 would tend to diverge as $[CH_3NC]$ increases. And in fact, if the data of Schneider and Rabinovitch (4) are plotted in the form of k_1 vs. $[CH_3NC]^{-1}$ there is some evidence of incipient divergence both at 200 and 230 °C; in contrast, k_1 is unchanged when the reaction is pressurized with carbon dioxide, and reduced by about 20% when pressurized with propane.

Three conclusions emerge: (*i*) the carbon dioxide experiments confirm Schneider and Rabinovitch's conclusion that self-heating is unimportant under these conditions; (*ii*) they also

[2]Reaction [3*a*] seems more likely in view of the unsaturated nature of the isocyanide group, but we never found any cyanogen in any of our reaction mixtures. B. K. Dunning of this laboratory has looked for evidence of reactions [3] and [3*a*] by photolyzing ICN (5) in the presence of CH_3NC; however, addition reactions (1) obscured all other processes, and no conclusions were reached.

suggest that reaction [1] is already at its high-pressure limit at a $[CH_3NC]$ concentration of 4×10^{-5} moles in 12 cc, i.e. 1.3 atm at 200 °C; (*iii*) the propane experiments show that at 200 °C, the high-pressure limiting rate constant $k_\infty \approx 5 \times 10^{-5}$ s^{-1} rather than the value 7.5×10^{-5} s^{-1} chosen by Schneider and Rabinovitch.

In view of the fact that over the past 10 years, the isocyanide (particularly methyl isocyanide) isomerization reaction has achieved central importance in the unimolecular reaction field (6), we believe it is urgent that independent corroboration of our results be obtained. If our findings are confirmed, then it would appear that history is repeating itself. The development of the theory of unimolecular reactions in the 1930's received considerable stimulus from the experimental study of a number of thermal reactions which were thought to be unimolecular reactions, but which eventually turned out to be free-radical chain reactions (7). Similarly, in the 1960's, theoretical advances have been stimulated by the study of the thermal isomerization of isocyanides; in this case, however, there is no doubt that these reactions do exhibit unimolecular reaction characteristics, but it may be that they will be found unsuitable reactions against which to make *quantitative* tests of the theory.

1. D. H. SHAW and H. O. PRITCHARD. Can. J. Chem. **45**, 2749 (1967).
2. C. K. YIP and H. O. PRITCHARD. Can. J. Chem. **47**, 4708 (1969).
3. D. H. SHAW and H. O. PRITCHARD. Can. J. Chem. **46**, 2721 (1968).
4. F. W. SCHNEIDER and B. S. RABINOVITCH. J. Amer. Chem. Soc. **84**, 4215 (1962).
5. C. A. GOY, D. H. SHAW, and H. O. PRITCHARD. J. Phys. Chem. **69**, 1504 (1965).
6. D. L. BUNKER. Theory of elementary gas reaction rates. Pergamon, London. 1966. Chap. 3.
7. A. F. TROTMAN-DICKENSON. Gas kinetics. Butterworths, London. 1955. p. 70.

Reinvestigation of the nature of the reactive intermediate in electrophilic bromine addition to styrenes

JAMES A. PINCOCK AND KEITH YATES
Department of Chemistry, University of Toronto, Toronto 5, Ontario

Received April 28, 1970

The rate constants for the electrophilic addition of bromine to a series of ring-substituted styrenes have been redetermined. The new ρ^+ value of -4.71 is discussed in terms of the intermediate involved for these substrates.

Canadian Journal of Chemistry, **48**, **2944** (1970)

It has been previously reported from this laboratory (1), that the rates of electrophilic addition of molecular bromine to a series of ring-substituted styrenes in acetic acid followed eq. [1].

$$[1] \quad -\mathrm{d}\frac{(Br_2)}{dt} = k_2\,(\text{styrene})\,(Br_2)^2 + k_3\,(\text{styrene})\,(Br_2)^2$$

The k_2 values (Table 1) previously obtained by a spectrophotometric method were found to correlate well with the substituent constants with $\rho = -2.21$. This low value of ρ (compared to values of approximately -4.2 for the solvolysis of benzyl derivatives and the chlorination of cinnamic acids) and the correlation with σ rather than σ^+ were interpreted in terms of a transition state leading to a cyclic bromonium ion intermediate. The reported $\Delta S^{\ddagger}$ values of approximately -30 e.u. were also in agreement with this interpretation.

However, in a more recent study by Rolston and Yates (2), values of k_2 were also reported for the reaction of bromine with a similar series of substituted styrenes. These values were obtained by measuring k_{obs} by a potentiometric method, as a function of [LiBr], and extrapolating to zero [LiBr] using eq. [2], where K is the equilibrium

$$[2] \quad (1 + K[\text{LiBr}])\,k_{obs} = k_2 + k_{Br_3^-}K[\text{LiBr}]$$

constant for tribromide ion formation (2). In this case values of k_2 (Table 1) either at ionic strength of 0.10 (kept constant by added $LiClO_4$) or at zero

Can. J. Chem. Downloaded from www.nrcresearchpress.com by 210.87.254.105 on 09/05/12
For personal use only.

suggest that reaction [1] is already at its high-pressure limit at a $[CH_3NC]$ concentration of 4×10^{-5} moles in 12 cc, i.e. 1.3 atm at 200 °C; (*iii*) the propane experiments show that at 200 °C, the high-pressure limiting rate constant $k_\infty \approx 5 \times 10^{-5}$ s^{-1} rather than the value 7.5×10^{-5} s^{-1} chosen by Schneider and Rabinovitch.

In view of the fact that over the past 10 years, the isocyanide (particularly methyl isocyanide) isomerization reaction has achieved central importance in the unimolecular reaction field (6), we believe it is urgent that independent corroboration of our results be obtained. If our findings are confirmed, then it would appear that history is repeating itself. The development of the theory of unimolecular reactions in the 1930's received considerable stimulus from the experimental study of a number of thermal reactions which were thought to be unimolecular reactions, but which eventually turned out to be free-radical chain reactions (7). Similarly, in the 1960's, theoretical advances have been stimulated by the study of the thermal isomerization of isocyanides; in this case, however, there is no doubt that these reactions do exhibit unimolecular reaction characteristics, but it may be that they will be found unsuitable reactions against which to make *quantitative* tests of the theory.

1. D. H. Shaw and H. O. Pritchard. Can. J. Chem. **45**, 2749 (1967).
2. C. K. Yip and H. O. Pritchard. Can. J. Chem. **47**, 4708 (1969).
3. D. H. Shaw and H. O. Pritchard. Can. J. Chem. **46**, 2721 (1968).
4. F. W. Schneider and B. S. Rabinovitch. J. Amer. Chem. Soc. **84**, 4215 (1962).
5. C. A. Goy, D. H. Shaw, and H. O. Pritchard. J. Phys. Chem. **69**, 1504 (1965).
6. D. L. Bunker. Theory of elementary gas reaction rates. Pergamon, London. 1966. Chap. 3.
7. A. F. Trotman-Dickenson. Gas kinetics. Butterworths, London. 1955. p. 70.

Reinvestigation of the nature of the reactive intermediate in electrophilic bromine addition to styrenes

James A. Pincock and Keith Yates
Department of Chemistry, University of Toronto, Toronto 5, Ontario

Received April 28, 1970

The rate constants for the electrophilic addition of bromine to a series of ring-substituted styrenes have been redetermined. The new ρ^+ value of -4.71 is discussed in terms of the intermediate involved for these substrates.

Canadian Journal of Chemistry, **48**, **2944** (1970)

It has been previously reported from this laboratory (1), that the rates of electrophilic addition of molecular bromine to a series of ring-substituted styrenes in acetic acid followed eq. [1].

$$[1] \quad -\mathrm{d}\frac{(Br_2)}{dt} = k_2\,(\text{styrene})\,(Br_2)^2 + k_3\,(\text{styrene})\,(Br_2)^2$$

The k_2 values (Table 1) previously obtained by a spectrophotometric method were found to correlate well with the substituent constants with $\rho = -2.21$. This low value of ρ (compared to values of approximately -4.2 for the solvolysis of benzyl derivatives and the chlorination of cinnamic acids) and the correlation with σ rather than σ^+ were interpreted in terms of a transition state leading to a cyclic bromonium ion intermediate. The reported $\Delta S^{\ddagger}$ values of approximately -30 e.u. were also in agreement with this interpretation.

However, in a more recent study by Rolston and Yates (2), values of k_2 were also reported for the reaction of bromine with a similar series of substituted styrenes. These values were obtained by measuring k_{obs} by a potentiometric method, as a function of [LiBr], and extrapolating to zero [LiBr] using eq. [2], where K is the equilibrium

$$[2] \quad (1 + K[\text{LiBr}])\,k_{obs} = k_2 + k_{Br_3^-}K[\text{LiBr}]$$

constant for tribromide ion formation (2). In this case values of k_2 (Table 1) either at ionic strength of 0.10 (kept constant by added $LiClO_4$) or at zero

Can. J. Chem. Downloaded from www.nrcresearchpress.com by 210.87.254.42 on 09/05/12
For personal use only.

TABLE 1

Second order rate constants, k_2, for the bromination of styrenes in acetic acid

Substituent	Temperature (°C)	$k_2 \times 10^2$ (M^{-1} s^{-1})* a	b	c	d
3-Cl	25.0	29.5	23	21.5±1.5	131
3,4-DiCl	25.0	12.3	8.9	11.1±1.0	65
	33.0	—	—	15.2±0.3	—
	40.0	—	—	19.4±0.4	—
	45.0	—	—	23.0±0.3	—
3-NO_2	25.0	6.2	1.2	0.961±0.005	6.7
4-NO_2	25.0	3.7	—	0.358±0.001	3.1
	45.0	11.8	—	0.995±0.006	—

*a, Values from ref. 1, ionic strength of 0.0; b, values from ref. 2, ionic strength of 0.0; c, present work, ionic strength of 0.0; d, values from ref. 2, ionic strength of 0.10.

ionic strength, correlated well with σ^+ giving ρ values of -1.21 and -4.26 respectively. Dubois and Schwarcs (3) have also obtained a ρ value of -4.30 for the bromination of styrenes in methanol at 0.20 *M* NaBr. Furthermore, results on the stereochemistry of the bromination of styrene derivatives (4, 5) showed that products are formed as a result of both *syn* and *anti* addition. This would not be expected from a cyclic bromonium ion intermediate. A weakly bridged intermediate lacking complete freedom of rotation was suggested, rather than an open ion, to account for the observation that product distributions were not independent of starting olefins (e.g. *cis*- or *trans*-β-methylstyrene).

No satisfactory explanation could be found for the large difference between the two ρ values based on either spectrophotometrically or potentiometrically obtained rate constants, since the only significant difference in the two investigations was the presence or absence of added electrolyte.

While studying the rates of bromine addition to some acetylenes (6, 7) by a spectrophotometric method, it became apparent that measurements made at 400 mμ, the maximum of the bromine absorbance band, did not always give reliable results. This was explained as follows. Additions to multiple bonds in nucleophilic solvents such as acetic acid often give solvent-incorporated products (8), and hence significant concentrations of HBr can be generated during the reaction. This complexes with the unreacted Br_2 to form tribromide ion. Since Br_3^- has a much higher extinction coefficient than Br_2 (in acetic acid, $\varepsilon_{Br_2} = 189$ and $\varepsilon_{Br_3^-} = 777$ at 390 mμ (2)), changes in optical density during reaction will no longer be directly proportional to changes in bromine concentration. An example of this effect is shown in Fig. 1 where plots of A/A_0 vs. time are given for the bromination of methylphenylacetylene at 400, 430, 460, and 480 mμ. By 480 mμ the effect of the tribromide absorbance has become negligible and hence rates can be measured at 490 mμ with confidence.

The results of Yates and Wright (1) had been obtained at 400 mμ (450 mμ for the nitrostyrenes). It therefore seemed possible that the unusual substituent plots from their data were a result of incorrect rate constants. The present method of obtaining k_2 values avoids the above difficulty (6) and, consequently, a re-evaluation of the k_2 values in acetic acid with no added electrolyte seemed desirable.

The k_2 values obtained[1] are given in Table 1. The results are the average of at least two determinations and the error quoted is the average deviation. The present k_2 values are in reasonably good agreement with those of Rolston and Yates (2), allowing for the experimental error involved in extrapolation to zero ionic strength. Furthermore, a salt effect of approximately seven is observed for all the compounds studied (whether spectrophotometrically or potentiometrically) compared with those at ionic strength of 0.10.

[1]At low bromine concentrations ($3 < 10^{-4}$ *M*) where the k_3 term in eq. [1] makes a negligible contribution to the total rate.

Can. J. Chem. Downloaded from www.nrcresearchpress.com by 210.87.254.42 on 09/05/12
For personal use only.

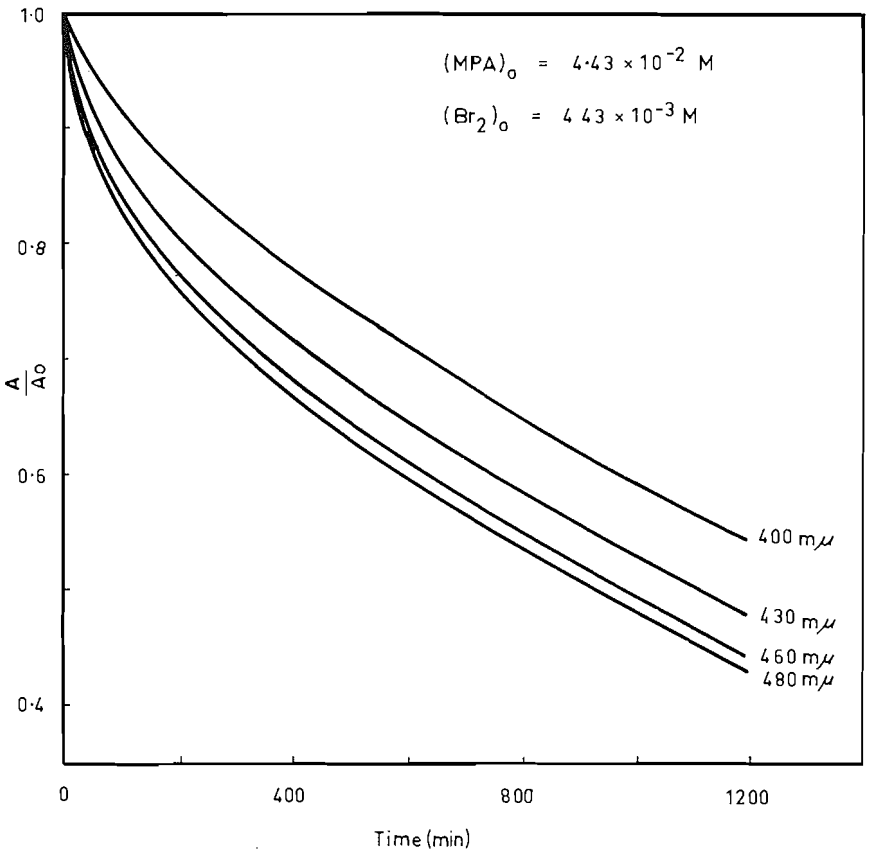

FIG. 1. Plots of A/A_0 vs. time (min) for the bromination of methylphenylacetylene in acetic acid at 400, 430, 460, and 480 mμ.

The results of Yates and Wright (1) fail to satisfy either of these requirements, especially those for the nitrostyrenes.

A plot of log k_2 vs. σ^+ (8) for the present values is given in Fig. 2.[2] The ρ value of -4.71 is in good agreement with those values obtained by Rolston and Yates (2) and Dubois and Schwarcs (3).

In view of the fact that the ρ value for the bromination of styrenes is now established as about -4.5, there no longer seems to be any justification for invoking cyclic bromonium ion transition states or intermediates for this type of substrate. The observation of different product distributions depending on whether the reactant is *cis*- or *trans*-β-methylstyrene (4, 5) is possibly a result of the differences in structure and reactivity of the initially formed ion pair intermediates, rather than a result of weak bridging. This revision of the mechanism for styrenes is important because several authors (4, 9, 10) have discussed in some detail the low ρ value of -2.2 reported earlier by Yates and Wright (1). Miller (9) has even stated that this type of kinetic study is an excellent way of demonstrating the importance of cyclic intermediates since the observation of *anti* stereospecific addition may only be consistent with, but not proof of, their existence.

Further, the activation parameters for 4-nitrostyrene ($\Delta H^{\ddagger} = 9.0$ kcal/mole, $\Delta S^{\ddagger} = -39$ e.u.) and 3,4-dichlorostyrene ($\Delta H^{\ddagger} = 6.1$ kcal/mole, $\Delta S^{\ddagger} = -42$ e.u.) were calculated from the rate constants in Table 1. The large negative $\Delta S^{\ddagger}$ values of approximately -30 e.u. reported previously (1) were reasonably interpreted in terms of a cyclic bromonium ion transition state. The values obtained here of -40 e.u. are even more negative and yet it now seems unlikely that cyclic

[2]The value of σ^+ for the 3,4-dichloro "substituent" was the same (0.476) as that used previously (2) for electrophilic addition of bromine to styrenes.

Can. J. Chem. Downloaded from www.nrcresearchpress.com by 210.87.254.42 on 09/05/12
For personal use only.

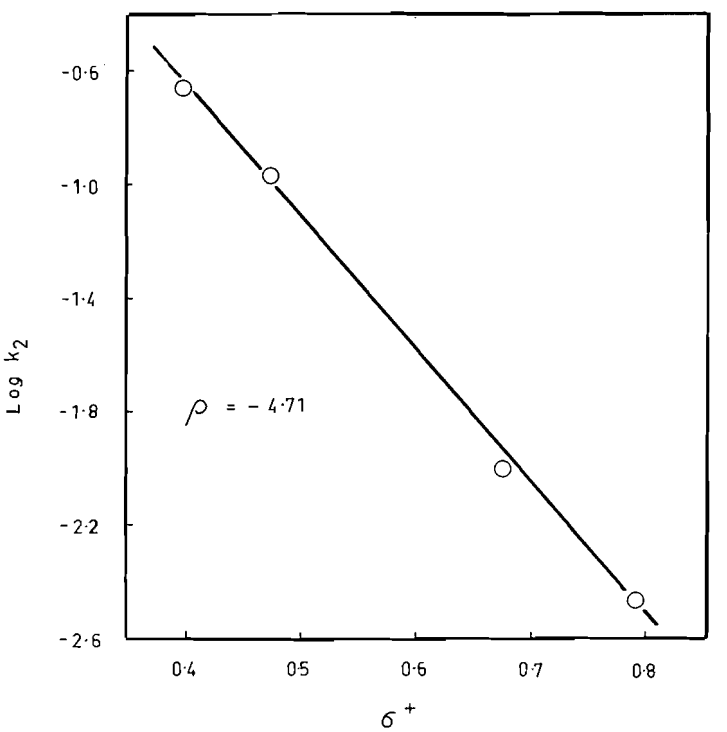

FIG. 2. Plot of log k_2 vs. σ^+ for the bromination of styrenes in acetic acid.

ion structures are important in these reactions. This further illustrates that large negative $\Delta S^{\neq}$ values in polar or ionic reactions are not necessarily a consequence of cyclic transition states.

Experimental

Reagents

Mallinckrodt analytical grade bromine was used without further purification. Commercial acetic acid was purified by the method described previously (1, 11). The four styrenes were commercially available compounds and were distilled before use.

Kinetics

The rates of bromine addition to the styrenes were measured on a Cary 16 Spectrophotometer by following the change in bromine absorbance at 490 mμ. Initial bromine concentrations were always less than 3×10^{-4} *M*. The reaction cell was a 10 cm cyclindrical cuvette equipped with a thermostatting jacket; cell temperature was controlled to ± 0.01 °C. The rate constants k_2 were obtained by plotting log $(A - A_\infty)$ vs. time, which yielded good first order plots.

The continued financial support of the National Research Council of Canada and the awards of an NRCC Studentship and an Ontario Graduate Fellowship to J.A.P. are gratefully acknowledged.

1. K. YATES and W. V. WRIGHT. Can. J. Chem. **45**, 167 (1967).
2. J. H. ROLSTON and K. YATES. J. Amer. Chem. Soc. **91**, 1483 (1969).
3. J.-E. DUBOIS and A. SCHWARCS. Tetrahedron Lett. **32**, 2167 (1964).
4. R. C. FAHEY and H.-J. SCHNEIDER. J. Amer. Chem. Soc. **90**, 4429 (1968).
5. J. H. ROLSTON and K. YATES. J. Amer. Chem. Soc. **91**, 1469 (1969).
6. J. A. PINCOCK and K. YATES. J. Amer. Chem. Soc. **90**, 5643 (1968).
7. J. A. PINCOCK. Ph.D. Thesis, University of Toronto, Toronto, Ontario, 1970.
8. H. C. BROWN and Y. OKAMOTO. J. Amer. Chem. Soc. **80**, 4979 (1958).
9. S. I. MILLER. Adv. in physical organic chemistry. Vol. 6. Academic Press, 1968. p. 185.
10. B. CAPON, M. J. PERKINS, and C. W. REES. Organic reaction mechanisms–1965. Interscience, 1966. p. 104.
11. J. H. ROLSTON and K. YATES. J. Amer. Chem. Soc. **91**, 1477 (1969).

Can. J. Chem. Downloaded from www.nrcresearchpress.com by 210.87.254.42 on 09/05/12
For personal use only.

Erratum: Radiation-induced oxidation of 2-propanol by hydrogen peroxide in aqueous solutions

C. E. BURCHILL AND I. S. GINNS
Department of Chemistry, University of Manitoba, Winnipeg 19, Manitoba

Received June 23, 1970

(Ref.: Can. J. Chem. **48**, 1232 (1970))

Canadian Journal of Chemistry, **48**, 2948 (1970)

In the final paragraph of p. 1235, reaction [2] is twice referred to as reaction [3]. Thus the first sentence of this paragraph should read "The rate constants for reactions [2] and [7] have been assessed ... reaction [7] must be considered in addition to reaction [2]."

Can. J. Chem. Downloaded from www.nrcresearchpress.com by 210.87.254.40 on 09/05/12
For personal use only.

2949-2

547m

Canadian Journal of Chemistry

Published by THE NATIONAL RESEARCH COUNCIL OF CANADA

VOLUME 48 OCTOBER 1, 1970 NUMBER 19

The microwave spectrum, dipole moment, and structure of cyclopropyl carbinol

A. BHAUMIK, W. V. F. BROOKS, S. C. DASS, AND K. V. L. N. SASTRY

Departments of Chemistry and Physics, University of New Brunswick, Fredericton, New Brunswick

Received April 30, 1970

The microwave spectra of cyclopropyl carbinol ($\overline{CH_2—CH_2—CH}—CH_2—OH$) and its deuterated (—OD) form were studied in the region of 8 to 35 gHz. Only one of the possible rotational isomers was identified. The measured rotational constants and dipole moments for $C_3H_5CH_2OH$ and $C_3H_5CH_2OD$ are, respectively, A (mHz): 12485.13, 12064.04; B (mHz): 3236.46, 3177.22; C (mHz): 2894.38, 2826.19; κ: −0.928665, −0.924001; μ_a (D): 1.81, 1.78; μ_b (D): 0.36, 0.32; μ_c (D): 0.31, 0.30; μ_{total} (D): 1.87, 1.84.

Rotation is apparently hindered by hydrogen bonding between the hydroxyl hydrogen and the electrons in the strained bonds of the cyclopropyl ring.

Canadian Journal of Chemistry, 48, 2949 (1970)

Introduction

Microwave spectroscopy has been used to study the molecular structure of a number of cyclopropyl compounds (1–4). Most of these have been semi-rigid molecules and the results have been consistent enough that the structure of the cyclopropyl group is reasonably well known. Cyclopropyl carbinol has a less well-defined structure since rotations of the entire carbinol group (relative to the ring) and of the OH group are possible. This work was undertaken to determine whether or not free rotation occurs in the molecule, whether one or more forms could be observed, and to investigate the conformations.

Experimental

The cyclopropyl carbinol was purchased from the Aldrich Chemical Company and it was used without further purification. The —OD molecule was formed by admitting vapors of both D_2O and the normal carbinol to the Stark cell.

The spectra were measured at room temperature (about 25 °C) and at −18 °C at pressures in the range 0.025 to 0.075 Torr. The spectrometer is a conventional Stark modulation instrument operating at 85 kc/s with oscilloscope display. The Stark field was calibrated with the OCS line $J = 1 \leftarrow 0$ (5).

Results and Discussion

Microwave Spectra

The most obvious feature of the spectrum of the normal molecule is a series of strong lines occurring in well-defined groups with readily resolved Stark lobes. These lines were assigned to *a*-type R transitions of an almost symmetric rotor. From these frequencies it was not possible to determine all three rotational constants precisely; but, with approximate constants, the frequencies of *b*- and *c*-type transitions could be predicted, and the predictions were accurate enough to help in identifying the much weaker *b* and *c* lines. The final rotational constants (Table 3) were determined by a least squares fitting procedure from the lines listed in Table 1.

The spectrum of the deuterated species is similar and was analyzed by the same method. One set of vibrational satellite lines was identified and assigned for each species (Table 2).

There are, in the region studied, a number of strong lines which were not assigned, but the Stark effects and general patterns suggest that these are lines of higher J of the same molecular species. It is possible, however, that some of the lines may be due to other geometrical isomers present at low concentrations or with small dipole moments.

Dipole Moments

Only quadratic Stark effects were observed. Stark coefficients were determined graphically from the plots of Stark shifts vs. the squares of the applied fields. Most of the Stark coefficients depend only upon μ_a, so that determination of

Can. J. Chem. Downloaded from www.nrcresearchpress.com by 210.87.254.40 on 09/05/12
For personal use only.

TABLE 1

Rotational assignment of the normal and deuterated species of cyclopropyl carbinol in the ground vibrational state

	Frequency (mHz)			
	$\overline{CH_2CH_2}CHCH_2OH$		$\overline{CH_2CH_2}CHCH_2OD$	
Transition	Obsd.	Calcd.	Obsd.	Calcd.
a-Type				
$2_{12} - 1_{11}$	11 919.92	11 919.60	11 655.89	11 655.80
$2_{02} - 1_{01}$	12 253.02	12 252.36	11 996.72	11 996.63
$2_{11} - 1_{10}$	12 603.86	12 603.75	12 357.54	12 357.86
$3_{13} - 2_{12}$	17 874.08	17 873.66	17 477.88	17 477.41
$3_{03} - 2_{02}$	18 355.08	18 355.30	17 969.69	17 969.52
$3_{22} - 2_{21}$	18 392.73	18 392.51	18 010.62	18 010.24
$3_{21} - 2_{20}$	18 429.39	18 429.73	18 050.94	18 050.96
$3_{12} - 2_{11}$	18 899.77	18 899.72	18 530.21	18 530.32
$4_{14} - 3_{13}$	23 821.50	23 821.04	23 291.97	23 291.75
$4_{04} - 3_{03}$	24 430.82	24 430.62	23 912.06	23 912.22
$4_{23} - 3_{22}$	24 516.32	24 516.11	24 005.60	24 005.72
$4_{32} - 3_{31}$	24 542.64	24 541.51	24 034.06	24 033.50
$4_{31} - 3_{30}$		24 542.46		24 034.61
$4_{22} - 3_{21}$	24 609.23	24 608.84	24 106.99	24 107.16
$4_{13} - 3_{12}$	25 188.21	25 188.39	24 694.32	24 694.76
$5_{15} - 4_{14}$	29 759.88	29 759.88	29 097.02	29 096.79
$5_{05} - 4_{04}$	30 469.70	30 469.96	29 815.51	29 815.72
$5_{24} - 4_{23}$	30 633.43	30 633.49	29 994.41	29 994.42
$5_{42} - 4_{41}$	30 675.00	30 674.89	30 040.68	30 039.72
$5_{41} - 4_{40}$		30 674.91		30 039.75
$5_{33} - 4_{32}$	30 684.64	30 684.57	30 050.64	30 050.21
$5_{32} - 4_{31}$	30 687.62	30 687.90	30 053.85	30 054.09
$5_{23} - 4_{22}$	30 817.47	30 817.71	30 195.01	30 195.74
$5_{14} - 4_{13}$	31 465.99	31 466.94	30 847.20	30 848.07
$6_{16} - 5_{15}$	35 688.79	35 688.62		
$6_{06} - 5_{05}$	36 467.15	36 466.39		
$6_{25} - 5_{24}$	36 743.04	36 743.13		
$6_{34} - 5_{33}$	36 831.97	36 831.92		
$6_{33} - 5_{32}$	36 840.44	36 840.77		
$6_{24} - 5_{23}$	37 061.71	37 061.69		
b-Type				
$4_{04} - 3_{13}$	15 994.60	15 996.35	15 857.93	15 858.34
$5_{23} - 5_{14}$			24 950.83	24 951.36
$7_{16} - 7_{07}$	15 072.53	15 072.35	14 916.65	14 916.33
$7_{25} - 7_{16}$			23 670.29	23 669.12
$8_{17} - 8_{08}$	16 964.29	16 964.37		
c-Type				
$2_{11} - 1_{01}$			21 594.96	21 595.71
$5_{05} - 4_{13}$	19 224.90	19 225.62		
$7_{16} - 6_{24}$	18 595.12	18 594.68		
$9_{09} - 8_{17}$	37 207.56	37 207.55		
$6_{25} - 6_{15}$			23 585.14	23 585.57
$7_{26} - 7_{16}$	23 606.44	23 606.81		
$8_{27} - 8_{17}$	22 332.32	22 331.60		

μ_b and μ_c is not straightforward. However, once good values of μ_a were known, relatively small trial values of μ_b and μ_c were used in calculations of Stark shifts in order to find which, if any, lines would have lobes especially sensitive to μ_b and μ_c. This was successful and the values of dipole components given in Table 4 are determined by a least squares program which, for each molecule, finds the set of dipole components which gives the best fit to a set of observed Stark coefficients. The same computer program does both the trial calculations and the final fitting. Most of the reported dipole moments for lighter alcohols are in the range 1.60 to 1.70 D (6), and methyl cyclopropane has a moment of 0.14 D (4). The relative magnitudes of the dipole

480220

Can. J. Chem. Downloaded from www.nrcresearchpress.com by 210.87.254.40 on 09/05/12
For personal use only.

TABLE 2

Rotational assignment of the normal and deuterated species of cyclopropyl carbinol in the excited vibrational state

	Frequency (mHz)			
	$\overline{CH_2CH_2}CHCH_2OH$		$\overline{CH_2CH_2}CHCH_2OD$	
Transition	Obsd.	Calcd.	Obsd.	Calcd.
a-Type				
$2_{12} - 1_{11}$	11 913.00	11 912.88		11 651.67
$2_{02} - 1_{01}$	12 241.86	12 241.87	11 990.64	11 991.41
$2_{11} - 1_{10}$	12 589.40	12 589.15	12 351.69	12 351.35
$3_{13} - 2_{12}$		17 863.69		17 471.28
$3_{03} - 2_{02}$		18 339.99	17 960.84	17 961.91
$3_{22} - 2_{21}$		18 376.53	18 002.95	18 002.26
$3_{21} - 2_{20}$		18 413.06	18 042.20	18 042.61
$3_{12} - 2_{11}$	18 877.50	18 877.93	18 520.88	18 520.61
$4_{14} - 3_{13}$	23 807.64	23 807.94	23 284.01	23 283.67
$4_{04} - 3_{03}$	24 411.89	24 410.98	23 902.60	23 902.50
$4_{23} - 3_{22}$	24 495.50	24 494.92	23 995.89	23 995.16
$4_{32} - 3_{31}$	24 520.74	24 519.87	24 022·77	24 022.68
$4_{31} - 3_{30}$		24 520.80		24 023.78
$4_{22} - 3_{21}$	24 585.52	24 585.97	24 096.07	24 095.67
$4_{13} - 3_{12}$	25 159.75	25 159.54	24 682.15	24 681.93
$5_{15} - 4_{14}$	29 743.44	29 743.79	29 086.75	29 086.86
$5_{05} - 4_{04}$	30 446.23	30 446.63	29 804.48	29 804.24
$5_{14} - 4_{13}$	31 430.65	31 431.22	30 831.92	30 832.22

components are superimposed upon the structure in Fig. 1.

Structure and Discussion

The structure is not, of course, adequately determined by the rotational constants of two isotopic species. However, if it is assumed that the geometries of the cyclopropyl and carbonyl groups are adequately known from previous work (1–8), then the principal unknown structural factors are the degrees of rotation about the C_{ring}—$C_{carbinol}$ and C—O bonds. The solution of Kraitchman's equations (9), using the normal and deuterated moments of inertia, gives the position of the hydroxyl hydrogen atom relative to the molecular center of mass. Once the hydroxyl hydrogen is placed, the oxygen position is also roughly fixed, and the general conformation is, therefore, known. A model constructed in this way gives fair agreement with the observed moments of inertia, but a small change in the C—O—H angle gives considerable improvement. The parameters of our final model are given in Table 5. Further adjustment of positions to give a better fit with observation seems to be of little value since there is no clear indication of which coordinates should be changed. The significant result is the general conformation rather than the exact

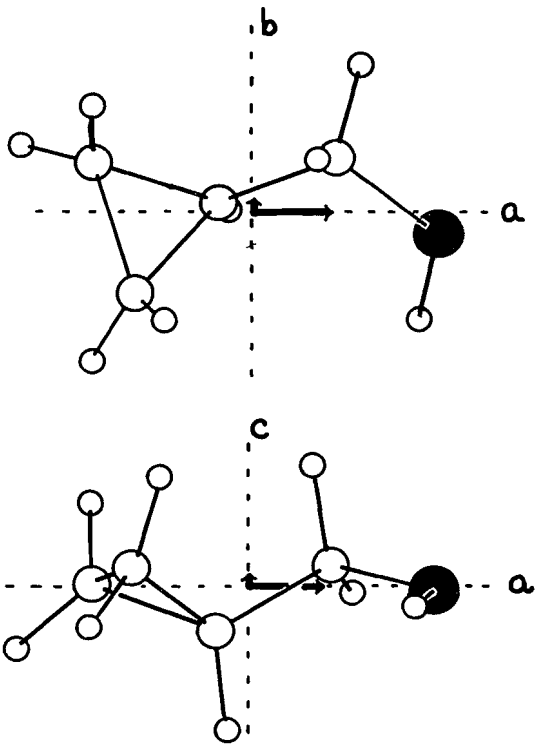

FIG. 1. Projection of cyclopropyl carbinol structure on the *a,b* and *a,c* planes of the principal axes. The relative values of μ_a, μ_b, and μ_c are shown as arrows; the directions of the arrows are conjectural.

Can. J. Chem. Downloaded from www.nrcresearchpress.com by 210.87.254.40 on 09/05/12
For personal use only.

Can. J. Chem. Downloaded from www.nrcresearchpress.com by 210.87.254.40 on 09/05/12
For personal use only.

TABLE 3

Rotational constants and principal moments of inertia of the normal and deuterated species of cyclopropyl carbinol

Species	Rotational constants (mHz)[a]				Principal moments of inertia (a.m.u. Å²)			
	A	B	C	κ	I_A	I_B	I_C	$-\Delta$
$\overline{CH_2CH_2}CHCH_2OH$								
Ground	12 485.13	3 236.46	2 894.38	−0.928665	40.478	156.151	174.606	22.023
Excited	(12 436)	3 231.82	2 893.69	−0.9291	(40.638)	156.375	174.648	(22.365)
$\overline{CH_2CH_2}CHCH_2OD$								
Ground	12 064.04	3 177.22	2 826.19	−0.924001	41.891	159.063	178.819	22.135
Excited	(12 084)	3 175.30	2 825.46	−0.9244	(41.822)	159.159	178.865	(22.116)

[a] ± 0.10.

TABLE 4

Stark effect and dipole moments of cyclopropyl carbinol

Transition	M	$\Delta\nu \times 10^4/E^2$ (mHz × cm²/V²) Obsd.	Calcd.
$\overline{CH_2CH_2}CHCH_2OH$			
$2_{12} - 1_{11}$	1	6.1000	5.8670
$2_{02} - 1_{1}$	1	0.1880	0.1897
$2_{11} - 1_{10}$	1	−5.5300	−5.6438
$3_{13} - 2_{12}$	1	0.1920	0.2027
	2	0.8320	0.8412
$3_{03} - 2_{02}$	0	−0.0368	−0.0419
	1	−0.0115	−0.0122
$3_{12} - 2_{11}$	1	−0.1710	−0.1923
	2	−0.6940	−0.7394
$4_{23} - 3_{22}$	0	0.0365	0.0358
$4_{22} - 3_{21}$	0	0.0269	0.0252
		$\mu_a = 1.81 \pm 0.01$ D	
		$\mu_b = 0.36 \pm 0.07$ D	
		$\mu_c = 0.31 \pm 0.04$ D	
		$\mu_t = 1.87 \pm 0.02$ D	
$\overline{CH_2CH_2}CHCH_2OD$			
$2_{12} - 1_{11}$	0	0.1856	0.1722
$2_{02} - 1_{01}$	1	0.1848	0.1846
$3_{13} - 2_{12}$	2	0.7618	0.7967
$3_{03} - 2_{02}$	0	−0.0449	−0.0400
$3_{12} - 2_{11}$	1	−0.1825	−0.1812
	2	−0.7149	−0.6954
$4_{23} - 3_{22}$	0	−0.0601	−0.0606
$4_{22} - 3_{21}$	0	0.2973	0.2972
		$\mu_a = 1.78 \pm 0.02$ D	
		$\mu_b = 0.32 \pm 0.01$ D	
		$\mu_c = 0.30 \pm 0.02$ D	
		$\mu_t = 1.84 \pm 0.02$ D	

TABLE 5

Structural parameters of model of cyclopropyl carbinol molecule

Parameter	Value[a]	Source
$C_{ring}—C_{ring}$	1.514	*b*
$C_{ring}—C_{carbinol}$	1.522	*b*
C—O	1.426	*c*
O—H	0.9451	*c*
$C_{ring}—H$	1.082	*d*
$C_{carbinol}—H$	1.091	*b*
∠ C—C—C (ring)	60°	Assumed
∠ H—C_{ring}—H	116°	*b*
∠ H—C_{ring}—$C_{carbinol}$	116°	Assumed
∠ C_{ring}—$C_{carbinol}$—X	109.45°	Assumed
∠ C—O—H	116.7°	*f*
∠ H—C_{ring}—$C_{carbinol}$—O[e]	±124.2°	*f*
∠ C_{ring}—$C_{carbinol}$—O—H[e]	∓32.3°	*f*

Can. J. Chem. Downloaded from www.nrcresearchpress.com by 210.87.254.40 on 09/05/12
For personal use only.

TABLE 5 (*Concluded*)

Calculated moments of inertia and observed–calculated difference values

Moments of inertia	$C_3H_5CH_2OH$		$C_3H_5CH_2OD$	
	Calculated	Obsd.−Calcd.	Calculated	Obsd.−Calcd.
I_a	40.4969	−0.0186	41.8683	0.0229
I_b	156.5645	−0.4134	159.8305	−0.7678
I_c	174.0228	0.5836	178.5867	0.2325

Coordinates of hydroxyl hydrogen in principal axes systems

Coordinate	Calculated	Observed[g]
$x(a)$	1.793	1.686±0.007
$y(b)$	1.175	1.182±0.010
$z(c)$	0.202	0.248±0.040

[a]Distances are given in Angstroms; 1 Å = 0.1 nm.
[b]Reference 4.
[c]Reference 8.
[d]Reference 7.
[e]The zero of these dihedral angles is taken as the coplanar *cis* configuration of the four atoms.
[f]Adjusted (one at a time) to give a best least squares fit with the measured rotational constants of normal and deuterated molecules. Estimated reliable to within ± 1.0°.
[g]Calculated from Kraitchman's equation and observed moments of inertia.

values of the bond distances and angles. There are actually two similar, mirror image structures, one of which is shown in Fig. 1.

The fact that the spectra can be interpreted in terms of rigid rotor models indicates that a relatively high barrier prevents rotations about the ring–carbinol and carbon–oxygen bonds. We propose that in addition to steric factors, there is an attraction between the hydroxyl hydrogen and the electrons of the nearest strained bond of the cyclopropyl ring. The model we are considering for the ring electrons is similar to what has been proposed by Walsh (10), and the attraction of these electrons for protons has been calculated by Hoffmann (11). Hoffmann also refers to the "quasi-π" character of cyclopropyl carbon–carbon bonds (12). Since π electrons seem to form intramolecular hydrogen bonds with hydroxyl and thiol hydrogens in allyl alcohol (13) and allyl mercaptan (14), the "quasi-π" electrons should behave in the same way although the forces may be weaker.

We are grateful to the National Research Council of Canada for the grants which have supported this work. We also thank the personnel of the University of New Brunswick Computing Centre for their assistance.

1. J. P. FRIEND and B. P. DAILEY. J. Chem. Phys. **29**, 577 (1958).
2. W. H. FLYGARE, A. NARATH, and W. D. GWINN. J. Chem. Phys. **36**, 200 (1962).
3. R. H. SCHWENDEMAN, G. D. JACOBS, and T. M. KRIGAS. J. Chem. Phys. **40**, 1022 (1964).
4. R. G. FORD and R. A. BEAUDET. J. Chem. Phys. **48**, 4671 (1968).
5. S. A. MARSHALL and J. WEBER. Phys. Rev. **105**, 1502 (1957).
6. E. V. IVASH and D. M. DENNISON. J. Chem. Phys. **21**, 1804 (1953); Phys. Rev. **89**, 895A (1953). C. P. SMYTH. Dielectric behavior and structure. McGraw-Hill, New York. 1955.
7. J. L. DUNCAN. J. Mol. Spectrosc. **25**, 451 (1968).
8. R. M. LEES and J. G. BAKER. J. Chem. Phys. **48**, 5249 (1968).
9. J. KRAITCHMAN. Amer. J. Phys. **21**, 17 (1953).
10. A. D. WALSH. Trans. Faraday Soc. **45**, 179 (1949).
11. R. HOFFMANN. J. Chem. Phys. **40**, 2480 (1964).
12. R. HOFFMANN. Tetrahedron Lett. 3819 (1965).
13. A. N. MURTY and R. F. CURL. J. Chem. Phys. **46**, 4176 (1967).
14. K. V. L. N. SASTRY, S. C. DASS, W. V. F. BROOKS, and A. BHAUMIK. J. Mol. Spectrosc. **31**, 54 (1969).

Can. J. Chem. Downloaded from www.nrcresearchpress.com by 210.87.254.40 on 09/05/12
For personal use only.

Can. J. Chem. Downloaded from www.nrcresearchpress.com by 210.87.254.42 on 09/05/12
For personal use only.

The photochemistry of aqueous solutions of Tl(III) perchlorate

C. E. BURCHILL AND W. H. WOLODARSKY[1]
Department of Chemistry, University of Manitoba, Winnipeg 19, Manitoba

Received May 22, 1970

In deaerated aqueous perchloric acid solution Tl(III) is reduced and 2-propanol oxidized to acetone in equivalent yields via a chain reaction initiated by light of 2537 Å. Initiation is attributed to a charge-transfer-to-metal excitation followed by dissociation

$$Tl(III)_{aq} \xrightarrow{h\nu} H^+ + Tl(II) + OH$$

The formation of Tl(II) in the primary process is demonstrated by flash photolysis. An upper limit of 0.36 ± 0.07 is estimated for the primary quantum yield.

Canadian Journal of Chemistry, **48**, 2955 (1970)

Introduction

A number of metal ions in solution display a strong absorption in the ultraviolet which is attributed to a charge-transfer excitation (1). Absorption of light in such a charge-transfer process is known to initiate a number of redox reactions (2). In the case of oxidizing metal ions, this initiation is envisaged as an electron transfer from a ligand to the metal ion in the excitation followed by dissociation to give a reduced metal ion and a free radical derived from the ligand. A large number of such processes have been described for ions of the transition and inner transition series. Relatively little study has been given to the corresponding photochemical processes for main-group metals, in part because the majority have only a single stable oxidation state. The photo-induced formation of X_2^- from Hg(II) halide complexes in aqueous solution has been attributed to such a charge-transfer process (3). The high-yield photo-induced exchange between Tl(III) and Tl(I) was explained by a chain mechanism (4) initiated by reaction 1.

$$[1] \qquad Tl(III)_{aq} \xrightarrow{h\nu} Tl(II)_{aq} + H^+ + OH$$

Recently (5), in a study of the radiation-induced oxidation of alcohols by Tl(III), it was proposed that the propagating step of the observed chain process was the reaction of a Tl(II) intermediate with the alcohol as in reaction 2.

$$[2] \qquad Tl(II)_{aq} + HROH \rightarrow Tl(I)_{aq} + H^+ + \cdot ROH$$

If the absorption of ultraviolet light by Tl(III) in acid aqueous solution leads to the dissociative process, reaction 1, it should be possible to initiate the same chain oxidation of alcohols as was observed under γ-irradiation. To test this proposal a study of the photo-reduction of Tl(III) in the presence of 2-propanol was undertaken.

The absorption spectrum of a species believed to be Tl(II) has been observed in the pulse radiolysis of aqueous Tl_2SO_4 solutions containing N_2O (6) and in γ-irradiated low temperature sulfuric acid glasses containing Tl_2SO_4 (7). From the position of the absorption maximum (260 nm) and the relatively large molar absorptivity ($5400\ M^{-1}\ cm^{-1}$) reported for this species, it seemed probable that it would be possible to observe the formation and decay of Tl(II) by the ultraviolet flash photolysis of aqueous Tl(III) solutions.

Experimental

Solutions of Tl(III) were prepared by dissolving Tl_2O_3 (Fisher, purified) in $HClO_4$ (Baker and Adamson, reagent, 70%) and triply distilled water to give a stock solution $2 \times 10^{-2}\ M$ in Tl(III) and $4\ M$ in $HClO_4$. Aliquots of this stock solution plus any other solutes were then diluted with triply distilled water to give solutions $5 \times 10^{-3}\ M$ in Tl(III) and $1.0\ M$ in $HClO_4$.

2-Propanol (Fisher, certified), *i*-propylamine (Eastman, high purity), and $TlClO_4$ (City Chemical Corp., purified) were used as received for the preparation of experimental solutions.

For steady-state photolysis experiments the light source was a Hanovia Z 1500–108 low pressure mercury arc with a Vycor envelope. The absorption by the envelope effectively eliminated the mercury emission line at 1849 Å while the lack of any significant absorption by Tl(III) solutions above 2800 Å ensured that reaction was initiated solely by the 2537 Å resonance emission.

Aliquots of the solution (10 ml) were degassed in 25 ml Pyrex bulbs using the freeze–pump–thaw technique. After degassing the solution was tipped into a cylindrical fused silica optical cell (of 4.2 cm o.d. and 1.00 cm light path) attached to a side arm and irradiated. Light from the

[1]Present address: Department of Chemistry, Queen's University, Kingston, Ontario.

Can. J. Chem. Downloaded from www.nrcresearchpress.com by 210.87.254.42 on 09/05/12
For personal use only.

lamp was roughly collimated by a series of masks. Spectrophotometric measurements gave a transmittance of 0.66 (34% absorption) at 2537 Å for solutions 5×10^{-3} *M* in Tl(III) and 1.0 *M* in $HClO_4$. Irradiations were carried out at ambient room temperature (25 ± 2 °C).

Actinometry was by the ferrioxalate method of Hatchard and Parker (8). The incident intensity was measured in silica cells, similar to those used for experimental solutions and identically positioned, first using the unfiltered light from the arc and then with a 4 mm thick Pyrex plate between the lamp and the cell. The difference was assumed to be the incident intensity, I_0, of the 2537 Å light (5.32×10^{-7} einstein l^{-1} s^{-1} for the majority of experiments). The light transmitted by the Pyrex filter was 10% of the total. Wire screens were introduced between the lamp and the sample to study the effect of varying light intensity. The rate of energy absorption from the light beam, I_a, was calculated from I_0 and the measured absorbance of the sample at 2537 Å.

The reaction was generally followed by measuring the concentration of acetone formed after each of a series of timed irradiations, using the salicylaldehyde method (5). Tl(III) concentrations were measured using *o*-phenylenediamine (5). Reduction of Tl(III) was held to less than 20% of the initial concentration to minimize the change in I_a as a result of the changing concentration.

The flash photolysis experiments were carried out at Atomic Energy of Canada's Whiteshell Nuclear Research Establishment using equipment which has been described elsewhere (9). Three flash lamps having Vycor jackets were arranged concentrically about the sample tube which had a diameter of 2.7 cm and a light path of 10.0 cm for the analyzing light. The Vycor envelopes of the flash lamps limited the exciting light to wavelengths mostly in excess of 2500 Å.

Results

(1) Flash Photolysis

A solution 5×10^{-3} *M* in Tl(III), 1×10^{-4} *M* in Tl(I), and 1.0 *M* in $HClO_4$, subjected to a flash showed a transient absorption in the region of 270 nm. This absorption decayed to the original base line in a time > 20 ms. The transient absorbance measured 100 μs after the flash is shown in Fig. 1. The absorption maximum is at 270 nm. A second order decay plot for the absorbance at 270 nm is shown in Fig. 2. The slope of such a plot gives $2k/\varepsilon l$ for a bimolecular decay. From Fig. 2, $2k/\varepsilon_{270} = (6.1 \pm 0.6) \times 10^4$ cm s^{-1}.

In a second series of experiments a solution containing 5×10^{-3} *M* Tl(III) and 5×10^{-2} *M* 2-propanol in 1.0 *M* $HClO_4$ was subjected to a flash. A transient absorption was observed at 270 nm which decayed with second order kinetics. For this experiment $2k/\varepsilon_{270}$ was estimated as $(1.3 \pm 0.2) \times 10^5$ cm s^{-1}.

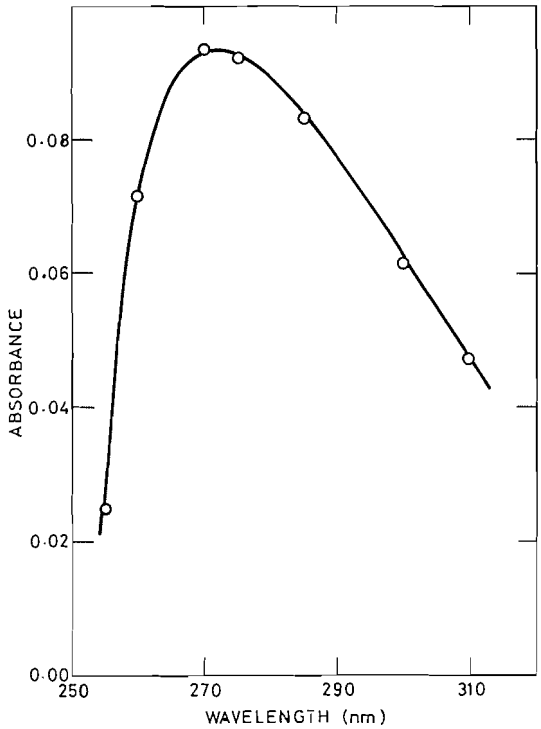

FIG. 1. Absorption spectrum of transient from 5×10^{-3} *M* $Tl(ClO_4)_3$ with 1×10^{-4} *M* $TlClO_4$ in 1.0 *M* $HClO_4$. Absorbance measured 100 μs after flash.

(2) Steady-State Photolysis

Under continuous illumination from the low pressure mercury arc Tl(III), in the presence of 2-propanol, was reduced with a quantum yield very much in excess of unity, indicative of a chain reaction. Acetone was formed in an equivalent yield. Because the acetone formation could be measured more precisely than the small reduction in Tl(III), only the acetone formation was measured in the majority of experiments. With no alcohol present there was little or no reduction of Tl(III). The light absorption by the solutions at 2537 Å was independent of the concentration of 2-propanol present and was not affected by the addition of *i*-propylamine. The addition of acetic acid or sulfuric acid caused a marked increase in the absorbance at 2537 Å.

In the presence of 2-propanol the quantum yield of acetone formation increased linearly with increasing alcohol concentration in the range $(1–10) \times 10^{-2}$ *M*, as shown in Fig. 3 for $I_a = 9.4 \times 10^{-8}$ einstein l^{-1} s^{-1}. With decreasing light intensity the quantum yield of acetone for-

Can. J. Chem. Downloaded from www.nrcresearchpress.com by 210.87.254.42 on 09/05/12
For personal use only.

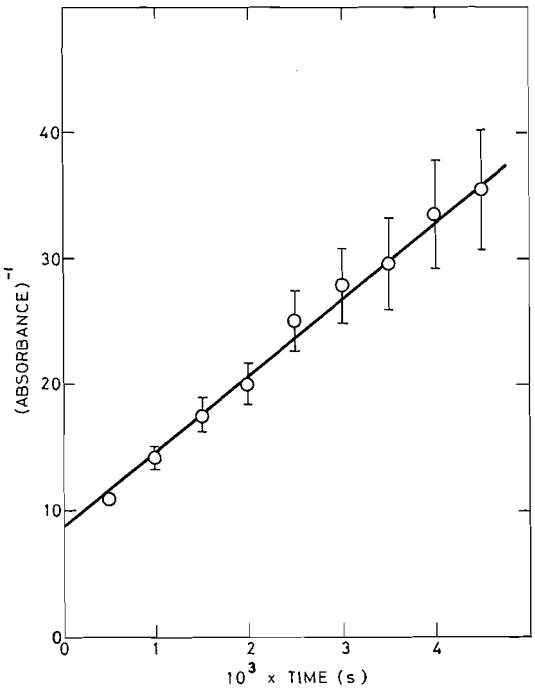

FIG. 2. Second order plot for decay of transient in Fig. 1. Analyzing light path = 10.0 cm.

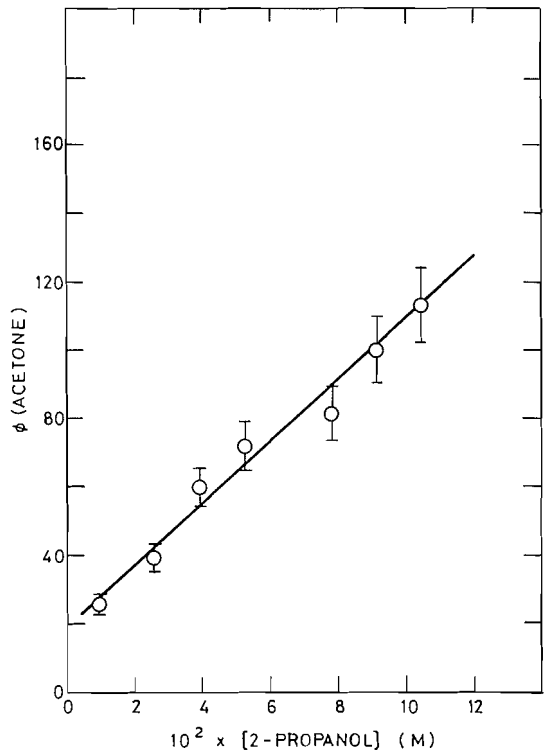

FIG. 3. Variation of quantum yield with 2-propanol concentration. [Tl(III)] = 5×10^{-3} *M*, $I_a = 9.4 \times 10^{-8}$ einstein l^{-1} s^{-1}.

mation increased and, as shown in Fig. 4, this variation was an inverse square root relationship for I_a in the range 1.81×10^{-7} to 1.91×10^{-8} einstein l^{-1} s^{-1}.

When 2-propanol was replaced by *i*-propylamine the quantum yield of Tl(III) reduction was reduced to a value less than unity and was essentially independent of the amine concentration in the range 0.02 to 0.10 *M*. The average quantum yield of Tl(III) reduction in the presence of *i*-propylamine was 0.36 ± 0.07.

Discussion

On the basis of the spectrophotometric data of Rogers and Waind (10) for the equilibrium system

[3] $$Tl^{3+}{}_{aq} \rightleftarrows TlOH^{2+} + H^+$$

the principal Tl(III) species in 1.0 *M* $HClO_4$ is $Tl^{3+}{}_{aq}$ (~ 90%) but the first hydrolysis product, $TlOH^{2+}$, absorbs most (*ca.* 80%) of the light at 254 nm. At the concentrations in which it was added or formed in the experiments described Tl(I) would not absorb a significant amount of energy. In the flash photolysis experiments the exciting light was not monochromatic but the sharp cutoff below 2500 Å by the Vycor jacket of the flash lamps would give a similar effect to that described above: absorption only by Tl(III) and principally by $TlOH^{2+}$.

In the flash photolysis the primary process proposed by Stranks and Yandell (4) would be the charge-transfer dissociation, reaction 4.

[4] $$Tl(OH)^{2+} \xrightarrow{h\nu} \phi_a Tl^{2+} + \phi_a OH$$

OH reacts with Tl^+ in a very rapid reaction (11) assumed to give Tl^{2+} as a product (6)

[5] $$OH + Tl^+ \rightarrow OH^- + Tl^{2+}$$

This reaction is sufficiently fast to be complete during the time of the flash (flash half-width ~ 25 μs). Thus the only transient expected after the flash is Tl^{2+}. The absorption maximum for the observed species (270 nm) is very close to that reported for Tl^{2+} by Cercek *et al.* (6) in neutral solution (260 nm) and by Brown and Dainton (7) in a sulfuric acid glass (267 nm). Tl^{2+} has been

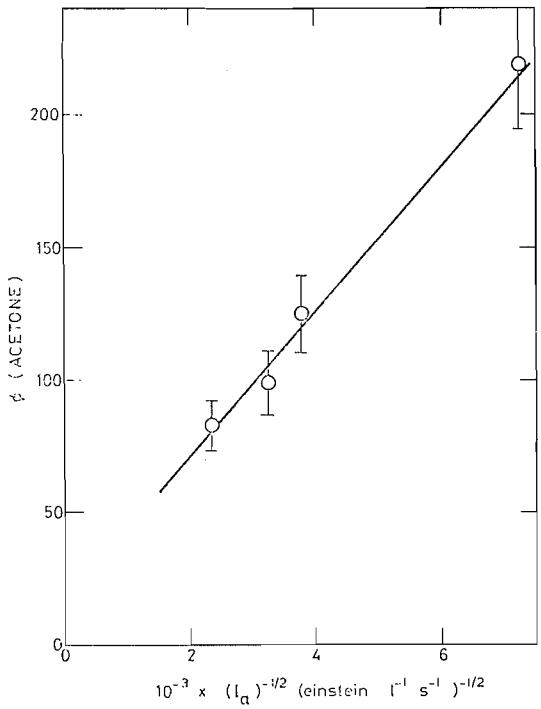

FIG. 4. Variation of quantum yield with intensity. $[Tl(III)] = 5 \times 10^{-3}$ *M*, $[(CH_3)_2CHOH] = 9.13 \times 10^{-2}$ *M*.

assumed to undergo a very rapid dismutation reaction (4–6, 12)

$$[6] \qquad 2Tl^{2+}_{aq} \rightarrow Tl^{+}_{aq} + Tl(III)_{aq}$$

The bimolecular decay observed for the transient is consistent with its being Tl^{2+} and the dismutation reaction is consistent with the observation of no net change under ultraviolet irradiation in the absence of an organic scavenger (4). In the pulse radiolysis experiments, Cercek *et al.* (6) observed a value of $2k/\varepsilon_{max}$ of 5.3×10^5 cm s^{-1} for the bimolecular reaction of the species assumed to be Tl^{2+}. This is nearly an order of magnitude greater than that obtained in this work ($2k/\varepsilon_{270} = (6.1 \pm 0.6) \times 10^4$ cm s^{-1}) and when it is recognized that the current work was carried out in a medium of much higher ionic strength (~ 1.0) the discrepancy is considerably greater. However, although the transients formed in the photochemical and radiation chemical experiments absorb light in the same spectral region they are not necessarily identical species. The pulse radiolysis studies were carried out in neutral solution where a Tl(II) species might be extensively hydrolyzed (as $TlOH^+$). Tl(II) formed in the 1.0 *M* $HClO_4$ medium used in the photochemical experiments would be much less likely to show any hydrolysis and consequently be present as Tl^{2+}_{aq}. This latter species could well have a maximum molar absorbancy greater than that of the hydrolyzed species and/or a dismutation rate constant less than that for $TlOH^+$. These results do not confirm absolutely that the species observed is Tl(II) but they do give considerable support to the supposition.

The steady-state photolysis is characterized by a linear dependence of acetone yields on 2-propanol concentration and a reciprocal square root intensity dependence. These characteristics are consistent with the chain mechanism proposed for the radiation-induced oxidation of 2-propanol by Tl(III). For the photo-induced reaction the analogous mechanism would be

$$[4] \qquad Tl(OH)^{2+} \xrightarrow{h\nu} \phi_a Tl^{2+} + \phi_a OH$$

$$[7] \qquad OH + (CH_3)_2CHOH \rightarrow H_2O + (CH_3)_2\dot{C}OH$$

$$[2] \qquad Tl^{2+} + (CH_3)_2CHOH \rightarrow Tl^{+} + H^{+} + (CH_3)_2\dot{C}OH$$

$$[8] \qquad (CH_3)_2\dot{C}OH + Tl^{3+} \rightarrow (CH_3)_2CO + H^{+} + Tl^{2+}$$

$$[6] \qquad 2Tl^{2+} \rightarrow Tl^{+} + Tl^{3+}$$

$$[9] \qquad \phi(\text{Acetone}) = \phi(-Tl^{3+}) = \phi_a + k_2\left(\frac{\phi_a}{k_6 I_a}\right)^{1/2}[(CH_3)_2CHOH]$$

which is in good agreement with the observed characteristics of the chain reaction. Equation 9 implies that the linear relationship between ϕ(acetone) and [2-propanol] should extrapolate to ϕ_a at zero alcohol concentration. Figure 3, however, shows a significantly higher intercept (~ 18). The origin of this discrepancy is not clear since, in the radiation-induced oxidation of 2-propanol by Tl(III), no such large intercept was observed and the precision of the photochemical results would seem to rule out so large a probable error in the intercept. We are unable to provide any satisfactory explanation for this phenomenon.

If the chain mechanism as outlined above applies even at the high radical concentrations after the flash, the initial concentration of Tl^{2+} would not be affected by the presence of 2-propanol and, as reaction 6 is the only one by which chain centers are removed, the kinetics of its decay should not be altered. When 2-propanol was present in the system exposed to a flash, the

Can. J. Chem. Downloaded from www.nrcresearchpress.com by 210.87.254.42 on 09/05/12
For personal use only.

Can. J. Chem. Downloaded from www.nrcresearchpress.com by 210.87.254.42 on 09/05/12
For personal use only.

initial absorbance at 270 nm was about 20% less than in its absence and the second order decay constant was increased by about a factor of 2. Although these experiments were of relatively low precision, these differences were outside the probable uncertainty. We consider it probable that the major portion of the absorbance at 270 nm does originate with Tl^{2+} but that, at the radical concentrations involved, termination may also occur via reactions such as [10] and [11] which would increase the effective rate of decay.

[10] $Tl^{2+} + (CH_3)_2\dot{C}OH \rightarrow Tl^+ + H^+ + (CH_3)_2CO$

[11] $2(CH_3)_2\dot{C}OH \rightarrow (CH_3)_2CHOH + (CH_3)_2CO$

By extrapolation of the intensity dependence of the Tl(III)/Tl(I) exchange Stranks and Yandell (4) estimated a value of $\phi_a = 0.5 \pm 0.3$. We propose that the quantum yield of Tl(III) reduction in the presence of *i*-propylamine (0.36 ± 0.07) represents an upper limit for ϕ_a. In the γ-radiolysis of aqueous solutions of Tl(III) and *i*-propylamine, $G(-Tl^{3+}) = 5.3 \pm 0.2$ (13). The stoichiometry of Tl(III) reduction by a purely non-chain process would be expected to be

[12] $G(-Tl^{3+}) = \frac{1}{2}(G_H + G_{OH}) + G_{H_2O_2}$

from the sequence

[13] $H + (CH_3)_2CHNH_3^+ \rightarrow H_2 + (CH_3)_2\dot{C}NH_3^+$

[14] $OH + (CH_3)_2CHNH_3^+ \rightarrow H_2O + (CH_3)_2\dot{C}NH_3^+$

[15] $(CH_3)_2CNH_3^+ + Tl^{3+} \xrightarrow{H_2O} (CH_3)_2CO + NH_4^+ + H^+ + Tl^{2+}$

[6] $2Tl^{2+} \rightarrow Tl^{3+} + Tl^+$

[16] $H_2O_2 + Tl^{3+} \rightarrow 2H^+ + O_2 + Tl^+$

Using values of $G_H = 3.7$, $G_{OH} = 3.0$, and $G_{H_2O_2} = 0.75$ (14) gives $G(-Tl^{3+}) = 4.1$. Thus, in the radiation reduction of Tl(III), *i*-propylamine gives little or no chain reaction and, if an analogous mechanism applies to the photoreduction, the observed yield of Tl(III) reduction would represent an upper limit of ϕ_a.

Accepting the chain mechanism previously outlined and using the value of $\phi_a = 0.36 \pm 0.07$ estimated above it is possible to estimate values of $k_2/(k_6)^{1/2}$ from the slopes of Figs. 3 and 4. From these data $k_2/(k_6)^{1/2}$ is 0.43 ± 0.05 and 0.49 ± 0.05, respectively. From the radiation chemical reduction (5) the corresponding ratio was calculated as 0.60 ± 0.04. In view of the uncertainty in ϕ_a the agreement is quite good.

It is clear from the results that the chain reduction of Tl(III) by 2-propanol initiated by ultraviolet light has a kinetic form similar to that induced by γ-irradiation. This, with the flash photolysis experiments, supports the contention that the primary event in the 2537 Å photolysis of Tl(III) in aqueous perchloric acid solution is a charge-transfer-to-metal dissociation leading to the formation of a Tl(II) species.

The authors gratefully acknowledge financial support for this work from the National Research Council of Canada. We also wish to acknowledge the generous assistance of the staff of the Whiteshell Nuclear Research Establishment, particularly Dr. Ajit Singh, in carrying out the flash photolysis experiments.

1. J. N. Murrell. Quart. Rev. **15**, 191 (1961).
2. A. W. Adamson, W. L. Waltz, E. Zinato, D. W. Watts, P. D. Fleischauer, and R. D. Lindholm. Chem. Rev. **68**, 541 (1968).
3. M. E. Langmuir and E. Hayon. J. Phys. Chem. **71**, 3809 (1967).
4. D. R. Stranks and Y. K. Yandell. J. Phys. Chem. **73**, 840 (1969).
5. C. E. Burchill and G. G. Hickling. Can. J. Chem. **48**, 2466 (1970).
6. B. Cercek, M. Ebert, and A. J. Swallow. J. Chem. Soc. A, 612 (1966).
7. D. M. Brown and F. S. Dainton. Trans. Faraday Soc. **62**, 1139 (1966).
8. C. G. Hatchard and C. A. Parker. Proc. Roy. Soc. Ser. A, **235**, 518 (1956).
9. A. Singh, A. R. Scott and F. Sopchyshyn. J. Phys. Chem. **73**, 2633 (1969).
10. T. E. Rogers and G. M. Waind. Trans. Faraday Soc. **57**, 1360 (1961).
11. M. Anbar and P. Neta. Int. J. Appl. Radiat. Isotop. **18**, 493 (1967).
12. H. A. Catherino and J. Jordan. Talanta, **11**, 159 (1964).
13. W. H. Wolodarsky. M.Sc. Thesis, University of Manitoba, Winnipeg, Manitoba. 1969.
14. E. Hayon. Trans. Faraday Soc. **61**, 734 (1964).

Can. J. Chem. Downloaded from www.nrcresearchpress.com by 210.87.254.42 on 09/05/12
For personal use only.

Studies of fluoroberyllate complexes in aqueous solution by ^{19}F nuclear magnetic resonance[1]

M. G. HOGBEN,[2] K. RADLEY, AND L. W. REEVES
The Chemistry Department, University of Waterloo, Waterloo, Ontario

Received May 5, 1970

Studies of aqueous solutions containing fluoride and beryllium ion in ratios between 5 and 0.5 were made by ^{19}F nuclear magnetic resonance at temperatures between the melting point of solutions and room temperature. Signals clearly identifiable as arising from BeF_4^{2-}, BeF_3^-, BeF_2, and BeF^+ were assigned. Chemical shifts and coupling constants J_{Be-F} are reported for all species and approximate equilibrium constants are determined from intensity measurements for the reactions $BeF_3^- \rightleftharpoons BeF_2 + F^-$, $BeF_2 \rightleftharpoons BeF^+ + F^-$, and $BeF^+ \rightleftharpoons Be^{2+} + F^-$.

Canadian Journal of Chemistry, **48**, 2960 (1970)

Introduction

Although aqueous beryllium fluoride chemistry has been studied by more classical techniques for some years, it has only recently (1) been analyzed by the nuclear magnetic resonance (n.m.r.) technique in reasonable detail. Everest (2), in his monograph on beryllium chemistry, reviews the electrochemical evidence for the presence of species BeF^+, BeF_2, BeF_3^-, and BeF_4^{2-} (3). The relative concentration of each of these fluoroberyllate ion complexes depends on the overall concentration ratio [F]/[Be] as well as p*H*. The complex ions are evidently hydrated in the manner $BeF_n(H_2O)_{4-n}^{(n-2)-}$.

Gutowsky and Hoffman (4) included BeF_2 in an early survey of chemical shifts of fluoride molecules. Francis and Lawrenson (5) made a qualitative study of the ^{19}F n.m.r. in tetrafluoroberyllate solutions and reported a chemical shift of +85.5 p.p.m. from an external trifluoroacetic acid reference (TFA) signal with a coupling constant $J_{Be-F} \simeq 33.7$ Hz for the species BeF_4^{2-}. A recent study by Reeves and co-workers (1) included among other things an equilibrium and kinetic study of the reaction

$$BeF_4^{2-} \rightleftharpoons [BeF_3(OH_2)]^- + F^-$$

in the region where concentrations of BeF_2 and BeF^+ are suppressed. The equilibrium constant of the above reaction was reported as $(8.0 \pm 2.0) \times 10^{-2}$ moles kg^{-1} and the kinetic analysis showed rapid fluoride exchange amongst all species with the slow process being the primary dissociation of the first fluoride ion from BeF_4^{2-}. Cursory studies of BeF_2 solutions were incorrectly interpreted because of the apparent absence of a signal for the fluoride ion. In this work an identification of ^{19}F resonances for all species BeF_4^{2-}, BeF_3^-, BeF_2, and BeF^+ are made and overall equilibrium data obtained.

Experimental

"Analar" ammonium fluoride was supplied by B.D.H. laboratories, beryllium fluoride by Alpha Inorganic Inc., and beryllium sulfate by Fisher Chemicals Ltd. Their purity was found to be quite adequate for the studies reported here. Solutions were prepared by weighing samples and adding water to the required volume. The ^{19}F n.m.r. spectra were recorded from a Varian H.R. 60 spectrometer tuned to 56.4 MHz for observation of ^{19}F. An external capillary of TFA was used as a reference. The variation of equilibrium concentration of the species observed was within the experimental error over the temperature range between the freezing point of the solutions and room temperature. It was convenient, therefore, to obtain the area of peaks as the solutions warmed after immersing in liquid nitrogen. Lower temperatures were desirable in order to slow down the fluoride exchange reactions and enable the resolution of quartets for each complex ion due to indirect spin–spin coupling of ^9Be of spin 3/2 with ^{19}F (1).

Results

Solutions of 1.0 *M* BeF_2 in water were made up with varying concentrations of additional NH_4F and $BeSO_4$. The overall ratio $[F^-]/[Be^{2+}]$ was varied between 5 and 0.5. The ambient temperature fluoride resonance of this series of samples showed broad resonances from +84 to +94 p.p.m. from TFA, resolving neither the different BeF_4^{2-}, BeF_3^-, BeF_2, and BeF^+ species nor their multiplet structure. No resonance due to

[1]This work was supported by research grants from the National Research Council of Canada to L.W.R.
[2]NRCC Postdoctorate Fellow, 1968–1970.

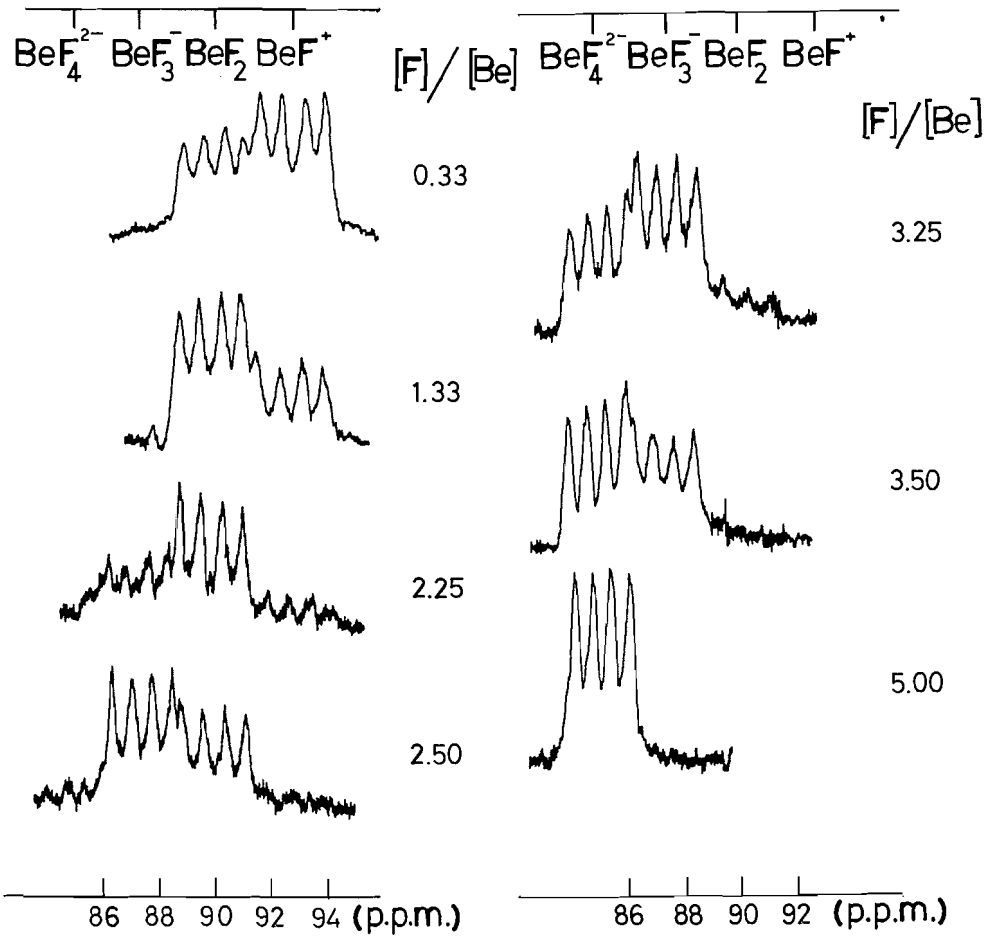

FIG. 1. Fluorine nuclear magnetic resonance spectra of fluoroberyllate complexes in aqueous solution.

fluoride was discerned at $\sim +37$ p.p.m. from TFA, from any of the above samples.

The spectra were improved, however, if the sample tube was cooled by quickly immersing it in liquid nitrogen, placed in the probe, and spectra taken while the sample warmed to room temperature (25 °C) from its melting point (~ -10 °C). In this way, four spectra were measured using the usual audio sideband technique, sweeping alternately up and downfield.

It should be mentioned that these varying temperature conditions did not affect the spectra to any noticeable extent. Differences in chemical shifts and coupling constants were less than the random errors encountered using the audio sideband technique. Differences in intensity measurements between spectra of different temperature could not be detected upon inspection and were less than the errors from cutting out the peaks. This agrees with previous work (1) in which no systematic change in equilibrium constant $[BeF_3^-][F^-]/[BeF_4^{2-}]$ with temperature was discerned, implying that ΔH of dissociation is close to zero.

At these low temperatures, the spectra of each species of BeF_4^{2-}, BeF_3^-, BeF_2, and BeF^+ are found to be 1:1:1:1 quartets (due to coupling to the Be with magnetic moment 3/2) with linewidths at half height of ~20–30 Hz. Selected spectra are shown in Fig. 1 for samples of different [F]/[Be] values. Chemical shifts and coupling constants for each species at each concentration are presented in Tables 1 and 2, respectively. It can be seen that each quartet is distinct from the

Can. J. Chem. Downloaded from www.nrcresearchpress.com by 210.87.254.42 on 09/05/12
For personal use only.

TABLE 1

Chemical shifts of the beryllium fluoride species*

[Additional ions] (M)†		Chemical shift (p.p.m. upfield for TFA)			
NH_4F	$BeSO_4$	BeF_4^{2-}	BeF_3^-	BeF_2	BeF^+
—	3.00			89.67	92.12
—	2.00			89.61	92.08
—	1.50			89.19	91.78
—	1.00		87.37	89.78	92.44
—	0.50		87.72	90.11	92.71
0.00	0.00		88.10	90.28	92.90
0.25			87.64	90.19	93.00
0.50			87.58	89.85	
0.75		85.04	87.35	89.78	
1.00		84.99	87.30	89.65	
1.25		84.84	87.09	89.29	
1.50		84.61	86.85		
2.00		84.51	86.66		
3.00		84.38			
	Range	84.4–85.0	86.7–88.1	89.3–90.3	91.8–93.0

*Concentration effect of BeF^+ opposite in sign to other species.
†All samples contained 1.0 M BeF_2 apart from additional fluoride and beryllium.

TABLE 2

Coupling constants for the beryllium fluoride species

Additional ions (M)		Coupling constant (Hz)			
NH_4F	$BeSO_4$	BeF_4^{2-}	BeF_3^-	BeF_2	BeF^+
	3.00				40.45
	2.00			38.98	40.86
	1.50			38.50	40.59
	1.00			38.60	40.02
	0.50			38.58	40.72
0.00	0.00			38.67	
0.25				38.62	
0.50			36.33	37.58	
0.75			36.57		
1.00			36.41		
1.25		34.29	36.44		
1.50		33.89	36.58		
2.00		33.72			
3.00		33.38			
	Mean	33.84	36.47	38.50	40.53

others since each species has characteristic chemical shift and coupling constant values. There can be no confusion as to the identity of each quartet.

The spectra of BeF_2 in water had been described as a broad resonance at +90.0 p.p.m. ascribed to "BeF_2 polymer" and a quadruplet at +92.2 p.p.m. from TFA ascribed to "BeF_2 monomer" (1). The present results show that these resonances correspond to those due to BeF_2 and BeF^+, respectively. Similarly the coupling constant for "BeF_2" monomer ($J_{Be-F} = 39.9$) agrees with that found for the species we identify as BeF^+. Our assignment of all these multiplets to the various species in Fig. 1 seems reasonable, since it explains the regular changes in chemical shift and coupling constants as each fluorine is replaced by water of solvation and also the regular way in which the intensity of each quartet changes with the [F]/[Be] ratio. The sample with highest [F]/[Be] ratio shows a single quartet due to BeF_4^{2-} and, as the [F]/[Be] ratio decreases, the intermediate species appear then disappear in

Can. J. Chem. Downloaded from www.nrcresearchpress.com by 210.87.254.42 on 09/05/12
For personal use only.

TABLE 3

Intensities and intensity ratios of beryllium fluoride species

[Additional ions] (*M*)*											
NH_4F	$BeSO_4$	[F]/[Be]	I_4	I_3	I_2	I_1	$\frac{I_4}{I_3}$	$\frac{I_3}{I_2}$	$\frac{I_2}{I_1}$	$\frac{K_2}{K_1}$	$\frac{K_3}{K_2}$
2.0	0.0	4.00	62.8	26.9			2.33				
1.50		3.50	41.7	56.7			0.737				
1.25		3.25	40.1	65.5			0.612				
1.00		3.00	12.3	70.0	45.8		0.176	1.53		0.11	
0.75		2.75	15.4	75.4	50.4		0.204	1.50		0.14	
0.50		2.50	9.8	57.7	64.8		0.170	0.891		0.19	
0.25		2.25		34.3	85.6	57.8		0.400	1.48		0.27
0.0	0.0	2.00		32.0	173.6	85.3		0.184	2.04		0.091
	0.50	1.33		20.2	123.0	136.2		0.164	0.903		0.18
	1.00	1.00		24.4	127.3	185.2		0.192	0.687		0.28
	1.50	0.80			112.9	251.1			0.450		
	2.00	0.67			97.3	229.7			0.424		
	3.00	0.50			65.9	242.9			0.271		

*All solutions contained 1.0 *M* BeF_2 apart from the additional fluoride and beryllium.

the expected fashion. The sample with lowest [F]/[Be] ratio contains predominantly BeF^+, but also BeF_2 and, presumably, Be^{2+}.

The intensities of each quartet were measured by photocopying the spectra onto good quality bond paper and cutting out the estimated portion due to each species and weighing. The results are presented in Table 3. Values of I_n are calculated from the weight (in mg) of the cut-out for $BeF_n^{(n-2)-}$ divided by n. Ratios of I_n represent the relative molarities of each species and are used in the calculation of equilibrium constants below.

Discussion

The system

$$BeF_4^{2-} \underset{+F^-}{\rightleftharpoons} BeF_3^- \underset{+F^-}{\rightleftharpoons} BeF_2 \underset{+F^-}{\rightleftharpoons} BeF^+ \underset{+F^-}{\rightleftharpoons} Be^{2+}$$

involves the following equilibria

$$K_1 = [BeF_3^-][F^-]/[BeF_4^{2-}]$$

$$K_2 = [BeF_2][F^-]/[BeF_3]^-$$

$$K_3 = [BeF^+][F^-]/[BeF_2]$$

$$K_4 = [Be^{2+}][F^-]/[BeF^+]$$

The first constant, K_1, has been calculated previously (1) to be $(8.0 \pm 2) \times 10^{-2}$ moles kg^{-1} assuming K_2, K_3, and K_4 to be zero. The concentrations and [F]/[Be] values in this study preclude a direct measurement of fluoride concentration and thus we are unable to calculate K_1 to K_4 directly. Assuming the previous value of K_1, however, the subsequent equilibrium constants are obtained from the following relationships

$$\frac{K_1}{K_2} = \frac{[BeF_3^-]^2}{[BeF_2][BeF_4^{2-}]} = \frac{I_3}{I_2}\cdot\frac{I_3}{I_4}$$

$$\frac{K_2}{K_3} = \frac{[BeF_2]^2}{[BeF^+][BeF_3^-]} = \frac{I_2}{I_1}\cdot\frac{I_2}{I_3}$$

$$\frac{K_3}{K_4} = \frac{[BeF]^2}{[Be^{2+}][BeF_2]} = \frac{I_1}{I_0}\cdot\frac{I_1}{I_2}$$

These computations are possible when at least three Be species are present in measurable amounts in the same sample. These ratios are presented in Table 3 and provide the following results

$$K_2 = (1.1 \pm 0.5) \times 10^{-2}$$

$$K_3 = (2 \pm 2) \times 10^{-3}$$

Substitution of these values into equations used to derive K_1 in ref. 1 shows that the resulting corrections to K_1 are within the accuracy quoted, thus validating our assumption.

Although the Be^{2+} concentration was not directly measured, its value could be deduced with acceptable accuracy. K_4 represents the equilibrium

$$BeF_2 + Be^{2+} \rightleftharpoons 2[BeF^+]$$

The following equations hold true if $[F^-]$, $[BeF_3^-]$, and $[BeF_4^{2-}]$ are negligible, which is reasonable for low [F]/[Be] ratios

Can. J. Chem. Downloaded from www.nrcresearchpress.com by 210.87.254.42 on 09/05/12
For personal use only.

Be balance

$$[BeF_2] + [Be^{2+}] + [BeF^+] = [\text{original } BeF_2] + [\text{added } Be^{2+}] = 1.0 + (1.5, 2.0, 3.0)$$

F balance

$$2[BeF_2] + [BeF^+] = 2\,[\text{original } BeF_2] = 2.0$$

Combining these two equations we get

$$[BeF_2][Be^{2+}]/[BeF^4]^2 = (0.500, 0.501, 0.494)$$

meaning

$$K_3/K_4 = 0.50$$

Therefore

$$K_4 = (1 \pm 1) \times 10^{-3}$$

1. J. Feeney, R. Haque, L. W. Reeves, and C. P. Yue. Can. J. Chem. **46**, 1389 (1968).
2. D. A. Everest. The chemistry of beryllium. Elsevier Publishing Co. 1964. Chap. 4.
3. M. Prytz. A. Anorg. Chem. **231**, 238 (1937).
4. H. S. Gutowsky and C. J. Hoffman. J. Chem. Phys. **19**, 1259 (1951).
5. P. E. Francis and I. J. Lawrenson. J. Inorg. Nucl. Chem. **26**, 1462 (1964).

Can. J. Chem. Downloaded from www.nrcresearchpress.com by 210.87.254.42 on 09/05/12
For personal use only.

The mercury-($^3P_1$)-photosensitized decomposition of formamide vapor[1]

J. C. BODEN[2] AND R. A. BACK
Division of Chemistry, National Research Council of Canada, Ottawa, Canada

Received May 12, 1970

The mercury-($^3P_1$)-photosensitized decomposition of formamide vapor has been studied briefly at 150 °C and pressures of about 1–30 Torr. Volatile products observed were CO, H_2, and NH_3. Three primary processes are postulated

$$Hg^* + NH_2CHO \rightarrow NH_3 + CO + Hg$$
$$\rightarrow NH_2CO + H + Hg$$
$$\rightarrow NHCHO + H + Hg$$

with estimated quantum yields of 0.53, 0.32, and 0.08, respectively. A dependence of product ratios on light intensity and formamide pressure is attributed to hydrogen-atom "cracking" reactions.

Canadian Journal of Chemistry, **48**, 2965 (1970)

Introduction

The photolysis of formamide vapor at 2062 Å has been studied recently in this laboratory (1, 2). Three major primary processes were thought to occur with estimated quantum yields as shown

[1] $NH_2CHO + h\nu \rightarrow NH_2 + CO + H$ (or HCO) ($\Phi = 0.35$)

[2] $\rightarrow H + NHCHO$ ($\Phi = 0.22$)

[3] $\rightarrow NH_3 + CO$ ($\Phi = 0.45$)

At temperatures below 200 °C, the secondary reactions

[4] $H + NH_2CHO \rightarrow H_2 + NH_2CO$

[5] $NH_2 + NH_2CHO \rightarrow NH_3 + NH_2CO$

and combination reactions of NH_2CO and NHCHO radicals completed the reaction mechanism.

The mercury-photosensitized decomposition is of obvious interest for comparison with the photolysis, and has not been investigated before.

Experimental

Apparatus, techniques, purification of formamide, and product analyses were all the same as used in the photolysis experiments (1, 2). The flat-spiral mercury resonance lamp (3) was operated at room temperature with a current of 30 mA, with a 7910 Corning filter to remove light of wavelengths below 2200 Å. The intensity of the 2537 Å light transmitted through the reaction vessel was measured by a type 935 phototube equipped with a suitable filter (4).

The mercury-photosensitized decomposition of propane at 150 °C and 300 Torr was used as an actinometer. The Phillips Research grade propane contained less than 0.01% olefin (by vapor phase chromatographic analysis), and the yield of H_2 was linear with time up to a conversion of 0.015%. Under these conditions, the quantum yield of hydrogen may be taken to be unity (5, 6). The evacuated heated cell was allowed to equilibrate with mercury at room temperature before reagent gases were admitted. The propane was saturated with mercury vapor at room temperature before admission; the formamide was not, because its low volatility did not permit contact with mercury at room temperature. The partial pressure of mercury vapor in the formamide system resulting from this procedure was somewhat irreproducible. In the quantum yield experiments, the light absorption was measured and taken into account. The yield was found to be generally less with formamide (~ 80%) than with propane (~ 98%), probably because of line broadening effects. Complete quenching of $Hg(^3P_1)$ in both systems was assumed in calculating quantum yields.

All experiments were done at 150 °C, a temperature at which the carbamyl (NH_2CO) radical is stable and free-radical chain decomposition does not occur (1, 2). As in the photolysis, corrections were made for the thermal "dark" reaction which accompanied the photosensitized decomposition.

Results and Discussion

The major products observed were CO, H_2, and NH_3, as in the direct photolysis. Much smaller amounts of HCN and CO_2 were detected under some conditions. Yields of individual products showed considerable scatter, probably due to varying mercury concentration, and as light absorption was not measured in most experiments, corrections could not be made. Product ratios, however, were consistent and reproducible. The ratio of CO to H_2 varied with formamide pressure (Fig. 1) and with the ab-

[1]NRCC No. 11 477.
[2]NRCC Postdoctorate Fellow, 1967–1969. Present address: British Petroleum Research Centre, Sunbury-on-Thames, Middlesex, England.

Can. J. Chem. Downloaded from www.nrcresearchpress.com by 210.87.254.42 on 09/05/12
For personal use only.

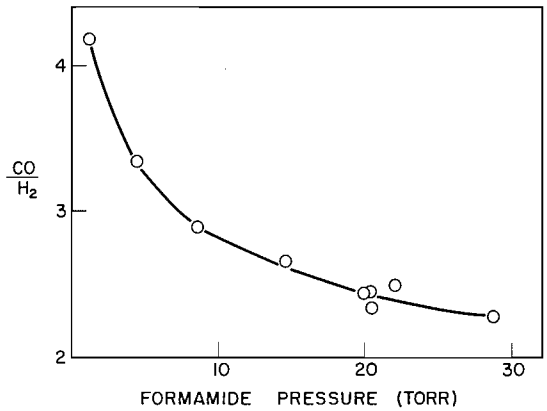

FIG. 1. The dependence of the CO/H_2 ratio on formamide pressure, at approximately constant absorbed light intensity of about 1.5×10^{-9} einsteins l^{-1} s^{-1}.

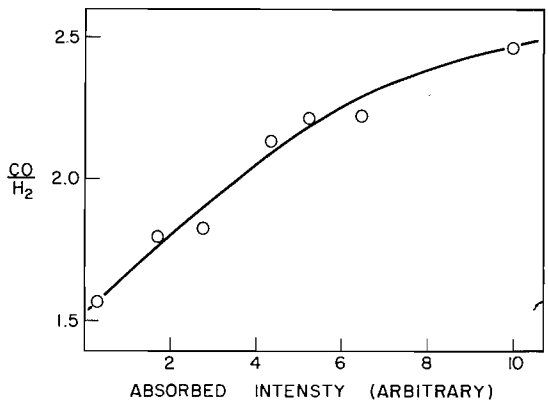

FIG. 2. The dependence of the CO/H_2 ratio on absorbed light intensity at a formamide pressure of 17.5 Torr.

sorbed intensity (Fig. 2), in marked contrast to the photolysis in which no such variation occurred (1). The yield of NH_3 was not measured in all the experiments, but appeared to be consistently about 70% of the CO. Quantum yields of CO and H_2 were measured under two conditions of pressure and light intensity, with careful monitoring of absorbed light intensity and are shown in Table 1.

The similarity of the products to those of the photolysis suggests that a similar mechanism is probably operative in the mercury-photosensitized decomposition. Before a detailed comparison can be made, however, the dependence of product ratios on pressure and intensity must be explained. The light intensity effect must axiomatically involve secondary rather than

TABLE 1

Quantum yields in the mercury-photosensitized decomposition of formamide vapor

Formamide pressure (Torr)	Absorbed light intensity (einstein/l s)	Φ_{CO}	Φ_{H_2}	Φ_{CO}/Φ_{H_2}
4.6	12×10^{-9}	0.77	0.20	3.85
17.4	1.5×10^{-9}	0.60	0.28	2.14

primary processes, and the most probable cause of both effects would appear to be an "atomic cracking" reaction analogous to those well established in low-pressure, high-intensity mercury-photosensitized decomposition of alkanes, and other low-pressure, high atom-concentration systems

[6] $H + NH_2CO \text{ (or } NHCHO) \rightarrow NH_2CHO^*$

[7] $NH_2CHO^* \rightarrow NH_3 + CO \text{ (or } NH_2 + HCO)$

[8] $NH_2CHO^* + M \rightarrow NH_2CHO + M$

where NH_2CHO^* is a vibrationally excited formamide molecule. Reaction 6 will compete with reaction 4 for H atoms, thus reducing the yield of H_2, with high light intensity favoring the former and high formamide pressure the latter. Reaction 7, which produces extra CO, competes with reaction 8, which regenerates formamide and is favored by high pressure. Quantitative treatment of the dependence of the CO/H_2 ratio on pressure and intensity in terms of this mechanism involves a number of unknowns and is not practical with the present data. Approximate linear dependence on $I^{1/2}$ and pressure$^{-1/2}$ can be predicted, and the plots in Fig. 3 support this prediction. It is also intuitively evident that at sufficiently high pressure or low light intensity, reaction 4 should become quantitative, and a common value of CO/H_2 should be attained. The curves in Fig. 3 in fact can both be extrapolated to 1.33, the value of CO/H_2 observed in the direct photolysis, but the extrapolation, especially of the pressure dependence data, is somewhat uncertain.[3]

From the extrapolations in Fig. 3 and the

[3]The apparent absence of reactions 6 to 8 in the direct photolysis appears to be due to the generally lower absorbed light intensities plus the fact that the highest absorbed intensities occurred at the highest pressures. Inhomogeneous absorption of mercury resonance radiation may also have accentuated the differences between the two systems.

Can. J. Chem. Downloaded from www.nrcresearchpress.com by 210.87.254.42 on 09/05/12
For personal use only.

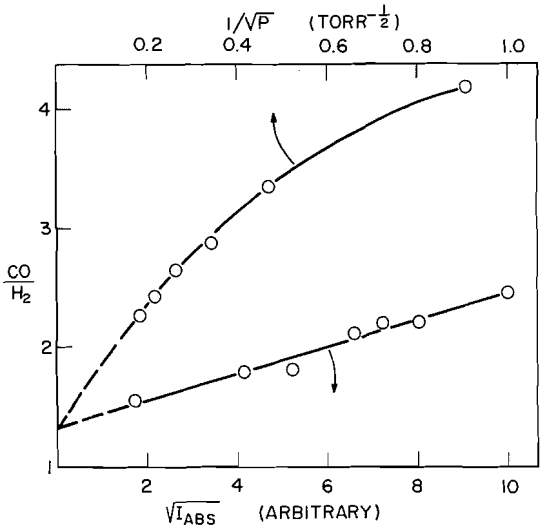

FIG. 3. Plots of the CO/H_2 ratio *vs.* (absorbed intensity)$^{1/2}$ and (formamide pressure)$^{-1/2}$.

quantum yields in Table 1 approximate limiting (low intensity – high pressure) values of $\Phi_{CO} = 0.53$ and $\Phi_{H_2} = 0.40$ may be estimated. These may reasonably be equated to primary yields of CO and H, respectively, as in the direct photolysis (1). The results suggest that 3 major primary dissociation reactions occurred in the mercury-photosensitized decomposition

$$[9] \quad H^* + NH_2CHO \rightarrow NH_3 + CO + Hg \qquad (\Phi = 0.53)$$

$$[10] \quad \rightarrow NH_2CO + H + Hg$$

$$[11] \quad \rightarrow NHCHO + H + Hg \qquad (\Phi = 0.40)$$

In the absence of evidence for collisional deactivation of primary excited species, a total primary quantum yield close to unity seems probable. Because $\Phi_{CO} + \Phi_{H_2} \simeq 1$, it is therefore suggested that CO and H arose from these separate primary processes rather than from a dissociation to $NH_2 + CO + H$ (or HCO) which would lead to $\Phi_{CO} + \Phi_{H_2} > 1$. Support for reaction 9 as the major source of CO comes from the higher yield of NH_3 (70% of the CO compared with 25% in the direct photolysis), since the reactions thought to be responsible for the loss of NH_3 would then be less important (1). Reaction 9 also seems the most reasonable way to account for the excess of CO ($\Phi = 0.53$) over H_2 derived from formyl H-atoms ($\Phi = 0.32$, see below). An argument against reaction 9 is that it violates spin conservation.

To assess the relative importance of reactions 10 and 11, experiments were done with NH_2CDO and ND_2CHO. Isotopic composition of the hydrogen produced is shown in Table 2.

TABLE 2

Isotopic composition of hydrogen from the mercury-photosensitized decomposition of NH_2CDO and ND_2CHO

Compound	Pressure (Torr)	Isotopic composition (%) H_2	HD	D_2
NH_2CDO	20.7	4	37	59
ND_2CHO	20.3	81	19	< 0.5
ND_2CHO	14.6	78	22	< 0.7

From a comparison of these data with those obtained from similar direct photolysis experiments (1), it may be estimated that the hydrogen atoms produced in the primary dissociation were 78% D from NH_2CDO and 83% H from ND_2CHO. Thus for NH_2CHO, reaction 10 probably occurs about 4 times more often than reaction 11, so that $\Phi_{10} = 0.32$ and $\Phi_{11} = 0.08$.

It also follows from the internal consistency of the data in Table 2 and those from the direct photolysis (1) that the hydrogen arose almost entirely from H atoms and not from a molecular process. Also worthy of note is the relatively small deuterium isotope effect in reactions 10 and 11, much smaller than usual for a mercury-photosensitized decomposition.

Tentative estimates of the quantum yields of the three suggested primary processes are $\Phi_9 = 0.53$, $\Phi_{10} = 0.32$, and $\Phi_{11} = 0.08$. Comparison with the direct photolysis (reactions 1 to 3) reveals somewhat more molecular dissociation to $NH_3 + CO$, and much less dissociation of the strong H—NHCHO bond in the mercury-photosensitized decomposition. Both differences may be attributed to the lower energy involved (112.6 *vs.* 138.5 kcal/mole). The major difference postulated between the two systems is the breaking of the $H—CO.NH_2$ bond (reaction 10) in the mercury-photosensitized process instead of the $NH_2—CHO$ bond (reaction 1), which is almost certainly weaker. Such preferential rupture of C—H bonds (instead of weaker C—C bonds, for example) is a common feature of mercury-photosensitized decompositions, and is usually attributed to the occurrence of a specific chemical interaction of the $Hg(^3P_1)$ atom rather than

Can. J. Chem. Downloaded from www.nrcresearchpress.com by 210.87.254.42 on 09/05/12
For personal use only.

simple energy transfer. It might be suggested that reactions 10 and 11 proceed by the former type of process and reaction 9 by the latter. The tentative nature of the interpretation and conclusions of the present study must be emphasized, however, and it is clear that much more work is required before the details of the decomposition can be established with certainty.

1. J. C. BODEN and R. A. BACK. Trans. Faraday Soc. **66**, 175 (1970).
2. R. A. BACK and J. C. BODEN. Trans. Faraday Soc. (To be published).
3. R. A. BACK and D. VAN DER AUWERA. Can. J. Chem. **40**, 2339 (1962).
4. J. G. CALVERT and J. N. PITTS. Photochemistry. John Wiley and Sons, Inc., New York. 1966. p. 729.
5. R. A. BACK. Can. J. Chem. **37**, 1834 (1959).
6. K. YANG. J. Amer. Chem. Soc. **86**, 3941 (1964).

Can. J. Chem. Downloaded from www.nrcresearchpress.com by 210.87.254.42 on 09/05/12
For personal use only.

Can. J. Chem. Downloaded from www.nrcresearchpress.com by 210.87.254.6 on 09/05/12
For personal use only.

The preparation and kinetics of complex formation of hexadimethylsulfoxidovanadium(III) perchlorate[1]

COOPER H. LANGFORD[2] AND FINE MAN CHUNG[3]
Department of Chemistry, Carleton University, Ottawa 1, Canada

Received November 20, 1969

We report the synthesis of the ion $V(DMSO)_6^{3+}$ and kinetics of its reactions with SCN^-, sulfosalicylic acid, and 2,2-bipyridine. The complex formation rates show some dependence on the ligand. The value of $\Delta S^{\ddagger}$ found for the reaction with bipyridine is quite negative. A definite mechanistic assignment cannot yet be made.

Canadian Journal of Chemistry, 48, 2969 (1970)

Introduction

Since Taube's suggestion in 1952 (1) that octahedral V(III) complexes might undergo ligand substitution by an associative mechanism because of the vacancy in the t_{2g} subshell, the chemistry of this system has appeared to be a critical test of theories of substitution. It is interesting that crystal field models also suggest associative reactions of V(III) complexes (2). In contrast, there is no evidence that d^0 ions of small radius are subject to nucleophilic attack (3). Recently, the reaction of $V(OH_2)_6^{3+}$ with NCS^- has been discussed (4, 5) and the substantial negative entropy of activation taken as evidence of associative activation. This contention is, apparently, not supported by results of Espenson (6) who has studied reactions of $V(OH_2)_6^{3+}$ with azide and failed to find a substantial nucleophilicity difference between the two ligands, N_3^- and NCS^-.

We have prepared $V(DMSO)_6(ClO_4)_3$ (DMSO = dimethylsulfoxide). It is a green crystalline material which detonates easily. Its reactions in DMSO solution with SCN^-, sulfosalicylic acid (SSA), and 2,2-bipyridine (bipy) are reported. Several other ligands gave no useful results because of small values of formation constants. Apparently, $V(DMSO)_6^{3+}$ is quite stable in DMSO solution.

Experimental

The complex salt $V(DMSO)_6(ClO_4)_3$ was prepared by addition of excess DMSO to an aqueous solution of V(II) perchlorate which was exposed to air. The solvent was evaporated and the crude $V(DMSO)_6(ClO_4)_3$ purified by several recrystallizations from DMSO under vacuum.

Anal. Calcd. for $VC_6H_{36}S_6Cl_3O_{18}$: C, 17.73; H, 4.44; S, 23.55; Cl, 13.31; V, 6.22. Found: C, 17.45; H, 4.52; S, 23.58; Cl, 12.84; V, 6.12.

The pure dry compound detonates easily.

Materials for reaction studies were reagent grade DMSO dried over 4 Å molecular sieve, reagent grade sodium thiocyanate and sodium perchlorate, reagent grade sulfosalicylic acid, and reagent grade 2,2-bipyridine. Reaction studies were carried out spectrophotometrically in cell chambers thermostatted (±0.02 °C) by circulating water. Most experiments were performed at 25 °C. Equilibrium studies were performed using a Gilford 240 visible–ultraviolet spectrophotometer. Kinetic studies were performed on a Durrum–Gibson stopped flow spectrophotometer. In all cases, data reported are based on the wavelength of maximum absorbance difference between the $V(DMSO)_6^{3+}$ ion and the product complex (within the range of the tungsten filament lamp of the instruments).

Equilibrium data were analyzed using the Newton–Arcand procedure (7). Kinetic data were recorded by photographing oscilloscope traces and were analyzed by the Guggenheim method (8) to give pseudo first order constants for rate of approach to equilibrium. All except T (temperature) dependence studies were made with metal concentration in excess over ligand concentration to ensure that only mono-complex formation was under observation. Ligand concentrations were chosen in the range $1\text{–}5 \times 10^{-4}$ M and $V(DMSO)_6^{3+}$ concentrations chosen in the range $1\text{–}2.5 \times 10^{-2}$ M except in studies of the reaction with SSA where metal ion concentrations were chosen in the range $4\text{–}7 \times 10^{-3}$ M. The reaction with thiocyanate was studied at an ionic strength of $\mu = 0.15$ maintained with $NaClO_4$. Data on the T dependence of one complex formation reaction was obtained from study of the reaction of 0.01 M $V(DMSO)_6^{3+}$ with 0.2 M bipyridine.

Nuclear magnetic resonance transverse relaxation times for DMSO protons in solutions of V^{3+} in DMSO were obtained from measurement of the width at half height of absorption signals on a JEOL C-60 spectrometer equipped with a variable temperature probe.

[1]We thank the National Research Council of Canada for financial support.

[2]Alfred P. Sloan Foundation Research Fellow 1968–1970.

[3]Northern Electric Predoctoral Fellow, 1969–1970.

Can. J. Chem. Downloaded from www.nrcresearchpress.com by 210.87.254.6 on 09/05/12
For personal use only.

Results

In all cases but for the experiments with bipyridine in excess over metal ion, the observations of complex formation are relevant to a system approaching equilibrium and described by reaction [1].

$$[1] \quad V(DMSO)_6^{3+} + L^{n-} \underset{k_r}{\overset{k_f}{\rightleftharpoons}} V(DMSO)_5L^{(3-n)+} + DMSO$$

For reaction [1] we have an equilibrium constant, K_{eq}, obtained from the Newton–Arcand analysis and a rate constant for approach to equilibrium, k_{eq}, obtained from the stopped flow data. We wish to resolve these observed constants into the second order rate constant for complex formation, k_f and the first order rate constant for complex dissociation k_r. This is accomplished by noting that for every (large) value of the metal concentration the rate constant for approach to equilibrium is pseudo first order and noting that the result for opposed first order reactions (the rate constant for approach to equilibrium is the sum of the forward and reverse rate constants) holds.

The analysis for a typical case is illustrated by data on the reaction of $V(DMSO)_6^{3+}$ with sulfosalicylic acid shown in Table 1. The results for all three ligands are collected in Table 2.

The temperature dependence of the complex formation reactions was not studied under the conditions relevant to the data in Table 2. The requirement for accurate determination of the temperature dependence of both K_{eq} and k_{eq} makes evaluation of $\Delta H^{\ddagger}$ and $\Delta S^{\ddagger}$ for the forward reaction an uncertain business. It was found that the reaction of $V(DMSO)_6^{3+}$ with *excess* bipyridine gave a trace corresponding to first order kinetics but associated with a larger absorbance change. The rate constant for this reaction at 25° (0.122 M^{-1} s^{-1}) is in fairly good agreement with the value of k_f quoted in Table 2 for the reaction with bipyridine (0.11 ± 0.01 M^{-1} s^{-1}). Therefore, the T dependence of this reaction with excess bipyridine was studied to give an estimate of the activation parameters for a case of complex formation in the range from 20 to 45 °C. Figure 1 shows the Arrhenius plot. It yields $\Delta H^{\ddagger}$ = 11.7 kcal/mole and $\Delta S^{\ddagger}$ = −25 e.u.

The one additional reaction which would be of great interest in the elucidation of the mechanisms employed by $V(DMSO)_6^{3+}$ is the solvent exchange process. Potentially, measurement of nuclear magnetic resonance (n.m.r.) transverse relaxation times (from line width at half height) as a function of T could provide this information (9). However, we found the DMSO proton line in this system underwent slight narrowing with increasing T over the range 20 to 140 °C. The apparent activation energy was less than 1 kcal $mole^{-1}$. Lines were relatively narrow. This suggests outer sphere relaxation only, modulated

TABLE 1

Reaction of $V(DMSO)_6^{3+}$ with SSA studied at 435 mμ*

$[V^{3+}]$ ($M \times 10^3$)	k_{eq} (pseudo first order) ($s^{-1} \times 10^3$)	k_f(M^{-1} s^{-1})
4.00	2.55	0.207
4.50	2.70	0.222
5.00	2.74	0.206
5.50	2.79	0.202
6.00	2.90	0.202
6.50	3.05	0.205
7.00	3.10	0.209

*$[V^{3+}]$ = 4–7 × 10^{-3} M; K_{eq} = 122 ± 10 M; [SSA] = 1 × 10^{-4} M. k_f (average) = 0.21 ± 0.01 M^{-1} s^{-1}; $k_r = k_f/K_{eq}$ = 1.7 × 10^{-3} s^{-1}.

TABLE 2

Rate and equilibrium constants for complex formation reactions of $V(DMSO)_6^{3+}$ at 25 °C

Ligand	K_{eq} (M^{-1})	k_f (M^{-1} s^{-1})	k_r (s^{-1})	Wavelength (mμ)
SCN^-*	143 ± 10	210 ± 10	1.5	356
Bipy	30.8 ± 1.0	0.11 ± 0.01	0.0036	366.5
SSA	122 ± 10	0.21 ± 0.01	0.0017	435

*Ionic strength for these experiments = 0.15 maintained with $NaClO_4$.

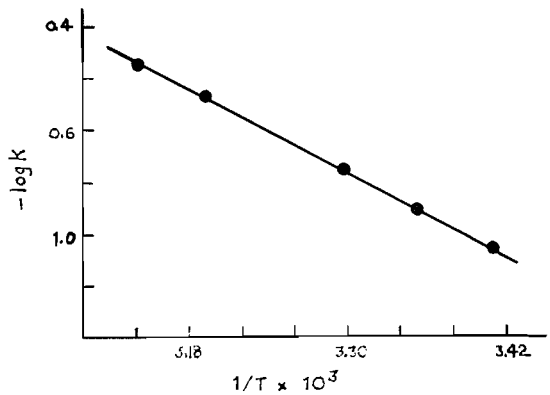

FIG. 1. Log of the rate constant (M^{-1} s^{-1}) for the reaction with excess bipyridine as a function of the reciprocal of the absolute temperature ($°K^{-1}$).

Can. J. Chem. Downloaded from www.nrcresearchpress.com by 210.87.254.6 on 09/05/12
For personal use only.

by the electronic relaxation time of the paramagnetic vanadium. It would appear that chemical exchange is not controlling up to 140°.

Discussion

It is probable that the reaction described in [1] should be written (3) as

$$[2]\quad V(DMSO)_6^{3+} + L \overset{K_E}{\rightleftharpoons} V(DMSO)_6^{3+},L \overset{k_1}{\underset{k_{-1}}{\rightleftharpoons}} V(DMSO)_5L + DMSO$$

In reaction [2], the first step is the rapid formation of the encounter complex (outer sphere complex or ion pair represented as $V(DMSO)_6^{3+},L$) which may be described by an equilibrium constant K_E. The second step is the slow replacement of a coordinated DMSO by L and its reverse reaction. The observed value of k_f is interpreted as

$$[3]\quad k_f = K_E k_1$$

The first mechanistically interesting question is whether k_1 varies significantly with variation of L indicating significant binding of L in the transition state and an associative mode of activation. This is a difficult question to answer. K_E must be estimated to get k_1 values for this purpose. Fuoss' equation (10) which includes steric and electrostatic factors in the estimation of K_E was used with an assumed distance of closest approach between $V(DMSO)_6^{3+}$ and L of 5 Å. (This distance has little more to justify it than that it has been used in other similar calculations (11) and that the relative values of K_E are not especially sensitive to the choice.) For a singly negative ion, the value estimated for K_E is approximately 7 at an ionic strength of 0.15. (Perhaps the value of K_E is too small since an extended Debye–Hückel expression had to be used for ionic strength correction.) The value of K_E for the neutral ligands is estimated to be 0.3. Using the K_E values from the simple calculations, estimated values of k_1 are: 30 s^{-1} (SCN^-), 0.4 s^{-1} (bipy), and 0.7 s^{-1} (SSA).

The differences among these three estimated first order rate constants should define a nucleophilicity order but that is not certain. It is worth noting that the two neutral nucleophiles in this study are significantly different; one is an N donor, the other an O donor yet the rate constants are close.

Ignoring the attempt to calculate K_E from a crude theoretical model, the observed second order rate constants may be compared to some results obtained in one other solvent of moderate dielectric constant for which appropriate data are available. Reactions of $Ni(CH_3OH)_6^{2+}$ with dithiooxalate^{2-}, SCN^-, and bipy have been reported by Pearson and Ellgen (12). At an ionic strength of 0.100 the second order rate constants are 2.5×10^5, 7.4×10^3, and 1.2×10^2 M^{-1} s^{-1}. These three cases are of charge type 2:2, 2:1, and 2:0. The methanol results are suggestively similar to those for the vanadium(III) reactions of charge types 3:1 and 3:0. Unfortunately, the Ni(II) results have been taken to imply dissociative substitution without any nucleophilic assistance from the entering ligand (12).

Another factor may be more mechanistically suggestive. Substantially negative values of $\Delta S^{\ddagger}$ have been taken as indicative of the associative mode of activation. The arguments are appealing although it must be admitted that the origins of $\Delta S^{\ddagger}$ are complex and an isolated value is dangerous ground on which to found a mechanistic hypothesis. Although the one $\Delta S^{\ddagger}$ result here supports the result of the study of $V(OH_2)_6^{3+}$ with SCN^- (4, 5), the dependence of rate on nucleophilicity of the entering ligand cannot be claimed to have been unambiguously demonstrated. Regrettably, our search for additional ligands to test only revealed that many complex formation equilibria favor $V(DMSO)_6^{3+}$.

1. H. Taube. Chem. Rev. **50**, 69 (1952).
2. F. Basolo and R. G. Pearson. Mechanics of inorganic reactions. 2nd ed. John Wiley and Sons, Inc., New York. 1967. p. 146.
3. C. H. Langford and T. R. Stengle. Ann. Rev. Phys. Chem. **19**, 193 (1968).
4. B. R. Baker, N. Sutin, and T. J. Welch. Inorg. Chem. **6**, 1948 (1967).
5. W. Kruse and D. Thusius. Inorg. Chem. 7, 464 (1968).
6. J. H. Espenson and J. R. Pladziewicz. Abstr. 156th Natl. Meeting Amer. Chem. Soc., Minneapolis, April 1969.
7. T. W. Newton and G. M. Arcand. J. Amer. Chem. Soc. **75**, 2449 (1953).
8. A. A. Frost and R. G. Pearson. Kinetics and mechanism. 2nd ed. John Wiley and Sons, Inc., New York. 1965. p. 49.
9. T. R. Stengle and C. H. Langford. Coord. Chem. Rev. **2**, 349 (1967).
10. R. M. Fuoss. J. Amer. Chem. Soc. **80**, 5059 (1958).
11. C. H. Langford and F. M. Chung. J. Amer. Chem. Soc. **96**, 4485 (1968).
12. R. G. Pearson and P. Ellgen. Inorg. Chem. **6**, 1379 (1967).

Can. J. Chem. Downloaded from www.nrcresearchpress.com by 210.87.254.40 on 09/05/12
For personal use only.

Thermogravimetric analysis of Ontario limestones and dolomites I. Calcination, surface area, and porosity

R. K. CHAN

Department of Chemistry, University of Western Ontario, London 72, Ontario

AND

K. S. MURTHI AND D. HARRISON

Chemical Research Department, Ontario Hydro Research Division, Toronto 18, Ontario

Received April 8, 1970

The calcination of natural Ontario limestones and dolomites in a flow of 100 cm^3/min of nitrogen at 745 °C required from 0.43 ± 0.03 to 0.35 ± 0.05 min/mg of 100 mesh samples, respectively. The nitrogen adsorption isotherm at 77 °K for all the calcined samples belonged to the type II isotherm of the B.D.D.T. classification. There was hardly any hysteresis between the adsorption and desorption branches which implied that most of the pores were relatively large in agreement with independent measurements of the most probable pore diameter by an Aminco mercury intrusion porosimeter (~0.1 μ). The B.E.T. surface areas ranged from 13.6 to 34.2 m^2/g of oxide calcined at 745 °C. The surface area decreased rapidly with increasing calcination temperature. At 1090 °C the surface area was less than 1 m^2/g. The surface area was also related to percentage calcination, percentage calcium oxide in the sample, and size of the sample. A sample of pure magnesium carbonate calcined at 565 °C had an inordinately large surface area of 174 m^2/g; pure calcium carbonate calcined at 745 °C, 15.2 m^2/g. Using a model of non-intersecting cylindrical or square capillaries for the pore configurations, one could calculate the surface area, porosity, and bulk density of the calcined samples with satisfactory agreement.

Canadian Journal of Chemistry, 48, 2972 (1970)

Introduction

There exists in Ontario an abundant, low cost, and readily accessible supply of limestone and dolomite. The present study is conducted to survey the chemical and physical properties of selected local supplies. The survey was made because of their potential application in controlling sulfur dioxide emission from the smoke stacks of fossil-fuel-fired electricity generating stations.

Experimental

The calcination of samples was carried out on the heated pan of a Cahn recording gram electrobalance. The schematic diagram of thermogravimetric analysis (TGA) apparatus with the concentric flow-through tube is shown in Fig. 1. The glass vacuum bottle was modified by replacing the standard taper joints with O-ring joints so that the flow-through tube could be removed and replaced frequently without disturbance to the delicate weighing mechanism and the weight calibration. The electrobalance was flushed constantly by a stream of dry nitrogen at 200 cm^3/min to prevent back-diffusion of gases from the flow-through tube.

The sample was ground in an unglazed porcelain mortar and pestle. The powder was stored in a small screw-cap glass vial. The size range of the powder was such that 70–80% of it was between 149 to 74 μ (100 and 200 mesh). The remaining 30–20% was finer. Baker reagent grade $CaCO_3$ and $MgCO_3$ were powdered precipitates all of which passed through a 200 mesh screen. Approximately 100 mg of a ground sample were placed in the quartz bucket and weighed accurately to the nearest 0.1 mg. Dry nitrogen at a flow rate of 100 cm^3/min passed over the sample. Because the inner diameter of the concentric flow-through tube was 20 mm, the linear velocity of flow at the calcination temperature of 745 °C was 1.8 cm/s, which caused an apparent weight loss of 0.1 mg. A Fisher Model 360 Linear Temperature Programmer was used to control the furnace temperature. The linearity of the program was ±1% and isothermal control was ±0.25%. For calcination, the furnace was heated up to 745 °C as quickly as possible. Because of the thermal inertia of the furnace, the heating period was approximately 11 min. The electromotive force (e.m.f.) equivalent to the weight change, and the e.m.f. equivalent to the temperature which was measured by a 26-gauge chromel–alumel thermocouple, were displayed simultaneously on a Hewlett–Packard two-channel strip chart recorder. One hundred mg full scale and 6 in. h^{-1} were convenient settings to display the rate of calcination. During calcination, the sample lost weight because of the thermal decomposition of carbonates.

After calcination, the sample of oxide was cooled to room temperature and evacuated at the same time for at least 4 h. The final vacuum was better than 10^{-4} Torr. The surface areas were determined gravimetrically by the B.E.T. method (1). The nitrogen adsorption isotherms at 77 °K for all the calcined samples belonged to the type II isotherm of the B.D.D.T. classification (2). The surface areas were calculated by eq. [1], which worked best for type II isotherms

$$[1] \qquad \frac{P}{X(P_0 - P)} = \frac{1}{X_m c} + \frac{c - 1}{X_m c} \cdot \frac{P}{P_0}$$

where X is the amount of nitrogen adsorbed, X_m the

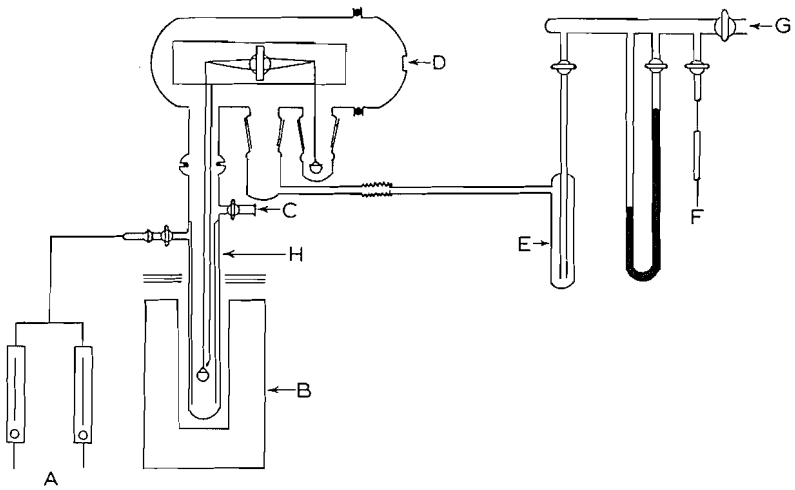

FIG. 1. Schematic diagram of TGA apparatus. *A*, Matheson low flow flowmeters and supplies of N_2 and SO_2; *B*, furnace controlled by Fisher model 360 linear temperature programmer; *C*, exhaust; *D*, to Cahn RG Electrobalance control unit and two-channel strip chart recorder; *E*, cold trap; *F*, capillary flowmeter and supply of N_2; *G*, to McLeod gauge, Hg diffusion pump, cold traps and mechanical pump; *H*, concentric flow-through tube.

monolayer capacity, ϵ is a measure of the net heat of adsorption, P and P_0 the pressure and saturated vapor pressure of nitrogen. When $P/X(P_0 - P)$ is plotted against P/P_0, a straight line is obtained in the range of $0.05 < P/P_0 < 0.35$ with slope $s = (c - 1)/(X_m c)$ and intercept $i = 1/(X_m c)$. Therefore, $X_m = 1/(s + i)$. X_m divided by the amount of calcined sample gives the monolayer capacity per gram of oxide, $\bar{X}_m$. The surface area, S, in m^2/g, is directly proportional to the monolayer capacity per gram,

$$[2] \qquad S = (\bar{X}_m N A/M) \times 10^{-20}$$

where N is the Avogadro's number, M molecular weight of nitrogen, A the average area in square Ångstrom units occupied per nitrogen molecule. The latter may be calculated from the density of liquid nitrogen at 77 °K. If the adsorbate molecules are assumed to be close-packed in the bulk liquid and on the surface of the adsorbent, the average area occupied per molecule would be given by

$$[3] \qquad A = 2\sqrt{3}\left(\frac{M}{4\sqrt{2}Nd}\right)^{2/3} \times 10^{16}$$

where d is density of liquefied adsorbate (3). For liquid nitrogen the density is 0.808 g/cm³ at 77 °K and A was calculated to be 16.2 Å².

The pore volume of calcined samples was measured by an Aminco 60 000 p.s.i. mercury intrusion porosimeter. As the pressure was increased stepwise, mercury was forced into progressively smaller pores. The amount of mercury intrusion was monitored as changing electrical capacitance of a receding mercury column. The uncertainty in the measurement of the intrusion volume was ±1%.

Results and Discussion

Nine samples from quarries located strategically around the Great Lakes were collected for this study (4). Table 1 gives the composition of these samples which were determined by the standard limestone analysis (5). The main undesirable impurities in the carbonate rocks are silica and alumina. These impurities combine with calcium oxide at elevated temperatures to form a slag which would reduce the pore volume and the amount of available active lime (6). Such impurities either occurred in the matrix or came from the material in the crevices and other strata excavated along with the limestone. Samples were chosen from quarries in which these impurities are low. When the limestone samples are decomposed essentially isothermally, the rate of decomposition seems to be controlled by some stage of the process occurring in the interface. However, at temperatures above 950 °C the rate of decomposition is governed by the rate of heat transfer across the layer of reaction product to the receding interface (7, and references therein). A correction was made to obtain the duration of decomposition under isothermal condition. Assuming constant rate of interface movement under isothermal condition, a plot of $[1 - (1 - \alpha)^{1/3}]$ against time should give a straight line for a spherical or cubic sample, where α is the fraction of decomposition. Extrapolation of $[1 - (1 - \alpha)^{1/3}]$ plot to zero yields the starting time of the isothermal decomposition. In contrast to the smooth decomposition of limestone, dolomite decomposes rapidly to calcium carbonate, magnesium oxide, and carbon dioxide on

Can. J. Chem. Downloaded from www.nrcresearchpress.com by 210.87.254.40 on 09/05/12
For personal use only.

TABLE 1

Chemical compositions of limestones and dolomites in weight %

Number	Sample source	Standard limestone analysis				
		CaO	MgO	R_2O_3	SiO_2	CO_2
1211	Beachville 1	54.7	0.6	0.2	0.1	43.5
1213	Uhthoff	52.1	1.2	1.2	2.5	42.0
1214	Picton	50.9	1.3	1.7	3.8	41.2
1217	Beachville 2	55.1	0.5	0.1	—	44.3
1212	Dundas	30.2	21.0	0.4	0.5	46.6
1215	Queenston	32.6	16.4	2.0	4.1	43.6
1216	Guelph	30.5	21.5	0.2	—	47.4
1218	Cayuga	29.1	19.0	1.5	4.4	44.1
1219	Acton	30.2	19.8	0.8	0.6	46.7

TABLE 2

Calcination of 100 mesh samples at 745 °C in 100 cm^3/min of nitrogen flow

Number	Wt. of sample (mg)	Oxide (%)	Duration for 100% calcination t (min)	$\frac{t}{\text{Wt. sample}}$ (min/mg)	Number	Wt. of sample (mg)	Oxide (%)	Duration for 100% calcination t (min)	$\frac{t}{\text{Wt. sample}}$ (min/mg)
Limestones					Dolomites				
1211	100.7	56.4	50	0.49	1212	101.4	52.9	41	0.40
1211	104.5	55.8	40	0.30	1212	109.9	53.1	46	0.42
1211	269.0	55.8	113	0.42	1212	276.0	52.9	108	0.39
1211	356.6	56.1	183	0.51	1215	101.5	56.1	29	0.29
1213	100.4	57.6	42	0.42	1215	108.8	55.7	39	0.36
1213	103.6	57.6	42	0.41	1216	100.4	52.3	26	0.26
1213	266.6	59.3	114	0.43	1218	100.4	55.5	40	0.40
1214	100.5	58.4	44	0.44	1218	112.5	56.3	48	0.42
1214	104.5	58.3	42	0.40	1219	100.0	52.9	28	0.28
1214	268.0	59.8	129	0.48	1219	117.4	52.7	31	0.26
1217	99.6	56.0	36	0.36					
1217	102.5	55.9	41	0.40					
$CaCO_3$	103.9	56.2	46	0.44					

heating to 745 °C in nitrogen, followed by a slower decomposition of the remaining calcium carbonate (8). Therefore, for dolomites the initial stage of decomposition was assumed to be due to decomposition of dolomite only and the correction to isothermal condition was applied accordingly. The starting time of the isothermal decomposition could be determined to an accuracy of ± 1 min. The rate and temperature of calcination for typical samples of limestone and dolomite are shown in Figs. 2 and 3. As expected, the durations for 100% calcination were longer for limestones (0.43 $\pm$ 0.03 min/mg) than for dolomites (0.35 $\pm$ 0.05 min/mg) because of the higher decomposition temperature of limestone samples. The results in Table 2 are depicted graphically in Fig. 4 in which each sample was assigned equal statistical weight.

After calcination the resultant oxides have lower molar volumes, larger surface areas, and greater porosities than the carbonates. According to Glasson (9), calcination of a carbonate entails the formation of an oxide having a pseudo-lattice of the carbonate and subsequent recrystallization to the normal cubic lattice of the oxide. If the temperature is high enough, sintering of the oxide will result. The surface areas of calcined samples were determined gravimetrically by the B.E.T. method (1). The nitrogen adsorption isotherms at 77 °K belong to the type II isotherm according to the B.D.D.T. classification (2). Representative adsorption isotherms and B.E.T. plots of limestone 1211 and dolomite 1212 are shown in Figs. 5 and 6. There is hardly any hysteresis between the adsorption and desorption branches, which implies that most of the pores are relatively large (ca. 0.1 μ, Table 3). For such large pore diameters, the hysteresis would occur

Can. J. Chem. Downloaded from www.nrcresearchpress.com by 210.87.254.40 on 09/05/12
For personal use only.

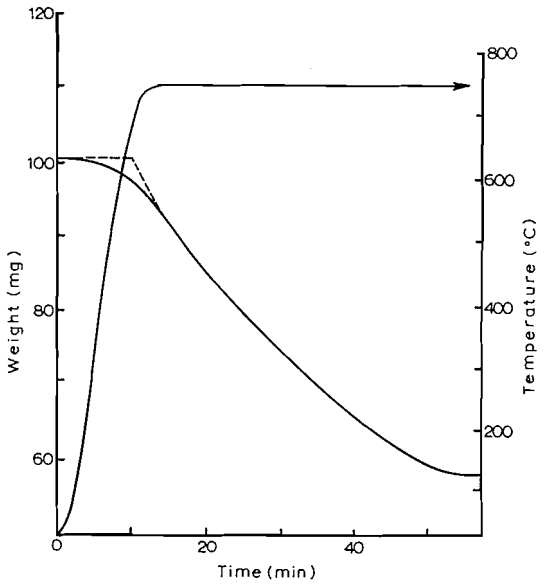

FIG. 2. Rate of calcination for limestone 1214. The dashed curve is corrected to isothermal condition.

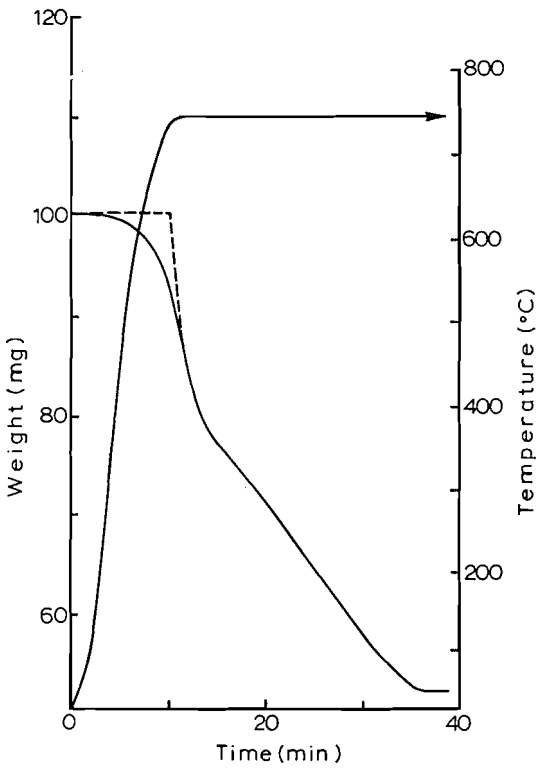

FIG. 3. Rate of calcination for dolomite 1216. The dashed curve is corrected to isothermal condition.

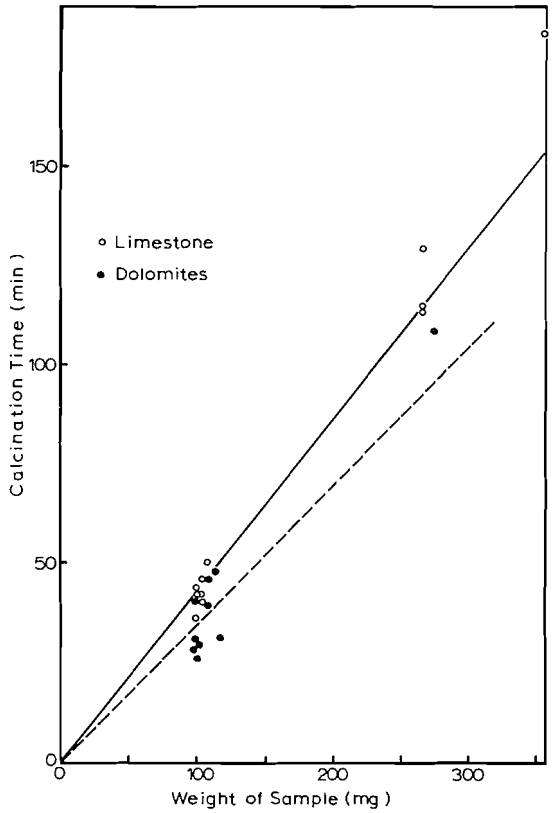

FIG. 4. Duration for complete decomposition vs. weight of sample. Solid and dashed lines represent the average slopes which are the durations per mg of limestone and dolomite, respectively.

near the saturated vapor pressure of the adsorbate (10). The surface areas of all samples calcined at 745 °C in 100 cm^3/min of nitrogen are given in Table 3. The pore volumes and most probable pore diameters of samples calcined at 837 °C were measured by an Aminco 60 000 p.s.i. mercury intrusion porosimeter. Typical results for limestone 1211 and dolomite 1212 are shown in Fig. 7. The histograms of pore size distribution are given in Fig. 8. The bulk density of a calcined sample is equal to the reciprocal of the sum of pore volume per gram and specific volume of crystalline oxide. The porosity is equal to pore volume times bulk density.

The surface area of a calcined sample can be estimated from pore volume and the most probable pore diameter when a simple model is used to represent the pore configurations. When the pores are assumed to be non-intersecting cylindrical capillaries (11), then

Can. J. Chem. Downloaded from www.nrcresearchpress.com by 210.87.254.40 on 09/05/12
For personal use only.

[4] surface area of pores $= \pi Dl$

[5] pore volume $= \pi(D/2)^2 l$

where D is the most probable pore diameter and l is the total length of the pores. Eliminating l from eqs. [4] and [5], one obtains

[6] surface area of pores $=$

$$\frac{4 \times \text{pore volume}}{\text{most probable pore diameter}}$$

The calculated surface areas are listed in column 3 of Table 3. It is worthwhile to point out that a similar model based on non-intersecting square capillaries with sides equal to D gives identical results. There is a correlation between the measured surface areas for samples calcined at 745 °C and calculated values at 837 °C. The slope of the correlation is 0.57 ± 0.10. When limestone 1211 was calcined at 745 °C the surface area was 24.6 m^2/g, and when it was calcined at 875 °C, 8.7 m^2/g. After it has been heated to 1090 °C for 20 min, the surface area was reduced to less than 1 m^2/g. The interpolated surface area at 837 °C is 12 m^2/g. The ratio of surface area at 837 °C to that at 745 °C is 0.49 which agrees with the slope, within the experimental errors. In addition, there is evidence of an inverse relationship between the most probable pore diameters and surface areas. Therefore, the simple models postulated for the pore configurations are reasonable.

The theoretical porosities of oxides obtained from calcination of limestone and dolomite are summarized in Table 4. The calculations are based on the X-ray data of the carbonates and oxides assuming no sintering has occurred during calcination (12).

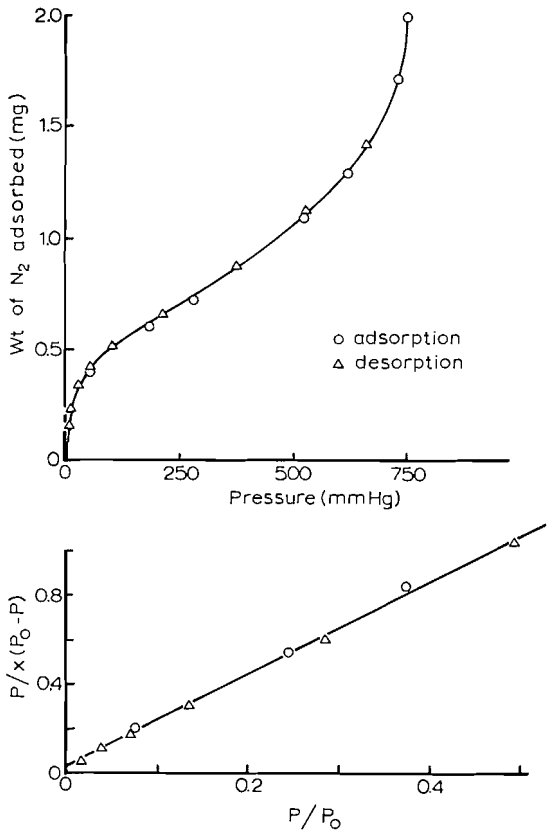

FIG. 5. Nitrogen adsorption isotherm at 77 °K and B.E.T. plot of limestone 1211: 356.3 mg of sample calcined at 875 °C for 12 min; 200.6 mg of oxide with surface area of 8.7 m^2g; X is the amount of nitrogen adsorbed in mg; P and P_0 are the pressure and saturated vapor pressure of nitrogen in mm Hg at 77 °K.

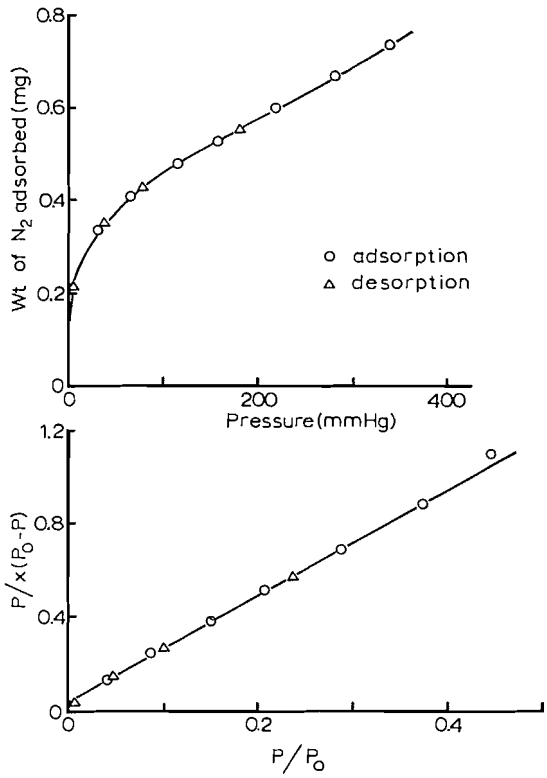

FIG. 6. Nitrogen adsorption isotherm at 77 °K and B.E.T. plot of dolomite 1212: 109.9 mg of sample calcined at 745 °C for 46 min; 58.4 mg of oxide with surface area of 26.4 m^2/g; X is the amount of nitrogen adsorbed in mg; P and P_0 are the pressure and saturated vapor pressure of nitrogen in mm Hg at 77 °K.

Can. J. Chem. Downloaded from www.nrcresearchpress.com by 210.87.254.40 on 09/05/12
For personal use only.

TABLE 3

Surface areas, pore volumes, most probable pore diameters, bulk densities, and porosities of calcined samples

Number	Surface area (m^2/g) Measured (745 °C)	Surface area (m^2/g) Calculated (837 °C)	Ratio of calcd. and meas. surface area (%)	Pore volume (cm^3/g)	Most probable pore diameter (μ)	Bulk density (g/cm^3)	Experimental porosity (%)
1211	24.6	14.2	0.577	0.32	0.090	1.61	51.6
1213	13.6	7.6	0.559	0.34	0.18	1.56	53.0
1214	14.7	9.0	0.612	0.38	0.17	1.47	55.8
1217	20.6	7.6	0.369	0.34	0.18	1.56	53.1
1212	26.4	12.0	0.454	0.42	0.14	1.41	59.3
1215	20.2	18.8	0.930	0.41	0.087	1.42	58.2
1216	30.1	16.2	0.538	0.40	0.099	1.45	58.0
1218	34.2	16.2	0.474	0.39	0.096	1.47	57.3
1219	26.1	15.5	0.595	0.33	0.085	1.61	53.1
$CaCO_3$	15.2						
$MgCO_3$	174*						

*$MgCO_3$ was calcined at 565 °C.

$$[7] \quad \text{theoretical porosity} = \frac{\text{molar volume of carbonate} - \text{molar volume of oxide}}{\text{molar volume of carbonate}} \times 100$$

The theoretical and experimental porosities agree satisfactorily for calcined limestone and dolomite samples. Such quantitative agreements imply little or no sintering of the sample calcined at 837 °C. It is interesting to compare the present results with those of limestones calcined at considerably higher temperatures. Boynton (13) listed calcination temperatures ranging from 930 to 1320 °C, retention times 46 to 474 min, bulk densities 1.72 to 2.67 g/cm^3, porosities 18.6 to 48.4%, volumetric shrinkages 12.1 to 44.2%, and surface areas less than 2 m^2/g.

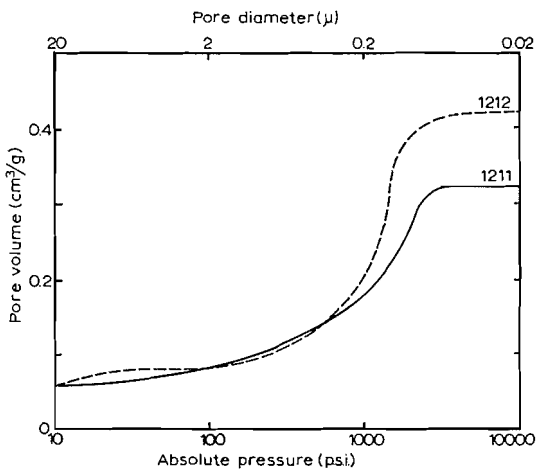

FIG. 7. Pore size distribution of limestone 1211 and dolomite 1212 calcined at 837 °C.

The higher porosity of magnesium oxide (Table 4) is expected to give a higher surface area (Table 3). Indeed, there exists some correlation between the surface areas and the percentage of calcium oxide in the samples. Pure magnesium

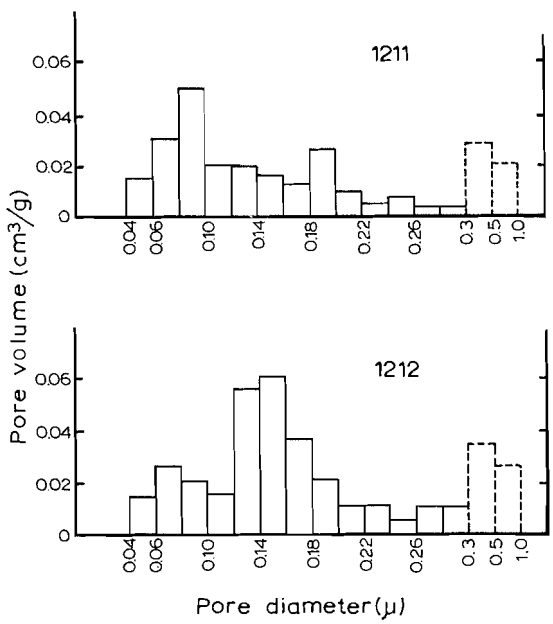

FIG. 8. Histograms of pore size distribution of limestone 1211 and dolomite 1212 calcined at 837 °C. The pore size ranges are 0.02 from 0.04–0.30 μ. The last 2 ranges are 0.3–0.5 μ and 0.5–1.0 μ.

Can. J. Chem. Downloaded from www.nrcresearchpress.com by 210.87.254.40 on 09/05/12
For personal use only.

TABLE 4

Porosities of oxides

Substance	Molar volume (cm^3/mole)	Porosity (%)	
		Theoretical	Experimental
$CaCO_3$	36.93		
CaO	16.76	54.62	54.4±1.2
$CaCO_3 \cdot MgCO_3$	64.34		
CaO, MgO	28.01	56.47	57.2±1.6
$MgCO_3$	28.02		
MgO	11.25	59.85	

carbonate calcined at 565 °C has an inordinately high surface area of 174 m^2/g (14). For limestone sample 1211, 83.5% calcination at 745 °C gives a surface area of 15.6 m^2/g; 100%, 24.6 m^2/g. In other words, 83.5% calcination attains only 63.5% of the final surface area. For a number of samples the surface areas have been measured for different sample sizes. According to data in Table 2, the surface areas decrease at an average rate of 3.4 ± 0.8 m^2/g for every 100 mg of sample. All these findings are in qualitative agreement with Glasson who found that surface areas increased non-linearly with percentage decomposition (9) but were correspondingly lower where larger samples required longer duration of calcination (15).

The authors wish to acknowledge the financial support of the Department of University Affairs and the Ontario Hydro, and to thank Mr. C. H. Clark, Engineer-in-Charge, Chemical Research Department and Mr. J. H. Waghorne, Director of Research of the Ontario Hydro for encouragement received to carry out this project.

1. S. BRUNAUER, P. H. EMMETT, and E. TELLER. J. Amer. Chem. Soc. **60**, 309 (1938).
2. S. BRUNAUER, L. S. DEMING, W. S. DEMING, and E. TELLER. J. Amer. Chem. Soc. **62**, 1723 (1940).
3. E. O. KRAEMER, J. W. WILLIAMS, and R. A. ALBERTY. *In* A treatise on physical chemistry. *Edited by* H. S. Taylor and S. Glasstone. 3rd ed. Van Nostrand Co. 1951. p. 604.
4. D. F. HEWITT. The limestone industries of Ontario. Ontario Department of Mines, Industrial Mineral Circular No. 5, 1960 and No. 13, 1964.
5. A. I. VOGEL. Quantitative inorganic analysis. 2nd ed. Longmans. 1951. p. 582.
6. P. NICHOLLS and W. T. REID. Trans. Amer. Soc. Mech. Engrs. **54**, 167 (1932).
7. T. R. INGRAHAM and P. MARIER. Can. J. Chem. Eng. **41**, 170 (1963).
8. P. D. GARN. Thermoanalytical methods of investigation. Academic Press. 1965. pp. 311 and 405.
9. D. R. GLASSON. J. Appl. Chem. **8**, 793 (1958).
10. S. J. GREGG and K. S. W. SING. Adsorption, surface area and porosity. Academic Press. 1967. Chap. 3.
11. D. H. EVERETT. The structure and properties of porous materials. Butterworths. 1958. p. 95.
12. R. C. WEAST (*Editor*). Handbook of Chemistry and Physics. 49th ed. 1968–1969. Chemical Rubber Co., Ohio. p. B-308.
13. R. S. BOYNTON. Chemistry and technology of lime and limestone. Interscience. 1966. p. 147.
14. D. R. GLASSON. J. Appl. Chem. **13**, 111 (1963).
15. D. R. GLASSON. J. Appl. Chem. **11**, 201 (1961).

Can. J. Chem. Downloaded from www.nrcresearchpress.com by 210.87.254.40 on 09/05/12
For personal use only.

Can. J. Chem. Downloaded from www.nrcresearchpress.com by 210.87.254.6 on 09/05/12
For personal use only.

Thermogravimetric analysis of Ontario limestones and dolomites. II. Reactivity of sulfur dioxide with calcined samples

R. K. CHAN

Department of Chemistry, University of Western Ontario, London 72, Ontario

AND

K. S. MURTHI AND D. HARRISON

Chemical Research Department, Ontario Hydro Research Division, Toronto 18, Ontario

Received April 8, 1970

Thermogravimetric analysis was done for representative calcined samples of Ontario limestones and dolomites in a 5% SO_2 controlled atmosphere. The SO_2 absorption vs. temperature curves showed three distinct regions. (*i*) A unimolecular chemisorption of SO_2 at room temperature. (*ii*) An intermediate temperature region between 200–450 °C where absorption of SO_2 was due to increased rate of SO_2 diffusion into the interior of CaO via grain boundaries. When the surfaces of these internal spaces were almost fully occupied the rate of SO_2 absorption decreased. Further absorption was due to diffusion of SO_2 into CaO lattice, which was a much slower process. (*iii*) A fast absorption region between 500–700°C, where a disproportionation of $CaSO_3$ into $CaSO_4$ and CaS took place which effectively broke down the original CaO structure to expose fresh layers of CaO. The amount of SO_2 absorption after 1 h at 745 °C corresponded to approximately 80% conversion of CaO to mainly $CaSO_4$ and CaS and smaller amount $CaSO_3$.

Finally, the calculations showed that the reaction of SO_2 with CaO was more exothermic than the reaction of SO_2 with MgO, which accounted for the faster rate of the former.

Canadian Journal of Chemistry, **48**, 2979 (1970)

Introduction

The present study was made to further our efforts to investigate methods for reducing the sulfur dioxide emission from the smoke stacks of fossil-fuel-fired boilers. The removal of sulfur dioxide by calcined limestones or dolomites is a solid–gas reaction. At the present time, no satisfactory methods have yet been developed to predict the kinetics of a heterogeneous reaction from first principles. It is necessary, therefore, to measure the reaction rates under controlled laboratory conditions that may approximate the situation in a steam boiler. The data obtained may be used to correlate with various physical and chemical properties of Ontario limestones and dolomites (1).

Experimental

Thermogravimetric analysis (TGA) was done with a Cahn RG electrobalance equipped with a controlled atmosphere accessory. A Fisher model 360 linear temperature programmer was used to control the furnace temperature. The anhydrous sulfur dioxide (99.80% min) and high purity grade nitrogen (99.9% min) were supplied by Matheson of Canada Ltd. The flows of nitrogen and of sulfur dioxide were controlled individually by a Matheson low-flow flowmeter with a range of 0.2 to 100 cm^3/min. The composition of sulfur dioxide in nitrogen was made up by adjusting the flow rates. The controlled atmosphere was preheated to the furnace temperature in the concentric arrangement of the flow-through tube. A schematic diagram of the TGA apparatus was given in Part I of this series (2). A quartz bucket containing the sample was suspended inside the flow-through tube. The temperature of a freshly calcined sample in an atmosphere of N_2 was adjusted to the desired temperature and then SO_2 was introduced. The size range of the powdered sample was 70–80% between 149 and 74 μ (100 and 200 mesh) and the remainder was finer particles. Baker reagent grade $CaCO_3$ and $MgCO_3$ were powdered precipitates that passed through a 200 mesh screen.

After absorption of SO_2, the sample was analyzed for the distribution of sulfur in the form of sulfate, sulfide, and sulfite according to the methods outlined by Foerster and Kubel (3). Addition of a concentrated solution of $MgCl_2$ to the sample and bubbling CO_2 through the mixture converted the sulfide to H_2S, which was absorbed by a slightly acidified solution of cadmium acetate. The resulting yellow CdS precipitate was determined gravimetrically. Next, the sulfite was decomposed to SO_2 by addition of dilute HCl. SO_2 was swept out by a stream of helium and absorbed by a molar solution of KOH. The resulting potassium sulfite was oxidized to sulfate by Br_2 and determined by the standard $BaSO_4$ method. Similarly, the remaining sulfate was determined as $BaSO_4$.

Results and Discussion

(A) 50% SO_2

Absorption took place at 745 °C in a flow of 85 cm^3/min of SO_2 and equal flow of N_2 by samples freshly calcined at the same temperature. Such a high concentration of SO_2 was used

Can. J. Chem. Downloaded from www.nrcresearchpress.com by 210.87.254.6 on 09/05/12
For personal use only.

mainly to see how fast and how much would be taken up under these extreme conditions. Approximately 100 mg samples were used. They required approximately 40 min for 100% calcination. Since the inner diameter of the flow-through tube was 20 mm, a total flow of 170 cm^3/min at 25 °C corresponded to a linear velocity of 3.1 cm/s at 745 °C. The rates of SO_2 absorption per mg of oxide for limestone and dolomite samples are given in Figs. 1 and 2. The absorption curves all showed similar characteristics: a straight portion which curved over to a plateau. The maximum rates for nine samples did not differ much. The average maximum rate of SO_2 absorption was 0.36 ± 0.2 mg/min per mg of oxide. The plateau was generally higher, the higher the CaO content of the sample. Pure $CaCO_3$ was the best absorbent, both on the basis of rate and on the total amount of SO_2 absorption. Pure $MgCO_3$ calcined at 490 °C showed little absorption of SO_2 in spite of its higher surface area and porosity (2).

Figure 3 shows the effect of sample size on SO_2 absorption. The maximum rate was hardly affected by a 35% increase of sample size but the plateau at 5 min was increased by 39%. The following is a probable explanation. Because of a reaction interface receding into the pile of oxide powder which had a packing density of approximately 1.1 g/cm^3 or 40% of the true density, the rate of absorption would probably be controlled by the interfacial area of the pile and the chemical processes in the interface at such a high rate of absorption.

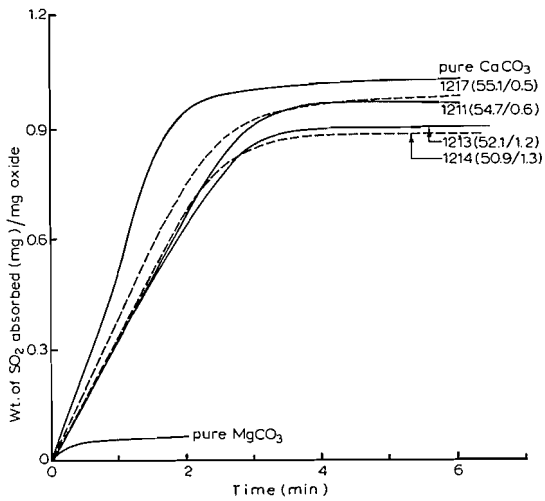

FIG. 1. Absorption of SO_2 at 745 °C in 50% SO_2 by freshly calcined limestone samples.

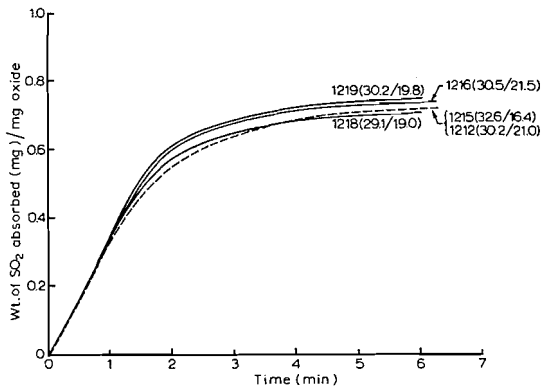

FIG. 2. Absorption of SO_2 at 745 °C in 50% SO_2 by freshly calcined dolomite samples.

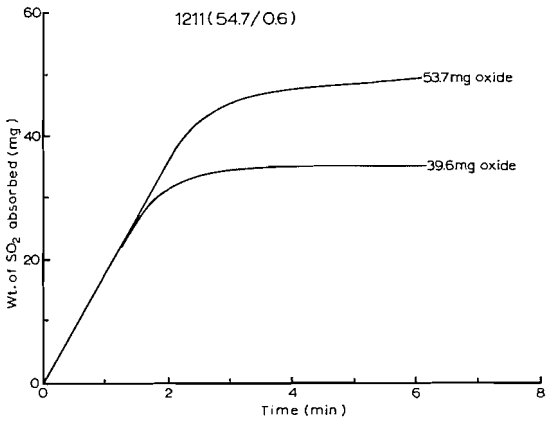

FIG. 3. Effect of sample size on the SO_2 absorption at 745 °C and in 50% SO_2.

(B) 5% SO_2

Absorption took place at 565 °C in 5% SO_2 in 100 cm^3/min of N_2 by samples calcined at 745 °C. The linear velocity of flow was 1.5 cm/s. The lower temperature and SO_2 concentration enabled more accurate rate measurements. Again, the absorption curves were similar to those in Figs. 1 and 2, and the maximum rates for nine samples did not differ much: $(4.58 \pm 0.15) \times 10^{-2}$ mg/min per mg of oxide.

For two limestone samples with substantially different initial B.E.T. surface areas, they were remeasured after SO_2 absorption. Sample 1211 had an initial surface area of 24.6 m^2/g. After absorbing 76% of SO_2 the surface area decreased to 3.3 m^2/g. On the other hand, after

Can. J. Chem. Downloaded from www.nrcresearchpress.com by 210.87.254.6 on 09/05/12
For personal use only.

31% of SO_2 absorption the surface area of sample 1214 decreased only from 14.7 to 8.8 m^2/g. Generally speaking, larger surface area was associated with a smaller most probable pore diameter (see Table 3 in Part I, 0.09 and 0.17 μ). Absorption of SO_2 into these smaller pores might destroy them and, consequently, eliminate a large percentage of the surface area. The larger pores in a lower surface area sample were not as susceptible to filling as the little pores.

(C) Thermogravimetric Analysis in 5% SO_2

In Fig. 4, TGA was run on representative samples of limestone 1211 and dolomite 1212. Approximately 100 mg of the samples were calcined at 745 °C in 100 cm^3/min of N_2. The average weight of these two calcined samples was 60.0 ± 0.1 mg. It was allowed to cool slowly for 1 h to room temperature followed by programmed heating at a rate of 10 °C/min in 5% SO_2 in 100 cm^3/min of N_2. All of the samples absorbed SO_2 rapidly at room temperature, of the order of 1 mg. For the limestone sample 1211 the rate of absorption rose gradually at 200 °C until it slowed down at 390 °C (~6 mg). For dolomite sample 1212 this intermediate temperature absorption region (~3 mg) was barely significant and it appeared also in a similar temperature region. They all possessed a high temperature region of fast absorption starting between 500–600 °C. As the furnace reached the isothermal zone of 745 °C, the SO_2 absorption was already starting to taper off, presumably due to almost complete conversion of CaO. The final amounts of SO_2 absorbed after 1 h at 745 °C for samples 1211 and 1212 were 51 and 44 mg, respectively.

The initial absorption at room temperature was caused by chemisorption of SO_2 in a monolayer. The area occupied by a SO_2 molecule is 19.3 $Å^2$, based on the assumption of closest packing of adsorbate molecules in the bulk liquid and on the surface of the adsorbent with the liquefied adsorbate density being 1.43 g/cm^3. The monolayer capacity is 0.55 mg/m^2. Using the surface areas of 24.6 and 26.4 m^2/g (2), the calculated amounts of SO_2 for a monolayer for limestone 1211 and dolomite 1212 are 0.81 and 0.87 mg compared with the observed values of 1.7 and 1.3 mg. The agreements are gratifying in view of the uncertainty regarding the configuration of SO_2 molecules on the CaO surface. The average area per SO_2 molecule, 19.3 $Å^2$, is only a rough guide. The actual area taken up by each SO_2 molecule depends on how the molecule interacts with the lattice sites of CaO on the surface. The interaction for a chemisorption is specific in contrast to the non-specific interaction in the case of a physical adsorption. Therefore, there is a strong possibility that the initial absorption is indeed a chemisorption because the isotherms at 25 °C have the shape of a type I isotherm according to the B.D.D.T. classification, which is similar to the chemisorption of O_2 on charcoal at −183 °C (4). The absorption took place rapidly: virtually complete in 1 min at 5% SO_2 or $P/P_0 \approx 0.01$ with an initial rate of 2.5 mg/min. Presumably, it forms a stable complex of $CaSO_3$ with CaO.

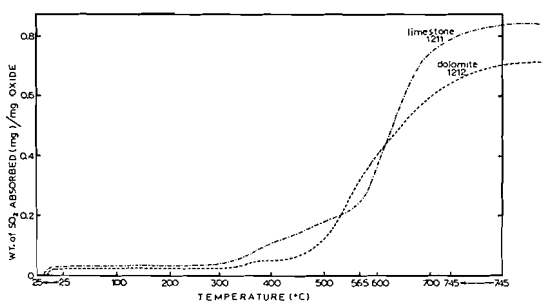

FIG. 4. 5% SO_2 TGA of representative limestone and dolomite samples calcined at 745 °C.

In the intermediate absorption region between 200–450 °C, the rate of SO_2 absorption on limestones samples increased from 200–390 °C and then slowed down at temperatures above 390 °C until disproportionation of $CaSO_3$ began at still higher temperatures. As the temperature is increased, the chemisorbed SO_2 on the surface may become mobile (5) and may be capable of diffusing into the interior of CaO via grain boundaries. During calcination cubic CaO is formed by rapid recrystallization from a pseudo-lattice of the carbonate (6). Thus, CaO is expected to be polycrystalline. When the surfaces of these internal spaces are almost fully occupied by a layer of chemisorbed SO_2, the rate of SO_2 absorption slows down. Further absorption is due to diffusion of SO_2 into CaO lattice which is a much slower process. Similar behavior has been observed in the absorption of CO_2 by CaO (11).

The fast absorption region starting between 500–600 °C is due to the disproportionation of

$CaSO_3$. According to Foerster and Kubel (3) in the vicinity of 650 °C, the following reaction takes place

[1] $$4\ CaSO_3\ (s) \rightarrow 3\ CaSO_4\ (s) + CaS\ (s)$$

When this happens the surface layers of $CaSO_3$ are disrupted to a very large extent, effectively breaking down the original CaO structure and exposing fresh layers of CaO. At higher temperatures a faint yellowish ring of elemental sulfur was observed to deposit on the inside of flow-through tube just above the asbestos furnace baffles, which may be due to the following reactions (7)

[2] $$CaS\ (s) + 2\ SO_2\ (g) \rightarrow CaSO_4\ (s) + S_2\ (g)$$

[3] $$CaSO_3\ (s) + \tfrac{1}{2}\ SO_2\ (g) \rightarrow CaSO_4\ (s) + \tfrac{1}{4}\ S_2\ (g)$$

For limestone sample 1211 after 1 h at 745 °C the distribution of sulfur was as follows: 69% in sulfate, 24% in sulfide, and 7% in sulfite. The sulfur ratio in sulfate and sulfide was 2.9. According to reactions [1], [2], and [3] the ratio should be slightly over 3. When the sample was heated for 1 h at 565 °C the distribution of sulfur was substantially different: 34% in sulfate, 11% in sulfide, and 55% in sulfite. The much higher proportion of sulfur in sulfite at a lower temperature is expected in view of the slower rate of disproportionation. Thus, at least the main features of the limestone TGA can be explained qualitatively.

(D) Thermodynamics

The enthalpies of reaction at 25 °C for the reaction of SO_2 with CaO and MgO are calculated from the thermochemical data of Rossini *et al.* (8), except the enthalpy of formation of $CaSO_3$ which is given by Wilcox and Bromley (9). The reaction of CaO with SO_2 is much more exothermic (−50 kcal/mole) than the corresponding reaction of MgO with SO_2 (−26 kcal/mole). Therefore, SO_2 will react with CaO at a faster rate than with MgO as observed experimentally in view of an empirical correlation between enthalpy of reaction and activation energy (10).

The authors wish to acknowledge the financial support of the Department of University Affairs and the Ontario Hydro, and to thank Mr. C. H. Clark, Engineer-in-Charge, Chemical Research Department and Mr. J. H. Waghorne, Director of Research of the Ontario Hydro for encouragement received to carry out this project.

1. D. F. Hewitt. The limestone industries of Ontario. Ontario Department of Mines, Industrial Mineral Circular No. 5, 1960 and No. 13, 1964.
2. R. K. Chan, K. S. Murthi, and D. Harrison. Can. J. Chem. This issue.
3. F. Foerster and K. Kubel. Z. Anorg. Allg. Chem. **139**, 261 (1924).
4. S. Brunauer, L. S. Deming, W. E. Deming, and E. Teller. J. Amer. Chem. Soc. **62**, 1723 (1940).
5. R. D. Shannon. Trans. Faraday Soc. **60**, 1902 (1964).
6. D. R. Glasson. J. Appl. Chem. **8**, 793 (1958).
7. R. S. Boynton. Chemistry and technology of lime and limestone. Interscience. 1966. p. 192.
8. F. D. Rossini *et al.* Selected Values of Chemical Thermodynamic Properties. Natl. Bur. Stds. Circ. 500 (1952).
9. D. E. Wilcox and L. A. Bromley. Ind. Eng. Chem. **55** (7), 32 (1963).
10. M. Boudart. Kinetics of Chemical Processes. Prentice-Hall. 1968. p. 190.
11. V. Boldyrev. Private communication.

Can. J. Chem. Downloaded from www.nrcresearchpress.com by 210.87.254.6 on 09/05/12
For personal use only.

Can. J. Chem. Downloaded from www.nrcresearchpress.com by 210.87.254.6 on 09/05/12
For personal use only.

The dielectric properties of 1,1-dichlorocyclohexane in a supercooled region

R. K. CHAN AND W. L. CLAYTON[1]
Department of Chemistry, University of Western Ontario, London, Ontario

Received April 29, 1970

From dielectric constant measurements of supercooled 1,1-dichlorocyclohexane in the anomalous dispersion region, the free energy, entropy, and enthalpy of activation for dielectric relaxation are found to be 4.05 kcal mole^{-1}, 123 cal °K^{-1} mole^{-1}, and 22.3 kcal mole^{-1}, respectively, at −125 °C. The calculated maximum free energy barrier of crystal nucleus formation based on simple nucleation theory is 3.64 kcal mole^{-1}. In view of the qualitative agreement between the experimental free energy of activation of dielectric relaxation and the calculated free energy of activation of nucleation, it is reasonable to conclude that the processes of molecular orientation and of crystal nucleus growth are similar. A calculation of the free energy barrier *vs.* crystal nucleus size diagram also predicts spontaneous crystallization when the radius of crystal nuclei exceeds 12.8 Å.

Canadian Journal of Chemistry, 48, 2983 (1970)

Introduction

Molecules with spheroidal shape, which pack with reasonable economy in free volume in liquid and crystallize into an anisotropic lattice, can often supercool to a large extent (1). The formation of a supercooled liquid is dependent on the two steps involved in crystallization. Formation of crystal nuclei in the liquid and growth of these nuclei must occur to form the crystal (2). If either of these is prevented, crystallization cannot take place and the liquid will supercool. Since the melting point of small crystals is lower than that of large crystals, crystal nuclei smaller than a certain size are unstable. The factor preventing the second step is a free energy barrier which prevents the movement of a molecule at the solid–liquid interface from a liquid-like position to a crystal-like position. The first effect will prevent crystallization over a temperature region just below the melting point and the second effect will prevent crystallization below that region. If either of these preventative measures is not effective, the supercooled liquid will crystallize spontaneously. As the temperature of a supercooled liquid is raised the molecules begin to gain additional molecular freedom until sufficient energy and volume are available for the molecules to rotate and begin to form crystal nuclei. The molecular motion in crystal growth has been shown by Richards (3) to be very similar to that in dipole orientation in an oscillating electric field. The free energy barrier to crystal growth and to dielectric relaxation are also very similar. Therefore, when crystal nucleus formation starts in the supercooled liquid, it will show a similar distribution of relaxation times to those of dipole relaxation. In the same manner, the enthalpy, free energy, and entropy of activation for the crystallization process can be found. When a temperature is reached at which the nuclei are stable and steady growth can occur, the supercooled liquid crystallizes spontaneously and exothermically to the stable crystalline phase.

[1]Present address: Imperial Oil Enterprises Ltd., Sarnia, Ontario.

Experimental

The dielectric constant was measured by a General Radio 1615-A transformer ratio arm capacitance bridge capable of 0.01% precision from 1–10 kHz and 0.2% up to 100 kHz. The automatic temperature control was ±0.1 °C (4). The stainless steel dielectric cell consisted of two 25 mm diameter parallel electrodes with a 4 mm spacing, which were enclosed completely by a guard electrode casing. It had a small volume of 2.3 cm^3 and a cell constant of 1.10 pF, calibrated by air, cyclohexane, and benzene.

The preparation of 1,1-dichlorocyclohexane was carried out at one tenth the scale and in the same manner as was done by Carroll *et al.* (5). The product was fractionated in a distillation column with a platinum spinning band. The portion boiling between 56–58 °C at 12 mm Hg was retained and had n_D = 1.4792 at 25 °C. The corresponding literature values were 1.4780 (5) and 1.4788 (6). A trace of 1-chlorocyclohexene was detected by i.r. and n.m.r. spectra, which could not be eliminated because 1,1-dichlorocyclohexane decomposed slowly at room temperatures to 1-chlorocyclohexene. Therefore, only freshly distilled samples were used for dielectric measurements.

Results

On quenching liquid 1,1-dichlorocyclohexane, the dielectric constants at 10 kHz followed a Debye $1/T$ temperature dependence (AB in Fig. 1). As the temperature reached B the viscosity became so large that the dielectric constants

TABLE 1

Dielectric constants of supercooled 1,1-dichlorocyclohexane at 10 kHz

Heating		Heating		Cooling		Heating	
T (°C)	ε	T (°C)	ε	T (°C)	ε	T (°C)	ε
−175.7	2.34	−159.2	2.50	−116.5	2.54	−142.3	2.32
−157.7	2.52	−151.6	2.53	−122.9	2.46	−130.0	2.42
−150.8	2.65	−139.6	4.04	−126.1	2.48	−125.5	2.48
−143.6	3.42	−130.3	11.22	−132.6	2.41	−115.7	2.53
−132.1	9.27	−126.7	13.40	−163.9	2.25	−104.1	2.52
−131.4	10.11	−124.9	13.68				
−128.0	13.05	−123.5	13.61				
		−120.0	12.07				
		−119.3	8.80				
		−118.7	4.26				
		−118.5	3.32				
		−117.4	2.71				
		−116.9	2.67				
		−113.6	2.58				
		−110.5	2.56				

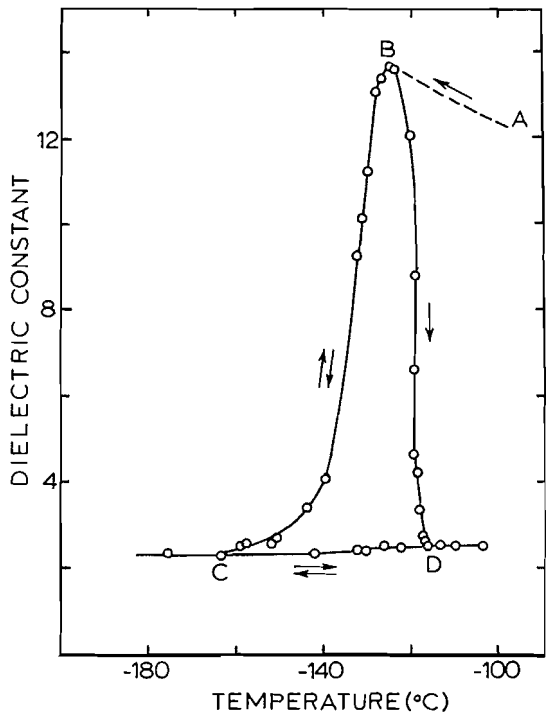

FIG. 1. Dielectric constant of 1,1-dichlorocyclohexane at 10 kHz *vs.* temperature.

showed anomalous dispersion in which the dielectric constants decreased rapidly from *B* to *C*. In other words, the molecular dipoles could no longer rotate to follow the oscillations of a 10 kHz applied field because dipolar interactions increased with increasing density and decreasing temperature. Consequently, the orientational polarization contribution to the dielectric constant diminished until only the atomic and electronic polarization contributions remained, and the dielectric constant approached the square of refractive index. The anomalous dispersion of dielectric constants could also be induced artificially by pressure. Danforth (7) confirmed experimentally that the same effect took place in liquid glycerol at 0 °C and 250 kHz when the pressure was raised to 6000 atm. As the temperature was raised slowly from *C* to *B*, the dielectric constant rose steeply. Further increase of temperature beyond *B* resulted in a drop of the dielectric constant which plunged rapidly with only moderate increase of temperature. In the region *BD*, crystallization of the supercooled 1,1-dichlorocyclohexane took place. Simultaneously, the temperature of the sample showed self-heating due to the release of latent heat of crystallization. If the temperature of the sample was quenched before the dielectric constant dropped to *D*, on subsequent heating the dielectric constant rose again at *C* to a peak which was lower than *B* and plunged again at temperatures above −125 °C. A smaller peak was observed after each thermal cycle. If the dielectric constant was allowed to drop to *D*, it followed *CD* on subsequent thermal cycles. The peak at *B* disappeared entirely which implied that crystallization was complete. The results are summarized in Table 1. Finally, the sample melted at −47 °C.

In the anomalous dispersion region *CB*, the real and imaginary parts of the dielectric con-

Can. J. Chem. Downloaded from www.nrcresearchpress.com by 210.87.254.6 on 09/05/12
For personal use only.

Can. J. Chem. Downloaded from www.nrcresearchpress.com by 210.87.254.6 on 09/05/12
For personal use only.

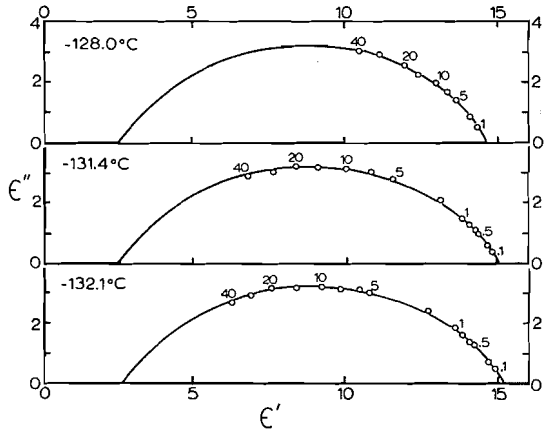

FIG. 2. Cole–Cole diagrams of supercooled 1,1-dichlorocyclohexane. The numbers refer to the frequency of measurements in kHz.

stants were measured at various frequencies. Figure 2 shows the Cole–Cole diagrams for three different temperatures. They are symmetrical arcs with a distribution parameter α equal to $\frac{1}{3}$ implying a wide distribution of dielectric relaxation times (8). The calculation of dielectric relaxation time was made by taking $\varepsilon_\infty = 2.6$ which was the dielectric constant of the crystalline phase. Table 2 shows the dielectric relaxation time, τ, as a function of temperature. The temperature dependence of τ can be obtained by application of absolute rate theory to the dipole rotation (1).

$$[1] \qquad \tau = \frac{h}{kT} e^{\Delta G^{\ddagger}/RT} = \frac{h}{kT} e^{-\Delta S^{\ddagger}/R} e^{\Delta H^{\ddagger}/RT}$$

where $\Delta G^{\ddagger}$, $\Delta S^{\ddagger}$, and $\Delta H^{\ddagger}$ are free energy, entropy, and enthalpy of activation. From Fig. 3, $\Delta H^{\ddagger}$ was estimated to be 22.3 $\pm$ 1 kcal mole^{-1}. $\Delta G^{\ddagger}$ and $\Delta S^{\ddagger}$ values are given in Table 3. Strictly speaking, ln $(T\tau)$ instead of ln τ should be used in Fig. 3. In practice, the temperature range is so small that it makes little difference.

TABLE 2

Dielectric relaxation times of supercooled 1,1-dichlorocyclohexane

Temperature (°C)	Relaxation time (s)
−139.6	2.02×10^{-3}
−132.7	1.50×10^{-5}
−132.2	1.19×10^{-5}
−132.1	1.43×10^{-5}
−131.4	9.81×10^{-6}
−131.3	7.69×10^{-6}
−131.1	6.63×10^{-6}
−130.3	4.50×10^{-6}
−130.3	6.07×10^{-6}
−129.7	3.59×10^{-6}
−129.3	2.50×10^{-6}
−128.8	1.99×10^{-6}
−128.1	1.70×10^{-6}
−128.0	2.16×10^{-6}
−127.9	1.57×10^{-6}
−127.6	1.29×10^{-6}
−126.7	1.35×10^{-6}
−124.9	8.37×10^{-7}

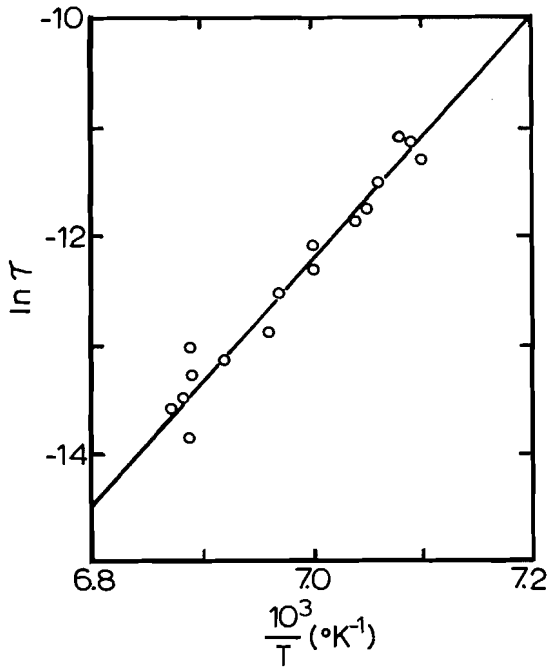

FIG. 3. Temperature dependence of dielectric relaxation time.

Discussion

The freedom of molecular rotation is restricted severely at low temperatures. This is evident from the absence of orientational polarization contribution to the dielectric constant. The formation and growth of crystal nuclei from a supercooled liquid entail rearrangements of molecules at the liquid–solid interface. In the anomalous dispersion region freedom of molecular rotation is much less restricted. It is reasonable to assume that formation and growth of crystal nuclei are likely to be favorable in the same temperature region.

An attempt is made to estimate the free energy barrier for the growth of crystal nuclei as a

TABLE 3

Free energy and entropy of activation

Temperature (°C)	$\Delta G^{\ddagger}$ (kcal mole^{-1})	$\Delta S^{\ddagger}$ (cal mole^{-1} deg^{-1})
−139.6	5.96	122
−132.7	4.91	124
−132.1	4.92	123
−131.1	4.74	124
−130.3	4.66	124
−129.3	4.52	124
−128.0	4.53	123
−126.7	4.43	122
−124.9	4.05	123

function of size. The continual growth of a crystal nucleus is contingent on a series of favorable molecular rotations as a result of energy fluctuations. The free energy barrier for the formation of one mole of crystal nuclei of radius r from the supercooled liquid can be expressed in terms of its bulk properties.

$$[2] \qquad \Delta G^* = 4\pi r^2 N\sigma + \tfrac{4}{3}\pi r^3 N(-\Delta \bar{G}_f)$$

where σ is the surface free energy per unit area of liquid–solid interface, $\Delta \bar{G}_f$ is the free energy of fusion per unit volume, and N is the Avogadro's number. The negative sign is introduced because $\Delta \bar{G}_f$ refers to *fusion* whereas $\Delta \bar{G}^*$ refers to *formation* of crystal nuclei. Introducing $\Delta \bar{G}_f = \Delta \bar{H}_f - T\Delta \bar{S}_f$ and $\Delta \bar{S}_f = \Delta \bar{H}_f/T_f$ where T_f is the temperature of fusion, into eq. 2, one gets

$$[3] \qquad \Delta G^* = (4\pi N\sigma)r^2 - \left[\frac{4}{3}\pi N\Delta \bar{H}_f\left(\frac{T_f - T}{T_f}\right)\right]r^3$$

A similar result has been obtained by Turnbull and Fisher for nucleation in condensed phases (9). For a supercooled liquid, *i.e.* $T_f > T$, $\Delta \bar{G}^*$ in eq. 3 goes through a maximum and becomes negative, which implies the existence of a critical size for the crystal nuclei (Fig. 4).

$$[4] \qquad \Delta G^*_{max} = \frac{16\pi}{3}\frac{\sigma^3 N}{\Delta \bar{H}_f^2}\left(\frac{T_f}{T_f - T}\right)^2$$

$$[5] \qquad r_{max} = \frac{2\sigma}{\Delta \bar{H}_f}\left(\frac{T_f}{T_f - T}\right)$$

The latent heat of fusion at the melting point of −47 °C is 1.65 kcal mole^{-1} measured by a Perkin–Elmer Differential Scanning Calorimeter. The liquid density is 1.156 g cm^{-3} at 20 °C (5). Using a coefficient of thermal expansion of

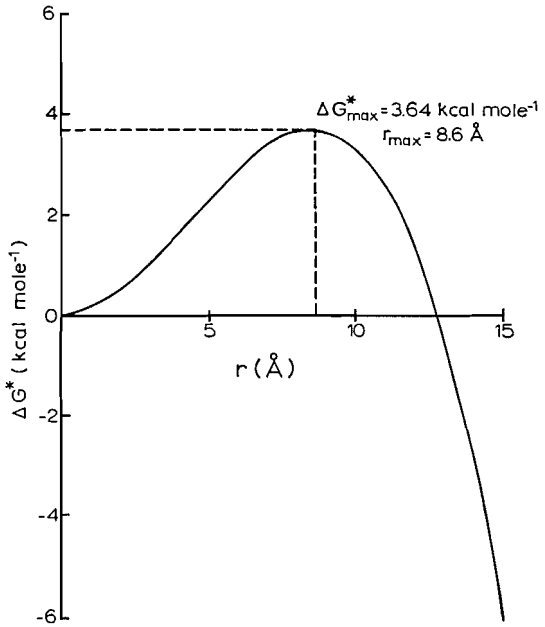

FIG. 4. Effect of crystal nucleus size on free energy barrier.

1.3 × 10^{-3} °C^{-1}, which is the average of ten widely different molecular liquids, the latent heat of fusion per cm^3, $\Delta \bar{H}_f$, is estimated to be 13.6 cal cm^{-3}. Based on the results of Turnbull and Fisher (9), De Nordwall and Staveley (10) established empirically for molecular liquids the following expression for surface free energy per unit area of liquid–solid interface.

$$[6] \qquad \sigma = \tfrac{1}{4}\Delta \bar{H}_f\left(\frac{V}{N}\right)^{\frac{1}{3}}$$

where V is the molar volume of liquid. Using eq. 6 and V = 121 cm^3 mole^{-1}, σ is estimated to be 8.33 erg cm^{-2}. When the estimated values of $\Delta \bar{H}_f$ and σ are substituted into eq. 1, at −125 °C where the rate of crystallization is appreciable, the free energy barrier of crystal nucleus formation at −125 °C becomes

$$[7] \qquad \Delta G^* = 0.151\, r^2 - 0.0118\, r^3$$

where ΔG^* and r are expressed in terms of kcal mole^{-1} and Å, respectively. In view of the approximations inherent in eq. 7, the numeric values of ΔG^* are not too important. However, the inference of a maximum free energy barrier and spontaneous crystallization is most significant (see Fig. 4). The maximum occurs at 3.64 kcal mole^{-1} and 8.6 Å. It is evident from

Can. J. Chem. Downloaded from www.nrcresearchpress.com by 210.87.254.6 on 09/05/12
For personal use only.

Fig. 4 that for crystal nuclei of radius smaller than 8.6 Å further growth is accompanied by an increasing free energy barrier, whereas for those larger than 8.6 Å, by a decreasing free energy barrier which becomes zero at $r = 12.8$ Å. Therefore, for crystal nuclei larger than the critical radius of 12.8 Å or more than 44 molecules, the free energy barrier is negative which implies spontaneous crystallization. The sharp drop of free energy barrier in Fig. 4 is consistent with the experimental observation that crystallization took place rapidly in the vicinity of -125 °C. The calculated free energy barrier maximum of 3.64 kcal mole^{-1} also agrees satisfactorily with the free energy of activation, 4.05 kcal mole^{-1} from dielectric relaxation measurements at -125 °C. Therefore, molecular rotations associated with dielectric relaxation and growth of crystal nucleus are related. According to Eyring's rate theory the large values of $\Delta S^{\ddagger}$ (Table 3), which are common in dielectric relaxation, are indicative of a highly co-operative process involving many molecules. In other words, when a molecule enters its transitional state, its neighboring molecules become disoriented and gain considerable freedom of their own (11).

The authors are grateful for the financial support from the National Research Council of Canada.

1. C. P. Smyth. Dielectric behavior and structure. McGraw-Hill Book Co., Inc., New York. 1955. pp. 177 and 63.
2. W. Kauzmann. Chem. Rev. **43**, 219 (1948).
3. W. T. Richards. J. Chem. Phys. **4**, 449 (1936).
4. R. K. Chan and H. A. Chew. Can. J. Chem. **47**, 2249 (1969).
5. B. Carroll, D. G. Kubler, H. W. Davis, and A. M. Whaley. J. Amer. Chem. Soc. **73**, 5382 (1951).
6. P. Bender, D. L. Flowers, and H. L. Goering. J. Amer. Chem. Soc. **77**, 3463 (1955).
7. W. E. Danforth. Phys. Rev. **38**, 1224 (1931).
8. K. S. Cole and R. H. Cole. J. Chem. Phys. **9**, 341 (1941).
9. D. Turnbull and J. C. Fisher. J. Chem. Phys. **17**, 71 (1949).
10. H. J. De Nordwall and L. A. K. Staveley. J. Chem. Soc. 224 (1954).
11. W. Kauzmann. Rev. Modern Phys. **14**, 12 (1942).

Can. J. Chem. Downloaded from www.nrcresearchpress.com by 210.87.254.6 on 09/05/12
For personal use only.

Can. J. Chem. Downloaded from www.nrcresearchpress.com by 210.87.254.105 on 09/05/12
For personal use only.

Molar polarizations of the constituents in a molecular complex system

R. K. CHAN AND S. C. LIAO
Department of Chemistry, University of Western Ontario, London, Ontario

Received May 4, 1970

A method of evaluating the molar polarizations of the constituents and the dipole moment of the complex simultaneously in a quaternary molecular complex system of A + B $\rightleftarrows$ AB in an inert solvent, S, is proposed on the basis of an empirical relationship between the specific polarization of the solution and the weight fraction of molecule A in combination with the mass action law and the mixture law of specific polarization. The validity of the method is tested by using the data obtained in Smith's papers for the systems of aniline in dioxane–benzene, *n*-butyl alcohol in pyridine–benzene, and pyridine in *n*-butyl alcohol – benzene. The agreement in dipole moment of the complex between the proposed and Smith methods for the first two systems verifies the applicability of the proposed method, which also gives consistent results for the second and third systems, while no value for the third system is given in Smith's paper.

Canadian Journal of Chemistry, **48**, 2988 (1970)

Introduction

The formation of a molecular complex is accompanied by intercomponent electron transfer, from donor to acceptor, resulting in corresponding changes of the electrical property of the components. The observed dipole moment of the complex which is different from its constituents plays a significant role in the intermolecular charge-transfer resonance theory proposed by Mulliken (1). The coefficients of the wave functions describing the complex at the ground and excited states can be evaluated experimentally with the aid of the dipole moment and the charge-transfer spectrum of the complex.

For the system containing a molecular complex, AB, formed by the intermolecular interaction between molecules A and B in an inert solvent, S, Few and Smith (2) reviewed previous works and derived a method for evaluating the equilibrium constant of the association process and the dipole moment of aniline–dioxane complex in benzene solution. This approach is based on the difference between the apparent molar polarization of aniline, calculated on the assumption of no complex formation of aniline in various mixtures of dioxane in benzene solvent, and the molar polarization of aniline at infinite dilution in benzene. It has also been applied to other systems such as *n*-butyl alcohol in pyridine–benzene, and pyridine in *n*-butyl alcohol – benzene (3). However, in the latter case, the Smith method gave no result for the dipole moment of the complex probably because of an almost zero intercept.[1]

[1]See the figure in ref. 3. The factor of 10^5 in abscissa should read 10^{-5}.

The Smith method, however, does not apply to the system in which a determination of the molar polarization of molecule A in the solvent cannot be carried out due to the insolubility of A in the solvent.[2]

The proposed method is based on the empirical dependence of the specific polarization of the complex solution on weight fraction of molecule A in solution, the mixture law of specific polarization, and the mass action law. It has also been tested with the data for three systems available in Smith's papers. The satisfactory agreement in the dipole moment of the complex between both methods indicates the applicability of the present method.

The proposed method supplies all the necessary molar polarizations for calculating the dipole moment of the complex from the experimental data. No individual effort is required to determine the molar polarizations of the reactants in a pure solvent.

Results and Discussion

The Benesi and Hildebrand equation (4), used principally for calculating the association constant of a molecular complex having a charge-transfer spectrum, has been derived on the basis of the combination of the Beer–Lambert law and the mass action law. It is possible to derive a similar equation for determining the dipole moment of a complex with the aid of the mixture

[2]The tetracyanoethylene (TCNE) complexes with methyl-substituted benzenes in carbon tetrachloride are the examples in which the insolubility of TCNE in carbon tetrachloride makes it impossible to determine the molar polarization of TCNE at infinitely dilute solution by extrapolation.

Can. J. Chem. Downloaded from www.nrcresearchpress.com by 210.87.254.105 on 09/05/12
For personal use only.

law of specific polarization and the mass action law for the system of A + B ⇄ AB in an inert solvent, S at equilibrium.

The weight fractions of species A, B, AB, and S may be expressed by $(w_A - \Delta w_A)$, $(w_B - \Delta w_B)$, $(\Delta w_A + \Delta w_B = \Delta w_{AB})$, and w_S, respectively; where w_i is the weight fraction of reactant and Δw_i the loss in weight fraction of the reactant i to form the complex AB. If the concentration of B is much larger than that of A, which is experimentally feasible, the concentration of complex will be negligibly small compared to that of B, i.e. $C_B \gg C_{AB}$. According to the mass action law, if the active masses of the species can be expressed in terms of their concentrations, the association constant, K_c, is given by

$$[1] \qquad K_c = \frac{C_{AB}}{C_B(C_A - C_{AB})} = \frac{\Delta w_{AB}/M_{AB}}{C_B(w_A - \Delta w_A)/M_A}$$

where M_i and C_i refer to the molecular weight and concentration of the ith component, respectively. Since $\Delta w_A/\Delta w_{AB} = M_A/M_{AB}$, therefore Δw_A, Δw_B, and Δw_{AB} can be expressed in terms of w_A.

$$[2] \qquad \Delta w_A = K_c C_B w_A/(1 + K_c C_B)$$

$$[3] \qquad \Delta w_B = \frac{M_B}{M_A}\frac{K_c C_B w_A}{(1 + K_c C_B)}$$

$$[4] \qquad \Delta w_{AB} = \frac{M_{AB}}{M_A}\frac{K_c C_B w_A}{(1 + K_c C_B)}$$

The specific polarization of a very dilute complex solution, p, consisting of the contribution from individual specific polarization, p_i, of the components including the complex, at infinite dilution in solvent can be written as

$$[5] \qquad p = p_A(w_A - \Delta w_A) + p_B(w_B - \Delta w_B) + p_{AB}(\Delta w_{AB}) + p_S w_S$$

If the concentration dependence of the specific polarization of the components is taken into consideration, higher order terms in w_A, w_B, and Δw_{AB} appear in eq. [5]. These terms will account for the curvatures in Figs. 3 and 5. Δw_B in eq. [5] cannot be neglected compared to w_B, otherwise it leads to the term P_B missing in eq. [6]. Substitution of eqs. [2] to [4] into eq. [5] gives

$$[6] \qquad p = p_B w_B + p_S w_S + \left(\frac{P_A + (P_{AB} - P_B)K_c C_B}{M_A(1 + K_c C_B)}\right) w_A$$

where P_i is the molar polarization of species i in the solvent. In addition, for a very dilute complex solution, $w_S = 1 - w_A - w_B$, then eq. [6] becomes

$$[7] \qquad p = p_S + (p_B - p_S)w_B + \left(\frac{(P_A - p_S M_A) + (P_{AB} - P_B - p_S M_A)K_c C_B}{M_A(1 + K_c C_B)}\right) w_A$$

If w_A is neglected regardless of the extent of dilution in the solution, it causes a significant error in eq. [7] in which the term $p_S M_A$ will be missing. Empirically, the specific polarization of a solution of A in a mixed solvent containing B and S can be expressed in terms of w_A.

$$[8] \qquad p = \frac{\varepsilon - 1}{\varepsilon + 2}\cdot\frac{1}{d} = C_1 + C_2 w_A + C_3 {w_A}^2$$

where ε and d are the dielectric constant and the density of the solution. Thus, the coefficients C_1 and C_2 can be deduced by comparison with eqs. [7] and [8].

$$[9] \qquad C_1 = p_S + (p_B - p_S)w_B$$

$$[10] \qquad C_2 M_A(1 + K_c C_B) = (P_A - p_S M_A) + (P_{AB} - P_B - p_S M_A)K_c C_B$$

Similarly, at different concentrations of B in a mixed solvent, the values of C_1 and $C_2 M_A(1 + K_c C_B)$ can be expressed also in terms of w_B and $K_c C_B$, respectively. Therefore, the molar polarization of solvent, P_S, and the molar polarization of B, P_B, in solvent are calculable from the slope and the intercept by plotting C_1 against w_B. P_A and P_{AB} at zero concentration in solvent are evaluated from the corresponding terms by plotting $C_2 M_A(1 + K_c C_B)$ against $K_c C_B$. The dipole moment of the molecular complex is obtained by assuming that the distortion polarization of the complex is equal to the sum of the distortion polarization of the components.

The proposed eqs. [8], [9], and [10] have been tested by using Smith's data for the systems of aniline in dioxane–benzene, *n*-butyl alcohol in pyridine–benzene, and pyridine in *n*-butyl alcohol – benzene solution. The association constants are taken from Smith's results: 128 and 2000 cm^3 $mole^{-1}$ for the 1:1 complex of aniline–

Can. J. Chem. Downloaded from www.nrcresearchpress.com by 210.87.254.105 on 09/05/12
For personal use only.

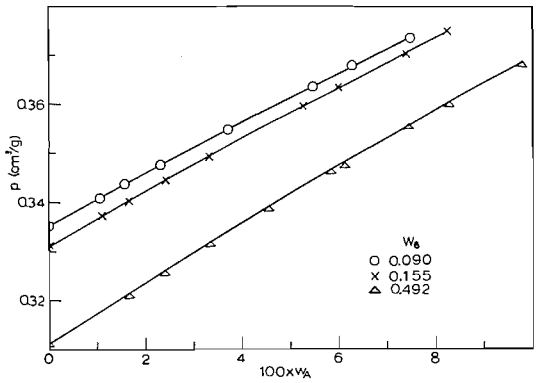

FIG. 1. Plot of p against w_A for aniline in dioxane–benzene at 25 °C.

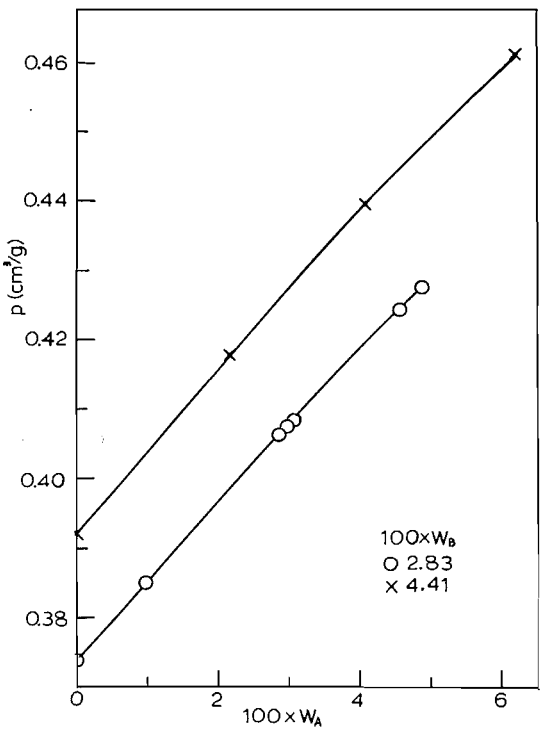

FIG. 2. Plot of p against w_A for n-butyl alcohol in pyridine–benzene at 25 °C.

dioxane and n-butyl alcohol – pyridine in benzene solution.

The plots of p against w_A for three systems are shown in Figs. 1, 2, and 3. At small values of w_A, the plots are linear which indicates the complete complexation between A and B in solution (5). Therefore, the linear relation of $p = C_1 + C_2 w_A$ is applied to this range and the results are indicated by (*a*) in Table 2. The results evaluated

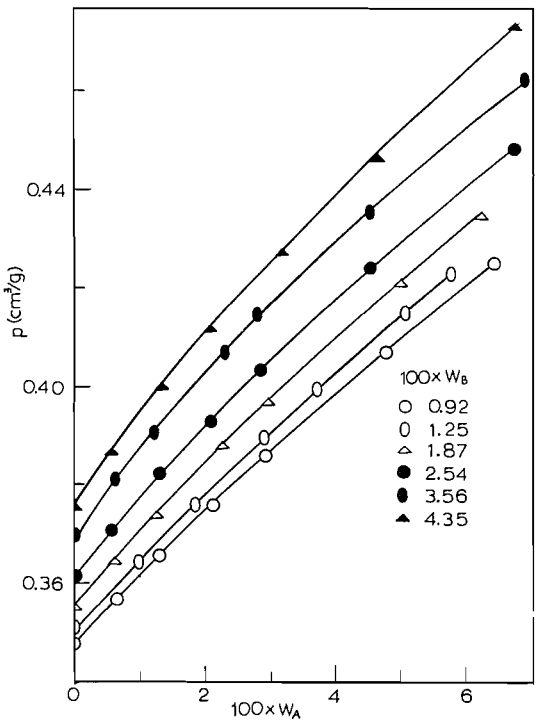

FIG. 3. Plot of p against w_A for pyridine in n-butyl alcohol – benzene at 25 °C.

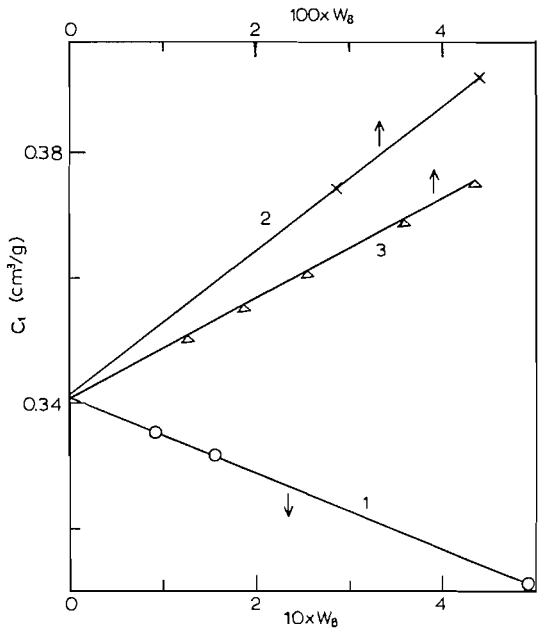

FIG. 4. Plot of C_1 against w_B for three systems in Table 2.

Can. J. Chem. Downloaded from www.nrcresearchpress.com by 210.87.254.105 on 09/05/12
For personal use only.

TABLE 1

Summary of results for eqs. [8], [9] and [10]

System	$100w_B$	C_1 (cm³/g)	C_2 (cm³/g)	$C_2M_A(1 + K_cC_B)$ (cm³/mole)	K_cC_B
1*	9.07	0.33538	0.53	55	0.1169
			(0.53)§	(55)	
	15.52	0.33150	0.54	61	0.2019
			(0.55)	(62)	
	49.21	0.31104	0.61	96	0.6751
			(0.64)	(100)	
2†	2.833	0.37432	1.11	134	0.6278
			(1.14)	(138)	
	4.410	0.39215	1.19	176	0.9792
		(0.3480)	(1.22)	(180)	
3‡	0.923	0.34797	1.37	132	0.2178
		(0.3480)	(1.37)	(132)	
	1.250	0.35062	1.41	144	0.2942
		(0.3508)	(1.42)	(145)	
	1.866	0.35558	1.55	176	0.4390
		(0.3559)	(1.50)	(171)	
	2.538	0.36102	1.66	210	0.5966
		(0.3614)	(1.59)	(201)	
	3.564	0.36932	1.80	262	0.8370
		(0.3699)	(1.72)	(250)	
	4.350	0.37544	1.93	309	1.0208
		(0.3761)	(1.83)	(292)	

*Aniline in dioxane–benzene.
†*n*-Butyl alcohol in pyridine–benzene.
‡Pyridine in *n*-butyl alcohol – benzene.
§Values in parentheses are calculated from $p = C_1 + C_2w_A + C_3w_A^2$. The rest of the values are from $p = C_1 + C_2w_A$.

TABLE 2

The dipole moments of the molecular complexes and molar polarizations of constituents at 25 °C*

System	A	B		P_S	P_B	P_A	P_{AB}	$_{c+a}P_{AB}$	$_oP_{AB}$	μ_{AB}
1	Aniline	Dioxane	(*a*)†	26.6	24.7	79	126	52	74	1.90
			(*b*)‡	26.6	24.7	78	141	52	89	2.04
			(*c*)§	26.6	24.6	78	124	52	72	1.88
2	*n*-Butyl alcohol	Pyridine	(*a*)†	26.7	117	84	262	46	216	3.25
			(*b*)‡	26.7	117	88	262	46	216	3.25
			(*c*)§	26.6	123	81	280	46	234	3.37
3	Pyridine	*n*-Butyl alcohol	(*a*)†	26.6	85	118	287	46	241	3.43
			(*b*)‡	26.6	86	125	260	46	214	3.24
			(*c*)§	26.6	81	123	—	—	—	—

*The unit of P_i is cm³ mole⁻¹ and μ_{AB} is Debye.
†(*a*) From $p = C_1 + C_2w_A$.
‡(*b*) From $p = C_1 + C_2w_A + C_3w_A^2$.
§(*c*) From Smith's papers and refs. 6 and 7.

from $p = C_1 + C_2w_A + C_3w_A^2$ are also given in parentheses in Table 1 and as (*b*) in Table 2. The data calculated for different values of w_B in a mixed solvent are shown in Table 1.

The calculated molar polarizations of the four components in each system and the dipole moments of the complexes are given in Table 2. The literature values are indicated by (*c*) in which the values of P_{AB}, μ_{AB} are from Smith's papers and the rest from the literatures (6, 7).

The linear plots of C_1 against w_B are shown in Fig. 4. The numeric codes refer to the systems in Table 2. The calculated molar polarizations of the constituents in a mixed solvent, P_S and P_B, are in good agreement with the values from the literatures.

The coefficient C_2 varies slightly, dependent on the use of the linear or quadratic expression for p–w_A, while C_1 is apparently independent of them at small w_A. Figure 5 shows the plots of $C_2M_A(1 + K_cC_B)$ against K_cC_B for the systems in Table 2. Hence, the molar polarizations of A

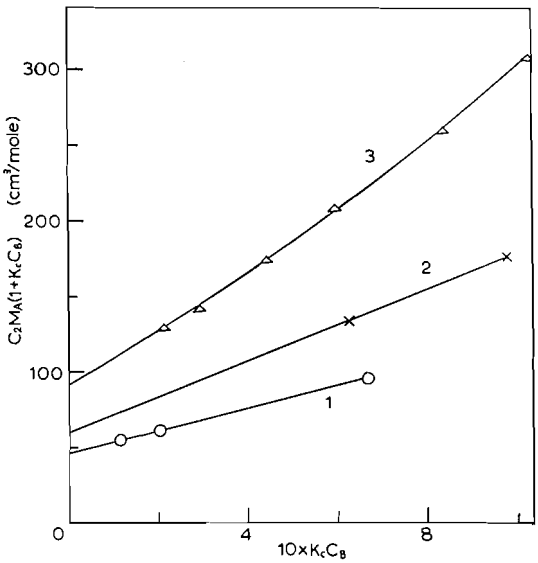

FIG. 5. Plot of $C_2M_A(1 + K_cC_B)$ against K_cC_B for three systems in Table 2.

and AB can be deduced. The agreements between the calculated dipole moments using the proposed method and Smith's values are in the order of 0.1 D which is very reasonable in view of the experimental difficulty. The μ_{AB} for pyridine in a mixed solvent of *n*-butyl alcohol and benzene is found to be 3.43 D by the proposed method, while no value is given in Smith's paper (3) because the difference between the molar polarization of the complex and the sum of molar polarizations of the two components assumed an unreasonably large value.

The consistent results in μ_{AB} of *n*-butyl alcohol – pyridine, deduced from the systems of *n*-butyl alcohol in pyridine–benzene and pyridine in *n*-butyl alcohol – benzene, indicate that the complex is existing as the same species in both systems (Table 2). Although the 0.2 D higher value in the latter system may be due to the effect of hydrogen bonding in a mixed solvent containing $\sim 10^{-2}$ in mole fraction of *n*-butyl alcohol, it seems more reasonable to attribute the difference to experimental errors.

For small w_A, the linear expression $p = C_1 + C_2w_A$ gives values of μ_{AB} which are in better agreement with the literature values than the quadratic expression (Table 2). Within the limit of a few percent error, the ratio of $w_A:w_B:w_S$ may be considered in the order of $10^{-4}:10^{-2}:1$, so that successive increments of w_A in a mixed solvent will not change w_B nor w_S in the solution significantly. For example, w_B changes about 7% from 0.044 in a mixed solvent to 0.041 in a solution; w_S from 0.956 to 0.879 with w_A increasing from 0 to 0.08 for the system of *n*-butyl alcohol in pyridine–benzene. The high values of w_A might cause a slight discrepancy in μ_{AB} calculated by the proposed method with respect to the accurate value.

We are grateful to the National Research Council of Canada for financial assistance.

1. R. S. MULLIKEN. J. Amer. Chem. Soc. **74**, 811 (1952).
2. A. V. FEW and J. W. SMITH. J. Chem. Soc. 2781 (1949).
3. D. CLEVERDON, G. B. COLLINS, and J. W. SMITH. J. Chem. Soc. 4499 (1956).
4. H. A. BENESI and J. H. HILDEBRAND. J. Amer. Chem. Soc. **71**, 2703 (1949).
5. MANSEL DAVIS. J. Chem. Educ. **46**, 17 (1969).
6. J. TIMMERMANS. Physico-chemical constants of pure organic compounds. Vol. 1–2. Elsevier Publ. Co., Amsterdam. 1965.
7. Landolt-Börnstein:Zahlenwerte und Funktionen aus Phy. Chem. Astron. Geophys. und Tech. Vol. II. Part 6, Springer–Verlag, Berlin. 1959.

Can. J. Chem. Downloaded from www.nrcresearchpress.com by 210.87.254.105 on 09/05/12
For personal use only.

Can. J. Chem. Downloaded from www.nrcresearchpress.com by 210.87.254.42 on 09/05/12
For personal use only.

Intermolecular forces in gaseous ammonia and in ammonia – nonpolar gas mixtures

C. S. LEE, J. P. O'CONNELL, C. D. MYRAT,[1] AND J. M. PRAUSNITZ
Department of Chemical Engineering, University of Florida, Gainesville, Florida 32601
and
Department of Chemical Engineering, University of California, Berkeley, California 94720

Received February 23, 1970

Intermolecular potential parameters for ammonia have been determined for the Stockmayer–Kihara function using experimental second virial coefficient, diffusivity and viscosity data of binary mixtures with argon, methane, nitrogen, and oxygen. The parameters $U_0/k = 215$ °K, σ(core-to-core) = 2.70 Å and $a^* = 0.2$ reproduce essentially all of the data nearly within experimental error and accurately reproduce pure ammonia transport properties. Upon considering both physical and chemical contributions to the second virial coefficient of ammonia, the apparent standard-state hydrogen-bond enthalpy for chemical dimerization is −3.2 kcal/mole while the vibrational entropy change is 20.2 cal/mole °K, indicating weak association.

Canadian Journal of Chemistry, 48, 2993 (1970)

In recent years, considerable effort has been expended in determining the form of the intermolecular potential for simple nonpolar substances from dilute gas properties, second virial coefficients, viscosity, diffusivity, thermal conductivity, and dielectric properties; agreement with experiment has generally been the criterion with which a given potential function was judged. Although it is not completely satisfactory, the Kihara potential with a spherical core has been successful in reproducing experimental data for several properties using a single set of parameters (1, 2). For more complex substances, particularly those containing permanent dipoles, little detailed examination of the potential has been made, probably because there is no rigorous theory for the transport properties of polyatomic substances, because there are few calculated values of the reduced equilibrium properties, and because accurate experimental data are scarce. In this work, we attempt to bring together as much knowledge as possible on the properties characterizing interactions of ammonia molecules with themselves and also with nonpolar gases such as argon, nitrogen, oxygen, and methane. We first summarize the properties which may be related to the intermolecular potential and discuss the various theories which provide the quantitative relations. We then analyze the experimental data which are available with respect to calculations based on the Stockmayer–Kihara potential function with a rigid spherical core. Finally, we discuss the consequences of the choice of potential parameters on hydrogen bonding in pure ammonia vapor.

[1]Present address: Van der Waals Laboratorium, University of Amsterdam, Netherlands.

Intermolecular Potential

For two particles which have permanent charge separations, the potential energy of interaction is written in terms of the multipole expansion about the two centers of charge (3). For complex molecules, the first approximation to the dipolar interaction, ϕ_{ij}^{d}, assumes ideal, point dipoles located at the centers of mass

$$[1]\quad \phi_{ij}^{d} = -(\mu_i\mu_j/r_{ij}^{3})[2\cos\theta_i\cos\theta_j - \sin\theta_i\sin\theta_j\cos(\psi_i - \psi_j)]$$

where μ is the measured dipole moment; r is the distance between the centers of mass; θ is the in-plane angle between the dipole vector and the vector from the center of i to the center of j; and ψ is the out-of-plane rotation of the dipole vectors.

The induction interaction, ϕ_{ij}^{i}, between a dipole (i) and an isotropically polarizable charge-distribution (j) is given by

$$[2]\quad \phi_{ij}^{i} = -\frac{\alpha_j\mu_i}{2r_{ij}^{6}}[3\cos^2\theta_i - 1] - \frac{\alpha_j\mu_i^{2}}{r_{ij}^{6}}$$

Finally, the nonpolar interaction between two polarizable charge distributions, ϕ_{ij}^{n}, is given by an empirical function such as the Kihara potential with a spherical core,

$$[3]\quad \phi_{ij}^{n} = \infty \qquad r < 2a_{ij}$$

$$\phi_{ij}^{n} = 4U_{0_{ij}}\left[\left(\frac{\sigma_{ij}}{r_{ij} - 2a_{ij}}\right)^{12} - \left(\frac{\sigma_{ij}}{r_{ij} - 2a_{ij}}\right)^{6}\right] \qquad r \geqslant 2a_{ij}$$

where $2a_{ij}$ is the core diameter and $2a_{ij} + \sigma_{ij}$ is the collision diameter, i.e., the center-to-center separation when $\phi_{ij}^{n} = 0$.

Can. J. Chem. Downloaded from www.nrcresearchpress.com by 210.87.254.42 on 09/05/12
For personal use only.

The total intermolecular potential energy is given by the sum of eqs. [1], [2], and [3]. Contributions to equilibrium properties from nonideal and non-central dipoles, quadrupoles and higher order moments and other induction forces can be taken into account (4, 5).

The spherically-symmetric induction interaction may be included approximately in the Kihara form of the dispersion interaction by modifying the potential parameters of eq. [3] (6)

$$[4]\quad U_{0_{ij}}' = U_{0_{ij}} \times \left[1 + \frac{\alpha_i\mu_j^2 + \alpha_j\mu_i^2}{4U_{0_{ij}}\sigma_{ij}^3(\sigma_{ij} + 2a_{ij})^3}\right]^2$$

$$[5]\quad \sigma_{ij}' = \sigma_{ij} \times \left[1 + \frac{\alpha_i\mu_j^2 + \alpha_j\mu_i^2}{4U_{0_{ij}}\sigma_{ij}^3(\sigma_{ij} + 2a_{ij})^3}\right]^{-1/6}$$

For the interaction of different molecular species, we use the following combination rules

$$[6]\quad a_{12} = (a_{11} + a_{22})/2$$

$$[7]\quad \sigma_{12} = (\sigma_{11} + \sigma_{22})/2$$

$$[8]\quad U_{0_{12}} = (U_{0_{11}}U_{0_{22}})^{1/2}$$

For spherical molecules, the first and second of these equations are of high accuracy. The third is an approximation which generally leads to calculated values of $U_{0_{12}}$ exceeding the correct values by a few percent (7).

Transport Properties

Chapman–Enskog kinetic theory (8) relates the dilute gas transport properties (viscosity, diffusivity, and thermal conductivity) to the spherically symmetric intermolecular potential of monatomic substances. For polar polyatomic molecules where inelastic and resonant collisions are important, Monchick and Mason (9) assumed that the two molecules retain the same configuration during a collision and the collision integrals are simple averages over all possible orientations with equal weight given to each orientation. The viscosity and diffusivity coefficients for interactions between like and unlike species are given by

$$[9]\quad \eta_{ij} = \frac{5}{16}\left(\frac{m_{ij}kT}{\pi}\right)^{1/2} \times f_\eta/\delta_{ij}^2\langle\Omega_{ij}^{(2,2)}\ (T^*, t^*)\rangle$$

$$[10]\quad D_{ij} = \frac{3}{8n}\left(\frac{kT}{\pi m_{ij}}\right)^{1/2} \times f_D/\delta_{ij}^2\langle\Omega_{ij}^{(1,1)*}(T^*, t^*)\rangle$$

where m_{ij} is the effective molecular mass $= 2m_im_j/(m_i + m_j)$; f_η and f_D are higher approximations obtained from kinetic theory; δ_{ij} is center-to-center distance parameter in the potential ($\delta_{ij} = \sigma_{ij} + 2a_{ij}$); n is molecular density; $T^* = kT/U_0$; $t^* = \mu^2/2U_0\delta^3$; and the $\langle\Omega^{(l,s)*}\rangle$ are average collision integrals presently available for the Stockmayer potential (eqs. [1] and [3] with $2a = 0$ (9)) and for the Kihara potential (eqs. [3] (1)), but not for the present Stockmayer–Kihara model.

In addition, Mason and Monchick (10) formulated expressions for thermal conductivity of pure gases which take into account the transfer of energy by internal degrees of freedom, particularly rotation. These expressions are based on modifications of Eucken's approximation and are of the form

$$[11]\quad \lambda = \frac{\eta}{M}\left(\frac{5}{2}C_{v\ trans} + \frac{\rho D_{int}}{\eta}C_{v\ int} - \frac{2}{\pi}\left(\frac{5}{2} - \frac{\rho D_{int}}{\eta}\right)^2\sum_k\frac{C_k}{Z_k}\right]$$

where M is the molecular weight; ρ is the density in mass per unit volume; D_{int} is the average coefficient for the diffusion of internal energy; $C_{v\ trans}$ and $C_{v\ int}$ are the translational and internal contributions to the molar heat capacity at constant volume; C_k is the molar heat capacity of an internal mode k; and Z_k is the number of collisions for relaxation of that mode. The value of D_{int} for nonpolar gases is often assumed equal to the self-diffusion coefficient, D. However, for polar molecules, "resonant exchange" of rotational energy may occur and a correction factor is included

$$[12]\quad D_{int} = D/(1 + Z'/Z_0)$$

For near-spherical tops like ammonia

$$[13]\quad Z'/Z_0 = 1.094 \times 10^8\frac{\rho D_{int}}{C_{int}T}\mu^2\left(\frac{\theta_B}{T}\right)^{1/2} \times \left(\frac{\theta_A}{T}\right)\left[1 - \frac{1}{4}\left(\frac{\theta_A - \theta_B}{\theta_B}\right)\right]^{-7/2}$$

where μ is the dipole moment in D; $\theta = h^2/8\pi kI_{rot}$; I_{rot} is the moment of inertia about the dipole axis (A) and the other two principal axes

Can. J. Chem. Downloaded from www.nrcresearchpress.com by 210.87.254.42 on 09/05/12
For personal use only.

(B) (assumed equal). In eq. [13], the units of ρ are g/cm^3; of D, cm^2/s; of T and θ, °K; and of C_{int}, cal/g-mole °K. For the thermal conductivity of binary mixtures, Brokaw (11) and Monchick *et al.* (12) have suggested similar formulas.

While the Mason and Monchick formulations are not exact, they are probably not far in error; therefore, in addition to providing an accurate predictive method, comparison of calculations from this theory with experimental data can lead to meaningful tests of potential models, particularly for simple, nearly-spherical molecules like ammonia.

The viscosity of binary mixtures can be calculated from eqs. [8.2–22] of Hirschfelder *et al.* (3).

Equilibrium Properties

The virial equation of state provides the link between the intermolecular potential and the compressibility factor

$$[14] \quad z = Pv/RT = 1 + B/v + C/v^2 + \ldots$$

where, for pure components, B, C, etc. are functions only of temperature and take into account interaction between two molecules, three molecules, etc. For mixtures the virial coefficients are functions of composition, e.g.,

$$[15] \quad B_{mix} = \sum_i \sum_j x_i x_j B_{ij}$$

where B_{ij} is the second virial coefficient for interaction between species i and species j. The statistical mechanical derivation of the virial equation gives for the second virial coefficients, for instance,

$$[16] \quad B_{ij} = (N_0/4) \int_0^\infty \int_0^{2\pi} \int_0^\pi \int_0^\pi r_{ij}^2 \times \{1 - \exp[-\phi_{ij}/kT]\} \sin\theta_i \sin\theta_j \times d\theta_i\, d\theta_j\, d(\psi_i - \psi_j)\, dr_{ij}$$

where N_0 is Avogadro's number; ϕ_{ij} is the intermolecular potential between species i and j as given by eqs. [1] and [3] using the modified parameters of eqs. [4] and [5].

For molecules containing permanent dipoles, tables of reduced second virial coefficients are available (1) for several potentials of the Stockmayer–Kihara core form (13, 14).

First-order contributions from angular-dependent induction forces and quadrupole forces are given by Buckingham and Pople (4),

$$[17] \quad B_{ang} = -\frac{2\pi N_0}{3}\delta^3 \left\{ q\left(\frac{U_0\tau^3}{60kT} + \frac{11q\tau^2}{80}\right) H_{12} + q\frac{U_0^3\tau^5}{65(kT)^3} H_{18} + \frac{Q^2}{U_0\delta^5}\left[\frac{\tau H_8}{32} + \frac{7Q^2H_{10}}{320U_0\delta^5}\right] + \ldots \right\}$$

where $q = \alpha/\delta^3$; $\tau = \mu^2/2U_0\delta^3$; Q is the quadrupole moment (assumed axially symmetric)

$$H_\kappa(y) = y^{(4.5-\kappa/6)} \sum_{m=0}^{\infty} \Gamma\left(\frac{6m + \kappa - 3}{12}\right) \frac{y^m}{m!}$$

$$y = 2\left(\frac{kT}{U_0}\right)^{-1/2}$$

When the dipole is assumed to be on the surface of the core, the first order effect of an off-center dipole on the second virial coefficient can be included through the equation of Lawley and Smith (5),

$$[18] \quad B_{\text{off-center}} = -\gamma^{*2}\tau(2\pi N_0\delta^3/3)H_8 + \ldots$$

where $\gamma^* = 2a/\delta = a^*/(1 + a^*)$. Higher order effects are not used for any of the angle-dependent forces because their sum for all effects tends to cancel. The calculated values of the second virial coefficient from eqs. [16]–[18] should be accurate to about 2 cc/g-mole except at very low temperatures.

If, in addition to the physical interactions of molecular collisions, chemical association can occur through hydrogen-bonding or other charge transfer mechanism, the compressibility at moderate pressures may deviate significantly from that calculated on the basis of physical interactions alone. We expect that the interactions of ammonia molecules with themselves involve hydrogen bonding (15) while interactions with nonpolar molecules do not (16–18). Thus, we expect that the parameters for the potential of eq. [3] should describe the cross coefficients and the pure ammonia dilute gas transport coefficients, but will lead to insufficiently negative values of the pure ammonia second virial coefficient.

Lambert, *et al.* (19, 20) have shown that for a weakly associated gas the second virial coefficient is of the form

$$[19] \quad B = B_{phys} + B_{chem} = B_{phys} - RTK_p$$

TABLE 1
Molecular parameters

Gas	U_0/k (°K)	σ (Å)	a^*	α (Å^3)	μ (D)	Reference
NH_3	215	2.70	0.20	2.24	1.47	This work
A	147.2	2.946	0.125	1.63	—	51
N_2	139.2	2.821	0.250	1.76	—	51
CH_4	230.5	2.754	0.280	2.60	—	1
O_2	194.3	2.373	0.310	1.60	—	1
Kr	215.6	3.062	0.150	2.46	—	51

where B_{phys} is the physical contribution (calculated from the intermolecular potential, eqs. [16]–[18]) and K_p is the chemical equilibrium constant for hydrogen-bonded dimer formation. A plot of $\ln K_p$ vs. $1/T$ yields the apparent standard enthalpy and entropy of association

$$[20] \qquad \ln K_p = -\Delta H^0/RT + \Delta S^0/R$$

For pure components, second virial coefficients are obtained from vapor-phase compressibility measurements. However, cross virial coefficients (B_{ij}) characterizing the interaction between unlike species can be obtained also from phase equilibrium data (1, 16, 18, 21). When the pressure is not large and the vapor mole fraction of the polar substance is small, B_{ij} can usually be determined to within ±5 cc/mole.

Comparisons with Data

Parameters used in our calculations are shown in Table 1. The ammonia quadrupole moment was assumed to be 0.3×10^{-26} e.s.u. (22). The nonpolar parameters for ammonia were chosen as "best" after comparison of data with calculations using many sets of parameters. This procedure is somewhat inefficient; however, since there is uncertainty in the weights to be given to the various data and in the possible experimental errors, simple least-squares fitting covers up the fact that a range of parameters is usually compatible with all data. The present choice of a single set as "best" is only a judgment until more complete and accurate data become available.

Calculations with the Kihara potential show that cross transport properties are insensitive to the energy parameter but sensitive to the center-to-center distance. On the other hand, cross virial coefficients are more sensitive to the energy parameter U_0, while only pure transport properties of polar substances are sensitive to the core size, through its pronounced effect on the reduced dipole moment.

A. Ammonia Nonpolar Systems

1. Virial Coefficients

B_{12} data for ammonia–argon were obtained at three temperatures from the vapor–liquid equilibrium data of Michels *et al.* (23). For data reduction, the third virial coefficient C_{122} (polar–nonpolar–nonpolar) was estimated by the method of Orentlicher and Prausnitz (24). Since the total pressure and the ammonia concentration were high, the analysis probably yields values of B_{ij} that are accurate to ±10–15 cc/g-mole. Michels (25) gives experimental values of B_{12} for ammonia with argon and with krypton at 298.15 °C obtained from volumetric measurements. B_{12} with argon from these measurements is about 20 cc/g-mole more negative than that obtained from equilibrium measurements.

The equilibrium data of Lurie and Gillespie (26) were used to provide B_{12} for ammonia with nitrogen at 318.15 °K. Compressibility data for ammonia–nitrogen mixtures by Lichtblau *et al.* (27) give additional cross coefficients at 350, 400, and 450 °C.

Kazarnovskii and Levchenko (28) have reported compressibility data for ammonia with methane. Because of the large uncertainties of the compressibility in the low density region, extrapolated values of the cross virial coefficients are uncertain (perhaps as high as ±20 cc/g-mole). Further, without accurate third virial coefficients, detailed comparison with experiment is not possible and these data cannot be weighed strongly.

Figure 1 and Table 2 summarize the comparisons. In general agreement between calculated and experimental results is good. In particular, the calculated values of B_{12} for NH_3 with Ar and N_2 reproduce the experimental vapor mole fraction of NH_3 within the experimental error despite some disagreement (up to 20 cc/g-mole) with the "best" experimental B_{12} values. The single value of B_{12} for ammonia with argon

Can. J. Chem. Downloaded from www.nrcresearchpress.com by 210.87.254.42 on 09/05/12
For personal use only.

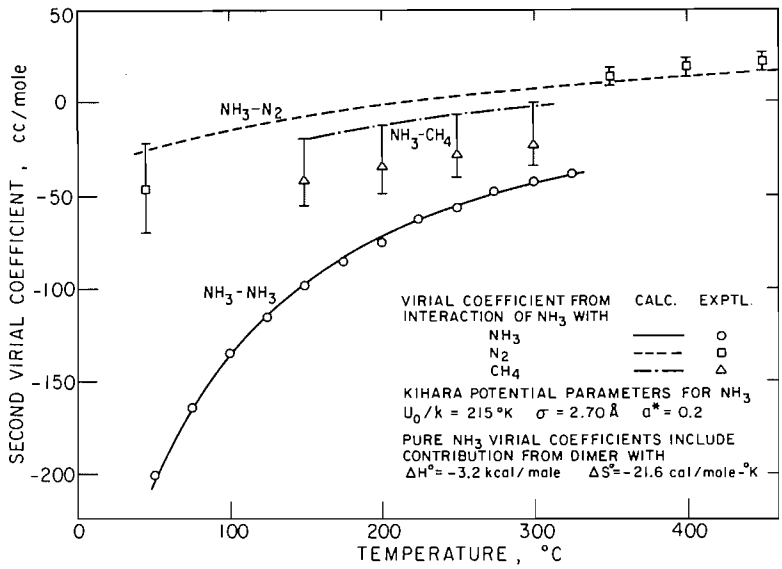

FIG. 1. Pure component and cross second virial coefficients for ammonia systems.

TABLE 2

Second cross virial coefficient for mixtures of ammonia with nonpolar gases

Gas	Type of data	Number of data points	Temperature range (°C)	Root mean square deviation* in B_{12}(cc/g-mole)	Reference
Argon	Equilibrium†	8	25–75	−10	23
	Volume of mixing	1	25	+10	25
Krypton	Volume of mixing	1	25	+3	25
Nitrogen	Equilibrium‡	7	45	+22	26
	Compressibility	12	350–450	−5	27
Methane	Compressibility	16	150–300	+19	28

*The sign indicates the direction in which the calculations are in error.
†Vapor–liquid data.
‡Vapor–solid ($BaCl_2 . 8NH_3$) data.

TABLE 3

Pure-component and binary diffusivities for ammonia systems

Gas	Number of data points	Temperature range (°C)	Root mean square deviation from experiment (%)	Reference
Ammonia	4	−40–173	+3.0	46, 47
Argon	4	−19–60	+8.4	29
Nitrogen	3	25–80	−2.2	30
Krypton	4	−19–60	+15.5	29

from compressibility data is not reproduced well but this inconsistency was previously noted by Michels (25). The uncertain ammonia–methane data of Kazarnovskii (28) are also not predicted accurately. These disagreements with unsure data lead to an uncertainty in U_0/k of perhaps 30 or 40 °K.

2. Transport Properties

Binary diffusion coefficients are available for ammonia with argon and for ammonia with krypton (29) and with nitrogen (30). They are shown in Table 3, which also gives a comparison with calculated values.

Agreement between calculated and experi-

Can. J. Chem. Downloaded from www.nrcresearchpress.com by 210.87.254.42 on 09/05/12
For personal use only.

TABLE 4

Comparison of calculated and experimental viscosities of ammonia with nonpolar gases

Gas	Number of data points	Temperature range (°C)	Root mean square deviation in η_{12} (%)	Root mean square deviation in η_{mix} (%)	References
Argon	13	20–30	−4.2	−1.5	32
	26	26–80	+11.0	+4.4	31
Nitrogen	25	24–200	4.0	1.0	33
	20	20–250	−0.6	0.2	34
Oxygen	15	20–200	2.1	0.7	34
Methane	35	14.5–80	3.6	1.1	31, 25

mental results is nearly within experimental error for the nitrogen system but disagreement with the diffusivity data for ammonia with argon, is the same as indicated by Brokaw (11). Since the ammonia–krypton diffusivity data and the ammonia–argon data were taken by the same investigators (29), and since the calculations do not agree well with experiment in both cases, it is likely that both sets of data are in error. Thus an overall comparison for D_{12} (such as that given below in Table 6) is probably not truly indicative of the accuracy of our theoretical model.

Two sets of viscosity data for ammonia–argon mixtures are available (31, 32). Unfortunately, although these workers essentially agree on the pure component values, the composition dependence (and thus the values of η_{12}) are markedly different. Two sets of viscosity data are available for ammonia–nitrogen mixtures (33, 34) and for ammonia–methane mixtures (31, 35). Here, agreement between experimenters is within experimental error. Trautz and Heberling (34) also have given a set of viscosity data for the ammonia–oxygen system.

Experimental and calculated viscosities are compared in Fig. 2 and Table 4. (When the calculated values were definitely too high or too low, the + or − signs have been used. No sign means no definite trend.) Except for one set of ammonia–argon viscosity data (31), the agreement is probably within experimental error. Based on this agreement, the uncertainty in the center-to-center distance is less than ±0.05 Å.

B. Pure Ammonia

1. Virial Coefficients

Cheh *et al.* (36) and O'Connell (13) have obtained the most recent set of second virial coefficients for ammonia from available compressibility measurements. Figure 1 and Table 5 present the complete set of virial coefficient data

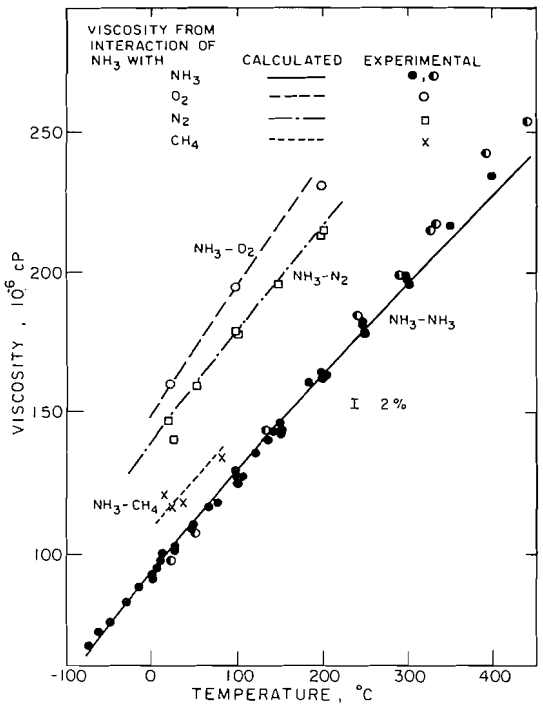

FIG. 2. Pure component and cross viscosities for ammonia systems.

used here. Also presented are the contributions from physical interactions and from a hydrogen-bonded dimer with a standard enthalpy of formation of −3.2 kcal/mole and an entropy of formation of −21.6 cal/mole °K. Using an analysis identical to that of Cheh *et al.* (36) for the ammonia–acetylene dimer,[2] the entropy of vibra-

[2]The basic conclusions of Cheh's work are unchanged when our final parameters are used in his analysis. Correcting an error in obtaining K_p from B_{chem} for unlike association (16) and a numerical error in eq. [18] in Cheh's work leads to ΔS_{vib}^0 of + 21.8 cal/mole °K and ΔH^0 of −2.06 kcal/mole for the ammonia–acetylene dimer.

Can. J. Chem. Downloaded from www.nrcresearchpress.com by 210.87.254.42 on 09/05/12
For personal use only.

TABLE 5

Second virial coefficients for ammonia (cc/g-mole)

Temperature (°C)	B_{phys}*	B_{chem}†	B_{calcd}	B_{exp}‡
50	−129.4	−77.8	−207.2	−201.5
75	−107.6	−58.7	−166.3	−164.5
100	−90.6	−46.2	−136.8	−137
125	−77.0	−37.6	−114.6	−116.5
150	−65.9	−31.5	−97.4	−99
175	−56.7	−27.0	−83.7	−86
200	−49.0	−23.6	−72.6	−74
225	−42.4	−21.0	−63.4	−63.5
250	−36.8	−18.9	−55.7	−56
275	−31.9	−17.2	−49.1	−48.5
300	−27.6	−15.8	−43.4	−42
325	−23.8	−14.7	−38.5	−38

*Calculated from the potential parameters $U_0/k = 215$ °K, $\sigma = 2.70$ Å, and $a^* = 0.2$.
†Calculated from $\Delta H^0 = -3.2$ kcal/mole and $\Delta S^0 = -21.6$ cal/mole °K.
‡Experimental values as smoothed by Cheh *et al.* (36) and O'Connell (13); root mean square deviation, 2.0 cc/mole.

tion of the ammonia–ammonia dimer $\Delta S_{vib}{}^0$, is 20.2 cal/mole °K, which indicates very weak hydrogen bonding according to Shepp and Bauer (37) and Slutsky and Bauer (38). We have assumed the N–N distance to be 3.38 Å as given by Mark and Pohland (ref. 39*a*, quoted from ref. 39*b*). Comparison of $\Delta S_{vib}{}^0$ for the ammonia–ammonia dimer with that for the ammonia–acetylene dimer suggests that these hydrogen bonds are similar.

Our calculated standard enthalpy of dimerization, −3.2 kcal/mole, is comparable to the previous values of −3.7 kcal/mole reported by Rowlinson (40) and −4.4 kcal/mole reported by Lambert *et al.* (20).

2. Transport Properties

Extensive measurements of the viscosity of ammonia over a wide temperature range are available (34, 41–45). Unfortunately, there is some disagreement at high temperatures. Figure 2 presents the data which were used as well as our calculated results. Since no collision integrals are available for the Stockmayer–Kihara model, the collision integral tables of Mason and Monchick for the Stockmayer potential (no core) were used with an empirical modification of the reduced dipole moment

$$t^{*\prime} = \mu^2/[\sqrt{8}U_0'\sigma'^{1.5}(\sigma' + 2a)^{1.5}]$$

The small core would also slightly affect the nonpolar contribution to the collision integral, but no quantitative estimate is available. The calculations suggest that some of the viscosity data are too high at high temperatures. Without the data of Braune and Linke (41), which are shown on Fig. 2 by half-filled circles, the deviation from experiment is reduced from 2.1 to 1.4%, but the uncertainties in the calculations are about as large as the experimental ones until collision integrals for the Stockmayer–Kihara model become available. The core size $2a = 0.54$ Å was adopted on the basis of agreement with viscosity at low temperatures but the uncertainty introduced by using approximate collision integrals may be as large as ± 0.2 Å.

Two sets of data are available for the self-diffusivity of ammonia (46, 47). Table 3 compares calculated values with experimental results (root mean square (r.m.s.) deviation 3.0%). It is likely that using exact collision integrals for the core model would decrease the disagreement.

Careful measurements of the thermal conductivity over a range of temperature are available (48, 49) and the agreement between various workers is the best for this property. Unfortunately, it also contributes the least to our analysis because of its additional parameter for the transfer of internal energy. Figure 3 compares calculated with experimental results (r.m.s. deviation 2.0%). The collision number was 1.8 and essentially independent of temperature. This value is identical to that found for water by a similar analysis (50).

Discussion

Although our parameters reproduce ammonia nonpolar transport properties satisfactorily, further accurate cross virial coefficient data may lead

Can. J. Chem. Downloaded from www.nrcresearchpress.com by 210.87.254.42 on 09/05/12
For personal use only.

TABLE 6

Potential parameters for ammonia

Source of parameters	U_0/k	σ	$2a/\sigma$	Root mean square deviations					
				B_{12}* (cc/mole)	B_{NH_3} (cc/mole)	D_{12}* (%)	D_{NH_3} (%)	η_{12}* (%)	η_{NH_3} (%)
Virial									
Rowlinson (40)	218†	2.69†	0	11.7	13.5	+22.4	+32.4	+20.1	+29.8
Viscosity									
Mason–Monchick (9)	323†	3.18†	0	27.3	−25.1	5.2	+3.1	6.5	2.0
This work	215	2.70	0.2	13.1	2.0‡	10.2	+3.0	5.2	2.1

*Mixture properties for ammonia with nonpolar gases: argon, krypton, nitrogen, methane, oxygen. See Tables 2–4. Inconsistent data for argon systems weighed equally with others.

†The original references did not take induction into account. These values of U_0/k and σ have had the spherically symmetric induction contribution removed.

‡Using dimer model with $\Delta H^0 = -3.2$ kcal/mole and $\Delta S^0 = -21.6$ cal/mole °K.

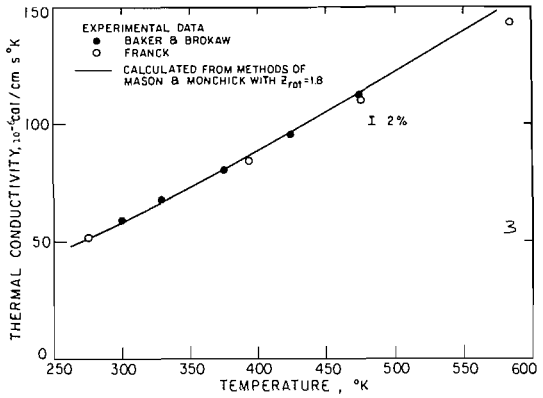

FIG. 3. Thermal conductivity of ammonia.

to another set of parameters, though only slightly different from the present ones. In any case, the present parameters describing the nonpolar interactions of ammonia molecules (and any expected changes) are more compatible with the structure and polarizability of ammonia than those obtained by previous workers and also are appropriately between the values which have been found for methane (1) and water (21).

Table 6, for instance, shows the parameters which various workers have obtained. Our parameters are significantly different because the potential model is more realistic and all experimentally available properties have been taken into account. In addition, the effects of induction on the properties and parameters were not previously taken into account in the explicit manner used here. This choice of parameters forces us to include hydrogen bonding for dense gas properties.

The success of our analysis indicates that we are using a viable method for determining a realistic description of the nonpolar forces of simple polar molecules as given by an analytic potential function of the Kihara type. Unfortunately, we have not been able to give a satisfactory test to the Monchick and Mason (9) expressions since we have had to modify empirically the collision integrals. However, it would seem that the Stockmayer potential without a core is probably as inadequate for even simple polar molecules as the Lennard–Jones potential has been shown to be for simple nonpolar substances. Work is in progress (52) to complete the collision integral calculations for the polar core model which can then be used in this type of analysis. It appears that the Monchick and Mason expressions lead to results for polar molecules at least as accurate as those used presently for nonpolar molecules, although it is likely that for large molecules, the presence of nonspherical repulsive forces may lead to appreciable error.

Conclusion

Our analysis of the dilute gas properties of ammonia and mixtures of ammonia with nonpolar gases suggests that the Stockmayer–Kihara potential function accurately describes the nonpolar interactions between ammonia and other molecules using the parameters $U_0/k = 215$ °K, $\sigma = 2.70$ Å, and $a^* = 0.2$. These parameters are not unique because some range about the above values may also yield nearly the same results. However, within this range, the values are more compatible with the structure of ammonia than those found previously.

Can. J. Chem. Downloaded from www.nrcresearchpress.com by 210.87.254.42 on 09/05/12
For personal use only.

It appears that the kinetic theory expressions of Monchick and Mason (9) are sufficiently accurate for predicting dilute gas transport properties for simple polar molecules since the agreement between experiment and calculations is at least as good as has been obtained previously for nonpolar molecules when a single set of parameters is used for both thermodynamic and transport properties. Weak hydrogen bonding exists between ammonia molecules, characterized by a standard enthalpy of dimerization of -3.2 kcal/mole and a standard entropy of dimerization of -21.6 cal/mole °K.

The authors are grateful for financial support from the Office of Saline Water, U.S. Department of Interior, and from the National Science Foundation.

1. J. P. O'Connell and J. M. Prausnitz. *In* Thermodynamic and transport properties at extreme pressures and temperatures. *Edited by* S. Gratch. ASME, New York. 1965. p. 19.
2. L. S. Tee, S. Gotoh, and W. E. Stewart. Ind. Eng. Chem. Funda. **5**, 363 (1966).
3. J. O. Hirschfelder, C. F. Curtiss, and R. B. Bird. Molecular theory of gases and liquids. John Wiley and Sons, Inc., New York. 1954.
4. A. D. Buckingham, and J. A. Pople. Trans. Faraday Soc. **51**, 1173 (1955).
5. K. P. Lawley, and E. B. Smith. Trans. Faraday Soc. **59**, 301 (1963).
6. J. P. O'Connell and J. M. Prausnitz. Ind. Eng. Chem. Funda. **8**, 453 (1969).
7. G. H. Hudson and J. C. McCoubrey. Trans. Faraday Soc. **56**, 761 (1960).
8. S. Chapman and C. G. Cowling. Mathematical theory of non-uniform gases. 2nd ed. Cambridge Press. 1952.
9. L. Monchick and E. A. Mason. J. Chem Phys. **35**, 1676 (1961).
10. E. A. Mason and L. Monchick. J. Chem. Phys. **36**, 1622 (1962).
11. R. S. Brokaw. *In* Proceedings of the International Seminar on the Transport Properties of Gases. *Edited by* J. Kestin and J. Ross. Brown University, Rhode Island, 1964. p. 77.
12. L. Monchick, A. N. G. Pereira, and E. A. Mason. J. Chem. Phys. **42**, 3241 (1965).
13. J. P. O'Connell. Ph.D. Thesis. University of California, Berkeley, California. 1967.
14. K. W. Suh and T. S. Storvick. J. Phys. Chem. **71**, 1450 (1967).
15. G. C. Pimentel and A. L. McClellan. The hydrogen bond. Reinhold, New York. 1960.
16. J. M. Prausnitz. Molecular thermodynamics of fluid-phase equilibria. Prentice–Hall, New Jersey. 1969. p. 142.
17. M. Rigby, J. P. O'Connell, and J. M. Prausnitz. Ind. Eng. Chem. Funda. **8**, 460 (1969).
18. J. S. Rowlinson. Liquids and liquid mixtures. 2nd ed. Plenum Press, New York. 1969.
19. J. D. Lambert, G. A. H. Roberts, J. S. Rowlinson, and V. J. Wilkinson. Proc. Roy. Soc. London Ser. A. **196**, 113 (1949).
20. J. D. Lambert and E. D. T. Strong. Proc. Roy. Soc. London, Ser. A. **200**, 566 (1950).
21. M. Rigby and J. M. Prausnitz. J. Phys. Chem. **72**, 330 (1968).
22. A. Duncan and J. A. Pople. Trans Faraday Soc. **49**, 217 (1953).
23. A. Michels, E. Dumoulin, and J. J. Van Dijk. Physica, **27**, 889 (1961).
24. M. Orentlicher and J. M. Prausnitz. Can. J. Chem. **45**, 373 (1967).
25. A. Michels. Nuovo Cimento, **9**, 358 (1958).
26. E. Lurie and L. J. Gillespie. J. Amer. Chem. Soc. **49**, 1146 (1927).
27. I. M. Lichtblau, R. H. Bretton, and B. F. Dodge. A.I.Ch.E. J. **10**, 486 (1964).
28. J. S. Kazarnovskii and C. T. Levchenko. J. Phys. Chem. U.S.S.R. **18**, 380 (1944).
29. B. N. Srivastava and I. B. Srivastava. J. Chem. Phys. **36**, 2616 (1962).
30. R. E. Bunde. Univ. of Wisconsin Naval Res. Lab. Rep. No. CM-850. Aug. 1955.
31. P. K. Chakraborti and P. Gray. Trans. Faraday Soc. **61**, 2422 (1965).
32. H. Iwasaki, J. Kestin, and A. Nagashima. J. Chem. Phys. **40**, 2988 (1964).
33. A. K. Pal and A. K. Barua. Indian J. Phys. **41**, 713 (1967).
34. M. Trautz and R. Heberling. Ann. Phys. **10**, 155 (1931).
35. G. Jung and H. Schmick. Z. Phys. Chem. **B7**, 130 (1930).
36. H. Y. Cheh, J. P. O'Connell, and J. M. Prausnitz. Can. J. Chem. **44**, 429 (1966).
37. A. Shepp and S. H. Bauer. J. Amer. Chem. Soc. **76**, 265 (1954).
38. L. Slutsky and S. H. Bauer. J. Amer. Chem. Soc. **76**, 270 (1954).
39. (*a*) H. Mark and E. Pohland. Z. Krist. **61**, 532 (1925). (*b*) G. C. Pimentel and A. L. McClellan. The hydrogen bond. Reinhold, New York. 1960.
40. J. S. Rowlinson. Trans. Faraday Soc. **45**, 974 (1949).
41. H. Braune and R. Linke. Zeit. Phys. Chem. **A148**, 195 (1930).
42. L. G. Burch and C. J. G. Raw. J. Chem. Phys. **47**, 2798 (1967).
43. R. S. Edwards and B. Worswick. Proc. Phys. Soc. **38**, 16 (1925).
44. R. Kiyama and T. Makita. Rev. Phys. Chem. Japan, **22**, 49 (1952).
45. A. B. Van Cleave and O. Maass. Can. J. Res. **13B**, 140 (1935).
46. C. E. Baker. J. Chem. Phys. **52**, 2159 (1970).
47. R. Paul and W. W. Watson. J. Chem. Phys. **45**, 2675 (1966).
48. C. E. Baker and R. S. Brokaw. J. Chem. Phys. **43**, 3519 (1965).
49. E. U. Franck. Z. Elektrochem. **55**, 636 (1951).
50. J. P. O'Connell and J. M. Prausnitz. Ind. Eng. Chem. Funda. In press.
51. A. E. Sherwood and J. M. Prausnitz. J. Chem. Phys. **41**, 429 (1964).
52. T. S. Storvick. Private communication.

Can. J. Chem. Downloaded from www.nrcresearchpress.com by 210.87.254.42 on 09/05/12
For personal use only.

Can. J. Chem. Downloaded from www.nrcresearchpress.com by 210.87.254.5 on 09/05/12
For personal use only.

Quantitative investigation of the ozonolysis reaction. XIV. A simple carbonium ion stabilization approach to the ozone cleavage of unsymmetrical olefins[1]

SÁNDOR FLISZÁR AND JEAN RENARD
Department of Chemistry, University of Montreal, Montreal, Quebec

Received February 17, 1970

The direction of ozone cleavage of selected unsymmetrical olefins $R_1R_2C{=}CR_3R_4$ to give (*a*) $R_1R_2CO + R_3R_4C^+OO^-$ and (*b*) $R_1R_2C^+OO^- + R_3R_4CO$ has been measured, with particular emphasis on the mode of participation of alkyl substituents in distributing the reaction paths *a* and *b*. The interpretation, in terms of substituent effects in stabilizing potential zwitterionic carbo-cations in the transition states corresponding to paths *a* and *b*, considers (*i*) the "hyperconjugative stabilization" of positive sites, where the stabilizing abilities of the substituents are in the order $CH_3 > C_2H_5 > i\text{-}C_3H_7 > tert\text{-}C_4H_9$, and (*ii*) the participation of inductive effects. The latter appear to be particularly important when the substituents on the two C atoms of the primary ozonide act in the same direction in favoring its electrocyclic cleavage. In the ozonolysis of monosubstituted ethylenes the inductive effects are predominant, i.e. the $R{-}C^+HOO^-$ formation is favored by the R groups in the order $tert\text{-}C_4H_9 > i\text{-}C_3H_7 > C_2H_5 > CH_3$, whereas in *trans*- and *cis*-1,2-disubstituted ethylenes "hyperconjugation" governs the direction of cleavage. The cleavage of selected 1,1-disubstituted, tri-, and tetrasubstituted ethylenes is also studied.

Canadian Journal of Chemistry, 48, 3002 (1970)

The primary ozonides **1** resulting from the 1,3-dipolar cyclo-addition (1) of ozone on a carbon–carbon double bond have been the object of recent studies, both experimental (2–5) and theoretical (6, 7).

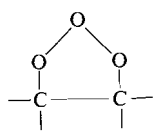

1

Their occurrence in the course of ozonolysis reactions (2, 4), their structure (**1**) (4, 5), and their conformations (6, 7) have been investigated. The (LCAO-MO) linear combination of atomic orbitals and molecular orbitals conformational analysis of a series of primary ozonides (7) confirmed the particularly unstable nature of *cis* primary ozonides bearing a *tert*-butyl substituent. However, even in the most favorable cases, as with the primary ozonide of *trans*-di-*tert*-butylethylene, the intermediates **1** are extremely unstable;[2] the *trans*-di-*tert*-butylethylene primary ozonide decomposes in an explosive way when "heated" up to $-60°$ (2). For the primary ozonide of 3-hexene, Greenwood's kinetic study of its decomposition at -100 °C indicated the reaction to be of first order (9).

According to Criegee's mechanism of ozonolysis (10), which is well supported by a great number of experimental verifications (11), the primary ozonides cleave into zwitterion and carbonyl compound. The proportions of the two possible ways of cleavage (*a* and *b*) have been the object of recent studies (Scheme 1).

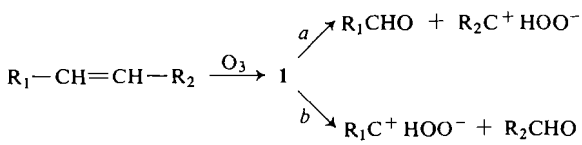

SCHEME 1

Transition states corresponding to the two possible ways of cleavage have been considered (12). These transition states could approach structure **2** corresponding to the cleavage following path *a*, and similar ones for path *b*. The participation of zwitterion structures **3** and **4** has been the object of recent discussions (6, 13, 14), but **5** has been rejected (15).

Because of the complexity of the reactions occurring in ozonolyses in inert solvents (CCl_4, hexane, for example), the cleavage of the primary ozonides of unsymmetrical olefins is studied adequately in the presence of a participating

[1]Abstracted from the Ph.D. Thesis of J. Renard, Université de Montréal, Montréal, Québec, 1969.

[2]The lower thermal stability of the 1,2,3-trioxolanes, as compared to their aliphatic O_3 analogs $R_3COOOCR_3$ is attributed to (*i*) the prevention of the normal skew conformation of the —O—O—O— chain by the constraint of the five-membered ring, and (*ii*) the assistance to its decomposition from concerted cleavage of the central C—C bond (8).

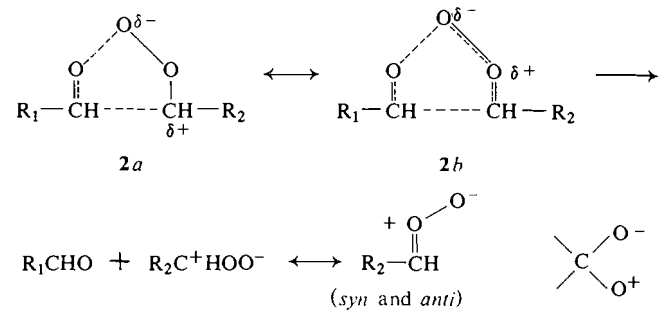

2a 2b

3 4 5

solvent, e.g. methanol or ethanol. In the presence of alcohol, the ozonolysis yields only four products which are well defined, i.e. two carbonyl compounds and two alkoxyhydroperoxides $R_1CH(OR)OOH$ and $R_2CH(OR)OOH$, the latter resulting from the attack of the alcohol ROH on the zwitterions. It has been shown, in all cases studied, that in the presence of enough methanol (or ethanol) the zwitterions are *quantitatively* trapped to give the corresponding alkoxyhydroperoxides (16, 17).[3] It has been also shown that the ozonolysis of 1 mole of olefin, in the presence of excess alcohol, results in the production of a total of 1 mole of the mixture of carbonyl compounds. This is in complete agreement with the stoichiometry of Criegee's mechanism (Scheme 1) (12, 16, 18).

Bailey's determinations (19) of the direction of cleavage of 1-substituted 1,2-dibenzoylethylenes, made by isolation of the ozonolysis products in the presence of methanol, have indicated that the inductive, rather than the resonance effects, play a role in distributing the proportions of cleavage. Similarly, Keaveney *et al.* (20) have measured the proportions of cleavage of styrene, propenylbenzene, and 2-methyl-propenylbenzene by isolation of the reaction products. The results indicated the predominant role of the inductive effect and a minor participation of resonance stabilization by the phenyl ring. The merits of direct isolation experiments are obvious. The disadvantage is clear, however, when the relative unstability of the hydroperoxides[4] is considered. Hence, only a poor precision can be obtained in using isolation techniques. Precision has been considerably improved by the use of non-destructive analytical methods for determining the amounts of reaction products, and because of this detailed studies on the factors governing the distribution of the paths of cleavage became possible (12, 16, 18, 22).

$$[1] \quad \log [x/(1-x)] = -(\Delta G_a^{\ddagger} - \Delta G_b^{\ddagger})/2.3RT = -\Delta\Delta G^{\ddagger}/2.3RT$$

$$[2] \quad \log [x/(1-x)] = -(\Delta G_{0,a}^{\ddagger} - \Delta G_{0,b}^{\ddagger})/2.3RT + (\rho_a - \rho_b)\sigma$$

Equation [2], which is derived from eq. [1] by standard methods (16*a*, 18, 23), was found to satisfactorily describe the proportions of ozone cleavage of a series of ring- and β-substituted

[3]P. Kolsaker and P. S. Bailey (38) have shown that methoxyhydroperoxides react with aldehydes in Baeyer–Villiger fashion when the reaction mixtures are allowed to stand for several days at room temperature, and are then heated to reflux until the peroxide is decomposed. It is important, therefore, to analyze for aldehyde immediately after completion of the ozonolysis. However, control analyses performed 2 h after the ozonolysis did not indicate any appreciable change in the aldehyde content. It is concluded that no reaction between aldehyde and methoxyhydroperoxide occurs under our experimental conditions.

[4]Razumovskii and Yurief (21) have taken advantage of the thermal instability of α-methoxyhydroperoxides; the direction of cleavage of some primary ozonides, including that of styrene, were determined by v.p.c. analyses of the thermal decomposition products of the methoxyhydroperoxides formed in methanolic ozonolyses. A study of the v.p.c. behavior of phenyl-methoxyhydroperoxide by means of a UCW 98 column at different temperatures indicates, however, that the production of the main decomposition product, the methyl benzoate, is neither quantitative nor very reproducible. These observations agree thus with the findings of Keaveney *et al.* (20) who reported five minor decomposition products, in addition to the ester, for the decomposition of phenyl-methoxyhydroperoxide. The work of Spencer *et al.* (39) also indicates that the ester production by thermal decomposition of α-methoxyhydroperoxides obtained by ozonation of unsaturated fatty acids is far from being quantitative. It is considered, therefore, that the method used by Razumovskii and Yurief is not very reliable, or accurate.

Can. J. Chem. Downloaded from www.nrcresearchpress.com by 210.87.254.5 on 09/05/12
For personal use only.

Can. J. Chem. Downloaded from www.nrcresearchpress.com by 210.87.254.5 on 09/05/12
For personal use only.

styrenes into (*a*) $RC_6H_4CHO + R_\beta C^+HOO^-$ and (*b*) $RC_6H_4C^+HOO^- + R_\beta CHO$. The proportion of cleavage following path *a* (with a rate constant k_a) is indicated by x, and, consequently, $1 - x$ is the proportion of cleavage following path *b*, with a rate constant k_b. $\Delta G_a^{\ddagger}$ and $\Delta G_b^{\ddagger}$ represent the Gibbs activation energies accompanying the formation of the transition states corresponding to paths *a* and *b*, respectively, and $\Delta G_{0,a}^{\ddagger}$ and $\Delta G_{0,b}^{\ddagger}$ the corresponding quantities for the compounds bearing no substituent in the phenyl ring; ρ and σ are Hammett's reaction and substituent constants.

In the study of ring- and β-substituted styrenes (16, 18), an interpretation of the Hammett relationship, eq. [2], and of the behavior of the β substituents in terms of transition states concludes that the zwitterion which is formed preferentially is the one whose environment is better able to stabilize the positive charge by increasing the electron density in the vicinity of the potential zwitterionic carbo-cation (in the transition state) via inductive and mesomeric effects. The relative efficiencies of the β substituents in stabilizing zwitterions can be placed in the order $COCH_3 > CH_3 > COOH > Ph > H > CH_2OH > COOCH_3$. The behavior of the groups $COCH_3$ and COOH which tend to stabilize the zwitterions $R_\beta C^+HOO^-$ despite the fact that they are electron-withdrawing groups is explained by resonance stabilization (18).

Similar results are also obtained in the study (12) of the cleavage of the primary ozonides of a series of *trans*-1,2-disubstituted ethylenes $R_\alpha CH{=}CHR_\beta$. The proportions of the two ways of cleavage to yield (*a*) $R_\alpha CHO + R_\beta C^+HOO^-$ and (*b*) $R_\alpha C^+HOO^- + R_\beta CHO$ obey eq. [3], which is derived from eq. [1], where x is the

$$[3] \quad \log [x/(1-x)] = [\Delta G_R^{\ddagger}(\alpha) - \Delta G_R^{\ddagger}(\beta)]/2.3RT$$

proportion of cleavage following path *a*, and $\Delta\Delta G^{\ddagger} = -\Delta G_R^{\ddagger}(\alpha) + \Delta G_R^{\ddagger}(\beta)$, the Gibbs activation energy difference between transition states of paths *a* and *b*. This equation enables the proportions of cleavage (x) following path *a* to be calculated from a table of values for the group contributions $\Delta G_R^{\ddagger}$ [$\Delta G_R^{\ddagger}(\alpha)$ for R_α and $\Delta G_R^{\ddagger}(\beta)$ for R_β] which, in most cases, are constant for each group, irrespective of the substituent on the other ethylenic carbon atom. The relative efficiencies of the groups (indicated by their $\Delta G_R^{\ddagger}$ values) in stabilizing zwitterions are in the order[5] $COCH_3$ (−0.34) > CH_3 (−0.28) > COOH (−0.18) > H (0.00) > OCH_3 (0.12) > CN (0.23) > CH_2OH (0.44) > CH_2I (0.59) > O—CO—CH_3 (0.68) > $COOCH_3$ (0.74) > CH_2Br (0.82) > CH_2Cl (0.95) > CH_2CN (1.07). For the phenyl group, however, no constant group contribution $\Delta G_R^{\ddagger}$ is observed.

The object of the present paper is to offer a generalization of the rationale which can prove helpful in predicting the direction of cleavage of a variety of mono-, di-, tri-, and tetra-substituted ethylenes by ozone, with particular emphasis on the study of the methyl, ethyl, *n*-propyl, *i*-propyl, and *tert*-butyl groups. The general approach is that of the stabilization of carbonium ions. The dependence of the distribution of the reaction paths on olefin geometry is also investigated, as are the temperature and solvent effects.

Temperature and Solvent Effects

The invariance of the direction of cleavage with temperature has been demonstrated (18) for styrene and *p*-chlorostyrene at 15, 25, and 35 °C and, for cinnamyl alcohol and anethole, at temperatures ranging from 0 to 35 °C. These relatively high temperatures were chosen because, owing to the extreme instability of the primary ozonides, it was considered that the participation of any possible side reaction (e.g. the reaction of alcohol or aldehyde with the primary ozonide) should be negligible, compared to the contribution of the unimolecular decomposition of the primary ozonide to give zwitterion and carbonyl compound. However, subsequent low temperature determinations of the proportions of cleavage of crotonic acid, 2-propen-1-ol, cyanoethylene, 2-buten-1-ol, and 1-chloro-2-butene indicated no significant change on varying the temperature of ozonolysis between −78 and 25 °C (12). Table 1 indicates the results obtained with styrene, *trans*-β-methylstyrene, *trans*-2-methyl-3-hexene, and *cis*-2,2-dimethyl-3-hexene at temperatures ranging from −78 to 25 °C.

According to these results, there is only a

[5]These $\Delta G_R^{\ddagger}$ values are indicated in kcal/mole, at 25 °C. The use of eq. [3] is illustrated by the following example. Let x be the proportion of $CH_3CHO + HOCH_2C^+HOO^-$ formed in the ozonolysis of CH_3—CH=CH—CH_2OH. Insertion of the appropriate $\Delta G_R^{\ddagger}$ values in eq. [3] gives: $\log [x/(1-x)] = (-0.28 - 0.44)/1.363$ and, hence, $x = 0.229$ [experimental 0.230 ± 0.005 (12)].

TABLE 1

Temperature dependence of the direction of cleavage of selected unsymmetrical olefins, in methanol

Olefin	Zwitterion considered	% Zwitterion formed* at temperatures (°C): 25	−15	−78
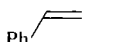	HC^+HOO^-	40.5±1	41.05±0.5	38.7±1
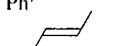	$CH_3C^+HOO^-$	81.7±1	82.05±1	83.6±1
	$C_2H_5C^+HOO^-$	65.5±1	64.50±1	66.3±1
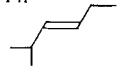	t-$C_4H_9C^+HOO^-$	63.4±1	62.8±1	67.7±1

*Referred to the olefin consumed. The results are indicated with a 95% confidence limit. The analytical methods used for determining the directions of cleavage are indicated in Table 8.

minor, if any, temperature effect on the direction of cleavage, except for the *cis*-2,2-dimethyl-3-hexene,[6] the only olefin, at present, for which a significant temperature effect on the direction of cleavage has been observed. Hence, from a consideration of the more general case for which the proportions of the two ways of cleavage are invariant with temperature, it follows from eq. [1] that $\partial(\Delta\Delta G^{\ddagger}/T)/\partial T = 0$ and, consequently, that $\Delta\Delta H^{\ddagger} = \Delta H_a^{\ddagger} - \Delta H_b^{\ddagger} = 0$. Equation [1] can thus be written as shown where $\Delta\Delta S^{\ddagger}$ ($=\Delta S_a^{\ddagger} -$

$$[4] \qquad \log [x/(1-x)] = \Delta\Delta S^{\ddagger}/2.3R$$

$\Delta S_b^{\ddagger}$) is the activation entropy difference between transition states corresponding to the paths of cleavage *a* and *b*. It appears, therefore, that the entropy factors, which may be related to the vibrational states of the transition states, primarily govern the direction of cleavage of the primary ozonides. In the case of *cis*-2,2-dimethyl-3-hexene, the $\Delta\Delta H^{\ddagger} = \Delta\Delta G^{\ddagger} + T\Delta\Delta S^{\ddagger}$ value can be estimated by using eq. [5]. By taking into consideration the uncertainties due to experimental errors, it is estimated that $\Delta\Delta H^{\ddagger} \lesssim 0.2$ kcal/mole.

$$[5] \quad \log [x/(1-x)]_{T_1} - \log [x/(1-x)]_{T_2} = \Delta\Delta H^{\ddagger}(T_1 - T_2)/2.3RT_1T_2$$

The effect of solvent in directing the proportions of cleavage has been investigated for the same four olefins. Methanol (3.0 *M*) solutions in carbon tetrachloride, ethyl acetate, *n*-hexane, and ether were used, as well as pure methanol and ethanol. The directions of cleavage were determined by nuclear magnetic resonance spectroscopy on 0.1 *M* olefin solutions, which were ozonized with about 75% of the theoretical amount of ozone, at 25 °C (Table 2).

These results clearly indicate that the direction of cleavage of primary ozonides is not affected by the solvent or by the alcohol which is used to quench the zwitterions.

Theoretical Considerations

The principal theoretical arguments which will be used in the discussion of the experimental results are summarized as follows. Since external factors, such as temperature of ozonolysis and solvent, do not affect the distribution of the two ways of cleavage, only substituent effects in directing the cleavage need to be considered. The heat of decomposition of the primary ozonide of *trans*-1,2-di-*tert*-butylethylene, as determined by calorimetric methods (2), is close to 40 kcal/mole. The cleavage of the primary ozonides is thus very exothermic. According to Hammond's postulate (24), for highly exothermic reactions the transition states are expected to possess structures close to that of the initial state (primary ozonide); there should be no regular tendency for the most stable products to be formed most rapidly in competitive reactions. The possible structures of the transition state **2** mentioned above closely resemble the initial state, the primary ozonide **1**.

[6]This olefin differs from the others in that its primary ozonide does not appear to possess a "stable" conformation; the attempt to assume a stable form is accompanied by the cleavage of the "primary ozonide" (7).

Can. J. Chem. Downloaded from www.nrcresearchpress.com by 210.87.254.5 on 09/05/12
For personal use only.

TABLE 2

Direction of cleavage of selected unsymmetrical olefins in different solvents, at 25 °C

Olefin	Zwitterion considered	% Zwitterion formed* in: CCl_4 MeOH (3 *M*)	CH_3COOEt MeOH (3 *M*)	*n*-C_6H_{14} MeOH (3 *M*)	Et_2O MeOH (3 *M*)	MeOH	EtOH
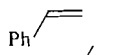	HC^+HOO^-	40.8±1	40.7±1	40.3±1	41.0±1	40.5±1	40.9±0.5
	$CH_3C^+HOO^-$	82.0±1	82.3±1	82.2±1	82.6±1	81.7±1	82.3±1
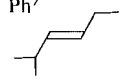	$C_2H_5C^+HOO^-$	65.2±1	65.8±2	64.9±0.5	65.6±1	65.5±1	64.5±1
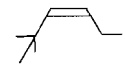	*t*-$C_4H_9C^+HOO^-$	64.0±1	63.1±1	63.1±0.5	62.3±1	63.4±1	62.7±1

*Referred to the amount of olefin used. The results are indicated with a 95% confidence limit.

It is considered that the proportions of the two ways of cleavage are governed by the relative stability of the corresponding transition states. The "hyperconjugative stabilization" and the dynamic (inductive) effects which participate in the formation of the transition states (or during the cleavage) are discussed in separate sections, for convenience. The resonance stabilization which, in some cases, may play an important role, as in the formation of the zwitterions R—C^+HOO^- with R = $COCH_3$ and COOH (18), will not be discussed further in the present paper, although it may be invoked occasionally. Attention will be focussed mainly on the behavior of aliphatic substituents such as the methyl, ethyl, *n*-propyl, *i*-propyl, and *tert*-butyl groups, for which effects other than resonance become important.

The arguments which will be used in the following section concern (*i*) the "hyperconjugative" relative stability of transition states corresponding to paths *a* and *b*, (*ii*) the charge transfer during the cleavage (inductive effects), and (*iii*) steric effects.

(*i*) *Relative "Hyperconjugative Stability" of the Transition States*

The transition states corresponding to paths *a* and *b* (Scheme 1) differ in the site of localization of the partial positive charge on one carbon atom in preference to the other in the 1,2,3-trioxolane ring. It is considered that the energies of the transition states are governed by the more or less efficient stabilization of the corresponding potential zwitterionic carbo-cations by neighboring groups.

The experimental results indicate that in some cases the formation of zwitterion is favored by substituents in the order CH_3 > C_2H_5 > *i*-C_3H_7 > *tert*-C_4H_9.[7] In line with the concepts which are commonly used, this order of stabilizing ability is designated, in the following, by "hyperconjugative stabilization" although, in the final analysis, organic chemists seem to disagree on what hyperconjugation really is. Indeed, all shades of meaning have contributed to obscure this concept; the common interpretation of the Baker–Nathan effect (29, 30) in terms of net electron release in the order CH_3 > . . . > *tert*-C_4H_9 and the conclusion (31) that "hyperconjugation of C—H bonds provides the most consistent and satisfactory explanation" has been seriously questioned (27, 32, 33). Hoffmann (34), in his study on the relative stabilities of alkyl carbonium ions, has pointed out the weakness of the usual argument that electron donation toward

[7]This order is the same as that observed in aromatic substitutions (e.g. bromation and benzoylation of R—Ph), in the solvolysis of R—Ph—CH_2Br, R—Ph—CH(Ph)Cl, R—CH=CH—CH_2Cl, as well as in some other reactions [Baker–Nathan effect (25)]. This effect is discussed in detail by Dewar (26) and has been interpreted in terms of (*i*) C—C or C—H hyperconjugation (25) or (*ii*) steric hindrance in the solvolysis (27). Dewar (26) considers that "there is in any case no reason for believing that hyperconjugation could account for the Baker–Nathan effect even if it were significant". Recent work (28) on the relative stabilities of trialkylcyclopropenyl cations also indicates that the relative ability of substituents to stabilize a cyclopropenyl cation is given by the order methyl > ethyl > *i*-propyl > *tert*-butyl.

Can. J. Chem. Downloaded from www.nrcresearchpress.com by 210.87.254.5 on 09/05/12
For personal use only.

Can. J. Chem. Downloaded from www.nrcresearchpress.com by 210.87.254.5 on 09/05/12
For personal use only.

a positive site is the effect that explains the relative stabilities of carbonium ions.

There is, however, one point which may be noteworthy: the net negative charge which is carried by a C atom is the greater the more H atoms are attached to it. Thus C in methyl carries a significantly higher negative charge than the central C atom in the *tert*-butyl group. Because of this, whichever the interpretation is that can be derived from this observation, it is equivalent to say that a zwitterionic carbo-cation is favored in a situation where the neighboring atoms are electron-richer or to say that zwitterions are favored by alkyl groups in the hyperconjugative order. The order of stability of carbonium ions also indicates that stability is the greater, the electron-richer are the neighboring atoms (34).

This is possibly a convenient way to look at hyperconjugation. However, any discussion of the nature of the hyperconjugative effect is beyond the scope of the present work. This concept is thus used in the following discussion of ozonolysis results with all the tacit reservations which may seem appropriate.[8]

(ii) Charge Transfer During the Cleavage. Inductive Effects

The cleavage of the primary ozonides **1** (viz. the transition states **2**) is believed to take place via an electron circulation, as indicated below. This dynamic effect which occurs in the transformation of the transition states to give the products zwitterion $RC^{+}OO^{-}$ and carbonyl compound is favored by electron releasing substituents R (inductive effect). The direction and amplitude of this electron circulation are related to the charge distribution in the transition state. The present considerations imply that electroneutrality is a good thing, i.e. the more the negative charge that can be donated to the positive site, the more the formation of the corresponding zwitterion is favored by its stabilization in the reacting transition state.

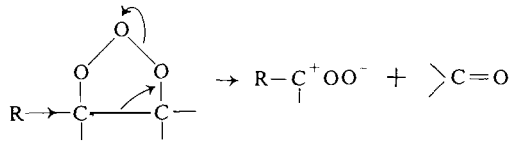

[8]A more detailed discussion of the hyperconjugative effect in correlation with charge distributions is considered in a forthcoming paper.

Clearly, as far as the participation of inductive effects of the substituents in distributing the reaction paths is concerned, the order operating in favoring the zwitterion formation is the usual one, i.e. *tert*-C_4H_9 > *i*-C_3H_7 > C_2H_5 > CH_3 > H.

(iii) Steric Effects

The cleavage of the primary ozonides is assumed to take place via a unimolecular process; this has been shown recently by Greenwood (9) in his kinetic study of the decomposition of 3-hexene primary ozonide. Hence, inhibition of either one of the two possible ways of cleavage by steric hindrance (as occurring in plurimolecular reactions) need not be considered. However, during the cleavage, a rehybridization of the carbon atoms of the 1,2,3-trioxolane ring from sp^3 to sp^2 takes place. This change of hybridization results in a modification of the steric interactions between the substituents. This change is the same for both carbon atoms in the transition state corresponding to path *a*. The same applies to path *b*. Hence, the steric effects which can be expected from the change in hybridization are the same for both reaction paths and are thus not likely to participate in distributing the proportions of cleavage.

The stereochemical dependence of the distribution of the reaction paths on olefin geometry is considered in the discussion of the experimental results obtained with *cis*-1,2-disubstituted ethylenes.

Results and Discussion

The experimental results are discussed in the following section by grouping the cases according to the parent olefins, i.e. (*i*) monosubstituted ethylenes, (*ii*) *trans*-1,2-disubstituted ethylenes, (*iii*) *cis*-1,2-disubstituted ethylenes, and (*iv*) 1,1-*di*substituted-, *tri*-, and *tetra*substituted ethylenes.

(i) Monosubstituted Ethylenes

The electronic effects which participate in directing the cleavage of primary ozonides are revealed by the results obtained with aliphatic monosubstituted ethylenes (Table 3).

These results can be interpreted as follows, in terms of a Taft linear free energy relationship (35). For the olefins $RCH{=}CH_2$ listed in Table 3, let x be the proportion of cleavage giving $RCHO + HC^{+}HOO^{-}$ with the rate constant k_a, and $1 - x$ the proportion of cleavage giving

TABLE 3

Direction of ozone cleavage of monosubstituted ethylenes

Olefin	Proportion of zwitterion $(1 - x)$	
$CH_2Cl—CH=CH_2$	0.17 ± 0.005	$CH_2Cl—C^+HOO^-$*
$CH_2Br—CH=CH_2$	0.20 ± 0.01	$CH_2Br—C^+HOO^-$*
$CH_2I—CH=CH_2$	0.27 ± 0.01	$CH_2I—C^+HOO^-$*
$CH_3—CH=CH_2$	0.62 ± 0.01	$CH_3—C^+HOO^-$
$C_2H_5—CH=CH_2$	0.63 ± 0.02	$C_2H_5—C^+HOO^-$
n-$C_3H_7—CH=CH_2$	0.60 ± 0.01	n-$C_3H_7—C^+HOO^-$
i-$C_3H_7—CH=CH_2$	0.64 ± 0.01	i-$C_3H_7—C^+HOO^-$
t-$C_4H_9—CH=CH_2$	0.70 ± 0.01	t-$C_4H_9—C^+HOO^-$
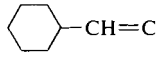	0.86 ± 0.01	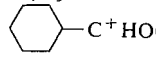

*Results extracted from ref. 12. The results are indicated with a 95% confidence limit.

RC^+HOO^- + HCHO with the rate constant k_b. Equation [6] then follows if both reactions are

$$[6] \qquad x/(1 - x) = k_a/k_b$$

of the same order, which is reasonable to assume. The dependence of the rate constants k on the substituents is given by the Taft relationship, eq. [7], where $k = k_0$ for R = CH_3 (i.e. $\sigma^* = 0$).

$$[7] \qquad \log k = \log k_0 + \rho^*\sigma^*$$

The substituent constant σ^* depends on R, irrespective of the direction of cleavage, but since two distinct reaction paths are considered, a distinct reaction constant ρ^* is associated with each path, i.e. ρ_a^* with path a and ρ_b^* with path b. Hence, the corresponding rate constants are given by eqs. [8] and [9].

$$[8] \qquad \log k_a = \log k_{0,a} + \rho_a^*\sigma^*$$

$$[9] \qquad \log k_b = \log k_{0,b} + \rho_b^*\sigma^*$$

The final eq. [10] is obtained from eqs. [6], [8], and [9].

$$[10] \qquad \log [x/(1 - x)] = \log (k_{0,a}/k_{0,b}) + (\rho_a^* - \rho_b^*)\sigma^*$$

The comparison of eq. [10] with the experimental results is illustrated in Fig. 1. It is noted that with respect to R = H (for which $x = 0.5$, because the cleavage of ethylene primary ozonide is necessarily symmetrical) the electron releasing substituents favor the formation of RC^+HOO^- since x (i.e. the proportion of RCHO formation) is less than 0.5, whereas the electron-withdrawing groups (with respect to H) behave in the opposite way (i.e. $x > 0.5$).

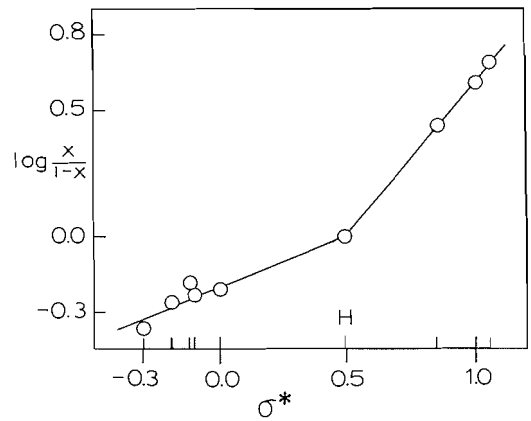

FIG. 1. Verification of eq. [10] for the ozone cleavage of mono-substituted ethylenes: log $[x/(1 - x)]$ vs. Taft's polar substituent constants σ^*. The experimental points are in the order *tert*-C_4H_9 ($\sigma^* = -0.3$), i-C_3H_7, n-C_3H_7, C_2H_5, CH_3 ($\sigma^* = 0.0$), H, CH_2I, CH_2Br, CH_2Cl.

The results indicate that the formation of the zwitterion is favored by the substituents R in the order *tert*-butyl > *i*-propyl > ethyl > methyl > H, i.e. in the order of increasing inductive effect. Hence, assuming that electroneutrality is favorable to zwitterion formation (as indicated by previous studies (16*a*, 18) on ring-substituted styrenes), the present results show that the inductive effects, rather than hyperconjugative stabilization, govern the distribution of the reaction paths. This is also indicated by the comparison of the results obtained with R = CH_2I, CH_2Br, and CH_2Cl; the more R is electron-withdrawing, the greater the proportion (x) of RCHO which is produced, i.e. the less the proportion of zwitterion RC^+HOO^-.

This predominant participation of inductive

Can. J. Chem. Downloaded from www.nrcresearchpress.com by 210.87.254.5 on 09/05/12
For personal use only.

Can. J. Chem. Downloaded from www.nrcresearchpress.com by 210.87.254.5 on 09/05/12
For personal use only.

effects can be visualized as follows. In Taft's scale of polar substituent constants σ^*, the alkyl substituents are described as electron-releasing groups with respect to H, which behaves like an electron attractor [$\sigma^*(H) = +0.490$]. Hence, the effects due to R and H (which are attached to different C atoms of the ring **1**) are codirectional in promoting the electron circulation which results in the preferential formation of RC^+HOO^-. These combined effects of R and H can be represented as follows, for the preferential cleavage.

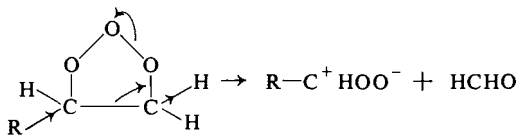

As discussed in the preceding section, the alkyl groups are placed in reverse order when their hyperconjugative stabilization abilities are compared to their inductive effects. In the *tert*-butyl group, for example, when compared to methyl, the gain in inductive effect is attenuated by the loss in hyperconjugative stabilizing ability. This results in lowering the *tert*-$C_4H_9C^+HOO^-$ formation, hence in an increase of the x value. A consideration of this mutual partial compensation of the effects may thus explain the relatively low value of the slope which is calculated by inserting the experimental values in eq. [10], i.e., $\rho_a^* - \rho_b^* \approx 0.43$.

If this interpretation is valid, the following behavior is to be expected for the halogenated alkyl groups. The inductive effects clearly indicate that the CH_2Cl group is the less favorable one from the point of view of zwitterion formation [$\sigma^* = 1.05(CH_2Cl), 1.00(CH_2Br), 0.85(CH_2I)$]. On the other hand, the electronegativity of the halogens increases in the order I, Br, Cl, and the negative charge on the C atom of the group is therefore expected to decrease as electronegativity of the halogen increases. Hence, the negative charge on the C atom of the substituent decreases in the order $CH_2I > CH_2Br > CH_2Cl$. If the correlation is correct that the hyperconjugative stabilizing ability is greater, the more the negative charge is carried by the central C atom, the lowest stabilizing ability is expected for CH_2Cl. The hyperconjugative and inductive effects thus operate in the same direction and any destabilization due to inductive effects is also enhanced by the concurrent decrease in hyperconjugative stabilization. From a consideration of these effects, a steeper slope of log $[x/(1-x)]$ *vs.* σ^* is expected for the halogenated alkyl groups than for the unsubstituted alkyl groups discussed previously. This is indeed observed (see Fig. 1), and the value $\rho_a^* - \rho_b^* = 1.2$ is calculated, by means of eq. [10], from the experimental results obtained with R = CH_2—halogen.

It is concluded, for mono-substituted ethylenes, that both inductive and hyperconjugative stabilization of carbonium ions participate in distributing the reaction paths; the inductive effect is, however, predominant. The inductive and hyperconjugative effects are opposite in order for the electron-releasing substituents *tert*-butyl, *i*-propyl, ethyl, and methyl, which results in a low value for $\rho_a^* - \rho_b^*$ (≈ 0.43); whereas these effects are concurrent for the CH_2—halogen groups, which results in a steeper slope ($\rho_a^* - \rho_b^* = 1.2$).

It must be borne in mind, however, that in any discussion of inductive and hyperconjugative effects in connection with eq. [10], such groups (e.g. $COCH_3$, COOH) (18) which may offer resonance stabilization of the positive site should not be included. Styrene is a typical example (16*a*, 18). In Taft's scale of polar constants σ^*, the phenyl group has an electron-withdrawing effect estimated at 0.600 with respect to the methyl group; and H, a similar effect estimated at 0.490. From a consideration of inductive effects only, the preferential formation of the zwitterion HC^+HOO^- should therefore be expected in the cleavage of styrene.[9] This is in variance with the experiments which show that this cleavage proceeds with the formation of 59% of PhC^+HOO^- and, consequently, 41% of HC^+HOO^- (16*a*). Hence, in the ozonolysis of styrene, the inductive effects do not seem to play the predominant role; the phenyl group appears to stabilize the zwit-

[9]Razumovskii *et al.* (21) held the point of view that the inductive effects govern primarily the ozone cleavage of styrene. Their determination of the direction of cleavage, which would support this view, is, however, in error (45% of PhC^+HOO^- formation, instead of 59%). Criticisms of the analytical method used have been indicated.[4] As shown in the Experimental section (Table 8), five different analytical methods have been used in the present work for determining the direction of cleavage of styrene, all of which give the same result. The latter is also confirmed by Keaveney's isolation experiments (20).

TABLE 4

Direction of cleavage (x) of the primary ozonides of selected *trans*-1,2-disubstituted ethylenes

R_1	R_2	Proportion of zwitterion	
CH_3	C_2H_5	0.56 ± 0.02	$CH_3—C^+HOO^-$
CH_3	n-C_3H_7	0.60 ± 0.03	
CH_3	i-C_3H_7	0.71 ± 0.01	
CH_3	t-C_4H_9	0.88 ± 0.01	
CH_3	Phenyl	0.82 ± 0.01	
CH_3	p-MeO-phenyl	0.68 ± 0.01	
C_2H_5	i-C_3H_7	0.655 ± 0.01	$C_2H_5—C^+HOO^-$
C_2H_5	t-C_4H_9	0.87 ± 0.01	

terionic positive charge (in the transition state) *via* a mesomeric effect, with the participation of its π electron-system and, possibly, also *via* an electromeric effect during the cleavage (16*a*, 20). The importance of these effects is increased by electron-releasing substituents in the phenyl ring, as indicated by the experiments. For ring-substituted styrenes, the results are suitably described by the Hammett relationship, eq. [2] (16*a*, 18).

(ii) trans-1,2-Disubstituted Ethylenes

Two series of *trans*-olefins $R_1CH{=}CHR_2$ have been investigated: (*i*) with $R_1 = CH_3$ and $R_2 = C_2H_5$, n-C_3H_7, i-C_3H_7, *tert*-C_4H_9, phenyl, and *p*-methoxyphenyl, and (*ii*) with $R_1 = C_2H_5$ and $R_2 = i$-C_3H_7 and *tert*-C_4H_9. The quantity x is defined as the proportion of cleavage giving $R_1CH(OCH_3)OOH + R_2CHO$. The experimental results are given in Table 4, with a confidence limit of 95%.

A correlation of these experimental values with Taft's polar substituent constants σ^* is attempted in Fig. 2. For the first series ($R_1 = CH_3$), 2-butene is chosen as reference compound, and 2-pentene for the second series, with $R_1 = C_2H_5$.

Figure 2 clearly indicates that the linear correlation which is anticipated by eq. [10] is not observed. In addition, the results also indicate that the methyl group is a better stabilizing agent than, say, *tert*-butyl; the 4,4-dimethyl-2-pentene is found to cleave with the formation of 88% of $CH_3C^+HOO^-$ and only 12% of *tert*-$C_4H_9C^+HOO^-$. Clearly, an inspection of the results in Table 4 reveals that the substituents favor the formation of the corresponding zwitterion in the order $CH_3 > C_2H_5 > n$-$C_3H_7 > i$-$C_3H_7 > tert$-C_4H_9, i.e. in the order expected from a consideration of the hyperconjugative stabilization

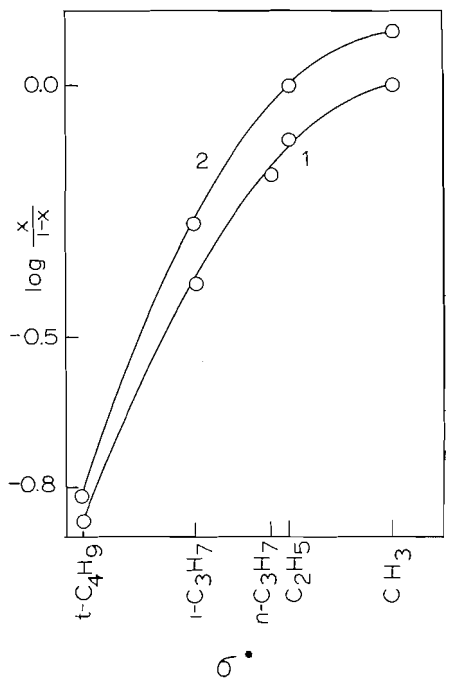

FIG. 2. A comparison of log $[x/(1-x)]$ with Taft's constants σ^* for *trans*-1,2-disubstituted ethylenes. $R_1 = CH_3$ (1); $R_1 = C_2H_5$ (2).

of positive sites. This effect thus seems to play the predominant role in directing the reaction paths.

For the dialkyl-substituted *trans*-ethylenes under consideration, the difference in electron releasing ability of the two groups is relatively small and ranges between the extremes of $\sigma^*(CH_3) = 0$ and $\sigma^*(tert\text{-}C_4H_9) = -0.300$. In addition, the electron circulation which is initiated by the inductive effects is opposite in direction for each substituent. This tends, therefore, to compensate (at least in part) the global effect due

Can. J. Chem. Downloaded from www.nrcresearchpress.com by 210.87.254.5 on 09/05/12
For personal use only.

Can. J. Chem. Downloaded from www.nrcresearchpress.com by 210.87.254.5 on 09/05/12
For personal use only.

to inductive properties of the substituents. In that, the *trans*-1,2-disubstituted ethylenes differ from the monosubstituted ethylenes, since, for the latter, the effects of R and H are codirectional, with σ^* ranging from -0.300 (*tert*-butyl) to $\sigma^*(H) = 0.490$.

The present results can thus be interpreted by considering that the inductive effects cancel each other, at least to an important extent, and that the contribution of the hyperconjugative stabilization of the positive sites in their respective transition states becomes therefore important. Since these are effects other than those described by Taft's σ^* constants, a linear relationship [10] is not to be expected. The order exhibited by the groups in stabilizing ability, which is the reverse of Taft's order, is readily understood in terms of hyperconjugative stabilization; the zwitterion which is formed preferentially is the one whose environment is electron-richer.

In the case of the *trans*-1-phenylpropene, the inductive effects of the phenyl and the methyl groups are in the same direction (18, 20) and, thus, strongly favor the formation of the zwitterion $CH_3C^+HOO^-$. The resonance stabilization by the phenyl group and the electromeric effect operate in the same direction, and are increased by electron-releasing substituents on the phenyl ring. These points have been discussed in detail for a number of substituted phenylethylenes $R—C_6H_4—CH=CH—R'$, and it was shown that the Hammett eq. [2] satisfactorily describes the experimental results (18).

(iii) cis-1,2-Disubstituted Ethylenes

The discussion of the results obtained with *cis*-olefins is attempted in the following section in terms of hyperconjugative and inductive effects, in a way similar to that considered for the *trans* isomers. For the *trans*-olefins it was considered that the inductive effects of the substituents in positions 1 and 2 cancel each other to a certain extent when the expected individual effects are similar, but no details have been given about the mode of this mutual partial compensation. Either it can be thought that each substituent favors individually the incipient carbonium ion to which it is attached and that the partial cancellation results because both substituents behave in a similar way or else, it may be assumed that each one of the substituents prevents the other from manifesting its inductive ability, i.e. from releasing electrons during the electrocyclic cleavage so as to favor the formation of the zwitterion to which it belongs.

Any attempt to discriminate between these two possibilities would be, at this stage, highly speculative. The interest of this point is, however, revealed by the question: how do opposite inductive effects in the 1,2,3-trioxolane ring compensate each other in *cis* primary ozonides, as compared to their *trans* isomers?

Because of the difficulty of giving *a priori* arguments to this question, the experimental results (Table 5) shall be examined and discussed.

An inspection of these results reveals that, with the exception of the olefins containing the *tert*-butyl group, the formation of the $CH_3C^+HOO^-$ zwitterion is favored with respect to the zwitterions $C_2H_5C^+HOO^-$, n-$C_3H_7C^+HOO^-$, and i-$C_3H_7C^+HOO^-$. In addition, the production of the methyl-zwitterion increases when C_2H_5 is replaced by n-C_3H_7 or i-C_3H_7. Hence, these substituents are found to favor the formation of their corresponding zwitterions in the order $CH_3 > C_2H_5 > n$-$C_3H_7 > i$-C_3H_7, i.e. in the order corresponding to a predominant hyperconjugative effect. A comparison of these results with those obtained with the corresponding *trans* isomers (Table 5) also indicates that the production of $CH_3C^+HOO^-$ is lower in the *cis* than in the *trans* cases.

In the cleavage of *cis* primary ozonides it would therefore appear (*i*) that the inductive effects of R_1 and R_2 cancel each other to a certain extent, leaving thus the hyperconjugative stabilization to be the predominant factor in directing the cleavage, and (*ii*) that this mutual partial cancellation of inductive effects is somewhat reduced in *cis* primary ozonides, with respect to their *trans* isomers.

For the smaller alkyl groups, up to i-C_3H_7, the

TABLE 5

Direction of ozone cleavage of selected *cis*-1,2-disubstituted ethylenes

R_1	R_2	Proportion of zwitterion	
CH_3	C_2H_5	0.52 ± 0.02	$CH_3C^+HOO^-$
CH_3	n-C_3H_7	0.54 ± 0.02	
CH_3	i-C_3H_7	0.57 ± 0.01	
CH_3	t-C_4H_9	0.38 ± 0.01	
C_2H_5	t-C_4H_9	0.368 ± 0.005	$C_2H_5C^+HOO^-$

Can. J. Chem. Downloaded from www.nrcresearchpress.com by 210.87.254.5 on 09/05/12
For personal use only.

general trends are thus similar in *cis* and *trans* primary ozonides. When R_2 is *tert*-butyl, however, the trend is reversed in *cis* primary ozonides since the *tert*-butyl group, rather than methyl or ethyl, appears to favor the formation of the corresponding zwitterion (Table 5). This result is not unexpected, for the following reasons.

Throughout the present work, the assumption is that the transition states resemble the initial state, i.e. the primary ozonide, when the latter is in its most stable conformation. Recent LCAO-EHMO calculations (7) indicate clearly that *cis* primary ozonides bearing a *tert*-butyl group do not appear to possess such a "stable" conformation; it would rather appear that the attempt to assume a stable form is accompanied by the cleavage of the "primary ozonide". These conclusions are drawn on the basis of (*i*) conformational analyses, (*ii*) unusual gross electron densities of the 1,2,3-trioxolane ring, and (*iii*) unusual Mulliken overlap populations for *cis* primary ozonides with a *tert*-butyl group. In addition, these conclusions agree with the experimental results of Durham and Greenwood (3) and Bailey and Thompson (4), which show that all *trans* primary ozonides, including that of 1,2-di-*tert*-butylethylene, can be observed, whereas only the *cis* primary ozonides bearing small substituents (e.g. those of 2-hexene and 2-pentene) can be observed. All attempts to observe the *cis*-1,2-di-*tert*-butylethylene primary ozonide have failed.

Hence, in the absence of any stable form of the *cis* primary ozonides under consideration, no transition state can correspond to it; there is nothing but cleavage, once the ozone is added on the double bond. Consequently, the whole process being a continuous evolution toward cleavage, it is expected that the inductive effect, rather than hyperconjugative stabilization, largely predominates in distributing the reaction paths. This is indeed indicated by the results observed with *cis*-4,4-dimethyl-2-pentene and *cis*-2,2-dimethyl-3-hexene, in which cases the zwitterion *tert*-C_4H_9—C^+HOO^- is preferred (62–63%).

There is still another point which merits attention. In any comparison of *trans* primary ozonides with their *cis* isomers it must be borne in mind that *trans* primary ozonides possess axial,axial or equatorial,equatorial conformation, whereas *cis* primary ozonides possess axial,equatorial conformation. Consequently, no conformational effect will participate in distributing the proportions of cleavage in *trans* primary ozonides, whereas in the *cis* isomers such a contribution of conformational effect may participate, since the contribution of a substituent when in axial or in equatorial position is not necessarily the same.

In a recent paper on the stereospecificity in ozonide and cross-ozonide formation, Bailey and co-workers (6) have offered several refinements to Criegee's theory of ozonolysis, involving the stereoselective decomposition of *cis* and *trans* primary ozonides to isomeric *syn* and *anti* zwitterions and the stereoselective recombination of these with aldehydes to give final ozonides. The stereochemical course of ozonide formation has been formulated into three general rules. Using the results reported in Table 5, it is now possible to discuss, in isolation, the Bailey–Bauld second rule, i.e. "an equatorial substituent is incorporated into a zwitterion moiety in preference to an axial substituent". The verification of this rule is made possible from the knowledge (*i*) of the substituent which prefers equatorial conformation, and (*ii*) of the proportion of cleavage giving the zwitterion retaining the equatorial substituent.

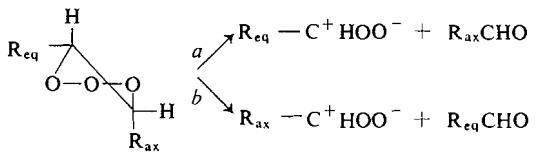

The preferential conformations which were established previously (7) from a consideration of the minimized total electronic energies are indicated in Table 6. The energy E_{eas} refers to the configuration with the small substituent in axial position, and E_{eab} to the configuration with the bulky group in axial position.

Inspection of these values reveals only a little difference between the two conformers of *cis*-2-pentene primary ozonide, slightly favoring the form having the ethyl group in equatorial position. Whilst in the primary ozonide of 2-hexene and 4-methyl-2-pentene the small methyl group prefers the equatorial position, the *tert*-butyl group directs the smaller substituent in axial position.

The preferential incorporation of a substituent into a zwitterion moiety can now be deduced from Tables 5 and 6. With the primary ozonide of 2-pentene, where both substituents exhibit little steric effects, and for which there appears to be a

TABLE 6

Total electronic energies and preferential conformation of primary ozonides of selected *cis* olefins (7)*

Parent olefin	$-E_{cas}$	$-E_{cab}$	$-E_{planar}$	Equatorial substituent
	(eV)			
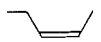	946.565	946.550	945.745	(C_2H_5)
	1048.463	1048.587	1047.789	CH_3
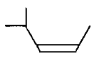	1049.510	1049.580	1048.680	CH_3
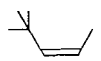	1147.234	1146.286	1143.065	t-C_4H_9
	1250.362	1249.378	1246.005	t-C_4H_9

*The results apply to the half-chair conformation of the 1,2,3-trioxolane ring, which is more stable than the envelope or planar forms.

small difference between the two conformers, a little less than 50% of zwitterion retaining the ethyl group is formed, although the equatorial position of the ethyl group seems to be slightly favored. However, in all the other cases, involving a substituent larger than the ethyl group, the comparison of the results in Tables 5 and 6 clearly indicates a significant preference for the equatorial substituent in the primary ozonide to be retained in the zwitterion moiety. This can be considered as an experimental evidence for the Bailey–Bauld second rule, for primary ozonides possessing sufficiently large substituents.

(iv) 1,1-Disubstituted, Trisubstituted, and Tetrasubstituted Ethylenes

The results indicated in Table 7 can be interpreted in terms of substituent effects in a way similar to that employed in the preceding sections.

If it is assumed that identical substituents in relative *trans* configuration on the C atoms of the 1,2,3-trioxolane ring mutually cancel their inductive abilities, similar directions of cleavage should be expected for the trimethylethylene and the propene primary ozonides. This is not the case, since 77 ± 3% of $(CH_3)_2C^+OO^-$ is produced in the cleavage of trimethylethylene primary ozonide, and only 62 ± 1% of $CH_3C^+HOO^-$ in the cleavage of propene. As indicated by Hoffmann's calculations (34), the secondary propyl-carbonium ion $(CH_3)_2CH^+$ is more stable than the ethyl-carbonium ion $CH_3CH_2^+$. Hence the efficient stabilization of the positive site by the two *gem* methyl substituents (in the transition state) is capable of explaining the higher yield of $(CH_3)_2C^+OO^-$, as compared to the production of $CH_3C^+HOO^-$ in the ozonolysis of propene.

A consideration of the results obtained with the olefins having $R_1 = R_2 = CH_3$ and $R_3 = CH_3$, C_2H_5, i-C_3H_7, or $tert$-C_4H_9 also illustrates the participation of the hyperconjugative stabilization of the positive site in the transition state. It is seen from this comparison that the proportion of $(CH_3)_2C^+OO^-$ zwitterion increases with increasing bulk of the R_3 substituent. Again, this is attributed to a decrease in stabilizing ability of the site leading to $R_3C^+HOO^-$ by the R_3 groups, in the order methyl > ethyl > isopropyl > *tert*-butyl, which corresponds to the situation where the hyperconjugative stabilization is predominant. The situation is thus similar to that of the *trans*-1,2-disubstituted ethylenes.

The high proportion (95 ± 2%) of $(CH_3)_2C^+$-HOO^- which is formed in the ozonolysis of 2-methyl-1-phenylpropene can be attributed to the great difference in inductive effects between the two electron-releasing *gem* methyl groups and the electron-withdrawing phenyl group; these effects are codirectional and thus favor the electrocyclic cleavage giving the aliphatic zwitterion. As in the case of the *trans*-1-phenylpropene, the stabilization of the positive site in the transition state by a mesomeric effect of the phenyl group does not compensate the inductive effect of the methyl group.

Can. J. Chem. Downloaded from www.nrcresearchpress.com by 210.87.254.5 on 09/05/12
For personal use only.

TABLE 7

Direction of cleavage of selected primary ozonides of 1,1-disubstituted, trisubstituted, and tetrasubstituted ethylenes

R_1	R_2	R_3	R_4	Proportion of zwitterion produced	
CH_3	CH_3	CH_3	H	0.77 ± 0.03	$(CH_3)_2C^+OO^-$
CH_3	CH_3	C_2H_5	H	0.81 ± 0.02	$(CH_3)_2C^+OO^-$
CH_3	CH_3	*i*-C_3H_7	H	0.97 ± 0.03	$(CH_3)_2C^+OO^-$
CH_3	CH_3	*t*-C_4H_9	H	1.000	$(CH_3)_2C^+OO^-$
CH_3	CH_3	C_6H_5	H	0.95 ± 0.02	$(CH_3)_2C^+OO^-$
cis-C_2H_5	CH_3	CH_3	H	0.891 ± 0.005	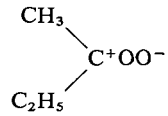
trans-C_2H_5	CH_3	CH_3	H	0.83 ± 0.01	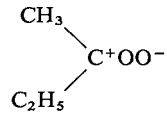
		CH_3	H	0.92 ± 0.02	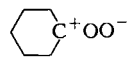
		CH_3	H	0.92 ± 0.01	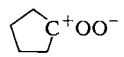
		H	H	0.968 ± 0.005	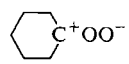
n-C_3H_7	CH_3	H	H	0.900 ± 0.005	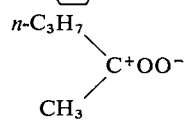
C_6H_5	C_6H_5	H	H	0.67 ± 0.01	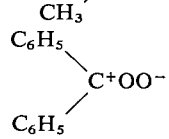
C_6H_5	C_6H_5	C_6H_5	H	0.71 ± 0.01	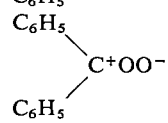
C_6H_5	CH_3	H	H	0.93 ± 0.01	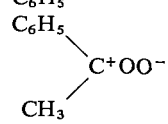
C_6H_5	CH_3	CH_3	CH_3	0.55 ± 0.01	$(CH_3)_2C^+OO^-$

A comparison of the results observed with the *cis* and *trans*-3-methyl-2-pentene and with trimethylethylene indicates that the replacement of a *gem* methyl group by ethyl favors the formation of $R_1R_2C^+OO^-$. This may be interpreted in terms of a participation of the inductive effect, which is more important for ethyl than methyl. As is shown in Table 7, this additional effect contributed by the ethyl group is more pronounced in the *cis* isomer, i.e. when ethyl and H are in relative *trans* configuration, than in *trans*-3-methyl-2-pentene, in which case the ethyl and the methyl groups are in *trans* position. This interpretation is, therefore, consistent with the one offered in the discussion of the *cis*-1,2-disubstituted ethylenes, in terms of an apparently better transmission of inductive effects in *trans* systems than in the corresponding *cis* isomers.

The high proportions of the ketonic zwitterions which are formed when R_1 and R_2 are replaced

Can. J. Chem. Downloaded from www.nrcresearchpress.com by 210.87.254.5 on 09/05/12
For personal use only.

Can. J. Chem. Downloaded from www.nrcresearchpress.com by 210.87.254.5 on 09/05/12
For personal use only.

by a cyclopentyl or cyclohexyl group may also be attributed to the participation of the inductive effect. The corresponding 1,1-disubstituted ethylenes, i.e. methylidene cyclohexane and 2-methyl-1-pentene, give rise to even higher proportions of ketonic zwitterion, under the influence of the electron-withdrawing inductive effect of the two methine-H atoms, as in the monosubstituted ethylenes.

The cleavage of the 2-methyl-3-phenyl-2-butene indicates that the methyl and phenyl groups in *gem* position have a global stabilizing ability which is only slightly lower than that exhibited by two *gem* methyl groups. The latter groups are excellent for their stabilizing property; this indicates that the phenyl group fully participates by resonance stabilization in the ozone cleavage of this tetrasubstituted ethylene. The excellent stabilizing ability of the *gem* phenyl–methyl pair is further confirmed by the direction of cleavage of the 2-phenylpropene, in which 93% of ketonic zwitterion is produced.

However, the relatively low proportion of ketonic zwitterion which is produced in the cleavage of 1,1-diphenylethylene (67%) suggests that the two *gem* phenyl groups possibly do not participate fully in the resonance stabilization. Ultraviolet spectroscopy (36) and theoretical calculations (37) agree in representing the molecule of 1,1-diphenylethylene having the two benzene rings in planes which are inclined with respect to the plane of the double bond. The resonance stabilization of a positive charge can only be fully efficient when the π orbitals of the phenyl ring are parallel to the vacant orbital of the carbonium ion. Since the two *gem* phenyl groups cannot be found in the same plane, the π orbitals of the two aromatic cycles cannot be simultaneously in the most efficient position for stabilizing the positive site in the transition state. Further studies are in progress to confirm this point.

Experimental

Ozonolysis Procedure

The technique of ozonolysis, using O_2–O_3 mixtures, together with the dosimetry of ozone, has been described previously (16*b*). The ozone output was varied between 0.07 and 0.2 mmole of O_3/min. The ozone used was limited to less than 80% of the theoretical amount, in order to prevent autoxidation of aldehydes to peracids; this autoxidation is enhanced by ozone in the absence of olefin.

The solvents used were methanol (for n.m.r. analyses), 3.0 *M* methanol in ethyl acetate (for polarographic analyses), and 1.0 or 3.0 *M* methanol in CCl_4 (for v.p.c. and i.r. analyses). In some cases other solvents were used (see Table 2). The initial olefin concentration was 0.1 *M* and, in most cases, 10 ml of solution were submitted to ozonolysis.

The time required for the ozonolysis never exceeded 15 min. It can therefore be assumed that the amounts of carbonyl compounds and alkoxyhydroperoxides, which were measured immediately after completion of the ozonolysis, had not been affected by secondary reactions, such as a slow decomposition of the hydroperoxides or an autoxidation of the aldehydes. This is confirmed by the observations reported below concerning the relative stability of the hydroperoxides under our experimental conditions.

Amounts of Hydroperoxides (Active Oxygen)

These amounts were measured by iodometry, as described previously (18). The analyses made under these conditions were very reproducible, providing they were carried out shortly after completion of the ozonolysis; the values found for the amounts of hydroperoxides decreased by only a few per cent 1 h after ozonolysis.

Gas Chromatographic Analyses

The v.p.c. was performed using a 5750 F & M gas chromatograph, with a flame detector. Columns (6 ft long) of Silicone Rubber UC W 98, Carbowax 20.000, or 20% diiso-propyl-phthalate were used. After the ozonization, the solvent loss due to evaporation during the ozonolysis was carefully compensated and 5-µl samples were injected in the gas chromatograph. The chromatograms were integrated by means of a planimeter; and the areas under the peak corresponding to the olefin which did not react and to the carbonyl compounds which were formed were compared to the areas under the peaks obtained under the same conditions using standard samples of the appropriate substances. The analyses were repeated a minimum of five times. Two different oven temperatures were used with no effect on the results. No v.p.c. pyrolysis occurred at sufficiently low oven temperature.

Polarographic Analyses

These analyses were made by means of a Metrohm E-261-R polarograph, as described in previous work (17).

Infrared Spectra

The i.r. spectra were recorded by means of a Perkin–Elmer 621 spectrometer, with the object of determining the intensities of the carbonyl bands in the region 1680–1720 cm^{-1}. The formation of hemiacetal of the aldehydes was checked using standard solutions of the aldehydes in the presence of 1.0 *M* CH_3OH.

Nuclear Magnetic Resonance Measurements

On completion of the ozonization, the solvent was evaporated and replaced by the minimum amount of CCl_4. The n.m.r. spectra were recorded, with tetramethylsilane as internal reference, using a Jeolco C-60 H and a Jeolco 4 H-100 spectrometer. The following signals are suitable for the determination of the direction of cleavage (17): methyl–H (1.3–1.4 δ), methoxy–H (3.35–3.50 δ), and the signal at 4.5–4.8 δ of the methine pro-

TABLE 8

Analytical methods used for determining the direction of cleavage

Olefin	Reaction products		Olefin consumed	
	Product	Method	Product	Method
	CH_3—$CH(OCH_3)OOH$ $CH_2(OCH_3)OOH$	n.m.r. n.m.r.		
	C_2H_5—$CH(OCH_3)OOH$ $CH_2(OCH_3)OOH$	Polarography	Active O	Iodometry
	n-C_3H_7—$CH(OCH_3)OOH$ $CH_2(OCH_3)OOH$	Polarography	Active O	Iodometry
	i-C_3H_7—$CH(OCH_3)OOH$ $CH_2(OCH_3)OOH$	Polarography	Active O	Iodometry
	t-C_4H_9—$CH(OCH_3)OOH$ $CH_2(OCH_3)OOH$	Polarography	Active O	Iodometry
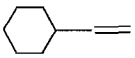	C_6H_{11}—CHO	v.p.c.	Olefin	v.p.c.
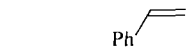	C_6H_5—$CH(OCH_3)OOH$ $CH_2(OCH_3)OOH$ $CH_2(OCH_3)OOH$ C_6H_5—CHO	n.m.r. Polarography i.r., v.p.c.	Active O Olefin	Iodometry v.p.c.
	CH_3—$CH(OCH_3)OOH$	Polarography	Active O	Iodometry
	CH_3—$CH(OCH_3)OOH$	Polarography	Active O	Iodometry
	CH_3—$CH(OCH_3)OOH$	Polarography	Active O	Iodometry
	CH_3—$CH(OCH_3)OOH$	Polarography	Active O	Iodometry
	CH_3—$CH(OCH_3)OOH$ i-C_3H_7—$CH(OCH_3)OOH$ i-C_3H_7—CHO	Polarography n.m.r. i.r.	Active O Olefin	Iodometry v.p.c.
	i-C_3H_7—$CH(OCH_3)OOH$ CH_3—$CH(OCH_3)OOH$	Polarography n.m.r.	Active O	Iodometry
	t-C_4H_9—$CH(OCH_3)OOH$ CH_3—$CH(OCH_3)OOH$	Polarography n.m.r.	Active O	Iodometry
	t-C_4H_9—$CH(OCH_3)OOH$ CH_3—$CH(OCH_3)OOH$	Polarography n.m.r.	Active O	Iodometry
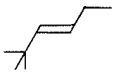	t-C_4H_9—$CH(OCH_3)OOH$ C_2H_5—$CH(OCH_3)OOH$	n.m.r.		
	t-C_4H_9—$CH(OCH_3)OOH$ C_2H_5—$CH(OCH_3)OOH$	n.m.r.		
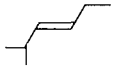	i-C_3H_7—$CH(OCH_3)OOH$ C_2H_5—$CH(OCH_3)OOH$	n.m.r.		
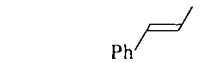	C_6H_5—CHO CH_3—$CH(OCH_3)OOH$ C_6H_5—$CH(OCH_3)OOH$ CH_3—$CH(OCH_3)OOH$	i.r., v.p.c. n.m.r. Polarography	Olefin Active O	v.p.c. Iodometry
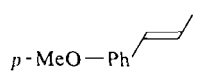	CH_3—$CH(OCH_3)OOH$	Polarography	Olefin	v.p.c.
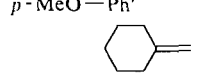		i.r.	Olefin	v.p.c.

Can. J. Chem. Downloaded from www.nrcresearchpress.com by 210.87.254.5 on 09/05/12
For personal use only.

TABLE 8 (*continued*)

Olefin	Reaction products: Product	Reaction products: Method	Olefin consumed: Product	Olefin consumed: Method
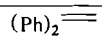	C_6H_5—CO—C_6H_5	i.r.	Olefin	u.v.
	C_6H_5—CO—CH_3	i.r.	Olefin	v.p.c.
	n-C_3H_7—CO—CH_3	i.r.	Olefin	v.p.c.
	CH_3—CO—CH_3	i.r.	Olefin	v.p.c.
	$(CH_3)_2$—C(OCH_3)OOH C_2H_5—CH(OCH_3)OOH	n.m.r.		
	i-C_3H_7—CHO	v.p.c.	Olefin	v.p.c.
	$(CH_3)_2$—C(OCH_3)OOH	n.m.r.		
	C_2H_5—CO—CH_3	v.p.c.	Olefin	v.p.c.
	C_2H_5—CO—CH_3	v.p.c.	Olefin	v.p.c.
		i.r.	Olefin	v.p.c.
		i.r.	Olefin	v.p.c.
	C_6H_5—CO—C_6H_5 C_6H_5—CHO	i.r.	Olefin	v.p.c.
	C_6H_5—CHO CH_3—CO—CH_3	i.r.	Olefin	v.p.c.
	C_6H_5—CO—CH_3 CH_3—CO—CH_3	i.r.	Olefin Active O	v.p.c. Iodometry

ton(s). From the integrated values of these signals, the direction of cleavage can be calculated by solving the appropriate system of equations.

Materials

The olefins were obtained from K & K Laboratories Inc. and Aldrich Chemical Co., Inc., or prepared by standard methods reported in the literature. Purifications were carried out, in many cases, by preparative v.p.c.

Analytical Methods

Analytical methods used to determine the direction of cleavage depend on the nature of the olefin investigated and the properties of the compounds formed upon ozonolysis. The specific products which were measured and the analytical methods used in each case are summarized in Table 8.

The financial support given by the National Research Council of Canada is gratefully acknowledged.

1. R. HUISGEN. Angew. Chem. **75**, 604, 742 (1963); Eng. ed. **2**, 565, 633. A. J. WHITWORTH, R. AYOUB, Y. ROUSSEAU, and S. FLISZÁR. J. Amer. Chem. Soc. **91**, 7128 (1969) and references contained therein.
2. R. CRIEGEE and G. SCHRÖDER. Chem. Ber. **93**, 689 (1960).
3. L. J. DURHAM and F. L. GREENWOOD. Chem. Commun. 24 (1968); L. J. DURHAM and F. L. GREENWOOD. J. Org. Chem. **33**, 1629 (1968).
4. P. S. BAILEY, J. A. THOMPSON, and B. A. SHOULDERS. J. Amer. Chem. Soc. **88**, 4098 (1966).
5. F. L. GREENWOOD. J. Org. Chem. **29**, 1321 (1964); F. L. GREENWOOD. J. Org. Chem. **30**, 3108 (1965).
6. N. L. BAULD, J. A. THOMPSON, C. E. HUDSON, and P. S. BAILEY. J. Amer. Chem. Soc. **90**, 1822 (1968).
7. J. RENARD and S. FLISZÁR. J. Amer. Chem. Soc. **92**, 2628 (1970).
8. P. D. BARTLETT and P. GÜNTHER. J. Amer. Chem. Soc. **88**, 3288 (1966).
9. F. L. GREENWOOD and L. J. DURHAM. J. Org. Chem. **34**, 3363 (1969).

Can. J. Chem. Downloaded from www.nrcresearchpress.com by 210.87.254.5 on 09/05/12
For personal use only.

10. R. CRIEGEE and G. WENNER. Ann. **564**, 9 (1949); R. CRIEGEE. Ann. **583**, 1 (1953); R. CRIEGEE. Record Chem. Progr. **18**, 111 (1957).
11. P. S. BAILEY. Chem. Rev. **58**, 926 (1958).
12. S. FLISZÁR and M. GRANGER. J. Amer. Chem. Soc. **92**, 3361 (1970).
13. S. FLISZÁR and J. CARLES. J. Amer. Chem. Soc. **91**, 2637 (1969).
14. S. FLISZÁR and J. CARLES. Can. J. Chem. **47**, 3921 (1969).
15. G. KLUTSCH, J. GRIGNON, J. RENARD, and S. FLISZÁR. Can. J. Chem. **48**, 1598 (1970).
16. (*a*) S. FLISZÁR and J. RENARD. Can. J. Chem. **45**, 533 (1967); (*b*) S. FLISZÁR, D. GRAVEL, and E. CAVALIERI. Can. J. Chem. **44**, 67, 1013 (1966).
17. J. RENARD and S. FLISZÁR. Can. J. Chem. **47**, 3333 (1969).
18. S. FLISZÁR and M. GRANGER. J. Amer. Chem. Soc. **91**, 3330 (1969).
19. P. S. BAILEY, S. B. MAINTHIA, and C. J. ABSHIRE. J. Amer. Chem. Soc. **82**, 6136 (1960).
20. W. P. KEAVENEY, M. G. BERGER, and J. J. PAPPAS. J. Org. Chem. **32**, 1537 (1967).
21. S. D. RAZUMOVSKII and YU. N. YURIEF. Zh. Org. Khim. **4**, 1716 (1968); Tetrahedron Lett. 3939 (1967).
22. W. P. KEAVENEY and J. J. PAPPAS. Tetrahedron Lett. 841 (1969).
23. K. J. LAIDLER. Chemical kinetics. McGraw-Hill Book Co., Inc., New York. 1965.
24. G. S. HAMMOND. J. Amer. Chem. Soc. **77**, 334 (1955).
25. J. W. BAKER and W. S. NATHAN. J. Chem. Soc. 1844 (1935).
26. M. J. S. DEWAR. Hyperconjugation. Ronal Press Co., New York. 1962.
27. W. M. SCHUBERT, J. M. CRAVEN, R. MINTON, and R. B. MURPHY. Tetrahedron, **5**, 194 (1959); W. M. SCHUBERT, R. B. MURPHY, and J. ROBINS. Tetrahedron, **17**, 199 (1962).
28. J. CIABATTONI and E. C. NATHAN, III. Tetrahedron Lett. 4997 (1969).
29. J. W. BAKER. Hyperconjugation. Oxford Univ. Press, London. (1953).
30. Conference on Hyperconjugation. Tetrahedron, **5**, 105–274 (1959).
31. E. BERLINER. Tetrahedron, **5**, 202 (1959).
32. W. M. SCHUBERT and W. A. SWEENEY. J. Org. Chem. **21**, 119 (1956); J. Amer. Chem. Soc. **76**, 4625 (1954); W. M. SCHUBERT, J. ROBINS, and J. L. HAUN. J. Amer. Chem. Soc. **79**, 910 (1957); W. M. SCHUBERT and J. ROBINS. J. Amer. Chem. Soc. **80**, 559 (1958); W. M. SCHUBERT, J. ROBINS, and J. M. CRAVEN. J. Org. Chem. **24**, 943 (1959).
33. W. M. SCHUBERT and R. MINTON. J. Amer. Chem. Soc. **82**, 6188 (1960).
34. R. HOFFMANN. J. Chem. Phys. **40**, 2480 (1964).
35. R. W. TAFT. J. Amer. Chem. Soc. **75**, 4231 (1953).
36. P. DUMPF and M. GILLOIS. Bull. Soc. Chim. **22**, 1350 (1955).
37. G. E. COATES and L. E. SUTTON. J. Chem. Soc. 567 (1942); A. PULLMANN, G. BERTHIER, and B. PULLMANN. Bull. Soc. Chim. **17**, 593 (1950); B. PULLMANN. *In* Théories électroniques de la chimie organique. *Edited by* Masson. Paris. 1952.
38. P. KOLSAKER and P. S. BAILEY. Acta Chem. Scand. **21**, 537 (1967).
39. G. F. SPENCER, R. KLEIMAN, F. R. EARLE, and I. A. WOLFF. Anal. Chem. **41**, 1874 (1969).

Can. J. Chem. Downloaded from www.nrcresearchpress.com by 210.87.254.5 on 09/05/12
For personal use only.

Can. J. Chem. Downloaded from www.nrcresearchpress.com by 210.87.254.6 on 09/05/12
For personal use only.

Infrared spectrum of HDO in aqueous solutions of perchlorates and tetrafluoroborates[1]

GEORGE BRINK[2] AND MICHAEL FALK
Atlantic Regional Laboratory, National Research Council of Canada, Halifax, Nova Scotia

Received April 10, 1970

The OH and OD stretching bands of HDO in aqueous solutions containing the ions ClO_4^- and BF_4^- are split into two components. The high-frequency component, *A*, does not shift with temperature. It is interpreted as due to OH groups involved in weak OH $\cdots ClO_4^-$ or OH $\cdots BF_4^-$ hydrogen bonds. This interpretation is in line with the corresponding OH frequencies of other systems containing ClO_4^- ions, such as methanolic solutions and crystalline hydrates. Solvent-separated ion pairs may account for the observed cation effect on band *A*. The low-frequency component, *B*, varies with temperature almost exactly like the corresponding band of pure water. It is interpreted to be due to those OH groups which are *not* associated with the anion. Components *A* and *B* are not resolved in solutions of most electrolytes because the distribution of strengths of interactions of OH groups with most anions overlaps that of OH $\cdots$ O interactions between water molecules.

Canadian Journal of Chemistry, **48**, 3019 (1970)

Introduction

The OH and OD stretching vibrations of HDO[3] in aqueous solutions of electrolytes generally give rise to broad, single-peaked bands which resemble the bands of HDO in pure water (1–4). Hartman (2) has shown that for aqueous solutions of perchlorate salts, however, the bands are split; a new high-frequency component appears near 3575 cm^{-1} for the OH stretching vibration of HDO. Kęcki and coworkers (5, 6) have shown that the corresponding OD stretching band of HDO appears between 2618 and 2634 cm^{-1} for various perchlorate salts.

In this paper we are presenting data on the concentration and temperature dependence of the OD stretching bands of HDO in aqueous solutions of $NaClO_4$ and $Mg(ClO_4)_2$. We also show that for aqueous solutions of the tetrafluoroborate ion, high-frequency components of the HDO stretching vibrations are observed and are similar to those of the perchlorate solutions. Further, the OH stretching band for solutions of $NaClO_4$ and $LiClO_4$ in methanol is similarly split. Our findings, together with the results of our recent study of crystalline hydrates of perchlorate salts (7) are discussed in connection with the effect of ions on the spectrum and structure of water.

[1]Issued as NRCC No. 11455.
[2]NRCC Postdoctorate Fellow, 1968–70.
[3]Isotopically dilute HDO has a far simpler vibrational spectrum than H_2O and D_2O, hence is preferable in structural studies (1).

Experimental

Samples of anhydrous sodium, lithium, barium, silver and magnesium perchlorates (G. F. Smith Chemical Co., Columbus, Ohio) were kept at 140° under vacuum for several days before being used. "AnalaR" grade methanol, dried over molecular sieves (Linde 1/16″ pellets), and doubly distilled H_2O were used. The D_2O was supplied by Merck, Sharp and Dohme, Montreal, and was of 99.7% isotopic purity. Sodium tetrafluoroborate (Alfa Inorganics, Beverly, Massachusetts) was recrystallized from aqueous solution; the insoluble material present was filtered off.

The BF_4^- ion is known to be hydrolyzed in water according to the equation $BF_4^- + H_2O = BF_3(OH)^- + HF$, to the extent of 5.5% in a 5.4 *M* solution of HBF_4 (8). However, the rate of hydrolysis of BF_4^- in neutral solutions is very slow (9) and we have not been able to detect any changes with time in the i.r. spectra of the aqueous solutions of $NaBF_4$.

A solution of HDO in H_2O was used for the quantitative study of the OD stretching band of aqueous perchlorate solutions. The concentration of HDO was about 2 moles/l, and was calculated by assuming the value of 3.8 for the equilibrium constant (10) for $H_2O + D_2O = 2HDO$ at 25°. The OD stretching vibration was studied in preference to the OH stretching vibration because of the difficulty of maintaining a constant low concentration of H_2O in D_2O. A concentration of about 2 moles/l HDO in D_2O was used for investigating the OH stretching bands qualitatively. Aqueous perchlorate solutions were prepared volumetrically and concentrations are expressed in moles/l solution.

Spectra were recorded on a Perkin-Elmer model 521 spectrophotometer. Cells with calcium fluoride windows and optical paths between 20 and 50 microns were used. A thermostated cell holder, which has previously been described (11), was used for the variable temperature spectra. The spectra of saturated solutions of $NaClO_4$ and $LiClO_4$ in methanol were obtained with capillary films between two calcium fluoride windows.

Can. J. Chem. Downloaded from www.nrcresearchpress.com by 210.87.254.6 on 09/05/12
For personal use only.

The OH and OD band profiles were obtained by subtraction of the spectra of the solution in pure H_2O or D_2O from the spectra of the solution which contained HDO.

Results

The absorptivities of the OD stretching bands of HDO in water are shown in Figs. 1 and 2 for a series of concentrations of $NaClO_4$ and $Mg(ClO_4)_2$. A shoulder on the high frequency side of the OD bands appears at low concentrations. This shoulder grows and becomes a well-defined peak as the solute concentration is increased. A similar set of curves was obtained for the OH stretching bands of HDO. The spectra in the OD stretching region agree with those reported by Kęcki *et al.* (5, 6); those in the OH region agree with the spectra of Hartman (2). We have also observed similar spectra for solutions of perchlorates of barium, lithium, and silver.

Figure 3 shows the absorptivities of the OD stretching band of HDO for a series of concentrations of $NaBF_4$. These curves contain a high-frequency feature similar to that found in the perchlorate solutions. If we consider that the two features in the spectra of the ClO_4^- and BF_4^- solutions correspond to two classes of OH groups, then the two components can be mathematically resolved. We shall refer to the high-frequency component as *A* and to the low-frequency component as *B*. We have assumed that both components have symmetrical band profiles described by the Gauss–Cauchy product function (12). Using the Band-Fit Optimization Program

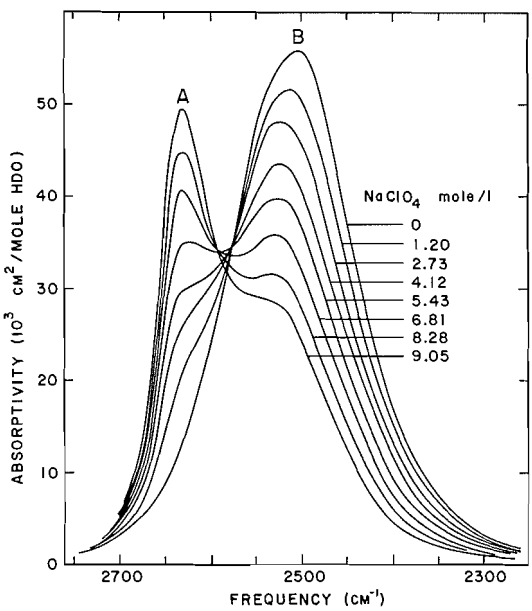

FIG. 1. Molar absorptivities of the OD stretching bands of HDO in aqueous $NaClO_4$ at 28°.

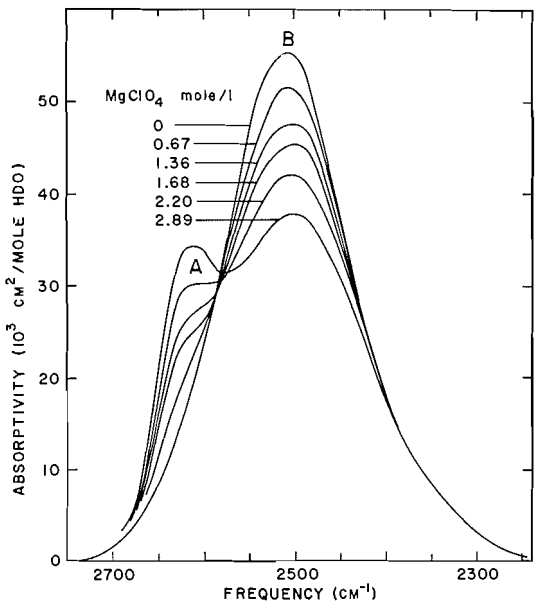

FIG. 2. Molar absorptivities of the OD stretching bands of HDO in aqueous $Mg(ClO_4)_2$ at 28°.

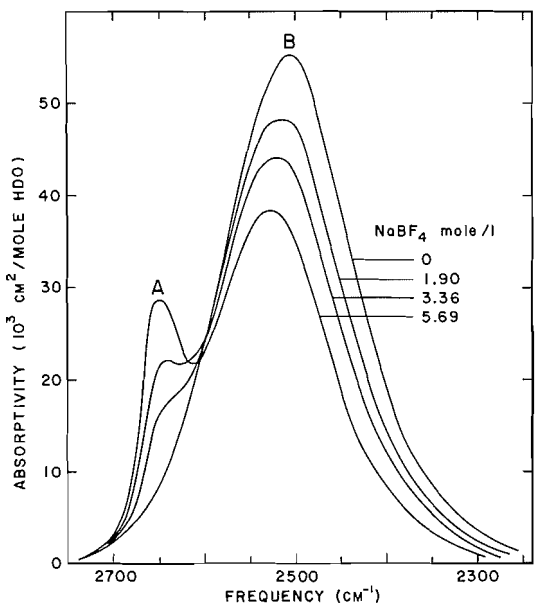

FIG. 3. Molar absorptivities of the OD stretching bands of HDO in aqueous $NaBF_4$ at 28°.

TABLE 1

Effect of perchlorate concentration on the peak frequencies, half-widths, and areas* of the component OD stretching bands of HDO at 28 °C

	Band *A*			Band *B*		
Concentration (mole/l)	ν_0 (cm^{-1})	Half-width (cm^{-1})	Area (10^6 cm/mole)	ν_0 (cm^{-1})	Half-width (cm^{-1})	Area (10^6 cm/mole)
$NaClO_4$						
0				2503	162	10.2
1.20	2628	52	0.3	2508	165	9.7
2.73	2630	53	0.6	2514	166	9.1
4.12	2629	54	0.9	2517	166	8.3
5.43	2629	55	1.3	2522	167	7.6
6.81	2630	53	1.5	2527	171	6.9
8.28	2629	54	1.9	2531	165	5.9
9.05	2629	54	2.2	2534	166	5.3
$Mg(ClO_4)_2$						
0				2503	162	10.2
0.67	2620	55	0.3	2503	173	9.9
1.36	2621	55	0.5	2503	180	9.6
1.68	2622	53	0.7	2502	188	9.4
2.20	2621	57	1.0	2501	190	9.0
2.89	2620	58	1.4	2500	196	8.6

*Area $= \frac{1}{cd}\int \log_{10}\left(\frac{T_0}{T}\right)_\nu d\nu$, where c is the total concentration of HDO in moles/l and d is the optical path in cm.

TABLE 2

Effect of sodium tetrafluoroborate concentration on the peak frequencies, half-widths, and areas of the component OD stretching bands of HDO at 28 °C

	Band *A*			Band *B*		
Concentration (mole/l)	ν_0 (cm^{-1})	Half-width (cm^{-1})	Area (10^6 cm/mole)	ν_0 (cm^{-1})	Half-width (cm^{-1})	Area (10^6 cm/mole)
0				2503	162	10.2
1.90	2644	38	0.3	2516	167	9.6
3.36	2646	42	0.6	2520	169	8.6
5.69	2649	43	1.0	2528	163	7.0

of Jones and Pitha (13) we have obtained the peak frequencies, half-widths, and areas (molar integrated absorptivities) of the two component bands, listed in Table 1. The same information is given in Table 2 for sodium tetrafluoroborate solutions. The standard deviation (root mean square of the residuals) of the fit for a curve was typically about 0.006 transmittance units. The areas of the resolved bands are only accurate to within 5% over most of the concentration range. At low perchlorate concentrations band *A* appears only as a small shoulder and the error in resolution is probably greater.

Table 3 shows the effect of temperature on the parameters of bands *A* and *B* of a nearly saturated solution of $NaClO_4$ and compares it with data for HDO in pure water. Band *B* undergoes a temperature shift similar to that of the corresponding HDO band in water, while band *A* remains nearly stationary. Figure 4 shows the effect of temperature on the OD band of a 7 mole/l (at 25°) solution of $NaClO_4$. The frequency shift and intensity change are considerable for band *B*, but very small for band *A*. The frequency of *A* varies from 2627 cm^{-1} at −11 to 2630 cm^{-1} at +75° while its absorbance, neglecting density changes, remains essentially constant at 0.323 ± 0.003.

Figure 5 compares the spectra of saturated solutions of $NaClO_4$ and $LiClO_4$ in methanol and of pure methanol. The $NaClO_4$ spectrum shows that the OH band contains *A* and *B* components. Resolution of the band for $NaClO_4$ gives component peak frequencies of 3541 and 3373 cm^{-1}, and half-widths of 93 and 268 cm^{-1}, compared with 3340 and 262 cm^{-1} for the OH stretching band of pure methanol. $LiClO_4$ is much more

Can. J. Chem. Downloaded from www.nrcresearchpress.com by 210.87.254.6 on 09/05/12
For personal use only.

TABLE 3

Effect of temperature on the peak frequencies and half-widths of bands of HDO in pure water and in 9 mole/l $NaClO_4$ solution

			$NaClO_4$			
	H_2O		Band *A*		Band *B*	
Temperature (°C)	ν_0 (cm^{-1})	Half-width (cm^{-1})	ν_0 (cm^{-1})	Half-width (cm^{-1})	ν_0 (cm^{-1})	Half-width (cm^{-1})
OH stretching band						
4	3387	250	3569	83	3430	255
28	3403	255	3572	84	3446	261
50	3419	259	3572	85	3456	265
OD stretching band						
4	2492	160	2627	52	2516	155
28	2503	162	2629	54	2531	165
50	2509	170	2629	56	2539	167

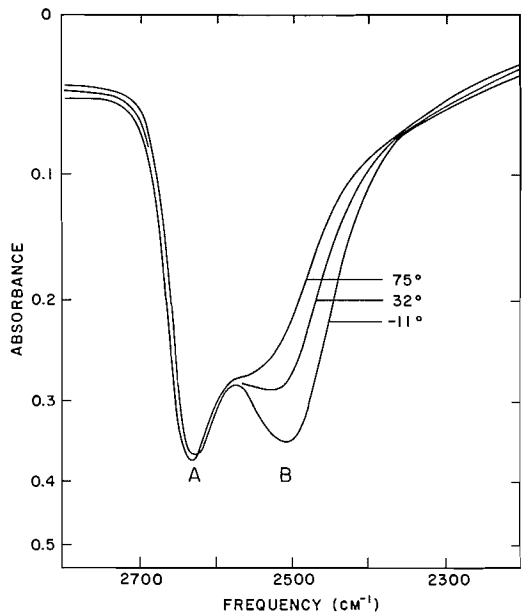

FIG. 4. Effect of temperature on the OD stretching bands of HDO in an approximately 7 mole/l solution of $NaClO_4$.

soluble in methanol than $NaClO_4$, and the OH band of the saturated $LiClO_4$ solution consists almost entirely of component *A*.

Discussion

Nature of Band A

The high frequency, relatively narrow half-width, and lack of appreciable temperature shift of band *A* are characteristic of OH groups which interact weakly with their environment (14). Thus Hartman's original assignment of this band to OH groups of water molecules weakly hydrogen-bonded to the ClO_4^- ions (2) appears reasonable. This assignment is consistent with the observation that the frequency of band *A* in aqueous solutions of perchlorates is almost identical to the stretching frequencies of HDO in crystalline $NaClO_4 \cdot H_2O$, $LiClO_4 \cdot 3H_2O$ and $Ba(ClO_4)_2 \cdot 3H_2O$. The water molecules in these compounds participate in $OH \cdots ClO_4^-$ hydrogen bonds, which although weak are well documented (7). The appearance of band *A* for solutions of perchlorate salts in methanol confirms the assignment of this band to $OH \cdots ClO_4^-$ interactions. Figure 6 shows that the frequency shifts of band *A* with respect to the frequencies of the vapor, CCl_4 solution, and pure liquid are nearly the same for HDO and for CH_3OH. Band *A* therefore appears to originate in the interactions of OH groups and ClO_4^- ions and is not a consequence of some special fit of the perchlorate ion into the structure of liquid water, as sometimes suggested (15).

Band *A* lies 146 cm^{-1} below the vapor frequency for OH stretching of methanol and 134 cm^{-1} below the vapor frequency for the OH stretching of HDO. Assuming a linear relation between the frequency shift and hydrogen-bond enthalpy [the Badger–Bauer rule (16)], one obtains about 2 kcal/mole for the enthalpy of the $OH \cdots ClO_4^-$ bonds (7). A non-linear correlation of frequency and enthalpy, which fits experimental data for HDO somewhat better (17), would give a slightly *higher* enthalpy value. The OD groups of HDO in liquid water at density of 1.0 g/cm^3 at 400° have almost the same OD frequency (18) as band *A* for HDO in aqueous $NaClO_4$. Whether the water–water bond at such high temperatures, or the water–perchlorate bonds in solution, are to be regarded as weak

Can. J. Chem. Downloaded from www.nrcresearchpress.com by 210.87.254.6 on 09/05/12
For personal use only.

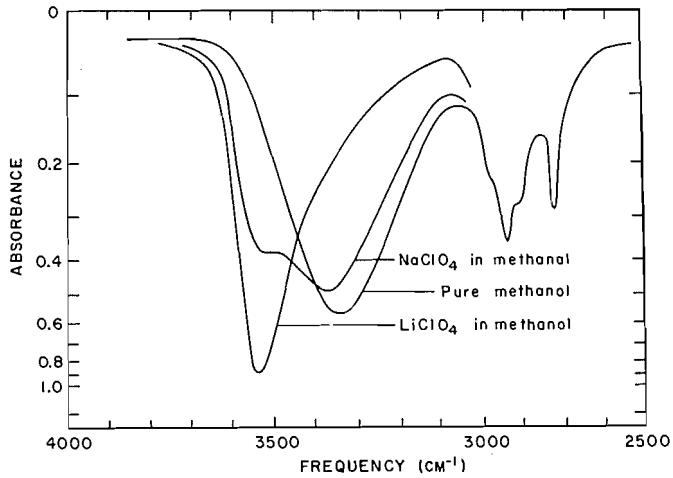

FIG. 5. Spectra in the OH and CH stretching regions of saturated solutions of $NaClO_4$ and $LiClO_4$ in methanol at 28°.

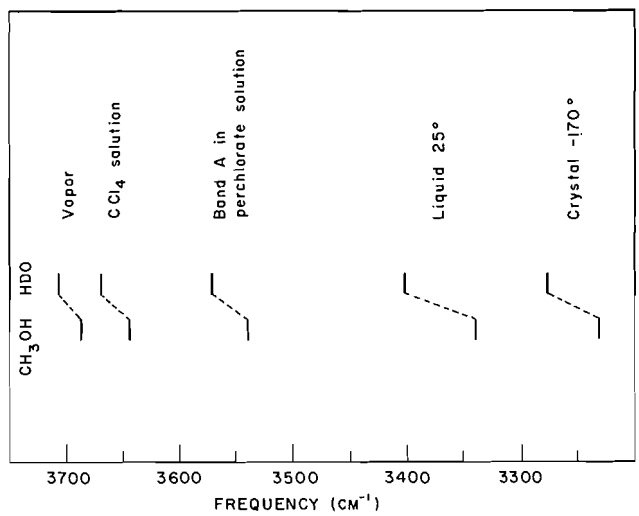

FIG. 6. The OH stretching peak frequencies of HDO and methanol in various environments.

hydrogen bonds or strong non-hydrogen-bonded interactions of the OH group is arbitrary (14).

The frequency of band *A* depends on the cation: for saturated solutions the OD frequency is 2629 cm^{-1} for $NaClO_4$, 2626 cm^{-1} for $Ba(ClO_4)_2$, 2625 cm^{-1} for $LiClO_4$, 2620 cm^{-1} for $Mg(ClO_4)_2$, and 2606 cm^{-1} for $AgClO_4$. We explain the cation effect by the formation of solvent-separated cation ... water ... anion pairs. Such pairing would cause the frequency of band *A* to vary with the cation but to remain independent of the perchlorate concentration for any particular cation. Solvent-separated ion pairs have often been postulated to occur in aqueous solution (19). Such pairs have been considered by Dryjański and Kęcki (6) as a possible explanation for the spectrum of the perchlorate solutions, but were rejected because of the lack of a discrete band *A* for solutions of sulfates. Our view is that the $OH\cdots SO_4^{2-}$ hydrogen bonds are sufficiently strong that the frequencies of the OH groups bonded to the sulfate ions merge with the broad band due to the other OH groups.

Nature of Band B

If band *A* corresponds to OH groups associated with the perchlorate ions, then band *B* must correspond to all the remaining OH groups

Can. J. Chem. Downloaded from www.nrcresearchpress.com by 210.87.254.6 on 09/05/12
For personal use only.

Can. J. Chem. Downloaded from www.nrcresearchpress.com by 210.87.254.6 on 09/05/12
For personal use only.

in solution. Its greater half-width is due to a wider variety of OH · · ·O bond strengths, and its lower peak frequency to a greater *average* hydrogen bond strength. For solutions of $NaClO_4$, band *B* shifts to higher frequencies with increasing concentration (Table 1), indicating a general weakening of hydrogen bonding. The shift for OD stretching is from 2503 cm^{-1} in pure water to 2534 cm^{-1} for a nearly saturated solution of $NaClO_4$. This shift is about the same as that observed for water when the temperature is raised by 100 °C (11, 18). $LiClO_4$ and $Ba(ClO_4)_2$ also cause band *B* to shift to higher frequencies with increasing concentration. $Mg(ClO_4)$, on the other hand, causes a slight shift of band *B* to lower frequencies with increasing concentration. The difference between Mg^{2+} and the other cations is probably due to the greater water-coordinating ability of Mg^{2+}, which may cause a small net strengthening of water–water hydrogen bonds.

The effect of increasing temperature on band *B* is to shift its maximum to higher frequencies and to decrease its intensity. This lost intensity is *not* gained by band *A*, which remains almost unchanged between −11 and +75° (Fig. 4). This indicates that the number of water molecules, or OH groups, surrounding the perchlorate ions does not vary greatly with temperature and that the already weak OH · · · ClO_4^- interactions do not weaken appreciably with higher temperature. The remaining OH groups, *i.e.* those giving rise to band *B*, have a wide distribution of hydrogen-bond strengths, which shifts under the influence of temperature in the same way as the corresponding distribution for pure water (11).

Effect of Ions on the Spectrum and Structure of Water

Most of the common anions are capable of forming hydrogen bonds with water, which are comparable in strength to water–water bonds. In aqueous solution one can therefore formally distinguish OH groups bonded to an anion from those bonded to a water molecule. The former should give rise to band *A* and the latter to band *B*, in analogy with the spectrum of perchlorate solutions. However, if the OH · · ·anion bonds are comparable in strength to the OH · · ·water bonds, and a wide variety of interactions of either type occurs, then we obtain bands *A* and *B* whose peaks differ by a small fraction of their half-width. Such peaks cannot be spectroscopically resolved (3, 4). Thus no splitting of the stretching bands of HDO can be observed for solutions of halide ions (1–4) and of oxyanions such as SO_4^{2-}, NO_3^-, NO_2^-, ClO_3^-, IO_4^-, and ReO_4^- (20). Only small overall shifts of these bands are observed.

The special property of the ClO_4^- ion which causes band *A*, due to OH · · ·anion bonds, and band *B*, due to OH · · ·water bonds, to become spectroscopically well separated, is the weakness of OH · · · ClO_4^- interactions. The distribution of strengths of these interactions is much narrower than that of OH · · ·water interactions, hence the band is relatively narrow (50–60 cm^{-1} half-width for OD stretching) compared with band *B* (160–170 cm^{-1} half-width for OD stretching). Bands *A* and *B* are resolved, because the half-width of *A* is smaller than their peak-to-peak distance of about 120 cm^{-1}. It should be noted that the half-width of 50 cm^{-1} for band *A* in solution is still 10 or 20 times greater than the half-widths of the OH stretching bands in crystalline $NaClO_4 \cdot H_2O$, $LiClO_4 \cdot 3H_2O$, and $Ba(ClO_4)_2 \cdot 3H_2O$ (7). This points to the essential difference between the crystalline solid and the solution: although the strengths of the OH · · · ClO_4^- interactions (reflected by the frequencies) are about the same, the order present in the crystal (reflected by the narrow band widths) is absent in solution.

The weakness of the OH · · ·perchlorate bonding is in line with the well-known low reactivity of the perchlorate ion, which has been explained by Nightingale (21) as due to the double bonding between the Cl and O atoms. This localizes the negative charge on the central chlorine atom, thereby rendering the charge less accessible for hydrogen bonding *i.e.* the π-bonds utilize the oxygen *p*-orbitals and render them unavailable for intermolecular bonding (21).

It is known that the tetrafluoroborate ion, BF_4^-, is structurally similar to the perchlorate ion, the salts with these two anions having similar properties, *e.g.* solubility (22). We have found that HDO in solutions of $NaBF_4$ shows the characteristically split OD and OH bands (Table 2). Band *B* almost exactly matches that of $NaClO_4$ solutions in frequency and half-width, while band *A* at 2644 to 2649 cm^{-1} lies about 20 cm^{-1} higher than that of $NaClO_4$ solutions. This shows that the OH · · · BF_4^- interactions are even weaker than OH · · · ClO_4^-.

The distinction between OH groups involved in

water–water interactions and those involved in water–anion interactions may be somewhat artificial. Large monovalent anions like Cl^-, Br^-, I^-, and particularly ClO_4^-, have charge densities too low to orientate water molecules rigidly. Thus many of the OH groups might be at the same time interacting with an anion and a water molecule. Our picture of two distinct types of interaction, and the division of the OH stretching band into the sub-bands *A* and *B* is thus an oversimplification, even in the cases of ClO_4^- and BF_4^- solutions, when two maxima are actually observed.

Addendum

The effects of the perchlorate ion on the Raman spectrum of water have been discussed at length by Walrafen (23). Walrafen holds that the perchlorate ion "does not form directed hydrogen bonds with water" and interprets band *A* as being due to "non-hydrogen-bonded OH groups". We prefer to consider the OH···perchlorate interactions as weak hydrogen bonds, this interpretation being more consistent with our experimental findings. It should be particularly noted that weak hydrogen bonds between water molecules and perchlorate ions occur in crystalline hydrates (see ref. 7 and the refs. therein) and that the frequency of band *A* in solutions is about the same as the OH stretching frequencies in such hydrates (7).

1. R. D. Waldron. J. Chem. Phys. **26**, 809 (1957).
2. K. A. Hartman. J. Phys. Chem. **70**, 270 (1966).
3. T. T. Wall and D. F. Hornig. J. Chem. Phys. **47**, 784 (1967).
4. H. R. Wyss and M. Falk. Can. J. Chem. **48**, 607 (1970).
5. Z. Kęcki, P. Dryjański, and E. Kozłowska. Rocz. Chem. **42**, 1749 (1968).
6. P. Dryjański and Z. Kęcki. Rocz. Chem. **43**, 1053 (1969).
7. G. Brink and M. Falk. Can. J. Chem. **48**, 2096 (1970).
8. C. A. Wamser. J. Amer. Chem. Soc. **70**, 1209 (1948); **73**, 409 (1951).
9. M. Anbar and S. Guttmann. J. Phys. Chem. **64**, 1896 (1960).
10. I. Kirshenbaum. Physical properties and analysis of heavy water. McGraw-Hill, New York, N.Y. 1951. p. 54.
11. M. Falk and T. A. Ford. Can. J. Chem. **44**, 1699 (1966).
12. K. S. Seshadri and R. N. Jones. Spectrochim. Acta, **19**, 1013 (1963).
13. J. Pitha and R. N. Jones. NRCC Bulletin No. 12 (1968).
14. K. Szczepaniak and M. Falk. Spectrochim. Acta, **26A**, 883 (1970).
15. J. L. Kavanau. Water and solute-water interactions. Holden-Day, San Francisco. 1964. p. 54.
16. R. M. Badger and S. H. Bauer. J. Chem. Phys. **5**, 839 (1937).
17. T. A. Ford and M. Falk. Can. J. Chem. **46**, 3579 (1968).
18. E. U. Franck and K. Roth. Discuss. Faraday Soc. **43**, 108 (1967).
19. Reference 15, p. 55.
20. G. Brink. Unpublished results.
21. E. R. Nightingale. J. Phys. Chem. **64**, 162 (1960).
22. N. V. Sidgwick. The chemical elements and their compounds. Vol. 1. Oxford. 1951. p. 410.
23. G. E. Walrafen. J. Chem. Phys. **52**, 4176 (1970).

Can. J. Chem. Downloaded from www.nrcresearchpress.com by 210.87.254.6 on 09/05/12
For personal use only.

Can. J. Chem. Downloaded from www.nrcresearchpress.com by 210.87.254.105 on 09/05/12
For personal use only.

The Raman spectrum and molecular structure of $Me_3SiOReO_3$ in the solid, liquid, solution, and gaseous phases

D. H. Boal and G. A. Ozin
Lash Miller Chemical Laboratories, University of Toronto, Toronto 181, Ontario

Received May 19, 1970

The Raman spectrum of $Me_3SiOReO_3$ is found to be essentially the same in all of the above phases, proving that the non-linear SiORe bridged structure found in the solid phase is retained in the other phases and is not just the result of crystal packing requirements. The interpretation of the spectrum of $Me_3SiOReO_3$ is found to be particularly straightforward as the vibrational data can be considered to be intermediate between that of the parent, non-linear molecules $(Me_3Si)_2O$ and $(O_3Re)_2O$. In the present work, assignments for the ReO and SiO bridge stretching modes are proposed.

Canadian Journal of Chemistry, 48, 3026 (1970)

Laser Raman spectroscopy is now recognized by the inorganic chemist as being a valuable aid towards structural and vibrational assignment. The availability of high energy lasers now means that molecules can often be investigated in the vapor phase as well as in all other phases.

The Raman data for molecular $Me_3SiOReO_3$ in its various phases is extremely relevant to the stereochemical consequences of replacing silicon by rhenium(VII) which, like silicon, also has vacant d orbitals. It has been found that SiOSi angles generally fall in the range 130–150° whereas the more limited data for ReORe angles has been found to vary from 180° in the linear Re(IV) anion (1) $(Cl_5ReOReCl_5)^{4-}$ to approximately 120° in liquid and gaseous rhenium heptoxide (2), $O_3ReOReO_3$.

The recent X-ray data (3) for $Me_3SiOReO_3$ shows the presence of a molecular species with a SiORe bridge angle[1] of 164 ± 5°. Some degree of d orbital participation in the bonding was invoked to rationalize the wide SiORe angle.

It was thus of considerable interest to investigate the vibrational spectrum of $Me_3SiOReO_3$ in all of its possible phases to try to determine whether the non-linear SiORe skeleton found for the molecule in the crystal was retained in its other phases and was not just the result of crystal packing requirements.[2] The present paper reports for the first time Raman data for trimethylsilylperhennate, $Me_3SiOReO_3$.

The sensitivity of metal–oxygen bridge stretching frequencies to changes in the angle of the bridge has been demonstrated on a number of occasions (5). Thus an essential part of our discussion depends on a satisfactory assignment of the SiO and ReO bridge stretching modes in $Me_3SiOReO_3$ and the "parent" compounds.

Our approach to the problem was to obtain the Raman spectrum and Raman polarization data for $Me_3SiOReO_3$ in all possible phases and to compare the frequencies with those of $(Me_3Si)_2O$ and $(O_3Re)_2O$ whose vibrational spectra have been satisfactorily assigned (6, 2).

The X-ray data (3) for $Me_3SiOReO_3$ shows the crystal to be monoclinic with the centrosymmetric space group $C2/c$ (C_{2h}^6) and having four molecules in the primitive unit cell. In the crystal, the SiC bonds are staggered with respect to the terminal ReO bonds and the molecule has an overall symmetry of approximately C_s. Although there are four molecules in the primitive

TABLE 1

Correlations for the normal modes of vibration of $Me_3SiOReO_3$

Approximate description*	C_{3v} residue	C_s molecule
$\nu SiMe + \nu ReO_t$	$2a_1$	$2a'$
$\nu SiMe + \nu ReO_t$	$2e$	$2a' + 2a''$
$\nu SiO_b + \nu ReO_b$	$2a_1$	$2a'$
$\delta SiMe + \delta ReO_t$	$2a_1$	$2a'$
$\delta SiMe + \delta ReO_t$	$2e$	$2a' + 2a''$
$\rho_r SiMe + \rho_r ReO_t$	$2e$	$2a' + 2a''$
$\rho_r SiMe + \rho_r ReO_t$	$2a_2$	$2a''$
$\rho_r Me$	$2a_1$	$2a'$
$\rho_r Me$	$2e$	$2a' + 2a''$
$\delta SiORe$	a_1	a'

*ν = stretch; δ = deformation; ρ_r = rock; ρ_t = torsion.

[1]The rhenium co-ordinates in $Me_3SiOReO_3$ were better defined than those of the light atoms because the heavy rhenium atom dominated the diffraction of X-rays and, as a result, the bond lengths and angles were not very precise.

[2]The recent X-ray crystal structure (4) for technicium heptoxide, Tc_2O_7, shows the presence of oxygen bridged molecules, linear at the oxygen atom. The bridge oxygen atom was required to lie on a center of symmetry in the crystal.

TABLE 2

The Raman Spectra of $Me_3SiOReO_3$ in the solid, liquid, solution, and gaseous phases, Re_2O_7 in the gaseous phase, and $(Me_3Si)_2O$ in the liquid phase*

		$Me_3SiOReO_3$					
Re_2O_7 (2) gas (360°)	$(Me_3Si)_2O$ (6) liquid	Solid	Liquid (100°)	Solution	Gas (180°)	C_s assignment	Approximate description of mode
1009 sp		1007 vs	1006 vsp	1007 vsp‡	1010 vsp	vReO	a'
972 m		959 m	960 mp	964 w‡	970 w	vReO	$a' + a''$
	1053†	931 wsh	915 wp	934 vw	926 wp	vSiO	a'
	518 sp						
	889 wp	857 w	857 vw			$\rho_r CH_3$	a''
		831 w	834 vwp			$\rho_r CH_3$	a'
	835 mp?			~807 wp		$\rho_r CH_3$ or vSiMe	a' or a''
		763 w	760 w				
	752 w	703 w	702 w			vSiMe	$a' + (a''?)$
	683 mp						
	658 msp	642 m	635 sp	638 msp	639 msp	vSiMe	a'
~800 vvw		446 w	475 mwp		~475 w§	vReO	a'
456 wp							
341 mbr		350 s	343 mp	344 msp	347 mp	δReO	$2a' + a''$
322 wsh p	335 wp	315 wsh	322 vwsh	326 wsh	328 wsh	δSiMe	a'
268 vw			293 wp		299 wp	ρ_rReO	a'
	248 msp	243 m	238 mp			δSiMe	$a' + a''$
	217 s						
185 ms	197 msh	193 vsbr	185 sp	190 msbr	180 msbrp	ρ_rReO	$a'' + a'$
177 wsh p	176 vs p					ρ_rSiMe	
		157 w?			150 vw?	ρ_rSiMe	a''
113 vvw		134 w				δReOSi or terminal torsions	
95 vvw							
50 mp		117 w					

*v = very, w = weak, m = medium, s = strong, sh = shoulder, br = broad, p = polarized.
†Observed only in infrared spectrum.
‡These refer to the recorded values in $(Me_3Si)_2O$ solution, as this region was obscured by benzene lines.
§Not resolved clearly from band due to Pyrex glass in the region 520–470 cm^{-1} as this was a high sensitivity scan.

unit cell, no correlation splitting of the vibrational modes of the molecule into $a_g + b_g$, Raman active crystal components was observed.

The main difference between the unsymmetrical bridge system found in $Me_3SiOReO_3$ and the symmetrical bridge systems found in $(Me_3Si)_2O$ and $(O_3Re)_2O$ lies in the fact that in the former the SiO and ReO bridge stretching modes are both totally symmetrical and can be expected to occur in the Raman spectrum as polarized lines. However, in the latter two species two bridge-stretching modes are still expected to occur (a high and low frequency mode), but only the lower frequency mode will be totally symmetrical.

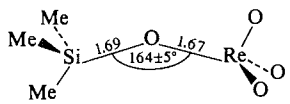

Let us consider $Me_3SiOReO_3$ to be a rigid molecule without free rotation of the terminal Me_3Si— and O_3Re— groups about the respective metal–oxygen bonds. Then we can expect $13a' + 8a''$ vibrational modes (below approximately 1100 cm^{-1}) associated with the basic $C_3SiOReO_3$ skeleton. In addition there will be methyl rocking modes associated with the Me_3Si group which under C_{3v} symmetry (for the residue) have the symmetry species $2a_1 + 2e$. These are expected to occur in the range 870–720 cm^{-1}.

If there is very little vibrational coupling across the SiORe bridge, as would be expected by analogy with previous results on symmetrical bridge systems, then one can consider the two halves of the molecule as separate C_{3v} residues. We then arrive at the correlations for the normal modes of vibration of $Me_3SiOReO_3$ (below approximately 1100 cm^{-1}) as shown in Table 1.

The lowering of the symmetry of the terminal groups from C_{3v} to C_s results in practice, in either a small splitting or slightly polarized character for some of the modes assignable to degenerate e modes of the C_{3v} residues. On this basis and taking into account the assignments for the related species $(Me_3Si)_2O$ and $(O_3Re)_2O$, we assign SiO and ReO bridge stretching modes in $Me_3SiOReO_3$ to polarized bands observed at 915

Can. J. Chem. Downloaded from www.nrcresearchpress.com by 210.87.254.105 on 09/05/12
For personal use only.

and 475 cm^{-1} (in the liquid) and 931 and 446 cm^{-1} (in the solid), respectively: *cf.* $(Me_3Si)_2O$ ν_{sym} 518 cm^{-1} and ν_{anti} 1053 cm^{-1}; $(O_3Re)_2O$ ν_{sym} 456 cm^{-1} and ν_{anti} ~ 800 cm^{-1}. Although the modes involving mainly stretching of the SiO and ReO bridge bonds both involve motion of the central oxygen atom and will be of mixed character, the above assignment is acceptable purely on a mass basis.

The remaining bands for $Me_3SiOReO_3$ are assigned as in Table 2 by analogy with the "parent" compounds whose Raman spectra are included in Table 2 for the purpose of comparison. The unassigned bands are the Me_3Si— and O_3Re— torsional modes and the totally symmetrical SiORe deformational mode, all of which are expected to occur below 180 cm^{-1}.

The changes in frequency of the bridge stretching modes are small and variable between phases and correspond to a decrease of approximately 10° (with respect to the solid) in the SiORe angle. The changes may be attributable to crystal packing requirements in the solid and intermolecular interactions in the liquid and solution phases. However, the internal consistency of the Raman spectra for $Me_3SiOReO_3$ between phases shows unambiguously that the molecular structure is retained in all phases with only slight variations in the SiORe bridge angle.

Experimental

Rhenium heptoxide was prepared by oxidizing rhenium metal powder under anhydrous conditions and then sublimation of the pale yellow product in vacuo. Hexamethyldisiloxane was dried by refluxing over CaH_2 and then distillation in vacuo. All solvents used, diethyl ether, chloroform, and benzene were also dried with CaH_2 by standard procedures.

Trimethylsilylperhennate, $Me_3SiOReO_3$, was prepared by refluxing Re_2O_7 in excess hexamethyldisiloxane under anhydrous conditions (7). The crystallized $Me_3SiOReO_3$ was further purified by vacuum sublimation (obs. m.p. 80.0 °C; lit. m.p. 79.5–80.5 °C).

Raman spectra were recorded on a Spex 1401 Raman spectrometer using ether argon–krypton or argon ion laser excitation. The spectra of liquid and gaseous $Me_3SiOReO_3$ were recorded at 100 and 180 °C, respectively, using cell and furnace designs similar to those described previously (2, 8).

Attempts to record laser Raman solution spectra in diethyl ether and chloroform were unsuccessful owing to rapid photodecomposition reactions. Solution data could, however, be obtained in hexamethyldisiloxane and benzene solution although photodecomposition reactions were still observed to be occurring very slowly in benzene solution. In order to identify any impurity bands, many solution spectra were recorded.

One of us (G.A.O.) would like to thank the National Research Council of Canada for financial support.

1. J. C. MORROW. Acta Cryst. **15**, 851 (1962).
2. I. R. BEATTIE and G. A. OZIN. J. Chem. Soc. (A), 2615 (1969).
3. G. M. SHELDRICK and W. S. SHELDRICK. J. Chem. Soc. (A), 2160 (1969).
4. B. KREBS. Angew. Chem. **81**, 328 (1969).
5. R. M. WING and K. P. CALLAHAN. Inorg. Chem. **8**, 781 (1969) and references therein.
6. I. F. KOZALEV, L. A. OZOLIN, M. G. VORONKOV, and L. A. ZHAGAT. Opt. Spectrosk. **3**, 301 (1967).
7. M. SCHMIDT and H. SCHMIDBAUER. Chem. Ber. **92**, 2667 (1959).
8. I. R. BEATTIE and J. HOARDER. J. Chem. Soc. (A), 2655 (1969).

Can. J. Chem. Downloaded from www.nrcresearchpress.com by 210.87.254.105 on 09/05/12
For personal use only.

Can. J. Chem. Downloaded from www.nrcresearchpress.com by 210.87.254.105 on 09/05/12
For personal use only.

The radiation chemistry of carbon monoxide at very high dose rates[1,2]

C. WILLIS AND O. A. MILLER

Physical Chemistry Branch, Chalk River Nuclear Laboratories, Atomic Energy of Canada Limited, Chalk River, Ontario

Received April 14, 1970

Carbon monoxide has been irradiated with single intense pulses from an electron accelerator at a dose rate of $\sim 2 \times 10^{27}$ eV g^{-1} s^{-1}. The yield of carbon dioxide obtained was $G(CO_2) = 0.7 \pm 0.1$ with a very small yield of carbon suboxide, $G(C_3O_2) \leq 0.02$.

Addition of propene reduces the carbon dioxide yield to almost zero while addition of propane has no effect. This suggests that propene is acting as an oxygen atom scavenger rather than as a quencher of an excited state of carbon monoxide. However, rate constant data do not support this suggestion and it is concluded that the residual yield of carbon dioxide observed at high dose rates arises from reaction 9

[9] $$CO^+ + CO \rightarrow CO_2 + C^+$$

where CO^+ is in an $A^2\Pi$ or $B^2\Sigma^+$ state.

Canadian Journal of Chemistry, 48, 3029 (1970)

Introduction

Some aspects of the radiation chemistry of carbon monoxide are well established. The products of radiolysis are carbon dioxide and a carbon–oxygen polymer with general formula $(C_{1.5\pm0.2}O)_n$ (1). The yield of carbon dioxide at low dose rates (10^{16}–10^{18} eV g^{-1} s^{-1}) is $G(CO_2) = 2.0 \pm 0.2$ (1–3) with $G(-CO) = 8 \pm 1$ (1, 4).[3] As the dose rate is increased, the yields of both carbon dioxide and polymer decrease to limiting values of $G(CO_2) = 0.6 \pm 0.2$ and[4] G(polymer) $\approx 1.5 \pm 0.5$ above 10^{21} eV g^{-1} s^{-1} (1, 5).

The mechanism associated with the production of these products has not been clearly defined. It is generally assumed that there is no ionic contribution to the yields (1, 3, 5) and that the species C_2O, O, C, and CO_2 arise predominantly from excited carbon monoxide molecules by reactions 1–3, where the excited electronic state of the carbon monoxide molecule involved is not necessarily the same for each reaction.

[1] $$CO^* \rightarrow C + O$$

[2] $$CO^* + CO \rightarrow C_2O + O$$

[3] $$CO^* + CO \rightarrow CO_2 + C$$

The dose rate effect was then explained (1, 5) in terms of reactions 4–8

[4] $$C + CO \rightarrow C_2O$$

[5] $$C_2O + CO \rightarrow C_3O_2$$

[6] $$C_2O + O \rightarrow 2CO$$

[7] $$C + O + M \rightarrow CO + M$$

[8] $$O + CO\ (+ M) \rightarrow CO_2\ (+ M?)$$

with reactions 6 and 7 becoming more important as the dose rate was increased. The residual limiting yield of $G(CO_2) = 0.6 \pm 0.2$ at the high dose rates was assumed to arise from direct production of carbon dioxide by reaction 3.

Attempts to measure yields of intermediates directly have been sparse. One notable exception is the work of Briggs and Clay (6, 7), who report measurements of the yield of oxygen atoms in a ^3P state in irradiated carbon monoxide. Using propene as an oxygen atom scavenger they concluded that $G(O^3P) = 1.41 \pm 0.22$, leading to about 75% of the observed yield of carbon dioxide at low dose rates and that ionic reactions are not involved in $O(^3P)$ atom formation. They could not preclude the possibility of $O(^1D)$ atoms as precursors of the $O(^3P)$ atoms measured.

In a previous publication we reported the observation of $C_2O(^3\Sigma)$ as a transient in the radiolysis of carbon monoxide (8). We speculated on the origins of $C_2O(^3\Sigma)$ and on its importance in the system. Because of this work and because

---

[1]AECL No. 3696.

[2]Presented in part at 52nd C.I.C. Conference, Montreal, June 1969.

[3]G value is the number of molecules of a species produced per 100 eV of energy absorbed. This yield of $G(-CO) = 8 \pm 1$ is the number of molecules of carbon monoxide consumed per 100 eV of energy absorbed, based on the overall equation

$$4\ CO \rightarrow CO_2 + C_3O_2$$

[4]The polymer yield is on the basis of $G(C)_{solid}$ (1).

Can. J. Chem. Downloaded from www.nrcresearchpress.com by 210.87.254.105 on 09/05/12
For personal use only.

of the lack of certainty of the mechanism for the dose rate effect, we have measured yields in carbon monoxide irradiated at very high dose rates.

Experimental

Irradiations

The irradiation source used was a Febetron 705. This is a pulsed electron accelerator which gives single electron pulses with a peak current of ~ 3000 A. Samples of gas were irradiated in 75 ml quartz cells with thin electron windows. The procedures involved have been reported elsewhere (9, 10).

Dosimetry

The energy absorbed in a cell was measured by nitrous oxide dosimetry taking $G(N_2) = 12.4 \pm 0.3$ at Febetron dose rates (10–12).

Analyses

The yields of carbon dioxide and carbon suboxide were measured using gas chromatography. The irradiated gas sample was expanded into two large liquid nitrogen traps and then slowly pumped through a "scrubbing" loop at liquid nitrogen temperature. The condensed gases were then transferred to the inlet loop of a Loenco 15C gas chromatograph equipped with hot-wire thermal conductivity detectors. A 3/16 in., 2 m column packed with Poropak Q was used. The efficiency of the overall method was established using synthetic mixtures of CO–CO_2. The sensitivity of the method was sufficient to measure the carbon dioxide yield in a single-pulse (1.7 Mrad) irradiation with an accuracy of about ± 5%.

Products were identified by mass-spectrometry. Characteristic peaks at $m/e = 68$ and 40 (13) were observed for carbon suboxide.

Polymer was formed in the high dose rate radiolysis of carbon monoxide. This was not the characteristic yellow-brown polymer observed in low dose rate radiolysis or photolysis (14) but was white and almost transparent. All polymer was removed from the cell by flaming to red heat in air after each experiment. No quantitative analysis of the polymer was attempted. Standard vacuum pyrolysis gave both carbon dioxide and carbon monoxide and left a black, carbon-like residue.

Materials

The carbon monoxide used was Matheson research grade gas. This was found to contain traces of oxygen, carbon dioxide, and a metal carbonyl. It was further purified by passing over copper "Flitters" (British Drug Houses) at 700 °C in a quartz tube to catalyze combination of the oxygen and carbon monoxide. This also served to pyrolyze the metal carbonyl. The carbon dioxide was removed by passing the gas through Linde 13X molecular sieve followed by a final scrubbing through a 1 mm i.d., 2 m long glass coil immersed in liquid nitrogen.

This procedure gave reproducible results whereas if any stage of the purification train was omitted, high, irreproducible yields of carbon dioxide were obtained. Very small traces of oxygen in particular gave increased yields of carbon dioxide similar to those reported for low dose rate radiolyses of carbon monoxide (2).

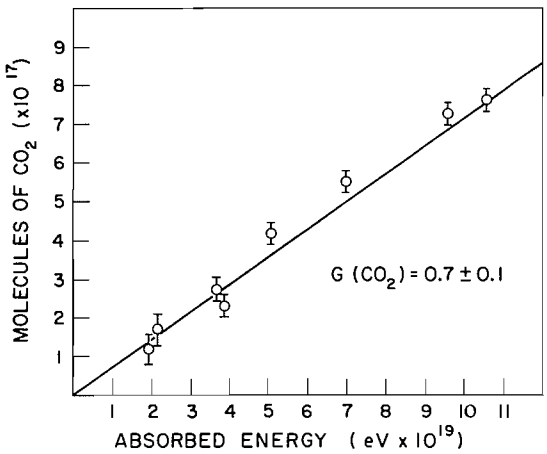

FIG. 1. Amount of carbon dioxide formed in the radiolysis of carbon monoxide at 10^{27} eV g^{-1} s^{-1}.

The propene and propane were Matheson research grade gases and were used without further purification other than outgassing thoroughly to remove non-condensible impurities.

Results

The amounts of carbon dioxide formed from high dose rate radiolysis of carbon monoxide at 760 Torr as a function of absorbed energy are shown in Fig. 1. The variation of absorbed energy was achieved by multiple pulse irradiations. As can be seen, the yield is independent of absorbed energy up to 10^{20} eV (1 to 8 pulses). The slope of the straight line gives $G(CO_2) = 0.7 \pm 0.1$.

Carbon suboxide was also formed in the radiolyses but in amounts not very much above the limit of detection of the gas chromatography method. The amount of carbon suboxide appeared to increase linearly with dose and $G(C_3O_2) \leqslant 0.02$.

Fairly small amounts of olefin added to the system rapidly reduced the yields of carbon dioxide. Figure 2 shows the effect of additions up to about 8 mole % added propene. The yields are not corrected for the increase in absorbed energy caused by the addition of propene. The limiting yield of carbon dioxide at high propene concentrations is $G(CO_2) = 0.02 \pm 0.02$.

Addition of up to 4.3 mole % propane had no effect on the carbon dioxide yield. The effects of propene and propane additions on the carbon dioxide yields are compared in Table 1. The mean yield in the presence of propane is identical with that observed in its absence.

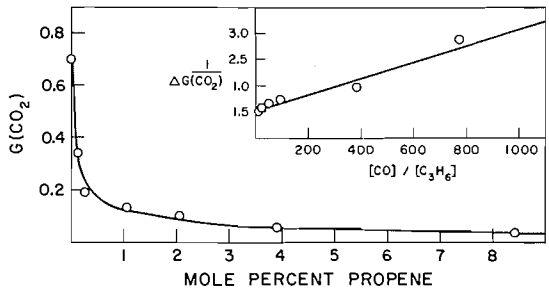

FIG. 2. Effect of propene on the yield of carbon dioxide in the radiolysis of carbon monoxide at 10^{27} eV g^{-1} s^{-1}. Inset shows Stern–Volmer plot of results.

TABLE 1

Comparison of effects of propene and propane on the carbon dioxide yield

Mole % additive	$G(CO_2)$ with added propene*	$G(CO_2)$ with added propane
0.0	0.70	0.70
0.6	0.16	0.62
1.3	0.11	0.75
2.6	0.07	0.69
4.3	0.05	0.70
		Mean 0.69

*Yields taken from Fig. 2.

Discussion

Carbon Dioxide Yield

The carbon dioxide yield, $G(CO_2) = 0.7 \pm 0.1$ at 10^{27} eV g^{-1} s^{-1} is in good agreement with the limiting yield of $G(CO_2) = 0.6 \pm 0.2$ reported by Anderson *et al.* (1) at a dose rate of 10^{21} eV g^{-1} s^{-1}.

There are four possible origins of this residual yield of carbon dioxide observed at high dose rates:

(*1*) Excited states of carbon monoxide

[3] $$CO^* + CO \rightarrow CO_2 + C$$

(*2*) Oxygen atoms in a ^3P state

[8] $$CO + O(^3P) \xrightarrow{(+ M)} CO_2$$

(*3*) Oxygen atoms in a ^1D state

[8′] $$CO + O(^1D) + M \rightarrow CO_2 + M$$

(*4*) CO^+ ions in states above ground

[9] $$CO^+ + CO \rightarrow CO_2 + C^+$$

As will be seen, we can eliminate the first three of these on fairly good grounds leaving the ionic mechanism as the remaining possibility.

(1) Excited States of Carbon Monoxide

It has been suggested that reaction 3 is the sole origin of the limiting yield of carbon dioxide at high dose rates (1).

The results shown in Fig. 2 show that $G(CO_2)$ can be almost completely suppressed by propene. It could be argued that this suppression is due to deactivation of CO* by the olefin, but it seems rather doubtful that such small amounts of olefin have so marked an effect. Small amounts of olefin do not suppress the formation of $C_2O(^3\Sigma)$ (15) in the pulse radiolysis of carbon monoxide where it is expected (8) to be formed from reaction 2. The lack of effect of propane on the carbon dioxide yields, shown in Table 1, strongly argues against deactivation as the explanation of the decrease in yields.

Slanger in a study of xenon-sensitized fluorescence of carbon monoxide (16) derives a value for the rate of reaction 3 as $k_3 = 1.2 \times 10^{-10}$ cm^3 molecule^{-1} s^{-1} based on known radiative lifetime data. If indeed deactivation of CO* were the explanation for the effect of propene then, using the relative rate constants obtainable from the Stern–Volmer plot in Fig. 2, propene would have to deactivate the excited carbon monoxide molecule with a rate constant some 300 times greater than the collision rate constant, which is not reasonable.

Reaction 3 probably does occur to a small extent in irradiated carbon monoxide. Slanger (16) observes radiation from $CO(d^3\Delta)$ and suggests deactivation of this by reaction 3. Bushmann and Groth (17), in studies of the radiolysis of carbon monoxide in both liquid and solid states, produce convincing evidence for reaction 3 but with very low yields which do not contradict the observations given in the present work.

(2) O(^{3}P) Atoms

It is possible that there could be residual oxygen atoms at high dose rates if reaction 10 is included in the reaction scheme. Under these

[10] $$C_2O + C_2O \rightarrow C_4O_2 \rightarrow \text{Polymer}$$

circumstances C_2O could be consumed independently of oxygen atoms and the residual oxygen atoms could then either react with the polymer or with carbon monoxide to form carbon dioxide.

Can. J. Chem. Downloaded from www.nrcresearchpress.com by 210.87.254.105 on 09/05/12
For personal use only.

Can. J. Chem. Downloaded from www.nrcresearchpress.com by 210.87.254.105 on 09/05/12
For personal use only.

In agreement with this, $C_2O(^3\Sigma)$ is known to disappear bimolecularly in both flash photolysis (18) and pulse radiolysis (8) systems.

The Stern–Volmer plot shown in Fig. 2 is based on the competition between propene and carbon monoxide for the precursor, (A), of carbon dioxide, reactions 11 and 12.

[11] $$CO + A \rightarrow CO_2$$

[12] $$C_3H_6 + A \rightarrow \text{no } CO_2$$

From the slope and intercept of the plot it can be derived that $k_{12}/k_{11} = 4 \times 10^2$.

Now if A is an $O(^3P)$ atom, using a value of $3.2 \pm 0.4 \times 10^{11}$ cm^3 mole^{-1} s^{-1} (19) for the rate constant of reaction of $O(^3P)$ with propene, then the rate constant for reaction 8 (which reaction 11 would then be equivalent to), based on the Stern–Volmer plot, would be 8×10^8 cm^3 mole^{-1} s^{-1}. Values in this range can be derived from high pressure combustion studies as has been discussed by Brabbs and Belles (20). However, Mahan and Solo (21), in a very careful study of the kinetics and light emission of the CO–$O(^3P)$ reaction, report $k_8 = 10^{10} \exp(-4000/RT)$ cm^3 mole^{-1} s^{-1} which at 25 °C is 9.0×10^6 cm^3 mole^{-1} s^{-1}. The work of Briggs and Clay (6, 7) where the yields of reaction 13 in carbon

[13] $$C_3H_6 + O(^3P) \rightarrow C_3H_6O \text{ type products}$$

monoxide were shown to be independent of propene concentration above 0.03 mole % propene, clearly contradicts these high values and supports that of Mahan and Solo.

(3) $O(^1D)$ Atoms

Reliable published rate constant data on the rate of reactions of $O(^1D)$ with C_3H_6, C_3H_8, and CO are not available, hence the possibility that the reduction of the CO_2 yield by propene reported here is due to reaction of $O(^1D)$ with C_3H_6 cannot be excluded. The lack of effect of C_3H_8 on the CO_2 yield appears, however, to exclude the possibility that the propyl alcohol formation during radiolysis of CO/C_3H_8 mixtures, observed by Briggs and Clay (6), is due to $O(^1D)$ formation; because no effect on $G(CO_2)$ is observed at propane contents where propyl alcohol formation is observed and $O(^1D)$ is known to react with CO to form CO_2 (22).

(4) CO^+ Ions

A possible source of carbon dioxide in irradiated carbon monoxide which cannot be discounted on present evidence is reaction 9.[5]

[9] $$CO^+ + CO \rightarrow CO_2 + C^+$$

On thermodynamic grounds, this reaction is not possible for CO^+ ions in a ground state ($X^2\Sigma^+$) but is possible for both CO^+ ($A^2\Pi$) and CO^+ ($B^2\Sigma^+$) (23). Reactions of $CO^+ + CO$ have been studied (23) and reaction 9 has been shown to occur with non-trivial cross-sections.

If this reaction 9 is the mode of formation of the residual carbon dioxide yield, the effect of propene would be explained by charge transfer[6] reaction

[15] $$CO^+ + C_3H_6 \rightarrow CO + C_3H_6^+$$

The equivalent reaction with propane would have to be slow.

Carbon Suboxide Yield

There is a small but certain yield of carbon suboxide formed in the radiolysis of carbon monoxide at the present dose rates. Presumably, it is formed via reaction 5

[5] $$C_2O + CO \rightarrow C_3O_2$$

It is well established that C_2O can exist in both singlet and triplet states of very different reactivities (24, 25) (probably $C_2O(^1\Delta)$ and $C_2O(^3\Sigma)$) and that deactivation of the singlet to the triplet, ground state is very slow indeed (24). The precursor of carbon suboxide in the high dose rate radiolysis of carbon monoxide is probably $C_2O(^1\Delta)$

[5′] $$C_2O(^1\Delta) + CO \rightarrow C_3O_2$$

In terms of spin conservation, it is expected that $C_2O(^3\Sigma)$ reacts much more slowly to form carbon suboxide than does $C_2O(^1\Delta)$. The yield of $C_2O(^1\Delta)$ can then be equated to the yield of carbon suboxide: that is $G(C_2O^1\Delta) = G(C_3O_2) \leqslant 0.02$. All $C_2O(^3\Sigma)$, at high dose rates will disappear via either reactions 6 or 10

[6] $$C_2O + O \rightarrow 2CO$$

[10] $$C_2O + C_2O \rightarrow C_4O_2 \rightarrow \text{Polymer}$$

---

[5]We should like to thank Dr. J. P. Briggs, Chemistry Division, National Research Council of Canada, Ottawa, for pointing out this possibility to us.

[6]Both charge transfer to C_3H_6 and C_3H_8 are thermodynamically exothermic. Ionizing potential (i.p.) for CO = 14.01 eV; C_3H_8 = 11.21 eV; C_3H_6 = 9.73 eV (see ref. 27).

This equating $G(C_2O^1\Delta)$ with $G(C_3O_2)$ neglects the possibility of disappearance of $C_2O(^1\Delta)$ by reaction 10′. If reaction 10′ were important,

[10′] $C_2O(^1\Delta) + C_2O(^1\Delta) \rightarrow$ polymer

then, at lower dose rates than those used in the present experiments, the yield of carbon suboxide should increase to a maximum yield equivalent to the total yield of $C_2O(^1\Delta)$.

Because of the uncertainty of their yields, the fates of carbon atoms, both singlet ($C(^1D)$, $C(^1S)$) and triplet ($C(^3P)$), in irradiated carbon monoxide remain uncertain. From the direct observation of the rate of disappearance of $C(^1S)$ by pulse radiolysis (8, 26) it would appear that carbon atoms do not react very rapidly with carbon monoxide. It is probable that they react with oxygen atoms at the present dose rates, reaction 7

[7] $C + O + M \rightarrow CO + M$

Alternatively, however, the carbon atoms may react to form polymer by some slow but undefined mechanism.

Conclusions

The observed yield of carbon dioxide and the effect of propene are tentatively explained in terms of reactions 9 and 15

[9] $CO^+ (A^2\Pi, \text{ or } B^2\Sigma^+) + CO \rightarrow CO_2 + C^+$

[15] $CO^+ + C_3H_6 \rightarrow CO + C_3H_6^+$

The other possible precursors of the residual yield of carbon dioxide observed at high dose rates, excited carbon monoxide, and $O(^1D)$ and $O(^3P)$ atoms, are eliminated on kinetic grounds.

The observed limiting yield of $G(C_3O_2) \leqslant 0.02$ is equated with the primary yield of $C_2O(^1\Delta)$ plus carbon atoms in singlet states.

1. A. R. Anderson, J. V. F. Best, and M. J. Willett. Trans. Faraday Soc. **62**, 595 (1966).
2. P. G. Clay, G. R. A. Johnson, and J. M. Warman. Discuss. Faraday Soc. **36**, 46 (1963).
3. S. Dondes, P. Harteck, and H. von Weyssenhoff. Z. Naturf. **19***a*, 13 (1963).
4. S. C. Lind and P. A. Rudolph. J. Chem. Phys. **33**, 705 (1960).
5. A. R. Anderson. Fundamental processes in radiation chemistry. *Edited by* P. Ausloos. J. Wiley, Publ., New York. 1968. p. 336.
6. J. P. Briggs and P. G. Clay. Int. J. Radiat. Phys. Chem. **1**, 67 (1969).
7. J. P. Briggs and P. G. Clay. Nature, **217**, 947 (1968).
8. C. Willis and C. Devillers. Chem. Phys. Lett. **2**, 51 (1968).
9. C. Willis, A. W. Boyd, and O. A. Miller. Can. J. Chem. **47**, 3007 (1969).
10. C. Willis, A. W. Boyd, and D. A. Armstrong. Can. J. Chem. **47**, 3783 (1969).
11. C. Willis, O. A. Miller, A. E. Rothwell, and A. W. Boyd. Advan. Chem. **81**, 539 (1968).
12. A. W. Boyd, C. Willis, and O. A. Miller. Can. J. Chem. **47**, 351 (1969).
13. K. D. Bayes. J. Amer. Chem. Soc. **84**, 4077 (1962).
14. R. N. Smith, R. A. Smith, and D. A. Young. Inorg. Chem. **5**, 145 (1966).
15. C. Willis and C. Devillers. Unpublished data.
16. T. G. Slanger. J. Phys. Chem. **48**, 586 (1968).
17. H. W. Buschmann and W. Groth. Chem. Phys. Lett. **2**, 245 (1968).
18. C. Devillers. Compt. Rend. **262***c*, 1485 (1966).
19. F. Kaufman. Prog. React. Kinet. **1**, 1 (1961).
20. T. A. Brabbs and F. E. Belles. 11th Symposium on Combustion, The Combustion Institute, Pittsburgh, Pennsylvania. 1967. p. 125.
21. B. H. Mahan and R. B. Solo. J. Chem. Phys. **37**, 2669 (1962).
22. O. F. Raper and W. B. DeMore. J. Chem. Phys. **40**, 1053 (1964).
23. J. J. Leventhal and L. Friedman. J. Chem. Phys. **46**, 997 (1967).
24. K. D. Bayes. J. Amer. Chem. Soc. **85**, 1730 (1963).
25. A. Forchioni and C. Willis. J. Phys. Chem. **72**, 3105 (1968).
26. G. M. Meaburn and D. Perner. Nature, **212**, 1042 (1966).
27. V. I. Vedeneyev, L. V. Gurvich, V. N. Kondrat'yev, V. A. Medredev, and Ye. L. Frankevich. Bond energies, ionization potentials, and electron affinities. (Translation) *Published by* Edward Arnold, London. 1966.

Can. J. Chem. Downloaded from www.nrcresearchpress.com by 210.87.254.105 on 09/05/12
For personal use only.

Can. J. Chem. Downloaded from www.nrcresearchpress.com by 210.87.254.5 on 09/05/12
For personal use only.

Branched-chain aminodeoxy sugars. Methyl 3-*C*-aminomethyl-2-deoxy-α-D-*ribo*-hexopyranoside and methyl 3-*C*-aminomethyl-2-deoxy-α-D-*arabino* hexopyranoside

ALEX ROSENTHAL AND KHONG-SENG ONG
Department of Chemistry, University of British Columbia, Vancouver, British Columbia

Received April 6, 1970

Addition of methyl 4,6-*O*-benzylidene-2-deoxy-α-D-*erythro*-hexopyranosid-3-ulose (**1**) to excess nitromethane and 1 molar equivalent of sodium methoxide in methanol gave methyl 4,6-*O*-benzylidene-2-deoxy-3-*C*-nitromethyl-α-D-*ribo*-hexopyranoside (**2**) and the *arabino* stereoisomer **3** in 63 and 22% yields, respectively. The proof of structure of the branched-chain deoxy nitro sugars is described. Debenzylidenation of the nitro sugars afforded the partially blocked nitro sugars **4** and **5**. Catalytic hydrogenation of the latter or of **2** and **3** yielded the branched-chain aminodeoxy sugars **7** and **9** (**7** characterized as its *N*-acetyl derivative and **9** as its *N*-2,4-dinitrophenyl derivative).

Canadian Journal of Chemistry, **48**, 3034 (1970)

We have recently reported in preliminary form (1) the synthesis of two branched-chain nitro sugars by an extension of the nitromethane synthesis (2) to methyl 4,6-*O*-benzylidene-2-deoxy-α-D-*erythro*-hexopyranosid-3-ulose (**1**). This paper describes the complete experimental details of this research and, in addition, reports the conversion of the nitro sugars into branched-chain aminodeoxy sugars.

Introduction of a branched-chain at C-3′ of the furanose ring of nucleosides has resulted in a striking modification of the biological activity of the nucleoside (3, 4).[1] Although aminoacyl nucleoside antibiotics (for example puromycin and amicetin) are known to be inhibitors of protein synthesis (5), there is no published report of the biological activity of aminoacyl nucleosides derived from branched-chain amino sugars. It therefore seemed of interest to develop a general method for the introduction of a branched-chain aminoalkyl group into sugars and to subsequently use these unusual sugars as intermediates in the synthesis of aminoacyl nucleosides.

Addition of 4,6-*O*-benzylidene-2-deoxy-α-D-*erythro*-hexopyranosid-3-ulose (**1**) (6) to an excess of nitromethane and 1 molar equivalent of sodium methoxide in methanol for 16 h at room temperature gave crystalline 4,6-*O*-benzylidene-2-deoxy-3-*C*-nitromethyl-α-D-*ribo*-hexopyranoside (**2**) and the *arabino* isomer (**3**) in 63 and 22% yields, respectively. Although the two nitro sugars were readily separable by fractional crystallization, chromatographic separations were very difficult because both had almost identical R_f's on silica gel G with different solvents as developers.

The structures of the nitro sugars **2** and **3** were ascertained by classical chemical conversions and were indicated on the basis of their circular dichroism (c.d.) spectra. The debenzylidenated nitro sugar **4** was converted by sulfonylation into the 6-*O*-*p*-toluenesulfonate **6**. The latter readily condensed with acetone to yield methyl 2-deoxy-3,4-*O*-isopropylidene-3-*C*-nitromethyl-6-*p*-tolylsulfonyl-α-D-*ribo*-hexopyranoside (**11**). This evidence confirms the presence of a *cis* glycol at C-3 and -4, and therefore compound **4** is undoubtedly methyl 2-deoxy-3-*C*-nitromethyl-α-D-*ribo*-hexopyranoside. On the other hand, the monosulfonate of **5** did not yield the corresponding 3,4-*O*-isopropylidene derivative; thus indicating that compound **5** is probably the *arabino* isomer. Based on the facts that the spectrum of the nitro sugar **2** showed a negative c.d. maxima, whereas the spectrum of its stereoisomer **3** exhibited a slight positive (essentially zero) maxima, it might be inferred that **2** and **3** are the *ribo* and *arabino* isomers, respectively (7).

Debenzylidenation of the nitro sugars **2** and **3** presented a problem of unexpected difficulty. Although removal of the benzylidene group from **2** and **3** was readily carried out with Dowex 50 W-X8 (H^+) resin to afford the nitro sugars **4** and **5** in high yield, it was essential that the reaction be stopped immediately after disappearance of the starting material (monitored by t.l.c.) to prevent isomerization of the product. Utilization of Reynn 101 (H^+) resin as the debenzylidenation reagent gave a much lower yield of product (about 27%). Use of aqueous acetic acid

[1]Biological tests were carried out on the nucleosides of the branched-chain sugars.

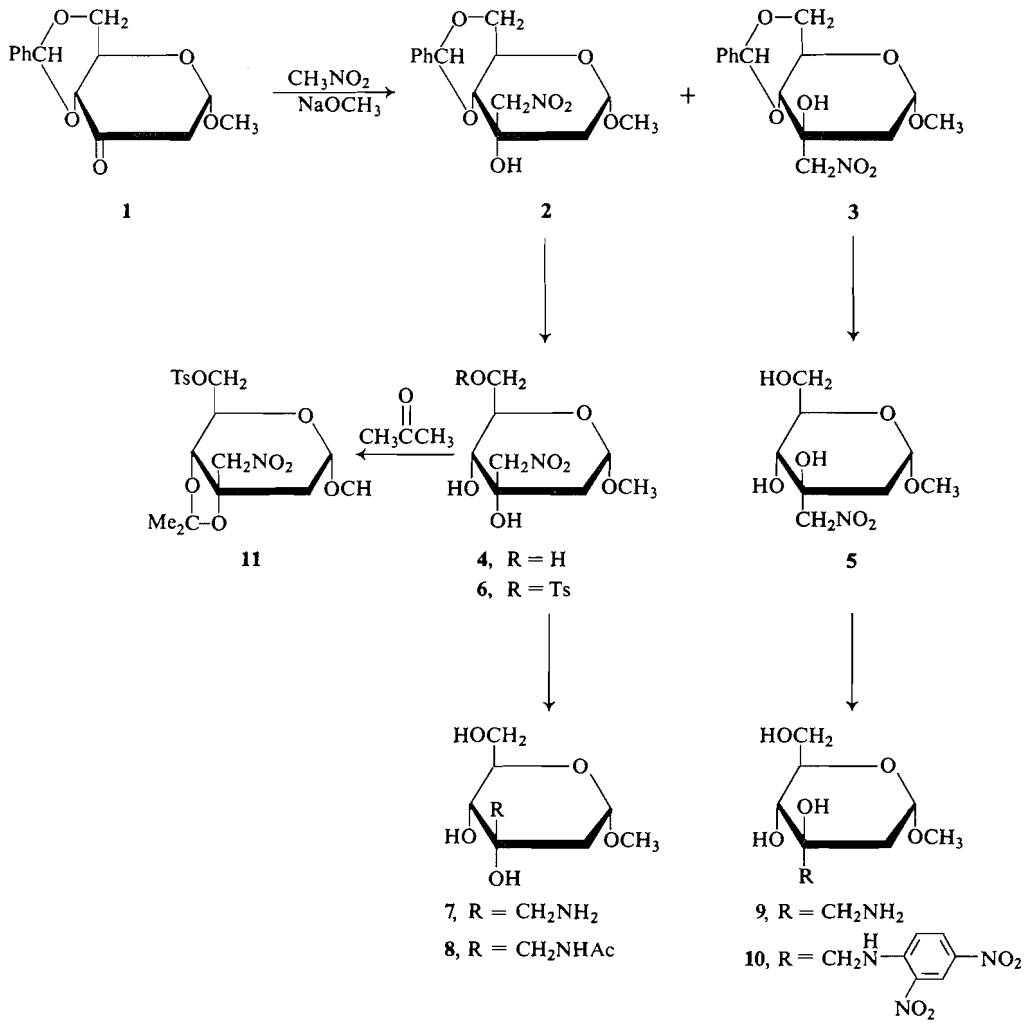

for the hydrolysis of **2** and **3** is to be avoided because mixtures of products were obtained. Catalytic debenzylidenation of **2** over 10% palladium-on-charcoal gave the free amino sugar **7**.

Sulfonylation of **4** with 1.1 molar equivalents of *p*-toluenesulfonyl chloride did not selectively sulfonylate the primary hydroxyl of **4**. A mixture of two monosulfonates was obtained which was separated by silica gel column chromatography with chloroform–ether as developer. The faster-moving sulfonate was deduced to be the 6-*O*-*p*-toluenesulfonate **6** on the basis of its n.m.r. spectrum (H-6 was shifted 42 c.p.s. downfield). No attempt was made to determine the structure of the slower-moving component as it was not needed in the determination of the structure of **2**.

Although the p.m.r. spectra of **2** and **3** could not be used to determine the structure of the nitro sugars (no hydrogen attached to C-3), their spectra were different enough to merit a brief discussion (see Experimental). The n.m.r. of the *arabino* isomer **3** showed the expected two quartets at τ 7.60 and 8.05 which are attributed to H-2*e* and -2*a* (8–10). Geminal hydrogens on C-2 of 2-deoxy pyranosides usually have large coupling ($J \simeq 14$ Hz), and there is usually a considerable downfield shift of H-2*e* with respect to H-2*a*. The downfield shift of H-2*e* of **3** is attributed to the strong deshielding effect of the nitromethyl group on C-3. On the other hand, the H-2*a* and -2*e* signals of the *ribo* stereoisomer **2** overlapped each other and occurred at τ 7.70–7.85. Because both stereoisomers **2** and **3** must

Can. J. Chem. Downloaded from www.nrcresearchpress.com by 210.87.254.5 on 09/05/12
For personal use only.

Can. J. Chem. Downloaded from www.nrcresearchpress.com by 210.87.254.5 on 09/05/12
For personal use only.

exist in a locked-chair conformation due to the benzylidene group on C-4 and -6, the upfield chemical shift of H-2*e* and downfield shift of H-2*a* of **2** might be due to a fortuitous equalization of the electronic effects of the nitromethyl and hydroxyl groups.

The branched-chain aminodeoxy sugars **7** and **9** were produced from the nitro sugars **2** and **3** in two different routes. In the first procedure the debenzylidenated nitro sugar **4** was reduced over pre-hydrogenated platinum oxide in the presence of hydrochloric acid to give in almost quantitative yield the aminodeoxy sugar **7** as a hydrate. After removal of water of hydration, **7** was converted into its *N*-acetyl derivative **8**. In the second procedure the blocked nitro sugar **2** was simultaneously debenzylidenated and reduced with hydrogen over 10% palladium-on-charcoal to yield the aminodeoxy sugar **7** in 86% yield. Similar deblocking of the nitro sugar **3** over Dowex 50 W-X8 (H^+) followed by catalytic reduction of the unblocked nitro sugar over platinum oxide gave the aminodeoxy sugar **9** in 75% yield. The latter was characterized as its *N*-2,4-dinitrophenyl derivative **10**.

Because the acetylated derivatives of the nitro sugars **2** and **3** proved to be unstable, no attempt was made to utilize them in nucleoside synthesis. The *N*-acetyl derivative of the aminodeoxy sugar could not be utilized because of the participation of the *N*-acetyl group to form a compound having nitrogen in the ring (11).

Experimental

General Considération

The n.m.r. spectra were obtained in chloroform-*d* solution (unless otherwise stated), with tetramethylsilane as the internal standard (set at τ 10) by using a Jeolco 60 or Varian HA-60 spectrometer (s, singlet; d, doublet; t, triplet; q, quartet; m, multiplet). The i.r. spectra were obtained with a Perkin–Elmer Model 457 spectrometer. The c.d. spectra were measured with a Jasco Model ORD/UV-5 spectropolarimeter. All melting points (micro hot stage) are corrected. Solutions were concentrated *in vacuo*. Silica gel G was used for t.l.c. and column chromatography. Elemental analyses were performed by the microanalytical laboratory of the University of British Columbia, Vancouver, B.C.

Reaction of Methyl 4,6-O-Benzylidene-2-deoxy-α-D-erythro-hexopyranosid-3-ulose (1) with Nitromethane to Yield Methyl 4,6-O-Benzylidene-2-deoxy-3-C-nitromethyl-α-D-ribo-hexopyranoside (2) and Methyl 4,6-O-Benzylidene-2-deoxy-3-C-nitromethyl-α-D-arabino-hexopyranoside (3)

A 1 *M* solution of sodium methoxide in methanol (5.3 ml, 5.3 mmoles) was added dropwise with stirring to a solution of compound **1** (1.35 g, 5.3 mmoles) in 35 ml of anhydrous nitromethane. The reaction mixture was stirred for 16 h at room temperature and then was deionized with IR 120 (H^+) resin and the filtrate was evaporated to a solid. The t.l.c. of the product on silica gel with 4:1 chloroform–ether revealed two spots with R_f's of 0.57 and 0.52. Fractional crystallization (twice) of the product from ethyl acetate – petroleum ether (b.p. 30–60°) gave methyl 4,6-*O*-benzylidene-2-deoxy-3-*C*-nitromethyl-α-D-*ribo*-hexopyranoside (**2**) (1.03 g, 63%); m.p. 192–194°; $[\alpha]_D^{22}$ +88° (*c* 2, chloroform); R_f 0.57; v (0.005 *M* CCl_4) 3600 (OH), 1550 (NO_2); c.d. (*c* 0.0006, methanol) $[\theta]_{285}$ −1100; τ ($CDCl_3$) 4.40 (s, CHPh), 5.1 (q, H-1), 5.4 (an AB system, $J_{a,b}$ = 13 Hz, methylene protons a and b on C-1′), 5.5–6.4 (m), 6.6 (s, OCH_3), 7.7 (q, H_{2e}, $J_{2e,2a}$ = 7 Hz), 7.85 (q, H_{2a}, $J_{2a,2a}$ = 7 Hz).

Anal. Calcd. for $C_{15}H_{19}NO_7$: C, 55.38; H, 5.89; N, 4.31. Found: C, 55.22; H, 5.88; N, 4.28.

After the combined mother liquors from the crystallizations of **2** were evaporated to dryness, the residue was dissolved in ethanol (25 ml) and water then added dropwise to the point of incipient turbidity. Methyl 4,6-*O*-benzylidene-2-deoxy-3-*C*-nitromethyl-α-D-*arabino*-hexopyranoside (**3**) crystallized after standing at 0° for several hours, 0.37 g (22%); m.p. 117–118°; $[\alpha]_D^{22}$ +69° (*c* 2, chloroform); v (0.005 *M* CCl_4), 3500 (OH); c.d. (*c* 0.002, methanol) $[\theta]_{270-280}$ 0; τ ($CDCl_3$) 4.45 (s, CHPh), 5.02 (an AB system, $J_{a,b}$ = 13 Hz, methylene protons a and b on C-1′), 5.18 (q, H-1), 5.3–6.38 (m), 6.6 (OCH_3), 7.6 (q, H_{2e}, $J_{2e,2a}$ = 14 Hz, $J_{2e,1e}$ = 1 Hz), 8.05 (q, H_{2a}, $J_{2a,2e}$ = 14 Hz, $J_{2a,1e}$ = 4.3 Hz).

Anal. Calcd. for $C_{15}H_{19}NO_7$: C, 55.38; H, 5.89; N, 4.31. Found: C, 55.26; H, 5.79; N, 4.38.

Attempted Preparation of Methyl 3-O-Acetyl-4,6-O-benzylidene-2-deoxy-3-C-nitromethyl-α-D-ribo-hexopyranoside

Compound **2** was allowed to react with acetic anhydride (0.5 ml) and *p*-toluenesulfonic acid monohydrate (0.022 g) at room temperature overnight. After addition of ice-cold aqueous sodium hydrogen carbonate the product was extracted with chloroform (3 × 50 ml). Work-up of the product in the usual way gave a mixture of three components. The major component (presumed to be the 3-*O*-acetate) was found to be unstable on silica with 9:1 benzene – ethyl acetate as developer. Treatment of **2** with acetic anhydride and pyridine gave unchanged starting material.

Debenzylidenation of 2 to Yield Methyl 2-Deoxy-3-C-nitromethyl-α-D-ribo-hexopyranoside (4)

The nitro sugar **2** (0.300 g) dissolved in 25 ml methanol was allowed to react under reflux for 1 h (or until no starting material remained) with methanol pre-washed Dowex 50WX-8(H^+) (1.2 g). Careful monitoring of the reaction was essential to avoid excessive isomerization of the product. The resin was removed by filtration and the residue evaporated to dryness. Water (10 ml) was added to the residue and the solution treated with a small amount of charcoal. After the water was evaporated from the filtrate the residue was treated with ethanol followed by benzene. The solvents were evaporated under vacuum to remove water. The residual syrup (0.202 g,

Can. J. Chem. Downloaded from www.nrcresearchpress.com by 210.87.254.5 on 09/05/12
For personal use only.

90%), was crystallized first from ethanol – light petroleum ether (b.p. 30–60°), and then from ethyl acetate – petroleum ether (b.p. 30–60°); m.p. 105–106°; $[\alpha]_D^{22}$ +85° (*c* 2, ethanol); τ (D_2O) 5.2 (q, H-1), 5.5 (CH_2NO_2), 6.32 (CH_2OH), 6.2–6.7 (overlapping peaks, H-5, H-4), 6.7 (s, OCH_3), 8.0–8.1 (H-2).

Anal. Calcd. for $C_8H_{15}NO_7$: C, 40.51; H, 6.32; N, 5.91. Found: C, 40.48; H, 6.44; N, 5.90.

An attempt to debenzylidenate **2** with 70% acetic acid on the steam bath for 30 min gave incomplete debenzylidenation. Two debenzylidenated products were formed.

Hydrogenation of **2** over platinum oxide in the presence of 0.1 *N* hydrochloric acid afforded a mixture of three products. One of the components was an amino sugar (positive ninhydrin test).

Debenzylidenation of **2** with Rexyn (101 H^+) resin gave 27% yield of **4**.

*Debenzylidenation of **3** to Yield Methyl 2-Deoxy-3-C-nitromethyl-α-D-arabino-hexopyranoside (**5**)*

The nitro sugar **3** was debenzylidenated in the same way as already described to give **5** as a syrup, $[\alpha]_D^{22}$ +126° (*c* 1, methanol).

Anal. Calcd. for $C_8H_{15}NO_7 \cdot 1/2H_2O$: C, 39.02; H, 6.55; N, 5.69. Found: C, 38.93; H, 6.52; N, 5.48.

*Catalytic Reduction of **4** to Yield Methyl 3-C-Aminomethyl-2-deoxy-α-D-ribo-hexopyranoside (**7**)*

The nitro sugar **4** (200 mg), dissolved in 0.1 *N* HCl (10 ml) was hydrogenated in the presence of prehydrogenated platinum oxide (100 mg) until no further up-take of hydrogen was observed. After filtration the solution was passed through a column of Dowex 50WX-8(H^+) (5 ml). The resin was washed with water until the eluent was neutral and chloride-free. Elution of the column with 0.6 *M* ammonium hydroxide, followed by evaporation of the basic eluent, gave 180 mg of the amino sugar 7 as a foam. This amino sugar was hygroscopic and was dried under high vacuum for 6 h prior to analysis, $[\alpha]_D^{22}$ +79° (*c* 2, water), τ (D_2O) 5.02 (q, H-1), 6.1–6.4 (m), 6.6 (s, OCH_3), 7.2 (d, CH_2NH_2).

Anal. Calcd. for $C_8H_{17}NO_5$: C, 46.31; H, 8.22; N, 6.76. Found: C, 46.11; H, 8.38; N, 6.71.

*Methyl 3-Acetamidomethyl-2-deoxy-α-D-ribo-hexopyranoside (**8**)*

The amino sugar **7** (0.100 g) was acetylated with a mixture of 0.2 ml of acetic anhydride and 5 ml of anhydrous methanol at room temperature for 3 h (until ninhydrin negative). After evaporation of the volatile components the residue was treated with several portions of toluene followed by subsequent evaporations to yield 0.087 g of **8** as a syrup, $[\alpha]_D^{22}$ +71° (*c* 3, water); τ (D_2O) 5.1 (q, H-1), 5.9–6.4 (m), 6.5 (s, CH_2NH_2), 6.68 (s, OCH_3), 7.98 (s, CH_3C), 7.8–8.5 (H-2).

*Catalytic Debenzylidenation and Reduction of **2** to Yield **7***

The blocked nitro sugar **2** (0.200 g) in 5 ml ethanol was allowed to react with hydrogen in the presence of 10% palladium-on-charcoal (0.100 g) in the usual way to yield **7** (0.110 g) in almost pure form.

When platinum oxide was used as a catalyst a mixture (as evidenced by its n.m.r. spectrum) of two products in almost equal amounts was obtained which were not separated.

*Methyl 2-Deoxy-3-C-methylamino-α-D-arabino-hexopyranoside (**9**) and Methyl 2-Deoxy-3-C-methyl(2,4-dinitroanilino)-α-D-arabino-hexopyranoside (**10**)*

The debenzylidenated nitro sugar **5** (0.26 g) was hydrogenated in 11 ml of 0.1 *N* HCl over platinum oxide (pre-reduced) in the usual way to give 0.176 g (75%) of the amino sugar **9** as a syrup, $[\alpha]_D^{22}$ +41° (*c* 2, ethanol); τ (D_2O) 4.98 (q, H-1), 6–6.4 (m), 6.52 (s, OCH_3), 6.78 (d, H-2, CH_2NH_2), 7.73 (H_{2e}, $J_{2e,2a}$ = 12 Hz, $J_{2e,1e}$ = 2 Hz), 8.13 (H_{2a}, $J_{2a,2e}$ = 12 Hz, $J_{2a,1e}$ = 4 Hz).

The amino sugar **9** (0.10 g) in 2 ml ethanol was allowed to react with 1-fluoro-2,4-dinitrobenzene (0.13 g) in the presence of sodium hydrogen carbonate (0.10 g) with stirring at room temperature until no starting material remained (monitored by t.l.c. with 9:1 benzene–ethanol as developer). After evaporation of the ethanol, water (2 ml) was added and the amino derivative extracted with chloroform. After evaporation of the chloroform, the residue was purified by preparative t.l.c. with 9:1 benzene–ethanol as developer. The product was crystallized from ethyl acetate – petroleum ether (b.p. 30–60°) to yield 0.035 g of crystalline material, m.p. 145–147°, $[\alpha]_D^{22}$ +139° (*c* 2, ethanol).

Anal. Calcd. for $C_{14}H_{19}N_3O_9$: C, 45.04; H, 5.13; N, 11.26. Found: C, 45.16; H, 5.08; N, 11.58.

*Methyl 2-Deoxy-3,4-O-isopropylidene-3-C-nitromethyl-6-O-p-tolylsulfonyl-α-D-ribo-hexopyranoside (**11**)*

To a solution of 0.300 g of the nitro sugar **4** in 5 ml of anhydrous pyridine was added 0.290 g (1.1 molar equivalent) of *p*-toluenesulfonyl chloride. The reaction mixture, protected from moisture, was kept at 0° for 3 h and then left overnight at room temperature. Two separate portions of toluene were added to the reaction mixture and were evaporated off to remove pyridine. Water (5 ml) was then added and the aqueous mixture extracted with chloroform (3 × 10 ml). The combined chloroform extract was washed with aqueous sodium hydrogen carbonate, water, and then dried (sodium sulfate). Evaporation of the filtrate gave a syrup (0.610 g). The t.l.c. of the residue, with 4:1 chloroform–ether as developer, showed the presence of two products but no starting material. Column chromatography of the residue on 60 g of silica gel (activity II) with 9:1 chloroform–ether as developer gave 0.135 g of the faster-moving sulfonate **6**, $[\alpha]_D^{22}$ +158° (*c* 2, chloroform) and 0.119 g of a slower-moving component, $[\alpha]_D^{22}$ +54° (*c* 2, chloroform) which was probably the 4-*O*-tosyl derivative of **4**; τ ($CDCl_3$) (of **6**) 5.16 (H-1, q), 5.35–5.5 (CH_2NO_2), 5.65 (d, CH_2OTs), 6.0–6.5 (overlapping peaks = 2H), 6.63 (s, OCH_3), 6.7–7.5 (OH, broad), 7.56 (s, $CH_3C_6H_4$), 7.7–8.2 (H-2); τ ($CDCl_3$ + D_2O) (of **6**), OH peaks disappeared.

The monosulfonate **6** (0.070 g) was allowed to react with stirring with anhydrous acetone (2 ml), anhydrous copper sulfate (0.160 g), and a trace of concentrated sulfuric acid overnight at room temperature. The course of the reaction was followed by t.l.c. with 4:1 chloroform–ether as developer. The reaction mixture was neutralized with solid barium carbonate. After filtration and evaporation of the filtrate the residue (0.065 g) was chromatographed on 6 g of silica gel (activity II) with 9:1 chloroform–ether to give 0.030 g of the 3,4-*O*-isopropylidene derivative **11**, $[\alpha]_D^{22}$ +83° (*c* 2, chloroform); τ ($CDCl_3$)

8.6 (d, CMe_2), 7.5–8.4 (H-2), 7.5 (s, $CH_3C_6H_4$), 6.65 (s, OCH_3), 5.6–6.1 (two m), 5.5 (s, CH_2NO_2), 5.25 (q, H-1), 2.17–2.7 (q, C_6H_4—CH_3).

Anal. Calcd. for $C_{18}H_{25}NO_9S \cdot 1/2H_2O$: C, 49.07; H, 5.95; N, 3.17. Found: C, 49.01; H, 6.14; N, 2.78.

This research was supported by the National Research Council of Canada.

1. A. Rosenthal and Khong-Seng Ong. Tetrahedron Lett. 3981 (1969).
2. H. H. Baer. Advan. Carbohyd. Chem. **24**, 67 (1969).
3. E. Walton, S. R. Jenkins, R. F. Nutt, M. Zimmerman, and F. W. Holly. J. Amer. Chem. Soc. **88**, 4524 (1966).
4. A. Rosenthal and L. Nguyen. J. Org. Chem. **34**, 1029 (1969).
5. J. J. Fox, K. A. Watanabe, and A. Block. Progr. in Nucleic Acid Res. and Mol. Biol. **5**, 251 (1966).
6. A. Rosenthal and P. Catsoulacos. Can. J. Chem. **46**, 2868 (1968).
7. C. Satoh, A. Kujomoto, and T. Okuda. Carbohyd. Res. **5**, 140 (1967).
8. R. U. Lemieux and S. Levine. Can. J. Chem. **42**, 1473 (1964).
9. S. Hanessian. Advan. Carbohyd. Chem. **21**, 143 (1966).
10. A. Rosenthal. Advan. Carbohydrate Chem. **23**, 59 (1968).
11. H. Paulsen and K. Todt. Advan. Carbohyd. Chem. **23**, 116 (1968).

Can. J. Chem. Downloaded from www.nrcresearchpress.com by 210.87.254.5 on 09/05/12
For personal use only.

Can. J. Chem. Downloaded from www.nrcresearchpress.com by 210.87.254.40 on 09/05/12
For personal use only.

Etude par résonance magnétique nucléaire à température variable de composés apparentés au méthylènecyclohexane

MICHEL BERNARD ET MAURICE ST-JACQUES
Département de Chimie, Université de Montréal, Montréal, Québec

Reçu le 27 avril 1970

Des modifications ont été observées dans le spectre r.m.n. à basse température des difluorométhylènecyclohexane, isopropylidènecyclohexane, et dichlorométhylènecyclohexane. Les barrières d'interconversion conformationnelles $\Delta F^{\ddagger}$ de ces composés ont été calculées et sont discutées.

Spectral modifications have been observed in the n.m.r. spectra of difluoromethylenecyclohexane, isopropylidenecyclohexane, and dichloromethylenecyclohexane. The free energy barriers for conformational interconversion in these compounds have been estimated and are discussed.

Canadian Journal of Chemistry, **48**, 3039 (1970)

Introduction

Les barrières d'inversion conformationnelles des cycles à six chaînons ont été largement étudiées au cours des dernières années par r.m.n. à basse température (1). Le comportement des systèmes cyclohexaniques possédant un seul atome de carbone hybridé sp^2 présente un grand intérêt, cette géométrie correspondant au squelette de la cyclohexanone.

Les travaux de Jensen et Beck (2) et Gerig et Rimerman (3) ont montré que l'inversion de la cyclohexanone ne pouvait être étudiée à l'aide de cette technique, l'énergie libre d'activation mise en jeu étant trop faible. Par contre, le ralentissement de l'inversion du méthylènecyclohexane (**1**) a été mis en évidence par ces auteurs à une température inférieure à -100 °C environ. D'après Gerig et Rimerman (3), la symétrie du spectre r.m.n. à basse température du tétradeutério-3,3,5,5 méthylènecyclohexane ainsi que les déplacements chimiques et les constantes de couplage dans le cas du dideutério-4,4 méthylènecyclohexane sont dus à une conformation chaise, voisine de celle du cyclohexane.

Dans le cadre d'une étude de l'influence de différents groupements exométhylèniques substitués sur la conformation privilégiée des dérivés du diméthylène-1,4 cyclohexane (4) nous avons préparé les composés **2**, **3**, et **4** pour nous en servir comme modèles.

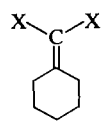

1 X = H
2 X = F
3 X = CH_3
4 X = Cl

Les résultats de l'étude r.m.n. à basse température de ces composés sont étroitement reliés à l'origine de l'inversion du cycle dans cette classe de composés et font l'objet du présent article.

Résultats

Les spectres r.m.n. du difluorométhylènecyclohexane (**2**), de l'isopropylidènecyclohexane (**3**), et du dichlorométhylènecyclohexane (**4**) ont présenté des modifications à basse température.

A la température de 24 °C, le spectre à 100 MHz de **2** (fig. 1) consiste en deux massifs non résolus centrés à $\delta = 2.09$ p.p.m. (quatre protons) et 1.53 p.p.m. (six protons). Ces signaux sont respectivement attribués aux protons des atomes de carbone en position 2 et 6, et à ceux des carbones en position 3, 4, et 5. Lorsque la température de l'échantillon est abaissée, les deux signaux s'élargissent et à partir de -126 °C, le spectre se transforme pour donner finalement à -150 °C quatre massifs larges centrés à 2.48, 2.36, 1.79, et 1.27 p.p.m.

Les pics centrés à 1.79 et 1.27 p.p.m. sont dus au dédoublement du signal centré à 1.53 p.p.m. à température ambiante. La largeur des raies est due à des couplages "spin–spin" importants entre les protons. La différence de déplacement chimique entre protons axiaux et équatoriaux à basse température $\Delta\nu = 0.52$ p.p.m. peut être comparée à la valeur de 0.48 p.p.m. observée dans le cas du cyclohexane (5). La température de coalescence observée est de -128 °C.

De même, le signal dû aux protons en α de la double liaison est dédoublé en un système du type AB (6) dont seule la moitié gauche peut être nettement observée à 2.48 et 2.36 p.p.m., l'autre moitié coincidant avec le pic des protons équa-

Can. J. Chem. Downloaded from www.nrcresearchpress.com by 210.87.254.40 on 09/05/12
For personal use only.

toriaux en position 3, 4, et 5 (1.79 p.p.m.). La constante de couplage entre protons géminés est d'environ 12.5 Hz, la différence de déplacement chimique entre proton axial et proton équatorial est de 65 Hz. La température de coalescence pour cette partie du spectre est de −126 °C.

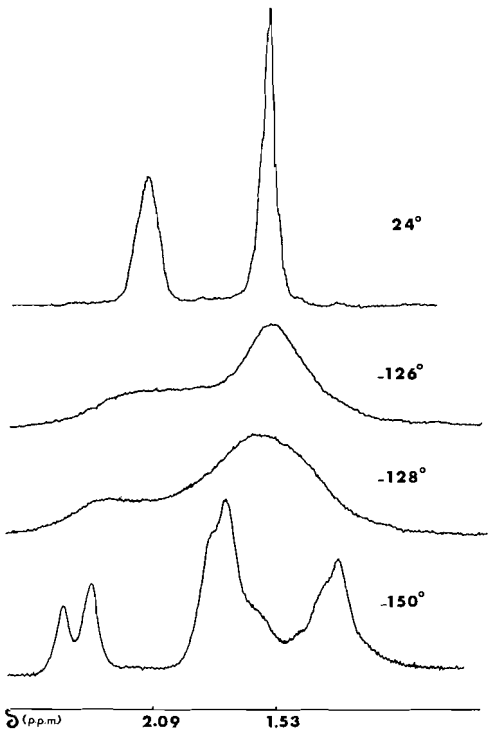

FIG. 1. Spectre r.m.n. à 100 MHz du difluorométhylènecyclohexane (**2**) à différentes températures. Concentration: 4% en volume dans un mélange CHF_2Cl (15%), $CH_2{=}CHCl$ (85%). L'échelle est en p.p.m. relativement au TMS.

La constante de vitesse de l'équilibre conformationnel est calculée pour chacune des températures de coalescence. Le changement d'allure du massif centré à 1.53 p.p.m. peut être considéré comme un système "à deux raies" avant coalescence, tel que l'équation: $k = \pi\Delta\nu/\sqrt{2}$ (7) permet une bonne estimation de la constante de vitesse. Pour un système AB coalescant en un singulet, l'équation utilisée est: $k = \pi(6J^2 + \Delta\nu^2)^{1/2}/\sqrt{2}$ (8) où $\Delta\nu$ est la différence de déplacement chimique à basse température et J, la constante de couplage. Il est donc possible de calculer $k = 159\ s^{-1}$ à −126 °C et $k = 116\ s^{-1}$ à −128 °C. L'énergie libre d'activation conformationnelle calculée à partir de ces valeurs est de 6.7 kcal/mole.[1] L'incertitude sur la valeur de $\Delta F^{\ddagger}$ est probablement de l'ordre de ±0.5 kcal/mole (2).

La fig. 2 représente le spectre à 100 MHz de **3** en fonction de la température. A température ordinaire, les protons du cycle donnent deux massifs centrés à 1.52 p.p.m. (six protons, positions 3, 4, et 5) et 2.16 p.p.m. (quatre protons, positions 2 et 6); les protons des groupes méthyles se trouvent à 1.64 p.p.m. (six protons). Lorsque la température décroît, les signaux centrés à 1.52 et 2.16 p.p.m. s'élargissent puis se dédoublent alors que la forme du signal des méthyles reste inchangée. A −159 °C, du fait de l'encombrement du spectre vers 1.65 p.p.m., une analyse précise des systèmes dédoublés n'a pu être entreprise. Les différences de déplacement chimique sont calculées dans l'hypothèse où le dédoublement des raies est symétrique par rapport au

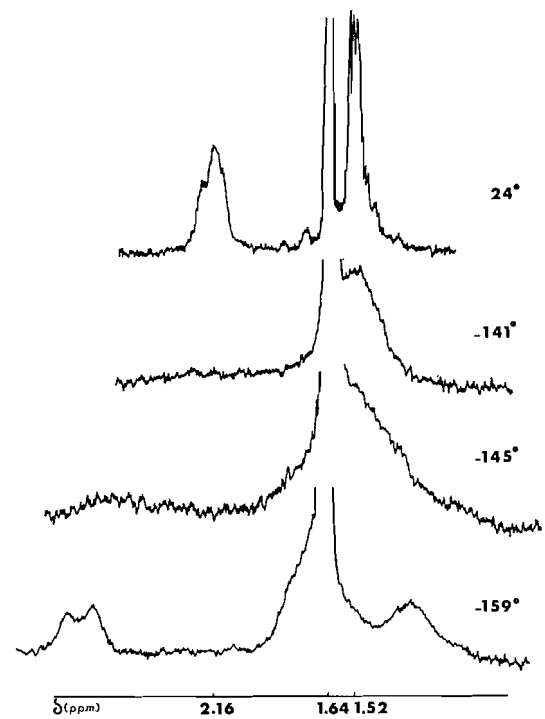

FIG. 2. Spectre r.m.n. à 100 MHz de l'isopropylidènecyclohexane (**3**) à différentes températures. Concentration: 3% dans CHF_2Cl (15%), $CH_2{=}CHCl$ (85%).

[1]L'énergie $\Delta F^{\ddagger}$ est calculée en utilisant un coefficient de transmission égal à 1/2 dans l'équation d'Eyring. L'énergie libre ainsi calculée correspond à la barrière d'inversion entre la forme chaise et une forme bateau, cette dernière représente un intermédiaire métastable au cours de l'interconversion conformationnelle.

Can. J. Chem. Downloaded from www.nrcresearchpress.com by 210.87.254.40 on 09/05/12
For personal use only.

signal correspondant à température ordinaire, soit en négligeant la variation possible du déplacement chimique avec la température.

A -159 °C, seule la moitié droite du système dû aux protons en position 3, 4, et 5 peut être observée à 1.24 p.p.m., la moitié gauche est trop proche du pic des protons méthyliques pour être distinguée. La coalescence a lieu à -146 °C pour cette partie du spectre, en utilisant $\Delta\nu \approx 55$ Hz, la constante de vitesse calculée est de 122 s^{-1} à cette température. De même, les protons en α de la double liaison montrent seulement un doublet vers 2.71 p.p.m. ($J \approx 12$ Hz), la moitié droite du système AB correspondant est vraisemblablement située dans la région 1.70–1.60 p.p.m. La température de coalescence observée est de -141 °C, avec un $\Delta\nu$ estimé à 110 Hz, la constante de vitesse est de 244 s^{-1}. L'énergie libre d'activation d'interconversion conformationnelle est de 5.8 ± 0.5 kcal/mole.

Enfin, le même type de modification a été observé dans le spectre à basse température de **4** (fig. 3). Le spectre r.m.n. à température ordinaire consiste en deux massifs non résolus centrés à $\delta = 2.33$ p.p.m. (quatre protons) et 1.51 p.p.m. (six protons). Les protons des carbones en position 3, 4, et 5 (1.51 p.p.m. à température ordinaire) donnent à -160 °C deux massifs centrés à 1.66 et 1.35 p.p.m. soit un $\Delta\nu \approx 0.31$ p.p.m. pour une température de coalescence de -157 °C. Etant donné la proximité de la coalescence, il semble qu'à -160 °C, la séparation entre les deux signaux n'ait pas atteint sa valeur maximale, probablement voisine de 0.50 p.p.m. L'enregistrement du spectre aux températures inférieures à -160 °C n'a pas été possible du fait de la cristallisation partielle de la solution. La constante de vitesse à la température de coalescence est de 110 s^{-1} environ, en utilisant $\Delta\nu = 50$ Hz.

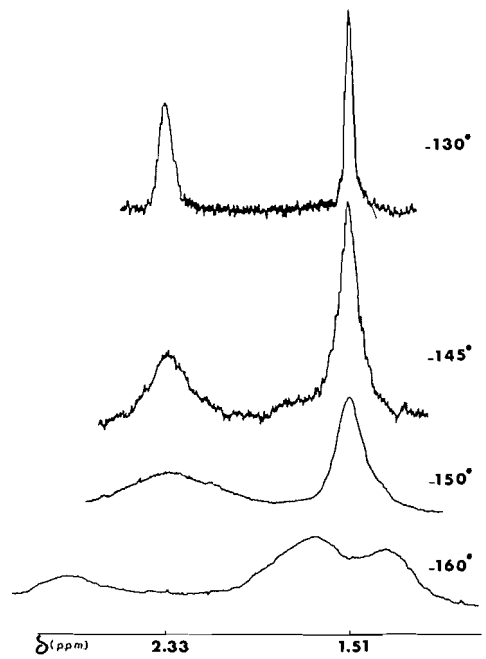

FIG. 3. Spectre r.m.n. à 100 MHz du dichlorométhylènecyclohexane (4) à différentes températures. Concentration: 2% dans CHF_2Cl (15%), $CH_2{=}CHCl$ (85%).

Les protons en α de la double liaison résonnent à 2.33 p.p.m. à la température ambiante; à -160 °C, seule la moitié gauche du système dédoublé peut être observée sous forme d'un massif centré vers 2.77 p.p.m. L'autre moitié forme un épaulement peu visible dans le massif centré à 1.66 p.p.m. La température de coalescence est de -152 °C, la valeur de k à cette température est de 200 s^{-1} avec $\Delta\nu \approx 90$ Hz. L'énergie libre d'activation conformationnelle est de 5.4 ± 0.5 kcal/mole pour **4**.

Discussion

Il a été établi que la conformation de **1** dans l'état fondamental est une forme chaise (3) et il est vraisemblable que ceci soit également le cas pour **2**, **3**, et **4**. Le processus d'interconversion conformationnelle responsable des modifications spectrales observées pour les molécules **1** à **4** est donc une inversion du cycle analogue à celle du cyclohexane (9, 10). Les énergies libre d'activation conformationnelle $\Delta F^{\ddagger}$ de ces composés sont rassemblées dans le tableau 1.

Gerig et Rimerman (3) ont comparé la différence de $\Delta F^{\ddagger}$ entre le cyclohexane et le méthylènecyclohexane, soit 2 kcal/mole environ, avec la différence entre les barrières de rotation

TABLEAU 1

Energies libres d'activation conformationnelles du cyclohexane, du méthylènecyclohexane, et de composés apparentés

Molécule	$\Delta F^{\ddagger}$ (kcal/mole)	Référence
Cyclohexane	10.3	10
1	8.4	3
2	6.7	Ce travail
3	5.8	Ce travail
4	5.4	Ce travail

interne autour du lien CH_3—C dans le propane et l'isobutène.

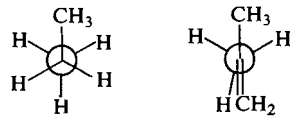

5 **6**

Les formules de projection **5** et **6** représentent la conformation la plus stable du propane et de l'isobutène. Les barrières de rotation interne pour un groupe méthyle sont de 3.3 kcal/mole pour le propane (11) et de 2.2 kcal/mole pour l'isobutène (12), soit une différence d'énergie de 1.1 kcal/mole. Le double de cette énergie, soit 2.2 kcal/mole (rotation autour de *deux* liens CH_3—C) est comparable à la différence des $\Delta F^{\ddagger}$ du cyclohexane et du méthylènecyclohexane (2 kcal/mole).

Les barrières de rotation interne des dérivés substitués en position 1 de l'isobutène n'étant pas connues, nous avons cherché à comparer les $\Delta F^{\ddagger}$ des molécules du tableau 1 aux barrières de rotation interne des groupes méthyles des composés du tableau 2.

La comparaison des barrières de rotation de l'éthane et du propane d'une part, du propène et de l'isobutène d'autre part, met en évidence pour chaque paire, des valeurs voisines de l'énergie de rotation. Ceci suggère l'existence d'une relation de similitude entre les dérivés substitués en position 1 du propène (tableau 2) et les dérivés correspondants de l'isobutène dont les barrières n'ont pas été déterminées jusqu'ici.

Le difluoro-1,1 propène et le fluoro-1 propène *cis* sont groupés pour montrer que l'atome en position *cis* exerce un effet déterminant sur la barrière de rotation du groupe méthyle, et donc, que les valeurs données pour le butène-2 *cis* et le chloro-1 propène *cis* donnent une bonne indication de la valeur de la barrière du diméthyl-2,3 butène-2 et celle du dichloro-1,1 propène. Dale (16) a suggéré que ce comportement était dû en grande partie à une répulsion entre les groupements *cis*.

Une comparaison qualitative des tableaux 1 et 2 montre que du point de vue énergétique, les substituants étudiés ici se retrouvent dans le même ordre dans les deux séries. D'un point de vue quantitatif, la corrélation entre les différences de $\Delta F^{\ddagger}$ d'inversion en série cyclohexanique et les barrières de rotation du groupe méthyle des molécules simples correspondantes du tableau 2

TABLEAU 2

Barrières de rotation du groupe méthyle déterminées par spectre de micro-onde

Molécule	Barrière de rotation (kcal/mole)	Références
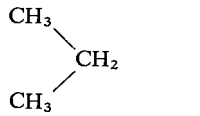	3.3	11
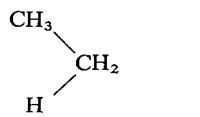	3.03	13
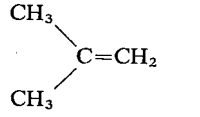	2.2	12
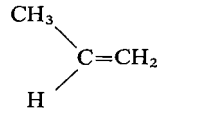	1.98	13
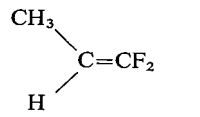	1.25	14
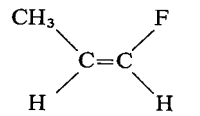	1.05	14
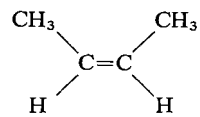	0.75	15
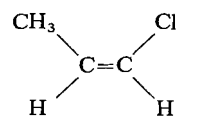	0.6	14

a pu être vérifiée de façon satisfaisante comme l'indique la fig. 4. Ce graphique montre qu'il existe bien une relation linéaire entre les énergies d'activation d'inversion[2] des méthylènecyclohexanes et les barrières de rotation interne des

[2]Les tentatives de détermination de l'entropie d'activation d'inversion $\Delta S^{\ddagger}$ pour le cyclohexane (10) ont conduit à des résultats souvent contradictoires. Il semble que pour les dérivés du méthylènecyclohexane, la valeur de $\Delta S^{\ddagger}$ soit faible (ref. 3) et que $\Delta F^{\ddagger}$ représente une bonne approximation de l'enthalpie d'activation $\Delta H^{\ddagger}$. En fait, des valeurs de $\Delta S^{\ddagger}$ voisines pour les composés **1** à **4** contribueraient aussi à la relation linéaire observée.

Can. J. Chem. Downloaded from www.nrcresearchpress.com by 210.87.254.40 on 09/05/12
For personal use only.

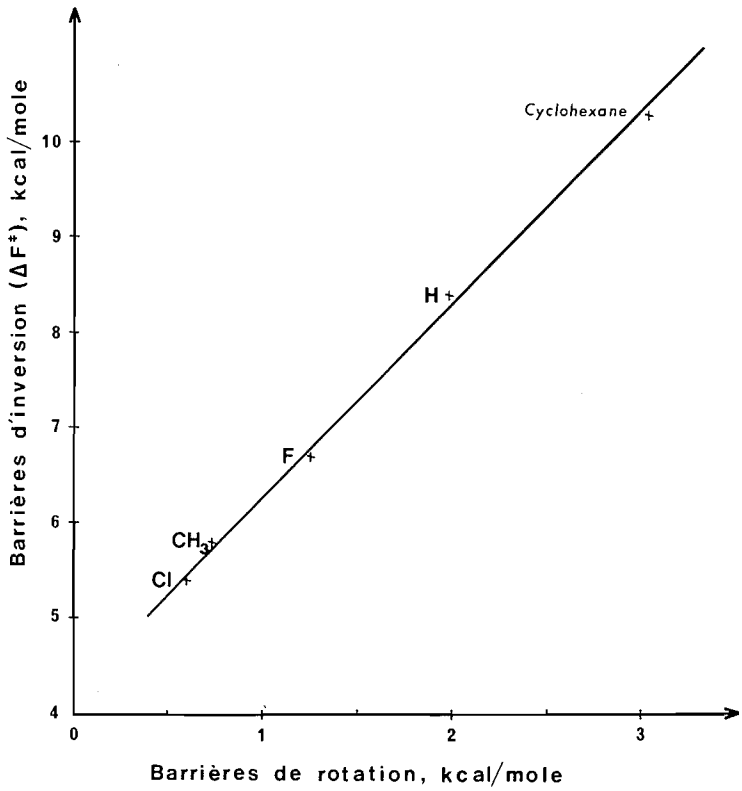

FIG. 4. Relation entre les barrières d'inversion ($\Delta F^{\ddagger}$) des méthylènecyclohexanes et les barrières de rotation interne du groupe méthyle en série propénique.

dérivés propéniques correspondants, en fonction des substituants, comme le calcul décrit plus haut pour **1** pouvait le laisser entrevoir.

Nous avons tenté d'étendre ce type de corrélation à la cyclohexanone ($\Delta F^{\ddagger} < 5$ kcal/mole) (2) en considérant la barrière de rotation interne de l'acétone (0.78 kcal/mole) (17) et celle de l'acétaldéhyde (1.16 kcal/mole) (13). Dans ce cas, la relation entre les énergies n'est plus vérifiée. Cette observation s'explique peut être à la lumière de la théorie qualitative avancée par Dale (16) sur l'origine de la barrière de rotation. Cet auteur suggère que la plus grande polarisabilité de la liaison C=O comparée à la liaison C=C est à l'origine d'un comportement différent pour les deux classes de composés, ce qui ne permet pas de comparaison directe.

La corrélation entre les barrières d'énergie des tableaux 1 et 2 rapportée dans la fig. 4 fait apparaître que la torsion des liaisons C(1)—C(2) et C(1)—C(6) dans les composés **1** à **4** joue un rôle important dans l'établissement de l'état de transition au cours de l'inversion du cycle. Cette conclusion suggère que l'inversion du cycle des composés **1** à **4** passe par un état de transition semblable à celui calculé pour la cyclohexanone (18) et qui peut être représenté schématiquement par la conformation **7**.

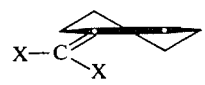

7

Partie expérimentale

Les spectres i.r. sont enregistrés sur un spectromètre Beckman modèle IR-8; le spectre est celui d'un film liquide de la substance pure, déterminé entre deux faces de NaCl.

Les analyses par c.p.g. ont été effectuées à l'aide d'un chromatographe Varian, modèle 90P-3 à détection thermique, utilisant l'hélium comme gaz vecteur. Les produits ont été purifiés en chromatographie préparative sur une colonne de carbowax 20M, 20% sur chromosorb P.

Les spectres r.m.n. ont été enregistrés sur un spectro-

Can. J. Chem. Downloaded from www.nrcresearchpress.com by 210.87.254.40 on 09/05/12
For personal use only.

mètre Jeol modèle JNM-4H-100. Les produits sont en solution peu concentrée dans un mélange de chlorure de vinyle et de chlorodifluorométhane, ce dernier étant utilisé pour fixer le champ magnétique. Le TMS est utilisé comme référence interne, les échantillons sont dégazés et scellés sous vide. La régulation de la température est réalisée à l'aide d'un contrôleur de température Jeol modèle JES-VT-3, préalablement calibré à l'aide d'un thermocouple. La vérification régulière de cette calibration a permis de déterminer l'incertitude maximale sur la température à $\pm$ 2 °C.

Le difluorométhylènecyclohexane (**2**) a été obtenu à partir de la cyclohexanone par la méthode décrite par Fuqua *et al.* (19). La synthèse du dichlorométhylènecyclohexane (**4**) a été effectuée d'après la méthode de Speziale et Ratts (20) en partant de la cyclohexanone. Les spectres i.r. et r.m.n. des composés **2** et **4** correspondent à ceux décrits dans la littérature (19, 20).

L'isopropylidènecyclohexane (**3**) a été préparé à partir de l'acide cyclohexanecarboxylique par la méthode décrite par Lautenschlaeger et Wright (21) pour la synthèse du bis(isopropylidène)-1,4 cyclohexane.

L'acide cyclohexanecarboxylique (0.06 moles) est estérifié à reflux par le méthanol dans le benzène en présence d'acide sulfurique. L'ester obtenu (95%) est traité par le chlorure de méthylmagnésium dans l'éther anhydre. Après hydrolyse, 5.5 g d'isopropylolcyclohexane (67%) sont isolés. L'acide formique est utilisé pour déshydrater cet alcool par chauffage à 100 °C pendant 10 min, les différents produits de déshydratation sont séparés et isolés en chromatographie préparative (température de la colonne: 150 °C).

L'isopropylidènecyclohexane (25%) est caractérisé par son spectre r.m.n. (fig. 2) et par son spectre i.r., ce dernier étant identique à celui décrit dans la littérature (22).

Les auteurs remercient Monsieur D. F. Williams pour l'enregistrement des spectres r.m.n. et le Conseil National de Recherches du Canada pour l'aide financière apportée sous forme de subventions et de bourse pour l'un d'entre nous (M.B.).

1. G. Binsch. Topics in stereochemistry. E. L. Eliel et N. L. Allinger, éditeurs. Vol. 3. Interscience Publishers Inc., New York, N.Y., 1968. p. 97.
2. F. R. Jensen et B. H. Beck. J. Amer. Chem. Soc. **90**, 1066 (1968).
3. J. T. Gerig et R. A. Rimerman. J. Amer. Chem. Soc. **92**, 1219 (1970).
4. M. St-Jacques et M. Bernard. Can. J. Chem. **47**, 2911 (1969).
5. F. A. Bovey, F. P. Hood, E. W. Anderson, et R. L. Kornegay. J. Chem. Phys. **41**, 2041 (1964).
6. J. W. Emsley, J. Feeney, et L. H. Sutcliffe. High resolution nuclear magnetic resonance spectroscopy. Vol. 1. The Pergamon Press Ltd., New York, N.Y., 1967. p. 310.
7. J. A. Pople, W. G. Schneider, et H. J. Bernstein. High resolution nuclear magnetic resonance. McGraw-Hill Book Inc., New York, N.Y., 1959. p. 223.
8. R. J. Kurland, M. B. Rubin, et W. E. Wise. J. Chem. Phys. **40**, 2426 (1964).
9. J. B. Hendrickson. J. Amer. Chem. Soc. **89**, 7047 (1967).
10. F. A. L. Anet et A. J. Bourn. J. Amer. Chem. Soc. **89**, 760 (1967).
11. E. L. Eliel, N. L. Allinger, S. J. Angyal, et G. A. Morrison. Conformational analysis. Interscience Publishers Inc., New York, N.Y., 1965. p. 9.
12. J. W. Laurie. J. Chem. Phys. **34**, 1516 (1961).
13. D. J. Millen. Progr. Stereochem. **3**, 146 (1962).
14. V. W. Weiss, P. Beak, et W. H. Flygare. J. Chem. Phys. **46**, 981 (1967).
15. T. N. Sarachman. J. Chem. Phys. **49**, 3146 (1968).
16. J. Dale. Tetrahedron, **22**, 3373 (1966).
17. R. Nelson et L. Pierce. J. Mol. Spectrosc. **18**, 344 (1965).
18. N. L. Allinger, J. A. Hirsch, M. A. Miller, et I. J. Tyminski. J. Amer. Chem. Soc. **91**, 337 (1969).
19. S. A. Fuqua, W. F. Duncan, et R. M. Silverstein. J. Org. Chem. **30**, 2543 (1965).
20. A. J. Speziale et K. W. Ratts. J. Amer. Chem. Soc. **84**, 854 (1962).
21. F. Lautenschlaeger et G. F. Wright. Can. J. Chem. **41**, 1972 (1963).
22. R. H. Siegmann, M. J. Beers, et H. O. Huisman. Rec. Trav. Chim. **83**, 67 (1964).

Can. J. Chem. Downloaded from www.nrcresearchpress.com by 210.87.254.40 on 09/05/12
For personal use only.

Can. J. Chem. Downloaded from www.nrcresearchpress.com by 210.87.254.105 on 09/05/12
For personal use only.

Photoaddition of α-diketones to olefins. Stereospecificity of the addition reaction

Y. L. CHOW, T. C. JOSEPH, H. H. QUON, AND J. N. S. TAM
Department of Chemistry, Simon Fraser University, Burnaby 2, British Columbia

Received March 9, 1970

Phenanthraquinone (PQ) photolytically adds to *cis*- and *trans*-alkenes to give a mixture of *cis*- and *trans*-1,4-dioxenes and two reduction products. The ratios of *cis*- to *trans*-1,4-dioxenes remain the same irrespective of the photoaddition to *cis*- or *trans*-alkenes and are 1:1 for 2-butenes, 6:4 for 3-hexenes, and 8:2 for cyclohexene. A triplet excited phenanthraquinone is proposed as the reactive species which initiates the addition leading to the intermediate diradical **10**. Depending on the nature of addenda the diradical **10** may be stabilized by a charge transfer structure in different conformations leading to the observed stereochemistry of the adducts. The PQ fails to add to fumaronitrile photolytically or thermally and thermally adds to 2-butenes only inefficiently. Biacetyl undergoes photoreduction readily in the presence of a large excess of cyclohexene.

Canadian Journal of Chemistry, **48**, 3045 (1970)

The formation in sunlight of 1,4-dioxenes by the addition of aromatic α-diketones and *o*-quinones to carbon–carbon double bonds was originally discovered by Schönberg (1). Due to limitations in both instrumentation and stereochemical knowledge at that time, much remains

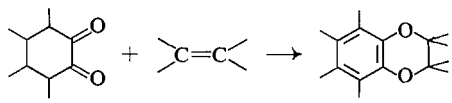

to be studied in terms of the reaction mechanism. A number of investigations concerning this photoaddition have since been published (2), but the major contribution was made by Schenck and his co-workers who studied the addition to various conjugated olefins and a few simple alkenes (3). Certain *o*-quinones are also known to add thermally to reactive carbon–carbon double bonds (3, 4).

The availability of n.m.r. spectroscopy, and the intense interest in the photochemistry of carbonyl compounds (5–8) in recent years, has led to clarification of some mechanistic aspects of this photoaddition. Several communications dealing with such aspects have been published (4, 9–11); they include perturbation molecular orbital calculation which predicts a concerted cycloaddition reaction (12). Some results published so far, however, do not agree completely. The purpose of this paper is to extend the results of our earlier communication (11) on the stereochemical study and to discuss the addition mechanism.

Results

Since phenanthraquinone (PQ) has been most widely studied as the addendum, the initial state of this investigation was aimed at clarifying the stereospecificity of its addition to simple olefins. PQ (E_T = 48 kcal/mole) (13, 14) is known[1] to be a triplet sensitizer for the isomerization of piperylene (16) and stilbenes (14). Simple olefins (E_T = 80 kcal/mole) (15) have been chosen in the hope of eliminating any complication from sensitized isomerization of olefins[2] during the photoaddition.

The photoaddition was carried out with a suspension of finely divided PQ in benzene in the presence of an olefin (concentration 0.1–0.001 *M*) under nitrogen atmosphere. Irradiation was provided by a Hanovia medium pressure lamp placed in a water cooled Pyrex finger. Although benzene limits the solubility of PQ, it also suppresses the photoreduction of a carbonyl compound to a ketyl radical since benzene is a poor hydrogen donating solvent; since the adducts are readily soluble in benzene, PQ dissolves as the photolysis proceeds. In benzene solution, PQ exhibits intense absorption at 420 mμ (ε, 1200) and a shoulder at 510 mμ (ε, 100). As solid PQ is consumed, the absorption at 400–500 mμ region slowly decreases to nil while a new peak at 350 mμ region increases. The t.l.c. analysis of the photolysis solution at regular intervals showed the progressive accumulation of photoproducts.

The products from the photoaddition to sym-

[1]From sensitization experiments, E_T of PQ has been estimated at 65 kcal/mole above the ground state (16). The figure of 48 kcal/mole represents the lowest triplet state and was obtained from phosphorescence spectroscopy (13, 14).

[2]During the photoaddition of benzophenone to 2-butenes, isomerizations of the latter are reported to be insignificant (17).

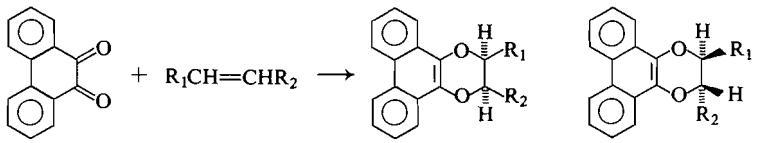

cis-**2** *trans*-**2**

a R_1 and $R_2 = CH_3-$
b R_1 and $R_2 = CH_3CH_2-$
c $R_1, R_2 = -(CH_2)_4-$

metrically disubstituted *cis*- and *trans*-alkenes (RCH=CHR) were partially separated to a mixture of 1,4-dioxene derivatives (**2**) and fractions containing at least two by-products; t.l.c. of the former showed a single spot readily separated from other materials in the photolysate. The crude 1,4-dioxenes were obtained in 30 to 75% yield and showed three n.m.r. multiplets of τ 1.4, 1:8, and 2.5 (ratio 2:2:4) due to the phenanthrene ring protons, and two multiplets in the τ 5.5–6.2 region equivalent to two protons due to the methine protons of —CH—O-linkage. The methine proton multiplet at lower field was assigned to the *cis*-isomer of 1,4-dioxene **2** and that at higher field to the *trans*-isomer (see Discussion) (18). The ratio of these two multiplets varied depending on the type of olefin but remained the same (within experimental error) with a pair of *cis*- and *trans*-olefins; thus the ratio of *cis*- to *trans*-1,4-dioxenes **2** is 6:4 from either *cis*- or *trans*-2-butenes, 2:1 from *cis*- or *trans*-3-hexenes and 8:2 from cyclohexene.

The PQ was shown to be completely consumed in the photolysis, but a small amount of this compound was always isolated in chromatography probably due to an air oxidation (14, 19) of 9,10-dihydroxyphenanthrene (**3**). The latter was formed as a by-product, through photoreduction of PQ. In agreement with this, a photolysate shown by u.v. and t.l.c. analysis to contain no PQ, after aeration exhibited the typical PQ absorption in the 420 mμ region, and the t.l.c. spot corresponding to PQ. Further, 9,10-*bis*-acetoxyphenanthrene was isolated and identified from a crude photolysis mixture after acetylation.

Another solid by-product in the photoaddition to cyclohexene was shown to be hydroxyketone **4***c*; the material showed i.r. absorptions at 3490 and 1695 cm^{-1}, and an n.m.r. multiplet in the τ 4.5 region equivalent to two olefinic protons. The vigorous conditions required for the acetylation, and the thermal instability, suggest the presence of a tertiary hydroxyl group. Lack of a bathochromic shift in the u.v. spectrum in the presence of sodium hydroxide confirms that the compound must have the structure **4***c* rather than structure **5** (20). Since both by-products were

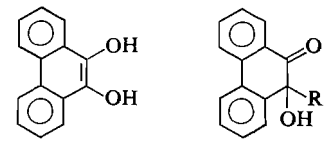

3 **4**

a R = H
b R = EtCH=CH—CH(CH$_3$)—
c R =

unstable, they were isolated and characterized as their acetates. The acetate of **4***c* showed u.v. absorptions (in EtOH) at 332, 253, and 244 mμ, similar to those of 9,10-dihydro-9-hydroxy-9-benzyl-10-ketophenanthrene at 242, 248 and 327 mμ (20). The corresponding by-product **4***b* from the photoaddition to *cis*-3-hexene was obtained as a solid, but could not be purified due to its instability. On completion of the photolysis, v.p.c. analyses of the remaining olefins showed that *trans*-3-hexene and *trans*-4-octene completely retained the initial stereochemistry but several percent of *cis*-3-hexene was isomerized to the *trans*-isomer during the irradiation.

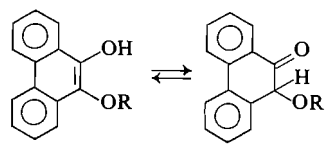

5 **5′**

The photoaddition to *cis*-2-butene gave a better yield of 1,4-dioxene derivative **2***a* (65–75%) than does the photoaddition to *trans*-2-butene

Can. J. Chem. Downloaded from www.nrcresearchpress.com by 210.87.254.105 on 09/05/12
For personal use only.

Can. J. Chem. Downloaded from www.nrcresearchpress.com by 210.87.254.105 on 09/05/12
For personal use only.

(yield 55–35%). The t.l.c. analysis also showed that more by-products (other than 1,4-dioxenes) were formed in the latter case. Fractional recrystallization of the dioxene fraction from both photoadditions afforded two crystalline products, m.p. 89–91 and 161–163°. The first of these, *cis*-1,4-dioxene **2***a*, showed the multiplet of methine protons (XX′ part of $A_3XX'A_3'$ system) at a lower field (τ 5.68) than the other material, *trans*-1,4-dioxene **2***a* (τ 6.07).

The photoadducts, *cis*-**2***a* and *trans*-**2***a*, were shown to be stable under the irradiation conditions. The *cis*:*trans* ratios described above, therefore, were kinetically controlled values. The mixture of 1,4-dioxenes **2***b* and **2***c* obtained from photoaddition to 3-hexenes, and to cyclohexene, could not be separated into *cis*- and *trans*-isomers. In these photoadditions, t.l.c. analysis showed that higher percentage of by-products were formed and that the yields of 1,4-dioxenes were consequently lower than **2***a*.

Although heating a mixture of PQ, *trans*-2-butene and benzene in a sealed tube at 120° for 4 h did not produce any reaction, about 5% of the dioxenes **2***a*, with a *cis*:*trans* ratio of 6:4, were obtained when the reaction mixture was kept at 145°. At higher temperatures, **2***a* was produced in trace amounts only, while the percentage of tars was increased. However, a thermal addition to *cis*-2-butene gave only a trace of the 1,4-dioxenes **2***a*, barely detectable by t.l.c. analysis.

Irradiation of a mixture of PQ and fumaronitrile in benzene under similar conditions, however, did not give any reaction; n.m.r. spectroscopy and v.p.c. analysis showed that the recovered nitrile fraction contained only fumaronitrile. The same reaction mixture, when heated at 145°, also failed to give an adduct, and the starting material was removed in nearly quantitative yield.

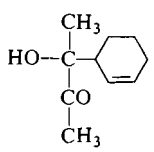

6

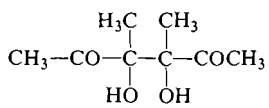

7

Unlike the well investigated 1,4-addition of *o*-quinones or aromatic diketones, photoaddition of aliphatic α-diketones does not appear to have been reported previously. When a solution of biacetyl and cyclohexene was irradiated under conditions similar to above, the absorption peak of biacetyl at 410 mμ disappeared gradually. The only photoproducts identified were 3-(2′-cyclohexenyl)-3-hydroxy-2-butanone (**6**, 19%) and a mixture of *meso*- and *dl*-3,4-dimethyl-3,4-dihydroxy-2,5-hexanedione (**7**, 38%) (21). The n.m.r. spectrum of **6** showed the alkyl methyl protons as two singlets, of equal intensity, at τ 8.74 ($\Delta\nu$ = 2 Hz), while the acetyl methyl protons showed a singlet at τ 7.84. This separation of the methyl signal indicated that the sample is a 1:1 mixture of two diastereoisomeric pairs, although t.l.c. analyses showed only one spot. All other spectroscopic data were in agreement with the proposed structure of **6**. The n.m.r. of the diastereoisomeric mixture of **7** showed two pairs of singlets due to *meso* and *dl*-isomers; the former was isolated by chromatography, and was shown to have the same spectral data as previously reported (21).

Discussion

Before one can discuss the stereochemical course of the 1,4-dioxene formation, it is desirable to put the stereochemical assignments of *cis*- and *trans*-1,4-dioxenes on a firmer basis. The assignments described above are based on the chemical shift relation (18), by which the methine protons of a *cis*-1,4-dioxene should resonate at a lower field than those of the *trans*-isomer, since the former has axial and equatorial C—H orientations while the latter has two axial orientations. This relation is derived from the well established rule that an axial proton resonates at a higher field than an equatorial proton in a cyclohexane system if other environmental factors are comparable (22).

Since it has recently been reported (23) that oxygen causes a very large lowering of the chemical shift of a 3-axial proton relative to that of the 3-equatorial proton in dioxane systems, a direct extension of this chemical shift rule to the dioxene system should be treated with caution. Ideally, the coupling pattern should be analyzed to obtain the coupling constants of the methine protons (24). Fortunately, the coupling patterns of the $A_3XX'A_3'$ systems in *cis*- and *trans*-2,3-dimethyl-1,4-dioxanes have been precisely analyzed (25) and bear close resemblance to those of our 1,4-dioxenes **2***a*. Using Anet's method (24)

Can. J. Chem. Downloaded from www.nrcresearchpress.com by 210.87.254.105 on 09/05/12
For personal use only.

of analysis and assuming that the $J_{AX'}$ values of the 1,4-dioxanes (−0.33 Hz for *trans* and −0.09 Hz for *cis*) found by Gatti *et al.* (25) are also applicable to our case, it can be shown[3] that the *trans*-1,4-dioxene **2***a* has $J_{AX} = 6.33$ Hz, $J_{XX'} = 7.62$ Hz and the *cis*-1,4-dioxene **2***a* has $J_{AX} = 6.39$ Hz and $J_{XX'} = 0.20 \pm 0.11$. These values are in agreement with the 1,4-dioxane systems (25), and confirm the *axial–axial* orientation of the methine protons in *trans*-**2***a* and the *axial–equatorial* in *cis*-**2***a*.

The fact that the PQ photoaddition to either *cis*- or *trans*-2-butenes (or 3-hexenes) gave an identical mixture of 1,4-dioxenes **2***a* (or **2***b*) proves (*i*) that the photoaddition is completely nonstereospecific, and (*ii*) that additions to both *cis*- and *trans*-alkenes take place via a common intermediate. PQ has been shown to be a good triplet sensitizer for 1,3-pentadienes (16) and stilbenes (14) in which intersystem crossing has been assumed to be very efficient. Two observations led us to believe that the photoaddition occurs from a triplet excited state of PQ. *Firstly*, the photoaddition takes place at a cyclohexene concentration of 10^{-3} *M*, which places the lifetime of the reactive state of PQ longer than 10^{-7} s if the reaction rate constant is assumed to be as high as that controlled by diffusion (10^{10} M^{-1} s^{-1}) (8). This lifetime ($> 10^{-7}$ s) is approaching to the upper limits of various reactions of the lowest singlet state of aryl ketones and does not unambiguously exclude the singlet state reaction. However, since the yields and ratio of photoproducts at this low concentration of cyclohexene are virtually unaltered from that at a higher concentration, the lifetime of the reactive PQ is considered to be far longer than 10^{-7} s and may well be in the region of a triplet excited carbonyl compound (8). *Secondly*, the yield of the 1,4-dioxene **2***c* decreased when the photoaddition to cyclohexene was run under an oxygen atmosphere. This appears to indicate a quenching of the reactive triplet state (7, 8) of PQ by oxygen, although other possibilities are not rigorously excluded.

There is good evidence that, in general, photoaddition (to form oxetanes) and photoreduction of the carbonyl compound take place from the $n \rightarrow \pi^*$ triplet state (26–28). Both pathways have been suggested to involve a triplet diradical (such as **8**) as the chemically reactive species (26–28). On the basis of this information, the reaction mechanism, Scheme 1, is proposed. The triplet excited state of PQ is visualized as a resonance hybrid of **8** and **9**, in which the contribution of **9** is expected to be the predominant one as a result of the closed shell (14 π-electrons) stabilization. The triplet diradical **10** is the logical candidate for the common intermediate in the addition and, therefore, ought to possess a lifetime long enough to allow the alkyl moiety to re-orient itself to attain a conformational equilibrium. The diradical **10**, after intersystem crossing, collapses to the same mixture of 1,4-dioxenes **2** regardless of the original stereochemistry of the olefin. The distribution of *cis*-**2** and *trans*-**2** is probably controlled by the conformational equilibrium during the triplet lifetime of **10** since combination of the singlet diradical must be a very rapid process. Formation of *cis*-**2***a* and *cis*-**2***b* in excess may reflect the relative stability of the *cis*-conformation in the half-closed ring **10**. For the diradical derived from cyclohexene, a cyclohexene ring inversion[4] is required in order to attain the equatorial orientation of the PQ moiety so that the *trans*- addition can take place. Since the activation energy for the ring inversion (10.5 kcal/mole) (29) is relatively high in comparison to that

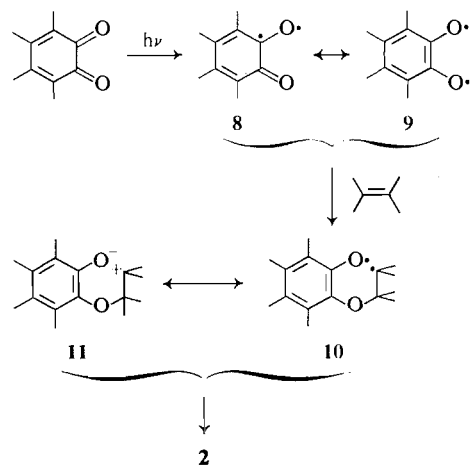

SCHEME 1

[3]We are grateful to Professor D. P. Chong who helped us to perform the calculation.

[4]This argument explicitly assumes an axial approach of PQ radical to the π-bond of cyclohexene leading to the axial orientation of the PQ group in **10**. This stereochemical course of a radical addition has ample precedent; one example is ref. 30*b*.

Can. J. Chem. Downloaded from www.nrcresearchpress.com by 210.87.254.105 on 09/05/12
For personal use only.

of the diradical combination, the latter process occurs faster than the former in this particular case. This probably explains why less stable *cis*-**2***c* is formed in large excess.

As partial charge transfer is characteristic for a radical pair (30*a*), the ionic structure **11** should contribute, as a resonance form, to a certain extent to the diradical depending on stabilization of the positive and negative charges. Thus the contribution of the charge transfer structure **11** must be very significant in the diradical derived from tetrachloro-*o*-quinone and stilbene since the positive and the negative poles are respectively stabilized by resonance (4). Interaction of the charges conceivably restricts the free rotation around the C_2—C_3 bond. The high stereospecificity observed in the addition of tetrachloro-*o*-quinone to stilbenes[5] (4) and some selectivity observed in the addition of PQ to stilbenes (9) are both in consonance with this proposal. It follows that in a PQ addition to a simple olefin the contribution of the charge transfer structure **11** is insignificant, resulting in complete non-stereospecific addition. This proposal is also in agreement with the observation that the *cis*:*trans* ratio[6] of **2***a* are very slightly susceptible to temperature change while that of the PQ addition to stilbenes is somewhat temperature dependent (9).

As photoreduction via a ketyl radical is typical of triplet excited carbonyl groups (6–8), the formation of **3** can readily be seen as a hydrogen transfer reaction from either **8** or **9**. However, the formation of **5** (or **5′**) is also to be expected from **9** (or **8**) via hydrogen transfer followed by the combination of the two radicals. These two types of addition reactions have been demonstrated (20). Since **5** (or **5′**) has also been shown to efficiently rearrange photolytically to **4** (20), it is reasonable that only the latter, and not the former, is isolated under the present photolysis condition.

Although it is of secondary importance as far as the present results are concerned, the lack of photosensitized isomerization of *trans*-alkenes in contrast to a small degree in the case of *cis*-3-hexene requires some comment. The energy level of the lowest singlet state of PQ can be estimated from the absorption peak of the longest wavelength (465 mμ), and is found to be approximately 56 kcal/mole. Since the lowest triplet energy of PQ is 48 kcal/mole (13, 14), it is difficult to see how a classical or a non-classical energy transfer (31) can take place either from singlet or triplet PQ to olefin. However, dissociation of the common intermediate **10** (from the ground state) to PQ and the olefin is possible and may explain the observed isomerization.[7] Further, if one assumes that the common intermediate **10** has lost a substantial amount of excess vibrational energy, it is not difficult to see that the regenerated olefin will have more stable *trans*-configuration. A lack of isomerization in a *trans*-alkene, therefore, does not necessarily contradict this proposed mechanism.[8]

The scope and limitations of the addition of PQ to a carbon–carbon double bond have been summarized (3). To this, several observations can now be added.

(*1*) From the failure of addition to fumaronitrile and other known examples (3), it can be concluded that PQ photoaddition does not take place with an electron deficient double bond.[9]

(*2*) Although the formation of an oxetane is a side reaction frequently observed in the photoaddition of PQ (3, 9, 10), it is now clear that the photoaddition to a simple olefin does not give the expected oxetane. Photoadditions to certain conjugated olefins have been shown to give oxetanes as the major product (3), but the factors favoring oxetane formation, are not clear.

---

[5]The addition takes place either by irradiation or thermolysis to give, in both cases, a high degree of stereoselectivity for which Professor D. Bryce-Smith has proposed the charge transfer structure **11** as the intermediate (4). The authors appreciate very much the discussion exchanged with Professor Bryce-Smith.

[6]Farid (9) has reported that the yields of *cis*-**2***a* were 57 and 70% respectively, when the photoaddition of PQ to *trans* and *cis*-2-butene were carried out with the light source > 390 mμ. Since we performed our photoaddition in a Pyrex apparatus (λ > 280 mμ), the discrepancy in the yields of **2***a* could be ascribed to the difference in the incipient light. It is, however, difficult to explain the formation of more *cis*-**2***a* (57%), than *trans*-**2***a*, from the addition to *trans*-2-butene in Farid's experiment.

[7]The general idea of this isomerization mechanism has been proposed by Schenck in another study (32) and has been proven to be important in certain cases (33).

[8]It should be pointed out that photosensitized isomerization in *cis*-2-pentene was found to be faster and more steady than *trans*-2-pentene using a carbonyl sensitizer (16).

[9]It is interesting to point out that alkyl ketones photolytically add to fumaronitrile stereospecifically for which a singlet addition mechanism has been suggested (17). The triplet state addition has been shown to be an electrophilic reaction (26–28).

Can. J. Chem. Downloaded from www.nrcresearchpress.com by 210.87.254.105 on 09/05/12
For personal use only.

(*3*) It is demonstrated that PQ does undergo thermal addition to a simple olefin, *albeit* extremely inefficiently, to give the 1,4-dioxenes **2**.

(*4*) In contrast to a facile 1,4-addition exhibited by photoexcited aromatic diketones (including *o*-quinones), it is demonstrated that a photoexcited alkyl α-diketone does not form a 1,4-dioxene derivative.

In the presence of cyclohexene, biacetyl undergoes the typical photoreduction of a carbonyl compound. It has been proposed that the triplet diradical of the keto group triggers inter and intramolecular hydrogen transfers (35, 36). This result is in agreement with the detailed studies of the photoreduction of biacetyl, reported recently by Turro and Engel (37).

Experimental

The n.m.r. spectra were taken with a Varian A56/60 spectrometer by dissolving the samples in $CDCl_3$ solution using TMS as the internal standard. The i.r. spectra were measured in a Perkin–Elmer 457 instrument, in Nujol mulls or liquid film. The u.v. spectra were recorded with a Unicam SP–800 spectrophotometer. Melting points were taken in a Fischer–Johns hot stage instrument and were uncorrected. Analyses were performed by Dr. A. Bernhardt, Engelskirchen, W. Germany.

Cyclohexene (b.p. 82–93°) and biacetyl (b.p. 89–90°) were distilled before reaction. Fumaronitrile and phenanthroquinone (Aldrich Co.), and 2-butenes (Mathieson), were used as supplied. The purities of *cis*- (96%) and *trans*-3-hexene (100%) and *trans*-4-octene (100%) were confirmed by v.p.c. analysis on a 30% $AgNO_3$ – TEG-firebrick column. The chromatographic fractions were analyzed by t.l.c. to check the purity.

Photoaddition

A mixture of PQ, and an olefin in benzene was photolyzed with a Hanovia medium pressure mercury lamp (100 or 450 W) in a Pyrex apparatus. PQ did not dissolve completely, and the suspension was stirred with a slow stream of purified nitrogen. The solid disappeared gradually as the reaction proceeded. The concentration of the olefin varied from 0.1 to 0.001 *M*. The lamp sleeve was cooled with tap water, and the reaction vessel with an ice bath. The progress of the reaction was traced by the disappearance of the PQ absorption in the 450 mμ region, and/or by t.l.c. analyses.

The crude product was chromatographed on a column of neutral alumina. The 1,4-dioxene adducts were eluted first with benzene, followed by other by-products, and finally by unreacted phenanthraquinone. The separation was followed by silicic acid t.l.c. analysis. The mixture of 1,4-dioxenes obtained in this manner showed a single spot on a t.l.c. plate with a higher R_f value than other by-products. Repeated chromatography was required to yield a pure fraction of the by-product.

Photoaddition to Cyclohexene

A suspension of PQ (3 g) and cyclohexene (6 ml) in benzene (160 ml) was photolyzed for 7.5 h. The t.l.c. trace during the photoaddition showed three components, due to by-products having intermediate R_f values between those of the dioxene adducts and PQ. Repeated chromatography of the crude product yielded the dioxene adduct **2***c* (1.3 g, 34%), a mixture (1.6 g), and compound **4***c* (90 mg, 2%).

The dioxene fraction could not be purified by column chromatography or preparative t.l.c. and gave, from an acetone light petroleum mixture, a non-crystalline solid;[10] i.r. 1610, 1500, 1450, 1240, 1010, 1080, and 715 cm^{-1}; n.m.r. τ 5.72 and 6.28 (both multiplets integrated to 2H with a ratio of 81.9); mass spectrum, *m/e*(%) 290(100), 274(17), 247(9), 231(13), 220(11), 210(54), 209(30), 194(17), 180(57), and 152(28).

Anal. Calcd. for $C_{20}H_{18}O_2$: C, 82.73; H, 6.25. Found: C, 82.52; H, 6.33.

The compound **4***c* was obtained as a solid and decomposed on heating to 160° but gave one spot on a t.l.c. analysis; i.r. 3500, 1695, 1605, 1200, 1015, 990, and 730 cm^{-1}; mass spectrum *m/e*(%) 211(14), 210(91), 209(12), 208(10), 181(52), 180(100), 152(50); u.v. λ_{max} 335 mμ in EtOH or EtOH–NaOH solution.

Part of the mixture (650 mg) was treated with acetic anhydride in pyridine under reflux for 4 h. The crude product was worked up in the usual manner and was chromatographed on a basic alumina column. The first fraction (150 mg) eluted with benzene, crystallized from ether, and recrystallized from benzene to give 9,10-bisacetoxyphenanthrene; m.p. 202–205° [lit. (38) 202°]; i.r. 1765 and 1200; n.m.r. τ 2.5 (8H) and 7.6 (6H, s); mass spectrum *m/e*(%) 294(19), 253(14), 252(57), 211(48), 210(100), 209(68), 197(35), and 182(42). A mixed m.p. of this material with an authentic sample prepared according to the known method (38) was not depressed.

The following three fractions (240 mg) eluted with benzene were combined, recrystallized from methanol three times, and sublimed to white crystals (the acetate of **4***c*); m.p. 155–158°; u.v. (EtOH), 244 mμ (ε 29 500), 253 (24 000), 332 (3050); i.r. 1740, 1685, 1600, 1485, 1240, 1040, 770, and 740 cm^{-1}; m.n.r. τ 4.2 (m, 2H), 7.30 (m, 1H), and 7.89 (s, 3H); mass spectrum *m/e*(%) 332(1), 274(2.4), 253(4.8), 211(17), 210(100), 209(44), 181(24), 153(6), 152(14), and 151(6).

Anal. Calcd. for $C_{22}H_{20}O_3$: C, 79.50; H, 6.06. Found: C, 79.37; H, 5.93.

The fractions (495 mg) eluted with 20% chloroform in benzene were combined and recrystallized to give PQ.

The ratios of the products were not altered significantly when one molar equivalent of cyclohexene was used, or when the concentration of cyclohexene was adjusted to 0.001 *M*. The yields of the crude dioxene, however, varied from 33 to 42%.

Photoaddition to 3-Hexenes

A suspension of PQ (505 mg) and *cis*-hexene (1 ml) in benzene (45 ml) was photolyzed for 19 h. The v.p.c. analyses of the solution showed that the content of *trans*-3-hexene was 3.5% at 0 h, and 7 ± 1% at the end of 6 h irradiation. The crude product was chromatographed to give a mixture of the dioxene adducts (426 mg, 60%), compound **4***b* (68 mg, 2%), and PQ (130 mg). The

[10]Pfundt and Schenck (3) reported m.p. 80° and 38% yield for the same photoadduct.

Can. J. Chem. Downloaded from www.nrcresearchpress.com by 210.87.254.105 on 09/05/12
For personal use only.

fractions of dioxene adducts exhibited two n.m.r. signals at τ 5.80 and 6.16 in the ratio of 2:1 although the t.l.c. analysis showed a single spot. A part of this fraction was sublimed at 180°/1 mm to afford a semi-crystalline light brown solid (**2***b*); m.p. 73–78°; i.r. 1630, 1610, 1500, 1100, 760, and 725 cm^{-1}; n.m.r. τ 8.88 (two q, J = 5.5 Hz, $\Delta\nu$ = 2 Hz), 8.33 (broad, J = 5.5 Hz), 6.16 (t, J = 4 Hz), and 5.80 (dd, J = 4.5 and 7 Hz); mass spectrum *m/e*(%) 292(10), 234(2), 210(10), 209(5), 208(4), 180(18), and 152(10).

Anal. Calcd. for $C_{20}H_{20}O_2$: C, 82.16; H, 6.89. Found: C, 82.50; H, 6.92.

Compound **4***b* was a non-crystalline solid and decomposed on sublimation; i.r. 3800, 1695, 1605, 1200, 1000, 770, and 734 cm^{-1}; n.m.r. τ 5.0 (broad m, 2H), 6.05 (OH, D_2O exchangeable), 9.25 (m, 6H); u.v. λ_{max} 330 mμ in EtOH or EtOH–NaOH solution.

The same photoaddition was run with *trans*-3-hexene (100% by v.p.c. analysis). Similar v.p.c. analyses of the solution during irradiation showed that no *cis*-3-hexene was formed during 6 h irradiation. The fraction of the dioxene adducts (70%) obtained by chromatography showed n.m.r. triplets at τ 5.80 and 6.16 in the ratio of 2:1. The i.r. and the mass spectra of this fraction are the same as that obtained from the addition to *cis*-3-hexene.

Photoaddition to 2-Butenes

A suspension of PQ (505 mg) and *cis*-2-butene (0.5 ml) in benzene (200 ml) was photolyzed for 4 h. The t.l.c. analysis during the reaction showed a major and minor spot, gradually increasing proportionally to PQ. Column chromatography gave a fraction of the dioxene adducts (422 mg, 66%) which exhibited a single t.l.c. spot; the integrated ratio of the n.m.r. multiplets at τ 5.68 and 6.07 was in the ratio of 57:43. The first crop of crystals from a cyclohexene solution of the adducts were recrystallized from cyclohexane three times, and sublimed to afford the *trans*-isomer of **2***a*: m.p. 162–163°; i.r. 1600, 1500, 1450, 1240, 1220, 1100, and 1180 cm^{-1}; n.m.r. (in pyridine) τ 8.55 (m, 6H) and 6.07 (m, 2H); M^+ 264.1218 (Calcd. for $C_{18}H_{16}O_2$: 264.1150).

Anal. Calcd. for $C_{18}H_{16}O_2$: C, 81.79; H, 6.10. Found: C, 81.56; H, 6.13.

The second crop of crystals obtained from the cyclohexane mother liquor was recrystallized from methanol several times to afford white crystals (*cis*-**2***a*): m.p. 89–91°; i.r. 1630, 1605, 1500, 1340, 1090, 1035, 760, and 725 cm^{-1}; n.m.r. (in pyridine) τ 5.63 (m, 2H) and 7.77 (m, 6H); M^+ 264.1218 (Calcd. for $C_{18}H_{16}O_2$: 264.1150).

When the photoaddition was run with *trans*-2-butene under the same conditions, the fraction of the dioxene adduct (250 mg) exhibited n.m.r. signals at τ 5.68 and 6.07 in the ratio of 58:42. The *trans*- and *cis*-adduct were isolated by recrystallization and were found to be identical with those isolated from the previous experiment. In this photoaddition an unstable by-product was also formed in *ca.* 10% yield, but this substance could not be purified. The t.l.c. analyses showed this compound to have the same R_f value as that of **3**. When the photolysate was aerated, the long wavelength absorption of PQ (450 mμ) appeared. A small amount of PQ was also isolated by chromatography.

A mixture of PQ (2.02 g), *trans*-2-butene (0.5 ml) and benzene (150 ml) was heated in an autoclave at 140° for 5 h, until there was no further decrease in pressure. The residue was treated with light petroleum and the light petroleum solution was chromatographed in the usual manner. The first fraction (111 mg) eluted with benzene showed an i.r. spectrum identical to that of the crude dioxene adduct as obtained in the photoreaction, with n.m.r. signals at τ 5.68 and 6.07 in the ratio of 6:4. When the mixture was heated to 165°, tar was formed, but only a trace of dioxene adducts was obtained.

Photoaddition to 4-Octene

The photolysis was repeated using pure *trans*-4-octene as the olefin. After 17 h irradiation the crude mixture was distilled at 120° bath temperature to give a distillate, whose v.p.c. analysis with a 30% SE-30 column showed no peak corresponding to *cis*-4-octene. The t.l.c. analysis of the residue showed that three products were formed in approximately the same proportion.

Addition to Fumaronitrile

A suspension of PQ (102 mg), fumaronitrile (44 mg) in benzene (45 ml) was photolyzed for 6 h. The t.l.c. analysis during the irradiation showed no significant change, but the u.v. trace showed a small increase in intensity at 310 mμ. The remaining residue from evaporation of the solvent was chromatographed in the usual manner to afford a crude fraction of the nitrile and PQ. The v.p.c. analysis of the nitrile fraction on 10% XF-1150 on a chromosorb W column showed that it contained only fumaronitrile (R_f = 15 min) and no maleonitrile (R_f = 9.5 min).

Phenanthraquinone (2.88 g) and fumaronitrile (1.36 g) in benzene (100 ml) were placed in a sealed tube. This mixture was heated for 45 h. On working up in the above manner, the starting materials were recovered.

Photoaddition of Biacetyl

A solution of redistilled biacetyl (834 mg), cyclohexene (0.85 ml), and benzene (125 ml) was photolyzed for 3 h. The reaction mixture was evaporated to give a residue (1.04 g). Chromatography of the residue on a silicic acid column gave an oily fraction (305 mg, 18%), and a mixture of oil and crystals (318 mg, 38%). The oily fraction was distilled at 100°/1 mm to give **6** u.v. end absorption; i.r. 3480, 1720, 1360, and 1110 cm^{-1}; n.m.r. τ 8.74 (two s, $\Delta\nu$ = 2 Hz, 3H), 7.84 (s, 3H), 4.22 (m, 1H), and 4.6 (m, 1H); mass spectrum, *m/e*(%) 150(3.5), 125(21), 88(23), 81(23), 59(28), and 43(100). The semicarbazone of **6** was recrystallized from ethanol; m.p. 187–189°.

Anal. Calcd. for $C_{11}H_{19}N_3O_2$: N, 18.65. Found: N, 18.77.

The mixture showed i.r. absorptions at 3450 and 1710 (broad) and n.m.r. signals τ 8.80, 7.67 (same intensity) and 8.72, 7.77 (same intensity). This fraction was recrystallized from light petroleum and sublimed (90°/5 mm) to give white needles of *meso*-3,4-dihydroxy-3,4-dimethyl-2,5-hexanedione (7); m.p. 91–94° [lit. (21), m.p. 95–96°]; n.m.r. (CCl_4) τ 5.6 (D_2O exchangeable), 7.65 (s, 3H), 8.80 (s, 3H) and the small signals due to the *dl*-isomer; i.r. 1695 and 3450 cm^{-1}.

We are grateful to the National Research Council of Canada for generous support by Operating and Capital Equipment (mass spectrometer) grants.

1. A. SCHÖNBERG and A. MUSTAFA. J. Chem. Soc. 67 (1944); Chem. Rev. **40**, 188 (1947).
2. P. DE MAYO. *In* Advances in organic chemistry. Vol. II. R. A. Raphael, E. C. Taylor, and H. Wynberg, *editors*. Interscience Publishers, Inc., New York, N.Y., 1960. p. 329.
3. G. PFUNDT and G. O. SCHENCK. *In* 1,4-Cycloaddition reaction. J. Hamer, *editor*. Academic Press, New York, N.Y., 1967. Chapt. 11.
4. D. BRYCE-SMITH and A. GILBERT. Chem. Commun. 1701, 1702 (1968).
5. R. O. KAN. Organic photochemistry. McGraw-Hill Book Co., New York, N.Y., 1966. Chapts. 3, 6.
6. D. C. NECKERS. Mechanistic organic photochemistry. Reinhold Publishing Co., New York, N.Y., 1967. Chapts. 6, 7.
7. J. G. CALVERT and T. N. PITTS, JR. Photochemistry. John Wiley and Sons, New York, N.Y., 1966.
8. N. J. TURRO. Molecular photochemistry. W. A. Benjamin Co., New York, N.Y., 1967. Chapts. 7, 8.
9. S. FARID. Chem. Commun. 1268 (1967).
10. S. FARID and K. H. SCHOLZ. Chem. Commun. 412 (1968).
11. Y. L. CHOW and T. C. JOSEPH. Chem. Commun. 604 (1968).
12. W. C. HERNDON and W. B. GILE. Chem. Commun. 497 (1969).
13. N. A. SHCHEGOLVA, D. A. SHIGORIN, and M. V. GORELIK. Zh. Fiz. Khim. **39**, 893 (1965).
14. J. J. BOHNING and K. WEBB. J. Amer. Chem. Soc. **88**, 2893 (1966).
15. D. F. EVANS. J. Chem. Soc. 1351 (1957).
16. G. S. HAMMOND, N. J. TURRO, and P. A. LEERMAKERS. J. Phys. Chem. **66**, 1144 (1962).
17. N. J. TURRO, P. WRIEDE, J. C. DALTON, D. ARNOLD, and A. GLICK. J. Amer. Chem. Soc. **89**, 3950 (1967).
18. G. PFUNDT and S. FARID. Tetrahedron, **22**, 2237 (1966).
19. P. RAMART-LUCAS, J. MATTI, T. GUILMART, and M. GRUMEY. Bull. Soc. Chem. Fr. 1215 (1961).
20. M. B. RUBIN and P. ZWITKOWITS. J. Org. Chem. **29**, 2362 (1964); Tetrahedron Lett. 2453 (1965).
21. F. RAMIREZ, N. RAMANATHAN, and N. B. DESAI. J. Amer. Chem. Soc. **85**, 3465 (1963).
22. R. U. LEMIEUX, R. K. KULLING, H. J. BERNSTEIN, and W. G. SCHNEIDER. J. Amer. Chem. Soc. **80**, 6098 (1958).
23. R. A. SPRAGG. J. Chem. Soc. (B), 1128 (1968).
24. F. A. L. ANET. J. Amer. Chem. Soc. **84**, 747 (1962); A. A. BOTHNER-BY and C. NAAR-COLIN. J. Amer. Chem. Soc. **84**, 743 (1965).
25. G. GATTI, A. L. SEGRE and C. MORANDI. Tetrahedron, **23**, 4385 (1967).
26. D. R. ARNOLD, R. L. HINMAN, and A. H. GLICK. Tetrahedron Lett. 1425 (1964).
27. N. C. YANG. Rev. Pure Appl. Chem. **9**, 591 (1964).
28. N. C. YANG, M. NUSSIM, M. J. JORGENSON, and S. MUROV. Tetrahedron Lett. 3657 (1964).
29. E. L. ELIEL. Stereochemistry of carbon compounds. McGraw-Hill Book Co., Inc., New York, N.Y., 1962. Chapt. 8.
30. (*a*) C. WALLING. Free radical in solution. John Wiley and Sons, Inc., New York, N.Y., 1957. p. 134. (*b*) P. D. READIO and P. S. SKELL. J. Org. Chem. **31**, 753, 759 (1966).
31. G. S. HAMMOND *et al.* J. Amer. Chem. Soc. **86**, 3197 (1964).
32. G. O. SCHENCK and R. STEINMETZ. Bull. Soc. Chem. Belg. **71**, 781 (1962).
33. N. C. YANG, J. L. COHEN, and A. SHANI. J. Amer. Chem. Soc. **90**, 3264 (1968); J. SALTIEL, K. K. NEUBERGER, and M. WRIGHTON. J. Amer. Chem. Soc. **91**, 3658 (1969).
34. C. H. KRAUCH, S. FARID, and G. O. SCHENCK. Chem. Ber. **98**, 3102 (1965); S. FARID, D. HESS, and C. H. KRAUCH. Chem. Ber. **100**, 3266 (1967).
35. H. L. J. BÄCKSTROM and K. SANDROS. Acta Chem. Scand. **12**, 3 (1958).
36. W. H. URRY and D. J. TRECKER. J. Amer. Chem. Soc. **84**, 118 (1962); W. H. URRY, D. J. TRECKER, and D. A. WINEY. Tetrahedron Lett. 609 (1962).
37. N. J. TURRO and R. ENGEL. J. Amer. Chem. Soc. **91**, 7113 (1969).
38. J. SCHMIDT and H. LUMPP. Chem. Ber. **43**, 787 (1910).

Can. J. Chem. Downloaded from www.nrcresearchpress.com by 210.87.254.105 on 09/05/12
For personal use only.

Can. J. Chem. Downloaded from www.nrcresearchpress.com by 210.87.254.5 on 09/05/12
For personal use only.

Cinétique de relaxation des complexes Ce(IV).alcool[1]

G. Boivin et M. Zador
Département de chimie, Université de Montréal, Montréal, Québec

Reçu le 12 mars 1970

La cinétique de relaxation des complexes Ce(IV).alcool a été étudiée. Les constantes de vitesse de formation et de dissociation ont été déterminées et dépendent de la nature de l'alcool: primaire > secondaire > tertiaire. De plus les constantes de vitesse augmentent avec l'acidité ce qui est discuté dans le mécanisme proposé.

Relaxation kinetics of Ce(IV).alcohol complexes has been studied. The rate constants of formation and dissociation have been determined and are found to depend on the nature of the alcohol: primary > secondary > tertiary. In addition, there is an increase in the rate with acidity; a mechanism is proposed to explain this.

Canadian Journal of Chemistry, 48, 3053 (1970)

Introduction

Le Ce(IV) est un oxydant très puissant; il oxyde diverses substances organiques telles que les alcools, les aldéhydes, les cétones etc.... (1). L'oxydation des alcools a fait l'objet de nombreuses études; le mécanisme accepté pour l'oxydation fait intervenir un complexe Ce(IV).alcool dans le mécanisme (2–7)

$$[1] \qquad \mathrm{Ce(IV)} + \mathrm{al} \overset{\text{rapide}}{\rightleftharpoons} \mathrm{Ce(IV).al}$$

$$[2] \qquad \mathrm{Ce(IV).al} \xrightarrow{\text{lente}} \text{Produits}$$

La formation du complexe étant très rapide, ne fut étudiée dans les travaux antérieurs qu'au point de vue de sa stoechiométrie et de sa constante d'équilibre (2–7). L'étude des réactions rapides de formation de complexes métal–ligand a connu ces dernières années un développement considérable dû, en partie, aux nouvelles techniques mises au point (8, 9).

Dans un très grand nombre de cas on admet un mécanisme à deux étapes dont la première est la formation rapide d'une paire d'ions de type complexe externe qui est suivi du départ lent d'une molécule d'eau et la rentrée du ligand dans la sphère interne du métal; la vitesse de cette deuxième étape est indépendante de la nature du ligand.

$$[3] \qquad \mathrm{M(H_2O)_n^{m+}} + \mathrm{L^{p-}} \overset{\text{rapide}}{\rightleftharpoons} [\mathrm{M(H_2O)_n^{m+} \ldots L^{p-}}]$$

$$[4] \qquad [\mathrm{M(H_2O)_n^{m+} \ldots L^{p-}}] \overset{\text{lente}}{\rightleftharpoons} \mathrm{M(H_2O)_{n-1}L^{m-p}} + \mathrm{H_2O}$$

Ce type de mécanisme a été proposé la première fois par Eigen (10); depuis il a été confirmé dans un grand nombre de cas qui sont résumés dans les articles de revues (11, 12).

En fait ce mécanisme représente un cas limite de la formation de complexes; on l'appelle mécanisme S_N1 limite. Ce mécanisme et d'autres mécanismes de formation de complexes ont été amplement discutés (12, 13).

Le mécanisme simple présenté par les éqs. 3 et 4 est dans certains cas compliqué par l'influence du p*H*. La vitesse de formation du complexe peut augmenter avec le p*H* à cause de la formation d'espèces hydrolysées telles que $FeOH^{2+}$ dont le groupe hydroxy facilite l'échange d'une molécule d'eau de coordination de l'ion Fe^{3+} (14). L'influence contraire du p*H*, donc une "catalyse acide", a été également observée due à la protonation du ligand (15–18).

La présente étude est consacrée aux complexes Ce(IV).alcool intermédiaires dans l'oxydation. L'étude a été effectuée par la méthode de relaxation dite de saut de température (T. Jump). Dans notre cas, l'équilibre 1 est constamment perturbé par la réaction 2, qui impose certaines limitations quant au choix des alcools ainsi que des concentrations des réactifs en général.

Partie Expérimentale

Réactifs

Le solvant est l'eau distillée. Les alcools ont été purifiés par les méthodes habituelles. Le Ce(IV) a été utilisé en solution dans l'acide perchlorique 6 *N* (G. F. Smith); le titre des solutions a été déterminé par iodométrie. Les autres solutions ont été préparées par gravimétrie. La force ionique des solutions a été maintenue constante par le perchlorate de lithium, étant donné que l'augmentation de la force ionique entraîne une diminution sensible des temps de relaxation.

[1]Présenté en partie au 52ème Congrès Annuel de l'Institut de Chimie du Canada, Montréal, mai 1969.

Can. J. Chem. Downloaded from www.nrcresearchpress.com by 210.87.254.5 on 09/05/12
For personal use only.

Appareillage

L'appareil de relaxation utilisée provient de la compagnie Messanlagen Studiengesellschaft m.b.H. Göttingen, Allemagne Fédérale. Le principe de l'appareil a été décrit dans la littérature (8). Le monochromateur utilisé est de marque Bausch et Lomb et l'oscillographe cathodique est un Tektronix modèle 535A. On a utilisé des cellules à électrode de platine d'un volume total de 7 ml avec un volume d'environ 1 ml entre les électrodes. Le condensateur d'une capacité de 0.05 μF peut-être chargé à 40 kV; dans ce cas la décharge est d'environ 42 J et le saut de température correspondant est d'environ 10 °C. Le compartiment à cellule est thermostaté et la température est mesurée à l'intérieur de la cellule à l'aide d'un thermocouple.

Manipulations

La solution étudiée est introduite dans la cellule et dès que la température est stabilisée on effectue la décharge pour minimiser la perturbation due à l'oxydation (éq. 2). La courbe de relaxation obtenue par photographie du signal sur l'oscillographe, est due au changement de densité optique de la solution à la longueur d'onde choisie. On a travaillé à des longueurs d'onde variant de 390 à 420 mμ pour obtenir le rapport signal/bruit optimum. L'erreur sur le temps de relaxation, τ, est d'environ 10%. Pour pouvoir interpréter quantitativement les résultats nous avons travaillé avec un grand excès d'alcool par rapport au Ce(IV). Dans ces conditions, seule la concentration en Ce(IV) varie à cause de la réaction 2; celle de l'alcool reste pratiquement constante et donc connue. On n'a observé aucune influence des ions Ce(III) sur le temps de relaxation.

Résultats

Dans les conditions expérimentales où le travail a été effectué, le Ce(IV) se trouve partiellement hydrolysé (19)

$$[5] \qquad Ce^{4+} + H_2O \rightleftharpoons CeOH^{3+} + H^+$$

A des longueurs d'onde d'environ 305 mμ les deux formes du Ce(IV) ont un coefficient d'absorption différent, donc en principe la réaction 5 peut-être étudiée. L'étude expérimentale n'a cependant pas montré de relaxation dans les limites de l'appareil ce qui permet d'estimer la limite supérieure du temps de relaxation de ce système à environ 10^{-6} s. Les solutions d'alcool n'ont pas présenté de relaxation.

Influence de l'alcool

Dans le cas d'un système Ce(IV).alcool on observe une seule relaxation avec un temps, τ, compris entre 5×10^{-3} et 10^{-5} s suivant les conditions expérimentales. A une température donnée et à des concentrations en Ce(IV) et H^+ constantes, l'inverse du temps de relaxation, τ^{-1}, est donnée par l'équation

$$[6] \qquad \tau^{-1} = k_d + k_f[al]$$

L'équation [6] est celle que l'on obtiendrait pour un mécanisme simple du type

$$[7] \qquad Ce^{4+} + al \underset{k_d}{\overset{k_f}{\rightleftharpoons}} Ce.al^{4+}$$

Le temps de relaxation de ce système 7 est donné par

$\tau^{-1} = k_d + k_f([\overline{al}] + [\overline{Ce(IV)}])$ où

$[\overline{al}]$ et $[\overline{Ce(IV)}]$

sont des concentrations à l'équilibre. Si on prend [Ce(IV)] ≪ [al] alors on obtient l'équation [6], obtenu justement dans ces conditions pour des raisons discutées plus haut. Nous avons vérifié que dans ce cas τ^{-1} est indépendant de la concentration du Ce(IV).

Une des droites de la fig. 1 représente la variation de τ^{-1} en fonction de la concentration en alcool à une acidité donnée et permet de vérifier l'équation [6] et de déterminer k_d et k_f.

Le tableau 1 résume les résultats obtenus dans des conditions identiques pour une série d'alcools à partir des temps de relaxation obtenus pour six concentrations en alcools comprises entre 0.02 et 0.4 *M*. L'erreur sur les temps de relaxation est d'environ 10%, bien que la reproductibilité soit meilleure que 5%; l'erreur sur les constantes de vitesse est d'environ 20%.

Les valeurs des k_f et k_d du tableau 1 sont dans

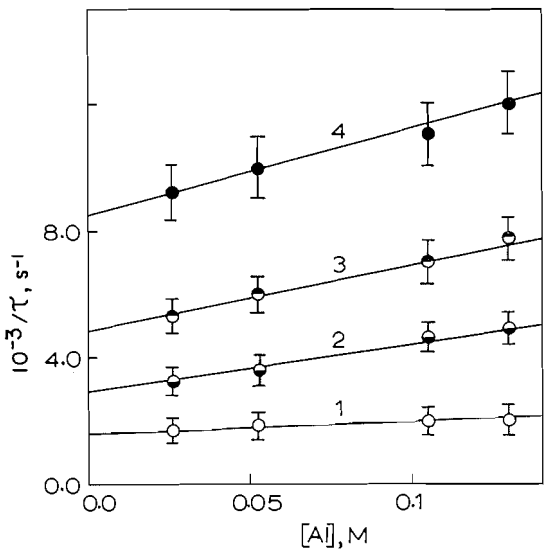

FIG. 1. Temps de relaxation du système Ce(IV). diméthyl-2,2 propanol-1. T = 10 °C; [Ce(IV)] = 0.005 *M*: force ionique = 1 *M*; *1*, $[HClO_4]$ = 0.1 *M*; *2*, $[HClO_4]$ = 0.3 *M*; *3*, $[HClO_4]$ = 0.5 *M*; *4*, $[HClO_4]$ = 0.7 *M*.

TABLEAU 1

Influence de la nature de l'alcool*

Alcool	k_d (s^{-1})	k_f (M^{-1} s^{-1})	K_c (M^{-1})	K_c (M^{-1})‡	K_c (M^{-1})§
Isobutanol	$2.3\ 10^4$	$8.3\ 10^4$	3.6 ± 1.4	—	—
Diméthyl-2,2 propanol-1	$5.0\ 10^3$†	$20.0\ 10^3$†	4.0 ± 1.6†	—	2.0 ± 0.5†
Butanol secondaire	$5.6\ 10^3$	$9.2\ 10^3$	1.7 ± 0.7	11	—
Butanol tertiaire	$1.2\ 10^2$	$3.7\ 10^2$	3.1 ± 1.2	13	1.5 ± 0.4‖

*T = 13 °C, Ce(IV) = 0.005 M, $HClO_4$ = 0.5 M.
†T = 10 °C.
‡Référence (21), T = ?, $[HClO_4]$ = 1.62 M.
§Méthode spectrophotométrique.
‖T = 25 °C.

l'ordre: isobutanol > butanol secondaire > butanol tertiaire et dépendent d'une manière très importante de la nature du ligand. Ceci est très différent des résultats obtenus dans le cas des complexes des métaux de transition (20). On a également porté au tableau les constantes de stabilité des complexes Ce(IV).alcool obtenu à partir des constantes de vitesse, $K_c = k_f/k_d$. En comparant ces constantes avec les valeurs publiées (21), à une concentration en acide perchlorique de 0.5 M, nous avons dû faire une correction en tenant compte de l'équation 5; l'augmentation de l'acidité entraîne le déplacement de l'équilibre 5 vers la gauche, causant une augmentation de la constante d'équilibre apparente de la formation du complexe Ce(IV).alcool dans lequel, comme il a été montré (5–7), seule l'espèce Ce^{4+} participe. La correction apportée à nos valeurs est de 20 à 50% d'après les valeurs extrêmes de 0.2 (22) et de 5.2 (19) de la constante d'hydrolyse publiées. Etant donné que même après correction l'écart était très important, nous avons vérifié les approximations faites dans l'étude des auteurs (21) et nous avons trouvé dans l'équation utilisée pour interpréter les résultats, qu'ils avaient négligé la quantité de Ce(IV) engagée dans le complexe. A une concentration de 0.1 M en Ce(IV) et en butanol tertiaire elle serait de 0.056 M avec la valeur de 13 M^{-1} pour la constante d'équilibre. Cette mauvaise approximation a comme conséquence des constantes d'équilibre beaucoup trop grandes. Pour écarter tout doute possible nous avons effectué une étude spectrophotométrique de la formation des complexes et nous avons trouvé des valeurs beaucoup plus près de celles obtenues par relaxation.

Influence de l'acidité

Au début de notre travail, nous avons envisagé l'étude de l'influence de l'acidité étant donné qu'elle intervient dans l'équilibre 5. L'étude a été réalisée entre 0.1 et 0.7 M en acide perchlorique; a très haute acidité. > 0.7 M, l'équation [8] est très déplacée vers la formation du Ce^{4+} et ne contribuant plus au saut celui-ci devient trop petit, tandis qu'a basse acidité, < 0.1 M, il y a formation d'espèces polynucléaires (19).

En effet l'acidité a une influence très importante; à une concentration en alcool donnée τ^{-1} augmente avec l'acidité.

L'étude systématique de l'influence de l'acidité est illustrée par les résultats présentés à la fig. 1 et on constate que k_f et k_d, donc pente et ordonnée à l'origine, augmentent avec l'acidité; l'ensemble des valeurs de ces constantes apparentes est résumé au tableau 2.

Le mécanisme le plus simple qui pourrait rendre compte des résultats expérimentaux est de trois étapes

[8] $$CeOH^{3+} + H^+ \underset{k_2}{\overset{k_1}{\rightleftharpoons}} Ce.H_2O^{4+} \text{ très rapide}$$

[9] $$Ce.H_2O^{4+} + al \underset{k_4}{\overset{k_3}{\rightleftharpoons}} (Ce.H_2O^{4+})al \text{ rapide}$$

TABLEAU 2

Influence de l'acidité*

(*a*) Diméthyl-2,2 propanol-1

$[HClO_4]$ (M)	10^{-3} k_d (s^{-1})		10^{-3} k_f (M^{-1} s^{-1})	
	10 °C	20 °C	10 °C	20 °C
0.1	1.6	2.5	3.5	8.0
0.3	3.2	4.4	12	14
0.5	5.0	5.5	20	22
0.7	8.5	9.0	30	32

(*b*) Butanol secondaire à 10 °C

$[HClO_4]$ (M)	10^{-3} k_d (s^{-1})	10^{-3} k_f (M^{-1} s^{-1})
0.1	1.9	2.5
0.3	2.7	7.5
0.5	4.6	15

*[Ce(IV)] = 0.005 M, force ionique = 1.0 M.

Can. J. Chem. Downloaded from www.nrcresearchpress.com by 210.87.254.5 on 09/05/12
For personal use only.

Can. J. Chem. Downloaded from www.nrcresearchpress.com by 210.87.254.5 on 09/05/12
For personal use only.

[10] $(Ce.H_2O^{4+})al + H^+ \underset{k_6}{\overset{k_5}{\rightleftharpoons}} Ce.al^{4+} + H_3O^+$ lente

où $Ce.H_2O^{4+}$ représente l'ion cérique avec la molécule d'eau de coordination qui est impliquée dans le mécanisme.

L'expression générale des temps de relaxation d'un tel système à trois étapes est extrêmement complexe et ne se prête pas à une vérification expérimentale; dans le calcul des temps de relaxation nous avons retenu les hypothèses suivantes: (*i*) l'étape 8 est très rapide par conséquent à l'équilibre; (*ii*) l'étape 9 est nettement plus rapide que l'étape 10 ce qui donne une expression simplifiée pour le temps de relaxation de ce système, identique à celle utilisée dans la littérature (8):

$$\tau^{-1} = a_{22} - a_{12} \cdot \frac{a_{21}}{a_{11}}$$

où les a_{ii} sont les coefficients du déterminant séculaire du système des étapes 9, 10, (*iii*) les concentrations des réactifs sont dans le rapport

$[H^+], [al] \gg$
$[Ce^{4+}], [CeOH^{3+}], [CeOH_2 \ldots al^{4+}], [Ce.al^{4+}]$

Tenant compte de ces hypothèses on obtient

$$[11] \quad \tau^{-1} = \frac{k_6([H^+] + K_{2,1})}{1 + K_{2,1}/[H^+] + K_{3,4}[al]} + \frac{(k_5 + k_6)K_{3,4}[H^+][al]}{1 + K_{2,1}/[H^+] + K_{3,4}[al]}$$

où

$$K_{3,4} = k_3/k_4$$

et

$$K_{2,1} = k_2/k_1$$

$K_{3,4}[al] \ll 1$, étant donné que la formation d'un complexe externe avec les alcools implique des intéractions électrostatiques beaucoup plus faibles que dans le cas de la formation d'une paire d'ions.

En introduisant le potentiel d'intéraction ion-dipole dans les relations utilisées par Eigen (23) et Hammes et Steinfeld (20), on a estimé la limite supérieure de $K_{3,4}$ à 0,2 pour une distance d'interaction de 4 Å. Le calcul exact n'est cependant pas possible car en plus des approximations habituelles concernant le potentiel d'interaction dans ce milieu, la constante diélectrique et la distance d'interaction, il faudrait utiliser le moment dipolaire du ligand, obtenu en phase gazeuse ou en solvant non-polaire, dans l'eau qui forme avec celui-là des ponts hydrogène.

Dans ces conditions l'équation 11 devient

$$[12] \quad \tau^{-1} = k_6[H^+] + k_5 \frac{K_{3,4}[H^+][al]}{1 + K_{2,1}/[H^+]}$$

Les figs. 2 et 3 montrent l'accord entre les valeurs de k_d et k_f expérimentales (les points) avec les courbes calculées à l'aide de l'éq. 12 en utilisant

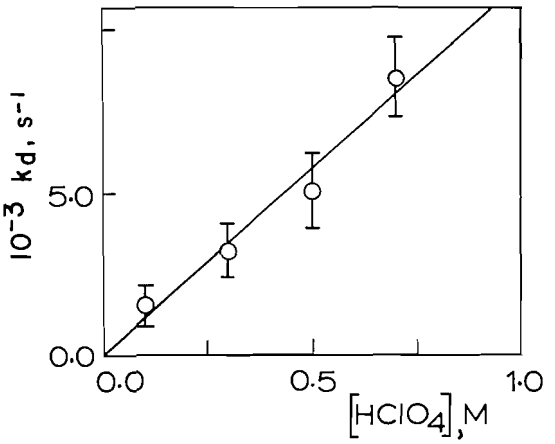

FIG. 2. Influence de l'acidité sur k_d: diméthyl-2,2 propanol-1; points expérimentaux et courbe calculée; $T = 10$ °C; [Ce(IV)] = 0.005 M; force ionique = 1 M.

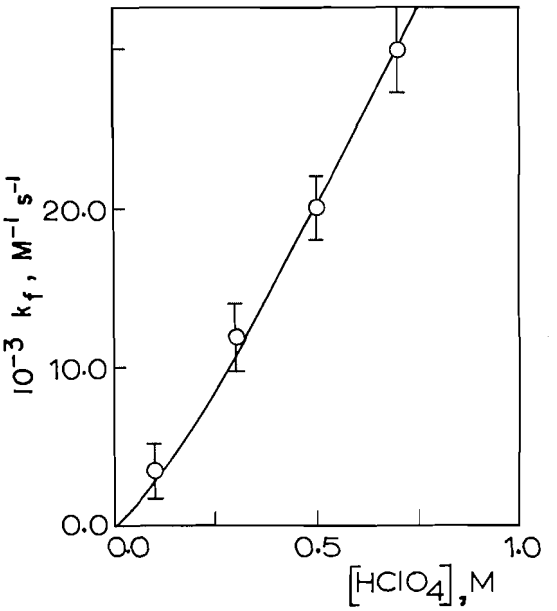

FIG. 3. Influence de l'acidité sur k_f: diméthyl-2,2 propanol-1; points expérimentaux et courbe calculée; $T = 10$ °C; [Ce(IV)] = 0.005 M; force ionique = 1 M.

TABLEAU 3

Comparaisons des $\tau_{exp.}$ et $\tau_{calc.}$

Diméthyl-2,2 propanol-1						Butanol secondaire			
		10 °C		20 °C				10 °C	
$[H^+]$ (*M*)	[al] (*M*)	10^4 $\tau_{exp.}$ (s)	10^4 $\tau_{calc.}$* (s)	10^4 $\tau_{exp.}$ (s)	10^4 $\tau_{calc.}$† (s)	$[H^+]$ (*M*)	[al] (*M*)	10^4 $\tau_{exp.}$ (s)	10^4 $\tau_{calc.}$‡ (s)
0.10	0.131	5.0	5.5	2.6	6.2	0.10	0.32	4.0	5.4
0.10	0.105	5.0	5.9	—	—	0.10	0.24	4.0	6.6
0.10	0.078	—	—	3.0	6.6	0.10	0.16	4.4	7.4
0.10	0.052	5.3	6.7	3.3	6.9	0.10	0.08	4.8	8.3
0.10	0.026	5.9	7.1	3.6	7.1	0.30	0.32	1.9	1.7
0.30	0.131	2.0	2.1	1.55	1.8	0.30	0.24	2.2	2.0
0.30	0.105	2.2	2.3	1.65	1.9	0.30	0.16	2.7	2.3
0.30	0.052	2.8	2.7	1.9	2.15	0.30	0.08	3.0	2.7
0.30	0.026	3.0	2.9	2.1	2.3	0.50	0.32	1.0	1.0
0.50	0.131	1.3	1.15	1.2	1.05	0.50	0.24	1.3	1.1
0.50	0.105	1.4	1.25	1.3	1.15	0.50	0.16	1.4	1.3
0.50	0.052	1.7	1.5	1.55	1.35	0.50	0.08	1.6	1.6
0.50	0.026	1.9	1.6	1.7	1.45	Butanol tertiaire 35 °C			
0.70	0.131	0.85	0.83	0.75	0.7	0.10	0.08	6.0	—
0.70	0.105	0.9	0.91	0.85	0.8	0.30	0.08	6.0	—
0.70	0.052	1.0	1.05	0.95	0.9	0.70	0.08	6.0	—
0.70	0.026	1.1	1.15	1.05	1.0	1.10	0.08	5.0	—

*$K_{2,1} = 0.1\ M$, $K_{3,4}k_5 = 4.3 10^4\ M^{-2}s^{-1}$, $k_6 = 1.1\ 10^4\ M^{-1}s^{-1}$.
†$K_{2,1} = 0.15\ M$, $K_{3,4}k_5 = 5.0\ 10^4\ M^{-2}s^{-1}$, $k_6 = 1.3\ 10^4\ M^{-1}s^{-1}$.
‡$K_{2,1} = 0.1\ M$, $K_{3,4}k_5 = 3.2\ 10^4\ M^{-2}s^{-1}$, $k_6 = 1.0\ 10^4\ M^{-1}s^{-1}$.

les paramètres du tableau 2. Bien que les valeurs de la fig. 3 seraient en accord avec une droite, il était impossible de trouver un mécanisme pouvant l'expliquer, car ceci impliquerait que l'on néglige le dénominateur dans l'éq. 12, c'est-à-dire que l'on ne tient pas compte de l'hydrolyse, pourtant bien établie, du Ce^{4+}. L'ensemble des résultats pour le diméthyl-2,2-propanol-1 et le butanol secondaire est présenté au tableau 3, et on constate que l'accord entre les temps de relaxation expérimentaux et calculés avec les paramètres du tableau 3 est satisfaisant.

Discussion

Le mécanisme proposé est plus complexe que celui généralement trouvé dans le cas des alcalino-terreux, les métaux de transition, et même dans le cas des complexes du Ce(III), qui se font par un mécanisme S_N1 (24) et dont il diffère sur deux points importants: (*i*) le départ d'eau (ou du ligand) est catalysé par H^+ (*ii*) la vitesse varie d'une manière notable avec la nature du ligand.

Influence de l'acidité

L'influence catalytique de H^+ est semblable à celle trouvée dans le cas de la dissociation de certains complexes (15–18). Bien que très défavorisée à cause de la répulsion électrostatique, la protonation de la molécule d'eau de coordination dans le complexe activé, rend la rupture de la liaison de transfert de charge Ce—O beaucoup plus facile et c'est ce dernier phénomène qui l'emporte.

Dans l'étude des réactions d'échange de protons des molécules d'eau de coordination de certains ions métalliques l'influence comparable de H^+ a été observée; l'interprétation des résultats a également fait intervenir une molécule d'eau de coordination protonée dans l'étape lente (25).

Toutefois dans le cas des complexes Ce(IV). alcool le mécanisme catalytique ne semble constituer qu'un cas limite. En effet l'éq. 12 ne permet pas l'interpréter les résultats dans le cas du butanol tertiaire où un mécanisme non-catalytique serait prépondérant. Même dans les cas du diméthyl-2,2 propanol-1 et du butanol secondaire on ne peut exclure ce mécanisme non-catalytique contribuant à raison de quelques pourcents aux temps observés et pouvant expliquer les écarts à basse concentration en H^+ du tableau 3, bien que ces résultats soient aussi influencés par un début de dimérisation du Ce(IV).

Influence de l'alcool

L'influence importante de la nature de l'alcool montre que contrairement aux complexes d'al-

Can. J. Chem. Downloaded from www.nrcresearchpress.com by 210.87.254.5 on 09/05/12
For personal use only.

calino-terreux, métaux de transition (24) on est ici en présence d'un mécanisme à un caractère SN2 non négligeable. Le fait que celle-ci soit à peu près identique sur les vitesses de formation et de dissociation des complexes ne peut pas être attribuée à une seule cause, par conséquent l'interprétation en est très spéculative. Le changement important de l'encombrement stérique de l'oxygène en passant de l'isobutanol au butanol tertiaire expliquerait assez bien la diminution de la vitessé de formation, à cause des intéractions répulsives avec l'ion central ainsi qu'avec les molécules d'eau de coordination. Toutefois si l'effet stérique était le seul à intervenir le même raisonnement mènerait à une diminution de la constante de stabilité. Les résultats expérimentaux montrent que tel n'est pas le cas et que la force de liaison de transfert de charge formée, plus grande dans le cas du butanol tertiaire, peut compenser cet effet et entraîner en même temps une diminution de la vitesse de dissociation. Il est à noter que l'effet stérique du ligand a déjà été mis en évidence dans le cas de formation de certains chélates (26).

Il est évident que les effets observés sont en partie dus aux changements de la couche de coordination secondaire de l'ion et aux changements de solvatation des alcools; mais ces derniers ne peuvent être évalués.

Nous remercions le Conseil National de Recherches du Canada pour l'octroi grâce auquel ce travail a pu être réalisé.

1. W. H. RICHARDSON. Oxydation in organic chemistry. Vol. 5A. *Edited by* K. B. Wiberg. Academic Press Inc., New York, 1965. p. 243.
2. F. R. DUKE et A. A. FLORIST. J. Amer. Chem. Soc. **71**, 2790 (1949).
3. F. R. DUKE et R. F. BREMER. J. Amer. Chem. Soc. **73**, 5179 (1951).
4. H. L. LINTZ et D. C. JOHNSON. J. Org. Chem. **32**, 556 (1967).
5. M. ARDON. J. Chem. Soc. 1811 (1957).
6. S. S. MUHAMMAD et K. V. RAO. Bull. Chem. Soc. Jap. **36**, 943 (1963).
7. B. SETHURAM et S. S. MUHAMMAD. Acta Chim. Acad. Sci. Hung. **46**, 125 (1965). D. PAQUETTE et M. ZADOR. Can. J. Chem. **46**, 3507 (1968).
8. M. EIGEN et L. DE MAEYER. Technique of organic chemistry. Vol. 8. *Edited by* A. Weissberger, Interscience, New York, 1963. G. H. CZERLINSKI. Chemical relaxation. Marcel Dekker Inc., New York, 1966.
9. E. F. CALDIN. Fast reactions in solution. John Wiley and Sons, Inc., New York, 1964.
10. M. EIGEN. Pure Appl. Chem. **6**, 97 (1963).
11. L. I. BUDARIN et K. B. YATSIMIRSKIL. Russ. Chem. Rev. **37** (3), 209 (1968).
12. A. MCAULEY et J. HILL. Quart. Rev. 18 (1969).
13. C. H. LANGFORD et H. B. GRAY. Ligand substitution processes. Benjamin, New York, 1966.
14. M. EIGEN. Advances in the chemistry of the coordination compounds. *Edited by* S. Kirschnner, MacMillan, New York, 1961. p. 371.
15. F. BASOLO, W. R. MATOUSH, et R. G. PEARSON. J. Amer. Chem. Soc. **78**, 4833 (1956).
16. S. C. CHAN. J. Chem. Soc. 2375 (1964).
17. J. H. BAXENDALE et P. GEORGE. Trans. Faraday Soc. **46**, 7361 (1950).
18. D. SEEWALD et N. SUTIN. Inorg. Chem. **2**, 643 (1963).
19. T. S. HARDWICK et E. ROBINSON. Can. J. Chem. **29**, 818 (1951).
20. G. G. HAMMES et J. J. STEINFELD. J. Amer. Chem. Soc. **84**, 4639 (1962).
21. H. G. OFFNER et D. A. SKOOG. Anal. Chem. **38**, 1520 (1966).
22. H. G. OFFNER et D. A. SKOOG. Anal. Chem. **37**, 1018 (1965).
23. M. EIGEN. Z. Electrochem. **64**, 115 (1960).
24. G. GEIER. Ber. Bunsenges. Phys. Chem. **69**, 617 (1965).
25. J. J. SWIFT et T. A. STEPHENSON. Inorg. Chem. **5**, 1100, (1966). J. J. SWIFT, T. A. STEPHENSON et G. R. STEIN. J. Amer. Chem. Soc. **89**, 1611 (1967).
26. K. KUSTIN, R. F. PASTERNACK et E. M. WEINSTOCK. J. Amer. Chem. Soc. **88**, 4610 (1966). A. KOWALAK, K. KUSTIN, R. F. PASTERNACK et S. PETRUCCI. J. Amer. Chem. Soc. **89**, 3121 (1967).

Can. J. Chem. Downloaded from www.nrcresearchpress.com by 210.87.254.5 on 09/05/12
For personal use only.

Can. J. Chem. Downloaded from www.nrcresearchpress.com by 210.87.254.42 on 09/05/12
For personal use only.

New preparation of benzo-2,1,3-oxadiazoles (benzofurazans)[1]

J. M. PROKIPCAK AND P. A. FORTE
Department of Chemistry, University of Guelph, Guelph, Ontario

Received March 10, 1970

A new procedure for the synthesis of substituted benzo-2,1,3-oxadiazoles (benzofurazans) has been established. The method involved the pyrolysis of substituted methyl *N*-(*o*-nitrophenyl)carbamates. A possible mechanism for the reaction is outlined.

Canadian Journal of Chemistry, **48**, 3059 (1970)

Previously it was reported (1) that the thermal decomposition of alkyl *N*-(*o*-nitrophenyl)carbamates yielded benzofurazan. Further investigation of the reaction has shown that this relatively simple procedure could be generally applicable as a synthetic route to benz-substituted benzofurazans (Table 1). The only apparent limitation would be the availability of the properly substituted starting carbamates.

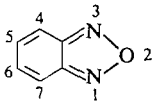

1

The preferred alkyl carbamate has been shown (1) to be the methyl carbamate. When the alkyl group was ethyl or isopropyl, side reactions involving olefin formation occurred. These were shown to be occurring by passing the gaseous products through a CCl_4–Br_2 solution. When different phenyl carbamates were used, benzofurazan formation was noticeably reduced or failed to occur (Table 2). In making use of this reaction for the preparation of benzofurazans it was necessary to prepare the substituted methyl-*N*-(*o*-nitrophenyl)carbamates. These carbamates were prepared in two different ways depending on the availability of the starting materials. Certain carbamates were readily obtained by reacting substituted *o*-nitroanilines with methyl chloroformate. Other carbamates were prepared by starting with the substituted *o*-nitrobenzoic acid and converting the acid to the acid chloride by using thionyl chloride. The acid chloride was then reacted with sodium azide (Curtius reaction) to yield the substituted *o*-nitrophenylisocyanate. Addition of absolute methanol to the isocyanate gave the substituted methyl carbamate.

In the absence of kinetic data the proposed mechanism is based on product yields (Table 1) and from the results of special reaction mixtures listed in Table 3. Attempts to run kinetics on the reaction in solvents such as diphenyl ether, dimethyl sulfoxide, hexamethylphosphoramide, and benzonitrile yielded only trace amounts of benzofurazans. Two tentative routes which could lead to the final products are shown in Scheme 1.

Both routes *1* and *2* require the formation of a cyclic intermediate; route *1* in the cyclization of the starting urethane and route *2* in the cyclization of the *o*-nitrophenylisocyanate once it has formed. In addition to the carbamate pyrolysis reactions, the following findings are of both preparative and mechanistic interest (Table 3). Pyrolysis of *o*-nitrophenylisocyanate itself resulted in a lower yield of benzofurazan than most of the studied carbamates. Also the yield of product was unaffected by the addition of base. However, addition of base to the pyrolysis of methyl *N*-(*o*-nitrophenyl)isocyanate which should facilitate breakdown of carbamate into isocyanate and alcohol (2) drastically reduced the yield of benzofurazan.

The experimental results obtained would favor the formation of the benzofurazans via route *1*. The cyclic intermediate formed then could break down to a nitrene-type intermediate similar to that proposed by Huisgen (3) as a feasible intermediate when benzofuroxan was formed from *o*-nitrophenyl azide according to eq. 1. Subsequent cyclization of the nitrene intermediate would yield benzofurazan. However, route *2* is probably operative and does lower the yields of benzofurazan due to undesirable side reactions.

[1]Taken from the thesis of Peter A. Forte presented to the Faculty of Graduate Studies, University of Guelph, Guelph, Ontario, as part of the requirements for the degree of Master of Science.

TABLE 1

The preparation of substituted benzofurazans*

Substituents				Melting points (°C)		
R_4	R_5	R_6	R_7	Observed	Reported	% Yield
CH_3	H	H	H	41.5–42.5	44	30
CH_3O	H	H	H	87.5–88.5	89–90	30
H	CH_3O	H	H	98–100	99	20
H	CH_3	H	H	35.5–36.5	37	50
H	H	H	H	51.5–52.5	55	50
H	Cl	H	H	41–42	44	40
H	NO_2	H	H	64–65	65	35
H†	CH_3	CH_3	H	83–85		48
H	H	CH_3	H	35.5–36.5	37	46
H	H	Cl	H	41–42	44	20
H	H	H	CH_3	41.5–42.5	44	50

*The general structure was 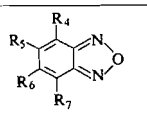

†Anal. Calcd. for $C_8H_8N_2O$: C, 64.85; H, 5.44; N, 17.35. Found: C, 64.55; H, 5.43; N, 17.09.

TABLE 2

The preparation and decomposition of substituted phenyl *N*-(*o*-nitrophenyl)carbamates*

X	Melting point (°C)	% Composition Calcd. C	H	N	Found C	H	N	% Yield benzofurazan
H	93–95	60.46	3.90	10.85	60.16	4.06	11.03	0
CH_3O	157–158	58.33	4.19	9.72	58.48	4.38	9.51	15
O_2N	174–176	51.49	2.99	13.86	51.62	2.64	14.01	0

*General Formula 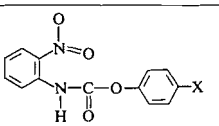

All the phenyl-*N*-*o*(nitrophenyl)carbamates were prepared by treating the *o*-nitrophenyl isocyanate with the corresponding phenol.

TABLE 3

Special reaction mixtures

Reactant(s)	Reaction temperature* (°C)	% Benzofurazan
o-Nitrophenylisocyanate	255	24†
o-Nitrophenylisocyanate; 18% MeO	190	28
o-Nitrophenylisocyanate; 79% MeO	190	26
Methyl *N*-(*o*-nitrophenyl)-carbamate; 2% MeO	250	20
Methyl *N*-(*o*-nitrophenyl)-carbamate; 70% MeO	200	0

*Reaction temperature is taken as the temperature where the evolution of CO_2 gas is at a constant rate.

†Previously reported (1) as 5%. An improved workup technique raised the yield over a series of runs.

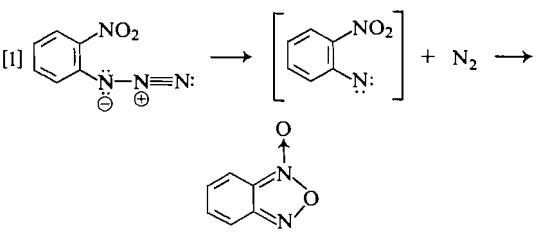

Experimental

All melting points were determined on the Fisher-Johns melting point apparatus and are uncorrected. Analyses were performed by Organic Microanalyses, 5757 Decelles Avenue, Montreal, Quebec. The n.m.r. spectra were measured on a Varian A60A instrument using tetramethylsilane as a standard and the i.r. spectra on a

Can. J. Chem. Downloaded from www.nrcresearchpress.com by 210.87.254.42 on 09/05/12
For personal use only.

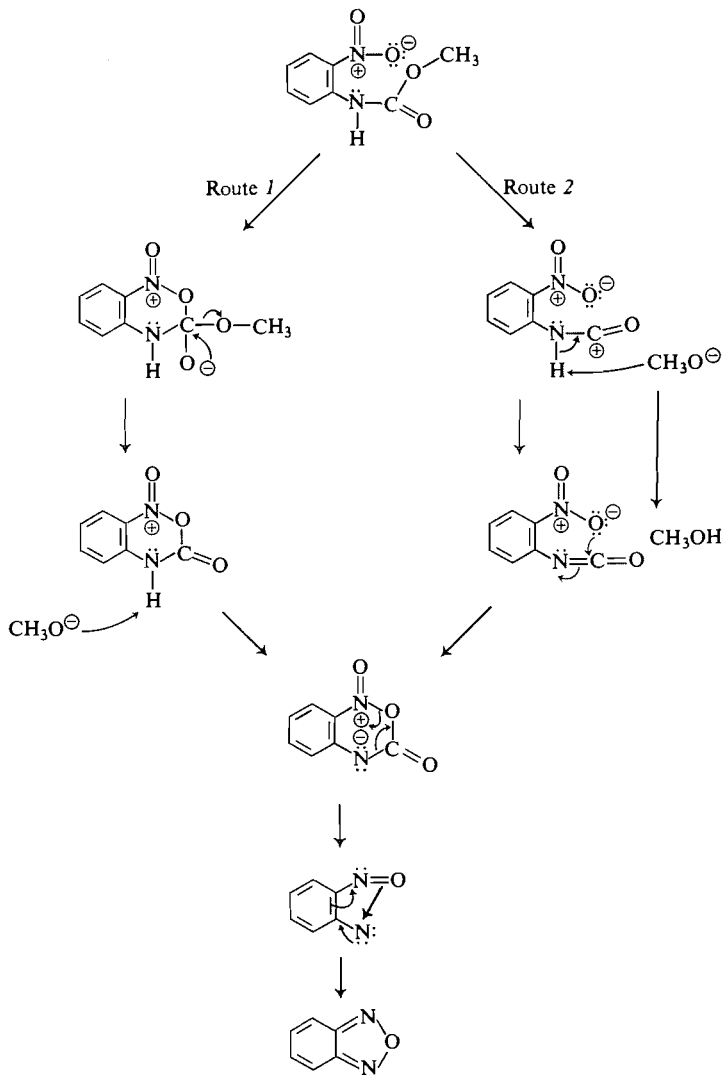

SCHEME 1

Beckmann IR5A. All product yields are based on an average of at least three runs.

Preparation of Substituted Methyl N-(o-Nitrophenyl)-carbamates

Method A: Preparation of Methyl N-(4-Methyl-2-nitrophenyl)carbamate

In a typical experiment, a slurry of 4-methyl-2-nitroaniline (50.0 g, 0.328 mole) and CCl_4 (400 ml) was made. To this 50.0 ml (61.1 g, 0.650 mole) of methyl chloroformate were added over a period of 30 min. The mixture was stirred continuously at room temperature for an additional hour. Pyridine (26.5 ml, 0.328 mole) was then added over a period of 1 h and the reaction mixture stirred at room temperature for an additional hour. The solid material which separated was removed by filtration. The CCl_4 from the remaining liquid was removed *in vacuo* whereupon an orange-yellow precipitate resulted. Recrystallization of this precipitate from hexane – carbon tetrachloride (9:1) gave 39.0 g (56%) of methyl *N*-(4-methyl-2-nitrophenyl)carbamate, m.p. 104–105° with the following spectral data: n.m.r. ($CDCl_3$) δ 9.54 (1 NH broad singlet which disappears on the addition of D_2O), 7.10–8.51 (3H multiplet), 3.80 (3H singlet), and 2.36 (3H singlet); i.r. (CCl_4) 3325 (—N—H), 1740 (—C(=O)—), and 1250 (—O—CH_3) cm^{-1}.

Anal. Calcd. for $C_9H_{10}N_2O_4$: C, 51.43; H, 4.80; N, 13.33. Found: C, 51.48; H, 4.83; N, 13.19.

Method B: Preparation of Methyl N-(5-Methyl-2-nitrophenyl)carbamate

The method of McElvain and Carney (4) was followed

Can. J. Chem. Downloaded from www.nrcresearchpress.com by 210.87.254.42 on 09/05/12
For personal use only.

TABLE 4

The preparation of methyl *N*-(substituted-2-nitrophenyl)carbamates*

Substituents				Method	Melting point (°C)	% Yield	Analysis: Calcd. (%)			Analysis: Found (%)		
R_4	R_5	R_6	R_7				C	H	N	C	H	N
CH_3	H	H	H	B	48–49.5	75	51.43	4.79	13.33	51.43	4.38	13.51
CH_3O	H	H	H	B	125–127	44	47.79	4.46	12.38	47.78	4.32	12.68
H	CH_3O	H	H	A	100.5–101	60	47.79	4.46	12.38	47.38	4.48	12.51
H	CH_3	H	H	A	104–105	56	51.43	4.80	13.33	51.48	4.83	13.19
H†	H	H	H		51–53	71	48.98	4.11	14.28	48.89	4.01	14.28
H‡	Cl	H	H	A	107.5–108	58	41.67	3.06	12.15	41.36	2.88	12.05
H	NO_2	H	H	B	125–127	58	39.84	2.92	17.42	40.13	3.23	17.66
H	CH_3	CH_3	H	A	81–82.5	57	53.57	5.39	12.49	53.84	5.36	12.31
H	H	CH_3	H	B	59–60	57	51.43	4.79	13.33	51.43	4.70	13.46
H§	H	Cl	H	B	63.5–65.5	24	41.67	3.06	12.15	41.70	2.96	12.01
H	H	H	CH_3	A	133–134	2.5	51.43	4.79	13.33	51.44	4.55	13.66

*The general structure was 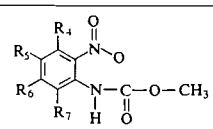

†Reference 1 for preparation.
‡Analysis for Cl: Calcd., 15.37; Found, 15.65.
§Analysis for Cl: Calcd., 15.37; Found, 15.31.

for the preparation of the acid chloride of 5-methyl-2-nitrobenzoic acid. 5-Methyl-2-nitrobenzoic acid (50.0 g, 0.277 mole) was dissolved in 600 ml of dry benzene and cooled to 13° by a cold water bath. To this solution 93.0 ml (132.0 g, 1.108 mole) of thionyl chloride were added slowly with stirring after which the solution was refluxed gently for 24 h. The solvent and excess thionyl chloride were removed *in vacuo* to give the crude acid chloride which was used in the unpurified form for preparing the isocyanate according to the method of Allain and Bell (5).

Sodium azide (27.0 g, 0.415 mole) was dissolved in 180 ml of distilled water and cooled to 10°. While stirring this solution, the acid chloride (dissolved in 150 ml of reagent acetone) was added at a rate such that the reaction temperature did not exceed 15°. After addition of the acid chloride, the reaction mixture was stirred at 18° for 3 h. A solid formed which was filtered off. The organic layer of the filtrate was separated and the solvent removed *in vacuo* whereupon a solid formed. This solid azide was combined with the original solid and was added in small portions to dry benzene which had been heated initially to 60°. The addition of the azide was exothermic and so no further warming was necessary. After complete addition the solution was allowed to stand at room temperature for 2 h.

To the benzene solution was added 20.0 ml anhydrous methanol and the solution was refluxed for 3 h. The solvent and excess methanol was removed *in vacuo* whereupon an oil resulted. Addition of hot hexane yielded 32.6 g (57%) of methyl *N*-(5-methyl-2-nitrophenyl)-carbamate, m.p. 59–60°, with the following spectral data: n.m.r. ($CDCl_3$) δ 9.90 (1 NH broad singlet which disappears on the addition of D_2O), 5.80–8.40 (3H multiplet), 3.82 (3H singlet), and 2.41 (3H singlet); i.r. (CCl_4) O ‖ 3325 (—N—H), 1745 (—C—), and 1250 (—O—CH_3) cm^{-1}.

Anal. Calcd. for $C_9H_{10}N_2O_4$: C, 51.43; H, 4.79; N, 13.33. Found: C, 51.43; H, 4.70; N, 13.46.

The remainder of the carbamates were prepared by one of the two methods given. Details are shown in Table 4.

Preparation of Substituted Benzofurazans

The method of preparation of the substituted benzofurazans was identical for all cases. The thermal decomposition of methyl *N*-(4-methyl-2-nitrophenyl)carbamate resulting in the formation of 5-methylbenzofurazan, CO_2, and methanol will be described as a typical method. The remainder of the benzofurazans were similarly prepared and these details are shown in Table 1.

Thermal Decomposition of Methyl N-(4-methyl-2-nitrophenyl)carbamate

Methyl N-(4-methyl-2-nitrophenyl)carbamate (8.9 g, 0.065 mole) was placed in a 50 ml two-necked conical flask fitted with a thermometer and a simple distillation set up consisting of a stillhead, condenser, and receiver. The flask contents were raised to 255° by means of a heating mantel. The evolution of CO_2 gas was detected by use of a limewater solution. After the evolution of gas ceased, the material in the pot was distilled at 0.2 mm pressure. All distillable material came off at a pot temperature less than 169° and solidified in the condenser. This solid was scraped out of the condenser and purified using a Nester-Faust sublimation apparatus. Pure 5-methylbenzofurazan, m.p. 35–36.5° (lit. (8) 37°) was obtained with the following spectral properties: n.m.r.

Can. J. Chem. Downloaded from www.nrcresearchpress.com by 210.87.254.42 on 09/05/12
For personal use only.

($CDCl_3$) δ 7.08–7.75 (multiplet) and 2.43 (singlet) with an integrated area ratio of 1:1 respectively; i.r. (CCl_4) showed strong absorption at 1630, 1530, 1460, 1440, 1410, 1370, 1315, 1155, 1040, 1010, 890, and 850 cm^{-1}.

The authors would like to acknowledge the National Research Council of Canada for financial support of this research. We also thank Mr. H. S. McKinnon for running all the n.m.r. spectra.

1. J. M. PROKIPCAK, P. A. FORTE, and D. D. LENNOX. Can. J. Chem. **47**, 2482 (1969).
2. T. MUKAIYAMA and Y. HOSHINO. J. Amer. Chem. Soc. **78**, 1946 (1956).
3. R. HUISGEN. Angew. Chem. Intern. **2**, 565 (1962).
4. S. M. MCELVAIN and T. P. CARNEY. J. Amer. Chem. Soc. **68**, 2599 (1946).
5. C. F. H. ALLAIN and A. BELL. Org. Syn. E. C. Horning, editor. Col. Vol. III. Wiley, New York, N.Y. 1955. p. 846.

Can. J. Chem. Downloaded from www.nrcresearchpress.com by 210.87.254.42 on 09/05/12
For personal use only.

Can. J. Chem. Downloaded from www.nrcresearchpress.com by 210.87.254.6 on 09/05/12
For personal use only.

Potassium fluoride catalyzed reactions between malononitrile and α,β-unsaturated ketones

J. W. ApSimon, J. W. Hooper, and B. A. Laishes
Department of Chemistry, Carleton University, Ottawa, Canada

Received April 23, 1970

The preparation and structure elucidation of the condensation products between malononitrile and a variety of α,β-unsaturated ketones using potassium fluoride as catalyst is described. If the carbonyl group of the α,β-unsaturated ketone is hindered, then Michael addition occurs. If, however, the carbonyl group is unencumbered, a Knoevenagel reaction appears to occur first which, in many cases, is then followed by conjugate addition and intramolecular condensation to yield compounds of unusual structure.

Canadian Journal of Chemistry, 48, 3064 (1970)

During the course of the work directed towards the total synthesis of pentacyclic triterpenes we required an intermediate of type **1**, intended to become ring E and part of ring D of the natural products, *e.g.*, β-amyrin (**2**). An obvious route was Michael addition of a two-carbon unit to 3,6,6-trimethyl-2-cyclohexenone (**3**).

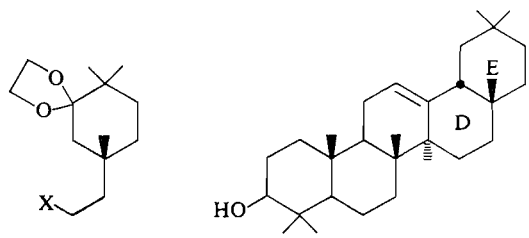

1 **2**

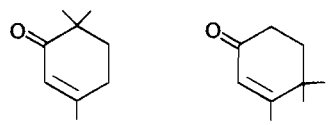

3 **4**

Base catalyzed condensation of methyl vinyl ketone with 3-methyl-2-butanone gave a mixture of ketone **3** and its isomer **4** (82:18). The structures of these ketones were established by comparing their physical constants, and the rates of formation of their semicarbazones, with the data of Buchman and Sargent (3) for the same compounds. These structural assignments were confirmed by the subsequent reactions of the ketones **3** and **4**.[1]

[1]Several reports of the preparation of ketones **3** and **4** exist (1–5) and the former has usually been the major product of condensations of the type described above. The substance obtained by Dauben *et al.* (5) and assigned structure **4** is probably ketone **3** judging from the spectral data given and its mode of formation.

Attempts to induce a Michael addition of diethyl malonate to **3** in the presence of various bases failed. Such an addition has been successful in the case of 3-methyl-2-cyclohexenone (7), but in low yields. Reports (8) of the use of anhydrous potassium fluoride as a catalyst in Michael and Knoevenagel reactions induced us to investigate its use in our case. We chose also to use the more acidic malononitrile, a substrate that probably also has smaller steric requirements than malonic ester.

The solvent choice for this reaction was critical. Thus, at room temperature in dimethylformamide (DMF) a slow reaction occurred between **3** and malononitrile. Heating at 100° did not appreciably alter the rate of Michael addition, rather, the i.r. spectra of aliquots indicated the formation of 1,2-addition products (Knoevenagel reaction) (2210 cm^{-1} unsaturated nitrile) (9, 14). Anhydrous potassium fluoride is only sparingly soluble in DMF (10) and it was reasoned that if its concentration in the reaction could be raised, then formation of the Michael adduct **5** might be facilitated. The reaction was carried out in mixtures of ethylene glycol and DMF (1:1) (11). Time studies showed that the concentration of a component absorbing at 1695 cm^{-1} (saturated ketone) was at a maximum after 2–2.5 h and thereafter steadily declined with regeneration of starting material and formation of the substance showing i.r. absorption at 2210 and 1615 cm^{-1} (C=C). Apparently the Michael reaction is reversible and subsequent removal of malononitrile by oligimerization (12) and formation of a Knoevenagel product displaces the equilibrium away from the Michael adduct. The optimum yield of Michael adduct **5** m.p. 68–69°, was 56% after 2–3 h. The i.r. spectrum of **5** showed absorp-

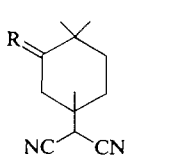

5 R = O

7 R = 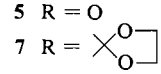

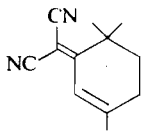

6

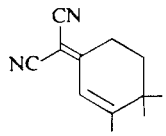

8

tions for saturated nitrile (2250 cm^{-1}) and saturated ketone (1695 cm^{-1}) and the n.m.r. spectrum showed signals for three tertiary methyl groups and a one proton singlet at δ 4.87 assigned to the methine proton α to the nitrile groups. Reaction for 24 h gave a reduced yield of **5** and an increase in the yield of Knoevenagel product **6**. Conversion of the contaminating Michael adduct to the corresponding ketal **7**, which readily crystallized out of the mixture, followed by distillation of the residues and crystallization of the distillate provided pure Knoevenagel product **6**, m.p. 67–68°. The u.v. spectrum of **6** showed a maximum at 306 nm (14) and the i.r. spectrum exhibited absorption at 2210 (unsaturated nitrile) and 1615 cm^{-1} (double bond). The n.m.r. spectrum included signals for the *gem*-dimethyl (δ 1.42), the vinylic methyl (δ 2.07), and the ethylenic proton (δ 6.58). Attempts to prepare this product by the normal ammonium acetate catalyzed Knoevenagel process (13) failed. Both **3** and **4** were recovered unchanged when treated with anhydrous KF in the solvent system used in the absence of malononitrile, thus eliminating the possibility of any rearrangement process during the addition reactions (6). Under similar conditions the Michael adduct **5** underwent reversion to **3** (85%), but not to **4**, with some formation of the Knoevenagel product **6**. The ketal **7** has since been converted into tosylate **1** (X = OTs) and this work will be reported in context with our triterpene syntheses.

The anhydrous KF catalyzed reaction of 3,4,4-trimethyl-2-cyclohexenone **4** with malononitrile gave essentially one substance identified as the Knoevenagel product **8**, m.p. 55–56°. Its i.r. spectrum showed absorptions at 2210 (unsaturated nitrile) and 1600 and 1545 cm^{-1} (double bonds) whilst the u.v. spectrum showed a typical maximum at 304.5 nm (14). The n.m.r. spectrum was consistent with this structure (see Experimental).

These early experiments suggested that if the carbonyl group of a 2-cyclohexenone is sterically hindered then a Michael reaction is favored; on the other hand, if the β-terminus is hindered and the carbonyl is relatively available, then a 1,2-addition takes place to give the Knoevenagel product. This idea was reinforced when testosterone was treated under the same reaction conditions to give only the dicyanoethylidene derivative **9**, m.p. 184°, with no evidence of the Michael product.

In order to investigate the scope of this reaction somewhat further we studied the behavior of several α,β-unsaturated ketones under the conditions described. The substrates examined and the products obtained are dealt with in turn.

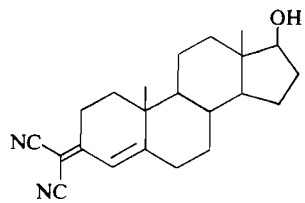

9

Pulegone (10)

Inspection of the structure of pulegone **10** shows an enone carbonyl group that is relatively hindered. Reaction with malononitrile in the presence of KF afforded a crystalline product $C_{13}H_{18}N_2O$ in 50% yield whose i.r. spectrum indicated NH_2 (3450 and 3320 cm^{-1}), C=C double bond (1640 cm^{-1}), and unsaturated nitrile (2180 cm^{-1}) (15), and what appeared at first to be a carbonyl absorption at 1710 cm^{-1}. That conjugate addition had occurred was indicated by the n.m.r. spectrum of the product where the signal for the isopropylidene methyl groups (δ 2.00 and 1.60 in pulegone) now appeared at δ 1.22. These data led us to consider a structure such as **11** or a closely related one for this adduct. However, the ready acid hydrolysis to an enol lactone, $C_{13}H_{17}NO_2$, ν_{max} 1755 cm^{-1}, which would appear to have structure **12**, suggested revision to structure **13**. The u.v. spectrum of the adduct showed a maximum at 269 nm (ε 5800) as well as strong end absorption, which is attributable to the enamino cyano system proposed for **11** or **13** (18, 21). Support for structure **13** was immediately available from the recent work of Wolinsky (16) who showed that the reaction of pulegone with ethyl acetoacetate gave compound **14**, and further in a large series of γ-pyrans of similar structure, strong absorption around 1710 cm^{-1} in the i.r. was observed (17). This

Can. J. Chem. Downloaded from www.nrcresearchpress.com by 210.87.254.6 on 09/05/12
For personal use only.

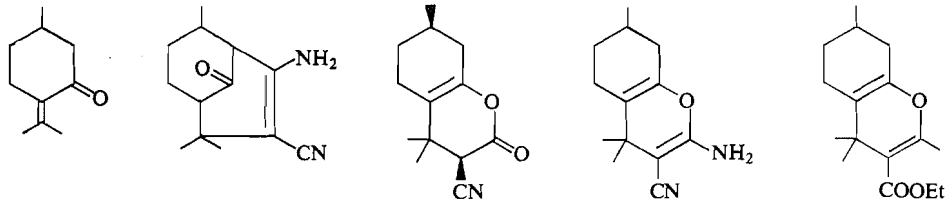

10 11 12 13 14

information enabled us to assign all spectral data in support of **13**. Further evidence was available from the mass spectrum[2] of **13**. Thus, the base peak is at M-15, corresponding to the loss of $-CH_3$ to yield the stable pyrilium ion **15** (16), (Scheme 1). There is one other major fragment at *m/e* 161 (11%) which can be accommodated by a reverse Diels–Alder process as shown to yield ion **16**, a process supported by a metastable peak of *m/e* 128.

The mass spectrum of enol lactone **12** is more complex with very intense fragments at *m/e* 204 (100%), 152 (95%), and 81 (71%). That at *m/e* 204 is doubtless loss of $-CH_3$ to yield ion **17**; however, an alternate fragmentation appears to lead to *m/e* 152 via a retro Diels–Alder pathway (Scheme 2) in which cleavage of the lactone, accompanied by loss of cyanoketene, yields ion **18** (19).[3]

The stereochemistry indicated in **12** is that favored since the new asymmetric center (H—C—CN) will probably be formed under equilibrating conditions and the cyano group would then be expected to take up a pseudo equatorial configuration.

3-Methyl-2-cyclohexenone (19)

In the case of 3-methyl-2-cyclohexenone (20) we chose a compound in which we felt that Knoevenagel reaction would be the major pathway. When the anhydrous KF catalyzed procedure with malononitrile was carried out, a 63% yield of a compound analyzing for $C_{16}H_{14}N_6$ was obtained, corresponding to a 3:1 condensation product with malononitrile. The i.r. spectrum of this material exhibited absorption bands for $-NH_2$, non-conjugated nitrile (2275 and 2255 cm^{-1}), conjugated nitrile (2200 cm^{-1}), and C=C (1650 cm^{-1}). Thus, there are apparently 3 types of cyano grouping present in the adduct. The u.v. spectrum (λ_{max} 274 nm, ε 35 300) indicated a similar chromophore (NC—C=C—NH_2) to that present in **13** (18). The n.m.r. spectrum of this adduct showed three exchangeable protons of which two appeared at δ 7.10 ($-NH_2$) and the other as a singlet at δ 4.85. The latter signal is assigned to the methine proton on $-CH(CN)_2$, the exchange being autocatalytic in the presence of the basic amino grouping in the adduct.[4] The methyl signal now appears at δ 1.48 as a singlet indicating that conjugate addition has probably occurred (δ 2.00 in **19**).

These data are consistent with two structures for the adduct, **23** or **24**, and at this stage we are unable to distinguish between these possibilities although apparently only one compound is formed.

The mode of formation that we favor for **23** or **24** is illustrated in Scheme 3 and is supported by the following. The Knoevenagel adduct of 3-methyl-2-cyclohexenone (**20**) was prepared and reacted for a short time with malononitrile in the presence of KF to yield 38% of the 1,6-addition product **21**. When this material was in turn treated under the same reaction conditions, the final product **23** or **24** could be detected. Intermediate **21** proved very difficult to purify rigorously for combustion analysis (as did many

[2]In the mass spectral data presented in this paper we discuss only those major fragments pertinent to the structural elucidation. No deuterium labelling work has been performed in support of the proposed fragmentation. However, in the majority of cases, the processes depicted are supported by metastable peaks, shown in the various schemes by m* on the arrows indicating the fragmentations. Ions are indicated as percentages of the base peak.

[3]The origin of the fragment *m/e* 81 must await further studies but we favor a species such as

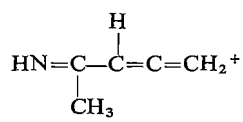

[4]This proton exchanges more slowly with D_2O than those whose signal appears at δ 7.10, but is accelerated by added base. Further, the normally non-exchangeable protons of malononitrile rapidly exchange with D_2O on addition of traces of diethylamine (n.m.r. evidence).

Can. J. Chem. Downloaded from www.nrcresearchpress.com by 210.87.254.6 on 09/05/12
For personal use only.

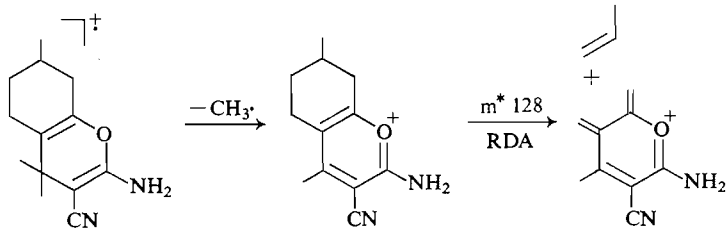

13 15 16

SCHEME 1

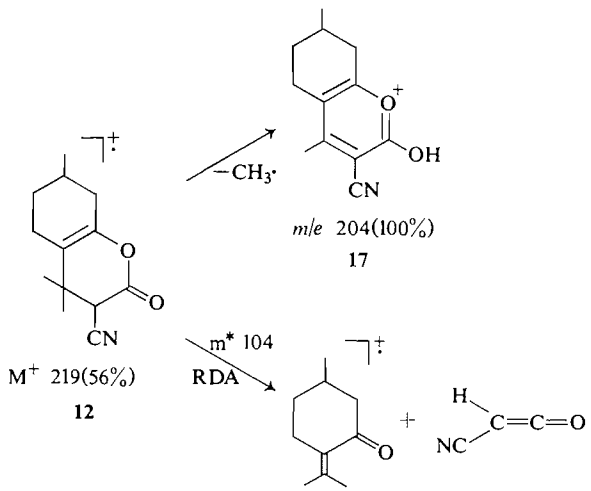

17 12 18

SCHEME 2

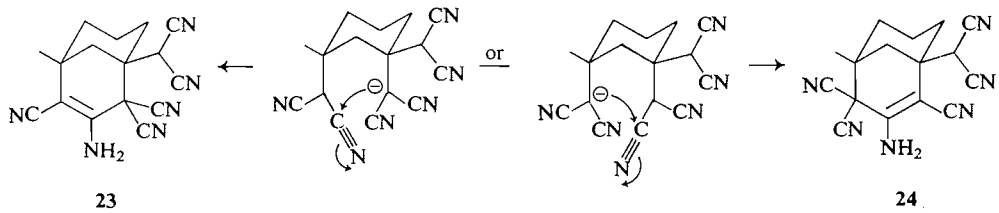

23 24

SCHEME 3

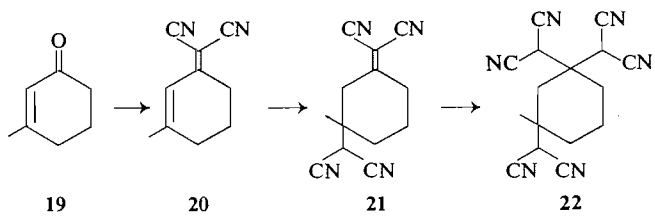

19 20 21 22

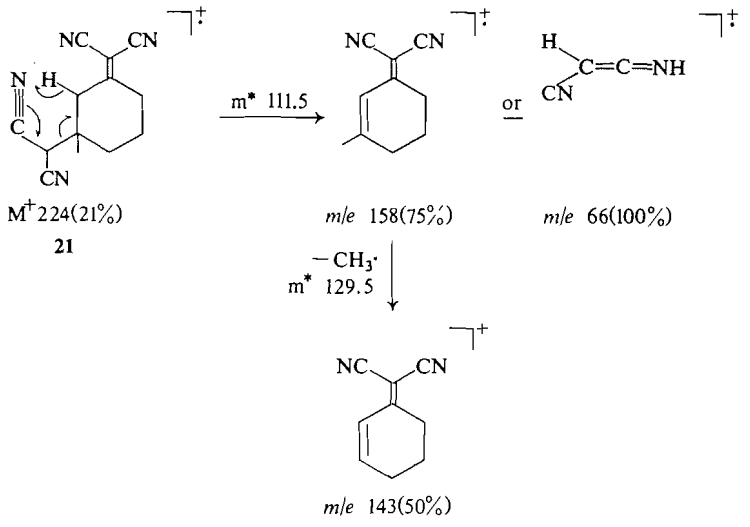

SCHEME 4

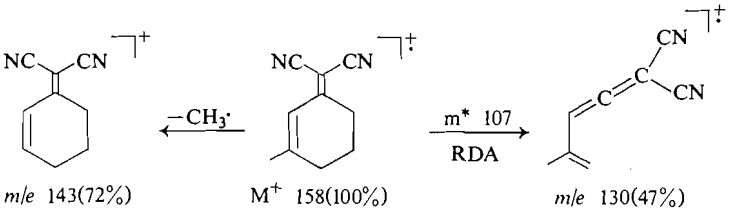

SCHEME 5

compounds in this study), however, all spectroscopic properties supported the formulation shown. Thus, the mass spectra of **20** and **21** proved useful in confirming their structures. That of **21** showed major fragments at *m/e* 158 (75%), 143 (50%), and 66 (100%) which can be readily assigned as indicated in Scheme 4 (21).

The mass spectrum of **20** was dominated by fragments at *m/e* 143 (72%) (M—CH_3) and 130 (47%) which is readily accounted for by the reverse Diels–Alder process as shown in Scheme 5.

The mass spectrum of the adduct **23** or **24** was very complex, but showed the base peak at *m/e* 66 and the next major fragment at *m/e* 225 (72%) as well as the parent ion at *m/e* 290 (7%). These ions can be accounted for on the basis of the proposed structure as shown (Scheme 6).

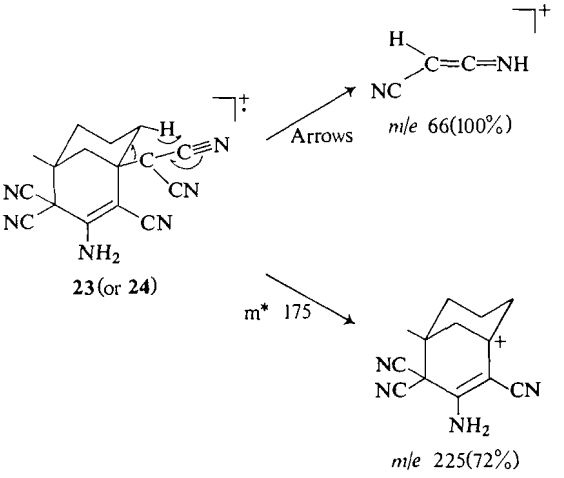

SCHEME 6

Mesityl Oxide (25)

On reaction with malononitrile in the presence of anhydrous KF, a modest yield of an adduct $C_{12}H_{12}N_4$ was obtained whose i.r. spectrum indicated the presence of both saturated (2220 cm^{-1}) and unsaturated nitrile (2190 cm^{-1}) as well as —NH_2. The simple n.m.r. spectrum showed a six-hydrogen singlet (2 × CH_3) at δ 1.25, indicating that conjugate addition had occurred, and a three-hydrogen doublet (J = 2 Hz) at δ 1.80 coupled with a one-hydrogen quartet at δ 5.15 suggesting a methyl group on a trisubstituted

Can. J. Chem. Downloaded from www.nrcresearchpress.com by 210.87.254.6 on 09/05/12
For personal use only.

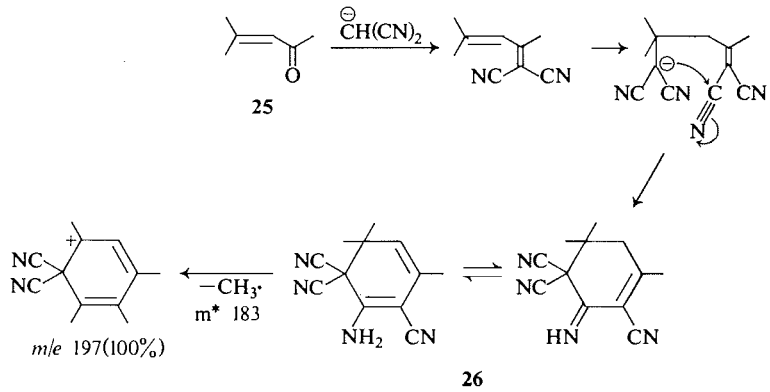

SCHEME 7

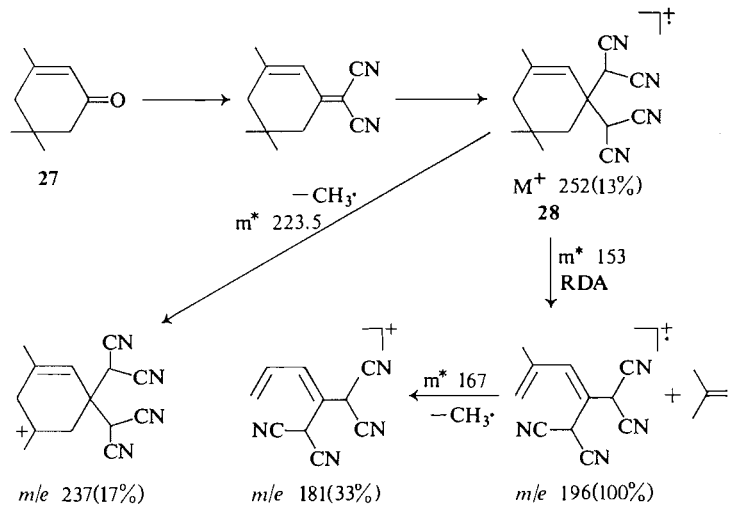

SCHEME 8

double bond. A two-hydrogen signal at δ 7.70 was exchangeable with D_2O. The u.v. spectrum showed maxima at 218 (ε 8900), 238 (ε 3500) and 325 nm (ε 4100). These data are consistent with structure **26** arising by the route shown in Scheme 7.

Structure **26** has been previously assigned to a condensation product of acetone and malononitrile (22, 23) and our physical properties corresponded closely to those reported. A sample of **26** prepared from acetone and malononitrile in the presence of piperidine (23) was identical to the mesityl oxide sample. The mass spectrum of **26** showed a base peak at *m/e* 197 corresponding to loss of —CH_3 probably arising as indicated.

Isophorone (27)

Isophorone reacted (under the conditions described) to yield a product analyzing for $C_{15}H_{16}N_4$, whose i.r. spectrum showed the absence of α,β-unsaturated ketone and NH_2 absorptions. A single saturated nitrile absorption at 2220 cm^{-1} was present. The n.m.r. spectrum showed retention of the olefinic double bond originally present in isophorone (methyl doublet at δ 2.05 and olefinic one-proton quartet at δ 6.63). The mass spectrum, M^+ 252, showed a base peak at *m/e* 196 (M-56) with other major fragments corresponding to M-15 (17%) and M-71 (33%). These data are consistent with the structure **28** for the adduct and the fragmentations indicated in Scheme 8.

D-*Carvone (29)*

The anhydrous KF catalyzed reaction gave a high yield of a pale yellow compound $C_{16}H_{16}N_4$ whose i.r. spectrum suggested the cyanoenamine grouping encountered previously (2170 cm^{-1})

Can. J. Chem. Downloaded from www.nrcresearchpress.com by 210.87.254.6 on 09/05/12
For personal use only.

Can. J. Chem. Downloaded from www.nrcresearchpress.com by 210.87.254.6 on 09/05/12
For personal use only.

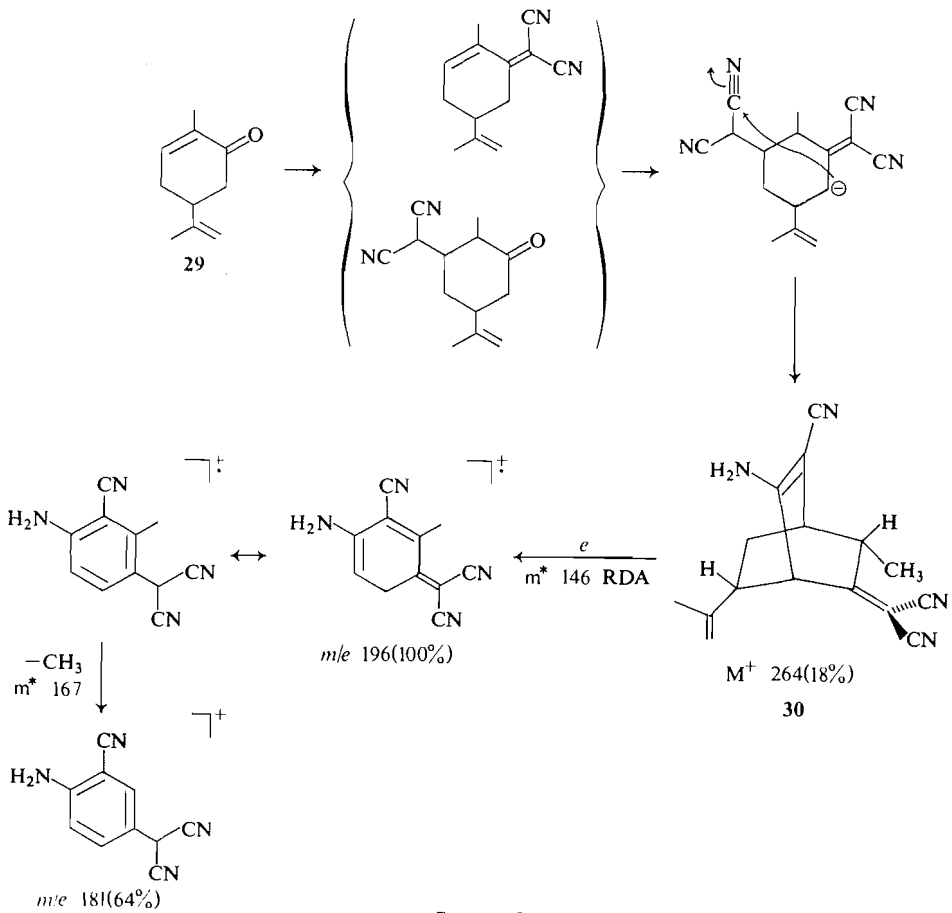

SCHEME 9

(*cf.* **13** and **24**) as well as the presence of another unsaturated nitrile (2230 cm^{-1}). The latter is probably present as part of a dicyanoethylidene group since the n.m.r. spectrum indicated that saturation of the enone double bond had occurred (methyl doublet at δ 1.18, and absence of olefinic proton signal). The isopropylidene side chain was unaffected. Two protons at δ 6.88 exchangeable with D_2O supported the presence of an $—NH_2$ grouping. This information, plus the physical data quoted in the Experimental, are consistent with structure **30**, the formation of which can be rationalized as shown in Scheme 9 which also indicates the proposed fragmentation of **30** on electron impact.

The formation of this adduct is apparently highly stereoselective since only one product could be isolated and we suggest the stereochemistry indicated in **30** for this material on the basis that the Michael reaction will proceed in a perpendicular manner via a 'pre-chair transition state' to **31** (24). Since this intermediate will be formed under equilibrating conditions the methyl group α to the dicyanoethylidene group will be expected to take up an axial position in preference to an equatorial one to relieve $A^{(1,3)}$ strain (25) and give **32**, whose anion can react in a boat form via cyclization and tautomerism of the resultant imino group to yield **30** in stereochemically pure form (Scheme 10).

Discussion

The competition between Michael and Knoevenagel reactions in the above cases is obviously very dependent on the steric environment of the α,β-unsaturated ketones under study. Where the carbonyl group of the enone is relatively unencumbered, the addition in a 1,2-sense occurs initially to yield the Knoevenagel product and, conversely, when the β-carbon terminus of the

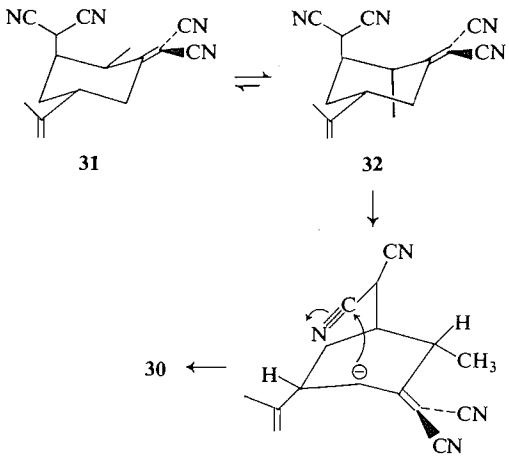

SCHEME 10

enone is readily available by comparison to the carbonyl group, 1,4-addition in a Michael sense is observed.

Apparently, once 1,2-addition has occurred the conjugated system is activated to further Michael addition resulting in multi-addition of the Michael donor, malononitrile anion. Thus, in the case of mesityl oxide, we favor the sequence of 1,2- followed by 1,6-addition and subsequent cyclization to **26**, whereas with 3-methyl-2-cyclohexenone (**19**) a further 1,4-addition is required before a precursor suitable for cyclization, **22**, is obtained. Isophorone would appear to undergo 1,2-addition by an activated Michael donor, but 1,6-addition is prohibited in this instance by the developing 1,3-diaxial interaction between one of the methyl groups of position 5 and the Michael addend approaching in a perpendicular manner from the top face to the terminus of the conjugated system (24), as shown in **33**. Approach of the malononitrile anion from the α face is less favored since this would involve a boat-like transition state. The alternate 1,4-Michael addition is thus favored, yielding **28**.

The formation of **13** from pulegone is readily explained via the intermediate enolate **34** which

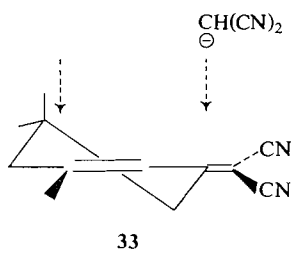

33

is formed close to one of the cyano groups on Michael addition.

The obtention of **30** from carvone necessitates formation of the anion **31**, although an alternate mechanism is that proceeding by way of the anion from Michael attack **35**, followed by enolate exchange to **36**, cyclization to **37**, then Knoevenagel reaction to **30**. Again the methyl group stereochemistry is predicted on the basis of relief of $A^{(1,3)}$ strain (25) under equilibrating conditions.

Our continuing work includes examination of the behavior of other α,β-unsaturated carbonyl systems under these reaction conditions as well as a deeper study of the utility of anhydrous potassium fluoride in organic synthesis. Variations in products on changing the molar ratios of ketones to malononitrile is also under study.[5]

Experimental

Melting points were determined on a Kofler hot stage and are corrected. Thin layer chromatography was performed with pre-coated plates (E. Merck, Silica Gel F-254, 0.25 mm thickness) and developed with ceric sulfate. The n.m.r. spectra were obtained on JEOLCO C-60 and Varian A-60 spectrometers with tetramethylsilane as an internal standard; chemical shifts are expressed on the δ scale. The following abbreviations are used to designate multiplicity of the n.m.r. signals: s, singlet; d, doublet; t, triplet; q, quartet; and m, multiplet. Optical rotations were measured in ethanol solution at 25° in 1 dm tubes on a Perkin-Elmer 141 automatic polarimeter. Infrared spectra were determined on a Perkin-Elmer 237B grating spectrophotometer and u.v. spectra (in ethanol) on a Perkin-Elmer 202 spectrophotometer. Gas–liquid chromatography was carried out on a Hewlett-Packard 402 gas chromatograph using an OV 210 on Diatoport S column at 150°. Mass spectra were determined on an A.E.I. MS 12 at the University of Liverpool or on a Thomson-Houston machine at l'Institut de Chimie, Strasbourg. Major fragments in the mass spectra are expressed as percentages of the base peak. Petrol ether is the fraction b.p. 60–110°.

3,6,6-Trimethyl-2-cyclohexenone (3) and 3,4,4-Trimethyl-2-cyclohexenone (4)

3-Methyl-2-butanone (178 g) in ether (225 ml) was added to a stirred solution of potassium hydroxide (50 g) in ethanol (190 ml) at 0° during 15 min. This was stirred for 10 min and then a solution of freshly distilled methyl vinyl ketone (156 g) in ether (1 l) was added during 3 h at 0°. The cooling bath was removed and the reaction was stirred for a further 45 min, then poured into water, and diluted with ether (500 ml). The ether layer was washed successively with water (× 3), dilute sulfuric acid, dilute sodium bicarbonate solution, and saturated salt solution

[5]In the present work no attempt was made to study these parameters in detail.

Can. J. Chem. Downloaded from www.nrcresearchpress.com by 210.87.254.6 on 09/05/12
For personal use only.

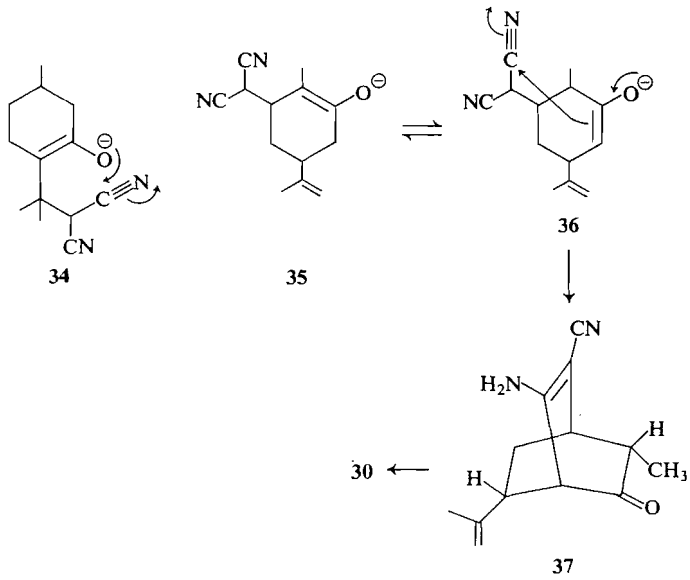

and then dried ($MgSO_4$) and evaporated to a red oil. Distillation of this afforded a mixture of **3** and **4** (88 g, 31%) b.p. 80–95°/7 mm (82:18 (±1.5) by g.l.c.).

A similar experiment in which the reaction mixture was stirred at room temperature for 48 h gave a mixture of **3** and **4** (28%) in the proportions 88.5:11.5 (±1.5) (by g.l.c.).

Redistillation of mixtures of **3** and **4** through a 25 cm Vigreux column gave early fractions containing pure **3**, b.p. 80–82°/8 mm; $n_D^{25°}$ 1.4781 (lit. b.p. 86°/13 mm (3), 86–88°/15 mm (2), 86–88°/13 mm (1) and $n_D^{25°}$ 1.4780 (3), $n_D^{22°}$ 1.4747 (2)); λ_{max} 231 nm (ε 12 900); ν_{max} (neat) 1670 (unsaturated C=O) and 1635 cm^{-1} (C=C); n.m.r. ($CDCl_3$) δ 1.05 (s, 6H, $(CH_3)_2$ at C-6), 1.80 (t, 2H, CH_2 at C-5), 1.93 (broad s, 3H, vinyl CH_3), 2.33 (t, 2H, CH_2 at C-4), and 5.73 (broad s, 1H, vinyl proton). Semicarbazone forms slowly m.p. 195–198° dec., lit. m.p. 201° (3).

Three redistillations of fractions rich in ketone **4** (by g.l.c.) produced pure material, b.p. 94–97°/7 mm; $n_D^{25°}$ 1.4878 (lit. b.p. 98°/13 mm (3), 93–95°/10 mm (4) and $n_D^{25°}$ 1.4889 (3), $n_D^{24°}$ 1.4840 (4)); λ_{max} 235 nm (ε 14 200); ν_{max} (neat) 1665 (unsaturated C=O) and 1615 cm^{-1} (C=C); n.m.r. ($CDCl_3$) δ 1.17 (s, 6H, $(CH_3)_2$ at C-4), 1.1–0.7 (m, 2H, CH_2 at C-5), 1.92 (broad s, 3H, vinyl CH_3), 2.38 (m, 2H, CH_2 at C-6), and 5.75 (broad s, 1H, vinyl proton). Semicarbazone forms rapidly m.p. 201–204° dec., lit. m.p. 206–207° (3, 4).

Reaction of 3,6,6-Trimethyl-2-cyclohexenone (3) with Malononitrile

To a stirred solution of the ketone **3** (26.2 g) in DMF (100 ml) containing malononitrile (75 g) was added a solution of anhydrous potassium fluoride (20 g) in ethylene glycol (100 ml). A red color developed in 1 min and the solution became warm. After 2.3 h the mixture was poured into water and extracted with ether (× 2). The organic layers were washed with water (× 5) and then with saturated salt solution, dried ($MgSO_4$), and evaporated to a brown oil. Distillation of this afforded the ketone **3** (10.0 g, 38% recovery) and a viscous oil which solidified on standing (13.5 g, 56% based on unrecovered **3**) b.p. 108–111°/0.1 mm, shown to be substantially pure Michael adduct **5** by i.r. and n.m.r. spectroscopy. This was recrystallized from petrol ether to give pure material (10.1 g) m.p. 68–69°; ν_{max} (Nujol) 2250 (saturated CN) and 1697 cm^{-1} (saturated C=O); n.m.r. ($CDCl_3$) δ 1.12 (s, 3H, CH_3 at C-3), 1.23 (s, 6H, $(CH_3)_2$ at C-6), 2.5–3.0 (m, 6H, CH_2 at C-2, C-4, and C-5), and 3.87 (s, 1H, —$CH(CN)_2$).

Anal. Calcd. for $C_{12}H_{16}N_2O$: C, 70.56; H, 7.90; N, 13.71. Found: C, 70.74; H, 7.92; N, 13.69.

The mother liquors showed weak i.r. absorption at 2210 and 1615 cm^{-1} indicating the presence of some Knoevenagel adduct **6**.

A similar experiment to the one above, in which the reaction mixture was stirred for 24 h and then worked up in the same way, afforded ketone **3** (3.6 g) and higher boiling fractions (13.2 g). From the latter, Michael adduct **5** (4.6 g) was obtained by crystallization from petrol ether. The mother liquors were evaporated and a solution of the residue in benzene (200 ml) and ethylene glycol (20 ml) containing *p*-toluenesulfonic acid (100 mg) was heated under reflux with water separation for 24 h, and worked up in the usual way. Several crops of the ketal **7** (4.3 g), m.p. 97–98°, were obtained from petrol ether; ν_{max} (Nujol) 2245 (saturated CN) and 1075 cm^{-1} (ketal); n.m.r. ($CDCl_3$) δ 0.90 (s, 3H, CH_3), 1.03 (s, 3H, CH_3), 1.28 (s, 3H, CH_3), 1.4–2.00 (m, 6H), 3.97 (s, 4H, —OCH_2—CH_2—O—), and 4.75 (s, 1H, —$CH(CN)_2$).

Anal. Calcd. for $C_{14}H_{18}N_2O_2$: C, 67.72; H, 8.12; N, 11.28. Found: C, 67.74; H, 8.08; N, 11.28.

The residue obtained after evaporation of the mother liquors was purified by short path distillation at 120°/0.1 mm and the distillate was recrystallized three times from petrol ether to give the Knoevenagel adduct **6** (0.6 g) m.p. 67–68°; λ_{max} 306 nm (ε 22 000); ν_{max} (Nujol) 2210

Can. J. Chem. Downloaded from www.nrcresearchpress.com by 210.87.254.6 on 09/05/12
For personal use only.

Can. J. Chem. Downloaded from www.nrcresearchpress.com by 210.87.254.6 on 09/05/12
For personal use only.

(unsaturated CN), 1615 and 1520 cm^{-1} (C=C); n.m.r. ($CDCl_3$) δ 1.42 (s, 6H, $(CH_3)_2$ at C-6), 1.68 (t, J = 6 Hz, 2H, CH_2 at C-5), 2.07 (broad s, 3H, vinyl CH_3), 2.33 (t, J = 6 Hz, 2H, CH_2 at C-4), and 6.58 (broad s, 1H, vinyl proton).

Anal. Calcd. for $C_{12}H_{14}N_2$: C, 77.40; H, 7.58; N, 15.05. Found: C, 77.65; H, 7.55; N, 14.91.

Reverse Michael Reaction of Adduct 5

The adduct **5** (0.5 g) was treated with anhydrous potassium fluoride (0.5 g) in DMF (3.5 ml) and ethylene glycol (3.5 ml) at room temperature for 18 h. The product was shown by g.l.c. and i.r. spectroscopy to contain the ketone **3** (85%), the Knoevenagel adduct **6** (12%), and the Michael adduct **5** (*ca.* 3%).

Attempted Preparation of the Knoevenagel Adduct 6 Using Ammonium Acetate as Catalyst

A solution of the ketone **3** (3.2 g), malononitrile (1.7 g), ammonium acetate (0.5 g), and acetic acid (0.25 g) in benzene (100 ml) was refluxed for 18 h with water separation (13). The product (3.0 g) was shown by g.l.c. and i.r. spectroscopy to be unchanged starting material.

Reaction of 3,4,4-Trimethyl-2-cyclohexenone (4) with Malononitrile

Reaction of the ketone **4** (2.0 g) with malononitrile (6.0 g) and anhydrous potassium fluoride (1.6 g) in DMF (8 ml) and ethylene glycol (8 ml) was carried out as described for the isomeric ketone **3**. After 3 h at room temperature this gave a yellow oil shown by g.l.c. and i.r. spectroscopy to consist of almost pure Knoevenagel adduct **8** (2.5 g, 93%). No trace of ketone **4** or of a Michael adduct could be detected. Short path distillation of this oil (125°/0.1 mm) and crystallization of the distillate from petrol ether afforded the Knoevenagel adduct **8** (1.65 g) m.p. 55–56°; λ_{max} 304.5 nm (ε 25 000); ν_{max} (Nujol) 2210 (unsaturated CN), 1600 and 1545 cm^{-1} (C=C); n.m.r. ($CDCl_3$) δ 1.13 (s, 6H, $(CH_3)_2$ at C-4), 1.70 (t, J = 6 Hz, 2H, CH_2 at C-5), 2.03 (d, J = 1.5 Hz, 3H, vinyl CH_3), 2.80 (t, J = 6 Hz, 2H, CH_2 at C-6), and 6.50 (m, 1H, vinyl proton).

Anal. Calcd. for $C_{12}H_{14}N_2$: C, 77.40; H, 7.58; N, 15.05. Found: C, 77.61; H, 7.60; N, 14.80.

Reaction of Pulegone 10 with Malononitrile

Reaction of pulegone (5.0 g) with malononitrile (6.5 g) and anhydrous potassium fluoride (3.6 g) in DMF (16 ml) and ethylene glycol (16 ml) for 10 h at room temperature was carried out in the usual way. The orange mixture was poured into water and the precipitate crystallized twice from methanol to give the pyran **13** (3.5 g), m.p. 131–132°, $[\alpha]_D$ = 85°; λ_{max} 220 (ε 8400) and 269 nm (ε 5800); ν_{max} (Nujol) 3450 and 3320 (NH_2), 2180 (unsaturated CN), 1710 (pyran), and 1640 cm^{-1} (C=C); n.m.r. ($CDCl_3$) δ 0.89 (d, J = 5.8 Hz, 3H, $CHCH_3$), 1.22 (s, 6H, $(CH_3)_2$ at C-4), and 4.28 (broad s, 2H, exchanges with D_2O, NH_2); mass spectrum M^+ 218 (6%), major fragments at *m/e* 203 (100%) and 161 (11%).

Anal. Calcd. for $C_{13}H_{18}N_2O$: C, 71.29; H, 8.31; N, 12.83. Found: C, 71.21; H, 8.30; N, 12.72.

Hydrolysis of Pulegone Adduct 13

A mixture of acetic acid (50 ml), water (200 ml), and the pyran **13** (5.0 g) was refluxed for 30 min, cooled, and extracted with ether (× 2). The combined organic layers were washed free of acetic acid, dried ($MgSO_4$), and evaporated to a yellow oil which crystallized from ethanol to give colorless prisms of the enol lactone **12** (3.0 g) m.p. 69–71°, $[\alpha]_D$ = 62°; λ_{max} 222 nm (ε 2500); ν_{max} (Nujol) 2250 (saturated CN), 1755 (lactone C=O), and 1690 cm^{-1} (C=C); n.m.r. ($CDCl_3$) δ 1.00 (d, J = 4.5 Hz, 3H, $CHCH_3$), 1.15 (s, 3H, CH_3), 1.26 (s, 3H, CH_3), and 3.61 (d, J = 2.0 Hz, 1H, —CH(CN)—C=O); mass spectrum M^+ 219, major fragments at *m/e* 204 (100%), 152 (95%), and 81 (71%).

Anal. Calcd. for $C_{13}H_{17}NO_2$: C, 71.21; H, 7.82; N, 6.39. Found: C, 70.95; H, 7.67; N, 6.56.

Reaction of 3-Methyl-2-cyclohexenone (19) and Malononitrile

3-Methyl-2-cyclohexenone (6.0 g), malononitrile (10.8 g), and anhydrous potassium fluoride (6.3 g) in DMF (18 ml) and ethylene glycol (18 ml) were reacted in the usual way for 10 h at room temperature. The mixture was poured into water and the product was isolated with ether to yield an orange solid which crystallized from methanol–water as pale yellow plates of the adduct **23** or **24** (10.2 g) m.p. 267–268° (sublimes at 240°); λ_{max} 274 nm (ε 35 300); ν_{max} (Nujol) 3420, 3335, 3260, and 3230 (all NH_2), 2275 (saturated CN), 2255 (saturated CN), 2200 (unsaturated CN), 1650 and 1610 cm^{-1} (C=C); n.m.r. ($(CD_3)_2CO$) δ 1.48 (s, 3H, CH_3), 4.85 (s, 1H, exchanges with D_2O, —$CH(CN)_2$), and 7.10 (broad s, 2H, exchanges with D_2O, NH_2); mass spectrum M^+ 290 (7%), major fragments at *m/e* 225 (72%) and 66 (100%).

Anal. Calcd. for $C_{16}H_{14}N_6$: C, 66.21; H, 4.86; N, 28.96. Found: C, 65.76; H, 4.76; N, 29.43.

Reaction of Knoevenagel Adduct 20 with Malononitrile

Adduct **20** was obtained by the literature methods (13) and had m.p. 88–89°; λ_{max} 302.5 nm (ε 25 000); ν_{max} 2220 (unsaturated CN), 1625 and 1615 cm^{-1} (C=C); n.m.r. ($CDCl_3$) δ 1.05 (s, 3H, vinyl CH_3), 6.62 (m, 1H, vinyl proton); mass spectrum M^+ 158 major fragments at *m/e* 143 (72%) and 130 (47%).

Adduct **20** (0.50 g), malononitrile (0.40 g), and anhydrous potassium fluoride (0.60 g) in DMF (5 ml) and ethylene glycol (5 ml) were reacted for 40 h at room temperature and worked up in the usual way to yield the adduct **23** or **24** (0.1 g) identical with a sample prepared from 3-methyl-2-cyclohexenone.

In another experiment Knoevenagel adduct **20** (2.0 g), malononitrile (1.6 g), and anhydrous potassium fluoride (7.2 g) in DMF (25 ml) were stirred together for 8 min at room temperature and then worked up in the usual way to afford the 1,6-addition product **21** (0.75 g) m.p. 111–113° (needles from ether). Attempts at recrystallization gave less pure material and combustion analyses were poor; ν_{max} (Nujol) 2240 (saturated CN), 2220 (unsaturated CN), and 1600 cm^{-1} (C=C); λ_{max} 302 nm (ε 23 100); n.m.r. ($CDCl_3$) δ 1.25 (s, 3H, CH_3), 2.78 (q, 2H, CH_2 at C-2), and 3.8 (s, 1H, —$CH(CN)_2$); mass spectrum M^+ 244, major fragments at *m/e* 158 (75%), 143 (50%), and 66 (100%).

Reaction of 1,6-Addition Product 21 with Malononitrile

Adduct **21** (0.20 g), malononitrile (0.10 g), and anhydrous potassium fluoride (0.05 g) in DMF (2.5 ml)

Can. J. Chem. Downloaded from www.nrcresearchpress.com by 210.87.254.6 on 09/05/12
For personal use only.

and ethylene glycol (2.5 ml) were reacted together for 3 h at room temperature. Routine workup gave **23** or **24** identical with an authentic sample.

Reaction of Testosterone with Malononitrile

Testosterone (8.0 g), malononitrile (5.6 g), and anhydrous potassium fluoride (3.2 g) in DMF (25 ml) and ethylene glycol (25 ml) were reacted for 30 min at room temperature and then poured into water. The product was isolated by ether extraction and crystallized from ethanol to give pale yellow plates of the Knoevenagel adduct **9** (5.9 g) m.p. 184–184.5°; $[\alpha]_D = +251°$; λ_{max} 309 nm (ε 30 000); ν_{max} (Nujol) 3600 (OH), 2225 (unsaturated CN), and 1600 cm^{-1} (C═C); n.m.r. ($CDCl_3$) δ 0.77 (s, 3H, CH_3 at C-18), 1.13 (s, 3H, CH_3 at C-19), and 6.44 (s, 1H, vinyl proton); mass spectrum M^+ 336.

Anal. Calcd. for $C_{22}H_{28}N_2O$: C, 78.53; H, 8.39; N, 8.33. Found: C, 78.23; H, 8.38; N, 8.27.

Reaction of Mesityl Oxide ***25*** *with Malononitrile*

Mesityl oxide (5 g, redistilled), malononitrile (3 g), and anhydrous potassium fluoride (3 g) in DMF (20 ml) and ethylene glycol (10 ml) were reacted together for 2 h at room temperature, poured into water, and kept at 0° overnight. The crystalline deposit was recrystallized from acetone to give needles of the adduct **26** (1.1 g) m.p. 171–174°; λ_{max} 218 (ε 8900), 238 (ε 3500), and 324 nm (ε 4100); ν_{max} (Nujol) 3400–3100 (NH_2), 2220 (saturated CN), 2190 (unsaturated CN), and 1640 cm^{-1} (C═C); n.m.r. ($(CD_3)_2SO$) δ 1.25 (s, 6H, $(CH_3)_2C$), 1.80 (d, $J = 1.5$ Hz, 3H, vinyl methyl), 5.15 (q, $J = 1.5$ Hz, 1H, vinyl proton), and 7.70 (broad s, 2H, exchanges with D_2O, NH_2); mass spectrum M^+ 212 (37%), major fragment at *m/e* 197 (100%).

Anal. Calcd. for $C_{12}H_{12}N_4$: C, 67.91; H, 5.70; N, 26.40. Found: C, 68.04; H, 5.92; N, 26.90.

Reaction of Isophorone ***27*** *with Malononitrile*

Isophorone (5 g), malononitrile (2.5 g), and anhydrous potassium fluoride (3.0 g) in DMF (15 ml) and ethylene glycol (15 ml) were reacted for 4 h at room temperature and then poured into water. The precipitate was recrystallized from methanol to give yellow prisms of the adduct **28** (2.1 g) m.p. 69–70°; λ_{max} no intense absorption above 210 nm; ν_{max} (Nujol) 2220 (saturated CN) and 1610 cm^{-1} (C═C); n.m.r. ($CDCl_3$) δ 1.02 (s, 6H, $(CH_3)_2C$), 2.05 (d, $J = 2$ Hz, 3H, vinyl CH_3), 2.20 (s, 2H, C—CH_2—C), 2.53 (s, 2H, C—CH_2—C), 3.48 (s, 1H, —$CH(CN)_2$), and 6.63 (q, $J = 2$ Hz, 1H, vinyl proton); mass spectrum M^+ 252 (13%), major fragments at *m/e* 237 (16%), 197 (100%), and 181 (33%).

Anal. Calcd. for $C_{15}H_{16}N_4$: C, 71.40; H, 6.39; N, 22.20. Found: C, 71.25; H, 6.16; N, 21.93.

Reaction of D*-Carvone* ***29*** *and Malononitrile*

D-Carvone (10 g), malononitrile (10 g), and anhydrous potassium fluoride (10 g) in DMF (30 ml) and ethylene glycol (30 ml) were reacted for 10 h at room temperature and then poured into water. The precipitate was recrystallized from methanol to yield pale yellow needles of adduct **30** (7.1 g) m.p. 208°; λ_{max} 252 (ε 15 700) and 346 nm (ε 1390); ν_{max} (Nujol) 3430, 3350, 3265, 3240 (all NH_2), 2230, 2170 (unsaturated CN), 1650 and 1600 cm^{-1} (C═C); n.m.r. ($(CD_3)_2SO$) δ 1.18 (d, $J = 6$ Hz, 3H, $CHCH_3$), 1.83 (s, 3H, vinyl CH_3), 4.95 (d, $J = 12$ Hz, 2H, CH_2), 3.95 (d, $J = 2.5$ Hz, 1H, C═C—CH—C═C), and 6.88 (broad s, 2H, exchanges with D_2O, NH_2); mass spectrum M^+ 264 (18%), major fragments at *m/e* 196 (100%) and 181 (64%).

Anal. Calcd. for $C_{16}H_{16}N_4$: C, 72.70; H, 6.10; N, 21.20. Found: C, 72.47; H, 6.02; N, 21.75.

We thank the National Research Council of Canada for generous financial assistance. One of us (J.W.A.) thanks the administrators of the C. D. Howe Memorial Foundation for a fellowship and G. Ourisson, Institut de Chimie, Strasbourg, Germany, for his hospitality during the period when some of this work was performed. We thank Miss Sandra Lawrence, Mrs. Sue Macaulay, and Mrs. Jill Hooper for expert technical assistance.

1. K. VON AUWERS and M. HESSENLAND. Ber. **41**, 1812 (1908).
2. J. M. CONIA and F. ROUESSAC. Bull. Soc. Chim. Fr. 1925 (1963).
3. E. R. BUCHMAN and H. SARGENT. J. Org. Chem. **7**, 140 (1942).
4. R. P. GHANDI, B. VIG, and S. M. MUKHERJI. J. Ind. Chem. Soc. **36**, 299 (1959).
5. W. G. DAUBEN, G. W. SHAFFER, and N. D. VIETMEYER. J. Org. Chem. **33**, 4060 (1968).
6. R. N. LACEY. J. Chem. Soc. 1639 (1960).
7. P. R. SHAFER, W. E. LOEB, and W. S. JOHNSON. J. Amer. Chem. Soc. **75**, 5965 (1953). R. D. MURRAY, W. E. PARKER, and R. A. RAPHAEL. Tetrahedron, **16**, 74 (1961). M. W. CRONYN and G. H. RIESSER. J. Amer. Chem. Soc. **75**, 1664 (1953).
8. H. BABA, H. MIDORIKAWA, and S. AOYAMA. J. Sci. Res. Inst. **52**, 99 (1958). M. IGARASHI, H. MIDORIKAWA, and S. AOYAMA. J. Sci. Res. Inst. **52**, 105 (1958). H. YASUDA, H. MIDORIKAWA, and S. AOYAMA. J. Sci. Res. Inst. **53**, 19 (1959). S. KANBE, H. YASUDA and H. MIDORIKAWA. J. Sci. Res. Inst. **58**, 118 (1964). S. KANBE and H. YASUDA. Bull. Chem. Soc. Japan. **39**, 2549 (1966). S. KANBE and H. YASUDA. J. Sci. Res. Inst. **58**, 148 (1964). L. RAND, D. HAIDKEWYCH, and R. J. DOLINSKI. J. Org. Chem. **31**, 1272 (1965). L. RAND, J. V. SWISHER, and C. J. CRONIN. J. Org. Chem. **27**, 3505 (1962). J. PATTERSON and M. BARNES. Bull. Chem. Soc. Jap. **40**, 2715 (1967). P. M. LELEAN and J. A. MORRIS. Chem. Commun. 239 (1968).
9. D. G. I. FELTON and S. F. D. ONT. J. Chem. Soc. 2170 (1955); see also, W. E. PARHAM and L. J. CZUBA. J. Org. Chem. **34**, 1899 (1969).
10. L. RAND, J. V. SWISHER, and C. J. CRONIN. J. Org. Chem. **27**, 3505 (1962).
11. L. F. FIESER and M. FIESER. Reagents for organic synthesis. John Wiley and Sons, New York, N.Y. 1967. p. 375.
12. F. FREEMAN. Chem. Rev. **69**, 591 (1969). J. D. ATKINSON and M. C. JOHNSON. J. Chem. Soc. (C), 2181 (1969).
13. A. C. COPE and K. E. HOYLE. J. Amer. Chem. Soc. **63**, 733 (1941). A. C. COPE, C. M. HOFMANN, C. WYCKOFF, and E. HARDENBERG. J. Amer. Chem. Soc. **63**, 3452 (1941). G. JONES. Org. React. Vol. 15. John Wiley and Sons, New York, N.Y. 1967. p. 204. H. JÄGER. Chem. Ber. **95**, 244 (1962).
14. H. HART and Y. C. KIM. J. Org. Chem. **31**, 2784 (1966).
15. C. R. GANELLIN and C. J. STOLZ. J. Chem. Soc. (C), 2132 (1969). H. JUNEK, B. HONISCHER, and H. STARK. Monatsh. Chem. **99**, 2121 (1968).

16. J. WOLINSKY and H. S. HAUER. J. Org. Chem. **34**, 380 (1969); cf. Y. L. CHOW and H. H. QUON. J. Org. Chem. **34**, 1465 (1969).
17. J. WOLINSKY and H. S. HAUER. J. Org. Chem. **34**, 3169 (1969). S. MASAMUME and N. T. CASTELLUCCI. J. Amer. Chem. Soc. **84**, 2452 (1962). H. W. WHITLOCK, JR. and N. A. CARLSON. Tetrahedron, **20**, 2101 (1964). M. J. JORGENSON. J. Org. Chem. **27**, 3224 (1962). J. FICINI and A. KRIEF. Tetrahedron Lett. 1427 (1969).
18. T. OISHI, M. OCHIAI, M. NAGAI, and V. BAN. Tetrahedron Lett. 497 (1968); cf. V. PRELOG and S. SZPILFOGEN. Helv. Chim. Acta, **28**, 1684 (1945); F. JOHNSON and J. P. HEESCHEN. J. Org. Chem. **29**, 3252 (1964).
19. A. K. DAS GUPTA, R. M. CHATTERJE, and K. R. DAS. J. Chem. Soc. (C), 2618 (1969).
20. D. S. TARBELL and A. H. HERZ. J. Amer. Chem. Soc. **75**, 1666 (1953).
21. F. W. MCLAFFERTY. Anal. Chem. **34**, 26 (1962).
22. J. K. WILLIAMS. J. Org. Chem. **28**, 1054 (1963).
23. M. R. S. WEIR and J. B. HYNE. Can. J. Chem. **41**, 2905 (1963). D. M. W. ANDERSON, F. BELL, and J. L. DUNCAN. J. Chem. Soc. 4705 (1961).
24. E. TOROMANOFF. Bull. Soc. Chim. Fr. 708 (1962). H. O. HOUSE and H. W. THOMPSON. J. Org. Chem. **28**, 360 (1965). R. A. ABRAMOVITCH and D. L. STRUBLE. Tetrahedron Lett. 289 (1966). N. L. ALLINGER and C. K. RIEW. Tetrahedron Lett. 1269 (1966). E. L. ELIEL, N. L. ALLINGER, S. J. ANGYAL, and S. A. MORRISON. Conformational analysis. Interscience Publishers. New York, N.Y. 1965. p. 314.
25. F. JOHNSON. Chem. Rev. **68**, 375 (1968). F. JOHNSON and S. K. MALHOTRA. J. Amer. Chem. Soc. **87**, 5492, 5513 (1963). F. JOHNSON and L. G. DUQUETTE. Chem. Commun. 1448 (1969).

Can. J. Chem. Downloaded from www.nrcresearchpress.com by 210.87.254.6 on 09/05/12
For personal use only.

Can. J. Chem. Downloaded from www.nrcresearchpress.com by 210.87.254.40 on 09/05/12
For personal use only.

Cobalt(II) and nickel(II) complexes of some bidentate imidazoline ligands. Stereochemically dependent delocalization in the imidazoline rings

A. B. P. Lever, B. S. Ramaswamy, S. H. Simonsen,[1] and L. K. Thompson
The Department of Chemistry, York University, Downsview (Toronto), Ontario

Received May 11, 1970

Tetrahedral and octahedral cobalt(II), and square and octahedral nickel(II) complexes of 1,2-bis(2′-imidazolin-2′-yl)benzene, 1,2-bis(2′-imidazolin-2′-yl)ethane, and some imidazoline ring methyl substituted ligands are reported. The structures are confirmed by three X-ray structural analyses, magnetism, and electronic and vibrational (conventional and far i.r.) spectroscopy. Both *cis* and *trans* octahedral complexes of the type $M(ligand)_2(NCS)_2$ [M = Co(II), Ni(II)] have been characterized, and none of these exhibit splitting of the ν(CN)(NCS) absorption in the i.r. spectrum at room temperature. Low temperature studies reveal splitting of the ν(CN) band in the *cis* isomers. Both ^{13}C and ^{15}N satellite absorption is identified. The delocalization of the double bond in the imidazoline rings in these complexes is discussed in terms of the i.r. and X-ray data.

Canadian Journal of Chemistry, 48, 3076 (1970)

We report here the metal complexing ability of some novel bidentate ligands containing imidazoline rings. Although the coordination chemistry of imidazole and its derivatives has been extensively investigated (1, 2), studies of its dihydro derivative are restricted to the chemistry of 2,2′-bi-2-imidazoline (3). Since the dihydro ligand is somewhat simpler than imidazole, being non-aromatic, it was thought that a study of its metal complexing ability might prove rewarding. The ligands 1,2-bis(2′-imidazolinyl)benzene (**1**, LP), the corresponding imidazoline ring methyl substituted derivative (**2**, LMP), 1,2-bis(2′-imidazolinyl)ethane (**3**, LE), and its ring methyl substituted derivative (**4**, LME) were synthesized by the phosphorus pentasulfide catalyzed reaction of ethylenediamine (or 1,2-propanediamine) with phthalodinitrile or succinonitrile, a standard route for the preparation of imidazolines (4). The ethane derivative LE has been reported (5) but the other ligands were previously unknown.

Reaction of the parent ligands with cobalt and nickel salts in alcohol led to the isolation of a series of square, tetrahedral, and octahedral complexes whose structures have been justified by electronic and vibrational spectra (conventional and far i.r.), magnetism, and X-ray structural analysis. The ring methyl substituted ligands exhibited great reluctance in forming complexes and few were characterized.

Experimental

The n.m.r. data were obtained in $CDCl_3$ with a Varian Associates A60 spectrometer using $SiMe_4$ as an internal calibrant. The u.v. spectra were recorded with a Cary 14 spectrometer and molecular weight data with a modified Gallenkamp Model 7665K semi-micro ebulliometer, calibrated with azobenzene and with benzoic acid. Infrared and far i.r. data were obtained with a Beckman IR 12 spectrometer, and magnetic susceptibilities, via the Gouy method with an Alpha 4 in. magnet calibrated with mercury cobalt tetrathiocyanate. Low temperature electronic and vibrational data were obtained with a Beckman VLT-2 Variable Temperature Cell, with quartz (electronic), or NaCl (i.r.) windows. Microanalyses were carried out by Galbraith Laboratories, Knoxville, Tennessee, and by A. B. Gygli, Toronto. Mass spectra were obtained with a Hitachi–Perkin Elmer model RMU-6 mass spectrometer. Melting points are uncorrected.

1,2-Bis(2′-imidazolin-2′-yl)benzene (1)

Method A

To 1,3-diiminoisoindoline (6) (7.25 g, 0.05 mole) dissolved in boiling absolute ethanol, was added ethylenediamine (6.2 g, 0.1 mole) and the mixture refluxed until evolution of ammonia had ceased. The bulk of the solvent was removed by distillation at reduced pressure until crystallization occurred. The white crystalline product (6.1 g, 60% yield) was recrystallized from benzene. The pure product melted at 174–175°.

Method B (Based on (7))

o-Dicyanobenzene (6.4 g, 0.05 mole), ethylenediamine (6.2 g, 0.1 mole), and a catalytic amount of phosphorus pentasulfide (20 mg) were mixed together. Upon application of heat (80°), vigorous evolution of ammonia occurred and the entire reaction mixture solidified. This product was crushed and recrystallized from benzene to yield the same product (7.9 g, 75% yield, mixed m.p. undepressed) as method *A*.

Anal. Calcd. for $C_{12}H_{14}N_4$ (mol. wt. 214): C, 67.3; H, 6.5; N, 26.15. Found (218 (ebullioscopic), 214 (mass spectrum)): C, 66.9; H, 6.65; N, 25.9.

The u.v. spectrum (in methanol) (wavenumbers, molar intensities in parentheses) 44 640 (11 500), 39 210 (3425) cm^{-1}; i.r. 3100(νNH), 1585, 1600(νCN) cm^{-1}; n.m.r. [τ(relative intensity)], 2.5 (4) (multiplet, aromatic CH), 4.0 (2) (broad, NH), 6.33 (8) (singlet, ring CH_2); mass peaks, *m/e* (relative intensities) 214(12)P, 185(48), 129(69), 102(55), 54(26), 42(46), 32(74), 30(51), 28(100).

[1]Department of Chemistry, University of Texas, Austin, Texas.

Can. J. Chem. Downloaded from www.nrcresearchpress.com by 210.87.254.40 on 09/05/12
For personal use only.

1,2-Bis(4'-methyl-2'-imidazolin-2'-yl)benzene (2)

Utilization of 1,2-diaminopropane *in lieu* of ethylenediamine in the preparation of LP (**1**) in either method *A* or *B* leads to the preparation of compound **2** (65% yield), m.p. 149–150°.

Anal. Calcd. for $C_{14}H_{18}N_4$ (mol. wt. 242): C, 69.4; H, 7.5; N, 23.1. Found (243 (ebullioscopic), 242 (mass spectrum)): C, 69.7; H, 7.7; N, 23.2. The u.v. spectrum (in methanol) (wavenumbers, molar intensities in parentheses) 44 640 (10 000), 39 210 (2770) cm^{-1}; i.r. 3125 (vNH), 1587, 1603(vCN) cm^{-1}; n.m.r. [τ(relative intensity)] 2.5 (4) (multiplet, aromatic CH), 4.15 (2) (broad, NH), 5.9–6.8 (6) (multiplet, ring CH, CH_2), 8.77 (6) (doublet, CH_3, $J = 6.0$ Hz); major mass peaks *m/e* (relative intensities) 242 (6) P, 227 (29), 170 (46), 129 (63), 102(43), 42(44), 41(39), 28(100).

1,2-Bis(2'-imidazolin-2'-yl)ethane (3)

This compound was prepared via method *B* using succinonitrile in place of *o*-dicyanobenzene. Recrystallization from benzene yielded the pure derivative **3** (60% yield), m.p. 203–204°, lit. m.p. 235° (5).

Anal. Calcd. for $C_8H_{14}N_4$ (mol. wt. 166): C, 57.8; H, 8.5; N, 33.7. Found (166 (mass spectrum)): C, 57.6; H, 8.3; N, 33.6. The i.r. 3160 (vNH), 1610(vCN) cm^{-1}; insufficiently soluble for n.m.r. study; major mass peaks, *m/e* (relative intensities) 166(27)P, 84(60), 83(35), 55(39), 54(90), 45(38), 42(49), 41(51), 33(37), 30(53), 28(100).

1,2-Bis(4'-methyl-2'-imidazolin-2'-yl)Ethane (4)

Method *B* was employed using 1,2-diaminopropane and succinonitrile. The compound (50% yield) melted at 161–162°.

Anal. Calcd. for $C_{10}H_{18}N_4$ (mol. wt. 194): C, 61.8; H, 9.3; N, 28.8. Found (194 (mass spectrum)): C, 61.8; H, 9.4; N, 28.9. The i.r. 3140 (vNH), 1605(vCN) cm^{-1}; n.m.r. [τ(relative intensity)] 4.71 (2) (singlet, NH), 6.0–6.9 (6) (multiplet, ring CH, CH_2), 7.47 (4) (singlet, bridge CH_2), 8.81 (6) (doublet, CH_3, $J = 6.5$ Hz); major mass peaks, *m/e* (relative intensities) 194 (5) P, 179 (20), 82 (24), 68(21), 54(47), 42(32), 41(38), 30(30), 28(100).

Hydrolytic Degradation

The compounds were hydrolyzed by refluxing in concentrated hydrochloric acid for 6 h. On cooling, phthalic acid, compound **1**, or succinic acid, compound **3**, was obtained and identified by its i.r. spectrum. The hydrochloric acid was removed at the pump leaving a white residue of the amine hydrochloride which was also identified by its i.r. spectrum. The weights of the products obtained were in accord with the structures proposed for each compound.

General Preparation of Metal Complexes of Imidazolines

The complexes reported in this paper, unless otherwise stated, were prepared by the following general technique.

Stoichiometric amounts of the metal salt and ligand were dissolved separately in hot absolute alcohol and filtered. The filtered solutions were heated and a hot solution of the ligand was added to the hot metal salt and the mixture heated with stirring for about 1 h. The metal complex which crystallized out was filtered, washed with ether, and dried under vacuum at 100 °C. The complexes were recrystallized by Soxhlet extraction with an appropriate solvent, and dried under reduced pressure at 100 °C.

Metal Complexes of 1,2-Bis(2'-imidazolin-2'-yl)-benzene (1, LP)

Dichloro Bis[(1,2-bis(2'-imidazolin-2'-yl)benzene]-nickel(II)

Soxhlet extraction of the product in methanol gave an orange crystalline product.

Anal. Calcd. for $C_{24}H_{28}Cl_2N_8Ni$: C, 51.6; H, 5.1; Cl, 12.7; N, 20.1; Ni, 10.5. Found: C, 51.45; H, 5.1; Cl, 12.7; N, 20.2; Ni, 10.5.

Dibromo Bis[1,2-bis(2'-imidazolin-2'-yl)benzene]-nickel(II)

Recrystallization from methanol gave an orange product.

Anal. Calcd. for $C_{24}H_{28}Br_2N_8Ni$: C, 44.5; H, 4.4; Br, 24.7; N, 17.3; Ni, 9.15. Found: C, 44.4; H, 4.2; Br, 24.1; N, 17.15; Ni, 9.2.

Diiodo Bis[1,2-bis(2'-imidazolin-2'-yl)benzene]-nickel(II)

Recrystallization from ethanol gave an orange crystalline product.

Anal. Calcd. for $C_{24}H_{28}I_2N_8Ni$: C, 38.9; H, 3.8; I, 34.3; Ni, 7.9. Found: C, 38.65; H, 3.8; I, 34.75; Ni, 7.9.

Diperchlorato Bis[1,2-bis(2'-imidazolin-2'-yl)-benzene]nickel(II)

Recrystallization from methanol gave an orange crystalline substance.

Anal. Calcd. for $C_{24}H_{28}Cl_2N_8NiO_8$: C, 42.1; H, 4.1; Ni, 8.6. Found: C, 42.3; H, 4.2; Ni, 8.7.

Dinitrato Bis[1,2-bis(2'-imidazolin-2'-yl)benzene]-nickel(II)

Recrystallization from methanol gave an orange crystalline substance.

Anal. Calcd. for $C_{24}H_{28}N_{10}NiO_6$: C, 47.2; H, 4.6; Ni, 9.6. Found: C, 47.0; H, 4.6; Ni, 9.6.

Dithiocyanato Bis[1,2-bis(2'-imidazolin-2'-yl)-benzene]nickel(II)

Recrystallization from methanol gave a mauve colored crystalline product.

Anal. Calcd. for $C_{26}H_{28}N_{10}NiS_2$: C, 51.7; H, 4.6; N, 23.2; Ni, 9.7; NCS, 19.2. Found: C, 51.7; H, 4.5; N, 23.1; Ni, 9.75; NCS, 19.1.

Dithiocyanato [1,2-bis(2'-imidazolin-2'-yl)benzene]-nickel(II)

The product could not be recrystallized as it is converted thereby to $(LP)_2Ni(NCS)_2$. The light brown precipitate was washed with hot ethanol and dried.

Anal. Calcd. for $C_{14}H_{14}N_6NiS_2$: C, 43.2; H, 3.6; Ni, 15.1; NCS, 29.8. Found: C, 43.2; H, 3.7; Ni, 15.1; NCS, 29.9.

Dithiocyanato Bis[1,2-bis(2'-imidazolin-2'-yl)-benzene]cobalt(II)

The ligand was used in excess. A buff colored product was obtained; on recrystallization from absolute alcohol orange crystals were produced.

Anal. Calcd. for $C_{26}H_{28}CoN_{10}S_2$: C, 51.7; H, 4.7; Co, 9.8; NCS, 19.2. Found: C, 52.2; H, 4.9; Co, 9.75; NCS, 19.25.

Dithiocyanato [1,2-Bis(2'-imidazolin-2'-yl)benzene]-cobalt(II)

Crystallization from acetonitrile gave a dark blue crystalline product.

Anal. Calcd. for $C_{14}H_{14}CoN_6S_2$: C, 43.2; H, 3.6; Co, 15.1; NCS, 29.8. Found: C, 43.35; H, 3.6; NCS, 29.40.

Can. J. Chem. Downloaded from www.nrcresearchpress.com by 210.87.254.40 on 09/05/12
For personal use only.

Dichloro [1,2-Bis(2'-imidazolin-2'-yl)benzene]-cobalt(II)

Crystallization from absolute ethanol gave a dark blue crystalline product.

Anal. Calcd. for $C_{12}H_{14}CoCl_2N_4$: C, 41.9; H, 4.1; Cl, 20.6; Co, 17.1; N, 16.3. Found: C, 41.8; H, 4.2; Cl, 20.9; Co, 17.15; N, 16.2.

Dibromo [1,2-Bis(2'-imidazolin-2'-yl)benzene]-cobalt(II)

Crystallization from methanol gave a dark blue crystalline product.

Anal. Calcd. for $C_{12}H_{14}Br_2CoN_4$: C, 33.3; H, 3.3; Br, 36.9; Co, 13.6; N, 12.9. Found: C, 33.4; H, 3.2; Br, 37.0; Co, 13.6; N, 13.0.

Diiodo [1,2-Bis(2'-imidazolin-2'-yl)benzene]-cobalt(II)

Crystallization from acetonitrile gave a dark blue crystalline product.

Anal. Calcd. for $C_{12}H_{14}CoI_2N_4$: C, 27.3; H, 2.7; Co, 11.2; I, 48.2; N, 10.6. Found: C, 27.7; H, 2.7; Co, 11.15; I, 48.4; N, 10.7.

Diperchlorato Bis[1,2-bis(2'-imidazolin-2'-yl)-benzene]cobalt(II)

Recrystallization from ethanol gave a violet product.

Anal. Calcd. for $C_{24}H_{28}Cl_2CoN_8O_8$: C, 42.0; H, 4.1; Co, 8.6. Found: C, 42.3; H, 4.2; Co, 8.4.

Dithiocyanato Bis[1,2-bis(4'-methyl-2'-imidazolin-2'-yl)benzene]nickel(II)

Recrystallization from absolute ethanol gave mauve colored crystals.

Anal. Calcd. for $C_{30}H_{36}N_{10}NiS_2$: C, 54.6; H, 5.5; Ni, 8.9; NCS, 17.6. Found: C, 54.5; H, 5.2; Ni, 9.1; NCS, 17.3.

Dithiocyanato Bis[1,2-bis(4'-methyl-2'-imidazolin-2'-yl)ethane]nickel(II)

Recrystallization from ethanol gave a brown product. Difficulty was experienced in obtaining adequate C and H analyses.

Anal. Calcd. for $C_{22}H_{36}N_{10}NiS_2$: Ni, 10.4; NCS, 20.6. Found: Ni, 10.2; NCS, 20.8.

Dithiocyanato Bis[1,2-bis(2'-imidazolin-2'-yl)ethane]-nickel(II)

A large excess of the ligand was necessary; a greenish-blue powder was obtained and recrystallized from ethanol to give green-blue crystals.

Anal. Calcd. for $C_{18}H_{28}N_{10}NiS_2$: C, 42.6; H, 5.6; Ni, 11.6; NCS, 22.9. Found: C, 42.7; H, 5.5; Ni, 11.5; NCS, 22.5.

Dibromo Bis[1,2-(2'-imidazolin-2'-yl)ethane]nickel(II)

Recrystallized from methanol to give a reddish-brown product.

Anal. Calcd. for $C_{16}H_{28}N_8Br_2Ni$: C, 34.9; H, 5.1; Br, 29.0; Ni, 10.7. Found: C, 34.6; H, 5.9; Br, 28.7; Ni, 10.5.

Dichloro Bis[1,2-(2'-imidazolin-2'-yl)ethane]-nickel(II)

A large excess of the ligand was used in the preparation to give a reddish-brown product. Recrystallization from ethanol gave reddish-brown crystals.

Anal. Calcd. for $C_{16}H_{28}N_8Cl_2Ni$: C, 41.6; H, 6.1; Cl, 15.3; Ni, 12.7. Found: C, 41.6; H, 6.4; Cl, 15.3; Ni, 12.6.

Diiodo Bis[1,2-bis(2'-imidazolin-2'-yl)ethane]-nickel(II)

Recrystallization from ethanol gave a reddish-brown crystalline product.

Anal. Calcd. for $C_{16}H_{28}I_2N_8Ni$: C, 29.8; H, 4.4; I, 39.4; Ni, 9.1. Found: C, 29.8; H, 4.5; I, 39.1; Ni, 9.4.

Diperchlorato Bis[1,2-bis(2'-imidazolin-2'-yl)ethane]-nickel(II)

Recrystallization from ethanol gave an orange product.

Anal. Calcd. for $C_{16}H_{28}Cl_2N_8NiO_8$: C, 32.6; H, 4.8; Ni, 9.9. Found: C, 32.7; H, 5.0; Ni, 10.15.

Dinitrato Bis[1,2-bis(2'-imidazolin-2'-yl)ethane]-nickel(II)

Recrystallization from ethanol gave a brick red crystalline product.

Anal. Calcd. for $C_{16}H_{28}N_{10}NiO_6$: C, 37.3; H, 5.5; Ni, 11.4. Found: C, 37.4; H, 5.6; Ni, 11.1.

Dithiocyanato Bis[1,2-bis(2'-imidazolin-2'-yl)-ethane]cobalt(II)

The complex was prepared by adding an excess of the ligand in ethanol to the metal salt and leaving the mixture in a shaker overnight. The light brown precipitate that separated out was recrystallized from absolute alcohol to give a brown crystalline product.

Anal. Calcd. for $C_{18}H_{28}CoN_{10}S_2$: C, 42.6; H, 5.6; Co, 11.6; NCS, 22.9. Found: C, 42.4; H, 5.5; Co, 11.4; NCS, 23.2.

Dithiocyanato [1,2-Bis(2'-imidazolin-2'-yl)ethane]-cobalt(II)

This was prepared by the general method but acetonitrile was used instead of ethanol. Recrystallized from ethanol to give a dark blue crystalline product.

Anal. Calcd. for $C_{10}H_{14}CoN_6S_2$: C, 35.2; H, 4.1; Co, 17.3; NCS, 34.0. Found: C, 35.4; H, 4.0; Co, 17.2; NCS, 33.7.

Dichloro [1,2-Bis(2'-imidazolin-2'-yl)ethane]-cobalt(II)

Recrystallized from methanol to give dark blue crystals.

Anal. Calcd. for $C_8H_{14}Cl_2CoN_4$: C, 32.5; H, 4.8; Cl, 23.95; Co, 19.9. Found: C, 32.4; H, 4.9; Cl, 23.5; Co, 19.0.

Dibromo [1,2-Bis(2'-imidazolin-2'-yl)ethane]-cobalt(II)

Recrystallized from methanol to give blue crystals.

Anal. Calcd. for $C_8H_{14}Br_2CoN_4$: C, 25.0; H, 3.7; Br, 41.5; Co, 15.3. Found: C, 24.8; H, 3.6; Br, 41.5; Co, 15.0.

Diiodo [1,2-Bis(2'-imidazolin-2'-yl)ethane]cobalt(II)

Recrystallized from ethanol to give bluish-red crystals. Difficulty was experienced in obtaining adequate C and H analyses.

Anal. Calcd. for $C_8H_{14}CoI_2N_4$: Co, 12.3; I, 53.0. Found: Co, 12.1; I, 53.1.

Diperchlorato Bis[1,2-bis(2'-imidazolin-2'-yl)ethane]-cobalt(II)

Recrystallized from methanol to give a violet crystalline product.

Anal. Calcd. for $C_{16}H_{28}Cl_2CoN_8O_8$: C, 32.6; H, 4.8; Co, 10.0. Found: C, 32.9; H, 4.8; Co, 9.7.

Can. J. Chem. Downloaded from www.nrcresearchpress.com by 210.87.254.40 on 09/05/12
For personal use only.

Results and Discussion

Characterization of the Ligands

The ligand LP was initially discovered through the reaction of ethylenediamine with 1,3-diiminoisoindoline, which we had hoped would generate an interesting tridentate ligand analogous to 1,3-di(2′-pyridyl)iminoisoindoline (8). Since LP was soon found to give rise to an interesting series of metal complexes, a more rational synthesis was sought.

Such a synthesis followed from a report in the Japanese patent literature (7) that nitriles will condense with ethylenediamine to yield imidazoline ring systems. Acetonitrile and *p*-dicyanobenzene had been investigated (7). Reaction of *o*-dicyanobenzene with ethylenediamine was found to proceed at 80° with the evolution of ammonia to yield the same derivative (**1**). Molecular weight studies and mass spectra indicate that the molecule is monomeric. The structure **1** is confirmed by i.r., n.m.r., mass spectroscopy (experimental) and X-ray spectroscopy (see below). The i.r. spectrum is consistent with the presence of an ortho disubstituted benzene derivative containing both NH and C—N groups. In the n.m.r. spectrum the $—CH_2—$ absorption is shifted to low field as a consequence of the adjacent nitrogen atoms. The presence of a singlet for the four methylene protons of each ring implies their chemical equivalence which is not at first sight expected on the basis of the structure **1**. It is likely that there is fast exchange of the hydrogen atoms resulting in the nitrogen atoms, and the methylene protons, becoming chemically equivalent. The compound may be further characterized by hydrolysis with hydrochloric acid under reflux, which leads to the formation of one equivalent of phthalic acid and two equivalents of ethylenediamine hydrochloride, identified by their i.r. spectra.

The cleavage pattern of imidazoline rings in the mass spectrometer (9) is similar to that of the related thiazoline ring system (10). The most intense fragments observed in the spectrum of compound **1** are recorded in the experimental section. The mass spectrum is quite consistent with the structure **1** proposed and with the earlier literature (9).

The *C*-methyl derivative of **1**, namely 1,2-bis(4′-methyl-2′-imidazolin-2′yl)benzene (**2**) was obtained through the reaction of 1,2-diaminopropane with *o*-dicyanobenzene. The i.r., n.m.r., and mass spectra of this derivative are quite consistent with the proposed structure (**2**). The methyl resonance is, as expected, split into a doublet by the adjacent hydrogen atom. The remaining resonances fall in the same regions as in the preceding compound **1**. The compound may be hydrolyzed with hydrochloric acid to yield phthalic acid and 1,2-diaminopropane hydrochloride in the appropriate ratio. In view of the intramolecular hydrogen exchange in solution and the likelihood of hydrogen bonding in the solid state, no distinction seems possible between the two alternate methyl substituted isomers, substitution in the 4′ or 5′ positions. A distinction may however be anticipated in the metal complexes of this ligand.

When succinonitrile was employed in place of *o*-dicyanobenzene, the aliphatic analogue of **1**, namely 1,2-bis(2′-imidazolin-2′-yl)ethane (**3**), was generated, ammonia being evolved. The i.r. and mass spectra of this complex confirm its identity. Whilst it was not soluble enough for an n.m.r. study, the n.m.r. spectrum of its methyl substituted derivative (below) provided further confirmation. Hydrolysis leads to the formation of succinic acid and ethylenediamine in the molar ratio 1:2. The primary bond breaking process in the mass spectrometer appears to be cleavage of the ethane bridge followed by breakdown of the rings.

Reaction of succinonitrile and 1,2-diaminopropane leads to the methyl derivative of **3**, namely 1,2-bis(4′-methyl-2′-imidazolin-2′-yl)-ethane (**4**). The n.m.r. spectrum of this compound shows a high field doublet assigned to the methyl groups split by the adjacent hydrogen atom and two sets of resonances attributable to the remaining protons. Those at low field of relative intensity 6 are assigned to the ring protons shifted downfield by the deshielding effect of the adjacent nitrogen atoms, and those at higher field (relative intensity 4) are attributed to the bridging methylene groups. The latter give rise to a singlet indicating the high symmetry of this compound, **4**. Hydrolysis of this compound gave the expected products.

Characterization of the Complexes

Several series of complexes were synthesized; complexes of nickel(II) were either square or octahedral, (or contained nickel species of both these stereochemistries), whilst the cobalt(II)

TABLE 1

Magnetic and i.r. data*

Type of complex	χ_g	μ_{eff}(BM)	ν(CN)†		ν(M–L)‡
Square					
$(LP)_2NiCl_2$	—	Dia	1582, 1598, 1614w	L	ni
$(LP)_2NiBr_2$	—	Dia	1580, 1600, (1615)	L	ni
$(LP)_2NiI_2$	—	Dia	1587, 1605	L	ni
$(LP)_2Ni(NO_3)_2$	—	Dia	(1582), 1599, (1608)	L	ni
$(LP)_2Ni(ClO_4)_2$	—	Dia	1585, 1603, 1617w	L	ni
$(LE)_2NiCl_2$	—	Dia	1600, 1631	H	435 (Ni—N)
$(LE)_2NiBr_2$	—	Dia	1603, 1620, (1635)	H	435 (Ni—N)
$(LE)_2NiI_2$	—	Dia	1595, 1627	H	429 (Ni—N)
$(LE)_2Ni(NO_3)_2$	—	Dia	1590, 1617, (1625)	H	436 (Ni—N)
$(LE)_2Ni(ClO_4)_2$	—	Dia	1602, 1626	H	435 (Ni—N)
Octahedral					
$(LP)_2Ni(NCS)_2$	6.25	3.12	(1590), 1615, (1620)	H	ni
$(LMP)_2Ni(NCS)_2$	6.00	3.21	(1592), 1610	?	ni
$(LE)_2Ni(NCS)_2$	7.62	3.14	1600, 1620	H	ni
$(LP)_2Co(NCS)_2$	16.37	4.93	1591, 1610br, (1621)	H?	ni
$(LE)_2Co(NCS)_2$	19.99	4.98	1601, 1614	H	ni
Tetrahedral					
$(LP)Co(NCS)_2$	19.56	4.31	1595, (1605)	L?	296, 315 (Co—NCS)
$(LP)CoCl_2$	22.71	4.36	1588, 1605	L?	310, 325 (Co—Cl)
$(LP)CoBr_2$	18.83	4.46	(1582), 1590	L	ni
$(LP)CoI_2$	16.25	4.58	(1570), 1590	L	214
$(LP)_2Co(ClO_4)_2$	11.05	4.35	1580, 1595	L	ni
$(LE)Co(NCS)_2$	20.59	4.13	1582, 1603	L	ni
$(LE)CoCl_2$	24.25	4.17	1586, 1602	L	293, 320 (Co—Cl)
$(LE)CoBr_2$	16.76	3.97	1585, 1602, (1615)	L	255 (Co—Br)
$(LE)CoI_2$	16.34	4.33	1589, 1602	L	204
$(LE)_2Co(ClO_4)_2$	12.31	4.23	1590br	L	ni
Mixed stereochemistry					
$(LP)Ni(NCS)_2$	5.47	2.35	1586, 1603, 1623w	L	ni
$(LME)_2Ni(NCS)_2$	3.33	2.27	1600, 1630, (1637)	H	ni

*The ν(NH) absorption is generally broad, in the range 3100 to 3400 cm^{-1} and in some cases the apparent peak centers shift from one sample preparation to another; we therefore do not report the data here.
†L and H refer to division of the complexes into two series according to whether they have low or high ν(CN) frequencies.
‡ni—no metal ligand vibrations have as yet been positively identified in these complexes.

complexes were octahedral or tetrahedral (Table 1). The gross stereochemistries of most of these complexes follow readily from their magnetism (Table 1), far i.r. spectra (Table 1), electronic spectra (Table 2), or conventional i.r. spectra (Table 1). In three cases X-ray structural analyses have been completed and the broad details are presented here. It is convenient to first discuss the cobalt and nickel derivatives grouped according to their stereochemistries.

Tetrahedral Cobalt(II) Complexes

These derivatives have electronic spectra and magnetism typical for their stereochemistry (11); solution of the appropriate secular determinants leads to *Dq* values for these ligands of 465 (LP) and 531 cm^{-1} (LE) (Table 2) (calculated from the perchlorates). These are somewhat higher than those of many other CoN_4 chromophores (8) but parallel closely the behavior of the imidazoles (1). The very distorted nature of these complexes renders a more sophisticated discussion of their crystal field strength rather futile. By comparison of their far i.r. spectra with those of the other complexes it is easy to distinguish the cobalt–halogen stretching frequencies (Table 1) which lie in the appropriate regions (12, 13). Cobalt–nitrogen stretching frequencies have not yet been unequivocally identified.

Square Planar Nickel(II) Complexes

Reaction of nickel halides, nitrate, or perchlorate with the ligands leads to the isolation of orange diamagnetic complexes in which the stereochemistry about the nickel(II) ion is evidently square. An X-ray determination of the structure of $(LP)_2Ni(ClO_4)_2$ has been completed and confirms a square planar stereochemistry. The gross details are shown in Fig. 1; detailed evidence for this structure will be presented else-

Can. J. Chem. Downloaded from www.nrcresearchpress.com by 210.87.254.40 on 09/05/12
For personal use only.

TABLE 2

Electronic spectra – mull transmittance spectra (cm^{-1})*

Type of complex*,‖						
Square						
$(LP)_2NiCl_2$		(21 000)	26 000			
$(LP)_2NiBr_2$		21 000	25 000	28 500		
$(LP)_2NiI_2$		21 000	25 000			
$(LP)_2Ni(ClO_4)_2$		(19 250)	21 100	25 000	26 350	
$(LP)_2Ni(NO_3)_2$		20 400	24 600			
$(LE)_2NiCl_2$		20 600	24 250			
$(LE)_2NiBr_2$		20 000	24 000			
$(LE)_2NiI_2$		(20 000)	23 500			
$(LE)_2Ni(ClO_4)_2$		(20 000)	24 200			
$(LE)_2Ni(NO_3)_2$		19 050	23 900	(28 600)		
Octahedral†		ν_1		ν_2	ν_3	Spin forbidden
$(LP)_2Ni(NCS)_2$		10 950		17 850	28 400	
	L.T.	10 100, 11 450		18 400	28 700	
$(LE)_2Ni(NCS)_2$		9750		16 350	29 600	
	L.T.	(9500), 10 400		17 000	28 200	13 320w, (22 200)
$(LMP)_2Ni(NCS)_2$		9830, 10 590		17 700		(13 000)
	L.T.	11 200		18 200		(13 200)
$(LP)_2Co(NCS)_2$		9750			(19 050), (20 000) 21 100	
	L.T.	10 150, (11 400)			(19 450), (20 450) 22 000	
$(LE)_2Co(NCS)_2$		8500, 9500			(19 500), 21 250	
	L.T.	(8450), 10 300			(19 050), 20 000 20 900, 22 000	
Tetrahedral‡		ν_2			ν_3	
$(LP)Co(NCS)_2$		(7150), 8000, 9900			15 700	16 950 18 550
$(LP)CoBr_2$		(6860), 7050, (7650), 9740			15 250	16 650 17 400
$(LP)CoCl_2$		(6300), 7240, 9750			15 100	16 100 17 300
$(LP)CoI_2$		5850, 6850, 9400			14 400	14 900 17 300
$(LP)_2Co(ClO_4)_2$		8000br			15 925	18 050 (19 270)
	L.T.	7970, (8695), (10 000)			15 925	18 020 (19 305)
$(LE)Co(NCS)_2$		(7550), 9150, (10 500)			16 500	17 700 (19 050)
$(LE)CoBr_2$		(6350), 7280, (7880), 9400			15 400	15 900 17 550
$(LE)CoCl_2$		7000, 8700, 9800			15 500	16 250 17 500
$(LE)CoI_2$		(8200), 9100, (10 000)			17 200	(17 700) (19 050)
$(LE)_2Co(ClO_4)_2$		9010br			(16 670)	17 390 19 050
	L.T.	9010, 10 150, (10 525)			(16 670)	17 510 19 190

*br = broad, L.T. = −196 °C, and ( ) shoulders.

†Assignments are as follows: octahedral nickel complexes, $\nu_1\ ^3T_{2g} \leftarrow {}^3A_{2g}$, $\nu_2\ ^3T_{1g} \leftarrow {}^3A_{2g}$, $\nu_3\ ^3T_{1g}(P) \leftarrow {}^3A_{2g}$; octahedral cobalt complexes, $\nu_1\ ^4T_{2g} \leftarrow {}^4T_{1g}$, $\nu_3\ ^4T_{1g}(P) \leftarrow {}^4T_{1g}$.

‡Tetrahedral cobalt complexes, $\nu_2\ ^4T_1 \leftarrow {}^4A_2$, $\nu_3\ ^4T_1(P) \leftarrow {}^4A_2$.

‖Low temperature data for complexes of mixed stereochemistry: $(LP)Ni(NCS)_2$ 6250, 15 550, 20 200, 26 670 cm^{-1}; $(LME)_2Ni(NCS)_2$ 10 200, 16 700, 20 600, 24 200 cm^{-1}.

where (14). The imidazoline rings cant in a propeller-like fashion around the NiN_4 plane and the benzene rings are almost perpendicular to this plane. Most of the corresponding nickel complexes with imidazole are paramagnetic (1), leading to the supposition that: (*i*) the crystal field strength of these bidentate ligands towards nickel(II) is substantially greater than that of the imidazoles or; (*ii*) the stereochemistry is sterically imposed. The crystal field strength of imidazole and its derivatives is of the order (1) of 1080 cm^{-1} (*Dq*) whilst the mean crystal field strengths in the octahedral complexes $(LP)_2Ni(NCS)_2$ and $(LE)_2Ni(NCS)_2$ are 1095 and 975 cm^{-1}, respectively. Thus the diamagnetism of the other nickel complexes cannot arise through electronic factors. It is clear both from molecular models and from the structure reported above that the conformation of the ligands causes considerable crowding above and below the molecular plane of the ligand; as a consequence of this crowding only small and strongly coordinating groups, such as the thiocyanate ion, can cause the nickel ion to take up an octahedral stereochemistry.

The electronic spectra of these complexes are all very similar, being essentially independent of the nature of the anion. The LP complexes have two bands near 21 000 and 25 000 cm^{-1}, whilst the LE complexes have a similar spectrum but shifted about 1000 cm^{-1} to lower energy. Thus

Can. J. Chem. Downloaded from www.nrcresearchpress.com by 210.87.254.40 on 09/05/12
For personal use only.

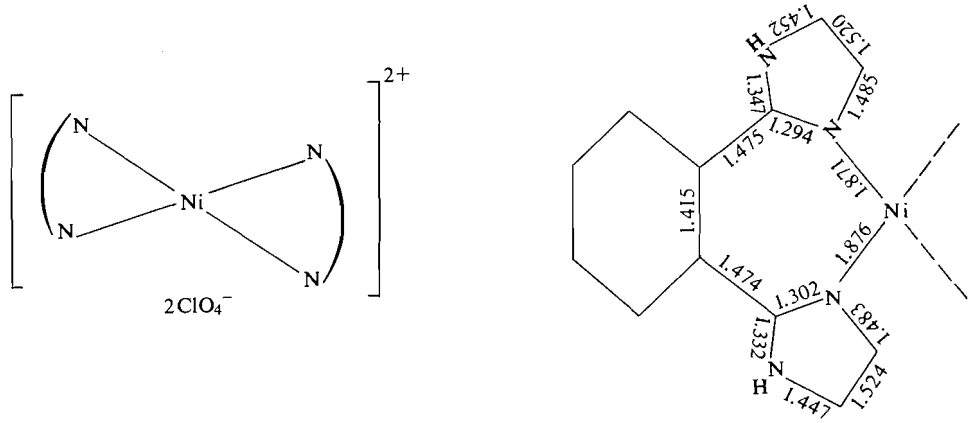

FIG. 1. The structure of $(LP)_2Ni(ClO_4)_2$. The space group is $P2_1/c$ and $R = 0.077$. The imidazoline rings cant in a propeller-like fashion about the NiN_4 plane and the benzene rings are approximately perpendicular to this plane. The angles at the nitrogen atom are close to 90°, and there are two molecules to the unit cell.

the LE ligand probably has a somewhat smaller crystal field towards square nickel than LP; the reverse of the situation towards tetrahedral cobalt(II). It is not possible to make unequivocal assignments of the spectra of square planar nickel complexes (11), and little can be said about these spectra except that the bands fall in the region anticipated for a square NiN_4 chromophore.

The far i.r. spectra of these complexes are very complicated. Comparison with the spectra of the tetrahedral and octahedral complexes, and with the free ligand, leads to the tentative assignment of a metal nitrogen stretching vibration near 430 cm^{-1} in the LE complexes.

The spectra of the LP complexes in the 400 cm^{-1} region are more complicated than those of the LE derivatives. Certain bands have been tentatively identified as metal nitrogen modes, as have additional bands between 400 and 200 cm^{-1} in both series of complexes. These will be published when further work has positively identified them (15). Nickel nitrogen stretching frequencies in square nickel amine complexes have not been characterized in the literature. It is pertinent that square nickel complexes of the imidazoles (1, 16) also have bands in the 400 cm^{-1} region which may be νNi—N in origin. A normal coordinate analysis of the square planar bis-(imidazolinato)nickel(II) has been reported (17) and a band at 445 cm^{-1} assigned to the nickel nitrogen stretching mode. Our own work (18) with an extensive series of metal ethylenediamine complexes, also suggests that this mode should be sought near 400 cm^{-1}.

Octahedral Cobalt(II) and Nickel(II) Complexes

Reaction of cobalt or nickel thiocyanates with the ligands leads to a series of octahedral complexes $L_2M(NCS)_2$ [L = LP, LE, LME, and M = Co(II) and Ni(II)]. All these derivatives have a single band near 2100 cm^{-1} assigned to the νCN stretching mode of the NCS groups and a band at 880–890 cm^{-1} assigned to the νC—S stretching vibration of a terminally nitrogen coordinated thiocyanate group. The νNCS bending frequency near 470 cm^{-1} is obscured by ligand absorption (Table 3).

The octahedral stereochemistry follows from the electronic spectra and magnetism of these complexes and is confirmed by X-ray structural analyses (14) of $(LP)_2Ni(NCS)_2$ and $(LE)_2Ni(NCS)_2$. The former complex, shown in Fig. 2, has a *cis* configuration, whilst the latter, shown in Fig. 3, has a *trans* configuration. In view of the crowding above and below the molecular plane of the square LP nickel complex, a *cis* configuration for the octahedral thiocyanate is by no means surprising. In this way the ligands will minimize their mutual interaction. In the case of LE, crowding above and below the molecular plane in a *trans* derivative would be less serious since the methylene bridges will be much less bulky than the benzene rings. The absence of a splitting in the ν(CN)(NCS) absorption in the *cis* complexes implies very little coupling between these thiocyanate group vibrations. This does not appear to be due to a lengthening in the nickel thiocyanate bond since the distance observed

Can. J. Chem. Downloaded from www.nrcresearchpress.com by 210.87.254.40 on 09/05/12
For personal use only.

TABLE 3

The i.r. spectra of the complex thiocyanates (cm^{-1})

Complex		ν(CN)* ^{13}C	ν(CN)* ^{15}N	ν(CN)* ^{12}C	ν(C—S)†
$(LP)_2Ni(NCS)_2$		2057w		2102s	885
	L.T.	2053wn	2088w	2105s, 2111s	nr
$(LMP)_2Ni(NCS)_2$		(2060)		(2098), 2105s	874, 886
	L.T.	(2060)		2106s, 2111s	nr
$(LP)Ni(NCS)_2$		2036w		2082s, 2120s	793
	L.T.	2039w		2084s, 2107m 2112m, 2126s	nr
$(LE)_2Ni(NCS)_2$		2053w	2079w	2100	880
	L.T.	2058wn	2075w	2103s	nr
$(LME)_2Ni(NCS)_2$				(2074), 2110s, (2138)	879
	L.T.			(2105), 2118s, (2127)	nr
$(LP)_2Co(NCS)_2$		2050w		2099s	886
	L.T.	2053wn	2073w	2098s, 2104s	nr
$(LE)_2Co(NCS)_2$		(2050)		2100s	(880)
	L.T.	2051wn		2102s	nr
$(LP)Co(NCS)_2$				2057s, 2075s	835
	L.T.	2022w		2060s, 2079s	nr
$(LE)Co(NCS)_2$				2081s, 2097s	832
	L.T.	2036w		2082s, 2099s	nr

*w = weak, s = strong, m = medium, ( ) shoulders, n = narrow sharp band, and L.T. = −196 °C.
†nr = not recorded at low temperature. The ν(NCS) bending modes near 470 cm^{-1} could not be distinguished from the ligand absorption.

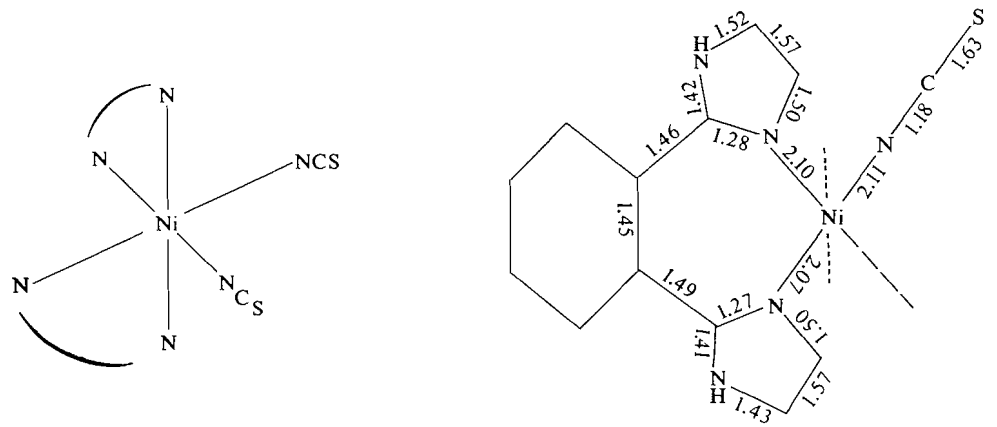

FIG. 2. The structure of $(LP)_2Ni(NCS)_2$. The space group is $C2/c$ (aniso.) and $R = 0.129$. The angles at the nickel atom are close to 90° and the Ni—NCS atoms are approximately collinear.

here is similar to that observed (19) in the complex $Ni(en)_2(NCS)_2$. This result emphasizes that caution should be exercised in assuming that the absence of a splitting of the ν(CN) mode in an octahedral dithiocyanate complex necessarily infers a *trans* geometry for that complex.

However, we were successful in resolving the CN stretching vibrations in this complex into two main components at liquid nitrogen temperature (Fig. 4); under similar low temperature conditions, no resolution of the CN stretching vibration of the *trans* complex was observed. Studies of the other complexes led to resolution of the stretching vibration in both the LP cobalt and nickel complexes and in the LMP nickel complex, but no resolution in the LE cobalt and nickel complexes. We are tempted to conclude therefore that the $(LP)_2M(NCS)_2$ and $(LMP)_2Ni(NCS)_2$ complexes contain a *cis* octahedral arrangement about the metal ion, whilst in the $(LE)_2M(NCS)_2$ complexes, a *trans* octahedron is present.

Can. J. Chem. Downloaded from www.nrcresearchpress.com by 210.87.254.40 on 09/05/12
For personal use only.

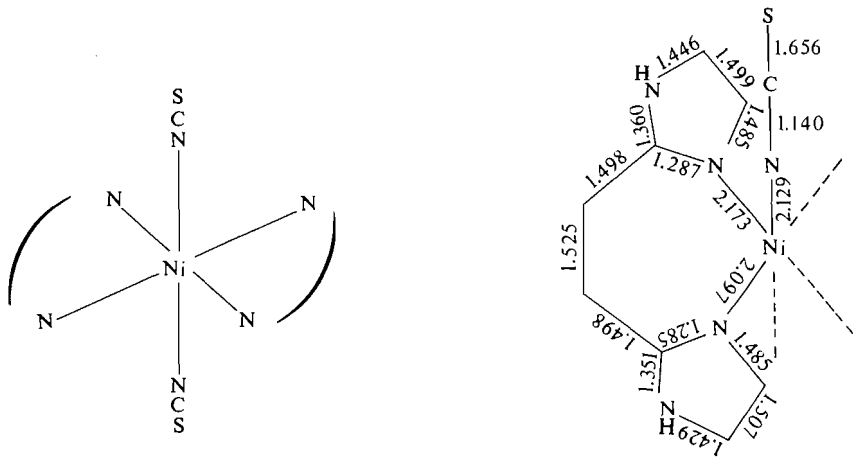

FIG. 3. The structure of $(LE)_2Ni(NCS)_2$. The space group is $P\bar{1}$ and $R = 0.045$.

In the tetrahedral $LCo(NCS)_2$ complexes the ν(CN)(NCS) stretching vibration is well resolved at room temperature, there being a splitting of some 16–18 cm^{-1} compared with about 6 cm^{-1} at liquid nitrogen temperature in the octahedral complexes (Table 3).

The somewhat higher crystal field strength of the LP ligand in the square complexes is also reflected in the octahedral complexes, the mean crystal field strengths having been cited above. As might be expected for a NiN_6 chromophore, there is no observable splitting of the first spin-allowed d–d transition (near 10 000 cm^{-1}) in the room temperature spectra of these complexes. At low temperature however (−196 °C, Table 2) some resolution into two components is observed. The splitting in the *trans* complex is seen to be 900 cm^{-1}, whilst that in the *cis* complex is 1350 cm^{-1}. This is rather surprising in that the splitting in *cis* isomers is expected to be about half that in the *trans* isomer, the crystal field strengths of the ligands concerned remaining constant (20). However, calculation reveals that this can be readily explained. In the LE complex the two bands concerned are assigned to the transitions from the $^3B_{1g}$ ground state to the ^3E_g and $^3B_{2g}$ excited states in D_{4h} symmetry. However, the relative order of these excited states is not immediately obvious. We calculate here the values of $10Dq_{LE}$ and $10Dq_{NCS}$ according to the two possible assignments (*i* and *ii*) shown in Table 4. A similar calculation may be carried out on the *cis* LP complex assuming it to possess pseudo D_{4h} symmetry (21).

Assignment *i* must be eliminated because the value for $10Dq_{NCS}$ exceeds that for the $Ni(NCS)_6^{4-}$ chromophore (about 10 800 cm^{-1}) (11) yet the nickel thiocyanate bonds are known to be somewhat long; assignment *ii* for $(LE)_2Ni(NCS)_2$ is quite consistent with the known facts. Assignment *iv* for $(LP)_2Ni(NCS)_2$ is rejected because the $10Dq_{LP}$ value lies well below $10Dq_{LE}$; from the square nickel complex spectra we know $10Dq_{LP}$ is greater than $10Dq_{LE}$. Thus assignments *ii* and *iii* are chosen. These are fully consistent in that $10Dq_{LP}$ exceeds $10Dq_{LE}$, the $10Dq_{NCS}$ values are low and of similar magnitude, and the actual assignments are inverted as expected for a pair of related *cis* and *trans* isomers.

Whilst the absolute values derived from such first order calculations should not be taken too seriously, they are sufficiently accurate to allow assignments to be made with confidence, and they do corroborate the conclusion from X-ray and i.r. data that the nickel thiocyanate bond lengths are somewhat long. The unexpectedly large splitting in the *cis* isomer is now substantiated. The spectra of the corresponding cobalt(II) derivatives show similar splittings; however, the presence of the $^4T_{1g}$ ground term (in O_h) renders this species intractable to calculation.

Other Complexes

Reaction of a deficiency of the ligand LP with nickel thiocyanate led to the isolation of a brown complex, $(LP)Ni(NCS)_2$. This complex has a magnetic moment of 2.35 BM, which is essen-

Can. J. Chem. Downloaded from www.nrcresearchpress.com by 210.87.254.40 on 09/05/12
For personal use only.

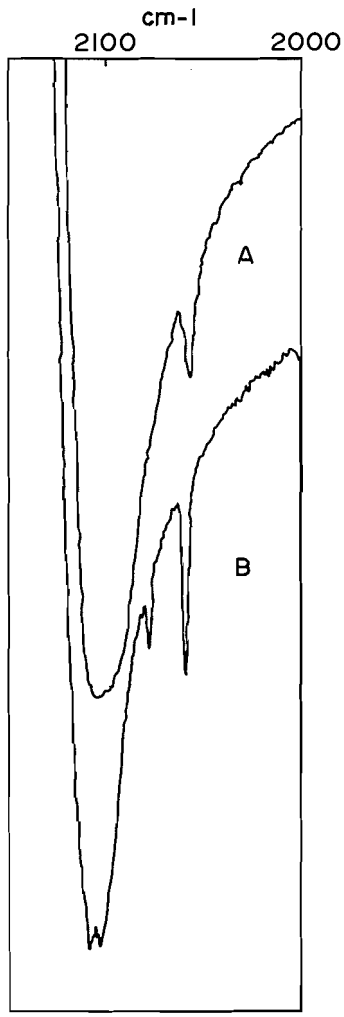

FIG. 4. The room temperature, *A*, and low temperature, *B*, spectra of $(LP)_2Ni(NCS)_2$ in the ν(CN)(NCS) region.

tially independent of temperature (room temperature down to −196 °C). The electronic spectrum exhibits bands consistent with the presence of the diamagnetic $(LP)_2Ni^{2+}$ chromophore, and, in addition, exhibits bands due to spin triplet nickel(II). These data are consistent with the formulation of this complex as $(LP)_2Ni^{2+}(Ni(NCS)_4)^{2-}$. Forster and Goodgame (22) have shown that the structure of the $Ni(NCS)_4^{2-}$ ion depends upon the cation, and may be either tetrahedral monomeric or octahedral polymeric. Comparison of their data with ours leads to the conclusion that the anion is polymeric in this complex. The complex shows multiple ν(CN) absorption near 2100 cm^{-1} (Table 3) consistent with hypothesis. Forster and Goodgame report magnetic moments of 3.24 and 3.33 BM for the polymeric ions they studied. Assuming a mean value of 3.3, our complex should theoretically exhibit a moment of 2.33 BM in excellent agreement with experiment.

TABLE 4

Possible ligand field assignments of nickel complexes

Assignment	$^3B_{2g}$ (cm^{-1})	^3E_g (cm^{-1})	$10Dq_{LE}$ (cm^{-1})	$10Dq_{NCS}$ (cm^{-1})
$(LE)_2Ni(NCS)_2$				
i	9 500	10 400	9 500	11 300
ii	10 400	9 500	10 400	8 600
$(LP)_2Ni(NCS)_2$			$10Dq_{LP}$	
iii	10 100	11 450	12 800	7 400
iv	11 450	10 100	8 750	8 600

Many attempts were made to prepare complexes of the methyl substituted ligands LMP and LME. These were for the most part unsuccessful. It was possible, however, to isolate complexes with nickel thiocyanate analyzing as $(LMP)_2Ni(NCS)_2$ and $(LME)_2Ni(NCS)_2$. The former complex is typical of the parent octahedral derivatives and is included within the discussion above. The latter complex, however, is brown and exhibits a temperature-independent reduced moment of 2.27 BM. Its electronic spectrum suggests the presence of the diamagnetic $(LME)_2Ni^{2+}$ cation, and a spin-triplet nickel species. It has a single ν(CN) absorption in the i.r. at 2110 cm^{-1} with an ill-defined shoulder at 2138 cm^{-1}. No resolution is achieved at low temperature. We are unable to adequately characterize this species at the present time.

Reaction of nickel thiocyanate with a deficiency of the ethane ligand LE led to the isolation of the olive green $(LE)Ni(NCS)_2$. Unfortunately it was not found possible to adequately purify this complex. However, the data obtained with the slightly impure derivative suggested its formulation as $(LE)_2Ni^{2+}Ni(NCS)_4^{2-}$ with the anion, in this case, a tetrahedral monomer.

Nature of the Imidazoline Rings

Of particular interest to this discussion are the NH stretching and bending vibrations and the CN stretching vibrations in the ligands and their complexes. Attempts were made to relate these frequencies with structural features in the com-

Can. J. Chem. Downloaded from www.nrcresearchpress.com by 210.87.254.40 on 09/05/12
For personal use only.

Can. J. Chem. Downloaded from www.nrcresearchpress.com by 210.87.254.40 on 09/05/12
For personal use only.

plexes. The NH and CN stretching modes are readily assigned near 3300 and 1600 cm^{-1}, respectively. The bending modes were identified by deuteration of the ligands and some of their complexes. Unfortunately no correlation was observed between the NH vibrations and any structural feature. Their variation appears random and this must undoubtedly arise as a consequence of marked changes in the extent of hydrogen bonding from one complex to another.

Systematic variations in the ν(CN) bands near 1600 cm^{-1} however, were observed. Both LP and LE exhibit two bands in this region assignable to this vibration; the LP complexes frequently have an additional shoulder or weak peak which is probably a benzene C=C vibration. The energy of the highest of these two bands appears to be a function of the stereochemistry of the complexes. Two series of derivatives may be detected, those with their highest ν(CN) vibration near 1620 cm^{-1}, and those with this band near 1600 cm^{-1}; whilst the separation is small, the division into two series is clear cut for most of the complexes.

Octahedral complexes of LP and LE and square nickel complexes of LE absorb at higher energy, whilst tetrahedral cobalt complexes of all the ligands, and square nickel complexes of LP absorb at lower energy. There is little doubt that in these complexes the ligand coordinates via the tertiary nitrogen atom rather than the secondary one. This is what would be expected and it is confirmed by the X-ray studies already completed. Given this situation two extreme structures may be postulated, **5** and **6**, containing localized and delocalized rings, respectively.

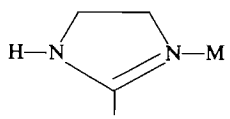

5

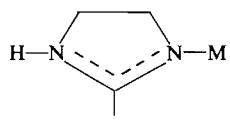

6

These would be distinguishable via X-ray studies since the former should yield two very different C—N bond distances, whilst the latter will not. In the i.r. spectra the νCN frequency is expected to occur at a higher energy in the former than in the latter. Given a classification of the complexes into two series according to νCN, as shown above, and in Table 1, it is tempting to conclude that the two series are distinguished according to the degree of delocalization in the imidazole rings. The X-ray structure of the square nickel LP complex shows that this does contain essentially delocalized rings as predicted by the i.r. spectrum. The octahedral LP complex, on the other hand, shows two very different C—N distances expected for an essentially localized structure also in agreement with the i.r. spectrum. The crystal structure of the LE octahedral nickel complex suggests delocalization of the ring, whilst the i.r. spectrum suggests localization. The discrepancy here may arise through the question of how much delocalization is needed before it will show up in each of the techniques. In an attempt to answer this question, the *N*-methyl derivative of LE was synthesized, and a few of its metal complexes prepared (15). The free ligand, which must necessarily contain a localized ring, has a νCN frequency at 1605 cm^{-1}, whilst the complexes absorb at about 1612 cm^{-1}. Thus coordination to a metal leads to an increase in the νCN frequency paralleling the behavior of pyridine (23). The ligand LE absorbs at 1610 cm^{-1}, and must surely be at least partially delocalized. Since coordination to a metal will increase the CN frequency as proven above, it follows that a CN frequency of around 1600 cm^{-1} is definitive of a highly delocalized imidazoline ring. However, a frequency above that of the free ligand, say around 1620 cm^{-1}, is ambiguous. It will not readily distinguish between a state midway between the two extremes and a completely localized structure.

Thus the tetrahedral complexes and the square nickel complexes with the ligand LP may be assigned structures involving delocalized rings, but accurate X-ray structures will be needed to identify the extent of delocalization in the other complexes. Certainly it is reasonable to suppose they will involve at least partial localization of the double bond in the imidazoline rings.

Additional X-ray structures are in progress and further discussion of this point will be deferred until the data are available.

Magnetism

The magnetic properties of these complexes are typical for the stereochemistries proposed. Worthy of comment are the rather low moments for the tetrahedral complexes of cobalt(II). To a first approximation tetrahedral complexes should exhibit a spin-only moment of 3.87 BM since they have an orbitally singlet ground state. How-

Can. J. Chem. Downloaded from www.nrcresearchpress.com by 210.87.254.40 on 09/05/12
For personal use only.

ever, moments of 4.4–4.9 BM are generally observed as a consequence of the mixing of the first orbital triplet excited state through spin–orbit coupling. In a highly distorted complex, such as those under discussion, the degeneracy of the excited state concerned will be lifted and its contribution to the ground state magnetic moment greatly reduced. This is evidently what is happening in these complexes. It is noteworthy that the LE complexes have a lower moment than their corresponding LP complexes in agreement with the increased ligand field strength (the excited state contribution to the moment being inversely proportional to the crystal field strength) (24).

Thiocyanate Stretching Frequencies

It has already been pointed out that the tetrahedral $CoL(NCS)_2$ complexes exhibit two ν(CN) stretching vibrations as expected, whilst both the *cis*- and *trans*-$ML_2(NCS)_2$ complexes exhibit only one band at room temperature. As indicated in Table 3, the spectrum of the *cis* isomers may be resolved into two bands at liquid nitrogen temperature. In addition the low temperature spectra have additional structure on the low energy edge of the main band (Table 3, Fig. 4). The very sharp band near 2060 cm^{-1} is a ^{13}C satellite predicted by a first order (diatomic oscillator) calculation to lie at about 2056 cm^{-1} (if main band is at 2100 cm^{-1}). The intensity is in line with the fact that the natural abundance of ^{13}C is 1.1%. The weaker band at 2070–2080 cm^{-1} is believed to be a ^{15}N satellite since its intensity is about one third that of the ^{13}C satellite and the natural abundance of ^{15}N is 0.37%. With the main band at 2100 cm^{-1} a first order calculation predicts the ^{15}N satellite at 2072 cm^{-1} in excellent agreement with the observations.

Electronic Spectra; Variations in Ligand Field Strengths of the Ligands

Closer inspection of the data for the square planar complexes reveals not only that the LP ligand exerts a stronger field than the LE ligand, but also that the nitrates are typical in having a band envelope displaced somewhat to lower energy. Both the nitrates behave in a similar fashion and it seems reasonable to propose that the nitrate groups are to be found along the *z* axis of the molecule, there being a weak axial nickel oxygen interaction.

The tetrahedral complexes of cobalt(II) exhibit spectra typical of strongly distorted tetrahedral chromophores (24) and provide thereby some justification for the low magnetic moments observed. Although it would be meaningless to calculate *Dq* and *B* parameters from these data, it is pertinent that the band envelopes for the LE complexes lie to somewhat higher energies than those for the LP complexes. This is particularly evident in the $(L)_2Co(ClO_4)_2$ derivatives. Thus in the tetrahedral complexes the LE ligand appears to exert a stronger ligand field than the LP, the converse of the situation in the square and octahedral cases.

In view of the close similarity in the donor characteristics of the two parent ligands, these differences in field strength are probably steric in origin. Because of the different angular constraints of the ethane *vs.* the phenyl bridge, the 'bite' of the two ligands will differ. The conclusion is that the LP ligand can more readily accommodate a 90° angle at the metal atom, than the LE ligand, whilst the LE ligand can more readily adopt a 109° angle than the LP.

Comparison of the X-ray data for the two octahedral complexes suggests that the nickel nitrogen bonds in the LE complex are slightly longer than those in the LP complex in agreement with the ligand field data. However at the present stage of refinement of the $(LP)_2Ni(NCS)_2$ complex, it is not yet certain that the differences are significant.

We are indebted to the National Research Council of Canada and the Department of University Affairs (Ontario) for financial support of this work, and Dr. D. N. Butler for useful discussions. S.H.S. is indebted to the Robert A. Welch Foundation for financial support.

1. D. M. L. Goodgame, M. Goodgame, and G. W. Rayner-Canham. Inorg. Chim. Acta, **3**, 406 (1969) and references therein.
2. C. E. Taylor and A. E. Underhill. J. Chem. Soc. 368 (1969) and references therein.
3. J. C. Wang and J. E. Bauman, Jr. Inorg. Chem. **4**, 1613 (1965).
4. A. Albert. Heterocyclic chemistry. 2nd ed. Athlone Press, London. 1968.
5. P. Oxley and W. Short. J. Chem. Soc. 497 (1947).
6. M. K. Lowery, A. J. Starshak, T. N. Esposito, R. C. Kreuger, and M. E. Kenney. Inorg. Chem. **4**, 128 (1965).
7. Natsuo Sawa and Masahiro Yasuda. Japan Patent No. 24 965 (1964); Chem. Abstr. **62**, 11820 (1965). idem, Japan Patent No. 1548 (1967); Chem. Abstr. **66**, 95042 (1967).
8. J. A. Elvidge and R. P. Linstead. J. Chem. Soc. 5000 (1952).

9. M. OHASHI, N. OHNO, and H. KAKISAWA. Org. Mass Spectry. **1**, 703 (1968).
10. D. L. KLAYMAN and G. W. A. MILNE. J. Org. Chem. **31**, 2349 (1966); D. L. KLAYMAN, A. SENNING, and G. W. A. MILNE. Acta Chem. Scand. **21**, 217 (1967).
11. A. B. P. LEVER. Inorganic electronic spectroscopy. Elsevier Publ. Co., Amsterdam. 1968.
12. R. J. H. CLARK. Halogen chemistry. Volume 3. *Edited by* V. GUTMAN. p. 85. 1967.
13. R. J. H. CLARK and C. S. WILLIAMS. Inorg. Chem. **4**, 350 (1965).
14. R. DAVIS, J. HALEY, and S. H. SIMONSEN. To be published.
15. A. B. P. LEVER and B. S. RAMASWAMY. To be published.
16. D. M. L. GOODGAME, M. GOODGAME, P. J. HAYWARD, and G. W. RAYNER-CANHAM. Inorg. Chem. **7**, 2447 (1968).
17. M. M. CORDES and J. L. WALTER. Spectrochim. Acta, **24A**, 1421 (1968).
18. A. B. P. LEVER and E. MANTOVANI. To be published.
19. B. W. BROWN and E. C. LINGAFELTER. Acta Cryst. **16**, 753 (1963).
20. A. B. P. LEVER. Coord. Chem. Rev. **3**, 119 (1968).
21. M. KEETON, A. B. P. LEVER, and D. H. BUSCH. Inorg. Chem. In press.
22. D. FORSTER and D. M. L. GOODGAME. Inorg. Chem. **4**, 823 (1965).
23. P. E. FIGGINS and D. H. BUSCH. J. Phys. Chem. **65**, 2236 (1961).
24. A. B. P. LEVER and S. M. NELSON. J. Chem. Soc. **A**, 859 (1966).

Can. J. Chem. Downloaded from www.nrcresearchpress.com by 210.87.254.40 on 09/05/12
For personal use only.

Can. J. Chem. Downloaded from www.nrcresearchpress.com by 210.87.254.42 on 09/05/12
For personal use only.

Vibrational spectra of phosphorus ligand derivatives of some alkyltricarbonyl-π-cyclopentadienylmolybdenum compounds

P. J. CRAIG[1]

Department of Chemistry, University of Calgary, Calgary 44, Alberta

Received May 5, 1970

Raman and infrared spectra of a series of complexes $RCOMo(CO)_2[L]\pi\text{-}C_5H_5$ (R = Me, Et, $\sigma\text{-}C_3H_5$, CH_2Ph; L = PPh_3, $P(OCH_2)_3CCH_3$) and of $ClMo(CO)_2[PPh_3]\pi\text{-}C_5H_5$ and $HW(CO)_2[P(OPh)_3]\pi\text{-}C_5H_5$ have been recorded. In this complementary study of complex metal carbonyl compounds, assignments are suggested for metal–carbon–oxygen deformation, metal–carbon stretching, metal–ring, and metal–phosphorus stretching vibrations. It is thought that the latter occur in the range 240–200 cm^{-1}, frequencies for phosphite complexes being lower than for the corresponding phosphine derivatives.

Canadian Journal of Chemistry, 48, 3089 (1970)

Introduction

Infrared (i.r.) spectra of metal carbonyl complexes have been extensively studied in the ν(CO) region, but only more recently has much attention been directed towards the lower frequency regions of the spectrum where δ(MCO) and ν(MC) vibrations occur. There are rather few reports of complementary Raman and i.r. studies of these regions for more complex metal carbonyls. Inferences concerning the relative π-bonding abilities of phosphorus ligands have been made as a result of observations on ν(CO) frequencies, but there are few direct observations of metal–phosphorus stretching frequencies in carbonyl compounds. In this work Raman and i.r. spectra of some molybdenum complexes in low frequency regions are compared, and suggestions are made concerning the origins of some vibrations. It should be realized that owing to the complexity of these molecules any detailed assignment of vibrations must be somewhat tentative, but nevertheless, useful information can be obtained from their vibrational spectra.

Experimental

The complexes were those reported previously (1). They were purified by recrystallization immediately before the spectra were recorded.

Infrared Spectra

The i.r. spectra were measured as Nujol mulls between CsI plates in the region 4000–200 cm^{-1} on a Perkin–Elmer 621 spectrophotometer. Between 350–33 cm^{-1} a Beckmann IR-11 instrument was used, with the sample supported on polythene windows. Spectra were also recorded in CS_2 solution in the relevant regions to confirm that bands reported did not arise through solid state effects. Accuracy was ± 2 cm^{-1} with the Perkin–Elmer and ± 3 cm^{-1} with the Beckmann (calibrated with polystyrene).

Raman Spectra

Raman spectra of the solids were obtained with a Cary 81 using helium–neon excitation. In some cases the laser beam gradually decomposed the sample. This was prevented by application of a film of glycerol to the sample surface to exclude air. Accuracy was ± 3 cm^{-1}, calibrated from the exciting line. Solution spectra were not obtained because of insufficient solubility.

Results and Discussion

Carbon–oxygen Stretching Vibrations

The i.r. spectra of solutions for this region have been reported (1). The stereochemistry of these complexes has been inferred from the relative intensities of the two terminal carbonyl stretching vibrations (1–4), and is supported by an X-ray study in one case (5). Raman spectra have not been reported previously. The ν(CO) modes are of medium intensity in the Raman spectrum, and the symmetric and asymmetric bands are of approximately equal intensity, though for the *trans* complexes the higher frequency (symmetric) vibration was usually the more intense. The ν(CO) vibrations of the acyl groups were extremely weak in the Raman effect and were sometimes not observed.

Metal–carbon–oxygen Deformation and Metal–carbon Stretching Vibrations

These occur in the range 700–300 cm^{-1} and for any one complex the δ(MCO) vibrations normally occur at higher frequencies (and are more intense in the i.r.) than the ν(MC) modes, which usually occur over a narrower frequency

[1]Present address: I.C.I. Petrochemical and Polymer Laboratory, P.O. Box 11, The Heath, Runcorn, Cheshire, England.

Can. J. Chem. Downloaded from www.nrcresearchpress.com by 210.87.254.42 on 09/05/12
For personal use only.

range below 500 cm^{-1} (6). More recent investigations into the Raman spectra of carbonyl complexes indicate that the ν(MC) vibrations often give rise to intense absorption bands, whereas the δ(MCO) modes may be very weak (7). For such complex and asymmetric compounds it can be pointed out that labelling of bands as pure δ(MCO) or ν(MC) is inaccurate, as all of these vibrations are to some extent mixed. However it is usually true that a particular absorption is mainly either δ(MCO) or ν(MC). (e.g. The symmetric ν(MC) mode of $CO(CO)_3NO$ is calculated to consist of 87% ν(MC) with the remainder being other modes of the correct symmetry mixed in (8).)

The i.r. work on Ph_3P derivatives of metal carbonyls is made more difficult by strong absorption of the ligand in the δ(MCO) and ν(MC) regions (9). For Ph_3P, these absorption bands are very weak in the Raman spectrum and though the δ(MCO) modes are also weak, the absence of an intense ligand band can aid identification of bands in the δ(MCO) region, e.g. for $EtCOMo(CO)_2[PPh_3]\pi\text{-}C_5H_5$.

The δ(MCO) and ν(MC) modes of $XFe(CO)_2\pi\text{-}C_5H_5$ (X = Cl, I, $SnBr_3$) and $X_3M(CO)_2\pi\text{-}C_5H_5$ (X = Cl, Br, I; M = Mo, W) containing $M(CO)_2$ groups have been identified using i.r. spectroscopy (10, 11). The i.r. and partial Raman data on these modes has been reported for $X_2Sn[Fe(CO)_2\pi\text{-}C_5H_5]_2$ (X = Cl, Br, I) (10). In most cases three bands assignable to δ(MCO) vibrations were observed. A detailed assignment of the δ(MCO) modes based on the "local symmetry" of the $M(CO)_2$ group has been made from i.r. studies of $LFe(CO)_2\pi\text{-}C_5H_5$ (L = PPh_3^+, I, $SnCl_2I$, $SnPh_3$) and *trans* $LMo(CO)_2[SnPh_3]\pi\text{-}C_5H_5$ (L = $P(OMe)_3$, PPh_3, $SbPh_3$) (12). Local symmetry of the $M(CO)_2$ group would lead to a prediction of three i.r.-active and four Raman-active δ(MCO) vibrations.

For the present series of complexes, vibrations that do not originate within the phosphine ligands were assigned to δ(MCO) or ν(MC) modes (after comparison with the spectra of the pure ligands). In these complexes i.r. spectra revealed in most cases three strong bands assignable to (mainly) δ(MCO) vibrations, with the formally i.r.-forbidden vibration usually appearing weakly. Fewer Raman bands were observed than predicted in nearly every case. Observations are presented in Tables 1–3.

In these complexes two bands not assignable to ligand vibrations occur, weakly in the i.r., quite strongly in the Raman, between 470 and 440 cm^{-1}, and it is suggested that these are the expected two ν(MC) vibrations. These are found in the same general region as in other π-cyclopentadienyl metal complexes with $M(CO)_2$ groups (10–12). The mode occurring at lower frequency is always very intense in the Raman spectrum, and is much stronger than the other vibration. Accordingly this lower frequency mode is preferred as the symmetric A_1 vibration because of its intensity (13). Hence the symmetric and asymmetric ν(CO) and ν(MC) vibrations appear to be in the reverse order.

Substitution of carbonyl groups by poorer π-bonding Ph_3P would be expected to lead to a lowering of the ν(CO) frequencies of the remaining carbonyl groups, with a simultaneous increase in the ν(MC) and δ(MCO) frequencies. Comparison with similar unsubstituted carbonyl complexes reveals this trend. (In $[\pi\text{-}C_5H_5Mo(CO)_3]_2$ the lowest frequency assignable to a ν(MC) vibration is observed at 411 cm^{-1}, in $PhCH_2Mo(CO)_3\pi\text{-}C_5H_5$ it occurs at 422 cm^{-1}.[2]) Within the present series, replacement of Ph_3P by the better π-bonding (14) phosphites would be expected to lower the ν(MC) and, to a lesser extent, the δ(MCO) frequencies. Such a lowering is observed for the highest frequency peak assigned to a ν(MC) vibration, supporting the assignment. Within the series of vibrations assigned to δ(MCO) there is a reduction of frequency on substitution of $P(OCH_2)_3CCH_3$ for Ph_3P in $CH_3COMo(CO)_2[L]\pi\text{-}C_5H_5$.

Little is known about metal–acyl vibrations in these and similar complexes. Two vibrations of the $MCOCH_3$ group are reported between 590 and 510 cm^{-1} for a series of *trans* $MX(COMe)[P(Et_3)]_2$ complexes (M = Pt, Pd; X = anionic ligand) (15). These are of weak to medium intensities compared to the very strong ν(C═O) vibration of the acetyl group. In the present series of complexes it is suggested that the metal–acetyl vibrations occur in the region of the δ(MCO) modes, and in the i.r. spectrum are obscured by them, and also by the strong ligand vibrations in this region.

Metal–π-cyclopentadiene Ring Vibrations

In most of these complexes three vibrations occur between 370 and 300 cm^{-1}, which cannot be easily assigned to ligand or metal–acyl

[2]Our own data, Nujol mulls.

Can. J. Chem. Downloaded from www.nrcresearchpress.com by 210.87.254.42 on 09/05/12
For personal use only.

TABLE 1

Suggested assignments for $XMo(CO)_2[L]\pi\text{-}C_5H_5$ complexes*

No.	Complex		δ(MCO)†				ν(MC)†	
I	$MeCOMo(CO)_2[PPh_3]\pi\text{-}C_5H_5$	i.r.	584 (4.7)	575 (4.4)	546 (sh)	540 (4.7)	468 (2.6)	440 (1.0)
		R	588 (4.0)		548 (1.5)		470 (3.0)	440 (10.0)
II	$EtCOMo(CO)_2[PPh_3]\pi\text{-}C_5H_5$	i.r.	581 (3.0)	560 (6.2)	535 (0.1)	525 (sh)	466 (1.6)	442 (1.0)
		R	580 (1.1)	561 (0.4)	540 (0.7)	523 (0.7)	468 (1.8)	449 (10.0)
III	$\sigma C_3H_5COMo(CO)_2[PPh_3]\pi\text{-}C_5H_5$	i.r.	579 (2.7)	559 (7.0)	540 (sh)	534 (8.7)	462 (1.7)	453 (1.0)
		R					460 (3.6)	449 (10.0)
IV	$PhCH_2COMo(CO)_2[PPh_3]\pi\text{-}C_5H_5$	i.r.	580 (2.3)	564 (4.0)		538 (3.7)	471 (1.7)	440 (1.0)
		R	584 (2.5)	561 (1.5)		540 (4.0)	471 (4.0)	442 (10.0)
V	$MeCOMo(CO)_2[P(OCH_2)_3CCH_3]\pi\text{-}C_5H_5$	i.r.	581 (3.3)	541 (6.3)		535 (6.7)	458 (5.3)	442 (1.0)
		R	582 (1.2)	544 (1.2)			462 (2.5)	442 (10.0)
VI	$EtCOMo(CO)_2[P(OCH_2)_3CCH_3]\pi\text{-}C_5H_5$	i.r.	580 (3.7)	558 (10.0)	535 (sh)		459 (3.5)	446 (1.0)
		R	583 (0.6)	559 (0.2)	539 (0.4)	521 (1.8)	462 (2.7)	448 (10.0)
VII	$ClMo(CO)_2[PPh_3]\pi\text{-}C_5H_5$	i.r.	590 (1.2)	568 (1.6)	543 (4.2)	536 (0.8)	460 (0.8)	442 (1.0)
		R			544 (3.1)		462 (7.5)	438 (10.0)
VIII	$HW(CO)_2[P(OPh)_3]\pi\text{-}C_5H_5$	i.r.	581 (3.5)	566 (1.9)	553 (sh)	531 (2.3)	470 (2.2)	445 (1.0)
		R					476 (12.1)	441 (10.0)

*Peak positions in cm^{-1}. Complexes I–VI are *trans*; VII and VIII are *cis*.
†Figures in parentheses are peak heights relative to the lower frequency ν(MC) vibration.

TABLE 2

Suggested assignments for $XMo(CO)_2[L]\pi\text{-}C_5H_5$ complexes*

Complex No.		ν(CO)			(Metal–ring)†			ν(MP)†
I	i.r.	1930 vs	1850 vs	1600 s	360 (0.7)	351 (0.9)		237 (0.8)
	R	1935 m	1847 m	1603 vvw	364 (12.6)	353 (12.0)		237 (3.0)
II	i.r.	1922 vs	1836 vs	1611 s	370 (0.3)	346 (1.2)	319 (0.5)	235 (1.0)
	R	1925 m	1843 m		370 (5.0)	347 (4.3)	322 (4.0)	236 (2.1)
III	i.r.	1924 vs	1830 vs	1613 s	368 (0.2)	349 (0.7)	312 (0.5)	235 (0.5)
	R	1929 w	1835 w			348 (10.0)	315 (3.4)	
IV	i.r.	1927 vs	1841 vs	1609 s	358 (0.2)	344 (0.5)	316 (0.3)	231 (0.6)
	R	1931 m	1851 m		366 (8.0)	347 (17.5)	318 (3.5)	229 (3.0)
V	i.r.	1956 vs	1860 vs	1616 s	366 (0.5)	351 (1.0)		
	R	1961 m	1861 m	1614 vw	366 (6.3)	349 (10.1)		210 (5.5)
VI	i.r.	1948 vs	1861 vs	1620 s	368 (0.4)	344 (0.7)	306 (1.0)	202 (0.9)
	R	1949 m	1869 m	1625 vw	372 (6.3)	351 (10.1)	307 (2.5)	203 (7.5)
VII	i.r.	1946 vs	1861 vs		358 (0.3)	344 (0.3)	313 (0.2)	235 (0.3)
	R	1960 m	1855 m		360 (10.0)	342 (15.0)		
VIII	i.r.	1951 vs	1882 vs		366 (1.0)	342 (0.4)	304 (0.4)	216 (0.5)
	R	1957 m	1870 m		365 (10.0)	342 (13.3)	307 (8.2)	

*Peak positions in cm^{-1}.
†Figures in parentheses are peak heights relative to the lower frequency ν(MC) vibration; see Table 1.

TABLE 3

Other vibrations of $XMo(CO)_2[L]\pi\text{-}C_5H_5$ complexes

Complex		Peak positions (cm^{-1})										
Ph_3P	i.r.	509 vs	498 vs	490 sh	423 w	412 w	391 vw	271 w	256 w	250 w	215 w	197 w
	i.r.	186 w	173 vw	143 vw	113 w							
	R	513 w	502 w	496 sh	425 vw	410 w	273 w	254 s	248 sh	214 s	199 m	189 m
	R	105 sh	79 sh									
$P(OCH_2)_3CCH_3$	i.r.	511 m	505 sh	467 m	409 m	330 s	288 w	266 m	121 vw			
$P(OPh)_3$	i.r.	499 s	466 sh	203 vw								
I	i.r.	512 vs	497 m	431 m	422 s	392 vw	288 m	278 w	260 vw	252 vw	221 w	207 m
	i.r.	199 m	138 m	115 w	90 w							
	R	517 w	497 m	430 sh	289 s	261 sh	251 w	215 w	200 s			
II	i.r.	514 vs	508 sh	495 m	433 w	419 m	390 vw	275 w	256 w	249 m	224 w	210 w
	i.r.	188 w	143 w	108 w								
	R	498 w	422 w	289 w	272 w	259 m	206 m					
III	i.r.	513 vs	509 sh	496 s	430 w	418 m	391 vw	303 sh	291 w	276 w	252 w	243 m
	i.r.	221 sh	204 w	192 w	144 w	106 w						
IV	i.r.	511 vs	497 m	460 w	435 w	420 m	390 vw	291 vw	272 w	255 w	251 vw	211 m
	i.r.	200 w	130 w	113 vw								
	R	510 vw	490 vw	289 w	270 w	254 w	191 m	174 w				
V	i.r.	512 s	499 s	410 w	284 w	271 m						
	R	510 w	411 vw	274 s	188 m	153 w						
VI	i.r.	512 s	498 s	410 m	272 w	259 w	224 vw	168 vw	151 vw	104 vw		
	R	412 vw	261 s	223 m	177 m							
VII	i.r.	513 vs	504 sh	488 vw	429 w	281 m	269 w	257 w	222 w	205 w	192 w	145 w
	i.r.	124 w										
VIII	i.r.	506 sh	492 vs	480 vs	320 vw	270 vw	184 vw	147 vw	120 w			

Can. J. Chem. Downloaded from www.nrcresearchpress.com by 210.87.254.42 on 09/05/12
For personal use only.

Can. J. Chem. Downloaded from www.nrcresearchpress.com by 210.87.254.42 on 09/05/12
For personal use only.

vibrations (because of their nearly constant positions in different compounds). These are thought to be metal–ring tilting and stretching modes. A mono-π-cyclopentadienyl complex would be expected to exhibit two tilting and one stretching mode, but usually the tilting vibrations are degenerate (16*a*). In the complexes showing three vibrations, it is tentatively suggested that the degeneracy of the tilting modes is removed either by the bulk of the acyl or ligand groups, or by the asymmetric nature of the (*cis*) complexes. The metal-ring vibrations are weak in the i.r. and very strong in the Raman spectrum.

Metal–phosphorus Stretching Vibrations

These have been reported to vary considerably for complexes with differing stereochemistries, electronic configurations, and oxidation states, and have been observed in the range 460–100 cm^{-1} (9, 16*b*). A number of assignments of ν(MP) vibrations in phosphorus–ligand substituted metal carbonyl complexes have been made. Frequencies (cm^{-1}) for some monotriphenylphosphine complexes are as follows: $Ni(CO)_3[PPh_3]$ (17), 192; $M(CO)_5[PPh_3]$ (M = Cr) 206, (M = Mo) 204 (9). Spectra of some phosphite–ligand substituted compounds indicate that, for monosubstituted derivatives, ν(MP) is lower than for the analogous phosphine complex; ν(MP) frequencies (cm^{-1}) are as follows: $Ni(CO)_3[P(OCH_2)_3CCH_3]$ (18), 143; $M(CO)_5[P(OCH_2)_3CCH_3]$ (M = Cr) 164, (M = Mo) 195, (M = W) 180 (18). For $Ni(CO)_{4-n}[PF_3]_n$ ν(MP) occurs between 260 and 190 cm^{-1} (19).

For the present series of complexes of π-bonding ligands with a transition metal in a low oxidation state, it would be reasonable to look for ν(MP) in the same general region as for the $M(CO)_5[PPh_3]$ derivatives. For the acyl series of Ph_3P complexes, where only the acyl group varies, ν(MP) would probably occur at very similar frequencies for each derivative. For this series no peak of fairly constant position occurred in the i.r. or Raman spectra in the range 450–300 cm^{-1} that could not be better assigned to Ph_3P, ν(MC), or metal–ring modes. The region below 150 cm^{-1} appeared unlikely to contain the ν(MP) mode, by analogy with other carbonyl complexes, and the vibrations that are found here are more suitably assigned to δ(CMC), δ(CMP), or ring–twisting modes.

The i.r. spectrum of pure Ph_3P was run between 300 and 150 cm^{-1} and agreed very closely with a published spectrum for this compound (20). The i.r. spectra of the complexes $RCOMo(CO)_2[PPh_3]\pi\text{-}C_5H_5$ (R = Me, Et, $\sigma\text{-}C_3H_5$, CH_2Ph) revealed one additional band compared to Ph_3P in this region, at about 230 cm^{-1}. The other vibrations all had close counterparts in the spectrum of Ph_3P, and so the band at 230 cm^{-1} is believed to be the ν(MP) vibration. No assignments were made which depended on enhanced intensities of bands already occurring in the ligand spectrum; these have been shown to be misleading in some cases (20). The Raman spectra of Ph_3P and the above complexes were compared in three cases (R = Me, Et, CH_2Ph) and an additional band was observed for the complexes coincident with the extra band noted in the i.r.

The i.r. spectrum[3] of $(PhO)_3P$ below 300 cm^{-1} revealed only a broad, weak band near 200 cm^{-1}. The complex $HW(CO)_2[P(OPh)_3]\pi\text{-}C_5H_5$ shows two bands near 200 cm^{-1}, a weak, broad absorption at about 180 cm^{-1}, and a stronger, sharp peak at 216 cm^{-1} which is assigned to ν(MP).

The ligand $P(OCH_2)_3CCH_3$ is reported (18) to have no i.r. vibrations between 250 and 120 cm^{-1}. For $MeCOMo(CO)_2[P(OCH_2)_3CCH_3]\pi\text{-}C_5H_5$ a peak which could be assigned to ν(MP) appeared in the Raman at 210 cm^{-1}. Raman and i.r. spectra of $EtCOMo(CO)_2[P(OCH_2)_3CCH_3]\pi\text{-}C_5H_5$ showed bands at 224 (weak) and 202 cm^{-1} (stronger), either of which could be assigned to ν(MP). Intuitively the lower frequency peak is preferred because of its intensity and because ν(MP) would not be expected to be higher in the Et compared to the Me derivative.

Assignments made on this basis would agree with a trend noted previously (18), that for monosubstituted derivatives higher ν(MP) frequencies are found for phosphine complexes than for the equivalent phosphites and since phosphites are generally thought to be more effective π-bonding ligands than phosphines (14) (and the ν(CO) frequencies observed for these compounds would suggest this), it is perhaps surprising that the observed trend in ν(MP) frequencies exists. It has been tentatively suggested that a coupling effect may be responsible (18).

[3]Our own data, liquid film spectrum.

NOTE ADDED IN PROOF: It has recently been suggested that the degeneracy of the ring-tilt mode is lifted in some (π-arene)$M(CO)_3$ complexes (21).

The author thanks Dr. M. Green (University of Bristol, Bristol, England) for advice and encouragement during the preparation of these complexes, and Drs. P. M. Boorman and T. W. Swaddle (University of Calgary, Calgary, Alberta) for provision of a post-doctoral fellowship and for very helpful discussions. The author would like to thank Dr. J. E. Bertie (University of Alberta, Edmonton, Alberta) for use of the Beckmann IR-11 in that Department.

1. P. J. CRAIG and M. GREEN. J. Chem. Soc. (A) 1978 (1968); A. BAINBRIDGE, P. J. CRAIG, and M. GREEN. J. Chem. Soc. (A) 2715 (1968); P. J. CRAIG and M. GREEN. J. Chem. Soc. (A) 157 (1969).
2. W. BECK, A. MELNIKOFF, and R. STAHL. Ber. **99**, 3721 (1966).
3. A. R. MANNING. J. Chem. Soc. (A) 1984 (1967).
4. A. R. MANNING. J. Chem. Soc. (A) 651 (1968).
5. M. R. CHURCHILL and J. P. FENNESSEY. Inorg. Chem. **7**, 953 (1968).
6. D. M. ADAMS. J. Chem. Soc. 1771 (1964).
7. D. M. ADAMS and A. SQUIRE. J. Chem. Soc. (A) 2817 (1968).
8. R. S. MCDOWELL, W. D. HORROCKS, JR., and J. T. YATES. J. Chem. Phys. **34**, 530 (1961).
9. See for example, A. A. CHALMERS, J. LEWIS, and R. WHYMAN. J. Chem. Soc. (A) 1817 (1967).
10. D. M. ADAMS, J. N. CROSBY, and R. D. W. KEMMITT. J. Chem. Soc. (A) 3056 (1968).
11. M. L. H. GREEN and W. E. LINDSELL. J. Chem. Soc. (A) 686 (1967).
12. A. R. MANNING. J. Chem. Soc. (A) 1670 (1968).
13. See for example, E. W. ABEL, P. J. HENDRA, R. A. N. MCLEAN, and M. M. QURASHI. Inorg. Chim. Acta, **3**, 77 (1969).
14. W. D. HORROCKS, JR. and R. C. TAYLOR. Inorg. Chem. **2**, 723 (1963).
15. D. M. ADAMS and G. BOOTH. J. Chem. Soc. 1112 (1962).
16. (*a*) D. M. ADAMS. Metal-ligand and related vibrations. Edward Arnold (Publishers) Ltd., London, 1967. p. 190; (*b*) p. 321.
17. W. F. EDGELL and M. P. DUNKLE. Inorg. Chem. **4**, 1629 (1965).
18. A. C. VANDENBROUCKE, JR., D. G. HENDRICKER, R. E. MCCARLEY, and J. G. VERKADE. Inorg. Chem. **7**, 1825 (1968).
19. A. LOUTELLIER and M. BIGORGNE. Bull. Soc. Chim. France, 3186 (1965).
20. A. BALLS, N. N. GREENWOOD, and B. P. STRAUGHAN. J. Chem. Soc. (A), 753 (1968).
21. D. M. ADAMS and A. SQUIRE. J. Chem. Soc. (A) 814 (1970).

Can. J. Chem. Downloaded from www.nrcresearchpress.com by 210.87.254.42 on 09/05/12
For personal use only.

Can. J. Chem. Downloaded from www.nrcresearchpress.com by 210.87.254.40 on 09/05/12
For personal use only.

The low frequency infrared and Raman spectroscopic studies of some uranyl complexes: the deformation frequency of the uranyl ion

J. I. BULLOCK
Department of Chemistry, University of Surrey, Guildford, Surrey, England

AND

F. W. PARRETT
Department of Chemistry, Royal Military College of Canada, Kingston, Ontario

Received April 23, 1970

A study of the low frequency vibrational spectra of compounds of the type $L_2UO_2(NO_3)_2$ (L = monodentate ligand), $MUO_2(NO_3)_3$ (M = monovalent cation), and $Cs_2UO_2X_4$ (X = Cl or Br) has shown that the deformation frequency of the uranyl group occurs in the region 274–245 cm^{-1} but detailed assignments of the U—O (nitrate) frequencies are not given since it is shown that structurally related complexes do not necessarily give similar low frequency infrared (i.r.) and Raman spectra.

Canadian Journal of Chemistry, 48, 3095 (1970)

Introduction

There are conflicting reports of the deformation frequency of the uranyl ion (UO_2^{2+}). For nitrato complexes Ferraro and Walker (1) assign an absorption at 140 cm^{-1} to this vibration whilst Topping (2) prefers 212 cm^{-1}. Recently Hart and Newbery (3, 4) have shown clearly that the vibration occurs near 260 cm^{-1} for some halide complexes. The halide–uranium vibrational modes were adequately assigned for the $UO_2X_4^{2-}$ ions in terms of the D_{4h} point group although the true symmetry (5) is lower than this for the chloride.

All of these authors assign only one i.r. band to the doubly-degenerate deformation mode, implying that the ion is linear in a variety of ligand environments. This assumption is fully justified by X-ray crystallographic results (6) and by i.r. and Raman studies (7, 8) of the stretching frequencies.

We report the i.r. and laser Raman spectra of $L_2UO_2(NO_3)_2$, $MUO_2(NO_3)_3$, and $Cs_2UO_2X_4$ showing that the UO_2^{2+} deformation mode is in the range 274 to 248 cm^{-1} and is i.r. active.

Experimental

Preparation and Analysis of the Complexes

Full details are given elsewhere (7, 8).

Spectroscopic Measurements

Infrared spectra (300–30 cm^{-1}) of the solid complexes were obtained as Nujol mulls between polyethylene plates using a Research and Industrial Instruments Ltd. FS-720 Fourier Spectrophotometer, the transformation to a spectrum being carried out by a digital computer using a program described in detail elsewhere (9). Raman spectra were determined on solid complexes using the Cary 81 Laser Raman spectrometer with He–Ne excitation. Many of the complexes are fluorescent and in some cases poor quality Raman spectra were obtained.

Results and Discussion

Table 1 shows the observed spectral results. In all cases a strong i.r. band is observed between 274 and 248 cm^{-1}. With the exceptions of $Cs_2UO_2Cl_4$ and $[(C_6H_5)_3PO]_2UO_2(NO_3)_2$ this has no strong, coincident Raman shift. A comparison of the spectra of $Cs_2UO_2Cl_4$ and $Cs_2UO_2Br_4$ shows that the strong Raman band at 267 cm^{-1} in the chloride is not present in the bromide but instead a strong shift at 172 cm^{-1} is observed which is accompanied by a strong i.r. absorption at 170 cm^{-1}. The Raman shifts are assigned (4) to U—X stretching vibrations whilst the i.r. bands at 254 cm^{-1} in the chloride and 248 cm^{-1} in the bromide are assigned (4) to the UO_2^{2+} deformation mode. In addition the bromide has a very weak Raman shift at 253 cm^{-1} which could be assigned to the doubly-degenerate UO_2^{2+} deformation since two bands at 248(s) and 258(sh) cm^{-1} occur in the i.r.

In the nitrato complexes there is a strong i.r. absorption near 250 cm^{-1} which we assign to the UO_2^{2+} deformation mode by comparison with

Can. J. Chem. Downloaded from www.nrcresearchpress.com by 210.87.254.40 on 09/05/12
For personal use only.

TABLE I

Infrared and Raman spectra (300–30 cm^{-1}) of the uranyl complexes*

$Cs_2UO_2Cl_4$		$Cs_2UO_2Br_4$		$KUO_2(NO_3)_3$		$NH_4UO_2(NO_3)_3$		$RbUO_2(NO_3)_3$		$CsUO_2(NO_3)_3$		
Infrared	Raman	Infrared	Raman	Infrared	Raman	Infrared	Raman	Infrared	Raman	Infrared	Raman	Assignments‡
—	267(s)	258(sh)	253(w)	—	—	278(sh)	—	—	—	269(sh)	—	
254(s)	—	248(s)	—	260(s)	—	266(s)	—	268(s)	—	262(s)	—	UO_2^{2+} deformation
236(m)	230(w)	192(w)	192(m)	—	—	—	—	—	—	252(m)	—	§
—	206(s)	170(s)	172(m)	234(m)	234(s)	—	231(m)	—	231(m)	—	—	‖
—	184(w)	158(w)	—	225(sh)	—	223(m)	—	223(s)	—	220(m)	224(m)	
—	131(m)	108(w)	109(w)	208(w)	—	205(s)	—	214(sh)	—	212(m)	—	
110(m)	—	—	83(m)	—	168(s)	157(m)	166(s)	—	165(s)	—	154(s)	Molecular
—	92(w)	—	75(sh)	128(w)	—	140(m)	—	—	—	142(w)	—	deformation
—	80(sh)	68(w)	—	—	107(m)	—	106(w)	112(m)	107(m)	116(w)	—	and
—	71(w)	—	45(w)	90(w)	78(w)	90(w)	—	82(s)	93(s)	100(w)	—	lattice modes
58(w)	—	—	—	—	—	—	—	—	61(s)	—	—	

$(C_2H_5)_4NUO_2(NO_3)_3$		$UO_2(NO_3)_2 \cdot 6H_2O$		$[(C_6H_5)_3PO]_2UO_2(NO_3)_2$†		$[(C_6H_5)_3AsO]_2UO_2(NO_3)_2$†		$[(C_2H_5O)_3PO]_2UO_2(NO_3)_3$		
Infrared	Raman	Infrared	Raman	Infrared	Raman	Infrared	Raman	Infrared	Raman	Assignments‡
—	—	—	—	296(w)	—	298(w)	—	268(sh)	—	
264(s)	—	248(s)	—	270(s)	—	274(s)	—	262(s)	—	UO_2^{2+} deformation
—	—	—	—	259(s)§	263(s)§	252(s)§	246(w)§	—	—	§
—	234(m)	226(w)	—	—	—	—	—	218(sh)	—	‖
224(m)	—	—	—	212(sh)	—	—	—	210(s)	—	
216(m)	218(m)	204(w)	209(s)	203(m)	—	190(m)	—	—	195(s)	
170(m)	—	166(w)	—	—	—	—	—	—	—	Molecular
—	138(s)	—	126(s)	142(w)	—	—	—	—	124(w)	deformation
—	—	—	—	98(w)	—	—	—	88(w)	93(m)	and
86(w)	—	—	—	73(w)	—	—	—	—	—	lattice modes
64(w)	—	—	—	—	—	—	—	—	—	

*s = strong, m = medium, w = weak, sh = shoulder.
†Poor quality Raman spectra were obtained for these compounds.
‡These assignments refer to the nitrato complexes only, for assignments of the halide spectra see ref. 4.
§Phenyl rocking modes.
‖These bands may be associated to some extent with U—O(NO_2) and U—O (ligand) stretching.

the halide spectra. As expected this has no coincident Raman shift. The stretching frequencies of the UO_2^{2+} ion vary little on changing the equatorial ligand environment (8). Frequencies below 170 cm^{-1} have been assigned to molecular deformation and lattice modes.

There have been several attempts (2, 10, 11) to predict the frequency, the pattern, and the nature of the vibrational modes of coordinated nitrate ions. All of these predict relatively simple patterns but since the mixing and coupling of vibrations and the unit cell dimensions were not rigorously considered observed spectra (12) are often more complicated. The uranyl nitrate complexes, which have bidentate nitrate groups, have up to nine i.r. and Raman active bands which could be assigned to "U—O" vibrations (8). It is tempting, therefore, to assign bands in the region 235–190 cm^{-1} to U—O stretching modes. However, structurally related ions, e.g., in the trisnitrato complexes, do not have identical spectra or the same total number of bands or bands of corresponding activity (see Table 1). The complete crystal structures of three of the complexes are known whilst there are partial structures for two of them (for $[(C_6H_5)_3PO]_2UO_2(NO_3)_2$ and $[(C_6H_5)_3AsO]_2UO_2(NO_3)_2$, see ref. 6*a*; $RbUO_2(NO_3)_3$, ref. 6*b*; $UO_2(NO_3)_2 \cdot 6H_2O$, ref. 6*c*; and $[(C_2H_5O)_3PO]_2UO(NO_3)_2$, ref. 6*d*). Not all contain the same number of molecules or ions per unit cell. In view of the general lack of precise crystallographic information and the reported variations in spectral properties, it would be unwise to assign bands in these complexes to the equatorial U—O modes or to use the spectra as a basis for the identification of bidentate nitrate groups in compounds of unknown structure.

1. J. R. Ferraro and A. Walker. J. Chem. Phys. **45**, 550 (1966).
2. G. Topping. Spectrochim. Acta, **21**, 1743 (1965).
3. F. A. Hart and J. E. Newbery. J. Inorg. Nucl. Chem. **30**, 318 (1968).
4. J. E. Newbery. Spectrochim. Acta, **25A**, 1699 (1969).
5. D. Hall, A. D. Rae, and T. N. Waters. Acta Cryst. **20**, 160 (1966).
6. (*a*) C. Panattoni, R. Graziani, U. Croatto, B. Zarli, and G. Bombieri. Inorg. Chim. Acta, **2**, 43 (1968); (*b*) G. A. Barclay, T. M. Sabine, and J. C. Taylor. Acta Cryst. **19**, 205 (1965); (*c*) J. E. Fleming and H. Lynton. Chem. Ind. 1416 (1960); (*d*) J. E. Fleming and H. Lynton. Chem. Ind. 1415 (1960).
7. J. I. Bullock. J. Inorg. Nucl. Chem. **29**, 2257 (1967).
8. J. I. Bullock. J. Chem. Soc. (A), 781 (1969).
9. F. W. Parrett. Lab. Pract. **19**, 68 (1970).
10. R. E. Hester and W. E. L. Grossman. Inorg. Chem. **5**, 1308 (1966).
11. R. H. Nuttall and D. W. Taylor. Chem. Commun. 1417 (1968).
12. J. I. Bullock and F. W. Parrett. Chem. Commun. 157 (1969).

Synthesis of *p*-*O*-(tetra-*O*-acetyl-α-D-glucopyranosyl)-penicillin G

T. L. Nagabhushan[1] and C. G. Chin

R & L Molecular Research Ltd., 8045 Argyll Road, Edmonton 82, Alberta

Received May 6, 1970

The synthesis of *p*-*O*-(tetra-*O*-acetyl-α-D-glucopyranosyl)-phenylacetic acid from tetra-*O*-acetyl-2-deoxy-2-nitroso-α-D-glucopyranosyl chloride and *t*-butyl-*p*-hydroxyphenylacetate and its coupling with 6-aminopenicillanic acid by way of the corresponding acid chloride to give *p*-*O*-(tetra-*O*-acetyl-α-D-glucopyranosyl)-penicillin G is described.

Canadian Journal of Chemistry, 48, 3097 (1970)

In view of high biological activity exhibited by a number of naturally occurring α-glycosides it is conceivable that a variety of non-glycosidic drugs may be beneficially modified for therapeutic application by conversion to α-glycosides. Such structural changes, whether they enhance the intrinsic biological activity of the drug or increase its effectiveness by improving the pharmacodynamic properties, could lead to clinically useful agents. Recent developments in α-glucoside synthesis (1–3) clearly indicate that an α-glucosidic linkage between the hydroxyl group of a desired aglycon and D-glucose can readily be established with a very high degree of stereoselectivity using dimeric 3,4,6-tri-*O*-

[1]Present address: Department of Chemistry, University of Alberta, Edmonton 7, Alberta.

Can. J. Chem. Downloaded from www.nrcresearchpress.com by 210.87.254.40 on 09/05/12
For personal use only.

the halide spectra. As expected this has no coincident Raman shift. The stretching frequencies of the UO_2^{2+} ion vary little on changing the equatorial ligand environment (8). Frequencies below 170 cm^{-1} have been assigned to molecular deformation and lattice modes.

There have been several attempts (2, 10, 11) to predict the frequency, the pattern, and the nature of the vibrational modes of coordinated nitrate ions. All of these predict relatively simple patterns but since the mixing and coupling of vibrations and the unit cell dimensions were not rigorously considered observed spectra (12) are often more complicated. The uranyl nitrate complexes, which have bidentate nitrate groups, have up to nine i.r. and Raman active bands which could be assigned to "U—O" vibrations (8). It is tempting, therefore, to assign bands in the region 235–190 cm^{-1} to U—O stretching modes. However, structurally related ions, e.g., in the trisnitrato complexes, do not have identical spectra or the same total number of bands or bands of corresponding activity (see Table 1). The complete crystal structures of three of the complexes are known whilst there are partial structures for two of them (for $[(C_6H_5)_3PO]_2UO_2(NO_3)_2$ and $[(C_6H_5)_3AsO]_2UO_2(NO_3)_2$, see ref. 6*a*; $RbUO_2(NO_3)_3$, ref. 6*b*; $UO_2(NO_3)_2 \cdot 6H_2O$, ref. 6*c*; and $[(C_2H_5O)_3PO]_2UO(NO_3)_2$, ref. 6*d*). Not all contain the same number of molecules or ions per unit cell. In view of the general lack of precise crystallographic information and the reported variations in spectral properties, it would be unwise to assign bands in these complexes to the equatorial U—O modes or to use the spectra as a basis for the identification of bidentate nitrate groups in compounds of unknown structure.

1. J. R. Ferraro and A. Walker. J. Chem. Phys. **45**, 550 (1966).
2. G. Topping. Spectrochim. Acta, **21**, 1743 (1965).
3. F. A. Hart and J. E. Newbery. J. Inorg. Nucl. Chem. **30**, 318 (1968).
4. J. E. Newbery. Spectrochim. Acta, **25A**, 1699 (1969).
5. D. Hall, A. D. Rae, and T. N. Waters. Acta Cryst. **20**, 160 (1966).
6. (*a*) C. Panattoni, R. Graziani, U. Croatto, B. Zarli, and G. Bombieri. Inorg. Chim. Acta, **2**, 43 (1968); (*b*) G. A. Barclay, T. M. Sabine, and J. C. Taylor. Acta Cryst. **19**, 205 (1965); (*c*) J. E. Fleming and H. Lynton. Chem. Ind. 1416 (1960); (*d*) J. E. Fleming and H. Lynton. Chem. Ind. 1415 (1960).
7. J. I. Bullock. J. Inorg. Nucl. Chem. **29**, 2257 (1967).
8. J. I. Bullock. J. Chem. Soc. (A), 781 (1969).
9. F. W. Parrett. Lab. Pract. **19**, 68 (1970).
10. R. E. Hester and W. E. L. Grossman. Inorg. Chem. **5**, 1308 (1966).
11. R. H. Nuttall and D. W. Taylor. Chem. Commun. 1417 (1968).
12. J. I. Bullock and F. W. Parrett. Chem. Commun. 157 (1969).

Synthesis of *p*-*O*-(tetra-*O*-acetyl-α-D-glucopyranosyl)-penicillin G

T. L. Nagabhushan[1] and C. G. Chin

R & L Molecular Research Ltd., 8045 Argyll Road, Edmonton 82, Alberta

Received May 6, 1970

The synthesis of *p*-*O*-(tetra-*O*-acetyl-α-D-glucopyranosyl)-phenylacetic acid from tetra-*O*-acetyl-2-deoxy-2-nitroso-α-D-glucopyranosyl chloride and *t*-butyl-*p*-hydroxyphenylacetate and its coupling with 6-aminopenicillanic acid by way of the corresponding acid chloride to give *p*-*O*-(tetra-*O*-acetyl-α-D-glucopyranosyl)-penicillin G is described.

Canadian Journal of Chemistry, 48, 3097 (1970)

In view of high biological activity exhibited by a number of naturally occurring α-glycosides it is conceivable that a variety of non-glycosidic drugs may be beneficially modified for therapeutic application by conversion to α-glycosides. Such structural changes, whether they enhance the intrinsic biological activity of the drug or increase its effectiveness by improving the pharmacodynamic properties, could lead to clinically useful agents. Recent developments in α-glucoside synthesis (1–3) clearly indicate that an α-glucosidic linkage between the hydroxyl group of a desired aglycon and D-glucose can readily be established with a very high degree of stereoselectivity using dimeric 3,4,6-tri-*O*-

[1]Present address: Department of Chemistry, University of Alberta, Edmonton 7, Alberta.

Can. J. Chem. Downloaded from www.nrcresearchpress.com by 210.87.254.42 on 09/05/12
For personal use only.

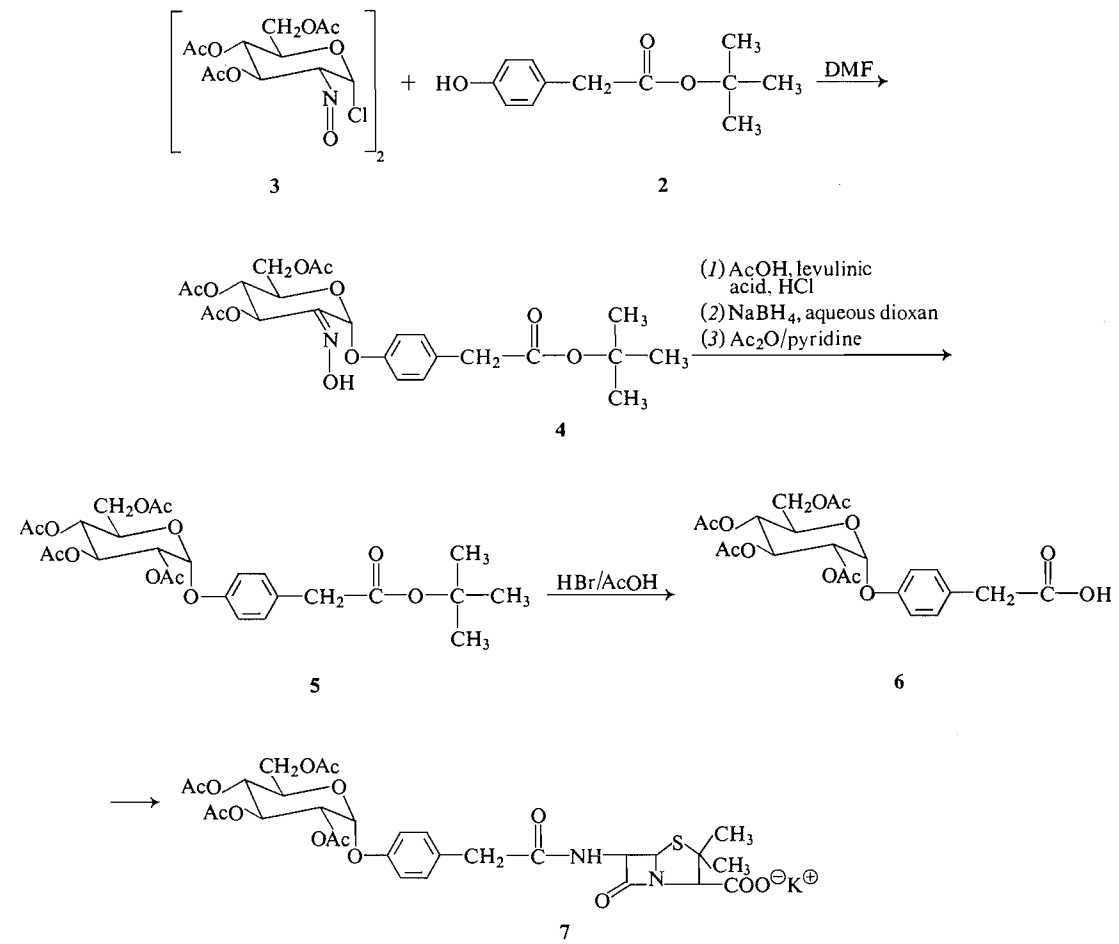

3 2 4 5 6 7

SCHEME 1

acetyl-2-deoxy-2-nitroso-α-D-glucopyranosyl chloride as the precursor (**3**). It was, therefore, apparent to us that this method could be applied to synthesize an α-glucosidic derivative of penicillin G so that a study of the effect of such a structural change on the biological property of the antibiotic could be undertaken. Although a large number of penicillin G derivatives have been made since 6-aminopenicillanic acid became available, to our knowledge the preparation of a derivative of this antibiotic containing the phenyl ring linked glycosidically to a sugar in the α-configuration has not been described. In this paper we wish to report the synthesis of one such derivative in which the phenylacetic acid side chain forms an α-glucoside at the para position.

The starting material in our synthesis, *t*-butyl *p*-hydroxyphenyl acetate (**2**), was prepared by reaction of the corresponding acid **1** with isobutylene in the presence of sulfuric acid in a manner analogous to that described for the preparation of di-*t*-butyl malonate from malonic acid (4). Condensation of this compound with dimeric 3,4,6-tri-*O*-acetyl-2-deoxy-2-nitroso-α-D-glucopyranosyl chloride (**3**) provided, as expected, the oximinoglycoside **4** (see Scheme 1). Hydrolysis of the oximino group of **4** under mild conditions followed by reduction of the resulting ketoglycoside by sodium borohydride yielded, after *O*-acetylation, *p*-*O*-(tetra-*O*-acetyl-α-D-glucopyranosyl)-*t*-butyl phenylacetate (**5**) (1). Removal of the *t*-butyl group of **5** with hydrobromic acid gave the corresponding acid **6** which was coupled with 6-aminopenicillanic acid by the modified acid chloride method to give the

Can. J. Chem. Downloaded from www.nrcresearchpress.com by 210.87.254.42 on 09/05/12
For personal use only.

Can. J. Chem. Downloaded from www.nrcresearchpress.com by 210.87.254.42 on 09/05/12
For personal use only.

penicillin **7** (5). Structural proof for compounds **4**–**7** was obtained by elemental analysis, infrared (i.r.) and nuclear magnetic resonance (n.m.r.) spectroscopy (see the Experimental). The new penicillin **7** exhibited strong antibacterial activity against Gram-positive microorganisms.

Experimental

Melting points are uncorrected. The i.r. spectra were recorded with a Perkin–Elmer model 137 "Infracord" spectrophotometer. The n.m.r. spectra were measured at 60 MHz with a Varian A-60 spectrometer. Chemical shifts refer, unless otherwise stated, to spectra measured in deuteriochloroform using tetramethylsilane as the internal standard. Optical rotations were determined with a Carl Zeiss Circular Polarimeter model 0.01°. Solutions were dried over anhydrous sodium sulfate and concentrated on a rotary evaporator at 45°.

t-Butyl p-Hydroxyphenylacetate (2)

This compound, m.p. 98–99°, was prepared in 54% yield from *p*-hydroxyphenylacetic acid (**1**) by application of a procedure described in the literature for the preparation of di-*t*-butyl malonate (4); ν_{max} (Nujol) 3325 (hydroxyl), 1690 cm^{-1} (*t*-ester carbonyl); n.m.r. data: τ 8.59 (*t*-butyl), 6.59 (methylene), 3.47 (hydroxyl).

Anal. Calcd. for $C_{12}H_{16}O_3$: C, 69.29; H, 7.75. Found: C, 69.14; H, 7.73.

p-O-(Tri-O-acetyl-2-oximino-α-D-arabino-hexopyranosyl)-t-butyl phenylacetate (4)

A solution of tri-*O*-acetyl-2-deoxy-2-nitroso-α-D-glucopyranosyl chloride dimer (**3**, 3.37 g) and the above ester **2** (3.12 g) in dry *N,N'*-dimethylformamide (11 ml) was set aside at room temperature for 65 h. The solvent was removed *in vacuo* (oil pump) and a solution of the residue in methylene chloride (100 ml) washed successively with water (2 × 30 ml), 0.05 *N* sodium hydroxide solution (2 × 50 ml) and water. After drying, the solvent was removed and the residue chromatographed on a column (3 × 55 cm) of silica gel (28–200 mesh) using ethyl acetate – *n*-hexane (1:3) as the developing solvent. After collecting 1.15 l, the solvent system was changed to ethyl acetate – *n*-hexane (1:1) whereupon the compound was eluted in the next 600 ml. The compound was isolated in the usual manner, crystallized from *n*-hexane, and recrystallized from chloroform – *n*-hexane to yield 2.4 g (47.5%), m.p. 113–114° and $[\alpha]_D^{24}$ +70.2° (*c*, 0.93 in chloroform); ν_{max} (Nujol) 3200 (oxime hydroxyl), 1725 (ester carbonyl), 1670 cm^{-1} (*t*-ester carbonyl); n.m.r. data: τ 8.59 (*t*-butyl), 8.02, 7.96 (*O*-acetyl), 6.55 (methylene), 3.4 (H-1, singlet), 4.06 (H-3, doublet $J_{3,4}$ = 9.0 c.p.s.), 4.77 (H-4, near triplet, $J_{4,5}$ = 10 c.p.s.), 0.9 (oxime hydroxyl).

Anal. Calcd. for $C_{24}H_{31}NO_{11}$: C, 56.58; H, 6.13; N, 2.74. Found: C, 56.32; H, 6.04; N, 2.51.

p-O-(Tetra-O-acetyl-α-D-glucopyranosyl)-t-butyl phenylacetate (5)

Levulinic acid (600 mg) and 1 *N* hydrochloric acid (1 ml) were added to a solution of **4** (500 mg) in acetic acid (3 ml). The mixture was stirred at room temperature for 17 h, poured into ice-water and partitioned between chloroform and water. The chloroform solution was freed of acids in the usual manner and concentrated to a sirup. The sirup was dissolved in dioxan (3 ml) and water (1.5 ml) and the solution was cooled with stirring in an ice-water bath. A solution of sodium borohydride (100 mg) in dioxan (1 ml) and water (1 ml) was added, dropwise, and the stirring continued for 0.5 h at ice temperature and then for 1 h at room temperature. Excess borohydride was destroyed with acetic acid and the solvents removed. The dried residue was acetylated with pyridine (10 ml) and acetic anhydride (3 ml) overnight at room temperature. Work-up in the usual manner provided a sirup which was crystallized from *n*-hexane, yield 45%, m.p. 105–108°; $[\alpha]_D^{24}$ +138.2° (*c*, 2.3 in chloroform); ν_{max} (Nujol) 1725 (carbonyl), 1675 (shoulder, *t*-ester carbonyl), 1600 cm^{-1} (phenyl); n.m.r. data: τ 8.57 (*t*-butyl), 7.96 (*O*-acetyl), 6.55 (methylene), 4.32 (doublet, H-1, $J_{1,2}$ = 3.5 c.p.s.), 5.0 (pair of doublets, H-2, $J_{2,3}$ = 9.5 c.p.s.), 4.30 (triplet, H-3, $J_{3,4}$ = 10.0 c.p.s.), 4.89 (triplet, H-4).

Anal. Calcd. for $C_{26}H_{34}O_{12}$: C, 57.99; H, 6.36. Found: C, 57.79; H, 6.52.

p-O-(Tetra-O-acetyl-α-D-glucopyranosyl)-phenylacetic acid (6)

To the ester **5** (4 g) was added a cold solution of 30–32% hydrogen bromide in glacial acetic acid (~4°, 16 ml) and the mixture was swirled until it was homogeneous (3–4 min). The solution was concentrated and on addition of ice-cold water a solid precipitated which was isolated and crystallized from chloroform – *n*-hexane to give 3.4 g (92%) of product m.p. 89–90°; $[\alpha]_D^{24}$ +150° (*c*, 1.2 in chloroform); ν_{max} (Nujol) 3550, 3400 (hydroxyl), 1725, 1700 cm^{-1} (broad, acetyl and acid carbonyl, respectively); n.m.r. data: τ 7.97 (acetyl), 6.42 (methylene), 4.3 (doublet, H-1, $J_{1,2}$ = 3.5 c.p.s.), 5.0 (pair of doublets, H-2, $J_{2,3}$ = 9.5 c.p.s.), 4.32 (triplet, H-3, $J_{3,4}$ = 9.5 c.p.s.), 4.89 (triplet, H-4).

Anal. Calcd. for $C_{22}H_{26}O_{12}$: C, 54.77; H, 5.39. Found: C, 54.35; H, 5.22.

p-O-(Tetra-O-acetyl-α-D-glucopyranosyl)-penicillin G as the Potassium Salt (7)

Ice-cold thionyl chloride (20 ml) was added to the acid **6** (3.2 g) and nitrogen bubbled through the solution. After 0.5 h at 0° and 0.5 h at room temperature, thionyl chloride was removed by co-distilling with benzene three times. A solution of the residue (3.3 g) in methylene chloride (20 ml) was added to triethylamine salt of 6-aminopenicillanic acid dissolved in methylene chloride (60 ml) containing triethylamine (0.65 g) and maintained at 0°. After 1 h the solvent was removed and work-up in the usual manner (5) afforded 3.4 g (73%) of **7**, m.p. >190° dec.; $[\alpha]_D^{24}$ +202° (*c*, 2.47 in chloroform); ν_{max} (Nujol) 1775 (β-lactam), 1750 (ester carbonyl), 1660 (amide), 1600 cm^{-1} (carboxylic acid); n.m.r. data (deuterium oxide, external tetramethylsilane): τ 8.54 (methyl), 8.09, 7.97 (*O*-acetyl), 5.82 (H-3 of the thiazolidine ring), 4.54 (β-lactam hydrogen).

Anal. Calcd. for $C_{30}H_{35}N_2O_{14}SK$: C, 50.12; H, 4.87; N, 3.89; S, 4.46. Found: C, 49.91; H, 4.78; N, 3.57.

The authors thank Professor R. U. Lemieux, Director of Research, for his advice and encouragement in the

conduct of this research and Miss K. Hayakawa and Messrs. A. Vanson and S. Cherwonka for their technical assistance.

1. R. U. LEMIEUX, R. SUEMITSU, and S. W. GUNNER. Can. J. Chem. **46**, 1040 (1968).
2. T. L. NAGABHUSHAN. Can. J. Chem. **48**, 257 (1970).
3. R. U. LEMIEUX, T. L. NAGABHUSHAN, and S. W. GUNNER. Can. J. Chem. **46**, 405 (1968).
4. A. L. MCCLOSKEY, G. S. FONKEN, R. W. KLUIKER, and W. S. JOHNSON. Org. Syn. Coll. Vol. IV. John Wiley and Sons, Inc., New York, N.Y. 1963. p. 261.
5. F. P. DOYLE, K. HARDY, J. H. C. NAYLER, M. J. SOULAL, E. R. STOVE, and H. R. J. WADDINGTON. J. Chem. Soc. 1453 (1962).

Acid dependence and ion pairing in the anation reactions yielding iron(III) monosulfate

F. L. BAKER AND W. MACF. SMITH
Department of Chemistry, Queen's University, Kingston, Ontario

Received May 12, 1970

Stopped-flow studies of the kinetics of the anation reaction yielding iron(III) monosulfate indicate a significant dependence of rate constant on acidity and also a dependence on iron concentrations. This is consistent with association constants for outer ion pair formation between the reactants which have about three times the Fuoss values.

Canadian Journal of Chemistry, **48**, 3100 (1970)

Introduction

The anation reaction of iron(III) ion with sulfate has been examined by Wendt and Strehlow (1) and Cavasino (2) by relaxation methods, by Davis and Smith (3) by continuous flow methods, and the data interpreted on the basis of the reaction scheme

$$\begin{array}{ccc} & K_e & \\ Fe^{3+} + SO_4^{2-} & \underset{k_{-1}}{\overset{k_1}{\rightleftharpoons}} & FeSO_4^+ \\ -H^+ \Big\downarrow \Big\uparrow +H^+ & & -H^+ \Big\downarrow \Big\uparrow +H^+ \\ FeOH^{2+} + SO_4^{2-} & \underset{k_{-2}}{\overset{k_2}{\rightleftharpoons}} & FeOHSO_4 \end{array} \qquad [1]$$

where the proton transfer reactions are fast compared to the anation reactions and the $Fe(OH)SO_4$ is in such small concentrations that its effects may be ignored. All investigations imply that at hydrogen concentrations less than 0.20 *M*, the contribution of the anation reaction involving Fe^{3+} and HSO_4^- is nearly negligible. However, Cavasino and also Wendt and Strehlow reported an acid dependence of rate which is interpretable in terms of the kinetic activity of $Fe(OH)^{2+}$ whereas the results of Davis and Smith seemed to imply an almost negligible dependence. We have further investigated this reaction using stopped-flow methods with the view of resolving the conflict and also to examine the effect of ion pairing and, from the kinetic data, to assess values of effective association constants for (outer) ion pairing. Our conditions do not include the range of lower acidities investigated by Cavasino, but they do cover a range of iron(III) concentrations greater than those examined by previous investigators. We ignore consideration of the reaction between $FeOH^{2+}$ and HSO_4^- which may not be distinguished from reaction 1 on the basis of reaction order and which Cavasino (2) considers does not contribute appreciably to the acid independent reaction.

Experimental

Solutions were prepared using distilled water which had been passed through Barnstead organic removal and mixed bead demineralizing ion exchange columns. Sodium perchlorate solution was prepared from G Frederick Smith's reagent grade 70% perchloric acid and British Drug Houses standard sodium hydroxide solution. Otherwise the preparation and analysis of solutions were as described previously (3).

Measurements were made at temperatures 15, 25, and 35 °C with the iron concentration at 2.175×10^{-2} *M*, sulfate at 0.75×10^{-3}, 1.5×10^{-3}, and 3.0×10^{-3} *M*, and perchloric acid ranging from 0.08 to 0.2 *M*. At 25 °C iron concentration ranged from 0.40×10^{-2} to 2.175×10^{-2} *M*. Ionic strength was adjusted with sodium perchlorate to 0.50 in all solutions.

Our stopped-flow equipment of local but conventional design yielded a photographic record of the position of the plungers of the driving syringes as well as a record of the intensity of the light transmitted through the reacting solution as they depend on time. An estimate of the transmission in the absence of outer ion pairing between iron(III) and sulfate was obtained by mixing

Can. J. Chem. Downloaded from www.nrcresearchpress.com by 210.87.254.42 on 09/05/12
For personal use only.

conduct of this research and Miss K. Hayakawa and Messrs. A. Vanson and S. Cherwonka for their technical assistance.

1. R. U. LEMIEUX, R. SUEMITSU, and S. W. GUNNER. Can. J. Chem. **46**, 1040 (1968).
2. T. L. NAGABHUSHAN. Can. J. Chem. **48**, 257 (1970).
3. R. U. LEMIEUX, T. L. NAGABHUSHAN, and S. W. GUNNER. Can. J. Chem. **46**, 405 (1968).
4. A. L. MCCLOSKEY, G. S. FONKEN, R. W. KLUIKER, and W. S. JOHNSON. Org. Syn. Coll. Vol. IV. John Wiley and Sons, Inc., New York, N.Y. 1963. p. 261.
5. F. P. DOYLE, K. HARDY, J. H. C. NAYLER, M. J. SOULAL, E. R. STOVE, and H. R. J. WADDINGTON. J. Chem. Soc. 1453 (1962).

Acid dependence and ion pairing in the anation reactions yielding iron(III) monosulfate

F. L. BAKER AND W. MACF. SMITH
Department of Chemistry, Queen's University, Kingston, Ontario

Received May 12, 1970

Stopped-flow studies of the kinetics of the anation reaction yielding iron(III) monosulfate indicate a significant dependence of rate constant on acidity and also a dependence on iron concentrations. This is consistent with association constants for outer ion pair formation between the reactants which have about three times the Fuoss values.

Canadian Journal of Chemistry, **48**, 3100 (1970)

Can. J. Chem. Downloaded from www.nrcresearchpress.com by 210.87.254.40 on 09/05/12
For personal use only.

Introduction

The anation reaction of iron(III) ion with sulfate has been examined by Wendt and Strehlow (1) and Cavasino (2) by relaxation methods, by Davis and Smith (3) by continuous flow methods, and the data interpreted on the basis of the reaction scheme

$$\begin{array}{ccc} & K_e & \\ Fe^{3+} + SO_4^{2-} & \underset{k_{-1}}{\overset{k_1}{\rightleftharpoons}} & FeSO_4^+ \\ -H^+\downarrow\uparrow+H^+ & & -H^+\downarrow\uparrow+H^+ \\ FeOH^{2+} + SO_4^{2-} & \underset{k_{-2}}{\overset{k_2}{\rightleftharpoons}} & FeOHSO_4 \end{array} \qquad [1]$$

where the proton transfer reactions are fast compared to the anation reactions and the $Fe(OH)SO_4$ is in such small concentrations that its effects may be ignored. All investigations imply that at hydrogen concentrations less than 0.20 *M*, the contribution of the anation reaction involving Fe^{3+} and HSO_4^- is nearly negligible. However, Cavasino and also Wendt and Strehlow reported an acid dependence of rate which is interpretable in terms of the kinetic activity of $Fe(OH)^{2+}$ whereas the results of Davis and Smith seemed to imply an almost negligible dependence. We have further investigated this reaction using stopped-flow methods with the view of resolving the conflict and also to examine the effect of ion pairing and, from the kinetic data, to assess values of effective association constants for (outer) ion pairing. Our conditions do not include the range of lower acidities investigated by Cavasino, but they do cover a range of iron(III) concentrations greater than those examined by previous investigators. We ignore consideration of the reaction between $FeOH^{2+}$ and HSO_4^- which may not be distinguished from reaction 1 on the basis of reaction order and which Cavasino (2) considers does not contribute appreciably to the acid independent reaction.

Experimental

Solutions were prepared using distilled water which had been passed through Barnstead organic removal and mixed bead demineralizing ion exchange columns. Sodium perchlorate solution was prepared from G Frederick Smith's reagent grade 70% perchloric acid and British Drug Houses standard sodium hydroxide solution. Otherwise the preparation and analysis of solutions were as described previously (3).

Measurements were made at temperatures 15, 25, and 35 °C with the iron concentration at 2.175×10^{-2} *M*, sulfate at 0.75×10^{-3}, 1.5×10^{-3}, and 3.0×10^{-3} *M*, and perchloric acid ranging from 0.08 to 0.2 *M*. At 25 °C iron concentration ranged from 0.40×10^{-2} to 2.175×10^{-2} *M*. Ionic strength was adjusted with sodium perchlorate to 0.50 in all solutions.

Our stopped-flow equipment of local but conventional design yielded a photographic record of the position of the plungers of the driving syringes as well as a record of the intensity of the light transmitted through the reacting solution as they depend on time. An estimate of the transmission in the absence of outer ion pairing between iron(III) and sulfate was obtained by mixing

Can. J. Chem. Downloaded from www.nrcresearchpress.com by 210.87.254.40 on 09/05/12
For personal use only.

solutions identical with those of a kinetic run except that sodium sulfate was replaced by sodium perchlorate. An estimate of the time elapsing between mixing and observation could be made from the rate of plunger movement and the geometry of the equipment. The wavelength of the spectrophotometric beam was identical with that used by Davis and Smith i.e. 305 mμ.

Results and Discussion

We have interpreted our results initially on the basis of the reaction Scheme 1, assuming a first order dependence of rate on the concentration of Fe^{3+}, $FeOH^{2+}$, SO_4^{2-}, and of $FeSO_4^+$ and that the concentration of Fe^{3+} was substantially constant. On the basis of these assumptions, relation 2 was obtained

$$[2] \quad \ln \frac{[FeSO_4^+]^* - [FeSO_4^+]}{[FeSO_4^+]^*} = k_{obs} Ft$$

where

$$k_{obs} = k_{1f} + k_{2f} \frac{K_h}{[H^+]}$$

and

$$F = \frac{1}{K_e} + \frac{[Fe^{3+}]}{1 + [H^+]/K_a}$$

where K_e is the association constant of $FeSO_4^+$; K_h the hydrolysis constant of Fe^{3+}; and K_a the acid ionization constant of HSO_4^-.

Therefore

$$[3] \quad \ln \frac{D_\infty - D_t}{D_\infty - D_0} = k_{obs} Ft$$

where D_0, D_∞, and D_t represent the optical densities of the reacting solution at zero time, equilibrium, and intermediate time t. The slope of the plot of $\ln (D_\infty - D_t)$ vs. t yields $k_{obs} F$.

Interpretation of the data using eq. [3] and the same values for the various constants as used by Davis and Smith yields the results summarized graphically in Fig. 1, where k_{obs} is plotted against $1/[H^+]$. A significant dependence of k_{obs} on acidity at 25 and 35 °C is apparent. There is also a dependence on the total iron concentration.

The dependence of k_{obs} on the iron(III) concentration is consistent with an effect due to a significant degree of ion pairing between iron(III) ion and sulfate and iron(III) ion and bisulfate, through which the outer ion pairs hold a significant fraction of uncomplexed sulfate and the rate constant falls to less than first order in iron(III).

We have interpreted the data, allowing for the effect of ion pairing, on the basis of the scheme given below, retaining the view that the reactions of proton transfer and outer ion pairing are relatively very rapid compared to the reactions with rate constants k_{01} and k_{02}.

$$[4] \quad \begin{array}{ccccc} & & Fe^{3+} \cdot HSO_4^- & & \\ & K_{031} & & & \\ & -HSO_4^- \downarrow\uparrow +HSO_4^- & & & \\ & & & & K_{OCl} \\ & Fe^{3+} + SO_4^{2-} & \overset{K_{032}}{\rightleftharpoons} & Fe^{3+} \cdot SO_4^{2-} & \underset{k_{-01}}{\overset{k_{01}}{\rightleftharpoons}} \; FeSO_4^+ \\ & -H^+ \downarrow\uparrow +H^+ & & & -H^+ \downarrow\uparrow +H^+ \\ & K_h & & & \\ & FeOH^{2+} + SO_4^{2-} & \overset{K_{022}}{\rightleftharpoons} & FeOH^{2+} \cdot SO_4^{2-} & \underset{k_{-02}}{\overset{k_{02}}{\rightleftharpoons}} \; FeOHSO_4 \end{array}$$

$Fe^{3+} \cdot SO_4^{2+}$, $Fe^{3+} \cdot HSO_4^-$, and $FeOH^{2+} \cdot SO_4^-$ represent outer sphere ion pairs.

The product $k_{01}K_{032}$ of this scheme is identifiable with k_{1f} of Scheme 1 and $k_{02}K_{022}K_h/[H^+]$ is identifiable with $k_{2f}K_h/[H^+]$. The relationship 2 still applies but

$$[5] \quad F = \frac{1}{K_{OCl}K_{032}} + \frac{[Fe^{3+}]}{1 + \frac{[H^+]}{K_a} + [Fe^{3+}]\left(K_{032} + K_{031}\frac{[H]}{K_a}\right)}$$

If significant ion pairing is occurring then the relation between $(K_{OCl}K_{032})$ and the values of the association constant (K_e) reported by Davis and Smith need re-interpretation. We have assumed that the extinction coefficient at $\lambda = 305$ mμ for iron(III) ion in the outer sphere complex is the same as that for free iron(III) ion, an assumption supported by the fact that plots of $\ln (D_\infty - D_t)/(D_\infty - D_0)$ extrapolated to zero time show intercepts with no significant deviation from zero. (A large difference in the extinction coefficients for iron(III) in the free form and in the outer ion pair would produce, in the presence of marked outer

Can. J. Chem. Downloaded from www.nrcresearchpress.com by 210.87.254.40 on 09/05/12
For personal use only.

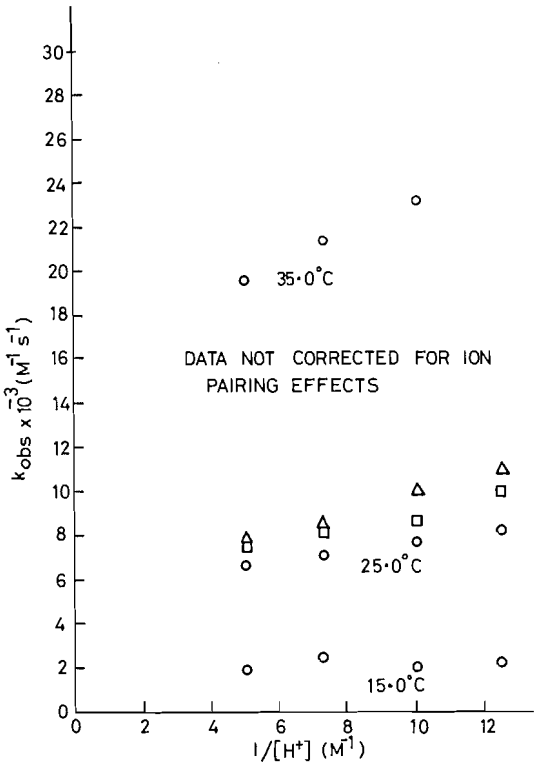

FIG. 1. Plot of k_{obs} against $1/[H^+]$. k_{obs} estimated without allowance for ion pairing. ○, Fe(III) = 2.175×10^{-2} M; □, Fe(III) = 0.80×10^{-2} M; △, Fe(III) = 0.40×10^{-2} M.

ion pairing, a considerable change in optical density after mixing but before anation.) On the basis of this assumption

$$[6] \qquad K_{032}K_{0C1} = K_e - K_{032}$$

where K_e is the association constant determined by Davis and Smith.

Values for $K_{032}K_{0C1}$ required for the interpretation of the kinetic data cannot be assessed solely from experimental data available but can be estimated for various assumed (or calculated) values for the outer pair association constant K_{032}. We have interpreted our data using eqs. 5 and 6 and various values for K_{032} and K_{031}. Values derived from the simple Fuoss (4) relationship, using a value for a (the distance of approach of the ions) of 5 Å, lead to decrease in the dependence of k_{obs} on the iron concentration but values three times the Fuoss values were required to yield values of k_{obs} which are independent of the iron concentration. The results of calculations using a value of 49.2 l mole^{-1} for K_{032} and 6.9 l mole^{-1} for K_{031} are shown in Fig. 2. The Fuoss values are 16.4 and 2.3 l mole^{-1}. It may be noted that the ion pair association constants K_{032} and K_{031} have been arbitrarily increased in the same ratio, also that the magnitude of the association constant ($K_{032}K_{0C1}$) is being simultaneously adjusted in accordance with eq. 6.

Our data for k_{obs} along with those of Davis and Smith for comparable conditions are displayed in Fig. 3. Only at 35 °C is the discrepancy marked. Table 1 contains the values of the equilibrium quotients K_a, K_h, and K_e used in interpreting the kinetic data. Table 2 contains values for k_{1f} and k_{2f} determined from the data applying to iron concentration of 0.02175 M (the only concentration used at 35 and 15 °C) and ignoring ion pairing and Table 3 the values for k_{1f} and k_{2f} determined from all data for 25 °C and considering ion pairing as indicated above. Our data relate to a narrower range of $[H^+]$ than do those of Cavasino and the uncertainty associated with the estimation of k_{2f} correspondingly larger.

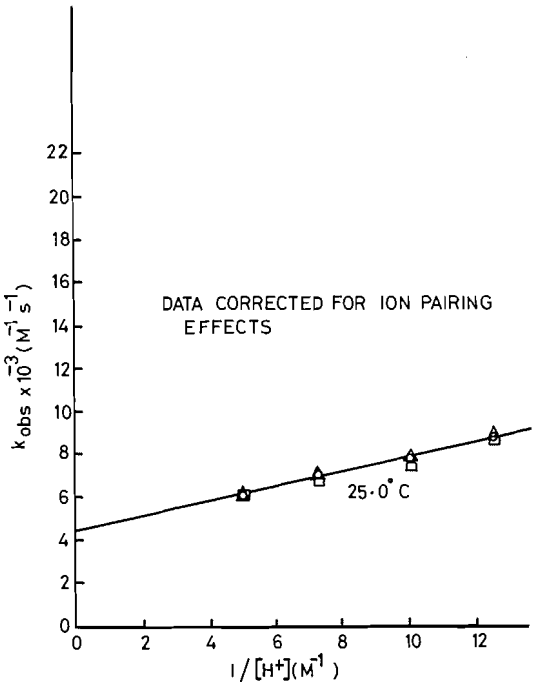

FIG. 2. Plot of k_{obs} against $1/[H^+]$ for data at 25 °C. k_{obs} estimated with allowance for ion pairing. ○, Fe(III) = 2.175×10^{-2} M; □, Fe(III) = 0.80×10^{-2} M; △, Fe(III) = 0.40×10^{-2} M.

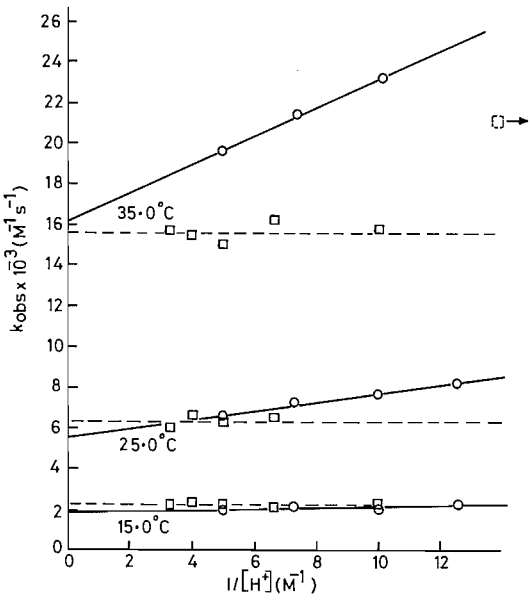

FIG. 3. Comparison of values for k_{obs} at various hydrogen ion concentrations obtained by Davis and Smith and by Baker and Smith. ○, Baker and Smith; □, Davis and Smith; ⬚, Davis and Smith's value for $1/[H^+] = 20\ M^{-1}$.

TABLE 1

Equilibrium quotients

Temperature (°C)	$K_a \times 10^2$ (M)	$K_h \times 10^3$ (M)	K_e (M^{-1})
15.0	5.40	1.18	149
25.0	4.33	1.90	205
35.0	3.36	3.20	280

TABLE 2

Rate constants k_{1f} and k_{2f} ignoring ion pairing and applying to iron(III) concentration of 0.02175 M

Temperature (°C)	$k_{1f} \times 10^{-3}$ (l mole^{-1} s^{-1})	$k_{2f} \times 10^{-4}$ (l mole^{-1} s^{-1})
15.0	1.65+0.28	4.5 ±2.3
25.0	5.64±0.40	10.9 ±0.2
35.0	16.3 ±0.4	21.7 ±1.8

However, it is apparent that our data do imply a significant dependence of rate constant on acidity that supports the view that the species $Fe(OH)^{2+}$ has significant kinetic activity. Our conditions of concentration are close to those of Cavasino only at the lowest iron concentration at 25 °C. For this condition our data (ignoring ion pairing) imply values for k_{1f} and k_{2f} of $(5.79 \pm 0.12) \times 10^3$ and $(21.7 \pm 1.8) \times 10^4$, respectively, whereas Cavasino's values are 4.6×10^3 and 23.1×10^4. It is notable that our values for k_{2f} estimated with allowance for ion pairing are greater than those obtained with ion pairing effects ignored but that the values for k_{1f} are somewhat reduced by allowance for ion pairing, a result which arises from the values of $K_{032}K_{0C1}$ being appreciably less than the values for K_e obtained by Davis and Smith.

TABLE 3

Rate constants k_{1f} and k_{2f} at 25 °C considering ion pairing

Temperature (°C)	$k_{1f} \times 10^{-3}$ (l mole^{-1} s^{-1})	$k_{2f} \times 10^{-4}$ (l mole^{-1} s^{-1})
25.0	4.35±0.17	18.7±1.0

The results referred to above were obtained using the values reported by Davis and Smith and our kinetic data interpreted on the basis of eq. 6. We have further scrutinized the original equilibrium data upon which the values of the association constants were based and have attempted a tentative re-interpretation retaining the conclusion of the earlier paper that $FeHSO_4^{2+}$ is formed to a negligible extent but introducing the assumption that $FeOHSO_4$ is present in significant amounts. The data may be interpreted on this basis with considerable internal consistency to imply a hydrolysis constant for

$$FeSO_4 \overset{H_2O}{\rightleftharpoons} FeOHSO_4 + H^+$$

of 4.33×10^{-2} at 25 °C; a value k_{1f} of 1.34×10^3 and a value for k_{2f} not significantly different from zero. However, the implication of marked hydrolysis of $FeSO_4^+$ seems decidely questionable and we are consequently planning further investigations of the protolytic reaction of the iron(III) sulfate system.

We thank the National Research Council of Canada for financial support of this work.

1. H. WENDT and H. STREHLOW. Z. Elektrochem. **66**, 228 (1962).
2. F. P. CAVASINO. J. Phys. Chem. **72**, 1378 (1968).
3. G. G. DAVIS and W. MACF. SMITH. Can. J. Chem. **40**, 1836 (1962).
4. R. M. FUOSS. J. Amer. Chem. Soc. **80**, 5059 (1958).

Can. J. Chem. Downloaded from www.nrcresearchpress.com by 210.87.254.40 on 09/05/12
For personal use only.

Effect of p*H* on the reaction of 1,3-dihydro-1-hydroxy-3-oxo-1,2-benziodoxole with 2-mercaptoethanol, 2-mercaptoethylamine, and glutathione

JAMES LESLIE
Department of Medicinal Chemistry, School of Pharmacy, University of Maryland, 636 West Lombard Street, Baltimore, Maryland 21201

Received March 23, 1970

The kinetics of the oxidation of 2-mercaptoethanol, 2-mercaptoethylamine, and glutathione with 1,3-dihydro-1-hydroxy-3-oxo-1,2-benziodoxole (**1**) have been examined at p*H* 4–5.6. The reaction is second-order, which can be explained by a rate-determining step involving the reaction of one molecule of the thiol with one molecule of **1**. The second-order rate constants vary in a linear manner with the reciprocal of the hydrogen ion activity. The ionic species involved in the reaction are discussed.

Canadian Journal of Chemistry, 48, 3104 (1970)

Can. J. Chem. Downloaded from www.nrcresearchpress.com by 210.87.254.6 on 09/05/12
For personal use only.

The reaction of 1,3-dihydro-1-hydroxy-3-oxo-1,2-benziodoxole (**1**), also known as *o*-iodosobenzoic acid, is frequently used as an enzyme inhibitor (1), and as a reagent for the quantitative analysis of sulfhydryl groups (2). The reaction of **1** with thiols is shown in eq. 1. Recently, it has been shown that the reaction of **1** with cysteine

[1] 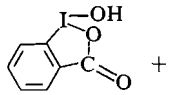 + 2RSH →

1

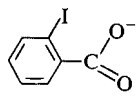 + H^+ + RSSR + H_2O

follows second-order kinetics (3) and a mechanism was postulated in which the initial step was the reaction of one molecule of each of the reactants facilitated by the formation of complexes of **1** with the charged amino- and carboxy-groups of cysteine in its zwitterionic form. In order to study the effect of p*H* on the rate of oxidation of the sulfhydryl group without the complications of the effect of amino- and carboxy-groups, the oxidation rate of 2-mercaptoethanol by **1** was examined. For comparison, however, the rate of reaction of **1** with glutathione, which contains a carboxy-group, and with 2-mercaptoethylamine, which contains an amino-group, was also measured.

Experimental and Results

The 1,3-dihydro-1-hydroxy-3-oxo-1,2-benziodoxole was prepared from *o*-iodobenzoic acid by oxidation with potassium permanganate (2). The product was reprecipitated from alkaline solution with carbon dioxide at least three times, and was greater than 99% pure as determined by the amount of iodine liberated from acidified potassium iodide. 2-Mercaptoethanol was obtained from Eastman Organic Chemicals. Rather than attempting to weigh precise amounts of this malodorous volatile liquid, stock solutions were prepared of the approximate required concentration, and the thiol content determined by spectrophotometric titration with *N*-ethylmaleimide (4). It was ascertained that no oxidation of the mercaptoethanol stock solution by dissolved oxygen occurred by repeated assay of the stock solution during any series of experiments. Glutathione and 2-mercaptoethylamine were obtained from Nutritional Biochemicals Corporation.

The kinetics of the oxidation of 2-mercaptoethanol and of 2-mercaptoethylamine were followed by measuring the acid liberated as a function of time. This was done automatically and recorded using a Radiometer SBR2/SBU1/TTA31 titration assembly. Measurements were made at 25 ± 1°. The use of this apparatus permitted the reaction to be followed at constant p*H*. In a typical experiment 7 ml of a 1 m*M* solution of the oxidant was added to the titration vessel, adjusted to the desired p*H* with a

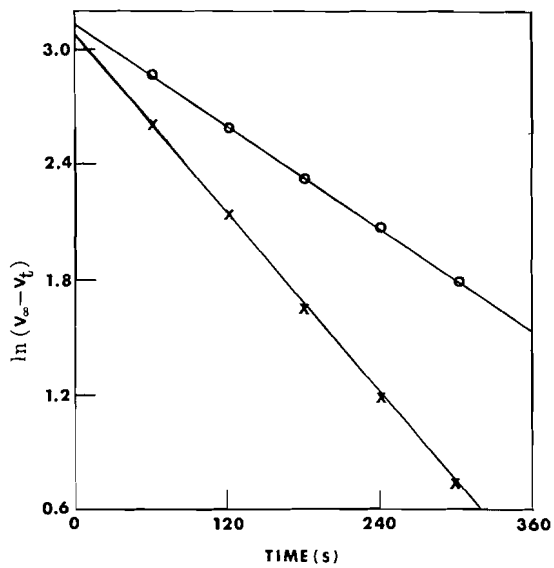

FIG. 1. First-order plots for the oxidation of 2-mercaptoethanol, 1.57×10^{-2} *M*, at p*H* 4.6 (○) and 2-mercaptoethylamine, 1.59×10^{-2} *M*, at p*H* 4.95 (×) by 1,3-dihydro-1-hydroxy-3-oxo-1,2-benziodoxole at 25°.

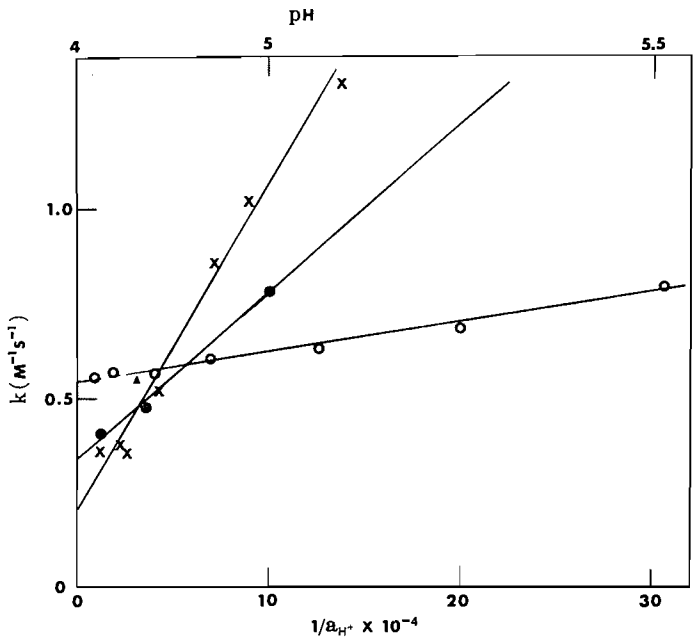

FIG. 2. Plots of the second-order rate constants for the oxidation of 2-mercaptoethanol (○, titrimetric method; ▲, spectrophotometric method), 2-mercaptoethylamine (×), and glutathione (●) by 1,3-dihydro-1-hydroxy-3-oxo-1,2-benziodoxole at 25° as a function of the hydrogen ion activity.

measured volume of 0.05 *N* NaOH, then 2 ml of thiol solution added, and the volume of 0.05 *N* NaOH required to maintain a constant p*H* was recorded as a function of time. In all experiments the amount of acid titrated at the completion of the reaction was consistent with eq. 1.

The thiol was always in excess over the 1,3-dihydro-1-hydroxy-3-oxo-1,2-benziodoxole. Although the reaction was followed to completion, only the data from the first 85% of the reaction were used in the analysis of the data because of the small differences between V_∞, the total volume of NaOH added by the end of the reaction, and V_t, the volume added at time t after the initiation of the reaction. Plots of $\ln (V_\infty - V_t)$ *vs.* t were linear; typical plots are shown in Fig. 1. This showed that the reaction had a first-order dependence on the oxidant, and pseudo first-order rate constants were obtained from the slopes of the linear plots. It was also found that these first-order rate constants were directly proportional to the concentration of thiol in the reaction mixture, indicating that the reaction was also first-order in thiol; this proportionality is shown in Table 1. The plot of the second-order rate constants, obtained by dividing the first-order rate constants by the thiol concentration, *vs.* the reciprocal of the hydrogen ion activity was linear, as shown in Fig. 2. For 2-mercaptoethanol, the intercept of this plot was 0.540, the slope was 7.87×10^{-7}, and the correlation coefficient was 0.996, as determined by least squares, and the corresponding values for 2-mercaptoethylamine were 0.210, 8.38×10^{-6}, and 0.991, respectively.

When the thiol has a carboxy-group, as in glutathione, the titrimetric procedure for following the reaction described above is not suitable because of the buffering effects of the carboxy-groups. Furthermore, the spectrophotometric method described by Wolf and Wu (3)

TABLE 1

Proportionality of first-order rate constant to the thiol concentration. Data presented are for 2-mercaptoethanol at p*H* 4.4. Proportionality is shown by constancy of values in third column

k (s^{-1}) $\times 10^2$	[2-mercapto-ethanol] $\times 10^2$	k/[2-mercapto-ethanol]
1.32	2.30	0.57
1.50	2.36	0.64
1.25	2.04	0.62
2.27	3.57	0.64
0.93	1.58	0.59

presents difficulties when used with buffer solutions in the p*H* range of interest in this study as it was observed that at constant p*H* the reaction rate increases as the buffer concentration increases. Caraway and Hellerman (5) have found that the oxidation of ascorbic acid by **1** is catalyzed by undissociated acids. However, in order to obtain results comparable to those obtained using the titrimetric procedure some measurements were made by the spectrophotometric procedure in acetate buffers. Absorbance changes were measured on a Beckman DU-2 spectrophotometer; otherwise, the procedure is as previously described (3). A typical second-order plot is shown in Fig. 3. It was observed that the second-order rate constant was a linear function of the acetic acid concentration in the buffer solution, at constant p*H*. For the oxidation of 2-mercaptoethanol at p*H* 4.5 the second-order rate constants were 0.595, 0.645, 0.737, and 0.853 M^{-1} s^{-1} in

Can. J. Chem. Downloaded from www.nrcresearchpress.com by 210.87.254.6 on 09/05/12
For personal use only.

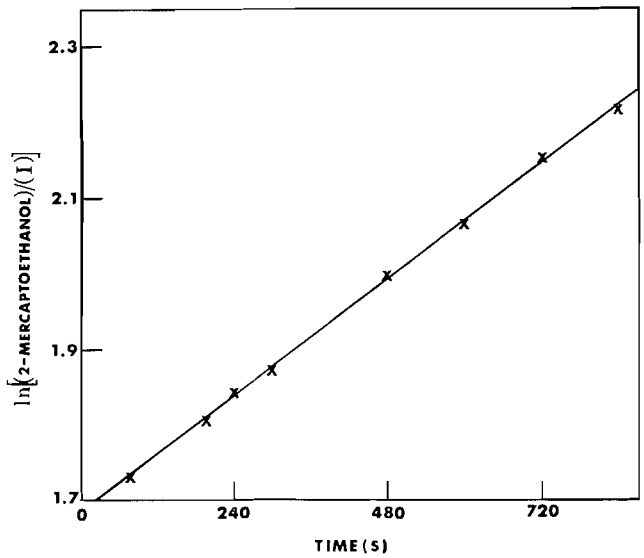

FIG. 3. Second-order plot for the oxidation of 2-mercaptoethanol by 1,3-dihydro-1-hydroxy-3-oxo-1,2-benziodoxole at 25°. Initial concentrations were 1.17×10^{-3} and 2.16×10^{-4} M, respectively, in 0.699 M acetate – acetic acid buffer at pH 4.42.

buffer solutions containing 0.0564, 0.108, 0.243, and 0.480 M acetic acid, respectively, and extrapolation to zero acetic acid concentration yielded a value of 0.55 M^{-1} s^{-1}. This rate constant at zero acetic concentration is consistent with the results obtained by the titrimetric method, as illustrated in Fig. 2. The oxidation of glutathione was carried out in a similar manner in acetate buffers at pH 4.05, 4.55, and 5.00, and the results are summarized in Table 2. Figure 2 shows the plot of the rate constants at zero acetic acid concentration *vs.* the reciprocal of the hydrogen ion activity; it is linear with an intercept of 0.339, a slope of 4.45×10^{-6}, with a correlation coefficient of 0.996.

TABLE 2

Rate constants for the oxidation of glutathione by 1,3-dihydro-1-hydroxy-3-oxo-1,2-benziodoxole in acetate buffers at 25°

pH	Buffer concentration (M)	k M^{-1} s^{-1}
5.00	0.0	(0.789)*
	0.233	0.926
	0.466	1.020
	0.931	1.293
4.55	0.0	(0.477)*
	0.233	0.574
	0.582	0.678
	1.164	1.145
4.05	0.0	(0.406)*
	0.233	0.543
	0.582	0.817
	1.164	0.989

*Extrapolated values.

Discussion

The rate equation for the oxidation of 2-mercaptoethanol, 2-mercaptoethylamine, and glutathione by 1,3-dihydro-1-hydroxy-3-oxo-1,2-benziodoxole is similar to that for the oxidation of cysteine (3). The second-order rate equation is consistent with a mechanism in which one molecule of thiol and one molecule of oxidant react in a rate-determining step, followed by subsequent fast reactions involving another thiol molecule. In the oxidation of cysteine (3) it was postulated that the charged amino- and carboxy-groups form complexes with the oxidant such that the sulfhydryl group is oriented to facilitate reaction with the iodine atom. Obviously this complex formation cannot occur in the oxidation of 2-mercaptoethanol and so it is likely that direct reaction occurs between the sulfhydryl group and the 1,3-dihydro-1-hydroxy-3-oxo-1,2-benziodoxole.

The pH dependence of the reaction rate can be explained by realizing that in the solutions used there exist ionized and unionized forms of the thiol (pK 8–10) and 1,3-dihydro-1-hydroxy-3-oxo-1,2-benziodoxole (pK 7.2), although under the conditions used in these experiments the unionized forms would greatly predominate. A rate equation may be written for this reaction as shown in eq. 2; RSH and RS^-, OX and OX^- are

Can. J. Chem. Downloaded from www.nrcresearchpress.com by 210.87.254.6 on 09/05/12
For personal use only.

$$[2] \quad -d(OX)/dt = k_1(RSH)(OX) + k_2(RS^-) \times (OX) + k_3(RSH)(OX^-) + k_4(RS^-)(OX^-)$$

$$[3] \quad k = k_a + k_b/a_{H^+} + k_c/(a_{H^+})^2$$

the unionized and ionized forms of the sulfhydryl compound and **1**, respectively. When the unionized forms predominate, as in the experiments described here, the observed second-order rate constant, k, may be expressed by eq. 3, in which the various rate constants are related thus: $k_a = k_1$, $k_b = k_2K_{SH} + k_3K_{OX}$, and $k_c = k_4K_{SH}K_{OX}$, where K_{SH} and K_{OX} are the dissociation constants of thiol and **1**, respectively, and a_{H+} is the hydrogen ion activity. These equations take into consideration only the sulfhydryl group of the thiol ionizing, and do not include the amino- or carboxy-group. Since it has been found that there is a linear relationship between the rate constant and the reciprocal of the hydrogen ion activity, the term involving the square of the hydrogen ion activity is negligible. Therefore, under the experimental conditions used it may be concluded that there is substantial reaction between the unionized forms of the sulfhydryl groups and the oxidant with a rate constant of k_1 equal to 0.54 M^{-1} s^{-1} for 2-mercaptoethanol, 0.21 M^{-1} s^{-1} for 2-mercaptoethylamine, and 0.34 M^{-1} s^{-1} for glutathione. It is not possible to separate values for k_2 and k_3 from the kinetic data, but k_b, obtained from the slope of the plots in Fig. 2, gives the overall dependence of the reaction rate on the pH. It can be seen that this is greatest for 2-mercaptoethylamine, and least for 2-mercaptoethanol. However, it is not possible to determine from the data the extent, if any, of participation by the amino- and carboxy-groups in the reaction.

The apparent simplicity of the kinetics of oxidation of thiols by 1,3-dihydro-1-hydroxy-3-oxo-1,2-benziodoxole is interesting in that the kinetics of the oxidation of thiols are usually complex and subject to a number of factors, including catalysis by traces of heavy metal ions and heterogeneous catalysis (6). Nothing was observed during the course of this work to indicate any unusual effects, and indeed, it was ascertained that EDTA had no effect on the reaction rate, indicating absence of catalysis by heavy metal ions. Although in much more concentrated solutions reactions other than the simple oxidation to disulfide may occur (2) the reaction appears to be kinetically simple in the dilute solutions used in this work.

1. J. L. Webb. Enzyme and metabolic inhibitors. Vol. II. Academic Press, New York, N.Y. 1966. p. 701.
2. F. P. Chinard and L. Hellerman. *In* Methods of biochemical analysis. Vol. 1. *Edited by* D. Glick. Interscience, New York, N.Y. 1954. p. 1.
3. W. Wolf and T. Wu. J. Pharm. Sci. **58**, 491 (1969).
4. N. M. Alexander. Anal. Chem. **30**, 1292 (1958).
5. W. T. Caraway and L. Hellerman. J. Amer. Chem. Soc. **75**, 5334 (1953).
6. R. Cecil and J. R. McPhee. Advan. Protein Chem. **14**, 292 (1959).

Thermal and photochemical rearrangements of methyl-substituted cyclopentadienes

Stewart McLean and D. M. Findlay
Department of Chemistry, University of Toronto, Toronto 181, Ontario

Received May 7, 1970

5,5-Dimethylcyclopentadiene undergoes a thermal rearrangement by migration of a methyl group, the kinetics of which have been studied, but no rearrangement product was observed on u.v. irradiation. However, methylcyclopentadiene is converted photochemically to 2-methylbicyclo[2.1.0]pentene, which is thermally unstable.

Canadian Journal of Chemistry, 48, 3107 (1970)

Rearrangements of suitably substituted cyclopentadienes represent processes which, under the appropriate reaction conditions, should be governed by the Woodward–Hoffman rules concerning the conservation of orbital symmetry (1), and can consequently be used to illustrate aspects of these rules. We have previously been concerned with demonstrating that thermally-induced hydrogen migrations taking place in cyclopentadienes are [1,5]-sigmatropic reactions with a very

Can. J. Chem. Downloaded from www.nrcresearchpress.com by 210.87.254.6 on 09/05/12
For personal use only.

$$[2] \quad -d(OX)/dt = k_1(RSH)(OX) + k_2(RS^-) \times (OX) + k_3(RSH)(OX^-) + k_4(RS^-)(OX^-)$$

$$[3] \quad k = k_a + k_b/a_{H^+} + k_c/(a_{H^+})^2$$

the unionized and ionized forms of the sulfhydryl compound and **1**, respectively. When the unionized forms predominate, as in the experiments described here, the observed second-order rate constant, k, may be expressed by eq. 3, in which the various rate constants are related thus: $k_a = k_1$, $k_b = k_2K_{SH} + k_3K_{OX}$, and $k_c = k_4K_{SH}K_{OX}$, where K_{SH} and K_{OX} are the dissociation constants of thiol and **1**, respectively, and a_{H+} is the hydrogen ion activity. These equations take into consideration only the sulfhydryl group of the thiol ionizing, and do not include the amino- or carboxy-group. Since it has been found that there is a linear relationship between the rate constant and the reciprocal of the hydrogen ion activity, the term involving the square of the hydrogen ion activity is negligible. Therefore, under the experimental conditions used it may be concluded that there is substantial reaction between the unionized forms of the sulfhydryl groups and the oxidant with a rate constant of k_1 equal to 0.54 M^{-1} s^{-1} for 2-mercaptoethanol, 0.21 M^{-1} s^{-1} for 2-mercaptoethylamine, and 0.34 M^{-1} s^{-1} for glutathione. It is not possible to separate values for k_2 and k_3 from the kinetic data, but k_b, obtained from the slope of the plots in Fig. 2, gives the overall dependence of the reaction rate on the pH. It can be seen that this is greatest for 2-mercaptoethylamine, and least for 2-mercaptoethanol. However, it is not possible to determine from the data the extent, if any, of participation by the amino- and carboxy-groups in the reaction.

The apparent simplicity of the kinetics of oxidation of thiols by 1,3-dihydro-1-hydroxy-3-oxo-1,2-benziodoxole is interesting in that the kinetics of the oxidation of thiols are usually complex and subject to a number of factors, including catalysis by traces of heavy metal ions and heterogeneous catalysis (6). Nothing was observed during the course of this work to indicate any unusual effects, and indeed, it was ascertained that EDTA had no effect on the reaction rate, indicating absence of catalysis by heavy metal ions. Although in much more concentrated solutions reactions other than the simple oxidation to disulfide may occur (2) the reaction appears to be kinetically simple in the dilute solutions used in this work.

1. J. L. Webb. Enzyme and metabolic inhibitors. Vol. II. Academic Press, New York, N.Y. 1966. p. 701.
2. F. P. Chinard and L. Hellerman. *In* Methods of biochemical analysis. Vol. 1. *Edited by* D. Glick. Interscience, New York, N.Y. 1954. p. 1.
3. W. Wolf and T. Wu. J. Pharm. Sci. **58**, 491 (1969).
4. N. M. Alexander. Anal. Chem. **30**, 1292 (1958).
5. W. T. Caraway and L. Hellerman. J. Amer. Chem. Soc. **75**, 5334 (1953).
6. R. Cecil and J. R. McPhee. Advan. Protein Chem. **14**, 292 (1959).

Thermal and photochemical rearrangements of methyl-substituted cyclopentadienes

Stewart McLean and D. M. Findlay
Department of Chemistry, University of Toronto, Toronto 181, Ontario

Received May 7, 1970

5,5-Dimethylcyclopentadiene undergoes a thermal rearrangement by migration of a methyl group, the kinetics of which have been studied, but no rearrangement product was observed on u.v. irradiation. However, methylcyclopentadiene is converted photochemically to 2-methylbicyclo[2.1.0]pentene, which is thermally unstable.

Canadian Journal of Chemistry, 48, 3107 (1970)

Rearrangements of suitably substituted cyclopentadienes represent processes which, under the appropriate reaction conditions, should be governed by the Woodward–Hoffman rules concerning the conservation of orbital symmetry (1), and can consequently be used to illustrate aspects of these rules. We have previously been concerned with demonstrating that thermally-induced hydrogen migrations taking place in cyclopentadienes are [1,5]-sigmatropic reactions with a very

Can. J. Chem. Downloaded from www.nrcresearchpress.com by 210.87.254.6 on 09/05/12
For personal use only.

Can. J. Chem. Downloaded from www.nrcresearchpress.com by 210.87.254.6 on 09/05/12
For personal use only.

low activation energy (2). A consequence of this facile hydrogen shift is that the study of alternative modes of rearrangement is made more difficult because both reactants and products may be undergoing rapid isomerization by hydrogen migration even at room temperature.

We examined, therefore, the thermal rearrangement of 5,5-dimethylcyclopentadiene (**1**), in which the hydrogen-shift isomerization is not

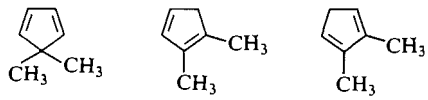

1 **2** **3**

possible and the corresponding methyl-shift isomerization would be expected to take place much less readily because, although strictly governed by the same symmetry rule, the orbital associated with the C—Me bond has a different spatial distribution from that of the C—H bond. In this case a temperature in excess of 200° was required to effect isomerization and the products were the 1,2- and 2,3-dimethylcyclopentadienes (**2** and **3**) (2) expected from a 1,2-methyl migration ([1,5]-sigmatropic reaction) followed by rapid hydrogen migration. The kinetics of the methyl migration were studied between 240 and 257 °C, in which range the first order rate law was obeyed and specific reaction rates for methyl migration (*i.e.* statistically corrected) were

$$k(\text{Me migration}) = (9.3 \times 10^{13}) \exp(-43\,300/RT)\ \text{s}^{-1}$$

in this limited range (with measurements at seven temperatures), the Arrhenius parameters, E_a = 43.3 kcal/mole (standard deviation 2.4) and ΔS = 3 e.u. (standard deviation 3), although rather imprecise, are similar to those obtained by others (3) for closely related processes. Outside this range the reaction was inconveniently slow for the technique employed or side reactions became appreciably competitive. When the reaction was carried out in the presence of cyclopentadiene-d_6, the rate of rearrangement was not appreciably changed, but there was a small incorporation (based on examination of the mass spectrum) of deuterium into the products. We can conclude, therefore, that at temperatures below 200° no significant amount of rearrangement of **1** by thermally-induced migration of the methyl group occurs; at higher temperatures the [1,5]-sigmatropic reaction involving the methyl group becomes important and at about 250° is the dominant process observed, while a radical process is a minor competitor in this temperature range, but probably becomes more significant at higher temperatures still.

We turned next to an examination of the behavior of **1** when subjected to photochemical excitation, since two rearrangements, methyl migration by a [1,3]-sigmatropic reaction and an electrocyclic reaction leading to the bicyclo-[2.1.0]pentene skeleton, are allowed by the Woodward–Hoffman rules, and either or both might be observed. The photochemical conversion of cyclopentadiene to bicyclo[2.1.0]pentene (**4**; $R_1 = R_2 = H$) itself has been observed previously (4), but several possible pathways can be suggested for this transformation and it has not yet been established that it does involve a simple electrocyclic process. One of our aims in continuation of the present work has been to carry out the rearrangement on cyclopentadienes suitably substituted to test the various alternatives. Unfortunately, in our hands, the irradiation of **1** in solution under a variety of reaction conditions afforded no rearrangement product whatsoever and unchanged **1** was the only volatile material recovered from the reaction mixture. However, we have been able to carry out conversion of cyclopentadiene to bicyclopentene under the conditions originally used by Brauman *et al.* (4)[1]; success in this conversion is critically dependent on the conditions used for the irradiation and isolation. Moreover, we have demonstrated that we can convert the equilibrium mixture of methylcyclopentadienes (2) by irradiation under similar conditions to a product which contains 2-methylbicyclo[2.1.0]pentene (**4**; R_1 = Me; R_2 = H); the 1-methyl isomer (**4**; R_1 = H; R_2 = Me) may also have been present, but only

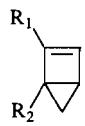

4

the 2-methyl isomer was obtained in a relatively pure state. The reaction mixture was subjected to v.p.c. and the component which produced a peak not found in the starting material was

[1]We are grateful to Professor Brauman for a detailed account of these reaction conditions.

collected. Its n.m.r. spectrum resembled that of bicyclopentene (**4**; $R_1 = R_2 = H$) but showed a methyl doublet ($J = 1.5$ Hz) at τ 8.34 and a narrow multiplet centered at τ 4.14 corresponding to the vinyl proton. This product was thermally unstable and the spectrum changed with time, the characteristic peaks of methylcyclopentadienes (2) replacing those of the photoproduct. At 47 °C this decay followed the first order rate law with a half life of about 4.5 h, a rate comparable with that of the thermal reversion of bicyclopentene to cyclopentadiene (5).

It seems probable, therefore, that our failure to obtain any observable rearrangement product in the photochemical reaction of **1** must be caused by the *gem*-dimethyl group in this compound. Since the methyl substituents can not significantly affect the photoexcitation process, they must either inhibit the bond-forming process leading to the bicyclopentene or increase the rate of the retrograde thermal reaction to such an extent that the product does not last long enough to be isolated. However, since it is clear that the reaction is observed with other cyclopentadienes only under very carefully specified conditions, we can not preclude the possibility that we simply failed to find the precise conditions required for a successful isomerization of **1**.

Experimental

Thermal Rearrangement of 5,5-Dimethylcyclopentadiene

Small samples of 5,5-dimethylcyclopentadiene (6) were sealed in evacuated tubes, placed in a thermostatted bath for the required time, and then rapidly cooled. The progress of the reaction was followed by v.p.c. analysis and the identity of the products was confirmed by converting samples to their *N*-phenylmaleimide adducts (7). The kinetic results were calculated by standard procedures (2).

Irradiation of 5,5-Dimethylcyclopentadiene

The procedures used were modeled on those described previously (4); in addition, the conditions were varied with respect to (*a*) the solvent (ethanol, 1-pentanol, and *iso*-octane), (*b*) the temperature (−35°–0°), (*c*) the length of time of irradiation (1–4 h), and (*d*) the use of a variety of v.p.c. conditions. In every case the only non-solvent peak identified in the v.p.c. was that of **1**.

Irradiation of Methylcyclopentadienes

A 3% solution of the isomeric methylcyclopentadienes (7) in decalin, cooled in an ice–salt bath, was irradiated by a Hanovia 450 W high-pressure mercury lamp for 1–3 h. The volatile products were distilled at 10^{-3} mm Hg and collected in a trap cooled with liquid nitrogen. When the products were examined by v.p.c. (6 ft UCON-LD-550-X column), peaks corresponding to solvent, starting materials, and at least one product were identified; treatment of the mixture with a solution of potassium *t*-butoxide in dimethyl sulfoxide followed by a further vacuum distillation, produced a mixture in which the relative amount of starting cyclopentadienes was diminished, and it was possible by preparative v.p.c. to isolate a product which, on the basis of the appearance in its n.m.r. spectrum of peaks at τ 4.14 (narrow multiplet), 8.0–8.5 (m), 8.34 (d; $J = 1.5$ Hz), in the ratio 1:4:3, was predominantly **4** ($R_1 = Me$; $R_2 = H$), but the spectrum included other peaks, attributed to small amounts of contaminants. When the sample was allowed to stand, the growth of peaks characteristic of methylcyclopentadienes could be observed. The kinetics of this process were followed by observing the decay as a function of time of the signals due to the methylbicyclopentene in a spectrometer with the probe temperature set at 47°.

We thank the National Research Council of Canada for financial support of this work.

1. R. B. WOODWARD and R. HOFFMANN. The conservation of orbital symmetry. Academic Press, New York, N.Y. 1970.
2. S. MCLEAN and P. HAYNES. Tetrahedron Lett. 2385 (1964); Tetrahedron, **21**, 2329 (1965). S. MCLEAN, C. J. WEBSTER, and R. J. D. RUTHERFORD. Can. J. Chem. **47**, 1555 (1969).
3. J. W. DE HAAN and H. KLOOSTERZIEL. Rec. Trav. Chim. Pays Bas, **84**, 1594 (1965). W. C. HERNDON and J. M. MANION. J. Org. Chem. **33**, 4504 (1968).
4. J. I. BRAUMAN, L. E. ELLIS, and E. E. VAN TAMELEN. J. Amer. Chem. Soc. **88**, 846 (1966).
5. J. I. BRAUMAN and D. M. GOLDEN. J. Amer. Chem. Soc. **90**, 1920 (1968).
6. R. S. ROUSE and W. E. TYLER. J. Org. Chem. **26**, 3525 (1961).
7. S. MCLEAN and P. HAYNES. Tetrahedron, **21**, 2313 (1965).

Can. J. Chem. Downloaded from www.nrcresearchpress.com by 210.87.254.6 on 09/05/12
For personal use only.

Trimethylsilyl-substituted cyclopentadienes

S. McLEAN AND G. W. B. REED[1]
Department of Chemistry, University of Toronto, Toronto 181, Ontario

Received May 7, 1970

An account is given of the migratory behavior of the silyl group and of hydrogen in trimethylsilyl-substituted cyclopentadienes. The reaction of trimethylsilylcyclopentadiene with dimethyl sulfoxide is described.

Canadian Journal of Chemistry, 48, 3110 (1970)

Can. J. Chem. Downloaded from www.nrcresearchpress.com by 210.87.254.40 on 09/05/12
For personal use only.

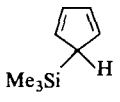

1

2

3

Trimethylsilylcyclopentadiene under ordinary conditions consists of a set of interconverting isomers (**1**, **2**, **3**) in which, at equilibrium, the 5-substituted isomer (**1**) predominates (85–90%). Isomerization within this set results from a series of 1,2 hydrogen shifts ([1,5]-sigmatropic reactions (1)) which occur at a rate comparable with those in alkylcyclopentadienes. In addition, 5-trimethylsilylcyclopentadiene is a "fluxional" molecule (2) in which the silyl group migrates about 10^6 times faster than the hydrogen does, and produces a degenerate set of molecules of structure **1**, distinguishable only if the ring sites are labelled. A methyl substituent on the ring does not migrate and can act as a label, but the thermodynamic and kinetic complexity of the system is increased even further. These dienes can be trapped as their Diels–Alder adducts by reaction with suitable dienophiles under a variety of conditions, but it can be anticipated that, when the thermodynamic and kinetic problems associated with direct and retrograde Diels–Alder reactions are superimposed on those already described, the distribution of isomers in the product does not necessarily reflect the equilibrium composition of the reactants.

The availability of vacant d orbitals on the silicon atom which can interact with the π-electrons of the diene system in **1** allows the sigmatropic process to follow a path that is not open when the migrating species is hydrogen or an alkyl group; this is undoubtedly the cause of the extremely facile migration of the silyl group and accounts for the kinetic results. However, the thermodynamic observation that isomer **1** is more stable than its isomers **2** and **3**, strongly contrasts with the situation in the alkylcyclopentadienes (3), and no ready answer to the interesting and significant questions it raises appears to be available. The attractive possibility that the interaction of the silicon and the π-system also stabilizes the ground state of the molecule is not supported by the evidence that the u.v. spectra (down to 185 mμ) of the trimethylsilyl derivatives of cyclopentadiene and methylcyclopentadiene are very similar to those of the parent hydrocarbons; the silyl compounds show a less pronounced absorption minimum near 210 mμ, but the positions and intensities of the maxima are almost identical. The most significant point may be, in fact, that the trimethylsilyl substituent appears to perturb the chromophore even less than an alkyl substituent does (3).

These conclusions are based on the studies we have made, because of our interest in the conclusions drawn in the original report (4) on this subject and their relationship to our own earlier work (3), of the n.m.r. spectra of trimethylsilyl derivatives of cyclopentadiene and methylcyclopentadiene, the temperature dependence of these spectra, and the formation of Diels–Alder adducts with a number of dienophiles at various temperatures (5). Our results are in substantial agreement with those reported (6) regarding the structures of the Diels–Alder adducts, and both our results and the conclusions we draw from them correspond closely with those in the very recent accounts (7, 8) of careful and thorough studies of the n.m.r. characteristics of the trimethylsilylcyclopentadienes.

The original report on this topic (4) led to the appearance of a number of publications on the subject and a considerable amount of confusion. The trimethylsilylcyclopentadiene system is clearly a complex one and it is now obvious that

[1]Taken from the M.Sc. Thesis of G. W. B. Reed, University of Toronto, Toronto, Ontario, January 1970.

some reports were based on incomplete results and some were simply in error. Particularly in the light of the most recent work (7, 8) it is now possible to get a consistent and satisfactory view of the whole situation, as outlined above, and to clear up the earlier confusion. However, the observation (9) that the n.m.r. spectrum of trimethylsilylcyclopentadiene in dimethyl sulfoxide is that of a non-fluxional molecule remains to be explained satisfactorily. We have confirmed the observation of a low-field multiplet with fine structure characteristic of a molecule with a long lifetime on the n.m.r. time-scale, but the explanation (9) that this results from an inhibition of silyl migration because of complex formation involving silicon d orbitals and dimethyl sulfoxide is wrong; the spectrum produced is that of cyclopentadienylidenedimethylsulfurane (**4**) which results from the vigorous exothermic reaction of

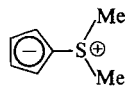

4

trimethylsilylcyclopentadiene with dimethylsulfoxide. We have isolated this interesting stable ylid (10), m.p. 131–133°, directly from this reaction, and the n.m.r. spectrum of the pure compound in $CDCl_3$ shows that the vinyl protons give rise to two multiplets centered at τ 3.58 and 3.74, slightly solvent-shifted from the corresponding signals in the dimethyl sulfoxide reaction mixture, and that the singlet due to the methyl groups is at τ 7.16, and was buried in the solvent peak in the reaction mixture. The other reaction product isolated was hexamethyldisiloxane, which is known to be a spontaneous transformation product of trimethylsilanol (11). It can be surmised that **4** is produced in a reaction in which the oxygen of the dimethyl sulfoxide attacks the silicon of **1**, the electron shifts, concerted or stepwise, summarized below, then lead to the protonated ylid and Me_3SiO^-, and a proton shift finally produces the ylid and trimethylsilanol.

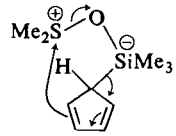

Experimental

Trimethylsilylcyclopentadiene (4) λ_{max} (MeOH) 240 mμ (ε 2500), λ_{max} (hexane) 240.5 mμ (ε 2400), λ_{min} (hexane) 212 mμ (ε 2100) (recorded on a Perkin Elmer model 350 spectrometer) was allowed to react with an equimolar amount of dry dimethyl sulfoxide at room temperature. The solution warmed up, became discolored, and formed two layers. After 3 h the layers were separated and the upper clear colorless layer was identified as hexamethyldisiloxane by direct comparison with an authentic sample. When ether was added to the lower dark-colored layer, a tan crystalline product separated (yield ~40%). This material, m.p. 131–133°, $C_7H_{10}S$ (by mass spectrometry), corresponded in m.p., u.v., and n.m.r. characteristics with those reported (10) for the ylid **4**.

Support of this work by the National Research Council of Canada is gratefully acknowledged. We thank Drs. Davison and Rakita for an account of their results (7) prior to their publication.

1. R. B. Woodward and R. Hoffmann. The Conservation of orbital symmetry. Academic Press, New York, N. Y. 1970.
2. F. A. Cotton. Account. Chem. Res. **1**, 257 (1969).
3. S. McLean and P. Haynes. Tetrahedron, **21**, 2313, 2329, 2343 (1965).
4. H. P. Fritz and C. G. Kreiter. J. Organometal. Chem. **4**, 313 (1965).
5. G. W. B. Reed. M.Sc. Thesis. University of Toronto, Toronto, Ontario. January, 1970, and unpublished results from this laboratory.
6. C. S. Kraihanzel and M. L. Losee. J. Amer. Chem. Soc. **90**, 4701 (1968).
7. A. Davison and P. E. Rakita. Inorg. Chem. **9**, 289 (1970).
8. A. J. Ashe. J. Amer. Chem. Soc. **92**, 1233 (1970).
9. Y. A. Ustynyuk, A. V. Kisim, and O. E. Oksinoid. Zh. Obshch. Khim. **38**, 391 (1968).
10. H. Behringer and F. Scheidl. Tetrahedron Lett. 1757 (1965).
11. C. Eaborn. Organosilicon compounds. Academic Press, New York, N.Y. 1960. p. 246.

Can. J. Chem. Downloaded from www.nrcresearchpress.com by 210.87.254.40 on 09/05/12
For personal use only.

Assignment and conformational properties of the sugar-ring hydroxyl protons of the common nucleosides[1]

D. B. DAVIES AND S. S. DANYLUK
Division of Biological and Medical Research, Argonne National Laboratory, Argonne, Illinois 60439

Received March 18, 1970

A 60 MHz proton magnetic resonance study has been made of the hydroxyl protons of the ribose and deoxyribose rings for the common nucleosides dissolved in mixtures of dry DMSO-d_6 and C_6D_6. Use of this solvent system permitted the detection and assignment of the exchange-free spin-coupled multiplets for the hydroxyl protons. The assignment was confirmed by spin-decoupling experiments.

Based on the magnitudes of the observed coupling constants, it is concluded that the O—$H_{5'}$ group is freely rotating around the $C_{5'}$—$O_{5'}$ bond. It is calculated that the O—$H_{3'}$ bond favors a *gauche* conformation relative to the $C_{3'}$—$H_{3'}$ bond, consistent with the preferred conformation found in the solid state for the $H_{3'}$—$C_{3'}$—$O_{3'}$—P bonds of the nucleoside 3′-phosphates. The conformation of the O—$H_{2'}$ bond relative to the $C_{2'}$—$H_{2'}$ bond demonstrates no preference for the *gauche* rotamer. Such a rotamer might be expected if a hydrogen-bond between the 2′-OH and the purine base exists in this solvent system, as well as in aqueous solutions where such an interaction has been postulated as a stabilizing influence for ribosides.

Canadian Journal of Chemistry, 48, 3112 (1970)

Introduction

High-resolution proton magnetic resonance (p.m.r.) studies have yielded valuable information about the structure and interactions of base-rings in nucleic acid derivatives (1–4). From this work a clear picture has emerged of the part played by base-rings in stabilizing the structure of nucleic acids in solution. It would be useful if the data for base-rings could be combined with similar results for the ribose and ribose–phosphate moieties. Since the sugar-ring hydroxyl protons might have an important influence on the conformation of the ribose–phosphate backbone of polynucleotides, this study has been concerned with the observation and assignment of signals for these protons.

The three ribose hydroxyl protons of a nucleoside are the O—$H_{2'}$, O—$H_{3'}$ and O—$H_{5'}$ protons shown in Fig. 1. In deoxyribose nucleosides the O—$H_{2'}$ group is replaced by a hydrogen.

Hydroxyl coupling constants are known to vary with polarity of the solvent (5, 6), electronegativity of neighboring substituent groups (5, 8), and the geometry of the molecule (6, 7, 9, 10). Bearing in mind these limitations, the stereochemical dependence of the vicinal H—C—O—H coupling constants has been calculated (11) as

$$J_{HCOH} = 10.4 \cos^2 \phi - 1.5 \cos \phi + 0.2$$

where J is the spin-coupling constant and ϕ the dihedral angle between vicinal protons.

[1]Work supported by the U.S. Atomic Energy Commission.

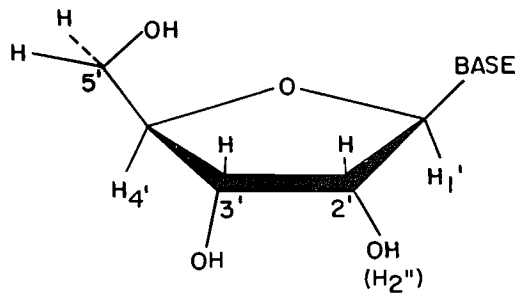

FIG. 1. Numbering scheme for the ribose and deoxyribose ring of the nucleosides.

If proton exchange processes are sufficiently minimized, then well-resolved multiplets arising from spin-coupling interactions with vicinal methine protons should be observed for hydroxyl protons of both ribose and deoxyribose nucleosides. Although separate hydroxyl signals were observed in an earlier study (12), the residual H_2O concentration in the dimethyl sulfoxide (DMSO) solvent was sufficiently high to prevent detection of fine structure in the signal.

Results

A typical spectrum for the ribose and hydroxyl protons of a nucleoside is illustrated by adenosine in Fig. 2. An assignment of the hydroxyl proton signals was carried out in the following manner. Comparison of the spectrum in the dried solvent system with that obtained previously in "wet" DMSO (12) permitted the assignment of multiplets at 5.26, 5.56, and 5.80 p.p.m. to hydroxyl protons. The remaining signals in the region of

Can. J. Chem. Downloaded from www.nrcresearchpress.com by 210.87.254.105 on 09/05/12
For personal use only.

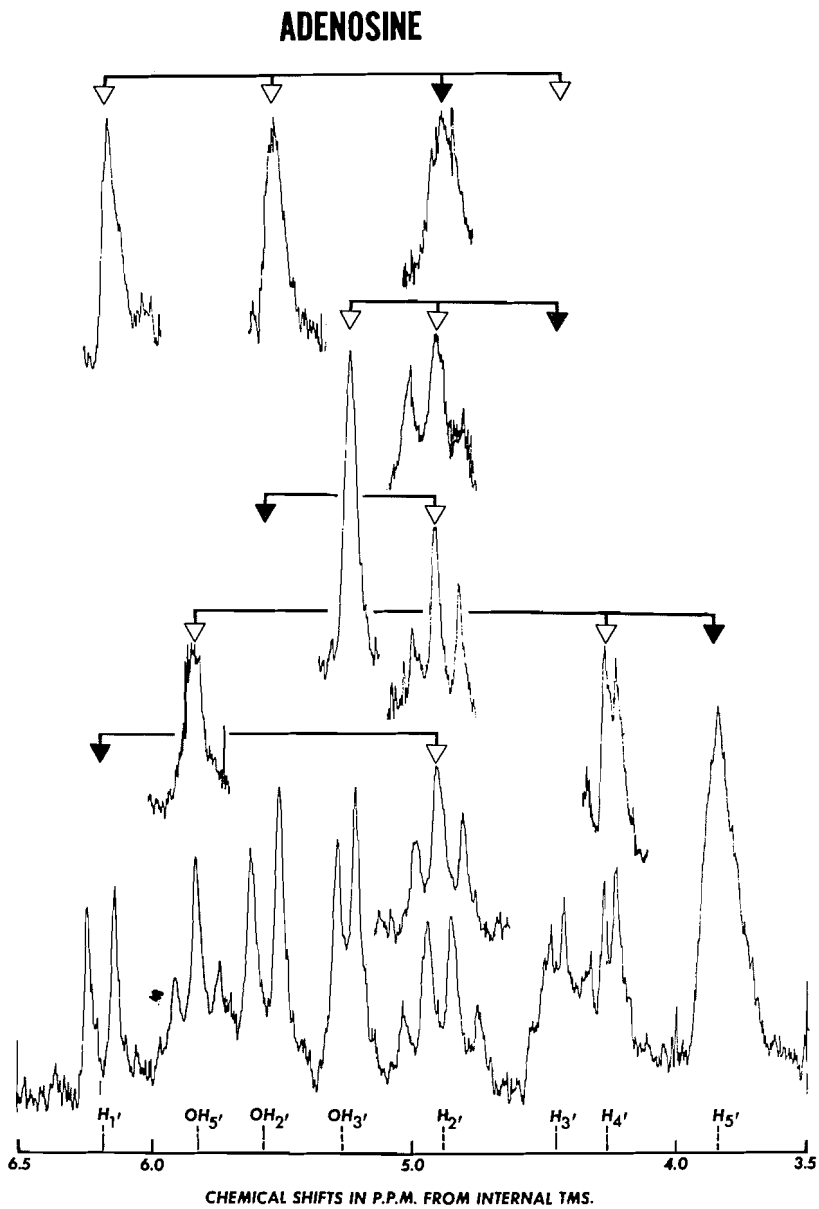

FIG. 2. Part of the 60 MHz n.m.r. spectrum of 0.1 *M* adenosine in 40% benzene–DMSO solution showing the proton resonance spectrum of the ribose ring and the double resonance spectra used in spectral analysis. The horizontal lines connect coupled signals with the solid arrow indicating the irradiating frequency and the open arrow showing the observing frequency in double resonance experiments.

the spectrum shown in Fig. 2 are due to ribose ring protons.

A further assignment of the signals to individual hydroxyl groups can be made by the use of double resonance techniques (13). For example, double resonance experiments establish the coupling scheme $C_1{\cdot}H_1{\cdot}$—$C_2{\cdot}H_2{\cdot}$—$OH_2{\cdot}$; cf. connected arrows in Fig. 2. Hence, an assignment of the doublet at 5.56 p.p.m. to the O—$H_2{\cdot}$ proton is possible. Similarly, an assignment may be made of the signals at 5.80 and 5.26 p.p.m. to the O—$H_5{\cdot}$ and O—$H_3{\cdot}$ protons respectively. As-

Can. J. Chem. Downloaded from www.nrcresearchpress.com by 210.87.254.105 on 09/05/12
For personal use only.

TABLE 1

Proton chemical shifts in p.p.m. (±0.002 p.p.m.) from TMS and spin-coupling constants ($J \pm 0.1$ Hz) of 0.1 *M* solutions of the nucleosides in various benzene–DMSO mixtures at 30 °C

Nucleoside*	% Benzene in solution	Proton chemical shifts (p.p.m. from TMS)							Spin-coupling constants (Hz)		
		$H_{2'}$	$H_{3'}$	$H_{5''}$†	$H_{5'}$†	$OH_{2'}$	$OH_{3'}$	$OH_{4'}$	$H_{2'}OH_{2'}$	$H_{3'}OH_{3'}$	$H_{5'}OH_{5'}$
T	5	~2.1	4.307	3.577	3.613	—	5.218	5.008	—	4.3	5.0
dC	5	~2.0	4.208	3.565	3.592	—	5.163	4.931	—	4.0	5.0
dA	5	~2.5	4.500	3.610	3.710	—	~5.3	~5.3	—	4.0	5.0
dG	5	~2.5	4.403	3.555	3.651	—	5.251	4.876	—	3.8	5.4
U	40	~4.01	~4.01	3.673	3.743	5.438	5.147	5.188	5.5‡	4.7‡	5.2
C	40	~4.16	~4.16	3.731	3.851	5.381	5.003	5.141	§	§	5.1
A	40	4.213	4.452	3.663	3.763	5.563	5.263	5.805	6.0	4.1	5.0
G	20	4.515	4.260	3.644	3.746	5.448	5.160	5.101	5.6	4.2	5.0

*Abbreviations: T = thymidine; dC = deoxycytidine, etc.
†Calculated from 220 MHz spectra.
‡220 MHz measurements at 22 °C.
§Cannot be determined due to virtual coupling ($H_{2'}$ and $H_{3'}$ have similar chemical shifts even at 220 MHz).

signment of the hydroxyl protons for the other purine riboside, guanosine, was made in an analogous manner.

The similar chemical shifts of the $H_{2'}$ and $H_{3'}$ proton resonances for the pyrimidine ribosides at 60 MHz means that the corresponding hydroxyl proton resonances do not exhibit first-order coupling and therefore the signals cannot be unambiguously assigned by spin-decoupling experiments. The chemical shifts of the $OH_{2'}$ and $OH_{3'}$ proton signals of uridine and cytidine were therefore assigned by comparison with the 60 MHz purine riboside spectra.[2]

A summary of the observed chemical shifts and coupling constants for all the nucleosides is given in Table 1.

Several points may be noted regarding the magnitudes of the coupling constants. A surprising constancy is observed for the $H_{5'}$—$OH_{5'}$ coupling constants for all the nucleosides. Moreover, the magnitude of this coupling, 5.0 ± 0.1 Hz, is close to the value observed for hydroxyl couplings in simple aliphatic alcohols. For aliphatic alcohols (methanol, ethanol, *t*-butyl alcohol) the hydroxyl coupling constants (5) obtained in CCl_4 and DMSO as solvents were 5.3 (± 0.3) Hz. The latter value is very close to the theoretical magnitude expected for a hydroxyl group rotating freely about the C—O bond (11). Accordingly, it is reasonable to conclude that the 5′-hydroxyl group of nucleosides is rotating freely (on the nuclear magnetic resonance (n.m.r.) time-scale) about the $C_{5'}$—$O_{5'}$ bond.

In contrast with the 5′-hydroxyl couplings, the $H_{3'}$—$OH_{3'}$ coupling constants vary for different nucleosides, although all of the couplings are significantly less than the value arising from a freely rotating hydroxyl group. A number of assumptions allow calculation of the relative rotamer populations from the observed hydroxyl group coupling constants. These assumptions are that the empirical relation (11) between vicinal coupling constant, J_{HCOH}, and dihedral angle, ϕ_{HCOH}, holds, that the observed J's are weighted time-averages for values given by the classical staggered rotational isomers (two *gauche* and one *trans* in this instance), and that the *gauche* and *trans* coupling constants for the different conformers are the same. The observed J is given by

$$J_{(obs)} = 2.1P_g + 12.1P_t$$

where P_g and P_t are the fractional populations of the *gauche* and *trans* conformers respectively. An observed coupling of 4.0 Hz for $J_{H_{3'}OH_{3'}}$ indicates that the O—$H_{3'}$ group exists for 80% of its time in a *gauche* conformation and 20% of its time in a *trans* conformation with respect to the $C_{3'}$—$H_{3'}$ bond. In the solid state the preferred conformation for the nucleoside 3′-phosphates is that in which the bond sequence $H_{3'}$—$C_{3'}$—$O_{3'}$—P assumes an approximately *gauche* conformation (15).

The $H_{2'}$—$OH_{2'}$ couplings are all only slightly

[2]Spectra for uridine and cytidine have now been measured at 220 MHz (14). At this frequency the shifts for $H_{2'}$ and $H_{3'}$ of uridine are sufficiently different so that the corresponding hydroxyl signals are close to first-order. For cytidine, however, the $H_{2'}$ and $H_{3'}$ chemical shifts are still very similar.

Can. J. Chem. Downloaded from www.nrcresearchpress.com by 210.87.254.105 on 09/05/12
For personal use only.

greater than that observed and calculated for a freely rotating hydroxyl group, and a calculation similar to the above indicates that the relative populations of the *gauche* and *trans* rotamers are only slightly different from the values expected for free rotation.

In aqueous solutions a hydrogen-bond interaction between the $OH_{2'}$ of the ribose ring and the N_3 atom of the purine ring has been suggested from chemical shift data (16). A Dreiding model of adenosine shows that for the ribose ring in an approximate $C_{2'}$ *endo* conformation, observed in DMSO solutions (14), such a hydrogen bond would result in a *gauche* orientation of the hydroxyl group relative to the $C_{2'}$—$H_{2'}$ bond, with a dihedral angle of approximately 45°. If this hydrogen-bond exists for a time comparable to the n.m.r. time-scale, one might expect to observe a $J_{H_{2'}OH_{2'}}$ of about 4.5 Hz. However, the observations in Table 1 demonstrate that there is no preference for a *gauche* rotamer in the purine ribosides. An intramolecular hydrogen bond between $OH_{2'}$ and N_3 is therefore considered unlikely in the present systems.

Experimental

The solvent system selected consisted of a mixture of DMSO-d_6 and C_6D_6. The proportions of these solvents in the binary mixture were adjusted to give the best resolution of the ribose and deoxyribose ring and hydroxyl protons. Extreme precaution was taken to eliminate trace amounts of water from solvents. Solvents were stored over molecular sieve (Linde 3A) and the nucleosides were pumped on a high-vacuum line for long periods to remove adsorbed water molecules. Solutions were made up in a dry box and sealed in n.m.r. tubes to prevent absorption of water vapor.

High-resolution spectra were measured at 30 °C for 0.1 *M* solutions of the common purine and pyrimidine nucleosides. Spectra were recorded at 60 MHz with a Varian DA 60I Internal-lock spectrometer locked on internal tetramethylsilane. Double resonance experiments were performed in the usual manner (13).

Since the $OH_{2'}$ and $OH_{3'}$ doublet signals were close to first-order, the chemical shifts and coupling constant values were estimated directly from the 60 MHz spectra. The pseudo-triplet of the $OH_{5'}$ proton resonance has further been analyzed by second-order analysis of the 220 MHz spectrum and the coupling constants checked by computer simulation (14). All the chemical shifts and coupling constants will be published in a paper dealing with the conformational properties of the pentose ring and the exocyclic carbinol group (14). The chemical shifts of the $C_{2'}$, $C_{3'}$, and $C_{4'}$ protons listed in Table 1 are estimated values sufficient for this discussion while the $C_{5'}$ chemical shifts are values derived from second-order analysis of the 220 MHz spectra.

1. P. O. P. Ts'o. Ann. N. Y. Acad. Sci. **153**, 784 (1969).
2. A. D. Broom, M. P. Schweizer, and P. O. P. Ts'o. J. Amer. Chem. Soc. **89**, 3612 (1967).
3. S. I. Chan and J. H. Nelson. J. Amer. Chem. Soc. **91**, 168 (1969).
4. S. S. Danyluk and F. E. Hruska. Biochem. **7**, 1038 (1968).
5. W. B. Moniz, C. F. Poranski, and T. N. Hall. J. Amer. Chem. Soc. **88**, 190 (1966).
6. C. P. Rader. J. Amer. Chem. Soc. **88**, 1714 (1966).
7. N. L. Bauld and Y. S. Rim. J. Org. Chem. **33**, 1303 (1968).
8. J. J. Uebel and H. W. Goodwin. J. Org. Chem. **31**, 2040 (1966).
9. R. D. Stolow and A. A. Gallo. Tetrahedron Lett. **29**, 3331 (1968).
10. B. Casu, M. Reggiani, G. G. Gallo, and A. Vigevani. Tetrahedron Lett. **22**, 3061 (1966).
11. R. R. Fraser, M. Kaufman, P. Morand, and S. Govil. Can. J. Chem. **47**, 403 (1969).
12. L. Gatlin and J. C. Davis. J. Amer. Chem. Soc. **84**, 4464 (1962).
13. R. A. Hoffman and S. Forsen. Progress in n.m.r. spectroscopy. Vol. 1, *Edited by* J. W. Emsley, J. Feeney, and L. H. Sutcliffe. Pergamon Press, London, 1966. Chapt. 2.
14. D. B. Davies and S. S. Danyluk. To be published.
15. M. Sundaralingham. Biopolymers. **7**, 821 (1969).
16. P. O. P. Ts'o, M. P. Schweizer, and D. P. Hollis. Ann. N.Y. Acad. Sci. **158**, 256 (1969).

Can. J. Chem. Downloaded from www.nrcresearchpress.com by 210.87.254.105 on 09/05/12
For personal use only.

Can. J. Chem. Downloaded from www.nrcresearchpress.com by 210.87.254.40 on 09/05/12
For personal use only.

Canadian Journal of Chemistry

Published by THE NATIONAL RESEARCH COUNCIL OF CANADA

VOLUME 48 OCTOBER 15, 1970 NUMBER 20

Vibrational spectra of some perfluoro-arsenates and antimonates with nitrogen heterocations

A. M. QURESHI AND F. AUBKE[1]

Department of Chemistry, The University of British Columbia, Vancouver 8, British Columbia

Received April 20, 1970

The infrared spectra from 4000–250 cm^{-1} and the laser Raman spectra of $NOAsF_6$, NO_2AsF_6, $N_2F_3AsF_6$, F_2NOAsF_6, $NOSbF_6$, NO_2SbF_6, $N_2F_3Sb_2F_{11}$, and $F_2NOSb_2F_{11}$ are recorded. Eight of the nine fundamentals expected for the $N_2F_3^+$ cation can be observed and are tentatively assigned. The vibrational spectra of the MF_5 adducts are in agreement with an ionic formulation; however, the mutual exclusion rule for infrared and Raman active vibrations appears to be relaxed and one of the fundamentals ν_5 [F_{2g}] is split into a doublet in almost all cases.

Canadian Journal of Chemistry, 48, 3117 (1970)

The interaction of the nitrogen oxyfluorides FNO (1), F_3NO (2, 3), and FNO_2 (4) and the binary fluorides N_2F_4 (5–7) and N_2F_2 (7–8*a–c*) with the strong Lewis acids AsF_5 and SbF_5 has been found to yield solid products, frequently with the reactants in a 1:1 molar ratio. These complexes are commonly regarded as ionic with the anions AsF_6^-, SbF_6^-, and $Sb_2F_{11}^-$ and the cations NO^+, NO_2^+, F_2NO^+, N_2F^+, and $N_2F_3^+$.

In the absence of detailed X-ray diffraction studies on any of these compounds, the claim of ionicity is primarily based on vibrational spectra, X-ray powder diagrams, and the solution behavior in polar solvents. The reported vibrational data are frequently incomplete and almost always limited to infrared studies extending primarily over the sodium chloride spectral region. Raman spectra on solid complexes are reported only for F_2NOAsF_6 (9) and N_2FAsF_6 (10). The present study reports the infrared spectra from 4000 to 250 cm^{-1} and the laser Raman spectra for the following complexes: $NOAsF_6$, NO_2AsF_6, $NOSbF_6$, NO_2SbF_6, F_2NOAsF_6, $F_2NOSb_2F_{11}$, $N_2F_3AsF_6$, and $N_2F_3Sb_2F_{11}$. Since vibrational spectra for N_2FAsF_6 (8, 10) and the related complex NF_4AsF_6 (11) have previously been reported, a comparison of the spectra for these nitrogen heterocation complexes is now possible. Inclusion of the spectra for $KAsF_6$ and $KSbF_6$ in this discussion should allow one to study the deviations from ideal octahedral symmetry, possibly due to site symmetry lowering or possible anion–cation interaction, resulting in a distortion of the MF_6 group and loss of O_h symmetry.

The following features would be expected: removal of degeneracies, relaxation of the mutual exclusion rule for Raman and infrared active vibrations, and a frequency shift compared to the potassium compounds. The fact that all compounds in this series gave very well resolved Raman spectra on polycrystalline samples provides a good basis for the intended discussion. Main emphasis will have to be placed on the spectra for the ideally highly symmetrical anions, since all cations involved are of relatively low symmetry (C_{2v}, C_2, and $D_{\infty h}$ etc.), where anion–cation interaction will primarily result in a frequency shift only. A meaningful study of these effects on the cations as, *e.g.*, carried out for the NO^+ cation (12) would require inclusion of a larger number of related complexes than are presently reported.

In addition, it was intended to provide a frequency assignment for the cation $N_2F_3^+$, at present only incompletely characterized, and to characterize the polymeric $Sb_2F_{11}^-$ in these complexes more fully.

[1]To whom correspondence should be addressed.

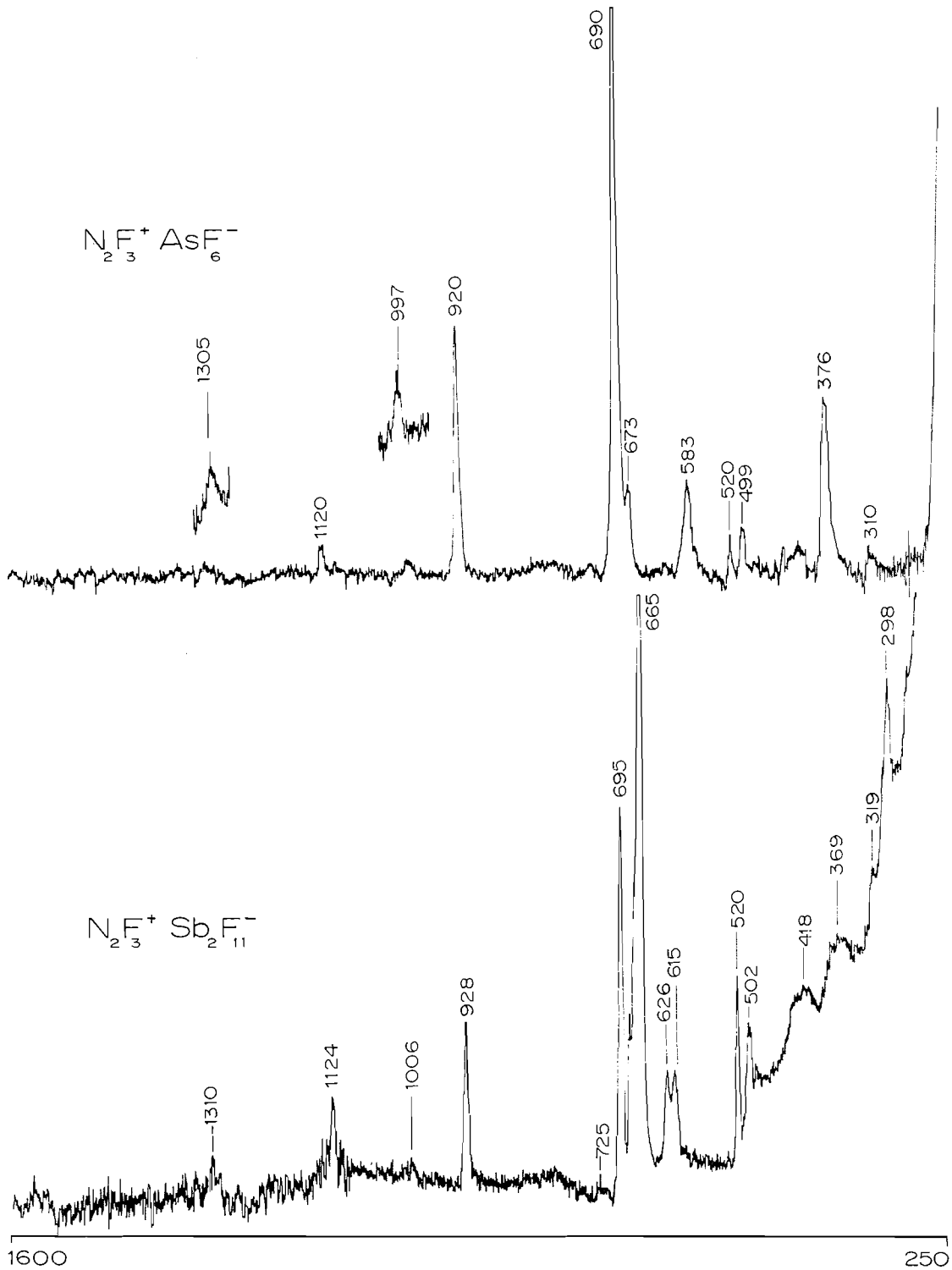

FIG. 1. Raman spectra of $N_2F_3AsF_6^+$ and $N_2F_3^+Sb_2F_{11}$.

Can. J. Chem. Downloaded from www.nrcresearchpress.com by 210.87.254.40 on 09/05/12
For personal use only.

Can. J. Chem. Downloaded from www.nrcresearchpress.com by 210.87.254.40 on 09/05/12
For personal use only.

Experimental

Materials and Preparations

Anhydrous HF (Matheson of Canada), AsF_5 (Peninsular Chemresearch), SbF_5 (Ozark Mahoning Co.), N_2F_4 (Air Products), and anhydrous SO_2 (Matheson of Canada) were all reagent grade. They were purified by repeated distillation in a monel vacuum line, their purity was checked by infrared spectroscopy. A sample of ONF_3 was obtained from Professor J. M. Shreeve of the University of Idaho.

Nitrosylchloride (13) and nitrylchloride (14) were prepared as described, and used after purification in the preparation of $NOAsF_6$, $NoSbF_6$, NO_2AsF_6, and NO_2SbF_6 according to Kuhn (15). The reactions in HF solution were carried out in Kel-F traps with monel fittings and valves. The interaction of ONF_3 and N_2F_4 with AsF_5 and SbF_5 were carried out in monel reaction cans equipped with Hoke valves as described in the original preparations. The reactions were followed by weight. All solid materials were handled in a dry box.

Infrared Spectra

A Perkin–Elmer 457 grating spectrophotometer was used for recording spectra in the 4000–250 cm^{-1} range. The region below 250 cm^{-1} was investigated with a Perkin–Elmer 421 spectrophotometer, fitted with a purging unit. Spectra of the ONF_2^+ and $N_2F_3^+$ complexes were obtained without using any mulling agent, Nujol and hexachlorobutadiene were employed for the rest. Silver chloride, cesium iodide, KSR-5 (Harshaw Chemical Corp.) and polyethylene windows were used.

Raman Spectra

A Cary 81 spectrophotometer equipped with a Spectra Physics model 125 He–Ne laser was used. The 6328 Å wavelength line was used as exciting light. The solid samples were contained in flat bottom Pyrex tubes with 6 mm o.d. The tubes were filled in a dry box and immediately flame sealed.

Results

The vibrational frequencies for $NOAsF_6$, NO_2AsF_6, $NOSbF_6$, NO_2SbF_6, $N_2F_3Sb_2F_{11}$, $N_2F_3AsF_6$, F_2NOAsF_6, and $F_2NOSb_2F_{11}$ are listed below together with estimated intensities. Tracings of the Raman spectra of $N_2F_3^+AsF_6^-$ and $N_2F_3^+Sb_2F_{11}^-$ and of the i.r. spectrum of $N_2F_3^+AsF_6^-$ are shown in Figs. 1 and 2.

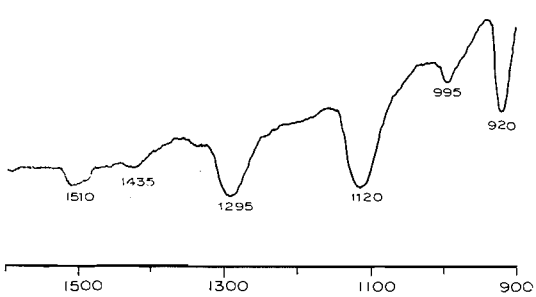

FIG. 2. Infrared spectrum of $N_2F_3^+AsF_6^-$.

$NOAsF_6$

Infrared: 2340 m, 1285 vw, 1150 w, 970 vw, 860 w, 820 vw, 695 vs, 565 vw, 385 s, 380 sh, w, 355 sh, w.

Raman: 2342 m, 693 vs, 582 m, 379 s, 370 m.

NO_2AsF_6

Infrared: 2385 m, b, 1300 vw, 1155 vw, 1030 w, 825 vw, 690 vs, 598 s, 560 vw, 385 vs, 380 w, sh, 370 w.

Raman: 1404 s, 693 vs, 582 m, 382 m, 370 m, sh,

ONF_2AsF_6

Infrared: 1855 s, 1165 s, 897 s, 820 vw, 720 w, sh. 692 vs, 650 sh, 595 s, 565 m, 373 w.

Raman: 1845 m, 1400 vw, 1167 w, 895 s, 800 vw 689 vs, 636 w, 584 w, sh, 573 s, 378 m, 372 w.

$N_2F_3AsF_6$

Infrared: 1510 w, 1435 ms, 1295 s, 1120 s, 995 m, 920 m, 830 w, 695 vs, 672 m, 595 m, sh, 515 m, 495 ms, 380 s, 305 m.

Raman: 1305 w, 1120 m, 997 m, 926 s, 690 vs, 673 m, 584 s, 520 m, 499 m, 370 ms, 376 ms, 310 m.

$KAsF_6$

Infrared: 698 vs, 382 sb.

Raman: 692 s, 580 m, 375 m.

$NOSbF_6$

Infrared: 2342 m, 1300 vw, 660 vs, 285 w, sh, 275 s.

Raman: 2345 m, 658 vs, 570 m, 294 w, 284 m.

NO_2SbF_6

Infrared: 2368 m, b, 1305 w, 1255 w, 660 vs, 601 m, sh, 285 w, sh, 273 s.

Raman: 1411 s, 661 vs, 576 w, 568 ms, 294 w, 283 m.

$ONF_2Sb_2F_{11}$

Infrared: 1856 s, 1165 s, 900 s, 725 s, sh, 710 w, sh, 690 vs, 680 s, sh, 665 s, 610 vw, sh, 565 m, 520 m, 285 w, sh, 270 w.

Raman: 1864 m, 1176 m, 902 vs, 699 m, sh, 680 s, sh, 665 vs, 614 vw, 570 w, 284 w, 296 w.

$N_2F_3Sb_2F_{11}$

Infrared: 1500 w, 1370 w, 1295 m, 1120 s, 1000 m, 920 ms, 730 w, sh, 705 s, 695 vs, 681 m, sh, 675 vs, 610 vw, 520 m, 500 m, sh, 380 vw, 335 w, 319 w, 280 m, b.

Raman: 1310 w, 1124 w, 1006 m, 928 s, 725 m, 695 m, sh, 670 w, sh, 665 vs, 615 vw, 520 m, 500 m, sh, 310 m, sh, 298 s, 220 m.

$KSbF_6$

Infrared: 1310 vw, 1160 w, 655 vs, 270 s.

Raman: 661 vs, 575 s, 294 m, 278 m.

Can. J. Chem. Downloaded from www.nrcresearchpress.com by 210.87.254.40 on 09/05/12
For personal use only.

Discussion

(a) *The Vibrational Assignment for the $N_2F_3^+$ Cation*

Previous assignments of the stretching modes for $N_2F_3^+AsF_6^-$ (5) and $N_2F_3^+Sb_2F_{11}^-$ (7) are based on infrared spectra in the AgCl region only. A medium-weak vibration at $\sim 1500\ cm^{-1}$ is assigned as ν_{NN} whereas vibrations at ~ 920, ~ 1100, and $\sim 1295\ cm^{-1}$ are regarded as N—F stretching modes. The proposed (5) resonance structure

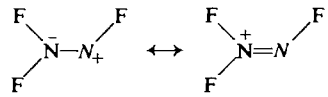

1 **2**

is primarily based on the non-equivalence of the three fluorine atoms in the ^{19}F nuclear magnetic resonance spectrum, obtained in SO_2 and HF solution as well as in the melt, indicating the absence of free rotation along the N—N molecular axis up to temperatures of + 120 °C and the likely presence of multiple bonding.

The symmetry of such a cation would be C_s or C_1, resulting in a maximum of nine infrared and Raman active vibrations for a 5-atom species. The Raman data should therefore provide a second set of identical vibrational frequencies and facilitate the interpretation. The vibrational spectra for both compounds together with a tentative assignment is found in Table 1. The previous assignment of the vibration at $\sim 1500\ cm^{-1}$ as ν_{N-N} is not confirmed by the Raman spectrum, where a corresponding band was not observed. It seems therefore appropriate to regard this vibration as a combination band. From a comparison with previously reported assignments in the N—F stretching region listed in Table 2, involving related molecules, it appears doubtful that such a vibration would be found as high up as $\sim 1300\ cm^{-1}$ even considering sp^2 hybridization for the NF bond together with some π-character as suggested by the structure **2**. In addition, a medium intensity band is found for both compounds at $\sim 1000\ cm^{-1}$, i.r. as well as Raman active, which can be assigned as N—F stretching mode. Such an absorption for $N_2F_3^+$ was previously also reported by Ruff (6). Thus the following assignment is suggested: ν_{NN} at 1300, $\nu_{as\ NF_2} \sim 1120$, $\nu_{sym\ NF_2} \sim 920$, and $\nu_{NF} \sim 1000\ cm^{-1}$. The N—N stretching mode appears to be closer to a value found for the hyponitrous ion (16) found at $1383\ cm^{-1}$ and different from the values reported for *cis*- and *trans*-N_2F_2, found at 1525 and $1523\ cm^{-1}$ (16, 17). This may indicate a weaker N—N bond in $N_2F_3^+$ than in both difluorodiazine isomers. This finding is best explained by invoking some contributions from structure **1**, which in turn would mean that the F_2N—N part of the ion would not be completely planar as suggested by structure **2**.

Assignment of the NF_2 stretching vibrations is in good agreement with the identical vibrations at 1162 and $905\ cm^{-1}$ for the ONF_2^+ cation, indicative of strong NF bonds and appreciable s-character of the NF bonds. The assignment of the $1000\ cm^{-1}$ vibration as due to the NF stretching is supported also by a similar position for *trans*-N_2F_2.

The remaining deformation modes are assigned, assuming C_1 symmetry for $N_2F_3^+$, in analogy to the assignment for N_2O_3 (19).

In conclusion it appears that the i.r. and Raman spectrum are consistent with an ionic formulation for the N_2F_3 group in both complexes, $N_2F_3AsF_6$ and $N_2F_3Sb_2F_{11}$. The differences in the band position for the cation in both salts are minor and within the estimated limit of accuracy.

TABLE 1

Frequencies of the $N_2F_3^+$ cation in cm^{-1}

$N_2F_3^+AsF_6^-$		$N_2F_3^+Sb_2F_{11}^-$		Assignment
Raman	Infrared	Raman	Infrared	
1305	1295	1310	1295	ν_1, ν_{N-N}
1120	1120	1124	1120	ν_6, $\nu_{as\ NF_2}$
997	995	1006	1000	ν_2, ν_{NF}
926	920	928	920	ν_3, $\nu_{s\ NF_2}$
673	672	670	675	ν_4, δ_{NNF}
520	515	520	520	ν_7, $\delta_{as\ NF_2}$
499	495	500	500	ν_5, $\delta_{s\ NF_2}$
310	305	310	319	ν_8
—	—	—	—	ν_9, torsion

TABLE 2

Nitrogen–fluorine stretching vibrations

Compound	$\nu_{antisym}$ (cm^{-1})	ν_{sym} (cm^{-1})	Reference
HNF_2	972	888	22
ONF_3	883	743	23
F_2NOSO_2F	913	1033	24
$ClNF_2$	854	930	25
$ONF_2^+AsF_6^-$	1165	897	This work
$NF_4^+AsF_6^-$	1159	813	11
$N_2F_3^+$	1124	920	This work
cis-N_2F_2	924		17
trans-N_2F_2	1000		18
$N_2F^+AsF_6^-$	1050		10

Can. J. Chem. Downloaded from www.nrcresearchpress.com by 210.87.254.40 on 09/05/12
For personal use only.

TABLE 3
Frequency assignment for the cations

(*a*) NO^+, symmetry $C_{\infty v}$

	ν_1			
	This work		Previous work	
Compound	Infrared	Raman	Infrared	Reference
$NOAsF_6$	2340	2342	2334	27
			2340	12
$NOSbF_6$	2342	2345	2339	27
			2385	12

(*b*) NO_2^+, symmetry $D_{\infty h}$

	This work			Previous work	
Compound	ν_1 (Raman	ν_2 (i.r.)	ν_3 (i.r.)	ν_2 (i.r.)	ν_3 (i.r.)
NO_2AsF_6	1404	598	2385	602*	2365*
NO_2SbF_6	1411	601	2368	597*	2375*
					2358†

*Reference 27.
†Reference 28.

(*c*) F_2NO^+, symmetry C_{2v}

	ν_1 (A_1)		ν_2 (A_1)		ν_3 (A_1)		ν_4 (B_1)		ν_5 (B_1)		ν_6 (B_2)	
Compound	Infrared	Raman	Infrared	Raman	Infrared	Raman	Infrared	Raman	Infrared	Raman	Infrared	Raman
F_2NOAsF_6*	897	895	1855	1845	565	573	1165	1167	650	636	720	—
F_2NOAsF_6†	898	902	1858	1863	569	573	1162	1169	645	634	720	—
F_2NOSbF_6, SbF_5*	900	902	1856	1864	565	570	1165	1176	665	665	710	—

*This work.
†Reference 9.

TABLE 4

Fundamental frequencies for the AsF_6^- and SbF_6^- ions in cm^{-1}

Compound	ν_1 (A_{1g})	ν_2 (E_g)	ν_3 (F_{1u})	ν_4 (F_{1u})	ν_5 (F_{2g})	Reference
(*a*) AsF_6^- Anion						
$KAsF_6$	692	580	698	382	375	This work
$NOAsF_6$	693	582*	695	385	379, 370	This work
NO_2AsF_6	693	582*	690	385	382, 370	This work
$N_2F_3AsF_6$	690	584	695	380	376, 370	This work
NF_4AsF_6	687	581†	709	406	378	11
ONF_2AsF_6	689	584*	692	373	378, 372	This work
N_2FAsF_6	688	579	~715	—	375	7, 10
(*b*) SbF_6^- Anion						
$KSbF_6$	661	575	655	270	294, 278	This work
$NOSbF_6$	658	570*	660	275	294, 284	This work
NO_2SbF_6	661	576, 568*	660	273	294, 283	This work

*Denotes a vibration found in the i.r. and Raman spectrum.
†Found in the i.r. spectrum only.

The remaining cations NO^+, NO_2^+, and ONF_2^+ are well established; the observed frequencies are listed in Table 3 and compared to previously reported values. Here again, all assignments are favoring an ionic formulation for the complexes.

The vibrational frequencies for the anions AsF_6^- and SbF_6^- are listed in Table 4, the potassium compounds are listed for comparison. It is surprising that ν_5 for $KSbF_6$ is split into two components of an approximate intensity ratio of 1:2. A similar observation was published recently (20). A previous assignment (21) of the i.r. active band ν_4 at 350 cm^{-1} for $LiSbF_6$ is not confirmed for the potassium compound where ν_4 is found at 270 cm^{-1}.

In general, the found range of the fundamental frequencies is very narrow for both the AsF_6^- and SbF_6^- compounds. The reported ν_4 for $NF_4^+AsF_6^-$ presents the only exception, but the assignment here may be questionable. Except for the potassium salts all compounds covered in this study show two departures from the expected behavior: (*a*) all ν_2 vibrations appear to be Raman and infrared active indicating a relaxation of the mutual exclusion rule. (*b*) the Raman active ν_5 (F_{2g}) is split into two components indicating a removal of degeneracy. The intensity ratio of both components is either 1:2 or 2:1. The ν_2 mode appears to be split into two components only for $NO_2^+SbF_6^-$

All departures from the expected behavior might be accounted for by a possible lowering of the site symmetry for the anion without having to invoke strong anion–cation interaction. Lower site symmetries are observed in a number of hexafluorosalts with alkali cations (for a detailed discussion see ref. 21). Since apparently the Raman active fundamentals ν_5 and ν_2 are most affected by such site symmetry effects, the importance of laser Raman spectroscopy in judging these effects becomes self evident.

In spite of these minor departures of the spectra from those expected for ideal octahedrons (more obvious for the SbF_6^- complexes) all compounds, perhaps with the possible exception of $NF_4^+AsF_6^-$, can be regarded as predominantly ionic complexes where appreciable anion–cation interaction is absent.

Two final comments remain to be made. The polyanion $Sb_2F_{11}^-$ has been identified previously in the system N_2F_4/SbF_5 without any detailed characterization. The vibrational frequencies assigned to this species are listed in Table 5 and are compared to previously reported values (30–32). Agreement with the reported i.r. spectrum of

TABLE 5

Vibrational frequencies of the $Sb_2F_{11}^-$ ion in cm^{-1}

$VO_2Sb_2F_{11}$ (30)	$Se_4Sb_2F_{11}$ (31)*		$N_2F_3Sb_2F_{11}$	
infrared	Infrared	Raman	Infrared	Raman
765				
730			730	725
705			705	
700			695	695
685			681	665
523				
275	272			
278	285		280	298
225	225	289		
	237			220

*No values above 500 cm^{-1} are reported.

Can. J. Chem. Downloaded from www.nrcresearchpress.com by 210.87.254.40 on 09/05/12
For personal use only.

$VO_2Sb_2F_{11}$ (30) is fair and allows one to identify this species. A suggested assignment is also found there (30) and will not be discussed at this point.

When F_3NO and SbF_5 are reacted, in departure from the normal synthesis (29), with the latter component in excess, the obtained vibrational spectrum contains bands attributable also to the $Sb_2F_{11}^-$ ion. The small amount of sample did not allow a more complete characterization of this compound. It is noteworthy that the cation frequencies of the F_2NO^+ ion are not strongly affected whether the anion is AsF_6^-, SbF_6^- (9), or the polyanion $Sb_2F_{11}^-$ as would be expected for dominantly ionic complexes.

Financial assistance by the National Research Council of Canada is gratefully acknowledged. We are indebted to Professor J. M. Shreeve of the University of Idaho for a sample of F_3NO used in this work. We would also like to thank Mr. A. Hardin for his assistance in obtaining infrared spectra in the low frequency range.

1. K. Stauber, H. Graf, and O. Ruff. Z. Anorg. Chem. **58**, 325 (1908).
2. N. Bartlett, J. Passmore, and E. J. Wells. Chem. Commun. 213 (1966).
3. W. B. Fox, J. S. Mackenzie, N. Vanderkooi, B. Sukornick, C. A. Wamser, J. R. Holmes, R. E. Eibeck, and B. B. Stewart. J. Amer. Chem. Soc. **88**, 2604 (1966).
4. S. J. Kuhn and G. A. Olah. J. Amer. Chem. Soc. **83**, 4564 (1961).
5. A. R. Young II, and D. Moy. Inorg. Chem. **6**, 178 (1967).
6. J. K. Ruff. J. Amer. Chem. Soc. **87**, 1140 (1965).
7. J. K. Ruff. Inorg. Chem. **5**, 1791 (1966).
8. (*a*) D. Moy and A. R. Young II. J. Amer. Chem. Soc. **87**, 1889 (1965). (*b*) H. W. Roesky, O. Glemser, and D. Bormann. Chem. Ber. **99**, 1589 (1966). (*c*) A. V. Pankratov and N. J. Savenkova. Russ. J. Inorg. Chem. **13**, 1345 (1968).
9. K. O. Christie and W. Maya. Inorg. Chem. **8**, 1253 (1969).
10. J. Shamir and J. Binenboym. J. Mol. Struct. **4**, 100 (1969).
11. K. O. Christie, J. P. Guertin, A. E. Pavlath, and W. Sawodny. Inorg. Chem. **6**, 533 (1967).
12. D. W. A. Sharp and J. Thorley. J. Chem. Soc. 3557 (1963).
13. G. Brauer. Handbook of preparative inorganic chemistry. 2nd ed. Academic Press Inc., New York. 1963. p. 511.
14. G. Brauer. Handbook of preparative inorganic chemistry. 2nd ed. Academic Press Inc., New York. 1963. p. 513.
15. S. J. Kuhn. Can. J. Chem. **45**, 3207 (1967).
16. D. J. Millen, C. N. Polydoropoulos, and D. Watson. J. Chem. Soc. 687 (1960).
17. S. T. King and J. Overend. Spectrochim Acta, **22**A, 689 (1966).
18. S. T. King and J. Overend. Spectrochim. Acta, **23**A, 61 (1967).
19. J. P. Devlin and I. C. Hisatsune. Spectrochim. Acta, **17**, 218 (1961).
20. M. Azeem, M. Brownstein, and R. J. Gillespie. Can. J. Chem. **47**, 4159 (1969).
21. G. M. Begun and A. C. Rutenberg. Inorg. Chem. **6**, 2213 (1967).
22. J. J. Comeford, N. E. Mann, L. J. Schoen, and R. Lide. J. Chem. Phys. **38**, 461 (1963).
23. E. C. Curtis, D. Pilipovich, and W. H. Moberly. J. Chem. Phys. **46**, 2904 (1967).
24. M. Lustig and G. H. Cady. Inorg. Chem. **2**, 388 (1963).
25. R. Ettinger. J. Chem. Phys. **38**, 2427 (1963).
26. D. Moy and A. R. Young. J. Amer. Chem. Soc. **87**, 1889 (1965).
27. R. D. Peacock and I. L. Wilson. J. Chem. Soc. (A) 2030 (1969).
28. D. Cook, S. J. Kuhn, and G. A. Olah. J. Chem. Phys. **33**, 1669 (1969).
29. C. A. Wamser, W. B. Fox, B. Sukornick, J. R. Holmes, B. B. Stewart, R. Juurik, N. Vanderkooi, and D. Gould. Inorg. Chem. **8**, 1249 (1969).
30. J. Weidlein and K. Dehnicke. Z. Anorg. Allg. Chem. **348**, 278 (1966).
31. R. J. Gillespie and G. P. Pez. Inorg. Chem. **8**, 1229 (1969).
32. F. O. Sladky, P. A. Bullinev, and N. Bartlett. J. Chem. Soc. A. 2179 (1969).

Can. J. Chem. Downloaded from www.nrcresearchpress.com by 210.87.254.40 on 09/05/12
For personal use only.

Crystallographic studies of cobalt arsenates II. Crystal structure of $Co_8As_3O_{16}$

N. KRISHNAMACHARI AND C. CALVO

Department of Chemistry and The Institute for Materials Research, McMaster University, Hamilton, Ontario

Received March 10, 1970

$Co_8As_3O_{16}$, the Co analogue of the mineral aerugite, crystallizes in the rhombohedral space group $R\bar{3}m$ with hexagonal unit cell parameters $a = 6.046(1)$ and $c = 28.062(8)$ Å, and $Z = 3$. The structure has been refined by a full matrix least squares technique using 613 reflections to a final R value of 0.080. The cations are in tetrahedral and octahedral interstices between layers of oxygen atoms nearly showing cubic closest packing. The structure has one third of the As ions in sites of point group symmetry $\bar{3}m$ with a nearly perfect octahedral environment of oxygen atoms. The remaining As ions lie in sites having the point group $3m$ and showing tetrahedral coordination to oxygen atoms. In the former case the mean As—O bond length is 1.84 Å while in the latter case it is 1.68 Å. The Co ions lie in positions having either $2/m$ or m symmetry with a mean Co—O bond length of 2.13 Å in each case. All the atoms have at least mirror symmetry about them. Some deviation from stoichiometry has been found and may indicate that some of the cobalt has been oxidized.

Canadian Journal of Chemistry, 48, 3124 (1970)

Introduction

In the first two studies in this series (1, 2), it was shown that cobalt oxide – arsenic pentoxide mixtures show a preference for structures based upon close packed layers of oxygen atoms. For a closest packed array of oxygen atoms, assumed to have ionic radii of 1.40 Å (3), the tetrahedral sites have the oxygen atoms displaced by 1.71Å from the center while the octahedral sites have the oxygen atoms displaced by 1.98 Å from the center. From recent structural studies it would appear that either As^{5+} (1, 2) or V^{5+} (4) could be readily accommodated in the tetrahedral sites while any of the cations among Mg^{2+}, Ni^{2+} Zn^{2+}, and Co^{2+} could be housed in the octahedral sites with only modest expansion. In contrast, in the extensively studied divalent metal ion phosphate structures only one example of a structure based on a closest packed array of oxygen atoms is found, that in the mineral sarcopside (5). On the other hand, the phosphate ion itself shows considerable regularity with a mean P—O bond length of 1.54 Å and nearly tetrahedral environment with a stable pentavalent oxidation state for the phosphorus.

In the first study of this series, concerned with the structure of $Co_3(AsO_4)_2$, the oxygen atom packing was symbolized as *ABAC*. These letters designated the arrangement of an entire layer of oxygen atoms by indicating in which holes in the antecedent layer the oxygen atom lie (1). No significant deviation from stoichiometry was noted. The average Co(II)—O bond length over three types of cation sites was 2.12 Å while the mean As—O bond length was 1.69 Å. In the second study (2), concerned with the structures of $Co_{5.9}As_{3.2}O_{16}$, an *AB* oxygen atom layer packing sequence was found with variable occupancy of both the Co and As sites in an olivine-like structure. Despite the fractional Co site occupancy the Co—O bond length did not differ from that found in $Co_3(AsO_4)_2$ although the As—O bond lengths appeared to shorten.

The preparation of the compound, whose study is the subject of this paper, was reported by Taylor and Heyding (6). They gave the stoichiometry as $6CoO.As_2O_5$, and suggested an orthorhombic cell for this and its Ni isomorph. In a subsequent study by Davis, Hey, and Kingsbury (7), the stoichiometry was given as nearly $Ni_9As_3O_{16}$ and it was suggested that about one-sixth of the As are in the trivalent oxidation state. They further suggested a close packed arrangement of oxygen atoms based upon $\sqrt{3}$ relationship between the monoclinic axis a and b.

The structures of CoO and Co_3O_4 are also based upon a cubic closest packing of oxygen atoms with the former oxide manifesting the rock salt structure and the latter the spinel structure (8). Unfortunately, Co_2O_3, where the Co is trivalent, as yet has not been prepared (9). The structure reported here is the first in this series based upon a cubic closest packing and the relationship between this packing and that in hexagonal closest packing is discussed along the lines recently set forth by Kamb (10) in considering the olivine-spinel stability.

Experimental

The crystals investigated were prepared by heating hydrated $Co_3(AsO_4)_2$ in air until the product fused. Two crystal forms were identified. The one with a deep pink color was shown to be $Co_3(AsO_4)_2$ while the second

Can. J. Chem. Downloaded from www.nrcresearchpress.com by 210.87.254.6 on 09/05/12
For personal use only.

Can. J. Chem. Downloaded from www.nrcresearchpress.com by 210.87.254.6 on 09/05/12
For personal use only.

crystal, dark purple in color, is the subject of this study. Preliminary photographs of this crystal using both Weissenberg and precession cameras indicated that it had space group symmetry of $C2$, Cm, or $C2/m$ with unit cell dimensions near those reported by Davis *et al.* (7) for aerugite. From density measurements and chemical analysis these authors concluded that the stoichiometry was $Ni_{18}As_6O_{32}$, although all their analyses showed low values for Ni. Such a result would suggest fractional occupancy of some of the cation sites in the monoclinic space group and this, together with a b-to-a ratio of $\sqrt{3}$, suggested a possible rhombohedral cell. A proposed transformation relating monoclinic cell dimensions (primed) to hexagonal lattice parameters (unprimed), involving the matrix equation

$$\begin{pmatrix} a \\ b \\ c \end{pmatrix} = \begin{pmatrix} -1/2 & -1/2 & 0 \\ 0 & 1 & 0 \\ 1 & 0 & 3 \end{pmatrix} \begin{pmatrix} a' \\ b' \\ c' \end{pmatrix}$$

proved to be correct. The crystals, with Laue symmetry $\bar{3}m$, thus have space group symmetry $R32$, $R3m$, or $R\bar{3}m$, since the only extinctions are those reflections with $-h + k + l \neq 3n$. Accurate unit cell parameters were determined from films calibrated with reflections from a single crystal of TiO_2 whose a and c lattice parameters were taken as 4.5929 and 2.9591 Å (11). The derived lattice parameters, $a = 6.046(1)$ and $c = 28.062(8)$ Å, together with the density results reported by Davis *et al.* (7) for aerugite suggested a molecular formula near $Co_{27}As_9O_{48}$ per unit cell.

Since the imaginary component of the atomic scattering factor for Co was reasonably large when CuKα radiation was employed, the first five layers of the [010] zone containing reflections hnl, $n = 0, 1, 2, 3, 4$, together with oscillation photographs about the b axis were examined for deviations from Friedel's law. Since no significant or systematic deviations could be detected the space group was assumed to be $R\bar{3}m$ initially.

Data of the type hnl, $n = 0, 1, 2, 3, 4$, (monoclinic cell) were collected using a manually oriented scintillation counter in conjunction with a Supper Weissenberg camera. The crystal was rocked through an ω angle of 2° while the intensity was recorded and each reflection was corrected for the background measured near the Bragg peak. The intensity was corrected for the effects of counter saturation. In addition reflections of the type $hk0$ (hexagonal), $hk0$, and $0kl$ (monoclinic cell) were measured with a Joyce–Lobel microdensitometer from integrated precession photographs. All these data were recorded with MoKα_1, α_2 radiation ($\lambda = 0.71069$ Å). The crystal used had the dimensions $0.01 \times 0.01 \times 0.15$ mm^3 which leads to a μR value of 1.0 and thus absorption corrections were deemed necessary and applied. Of the 1226 reflections measured 613 were non-symmetry related and of these 386 had sufficient intensity to be detected.

The c axis length, at 28.062 Å, is smaller than 12 layers of close packed oxygen atoms based upon $3 \times$ the b axis length (9.675 Å) in $Co_3(AsO_4)_2$, where Co in octahedral sites and As in tetrahedral sites lie between the same oxygen atom layers. It was considered likely, therefore, that the tetrahedrally coordinated As would lie in layers between oxygen atom layers devoid of cobalt ions.

The structure was derived from Patterson functions calculated at intervals of 5/60 along the b axis. The Patterson function, $P(U,V,W)$, had relatively large peaks at sections $V = 0$ and 1/2 at $U,W = (0,0)$, (1/2,0), and (1/4,1/4) and at sections $V = 1/4$ and 3/4 at $U,W = (0,1/4)$, (1/4,0) and (1/2,1/4). A trial structure with cations located at $x,z = (0,0)$, (1/2,0), and (1/4,1/4) at level $y = 0$ and 1/2 and $x,z = (0,1/4)$, (1/4,0), and (1/2,1/4) at levels $y = 1/4$ and 3/4 gave a reasonable interpretation of the Patterson function. This model, based upon the monoclinic cell, without distinguishing between Co and As accounted for all the cations and would suggest that all the cations lay in either sites of octahedral or tetrahedral coordination. A three-dimensional electron density map, computed with the signs determined for the structure factors based upon this trial structure, indicated that the atom at (1/4,1/2,1/4) had been incorrectly located and instead an atom should be placed near (0.3,0.5,0.4). A significant improvement was noted in the subsequent structure factor calculations. The atom coordinates were now transformed to those corresponding to a trigonal cell and these positions adjusted to correspond with the demands of the higher symmetry. The cations, save for the last one located, lay at levels roughly 5/60 apart. These were identified with Co ions and the remaining cations regarded as As ions. The former were found to lie in sites having, as their point group symmetry, either $\bar{3}m$, $2/m$, or m, while the As ion lay in a site showing $3m$ symmetry. Oxygen atoms were now inserted between Co ion layers showing cubic closest packing with four oxygen atoms per layer. The stoichiometry at this point corresponded to $Co_{30}As_6O_{48}$. This structure was refined through one cycle of least squares using isotropic temperature factors and the resulting parameters used to calculate cation–oxygen atom distances. Since the Co on the site having $\bar{3}m$ symmetry showed a Co—O distance of 1.8 Å, this atom was considered to actually be an As ion. This identification caused the value of the residual to drop from 0.18 to 0.15. The structure was then refined using a full matrix least squares program written by J. S. Stephens. In addition to the positional parameters, the anisotropic thermal components and seven scale constants were refined. Common reflections from different batches were averaged and assigned to one of the batches from which they arose without prejudice. Weights, ω, were chosen so that the value of $\omega(|F_o| - |F_c|)^2$ would be independent of the magnitude of F_o, the observed structure factor. The function used was $\omega = (60 + 0.032\,|F_o| + 0.0077\,|F_o|^2)^{-1}$ except for those reflections whose calculated value was less than the minimum observable, in which case the weight was set equal to zero. The atomic scattering curve for Co^{2+} was taken from the tables listed by Cromer and Waber (12) while those for As^{5+} and O^- were taken from the International Tables (13). In the case of cobalt and arsenic, the curves were corrected for dispersion. When the minimum of 0.12 had been obtained in

$$R_2 = \left(\frac{\sum \omega(F_o - F_c)^2}{\sum \omega F_o^2} \right)^{1/2}$$

the values of the multiplicities in the Co and As sites were varied. Since the multiplicity of neither As ion deviated

Can. J. Chem. Downloaded from www.nrcresearchpress.com by 210.87.254.6 on 09/05/12
For personal use only.

TABLE 1

Atomic parameters for $Co_8As_3O_{16}$*

Atom	Site symmetry		Atoms/ unit cell	Fractional coordinates			Thermal parameters (Å²)†					
				x	y	z	U_{11}	U_{22}	U_{33}	U_{12}	U_{13}	U_{23}
Co(1)	$2/m$	12(e)‡	7.8(2)	0	1/2	0	0.014(2)	U_{11}	0.019(1)	$\frac{1}{2}U_{11}$	−0.001(1)	$2U_{13}$
Co(2)	m	24(h)	15.6(2)	−0.1652(5)	−x	0.9116(1)	0.012(1)	U_{11}	0.016(1)	0.005(1)	−0.001(1)	$-U_{13}$
As(1)	$\bar{3}m$	3(a)	3	0	0	0	0.009(1)	U_{11}	0.006(1)	$\frac{1}{2}U_{11}$	—	—
As(2)	$3m$	6(c)	6	0	0	0.8079(1)	0.008(1)	U_{11}	0.013(1)	$\frac{1}{2}U_{11}$	—	—
O(1)	m	18(h)	18	0.1432(23)	−x	−0.0377(4)	0.015(7)	U_{11}	0.015(8)	0.019(4)	−0.000(3)	$-U_{13}$
O(2)	$3m$	6(c)	6	0	0	0.3743(7)	0.014(8)	U_{11}	0.013(6)	$\frac{1}{2}U_{11}$	—	—
O(3)	$3m$	6(c)	6	0	0	0.1318(6)	0.005(6)	U_{11}	0.013(7)	$\frac{1}{2}U_{11}$	—	—
O(4)	m	18(h)	18	0.4860(25)	−x	−0.1224(3)	0.015(7)	U_{11}	0.015(3)	0.006(4)	0.001(4)	$-U_{13}$

*Estimated standard deviations are in parentheses.

†The thermal parameters have been obtained from $\beta_{ij} = 2\pi^2 b_i b_j U_{ij}$ where the β_{ij}'s appear as a thermal effect through exp $[-(\beta_{11} h^2 + 2\beta_{12} hk + ...)]$ in the structure factor expression and b_i are reciprocal lattice vectors.

‡The letters follow the convention set forth by ref. 18.

Can. J. Chem. Downloaded from www.nrcresearchpress.com by 210.87.254.6 on 09/05/12
For personal use only.

significantly from the value required to fill the site these values were reset to that required by the space group and left unvaried. The value of R then settled to 0.080 while R_2 was 0.102 when the refinement was terminated. The values of the final positional and thermal parameters are given in Table 1. The estimated standard deviations were computed from the elements of the inverse matrix obtained in the least squares refinement. In Table 2, the calculated structure factors and the observed ones are compared. The final composition corresponds to $Co_{23.4}As_9O_{48}$ with an estimated standard deviation of 0.4 Co atoms per cell.

As a final test for the correctness of the space group, and therefore the structure, the Patterson function was interpreted so as to satisfy the requirements of the $R32$ space group. The oxygen atoms were then inserted as above and the structure refined. The final value of R_1 was 0.091 and of R_2 was 0.111. Since this model contained about 25% more parameters than did the model in $R\bar{3}m$, it was rejected. A model showing $R3m$ symmetry was also rejected since it yielded R and R_2 values larger than either of the above models.

Description of the Structure

The structure of $Co_{23.4}As_9O_{48}$ consists of 12 layers of nearly ideally cubic closest packed oxygen atoms. The As ion at the origin sits in a site surrounded by six oxygen atoms and shows no significant deviation from regularity. All the As(1)—O bond lengths are symmetry related with the value 1.84(1) Å, while the angles lie within 1σ(σ = estimated standard deviation) of their ideal value. This As(1)–O_6 group shares its 12 edges with 12 different CoO_6 octahedra. Six of these cobalt ions, Co(1), lie in the same plane as As(1). The As(1)–O_6 and Co(1)–O_6 groups form sheets of edge shared octahedra in the *ab* plane as shown in Fig. 1. These sheets also occur in the thortveitite-series of structures, where the As(1) site is empty, as for example in $Mg_2As_2O_7$ (14). The Co(1)–O_6 octahedra deviate substantially from ideality, showing a range of Co—O bond distance from 2.09 to 2.16 Å. The greatest irregularity results from the short edge shared with As(1) resulting in an O(1)—Co(1)—O(1) bond angle of 74°. A similar effect is found in the Co(2)–O_6 group where the angle subtending the shared edge is contracted to 74°. The Co(2)—O bond lengths range from 2.06 to 2.21 Å and both types of cobalt ions show a mean Co—O bond length of 2.13 Å. These bond lengths and angles are to be found in Table 3.

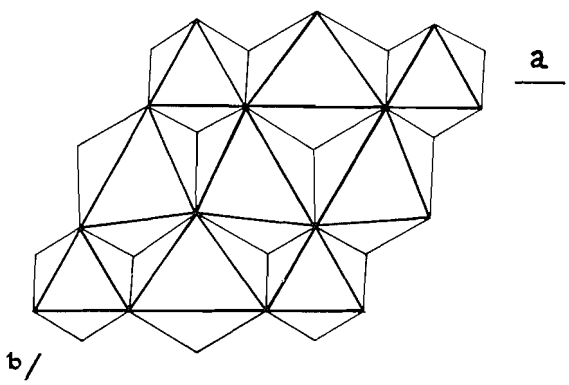

FIG. 1. The arrangement of the edge sharing AsO_6 and CoO_6 octahedra lying near the plane $z = 0$ is shown in projection down the c axis of the hexagonal cell. The smaller octahedra represent AsO_6 while the larger represent CoO_6. The oxygen atoms are at the corners of the octahedral groups.

Co(2) lie between the oxygen atoms composing the sheets of octahedra of Fig. 1 and the next layer of oxygen atoms. Three Co(2)–O_6 groups lie on one side of the sheet, each sharing an edge with As(1), two edges with two Co(1) ions, and two edges with the other two Co(2) ions in the array. These three Co(2)–O_6 groups all share one common oxygen atom and that one lies on the three fold axis as is shown in Fig. 2. The oxygen atoms of the upper face of the Co(2)–O_6 octahedra, that is, the one parallel to the *a–b* plane but on the side furthest removed from As(1) are each shared with three different As(2)–O_4. The As(2) ion lies above the plane of the oxygen atoms. These As ions lie in planes separating oxygen atoms layers which contain no other cations. This results in a contracted c axis as suggested above. The As(2)–O_4 tetrahedra corner share three of its oxygen atoms each with two different Co(2). The oxygen atom that lies on the three fold axis, O(3), is the oxygen atom shared by the three Co(2) ions as described above and related to that one by an inversion followed by the rhombohedral centering. The As—O bond lengths about As(2) are all 1.68 Å, while the O—As—O angle deviates from regularity by about four standard deviations. A view of the structure projected down the c axis is shown in Fig. 3.

Discussion

The ideal composition of this compound, that is with all sites fully occupied, is $Co_{27}As_9O_{48}$. The composition determined by refining the

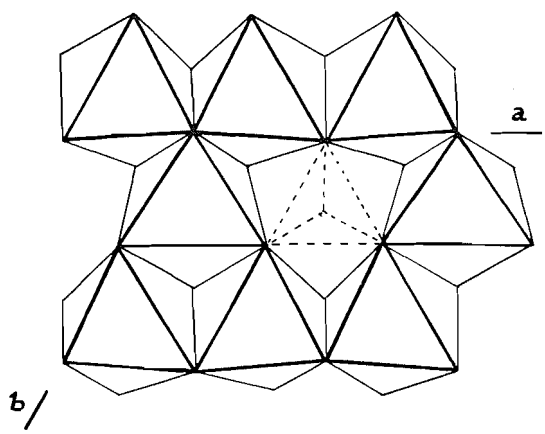

FIG. 2. The arrangement of edge sharing Co(2)–O_6 groups in the layer near $z = 0.14$ is shown as viewed down the c axis of the hexagonal cell. The c axis passes through the intersection of the three octahedra in the upper left corner. The tetrahedrally coordinated As site, shown with dashed lines, lies above the upper plane of oxygen atoms and shares three such atoms with three Co_6 groups. The remaining oxygen atom arises from the next layer of oxygen atoms.

Can. J. Chem. Downloaded from www.nrcresearchpress.com by 210.87.254.6 on 09/05/12
For personal use only.

TABLE 2

Observed and calculated structure factors for $Co_8As_3O_{16}$

UNOBSERVED REFLECTIONS ARE MARKED WITH AN ASTERISK (*), AND UNRELIABLE REFLECTIONS WITH THE SYMBOL ($).

H	L		|FOBS|	|FCALC|
[illegible]				
6	-2		51	58
6	1		107	106
6	4		159	148
6	7	*	43	36
6	10		43	38
6	-11		71	79
6	13		57	49
6	16		205	204
6	19	*	45	11
6	22	*	46	16
6	25		114	113
6	28		49	47
6	31	*	49	40
6	34	*	49	10
6	37		81	100
-7	12		43	47
-7	15		92	100
-7	18	*	42	20
-7	21		63	66
7	-13	*	47	32
7	-10		73	69
7	8		62	68
7	11		57	53
-8	14	*	44	18
-8	17		119	110
-8	20		128	128
-8	23	*	46	18
-8	29		53	58
-8	32		97	101
-8	35	*	49	2
-8	38	*	49	18
-8	41		77	87
-8	44	*	48	13
-8	47	*	47	17
-8	50	*	45	12
-8	53		60	48
8	-15		49	53
8	-12		91	74
8	-9		61	69
8	0		170	157
8	3	*	48	0
8	9		59	60
8	15		61	59
8	21		104	101
8	24		65	56
-9	31		49	58
-10	21		84	94
-10	24		58	52
10	-16		82	78
10	11	*	47	29
H	L		K = 3	
0	6		209	164
0	9		78	79
-0	12		88	96
-0	21		84	99
-0	24		63	64
-0	27		53	58
-0	30		46	44
0	33		65	68
-1	5		128	113
-1	8		199	196
-1	11		151	144
1	4		63	63
-2	1	*	32	22
-2	7	*	25	7
-2	16		62	61
-2	22		69	75
-2	25	*	34	25
-2	28		61	63
-2	31		101	113
2	2	*	28	17
2	5		141	125
2	8		123	128
2	11		85	77
2	14		37	28
2	17		66	60
2	20	*	34	11
2	23	*	35	6
2	26		89	89
-3	9	*	33	15
-3	12		71	81
-3	21		53	61
-3	27		65	76
-3	30		55	57
-3	33		45	43
-3	36		57	54
3	0		77	72
3	3		54	52
3	6		121	110
3	21		56	62
-4	26		87	96
4	4		33	28
4	13		60	47
4	16		43	48
-5	7		60	52
-5	10		164	144
-5	13		106	105
-5	19	*	33	3
-5	22		69	74
-5	25	*	36	15
-5	28		38	38
-5	31		74	86
5	-10		80	79
5	5		69	68
5	8		44	47
5	11		62	62
-6	9	*	40	16
-6	12		65	71
-6	15		81	83
-6	18	*	37	29
-6	24		42	40
-7	11		86	82
H	L		K = 4	
-0	14		53	45
-0	17		215	210
-0	20		221	214
-0	23		54	47
-0	26		60	69
-0	29		87	103
-0	35	*	46	1
-0	38	*	48	29
-0	41		136	139
-0	44	*	50	14
-0	47	*	51	18
-0	50	*	51	16
-0	53		85	68
-0	56	*	42	28
-1	1		64	63
-1	13		117	100
-1	16		62	52
-1	19	*	30	3
-1	22		71	75
-1	25	*	36	4
-1	28		53	53
-1	31		93	94
-1	34	*	43	26
-1	37		40	34
-1	40	*	41	9
-1	43	*	43	29
-1	46	*	43	35
-1	49	*	44	29
-1	52	*	44	35
-1	55	*	43	1
-1	58	*	42	15
1	0		76	58
1	3		62	49
1	6		169	137
1	12		61	68
1	15		95	83
1	18	*	37	25
1	21		54	55
1	27		62	63
1	30		48	48
1	33	*	39	34
1	36	*	41	42
1	39	*	48	5
-2	0		727	683
-2	15		128	123
-2	18		97	106
-2	21		274	279
-2	27	*	38	40
-2	30		39	40
-2	36		118	115
-2	42		68	65
-2	45		71	72
-2	48		61	58
-2	51	*	44	13
-2	54	*	44	24
-2	57		89	74
-2	60	*	43	0
2	1		181	165
2	4		242	220
2	10		44	40
2	16		334	311
2	19	*	37	4
2	25		159	169
2	34	*	43	16
2	37		119	129
2	40		62	61
2	43	*	46	1
2	49	*	44	51
-3	2	*	36	8
-3	8		153	137
-3	11		116	106
-3	17		42	43
-3	20	*	33	10
-3	23	*	35	10
-3	29		45	47
-3	32		38	37
-3	35	*	39	27
-3	38	*	40	16
-3	41	*	42	9
-3	44	*	43	22
3	-7	*	34	9
3	2	*	34	2
3	5		58	61
3	8		88	95
3	14	*	36	36
3	17	*	37	2
3	20	*	38	19
3	23	*	39	19
3	26		71	74
3	32	*	42	12
3	35	*	43	26
3	38	*	44	16
3	41	*	44	13
-4	10		48	42
-4	13		106	110
-4	16		419	418
-4	34	*	45	21
-4	37		140	153
-4	40		70	76
-4	46		49	56
-4	49		58	60
-4	52		44	45
-4	55	*	43	20
4	0		276	275
4	3	*	36	12
4	6	*	36	21
4	9		100	105
4	12		122	114
4	15		76	79
4	18		43	49
4	21		147	153
4	24		96	95
4	30	*	43	24
4	33		70	75
4	36		71	78
-5	6		147	121
-5	9		47	46
-5	12		70	75
-5	15		115	115
-5	18	*	37	27
-5	21		70	78
-5	27		44	50
-5	30		38	38
-5	36	*	41	33
-5	39	*	42	2
5	-11		42	42
5	-8		64	59
5	7	*	40	26
5	10		73	76
5	13		59	52
5	16	*	41	19
5	19	*	42	0
5	22	*	43	42
-6	8		248	236
-6	11		106	115
-6	14		43	34
-6	17		158	158
-6	20		173	175
-6	23	*	38	32
-6	35	*	44	2
-6	38	*	45	24
-6	41		105	116
-6	44	*	46	13
-6	47	*	46	18
-6	50	*	46	14
-6	53		65	61
-6	56	*	43	24
6	-4		118	108
6	-1		81	82
6	5		92	100
6	8		98	88
6	14	*	43	13
6	17		68	74
6	20		95	95
6	23	*	44	8
6	26	*	44	40
6	32		71	76
-7	10		118	105
-7	19	*	37	16
-7	22	*	38	42
-7	25	*	39	17
-7	28	*	40	42
-7	31		60	77
-7	34	*	42	25
-7	37		43	36
-7	40	*	44	2
-7	43	*	44	16
-7	46	*	44	24
-7	49	*	43	27
-7	52	*	42	23
-8	27	*	42	22
8	4		78	72
8	7	*	44	22
8	10	*	43	25
8	13	*	43	21
8	16		88	92
8	19	*	42	8
8	22	*	42	10
-9	14	*	41	14
-9	17	*	42	30
-9	20	*	42	9
-9	23	*	43	4
-9	32	*	44	26
-9	38	*	44	6
-10	16		140	141
-10	19	*	44	8
-10	22	*	44	14
-10	25		74	86
-11	18	*	44	16
H	L		K = 7	
-4	1	*	35	10
H	L		K = 8	
-5	2	*	30	6

* Indicates an unobserved reflection with F_o as its maximum possible value and $ indicates an unreliable reflection probably because of extinction.

TABLE 3

Bond distance and angles in $Co_8As_3O_{16}$*

(*a*) $Co(1)-O_6$ group

Bond	Distance (Å)	Bonds	Angle (deg)
Co(1)—O(1)	4 × 2.16(1)	O(1)—Co(1)—O(1)[a]	73.9(4)
—O(2)[e]	2 × 2.09(1)	—O(2)[e]	91.2(4)

(*b*) $Co(2)-O_6$ group

Bond	Distances (Å)	Bonds	Angle (deg)	Bonds	Angle (deg)
Co(2)—O(4)[a]	2.06(1)	O(4)[a]—Co(2)—O(2)[g]	88.0(4)	O(2)[g]—Co(2)—O(3)[c]	178.0(6)
—O(2)[g]	2.21(1)	—O(3)[c]	93.2(4)	—O(1)[a]	88.0(5)
—O(3)[c]	2.12(1)	—O(1)[a]	163.9(3)	—O(1)[b]	88.0(5)
—O(1)[a]	2.16(1)	—O(1)[b]	90.4(3)	—O(4)[b]	88.0(4)
—O(1)[b]	2.16(1)	—O(4)[b]	105.1(5)	O(3)[c]—Co(2)—O(1)[a]	90.4(5)
—O(4)[b]	2.06(1)	O(1)[a] —O(1)[b]	73.9(4)	—O(1)[b]	90.4(4)
		—O(4)[b]	90.4(4)	—O(4)[b]	93.2(5)
		O(1)[b] —O(4)[b]	163.9(5)		

(*c*) $As(1)-O_6$ group

Bond	Distances (Å)	Bonds	Angle (deg)
As(1) —O(1)	6 × 1.84(1)	O(1)—As(1)—O(1)	89.9(5)

(*d*) $As(2)-O_4$ group

Bond	Distances (Å)	Bonds	Angle (deg)
As(2)—O(3)[c]	1.69(2)	O(3)[c]—As(2)—O(4)[f]	108.3(4)
—O(4)[f]	3 × 1.68(1)	O(4)[f]—As(2)—O(4)[h]	110.6(5)

*The letter designates the transformations to be applied to the positions listed in Table 1 in order to derive the appropriate oxygen atom positions. Lattice translations are not included. Superscripts denote the following: *a*, $-y, x-y, z$; *b*, $y-x, -x, z$; *c*, $-x, -y, -z$; *d*, $y, y-x, -z$; *e*, $x+\frac{1}{3}, y+\frac{2}{3}, z+\frac{2}{3}$; *f*, $-x+\frac{1}{3}, -y+\frac{2}{3}, -z+\frac{2}{3}$; *g*, $-x+\frac{2}{3}, -y+\frac{1}{3}, -z+\frac{1}{3}$; *h*, $y+\frac{1}{3}, y-x+\frac{2}{3}, -z+\frac{2}{3}$.

X-ray data corresponds to $Co_{23.4}As_9O_{48}$, where it has been assumed that the oxygen atom sites are fully occupied. The estimated standard deviation on the number of cobalt ions per unit cell is 0.4. The deficiency in Co content is randomly distributed among the Co sites.

Davis *et al.* (7) concluded that the theoretical composition of aerugite corresponds to $Ni_{27}As_9O_{48}$ but their chemical analysis on natural and synthetic materials suggested an atom ratio of Ni to As varying between 2.59 and 2.95. The number of arsenic atoms per unit cell of aerugite varied from 8.58 to 9.44 while the number of Ni atoms lay between 23.65 to 25.72 with low values of Ni correlated with high values of As. These authors obtained evidence for some As^{3+} in their aerugite samples but its atomic ratio to the total As was near 0.2/5.7 rather than the 1/6 their formula suggests. It is interesting, however, that the ratio of octahedral As to total As in the structure of $Co_{24}As_9O_{48}$ is 1/3. It is difficult to decide purely on crystallographic grounds whether the octahedral As is to be designated 3^+ or 5^+. The average As—O bond length in octahedral coordination found in $As_2O_5 \cdot 5/3H_2O$ is 1.85 Å (15) and corresponds very closely to the value expected when changing from an octahedral to a tetrahedral packing of oxygen atoms. The crystallography of As^{3+} has not been extensively investigated and therefore there are no well refined and characterized structures for comparison, although As^{3+} does seem to prefer a triangular coordination geometry.

Charge balancing considerations are inclusive. If one assumes a -2 charge on the oxygen atoms then with all the As as $+5$ and all the Co as $+2$ the cell comes within 5 charges of charge neutrality. This deviation ($\sim 5\sigma$) seems significant in terms of the σ on the cobalt composition. Thus some of the Co must be oxidized to the trivalent state in this formulation. On the other hand if As(1), one-third of the total As, were to be

Can. J. Chem. Downloaded from www.nrcresearchpress.com by 210.87.254.6 on 09/05/12
For personal use only.

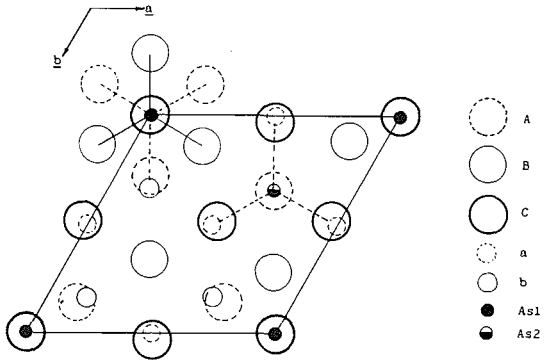

FIG. 3. That portion of the structure of $Co_8As_3O_{16}$ that lies between $z = -0.05$ and $z = 0.15$ is shown in projection down the c axis of the hexagonal cell. The larger circles are oxygen atoms with A at $z = -0.04$, B at $z = 0.04$, and C at $z = 0.13$; the cobalt ions are represented by the next larger circles with type a at $z = 0$ and type b at $z = 0.14$. The As—O bonds are shown as dashed lines.

assigned as trivalent and the remainder pentavalent, then Co(1), one-third of the total Co could be trivalent with the remainder divalent, and the cell would be neutral to within two units of charge. The bond lengths about the two Co ions do not differ and therefore they provide no confirmation for this charge assignment. A similar situation has arisen in the olivine-like cobalt arsenates (2) and may be a result of charge sharing amongst the Co ions.

Finally these crystals were grown together with $Co_3(AsO_4)_2$ where deviations from the nominal charge of As equal to 5+ and Co equal to 2+ are unnecessary. The reaction that occurs is the decomposition of orthoarsenate with the resultant loss of As_2O_5 as

$$3CoO \cdot As_2O_5 \rightarrow 6CoO \cdot As_2O_5 + As_2O_5$$

However, the As_2O_5 decomposes in air giving rise to the reaction

$$As_2O_5 \rightarrow As_2O_3 + O_2 \quad (16)$$

Thus trivalent As may be expected to appear in the system. Since pure CoO is converted to Co_3O_4 upon heating (9) it is possible that some Co^{3+} might also exist in our system. If the proposed changes do take place then the fact they do so in both Ni and Co systems is interesting in the light of the greater relative stability of trivalent state in Co. It would be of considerable value to investigate the structure of the $6MgO \cdot As_2O_5$ compound prepared by Travnicek, Kroger, Botden, and Zalm (16) since its powder pattern, compared to that of aerugite, suggests they would have similar structures. It would probably be necessary to grow the crystals in a flux to prevent decomposition, since the melting temperatures of the Mg compounds are generally substantially higher than their Co analogues.

Kamb (10) has suggested that structures can be stabilized by the contraction of edges shared between the polyhedral units composing the structure. This is a consequence of the repulsion of the positively-charged cations. In the close packed structures with stoichiometry AB_2O_4 a small ion, A, in the tetrahedral site leads to a natural shortening of the relevant shared edges relative to the unshared edges in the olivine structure. In the spinel form this change results in a lengthening of the shared edges. The relevant shared edges are between the BO_6 octahedra and the AO_4 tetrahedra in the former case and between octahedra in the latter. Thus, if all the other effects nearly cancel, it will be the ratio of the B—O bond length to the A—O bond length that determines which of these phases will appear. These arguments, in fact, should apply to any close packed arrangement with the hexagonally close packed arrangement being olivine-like while the cubic close packed ones are spinel-like. As has previously been shown (4), the cobalt arsenate phases have the bond length ratio B—O/A—O greater than 1.25 and are based upon hexagonally closed-packed layers while the orthovanadates of Mg (4) and Zn (17) have this ratio below 1.23. The compound at hand has both Co and one third of the As in octahedrally coordinates sites and thus the relevant parameter would require a weighted mean of the two ratios. If the weights are chosen in proportion to their number the ratio, B—O/A—O, obtained is 1.24. Although the AsO bond lengths do not appear lengthened by the strain of sharing every edge with a CoO_6 octahedron the angles subtended by the shared edge at the cobalt is 74° in both Co(1)–O_6 and Co(2)–O_6. If the cation repulsion across these edges is really significant presumably it could help drive As^{5+} to As^{3+} for the As in the octahedral site, since then the cation charges giving rise to the repulsion are changed from +5 and $+2\frac{1}{8}$ to +3 and $+2\frac{3}{8}$.

The authors acknowledge the support of the National Research Council of Canada.

Can. J. Chem. Downloaded from www.nrcresearchpress.com by 210.87.254.6 on 09/05/12
For personal use only.

1. N. KRISHNAMACHARI and C. CALVO. Can. J. Chem. **48**, 881 (1970).
2. N. KRISHNAMACHARI. Ph.D. thesis, McMaster University, Hamilton, Ontario. 1970.
3. L. PAULING. Nature of the chemical bond. Cornell University Press, Ithaca. 1948.
4. N. KRISHNAMACHARI and C. CALVO. To be published.
5. M. E. MROSE and D. E. APPLEMAN. Amer. Crystallogr. Ass., Annual Meeting, Program and Abstr., University of Colorado, Boulder, Colorado. (1961).
6. J. B. TAYLOR and R. D. HEYDING. Can. J. Chem. **36**, 597 (1958).
7. R. J. DAVIS, M. H. HEY, and A. W. G. KINGSBURY. Miner. Mag. **35**, 72 (1965).
8. A. F. WELLS. Structural inorganic chemistry. Oxford at the Clarendon Press. 1962.
9. F. A. COTTON and G. WILKINSON. Advanced inorganic chemistry. Interscience Publ. 1962.
10. B. KAMB. Amer. Miner. **53**, 1439 (1968).
11. D. T. CROMER and K. HERRINGTON. J. Am. Chem. Soc. **77**, 4708 (1955).
12. D. T. CROMER and J. T. WABER. Acta Cryst. **18**, 1041 (1965).
13. International tables for X-ray crystallography. Vol. III. Kynoch Press, Birmingham. 1962.
14. C. CALVO and K. NEELAKANTAN. Can. J. Chem. **48**, 890 (1970).
15. J. R. PARTINGTON. General and inorganic chemistry for university students. Macmillan and Co., Ltd., London. 1951. p. 628.
16. M. TRAVNICEK, F. A. KROGER, P. J. BOLDEN, and P. ZALM. Physica, **18**, 33 (1946).
17. R. GOPAL and C. CALVO. To be published.
18. International tables for X-ray crystallography. Vol. I. Kynoch Press. Birmingham. 1965.

Can. J. Chem. Downloaded from www.nrcresearchpress.com by 210.87.254.6 on 09/05/12
For personal use only.

Can. J. Chem. Downloaded from www.nrcresearchpress.com by 210.87.254.105 on 09/05/12
For personal use only.

Acenaphthene I. The preparation of derivatives of 4,5-diamino naphthalic anhydride[1]

LOUIS A. JONES,[2] CHARLES T. JOYNER, HONG KI KIM, AND ROBERT A. KYFF[3]
Department of Chemistry, North Carolina State University, Raleigh, North Carolina 27607

Received April 22, 1970

The preparation of 5-nitroacenaphthene (**2**) using several nitrating agents resulted in a product which was found to be contaminated with 20–30% of the 3-nitro isomeride. Separation was accomplished by t.l.c. and the n.m.r. spectra of the isomers are now reported. A new synthesis of 4,5-dinitronaphthalic anhydride (**5**) and an improved preparation of the dimethyl and diethyl esters of 4-nitronaphthalic anhydride and **5** is described. The esters were converted to the corresponding diamino derivatives by high pressure hydrogen–Pd reduction.

Canadian Journal of Chemistry, **48**, 3132 (1970)

Acenaphthene (**1**) has been used as a convenient starting material for the preparation of 5-nitroacenaphthene (**2**) which can be oxidized to the 4-nitronaphthalic anhydride (**3**). It has been

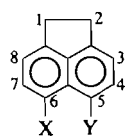

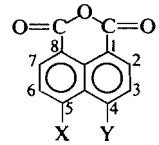

1 X = Y = H
2 X = H; Y = NO_2
4 X = NO_2; Y = NO_2

3 X = H; Y = NO_2
5 X = NO_2; Y = NO_2

reported that the nitro group can be reduced to the amine although the literature is in conflict (1). For nitration, mixtures such as glacial acetic acid – nitric acid (2), concentrated sulfuric acid – nitric acid (2*d*, 3) and $UO_2(NO_3)_2 \cdot H_2O \cdot N_2O_4$ (4*a*) have been used successfully to prepare **2** in 75–85% yield. Oxidation to **3** using glacial acetic acid and sodium dichromate occurs in yields of 59% (2, 5). In our studies of the published methods of nitration, modification of Sachs and Mosebach's procedure (2*a*, *b*) gave superior results. However, in all methods used to prepare **2**, the n.m.r. spectra suggested that 20–30% of the 3-nitro isomer was present and extensive recrystallization failed to improve the melting point or the n.m.r. pattern. A search of the literature revealed that only **2** has been considered to be the product of nitration of acenaphthene using acetic acid – nitric acid. Use of benzoyl-nitrate as the nitrating agent has been reported to produce 3-nitroacenaphthene (41%) while diacetylorthonitric acid gave a 22% yield (6). In our hands, attempts to resolve the mixture by column chromatography, sublimation, and zone refining were unsuccessful but t.l.c. afforded separation. Preparative t.l.c. gave two compounds, pure **2** and the 3-nitro isomeride and the n.m.r. spectra, when combined, gave the original spectrum of impure **2** (Fig. 1). Reduction of impure **2** to the amine gave the pure 5-amino derivative after two recrystallizations from ethanol as indicated by comparison with the product derived from the t.l.c. purified compound.

Attempts to oxidize impure **2** to **3** by neutral sodium dichromate under high pressure (7) and also by the Cornforth reagent (8) resulted in complete degradation in the former case and less than 10% yield in the latter. Although it has been reported (2*b*, 4*b*) that 4-nitronaphthalic acid is the original product of oxidation which then dehydrates to **3**, only **3** was obtained on acetic acid – sodium dichromate oxidation and t.l.c. indicated no 3-nitro isomer survived the oxidation. Attempted reduction (1) of **3** to the amine gave only an amorphous yellow–orange powder of an indefinite m.p., and the i.r. and n.m.r. spectra suggested some polymerization had occurred as indicated by diffuse N—H and poorly defined anhydride carbonyl absorptions.

The preparation of 4,5-dinitronaphthalic anhydride (**5**) has been accomplished with acetic anhydride – nitric acid and oxidation was carried out as previously described (2*b*). However, the extensive length of time required for stepwise preparation of **5** prompted an investigation into quicker methods of nitration and oxidation.

[1]The financial support from NASA Grant NGR 34-002-056 is gratefully acknowledged as is the technical assistance of C. H. McDonald and Miss Gail Gescheidle.
[2]To whom inquiries should be sent.
[3]Present address: IBM Research Laboratories, Essex Junction, Vermont.

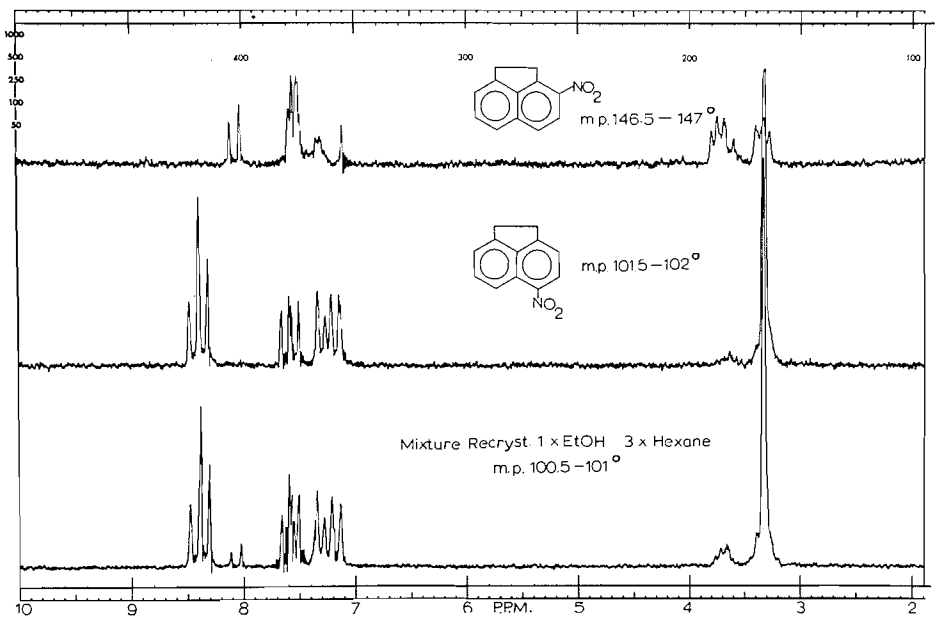

FIG. 1. Nitration products of acenaphthene. Run on an HA-100 in $CDCl_3$ with 1% TMS.

Oxidation with concentrated nitric acid under reflux conditions overnight showed that **4** → **5** occurred in 24% yield and **2** → **5** gave a 22% yield. Starting with **1** and refluxing for 16–18 h gave *ca.* 25% yield of pure **5** and it seems reasonable therefore that the pathway follows **1** → **2** → **4** → **5** under the *in situ* nitrating–oxidizing conditions. It should be noted that no nitrated product other than **5** was found nor was there any evidence for the formation of any of the corresponding acid, contrary to published results (*2b*). Attempts to reduce the nitro groups to amines using Pd–H_2 under pressure or $SnCl_2$–HCl (*2b*, 5) resulted in a brown powder of indeterminate m.p. and an i.r. spectrum completely lacking in the two carbonyl stretching vibrations characteristic of anhydrides.

It was considered desirable to determine if the esters of **3** and **5** could be successfully reduced to give the corresponding amines. Several methods of esterification were investigated including the formation of the acid chlorides but yields were too low to be practicable. The procedure of Bickoff *et al.* (9) (*i.e.*, refluxing an acetone solution of **3** or **5** with dialkylsulfate and potassium carbonate) resulted in low yields of the desired esters. However, when the corresponding alcohol was used as the solvent and the anhydride refluxed overnight with the dialkylsulfate and potassium carbonate, yields were considerably improved. In this manner, a 76% yield of 4-nitronaphthalic-1,8-dimethyl ester (**4**), 69% of 4-nitronaphthalic-1,8-diethyl ester (**7**), 90% of 4,5-dinitronaphthalic-1,8-dimethyl ester (**8**), and 51% of 4,5-dinitronaphthalic-1,8-diethyl ester (**9**) was obtained. An 18.4% yield of **6** has been previously reported from refluxing the potassium salt of **3** with dimethylsulfate (*2b*).

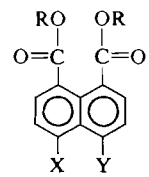

6 R = Me; X = H; Y = NO_2 **6***a* Y = NH_2
7 R = Et; X = H; Y = NO_2 **7***a* Y = NH_2
8 R = Me; X = Y = NO_2 **8***a* X = Y = NH_2
9 R = Et; X = Y = NO_2 **9***a* X = Y = NH_2

Reduction was attempted via $SnCl_2$–HCl (5), Fe–HCl (1*a*), and PtO_2–H_2 in ethanol (10), and in the latter case a blue precipitate was formed which was not investigated further. However, in all cases, the yield was small. Successful conversion of **6**, **7**, **8**, and **9** to the corresponding amines occurred by the Pd–H_2 reduction of the heterogeneous nitronaphthalic ester–benzene system under high pressure and moderate temperature.

Can. J. Chem. Downloaded from www.nrcresearchpress.com by 210.87.254.105 on 09/05/12
For personal use only.

Can. J. Chem. Downloaded from www.nrcresearchpress.com by 210.87.254.105 on 09/05/12
For personal use only.

Experimental[4]

Acenaphthene (**1**) (practical, Aldrich Chemical Co., Inc.) was conveniently purified by batch chromatography on alumina using hexane as the elutant. Approximately 750 g of alumina slurried in hexane was added to a column 9.5 × 80 cm and on this was placed 2 kg of practical **1**. Hexane was continuously run through the bed until all of **1** disappeared and the collected elutant stripped off under vacuum; m.p. 95 °C, n.m.r. δ 3.18 (4H, s, cycloaliphatic H), 6.53–8.00 (6H, m, aromatic H).

5-Nitroacenaphthene (2)

The procedure used was similar to that of previous workers (*2a*, *b*). A mixture of 400 g of **1** and acetic acid (3.2 l) was cooled to 15 °C in an ice bath and nitric acid (180 g, $d = 1.42$) was added with stirring at such a rate as to maintain a temperature of 15–20 °C. After 1 h, the precipitate was filtered, washed with acetic acid, and recrystallized from hexane. This gave 340 g (66%) of impure (*ca.* 20% of 3-nitroacenaphthene) 5-nitroacenaphthene (**2**). A portion of this was successively recrystallized from ethanol and hexane to give yellow–green needles, m.p. 101–105 °C, lit. m.p. 101–102 °C (*2b*). Qualitative t.l.c. (Barkerflex Silica Gel 1 B, hexane:ether 3:1 v/v) showed the 3-nitro isomer to have the larger R_f and preparative t.l.c. (silica gel HF, 40 × 20 cm glass plates, hexane:ether, 3:1 v/v) separated the two bands. The n.m.r. spectra are shown in Fig. 1 and integrate correctly; 3-nitroacenaphthene m.p. 146.5–147 °C, lit. m.p. 151.5 °C (6).

Anal. Calcd. for $C_{12}H_9NO_2$ (mol. wt. 199.14): C, 72.36; H, 4.52; N, 7.04. Found: C, 72.21; H, 4.58; N, 6.94.

Impure **2** (0.5 g) was refluxed with 2 ml of hydrazine hydrate and 0.05 g of 10% Pd on carbon in 50 ml of ethanol for 2 h, and filtration, followed by evaporation, gave impure 5-aminoacenaphthene. This was recrystallized twice from ethanol to give 0.3 g (71%) of pure compound, m.p. 106 °C, lit. m.p. 104 °C (11). The t.l.c. purified **2** was treated similarly and the product melted at 106.5 °C; mixed m.p. showed no depression. The n.m.r. and i.r. spectra were identical and t.l.c. showed no impurities present; i.r. 1330 (NO_2 sym. stretch) and 1520 cm^{-1} (NO_2 asym. stretch); n.m.r. δ 3.30 (4H, s, methylene H), 3.65 (2H, s, amine H), 6.60–7.60 (5H, m, aromatic H).

4-Nitronaphthalic Anhydride (3)

The solid from above was added to acetic acid (5.2 l) containing technical sodium dichromate (3200 g) and the mixture was heated on a boiling water bath for 5 h. The solution was poured into water and the orange crystals were filtered and dissolved in 3% potassium carbonate solution. This was filtered and the filtrate was acidified with hydrochloric acid, producing a light tan precipitate. After filtration, water washes, and drying, a total of 301 g of **3** (48%), m.p. 228–229 °C, was obtained, lit. m.p. 228–229 °C (*2b*). No 2-nitro compound was indicated by t.l.c.; i.r. (KBr) 1300 (NO_2 sym. stretch), 1525 (NO_2 asym. stretch), 1760 (C=O sym. stretch), and 1790 cm^{-1} (C=O asym. stretch).

5,6-Dinitroacenaphthene (4)

Compound **1** (90.5 g) was added slowly to 700 ml of nitric acid – acetic anhydride (2:5 v/v). The mixture was stirred for two h (28.0–68.5 °C) and then heated to 93.0 °C for 1 h, and then diluted with water and filtered. The resulting precipitate was recrystallized from glacial acetic acid and toluene, yielding 32 g of **4** (20%), reddish-brown needles, m.p. 213–214 °C; lit. m.p. 210–212 °C (11). Qualitative t.l.c. indicated only one compound; i.r. (KBr) 1325 (NO_2), 1515 (NO_2) cm^{-1}; n.m.r. (DMSO) δ 3.55 (4H, s, methylene H) and 6.75–7.63, (4H, AB pattern, aromatic H).

4,5-Dinitronaphthalic Anhydride (5)

To a vigorously stirred sample of 150 g of **1** in cold acetic acid (900 ml, 15 °C) was added 405 ml of nitric acid ($d = 1.5$) slowly in small portions such that the temperature did not rise above 20 °C. The yellow mixture was stirred for 1 h at 15–20 °C and heated to 80 °C for an additional 20 min. Nitric acid (2.5 l, $d = 1.42$) was then added and the mixture refluxed for 16–18 h, cooled, and filtered. The light yellow crystals obtained were washed with water until neutral and then dried. A 73.5 g sample (26%) of **5**, m.p. 324–326 °C, was obtained, lit. m.p. 323–324 °C (*2b*), i.r. (KBr) 1330 (NO_2), 1530 (NO_2), 1750 (C=O), and 1780 cm^{-1} (C=O).

4-Nitronaphthalic-1,8-dimethylester (6)

A 146 g sample of **3** was added to methanol (2.5 l) and 114 ml of dimethylsulfate. The mixture was refluxed, 91 g of potassium carbonate added, and refluxing continued overnight. The addition of water caused a tan precipitate to form and, following filtration, the solid was washed and dried to give 131.4 g of **6** (76%), m.p. 125–126 °C, i.r. (KBr) 1280 (C—O), 1345 (NO_2), 1525 (NO_2) and 1725 cm^{-1} (C=O); n.m.r., δ 3.85 (6H, s, methyl), 7.30–8.60 (5H, m, aromatic H).

Anal. Calcd. for $C_{14}H_{11}NO_6$ (289.26): C, 58.13; H, 3.84; N, 4.84. Found: C, 58.27; H, 3.76; N, 4.76.

4-Aminonaphthalic-1,8-dimethylester (6a)

A mixture of 131.4 g of **6**, benzene (1 l), and 6.5 g of Pd catalyst was placed in a 2 l high pressure apparatus which was sealed, flushed three times with 200 p.s.i. hydrogen, and then filled to 1100 p.s.i. hydrogen. Stirring and heating to 75 °C initiated the reaction which continued for 5 min. The maximum temperature reached was 110 °C, at which point the mixture was cooled to room temperature, excess hydrogen released, and the mixture was filtered to recover catalyst. The filtrate was stripped of benzene and the gum-like yellow–brown product dissolved in 600 ml of methanol. Concentrated hydrochloric acid (300 ml) was added and the precipitated white salt was filtered and washed twice with acetone. After drying, 94.2 g of the salt was obtained. This was dissolved in water and the solution made basic and exhaustively extracted with ether. The ether was partially evaporated in air, cooled in an acetone – Dry Ice bath, and filtered to give 64.9 g (55%) of **6***a*, m.p. 86–90 °C;

[4]Melting points were determined on a Thomas Hoover capillary melting point apparatus and elemental analyses, by Galbraith Laboratories, Inc., Knoxville, Tennessee. The u.v. spectra were determined on a Perkin–Elmer Model 202 ultraviolet-visible spectrophotometer. The n.m.r. spectra of all the compounds were run in deuterochloroform with TMS as an internal standard on a Varian T-60 n.m.r. spectrophotometer except where otherwise noted. The i.r. spectra were run on a Perkin–Elmer 521 i.r. spectrophotometer.

Can. J. Chem. Downloaded from www.nrcresearchpress.com by 210.87.254.105 on 09/05/12
For personal use only.

i.r. (Nujol) 1250 (C—O), 1725 (C=O), and 3340 cm^{-1} (NH_2); n.m.r. δ 3.80 (6H, s, methyl H), 4.38 (2H, s, amine H), 6.50–7.90 (5H, m, aromatic H).

Anal. Calcd. for $C_{14}H_{13}NO_4$ (259.28): C, 64.84; H, 5.06; N, 5.40. Found: C, 64.90; H, 5.03; N, 5.35.

4-Nitronaphthalic-1,8-diethyl Ester (7)

Compound **3** (24.4 g), 500 ml of ethanol, 13.4 ml of diethyl sulfate, were refluxed, and potassium carbonate (7.6 g) added. Refluxing was continued for 2 h and then an additional 13.4 ml of diethyl sulfate and 7.6 g of potassium carbonate was added and refluxing continued for an additional 3 h after which the hot mixture was filtered. The filtrate was diluted with water and the precipitate was filtered, washed, and dried to give 21.8 g (69%) of yellow–green crystals, m.p. 83.0 °C; i.r. (KBr) 1275 (C—O), 1335 (NO_2), 1530 (NO_2), and 1715 cm^{-1} (C=O); n.m.r., δ 1.50 (6H, t, methyl H), 4.50 (4H, q, methylene H), 7.58–8.56 (5H, m, aromatic H).

Anal. Calcd. for $C_{16}H_{15}NO_6$ (317.30): C, 60.56; H, 4.77; N, 4.42. Found: C, 60.41; H, 4.66; N, 4.54.

4-Aminonaphthalic-1,8-diethyl Ester (7a)

A mixture of 100 g of **7**, benzene (1 l), and 5 g of Pd catalyst was placed in a prepared high pressure apparatus (*vide ante*). The mixture was stirred constantly and heated at 125 °C for 1 h, cooled to room temperature, and treated as previously described. The filtrate, stripped of benzene, produced a brown gummy substance which dissolved in 700 ml carbon tetrachloride and resulted in the formation of a yellow precipitate when cooled to 0 °C. Filtration yielded 72 g (80%) of yellow crystals, m.p. 127–130 °C. Recrystallization from EtOH–H_2O (1:1) yielded 64.8 g (72%) of **7a**, m.p. 132–132.5 °C; i.r. (Nujol) 1260 (C—O), 1740 (C=O), and 3380 cm^{-1} (NH_2); n.m.r. δ 1.38 (6H, t, methyl H), 4.38 (4H, q, methylene H), 4.60 (2H, s, amine H), 7.20–8.08 (5H, m, aromatic H).

Anal. Calcd. for $C_{16}H_{17}NO_4$ (287.34): C, 66.85; H, 5.96; N, 4.87. Found: C, 66.72; H, 5.96; N, 4.84.

4,5-Dinitronaphthalic-1,8-dimethyl Ester (8)

Methanol (3 l) containing 172.4 g of **5**, and dimethyl sulfate (114 ml) were refluxed and 91.2 g of potassium carbonate was added. After refluxing for 2 h, 22.8 g of potassium carbonate and 28.5 ml of dimethyl sulfate was added and the mixture refluxed for an additional 3 h and filtered while hot. The precipitate was washed once with methanol and 3 times with water and dried, yielding 180 g (90%), m.p. 247–249 °C; lit. m.p. 236–240 °C (2*b*); i.r. (KBr) 1270 (C—O), 1340 (NO_2), 1540 (NO_2), and 1715 cm^{-1} (C=O); n.m.r. δ 3.99 (6H, s, methyl), 8.28 (4H, AB pattern, aromatic H).

Anal. Calcd. for $C_{14}H_{10}N_2O_8$ (334.26): C, 50.30; H, 3.02; N, 8.38. Found: C, 50.20; H, 3.11; N, 8.33.

4,5-Diaminonaphthalic-1,8-dimethyl Ester (8a)

A mixture of 100 g of **8**, benzene (1 l), and 10 g of Pd catalyst was placed in a high pressure reaction apparatus and reduced as previously described. The reaction proceeded for 15 min at 75 °C. After cooling, the mixture was filtered and the dark green precipitate boiled in methanol, filtered hot, and the filtrate cooled to −4 °C. Filtration gave 45.5 g (55%) of light yellow – green crystals of 4,5-diaminonaphthalic-1,8-dimethyl ester (**8a**) m.p. 213.5–215.0 °C; i.r. (Nujol) 1250 (C—O), 1680 (C=O), 3370 (NH_2), and 3400 cm^{-1} (NH_2); n.m.r. (on a HA-100, in DMSO-d_6): δ 3.68 (6H, s, methyl H), 6.38 (4H, s, amine H), 7.15 (4H, AB pattern, aromatic H).

Anal. Calcd. for $C_{14}H_{14}N_2O_4$ (274.30): C, 61.30; H, 5.15; N, 10.22. Found: C, 61.42; H, 4.97; N, 10.09.

4,5-Dinitronaphthalic-1,8-diethyl Ester (9)

Ethanol (250 ml), 17.3 g of **5**, and diethyl sulfate (9 ml) were refluxed and 5.25 g of potassium carbonate added and refluxed for 2 h. An additional 5.25 g of potassium carbonate and 9 ml of diethyl sulfate was added after a 2 h reflux, refluxing continued for an additional **3** h and filtered while hot. The light tan crystalline precipitate was washed several times with water and dried, yielding 11 g (50.7%) of 4,5-dinitronaphthalic-1,8-diethyl ester (**9**) m.p. 155–157 °C, lit. m.p. 156.5–157 °C (2*b*); i.r. (KBr) 1260 (C—O), 1350 (NO_2), 1545 (NO_2) and 1725 cm^{-1} (C=O); n.m.r. δ 2.48 (6H, t, methyl H), 4.42 (4H, q, methylene H), 8.28 (4H, AB pattern, aromatic H).

Anal. Calcd. for $C_{16}H_{14}N_2O_8$ (362.32): C, 53.04; H, 3.90; N, 7.73. Found: C, 52.96; H, 3.91; N, 7.56.

4,5-Diaminonaphthalic-1,8-diethyl Ester (9a)

A mixture of 50 g of **9**, 500 ml of benzene, and 5 g of Pd catalyst was reduced as previously described at 100 °C overnight. After filtering the mixture, the precipitate was dissolved in 700 ml of boiling ethanol and filtered for catalyst removal. Upon cooling, brown crystals were obtained which were dried to yield 15.9 g (39%), m.p. 166–167 °C, lit. m.p. 167.0–167.5 °C (2*b*); i.r. (Nujol), 1240 (C—O), 1690 (C=O), 3380 cm^{-1} (NH_2); n.m.r. δ 1.36 (6H, t, methyl H), 4.30 (4H, q, methylene H), 4.83 (4H, s, amine H), 7.10 (4H, AB pattern, aromatic H).

1. (*a*) F. Anselm and F. Zuckmayer. Ber. **32**, 3283 (1899). (*b*) C. Graebe. Ann. **327**, 84 (1903). (*c*) M. Okazaki and N. Ishikawa. Yûki Gôsei Kagaku Kyôkai Shi, **14**, 398 (1956).
2. (*a*) F. Sachs and G. Mosebach. Ber. **44**, 2852 (1911). (*b*) I. Honda and M. Okazaki. J. Soc. Org. Syn. Chem. Japan, **7**, 25 (1950). (*c*) M. Okazaki, T. Tanaka, and S. Taniguchi. Yûki Gôsei Kagaku Kyôkai Shi, **14**, 344 (1956). (*d*) M. M. Dashevski. Zhur. Priklad Khim. **32**, 2749 (1959).
3. T. Ishii and Y. Yamazaki. Mem. Fac. Technol. Tokyo Metropol. Univ. **1**, 21 (1951).
4. (*a*) J. R. Lacher, K. Ensley, and A. Tenge. J. Org. Chem. **24**, 1347 (1959). (*b*) M. Okazaki, Y. Suhara, and M. Fujiyama. Yûki Gôsei Kagaku Kyôkai Shi, **14**, 394 (1956).
5. M. Okazaki and I. Ishikawa. Yûki Gôsei Kagaku Kyôkai Shi, **14**, 398 (1956).
6. G. T. Morgan and H. A. Harrison. J. Soc. Chem. Ind. 413T (1930).
7. (*a*) S. Kato, H. Hashimoto, and H. Sugiyama. Yûki Gôsei Kagaku Kyôkai Shi, **14**, 723 (1956). (*b*) L. Friedman, D. L. Fishel, and H. Schecter. J. Org. Chem. **30**, 1453 (1965).
8. R. H. Cornforth, J. W. Cornforth, and G. Popják. Tetrahedron, **18**, 1351 (1962).
9. E. M. Bickoff, R. L. Lyman, A. L. Livingston, and A. N. Booth. J. Amer. Chem. Soc. **80**, 3969 (1958).
10. R. Adams and F. L. Cohen. Org. Syn. Coll. Vol. **1**, 240 (1944).
11. M. P. Cava, K. E. Merkel, and R. H. Schlessinger. Tetrahedron, **21**, 3059 (1965).
12. H. J. Richter. J. Org. Chem. **21**, 619 (1956).

Can. J. Chem. Downloaded from www.nrcresearchpress.com by 210.87.254.40 on 09/05/12
For personal use only.

Cyanoethylations and Michael additions. IV.[1] The synthesis of allylic cyclohexenols by γ-cyanoethylation of α,β-unsaturated aldehydes and ketones. Part IV[2,3]

CH. R. ENGEL AND L. RUEST
Department of Chemistry, Laval University, Quebec, Quebec

Received April 24, 1970

The cyclo-γ-cyanoethylation of 3β-acetoxy-D-homo-5α-pregn-17*a*-en-21-al is reported. It is shown that the orientation of the cyanoethylation of 2-cycloalkyl-substituted ethenals does not significantly depend on the ring size of the cycloalkyl substituent. It is further shown that the stereochemistry of the cyclohexadienonitrile obtained by dehydration of the main reaction products seems to be, in the case of a fusion to a six-membered ring, in agreement with Moscowitz' rule relating the helicity of the chromophore to the sign of its Cotton effect, in contradistinction to the situation in the case of a system in which one of the double bonds of the chromophore is exocyclic to a five-membered ring.

Canadian Journal of Chemistry, **48**, 3136 (1970)

In previous publications of this series (3, 4, *cf.* also 5) we reported the first cyclo-γ-cyanoethylation of an α,β-unsaturated carbonyl system which led in high yield, in a single operation, to allylic α′-cyano hexenols. Evidently, such a reaction would present synthetic interest if its generality could be established, if, in particular, one could foresee when to expect α-substituted products, and when to expect cyclized γ-addition products. Indeed, in practically all previous examples of Michael-type additions, in which the carbanion is derived from an α,β-unsaturated polar system (such as an α,β-unsaturated carbonyl compound), addition occurs in the α-position (*cf.* 3, 4). It has now been suggested to us[4] that the orientation of such additions may be related to the difference in stability of five- and six-membered rings with endocyclic, respectively exocyclic unsaturations (6, *cf.* also 7–10).

In order to investigate such a hypothesis and also to contribute to the determination of the degree of generality of the cyclo-γ-cyanoethylation, we studied the cyanoethylation of 3β-acetoxy-D-homo-5α-pregn-17*a*-en-21-al (**5**), the D-homo analog of the first aldehyde which had been subjected to such a reaction.[5]

Aldehyde **5** was synthesized from 3β-acetoxy-D-homo-5α-androstan-17*a*-one (**2**)[6] exactly like the lower homolog of the normal steroid series (3, 4). Ethoxyacetylenation of ketone **2** led, after reacetylation, to the 17α- and 17β-ethoxyacetylene derivatives **3**A and B which were reduced to the epimeric ethoxyethylene derivatives **6**A and B, both of which were readily rearranged to aldehyde **5**, the total yield of the sequence of reactions amounting to 75%.[7]

Cyanoethylation in benzene with a sodium

---

[1]For paper III of this series *cf.* ref. 1.

[2]This publication represents part XXXIII in the series on Steroids and Related Products. For paper XXXII see ref. 1.

[3]Abbreviated from the doctoral thesis of L. Ruest, submitted to the School of Graduate Studies of Laval University, Quebec, Quebec in 1969 and from the "thèse de doctorat d'Etat ès sciences", University of Paris, Paris, France, registered at the C.N.R.S. under the number A.O. 1987. For a preliminary report see ref. 2.

[4]We thank Prof. V. Prelog, Zurich, and Prof. H. Favre, Montreal, for interesting discussions in which they drew such a consideration to our attention.

[5]The choice of aldehyde **5** was motivated by the desire to arrive at valid conclusions concerning the inference of the ring size of the ethenal substituent on the orientation of the reaction. We also studied the reaction of *trans*-decal-1-yledenethanal with acrylonitrile which leads predominantly to cyclized γ-cyanoethylation products (2, 11).

[6]The D-homo ketone **2** (12) was prepared in a classical fashion from 3β-acetoxy-5α-androstan-17-one (**1**), which was transformed with potassium cyanide, under the reaction conditions used by Allinger and Greenberg (13), to a mixture of the 17-epimeric 17-cyanohydrins (13), which was reduced with platinum and hydrogen to a mixture of the corresponding 17-aminomethyl 17-alcohols (13, 14). Tieffeneau rearrangement (15, *cf.* also 14) led to the desired ketone **2** and its 17-oxo isomer (14), which were separated by chromatography on alumina.

[7]The isomeric ethoxyacetylene derivatives **3**A and B could be separated by chromatography on alumina. Their respective stereochemistry in position 17a was determined by n.m.r. spectroscopy, the 18-methyl group of the isomer with a β-configuration of the ethoxyacetylene substituent being strongly deshielded. The stereochemistry of the ethoxyvinyl derivatives **6**A and B was also deduced by n.m.r. analysis, the olefinic 20-proton of the derivative with a β-configuration of the ethoxyvinyl group appearing 29 Hz up-field from the signal of the olefinic proton of its epimer.

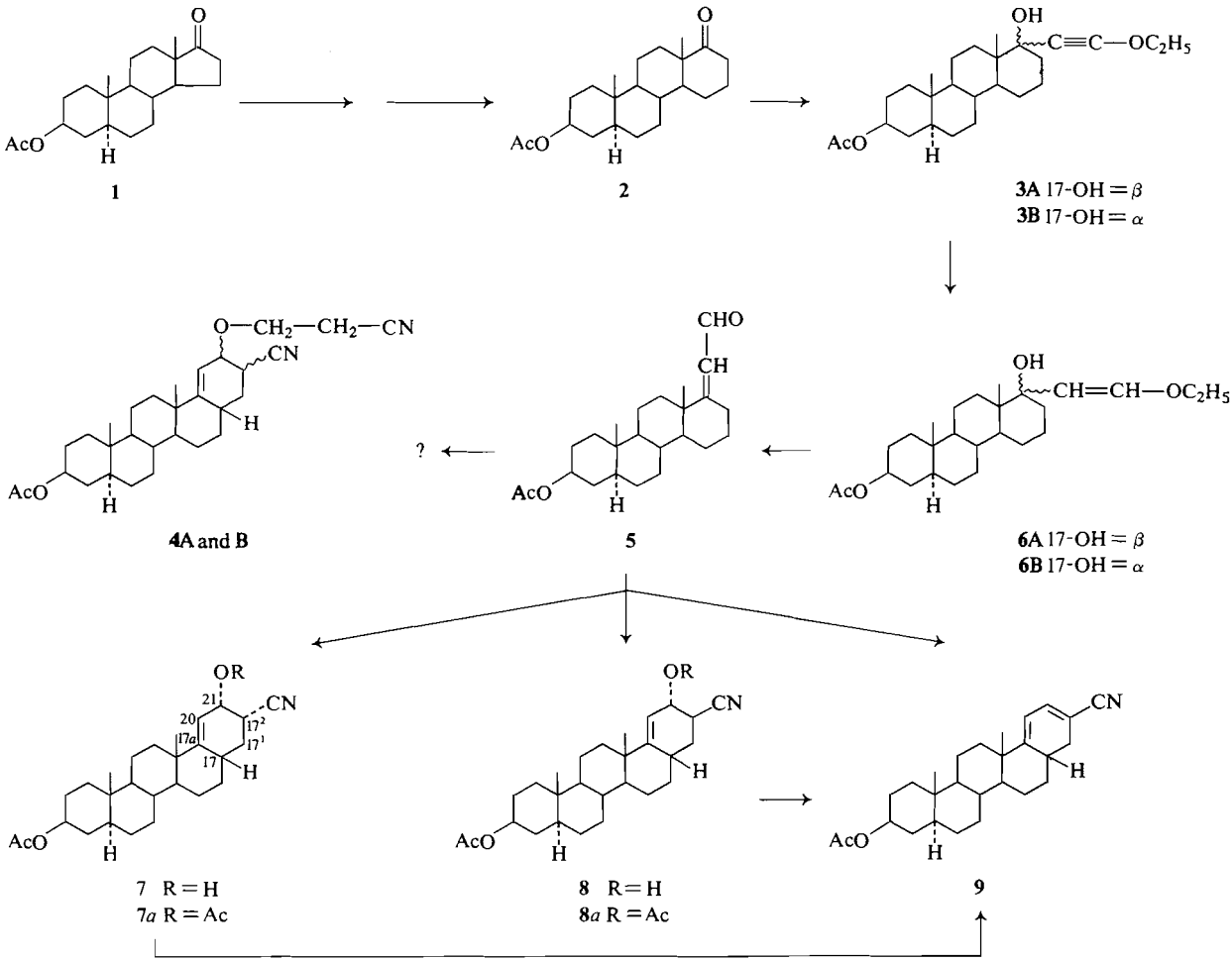

amylate catalyst under conditions identical to those used for the reaction of the lower homolog (4), led to a mixture from which 15% of the starting material was recovered and which consisted mostly of cyclized γ-cyanoethylation products. The two epimeric cyano alcohols **7** and **8** were isolated in 55% yield, in a proportion of 4:3, the dienonitrile **9** in 18% yield.[8] We also obtained in 6% yield a mixture of nitriles to which we tentatively assign the structures of isomeric dicyanoethylated products, arising from an additional oxygen-cyanoethylation (cf. **4**A and B). The proofs of structure of the various products follow those reported in the case of the cyanoethylation of the lower homologs of the normal steroid series (4). The elemental analyses of the main cyanoethylation products **7**, **8**, and **9** correspond to a mono-addition of acrylonitrile. The spectra of the acetoxy hydroxy nitriles **7** and **8** reveal an acetoxy group, a hydroxy group, a non-conjugated nitrile function, and a trisubstituted double bond. In the n.m.r. spectra one sees the couplings of the olefinic 20-proton of the alcohols **7** and **8** with the 21-proton and the allylic 17-proton; the chemical shift of the 21-proton is indicative of its vicinity to the double bond.[9] These data are compatible with structures **7** and **8** but not with structures of products arising from an α-cyanoethylation, followed by a cyclization.[10]

[8]These yields take into account the recovery of starting material.

[9]For details see Experimental.

[10]The i.r. absorptions of the isolated double bonds of compounds **7** and **8** [ν_{max} ($CHCl_3$) 1642 cm^{-1}] correspond well to those of cyclohexenes, the double bonds of which are exocyclic to another six-membered ring and differ therefore from those of the homologous products of the normal steroid series in which the double bond is exocyclic to a five-membered ring (4).

Can. J. Chem. Downloaded from www.nrcresearchpress.com by 210.87.254.40 on 09/05/12
For personal use only.

Can. J. Chem. Downloaded from www.nrcresearchpress.com by 210.87.254.40 on 09/05/12
For personal use only.

In the case of alcohol **8**, the structure was confirmed by oxidation with Jones' reagent (16) to the α,β-unsaturated ketone **10** whose spectral characteristics (*cf.* Experimental) are in perfect agreement with those expected for a conjugated cyclohexenone substituted in position α′ by a nitrile function, and which are not compatible with those of a four-membered ring ketone (*cf.* 4).[11, 12]

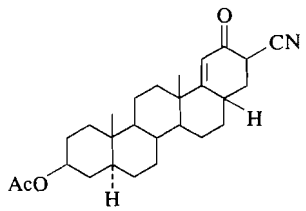

10

Both the elemental composition of dienonitrile **9** and its spectral characteristics are compatible only with the suggested structure. We refer to the Experimental for the description of the spectra, and for their interpretation to the discussion of the absolutely analogous spectra of the lower homologs of dienonitrile **9**.

In order to correlate dienonitrile **9** to the hydroxy nitriles **7** and **8**, we treated the diacetates **7***a* and **8***a* with sodium methoxide in methanol; after reacetylation, the acetoxy dienonitrile **9** was obtained in both instances, in 75% yield in the case of diacetate **7***a*, in 40% yield in the case of diacetate **8***a*.

The minor reaction products **4**A and B were unstable. Therefore no analytical results are available. The structures tentatively suggested and which correspond to analogous products identified in the case of the cyanoethylation of *trans*-decal-1-ylidenethanal (11), were based on the interpretation of their spectral characteristics. Their i.r. spectra (taken in KBr) show the usual acetate absorption and that of an isolated double bond, as well as a non-conjugated nitrile band, the intensity of which would correspond to two nitrile functions. There also appear at 1130 and 1100 cm^{-1} peaks which can be attributed to the ether function. In the n.m.r., the olefinic proton in position 20 appears as a large triplet (J = 6.0 Hz), centered at 5.28 δ, with a half-band width of 2–3 Hz; this corresponds well to the coupling of this proton with the protons in positions 17 and 21. At 3.63 and 2.75 δ appear two triplets (J = 6.5 Hz), each corresponding to two protons, which we assign to the two methylene groups of the ether function. This assignment corresponds to values from the literature (17). The formation of such nitriles can readily be rationalized by the assumption of an additional oxygen-cyanoethylation.

[11]The position of the i.r. absorption band of the double bond corresponds again to that of a conjugated cyclohexenone, the double bond of which is exocyclic to a six-membered ring and thus differs from that of the lower homolog (4) in which this double bond is exocyclic to a five-membered ring.

[12]In accord with structure **10**, the olefinic proton appears in the n.m.r. as a doublet centered at 6.02 δ (J = 2.5 Hz), which confirms that this proton is solely coupled with the only allylic proton of position 17.

Stereochemistry

In this study, the determination of the stereochemistry of the various products was not our prime concern. However, the available spectral data, combined with the consideration of certain chemical results, allow, in our opinion, dependable stereochemical assignments.

The formation of only one dienonitrile (**9**) in the dehydroacetylation of both diacetoxy nitriles **7***a* and **8***a*, seems to indicate the identity of configuration in position 17 of the three main reaction products, if one may extrapolate the findings from the normal steroid series, for which it has been established that under the reaction conditions no isomerization occurs during dehydroacetylation (4). In the preceding communication of this series (1), we have put forward indirect evidence for a 16β-hydrogen configuration of the main cyclo-γ-cyanoethylation products of the lower homolog of aldehyde **5**. In another paper (4), we have established the configuration of these products on the grounds of an n.m.r. analysis, principally by showing that in the hydroxy nitriles analogous to structures **7** and **8** and in their derivatives the 18-methyl group is deshielded when the nitrile function is axial and *cis* to the angular hydrogen at the D/E ring junction (in position 16 in the normal steroid series, which corresponds to position 17 in the D-homo series). In the case of the hydroxy nitriles **7** and **8** and of their acetates **7***a* and **8***a* of the D-homo series we observe again that the isomers **8** and **8***a*, in which the nitrile functions are axial and *cis* to the 17-hydrogen (see below), the 18-methyl group is more deshielded than in the case of their epimers **7** and **7***a* in which the nitrile group is equatorial and *trans* to the 17-hydrogen.

Can. J. Chem. Downloaded from www.nrcresearchpress.com by 210.87.254.40 on 09/05/12
For personal use only.

This again can be rationalized by the assumption of a *cis*-relationship of the nitrile group of compounds **8** and **8***a* and the 18-methyl group, which implies a *cis*-relationship of the 17-hydrogen and the 18-methyl group and thus a 17β-hydrogen configuration.

Furthermore, the spin coupling of the olefinic 20-proton of dienonitrile **9** with the proton in position 17 is indicative of an axial conformation of the latter, which is possible only if it is β, provided that ring D has the preferred chair conformation. The assignment of a 17β-hydrogen configuration is in perfect agreement with Moscowitz' rule (18) relating the helicity of a conjugated homodiene to the sign of its Cotton effect, since the observed Cotton effect of dienonitrile **9** is strongly positive, which should indicate a right-handed helicity and therefore a 17β-hydrogen configuration. This is noteworthy because the assigned 16β-hydrogen configuration of the lower homolog of dienonitrile **9** (14) and of the dienonitrile obtained by cyclo-γ-cyanoethylation of a parent methyl ketone (2, 19) is in opposition to Moscowitz' rule. One might tentatively take into consideration that the exceptions to Moscowitz' rule are in relation to the fact that in the dienes in question one of the conjugated double bonds is exocyclic to a 5-membered ring. The fact that the polar nitrile group is not responsible for this exception is demonstrated by the "normal" Cotton effect of dienonitrile **9**.[13]

The facile dehydroacetylation of the diacetoxy nitrile **7***a* suggests a *trans*-diaxial arrangement of the 21-oxygen function and the 17^2-hydrogen. The relative difficulty in dehydroacetylating diacetate **8***a* could suggest a *cis*-arrangement of the corresponding groups, if the situation were analogous to that in the normal steroid series (4). This is borne out by the n.m.r. spectra. The 21-proton of alcohols **7** and **8** appears as a multiplet centered at 4.33 δ with a half-band width of 6.0 Hz. In the case of the diacetoxy derivative **7***a* this proton appears as a multiplet of the same nature centered at 5.37 δ, and in the case of the diacetate **8***a* as a multiplet centered at 5.36 δ. According to Bhacca and Williams (21), this indicates an equatorial or quasi-equatorial conformation of this proton; this, in turn, corresponds to a β-configuration of this proton if ring E exists in the thermodynamically favorable half-chair conformation. The olefinic 20-proton of the hydroxy nitrile **7** appears as a doublet of doublets at 5.65 δ with coupling constants of 4.5 and 2.0 Hz, the latter arising from the allylic coupling with the 17-proton. The coupling constant of 4.5 Hz thus arises from the coupling with the proton in position 21 and this coupling constant should correspond to a dihedral angle of approximately 40°. Such an angle is possible only in the case of a half-chair conformation of ring E and an equatorial conformation of the 21-proton which must therefore be β. The situation is analogous in the case of alcohol **8** where the 20-proton appears as a doublet of doublets at 5.63 δ with coupling constants of 5.0 and 2.0 Hz. The alcohols **7** and **8** and their derivatives must therefore be epimeric in position 17^2. Now, the 17^2-proton of alcohol **7** appears as a doublet of triplets centered at 2.72 δ with coupling constants of 12.5 and 3.5 Hz; the larger coupling constant must correspond to diaxial coupling (with the axial 17^1-proton), thus the proton in position 17^2 must be axial, the nitrile group equatorial. The data from the spectrum of the diacetate **7***a* (*cf.* Experimental) are fully confirmatory. By exclusion, it follows that the conformation of the nitrile function of alcohol **8***a* must be axial, its configuration β. This is confirmed by the fact that the 17^2-proton of alcohol **8** and of its acetate **8***a* is more shielded (by 0.18 p.p.m.) than the corresponding proton of alcohol **7** and of the acetoxy derivative **7***a*. Furthermore, the 17^2-proton of compounds **8** and **8***a* shows no vicinal diaxial coupling. The *cis*-relationship between the axial nitrile group of alcohol **8** and acetate **8***a* with the 18-methyl group, apparent from the deshielding effect of this substituent on the methyl signal, has already been pointed out; similarly, the axial 17β-proton of

[13]The non-determining role of the polar group conjugated with the diene moiety became already probable on the basis of the reduction of the dienone **i** [obtained either by a Diels–Alder addition of methyl vinyl ketone to the lower homolog of aldehyde **5** (1) or by the action of methyllithium on the lower homolog of dienonitrile **9** (20)] to the corresponding hydroxy diene, which still exhibits an "abnormal" Cotton effect.

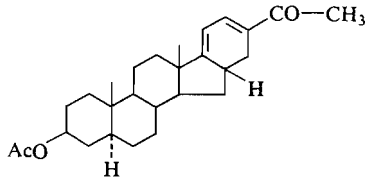

i

Can. J. Chem. Downloaded from www.nrcresearchpress.com by 210.87.254.40 on 09/05/12
For personal use only.

compounds **8** and **8***a* is more deshielded than the 17β-proton of the isomers **7** and **7***a*.

The 17^2-proton of ketone **10** appears as a triplet, centered at 3.37 δ, with a coupling constant of 3.5 Hz which cannot arise from a diaxial coupling; therefore, this proton must be equatorial, the nitrile function axial; this in turn indicates a β-configuration of this nitrile substituent if ring E has a half-chair conformation, an assumption in agreement with the positive Cotton effect in the region corresponding to the $n \rightarrow \pi^*$ transition (22).

The stereochemically most significant finding seems the congruency of the n.m.r. data with the determination of configuration in position 17 on the basis of Moscowitz' rule, applied to dienonitrile **9**.

In summary, we have shown that the previously observed cyclo-γ-cyanoethylation of 3β-acetoxy-5α-pregn-17-en-21-al (3, 4) was not an isolated case, that the reaction proceeded in excellent yields also in the case of the D-homo analog **5**, and that the size of the ring to which the ethenal moiety is attached seems to play no decisive role in orientating the addition to the γ-position. Together with the experiments in the normal steroid series and with those in the decaline series (2, 11), the present investigation contributes to establish sufficient generality for the cyclo-γ-cyanoethylation of α,β-unsaturated aldehydes of type **5** to permit the hope that it might become useful for the synthesis of polyfunctional polycyclic systems.

Experimental[14]

3β-Acetoxy-D-homo-5α-androstan-17a-one (2) and 3β-Acetoxy-D-homo-5α-androstan-17-one

According to the method of Allinger and Greenberg (13), 25 g of 3β-acetoxy-5α-androstan-17-one (**1**), m.p. 116–117°, was treated with 150 g of potassium cyanide and 160 ml of acetic acid in 835 ml of methanol. The crude reaction product (26.81 g) was dissolved in 675 ml of acetic acid and hydrogenated at atmospheric pressure over 6 g of platinum oxide, 4.2 l of hydrogen being absorbed. The product was filtered, the filtrate reduced *in vacuo* to 50 ml and diluted with 600 ml of ice water. To the stirred mixture, 11.5 g of sodium nitrite in 100 ml of water was added dropwise, in the cold. After 2 h at 0°, the mixture was kept 15 h at room temperature and precipitated in water. The usual work-up gave 26.38 g of a partly crystalline residue which was chromatographed on 700 g of aluminum oxide. Elutions with petroleum ether – benzene (4:1) gave 13.92 g (55%) of *3β-acetoxy-D-homo-5α-androstan-17a-one (2)*, m.p. 122–123°. A sample was recrystallized three times from ether–hexane for analysis; m.p. 124.5–125°; $[\alpha]_D^{25}$ −45.0° (*c*, 1.00 in $CHCl_3$) [lit. (12*a*): m.p. 124–125°; $[\alpha]_D$ −45° (CH_3OH)]; ν_{max} (KBr) 1740 (acetate), 1700 (ketone), 1240 cm^{-1} (acetate); n.m.r.: δ ($CDCl_3$) 0.84 (s) (19-CH_3), 1.08 (s) (18-CH_3), 2.00 (s) (CH_3COO), 2.28 (m) (17-CH_2), 4.70 (m) (3α-H).

Anal. Calcd. for $C_{22}H_{34}O_3$: C, 76.26; H, 9.89. Found: C, 76.32; H, 9.95.

Elutions with petroleum ether – benzene (1:1) gave 5.63 g (23%) of *3β-acetoxy-D-homo-5α-androstan-17-one*, m.p. 104–107°. For analysis, a sample was recrystallized four times from ether–hexane; m.p. 111.5–112°; $[\alpha]_D^{25}$ −4.5° (*c*, 1.00 in $CHCl_3$) [lit. (12*b*): m.p. 102–104°; $[\alpha]_D$ −3.7° (dioxane)]; ν_{max} (KBr) 1745 (acetate), 1715 (ketone), 1255 cm^{-1} (acetate); n.m.r.: δ ($CDCl_3$) 0.78 (s) and 0.82 (s) (18- and 19-CH_3), 2.00 (s) (CH_3COO), 2.05–2.28 (m) (16- and 17*a*-CH_2), 4.70 (m) (3α-H).

Anal. Calcd. for $C_{22}H_{34}O_3$: C, 76.26; H, 9.89. Found: C, 76.03; H, 9.93.

3β-Acetoxy-17aβ-hydroxy-17aα-ethoxyethynyl-D-homo-5α-androstane (3A) and 3β-Acetoxy-17aα-hydroxy-17aβ-ethoxyethynyl-D-homo-5α-androstane (3B)

To a Grignard solution prepared from 10.3 g of magnesium, 39 ml of ethyl bromide, and 375 ml of absolute ether, a solution of 32 g of ethoxyacetylene in 240 ml of absolute ether was added in the course of 30 min. The mixture was refluxed for 1.5 h and subsequently there was added, at room temperature, 11.87 g of 3β-acetoxy-D-homo-5α-androstan-17a-one (**2**) in 210 ml of absolute ether, in the course of 30 min. The mixture was refluxed for 1 h and worked-up in the usual fashion (4). The reaction product was dissolved in 60 ml of pyridine and 24 ml of acetic anhydride was added. After 15 h at room temperature the product was worked-up, as usual. The product (17.6 g) was chromatographed on 450 g of aluminum oxide. Petroleum ether – benzene (9:1 and 4:1) eluted 7.34 g (51%) of *3β-acetoxy-17aβ-hydroxy-17aα-ethoxyethynyl-D-homo-5α-androstane (3A)*, m.p. 117–119°. A sample was recrystallized three times from ether–hexane for analysis; m.p. 124–125°; $[\alpha]_D^{25}$ −25.0° (*c*, 1.00 in $CHCl_3$); ν_{max} (KBr) 3540 (hydroxyl), 2250 (triple bond), 1730 and 1246 (acetate), 1125 (ether), 1038 cm^{-1} (acetate and alcohol); n.m.r.: δ ($CDCl_3$) 0.80 (s) (19-CH_3), 0.88 (s) (18-CH_3), 1.39 (t, J = 7.0 Hz) (O—CH_2—CH_3), 1.95 (s) (exchanged with D_2O) (17*a*β-OH), 2.00 (s) (CH_3COO), 4.12 (q, J = 7.0 Hz) (O-CH_2-CH_3), 4.70 (m) (3α-H).

[14]The melting points were taken in evacuated capillaries and the temperatures were corrected. For column chromatography, neutral aluminum oxide Woelm, activity III, and Davison's silica gel 923 were employed. The t.l.c. was performed with Merck–Darmstadt silica gel. The i.r. spectra were recorded on a Beckman IR-4 spectrophotometer and the u.v. spectra on a Beckman DK-1A instrument. The n.m.r. spectra were recorded on a Varian A-60 spectrometer, tetramethylsilane serving as internal standard and deuteriochloroform as solvent. The rotatory dispersion curves were registered on a Jasco ORD/UV 5 spectropolarimeter, the mass spectra were taken on a Varian M-66 mass spectrometer. The microanalyses were performed by the late Mr. A. Bernhardt, Max Planck Institute for Coal Research, Mülheim, Germany, and by Dr. F. Pascher, Bonn, Germany, to whom we are much indebted.

Can. J. Chem. Downloaded from www.nrcresearchpress.com by 210.87.254.40 on 09/05/12
For personal use only.

Anal. Calcd. for $C_{26}H_{40}O_4$: C, 74.96; H, 9.68. Found: C, 75.05; H, 9.79.

Petroleum ether – benzene (1:1) and pure benzene eluted 4.71 g (33%) of *3β-acetoxy-17aα-hydroxy-17aβ-ethoxyethynyl-D-homo-5α-androstane (3B)*, m.p. 142–143°. A sample was recrystallized twice from ether–hexane for analysis; m.p. 143–144°; $[\alpha]_D^{25}$ +23.0° (*c*, 1.00 in $CHCl_3$); ν_{max} (KBr) 3505 (hydroxyl), 2245 (triple bond), 1723 and 1260 (acetate), 1130 (ether), 1028 cm^{-1} (acetate and alcohol); n.m.r.: δ ($CDCl_3$) 0.78 (s) (19-CH_3), 0.94 (s) (18-CH_3), 1.32 (t, J = 7.0 Hz) (O—CH_2—CH_3), 1.98 (s) (exchanged with D_2O) (17*a*α-OH), 1.98 (s) (CH_3COO), 4.03 (q, J = 7.0 Hz) (O—CH_2—CH_3), 4.70 (m) (3α-H).

Anal. Calcd. for $C_{26}H_{40}O_4$: C, 74.96; H, 9.68. Found: C, 74.94; H, 9.73.

3β-Acetoxy-17aβ-hydroxy-17aα-ethoxyvinyl-D-homo-5α-androstane (6A)

A quantity of 5.39 g of 3β-acetoxy-17*a*β-hydroxy-17*a*α-ethoxyethynyl-D-homo-5α-androstane (**3A**), m.p. 122–124°, was hydrogenated in 130 ml of pyridine with 1.82 g of a 2.5% palladium – on – calcium carbonate catalyst, 325 ml of hydrogen being absorbed in 10 min. The usual work-up gave 5.49 g of the vinyl derivative **6A**, m.p. 138–140°. For analysis, a sample was recrystallized twice from ether–hexane; m.p. 142–143°, $[\alpha]_D^{25}$ −36° (*c*, 1.00 in $CHCl_3$); ν_{max} (KBr) 3600 (hydroxyl), 1740 (acetate), 1655 (double bond), 1250 (acetate), 1122 and 1115 (ether), 1037 cm^{-1} (acetate and alcohol); n.m.r.: δ ($CDCl_3$) 0.81 (s) (19-CH_3), 0.95 (s) (18-CH_3), 1.26 (t, J = 7.0 Hz) (O—CH_2—CH_3), 1.99 (s) (CH_3COO) 3.83 (q, J = 7.0 Hz) (O—CH_2—CH_3), 4.18 (s) (17*a*β-OH), 4.63 (m) (3α-H), 4.87 (d) and 6.01 (d) (AB system, J = 7.0 Hz) (20-H and 21-H).

Anal. Calcd. for $C_{26}H_{42}O_4$: C, 74.60; H, 10.11. Found: C, 74.58; H, 10.13.

3β-Acetoxy-17aα-hydroxy-17aβ-ethoxyvinyl-D-homo-5α-androstane (6B)

A quantity of 4.56 g of 3β-acetoxy-17*a*α-hydroxy-17*a*β-ethoxyethynyl-D-homo-5α-androstane (**3B**), m.p. 142–143°, was hydrogenated with 1.54 g of a 2.5% palladium – on – calcium carbonate catalyst in 110 ml of pyridine at atmospheric pressure. The crystalline reaction product (4.57 g) melted at 122–126°. Three recrystallizations from ether–hexane gave an analytical sample, m.p. 146–147°; $[\alpha]_D^{25}$ −29° (*c*, 1.00 in $CHCl_3$); ν_{max} (KBr) 3550 (hydroxyl), 1739 (acetate), 1659 (double bond), 1246 (acetate), 1108 (ether), 1025 cm^{-1} (acetate and alcohol); n.m.r.: δ ($CDCl_3$) 0.78 (s) (19-CH_3), 0.82 (s) (18-CH_3), 1.24 (t, J = 7.0 Hz) (O—CH_2—CH_3), 4.13 (s) (17*a*α-OH), 4.40 (d) and 5.95 (d) (AB system, J = 7.0 Hz) (20-H and 21-H).

Anal. Calcd. for $C_{26}H_{42}O_4$: C, 74.60; H, 10.11. Found: C, 74.59; H, 10.21.

3β-Acetoxy-D-homo-5α-pregn-17a-en-21-al (5)

(a) From 3β-Acetoxy-17aβ-hydroxy-17aα-ethoxyvinyl-D-homo-5α-androstane (6A)

To a solution of 7.2 g of 3β-acetoxy-17*a*β-hydroxy-17*a*α-ethoxyvinyl-D-homo-5α-androstane (**6A**), m.p. 138–140°, in 160 ml of dioxane, 50 ml of 2 *N* hydrochloric acid was added and the mixture was stirred for 30 min at room temperature. The crystalline reaction product was filtered, washed with water, and dried. Thus, 5.36 g of aldehyde **5**, m.p. 172–174°, was obtained. A sample was recrystallized twice from ether–hexane for analysis; m.p. 175–176°; $[\alpha]_D^{25}$ −99.5° (*c*, 1.00 in $CHCl_3$); λ_{max} (EtOH) 243 nm (ε 17150); ν_{max} (KBr) 2750 (C—H of aldehyde), 1745 (acetate), 1672 and 1614 (Δ^{17}-21-aldehyde doublet), 1240 and 1022 cm^{-1} (acetate); n.m.r.: δ ($CDCl_3$) 0.83 (s) (19-CH_3), 1.06 (s) (18-CH_3), 2.00 (s) (CH_3COO), 2.20 (m) (17α-H), 3.32 (d, large, J = 14.0 Hz) (17β-H), 4.68 (m) (3α-H), 5.87 (d of t, J_α = 8.0 Hz, J_t = 0.9 Hz) (20-H), 10.11 (d, J = 8.0 Hz) (21-H).

Anal. Calcd. for $C_{24}H_{36}O_3$: C, 77.37; H, 9.74. Found: C, 77.48; H, 9.80.

(b) From 3β-Acetoxy-17aα-hydroxy-17aβ-ethoxyvinyl-D-homo-5α-androstane (6B)

A quantity of 4.29 g of 3β-acetoxy-17aα-hydroxy-17aβ-ethoxyvinyl-D-homo-5α-androstane (**6B**), m.p. 122–126°, was treated as under (*a*) with hydrochloric acid and gave 3.56 g of pure aldehyde **5**, m.p. 174–175°, identified by the determination of a mixture melting point and the comparison of its i.r. spectrum with that of the product described under (*a*).

The washings of the crystals of experiments (*a*) and (*b*) were extracted with ether, the ethereal layer was washed with cold saturated sodium bicarbonate solution and with water and was dried over sodium sulfate. Evaporation of the solvent gave 1.2 g of a crude product which was chromatographed on 30 g of aluminum oxide. Elutions with petroleum ether – benzene (9:1, 4:1, and 1:1) gave 680 mg of aldehyde **5**, m.p. 172–174°.

Cyanoethylation of 3β-Acetoxy-D-homo-5α-pregn-17a-en-21-al (5)

To a stirred solution of 3.5 g of aldehyde **5**, m.p. 174–175°, in 34 ml of absolute benzene, 0.56 ml of a 1.9 *N* solution of *t*-sodium amylate in benzene was added in a nitrogen atmosphere. To this mixture there was added, within 10 min, dropwise and with stirring, 11.8 ml of a 0.83 *M* acrylonitrile solution in benzene. The reaction mixture was stirred at 24° for 3 h, at 55° for 5 h, and at room temperature for 12 h. The product was poured into 600 ml of ice water containing 6 ml of an aqueous 0.1 *M* acetic acid solution. The precipitate was extracted with ether, the ethereal layer was washed with water, and dried over sodium sulfate. Evaporation of the solvent gave 3.88 g of a product which was chromatographed on 500 g of silica gel.

Elutions with benzene – ethyl acetate (96:4) gave 600 mg of *3β-acetoxy-17α-ethyl-17²-cyano-17²,21-cyclo-D-homo-5α-pregna-17a,21-diene (9)*, m.p. 258–261°. A sample was recrystallized three times from dichloromethane–ether–hexane for analysis; m.p. 264–264.5°; $[\alpha]_D^{25}$ +105.0° (*c*, 0.95 in $CHCl_3$); λ_{max} (EtOH) 297 nm (ε 11 620); ν_{max} (KBr) 3050 (vinylic hydrogens), 2190 (conjugated nitrile), 1735 (acetate), 1638 and 1568 (conjugated double bonds), 1247 cm^{-1} (acetate); n.m.r.: δ ($CDCl_3$) 0.82 (s) (19-CH_3), 1.08 (s) (18-CH_3), 2.02 (s) (CH_3COO), 2.25 (m) (17¹-CH_2), 2.35 (m) (17β-H), 4.68 (m) (3α-H), 5.84 (d of d, J = 6.0 and 2.5 Hz) (20-H), 6.67 (d of d, J = 6.0 and 2.0 Hz) (21-H); optical rotatory dispersion (o.r.d.) (*c*, 0.001 in CH_3OH): $[\alpha]_{400}$ +200, $[\alpha]_{350}$ +600, $[\alpha]_{320}$ +2300 (max), $[\alpha]_{300}$ 0, $[\alpha]_{290}$ −3000, $[\alpha]_{264}$ −5500 (min), $[\alpha]_{250}$ −5400°

Can. J. Chem. Downloaded from www.nrcresearchpress.com by 210.87.254.40 on 09/05/12
For personal use only.

(positive Cotton effect); mass spectrum: *m/e* 407 (M^+), 392, 347, 332.

Anal. Calcd. for $C_{27}H_{37}O_2N$: C, 79.56; H, 9.15; N, 3.44. Found: C, 79.34; H, 9.04; N, 3.39.

Elutions with benzene – ethyl acetate (94:6) gave 525 mg of starting material, *aldehyde* **5**, m.p. 172–174°.

Elutions with benzene – ethyl acetate (92:8) gave oily fractions (195 mg) which could not be crystallized and to which we assign tentatively the structures of isomeric *3β-acetoxy-17α-ethyl-17²ξ-cyano-21-(2¹-cyanoethoxy)-17²,21-cyclo-D-homo-5α-pregn-17a-enes (4A and B)*; ν_{max} (KBr) 2230 (non-conjugated nitrile), 1740 (acetate), 1670 (double bond), 1245 (acetate), 1130 and 1100 cm^{-1} (ether); n.m.r.: δ ($CDCl_3$) 0.82 (s) (19-CH_3), 0.97 (s) (18-CH_3), 2.00 (CH_3COO), 2.30 (m) (17-H, 17¹-CH_2, 17²-H), 2.57 (t, J = 6.5 Hz) (CH_2-CN), 3.63 (t, J = 6.5 Hz) (O—CH_2), 4.09 (t, J = 6.0 Hz) (21-H), 5.28 (t, large, J = 6.0 Hz) (20-H).

The following chromatogram fractions (1.92 g), eluted with benzene – ethyl acetate (90:10 to 50:50), were combined and rechromatographed on 45 g of aluminum oxide. Petroleum ether – benzene (1:9) and pure benzene eluted 810 mg of *3β-acetoxy-21α-hydroxy-17α-ethyl-17²β-cyano-17²,21-cyclo-D-homo-5α-pregn-17a-ene (8)*, m.p. 205–207°. A sample was recrystallized twice from ether–hexane for analysis; m.p. 213–214°; $[\alpha]_D^{25}$ +43.0° (*c*, 1.00 in $CHCl_3$); ν_{max} (KBr) 3460 (hydroxyl), 2220 (non-conjugated nitrile), 1740 (acetate), 1652 (double bond), 1245 (acetate), 1036 and 1019 (acetate and alcohol); ν_{max} ($CHCl_3$) 3600, 3460, 2240, 1724, 1642, 1255, 1027, and 1006 cm^{-1}; weak coloration with tetranitromethane; n.m.r.: δ ($CDCl_3$) 0.80 (s) (19-CH_3), 1.01 (s) (18-CH_3), 2.00 (s) (CH_3COO), 2.36 (m) (exchanged with D_2O) (21-OH), 2.90 (t, J = 3.8 Hz) (17²α-H), 4.33 (m, *w*/2 6.0 Hz) (21β-H), 4.70 (m) (3α-H), 5.63 (d of d, J = 5.0 and 2.0 Hz) (20-H).

Anal. Calcd. for $C_{27}H_{39}O_3N$: C, 76.19; H, 9.24; N, 3.29. Found: C, 76.03; H, 9.42; N, 3.31.

In the secondary chromatogram, benzene–ether (20:1 and 9:1) eluted 1.08 g of *3β-acetoxy-21α-hydroxy-17α-ethyl-17²α-cyano-17²,21-cyclo-D-homo-5α-pregn-17a-ene (7)*, m.p. 236–238°. A sample was recrystallized twice from ether–hexane for analysis; m.p. 241–242°; $[\alpha]_D^{25}$ −24.0° (*c*, 1.10 in $CHCl_3$); ν_{max} (KBr) 3465 (hydroxyl), 2225 (non-conjugated nitrile), 1744 (acetate), 1655 (double bond), 1240 (acetate), 1032 and 1000 cm^{-1} (acetate and alcohol); ν_{max} ($CHCl_3$) 3600, 3455, 2240, 1722, 1642, 1255, 1027, and 1007 cm^{-1}; n.m.r.: δ ($CDCl_3$) 0.81 (s) (19-CH_3), 1.00 (s) (18-CH_3), 2.00 (s) (CH_3COO), 2.35 (m) (exchanged with D_2O) (21-OH), 2.72 (d of t, J_d = 12.5 Hz, J_t = 3.5 Hz) (17²β-H), 4.33 (m, *w*/2 6.0 Hz) (21β-H), 4.70 (m) (3α-H), 5.65 (d of d, J = 4.5 and 2.0 Hz) (20-H).

Anal. Calcd. for $C_{27}H_{39}O_3N$: C, 76.19; H, 9.24; N, 3.29. Found: C, 75.99; H, 9.20; N, 3.28.

The final fractions of the original chromatogram, eluted with benzene – ethyl acetate (25:75) mixtures and with pure ethyl acetate consisted of complex cyanoethylation products (375 mg) which could not be separated by chromatography; ν_{max} (KBr) 3400 (large), 2240, 1740, 1720, 1700, 1680, 1670, 1630, 1245, 1180, 1100, and 1030 cm^{-1}.

In toto, there were obtained 600 mg (18%) of dienonitrile **9**, 1.08 g (31%) of hydroxy nitrile **7**, 810 mg (24%) of hydroxy nitrile **8**, 195 mg of oxygen-cyanoethylated products (**4A** and B), and 375 mg of unidentified products. The total yield of γ-cyanoethylation products amounted to 79% (the recovery of starting material **5** being taken into account when calculating the yields).

3β,21α-Diacetoxy-17α-ethyl-17²α-cyano-17²,21-cyclo-D-homo-5α-pregn-17a-ene (7a)

Acetylation at room temperature, under the usual conditions, of 68 mg of hydroxy nitrile **7**, m.p. 238–240°, with 1.3 ml of acetic anhydride in 2.5 ml of pyridine, gave 71 mg of the diacetate **7a**, m.p. 166–169°. A sample was recrystallized twice from ether–hexane for analysis; m.p. 176.5–177°; $[\alpha]_D^{25}$ −64.0° (*c*, 1.00 in $CHCl_3$); ν_{max} (KBr) 2245 (non-conjugated nitrile), 1745 (acetates), 1655 (double bond), 1260, 1235, 1055, 1035, and 1018 cm^{-1} (acetates); n.m.r.: δ ($CDCl_3$) 0.78 (s) (19-CH_3), 0.97 (s) (18-CH_3), 1.97 (s) (3β-CH_3COO), 2.07 (s) (21α-CH_3COO), 2.30 (m) (17β-H), 2.80 (d of t, J_d = 12.5 Hz, J_t = 3.5 Hz) (17²β-H), 4.67 (m) (3α-H), 5.37 (m, *w*/2 6.0 Hz) (21β-H), 5.61 (d of d, J = 5.0 and 2.0 Hz) (20-H).

Anal. Calcd. for $C_{29}H_{41}O_4N$: C, 74.48; H, 8.84; N, 3.00. Found: C, 74.50; H, 8.81; N, 3.05.

3β,21α-Diacetoxy-17α-ethyl-17²β-cyano-17²,21-cyclo-D-homo-5α-pregn-17a-ene (8a)

Acetylation of 18 mg of cyano alcohol **8**, m.p. 209–211°, with 0.5 ml of acetic anhydride in 1.0 ml of pyridine gave 21 mg of diacetate **8a**, m.p. 179–180°. The product was recrystallized twice from ether–hexane for analysis; m.p. 180–181°; $[\alpha]_D^{25}$ −47.7° (*c*, 1.01 in $CHCl_3$); ν_{max} (KBr) 2230 (non-conjugated nitrile), 1742 (acetates), 1655 (double bond), 1245, 1230, 1065, and 1025 cm^{-1} (acetates); n.m.r.: δ ($CDCl_3$) 0.80 (s) (19-CH_3), 1.00 (s) (18-CH_3), 2.00 (s) (3β-CH_3COO), 2.05 (s) (21α-CH_3COO), 2.63 (m) (17β-H), 2.98 (large triplet, J = 3.8 Hz) (17²α-H), 4.68 (m) (3α-H), 5.36 (m, *w*/2 6.0 Hz) (21β-H), 5.57 (d of d, J = 5.0 and 2.0 Hz) (20-H).

Anal. Calcd. for $C_{29}H_{41}O_4N$: C, 74.48; H, 8.84; N, 3.00. Found: C, 74.54; H, 8.90; N, 3.04.

Dehydroacetylation of the Diacetoxy Nitrile 7a

To a solution of sodium methylate prepared from 80 mg of sodium and 5 ml of methanol, 39 mg of diacetate **7a**, m.p. 172–174°, in 0.5 ml of absolute benzene was added. The mixture was refluxed for 1 h and poured into ice water. The precipitate was extracted with ether, the ethereal layer was washed with water and dried over sodium sulfate. Evaporation of the solvent gave 37 mg of a residue which was dissolved in 2.0 ml of pyridine to which 1.0 ml of acetic anhydride was added. The product was worked-up after 15 h. The amorphous material obtained was subjected to preparative t.l.c. (petroleum ether – ether 1:1); thus, 25 mg (75%) of *dienonitrile* **9**, m.p. 259–261°, $[\alpha]_D^{25}$ +101.0° (*c*, 1.00 in $CHCl_3$), and 12 mg of starting material, *diacetate* **7a**, m.p. 174–175°, were isolated. The structures of the products were determined by comparison of their i.r. spectra with those of authentic samples and by the determination of mixture melting points.

Dehydroacetylation of Diacetoxy Nitrile 8a

Under the conditions described for the analogous reaction of diacetate **7a**, 30 mg of diacetate **8a**, m.p.

179–180°, were dehydroacetylated. After reacetylation, the product was subjected to preparative t.l.c. and 10 mg (40%) of *dienonitrile* **9**, m.p. 260–262°; $[\alpha]_D^{25}$ +103.0° (*c*, 1.00 in $CHCl_3$), and 20 mg of starting material, *diacetate* **8a**, m.p. 179–180°, were isolated. The identity of the products was determined as described above.

*3β-Acetoxy-17α-ethyl-17²β-cyano-17²,21-cyclo-D-homo-5α-pregn-17a-en-21-one (**10**)*

To a stirred solution of 18 mg of hydroxy nitrile **8**, m.p. 209–211°, in 2 ml of absolute acetone, 0.075 ml of Jones' reagent (16) was added. The mixture was stirred for 2 min and poured into ice water. The precipitate was extracted with ether, the ethereal layer was washed with cold water and dried over sodium sulfate. Removal of the solvent gave 17 mg of the cyano ketone **10**, m.p. (dec.) 198–201°; $[\alpha]_D^{25}$ −45.0° (*c*, 0.82 in $CHCl_3$); λ_{max} (CH_3OH) 245 nm (ε 11 200); ν_{max} (KBr) 2240 (non-conjugated nitrile), 1738 (acetate), 1684 and 1605 (Δ^{17}-21-keto doublet), 1252 and 1032 cm^{-1} (acetate); n.m.r.: δ ($CDCl_3$) 0.77 (s) (19-CH_3), 1.04 (s) (18-CH_3), 1.95 (s) (CH_3COO), 2.77 (m) (17β-H), 3.37 (t, J = 3.5 Hz) (17²α-H), 4.61 (m) (3α-H), 6.02 (d, J = 2.5 Hz) (20-H); o.r.d. (*c*, 0.04 in CH_3OH): $[\alpha]_{600}$ −20, $[\alpha]_{450}$ 0, $[\alpha]_{400}$ −10, $[\alpha]_{380}$ −80, $[\alpha]_{356}$ −160, $[\alpha]_{344}$ 0, $[\alpha]_{320}$ +640, $[\alpha]_{300}$ +920, $[\alpha]_{290}$ +1160, $[\alpha]_{280}$ +1860°; (*c*, in CH_3OH): $[\alpha]_{344}$ 0, $[\alpha]_{310}$ +240, $[\alpha]_{286}$ +380, $[\alpha]_{254}$ +1520 (max), $[\alpha]_{244}$ 0, $[\alpha]_{230}$ −2240 (min), $[\alpha]_{218}$ −1200° (negative Cotton effect); mass spectrum: *m/e* 423 (M^+), 408, 397, 370, 363, 348, and 309.

We acknowledge with gratitude the excellent cooperation of Mrs. J. Capitaine and the devoted technical assistance of Mr. D. Capitaine and Mrs. G. Pelletier. Sincere thanks are due to the National Research Council of Canada and to Ayerst Laboratories, Montreal, Quebec, for financial assistance; we also thank the latter organization for a generous gift of starting material. One of us (L.R.) expresses his gratitude to the National Research Council of Canada for scholarships during the years 1965–1968.

1. S. Bory and Ch. R. Engel. Bull. Soc. Chim. Fr. In press.
2. Ch. R. Engel, J. Lessard, L. Ruest, and S. Bory. Abstr. of Commun., 5th International symposium on the chemistry of natural products. London, England. 1968. pp. 358–359.
3. Ch. R. Engel and J. Lessard. J. Amer. Chem. Soc. **85**, 638 (1963).
4. Ch. R. Engel and J. Lessard. Can. J. Chem. **48**, 2819 (1970).
5. Ch. R. Engel and J. Lessard. Abstr. of Commun., 2nd International symposium on the chemistry of natural products. Prague, Czechoslovakia. 1962. p. 34.
6. H. C. Brown. J. Org. Chem. **22**, 439 (1957).
7. H. C. Brown, J. H. Brewster, and H. Schechter. J. Amer. Chem. Soc. **76**, 467 (1954).
8. J. B. Bream, D. C. Eaton, and H. B. Henbest. J. Chem. Soc. 1974 (1957).
9. R. B. Turner and R. H. Garner. J. Amer. Chem. Soc. **79**, 253 (1957).
10. R. Fleck. J. Org. Chem. **22**, 439 (1957).
11. (*a*) J. Lessard and Ch. R. Engel. Ann. ACFAS, **30**, 53 (1964); (*b*) J. Lessard and Ch. R. Engel. Ann. ACFAS, **34**, 42 (1967); (*c*) J. Lessard and Ch. R. Engel. Unpublished results.
12. (*a*) M. W. Goldberg and R. Monnier. Helv. Chim. Acta, **23**, 376 (1940); (*b*) M. W. Goldberg and E. Wydler. Helv. Chim. Acta, **26**, 1142 (1943).
13. N. L. Allinger and S. Greenberg. J. Org. Chem. **25**, 1399 (1960).
14. (*a*) D. A. Prins and C. W. Shoppee. J. Chem. Soc. 494 (1946); (*b*) L. Ruzicka, Pl. A. Plattner, H. Heusser, and J. Pataki. Helv. Chim. Acta, **29**, 936 (1946).
15. M. Tiffeneau, P. Weill, and B. Tchoubar. C. R. Acad. Sci. **205**, 54 (1937).
16. (*a*) K. Bowden, J. M. Heilbron, E. R. H. Jones, and B. C. L. Weedon. J. Chem. Soc. 39 (1946); (*b*) A. Bowers, T. G. Halsall, E. R. H. Jones, and A. J. Lemin. J. Chem. Soc. 2548 (1953).
17. (*a*) A. D. Cross, E. Denot, H. Carpio, R. Acedevo, and P. Crabbé. Steroids, **5**, 557 (1965); (*b*) N. S. Bhacca, L. F. Johnson, and J. N. Shoolery. NMR spectra catalog. Varian Associates. National Press. 1962. Spectrum 69.
18. A. Moscowitz, E. Charney, U. Weiss, and H. Ziffer. J. Amer. Chem. Soc. **85**, 1976 (1963).
19. Ch. R. Engel, V. S. Salvi, and L. Ruest. Can. J. Chem. In press.
20. J. Lessard and Ch. R. Engel. Unpublished results.
21. N. S. Bhacca and D. H. Williams. Applications of n.m.r. spectroscopy in organic chemistry. Holden-Day Inc., San Francisco. 1964. p. 79.
22. C. Djerassi, R. Records, E. Bunnenberg, K. Mislow, and A. Moscowitz. J. Amer. Chem. Soc. **84**, 870 (1962).

Can. J. Chem. Downloaded from www.nrcresearchpress.com by 210.87.254.40 on 09/05/12
For personal use only.

Can. J. Chem. Downloaded from www.nrcresearchpress.com by 210.87.254.5 on 09/05/12
For personal use only.

Lignans of western red cedar (*Thuja plicata* Donn). X. γ-Thujaplicatene

BRUCE F. MACDONALD AND G. M. BARTON

Department of Fisheries and Forestry, Canadian Forestry Service, Forest Products Laboratory, Vancouver, British Columbia

Received May 20, 1970

The structure of the tenth in the series of novel lignans from the heartwood of western red cedar (*Thuja plicata* Donn) has been determined as 2-(3″,4″-dihydroxy-5″-methoxybenzylidene)-3-(4′-hydroxy-3′-methoxybenzyl)-butyrolactone (γ-thujaplicatene) (**1**) by spectrometric methods and comparison with synthetic derivative reactions. The discovery of this lignan with a double bond conjugated with an aromatic ring confirms previously suggested biosynthetic routes to the cedar lignans.

Canadian Journal of Chemistry, **48**, 3144 (1970)

Introduction

Previous work has elucidated the structural relationship of nine lignans present in the heartwood of western red cedar (*Thuja plicata* Donn), two of which were 4-aryltetrahydronaphthalenes, five were substituted dibenzyl butyrolactones, the eighth was a 4-aryl-α-naphthol lactone, and the ninth was an aromatized naphthalene (1).

The new lignan is the first member of this series of lignans (1) which possesses a double bond conjugated with the aromatic nucleus. 2-(3″,4″-dihydroxy-5″ methoxy benzylidene)-3-(4′-hydroxy-3′-methoxy-benzyl)-butyrolactone, given the trivial name γ-thujaplicatene, provides one of the intermediate structures in the suggested biosynthesis of western red cedar lignans (2).

γ-Thujaplicatene was separated by extracting western red cedar meal with ethyl acetate which after evaporation of the solvent was triturated with chloroform. The chloroform solubles were column chromatographed on polyamide (Woelm) and γ-thujaplicatene purified on a cellulose column.

The i.r., n.m.r., and blue fluorescence under short-wave u.v. light indicated a structure similar to a naphthalene or conjugated double bond with a benzene ring of the thujaplicatin type. The u.v. spectrum of γ-thujaplicatene, which showed peaks at 338 and 288 mμ, was not indicative of plicatinaphthalene (1) which has peaks at 356, 315, and 259 mμ, or of the apopicropodophyllin series whose peaks are 310, 290, and 350 mμ for the α, β and γ positions of the double bond respectively (3). Attempts to shift the conjugated double bond of γ-thujaplicatene to the β position by use of piperidine acetic acid (3) were unsuccessful, indicating that the position of the bond remained unchanged.

γ-Thujaplicatene gave a positive test with the ferric–ferri-cyanide reagent (4). When chromatographed on molybdic acid-treated paper with butanol – acetic acid – water it showed a considerably reduced R_f value (0.61) and a yellow color indicating the presence of pyrocatechol group when compared with untreated paper R_f (0.80).

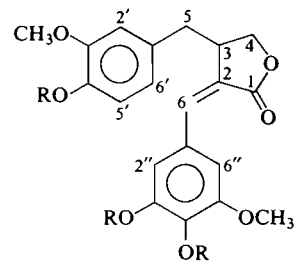

1 R = H
2 R = CH_3
3 R = Ac

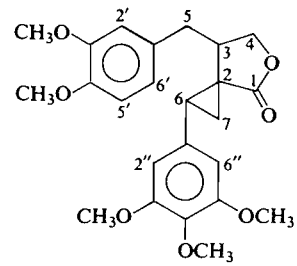

4

The structure of the γ-thujaplicatene was inferred from a double-focusing high-resolution mass spectrum of the acetylated derivative (**3**) which showed a molecular weight of *m/e* 498, but the intensity of the parent ion peak was too low for isotopic work. A study of the fragmentation showed the compound could not be of the plicatin series as the peak at 269 indicative of closed-ring lignans (5) was missing. The major

Can. J. Chem. Downloaded from www.nrcresearchpress.com by 210.87.254.5 on 09/05/12
For personal use only.

fragmentation peaks at *m/e* 235 and 137 indicated the open structure similar to those of the thujaplicatin series (6). Acetyl groups were accounted for by peaks at *m/e* 456, 414, and 277, giving further evidence of γ-thujaplicatene.

The n.m.r. spectra of the methylated (**4**) and the acetylated (**3**) derivative confirmed the presence of two methoxyl and three hydroxyl groups in the original thujaplicatene. The n.m.r. spectra in deuterated solvents of γ-thujaplicatene and its triacetyl derivative (**3**) showed the expected chemical shifts. An important feature of the acetyl spectrum was a clearly defined AB eight-line pattern which previously had not been observed in this lignan series. Determination of the geminal protons coupling constant of this AB pattern (J_{AB} = 16 MHz) provided additional proof that they belonged to C-5, since the coupling constant for C-4 protons in a γ-lactone would be only 9 MHz (7). The n.m.r. of the methylated derivative (**4**) was markedly different in all regions, as was its i.r. which showed a loss of the 1635 band attributed to a conjugated double bond and a shift of the lactone band from 1744 to 1767 cm^{-1}. Correspondingly, there was a loss of the absorption band at 338 mu in the u.v. spectrum of the methylated product. These differences in spectra suggested that diazomethane had added on across the double bond (8) as well as methylating the three phenolic hydroxyl groups. Confirmation of this was obtained from the mass spectrum which showed a parent ion peak at *m/e* 428 indicative of structure **4**.

Final confirmation of the structures of γ-thujaplicatene (**1**) and its methylated cyclo-addition product **4** was obtained by treating synthetic methylated γ-thujaplicatene (**2**) (8) with diazomethane for 40 hours. After crystallization from ether, the cyclo-addition product gave an identical quantitative i.r. spectrum with the similarly treated natural product.

Experimental

The following equipment and materials were used: m.p., Fisher–Johns heated block (uncorrected); i.r. spectra, Perkin–Elmer 521 grating spectrometer (KBr disks); u.v. spectra, Beckman DK-2 spectrophotometer (ethanol); n.m.r., Varian HA-100 (tetramethylsilane σ = 0 as internal standard in the solvents shown). High resolution mass spectrum by Morgan–Schaffer, Montreal. The t.l.c. values were obtained with silica gel G (Merck) as absorbent, benzene – ethanol – acetic acid (90:10:1) as developer, with u.v. light followed by nitric acid – sulfuric acid (1:1) spray and heat as detector. Papergrams were developed with 2% aqueous acetic acid and detected with potassium ferri-cyanide – ferric chloride reagent (mixed 1% solutions).

γ-Thujaplicatene (1)

Western red cedar wood meal was soxhlet extracted with ethyl acetate, dried, and the residue triturated several times with hot chloroform. The evaporated chloroform solubles were dissolved in a minimum quantity of methanol and extracted with petroleum ether (3 × 400 ml) to remove thujaplicins, thujic acid, methyl thujate and other terpenoids. The remaining methanol solubles were chromatographed on a polyamide (Woelm) column (3 cm × 40 cm) eluting with benzene followed by a gradient elution with ethanol. The fractions were monitored by both t.l.c. and paper chromatography. γ-Thujaplicatene gave a single spot R_f 0.23 in the former and a blue fluorescent streak (short wave u.v.) R_f 0.16 to 0.29 in the latter. Final purification was achieved by eluting from a cellulose column with water. The spectra gave: λ_{max} in mμ (log ε) 338 (4.02) and 288 (3.39) shifting in alkaline media to 292 (4.19) and 248 (3.89); ν_{max} 3380 (broad hydroxyl), 1720 (lactone), 1635 and 1585 (double bond conjugated with aromatic ring) cm^{-1}; n.m.r. (deuterioacetone) *2.60* (1H, singlet, C-6), 3.08–3.41 (5H, multiplet, aromatic), 4.20–5.00 (3H, broad singlet, hydroxyls), 5.78 (2H, doublet, C-4), 6.15 (6H, singlet, methoxyls), 6.92–7.59 (2H, AB part of ABX, J_{AB} = 16 MHz, C-5) τ units. (C-3 proton hidden under methoxyl peak).

Triacetyl Thujaplicatene (3)

γ-Thujaplicatene (150 mg) was dissolved in pyridine (15 ml) and acetic anhydride (10 ml) and left standing 3 h. The reaction mixture was heated on a steam bath for 1 h. The product was added with stirring to ice water (250 ml), filtered, and washed with 2% hydrochloric acid (100 ml). The crude acetate (110 mg) was purified on an alumina column using gradient elution with benzene chloroform. The column was monitored by silica gel t.l.c. (R_f 0.53) and the best fraction crystallized from ethanol to yield 42 mg m.p. 148–149°. The spectra gave: ν_{max}, no hydroxyl band, 1756 (lactone shoulder), 1770–1740 (acetyl), 1640 (double bond conjugated with aromatic ring) cm^{-1}; n.m.r. (deuteriochloroform), 2.60 (1H, singlet, C-6), 2.97–3.40 (5H, multiplet, aromatic), 5.82 (2H, doublet, C-4), 6.89–7.57 (2H, AB part of ABX, J_{AB} = 16 MHz, C-5) 6.22 and 6.24 (3H each, singlets, methoxyls), 7.44 and 7.76 (3H and 6H, singlets, acetyls) τ units (C-3 proton hidden under methoxyl peak); mass spectrum, parent ion = 498 (0.3%), base peak 137, 456 (10%), 414 (10%), 277 (10%), 237 (39%).

Trimethyl Thujaplicatene Cyclo-addition Compound (4)

γ-Thujaplicatene (100 mg) was dissolved in methanol (15 ml) and diazomethane in ether (5 ml) was added at intervals to keep the color yellow for 40 h at room temperature in a stoppered reaction flask. Experiments using less time produced a mixture that could not be separated by silica or alumina chromatography. The reaction was monitored using methods followed for the acetylated compound. This product was crystallized from chloroform–ethanol (1:4) followed by ether to yield 20 mg, m.p. 95°–96°. The spectra gave: λ_{max} in mμ (log ε)

277 (3.80); ν_{max}, no hydroxyl band, 1585 (aromatic) cm^{-1}; and an identical quantitative i.r. spectrum to that obtained from an i.r. analysis of the compound resulting from treatment of synthetic trimethyl thujaplicatene (**2**) (8) with diazomethane for 40 h; mass spectrum, parent ion = 428 (30%), base peak 151, 277 (90%).

The authors wish to thank Dr. Koji Murakami, Kyoto University, Kyoto, Japan, for samples of his synthetic methylated compound and Dr. L. D. Hall, University of British Columbia, Vancouver, B.C., for his helpful advice on interpreting n.m.r. spectra.

1. H. MacLean and B. F. MacDonald. Can. J. Chem. **47**, 4495 (1969).
2. E. P. Swan, K. S. Jiang and J. A. F. Gardner. Phytochem. **8**, 345 (1969).
3. A. W. Schrecker and J. L. Hartwell. J. Amer. Chem. Soc. **74**, 5676 (1952).
4. G. M. Barton, R. S. Evans, and J. A. F. Gardner. Nature, **170**, 249 (1952).
5. A. Pelter. J. Chem. Soc. (C), 74 (1968).
6. H. MacLean and K. Murakami. Can. J. Chem. **44**, 1541 (1966).
7. J. B. Lawry and N. V. Riggs. Tetrahedron Lett. **39**, 2911 (1964).
8. C. R. Noller. Chemistry of organic compounds. 2nd Ed. W. B. Saunders Co., London. 1957. p. 835.

Can. J. Chem. Downloaded from www.nrcresearchpress.com by 210.87.254.5 on 09/05/12
For personal use only.

Can. J. Chem. Downloaded from www.nrcresearchpress.com by 210.87.254.6 on 09/05/12
For personal use only.

Synthesis of 5-substituted ether derivatives of 5-hydroxymethyldeoxyuridine and their α-anomers[1]

G. L. Bubbar and V. S. Gupta[2]
Department of Physiology, Western College of Veterinary Medicine, University of Saskatchewan, Saskatoon, Saskatchewan

Received March 6, 1970

The synthesis and properties of ether derivatives **6***a–d* of 5-hydroxymethyldeoxyuridine and their corresponding α-anomers **7***a–d* are described. Acid-catalyzed etherification of 5-hydroxymethyluracil (**1**) gave the corresponding 5-alkoxymethyluracils **2***a–e* in excellent yields. Treatment of compounds **2***a–e* with trimethylchlorosilane gave bis(trimethylsilyl)pyrimidines **3***a–e* in high yields which, upon condensation with 3,5-di-(*O-p*-toluoyl)-2-deoxy-D-ribofuranosyl chloride, furnished an anomeric mixture of substituted nucleosides, β-anomers **4***a–e* and α-anomers **5**(*a–e*). The nucleosides with β-configuration were the major products in each case and were recovered as crystalline solids in good yields. Deblocking of compounds **4***a–d* by alcoholysis resulted in the corresponding ether derivatives **6***a–d*. From mother liquors, two substituted α-anomers, **5***a, b* were isolated as crystalline solids in small yields. Compounds **7***c, d* were obtained from mother liquors after hydrolysis by using preparative t.l.c. The structures were confirmed on the basis of p.m.r. studies, u.v. and i.r. absorption spectra, and elemental analysis. The compounds **2***a–e* and **6***a–d* did not inhibit thymidylate synthetase at a concentration of 2.5 m*M*.

Canadian Journal of Chemistry, 48, 3147 (1970)

The hydroxymethylpyrimidine deoxyribonucleotides are unique constituents of viral DNA (1–5); furthermore, 5-substituted pyrimidines have been suggested as possible intermediates during the transformation of thymine to RNA pyrimidines (6). The hydroxymethylation of pyrimidine deoxyribonucleotides is carried out by specific hydroxymethylases; the hydroxymethyl group originates from the C_1-unit of 5,10-methylene tetrahydrofolic acid (7, 8). In this communication we report the synthesis of 5-substituted ether derivatives of 5-hydroxymethyldeoxyuridine and their corresponding α-anomers (Scheme 1). We have prepared these compounds for the study of the bulk tolerance of thymidylate synthetase to substituents on the 5-position of the pyrimidine ring.

The conversion of 5-hydroxymethyluracil (**1**) was successfully modified (9) to obtain 5-alkoxymethyluracils **2***a–e* in excellent yields (92–97%). These ethers **2**(*a–e*) on treatment with trimethylchlorosilane in the presence of triethylamine (10) gave the corresponding bis(trimethylsilyl) derivatives **3***a–e* in high yields (70–90%). The structure of silyl ethers **3***a–e* was confirmed by i.r. and p.m.r. spectra. Condensation of **3***a–e* with 3,5-di-(*O-p*-toluoyl)-2-deoxy-D-ribofuranosyl chloride by a modified silyl condensation procedure (11) at 185–195° yielded an anomeric mixture[3] of the corresponding blocked β-anomers **4***a–e*, and α-anomers, **5***a–e*; the β-anomers predominated in all cases.[4] After removal of the silyl groups by aqueous ethanol, β-anomers IV (a–e), were isolated from the reaction mixture as crystalline solids in good yields (45–72%). The β-configuration was assigned to 5-alkoxymethyl deoxyribonucleosides **4** (*a–e*) on the basis of a characteristic triplet in the p.m.r. spectrum; it exhibited a coupling constant ($J_{1',2'} = J_{1',2''}$ of 7.0 ± 0.1) c.p.s. for the anomeric proton at δ 6.30–6.35. Treatment of the substituted nucleosides **4***a–e* with hot sodium methoxide in methanol or with ethanolic sodium hydroxide at room temperature gave the corresponding 5-alkoxymethyl derivatives of deoxyuridine **6***a–e* in excellent yields (75–85%). In compounds **6***a–e* the signal of the anomeric hydrogen (1′-H) appeared in the form of a triplet as δ 6.16 with a coupling constant of $J_{1',2'} = J_{1',2''} = 6.95 \pm 0.1$ c.p.s. This triplet due to the anomeric proton (1′-H) is characteristic of deoxyribonucleosides having the β-configuration (15, 16).[5] Signals of other protons appeared

[1]This work was supported by the Medical Research Council of Canada (Grant MA-3136).

[2]To whom all enquiries should be sent.

[3]Since the *trans*-rule is not obeyed in the case of deoxyribonucleosides, both anomers are formed during the condensation reaction (12).

[4]The silyl condensation method has been observed previously to favor the β-configuration (13).

[5]Thymidine, whose β-configuration has been unequivocally established (14), exhibited a triplet at δ 6.16 (see also Lemieux (15) for a detailed discussion of the theoretical basis of the p.m.r. spectra of thymidine and its α-anomer.

Can. J. Chem. Downloaded from www.nrcresearchpress.com by 210.87.254.6 on 09/05/12
For personal use only.

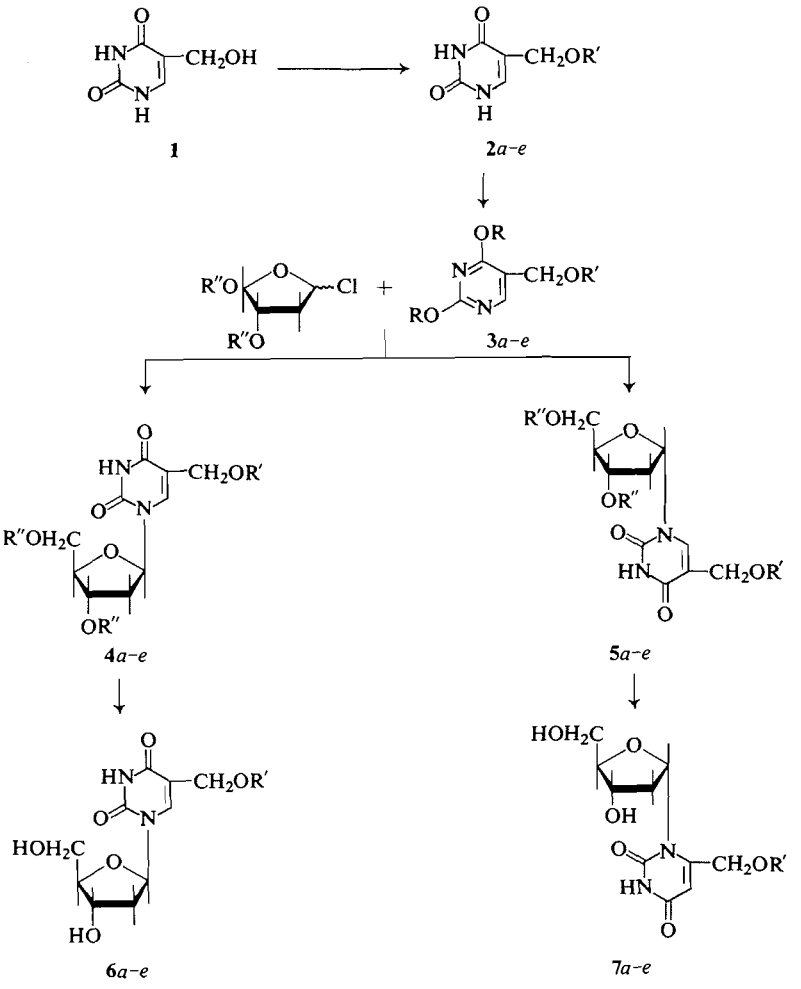

SCHEME 1

at the expected positions and the observed integration ratios were equal to calculated values.

Further proof of the structural assignment and configuration for the compounds **6***a–e* was obtained by the synthesis in poor yield of **6***c* by essentially the same procedure as used by Baker *et al.* (17) for the preparation of **6***b*.[6] The mixture m.p., R_f value, u.v. and p.m.r. spectra, and specific rotation of **6***c* prepared by this procedure

[6]5-Hydroxymethyl deoxyuridine was poorly soluble in the higher alcohols and preparation of compounds **6***c–e* by this procedure resulted in low yield (<10%).

Can. J. Chem. Downloaded from www.nrcresearchpress.com by 210.87.254.6 on 09/05/12
For personal use only.

and the silyl condensation method were identical.

The two substituted α-anomers, 1-[2-deoxy-3,5-di-(*O*-*p*-toluoyl)-α-D-ribofuranosyl]-5-methoxymethyluracil (**5***a*) and 1-[2-deoxy-3,5-di-(*O*-*p*-toluoyl)-α-D-ribofuranosyl]-5-ethoxymethyluracil (**5***b*), were recovered as crystalline solids in small amounts from the mother liquors.[7] In these compounds, **5***a*, *b*, the anomeric hydrogen (1′-H) exhibited a broad doublet at δ 6.60 and on raising the temperature to 70°, it split into a quartet (coupling constant = $J_{1',2''}$ = 3.20 and $J_{1',2'}$ = 7.25 c.p.s.). After deblocking, 1-(2-deoxy-α-D-ribofuranosyl)-5-propyloxymethyluracil (**7***c*) and 1-(2-deoxy-α-D-ribofuranosyl)-5-butyloxymethyluracil (**7***d*) were isolated by preparative t.l.c. In compounds **7***a–d*, the signal of the anomeric hydrogen (1′-H) appeared as a quartet at δ 6.48 (coupling constant = $J_{1',2''}$ = 3.2 and $J_{1',2'}$ = 7.8 c.p.s.). The quartet due to the anomeric hydrogen (1′-H) is characteristic of deoxyribonucleosides having the α-configuration (15, 16).

It is noteworthy that compounds **6***a–d* and their corresponding α-anomers, **7***a–d* did not obey Hudson's rules of isorotation. These observations are consistent with the phenomenon previously observed with other pyrimidine deoxyribonucleoside anomers (16, 18–20).

The compounds **2***a–e* and **6***a–d* failed to inhibit thymidylate synthetase of pig thymus gland at a concentration of 2.5 m*M*.

Experimental

Melting points were determined with a GallenKamp apparatus and are uncorrected. Specific rotations were measured (1 dm tube) with a Perkin–Elmer model 141 automatic digital readout polarimeter. The p.m.r. spectra were recorded on a Varian Associates A-100 spectrometer. All compounds were dissolved in dimethylsulfoxide (DMSO-d_6). The i.r. spectra were measured with a Perkin–Elmer model 421 spectrophotometer. A Unicam spectrophotometer, model SP-800, was used to measure the complete u.v. absorption spectra. Microanalyses were performed by the College of Pharmacy and the Prairie Regional Research Laboratory, Saskatoon, Saskatchewan. Silica gel (HF_{254}), was purchased from E. Merck, Darmstadt, Germany. The t.l.c. was carried out on silica gel plates (0.3 mm) at room temperature and spots were detected under u.v. illumination. Paper chromatograms were run overnight on Whatman No. 1 paper. Solvents used (by volume) were: (*A*) *n*-butanol – glacial acetic acid – water (4:1:5), upper phase; (*B*) *i*-propanol – NH_4OH – water (7:1:2); (*C*) $CHCl_3$–MeOH (8:2). All evaporations under reduced pressure were performed on rotary evaporator at 35°.

5-Hydroxymethyluracil (**1**) was prepared by base-catalyzed hydroxymethylation of uracil (9) and 5-hydroxymethyldeoxyuridine was synthesized by the method of Baker *et al.* (17).

Ether Derivations of 5-Hydroxymethyluracil (2a–e)

The ether derivatives of **1** were synthesized by the following modification of the procedure of Cline *et al.* (9). To 100 ml of each alcohol containing 1 ml of concentrated HCl was added 2 g of **1**. The suspension was stirred at room temperature for 15 min, and then kept on a steam bath for 3–4 h. The reaction mixture became homogeneous after 30–45 min in all instances, and t.l.c. of a sample (90 min or thereafter) using silica gel in solvent *C* for development showed only a single quenching spot. The reaction mixture was refrigerated and filtered to remove the crystals (yield 85–88%). Mother liquors on concentration gave an additional yield (5–10%) of the pure products. The m.p., total yields of the crystalline material, and $R_f \times 100$ values in solvents *A*, *B*, and *C*, respectively, were: for 5 methoxymethyluracil (**2***a*), 203–204° (lit. (9) 203–204°), 97.7%, 30, 46, 37; 5-ethoxymethyluracil (**2***b*), 212–213° (lit. (9) 212–213°), 97.2%, 54, 61, 68; 5-propyloxymethyluracil (**2***c*), 221–222°, 95%, 77, 78, 73; 5-butyloxymethyluracil (**2***d*), 215–217° (lit. (9) 215–217°), 94%, 81, 78, 79; and 5-benzyloxymethyluracil (**2***e*), 205–206° (lit. (16) 202–203°), 94.5%, 81, 84, 88.

Bis(trimethylsilyl) Derivatives of 5-Alkoxymethyluracil (3a–e)

To a suspension (12.4 mmoles) of each uracil ether **2***a–e* in anhydrous benzene (25 ml), was added trimethylchlorosilane (4.07 g, 37.5 m*M*). Triethylamine (3.79 g, 37.5 m*M*) in benzene (10 ml) was then added dropwise and the reaction mixture was stirred overnight at room temperature. The precipitated triethylamine hydrochloride was collected by filtration and washed with benzene (3 × 5 ml). The filtrate and washings were combined and the solvent was evaporated under reduced pressure. The viscous oily liquid of each silyl pyrimidine was distilled under high vacuum to yield compounds **3***a–e*. In the i.r. spectrum (liquid film) the silyl pyrimidines exhibited absorption bands at 1250 (vs), 835 (s), 753 (vs), $Si(CH_3)_3$; 1037 (vs), Si—O—C; 1087–1092 (s), Si—O—C and C—O—C and 1595 cm^{-1} (s), pyrimidine ring (10, 21). The physical properties and yields of these compounds are summarized in Table 1.

1-[2-Deoxy-3,5-di-(O-p-toluoyl)-β-D-ribofuranosyl]-5-alkoxymethyluracil (4a–e)

Anhydrous **3***a–e* (5 m*M*) and 3,5-di-(*O*-*p*-toluoyl)-2-deoxy-D-ribofuranosyl chloride (1.94 g, 5 m*M*) (22) were mixed and introduced into a preheated (to 170°) oil bath. After the halogenose melted, it was flushed with a gentle stream of nitrogen, the temperature of the oil bath was rapidly increased, and the reaction mixture was kept at 185–195° for an additional 30 min. The gummy residue

[7]The poor yield of α-anomers can be attributed to the high stereospecificity of the silyl condensation method for β-configuration, *vide supra* (13).

TABLE 1

Physical properties and yields of the trimethylsilyl pyrimidines

Compound	Boiling point (°C/mm Hg)	Yield (%)	Proton magnetic resonance data* of ether linkage δ (p.p.m.)
Bis(trimethylsilyl)-5-methoxy methyluracil (*3a*)	120/0.3	72	5.53 (3H,s,OCH_3)†
Bis(trimethylsilyl)-5-ethoxymethyluracil (*3b*)	120/0.1	88	5.67 (2H,q,—OCH_2—), 3.39 (3H,t,—CH_3)
Bis(trimethylsilyl)-5-propyloxymethyluracil (*3c*)	133/0.15	80	5.62 (2H,t,—OCH_2—), 3.62 (2H,se,—CH_2—), 3.16 (3H,t,—CH_3)
Bis(trimethylsilyl)-5-butyloxymethyluracil (*3d*)	137/0.1	72	5.62 (2H,t,—OCH_2—), 3.69 (4H,m,—CH_2—CH_2—), 3.12 (3H,t,—CH_3)
Bis(trimethylsilyl)-5-benzyloxymethyluracil (*3e*)	152–154/2	87	6.56 (2H,s,—OCH_2—); 7.22 (5H,m,5-phenyl protons)‡

*Formic acid external. Abbreviations: singlet (s), doublet (d), triplet (t), quartet (q), sextet (se) and multiplet (m).
†In addition the signals common in compounds *3a–e* were at δ 2.57 ± 0.02 (9H, s, 2 or 4 ($3CH_3$), 2.61 ± 0.02 (9H, s, 2 or 4 $(3CH_3)_3$ and 6.60 ± 0.12 (2H, s, 5-CH_2—with ring) p.p.m. The signal of the hydrogen (H_6) of the pyrimidine ring was located by using TMS (internal) and in *3a–e* appeared at δ 1.86 ± 0.02 p.p.m.
‡Located by using TMS (internal).

TABLE 2

Properties of 3,5-disubstituted pyrimidine 2-deoxy-D-ribonucleosides

Compound	$[\alpha]_D^{25°}$ $CHCl_3$ (Concentration)*	Ultraviolet absorption data EtOH (95%) λ_{max} (mμ)	$\varepsilon_{max} \times 10^4$	Proton magnetic resonance data of ether linkage δ (p.p.m.)
4*a*	−71.10° (1.28)	241.5	3.8	3.11 (3H,s,—OCH_3)†
5*a*	< +1.0 (0.015)	242.0	3.4	3.50 (3H,s,—OCH_3)‡
4*b*	−52.9° (1.39)	241.5	3.8	3.30 (2H,q,—OCH_2—), 1.0 (3H,t,—CH_3)†
5*b*	< +1.0 (0.025)	242.0	3.17	3.70 (2H,q,—OCH_2—), 1.35 (3H,t,—CH_3)‡
4*c*	−61.4° (1.14)	241.0	3.75	3.20 (2H,q,—OCH_2—), 1.31 (2H,se,—CH_2—), 0.78 (3H,t,—CH_3)†
4*d*	−65.0° (1.17)	240.0	3.75	3.23 (2H,q,—OCH_2—), 1.1–1.46(4H,m,—CH_2—CH_2—) 0.81 (3H,t,—CH_3)†
4*e*	−68° (1.24)	242.0	3.20	4.35 (2H,s,—OCH_2—), 7.29 (5H,s,phenyl ring at 5-position)†

*Concentration = g/ml.
†TMS internal.
‡TMS external.

was dissolved in 30 ml of ethanol (95%), refluxed for 30 min, and filtered hot through charcoal–Celite. The charcoal–Celite mixture was washed with hot ethanol (3 × 20 ml), filtrate and washings were combined, solvent was reduced in volume to 25 ml, and refrigerated. The crystals were collected by filtration and upon crystallization from ethanol and then methanol, yielded the substituted nucleosides **4***a–e* as white needles. The total amount of blocked nucleosides formed (based on the amounts of *3a–e* used), m.p., and yields of the crystalline material based on total nucleoside formed were: for 1-[2-deoxy-3,5-di-(*O-p*-toluoyl)-β-D-ribofuranosyl]-5-methoxymethyluracil (**4***a*), 70%, 170–172°, 45%; 1-[2-deoxy-3,5-di-(*O-p*-toluoyl)-β-D-ribofuranosyl]-5-ethoxymethyluracil (**4***b*), 73%, 183–185° (lit. (16), 185–186°), 54%; 1-[2-deoxy-3,5-di-(*O-p*-toluoyl)-β-D-ribofuranosyl]-5-propyloxymethyluracil (**4***c*), 86%, 187–188°, 68.7%; 1-[2-deoxy-3,5-di-(*O-p*-toluoyl)-β-D-ribofuranosyl]-5-butyloxymethyluracil (**4***d*), 88%, 160–162° (lit. (16) 162–163°), 60%; and 1-[2-deoxy-3,5-di-(*O-p*-toluoyl)-β-D-ribofuranosyl]-5-benzyloxymethyluracil (**4***e*), 60.5%, 142–143° (lit. (16) 141–142°), 44.8%. The chromatography (t.l.c.) of the mother liquors after deblocking indicated that the major constituent (*ca.* 80%) in every case was the β-anomer. However, none of the substituted nucleosides **4***a–e* could be induced to crystallize even after long standing. The physical properties are summarized in Table 2 and the signals of protons common to **4***a–e* in the p.m.r. spectra appeared at δ 7.66 (1H, s, 6-H), 11.40–11.45 (1H, s, 3-NH), 3.94 ± 0.02 (2H, s, 5-CH_2—with ring), 6.35 (1H, t, $J_{1',2'} = J_{1',2''}$ = 7.0 c.p.s., 1′-H), 5.62 (1H, m, 3′-H), 4.57 (2H, s, 5′-CH_2— and 4.47, m, 4′-H overlapped with 5′-CH_2—), 2.37–2.60 (2H, m, solvent and 2′, 2″-H), 7.87 and 7.95

Can. J. Chem. Downloaded from www.nrcresearchpress.com by 210.87.254.6 on 09/05/12
For personal use only.

Can. J. Chem. Downloaded from www.nrcresearchpress.com by 210.87.254.6 on 09/05/12
For personal use only.

(4H, α, 2 sets, 3-H and 5-H of two phenyl rings), 7.28, 7.38 (4H, d, 2 sets, 2-H and 6-H of two phenyl rings), 2.40 (6H, s, two *p*-methyl groups of benzene) p.p.m.

Anal. Calcd. for **4***b*, $C_{28}H_{30}N_2O_8$ (522.5): C, 64.35; H, 5.79; N, 5.36. Found: C, 64.20; H, 5.83; N, 5.37.

1-[2-Deoxy-3,5-di-(O-p-toluoyl)-α-D-ribofuranosyl]-5-methoxymethyluracil (5a)

Mother liquors left after removal of the β-anomer, **4***a*, were combined, dried, and the residue (575 mg) was shaken with warm benzene (3 × 10 ml), filtered, concentrated until turbid, and left overnight at room temperature. The crystalline mass (160 mg; m.p. 140–145°) was filtered and recrystallized twice from methanol to give **5***a*, as white shining needles (85 mg); m.p. 160–161°. The physical properties are given in Table 2 and common proton signals for compounds **5***a*, *b* in the p.m.r. spectra were, at δ 11.75 (1H, s, 3-NH), 8.29 (1H, s, 6-H), 4.38 (2H, s, 5-CH_2—with ring), 6.59 (1H, d, broad) which, at 70°, split into a quartet, 1′-H), 3.18–3.38 (1H, m, 2′-H), 2.74–2.88 (1H, m, 2′′-H and the solvent), 5.90 (1H, d, 3′-H), 5.37 (1H, t, 4′-H), 4.79 (2H, d, 5′-CH_2), 7.59, 7.67 (4H, d, 2 sets, two phenyl rings 2-H and 6-H), 8.11, 8.17 (4H, d, 2 sets, two phenyl rings 3-H and 5-H), and at 2.70 (6H, s, two-*p*-methyl groups attached to benzene rings) p.p.m.

1-[2-Deoxy-3,5-di-(O-p-toluoyl)-α-D-ribofuranosyl]-5-ethoxymethyluracil (5b)

The solvent was evaporated from the mother liquors and the residue (830 mg) was dissolved in boiling ether (50 ml). On cooling, the crystals (575 mg; m.p. 112–146°) were filtered and twice recrystallized from ether to give **5***b* as a fine microcrystalline powder (165 mg, m.p. 117–118°).

Anal. Calcd. for $C_{28}H_{30}N_2O_8$ (522.5); C, 64.35; H, 5.79; N, 5.36. Found: C, 64.20; H, 5.83; N, 5.39.

Physical properties are summarized in Table 2.

1-(2-Deoxy-β-D-ribofuranosyl)-5-alkoxymethyluracil (6a–d)

300 mg each of compound **4***a–d* was dissolved in 4.0 ml of NaOH (2 *N*) containing EtOH (8.0 ml) and the solution was left at room temperature overnight. After dilution with water (3 ml), Dowex 50 (H^+; X_8; 200–400 mesh) was added and the resulting solution at p*H* 4–5 was stirred for 30 min at room temperature. The resin was filtered, washed with water (3 × 4 ml), and the combined filtrate was evaporated to dryness. The residue was triturated with water (20 ml) and precipitated toluic acid was collected by filtration; mother liquors were freed of residual toluic acid by extraction with ether (2 × 25 ml). The aqueous phase on evaporation gave **6***a–d* as an amorphous white powder (yield 80–92%). The solvent of crystallization, yields of crystalline material, m.p., and R_f × 100 values in solvents *A* and *B*, respectively, were: for 1-(2-deoxy-β-D-ribofuranosyl)-5-methoxymethyluracil (**6***a*), EtOAc-cyclohexane, 45%, 120–125°, 55, 57; 1-(2-deoxy-β-D-ribofuranosyl)-5-ethoxymethyluracil (**6***b*), EtOAc–MeOH, 54%, 136–137° (lit. (17) 135–136°), 67, 66; 1-(2-deoxy-β-D-ribofuranosyl)-5-propyloxymethyluracil (**6***c*), EtOAc–ether, 68%, 127–128°, 76, 73; 1-(2-deoxy-β-D-ribofuranosyl)-5-butyloxymethyluracil (**6***d*), EtOAc–ether, 75%, 119–121°, 83, 79. The physical properties of compounds **6***a–d* are summarized in Table 3; signals for common protons in the p.m.r. spectra were, at δ 11.38 (1H, s, 3-NH), 7.92 (1H, s, 6-H), 4.03 (2H, s, 5-CH_2—with ring), 6.16 (1H, t, $J_{1',2'} = J_{1',2''} = 6.95$ c.p.s., 1′-H), 2.09 (2H, q, 2′, 2′′-H), 4.23 (1H, t, 3′-H), 5.21 (1H, d, proton of hydroxyl 3′-CHOH), 3.77 (1H, q, 4′-H), 3.57 (2H, s, (broad), 5′-CH_2—), 4.99 (1H, t, proton of hydroxyl group 5-CH_2OH). Each mother liquor showed a homogeneous quenching spot on paper chromatograms in solvents *A* and *B* and R_f values were the same; the crystalline products were not obtained in significant quantity even on long standing, however.

Direct Synthesis of 6c (17)

5-Hydroxymethyl deoxyuridine (500 mg) was suspended in *n*-propanol (50 ml) containing concentrated HCl (0.1 ml). The reaction mixture was stirred at room temperature for 30 min and then kept on a steam bath for 4 h. Solvent was removed *in vacuo*, the residue was taken up in MeOH (5 ml) and examined by paper chromatography (solvent *A*). In addition to **6***c* (R_f 0.76, major spot), there were two minor quenching spots: R_f 0.34, starting material (15%) and R_f 0.05, probably polymerized material (5%). The product did not crystallize and was therefore chromatographed on a column (2 × 25 cm) of silica gel packed in benzene. Elution was begun with $CHCl_3$ (200 ml) and followed with $CHCl_3$–MeOH (95:5, 500 ml); 25 ml fractions were collected and monitored by t.l.c. (solvent *C*). Fractions containing mostly **6***c* (tubes no. 15–28) were combined and evaporated *in vacuo*. The residue (112 mg) after crystallization from ethyl acetate – ether gave **6***c* as a microcrystalline solid (75 mg). The physical properties of this product were identical with those of **6***c* obtained by the condensation method. Mother liquors on standing at 4° gave an additional amount (20 mg) of material with a slightly lower m.p. 121–123°, but it was chromatographically homogeneous.

1-(2-Deoxy-α-D-ribofuranosyl)-5-methoxymethyluracil (7a)

The reaction mixture, consisting of 300 mg **5***a*, MeONa (150 mg), and anhydrous MeOH (6.0 ml), was refluxed for 30 min, deionized, and worked up as described under **6***a*. The residue (150 mg) was twice crystallized from ethylacetate and **7***a* was recovered as a fine microcrystalline solid (85 mg), m.p.149–150°, R_f (*A*, *B*), 51, 73; signals common to compounds **7***a–d* in p.m.r. were: at δ 11.65 (1H, s, 3-NH), 8.27 (1H, s, 6-H), 4.42 (2H, s, 5-CH_2—with ring), 6.47 (1H, q, $J_{1',2''} = 3.0 \pm 0.2$ c.p.s. and $J_{1',2'} = 7.5 \pm 0.1$ c.p.s., 1′-H); 2.78–3.06 (1H, m, partially buried under the solvent, 2′-H), 2.17 and 2.32 (1H, two triplets, 2′′-H), 4.53 (2H, m, 3′-H and 4′-H), 5.66 (1H, s (broad), proton of the hydroxyl group 3′-CHOH), 5.18 (1H, t, proton of the hydroxyl group 5′-CH_2OH), 3.75 (2H, t, overlapped with DOH, 5′-CH_2—) p.p.m. Mother liquors on prolonged standing at 4° gave an additional quantity (30 mg) of **7***a*. This product was chromatographically homogeneous but the m.p. (146–149°) was slightly lower. The physical properties and analytical values of compounds **7***a–d* are given in Table 3.

Can. J. Chem. Downloaded from www.nrcresearchpress.com by 210.87.254.6 on 09/05/12
For personal use only.

TABLE 3

Properties of pyrimidine 2-deoxy-D-ribonucleosides

Compound	$[\alpha]_D^{25°}$ EtOH, 95% (Concentration)*	Ultraviolet absorption data 0.1 *M* HCl (p*H* 1.0) λ_{max} (mμ)	$\varepsilon_{max} \times 10^3$	Proton magnetic resonance data of ether linkage δ (p.p.m.)	Analyses Formula (mol. wt.)	Calcd. (%)	Found (%)
6*a*	+21.7° (0.01)	206 264	11.4 10.7	3.50(3H,s,OCH_3)†	$C_{11}H_{16}N_2O_6$ (272.26)	C,48.52; H, 5.92; N,10.28	C,48.35; H,5.95; N,10.40
6*b*	+21.9° (0.096)	208 264	11.8 11.3	3.34(2H,q,—OCH_2—), 1.10 (3H,t,—CH_3)‡	$C_{12}H_{18}N_2O_6$ (286.17)	C,50.32; H, 6.34; N,9.78	C,50.25; H,6.28; N,9.75
6*c*	+21.7° (0.012)	208 264	11.9 11.5	3.35 (2H,q,—OCH_2—overlapped with DOH of solvent), 1.32–1.37 (2H,se,—CH_2—), 0.87 (3H,t,—CH_3)†	$C_{13}H_{20}N_2O_6$ (300.32)	C,51.99; H, 671; N,9.32	C,52.1; H,6.74; N,9.40
6*d*	+19.0° (0.01)	207 264	10.7 10.3	3.36 (2H,q,—OCH_2—overlapped with DOH of solvent), 1.13–1.61 (4H,m,—CH_2—CH_2—), 0.87 (3H,t,)	$C_{14}H_{22}N_2O_6$ (314.35)	C,53.49; H, 7.05; N,8.91	C,53.20; H,7.15; N,9.05
7*a*	+9.0° (0.04)	207 263.5	10.5 9.8	3.61(3H,s,5-OCH_3)‡	$C_{11}H_{16}N_2O_6$ (272.26)	C,48.52; H, 5.92; N,10.28	C,48.75; H,5.80; N,10.50
7*b*	+7.8° (0.02)	207 263.5	10.9 10.4	3.75(2H,q,—OCH_2—), 1.48 (3H,t,—CH_3)	$C_{12}H_{18}N_2O_6$ (286.17)	C,50.32; H, 6.34; N,9.78	N,9.85
7*c*	+6.7° (0.015)	204 263.5	9.6 8.5	3.58(2H,q,partially buried under DOH,—OCH_2—), 1.40–1.84 (2H,m,—CH_2)	$C_{13}H_{20}N_2O_6$ (300.32)	C,51.99; H, 6.71; N,9.32	C,52.3; H,6.84; N,9.10
7*d*	+7.75°	208.5	8.6	3.60(2H,q,—OCH_2—), 1.40–1.84 (4H,m,—CH_2—CH_2—)	$C_{14}H_{22}N_2O_6$ (314.35)	C,53.49; H, 7.05; N,8.91	N,8.87

*Concentration = g/ml.
†TMS internal.
‡TMS external.

1-(2-Deoxy-α-D-ribofuranosyl)-5-ethoxymethyluracil (7b)

The reaction mixture, consisting of **5***b* (100 mg), MeOH (1.5 ml), and MeONa (50 mg), was worked up as described under **6***a*. The residue (52 mg) was dissolved in ethyl acetate and precipitated twice with cyclohexane (43 mg); R_f (*A*,*B*) 50, 71 (see Table 3 for other physical properties).

1-(2-Deoxy-α-D-ribofuranosyl)-5-propyloxymethyluracil (7c)

Mother liquors left after the removal of 4*c* were dried, the white fluffy residue (0.6 g) was suspended in MeOH (15 ml) containing NaOMe (400 mg), refluxed for 30 min and worked up as described under **6***a*. The aqueous layer was concentrated to dryness, the residue was dissolved in MeOH (10 ml), spread on silica gel plates (6, 20 × 20 cm, 0.65 mm) which were developed three times with $CHCl_3$–MeOH (9:1). The respective zones were marked under u.v. illumination and the nucleoside was extracted with hot methanol. After removal of solvent, the residue (60 mg) was dissolved in EtOAc and precipitated twice with cyclohexane (49 mg), R_f, 49, 74 (solvents *A* and *B*).

1-(2-Deoxy-α-D-ribofuranosyl)-5-butyloxymethyluracil (7d)

After recovery of **4***d*, the mother liquors were dried *in vacuo*, and the residue (0.82 g) was hydrolyzed using MeONa (0.4 g) in anhydrous MeOH (20 ml) and worked up as described under **6***a*. The precipitate (300 mg) was dissolved in MeOH (5 ml) and purified using preparative t.l.c. (*vide supra*). The gum remaining after the removal of methanol was dissolved in EtOAc and precipitated twice with cyclohexane to give a white fluffy powder (44 mg); R_f, 51, 75 in solvents *A* and *B*. The analysis and physical properties are given in Table 3.

Assay of Thymidylate Synthetase

The direct spectrophotometric assay (23) was used for determining the activity of thymidylate synthetase. The contents of the reaction mixture and assay conditions were the same as described by Wahba and Friedkin (23), except that deoxyuridylate was used at a concentration of 50 μm. For inhibition experiments, the enzyme was pre-incubated with each compound for 10 min and then other co-factors were added. The reaction was run at room temperature.

The authors gratefully thank Drs. J. C. MacDonald (PRL) for allowing use of the polarimeter, J. R. Dimmock (Pharmacy College) for microanalysis facilities, and F. M. Loew (Veterinary College) for helpful suggestions in the preparation of this manuscript; Mr. T. Mazurek for measuring the p.m.r. spectra and Mr. B. Haid for recording the i.r. spectra.

1. J. G. Flaks and S. S. Cohen. J. Biol. Chem. **234**, 3501 (1959).
2. R. G. Kallen, M. Simon, and J. Marmur. J. Mol. Biol. **5**, 248 (1963).
3. S. Okubo, B. Strauss, and M. Stodolsky. Virol. **24**, 552 (1964).
4. J. J. Pene and J. Marmur. Fed. Proc. **23**, 318 (1964).
5. D. H. Roscoe and R. G. Tucker. Biochem. Biophys. Res. Commun. **16**, 106 (1964).
6. M. T. Abbott, R. J. Kadner, and R. M. Fink. J. Biol. Chem. **239**, 156 (1964).
7. D. H. Roscoe and R. G. Tucker. Virol. **29**, 157 (1966).
8. A. H. Alegria, F. M. Kahan and J. Marmur. Biochem. **7**, 3179 (1968).
9. R. E. Cline, R. M. Fink, and K. Fink. J. Amer. Chem. Soc. **81**, 2521 (1959).
10. T. Nishimura and I. Iwai. Chem. Pharm. Bull. Tokyo, **12**, 352 (1964).
11. T. Nishimura and B. Schimizu. Agr. Biol. Chem. Tokyo, **28**, 224 (1964).
12. B. R. Baker. The chemistry and biology of purines. Ciba Foundation Symposium. Churchill, London. 1957. p. 123.
13. H. G. Stout and R. K. Robins. J. Org. Chem. **33**, 1219 (1968).
14. A. M. Michelson and A. R. Todd. J. Chem. Soc. 816 (1955).
15. R. U. Lemieux. Can. J. Chem. **39**, 116 (1961).
16. R. Brossmer and E. Rohm. Hoppe-Seyler's Zeitsch. Phys. Chem. **348**, 1431 (1967).
17. B. R. Baker, T. J. Schwan, and D. V. Santi. J. Med. Chem. **9**, 66 (1966).
18. J. J. Fox, N. C. Yung, I. Wempen, and M. Hoffer. J. Amer. Chem. Soc. **83**, 4066 (1961).
19. J. Farkas, L. Kaplan, and J. J. Fox. J. Org. Chem. **29**, 1469 (1964).
20. R. U. Lemieux and M. Hoffer. Can. J. Chem. **39**, 110 (1961).
21. L. J. Bellamy. The infrared spectra of complex molecules. 2nd ed. John Wiley and Sons, Inc., New York, N.Y. 1958. p. 115 and 334.
22. M. Hoffer. Chem. Ber. **93**, 277 (1960).
23. A. J. Wahba and M. Friedkin. J. Biol. Chem. **236**, PC11 (1961).

Can. J. Chem. Downloaded from www.nrcresearchpress.com by 210.87.254.6 on 09/05/12
For personal use only.

Can. J. Chem. Downloaded from www.nrcresearchpress.com by 210.87.254.6 on 09/05/12
For personal use only.

Déplacement chimique du proton en résonance magnétique nucléaire. I. Calcul du terme diamagnétique en vue de son utilisation à l'étude de la structure des molécules. Application aux éthers vinyliques

FRANÇOIS TONNARD
Groupe de Physicochimie Structurale, Equipe Associée au C.N.R.S. n° 15, Faculté des Sciences, 35-Rennes-Beaulieu

SIMONE ODIOT
Laboratoire de Physique Expérimentale Moléculaire, 9, Quai Saint-Bernard Paris (5ème)

ET

MARYVONNE L. MARTIN
Laboratoire de Chimie Organique Physique, Faculté des Sciences 44-Nantes,

Reçu le 7 novembre 1969

On a établi une formule permettant de calculer le terme diamagnétique de la constante d'écran d'un proton à partir de la charge l.c.a.o. sur ce proton et sur le carbone auquel il est lié. Cette formule a été appliquée aux protons de quelques éthers vinyliques, ce qui a permis d'obtenir des indications sur la conformation du groupement éthoxyle dans ces molécules.

A relation between the diamagnetic term for a proton bonded to a carbon atom and the linear combination of atomic orbital charges on C and H is established. Proton diamagnetic terms of some vinyl ethers are calculated, and the conformation of ethoxy group in these molecules studied.

Canadian Journal of Chemistry, 48, 3154 (1970)

Introduction

De nombreux travaux ont été réalisés pour établir l'expression théorique de la constante d'écran (1 à 11). Les formules obtenues sont plus ou moins simples selon que la méthode utilisée consent des approximations plus ou moins sévères. Ces expressions se ramènent toujours à une somme de deux termes: l'un, diamagnétique, engage une distribution électronique à symétrie sphérique, l'autre, dit paramagnétique, rend compte de la perte de symétrie au niveau de la molécule.

Les études théoriques sont basées soit sur la méthode des variations soit sur celle des perturbations. Nous avons montré par ailleurs (12) que, ces deux méthodes étant équivalentes, elles conduisent à des expressions identiques à condition que les approximations faites dans les deux cas soient de même nature. Si l'on néglige la corrélation électronique, la constante d'écran σ peut s'écrire sous la forme

$$[1] \quad \sigma = \frac{e^2}{6mc^2} \times \sum_{i=1}^{n} \left\langle \phi_i(u) \left| \frac{\boldsymbol{r}_i \cdot (2\boldsymbol{r}_i - \mathrm{Rot}\, \boldsymbol{G}_i(u))}{r_i^3} \right| \phi_i(u) \right\rangle$$

avec

$$[2] \quad \nabla_i^2(\phi_i(u)\boldsymbol{G}_i(u)) - \boldsymbol{G}_i(u)\nabla_i^2\phi_i(u) = -2\boldsymbol{\nabla}_i\Lambda(\phi_i(u)\cdot\boldsymbol{r}_i)$$

Le terme diamagnétique est décrit par les seules fonctions ϕ_i non perturbées, alors que le terme paramagnétique introduit les vecteurs $\boldsymbol{G}_i$, solutions des équations [2]. Les difficultés que soulève la résolution de ces équations limitent l'application de la formule [1] à des systèmes tels que H_2, CH_4, C_2H_2, ... (13–15). En outre, nous remarquons (12) que si l'expression formelle du terme diamagnétique est indépendante de la corrélation électronique, celle du terme paramagnétique, au contraire, devient très complexe lorsque l'hamiltonien tient compte implicitement de l'interaction coulombienne des électrons (16).

Pour ces raisons, nous renonçons au calcul direct du terme paramagnétique, dans la mesure où nous étendons le domaine d'application de la théorie du déplacement chimique à l'étude des molécules organiques courantes. En conséquence nous proposons de déterminer indirectement la contribution paramagnétique au déplacement chimique par la différence

$$[3] \quad \delta_p = \delta_{exp} - \delta_d$$

Can. J. Chem. Downloaded from www.nrcresearchpress.com by 210.87.254.6 on 09/05/12
For personal use only.

Notre centre d'intérêt se déplace alors vers la recherche d'expressions du terme diamagnétique en fonction de paramètres électroniques calculables de façon simple et précise.

Bonham et Strand (17), Malli et Fraga (18) ont calculé ce terme pour les atomes libres. Pour les atomes engagés dans une molécule, Flygare et Goodisman (19) ont proposé une formule empirique qui utilise les valeurs de δ_d pour l'atome libre.

Nous avons proposé une expression de la contribution diamagnétique directement utilisable (20). Elle concerne un proton porté par un carbone, mais est limitée au cas d'une molécule non saturée dont les grandeurs physicochimiques dépendent surtout du mouvement des électrons délocalisés. Cette formule, de type π, relie le terme diamagnétique aux seules charges π (au sens l.c.a.o.) des carbones voisins. Elle a été appliquée avec succès à une étude de l'encombrement stérique sur une série de nitro-naphtalènes substitués (21).

L'objet de la première partie de ce travail est de développer une formule générale du terme diamagnétique d'un proton chimiquement lié à un carbone appartenant à une molécule dans laquelle tous les électrons de valence, localisés ou non, ont la même importance vis à vis des grandeurs étudiées. Le terme diamagnétique est relié par cette formule de type π–σ aux densités en électrons de valence sur la liaison C—H considérée, densités que l'on peut calculer par application de la méthode CNDO/2 (22).

Dans la deuxième partie, la contribution paramagnétique évaluée à l'aide de la formule [3] permet d'apprécier l'importance relative des effets électroniques et d'apporter des renseignements stéréochimiques. Nous illustrons ce processus d'analyse des résultats expérimentaux par l'étude d'éthers vinyliques. Nous calculons l'influence de la configuration *cis* ou *trans* sur la distribution électronique, donc sur le terme diamagnétique, et montrons que l'examen du terme paramagnétique apporte des informations sur la conformation au niveau des liaisons C—O.

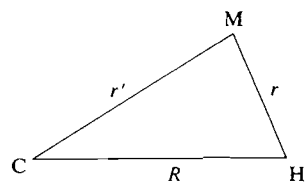

FIG. 1. Définition de r, r' et R.

1. Expression du terme diamagnétique

Considérons un fragment C—H et un point courant M situé à une distance r de H et r' de C (Fig. 1). Soit R la distance entre C et H. Comme le potentiel-vecteur dû au champ magnétique extérieur garde la même expression dans n'importe quel système de coordonnées on peut l'exprimer en fonction de r', ce qui donne pour le terme diamagnétique

$$\sigma_d = \frac{e^2}{3mc^2} \sum_i \left\langle \phi_i \left| \frac{\boldsymbol{r}\cdot\boldsymbol{r}'}{r^3} \right| \phi_i \right\rangle \qquad [4]$$

Dans une méthode l.c.a.o., ϕ_i est une combinaison linéaire d'orbitales atomiques χ_μ

$$\sigma_d = \frac{e^2}{3mc^2} \sum_{\mu,\nu} P_{\mu\nu} \left\langle \chi_\mu \left| \frac{\boldsymbol{r}\cdot\boldsymbol{r}'}{r^3} \right| \chi_\nu \right\rangle \qquad [5]$$

avec

$$P_{\mu\nu} = \sum_i \eta_i C_\mu{}^i C_\nu{}^i \qquad [6]$$

où η_i représente le nombre d'occupation de l'orbitale moléculaire. On voit qu'il est possible d'exprimer σ_d en fonction des quantités $P_{\mu\nu}$ du fragment C—H étudié: il suffit pour cela de calculer l'intégrale de [5] pour les différentes orbitales atomiques χ_μ de ces deux atomes.

(a) $\chi_\mu = \chi_\nu = 1s_H$

Dans ce cas on évalue l'effet de l'électron de l'atome d'hydrogène sur la constante d'écran de cet atome. L'orbitale de Slater $1s_H$ de l'hydrogène s'écrit

$$1s_H = (Z^3/\pi)^{1/2} e^{-Zr} \qquad [7]$$

Le coefficient de P_{HH} dans la formule [5] est alors, en prenant $Z = 1.2$ (22)

$$[8] \qquad I_{1s_H 1s_H} = \frac{e^2}{3mc^2}\left\langle 1s_H \left| \frac{1}{r} \right| 1s_H \right\rangle = \frac{Ze^2}{3mc^2}$$

$$[9] \qquad \boxed{I_{1s_H 1s_H} = 21.30 \times 10^{-6}}$$

(b) $\chi_\mu = \chi_\nu = 2s_C$

Dans la suite des calculs nous utiliserons les coordonnées elliptiques : $\lambda = (r + r')/R$, $\mu = (r - r')/R$ et ϕ.

Rappelons que, dans ce système de coordonnées, l'élément différentiel a pour expression

$$[10] \qquad d\tau = (R^3/8)(\lambda^2 - \mu^2)d\lambda d\mu d\phi$$

et le produit scalaire $\boldsymbol{r}\cdot\boldsymbol{r}'$ a pour valeur

$$[11] \qquad \boldsymbol{r}\cdot\boldsymbol{r}' = (R^2/4)(\lambda^2 + \mu^2 - 2)$$

L'orbitale de Slater $2s_C$ du carbone s'écrit alors

$$[12] \qquad 2s_C(r') = \left(\frac{Z'^5}{96\pi}\right)^{1/2} r' e^{-Z'r'/2} = \left(\frac{Z'^5}{96\pi}\right)^{1/2} \frac{R}{2}(\lambda - \mu)\, e^{-(Z'R/4)(\lambda-\mu)}$$

Il faut donc calculer l'intégrale

$$[13] \qquad I_{2s_C 2s_C} = \frac{e^2}{3mc^2} \cdot \frac{Z'^5}{96\pi} \cdot \frac{R^4}{16} \iiint e^{-(Z'R/2)(\lambda-\mu)} \frac{(\lambda^2 + \mu^2 - 2)(\lambda - \mu)^3}{(\lambda + \mu)^2} d\lambda d\mu d\phi$$

λ variant de 1 à ∞, μ de -1 à $+1$ et ϕ de 0 à 2π.

Cette intégrale se calcule analytiquement par intégration par parties sur les lignes λ = cte puis μ = cte. En posant $a = Z'R/2$, on obtient

$$[14] \qquad I_{2s_C 2s_C} = \frac{Z'e^2}{12mc^2} e^{-2a}(1 + 2a + 2a^2 + \tfrac{4}{3}a^3)$$

d'où pour $Z' = 3.25$ et $R = 2.060$ u.a.

$$[15] \qquad \boxed{I_{2s_C 2s_C} = 1.43 \times 10^{-6}}$$

(c) $\chi_\mu = \chi_\nu = 2p\sigma_C$

Nous appelons $2p\sigma_C$ l'orbitale 2p du carbone qui est dirigée suivant la liaison C—H. On a, en coordonnées polaires

$$[16] \qquad 2p\sigma_C = \left(\frac{Z'^5}{32\pi}\right)^{1/2} r' \cos\theta\, e^{-Z'r'/2}$$

En coordonnées elliptiques de pôles C et H

$$[17] \qquad r' \cos\theta = (R/2)(1 - \lambda\mu)$$

d'où

$$[18] \qquad 2p\sigma_C = \left(\frac{Z'^5}{32\pi}\right)^{1/2} \frac{R}{2}(1 - \lambda\mu)\, e^{-(Z'R/4)(\lambda-\mu)}$$

et l'intégrale à calculer est

$$[19] \qquad I_{2p\sigma_C 2p\sigma_C} = \frac{e^2}{3mc^2} \cdot \frac{Z'^5}{32\pi} \cdot \frac{R^4}{16} \iiint e^{-(Z'R/2)(\lambda-\mu)} \frac{(1 - \lambda\mu)^2(\lambda^2 + \mu^2 - 2)(\lambda - \mu)}{(\lambda + \mu)^2} d\lambda d\mu d\phi$$

En intégrant à nouveau par parties

Can. J. Chem. Downloaded from www.nrcresearchpress.com by 210.87.254.6 on 09/05/12
For personal use only.

[20] $$I_{2p\sigma_C 2p\sigma_C} = \frac{Z'e^2}{12mc^2}\left[-\frac{12}{a^3} + e^{-2a}\left(4a^3 + 6a^2 + 10a + 17 + \frac{24}{a} + \frac{24}{a^2} + \frac{12}{a^3}\right)\right]$$

d'où

[21] $$\boxed{I_{2p\sigma_C 2p\sigma_C} = 0.33 \times 10^{-6}}$$

(d) $\chi_\mu = \chi_\nu = 2p\pi_C$

Nous désignons par $2p\pi_C$ une orbitale 2p du carbone dirigée perpendiculairement à la liaison C—H. Les deux orbitales $2p\pi$ ont pour expression

[22] $$2py_C = \left(\frac{Z'^5}{32\pi}\right)^{1/2} \cdot \frac{R}{2}[(\lambda^2 - 1)(1 - \mu^2)]^{1/2} e^{-(Z'R/4)(\lambda-\mu)} \cos\phi$$

[23] $$2pz_C = \left(\frac{Z'^5}{32\pi}\right)^{1/2} \cdot \frac{R}{2}[(\lambda^2 - 1)(1 - \mu^2)]^{1/2} e^{-(Z'R/2)(\lambda-\mu)} \sin\phi$$

On aura, par exemple pour $2py_C$

[24] $$I_{2py_C 2py_C} = \frac{e^2}{3mc^2} \cdot \frac{Z'^5}{32\pi} \cdot \frac{R^4}{16} \times \iiint e^{-(Z'R/2)(\lambda-\mu)} \frac{(\lambda^2 - 1)(1 - \mu^2)(\lambda^2 + \mu^2 - 2)(\lambda - \mu)}{(\lambda + \mu)^2} \cos^2\phi \, d\lambda d\mu d\phi$$

L'intégrale $I_{2pz_C 2pz_C}$ ne diffère de [24] que par le changement de $\cos^2\phi$ en $\sin^2\phi$; on a donc $I_{2pz_C 2pz_C} = I_{2py_C 2py_C}$ et leur valeur commune est

[25] $$I_{2p\pi_C 2p\pi_C} = \frac{Z'e^2}{12mc^2}\left[\frac{6}{a^3} - e^{-2a}\left(2a + 7 + \frac{12}{a} + \frac{12}{a^2} + \frac{6}{a^3}\right)\right]$$

Soit

[26] $$\boxed{I_{2p\pi_C 2p\pi_C} = 1.98 \times 10^{-6}}$$

Lorsque l'axe Ox n'est pas dirigé suivant la liaison C—H, on doit effectuer une rotation d'un angle α. On a alors

[27] $$I_{2px_C 2px_C} = I_{2p\sigma_C 2p\sigma_C} \sin^2\alpha + I_{2p\pi_C 2p\pi_C} \cos^2\alpha$$

[28] $$I_{2py_C 2py_C} = I_{2p\sigma_C 2p\sigma_C} \cos^2\alpha + I_{2p\pi_C 2p\pi_C} \sin^2\alpha$$

[29] $$I_{2pz_C 2pz_C} = I_{2p\pi_C 2p\pi_C}$$

(e) $\chi_\mu = 1s_H$; $\chi_\nu = 2s_C$

En coordonnées elliptiques, l'orbitale $1s_H$ s'écrit

[30] $$1s_H = \left(\frac{Z^3}{\pi}\right)^{1/2} e^{-(ZR/2)(\lambda-\mu)}$$

et l'expression à calculer est donc

[31] $$I_{1s_H 2s_C} = \frac{e^2}{3mc^2} \cdot \left(\frac{Z^3 Z'^5}{96}\right)^{1/2} \cdot \frac{R^3}{8\pi} \times \iiint e^{-(ZR/2)(\lambda+\mu)} e^{-(Z'R/4)(\lambda-\mu)} \frac{(\lambda^2 + \mu^2 - 2)(\lambda - \mu)^2}{(\lambda + \mu)^2} d\lambda d\mu d\phi$$

Une intégration par parties, sur les lignes λ = cte par exemple, ramène cette intégrale à une forme plus simple dans laquelle le dénominateur en $\lambda + \mu$ est au premier degré. On doit alors réaliser un calcul numérique utilisant, le cas échéant, les formules de récurrence données par Guy *et al.* (23)

Can. J. Chem. Downloaded from www.nrcresearchpress.com by 210.87.254.6 on 09/05/12
For personal use only.

pour les intégrales du type

[32] $$I_{m,n}(a,b) = \iint e^{-a\lambda}\, e^{-b\mu}\, \frac{\lambda^m \mu^n}{\lambda + \mu}\, d\lambda d\mu$$

On obtient ainsi

[33] $$\boxed{I_{1s_H 2s_C} = 2.39 \times 10^{-6}}$$

(f) $\chi_\mu = 1s_H$; $\chi_\nu = 2p\sigma_C$

On doit alors évaluer l'intégrale

[34] $$I_{1s_H 2p\sigma_C} = \frac{e^2}{3mc^2} \cdot \left(\frac{Z^3 Z'^5}{32}\right)^{1/2} \cdot \frac{R^3}{8\pi} \times \iiint e^{-(ZR/2)(\lambda+\mu)}\, e^{-(Z'R/4)(\lambda-\mu)}\, \frac{(1-\lambda\mu)(\lambda^2+\mu^2-2)(\lambda-\mu)}{(\lambda+\mu)^2}\, d\lambda d\mu d\phi$$

Cette intégration se fait sans difficulté de la même manière que pour $I_{1s_H 2s_C}$ et on obtient

[35] $$\boxed{I_{1s_H 2p\sigma_C} = 3.07 \times 10^{-6}}$$

Lorsque l'une des orbitales est $2p\pi_C$, l'autre étant différente, l'intégration de 0 à 2π sur $\sin\phi$ et $\cos\phi$ entraine une annulation de I. On a donc

[36] $$I_{1s_H 2p\pi_C} = I_{2s_C 2p\pi_C} = I_{2p\sigma_C 2p\pi_C} = 0$$

Si l'axe Ox fait un angle α avec la liaison C—H, on a:

[37] $$I_{1s_H 2px_C} = I_{1s_H 2p\sigma_C} \cos\alpha$$

[38] $$I_{1s_H 2py_C} = -I_{1s_H 2p\sigma_C} \sin\alpha$$

(g) $\chi_\mu = 2s_C$; $\chi_\nu = 2p\sigma_C$

[39] $$I_{2s_C 2p\sigma_C} = \frac{e^2}{3mc^2} \cdot \frac{Z'^5}{32\sqrt{3}} \cdot \frac{R^4}{16} \iiint e^{-(Z'R/2)(\lambda-\mu)}\, \frac{(1-\lambda\mu)(\lambda^2+\mu^2-2)(\lambda-\mu)^2}{(\lambda+\mu)^2}\, d\lambda d\mu d\phi$$

[40] $$I_{2s_C 2p\sigma_C} = \frac{Z'e^2}{12\sqrt{3}mc^2}\left[-\frac{5}{a^2} + e^{-2a}\left(4a^3 + 6a^2 + 8a + 10 + \frac{10}{a} + \frac{5}{a^2}\right)\right]$$

[41] $$\boxed{I_{2s_C 2p\sigma_C} = -1.07 \times 10^{-6}}$$

Lorsque l'axe Ox fait un angle α avec la liaison C—H, on a

[42] $$I_{2s_C 2px_C} = I_{2s_C 2p\sigma_C} \cos\alpha$$

[43] $$I_{2s_C 2py_C} = -I_{2s_C 2p\sigma_C} \sin\alpha$$

On constate, d'après [20] et [25], que l'effet global des orbitales $2p_x$, $2p_y$ et $2p_z$ est égal à trois fois l'effet de l'orbitale 2s. Si l'on calcule, pour un atome de carbone C′ non chimiquement lié au proton considéré, l'intégrale $I_{2s_C' 2s_C}$, on trouve, dans le cas d'un carbone aromatique par exemple, que pour le plus proche voisin ($R = 4.068$ u.a.)

[44] $$I_{2s_C' 2s_C'} = 0.013 \times 10^{-6}$$

ce qui nous permet de dire que la contribution des atomes non chimiquement liés est négligeable.

Finalement, la formule qui relie le terme diamagnétique de la constante d'écran d'un proton aux charges l.c.a.o. sur le groupement C—H est la suivante

[45] $$\boxed{\begin{aligned}\sigma_d = {} & 21.30P_{HH} + 1.43P_{2s_C 2s_C} + (0.33\cos^2\alpha + 1.98\sin^2\alpha)P_{xx} + (0.33\sin^2\alpha \\ & + 1.98\cos^2\alpha)P_{yy} + 1.98P_{zz} + 2.39P_{1s_H 2s_C} + 3.07\cos\alpha P_{1s_H 2px_C} - 3.07\sin\alpha P_{1s_H 2py_C} \\ & - 1.07\cos\alpha P_{2s_C 2px_C} + 1.07\sin\alpha P_{2s_C 2py_C}\end{aligned}}$$

Can. J. Chem. Downloaded from www.nrcresearchpress.com by 210.87.254.6 on 09/05/12
For personal use only.

Can. J. Chem. Downloaded from www.nrcresearchpress.com by 210.87.254.6 on 09/05/12
For personal use only.

2. Application à l'étude de quelques éthers vinyliques

Afin d'appliquer le processus d'analyse précédent, nous avons entrepris une étude préliminaire de l'influence d'un substituant alcoxy sur les déplacements chimiques de protons éthyléniques. Cette étude a pour but de préciser notamment dans quelle mesure le terme diamagnétique participe aux écarts $\Delta\delta$ observables entre les configurations *cis–trans*. L'évaluation du terme paramagnétique doit ensuite renseigner sur la stéréochimie au niveau de la liaison C–O. Ce travail sera poursuivi en série diénique.

Les éthers vinyliques $CH_2{=}CH{-}OR$ ont déjà fait l'objet de plusieurs études par résonance magnétique nucléaire (r.m.n.) (24–26). La comparaison de leurs déplacements chimiques à celui de l'éthylène fait ressortir un effet diamagnétique important de OR sur le proton H_B situé en *trans* (1.25 p.p.m. pour $R = CH_3$ et 1.42 p.p.m. pour $R = C_2H_5$) (26). Ce phénomène a été attribué à une influence de la conjugaison de la paire libre de l'oxygène plutôt qu'à une contribution d'anisotropie; cette dernière est en effet présumée faible en raison de la distance O . . . H_B relativement élevée.

D'autres recherches s'intéressent au problème de la conformation de la liaison C—O. En admettant une hybridation trigonale de l'oxygène on peut envisager les schémas conformationnels suivants

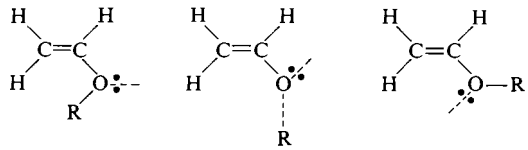

a *b* *c*

Les structures *a* et *c* sont planes "s *cis*" et "s *trans*" respectivement, la forme *b* étant non plane. Ces isomères, qui se transforment mutuellement par rotation de O—R autour de la liaison C—O peuvent être définis par l'angle θ que forment le plan COR et le plan éthylénique. Les structures *a* et *c* sont caractérisées par $\theta = 0°$ et $\theta = 180°$ respectivement. Selon des études de l'éther de vinyle et méthyle gazeux, par spectroscopies infrarouge (27) et de microondes (28), l'isomère s *cis a* est le plus stable à température ordinaire. D'autre part, des résultats r.m.n. indiquent qu'une forme non plane est favorisée par l'introduction de substituants R encombrants (29).

Nous avons entrepris l'étude théorique de ces problèmes en examinant les paramètres des dérivés éthoxylés **3** à **6**, les molécules d'éthylène (**1**) et de propène (**2**) étant prises pour références.

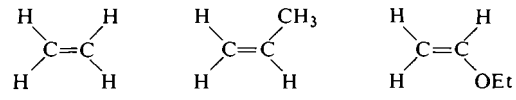

1 **2** **3**

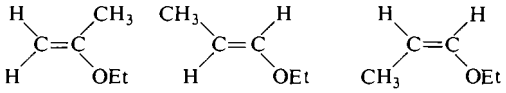

4 **5** **6**

Dans cette série nous considèrerons des molécules qui ne diffèrent l'une de l'autre que par la présence d'un substituant. Nous pourrons ainsi estimer systématiquement les contributions paramagnétiques propres au substituant. En se référant à la molécule non substituée, on a

$$[46]\quad \Delta\delta_p = \delta_p^{\text{éch}} - \delta_p^{\text{réf}} = (\delta^{\text{éch}} - \delta^{\text{réf}})_{\text{exp}} + (\sigma_d^{\text{éch}} - \sigma_d^{\text{réf}})_{\text{calc}} = \Delta\delta_{\text{exp}} + \Delta\sigma_{d\,\text{calc}}$$

Dans cette expression les composés **3** à **6** constituent les échantillons et **1**, **2** les références.

(a) Calcul du terme diamagnétique

Afin d'évaluer le terme diamagnétique nous avons calculé les indices théoriques π et σ par la méthode CNDO/2 (22). Les calculs ont été réalisés pour les trois conformations s *cis a*, non plane *b* et s *trans c* du système C=C—O—Et et pour une même géométrie du squelette. Ces indices théoriques, dont une partie est rassemblée dans le tableau 1, ont ensuite été utilisées pour déterminer les termes diamagnétiques σ_d au moyen de la formule [45] (tableaux 2 à 4). Dans ces tableaux, nous précisons de plus les énergies totales CNDO/2, E_T, relatives aux différentes structures étudiées.

L'examen des charges théoriques appelle différentes remarques: les charges π, P_{zz}, et les charges totales P_{CC} sur les carbones traduisent convenablement les variations attendues sur la base des effets inductif $-I$ et mésomère $+M$ de l'atome d'oxygène. Une relation simple du type $\delta_{\text{exp}} = kq$ s'applique donc approximativement.

TABLEAU 1

Valeurs de charges théoriques, calculées par la méthode CNDO/2, dans quelques éthers vinyliques*

Structure	Conformation	$P_{HH}(A)$	$P_{HH}(B)$	$P_{HH}(C)$	$P_{zz}(C_1)$	$P_{zz}(C_2)$	$P_{C_1C_1}$	$P_{C_2C_2}$
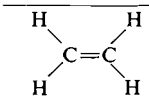 **1**			0.987		1.000		4.026	
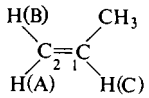 **2**		1.000	0.991	0.985	0.975	1.038	3.987	4.048
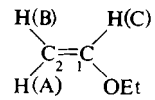 **3**	(*a*)	0.977	0.983	0.994	0.957	1.109	3.845	4.119
	(*b*)	0.974	0.981	1.004	0.958	1.085	3.842	4.105
	(*c*)	0.967	0.972	0.996	0.976	1.080	3.841	4.103
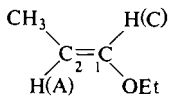 **5**	(*a*)	0.974	—	0.994	0.990	1.081	3.866	4.074
	(*b*)	0.971	—	1.004	0.992	1.057	3.864	4.060
	(*c*)	0.966	—	0.996	1.013	1.050	3.866	4.055

*Les $P_{HH}(i)$ désignent les charges sur les hydrogènes, P_{zz} les charges π et $P_{C_iC_i}$ les charges totales sur les carbones se raffortent aux conformations; (*a*), (*b*), et (*c*).

TABLEAU 2

Analyse des déplacements chimiques du proton H_C (30)*

Structure	δ_{exp}	σ_d	$\Delta\delta_{exp}$	$\Delta\sigma_d$	$\Delta\delta_p$	E_T
1	5.35	30.59	1.04	−0.11	0.93	−1219.6
3 (*a*)	6.39	30.48				
2	4.96	30.75	1.14	−0.22	0.92	−1419.9
5 (*a*)	6.10	30.53				
2	4.87	30.94	0.96	−0.27	0.69	−1417.1
6 (*a*)	5.83	30.67				
1	5.35	30.59	1.04	0.11	1.15	−1219.5
3 (*b*)	6.39	30.70				
2	4.96	30.75	1.14	0.01	1.15	−1419.9
5 (*b*)	6.10	30.76				
2	4.87	30.94	0.96	0.02	0.98	−1419.9
6 (*b*)	5.83	30.96				
1	5.35	30.59	1.04	−0.06	0.98	−1210.2
3 (*c*)	6.39	30.53				
2	4.96	30.75	1.14	−0.14	1.00	−1410.6
5 (*c*)	6.10	30.61				
2	4.87	30.94	0.96	−0.13	0.83	−1410.6
6 (*c*)	5.83	30.81				

*$\Delta\delta_{exp} = \delta_{éch} - \delta_{réf}$; $\Delta\sigma_d = \sigma_{d\,éch} - \sigma_{d\,réf}$; $\Delta\delta_p = \delta_{p\,éch} - \delta_{p\,réf}$; δ et σ sont exprimés en p.p.m. E_T en kcal mole^{-1}.

Cependant l'étude theorique approfondie que nous avons entreprise (section 1) montre que, pour évaluer le terme diamagnétique σ_d on doit en fait tenir compte de l'ensemble de la répartition électronique au voisinage du proton considéré; les résultats rassemblés dans les tableaux 2 à 4 montrent que $\Delta\sigma_d$ calculé reste relativement faible. La validité de ce calcul est évidemment tributaire de la précision avec laquelle sont obtenus les paramètres P_{HH} qui participent de façon importante au terme diamagnétique; bien que nous ayons eu recours à une méthode élaborée, une erreur absolue notable n'est pas exclue.

Une dépendance nette de $\Delta\sigma_d$ en fonction de la géométrie moléculaire se dégage de l'ensemble des résultats. Cette contribution est influencée notamment par l'orientation des paires libres de l'oxygène; ainsi un groupement R situé dans le

Can. J. Chem. Downloaded from www.nrcresearchpress.com by 210.87.254.6 on 09/05/12
For personal use only.

TABLEAU 3

Analyse des déplacements chimiques du proton H_A*

Structure	δ_{exp}	σ_d	$\Delta\delta_{exp}$	$\Delta\sigma_d$	$\Delta\delta_p$	E_T
1	5.35	30.59				
3 (*a*)	4.08	30.58	−1.27	−0.01	−1.28	−1219.6
2	4.87	30.94				
4 (*a*)	3.72	30.83	−1.15	−0.11	−1.26	−1419.9
2	5.73	30.45				
5 (*a*)	4.61	30.40	−1.12	−0.05	−1.17	−1419.9
1	5.35	30.59				
3 (*b*)	4.08	30.47	−1.27	−0.12	−1.39	−1219.5
2	4.87	30.94				
4 (*b*)	3.72	30.82	−1.15	−0.12	−1.27	−1419.8
2	5.73	30.45				
5 (*b*)	4.61	30.31	−1.12	−0.14	−1.26	−1419.9
1	5.35	30.59				
3 (*c*)	4.08	30.31	−1.27	−0.28	−1.55	−1210.2
2	4.87	30.94				
4 (*c*)	3.72	30.67	−1.15	−0.27	−1.42	−1410.6
2	5.73	30.45				
5 (*c*)	4.61	30.18	−1.12	−0.27	−1.39	−1410.6

*$\Delta\delta_{exp} = \delta_{éch} - \delta_{réf}$; $\Delta\sigma_d = \sigma_{d\,éch} - \sigma_{d\,réf}$; $\Delta\delta_p = \delta_{p\,éch} - \delta_{p\,réf}$; δ et σ sont exprimés en p.p.m. et E_T en kcal mole^{-1}.

TABLEAU 4

Analyse des déplacements chimiques du proton H_B*

Structure	δ_{exp}	σ_d	$\Delta\delta_{exp}$	$\Delta\sigma_d$	$\Delta\delta_p$	E_T
1	5.35	30.59				
3 (*a*)	3.88	30.71	−1.47	0.12	−1.35	−1219.6
2	4.96	30.75				
4 (*a*)	3.72	30.88	−1.24	0.13	−1.11	−1419.9
2	5.73	30.45				
6 (*a*)	4.26	30.45	−1.47	0	−1.47	−1417.1
1	5.35	30.59				
3 (*b*)	3.88	30.63	−1.47	0.04	−1.43	−1219.5
2	4.96	30.75				
4 (*b*)	3.72	30.79	−1.24	0.04	−1.20	−1419.8
2	5.73	30.45				
6 (*b*)	4.26	30.48	−1.47	0.03	−1.44	−1419.9
1	5.35	30.59				
3 (*c*)	3.88	30.41	−1.47	−0.18	−1.65	−1210.2
2	4.96	30.75				
4 (*c*)	3.72	30.59	−1.24	−0.16	−1.40	−1410.6
2	5.73	30.45				
6 (*c*)	4.26	30.29	−1.47	−0.16	−1.63	−1410.6

*$\Delta\delta_{exp} = \delta_{éch} - \delta_{réf}$; $\Delta\sigma_d = \sigma_{d\,éch} - \sigma_{d\,réf}$; $\Delta\delta_p = \delta_{p\,éch} - \delta_{p\,réf}$; δ et σ sont exprimés en p.p.m. et E_T en kcal mole^{-1}.

plan de la molécule introduit une diminution de la valeur de $\Delta\sigma_d$ relative au proton C alors qu'un groupement R hors plan peut entrainer une légère augmentation (tableau 2). On constate d'autre part, que le terme diamagnétique dépend de la disposition des protons géminés en β par rapport au substituant: OR introduit un écran diamagnétique plus important en *trans* (H_B) qu'en *cis* (H_A).

(b) Terme paramagnétique et structure moléculaire

Les termes paramagnétiques $\Delta\delta_p$ déduits de la formule [46] sont rassemblés dans les tableaux 2 à 4. A géométrie identique on attend en première approximation[1] des contributions caractéris-

[1]Les contributions à $\Delta\delta_p$ associées par exemple aux champs électriques intramoléculaires (31) dépendent en fait de la répartition des charges.

Can. J. Chem. Downloaded from www.nrcresearchpress.com by 210.87.254.6 on 09/05/12
For personal use only.

Can. J. Chem. Downloaded from www.nrcresearchpress.com by 210.87.254.6 on 09/05/12
For personal use only.

tiques de OEt sensiblement constantes en chacune des positions H_A, H_B ou H_C respectivement. A l'inverse, des valeurs $\Delta\delta_p$ notablement différentes pour une même position sont probablement l'indice d'une modification conformationnelle au niveau de la liaison C—O. La comparaison des résultats (tableaux 2 à 4) autorise les conclusions suivantes:

(1) Si, quelle que soit la conformation, les effets paramagnétiques de OEt sur H_C sont sensiblement identiques dans les molécules **3** et **5**, la structure **6** est nettement différenciée; ceci incite à attribuer au systéme HC—OEt de **6** une conformation différente de celle qu'il adopte dans les composés **3** et **5**; un changement de configuration *cis–trans* est probablement associé à une modification de l'équilibre conformationnel.

(2) Selon les énergies totales E_T la conformation non plane serait privilégiée dans **6**. Par contre les molécules **3**, **4** et **5** seraient soient planes s *cis* soit non planes, la seconde hypothèse étant alors exclue dans **3** et **5** en raison de la remarque *1*.

(3) L'effet paramagnétique de OEt sur H_C dans un composé **6** non plan est voisin des valeurs relatives aux molécules **3** et **5** planes s *cis* (tableau 2).

(4) Quel que soit le modèle adopté, les paramètres $\Delta\delta_p$ relatifs au proton H_A de **3**, **4** et **5** sont peu différents (tableau 3); l'équilibre conformationnel resterait donc assez voisin dans ces trois composés. Cependant le tableau 4 montre que $\Delta\delta_p(H_B)$ de **4** se distingue nettement de $\Delta\delta_p(H_B)$ de **3**. L'hypothèse de légères déformations angulaires ou de modifications conformationnelles du CH_3, dans **4** par rapport à **2**, peut notamment être avancée (31); un tel phénomène est en effet susceptible d'influencer de façon prépondérante le proton H_B situé en *cis* du CH_3 dans **4**.

En résumé, ces considérations sont en faveur de structures conformationnelles différentes dans les isomères *cis* et *trans*. L'existence d'un faible couplage du type $J_{H-C-O-C-H}$ dans le composé CH_3 CH=CH—OCH_3 de configuration *trans* et son absence apparente dans l'isomère *cis* corroborent ces conclusions (30). En effet les couplages à longue distance sont généralement mieux transmis lors d'une disposition "zig-zag" plane analogue à celle qui caractérise la conformation s *cis*. Les composés **3**, **4** et **5** présenteraient donc une géométrie préférentiellement plane s *cis* (*a*), alors que le composé **6** serait en majorité s *trans* ou non plan, la seconde alternative étant étayée par la comparaison des énergies totales. En ce qui concerne le dérivé **3**, ces conclusions sont en accord avec les résultats relatifs à l'éther de vinyle et de méthyle (27, 28). Des informations supplémentaires sont recherchées par spectroscopies ultraviolette et infrarouge.

Conclusion

Dans le souci de rendre les expressions théoriques du déplacement chimique applicables à la discussion des problèmes structuraux courants en chimie organique, nous avons cherché à les expliciter en fonction de paramètres calculables pratiquement.

Les formules issues du développement de l'équation de Ramsey dans le cadre des théories de perturbations et variations sont identiques et constituées d'un terme diamagnétique et d'un terme paramagnétique (formule [1]). La seconde contribution fait appel à des grandeurs difficiles à évaluer de façon rigoureuse ou même approchée et nous nous sommes limités au développement du terme diamagnétique σ_d. Celui-ci s'exprime en fonction de charges électroniques l.c.a.o. qui s'obtiennent par les méthodes habituelles de la chimie quantique (formule [45]). La précision de son évaluation dépend donc de la qualité de la méthode employée. Le terme paramagnétique est ensuite déterminé par application de la formule [3]. La discussion des termes $\Delta\sigma_d$ et $\Delta\delta_p$ ainsi évalués permet de préciser les contributions des effets électroniques et spatiaux associées à des changements de substituants ou de géométrie, et donc de renseigner sur la structure moléculaire. Nous avons appliqué ce processus d'analyse à l'étude de quelques éthers vinyliques; les charges électroniques calculées par la méthode CNDO/2 conduisent à des termes diamagnétiques qui dépendent de la configuration de la double liaison et de la conformation au niveau de la liaison C—O. L'effet prédominant du substituant OEt semble introduit cependant par le terme paramagnétique. Les résultats obtenus sont en faveur d'une conformation préférentiellement plane s *cis* du système C=C—O—C_2H_5 dans l'éther de vinyle et d'éthyle **3**, dans son dérivé méthylé sur le carbone en α de OEt **4** et dans l'éther de propényle et d'éthyle *trans* **5**; par contre, la structure est probablement en majorité non plane si le substituant méthyle en β est disposé en *cis* par rapport à OEt **6**.

Nous remercions le Professeur G. Klopman pour les discussions fructueuses que nous avons eues avec lui.

Ce travail se situe dans la perspective de recherche qui a reçu le soutien n° 296 de l'O.T.A.N.

1. N. F. RAMSEY. Phys. Rev. **78**, 699 (1950).
2. A. SAIKA et C. P. SLICHTER. J. Chem. Phys. **22**, 261 (1954).
3. J. A. POPLE. Proc. Roy. Soc. **A239**, 541 et 550 (1957).
4. H. M. MCCONNEL. J. Chem. Phys. **27**, 226. (1957).
5. T. P. DAS et R. BERSOHN. Phys. Rev. **104**, 849 (1956).
6. B. MCGARVEY. J. Chem. Phys. **26**, 221 (1957).
7. M. J. STEPHEN. Proc. Roy. Soc. **A242**, 264 (1957).
8. J. A. POPLE. Mol. Phys. **1**, 175 (1958).
9. R. MCWEENY. Mol. Phys. **1**, 311 (1958).
10. J. R. DIDRY, F. CABARET, et J. GUY. J. Phys. Rad. **23**, 65 (1962).
11. J. A. POPLE. J. Chem. Phys. **37**, 53 (1963).
12. F. TONNARD et S. ODIOT. Int. J. Quantum Chem. A paraître.
13. J. I. MUSHER. *Dans* Advances in magnetic resonance. Vol. **2**. Academic Press, Inc., New York. 1966. p. 177.
14. J. R. DIDRY. Thèse, Paris, 1963.
15. F. CABARET. Thèse, Paris, 1963.
16. R. M. STEVENS, R. M. PITZER, et W. N. LIPSCOMB. J. Chem. Phys. **38**, 550 (1963).
17. R. A. BONHAM et T. G. STRAND. J. Chem. Phys. **40**, 3447 (1964).
18. G. MALLI et S. FRAGA. Theor. Chim. Acta, **5**, 275 (1966).
19. W. H. FLYGARE et J. GOODISMAN. J. Chem. Phys. **49**, 3122 (1968).
20. S. ODIOT et F. TONNARD. C.R. Acad. Sci. **262**, 1181 (1966).
21. S. ODIOT, J. C. RICHER, et F. TONNARD. Can. J. Chem. **47**, 2805 (1969).
22. J. A. POPLE, D. P. SANTRY, et G. A. SEGAL. J. Chem. Phys. **43**, S129 (1965). J. A. POPLE et G. A. SEGAL. J. Chem. Phys. **44**, 3289 (1966).
23. J. GUY, A. SALES, et J. R. DIDRY. J. Phys. Rad. **23**, 149 (1962).
24. J. FEENEY, A. LEDWITH, et L. H. SUTCLIFFE. J. Chem. Soc. 2021 (1962).
25. J. FEENEY et L. H. SUTCLIFFE. Spectrochim. Acta. **24A**, 1135 (1968).
26. R. T. HOBGOOD, G. S. REDDY et J. H. GOLDSTEIN. J. Phys. Chem., **67**, 110 (1963).
27. N. L. OWEN et N. SHEPPARD. Trans. Faraday Soc. **60**, 634 (1964).
28. P. CAHILL, L. P. GOLD, et N. L. OWEN. J. Chem. Phys. **48**, 1620 (1968).
29. K. HATADA, M. TAKESHITA, et H. YUKI. Tetrahedron Lett. **44**, 4621 (1968).
30. J. P. DORIE. Thèse. en cours.
31. R. F. ZURCHER. *Dans* Progress in NMR spectroscopy. Vol. 2. *Edité par* Emsley, Feeney, et Sutcliffe, 1967.

Can. J. Chem. Downloaded from www.nrcresearchpress.com by 210.87.254.6 on 09/05/12
For personal use only.

Can. J. Chem. Downloaded from www.nrcresearchpress.com by 210.87.254.6 on 09/05/12
For personal use only.

The ternary system silver–indium–aluminum

A. N. CAMPBELL AND R. WAGEMANN

Department of Chemistry, University of Manitoba, Winnipeg, Manitoba

Received April 30, 1970

A number of alloys have been examined microscopically. From these observations, from the equilibrium diagrams of the component binary systems, and from the application of the phase rule, a room temperature isothermal section has been deduced. Three vertical sections through the ternary system have been partially constructed from differential thermal analysis. These data show that invariant planes occur at 143, 148, 241, and 506 °C. From the information obtained from the vertical sections and the room temperature isothermal section, isothermal sections have also been proposed at 143 and 148°. The transformation at the 143 °C invariant plane is a ternary eutectic, at 148° a ternary peritectic, and the other transformations at 241 and 506° are also ternary peritectics.

Some evidence indicates that the ξ-phase of Ag–Al system and the γ-phase of Ag–In system link up through the ternary system forming a single phase region, and that such may also be the case with the phases μ and α′ of the systems Ag–Al and Ag–In, respectively. The phases ε and φ of the system Ag–In do not appear to be capable of dissolving aluminum appreciably.

Canadian Journal of Chemistry, 48, 3164 (1970)

Introduction

This paper is a continuation of our work on the system Ag–In–Al. Previous papers have dealt with two of the component binary systems. The system Al–In is very simple, its main feature of interest being an extensive solubility gap. We have determined the limits of this gap up to the critical solution temperature of 945° (1).

The system Ag–Al is more complicated, exhibiting a eutectic, two peritectics, and five different solid phases. The system is well established (2) and we saw no reason to question it.

The third binary system Ag–In is the most complicated and still somewhat in doubt. We therefore subjected this system to a lengthy experimental investigation; the results have been published (3). Reference should be made to this paper for a bibliography and a discussion of our results and those of our predecessors. The experimental techniques, which are those of the present paper, are also described.

In the present study, the nomenclature of the binary system Ag–In has been retained, wherever possible, to describe the ternary phases. For example, the hexagonal phase ξ of the binary system Ag–Al is isomorphous with the γ-phase in the system Ag–In. The phase-field in the ternary system which connects these two phases in the binary systems is designated γ. However, when this phase is referred to in the binary system Ag–Al the symbol ξ is retained in accordance with the original nomenclature of this binary system. The symbol σ has been introduced to designate the aluminum-α solid solution.

Three isothermal sections of the ternary system were constructed at room temperature, 143 and 148 °C, respectively. The room temperature isotherm was drawn on the basis of experimental data. The two other isothermal sections were drawn on the basis of a knowledge of the type of equilibria that exist in the system, the data from the vertical sections, the room temperature isothermal section, and some reasonable assumptions.

Thermal Analysis

In order to study the ternary system we investigated alloys lying on vertical sections of the solid model. The composition of these sections is shown in Fig. 1. In all, we investigated 105

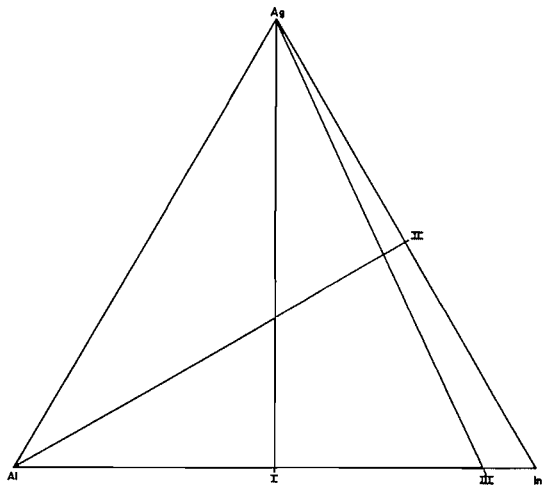

FIG. 1. Plan of "vertical sections".

Can. J. Chem. Downloaded from www.nrcresearchpress.com by 210.87.254.6 on 09/05/12
For personal use only.

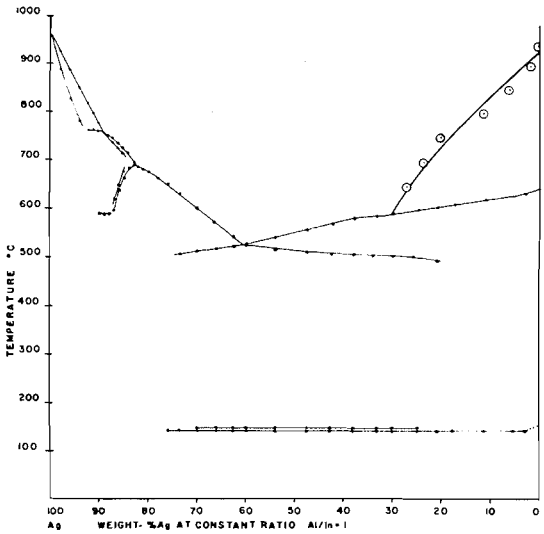

FIG. 2. Vertical section I.

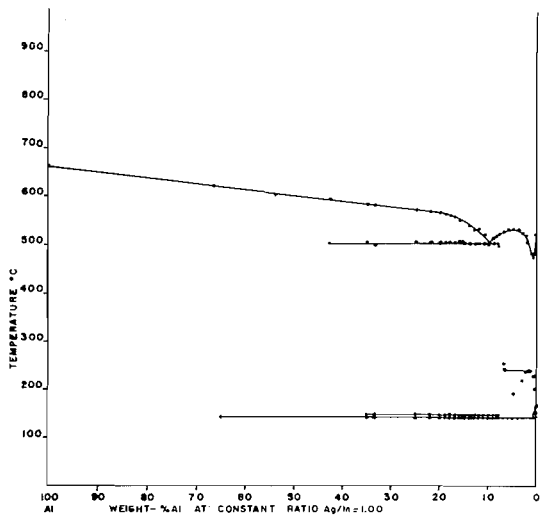

FIG. 3. Vertical section II.

alloys by differential thermal analysis from which these sections were constructed, as shown in Figs. 2, 3, and 4. The data for these sections as well as the X-ray and other pertinent data are to be found in the Depository of Unpublished Data.[1] Such sections are, of course, not pseudo-binary since in general, when a solid phase separates, the composition of the residual melt moves away from that of the vertical section.

[1]Photocopies may be obtained free of charge, upon request, from the Depository of Unpublished Data, National Science Library, National Research Council of Canada, Ottawa 2, Canada.

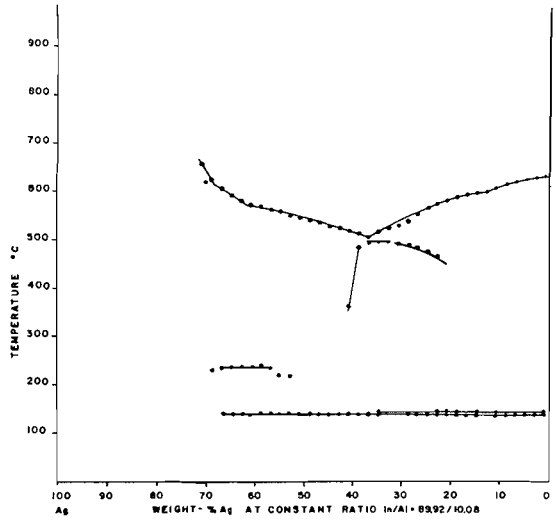

FIG. 4. Vertical section III.

Despite this limitation, the vertical sections yield much information about the ternary system. For example, the identity of some phases that must participate in the isothermal equilibria at 143 and 148 °C was established, as well as the type of equilibrium that must exist at these temperatures. The extent of the isothermal planes was roughly delineated with the use of these sections. If no metastability occurred the extent of these planes could be established accurately from these vertical sections. In general, it was possible to construct the room temperature isothermal section with a relatively small number of annealed alloys, with the aid of these vertical sections. Differential thermal analysis is, of course, much less laborious and time consuming than the preparation of microsections.

The Room Temperature Isothermal Section

At room temperature all phases are solid. We suggest that three three-phase areas exist, *viz.*, ($\sigma + \phi + \varepsilon$), ($\sigma + \gamma + \varepsilon$), and ($\sigma + \phi$ + In). Obviously, a two-phase area ($\sigma + \phi$) must exist separating the two three-phase areas to which σ and ϕ are common. We show, by means of a dotted line, that this area exists but we have no experimental data for it. The phase boundaries have been drawn very tentatively, in accordance with the microstructure of annealed alloys, shown in the photomicrographs of Plates 1 to 11. This isothermal section is shown in Fig. 5.

The phases were identified under the microscope by their characteristic appearance when

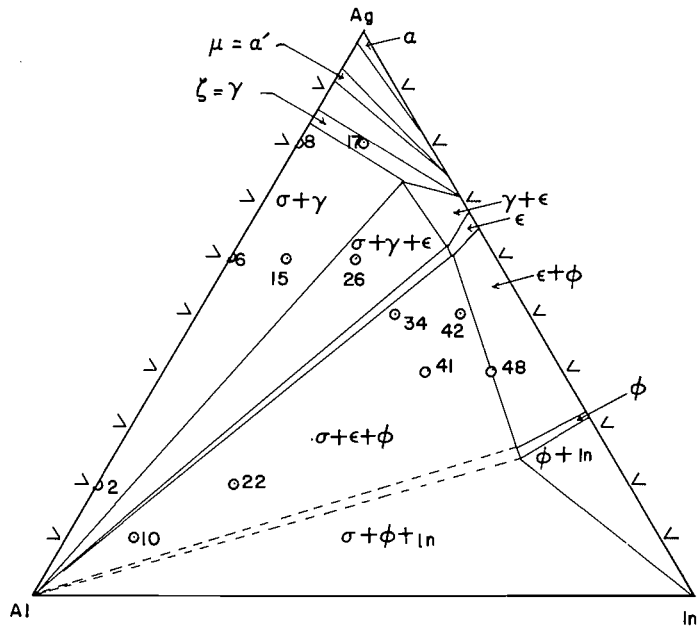

FIG. 5. Isothermal section at room temperature.

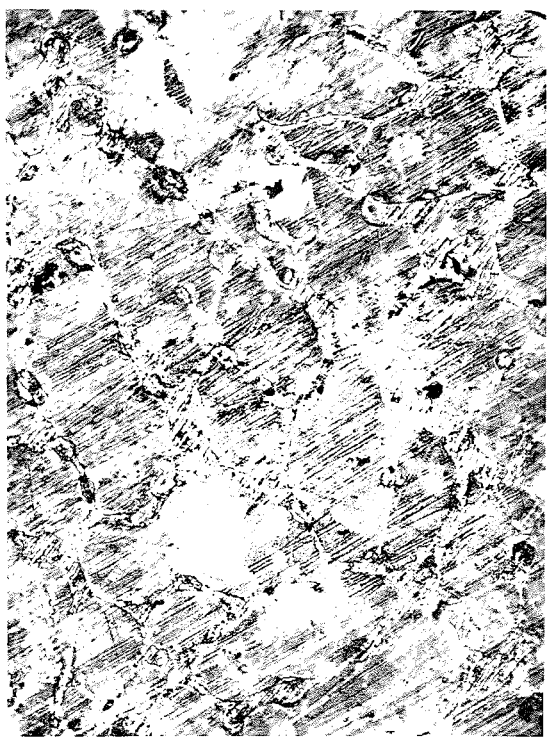

PLATE 1. Alloy No. 8. Composition: 80.00% Ag, 20.00% Al. Annealed at 135 °C for three weeks. Grain of ξ-phase separated by the eutectic matrix. Magnification approximately 80 ×.

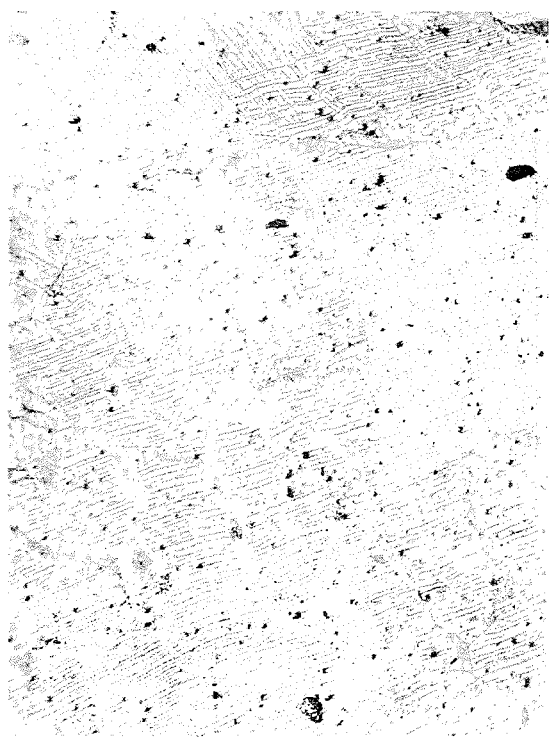

PLATE 2. Alloy No. 6. Composition: 60.00% Ag, 40.00% Al. Annealed at 135 °C for three weeks. Consists nearly completely of eutectic of the lamellar type. Magnification approximately 80 ×.

Can. J. Chem. Downloaded from www.nrcresearchpress.com by 210.87.254.6 on 09/05/12
For personal use only.

Can. J. Chem. Downloaded from www.nrcresearchpress.com by 210.87.254.6 on 09/05/12
For personal use only.

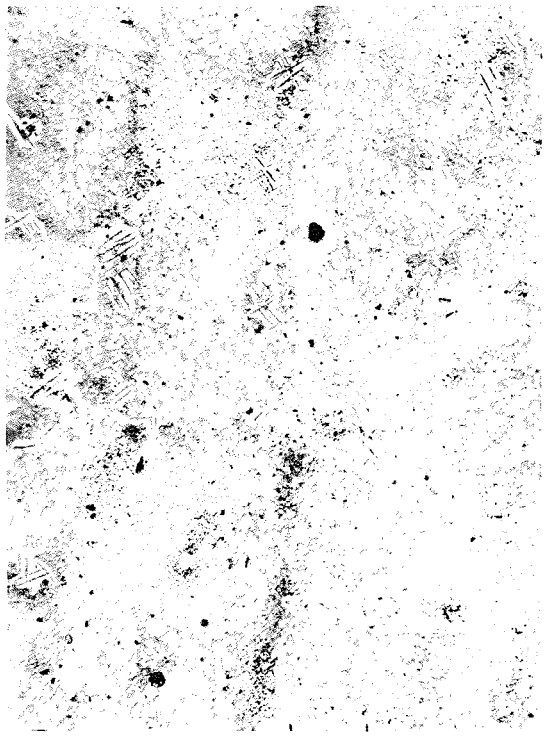

PLATE 3. Alloy No. 2. Composition: 20.00% Ag, 80.00% Al. Annealed at 135 °C for three weeks. Needle-like ξ-phase precipitate at the grain boundaries can be seen. Magnification approximately 80 ×.

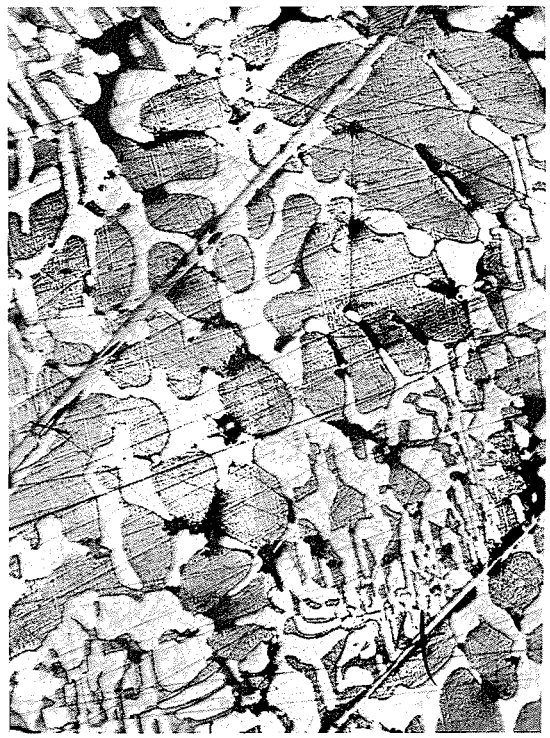

PLATE 4. Alloy No. 15. Composition: 60.00% Ag, 30.00% Al, 10.00% In. Annealed at 135 °C. for three weeks. Evidently it is a two-phase alloy. Darker γ-phase grains are separated by σ-phase (lighter areas). Magnification approximately 80 ×.

suitably etched. For the purpose of reference some Ag–Al alloys were examined (Plates 1–3) in order to discover the change in appearance of the microstructure when indium is added. Throughout the ternary system the σ-phase had a spongy appearance and was easily scratched. The physical characteristics of this phase did not change noticeably regardless of the gross composition of the alloy, and this indicates that silver and indium have a very limited solubility in this phase. The ε-phase and the ϕ-phase were also easily identified in the ternary system since their physical characteristics such as etching properties and hardness changed little when aluminum was added. Again, this indicates that the solubility of aluminum in these phases is small.

The alloy shown in Plate 4 consists of two phases σ, γ with no eutectic present, such as is found in the binary alloys shown in Plates 1 and 2. The alloys shown in Plates 6–9 and 11 all consist of three phases (σ + ε + ϕ). These alloys differ only in the proportion of these phases. The presence of a small amount of metastable indium is discernible in Plate 7. The alloy in Plate 11 has little σ-phase and must therefore be near the (ε + ϕ) boundary, while the alloy in Plate 10 shows only traces of σ-phase and therefore lies approximately on the boundary. The ξ-phase of the system Ag–Al and the γ-phase of the system Ag–In are both close packed hexagonal with similar cell edges, *viz.*, $a = 2.961$ Å, $c = 4.778$ Å, for γ (3); $a = 2.865$ Å, $c = 4.653$ Å, for ξ (7). An alloy of composition 80.00% Ag, 10.00% Al, 10.00% In,[2] was annealed for three weeks at 135 °C. When examined under the microscope this alloy appeared homogeneous. In view of this, it appears that the ξ-phase and the α-phase of the respective binary systems are connected in the ternary system by a single-phase field namely, γ.

The 143 °C Isothermal Section

This section is shown in Fig. 6. The transformation at this temperature is of the ternary eutectic type: L ⇄ ϕ + σ + In. The composition

[2]Compositions are in weight percent throughout.

PLATE 5. Alloy No. 26. Composition: 60.00% Ag, 20.00% Al, 20.00% In. Annealed for three weeks at 135 °C. Careful scrutiny shows that three phases are present, σ, γ, and ε. Magnification approximately 80 ×.

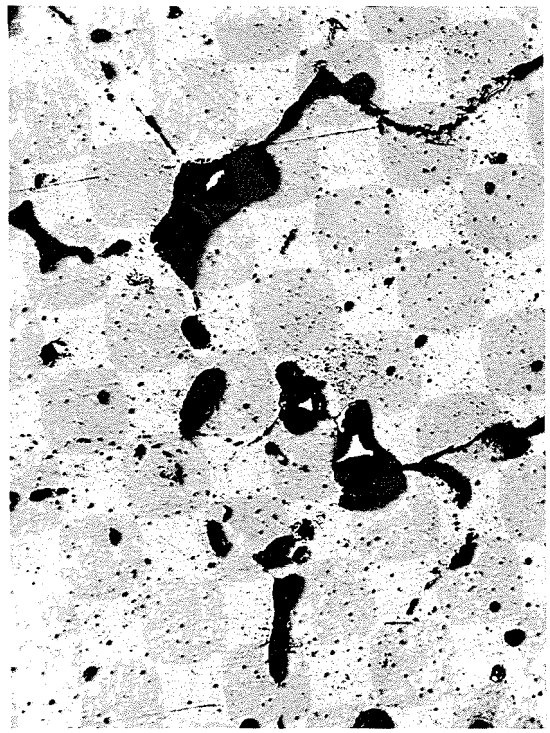

PLATE 6. Alloy No. 10. Composition: 10.00% Ag, 80.00% Al, 10.00% In. Annealed at 135 °C for three weeks. The major phase is σ-phase. A small amount of ϕ-phase is present (grey) and a very small amount of ε-phase (light) is also present. Magnification approximately 80 ×.

of the liquid in equilibrium with the three solids was estimated from the intersection of the eutectic troughs as 95% In, 4% Ag, 1% Al. Due to the very narrow range of homogeneity of the ϕ-phase the two-phase field (ϕ + σ), is not shown in this section. The three-phase field (ε + σ + ϕ) adjoining the invariant plane represents a limiting case.

The compositions of the three solids, σ, ϕ, In, as shown in Fig. 6, are very nearly the same as the compositions of these phases in the respective binary systems. This is borne out by the fact that the 143 °C arrest line (eutectic) in vertical section II (Fig. 3) abuts on the binary system Ag–In, which evidently suggests that ϕ does not incorporate aluminum at this temperature. With regard to the σ-phase (aluminum-α solid solution), we note that the solubility of silver (2) or indium (1) in aluminum is very small at this temperature. It is reasonable to assume, we think, that the solubility of these metals in aluminum in the ternary system is not greater than in the respective binary systems. The approximate termination of the 143 °C arrest line on the binary Al–In, in vertical sections I and III (Figs. 2 and 4) does indicate that the σ-phase is nearly pure aluminum. The ε-phase has a composition range of 2% in the binary system Ag–In (3, 8) and, since the 148 °C arrest line (peritectic) in vertical section II (Fig. 3) terminates at approximately 8% Al, the solubility of aluminum in ε can only be small, and the field of homogeneity of ε in the ternary system must therefore be small at this temperature.

The 148 °C Isothermal Section (Containing the Invariant Plane)

This section is shown in Fig. 7. From the location and direction of the ternary troughs, as deduced from the vertical sections, it is known that a peritectic type of equilibrium exists at this temperature. We deduced the nature and approximate composition of the equilibrium phases as follows: The vertical sections show that the binary arrest line at 166°, for the system Ag–In

Can. J. Chem. Downloaded from www.nrcresearchpress.com by 210.87.254.6 on 09/05/12
For personal use only.

Can. J. Chem. Downloaded from www.nrcresearchpress.com by 210.87.254.6 on 09/05/12
For personal use only.

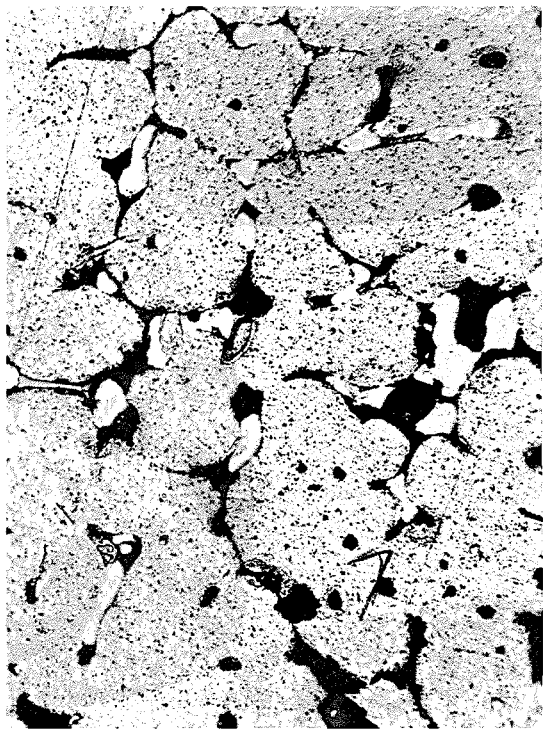

PLATE 7. Alloy No. 22. Composition: 20.00% Ag, 60.00% Al, 20.00% In. Annealed at 135 °C for three weeks. It is a three-phase alloy with σ (major), ε (small light areas) and some ϕ-phase (smooth grey) present. Some metastable In-phase is also present. Magnification approximately 80 ×.

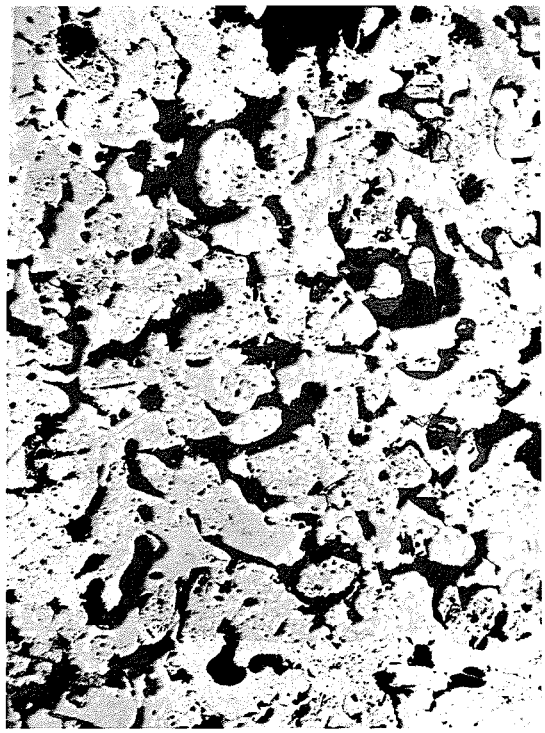

PLATE 8. Alloy No. 34. Composition: 50.00% Ag, 20.00% Al, 30.00% In. Annealed at 135 °C for three weeks. Three phases are present: σ (light "spongy"), ε (light smooth), and ϕ (smooth grey). Magnification approximately 80 ×.

terminates on the invariant plane at 148° which means that three phases of the four equilibrium phases must be L, ε, and ϕ. The fourth phase is σ since it coexists with solid In at room temperature and also with liquid indium, and no phases other than those present in the respective binary systems occur in the ternary system between room temperature and 166 °C. The equilibrium at 148 °C is therefore $L + \varepsilon \rightleftarrows \sigma + \phi$.

The composition of the liquid in equilibrium with the three solid phases is 89% In, 5% Ag, 6% Al with an error of ±2% in indium or aluminum and negligible error in silver. This was established by chemical analysis of the liquid of five different alloys, differing widely in gross composition. The alloys were first annealed at 135 °C for three weeks and then heated to 150 °C, and kept at this temperature for approximately 1 h. Droplets of liquid oozed out of the alloy after it was heated to this temperature. The alloy was then cooled to room temperature and the solidified globules were collected and analyzed by titration and polarography. In this analysis the error in composition of the equilibrium liquid due to the 2° rise in temperature of the liquid from equilibrium is negligible. The extent of the isothermal plane had to be such that the 148 °C "isotherms" of vertical sections II and III (Figs. 3 and 4) when transferred to this plane would fall within the area of this isothermal plane. The directions of the boundaries were also fixed to some extent by the requirement of thermodynamic stability of all phases.

Since the difference in temperature between this section and that at 143 °C is only 5 °C, it is not surprising that, apart from the invariant planes, there is considerable similarity between the two sections. The composition of the solids at this temperature is assumed to be practically the same as at 143 °C.

The μ-Phase and the α′-Phase

We have recently found that at the composition Ag_3In an α′-phase exists in the system Ag–In,

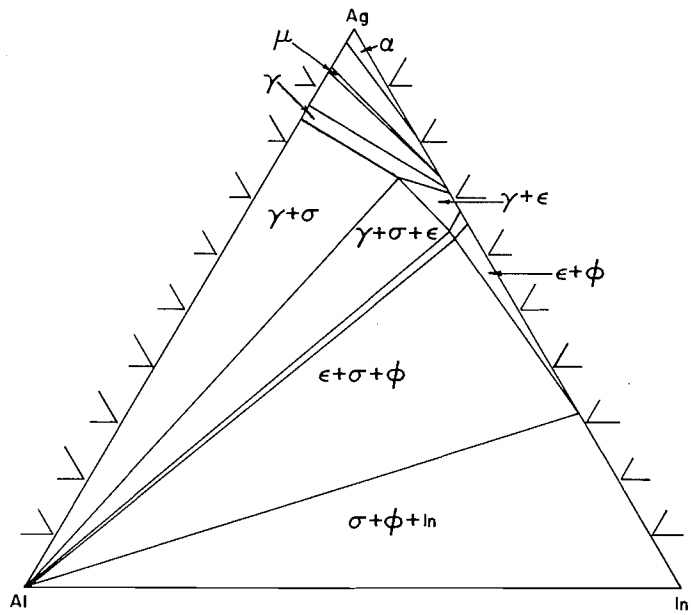

FIG. 6. Isothermal section at 143 °C.

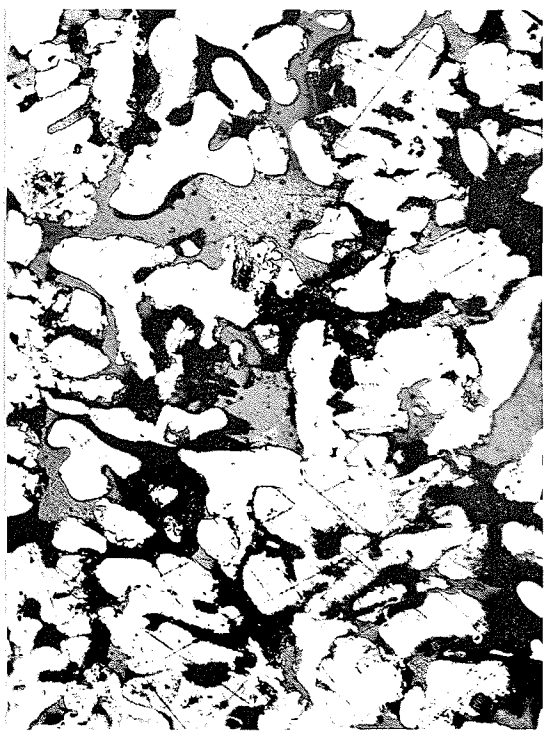

PLATE 9. Alloy No. 41. Composition: 40.00% Ag, 20.00% Al, 40.00% In. Annealed at 135 °C for three weeks. Three phases are present: σ (light scratched), ε (light smooth), and φ (dark grey smooth). Magnification approximately 80 ×.

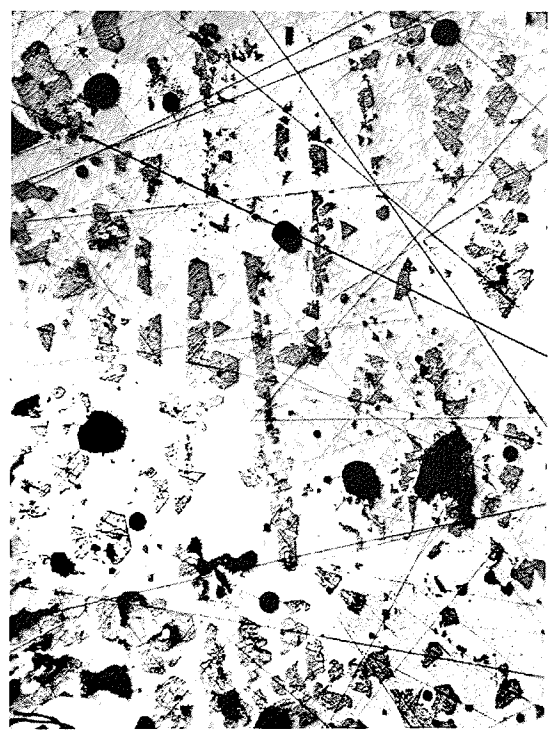

PLATE 10. Alloy No. 48. Composition: 40.00% Ag, 10.00% Al, 50.00% In. Annealed at 135 °C for three weeks. This alloy consists of ε-phase, φ-phase (brown), and a very small amount of σ-phase. The black areas are holes. Magnification approximately 80 ×.

Can. J. Chem. Downloaded from www.nrcresearchpress.com by 210.87.254.6 on 09/05/12
For personal use only.

Can. J. Chem. Downloaded from www.nrcresearchpress.com by 210.87.254.6 on 09/05/12
For personal use only.

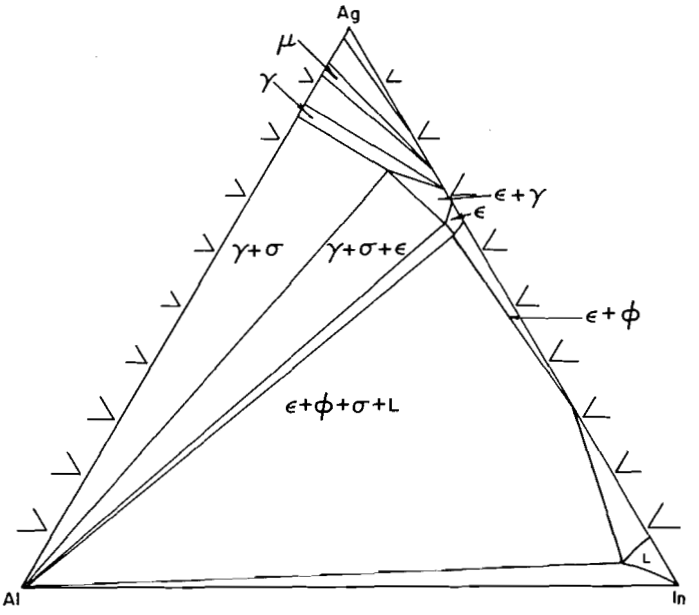

FIG. 7. Isothermal section at 148 °C.

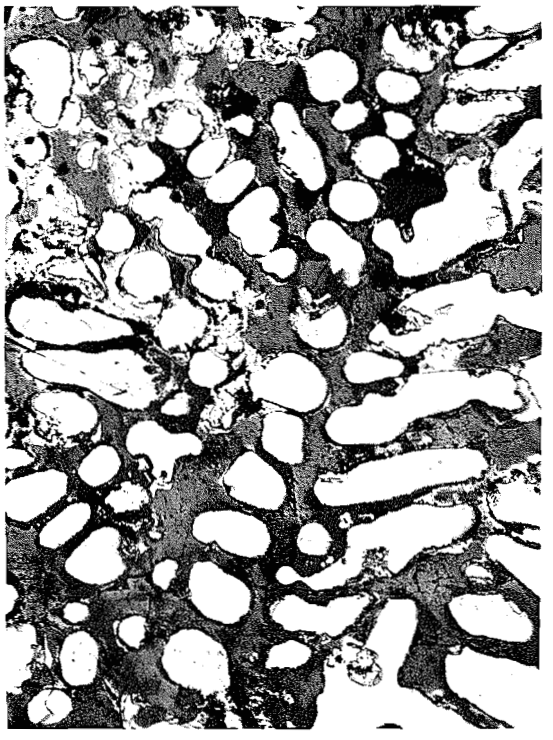

PLATE 11. Alloy No. 42. Composition: 50.00% Ag, 10.00% Al, 40.00% In. Annealed at 135 °C for three weeks. This alloy consists of ε-phase (light areas) within the φ-phase (grey) and a small amount of σ-phase. Magnification approximately 80 ×.

which is structurally closely related to the terminal Ag-α phase of that system (3). The cubic α′-phase has the same cell edge as the terminal Ag-α phase *viz.* 4.144 Å, but the two types of atoms occupy definite sites on the lattice. The silver atoms occupy the face-centered positions and the indium atoms occupy the corner positions of the cubic lattice.

In the system Ag–Al, the μ-phase exists at the composition Ag_3Al, which is reported as cubic (β-manganese) with a cell edge of 6.916 Å (4).

We have examined the powder X-ray diffraction data of Obinata and Hagiya (4*b*), and find that we can index all their diffraction lines, except two weak lines, on a smaller cubic cell edge, *viz.* 4.051 Å, if we allow for the presence of ξ-phase. The μ-phase is formed at 448 °C by a peritectoid reaction from ξ and (Ag-α) phases. That ξ could be present in such an alloy at room temperature is reasonable since peritectoid reactions are slow and are frequently responsible for the presence of metastable phases.

We suggest that in the system Ag–Al, the μ-phase is related to the terminal Ag-α phase in the same way that the α′-phase in the system Ag–In is related to the terminal Ag-α phase. If the two phases, α′ and μ have the same crystal structure and very similar cell edges, *viz.* $a = 4.144$ Å for α′ and $a = 4.051$ Å for μ, we would expect that aluminum and indium atoms are inter-

changeable on the two lattices, and that the two phases would be joined by a homogeneous phase-field in the ternary system as we have shown in the isothermal sections.

Against this view it may be urged that the atom positions for Ag and Al in the β-Mn structure have actually been determined by Fagerber and Westgren (5) and that their results rule out an α′ structure. Neither can we account for the two faint lines in the diffraction pattern. If indeed α′ and μ do not have the same structure, then the homogeneous field which we have labelled α′ will have to be replaced by two small fields, making this a heterogeneous area.

Other Aspects of the Ternary System

The two peritectic reaction arrests at 780 and 695° in the Ag–Al and Ag–In systems, respectively, form a connecting reaction surface through the ternary system. This is evident from vertical Section I, Fig. 2. Similarly the 610° peritectic halt of the binary Ag–Al system and the 670° peritectic arrest of the Ag–In system form a connecting reaction surface through the ternary system. The 727° arrest of the Ag–Al system and 660° arrest of the Ag–In system are similarly connected. This is again evident from Fig. 2. Thus the high temperature β-phase (body-centered cubic) which exists in the binary system Ag–In and Ag–Al, respectively, forms a connecting homogeneous volume through the ternary system. This is not surprising since the β-phases of the two binary systems have the same crystal structure and the cell edges are comparable, *viz.* $a = 3.3682$ Å (6) for β (Ag–In), *i.e.* Ag_3In, at 648° and $a = 3.3002$ Å (6) for β (Ag–Al), *i.e.* Ag_3Al, at 700°. This means that In and Al atoms are interchangeable on the lattice sites of the body-centered cubic structure.

The three-phase equilibrium of the binary system Ag–Al, at 566° (peritectic) terminates in the ternary system in an invariant plane at 506° (vertical section II, Fig. 3). From vertical section III, Fig. 4, it appears that an invariant plane also exists at 241°.

1. (*a*) E. RAUB and M. ENGEL. Metallforsch. **1**, 148 (1946). (*b*) S. VALENTINER and I. PUZICHA. Metallforsch. **2**, 127 (1947). (*c*) A. N. CAMPBELL, L. B. BUCHANAN, J. M. KUZMAK, and R. H. TUXWORTH. J. Amer. Chem. Soc. **74**, 1962–1966 (1952). (*d*) A. N. CAMPBELL and R. WAGEMANN. Can. J. Chem. **44**, 657 (1966).
2. M. HANSEN. Constitution of binary alloys. 2nd ed. McGraw-Hill Book Co., Inc., Toronto. 1958.
3. A. N. CAMPBELL, R. WAGEMANN, and R. B. FERGUSON, Can. J. Chem. **48**, 1703 (1970).
4. (*a*) A. WESTGREN and A. J. BRADLEY. Phil. Mag. **6** (7), 280–288 (1928). (*b*) I. OBINATA and M. HAGIYA. Kinzoku-No-Kenkyo, **12**, 419–429 (1935). (*c*) S. ISHIDA, H. TAJIRI, and M. KARASAWA. Rep. Aeronaut. Res. Inst. Tokyo, Imp. Univ., **13**, 77 (1937). (*d*) M. KATO and S. NAKAMURA. J. Chem. Soc. Japan, **58**, 694–705 (1937).
5. FAGERBER and A. WESTGREN. Metalwirt. **14**, 265 (1935).
6. (*a*) W. B. PEARSON. Handbook of lattice spacings and structure of metals. Pergamon Press, London. 1958. (*b*) D. P. MORRIS and I. WILLIAMS. Acta Cryst. **14**, 74 (1961).
7. R. F. MEHL and C. S. BARRETT. Amer. Inst. Mining Met. Eng. Metals Division Tech. Publ. No. 353. 1930. p. 18.
8. (*a*) V. M. GOLDSCHMIDT. Z. Phys. Chem. **133**, 397 (1928). (*b*) W. H. HUME-ROTHERY, G. W. MABBOTT, and K. M. CHANNEL-EVANS. Phil. Trans. Roy. Soc. London, **A233**, 1–97 (1934). (*c*) L. L. FREVEL and E. OTT. J. Amer. Chem. Soc. **57**, 228 (1935). (*d*) F. WEIBKE and H. EGGERS. Anorg. Allgem. Chem. **222**, 145 (1935). (*e*) E. HELLNER and F. LAVES. Z. Naturforsch. **2A**, 177 (1947). (*f*) E. HELLNER. Z. Metallkunde, **42**, 17–19 (1951).

Can. J. Chem. Downloaded from www.nrcresearchpress.com by 210.87.254.6 on 09/05/12
For personal use only.

Can. J. Chem. Downloaded from www.nrcresearchpress.com by 210.87.254.6 on 09/05/12
For personal use only.

Vapor pressures and vapor ⇄ liquid equilibria in the systems: (*1*) acetone – chloroform, (*2*) acetone – carbon tetrachloride, (*3*) benzene – carbon tetrachloride

A. N. Campbell and G. M. Musbally
Department of Chemistry, University of Manitoba, Winnipeg, Manitoba

Received May 20, 1970

The saturation vapor pressures of ten mixtures of the binary systems (*1*) acetone – chloroform, (*2*) acetone – carbon tetrachloride, and (*3*) benzene – carbon tetrachloride have been determined, from 100 to 230° for system *1* and from 100° up to the highest temperature at which liquid and vapor coexist for systems *2* and *3*. The system acetone – chloroform could not be studied at higher temperatures because of decomposition.

The gas–liquid critical temperatures of the three binary systems have been determined by the disappearance of meniscus method. The orthobaric compositions of the vapor–liquid equilibria of the binary systems have been measured from 100 to 180° for system *1* and from 100° to the critical region for systems *2* and *3*, using a glass bomb enclosed in a steel bomb.

From the vapor–liquid composition curves and the vapor pressure curves at constant temperatures (100, 150, 160, 170, and 180°), the existence of an azeotrope in the system acetone–chloroform at these temperatures, and having a composition of 36.2 mole % acetone at 100°, was confirmed. The composition of the azeotrope shifts towards lower acetone content as the temperature is raised. Azeotropes were not found in the systems acetone – carbon tetrachloride and benzene – carbon tetrachloride, over the ranges of temperature and pressure of this research.

The data of the binary systems were treated thermodynamically to yield the liquid phase activity coefficients and, as suggested by Chueh and Prausnitz, the Redlick–Kwong equation was used in a modified form to obtain the fugacity coefficients of components in the vapor phase. Several liquid phase parameters, such as the binary interaction constant, Henry's constant, and dilation constant have been calculated, using the van Laar equation as modified by Chueh and Prausnitz.

Canadian Journal of Chemistry, 48, 3173 (1970)

Introduction

Although most of the common liquids have been investigated at high temperatures, the thermodynamic treatment of mixtures has been largely limited to those of the paraffins. The reason for this is obviously the difficulties of the technique. Acetone, chloroform, benzene, and carbon tetrachloride were chosen for this study because they have been extensively investigated at low temperatures; the vapor ⇄ liquid equilibrium compositions have been determined for the binary systems between 10 and 55° and the vapor pressures at 25°. Chatterjee and Campbell (1) have recently determined the orthobaric densities and vapor pressures of the pure liquids, up to the critical region.

In addition to investigating the vapor pressures and vapor ⇄ liquid compositions, of the three binary systems, we have determined the critical temperatures of each system, as a function of composition. Rowlinson (2) points out that the critical temperature of a simple mixture is one of the most direct sources of information about the energy of interaction of two unlike molecules.

The system acetone – chloroform has been thoroughly investigated at low temperatures. Campbell, Kartzmark, and Friesen (3) reported H^E values for 25° and Campbell and Kartzmark (4) showed that a compound of acetone and chloroform exists in the liquid state; from their data on heats of mixing they calculated the enthalpy of the hydrogen bond. The vapor pressures and vapor ⇄ liquid compositions, at temperatures ranging from 15 to 55°, have been studied by many workers, including Zawidski (5) and Rock and Schröder (6). A complete review of the work done on this system is given by Chatterjee and co-workers (7).

The vapor ⇄ liquid compositions of the system benzene – carbon tetrachloride, at temperatures ranging from 25 to 45°, have been investigated by at least 12 different investigators, including Young (8), Scatchard, Wood, and Mochel (9), and Fowler and Lim (10). The existence or nonexistence of an azeotrope has been a question for more than 50 years. Young (8) first suggested the possibility of an azeotrope of composition 91.65 mole % carbon tetrachloride at 760 mm Hg pressure. Scatchard, Wood, and Mochel (9) investigated this system under isobaric and isothermal conditions at 760 mm and 40° but failed to find any azeotrope. Campbell and Dulmage

Can. J. Chem. Downloaded from www.nrcresearchpress.com by 210.87.254.6 on 09/05/12
For personal use only.

(11) found that the vapor phase is never richer in benzene than the liquid phase, that is, there is no reversal of composition as there would be in passing through an azeotropic point.

Vapor ⇄ liquid compositions of the system acetone – carbon tetrachloride have been measured at 0° by Gerrits (12), at 50° by Severns *et al.* (13), and by many other workers at relatively low temperatures. Brown and Smith (14) carried out vapor ⇄ liquid measurements at 45° and concluded that an azeotrope exists, under a pressure of 513.2 mm at a mole fraction of acetone of 0.964. Ellis and Rose (15) have measured the vapor pressures of this system over the temperature range 5–25°.

Experimental

Purification of Materials

Organic impurities were removed from spectroanalyzed acetone by treating it with silver nitrate solution, followed by sodium hydroxide. After shaking, the solution was filtered and distilled from anhydrous calcium sulfate. The portion distilling between 56.1 and 56.2°, under an atmospheric pressure of 746 mm Hg, was collected. A fresh batch was prepared every week.

Since it is notorious that chloroform decomposes when exposed to air and light, a fresh batch of this substance was prepared every 3 days. To remove ethanol, chloroform was shaken several times with concentrated sulfuric acid and then washed with water. The product was then dried with calcium chloride and distilled from phosphorus pentoxide. The final distillate was stored in a closed cupboard, in brown bottles wrapped in black paper.

Thiophene-free benzene was shaken with successive portions of concentrated sulfuric acid until a yellow color was no longer produced in the acid layer, then with water, dilute sodium hydroxide, and again with water. It was finally dried over phosphorus pentoxide and distilled from metallic sodium.

Carbon tetrachloride was boiled with dilute potassium hydroxide solution, then shaken with alkaline potassium permanganate solution, and finally distilled from barium oxide. The refractive indices and densities (at 25°) of our products were:

Substance	n_D^{25}	d_4^{25}
Acetone	1.3561	0.7880
Chloroform	1.4433	1.4805
Benzene	1.4979	0.8734
Carbon tetrachloride	1.4576	1.5842

Method of Analysis of Mixtures

Mixtures were analyzed refractometrically or by density, after preparation of calibration curves. Generally, the error of analysis was about 0.1%.

Determination of Critical Temperature

If a sealed tube containing liquid and vapor is heated uniformly, and if the overall density is not too different from the critical density, it is observed that the meniscus becomes flatter and fainter until the critical temperature is reached, when the meniscus disappears in the body of the tube. It had been observed by many workers, including ourselves, that it is not necessary that the overall density be exactly the critical density for these phenomena, including the occurrence of fluctuating striae, to be observed. There has been much discussion as to whether the temperature of disappearance of the meniscus is the true critical temperature, but, at all events, it is what we describe here as such. The method indicated above was the one chosen by us for the investigation of the systems (*1*) acetone – chloroform, (*2*) benzene – carbon tetrachloride, (*3*) acetone – carbon tetrachloride. The experimental tubes were 15 cm long and had an internal diameter of 2 mm. The internal volume of each tube was determined as a function of length. The pure liquid components were degassed by repeated freezing in liquid nitrogen and pumping off to a high vacuum line. Still under vacuum a suitable amount of liquid *1* was transferred to the capillary tube. The length of the tube occupied by liquid was measured with a cathetometer and the mass determined from the known density.

The second liquid was then distilled into the capillary and the height again measured. Any change in volume on mixing was considered to be negligible for our purposes. The tube was then sealed while in liquid nitrogen.

The tube with its contents of known composition was then placed in a thermostat at 200 °C. Temperature was controlled with a solid state proportional temperature controller. Up to a temperature of 225°, Dow Corning Silicone Oil 550 was used as thermostat liquid. Above this temperature, the eutectic mixture of potassium, sodium, and lithium nitrates was used. To prevent corrosion in the latter case, the temperature sensor was a thermistor sheathed in stainless steel and the heating element was encased in a non-corrosive nickel–chrome–iron alloy.

The temperature of the thermostat was then re-adjusted at higher temperatures. As the critical temperature was approached, the temperature intervals were reduced. The meniscus was viewed through a telescope placed at a distance of 2 m. The temperature at which the meniscus disappeared was measured with a copper–constantan multiple junction thermocouple. The bath was then allowed to cool slowly and the temperature of reappearance of the meniscus noted. The mean of these two temperatures was taken as the correct temperature. The reproducibility was 0.05 to 0.1°.

Measurement of Equilibrium Vapor–Liquid Compositions

This has been described previously (1).

Measurement of Vapor Pressure

The method has been described previously (1).

Not more than 30 min could be allowed for the establishment of equilibrium, because chemical decomposition became appreciable with time. To avoid this incipient decomposition as far as possible, two sets of experiments were carried out. In one, the temperature was raised from 100 to 190° and then a fresh filling was used for the range 200 to 280°. Because the volume of

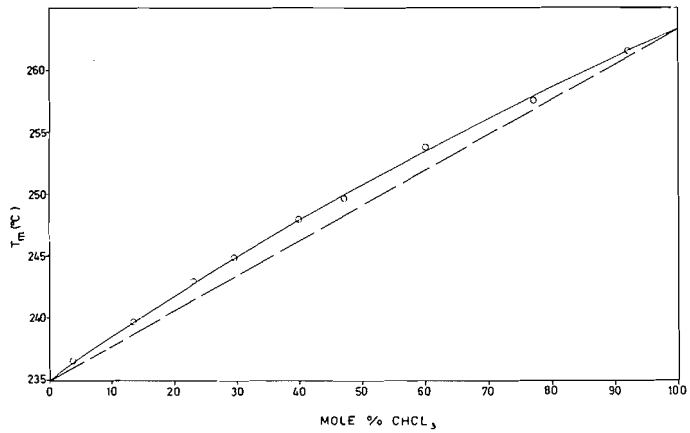

FIG. 1. Gas ⇄ liquid critical temperatures of the acetone–chloroform system as a function of mole% chloroform.

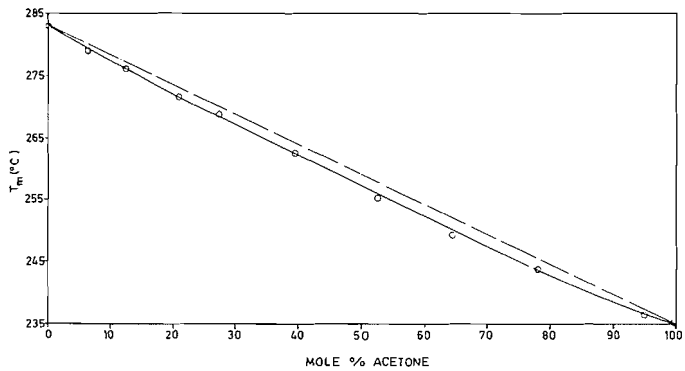

FIG. 2. Gas ⇄ liquid critical temperatures of the acetone carbon tetrachloride system as a function of mole% acetone.

the vapor phase was always much smaller than that of the liquid, we thought ourselves justified in assuming that the composition of the liquid did not change appreciably with temperature.

Results

Critical Temperatures

A. Pure Liquids

Critical temperatures of pure liquids are listed in Table 1.

B. Binary Systems

Acetone–Chloroform

The gas ⇄ liquid critical temperatures have been determined over the whole concentration range. These data, together with most of the other extensive data of this paper, are to be found in the Depository of Unpublished Data of the National Research Council of Canada.[1] The results are expressed graphically in Fig. 1, which represents critical temperature *vs.* mole% $CHCl_3$. Chloroform and mixtures having high chloroform content develop a yellowish color on prolonged heating. For this reason, tubes containing such mixtures were not introduced into the bath until the temperature was only a few degrees below the critical point.

TABLE 1

Critical temperatures of pure liquids

Substance	Critical temperature (°C)
Acetone	235.0±0.1
Carbon tetrachloride	283.2±0.1
Benzene	288.0±0.1
Chloroform	263.2±0.1

Acetone – Carbon Tetrachloride

The data are expressed graphically in Fig. 2.

[1]Photocopies may be obtained free of charge, upon request, from the Depository of Unpublished Data, National Science Library, National Research Council of Canada, Ottawa 2, Canada.

Can. J. Chem. Downloaded from www.nrcresearchpress.com by 210.87.254.6 on 09/05/12
For personal use only.

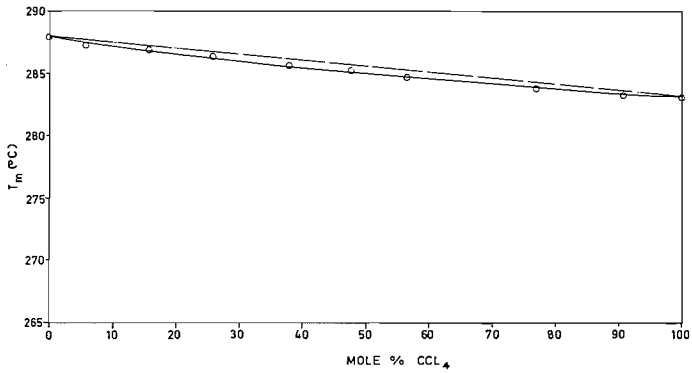

FIG. 3. Gas ⇄ liquid critical temperatures of the benzene – carbon tetrachloride system as a function of mole% carbon tetrachloride.

Benzene – Carbon Tetrachloride

The data are expressed graphically in Fig. 3.

Vapor ⇄ Liquid Equilibrium Compositions

Acetone–Chloroform

The vapor ⇄ liquid equilibrium compositions of this system have been determined at 100, 150, 160, and 180°. The data are to be found in the Depository of Unpublished Data. A typical graph, that for 160°, is given as Fig. 4.

Acetone – Carbon Tetrachloride

The data have been obtained for 100, 150, 200, 250, and 270°. A typical graph, that for 200°, is shown as Fig. 5.

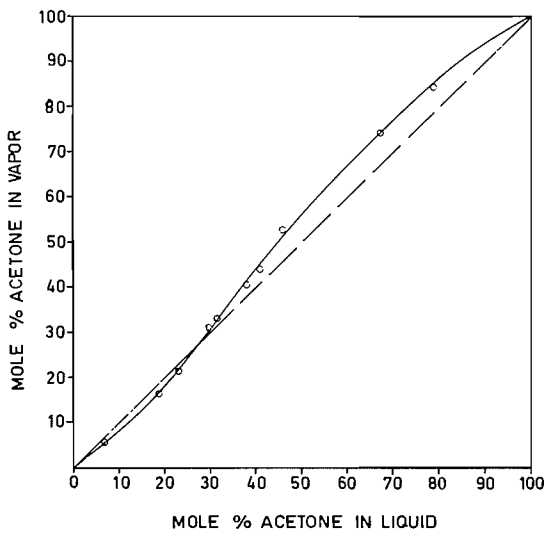

FIG. 4. The vapor–liquid equilibrium composition curve of the system acetone–chloroform at 160 °C.

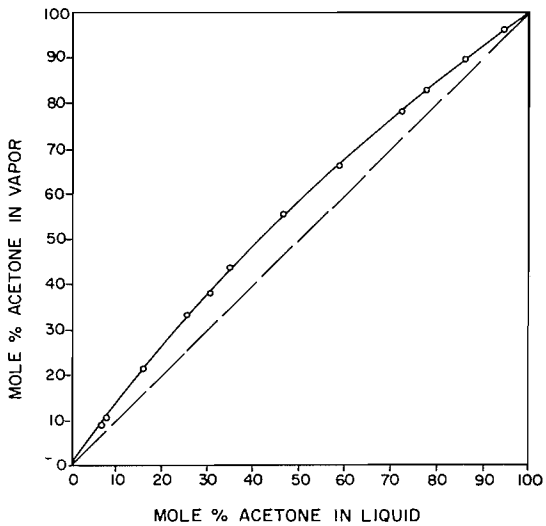

FIG. 5. The vapor–liquid equilibrium composition curve of the system acetone – carbon tetrachloride at 200 °C.

Benzene – Carbon Tetrachloride

The data have been obtained for 100, 108, 150, 200, 250, and 270°. The data for 150°, which are typical, are plotted in Fig. 6.

Vapor Pressures

Acetone–Chloroform

The saturation vapor pressures have been determined over the whole concentration range in the temperature interval 100 to 180°. The figures, together with all other vapor pressures, are to be found in the Depository of Unpublished Data. The results for mixtures containing 7.50 and 80.01 mole% acetone are expressed graph-

Can. J. Chem. Downloaded from www.nrcresearchpress.com by 210.87.254.6 on 09/05/12
For personal use only.

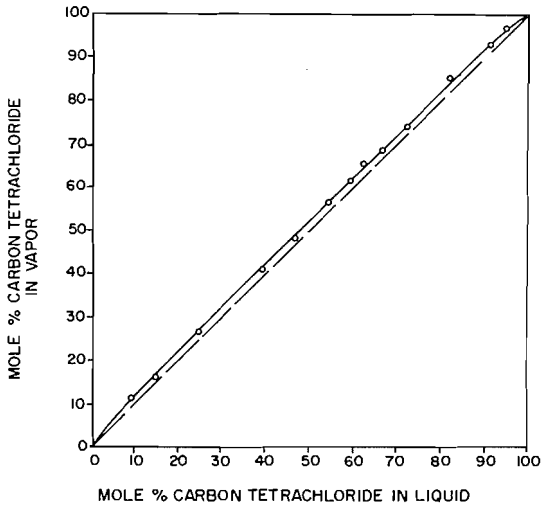

FIG. 6. The vapor–liquid equilibrium composition curve of the system benzene – carbon tetrachloride at 150 °C.

ically in Fig. 7. All intermediate compositions lie between these two limits.

Acetone – Carbon Tetrachloride

Figure 8 shows the plots of vapor pressure *vs.* temperature for different constant compositions, at the bubble-points of the system.

Benzene – Carbon Tetrachloride

Ten mixtures of different compositions were investigated between the temperatures of 100 and 270°. Figure 9 shows the relation between temperature and pressure for two of these mixtures: the pressures are very similar for all mixtures, despite the fact that the compositions of the ten mixtures varied from 5.00 to 97.21 mole% carbon tetrachloride.

Discussion

Thermodynamic Analysis

Thermodynamic reduction and correlation of vapor ⇄ liquid equilibrium data are common at low pressures but, at high pressures, little attempt has been made to reduce such data with thermodynamically significant functions. In high pressure phase equilibria it is not possible to make the simplifying assumptions commonly made at low pressures; in such systems both phases, vapor and liquid, exhibit large deviations from ideal behavior.

We have treated our experimental data by the method of Chueh and Prausnitz (16). Vapor pressure non-idealities are expressed as fugacity coefficients (ϕ_i) and the liquid phase non-idealities as activity coefficients (γ_i). The Redlich–Kwong equation, modified by the introduction of binary interaction constants, has been used for vapor phase properties. The van Laar equation, modified to allow for the rapid change of liquid molar volume which occurs in the critical region, has been used to represent the effect of composition on liquid phase properties.

The parameters we have determined are:

(*1*) Henry's constant, $H_{2(1)}{}^{P_0}$.

(*2*) The binary interaction constants $\alpha_{22(1)}$, defined by the equation

$$g^E/RT(x_1q_1 + x_2q_2) = -\alpha_{22(1)}\phi_2{}^2$$

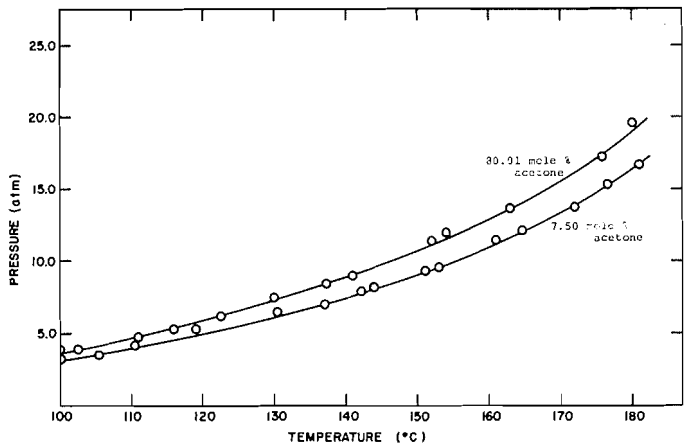

FIG. 7. Bubble point pressures of constant composition mixtures as function of temperature of the system acetone–chloroform.

Can. J. Chem. Downloaded from www.nrcresearchpress.com by 210.87.254.6 on 09/05/12
For personal use only.

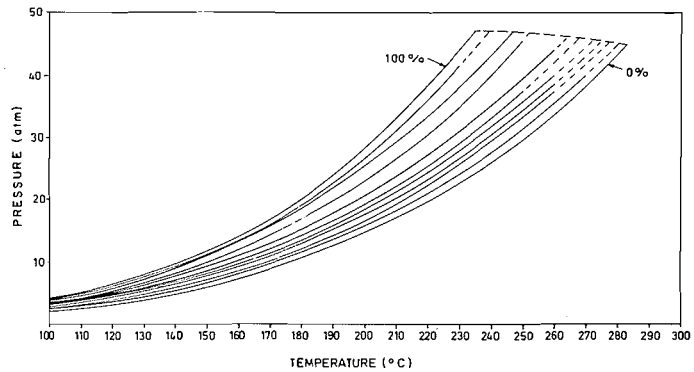

FIG. 8. Bubble point pressures of critical composition mixtures as functions of temperature of the system acetone – carbon tetrachloride. The compositions are 0.0, 6.22, 15.01, 24.89, 34.11, 46.80, 52.01, 72.02, 58.20, 86.70, and 100 mole% acetone.

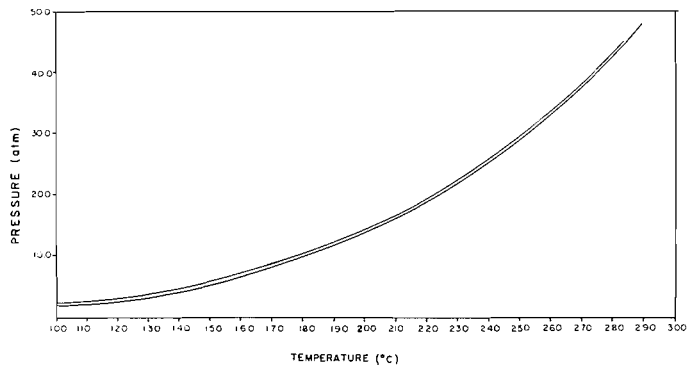

FIG. 9. Bubble point pressures of mixtures of constant composition of the system benzene – carbon tetrachloride. The lower curve represents a mixture containing 5.00 mole% carbon tetrachloride, the upper a mixture containing 97.21 mole% carbon tetrachloride, curves of the remaining eight mixtures lie in between.

α_{12}, defined by the equation

$$g^E/RT(x_1V_{C_1} + x_2V_{C_2}) = \alpha_{12}\phi_1\phi_2$$

where g^E = molar excess Gibbs energy, q_1, q_2 = the effective molal volumes; V_{C_1}, V_{C_2} = the critical molal volumes.

(*3*) The dilation constant.

For a given binary system, the above parameters depend only on temperature, so that isothermal experimental data are required. From the large scale plots of P *vs.* T, for fixed liquid compositions and of vapor ⇄ liquid equilibrium compositions, P–x–y data were read off for each isotherm. These data were then treated by the programs of Chueh and Prausnitz (16) and the analysis carried out, using an IBM 360/65 computer. As all details are given in ref. 16, there is no need to repeat them here.

Thermodynamic Consistency Test of the Vapor ⇄ Liquid Equilibrium Data

Vapor ⇄ liquid equilibrium data are said to be thermodynamically consistent when they satisfy the Gibbs–Duhem equation. When the data satisfy this equation, it is probable, but by no means certain, that they are correct. However, if they do not satisfy this equation, they are certainly incorrect. Thermodynamic consistency tests have been described by many authors; a good review is given in the monograph by van Ness (17).

Chueh, Muirbrook, and Prausnitz (18) have described a consistency test which is an extension to isothermal high pressure data of the integral (area) test given by Redlich and Kister (19) and by Herington (20) for isothermal low pressure data. Again details are out of place here. Chueh

Can. J. Chem. Downloaded from www.nrcresearchpress.com by 210.87.254.6 on 09/05/12
For personal use only.

Can. J. Chem. Downloaded from www.nrcresearchpress.com by 210.87.254.6 on 09/05/12
For personal use only.

and Prausnitz (16) have replaced the data plotting procedure by a regression analysis. Chueh and Prausnitz use the criterion that if the average deviation of the activity coefficients γ_1 and γ_2 differ by more than 3%, the data are inconsistent.

Discussion of Results

Chloroform–Acetone

Figure 1, which is a plot of T_m, the temperature of disappearance of meniscus, *vs.* mole% chloroform, shows that the system chloroform–acetone deviates from ideality. This has been observed previously by many workers, including Swietoslawski and Kreglewski (21) and Chatterjee and co-workers (7). The deviation from ideality is also apparent in the vapor pressure plots. The negative deviation from Raoult's law has been explained by the fact that a 1:1 hydrogen bonded compound exists in this system, and Campbell and Kartzmark (4) have determined the enthalpy of the hydrogen bond as -2.7 kcal mole^{-1}. We doubt, however, if this compound continues to exist under critical conditions.

The existence of an azeotrope has been confirmed from the vapor ⇄ liquid equilibrium composition curves, e.g. Fig. 4. It was found that the composition of the azeotrope, a negative azeotrope in the terminology of Rowlinson (2), which is 36.2 mole% acetone at 100°, shifts towards lower acetone content as the temperature is raised (Table 2). Rock and Schröder (6) came to the same conclusion from their study of this system at 10 to 55°. This observation also agrees with the well known fact that an increase of temperature of a negative azeotrope decreases the mole fraction of the component whose vapor pressure increases more rapidly with temperature. This system was investigated only up to 180 °C, at which temperature the azeotrope still exists, but it is known (22) that the azeotrope does not exist up to the critical point.

The experimental data for vapor ⇄ liquid composition and saturation vapor pressure of this binary system were treated to yield the fugacity coefficients, ϕ_1 and ϕ_2, and the activity coefficients, γ_1 and γ_2, of the two components, in the vapor and liquid phases, respectively. For this purpose we used the programs of Chueh and Prausnitz (16). Here again, most of the results are to be found in the Depository of Unpublished Data but a sample calculation (for 160°) is given in Table 3. The second round of fitting has been omitted since it was identical with the first round. From Table 3 it is seen that, though $\gamma_i \to 1$, as $x_i \to 1$, the system acetone–chloroform is not ideal at the temperatures and pressures of this work. The activity coefficients have been plotted as functions of mole fraction acetone in the liquid phase, for 160° only, in Fig. 10. The curves for the other temperatures are similar. The deviations between the experimental values of the activity coefficients and the calculated values are rather large but this is discussed later.

TABLE 2

Dependence of azeotropic composition on temperature in the system $CHCl_3$(1) – acetone(2)

Temperature (°C)	Azeotropic composition (mole fraction acetone)
100	0.362
150	0.347
160	0.292
170	0.235
180	0.209

Carbon Tetrachloride (1) – Acetone (2)

The plot of T_m, the temperature of disappearance of the meniscus, *vs.* mole% acetone (Fig. 2) for this system shows a slight deviation from ideality but the vapor pressure plots show neither maximum nor minimum. The vapor ⇄ liquid equilibrium curves (*e.g.* Fig. 5) also do not indicate the existence of an azeotrope. Brown and Smith (14), who studied the vapor ⇄ liquid equilibria of this system at 45°, claim the existence of an azeotrope at a mole fraction acetone of 0.964 and a pressure of 513.2 mm Hg. In our work, the vapor was found always to be richer in acetone, that is, we did not find an azeotrope. If an azeotrope exists at 45°, it must disappear at higher temperatures.

Thermodynamic analysis of this system was carried out in two parts. Data reduction for the isotherms at 150 and 200° were carried out using a one-parameter model for the excess Gibbs energy with $\eta_2(1) = 0$. The results for 150° are shown in Table 4. The Table shows that $\gamma_i \to 1$ as $x_i \to 1$ for this system. Figure 11 is a graphical representation of the activity coefficients as a function of mole fraction of acetone in the liquid phase. The differences between the experimental values for the activity coefficients and their calculated values are small; in other words, this

TABLE 3

Thermodynamic analysis of the system $CHCl_3$ (**1**) – acetone (**2**) at 160 °C*

x_2	y_2	Volume fraction of component **2** in the liquid phase	P (atm)	$\overline{V}_1^L$ (cc/mole)	$\overline{V}_2^L$ (cc/mole)	Poynting correction for γ_1	Poynting correction for γ_2	γ_1^{PO}(exp)	γ_2^{PO}(exp)
0.235	0.225	0.214	11.40	112.1	104.7	1.036	1.034	0.851	0.668
0.313	0.320	0.288	11.36	111.9	104.3	1.036	1.033	0.829	0.711
0.416	0.465	0.387	11.64	111.6	103.7	1.037	1.034	0.784	0.792
0.540	0.630	0.510	12.00	111.2	103.0	1.038	1.035	0.707	0.846
0.800	0.867	0.780	12.96	110.1	101.6	1.041	1.037	0.624	0.835
0.929	0.960	0.920	13.58	109.2	100.8	1.042	1.039	0.550	0.926

x_2	y_2	ϕ_1	ϕ_2	γ_1^{PO}(calcd)	γ_1(exp) − γ_1(calcd)	γ_2^{PO}(calcd)	γ_2(exp) − γ_2(calcd)
0.235	0.225	0.882	0.865	0.964	−0.113	0.652	0.015
0.313	0.320	0.883	0.865	0.937	−0.107	0.704	0.006
0.416	0.465	0.880	0.860	0.889	−0.105	0.771	0.020
0.540	0.630	0.878	0.855	0.816	−0.109	0.847	−0.000
0.800	0.867	0.870	0.843	0.622	0.001	0.967	−0.131
0.929	0.960	0.865	0.835	0.517	0.033	0.995	−0.069
				Ave. deviation	0.078	Ave. deviation	0.040

*Correction to geometric mean $K_{12} = 0.010$; $2\tau_{12}/(T_{c_1} + T_{c_2}) = 0.008$; $2v_{12}/(V_{c_1} + V_{c_2}) = 0.035$; reference fugacity 1 = 11.55 atm reference fugacity 2 = 13.66 atm; α_{12}, interaction constant of 1 and 2 = −0.0032 mole/cc.

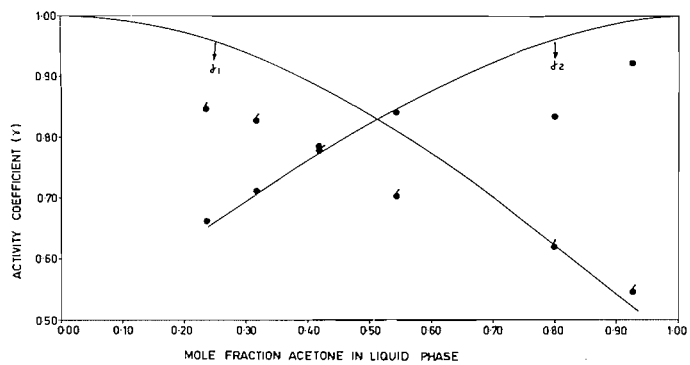

FIG. 10. Activity coefficients *vs.* mole fraction acetone in liquid phase of the systems chloroform–acetone at 160 °C.

system responds better to the solution model of Chueh and Prausnitz (16). This system is nearly ideal at 150°, since the activity coefficients are very nearly equal to one, but at 200° the deviations from ideality are larger. The deviations are positive at 150° and negative at 200°.

Data reductions for the system at 250 and 270° were carried out using a two parameter dilated van Laar model for the excess Gibbs energy and the unsymmetric convention of normalization for activity coefficients. As can be seen from Table 5, the program calculates $f_2^{(P)}/x_2$ *vs.* x_2 for each point and, by extrapolating the plot of $\ln f_2^{(P)}/x_2$ *vs.* x_2 (Fig. 12), Henry's constant of (**2**) in (**1**) is obtained, $H_{2(1)}$. The program also prints out the saturation pressure of component **1**, liquid partial molal volumes of both components at infinite dilution, the reference fugacity of component **1** at zero pressure, the molal volumes of the saturated liquid mixture, for each concentration, and the corrected reduced temperatures of the liquid mixture for each concentration (Table 5). This information is then used to evaluate the self-interaction constant, $\alpha_{22(1)}$ and the dilation constant $\eta_2(1)$ of the dilated van Laar model.

Benzene (1) – Carbon Tetrachloride (2)

The plot of T_m *vs.* composition (Fig. 3) for this system deviates only slightly from straight line

Can. J. Chem. Downloaded from www.nrcresearchpress.com by 210.87.254.6 on 09/05/12
For personal use only.

TABLE 4

Thermodynamic analysis of the system CCl_4 (1) – acetone (2) at 150 °C*

x_2	y_2	Volume fraction of component 2 in the liquid phase	P (atm)	$\bar{V}_1^L$ (cc/mole)	$\bar{V}_2^L$ (cc/mole)	Poynting correction for γ_1	Poynting correction for γ_2	γ_1^{PO}(exp)	γ_2^{PO}(exp)
0.249	0.372	0.206	8.67	121.0	98.4	1.030	1.024	0.99	1.11
0.341	0.476	0.288	9.28	121.3	97.9	1.033	1.026	1.01	1.09
0.468	0.581	0.407	9.92	122.0	97.3	1.035	1.028	1.06	1.03
0.520	0.631	0.458	10.28	122.4	97.1	1.036	1.029	1.07	1.03
0.582	0.692	0.521	10.42	122.9	96.9	1.037	1.029	1.03	1.02
0.720	0.806	0.668	10.94	124.6	96.7	1.040	1.031	1.01	1.00
0.867	0.906	0.836	11.26	127.0	96.9	1.042	1.031	1.06	0.96

x_2	y_2	ϕ_1	ϕ_2	γ_1^{PO}(calcd)	γ_1(exp) − γ_1(calcd)	γ_2^{PO}(calcd)	γ_2(exp) − γ_2(calcd)
0.249	0.372	0.872	0.892	1.00	−0.01	1.09	0.02
0.341	0.476	0.865	0.883	1.00	0.01	1.06	0.03
0.468	0.581	0.857	0.874	1.00	0.06	1.03	0.00
0.520	0.631	0.853	0.869	1.01	0.05	1.02	0.01
0.582	0.692	0.852	0.866	1.01	0.02	1.02	0.00
0.720	0.806	0.847	0.859	1.02	−0.01	1.00	0.00
0.867	0.906	0.846	0.854	1.03	0.03	1.00	−0.05
				Ave. deviation	0.026	Ave. deviation	0.019

*Correction to geometric mean $K_{12} = 0.01$; $2\tau_{12}/(T_{c_1} + T_{c_2}) = -0.033$; $2v_{12}/V_{c_1} + V_{c_2}) = -0.124$; reference fugacity 1 = 6.07 atm; reference fugacity 2 = 10.14 atm; α_{12}, interaction constant of 1 and 2 = −0.0087 mole/cc.

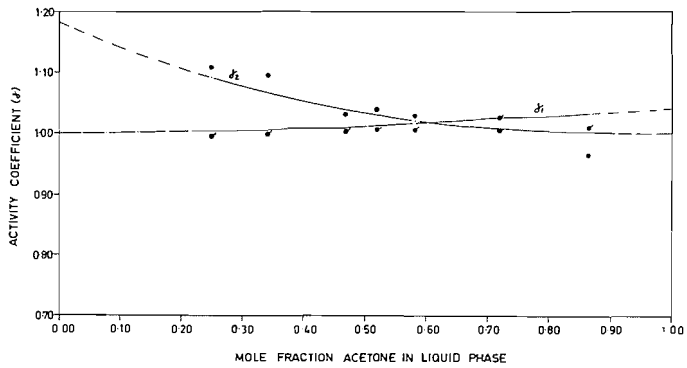

FIG. 11. Activity coefficients *vs.* mole fraction acetone in liquid phase for the system carbon tetrachloride – acetone at 150 °C.

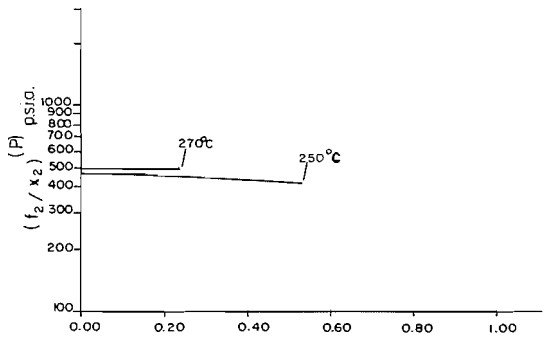

FIG. 12. Plot of Henry's constant $H_{2(1)}^{ps}$.

behavior. The vapor ⇄ liquid equilibrium composition curves (Fig. 6) do not suggest the existence of an azeotrope, since the vapor is always richer in carbon tetrachloride than the liquid.

Since the volatilities of the two pure components are very similar, no dilation constant is required and the binary system can be treated, using a one-parameter model for the excess Gibbs energy. Therefore, data reduction for this system was carried out using the symmetric convention for activity coefficients. The thermodynamic analyses for 150, 200, 250, and 270° are to be found in Depository but that for 200° is given as Table 6.

Can. J. Chem. Downloaded from www.nrcresearchpress.com by 210.87.254.6 on 09/05/12
For personal use only.

Can. J. Chem. Downloaded from www.nrcresearchpress.com by 210.87.254.6 on 09/05/12
For personal use only.

TABLE 5

Thermodynamic analysis of the system carbon tetrachloride (**1**) – acetone (**2**) at 250 °C*

$\frac{f_2}{x_2}$ (atm)	Saturation pressure of **1** (atm)	x_2	y_2	P (atm)	Molal volume of saturated liquid mixture (cc/mole)	ϕ_1	ϕ_2	$\bar{V}_1^L$ (cc/mole)	$\bar{V}_2^L$ (cc/mole)	Corrected T_R of liquid mixture
32.45	1.933	0.062	0.079	31.42	173.23	0.7455	0.8107	173.58	167.95	0.9756
32.69	3.953	0.150	0.185	33.44	175.24	0.7298	0.7925	176.09	170.44	0.9817
31.82	4.943	0.249	0.295	34.43	180.82	0.7234	0.7802	181.65	178.32	0.9891

x_2	Vol. fraction of component **2** in the liquid phase	Poynting correction for γ_1	Poynting correction for γ_2	γ_1^{PO}(exp)	γ_2^{PO}(exp)	γ_1^{PO}(calcd)	γ_1(exp) − γ_1(calcd)	γ_2^{PO}(calcd)	γ_2(exp) − γ_2(calcd)
0.062	0.0492	1.1355	1.1309	0.7864	0.9919	0.8876	−0.1012	0.9726	0.0193
0.150	0.1214	1.1471	1.1420	0.7921	0.9891	0.8721	−0.1200	0.9801	0.0090
0.249	0.2061	1.1569	1.1538	0.7847	0.9533	0.8412	−0.0565	0.9856	−0.0323
							Ave. deviation 0.0926		Ave. deviation 0.0202

*Henry's constant at the saturation pressure of solvent determined graphically from above data in upper table = 32.46 atm. Reference fugacity **1** = 25.75 atm; saturation pressure **1** = 29.49 atm; liquid partial molal volume **1** at infinite dilution = 172.53 cc/mole; $\bar{V}_2^{\infty}$ = 167.22 cc/mole; $\alpha_{22(1)}$, self-interaction constant of molecules **2** in the environment of molecules **1** = −0.001788 mole/cc; $\eta_{2(1)}$, dilation constant of solute **2** in solvent **1** = 1.2868; Henry's constant at zero pressure = 28.98 atm.

TABLE 6

Thermodynamic analysis of the system C_6H_6 (1) – CCl_4 (2) at 200 °C*

x_2	y_2	Volume fraction of component 2 in the liquid phase	P (atm)	$\bar{V}_1^L$ (cc/mole)	$\bar{V}_2^L$ (cc/mole)	Poynting correction for γ_1	Poynting correction for γ_2	γ_1^{PO}(exp)	γ_2^{PO}(exp)
0.103	0.104	0.110	14.12	118.3	151.8	1.044	1.056	0.973	0.807
0.165	0.168	0.176	14.20	117.5	150.3	1.043	1.056	0.971	0.817
0.244	0.248	0.258	14.23	116.6	148.5	1.043	1.056	0.971	0.817
0.326	0.332	0.343	14.29	115.9	146.8	1.043	1.055	0.972	0.821
0.520	0.582	0.539	14.34	114.5	143.2	1.043	1.054	0.858	0.903
0.621	0.684	0.639	14.40	114.1	141.6	1.043	1.053	0.825	0.892

x_2	y_2	ϕ_1	ϕ_2	γ_1^{PO}(calcd)	γ_1(exp) – γ_1(calcd)	γ_2^{PO}(calcd)	γ_2(exp) – γ_2(calcd)
0.103	0.104	0.832	0.852	0.993	−0.020	0.760	0.047
0.165	0.168	0.832	0.850	0.984	−0.012	0.786	0.031
0.244	0.248	0.832	0.849	0.966	0.005	0.816	0.000
0.326	0.332	0.832	0.848	0.941	0.030	0.845	−0.024
0.520	0.582	0.833	0.845	0.894	−0.035	0.902	0.001
0.621	0.684	0.833	0.844	0.856	−0.030	0.935	−0.042
			Ave. deviation	0.022		Ave. deviation 0.024	

*Correction to geometric mean $K_{12} = 0.010$; $2\tau_{12}/(T_{c_1} + T_{c_2}) = -0.003$; $2v_{12}/(V_{c_1} + V_{c_2}) = -0.040$; reference fugacity 1 = 11.62 atm; reference fugacity 2 = 14.24 atm; α_{12}, interaction constant of 1 and 2 = −0.00201 mole/cc.

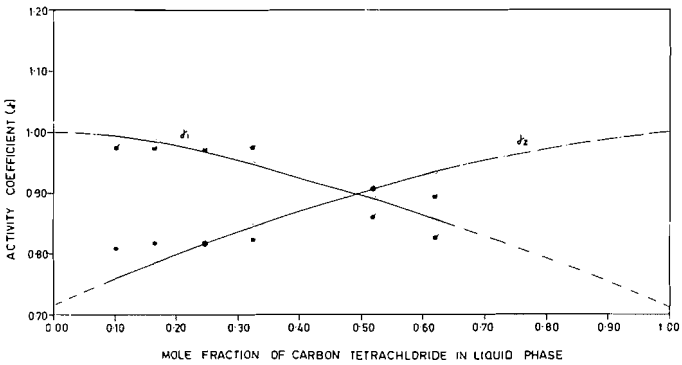

FIG. 13. Activity coefficients *vs.* mole fraction carbon tetrachloride in liquid phase for the system benzene – carbon tetrachloride at 200 °C.

The deviation of the activity coefficients from unity is not large but the system cannot be described as ideal. Since this system consists of two non-polar components, it would seem to be the ideal one whereby to test the solution model of Chueh and Prausnitz (16). Table 6 shows that the differences between experimental and calculated values of the activity coefficients are very small. An example of the plot of activity coefficients *vs.* mole fraction carbon tetrachloride (for 200°) is given as Fig. 13.

Comparison of Systems

The system acetone–chloroform shows negative deviation from Raoult's law and Campbell and Kartzmark (4) have shown that a 1:1 compound exists in the solid (and to some extent in the liquid) state. Many theoretical and semi-theoretical treatments of this system have been attempted (23, 24). Although there is no doubt of the hydrogen bonding, at room temperature, as indicated by the results of ultraviolet spectroscopy (24) and proton magnetic resonance (25), the attempt to construct a theory is complicated by the fact that both acetone and chloroform are associated in the pure state.

Our results (*e.g.* Table 3) show that the one parameter model of the van Laar equation is not successful in reproducing activity coefficients of the system acetone–chloroform at temper-

Can. J. Chem. Downloaded from www.nrcresearchpress.com by 210.87.254.6 on 09/05/12
For personal use only.

atures 150, 160, 170, and 180°; that is, at temperatures at which both components can exist in the liquid state. The dilated van Laar model of Chueh and Prausnitz (16) is based on the assumption that the non-ideality of liquid mixtures is due to the interaction of solute molecules with each other in the environment of the solvent molecules and not to interaction between solute and solvent molecules. It is doubtful if such a concept applies to the acetone–chloroform system. Furthermore, Prausnitz and Chueh's theory applies mostly to non-polar or slightly polar components, but both acetone and chloroform are polar compounds.

Neither does the solution model of Prausnitz and Chueh apply in strictness to the system acetone – carbon tetrachloride. Table 4 shows that the one-parameter model of the van Laar equation is fairly successful in reproducing activity coefficients for the temperatures 150 and 200°, but the two-parameter model applied at temperatures where one of the components (acetone) is supercritical (Table 5) is apparently not very successful. The same conclusion was reached by Campbell and Chatterjee (1) who used the two-parameter model for the system acetone–benzene at temperatures higher than 200°.

The system benzene – carbon tetrachloride consisting of two non-polar components should be the ideal system for testing the solution model of Prausnitz. It has been shown, however (26), that the deviation of physical properties from the mixture rule in this system can be ascribed to the association of carbon tetrachloride.

Our results (*cf.* Table 6) show that the one-parameter solution model gives thermodynamically consistent results for the activity coefficients at 150, 200, 250, and 270°, but we are at a loss to explain why the activity coefficients are so far removed from unity. Interaction between benzene molecules and carbon tetrachloride molecules might constitute an explanation if there were any reason to suppose such an interaction. It is interesting that, according to Ho, Boshko, and Lu (27), at lower temperatures this system shows very slight positive deviations from Raoult's law but there does seem to be a tendency for these to become less positive as the temperature rises.

1. A. N. CAMPBELL and R. M. CHATTERJEE. Can. J. Chem. **47**, 3893 (1969); **48**, 277 (1970).
2. J. S. ROWLINSON. Liquids and liquid mixtures. Butterworths Scientific Publ., London. 1959.
3. A. N. CAMPBELL, E. M. KARTZMARK, and H. FRIESEN. Can. J. Chem. **39**, 735 (1961).
4. A. N. CAMPBELL and E. M. KARTZMARK. Can. J. Chem. **38**, 652 (1960).
5. J. V. ZAWIDSKI. Z. phy. Chem. **35**, 129 (1900).
6. H. ROCK and W. SCHRÖDER. Z. phy. Chem. (Frankfurt) **11**, 41 (1957).
7. A. N. CAMPBELL, E. M. KARTZMARK, and R. M. CHATTERJEE. Can. J. Chem. **44**, 1183 (1966).
8. S. YOUNG. Distillation principles and processes. MacMillan, London. 1922.
9. G. SCATCHARD, S. E. WOOD, and J. M. MOCHEL. J. Amer. Chem. Soc. **70**, 1723 (1948).
10. R. T. FOWLER and S. C. LIM. J. Appl. Chem. **6**, 75 (1956).
11. A. N. CAMPBELL and W. J. DULMAGE. J. Amer. Chem. Soc. **70**, 1723 (1948).
12. G. C. GERRITS. Proc. Acad. Sci. Amsterdam. **7**, 167 (1904).
13. W. H. SEVERNS, A. SESONSKE, R. H. PERRY, and R. L. PIGFORD. J. Amer. Inst. Chem. Eng. **1**, 401 (1955).
14. I. BROWN and F. SMITH. Aust. J. Chem. **10**, 423 (1957).
15. S. R. M. ELLIS and L. M. ROSE. Birmingham Univ. Chem. Eng. **14**, (2) 45 (1963).
16. P. L. CHUEH and J. M. PRAUSNITZ. Ind. Eng. Chem. **60**, 35 (1968); Computer calculations for high pressure vapor liquid equilibria. Prentice-Hall. 1968.
17. H. C. VAN NESS. Classical thermodynamics of non-electrolyte solutions. Pergamon Press, New York. 1964.
18. P. L. CHUEH, N. K. MUIRBROOK, and J. M. PRAUSNITZ. Amer. Inst. Chem. Eng. J. **11**, 1097 (1965).
19. O. REDLICH and A. T. KISTER. Ind. Eng. Chem. **40**, 345 (1948).
20. E. F. G. HERINGTON. Nature, **160**, 610 (1947).
21. W. SWIETOSLAWSKI and A. KREGLEWSKI. Bull. de l'Acad. Polonaise des Sci. Sciences Cl III—Vol. II, No. 4 (1954), 187.
22. J. P. KUENEN and W. G. ROBSON. Phil. Mag. **3**, 149, 622 (1902).
23. J. A. BARKER and F. J. SMITH. J. Chem. Phys. **22**, 375 (1954).
24. A. MUNSTER. Trans. Faraday Soc. **46**, 165 (1950).
25. C. M. HUGGINS, G. C. PIMENTEL, and J. N. SHOOLERY. J. Chem. Phys. **23**, 1244 (1955).
26. A. SCHULZE. Z. phy. Chem. **86**, 309 (1913).
27. J. C. K. Ho, O. BOSHKO, and B. C. Y. LU. Can. J. Chem. Eng. **39**, 205 (1961).

Can. J. Chem. Downloaded from www.nrcresearchpress.com by 210.87.254.6 on 09/05/12
For personal use only.

Can. J. Chem. Downloaded from www.nrcresearchpress.com by 210.87.254.5 on 09/05/12
For personal use only.

Copper(II) derivatives of the stereochemically adaptive ligands 1,2-bis(2′-pyridyl)ethane and bis(2-pyridyl)disulfide

M. KEETON, A. B. P. LEVER, AND B. S. RAMASWAMY
Department of Chemistry, York University, Downsview, Ontario

Received May 25, 1970

Tetrahedral, square, square pyramidal, and tetragonally distorted octahedral complexes of copper(II) with the title ligands are characterized by electronic and vibrational spectroscopy (at ambient and low temperature) and magnetism. The infrared spectra are utilized to infer information about the conformation of the ligands in these complexes. The variation in structural types observed is believed to be a consequence of the stereochemical adaptability of these ligands to the electronic demands of the metal ion.

Canadian Journal of Chemistry, **48**, 3185 (1970)

We recently reported (1) the structural and physical characteristics of the cobalt(II), nickel(II), zinc, and mercury(II) complexes of the title ligands (**1**, **2**). Four, five, and six coordinate complexes were synthesized and the coordinating abilities of the two closely related ligands compared. The ability of the ligands to form complexes in various different geometries is, for complicated ligands such as these, moderately uncommon, and betokens unusual adaptability

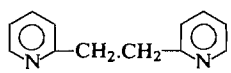

1

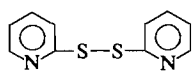

2

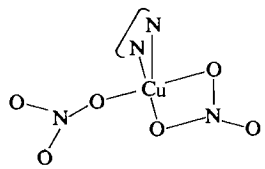

3

to different environments. With an ion such as cobalt(II) whose stereochemical requirements are quite severe, only tetrahedral complexes were observed. However, with nickel(II), an ion for which the energy barriers from one stereochemistry to another are moderately small, tetrahedral, square, and five coordinate complexes were observed. It was anticipated that with copper(II), an ion whose ability to form variable and distorted stereochemistries is quite remarkable (2), an even wider range of derivatives of these ligands could be prepared. This paper shows that this is indeed the case.

Experimental

Electronic spectra were recorded as transmittance through Nujol mulls with an Applied Physics Cary 14 spectrophotometer. Infrared data were recorded with a Beckman IR 12 spectrophotometer. The low temperature far infrared spectra were obtained via transmittance through thin polythene films obtained by compression of a mixture of the complex and a low melting polythene wax. A Beckman VLT-2 variable temperature cell was used to cool the samples down to liquid nitrogen temperature. Room temperature far infrared data were obtained as Nujol mulls on polythene plates. Magnetic measurements were made via both the Faraday and Gouy methods using a 4 in. Alpha magnet, the system being calibrated with mercury tetrathiocyanatocobaltate(II). Metal and halogen analyses are by the authors and C and H analyses by Galbraith Laboratories of Knoxville, Tenn. or A. B. Gygli of Toronto.

Preparation of the Complexes

The ligands were obtained as previously described (1).

Complexes of 1,2-bis(2′-Pyridyl)ethane

(LE)$CuCl_2$

Equimolar solutions of the ligand and metal salt in ethanol were mixed in the hot; a light green microcrystalline precipitate formed rapidly on cooling, in high yield. Recrystallization could be effected from ethanol.

Anal. Calcd. for $C_{12}H_{12}Cl_2CuN_2$: C, 45.2; H, 3.8; Cl, 22.2; Cu, 19.9. Found: C, 45.3; H, 3.9; Cl, 22.2; Cu, 19.6.

(LE)$CuBr_2$

Prepared in the same fashion as the chloride. The complex is dark green and is not very stable towards recrystallization.

Anal. Calcd. for $C_{12}H_{12}Br_2CuN_2$: C, 35.4; H, 3.0; Br, 39.2; Cu, 15.6. Found: C, 35.3; H, 3.1; Br, 39.0; Cu, 15.3.

Can. J. Chem. Downloaded from www.nrcresearchpress.com by 210.87.254.5 on 09/05/12
For personal use only.

(LE)$_2$Cu(ClO$_4$)$_2$

Ethanol solutions of copper perchlorate and the ligand were mixed in a 1:2 *M* ratio, and the mixture allowed to stand at room temperature. After several hours, a maroon red crystalline product was formed. The complex was recrystallized from ethanol and dried in a desiccator.

Anal. Calcd. for $C_{24}H_{24}Cl_2CuN_4O_8$: C, 45.7; H, 3.8; Cu, 10.1. Found: C, 45.2; H, 4.0; Cu, 10.1.

(LE)Cu(NO$_3$)$_2$

Copper nitrate and the ligand were each dissolved in ethanol in equimolar amounts and then mixed. A deep blue crystalline product was formed immediately. Recrystallization may be readily effected from acetonitrile.

Anal. Calcd. for $C_{12}H_{12}CuN_4O_6$: C, 38.8; H, 3.25; Cu, 17.1. Found: C, 38.8; H, 3.4; Cu, 17.0.

(LE)Cu$_2$(OAc)$_4$

Copper acetate was extracted from a soxhlet thimble by a boiling solution of the ligand in ethanol. The crystals which eventually formed in the boiler were purified by further soxhlet extraction to yield the pure green complex.

Anal. Calcd. for $C_{20}H_{24}Cu_2N_2O_8$: C, 43.9; H, 4.4; Cu, 23.3. Found: C, 44.1; H, 4.2; Cu, 23.35.

bis(2-Pyridyl)disulfide Complexes

(LS)CuCl$_2$

Yellow Green Isomer

When cold equimolar solutions of the ligand and copper chloride are mixed in ethanol, a yellow green precipitate is immediately produced. This was filtered, washed with ethanol, and dried at room temperature. It is converted into the dark blue isomer when heated or mulled intensely or on prolonged standing (several weeks).

Anal. Calcd. for $C_{10}H_8CuCl_2N_2S_2$: C, 33.9; H, 2.3; Cl, 20.0; Cu, 17.9. Found: C, 33.9; H, 3.6; Cl, 20.1; Cu, 17.9.

Dark Blue Isomer

This is most conveniently prepared by mixing the reactants in equimolar proportions in hot ethanol and refluxing momentarily.

Anal. Calcd. for $C_{10}H_8CuCl_2N_2S_2$: C, 33.9; H, 2.3; Cl, 20.0; Cu, 17.9. Found: C, 34.05; H, 2.65; Cl, 20.3; Cu, 17.7.

(LS)CuBr$_2$

This was prepared after the same manner as the chloride. A dark red product was obtained from the hot solution. The complex is unstable on standing (towards reduction to Cu(I)) and cannot be recrystallized.

Anal. Calcd. for $C_{10}H_8Br_2CuN_2S_2$: C, 27.1; H, 1.8; Br, 36.0; Cu, 14.3. Found: C, 27.0; H, 1.9; Br, 36.3; Cu, 13.9.

(LS)Cu(NO$_3$)$_2$

Equimolar quantities of the ligand and copper nitrate were dissolved in warm ethanol and the solution filtered. The resulting clear pale green solution was maintained at the boiling point for some hours. During this period, olive green crystals of the product slowly appeared. They may be recrystallized from alcohol. An accurate C and H analysis could not be achieved.

Anal. Calcd. for $C_{10}H_8CuN_4O_6S_2$: C, 29.4; H, 2.0; Cu, 15.6. Found: C, 30.6; H, 2.4; Cu, 15.6.

Results and Discussion

The ethane and sulfide ligands (**1**, **2**), labelled LE and LS, respectively, form a range of copper(II) complexes which differ markedly from one another, as is immediately evident from their electronic spectra (Figs. 1–3). The complexes, together with their magnetic and spectroscopic (electronic) properties, are shown in Table 1. Far infrared data are presented in Table 2.

In the earlier paper (1) it was demonstrated that the metal complexes could be divided into three series, I, II, and III, according to the complexity of their infrared spectra in several regions

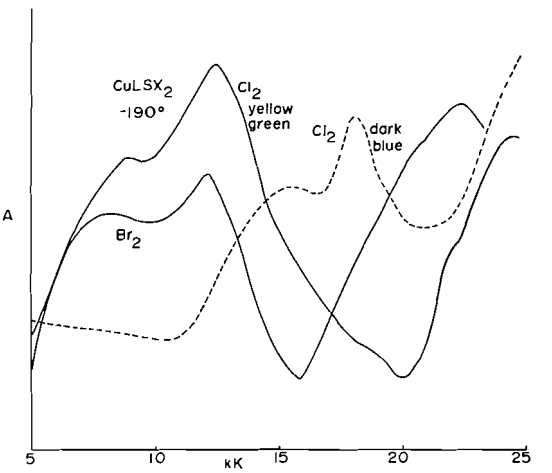

FIG. 1. The electronic transmittance spectra (at −190 °C) of the complexes $CuLSX_2$ (X = Cl, yellow green and dark blue isomers, and Br).

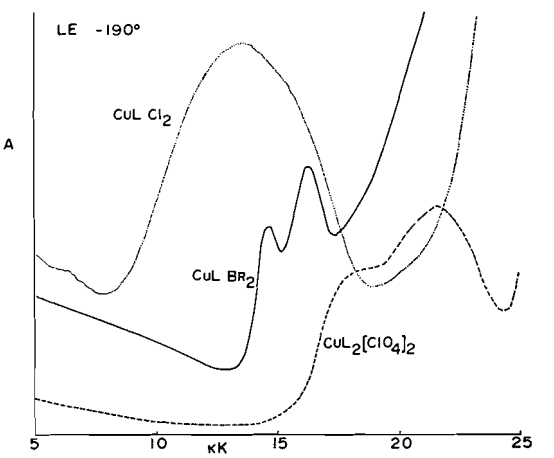

FIG. 2. The electronic transmittance spectra (at −190 °C) of the complexes $CuLEX_2$ (X = Cl and Br) and $Cu(LE)_2(ClO_4)_2$.

TABLE 1

Magnetic data and electronic spectra*

Complex	$\chi M'$*	μ (B.M., 22 °C)	Temperature†	Electronic spectrum‡ (cm^{-1})			
1,2-Bis(2′-pyridyl)ethane complexes							
(LE)$CuCl_2$	1560	1.92	r.t.	13 335			
			l.t.	13 335			
(LE)$CuBr_2$	1536	1.90	r.t.	(14 710)	15 870		
			l.t.	14 600	16 130		
(LE)$Cu(NO_3)_2$	1592	1.94	r.t.	(13 795)	16 025		
			l.t.	14 025	16 670		
(LE)$Cu_2(OAc)_4$	892	1.45	r.t.		13 795	26 670	
			l.t.	(11 110)	14 285	27 400	(29 630)
$(LE)_2Cu(ClO_4)_2$	1633	1.96	r.t.	(17 390)	21 050		
			l.t.	18 180	21 620		
Bis(2-pyridyl)disulfide complexes							
(LS)$CuCl_2$	§	§	r.t.	(8890)	12 060		
(Yellow green)			l.t.	8835	12 500	(22 820)w	
(LS)$CuCl_2$	1329	1.77	r.t.	15 700	18 150		
(Dark blue)			l.t.	16 000	18 690		
(LS)$CuBr_2$	1314	1.76	r.t.	8000	11 430	22 220	
			l.t.	7925br	11 960	22 730	
(LS)$Cu(NO_3)_2$	1325	1.77	r.t.	13 795			
			l.t.	14 145			

*Molar susceptibility corrected for diamagnetism of the ligands.
†r.t. = room temperature spectra; l.t. = spectra at liquid nitrogen temperature.
‡Shoulders are indicated in parentheses.
§Not possible to obtain magnetic data because grinding converts sample to the dark blue isomer.

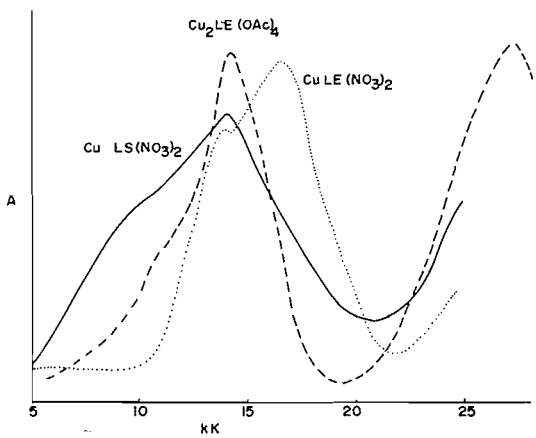

FIG. 3. The electronic transmittance spectra (at −190 °C) of the complexes $Cu_2LE(OAc)_4$, $CuLE(NO_3)_2$, and $CuLS(NO_3)_2$.

characteristic of pyridine. It was concluded that in the series I complexes the ligands were bidentate with a *cis* conformation, whilst in the series II complexes a *gauche* bidentate conformation, with respect to the bridging atoms, was present. The series III complexes had more complicated spectra which were assigned to a bidentate ligand in which the two pyridine residues, though both coordinated, were not chemically equivalent. Of particular importance to the discussion of the conformations of the ligands were the C—C out-of-plane deformations near 400 cm^{-1}. The free ligands and all the nickel, cobalt, zinc, and mercury complexes show at least two bands; the appearance of at least two bands arises from a *cis* rather than a *trans* arrangement of the pyridine residues about the bridging atoms. Azopyridine metal complexes (3) exhibited one or two C—C deformation frequencies near 400 cm^{-1}, one for a *trans* coordinating ligand with both pyridine residues coordinating, and two when one pyridine residue was uncoordinated.

Certain of the copper complexes, in contradistinction to the other complexes of LS and LE alluded to above, also only exhibit a single C—C deformation near 400 cm^{-1} and are expected therefore to have a *trans* configuration about the bridging atoms. Whilst this is a hypothesis rather than a strict rule, it is surely significant that the complex (LE)$Cu_2(OAc)_4$ has such a spectrum. This complex is formulated with dimeric copper acetate residues bridged by the ligand in a *trans* configuration. It is difficult to see how the dimeric units could readily be bridged by the ligand if the latter has a *cis* conformation. The intraligand steric interaction would surely exclude this possibility.

Can. J. Chem. Downloaded from www.nrcresearchpress.com by 210.87.254.5 on 09/05/12
For personal use only.

TABLE 2

Low temperature far infrared spectra (460-200 cm^{-1})

Complex	Series number*	Far infrared spectrum‖									
1,2-Bis(2′-pyridyl)ethane complexes											
(LE)$CuCl_2$	III	210m	276vs	296vs	(298)	333m	398s	435s	450s		
(LE)$CuBr_2$	I	215w	(255)	263s	274s	297m	420m	448s			
(LE)$Cu(NO_3)_2$	III	207m	212m	220m	243s	296vs	332vs	399s	429s	441s	
(LE)$Cu_2(OAc)_4$	IV	240m	270s	348s	364s	421s†	424s†				
$(LE)_2Cu(ClO_4)_2$	II	202m	248m	254m	270s	278s	308m	318m	401s	442vs	
Bis(2-pyridyl)disulfide complexes											
(LS)$CuCl_2$ (yg)§	IV	235m‡	285m	335s	423m						
(LS)$CuCl_2$ (db)§	I	211m	243s	252s	260s	274s	323vs	368m	374s	427s	441
(LS)$CuBr_2$	II	235m	245w	258s	263s	299w	318s	342m	424s	434s	
(LS)$Cu(NO_3)_2$	II	240s	291s	296s	364vs	390m	427s	449m			

*Infrared series to which complex belongs (see ref. 1 and text).
†Coalesce to one band at 417 cm^{-1} at room temperature.
‡Room temperature spectrum; complex isomerizes to blue form under conditions necessary to prepare low temperature sample.
§yg, Yellow green isomer; db, dark blue isomer.
‖Shoulders are indicated in parentheses.

The far infrared spectra of the previously reported complexes were assigned relatively easily (1), the varying stereochemistries occurring in this series of copper complexes, however, provide spectra which are not so readily interpreted. In order to facilitate this interpretation all the spectra were recorded at liquid nitrogen temperature when highly resolved spectra are generally obtained. It is convenient to discuss the complexes individually henceforth.

1,2-bis(2′-Pyridyl)ethane Complexes

(LE)$Cu_2(OAc)_4$

The presence of the well-known dimeric $Cu_2(OAc)_4$ unit is inferred by the analytical data and confirmed unequivocally by the magnetism, electronic, and vibrational spectra of the complex. The moment of 1.45 B.M. is exactly that expected (4) for a dimeric copper acetate moiety with axially coordinated pyridine residues. The electronic spectrum parallels those of other axially amine substituted copper acetate dimer chromophores (5, 6) both at room temperature and at low temperature. The low temperature far infrared spectrum is also very similar to that of related derivatives, a discussion of which will be published elsewhere (7).

The presence of only one C—C deformation frequency at 417 cm^{-1} suggests a *trans* conformation for the ligand, and indeed, as indicated above, if the ligand is to bridge dimer units, a *cis* conformation is highly unlikely. It is interesting that at low temperatures the band at 417 splits into two bands lying at 421 and 424 cm^{-1}. This may be a site symmetry effect or may imply that the two pyridine residues are not strictly equivalent.

This derivative is closely related to the corresponding complex formed between copper acetate and azopyridine (LN), namely, (LN)$Cu_2(OAc)_4$ which has essentially identical physical properties (3). All attempts to prepare the corresponding complex with bis(2′-pyridyl)disulfide were unsuccessful.

(LE)$CuCl_2$

The infrared spectrum of this complex places it into series III in which both pyridine residues are deemed to be coordinating but are not chemically equivalent. The electronic spectrum of this complex is fairly typical of a tetragonally distorted octahedron (8) which would be achieved via chlorine bridges. This is supported by consideration of the far infrared spectrum, comparison of which with those of other LE derivatives suggests assignment of the very strong band at 296 cm^{-1} to a terminal copper chlorine stretching mode, whilst the band at 210 cm^{-1} is probably a bridging copper chlorine vibrational frequency. These bands are in good agreement with those found in the spectrum of $CuPy_2Cl_2$ (295 and 234 cm^{-1} (9)) which is known to have a tetragonally distorted octahedral structure with long copper chlorine bridging bonds (10) connecting the planar $CuPy_2Cl_2$ units.

The presence of a series III infrared spectrum requires that the pyridine residues of the ligand span equatorial and axial sites of the tetragonally distorted octahedron. The lowest C—C deforma-

Can. J. Chem. Downloaded from www.nrcresearchpress.com by 210.87.254.5 on 09/05/12
For personal use only.

Can. J. Chem. Downloaded from www.nrcresearchpress.com by 210.87.254.5 on 09/05/12
For personal use only.

tion frequency, observed at 398 cm^{-1} is only 4 cm^{-1} higher than that of the free ligand. The energy of the C—C deformation frequency is known to increase with increasing metal–ligand interaction (11). Thus the small increase in frequency of the lowest energy band is associated with a weakly coordinated pyridine residue, presumably the one along the long bonded axis. This behavior parallels that of the five coordinate nickel complexes previously described (1). The complex exhibits a broad band centered at about 13 300 cm^{-1} in its electronic spectrum; this is somewhat below the corresponding band in the electronic spectrum of $CuPy_2Cl_2$ (namely 14 600 cm^{-1} (12)). The somewhat lower energy of the LE complex is fully in agreement with the structure proposed since, whilst the pyridine complex has an in-plane CuN_2Cl_2 chromophore with two long copper chlorine interactions, the LE complex is postulated to have an in-plane $CuNCl_3$ chromophore (via halogen bridging) with a long copper chlorine and a long copper pyridine interaction.

(LE)$CuBr_2$

This complex has a series I infrared spectrum and therefore should contain a bidentate LE ligand in the *cis* conformation. The structure of the complex may be deduced by consideration of its electronic spectrum. The relatively high energy of the absorption bands excludes a tetrahedral formulation, which would give rise to absorption near or below 10 000 cm^{-1} (8, 13). A square planar complex with no near neighbors along the four fold axis would be expected to absorb at a rather higher energy and should show only one broad band. Moreover such complexes are rare with halogen ligands in the absence of a pronounced steric interaction suppressing axial coordination. By analogy with the chloro complex above, a six coordinate tetragonally distorted octahedron is also eliminated since it would be expected to absorb near or below 14 000 cm^{-1}. A five coordinate structure, on the other hand, with an essentially square pyramidal chromophore would be consistent with the observed data. The complex [Cu(1,3-propanediamine)$_2$-H_2O]$^{2+}$$SO_4^{2-}$ has such a chromophore with a CuN_4O microsymmetry. It exhibits a band at 17 900 cm^{-1} with weaker absorption near 16 000 cm^{-1} (8). (LE)$CuBr_2$ is proposed to have a polymeric CuN_2Br_3 square pyramidal chromophore, giving rise to a shift in the band envelope to lower energies relative to the CuN_4O chromophore. A trigonal bipyramidal arrangement is excluded because it would certainly absorb at much lower energies (8, 14). Further support is forthcoming from consideration of some five coordinate square pyramidal copper complexes of a polyfunctional phthalazine ligand, which we have recently reported (15). A copper phthalazine complex with a CuN_2Br_2O chromophore in a square pyramidal array absorbs at 16 300 cm^{-1}, closely similar in energy to the spectrum of the above complex. In this case the low temperature study failed to resolve the low energy tail. Comparison of the far infrared spectra of the LE chloro and bromo complexes enables the tentative assignment of the strong band at 263 cm^{-1} to a copper–bromine stretching frequency. The corresponding band in the five coordinate phthalazine complex alluded to above is at 265 cm^{-1} (16).

(LE)$Cu(NO_3)_2$

This brilliant blue complex has a spectrum essentially similar to that of the previously described bromo complex, but with the main band shifted some 500 cm^{-1} to higher energy. Similar arguments may be employed to suggest that this complex is also five coordinate and square pyramidal (**3**). It differs from the bromide, however, in a number of interesting ways. Firstly, its infrared spectrum places it into series III, implying that the ligand spans equatorial and axial sites; secondly, five coordination may be achieved without recourse to bridging ligands. The presence of an axially coordinated, and apparently weakly coordinated, pyridine residue is indicated by the C—C out-of-plane deformation band at 399 cm^{-1} similar in energy to the copper chloride complex described above. The infrared spectrum in the regions associated with absorption by the nitrate group (17, 18) are exceedingly complex, much more so than in the corresponding (LS)$Cu(NO_3)_2$ derivative described below. It is concluded, therefore, that the two nitrate groups are inequivalently coordinated as required by structure (**3**). Two very intense bands in the infrared spectrum at 296 and 332 cm^{-1} are tentatively assigned to Cu—O(NO_3) stretching vibrations. Interestingly the complex is soluble in, and quite stable to, water.

(LE)$_2Cu(ClO_4)_2$

The very high energy electronic absorption of this complex, 21 620 and 18 180 cm^{-1} (at low

Can. J. Chem. Downloaded from www.nrcresearchpress.com by 210.87.254.5 on 09/05/12
For personal use only.

temperature) argues cogently for a square coplanar structure with a CuN_4 chromophore and no near neighbors along the four fold axis. The complex has a series II infrared spectrum suggesting the presence of bidentately coordinated LE ligands in a *gauche* conformation, and in this respect is similar to the corresponding $(LE)_2Ni(ClO_4)_2$ complex (1). It is difficult to rationalize, however, the very low energy of the first C—C deformation frequency (395 cm^{-1}). This implies a weak copper–pyridine interaction, yet there is no cause to postulate this.

bis(2-Pyridyl)disulfide Complexes

(LS)$CuCl_2$

This complex exists in two isomeric forms: a yellow green isomer isolated from a reaction of the constituents in the cold, and a dark blue isomer obtained on heating. The yellow green isomer is converted into the dark blue isomer by pressure (extensive mulling) or by heat.

Yellow Green Isomer

This complex has a very simple infrared spectrum with only one pyridine ring breathing vibrational frequency at 1024 cm^{-1}, and only one C—C deformation frequency at 424 cm^{-1}. Following the earlier classification (1), this may be labelled a series IV spectrum; the ligand is expected to exist in a *trans* geometric form, and will presumably bridge copper atoms in a polymeric array.

The electronic spectrum consists of two components at relatively low energy (8835 and 12 500 cm^{-1}, with the higher energy band of higher intensity); following the arguments above a square or square pyramidal structure is excluded. The energies would appear to be of the correct order of magnitude for a tetragonally distorted octahedron [*cf.* (LE)$CuCl_2$]. The only other alternative formulation is a trigonal bipyramidal arrangement, expected to absorb near 12 000 cm^{-1} (8, 14). Consideration of model compounds of each of these structural types (8) reveals that the octahedral complexes have their most intense absorption in the visible region with a lower intensity tail to lower energy which may or may not be resolved into an additional lower intensity band. The trigonal bipyramidal complexes, on the other hand (8, 14), generally exhibit two components, with the *lower energy* component of higher intensity. Thus the yellow green isomer would appear, if this criterion is valid, to have a tetragonally distorted octahedral structure. Since the ligand belongs to series IV, a polymeric structure is envisaged with both halogen and ligand bridges. Since the C—C deformation frequency is relatively high the ligand probably coordinates in the equatorial plane of the distorted octahedron. The far infrared spectrum does not convey very much information except that its simplicity, relative to the other isomer suggests high symmetry. The band at 335 cm^{-1} is strong and suggestive of a copper–chlorine stretching vibration; however, this vibration is not expected at so high a frequency if the structure is adjudged correctly. Instead this band may be a ligand band (the free ligand absorbs at 347 cm^{-1}).

Dark Blue Isomer

This complex absorbs at a much higher energy in its electronic spectrum, higher than any other complex except $Cu(LE)_2(ClO_4)_2$. It is probable therefore that the complex is *cis* square coplanar; the infrared spectrum puts the complex into series 1 with a bidentate ligand of *cis* conformation. The far infrared spectrum is fairly complicated with a strong band at 323 cm^{-1} which should be assigned to a copper chlorine stretching frequency. In this case an additional band is observed at 368 cm^{-1} (absent in the yellow green isomer) which is probably the ligand vibration alluded to above. The electronic and vibrational data are very similar to those of the complex $(2\text{-Br-pyridine})_2CuCl_2$ which is also believed to be square planar (19). This latter complex has a Cu—Cl stretching vibration at 333 cm^{-1} (20) and absorbs in the visible region at 15 250 and 18 700 cm^{-1} (12). The possibility of a very weakly coordinated chlorine atom, from a neighboring molecule, being present along the axis to form a five coordinate derivative should be considered in view of the fact that the LS ligand appears to be in a *cis* configuration rather than the *gauche* configuration which might have been anticipated. The complex $(4\text{-methylpyridine})_2CuCl_2$ does in fact have this kind of five coordinate structure (a plane with a long fifth bond) (21); it absorbs in the visible region at 14 950 cm^{-1} (12) and has its Cu—Cl stretching vibration in the far infrared region at 299 cm^{-1} (22). Thus a similar five coordinate structure for (LS)$CuCl_2$ (dark blue) seems very unlikely.

(LS)$CuBr_2$

The relatively low energy of the electronic absorption of this complex would indicate a

Can. J. Chem. Downloaded from www.nrcresearchpress.com by 210.87.254.5 on 09/05/12
For personal use only.

tetrahedral (or distorted tetrahedral) or five coordinate trigonal bipyramidal structure as the most likely structures. Both are expected to give multiple absorption in this region, although a regular tetrahedral stereochemistry might absorb at lower energies (13). Of key significance to the elucidation of the structure of this complex is the broad band near 22 000 cm^{-1} which can only be ascribed to a bromine-to-copper charge transfer band. The energy of this band will increase with increasing coordination number of the metal ion (23). A trigonal bipyramidal copper complex with bromine ligands exhibits a Br $\rightarrow$ Cu transition near 27 000 cm^{-1} whilst the tetrahedral $CuBr_4^{2-}$ ion has comparable absorption (24) from 17 000 cm^{-1}. Since the transition is from a π orbital on the bromine atom to the $d_{x^2-y^2}$ orbital of the copper ion, distortion of the tetrahedron via flattening towards a square structure will increase the energy of the d–d transitions (25) and simultaneously raise the energy of the bromine-to-metal charge transfer band. The data would therefore be totally consistent with a flattened tetrahedral structure for this complex. There is no obvious mechanism by which, in a five coordinate trigonal bipyramidal complex, the charge transfer band could decrease in energy by some 5000 cm^{-1}; both five coordinate square pyramidal or octahedral bromine copper complexes would be expected to exhibit charge transfer appreciably above 22 000 cm^{-1}. The far infrared spectra of copper bromo complexes have been fairly extensively studied. Tetrahedral complexes of the type L_2CuBr_2 are expected to absorb in the region 219–229 cm^{-1} (26), whilst square complexes absorb at higher energies and may exhibit bands as high as 266 cm^{-1} [*e.g.* $(quinoline)_2CuBr_2$ (27)]. The complex under discussion shows several bands in the region 219–266 cm^{-1}, but it is not possible to unequivocally identify the metal–bromine absorption. The complex has a series II infrared spectrum, suggesting the presence of a bidentately bound ligand group with a *gauche* conformation similar to some zinc and cobalt tetrahedral complexes described earlier (1). The complex is not very stable, decomposing to a copper(I) derivative on standing (several days). There is also evidence for a light colored isomer of this complex which is formed when the reactants are mixed in the cold; however, it is converted very rapidly to the brown form and cannot be characterized. The electronic spectra of the $(LS)CuCl_2$ (yellow green) and $(LS)CuBr_2$ are at first sight very similar (Fig. 2), which might suggest that they have similar structures. However, this is not the case. The splitting of the electronic absorption bands is appreciably greater in the case of the bromide, the two complexes belong to two different infrared series, and the far infrared spectra are very different. It is probable that the very unstable light colored bromo complex is structurally related to the yellow green chloride isomer.

$(LS)Cu(NO_3)_2$

This pale green complex, unlike its LE analog, has a series II infrared spectrum suggestive of equivalently bound pyridine residues. It also differs from the earlier complex in having much simpler absorption in the NO_3^- absorption regions. Consequently, it is probable that both nitrate groups are similarly bound. The complex does not absorb at nearly so high an energy as $(LE)Cu(NO_3)_2$; indeed, the spectrum is very similar to that of the yellow green $(LS)CuCl_2$ but is displaced slightly to higher energy. Accepting that the two nitrate groups are equivalently bound, then a coordination number of four is required if the nitrates are unidentate and six if bidentate. A coordination number of four can be clearly eliminated by consideration of the electronic spectrum (a tetrahedral complex would not absorb at so high an energy, a square complex would absorb at a higher energy, and a distorted version would probably have a more grossly split spectrum *cf.* $(LS)CuBr_2$). A six coordinate octahedral complex with bidentate nitrate groups (III) presumably tetragonally distorted along one O—Cu—O axis would seem compatible with the observed facts. The complex is typical in having three bands near 400 cm^{-1}, which is generally only the case with series III complexes. However, the simplicity of the rest of the infrared spectrum is incompatible with the presence of non-equivalently bound pyridine residues.

Magnetism

The magnetic properties of copper complexes rarely provide much information concerning their stereochemistry. Most complexes have moments in the range 1.73–2.00 B.M. if magnetically dilute. Tetrahedral complexes, having an orbital triplet ground state, should theoretically have moments exceeding 2.00 B.M. but rarely do, because distortion almost invariably

removes the degeneracy of this ground state. Consideration of the data in Table 1 clearly shows that, whilst all the LE complexes have moments near 1.9 B.M., the LS complexes have moments near 1.8. The difference, though not very large, is significant. Moments above 1.73 B.M. in copper complexes which do not have orbital triplet ground terms, are achieved by the mixing in of excited orbitally degenerate terms into the ground state. This mixing process is directly proportional to the spin–orbit coupling coefficient (very large for Cu(II)) and inversely proportional to the energy separation between the ground state and excited term concerned. Since the stereochemistries vary throughout the complexes studied, so will the energy separation between ground and excited states. Further complexes are needed to see whether the difference between the two ligands is real, but it does seem as if the ligand LS causes a larger decrease in the spin–orbit coupling coefficient than does the ligand LE.

Summary

The extraordinary adaptability of these ligands to the electronic demands of the metal ion has been demonstrated by the existence of cobalt(II), nickel(II), copper(II), zinc, and mercury complexes in a wide range of stereochemistries. A linear two coordinate complex was observed with mercury (1) whilst four coordinate square and tetrahedral, five coordinate square pyramidal (and possibly trigonal bipyramidal), six coordinate octahedral, and tetragonally distorted octahedral complexes were observed with the other ions.

The rationale for this behavior stems from the extreme flexibility of these ligands. They can adopt a conformation which will allow a wide range of possible angles to be subtended at the metal ion, and can therefore coordinate in various stereochemical modes. It is also likely that the high polarizability of the electron cloud on the pyridine residues will allow the metal–nitrogen bond lengths to vary somewhat without a serious loss in bond energy.

Hopefully, X-ray structures of some of these complexes can be obtained in the future to clarify the bonding modes and substantiate the structures proposed.

We are indebted to the National Research Council of Canada for financial support.

1. M. KEETON and A. B. P. LEVER. Inorg. Chem. In press.
2. F. A. COTTON and G. WILKINSON. Advanced inorganic chemistry. 2nd ed. John Wiley and Sons Inc., New York. 1966.
3. D. A. BALDWIN, A. B. P. LEVER, and R. V. PARISH. Inorg. Chem. **8**, 107 (1969).
4. E. KOKOT and R. L. MARTIN. Inorg. Chem. **3**, 1306 (1964).
5. M. KATO, H. B. JONASSEN, and J. C. FANNING. Chem. Rev. **64**, 99 (1964).
6. A. B. P. LEVER, F. J. C. ROSSOTTI, D. H. SCHÄRER, and B. J. EDMONDSON. J. Chem. Soc. A, In press.
7. A. B. P. LEVER and B. S. RAMASWAMY. To be published.
8. B. J. HATHAWAY and D. E. BILLING. Coord. Chem. Rev. In press.
9. R. J. H. CLARK and C. S. WILLIAMS. Inorg. Chem. **3**, 350 (1965).
10. J. D. DUNITZ. Acta Cryst. **10**, 307 (1957).
11. N. S. GILL, R. H. NUTTALL, D. E. SCAIFE, and D. W. A. SHARP. J. Inorg. Nucl. Chem. **18**, 79 (1961).
12. W. LUDWIG and F. GASSER. Helv. Chim. Acta, **52**, 107 (1969).
13. D. M. L. GOODGAME and F. A. COTTON. J. Chem. Soc. 2298 (1961).
14. M. CIAMPOLINI and N. NARDI. Inorg. Chem. **5**, 41 (1966).
15. L. K. THOMPSON, V. T. CHACKO, J. A. ELVIDGE, A. B. P. LEVER, and R. V. PARISH. Can. J. Chem. **47**, 4141 (1969).
16. J. DONINI, A. B. P. LEVER, and E. MANTOVANI. To be published.
17. C. C. ADDISON and W. B. SIMPSON. J. Chem. Soc. 598 (1965).
18. A. B. P. LEVER. Inorg. Chem. **4**, 1042 (1965).
19. M. KEETON, A. B. P. LEVER, and B. S. RAMASWAMY. Spectrochim. Acta. In press.
20. W. R. MCWHINNIE. J. Inorg. Nucl. Chem. **27**, 2573 (1965).
21. V. F. DUCKWORTH, D. P. GRADDON, N. C. STEPHENSON, and E. C. WATTON. Inorg. Nucl. Chem. Lett. **3**, 557 (1967).
22. C. W. FRANK and L. B. ROGERS. Inorg. Chem. **5**, 615 (1966).
23. A. B. P. LEVER. Inorganic electronic spectroscopy. Elsevier Publ. Inc., Amsterdam. 1968.
24. C. K. JØRGENSEN. Advan. Chem. Phys. **5**, 33 (1963).
25. L. SACCONI and M. CIAMPOLINI. J. Chem. Soc. 276 (1964).
26. R. J. H. CLARK. *In* Halogen chemistry. Vol. 3. *Editor* V. Gutmann. Academic Press, New York. 1968. p. 85.
27. M. GOLDSTEIN, E. F. MOONEY, A. ANDERSON, and H. A. GEBBIE. Spectrochim. Acta, **21**, 105 (1965).

Can. J. Chem. Downloaded from www.nrcresearchpress.com by 210.87.254.5 on 09/05/12
For personal use only.

Can. J. Chem. Downloaded from www.nrcresearchpress.com by 210.87.254.5 on 09/05/12
For personal use only.

The photo-electron spectrum of XeF_2

BURKHARD BREHM, MICHAEL MENZINGER,[1] AND CHRISTIAN ZORN
Physikalisches Institut, University of Freiburg i.Br., Germany

Received May 4, 1970

Six electronic states of XeF_2^+ have been found in the photo-electron spectrum of XeF_2. The adiabatic ionization potentials, vertical ionization potentials, and relative ionization probabilities for these states are compared with theoretical predictions and an attempt is made to assign the states in terms of molecular orbitals.

Canadian Journal of Chemistry, 48, 3193 (1970)

Introduction

The discovery (1) of the xenon fluorides in 1962 was soon followed by an extensive discussion of the electronic structure of these compounds (2, 3). Several different theoretical approaches were used out of which the linear combination of atomic orbitals and molecular orbitals (l.c.a.o.-m.o.) scheme (3–7) appears to be the most successful in explaining properties such as molecular geometry, thermochemical data, visible and ultraviolet-absorption spectra, and magnetic properties.

We report the photo-electron spectrum of XeF_2, which gives direct information about some low lying electronic states of the XeF_2^+ ion and within the approximation of Koopmanns' theorem (8) about the binding energy and bonding properties of the molecular orbitals occupied in XeF_2.

Experimental

The spectrometer, which has been described previously (9) employs a planar retarding field and an einzellens for collimation of the electron beam prior to the retarding field. The electrons produced by 584 Å resonance radiation of a He discharge lamp are counted and registered in the 400 channels of a multichannel analyzer which is swept in the multiscaling mode synchronously with a sawtooth voltage applied to the retarding field grid and the einzellens. The XeF_2 gas emerged from a multichannel jet of sintered glass. The resolving power, as measured by the 10 to 90% step width of electrons from Ar or Xe is 10 meV, although this resolution apparently has not been reached in this study, probably due to surface changes caused by the reactive gas under investigation.

Figure 1 shows a photo-electron spectrum of XeF_2. Upon initial admission of the gas the two steps at 12.13 and 13.43 eV were ten times as large as in Fig. 1. By addition of some Xe gas it could be proven that these two steps are due to Xe-atoms formed by decomposition of the xenon fluoride probably at the walls of the gas inlet system. After conditioning for 1 h these two steps had decreased to the size displayed in Fig. 1 where they serve as a convenient internal standard for the energy calibration.

Six steps corresponding to different electronic states of the XeF_2^+ ion are found and there seems to be a seventh structure at the high ionization energy end. It occurs at the low electron energy end of the spectrum where the bad signal-to-noise ratio and an appreciable background of slow electrons make the investigation of the spectrum difficult. Table 1 summarizes the experimental findings.

Theory

The Results of Linear Combination of Atomic Orbitals and Molecular Orbitals

Before discussing the electronic state assignment in terms of the various molecular orbitals, a short summary of the theoretical predictions (6) may be appropriate. Taking only the three 5p orbitals of Xe and the six 2p orbitals of the two F atoms as a basis set, the following molecular orbitals (m.o.) can be formed: there is one σ_g orbital which is the difference of the two fluorine $2p_\sigma$ atomic orbitals (a.o.). Symmetry excludes any contribution of the Xe 5p orbitals. The same is true of the only π_g orbital which is the difference of the two fluorine $2p_\pi$ orbitals. These two orbitals should be non-bonding and close together on the orbital energy scale. If the band intensities are assumed to be approximately proportional to the degeneracies of the vacated orbitals, an intensity ratio of 2:1 in favor of the π_g orbital is expected.

Two σ_u orbitals can be formed out of the sum of the two $2p_\sigma$ a.o. of fluorine and the Xe $5p_\sigma$ a.o., one of which should be strongly bonding (low energy) and the other strongly anti-bonding (high energy). The contribution of the Xe a.o. should be larger for the anti-bonding σ_u orbital because of the lower ionization energy of Xe.

[1]Present address: Department of Chemistry, University of Toronto, Toronto 181, Ontario.

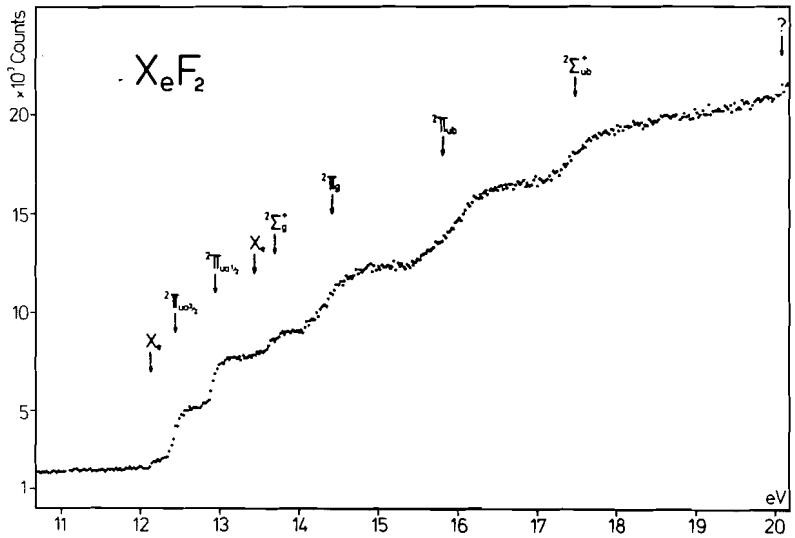

FIG. 1. The photo-electron spectrum of XeF_2, 584 Å. The contents of consecutive channels of a multichannel analyzer are plotted as a function of the difference of the photon energy and the electron energy $h\nu - E_{el}$.

TABLE 1

Observed transitions and their assignments

Ionization potential (eV)		Relative step height	Width (eV)	Molecular orbital classification
Adiabatic	Vertical			
12.33 ± 0.02	12.44	1	0.2	π_{ua}, $\Omega = 3/2$
12.83 ± 0.02	12.94	1	0.2	π_{ua}, $\Omega = 1/2$
13.58 ± 0.05	13.68	0.43	0.3 (?)	σ_g
14.06 ± 0.05	14.36	1.3	0.7	π_g
15.40 ± 0.05	15.9 (?)	1.6	1.0	π_{ub}, $\Omega = 3/2$, and $1/2$
17.10 ± 0.1	17.5	1.1	1.0	σ_{ub}
20.05 ± 0.1	?	?	?	?

Finally two π_u orbitals can be formed out of the sum of the two F $2p_\pi$ a.o. and the Xe $5p_\pi$ a.o. Again one should be bonding and the other anti-bonding, but the binding of these orbitals is expected to be small due to the small overlap. The intensity of the ionization process eliminating an electron from a π orbital is expected to be roughly twice as large as in the case of a σ orbital, but deviations from this rule are not uncommon.

The spin–orbit coupling can split only the two π_u orbitals into $\pi_{u1/2}$ and $\pi_{u3/2}$ components, since the π_g orbital is localized on the F atoms which are too small to cause measurable spin–orbit effects. Altogether, there are eight molecular orbitals (π_g is doubly degenerate), the order of which with decreasing ionization energy from left to right is: $(\sigma_{ub})^2$, $(\pi_{u1/2b})^2$, $(\pi_{u3/2b})^2$, $(\pi_g)^4$, $(\sigma_g)^2$, $(\pi_{u1/2a})^2$, $(\pi_{u3/2a})^2$, (σ_{ua}), where "a" stands for anti-bonding and "b" for bonding. As there are only 16 valence electrons to be accommodated by the basis set chosen thus the σ_{ua} orbital is left unoccupied for the ground state of XeF_2. This leads to an atomic net charge distribution with about +1 around the Xe atom and −1/2 around each F atom (3, 6). The order of the σ_g and π_g orbitals is practically undetermined within this approximation. The ionic states in a photo-electron spectrum should correspond to the electronic states generated by removing one electron out of either one of the occupied orbitals.

Interpretation of the Results

A. Energetic Position and Relative Intensity

Comparing these predictions with the measurements (see Fig. 1) the first two steps at 12.44 and 12.94 eV, essentially equal in size and shape,

Can. J. Chem. Downloaded from www.nrcresearchpress.com by 210.87.254.5 on 09/05/12
For personal use only.

Can. J. Chem. Downloaded from www.nrcresearchpress.com by 210.87.254.5 on 09/05/12
For personal use only.

can safely be assigned to the electronic states produced by ionization from the $\pi_{u3/2a}$ and the $\pi_{u1/2a}$ orbitals. Their small width also supports the prediction that these orbitals are only slightly anti-bonding.

Our value for the first ionization potential of XeF_2 12.33 eV agrees with the photo-ionization result of Morrison *et al.* (10), 12.28 eV. The 0.05 eV difference between the two numbers is caused by a difference in the interpretation of the curves. In both measurements the ionization starts with a small foot at 12.28 eV. We believe that this small foot is due to ionization processes of molecules in vibrationally excited states, because at 300 °K the majority of the molecules is in vibrationally excited states due to the relatively low vibrational frequencies (11). This assumption can be proven or disproven by measurements of the onset of the ionization at different gas temperatures. The apparent disagreement with the value 11.5 ± 0.1 eV given by Wilson *et al.* (7) seems to indicate that these authors have overestimated the precision of their extrapolation procedure based on four bands out of a Rydberg series.

Of the two next steps which are expected to correspond to the two "gerade" orbitals the smaller one at 13.68 eV can only involve the transition to the $(\sigma_g)^{-1}$ state of the ion while the large step comes from $(\pi_g)^{-1}$ state of the ion. The next broad step at 15.9 eV is assigned to the $(\pi_{ub})^{-1}$ state and gives an indication of the strongly overlapping spin orbit doublet $\Omega = 1/2$, $\Omega = 3/2$. This leaves the step at 17.5 eV to the $(\sigma_{ub})^{-1}$ ionic state.

B. Bonding Character of the Orbitals

While the energetic order and relative ionization probabilities of the ion states seem to be in rough agreement with the expectations, an evaluation of the width of the observed structures in terms of bonding properties of the m.o.'s leads to some difficulties. The l.c.a.o.-m.o. model predicts strong bonding only for the σ_{ub} m.o., while the other orbitals should be non-bonding (σ_g, π_g), or only slightly bonding (π_{ub}), or slightly anti-bonding (π_{ua}), but only the first two steps identified as $(\pi_{ua})^{-1}$, $\Omega = 3/2$ and $(\pi_{ua})^{-1}$, $\Omega = 1/2$ are in agreement with this. The predictions of the bonding properties of the m.o. based on qualitative m.o. arguments have to be taken with caution, however, especially in molecules, where ionic binding makes an important contribution to the stability of the molecule as in XeF_2 (6).

As has been mentioned before, the charge distribution in XeF_2 is believed to be +1 at the Xe atom and −1/2 at each F atom. Ionization of an electron out of an m.o. localized on the two F atoms will decrease the net charge of these atoms to zero eliminating the ionic contribution to the binding. So, within this simple model, the ionization of an electron from the σ_g or π_g orbital will behave like the ionization of an electron from a bonding orbital in spite of the fact that these orbitals can have no interaction with any of the 5p a.o. of Xe. An application of this argument to the two π_u electrons suffers from the lack of information about the relative contribution of the Xe a.o. and the F a.o. to these m.o. If one simply takes point charges, one finds that the attractive forces are increased as one removes an electron from an orbital where the contribution of the Xe a.o. is more than 63%; in the other case the forces are decreased. This is consistent with the experiment, if the π_{ua} m.o. has about 60% Xe a.o., while the π_{ub} m.o. has about 40% Xe a.o. contribution.

C. Spin–Orbit Coupling

The observed spacing between the two components of the $(\pi_{ua})^{-1}$ state of XeF_2^+ (0.5 eV) can be compared with the splitting of the two ^2P states of Xe^+ (1.3 eV). Since the expectation value of the spin orbit coupling operator is large only around the nucleus and the inner shells of the Xe atom, the part of the wave function around the Xe nucleus determines the spin–orbit splitting. Within the "almost closed shell" approximation widely used for atoms and within the one-electron m.o. approximation, the π_{ua} m.o. must be compared with the 5p a.o. of Xe in the vicinity of the Xe nucleus. They should be very similar, except for a normalization factor λ^2 giving the relative contribution of the Xe a.o. to the m.o., because the binding energy of the two electrons compared is fortunately the same while the difference in net charges influences mainly the outer shells and not the inner shells of Xe, where the spin–orbit coupling takes place. If one furthermore assumes that in the molecule the orbital angular momentum is more strongly coupled to the molecular axis than to the spin (Hund's case *a*), the ratio of the molecular spin–orbit splitting to atomic spin–orbit splitting comes out to be $\frac{2}{3}\lambda^2$. This leads to $\lambda^2 = 0.58$ or 58% if one takes the

Can. J. Chem. Downloaded from www.nrcresearchpress.com by 210.87.254.5 on 09/05/12
For personal use only.

experimental numbers given above. This value of 58% Xe a.o. contribution to the π_{ua} m.o. is in amazing agreement with the other simple model presented above to rationalize the bonding characteristics of the m.o.'s.

If one accepts that the π_{ua} m.o. has 60% contribution of the Xe a.o., the π_{ub} m.o. must be about 40% a.o. due to the orthogonality requirement. From this one could predict a spin–orbit splitting of 0.37 eV, but the interaction of the $\Omega = 1/2$ component of the π_{ub} m.o. with the close by (1.7 eV) σ_{ub} m.o. induced by the spin–orbit coupling and the effect of the different energy of the π_{ub} m.o. as compared to the Xe 5p a.o. on the wave function in the vicinity of the Xe nucleus cannot easily be taken into account. As a result the value of 0.37 eV for the spin–orbit splitting of the π_{ub} orbital can only be taken as a rough guess, but together with the argument about the "bonding properties" of this orbital the possibility to clearly resolve the two spin–orbit components of this state appears to be plausible.

Even though both theoretical models are quite crude they seem to lead to a consistent interpretation of all experimental results.

D. Contribution of Other Atomic Orbitals

Aside from the structure observed at 20 eV, the energetic order of the σ_g and π_g orbital seems to make the consideration of the interaction of the orbitals discussed so far with other atomic orbitals worthwhile, even though they are either 10 eV or more below (Xe 5s, Xe 4d, F 2s) or 10 eV or more above (Xe 6s, Xe 4f, F 3s) the orbital energies used in the present basis set. Calculations indicate (6) that the F 2s orbitals show the largest interactions. These F 2s orbitals generate one σ_g m.o. and one σ_u m.o. which would have the effect of a small upward shift of the σ_g and σ_u m.o.'s discussed here. This may be the reason why the σ_g orbital has a lower ionization potential than the π_g orbital.

It is not easy to see which of the additional orbitals can be taken to explain the structure observed at 20 eV. This question must be left open until better calculations or photo-electron spectra produced with more energetic radiation give enough information about the lower molecular orbitals of XeF_2.

NOTE ADDED IN PROOF: After submission of the manuscript an article by Brundle, Robin, and Jones (12) about the photo-electron spectrum of XeF_2 appeared. These authors found some vibrational structure around the ionization threshold and detected the S—O splitting of the π_u level at 15.8 eV and the structure at 20 eV using the 304 Å radiation of He^+. Their results are in very good agreement with the results given in this article; some small deviations in the numbers given for the 2., 5. and 6. adiabatic ionization potential (i.p.) appear to be due to differences in the evaluation procedures. Subtraction of estimated contributions from hot bands resulted in the somewhat higher values given in this article for the 5. and 6. adiabatic i.p. The structure at the 2. i.p., after subtraction of the hot band contribution, seems to be broadened either by unresolved vibrational structure or by pre-dissociation, as Brundle *et al.* (12) suggest. Both effects would, however, tend to shift the peak of the ionization probability away from the adiabatic i.p. toward higher energies. In addition the definition of an "adiabatic ionization potential" itself loses precision, if broadening due to pre-dissociation is assumed.

We thank Dr. J. Heitz and Dr. J. P. Adloff of the Centre des Recherches Nucléaires in Strasbourg, France, for providing us with a XeF_2 sample. The award of an Alexander von Humboldt Fellowship and financial support through the National Research Council of Canada to one of us (M.M.) is gratefully acknowledged.

1. C. L. CHERNIK *et al.* Science, **138**, 136 (1962). N. BARTLETT. Proc. Chem. Soc. 218 (1962).
2. HYMAN (*Editor*). Noble gas compounds. University of Chicago Press, Chicago, Illinois. 1963.
3. C. A. COULSON. J. Chem. Soc. 1442 (1964).
4. R. E. RUNDLE. J. Chem. Soc. **85**, 112 (1963).
5. L. L. LOHR and W. N. LIPSCOMB. J. Amer. Chem. Soc. **85**, 240 (1963).
6. J. G. MALM, H. SELIG, J. JORTNER, and S. A. RICE. Chem. Rev. **65**, 199 (1965).
7. G. G. WILSON, J. JORTNER, and S. A. RICE. J. Amer. Chem. Soc. **85**, 813 (1963).
8. J. KOOPMANNS. Physica, **1**, 104 (1933).
9. R. SPOHR and E. VON PUTTKAMER. Z. Naturf. **22**a, 409 (1967).
10. J. D. MORRISON, A. J. C. NICHOLSON, and T. A. O'DONNELL. J. Chem. Phys. **49**, 959 (1968).
11. S. REICHMANN and F. SCHREINER. J. Chem. Phys. **51**, 2355 (1969).
12. C. R. BRUNDLE, M. B. ROBIN, and G. R. JONES. J. Chem. Phys. **52**, 3383 (1970).

Can. J. Chem. Downloaded from www.nrcresearchpress.com by 210.87.254.105 on 09/05/12
For personal use only.

Cu^{2+} – fulvic acid chelation equilibrium in 0.1 *m* KCl at 25.0 °C

DONALD S. GAMBLE, M. SCHNITZER, AND I. HOFFMAN
Analytical Chemistry Research Service[1] *and Soil Research Institute*,[2] *Research Branch, Canada Department of Agriculture, Ottawa, Canada*

Received June 9, 1970

Cu^{2+} reacts with fulvic acid to form a site-bound chelate on the fulvic acid polymer molecules. It is deduced from literature evidence that this chelate is the same type that Cu^{2+} forms with salicylic acid. This is supported by a Job's continuous variations plot. The mass action quotient for the chelate formation in 0.1 *m* KCl at 25.0 °C has been measured as a function of the degree of ionization of the chelating carboxyl groups. The strength of the Cu^{2+} – fulvic acid chelate is comparable to that of other bidentate Cu^{2+} chelates.

Canadian Journal of Chemistry, **48**, 3197 (1970)

Introduction

Humic materials constitute a group of aromatic polymers ranging from low molecular weight, soluble polyelectrolytes to high molecular weight cation exchangers (1–3). The various soluble, colloidal, and ion exchange fractions have similar polymer backbones and weak acid functional groups. Their range of polyelectrolyte and ion exchange properties is therefore quite comparable to that of synthetic polyelectrolyte systems, such as polyacrylic and polymethacrylic acid (4–7), which are extensively described in the literature. An important difference is that unlike synthetic chain polymers, humic materials such as fulvic acid consist of irregular two or three dimensional arrays of condensed and broken aromatic rings, with no identifiable monomer units.

As is the case with the polyacrylic acids (8, 9), both soluble and crosslinked humic acid fractions complex metal ions (10, 11). The common practice (12, 13) of using soluble polyelectrolytes as model systems for predicting ion exchanger properties should therefore apply to the humic materials.

This investigation of the Cu^{2+}– fulvic acid complexing equilibrium accordingly has the following objectives: (*1*) to re-evaluate the evidence for the nature of the complexing sites and of the complex, in the light of recently available fulvic acid ionization data; (*2*) to confirm the number of Cu^{2+} complexing sites per gram of fulvic acid that earlier work had indicated; (*3*) to measure the Cu^{2+} – fulvic acid complexing equilibrium as a function of the degree of ionization of the carboxyl groups at the complexing sites.

[1]Contribution No. 126.
[2]Contribution No. 336.

The Complexing Reaction

Fulvic acid has three general types of functional groups that influence any metal ion – fulvic acid complexing study: (*a*) phenolic OH groups, which remain unneutralized except by prolonged reaction with concentrated strong base (14); (*b*) Type I carboxyl groups, defined as those ortho to the phenolic groups, which are about 80% ionized at 10^{-3} *m* H^+ and virtually all ionized at 10^{-5} *m* H^+; (*c*) Type II carboxyl groups, which probably include some that are meta to the phenolic groups, and are nearly unionized at 10^{-3} *m* H^+, and about 43% ionized at 10^{-5} *m* H^+. A previous report (15) gives the ionization equilibria and numbers of Type I and Type II carboxyl groups per gram of fulvic acid, for the sample used in this work.

The familiar Cu^{2+} chelation reactions of salicylic acid and phthalic acid (16) suggest that reactions 1 and 2 are both possible with humic acids.

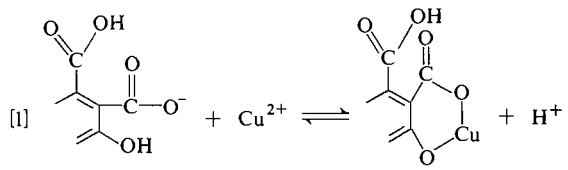

By heavily loading fulvic acid with Fe^{3+} and Al^{3+}, Schnitzer and Skinner (17) evidently complexed more metal ion per gram of fulvic acid than could be accounted for by reaction 1. Reaction 2 must therefore have occurred, either alone or together with [1]. The trace Cu^{2+} concentrations generally

Can. J. Chem. Downloaded from www.nrcresearchpress.com by 210.87.254.105 on 09/05/12
For personal use only.

found in nature will not cause such loading, however. The available evidence indicates that under natural conditions reaction 1 will occur. This evidence comes from two types of experiments.

(1) Selective Blocking of Metal Complexing Funcional groups

In 1957 Himes and Barber (18) found that the blocking of noncarboxylic acid functional groups reduced Zn^{2+} retention just as effectively as did the blocking of carboxyl groups. From this they concluded that the carboxyl groups did not constitute independent complexing sites. Himes and Barber suspected the existence of bidentate chelating sites as seen in reaction 1.

Schnitzer and Skinner (19) exploited this technique more fully in 1965, using Cu^{2+}, Fe^{3+}, and Al^{3+}. The Type I and Type II carboxyl groups, and the phenolic and alcoholic OH groups were blocked in various combinations. This was followed by metal retention measurements effected with cation exchanger in an aqueous acetone solvent. Their results were as follows. (*a*) The largest reduction in metal ion retention by the fulvic acid occurred when carboxyl groups and phenolic OH groups were both blocked. (*b*) The second largest effect was obtained when either carboxyl groups or phenolic groups were blocked. (*c*) No effect resulted from the blocking of alcoholic OH groups.

There was a residual metal ion retention, even for case (*a*). The probable reason for this was that the aqueous acetone solvent was required for fulvic acid with blocked functional groups. The resulting loss of metal ion solubility limited the amount of complexed metal ion to about 1 mole% of the total carboxyl groups of the unmodified fulvic acid. If the blocking of the functional groups were, for example, only 99.5% effective, then the observed residual metal ion retentions could be explained. The residual metal ion retentions of cases (*a*) and (*b*) are, therefore, compatible with reaction 1. The results obtained by Schnitzer and Skinner, therefore, lead to two conclusions. Firstly, at least 50% of the retained Cu^{2+} was chelated according to reaction 1. Secondly, because of the small amounts of metal bound per gram of fulvic acid and the possibility of incomplete blocking, the residual metal ion retentions cannot be interpreted as evidence for complexing at other sites. For example, reaction 2 cannot be assumed to apply.

(2) The Effect of Added Cu^{2+} on the Titration of Humic Materials

In 1959, Beckwith examined the effect of added Cu^{2+} on the potentiometric titration of a humic material (1), after first testing this procedure with salicylic and citric acids. All three samples gave the same result. That is, the Cu^{2+} released an otherwise untitratable H^+ from the fulvic acid. Within the limits of what was likely their experimental error, Khanna and Stevenson (10) found the same effect of Cu^{2+} on the titration curves of fulvic acid in 1962. Although referring to "nitrogenous materials" in their humic polymer fractions, Khanna and Stevenson did not consider that α-amino groups had made any significant contribution to complexing.

With further confirmation of these titration results by Schnitzer and Skinner in 1963 (17), reaction 1 is assumed to be the correct description of the Cu^{2+} – fulvic acid chelation reaction. From this it follows by definition that the number of bidentate chelating sites is identical to the number of Type I carboxyl groups.

Formulation of the Problem

The chemical assumptions described in the previous report (15) for Type I carboxyl groups apply, by definition, to the bidentate chelating sites which consist of the Type I chelating site and the ortho phenolic OH.

The chelation equilibrium defined for all of the chelating sites is accordingly described by eqs. 3 and 4.

$$[3] \qquad AH^- + Cu^{2+} \overset{\bar{K}_4}{\rightleftharpoons} ACu + H^+$$

$$[4] \qquad \bar{K}_4 = m_c m_H / m_{AH} m_M$$

where m_c, m_H, m_{AH}, and m_M stand for the molality of the site-bound, bidentate Cu(II) chelate, H^+, the singly ionized bidentate chelating sites, and Cu^{2+}, respectively; and $\bar{K}_4$ is the mass action quotient for chelate formation. Like the Type I carboxyl groups, the bidentate chelating sites are assumed to be similar but inherently chemically non-identical. The chelation equilibrium may therefore be written for the ith infinitesimal increment of chelating sites as follows

$$[5] \qquad A_iH^- + Cu^{2+} \overset{K_{4_i}}{\rightleftharpoons} A_iCu + H^+$$

$$[6] \qquad K_{4_i} = m_{c_i} m_H / m_{A_iH} m_M$$

For k such infinitesimal increments one has the totals given by eqs. 7 and 8.

Can. J. Chem. Downloaded from www.nrcresearchpress.com by 210.87.254.105 on 09/05/12
For personal use only.

[7] $$m_c = \sum_{i=0}^{k} m_{c_i}$$

[8] $$m_{AH} = \sum_{i=0}^{k} m_{A_iH}$$

The rest of the argument is essentially the same as that presented earlier for the weak acid ionization equilibria of fulvic acid (15). The above equations give [9], from which it is seen that $\bar{K}_4$ is a weighted average of all of the K_{4_i} values.

[9] $$\bar{K}_4 = \sum_{i=0}^{k} m_{A_iH}K_{4_i} \Big/ \sum_{i=0}^{k} m_{A_iH}$$

By definition, the number of bidentate chelating sites is identical to the number of Type I carboxyl groups. Therefore, if m_L = molality of ionized Type I carboxyl group, m_{LH} = molality of unionized Type I carboxyl group, m_{AH_2} = molality of unionized bidentate chelating sites, then m_T is defined as

$$m_T = m_L + m_{LH} = m_{AH} + m_{AH_2}$$

If α_1 = mole fraction of Type I carboxyl groups, including mole fraction ionized ($\alpha_1 = m_L/m_T$ = degree of ionization), we have

$$\alpha_1 = m_L/m_T \equiv m_{AH}/m_T$$

and

$$[\Delta\alpha_1]_i = m_{L_i}/m_T = m_{A_iH}/m_T$$

Again following the reasoning referred to above, the final results are given by eqs. 10 and 11.

[10] $$\bar{K}_4 = \frac{1}{\alpha_1}\int_0^{\alpha_1} K_4(\alpha_1)\,d\alpha_1$$

[11] $$K_4(\alpha_1) = \delta m_c m_H/m_M \delta m_{LH} = d(\alpha_1\bar{K}_4)/d\alpha_1$$

In principle, therefore, the K_4 which characterizes the infinitesimal mole fraction increment of chelating sites at any α_1 can be calculated from eq. 11.

Ion Exchange Method of Complexing Measurement

Cation exchange methods of complexing measurement have been fully reviewed, both by Helfferich (20) and by Marcus (21). Equilibrium distributions of Cu^{2+} between the ion exchange and solution phases have been used here. The required ion exchange calibration curve, eq. 12, is obtained in the absence of ligand.

[12] $$m_M = m_M(R)$$

where R is the Cu^{2+} content of the cation exchange resin, in moles of Cu^{2+} per gram of dry K^+ form resin. For small metal ion concentrations and low resin loadings, [12] will generally be a linear function. With the presence of background electrolyte, low ligand concentration, and no metal ion hydrolysis, it will also be independent of m_H and c_A, where $c_A = m_T + m_c$ = molality of total bidentate chelating sites. Literature data for Cu^{2+} hydrolysis equilibria (22) were used to estimate the extent of hydrolysis at 10^{-4} *m* H^+. This was found to be negligible. The chelation experiment consists of measuring the total concentration of Cu^{2+} in solution as a function of R, total ligand concentration, and H^+ concentration. That is, the empirical relationship of eq. 13 is determined.

[13] $$c_1 = f_1(R,c_A,m_H)$$

The concentrations of site-bound chelate and of ionized, unreacted chelating sites are then calculated from eqs. 14 and 15.

[14] $$m_c = c_1 - m_M$$

[15] $$m_{AH} = \alpha_1(c_A - m_c)$$

where

$c_1 = m_M + m_c$
= molality of total Cu(II) in solution

Experimental

(a) Chemicals

Fulvic acid Batch No. *4*: a previous report (15) gives a general description of this sample, together with measurements of the numbers of Type I and Type II carboxyl groups per gram, and of their respective ionization equilibria in 0.1 *m* KCl at 25 °C.

Cu metal foil: Analar, 99.99% pure, no acid-insoluble residue. It was washed with diethyl ether and with dilute HCl, and dried to constant weight at 100 °C.

Cation exchange resin: Bio-Rad AG50W-X8, 20 to 50 U.S. mesh size, Na^+ form, 5.1 milliequivalents per dry gram. Two batches were thoroughly mixed, and converted to the K^+ form. The resin was washed with 0.1 *m* KCl, and stored under this solution until used.

KCl: Fisher Certified A.C.S. reagent crystals: dried to constant weight.

H_2O_2: British Drug Houses Analar Reagent, 30 *w/v*%.

H_2O: refluxed for 4 h with acid dichromate, and redistilled.

HCl: Fisher 0.1 *N* standardized solution.

HCl: Allied Chemical C.F., 37.0 to 38.0%.

H_2SO_4: Allied Chemical C.F., specific gravity, 1.84.

HNO_3: Allied Chemical C.P.

$HClO_4$: Allied Chemical, 70 to 72% solution.

Can. J. Chem. Downloaded from www.nrcresearchpress.com by 210.87.254.105 on 09/05/12
For personal use only.

(b) Apparatus

Techtron Pye Type AA3 atomic absorption spectrophotometer: with Cu lamp, $\lambda = 3247$ Å.

Beckman Research Model p*H* meter: with Sargent combination electrode No. S-30072-15.

Constant temperature bath: 25.00 ± 0.05 °C.

Sargent thermometer: Hg-in-glass, total immersion, range 0 to 50 °C; graduations 0.1–0.015 °C, correction at 25 °C. Serial No. 580210A. Calibrated by Division of Applied Physics, National Research Council of Canada.

Orion 94-29 solid state copper specific ion electrode: used with Beckman 39071 frit junction calomel reference electrode, with Orion filling solution 90-00-01.

(c) Job's Continuous Variations, with Cu^{2+} and Bidentate Chelating Sites

Cu^{2+} and fulvic acid stock solutions were prepared having 1×10^{-4} *m* $Cu(NO_3)_2$ and 1×10^{-4} *m* chelating sites, respectively. Both had 1×10^{-4} *m* H^+. A set of Job's variations samples were prepared volumetrically in the usual way. Cu^{2+} standard solutions were also prepared volumetrically. Two sets of voltage measurements were made on the samples with the Orion Cu^{2+} electrode, and averaged. The same was done with the standards.

(d) Cu^{2+}–K^+ Ion Exchange Calibration Curve

Cu^{2+} standard stock solutions were prepared gravimetrically, having 0.1 *m* KCl. Cu metal foil was weighed and dissolved to give Cu^{2+} molalities about 1.2×10^{-4}, accurate to at least four significant figures.

Portions of wet resin and stock solution were weighed into flasks to give 20 to 65 g samples. These had solution-to-resin dry weight ratios ranging from 21 to 214. A total of 51 such samples were run in four sets. Each set was shaken at ambient temperatures for one week, and then thermostatted for one week at 25.00 ± 0.05 °C. A time study had demonstrated a one week ion exchange equilibration time. Upon equilibration, the two phases were quickly separated on filtering funnels, and the resin beads were freed from external electrolyte and dried to constant weight at about 110 °C.

(e) Ion Exchange Chelation Measurements

A standard stock solution was prepared gravimetrically for each of two sets of experiments. These were made using Cu metal foil, and contained 0.1 *m* KCl. One had 1.908×10^{-4} total Cu(II) and 4.49×10^{-4} *m* total chelating sites, and the other had 1.800×10^{-4} *m* total Cu(II) and 4.26×10^{-4} *m* total chelating sites.

The samples were prepared, equilibrated, and separated as described above. Their weights ranged from 20 to 83 g, with solution to dry resin weight ratios of 34 to 136.

(f) Chemical Analyses

The H^+ molalities of the equilibrated, freshly separated solution phases were measured essentially as described in the preceding report (15).

Dried, weighed ion exchange beads were destroyed by perchloric digestion. H_2O_2 digestion was used to remove fulvic acid from complexing solutions. Weighed sample solutions were prepared from the digests and from the ion exchange calibration solutions, for atomic absorption measurements. Sample and standard solutions were made up so as to avoid errors from viscosity and density effects. Standard curves were fitted by the method of least squares.

Results and Calculations

(1) Job's Continuous Variations Method

The variations curve in Fig. 1 has a blunt maximum because a relatively small fraction of the chelating sites had reacted. For example, at $X_m = 0.5$, about 25% of them were chelated. A 1:1 mole ratio of Cu^{2+} to bidentate chelating sites is nevertheless indicated.

(2) Chelate Formation Equilibrium

The Cu^{2+}–K^+ ion exchange calibration curve was calculated using 51 data points from 4 sets of experiments. A straight line was found by the method of least squares to give the best description of these measurements. The calibration curve is described in Table 1. As expected, the ion

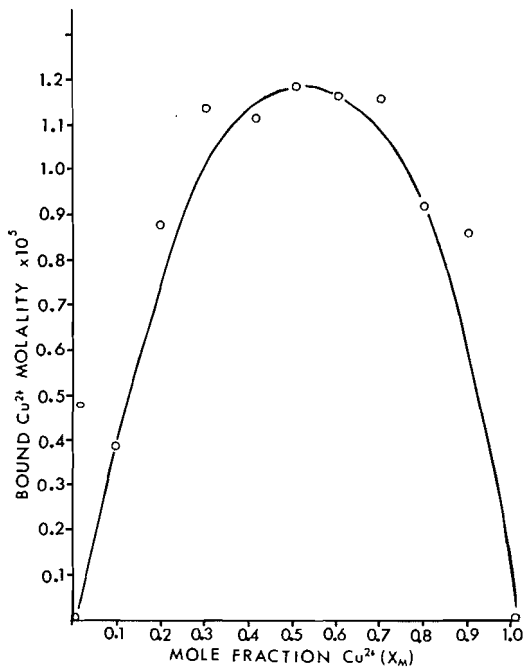

FIG. 1. Cu^{2+}–Fulvic acid chelate composition. Job's continuous variations, with mole fractions of Cu^{2+} and bidentate chelating sites. Total concentration of reactants, 1×10^{-4}; 1×10^{-4} *m* H^+. No KCl.

TABLE 1

Cu^{2+}–K^+ ion exchange calibration curve

$[KCl] = 0.1$ *m*
$T = 25.00$ °C
$m_M \times 10^6 = 0.9913 + 7.784(R \times 10^5)$
$\sigma = \pm 0.56$
Error in $m_M = \pm 8\%$
$2.7 \times 10^{-6}\ m \leqslant m_M \leqslant 1.9 \times 10^{-5}\ m$
2.5×10^{-6} mole/g $\leqslant R \leqslant 2.2 \times 10^{-5}$ mole/g

TABLE 2

Ion exchange measurements: Cu^{2+} – fulvic acid complexing*

Samples C94 to C108

$c_1 \times 10^5 = 1.844 + 0.02139\,Y$
$\sigma = \pm 0.13$; error in c_1 is $\pm 3\%$
$R \times 10^5 = 0.01865 + 0.01600\,Y - 0.000024\,Y^2$
$\sigma = \pm 0.012$; error in R is $\pm 1\%$
$2.61 \times 10^{-5}\,m \leqslant c_1 \leqslant 4.27 \times 10^{-5}\,m$
0.538×10^{-5} (mole/g) $\leqslant R \leqslant 1.56 \times 10^{-5}$ (mole/g)
$4.49 \times 10^{-4}\,m \leqslant m_H \leqslant 6.52 \times 10^{-4}\,m$

Samples C79 to C93

$c_1 \times 10^5 = -0.1162 + 0.05766\,Y - 0.000415\,Y^2 + 0.000001\,Y^3$
$\sigma = \pm 0.067$; error in c_1 is $\pm 3\%$
$R \times 10^5 = -0.006555 + 0.01814\,Y - 0.000026\,Y^2$
$\sigma = \pm 0.020$; error in R is $\pm 1\%$
$1.38 \times 10^{-5}\,m \leqslant c_1 \leqslant 3.72 \times 10^{-5}\,m$
0.585×10^{-5} (mole/g) $\leqslant R \leqslant 1.95 \times 10^{-5}$ (mole/g)
$2.40 \times 10^{-3}\,m \leqslant m_H \leqslant 3.23 \times 10^{-3}\,m$

*[KCl] = 0.1 m; T = 25.00 °C; Y = composition of the experimental sample, in grams of stock solution per gram of dry K^+ form resin.

exchange calibration measurements were independent of acid concentration over the range 1.66×10^{-4} to 2.58×10^{-3} m H^+.

The chelation data were fitted to c_1 *vs.* Y and R *vs.* Y polynomials by the method of least squares. In each case the function giving the best fit was chosen for subsequent calculations. Table 2 gives the results and experimental conditions for each of the two sets of ion exchange chelation samples. The mass action quotient for chelate formation, $\bar{K}_4$, was calculated directly using the polynomials in Table 2, the ion exchange calibration curve, and the concentrations of total chelating sites. The degrees of ionization of the Type I and Type II carboxyl groups were calculated from the measured H^+ molalities, using the weak acid ionization data previously reported for this fulvic acid sample (15). All ion exchange sample dry weights were corrected to the weights of pure K^+ form. These corrections were generally small.

The Cu^{2+} – fulvic acid chelate formation results are presented in Table 3.

(3) Experimental Errors

(a) Cu^{2+}–K^+ Ion Exchange Calibration Curve

The experimental errors in the atomic absorption measurements were ± 0.5 to $\pm 1\%$. Including those required for both standards and samples, the atomic absorption measurements contributed ± 1 to $\pm 2\%$ error to the Cu^{2+} analyses. The scatter in the Cu^{2+} material balance for each of the four sets of samples averaged about $\pm 4\%$. The four sets of samples showed randomly occurring systematic errors of similar magnitude, giving a total error in the m_1 *vs.* R calibration curve of $\pm 8\%$.

(b) Cu^{2+} – Fulvic Acid Chelation Experiments

The atomic absorption errors were as described above. For samples C94 to C108, the error in the Cu^{2+} material balance was $\pm 2\%$, and for samples C79 to C93 it was $\pm 2.6\%$. The errors in c_1, R, and m_H may be found in Tables 2 and 3.

The previously reported errors (15) in the Type I and Type II carboxyl ionization data, and in the number of Type I carboxyl groups per gram for fulvic acid Batch No. *4* were ± 2, ± 20, and 0.7%, respectively. The errors in $\bar{K}_4$, α_1, and α_2 were calculated from these errors (α_2 = degree of ionization of Type II carboxyl groups).

Discussion

The Job's variations plot agrees with the number of Type I carboxyl groups per gram of fulvic acid that was measured by titration (15). The postulated composition of the site-bound chelate is also substantiated. A sharper peak could have been obtained with somewhat higher concentrations of reactants. Such concentrations would have less relevance to conditions existing in nature, however. Schnitzer and Hansen (24) and Schnitzer and Skinner (17) have done Job's variations experiments based on moles of Cu^{2+}

Can. J. Chem. Downloaded from www.nrcresearchpress.com by 210.87.254.105 on 09/05/12
For personal use only.

TABLE 3

Cu^{2+} – fulvic acid chelate formation equilibrium*

$\bar{K}_4$	α_1	α_2 ±20	Total Cu^{2+} ($m \times 10^5 \pm 3\%$)	H^+ ($m \times 10^4 \pm 1\%$)	Total chelating sites ($m \times 10^4 \pm 0.7\%$)
5.0±17%	0.871±0.2%	0.072	2.59	4.47	
4.8	0.865	0.068	2.75	4.77	
4.7	0.861	0.066	2.86	4.97	
4.7	0.861	0.065	2.88	5.01	
4.6	0.856	0.063	3.03	5.26	
4.6	0.853	0.061	3.15	5.43	
4.6	0.851	0.060	3.22	5.53	
4.6	0.849	0.059	3.32	5.66	4.26
4.6	0.846	0.058	3.4	5.79	
4.6	0.843	0.057	3.6	5.96	
4.6	0.840	0.055	3.8	6.16	
4.6	0.838	0.055	3.9	6.25	
4.5	0.836	0.054	4.1	6.37	
4.5±20%	0.834±0.2%	0.053	4.3	6.50	
13. ±28%	0.67 ±5%	0.016	1.41	23.9	
13.	0.67	0.016	1.54	24.8	
14.	0.66	0.015	1.62	25.3	
14.	0.66	0.015	1.80	26.4	
15.	0.65	0.014	1.88	26.9	
15.	0.65	0.014	2.01	27.7	
15.	0.65	0.014	2.09	28.1	
15.	0.64	0.013	2.26	28.9	4.49
15.	0.64	0.013	2.50	30.0	
14.	0.63	0.013	2.73	30.7	
14.	0.63	0.012	3.07	31.4	
14.	0.63	0.012	3.18	31.6	
14.	0.63	0.012	3.4	32.0	
14.	0.63	0.012	3.5	32.1	
15. ±31%	0.63 ±5%	0.012	3.6	32.3	

*[KCl] = 0.1 *m*; T = 25.00 °C.

and moles of number-average polymer molecules rather than moles of chelating sites. In both cases a 1:1 mole ratio was found. Since the average polymer molecule has about three chelating sites, this result is to be expected if less than 1/3 of the chelating sites have reacted. In discussing the nature of the Cu^{2+} – fulvic acid chelate, Geering and Hodgson (25) noted that the complexing reaction releases an otherwise non-titratable H^+, and that the complex is more strongly formed than would be expected if only one functional group were bound to each metal ion. They postulated the existence of a chelate ring, but suggested that a phosphate acid group and a carboxyl group might constitute the bidentate chelating sites. If their suggestion were correct, then the displaced H^+ would be titratable in the absence of Cu^{2+}.

On the basis of reaction 1, $\bar{K}_4$ might be expected to be an increasing function of α_1. If any such trend exists, it has been obscured in the present case by other effects. For example, 0.1 *m* KCl, which was used to reduce the risk of ligand sorption by the ion exchange beads, may have resulted in some K^+–polyelectrolyte ion pairing, and some cupric chloride complex formation. The net effect of these on the $\bar{K}_4$ *vs.* α_1 curve is unknown.

Cu^{2+} chelation data recalculated from the literature have been compiled in Table 4, for comparison with the present results. Although estimates of experimental errors were unfortunately not provided for any of the literature data, they set the present results into perspective. Some of the synthetic polymers (ethylene – maleic acid copolymer and crosslinked polyacrylic acid) having dicarboxyl chelating sites, show Cu^{2+} chelating strengths that fall within the range of the present fulvic acid values. The Cu^{2+} – fulvic acid values obtained by Schnitzer and Hansen (24) for fulvic acid have a wide range that encompasses the results presented here. As expected, salicylic and phthalic acids form weaker Cu^{2+} chelates than do the polymeric materials. The unexpectedly low values for peat might have been caused, at least partly, by the assumption by Coleman *et al.* (11) that every carboxyl group participated in a chelating site. The weak acid ionization and

Can. J. Chem. Downloaded from www.nrcresearchpress.com by 210.87.254.105 on 09/05/12
For personal use only.

TABLE 4

Cu^{2+} chelation data*

Complexing agent	AH^-	$\bar{K}_1$	$\bar{K}_2$	H^+ concentration (M)	Salt	$\bar{K}_4$	Reference number
Ethylene-maleic acid copolymer	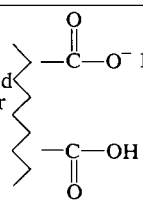	$10^{-4.97}$	$10^{-9.60}$		$\mu \rightarrow 0$	11.1	23
Polyacrylic acid	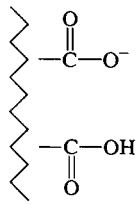	$10^{-6.17}$ $10^{-4.91}$ $10^{-4.30}$			0.0 M 0.2 M $NaNO_3$ 2.0 M $NaNO_3$	0.13 0.13 0.31	8
Polyacrylic acid crosslinked gel	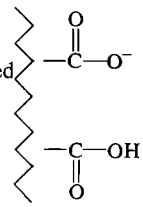	$10^{-5.30}$		$10^{-3.28}$	1.0 M $NaNO_3$	5.0 to 0.73	9
Salicylic acid	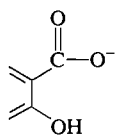	$10^{-2.9}$	$10^{-13.1}$		$\mu = 0.1$	0.0032	16
Phthalic acid	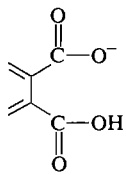	$10^{-2.8}$	$10^{-5.1}$		$\mu = 0.1$	0.010	16
Fulvic† acid	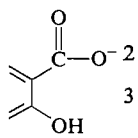	2.2×10^{-3} 3.6×10^{-3}	2.5×10^{-5} 3.9×10^{-5}	10^{-5} 10^{-3} 10^{-3} 10^{-3}	0.1 M KCl 0.00 M KCl 0.10 M KCl 0.15 M KCl	0.033 20. 0.90 0.20	24
Peat	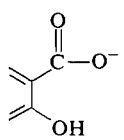	$10^{-5.5}$ $10^{-4.8}$ $10^{-4.3}$			0.01 M KNO_3 0.1 M KNO_3 1.0 M KNO_3	0.058 0.090 0.13	11

*Generally, literature results were found expressed on the molar scale. However, for the concentrations used, $M \approx m$.
†$\bar{K}_1$ and $\bar{K}_2$ estimated using data from ref. 15.

Can. J. Chem. Downloaded from www.nrcresearchpress.com by 210.87.254.105 on 09/05/12
For personal use only.

Cu^{2+} chelation properties of peats need to be re-examined in the light of recent results.

The biggest single source of experimental error in this work occurred in the ion exchange measurement of total Cu^{2+} concentration in the solution phase. Because this is the case for both the ion exchange calibration curve and the chelation samples, the $\bar{K}_4$ values have two error contributions from this source. For this reason the Cu^{2+} specific ion solid state electrode, which became available when this work was well advanced, should make possible a substantial reduction in the experimental error in $\bar{K}_4$. This in turn might make practical the calculation of K_4 according to eq. 11.

Mr. J. G. Desjardins and Mr. D. A. Hindle rendered experimental assistance. This work depended especially on the dedicated efforts of Mr. K. A. Wilson at the bench.

1. R. S. Beckwith. Nature, **184**, 745 (1959).
2. F. E. Broadbent and G. R. Bradford. Soil Sci. **74**, 447 (1952).
3. M. Schnitzer and S. I. M. Skinner. Isotopes and radiation in soil organic-matter studies. International Atomic Energy Agency, Vienna, (1968). p. 41.
4. R. Arnold and J. Th. G. Overbeek. Rec. Trav. Chim. **69**, 192 (1950).
5. Harry P. Gregor and Michael Frederick. J. Polymer Sci. **23**, 451 (1957).
6. Frederick T. Wall. J. Phys. Chem. **61**, 1344 (1957).
7. M. Mandel, J. C. Leyte, and M. G. Stadhouder. J. Phys. Chem. **71**, 603 (1967).
8. Harry P. Gregor, Lionel B. Luttinger, and Ernest M. Loebl. J. Phys. Chem. **59**, 34 (1955).
9. Richard L. Gustafson and Joseph A. Lirio. J. Phys. Chem. **72**, 1502 (1968).
10. S. S. Khanna and F. J. Stevenson. Soil Sci. **93**, 298 (1962).
11. N. T. Coleman, A. C. McClung, and David P. Moore. Science, **123**, 330 (1956).
12. Jacob A. Marinsky. Interpretation of ion-exchange. Vol. 1. *Edited by* Jacob A. Marinsky. Marcel Dekker Inc., New York. 1966. Chap. 9.
13. Donald S. Gamble. Doctoral Dissertation, State University of New York at Buffalo. 1965.
14. M. Schnitzer and J. G. Desjardins. Soil Sci. Soc. Amer. Proc. **26**, 362 (1962).
15. Donald S. Gamble. Can. J. Chem. **48**, 2662 (1970).
16. Anders Ringbom. Complexation in analytical chemistry. Interscience Publ. Inc., New York. 1963.
17. M. Schnitzer and S. I. M. Skinner. Soil Sci. **96**, 86 (1963).
18. Frank L. Himes and Stanley A. Barber. Soil Sci. Amer. Proc. **21**, 368 (1957).
19. M. Schnitzer and S. I. M. Skinner. Soil Sci. **99**, 278 (1965).
20. Friedrich Helfferich. Ion exchange. McGraw-Hill Book Co., Inc., 1962. p. 202.
21. Y. Marcus. Ion-exchange studies of complex formation. Vol. 1. *Edited by* Jacob A. Marinsky. Marcel Dekker Inc., New York. 1966. Chap. 3.
22. Jannik Bjerrum, Gerold Schwarzenbach, and Lars Gunnar Sillen. Stability constants of metal-ion complexes with solubility products of inorganic substances. Part II: Inorganic ligands. The Chem. Soc. London, 1958.
23. Betty J. Felber, Ernest M. Hodnett, and Neil Purdie. J. Phys. Chem. **72**, 2496 (1968).
24. M. Schnitzer and E. H. Hansen. Soil Sci. **109**, 333 (1970).
25. H. R. Geering and J. F. Hodgson. Soil Sci. Soc. Amer. Proc. **33**, 54 (1969).

Can. J. Chem. Downloaded from www.nrcresearchpress.com by 210.87.254.105 on 09/05/12
For personal use only.

Pyrolysis of dimethylzinc and dimethylzinc-d_6 by the toluene carrier method

A. N. DUNLOP[1] AND S. J. W. PRICE
Department of Chemistry, University of Windsor, Windsor, Ontario

Received June 22, 1970

The pyrolysis of dimethylzinc has been studied over the temperature range 823–1015 °K using toluene to alkyl ratios from 51:1 to 121:1 and total pressure of 17 to 169 mm. The decomposition occurs in two steps

[1] $$Zn(CH_3)_2 \rightarrow ZnCH_3 + CH_3$$

[2] $$ZnCH_3 \rightarrow Zn + CH_3$$

By extrapolation to infinite pressure

$$\log k_1/s^{-1} = 13.3 - (54\,000 \pm 2000/4.58T)$$

and at 10 cm pressure

$$\log k_2/s^{-1} = 6.6 - (31\,000 \pm 1000/4.58T)$$

Assuming E_2 must be increased by 2–4 kcal mole^{-1} to obtain E_2 at infinite pressure $D_1 + D_2 = 88 \pm 4$ kcal mole^{-1}; *cf.* 86 ± 3 kcal mole^{-1} from thermochemistry. When dimethylzinc-d_6 is used only traces of CD_4 are produced. This indicates that the non free radical decomposition of methylzinc, suggested by the results of a previous sealed ampoule study, is not a significant process under the present experimental conditions.

Canadian Journal of Chemistry, **48**, 3205 (1970)

Introduction

The pyrolysis of dimethylzinc has previously been studied by the toluene carrier method (1), in sealed ampoules using cyclohexane as a radical scavenger (2) and by an argon carrier technique (3). The toluene carrier study indicated a stepwise decomposition in which both $Zn(CH_3)_2$ and $ZnCH_3$ decomposed by a free radical mechanism. The activation energy for the first step, the decomposition of $Zn(CH_3)_2$ into $ZnCH_3$ and CH_3, was obtained in a pressure dependent region using rate constants which were calculated without taking into account those methyl radicals which combined with benzyl radicals to form ethylbenzene. The activation energy of the second step, the decomposition of $ZnCH_3$ into Zn and CH_3, was determined in essentially the second order region. Again the rate constants did not allow for ethylbenzene formation and, in addition, contained a further uncertainty because of the corrections that had to be made to allow for decomposition of the toluene carrier.

The sealed ampoule study was carried out at much lower temperatures (250–400 °C, *cf.* 573–825 °C in the toluene carrier work) and used both $Zn(CH_3)_2$ and $Zn(CD_3)_2$. From the 1:1 yield of CH_3D to CH_4 when $Zn(CH_3)_2$ was studied in the presence of C_6D_{12}, it was concluded that $ZnCH_3$ decomposed by some process that did not involve the release of free methyl radicals. A detailed mechanism was not given but it was proposed that the first step was probably the formation of $(ZnCH_3)_2$.

The argon carrier work was a preliminary survey to test the feasibility of studying the pyrolysis by leaking a small part of the reaction stream directly into a mass spectrometer (3). The temperature control of the reactor was inadequate for a detailed kinetic study although the limited results reported are in approximate agreement with the toluene carrier work.

In the present investigation, $Zn(CD_3)_2$ has been used to ascertain if any processes occur which produce CD_4 and to eliminate the necessity of making a correction for the decomposition of toluene. In the first bond region, where the decomposition of the carrier is negligible, $Zn(CH_3)_2$ was used and an attempt was made to collect sufficient data to allow an approximate extrapolation to infinite pressure.

Experimental

Materials

(*a*) Toluene from sulfonic acid (Eastman Organic X325) was prepared for use by refluxing over sodium under vacuum for 24 h and then degassing twice by bulb-to-bulb distillation.

(*b*) Dimethylmercury was prepared by adding methyl

[1]Present address: Department of Chemical Engineering and Applied Chemistry, University of Toronto, Toronto, Ontario.

Can. J. Chem. Downloaded from www.nrcresearchpress.com by 210.87.254.105 on 09/05/12
For personal use only.

TABLE 1

Pyrolysis of dimethylzinc, second bond

Temperature (°K)	P (mm)	t_c (s)	Toluene/Alkyl (molar ratio)	Alkyl*	CD_3H	CD_4	C_2D_6	Ethylbenzene-d_3	Styrene-d_2	k_2 (s^{-1})
				(moles × 10^5)						
1014.6	105	2.07	102	75.1	112.4	Trace	0.304	1.5	21.9	0.80
	54	3.63	74	42.8	63.3	0.399	0.108	2.5	9.4	0.40
997.4	85	3.55	78	51.9	77.9	0.055	0.028	4.6	10.5	0.44
948.4	105	4.01	70	84.7	115.4	Trace	0.136	10.2	6.4	0.21
	85	3.42	85	75.6	104.6	Trace	0.128	10.6	4.4	0.25
	56	3.53	93	49.8	62.9	Trace	0.118	7.6	2.1	0.17
924.6	106	3.51	93	75.7	98.8	Trace	0.134	8.4	2.4	0.17
	56	3.38	102	48.9	58.0	Trace	0.117	6.6	1.1	0.13
	17	3.25	53	63.6	75.5	Trace	0.081	3.0	1.5	0.07†

Temperature (°K)	P (mm)	t_c (s)	Toluene/Alkyl (molar ratio)	Alkyl‡	CH_4§	C_2H_6§	Ethylbenzene§	Styrene§	k_2 (s^{-1})
				(moles × 10^5)					
900.1	164	3.98	85	70.5	85.4	0.090	6.0	1.8	0.13
	140	4.23	89	67.3	85.6	0.084	6.4	1.7	0.14
	104	3.66	90	57.4	63.9	0.062	5.4	0.9	0.09
	54	3.70	90	35.9	36.1	0.064	3.9	0.4	0.05

*Dimethylzinc-d_6.
†Rate data obtained at 930 °K, k_2 corrected to 924.6 °K.
‡Dimethylzinc.
§Corrected for the contribution from toluene decomposition. Values of k_2 at 900.1 °K are from consecutive order calculations.

magnesium iodide to an ether slurry of mercuric chloride (4).

(*c*) Dimethylzinc was prepared by refluxing zinc metal with dimethylmercury under a nitrogen atmosphere (5). The product (b.p. 41 °C at 712 mm) was degassed and stored under its own vapor pressure at −78 °C.

(*d*) The preparation of dimethylzinc-d_6 (b.p. 41.4 °C at 714 mm) followed the procedure under (*b*) and (*c*), except methyliodide-d_3 was used in the preparation of the Grignard reagent.

Apparatus and Procedure

The experiments were carried out using the same system previously used in studying the decomposition of dimethylmercury in a benzene carrier (4). The gaseous products were analyzed using a Perkin–Elmer 154 gas chromatograph equipped with a 1/4 in. × 6 ft silica gel column. The column was maintained at 80 °C and a helium flow rate of 20 cc/min was used.

The liquid products condensed along with the toluene in an acetone – Dry Ice trap were analyzed using a Perkin–Elmer model 800 gas chromatograph equipped with a 150 ft × 0.02 in. inside diameter Golay Column coated with poly(propylene glycol) (isothermal operation at 60 °C, inlet pressure of N_2 carrier is 7 lb).

The mass spectrometric analyses were carried out using an AEI MS10c2 mass spectrometer. Samples were handled in a conventional vacuum system and were admitted to the mass spectrometer through a porous leak. The yields of CH_4, CD_3H, CD_4, C_2H_6, and C_2D_6 were based on m/e = 15, 19, 20, 29, and 36, respectively. No appreciable background subtraction was required at any of these masses. The m/e = 20 peak was corrected for the contribution from $^{13}CD_3H$ and a small correction for CDH was required at m/e = 15.

Analysis for $C_6H_5CH_2CD_3$ and $C_6H_5CHCD_2$ in the total ethylbenzene and styrene, respectively, was carried out on the appropriate fractions obtained by gas chromatography. In the ethyl benzene fraction m/e = 106 was used for ethylbenzene and m/e = 109 for ethylbenzene-d_3. In the styrene fraction m/e = 104 was used for styrene and m/e = 106 for styrene-d_2.

Results and Discussion

The experimental results are given in Tables 1 and 2. It is clear from the very small yields of CD_4 that the apparent molecular elimination of methane encountered in the sealed ampoule work (2) did not occur to any significant extent in the toluene carrier system. The results may be discussed in terms of the following mechanism. It is assumed that all reactions shown for $Zn(CH_3)_2$, $ZnCH_3$, and CH_3 apply equally well to $Zn(CD_3)_2$, $ZnCD_3$, and CD_3 since only secondary isotope effects are involved.

[1] $$Zn(CH_3)_2 \rightarrow ZnCH_3 + CH_3$$

[2] $$ZnCH_3 \rightarrow Zn + CH_3$$

[3] $$CH_3 + C_6H_5CH_3 \rightarrow CH_4 + C_6H_5CH_2$$

[4] $$2CH_3 \rightarrow C_2H_6$$

[5] $$ZnCH_3 + C_6H_6CH_2 \rightarrow C_6H_5CH_2ZnCH_3$$

[6] $$2ZnCH_3 \rightarrow (ZnCH_3)_2$$

[7] $$2C_6H_5CH_2 \rightarrow \text{Dibenzyl}$$

[8] $$CH_3 + C_6H_5CH_2 \rightarrow C_6H_5C_2H_5$$

[9] $$C_6H_5C_2H_5 \rightarrow C_6H_5C_2H_3 + H_2$$

Can. J. Chem. Downloaded from www.nrcresearchpress.com by 210.87.254.105 on 09/05/12
For personal use only.

TABLE 2

Pyrolysis of dimethylzinc, first bond

Temperature (°K)	P (mm)	t_c (s)	Toluene / Alkyl (molar ratio)	Alkyl*	CH_4†	C_2H_6†	Ethylbenzene†	Styrene‡	k_1 (s^{-1})
				(moles × 10^5)					
874.6	169	4.38	109	92.9	82.7	0.076	3.6	0.64	0.310
	140	4.45	92	89.3	74.1	—	4.1	0.68	0.290
	85	3.88	84	87.8	52.2	0.380	2.9	0.28	0.230
	54	3.62	92	60.7	32.3	0.032	1.7	0.11	0.210
860.4	153	3.77	77	79.6	39.5	0.060	1.7	0.20	0.166
	105	4.60	67	64.7	31.1	0.050	1.8	0.16	0.135
	28	3.23	67	44.8	9.5	0.024	0.7	0.02	0.079
848.2	140	2.74	121	65.2	14.4	0.018	1.0	0.14	0.092
	102	3.54	85	65.1	17.9	0.019	1.0	0.08	0.090
	53	3.43	103	51.8	10.9	0.020	0.6	0.05	0.071
	22	3.30	61	52.6	8.6	0.019	0.8	0.03	0.059
834.4	162	3.66	96	90.4	17.2	0.011	0.7	0.05	0.055
	108	4.02	82	77.6	13.1	0.016	0.5	0.04	0.045
	24	3.48	51	57.2	5.7	0.014	0.3	0.02	0.030
822.7	145	2.80	129	71.7	7.6	0.003	0.8	0.20	0.041
	108	4.62	75	62.4	9.7	—	0.7	0.10	0.037
	104	4.10	74	47.8	6.9	0.009	0.7	0.08	0.039
	51	3.60	90	36.7	3.9	0.010	0.5	0.08	0.032
	26	3.07	71	41.9	3.0	0.007	0.4	0.08	0.027

*Dimethylzinc.
†Correction for toluene decomposition negligible. Note: in a run using $Zn(CD_3)_2$ at 874 °K and 17 mm pressure (approximately 40% decomposition first bond) the ratio of CD_3H to CD_4 was 1000:1.)

Reactions 3, 4, 7, 8, 9 and other minor processes which produced traces of ethylene and xylenes in the present work are characteristic of toluene carrier work in which appreciable quantities of CH_3 are released. The characteristic break in the Arrhenius plot of $k_3/k_4^{1/2}$ shown in Fig. 1 is indicative of a stepwise decomposition, in which reaction 2 is occurring to a major extent only at temperatures where reaction 1 is essentially complete (1, 6, 7). The values of k_2 in Table 1 at 924.6 °K and up were therefore calculated on the assumption that

$$\text{fraction } ZnCD_3 \text{ decomposed} = \frac{\text{moles } [CD_3H + C_6H_5CH_2CD_3 + C_6H_5CHCD_2] + 2 \times \text{moles } C_2D_6 - \text{moles } Zn(CD_3)_2}{\text{moles } Zn(CD_3)_2}$$

Extrapolated values of k_2 were then used to calculate the values of k_1 shown in Table 1 by successive approximations from the expression

$$\text{moles product} = \text{moles } Zn(CH_3)_2 \text{ used} \times \left\{2 - \frac{k_1}{k_1 - k_2}[\exp(-k_1 t) + \exp(-k_2 t)] - 2\frac{k_2}{k_2 - k_1}\exp(-k_1 t)\right\}$$

where moles product = moles $[CH_4 + C_6H_5C_2H_5 + C_6H_5C_2H_3] + 2 \times$ moles C_2H_6. At 874.6 °K and 169 mm, approximately 20% of the products are from second bond decomposition while at the lowest temperature used, 822.7 °C, only about 4% of the products are from this source. At 900 °K the assumption inherent in the method used to calculate k_2 that reaction 1 is complete in a negligible fraction of the reaction zone is not valid so that consecutive reaction calculations were also done to obtain the values of k_2 at this temperature.

Reactions 5 and 6 are tentatively proposed as reasonable reactions for removal of $ZnCH_3$ that does not undergo decomposition. Both reactions would probably occur primarily in the outlet tube as the products should have little stability at the temperature of the reaction zone. The dimer produced in reaction 6 might reasonably be expected to reach the acetone – Dry Ice trap used to condense toluene, unreacted alkyl, ethylbenzene, and styrene. The bulk of the $C_6H_5CH_2$-$ZnCH_3$ would probably deposit in the outlet tube along with dibenzyl. Zinc analyses were carried

Can. J. Chem. Downloaded from www.nrcresearchpress.com by 210.87.254.105 on 09/05/12
For personal use only.

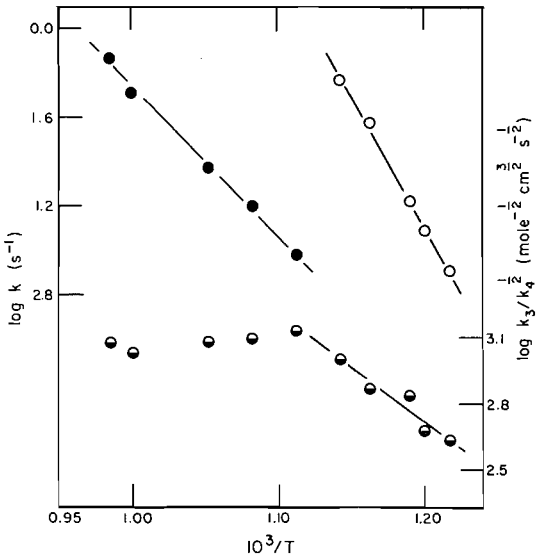

FIG. 1. Arrhenius plots for dimethylzinc (k_1), methylzinc (k_2), and the reaction of methyl radicals with toluene (expressed in terms of $k_3/k_4^{1/2}$). ○, k_1 at infinite pressure; ●, k_2 at 10 cm pressure; ◒, $k_3/k_4^{1/2}$ at 10 cm pressure.

out on a number of runs by EDTA titration using Eriochrome Black T as indicator.

The small quantities of zinc (20–30 mg) and the volatility of the alkyl made accurate analysis difficult. However, in 8 runs in the first bond region, the quantity of zinc found in the acetone – Dry Ice trap led to a material balance for zinc of 95 ± 10% (based on the assumption that the only zinc compound reaching the trap was unreacted $Zn(CH_3)_2$). This is consistent with the expectation that most of the $C_6H_5CH_2ZnCH_3$ would not be expected to get to the trap and indicates that reaction 6 is probably not a major process. Analyses carried out on samples from the second bond region showed only 0–5% of the zinc got through to the trap. As well, after all the runs were completed, the reaction vessel was removed, and analysis of the zinc metal present compared favorably with the amount of zinc that would be expected from second bond decomposition calculated on the basis of the mechanism (1.16 g expected; 1.20 g found).

The apparatus used in the present work is not suitable for use over a wide range of pressure. However, an attempt was made to cover a sufficient range of conditions to obtain an estimate of E_1 at infinite pressure. The required values of k_1 at infinite pressure were obtained by extrapolation of approximately linear $1/k$ *vs.* $(1/P)^x$ curves (8). The best linearity was obtained in the present work when $x = 0.6$. The resulting Arrhenius plot is shown in Fig. 1. Least squares analysis gives

$$k_1^{\infty}/s^{-1} = 2.0 \times 10^{13} \exp(-54\,000/1.987T)$$

An estimated uncertainty of ±2 kcal mole^{-1} should be assigned to E_1.

Similarly, the plot of k_2 at 10 cm yields

$$k_2^{10\ cm}/s^{-1} = 3.5 \times 10^{6} \exp(-31\,000/1.987T)$$

with an estimated uncertainty of ±2 kcal mole^{-1}. The value of E_2 at infinite pressure should probably be 2–4 kcal mole^{-1} above the 10 cm value. The value of A_2 is of the same order of magnitude as previously reported and is quite reasonable for a unimolecular reaction that is occurring close to its second order region (1).

The infinite pressure activation energies should be a good approximation to the corresponding bond dissociation energies. Thus, $D[CH_3Zn—CH_3] = D_1 = 54 \pm 2$ kcal mole^{-1} and $D[Zn—CH_3] = D_2 = 34 \pm 2$ kcal mole^{-1}. Hence, $D_1 + D_2 = 88 \pm 4$ kcal mole^{-1}. From the heat of formation of dimethylzinc (9, 10), of the zinc atom (11), and of the methyl radical (12) $D_1 + D_2 = 86 \pm 3$ kcal mole^{-1}. The agreement between the kinetic and thermochemical estimates substantiates the conclusion drawn from the original toluene carrier study (1) that when methylzinc undergoes decomposition the zinc atom is released in its ground state.

This work has been supported by a grant from the National Research Council of Canada.

1. S. J. W. PRICE and A. F. TROTMAN-DICKENSON. Trans. Faraday Soc. **53**, 1208 (1957).
2. I. LAMBERT. J. Chim. Phys. **62**, 516 (1965).
3. D. C. TOPOR. J. Chim. Phys. **63**, 347 (1966).
4. M. KRECH and S. J. PRICE. Can. J. Chem. **41**, 224 (1963).
5. L. H. LONG and J. CATTANACH. J. Inorg. Nucl. Chem. **20**, 341 (1961).
6. M. G. JACKO and S. J. W. PRICE. Can. J. Chem. **41**, 1560 (1963).
7. M. G. JACKO and S. J. W. PRICE. Can. J. Chem. **42**, 1198 (1964).
8. I. OREF and B. S. RABINOVITCH. J. Phys. Chem. **72**, 4488 (1968).
9. L. H. LONG and R. G. W. NORRISH. Phil. Trans. A. **241**, 587 (1949).
10. A. S. CARON, K. HARTLEY, and H. A. SKINNER. Trans. Faraday Soc. **45**, 1159 (1949).
11. T. COTTRELL. The strength of chemical bonds. Butterworths, Publ., London. 1954.
12. Handbook of chemistry and physics. 47th ed. The Chemical Rubber Co., Cleveland, Ohio. 1966–1967.

Can. J. Chem. Downloaded from www.nrcresearchpress.com by 210.87.254.105 on 09/05/12
For personal use only.

Can. J. Chem. Downloaded from www.nrcresearchpress.com by 210.87.254.6 on 09/05/12
For personal use only.

The pyrolysis of trimethylarsine

S. J. W. PRICE AND J. P. RICHARD
Department of Chemistry, University of Windsor, Windsor, Ontario

Received June 22, 1970

The pyrolysis of trimethylarsine has been studied in a toluene carrier flow system from 764 to 858 °K using total pressures from 6.35 to 35.5 mm. Contact times varied from 0.9 to 3.7 s and the amount of decomposition, from 1.2 to 73%. The progress of the reaction was followed by measuring the amount of methane, ethane, ethylene, and ethylbenzene formed. No heterogeneous reaction was detected and the first order rate constants appear to have been determined at approximately the high pressure limit. In seven runs the undecomposed alkyl was also measured. The quantity found was in agreement with the product analysis if three methyl radicals are released for each molecule undergoing reaction.

Least squares analysis of the results gives

$$\log_{10} k/s^{-1} = 15.82 - (62\,800 \pm 800)/2.3RT$$

The activation energy should be a good approximation to $D[(CH_3)_2As—CH_3]$. The product analysis and the values of $k_4/k_5^{1/2}$ are consistent with the simple consecutive release of three methyl radicals but thermodynamic and kinetic considerations may preclude this possibility.

Canadian Journal of Chemistry, 48, 3209 (1970)

Introduction

The pyrolysis of trimethylarsine in a static system has been reported by Ayscough and Emeleus (1). They found the reaction to be homogeneous and of the first order with an activation energy of 54.6 ± 1.8 kcal/mole ($\log_{10} k = 12.77 - 54\,600/2.3RT$). It was assumed that the eventual fate of $(CH_3)_2AsCH_2$ had no appreciable effect on the observed rate and the activation energy was associated with $D[(CH_3)_2As—CH_3]$.

The present toluene carrier work was undertaken to study the pyrolysis of trimethylarsine under conditions such that no significant attack by methyl radicals on the parent alkyl should occur.

Experimental

Materials

(*a*) Trimethylarsine was prepared by the reaction of CH_3MgI in butyl ether with $AsCl_3$. The complex formed was decomposed by gradually heating to 120–150 °C (2). The fraction boiling at 50–52 °C was separated, refractionated, and degassed. Vapor pressure data for the final product over the temperature range −14 to 20 °C may be represented by $\log P/mm = -1574/T + 7.749$. This equation gives an extrapolated standard boiling point of 50.2 °C, in excellent agreement with literature values of 50.1–50.3° (1) and 50.4° (3).

(*b*) Toluene from sulfuric acid (Eastman Organic X325) was used. Gas chromatographic analysis detected traces of higher hydrocarbons (xylenes, ethylbenzene). These were reduced to less than 40 p.p.m. by a fractional distillation in which a large tail fraction was discarded. Prior to use, the toluene was dried by refluxing over sodium metal for 24 h and then degassed by bulb-to-bulb distillation.

Apparatus and Procedure

The experiments were carried out in a system similar to that used in previous work (4). The reaction vessel had a volume of 156 cc. To test for surface effects a vessel was packed with small quartz tubes. This vessel had a volume of 117 cc and a surface to volume ratio 18 times that of the unpacked vessel. Both vessels were treated with hot concentrated nitric acid before use. The residual acid was baked out under vacuum after the vessels were installed in the reaction system.

The gaseous products were analyzed using a Perkin–Elmer model 154 gas chromatograph equipped with a 1/4 in. × 6 ft silica gel column. The column was maintained at 80 °C, and a helium flow rate of 20 cm^3 per min was used.

The liquid products which condensed along with the toluene in an acetone – Dry Ice trap were analyzed using a Perkin-Elmer model 800 gas chromatograph equipped with a 150 ft × 0.02 in. i.d. Golay column coated with poly(propylene glycol). (Isothermal operation at 60 °C, inlet pressure of nitrogen carrier was 7 lb.)

After a number of runs, the grey deposit at the outlet of the reaction zone was dissolved in nitric acid and analyzed for arsenic by titration with iodine (5). The results indicated that this deposit is essentially pure arsenic (98.4% As found).

Results and Discussion

The experimental results are given in Tables 1 and 2. They may be discussed in terms of the following mechanism

[1] $As(CH_3)_3 \rightarrow As(CH_3)_2 + CH_3$

[2] $As(CH_3)_2 \rightarrow AsCH_3 + CH_3$

[2*a*] $2As(CH_3)_2 \rightarrow As(CH_3)_3 + AsCH_3$

[3] $AsCH_3 \rightarrow As + CH_3$

[3*a*] $2As(CH_3) \rightarrow As(CH_3)_2 + As$

TABLE 1

Experimental data for pyrolysis of $As(CH_3)_3$

T (°K)	t_c (s)	P (mm)	T/A* ratio	$As(CH_3)_3$ used	CH_4	C_2H_6	C_2H_4	Ethyl-benzene	k_1 (s^{-1})
				(moles × 10^4)					
858.0	1.94	24.7	61.3	3.549	5.028	0.179	0.111	2.132	0.668
858.0	1.71	26.5	49.9	5.282	7.490	0.345	0.172	2.267	0.667
858.0	1.18	24.8	64.5	5.606	6.362	0.264	0.140	1.782	0.643
858.2	0.99	21.2	61.8	5.940	6.225	0.284	0.124	1.654	0.674
852.6	1.47	22.3	112.5	7.064	9.594	0.261	0.131	1.092	0.530
852.7	1.59	21.0	60.0	3.807	4.491	0.198	0.095	1.445	0.533
852.7	1.46	25.2	52.8	5.606	6.764	0.295	0.138	1.646	0.548
852.7	1.52	20.9	51.0	6.964	8.092	0.386	0.180	2.278	0.527
852.6	2.16	23.2	32.0	5.690	8.131	0.434	0.201	2.362	0.541
840.6†	1.06	23.4	56.4	5.140	3.328	0.107	0.071	0.650	0.311
836.5	3.47	35.5	17.1	9.989	13.202	0.861	0.391	2.501	0.270
835.4	1.66	24.5	32.4	7.889	5.281	0.302	0.132	1.495	0.234
836.1	2.02	20.4	112.4	3.190	2.941	0.071	0.045	0.703	0.256
836.5	3.70	20.1	15.3	5.856	7.040	0.561	0.277	2.145	0.260
836.5	1.25	13.1	55.2	3.349	1.925	0.085	0.037	0.578	0.255
836.4	1.33	11.6	39.5	3.849	1.941	0.121	0.047	0.607	0.215
836.5	1.82	6.3	33.6	10.814	6.272	0.439	0.190	1.958	0.190
811.5	1.70	26.0	35.1	11.697	3.575	0.137	0.044	0.863	0.0863
811.5	1.74	24.9	33.1	11.613	3.553	0.145	0.043	0.779	0.0834
810.5	1.31	21.5	58.5	5.107	1.215	0.031	0.003	0.223	0.0792
810.3	1.36	22.8	35.5	8.506	1.942	0.065	0.012	0.386	0.0752
804.7†	1.21	19.8	55.9	4.032	0.718	0.017	0.005	0.091	0.0606
804.7†	1.25	19.8	51.5	4.223	0.801	0.019	0.005	0.092	0.0617
782.1†	1.33	19.4	68.5	3.015	0.192	0.002	0.001	0.038	0.0199
774.3	1.84	23.6	30.7	11.788	0.735	0.012	0.001	0.117	0.0137
774.1	1.84	23.9	29.7	12.305	0.685	0.013	0.002	0.123	0.0125
764.6	1.85	24.3	31.9	11.747	0.391	0.005	0.000	0.066	0.00722
764.5	1.84	21.4	26.2	12.580	0.406	0.008	0.000	0.061	0.00697
764.5	1.89	22.3	23.9	18.645	0.661	0.011	0.000	0.086	0.00735
764.3	1.85	24.5	31.4	12.047	0.403	0.005	0.000	0.046	0.00690

*Molar ratio of toluene to $As(CH_3)_3$ at the inlet of the reaction vessel. Initial concentrations may be calculated from this figure, the total pressure (P) and the temperature of the reaction zone (T).
†Packed vessel runs.

[4] $CH_3 + C_6H_5CH_3 \rightarrow CH_4 + C_6H_5CH_2$

[5] $2CH_3 \rightarrow C_2H_6$

[6] $CH_3 + C_6H_5CH_2 \rightarrow C_6H_5C_2H_5$

plus the usual reactions leading to small quantities of ethylene and traces of xylenes and styrene. Values of k_1 were calculated from the usual first order equation

$$k = \frac{2.303}{t_c} \log \frac{1}{1 - x}$$

where t_c is the average residence time in the reaction zone and the fraction decomposed, x, is given by

$$x = \frac{\text{moles } CH_4 + \text{moles ethylbenzene} + 2(\text{moles } C_2H_6 + \text{moles } C_2H_4)}{3(\text{moles } As(CH_3)_3) \text{ used}}$$

The only volatile arsenic containing compound that could be found by either flame or electron capture gas chromatography following a run was the parent alkyl. The only involatile products were dibenzyl and a grey deposit at the outlet of the furnace which, as previously mentioned, was 98.4% arsenic. These facts, coupled with the distribution of products shown in Table 1 and the agreement shown in Table 2 between the percent decomposition calculated from product analysis and from the differences between the quantity of alkyl used and the residual alkyl, indicate that reaction 1 is the rate controlling step in a sequence of reactions that produces three methyl radicals and free arsenic. The simple linear nature of the Arrhenius plot of $k_4/k_5^{1/2}$ shown in Fig. 1 is further supporting evidence (6).

All contact times used should be such that

Can. J. Chem. Downloaded from www.nrcresearchpress.com by 210.87.254.6 on 09/05/12
For personal use only.

TABLE 2

Percent decomposition by product analysis and alkyl recovery

T (°K)	Percent decomposition: Product analysis	Alkyl recovery*
858.0	72.7	67.1
852.7	55.2	53.8
852.6	54.1	53.4
840.6	28.1	27.4
836.5	60.8	63.0
836.4	25.0	20.1
774.3	2.5	1.6

*From gas chromatographic analysis of the toluene trapped at the outlet of the reaction vessel in a trap cooled by acetone – Dry Ice. Conditions used were the same as those for ethylbenzene analysis. Analyses were carried out immediately following the run and fresh standard solutions were used. The solutions have limited stability and care must be taken to avoid loss of alkyl by evaporation.

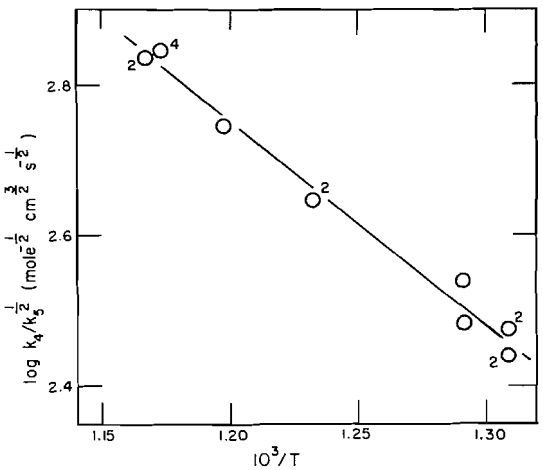

FIG. 1. Arrhenius plot of $k_4/k_5^{1/2}$. Numerals denote the number of runs averaged to obtain the given point. Total pressure 21–26 mm.

thermal equilibrium and diffusion problems should not be significant (7). The experimental results at 858 °K support this conclusion.

The negligible effect on k_1 of a variation by a factor of 3.7 in concentration at 852 °K and by a factor of 7.2 at 836 °K indicates that the decomposition is first order. The agreement in Fig. 2 between the four experiments in the packed vessel and those in the unpacked vessel shows that no detectable surface reactions are occurring. Least squares analysis of the points used to obtain this plot gives

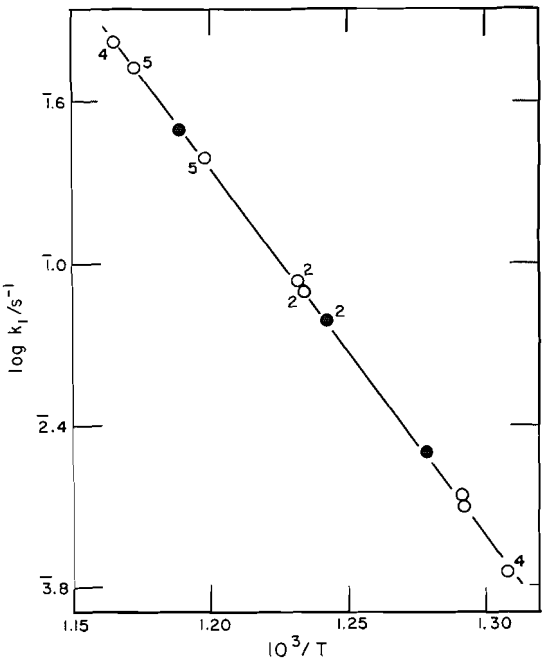

FIG. 2. Arrhenius plot for k_1. Numerals denote the number of runs averaged to obtain the given point. ○, runs in unpacked reaction vessel; ●, runs in packed reaction vessel.

$$\log k_1/s^{-1} = 15.82 - (62\,800 \pm 800)2.3RT$$

From the runs at 836 °K it is apparent that above approximately 13 mm total pressure the values of k_1 are essentially the high pressure limiting values. The observed activation energy should therefore be a reasonable measure of $D[(CH_3)_2\text{-As—}CH_3]$.

From $\Delta H_f^\circ{}_{298}$ [As$(CH_3)_{3,g}$] = 3.7 kcal mole^{-1} (3), $\Delta H_f^\circ{}_{298}$ [$CH_{3,g}$] = 33.2 kcal mole^{-1} (8), and $\Delta H_f^\circ{}_{298}$ [As, g] = 72.3 kcal mole^{-1} (8) the sum of the dissociation energies for reactions 1, 2, and 3 should be approximately 168 kcal mole^{-1}. Therefore, with D_1 = 63 kcal mole^{-1}, $D_2 + D_3$ = 105 kcal mole^{-1}. At the temperatures and pressures used, the A factor for reaction 2 should have a maximum value of about 10^{15} and, in all likelihood, would be considerably lower. If reaction 1 is to be rate controlling, k_1 must be significantly smaller than k_2. Taking the rather conservative estimate that k_2 must be at least twice k_1 leads to what should probably be considered an absolute maximum value of D_2 = 59 kcal mole^{-1}. This then requires that $D_3 \geqslant 46$ kcal mole^{-1} and for $k_3 = 2k_2$ the minimum value of A_3 would be

Can. J. Chem. Downloaded from www.nrcresearchpress.com by 210.87.254.6 on 09/05/12
For personal use only.

about 10^{12} s^{-1}, a value which is probably at least a power of ten greater than that expected (6).

Obviously the preceding discussion does not rule out completely the possibility that reactions 2 and 3 occur and, in fact, based on experience with other alkyls, reaction 2 is probably much more likely than reaction 2*a*. The regeneration of $As(CH_3)_3$ by either reaction 2*a* or by recombination of CH_3 with $As(CH_3)_2$ is probably negligible. To the extent that it does occur, the reported value of $D[(CH_3)_2As—CH_3]$ may be slightly low. There does seem to be a distinct possibility that the decomposition of methylarsine must occur largely by reaction 3*a* or some other similar process.

This work has been supported by a grant from the National Research Council of Canada.

1. P. B. Ayscough and H. J. Emeleus. J. Chem. Soc. 3381 (1954).
2. R. A. Zingdro and A. Merijanian. Inorg. Chem. **3**, 580 (1964).
3. L. H. Long and J. F. Sackman. Trans. Faraday Soc. **52**, 1201 (1956).
4. M. Krech and S. J. Price. Can. J. Chem. **41**, 224 (1963).
5. A. Vogel. Quantitative inorganic analysis. 3rd ed. Longmans. 1961.
6. M. G. Jacko and S. J. W. Price. Can. J. Chem. **42**, 1198 (1964).
7. M. F. R. Mulcahy and M. R. Pethard. Aust. J. Chem. **16**, 527 (1961).
8. Selected values of chemical thermodynamic properties. Natl. Bur. Std. U.S. Tech. Notes, No. 270-3. 1968.

Can. J. Chem. Downloaded from www.nrcresearchpress.com by 210.87.254.6 on 09/05/12
For personal use only.

Mass spectral studies of metal chelates. VI. Mass spectra and appearance potentials of β-diketonates of copper(II)[1,2]

C. REICHERT[3] AND J. B. WESTMORE
Department of Chemistry, University of Manitoba, Winnipeg, Manitoba

Received April 1, 1970

The mass spectra of several copper complexes of β-diketones are discussed. The extent of fragmentation of the molecular ions depends upon the nature of the substituents on the chelate ring, being larger for electron-withdrawing, and smaller for electron-releasing substituents. In a number of fragmentations, migration of an aryl group to the copper atom occurs. Hydrogen atom migrations are also observed in some fragmentations. Attempts are made to correlate the appearance potentials of the molecular ions with acid dissociation constants of the β-diketones, formation constants and polarographic reduction potentials of the complexes, and Hammett σ constants of the substituents.

Canadian Journal of Chemistry, **48**, 3213 (1970)

Can. J. Chem. Downloaded from www.nrcresearchpress.com by 210.87.254.5 on 09/05/12
For personal use only.

Introduction

Recently, mass spectrometric investigations of transition metal complexes of β-diketones have been reported. These studies included the mass spectra of acetylacetonates (2–6), various β-diketonates of chromium(III) (7), copper(II) (8), various metal complexes of dibenzoylmethane (9), lanthanide complexes of hexamethylacetylacetone (10), and fluorine-substituted acetylacetonates (11). The effect of variation in metal or ligand upon appearance potentials has also been investigated (1, 5–8, 10, 12).

In this paper we report the mass spectra of several copper(II) β-diketonates (see Table 1), the appearance potentials of the molecular ions, and, in a few cases, of fragment ions. Mass spectra for only three of these compounds, *viz.* **1** (2, 8), **3** (8), and **12** (9) and appearance potentials for four compounds, *viz.* **1**, **3–5** (8) have been reported previously by other workers.

Experimental

The copper β-diketonates were prepared by the aqueous solution synthesis of Fernelius and Bryant (13). In this method, an alcoholic solution of the purified β-diketone is mixed with an aqueous solution of copper acetate. The complex usually precipitated from the solution although in some cases it was necessary to add a few drops of ammonium hydroxide before the diketone would react. The mixed ligand complex, **5**, Cu(acac)(hfacac) was prepared by the method described by Farona *et al.* (14), in which an equimolar mixture of acetylacetone and hexafluoroacetylacetone was added to a small excess of basic copper carbonate suspended in chloroform. The unreacted material was filtered off and the solvent was evaporated. All complexes were purified by fractional sublimation at reduced pressure. If, like $Cu(acac)_2$ the complexes are square planar (15), then the unsymmetrically substituted chelates can exist in *cis* and *trans* forms. A determination of the geometry of the complexes obtained in these preparations appears not to have been undertaken.

3-Methyl-2,4-pentanedione was prepared by the method of Morgan and Rawson (16), by reaction of sodium ethoxide with acetylacetone, and reaction of the sodium acetylacetonate produced with methyl iodide in a sealed tube at 100° for several hours. The 3-methyl-2,4-pentanedione was distilled from the reaction mixture, at reduced pressure.

3-Phenyl-2,4-pentanedione was prepared by Hauser's method (17). A mixture of 0.4 mole of phenylacetone, 0.8 mole of acetic anhydride, and 0.12 mole of *p*-toluenesulfonic acid was stirred for 5 min and saturated at 0–10° with boron trifluoride for 3–4 h. The mixture was then allowed to warm to room temperature over a 3 h period, then poured into a solution of sodium acetate and refluxed to hydrolyze the boron fluoride complexes. The mixture was cooled and extracted with ligroin. The product was purified by recrystallization from ligroin. The remaining β-diketones were purchased as follows: acetylacetone, 2-thenoyltrifluoroacetone, Fisher Scientific Co.; trifluoroacetylacetone, hexafluoroacetylacetone, Peninsular Chemresearch Inc.; dibenzoylmethane, benzoylacetone, Aldrich Chemical Co.; benzoyltrifluoroacetone, 2-naphthoyltrifluoroacetone, 2-furoyltrifluoroacetone, Eastman Organic Chemicals. The β-diketones were purified by distillation, or by recrystallization from a suitable solvent, as appropriate.

Deuteration of the complexes at the bridging carbon atom was achieved by shaking the complex with a solution of NaOD in D_2O (9).

The mass spectra were obtained on a Hitachi Perkin–Elmer RMU-6D single focussing mass spectrometer. The samples were introduced by the direct insertion method. The temperature of the ion source was about 150°. The

---

[1]See ref. 1 for Part V.

[2]Presented, in part, at the 21st Annual Southeastern Regional Meeting of the American Chemical Society, Richmond, Va, November, 1969.

[3]Present address: Department of Chemistry, University of Western Ontario, London, Ontario.

TABLE 1

Copper β-diketonates studied

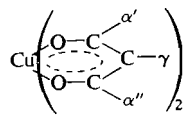

Compound	β-Diketone	α′	α″	γ
1	Acetylacetone	CH_3	CH_3	H
2	3-Methyl-2,4-pentanedione	CH_3	CH_3	CH_3
3	Trifluoroacetylacetone	CH_3	CF_3	H
4	Hexafluoroacetylacetone	CF_3	CF_3	H
5*	Acetylacetone	CH_3	CH_3	H
	Hexafluoroacetylacetone	CF_3	CF_3	
6	Benzoylacetone	CH_3	Ph	H
7	3-Phenyl-2,4-pentanedione	CH_3	CH_3	Ph
8	Benzoyltrifluoroacetone	CF_3	Ph	H
9	2-Furoyltrifluoroacetone	CF_3	2-Furyl	H
10	2-Thenoyltrifluoroacetone	CF_3	2-Thenyl	H
11	2-Naphthoyltrifluoroacetone	CF_3	2-Naphthyl	H
12	Dibenzoylmethane	Ph	Ph	H

*5 is the mixed ligand complex Cu(acac) (hfacac).

masses of the ions at high mass were verified by the simultaneous introduction into the ion source of perfluorokerosene, which gives ions of known mass, at small intervals, to masses beyond 1000. Appearance potentials were determined, as described previously (5), by the semilogarithmic method (18) using xenon as a standard.

Results and Discussion

The Mass Spectra

The relative intensities of all copper-containing ions (with the exception of those having a relative intensity of less than 1%) are shown in Table 2. Intensities of non-copper-containing ions are not recorded. They tend to be variable, are usually quite low (the sum of their intensities was less than 20% of the total ion current for all compounds except **11** and **12**, when this sum was between 30 and 40%) and are considered to be of little diagnostic value.

The general features of the mass spectra of metal β-diketonates have been interpreted in terms of the relative stabilities of odd- or even-electron ions, and the tendency of the metal to undergo valency change (1, 2, 5, 7, 8), *i.e.* upon the ability of the metal to stabilize the molecular ion through metal-to-ligand charge-transfer (metal d-orbital expansion) (1). Thus, a bis-β-diketonate will produce a molecular ion which we formally represent as the odd-electron species **1** (see Fig. 1), since we have presented data which suggest that ionization causes the removal of an electron from a ligand-dominated molecular orbital (1, 5, 7). The subsequent fragmentation of the molecular ion will depend upon the nature of the α and γ substituents as well as upon the nature of M. Expected fragmentations involve homolytic fission of the C—α or C—γ bonds with assumed transfer of one electron from the bond to the half-filled bonding ligand π orbital, to give species which we formally represent as the even-electron species **2**, **3**, and **4**. Unless **1** can be stabilized by release of electron density to the ring from M, or from the α or γ substituents, appreciable π-stabilization of **2**, **3**, and **4** relative to **1** would be expected, and the reaction should occur readily, resulting in major ion peaks for one or more of these ions. No formal valency change of the metal is required in this reaction. These reactions should be enhanced if the C—α or C—γ bonds are weak or if the α and γ substituents are electron-attracting. These reactions will occur less readily if electron release to the chelate ring of **1** can occur. Probably the most important way in which the electron release occurs is via π-interactions. The π-stabilization can occur either (*a*) by metal-to-ligand charge-transfer via the metal d orbitals, if permitted by symmetry, or (*b*) by delocalization of the positive charge on the chelate ring into the α or γ substituents. In case (*a*) the amount of stabilization should parallel the ease of oxidation of the metal. Thus, on the basis of appearance potential measurements, substantial π-stabilization of **1** was proposed for $Fe(acac)_2$, $Fe(tfacac)_2$, and $Fe(hfacac)_2$, while for the corresponding Cu(II)

Can. J. Chem. Downloaded from www.nrcresearchpress.com by 210.87.254.5 on 09/05/12
For personal use only.

Can. J. Chem. Downloaded from www.nrcresearchpress.com by 210.87.254.5 on 09/05/12
For personal use only.

TABLE 2

Relative intensities of copper-containing ions in the mass spectra of copper β-diketonates, at an electron energy of 50 V and an ionization chamber temperature of 150 °C*

		Relative intensity†											
	Compound	**1**	**2**	**3**	**4**	**5**	**6**	**7**	**8**	**9**	**10**	**11**	**12**
	α′	CH_3	CH_3	CH_3	CH_3	CH_3, CF_3	CH_3	CH_3	CF_3	CF_3	CF_3	CF_3	Ph
	α″	CH_3	CH_3	CF_3	CF_3	CH_3, CF_3	Ph	CH_3	Ph	2-Furyl	2-Thenyl	2-Naphthyl	Ph
Ion	γ	H	CH_3	H	H	H	H	Ph	H	H	H	H	H
L_2Cu^+ (*a*)		48 (12)	26 (10)	5 (2)	9 (4)	22 (8)	100 (30)	62 (21)	100 (40)	100 (35)	100 (32)	73 (20)	89 (38)
$(L_2Cu - CH_3)^+$ (*b*)		35		1		5	11						
$(L_2Cu - CF_3)^+$ (*c*)				11	24[a]	13			31	42	35[a]	9	
$(L_2Cu - H_2O)^+$		< 1					6[a]			5[a]			10[a]
$(L_2Cu - CH_2CO)^+$		10[a]		8									
$(L_2Cu - CFO)^+$				8[a]					5	4[a]	5	4	
$(L_2Cu - PhCO_2H)^+$													14
$(L_2Cu - 2CH_3)^+$ (*d*)		35				2	5						
$(L_2Cu - 2CF_3)^+$ (*e*)‡					23[c]								
$LCuAr^+$ (*f*)‡									28[c]	26[c]	45[c]	11	
$(L_2Cu - 138)^+$‡				27**		8							
$LCuH^+$		35‖	38				30[a]	100[a]	14[a]	7	9[a]	62[a]	
LCu^+ (*g*)		50[bd]	39	8	1.5	73§	26[a]	20[a]	7[a]	9	6[a]	6[a]	
$(LCu - H)^+$		5	100				35[a]	16[a]	13[a]	13	19[a]	100[a]	100
$(LCu - CH_3)^+$ (*h*)		100[a]	35	10		100§	28	71[a]					
$(LCu - CF_3)^+$ (*i*)				100[f]	100[a]				30[a]	76	76[f]	57	
$(LCu - Ph)^+$							25						21
$(LCu - 42)^+$							42						
$(LCu - 2CH_3)^+$		12[d]						14					
$CuAr^+$							14		12	3	11	36	
$CuOCCH_2^+$		50		59[f]									
$CuOCCH^+$		8		18	11								
Cu^+		10	21[h]	44	82[f]	70	10	8	13		9	11	

*Identified metastable transitions are indicated by superscripts which relate the daughter ion to its precursor as labelled in column **1**.
†Numbers in parentheses are the percentage of the total ion current of the copper-containing ions carried by the molecular ion.
‡These ions have the same mass. Assignments for **3** and **4** have been discussed previously (1), and for **8**, **9** and **10** by deuterium labelling (see Table 3).
§L = acac.
‖Incorrectly reported in ref. 6.
**A metastable peak was detected for the transition $LCu\alpha''^+ \rightarrow L^+ + Cu\alpha''$.

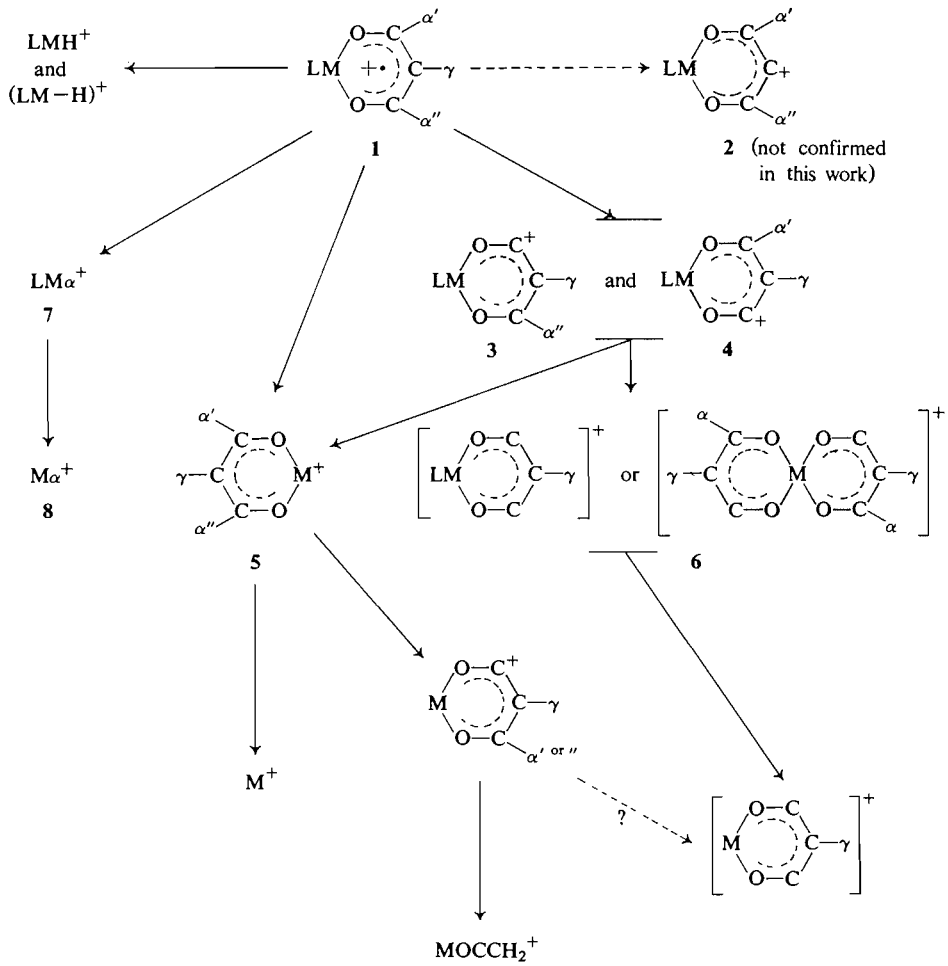

FIG. 1. Major fragmentation pathways for bis-β-diketonate complexes, with special reference to copper complexes.

chelates the stabilization was quite small (1), consistent with the much greater ease of oxidation of Fe(II) to Fe(III) than of Cu(II) to Cu(III). In view of this apparently limited ability of copper to stabilize the molecular ions, **1**, the series of complexes listed in Table 1 forms an excellent series in which to study the ability of substituents on the chelate ring to stabilize **1** via their effects on the mass spectra. Thus, in case (*b*) the delocalization of the positive charge on the ring could be accomplished via π donation from the α or γ substituents. This donation would be expected to occur most readily if the α or γ substituents have lone pair electrons, or have aromatic character.

The data presented in Table 2 are consistent with the above suggestions. Thus, when one or more of the α or γ substituents have aromatic character, as in compounds **6–12**, the molecular ions represent a significantly larger proportion of the total ion current. This remains true even when the intensities of non-copper-containing ions are taken into account. Also, there is generally less extensive fragmentation than for compounds **1–5**, in which only aliphatic groups are bonded to the chelate ring. For compounds **6–11**, which have one aromatic and one aliphatic substituent, the aliphatic substituent is lost more readily on fragmentation. In fact, there is no example in which the aromatic substituent is eliminated. This is consistent with the expected greater strength of the bond of an aromatic group to the chelate ring. In this group of compounds the fission of a C—γ bond has not been confirmed.

Can. J. Chem. Downloaded from www.nrcresearchpress.com by 210.87.254.5 on 09/05/12
For personal use only.

TABLE 3

Increase in mass of selected ions upon γ-deuteration of some copper β-diketonates

Ion	Mass change with respect to				
	6	**8**	**9**	**10**	**12**
L_2Cu^+	+2	+2	+2	+2	+2
$LCuAr^+$	—	+1	+1	+1	—
$LCuH^+$	+1 (40%) +2 (60%)	+1 (56%) +2 (44%)	+1	+1 (44%) +2 (56%)	—
LCu^+	+1	+1	+1	+1	—
$(LCu - H)^+$	0	0	+1	0	0
$(LCu - CH_3)^+$	+1	—	—	—	—
$(LCu - CF_3)^+$	—	+1	+1	+1	—
$(LCu - Ph)^+$	+1	—	—	—	+1
$(LCu - 42)^+$	+1	—	—	—	—

Alternatively, the molecular ion may decompose to the species **5**, LCu^+, by elimination of a ligand radical. **1** is not necessarily the only precursor of **5** as shown by the detection of metastable peaks for the reactions $(L_2Cu-CH_3)^+ \rightarrow LCu^+$ and $(L_2Cu-2CH_3)^+ \rightarrow LCu^+$ for compound **1**, $Cu(acac)_2$.

In the spectra of compounds containing the CF_3 substituent are ions labelled as $(L_2Cu-138)^+$ in Table 2. These could be due to loss of two $\cdot CF_3$ radicals, or loss of $CF_3COCHCO$ (or $\cdot CF_3 + COCHCO$) from the molecular ion. The identity of this ion can be clarified by using ligands deuterated at the central carbon atom. In this way it has been shown (1) that for compound **4** this ion, **6**, corresponds to loss of two $\cdot CF_3$ radicals and for compound **3** both processes occur with approximately equal probability. For compounds **8–11**, the latter process is expected since (*a*), the aromatic groups should stabilize the molecular ions and effectively strengthen the C—CF_3 bond, and (*b*), the $(L_2Cu - 138)^+$ ion corresponds to species **7** in which migration of the aromatic group has occurred. The aromatic group can stabilize the ion by partial delocalization of the positive charge into its π-system. Further support for the aromatic group migration is given by the presence of $CuAr^+$, **8**, ions in the spectra of these compounds. Ions of this type have also been observed in other work on copper compounds (19, 20). These expectations are confirmed by the data of Table 3.

In many of the spectra, especially of the compounds containing an aromatic substituent, there are, apart from the LCu^+ species, ions which differ from it by one hydrogen atom, namely, the $LCuH^+$ and $(LCu - H)^+$ species. In the formation of this latter pair of ions a hydrogen atom migration is indicated and the origin of the hydrogen atom is of some interest. This can be partially clarified by deuteration of the central carbon atom of the ligand, although in some cases specific deuteration of the aryl substituents would be necessary. The effects of this deuteration on the mass spectra are shown in Table 3.

Lacey, MacDonald, and Shannon (9) found that for compound **12** the hydrogen atom transferred into the neutral product, HL, originated from the bridging position of the ligand. We agree with this finding and note that a similar result is obtained for compounds **6**, **8**, and **10**. For the Co(II) and Ni(II) complexes of dibenzoylmethane they also found that the hydrogen atom transferred in the formation of the LMH^+ ion originated from the ortho position of the phenyl substituent. The results in Table 3 indicate that for compounds **6**, **8**, and **10**, there are competing reactions in which a hydrogen atom is transferred either from the bridging carbon atom, or from the aromatic substituent. Since the relative intensities of the group of peaks $LCuH^+$, LCu^+, and $(LCu - H)^+$ are independent of electron energy, even to just above the ionization threshold, it is likely that they have a common precursor, possibly a molecular ion in which ring opening has occurred. Following the rationalizations of Lacey, MacDonald, and Shannon (9) we may speculate that these ions are formed by the sequences of reactions given in Fig. 2, in which it is possible to write reasonable canonical forms for all species involved except for the neutral $(L - H)$ species (which is also formed for compound **1**). It is interesting to note that one of the canonical forms of $(LCu - H)^+$ formally involves Cu(I). The corresponding ion is absent in the mass spectra of the benzoylacetonates of

Can. J. Chem. Downloaded from www.nrcresearchpress.com by 210.87.254.5 on 09/05/12
For personal use only.

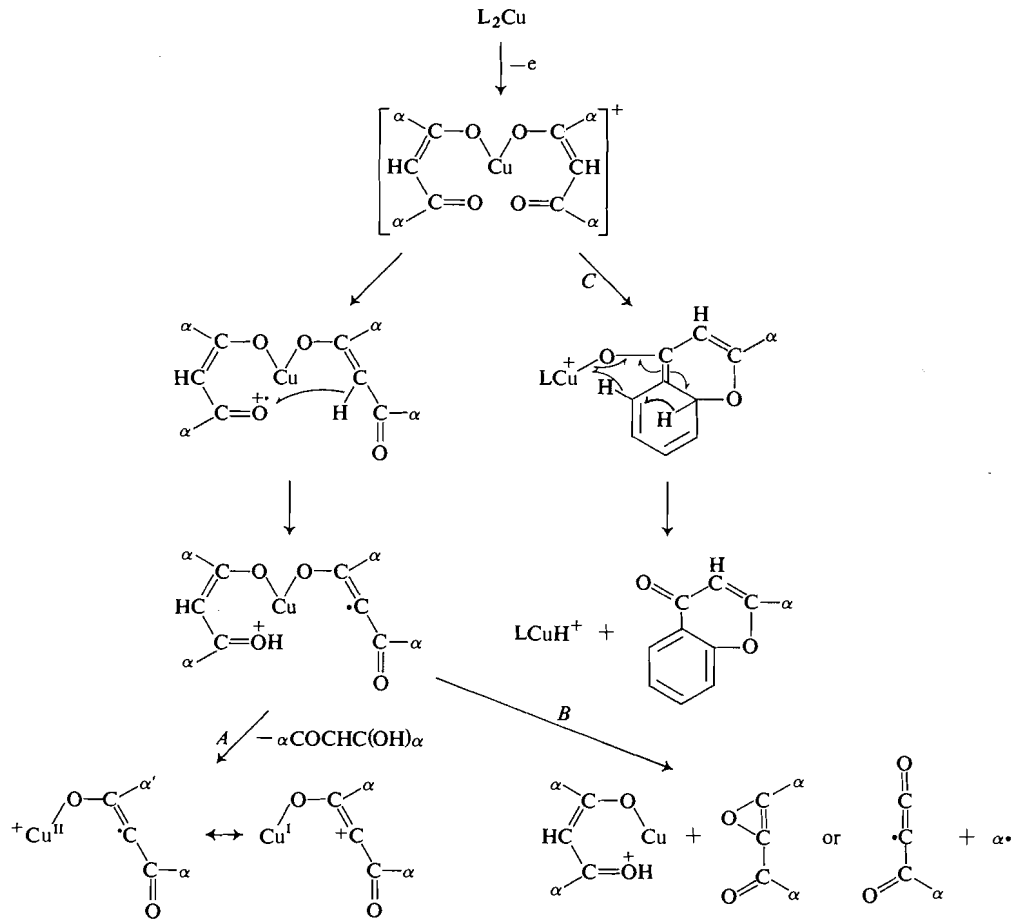

FIG. 2. Possible fragmentation pathways to the $LCuH^+$ and $(LCu - H)^+$ ions. In pathways *A* and *B* the migrating H atom comes from the bridging carbon atom; in pathway *C* it comes from the aryl group.

Co(II) and Ni(II), metals in which the +1 oxidation state is much less stable. (The only major peaks we have observed in the spectra of these latter compounds are L_2Co^+ (100%), $(L_2Co - CF_3)^+$ (81%), LCo^+ (17%), and L_2Ni^+ (100%), $(L_2Ni - CF_3)^+$ (62%), $LNiH^+$ (11%), $LiNi^+$ (15%).

Other fragmentations which occur are given in Fig. 1. These have been discussed previously (2, 5, 9). In many cases support for a proposed fragmentation is given by the detection of a metastable peak (see Table 2).

Appearance Potentials

All of the chelates gave abundant molecular ions, and consequently it was possible to measure the appearance potentials of the complete series of compounds with a reproducibility of ±0.05 V and a probable accuracy of ±0.1 V. The appearance potentials of the molecular ions are shown in Table 4. In a few cases the appearance potentials of the LCu^+ ions are also shown.

In previous papers (1, 5, 7) we have suggested, in agreement with other workers (8, 12), that the appearance potential of the molecular ion depends much more upon the nature of the ligand than upon the nature of the metal, and that ionization of the molecule results in the removal of an electron from a ligand-dominated orbital. The present results are consistent with this proposal since the variations in the appearance potentials can be related to electronic effects in the ligand. Thus, in Table 5 are tabulated data relating to acid dissociation constants of the ligands, formation constants between the ligands and copper, and polarographic half-wave poten-

Can. J. Chem. Downloaded from www.nrcresearchpress.com by 210.87.254.5 on 09/05/12
For personal use only.

TABLE 4

Appearance potentials of copper β-diketonates

β-Diketone	Appearance potential (V)		
	This work		Literature value (8)
	L_2Cu^+	LCu^+	L_2Cu^+
1 Acetylacetone	8.31±0.05	13.1±0.1	7.75±0.05
2 3-Methyl-2,4-pentanedione	7.97±0.05	10.8±0.1	—
3 Trifluoroacetylacetone	9.05±0.05	13.1±0.1	8.61±0.05
4 Hexafluoroacetylacetone	9.86±0.05	—	9.68±0.01
5 Acetylacetone / Hexafluoroacetylacetone	9.03±0.05	—	8.65±0.01
6 Benzoylacetone	8.37±0.05	10.7±0.1	—
7 3-Phenyl-2,4-pentanedione	8.05±0.05	—	—
8 Benzoyltrifluoroacetone	9.06±0.05	—	—
9 2-Furoyltrifluoroacetone	8.89±0.05	—	—
10 2-Thenoyltrifluoroacetone	8.90±0.05	—	—
11 2-Naphthoyltrifluoroacetone	8.39±0.05	—	—
12 Dibenzoylmethane	8.28±0.05	10.3±0.1	—

TABLE 5

Acid dissociation constants of the β-diketone, and formation constants and polarographic half-wave potentials of copper β-diketonates, all in aqueous 75 volume% dioxane

β-Diketone	pK_a (21)	Log K_1K_2 (21)	$E_{1/2}$ (22, 23)
1 Acetylacetone	12.75	22.6	−0.502
2 3-Methyl-2,4-pentanedione	—	—	−0.559
3 Trifluoroacetylacetone	8.7	17.2	−0.169
4 Hexafluoroacetylacetone	6.0	8*	+0.038
6 Benzoylacetone	12.85	23.0	−0.381
7 3-Phenyl-2,4-pentanedione	—	—	−0.497
8 Benzoyltrifluoroacetone	9.3	18.8	−0.150
9 2-Furoyltrifluoroacetone	8.5	17.2	−0.130
10 2-Thenoyltrifluoroacetone	9.1	19.0	−0.137
11 2-Naphthoyltrifluoroacetone	9.3	18.4	—
12 Dibenzoylmethane	13.75	25.0	−0.379

*Estimated value, log K_1 = 4.3.

tials of the copper complexes. These results were all obtained in a 75 volume% dioxane/water solvent. It should be noted that the polarographic reduction waves were not reversible and hence do not give equilibrium data, but in spite of this, a correlation between the $E_{\frac{1}{2}}$ values of the aliphatic-substituted chelates with acid dissociation constants of the ligand and with Hammett σ constants has been noted to exist (23). Earlier, a correlation between acid dissociation constants and chelate formation constants had been noted (21). In Fig. 3 the ionization potentials are plotted against the data of Table 5. In each plot, a straight line can be drawn so that most of the points lie fairly close to it. In each case the biggest deviation from the line occurs for compound **11**, which contains the naphthyl substituent.

The appearance potentials of the molecular ions shown in Table 4 can also be compared with ionization potentials of some appropriate aromatic compounds which are listed in Table 6. There is much experimental evidence for the quasi-aromatic nature of the chelate ring in metal β-diketonate complexes (see ref. 7 and references therein). With respect to the chelates, the main points to note are as follows: (*a*) substitution of CF_3 for CH_3 raises the appearance potential by approximately 0.7 V (compare compounds **1**, **3**, and **4**, and also **6** and **8**); (*b*) substitution of CH_3 for H lowers the appearance potential by approximately 0.3 V (compare compounds **1** and **2**); (*c*) substitution of Ph for CH_3 has only a small effect on the appearance potentials (compare compounds **1**, **6**, and **12**, com-

Can. J. Chem. Downloaded from www.nrcresearchpress.com by 210.87.254.5 on 09/05/12
For personal use only.

TABLE 6

Ionization potentials determined by the photoionization method for selected aromatic compounds (24–26)

Compound	Ionization potential (V)	Compound	Ionization potential (V)
Benzene	9.245	Trifluoromethylbenzene	9.68
Furan	8.89	1,2,3-Trimethylbenzene	8.48
Thiophene	8.91	1,2,4-Trimethylbenzene	8.27
Toluene	8.82	1,3,5-Trimethylbenzene	8.39
o-Xylene	8.56	Naphthalene	8.12
m-Xylene	8.56	Biphenyl	8.27
p-Xylene	8.45		

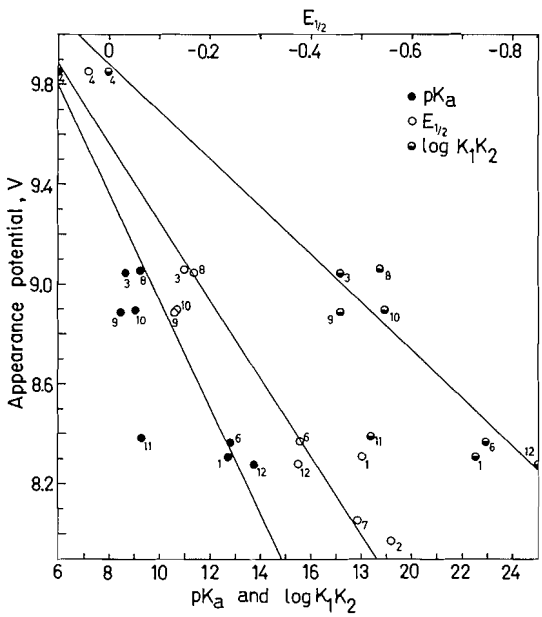

FIG. 3. Plot of appearance potential against pK_a (of the β-diketone), log K_1K_2 and polarographic half-wave potential of the complex. (Numbers beside points refer to complexes listed in Table 1.)

pounds **2** and **7**, and **3** and **8**); (*d*) substituent of 2-furyl or 2-thenyl for CH_3 lowers the appearance potential by approximately 0.15 V (compare compounds **3**, **9**, and **10**); (*e*) substitution of 2-naphthyl for CH_3 lowers the appearance potential by approximately 0.65 V (compare compounds **3** and **11**).

The variations of appearance potential under points (*a*) and (*b*) are similar to those observed in a previous study (7) on β-diketonates of Cr(III), and are consistent with variations to be expected for substituents bonded to a quasi-aromatic ring (compare ionization potentials of benzene, toluene, xylene, trimethylbenzene, and trifluoromethylbenzene given in Table 6). Under points (*c*) and (*d*) the effects of the phenyl, 2-furyl, and 2-thenyl substituents are smaller than expected when the ionization potentials of benzene, toluene, and biphenyl are compared. This suggests that conjugation between the chelate ring and the aryl substituent is smaller than in biphenyl although, except for compound **7** there appears to be no steric reason why the aryl substituent cannot become coplanar with the chelate ring. It may be significant that the appearance potentials of compounds **8**, **9**, and **10** are similar to those of benzene, furan, and thiophene, respectively. On the other hand substitution of the 2-naphthyl substituent for a methyl group (point (*e*)) produces a significant lowering of the appearance potential. Recalling that electron impact appearance potentials are often 0.3–0.4 V higher than ionization potentials determined by the photoionization method, it seems probable that ionization of compound **11** removes an electron from an orbital dominated by the naphthyl substituent. The energy of such an orbital may also be lowered slightly (*i.e.* the ionization potential should be raised) by the inductive effect of the electron-attracting CF_3 substituent. If, in fact, ionization occurs by removal of an electron from the highest energy, occupied ligand-dominated orbital, this would explain the deviation of the appearance potential of compound **11** from the straight lines of Fig. 3. In compounds **1**–**7** and **12** this orbital should be localized mainly on the chelate ring. In compounds **8**–**10** the chelate ring and aryl orbitals are expected to have similar energies. In compound **11** the naphthyl dominated orbitals should have the highest energies. The acid dissociation constants and complex formation constants are of course dependent upon the electron density at the oxygen atoms

Can. J. Chem. Downloaded from www.nrcresearchpress.com by 210.87.254.5 on 09/05/12
For personal use only.

Can. J. Chem. Downloaded from www.nrcresearchpress.com by 210.87.254.5 on 09/05/12
For personal use only.

which may reasonably correlate with the energies of chelate ring-dominated orbitals.

The appearance potential of the mixed ligand chelate, compound **5**, Cu(acac)(hfacac), is of interest (see ref. 8). In agreement with these authors we find a value close to that for compound **3**, *i.e.* close to the mean appearance potential value of compounds **1** and **4**. This is contrary to the expected result if ionization causes removal of an electron from an orbital dominated by the acac ring, *i.e.* the ligand orbital expected to have the highest energy. We were not able to detect any upward breaks in the ionization efficiency curve near threshold. A break might be expected at the onset of ionization of the hfacac ring. We are therefore in agreement with an earlier statement (8), namely, that the energy of the orbital from which the electron is removed is controlled about equally by substituents in both rings.

In Fig. 4 an attempt has been made to correlate the appearance potentials with substituent effects as given by Hammett σ constants. It is realized

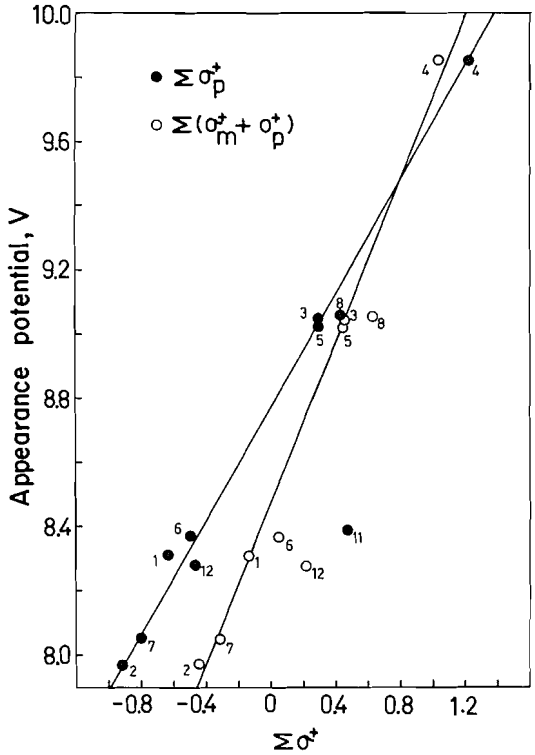

FIG. 4. Plot of appearance potential against $\Sigma\sigma_p^+$ and $\Sigma(\sigma_m^+ + \sigma_p^+)$ for the substituents. (Numbers beside points refer to complexes listed in Table 1.)

that the presence of the copper and oxygen atoms will mean that the chelate ring will not be truly aromatic. The σ^+ constants of Brown and Okamoto (27) have been used although use of the σ values of McDaniel and Brown (28) leads to the same conclusions. In one plot the values used have been selected with respect to the position of the substituent relative to the copper atom, *i.e.* σ_m^+ values for α-substituents, σ_p^+ values for γ-substituents; in the other plot σ_p^+ values have been used. The first set of values should relate to the electron density near the copper atom, the second set to the electron density on the chelate ring. The σ^+ values used for each compound are the sum of the individual values for each substituent. In both plots a good linear correlation is obtained for the aliphatic-substituted chelates but the aromatic substituted chelates fall below this line, as noted by Streitweiser for substituted benzenes (29). The naphthyl substituent lies so far below the line that a different mechanism of ionization is indicated.

The appearance potentials of compounds **1**, **3**, **4**, and **5** have been reported previously (8). The values, although obtained in a similar instrument, were 0.2–0.6 V lower than our values, probably because a different method of obtaining the appearance potentials was used. The electron energies were calibrated via benzene and anthracene using ionization potentials obtained by the photoionization method. Electron impact values are usually higher and this may account for most of the discrepancy.

NOTE ADDED IN PROOF: In a recent communication (30) preliminary results on the measurement of the ionization potentials of some hexafluoroacetylacetonates by photoelectron spectroscopy have been reported. These values may differ from appearance potentials determined by electron impact and may extend discussions on ionization mechanisms of metal chelates and related compounds.

We thank the National Research Council of Canada for financial assistance.

1. C. REICHERT, G. M. BANCROFT, and J. B. WESTMORE. Can. J. Chem. **48**, 1362 (1970).
2. C. G. MACDONALD and J. S. SHANNON. Aust. J. Chem. **19**, 1545 (1966).
3. J. MACKLIN and G. DUDEK. Inorg. Nucl. Chem. Lett. **2**, 403 (1966).

4. S. SASAKI, Y. ITAGAKI, T. KUROKAWA, K. NAKANISHI, and A. KASAHARA. Bull. Chem. Soc. Japan. **40**, 76 (1967).
5. G. M. BANCROFT, C. REICHERT, and J. B. WESTMORE. Inorg. Chem. **7**, 870 (1968).
6. C. REICHERT and J. B. WESTMORE. Inorg. Chem. **8**, 1012 (1969).
7. G. M. BANCROFT, C. REICHERT, J. B. WESTMORE, and H. D. GESSER. Inorg. Chem. **8**, 474 (1969).
8. H. F. HOLTZCLAW, R. L. LINTVEDT, H. E. BAUMGARTEN, R. G. PARKER, M. M. BURSEY, and P. F. ROGERSON. J. Amer. Chem. Soc. **91**, 3774 (1969).
9. M. J. LACEY, C. G. MACDONALD, and J. S. SHANNON. Org. Mass Spectrom. **1**, 115 (1968).
10. J. D. MCDONALD and J. L. MARGRAVE. J. Less-Common Metals, **14**, 236 (1968).
11. C. REICHERT, J. B. WESTMORE, and H. D. GESSER. Chem. Commun. 782 (1967).
12. S. M. SCHILDCROUT, R. G. PEARSON, and F. E. STAFFORD. J. Amer. Chem. Soc. **90**, 4006 (1968).
13. W. C. FERNELIUS and B. E. BRYANT. Inorganic syntheses. Vol. 5. McGraw-Hill, Co., Inc., New York. 1957. p. 105.
14. M. F. FARONA, D. C. PERRY, and H. A. KUSKA. Inorg. Chem. **7**, 2415 (1968).
15. S. SHIBATA and K. SONE. Bull. Chem. Soc. Japan. **29**, 852 (1956).
16. G. T. MORGAN and E. A. RAWSON. J. Soc. Chem. Ind. **44**, 462 (1925).
17. (*a*) C. R. HAUSER, F. W. SWAMER, and J. T. ADAMS. Organic reactions. Vol. 8. *Edited by* R. Adams. John Wiley and Sons, Inc., New York. 1954. p. 59. (*b*) C. R. HAUSER and R. M. MANYIK. J. Org. Chem. **18**, 588 (1953). (*c*) J. T. ADAMS and C. R. HAUSER. J. Amer. Chem. Soc. **67**, 284 (1945).
18. F. W. LOSSING, A. W. TICKNER, and W. C. BRYCE. J. Chem. Phys. **19**, 1254 (1951).
19. C. REICHERT, D. K. C. FUNG, D. C. K. LIN, and J. B. WESTMORE. Chem. Commun. 1094 (1958).
20. D. C. K. LIN and J. B. WESTMORE. Unpublished results.
21. L. G. VAN UITERT, W. C. FERNELIUS, and B. E. DOUGLAS. J. Amer. Chem. Soc. **75**, 457 (1953).
22. H. F. HOLTZCLAW, JR., A. H. CARLSON, and J. P. COLLMAN. J. Amer. Chem. Soc. **78**, 1838 (1956).
23. R. L. LINDVEDT, H. D. RUSSELL, and H. F. HOLTZCLAW, JR. Inorg. Chem. **5**, 1603 (1966).
24. K. WATANABE. J. Chem. Phys. **26**, 542 (1957).
25. K. WATANABE, T. NAKAYAMA, and J. MOTTL. Final report on ionization potentials of molecules by a photoionization method. Report OOR 1624, Office of Technical Services, Washington, D.C., 1959.
26. R. W. KISER. Tables of ionization potentials. U.S. Atomic Energy Commission Report TID-6142, 1960.
27. H. C. BROWN and Y. OKAMOTO. J. Amer. Chem. Soc. **80**, 4979 (1058).
28. D. M. MCDANIEL and H. C. BROWN. J. Org. Chem. **23**, 420 (1958).
29. A. STREITWIESER, JR. Prog. Phys. Org. Chem. **1**, 1 (1963).
30. D. R. LLOYD. Chem. Commun. 868 (1970).

Can. J. Chem. Downloaded from www.nrcresearchpress.com by 210.87.254.5 on 09/05/12
For personal use only.

The effect of pressure on the hydrolysis equilibria of aqueous metal ions

T. W. SWADDLE AND PI-CHANG KONG
Department of Chemistry, University of Calgary, Calgary 44, Alberta

Received June 11, 1970

The molal acid dissociation ("hydrolysis") constant K_m of aqueous hexaaquochromium(III) ion, at 25.0° and ionic strength 0.5 *m*, has been determined spectrophotometrically as a function of pressure P up to 3 kbar. K_m increases with P (kbar) in accordance with the equation

$$\ln K_m = 0.151\,P - 9.474$$

The molal volume change is -3.8 ± 0.7 cm^3 mole^{-1}, and the enthalpy and entropy changes at 1 bar are 9.3 kcal mole^{-1} and 12.1 cal deg^{-1} mole^{-1}. Compressions of 0.1, 0.5, and 1.0 *M* aqueous perchloric acid, lithium perchlorate, and sodium perchlorate up to 4 kbar have also been measured.

Canadian Journal of Chemistry, **48**, 3223 (1970)

Can. J. Chem. Downloaded from www.nrcresearchpress.com by 210.87.254.42 on 09/05/12
For personal use only.

Introduction

The experimental data relating to the effect of pressure on the dissociation of electrically neutral weak acids (eq. 1) and bases (eq. 2) in aqueous solution have been reviewed by Hamann (1, 2) and Weale (3).

[1] $$HA = H^+ + A^-$$

[2] $$B + H_2O = HB^+ + OH^-$$

However, data relating to the effects of pressure on the acid dissociation ("hydrolysis") constants K of aqueous metal ions (eq. 3) are virtually non-existent.

[3] $$M(H_2O)_x^{n+} = M(H_2O)_{x-1}OH^{(n-1)+} + H^+$$

This information is needed if we are to utilize the pressure dependence of the kinetics of substitution (4) and oxidation–reduction (5) reactions of aqueous metal ions as a mechanistic criterion. The pressure dependence of metal ion hydrolysis is also of considerable interest *per se*, with reference to theories of the volumetric and piezometric properties of aqueous ions (1–3, 6), and also in connection with the chemistry of metal ions in pressurized high-temperature aqueous systems, in which hydrolysis is of major importance.

We have therefore investigated the hydrolysis of the hexaaquochromium(III) ion (eq. 4) as a function of pressure up to 3 kbar.

[4] $$Cr(H_2O)_6^{3+} = Cr(H_2O)_5OH^{2+} + H^+$$

This system was chosen because chromium(III) species react conveniently slowly in substitution reactions, so that they are ideally suited for kinetic studies, and furthermore one can study the extremely rapid equilibrium [4] close to ambient temperature over a convenient period of time without complications arising from hydrolytic polymerization (reaction 5), which is essentially a substitution process.

[5] $$2Cr(H_2O)_5OH^{2+} = (H_2O)_4Cr(OH)_2Cr(OH_2)_4^{4+} + 2H_2O \text{ (etc.)}$$

High pressures place considerable restrictions on the experimental methods available for the determination of the hydrolysis constant K of reaction 4. We have developed a spectrophotometric method, based on that of Emerson and Graven (7), which utilizes the ligand-field absorption band of $Cr(H_2O)_5OH^{2+}$ centered on 435 mμ at room temperature and pressure; the corresponding band of $Cr(H_2O)_6^{3+}$ has a maximum at 407 mμ with half the intensity of the $Cr(H_2O)_5OH^{2+}$ peak.

It is customary, in high-pressure studies, to express concentrations on the molal or mole-fraction scales, since these are independent of pressure. However, volume can be an important variable, and we have therefore also measured the compressions of some aqueous electrolyte solutions commonly used to provide media of constant ionic strength.

Experimental

Materials

Baker Analyzed perchloric acid and fresh Fisher reagent-grade $Cr(NO_3)_3.9H_2O$ were used without further purification; Fisher sodium perchlorate was recrystallized before use. Lithium perchlorate trihydrate was made from Baker Analyzed lithium carbonate. Deionized distilled water was used throughout.

Compression Studies

Mercury piezometers, as described by Adams (8), were used, following the recommendations of Newitt and

Can. J. Chem. Downloaded from www.nrcresearchpress.com by 210.87.254.42 on 09/05/12
For personal use only.

Weale (9). The piezometers were contained in a thick-walled stainless-steel pressure vessel which was immersed in a thermostatic oil bath (25.00 ± 0.02 °C), and pressure was applied with hydraulic oil from an air-driven mechanical pump (Autoclave Engineers, Inc., Erie, Pa.). Pressures at the pressure-vessel head were measured with an accuracy of ± 5 atm with a 40 cm diameter Heise Bourdon gauge (0–4100 atm, calibrated against a deadweight pressure balance), which was fitted with a microswitch to activate the pump to maintain a preselected pressure. Compressions were measured at 250 atm intervals up to 1000 atm, and thereafter at 500 atm intervals to 4000 atm, except 3500 atm.

The compressions so measured were reproducible to within 1%; the compression of water at 1000 atm was measured occasionally as a check and found to be within 1% of Gibson and Loeffler's (10) value of 0.0399. The accuracy of the compression data is thus of the order of ± 1%, except at the lowest pressures, which were less easily controllable.

Determination of K at Atmospheric Pressure

The procedure followed was similar to that described by Emerson and Graven (7). Chromium nitrate solution (*ca.* 0.0667 *M*, 25.0 ml) and sodium perchlorate solution (1.6 *M*, 25.0 ml) were mixed in a 100 ml graduated flask, brought to the desired temperature, and treated slowly under vigorous magnetic stirring with 45 ml of a tempered aqueous solution containing 1.0–9.0 ml of 0.1 *M* sodium hydroxide. It was imperative to avoid the formation of pockets of high p*H* in the mixture, otherwise hydrolytic polymerization resulted and led to inconsistent K_a values. The solutions were made to the mark with water.

The p*H* of stirred, thermostatted samples of the solutions was measured with a Beckman Research Model p*H* meter fitted with a Beckman No. 41263 glass electrode. The reference electrode was an Orion No. 90-02-00 double junction calomel electrode with ammonium nitrate solution as the connecting electrolyte. The assembly was standardized against 0.0500 *M* potassium hydrogen phthalate solution, for which p*H* = 4.005 at 5 and 25° (11). The p*H* of a chromium(III) solution was monitored continuously while the optical absorbance of separate samples of the same solution was being measured on a Cary Model 15 spectrophotometer at 450, 440, 430, and 420 mμ in a conventional 2.00 cm cell or in the high-pressure spectrophotometer cell (see below) at atmospheric pressure.

Temperature control (± 0.1°) of the optical cell was achieved with a thermostatable cell compartment (Cary No. 1540500) which was augmented with a thermostatable cell jacket (Cary No. 1540750) when the conventional cells were used. A solid aluminum mounting-block was used to improve thermal contact between the high-pressure cell and the compartment walls. Solution temperatures were measured with calibrated thermistor thermometer probes (Atkins Technical).

The total chromium content of the solutions was determined spectrophotometrically as CrO_4^{2-}, after oxidation with alkaline hydrogen peroxide.

Spectrophotometry at High Pressures

The spectrum of hexaaquochromium(III) nitrate in 0.4 *M* perchloric acid was studied as a function of pressure over the wavelength range 700–350 mμ using a Cary Model 15 spectrophotometer and an Aminco No. 41-11551 high-pressure spectrophotometer cell with sapphire windows and a Hastelloy C interior. The optical path length in the solution cavity was 2.0 cm. Pressure was transmitted with hydraulic oil from a hand-pump through a 10:1 intensifier (Autoclave Engineers, Inc.) designed for service to 5 kbar.

To avoid direct contact between the hydraulic oil and the solution under investigation, pressure was transmitted to the solution through a separator vessel (Aminco), which consisted of a Hastelloy-C-lined cylinder containing a free piston. The pressure was measured at the separator, with a 40 cm Heise Bourdon gauge (0-4100 bar, ± 4 bar).

Determination of K at High Pressures

The high-pressure spectrophotometer cell was brought to the desired temperature (± 0.05°) before filling it with the thermostatted solution (freshly prepared and analyzed as described for experiments at atmospheric pressure) and was placed in the thermostatted cell compartment of the spectrophotometer. The temperature of the cell was measured using a calibrated thermistor inserted in a narrow well drilled close to the solution cavity. Good temperature control (± 0.1°) was maintained throughout each experiment at 25°, but some difficulty was experienced in maintaining constant temperatures near 5°.

The optical absorbances of the solutions were measured at 450, 440, 430, and 420 mμ at 500 bar intervals up to 3 kbar. Pressure was increased slowly (over about 5 min for each 500 bar interval); optical measurements extended over about 5 min in each case and absorbance readings were steady to within 0.001 unit. The optical measurements were repeated while decreasing the pressure from 3 kbar over the same 500 bar intervals, and were the same (± 0.002) as those obtained while increasing the pressure.

The efficiency of temperature equilibration between the solution and the high-pressure spectrophotometer cell was checked by injecting water (25, 35, and 45°) into the cell (23°) and recording the cell and solution temperatures (± 0.1°) with thermistors as a function of time. The liquid temperature decayed approximately exponentially to the constant temperature of the cell, with a half-period of about 60 s, so that a 10° differential effectively disappeared within 7 min.

Results

Compression Studies

We define the compression k of a liquid at a pressure P as

$$k = (V_0 - V_p)/V_0, \quad [6]$$

where V_0 and V_p are the specific volumes of the liquid at atmospheric pressure and pressure P, respectively. Our data were analyzed with a least-squares computer program in terms of the modified Tait equation

$$k = \rho \log_{10} (1 + P/\pi) \quad [7]$$

TABLE 1
Parameters in Tait eq. 7

Solute	Concentration (M)	k_{obs} 1000 (atm)	ρ	π (katm)	π (kbar)
$HClO_4$	0.1	0.0403	0.261	2.32	2.35
	0.5	0.0396	0.250	2.26	2.29
	1.0	0.0390	0.253	2.37	2.40
$LiClO_4$	0.1	0.0393	0.245	2.19	2.22
	0.5	0.0389	0.247	2.27	2.30
	1.0	0.0372	0.265	2.64	2.68
$NaClO_4$	0.1	0.0394	0.266	2.46	2.49
	0.5	0.0379	0.239	2.24	2.27
	1.0	0.0354	0.252	2.58	2.61
NaCl*	1.0	0.0365	0.293	3.01	3.05
None	—	0.0402	0.321	3.02	3.06

*Interpolated from data of Adams (8).

where ρ and π are constants for a given liquid and temperature. Table 1 lists averaged values of k measured at 1000 atm and values of ρ and π which reproduce the experimental data to within about ± 1% over the range 750–4000 atm. The measurements made at 250 and 500 atm were less reliable than those at higher pressures and consequently the fit was somewhat poorer. In all cases, however, the Tait parameters of Table 1 reproduce the observed k values to within 0.0010, and are therefore accurate enough for volumetric calculations at least.

The four-parameter equation proposed by Adams (8) gave a closer fit of the data than did eq. 7, but convergence of the computation was not achieved in all cases.

Determination of K at Atmospheric Pressure

If α and β are the molar absorbance indices of $Cr(H_2O)_6^{3+}$ and $Cr(H_2O)_5OH^{2+}$, respectively, and C is the total chromium(III) concentration, then the optical absorbance A (per cm path length) is given (7) by eq. 8.

$$[8] \quad A = (\alpha[H^+] + \beta K)C/(K + [H^+])$$

In our experiments $[H^+]$ is the activity of hydrogen-ion at ionic strength 0.5 M, as measured with a glass electrode. The spectrum of $Cr(H_2O)_6^{3+}$ in 0.4 M perchloric acid gave α. For each series of measurements at a given temperature T and wavelength λ, nine pairs of corresponding $[H^+]$ and A values were fitted to eq. 8 with a least-squares computer program, and values of K and β were obtained with typical standard deviations of ± 8 and ± 3%, respectively (Table 2). These nine data pairs referred to solutions, the optical absorbance of which was constant (± 0.002) and the pH of which did not decrease by more than 0.010 pH unit over 2 h, i.e., to solutions for which hydrolytic polymerization (eq. 5) was negligible in the time-span of these experiments and those conducted at high pressure. At 25°, these criteria placed the upper limit of pH at 3.90, while the lower limit (pH 2.96) was set by those solutions to which no sodium hydroxide had been added.

TABLE 2
Hydrolysis constant K of $Cr(H_2O)_6^{3+}$ and molar absorbancy indices α and β of $Cr(H_2O)_6^{3+}$ and $Cr(H_2O)_5OH^{2+}$, at atmospheric pressure and ionic strength 0.5 M

T,°C	λ, mμ	α	β	10^5 K, M
5.4	450	6.2	26.1	2.35
	440	8.5	27.9	2.48
	430	11.5	29.2	2.37
	420	14.0	26.8	2.41
23.0	450	6.5	27.6	6.70
	440	8.9	30.4	6.56
	430	11.8	30.8	6.55
	420	14.3	28.4	6.32
25.0	450	7.0	27.9	7.10, 7.41
	440	8.5	30.5	7.06, 7.45
	430	12.5	—	—
	420	15.0	—	—

The averaged K data of Table 2, together with that of Bjerrum and Jørgensen (12) for 20.0° and the same ionic strength, give a good linear plot of ln K *vs.* T^{-1}, from which we find $\Delta H^0 = 9.2_5$ kcal mole^{-1}; this compares favorably with $\Delta H^0 = 9.4 \pm 0.4$ kcal mole^{-1} reported by Postmus and King (13). It follows that tempera-

Can. J. Chem. Downloaded from www.nrcresearchpress.com by 210.87.254.42 on 09/05/12
For personal use only.

Can. J. Chem. Downloaded from www.nrcresearchpress.com by 210.87.254.42 on 09/05/12
For personal use only.

ture fluctuations of 0.2° in our experiments would result in an error in K of 1.0%, which is negligible.

Spectrum of Hexaaquochromium(III) Ion at High Pressures

Compression to 4 kbar of a solution of chromium(III) nitrate in 0.1 M perchloric acid resulted in shifts of the 570 and 407 mμ maxima of $Cr(H_2O)_6^{3+}$, and the 300 mμ maximum of NO_3^-, of approximately 5, 4, and 2 mμ toward shorter wavelengths. The intensities of these maxima at 4 kbar exceeded the values, calculated from atmospheric pressure data on the basis of compression alone, by 11, 7, and 4%, respectively, although the bandwidths were not appreciably affected. Absorbances on the red side of the bands, notably in the region 430–450 mμ, were not so much affected by pressure, because the compressional increase in intensity is partly counteracted by the hypsochromic shift of the band. Nevertheless, it became clear that absorbance indices at high pressures must be determined experimentally.

Determination of K at High Pressure

In principle, absorbance data obtained for chromium(III) solutions at high pressure can be analyzed in terms of eq. 8 to yield the high-pressure parameters K_p and β_p. The absorbancy index α_p of $Cr(H_2O)_6^{3+}$ was obtained as above (uncorrected for compression of the medium), but $[H^+]_p$ could not conveniently be measured directly. However, for any given solution for which the pH, C, and K at atmospheric pressure are known, the material balance of eq. 4 determines $[H^+]_p$ in terms of $[Cr(H_2O)_6^{3+}]_p$ and $[Cr(H_2O)_5OH^{2+}]_p$, and these in turn can be expressed as functions of C_p, α_p, β_p, and K_p. It is convenient to define a function F for a solution at atmospheric pressure.

$$[9] \qquad F = [H^+] + C[H^+]/(K + [H^+])$$

If all concentrations, absorption indices, and K are on the *molal* scale, K_p and β_p can be calculated from eq. 10 (in which the subscripts P have been dropped for clarity).

$$[10] \qquad F = \frac{A\alpha K - A\beta K - A^2 + A\alpha C - \alpha\beta CK + K\beta^2 C + A\beta C - \alpha\beta C^2}{\alpha^2 C - A\alpha - \alpha\beta C + A\beta}$$

In practice, experimental values of A, α, C, and F were left in molar units valid at atmospheric pressure for fitting to eq. 10 with a least-squares computer program, and the values of K so obtained for each pressure were subsequently converted to K_m (molal units) using the measured density of the solutions (1.032 g cm^{-3} at atmospheric pressure). True molar hydrolysis constants, K_c, were calculated from the raw K values using the compression data of Table 1, it having been established that the compressions of the solutions were virtually identical with those of 0.5 M sodium perchlorate. The results are summarized in Table 3; the K_m values are the average of four determinations at different wavelengths, the standard deviation in K_m being about 9% in all cases.

The molal values of β calculated from eq. 10 at each pressure had standard deviations of 2% in all cases, and increased uniformly with pressure. The molar values of β at 440 mμ were essentially constant, within the experimental uncertainty, but this was probably fortuitous, since the 435 mμ maximum of $Cr(H_2O)_5OH^{2+}$ appeared to move toward the violet with increasing pressure.

TABLE 3

Molal (K_m) and molar (K_c) hydrolysis constants for hexaaquochromium(III) ion*

P, bars	10^5K_m, m	10^5K_c, M
1	7.4	7.3
500	8.1	7.8
1000	9.5	8.9
1500	10.2	9.4
2000	10.0	9.2
2500	11.0	9.9
3000	12.1	10.8

*T = 25.0°, ionic strength = 0.5 M.

A similar set of experiments was run at 5.4°, with a view to eliminating any possibility of hydrolytic polymerization, but the K values calculated from eq. 10 had unacceptably large standard deviations, because of difficulties in controlling the temperature and preventing condensation of water vapor on the optical surfaces (despite flushing the cell compartment with dry nitrogen at 5°). However, a general

Can. J. Chem. Downloaded from www.nrcresearchpress.com by 210.87.254.42 on 09/05/12
For personal use only.

increase in K_m with pressure, of the same order of magnitude as at 25°, was noted.

At either temperature, heating of the solution by compression could constitute a major source of error. However, the rate of relaxation of a temperature differential was sufficiently rapid that any significant temperature deviations would have been manifested by inconstant optical absorbance readings. Furthermore, it is extremely improbable that such good agreement between absorbance measurements made with ascending pressure and those made with descending pressure would have been achieved, had re-equilibration of the solution and cell temperatures not occurred within the course of measurements at a given pressure.

Discussion

Pressure Dependence of K

The data collected by Hamann (1, 2) and by Weale (3) show that dissociations of electrically neutral aqueous acids HA (reaction 1) are accompanied by a marked contraction in volume i.e., dissociation of HA is strongly favored by increasing pressure. The magnitude of the molal volume change ΔV^0 varies considerably with HA, but a value of -13 cm^3 mole^{-1} is typical. For mononegative acids HA^-, ΔV^0 is typically about -28 cm^3 mole^{-1}. These data suggest that, if the Drude–Nernst equation (2) is applicable, i.e., if the "electrostrictive" volume change ΔV_{el} is essentially proportional to $-\Delta Z^2$ for the reaction, then ΔV^0 is made up very largely of ΔV_{el} for the ionization of HA ($\Delta Z^2 = +2$) and HA^- ($\Delta Z^2 = +4$). Again, for the dissociation of weak, electrically neutral aqueous bases B (reaction 2), ΔV^0 is typically about -27 cm^3 mole^{-1}, so that, using $\Delta V^0 = -21.3$ cm^3 mole^{-1} for the autoprotolysis of water (14), we estimate $\Delta V^0 = +6$ cm^3 mole^{-1} for the acid dissociation of BH^+, which is not inappropriate for $\Delta Z^2 = 0$.

These considerations lead to the expectation that for the hydrolysis of $Cr(H_2O)_6^{3+}$, for which $\Delta Z^2 = -4$ (reaction 4), ΔV^0 might be about $+25$ cm^3 mole^{-1}. Adamson and Stranks (5) have predicted $\Delta V^0 \sim +20$ cm^3 mole^{-1} for the analogous hydrolysis of thallium(III), on the basis of Noyes' treatment (6). Finally, Hepler's correlation (15) of ΔV^0 with ΔS^0 for the dissociation of a variety of aqueous acids predicts $\Delta V^0 \sim +18$ cm^3 mole^{-1}, since our temperature-dependence studies give $\Delta S^0 = +12.1$ cal deg mole^{-1} at 25° and ionic strength 0.5 M.

It is therefore surprising to find that the data of Table 3 require a *small, negative* value of ΔV^0. Within the limits of the 9% uncertainty in K, one can represent the data of Table 3 by eq. 11, which is a least-squares fit (K in molal units, P in kilobars).

$$[11] \qquad \ln K = 0.151P - 9.474$$

This implies that ΔV^0 is -3.8 ± 0.7 cm^3 mole^{-1} and is essentially independent of the pressure. A precedent for a ΔV^0 value of this magnitude for metal-ion hydrolysis can be found in Spiro, Revesz, and Lee's (16) dilatometric value of $\Delta V^0 = +20.6$ cm^3 mole^{-1} for reaction 12 at low ionic strength and atmospheric pressure; combination of this value with $\Delta V^0 = -21.3$ cm^3 mole^{-1} for the autoprotolysis of water under similar conditions (14) leads to $\Delta V^0 = -0.7$ cm^3 mole^{-1} for reaction 13, which is closely analogous to reaction 4.

$$[12] \quad Co(NH_3)_5OH_2^{3+} + OH^- = Co(NH_3)_5OH^{2+} + H_2O$$

$$[13] \quad Co(NH_3)_5OH_2^{3+} = Co(NH_3)_5OH^{2+} + H^+$$

The failure of ΔV^0 for reactions such as [4] and [13] to correlate with ΔV^0 for the dissociation of simple protonic acids probably originates in the effective spreading of the triple positive charge of the aqueous metal ion over the surface of an unusually large sphere, since the central cation is complexed with aquo (or ammine) ligands. Thus, the reduction of the formal charge of this large species by one unit, together with the creation of a free aqueous proton, may not result in a significant dissipation of charge density, so that ΔV_{el} may be much less positive than predicted on the basis of naive applications of the Drude–Nernst equation.

Compression Data

These data were obtained for purely utilitarian purposes, and do not merit detailed theoretical attention. It is sufficient to note that the compressions decrease with increasing concentration of a given electrolyte, and also decrease in the order $HClO_4 > LiClO_4 > NaClO_4$. The compressions of 1.0 M sodium chloride (estimated by interpolation from the data of Adams (8))

and 1.0 *M* sodium perchlorate are similar, as are those of water and 0.1 *M* perchloric acid, although the parameters of the Tait equation differ considerably in these pairs.

We thank Atomic Energy of Canada, Ltd., for financial support of this work through Whiteshell Nuclear Research Establishment, and Dr. G. Guastalla for his contributions in the construction of the apparatus and in some preliminary experiments.

1. S. D. HAMANN. The physicochemical effects of pressure. Butterworths Scientific Publications, London. 1957. pp. 149–159.
2. S. D. HAMANN. High pressure physics and chemistry. Vol. 2. *Edited by* R. S. Bradley. Academic Press, New York. 1963. p. 146ff.
3. K. E. WEALE. Chemical reactions at high pressures. E. and F. N. Spon, Ltd., London. 1967. pp. 121–126.
4. K. R. BROWER. J. Amer. Chem. Soc. **90**, 5401 (1968).
5. M. G. ADAMSON and D. R. STRANKS. J. Chem. Soc. **D** (Chem. Commun.) 648 (1967).
6. R. M. NOYES. J. Amer. Chem. Soc. **86**, 971 (1964).
7. K. EMERSON and W. M. GRAVEN. J. Inorg. Nucl. Chem. **11**, 309 (1959).
8. L. H. ADAMS. J. Amer. Chem. Soc. **53**, 3769 (1931).
9. D. M. NEWITT and K. E. WEALE. J. Chem. Soc. 3092 (1951).
10. R. E. GIBSON and O. H. LOEFFLER. J. Amer. Chem. Soc. **63**, 898 (1941).
11. A. I. VOGEL. A textbook of quantitative inorganic analysis. 3rd ed. J. Wiley and Sons, Inc., New York. 1961. p. 911.
12. J. BJERRUM and E. JØRGENSEN. J. Inorg. Nucl. Chem. **8**, 313 (1958); Acta Chem. Scand. **12**, 1047 (1958).
13. C. POSTMUS and E. L. KING. J. Phys. Chem. **59**, 1208 (1955).
14. A. BODANSZKY and W. KAUZMANN. J. Phys. Chem. **66**, 177 (1962).
15. L. G. HEPLER. J. Phys. Chem. **69**, 965 (1965).
16. T. G. SPIRO, A. REVESZ, and J. LEE. J. Amer. Chem. Soc. **90**, 4000 (1968).

Can. J. Chem. Downloaded from www.nrcresearchpress.com by 210.87.254.42 on 09/05/12
For personal use only.

Can. J. Chem. Downloaded from www.nrcresearchpress.com by 210.87.254.40 on 09/05/12
For personal use only.

Infrared spectra and the molecular conformations of some aliphatic amines

P. J. KRUEGER AND J. JAN
Department of Chemistry, University of Calgary, Calgary 44, Alberta

Received July 31, 1969[1]

The presence of two CD stretching bands for $(CH_3)_2CDNH_2$ in dilute CCl_4 solution is interpreted in terms of two conformations differing in enthalpy by 0.12 ± 0.02 kcal/mole. The low frequency component is assigned to the thermodynamically more stable conformer with the CD bond *trans* to the N lone pair. Similar rotational isomerism is observed in $CH_3CD_2NH_2$ and $CD_3CH_2NH_2$. Band contours for the NH stretching vibration in some *N*-alkyl anilines reported previously are also interpreted in terms of rotational isomerism and a change in hybridization of the N atom when the lone pair is *trans* to an α-CH bond, which results in an increase in ν_{NH} and a decrease in ν_{CH}.

Canadian Journal of Chemistry, 48, 3229 (1970)

Introduction

In some recent publications dealing with restricted rotation about the C—N bond and rotational isomerism in amines (1, 2) the doublet character of the NH stretching vibration was attributed largely to variations in the steric effect of R in $CH_3—CH_2—NH—R$ in different molecular conformations. This paper provides further evidence for rotational isomerism in amines, and re-interprets the doubling of the NH bands in secondary amines. Following the arguments advanced in the interpretation of the i.r. spectra of some quinolizidine alkaloids (3) and cyclic imines (4), conformers with an α-CH bond *trans* to a lone pair of electrons on N are considered to be subject to a "lone pair-bond" interaction (5) which is equivalent to a specific partial electron delocalization from N into the N—C bond (6). This can also be described as a change in hybridization at N which leads to an increase in ν_{NH} and a decrease in ν_{CH}.

Experimental

Spectra were obtained in a conventional manner using a Perkin–Elmer Model 621 spectrophotometer and matched 2.0 or 5.0 cm quartz (Infrasil) cells to avoid complications due to association. Temperature dependence studies were carried out in standard 1 mm cells. Spectroscopic quality CCl_4 was used as solvent. The spectra of aromatic amines were obtained in 2.0 cm cells at concentrations of the order of 0.004–0.005 *M*, while aliphatic amines were investigated at pathlengths of 5.0 cm, using 0.01–0.02 *M* concentrations.

The $(CH_3)_2CDNH_2$ was prepared by $LiAlD_4$ (Bio Rad Laboratories, 99 atom % D) reduction of acetone oxime, followed by equilibration of the amino protons (17). The n.m.r. spectrum of the product showed that the CH septet found at 6.96 τ in the normal compound was gone, and the methyl doublet centered at 9.00 τ had collapsed into a singlet. The $CH_3CD_2NH_2$ was prepared by $LiAlD_4$ reduction of acetonitrile; here the normal methyl triplet at 8.95 τ had collapsed to a singlet. An analogous reduction of CD_3CN (Merck, Sharpe and Dohme of Canada, Ltd., 99 atom % D) with $LiAlH_4$ gave $CD_3CH_2NH_2$, in which the n.m.r. quartet of the methylene group found in normal ethylamine had collapsed to a single line at 7.30 τ.

All other compounds used were commercial products purified by distillation or sublimation.

Results and Discussion

2-Propylamine-2-C-d$_1$

Rotational isomerism in $(CH_3)_2CDNH_2$ is firmly established through the appearance of two ν_{CD} bands (2156 and 2081 cm^{-1}) in dilute CCl_4 solution (Fig. 1 and Table 1). The high frequency component, which has shoulders on both sides, corresponds to conformer **1** with a "free" or "normal" CD bond, while the low frequency component corresponds to conformer **2** with a lone pair/α-CD interaction.

In conformer **2** the decrease in ν_{CD} can be understood in terms of the following electron shifts which result in a decrease of the CD stretching force constant accompanied by an increase in the s-character of the NH bonds.[2] Hamlow *et al.* (6) have rationalized this *trans* interaction in terms of partial participation of the lone pair in a σ* C—H(D) orbital on the adjacent carbon atom. In effect, this allows some overlap

[1]Revision received June 22, 1970.

[2]This should result in a corresponding *increase* in ν_{NH} as that stretching force constant increases. While this has been observed in secondary amines (4) and is discussed further later in this paper, a doubling of the NH_2 ν_{asym} and ν_{sym} stretching vibrations in primary aliphatic amines cannot be detected. However, both bands are inherently very broad and this feature may be masked. Some spectra were obtained of the "secondary amine" NH stretching vibration in *n*-propylamine-NHD at various levels of deuteration in an attempt to resolve two components. The results were inconclusive, although the NH band is broad.

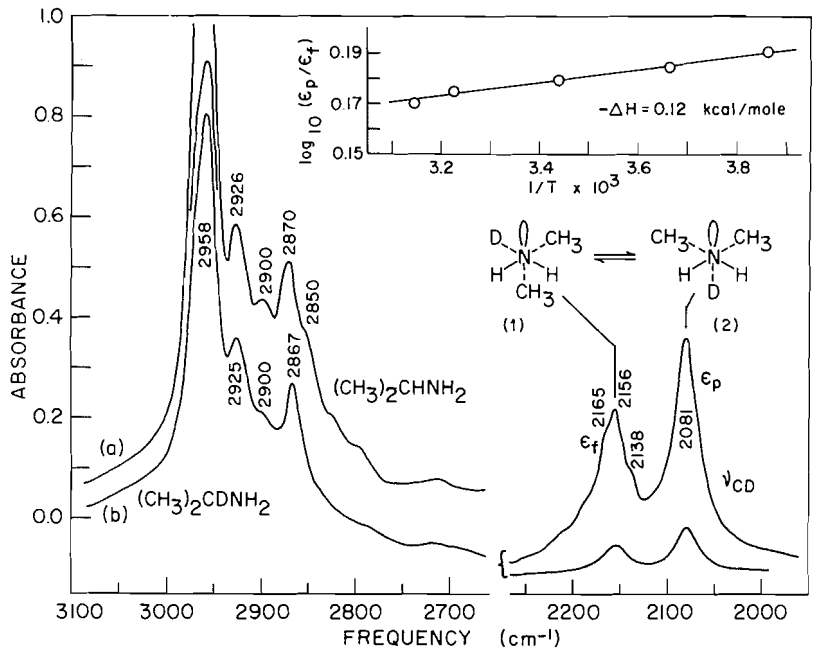

FIG. 1. Infrared spectra of (*a*) $(CH_3)_2CHNH_2$ and (*b*) $(CH_3)_2CDNH_2$ in the CH and CD stretching regions (dilute CCl_4 solutions) and temperature dependence of conformational equilibrium.

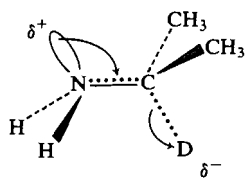

between the σ* orbital and the lone pair orbital, generating some C⋯N double bond character. This postulated orbital interaction has been used to explain the decrease in ν_{CH} in the i.r. and the increased shielding of the α-proton in n.m.r. spectra (6, 7).

From the temperature dependence of the peak heights of the CD bands a value of $\Delta H = 0.12 \pm 0.02$ kcal/mole is obtained, with conformer **2** being thermodynamically more stable. Stabilization by means of the *trans* lone pair/α-CD interaction is therefore suggested.

The "normal" CD peak is flanked by two shoulders at 2165 and 2138 cm^{-1}, respectively, both of which become more prominent at lower temperature. An additional weak band appears at 2110 cm^{-1} at low temperatures. The features associated with the main CD band of **1** at 2156 cm^{-1} could arise from sub-minima in the potential energy function which do not coincide with the traditional exact staggering of bonds on adjacent atoms.[3] Recent calculations by Scott and Scheraga (9) have demonstrated that even in propane the rotations about the two C—C bonds are correlated due to near-neighbor nonbonded interactions. For long chain molecules (C_5 and beyond) their calculations indicate that the traditional procedure of assuming that each bond in a hydrocarbon molecule can exist in three rotational isomeric states is an oversimplification, and that more minima occur.

If such additional energy minima exist for rotation about C—C bonds, then it is even more likely that they exist for rotation about a C—N bond where the C has two methyl substituents (with energy minima for rotation about the C—C bond) and the N a lone pair of electrons. It may also be significant that these additional bands are associated with the main CD band of **1**, where rotation about the C—N bond is postulated to be less restricted than in **2**. In **2** it is proposed that the lone pair interaction with the C—N and C—D bonds stabilizes a more rigid *trans* geometry of

[3]While rotation in solution has been well-documented (8), it appears unlikely that the contours observed can arise from rotation of a molecule as large as this. Also, the temperature dependence of the shoulders and the fact that the CD band of **2** does not have shoulders cannot be accounted for in this way.

Can. J. Chem. Downloaded from www.nrcresearchpress.com by 210.87.254.40 on 09/05/12
For personal use only.

TABLE 1

Methyl and methylene stretching frequencies in amine conformers (cm^{-1})

Mode	Conformer	$(CH_3)_2CHNH_2$	$(CH_3)_2CDNH_2$	$CH_3CH_2NH_2$	$CH_3CD_2NH_2$	$CD_3CH_2NH_2$	ν_{CH}/ν_{CD}
Asym. CH_3		2958, 2926	2958, 2925				
Sym. CH_3		~2900, 2870	2900, 2867				
CH(D)	1	~2900	2156				~1.345
CH(D) "pert."	2	2850	2081				1.370
Asym. $CH_3(CD_3)$	3			2961	2958	2225	1.331
Asym. $CH_3(CD_3)$ "pert."	4, 4′			2924	2928	2214	1.321
Sym. $CH_3(CD_3)$	3			2896	2894	2118	1.367
Sym. $CH_3(CD_3)$ "pert."	4, 4′			2860	2862	2073	1.380
Asym. $CH_2(CD_2)$	3			2938	2207	2930	1.331
Asym. $CH_2(CD_2)$ "pert."	4, 4′			2906	2175	2911	1.336
Sym. $CH_2(CD_2)$	3			—	2116	2875	1.359
Sym. $CH_2(CD_2)$ "pert."	4, 4′			2840	2077	2845	1.367

the conformer. These satellite bands are also found in $(CH_3)_2CDOH$ and $(CH_3)_2CDSH$ (10).

Recently Brignell *et al.* (11) have evaluated a scheme of "standard intramolecular interactions" on the basis of which energy differences between conformations may be estimated. In terms of this scheme, conformer **1** suffers three "propane interactions" and an "ethylamine interaction", whereas **2** undergoes two "propane interactions" and two "ethylamine interactions", predicting that the free energy of **1** should exceed that of **2** by 0.2 kcal/mole. Since this is a crude approximation, the agreement with the experimental ΔH value is acceptable.[4]

Assignments in the CH and CD stretching region of $(CH_3)_2CHNH_2$ and $(CH_3)_2CDNH_2$ are given in Table 1.

Ethylamine-1-C-d_2 and Ethylamine-2-C-d_3

The *trans* lone pair/α-CH interaction was investigated further with regard to its effect on the characteristic ν_{asym} and ν_{sym} stretching vibrations of the methylene group in a compound where the force constant of only one of the CH bonds is lowered, while the other remains unchanged (or is increased since it is bonded to a C atom with partial sp^2 character). Methyl and methylene stretching vibrations are separated cleanly in $CH_3CD_2NH_2$ and $CD_3CH_2NH_2$, as shown in Fig. 2.

Four CD stretching vibrations are observed for $CH_3CD_2NH_2$, and these are interpreted as ν_{asym} and ν_{sym} modes of a "normal" CD_2 group as in conformer **3**, and corresponding modes shifted to lower frequencies arising from "perturbed" CD_2 groups in the mirror-image conformers **4** and **4′**. The four corresponding CH_2 vibrations can be identified in $CD_3CH_2NH_2$, and hence the complex CH stretching absorption of $CH_3CH_2NH_2$ becomes much more intelligible (Table 1). Conformers **4** and **4′** appear to be thermodynamically more stable than **3** although no accurate enthalpy differences were obtained.

The CD_3 group in $CD_3CH_2NH_2$ also gives rise to two ν_{asym} and two ν_{sym} stretching bands (Fig. 2*c*). This is consistent with the conformers presented, as the methyl groups in **4** and **4′** are likely to be influenced more directly by the lone pair than in **3**, and they are also attached to methylene carbon atoms of slightly different character. However, it must also be borne in mind that the ν_{asym} CH stretching vibration of methyl groups is known to split into two components in some cases because of an unsymmetrical local environment which removes the degeneracy (12).

Conformers **3** and **4** are clearly distinguishable in the skeletal region, where Wolff and Ludwig (13) have shown that the "symmetric" CCN stretching vibrations lie at 881 and 891 cm^{-1}, respectively, in the Raman spectrum of the vapor. A doublet was also resolved in the Raman spectrum of the liquid at low temperatures. The high frequency component is about twice as intense as the low frequency component, in keeping with the statistical weighting of two for **4**. These observations are in agreement with a higher C—N bond order in **4** than in **3**.

N-Alkylanilines

In *N*-alkylanilines the NH stretching bands are

[4]Assuming that the entropy difference between **1** and **2** is small.

Can. J. Chem. Downloaded from www.nrcresearchpress.com by 210.87.254.40 on 09/05/12
For personal use only.

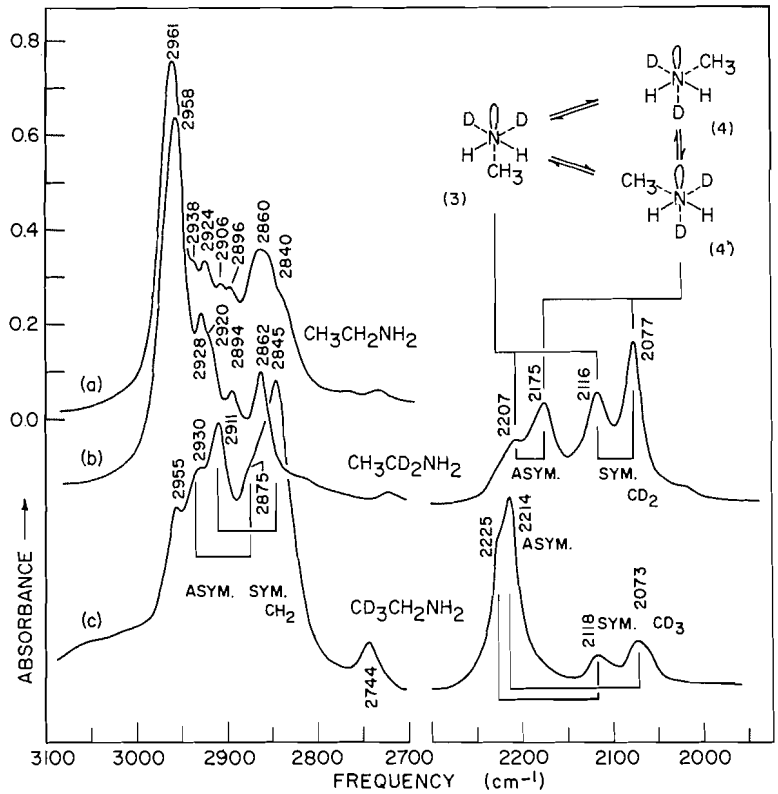

FIG. 2. Infrared spectra of (*a*) $CH_3CH_2NH_2$, (*b*) $CH_3CD_2NH_2$, and (*c*) $CD_3CH_2NH_2$ in the CH and CD stretching regions (dilute CCl_4 solutions).

considerably narrower than in alkyl amines, and shoulders on these bands in certain compounds have been noted previously (1, 2). Extensive delocalization of the lone pair into the aromatic ring reduces the intensity of the "perturbed" NH band (at higher frequency than the normal NH band), and possibly also the population of conformer **5′** relative to **6**,[5] assuming that **5** is not populated because of steric interference of the methyl group with an *ortho* ring H atom. The high frequency NH component therefore only appears as a shoulder on the main band (Fig. 3 and Table 2), except where it is the only band expected, as in *N*-methylaniline. Here all conformers are equivalent (R = H) and of the type **5′**, which is consistent with a single NH band at 3438 cm^{-1}, while in *N*-*t*-butylaniline this interaction is entirely precluded and a single low frequency band at 3418 cm^{-1} is observed, consistent with conformers essentially of the type **6**. *N*-Isopropylaniline appears to be similar to *N*-*t*-butylaniline, and conformer **7′** is probably

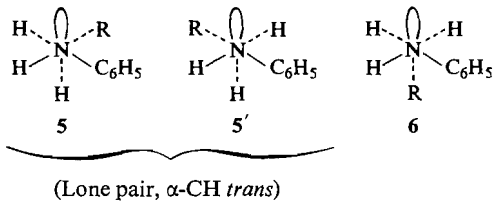

[5]The extinction coefficient of ν_{NH} in **5′** is likely to be greater than in **6**, so that relative band intensities cannot be related directly to conformer populations.

TABLE 2

NH Stretching frequencies in *N*-alkylaniline conformers*

Substituents	ν_{NH} (cm^{-1}) Conformer **5′**	Conformer **6**
p-Cl—N—Et	3435 (sh)	3418
N—Et	3435 (sh)	3417
m-Me—N—Et	3435 (sh)	3412
N—Me	3438	—
N-*i*-Pr	—	3415†
N-*t*-Bu	—	3418†

*Apparent frequency positions of overlapped bands.
†Conformer 7′, or equivalent.

Can. J. Chem. Downloaded from www.nrcresearchpress.com by 210.87.254.40 on 09/05/12
For personal use only.

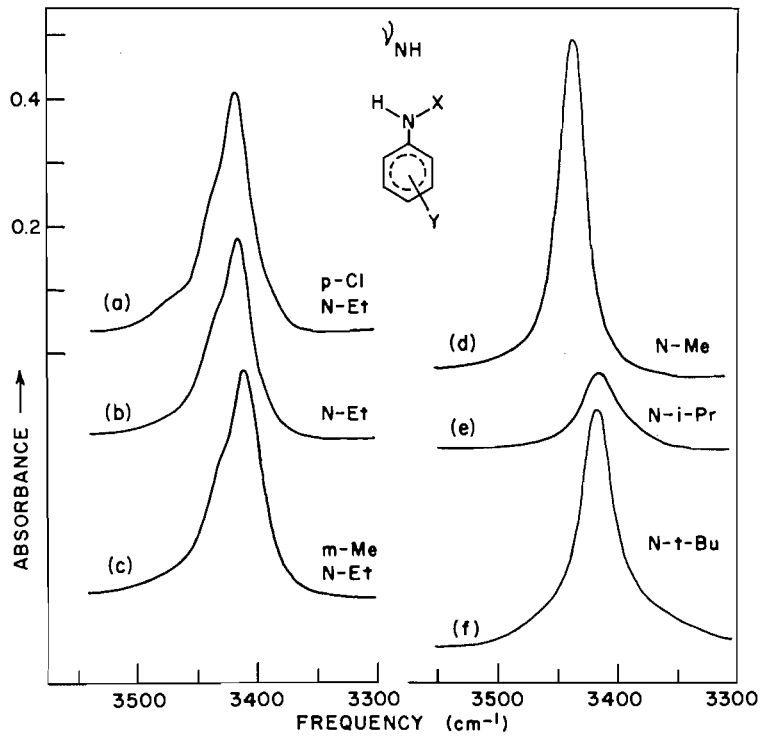

FIG. 3. Fundamental NH stretching vibrations of *N*-alkylanilines in dilute CCl_4 solution: (*a*) *p*-chloro-*N*-ethylaniline, (*b*) *N*-ethylaniline, (*c*) *m*-methyl-*N*-ethylaniline, (*d*) *N*-methylaniline, (*e*) *N*-*i*-propylaniline, and (*f*) *N*-*t*-butylaniline.

favored because of greater steric interference between a methyl group and the ring H atom in **7** and **8**. While a shoulder at 3395 cm^{-1} on the

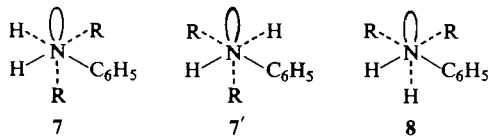

7 **7′** **8**

(Lone pair, α-CH *trans*)

main NH band of *N*-isopropylaniline has been noted (1, 2), we find this small and its relation to another type of conformer not consistent with the spectra in the CH region.

Figure 4 shows that only in *N*-alkylanilines in which conformers are expected with a *trans* N lone pair/α-CH relationship is significant CH absorption found below ~2860 cm^{-1} ("Bohlmann" band region, *cf.* ref. 7). Thus *N*-*t*-butylaniline and *N*-ethylbenzamide (lone pair delocalized into the amide system) have the lowest CH bands at 2868 and 2875 cm^{-1}, respectively. *N*-Isopropylamine behaves like *N*-*t*-butylaniline, for reasons suggested above. In *N*-methylaniline all three equivalent conformations contribute to the most intense CH band displaced downward to 2814 cm^{-1} ("perturbed" ν_{sym} of CH_3).[6] In *N*-ethylanilines the relatively weak CH absorption below ~2860 cm^{-1} is consistent with reduced electron density on N and the high population of conformer **6**, which has "normal" CH stretching frequencies.

The strong band near 2800 cm^{-1} in *N*-methylaniline has been used as a "characteristic group frequency" for the N—CH_3 group for some time (see ref. 14 for a review of the literature and a discussion of correlations). Its absence when the lone pair is delocalized has also been noted. This investigation supports the assignment of this band to a shifted ν_{sym} stretching mode of the CH_3 group and not to an overtone of the sym-CH_3 deformation mode. The absence of this band when the N lone pair is delocalized is then simply explained because the CH_3 stretching modes

[6]The "perturbed" ν_{asym} CH stretching vibrations of CH_3 and CH_2 groups are more difficult to locate since they are probably displaced less, and remain in the complex normal CH region.

Can. J. Chem. Downloaded from www.nrcresearchpress.com by 210.87.254.40 on 09/05/12
For personal use only.

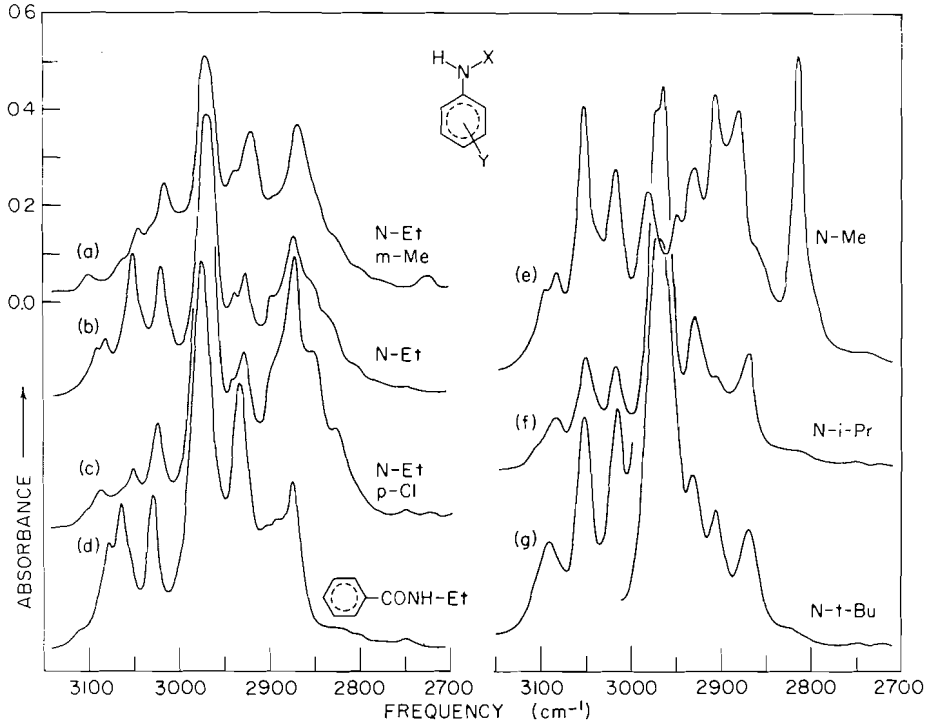

FIG. 4. Fundamental CH stretching vibrations in dilute CCl_4 solution: (*a*) *m*-methyl-*N*-ethylaniline (*b*) *N*-ethylaniline, (*c*) *p*-chloro-*N*-ethylaniline, (*d*) *N*-ethylbenzamide, (*e*) *N*-methylaniline, (*f*) *N*-*i*-propylaniline, and (*g*)*N*-*t*-butylaniline.

TABLE 3

Substituent effects on "perturbed" CH and NH stretching vibrations in *n*-alkyl amino compounds (measurements in dilute CCl_4 solution)

Compound	"Pert." ν_{sym} CH_3 stretch (cm^{-1})
$H_2N—NH—CH_3$	2780 (s)
$N—CH_3$	2780
$H_2N—CH_3$	2807
$H_2N—NH—CH(CH_3)_2$	2850 (w)

X	Hammett σ	"Pert." ν_{sym} CH_3 stretch (cm^{-1})	ν_{NH} (cm^{-1})*†	$\frac{1}{2}(\nu_{asym} + \nu_{sym})$ NH_2†	Δ (cm^{-1})‡
	X—⟨⟩—NH—CH_3			X—⟨⟩—NH_2	
p-$NHCH_3$	−0.84	2805	3418	3410	8
p-NH_2	−0.66	2806	3429	3414	15
p-OH	−0.37	2802	3425	3421	4
H	0	2813	3443	3439	4
p-COOH	+0.41	2821	3448	3454	−6
p-NO_2	+1.27	2825	3451	3463	−12

*"Perturbed" NH frequency; three equivalent conformers.
†From ref. 15, supplemented by new measurements.
‡$\Delta = \nu_{NH(CH_3)} - [\frac{1}{2}(\nu_{asym} + \nu_{sym})_{NH_2}]$ (cm^{-1}) .

Can. J. Chem. Downloaded from www.nrcresearchpress.com by 210.87.254.40 on 09/05/12
For personal use only.

Can. J. Chem. Downloaded from www.nrcresearchpress.com by 210.87.254.40 on 09/05/12
For personal use only.

occur in the normal CH region. The presence of two bands in the ranges 2825–2810 and 2775–2765 cm^{-1} as a "characteristic" feature of alkyl-$N(CH_3)_2$ (14) arises because of coupling of the vibrations of the two CH_3 groups through the N lone pair.

Substituent Effects

While the ring substituent effect on ν_{NH} in the *N*-ethylanilines is too small to be observed in the limited range of compound type investigated, it is evident from the "perturbed" ν_{sym} CH_3 stretching frequencies in *N*-methylanilines presented in Table 3. This frequency increases (*i.e.* becomes more "normal") as ring substituents become more electron-withdrawing. At the same time the anticipated increase in the "perturbed" ν_{NH}, which is clearly noticeable for strongly electron-donating ring substituents, disappears progressively as the *trans* lone pair/α-CH interaction falls off with the withdrawal of N electron density into the aromatic ring. Thus, while ν_{NH} in *N*-methylanilines with electron-donating ring substituents, *e.g.* in *p*-hydroxyaniline, is *greater* than $\frac{1}{2}(\nu_{asym} + \nu_{sym})$ for NH frequencies of corresponding anilines, it falls progressively as the Hammett σ value of substituents increases until it is *smaller* than $\frac{1}{2}(\nu_{asym} + \nu_{sym})$ for corresponding anilines, *e.g.* in *p*-nitroaniline (see Table 3).[7]

The substituent effect in aliphatic amines is demonstrated in Fig. 5, which shows the "perturbed" ν_{sym} stretching mode of CH_3 in CH_3NH_2 at 2807 cm^{-1}, while it is lowered to 2779 cm^{-1} in H_2NNHCH_3 where the electron density on the N atom adjacent to the methyl group is increased. *N*-Isopropylhydrazine shows weak "perturbed" CH absorption at 2850 cm^{-1}, as a broadening of the 2861 cm^{-1} band, which is consistent with the fact that only one of the three conformers which arise from rotation about the N—C bond has a *trans* lone pair/α-CH relationship.

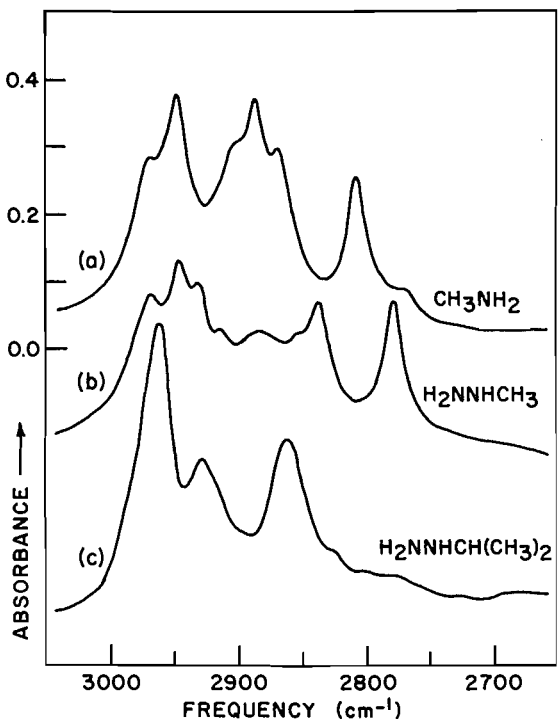

FIG. 5. Fundamental CH stretching vibrations in dilute CCl_4 solution: (*a*) methylamine, (*b*) *N*-methyl hydrazine, and (*c*) *N*-*i*-propyl hydrazine.

This research was supported by the U.S. Army Research Office, Durham, North Carolina, U.S.A., under Grant No. DA-ARO-D-31-124-G658.

1. M. OKI and K. MUTAI. Bull. Chem. Soc. Japan, **33**, 784 (1960).
2. A. PERRIER-DATIN, P. SAUMAGNE, and M. L. JOSIEN. Compt. Rendus, **259**, 1825 (1964).
3. J. SKOLIK, P. J. KRUEGER, and M. WIEWIOROWSKI. Tetrahedron, **24**, 5439 (1968).
4. P. J. KRUEGER and J. JAN. Can. J. Chem. This issue.
5. D. HADZI, J. JAN, and A. OCVIRK. Spectrochim. Acta, **25A**, 97 (1969).
6. H. P. HAMLOW, S. OKADA, and N. NAKAGAWA. Tetrahedron Lett. 2553 (1964).
7. F. BOHLMANN. Ber. **91**, 2157 (1958).
8. W. J. JONES and N. SHEPPARD. *In* Spectroscopy. *Edited by* M. J. Wells. Conference Report of the Hydrocarbon Research Group of the Institute of Petroleum, London. 1962. pp. 181–203.
9. R. A. SCOTT and H. A. SCHERAGA. J. Chem. Phys. **44**, 3054 (1966).
10. P. J. KRUEGER, J. JAN, and H. WIESER. J. Mol. Struct. **5**, 375 (1970).
11. P. J. BRIGNELL, K. BROWN, and A. R. KATRITZKY. J. Chem. Soc. (B), 1462 (1968).
12. H. WIESER, W. G. LAIDLAW, P. J. KRUEGER, and H. FUHRER. Spectrochim. Acta, **24A**, 1055 (1968), and references cited therein.
13. H. WOLFF and H. LUDWIG. Ber. der Bunsengesellschaft fuer phys. Chem. **68**, 143 (1964).
14. L. J. BELLAMY. Advances in infrared group frequencies. Methuen and Co., Ltd., London. 1968. pp. 4–5.
15. (*a*) P. J. KRUEGER and H. W. THOMPSON. Proc. Roy. Soc. Ser. A. **243**, 143(1957). (*b*) P. J. KRUEGER. Can. J. Chem. **40**, 2300 (1962). (*c*) P. J. KRUEGER. Can. J. Chem. **45**, 2135 (1967).
16. H. J. BERNSTEIN. Spectrochim. Acta, **18**, 161 (1962).
17. R. B. WAGNER and H. D. ZOOK. Synthetic Organic Chemistry. John Wiley and Sons, Inc., N.Y. 1953. p. 658.

[7]It has been shown that the arithmetic mean of ν_{asym} and ν_{sym} stretching frequencies of XH_2 groups is a good measure of the XH stretching force constant (16).

Can. J. Chem. Downloaded from www.nrcresearchpress.com by 210.87.254.6 on 09/05/12
For personal use only.

Conformational equilibria in some cyclic imines: NH and CH stretching vibrations and the axial lone pair

P. J. KRUEGER AND J. JAN
Department of Chemistry, University of Calgary, Calgary 44, Alberta

Received July 31, 1969[1]

The fundamental NH and CH stretching vibrations of a number of cyclic imines have been examined in dilute CCl_4 solution. A *trans* orientation of the N lone pair orbital and one or more hydrogen atoms on adjacent carbons lowers the relevant ν_{CH} ("Bohlmann" bands) and raises ν_{NH}, reflecting an increase in the s-character of the CH bond(s), consistent with a partial delocalization of the lone pair electrons into the CN bond. Conformations in which this interaction occurs are thermodynamically favored, and the ΔH values for the lone pair axial–equatorial equilibrium in piperidine, pyrrolidine, and indolene are estimated to be 0.4, 0.2, and 0.1 kcal/mole, respectively, in dilute CCl_4 solution.

The effects of hetero ring size, *N*-substitution, α-methyl substitution, and the solvent environment are investigated.

Canadian Journal of Chemistry, 48, 3236 (1970)

Introduction

Conformational problems which arise from different orientations of the nitrogen atom lone pair orbital in heterocyclic compounds (1*a*) have received much attention in the case of six-membered rings like piperidine or morpholine, and a variety of methods like i.r. spectroscopy (2–12), n.m.r. spectroscopy (12–22), microwave spectroscopy (23), and dipole moment measurements (24–30) have been employed. The results of these studies have not been uniformly consistent. A comparative review has appeared recently (31), and there has been a full discussion of the question of the "size" of the lone pair on N with respect to other substituents (32, 33). A simple quantitative approach to intramolecular interactions in saturated heterocycles has been achieved (34, 35), from which axial–equatorial equilibria can be predicted.

This investigation shows that the low frequency CH stretching vibrations identified by Bohlmann in some cyclic imines (36) arise in conjunction with a secondary *increase* in the NH stretching frequency, supporting a decrease in the N atom charge density and a partial delocalization of charge into the CN bond (37, 38) when one or more α-CH bonds are *trans* to the lone pair. The hybridization of N in this molecular conformation therefore differs from the hybridization in conformations where no α-CH bond(s) bear this geometrical relation to the lone pair.

It has been possible to assess the spectral changes arising when the electron density on N is altered, and to make some specific vibrational assignments concerning the origin of CH absorption bands below ~2850 cm^{-1} through the use of specifically deuterated species.

[1]Revision received June 22, 1970

Experimental

Except where otherwise noted, all the compounds used were commercial products which were purified prior to use and had acceptable physical constants, or they were prepared by standard methods. The deuterated materials α-d_2-piperidine, α-d_2-pyrrolidine, and α,α′-d_4-pyrrolidine were prepared by $LiAlD_4$ reduction of α-piperidone, α-pyrrolidone, and succinimide respectively. A deuteration level of 95% or better was indicated by n.m.r. spectra.

Spectroscopic measurements were made with a Perkin–Elmer Model 621 i.r. spectrophotometer, and a few spectra were obtained with a Cary Model 81 laser Raman spectrometer. Commercial "spectroquality" CCl_4 was used as a solvent for i.r. measurements at path lengths from 2.0–10.0 cm, except in the CD stretching region where shorter path lengths are required. Spectra in deuterated solvents were also obtained at shorter pathlengths.

A complete list of absorption frequencies is filed in the Depository of Unpublished Data, National Science Library, NRCC, Ottawa, Canada.

Results and Discussion

Piperidine

Figure 1 shows the spectrum of piperidine and α-d_2-piperidine in the CH and CD stretching regions. Piperidine exhibits normal ν_{asym} and ν_{sym} CH_2 stretching vibrations[2] at 2933 and 2850

[2]The α-, β-, and γ-methylene vibrations in the lone pair equatorial form and the β- and γ-methylene vibrations in the lone pair axial form are likely superimposed to a high degree, leading to relatively broad bands.

Can. J. Chem. Downloaded from www.nrcresearchpress.com by 210.87.254.6 on 09/05/12
For personal use only.

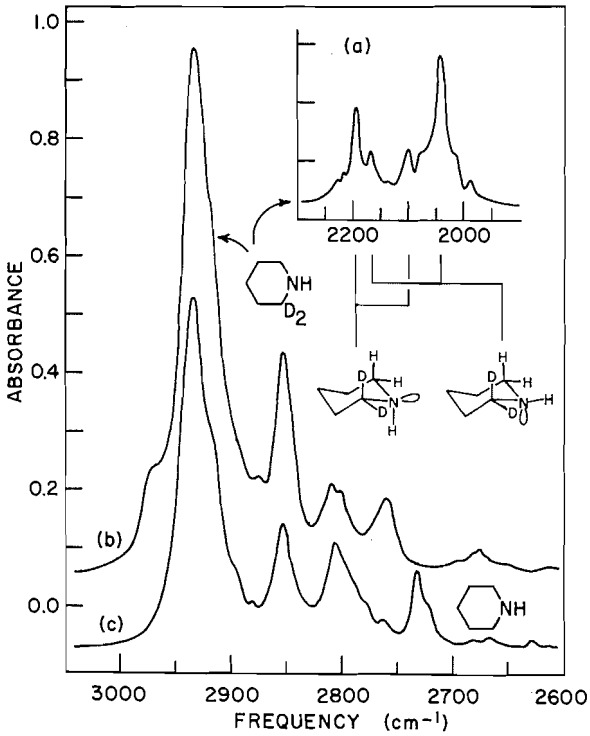

FIG. 1. Methylene stretching vibrations in the i.r. spectra of (*a*), (*b*) α-d_2-piperidine, and (*c*) piperidine (CCl_4 solutions; 2 cm cells in CH stretching region and 0.1 cm cells in CD stretching region).

cm^{-1} respectively, and all other piperidines investigated show similar absorptions. Deuteration of one α-methylene group removes the shoulders at 2915 and 2895 cm^{-1} from ν_{asym}, and replaces the low frequency bands at 2730 and 2803 cm^{-1} with an intermediate band at 2760 cm^{-1}.

These spectral features can be accounted for in terms of a *trans* diaxial lone pair/α-CH interaction, and consequent coupling of the two α-CH_2 group vibrations in the piperidine conformation with an axial lone pair. Figure 2 shows the vibrations that might be expected. The bands at 2915 and 2895 cm^{-1} can be explained as the two components of ν_{asym}, and the bands at 2803 and 2730 cm^{-1} as the two ν_{sym} components.[3] Insertion of one α-CD_2 group breaks the coupling

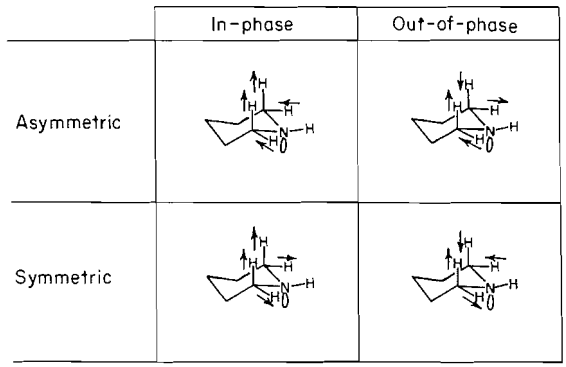

FIG. 2. Projected coupling of asymmetric and symmetric CH stretching vibrations in piperidine conformation with axial lone pair.

and accounts for the appearance of the 2760 cm^{-1} band, while the shoulders at 2915 and 2895 cm^{-1} also become less marked.

In the CD stretching region the interpretation is guided by spectroscopic studies of $CH_3CD_2NH_2$ (38) which show that "normal" ν_{asym} and ν_{sym} frequencies arise from the conformation which does not have a *trans* lone pair/α-CD interaction, while the CD_2 frequencies are lowered by 32 and 39 cm^{-1} respectively if such an interaction is present. This is in agreement with calculations for an XH_2 group showing that ν_{sym} is lowered by more than ν_{asym} if one of the HX force constants is progressively reduced (39). The four main CD bands in α-d_2-piperidine are therefore interpreted as shown in Table 1.[4]

The shifted ν_{sym} band at 2043 cm^{-1} is unusually intense, which may reflect the high degree of interaction between the axial lone pair on N and the axial α-CD bond, and the greater involvement of the lone pair in ν_{sym} relative to ν_{asym} (40). No quantitative conclusions can be based on the CH and CD stretching frequencies regarding the relative proportions of lone pair axial and lone pair equatorial conformers, but it is clear that both exist in piperidine in CCl_4 solution.

Measurements in the NH stretching region are collected in Fig. 3. Piperidine (curve *e*, at concentration 3×10^{-3} moles/l) has a main NH band at 3343 cm^{-1} with a shoulder at 3315 cm^{-1}. The dominant high frequency component is assigned to the NH equatorial (lone pair axial) conforma-

[3]The band at 2803 cm^{-1} appears to be overlapped with other absorptions and therefore does not disappear entirely on deuteration but is only reduced in intensity relative to the main CH bands. Both the 2803 and the 2730 cm^{-1} bands were noted in the Raman spectrum of piperidine. The appearance of "Bohlmann bands" in Raman spectra has not been reported to date.

[4]It is recognized that equatorial CD bonds of —CHD groups absorb about 30 cm^{-1} higher than axial CD bonds in cyclohexanes (1*c*), reflecting slight non-equivalence of the two bonds of CH_2 (or CD_2) groups.

TABLE 1

Main CD bands in α-d_2-piperidine

	ν_{asym} (cm^{-1})	(ν_{CH}/ν_{CD})	ν_{sym} (cm^{-1})	(ν_{CH}/ν_{CD})
Lone pair equatorial	2194	1.337	2100	1.358
Lone pair axial	2164	1.347	2043	1.346

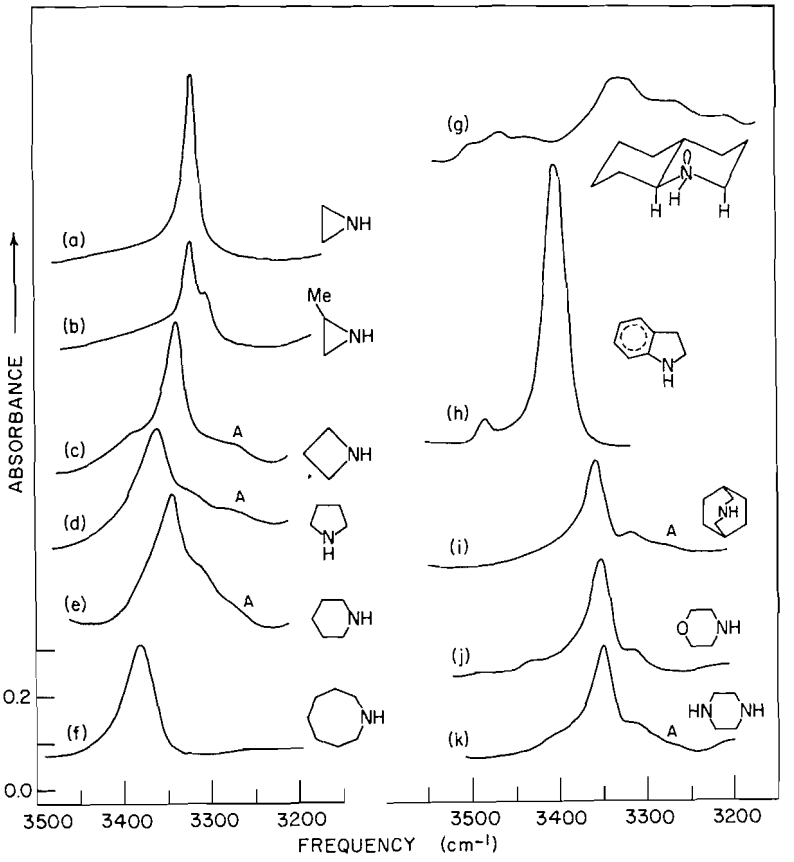

FIG. 3. Infrared spectra in the NH stretching region: (*a*) aziridine, (*b*) propyleneimine, (*c*) azetidine, (*d*) pyrrolidine, (*e*) piperidine, (*f*) heptamethyleneimine, (*g*) *trans*-decahydroquinoline, (*h*) indoline, (*i*) 3-azabicyclo[3.2.2]nonane, (*j*) morpholine and (*k*) piperazine (A = association bands; measurements in dilute CCl_4 solution at 5 or 10 cm path length).

tion, and the increase in frequency ascribed to the partial loss of charge from the N atom. The low frequency component is assigned to the NH axial form. Baldock and Katritzky (5, 6) have recently made similar assignments for piperidine based on gas phase and CCl_4 solution spectra in the first overtone NH region. In the gas phase they conclude that the NH equatorial form of piperidine predominates (*ca.* 60%) with $\Delta H = 0.53 \pm 0.13$ kcal/mole, and that the same holds for CCl_4 solutions with $\Delta H = 0.6 \pm 0.2$ kcal/mole. Our own estimate of ΔH based on badly overlapped NH bands in solution is 0.4 kcal/mole, with the lone pair axial form being the more stable form.

Alkyl Piperidines

The spectrum of 2,2,6,6-tetramethylpiperidine has only CH_3 and normal CH_2 stretching vibrations, the lowest of which lies at 2840 cm^{-1}, in marked contrast to the 2803 and 2730 cm^{-1}

Can. J. Chem. Downloaded from www.nrcresearchpress.com by 210.87.254.6 on 09/05/12
For personal use only.

Can. J. Chem. Downloaded from www.nrcresearchpress.com by 210.87.254.6 on 09/05/12
For personal use only.

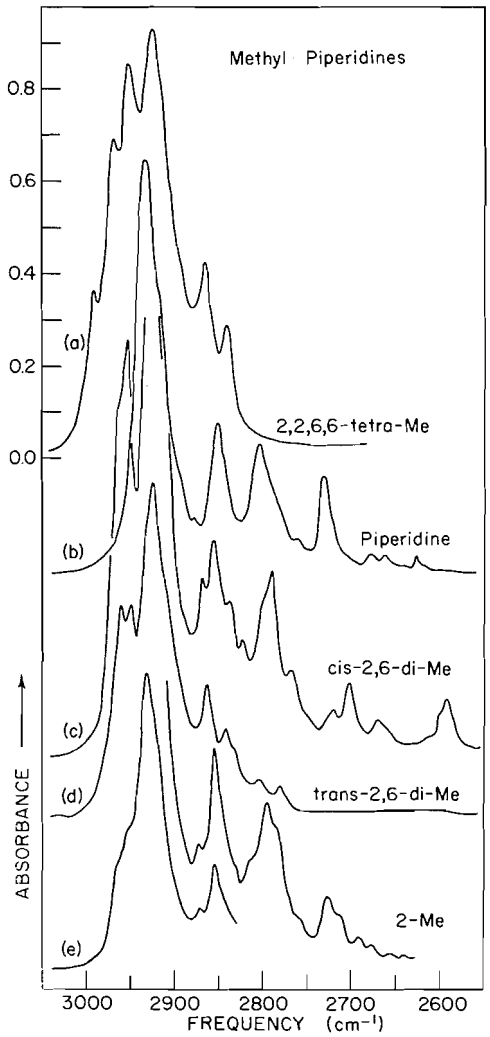

FIG. 4. Infrared spectra of α-methyl piperidines in the CH stretching region: (*a*) 2,2,6,6-tetramethylpiperidine, (*b*) piperidine, (*c*) *cis*-2,6-dimethylpiperidine, (*d*) *trans*-2,6-dimethylpiperidine, (*e*) 2-methylpiperidine.

bands of piperidine (Fig. 4*a* and *b*). Booth *et al.* (18) have recently shown from n.m.r. measurements that *cis*-2,6-dimethylpiperidine has its two methyl groups in the equatorial conformation. Shifted CH absorption at 2790 and 2701 cm^{-1} confirms that the α-CH bonds are axial[5] (Fig. 4*c*), particularly when compared with the corresponding *trans*-2,6-dimethylpiperidine (Fig. 4*d*) which only has weak CH absorption below 2840 cm^{-1} consistent with one axial tertiary α-CH group.[6] 2-Methylpiperidine exhibits absorption similar to that of piperidine, which would be expected with the methyl group in an equatorial position.

Measurements in the fundamental NH stretching region were in general agreement with those reported by Baldock and Katritzky (6) for the first overtones. Because the interpretation of the fundamental region is complicated by the presence of combination bands no such data are reported here. Only a single ν_{NH} band at 3312 cm^{-1} was observed in 2,2,6,6-tetramethylpiperidine; this corresponds to the low frequency component in those cases with α-CH groups, as expected.

N-Substituent Effects

The effect of substitution on N is summarized in Fig. 5 and in Table 2, which also gives some tentative assignments. In *N*-benzoylpiperidine the lone pair on N is withdrawn and no absorption occurs below 2855 cm^{-1} (Fig. 5*j*). The *N*-*p*-tolyl group does not withdraw charge from N as effectively, and weak absorption below 2855 cm^{-1} remains (Fig. 5*h*). Although piperidine-*N*-oxide is held to exist as the *N*-hydroxypiperidine, its spectrum also shows only very weak absorption below 2855 cm^{-1} (Fig. 5*i*).

On the other hand, electron-donating substituents enhance the perturbed in-phase and out-of-phase α-CH_2 bands near 2780 and 2730 cm^{-1}, relative to the normal CH bands. The particular compounds investigated were *N*-amino-, *N*-*t*-butyl-, *N*-methyl-, and *N*-methyl-4-hydroxypiperidine (Fig. 5*a–d*).[7]

N-Chloropiperidine is a special case with a relatively intense CH band at 2830 cm^{-1}; in view of the absence of absorption near 2730 cm^{-1}, its assignment to "perturbed" α-CH_2 groups is uncertain.

trans-Decahydroquinoline

According to Booth and Bostock (16) this compound is expected to exist entirely in the conformation shown in Fig. 5*f*. The perturbed CH bands at 2794 and 2740 cm^{-1} are consistent with this conformation and an appreciable proportion of axially oriented lone pairs on N.

[5]In-phase and out-of-phase coupling in the lone pair axial conformation.

[6]We thank Dr. H. Booth for making samples of *cis*- and *trans*-2,6-dimethylpiperidine available.

[7]In *N*-methylpiperidines the band at 2780 cm^{-1} is enhanced by ν_{sym} of the CH_3 group, which is expected to have one CH bond *trans* to the lone pair.

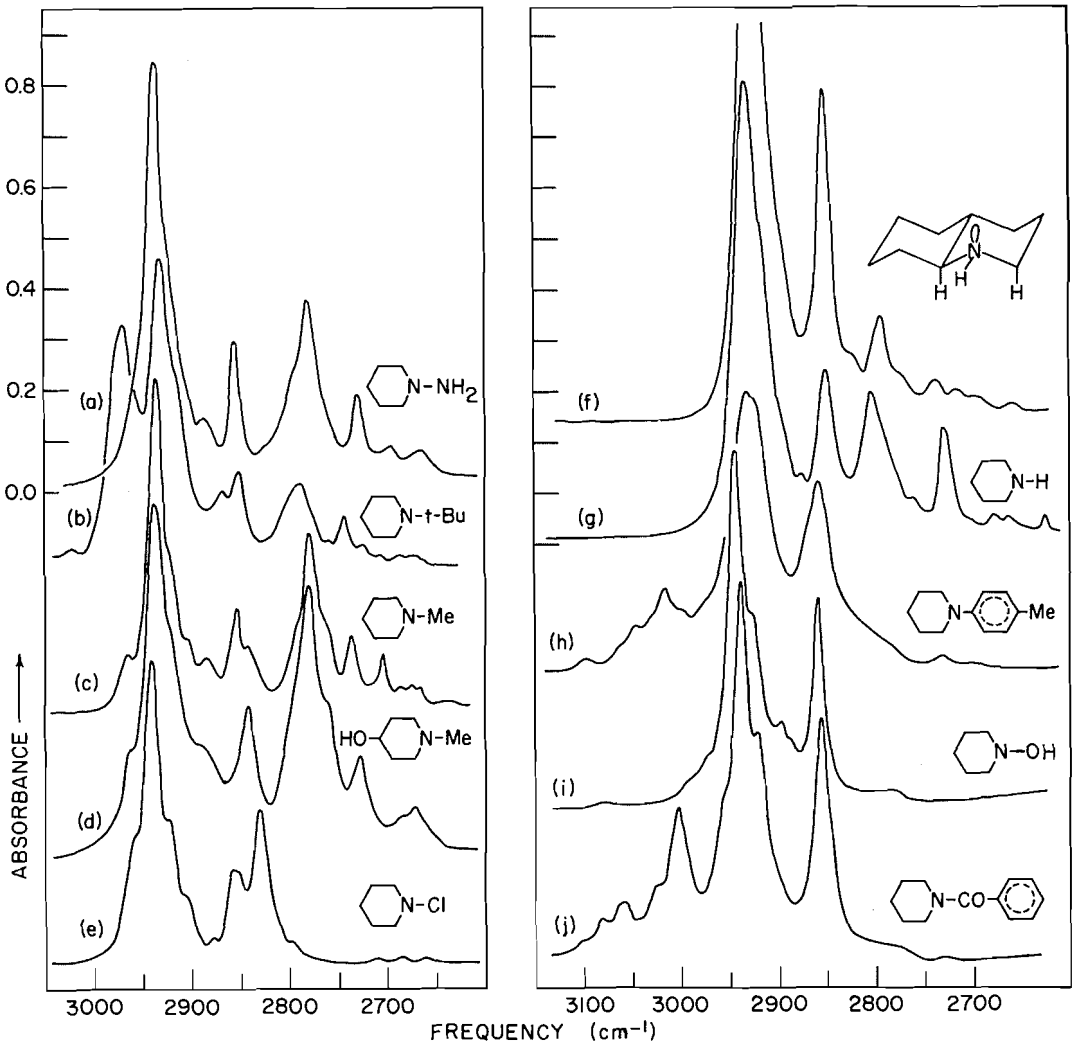

FIG. 5. Infrared spectra of *N*-substituted piperidines in the CH stretching region: (*a*) *N*-aminopiperidine, (*b*) *N*-*t*-butylpiperidine, (*c*) *N*-methylpiperidine, (*d*) *N*-methyl-4-piperidinol, (*e*) *N*-chloropiperidine, (*f*) *trans*-decahydroquinoline, (*g*) piperidine, (*h*) *N*-*p*-tolylpiperidine, (*i*) *N*-nitrosopiperidine, (*j*) *N*-benzoylpiperidine.

However, from Fig. 3*c* it appears that the NH band is a doublet (~3336 and ~3316 cm^{-1}), which indicates equatorial as well as axial lone pair orientation.

Piperazines

Relative to piperidines the piperazines exhibit more intense perturbed CH bands, which in some cases are stronger than the normal CH bands (Fig. 6). *N*,*N*-Diamino-piperazine and *N*-amino-*N'*-methylpiperazine fall into the latter category. This is expected since the substituents are strong electron donors, and all the CH_2 groups are adjacent to a N atom.

The CH absorption of piperazine is undoubtedly complicated by the existence of conformers with axial–axial, axial–equatorial, and equatorial–equatorial lone pair combinations (25). The spectrum of *N*,*N'*-diaminopiperidine is simpler than that of piperidine, since the substituents are probably largely in equatorial orientations, yielding a conformer with two intensified axial lone pairs. Nevertheless, the presence of a ν_{asym} CH_2 stretching band in the normal position

Can. J. Chem. Downloaded from www.nrcresearchpress.com by 210.87.254.6 on 09/05/12
For personal use only.

TABLE 2

Methylene stretching vibrations of some six-membered *N*-heterocycles (in cm^{-1}; measurements in dilute CCl_4 solution)

Compound	Asymmetric mode		Symmetric mode	
	Normal	Perturbed*	Normal	Perturbed*
Piperidine (P)	2933	2915 sh, 2895 sh	2850	2803, 2730
2-Methyl P	2930	2915 sh	2855	2795, 2728
trans-2,6-Dimethyl P	2925	~2895 sh†	2842	2803†
cis-2,6-Dimethyl P	2925	2910 sh	2855	2790, 2701
2,2,6,6-Tetramethyl P	2925	—	2840	—
N-Amino P	2937	2920 sh, 2887	2855	2781, 2729
N-*t*-Butyl P	2932	2915 sh	2850	2787, 2743
N-Methyl P	2935	2920 sh, 2903 sh	2852	(2779)‡, 2735, 2709
N-Methyl-4-piperidinol	2939	2920 sh, 2889 sh	2842	(2780)‡, 2728
N-Chloro P	2941	2925 sh, 2905 sh	2855	2830 (?)
N-*p*-Tolyl P	2932	—	2859	—
Piperidine-*N*-oxide	2944	—	2859	—
N-Benzoyl P	2938	—	2855	—
Piperazine (Pz)	2944	2918, 2911, 2883	2855 sh	2825, 2812, 2749, 2733, 2723
N-Methyl-*N'*-amino Pz	2938	2912, 2877	2842	2810, (2796)‡, 2766, 2738
1,4-Diamino Pz	2938	2911, 2877	2828	2809, 2737
N,*N'*,*N''*-Trimethylhexahydro-*s*-triazine	2940	2892	2841	2787, 2772, 2724

*Belonging to α-CH_2 groups in lone pair axial conformer.
†Tertiary α-CH group(s) only.
‡ν_{sym} of *N*-CH_3 group.

(2938 cm^{-1}) indicates that at least some molecules have an axial substituent (equatorial lone pair).

The NH stretching region, with a main band at 3351 cm^{-1} and a shoulder at 3314 cm^{-1}, shows strong preference for the axial orientation of lone pairs in piperazine (Fig. 3*k*).

1,3,5-Trimethylhexahydro-*s*-triazine is expected to show a conformational preference for equatorial substituents (41). Again the CH region is complicated because each methylene is adjacent to two N atoms, of which a significant number must have axial substituents to account for the normal ν_{asym} CH_2 intensity at 2940 cm^{-1}. However, *trans* diaxial lone pair/α-CH interactions (plus vibrational coupling) account for the intense and complicated absorption below 2835 cm^{-1}.

Pyrrolidines

By analogy with tetrahydrofuran (42) the nonplanar semi-chair conformation appears most reasonable for pyrrolidine (Fig. 7). In conformation (**1**) an α-CH bond at C-1 is *trans* to the N lone pair while none of the hydrogens at C-4 are *trans*. With inversion at N to form conformer **2**, none of the α-CH bonds are *trans* to the lone pair. A principal difference between piperidine and pyrrolidine should therefore be the absence of coupling between α-CH_2 groups in the latter.

The relevant frequencies and assignments are tabulated in Table 3. Pyrrolidine exhibits a shoulder at 2930 and a band at 2821 cm^{-1} corresponding to ν_{asym} and ν_{sym} of a "perturbed" α-CH_2 group. In the α-CD_2 compound the 2930 cm^{-1} is largely gone (leading to resolution of an underlying weak band at 2911 cm^{-1}), and the 2821 cm^{-1} band is reduced to a shoulder. In the α,α'-di-CD_2 compound both bands are eliminated.

In the CD stretching region pyrrolidine-α-d_2 has "normal" CD_2 stretching frequencies at 2215 and 2110 cm^{-1} (ν_{asym} and ν_{sym}, respectively) arising from **2** with the CD_2 group at either C-1 or C-4, and from **1** with the CD_2 group at C-4. "Perturbed" ν_{asym} and ν_{sym} CD_2 frequencies at 2195 and 2088 cm^{-1}, respectively, must arise from **1** with a 1-CD_2 group; since these bands are relatively more intense conformer **1** with the *trans* lone pair/α-CH interaction seems to be favored over **2**. The weak CD absorption at 2137 cm^{-1} is probably due to —CHD impurity.

Can. J. Chem. Downloaded from www.nrcresearchpress.com by 210.87.254.6 on 09/05/12
For personal use only.

Can. J. Chem. Downloaded from www.nrcresearchpress.com by 210.87.254.6 on 09/05/12
For personal use only.

TABLE 3

Methylene stretching frequencies in pyrrolidines (cm^{-1})

	CH_2				CD_2			
	Asymmetric		Symmetric		Asymmetric		Symmetric	
Compound	Normal	Perturbed	Normal	Perturbed	Normal	Perturbed	Normal	Perturbed
Pyrrolidine	2962	2930 sh	2872	2821	—	—	—	—
Pyrrolidine-α-d_2	2960	?	2874	2820 sh	2215	2195	2110	2088
(ν_{CH}/ν_{CD})					(1.336)	(1.335)	(1.361)	(1.351)
Pyrrolidine-α,α′-d_4	2956	—	2873	—	2215	2195	2110	2087
(ν_{CH}/ν_{CD})					(1.336)	(1.335)	(1.361)	(1.352)
N-Aminopyrrolidine	2957	2928	2875	2789	—	—	—	—

Can. J. Chem. Downloaded from www.nrcresearchpress.com by 210.87.254.6 on 09/05/12
For personal use only.

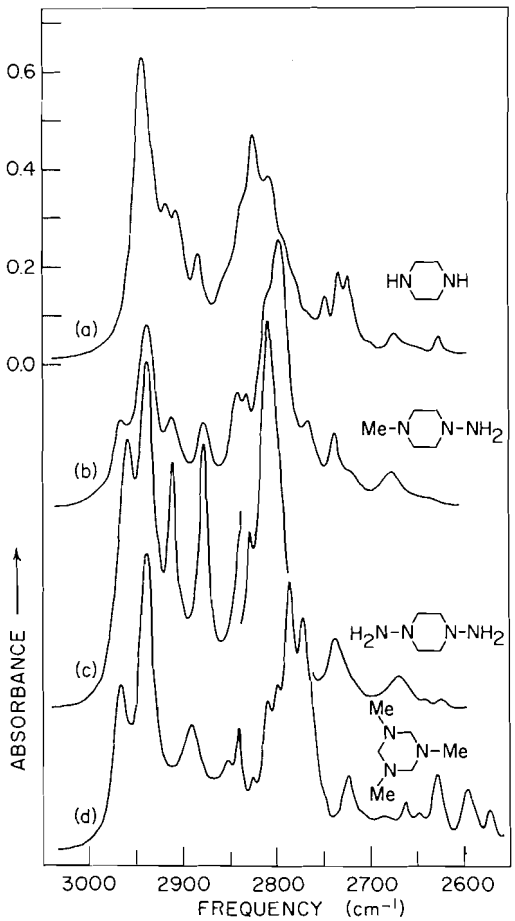

FIG. 6. Infrared spectra in the CH stretching region: (*a*) piperazine, (*b*) 1-amino-4-methylpiperazine, (*c*) 1,4-diaminopiperazine, (*d*) 1,3,5-trimethyltriazine.

In pyrrolidine-α,α'-d_4 the same four bands appear, with no new features such as would be expected if two α-CD bonds were *trans* to the lone pair. Although the asymmetric CD_2 band was more difficult to resolve, the apparent peak at 2207 cm^{-1} shows both high and low frequency shoulders consistent with the spectrum of the α-CD_2 compound.

In the NH stretching region pyrrolidine has a main band at 3362 cm^{-1} with a shoulder at 3320 cm^{-1} (Fig. 3*c*), confirming that **1** is favored over **2**. From the temperature dependence of these bands the enthalpy difference is estimated as ~ 0.2 kcal/mole.

The intensity of the perturbed ν_{sym} CH_2 stretching vibration at 2789 cm^{-1} in *N*-amino-pyrrolidine is almost equal to that of the normal ν_{asym} CH_2 band (Fig. 8*e*). This spectrum provides further evidence that only one "Bohlmann band" is induced below 2850 cm^{-1} in pyrrolidine, even if the electron density on N is increased. The perturbed ν_{asym} CH_2 stretching vibration is tentatively assigned to the band at 2928 cm^{-1} in the *N*-amino compound.

If the electron density is removed from N, as in indoline (Fig. 8*b*), the CH absorption below 2850 cm^{-1} is reduced to two very weak bands at 2796 and 2708 cm^{-1}. Figure 3*h* shows that in the NH stretching region the conformer with the pyrrolidine ring of type **1** and having the aromatic ring fused on the C-4 side now absorbs only very weakly at 3483 cm^{-1}, while the conformer with the pyrrolidine ring of the type **2** having the lone pair delocalized into the fused aromatic ring is much more abundant and absorbs strongly at 3403 cm^{-1}. Both bands can be shifted by deuteration. Conformer **1** is more stable than conformer **2** by ~ 0.1 kcal/mole in dilute CCl_4 solution.

Morpholine

The CH stretching region of morpholine (Fig. 8*a*) is surprisingly like that of piperazine, with the exception of changes in relative intensities. This suggests that the lone pair orbitals on oxygen may play a similar role to those on nitrogen in shifting certain CH bands. This effect has been investigated further in this laboratory, using simpler model compounds (43).

In the NH stretching region (Fig. 3*j*) morpholine shows the same strong preference for axial orientation of the lone pair as piperazine.[8]

3-Azabicyclo[3.2.2]nonane

The weak CH absorption below 2850 cm^{-1} (Fig. 8*c*) suggests that some molecules exist in a conformation where *trans* N lone pair/α-CH_2 interaction is possible. This is consistent with molecular models. In the NH region the spectrum resembles that of morpholine (Fig. 3*j*).

Effect of Heterocyclic Ring Size

The i.r. spectra of cyclic imines of ring size 3–7 have been investigated (44), and the increase in ν_{CH} as ring size decreases is well known. The frequency assignments for 3-membered hetero-

[8]In agreement with recent conclusions by Baldock and Katritzky (6) for morpholine in the gas phase and in dilute CCl_4 solution.

Can. J. Chem. Downloaded from www.nrcresearchpress.com by 210.87.254.6 on 09/05/12
For personal use only.

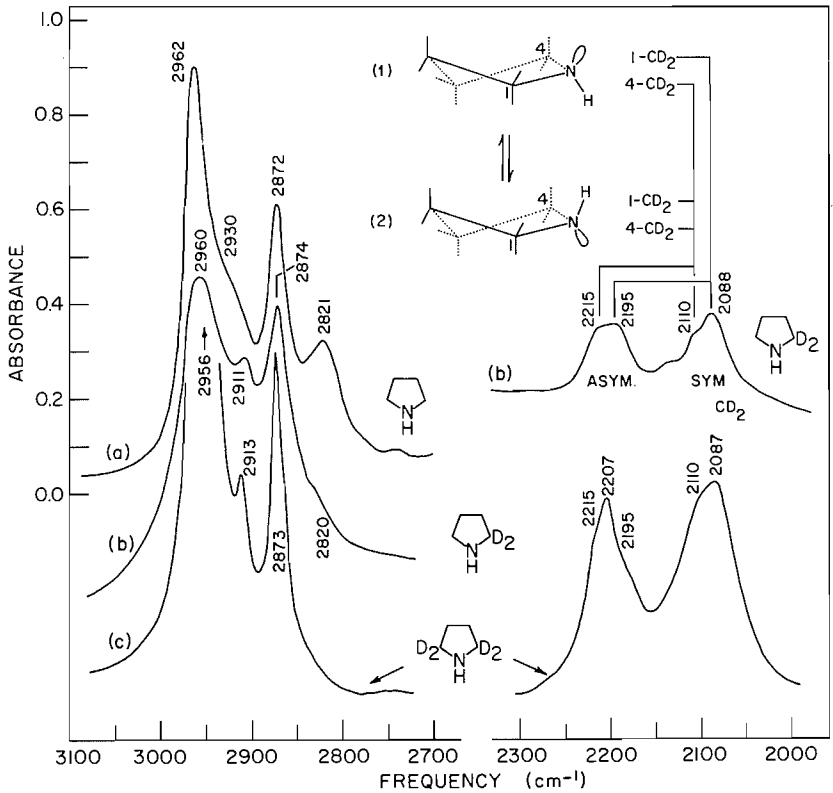

FIG. 7. Methylene stretching vibrations in the i.r. spectra of (*a*) pyrrolidine, (*b*) α-d_2-pyrrolidine, and (*c*) α,α′-d_4-pyrrolidine.

cyclic rings are firmly based (45), and the bands at 2935, 2903, and 2896 cm^{-1} in ethyleneimine (aziridine) must be overtones and/or combination bands (Fig. 9*a*). Similar absorptions are observed in 2-methylaziridine (Fig. 9*b*), although a doublet ν_{NH} is observed for the latter (Fig. 3*a* and *b*) because of *cis–trans* isomerism of the CH_3 group and the NH (46). The ν_{NH} components at 3322 and 3305 cm^{-1} are shifted to 2465 and 2453 cm^{-1} on deuteration.

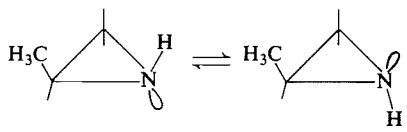

3
CH_3/NH *cis*
(Low frequency ν_{NH})

4
CH_3/NH *trans*
(High frequency ν_{NH})

By analogy with mono-substituted cyclobutanes (47), azetidine should exist in two conformations with lone pair orientations that are essentially "axial" and "equatorial" and this is borne out by NH and CH frequencies (Figs. 3*c* and 9*c*).

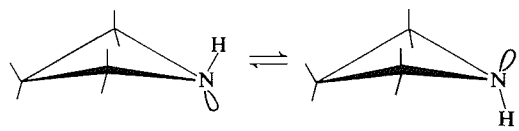

5
Lone pair "axial"
(two *trans* CH/lone pair interactions)
high frequency ν_{NH}(3387 cm^{-1})

6
Lone pair "equatorial"
(no *trans* CH/lone pair interaction)
low frequency ν_{NH}(3339 cm^{-1})

The lowest CH frequency (2859 cm^{-1}) has the highest intensity, and this band is tentatively related to the quasi-*trans* orientation of α-CH bonds to the lone pair in **5**. It should be noted that the electron donor ability of N in cyclic imines is

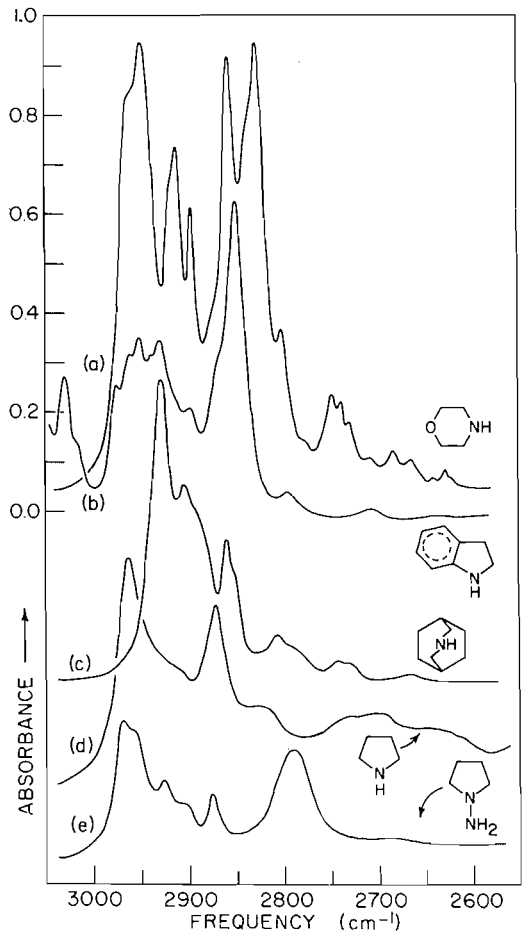

FIG. 8. Infrared spectra in the CH stretching region: (*a*) morpholine, (*b*) indoline, (*c*) 3-azabicyclo[3.2.2] nonane, (*d*) pyrrolidine, (*e*) *N*-aminopyrrolidine.

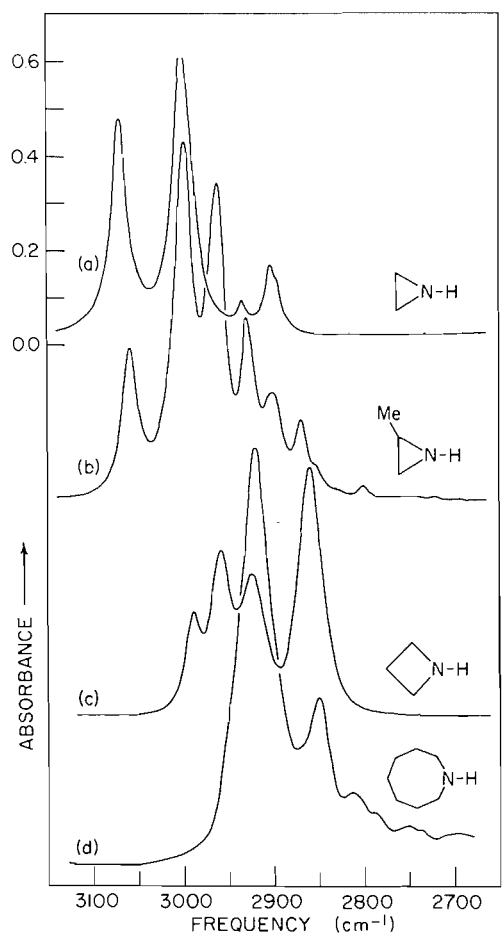

FIG. 9. Infrared spectra in the CH stretching region: (*a*) aziridine, (*b*) 2-methylaziridine, (*c*) azetidine, (*d*) heptamethyleneimine.

known to follow the ring size order 4 > 5 > 6 > 7 > 3 (48). In *N*-benzoyl azetidine where the lone pair has been delocalized the lowest frequency CH band is found at 2885 cm^{-1}.

The only large ring imine investigated was heptamethyleneimine, which has normal ν_{asym} and ν_{sym} CH_2 modes at 2920 and 2850 cm^{-1}, respectively, and weak absorption below 2850 cm^{-1} (Fig. 9*d*). In the NH region the main band at 3381 cm^{-1} shows some asymmetry on the high frequency side.

Solvent Effect Studies

The ν_{CD} shift of $CDCl_3$ when amines are added to it until the "free" CD band at 2252 cm^{-1} disappears (49) shows a dual basicity for piperidine and *N*-alkylpiperidines (Fig. 10). Similar spectra are obtained if CCl_4 is used as a ternary solvent. The relative intensities for the two CD···N bands do not, however, represent the relative proportions of the less basic (lone pair axial, $\Delta\nu_{CD} \approx 33\ cm^{-1}$) and more basic (lone pair equatorial, $\Delta\nu_{CD} \approx 75\ cm^{-1}$) forms under these conditions. Lord *et al.* (50) have shown that the integrated ν_{CD} intensity of $CDCl_3$ increases dramatically on hydrogen bond formation, e.g. for $\Delta\nu_{CD} = 36\ cm^{-1}$ on hydrogen bond formation with pyridine the CD band intensity increases more than 20-fold. Thus Fig. 10 grossly accentuates the low frequency CD···N band (lone pair

Can. J. Chem. Downloaded from www.nrcresearchpress.com by 210.87.254.6 on 09/05/12
For personal use only.

Can. J. Chem. Downloaded from www.nrcresearchpress.com by 210.87.254.6 on 09/05/12
For personal use only.

TABLE 4

Peak intensities of CH bands in piperidines* relative to 2935 cm^{-1} (normal asymmetric CH_2 stretch) set at 1.00

	Piperidine			*N*-Methylpiperidine			
Solvent	2850 cm^{-1}†	2803 cm^{-1}	2730 cm^{-1}	2852 cm^{-1}†	2779 cm^{-1}‡	2735 cm^{-1}	2709 cm^{-1}
CCl_4	0.37	0.31	0.24	0.30	0.53	0.22	0.16
Pure liquid	0.56	0.42	0.32	0.45	0.68	0.37	0.28
Solid film (−135 °C)	0.31	0.32	0.32	—	—	—	—
$CDCl_3$	0.38	0.28	0.12	0.37	0.51	0.17	0.13
$(CD_3)_2C{=}O$	0.44	0.27	0.07	0.34	0.48	0.20	0.09
$CD_3C{\equiv}N$	0.44	0.27	0.16	0.36	0.52	0.23	0.17
$(CD_3)_2S{=}O$	0.48	0.28	0.20	0.39	0.53	0.27	0.19
CD_3OD§	0.45 (2856)	≪0.28 (2833 broad, overlapped)	0.09 (2747)	0.48 (2857)	0.45 (2803)	0.16 (2741)	0.07 (2710)

*Frequencies slightly solvent dependent; values cited in dilute CCl_4 solution.
†Normal symmetric CH_2 stretching vibration of N lone pair equatorial conformer.
‡ν_{sym} of *N*-CH_3 group.
§Reference bands shifted very little, other bands moved to higher frequencies as indicated.

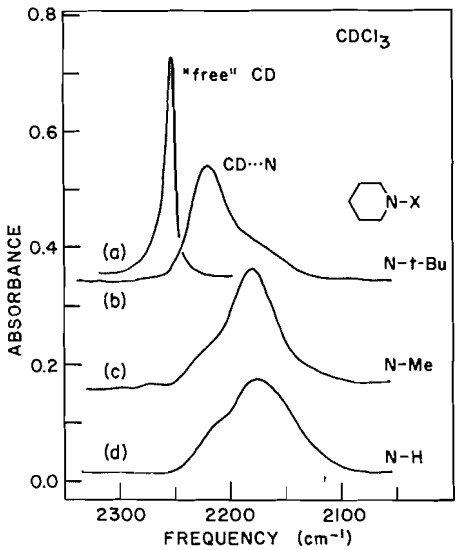

FIG. 10. Fundamental CD stretching vibrations of $CDCl_3$: (*a*) in dilute CCl_4, (*b*) in *N*-*t*-butylpiperidine, (*c*) in *N*-methylpiperidine, and (*d*) in piperidine.

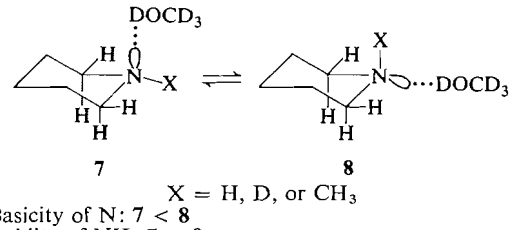

7 8

X = H, D, or CH_3

Basicity of N: 7 < 8
Acidity of NH: 7 > 8
Steric hindrance of N—CH_3: 7 > 8
Steric hindrance to solvent attack on lone pair: 7 > 8
Polarity of conformer: 7 < 8
Thermodynamic stability: 7 > 8

FIG. 11. Projected properties of N lone pair axial and equatorial conformers in piperidine and *N*-methylpiperidine.

equatorial form). Nevertheless it provides some further evidence that the lone pair axial conformer is *less* basic than the lone pair equatorial conformer.

While the concentration of axially oriented *t*-butyl groups is normally considered to be negligible (1*b*), *N*-*t*-butylpiperidine appears to have some, although if $\varepsilon_{CD\cdots N}^{axial}$ (2170 cm^{-1}) > $\varepsilon_{CD\cdots N}^{equatorial}$ (2219 cm^{-1}) a very small percentage of axial *t*-butyl groups could account for the observed spectrum.

For piperidine and *N*-methylpiperidine in which *ca.* 60 and 66%, respectively, of the *N*-substituent are now deemed to be equatorial in benzene solution (6), the low frequency CD···N chloroform complex band predominates, but probably only because of its intrinsically greater extinction coefficient.

The axial–equatorial equilibrium in piperidines is expected to show some solvent sensitivity, and CH spectra were obtained for piperidine and *N*-methylpiperidine in a variety of deuterated solvents (Table 4). The projected properties of the two conformers are summarized in Fig. 11.

Since only peak height ratios for these overlapped bands are readily obtained, the data can only be interpreted qualitatively. The 2730 cm^{-1} band in piperidine assigned to the lone pair axial form has the highest relative intensity in the pure liquid and in low temperature solid film spectra. In the glassy film spectrum, where the resolution is improved, the 2850 cm^{-1} normal ν_{asym} CH_2 band has the lowest relative intensity. In the crystalline state the concentration of the lone pair axial form has previously been held to increase (3). In dimethyl sulfoxide-d_6, acetonitrile-d_3, chloroform-*d*, acetone-d_6, and methanol-d_4 the 2730 cm^{-1} piperidine band is relatively less intense than in CCl_4 solution, and decreases in the order given. In all cases except the low temperature solid film the 2850 cm^{-1} band is relatively more intense than in CCl_4 solution. These changes can be explained by increased stabilization of the more polar conformer (N lone pair equatorial) in polar solvents, and in the case of $CDCl_3$ and CD_3OD, also by preferential stabilization of the lone pair equatorial form by hydrogen bonding. Obviously a number of factors must be involved, some of which are mentioned in Fig. 11.

While the CH frequencies are not markedly solvent dependent, the CD_3OD solution appears exceptional. The frequency of the normal ν_{asym} CH_2 reference band is hardly altered but all the others are shifted to higher frequencies (Table 4). This is consistent with hydrogen bonding in the lone pair axial form, thereby reducing the effective charge on N and in turn making the α-CH_2 bands in this conformer more normal.

N-Methylpiperidine shows roughly similar behavior in deuterated solvents, although the relative decrease in the 2709 cm^{-1} band with respect to the value in CCl_4 solution is not as

Can. J. Chem. Downloaded from www.nrcresearchpress.com by 210.87.254.6 on 09/05/12
For personal use only.

great. In CD_3CN no significant change in the low frequency band is noted, and in $(CD_3)_2SO$ a small increase is observed. The lower solvent sensitivity of the conformational equilibrium in *M*-methylpiperidine may arise from the fact that the N lone pair can always be *trans* to at least one CH bond (of the methyl group) in both conformations, plus the greater steric hindrance in the *N*-methyl axial position.

The assistance of Miss Marelle Law with some of the experimental measurements is gratefully acknowledged. This work was supported by the U.S. Army Research Office, Durham, North Carolina, U.S.A., under Grant No. DA-ARO-D-31-124-G658.

1. E. L. Eliel, N. L. Allinger, S. J. Angyal, and G. A. Morrison. Conformational analysis. Interscience Publishers, New York, N.Y. 1966. (*a*) p. 244–255, (*b*) p. 49, (*c*) p. 144.
2. G. Levi. C.R. **261**, 4007 (1965).
3. O. S. Anisimova, A. N. Kost, Y. A. Pentin, and L. G. Yudin. Vestn. Mosk. Univ. Ser. II Khim. **21**, 19 (1966). Chem. Abstr. **66**, 23941*j* (1967).
4. T. V. Titova, O. S. Anisimova, and Y. A. Pentin. Opt. Spectrosc. **23**, 495 (1967).
5. R. W. Baldock and A. R. Katritzky. Tetrahedron Lett. 1159 (1968).
6. R. W. Baldock and A. R. Katritzky. J. Chem. Soc. (B) 1470 (1968).
7. T. Masamune. Chem. Commun. 244 (1968).
8. T. Masamune and M. Takasugi. Chem. Commun. 625 (1967).
9. T. Masamune, M. Takasugi, and M. Matsuki. Bull. Chem. Soc. Jap. **41**, 2466 (1968).
10. F. Moll. Tetrahedron Lett. 5201 (1968).
11. C. Y. Chen and R. J. W. Lefevre. Tetrahedron Lett. 1611 (1965).
12. J. B. Lambert, R. G. Keske, R. E. Carhart, and A. P. Jovanovich. J. Amer. Chem. Soc. **89**, 3761 (1967).
13. M. J. T. Robinson. Tetrahedron Lett. 1153 (1968).
14. J. B. Lambert and R. G. Keske. J. Amer. Chem. Soc. **88**, 620 (1966).
15. P. J. Brignell, A. R. Katritzky, and P. L. Russell. Chem. Commun. 723 (1966).
16. H. Booth and A. H. Bostock. Chem. Commun. 177 (1967).
17. H. Booth. Chem. Commun. 802 (1968).
18. H. Booth, J. H. Little, and J. Feeney. Tetrahedron, **24**, 279 (1968).
19. R. K. Harris and R. A. Spragg. Chem. Commun. 314 (1966).
20. P. J. Brignell, A. R. Katritzky, and P. L. Russell. J. Chem. Soc. (B) 1459 (1968).
21. H. Booth and J. H. Little. Tetrahedron, **23**, 291 (1967).
22. J. B. Lambert and R. G. Keske. Tetrahedron Lett. 2023 (1969).
23. P. J. Buckley, C. C. Costain, and J. E. Parkin. Chem. Commun. 668 (1968).
24. M. Aroney and R. J. W. Lefevre. J. Chem. Soc. 3002 (1958).
25. N. L. Allinger, J. G. D. Carpenter, and F. M. Karkowski. Tetrahedron Lett. 3345 (1964).
26. N. L. Allinger, J. G. D. Carpenter, and F. M. Karkowski. J. Amer. Chem. Soc. **87**, 1232 (1965).
27. R. J. Bishop, L. E. Sutton, D. Dineen, R. A. Y. Jones, A. R. Katritzky, and R. J. Wyatt. J. Chem. Soc. (B) 493 (1967).
28. N. W. J. Pumphrey and M. J. T. Robinson. Chem. Ind. 1903 (1963).
29. M. J. Aroney, C. Y. Chen, R. J. W. Lefevre, and J. D. Saxby. J. Chem. Soc. 4269 (1964).
30. M. J. Aroney and R. J. W. Lefevre. J. Chem. Soc. 3002 (1958); 2161 (1960).
31. F. G. Riddell. Quart. Rev. **21**, 364 (1967).
32. N. L. Allinger, J. A. Hirsch, and M. A. Miller. Tetrahedron Lett. 3729 (1967).
33. N. L. Allinger and J. C. Tai. J. Amer. Chem. Soc. **87**, 1227 (1965).
34. A. R. Katritzky. Bull. Soc. Chim. Fr. 3585 (1967).
35. P. J. Brignell, K. Brown, and A. R. Katritzky. J. Chem. Soc. (B) 1462 (1968).
36. F. Bohlmann. Ber. **91**, 2157 (1958).
37. H. P. Hamlow, S. Okuda, and N. Nakagawa. Tetrahedron Lett. 2553 (1964).
38. P. J. Krueger and J. Jan. Can. J. Chem. This issue.
39. H. Wolff and D. Staschewski. Z. Elektrochem. **66**, 140 (1962).
40. P. J. Krueger. Can. J. Chem. **40**, 2300 (1962).
41. R. F. Farmer and J. Hamer. Tetrahedron, **24**, 829 (1968).
42. D. Gagnaire and P. Vottero. Bull. Soc. Chim. Fr. 2779 (1963). J. C. Evans and J. C. Wahr. J. Chem. Phys. **31**, 655 (1959).
43. P. J. Krueger, J. Jan, and H. Wieser. J. Mol. Struct. **5**, 375 (1970).
44. Y. N. Sheinker and E. M. Peresleni. Zh. Fiz. Khim. **32**, 2112 (1958).
45. A. R. Katritzky and A. P. Ambler. *In* Physical methods in heterocyclic chemistry. Vol. 1. *Edited by* A. R. Katritzky. Academic Press, New York, N.Y. 1963. pp. 176–178.
46. A. Lattes, R. Martino, and R. Mathis-Noel. C.R. **263C**, 49 (1966).
47. (*a*) W. G. Rothschild. J. Chem. Phys. **45**, 1214 (1966). (*b*) J. R. Durig and W. H. Green. J. Chem. Phys. **47**, 673 (1967). (*c*) J. R. Durig and A. C. Morrissey. J. Chem. Phys. **46**, 4854 (1967).
48. E. Lippert and H. Prigge. Ber. Bunsenges. Phys. Chem. **67**, 554 (1963).
49. E. W. Abel, D. A. Armitage, and G. R. Willey. Trans. Faraday Soc. **60**, 1257 (1964).
50. R. C. Lord, B. Nolin, and H. D. Stidham. J. Amer. Chem. Soc. **77**, 1365 (1955).

Can. J. Chem. Downloaded from www.nrcresearchpress.com by 210.87.254.6 on 09/05/12
For personal use only.

Can. J. Chem. Downloaded from www.nrcresearchpress.com by 210.87.254.5 on 09/05/12
For personal use only.

Thermodynamics of proton dissociations from imidazolium ion, 6-uracilcarboxylic acid, and protonated hypoxanthine in aqueous solution

EARL M. WOOLLEY, RICHARD W. WILTON, AND LOREN G. HEPLER
Department of Chemistry, The University of Lethbridge, Lethbridge, Alberta

Received May 22, 1970

Equilibrium constants have been determined potentiometrically for proton dissociations from imidazolium ion, 6-uracilcarboxylic acid (pK_1 and pK_2), and protonated hypoxanthine (pK_1, pK_2, and pK_3) in aqueous solution at 25 °C and used for calculation of ΔG° values for the corresponding reactions. Enthalpies of these same proton dissociations have been measured calorimetrically and combined with the ΔG° values to yield ΔS° values for these reactions.

Canadian Journal of Chemistry, 48, 3249 (1970)

Introduction

Thermodynamic data for proton dissociation reactions in aqueous solution are useful for such calculations as extent of ionization, pH of buffer solution, and change of equilibrium constant with change in temperature. These data have also led to increased understanding of relations between structure, substituent effects, and reactivity of many molecules and ions in solution (1–3). Knowledge of solute–solvent interactions and thence improved understanding of solvent properties has also been derived from previous studies of thermodynamics of proton dissociation reactions (1–4). In addition to these general reasons for interest in thermodynamics of proton dissociation reactions, there are specific reasons for investigation of certain acids. Pyrimidines and related compounds are present in living systems and are well known as important components of nucleic acids. Earlier workers have carried out measurements related to ours because of the biochemical importance of these kinds of compounds (5–7).

We have made potentiometric and calorimetric measurements leading to pK, ΔG°, ΔH°, and ΔS° values for proton dissociations from imidazolium ion, 6-uracilcarboxylic acid, and protonated hypoxanthine in aqueous solution at 25 °C. Our results are discussed in relation to similar results of earlier workers. We have also used imidazole as a test compound in investigating relative advantages of "traditional" and titration calorimetry.

Experimental

Imidazole, 6-uracilcarboxylic acid monohydrate (also called orotic acid), and hypoxanthine were all obtained (A Grade) from California Biochemical Corp. Different samples of imidazole were further purified by zone melting, by recrystallization from benzene, and by recrystallization from petroleum ether. Several samples of hypoxanthine and 6-uracilcarboxylic acid were purified by recrystallization from water. Calorimetric results obtained with different samples of the same compound were identical within our quoted uncertainties.

Carbonate-free NaOH solutions and HCl solutions were prepared and standardized by usual methods (8). All measurements were made with boiled, doubly distilled water and precautions were taken to minimize subsequent contamination with CO_2.

The "best" pK value for ionization of imidazolium ion was taken from the results of hydrogen electrode measurements by Datta and Grzybowski (9). Our measurements with a glass electrode were in agreement with this value.

We have obtained pK_1 and pK_2 values for 6-uracilcarboxylic acid and pK_1, pK_2, and pK_3 values for protonated hypoxanthine by way of pH titration measurements in which we used a glass electrode (1). We also obtained pK_1 for 6-uracilcarboxylic acid by a difference potentiometric method using a glass electrode (10).

All calorimetric measurements were made with an LKB Precision Calorimetry System. The titrant for titration calorimetric measurements was supplied by a Metrohm Dosimat automatic titrator. All measurements refer to 25.0 °C, with results reported in terms of the defined calorie (1 cal = 4.1840 J).

Results and Discussion

Heats of solution of imidazole in 1.5×10^{-4} M NaOH and in dilute HCl are reported in Tables 1

TABLE 1
Heats of solution of imidazole, eq. 1

g Imidazole/100 ml	ΔH_1/(kcal mole^{-1})*
0.08193	3.080
0.12020	3.091
0.12261	3.082
0.14132	3.094
0.68348	3.092

*Average ΔH_1 = 3.088 kcal mole^{-1}, with average deviation = 0.005 kcal mole^{-1}.

Can. J. Chem. Downloaded from www.nrcresearchpress.com by 210.87.254.5 on 09/05/12
For personal use only.

TABLE 2

Heats of solution of imidazole in aqueous HCl, eq. 2

g Imidazole/ 100 ml	mmole HCl/100 ml	ΔH_2/ (kcal mole^{-1})*
0.08323	1.956	−5.622
0.08744	1.956	−5.615
0.09988	1.956	−5.637
0.10426	2.738	−5.621
0.10847	1.956	−5.617
0.12252	1.956	−5.603

*Average $\Delta H_2 = -5.619$ kcal mole^{-1}, with average deviation = 0.008 kcal mole^{-1}.

and 2. Calorimetric reactions are represented by eqs. 1 and 2, in which we use Im and ImH^+ for

[1] $$Im(c) = Im(aq) \qquad \Delta H_1$$

[2] $$Im(c) + H^+(aq) = ImH^+(aq) \qquad \Delta H_2$$

imidazole and imidazolium ion. These data lead us to $\Delta H_1^\circ = 3.09$ kcal mole^{-1} and to $\Delta H_2^\circ = -5.62$ kcal mole^{-1}, which we combined to obtain $\Delta H_3^\circ = 8.71$ kcal mole^{-1} for the proton ionization represented by eq. 3. We estimate that the *total* uncertainty (chemical impurities, calorimetric errors, heats of dilution) in this ΔH_3° is less than $\pm$ 0.04 kcal mole^{-1}.

[3] $$ImH^+(aq) = Im(aq) + H^+(aq) \qquad \Delta H_3$$

Two calorimetric titration runs in which 0.2445 *M* HCl was titrated into 0.01400 *M* imidazole led to $\Delta H_3^\circ = 8.70$ kcal mole^{-1}, with our estimate of the *total* uncertainty in this value being $\pm$ 0.12 kcal mole^{-1}.

We have also made calorimetric measurements of the heats to be associated with eqs. 1 and 2 in solutions maintained at ionic strength of 0.20 *M* with NaCl and have combined these results to obtain ΔH_3 (I = 0.20) = 8.81 kcal mole^{-1}, with *total* uncertainty estimated to be $\pm$ 0.04 kcal mole^{-1}.

The p*K* values at several temperatures obtained by Datta and Grzybowski (9) led these investigators to report $\Delta H_3^\circ = 8.79 \pm 0.03$ kcal mole^{-1}. Christensen *et al.* (11) have made calorimetric measurements in which aqueous imidazole was titrated with aqueous acetic acid. Their results yielded p*K* for reaction (3) and also led them to report $\Delta H_3^\circ = 8.78 \pm 0.04$ kcal mole^{-1}. Calorimetric measurements by Wadso (12) have led him to report ΔH_3 (I = 0.20) = 8.79 $\pm$ 0.03 kcal mole^{-1}.

All of the reported ΔH_3 values are summarized in Table 3. It is an indication of the considerable progress in investigation of thermodynamics of ionization reactions that these values range only from 8.70 to 8.81 kcal mole^{-1}.

TABLE 3

Heats of proton ionization from imidazolium ion

Method	ΔH (kcal mole^{-1})	Reference
"Traditional" calorimetry, I = 0	8.71 ± 0.04*	This work
Titration calorimetry, I = 0	8.70 ± 0.12*	This work
Titration calorimetry, I = 0	8.78 ± 0.04†	11
dpK/dT	8.79 ± 0.03†	9
"Traditional" calorimetry, I = 0.20	8.81 ± 0.04*	This work
"Traditional" calorimetry, I = 0.20	8.79 ± 0.03†	12

*We use ± to indicate estimated *total* uncertainties, rather than average deviations, standard deviations, etc.
†The ± values cited are those given by the original authors.

The values calculated from dpK/dT (9) and obtained by calorimetric titration with acetic acid (11) are in excellent agreement, both being larger than our ΔH_3° values. Our analysis of uncertainties in the reported p*K* values (9) and subsequent calculations leading to ΔH_3° *suggests* that the *total* uncertainty is larger than the $\pm$ 0.03 kcal mole^{-1} originally reported. On this basis we therefore say that this ΔH_3° value is in satisfactory agreement with all of the other values listed in Table 3. Our results and those of Wadso (12) that refer to solutions with I = 0.20 *M* are in agreement with each other, but are not directly applicable to evaluation of the best ΔH_3° value referring to solutions with I = 0. But the excellent agreement of these independent calorimetric ΔH values does provide support for our assessment of our uncertainties.

In calculating ΔH_3° from results of their calorimetric titration measurements, Christensen *et al.* (11) used $\Delta H^\circ = -0.01$ kcal mole^{-1} for proton ionization from aqueous acetic acid. There is some evidence (2) that the "best" ΔH° value for this reaction is a little more negative than their −0.01 kcal mole^{-1}. Recalculation of their results with a more negative ΔH° for ionization of aqueous acetic acid decreases the derived ΔH_3° and can account for all of the difference between the values cited in Table 3.

On the basis of considerations cited above and because we were able to draw upon useful advice from earlier workers (11, 12), we believe that our $\Delta H_3^\circ = 8.71 \pm 0.04$ kcal mole^{-1} from "tradi-

TABLE 4

Thermodynamics of proton ionizations in aqueous solution at 298 °K*

Acid	pK	$\Delta G°$ (kcal mole^{-1})	$\Delta H°$ (kcal mole^{-1})	$\Delta S°$ (cal deg^{-1} mole^{-1})
Imidazolium ion	6.993 (±0.002)	9.545 (±0.003)	8.71 (±0.04)	−2.8 (±0.1)
6-Uracilcarboxylic acid				
1st	1.8 (±0.2)	2.4 (±0.3)	0.5 (±0.5)	−6.4 (±3)
2nd	9.55 (±0.15)	13.0 (±0.2)	8.7 (±0.7)	−14.4 (±3)
Protonated hypoxanthine				
1st	1.9 (±0.15)	2.6 (±0.2)	2.5 (±0.3)	0.3 (±2)
2nd	8.8 (±0.15)	12.0 (±0.2)	8.0 (±0.3)	−13.4 (±2)
3rd	12.0 (±0.2)	16.4 (±0.3)	10.0 (±0.5)	−21.5 (±3)

*We have used ± to indicate our estimates of *total* uncertainty (chemical purity, measurement errors, heats of dilution, etc.) rather than average or standard deviation.

tional" calorimetry is the "best" value for this proton ionization reaction. We combine this $\Delta H_3°$ with $\Delta G_3° = 9.545$ kcal mole^{-1} from pK = 6.993 (9) to obtain $\Delta S_3° = -2.8 \pm 0.1$ cal deg^{-1} mole^{-1}.

Because 6-uracilcarboxylic acid and hypoxanthine are only slightly soluble and dissolve slowly, it was found to be more convenient to investigate the proton ionization properties of these compounds by titration calorimetry than by "traditional" calorimetry. In all such measurements we titrated 95.00 ml of dilute (M = 0.0032 to 0.0061) organic solute with standardized aqueous HCl or standardized aqueous NaOH. Results of these measurements are reported in Table 4 where we also list our pK values and the derived $\Delta G°$ and $\Delta S°$ values. Included in Table 4 are the "best" values for imidazole cited earlier in this paper.

Equilibrium constants and other thermodynamic data for proton ionization reactions refer to well-defined reactions, but do not necessarily provide evidence concerning the structures of the species involved in the reaction. For example, the data reported here for proton ionization from imidazolium ion refer quite explicitly to the reaction represented by eq. 3. These data, however, do not tell us (at least, do not tell us directly) to which nitrogen the "extra" proton is attached in imidazolium ion. Similarly, the thermodynamic data for 6-uracilcarboxylic acid refer explicitly to loss of one proton from the neutral acid and loss of another proton from the anion formed as a result of loss of the first proton. But these data do not necessarily tell us which proton is involved in either ionization reaction, nor do these data necessarily tell us whether the enol or keto form is predominant. Similar considerations also apply to the successive proton ionizations from protonated hypoxanthine. On the other hand, it is clear from earlier investigations (2, 5–7) that we can expect considerable guidance from thermodynamic data in making decisions about these and similar questions, once we have data for related heterocyclic acids and bases.

It is commonly believed, partly on the basis of resonance stabilization arguments, that the structure of imidazolium ion may be represented by **1**.

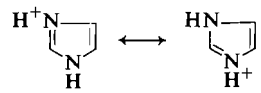

1

Dolman (13) has recently obtained spectroscopic evidence to support this formulation. On the basis of comparison of data in Table 4 for imidazolium ion with similar data (2) for other nitrogen-containing compounds, we conclude that the thermodynamic data are consistent with this formulation.

The data in Table 4 for the first ionization of 6-uracilcarboxylic acid (**2**) are consistent with

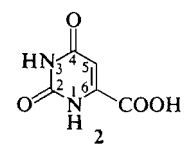

2

other data (2) for ionization of highly polar carboxylic acids. We have a less satisfactory basis for similar comparisons for the second ionization, but suggest that the second proton ionization is from the 3 position rather than the 1 position. We have pictured 6-uracilcarboxylic

Can. J. Chem. Downloaded from www.nrcresearchpress.com by 210.87.254.5 on 09/05/12
For personal use only.

acid in the keto form, although the enol form might be predominant.

We represent protonated hypoxanthine by **3** in

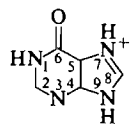

3

which the positive charge may be distributed between the 7 and 9 positions. It seems reasonable to suggest that the first proton ionization refers to loss of a proton from either the 7 or 9 position, while the second proton is lost from the 1 position and the third from either the 7 or 9 position. Again, we have drawn the keto structure.

Our experience with numerous measurements on imidazole and critical comparisons (14) of earlier results obtained in different ways lead us to make the following comments. First, titration calorimetry is probably the quickest and easiest way to determine reliable ΔH° values for most proton ionization reactions. Secondly, "traditional" reaction calorimetry can lead to more accurate ΔH° values, usually after expenditure of greater effort and more time. Finally, we believe that uncertainties in ΔH° values obtained calorimetrically are easier to assess and likely to be smaller than uncertainties in ΔH° values derived from proton ionization constants at several temperatures and the van't Hoff equation.

This research has been supported by the National Research Council of Canada and the University of Lethbridge Research Committee, Lethbridge, Alberta. We are grateful to C. Bender, J. Christensen, D. Dolman, R. Izatt, R. Meintzer, and I. Wadso for their helpful comments.

1. E. J. KING. Acid-base equilibria. Pergamon Press, Inc., Oxford, England. 1965.
2. J. W. LARSON and L. G. HEPLER. *In* Solute-solvent interactions. J. F. Coetzee and C. D. Ritchie, editors. Marcel Dekker, Inc., New York, N.Y. 1969.
3. L. G. HEPLER. J. Amer. Chem. Soc. **85**, 3089 (1963); L. G. HEPLER. J. Phys. Chem. **68**, 2645 (1964); J. W. LARSON and L. G. HEPLER. J. Org. Chem. **33**, 3961 (1968). (Note that the misprinted equation 17 in the latter paper should have a fraction on the right side that reduces to ~0/0.)
4. L. G. HEPLER. J. Phys. Chem. **69**, 965 (1965).
5. R. M. IZATT, J. H. RYTTING, L. D. HANSEN, and J. J. CHRISTENSEN. J. Amer. Chem. Soc. **88**, 2641 (1966); **87**, 2760 (1965); J. J. CHRISTENSEN, J. H. RYTTING, and R. M. IZATT. J. Amer. Chem. Soc. **88**, 5105 (1966).
6. R. M. IZATT and J. J. CHRISTENSEN. J. Phys. Chem. **66**, 359, 1030 (1962).
7. J. J. CHRISTENSEN, J. H. RYTTING, and R. M. IZATT. J. Phys. Chem. **71**, 2700 (1967).
8. E. H. SWIFT. Introductory quantitative analysis. Prentice-Hall, Inc., New York, N.Y. 1950.
9. S. P. DATTA and A. K. GRZYBOWSKI. J. Chem. Soc. (B) 136 (1966).
10. J. O. FROHLIGER, R. A. GARTSKA, H. W. IRWIN, and O. W. STEWARD. Anal. Chem. **40**, 1408 (1968).
11. J. J. CHRISTENSEN, D. P. WRATHALL, and R. M. IZATT. Anal. Chem. **40**, 175 (1968).
12. I. WADSO. Acta Chem. Scand. **16**, 479 (1962).
13. D. DOLMAN. Personal Commun. 1970.
14. L. G. HEPLER and E. M. WOOLLEY. International symposium on calorimetry in chemistry and biology. Guildford, England. 1969.

Can. J. Chem. Downloaded from www.nrcresearchpress.com by 210.87.254.5 on 09/05/12
For personal use only.

Branched-chain 2-deoxy sugars. V. Application of the Wittig reaction to methyl 3,4-*O*-isopropylidene-β-D-*erythro*-pentopyranosid-2-ulose and attempted synthesis of nucleosides of 2-deoxy-2-*C*-methylpentoses

ALEX ROSENTHAL AND MATEJ SPRINZL
Department of Chemistry, University of British Columbia, Vancouver 8, British Columbia
Received April 24, 1970

Oxidation of methyl 3,4-*O*-isopropylidene-β-D-arabinopyranoside (**1**) with ruthenium tetroxide afforded methyl 3,4-*O*-isopropylidene-β-D-*erythro*-pentopyranosid-2-ulose (**2**) in 78% yield. Condensation of methylenetriphenylphosphorane with **2** in the presence of *n*-butyllithium yielded methyl 3,4-*O*-isopropylidene-2-deoxy-2-*C*-methylene-β-D-*erythro*-pentopyranoside (**3**) in 55% yield. Reduction of the latter with 10% palladium-on-charcoal gave a 7:1 mixture of two isomeric 2-deoxy-2-*C*-methylpentoside derivatives in 95% yield: the preponderant product had the D-*ribo* configuration. The fully blocked methyl glycosides were de-isopropylidenated with methanolic hydrogen chloride to yield **6** and **7** and these were converted into the *p*-toluoyl esters (**8**) and (**9**). Attempts to utilize the latter in the synthesis of nucleosides of 2-deoxy-2-*C*-methyl pentoses were unsuccessful.

Canadian Journal of Chemistry, 48, 3253 (1970)

Introduction

Until 1967 there were few useful synthetic routes for the preparation of branched-chain deoxy sugars possessing a hydrogen and a *C*-alkyl, hydroxyalkyl, or aminoalkyl substituent on the same carbon (1–3). During the past few years the Wittig reaction has been successfully applied to several 3-keto sugar derivatives to afford unsaturated sugar derivatives; the latter have been readily converted stereoselectively in high yield into the aforementioned type of branched-chain deoxy sugars (4–7). There is also a report of a light-induced addition of 1,3-dioxolan to an unsaturated carbohydrate in the presence of acetone to afford a branched-chain sugar (8). Although sodium cyanide and hydrogen cyanide have been used to open carbohydrate epoxides (9, 10), and the oxo reaction has been applied to unsaturated carbohydrates (11) to afford branched-chain sugars, these routes give complex mixtures of products. A more promising supplementary route to the branched-chain amino sugars has been provided via the nitromethane addition to keto sugar derivatives and the nitroethane addition to dialdehydo sugar derivatives (12).

In continuation of our studies on the synthesis of branched-chain sugars and their subsequent utilization in the preparation of 3′-deoxy-3′-*C*-methyl (and hydroxyalkyl) sugar nucleosides (6, 13) we now wish to report an extension of the Wittig reaction to a 2-keto sugar derivative to afford two novel isomeric 2-*C*-methylpentoside derivatives.

Results and Discussion

Oxidation of methyl 3,4-*O*-isopropylidene-β-D-arabinopyranoside (**1**) with ruthenium tetroxide, according to a slight modification of the procedure of Lawton *et al.* (14), afforded methyl 3,4-*O*-isopropylidene-β-D-*erythro*-pentopyranosid-2-ulose (**2**) (see Scheme 1), which was obtained as the hydrate in crystalline form in 78% yield. Distillation of anhydrous benzene from the hydrate converted the latter into the keto sugar (**2**). Methyl 3,4-*O*-isopropylidene-β-L-*erythro*-pentopyranosid-2-ulose has been prepared by ruthenium tetroxide oxidation of the appropriate glycoside in 40% yield (15), whereas the D-enantiomer of the latter was prepared in 80% yield (16). Treatment of **1** with methylsulfoxide – phosphorus pentoxide (17) as oxidant gave a 40% yield of the keto sugar (**2**); utilization of methyl sulfoxide – acetic anhydride as oxidant (18) raised the yield to 55%. Reaction of methyltriphenylphosphonium bromide with *n*-butyllithium in hexane (19) with the 2-keto sugar (**2**) afforded the branched-chain unsaturated sugar, methyl 3,4-*O*-isopropylidene-2-deoxy-2-*C*-methylene-β-D-*erythro*-pentopyranoside (**3**), in 55% yield. Contaminants accompanying **3** were removed by chromatography on silica gel, with 10:1 benzene – ethyl acetate as eluent. The unsaturated sugar (**3**) was stable and could be distilled under reduced pressure. Substitution of tetrahydrofuran for ether as solvent in the Wittig reaction led to a significant decrease in yield of **3** and also led to partial degradation of the product. When methylenetriphenylphos-

Can. J. Chem. Downloaded from www.nrcresearchpress.com by 210.87.254.42 on 09/05/12
For personal use only.

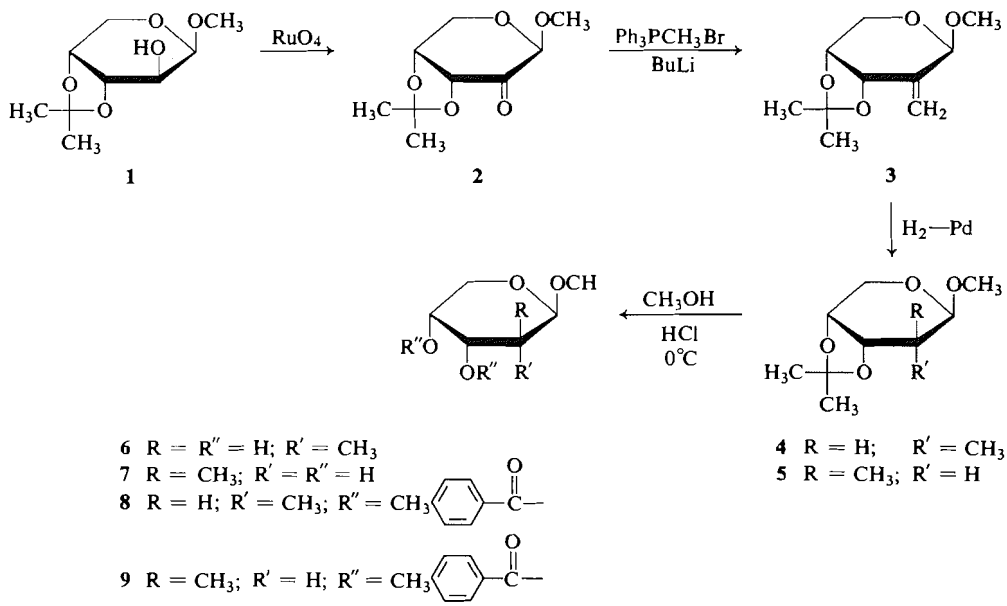

SCHEME 1

phorane was obtained by allowing methyltriphenylphosphonium bromide in methyl sulfoxide to react with sodium hydride, according to a previously published procedure (6), then **3** was obtained in 3% yield.

Hydrogenation of the unsaturated sugar (**3**), with 10% palladium-on-charcoal as catalyst, gave a 7:1 mixture of *ribo* and *arabino* epimers, namely, methyl 2-deoxy-2-*C*-methyl-3,4-*O*-isopropylidene-β-D-*ribo* (**4**) and *arabino* (**5**) pyranoside in a combined yield of 95%. This mixture was separated by silica gel column chromatography with 50:1 benzene – ethyl acetate as developer. When Wilkinson catalyst (20) (triphenylphosphine ruthenium chloride) was used as catalyst, a 7:4 mixture of 2-*C*-methylribo- (**4**) and -arabinopentosides was obtained. The structures of **4** and **5** were readily deduced from their n.m.r. spectra in chloroform-*d*. The *ribo*-isomer (**4**) showed a 1-proton doublet at τ 5.62 with $J = 8$ Hz, which collapsed to a singlet on irradiation of H-2 at τ 8.3, that was assigned to H-1. The large geminal coupling of the axial anomeric hydrogen with the C-2 hydrogen indicates strongly that H-2 must be in an axial orientation, and therefore, the C-2 methyl group is in an equatorial orientation and **4** must be the *ribo*-isomer. On the other hand, the n.m.r. of **5** showed a 1-proton doublet at τ 5.51 with $J = 3$ Hz. The much smaller $J_{1,2}$ of compound **5** than of compound **4**, indicates that H-2 of **5** must be in an equatorial orientation, and therefore compound **5** must be methyl 2-deoxy-3,4-*O*-isopropylidene-β-D-arabinopyranoside.

Hydrolysis of **4** and **5** to afford the branched-chain methyl glycosides **6** and **7** posed a problem of unexpected difficulty. Hydrolysis of **4** and **5** with about 0.01 *M* hydrogen chloride in anhydrous methanol must be done under careful surveillance by t.l.c. monitoring. For optimal yield of product, the reaction mixture was kept at 0° for 2 h. Purification of the product was achieved by silica gel column chromatography with 10:1 benzene – ethyl acetate as eluent. Utilization of Dowex 50 (H^+) resin in methanol for removal of the isopropylidene group gave a mixture of at least four products which could not be separated by column chromatography. Complete hydrolysis of **4** and **5** was achieved in 5 min with 90% trifluoroacetic acid to afford 2-deoxy-2-*C*-methyl-D-*ribo*-(and *arabino*)pentose as evidenced by their n.m.r. spectra. The free sugars were accompanied by impurities which could not be removed and as a consequence no attempt was made to characterize the free sugars.

As the primary objective of the research outlined herein was to prepare 2′-*C*-methyl pyranosyl (and furanosyl) nucleosides, the next step was the

Can. J. Chem. Downloaded from www.nrcresearchpress.com by 210.87.254.42 on 09/05/12
For personal use only.

Can. J. Chem. Downloaded from www.nrcresearchpress.com by 210.87.254.42 on 09/05/12
For personal use only.

conversion of the methyl glycosides **6** and **7** into suitably blocked pyranosyl sugar halides. When the *p*-nitrobenzoyl group was used as a blocking group the *p*-nitrobenzoates of sufficient analytical purity for nucleoside synthesis could not be obtained. Treatment of **6** and **7** with *p*-toluoyl chloride in pyridine afforded the *p*-toluoyl esters **8** and **9** (crystalline) which appeared to have the correct structure (as judged from their n.m.r. spectra) but which gave elemental analysis which deviated slightly from the theoretical values (about 1%). These toluoyl esters were allowed to react with hydrogen bromide or hydrogen chloride in methylene chloride to afford the pyranosyl halide which was immediately allowed to react with 6-benzamidochloromercuripurine by an already published procedure (21) to afford a mixture of products. This mixture, after the usual work-up, was partially separated by preparative silica gel G t.l.c. with 1:1 benzene – ethyl acetate as developer to afford trace quantities of impure 2′-deoxy-2′-*C*-methylribo-β(and α)pyranosyl adenine nucleosides. The great difficulty in obtaining sufficient quanties of nucleosides for analysis and the recent publication (22) of nucleosides from 2-*C*-methyl-2-deoxy-*erythro*-D-pentose led us to abandon further work on the project.

Experimental

General considerations were similar to those previously described (6, 13).

Methyl 3-4-O-Isopropylidene-β-D-arabinopyranoside (1)

The title compound (**1**) was prepared from D-arabinose in 59% yield, b.p. 94° (at 0.75 mm pressure); $[\alpha]_D^{22}$ −202° (*c* 1, chloroform), according to a procedure used for the preparation of the L-enantiomer (23, 24), and agrees with the physical constants given for the enantiomer.

Methyl 3,4-O-Isopropylidene-β-D-erythro-pentopyranosid-2-ulose (2)

To a solution of methyl 3,4-*O*-isopropylidene-β-D-*arabino*-pyranoside (**1**) (4 g) in carbon tetrachloride (75 ml) was added water (15 ml), sodium hydrogen carbonate (1 g), and ruthenium dioxide (80 mg). Sodium metaperiodate (1.2 equiv of 5% aqueous solution) was added dropwise in small aliquots to the vigorously stirred solution (it is important to avoid adding excess of oxidant and to add the oxidant only when the color of the solution changes). After any excess oxidant was destroyed, by the addition of a few drops of isopropyl alcohol, the precipitated ruthenium compound was removed by filtration. The water layer was then extracted with chloroform (7 × 30 ml). This combined extract was now added to the carbon tetrachloride layer and evaporated to yield 3.2 g (78%) of the hydrate of the ketose (**2**). Recrystallization of this hydrate from methanol afforded 2.8 g of the ketose hydrate, m.p. 114°; $[\alpha]_D^{22}$ −161° (*c* 1, ethanol); ν(Nujol) 3600 (OH). The hydrate was converted to the ketose **2** by distilling benzene from it; ν(Nujol) 1750 (carbonyl).

When **1** was oxidized with methyl sulfoxide in the presence of phosphorus pentoxide (17) the yield of ketose (**2**) was 40%. Compound **1** was also converted into **2** in 55% yield using methyl sulfoxide – acetic anhydride as oxidant (18).

Application of the Wittig Reaction to 2 to Yield Methyl 3,4-O-Isopropylidene-2-deoxy-2-C-methylene-β-D-erythro-pentopyranoside (3)

Methyltriphenylphosphonium bromide (10.95 g) was added in small portions with stirring to a solution of *n*-butyllithium in hexane (13.2 ml of 2.25 *M*) and ether (50 ml) contained in a nitrogen-filled dry box. After the reactants were stirred for 4 h, a solution of the ketose (**2**) (6 g dissolved in 50 ml of ether) was added dropwise to the ylide and the reaction allowed to proceed for an additional 2 h. The reaction mixture was filtered and the filtrate extracted with water (3 × 10 ml) until the last aqueous extract was neutral. The combined ether extracts were dried with magnesium sulfate, filtered, and the filtrate evaporated to a syrup (3.3 g, 55%). Silica gel column chromatography of this syrup with 10:1 benzene – ethyl acetate as developer gave 1.7 g of pure unsaturated sugar **3**. The analytical sample was prepared by distillation at 80° at 0.005 atm pressure; $[\alpha]_D^{22}$ −176° (*c* 2, chloroform); τ ($CDCl_3$) 4.6 (m, methylene group), 4.9 (t, H-1), 5.2 (d, H-3), 5.8 (d, H-4), 6.2 (d, H-5), 6.55 (s, OCH_3), 8.5 (d, CMe_2).

Anal. Calcd. for $C_{10}H_{16}O_4$: C, 60.00; H, 8.07. Found: C, 60.12; H, 8.14.

When the ketose **2** was allowed to react with the same ylide in methyl sulfoxide containing sodium hydride according to a previously published procedure (6), then a 3% yield of **3** was obtained. Use of *n*-butyllithium in tetrahydrofuran led to considerable cleavage of the glycosidic bond of **2**.

Hydrogenation of 3 to Yield Methyl 2-Deoxy-2-C-methyl-3,4-O-isopropylidene-β-D-ribopyranoside (4) and Methyl 2-Deoxy-2-C-methyl-3,4-O-isopropylidene-β-D-arabinopyranoside (5)

(a) Using Pd–C as Catalyst

The unsaturated sugar **3** (0.4 g) in 20 ml of methanol was hydrogenated using 10% palladium-on-charcoal as catalyst; 1 mol equiv of gas was absorbed in 1 h. The catalyst was removed by filtration through Celite and the filtrate was then evaporated to a syrup (0.38 g, 95%). The ratio of isomers **4** and **5** was 7:1 as evidenced by n.m.r.

The mixture of isomers **4** and **5** (2.65 g) was separated by chromatography on silical gel (40 g, activity grade II) with 50:1 benzene – ethyl acetate as developer. The slower moving zone (1.61 g, *ribo*-pentoside (**4**)) had an R_f 0.50 with 10:1 benzene – ethyl acetate as developer and a b.p. of 60–65° at 12 mm pressure; $[\alpha]_D^{22}$ −81° (*c* 2, chloroform); τ ($CDCl_3$) 5.62 (d, H-1, $J_{1,2}$ = 8 Hz), 5.8 (m, one H), 6.35 (m, two H), 6.6 (s, OCH_3), 8.3 (m, H-2), 8.6 (CMe_2), 8.85 (d, J = 6 Hz, Me-2).

Anal. Calcd. for **4**, $C_{10}H_{18}O_4$: C, 59.40; H, 8.97. Found: C, 59.34; H, 9.06.

Can. J. Chem. Downloaded from www.nrcresearchpress.com by 210.87.254.42 on 09/05/12
For personal use only.

The faster moving zone (0.32 g of *arabino*-pentoside (**5**) had an R_f 0.55 and b.p. of 60–65° at 12 mm pressure; $[\alpha]_D^{22}$ −78° (*c* 2, chloroform); τ ($CDCl_3$) 5.5 (d, H-1, $J_{1,2}$ = 3 Hz), 5.9–6.3 (m, equal to 4H), 6.65 (s, OCH_3), 8.2 (m, H-2), 8.55 (d, CMe_2), 8.95 (d, J = 6.5 Hz, Me-2). For analysis **5** was distilled under reduced pressure.

Anal. Calcd. for **5**, $C_{10}H_{18}O_4$: C, 59.40; H, 8.91. Found: C, 59.30; H, 9.02.

(b) Using Triphenylphosphine Ruthenium Chloride (Wilkinson Catalyst)

The unsaturated sugar **3** (0.66 g) was dissolved in benzene (50 ml) and hydrogenated in the presence of triphenylphosphine ruthenium chloride (0.2 g) (20) at 20° at atmospheric pressure for 3 days. After the solvent was removed under reduced pressure, petroleum ether (20 ml, b.p. 30–60°) was added. The precipitate was removed by filtration, washed with petroleum ether (2 × 10 ml), and the filtrate evaporated under reduced pressure to yield 0.60 g (91%) of a 7:4 mixture of the isomers **4** and **5**.

*Partial Hydrolysis of **4** to Yield Methyl 2-Deoxy-2-C-methyl-β-D-ribopyranoside (**6**)*

Methyl 3,4-*O*-isopropylidene-2-deoxy-2-*C*-methyl-β-D-ribopyranoside (**4**) (0.32 g) was dissolved in an ice-cold solution of 5 ml anhydrous methanol containing 0.01 *M* anhydrous hydrogen chloride. After the reaction mixture was kept at 0° for 2 h, it was neutralized with an excess of solid sodium hydrogen carbonate, filtered, and the filtrate evaporated to yield a syrup (0.22 g, 87%). This syrup was chromatographed on 20 g silica gel (activity grade II) with 10:1 benzene – ethyl acetate as developer to afford 0.181 g of a homogeneous powder (by t.l.c.), R_f 0.25 on silica gel G with 10:1 benzene – ethyl acetate as developer; $[\alpha]_D^{22}$ −151° (*c* 1, chloroform); τ ($CDCl_3$) 5.6 (d, H-1, $J_{1,2}$ = 8 Hz), 6.1–6.5 (m, H-5, H-4, H-3), 6.6 (OCH_3), 7.2 (s, OH), 8.3 (m, H-2), 8.9 (d, J = 7 Hz, CH_3).

*Methyl 2-Deoxy-2-C-methyl-β-D-arabinopyranoside (**7**)*

The arabino sugar **5** (0.100 g) was partially hydrolyzed according to the same procedure used for the hydrolysis of **4**. The product was, however, not purified by column chromatography but was crystallized from petroleum ether (b.p. 30–60°) to give 0.054 g (67%) of crystalline methyl 2-deoxy-2-*C*-methyl-β-D-arabinopyranoside, R_f 0.7 with 10:1 benzene–ethyl acetate as developer; m.p. 136°; $[\alpha]_D^{22}$ − 24° (*c* 2, chloroform); τ ($CDCl_3$) 5.45 (d, H-1, $J_{1,2}$ = 3 Hz), 6.0–6.5 (m, H-5, H-4, H-3), 6.65 (s, OCH_3), 8.0 (s, OH, overlapping H-2), 7.8–8.2 (m, H-2), 9.0 (d, J = 7 Hz, CH_3).

Anal. Calcd. for $C_7H_{14}O_4$: C, 51.84; H, 8.70. Found: C, 51.66; H, 8.67.

*Attempted Complete Hydrolysis of Sugars **4** and **5** with Trifluoroacetic Acid to Yield 2-Deoxy-2-C-methyl-D-ribo-pentose and 2-Deoxy-2-C-methyl-D-arabino-pentose*

The blocked *ribo*-isomer **4** (0.49 g) was allowed to react at room temperature for 5 min with 90% trifluoroacetic acid (5 ml). The solution was immediately evaporated at 30° at 1 mm pressure. The syrup was triturated with ether and the white precipitate was isolated by decantation, yield 0.35 g. The main component had $R_{Glucose}$ 1.7 on paper with 8:2:2 ethyl acetate – pyridine – water as developer (several additional spots were visible). The sugar gave a positive Fehling's test. τ (D_2O) of the *ribo* free sugar 4.8–5.3 (m, H-1, poorly resolved), 5.5–6.7 (m, H-5, H-4, H-3), 7.5–8.3 (m, H-2), 8.8–9.1 (three d, CH_3). The free sugar was probably a mixture of α- and β-anomers of both pyranose and furanose sugars.

Similar treatment of the *arabino*-isomer (**5**) gave mainly one reducing sugar having $R_{Glucose}$ 1.7 which in D_2O solution probably existed as an anomeric mixture of pyranose and furanose sugars.

*Methyl 2-Deoxy-2-C-methyl-3,4-di-O-p-toluoyl-β-D-ribopyranoside (**8**)*

To an ice-cold solution of compound **6** (0.282 g) in anhydrous pyridine (8 ml) was added with mixing freshly distilled *p*-toluoyl chloride (0.5 ml). After the reaction mixture stood overnight at room temperature, water (10 ml) was added, and then the mixture was extracted with chloroform (3 × 15 ml). The combined chloroform extracts were washed with saturated aqueous sodium hydrogen carbonate, water, dried with magnesium sulfate, filtered, and the filtrate evaporated under reduced pressure to yield a syrup (0.65 g). This syrup was chromatographed on 50 g silica gel (grade II) with 50:1 benzene – ethyl acetate as developer to afford chromatographically pure **8** (0.530 g, 73%), R_f 0.7 (10:1 benzene – ethyl acetate); $[\alpha]_D^{22}$ −62° (*c* 1, chloroform); τ ($CDCl_3$) 2.0 (m), 2.7 (m), 4.22 (t, equal to one H), 4.55 (m, equal to one H), 5.35 (d, H-1, $J_{1,2}$ = 6 Hz), 5.9 (m, equal to three H), 6.45 (s, OCH_3), 7.6 (d, toluoyl CH_3), 2.1 (m, H-2), 8.8 (d, *C*—$2CH_3$, J = 7 Hz).

*Methyl 2-Deoxy-2-C-methyl-3,4-di-O-p-toluoyl-β-D-arabinopyranoside (**9**)*

The arabinopyranoside **7** was allowed to react with *p*-toluoyl chloride in the same manner as described for the preparation of **8** to afford **9** in 69% yield. Compound **9** was recrystallized from methanol–ether, m.p. 84–85°; R_f = 0.7; $[\alpha]_D^{22}$ −69° (*c* 1, chloroform); τ ($CDCl_3$) 2.0 (m), 2.7 (m), 4.45 (t, equal to one H), 4.6 (d, equal to one H), 5.23 (d, H-1, $J_{1,2}$ = 3 Hz), 5.95 (m, equal to two H), 6.58 (s, OCH_3), 7.6 (d, toluoyl CH_3), 8.7 (m, H-2), 8.95 (d, *C*—$2CH_3$, J = 7 Hz). The elemental analysis of **9** deviated by about 1% from the theoretical values, but the n.m.r. spectrum of **9** was in complete accord with the title compound.

Attempted Synthesis of 9-(2′-Deoxy-2′-C-methyl-β-(and α)-D-arabino(and ribo)pyranosyl)adenine

The blocked methyl arabinopyranoside (**9**) was converted into the blocked pyranosyl bromide by reaction with hydrogen bromide in methylene chloride at 0° and subsequently immediately condensed with 6-benzamidochloromercuripurine in the presence of cadmium carbonate according to a procedure already published (21). A mixture of α- and β-blocked nucleosides as syrups was obtained in very low yield having R_f of 0.4 and 0.3 on silica gel G with 1:1 benzene–ethyl acetate as developer; $[\alpha]_D^{22}$ (faster component) −94° (*c* 0.2 chloroform), $[\alpha]_D^{22}$ (slower component) −62° (*c* 0.2, chloroform); τ ($CDCl_3$) (faster component) 3.6 (d, probably H-1′, $J_{1',2'}$ = 3 Hz), 7.5 (d, *p*-toluoyl CH_3),

8.95 (d, C-2′-CH_3, J = 7 Hz); τ ($CDCl_3$) (slower component) 4.15 (d, probably H-1′, $J_{1',2'}$ = 1.5 Hz), 7.6 (d, *p*-toluoyl CH_3), 9.3 (d, C-2′-CH_3, J = 7 Hz).

Insufficient quantity of nucleosides was obtained for satisfactory analyses.

Attempts to use the blocked methyl ribopyranoside (**8**) as an intermediate in the nucleoside synthesis gave only trace amounts of nucleosides. Attempts to convert the *p*-nitrobenzoyl esters of **6** and **7** into nucleosides were also unsuccessful.

This research was supported by the National Research Council of Canada.

1. W. G. Overend. Chem. Ind. London. 342 1963.
2. L. Hough and A. C. Richardson. In Rodd's chemistry of carbon compounds. Edited by S. Coffey. Vol. I. Part F. Elsevier Publishing Co., Amsterdam, 1967. pp. 529–543.
3. J. S. Brimacombe. Angew. Chem. Int. Edit. **8**, 401 (1969).
4. A. Rosenthal and L. (Benzing) Nguyen. Tetrahedron Lett. 2393 (1967). A. Rosenthal and P. Catsoulacos, Can. J. Chem. **46**, 2868 (1968).
5. D. G. Lance and W. A. Szarek. Carbohyd. Res. **10**, 306 (1969). W. A. Szarek, J. S. Jewell, I. Szczerek, and J. K. N. Jones. Can. J. Chem. **47**, 4473 (1969). E. A. Williams, W. A. Szarek, and J. K. N. Jones. Can. J. Chem. **47**, 4467 (1969).
6. A. Rosenthal and Matej Sprinzl. Can. J. Chem. **47**, 3941, 4477 (1969).
7. A. Rosenthal and D. Baker. Tetrahedron Lett. 397 (1969).
8. J. S. Jewell and W. A. Szarek. Tetrahedron Lett. 43 (1969).
9. N. R. Williams. Chem. Commun. 1012 (1967).
10. B. E. Davison, R. D. Guthrie, and A. T. McPhail. Chem. Commun. 1273 (1968).
11. A. Rosenthal and H. J. Koch. J. Amer. Chem. Soc. **90**, 2181 (1968). A. Rosenthal. Advan. Carbohyd. Chem. **23**, 59 (1969).
12. A. Rosenthal and K. S. Ong. Tetrahedron Lett. 3981 (1969). G. J. Lourens. Tetrahedron Lett. 3733 (1969). A. Rosenthal, K. S. Ong, and D. Baker. Carbohyd. Res. **13**, 113 (1970). H. H. Baer and K. S. Ong. Can. J. Chem. **46**, 2511 (1968).
13. A. Rosenthal and L. Nguyen. J. Org. Chem. **34**, 1029 (1969).
14. B. T. Lawton, W. A. Szarek, and J. K. N. Jones. Carbohyd. Res. **10**, 456 (1969).
15. P. J. Beynon, P. M. Collins, P. T. Doganges, and W. G. Overend. J. Chem. Soc. (C), 1131 (1966).
16. V. M. Parikh and J. K. N. Jones. Can. J. Chem. **43**, 3452 (1965).
17. K. Onodera, S. Hirano, and N. Kashimura. J. Amer. Chem. Soc. **87**, 4651 (1965).
18. W. Sowa and G. H. S. Thomas. Can. J. Chem. **44**, 836 (1966).
19. G. Wittig and U. Schoellkopf. Org. Syn. **40**, 66 (1960).
20. J. F. Young, J. A. Osborn, F. H. Jardine, and G. Wilkinson. Chem. Commun. 131 (1965).
21. A. Rosenthal, M. Sprinzl, and H. J. Koch. Can. J. Chem. **47**, 3263 (1969).
22. J. J. K. Novák, J. Šmejkal and F. Šorm. Tetrahedron Lett. 1627 (1969).
23. J. W. Pratt, N. K. Richtmyer, and C. S. Hudson. J. Amer. Chem. Soc. **74**, 2200 (1952).
24. J. Honeyman. J. Chem. Soc. **212**, 990 (1946).

Can. J. Chem. Downloaded from www.nrcresearchpress.com by 210.87.254.42 on 09/05/12
For personal use only.

Can. J. Chem. Downloaded from www.nrcresearchpress.com by 210.87.254.40 on 09/05/12
For personal use only.

Reactivities of ions and ion-pairs in the base-catalyzed reaction of phenyl glycidyl ether and benzoic acid in various solvents

YOSHIO TANAKA, AKIRA OKADA, AND MITSUO SUZUKI
Research Institute for Polymers and Textiles, 4 Sawatari, Kanagawa, Yokohama, Japan

Received February 20, 1970

The conductance of pyridinium benzoate has been measured in various solvents such as nitrobenzene, benzonitrile, *o*-dichlorobenzene, monochlorobenzene, and toluene, and its dissociation constant, K, was determined, using the Kraus and Bray's equation with the Λ_0 value estimated from Walden and Ulich's rule and Stokes's law. The logarithm of K was found to be linear with the reciprocal of the dielectric constant, ε, or with the Kirkwood–Laidler–Eyring function, $(\varepsilon - 1)/(2\varepsilon + 1)$. Kinetic studies for pyridine-catalyzed reaction between phenyl glycidyl ether and benzoic acid were also made in these solvents. Both the free ions and ion-pairs including the molecular addition complex participate in the reaction. The apparent rate constants, k'', of the reaction were shown to be linear with $1/(K/c)^{1/2}$, c being the concentration of pyridinium benzoate. The intercepts of such lines give the rate constant for formation of ion-pairs, k_i, and the slopes yield the rate constant for formation of free ion, k_f. The free ion rate constant increases fairly rapidly as the dielectric constant decreases, while the ion-pair reaction constant drifts downward comparatively slowly. A plot of the logarithm of k_f or $k_f(K/c)^{1/2}$ against $1/\varepsilon$ or $(\varepsilon - 1)/(2\varepsilon + 1)$ is found to be linear, but the plots of log k_i against the same function are curved. The tangent of the curve is steeper for polar solvents than for non-polar solvents. The results have been compared with those predicted from classical dielectric theory.

Canadian Journal of Chemistry, 48, 3258 (1970)

Introduction

The ring-opening reaction of an epoxide by acidic and basic catalysts is usually assumed to involve some form of ionic intermediate (1), the preferred being the ion pair (2). It is therefore essential for the understanding of the intricacies of this process to know the detailed structure of these species.

In previous papers (3–5), the rate of the tertiary amine catalyzed reaction of phenyl glycidyl ether (PGE) and benzoic acid (BA) was suggested to depend on the structural alteration of the hydrogen bond in the transition state due to the structural changes in the catalyst and the reactants. It was also suggested that the proton transfer from the molecular addition compound or the ion-pair to the epoxide through the activated complex or the transition state species, in various pure and mixed solvents, was affected by the dielectric character and the hydrogen bonding abilities of these solvents.

Consideration of the probable concentration of the active species, and the wide range of dielectric constants of the solvents used leads to some questions if the ion-pair, as defined by Fuoss and Kraus (6), is always the predominant species. It is generally agreed that dissociation into free ions is negligible in such non-polar solvents as hydrocarbons, but when the dielectric constant is 10 or above in solvents such as chlorinated hydrocarbons and nitrobenzene, the possibility that free ions are the major species should be considered.

The problem is far from simple. Ionic species may exist in a great variety of forms such as free ions, ion-pairs, triple ions, quadruplets, and as still higher aggregates. It is, then, difficult to determine the state of the ions in normal ionic reactions owing to the transitory nature of the reacting species. In order to demonstrate the transition from one type of behavior to another for the ring-opening reaction of epoxide, the rate constant for the pyridine-catalyzed reaction between PGE and BA, and the ion association constants, have been measured in pure solvents such as nitrobenzene, benzonitrile, *o*-dichlorobenzene, monochlorobenzene, and toluene.

Experimental Section

Materials

Reagent grade PGE was dried over calcium hydride for several days and distilled at reduced pressure. The fraction boiling at 103° (6 mm) was collected for use. Reagent grade BA was recrystallized from its aqueous solution and dried over phosphorus pentoxide. Pyridine was distilled after refluxing with barium oxide (7). Reagent grade toluene was shaken successively with concentrated sulfuric acid and aqueous sodium bicarbonate solution, dried with calcium chloride, and stored over calcium hydride; before use, it was distilled fractionally, and the fraction boiling at 110.0–110.5° was collected and used. Monochlorobenzene was purified (8) by shaking repeatedly with portions of sulfuric acid

Can. J. Chem. Downloaded from www.nrcresearchpress.com by 210.87.254.40 on 09/05/12
For personal use only.

until the acid no longer became colored. It was then washed with water and with a dilute sodium bicarbonate solution, dried with calcium chloride, and fractionally distilled through a 40 cm column. A fraction boiling at 131.5° was collected and used. *o*-Dichlorobenzene was distilled through a 60 cm Widmer column and the middle fraction boiling at 179–180° was collected (9). A commercial nitrobenzene was dried with calcium chloride and fractionated at reduced pressure. The nitrobenzene was freshly distilled for each series of measurements, only the middle fraction being used (10). Reagent grade benzonitrile was purified (11) by steam distillation, and the distillate was washed with sodium carbonate solution, dissolved in ether, washed with water, and dried over calcium chloride. The solution was filtered and the ether was removed by distillation. The residue was fractionally distilled under reduced pressure.

Reaction Procedure

Reaction apparatus, procedure, and analytical methods for epoxide and acid in kinetic measurements, have been described previously (3, 12). A reaction flask containing BA and the solvent was heated to the desired temperature and to this were added solutions of PGE and of pyridine preheated to the same temperature. In all cases, the time was measured from the moment of mixing the acid and amine. Aliquots (3 or 4 ml) of the reaction mixtures were taken for analysis at convenient intervals. The acid and epoxy contents of the sample were determined respectively by direct neutralization method (13) and by the method of Durbetaki (14). The initial concentrations of PGE, BA, and pyridine were 0.250–2.00 $\times 10^{-1}$, 0.250–2.00 $\times 10^{-1}$, and 0.16–2.48 $\times 10^{-2}$ *M*, respectively. The temperature of the reaction mixtures was kept constant to $\pm 0.2°$.

Direct current measurements were made using a Takeda Riken TR-84M vibrating reed electrometer with a TR-300B power supply. Calibrated 10^8 and 10^{10} ohm standard resistances, Takeda Riken TR-45, were used in parallel with a conductivity cell. The cell, consisting of a 100 ml cylinder with the electrode assembly, had a cell constant of about 0.134. The measurements were made in an oil-bath held at 25.0 ± 0.01°. The specific conductivities of these solvents were found to be: 3.2 $\times 10^{-10}$ for nitrobenzene, 7.4 $\times 10^{-10}$ for benzonitrile, 2.6 $\times 10^{-10}$ for *o*-dichlorobenzene, 8.1 $\times 10^{-12}$ for monochlorobenzene, and 3.6 $\times 10^{-14}$ mho cm^{-1} for toluene, and therefore corrections had to be introduced when determining the conductances of the diluted solutions in benzonitrile, monochlorobenzene, and toluene.

Results and Discussion

From the electrical conductivity measurements of the solutions, concentration dependences of the equivalent conductances, Λ, were calculated and these results are given in Table 1. A range of dielectric constant was chosen in which the conductance is sensitive to the dielectric constant. The conductance at a given pyridinium benzoate concentration changes by several orders of magnitude in going from ε = 2.38 to 34.8. This behavior is shown on log Λ − log *c* plots in Fig. 1, where *c* is the concentration of pyridinium benzoate. In all cases, the points are found to lie close to lines of slope −1/2 which is the behavior expected from salts existing mainly as ion-pairs in equilibrium with free ions in low concentration (15). In this case, we may test the results by the Kraus and Bray method (16) which assumes that the effects of interionic attraction are negligible. They derived eq. [1] so

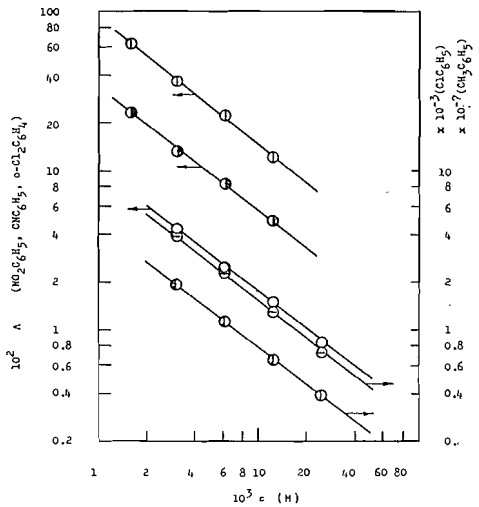

FIG. 1. Conductance for pyridinium benzoate in various solvents plotted as log Λ against logarithm of concentration: ◑, in nitrobenzene; ◑, in benzonitrile; ○, in *o*-dichlorobenzene; ◐, in monochlorobenzene; ◓, in toluene.

$$[1] \qquad 1/\Lambda = 1/\Lambda_0 + c\Lambda/K\Lambda_0^2$$

that in the plot of $1/\Lambda$ against $c\Lambda$, the slope of a line is $1/K\Lambda_0^2$ and the intercept is $1/\Lambda_0$, where *K* is the ion-pair dissociation constant and Λ_0 is the equivalent conductance at zero concentration. The results plotted in this manner gave straight lines in all cases. If the equivalent conductance at infinite dilution, Λ_0, is known, it is possible to evaluate the ion dissociation constant, *K*, but unfortunately the intercept was too small to be read accurately from the data because of the low degree of dissociation. Fuoss and Accascina (15) derived eq. [2], but

$$[2] \qquad F/\Lambda = 1/\Lambda_0 + (cf^2\Lambda/F)/(K\Lambda_0^2)$$

this cannot be used here because of the high concentration of the salt ($>3 \times 10^{-7}\varepsilon$)[3]. Therefore calculations involving Walden and Ulich's rule (17), and Stokes's law (18) were used to obtain a fair approximation of Λ_0.

Can. J. Chem. Downloaded from www.nrcresearchpress.com by 210.87.254.40 on 09/05/12
For personal use only.

TABLE 1

Ion dissociation constant of pyridinium benzoate, and rate constant for pyridine-catalyzed reaction between phenyl glycidyl ether (PGE) and benzoic acid (BA) at 81° in various solvents

Concentration							
Pyridine (10^{-2} M)	PGE & BA* (10^{-1} M)	Λ (mho cm^2)	K† (M)	Third-order rate constant, k'' (M^{-2} s^{-1})	Ion-pair rate constant, k_i‡ (M^{-2} s^{-1})	Free ion rate constant, k_f‡ (M^{-2} s^{-1})	$k_f(K/c)^{1/2}$ (M^{-2} s^{-1})
In nitrobenzene ($\kappa = 1.00$–1.50×10^{-6} mho cm^{-1})							
1.24	2.00	1.21×10^{-1}	9.74×10^{-8}	6.81×10^{-3}	5.82×10^{-3}	4.7×10^{-1}	1.0×10^{-3}
0.62	1.00	2.23		7.35			1.5
0.31	0.50	3.65		7.90			2.1
0.16	0.25	6.25		8.74			2.9
In benzonitrile ($\kappa = 3.74$–6.00×10^{-7} mho cm^{-1})							
1.24	2.00	4.84×10^{-2}	6.50×10^{-9}	5.50×10^{-3}	4.58×10^{-3}	1.2	0.92×10^{-3}
0.62	1.00	8.23		6.02			1.4
0.31	0.50	13.2		6.54			2.0
0.16	0.25	23.4		7.21			2.6
In *o*-dichlorobenzene ($\kappa = 1.34$–2.05×10^{-7} mho cm^{-1})							
2.48	2.00	8.27×10^{-3}	2.85×10^{-10}	3.69×10^{-3}	3.40×10^{-3}	3.8	0.29×10^{-3}
1.24	1.00	15.0		4.08			0.68
0.62	0.50	24.8		4.37			0.97
0.31	0.25	43.2		4.63			1.2
In monochlorobenzene ($\kappa = 5.98$–9.56×10^{-9} mho cm^{-1})							
2.48	2.00	3.86×10^{-4}	2.71×10^{-13}	2.87×10^{-3}	2.70×10^{-3}	7.6×10	0.17×10^{-3}
1.24	1.00	6.45		3.14			0.44
0.62	0.50	11.2		3.30			0.60
0.31	0.25	19.3		3.53			0.83
In toluene ($\kappa = 1.20$–1.78×10^{-12} mho cm^{-1})							
2.48	2.00	7.18×10^{-8}	5.78×10^{-21}	2.34×10^{-3}	2.30×10^{-3}	2.0×10^{5}	0.04×10^{-3}
1.24	1.00	12.9		2.41			0.11
0.62	0.50	22.6		2.50			0.20
0.31	0.25	38.7		2.60			0.30

*Equimolar amounts of PGE and BA were used.
†Calculated by Kraus and Bray's equation (16) (eq. [1]) using the slope of the line for the plot of $1/\Lambda$ against $c\Lambda$. The Λ_0 values were estimated by Walden and Ulich's rule (17) and Stokes' law (18), and given in Table 2.
‡Obtained graphically in Fig. 2.

TABLE 2

Limiting conductivities of pyridinium cation, benzoate anion, and pyridinium benzoate in various solvents*

Solvent			Λ_0^+ for $C_5H_5NH^+$ (mho cm^2)	Λ_0^- for $C_6H_5COO^-$ (mho cm^2)	Λ_0 for $C_5H_5NH^+{}^-OCOC_6H_5$ (mho cm^2)
	ε†	η at 25° (cP)			
Nitrobenzene	34.8	1.811‡	18.8††	16.0‡‡	34.8
Benzonitrile	25.2	1.228§	27.7	23.6	51.3
o-Dichlorobenzene	9.93	1.00‖	34.0	29.0	63.0
Monochlorobenzene	5.62	0.752¶	45.2	38.6	83.8
Toluene	2.38	0.5516**	61.6	52.6	114.2

*By calculations involving Walden and Ulich's rule (17), and Stokes's law (18). See text.
†See ref. 32.
‡Reference 22.
§Obtained graphically with the data of J. Timmermans and Mme. Hennaut-Roland (33).
‖Estimated by Stokes' law (18) with the data of benzonitrile and monochlorobenzene.
¶Obtained graphically with the data of T. Titani (34).
**See ref. 35.
††Reference 22.
‡‡The value for picrate anion (22). See text.

Since these solvents have often been used for conductivity measurements, it is possible to obtain Λ_0 from the literature if Walden's rule is valid in these solvents. This rule is fairly true when the ions are large as tetrabutylammonium ion while small ions show considerable deviations when tested by conductances in a variety of solvents (15, 19). Elliott and Fuoss (20) suggested that the abnormally higher mobility of the ions is due to slipping in which small ions can pass between certain configurations of large solvent molecules without displacing them. These solvents have similar molecular volumes;[1] 106.3 for toluene, 101.6 for monochlorobenzene, 112.4 for *o*-dichlorobenzene, 102.5 for benzonitrile, 102.3 for nitrobenzene, and 80.9 and 96.4 cm^3 for pyridine and benzoic acid, respectively at 25°. Thus this kind of slipping effect should be absent, negligibly small, or constant in magnitude.

The limiting conductivity $\Lambda_0 = \Lambda_0^+ + \Lambda_0^-$, where Λ_0^+ and Λ_0^- denote the limiting conductivities of the pyridinium cation and benzoate anion. The Λ_0^+ values for pyridinium cation in various solvents are known (22, 23). Therefore, to complete our task, we have only to determine Λ_0^- for benzoate anion. Walden's rule is not valid, but should be nearly true for pyridinium cation for which Λ_0^+ values in various solvents are given in Table 2. The limiting conductivity for benzoate anion cannot be found in the literature, so it is assumed to be similar to that for picrate anion. In this study, the limiting conductivity for picrate anion was taken as the Λ_0^- value for benzoate anion as shown in Table 2. No simple application of Walden–Ulich's rule (17) can be made to the anion (15, 19), but the product $\eta\Lambda_0^-$ for picrate anion are almost constant at 0.290 and 0.297 mho dyne s in nitrobenzene and pyridine, which are estimated by applying Stokes's law (18) to Λ_0^- values of 16.0 and 33.7 mho cm^2 given by Witschonke and Kraus (22) and by Burgess and Kraus (23), where η is the viscosity of the solvent. The values of viscosities and dielectric constants were taken from the literature and are shown with the resultant Λ_0 values in Table 2. The limiting conductivities (22) of the pyridinium and benzoate ions were taken as 18.8 and 16.0 mho cm^2, respectively, in nitrobenzene, for which viscosity was taken as 1.811 cP (22) (25°). Using these values, 0.340 and 0.290 mho dyne s were obtained as the products $\eta\Lambda_0^+$ and $\eta\Lambda_0^-$, respectively, which give Λ_0^+ and Λ_0^- values shown in Table 2. The estimated values of Λ_0 for the pyridinium benzoate salt are thus 34.8, 51.3, 63.0, 83.8, and 114 mho cm^2 in nitrobenzene, benzonitrile, *o*-dichlorobenzene, monochlorobenzene, and toluene. These values of Λ_0, when inserted in eq. [1], give the ion-pair dissociation constants, K, shown in Table 1.

We suggest that the pyridine-salt of benzoic acid may exist in two forms, a molecular addition compound, $C_5H_5N \cdot HOCOC_6H_5$, and a salt-like form, $C_5H_5NH^+ \cdot {}^-OCOC_6H_5$. This concept may be compared to that of Pedersen (24), who suggested that the two forms of aniline picrate with different solubilities might be a

[1]Calculated from the densities listed in ref. 21.

Can. J. Chem. Downloaded from www.nrcresearchpress.com by 210.87.254.40 on 09/05/12
For personal use only.

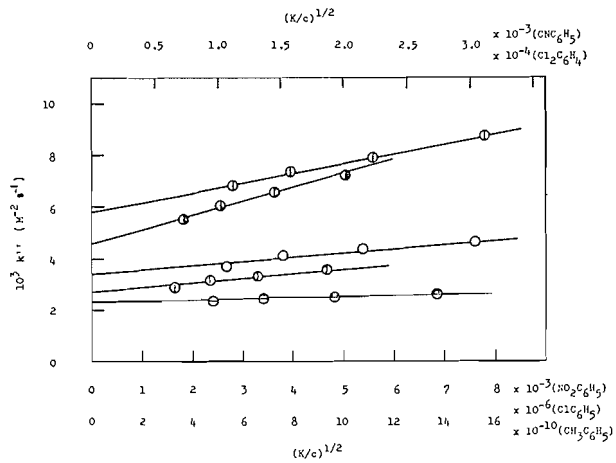

FIG. 2. Dependence of the third-order rate constant, k'', for the pyridine-catalyzed reaction between phenyl glycidyl ether and benzoic acid on pyridinium benzoate concentration in various solvents: ⓘ, nitrobenzene; ◑, benzonitrile; ○, *o*-dichlorobenzene; ◐, monochlorobenzene; ◓, toluene.

molecular addition compound and electrolyte, and of Elliott and Fuoss (20) who assumed two isomeric polar and non-polar structures for amine picrates and heavy metal cyanides (25). The non-polar molecular addition compound of BA with pyridine may undergo dissociation into free acid and base when dissolved in these solvents. Such dissociation, however, should be repressed by addition of either acid or base, as the acid–base dissociation of pyridinium picrate is completely repressed on addition of 0.001 *M* acid (22). Pyridinium benzoate in the salt-like form may exist in two ionic forms in solution, viz., contact or intimate ion-pairs and solvent-separated ion-pairs, as $Co(NH_3)_5SO_4^+$ in water (26) and the fluorenyl salts in solvents such as tetrahydrofuran, dioxane, and dimethyl sulfoxide (27). The problem of possible forms of ion-pairs will be investigated further.

The reaction in these solvents was found to be third-order, being first-order in each of the three reactants, pyridine, PGE, and BA, as mentioned previously (5), and the observed reaction rate was expressed as eq. [3], where k'' is the third-

$$[3] \quad d[PGE]/dt = d[BA]/dt = -(k''[P] + k')[PGE][BA]$$

order rate constant, k' is the second-order rate constant for the uncatalyzed reaction, and [P], [PGE], and [BA] are the concentration of pyridine, PGE, and BA, respectively. The apparent termolecular rate constant, k'', of this reaction was determined for initial concentrations of pyridine ranging from 0.16×10^{-2} to 2.48×10^{-2} *M* with the various concentrations of PGE and BA ($0.25–2.00 \times 10^{-1}$ *M*), as given in Table 1. The observed increase of k'' on dilution may arise from the ionic dissociation of ion-pairs. If ion-pairs such as $C_5H_5NH^+ \cdot {}^-OC\text{-}OC_6H_5$, and free ions $C_6H_5CO_2^-$ and $C_5H_5\text{-}NH^+$, participate in this reaction with respective rate constants of k_i and k_f, and if the free ions react faster than ion-pairs with PGE, then the observed k'' is given by eq. [4] (28), where α is the fraction of reactant dissociated. For $\alpha <$

$$[4] \quad k'' = (1 - \alpha)k_i + \alpha k_f$$

0.05, the approximations $(1 - \alpha) = 1$ and $\alpha = (K/c)^{1/2}$ are valid, and thus, eq. [5] is obtained.

$$[5] \quad k'' = k_i + k_f(K/c)^{1/2}$$

In eq. [5], K denotes the dissociation constant of the relevant ion-pairs. Hence, plots of k'' against $(K/c)^{1/2}$ should result in straight lines, and indeed, such lines are shown in Fig. 2, supporting, therefore, the proposed explanation for the variations of k'' on dilution. The slopes of these lines give k_f values, and their intercepts lead to k_i, the ion-pair rate constants.

The free energy of an ionic reaction, or its free energy of activation, is commonly found to involve a term representing electric work, the magnitude of which depends on the dielectric constant of the medium. For reactions between ions, the electrostatic energy is proportional to

Can. J. Chem. Downloaded from www.nrcresearchpress.com by 210.87.254.40 on 09/05/12
For personal use only.

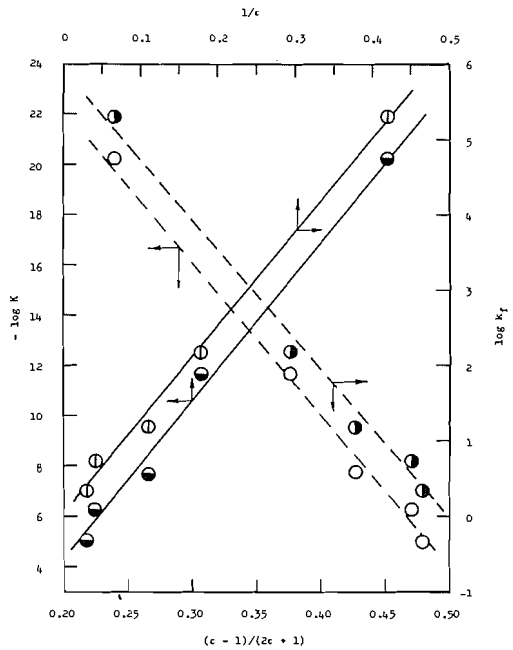

FIG. 3. Dependencies of the ion-pair dissociation constant, K, and of the rate constant of free ion, k_f, on dielectric constant: ○ And ◒, log K; ◑ and ⓘ, log k_f.

the reciprocal of the dielectric constant, ε. The dissociation of the ion-pair, pyridinium benzoate, into free ions, pyridinium cation and benzoate anion, is a typical example of such a situation, and as shown in Fig. 3. With due allowance for the large uncertainties in dissociation constants, K, the plots appear to be linear. As the interaction energy falls relatively slowly with ionic separation, use of the bulk dielectric constant is moderately successful, though it is found to be a poor measure of the electric properties of a medium in the immediate vicinity of ion-pairs (15). Where dipoles are concerned, the interaction energy falls off more rapidly with distance, and use of the bulk dielectric constant is likely to be less realistic, for much of the interaction energy occurs at small separations where saturation effects are important. It seems, therefore, that the involvement of further neighboring molecules must be appreciable, or the reaction field of the dipole must be considered. Moelwyn–Hughes (28) has suggested, that for dipole interactions, (ε + 2)/3ε is a more appropriate dielectric function. Kirkwood (29) and Laidler and Eyring (30) considered the medium surrounding the cavity in which the reaction takes place and have used the function (ε − 1)/(2ε + 1). However, since in the investigated range of ε, all three dielectric functions are almost linearly related and, in fact, give equally good fits when plotted against the logarithm of the dissociation constant, it is not yet feasible to discriminate among these approaches.

The free ion reaction constant rises fairly rapidly as the dielectric constant decreases, but the ion-pair rate constant drifts down comparatively slowly. The rate constants measured for overall reaction are all reproducible to ±3% or better in duplicate determinations, but in spite of this uncertainty, some effects of dilution and solvents are evident. The free ion rate constants in these solvents are given in Table 1 and presented in Fig. 3 as a plot of the logarithm of k_f vs. (ε − 1)/(2ε + 1) or 1/ε. The experimental points conform fairly well to a linear relation. The linearity of similar plots is also found when the above dielectric functions are plotted against the logarithm of the $k_f(K/c)^{1/2}$ value, as shown in Fig. 4. The results in Table 1 and Fig. 3 may

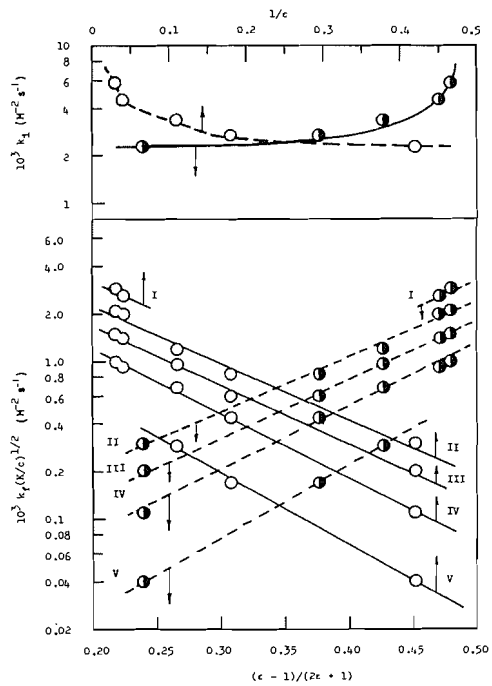

FIG. 4. Dependencies of the rate constant of ion-pairs, k_1, and of $k_f(K/c)^{1/2}$ on dielectric constant, in various pyridinium benzoate concentrations: I, 0.16; II, 0.31; III, 0.62; IV, 1.24; V, 2.48×10^{-2} M.

Can. J. Chem. Downloaded from www.nrcresearchpress.com by 210.87.254.40 on 09/05/12
For personal use only.

indicate that the lower reactivity of the free ions in polar solvents such as nitrobenzene is due to participation of several molecules of solvent. The reaction of the free pyridinium cation or benzoate anion can only be observed over a limited kind of solvent or a limited range of solvent composition (5), and the results are very sensitive to errors in measurement of both K and the slopes of the lines in Fig. 2. The major reason for the rapid decrease in the importance of the free ion reaction is not a decrease in reactivity, but a rapid decrease in free ion concentration as the medium becomes less polar.

In contrast to the dissociation process and the contribution of the free ion reaction, the reactivity of the pyridinium benzoate ion-pair or the molecular addition complex, $C_5H_5N \cdot HOCOC_6H_5$, cannot be accounted for in these simple terms. As shown in Fig. 4, the plots of logarithm of k_i against $1/\varepsilon$ or $(\varepsilon - 1)/(2\varepsilon + 1)$ deviate substantially from linearity. The tangent of the curve shown in Fig. 4 is steeper for the polar solvent than for the non-polar solvent. This may indicate that the higher reactivity of the ion-pairs in polar solvents is due to participation of several molecules of solvent in the transition state of the reaction. A majority of ion-pairs may be present as less reactive contact ion-pairs of molecular addition compounds (4, 5) with only a small fraction existing as highly reactive, solvent-separated ion-pairs. This aspect will be investigated further. Alternatively, the increase in the ion-pair rate constant at higher dielectric constants formally corresponds to an increase in dipole moment in transition state formation as mentioned before (5, 31).

1. (*a*) S. WINSTEIN and R. B. HENDERSON. Heterocyclic compounds. Vol. 1. *Edited by* R. Elderfield. John Wiley & Sons Inc., New York, 1950. p. 1. (*b*) R. E. PARKER and N. S. ISAACS. Chem. Rev. **59**, 737 (1959).
2. C. G. SWAIN. J. Amer. Chem. Soc. **74**, 4108 (1952).
3. H. KAKIUCHI and Y. TANAKA. J. Org. Chem. **31**, 1559 (1966).
4. Y. TANAKA. J. Org. Chem. **32**, 2405 (1967).
5. Y. TANAKA and H. TAKEUCHI. Tetrahedron, **24**, 6433 (1968).
6. R. M. FUOSS and C. A. KRAUS. J. Amer. Chem. Soc. **55**, 1019 (1933).
7. R. G. PEARSON and F. V. WILLIAMS. J. Amer. Chem. Soc. **75**, 3073 (1953).
8. K. B. MCALPINE and C. P. SMYTH. J. Chem. Phys. **3**, 55 (1935).
9. E. M. MOORE and M. E. HOOBS. J. Amer. Chem. Soc. **71**, 411 (1949).
10. H. M. ROBERTS and C. R. BURY. J. Chem. Soc. 2037 (1923).
11. A. R. MARTIN. J. Chem. Soc. 3270 (1928).
12. H. KAKIUCHI and Y. TANAKA. Kobunshi Kagaku, **20**, 619 (1963).
13. E. R. BISHOP, E. B. KITTREDGE, and J. H. HILDEBRAND. J. Amer. Chem. Soc. **44**, 135 (1922).
14. A. J. DURBETAKI. Anal. Chem. **28**, 2000 (1956).
15. R. M. FUOSS and F. ACCASCINA. Electrolytic Conductance. Interscience Publishers, Inc., New York, N.Y., 1959.
16. C. A. KRAUS and W. C. BRAY. J. Amer. Chem. Soc. **35**, 1315 (1913); Chem. Abstr. **8**, 854 (1914).
17. P. WALDEN and H. ULICH. Z. Phys. Chem. **107**, 219 (1923).
18. R. W. GURNEY. Ionic processes in solution. McGraw–Hill Book Company, Inc., New York, N.Y., 1953.
19. C. B. MONK. Electrolytic dissociation. Academic Press, London, 1961.
20. M. A. ELLIOTT and R. M. FUOSS. J. Amer. Chem. Soc. **61**, 294 (1939).
21. Landolt–Bornstein Physikalische Tabellen.
22. C. R. WITSCHONKE and C. A. KRAUS. J. Amer. Chem. Soc. **69**, 2472 (1947).
23. D. S. BURGESS and C. A. KRAUS. J. Amer. Chem. Soc. **70**, 706 (1948).
24. K. J. PEDERSEN. J. Amer. Chem. Soc. **56**, 2615 (1934).
25. E. C. FRANKLIN and C. A. KRAUS. J. Amer. Chem. Soc. **27**, 197 (1905).
26. H. TAUBE and F. A. POSEY. J. Amer. Chem. Soc. **75**, 1463 (1953).
27. T. E. HOGEN-ESCH and J. SMID. J. Amer. Chem. Soc. **82**, 307 (1966).
28. E. A. MOELWYN-HUGHES. The kinetics of reactions in solution. 2nd Edition. Oxford, Clarendon Press, 1947.
29. J. KIRKWOOD. J. Chem. Phys. **24**, 233 (1939).
30. K. J. LAIDLER and H. EYRING. Ann. N.Y. Acad. Sci. **39**, 303 (1940).
31. S. GLASSTONE, K. J. LAIDLER, and H. EYRING. The theory of rate processes. McGraw–Hill Book Company, Inc., New York, N.Y., 1941.
32. A. A. MARYOTT and E. A. SMITH. Table of dielectric constants of pure liquids. NBS Circular 514, Aug. 1951.
33. J. TIMMERMANS and MME HENNAUT–ROLAND. J. Chim. Phys. **32**, 501, 589 (1935); Chem. Abstr. **30**, 2072 (1936).
34. T. TITANI. Bull. Inst. Res. Japan, 671 (1927); Bull. Chem. Soc. Japan, **2**, 95, 161, 196, 225 (1927).
35. American Petroleum Institute Research Project 44, Pittsburgh, Pennsylvania. Carnegie Institute of Technology. Selected values of properties and related compounds, Table 5c, Nov. 30, 1949.

Can. J. Chem. Downloaded from www.nrcresearchpress.com by 210.87.254.40 on 09/05/12
For personal use only.

Can. J. Chem. Downloaded from www.nrcresearchpress.com by 210.87.254.105 on 09/05/12
For personal use only.

Photochemical rearrangement of diene endoperoxides[1, 2]

K. K. MAHESHWARI, P. DE MAYO, AND D. WIEGAND
Department of Chemistry, University of Western Ontario, London, Ontario

Received June 23, 1970

It has been shown that the direct irradiation of cyclic peroxides such as ascaridole, and those derived from cyclohexadiene, 1,3,5,5-tetramethylcyclohexadiene, and levopimaric acid methyl ester rearrange on irradiation. The bisepoxides are obtained, as in the thermal rearrangement, together with, where the structure permits, the ketoepoxide. The reaction can be induced by triplet–triplet energy transfer.

Canadian Journal of Chemistry, **48**, 3265 (1970)

The discovery (1, 2) in nature of a *cis* bisepoxide, crotepoxide (**1**) raised the problem of a general mode of synthesis of substances containing such functional groups. An obvious method was the thermal rearrangement of endoperoxides. The most studied of these is ascaridole (**2**), which on such treatment has been shown (3, and references there cited) to give isoascaridole (**3**), but other examples are available in alicyclic chemistry (4, 5). An objection to the use of this procedure was that the temperature needed (*ca.* 140°) might well be such as to lead to decomposition of the product should it be substituted with sensitive groups. An alternative mode of rearrangement was therefore sought.

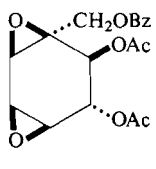

1

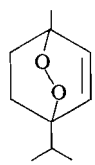

2

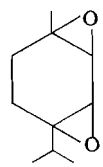

3

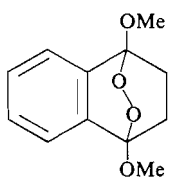

4

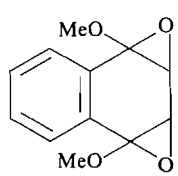

5

The photolytic rearrangement of peroxides derived from the oxidation of acenes has been a subject of study by Dufraisse, Rigaudy and their school (6, 7 and references cited). Recently the rearrangement has been extended into the naphthalene series (8), as exemplified by the transformation of **4** into **5**. It was therefore possible that the simple endoperoxides of type **2** might also rearrange. The irradiation of acyclic peroxides was already known (9, 10) to lead to photolysis, and evidently if the intermediate species so generated were the same as in the thermolysis then the same transformation should be expected (11).

Indeed, it was found that ascaridole (**2**) and peroxides derived from 1,3,5,5-tetramethylcyclohexadiene (**6**), cyclohexadiene (**7**), and levopimaric acid methyl ester (**8**) all behaved in essentially the same manner on irradiation through Pyrex or at 366 nm as on heating. In all cases a bisepoxide was obtained, but this was accompanied, where the structure permitted, by the corresponding ketoepoxide. The latter was unstable with respect to the corresponding keto alcohol, and chromatographic treatment usually yielded the latter.

A number of incidental points of interest emerge. Ascaridole has, as have most peroxides, a long tail in the u.v. absorption spectrum which reaches beyond 360 nm. In ascaridole this absorption is intensified somewhat as compared with normal peroxides and there appears to be a maximum at 233 nm of low intensity ($\varepsilon \sim 166$). The origin of this is conjectural, but it presumably implies interaction of the oxygen lone pairs with the double bond, perhaps in the antibonding orbital. It was possible that this interaction might allow the conversion of ascaridole to isoascaridole without passing through any intermediate biradical. This would then suggest participation of

[1]Photochemical synthesis: Part 34.
[2]Publication No. 10 from the Photochemistry Unit.

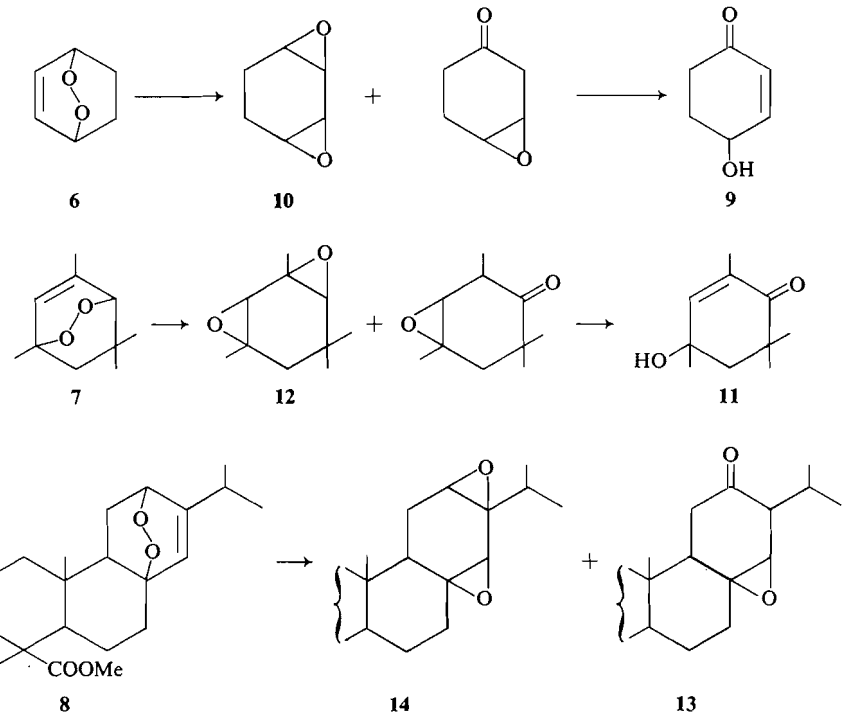

some excited singlet state. Some qualitative experiments were undertaken to ascertain if this were so.

It was found, however, that irradiation of solutions of ascaridole or of **8** in the presence of any of the sensitizers, Michler's ketone, phenanthrene, or triphenylamine (such that the sensitizers absorbed essentially all the light), gave a faster conversion to products than did direct irradiation under the same conditions. Presumably, then, the triplet was a possible pathway though not necessarily the only one. However, the complementary quenching experiments were more difficult to perform. Essentially the problem was to find a quencher which did not absorb more than the peroxide. The acyclic dienes were possible candidates and indeed appeared to quench the reaction. But careful measurements of the extinction coefficient near 366 nm indicated that the dienes had residual absorption which required quantitative yield measurement to give decisive information. A similar experiment was performed with di-*tert*-butyl nitroxide as quencher by irradiation at 334 nm. In this case the yields were estimated by t.l.c. using a densitometer. The results (see the Experimental section) indicated, apparently beyond the limits of error, that quenching was occurring. Such a result is surprising and cannot be regarded as definitive since a number of points remain unclear. The possibility of singlet quenching, known to be possible with di-*tert*-butyl nitroxide (19) cannot be excluded. Assuming diffusion controlled quenching the lifetime of a species showing the degree of "quenchedness" observed can be calculated to be of the order of 10^{-9}–10^{-10} s.

The absorption spectrum of peroxides may result from the overlapping of two lone-pair orbitals with resulting splitting of so-formed π levels into bonding and antibonding, both filled. The transition may then be $\pi^* \rightarrow \sigma^*$. The quenching then requires that this state be not immediately dissociating, but yet that it may efficiently become so, since the quantum yield of peroxy radicals from di-*tert*-butyl peroxide and other peroxides is unity even in solution. The significance of the experiment is thus unclear.

The nature of the products suggests that when the biradical is formed, and a methine hydrogen(s) exist on the carbon(s) bearing oxygen addition (to give **15**) to the double bond takes place faster than hydrogen migration (Scheme 1). For the second step, if the reaction proceeds via a triplet, a spin inversion is required. It may be that this

Can. J. Chem. Downloaded from www.nrcresearchpress.com by 210.87.254.105 on 09/05/12
For personal use only.

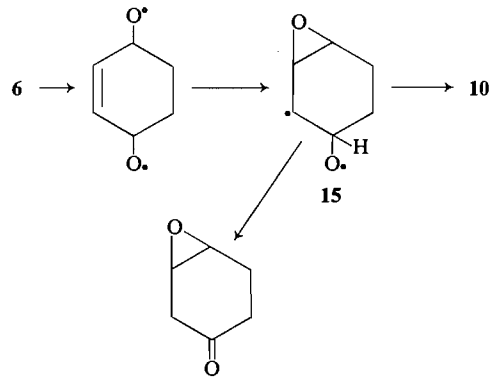

SCHEME 1

delays the closure to the bisepoxide sufficiently to allow the hydrogen migration to compete.[3]

An alternative possible explanation is that the bisepoxide is first formed and is then further rearranged. The thermal rearrangement of epoxides to ketones has been observed as have exceptions (12), but such rearrangements are not known to occur photochemically with light of such long wavelength[4] in the absence of an additional vicinal chromophore (such as a ketone carbonyl). In control experiments the bisepoxides appeared stable, which suggests that the 1,3-biradical **15** rearranges directly to the ketoepoxide at least in the photochemical process. That the relative proportions of the products have a rough parallel in the thermal and photochemical processes suggests that the same is true for the thermal process. In addition thermal or photochemical rearrangement of the bisepoxides should not be restricted to just one of the pair, nor restrict the direction of opening to essentially one sense.

Experimental

Ascaridole

Ascaridole was distilled (56–57° at 0.17 mm) and gave a single spot on t.l.c. It showed λ_{max} 233 nm, ε 188. It was further purified by the method of Halsall (14). Repeated purification gave material with ε = 166 which was unchanged on further chromatography. Isoascaridole was prepared by heating a solution of ascaridole in refluxing xylene for 4 h followed by chromatography.

[3]This raises the interesting possibility that the ketone may first be formed in the triplet state.

[4]The irradiation of epoxides at 254 mm has been recorded (13) but beyond this wavelength there is insufficient absorption for reaction to occur under normal conditions of irradiation.

Irradiation of Ascaridole

(*a*) A solution of 100 mg ascaridole in cyclohexane (10 ml) was degassed by nitrogen purge (30 min). The solution was then irradiated through Pyrex for 6 h (85 W G.E. mercury medium pressure arc). The t.l.c. indicated the absence of ascaridole and the presence of isoascaridole as the only detectable substance. The isolated oil (85%) was identified as isoascaridole by comparison of i.r. and n.m.r. spectra which were identical.

Irradiation of ascaridole in methanol gave identical results.

(*b*) Solutions of ascaridole (32 mg) in (*i*) cyclohexane (*ii*) dioxan and dioxan containing (*iii*) 150 mg phenanthrene, (*iv*) 100 mg Michler's ketone, (*v*) 160 mg triphenylamine, (*vi*) 5 mg hexadiene-2,4, (*vii*) 11 mg hexadiene-2,4, and (*viii*) 22 mg hexadiene 2,4 were simultaneously irradiated on a merry-go-round (15) using a 450 W medium pressure mercury source and filters (Corning 760 and 052) to permit transmission in the 366 nm region. After 3 h irradiation the presence of isoascaridole was detectable in small amounts by t.l.c. in tubes (*i*) and (*ii*), and in decreasing amounts in tubes (*vi*) to (*viii*). In the latter the isoascaridole was barely detectable. Tubes (*iii*) to (*v*) showed the presence of large amounts of isoascaridole. In the case of tube (*iv*) the products were isolated and the isoascaridole (yield ~ 50%) identified by comparison of its i.r. spectrum with that of an authentic specimen. Control experiments showed that isoascaridole itself was stable under the conditions of the experiment.

(*c*) Solutions of ascaridole (*ca.* 125 mg) in methanol (5 ml) were prepared and di-*t*-butyl nitroxide (*ca.* 35 mg) added to half, such that greater than 90% of the incident light was absorbed by the ascaridole. The light from the 200 W high pressure mercury arc was passed through the following filters (*i*) $NiSO_4.6H_2O$ (saturated solution), 2 cm, (*ii*) CS 7-51, (*iii*) naphthalene, 12.8 g/l isooctane, 1 cm. This system gave 30% transmission at 334 nm <2% at 320 nm and <5% at 355 nm. The product was estimated by t.l.c., standardized charring and relative intensities measured on the plates by a densitometer after moistening with Nujol. The irradiation was followed over 13 h. The amount of quenching at the end of this time in two separate experiments was 30 and 45% where reproducibility of the analysis appeared to be ±10%. The agreement between the separate experiments is not good, but the fact of quenching appears to be beyond experimental error.

Cyclohexa-1,3-diene Endoperoxide

This was prepared by the method of Murray and Kaplan (16). The endoperoxide was first obtained as a waxy solid, but after sublimation was crystalline in form. However, some benzenoid material was present. The procedure of Foote *et al.* (17) also, in our hands gave material having some benzenoid absorption. Separation by t.l.c. eliminated this impurity but some diene absorption (λ_{max} ~230 nm) remained. This could not effectively be further purified and was used as such.

Irradiation

(*a*) A solution of 125 mg of the endoperoxide (**6**) in 25 ml cyclohexane was irradiated as described for ascaridole (1.5 h). The mixture was separated by t.l.c.

Can. J. Chem. Downloaded from www.nrcresearchpress.com by 210.87.254.105 on 09/05/12
For personal use only.

Can. J. Chem. Downloaded from www.nrcresearchpress.com by 210.87.254.105 on 09/05/12
For personal use only.

(eluant ether:benzene, 1:4). Two main products were isolated:

(*i*) The alcohol (**9**) (28 mg; 22%), ν_{max} ($CHCl_3$) 3600, 3400, 1680 cm^{-1}; λ_{max} (cyclohexane) 220 nm (ε 6700). Vinylic protons were present in the n.m.r. spectrum at δ 6.95 and 5.92. These protons were not present in the n.m.r. spectrum of the crude irradiation mixture.

Anal. Calcd. for $C_6H_8O_2$: C, 64.27; H, 7.19. Found: C, 63.87; H, 7.29.

(*ii*) The bisepoxide (**10**) (35 mg; 27%). This substance was optically transparent (210–300 nm) and showed no hydroxyl or carbonyl absorption in the i.r. spectrum. The n.m.r. spectrum showed signals in the region δ 3.0–3.3 for four protons and at 1.77 for a similar number.

Anal. Calcd. for $C_6H_8O_2$: C, 64.27; H, 7.19. Found: C, 63.71; H, 7.48.

(*b*) Irradiation of a nitrogen-flushed solution of 102 mg of the endoperoxide in 20 ml methanol at $-70°$ for 7 h gave **9** and **10** in 24 and 29% yield respectively.

Thermal Rearrangement

A solution of 245 mg of the endoperoxide in 6 ml xylene was refluxed for 3 h. The reaction product, which appeared cleaner than that obtained by irradiation, consisted essentially of **9** and **10**. Separation by t.l.c. gave 45 and 36% respectively, of these substances.

1,3,5,5-Tetramethyl-1,3-cyclohexadiene Endoperoxide

The diene (2 g) in 200 ml methanol containing 35 mg Rose Bengal was irradiated (300 W tungsten lamp) with the concomitant passage of oxygen. The endoperoxide (**7**) was partly purified by chromatography and t.l.c. (0.82 g; 41%) but contained small amounts of a heteroannular diene (λ_{max} 236) which was a contaminant of the starting material.

Irradiation

A solution of 200 mg endoperoxide in 200 ml cyclohexane on irradiation (6 h) gave two major products and several substances in minor amounts which were not further investigated. The two main products were isolated by t.l.c. One was the enone **11**, ν_{max} ($CHCl_3$) 3600, 3400, and 1685 cm^{-1}; λ_{max} (MeOH) 228 nm (ε 7600).

Anal. Calcd. for $C_{10}H_{16}O_2$: C, 71.39; H, 9.59. Found: C, 70.75; H, 9.30.

The second substance was the bisepoxide (**12**) n.m.r ($CDCl_3$) δ: 2.88H (1H, S), 2.56 (1H, S), 1.53 (3H, S), 1.31 (3H, S), 1.02 (3H, S), and 0.97 (3H, S).

The methylene group appeared as an AB centered approximately at 1.42 ($J \sim 15$ Hz), but only the outside two of the four peaks were resolved, one of the center two being a shoulder on the 1.31 singlet and the other being observed by the 1.53 singlet.

Anal. Calcd. for $C_{10}H_{16}O_2$: C, 71.39; H, 9.59. Found: C, 71.48; H, 9.77.

Methyl Levopimarate Endoperoxide (8)

(*a*) This was prepared by the method of Schuller and Lawrence (18). Irradiation of 210 mg in 60 ml cyclohexane (5 h) gave two main products. Separation by t.l.c. gave: (*i*) 78 mg of **13** (30%) m.p. 147–148°. Recrystallization from methanol gave material of m.p. 149–150°; ν_{max} (CCl_4) 1725, 1705, 1245 cm^{-1}.

Anal. Calcd. for $C_{21}H_{32}O_4$: C, 72.38; H, 9.26. Found: C, 72.60; H, 9.31.

(*ii*) The bisepoxide, **14**, 63 mg (31%), m.p. 118–119° unchanged on further crystallization from methanol ν_{max} (CCl_4) 1725, 1245 cm^{-1}.

Anal. Calcd. for $C_{21}H_{32}O_4$: C, 72.38; H, 9.26. Found: C, 72.53; H, 9.45.

(*b*) Thermal rearrangement of 75 mg of the endoperoxide in 7 ml refluxing xylene for 8 h gave **13** and **14** in 41 and 29% yields respectively.

(*c*) Solutions of the endoperoxide (35 mg) in (*i*) cyclohexane, (*ii*) dioxane, and dioxane containing (*iii*) 120 mg Michler's ketone, (*iv*) 150 mg phenanthrene, and (*v*) 150 mg triphenylamine were irradiated on a merry-go-round as described for ascaridole. After 2 h the presence of the irradiation products was readily detectable in tubes (*iii*) to (*v*) but not in (*i*) and (*ii*). After 6 and 18 h the difference was more marked (at least a factor of 10).

1. S. M. Kupchan, R. J. Hemingway, P. Coggon, A. T. McPhail, and G. A. Sim. J. Amer. Chem. Soc. **90**, 2982 (1968).
2. S. M. Kupchan, R. J. Hemingway, and R. M. Smith. J. Org. Chem. **34**, 3898 (1969).
3. G. Jacob and G. Ourisson. Bull. Soc. Chem. Fr. 734 (1958).
4. E. J. Agnello, R. Pinson, and G. D. Laubach. J. Amer. Chem. Soc. **78**, 4756 (1956).
5. D. Brown, B. T. Davis, T. G. Halsall, A. R. Hands, J. V. Hatton, and R. E. Richards. J. Chem. Soc. 4492 (1962).
6. J. Rigaudy, N. C. Cohen, and N. K. Cuong. C. R. 1851 (1967).
7. J. Rigaudy, C. Delatang, D. Sparfel, and N. K. Cuong. C. R. 1714 (1968).
8. J. Rigaudy. Pure Appl. Chem. **16** No. 1, 169 (1968).
9. G. R. McMillan. J. Amer. Chem. Soc. **83**, 3018 (1961).
10. P. J. Krusic and J. K. Kochi. J. Amer. Chem. Soc. **90**, 7155 (1968).
11. W. Bergmann, F. Hirschmann, and E. L. Skau. J. Org. Chem. **4**, 29 (1939).
12. D. L. Garin. J. Org. Chem. **34**, 2355 (1969).
13. R. J. Gritter and E. C. Sabatino. J. Org. Chem. **29**, 1965 (1967).
14. D. Brown, B. T. Davis, T. G. Halsall, and A. R. Handa. J. Chem. Soc. 4492 (1962).
15. F. G. Moses, R. S. H. Liu, and B. M. Monroe. Mol. Photochem. **1**, 245 (1969).
16. R. W. Murray and M. L. Kaplan. J. Amer. Chem. Soc. **90**, 537 (1968).
17. C. S. Foote, S. Wexler, W. Ando, and R. Higgins. J. Amer. Chem. Soc. **90**, 975 (1968).
18. W. H. Schuller and R. V. Lawrence. J. Amer. Chem. Soc. **80**, 1438 (1958).
19. L. A. Singer, G. A. Davis, and U. P. Muraldharan. J. Amer. Chem. Soc. **91**, 897 (1969).

On the deexcitation of the singlet excited oxygen atoms

HIDEO YAMAZAKI
Laboratory of Physical Chemistry, Tokyo Institute of Technology, Meguro-ku, Tokyo, Japan

Received May 8, 1970

The relative efficiency of a number of gases for the collisional deexcitation or chemical reaction with the singlet excited oxygen atoms $O(^1D_2)$ was studied by a competitive technique. Excited oxygen atoms were produced by the photolysis of nitrous oxide at 2139 Å and of ozone at 3132 Å. The order of the relative efficiency of the foreign gases is $CO_2 \cong Xe > CO > N_2 > Kr > Ar$ in the photolysis of nitrous oxide and $N_2O \cong CO_2 > Xe > Ne$ in the case of ozone. These trends are consistent with the previous results.

Canadian Journal of Chemistry, **48**, 3269 (1970)

Can. J. Chem. Downloaded from www.nrcresearchpress.com by 210.87.254.42 on 09/05/12
For personal use only.

Introduction

A considerable number of investigations of the deexcitation of the excited oxygen atoms $O(^1D_2)$ has been carried out by various methods, such as the kinetic method with product analysis (1–17), the measurement of chemiluminescence (18–24), and flash photolysis (25). However, some of these data are still not mutually consistent. It is therefore important to study these processes by as many independent techniques as is experimentally feasible. In the present work an attempt has been made to obtain the relative efficiency of deexcitation of the excited oxygen atoms and of their reaction with various gases by measuring the rate of formation of NO in their reaction with N_2O. In a second method, the destruction of O_3 in the presence of H_2 by the chain reaction initiated by the excited oxygen atoms has been used to assure that the excited oxygen atoms are indeed $O(^1D)$. In the presence of deactivating gases, the rates of these reactions are decreased and the relative rates of the deexcitation or the reaction of the excited oxygen atoms can be determined.

Experimental

The apparatus consisted of a mercury free vacuum system with the quartz reaction vessel of 2.5 cm in diameter and 14 cm in length. Phillips 93106E Zinc lamp (25 W) was used as a light source for the photolysis of N_2O. Its main spectral line was 2139 Å and the intensity of light was measured by a phototube with Pd surface. For the photolysis of O_3 a Toshiba H400P medium pressure mercury lamp (100 W) was used with a Toshiba UV31 filter; the main transmitted line was 3132 Å. Research grade rare gases and other gases were obtained from Takachihoshoji Co. Ozone was synthesized by the 1849 Å photolysis of pure oxygen in a circulating system with a liquid nitrogen trap. After pumping out the residual oxygen from the trap, O_3 was transferred to the reaction vessel.

The excited oxygen atoms were formed by the photolysis of N_2O at 2139 Å or by the photolysis of O_3 at 3132 Å. The formation of NO was detected as one of the reaction products between the excited oxygen atoms and N_2O. The changes in the intensity of the absorption spectrum of NO and O_3 were measured by Cary 14 spectrophotometer and Shimadzu MPS-50 spectrophotometer. The relative amounts of nitric oxide produced were measured by the absorption of the γ-band of NO with Cary 14 spectrophotometer with a slide wire expansion of the 0.1 absorbance to the full scale. Since the γ-band spectrum is very sharp, an atmosphere of He was added before the measurements to broaden the band and the slit of the spectrophotometer was made as narrow as possible so that the absorption varied linearly with the concentration in the quantitative measurements. The changes in the concentration of O_3 were measured by absorption at 2600 Å.

Results and Discussion

In the photolysis of N_2O the deexcitation and the scavenging of the excited oxygen atoms (O^*) can be represented by the following reaction scheme[1]

[1] $N_2O + h\nu \rightarrow N_2 + O^*$

[2*a*] $O^* + M \rightarrow O(^3P) + M$

[2*b*] $O^* + S \rightarrow SO$

[3*a*] $O^* + N_2O \rightarrow N_2 + O_2$

[3*b*] $O^* + N_2O \rightarrow 2NO$

[1]A primary split of N_2O into $N(^4S)$ and $NO(X^2\Pi)$ also occurs to a smaller extent at the shorter wavelength of 1830 Å (26, 27), and is also energetically possible at 2138 Å. The reactions of $N(^4S)$ with N_2O, CO, and CO_2 are immeasurably slow at room temperature (28, 29) and that with O_2 has a considerable energy of activation (28). On the other hand the reaction $N(^4S) + NO \rightarrow N_2 + O(^3P)$ has a rate coefficient of 2×10^{-11} cm^3/molecule s (30). Therefore, this effect on the production of NO can be ignored, even if the primary split takes place to some extent at 2138 Å. However, there is no indication that a split into N and NO occurs at 2138 Å since nitrosoalkanes have not been detected as products in the photolysis of N_2O at 2138 Å in the presence of hydrocarbons such as propane (8), isobutane (14), and neopentane (15, 16).

Can. J. Chem. Downloaded from www.nrcresearchpress.com by 210.87.254.42 on 09/05/12
For personal use only.

where M is a deactivating gas, and S is a scavenger of the excited oxygen atoms.

In the photolysis of N_2O at 2139 Å, there is still some possibility of production of $O(^1S)$ as well as $O(^1D)$, although the calculated available energy is 133 kcal/mole while the minimum required energy to form $O(^1S)$ is 135 kcal/mole. The steady state treatment gives the following relation between $1/R_{NO}$ and [M] (for S = 0)

$$[1] \qquad 1/R_{NO} = \frac{k_{2a}}{2k_1k_{3b}}\frac{[M]}{[N_2O]} + \frac{(k_{3a} + k_{3b})}{2k_1k_{3b}}$$

Equation 1 can be rearranged to give

$$[2] \qquad \frac{(1/R_{NO})}{(1/R_{NO})_0} = 1 + \frac{k_{2a}}{(k_{3a} + k_{3b})}\frac{[M]}{[N_2O]}$$

where $(1/R_{NO})_0$ is the value at [M] = 0. From the linear plots of $(1/R_{NO})/(1/R_{NO})_0$ against $[M]/[N_2O]$ the relative efficiencies of the deexcitation are obtained. For a scavenging process, k_{2a} and [M] in eqs. 1 and 2 are replaced by k_{2b} and [S].

Several straight line plots of eq. 2 were obtained, as shown in Fig. 1 and their slopes gave the relative efficiencies of the deexcitation and the scavenging of the excited oxygen atoms by various simple molecules. The relative efficiencies are shown in the first column in Table 1. These relative values of the rates of destruction of the excited oxygen atoms are practically coincident with the previous results (6–9, 15).

When $O(^1D_2)$ oxygen atoms are produced by the photolysis of ozone in the presence of a larger amount of H_2 (so that $O(^1D_2)$ atoms do not react with O_3 to any significant extent), the reaction mechanism proposed by Norrish and Wayne (11) may be applied.[2] The excited atoms will be consumed in reaction

$$[2c] \qquad O^* + H_2 \rightarrow OH + H$$

[2]In the photolysis of O_3 at 3132 Å $O(^3P)$ is also produced (31), but the reaction of $O(^3P)$ with H_2 is very slow and is not likely to produce vibrationally excited hydroxyl radicals, OH*, as chain initiators. Furthermore, the rate of reaction of O_3 with any $O(^3P)$ formed in the primary split of O_3 is independent of pressure of foreign gases introduced. The OH* produced by $O(^1D)$ (10, 11, 32) in reaction 2*c* is also deactivated by the various gases introduced. However, the effect of such a deactivation of OH* on the course of the reaction is evidently not large since addition of Ne and Ar, which have almost the same mass as OH, did not affect the rate of decomposition of O_3 (Fig. 2). However, a slight increase in the relative efficiencies of deactivation by polyatomic gases, CO_2 and N_2O, may be partially due to deactivation of OH*.

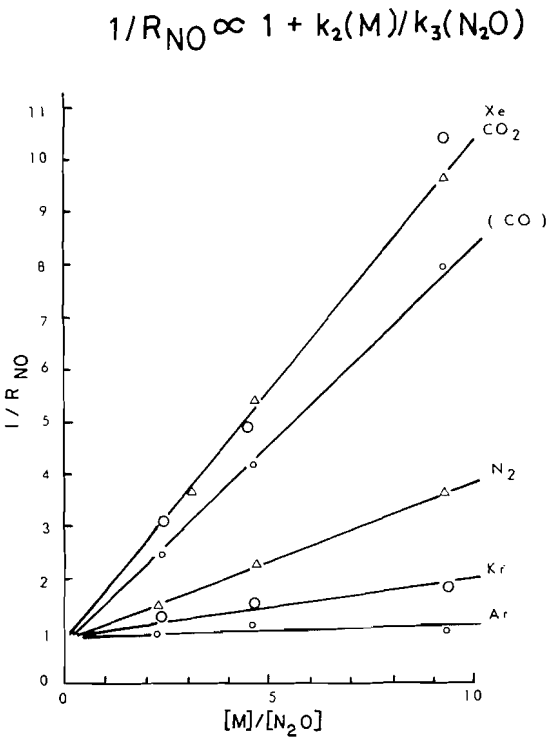

FIG. 1. The relative reciprocal rate of formation of NO plotted against the reduced concentration of foreign gases.

TABLE 1

Relative rate constants for the reaction or deexcitation of the excited oxygen atoms

M	Relative rate constants: N_2O Photolysis	Relative rate constants: O_3 Photolysis
Ne		0.0
Ar	0.01	0.0
Kr	0.09	
Xe	1.00	0.6
N_2	0.29	
CO_2	1.00	1.0
N_2O	1.06	1.0*, 1.1†
CO	0.79	

*Evaluated by assuming $\phi_0 = k_{2c}/k(O_3) = \infty$ in eq. 3.
†Evaluated by assuming $\phi_0 = 4$.

and, when M or N_2O are present, in reactions 2*a*, 3*a*, and 3*b* as well. Further reactions involved in the decomposition of ozone and chain termination are

$$[4] \qquad H + O_3 \rightarrow OH + O_2$$

$$[5] \qquad OH + O_3 \rightarrow HO_2 + O_2$$

Can. J. Chem. Downloaded from www.nrcresearchpress.com by 210.87.254.42 on 09/05/12
For personal use only.

[6] $HO_2 + O_3 \rightarrow 2O_2 + OH$

[7] $O(^3P) + O_3 \rightarrow 2O_2$

[8] $NO + O_3 \rightarrow NO_2 + O_2$

[9] $OH \rightarrow$ Termination

[10] $HO_2 \rightarrow$ Termination

Since in the chain process $k_6(O_3) \gg k_{10}$, and assuming approximately that $k = 4k_5k_{2c}/(k_9 + k_{10}k_5/k_6)$ remains constant in all the experiments carried out, steady state treatment gives the following general expression, valid when both M and N_2O are present

$$[3] \quad \frac{1}{\phi - 2} = \left\{ \frac{k_{2c}}{k[O_3]} + \frac{k_{2a}[M]}{k[O_3][H_2]} + \frac{(k_{3a} + k_{3b})[N_2O]}{k[O_3][H_2]} \right\} \Big/ \left\{ 1 + \frac{(k_{3b} - k_{3a})[N_2O]}{k[O_3][H_2]} \right\}$$

where ϕ is the quantum yield of decomposition of ozone. The light absorption in the reaction vessel is proportional to the O_3 pressure for sufficiently small absorption by O_3 at 3132 Å. The decrease of O_3 is then a first order reaction in O_3 concentration, assuming that ϕ remains approximately constant in the course of the reaction at the relatively small conversions of O_3 used, i.e.

$$[4] \quad [O_3(t)] = [O_3(0)] \exp \{ - \phi \alpha I_0 V t \}$$

where α is the absorption coefficient of O_3 at 3132 Å, I_0 the light intensity, and V the volume of the reaction vessel.

The experimental results, given in Fig. 2, show the first order decay of O_3 in the presence of various gases at constant pressure ([M] = 250, $[H_2] = 10$, $[O_3] = 0.3$ Torr). The slopes gave the values of ϕ from which the relative rates of deexcitation of $O(^1D_2)$, shown in the second column of Table 1, were evaluated from the appropriately simplified forms of eq. 3. In the case of Ne, Ar, Xe, and CO_2, $[N_2O] = 0$, and in the case of N_2O, [M] = 0. In the latter case, eq. 3 can be written in the form

$$[5] \quad \frac{1}{\phi - 2} = \frac{k_{2c}}{k[O_3]} + \frac{(k_{3a} + k_{3b})}{k} \times \left[1 - \frac{k_{3b} - k_{3a}}{k_{3b} + k_{3a}} \frac{1}{\phi - 2} \right] \frac{[N_2O]}{[O_3][H_2]}$$

and the required value of k_{3b}/k_{3a} has been assumed to be 2, as most of the experimental data in the literature seem to indicate.

The results in Table 1 are quite consistent with the various data on the deexcitation of the excited oxygen atoms (9, 15). Thus, the excited oxygen atoms produced in the photolysis of N_2O, O_3, and NO_2 all show very similar kinetic behavior for deexcitation. It is most likely that in all these cases the excited oxygen atoms are $O(^1D)$. The reaction with CO has been studied by flash photolysis (25), which showed that the rate was quite fast, in qualitative agreement with the present finding. The data obtained in the chemiluminescence experiments (18–23) do not always agree with the results of the kinetic methods (1–17). Further investigation will be necessary in order to reconcile these disagreements.

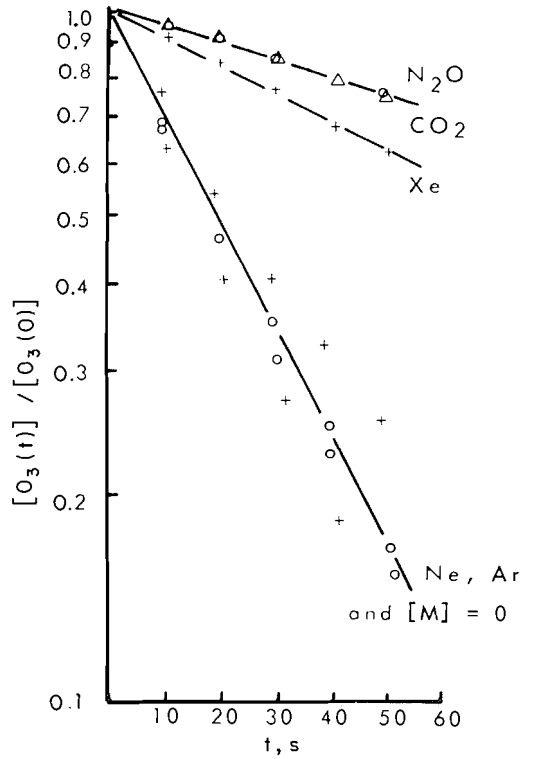

FIG. 2. First order decay of O_3 in the presence of foreign gases.

The author wishes to thank Dr. R. J. Cvetanović, National Research Council of Canada, Ottawa, for his careful examination of the manuscript, Professor S. Shida, Tokyo Institute of Technology, for his continued

interest in this work, and also Dr. M. Izawa, National Institute of Radiological Sciences, for the use of various experimental equipment.

1. W. B. DeMore and O. F. Raper. J. Chem. Phys. **37**, 2048 (1962).
2. O. F. Raper and W. B. DeMore. J. Chem. Phys. **40**, 1053 (1964).
3. W. B. DeMore and O. F. Raper. J. Chem. Phys. **44**, 1780 (1966).
4. W. B. DeMore and O. F. Raper. J. Chem. Phys. **46**, 2500 (1967).
5. W. B. DeMore. J. Chem. Phys. **47**, 2777 (1967).
6. H. Yamazaki and R. J. Cvetanović. J. Chem. Phys. **39**, 1902 (1963).
7. H. Yamazaki and R. J. Cvetanović. J. Chem. Phys. **40**, 582 (1964).
8. H. Yamazaki and R. J. Cvetanović. J. Chem. Phys. **41**, 3703 (1964).
9. K. F. Preston and R. J. Cvetanović. J. Chem. Phys. **45**, 2888 (1966).
10. R. G. W. Norrish and R. P. Wayne. Proc. Roy. Soc. London, Ser. A. **288**, 200 (1965).
11. R. G. W. Norrish and R. P. Wayne. Proc. Roy. Soc. London, Ser. A. **288**, 361 (1965).
12. P. Warneck. J. Chem. Phys. **43**, 1849 (1965).
13. D. Katakis. J. Chem. Phys. **47**, 541 (1967).
14. G. Paraskevopoulos and R. J. Cvetanović. J. Chem. Phys. **50**, 590 (1969).
15. G. Paraskevopoulos and R. J. Cvetanović. J. Amer. Chem. Soc. **91**, 7572 (1969).
16. G. Paraskevopoulos and R. J. Cvetanović. J. Chem. Phys. **52**, 5821 (1970).
17. W. B. DeMore. J. Chem. Phys. **52**, 4309 (1970).
18. R. A. Young, G. Black, and A. Y. M. Ung. J. Chem. Phys. **45**, 2702 (1966).
19. R. A. Young and A. T. M. Ung. J. Chem. Phys. **44**, 3038 (1966).
20. R. A. Young and G. Black. J. Chem. Phys. **47**, 2311 (1967).
21. R. A. Young, G. Black, and T. G. Slanger. J. Chem. Phys. **49**, 4758 (1968).
22. R. A. Young, G. Black, and T. G. Slanger. J. Chem. Phys. **49**, 4769 (1968).
23. J. F. Noxon. J. Chem. Phys. **52**, 1852 (1970).
24. R. F. Hampson, Jr., and H. Okabe. J. Chem. Phys. **52**, 1930 (1970).
25. M. Clerc and F. Barat. J. Chem. Phys. **46**, 107 (1967).
26. J. P. Doering and B. H. Mahan. Chemical reactions in the lower and upper atmosphere. Interscience Publ. Inc., New York. 1961. P. 327.
27. J. P. Doering and B. H. Mahan. J. Chem. Phys. **36**, 1682 (1962).
28. B. Brocklehurst and K. R. Jennings. Progr. React. Kinet. **4**, 1 (1967).
29. F. Kaufman and J. R. Kelso. J. Chem. Phys. **28**, 510 (1958).
30. L. F. Phillips and H. I. Schiff. J. Chem. Phys. **36**, 1509 (1962).
31. I. T. N. Jones and R. P. Wayne. J. Chem. Phys. **51**, 3617 (1969).
32. W. B. DeMore. J. Chem. Phys. **46**, 813 (1967).

Can. J. Chem. Downloaded from www.nrcresearchpress.com by 210.87.254.42 on 09/05/12
For personal use only.

Can. J. Chem. Downloaded from www.nrcresearchpress.com by 210.87.254.42 on 09/05/12
For personal use only.

Stereoselective synthesis of (±)epihinesol (agarospirol)[1]

M. MONGRAIN,[2] J. LAFONTAINE,[3] A. BÉLANGER,[2] AND P. DESLONGCHAMPS
Laboratoire de synthèse organique, Départment de chimie, Université de Sherbrooke, Sherbrooke, Québec
Received June 18, 1970

An efficient stereoselective synthesis of (±)epihinesol (**1**) (agarospirol) is described.

Canadian Journal of Chemistry, 48, 3273 (1970)

Current interests in degradative and synthetic studies on spiro[4.5]decane sesquiterpenes (1) prompt us to report a total synthesis of epihinesol **1** (1*c*, *d*).

The readily available keto ester **2** (2) was first converted into the dienone **4** (b.p. 65–68 °C (0.8 mm); ν_{max} 1665 cm^{-1}; τ 4.09 (1H, broad singlet), 4.56 (1H, singlet), 4.64 (1H, multiplet), 7.91 (3H, doublet, J = 1.5 Hz), and 8.80 (3H, doublet, J = 7 Hz); λ_{max} (EtOH) 273 mμ (ε = 16 300)) via the corresponding ketal ester and ketal alcohol **3** in 72% overall yield.

Michael addition with sodiomalonate followed by hydrolysis decarboxylation and reesterification with diazomethane gave the enone ester **5** (65% overall yield from **4**).

After protection of the ketonic carbonyl which was accompanied by migration of the double bond, the resulting ester was hydrolyzed to the crystalline acid (m.p. 72–73 °C). Conversion to the diazoketone **6** was then accomplished by standard procedures.

Copper-catalyzed internal cyclization (3) of the diazoketone **6** proceeded in a highly stereoselective manner to give **7***a* (10%) and *b* (90%)[4] (40% overall yield from **5**).

On being subjected to the following sequence of reactions: carbomethoxylation (→ **8**), borohydride reduction (→ **9**), Grignard reaction (→ **10**) and aqueous acid treatment, the mixture **7***a* and *b* gave the spiroketone **11** (m.p. 65–66 °C). Crude spiroketone **11** was further reduced to the diol **12** (m.p. 118–120 °C) which can be conveniently purified by direct crystallization (40% overall yield from **7***a* and *b*). The diol **12** was then converted in a quantitative yield into the monoacetate **13** (m.p. 79–80 °C).

Hydrogenolysis of the allylic acetate grouping (4) and specific reduction of the cyclopentene double bond was realized in a single operation giving epihinesol **1** almost quantitatively by treatment of **13** with lithium in ethylamine (5). Analogous reduction of the diol **12** also gave epihinesol (**1**), albeit in inferior yield (*ca.* 55%). The synthetic acetate **14** was found to be identical in all respect with an authentic sample of epihinesol acetate (1*a*, *b*).[5,6]

All new compounds reported in this communication gave satisfactory elemental analysis and spectroscopic data.

[1]Support for this work by the National Research Council of Canada, Ottawa, Canada, and by the "Ministère de l'Education" (Québec) is gratefully acknowledged. Collaboration at the initial stage of this project with Dr. J. S. Wilson is deeply appreciated.

[2]Holder of an NRCC Studentship (Canada) 1968–1970.

[3]Holder of a "bourse du Ministère de l'Education" (Québec) 1966–1969.

[4]Assignment of stereostructures of the two chromatographically separated isomers 7*a* and 7*b* will be presented in details in our forthcoming full publication. Professor G. Stork has kindly informed us that the identical reaction (**6** → 7*a*, *b*) has been carried out in his laboratories and similar conclusions were reached (P. McCurry (7)).

[5]We thank Professor James A. Marshall who kindly made this identification.

[6]Epihinesol (isopropylol epimer of hinesol) could very well be identical to agarospirol (1*d*) on the basis of biogenetic considerations (6). This conjecture is now strengthened by the identity of the n.m.r. spectrum of the crystalline epoxide **15** (m.p. 94–95 °C) with agarospirol epoxide. We thank Professor S. C. Bhattacharyya for this identification. However, the n.m.r. spectrum of our synthetic epihinesol differs from the one recorded in Bhattacharyya's paper in such a way that we suspect the natural "agarospirol" used by the Indian workers was probably contaminated. This was further hinted by our experience of quantitative epoxidation of epihinesol to a single product. We have not been able to secure a sample of authentic agarospirol.

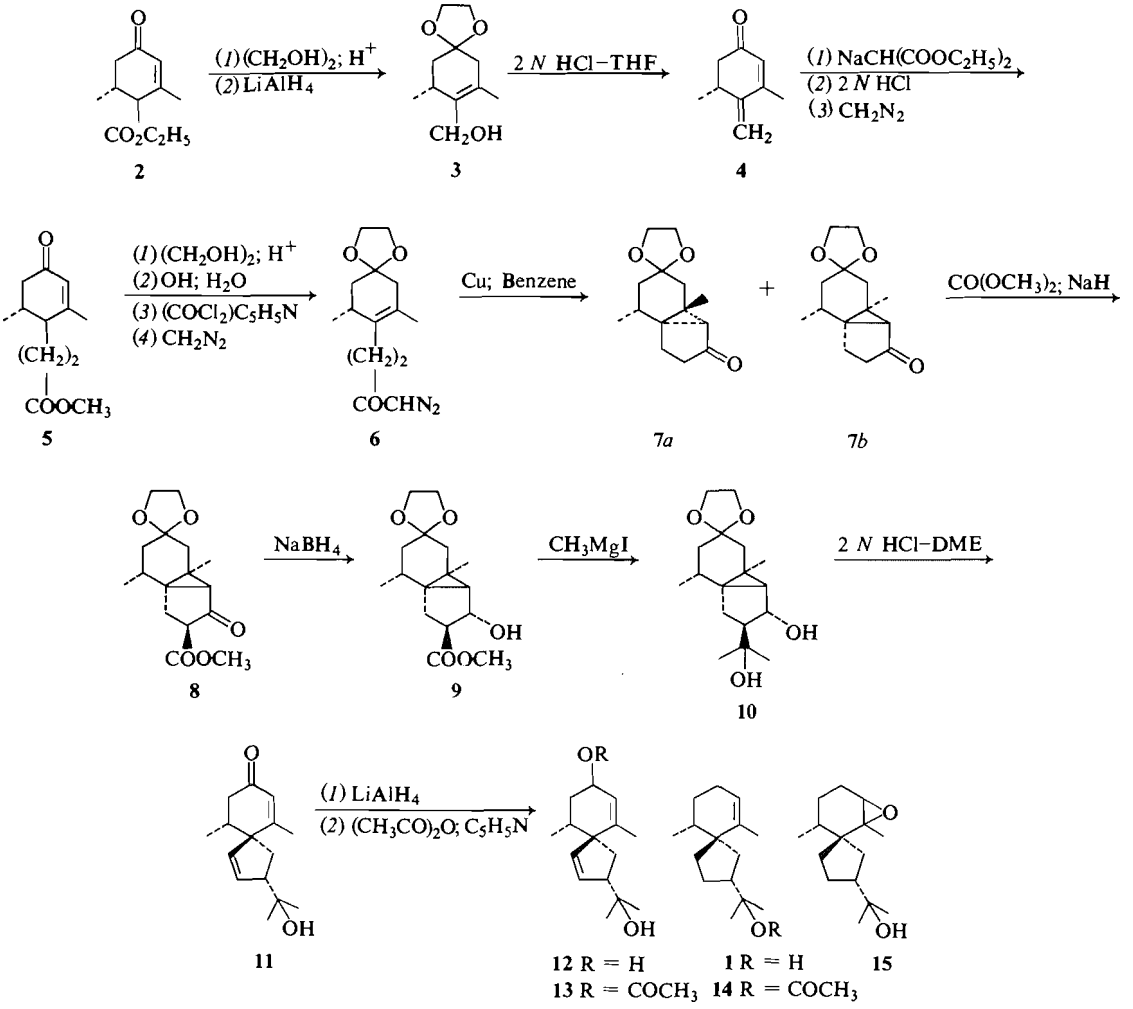

1. (*a*) J. A. MARSHALL, N. H. ANDERSEN, and P. C. JOHNSON. J. Amer. Chem. Soc. **89**, 2748 (1967); J. A. MARSHALL and P. C. JOHNSON. J. Amer. Chem. Soc. **89**, 2750 (1967). (*b*) J. A. MARSHALL and P. C. JOHNSON. Chem. Commun. 391 (1968); J. Org. Chem. **35**, 192 (1970); A. P. JOHNSON. International Symposium of Synthetic Methods and Rearrangements in Alicyclic Chemistry. Oxford, July 22–24, 1969. Abstract p. 13. (*c*) J. A. MARSHALL and S. F. BRADY. Tetrahedron Lett. 1387 (1969). (*d*) K. R. VARMA, M. L. MAHESHWARI, and S. C. BHATTACHARYYA. Tetrahedron, **21**, 115 (1965). (*e*) P. C. MUKHARJI and P. K. SEN GUPTA. Chem. Ind. 533 (1970).
2. E. C. HORNING, M. O. DENEKAS, and R. E. FIELD. Organic synthesis. Coll. Vol. 3. John Wiley and Sons, New York, N.Y., 1955. p. 317.
3. G. STORK and J. FICINI. J. Amer. Chem. Soc. **83**, 4678 (1961).
4. A. S. HALLSWORTH, H. B. HENBEST, and T. I. WRIGLEY. J. Chem. Soc. 1969 (1957).
5. R. A. BENKESER, J. J. HAZDRA, R. F. LAMBERT, and P. W. RYAN. J. Org. Chem. **24**, 854 (1959).
6. J. A. MARSHALL and S. F. BRADY. The chemistry of spiro[4.5]decane sesquiterpenes. *In* Topics in carbocyclic chemistry. Vol. II. *Edited by* D. Lloyd. Logos Press, 1970.
7. P. MCCURRY. Ph.D. Thesis. Columbia University, New York, N.Y., 1970.

Can. J. Chem. Downloaded from www.nrcresearchpress.com by 210.87.254.42 on 09/05/12
For personal use only.

Can. J. Chem. Downloaded from www.nrcresearchpress.com by 210.87.254.6 on 09/05/12
For personal use only.

Canadian Journal of Chemistry

Published by THE NATIONAL RESEARCH COUNCIL OF CANADA

VOLUME 48 NOVEMBER 1, 1970 NUMBER 21

Notes for authors of papers presenting the results of X-ray crystal-structure analysis[1]

The crystallographic nomenclature should correspond to that given in the *International Tables for X-Ray Crystallography*, Vol. I (1).

The following primary crystallographic data should be given: chemical formula, formula weight, unit cell dimensions, unit cell volume, observed density, number of formula units in cell, calculated density, working temperature, and the assumed value for the wavelength or other reference parameter used in calculating the cell dimensions. All measured quantities should be accompanied by an estimate of the accuracy, and the basis for the estimate should be stated. The crystal data should be presented in a condensed form, such as:

$C_6H_4N_2O_4$ f.w. = 168.1
Orthorhombic, a = 13.20(3), b = 13.97(3), c = 3.800(5)Å, V = 700.7 Å^3, ρ_0 = 1.57(1), Z = 4, ρ_c = 1.583, (20 °C; CuKα_1, λ = 1.54050 Å).

(The formula and formula weight may, if more convenient, be given elsewhere in the paper).

Authors are reminded that for presentation in such compilations as *Crystal Data* (2), certain conventions regarding the choice of unit cell are mandatory. Confusion in the literature can be avoided if these conventions are adopted in primary publication. Full details are given in *Crystal Data*, and in the *International Tables for X-Ray Crystallography*, Vol. II (1).

The space group should be reported in the Hermann–Mauguin notation. If the setting differs from the standard setting in the *International Tables for X-Ray Crystallography*, Vol. I (1), the corresponding Schoenflies symbol and the systematic absences should be given also. If there is any ambiguity in the choice of space group, the manner of its resolution should be stated. It must be emphasized that the space-group symbol given, and the origin implied by the symbol, should correspond to the setting and origin actually used.

The following information pertaining to the measurement of intensity data should be given: method of recording and measurement, the region of reciprocal space explored, and the number of accessible and observed reflections in this region, specimen size and shape, the radiation used, and details of any special corrections such as absorption or extinction.

The final refinement should be reported in sufficient detail to enable the reader to assess its reliability and completeness, and if necessary, to repeat or extend it. The origin of the scattering factors used should be specified, together with details of any corrections for anomalous scattering. A suitable table of observed and calculated structure amplitudes must accompany the paper; it should include the calculated structure amplitudes of unobserved reflections in the region of reciprocal space explored. This table will not be published, but will be placed in the Depository of Unpublished Data, National Science Library, National Research Council of Canada, Ottawa 7, which will supply copies on request. It must, therefore, be suitable for limited duplication and circulation. A final agreement index ($R = \sum| |F_0| - |F_c| |/ \sum |F_0|$) should be given and defined with respect to the treatment of unobserved reflections. For least-squares refinement, any approximation (*e.g.*, block-diagonal) should be specified, as should the quantity minimized. The weighting scheme should be given, and should include a statement of any reflections assigned zero weight. If the weighting scheme cannot be specified by a function (as, for example, when the weights are based on the total counts recorded for the reflec-

[1]These notes have been read and approved by the Canadian National Committee for Crystallography, at Ottawa, July 3, 1970.

TABLE 1

Final parameters (e.s.d.'s) × 10^4

$\pm|x, y, z; \frac{1}{2}+x, \frac{1}{2}-y, z|$

T.F. = $\exp\{-2\pi^2(a^{*2}h^2U_{11}+\cdots+2a^*b^*hkU_{12}+\cdots+)\}$

	x	y	z	U_{11}	U_{22}	U_{33}	U_{12}	U_{13}	U_{23}
C(1)	1268(6)	4171(2)	9020(4)	175(5)	350(10)	217(7)	41(4)	−26(2)	2(4)
C(2)	etc.								

tion, or other data unavailable to the reader), individual weights should be included in the table of structure amplitudes. Where possible, the correctness of the reported structure should be checked by a method independent of that used for refinement (*e.g.*, by a difference–Fourier synthesis) and the result of this procedure briefly reported.

The final structural parameters (positional and thermal) should be given in a single table, with the coordinates expressed as fractions of the cell edges. If the space-group setting is non-standard, a statement of the equivalent positions should be given also. The table should preferably include, or at least be accompanied by, an estimate of the standard deviations of the parameters. The asymmetric unit defined by the coordinates should, where possible, specify a single molecule or other appropriate chemical entity. Temperature factors should be defined explicitly in terms of the parameters given. Atoms of the same chemical species should be distinguished by appended arabic numerals in parentheses. Subscripts are not acceptable, as they may lead to confusion in chemical contexts. In order to conserve space, the parameters should be multiplied by appropriate powers of ten. A suitable (but not mandatory) format for the table of parameters is:

The volume of information required for compliance with these notes is formidable, and it is essential that the presentation be concise and relevant. It should not be a narrative account of the progress of the analysis, or a discussion of method, unless these elements have a direct bearing on the chemical conclusions.

1. International tables for X-ray crystallography. Vols. I–III. Kynoch Press, Birmingham. 1952, 1959, 1962.
2. Crystal Data, determinative tables. 2nd ed. Monograph 5, American Crystallographic Association. 1963.

Can. J. Chem. Downloaded from www.nrcresearchpress.com by 210.87.254.6 on 09/05/12
For personal use only.

Can. J. Chem. Downloaded from www.nrcresearchpress.com by 210.87.254.105 on 09/05/12
For personal use only.

The radiolysis of ethane. II. Liquid phase at 195 °K; effect of electron and positive ion scavengers

P. T. HOLLAND AND J. A. STONE
Chemistry Department, Queen's University, Kingston, Ontario

Received April 30, 1970

H atoms and $\cdot C_2H_5$ radicals in the radiolysis of liquid ethane have both ionic and non-ionic precursors. The use of SF_6 as an electron scavenger leads to very low C_2H_4 yields which is consistent with the addition of $\cdot SF_5$ radicals to this product. H and D atoms produced by neutralization of ND_3H^+ can either add to C_2H_4 or abstract from C_2H_6 at 195 °K.

Canadian Journal of Chemistry, **48**, 3277 (1970)

Introduction

In a previous paper (1) we showed that the product yields obtained in the radiolysis of liquid ethane at 195 °K are quantitatively explicable in terms of the reactions of H atoms and ethyl and methyl radicals. Initial G values for all major products and radical intermediates were determined. However, the precursors of these radicals were not determined. In this paper we report the effects of an electron scavenger, SF_6, and a proton acceptor, ND_3, on the radiolysis of liquid ethane from which we estimate the ionic contribution to radical formation. The results of these studies emphasize again the problems caused by H atom addition to product olefin in the quantitative interpretation of experimental data obtained from the radiolysis of ethane at low temperature. Because of this self-scavenging the number of electrons scavenged cannot be determined simply from the decrease in $G(H_2)$. A mechanism consistent with experimental results requires the formation of $\cdot SF_5$ subsequent to electron capture by SF_6.

Experimental

Ethane purification, sample preparation, irradiation, and product analysis were as described previously (1). SF_6 (Matheson, 99.8%) and ND_3 (Merck, Sharpe and Dohme of Canada, Ltd. 98% D) were subject to trap-to-trap distillation before use. The analysis of the isotopic hydrogens was performed with an AEI MS-10 mass spectrometer.

Results and Discussion

Sulfur Hexafluoride as an Electron Scavenger

SF_6 has seen wide use as a specific electron scavenger in organic systems even though its fate following electron capture is not known. In liquid cyclohexane at 298 °K, it reduces $G(H_2)$ but at the same time does not lead to increased yields of the usual radiolytic products from the hydrocarbon alone as does either N_2O (2, 3) or some perfluorinated hydrocarbons (4). Sagert and Blair (3) studied the radiolysis of cyclohexane–SF_6 mixtures in the solid phase at 77 °K and concluded that (*a*) the chemistry of the system is complex and (*b*) no cyclohexyl radicals appear to be formed when the neutralization step $c\text{-}C_6H_{12}^+ + SF_6^-$ occurs. Van Ingen and Cramer (5) disagree with this latter conclusion. We are not aware of any results reported for the radiolysis of solutions of SF_6 in liquid hydrocarbons at reduced temperatures.

Figure 1 shows the yields of the major products ($G > 0.1$) as functions of dose in the radiolysis of liquid ethane containing 1.5 mole% SF_6. No fluorinated products were observed although Bakale (6) has reported detecting C_2H_5F in unknown yield in this system. No authentic sample was available as standard and it may be that such a product would not be eluted from the columns used in our chromatographic analyses. The curves in Fig. 1 are to be compared with those for ethane in the absence of SF_6 (Figs. 1 and 2 of ref. 1). While the yields of CH_4, C_3H_8, and $n\text{-}C_4H_{10}$ show similar dose dependences in the presence and absence of SF_6, the H_2 and C_2H_4 yields do not. The ethylene concentration is constant at 2×10^{16} molecules/g from 1 to 7 $\times 10^{19}$ eV/g in the presence of SF_6 whereas in its absence a steady increase in concentration ($G = 0.7$) occurs at doses above 4×10^{19} eV/g. The hydrogen yield in the presence of SF_6 shows much less curvature with dose than it does in its absence.

These results can be rationalized in terms of the

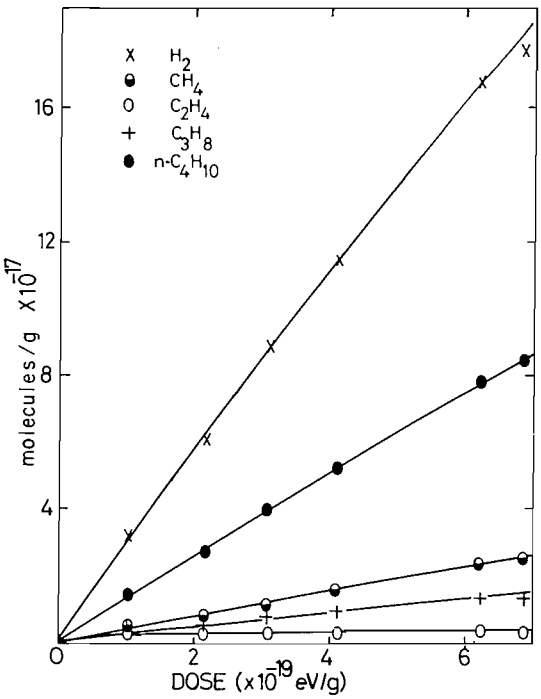

FIG. 1. Product yields from liquid ethane containing 1.5 mole% SF_6 at 195 °K.

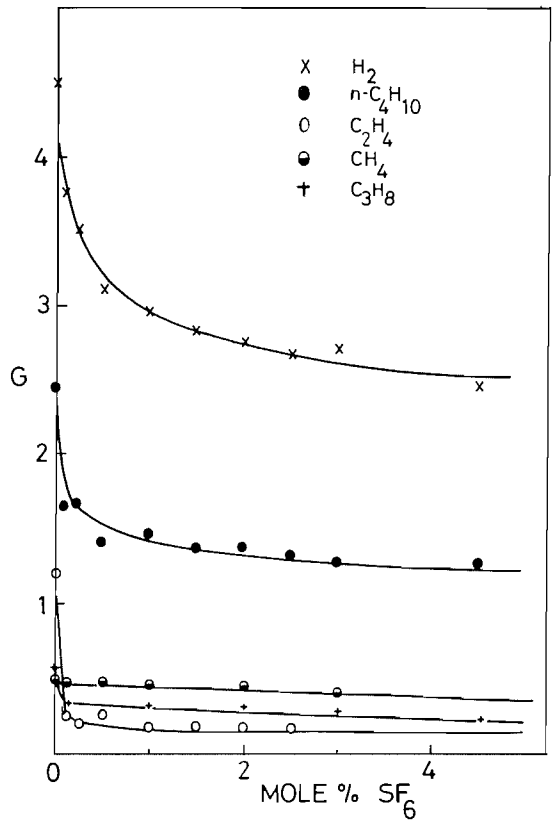

FIG. 2. The effect of SF_6 on product yields from liquid ethane (dose = 2.1×10^{19} eV/g).

free radical mechanism, involving $\cdot H$ and $\cdot C_2H_5$, operating in liquid ethane (1, 7)

[1] $\quad H\cdot + C_2H_6 \rightarrow H_2 + \cdot C_2H_5$

[2] $\quad H\cdot + C_2H_4 \rightarrow \cdot C_2H_5$

[3*a*] $\quad 2\cdot C_2H_5 \rightarrow C_2H_4 + C_2H_6$

[3*b*] $\quad \rightarrow n\text{-}C_4H_{10}$

At very low dose, reaction 2 is negligible compared with [1] and $G(C_2H_4) = 2.96$. Since $G(H\cdot) = 2.3$ then at doses above 4×10^{19} eV/g, when all H atoms disappear by reaction 2, $G(C_2H_4) \approx 2.96 - 2.3 \approx 0.7$. The low, constant concentration of C_2H_4 (Fig. 1) shows that in the presence of SF_6, C_2H_4 is being removed at the same rate as that at which it is formed *i.e.* either $G(H\cdot) > G(C_2H_4)$ or C_2H_4 is being removed in a secondary reaction. The latter contention is supported by the C:H balance as discussed later.

The effect of increasing SF_6 concentration on product yields at a dose of 2.1×10^{19} eV g^{-1} is shown in Fig. 2. The values for $G(C_2H_4)$ show that the steady state concentration of ethylene changes little with SF_6 concentration. In pure ethane a good C:H balance for products of 1:3.05 was obtained from which, with the aid of H atom scavenging experiments with cyclopentene, it was deduced that at very low dose $g(H\cdot) = 2.3$ and $g(\cdot C_2H_5) = 5.8$ (1). Such calculations are not possible in the ethane/SF_6 system since the C:H balance is poor (e.g. 1:3.3 for 1.5 mole% SF_6 at 2×10^{19} eV/g). Carbon-rich products are unaccounted for. If plausible assumptions as to the nature of these missing products can be made then due allowance may be made in the product balance and estimates of the role of ionic precursors in the formation of reaction intermediates may be made.

Capture of thermalized electrons by SF_6 in the gas phase yields mainly SF_6^- (8).

[4] $\quad e + SF_6 \rightarrow SF_6^-$

The reaction of SF_6^- and $C_2H_6^+$ must lead to chemical reaction in some of the encounters, otherwise the C:H balance would be as good in the presence of SF_6 as in its absence. The most

Can. J. Chem. Downloaded from www.nrcresearchpress.com by 210.87.254.105 on 09/05/12
For personal use only.

Can. J. Chem. Downloaded from www.nrcresearchpress.com by 210.87.254.105 on 09/05/12
For personal use only.

probable neutralization reaction is (5)

[5] $SF_6^- + C_2H_6^+ \rightarrow \cdot SF_5 + HF + \cdot C_2H_5$

In the absence of SF_6, neutralization of RH^+ would lead mainly to either C_2H_4 or n-C_4H_{10} and H_2 ([6*a*] or [6*b*] followed by [3*a*] or [3*b*]).

[6*a*] $e + C_2H_6^+ \rightarrow C_2H_6^* \rightarrow \cdot C_2H_5 + H\cdot$

[6*b*] $\rightarrow C_2H_4 + H_2$

Reaction 5 produces one ethyl radical without any H or H_2 and so cannot lead to a deficit of carbon in the material balance even if this $\cdot C_2H_5$ disappears by combination with $\cdot SF_5$. No plausible reaction scheme involving charge neutralization and radical–radical reactions can lead to a surplus. It is most probable that a reaction product, namely ethylene, is disappearing in a secondary reaction. This cannot be wholly due to H atom scavenging since this does not change the C:H balance of the products. Two possible reactions which might occur subsequent to reaction 5 are addition of either HF or $\cdot SF_5$ to ethylene.

[7] $HF + C_2H_4 \rightarrow C_2H_5F$

[8] $\cdot SF_5 + C_2H_4 \rightarrow \cdot C_2H_4SF_5$

Little is known about reaction 7 although it is described as a preparative method for C_2H_5F (9). Radiolysis of solutions of perfluorocyclohexane in n-hexane give high yields of HF which are little changed by the addition of olefin (10). In two experiments we find $G(C_2H_4) = 0.71$ and 0.62, respectively, for 0.5 and 2 mole% c-C_6F_{12} in C_2H_6. Reaction 7 therefore appears improbable in the C_2H_6/SF_6 system.

Van Ingen and Cramer (5) have explained the high G value for *cis–trans* isomerization of 2-pentene in γ-irradiated liquid cyclohexane containing SF_6 in terms of the reversible addition of $\cdot SF_5$.

[9] $\cdot SF_5 + cis\text{-2-pentene} \rightleftharpoons SF_5C_5H_{10}\cdot \rightleftharpoons \cdot SF_5 + trans\text{-2-pentene}$

This is supported by the work of Sidebottom, Tedder, and Walton (11) who estimate for the gas phase reaction

[10] $\cdot SF_5 + C_2H_4 \underset{k_{-10}}{\overset{k_{+10}}{\rightleftharpoons}} SF_5C_2H_4\cdot$

$k_{+10} \approx 4 \times 10^5 \exp(1900/RT) M^{-1}\ s^{-1}$ while k_{-10} has an activation energy of 8.5 kcal mole^{-1}. At 195 °K the forward reaction may be possible and can remove ethylene but the reverse reaction will be too slow to compete with addition or disproportionation with $\cdot C_2H_5$ radicals.

[11*a*] $SF_5C_2H_4\cdot + \cdot C_2H_5 \rightarrow SF_5C_2H_5 + C_2H_4$

[11*b*] $\rightarrow SF_5C_2H_3 + C_2H_6$

[11*c*] $\rightarrow SF_5C_4H_9$

Reaction 11*a* would lead to the regeneration of some ethylene but as an approximate value for the removal of ethylene by secondary reaction we may take the number of moles of C_2H_4 required to bring the C:H ratio back to the value observed for pure ethane; 0.8 G units are required at 1.7 mole% SF_6. The yield of ethylene when protected by another olefin from both $\cdot SF_5$ and H atom attack should be at least this value. Figure 3 shows the effect of small concentrations of c-C_5H_8 on liquid ethane containing 1.7 mole% SF_6. The "protected" yield of C_2H_4 is 1.25 which is to be compared with the value of 2.6 in the absence of SF_6.

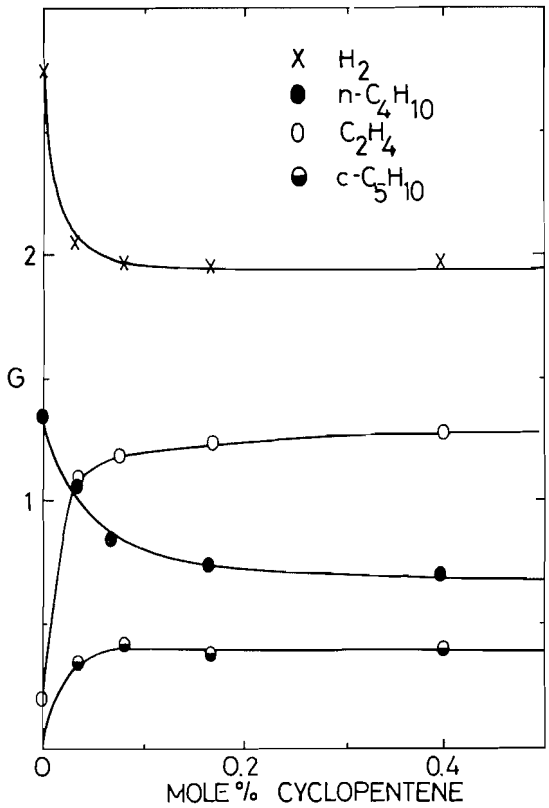

FIG. 3. The effect of cyclopentene on product yields from liquid ethane containing 1.7 mole% SF_6 (dose = 3×10^{19} eV/g).

TABLE 1

Product yields in the system C_2H_6/ND_3 (2×10^{19} eV/g)

Mole% ND_3	$G(H_2)$	$G(HD)$	$G(D_2)$	$G(C_2H_4)$	$G(n\text{-}C_4H_{10})$
0	4.70	0	0	1.20	2.42
0.012	4.48	0.07	0	1.19	2.47
0.25	4.30	0.15	0.002	1.12	2.50
0.50	4.19	0.21	0.008	0.93	2.64
0.8	4.01	0.28	0.02	—	2.62

In a previous paper (1) we showed how mass balance equations may be written for C_2H_4 and n-C_4H_{10} in the presence and absence of cyclopentene. The solution of these equations gives the yields of the radical intermediates $\cdot C_2H_5$ and $\cdot H$ and the yields of H_2 and C_2H_4 arising from processes not susceptible to radical scavengers. We performed these calculations for the systems C_2H_6/1.7 mole% SF_6 and C_2H_6/1.7 mole% SF_6/0.1 mole% c-C_5H_8 and obtained $g(H\cdot) = 1.33$, $g(\cdot C_2H_5) = 2.18$, $G_m(C_2H_4) = 1.33$, and $G_m(H_2) = 1.93$. (Here G_m denotes a yield from sources other than scavengeable radicals and ions.) We assume that the $\cdot SF_5$ and $SF_5C_2H_4\cdot$ radicals react with $\cdot C_2H_5$ *i.e.* the $\cdot C_2H_5$ radicals produced in reaction 5 need not be included in the mass balance. In the absence of a detailed knowledge of the fate of the fluorinated radicals this is a reasonable approximation since the major radical is $\cdot C_2H_5$ and C_2H_4 regeneration via [11*a*] does not affect the mass balance. The yield of n-C_4H_{10} not scavengeable by normal concentrations of either radical or ionic scavengers which was required in the calculation was taken as 0.28, a value obtained in liquid C_2H_6 containing 8 mole% D_2S.

1.7 mole% SF_6 does not scavenge all electrons, but from the declining $G(H_2)$ values in Fig. 2 we estimate that approximately 83% of the total decrease expected at high SF_6 concentration has occurred. If the reasonable assumption is made that the declining radical yields follow $G(H_2)$ then, allowing for a further 17% decrease in yield reductions and taking into account that in pure C_2H_6 $g(H\cdot) = 2.3 \pm 0.2$ and $g(\cdot C_2H_5) = 3.5 \pm 0.4$ (from ref. 1 where $g(\cdot C_2H_5)$ is given erroneously as 3.18 ± 0.4), the fully electron scavenged system has $g(H\cdot) = 1.1$ and $g(\cdot C_2H_5) = 1.9$. The ionic yields are therefore 1.2 and 1.6, respectively. The total decomposition due to ionic reactions is ~3.2 molecules per 100 eV absorbed. These values are approximate because of the lack of detailed knowledge of the system, however, they do show that both radicals are produced by ionic and non-ionic mechanisms each contributing about 50% of the yields. We have been able to make one check on the non-ionic yield of $H\cdot$. At very low concentrations of D_2S in liquid ethane $G(HD) = g(H\cdot)$ (1). The addition of 2 mole% SF_6 causes this value to fall to ~1.0 confirming that about 50% of the thermalized $H\cdot$ atoms formed in liquid C_2H_6 have ionic precursors. The only comparable measurement was by Asmus, Warman, and Schuler who found that in liquid cyclohexane at 298 °K, 60% of the thermalized $H\cdot$ atoms have ionic precursors (12).

Positive Ion Scavenging by ND_3

Williams (13) has shown that ND_3 may be used as an efficient ion scavenger in irradiated paraffins. The proton affinity of ND_3 is 59 kcal mole^{-1} greater than that of $\cdot C_2H_5$ (14) so that the proton transfer reaction

$$[12] \qquad C_2H_6^+ + ND_3 \rightarrow \cdot C_2H_5 + ND_3H^+$$

should be facile. Table 1 shows the yields of major products from the radiolysis of low concentrations of ND_3 in C_2H_6 at a dose of 2.0×10^{19} eV/g. ND_3 appears to have a very limited solubility in ethane at 195 °K since attempts to prepare solutions containing 1 mole% or more always resulted in a two phase system.

As the concentration of ND_3 increases, $G(HD)$ increases but $G(H_2 + HD)$ decreases. At room temperature $G(H_2 + HD)$ remains constant for ND_3 in c-C_6H_{12}. This is consistent with the self-scavenging at the lower temperature of H and D atoms formed by

$$[13a] \qquad ND_3H^+ + e \rightarrow ND_2H + D\cdot$$

$$[13b] \qquad \rightarrow ND_3 + H\cdot$$

The H and D atoms will either abstract from C_2H_6 or be scavenged by the C_2H_4 produced. The ratio of abstraction to addition will change as the olefin concentration builds up. In pure ethane up to a dose of 2.0×10^{19} eV g^{-1} the

Can. J. Chem. Downloaded from www.nrcresearchpress.com by 210.87.254.105 on 09/05/12
For personal use only.

TABLE 2

Estimates of G(ions scavenged by ND_3) in C_2H_6

Mole% ND_3	$\left(\frac{1}{0.45} \times \frac{4}{3}\right)G(HD)$	$\Delta G(H_2) + \left(\frac{1}{0.45} \times \frac{1}{3}\right)G(HD)$
0.012	0.21	0.25
0.25	0.44	0.49
0.50	0.62	0.64
0.80	0.82	0.87

hydrogen yield curve shows (see Fig. 1 of ref. 1) that on the average 55% of the H atoms produced are scavenged by C_2H_4 while 45% abstract. In the presence of ND_3 the C_2H_4 concentration is decreased (Table 1), due partly to the production of more hydrogen atoms (H and D) and probably partly to the reduced formation of C_2H_4 having ionic precursors. As an approximation, since the forms of the C_2H_4 or H_2 yield *vs.* dose curves other than those for pure C_2H_6 are not known, we will assume that the ratio of addition to abstraction remains equal to that in pure C_2H_6 at the same dose. If we take the ratio k_{13a}/k_{13b} to be the statistical ratio of 3:1 then G(ions scavenged) by reaction 12 will be (1/0.45) × (4/3)G(HD). Another measure of the number of ions scavenged will be the decrease in H_2. At room temperature for ND_3 in cyclohexane $\Delta G(H_2) = G(HD) = \frac{3}{4}\ G$(ions scavenged) (13). At 195 °K in C_2H_6 G(ions scavenged) will be given approximately by $\Delta G(H_2)$ + (1/0.45) G(HD) × (1/3). The values of these two estimates of ions scavenged at different ND_3 concentrations are presented in Table 2. The agreement is good within the limits of the approximation of no change in the addition/abstraction ratio with change in olefin yield.

If all ions scavenged normally lead to H atom production in pure ethane, then ΔG(hydrogen) *i.e.* $\Delta G(H_2 + HD + D_2) = 0$ for all ND_3 concentrations. G(hydrogen) decreases while $G(C_2H_4)$ decreases and $G(n\text{-}C_4H_{10})$ increases (Table 1). The results are consistent with those obtained with SF_6. When reactions 6*a* and 6*b* are superceded by reactions 12 and 13 the yield of hydrogen atoms (H and D) increases, and therefore a larger fraction of the hydrogen yield is scavengeable, and hence G(hydrogen) decreases while $G(C_2H_4)$ decreases and $G(n\text{-}C_4H_{10})$ increases.

The generation of D and H atoms by neutralization of the ammonium ion and the subsequent decrease in $G(H_2 + HD)$ compared with $G(H_2)_{initial}$ is confirmation of the previous descriptions (1, 7) of the behavior of hydrogen atoms in liquid ethane at 195 °K.

We thank the National Research Council of Canada and Atomic Energy of Canada Ltd. (Commercial Products) for financial assistance.

1. P. T. HOLLAND and J. A. STONE. Can. J. Chem. **48**, 1078 (1970).
2. R. BLACKBURN and A. CHARLESBY. Nature, **210**, 1036 (1966).
3. N. H. SAGERT and A. S. BLAIR. Can. J. Chem. **45**, 1351 (1967).
4. N. H. SAGERT. Can. J. Chem. **46**, 95 (1968).
5. J. W. F. VAN INGEN and W. A. CRAMER. J. Phys. Chem. **74**, 1134 (1970).
6. G. BAKALE. Ph.D. Thesis. Case Western Reserve University, 1968. p. 170.
7. G. BAKALE and H. A. GILLIS. J. Phys. Chem. **73**, 2178 (1969).
8. W. M. HICKAM and R. E. FOX. J. Chem. Phys. **25**, 642 (1956).
9. A. V. GROSSE and G. B. LINN. J. Org. Chem. **3**, 26 (1938).
10. L. A. RAJBENBACH. J. Phys. Chem. **73**, 356 (1969).
11. H. W. SIDEBOTTOM, J. M. TEDDER, and J. C. WALTON. Trans. Faraday Soc. **65**, 2103 (1969).
12. K-D. ASMUS, J. M. WARMAN, and R. H. SCHULER. J. Phys. Chem. **74**, 246 (1970).
13. T. F. WILLIAMS. J. Amer. Chem. Soc. **86**, 3954 (1964).
14. G. R. FREEMAN. Rad. Res. Rev. **1**, 1 (1968).

Can. J. Chem. Downloaded from www.nrcresearchpress.com by 210.87.254.105 on 09/05/12
For personal use only.

Can. J. Chem. Downloaded from www.nrcresearchpress.com by 210.87.254.40 on 09/05/12
For personal use only.

Radiolysis of liquid hydrocarbons containing deuterium sulfide

J. A. STONE AND P. T. HOLLAND[1]
Chemistry Department, Queen's University, Kingston, Ontario
Received June 4, 1970

The radiolysis of hydrocarbons containing dissolved D_2S leads to HD, D_2, and H_2 formation, the total hydrogen yields being greater than those in the absence of D_2S. A limiting yield of HD is attained at low D_2S concentrations (~5 mole%) in all solvents studied. This limiting yield is equal to $G(H\cdot)$ in ethane at 195 °K but not in *c*-C_6H_{12} at 298 °K when $G(HD)$ is much greater than accepted values of $G(H\cdot)$. D_2S behaves as both an electron and a positive ion scavenger, most of the D_2 and probably some of the HD being formed in these processes. The use of D_2S to determine H atom and ion yields in irradiated alkanes is not recommended.

Canadian Journal of Chemistry, **48**, 3282 (1970)

Introduction

Meissner and Henglein (1) have suggested that deuterium sulfide possesses admirable properties as a scavenger for the study of transient species in the radiolysis of saturated hydrocarbons. They studied the yields of isotopic hydrogens in the *n*-hexane/deuterium sulfide system in the liquid phase, mainly at room temperature; we here present an outline of the radiolytic mechanism they propose as an explanation of the yields obtained.

Two types of thermalized H atoms can be recognized in *n*-hexane; those formed without ionic precursors

[1] $n\text{-}C_6H_{14} \rightsquigarrow n\text{-}C_6H_{14}^* \rightarrow n\text{-}C_6H_{13}\cdot + H\cdot$

are designated H_α while those which have ionic precursors

[2] $n\text{-}C_6H_{14} \rightsquigarrow n\text{-}C_6H_{14}^+ + e \rightarrow n\text{-}C_6H_{14}^* \rightarrow n\text{-}C_6H_{13}\cdot + H\cdot$

are designated H_β.

H atoms can abstract D from D_2S to yield HD,

[3] $H\cdot + D_2S \rightarrow HD + DS\cdot$

so that the yield of this product is a measure of the number of H atoms scavenged.

Charge transfer from $n\text{-}C_6H_{14}^+$ to D_2S occurs and, following neutralization of D_2S^+, D_2 is produced

[4] $n\text{-}C_6H_{14}^+ + D_2S \rightarrow n\text{-}C_6H_{14} + D_2S^+$

[5] $D_2S^+ + e \rightarrow D_2 + S$

The D_2 yield is therefore a measure of the number of ions scavenged. At high D_2S concentration (~ 10 mole %) almost all ions are scavenged and $G(D_2) \approx 3$. When this occurs no H_β atoms are formed and so a limiting yield of HD is obtained which is a measure of H_α. For *n*-hexane this limiting yield is 1.5 G.

The above scheme is very attractive in that it appears possible, simply by measuring isotopic hydrogen yields, to obtain much information about reactive intermediates in irradiated hydrocarbons. We have examined the yields of the isotopic hydrogens obtained when D_2S is irradiated in cyclohexane, *n*-hexane, and cyclopentane at 298 °K and in liquid ethane at 195 °K. In all cases the variations of yields with D_2S concentration are similar to those obtained by Meissner and Henglein. We find, however, that the above simple interpretation of these yields is not valid. The HD yield always has ionic precursors and in addition D_2S appears to behave as an electron scavenger.

Experimental

Cyclohexane (Fisher Spectranalysed), cyclopentane (Phillips Research Grade), and *n*-hexane (Phillips Pure Grade) were usually used as received. Treatment with concentrated sulfuric acid followed by distillation, or storage over sodium had no effect on the experimental results obtained. Ethane (Phillips Research Grade) was purified as described previously (2). D_2S (Stohler Isotope Chemicals) was 98 atom % in D and was used after degassing under vacuum.

Samples for room temperature irradiation were contained under vacuum in Pyrex tubes, 0.6 cm o.d., sealed off so that the gas volume was negligibly small (less than 3% of the liquid volume). All these samples contained 2 ml of the liquid hydrocarbon plus the appropriate amount of D_2S and any other solute required. The preparation of the liquid ethane samples has been described (2).

Samples were irradiated in a ^{60}Co Gammacell 220 (Atomic Energy of Canada Limited) to total doses of about 10^{19} eV/g. Except for those samples containing very low concentrations of D_2S when a large fraction

[1]Present address: Space Sciences Laboratory, University of California, Berkeley, California 94720.

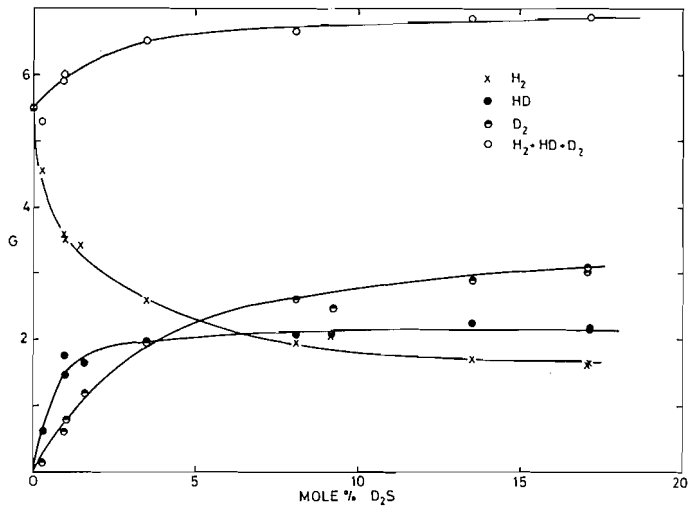

FIG. 1. Hydrogen yields from c-C_6H_{12}/D_2S solutions at 298 °K (dose = 9.6×10^{18} eV/ml).

was used up, the yields showed no dose dependence up to at least 2.5×10^{19} eV/g.

The hydrogen was separated from other products by pumping through solid nitrogen traps and was then measured volumetrically. Isotopic analysis was performed with a calibrated mass spectrometer (AEI MS-10).

Results

The addition of D_2S to all the hydrocarbons studied resulted in (*a*) a reduction in $G(H_2)$ and the formation of HD and D_2 and (*b*) the total hydrogen yield (H_2 + HD + D_2) being greater than $G(H_2)$ for the hydrocarbon alone. Our results for the n-C_6H_{14}/D_2S system are in agreement with those of Meissner and Henglein (1).

The hydrogen yields for the c-C_6H_{12}/D_2S system at 298 °K are shown in Fig. 1. In this, as in all other figures and tables, G values are calculated from the total absorbed dose. In the presence of SF_6 as electron scavenger all yields are reduced, the D_2 much more than the others. There is no substantial difference between results obtained with either 1.5 or 2 mole % SF_6. Table 1 shows the reduction in yields brought about by this lower concentration of SF_6 for a series of c-C_6H_{12}/D_2S samples.

The products of neutralization of SF_6^- and hydrocarbon positive ions have not been identified and so the effect of D_2S on the extent of electron scavenging by this solute cannot be studied. However, N_2O captures electrons with about the same efficiency as SF_6 and gives a measurable product, N_2. Figure 2 shows the

TABLE 1

The effect of 1.5 mole % SF_6 on the isotopic hydrogens in c-C_6H_{12}/D_2S solutions

Mole % D_2S	$\Delta G(H_2)$	ΔG(HD)	$\Delta G(D_2)$
1.9	1.0	1.2	1.1
2.8	0.8	1.1	1.5
3.6	0.7	1.0	1.7
9	0.4	0.8	2.2
16	0.3	0.8	2.4

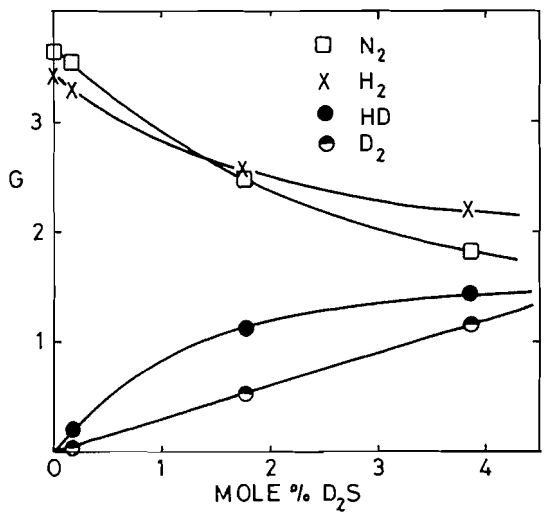

FIG. 2. The effect of D_2S on the N_2 yields from 0.3 mole % N_2O in c-C_6H_{12} at 298 °K (dose = 4.3×10^{19} eV/ml).

Can. J. Chem. Downloaded from www.nrcresearchpress.com by 210.87.254.40 on 09/05/12
For personal use only.

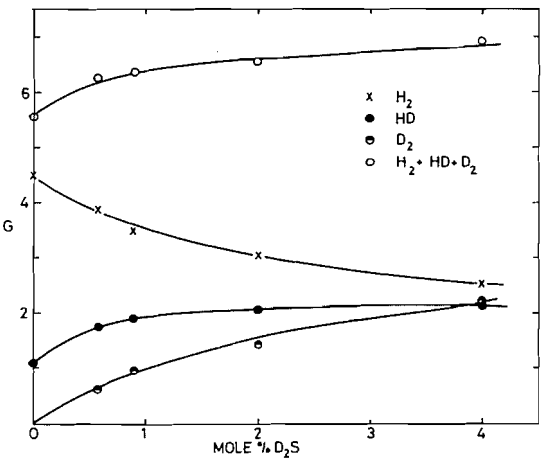

FIG. 3. The effect of D_2S on hydrogen yields from c-C_6H_{12}/2.44 mole % ethanol-d solutions at 298 °K (dose = 1.05×10^{19} eV/ml).

effect of increasing concentrations of D_2S on the N_2 yield from c-C_6H_{12} containing 0.3 mole % N_2O. A similar figure for the n-$C_6H_{14}/N_2O/D_2S$ system has been published (3); in that case the D_2S concentration was extended to 8 mole %. The results are essentially the same in the two hydrocarbons.

Perfluorocyclohexane also gives a measurable product, c-$C_6F_{11}H$, subsequent to its capture of thermalized electrons (4). A cyclohexane solution 0.27 mole % in c-C_6F_{12} and 3.3 mole % in D_2S was irradiated to the same total dose as a solution containing the same amount of c-C_6F_{12} but no D_2S. The height of the c-$C_6F_{11}H$ chromatographic peak was decreased by 50% when D_2S was present. No c-$C_6F_{11}H$ was available as standard but if Sagert's value of $G(c\text{-}C_6F_{11}H) \approx 1.5$ at 0.27 mole % c-C_6F_{12} (4) is used, the reduction in yield is 0.75 G.

The effect of positive ion scavengers was also studied. Figure 3 shows the effect of D_2S on hydrogen yields from solutions of c-C_6H_{12} containing 2.44 mole % of ethanol-d. Similar results were obtained with c-C_5H_{10} as solvent.

α-Methyltetrahydrofuran (MTHF) in low concentration rapidly reduces $G(D_2)$ from 0.8 mole % D_2S in n-hexane while the HD yield is less readily reduced as shown in Table 2. Cyclopropane had a negligible effect on either G(HD) or $G(D_2)$ from c-C_6H_{12}/D_2S and c-C_5H_{10}/D_2S solutions as shown in Table 3. Neopentane is a positive ion scavenger in cyclopentane (5) yielding methane as an easily measured product. The

TABLE 2

The effect of α-methyltetrahydrofuran on the isotopic hydrogens in n-C_6H_{14}/0.8 mole % D_2S solutions

Mole % MTHF	$G(H_2)$	G(HD)	$G(D_2)$
0	3.30	1.12	0.88
1.26	4.07	1.04	0.17
3.11	4.02	1.00	0.14
5.46	4.36	0.73	0.06

TABLE 3

Isotopic hydrogen yields from c-C_6H_{12}/D_2S and n-C_6H_{14}/D_2S solutions containing c-C_3H_6

Solvent	Mole % D_2S	Mole % c-C_3H_6	$G(H_2)$	G(HD)	$G(D_2)$
c-C_6H_{12}	1.8	0	3.42	1.64	1.22
c-C_6H_{12}	1.8	4.0	3.22	1.52	1.21
c-C_5H_{10}	1.6	0	3.60	1.23	0.84
c-C_5H_{10}	1.6	3.7	3.41	1.21	0.88

TABLE 4

Hydrogen and methane yields from c-C_5H_{10}/D_2S/5 mole % $C(CH_3)_4$ solutions (dose = 1.1×10^{19} eV/ml)

Mole % D_2S	$G(H_2)$	G(HD)	$G(D_2)$	$G(CH_4)$	$G(CH_3D)$
0	4.91	—	—	0.56	—
2.0	2.84	1.45	1.05	0.20	0.15
5.0	2.61	1.79	1.77	0.17	0.21

effect of D_2S on the methane yield from a solution 5 mole % in neopentane is shown in Table 4. The olefins, ethylene, and propylene, decrease G(HD) from n-C_6H_{14}/D_2S *e.g.* 2.6 mole % C_2H_4 reduces G(HD) from 1.75 to 0.77 at a D_2S concentration of 1.5 mole %. At the same time $G(D_2)$ is not affected.

The yields of isotopic hydrogens from liquid C_2H_6/D_2S solutions at 195 °K are qualitatively similar to those described above. Figure 4 shows the isotopic hydrogen yields for D_2S concentrations up to 8 mole % while Fig. 5 shows the effect of 2 mole % SF_6 on these yields. The effect of D_2S on the N_2 yields from liquid ethane containing 0.31 mole % N_2O is presented in Fig. 6.

Discussion

The yields of isotopic hydrogens in c-C_6H_{12} and C_2H_6 (Figs. 1 and 4) show similar dependence on D_2S concentration to those for n-hexane (1) and appear at first sight to be consistent with

Can. J. Chem. Downloaded from www.nrcresearchpress.com by 210.87.254.40 on 09/05/12
For personal use only.

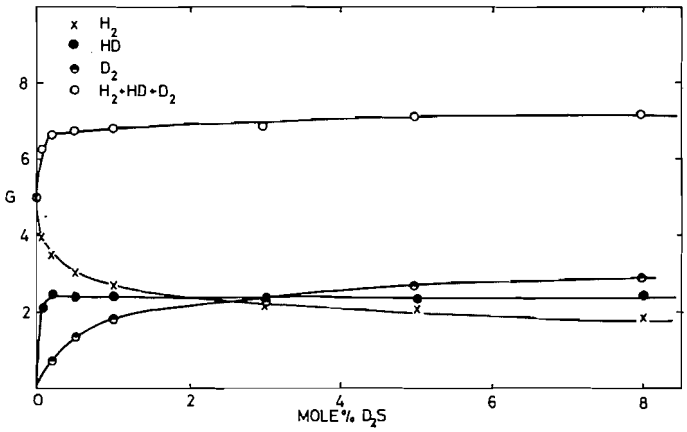

FIG. 4. Hydrogen yields from C_2H_6/D_2S solutions at 195 °K (dose = 2×10^{19} eV/g).

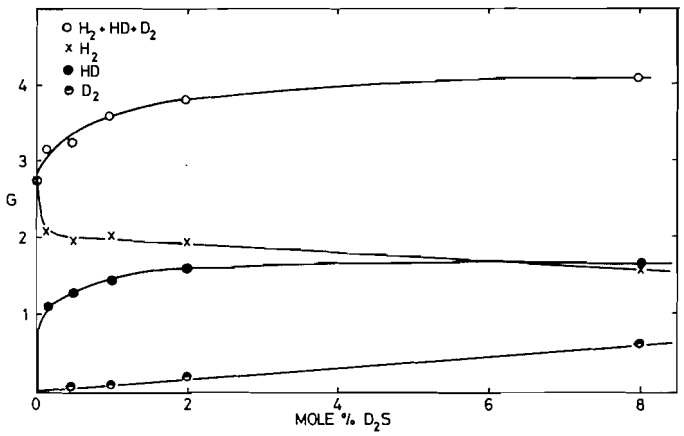

FIG. 5. The effect of 2 mole % SF_6 on hydrogen yields from C_2H_6/D_2S solutions at 195 °K (dose = 1.9×10^{19} eV/g).

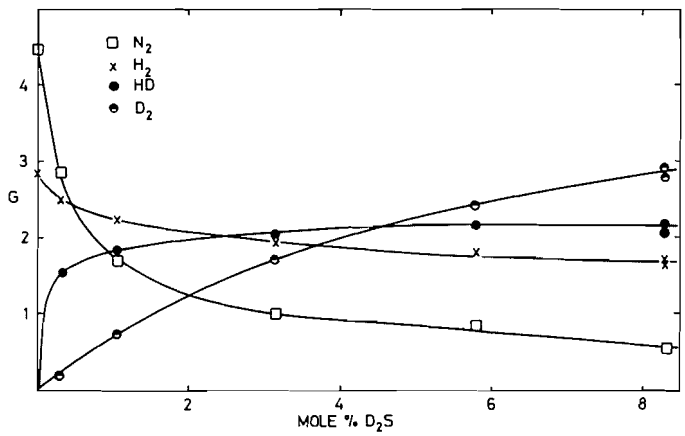

FIG. 6. The effect of D_2S on the N_2 yields from 0.31 mole % N_2O in C_2H_6 at 195 °K (dose = 1.4×10^{19} eV/g).

Can. J. Chem. Downloaded from www.nrcresearchpress.com by 210.87.254.40 on 09/05/12
For personal use only.

Can. J. Chem. Downloaded from www.nrcresearchpress.com by 210.87.254.40 on 09/05/12
For personal use only.

the reaction scheme outlined in the introduction. The HD yield reaches a limiting value at about 5 mole % D_2S in *c*-C_6H_{12} but at a much lower concentration (< 0.2 mole %) in liquid ethane at 195 °K. This is as expected since at the lower temperature the abstraction of H from the solvent by H atoms is very slow compared with reaction 3 (2). The D_2 yields increase much more slowly with increasing D_2S concentration than do the HD yields, this is consistent with the relative efficiencies of H atom and positive ion scavenging. The H_2 yields decrease continuously as HD and D_2 increase while the total yield of hydrogen (H_2 + HD + D_2) increases.

The Formation of HD

At the highest D_2S concentrations only H_α atoms should contribute to HD formation and the limiting value of G(HD) should equal $G(H_\alpha)$. In *n*-hexane we find, in agreement with Meissner and Henglein, that this limiting value is ~1.5. However, 1.4 mole % SF_6 will reduce G(HD) from 1.47 to 0.78 in *n*-hexane containing 2.9 mole % D_2S. The limiting HD yields in *c*-C_6H_{12} and C_2H_6 are also reducible by SF_6 (Table 1 and Fig. 5). The limiting yield must therefore either have contributions from both H_α and H_β or there must be another means by which HD may be formed. If the former were the case and $G(D_2)$ does represent the degree to which positive ion scavenging, a less efficient process than H atom scavenging, occurs then G(HD) should decline with increasing D_2S concentration. This apparently does not occur. However, Table 1 and Fig. 5 show that a fixed concentration of SF_6 is more efficient in decreasing G(HD) at low than at high D_2S concentrations. In the absence of SF_6 the apparently constant HD yield therefore has contributions from at least two sources, one of which is declining with increasing D_2S while the other increases. This is discussed later.

Reliable values for $G(H\cdot)$ in liquid hydrocarbons are scarce since most so called H atom scavengers also react with electrons or positive ions. Rajbenbach and Kaldor (6) from a kinetic analysis of hydrogen yields from *c*-C_4F_8/*n*-C_6H_{14} solutions in the presence and absence of hexene-1 find G(thermal hydrogen atom) = 1.4 in *n*-C_6H_{14}. This value is numerically in agreement with the limiting HD yield from D_2S in *n*-C_6H_{14} but Rajbenbach and Kaldor's analysis is based on the supposition that thermalized H atoms do not have ionic precursors. Since about 50% of the HD yield is suppressible by SF_6 the agreement between the two sets of results appears to be fortuitous. This does not rule out the possibility that $G(H\cdot)$ is actually close to 1.4 in *n*-hexane.

Asmus *et al.* (7) have found from a careful study of H atom scavenging by C_2H_4 in liquid *c*-C_6H_{12}, and after making allowance for positive charge scavenging, that $G(H\cdot)$ in liquid *c*-C_6H_{12} is 1.46. Of this, 0.89 G can be ascribed to H_β and 0.57 G to H_α. Figure 1 shows that the limiting HD yield would give $G(H\cdot) = 2.2$. Even in the presence of 1.5 mole % SF_6 G(HD) = 1.3 which should equal $G(H_\alpha)$. The two sets of data are inconsistent. The lower value of 1.46 is supported by the work of Hagemann and Schwarz (8) who used α-chlorotoluene to obtain $G(H\cdot)$ = 1–1.5 and by the work of Sauer and Mani (9) who obtained $G(H) \sim 1.4 \pm 0.2$ by measuring the yield of the cyclohexadienyl radical from solutions of benzene in cyclohexane. The only value of $G(H\cdot)$ close to 2.2 is that of ~ 2.0 by Holroyd (10) who also used C_2H_4 as scavenger but a less direct method than Asmus *et al.* for the measurement of the resulting $\cdot C_2H_5$ radicals. The more direct method should give the better value for $G(\cdot C_2H_5)$ and hence $G(H\cdot)$. We conclude that the limiting yield of HD in the D_2S/*c*-C_6H_{12} system does not equal $G(H\cdot)$, let alone $G(\cdot H_\alpha)$.

Two determinations of $G(H\cdot)$ in liquid ethane at 195 °K, both employing scavenging of H atoms by olefins, gave $G(H\cdot) = 2.3 \pm 0.2$ (2, 11). At this low temperature only very small concentrations of olefin are required to scavenge all H atoms since H atom abstraction from solvent is slow. Figure 4 shows that the addition of a very small amount of D_2S gives immediately a limiting G(HD) ≈ 2.3. Under these circumstances G(HD) = $G(H\cdot)$ and $G(H_2 + HD + D_2) = 5.9$, the calculated value of $G(H_2)$ for pure ethane at very low dose. With increasing D_2S concentration G(HD) remains constant, but this yield has at least two precursors as discussed earlier. Once again the limiting G(HD) value cannot be equated with $G(H_\alpha)$ alone.

The Yield of D_2

$G(D_2)$ is greater than can be accounted for by direct radiolysis of D_2S. $G(H_2)$ for liquid H_2S at both 298 and 195 °K is 9.4 (12). $G(D_2)$ from liquid D_2S will probably be about 20% less. It is

Can. J. Chem. Downloaded from www.nrcresearchpress.com by 210.87.254.40 on 09/05/12
For personal use only.

impossible to calculate a priori how much D_2 is formed by direct radiolysis in a hydrocarbon/D_2S mixture and therefore no corrections have been applied to the total D_2 yields shown in the figures. The non-ionic contribution may be estimated from the SF_6 scavenging experiments. There is little change in $G(D_2)$ when the SF_6 content of a c-C_6H_{12}/D_2S solution is changed from 1.5 to 2.0 mole %. This is as expected since as shown by the H_2 yield (13) almost all scavengeable electrons have been captured at these concentrations. This residual D_2 yield may be ascribed mainly to direct radiolysis of D_2S yielding either D_2 directly or D atoms which are subsequently scavenged by D_2S. At the highest D_2S concentrations there may be some contribution from electron scavenging by D_2S (see later). Therefore, at 8 mole % D_2S the yields of D_2 from "indirect" action are 3.0 in C_2H_6, 2.5 in n-C_6H_{14}, and 2.2 in c-C_6H_{12}. The D_2 yield increases more rapidly with increasing D_2S concentration in C_2H_6 than in either n-C_6H_{14} or c-C_6H_{12} while $G(D_2)$ for a given concentration of D_2S in n-C_6H_{14} is always ~ 0.3 units above that in c-C_6H_{12}.

The gas phase photoionization potentials of D_2S, C_2H_6, n-C_6H_{14}, and c-C_6H_{12} are 10.46, 11.65, 10.18, and 9.88 eV, respectively (14). Therefore exothermic charge transfer from the molecular ion to D_2S in the gas phase is possible only with C_2H_6. Ionization potentials of hydrocarbons are lower in the liquid phase (15) but evidence favors the retention of the relative order of values (16). If the reduction in $G(D_2)$ by SF_6 is due to prevention of D_2 formation after exothermic charge transfer then the ionization potential of D_2S must be decreased to a greater extent than those of the hydrocarbons.

MTHF is very efficient in reducing $G(D_2)$ (Table 2) and at higher concentrations reduces G(HD). Since the D_2 yields from D_2S/n-C_6H_{14} solutions, when interpreted in terms of positive ion scavenging, show that D_2S is a more efficient scavenger than either ND_3 or C_2H_5OD (17), the results of Table 2 suggest that MTHF is even more efficient than D_2S. We do not see why this should be. Similarly the D_2 yields from D_2S/C_2H_5OD/c-C_6H_{12} solutions are only slightly higher than those in the absence of C_2H_5OD (Figs. 1 and 3). The slight increase is probably due to scavenging of D atoms produced by neutralization of $C_2H_5ODH^+$. Interpretation of experimental results in these systems may be complicated to some extent by proton or deuteron transfer between the solutes subsequent to charge transfer but prior to charge neutralization. The results do not, however, appear to support simple competition between the added solutes.

This conclusion is supported by the lack of effect of c-C_3H_6 or olefins on the D_2 yield. 4 mole % c-C_3H_6 decreases $G(H_2)$ in c-C_6H_{12} by ~ 1 G unit (7) which implies the scavenging of this number of positive ions. However, Table 3 shows that this concentration has little effect on the isotopic hydrogens from a solution 1.8 mole % in D_2S. The same applies in c-C_5H_{10} as solvent. Ion scavenging by c-C_3H_6 in c-C_6H_{12} leads to $\sim 60\%$ C_3H_8 by H_2 transfer and $\sim 40\%$ $\cdot C_3H_7$ (18). It would, therefore, be expected that c-C_3H_6 would reduce $G(D_2)$ since the c-$C_6H_{10}^+$ ion, (or c-$C_5H_8^+$ in c-C_5H_{10}) resulting from H_2 transfer should not be scavenged by D_2S (1.5 mole % D_2S in c-C_6H_{10} at 298 °C yielded essentially no D_2 ($G \sim 0.01$)). Ethylene and propylene in concentrations at which charge scavenging has been observed (19) do not affect $G(D_2)$. Similarly we find that benzene does not affect $G(D_2)$ from D_2S/C_2H_6 solutions at 195 °K.

The reduction in G(methane) upon the addition of D_2S to a solution of neopentane in cyclopentane (Table 4) is evidence that charge transfer can be inhibited by D_2S. There is a marked reduction in G(methane) for the addition of 2 mole % D_2S but essentially no further decrease when the concentration is increased to 5 mole %. (G(methane) from direct radiolysis of neopentane should be no greater than 0.19.) This does not correlate with the $\sim 70\%$ increase in $G(D_2)$ over the same concentration range if it is all attributable to ion scavenging.

In summary, it appears that the D_2 yield may arise in part from positive ion scavenging but experiments with a second positive ion scavenger lead to results which are not easily interpretable. In particular MTHF appears to be much too efficient relative to D_2S while c-C_3H_6 and olefins appear relatively inefficient.

The Total Hydrogen Yield

D_2S increases the total hydrogen yield in all three solvents. This increase is most marked in liquid ethane due to scavenging of H atoms which, at the doses employed, normally add to product

Can. J. Chem. Downloaded from www.nrcresearchpress.com by 210.87.254.40 on 09/05/12
For personal use only.

ethylene (2, 11). Even in this system $G(H_2 + HD + D_2)$ soon exceeds the value of 5.95 estimated for $G(H_2)$ at very low dose when no addition to olefin occurs (2). Meissner and Henglein (1) attribute the increase in total hydrogen to the scavenging of positive ions which do not normally lead to H_2 production in the pure hydrocarbon. We reject this explanation since neither ND_3 (20) nor C_2H_5OD (21) lead to such an increase. There is no reason why these two solutes should not be equally as efficient as D_2S in scavenging ions and producing an equivalent number of hydrogen molecules, indeed they are assumed to react upon the first encounter.

Increased hydrogen yields in non-branched liquid hydrocarbons are associated with electron scavengers such as HCl (22) or HI (23). That the increased total hydrogen yield from D_2S/hydrocarbon mixtures might also be associated with such an occurrence was one reason for examining the electron scavenging properties of D_2S

D_2S as an Electron Scavenger

When liquid hydrocarbons containing N_2O are irradiated, $G(N_2) > G$(electrons scavenged) (24). The increased N_2 yield is due to secondary reaction, for example, it has been suggested that O^- produced by dissociative electron capture may react further (25)

$$[5] \qquad e + N_2O \rightarrow N_2O^- \rightarrow N_2 + O^-$$

$$[6] \qquad O^- + N_2O \rightarrow N_2 + O_2^-$$

The reaction mechanism is not known with certainty but the above two equations may be taken as a guide to the overall stoichiometry. The extent of reaction 6 will depend upon N_2O concentration and $G(N_2)$ will lie in the range G(e) to $2G$(e). D_2S may interfere with the secondary reaction and so reduce $G(N_2)$. However, Figs. 2 and 6 show that $G(N_2)$ is, at the highest D_2S concentrations, reduced to a value less than one-half its initial one. Competition of D_2S and N_2O for electrons must be occurring, more especially at the lower temperature in liquid C_2H_6. The reduction in $G(c\text{-}C_6F_{11}H)$ in the $c\text{-}C_6H_{12}/c\text{-}C_6F_{12}$ system supports the assignment of electron scavenging properties to D_2S.

Acceptance of electron capture by D_2S in liquid hydrocarbons requires its reconciliation with the 1.56 eV activation energy (26) required in the gas phase for

$$[7] \qquad e + H_2S \rightarrow HS^- + H\cdot$$

This reaction could be energetically feasible under any of the following circumstances:

(*a*) If the affinity of D_2S for thermalized electrons is far different in the gas phase from that in the liquid phase. We have no data on such effects but French and Willard (27) report observing $\cdot CH_3$ probably from thermal electron capture by CH_3F in solid 3-methylpentane at 77 °K, a process which does not occur in the gas phase.

(*b*) If non-thermalized electrons are captured. This might occur at the highest D_2S concentrations employed but will be improbable in the more dilute solutions where a large part of the increase in G(total hydrogen) occurs.

(*c*) If thermal electron capture is aided by solvation of the anion. Meissner and Henglein (1) have argued against this on the basis of the low dielectric constants of hydrocarbons. However, the dielectric constant of the solution will be raised by added D_2S ($\varepsilon = 9.05$ for H_2S in the liquid phase at −78.5 °C (28)). Also the solution may not be homogeneous on the molecular level and clusters of D_2S molecules may be present, since the dipole moment of H_2S is 0.9 D. Solvation of the DS^- would therefore probably be by D_2S molecules rather than by hydrocarbon.

Comparison of Figs. 4 and 6 shows that at 8 mole % D_2S, $G(H_2)$, G(HD), and $G(D_2)$ are only slightly lower in the presence of 0.31 mole % N_2O than in its absence. Therefore, electron capture by D_2S in C_2H_6 at 195 °K leads to D_2 and probably to HD formation since Fig. 6 shows $\Delta G(N_2) = 4$, *i.e.* D_2S is scavenging a maximum of 4 and a minimum of 2 G units of electrons. In *n*-hexane G(electrons scavenged) at 8 mole % D_2S has a minimum value of 0.5 and a maximum of 3.0 G (3). Electron capture is most efficient in ethane at 195 °K.

A Possible Mechanism for D_2 and HD Formation

Our results are consistent with both electron capture and positive charge scavenging by D_2S in addition to H atom scavenging. If we interpret the dependence of the D_2 yield on D_2S concentration solely in terms of electron scavenging then D_2S is an inefficient electron scavenger compared to *e.g.* N_2O or $c\text{-}C_6F_{12}$ (a Stern–Vollmer type plot of the results in Fig. 6 after allowing for complete quenching of reaction 6 by D_2S suggests it would be six times less efficient

Can. J. Chem. Downloaded from www.nrcresearchpress.com by 210.87.254.40 on 09/05/12
For personal use only.

than N_2O). Interpretation of the yields solely in terms of positive charge scavenging shows D_2S to be an extremely efficient charge scavenger (Freeman (17) has suggested that this is due to a "loose association" between D_2S and an electron which reduces the mobility of the latter and therefore allows a longer time for positive charge transfer). We suggest that D_2S participates in both charge and electron scavenging, both of which lead to D_2, and most probably HD, formation. A possible reaction scheme is

[8] $RH^+ + D_2S \rightarrow RH + D_2S^+$

[9] $e + D_2S \rightarrow DS^- + D\cdot$

[10] $D\cdot + D_2S \rightarrow D_2 + DS\cdot$

[11] $D\cdot + RH \rightarrow HD + R\cdot$

[12*a*] $e + D_2S^+ \rightarrow D_2 + S$

[12*b*] $\rightarrow D\cdot + D\cdot + S$

[13] $DS^- + RH^+ \rightarrow$ No hydrogen

Reaction 12*b* is exothermic by ~ 2 eV if a decrease of ~ 1 eV below the gas phase ion recombination energy is allowed for the change of phase density (29). This reaction would lead to the increased total hydrogen yield observed. At higher D_2S concentrations it would be superceded by neutralization of D_3S^+ formed by deuteron transfer

[14] $D_2S^+ + D_2S \rightarrow D_3S^+ + DS\cdot$

[15*a*] $D_3S^+ + e \rightarrow D\cdot + D_2S$

[15*b*] $\rightarrow \cdot D + \cdot D + DS\cdot$

Reaction 15*b* is also exothermic but to a lesser extent than [12*b*]. If [12*b*] but not [15*b*] occurs then the total hydrogen yield should decrease with increasing D_2S concentration. This is not observed and so either both or neither reactions occur.

As written, no hydrogen is formed by neutralization of RH^+ by DS^-. This is by analogy with similar reactions of electron scavengers, *e.g.* N_2O or SF_6. We have no evidence that this is correct and it may be that the increased total hydrogen yield is due to hydrogen production in this reaction.

Although Meissner and Henglein (1) suggest charge transfer (reaction 8) as the only major reaction of molecular ions with D_2S, proton transfer may also occur. Bone and Futrell (30) have shown that in the gas phase deuteron transfer is the predominant reaction between $C_3D_8^+$ and H_2S. The proton affinity of H_2S is 178 kcal mole^{-1} (31) while those of $\cdot C_2H_5$ and c-$C_6H_{11}\cdot$ are 143 and ~ 174 kcal mole^{-1}, respectively (29). The proton affinity of n-$C_6H_{13}\cdot$ will be in this range. We can, therefore, also expect the following reactions to occur

[16] $RH^+ + D_2S \rightarrow R\cdot + HD_2S^+$

[17*a*] $HD_2S^+ + e \rightarrow H\cdot + D_2S$

[17*b*] $\rightarrow D\cdot + HDS$

At the highest D_2S concentrations the H and D, after thermalization, will give HD and D_2, respectively. This may account in part for the yield of HD scavengeable by SF_6 and also for the difference in D_2 and HD yields obtained in c-C_6H_{12} and n-C_6H_{14}, since, due to the difference in their ionization potentials there may be a difference in the relative rates of reactions 8 and 16. In c-C_6H_{12} the D_2 yield is lower and the HD yield is higher at a given D_2S concentration compared with those in n-C_6H_{14}.

The above reaction scheme is qualitatively consistent with many of our experimental results but a quantitative description will be impossible until methods of unambiguously measuring the yields of HD and D_2 from each reaction can be devised. For example SF_6 may reduce the D_2 yield either by competing with D_2S for electrons (reaction 9) or by suppressing D_2 production via reactions 12 or 17. In either case all that is observed is a reduction in $G(D_2)$.

We have no explanation for the lack of effect of c-C_3H_6 or other olefins on the D_2 yields. The high efficiency of MTHF in reducing $G(D_2)$ suggests that it reacts in more than one way *e.g.* (*a*) by competitive positive ion scavenging; (*b*) by deuteron transfer from either D_2S^+, D_3S^+, or D_2HS^+; (*c*) by interfering with D_2S clustering which aids electron capture by D_2S (reaction 7). Deuteron bonding —S—D···O— will disrupt the clustering of D_2S alone. (MTHF has no affinity for thermalized electrons since 4 mole % MTHF did not change $G(N_2)$ from 0.31 mole % N_2O in c-C_6H_{12}.)

Our results show that the simple interpretation of Meissner and Henglein of the HD and D_2 yields in terms of H atom and ion scavenging respectively is not valid. The system is much more complex than their simple picture and the use of D_2S as a scavenger in liquid alkanes does not yield readily interpretable results.

NOTE: A referee has suggested that associative electron capture to yield D_2S^- followed by $D_2S^- + RH^+ \rightarrow HD, D_2$ may also explain our results without the requirement of dissociative electron capture. Associative electron capture has not been observed in the gas phase but a brief communication reporting its detection in solid H_2S and D_2S at 77 °K has been published (32). The energetics of this capture are not known and further speculation is not warranted. We do question whether the above neutralization reaction could lead to the large D_2 yields observed; dissociative electron capture can explain these yields.

The authors thank the National Research Council of Canada and Atomic Energy of Canada Limited, Commercial Products for financial assistance. One of us (P.T.H.) gratefully acknowledges the receipt of a National Research Council of Canada postgraduate fellowship.

1. G. MEISSNER and A. HENGLEIN. Ber. Bunsenges. Phys. Chem. **69**, 264 (1965).
2. P. T. HOLLAND and J. A. STONE. Can. J. Chem. **48**, 1078 (1970).
3. P. T. HOLLAND and J. A. STONE. J. Phys. Chem. **73**, 4397 (1969).
4. N. H. SAGERT. Can. J. Chem. **46**, 95 (1968).
5. J. A. STONE. Chem. Commun. 1677 (1968).
6. L. A. RAJBENBACH and U. KALDOR. J. Chem. Phys. **47**, 242 (1967).
7. K.-D. ASMUS, J. M. WARMAN, and R. H. SCHULER. J. Phys. Chem. **74**, 246 (1970).
8. R. J. HAGEMANN and H. A. SCHWARZ. J. Phys. Chem. **71**, 2694 (1967).
9. M. C. SAUER and I. MANI. J. Phys. Chem. **72**, 3856 (1968).
10. R. A. HOLROYD. J. Phys. Chem. **70**, 1341 (1966).
11. G. BAKALE and H. A. GILLIS. J. Phys. Chem. **73**, 2178 (1969).
12. G. MEISSNER and A. HENGLEIN. Z. Naturforsch. **20b**, 1005 (1965).
13. N. H. SAGERT and A. S. BLAIR. Can. J. Chem. **45**, 1351 (1967).
14. K. WATANABE, T. NAKAYAMA, and J. MOTTL. U.S. dept. com. office technical service Report. **158**, 319 (1959).
15. C. VERMILE, F. MULLER, M. MATHESON, and S. LEACH. Bull. Soc. Chim. Belg. **71**, 837 (1962).
16. J. A. STONE, A. R. QUIRT, and O. A. MILLER. Can. J. Chem. **44**, 1175 (1966).
17. G. R. FREEMAN. J. Chem. Phys. **46**, 2822 (1967).
18. S. J. RZAD and R. H. SCHULER. J. Phys. Chem. **72**, 228 (1968).
19. P. AUSLOOS, A. A. SCALA, and S. G. LIAS. J. Amer. Chem. Soc. **89**, 3677 (1967).
20. F. WILLIAMS. J. Amer. Chem. Soc. **86**, 3954 (1964).
21. J. W. BUCHANAN and F. WILLIAMS. J. Chem. Phys. **44**, 4377 (1966).
22. P. J. DYNE. Can. J. Chem. **43**, 1080 (1965).
23. J. R. NASH and W. H. HAMILL. J. Phys. Chem. **66**, 1097 (1962).
24. W. V. SHERMAN. J. Chem. Soc. (A), 599 (1966).
25. G. R. A. JOHNSON and J. M. WARMAN. Trans. Faraday Soc. **61**, 1709 (1965).
26. K. JÄGER and A. HENGLEIN. Z. Naturforsch. **21a**, 1251 (1966).
27. W. G. FRENCH and J. E. WILLARD. J. Phys. Chem. **74**, 240 (1970).
28. Handbook of chemistry and physics. 50th ed. The Chemical Rubber Company, Cleveland, Ohio, U.S.A. 1970. p. E-61.
29. G. R. FREEMAN. Rad. Res. Rev. **1**, 1 (1968).
30. L. I. BONE and J. H. FUTRELL. J. Chem. Phys. **47**, 4366 (1967).
31. J. L. BEAUCHAMP and S. E. BUTTRILL. J. Chem. Phys. **48**, 1783 (1968).
32. J. E. BENNET, B. MILE, and A. THOMAS. Chem. Commun. 182 (1966).

Can. J. Chem. Downloaded from www.nrcresearchpress.com by 210.87.254.40 on 09/05/12
For personal use only.

The kinetics of hydration of tricalcium silicate

K. G. McCurdy and B. P. Erno
Chemistry Department, University of Lethbridge, Lethbridge, Alberta
Received June 15, 1970

An investigation has been made of the kinetics of hydration of tricalcium silicate at several temperatures in a large excess of water in the presence of various added ions. The rate data have been interpreted by a reaction mechanism which involves: (*a*) the first order hydration of tricalcium silicate to form an intermediate product, $1.5CaO \cdot SiO_2$, which can react by two pathways, (*b*) the direct first order decomposition of intermediate, $1.5CaO \cdot SiO_2$, to form lime and silica or (*b'*) complexing of intermediate with silica and subsequent decomposition to form lime and silica. This reaction mechanism predicts the rate of production of base during the hydration. The effect of various added ions is interpreted in terms of the proposed mechanism.

Rate constants and activation energies for the various steps in the proposed mechanism are reported.

Canadian Journal of Chemistry, 48, 3291 (1970)

Can. J. Chem. Downloaded from www.nrcresearchpress.com by 210.87.254.6 on 09/05/12
For personal use only.

Introduction

Tricalcium silicate contains calcium (Ca^{2+}), oxygen (O^{2-}) ions, and silicate (SiO_4^{4-}) groups (1) which hydrate during dissolution as represented by

$$[1]\quad 3Ca^{2+}(c) + O^{2-}(c) + SiO_4^{4-}(c) + nH_2O\,(l) \rightarrow 3Ca^{2+}(aq) + 4OH^-(aq) + H_2SiO_4^{2-}(aq)$$

Numerous studies have been made of the stoichiometry and thermochemistry of hydration of tricalcium silicate, Ca_3SiO_5. Extensive reviews of the investigations on this system are available (2).

While a considerable amount of some kinds of information on the hydration of tricalcium silicate has been published, there is little information available on the rate of hydration of Ca_3SiO_5. The few published data refer to widely varying experimental conditions and are therefore difficult to compare or interpret.

Kantro, Brunauer, and Weise (3) have investigated the disappearance of unhydrated tricalcium silicate and the development of surface as a function of time in paste systems of tricalcium silicate. Their proposed mechanism involves: (*a*) the formation of a gel coating on the surface of the unhydrated silicate, (*b*) the splitting off of thin sheets from the gel surface, and (*c*) the conversion of the thin sheet into stable tobermorite.

A kinetic investigation of the influence of silica on the hydration of Ca_3SiO_5 led Stein and Stevels (4) to conclude that their results were consistent with the results of Kantro *et al.* (3). The acceleration of the rate of hydration of Ca_3SiO_5 in the presence of amorphous silica was explained in terms of an increased rate of conversion of a first formed protective hydrate into a less protective one.

Greenberg and Chang (5) investigated the hydration of tricalcium silicate and interpreted their data as supporting a solution theory for hydration. They could not fit their data to either a simultaneous solution and precipitation mechanism or to a mechanism in which the rate of solution was controlled by diffusion of ions into solution. An alternative method of interpreting their data was proposed by Stein and Stevels (6), who suggested that the data could be interpreted either in terms of recrystallization of the calcium silicate hydrates or changing reactivity of the Ca_3SiO_5.

In the present work, we have measured the rate of hydration of tricalcium silicate in dilute hydroxide solutions under conditions of constant p*H*, ranging from 7.5 to 10.6. The effect of temperature and added salts was studied as well as a small range of weight solid to weight solvent ratios.

This heterogeneous chemical reaction is of interest because there has been little progress made on the understanding of heterogeneous chemical kinetics particularly for solution–solid reactions. The reaction is also of fundamental interest to cement technologists because the rate of hydration of tricalcium silicate is important to an understanding of cement chemistry.

Experimental

Materials

The tricalcium silicate used in these experiments was kindly supplied by the Portland Cement Association, Skokie, Illinois. The preparation was numbered B-101 and the analysis reported as: CaO 73.87%, Al_2O_3 0.13%, and SiO_2 26.14%. They also supplied the calculated com-

position as: tricalcium silicate 96.77%, dicalcium silicate 1.81%, tricalcium aluminate 0.34%, and free lime as 1.08%. The tricalcium silicate had a Blaine surface area (ASTM designation C-204-51) of about 3310 $cm^2\ g^{-1}$.

All solutions were prepared using doubly distilled water.

Fisher Certified Reagent chemicals were used throughout.

Equipment

The p*H* stat used was a Radiometer titrigraph SBR2C/SBU1 composed of TTT1 automatic titrator, SBR2 recorder, and SBU1 syringe burette. The titrant was delivered from a calibrated ½ ml syringe. A Radiometer G202C glass electrode and a K401 calomel reference electrode were used to monitor the p*H*.

Procedure

The reactions were carried out with 10 ml solution in a reaction vessel in which an access port above the solution was available for the introduction of the tricalcium silicate, usually 10 mg. The reaction cell was thermostated to 25 ± 0.05 °C, unless otherwise indicated. A stream of nitrogen was bubbled through water and then through the reaction solution.

In a typical experiment, 10 ml of solution were pipetted into the reaction vessel. The stat was set to maintain the p*H* of the solution, which had been preadjusted with $Ca(OH)_2$ solution to the desired p*H* value. After thermal equilibrium had been attained, the tricalcium silicate was introduced through the access port by means of a small funnel. The stat began to record the volume of standardized HCl solution required to maintain the p*H* of the solution at the preset value.

The hydration was followed by the stat until no further HCl was required for a 5 min interval. In all cases in these investigations, reactions were complete in 30 min.

Theory

Chemical System

Reaction 1 indicates that as the hydration of tricalcium silicate proceeds, the solution becomes increasingly basic. The silicic acid produced in the reaction will be distributed in solution as H_4SiO_4, $H_3SiO_4^-$, and $H_2SiO_4^{2-}$ as a function of the p*H* of the solution and the dissociation constants of silicic acid. The values used for the ionization of silicic acid (7, 8) were $pK_1 = 9.77$ and $pK_2 = 11.8$.

The amount of Ca_3SiO_5 that reacted was calculated from the number of equivalents of acid involved in neutralizing the products of the reaction, with consideration given to the ionization of silicic acid. The amount of acid required is usually less than the theoretical amount required to titrate all the Ca_3SiO_5. It was assumed that the unreacted material was unhydrated Ca_3SiO_5.

Since the p*H* of the reaction solution was held constant, calculations are readily made which show that the solution is never saturated with $Ca(OH)_2$; $K_{sp} = 8.25 \times 10^{-6}$ (5).

The solution does become saturated with CaH_2SiO_4, $K_{sp} = 10^{-7}$ (4), in the later stages of reaction. The experimental evidence of Greenberg (5) indicates that at the p*H* and the times involved in the present investigation the amount of this species formed would be negligible.

The hydration of tricalcium silicate produces a hydrate of variable lime–silica ratio. This species is denoted as $r CaO \cdot SiO_2$, where r is the molar lime–silica ratio in the hydrate. Graphs of the value of r *vs.* the equilibrium concentration of lime are available (2). Under the experimental conditions of the present investigation no calcium silicate hydrate is precipitated.

Results

The experimental conditions including p*H*'s, addant conditions, and temperatures used in the present investigation are given in Table 1. All experiments, except those listed below, were initiated by the addition of 10 mg of tricalcium silicate to 10 ml of dilute calcium hydroxide solution. Series 26, 5 mg of tricalcium silicate; Series 27, 15 mg of tricalcium silicate; Series 28, 20 mg of tricalcium silicate.

Kinetics and Mechanism–Reaction Order

Heterogeneous solid–liquid reactions are generally studied by examination of weight of solid (w_t) remaining at various extents of reaction (9–12). The values of weight solid that had dissolved at various times $(w_{sol.})_t$ were determined from the volume of standardized acid required to titrate the liberated base at that time. The weight of solid remaining at any time, w_t, was set equal to $[w_0 - (w_{sol.})_t]$.

The series of experiments in which the weight ratio of solid to liquid was varied was analyzed by plotting the initial rate of liberation of base *vs.* the initial weight of tricalcium silicate. The initial reaction velocity was found to be proportional to the first power of the weight of tricalcium silicate. Attempts to apply first order kinetics over the entire extent of any reaction were unsuccessful, suggesting a more complicated reaction scheme.

Previous investigators (13) of this system, using a ball mill hydration method and a higher solid to liquid ratio, had suggested the formation of an intermediate, $1.5CaO \cdot SiO_2$, denoted "Hydrate III". Using this proposal, an analysis was

Can. J. Chem. Downloaded from www.nrcresearchpress.com by 210.87.254.6 on 09/05/12
For personal use only.

TABLE 1

Experimental conditions for the hydration of tricalcium silicate in dilute calcium hydroxide solution

Series number	pH	Initial experimental conditions	Temperature (°C)	Number of experiments averaged
1	10.6	0.22×10^{-3} M $Ca(OH)_2$	25	10
2	9.8	0.132 M $CaCl_2$	25	10
3	9.7	0.302 M $CaCl_2$	25	10
4	10.2	0.409 M $Ca(NO_3)_2$	25	10
5	9.8	0.399 M $Ca(NO_3)_2$	25	10
6	9.8	0.206 M $Ca(NO_3)_2$	25	10
7	9.6	0.102 M $Ca(NO_3)_2$	25	10
8	9.6	0.135 M $Ca(C_2H_3O_2)_2$	25	10
9	10.0	0.261 M $Ca(C_2H_3O_2)_2$	25	10
10	10.0	0.394 M $Ca(C_2H_3O_2)_2$	25	9
11	9.8	0.520 M $Ca(C_2H_3O_2)_2$	25	8
12	10.0	0.616 M $Ca(C_2H_3O_2)_2$	25	10
13	10.4	0.163×10^{-3} M $Ca(OH)_2$	15	4
14	10.2	0.163×10^{-3} M $Ca(OH)_2$	25	4
15	10.0	0.163×10^{-3} M $Ca(OH)_2$	35	4
16	9.8	0.163×10^{-3} M $Ca(OH)_2$	45	3
17	9.6	0.163×10^{-3} M $Ca(OH)_2$	55	3
18	10.5	0.195×10^{-3} M $Ca(OH)_2$	15	5
19	10.3	0.195×10^{-3} M $Ca(OH)_2$	25	5
20	9.9	0.195×10^{-3} M $Ca(OH)_2$	35	5
21	9.7	0.195×10^{-3} M $Ca(OH)_2$	45	5
22	9.5	0.195×10^{-3} M $Ca(OH)_2$	55	5
23	9.1	0.195×10^{-3} M $Ca(OH)_2$	65	5
24	8.8	0.195×10^{-3} M $Ca(OH)_2$	75	3
25	10.6	0.290×10^{-3} M $Ca(OH)_2$	25	4
26	10.6	0.290×10^{-3} M $Ca(OH)_2$	25	4
27	10.6	0.290×10^{-3} M $Ca(OH)_2$	25	4
28	10.6	0.290×10^{-3} M $Ca(OH)_2$	25	4
29	7.5	Trace $Ca(OH)_2$	1	2
30	7.5	Trace $Ca(OH)_2$	10	2
31	7.5	Trace $Ca(OH)_2$	20	2
32	7.5	Trace $Ca(OH)_2$	30	3
33	7.5	Trace $Ca(OH)_2$	40	2
34	7.5	Trace $Ca(OH)_2$	50	2
35	9.5	Trace $Ca(OH)_2$	25	2
36	9.5	Trace $Ca(OH)_2$	25	1
37	9.5	Saturated with SiO_2	25	1
38	9.5	Saturated with SiO_2	25	2
39	10.0	Trace $Ca(OH)_2$	25	2
40	10.2	0.021 M $Ca(Cl)_2$	25	2

attempted using a system of consecutive first order reactions.

$$3CaO\cdot SiO_2(s) \xrightarrow{k_1} 1.5Ca^{2+}(aq) + 3OH^-(aq) + 1.5CaO\cdot SiO_2(s)$$

$$1.5CaO\cdot SiO_2(s) \xrightarrow{k_2} 1.5Ca^{2+}(aq) + 3OH^-(aq) + SiO_2$$

The notation SiO_2 is used to represent the total silica in solution, realizing that it is distributed in solution among H_4SiO_4, $H_3SiO_4^-$, and $H_2SiO_4^{2-}$. All calculations included corrections for the formation of these species.

The above reaction scheme was found to be unsuccessful at large extents of reaction.

It has been proposed that tricalcium silicate liberates lime on coming in contact with water (14). Kantro *et al.* (3) proposed that the initial product of the hydration of tricalcium silicate was a lime-rich intermediate that was converted to a lime-poor intermediate and ultimately to hydration products. Stein and Stevels (4) found that amorphous silica increased the rate of hydration of tricalcium silicate. In an attempt to satisfy these requirements, the following reaction scheme was proposed.

$$3CaO\cdot SiO_2(s) \xrightarrow{k_1} 1.5Ca^{2+}(aq) + 3OH^-(aq) + 1.5CaO\cdot SiO_2(s)$$

$$1.5CaO\cdot SiO_2(s) \xrightarrow{k_2} 1.5Ca^{2+}(aq) + 3OH^-(aq) + SiO_2$$

Can. J. Chem. Downloaded from www.nrcresearchpress.com by 210.87.254.6 on 09/05/12
For personal use only.

Can. J. Chem. Downloaded from www.nrcresearchpress.com by 210.87.254.6 on 09/05/12
For personal use only.

$$1.5CaO\cdot SiO_2(s) + SiO_2 \overset{K_3}{\rightleftharpoons} 1.5CaO\cdot SiO_2\cdot SiO_2$$

$$1.5CaO\cdot SiO_2\cdot SiO_2(s) \xrightarrow{k_4} 1.5Ca^{2+}(aq) + 30H^-(aq) + 2SiO_2$$

The reaction with rate constant k_1 is assumed first order in weight of Ca_3SiO_5.[2]

$$-\frac{d(Ca_3SiO_5)_s}{dt} = k_1(Ca_3SiO_5)_s^1 = \frac{1}{3}\frac{d[OH^-]}{dt}$$

Integration of this expression yields

$$\ln \frac{[OH_{01}^-]}{[OH_{01}^- - OH_{t1}^-]} = 3k_1t$$

where OH_{t1}^- is the base liberated from the first reaction at time t and OH_{01}^- is the total amount of hydroxide that would be generated by completion of the first reaction. Only one-half the total amount of the base in the reacting tricalcium silicate is released during this step.

The overall rate of formation of base $d[OH^-]_T/dt$, is

$$[2] \quad \frac{d[OH^-]_T}{dt} = 3k_1([OH_{01}^-] - [OH_{t1}^-]) + 3k_2(1.5CaO\cdot SiO_2) + 3k_4(1.5CaO\cdot SiO_2\cdot SiO_2)$$

If we define θ as the fraction of $1.5CaO\cdot SiO_2$ that is complexed at any time, then $(1 - \theta)$ is the fraction of $1.5CaO\cdot SiO_2$ that is not complexed. If it is assumed that the equilibrium denoted by K_3 is a rapid reaction, then it is easily shown that

$$\theta = \frac{K_3[SiO_2]}{1 + K_3[SiO_2]}$$

if the silica is adsorbed on the $1.5CaO\cdot SiO_2$ intermediate which is on the unhydrated Ca_3SiO_5 and one silica is adsorbed per $1.5CaO\cdot SiO_2$.

The rate eq. 2 above can be rewritten to give

$$[3] \quad \frac{d[OH^-]_T/dt - 3k_1([OH_{01}^-] - [OH_{t1}^-])}{(1.5CaO\cdot SiO_2)[3]} = k_2(1 - \theta) + k_4\theta$$

The value of the rate constant k_1 was obtained from the amount of lime liberated at $\frac{1}{2}$ min. At this time the amount of product formed from $1.5CaO\cdot SiO_2$ is negligible since its concentration is low.

From the stoichiometric equations of the proposed mechanism, it is possible to write a computer program which will allow calculation of the total concentrations of $1.5CaO\cdot SiO_2$ and SiO_2 at any time, as well as the base produced from the first step at any time. The value of $d[OH^-]_T/dt$ was determined by drawing slopes of the plot of base produced *vs.* time at $\frac{1}{2}$ min intervals. The left hand side of eq. 3 above can then be calculated at various times. The right hand side of eq. 3, when we substitute for θ, becomes

$$k_2\left(1 - \frac{K_3[SiO_2]}{1 + K_3[SiO_2]}\right) + k_4\left(\frac{K_3[SiO_2]}{1 + K_3[SiO_2]}\right)$$

At the beginning of the reaction when the concentration of SiO_2 is low and $K_3[SiO_2]$ is small compared to unity, the right hand side of the equation becomes

$$k_2 - k_2K_3[SiO_2] + k_4K_3[SiO_2]$$

Plots of the left hand side of eq. 3 against the concentration of SiO_2 should give a straight line of intercept k_2 and slope $(-k_2K_3 + k_4K_3)$, K_3 cannot be determined if k_2 is equal to k_4. At later stages in the reaction when the concentration of SiO_2 becomes large, and $K_3[SiO_2]$ is large compared to unity, a plateau region should be observed with a value of k_4.

Using this type of analysis the values for k_1, k_2, K_3, and k_4 reported in Table 2 were obtained.

A measure of the reproducibility of the data can be best made by considering experiments numbered 1, 14, 19, 25, 35, 36, and 39. These experiments were conducted at low concentrations of added ions and over a small pH range. The average values of the kinetic parameters with their standard deviations are: $k_1 = 0.746 \pm 0.033$, $k_2 = 0.185 \pm 0.064$, $K_3 = 706 \pm 131$, and $k_4 = 0.152 \pm 0.015$. The results for k_1 and k_4 can be considered to be reliable to ± 5–10%. Errors in k_2 and K_3 are considerably larger and should be considered reliable only to ± 20–30%. Typical plots for the determination of k_2, K_3, and k_4 have been given in Fig. 1.

The contributions of base from each of the reaction steps are plotted in Fig. 2. The experimental amount of base produced is plotted for comparison.

[2]Parentheses denote solid in moles per liter; square brackets denote concentration in moles per liter.

TABLE 2

Kinetic parameters for the hydration of tricalcium silicate

Series number	Tricalcium silicate reacted (μmoles)	k_1 (min^{-1})	k_2 (min^{-1})	K_3 ($molar^{-1}$)	k_4 (min^{-1})
1	39.57	0.776	0.082	723	0.137
2	31.41	0.548	0.700	1060	0.430
3	22.58	0.824	0.275	911	0.315
4	28.96	0.568	0.103	911	0.150
5	36.08	0.506	0.114	925	0.152
6	37.22	0.546	0.091	584	0.156
7	39.04	0.671	0.114	703	0.205
8	40.07	0.682	0.119	426	0.201
9	38.38	0.612	0.082	871	0.150
10	37.35	0.497	0.062	519	0.111
11	38.33	0.488	0.132	1401	0.148
12	37.35	0.486	0.075	771	0.120
13	43.8	0.479	0.040	871	0.092
14	40.69	0.788	0.104	901	0.142
15	42.96	1.016	0.118	554	0.172
16	40.98	1.435	0.192	594	0.300
17	42.77	2.156	0.372	1307	0.400
18	48.48	0.513	0.060	1208	0.087
19	51.15	0.824	0.159	299	0.111
20	41.05	1.165	0.246	468	0.200
21	38.31	1.710	0.425	711	0.280
22	38.45	2.333	0.470	—	0.470
23	36.68	3.525	0.950	337	0.520
24	35.43	4.800	1.19	309	0.460
25	39.51	0.787	0.088	1358	0.110
26	21.18	0.935	0.140	880	0.202
27	59.57	0.768	0.083	962	0.102
28	75.61	0.760	0.063	—	0.063
29	41.05	0.321	0.252	935	0.109
30	42.93	0.414	0.315	435	0.160
31	41.09	0.809	0.349	591	0.285
32	41.54	1.009	0.510	310	0.350
33	40.81	1.824	0.622	252	0.420
34	37.83	1.866	0.732	339	0.495
35	34.89	0.573	0.400	484	0.200
36	39.45	0.754	0.250	513	0.210
37	35.66	0.461	0.250	966	0.190
38	38.73	0.517	0.255	842	0.210
39	40.82	0.721	0.215	667	0.156
40	42.99	0.834	0.235	687	0.185

The activation energies for the reaction steps 1, 2, and 4 are given in Table 3.

The calculated amounts of $1.5CaO \cdot SiO_2$ and SiO_2 at various times are given in Fig. 3.

Discussion

A review of the published material on the kinetics of the hydration of tricalcium silicate indicates that the results have been obtained under various experimental conditions. The materials used in the preparation, the method of preparation, the purity and particle size distribution of the tricalcium silicate all undoubtedly have an effect on its rate of hydration. Also to be considered are the weight ratio of water to tricalcium silicate, the method of determining the extent of the reactions, and the experimental environment of the reactions including temperature, p*H*, and the presence of extraneous ions. These effects make comparison and interpretation of the results of different investigators difficult. The present investigation was undertaken with an appreciation of the above problems and an attempt was made to control their effects. The reactions were conducted with a homogeneous sample of tricalcium silicate using conditions of high water to solid ratio. The temperature of the reaction was controlled and more significantly the p*H* of the media was not allowed to change with the extent of the reaction.

Can. J. Chem. Downloaded from www.nrcresearchpress.com by 210.87.254.6 on 09/05/12
For personal use only.

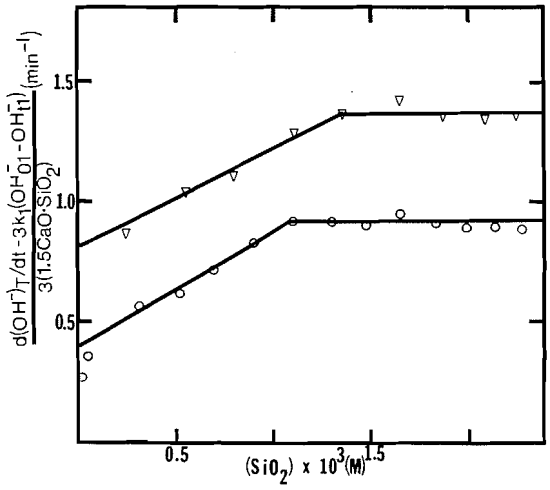

FIG. 1. Typical plots of eq. 3 for the determination of k_2, K_3, and k_4. ○, series 13; △, series 1.

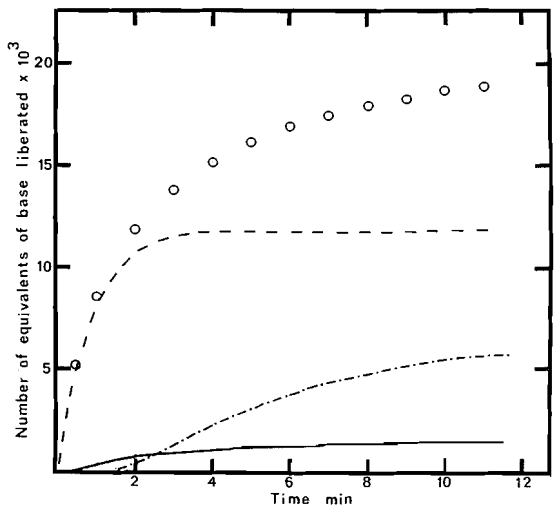

FIG. 2. Experimental plot ○, and its resolved components k_1 -----, k_2——, and k_4 ·-·-· in equivalents of base liberated as a function of time.

The problem of the method of determining the extent of the reaction has been thoroughly reviewed (2). Determination of the base liberated from the tricalcium silicate at various times has been criticized because it has been suggested that the reaction products in the early stages differ from those formed in the later stages (15). These criticisms apply mainly to those experiments where a calcium silicate hydrate is produced, and the K_{sp}'s of $Ca(OH)_2$ and CaH_2SiO_4 are exceeded, as occurs when the pH is allowed to vary and

TABLE 3

Calculated activation energies for the hydration of tricalcium silicate

Series	E_1(kcal/mole)	E_2(kcal/mole)	E_4(kcal/mole)
13–17	7.47	10.27	7.00
18–24	7.19	8.50	7.00
29–34	5.11	4.04	6.69

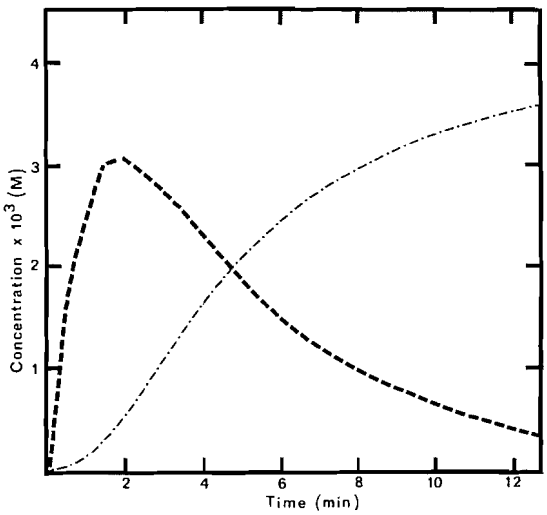

FIG. 3. Plot of $[1.5CaO \cdot SiO_2]$ ----- and $[SiO_2]$ ·-·-· as a function of time, series 1.

lower liquid to solid ratios than the present ratios are investigated.

Greenberg and Chang (5) have suggested that under their experimental conditions, where the pH increased with the extent of the reaction, that more than 0.5 g of tricalcium silicate per liter may not lead to complete dissolution of the tricalcium silicate. In the present work, the extent of the reaction is quite high (see Table 2); in the calculations in this work, it was assumed that the unreacted material was tricalcium silicate.

The data were analyzed according to several previously proposed mechanisms before the present mechanism was accepted. These mechanisms included: (*a*) rate of solution controlled by the rate of diffusion of ions into solution (5), (*b*) simultaneous solution and precipitation (5), (*c*) third order kinetics (16, 17), (*d*) diffusion mechanism (18), (*e*), 4/3 order kinetics (11), and (*f*) 2/3 order kinetics (13). None of these were found to fit the experimental data to any appreciable extent of reaction. Other methods of analysis attempted were two parallel first order reactions

Can. J. Chem. Downloaded from www.nrcresearchpress.com by 210.87.254.6 on 09/05/12
For personal use only.

producing a common product (19) lime and silica, and consecutive irreversible first order kinetics (20).

$$3CaO \cdot SiO_2 \rightarrow 1.5CaO \cdot SiO_2 + 1.5CaO$$
$$\downarrow$$
$$1.5CaO + SiO_2$$

Neither of these gave acceptable results.

Intermediates

The mechanism proposed in the present paper suggests an intermediate product, $1.5CaO \cdot SiO_2$, formed by a first order reaction of $3CaO \cdot SiO_2$. Other species, $1CaO \cdot SiO_2$ and $2CaO \cdot SiO_2$ were also proposed; however, both of these intermediates gave results which were not as acceptable as the $1.5CaO \cdot SiO_2$ species. The $1CaO \cdot SiO_2$ proposal gave results which were totally unacceptable since it could not account for the amount of lime in the system at any time except at very short intervals (0.5 min) and at very high percentages of reaction. The intermediate $2CaO \cdot SiO_2$ gave better results than the $1CaO \cdot SiO_2$ but not as good as the $1.5CaO \cdot SiO_2$ intermediate. It is possible that there is a species with a lime–silica ratio between 1.5 and 2.0 that would give better results but the kinetic analysis is not precise enough to differentiate between these limits. Kantro *et al.* (13) proposed a hydration mechanism involving a first formed intermediate $3CaO \cdot SiO_2 yH_2O$ which is converted to a hydrate intermediate $1.5CaO \cdot SiO_2$ designated "Hydrate III". The experimental method used in the present investigation would not detect the formation of $3CaO \cdot SiO_2 yH_2O$; however, its existence would add a fast reaction prior to the first reaction step (k_1) and not affect the rest of the kinetic analysis. Kawada and Nemoto (14) also suggested an immediate liberation of lime from tricalcium silicate when it comes into contact with water forming an intermediate product.

Autocatalysis

Previous investigations (21) of the hydration of $3CaO \cdot SiO_2$ pastes exhibited an increasing rate of heat evolution during the first hours of hydration followed by a decrease in the rate of heat evolution. Similar heat evolution patterns (22, 23) occur in cement pastes which contain a high percentage of tricalcium silicate. Angstadt and Hurley (24), using an X-ray diffraction technique, found that the amount of $3CaO \cdot SiO_2$ in cement pastes decreased slowly at first during hydration, decreased more rapidly during the time period of maximum heat evolution and then slowed down. Kantro, Brunauer, and Weise (3) found similar results on $3CaO \cdot SiO_2$ pastes. The hypothesis proposed for these effects has been discussed by Stein and Stevels (4). The proposed mechanism can account for autocatalysis via the silica complexing step.

The present results do not cover a sufficiently wide range of pH's to allow calculation of the particular silica species involved in the autocatalysis.

Mechanism

The present results support the results of Kantro *et al.* (3) and Stein and Stevels (4). The tricalcium silicate, when it comes into contact with water liberates base forming an intermediate, $1.5CaO \cdot SiO_2$. This intermediate reacts by either of two possible paths; in the absence of silica, a simple first order reaction forming lime and silica. As soon as silica is formed, the intermediate has an alternative path, silica is adsorbed on the surface of the intermediate and then this complex decomposes to form lime and silica. Kantro *et al.* (3) have proposed a high lime initial product, first hydrate, (f.h.), formed during the hydration of tricalcium silicate. They suggest that this high lime product is converted by splitting off layers of gel into another intermediate, second hydrate, (s.h.), which has a lower lime silica ratio. Stein and Stevels (4) suggest that there is electron microscope evidence for the ultimate conversion of this second hydrate into reaction products.

Reactions which are first order with respect to powder weight have previously been proposed (9–11, 25). Granquist (9) has studied the acid dissolution of bentonite and proposed that the reaction is first order in weight of bentonite. A cylindrical model with edge attack gave the best fit to his experimental data. This model predicts a second order surface dependency. He proposed that the reaction proceeds through H^+ adsorbed on the reactive surface and gave the following process

$$[\text{lattice components}]_{\text{surface}} + [H^+]_{\text{surface}} \rightarrow \text{products}$$

The concentrations of both reactants (lattice components in the surface and adsorbed H^+) are proportional to the surface, and the rate of dissolution becomes second order with respect to lattice surface.

Can. J. Chem. Downloaded from www.nrcresearchpress.com by 210.87.254.6 on 09/05/12
For personal use only.

Can. J. Chem. Downloaded from www.nrcresearchpress.com by 210.87.254.6 on 09/05/12
For personal use only.

The present results are not complete enough to determine this second order surface dependence. Investigations on surface effects are now underway in this laboratory.

Effect of Addants

In the present investigations, the rate of reaction was monitored by titrating the liberated base with standardized hydrochloric acid. Series 39 and 40 were performed to investigate whether the chloride added during the titration influenced the rate of the reaction. Experiment 40 was initiated in a solution in which the initial chloride concentration was approximately equal to the value it would have when the base had been completely neutralized at the end of the reaction. Experiment 39 is a control experiment started without any initial chloride. The results of these experiments are within the expected experimental error of the measurements, and chloride at least at this low concentration does not influence the progress of the reaction.

When the concentration of added salt is high, the rate constants k_1 and k_4 decrease with increasing concentration of the salt. Previous results (2*a*) have indicated that added $CaCl_2$ accelerates the hydration of tricalcium silicate. The mechanism proposed in this work can account for this acceleration by removal of hydroxide and precipitation with calcium ion, particularly if further investigations indicate a pH dependance of k_1. The parameters K_3 and k_2 are not affected by the presence of added salt.

The series numbered 36, 37, 38, and 39 form a set in which the effect of silica on the rate of hydration of tricalcium silicate can be evaluated. The experimental results indicate that reactions started in a solution that was saturated with silica are not appreciably different than those in the absence of initial silica. Stein and Stevels (4) found that silica accelerated the hydration of tricalcium silicate in suspension and in paste studies and suggested that the silica lowers the calcium and hydroxide concentrations in the medium and increases the rate of conversion of the first hydrate into a second hydrate. In our experiments with the high excess of solvent, the calcium concentration and the hydroxide concentration are low enough that the addition of silica does not assist the rate of the reaction by further lowering of the calcium concentration.

Series in which comparable experimental conditions were used indicate that the rate constant values increased with increasing acidity of the solution. A more thorough examination of this effect is underway.

Effect of Weight Solid – Weight Liquid Ratio

The series 25, 26, 27, and 28 were undertaken to investigate the effect of various weight ratios over a small ratio range.

The results suggest that k_1 is large when 5 mg of tricalcium silicate are dissolved in 10 ml of solvent; however, this result is subject to considerably larger experimental error than the others and k_1 may be taken as essentially constant as the weight of solid per unit weight solvent is increased. Both k_2 and k_4 are diminished as the weight of solid is increased. The ratio of k_4/k_2 decreases from 1.44 to 1.00 as the amount of solid is increased, supporting the proposal of inhibition of adsorption by added salts of calcium. The mechanism proposes that the calcium ion concentration increases more rapidly in the initial stages of reaction as the weight solid – weight liquid ratio increases.

Temperature Dependence

The activation energies of the various steps in the mechanism are reported in Table 3. The effect of temperature on K_3 is slight and indicates a low heat of complexing of silica with the intermediate. The series labelled 13–17 and 18–24 have different pH's at the different temperatures studied but do indicate an increasing rate constant with increasing temperature. Series 29–34 were conducted at a low pH which was constant for all temperatures. The activation energies seem to be lower for this lower pH series. Previous investigators have reported various activation energies for the reaction. Knoblauch (16) and Schwiete and Muller-Hesse (17) proposed a third order rate equation for the hydration of tricalcium silicate and calculated a 2.1 Kcal/mole activation energy.

Studies are now being carried out in this laboratory on the effect of pH and particle size on the kinetics of hydration of tricalcium silicate.

K. G. M. is indebted to the National Research Council of Canada for financial assistance. The continuing financial support of the University of Lethbridge Research Committee is greatly appreciated. The authors wish to thank the Departments of Physics and Mathematics for use of their computing facilities.

1. J. D. BERNAL, J. W. JEFFERY, and H. F. W. TAYLOR. Mag. Concrete Res. **11**, 49 (1952).
2. S. BRUNAUER and S. A. GREENBERG. Proceedings of the 4th International Symposium on the Chemistry of Cements, Washington, D.C. 1960. p. 135.
2*a*. L. E. COPELAND and D. L. KANTRO. Fifth International Symposium on the Chemistry of Cement, Tokyo, Japan. 1968.
2*b*. R. KONDO and S. UEDA. Fifth International Symposium on the Chemistry of Cement, Tokyo, Japan. 1968.
3. D. L. KANTRO, S. BRUNAUER, and C. H. WEISE. J. Phys. Chem. **66**, 1804 (1962).
4. H. N. STEIN and J. M. STEVELS. J. Appl. Chem. **14**, 338 (1964).
5. S. A. GREENBERG and T. N. CHANG. J. Phys. Chem. **69**, 553 (1965).
6. H. N. STEIN and J. M. STEVELS. J. Phys. Chem. **69**, 2489 (1965).
7. S. A. GREENBERG and E. W. PRICE. J. Phys. Chem. **61**, 1539 (1957).
8. S. A. GREENBERG. J. Amer. Chem. Soc. **80**, 6508 (1958).
9. W. T. GRANQUIST. Proc. 6th Natl. Conf. Clay Minerals. 1959. p. 292.
10. M. C. GASTOUCHE and G. G. SUMNER. Science of Ceramics. Academic Press, New York. 1962. pp. 1, 121.
11. A. PACKTER and H. S. DHILLON. J. Chem. Soc. (A). 2588 (1969).
12. NUMAN ABDUL-LATIF and C. E. WEAVER. Clays and Clay Minerals, **17**, 169 (1969).
13. D. L. KANTRO, S. BRUNAUER, and C. H. WEISE. J. Colloid. Sci. **14**, 363 (1959).
14. N. KAWADA and A. NEMOTO. Zement-Kalk-Gips. No. 2, 65 (1967).
15. A. VAN BEMST. Bull. Soc. Chim. Belges. **64**, 333 (1955).
16. H. KNOBLAUCH. Tonindustrie Zeitung. **82**, 36 (1958).
17. H. E. SCHWEITE and H. MULLER-HESSE. Zement u. Beton. No. **16**, 25 (1959).
18. H. ZUR. STRASSEN. Zement u. Beton. No. **16**, 32 (1959).
19. A. A. FROST and R. G. PEARSON. Kinetics and mechanism. 2nd ed. John Wiley and Sons, Inc., New York. 1961. p. 162.
20. C. G. SWAIN. J. Amer. Chem. Soc. **66**, 1696 (1944).
21. L. H. FORBRICH. J. Amer. Concrete Inst. **12**, 161 (1940).
22. L. R. LERCH. Proc. Amer. Soc. Test. Materials, **46**, 1252 (1946).
23. H. N. STEIN. J. Appl. Chem. **11**, 474, 482 (1961).
24. R. L. ANGSTADT and F. R. HURLEY. Nature, London. **197**, 688 (1963).
25. A. PACKTER. Chem. and Ind. 1384 (1955).

Can. J. Chem. Downloaded from www.nrcresearchpress.com by 210.87.254.6 on 09/05/12
For personal use only.

Can. J. Chem. Downloaded from www.nrcresearchpress.com by 210.87.254.105 on 09/05/12
For personal use only.

The kinetics of the thermal insertion reaction of tin(II) halides with cyclopentadienyliron dicarbonyl dimer

P. F. Barrett and Kenneth K. W. Sun
Department of Chemistry, Trent University, Peterborough, Ontario

Received June 18, 1970

The kinetics of the thermal insertion reaction of $SnBr_2$ and $SnCl_2$ with the metal–metal bonded dimer $[\pi\text{-}C_5H_5Fe(CO)_2]_2$ have been studied by following the change in the visible spectrum. The kinetic data are consistent with a two-stage mechanism involving the formation of a carbonyl-bridged intermediate followed by nucleophilic attack by the halides on this intermediate. The formation of the intermediate requires an activation enthalpy of 38.0 ± 1.0 kcal/mole, and an activation entropy of 45.5 ± 1.5 cal $mole^{-1}$ deg^{-1}. The activation energy required to break the Fe—Fe bond is estimated to be about 32 kcal/mole.

Canadian Journal of Chemistry, **48**, 3300 (1970)

Since the relatively recent discovery of the existence of covalent metal–metal bonds in compounds containing d-block elements, there has been considerable interest in the synthesis and structure of metal–metal bonded carbonyl or substituted carbonyl compounds. Although the insertion reaction of a lower valent metal halide such as $SnCl_2$, GeI_2, or InBr with a metal carbonyl dimer is a well established method for forming metal–metal bonds between main group IV and transition metal atoms (1–6), very little kinetic data are available to date for such insertion reactions into metal–metal bonds. The kinetics of the insertion reaction of tin(II) halides with hexacarbonylbis(tri-*n*-butyl-phosphine) dicobalt (7) have been previously investigated. In this paper we report the kinetic data for the thermal insertion reaction of $SnCl_2$ and $SnBr_2$ with $[\pi\text{-}C_5H_5Fe(CO)_2]_2$.

The structure of $[\pi\text{-}C_5H_5Fe(CO)_2]_2$ in solution has been the subject of debate for some time. It is now believed that the solution contains *cis*-bridged and *trans*-bridged species in comparable quantities which interconvert rapidly via a non-bridged intermediate (8). The insertion of tin(II) halides into the Fe—Fe bond is well substantiated (1, 2) and X-ray crystallographic studies of $[\pi\text{-}C_5H_5Fe(CO)_2]_2SnCl_2$ (9) show that this compound is indeed Fe—Sn—Fe bonded.

Experimental and Results

Materials

All chemicals were purchased from either Alfa Inorganics Inc. or Fisher Scientific Co. Cyclopentadienyliron dicarbonyl dimer, $[\pi\text{-}C_5H_5Fe(CO)_2]_2$, was purified by recrystallization from methanol. Anhydrous tin(II) chloride was prepared by dehydrating the dihydrate with acetic anhydride (10). Anhydrous tin(II) bromide was prepared in a similar manner except that the preparation was carried out in an atmosphere of nitrogen in a dry bag. Both anhydrous $SnCl_2$ and $SnBr_2$ were stored in vacuo over phosphorus pentoxide. Tetrahydrofuran was purified by refluxing over sodium wire, and was freshly distilled before use in the kinetic runs.

Kinetics

With stannous halides in excess, the thermal reactions were studied in the temperature range 35–55 °C. A weighed amount of the tin(II) halide was transferred into a 10 ml volumetric flask and was dissolved and made up with freshly distilled tetrahydrofuran, THF. The solution was warmed up to the desired temperature before completely filling a 1 cm silica cell which contained an estimated amount of the complex, $[\pi\text{-}C_5H_5Fe(CO)_2]_2$, required to give an approximately 2–4 × 10^{-3} *M* solution. The cell was tightly stoppered and immediately placed in a thermostated cell holder, making sure that no air bubbles were trapped inside. The change in the visible spectrum of the reaction mixture was recorded on a Unicam SP800 spectrophotometer, or the decrease in the optical density at 550 mμ was measured with a Gilford 2400 spectrophotometer. The infrared spectrum of the reaction products showed no bridging carbonyl frequencies. The slow decomposition of $[\pi\text{-}C_5H_5Fe(CO)_2]_2$ in THF was also followed in a similar manner.

In all cases the reaction solutions were handled so that they were exposed to a minimum of air and light. Exposure to air resulted in varying degrees of oxidation of the tin(II) halide and the complex, and hence led to irreproducibility of the kinetics. The rates of the reactions were found to be greatly accelerated during exposure to laboratory light.

Pseudo first order kinetics were observed in all cases with $SnBr_2$ and $SnCl_2$ and the plots of log (o.d.$_t$ − o.d.$_\infty$), where o.d.$_t$ and o.d.$_\infty$ are the optical densities at 550 mμ at times *t* and ∞, respectively, against time were linear for approximately 50% reaction. The observed pseudo first order rate constants, k_{obs}, are plotted in Figs. 1 and 2 as a function of the tin(II) halide concentration. In Fig. 1, the line drawn through the experimental points is a theoretical one calculated on the basis of rate parameters derived by a least-squares treatment (11).

Can. J. Chem. Downloaded from www.nrcresearchpress.com by 210.87.254.105 on 09/05/12
For personal use only.

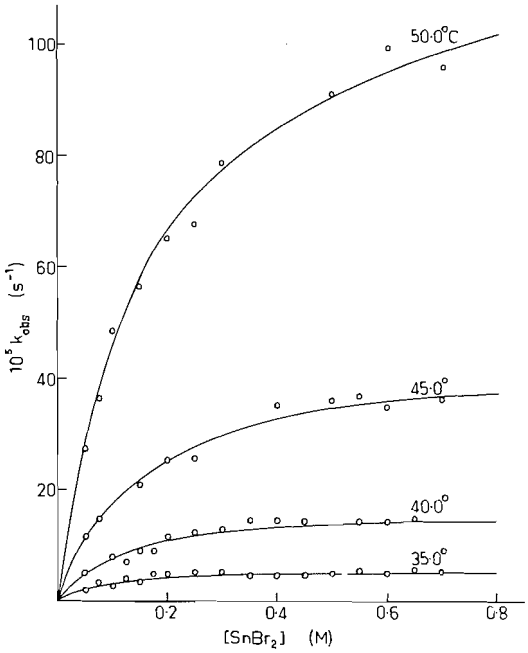

FIG. 1. Plot of the observed pseudo first order rate constant *vs.* tin(II) bromide concentration for the thermal reaction $[\pi\text{-}C_5H_5Fe(CO)_2]_2 + SnBr_2 \rightarrow [\pi\text{-}C_5H_5Fe(CO)_2]_2SnBr_2$ in THF. The curves drawn through the experimental points are theoretical lines calculated from the rate constants in Table 1.

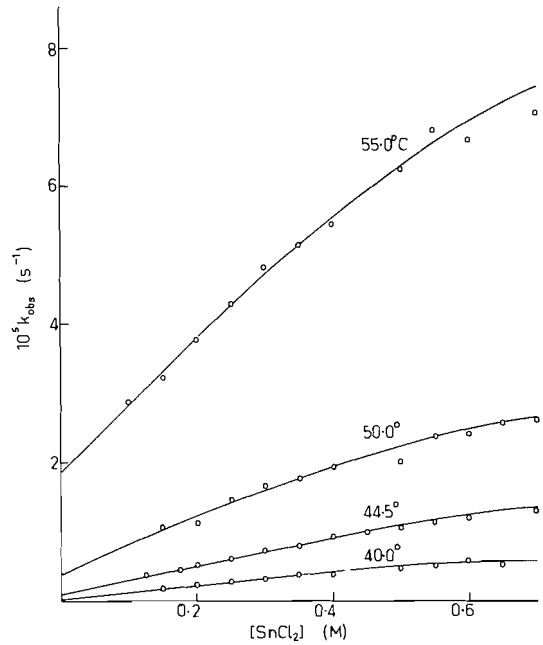

FIG. 2. Plot of the observed pseudo first order rate constant *vs.* tin(II) chloride concentration for the thermal reaction $[\pi\text{-}C_5H_5Fe(CO)_2]_2 + SnCl_2 \rightarrow [\pi\text{-}C_5H_5Fe(CO)_2]_2SnCl_2$ in THF.

Discussion

Figure 1 shows the variation of the pseudo first order rate constant k_{obs} with the concentration of tin(II) bromide for the thermal reaction of $[\pi\text{-}C_5H_5Fe(CO)_2]_2$ with excess $SnBr_2$ in THF at temperatures as indicated on the curves. It can be seen that at low concentrations of $SnBr_2$, k_{obs} increases with increasing concentration, while at high concentrations, the rate levels off and k_{obs} becomes independent of the concentration of $SnBr_2$. Such behavior is consistent with a two-stage mechanism which may be written as follows

$$A_2 \underset{k_{-1}}{\overset{k_1}{\rightleftharpoons}} A_2^* \xrightarrow[B]{k_2} ABA$$

where A_2 represents the iron complex dimer $[\pi\text{-}C_5H_5Fe(CO)_2]_2$, and A_2^* is a reactive intermediate, produced from A_2 which can either return to A_2 by a first order process or react with B (tin(II) bromide) by a bimolecular reaction to form the insertion product ABA. It is interesting to note that no second order contribution to the rate was observed as was the case in the substituted cobalt carbonyl system (7).

If B is present in large excess and the concentration of A_2^* remains small, the steady state approximation may be used for the concentration of A_2^*. This yields the rate equation

$$[1] \quad -\frac{dA_2}{dt} = \frac{k_1k_2[B]/k_{-1}}{1 + k_2[B]/k_{-1}}[A_2] = k_{obs}[A_2]$$

Thus at low values of [B], k_{obs} varies linearly with [B] but at high concentrations, k_{obs} should reach a limiting value equal to k_1. The test of eq. 1 is the plot of $1/k_{obs}$ *vs.* 1/[B] because [1] can be rearranged to give

$$[2] \quad 1/k_{obs} = 1/k_1 + k_{-1}/k_1k_2[B]$$

This plot should be a straight line with slope k_{-1}/k_1k_2 and intercept $1/k_1$. Figure 3 shows that plots of this type for the thermal reaction of $[\pi\text{-}C_5H_5Fe(CO)_2]_2$ with $SnBr_2$ do fit eq. 2. The kinetic parameters together with their standard deviations shown in Table 1 were obtained from a least-squares treatment of these plots assuming equal uncertainties for all values of k_{obs}. The

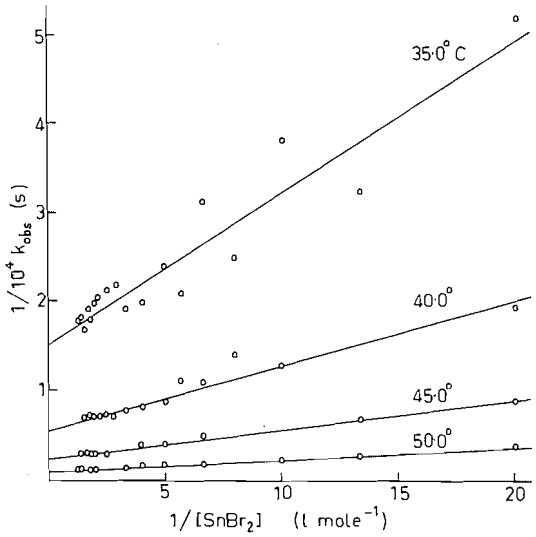

FIG. 3. Plot showing linear relationship between values of $1/k_{obs}$ and $1/[SnBr_2]$ taken from Fig. 1. The straight lines are least-squares plots and lead to the rate constants given in Table 1.

TABLE 1

Kinetic parameters for the $SnBr_2$ thermal reaction*

Temperature (°C)	$10^5 k_1$ (s^{-1})	k_{-1}/k_2 (mole l^{-1})
50.0	122 ±5	0.17±0.01
45.0	44.2 ±1.9	0.15±0.01
40.0	17.5 ±1.3	0.13±0.01
35.0	6.55±0.45	0.11±0.01

*The uncertainties are standard deviations; $\Delta H_1^{\neq} = 38.0 \pm 1.0$; $\Delta H_{-1}^{\neq} - \Delta H_2^{\neq} = 5.4 \pm 1.4$ kcal mole^{-1}; $\Delta S_1^{\neq} = 45.5 \pm 1.5$; $\Delta S_{-1}^{\neq} - \Delta S_2^{\neq} = 13 \pm 4$ cal mole^{-1} deg^{-1}.

values for activation enthalpies and entropies, and their standard deviation were obtained from k_1 and k_{-1}/k_2 values by means of a weighted least-squares treatment (11).

The plots in Fig. 2 indicate that the observed pseudo first order rate constants for the $SnCl_2$ reaction also increase with increasing $SnCl_2$ concentration but level off much more slowly than in the $SnBr_2$ case so that much higher concentrations of $SnCl_2$ would be necessary to reach the limiting rate. This type of behavior was also noted in the insertion reactions of the substituted cobalt carbonyl (7). The non-zero intercepts in Fig. 2 may be attributed to simultaneous decomposition of $[\pi\text{-}C_5H_5Fe(CO)_2]_2$ caused by traces of oxygen present in the THF even though the solvent was freshly distilled before use. The observed rate constants for the decomposition of $[\pi\text{-}C_5H_5Fe(CO)_2]_2$ in THF under the same conditions as the insertion reactions were estimated by independent experiments and found to be of the same order of magnitude as the intercepts in Fig. 2. Presumably decomposition also occurs in the $SnBr_2$ reactions but its rate is negligible compared with the much greater rate of the main insertion reaction.

Because of the very slight curvature of the plots in Fig. 2 and the uncertainty in the contribution due to decomposition, it was not possible to obtain reliable values for the limiting rate constants k_1. However, at low concentrations of B, eq. 1 reduces to eq. 3

$$[3] \qquad k_{obs} = k_1 k_2 / k_{-1}[B]$$

and the slope of the near-linear portion of the plots in Fig. 2 at low concentrations of $SnCl_2$ should equal $k_1 k_2 / k_{-1}$. Assuming that the limiting rate constants k_1 are the same as those found for the $SnBr_2$ reactions, and using the values for $k_1 k_2 / k_{-1}$ determined from a least-squares treatment of the k_{obs} *vs.* $[SnCl_2]$ plots at $SnCl_2$ concentrations up to 0.3 *M*, the k_{-1}/k_2 ratios were evaluated and are recorded in Table 2. The values for the activation enthalpies and entropies and their standard deviations were obtained from these k_{-1}/k_2 values by means of a weighed least-squares treatment.

Since the dimer $[\pi\text{-}C_5H_5Fe(CO)_2]_2$ exists mainly as carbonyl-bridged species **1** in solution, it seems reasonable to postulate that a carbonyl-bridged species, **2**, is formed as the intermediate during the insertion reaction similar to intermediates that have been suggested might be involved in the reactions of $Mn_2(CO)_{10}$ (12) and the insertion reactions of the substituted cobalt carbonyl system (7). The activation energy re-

TABLE 2

Kinetic parameters for the $SnCl_2$ thermal reaction*

Temperature (°C)	$10^5 k_1$† (s^{-1})	k_{-1}/k_2 (mole l^{-1})
55.0	322 ±6	33±2
50.0	122 ±5	29±5
44.5	44.2±1.9	21±1
40.0	17.5±1.3	17±1

*The uncertainties are standard deviations; $\Delta H_{-1}^{\neq} - \Delta H_2^{\neq} = 8.7 \pm 1.2$ kcal mole^{-1}; $\Delta S_{-1}^{\neq} - \Delta S_2^{\neq} = 34 \pm 4$ cal mole^{-1} deg^{-1}.

†Values are obtained from the $SnBr_2$ thermal reaction at 50.0, 45.0, and 40.0 °C, and the value for k_1 and its standard deviation at 55.0 °C are estimated.

Can. J. Chem. Downloaded from www.nrcresearchpress.com by 210.87.254.105 on 09/05/12
For personal use only.

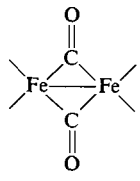

1

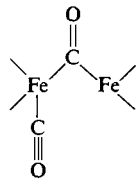

2

quired to break the two carbonyl bridges of the dimer **1** has been estimated to be about 13 ± 2 kcal/mole (8). The value of 38 ± 1 kcal/mole for $\Delta H_1^{\ddagger}$ may be reasonably considered to be the energy required to break one carbonyl bridged bond and an iron–iron bond, so that if the energy required to rupture one carbonyl bridge is about 6–7 kcal/mole, an estimate of about 32 kcal/mole can be made for the energy of the Fe—Fe bond on the basis of this mechanism.

The rather large value of $\Delta S_1^{\ddagger}$ is consistent with a mechanism which involves the conversion of the rigid dimer molecule **1** containing a metal–metal bond and two bridging carbonyl groups to a singly bridged species **2** in which two of the links between iron atoms have been broken. Although the $\Delta H_1^{\ddagger}$ is greater in the iron case than in the cobalt system, this more favorable entropy term results in higher values for k_1 in the iron case over the temperatures studied.

The second step in the proposed mechanism can be thought of as involving initially the nucleophilic attack of the tin(II) halide on the coordinatively unsaturated iron atom of the intermediate forming a four-centered transition state as depicted in **3**. The much lower values of k_{-1}/k_2 for the $SnBr_2$ reaction compared with the $SnCl_2$

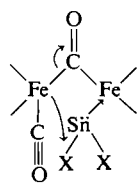

3

reaction indicate that k_2 for the $SnBr_2$ reaction is much greater than for the $SnCl_2$ reaction and this is consistent with the expectation that the "softer" $SnBr_2$ should be more nucleophilic towards the metal carbonyl intermediate (13). The similarity in the values for $\Delta H_{-1}^{\ddagger} - \Delta H_2^{\ddagger}$ for the two reactions however shows that the entropy of activation must be the important factor in establishing the rate differences and this is borne out by the fact that $\Delta S_2^{\ddagger}$ is about 21 e.u. lower for the $SnCl_2$ reaction than for the $SnBr_2$ reaction as calculated from the $\Delta S_{-1}^{\ddagger} - \Delta S_2^{\ddagger}$ values.

Although the data are consistent with, and have been interpreted according to a mechanism involving a single carbonyl bridged intermediate, the structure of this intermediate is by no means certain. The formation of a pair of π-$C_5H_5Fe(CO)_2$ radicals trapped in a solvent cage as an intermediate, similar to the suggestion put forward for the insertion reactions of $[Co(CO)_3PBu_3]_2$, is not inconceivable, but would appear to be a higher energy and less favorable pathway than that in which only one, rather than both of the carbonyl bridges is broken. An intermediate formed simply by the rupture of the Fe—Fe bond leaving the carbonyl bridges intact would seem unreasonable in view of the rather large $\Delta S_1^{\ddagger}$ observed for the reaction.

The authors are grateful for the assistance of Mr. W. J. Perry for performing some of the kinetic experiments, and are indebted to the Department of University Affairs of the Province of Ontario and the National Research Council of Canada for financial support.

1. F. Bonati and G. Wilkinson. J. Chem. Soc. 179 (1964).
2. D. J. Patmore and W. A. G. Graham. Inorg. Chem. **5**, 1405 (1956); **5**, 1586 (1966).
3. F. Bonati, S. Cenini, D. Morelli, and R. Ugo. J. Chem. Soc. A, 1052 (1966).
4. F. G. A. Stone, N. F. Flitcroft, D. A. Harbourne, I. Paul, and P. M. Tucker. J. Chem. Soc. A, 1130 (1966).
5. J. K. Ruff. Inorg. Chem. **6**, 2080 (1967).
6. J. Hoyano, D. J. Patmore, and W. A. G. Graham. Inorg. Nucl. Chem. Lett. **4**, 201 (1968).
7. P. F. Barrett and A. J. Poë. J. Chem. Soc. A, 429 (1968).
8. J. G. Bullitt, F. A. Cotton, and T. J. Marks. J. Amer. Chem. Soc. **92**, 2155 (1970) and references therein.
9. J. E. O'Connor and E. R. Corey. Inorg. Chem. **6**, 968 (1967).
10. G. Brauer (*Editor*) Handbook of preparative inorganic chemistry. Vol. 1. Academic Press, New York. 1963. p. 728.
11. J. Mandel. The statistical analysis of experimental data. Interscience Publ., New York. 1964. pp. 141–144, and pp. 272–278.
12. L. I. B. Haines, D. Hopgood, and A. J. Poë. J. Chem. Soc. A, 421 (1968).
13. R. G. Pearson. J. Amer. Chem. Soc. **85**, 2533 (1963).

Can. J. Chem. Downloaded from www.nrcresearchpress.com by 210.87.254.105 on 09/05/12
For personal use only.

Can. J. Chem. Downloaded from www.nrcresearchpress.com by 210.87.254.40 on 09/05/12
For personal use only.

Structure of thallium amalgams and their reaction with oxygen

W. T. Foley, Masaaki Nemori, and James D. MacNeil
Department of Chemistry, St. Francis Xavier University, Antigonish, Nova Scotia

Received[1] September 17, 1969

The stoichiometry was determined for the oxide formed by bubbling oxygen through thallium amalgam until the wt.% thallium in the amalgam was reduced by about 2%. The composition of the oxide depended upon the wt.% Tl in the amalgam. In the most dilute amalgams the oxide approached the formula Tl_2O and as the wt.% Tl increased the oxide became richer in thallium(III). Between 20 and 29 wt.% Tl the oxide approximated Tl_3O_2 and for alloys richer in thallium the oxide became richer in thallium(III). When the wt.% Tl in the alloy was 41.0 the ratio of thallium to oxygen in the oxide was 1.19. It is suggested that the experimental results indicate the existence of shortrange order in the liquid.

Canadian Journal of Chemistry, **48**, 3304 (1970)

This is a report on an experimental study to test the hypothesis that short-range order exists in liquid thallium amalgams. There is considerable evidence to support the view that intermetallic compounds retain some of their solid-state characteristics on melting (1). The equilibrium diagram of the mercury–thallium system (2, 3) reveals the existence of an intermediate phase about the Tl_2Hg_5 composition (28.9 wt.% thallium) and this intermediate phase at −79 °C extends from 21.4 to 30.7 wt.% thallium and at 0 °C it extends to 33.7 wt.% thallium. There are also two eutectics at 8.7 and 40.5% with temperatures of −59 and 0.6 °C, respectively. There is a maximum in the liquidus curve of the intermediate phase at 14.5 °C.

Smallman and Frost (4) made an X-ray investigation of the structure of liquid mercury and liquid mercury–thallium alloys at 17 °C and their analysis of the intensity and atomic distribution curves indicated a more orderly arrangement of the atoms in the liquid at a composition corresponding to Tl_2Hg_5 than at any other composition. Halder *et al.* (5) made a complete reinvestigation of the Hg–Tl system at 25 °C by X-ray diffraction methods and their findings did not confirm the work of Smallman and Frost.

Ward and Wilson (6) measured the e.m.f. of concentration cells of thallium amalgams over a range of temperatures and calculated the partial molar entropy of solution of thallium, and, from the variation of this thermodynamic property, they deduced that there was short-range order in the liquid at a composition close to that of Tl_2Hg_5.

Foley *et al.* (7–9), in studies of mutual and tracer diffusion, found that when diffusion coefficients were plotted against mole fraction of thallium a minimum occurred at a composition corresponding to Tl_2Hg_5. Clair *et al.* (10) have made a calorimetric study of the mercury–thallium system at the temperature of the melting point of Tl_2Hg_5, and they also determined the entropy of fusion. They assert that the difference between the calculated and measured values of the entropy of fusion can be interpreted as evidence supporting the existence of short-range order in the liquid.

Addison *et al.* (11), for the systems they studied, have found that there exists a direct correlation between the liquidus curve for a binary metal solution, and the chemical reactivity of the liquid mixture, and that large and sudden changes in chemical reactivity are predictable from the phase diagram. This paper is a report on the reactivity of thallium amalgam towards oxygen and the relation existing between this reactivity and the phase diagram.

Experimental

Thallium amalgam was prepared in a manner previously described (9). The apparatus used in the oxidation studies is shown in Fig. 1. The amalgam was stored in flask A until the apparatus had been pumped down to a pressure of 1 mTorr. About 200 g of amalgam was transferred to the reaction chamber, and oxygen, dried by passage through a tower containing anhydrous magnesium perchlorate, was admitted to the apparatus, which was then isolated from the manifold by means of the stopcock. The pressure and temperature of the oxygen was recorded and then mercury from the levelling bulb was permitted to flow into the apparatus. A reversible electric motor was used to raise and lower repeatedly the levelling bulb, thus forcing the oxygen to bubble through the amalgam.

The oxide which first formed when the oxygen was bubbled through the amalgam was cobalt-blue in color

[1]Revision received June 30, 1970.

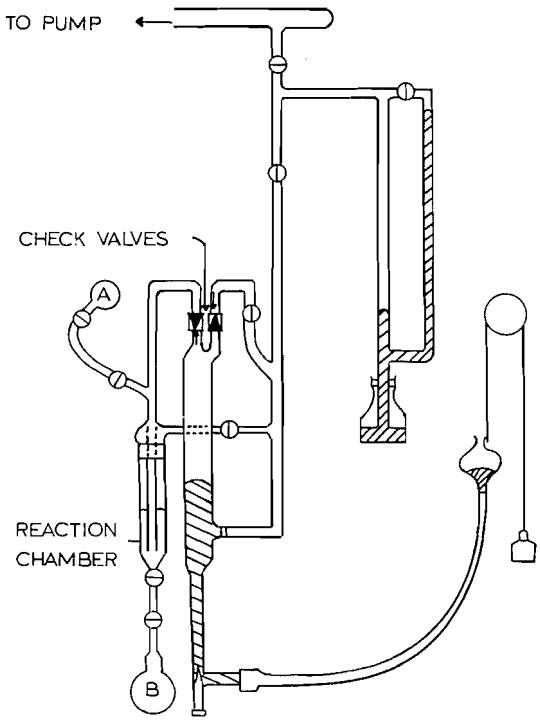

FIG. 1. Oxidation apparatus.

(if this blue oxide were exposed to the laboratory air it changed in color to brownish black). However, as the oxidation proceeded beyond the initial stages, the surface of the amalgam in the flask became greyish-black in color. This surface coat on quiescent amalgam rendered the amalgam inert towards further attack by oxygen. In the early stages of the addition of oxygen, the gas, neglecting that portion of it which reacted with the thallium, bubbled through the amalgam, and the bubbling sounds could be heard about 30 ft away, but as time went on the bubbling sound was replaced by a feeble pulsing sound, and finally the gas passed through the mixture of alloy and oxide noiselessly. When the hand was placed on the reaction flask only a faint throb could be felt as the oxygen was forced through the reaction vessel. At this time the reaction between the oxygen and the alloy had come to a virtual halt, and the absolute wt.% decrease in the thallium content of the amalgam was between 1.5 and 2.0 percentage points. The rate of uptake of the oxygen by the amalgam decreased rather steadily with time. The reaction time varied from about 40 h for the concentrated amalgams to about 70 h for the dilute amalgams. The heat of formation of thallium(I) oxide is -44 kcal and, since the amount of thallium oxide formed was less than one hundredth of a mole, cooling of the apparatus was not a problem. The enclosure of the apparatus was maintained at 23 ± 1 °C. When gas pressures were being determined, the temperature was held to within 23 ± 0.1 °C.

Before the actual kinetic experiments were begun some preliminary observations were made on the reaction products, and for this purpose the reaction vessel was removed after about 200 ml of oxygen had reacted, and an amount of liquid metal which corresponded to about half of the original charge of metal was poured out of the vessel and it was readily filtered clean by passage through a pin-hole in a filter paper supported in a funnel. The remainder of the metal and oxide had to be scraped from the reaction vessel with a spatula and this material was somewhat resilient and it could not be filtered through a pin-hole. When it was centrifuged for 25 min in a Clay–Adams clinical centrifuge at 4000 r.p.m., there was no separation of the oxide from the liquid metal. It was concluded that this material was possibly in the colloidal state. When this portion of the reaction product was stirred while covered with dilute sodium hydroxide, the bottom layer became beautifully clean thallium amalgam, readily filterable through a pin-hole, and the top aqueous layer was rich in thallium (1).

The extreme difficulty of separating the reactive liquid metal from the oxide by physical means made an X-ray examination of the oxide a rather formidable task especially since the scattering power of thallium is virtually the same as that of mercury. The thallium content of the amalgam both before and after oxidation was determined by the method of Foley and Osyany (11), and these data along with the value of the volume of oxygen consumed permitted the calculation of the composition of the oxide.

The procedure adopted was as follows. The oxidation was permitted to take place until about 200 ml of oxygen were consumed and this corresponded to a change in thallium composition of 1.5 to 2.0 percentage points. Before a final reading of the temperature and pressure of the oxygen was taken, the mercury was restored to the levelling bulb. The unreacted oxygen was then pumped off. When the stopcock at the base of the reaction chamber was opened, about half of the amalgam remaining ran into flask B. The stopcock at the base of the reaction chamber was closed, and the apparatus was filled with nitrogen gas. Flask A was replaced by a flask containing 1 *N* NaOH which had been degassed by successive freeze–thaws. When the sodium hydroxide was added to the reaction chamber, the amalgam fell to the bottom, and with the exception of a few grams, it was transferred to flask B.

The precision of the chemical analysis and of the measurement of the volume of oxygen consumed was such that the ratio of the number of atoms of thallium to oxygen would be reproducible to ± 0.03 units. The sodium hydroxide solution could permit thallium oxide to react with the thallium in the amalgam. Two important electrode potentials are

$$[1] \quad Tl^+ + e^- = Tl \qquad E_0 = -0.3363 \text{ V}$$

$$[2] \quad Tl(OH)_3(s) + 2e^- = 2OH^- + TlOH(s) \qquad E_0 = -0.05 \text{ V}$$

The potential for reaction 1 is dependent upon the logarithm of the activity of thallium in the amalgam. Thus from thermodynamic considerations one would expect that $Tl(OH)_3$, if it were present, would be unstable in the presence of thallium amalgam.

Can. J. Chem. Downloaded from www.nrcresearchpress.com by 210.87.254.40 on 09/05/12
For personal use only.

Can. J. Chem. Downloaded from www.nrcresearchpress.com by 210.87.254.40 on 09/05/12
For personal use only.

In addition to the possibility of the amalgam reacting with the thallium(III) oxide if present, there is the certainty that the thallium amalgam reacts with solutions containing dissolved oxygen.

To determine whether the amalgam reacted with the thallium oxide while the sodium hydroxide was present, two chemical analyses were performed. The amalgam which was withdrawn before the addition of the caustic solution was analyzed, and an analysis was made of the amalgam that was withdrawn after the addition of the base. The difference in concentration of the two samples was less than 0.1 wt.% thallium each time. The amalgam that was recovered after the addition of the sodium hydroxide solution was richer in thallium. A difference in thallium concentration of 0.10 wt.% thallium would make a difference of no more than 0.05 in the thallium-to-oxygen ratio. The fact that the two batches of amalgam yielded almost the same analytical result does not preclude the possibility that the amalgam had reacted with the oxide, because at the beginning of the oxidation some of the amalgam may have been trapped by the dispersing action of the oxide and thus be protected from further attack by oxygen. One can presume that errors resulting from the interaction of the amalgam and the oxide during the separation of the phases are more likely to occur with amalgams of high thallium concentration and that these errors would tend to inflate the calculated value of the ratio of thallium-to-oxygen in the oxide product. The experimental results show that the highest ratio of thallium-to-oxygen occurred in the oxide from the most dilute amalgam.

There still remained the possibility that some of the oxygen was retained by the reaction product by adsorption. To test for adsorption, the residual oxygen at the conclusion of an experiment was allowed to expand into an evacuated flask of known volume which was attached at the place where flask A had been located. This procedure was repeated many times until a very low pressure of oxygen was reached. The original volume, temperature, and pressure of the residual oxygen was known. Since the final low pressure of the oxygen agreed exactly with the calculated pressure, it was concluded that there was no oxygen adsorbed by the reaction products. The experimental results obtained are displayed in Fig. 2.

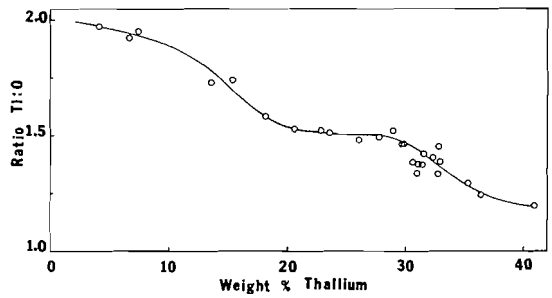

FIG. 2. Ratio of thallium to oxygen in oxide as a function of amalgam composition.

Discussion

The results indicate that in very dilute amalgams the formula of the oxide approaches a limiting value of Tl_2O. As the amalgam becomes richer in thallium the proportion of thallium(III) in the oxide increases except in the composition range between 21 and 29 wt.% thallium in which region the formula of the oxide corresponds fairly closely to Tl_3O_2. Thus there is a correlation between the reactivity of the alloys and the intermediate α phase. The work of Addison and co-workers (1, 12) has shown that in the case of the reaction of nitrogen with liquid alloy of barium and sodium the product changed sharply in composition to Ba_2N from Ba_3N at a composition of the alloy of about 8 atomic % of barium. What is remarkable is that there is a break at this same composition in the liquidus curve of the sodium–barium phase diagram. No such abrupt break in oxide composition occurred in the mercury–thallium system at compositions corresponding to the extremities of the intermediate phase. It is noteworthy that as the concentration of thallium in the amalgam diminishes, the effect of the mercury seems to inactivate two of the three thallium electrons. In a study of the nitrogen with lithium amalgams (13), it is shown that as the concentration of lithium diminishes, the mercury is able to inactivate the single valency electron. Taken together, these results have more interest than when taken separately.

Grateful acknowledgment is made by W. T. Foley of the grant-in-aid of research from the National Research Council of Canada.

1. C. C. ADDISON, B. M. DAVIES, R. M. LINTONBON, and R. J. PULHAM. Chem. Commun. 211 (1967).
2. M. HANSEN. Constitution of binary alloys. 2nd ed. McGraw-Hill Book Co., New York. 1958. p. 843.
3. W. T. FOLEY, REBECCA FAI-YING CHIU, and JOHN R. DELOREY. Can. J. Chem. **46**, 1197 (1968).
4. R. E. SMALLMAN and B. R. T. FROST. Acta Metal, **4**, 611 (1956).
5. N. C. HALDER, R. J. METZGER, and C. N. J. WAGNER. J. Chem. Phys. **45**, 1259 (1966).
6. R. G. WARD and J. R. WILSON. Nature, **182**, 334 (1958).
7. W. T. FOLEY and L. E. REID. Can. J. Chem. **41**, 1782 (1963).
8. W. T. FOLEY and MICHAEL T. H. LIU. Can. J. Chem. **42**, 2607 (1964).
9. W. T. FOLEY and KATHLEEN O'SULLIVAN. Can. J. Chem. **45**, 855 (1967).
10. YVON CLAIRE, ROBERT CASTANET, HENRI TACHOIRE, and MARC LAFFITTE. Centre de Recherche de Micro-calonimétrie et de Thermochimie du C.N.R.S. Marseille. Private communication.
11. W. T. FOLEY and J. M. OSYANY. Anal. Chem. **33**, 1657 (1961).
12. C. C. ADDISON. Endeavour, **98**, 91 (1967).
13. C. C. ADDISON and B. M. DAVIES. J. Chem. Soc. (A), 1831 (1969).

Nuclear spin – lattice relaxation and molecular association in acetone/water mixtures

L. W. REEVES[1] AND C. P. YUE
Department of Chemistry, University of Waterloo, Waterloo, Ontario
Received July 2, 1970

Nuclear spin – lattice relaxation times T_1 of protons have been measured as a function of concentration at room temperature for H_2O/CD_3COCD_3 and CH_3COCH_3/D_2O solutions. The results show that T_1 reaches a minimum at ~ 0.8 mole fraction of water in both solutions. This is interpreted in terms of molecular association between water and acetone molecules by hydrogen bonding.

Theoretical values for $(1/T_1)_{rot}$ and $(1/T_1)_{trans}$ are also calculated from rotational and translational correlation times using Stokes' model and the microviscosity model. Comparison with the experimental T_1's shows that both models are inadequate to describe the system.

Contributions to the overall $(1/T_1)$ from $(1/T_1)_{rot}$ and $(1/T_1)_{trans}$ are analyzed. It is found that the rotational motion dominated the relaxation process. The use of two different interaction parameters λ and η^c to describe molecular association is discussed.

Canadian Journal of Chemistry, **48**, 3307 (1970)

Can. J. Chem. Downloaded from www.nrcresearchpress.com by 210.87.254.40 on 09/05/12
For personal use only.

Introduction

The study of nuclear spin – lattice relaxation time T_1 in liquids can provide useful information about motions of molecules in the liquid. As is known, $(1/T_1)$ can be written as

$$[1] \qquad (1/T_1) = (1/T_1)_{rot} + (1/T_1)_{trans}$$

where $(1/T_1)_{rot}$ is the contribution due to random rotational motion and $(1/T_1)_{trans}$ is the contribution due to translational motion of the molecules. Separation of these two terms leads to an understanding of the nature of the motion of molecules and the relaxation mechansim. The study of molecular association in solution by measuring T_1 has been demonstrated by Giulotto *et al.* (1) and Murthy and Spence (2).

The basic theory of nuclear magnetic relaxation and interaction of nuclear spins with their environment has been well developed (3, 4). Different models have been used to relate T_1 with the viscosity of liquids (3, 5, 6). Unfortunately, none of the proposed models is applicable to all kinds of solutions. In this paper, we only apply Stokes' model and the microviscosity model (5) to calculate rotational and translational correlation times. The results will be discussed in a later section.

Various physical properties of the acetone/water solution have been studied (7–10). The results show that water and acetone molecules interact strongly and as a consequence there are large deviations from the ideal solution behavior. The present work is an additional proof for molecular association between water and acetone molecules corresponding to a maximum at concentrations of about 0.8 mole fraction of water. In fact, Neronov and Drabkin (10) came to the same conclusion from their measurement of the self-diffusion coefficient of protons in acetone/water solutions by the spin-echo method.

[1]To whom all correspondence should be addressed.

Theory

The theory for dipole–dipole relaxation is now well-understood. Detailed derivations of the nuclear spin – lattice relaxation time T_1 with contributions from both the inter- and intramolecular dipole–dipole interactions can be found in literature (3, 4, 11). The intermolecular dipole–dipole contribution is mainly due to the relative translational motion of the molecules, while the intramolecular contribution depends on the tumbling motion of the molecules or rotation of internal groups of atoms. The expressions used for $(1/T_1)_{rot}$ (3, 12) and $(1/T_1)_{trans}$ (3) in this work are

$$[2] \qquad \left(\frac{1}{T_1}\right)_{rot} = \tfrac{3}{2}\hbar^2\gamma^4 \sum_j d_{ij}^{-6}\tau_{rot}$$

$$[3] \qquad \left(\frac{1}{T_1}\right)_{trans} = \frac{1}{10} \cdot \frac{\pi N\hbar^2\gamma^4}{a} \cdot \tau_{trans}$$

γ is the gyromagnetic ratio, d is the separation between different spins, a is the molecular radius, τ_{rot} and τ_{trans} are the rotational and translational correlation times, and N is the number of spins per unit volume.

Can. J. Chem. Downloaded from www.nrcresearchpress.com by 210.87.254.40 on 09/05/12
For personal use only.

The rotational and translational correlation times τ_{rot} and τ_{trans} can be evaluated by different models. τ_{rot} is related to the diffusion coefficient D_r by

$$[4] \qquad \tau_{rot} = 1/6D_r$$

where

$$D_r = kT/\beta$$

and β is the "friction drag" constant for rotation for a spherical molecule in a viscous medium.

In Stokes' model, $\beta = 8\pi\eta a^3$, where η is the viscosity of the medium. Equation 4 now has the following form

$$[5] \qquad \tau_{rot(S)} = (4/3)\,\pi\eta a^3/kT$$

The subscript rot(S) denotes the Stokes' model.

The microviscosity model developed by Gierer and Wirtz (5) has a different value for β; it is related to the spherical shell of solvent molecules with thickness $2r_1$ surrounding a solute molecule.

$$[6] \qquad \beta = 8\pi\eta a^3\left[6\frac{r_1}{a} + \frac{1}{\left(1+\frac{r_1}{a}\right)^3}\right]^{-1}$$

With the above value for β, τ_{rot} is expressed by

$$[7] \qquad \tau_{rot(M)} = \frac{4\pi\eta a^3}{3kT}\left[6\frac{r_1}{a} + \frac{1}{\left(1+\frac{r_1}{a}\right)^3}\right]^{-1}$$

The subscript M denotes the microviscosity model.

The translational correlation time τ_{trans} is defined by

$$[8] \qquad \tau_{trans} = \frac{2a^2}{kT}\beta$$

where

$$\beta = 6\pi\eta a$$

in Stokes' model and

$$\beta = 6\pi\eta a\left[1.5\frac{r_1}{a} + \frac{1}{1+\frac{r_1}{a}}\right]^{-1}$$

in the microviscosity model. This leads to the following expressions

$$[9] \qquad \tau_{trans(S)} = \frac{12\pi\eta a^3}{kT}$$

$$[10] \qquad \tau_{trans(M)} = \frac{12\pi\eta a^3}{kT}\left[1.5\frac{r_1}{a} + \frac{1}{1+\frac{r_1}{a}}\right]^{-1}$$

The molecular radius a is evaluated by assuming a hexagonal closed-packed structure for the solutions, and using the expression

$$[11] \qquad \tfrac{4}{3}\pi a^3 N_0 = 0.74V_m$$

where $N_0 = 6.023 \times 10^{23}$ mole^{-1} and V_m is the molar volume.

For a binary solution with one perdeuterated component, the experimental proton spin–lattice relaxation time is given by

$$[12] \qquad \left(\frac{1}{T_1}\right)_{exp} = \left(\frac{1}{T_1}\right)_{rot} + \left(\frac{1}{T_1}\right)_{trans}\{x + (1-x)R\}$$

where x is the mole fraction and $R \simeq 0.042$ to account for the contribution due to the perdeuterated molecules.

Two other models developed by Moniz *et al.* (13) and Hill (6) are not used in this work. The model of Hill is only applicable rigorously to non-polar liquids.

Experimental

The binary solutions were prepared by mixing weighed amounts of pure liquids. Doubly distilled H_2O was used. Deuterated compounds were supplied by Merck, Sharp and Dohme of Canada Limited. Spectro grade acetone supplied by Eastman Organic Chemicals was used. The samples were carefully degassed by a series of freeze–pump–thaw cycles. Values of T_1 were obtained by the usual $\pi,\pi/2$ pulse method on a spin-echo spectrometer (14) operated at 40 Mc/s at room temperature (~25 °C). Experimental error of T_1 is about 5%.

Results and Discussions

We plot in Figs. 1 and 2 the values of experimental $1/T_1$ as a function of mole fraction. In

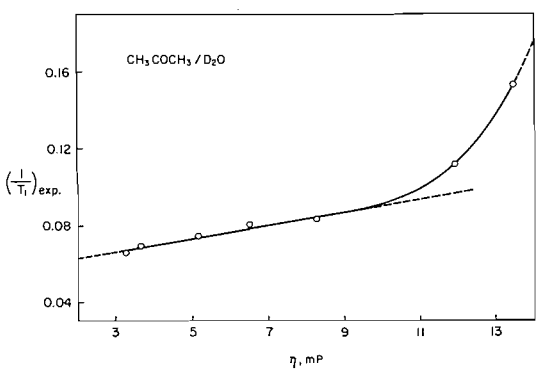

FIG. 1. Relaxation rates for acetone protons in acetone/H_2O mixtures as a function of viscosity.

TABLE 1

Physical properties of H_2O/CD_3COCD_3 solutions at room temperature (~25 °C)

Mole fraction H_2O	η* (mP)	$D_w \times 10^5$† (s/cm^2)	d‡ (g/cc)	$N \times 10^{22}$§	$(1/T_1)_{exp}$ ‖ (s^{-1})
0.90	11.80	1.74	0.9618	2.38	0.377
0.80	13.40	1.51	0.9253	1.68	0.422
0.60	8.85	1.89	0.8744	0.94	0.357
0.50	6.80	2.22	0.8515	0.66	0.314
0.40	5.43	2.65	0.8356	0.48	0.299
0.20	3.72	3.49	0.8065	0.20	0.203

*For viscosity data, see ref. 8.
†Self-diffusion coefficient for H_2O, see ref. 9.
‡Density of the solution, see ref. 7.
§Spin density, number of spins/unit volume.
‖Present work.

TABLE 2

Physical properties of CH_3COCH_3/D_2O solutions at room temperature (~25 °C)

Mole fraction CH_3COCH_3	η* (mP)	$D_a \times 10^5$† (s/cm^2)	d‡ (g/cc)	$N \times 10^{21}$§	$(1/T_1)_{exp}$ ‖ (s^{-1})
0.10	11.85	0.98	0.9603	2.67	0.112
0.20	13.43	1.08	0.9275	4.29	0.153
0.43	8.25	1.81	0.8680	6.35	0.083
0.53	6.50	2.25	0.8486	6.87	0.081
0.63	5.14	2.77	0.8311	7.27	0.074
0.81	3.65	3.56	0.8047	7.79	0.069
0.91	3.26	4.03	0.7935	7.97	0.066

*For viscosity data, see ref. 8.
†Self-diffusion coefficient for CH_3COCH_3, see ref. 9.
‡Density of the solution, see ref. 7.
§Spin density, number of spins/unit volume.
‖Present work.

TABLE 3

Comparison of theoretical and experimental relaxation time T_1 and molecular interaction parameters in H_2O/CD_3COCD_3 solution

Mole fraction	$(1/T_1^S)$*	$(1/T_1^M)$†	$(1/T_1)_{exp}$	γ‡	η^e§
0.90	0.433	0.066	0.377	4.24	3.3590
0.80	0.456	0.063	0.422	3.79	5.6081
0.60	0.279	0.034	0.337	1.73	2.2060
0.50	0.209	0.024	0.314	1.09	0.8231
0.40	0.164	0.018	0.279	0.62	0.0060
0.20	0.111	0.012	0.203	−0.07	−0.5080

*Values obtained from Stokes' model.
†Values obtained from microviscosity model.
‡Intermolecular interaction parameter, see ref. 15.
§Excess viscosity, see ref. 8.

the CH_3COCH_3/D_2O solution, $1/T_1$ reaches a maximum at about 0.2 mole fraction of acetone, and it varies linearly with the mole fraction of acetone in the region from 0.40 to 1.00. In the H_2O/CD_3COCD_3 solution, $1/T_1$ varies linearly with the mole fraction of H_2O from 0.00 to 0.60, and a maximum is reached at about 0.80 mole fraction of H_2O. A plot of $1/T_1$ *vs.* viscosity for the CH_3COCH_3/D_2O solution is shown in Fig. 1. It shows that $1/T_1$ is linearly proportional to the viscosity η of the solution up to $\eta = 8.5$ mP as predicted from the B.P.P. equation (3), but afterwards it varies non-linearly with viscosity.

Some physical properties with $(1/T_1)_{exp}$ of these two solutions are shown in Tables 1 and 2. It is interesting to note that the viscosity η has a larger value at ~0.80 mole fraction of H_2O in these two solutions. Self-diffusion coefficient of water in H_2O/CD_3COCD_3 solution at 0.80 mole fraction is also small as compared to values at other concentrations.

The change of $1/T_1$ with mole fraction in these

Can. J. Chem. Downloaded from www.nrcresearchpress.com by 210.87.254.40 on 09/05/12
For personal use only.

TABLE 4

Comparison of theoretical and experimental relaxation from T_1 and molecular interaction parameters in CH_3COCH_3/D_2O solution

Mole fraction	$(1/T_1^S)$*	$(1/T_1^M)$†	$(1/T_1)_{exp}$	γ‡	η^e§
0.10	1.394	0.350	0.112	4.19	3.4330
0.20	1.587	0.402	0.153	3.85	5.6020
0.43	0.990	0.257	0.083	1.54	1.7863
0.53	0.786	0.206	0.081	0.99	0.6253
0.63	0.626	0.166	0.074	0.53	−0.1187
0.81	0.451	0.122	0.069	−0.09	−0.4879
0.91	0.407	0.111	0.066	−0.03	−0.3189

*Values obtained from Stokes' model.
†Values obtained from microviscosity model.
‡Intermolecular interaction parameter, see ref. 15.
§Excess viscosity, see ref. 8.

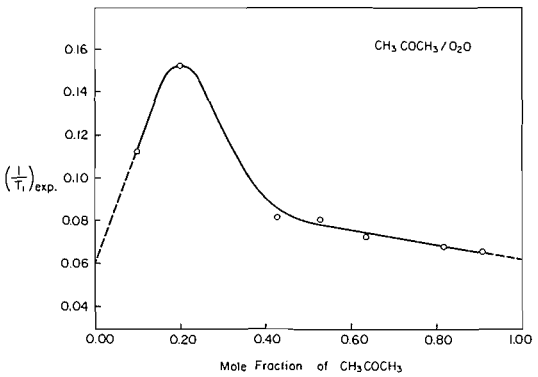

FIG. 2. Relaxation rates for acetone protons in acetone/D_2O mixtures; temperature, ~25 °C

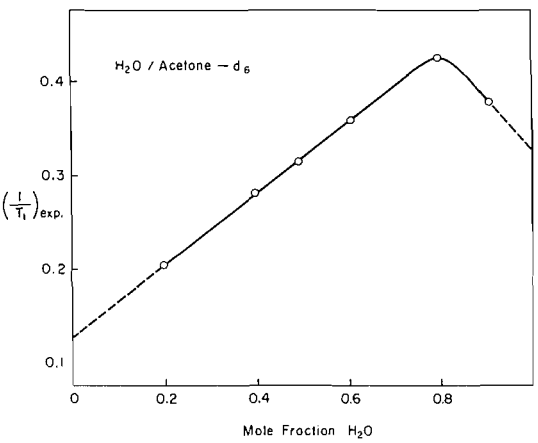

FIG. 3. Relaxation rates for water protons in acetone-d_6/H_2O mixtures; temperature, ~25 °C.

two solutions is similar to the change of viscosity with mole fraction. In fact, the curves plotted in Figs. 2 and 3 are similar to the viscosity – mole fraction curve in H_2O/CH_3COCH_3 solution in ref. 8. The non-linear region in these curves is interpreted as due to strong molecular association between water and acetone molecules. Excess viscosity η^e defined by

$$[13] \qquad \eta^e = \eta - \sum_i x_i \eta_i$$

has been used as a measure of the strength of hydrogen bonding formed between components in the solution (8). The subscript i in eq. 13 refers to the ith component, x_i is the mole fraction,

TABLE 5

Calculated rotational and translational correlation times ($\tau \times 10^{-12}$ s) for H_2O in H_2O/CD_3COCD_3 solutions at room temperature (~25 °C)*

Mole fraction H_2O	τ_{rot}^S	τ_{rot}^M	τ_{trans}^S	τ_{trans}^M
0.90	6.35	0.66	57.13	20.56
0.80	7.21	0.75	64.88	23.35
0.60	4.76	0.49	42.85	15.42
0.50	3.66	0.38	32.92	11.85
0.40	2.92	0.30	26.29	9.46
0.20	2.00	0.21	18.01	6.48

*Superscript S indicates Stokes' model is used; superscript M indicates microviscosity model is used.

TABLE 6

Calculated rotational and translational correlation times ($\tau \times 10^{-12}$ s) for CH_3COCH_3 in CH_3COCH_3/D_2O solution at room temperature (~25 °C)*

Mole fraction CH_3COCH_3	τ_{rot}^S	τ_{rot}^M	τ_{trans}^S	τ_{trans}^M
0.10	25.88	6.48	232.90	149.80
0.20	29.33	7.35	264.00	169.80
0.43	18.02	4.51	162.20	104.30
0.53	14.20	3.56	127.80	82.17
0.63	11.23	2.81	101.00	64.98
0.81	7.97	2.00	71.75	46.14
0.91	7.14	1.79	64.28	41.34

*Superscript S indicates Stokes' model is used; superscript M indicates microviscosity model is used.

Can. J. Chem. Downloaded from www.nrcresearchpress.com by 210.87.254.40 on 09/05/12
For personal use only.

TABLE 7

Theoretical values of $(1/T_1)_{rot}$ and $(1/T_1)_{trans}$ of protons calculated from different models in H_2O/CD_3COCD_3 solution*

Mole fraction H_2O	$(1/T_1^S)_{rot}$	$(1/T_1^M)_{rot}$	$(1/T_1^S)_{trans}$	$(1/T_1^M)_{trans}$
0.90	0.348	0.036	0.092	0.033
0.80	0.396	0.041	0.074	0.027
0.60	0.261	0.027	0.027	0.010
0.50	0.201	0.021	0.015	0.005
0.40	0.160	0.017	0.008	0.003
0.20	0.110	0.011	0.002	0.001

*Superscript S indicates values calculated from Stokes' model; superscript M indicates values calculated from microviscosity model.

TABLE 8

Theoretical values of $(1/T_1)_{rot}$ and $(1/T_1)_{trans}$ of protons calculated from different models in CH_3COCH_3/D_2O solution*

Mole fraction CH_3COCH_3	$(1/T_1^S)_{rot}$	$(1/T_1^M)_{rot}$	$(1/T_1^S)_{trans}$	$(1/T_1^M)_{trans}$
0.10	1.390	0.348	0.031	0.020
0.20	1.575	0.395	0.057	0.036
0.43	0.968	0.242	0.052	0.033
0.53	0.763	0.191	0.044	0.028
0.63	0.603	0.151	0.037	0.024
0.81	0.428	0.107	0.028	0.018
0.91	0.384	0.096	0.026	0.016

*Superscript S indicates values calculated from Stokes' model; superscript M indicates values calculated from microviscosity model.

η_i is the viscosity of the ith component when it is pure. Large positive value of η^e indicates strong hydrogen bonding formation, and this is true for the acetone/water solution in the region that corresponds to 0.6 ~ 1.00 mole fraction of H_2O. Calculated values of η^e are listed in Tables 3 and 4.

Another intermolecular interaction parameter γ was suggested by Grunberg and Nissan (15). For a binary solution, it is defined by the expression

$$[14] \quad \ln \eta = X_1 \ln \eta_1 + X_2 \ln \eta_2 + X_1 X_2 \gamma$$

γ is proportional to w/RT where w is the interchange energy. Values of γ are also listed in Tables 3 and 4. It seems that γ is not a proper measure of the strength of intermolecular interaction between two different components in the solution.

Reduction in the translational mobility of molecules can also serve as a measure of the degree of molecular association. Neronov and Drabkin (10) measured self-diffusion coefficients in acetone/water solution by the proton spin-echo method. They found a minimum for the proton self-diffusion coefficient corresponding to a concentration of about 0.80 mole fraction of water. They indicated that this was due to molecular association. The mobilities of molecules of different types approached one another in value. The reduction in the translational mobility due to molecular association is also reflected by the calculated correlation times as shown in Tables 5 and 6. Both the rotational and translational correlation times in the region corresponding to maximum molecular association are larger than values at other concentrations. This is clearly due to the reduction of mobilities of molecules by molecular association, resulting in the correlation times for the translational and rotational motion of the molecules increasing in value.

Tables 7 and 8 show the calculated $(1/T_1)_{rot}$ and $(1/T_1)_{trans}$ from the Stokes' model and the micro viscosity model. $(1/T_1)_{rot}$ is much larger

TABLE 9

Relaxation times from extrapolation

Compound	T_1	T_{1rot}
H_2O	3.45 (3.6)*	6.25 (5.26)†
CH_3COCH_3	15.80 (15.5)‡	16.30 (19.0)‡

*Reference 16.
†Theoretical value, ref. 17.
‡Reference 18.

Can. J. Chem. Downloaded from www.nrcresearchpress.com by 210.87.254.40 on 09/05/12
For personal use only.

than $(1/T_1)_{trans}$ and contributes a major part to the overall $1/T_1$. Contribution from the intermolecular dipole–dipole interaction is small in the region of molecular association. Values of calculated $1/T_1$ from these two models are also shown in Tables 3 and 4 and compared with the experimental results. Both models are inadequate to describe the motions of molecules in the binary solution but molecular association is clearly illustrated. T_1 and $(T_1)_{rot}$ for water and acetone obtained by extrapolation are shown in Table 9 and they are in good agreement with literature values.

This research was supported by the National Research Council of Canada.

1. L. GIULOTTI, G. LANZI, and L. TOSCA. J. Chem. Phys. **24**, 632 (1956).
2. C. R. K. MURTHY and R. D. SPENCE. J. Chem. Phys. **33**, 945 (1960).
3. N. BLOEMBERGEN, E. M. PURCELL, and R. V. POUND. Phys. Rev. **73**, 679 (1948).
4. A. KUBO and K. TOMITA. J. Phys. Soc. Jap. **9**, 888 (1954).
5. A. GIERER and K. WIRTZ. A. Naturforsch. **A, 8**, 532 (1953).
6. N. E. HILL. Proc. Phys. Soc. **B, 67**, 149 (1954).
7. R. J. FORT and W. R. MOORE. Trans. Faraday Soc. **61**, 2102 (1965).
8. R. J. FORT and W. R. MOORE. Trans. Faraday Soc. **62**, 1112 (1966).
9. D. W. MCCALL and D. C. DOUGLASS. J. Phys. Chem., **71**, 987 (1967).
10. YU. I. NERONOV and G. M. DRABKIN. J. Struct. Chem. **7**, 624 (1966).
11. A. ABRAGAM. The Principles of Nuclear Magnetism, Oxford Univ. Press. 1961.
12. H. S. GUTOWSKY and D. E. WOESSNER. Phys. Rev. **104**, 843 (1956).
13. W. B. MONIZ, W. A. STEELE, and J. A. DIXON. J. Chem. Phys. **88**, 2418 (1963).
14. K. H. ABRAMSON, P. T. INGLEFIELD, E. KRAKOWER, and L. W. REEVES. Can. J. Chem. **44**, 1685 (1966).
15. L. GRUNBERG and A. M. NISSAN. Nature, **164**, 799 (1949).
16. J. G. POWLES and D. CUTLER. Nature, **184**, 1123 (1959).
17. N. BLOEMBERGEN, E. M. PURCELL, and R. V. POUND. Phys. Rev. **73**, 679 (1948).
18. G. BONERA and A. RIGAMONTI. J. Chem. Phys. **42**, 171 (1965).

Can. J. Chem. Downloaded from www.nrcresearchpress.com by 210.87.254.40 on 09/05/12
For personal use only.

Can. J. Chem. Downloaded from www.nrcresearchpress.com by 210.87.254.42 on 09/05/12
For personal use only.

Kinetics of the pyrolysis of propylene. Part II

M. SIMON AND M. H. BACK
Chemistry Department, University of Ottawa, Ottawa, Canada

Received June 5, 1970

Analysis of the products of the pyrolysis of propylene in the initial stages shows that products of molecular weight up to C_9 are primary products of major significance below about 850 °K and above about 200 Torr. As these products accumulate in the system, their dissociation causes secondary initiation and a rapid increase in pressure. Measurements of the initial rate of decrease in pressure and of the final maximum rate of increase in pressure of the reaction are consistent with this interpretation of the mechanism.

Canadian Journal of Chemistry, 48, 3313 (1970)

Introduction

In Part I of this study of the pyrolysis of propylene (1) a mechanism for the reaction was proposed in which two main features were emphasized. The first was the bimolecular initiation step

$$2C_3H_6 \rightarrow C_3H_5 + C_3H_7$$

which was deduced from the order and activation energy of the rate of formation of the main products. The second was the formation of primary products of molecular weight higher than C_6 in the initial stages of the reaction. At temperatures below about 850 °K the pressure change calculated from the products measured, which did not include compounds of molecular weight greater than C_6, was significantly smaller than that actually measured, both in the initial and in the later stages of the reaction. The mechanism was therefore formulated to allow for the initial production of these "polymers". The significance of the formation of these polymers was that they were the unstable intermediates responsible for the observed induction period of the over-all rate. The increase in rate after the short induction period was caused by the secondary initiation provided by the decomposition of these polymers. Analysis of these products was not attempted with the technique described in Part I but now a qualitative analysis using a slightly modified technique has confirmed their presence and the results are reported in the present paper.

Many studies of the pressure change accompanying the pyrolysis of propylene have been made in the temperature range 820–910 °K and at pressures between 50 and 500 Torr (2–4). All these studies reported a sigmoidal form of pressure–time curve and measurements were made at the point of maximum rate after the induction period. The kinetics of the reaction in this region are likely to be complex, considering the suggestion that initiation is largely from secondary dissociation of products and measurements of the initial pressure change seemed essential to the understanding of the mechanism. To do this the pyrolysis was studied in a lower temperature region where the induction period is longer and the initial decrease in pressure is measurable.

In their discussion of the pyrolysis of propylene, Amano and Uchiyama (5) defined zones of polymerization and decomposition on a pressure–temperature diagram separated by a curve corresponding to the equivalence of the two rates

$$C_3H_5 + C_3H_6 \rightarrow \text{Polymer} + H$$

$$C_3H_5 \rightarrow C_3H_4 + H$$

Our studies concur with this general view and attempt to describe the polymerization rate more specifically in terms of elementary rates and to show its dependence on conditions of temperature and pressure.

Experimental

Analysis

The apparatus and procedure have been described in Part I. To collect the products of molecular weight higher than C_6 the reaction vessel was modified to be detachable and after filling with propylene was sealed off under vacuum. After the appropriate reaction time the vessel was removed from the furnace and a small side finger was immersed in liquid nitrogen. After all the condensable products had condensed in this small tube the vessel was opened, and the total amount of liquid collected (a few microliters) was injected into the gas chromatograph for analysis. It was assumed that this sample contained all the products of molecular weight greater than C_5, but the error introduced by this assumption was probably quite large, and may be the main source of the scatter observed in the yields of the products. A 3-ft column of silica gel and alumina programmed at 7.5°/min up to 250 °C separated the products according to carbon number. For further separation the peaks were

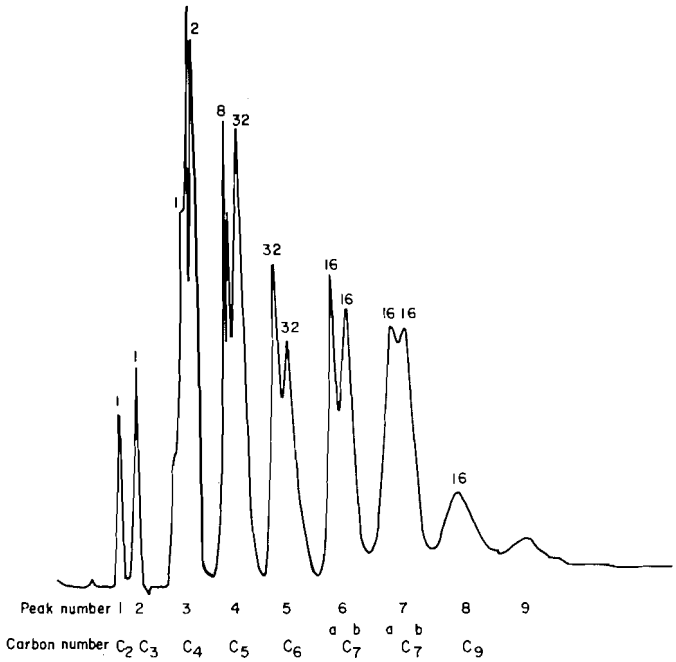

FIG. 1 Typical analysis chromatogram showing the separation of the products obtained on the silica gel column.

collected and analyzed isothermally on a 9-ft column of 30% tricresyl phosphate on Chromosorb P. Finally, the mass spectrum of each peak was measured.

Pressure Measurements

The pressure was measured with a Texas Instrument fused quartz spiral gauge Model 145. The sensitivity of the gauge was 2.58 Torr/deg. The position of the spiral could be estimated to 0.001° so that the instrument was capable of detecting changes in pressure of about 0.003 Torr. The temperature of the reaction vessel was recorded as the pressure measurements were made and corrections made accordingly. The volume of the gauge and connecting tubing was determined by measuring the change in pressure of an inert gas as the temperature of the reaction vessel was changed. The correction to the observed pressure change from this factor was 28%. The reaction vessel was connected to the apparatus with a Hoke stainless steel diaphragm seal valve which eliminated loss of propylene through absorption in stopcock grease. The scatter in the data gave an error of about 5% in any one determination of the initial rate, but the reproducibility was only about 30% at temperatures up to about 800 °K. At temperatures higher than 820 °K the initial decrease in pressure was too small to measure with confidence. The reproducibility of the maximum rate was about 20% at 800 °K but the error became much less at higher temperatures.

Results

Analysis

A typical chromatogram is shown in Fig. 1 with the carbon number indicated for each peak. Peaks numbered 6 and 7 each gave two main peaks when analyzed on the tricresyl phosphate column (as also shown from the silica gel column), while peak number 8 gave only one main peak. Each of these peaks, of course, may contain more than one isomer. Complete analysis of the higher molecular weight compounds was not attempted since the number of possible isomers is very large. Nevertheless the mass spectra of these peaks established the molecular weight and gave indication of the most probable constituents. These are listed in Table 1. The total yield of C_7 products (excepting toluene) was about half the total yield of C_6 products, while

TABLE 1

Peak number (from Fig. 1)	Molecular formula	Most probable constituents
6*a*	C_7H_{12}	4-Methyl-2-hexyne 1-Heptyne
6*b*	C_6H_6	Benzene
7*a*	C_7H_{12}	1-Methylcyclohexene 4-Methylcyclohexene 3-Methylcyclohexene
7*b*	C_7H_8	Toluene
8	C_9H_{16}	*cis*-Hexahydroindan 3,3,5-Trimethylcyclohexene *cis*-Cyclononene

Can. J. Chem. Downloaded from www.nrcresearchpress.com by 210.87.254.42 on 09/05/12
For personal use only.

Can. J. Chem. Downloaded from www.nrcresearchpress.com by 210.87.254.42 on 09/05/12
For personal use only.

the yield of C_9 products was about 1/5. These estimates are approximate and are based on peak height only. The analysis was not sufficiently accurate to calculate a pressure–time curve and pressure measurements were, in any case, not made under the same conditions as the analysis. It can be concluded only that the amounts of products of molecular weight higher than C_6 are roughly what was expected from the pressure measurements and the analysis under other conditions.

The ratios of the yields of products of molecular weight higher than C_6 to the total yield of C_6 products were obtained from the peak heights observed from the temperature-programmed analysis on the silica gel – alumina column. The ratios of peaks number 6*a*, 7*a*, and 8 to the total C_6 product were, within the errors involved, constant with time, showing these products to be primary. The benzene and toluene appeared to be secondary. The yield of the C_9 products approached a maximum value at fairly short reaction times. These higher molecular weight products thus appear less stable than the lighter products.

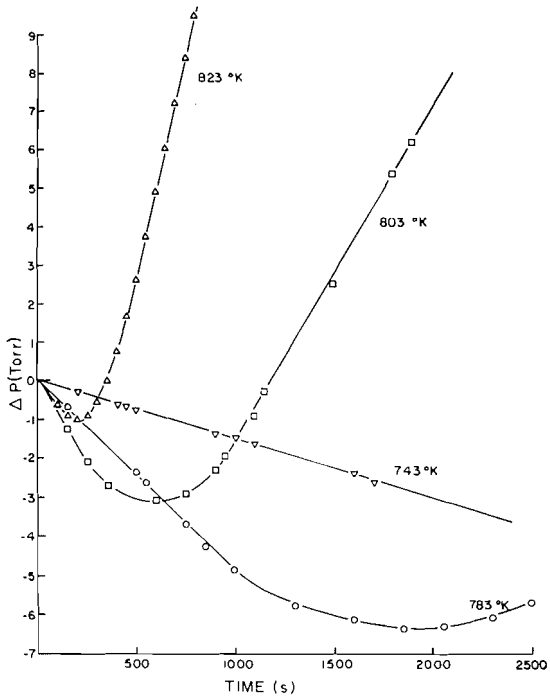

FIG. 2. Pressure–time curves. Initial pressure of propylene 600 Torr.

Pressure Measurements

At each temperature except the highest (873 °K) the pressure decreased initially, went through a minimum value and then increased, eventually reaching a constant rate. Typical pressure–time curves are shown in Fig. 2. The initial rate of pressure decrease became greater as the temperature was increased and the minimum value occurred at shorter reaction times. Consequently, the initial rate became more difficult to measure as the temperature was increased and was unreliable above about 810 °K. At the lowest temperature studied, 743 °K, the reaction was not allowed to proceed for a time sufficient to observe the maximum rate. Both initial and maximum rates could be measured only at temperatures between 783 and 803 °K.

The initial rate of pressure decrease, R_i, was second order in propylene. At temperatures below 783 °K the order increased at lower pressures. Typical results are shown in Fig. 3. The maximum rate of pressure increase, R_m, was approximately equal to the initial rate at pressures above about 400 Torr, but was greater than the initial rate at lower pressures. Figure 3 shows this behavior at 793 °K. At higher temperatures the maximum rate was of 1.5 order, in agreement with previous measurements. Values of the initial and maximum rates at high pressures are given in Table 2.

Discussion

The analysis confirms the conclusion reached in Part I, from the measurement of the pressure changes accompanying the reaction, that primary products of molecular weight higher than C_6 are formed in the pyrolysis of propylene. The following reactions represent the framework of the mechanism in the initial stages of the pyrolysis but do not include many of the decompositions and isomerizations that occur. These reactions emphasize the features mentioned in the Introduction and do not attempt to account for the formation of all the products.

[1] $2C_3H_6 \rightarrow C_3H_5 + C_3H_7$

[2] $C_3H_7 + C_3H_6 \rightarrow C_3H_8 + C_3H_5$

[3] $C_3H_7 + C_3H_6 \rightarrow C_6H_{13}$

[4] $C_3H_7 \rightarrow CH_3 + C_2H_4$

[5] $C_3H_5 + C_3H_6 \rightarrow C_6H_{11}$

[6] $C_6H_{11} + C_3H_6 \rightarrow C_6H_{10} + C_3H_7$

[7] $C_6H_{11} + C_3H_6 \rightarrow C_6H_{12} + C_3H_5$

[8] $C_6H_{11} + C_3H_6 \rightarrow C_9H_{17}$

[9] $C_9H_{17} \rightarrow C_7H_{12} + C_2H_5$

[10] $C_9H_{17} \rightarrow C_9H_{16} + H$

By continuing addition and abstraction reactions starting with the allyl and propyl radicals the compounds of molecular weight C_6 and higher in multiples of three may be formed as primary products. There is some indirect evidence to suggest that the higher molecular weight compounds are formed mainly from the chain propagated by allyl radicals and that the lower molecular weight compounds arise from reactions of the propyl radicals. Since the higher radicals are increasingly unstable their decomposition reactions will compete with further addition reactions, thus limiting the molecular weight of the products and providing a mechanism for formation of products with carbon number other than a multiple of three.

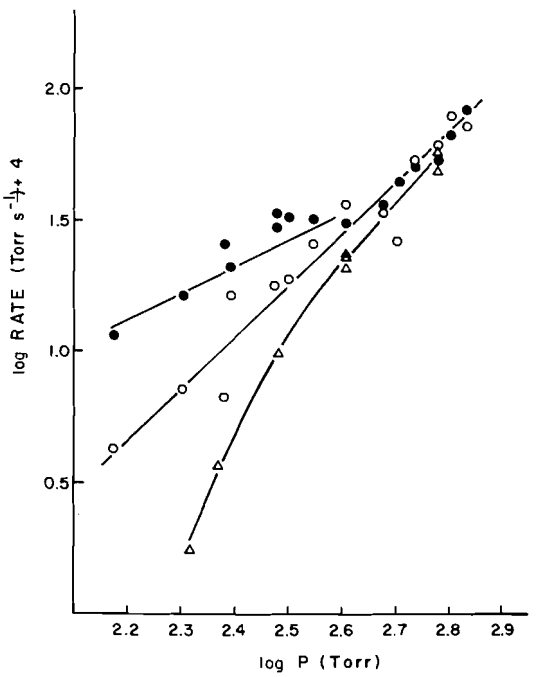

FIG. 3. Logarithm of the initial rate and of the maximum rate as a function of the logarithm of the initial pressure. ●, R_m; ○, R_i at 793 °K; △, R_i at 783 °K.

TABLE 2

Comparison of initial and maximum rates

T (°K)	Pressure (Torr)	R_i (Torr/s × 10^3)	R_m (Torr/s × 10^3)
783	400	2.0	1.8
793	630	8.0	6.8
803	590	7.1	8.7

The rate of change of pressure was almost unaffected by changing the surface/volume ratio by a factor of 8.5. Nevertheless the rates of formation of several of the products were considerably increased when the reaction occurred in the packed vessel (1). The reactions occurring on the surface must be those which form both low and high molecular weight products with the result that the net pressure change observed in the packed vessel is very similar to that observed in the unpacked vessel. The results of this study do not provide sufficient evidence to decide which reactions might be heterogeneous but they do illustrate that pressure measurements alone cannot provide a basis for testing the homogeneity of a reaction.

The formation of products of molecular weight higher than C_3 causes a decrease in pressure according to the following stoichiometry

[11] $$-dP/dt = \tfrac{1}{3}\,\text{Rate } C_4 + \tfrac{2}{3}\,\text{Rate } C_5 + \text{Rate } C_6 + \tfrac{4}{3}\,\text{Rate } C_7 + \tfrac{5}{3}\,\text{Rate } C_8 + 2\,\text{Rate } C_9$$

These products will subsequently be referred to as polymers. At low temperatures the initial rates of formation of C_4 and C_5 products other than cyclopentadiene were smaller and the initial decrease in pressure may therefore be expressed as

[12] $$-(dP/dt)_i = \text{Rate(Polymers)}_i = f(\text{Rate } C_6)_i$$

where f is a constant greater than one which takes into account the formation of cyclopentadiene and the primary products of molecular weight higher than C_6.

The formation of products of molecular weight smaller than C_3 causes an increase in pressure. Such products were almost entirely methane and ethylene and since these were formed in almost equivalent amounts the increase in pressure may be described as follows,

[13] $$+dP/dt = \tfrac{1}{2}\,\text{Rate } (CH_4 + C_2H_4)$$

The initial change in pressure observed as the reaction proceeds may thus be expressed as

Can. J. Chem. Downloaded from www.nrcresearchpress.com by 210.87.254.42 on 09/05/12
For personal use only.

Can. J. Chem. Downloaded from www.nrcresearchpress.com by 210.87.254.42 on 09/05/12
For personal use only.

$$[14] \quad (dP/dt)_i = \tfrac{1}{2}\,\text{Rate}\,(CH_4 + C_2H_4)_i - f(\text{Rate}\ C_6)_i$$

If the rate of formation of polymer exceeds that of the lower molecular weight products then a decrease in pressure is observed.

Equations 11 and 13 represent a consideration of the carbon stoichiometry only. Provided molecular hydrogen is not formed, and the measured yields were very small, it is not necessary to consider the fate of the hydrogen. Products rich in hydrogen, with respect to propylene, are balanced by products deficient in hydrogen, and although these are not all identified the pressure measurement represents the sum of the moles of each.

In Part I it was shown that the initial rate of formation of the C_6 products was close to the rate of the initiation reaction and it was concluded that the mechanism did not involve a long chain process. If all the allyl and propyl radicals formed C_6 products by reactions such as 3, 6, and 7, the initial rate of formation of C_6 products would equal $2k_1(C_3H_6)^2$. Some of the propyl radicals dissociate to yield lighter products, making the constant less than 2, and some of the C_6 radicals react to form higher molecular weight products, making the constant greater than 2. Furthermore some of the C_6 products may be formed by combination of C_3 radicals. If all the C_6 products were formed in this way their rate of formation would equal $k_1(C_3H_6)^2$. Therefore, a reasonable expression for the initial rate of formation of C_6 products is

$$[15] \quad (\text{Rate}\ C_6)_i = \alpha k_1(C_3H_6)^2$$

where α lies between 1 and 2 and k_1 is the rate constant for the initiation reaction. A fraction of the propyl radicals, $\beta = k_4/[k_4 + (k_2 + k_3)(C_3H_6)]$ decompose to yield methane and ethylene so that the initial rate of formation of methane and ethylene may be written as $\beta k_1(C_3H_6)^2$. The initial rate of change of pressure may be expressed as

$$[16] \quad (dP/dt)_i = \beta k_1(C_3H_6)^2 - \alpha f k_1(C_4H_6)^2 = (\beta - \alpha f)k_1(C_3H_6)^2$$

where β includes the factor of 1/2 from eq. 14, At low temperatures the pressure decreased initially, showing that the fraction β is smaller than the product αf. The initial rate of decrease of pressure was second order at high pressures but at lower initial pressures of propylene and lower temperatures this rate fell below the rate projected from the second-order region (Fig. 3). The fraction of product formed of molecular weight higher than C_6 is very likely a function of pressure and if this fraction becomes smaller at lower pressures the rate of decrease of pressure will be proportionately smaller. The analyses of the higher molecular weight products were not extensive enough to show this effect but such an assumption appears reasonable.

The activation energy of the initial rate was 35 kcal/mole. This is considerably less than the temperature coefficient of k_1 and indicates that the constants β, α, and f must be temperature dependent. Both f and α are measures of the extent of formation of products of molecular weight greater than C_6 and are inversely related to each other. Their individual effects will largely cancel. The factor β, although not large, will increase with temperature, having an activation energy of at most 32 kcal/mole (6). This factor acts in the opposite direction to k_1 which causes the initial pressure decrease to become larger as the temperature is increased. Thus the observed temperature coefficient for the initial rate of pressure decrease would be expected to be between the activation energy for k_1, 52 kcal/mole, and the difference between the activation energy for k_1 and for k_4, about 20 kcal/mole. The fact that the observed temperature coefficient was 35 kcal/mole shows that a considerable fraction of propyl radicals dissociate to yield lighter products.

As the higher molecular weight products accumulate in the system they begin to decompose and yield a variety of new products. The main products whose rate increases rapidly in this region are methane and ethylene. If the rate of initiation remains sufficiently fast to keep the chain length very short the rates of formation of methane and ethylene may be set equal to the rate of decomposition of the polymers.

$$[17] \quad \text{Rate}\,(CH_4 + C_2H_4) = k_d(C_6) + k_d'(C_7) + k_d''(C_9)$$

where k_d is the rate constant for dissociation. For simplicity this sum may be represented as follows

$$[18] \quad \text{Rate}\,(CH_4 + C_2H_4) = gk_d(C_6)$$

where g is a constant, since the kinetic characteristics of the higher primary products are probably

Can. J. Chem. Downloaded from www.nrcresearchpress.com by 210.87.254.42 on 09/05/12
For personal use only.

similar. The total rate of formation of methane and ethylene is therefore the sum of this rate and the initial rate.

$$[19] \quad \text{Rate } (CH_4 + C_2H_4) = \beta k_1(C_3H_6)^2 + gk_d(C_6)$$

The rate of formation of polymer may be written as

$$[20] \quad \text{Rate (Polymer)} = \alpha f k_1(C_3H_6)^2 - gk_d(C_6)$$

The rate of change of pressure may thus be expressed as

$$[21] \quad dP/dt = 2gk_d(C_6) - (\alpha f - \beta)k_1(C_3H_6)^2$$

where the concentration of polymer products is the only variable with time. The rate of change of C_6 and higher molecular weight products with time is equal to their initial rate of formation, eqs. 12, 15, minus their rate of dissociation, eq. 17.

$$[22] \quad d(C_6)/dt = \alpha f k_1(C_3H_6)^2 - gk_d(C_6)$$

and the concentration at any time is

$$[23] \quad (C_6) = (\alpha f k_1/gk_d)(C_3H_6)^2[1 - e^{-gk_d t}]$$

The rate of change of pressure therefore becomes

$$[24] \quad dP/dt = k_1(C_3H_6)^2[2\alpha f(1 - e^{-gk_d t}) - \alpha f + \beta]$$

In the initial stages of the reaction, when t is small,

$$[25] \quad dP/dt = (\beta - \alpha f)k_1(C_3H_6)^2$$

which is identical to eq. 16. At long reaction time when the steady state concentration of polymers is attained and the rate is a maximum,

$$[26] \quad dP/dt = (\beta + \alpha f)k_1(C_3H_6)^2$$

If β is small compared to αf the maximum rate will be equal to the initial rate but opposite in sign. Figure 3 and Table 2 show that the initial and maximum rates are close at high pressures but that the maximum is greater than the initial rate at low pressures.

There are several factors which could cause the maximum rate to exceed the initial rate. First, the decomposition of the propyl radical would likely become more important relative to its other reactions at low pressures. This would increase β relative to αf. Secondly, the assumption was made that the reaction in the region where secondary initiation is important is still essentially a radical non-chain reaction. If the chain length in the region of maximum rate is greater than in the initial stages then the maximum rate will be greater than the initial rate by the extent of this difference. Changes in the rate of initiation would affect both initial and maximum rates in the same way but the main propagation steps in each region will not be the same, and if these change with pressure in different ways the chain length would be different in the two regions.

It seems, therefore, that the maximum rate may very likely be greater than the initial rate and only where the simplest mechanism applies will they be similar. The increase in the maximum rate relative to the initial rate as the pressure is lowered causes the observed order of the maximum rate to be considerably lower than the order of the initial rate. From the present measurements the order of the maximum rate was close to 1.5, in agreement with previous measurements. It is apparent from the results of this study that this measured order does not allow deductions about the initiation and termination steps of the reaction. The fact that the initial and maximum rates are similar at high pressures shows that the mechanism in the region of maximum pressure increase is a radical reaction of very short chain length and not, as previously supposed, a very long chain reaction. Only in the lower pressure region does the chain length become appreciable.

At the minimum in the pressure, where the rate of change of pressure is zero,

$$[27] \quad (\alpha f + \beta)/2\alpha f = e^{-gk_d t}$$

In the region where the initial and maximum rates are equal, where β is small compared to αf,

$$[28] \quad gk_d = \ln 2/t$$

Measurements of the time at which $dP/dt = 0$ will give gk_d. This rate constant was found to increase as the pressure was lowered but approached a constant value at the higher pressures. This increase in gk_d, or decrease in t(min), at low pressures is the result of the increase in the maximum rate relative to the initial rate, since eq. 28 holds only where $R_i = R_m$. An Arrhenius plot of gk_d is given in Fig. 4. The expression for gk_d obtained from this graph is

$$gk_d = 1 \times 10^{15} e^{-66000/RT} s^{-1}$$

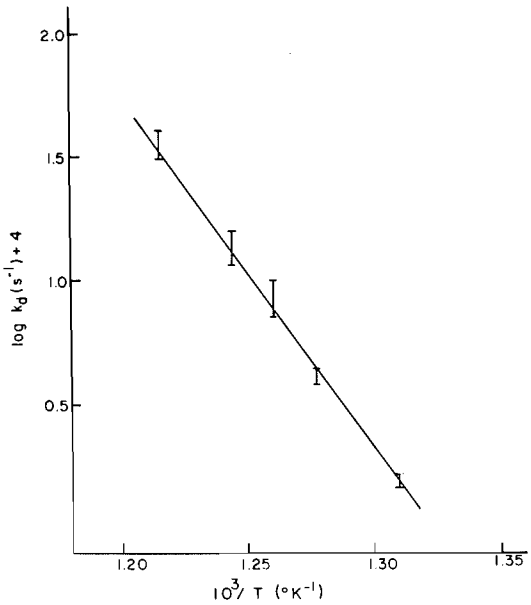

FIG. 4. Arrhenius plot of k_d.

This is a reasonable value for the rate of dissociation of a high molecular weight olefin, keeping in mind that the factor g is greater than one. The parameters are, however, only approximate since the factor g is complex and may itself be a function of temperature.

In summary, the polymerization and decomposition of propylene in the temperature range 740–850 °K and the pressure range 100–600 Torr is a radical reaction of very short chain length. Initiation occurs by the bimolecular reaction of propylene to give propyl and allyl radicals. Addition of the radicals to propylene gives primary products of molecular weight as high as C_9, causing the pressure in the system to decrease in the initial stages. As these products accumulate in the system their rate of decomposition becomes comparable to the rate of initiation by propylene and secondary initiation occurs. This secondary initiation yields methane and ethylene as the major products and consequently an increase in pressure is observed in the later stages of the reaction.

The authors thank the National Research Council of Canada for generous financial assistance.

1. M. SIMON and M. H. BACK. Can. J. Chem. **48**, 317 (1970).
2. K. U. INGOLD and F. J. STUBBS. J. Chem. Soc. 1749 (1951).
3. K. J. LAIDLER and B. W. WOJCIECHOWSKI. Proc. Roy. Soc. Ser. A. **259**, 257 (1960).
4. A. S. KALLEND, J. H. PURNELL, and B. C. SHURLOCK. Proc. Roy. Soc. Ser. A. **300**, 120 (1967).
5. A. AMANO and M. UCHIYAMA. J. Phys. Chem. **68**, 1133 (1964).
6. M. C. LIN and K. J. LAIDLER. Can. J. Chem. **44**, 2927 (1966).

Can. J. Chem. Downloaded from www.nrcresearchpress.com by 210.87.254.42 on 09/05/12
For personal use only.

Can. J. Chem. Downloaded from www.nrcresearchpress.com by 210.87.254.42 on 09/05/12
For personal use only.

Liquid phase photolysis of cyclobutanone[1]

R. F. KLEMM
Research Council of Alberta, Edmonton 7, Alberta

Received May 4, 1970

The photolysis of cyclobutanone has been examined at 3260, 3130, and 2537 Å in a variety of solvents and as a pure liquid. Both decarbonylation and photocleavage to C_2H_4 and CH_2CO occur with substantial yield in a manner which appears to be somewhat at variance with the currently accepted gas phase mechanism. While C_2H_4/(cyclopropane + propylene) is relatively insensitive to photon energy, there is a significant wavelength dependence in the rate of propylene formation suggesting that the photoreactions of cyclobutanone occur at rates comparable with relaxation times in solution.

Canadian Journal of Chemistry, 48, 3320 (1970)

The mechanism of the gas phase photolysis of cyclobutanone (CB) has received considerable attention (1). In the wavelength region 3130–2500 Å it is currently accepted that decarbonylation occurs after intersystem crossing to the n,π^* triplet (T_1). Adiabatic internal conversion converts the remainder of the initially formed n,π^* singlet (S_1) to the excited ground singlet, which then yields the same products as observed in pyrolysis, primarily ethylene and ketene. Formation of C_2H_4 and ketene are reduced by collisional quenching particularly at long wavelengths. The rates of intersystem crossing (isc), internal conversion (ic), and decomposition are of such magnitude as to preclude the observation of fluorescence or phosphorescence in the gas phase (2, 3). This interpretation is illustrated by eq. 1, where the asterisk denotes vibrational excitation.

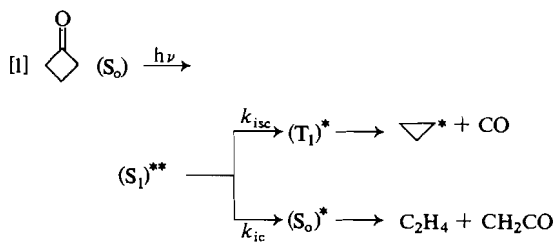

Since no study has been reported of the liquid phase photolysis of CB other than that of Turro and Southam (4) dealing with various photoinduced ring expansions, it was of interest to compare the photolytic behavior of CB in solution with that in the vapor. If indeed C_2H_4 and ketene arise from a hot ground state molecule, as in the gas phase, then one would anticipate ethylene formation to be efficiently quenched in the liquid while the decomposition of $(T_1)^*$ would depend on the relative rates of decomposition and quenching of T_1 by the solvent. It was on the basis of these considerations that the present investigation was begun.

Results and Discussion

Our concern was primarily with ethylene, propylene, and cyclopropane as a function of system variables. Ketene was noted as an interfering gas chromatography peak in preliminary work, but was irreversibly absorbed by the squalane column routinely employed. It is a product which has been confirmed as methyl acetate by Turro and Southam (4). Up to approximately 10% reaction in heptane g.c. analysis failed to reveal any products other than those mentioned above. Moreover, up to 1% reaction the yields of these products were found to increase linearly with irradiation time (as shown in Fig. 1) implying that they are formed directly from CB. All subsequent data were obtained under these conditions of linear yield. In Table 1 quantum yield data are presented for the formation of ethylene and cyclopropane in a variety of solvents at 3130 Å. Propylene was also observed and found to be approximately 0.6% of the cyclopropane in all solvents at 3130 Å. The first four solvents are of similar low dielectric strength but increasing strength as Lewis bases. The other solvents were chosen either because they illustrated a range of polarities or because of their diagnostic sensitivity toward triplet species (1,3-cyclohexadiene, piperylene, iso-propanol (5–9)).

The quantum yields in Table 1 have been

[1]Contribution No. 497 from the Research Council of Alberta, Edmonton, Alberta.

TABLE 1

Solvent dependence of product yields at 3130 Å; all solutions 0.25 *M* in CB

Solvent	3130 Å			
	$\frac{C_2H_4}{\text{cyclopropane + propylene}}$	$\phi_{C_2H_4}$	$\phi_{\text{cyclopropane}}$	ϕ_{TOTAL}
n-Heptane	1.3	0.18_5	0.14_5	0.33
c-Hexane	1.4	0.18_5	0.13	0.32
Benzene	1.8_5	0.18_5	0.10	0.28
1,4-Dioxane	2.2	0.18	0.08	0.26
1,3-Cyclohexadiene	1.6_5	0.094	0.056	0.15
Piperylene	1.4_5	0.17	0.12	0.29
t-Butanol	1.7	0.17	0.10	0.27
i-Propanol	1.7	0.18	0.11	0.29
Methanol	1.8_5	0.14_5	0.08	0.22
Acetonitrile	2.1	0.18	0.085	0.26

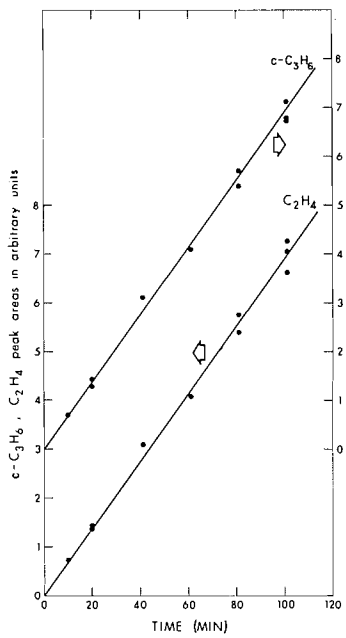

FIG. 1. C_2H_4 and cyclopropane yields as a function of irradiation time. 3130 Å, 0.25 *M* CB in *n*-heptane.

measured relative to a quantum yield for the disappearance of 2-hexanone equal to 0.33 mole/Einstein (9) and therefore are of uncertain reliability; they do establish an order of magnitude which indicates the liquid phase photolysis to be a non-trivial process. The error limits on the relative rates of product formation among the various solvent systems are ±5%, while values of ethylene/(cyclopropane + propylene) have an error of ±3%. The error in cyclopropane/propylene may be larger in those cases where the amount of propylene is small compared with cyclopropane.

The effect of photon energy on the quantities C_2H_4/(cyclopropane + propylene) and cyclopropane/propylene are given in Table 2 *a* for 0.25 *M* CB in *n*-heptane.[2] Included in this table is an experiment wherein an *n*-heptane solution 1.3 *M* in benzene and 0.05 *M* in CB was irradiated at 2537 Å. These data are taken to represent photosensitized decomposition of CB by singlet benzene. A value of cyclopropane/propylene close to that obtained by direct photolysis at 2537 Å tends to act as internal confirmation of this supposition. Normally all experiments were conducted in 12 mm i.d. Pyrex or quartz cells. However, preliminary experiments were carried out in 2 mm i.d. tubes where values of C_2H_4/(cyclopropane + propylene) were consistently 10% higher than those from the larger cells. Because of a limited supply of cyclobutanone the data in Table 2*b* were obtained from the smaller tubes and for that reason are likely high by 10% relative to all other values of this parameter reported here. While solutions of CB in benzene, cyclohexadiene, and piperylene were always degassed, for the remaining solvents the same results could be obtained from either aerated or thoroughly degassed solutions.

It is apparent that both decomposition reactions proceed with high yield in all solvents. In view of the rapid vibrational quenching in solution it is inconceivable that significant amounts

[2]In solution at 3260 Å Hemminger *et al.* (1*b*) report a value of 1.25 for C_2H_4/cyclopropane, supporting the figure we report in Table 2 *a*.

Can. J. Chem. Downloaded from www.nrcresearchpress.com by 210.87.254.42 on 09/05/12
For personal use only.

TABLE 2

Energy dependence of C_2H_4/(cyclopropane + propylene) and cyclopropane/propylene; (*a*) 0.25 *M* CB in *n*-heptane; (*b*) CB neat

	a		*b*	
	$\frac{C_2H_4}{\text{cyclopropane + propylene}}$	$\frac{\text{cyclopropane}}{\text{propylene}}$	$\frac{C_2H_4}{\text{cyclopropane + propylene}}$	$\frac{\text{cyclopropane}}{\text{propylene}}$
3260 Å (88 kcal/mole)	1.3	140	2.0	260
3130 Å (91 kcal/mole)	1.3	170	2.0	240
*Benzene sensitization at 2537 Å	1.1	34		
2537 Å (112 kcal/mole)	1.1	15	1.8	16

*1.3 *M* Benzene, 0.05 *M* CB in *n*-heptane.

of ethylene and ketene could be formed (as in the gas phase photolysis) via the vibrationally excited ground singlet state. Hence another route to ethylene must be open to CB (S_1) in solution.

The following arguments furthermore suggest neither set of products originate from a species which could be described as the CB (T_1) proposed to participate in the gas phase photolysis. The rate of ethylene production (Table 1) is independent of the solvent with the exception of methanol, in which solvent Turro and Southam report (and we confirm) 8% of the total photoreaction of CB involves reaction with methanol leading to α-methoxy tetrahydrofuran (4). Although the cyclohexadiene was carefully purified by preparative gas chromatography, it still absorbed close to 50% of the incident light at 3130 Å with a 12 mm i.d. cell, supporting a similar experience reported by Schenk *et al.* (10). Correcting the quantum yields for C_2H_4 and cyclopropane to account for this would give product yields in accord with the other systems. Thus neither the rate of C_2H_4 production nor that of cyclopropane changes in any discontinuous way in those solvents normally considered efficient triplet quenchers, namely cyclohexadiene, piperylene, and isopropanol. Additionally, no *trans*-piperylene was observed when the solvent was *cis*-piperylene, nor was there evidence of acetone or cyclobutanol in the solvent isopropanol (7). It has been shown (11) that the quantum yield for the photosensitized dimerization of cyclohexadiene is 1.0 and that a constant 3:1:1 ratio of possible cyclohexadiene dimers is obtained as long as the sensitizer triplet energy is greater than 53 kcal/mole which most certainly is the case for CB. The above dimer ratio was not obtained when CB was photolyzed in cyclohexadiene, and the dimers observed proved to be characteristic of the direct photolysis of cyclohexadiene, concurring with the results of Schenk *et al.* (10). Attempts to sensitize the formation of CB (T_1) using acetone as donor also failed. In this case an acetone triplet energy of 78 kcal/mole and a value of 75 kcal/mole for CB(T_1) were used (12). On the basis of these values and the quantitative ($\phi_{ST} = 1.0$) formation of triplet acetone in solution ($\tau \simeq 10^{-6}$ s) (13), diffusion controlled energy transfer from triplet acetone was anticipated to afford at least CB decarbonylation products. Only a small amount of CH_4 was detected (14).

Lee and Lee favor a CB(T_1) lifetime with respect to decarbonylation in the gas phase of approximately 10^{-11} s, based upon a constant rate of C_3 formation at pressures up to 1500 Torr (1). The lack of any evidence to support either quenching of triplet CB or sensitization of or by such a species in the present work could only occur if such a triplet had a lifetime comparable with relaxation times in solution ($\approx 10^{-12}$ to 10^{-13} s). On this basis the existence of such a bound state in the solution photochemistry of CB becomes exceedingly doubtful.

In sum, the data suggest that the reaction mechanism in solution is incompatible with the accepted gas phase mechanism for CB photolysis. It is not possible to define whether this is due to a major difference in the mode of decomposition in the two phases or to an imperfect gas phase mechanism. In discussing the liquid phase results no gas phase data will be considered; however, the following liquid phase observations are considered relevant: (*1*) A rate of ethylene formation which is independent of solvent. (*2*) A rate of cyclopropane formation which depends upon the solvent. When combined with (*1*) this implies a solvent-dependent total quantum yield. (*3*) A C_2H_4/(cyclopropane + propylene) ratio which varies only slightly with wavelength. (*4*) A

Can. J. Chem. Downloaded from www.nrcresearchpress.com by 210.87.254.42 on 09/05/12
For personal use only.

Can. J. Chem. Downloaded from www.nrcresearchpress.com by 210.87.254.42 on 09/05/12
For personal use only.

wavelength-dependent rate of propylene production.

The solvent-independent rate of C_2H_4 formation combined with a solvent-dependent rate of cyclopropane formation implies that the two sets of products do not arise from the same immediate precursor. The constant rate of ethylene formation on the other hand does suggest the common ancestor (S_1*) of both sets of products must react by competitive processes which are equally solvent sensitive. Although photo-reactions in solution are normally not wavelength dependent, there is definite evidence in the cyclopropane/propylene ratio (Table 2) for energy carry-over from the initial photon-substrate interaction, which is independent of concentration and light intensity. In the gas phase it is believed that propylene arises from rearrangement of vibrationally excited cyclopropane. In the liquid phase such a process would be so efficiently quenched as to rule out the observation of any propylene. Hence, it is assumed that propylene comes from the cyclopropane precursor and that the reactions leading to cyclopropane and propylene formation occur at rates comparable to relaxation rates in solution. It is unfortunate that the small amount of propylene (~0.6%) makes it impossible to decide whether its production is solvent sensitive at 3130 Å; the limited data at 2537 Å are also inconclusive on this point. Such information would have been useful in deciding whether propylene in fact does originate from the immediate cyclopropane precursor.

The significant change in cyclopropane/propylene with photon energy is to be contrasted with the relative insensitivity of C_2H_4/(cyclopropane + propylene) to changes in this parameter. This suggests both processes (decarbonylation and ethylene formation) have about the same energy sensitivity and perhaps invariant quantum yields. In the gas phase such a distribution of products is explained by two competing electronic transitions, internal conversion and intersystem cross-over. Internal conversion followed by total quenching no doubt accounts for the fractional total quantum yield observed in the present work. In solution two electronic processes which might lead to the observed products are cross-over from $CB(S_1)$ to the repulsive surfaces representing $\cdot CH_2COCH_2CH_2\cdot$ and $\cdot CH_2CH_2CH_2CO\cdot$, the former being responsible for ethylene formation and the latter the source of cyclopropane and propylene. Stereochemical studies are required to define further whether these processes occur in concerted or stepwise fashion.

Experimental

The CB was an Aldrich chemical used directly from the bottle upon verification of its purity. *n*-Heptane, acetone, and benzene were spectrograde chemicals; other solvents were the best dried reagent grades and known to be free of the products observed in CB photolysis. *cis*-Piperylene and 1,3-cyclohexadiene were purified by gas chromatography. Photolyses were done in 12 mm i.d. Pyrex or quartz tubes as well as tubes of 2 mm i.d.

Experimental wavelengths were obtained and isolated in the following fashion:

3260 Å: Cadmium low pressure lamp with Corning filters 0–54 (2) and 1–64. Less than 0.1% 3130 Å through Pyrex cell.

3130 Å: Medium pressure mercury lamp with Corning filters 0–54 plus 7–54 passed less than 1% 3020 Å through a Pyrex cell.

2537 Å: Low pressure mercury lamp and quartz cell preceded by a 2 mm thick 7910 Vycor plate and 1 cm thick Cl_2 gas filter cell.

Analyses for C_2H_4, propylene, and cyclopropane were done by aliquot syringe injections on a squalane column and F.I.D.

The author wishes to acknowledge the assistance provided by G. Fried and L. Schallig in carrying through portions of the experimental work. The many discussions with Dr. A. T. Blades have also been of particular value.

1. (*a*) NORMAN LEE and E. K. C. LEE. J. Chem. Phys. **50**, 2094 (1969) and references quoted therein; (*b*) JOHN C. HEMMINGER, CRAIG F. RUSBULT, and E. K. C. LEE. J. Amer. Chem. Soc. in press.
2. T. HOWARD MCGEE. J. Phys. Chem. **72**, 1621 (1968).
3. R. J. CAMPBELL, E. W. SCHLAG, and B. W. RISTOW. J. Amer. Chem. Soc. **89**, 5098 (1967).
4. N. J. TURRO and R. M. SOUTHAM. Tetrahedron Lett. 545 (1967) and references quoted therein.
5. A. SINGH and G. R. FREEMAN. J. Phys. Chem. **69**, 666 (1965).
6. P. DUNION and C. N. TRUMBORE. J. Amer. Chem. Soc. **87**, 4211 (1965).
7. R. SIMONAITIES, C. W. COWELL, and J. N. PITTS. Tetrahedron Lett. 3751 (1967).
8. DONALD VALENTINE, NICHOLAS J. TURRO, JR., and GEORGE S. HAMMOND. J. Amer. Chem. Soc. **86**, 5202 (1964).
9. D. ROBERT COULSON and N. C. YANG. J. Amer. Chem. Soc. **88**, 4511 (1966).
10. G. O. SCHENK, *et al.* Z. Naturforsch. **19b**, 18 (1964).
11. NICHOLAS J. TURRO. Molecular photochemistry. W. A. Benjamin Inc., New York, N.Y. 1967. p. 212.
12. NICHOLAS J. TURRO. *In* Technique of organic chemistry. A. Weissberger and P. A. Leermakers, Editors. Vol. XIV. Interscience Publishers, New York, N.Y. 1969.
13. RAYMOND F. BORKMAN and DAVID R. KEARNS. J. Amer. Chem. Soc. **88**, 3467 (1966).
14. R. PIECK and E. W. R. STEACIE. Can. J. Chem. **33**, 1304 (1955).

Can. J. Chem. Downloaded from www.nrcresearchpress.com by 210.87.254.105 on 09/05/12
For personal use only.

The hydrogenation of allene. III. The reaction of allene with hydrogen catalyzed by nickel, copper, and their alloys

R. S. MANN AND A. M. SHAH
Department of Chemical Engineering, University of Ottawa, Ottawa, Canada

Received May 4, 1970

The reaction between allene and hydrogen over unsupported nickel, copper, and their alloys has been investigated in a static constant volume system between 26 and 131 °C for a wide reactant ratios. The orders of reaction with respect to hydrogen and allene were one and zero, respectively, and temperature independent. The reaction over metals and their alloys is largely simple hydrogenation, the early stages being principally a selective formation of propylene, with small yields of reduced polymers of allene. The overall activation energies varied between 4.8 and 11.8 kcal/g-mole. Selectivity was highest with copper and least with nickel. The amount of allene polymerized was not related in any particular way to the copper content of alloy.

Canadian Journal of Chemistry, **48**, 3324 (1970)

Introduction

The kinetics of catalytic hydrogenation of olefins and alkynes has been extensively studied in the past. However, very little work has been reported about the hydrogenation of allene over metals and their alloys. Bond and Sheridan (1) studied the hydrogenation of allene over pumice supported nickel, palladium, and platinum catalysts. Mann and To (2) have reported the kinetics of allene hydrogenation over pumice supported transition metal catalysts. Recently, Mann and Tiu (3) investigated the kinetics of allene hydrogenation, catalyzed by unsupported nickel, iron, and cobalt catalysts. They found that the reaction orders were one and zero with respect to hydrogen and allene, respectively, and that the selectivity was highest with nickel, and least with cobalt. In the present study, we have examined the hydrogenation of allene over nickel, copper, and their alloys. Here we report the kinetics of the reaction, and the yields of propylene and propane over a wide range of conditions.

Experimental

The apparatus and experimental techniques were the same as described by Mann and Naik (4). Homogeneous nickel–copper alloys, pure nickel, and copper powders were prepared by the method of Best and Russell (5). The mixed basic carbonates (in case of alloys), or basic carbonates (for nickel and copper) precipitated by ammonium bicarbonate from their nitrate solutions, containing appropriate quantities of the nitrate, were dried at 105 °C overnight. The basic carbonates were decomposed to oxides by calcination at 500 °C in a muffle furnace, and then reduced in a hydrogen stream for 24 h at 400 °C. Quantitative analysis of the products was carried out by means of Fisher gas partitioner, maintained on the top of a Fisher thermal stabilizer, maintained at 40 °C, as described by Mann and Khulbe (6). The two columns employed were a 14 ft long 30% hexamethylphosphramide (HMPA) on 60–80 mesh Fisher columnpak and a blank. Helium at the rate of 60 ml/min at a pressure of 20 p.s.i.g. was used as the carrier gas.

The amount of polymers formed (allene lost) was calculated as the difference between the initial allene pressure and the pressure of hydrocarbons in the products. The pressure of hydrocarbons was the sum of the unreacted allene, propylene, and propane in the products. These polymers could not be detected by HMPA column under the experimental conditions.

X-Ray analysis of the reduced nickel–copper oxides showed that solid solutions closely corresponding to the expected compositions were indeed formed. None of the alloys contained detectable free metal, and all had face centered cubic structure. The lattice constants and calculated composition for these catalysts are given in Table 1. These checked very well with the expected values. Surface areas of these catalysts were determined by B.E.T. method and are given in Table 1.

Results

(a) Pressure–Time Curves

The various types of pressure–time curves observed in the hydrogenation of allene over supported and unsupported metals of the eighth group have been discussed in detail previously (2, 3). The pressure–time curves observed in the present investigation of hydrogenation of allene (Fig. 1) were of Type III (curve *AD* and *AE*) regardless of (*i*) the initial reactant ratio, (*ii*) the order of admission of the reactant, and (*iii*) the temperature. However, in the case of 80% Ni – 20% Cu catalyst a bilinear type of pressure–time curve (Type II, curve *ABC*) was always obtained for hydrogen/allene ratio greater than 1. A similar type of curve was also observed by Bond and Wells (7) in acetylene hydrogenation over alumina

TABLE 1

Characteristics of the catalysts, reaction orders, and activation energies*

Catalyst Ni–Cu alloy							Average reaction order		
Composition (% Cu)	Weight (g)	Lattice parameter (Å)	Surface area (m^2/g)	Temperature range (°C)	Specific rate k (min^{-1} m^{-2})	Activation energy E (kcal/g-mole)	n (± 0.008)	m (± 0.05)	$\log_{10} A$
0	0.1098 (0.0515)†	3.521	0.34	55–116 (88–112)	0.1033	6.79	0.994	0.00	3.0012
10	0.1038 (0.0520)†	3.530	2.09	26–108 (106–128)	0.2040	6.10	0.997	0.00	3.6327
20	0.1102 (0.1500)†	3.538	2.42	26–55 (47–123)	0.2164	5.61	0.990	0.00	3.4005
30	0.2530	3.543	1.39	40–66	0.0947	5.22	0.990	0.00	2.5447
50	0.4208	3.570	1.12	36–116	0.1041	4.82	0.990	0.00	2.2298
75	0.6958	3.590	5.20	62–124	0.0070	7.89	1.000	0.00	3.8161
100	1.0019	3.610	0.96	83–131	0.0051	11.77	0.990	0.00	5.4145

*n = reaction order with respect to hydrogen; m = reaction order with respect to allene; k = specific reaction rate in min^{-1} m^{-2} at 60 °C; $r_0 = kP_{H_2}{}^nP_{C_3H_4}{}^m$; A = frequency factor in min^{-1} g^{-1}.

†Amount of catalyst used during analysis.

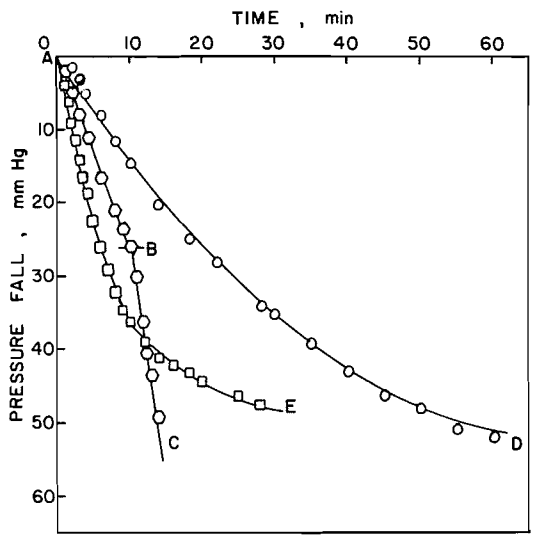

FIG. 1. Pressure–time curves, curve AD Cu powder P_{H_2} = 50 mm Hg, $P_{C_3H_4}$ = 50 mm Hg, T = 131.0 °C; curve ABC Ni = 80%, Cu = 20%, P_{H_2} = 80 mm Hg, $P_{C_3H_4}$ = 50 mm Hg, T = 55.0 °C; curve AE Ni powder P_{H_2} = 100 mm Hg, $P_{C_3H_4}$ = 50 mm Hg, T = 116.0 °C.

supported platinum catalyst, and by Mann and Khulbe (6, 8, 9) in the methylacetylene hydrogenation over cobalt and nickel–copper alloys and in the ethylacetylene hydrogenation over nickel. In the first stage (AB) the reaction was mainly the hydrogenation of allene to propylene and in the second region (BC) subsequent hydrogenation of propylene to propane. In the region BC the rate was accelerated.

(b) Orders of Reaction by the Initial Rate Method

Using a fixed allene pressure (50 mm) and a wide range of hydrogen pressure (30–200 mm) the order of reaction with respect to hydrogen (n) was determined at several temperatures. Similarly, the reaction order with respect to allene (m) was determined at different temperatures using a fixed hydrogen pressure (50 mm) and varying allene pressure (40–130 mm). The reaction orders with respect to hydrogen and allene were 1 and 0, respectively, and were temperature independent (Table 1).

(c) Temperature Dependence of Rate Constants

Plots of $\log_{10}$ specific reaction rate against the reciprocal of absolute temperature were good straight lines over a wide range of temperatures for all catalysts, satisfying the Arrhenius equation. The apparent activation energies for all the catalysts are given in Table 1 (Fig. 2).

A very satisfactory "compensation effect" exists between all the activation energies and the logarithmic frequency factors (Fig. 3).

(d) The Dependence of Activity on Composition of Nickel–Copper Alloys

The hydrogenation of allene has been investigated over seven different unsupported nickel–

Can. J. Chem. Downloaded from www.nrcresearchpress.com by 210.87.254.105 on 09/05/12
For personal use only.

Can. J. Chem. Downloaded from www.nrcresearchpress.com by 210.87.254.105 on 09/05/12
For personal use only.

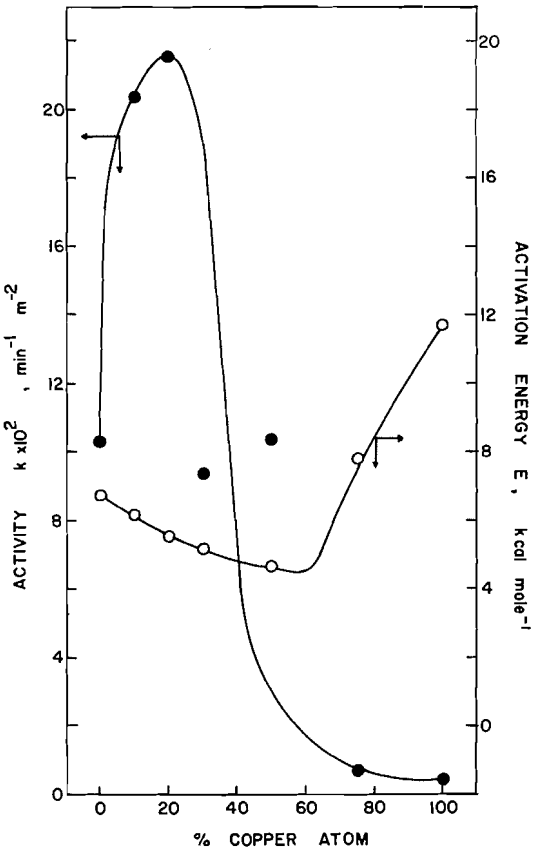

FIG. 2. Effect of copper content of the binary Ni–Cu alloys on the activity and the activation energy.

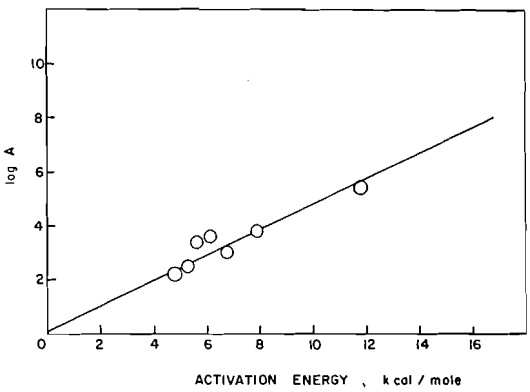

FIG. 3. Activation energy *vs.* $\log_{10} A$.

copper alloys. The results are summarized in Table 1. The striking feature of these results is that the catalytic activity rapidly increased with the slight increase of copper content (up to 20% Cu) in the alloy, and then decreased with increased copper content (Fig. 2). Similar behavior was observed by Mann and Khulbe (8) in methylacetylene hydrogenation over nickel–copper alloys. However, Best and Russell (5) observed the maximum activity in the hydrogenation of ethylene over nickel–copper alloys in the copper rich region.

(e) Course of Reaction and Dependence of Selectivity upon Pressure-fall

The course of reaction and the dependence of selectivity upon pressure fall was studied for hydrogen/allene ratios of 1 and 2 over various catalysts by analyzing the reaction products at different pressure falls. The selectivity (S) has been defined as the ratio of propylene to propylene plus propane. Thus

$$S = \frac{P_{\text{propylene}}}{P_{\text{propylene}} + P_{\text{propane}}}$$

The product distribution during the course of reaction for hydrogen/allene ratio of 2 is shown in Fig. 4 (A) and (B). Propylene, propane, and some polymers were observed as the initial products of the reaction, propylene being the major product. Figure 5 shows the dependence of selectivity upon the pressure fall for different alloys, for hydrogen/allene ratio of 2. Selectivity decreased with the pressure fall for all alloys. However, it was independent of pressure fall for all alloy compositions for hydrogen/allene ratio of 1. The amount of allene polymerized increased with the progress of the reaction for hydrogen/allene ratio of 1 and 2.

(f) The Dependence of Selectivity upon Initial Pressures of Hydrogen and Allene

Measurements were made of the selectivity of nickel, copper, and nickel–copper alloy catalysts at several temperatures as a function of initial hydrogen pressure by using a fixed allene pressure (50 mm) and varying hydrogen pressure between 40–190 mm. The products were analyzed when the total pressure fall was equal to 30 mm. The results are shown in Fig. 6. The selectivity was independent of initial hydrogen pressure for copper, but it decreased with increased hydrogen pressure for all other catalysts. While the amount of allene polymerized was independent of initial hydrogen pressure for the catalysts containing 30 and 50% copper, it increased with increased hydrogen pressure for other catalysts.

Similarly the variation of the selectivity with

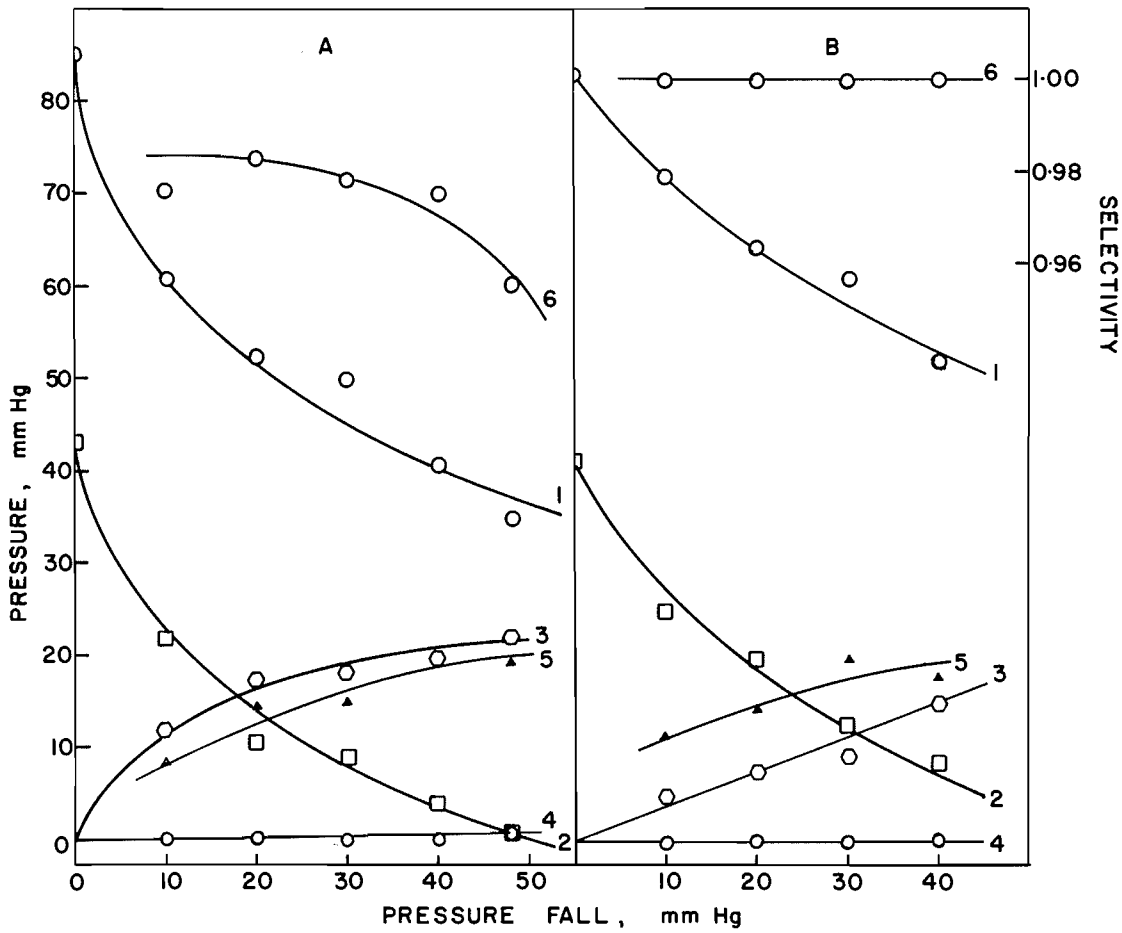

FIG. 4. Distribution of products during the course of reaction, $P_{H_2} = 100$ mm, $P_{C_3H_4} = 50$ mm. Ni powder, $T = 112.0$ °C; Cu powder, $T = 131.0$ °C. Curve *1*, hydrogen; curve *2*, allene; curve *3*, propylene; curve *4*, propane; curve *5*, polymer; curve *6*, selectivity.

allene pressure was determined by using a fixed hydrogen pressure (50 mm) and varying allene pressure (40–160 mm) and analyzing the products for a total pressure fall of 20 mm (Fig. 7). The selectivity was independent of allene pressure for all catalysts. The amount of allene polymerized, increased with increased allene pressures for nickel, copper, and the alloy containing 10% copper. For all other catalysts, it was independent of initial allene pressure.

(g) The Dependence of Selectivity upon Temperature

The temperature dependence of the selectivity for hydrogen/allene ratios of 1 and 2 was studied by analyzing the products at several temperatures at the pressure fall of 20 mm of total pressure. The results of the investigation are shown in Fig. 8. While the selectivity increased with increasing temperature for 20% copper, it decreased with increasing temperature for nickel for hydrogen/allene ratios of 1 and 2. For others, the selectivity was temperature independent when hydrogen/allene ratio was 1. When the hydrogen/allene ratio was 2, while the selectivity increased with increasing temperature for the alloys containing 50 and 75% copper, it decreased with increasing temperatures for the catalysts containing 10 and 30% copper. For copper the selectivity was one, and independent of temperature for hydrogen/allene ratios of 1 and 2. The extent of allene polymerization increased with increased temperature for all catalysts for hydrogen/allene ratio of 1. While it was independent of temperature for

Can. J. Chem. Downloaded from www.nrcresearchpress.com by 210.87.254.105 on 09/05/12
For personal use only.

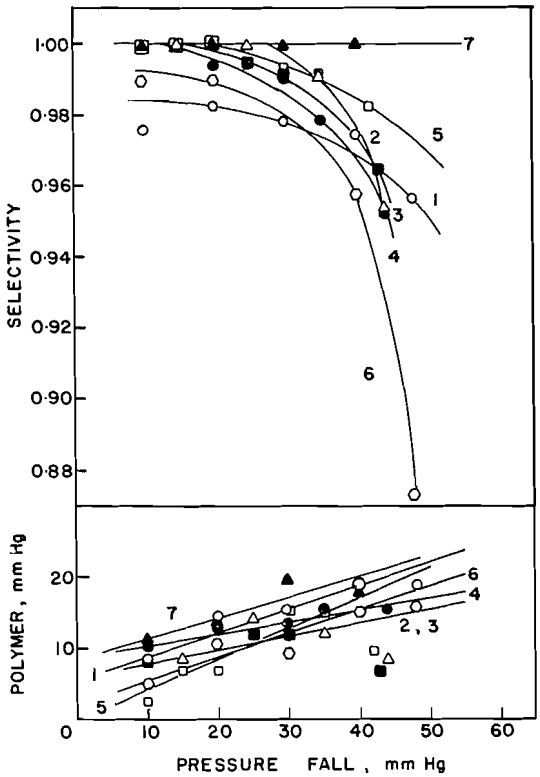

FIG. 5. Dependence of selectivity upon pressure fall, P_{H_2} = 100 mm, $P_{C_3H_4}$ = 50 mm. Curve *1*, Ni powder, ○, T = 112.0 °C; curve *2*, Ni = 90%, Cu = 10%, △, T = 128.0 °C; curve *3*, Ni = 80%, Cu = 20%, ■, T = 123.0 °C; curve *4*, Ni = 70%, Cu = 30%, ●, T = 123.0 °C; curve *5*, Ni = 50%, Cu = 50%, □, T = 116.0 °C; curve *6*, Ni = 25%, Cu = 75%, ⬡, T = 84.0 °C; curve *7*, Cu powder, ▲, T = 131.0 °C.

copper, it increased with increased temperature for other catalysts for hydrogen/allene ratio of 2.

(h) Polymerization

The amount of allene polymerized was calculated from the allene loss during the reaction. There seems to be no direct relationship between the polymer formation and alloy composition. However, the amount of allene polymerized was higher for pure metals (Ni, Cu) than for their alloys.

Discussion

The first order reaction with respect to hydrogen and zero order with respect to allene indicate that the latter was the more strongly adsorbed reactant and its surface coverage was high, whereas hydrogen was weakly adsorbed in comparison and its surface coverage was correspondingly low.

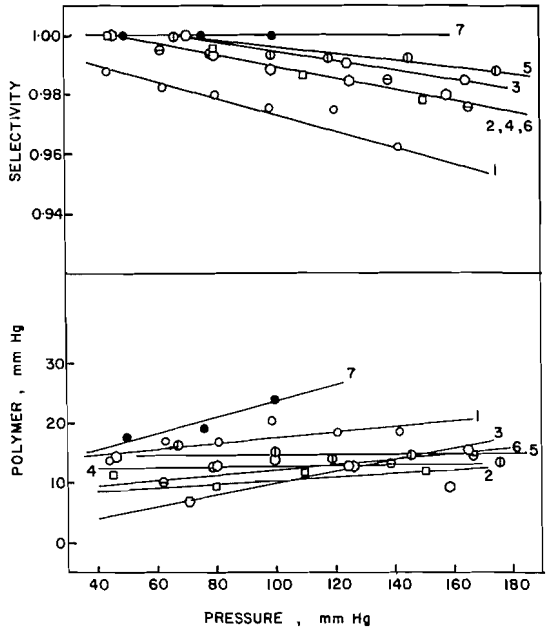

FIG. 6. Dependence of selectivity upon hydrogen pressure. Curve *1*, Ni powder, ○, T = 112.0 °C; curve *2*, Ni = 90%, Cu = 10%, □, T = 128.0 °C; curve *3*, Ni = 80%, Cu = 20%, ⬡, T = 123.0 °C; curve *4*, Ni = 70%, Cu = 30%, ⬡, T = 123.0 °C; curve *5*, Ni = 50%, Cu = 50%, ⊙, T = 116.0 °C; curve *6*, Ni = 25%, Cu = 75%, ⊖, T = 124.0 °C; curve *7*, Cu powder, ●, T = 131.0 °C.

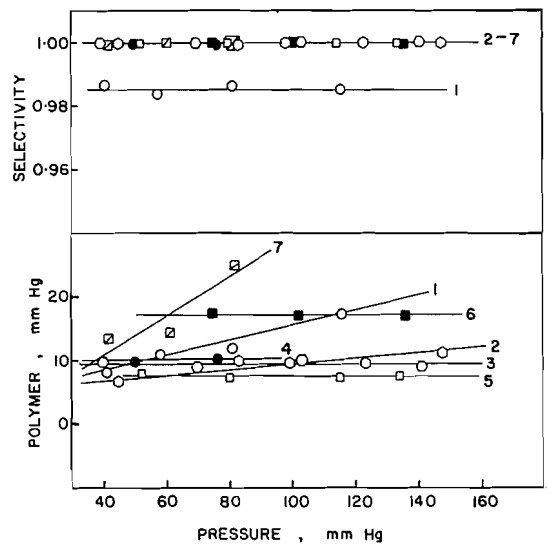

FIG. 7. Dependence of selectivity upon allene pressure. Curve *1*, Ni powder, ○, T = 112.0 °C; curve *2*, Ni = 90%, Cu = 10%, ⬡, T = 128.0 °C; curve *3*, Ni = 80%, Cu = 20%, ⬡, T = 123.0 °C; curve *4*, Ni = 70%, Cu = 30%, ●, T = 123.0 °C; curve *5*, Ni = 50%, Cu = 50%, □, T = 116.0 °C; curve *6*, Ni = 25%, Cu = 75%, ■, T = 124.0 °C; curve *7*, Cu powder, ⊠, T = 131.0 °C.

Can. J. Chem. Downloaded from www.nrcresearchpress.com by 210.87.254.105 on 09/05/12
For personal use only.

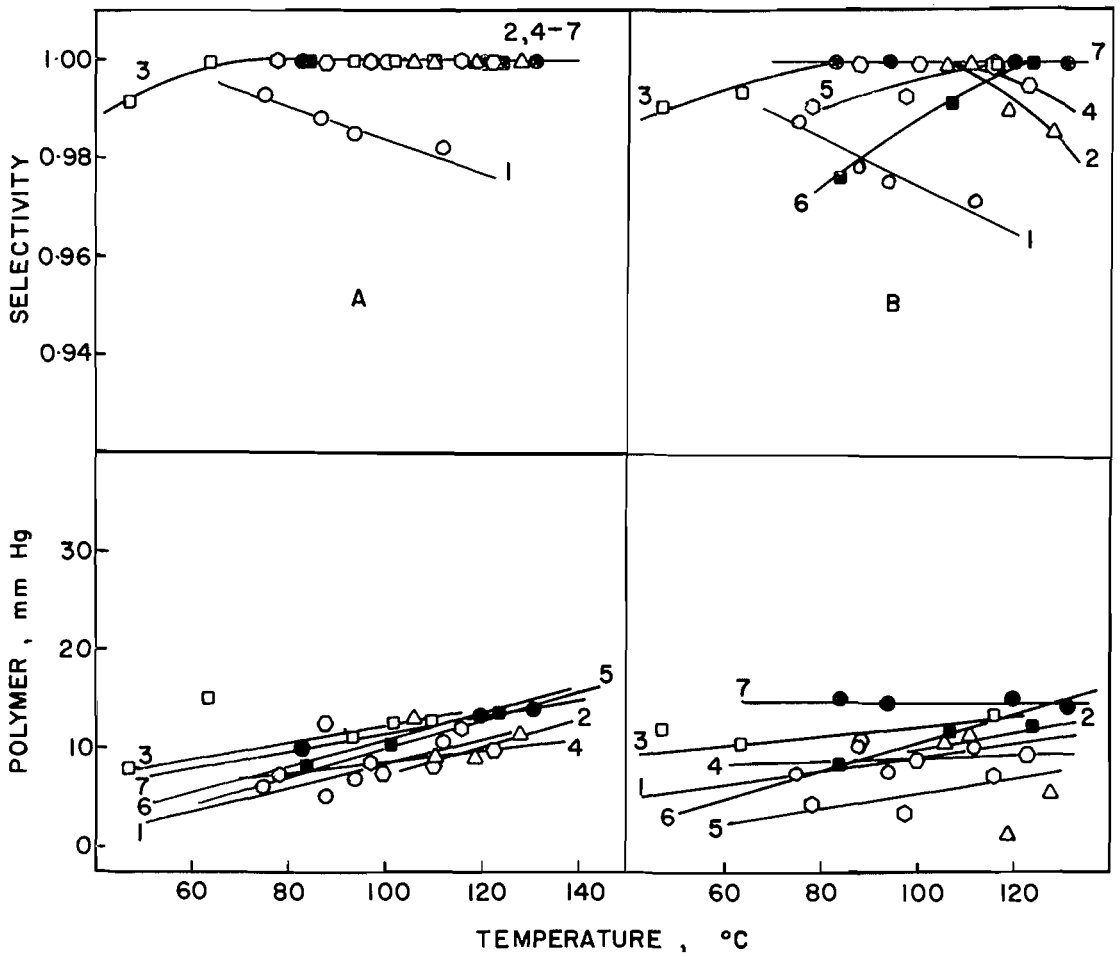

FIG. 8. Dependence of selectivity upon temperature: *A*: P_{H_2} = 50 mm; $P_{C_3H_4}$ = 50 mm; *B*: P_{H_2} = 100 mm; $P_{C_3H_4}$ = 50 mm. Curve *1*, Ni powder, ○; curve *2*, Ni = 90%, Cu = 10%, △; curve *3*, Ni = 80%, Cu = 20%, □; curve *4*, Ni = 70%, Cu = 30%,⬡; curve *5*, Ni = 50%, Cu = 50%,⬡; curve *6*, Ni = 25%, Cu = 75%, ■; curve *7*, Cu powder, ●.

The activation energy for the unsupported nickel (6.8 kcal/g-mole) compares well with the previously reported (3) value (6.5 kcal/g-mole) for allene hydrogenation. However, no comparison is possible for the activation energies for other catalysts (for allene hydrogenation) due to lack of availability of the published data.

A sudden increase in the activity of the nickel catalyst was observed with slight addition of copper. The activity appeared to increase on small addition of copper (Fig. 2) pass through a maximum for about 20% copper, and then decrease with further addition of copper. Several investigators (5, 8, 10, 11) have observed similar phenomenon. According to Dowden *et al.* (12) the holes in d-band are responsible for the catalytic activity of the transition metals. Dowden *et al.* regulated the concentration of d-holes by making alloys. The X-ray analysis of the alloys revealed that the alloys were homogeneous solid solutions. The catalytic activity of nickel–copper alloys in hydrogenation reactions has been investigated by several workers (13, 14). However, their results were not always in agreement with each other. For instance, it has been reported that the catalytic activity decreases progressively, as the concentration of d-holes falls until a sudden decrease marks the filling of the d-band or in some cases it exhibits one or two maxima depending on the catalyst (15). Takai *et al.* (14)

Can. J. Chem. Downloaded from www.nrcresearchpress.com by 210.87.254.105 on 09/05/12
For personal use only.

Can. J. Chem. Downloaded from www.nrcresearchpress.com by 210.87.254.105 on 09/05/12
For personal use only.

investigated the catalytic activities for the liquid phase hydrogenation of maleic acid, allyl alcohol, and acetone over nickel–copper alloys. They observed an increase in the activity on small addition of copper. They interpreted the activity pattern for the catalyst containing 5–60% copper on the basis of Dowden's theory for maleic acid and allyl alcohol hydrogenation. But in case of acetone, the activity was independent of d-holes. However, Campbell and Emmett (15), while studying the hydrogenation of ethylene over nickel–copper films, observed a minimum in the activity composition curve for an alloy containing approximately 25–30% nickel.

Considering the catalyst structure, it was found that the catalytic activity of copper catalyst having a face centered cubic structure was nearly zero, whereas nickel having the same face centered cubic structure was much more active than copper. According to Beeck's (16) correlation between the catalytic activity of metals and their lattice parameters, the activity of the series of alloys would be expected to increase markedly between pure nickel and copper. The results of the present investigation are contrary to this also.

Takeuchi *et al.* (17) observed that though the activity pattern observed in the hydrogenation of ethylene and benzene over massive nickel–copper alloys was similar to the one predicted by Dowden *et al.*, it was quite complicated over granular alloys. They have also shown that the heat of adsorption of hydrogen and the catalytic activity of the hydrogenation of ethylene are closely related to the composition of the alloy. In another paper, Takeuchi (18) attempted to correlate the heat of adsorption of hydrogen with the rate of hydrogenation of ethylene and the activation energy. Takai and Yamanaka (14) found that the ability of nickel metal to absorb hydrogen increased with increasing amount of copper with a maximum for an alloy containing about 80% copper. It then rapidly decreased with further addition of copper. Recently Takeuchi *et al.* (19) measured the electric resistance of nickel–copper alloys, but they could not get a simple relationship between the electric resistance and the catalytic activity. There appears to be no relationship between the heat of adsorption and electric resistance with the activity of the catalysts in the allene hydrogenation.

Considering the concentration of d-band holes, Bond and Mann (20) and Mann and Khulbe (8) have suggested three idealized possible forms of activity pattern in the activity–composition diagram. In one of the activity patterns, case *B*, it is suggested that as the d-band is filled, the binding strength decreases, and the activity increases reaching a maximum before the d-band is completely filled. As soon as the d-band is completely filled, the activity becomes very nearly equal to that of copper. This type of pattern has been confirmed by Couper and Eley (21) in the para-hydrogen conversion over palladium–gold alloys and by Mann and Khulbe (8) in the methylacetylene hydrogenation over nickel–copper alloys. The results of the present investigation are also very similar. However, there may be several other factors present. These opposing effects may lead to an earlier maximum.

While the selectivity increased with increased amount of copper, the activity increased to a maximum at about 20% copper, and thereafter decreased. It was observed that the selectivity and the activity are not related. It appears that besides the activity, some other factors, such as different types of active centers, lattice defects, may play an important role in controlling the selectivity.

The experimental results largely confirm the expected similarity between the hydrogenation of acetylene, methylacetylene, and allene. Hence, it may be presumed that the reaction mechanism is the same.

The authors are grateful to the National Research Council of Canada for the financial support of the project, through grant no. A-1125 (to R.S.M.) and a post graduate scholarship (to A.M.S.) and to Messrs. J. F. Rowland and R. K. Collings of Energy, Mines, and Resources Department, for X-ray analysis and the surface area measurements of the nickel–copper alloys, respectively.

1. G. C. Bond and J. Sheridan. Trans. Faraday Soc. **48**, 658 (1962).
2. R. S. Mann and D. E. To. Can. J. Chem. **46**, 161 (1968).
3. R. S. Mann and D. E. Tiu. Can. J. Chem. **46**, 3249 (1968).
4. R. S. Mann and S. C. Naik. Can. J. Chem. **45**, 1023 (1967).
5. R. J. Best and W. W. Russell. J. Amer. Chem. Soc. **76**, 838 (1954); **85**, 2881 (1963).
6. R. S. Mann and K. C. Khulbe. Can. J. Chem. **45**, 2755 (1967).
7. G. C. Bond and P. B. Wells. J. Catal. **4**, 211 (1965).
8. R. S. Mann and K. C. Khulbe. Can. J. Chem. **46**, 623 (1968).
9. R. S. Mann and K. C. Khulbe. J. Catal. **10**, 401 (1968).

10. W. K. HALL and P. H. EMMETT. J. Phys. Chem. **63**, 1102 (1959).
11. G. M. SCHWAB and W. BRENNECKE. Z. Phs. Chem. **824**, 393 (1933).
12. D. A. DOWDEN and P. W. REYNOLDS. Discuss. Faraday Soc. **8**, 184 (1950).
13. E. TAKAI. Sci. Papers Inst. Phys. Chem. Res. Japan, **62**, 24 (1968).
14. E. TAKAI and T. YAMANAKA. Sci. Papers Inst. Phys. Chem. Res. Japan, **55**, 194 (1961).
15. J. B. CAMPBELL and P. H. EMMETT. J. Catal. **7**, 252 (1967).
16. O. BEECK. Rev. Mod. Phys. **17**, 61 (1945).
17. T. TAKEUCHI, I. SAKAGUCHI, I. MIYOSHI, and T. TAKABATAKO. Bull. Chem. Soc. Japan, **35**, 1390 (1962).
18. T. TAKEUCHI. Bull. Chem. Soc. Japan, **38**, 322 (1965).
19. T. TAKEUCHI, Y. TEZUCKA, and O. TAKAYASU. J. Catal. **14**, 126 (1969).
20. G. C. BOND and R. S. MANN. J. Chem. Soc. 3566 (1959).
21. A. COUPER and D. D. ELEY. Discuss. Faraday Soc. **8**, 172 (1950).

Can. J. Chem. Downloaded from www.nrcresearchpress.com by 210.87.254.105 on 09/05/12
For personal use only.

Can. J. Chem. Downloaded from www.nrcresearchpress.com by 210.87.254.42 on 09/05/12
For personal use only.

Kinetics and mechanism of electrophilic bromination of acetylenes

JAMES A. PINCOCK AND KEITH YATES
Department of Chemistry, University of Toronto, Toronto 181, Ontario

Received June 16, 1970

The rates of addition of molecular bromine in acetic acid to a number of acetylenes have been found to follow the general equation

$$-\mathrm{d(Br_2)}/\mathrm{d}t = [\text{acetylene}](k_2[\mathrm{Br_2}] + k_3[\mathrm{Br_2}]^2 + k_{\mathrm{Br}^-}[\mathrm{Br_2}][\mathrm{Br}^-])$$

In the absence of bromide ion and at low bromine concentrations ($< 2 \times 10^{-4}$ *M*), only the k_2 process is observable. These k_2 values for a series of ring-substituted phenylacetylenes are correlated well with σ^+ values and give a ρ value of -5.17 which is interpreted in terms of a transition state leading to a vinyl cation intermediate. As expected from this intermediate, both *cis* and *trans* dibromide products are formed and the bromoacetates are only of the Markownikoff type (1-acetoxy-1-phenylethylene derivatives). An ion pair scheme has been presented to account for the variation in product composition with substrate structure.

In contrast to these results for phenylacetylenes, a cyclic bromonium ion intermediate is postulated for alkyl acetylenes on the basis of only *trans* dibromide formation for 3-hexyne and 1-hexyne.

The k_{Br^-} values have also been obtained for the ring-substituted phenylacetylenes as well as 3-hexyne. For all the substrates studied, this k_{Br^-} process represents a bromide ion catalyzed attack of molecular bromine in an Ad_E3 mechanism. Thus only *trans* dibromide products are formed from this rate process. The non-linear σ^+ plot for these values has been interpreted in terms of change in transition state structure with substituent.

Canadian Journal of Chemistry, **48**, 3332 (1970)

Introduction

As recent reviews by de la Mare and Bolton (1) and Fahey (2) indicate, the electrophilic addition of bromine to acetylenes has received much less attention than the corresponding reaction with olefins. Furthermore, the results available are so incomplete and, in some cases contradictory, that little confidence can be placed in any of the postulated mechanisms. Thus, Robertson *et al.* (3) have suggested that the rate equation for the addition of bromine to several substituted acetylenes in acetic acid is similar to that observed for olefins (first order in substrate and both first and second order in bromine) and that the overall rates are in the expected order for an electrophilic process. In contrast, Sinn *et al.* (4) have measured rates for the bromination (by a process second order in bromine) of diphenylacetylenes in bromobenzene, that are best interpreted in terms of a nucleophilic reaction. Only slightly more information is available on the stereochemistry of the products of this addition reaction. Bergel'son and Nazarov (5) have reported that the addition of bromine to 3-hydroxypropyne, 3-hydroxy-3-methylbutyne, propyne, and acetylene gives exclusively *trans* addition under conditions that favor an ionic reaction. On the other hand, results for the bromination of diphenylacetylene by molecular bromine (6) and *N*-bromosuccinimide (7) in acetic acid indicate non-stereospecific addition.

As the limited results available demonstrate, a systematic examination of product stereochemistry under conditions of known kinetic control is necessary before any definite mechanism for the addition of bromine to acetylenes can be postulated. Therefore, in the present work, rates and product compositions are presented for the bromination of a number of phenyl and alkyl acetylenes in acetic acid with and without added bromide ion salts. The choice of this solvent system was made on the basis that the results would then be directly comparable with similar results for olefin substrates where the main details of the reaction are well understood (1, 2, 8, 9).

Results and Discussion

(1) Rates in the Absence of Bromide Ion Salts

Robertson *et al.* (3) have reported that the addition of bromine to acetylenes in acetic acid follows the rate eq. 1. In agreement with this

$$[1] \quad -\mathrm{d}[\mathrm{Br_2}]/\mathrm{d}t = [\text{acetylene}](k_2[\mathrm{Br_2}] + k_3[\mathrm{Br_2}]^2)$$

equation, curved rate plots were obtained when either simple first or second order dependence on bromine concentration was assumed for the

Can. J. Chem. Downloaded from www.nrcresearchpress.com by 210.87.254.42 on 09/05/12
For personal use only.

TABLE 1

Second order rate constants, k_2, for the bromination of acetylenes in acetic acid

Substrate	n*	Temperature (°C)	$k_2 \times 10^3$† (M^{-1} s^{-1})
3-Hexyne	3	17.9	4.18±0.20
	3	24.8	5.84±0.10
	3	39.8	12.4±0.5
1-Hexyne	3	24.8	0.174±0.011
t-Butylacetylene	3	24.8	0.285±0.013
4-Me PA‡	3	24.8	247±8
3,4-Benzo PA‡	3	24.8	153±1
4-F PA‡	3	24.8	11.3±0.3
3-Me PA‡	4	24.8	14.3±0.8
PA‡	3	24.8	4.33±0.06
	3	39.8	11.6±0.3
4-Cl PA‡	3	24.8	1.54±0.16
4-Br PA‡	3	24.8	1.13±0.03
	3	39.8	3.27±0.04
Methylphenyl-acetylene	2	17.3	1.37±0.02
	5	24.8	2.46±0.06
	3	29.9	3.63±0.07
	4	39.8	6.8±0.3

*n is the number of determinations.
†The errors quoted are the average deviations.
‡PA represents phenylacetylene.

bromination of methylphenylacetylene at a bromine concentration of approximately 1×10^{-2} M. However, by working at low bromine concentration (less than 3×10^{-4} M) only the first term in eq. 1 makes a significant contribution to the observed rate. Using pseudo-order conditions ([acetylene] $\gg$ [Br_2]), excellent first order plots of log $(A - A_\infty)$ values *vs.* time were obtained. The rate constants, k_2, for the acetylenes studied are listed in Table 1.

Using the values of k_2 for methylphenylacetylene, the rate constants, k_3, can be evaluated from kinetic runs at higher bromine concentration where both k_2 and k_3 contribute to the overall rate equation. Integration of eq. 1 and rearranging gives eq. 2, where $\log Y = k_2't/2.303$, $k_2' = k_2$ [acetylene], $k_3' = k_3$ [acetylene] and

$$[2] \qquad k_3' = \frac{k_2'\left(\frac{[Br_2]}{[Br_2]_0} Y - 1\right)}{[Br_2](1 - Y)}$$

$[Br_2]_0$ is the bromine concentration at $t = 0$. The k_3' values can be calculated for each value of [Br_2] and t. These values are then averaged to obtain k_3' and, hence, k_3 for any given run. The results for methylphenylacetylene are shown in Table 2. As the average deviations indicate, these are less reliable rate constants than those obtained by a graphical method. However, the accuracy is sufficient to justify accepting eq. 1 as the general rate expression for the bromination of acetylenes in acetic acid. Values of k_3 were not determined for the other acetylenes.

TABLE 2

Third order rate constants, k_3, for the bromination of methylphenylacetylene in acetic acid

Temperature (°C)	n*	k_3† (M^{-2} s^{-1})
17.3	3	2.3±0.2
24.8	7	2.6±0.2
29.2	3	3.2±0.2
39.8	3	3.6±0.1

*n is the number of determinations.
†The errors quoted are the average deviations.

The effect of substituents on the k_2 values of the bromination reaction can be evaluated from the Hammett plot in Fig. 1. The ρ value (*vs.* σ^+) is −5.17 (correlation coefficient, 0.997). The σ^+ values are those given by Brown and Okamoto (10). Their listing does not, however, include a value for the 3,4-benzo group (β-naphthylacetylene). In a recent study of substituent effects in polycyclic aromatic compounds (11), values of σ^+ ranging from −0.135 to −0.280 are quoted for this group, implying that the value may reflect the operation of variables that differ from reaction to reaction. Using the rate constant of 153×10^{-3} M^{-1} s^{-1} obtained for β-naphthylacetylene, a σ^+ value of −0.28 can be obtained from the log k_2 *vs.* σ^+ correlation for the other substituents. In effect, this determines a value of σ^+ for the 3,4-benzo substituent which will be used in a correlation described below. The value of −0.28 is similar to those for aromatic nitration (−0.28) and bromination (−0.27). Since the addition reaction is a side chain reaction, the lower values of −0.20 or −0.135 obtained for the solvolysis of side chain derivatives might seem more reasonable. However, the point would then deviate markedly from the correlation in Fig. 1.

Although Sinn *et al.* have concluded that the bromination of diphenylacetylene derivatives is a nucleophilic reaction (4), the large negative ρ value and the good σ^+ correlation clearly demonstrate that the bromination of phenylacetylenes in acetic acid is an electrophilic reaction. The two cases are, however, not strictly comparable since in bromobenzene the reaction

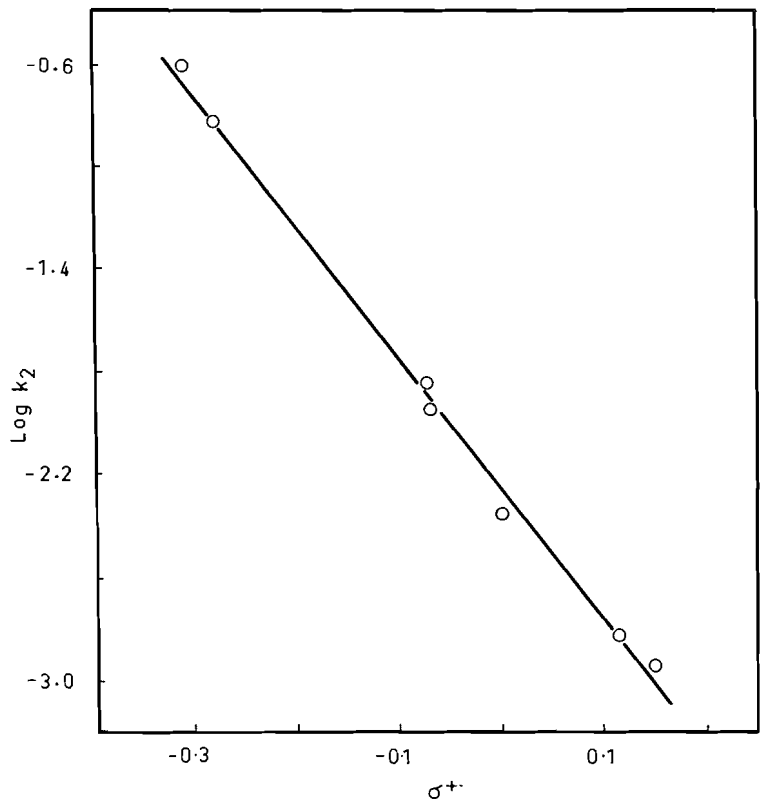

FIG. 1. Plot of log k_2 *vs.* σ^+ for the bromination of phenylacetylenes in acetic acid.

is second order in bromine whereas the rate constants obtained in this work are for the simpler first order in bromine process. In the corresponding olefin systems, the ρ^+ values are also quite different. Thus, for the bromination of styrenes in acetic acid ρ^+ value for the k_2 rate constants is approximately -4.5 (9, 12) whereas for the stilbenes the values for the k_3 process (13) are -0.67 in carbon tetrachloride and -1.99 in bromobenzene.

The ρ^+ value of -5.2 for the bromination of acetylenes in acetic acid can be compared with values for similar systems. The hydration of acetylenes has a ρ^+ value of approximately -4.5 (14, 15). As well, a ρ^+ value of -3.6 has been obtained by Miller and Kaufman (16) for the solvolysis of triaryliodoethylenes. These reactions have been interpreted in terms of transition states leading to vinyl cation intermediates. The similarity of these ρ^+ values to that for the bromination of acetylenes is therefore strongly indicative of rate determining formation of a vinyl cation **2** through a transition state resembling **1**, as shown in eq. 3. The bromination of olefins in acetic acid is also believed to proceed by a mechanism involving rate determining formation of a carbonium ion (1). The two systems, olefins and acetylenes, might therefore be expected to exhibit a similar substituent dependence. The ρ^+ value of approximately -4.5 (9, 12) for styrenes is therefore in agreement with the suggested rate determining step in eq. 3.

[3] $$\mathrm{Ph{-}C{\equiv}C{-}R} \xrightarrow[\mathrm{HOAc}]{\mathrm{Br_2}} \left[\mathrm{Ph{-}C^{+\delta}{\equiv}C{-}R \quad Br \quad Br^{-\delta}}\right] \xrightarrow{-\mathrm{Br}^-} \mathrm{Ph{-}\overset{+}{C}{=}C{-}R \quad Br}$$

1 **2**

Can. J. Chem. Downloaded from www.nrcresearchpress.com by 210.87.254.42 on 09/05/12
For personal use only.

Can. J. Chem. Downloaded from www.nrcresearchpress.com by 210.87.254.42 on 09/05/12
For personal use only.

As the great number of recent publications indicate (17, 18), there has been a considerable upsurge in interest in the structure, reactivity and stability of vinyl cations. The results available imply that linear structures of the type **2** with sp hybridization at the cationic center are favored

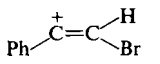

3a

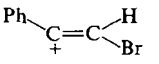

3b

over either of the bent forms ***3a*** or ***3b*** with sp^2 hybridization. This has been confirmed by theoretical molecular orbital calculations which show the bent structure to be less stable than the linear one by approximately 50–60 kcal/mole (19, 20). As well, the high negative ρ^+ values for reactions where vinyl cations are generated adjacent to phenyl rings (*vide supra*) suggests that the phenyl ring is directly conjugated with the positive charge on the α-carbon atom as in ***4a*** rather than with the remaining π-bond of the vinyl system as in ***4b***. In the discussion that

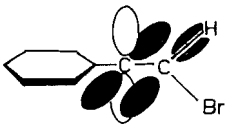

4a

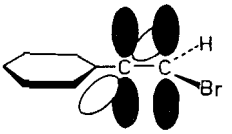

4b

follows, therefore, the structure of the cationic intermediate is assumed to be ***4a*** although, for simplicity, it will be drawn as shown in **2**.

The activation parameters for several of the acetylenes are shown in Table 3. These values are obtained from a least-squares fit of the data to a plot of log (k_2/T) *vs.* $1/T$ according to eq. 4 (21). For the phenylacetylenes, the entropy values

$$[4]\quad \log\frac{k_2}{T} = \left[\log\frac{k}{h} + \frac{1}{2.303}\frac{\Delta S^{\ddagger}}{R}\right] - \frac{\Delta H^{\ddagger}}{2.303R}\left(\frac{1}{T}\right)$$

of approximately −30 e.u. are consistent with the rate determining step proposed earlier (eq. 3). Thus, Wiberg (22) has estimated that, for a bimolecular reaction, an entropy change of −20 e.u. is expected because of loss of translational and rotational degrees of freedom. The excess over this estimate is presumably a result of restriction of solvent motion because of solvation changes as the reaction proceeds from neutral ground state molecules to a dipolar transition state. Similar values of −28 e.u. have been reported for the corresponding styrene substrates (23) but revised values of approximately −40 e.u. have been obtained more recently (12). A similar decrease to that observed for the entropy and enthalpy values of the k_3 process for methylphenylacetylene ($\Delta H^{\ddagger}$ = 3.0 kcal/mole and $\Delta S^{\ddagger}$ = −51 e.u. compared with $\Delta H^{\ddagger}$ = 12.3 kcal/mole and $\Delta S^{\ddagger}$ = −29 e.u. for the k_2 process) has also been previously observed for olefin substrates (24). Both these changes can be explained in terms of the usual mechanism postulated for this third order process: a bromine-assisted heterolysis of the bromine–bromine bond as in eq. 5 (1). The more negative entropy value is a reflection of the unfavorable nature of such a termolecular transition state. As well, the second molecule of bromine is acting as a catalyst in the breaking of the bromine–bromine bond and, hence, dispersing the negative charge of the bromide ion released. This should give a lower enthalpy of activation as observed. The

TABLE 3

Activation parameters for acetylenes

Substrate	$\Delta H\ddagger$* (kcal/mole)	$\Delta S\ddagger$* (e.u.)
Methylphenylacetylene, k_2	12.3±0.3	−(29±1)
PA,† k_2	11.7	−31
4-Br PA,† k_2	12.5	−30
3-Hexyne, k_2	8.4±0.2	−(41±1)
Methylphenylacetylene, k_3	3.0±0.2	−(51±1)

*Values quoted with no error are from rate constants at only two temperatures. The errors quoted are evaluated from the standard deviations of the slope and intercept of the least-squares line.
†PA represents phenylacetylene.

[5]

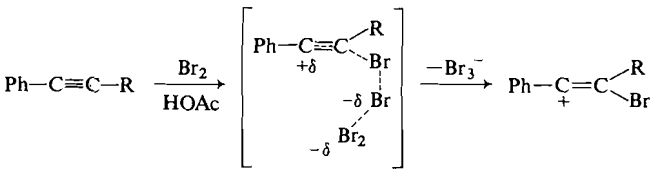

5

[6] 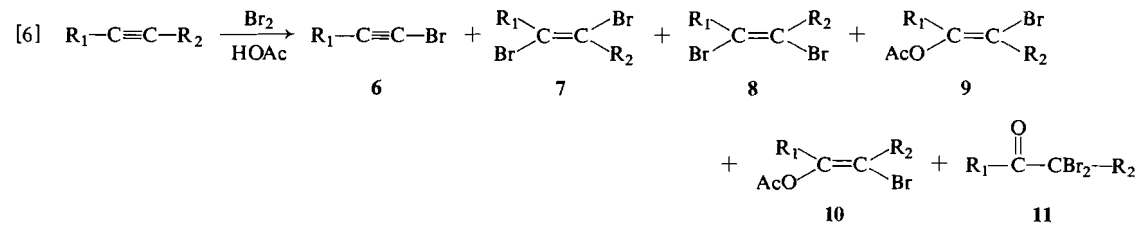

lower value of -40 e.u. for 3-hexyne compared to those of -30 e.u. for the phenylacetylenes will be discussed later.

The relative reactivity of olefins and acetylenes in electrophilic bromine additions can be estimated from the rate constants in Table 1 and those available in the literature for olefins.[1] Thus, the ratio for styrene:phenylacetylene is 2×10^3 and for 3-hexene:3-hexyne is 1.4×10^5. Perrin (25) has suggested that, for substrates that react via open ions rather than cyclic "bromonium" ion transition states, the reactivity of olefins and acetylenes might be similar. The reactivity factor of 2×10^3 for styrene over phenylacetylene does not agree with this hypothesis. However, the two substrates, 3-hexene and 3-hexyne, are believed to react via cyclic ions (*vide infra*) and in this case the reactivity ratio is 1.4×10^5. Perhaps this extra factor of approximately 10^2 may be accounted for in terms of Perrin's argument.

(2) Products of the Addition of Bromine to Acetylenes

The products for the addition of bromine to acetylenes in acetic acid are outlined, for the general case, in eq. 6. The bromoacetylene **6** is only formed if the acetylene is a terminal one, i.e. R_2 is H. The bromoacetates **9** and **10** are regiospecific in the Markownikoff sense so that for phenylacetylene derivatives only 1-acetoxy-1-phenyl products were observed. The dibromoketone (**11**) is formed by the reaction of bromine with the bromoacetates **9** and **10** and consequently can be regarded as a secondary reaction product. Fahey and Lee (26) have observed a similar reaction of the enol acetates formed from the addition of HCl to methylphenylacetylene in acetic acid. The bromoacetates themselves were not well characterized because they could not be separated by g.l.c. methods. Because of this problem, as well as the secondary reaction with bromine to form the ketone **11**, all three of the products, **9**, **10**, and **11**, are classified under one heading as solvent-incorporated (SI) products.

The results for methylphenylacetylene are shown in Table 4 and for the other acetylenes in Table 5. All of the products are formed under conditions of kinetic control since no isomerization or reaction of the dibromides (to form either bromoacetates or tetrabromides) was observed under the reaction conditions.

The results for methylphenylacetylene in Table 4 will be discussed first since the experimental results for this substrate are more complete. At the bromine concentrations shown, both the terms first order in bromine and that second order in bromine from eq. 1 are contributing to product formation. From the integrated form of eq. 2, one can derive eq. 7, where P_2 is

$$[7] \quad \frac{P_2}{P_2 + P_3} = \frac{k_2}{k_3[\mathrm{Br_2}]_0} \ln \frac{k_2 + k_3[\mathrm{Br_2}]_0}{k_2}$$

amount of product formed from the k_2 process and P_3 the amount from the k_3 process. In other words, the fraction of the product from the k_2 process, $P_2/(P_2 + P_3)$, is determined only by the rate constants k_2 and k_3 and $[\mathrm{Br_2}]_0$. Over the range of $[\mathrm{Br_2}]_0$ shown in Table 4 this ratio varies from 0.24 to 0.40 (using $k_2 = 2.46 \times 10^{-3}\ M^{-1}\ \mathrm{s}^{-1}$ in Table 1 and $k_3 = 2.7\ M^{-2}\ \mathrm{s}^{-1}$ in Table 2). Since no change in the product ratio (within experimental error) is observed, both k_2 and k_3 must lead to the same product distribution. This is also confirmed by the observation that the product distribution remains effectively constant for samples taken at 50, 75, and 100% conversion with initial bromine concentration of $6.66 \times 10^{-3}\ M$ even though the fraction of products from each rate process will be different for each sample. These results imply that the product forming intermediate is the same for both k_2

[1]The k_2 value for styrene is from ref. 9 at zero bromide ion concentration. The k_2 value for 3-hexene is estimated from data obtained by R. S. McDonald in this laboratory.

Can. J. Chem. Downloaded from www.nrcresearchpress.com by 210.87.254.42 on 09/05/12
For personal use only.

TABLE 4

Product distribution for the bromination of methylphenylacetylene

$[MPA]_0$ ($M \times 10^2$)	$[Br_2]_0$ ($M \times 10^3$)	Salt 0.10 M	T*	C*	SI*
			(%) by g.l.c.†		
11.1	10.3	—	59	14	27
8.55	8.4	—	56	13	31
10.6	6.3	—	56	14	30
8.96	4.56	—	58	12	30
3.34	3.78	—	59	14	27
1.40	6.66‡	—	62	12	26
	§	—	61	13	26
	‖	—	59	13	28
7.61	5.14	LiBr	97	<0.5	3
3.37	3.78	LiBr	98	<0.5	2
10.0	5.82	$LiClO_4$	49	10	41
7.91	3.96	$LiClO_4$	53	10	37

*T is *trans* dibromide, C is *cis* dibromide and SI is solvent-incorporated products **9**, **10**, and **11**.
†All results are from areas of g.l.c. peaks. Estimated accuracy is ±1 to ±2%.
‡, §, ‖All from the same reaction at 50, 75, and 100% reaction respectively.

TABLE 5

Product distribution for the bromination of acetylenes

Substrate and conditions*	BrA†	T†	C†	SI†
		(%) by g.l.c.‡		
4-Me phenylacetylene, HOAc	—	56	44	—
0.10 LiBr —	—	81	19	—
0.06 LiBr, 0.04 $LiClO_4$	—	73	27	—
0.02 LiBr, 0.08 $LiClO_4$	—	59	41	—
— 0.10 $LiClO_4$	—	42	58	—
Phenylacetylene, HOAc	25	42	19	14
0.10 LiBr —	—	>99	—	—
— 0.10 $LiClO_4$	—	52	21	27
3-Hexyne, HOAc	—	72§	—	—
0.10 LiBr —	—	>99	—	—
1-Hexyne, HOAc	—	>99	—	—

*Salt values are in molarity.
†BrA is bromoacetylene, T is *trans* dibromide, C is *cis* dibromide and SI is solvent-incorporated products **9**, **10**, and **11**.
‡All results are from areas of g.l.c. peaks. Estimated accuracy is ±1 to ±2%.
§28% of the product was an unknown compound which was not BrA, C, or SI.

and k_3 as has been postulated for olefins (1). For the other substrates in Table 5 the ratio of $P_2/(P_2 + P_3)$ cannot be calculated because k_3 is unknown. However, by analogy with methylphenylacetylene, the products are assumed to be the same for both rate processes.

The product results in the absence of lithium bromide will be discussed first. For the phenylacetylene derivatives, the non-stereospecific formation of dibromides as well as the formation of large amounts of solvent-incorporated products clearly point to a reactive intermediate, the vinyl cation, which reacts in a fast step with either bromide ion or the solvent acetic acid. This is in agreement with the kinetic results. The ratio of the various products will be dependent on the structure and reactivity of this intermediate cation. In a non-dissociating solvent, like acetic acid, ion pairing phenomena are extremely important as the early work of Winstein *et al.* on solvolysis demonstrated (27). Recently, several authors (26, 28, 29) have had some success in explaining product composition for addition reactions in terms of the various ion pairs possible. Figure 2 shows the completely general approach for the addition of bromine to phenylacetylenes.

The advantage of this type of scheme is, of

Can. J. Chem. Downloaded from www.nrcresearchpress.com by 210.87.254.42 on 09/05/12
For personal use only.

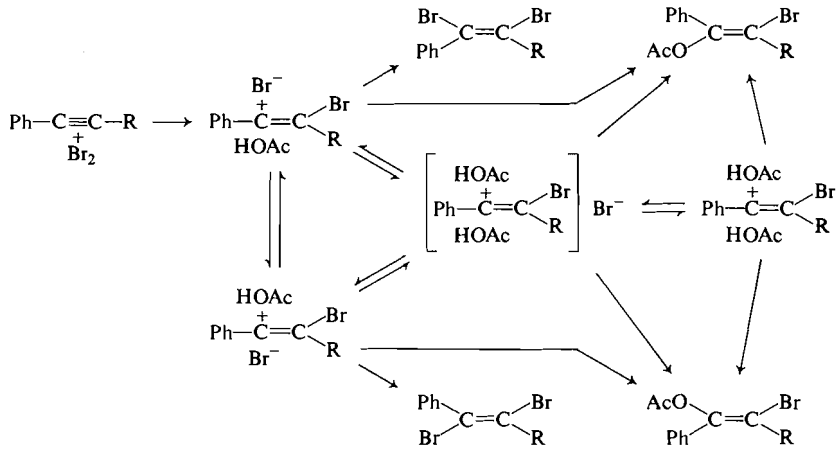

FIG. 2. General ion pair scheme for the addition of bromine to phenylacetylenes in acetic acid.

[8] 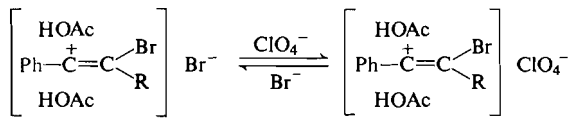

12 13

course, that any combination of products can usually be rationalized although there may only be rather tenuous arguments for invoking the particular ion pairs necessary. Perhaps the best approach would be to realize that, on the basis of the limited results available, any conclusions must be considered as speculative. The results for the phenylacetylenes will illustrate the difficulties involved.

The first point to note is that 4-methylphenylacetylene behaves quite differently from phenylacetylene and methylphenylacetylene. Thus, the 4-methyl compound gives no solvent-incorporated or elimination products. Furthermore, added $LiClO_4$ has little effect on the *trans*:*cis* dibromide ratio for the unsubstituted compounds (52:21 changes to 42:19 for phenylacetylene) whereas the ratio is significantly altered for the 4-methyl case (56:44 becomes 42:58 on addition of $LiClO_4$).

$LiClO_4$ is believed (27) to interact with solvent-separated ion pairs as shown in eq. 8. The perchlorate ion pair **13** is more likely to yield solvent-incorporated products than the bromide ion pair **12**. Consequently, the addition of $LiClO_4$ might be expected to increase the amount of bromoacetate product if solvent-separated ion pairs are important in these reactions. This effect is observed for the unsubstituted phenylacetylenes. However, this increased reaction with the solvent does not affect the *trans*:*cis* dibromide ratio for these substrates. There seem to be two possible interpretations of this result. First, there may be no return of solvent-separated ion pairs to intimate ion pairs. Thus, once dissociation occurs, the only product is a bromoacetate and the formation of dibromides is determined only by the relative reactivity of **14** and **15**. The effect of $LiClO_4$ must then be

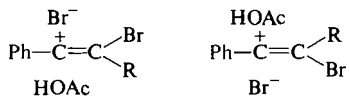

14 15

visualized as enhancing the dissociation of intimate ion pairs to solvent-separated ion pairs by increasing the polarity of medium. The capture of solvent-separated ion pairs by $LiClO_4$ would only be a secondary effect and not the major contributor to increased bromoacetate production. The second possibility is that there is return from solvent-separated ion pairs to intimate ion pairs. In this case, the same behavior must be exhibited by ions that are returning as those that did not dissociate. In other words **14** and **15**

Can. J. Chem. Downloaded from www.nrcresearchpress.com by 210.87.254.42 on 09/05/12
For personal use only.

Can. J. Chem. Downloaded from www.nrcresearchpress.com by 210.87.254.42 on 09/05/12
For personal use only.

equilibrate faster than they react to form dibromides. It is interesting to note at this point that Poutsma and Kartch (28) have concluded that an initially formed "*cis*" ion pair like **14** can rearrange to a "*trans*" ion pair like **15** without the intervention of solvent-separated ion pairs. This type of rearrangement is, of course, necessary in this second hypothesis.

The first of these interpretations seems preferable on the basis of the results for 4-methylphenylacetylene. The 4-methylphenylvinyl cation is more stable than the corresponding unsubstituted ions. Thus, it only reacts with bromide ion and not with the less nucleophilic acetic acid. However, since it is a more stable ion, solvent-separated ion pairs must also be important in its reaction scheme. Therefore, some of the dibromides must be formed from intimate ion pairs that are the result of return from solvent-separated ion pairs. Since the ratio of *trans*:*cis* dibromide changes on the addition of $LiClO_4$, ions returning from **13** through **12** to the intimate ion pairs give a different ratio of dibromides than those initially formed. This observation would seem to preclude complete equilibration of the intimate ion pairs.

In summary then, for phenylacetylene and methylphenylacetylene, the dibromides are probably formed from collapse of the initially formed intimate ion pairs. A similar conclusion has been reached for the bromination of β-methylstyrenes where added $LiClO_4$ also increases the bromoacetate products but does not affect the *trans*:*cis* ratio (8). The opposite conclusion has been reached by Fahey and Lee (26) for the addition of HCl to methylphenylacetylene since their scheme indicates that return of solvent-separated ion pairs to intimate ion pairs is important. This situation is more comparable to the scheme suggested here for 4-methylphenylacetylene.

On the basis of the results available, there seems to be no simple explanation for the observed dibromide ratios for these phenylacetylenes. More information is necessary on the stereochemistry of bromoacetate formation which presumably affects the amount of dibromide formed from the intimate ion pairs **14** and **15**. As well, the formation of bromophenylacetylene is more probable from **15** since the basic bromide ion is better situated for hydrogen abstraction than in **14**. This side reaction may well interfere with the "normal" reactivity of the two ion pairs.

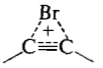

16

The results in Table 5 for the alkyl acetylenes are quite different than those for the phenylacetylenes. For both 3-hexyne and 1-hexyne only *trans* dibromides are observed. This is in agreement with the results of Bergel'son and Nazarov (5) for some other alkyl acetylenes and is good evidence that these alkynes react via an Ad_E2 (2) cyclic "bromonium" ion mechanism with an intermediate like **16**. This type of mechanism has been firmly established for the addition of sulfenyl halides since no *cis* addition has ever been observed (30, 31). There are several factors in favor of this interpretation. First of all, from solvolysis studies, alkyl vinyl cations are less stable than phenyl vinyl cations (17, 18) and, therefore, participation by bromine should be more favorable in the alkyl case. Second, the more negative entropy of activation value of -40 e.u. (Table 3) for 3-hexyne compared to that of -30 e.u. for the phenylacetylenes is consistent with a loss of degrees of freedom because of a more ordered transition state. Finally, the complete absence of solvent-incorporated products is also observed for the bromination of *cis*- and *trans*-2-butene in acetic acid (8). These olefins also react via cyclic bromonium ion intermediates.

The final point to be mentioned in this discussion of the products of addition is the change on the addition of LiBr. There is a marked decrease in bromoacetate product and a large increase in *trans* dibromide formation. An examination of the kinetics under these conditions is necessary before a mechanistic interpretation can be made.

(3) Rates in the Presence of Bromide Ion Salts

As the review by de la Mare and Bolton indicates (1), the kinetics of bromine addition to olefins in the presence of added bromide ion have been interpreted in a number of ways. More recent work (9, 32), although providing more results, has done little to clarify the problem. Before discussing this more fully, the main details of the kinetics will be briefly outlined.

If both tribromide ion and molecular bromine are electrophiles, the rate of consumption of bromine is given by eq. 9 where $[Br_2]_T$ is the total

TABLE 6

Second order rate constants,* $k_0 \times 10^3$, for the bromination of phenylacetylenes with added LiBr

LiBr (M)	$LiClO_4$ (M)	4-Me PA†	3,4-Benzo PA†	4-F PA†	PA†	4-Br PA†	3-Cl PA†	MPA‡
0.10	—	211±4	87.6±0.2	19.5±0.6	14.2±0.1	6.75±0.12	2.46±0.05	29.3±1.0
0.08	0.02	210±2	89.6±0.6	19.7±1.1	13.6±0.2	6.49±0	—	27.8±0.8
0.06	0.04	229±2	92.3±0.3	19.1±0.6	12.9±0.2	6.48±0.06	—	25.4±0.6
0.04	0.06	263±3	98.0±0.7	18.1±0.3	12.8±0.3	6.27±0.15	—	24.6±0.3
0.02	0.08	313±1	116±6	16.0±0.1	11.7±0.2	5.11±0	—	19.2±0.4

*k_0 values in units of $M^{-1}s^{-1}$.
†PA stands for phenylacetylene.
‡MPA stands for methylphenylacetylene.

TABLE 7

Second order rate constants* for the bromination of 3-hexyne and t-butylacetylene with added LiBr

LiBr (M)	$LiClO_4$ (M)	K (M^{-1})	$[1 + K(Br^-)]$	$k_0 \times 10^3$ 3-Hx†	$k_0 \times 10^3$ TBA‡
0.10	—	92	10.2	474±7	1.01±0.02
0.08	0.02	93.7	8.50	494±6	—
0.07	0.03	95.6	7.69	491±5	0.981±0.002
0.06	0.04	99.4	6.96	488±2	0.983±0
0.04	0.06	108	5.31	471±2	0.948±0.02
0.03	0.07	114	4.41	448±1	—
0.02	0.08	120	3.40	396±3	0.780±0.01
0.01	0.09	128	2.28	329±1	—

*k_0 values are in units of $M^{-1}s^{-1}$.
†3-Hexyne.
‡t-Butylacetylene.

[9] $$-d[Br_2]_T/dt = [\text{acetylene}](k_2[Br_2]_F + k_{Br_3^-}[Br_3^-])$$

bromine concentration and $[Br_2]_F$ is the free bromine, uncomplexed as tribromide ion. The two are related by eq. 10 where K is the equilibrium

[10] $$[Br_2]_T = (1 + K[Br^-])\,[Br_2]_F$$

constant for tribromide ion formation. Substitution of eq. 10 into eq. 9, integrating and rearranging gives eq. 11 where k_0 is the observed second order rate constant.

[11] $$k_0 = \frac{k_2 + k_{Br_3^-}K[Br^-]}{1 + K[Br^-]}$$

An alternative equation can be derived assuming that molecular bromine is the only electrophile but a bromide ion catalyzed process is possible as in eq. 12. Substituting eq. 10 into eq. 12, again integrating and rearranging gives eq. 13. As shown, eqs. 11 and 13 are kinetically indistinguishable, with $k_{Br^-} = Kk_{Br_3^-}$.

[12] $$-\frac{d[Br_2]_T}{dt} = [\text{acetylene}](k_2[Br_2]_F + k_{Br^-}[Br_2]_F[Br^-])$$

[13] $$k_0 = \frac{k_2 + k_{Br^-}[Br^-]}{1 + K[Br^-]}$$

Dubois *et al.* have discussed in considerable detail (32*b*) the problems in obtaining the rate constants k_2 and k_{Br^-} (or $k_{Br_3^-}$) from these equations using the usual plots of $(1 + K[Br^-])\,k_0$ *vs.* $[Br^-]$. However, there should be little difficulty if salt concentrations of up to only 0.10 M are used. Thus, the $k_{Br_3^-}$ values at either variable ionic strength or constant ionic strength agree well for the styrenes studied by Rolston and Yates (9).

The k_0 values for the phenylacetylene derivatives are given in Table 6. The values for 3-hexyne and t-butylacetylene are shown in Table 7 along with the K values (9) and the derived parameters necessary for $(1 + K[Br^-])\,k_0$ *vs.* $[Br^-]$ plots. The rate constants were obtained from the excellent linear plots of log $(A - A_\infty)$ values at

Can. J. Chem. Downloaded from www.nrcresearchpress.com by 210.87.254.42 on 09/05/12
For personal use only.

TABLE 8

Separated rate constants for the phenylacetylene derivatives

Substrate	k_{Br^-}* (M^{-2} s^{-1})	$k_2 \times 10^3$* (M^{-1} s^{-1})	$\frac{k_{Br^-}[Br^-]}{k_2}$§
4-Me PA†	12.8±0.9	826±61	1.5
3,4-Benzo PA†	7.85±0.47	128±31	6.1
4-F PA†	1.80±0.06	21.9±3.6	8.2
PA†	1.29±0.03	14.2±2.2	9.1
4-Br PA†	0.625±0.027	6.51±1.78	9.6
3-Cl PA†	0.251±0.005	—	—
MPA‡	2.88±0.03	8.1±7.6	35

*Errors quoted are obtained from the standard deviations of the least-squares line.
†PA represents phenylacetylene.
‡MPA represents methylphenylacetylene.
§Calculated at 0.10 *M* LiBr.

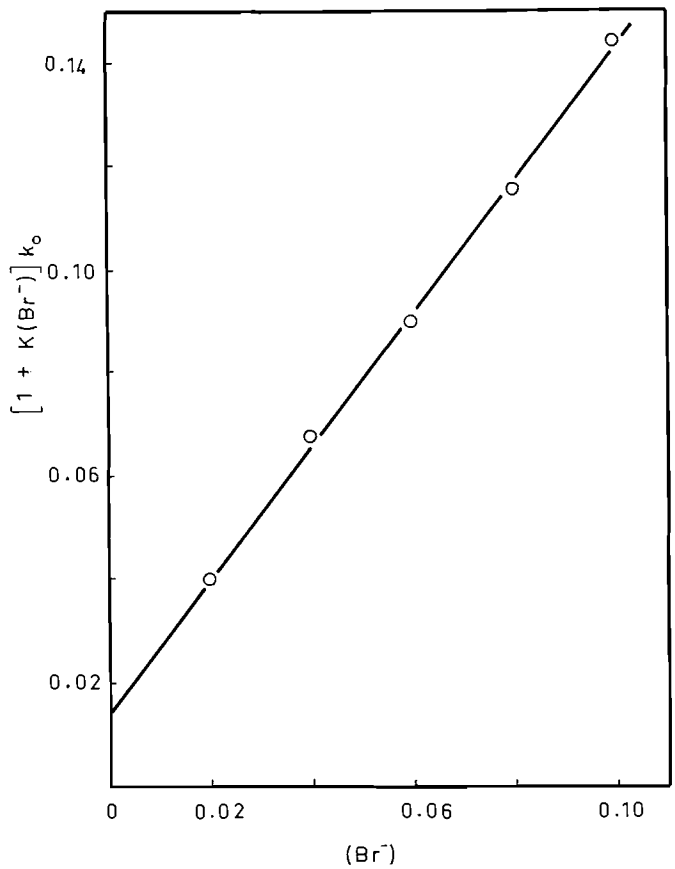

FIG. 3. Plot of $[1 + K(Br^-)]\,k_0$ *vs.* (Br^-) for phenylacetylene.

320 mμ vs. time. The values listed are the average of two runs and the error quoted is the average deviation.

The least-squares slope (k_{Br^-}) and intercept (k_2) for the $(1 + K[Br^-])\,k_0$ *vs.* $[Br^-]$ plots are shown in Table 8 for the phenylacetylenes. A sample plot for phenylacetylene is shown in Fig. 3. In general, the errors in the intercepts (k_2) are quite large because they are so close to the origin. Since these values have already been independently measured (Table 1) no attempt was made to use those obtained by extrapolation.

Can. J. Chem. Downloaded from www.nrcresearchpress.com by 210.87.254.42 on 09/05/12
For personal use only.

Can. J. Chem. Downloaded from www.nrcresearchpress.com by 210.87.254.42 on 09/05/12
For personal use only.

Now that the rate constants are known for the two rate processes occurring in the presence of added bromide ion, the ratio of the products obtained from each can be calculated. This ratio is equal to $k_{Br^-}[Br^-]/k_2$ for the bromide ion catalyzed case. These values are shown for the phenylacetylenes in Table 8 (bromide ion concentration is 0.10 M).

In view of the magnitude of this ratio for some substrates ($k_{Br^-}[0.10]/k_2 = 9.1$ for phenylacetylene) it is no longer surprising that the product ratios shown in Tables 4 and 5 change in the presence of added bromide ion. The reaction is now being dominated by a different kinetic process and the molecular bromination, k_2, is only a minor contributor.

The problem of distinguishing between the above two mechanisms (the tribromide ion and the bromide ion catalyzed) has been discussed in some detail in a preliminary communication on this work (33) and only the more recent results will be mentioned here. The data obtained by Rolston and Yates (8, 9) for the bromination of styrenes in acetic acid have been interpreted in terms of an electrophilic attack by tribromide ion mainly on the basis of product composition. The major objection to this conclusion is that for unreactive substrates, like 3- and 4-nitrostyrene, $k_{Br_3^-} > k_2$. It is surprising that tribromide ion becomes a better electrophile than molecular bromine, especially for unreactive substrates. Conversely, one would expect the bromide ion catalyzed process to become more favorable as the reactivity decreased. Finally, Dubois *et al.* (32) have given a lengthy discussion of this problem for the kinetics of a series of substituted olefins in methanol. The possibility of tribromide as an electrophile was rejected for the same reason mentioned above, that for unreactive compounds its reactivity would be equal to that of bromine.

Furthermore, the bromide ion catalyzed process as proposed here was also rejected. However, the argument used in this case assumes that the rate determining step of the molecular bromination is the formation of the π-complex between the olefin and bromine. All other authors (1) and even Dubois in other papers (34) have postulated a rate determining break-down of this complex. The reason for not considering the bromide ion catalyzed mechanism is therefore far from convincing. At any rate, Dubois *et al.* conclude that for the more reactive substrates the process with an order in bromide ion is simply a salt effect on the molecular bromine process. For the less reactive cases, a mechanism involving pre-equilibrium formation of a complex between the olefin and bromide ion followed by an electrophilic attack of molecular bromine on the negatively charged complex in the rate determining step is suggested.

As discussed previously for methylphenylacetylene (33), the case for acetylenes seems to be much more definite. The marked decrease in bromoacetate formation and the increase in *trans* dibromide in the presence of bromide ion is consistent with a bromide ion catalyzed process proceeding through a transition state like **17**. This

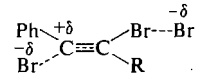

17

type of change in dibromide and solvent-incorporated products would not be expected for electrophilic attack by tribromide ion. Of particular interest is the product distribution for 4-methylphenylacetylene where both k_2 and k_{Br^-} are competitive even at 0.10 M LiBr. The ratio of *trans*:*cis* dibromide of 42:58 in 0.10 M $LiClO_4$ can be used for the product distribution of k_2 at ionic strength of 0.10. Assuming k_{Br^-} gives only *trans* dibromide, as is reasonable, a comparison of the calculated $k_{Br^-}[Br^-]/k_2$ ($k_{Br^-} = 12.8\,M^{-2}\,s^{-1}$ and $k_2 = 0.826\,M^{-1}\,s^{-1}$ in Table 8) and the observed ratio is shown in Table 9. The agreement is very good considering the errors involved in the rate constant and product composition determinations.

In summary this is one of the few cases where a clear-cut decision can be made between these two mechanisms. The bromide ion catalyzed process is obviously preferred for acetylenes over direct electrophilic attack by tribromide ion.

In view of the quite different transition state,

TABLE 9

Calculated and observed % *trans* dibromide for the bromination of 4-methylphenylacetylene

LiBr (M)	$LiClO_4$ (M)	(%) *trans* (observed)	(%) *trans* (calculated)
0.10	—	81	79
0.06	0.04	73	70
0.02	0.08	59	56

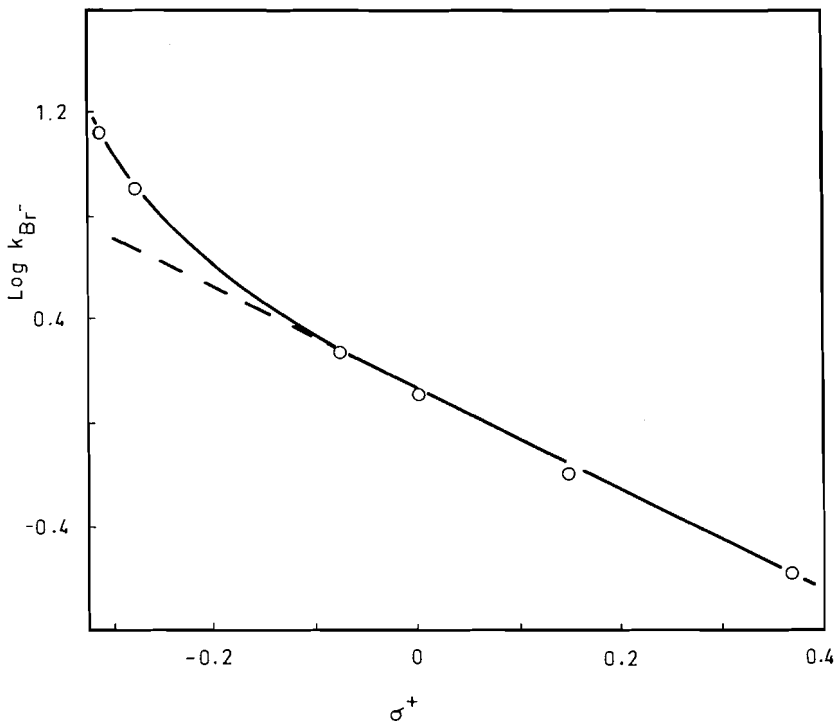

FIG. 4. Plot of log k_{Br^-} *vs.* σ^+ for bromination of phenylacetylenes in acetic acid.

17, postulated for the k_{Br^-} process compared to the molecular bromine, k_2, process substituent effects should also be quite different. This is shown by the Hammett $\rho\sigma^+$ plot shown in Fig. 4 for the k_{Br^-} values from Table 8. (As mentioned above the σ^+ value for the 3,4-benzo substituent was determined as -0.28 from the linear log k_2 *vs.* σ^+ correlation (Fig. 1).) The plot is curved and furthermore the effect of substitution is much less than for the k_2 process since the slope is approximately -1.9 for four substrates of lower reactivity.

Non-linear Hammett plots have generally been regarded as a criterion for a change in mechanism (35). However, this cannot be the case here since the product distribution for the 4-methyl compound is successfully explained by assuming the same Ad_E3 (2) *trans* mechanism (Table 9) as the unsubstituted compound. The curvature may be explained by another approach. The transition state **17** involves synchronous bond formation with both an electrophile (bromine) and a nucleophile (bromine ion). Presumably, as the substituent becomes more electron donating, bond formation between the electrophile and the substrate may have proceeded further than bond formation between the nucleophile and the substrate because positive charge build-up on the α-carbon atom is more favorable. Conversely, for electron withdrawing substituents nucleophile–substrate bonding may have proceeded further. The overall result would be that both types of substituent would have a rate accelerating effect and the Hammett plot would be concave upwards. This type of behavior has been observed previously for the reaction of benzyl halides with nucleophiles (36, 37). Unfortunately, this explanation is not certain because over the range of substituents used no minimum was reached. The possibility is currently being examined further in this laboratory.

As a final point on the reactivity of acetylenes in the presence of bromide ion, the rate constants for the alkyl acetylenes in Table 7 should be mentioned. The results for *t*-butylacetylene are quite straight-forward and a plot of $(1 + K[Br^-])\,k_0$ *vs.* $[Br^-]$ gives the two rate constants, $k_{Br^-} = (8.31 \pm 0.26) \times 10^{-2}\ M^{-1}\ s^{-1}$ and $k_2 = (18.5 \pm 1.8) \times 10^{-4}\ M^{-1}\ s^{-1}$. Bergel'son and Nazarov (5) have observed that *t*-butylacetylene gives exclusively *trans* dibromide in the presence of LiBr in acetic acid so this substrate

Can. J. Chem. Downloaded from www.nrcresearchpress.com by 210.87.254.42 on 09/05/12
For personal use only.

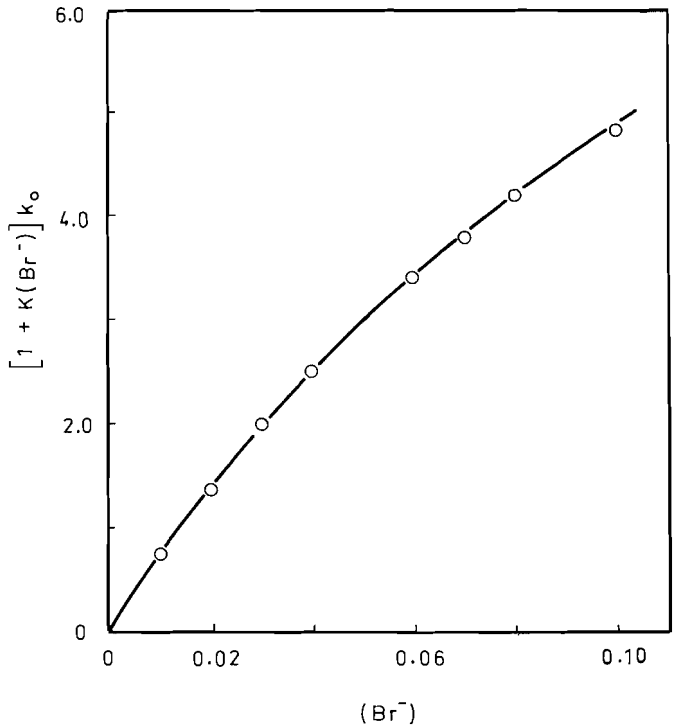

FIG. 5. Plot of $[1 + K(Br^-)]\ k_0$ *vs.* (Br^-) for 3-hexyne.

seems completely analogous to the phenylacetylenes for the bromide ion catalyzed case. The rate constants for 3-hexyne are somewhat different. Thus, a plot of $(1 + K[Br^-])\ k_0$ *vs.* $[Br^-]$ is decidedly curved as shown in Fig. 5. There are no changes in product composition for 3-hexyne in the presence of bromide ion since in both cases only *trans* dibromide is formed (Table 5). We have not as yet arrived at a completely satisfactory explanation for this curvature.

Experimental

All melting points and boiling points are uncorrected. The i.r. spectra were recorded on a Perkin–Elmer model 137B spectrophotometer: spectra of liquids were taken as thin films on sodium chloride discs and those of solids as solutions in CCl_4. Only bands used for identification purposes are reported. The n.m.r. spectra were recorded on a Varian model A-60 spectrometer. Samples were approximately 20% in CCl_4, with 1% tetramethylsilane as reference. Line positions (δ) are in p.p.m. downfield from this reference. The g.l.c. was carried out on either a Wilkens model A-705 "Autoprep" instrument or a Wilkens model 600D "Hy-Fi" instrument both equipped with flame ionization detectors. Peak areas were measured with a disc integrator on the former instrument and by the product of height times width at half peak height on the latter. Columns and conditions (column temperature, flow rate) will be outlined for the individual cases. Microanalyses were performed by A. Gygli, Toronto, Ontario.

Dipole moments were measured on a Wissenschaftliche–Technische Werkstätten Type DMO1 Dipolmeter as used previously in this laboratory (38). The instrument was not recalibrated but the measured dielectric constant of benzene (2.2726 to 2.2735) was in good agreement with that quoted (2.2730) in the previous work. The Halverstadt–Kumler equation (39) was used to obtain total molar polarizations, and electron polarizations were estimated from Vogel's values (40). No correction was made for atom polarization. The dipole moments were then obtained from the Debye equation (41).

Bromine – Acetic Acid Solutions

Acetic acid was purified by the method used previously in this laboratory (9). Bromine (Mallinckrodt) was used without further purification. Anhydrous LiBr and $LiClO_4$ were dried at 100 °C and 1 mm over P_2O_5 for at least 48 h. Stock 1.0 *M* solutions of these salts were prepared by weighing in a dry box to prevent the absorption of atmospheric water. Aliquots of the stock solutions were then used to prepare solutions of the desired concentration for kinetic and product studies.

Bromine concentrations in acetic acid were determined by titration with $Na_2S_2O_3$ (standardized against KIO_3) as described by Vogel (42) using the "dead-stop" end point technique (43). For more convenient work, as well

Can. J. Chem. Downloaded from www.nrcresearchpress.com by 210.87.254.42 on 09/05/12
For personal use only.

Can. J. Chem. Downloaded from www.nrcresearchpress.com by 210.87.254.42 on 09/05/12
For personal use only.

as for some of the kinetics, extinction coefficients in acetic acid were determined. The values at 490 mμ and the temperatures given are: 17.2 °C, 58.6 ± 0.1; 24.8 °C, 60.5 ± 0.3; 29.9 °C, 61.3 ± 0.1; 39.8 °C, 63.6 ± 0.3. The errors quoted are the average deviation for at least five points.

Kinetic Measurements in Acetic Acid

(a) Spectrophotometric Method

The rates of molecular bromination, k_2, for the acetylenes were measured on a Cary 16 spectrophotometer by following the change in bromine absorbance with time at 490 mμ. The maximum of this band (405 mμ) was not used for the reason described previously (12). Since low concentrations of bromine were necessary (less than 3×10^{-4} *M*) a 10 cm cylindrical cell equipped with a circulating jacket was used. The temperature of the cuvette was controlled to ±0.1 °C with circulating water.

The kinetics for methylphenylacetylene bromination were also measured at higher bromine concentration (2.0 to 5.0 $\times 10^{-3}$ *M*) using 1 cm cuvettes and the Cary 16 constant temperature cell holder for thermostatting.

(b) Spectrophotometric Method: Added Salts

The rates for the acetylenes were also measured on the Cary 16 spectrophotometer at LiBr concentrations varying from 0.01 to 0.10 *M*. Ionic strength was kept constant at 0.10 by addition of $LiClO_4$. The 1 cm cuvette was used and the change in absorbance at 320 mμ (335 mμ for β-naphthylacetylene and 380 mμ for *t*-butylacetylene) was followed.

Preparation and Purification of Acetylenes

Methylphenylacetylene, phenylacetylene, 3-hexyne, 1-hexyne, and *t*-butylacetylene were commercial compounds and were purified by distillation in a 24″ Nester-Faust spinning band still. The substituted phenylacetylenes (except β-naphthylacetylene) were prepared by the methods described previously (44). β-Naphthylacetylene was also prepared by the treatment of β-naphthylmethyl ketone with PCl_5 followed by base catalyzed dehydrohalogenation with KOH in ethanol. The product was purified by sublimation to give a white crystalline solid: m.p. 37–38 °C. The n.m.r. spectrum showed peaks at 3.0 (s, 1.0H) and 7.1–8.0 δ (multiplet, 7.4H).

Anal. Calcd. for $C_{12}H_8$: C, 94.70; H, 5.30. Found: C, 94.80; H, 5.33.

Products of Acetylene Bromination

(a) Methylphenylacetylene(MPA)

Bromine (6.9 g, 0.043 mole) in 50 ml of acetic acid was dropped into 5 g (0.043 mole) of MPA in 50 ml of acetic acid. The reaction mixture was left stirring for 10 h, then poured into 200 ml of water and extracted with two 50 ml portions of pentane. The extract was washed with 5% $NaHCO_3$ and then dried over $MgSO_4$. Concentration on the rotary evaporator gave 9.6 g of a mixture consisting of *trans*-1,2-dibromophenylpropene (81%), *cis*-1,2-dibromophenylpropene (8%), *trans*- and *cis*-1-acetoxy-2-bromo-1-phenylpropene, and 1,1-dibromoethylphenyl ketone (the last three combined are 10%) plus some unreacted acetylene. The ratio of the products was determined by g.l.c. on a 1/4″ × 5′ 5% DEGS on Chromosorb G column (140 °C, 60 ml/min).

The compounds were characterized as follows. The dibromides could be separated from the ketone and bromoacetates by column chromatography on Florisil with pentane eluant. Pure samples of the dibromides were then obtained by preparative g.l.c. on a 3/8″ × 12′ 5% Carbowax on Chromosorb G column (170 °C, 150 ml/min).

Anal. Calcd. for $C_9H_8Br_2$: C, 39.17; H, 2.92; Br, 57.91. Found for *trans* dibromide: C, 39.57; H, 2.99; Br, 57.86. Found for *cis* dibromide: C, 39.47; H, 3.07; Br, 57.55.

The stereochemistry of the dibromides was established by the measured dipole moment values of 0.1 D for the *trans* compound and 2.2 D for the *cis* isomer. This corresponds well with values given by McClelland (45) of 1.77 D for *cis*-1,2-dibromoethylene and 0.0 D for *trans*-1,2-dibromoethylene. This agreement is substantiated by the n.m.r. spectra. The *trans* dibromide shows 2.58 (s, 3.0H), and 7.33 δ (s, 5.2H) while the *cis* dibromide gives 2.22 (s, 3.0H) and 7.33 δ (s, 5.3H) in agreement with the observation that, for β-methylstyrene derivatives, methyl groups *cis* to phenyl absorb at higher field than those *trans* to phenyl (30). In addition the i.r. spectrum of the *cis* isomer has a band at 6.18 μ whereas the *trans* dibromide has only a very weak absorbance in this C=C stretch region.

1,1-Dibromoethylphenyl ketone was synthesized by acid catalyzed bromination of propiophenone. This sample had identical spectral properties to one obtained from the reaction mixture. The ketone could also be prepared by the reaction of bromine with a mixture of *trans* and *cis*-1-acetoxy-2-bromo-1-phenylpropene. This mixture was obtained by molecular distillation of the appropriate fraction from the column chromatography of the crude products from the bromination of MPA.

Anal. Calcd. for $C_{11}H_{11}O_2Br$: C, 51.78; H, 4.35; Br, 31.33. Found for mixture: C, 51.93; H, 4.21; Br, 31.29.

The n.m.r. spectrum of this mixture showed 2.10 (s, 1.8), 2.15 (s, 1.2H), 2.33 (s, 1.9H), 2.37 (s, 1.3H), and 7.25–7.45 δ (m, 5.0H) and indicated the two bromoacetates were there in the ratio of 1.85:1.25 but no assignment of stereochemistry was made. Unfortunately the two isomers could not be separated by g.l.c. The bromoacetates could also be synthesized by the addition of NBS to MPA in acetic acid as described by Jovtscheff (7). This reaction gave a mixture of the dibromoketone (57%) and the *trans* and *cis* bromoacetates (43%) as determined by n.m.r. analysis.

To establish that the products reported in Table 4 are kinetically controlled, a check for dibromide isomerization was made. Neither the *trans* or the *cis* dibromide showed any sign of reaction or isomerization when subjected to the reaction conditions. However, as mentioned above the bromoacetates do react with bromine. Because of this problem and the difficulty in separating and identifying the bromoacetates, these three products were combined as "solvent-incorporated" products (Table 4).

(b) Phenylacetylene (PA)

Bromine (12.0 g, 0.075 mole) in 50 ml of acetic acid was added slowly to 7.5 g (0.075 mole) of PA in 50 ml of acetic acid. The reaction was left to stand for 3 h and then poured into water and extracted with two 50 ml

Can. J. Chem. Downloaded from www.nrcresearchpress.com by 210.87.254.42 on 09/05/12
For personal use only.

portions of pentane. The extract was washed with 5% $NaHCO_3$ and dried over Na_2SO_4. After removal of the pentane, analysis on a 1/4″ × 5′ 5% DEGS on Chromosorb G column (150 °C, 50 ml/min) gave four products: bromophenylacetylene (26%), *trans*-1,2-dibromophenylethylene (43%), *cis*-1,2-dibromophenylethylene (17%), and 1-acetoxy-2-bromophenylethylene (14%). The bromoacetate could again be separated from the other components by column chromatography on Florisil with pentane eluant. Pure samples of the bromoacetylene and the dibromides were then prepared by preparative g.l.c. on a 3/8″ × 12′ 5% Carbowax on Chromosorb G column (175 °C, 175/min).

A sample of bromophenylacetylene was prepared independently by the reaction of PA with NaOBr (46). This compound had identical retention time, n.m.r. and i.r. spectra with the compound from the addition reaction.

The dibromides were characterized as follows.

Anal. Calcd. for $C_8H_6Br_2$: C, 36.68; H, 2.31; Br, 61.01. Found for *trans* dibromide: C, 36.66; H, 2.43; Br, 61.37. Found for *cis* dibromide: C, 36.81; H, 2.45; Br, 61.02.

The dipole moments were 0.6 D for the *trans* isomer and 2.1 D for the *cis* in agreement with the observation that *cis* dibromides have considerably higher dipole moments than the *trans* forms (*vide supra*). This assignment is also verified by n.m.r. spectra. The *trans* isomer gave 6.72 (s, 1.0H), 7.1–7.6 δ (m, 5.2H) whereas the *cis* isomer showed 6.90 (s, 1.0H), 7.0–7.5 δ (m, 5.1H). Again, protons *cis* to phenyl appear at lower field than those *trans* to phenyl for styrene derivatives (30).

1 - Acetoxy - 2 - bromophenylethylene was prepared independently by the reaction of NBS with PA in acetic acid (7). This reaction gave 52% of the bromoacetate product and 48% of α,α-dibromoacetophenone. A pure sample of the bromoacetate was obtained by preparative g.l.c. on a 3/8″ × 12′ 5% Carbowax or Chromosorb G column (175 °C, 175 ml/min). This sample was identical to that obtained from the addition of Br_2 to PA.

Anal. Calcd. for $C_{10}H_9Br_2O_2$: C, 49.82; H, 3.76; Br, 33.15. Found: C, 50.02; H, 3.7; Br, 32.97.

The n.m.r. spectrum for the bromoacetate was 2.20 (s, 3.1H), 6.50 (s, 1.0H), and 6.7–7.5 δ (m, 5.3H). The g.l.c. and n.m.r. analysis indicated only one of the bromoacetate isomers but its stereochemistry is unknown.

A check of both the *trans* and *cis* dibromides in acetic acid under the reaction conditions indicated no isomerization or reaction to form either tetrabromides or bromoacetates.

(c) 4-Methylphenylacetylene (4-Me PA)

Bromine (2.07 g, 0.013 mole) in 15 ml of CCl_4 was dropped slowly into 1.5 g (0.013 mole) of 4-Me PA in 15 ml of CCl_4. The solvent was then removed on the rotary evaporator. The g.l.c. analysis on the 1/4″ × 5′ 5% DEGS on Chromosorb G column (150 °C, 50 ml/min) showed only two compounds: *trans*-1,2-dibromo-(4-methylphenyl)ethylene (30%) and *cis*-1,2-dibromo-(4-methylphenyl)ethylene (70%). The two isomers could not be separated completely by preparative g.l.c. because they isomerized under the high temperatures required (190 °C) for reasonable retention times on the preparative column. However, a sample containing 43% *trans* and 57% *cis* was sent for analysis.

Anal. Calcd. for $C_9H_8Br_2$: C, 39.16; H, 2.92; Br, 57.91. Found: C, 38.85; H, 2.89; Br, 57.98.

This sample was obtained by distillation, t = 108–111 °C (1 mm). The stereochemistry of the two isomers was established by n.m.r. only. The olefinic proton of the *cis* isomer is at 6.93 δ; that of the *trans* isomer at 6.70 δ in agreement with the previous assignment for the phenylacetylene dibromides (*vide supra*).

No other products were obtained for the addition of Br_2 to 4-Me PA in either acetic acid or CCl_4.

(d) 3-Hexyne

Bromine (10.0 g, 0.061 mole) in 20 ml of acetic acid was dropped slowly into 5 g (0.061 moles) of 3-hexyne in 20 ml of acetic acid. The reaction mixture was poured into water, extracted with pentane, washed with 5% $NaHCO_3$ solution, and dried over $MgSO_4$. Removal of the pentane gave 13.5 g (90% yield) of product that by g.l.c. analysis was greater than 99% *trans*-3,4-dibromo-3-hexene. Analysis was carried out on the 1/4″ × 5′ 5% DEGS on Chromosorb G column (105 °C, 55 ml/min). Preparative g.l.c. on a 3/8″ × 13′ Tide (8) column (155 °C, 100 ml/min) gave the pure compound.

Anal. Calcd. for $C_6H_{10}Br_2$: C, 29.78; H, 4.18; Br, 66.05. Found: C, 30.31; H, 4.18; Br, 65.39.

The i.r. spectrum showed an absorption band in the C=C region. The n.m.r. spectrum was 1.10 (t, J = 7.5 c.p.s., 3.0H), 2.65 δ (q, J = 7.5 c.p.s., 2.0H).

In order to confirm that no *cis*-3,4-dibromo-3-hexene was being formed, a sample was prepared by acetophenone photo-sensitized isomerization of the *trans* compound in benzene. The g.l.c. analysis indicated a *trans*:*cis* ratio of 3.9 after 48 h. The dibromides were separated by preparative g.l.c. on a 3/8″ × 12′ 5% DEGS on Chromosorb G column (160 °C, 120 ml/min). The i.r. spectrum of the *cis* isomer showed a band at 6.3 μ in the C=C region and the n.m.r. spectrum was 1.16 (t, J = 7.5 c.p.s., 3.0H), 2.57 δ (q, J = 7.5 c.p.s., 1.9H).

Samples of 4,4-dibromo-3-hexanone and 3-acetoxy-4-bromo-3-hexene was also prepared by the reaction of NBS with 3-hexyne in acetic acid (7). Neither of these compounds were found to be formed in the molecular bromine reaction.

(e) 1-Hexyne

Bromine (20.0 g, 0.125 mole) in 30 ml of acetic acid was dropped slowly into 10 g (0.125 mole) of 1-hexyne in acetic acid and the reaction was left stirring for 12 h. The reaction was then poured into water and extracted with pentane. The extract was washed with 5% aqueous $NaHCO_3$, dried over Na_2SO_4, and then the pentane removed on the rotary evaporator. The yield was 24.4 g (80%) of a mixture of *trans*-1,2-dibromo-1-hexene (72%) and *cis*-1,2-dibromo-1-hexene (28%). The analysis was carried out on the 1/4″ × 5′ 5% DEGS on Chromosorb G column (105 °C, 50 ml/min).

Anal. Calcd. for $C_6H_{10}Br_2$: C, 29.99; H, 4.12; Br, 66.39. Found for the mixture: C, 29.78; H, 4.12; Br, 66.05.

The dibromides were separated by preparative g.l.c. on a 3/8″ × 12′ 5% DEGS on Chromosorb G column (120 °C, 100 ml/min). The i.r. spectrum of the *cis* isomer had a C=C stretch band at 6.23 μ whereas the *trans* isomer showed only a very weak band. The n.m.r. spectrum of the *trans* isomer was 1.00 (3, J = 7 c.p.s.,

Can. J. Chem. Downloaded from www.nrcresearchpress.com by 210.87.254.42 on 09/05/12
For personal use only.

3.3H), 1.2–1.8 (m, 4.2H), 2.60 (t, $J = 7$ c.p.s., 2.0H), and 6.20 δ (s, 1.0H). That of the *cis* was 0.92 (t, $J = 7$ c.p.s., 3.2H), 1.2–1.8 (m, 4.2H), 2.50 (t, $J = 7$ c.p.s., 2.1H), and 6.55 δ (t, $J = 1$ c.p.s., 1.0H). The coupling across the double bond between the vinyl and methylene protons is therefore somewhat larger for the *cis* compound (1 c.p.s.) than for the *trans* case (negligible). This effect has been observed previously (47, 48).

No other products were observed for the bromination of 1-hexyne in acetic acid.

Product Ratio Determinations

The procedures involved in the characterization of the reaction products were, in general, large scale reactions where the bromine concentrations are quite high. However, for accurate product determinations this procedure is undesirable because the k_3 kinetic process which would be dominant under these conditions is only well characterized for methylphenylacetylene (Table 2). Two procedures were used to ensure lower bromine concentration.

For reactive acetylenes, an acetic acid – bromine solution was dropped slowly into an acetylene solution so that the bromine concentration remained low because of rapid reaction. This procedure has the advantage that enough product can be obtained to compare g.l.c. and n.m.r. analysis. In all cases where this was possible, good agreement was obtained. As an example, for 4-methylphenylacetylene, 0.740 g of Br_2 in 10 ml of acetic acid was added slowly to 0.507 g of acetylene in 10 ml of acetic acid. Work-up yielded 1.06 g (85% yield). The g.l.c. analysis gave a *trans*:*cis* ratio of 1.31 whereas n.m.r. analysis indicated 1.25.

For less reactive acetylenes, stock solutions of known concentration were mixed and reaction allowed to go to completion. Since again bromine concentrations were kept low ($< 1.0 \times 10^{-2}$ *M*), only enough product for g.l.c. analysis was obtained.

In either case the reactions were worked-up by pouring into water, extracting with pentane, washing the extract with 5% $NaHCO_3$, drying over $MgSO_4$, filtering, and evaporating at room temperature on a rotary evaporator. For all the acetylenes the product ratios were determined on the 1/4″ × 5′ 5% DEGS on Chromosorb G column. Column conditions and retention times are given in the section on preparation and characterization of the compounds. Ratios are determined by peak areas, and reproducibility of the results in any given run or from run to run is estimated at ±1 to ±2%.

The financial assistance of the National Research Council of Canada is gratefully acknowledged. As well, one of us (J.A.P.) would like to thank NRCC for a studentship (1966–1969) and the Province of Ontario for a Graduate Fellowship (1969–1970).

1. P. B. D. de la Mare and R. Bolton. Electrophilic additions to unsaturated systems. Elsevier Publishing Co., 1966.
2. R. C. Fahey. The stereochemistry of electrophilic additions to olefins and acetylenes. *In* Topic in stereochemistry. Vol. III. Interscience. 1968. p. 237.
3. P. W. Robertson, W. E. Dasent, R. M. Milburn, and W. H. Oliver, J. Chem. Soc. 1628 (1950).
4. H. Sinn, S. Hopperdietzel, and D. Sauermann. Monatsh. Chem. **96**, 1036 (1965).
5. L. D. Bergel'son and I. N. Nazarov. Izv. Akad. Nauk. S.S.S.R., Otd. Khim. Nauk. **887**, 896 (1960).
6. J. L. Miller. Diss. Abst. **24**(11), 4403 (1964).
7. A. Jovtsceff and S. L. Spassov. Monatsh. Chem **98**, 2272 (1967).
8. J. H. Rolston and K. Yates. J. Amer. Chem. Soc. **91**, 1469 (1969).
9. J. H. Rolston and K. Yates. J. Amer. Chem. Soc. **91**, 1483 (1969).
10. H. C. Brown and Y. Okamoto. J. Amer. Chem. Soc. **80**, 4979 (1958).
11. B. G. van Leuwen and R. J. Ouellette. J. Amer. Chem. Soc. **90**, 7056 (1968).
12. J. A. Pincock and K. Yates. Can. J. Chem. **48**, 2944 (1970).
13. G. Heublein and E. Schütz. Z. Chem. **9**, 147 (1969).
14. D. S. Noyce *et al.* J. Amer. Chem. Soc. **87**, 2295 (1965); J. Amer. Chem. Soc. **89**, 6225 (1967); J. Amer. Chem. Soc. **90**, 372 (1968).
15. R. W. Bott, C. Eaborn, and D. R. M. Walton. J. Chem. Soc. 384 (1965).
16. L. L. Miller and D. A. Kaufman. J. Amer. Chem. Soc. **90**, 7282 (1968).
17. Z. Rappoport and A. Gal. J. Amer. Chem. Soc. **91**, 5246 (1969) and references therein.
18. D. R. Kelsey and R. G. Bergman. J. Amer. Chem. Soc. **92**, 228 (1970) and references therein.
19. R. Sustmann, J. E. Williams, M. J. S. Dewar, L. C. Allen and P. von R. Schleyer. J. Amer. Chem. Soc. **91**, 5350 (1969).
20. A. C. Hopkinson, K. Yates, and I. G. Csizmadia. J. Chem. Phys. In press.
21. K. J. Laidler. Chemical kinetics. McGraw-Hill, 1965 p. 89.
22. K. B. Wiberg. Physical organic chemistry. J. Wiley and Sons, 1964. p. 386–388.
23. K. Yates and W. V. Wright. Can. J. Chem. **45**, 167 (1967).
24. I. K. Walker and P. W. Robertson. J. Chem. Soc. 1517 (1939).
25. See ref. 2, p. 328.
26. R. C. Fahey and D. J. Lee. J. Amer. Chem. Soc. **88**, 5555 (1966).
27. S. Winstein, B. Appel, R. Baker and A. Diaz. Chem. Soc. Special Publication. **19**. 109 (1964).
28. M. L. Poutsma and J. L. Kartch. J. Amer. Chem. Soc. **89**, 6595 (1967).
29. (*a*) M. C. Cabaleiro and M. D. Johnson. J. Chem. Soc. *B*, 565 (1967). (*b*) M. D. Johnson and E. N. Trachtenburg. J. Chem. Soc. *B*, 827 (1966).
30. G. H. Schmid and M. Heinola. J. Amer. Chem. Soc. **90**, 3466 (1968).
31. G. Modena *et al.* J. Org. Chem. **34**, 2020 (1969) and preceding papers in the series.
32. (*a*) J.-E. Dubois *et al.* Bull. Soc. Chim. Fr. 2086 (1968); (*b*) J. Chim. Phys. 2009 (1968).
33. J. A. Pincock and K. Yates. J. Amer. Chem. Soc. **90**, 5643 (1968).
34. J.-E. Dubois *et al.* Bull. Soc. Chim. Fr. 3797 (1968) and preceding papers.
35. P. R. Wells. Linear free energy relationships. Academic Press, 1968.
36. C. G. Swain and W. P. Langsdorf. J. Amer. Chem. Soc. **73**, 2813 (1951).
37. K. Bowden and R. S. Cook. J. Chem. Soc. *B*, 1529 (1968).
38. B. F. Scott. Ph.D. Thesis. University of Toronto, Toronto, Ontario. 1967.

39. I. F. HALVERSTADT and W. D. KUMLER. J. Amer. Chem. Soc. **64**, 2988 (1942).
40. A. I. VOGEL. A Textbook of organic chemistry. 3rd Ed. Longmans, 1961. p. 1035.
41. P. DEBYE. Physik Z. **13**, 97 (1912).
42. A. I. VOGEL. Quantitative inorganic analysis. 3rd Edition. Longmans, 1961. p. 348.
43. (a) C. W. FOULK and A. T. BOWDEN. J. Amer. Chem. Soc. **48**, 2045 (1926). (b) N. H. FURMAN and E. B. WILSON. J. Amer. Chem. Soc. **50**, 277 (1928).
44. A. D. ALLEN and C. D. COOK. Can. J. Chem. **41**, 1084 (1963).
45. A. L. MCCLELLAN. Tables of experimental dipole moments. W. H. Freeman and Co., 1963. p. 53.
46. S. I. MILLER, G. R. ZIEGLER, and R. WIELESECK. Organic synthesis. W. G. Dauben, editor. Vol. 45. J. Wiley and Sons, 1965. p. 86.
47. A. A. BOTHNER-BY, C. NAAR-COLIN, and H. GÜNTHER. J. Amer. Chem. Soc. **84**, 2748 (1962).
48. J. W. EMSLEY, J. FEENEY, and L. H. SUTCLIFFE. High resolution nuclear magnetic resonance spectroscopy. Vol. 1. Pergamon Press. p. 730.

Can. J. Chem. Downloaded from www.nrcresearchpress.com by 210.87.254.42 on 09/05/12
For personal use only.

Can. J. Chem. Downloaded from www.nrcresearchpress.com by 210.87.254.40 on 09/05/12
For personal use only.

Mechanism of decarboxylation of substituted anthranilic acids at high acidity

G. E. DUNN AND S. K. DAYAL
Department of Chemistry, University of Manitoba, Winnipeg 19, Manitoba

Received March 12, 1970

The rates of decarboxylation of 4-methyl-, 4-methoxy-, and unsubstituted anthranilic acids have been determined in aqueous buffers over the p*H* range 2.5–3.8. Electron-releasing substituents increase the rates of ring-protonation about equally for an acid and its anion, and decrease the ratio of decarboxylation to deprotonation of the protonated acid. Rates, ^{13}C-carboxyl kinetic isotope effects, and deuterium solvent isotope effects have been determined for the decarboxylation of anthranilic acid in aqueous sulfuric acid up to 10 *M*. No evidence for decarboxylation by cleavage of the unionized carboxyl group was obtained.

Canadian Journal of Chemistry, **48**, 3349 (1970)

In previous papers (1, 2) it was proposed that the general mechanism for decarboxylation of substituted anthranilic acids is as shown in eq. 1,

[1]

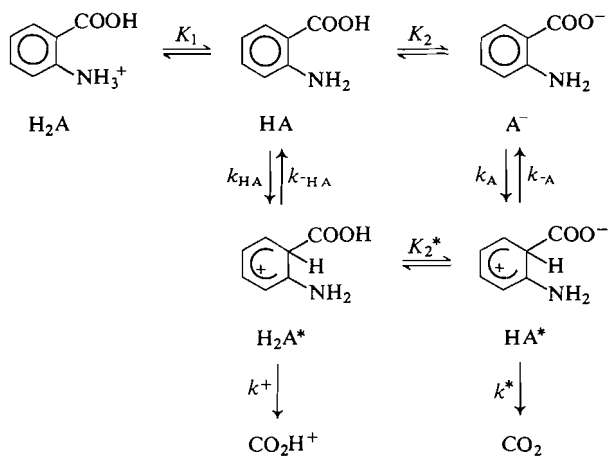

where HA can be either unionized acid, as shown, or zwitterion and for which the overall rate constant is given by eq. 2. For 4-methoxyanthranilic acid at 60° there is no ^{13}C-carboxyl kinetic isotope effect at low acidity, so k_{-A} is small compared to k^* and, because there is such an isotope effect at high acidity, k^+ is small compared to k_{-HA} (2). Hence, eq. 2 reduces to eq. 3. It was also shown that for 4-methoxyanthranilic acid in up to 2 *M* HCl, $k^+[H^+]$ is negligible compared to $k^*K_2^*$ (2), leading to the rate expression, eq. 4, which fits the rate data from p*H* 3.8 to 0.

$$[2] \quad k = \frac{k_A K_1 K_2 + k_{HA} K_1 [H^+]}{K_1 + [H^+]} \times \frac{k^* K_2^* + k^+ [H^+]}{(k^* + k_{-A}) K_2^* + (k^+ + k_{-HA})[H^+]}$$

$$[3] \quad k = \frac{k_A K_1 K_2 + k_{HA} K_1 [H^+]}{K_1 + [H^+]} \times \frac{k^* K_2^* + k^+ [H^+]}{k^* K_2^* + k_{-HA} [H^+]}$$

$$[4] \quad k = \frac{k_A K_1 K_2 + k_{HA} K_1 [H^+]}{K_1 + [H^+]} \times \frac{1}{1 + \frac{k_{-HA}}{k^* K_2^*} [H^+]}$$

The question then arises whether the $k^+[H^+]$ term may become significant at higher values of $[H^+]$. An evaluation of the k^*/k^+ ratio, or the establishment of a lower limit for it, would be of interest as a measure of the relative reactivities of CO_2 and CO_2H^+ as electrophilic leaving groups.

In order to work at higher acidities it is necessary to allow for the fact that $[H^+]$ in eqs. 2 and 3 actually represents hydrogen ion activity, which

Can. J. Chem. Downloaded from www.nrcresearchpress.com by 210.87.254.40 on 09/05/12
For personal use only.

can not be approximated by hydrogen ion concentrations at values higher than those used in the previous work (1). The common practice in such situations is to replace hydrogen ion concentration $[H^+]$, by the Hammett acidity function h_0 (3), so that a reaction which obeys the simple kinetic expression

$$k = k_H[H^+]$$

at low acidities, would be expected to fit the equation

$$k = k_H h_0$$

at high acidities. Since h_0 increases much more rapidly than $[H^+]$ it is convenient to use $H_0 = -\log h_0$ (3) and to test the fit of the data to the above equation by plotting $\log k$ against $-H_0$, which should give a straight line of unit slope. In fact, however, it is commonly observed that although such plots give straight lines they often have non-unit slopes (3). This implies that the ratio $\gamma^\ddagger/\gamma$ of the activity coefficients of transition and ground states in the reaction investigated is not equal to the ratio γ_{BH^+}/γ_B of the protonated and unprotonated forms of the indicators used to set up the acidity function, but that the two ratios are linearly related. In other words, different acid-catalyzed reactions may require different acidity functions to describe them but, since most acidity functions are proportional to H_0 (4), the rates of most acid-catalyzed reactions will fit the relationship given by eq. 5, where n is often, but not

$$[5] \quad \log k = \log k_H - nH_0 \quad \text{or} \quad k = k_H(h_0)^n$$

always, unity. It is important to note that a linear plot of $\log k$ *vs.* $-H_0$ with non-unit slope corresponds to a curved plot of k *vs.* h_0.

Willi *et al.* have reported (5) that the decarboxylation of anthranilic acid fits eq. 4 up to $H_0 = -1.4$ (4 *M* HCl) so that there is no evidence for cleavage of CO_2H^+ in this acid. Similarly, Longridge and Long (6) find only CO_2 cleavage from azulene-1-carboxylic acid up to $H_0 = -2.8$ (6 *M* $HClO_4$). For *p*-aminobenzoic acid, however, Willi and Vilk find some deviation from eq. 4 beginning at $H_0 = -0.68$ (2 *M* HCl) which is explained as a small contribution from the term $k^+[H^+]$ of eq. 3 corresponding to cleavage of CO_2H^+ (7). However, they used h_0 for $[H^+]$ in eq. 4 so that the deviation from linearity may result from a non-unit value of n in eq. 5. In fact, if their data are replotted in logarithmic form the curvature disappears.

There is, therefore, as yet no compelling evidence for decarboxylation of a carboxylic acid in its unionized form. It was the object of the present work to look for such evidence. Two approaches were used; first, investigation of the effects of substituents on the various rate constants of eq. 3 with the hope of gaining information which would make it possible to choose a carboxylic acid for which cleavage of CO_2H^+ would be readily demonstrable and, second, examination of the effect of increasing acidity on the rate of decarboxylation at high acidities.

Results and Discussion

Equation 3 describes the general dependence of rate of decarboxylation upon acidity according to the mechanism of eq. 1. This rather complex rate expression can be simplified to a straight-line equation in three separate regions of acidity. At low acidity (pH greater than 1) there is no appreciable ^{13}C-carboxyl kinetic isotope effect in the decarboxylation of anthranilic (8) or 4-methoxyanthranilic acids (2). Consequently, the right-hand fraction in eq. 3 must equal unity at low acidities, since the rate constants for carbon–carbon bond breaking, k^* and k^+, appear only in this fraction. Then eqs. 2 and 3 reduce to eq. 6.

$$[6] \quad k\left(1 + \frac{[H^+]}{K_1}\right) = k_A K_2 + k_{HA}[H^+]$$

At intermediate acidities, where $[H^+]$ exceeds K_1 and $k_A/k_{HA}K_2$, the left-hand side of eq. 3 reduces to $k_{HA}K_1$. If it is then assumed that $k^+[H^+]$ is negligible compared to $k^*K_2^*$, as was shown to be true for the 4-methoxy acid at 60° (1), eq. 3 becomes eq. 7.

$$[7] \quad \frac{1}{k} = \frac{1}{k_{HA}K_1} + \frac{k_{-HA}}{k_{HA}K_1} k^*K_2^*[H^+]$$

At higher acidities, where $[H^+] \gg k^*K_2^*/k_{-HA}$, and still assuming $k^+[H^+]$ is negligible, eq. 3 can be reduced to eq. 8.

$$[8] \quad k = \frac{k_{HA}K_1}{k_{-HA}} \frac{k^*K_2^*}{[H^+]}$$

Of these three straight-line equations, only eq. 6 is applicable at acidities low enough to permit using hydrogen ion concentration as an approximation for activity. In eqs. 7 and 8, $[H^+]$ should be replaced by $(h_0)^n$. This makes the region of intermediate acidities (eq. 7) difficult to handle, since it contains three unknowns of which one (n)

TABLE 1

Rates of decarboxylation of anthranilic acids in phthalate buffer at 80 °C, $\mu = 0.1$

Anthranilic		4-Methyl-		4-Methoxy-	
pH	$k \times 10^6$ (s^{-1})	pH	$k \times 10^5$ (s^{-1})	pH	$k \times 10^4$ (s^{-1})
2.53	2.07	2.53	1.67	2.48	2.67
2.88	1.76	2.86	1.50	2.81	2.09
3.13	1.60	3.14	1.18	3.26	1.40
3.29	1.54	3.29	0.959	3.53	1.32
3.54	1.43	3.56	0.863	3.81	1.15
		3.84	0.840		

TABLE 2

Rate and equilibrium constants for the decarboxylation of anthranilic acids

T (°C)	Equation	Constant	Anthranilic	4-Methyl-	4-Methoxy-
25		K_1 (M)	6.72×10^{-3}	4.51×10^{-3}	8.74×10^{-3}
25		K_2 (M)	1.40×10^{-5}	8.45×10^{-6}	1.33×10^{-5}
80	6	k_A ($s^{-1} M^{-1}$)	0.096	0.82	8.3
80	6	k_{HA} ($s^{-1} M^{-1}$)	5.7×10^{-4}	8.9×10^{-3}	7.8×10^{-2}

is an exponent. At high acidities eq. 8 can be used in the straight-line form, eq. 9.

$$[9] \quad \log k = nH_0 + \log \frac{k_{HA}K_1}{k_{-HA}} k^*K_2^*$$

Anthranilic acid and its 4-methyl and 4-methoxy derivatives were chosen for examination of the substituent effect because electron-attracting substituents reduce the rate of decarboxylation to values inconvenient for measurement (1). Table 1 shows rates of decarboxylation at 80° as a function of pH. The k_A and k_{HA} values obtained by plotting the data of Table 1 in eq. 6 are shown in Table 2. Since the pH data of Table 1 were obtained at 25°, as were the available values of K_1 and K_2 (9), the k_A and k_{HA} results shown in Table 2 are only approximate. However, they should not be in error by more than a factor of two, and the errors will be in the same direction for all three acids, so comparisons between the rate constants for protonation of neutral acid, k_{HA}, and of anion, k_A, should be valid. Both increase by a factor of about 10 each time the 4-substituent is changed from hydrogen to methyl to methoxy, so that the ratio of rates of protonation of acid and anion is only slightly affected by 4-substituents. Since K_1 and K_2 are also not much affected by substituents (9), it is evident that substituents will have little influence on the ratio of rates of formation of the protonated intermediates derived from acid and anion, respectively.

To see the effects of substituents upon the rates of decarboxylation of the protonated intermediates it is necessary to work at higher acidities where C—C bond breaking becomes part of the rate-determining process. Since the region of intermediate acidity is difficult to analyze, attention was directed to the region of high acidity where eqs. 8 and 9 apply. Equation 9 was derived on the assumption that $k^+[H^+]$ is negligible. Consequently, a plot of log k *vs.* H_0 should give a straight line if the assumption is correct. If, in fact, cleavage of the unionized carboxyl group occurs, then the rate will decrease less rapidly with increasing acidity than eq. 9 predicts. Consequently, an upward curvature of the plot would indicate CO_2H^+ decarboxylation.

Rates become inconveniently low at high acidities so the reaction temperature was increased to 115°. Under these conditions the 4-methoxy acid gave erratic and irreproducible results, possibly because of cleavage of the methoxy group. Anthranilic acid behaved well, however, and the rates in moderately concentrated sulfuric acid solutions are reported in Table 3. Figure 1 shows that the data do not deviate from eq. 9, so it must be concluded that CO_2H^+ decarboxylation is unimportant in sulfuric acid up to at least 60%. In sulfuric acid more

Can. J. Chem. Downloaded from www.nrcresearchpress.com by 210.87.254.40 on 09/05/12
For personal use only.

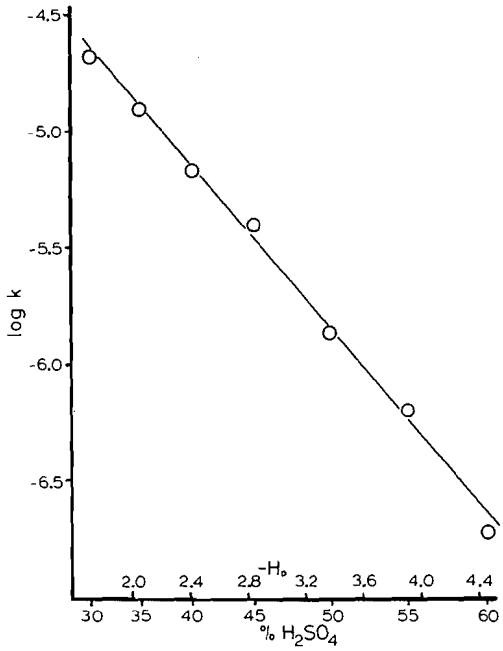

FIG. 1. Rates of decarboxylation of anthranilic acid in sulfuric acid solutions at 115 °C.

TABLE 3

Rates of decarboxylation of anthranilic acid in sulfuric acid at 115 °C

H_2SO_4 (%)	H_0	$k \times 10^6$ (s^{-1})
30	−1.72	21.1
35	−2.06	12.7
40	−2.4	7.26
45	−2.85	3.96
50	−3.38	1.35
55	−3.91	0.620
60	−4.46	0.152

concentrated than this, anthranilic acid becomes significantly protonated on the functional group and is half-protonated at about 72% sulfuric acid (10).

Figure 1 yields a value of 0.7 for the slope, n, thus confirming that a treatment which assumed unit slope would be unreliable. The intercept gives 3.6×10^{-4} s^{-1} as the value of $k_{HA}K_1k^*K_2^*/k_{-HA}$. If the value of $k_{HA}K_1$ derived from eq. 6 at ionic strength 0.1 could be applied in 30–60% sulfuric acid, this would yield a value of about 0.01 for the ratio of deprotonation to decarboxylation of ring-protonated anthranilic acid. Obviously, the solvents are very different, but 0.01 may be taken as indicative of the order of magnitude of the ratio.

Another approach to the substituent effect on the ratio of deprotonation to decarboxylation is through kinetic isotope effects. Since the only rate constants affected by C-isotopic substitution in the carboxyl group are those for the C—C breaking steps, k^* and k^+, there will be no ^{13}C-carboxyl kinetic isotope effect until $k_{-HA}[H^+]/k^*K_2^*$ in eq. 4 approaches unity. For 4-methoxyanthranilic acid this has been shown to occur at $[H^+] \sim 0.2$ M (1), so that there is a large carbon isotope effect at $[H^+] = 2$ M (2). On the other hand, the value of 0.01 for $k_{-HA}/k^*K_2^*$ in anthranilic acid indicates that for this acid the carbon isotope effect will not become important until $(h_0)^n \sim 100$; that is, until the sulfuric acid concentration reaches about 4.5 M. This prediction agrees with the observation by Stevens *et al.* that there is no detectable isotope effect for anthranilic acid up to 1 M sulfuric acid. The prediction is confirmed by the data of Table 4. In 2 M sulfuric acid the carbon isotope effect is negligible, but in 10 M sulfuric acid it is large.

It is therefore possible to conclude that, although electron-releasing substituents increase the rate of ring-protonation of anthranilic acids, they also increase the ratio of ring-deprotonation to decarboxylation of the ionized carboxyl group. It thus appears possible that decarboxylation of the unionized carboxyl group might reasonably be sought among acids with several electron-releasing substituents. It is unfortunate that 4-methoxyanthranilic acid is not stable at the high acidities required.

The change in carbon isotope effect with acidity reflects the change in mechanism from

TABLE 4

^{13}C-Carboxyl kinetic isotope effect in the decarboxylation of anthranilic acid in sulfuric acid at 115 °C

H_2SO_4 (M)	% Reaction	Mass ratio, 45/44	Mean	$100\left(\frac{k_{12}}{k_{13}} - 1\right)$
2.0	100	0.010384 0.010382	0.010383	—
2.0	15	0.010372 0.010370 0.010371 0.010372	0.010371	0.1
10.0	15	0.010036 0.010041 0.010020 0.010064 0.010019 0.010051	0.010038	3.7

Can. J. Chem. Downloaded from www.nrcresearchpress.com by 210.87.254.40 on 09/05/12
For personal use only.

TABLE 5

Solvent deuterium isotope effect in the decarboxylation of anthranilic acid in sulfuric acid at 115 °C

Sulfuric acid (M)	k (s^{-1}) H_2SO_4–H_2O	k (s^{-1}) D_2SO_4–D_2O	k_H/k_D
1.71	7.62×10^{-5}	2.13×10^{-5}	3.57
2.56	4.45×10^{-5}	1.40×10^{-5}	3.20
5.50	7.48×10^{-6}	2.30×10^{-6}	3.21
7.50	1.51×10^{-6}	5.04×10^{-7}	3.07

slow protonation (eq. 6) to slow CO_2 cleavage (eq. 8) but it can hardly be used to detect the onset of CO_2H^+ cleavage, because the differences in ^{13}C-isotope effect between CO_2 and CO_2H^+ cleavage will no doubt be too small to detect. However, a change from slow CO_2 cleavage ($k^*K_2^*$) to slow CO_2H^+ cleavage (k^+) would be accompanied by the disappearance of the ionization constant K_2^* from the rate expression (eq. 8). It would therefore appear possible to detect the change by means of a solvent deuterium isotope effect.

Table 5 shows the rates of decarboxylation of anthranilic acid in H_2O–H_2SO_4 and D_2O–D_2SO_4 solutions of concentrations such that eq. 8 should apply. Since $H_0 = D_0$ at the same acid concentrations (11), the rate ratios should reflect the solvent deuterium isotope effects on the various rate and equilibrium constants in the rate expression. The rate ratio k_{HA}/k_{-HA} in eq. 8 represents the equilibrium constant for ring-protonation of anthranilic acid, while K_1 and K_2^* are equilibrium constants for deprotonations. It would therefore be expected that k_{HA}/k_{-HA} will increase in deuteriated solutions while K_1 and K_2^* will decrease by a factor of about 2–3 (12). The overall effect of deuteriation of the solvent should therefore be a decrease in rate, as observed.

If $k^*K_2^*/[H^+]$ were to become small compared to k^+, K_2^* would disappear from eq. 8, leading to a decrease in the rate ratio k_H/k_D. However, this is not observed. When the experimental uncertainty of about 2% in each rate constant is combined with some additional uncertainty in reproducing acid concentrations in the two solvents, the combined uncertainties in the rate ratio k_H/k_D are at least 5%. Within this error, Table 5 shows the solvent deuterium isotope effect to be constant.

It may reasonably be concluded, therefore, that there is no evidence for cleavage of CO_2H^+ in acidities up to at least $H_0 = -4$. This means that $k^*K_2^*/k^+ > 10^4$. Although K_2^* is unknown it is probably considerably less than 1, so that the rate constant for CO_2 cleavage, k^*, must be greater than that for CO_2H^+ cleavage, k^+, by 10^5 or more.

Experimental

Preparation and purification of the three anthranilic acids have been previously described (9). Standardized solutions of perchloric and sulfuric acids were diluted by weight. Rates were determined by the ampoule technique, following concentration changes by measuring absorbance on a Beckman Model DU spectrophotometer in alkaline solution at 320 nm for 4-methoxy-, at 315 nm for 4-methyl-, and at 310 nm for anthranilic acid. Excellent first-order plots were obtained to more than three half lives. ^{13}C-Isotope effects were determined as described previously (2), except that the percent reaction was calculated from the amount of unreacted starting material measured spectrophotometrically. Mass ratios, $^{13}CO_2/^{12}CO_2$, were determined with a mass spectrometer, MAT Model GD150, having dual collectors.

The authors are grateful to Mr. W. D. Buchannon for the mass spectral measurements, and to the National Research Council of Canada for financial support.

1. G. E. Dunn, P. Leggate, and I. E. Scheffler. Can. J. Chem. **43**, 3080 (1965).
2. G. E. Dunn and J. Buccini. Can. J. Chem. **46**, 563 (1968).
3. F. A. Long and M. A. Paul. Chem. Rev. **57**, 935 (1957).
4. K. Yates and R. A. McClelland. J. Amer. Chem. Soc. **89**, 2686 (1967).
5. A. V. Willi, C. M. Won, and P. Vilk. J. Phys. Chem. **72**, 3142 (1968).
6. J. L. Longridge and F. A. Long. J. Amer. Chem. Soc. **90**, 3092 (1968).
7. A. V. Willi and P. Vilk. Z. Phys. Chem. Frankfurt, **59**,189 (1968).
8. W. H. Stevens, J. M. Pepper, and M. Lounsbury. Can. J. Chem. **30**, 529 (1952).
9. P. Leggate and G. E. Dunn. Can. J. Chem. **43**, 1158 (1965).
10. R. I. Zalewski and G. E. Dunn. Can. J. Chem. **46**, 2469 (1968).
11. E. Hogfeldt and J. Bigeleisen. J. Amer. Chem. Soc. **82**, 15 (1960).
12. W. J. Albery. Progr. in Reac. Kinetics, **4**, 353 (1967).

Can. J. Chem. Downloaded from www.nrcresearchpress.com by 210.87.254.40 on 09/05/12
For personal use only.

Can. J. Chem. Downloaded from www.nrcresearchpress.com by 210.87.254.5 on 09/05/12
For personal use only.

The H_- acidity function for dimethylformamide–water

E. BUNCEL AND E. A. SYMONS
Department of Chemistry, Queen's University, Kingston, Ontario

AND

DOUGLAS DOLMAN AND ROSS STEWART
Department of Chemistry, University of British Columbia, Vancouver, British Columbia

Received February 2, 1970

The H_- acidity function has been determined for *N*,*N*-dimethylformamide–water mixtures containing tetramethylammonium hydroxide by the Hammett indicator method. Basicity in the aqueous dimethylformamide system exceeds that in aqueous tetramethylenesulfone but is slightly less than in aqueous dimethylsulfoxide, at equivalent molar compositions of solvent and base. However, the basic aqueous dimethylformamide solvent system is only of limited utility as a result of reaction of hydroxide ion with the dimethylformamide.

Canadian Journal of Chemistry, **48**, 3354 (1970)

Introduction

There has been an increasing interest recently in the properties of strongly basic systems and particularly in the utilization of dipolar aprotic media in achieving such systems. The H_- acidity function, as defined by Hammett (1), measures the proton abstracting ability of a medium toward a neutral, weakly acidic, substrate AH.

$$[1] \qquad H_- = -\log a_{H^+}\frac{f_{A^-}}{f_{HA}} = pK_a - \log\frac{[A^-]}{[HA]}$$

In eq. [1], a_{H^+} is the hydrogen ion activity in solution, f_{A^-}, f_{HA} are activity coefficients, pK_a is the dissociation constant and $[A^-]/[HA]$ is the ionization ratio, often termed the indicator ratio. In very dilute aqueous solution $H_- = pH$ but above 1 *M* base the H_- scale increases more rapidly than the pH scale; an aqueous 10 *M* NaOH solution has a basicity corresponding to $H_- = 16.4$ (2). Solutions of even higher basicity are available by replacing, in part, the aqueous component of the medium with a dipolar aprotic solvent such as dimethylsulfoxide (DMSO) and keeping the hydroxide ion concentration quite low. For example a 50 mole% aqueous DMSO solution, 0.01 *M* in Me_4NOH, has $H_- = 17.3$ (3). The enhanced basicity of such media has been attributed to increased hydroxide ion activity and concurrent decreased water activity (4).

A number of dipolar aprotic media in combination with water or alcohols have been studied in the H_- context, including tetramethylenesulfone–water (3, 5), pyridine–water (3), DMSO–water (3), DMSO–methanol (6), and DMSO–ethanol (7). Summaries of data for these and other basic systems (including amines) are available (8, 9).

N,*N*-Dimethylformamide (DMF) as a typical dipolar aprotic solvent (10), has the property of greatly enhancing the rates of reactions involving anionic or basic reagents (10–13). Since in previous work we had used aqueous DMF media for proton abstraction, in 1,3-dinitrobenzene (14), 1,3,5-trinitrobenzene (15, 16), and 2,4,6-trinitrotoluene (17), a knowledge of the basicity of such solutions was desirable. Hence, an H_- study was undertaken and is presently reported.

Experimental

Reagents

DMF (Fisher Certified Reagent) was purified by vacuum distillation from phosphorus pentoxide after standing over Linde Type 4A molecular sieves (18). The middle fraction, b.p. 38–41° over the pressure range 6–8 mm, was collected and stored in the dark at room temperature under nitrogen. The presence of dimethylamine impurity in the distilled DMF was estimated by adding ca. 25 mg of 1,3,5-trinitrobenzene to 1–2 ml of solvent and noting the color of the resulting solution. Pure solvent yielded a pale yellow solution whereas the presence of dimethylamine gave various shades of orange, as a result of complex formation (19).

Distilled water used to prepare the DMF–water mixtures was degassed by boiling for 1 h and bubbling nitrogen through during subsequent cooling.

Tetramethylammonium hydroxide solutions were obtained by dilution of a 25% aqueous solution (Matheson, Coleman and Bell) followed by titration with standard acid. Sodium hydroxide solutions were prepared similarly. The resulting stock solutions of bases were stored in sealed polyethylene bottles equipped with rubber syringe caps.

TABLE 1

The pK_a data and spectral characteristics of the H_- indicators in DMF–water

Indicator	Neutral form* λ_{max} mμ	ε	Mole% DMF	Anionic form* λ_{max} mμ	ε	pK_a Observed	Literature (ref.)
2,4-Dinitrodiphenylamine (**1**)	364	17 100	58.8	432	19 100	(13.84)‡	13.84 (4)
2,4-Dinitro-4′-aminodiphenylamine (**2**)	378	12 700	62.6	488	17 000	14.61	14.64 (3)
4-Nitrodiphenylamine (**3**)	400	22 200	76.7	502	36 400	15.64	15.67 (4)
4-Chloro-2-nitroaniline (**4**)	420	5 400	84.2	515	8 400†	16.93	17.08 (4)
2-Nitrodiphenylamine (**5**)	430	6 200	84.2	541	9 100†	17.99	17.91 (4)
4-Methylsulfonyldiphenylamine (**6**)	317	22 000	84.2	378	30 000†	18.62	18.80 (4)
2,3,5,6-Tetrachloroaniline (**7**)	314	3 600	84.2	372	4 400†	19.02	19.22 (4)

*The spectrum of the neutral form of the indicator was taken in the medium given (third column). The composition of this medium was chosen in such a manner that in the presence of 0.019 *M* tetramethylammonium hydroxide the indicator would be completely ionized.
†Potassium *t*-butoxide was added to generate the anionic form.
‡Indicator **1** is used as the anchor indicator (4).

The indicators used (3, 4) were purified by recrystallization and/or column chromatography and had the following m.p. (uncorrected) and absorption maxima. 2,4-Dinitrodiphenylamine (**1**), m.p. 156.5–157.0°, ε (352 mμ) 17 600 in 95% EtOH. 2,4-Dinitro-4′-aminodiphenylamine (**2**), m.p. 181.5–183.5°, ε (375 mμ) 14 600 in sulfolane. 4-Nitrodiphenylamine (**3**), m.p. 133.5–135.0°, ε (393 mμ) 21 400 in 95% ethanol. 4-Chloro-2-nitroaniline (**4**), m.p. 117.0–117.5°, ε (422 mμ) 4570 in water. 2-Nitrodiphenylamine (**5**), m.p. 75.0–75.5°, ε (425 mμ) 6540 in 95% ethanol. 4-Methylsulfonyldiphenylamine (**6**), m.p. 170–170.5°, ε (308 mμ) 24 600 in 95% ethanol. 2,3,5,6-Tetrachloroaniline (**7**), m.p. 108.5–109.0°, ε (308 mμ) 4040 in 95% ethanol.

Procedures

A series of DMF–water mixtures of known compositions were prepared by introducing into 50 ml volumetric flasks the two components, first a known volume of DMF and then making up to mark with water, and weighing after each addition. Stock solutions of the indicators were made up in pure DMF. The main body of indicator measurements was taken using tetramethylammonium hydroxide as base (0.019 *M*). Sodium hydroxide (0.019 *M*) was used for a limited range of solvent compositions with identical procedures.

Spectral measurements were taken by means of a 1 cm quartz cell placed in the thermostatted (25°) cell compartment of a Bausch and Lomb Spectronic 600 spectrophotometer coupled to a Sargent SRL Recorder. The cell was filled under nitrogen by means of syringes through a silicone rubber disc (3). First 3.0 ml of a given DMF–water mixture was introduced, followed by 25 μl of indicator stock solution in DMF ($3–23 \times 10^{-3}$ *M* depending on the extinction coefficient) and the absorbance at λ_{max} was measured. A 29.2 μl aliquot of the 2.09 *N* Me_4NOH solution was then added and the spectrum recorded. In general the absorbance decreased with time, as a result of reaction of hydroxide with DMF (basic hydrolysis (20)) and extrapolation at constant λ was required to obtain zero time absorbance values. Measurements were performed in duplicate.

Indicator measurements as a function of Me_4NOH concentration were performed similarly but now the DMF–water composition was kept constant and stock base solutions of varying concentrations were added in constant volume.

Ionization Ratio Data

Evaluation of the indicator ionization ratio $I = [A^-]/[HA] = (\varepsilon - \varepsilon_{HA})/(\varepsilon_{A^-} - \varepsilon)$, requires availability of the extinction coefficient of the neutral form (ε_{HA}), of the ionized form (ε_{A^-}), as well as the extinction in a medium where the indicator is partly ionized (ε), all values referring to a particular wavelength. The value of ε_{HA} was recorded in the DMF–water medium of composition such that addition of Me_4NOH (final concentration 0.019 *M*) resulted in complete ionization and thus also yielded ε_{A^-}. Since beyond *ca.* 75 mole% DMF, Me_4NOH became increasingly insoluble, for the weaker indicator acids ε_{A^-} values were obtained by addition of solid potassium *t*-butoxide (Alfa Inorganics) to ca. 85 mole% DMF in small amounts until a maximum absorbance was obtained. The extinction data (ε_{HA}, ε_{A^-}) for the various indicators and the media in which the values were obtained are given in Table 1. Measurement of indicator ratios was usually confined to *I* values ranging between 0.1 and 10.

Results

The ionization ratios determined for each indicator over the solvent composition range resulting from 10 to 90% ionization in 0.019 *M* Me_4NOH were used to construct curves of log *I* vs. mole% DMF. By means of the normal stepwise overlap procedure (1, 21) and using the relationship $pK_2 - pK_1 = \log I_1 - \log I_2$ the p*K*'s of the various indicators were evaluated relative to the standard indicator 2,4-dinitrodiphenylamine, pK_a 13.84 (3). The resulting pK_a values are listed in Table 1. The H_- values were then calculated from the pK_a and log *I* values (eq. [1]) for each indicator and solvent composition. The H_- values over the entire range of solvent compositions, averaged for the various indicator measurements, are recorded in Table 2.

Can. J. Chem. Downloaded from www.nrcresearchpress.com by 210.87.254.5 on 09/05/12
For personal use only.

TABLE 2

The H_- values for dimethylformamide–water mixtures containing 0.019 M tetramethylammonium hydroxide

Mole % DMF	Average H_- value	Deviation from the mean	Particular indicators
0.00	12.28	—	(pH)
5.29	12.87	—	**1***
7.83	13.15	—	**1**
10.47	13.45 (13.41)†	—	**1**
14.92	13.95 (13.93)†	±0.01	**1, 2**
19.82	14.42 (14.41)†	±0.03	**1, 2**
24.50	14.80 (14.76)†	±0.03	**1, 2, 3**
29.34	15.20 (15.12)†	±0.02	**2, 3**
34.69	15.58 (15.53)†	±0.02	**2, 3**
39.31	15.95 (15.91)†	—	**3**
43.98	16.30 (16.20)†	±0.01	**3, 4**
49.61	16.70 (16.61)†	±0.03	**3, 4**
54.02	17.08 (16.97)†	±0.03	**4, 5**
58.77	17.49 (17.28)†	±0.01	**4, 5**
62.62	17.82 (17.54)†	±0.02	**4, 5, 6**
67.09	18.29 (17.81)†	±0.02	**5, 6, 7**
70.90	18.67	±0.02	**5, 6, 7**

*Extrapolated value from log I — mole% DMF plot for indicator **1**.
†H_- values in media containing 0.019 M NaOH (see text on solubility consideration). The data were obtained using indicators **1**, **3**, and **4** only.

Plots of log I vs. H_- for all the indicators are given in Fig. 1; the slopes range between 0.99 and 1.00.

Some H_- measurements were carried out in which the solvent composition was kept constant and the tetramethylammonium hydroxide concentration varied. The results, for three solvent compositions, are given in Table 3. If the equation $\Delta H_- = \log [OH^-]_2/[OH^-]_1$ holds, as previously noted for $[OH^-] < 1$ M in media of relatively high water content (8), then a plot of H_- vs. log $[OH^-]$ should be linear with unit slope. The data for the 15.9 mole% DMF medium with indicator **1** show significant deviation in this plot[1] above 0.05 M Me_4NOH. It is possible that the cause of this deviation is that the two activating nitro groups in **1** cause this indicator to be susceptible to addition of OH^- to aromatic carbon to form a Meisenheimer type adduct (22, 23) at high base concentrations. It is noteworthy that Ritchie and Uschold (24) made the following observation in titrating this same indicator in pure DMSO. Upon the addition of one equivalent of base to the indicator solution a good end-point was observed but excess base caused the solution color to change from reddish brown (believed to be due to the anion) to a bright red–orange (species unknown). This color change was accompanied by a second break in the titration curve.

[1]The data of Table 3 were plotted, H_- *vs.* log $[OH^-]$, and lines of unit slope were drawn, the deviation being estimated visually. If the lines are drawn through the actual data, one then obtains slope values of 0.88, 1.00, and 1.21, for the 15.9, 32.6, and 55.5 mole% DMF compositions, respectively.

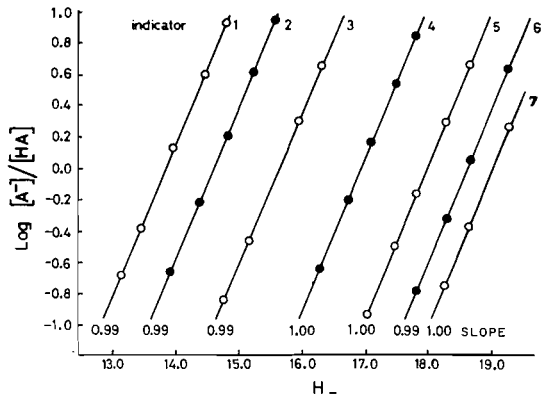

FIG. 1. Plots of log [ionization ratio] vs. H_- for the indicators used in determining the H_- function for the DMF–water system containing 0.019 M Me_4NOH. The indicators are numbered as in Table 1.

Indicator measurements in which sodium hydroxide was used as base were explored but were limited by solubility considerations. The H_- values, obtained as for the tetramethylammonium hydroxide system, are given in Table 2. The two sets of results agree initially but above *ca.* 50 mole% DMF the NaOH data exhibit increasing deviation from the Me_4NOH data, apparently as the result of decreasing solubility of sodium hydroxide in DMF solutions of relatively low water content. The low solubility of sodium hydroxide in DMF solutions was noted previously (10).

TABLE 3

The H_- values as a function of $[Me_4NOH]$ at constant medium compositions

$[Me_4NOH]$ (M)	H_- (mole% DMF)		
	H_- (15.9)*	H_- (32.6)†	H_- (55.5)‡
0.0066	13.63	14.97	16.74
0.0134	13.94	15.27	17.13
0.0274	14.22	15.56	17.44
0.0725	14.53	15.99	17.95
0.138	14.69	16.27	—
0.296	—	16.62	—

*Data obtained using indicator **1**.
†Indicator **3** used.
‡Indicator **4** used.

Can. J. Chem. Downloaded from www.nrcresearchpress.com by 210.87.254.5 on 09/05/12
For personal use only.

TABLE 4

Selected H_- data for aqueous binary mixtures with several dipolar aprotic solvents, each with 0.011 M tetramethylammonium hydroxide

Mole% dipolar aprotic component	Aqueous pyridine*	Aqueous tetramethylene sulfone*	Aqueous dimethylformamide†	Aqueous dimethylsulfoxide*
20	13.75	13.22	14.20	14.48
40	14.76	14.25	15.75	16.50
60	15.31	15.56	17.34	18.50

*Data from ref. 3
†Data from present work recalculated to allow for change in base concentration

Discussion

The validity of acidity function measurements has been tested in the past by several criteria. One criterion concerns the nature of log $I - H_-$ plots. In the present work the linearity of these plots (Fig. 1) and their unit slope provides a good indication of the validity of the overlap procedure for this series of aniline and diphenylamine indicators. Another criterion is the requirement of constancy of indicator pK_a values, independent of the nature of the medium (see also ref. 12). The pK's obtained in the aqueous DMF media (Table 1) agree within 0.2 pK units with literature values, which is within the acceptable limit (8). Since the pK's are determined in a step-wise manner, a possible error of 0.2 pK units in indicator **6** would automatically result in corresponding error in **7**.

Comparative H_- data for several solvent systems at constant (mole%) medium composition are presented in Table 4. It is seen that the effectiveness of the dipolar aprotic component in enhancing medium basicity decreases in the order DMSO > DMF > tetramethylene sulfone > pyridine. The dielectric constant of tetramethylene sulfone is greater than that of DMF (44.0 vs. 36.7) so that dielectric constant is not a main factor in determining solution basicity. The dominant factor is most likely hydrogen-bonding (4, 10, 12), resulting in desolvation of hydroxide ion. The evidence indicates that DMF is a poor hydrogen-bond donor toward hydroxide ion but a strong hydrogen-bond acceptor from solvent water. In these properties DMF and DMSO are about comparable, though DMSO excels slightly.

The relatively facile reaction (20) of hydroxide ion with DMF liberating dimethylamine and formate ion is of consequence in affecting the utility of this basic system. The aqueous DMF system may still be of value for conducting certain reactions involving hydroxide ion, albeit of limited value.

Financial support from the National Research Council of Canada is gratefully acknowledged. E.A.S. and D.D. were the holders of NRCC Scholarships.

1. L. P. HAMMETT. Physical organic chemistry. McGraw-Hill Book Co., Inc., New York. 1940. Ch. 9.
2. G. SCHWARZENBACH and R. SULZBERGER. Helv. Chim. Acta, **27**, 348 (1944).
3. R. STEWART and J. P. O'DONNELL. Can. J. Chem. **42**, 1681 (1964).
4. D. DOLMAN and R. STEWART. Can. J. Chem. **45**, 911 (1967).
5. C. H. LANGFORD and R. L. BURWELL, JR. J. Amer. Chem. Soc. **82**, 1503 (1960).
6. R. STEWART, J. P. O'DONNELL, D. J. CRAM, and B. RICKBORN. Tetrahedron, **18**, 917 (1962).
7. K. BOWDEN and R. STEWART. Tetrahedron, **21**, 261 (1965).
8. K. BOWDEN. Chem. Rev. **66**, 119 (1966).
9. C. H. ROCHESTER. Quart. Rev. **20**, 511 (1966).
10. A. J. PARKER. Quart. Rev. **16**, 163 (1962).
11. J. J. DELPEUCH. Bull. Soc. Chim. France, 1624 (1966).
12. C. D. RITCHIE. Solute–solvent interactions. Edited by J. F. Coetzee and C. D. Ritchie. Marcel Dekker, New York. 1969. Ch. 4.
13. A. J. PARKER. Chem. Rev. **69**, 1 (1969).
14. E. BUNCEL and A. W. ZABEL. J. Amer. Chem. Soc. **89**, 3082 (1967).
15. E. BUNCEL and E. A. SYMONS. Can. J. Chem. **44**, 771 (1966).
16. E. BUNCEL and E. A. SYMONS. Chem. Commun. 771 (1967).
17. E. BUNCEL, K. E. RUSSELL, and J. WOOD. Chem. Commun. 252 (1968).
18. C. D. RITCHIE and G. H. MEGERLE. J. Amer. Chem. Soc. **89**, 1447 (1967).
19. M. R. CRAMPTON and V. GOLD. J. Chem. Soc. (B) 23 (1967).
20. E. BUNCEL and E. A. SYMONS. Chem. Commun. 164 (1970).
21. M. A. PAUL and F. A. LONG. Chem. Rev. **57**, 1 (1957).
22. R. FOSTER and C. A. FYFE. Rev. Pure Appl. Chem. Australia. **16**, 61 (1966).
23. E. BUNCEL, A. R. NORRIS, and K. E. RUSSELL. Quart. Rev. **22**, 123 (1968).
24. C. D. RITCHIE and R. E. USCHOLD. J. Amer. Chem. Soc. **90**, 2821 (1968).

Can. J. Chem. Downloaded from www.nrcresearchpress.com by 210.87.254.5 on 09/05/12
For personal use only.

Can. J. Chem. Downloaded from www.nrcresearchpress.com by 210.87.254.105 on 09/05/12
For personal use only.

Systèmes métaux alcalins–oxygène. 3ème Partie.[1] Polymorphisme du monooxyde de potassium K_2O

PH. TOUZAIN ET F. BRISSE
Département de chimie, Université de Montréal, Montréal, Québec

ET

M. CAILLET
Service des Rayons X, Ecole Nationale Supérieure d'Electrochimie et d'Electrométallurgie de Grenoble, Grenoble, France

Reçu le 8 avril 1970

Le monooxyde de potassium de structure connue ($K_2O\gamma$: cubique faces centrées, $a = 6.436$ Å) présente deux transformations cristallines réversibles du 1er ordre successivement aux températures de 317 et 372 °C. Ces transformations ont été suivies par analyse thermique différentielle. Les nouvelles formes sont : K_2O β (entre 317 et 372 °C), cubique simple ($a = 12.125$ Å) et K_2O α (de 372 °C jusqu'au point de fusion), rhomboédrique ($a = 12.543$ Å, $\alpha = 91.47°$). Une transformation ordre–désordre est notée à 446 °C, température à laquelle se situe approximativement le début de la dismutation de K_2O en K_2O_2 et K.

First order reversible transitions occur in potassium monoxide successively at 317 and 372 °C. These transitions have been observed by differential thermal analysis. The known form is γ-K_2O, face-centered cubic, $a = 6.436$ Å. The new forms are β-K_2O between 317 and 372 °C, primitive cubic, $a = 12.125$ Å and α-K_2O from 372 °C to the melting point, rhombohedral, $a = 12.543$ Å, $\alpha = 91.47°$. An order–disorder transformation occurs at 446 °C. It is at approximately this temperature that K_2O begins to disproportionate into K_2O_2 and K.

Canadian Journal of Chemistry, 48, 3358 (1970)

Le monooxyde de potassium, K_2O, n'était connu jusqu'ici que sous une seule forme cristalline de structure cubique faces centrées contenant quatre groupements formulaires dans une maille de 6.436 Å (1). L'analyse thermique différentielle de ce composé nous a permis de mettre en évidence et de suivre deux transformations réversibles aux températures de 317 et 372 °C respectivement. Une troisième transformation beaucoup moins nette est perceptible à la température de 446 °C (2).

Partie expérimentale

Toutes les manipulations concernant le monooxyde de potassium sont effectuées dans une boîte à gants sous atmosphère d'azote anhydre et exempt d'oxygène. Le monooxyde de potassium est préparé, suivant la méthode décrite par Rengade (3), par oxydation ménagée du potassium suivie d'une distillation sous vide, à 250–300 °C, du potassium en excès. Une série d'échantillons de K_2O est recuite en tubes capillaires scellés sous azote à diverses températures au dessus de 317 °C. Certains échantillons sont refroidis lentement tandis que d'autres sont refroidis brusquement par immersion dans l'azote liquide. Ces échantillons sont alors rapidement examinés aux rayons X par la méthode Debye–Scherrer. D'autres sont maintenus à 330, 390, 450 et 500 °C pendant 24 h avant d'être examinés dans une chambre de diffraction à haute température, UNICAM de 190 mm de diamètre. Tous les films de poudre sont pris avec la radiation K_α du cuivre de longueur d'onde λ Cu $K_\alpha = 1.54178$ Å. Les mesures de conductibilité électrique sont effectuées avec un pont de Wheatstone Wayne Kerr, en courant alternatif de fréquence de 1592 c/s. L'oxyde K_2O en poudre est placé au contact de deux électrodes de tungstène dans un tube de verre Pyrex.

[1]Pour la deuxième partie, voir référence 2.

Résultats et discussions

Les spectres de diffraction X obtenus à température ambiante confirment la maille cubique faces centrées (tableau 1). Les échantillons refroidis lentement présentent le même spectre. Par contre, pour les échantillons trempés, un certain nombre de nouvelles raies s'ajoutent au spectre de la forme cubique faces centrées.

Ces nouvelles formes cristallines n'étant pas suffisamment stables à température ordinaire, on a obtenu leurs diagrammes de rayons X à hautes températures. Deux nouvelles formes cristallines de K_2O ont pu être caractérisées : (*i*) K_2O β entre 317 et 372 °C, cubique simple, $a = 12.125 \pm 0.010$ Å à 330 °C. (*ii*) K_2O α de 372 °C jusqu'au point de fusion à 646 °C, rhomboédrique, $a = 12.543 \pm 0.010$ Å, $\alpha = 91.47° \pm 0.10°$ à 450 °C (dans le système héxagonal : $a_H = 17.964$, $c_H = 21.165$ Å). Les données fournies par les spectres Debye–Scherrer des nouvelles variétés cristallines sont indiquées sur les tableaux 2 et 3.

Can. J. Chem. Downloaded from www.nrcresearchpress.com by 210.87.254.105 on 09/05/12
For personal use only.

TABLEAU 1

$K_2O\gamma$ cubique faces centrées*

d calculées en Å	Intensité calculée	*hkl*
3.71	9	111
3.22	35	200
2.28	100	220
1.95	7	311
1.86	13	222
1.61	22	400
1.47	3	331
1.44	21	420
1.31	53	422
1.23	3	511, 333
1.13	20	440

*a = 6.436 ± 0.003 Å à 20 °C; d'après Zintl et coll.

TABLEAU 2

K_2O β cubique simple*

d en Å		Intensité	
Observées	Calculées	observée	*hkl*
2.944	2.941	80	322, 410
2.864	2.858	60	330, 411
2.770	2.782	80	331
2.715	2.711	40	420
2.586	2.585	10	332
2.382	2.378	100	431, 510
1.831	1.828	60	622
1.787	1.788	40	631
1.668	1.665	40	641
1.637	1.650	20	552, 633, 721
1.525	1.516	20	800

*a = 12.125 ± 0.010 Å à 330 °C.

La transformation à 317 °C (γ–β) est assez lente; elle n'est complète qu'au bout de 24 h environ. Par contre, la transformation à 372 °C (β–α) est plus rapide.

La transition à 446 °C n'est pas due à un changement de système cristallin. Elle correspond à une transformation du 2ème ordre, le cristal passant lentement de la forme ordonnée α′ à la forme désordonnée α. Les spectres Debye–Scherrer sont dans les deux cas identiques, à l'exception de quelques raies de surstructure qui disparaissent au passage de la forme ordonnée à la forme désordonnée, tandis que les intensités d'autres raies augmentent légèrement. Un tel phénomène a déjà été observé dans le cas de la transition ordre–désordre du chlorure de strontium (4).

On n'observe pas de raies dans la phase β correspondant aux raies de forte intensité de la phase γ ce qui indique que ces deux phases ne dérivent pas directement l'une de l'autre. La transition γ–β apparait alors comme une reconstitution complète du réseau cristallin.

Au contraire, nous noterons une certaine analogie entre les deux formes β et α : (*a*) D'une part, les volumes de leurs mailles sont du même ordre de grandeur : $V_\beta = 1785\,Å^3$ et $V_\alpha = 1971\,Å^3$ contre $V_\gamma = 267\,Å^3$. (*b*) D'autre part, on observe une correspondance entre les distances réticulaires des deux phases pour les raies d'intensités les plus fortes.

Ceci indiquerait que la phase α dérive de la phase β par une légère distortion de son réseau cristallin.

Les mesures de densité de K_2O en fonction de la température n'ont pas été entreprises du fait de la très grande difficulté expérimentale de ces mesures à hautes températures. Le passage d'une variété à l'autre devrait cependant n'entraîner qu'une faible variation de densité. En supposant celle-ci à peu près égale ou légèrement inférieure à la densité de la forme γ, basse température ($d_\gamma = 2.33$ g/cm^3 (1, 3)), les deux nouvelles formes comprendraient 24 groupements formulaires par maille; leurs densités calculées seraient alors $d_\beta = 2.10$ et $d_\alpha = 1.90$ g/cm^3.

Selon cette hypothèse, les volumes formulaires de ces phases seraient : $v_\gamma = 66.7\,Å^3$, $v_\beta = 74.3\,Å^3$, $v_\alpha = 82.1\,Å^3$. Les variations de volume Δv n'étant pas nulles et les entropies de transition ΔS n'étant pas nulles non plus (pics endothermiques des courbes d'analyse thermique différentielle (2)), les transitions cristallines à 317 et 372 °C sont probablement toutes deux du 1er ordre.

Les mesures de conductibilité électrique sur l'oxyde K_2O n'ont pas permis de distinguer avec netteté ces transitions cristallines. On note simplement un léger décalage positif de la conductibilité vers 365–380 °C (β–α).

Par contre, l'analyse thermogravimètrique de K_2O décrite antérieurement (2), montre que, sous vide, une importante volatilisation de potassium métallique se produit à partir de 430–440 °C (fig. 1) laissant du peroxyde K_2O_2. La transformation ordre–désordre, observée à 446 °C par ATD, confirmée par les rayons X, apparait comme étant une étape conduisant à la dismutation de l'oxyde selon :

$$2\,K_2O \rightarrow 2\,K + K_2O_2$$

Notons (fig. 1) que la masse de l'échantillon augmente légèrement de 1% avant d'atteindre la température de dismutation. L'absorption des

TABLEAU 3

$K_2O\alpha$ rhomboédrique*

d en Å		Intensité à			*hkl*	
Observées	Calculées	390 °C	450 °C	500 °C	Rhomb.	Hexagonal
7.060	7.055	40	40	60	111	003
4.480	4.491	20	20	0	$20\bar{2}$	220
3.980	3.995	20	20	20	$30\bar{1}$	312
3.780	3.788	20	20	20	$31\bar{1}$	223
3.630	3.650	10	0	0	$22\bar{2}$	042
3.535	3.528	20	20	20	222	006
3.290	3.283	0	10	0	321	116
3.090	3.078	100	100	100	$22\bar{3}$	051
3.054	3.059	0	0	10	$32\bar{2}, 40\bar{1}$	143, 413
3.023	3.022	10	10	0	410	315
2.955	2.959	10	10	20	$41\bar{1}$	324
2.870	2.864	40	80	80	$33\bar{1}$	045
2.820	2.818	80	60	0	331	027
2.750	2.756	60	20	0	$41\bar{2}$	333
2.610	2.608	0	20	10	332	018
2.445	2.446	40	40	40	$43\bar{1}$, 510	146, 416
2.365	2.358	40	40	40	$32\bar{4}$	161
	2.351				333	009
2.315	2.315	40	40	20	$51\bar{2}$	612
	2.307				520	327
2.220	2.210	20	20	20	$41\bar{4}$	351
	2.210				$52\bar{2}$	701
2.115	2.114	40	40	40	$43\bar{4}$	262
	2.108				$53\bar{1}$	247
2.070	2.070	20	40	40	$60\bar{1}$	615
	2.061				$52\bar{3}$, 325	710, 170
2.010	2.015	10	20	20	611	508
1.867	—	0	10	10	—	—
1.712	—	0	0	10	—	—
1.590	—	20	20	10	—	—
1.485	—	10	10	10	—	—

*a = 12.543 ± 0.010 Å, α = 91.47 ± 0.10° à 450 °C; indéxé en hexagonal: a = 17.964, c = 21.165 Å.

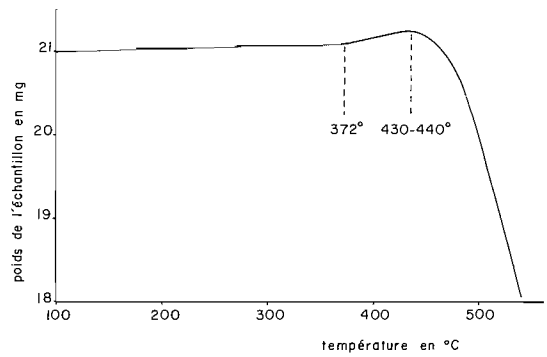

FIG. 1. Thermogravimètrie du monooxyde de potassium sous un vide de 10^{-4} mm Hg et avec une vitesse de chauffe de 8–10 °C/min.

gaz résiduels tels H_2O et O_2 en est naturellement la cause. Cependant, il est intéressant de remarquer que l'augmentation de masse, qui est faible aux basses températures (0.4% entre 20 et 372 °C), devient nettement plus importante à partir de 372 °C, température de transition entre les phases β et α'. Ce résultat semble indiquer que la forme α' est chimiquement plus active que la forme β.

Le schéma des transformations successives de K_2O, en fonction de la température, est le suivant :

$$K_2O \text{ c.f.c. } (Z = 4) \xrightarrow{317\ ^\circ C} K_2O \text{ c. simple } (Z = 24)$$

$$\xrightarrow{372\ ^\circ C} K_2O \text{ rhomb. } (Z = 24)$$

$$\xrightarrow{446\ ^\circ C} K_2O \text{ rhomb. dés. } (Z = 24) + \text{dismutation partielle en } K_2O_2 + 2K$$

$$\xrightarrow{646\ ^\circ C} \text{préfusion de } K_2O \text{ (fusion réelle à environ 685 °C)}$$

On constate d'après ce schéma que le désordre va croissant au fur et à mesure que la température croît, pour finalement conduire à une fusion d'autant plus progressive que le produit s'était décomposé au préalable.

Pour confirmer cette idée, il serait nécessaire de déterminer la position des atomes dans les deux nouvelles structures, le sens des déplacements des

Can. J. Chem. Downloaded from www.nrcresearchpress.com by 210.87.254.105 on 09/05/12
For personal use only.

atomes dans la transition ordre–désordre, et aussi de mesurer la variation de la capacité calorifique C_p de K_2O en fonction de la température; cela nous permettrait en particulier de savoir si la transformation à 446 °C est une transformation ordre–désordre relativement rapide ou si elle fait partie d'un phénomène de transition diffuse s'étendant sur un domaine de température plus large et reflétant le désordre graduel des cations potassium. Cette transition diffuse serait à rapprocher des résultats relatifs aux composés AB_2 à structure du type fluorine et antifluorine comme K_2S, $SrCl_2$ et CaF_2 (5), K_2O appartenant à cette catégorie par sa structure antifluorine à basse température.

Nous remerçions le Conseil National des Recherches du Canada pour l'aide financière apportée à ce travail et le Centre de Calcul de l'Université de Montréal. Les auteurs remercient également le Professeur A. Beauchamp du département de chimie de l'Université de Montréal ainsi que F. Natola pour son assistance technique.

1. E. ZINTL, A. HARDER et B. DAUTH. Z. Elektrochem. **40**, 588 (1934).
2. F. NATOLA et PH. TOUZAIN. Can. J. Chem. **48**, 1955 (1970).
3. E. RENGADE. Ann. Chim. Phys. **11**, 425 (1907).
4. U. CROATTO et M. BRUNO. Gazz. Chim. Ital. **76**, 246 (1946).
5. A. S. DWORKIN et M. A. BREDIG. J. Phys. Chem. **72**, 1277 (1968).

Can. J. Chem. Downloaded from www.nrcresearchpress.com by 210.87.254.105 on 09/05/12
For personal use only.

Can. J. Chem. Downloaded from www.nrcresearchpress.com by 210.87.254.42 on 09/05/12
For personal use only.

Effets de solvant sur les fréquences des vibrateurs CD et CH de quelques haloformes

INGA ROSSI, NGUYEN-VAN-THANH, CLAUDE BRODBECK ET CLAUDE HAEUSLER[1]

Laboratoire d'Infrarouge, Chimie Physique, Faculté des Sciences de Paris, Bâtiment 350 (91) Orsay, France (Equipe de recherche associée au C.N.R.S.)

Reçu le 17 mars 1970

Les fréquences des bandes fondamentales et harmoniques des vibrateurs C—D et C—H ont été mesurées pour les molécules $CDCl_3$, $CHCl_3$ et $CHBr_3$ à l'état dissous dans quelques solvants non polaires ou légèrement polaires.

On a remarqué que l'anharmonicité mécanique de ces vibrations est forte et dépend de la nature du solvant. C'est ainsi que l'approximation $\Delta\omega/\omega \simeq \Delta\nu/\nu$ n'est plus valable pour les oscillateurs considérés dans ce travail.

L'énergie d'interaction entre soluté et solvant est la somme des énergies d'induction, de dispersion et d'orientation (pour les solvants polaires). Les calculs basés sur un modèle cellulaire de l'état liquide ont montré que l'énergie d'induction est peu importante par rapport à l'énergie de dispersion qui est fortement responsable du déplacement des fréquences observées.

The frequencies of the fundamental C—D and C—H stretching band and the overtones have been measured for $CDCl_3$ and $CHBr_3$ in some nonpolar and some slightly polar solvents.

We have pointed out that the mechanical anharmonicity of these vibrations is strong and solvent-dependent. Therefore, the approximation $\Delta\omega/\omega \simeq \Delta\nu/\nu$ is not valid for the vibrators considered in this work.

The solute–solvent interaction energy is the sum of induction, dispersion, and orientation energies (for polar solvents). Calculations based on the cell model for the liquid state showed that induction energy is of slight influence with respect to dispersion energy, which is greatly responsible for the observed frequency shift.

Canadian Journal of Chemistry, 48, 3362 (1970)

Introduction

Dans le cadre des travaux consacrés à l'étude des interactions moléculaires entre soluté et solvant non complexant, on a déterminé les fréquences des bandes fondamentales ν_1 et harmoniques $n\nu_1$ des molécules $CDCl_3$, $CHCl_3$ et $CHBr_3$ à l'état dissous dans différents solvants non polaires et faiblement polaires. Les quatre solvants utilisés (CCl_4, C_2Cl_4, CS_2 et CCl_3Br) sont parfaitement transparents dans le domaine d'absorption des vibrateurs CH. L'analyse des bandes ν_1 et $2\nu_1$ de $CHCl_3$ et $CHBr_3$ relatives à l'état gazeux, a fait l'objet d'une publication récente (1). Les bandes ν_1, $2\nu_1$ et $3\nu_1$ de $CDCl_3$ à l'état gazeux sont également étudiées dans le présent travail.

La théorie de Buckingham (2–4) relative aux effets de solvant sur les fréquences de vibration des molécules diatomiques, prévoit que le déplacement $\Delta\nu$ de fréquence, dû au solvant, est proportionnel au nombre quantique v de vibration du niveau excité, si l'on suppose que la constante d'anharmonicité mécanique du soluté est la même pour les états gazeux et dissous.

Mais récemment plusieurs auteurs (5, 6) ont montré que pour certains vibrateurs XH, la constante d'anharmonicité dépend de la nature du solvant.

Le modèle cellulaire rend compte d'une manière assez satisfaisante de certains effets de solvant. L'hypothèse de l'analogie cristalline est alors faite pour obtenir une fonction de distribution des molécules de solvant à l'état liquide (7).

Il s'agit dans le présent travail de vérifier les relations obtenues par Buckingham, et d'en déterminer les limites de validité dans le cas des vibrateurs CD et CH.

Conditions expérimentales

Les spectres ont été obtenus sur un spectromètre de type PFUND à réseau échelette de 240 traits/mm fonctionnant dans les ordres 1, 2 et 3.

Selon le domaine spectral exploré, les détecteurs sont des cellules photorésistantes, soit au sulfure de plomb, soit au tellurure de plomb. Ces cellules sont refroidies respectivement à la température de la neige carbonique et à celle de l'azote liquide.

[1]Laboratoire de Chimie Physique Moléculaire, Faculté des Sciences de Rennes, France (35).

La fonction d'appareil est une fonction triangle (8), dont la largeur à mi-hauteur est de 0.5 cm^{-1} à 2000 cm^{-1}, de 1.0 cm^{-1} à 4000 cm^{-1} et de 1.5 cm^{-1} à 6000 cm^{-1}.

L'étalonnage du domaine spectral en nombre d'onde se fait par la méthode de Poggendorff. Nous avons repéré les bandes d'absorption des haloformes considérés par rapport aux raies de vibration–rotation des molécules suivantes: à 2300 cm^{-1}, CO_2 (9); 3000 cm^{-1}, HCl (10); 4500 cm^{-1}, HI (11); 6000 cm^{-1}, CH_4 (12); 6500 cm^{-1}, HI (13).

Les cuves à section circulaire avaient une épaisseur variant de 0.5 à 2 cm pour l'étude des solutions; pour l'étude de $CDCl_3$ gazeux deux cuves de longueur égale à 10 cm et 100 cm respectivement ont été utilisées. La concentration des solutions était de l'ordre de 10^{-5} mole/cm^3.

Rappels théoriques

A. Expression du déplacement de fréquence

A l'état gazeux, pour une molécule diatomique, l'hamiltonien de vibration peut se mettre sous la forme

$$\mathcal{H}_v = \mathcal{H}_v^{(0)} + \mathcal{H}_v^{(a)}$$

L'hamiltonien $\mathcal{H}_v^{(0)}$, relatif à l'oscillateur harmonique (14) s'écrit

$$[1] \qquad \mathcal{H}_v^{(0)} = hc\,\frac{\omega_e}{2}\left(\frac{p^2}{\hbar^2} + q^2\right)$$

où ω_e est la fréquence harmonique exprimée en cm^{-1}; q, la coordonnée normale sans dimension, p, le moment de quantité de mouvement.

L'hamiltonien perturbateur peut s'écrire

$$[2] \qquad \mathcal{H}_v^{(a)} = \mathcal{H}_v - \mathcal{H}_v^{(0)} = K_3q^3 + K_4q^4 + \cdots + K_nq^n + \cdots$$

Les termes K_3q^3, K_4q^4, $\cdots$ qui résultent de l'anharmonicité mécanique de la vibration sont infiniment petits les uns par rapport aux autres, de sorte que l'on a

$$\frac{hc\omega_e}{2}q^2 \gg K_3q^3 \gg K_4q^4 \gg \cdots \gg K_{n-1}q^{n-1} \gg K_nq^n \gg \cdots$$

Quand la molécule diatomique se trouve à l'état dissous, il faut tenir compte de l'énergie d'interaction entre la molécule de soluté et le solvant. L'énergie d'interaction U peut être exprimée en fonction de certaines grandeurs microscopiques du soluté et du solvant.

On peut adopter un modèle cellulaire dans lequel la molécule de soluté prend la place d'une molécule de solvant, et se trouve ainsi placée dans une enceinte constituée par les molécules de solvant environnantes. Les positions moyennes des molécules de solvant et celle de la molécule de soluté sont situées aux noeuds d'un réseau cubique à faces centrées (système, en particulier, dans lequel cristallise le solvant CCl_4). On désigne par a_s, la distance minimale entre deux noeuds consécutifs d'une maille unitaire.

Buckingham (4) exprime l'énergie intermoléculaire comme une fonction de deux variables τ et q

$$[3] \qquad \mathcal{U}(\tau, q) = \mathcal{U}_e(\tau) + \frac{1}{1!}\left[\frac{\partial\mathcal{U}(\tau)}{\partial q}\right]_e q + \frac{1}{2!}\left[\frac{\partial^2\mathcal{U}(\tau)}{\partial q^2}\right]_e q^2 + \cdots + \frac{1}{n!}\left[\frac{\partial^n\mathcal{U}(\tau)}{\partial q^n}\right]_e q^n + \cdots$$

τ représente l'ensemble des variables qui permettent de fixer la position et l'orientation de la molécule de soluté à l'intérieur de la maille.

En fait, il y aurait lieu en toute rigueur de tenir compte de l'ensemble des orientations possibles de la molécule au sein de la maille considérée. Mais dans ce cas, le calcul rigoureux de la fonction $\mathcal{U}(\tau,q)$ devient très laborieux. On se propose donc d'expliciter $\mathcal{U}$, seulement en fonction de la variable q. Ceci revient à raisonner sur une valeur moyenne du paramètre τ, caractéristique de la position et de l'orientation de la molécule étudiée.

L'hamiltonien de vibration de la molécule à l'état dissous s'écrit alors

$$[4] \qquad \mathcal{H}_v = \mathcal{H}_v^{(0)} + \mathcal{H}_v^{(a)} + \mathcal{U}$$

Can. J. Chem. Downloaded from www.nrcresearchpress.com by 210.87.254.42 on 09/05/12
For personal use only.

Can. J. Chem. Downloaded from www.nrcresearchpress.com by 210.87.254.42 on 09/05/12
For personal use only.

TABLEAU 1

Contributions diagonales et non diagonales de $(\mathscr{H}_v/hc)$

Opérateurs		Expression des éléments diagonaux et non diagonaux de $(\mathscr{H}_v/hc)$ en fonction du nombre quantique v	
$\frac{\mathscr{H}_v^{(0)}}{hc}$	$\frac{\omega_e}{2}\left(\frac{p^2}{\hbar^2}+q^2\right)$	$\frac{E_v^{(0)}}{hc}$	$\left\langle v\left\vert\frac{\mathscr{H}_v^{(0)}}{hc}\right\vert v\right\rangle$	$\omega_e(v+\frac{1}{2})$
$\frac{\mathscr{H}_v^{(1)}}{hc}$	$u'q+k_3q^3$	$\frac{E_v^{(1)}}{hc}$	$\left\langle v\left\vert\frac{\mathscr{H}_v^{(1)}}{hc}\right\vert v\right\rangle$	0
$\frac{\mathscr{H}_v^{(2)}}{hc}$	$\frac{u''}{2}q^2+k_4q^4$	$\frac{E_v^{(2)}}{hc}$	$\left\langle v\left\vert\frac{\mathscr{H}_v^{(2)}}{hc}\right\vert v\right\rangle$	$\frac{3}{2}k_4(v+\frac{1}{2})^2+\frac{u''}{2}(v+\frac{1}{2})+\frac{3}{8}k_4$
			$\sum_{k\neq v}\frac{\left(\left\langle v\left\vert\frac{\mathscr{H}_v^{(1)}}{hc}\right\vert k\right\rangle\right)^2}{E_v^{(0)}-E_k^{(0)}}$	$-\frac{15}{4}\frac{k_3^2}{\omega_e^2}(v+\frac{1}{2})^2-3\frac{k_3u'}{\omega_e}(v+\frac{1}{2})-\left(\frac{u'^2}{2\omega_e}+\frac{7}{16}\frac{k_3^2}{\omega_e}\right)$
$\frac{\mathscr{H}_v^{(3)}}{hc}$	$\frac{u'''}{3!}q^3+k_5q^5$	$\frac{E_v^{(3)}}{hc}$	$\left\langle v\left\vert\frac{\mathscr{H}_v^{(3)}}{hc}\right\vert v\right\rangle$	
			$\sum_{k\neq v}\left[2\frac{\langle v\vert(\mathscr{H}_v^{(1)}/hc)\vert k\rangle\langle k\vert(\mathscr{H}_v^{(2)}/hc)\vert l\rangle}{E_v^{(0)}-E_k^{(0)}}-\frac{(\langle v\vert(\mathscr{H}_v^{(1)}/hc)\vert k\rangle)^2\langle v\vert(\mathscr{H}_v^{(1)}/hc)\vert v\rangle}{(E_v^{(0)}-E_k^{(0)})^2}\right]$	0
			$\sum_{k,l\neq v}\frac{\langle v\vert(\mathscr{H}_v^{(1)}/hc)\vert k\rangle\langle k\vert(\mathscr{H}_v^{(1)}/hc)\vert l\rangle\langle l\vert(\mathscr{H}_v^{(1)}/hc)\vert v\rangle}{(E_v^{(0)}-E_k^{(0)})(E_v^{(0)}-E_l^{(0)})}$	
			$\langle v\vert(\mathscr{H}_v^{(4)}/hc)\vert v\rangle$	$\frac{5}{2}k_6(v+\frac{1}{2})^3+\frac{u''''}{16}(v+\frac{1}{2})^2+\frac{25}{8}k_6(v+\frac{1}{2})+\frac{u''''}{64}$
			$\sum_{k\neq v}2\frac{\langle v\vert(\mathscr{H}_v^{(1)}/hc)\vert k\rangle\langle k\vert(\mathscr{H}_v^{(3)}/hc)\vert v\rangle}{E_v^{(0)}-E_k^{(0)}}$	$-\frac{35}{2}\frac{k_3k_5}{\omega_e}(v+\frac{1}{2})^3-\left(\frac{5}{4}\frac{k_3u'}{\omega_e}+\frac{15}{2}\frac{k_5u'}{\omega_e}\right)(v+\frac{1}{2})^2$

Can. J. Chem. Downloaded from www.nrcresearchpress.com by 210.87.254.42 on 09/05/12
For personal use only.

TABLEAU 1 (*Concluded*)

Contributions diagonales et non diagonales de $(\mathscr{H}_v/hc)$

Opérateurs			Expression des éléments diagonaux et non diagonaux de $(\mathscr{H}_v/hc)$ en fonction du nombre quantique v
			$-\left(\frac{u'u'''}{2\omega_e}+\frac{95}{8}\frac{k_3k_5}{\omega_e}\right)(v+\frac{1}{2})-\left(\frac{15}{8}\frac{u'k_5}{\omega_e}+\frac{7}{48}\frac{k_3u'''}{\omega_e}\right)$
$\frac{\mathscr{H}_v^{(4)}}{hc}$	$\frac{u''''}{4!}q^4+k_6q^6$	$\frac{E_v^{(4)}}{hc}$	$\sum_{k\neq v}-\frac{(\langle v\vert(\mathscr{H}_v^{(1)}/hc)\vert k\rangle)^2\langle v\vert(\mathscr{H}_v^{(2)}/hc)\vert v\rangle}{(E_v^{(0)}-E_k^{(0)})^2}$
			$-\frac{41}{12}\frac{k_3{}^2k_4}{\omega_e{}^2}(v+\frac{1}{2})^5$
			$-\left[\frac{41}{36}\frac{k_3{}^2u''}{\omega_e{}^2}+\frac{9}{2}\frac{k_3k_4u'}{\omega_e{}^2}\right](v+\frac{1}{2})^4$
			$-\left[\frac{29}{8}\frac{k_3{}^2k_4}{\omega_e{}^2}+\frac{3}{2}\frac{k_3u'u''}{\omega_e{}^2}+\frac{3}{2}\frac{k_4(u')^2}{\omega_e{}^2}\right](v+\frac{1}{2})^3$
			$-\left[\frac{9}{4}\frac{k_3k_4u'}{\omega_e{}^2}+\frac{1}{2}\frac{(u')^2u''}{\omega_e{}^2}+\frac{133}{144}\frac{k_3{}^2u''}{\omega_e{}^2}\right](v+\frac{1}{2})^2$
			$-\left[\frac{3}{8}\frac{k_4(u')^2}{\omega_e{}^2}+\frac{3}{8}\frac{k_3u'u''}{\omega_e{}^2}+\frac{133}{192}\frac{k_3{}^2k_4}{\omega_e{}^2}\right](v+\frac{1}{2})$
			$-\frac{9}{32}\frac{k_3k_4u'}{\omega_e{}^2}$
			$\sum_{k\neq v}\frac{(\langle v\vert(\mathscr{H}_v^{(2)}/hc)\vert k\rangle)^2}{E_v^{(0)}-E_k^{(0)}}$
			$-\frac{17}{4}\frac{k_4{}^2}{\omega_e}(v+\frac{1}{2})^3-\frac{3}{2}\frac{k_4u''}{\omega_e}(v+\frac{1}{2})^2$
			$-\left(\frac{67}{16}\frac{k_4{}^2}{\omega_e}+\frac{(u'')^2}{8\omega_e}\right)(v+\frac{1}{2})-\frac{3}{8}\frac{k_4u''}{\omega_e}$
			+ termes d'ordre supérieur négligeables $\cdots$ $\cdots$

En considérant $(H_v^{(a)} + \mathcal{U})$ comme une perturbation infiniment petite devant $\mathcal{H}_v^{(0)}$, on obtient par la méthode des perturbations les valeurs de l'énergie jusqu'à l'ordre n.

L'énergie de vibration E_v est donnée par

$$[5] \qquad E_v = E_v^{(0)} + E_v^{(1)} + E_v^{(2)} + E_v^{(3)} + E_v^{(4)} + \cdots$$

Dans le tableau 1 figurent les différents termes $\mathcal{H}_v(^1)$, $\mathcal{H}_v^{(2)}$, $\mathcal{H}_v^{(3)}$ et $\mathcal{H}_v^{(4)}$ des hamiltoniens perturbateurs par rapport à l'hamiltonien $\mathcal{H}_v^{(0)}$ d'ordre zéro et les expressions des énergies $E_v^{(0)}$, $E_v^{(1)}$, $E_v^{(2)}$, $E_v^{(3)}$ et $E_v^{(4)}$.

Le terme spectral de vibration développé jusqu'à l'ordre quatre pour une molécule diatomique à l'état gazeux s'exprime par la relation suivante

$$[6] \qquad G_v^{gaz} = \frac{E_v^{gaz}}{hc} = (\omega_e - W)(v + \tfrac{1}{2}) - X(v + \tfrac{1}{2})^2 + Y(v + \tfrac{1}{2})^3 + c$$

Le terme spectral relatif à l'état dissous s'écrit

$$[7] \qquad G_v^{sol} = \frac{E_v^{sol}}{hc} = (\omega_e - W - \overline{W})(v + \tfrac{1}{2}) - (X + \overline{X})(v + \tfrac{1}{2})^2 + (Y + \overline{Y})(v + \tfrac{1}{2})^3 + c + \bar{c}$$

Dans le cas de la molécule $CDCl_3$ où les trois bandes ν_1, $2\nu_1$ et $3\nu_1$ sont étudiées, on néglige les termes d'ordre supérieur à $(v + \frac{1}{2})^3$. Pour les molécules $CHCl_3$ et $CHBr_3$ où seules les deux bandes ν_1 et $2\nu_1$ ont pu être étudiées, on se limite au terme en $(v + \frac{1}{2})^2$.

Les grandeurs intervenant dans l'équation 7 sont données par les relations suivantes

$$[8] \qquad W = -\frac{25}{8}k_6 + \frac{95}{8}\frac{k_3k_5}{\omega_e} + \frac{67}{16}\frac{k_4^2}{\omega_e}$$

$$\overline{W} = -\frac{1}{2}\left(\frac{\partial^2 u}{\partial q^2}\right)_e + \frac{3k_3}{\omega_e}\left(\frac{\partial u}{\partial q}\right)_e + \frac{1}{2\omega_e}\left(\frac{\partial u}{\partial q}\right)_e\left(\frac{\partial^3 u}{\partial q^3}\right)_e + \frac{1}{8\omega_e}\left(\frac{\partial^2 u}{\partial q^2}\right)_e^2$$

$$[9] \qquad X = -\frac{3}{2}k_4 + \frac{15}{4}\frac{k_3^2}{\omega_e}$$

$$\overline{X} = -\frac{1}{16}\left(\frac{\partial^4 u}{\partial q^4}\right)_e + \frac{5}{4}\frac{k_3}{\omega_e}\left(\frac{\partial u}{\partial q}\right)_e + \frac{15}{2}\frac{k_5}{\omega_e}\left(\frac{\partial u}{\partial q}\right)_e + \frac{3}{2}\frac{k_4}{\omega_e}\left(\frac{\partial^2 u}{\partial q^2}\right)_e$$

$$[10] \qquad Y = \frac{5}{2}k_6 - \frac{35}{2}\frac{k_3k_5}{\omega_e} - \frac{17}{4}\frac{k_4^2}{\omega_e}$$

en posant

$$\frac{\mathcal{U}}{hc} = u, \quad \frac{1}{hc}\left(\frac{\partial \mathcal{U}}{\partial q}\right)_e = \left(\frac{\partial u}{\partial q}\right)_e, \quad \frac{1}{hc}\left(\frac{\partial^2 \mathcal{U}}{\partial q^2}\right)_e = \left(\frac{\partial^2 u}{\partial q^2}\right)_e, \quad \frac{K_3}{hc} = k_3, \quad \frac{K_4}{hc} = k_4, \ldots$$

les grandeurs u, $(\partial u/\partial q)_e \cdots$ et k_3, $k_4 \cdots$ sont exprimées en cm^{-1}.

Afin d'alléger l'exposé, la grandeur $\overline{Y}$ ($\overline{Y} \ll Y$) de l'équation 7 dont l'expression est assez complexe, n'est pas explicitée. $\overline{W}$, $\overline{X}$ et $\overline{Y}$ dépendent du potentiel intermoléculaire $\mathcal{U}$.

On retrouve ainsi une expression analogue à celle donnée par Durocher et Sandorfy (5), mais non identique. Des différences apparaissent entre les deux expressions obtenues pour G_v. Elles proviennent de la manière dont sont groupés les différents termes qui interviennent dans les différents hamiltoniens $\mathcal{H}_v^{(1)}$, $\mathcal{H}_v^{(2)}$, $\mathcal{H}_v^{(3)}$ et $\mathcal{H}_v^{(4)}$ (cf. tableau 1).

En effet, nous avons fait un choix tel que

(*a*) d'une part, l'hamiltonien de la molécule diatomique à l'état dissous puisse s'écrire

$$\mathcal{H}_v = \mathcal{H}_v^{(0)} + \lambda\mathcal{H}_v^{(1)} + \lambda^2\mathcal{H}_v^{(2)} + \cdots + \lambda^n\mathcal{H}_v^{(n)} + \cdots$$

où λ est un paramètre ne définissant que l'ordre de grandeur des différents termes $\mathcal{H}_v^{(1)}$, $\mathcal{H}_v^{(2)}$, $\mathcal{H}_v^{(3)}$ et $\mathcal{H}_v^{(4)}$, $\cdots$ dont la convergence vers zéro est supposée *rapide*.

Can. J. Chem. Downloaded from www.nrcresearchpress.com by 210.87.254.42 on 09/05/12
For personal use only.

(*b*) d'autre part, tout terme d'ordre pair $\mathscr{H}_v^{(2n)}$ ne contienne que des éléments d'ordre pair en q, et que tout terme d'ordre impair $\mathscr{H}_v^{(2n+1)}$ ne renferme que des éléments d'ordre impair en q. Ceci présente l'avantage que les énergies d'ordre impair $E_v^{(1)}$ et $E_v^{(3)}$ sont nulles.

Tandis que Foldes et Sandorfy (15) traite le potentiel perturbateur

$$H_v' = H_v - H_v^{(0)}$$

comme un tout, et définit les ordres de perturbation suivant l'ensemble des termes non négligés dans l'équation séculaire. Ceci peut se justifier par le fait que les termes en K_3, K_4, ⋯ présentent une convergence *lente* dans le cas des systèmes soluté-solvant renfermant des liaisons hydrogène.

Dans le cas des haloformes, le calcul de la localisation de l'énergie correspondant à la vibration de valence ν_1 montre que pratiquement toute l'énergie se trouve localisée dans la vibration de la liaison CH (16) et que la molécule peut alors être considérée comme un oscillateur diatomique. Il semble donc légitime de considérer la molécule d'haloforme comme un simple dipôle oscillant H—(CX_3), où, du reste, la masse des trois atomes d'halogène joue un rôle négligeable. Dans ce cas, le moment dipolaire à prendre en considération est $\mu^{(C-H)}$ associé à la vibration C—H.

L'expression générale des nombres d'onde correspondant à la transition $(v = v') \leftarrow (v = v'')$ est la suivante

[11] $$\nu_{v' \leftarrow v''} = G(v') - G(v'')$$

Pour simplifier l'écriture, on désignera les nombres d'onde relatifs à l'état gazeux et à l'état dissous respectivement par $\nu^0_{v' \leftarrow v''}$ et $\nu_{v' \leftarrow v''}$. D'après les relations 6 et 7 on déduit les expressions donnant les nombres d'onde relatifs aux déplacements de fréquence $\Delta\nu$ des bandes du soluté lors du passage de la molécule de l'état gazeux à l'état dissous

$$\Delta\nu_{1\leftarrow 0} = \nu^0{}_{1\leftarrow 0} - \nu_{1\leftarrow 0} = \overline{W} + 2\overline{X} - \frac{13}{4}\overline{Y}$$

[12] $$\Delta\nu_{2\leftarrow 0} = \nu^0{}_{2\leftarrow 0} - \nu_{2\leftarrow 0} = 2\overline{W} + 6\overline{X} - \frac{31}{2}\overline{Y}$$

$$\Delta\nu_{3\leftarrow 0} = \nu^0{}_{3\leftarrow 0} - \nu_{3\leftarrow 0} = 3\overline{W} + 12\overline{X} - \frac{171}{4}\overline{Y}$$

A partir de ces dernières relations, on prévoit que

(*a*) les déplacements de fréquence $\Delta\nu_{1\leftarrow 0}$, $\Delta\nu_{2\leftarrow 0}$ et $\Delta\nu_{3\leftarrow 0}$ ne sont pas proportionnels au nombre quantique de vibration $v = 1, 2, 3$, car ils dépendent de $\overline{W}$, $\overline{X}$ et $\overline{Y}$.

(*b*) la constante d'anharmonicité $(X + \overline{X})$ est fonction de la nature du solvant.

Buckingham (2–4) au contraire, a prévu que les déplacements de fréquence $\Delta\nu_{1\leftarrow 0}$, $\Delta\nu_{2\leftarrow 0}$ et $\Delta\nu_{3\leftarrow 0}$ sont dans le rapport 1:2:3 en supposant que l'anharmonicité de la molécule en solution est la même que celle de la molécule à l'état gazeux.

Ayant choisi un potentiel intermoléculaire $\mathscr{U}$, on peut donc atteindre l'expression des grandeurs $\overline{W}$, $\overline{X}$ et $\overline{Y}$. Il est alors possible de comparer les valeurs théoriques ainsi obtenues, aux valeurs expérimentales de ces mêmes grandeurs déterminées à partir des relations 12, c'est-à-dire à partir des fréquences observées.

La comparaison est facile à effectuer en ce qui concerne $\overline{W}$ (relation 8). En effet, on voit que dans l'expression de $\overline{W}$ les termes prépondérants sont les deux premiers. On peut donc en première approximation négliger les deux derniers termes intervenant dans [8], et la valeur de $\overline{W}_{\text{théorique}}$ ainsi obtenue peut être valablement comparée à la valeur expérimentale.

Au contraire, en ce qui concerne $\overline{X}$, on doit prendre en considération plusieurs termes qui sont fonction de $(\partial u/\partial q)_e$, $(\partial^2 u/\partial q^2)_e$ et $(\partial^4 u/\partial q^4)_e$. Le calcul est donc ici plus délicat.

De surcroît, si la valeur expérimentale de $\overline{W}$ peut être obtenue avec une précision acceptable, celle de $\overline{X}$ est déjà beaucoup moins précise et $\overline{Y}$, qui est un terme inférieur à $\overline{X}$, l'est encore moins.

Comme le déplacement de fréquence harmonique $\Delta\omega$ est égal à $\overline{W}$ d'après les relations 6 et 7, nous

Can. J. Chem. Downloaded from www.nrcresearchpress.com by 210.87.254.42 on 09/05/12
For personal use only.

nous proposons d'évaluer le déplacement relatif de fréquence harmonique $\Delta\omega/\omega_e$ au lieu de $\Delta\nu/\nu$ dont l'expression est une fonction de $\overline{W}$, $\overline{X}$ et $\overline{Y}$.

B. Expression du déplacement relatif de fréquence harmonique $\Delta\omega/\omega_e$

Le déplacement de fréquence harmonique s'écrit

$$\Delta\omega = \omega_e^{gaz} - \omega_e^{sol} = \overline{W} \qquad [13]$$

avec

$$\omega_e^{sol} = \omega_e - \overline{W},$$

relatif à l'état dissous.

L'expression du déplacement relatif de fréquence harmonique $\Delta\omega/\omega_e$ est donnée par la relation

$$\frac{\Delta\omega}{\omega_e} = -\frac{1}{2\omega_e}\left(\frac{\partial^2 u}{\partial q^2}\right)_e + \frac{3k_3}{\omega_e^2}\left(\frac{\partial u}{\partial q}\right)_e + \frac{1}{2\omega_e^2}\left(\frac{\partial u}{\partial q}\right)_e\left(\frac{\partial^3 u}{\partial q^3}\right)_e + \frac{1}{8\omega_e^2}\left(\frac{\partial u}{\partial q}\right)_e^2$$
$$\simeq -\frac{1}{2\omega_e}\left(\frac{\partial^2 u}{\partial q^2}\right)_e + \frac{3k_3}{\omega_e^2}\left(\frac{\partial u}{\partial q}\right)_e \qquad [14]$$

C. Expression du potentiel intermoléculaire $\mathcal{U}$

Dans la relation 14 interviennent les dérivées première et seconde du potentiel intermoléculaire $\mathcal{U}$. Différents types de forces dérivent de ce potentiel: les forces d'induction, de dispersion et d'orientation. Les forces d'orientation étant négligeables pour les solvants non polaires ou faiblement polaires, on peut donc écrire

$$\Delta\omega^{observée} \simeq \Delta\omega^{induction} + \Delta\omega^{dispersion}$$

C.1. Choix d'un potentiel d'induction

Si nous assimilons l'oscillateur CD ou CH à un dipôle non polarisable placé au centre d'une maille unitaire d'un réseau c.f.c., représentant la distribution moléculaire au sein du liquide, l'énergie d'interaction du dipôle avec le solvant est donnée en première approximation par l'expression due à Debye (17):

$$\mathcal{U}^{induction} = -\tfrac{1}{2}\mu^2\frac{\alpha_s}{\varepsilon_s^2}\sum\frac{1}{R^6} = -\tfrac{1}{2}(\mu_e + \mu_t)^2\frac{\alpha_s}{\varepsilon_s^2}\frac{14.45}{a_s^6} \qquad [15]$$

La sommation porte sur toutes les molécules de solvant (18).

Dans l'expression de $\mathcal{U}^{induction}$ nous n'introduisons pas un facteur d'orientation, car nous supposons que la molécule de soluté peut tourner librement; μ est le moment dipolaire de la liaison CH du soluté à l'état gazeux; μ_e, sa valeur à l'équilibre, μ_t, est donnée par

$$\mu_t = \sum_{j=1}\frac{1}{j!}\left(\frac{\partial^j\mu}{\partial q^j}\right)_e q^j$$

α_s est la polarisabilité moyenne moléculaire du solvant; ε_s, sa constante diélectrique; R, la distance qui sépare la molécule de soluté d'une molécule de solvant; a_s, la distance minimum entre deux molécules du liquide.

Le potentiel $\mathcal{U}^{induction}$ peut se mettre sous la forme

$$\mathcal{U}^{induction} = \mathcal{U}_e + \frac{1}{1!}\left(\frac{\partial\mathcal{U}^{ind}}{\partial q}\right)_e q + \frac{1}{2!}\left(\frac{\partial^2\mathcal{U}^{ind}}{\partial q^2}\right)_e q^2 + \cdots + \frac{1}{n!}\left(\frac{\partial^n\mathcal{U}^{ind}}{\partial q^n}\right)_e q^n + \cdots$$

avec

$$\left(\frac{\partial\mathcal{U}}{\partial q}\right)_e^{ind} = -\mu_e\left(\frac{\partial\mu}{\partial q}\right)_e\frac{\alpha_s}{\varepsilon_s^2}\cdot\frac{14.45}{a_s^6}$$
$$\frac{1}{2}\left(\frac{\partial^2\mathcal{U}}{\partial q^2}\right)_e^{ind} = -\frac{1}{2}\left[\left(\frac{\partial\mu}{\partial q}\right)_e^2 + \mu_e\left(\frac{\partial^2\mu}{\partial q^2}\right)_e\right]\frac{\alpha_s}{\varepsilon_s^2}\frac{14.45}{a_s^6} \qquad [16]$$

Can. J. Chem. Downloaded from www.nrcresearchpress.com by 210.87.254.42 on 09/05/12
For personal use only.

Can. J. Chem. Downloaded from www.nrcresearchpress.com by 210.87.254.42 on 09/05/12
For personal use only.

En combinant les équations 14 et 16 on obtient finalement

[17]
$$\frac{\Delta\omega^{\text{ind}}}{\omega} \simeq -\frac{1}{2hc\omega_e}\left(\frac{\partial^2 \mathscr{U}^{\text{ind}}}{\partial q^2}\right)_e + \frac{3K_3}{hc\omega_e^2}\left(\frac{\partial \mathscr{U}^{\text{ind}}}{\partial q}\right)_e$$
$$\simeq \frac{1}{2hc\omega_e}\left[\left(\frac{\partial\mu}{\partial q}\right)_e^2 + \mu_e\left(\frac{\partial^2\mu}{\partial q^2}\right)_e - \frac{6K_3}{\omega_e}\mu_e\left(\frac{\partial\mu}{\partial q}\right)_e\right]\frac{\alpha_s}{\varepsilon_s^2}\frac{14.45}{a_s^6}$$

Le calcul des quantités $(\partial\mathscr{U}^{\text{ind}}/\partial q)_e$ et $(\partial^2\mathscr{U}^{\text{ind}}/\partial q^2)_e$ nécessite la connaissance des grandeurs a_s, $(\partial\mu/\partial q)_e$ et $(\partial^2\mu/\partial q^2)_e$.

La distance intermoléculaire a_s est obtenue à l'aide de la relation suivante

[18]
$$a_s = \left(\frac{\sqrt{2}M}{dN}\right)^{1/3}$$

où M désigne la masse moléculaire de la molécule de solvant; d, la densité du solvant (g cm^{-3}); N, le nombre d'Avogadro.

Pour obtenir les valeurs de $(\partial\mu/\partial q)_e$ et $(\partial^2\mu/\partial q^2)_e$, on utilise la méthode de Herman et Shuler (19).

C.1.1. Détermination de $(\partial\mu/\partial q)_e$ *et* $(\partial^2\mu/\partial q^2)_e$

L'intensité intégrée d'une bande d'une molécule à l'état gazeux s'exprime sensiblement par la relation suivante

[19]
$$A_{v'\leftarrow v''}^{\text{gaz}} = \frac{8\pi^3}{3hc}\nu_{v'\leftarrow v''}^{\text{gaz}}|R^{v'\leftarrow v''}|^2$$

où $R^{v'\leftarrow v''}$ représente l'élément matriciel de transition entre les niveaux d'énergie v' et v'', relatifs à un vibrateur anharmonique. $R^{v'\leftarrow v''}$ peut s'écrire sous la forme

$$R^{v'\leftarrow v''} = \int_\tau \Psi_{v'}{}^*\mu\Psi_{v''}\mathrm{d}\tau$$

ou en utilisant le développement en série de $\mu(q)$

$$R^{v'\leftarrow v''} = \sum_j \frac{1}{j!}\left(\frac{\partial^j\mu}{\partial q^j}\right)_e \int \Psi_{v'}(q)q^j\Psi_{v''}(q)\mathrm{d}q$$
$$= \sum_j \frac{1}{j!}\left(\frac{\partial^j\mu}{\partial q^j}\right)_e R_j{}^{v'\leftarrow v''}$$

On ne retiendra dans le développement de $R^{v'\leftarrow v''}$ que les deux premiers termes; il vient alors

$$R^{v'\leftarrow v''} \simeq \left(\frac{\partial\mu}{\partial q}\right)_e R_1{}^{v'\leftarrow v''} + \frac{1}{2}\left(\frac{\partial^2\mu}{\partial q^2}\right)_e R_2{}^{v'\leftarrow v''}$$

Les termes $R_j{}^{v'\leftarrow v''}$ s'expriment en fonction des constantes moléculaires (B_e, ω_e, α_e, X et r_e) et du nombre quantique v''. Les valeurs de B_e et α_e sont celles qui ont été calculées pour la molécule diatomique fictive correspondant à H—(CX_3).

La connaissance des quantités A et ν nous permet d'obtenir d'après la relation 19 la valeur absolue de $R^{v'\leftarrow v''}$. Nous sommes ainsi conduits à résoudre pour une molécule donnée le système d'équations suivant

[20]
$$R^{1\leftarrow 0} = \left(\frac{\partial\mu}{\partial q}\right)_e R_1{}^{1\leftarrow 0} + \frac{1}{2}\left(\frac{\partial^2\mu}{\partial q^2}\right)_e R_2{}^{1\leftarrow 0}$$
$$R^{2\leftarrow 0} = \left(\frac{\partial\mu}{\partial q}\right)_e R_1{}^{2\leftarrow 0} + \frac{1}{2}\left(\frac{\partial^2\mu}{\partial q^2}\right)_e R_2{}^{2\leftarrow 0}$$

pour toutes les combinaisons de signes possibles (tableau 2).

Les quantités $(\partial\mu/\partial r)_e$ devant être les mêmes pour les deux molécules diatomiques fictives corres-

TABLEAU 2

Valeurs expérimentales des coefficients $\left(\frac{\partial\mu}{\partial q}\right)_e$, $\left(\frac{\partial^2\mu}{\partial q^2}\right)_e$ et $\left(\frac{\partial\mu}{\partial r}\right)_e$

Molécule	B_e* (cm^{-1})	α_e* (cm^{-1})	r_e (Å)	$A_{1\leftarrow0}$ cm $mole^{-1}$ $\times 10^{-4}$	$A_{2\leftarrow0}$ cm $mole^{-1}$ $\times 10^{-4}$	$\left(\frac{\partial\mu}{\partial q}\right)_e$ ($D\times10^2$)	$\left(\frac{\partial^2\mu}{\partial q^2}\right)_e$ ($D\times10^2$)	$\left(\frac{\partial\mu}{\partial r}\right)_e$ ($D/Å\times10^2$)
$CDCl_3$	7.266	0.0737	1.073	0.318	5.082	+0.03 −0.03 +0.62 −0.62	+1.91 −1.91 −1.83 +1.83	+0.37 −0.37 +7.30 −7.30
$CHCl_3$	14.639	0.2057	1.073	1.593†	10.300†	+0.19 −0.19 +1.06 −1.06	+2.38 −2.38 −2.20 +2.20	+1.81 −1.81 +10.22 −10.22
$CHBr_3$	14.639	0.2221	1.073	30.360†	6.224†	+2.35 −2.35 +3.04 −3.04	+2.16 −2.16 −1.38 +1.38	+22.86 −22.86 +29.58 −29.58

*Les valeurs de B_e et α_e sont celles qui ont été calculées pour la molécule diatomique fictive correspondant à H—(CX_3).
†Référence 1.

pondant à D—(CCl_3) et H—(CCl_3), nous avons choisi comme combinaison de signes, celle qui redonnait sensiblement la même valeur pour les quantités $(\partial\mu/\partial r)_e$ du chloroforme et du chloroforme deuteré (tableau 2).

En adoptant la valeur $\mu_e^{C-H} = 0.7$ D (20) et en remarquant que le déplacement de fréquence $\Delta\omega$ est positif, on peut en déduire d'après l'équation 17, que μ_e et $(\partial^2\mu/\partial q^2)_e$ sont de même signe. Nous retenons finalement le développement suivant

pour $CDCl_3$

$$\mu^{C-D}(q) = 0.7 - 0.62 \times 10^{-2}q + 0.91 \times 10^{-2}q^2$$

pour $CHCl_3$

$$\mu^{C-H}(q) = 0.7 - 1.06 \times 10^{-2}q + 1.10 \times 10^{-2}q^2$$

pour $CHBr_3$

$$\mu^{C-H}(q) = 0.7 - 3.04 \times 10^{-2}q + 0.69 \times 10^{-2}q^2$$

Ainsi avec ces valeurs numériques, la quantité $(\Delta\omega/\omega_e)^{induction}$ peut être calculée d'après la relation 17 (cf. tableau 3).

C.2. Choix d'un potentiel de dispersion

L'énergie d'interaction due aux forces de dispersion du dipôle avec le solvant est donnée en première approximation par l'expression obtenue par Kirkwood (21) et Muller (22):

$$\mathscr{U}^{dispersion} = \frac{1}{2}\frac{\alpha\alpha_s}{\left(\frac{\alpha}{\chi^m} + \frac{\alpha_s}{\chi_s^m}\right)} 6mc^2 \sum \frac{1}{R^6}$$

[21]

$$\simeq (\alpha\chi^m)^{1/2}(\alpha_s\chi_s^m)^{1/2}\tfrac{3}{2}mc^2\,\frac{14.45}{a_s^6}$$

où α et χ^m désignent respectivement le polarisabilité moléculaire et la susceptibilité diamagnétique moléculaire du soluté α_s et χ_s^m sont les quantités correspondantes pour le solvant (23).

La polarisabilité α de la liaison CH est une fonction de q

$$\alpha = \alpha_e + \left(\frac{\partial\alpha}{\partial q}\right)_e + \frac{1}{2!}\left(\frac{\partial^2\alpha}{\partial q^2}\right)_e + \cdots$$

Entre χ^m et α existe la relation suivante due à Kirkwood

Can. J. Chem. Downloaded from www.nrcresearchpress.com by 210.87.254.42 on 09/05/12
For personal use only.

[22] $$\chi^m = -\frac{ne^2\sqrt{a_0}}{4mc^2}(Z\alpha)^{1/2}$$

a_0 = rayon de Bohr, e = charge élementaire de l'électron, n = nombre de molécules par gramme, Z = nombre d'électrons de la molécule.

En dérivant $\mathcal{U}^{dispersion}$ par rapport à la coordonnée normale q de la molécule de soluté, et en tenant compte du fait que χ^m est proportionnel à $\alpha^{1/2}$, on obtient les relations suivantes

[23] $$\left(\frac{\partial \mathcal{U}}{\partial q}\right)_e^{disp} = \frac{3}{4}\left(\frac{\partial \alpha}{\partial q}\right)_e\left(\frac{\chi_e{}^m}{\alpha_e}\right)^{1/2}(\alpha_s\chi_s{}^m)^{1/2}\cdot\tfrac{3}{2}mc^2\cdot\frac{14.45}{a_s{}^6}$$

[24] $$\left(\frac{\partial^2 \mathcal{U}}{\partial q^2}\right)_e^{disp} = \frac{3}{4}\left[\left(\frac{\partial^2\alpha}{\partial q^2}\right)_e - \frac{1}{4\alpha_e}\left(\frac{\partial\alpha}{\partial q}\right)_e^2\right]\left(\frac{\chi_e{}^m}{\alpha_e}\right)^{1/2}(\alpha_s\chi_s{}^m)^{1/2}\cdot\tfrac{3}{2}mc^2\cdot\frac{14.45}{a_s{}^6}$$

Le calcul de $(\partial\mathcal{U}/\partial q)_e^{disp}$ et $(\partial^2\mathcal{U}/\partial q^2)_e^{disp}$ nécessite la connaissance des grandeurs $(\partial\alpha/\partial q)_e$, α_e et $\chi_e{}^m$ relative à la molécule de soluté. Nous avons calculé la valeur de $(\partial\alpha/\partial q)_e$ à partir de la valeur de $(\partial\alpha/\partial r)_e$ publiée par Holzer (24): la relation entre q et $(r - r_e)$ est la suivante

$$q = \left(\frac{\omega_e}{2B_e}\right)^{1/2}\left(\frac{r - r_e}{r_e}\right)$$

où B_e est la constante rotationnelle de la molécule diatomique fictive correspondant à H—(CX_3). A l'heure actuelle, nous ne disposons pas de valeur expérimentale de $(\partial^2\alpha/\partial r^2)_e$.

Ne disposant pas de valeur expérimentale $\chi_{(C-H)}{}^m$, nous sommes conduits à déterminer le rapport $\chi_e{}^m/\alpha_e$ à partir des quantités moléculaires correspondantes.

Les expressions 23 et 24 nous permettent de calculer les valeurs de $\Delta\omega^{disp}$ (voir tableau 3).

TABLEAU 3

Valeurs calculées et observées de $(\Delta\omega/\omega)$

Mélange	$\Delta\omega/\omega \times 10^3$ Induction	Dispersion	Observé
$CDCl_3$—CCl_4	0.007	1.036	3.9
$CDCl_3$—C_2Cl_4	0.007	1.094	3.8
$CDCl_3$—CCl_3Br	0.006	1.088	4.6
$CHCl_3$—CCl_4	0.006	1.099	2.8
$CHCl_3$—C_2Cl_4	0.005	1.161	2.7
$CHCl_3$—CS_2	0.010	2.036	7.0
$CHCl_3$—CCl_3Br	0.005	1.155	3.1
$CHBr_3$—CCl_4	<0.001	1.116	4.4
$CHBr_3$—C_2Cl_4	<0.001	1.179	4.1
$CHBr_3$—CS_2	≃0.001	2.067	8.5
$CHBr_3$—CCl_3Br	<0.001	1.173	4.7

Résultats expérimentaux

Les résultats expérimentaux relatifs aux molécules $CDCl_3$, $CHCl_3$ et $CHBr_3$ sont relatés respectivement dans les tableaux 4, 5 et 6.

Dans ces tableaux figurent (*a*) les fréquences d'absorption $\nu_{v\leftarrow 0}$ et les déplacements de fréquence $\Delta\nu_{v\leftarrow 0}$; (*b*) les constantes moléculaires X et ω_e (déterminées pour les molécules $CHCl_3$ et $CHBr_3$ dans un travail antérieur (1) et les valeurs de $\overline{X}$ et $\overline{W}$ calculées à l'aide des équations (12). Pour $CHCl_3$ et $CHBr_3$, nous calculons $\overline{X}$ et $\overline{W}$ à partir des transitions $1 \leftarrow 0$ et $2 \leftarrow 0$. Pour $CDCl_3$, on a déterminé $\overline{X}$, $\overline{Y}$ et $\overline{W}$ à partir des transitions $1 \leftarrow 0$, $2 \leftarrow 0$ et $3 \leftarrow 0$.

L'imprécision des mesures sur les fréquences fondamentale ν_1 et harmoniques $2\nu_1$ et $3\nu_1$ était respectivement de 0.3, 0.6, et 1 cm^{-1}.

Des valeurs obtenues par Lascombe *et al.* (25), Anttila (26) et Durocher et Sandorfy (5) sont indiquées dans les tableaux 4, 5 et 6.

Discussion

D'après les tableaux 4, 5 et 6, on remarque que le déplacement $\Delta\nu_{v\leftarrow 0}$ n'est pas proportionnel au nombre quantique v. En effet, d'après la relation 12, $\Delta\nu_{v\leftarrow 0}$ est fonction des quantités $\overline{W}$, $\overline{X}$ et $\overline{Y}$. Les grandeurs $\overline{W}$, $\overline{X}$ et $(-\overline{Y})$ étant toujours positives pour les molécules $CDCl_3$, $CHCl_3$, $CHBr_3$, le déplacement est systématiquement supérieur à $v.\overline{W}$.

Ayant choisi un potentiel intermoléculaire $\mathcal{U}$, on peut déterminer l'expression de $\overline{W}$ donnée par la relation 14

$$\Delta\omega = \overline{W} \simeq -\frac{1}{2}\left(\frac{\partial^2 u}{\partial q^2}\right)_e + \frac{3k_3}{\omega_e}\left(\frac{\partial u}{\partial q}\right)_e$$

La valeur théorique de $\overline{W}$ peut alors être comparée à sa valeur expérimentale.

Can. J. Chem. Downloaded from www.nrcresearchpress.com by 210.87.254.42 on 09/05/12
For personal use only.

TABLEAU 4

Fréquences d'absorption $\nu_{1\leftarrow0}$, $\nu_{2\leftarrow0}$, $\nu_{3\leftarrow0}$ et déplacements de fréquences $\Delta\nu_{1\leftarrow0}$, $\Delta\nu_{2\leftarrow0}$, $\Delta\nu_{3\leftarrow0}$ du D-Chloroforme

Solvant	$\nu_{1\leftarrow0}$ (cm^{-1})	$\nu_{2\leftarrow0}$ (cm^{-1})	$\nu_{3\leftarrow0}$ (cm^{-1})	$\Delta\nu_{1\leftarrow0}$ (cm^{-1})	$\Delta\nu_{2\leftarrow0}$ (cm^{-1})	$\Delta\nu_{3\leftarrow0}$ (cm^{-1})
Gaz	2263.9 2264 (25)	4460.63 (26)	6588.5			
CCl_4	2252.4 2253.5 (25)	4435.2	6549.5	11.5	25.4	39.0
C_2Cl_4	2252.0	4433.7	6550.0	11.9	26.9	38.5
CCl_3Br	2250.3	4430.6	6547.5	13.6	30.0	41.0

Constantes moléculaires du D-Chloroforme gazeux et dissous

Solvant	X (cm^{-1})	$\bar{X}$ (cm^{-1})	Y (cm^{-1})	$\bar{Y}$ (cm^{-1})	ω_e (cm^{-1})	$\bar{W}$ (cm^{-1})
Gaz	32.4		−0.267		2329.6	
CCl_4		3.2		−0.5		6.5
C_2Cl_4		6.4		−1.1		2.6
CCl_3Br		7.6		−1.4		3.0

TABLEAU 5

Fréquences d'absorption $\nu_{1\leftarrow0}$, $\nu_{2\leftarrow0}$ et déplacements de fréquence $\Delta\nu_{1\leftarrow0}$, $\Delta\nu_{2\leftarrow0}$ du chloroforme

Solvant	$\nu_{1\leftarrow0}$ (cm^{-1})	$\nu_{2\leftarrow0}$ (cm^{-1})	$\Delta\nu_{1\leftarrow0}$ (cm^{-1})	$\Delta\nu_{2\leftarrow0}$ (cm^{-1})
Gaz	3032.9 (1) 3033 (5)	5941.4 (1) 5943 (5)		
CCl_4	3018.2 (8) 3021 (5)	5906.2 5904 (5)	14.7 12 (5)	35.2 39 (5)
C_2Cl_4	3018.1	5905.4	14.8	36.0
CS_2	3007.1 (8) 3011 (5)	5886.1 5888 (5)	25.8 22 (5)	55.3 55 (5)
CCl_3Br	3015.8	5900.0	17.1	41.4

Constantes moléculaires du chloroforme gazeux et dissous

Solvant	X (cm^{-1})	$\bar{X}$ (cm^{-1})	ω_e (cm^{-1})	$\bar{W}$ (cm^{-1})
Gaz	62.2 (1)		3157.3 (1)	
CCl_4		2.9		8.9
C_2Cl_4		3.2		8.4
CS_2		1.9		22.1
CCl_3Br		3.6		9.9

Pour le potentiel d'induction choisi, la valeur théorique de $\bar{W}_{\text{induction}}$ est sensiblement égale au premier terme en $(\partial^2 u/\partial q^2)_e$. Comme le déplacement $\Delta\omega$ est positif, les grandeurs μ_e et $(\partial^2\mu/\partial q^2)_e$ sont de même signe d'après la relation 17.

Mais pour le potentiel de dispersion choisi, la valeur théorique de $\bar{W}_{\text{dispersion}}$ se réduit au second terme en $(\partial u/\partial q)_e$. $\Delta\omega$ étant toujours positif, et, dans notre cas, k_3 négatif, la quantité $(\partial u/\partial q)_e$ est alors négative. D'après la relation 23 on déduit que $(\partial\alpha/\partial q)_e$ est aussi négatif.

D'après le tableau 3, on peut remarquer que les forces de dispersion sont plus importantes que celles d'induction. L'effet d'induction n'est d'ailleurs notable que dans le cas où la molécule présente une anharmonicité électrique importante (molécules $CHCl_3$ et $CDCl_3$). Notons que l'énergie d'induction a été sous-estimée, dans nos calculs, car nous avons négligé la polarisabilité de la molécule de soluté.

Ces résultats recoupent les calculs de Le Men (27). Celui-ci a en effet évalué les diverses contributions possibles aux interactions binaires entre une molécule dissoute et une molécule de solvant. En appliquant ce calcul au mélange HCl–CCl_4, il avait déjà mis en évidence que le terme de dispersion est le terme prépondérant.

Mais les contributions des forces de dispersion dans le cas des mélanges étudiés sont encore faibles, car elles ne représentent que les 30% de la

Can. J. Chem. Downloaded from www.nrcresearchpress.com by 210.87.254.42 on 09/05/12
For personal use only.

TABLEAU 6

Fréquences d'absorption $\nu_{1\leftarrow 0}$, $\nu_{2\leftarrow 0}$ et déplacements de fréquence $\Delta\nu_{1\leftarrow 0}$, $\Delta\nu_{2\leftarrow 0}$ du bromoforme

Solvant	$\nu_{1\leftarrow 0}$ (cm^{-1})	$\nu_{2\leftarrow 0}$ (cm^{-1})	$\Delta\nu_{1\leftarrow 0}$ (cm^{-1})	$\Delta\nu_{2\leftarrow 0}$ (cm^{-1})
Gaz	3048.3 (1)	5964.9 (1)		
CCl_4	3029.8 (8)	5923.2	18.5	41.7
C_2Cl_4	3029.8	5922.2	18.5	42.7
CS_2	3018.2 (8)	5901.5	30.1	63.4
CCl_3Br	3027.2	5916.4	21.1	48.5

Constantes moléculaires du bromoforme gazeux et dissous

Solvant	X (cm^{-1})	$\bar{X}$ (cm^{-1})	ω_e (cm^{-1})	$\overline{W}$ (cm^{-1})
Gaz	65.9 (1)		3180.1 (1)	
CCl_4		2.4		13.8
C_2Cl_4		2.9		12.8
CS_2		1.6		26.9
CCl_3Br		3.2		14.8

valeur expérimentale. Il apparaît plusieurs raisons à cet écart: (*a*) d'une part, le dipôle considéré n'est certainement pas situé au centre de la maille unitaire, compte tenu des paramètres géométriques de la molécule (r_{C-H} = 1.07 Å, r_{C-X} = 1.80 Å); (*b*) d'autre part, nous avons assimilé la molécule d'haloforme à un simple dipôle H—(CX_3). Il en résulte que les valeurs calculées des grandeurs $(\partial\mu/\partial q)_e$, $(\partial^2\mu/\partial q^2)_e$ et $(\partial\alpha/\partial q)_e$ qui interviennent dans le calcul du potentiel intermoléculaire $\mathcal{U}$, ont été obtenues à partir de la valeur de la constante rotationnelle B_e, relative à cette molécule diatomique fictive; (*c*) enfin, il faudrait en toute rigueur tenir compte des interactions moléculaires à court rayon d'action, en particulier des forces de répulsion.

Nous tenons à remercier M. A. Levy, Maître-Assistant, dont les conseils précieux nous ont permis de mener à bien ce travail.

1. I. Rossi, Nguyen-Van-Thanh, et C. Haeusler. Can. J. Chem. **47**, 3319 (1969).
2. A. D. Buckingham. Proc. Roy. Soc. A, **248**, 169 (1958).
3. A. D. Buckingham. Proc. Roy. Soc. A, **255**, 32 (1960).
4. A. D. Buckingham. Trans. Faraday Soc. **56**, 753 (1960).
5. G. Durocher et C. Sandorfy. J. Mol. Spectrosc. **22**, 347 (1967).
6. P. V. Huong, M. Perrot, et G. Turrel. J. Mol. Spectrosc. **28**, 341 (1968).
7. A. D. May, G. Varghese, J. C. Stryland, et H. L. Welsh. Can. J. Phys. **42**, 1058 (1964).
8. I. Rossi, A. Levy, et C. Haeusler. Can. J. Chem. **46**, 2103 (1968).
9. IUPAC Tables of wavenumbers for the calibration of IR spectrometers. London, Butterworths, 1961.
10. D. H. Rank, D. P. Eastman, B. S. Rao, et T. A. Wiggins. J. Opt. Soc. Amer. **52**, 1 (1962).
11. C. Haeusler et C. Meyer. C. R. Acad. Sci. **259**, 1067 (1964).
12. K. Fox. J. Mol. Spectrosc. **9**, 381 (1962).
13. C. Haeusler, Nguyen-Van-Thanh, et P. Barchewitz. J. Phys. **24**, 289 (1963).
14. P. Barchewitz. Spectroscopie Infrarouge, 1. Paris, Gauthier-Villars, 1961.
15. A. Foldes et C. Sandorfy. J. Mol. Spectrosc. **20**, 262 (1966).
16. A. Lecuyer, M. M. Denariez, et P. Barchewitz. J. Chim. Phys. **60**, 412 (1963).
17. J. H. Hildebrand et R. L. Scott. The solubility of nonelectrolytes. Dover Publishing Co., New York. 1964.
18. J. O. Hirschfelder, C. F. Curtiss, et R. B. Bird. Molecular theory of gases and liquids. p. 1040. New York, John Wiley, 1954.
19. R. C. Herman et K. E. Shuler. J. Chem. Phys. **22**, 481 (1954).
20. M. M. Denariez et A. Lecuyer. J. Chim. Phys. **60**, 421 (1963).
21. J. G. Kirkwood. Phys. Z. **33**, 57 (1932).
22. A. Muller. Proc. Roy. Soc. A, **154**, 624 (1936).
23. R. Ulbrich. Z. Naturforsch. **23A**, 1323 (1968).
24. W. Holzer. J. Mol. Spectrosc. **27**, 522 (1968).
25. J. Lascombe, J. Devaure, et M. L. Josien. J. Chim. Phys. **61**, 1271 (1964).
26. R. Anttila. Ann. Acad. Sci. Fenn. Ser. A, **254**, 7 (1967).
27. J. F. Le Men. Thèse Doctorat d'Etat, Besançon, France. 1967.

Can. J. Chem. Downloaded from www.nrcresearchpress.com by 210.87.254.42 on 09/05/12
For personal use only.

Can. J. Chem. Downloaded from www.nrcresearchpress.com by 210.87.254.40 on 09/05/12
For personal use only.

Mechanism of a base-catalyzed carbonium ion rearrangement

T. S. SORENSEN, I. J. MILLER, AND C. M. URNESS
The Department of Chemistry, University of Calgary, Calgary, Alberta

Received May 7, 1970

The rearrangement of *cis*-1,2,3,4,5-pentamethylcyclopentenyl cation to the *trans* isomer in aqueous sulfuric acids has been found to follow H_0 with unit slope (d log $k_{rearr.}$ = dH_0). This rearrangement involves the intermediacy of a neutral compound, 1,2,3,4,5-pentamethylcyclopentadiene, which on reprotonation is only partly efficient in leading to the *trans* ion product. Under both steady-state intermediate and direct protonation conditions, this diene protonates to give about 55% of the *cis* ion and only 45% of the thermodynamically more stable *trans* isomer.

Canadian Journal of Chemistry, 48, 3374 (1970)

Introduction

A number of directly observable carbonium ion rearrangements are base-catalyzed and in this category are two distinct types:

(*1*) rearrangements involving a base-catalyzed proton transfer, where, for aqueous sulfuric acid solvents, the plots of log $k_{rearr.}$ *vs.* H_0 (a convenient indication of acid "strength") are approximately linear and approximately of unit slope (1);

(*2*) rearrangements, as above, where the plot is approximately linear but of slope about 0.5 (2, 3).

This paper reports on a rearrangement belonging to category *1*, namely, the interconversion of *cis*- and *trans*-1,2,3,4,5-pentamethylcyclopentenyl cations (**1** and **2** respectively) in aqueous sulfuric acids.

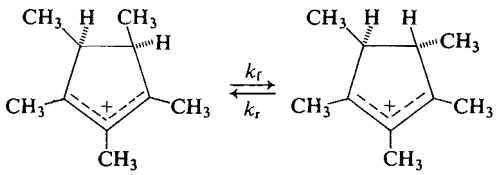

1 **2**

Results and Discussion

Ions **1** and **2** can be prepared quantitatively, *in situ*, in 84–100% aqueous sulfuric acid, each in about 90–95% geometric purity. The analytical procedure, using n.m.r. spectroscopy, for determining the relative amounts of **1** and **2** in mixtures, has been published (4). The *cis* ion **1** – *trans* ion **2** equilibrium (**2**/**1**) favors the *trans* isomer ($K = 3.9 \pm 0.3$) and the most accurate kinetic data are obtained naturally by measuring the *cis* → *trans* conversion. The rates have been plotted assuming reversible first order kinetics (however, see later) and the pseudo-first order rate constants (k_f) for 25 °C are given in Table 1, varying in turn the percent water in the sulfuric acid, the effect of added bisulfate ion and finally, the effect of changing the (**1** + **2**) total carbonium ion concentration. Since carbonium ions **1** and **2** are prepared from alcohols, the percent sulfuric acid figures in Table 1 have been corrected using either of the eqs. 1 or 2, the latter in the case of the 100% acid. The water is further protonated but this is an equilibrium of the sulfuric acid. The percent sulfuric acid figures quoted in column 2 of Table 1 are the same therefore as if one had prepared the solutions by adding carbonium ion bisulfate to the acid solvent.

[1] $ROH + H_2SO_4 \rightarrow R^+ + \text{“}H_2O\text{”} + HSO_4^-$

[2] $ROH + SO_3 \rightarrow R^+ + HSO_4^-$

The reaction is quite obviously of the base-catalyzed variety since the rate increases by a factor of about 100 in going from 100 to 88% aqueous sulfuric acid. Using the data for the 10% carbonium ion concentration solutions and plotting these against H_0, one obtains a slope of 0.99 (Fig. 1).[1]

As one lowers the concentration of the carbonium ion in the acid solutions there is a steady decrease in the rate of the equilibration reaction. This can be explained in part because the sulfuric acid solvent in the lower carbonium ion concentration solutions is less "diluted" during the ion preparation (see column 2 in Table 1). Comparing a 10 and 1% carbonium ion solution, using the slope of 0.99 for log k_f *vs.* H_0 and using

[1]The point for 100% acid deviates greatly from this line. We have used the H_0 value quoted by R. Gillespie (9) for 100% sulfuric acid. It is perhaps questionable to use this value (−12.1) for a solution which is 10% by volume in carbonium ion.

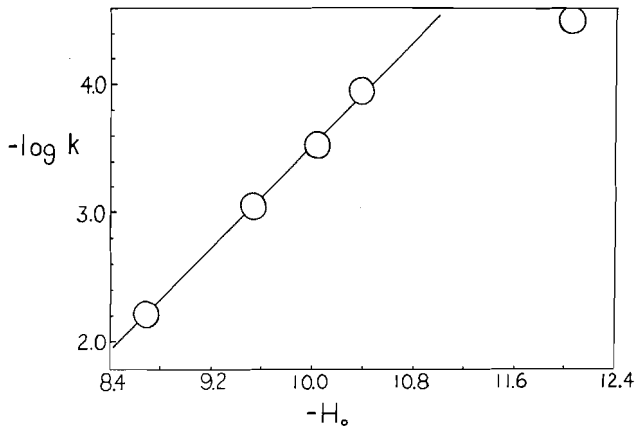

FIG. 1. Experimental values of $-\log k_f$ at 25° plotted against $-H_0$. The slope is 0.99.

TABLE 1

Kinetics for **1** ⇄ **2** at 25°

Original % H_2SO_4	Corrected % H_2SO_4	Added HSO_4^- (M)	Total HSO_4^- (M)	Ion concentration (% w/v)*	k_f (s^{-1})†
100.6	100.0	0	0.65	10	3.2×10^{-5}
		0.50	1.15	10	4.9×10^{-5}
		0.82	1.57	10	6.3×10^{-5}
98.7	98.0	0	2.68	10	6.9×10^{-5}
		0.63	3.31	10	1.2×10^{-4}
		1.12	3.80	10	1.3×10^{-4}
		1.18	3.86	10	1.4×10^{-4}
97.0	96.9	0	3.25	1	5.6×10^{-5}
		0.60	3.85	1	6.4×10^{-5}
	96.8	0	3.43	2.5	7.2×10^{-5}
	96.6	0	3.78	5	1.1×10^{-4}
	96.4	0	4.12	7.5	1.7×10^{-4}
	96.2	0	4.50	10	1.8×10^{-4}
		1.10	5.60	10	2.3×10^{-4}
94.2	93.3	0	7.33	10	5.4×10^{-4}
89.4	88.4	0	10.82	10	4×10^{-3}‡

*Weight of alcohol in g/volume of acid in ml × 100.
†The error is estimated as at least ±10% based on the scatter from, in most cases, four determinations.
‡Probably ±20%, since the n.m.r. resolution is much poorer in this acid.

an original sulfuric acid concentration of 97.0%, one might predict a rate decrease by a factor of about 0.75 (the relative difference in H_0 for the dilution values of 96.9 and 96.2% sulfuric acid, corresponding to the 10 and 1% carbonium ion concentrations respectively). The actual decrease is a factor of about 0.3. However, decreasing the carbonium ion concentration also decreases the bisulfate ion concentration and since this ion may act as a base in the equilibration reaction, the rate decrease may be more than that estimated above, the log k_f *vs.* H_0 correlation being based on 10% carbonium ion concentrations in each case. For this reason, a study was made of the effect of added bisulfate ion on the reaction rate. With 96% sulfuric acid, the effect is not large, for example, using a 10% carbonium ion concentration and adding 1.1 M bisulfate ion (a relative increase of 1.24) the rate increases by a factor of about 1.3 (Table 1). With higher percent sulfuric acid solvents, the relative rate increase with added bisulfate ion is roughly the same. Increasing the bisulfate ion concentration also increases the water concentration (eq. 3). Since both species probably act as bases it is difficult to effect an evaluation of the individual rate constants for water and bisulfate ion base catalysis.

[3] $H_2O + H_2SO_4 \rightleftarrows HSO_4^- + H_3O^+$

Can. J. Chem. Downloaded from www.nrcresearchpress.com by 210.87.254.40 on 09/05/12
For personal use only.

Can. J. Chem. Downloaded from www.nrcresearchpress.com by 210.87.254.40 on 09/05/12
For personal use only.

A crude separation indicates that in 96% sulfuric acid, water, and bisulfate ion catalysis are about equal. The catalytic constants are however quite different since bisulfate ion is present in much larger concentrations. Further experiments will be needed to prove this particular point.

The effect on the kinetics of decreasing the total carbonium ion concentration still seems rather large and the following process may be occurring in the more concentrated carbonium ion solutions, the diene being produced as an intermediate in the bisulfate ion or water-catalyzed reactions. This second order process

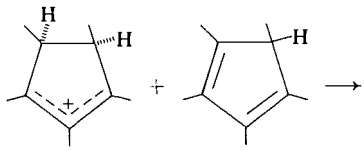

cis

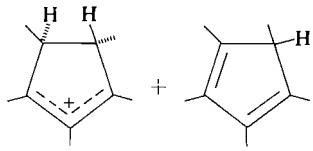

trans

would not be completely catalytic since one would expect the diene concentration to decrease somewhat during the course of the reaction. The experimental data are not accurate enough however to pick up any deviation in the first order plot.

We next turned our attention to the more detailed aspects of the reaction mechanism and Scheme 1 was used as working model, where

$$k_f \text{ (Table 1)} = \frac{k_1 k_{-2}}{k_{-1} + k_{-2}}$$

$$\text{and } k_r = \frac{k_2 k_{-1}}{k_{-1} + k_{-2}}$$

using the steady-state approximation for the diene, all of these being pseudo-first order rate

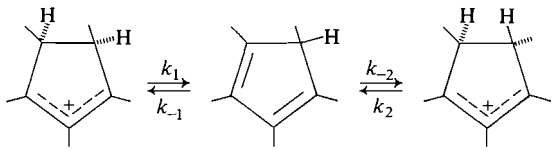

1 **2**

SCHEME 1

constants. Each reaction corresponds to a proton transfer; the slow steps (k_1 and k_2) with proton transfer from the carbonium ion to the base (probably water or bisulfate ion), the fast steps (k_{-1} and k_{-2}) with proton transfer from the acid (H_3O^+ or sulfuric acid) to the diene. Three different methods of attack were used in evaluating these rate constants; one gives k_1 (and k_2) directly while the other two give the k_{-1}/k_{-2} ratio directly. Each method, however, is indirect in the sense that these rate constants are not obtained under the identical conditions used to obtain k_f. In fact, all three methods give rate constants which agree very well with one another and give strong support therefore for the significance of each single method.

Two of the methods involve the preparation of **1** and, independently, **2**, in deuteriosulfuric acid solvent (D_2SO_4). Three separate aqueous (D_2O) concentrations of D_2SO_4 were used in the study (99.0, 95.0, and 92.2%). The rate of the H–D substitution from the solvent into the methyl groups is insignificant under the conditions used in this study.

During the course of the reactions of **1** (or **2**) in D_2SO_4, a total of six species can in theory exist in solution. These are, besides **1** and **2**, the corresponding mono-D carbonium ions, **1**-D and **2**-D, and the di-D ions, **1**-D_2 and **2**-D_2. One

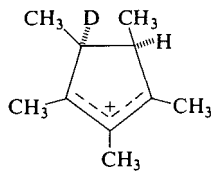

1-D

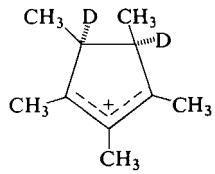

1-D_2

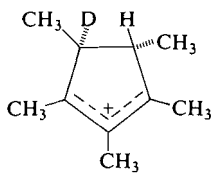

2-D

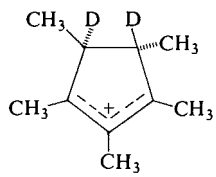

2-D_2

cannot independently measure all six species in the n.m.r. spectrum since the methyl resonance in the grouping

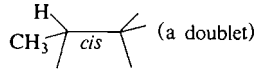

Can. J. Chem. Downloaded from www.nrcresearchpress.com by 210.87.254.40 on 09/05/12
For personal use only.

has the same chemical shift in **1** and **1**-D (double intensity in **1**). Exactly the same problem also occurs in the *trans* ions, **2** and **2**-D. Also the methyl resonance of the grouping

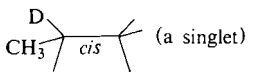

has the same chemical shift in **1**-D and **1**-D_2 (double intensity in **1**-D_2). In the *trans* ions, **2**-D and **2**-D_2, the situation is again entirely analogous. At short reaction times, however, **1**-D_2 and **2**-D_2 exist in only small concentrations and one can take the initial appearance of the

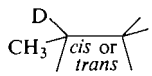

methyl group signal in the n.m.r. spectrum to indicate the concentrations of **1**-D and **2**-D. Typical n.m.r. spectra, at 100 MHz, obtained after short reaction times, starting from the *cis* ion **1** (Fig. 2*a*), and the *trans* ion **2** (Fig. 2*b*) are illustrated, together with the identification of the peaks involved. Note that in *both cases* the concentration of the mono-D *cis* ion (**1**-D) is initially *fractionally* larger than that of the mono-D *trans* ion (**2**-D). One can measure this ratio at

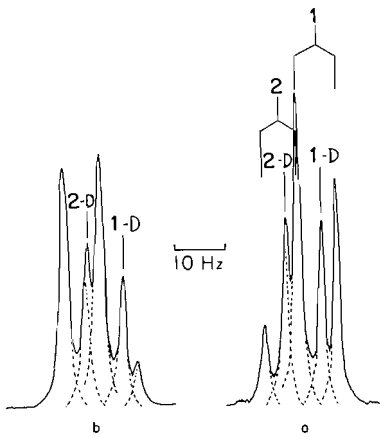

FIG. 2. (*a*) The C-4 and C-5 methyl n.m.r. region of (initially mainly) ion **1** in 95.0% D_2SO_4 solvent at 100 MHz. The measurement was made after *ca.* 40% deuterium incorporation had occurred. The chemical shift value of these methyl groups in **1**-D and **2**-D appears to be subject to a small isotope effect, shifting the resonance to slightly higher fields compared to these same groups in **1** and **2**.

(*b*) The C-4 and C-5 methyl n.m.r. region of (initially mainly) ion **2** in 95.0% D_2SO_4 solvent at 100 MHz. The measurement was made after *ca.* 30% deuterium incorporation had occurred.

low overall H–D conversions to obtain the k_{-1}/k_{-2} ratio, as is shown by the following schematic (Scheme 2). Using duplicate data for all three aqueous D_2SO_4 concentrations and starting initially with either **1** or **2**, one obtains average values of 50–55% **1**-D and 45–50% **2**-D, giving a $k_{-1}(D)/k_{-2}(D)$ ratio of 1.0–1.2.

In addition to determining the initial **1**-D/**2**-D ratio, it is possible to measure the overall disappearance of the n.m.r. methyl peak associated with either

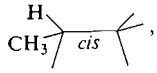

starting from **1**, or

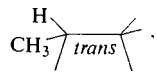

starting from **2**. The rate constant associated with this process is not identical with $k_1(D)$ or $k_2(D)$ as can probably be best seen from an examination of Scheme 2 (using **1** as an example). All reaction proceeding via k_{-2} results in the loss of the

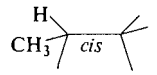

methyl signal but that portion of the reaction proceeding via k_{-1} still retains *one*

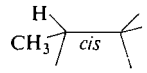

methyl grouping and as previously mentioned, this resonance coincides with that of **1**. In order to evaluate $k_1(D)$, we have subtracted the

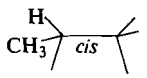

methyl area of **1**-D from the total peak area of this group. This is easily done because the amount of **1**-D formed is independently known from the appearance of the

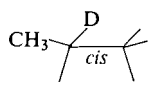

methyl resonance. One must also operate in the low H–D exchange region to ensure that **1**-D_2 is not formed in significant amounts. The rate constants (first order) for the corrected dis-

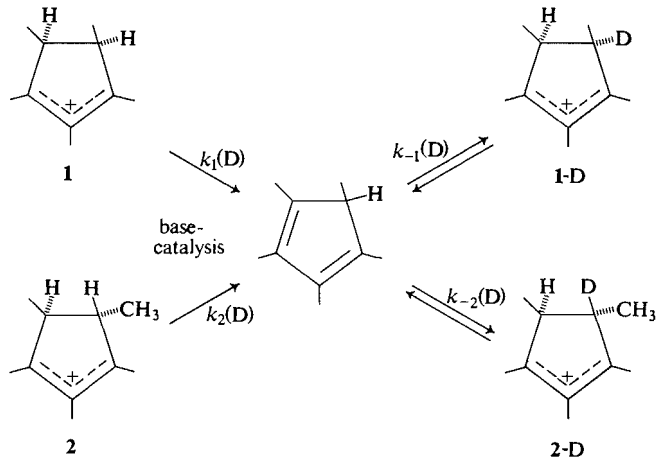

SCHEME 2

TABLE 2
Kinetics in D_2SO_4 solvents at 25°

% D_2SO_4	k_1(D)*(s^{-1})	k_2(D)*(s^{-1})	k_1(D)/k_2(D)	Kk_{-1}/k_{-2}†
99.0	1.5×10^{-4}	3.6×10^{-5}	4.2	4.7
95.0	9.6×10^{-4}	2.4×10^{-4}	4.0	4.7
92.2	2.8×10^{-3}	8.9×10^{-4}	3.1	4.7

*The errors are estimated as ±20% based on the reproducibility of duplicate experiments.
†Using $k_{-1}/k_{-2} = 1.2$.

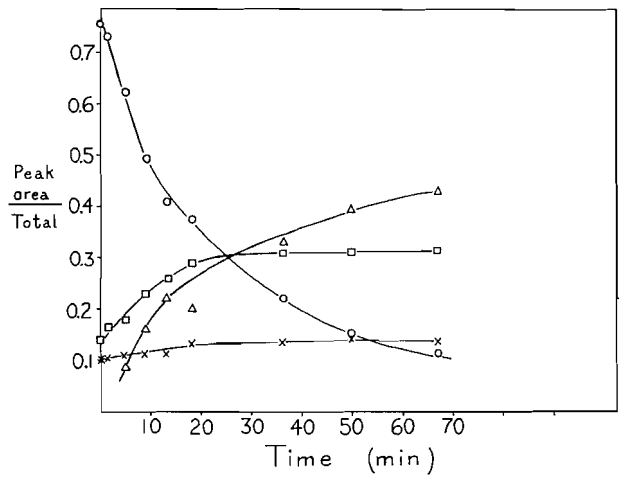

FIG. 3. The change in the relative areas associated with the following n.m.r. peaks, as a function of time, starting initially with mainly ion **1** in 95.0% D_2SO_4 at 25°; ○, the doublet of CH_3 (H, *cis*); □, the singlet of CH_3 (D, *cis*); X, the doublet of CH_3 (H, *trans*); △, the singlet of CH_3 (D, *trans*).

Can. J. Chem. Downloaded from www.nrcresearchpress.com by 210.87.254.40 on 09/05/12
For personal use only.

TABLE 3

Direct addition experiments with pentamethylcyclopentadiene

Temperature* of ion preparation (°C)	Acid	% *cis*	% *trans*
−5	96% H_2SO_4	51–57	43–49
−5	100% H_2SO_4	58–60	40–42
−5	96% D_2SO_4	50–53	47–50
−40	CF_3SO_3H	59–64	36–41
0	CF_3SO_3H	44–45	55–56
−80	$ClSO_3H$	55	45
0	$ClSO_3H$	44–45	55–56
−80	$ClSO_3H$ + 20% $Cl_2S_2O_5$	57–59	41–43
0	$ClSO_3H$ + 20% $Cl_2S_2O_5$	48–61	39–52
−80	FSO_3H	62	38
0	FSO_3H	54–61	39–46
−80	1:1 FSO_3H–SbF_5	53–55	45–47
0	1:1 FSO_3H–SbF_5	49–51	49–51

*Cooling bath temperature; solutions occasionally froze and had to be warmed slightly from time to time.

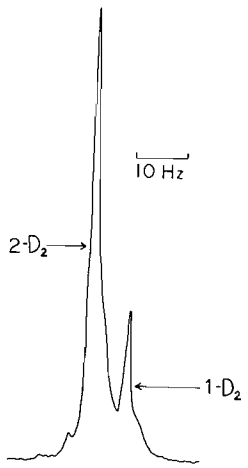

FIG. 4. The C-4 and C-5 methyl n.m.r. region at 100 MHz in 95.0% D_2SO_4, showing the final equilibrium mixture of **2**-D_2 and **1**-D_2 obtained.

appearance of **1** (k_1(D)) are listed in Table 2, as a function of the percent aqueous D_2SO_4 used as a solvent. The corresponding values for the disappearance of **2** (k_2(D)) are also given in Table 2.

At longer reaction times, the areas associated with the four different n.m.r. groupings (Fig. 2) continue to change and in Fig. 3, we show, as an example, the change in the area of these peaks as a function of time for ion **1** in 95.0% D_2SO_4. The final equilibrium result is shown in Fig. 4, yielding a **2**-D_2/**1**-D_2 ratio of 4 ± 1, within experimental error of that found for the protium compounds (**2**/**1**).

Since the diene proposed as an intermediate in these reactions is a completely accessible organic compound, we next measured the initial ratios of **1** and **2** obtained when the diene, 1,2,3,4,5-pentamethylcyclopentadiene, was added to a number of strong acids, including the solvent systems used for the kinetic measurements. In all cases, the ratios are measured under conditions where it can be shown that no subsequent (to protonation) *cis* ⇄ *trans* reaction occurs. The measurements were made in several cases at two different temperatures. The results are given in Table 3. Within experimental error (ca. ± 3%), the ion ratios (**2**/**1**), obtained in 96% H_2SO_4 or D_2SO_4 are identical to those found by the kinetic method in the H–D exchange work.

At low temperatures, in other solvents, some of the ratios are found to favor the *cis* ion by an even greater amount. These ratios are to be compared in all cases with the thermodynamic K of 3.9 favoring the *trans* isomer. The direct protonation results are also useful in providing information concerning the k_{-1}/k_{-2} ratio for acid solvents (FSO_3H, $ClSO_3H$, CF_3SO_3H,[2] 1:1 SbF_5–FSO_3H) for which one cannot reasonably use the H–D substitution method, because the rate of this reaction is simply too slow in these cases.

The three measurements, k_{-1}/k_{-2} (direct pro-

[2]The amount of the *cis* ion **1**, formed in this acid solvent by the direct addition of the diene, is much greater than that produced in the "stereospecific" dienylic cation cyclization reactions (4).

Can. J. Chem. Downloaded from www.nrcresearchpress.com by 210.87.254.40 on 09/05/12
For personal use only.

TABLE 4

Calculation of k_1 and k_2 at 25° and comparison with $k_1(D)$ and $k_2(D)$

% Acid	$k_f(s^{-1})$*	k_1(calcd.)†	$k_1(D)$‡	k_2(calcd.)§	$k_2(D)$‡
98.0	6.2×10^{-5}	1.5×10^{-4}	3×10^{-4}	3.2×10^{-5}	6×10^{-5}
96.2	1.8×10^{-4}	4.0×10^{-4}	6.4×10^{-4}	8.5×10^{-5}	1.5×10^{-4}
93.3	5.4×10^{-4}	1.2×10^{-3}	1.7×10^{-3}	2.5×10^{-4}	5.8×10^{-4}

*From Table 1.

†k_1 (calcd.) $= k_f \left(\frac{k_{-1} + k_{-2}}{k_{-2}}\right)$, using $k_{-1}/k_{-2} = 1.2$.

‡Since these measurements were not made in the same percentage sulfuric acid as were k_f (see Table 2), we have extrapolated the values of $k_1(D)$ and $k_2(D)$ from Table 2 to the same acid concentrations employed in the k_f measurement. This was done by making a graph of $k_1(D)$ and $k_2(D)$ *vs.* % D_2SO_4, using in each case the three points from Table 2, and then directly reading off this graph the above values.

§k_2 (calcd.) $= \frac{k_f}{K}\left(\frac{k_{-1} + k_{-2}}{k_{-1}}\right)$, using $k_{-1}/k_{-2} = 1.2$.

tonation), $k_{-1}(D)/k_{-2}(D)$ and $k_1(D)$ or $k_2(D)$, are independent in derivation but may be related to one another through k_f or k_r, *viz.* eq. 4. An obvious discrepancy arises in trying to fit both

$$[4] \quad \frac{k_{-1}}{k_{-2}} = \frac{k_1}{k_f} - 1 \quad \text{and} \quad \frac{k_{-1}}{k_{-2}} = \frac{k_r}{k_{-2} - k_r}$$

the $k_1(D)$ and $k_2(D)$ data and the k_{-1}/k_{-2} data to these equalities. This is shown in Table 4. The problem almost certainly arises from the equating of k_1 and $k_1(D)$ since it would not be at all unexpected to find a kinetic isotope effect operating (H_2O *vs.* D_2O, HSO_4^- *vs.* DSO_4^-, and H_2SO_4 solvent *vs.* D_2SO_4 solvent). The value of the k_{-1}/k_{-2} ratio, from the two independent measurements, is the same, and this ratio in any case would not be expected to show a significant isotope effect.

Further support for this interpretation comes from a comparison of $k_1(D)$ and $k_2(D)$ listed as $(k_1(D)/k_2(D))$, shown in Table 2, which should and does equal $K\frac{k_{-1}}{k_{-2}}$. Thus, even though k_1 and $k_1(D)$ or k_2 and $k_2(D)$ differ in absolute value, the ratios are the same because the isotope effects, as expected, cancel, *i.e.* $\frac{k_1(D)}{k_2(D)} = \frac{k_1}{k_2}$.

Although one can accurately obtain the k_{-1}/k_{-2} ratio, it is possible only to obtain an order of magnitude value for k_{-1} or k_{-2}. Deno *et al.* (5) have reported a value of -1.9 for the pK_a of 1,3-dimethylcyclopentenyl cation. Equilibrium measurements in this laboratory have shown that a 2-methyl substituent is stabilizing (over 2-H) by a factor of at least 100 (6). Using this minimum figure, the pK_a of **1** or **2** can be estimated as 0. Attempts to directly measure the pK_a of **1** − **2** were unsuccessful because of solubility problems and because the diene has a rather broad u.v. maximum which appears to merge with that of the ion. Using the data for the 1% carbonium ion concentration in 96.9% sulfuric acid, one calculates k_1 under these conditions, eq. 5. The treatment is simplified if one ignores

$$[5] \quad k_1 = k_f/k_{-2}(k_{-1} + k_{-2}) = 1.2 \times 10^{-4}\ s^{-1} \text{ at } 25°$$

the fact that one has two ions in equilibrium with the diene and for this order of magnitude calculation we will assume that only **1** is present. The acidity function value, H_0, for 96.9% sulfuric acid is -10.20 (7) and if one assumes that the [diene]/[ion$^+$] equilibrium follows H_0, as is reported for similar compounds by Deno *et al.* (5), then one would calculate log K for the [diene]/[ion$^+$] ratio, in this acid, as about -10. This then yields k_{-1} = about $1 \times 10^6\ s^{-1}$.

The temperature dependence of k_f in 96.2% sulfuric acid (0, 25, 45, 59 °C) was used to calculate an activation energy of 21 kcal/mole for the reaction of the *cis* ion **1** going to the *trans* ion **2**. If one uses approximately this same value for the activation energy of the reaction represented by k_1, one calculates an activation energy of about 8 kcal/mole for the reverse reaction (using a $K = e^{\frac{-\Delta F}{RT}}$ value of 1×10^{-10} (see above) and $\Delta H \sim \Delta F$).

The rate of the reverse reaction, given by k_{-1}, cannot be very dependent on the "acidity" of the medium (H_0) over the acid range studied. Log k_f follows H_0 with unit slope (Experimental) and since $k_f = \frac{k_1 k_{-2}}{k_{-1} + k_{-2}}$, and since k_{-1}/k_{-2} (Table 3) does not appear to vary with the "acidity" of the solvent, then k_1 must follow H_0 with unit slope. The previous assumption that K

Can. J. Chem. Downloaded from www.nrcresearchpress.com by 210.87.254.40 on 09/05/12
For personal use only.

for [diene]/[ion$^+$] follows H_0 then requires k_{-1} to be relatively constant, where $K = k_1/k_{-1}$.

Experimental

The purification of the acid solvents, the method of adding the organic compound to the acids and the method of analyzing for **1** and **2** in mixtures have been reported previously (4). Particular care was taken to prepare the ion solutions under anhydrous conditions and in each case the n.m.r. tubes were sealed with tape. All of the kinetic measurements were carried out in the n.m.r. tubes at 100 MHz using a Varian Associates HA-100 spectrometer, operated in the field sweep mode and using the acid solvent peak as a lock signal.

The temperature control for most of the kinetic experiments is good. The samples spend most of their time in a constant temperature bath (25 ± 0.1 °C) and only a small amount of time in transit (room temperature 25 ± 1 °C) or in the n.m.r. probe (25 ± 1 °C). The much faster kinetic measurements in 88.4 and 93.3 % sulfuric acid were however carried out entirely within the n.m.r. probe and are less accurate.

The deuteriosulfuric acid of 99% isotopic purity was obtained from Fluka AG. Dilutions were made with deuterium oxide of 99.5% isotopic purity. The concentration of carbonium ion in these experiments was 10% w/v, defined as in Table 1. Using the alcohol as a carbonium ion precursor introduces one proton/molecule of carbonium ion into the solvent, so that the isotope ratio at the time of the initial H–D substitution process is about 1:36 (H/D), of no consequence in the experiments described.

Bisulfate ion additions were made by adding anhydrous sodium sulfate to the sulfuric acid. A small correction was necessary in each case to take into account the resulting small decrease in sulfuric acid concentration ($H_2SO_4 + SO_4^{2-} \rightarrow 2HSO_4^-$). At least two and usually four duplicate runs were made for each set of conditions.

Bisulfate ion concentrations at any percent sulfuric acid were obtained by plotting selected values of $[HSO_4^-]$ *vs.* % sulfuric acid (using the data of Robertson (8)).

All organic compounds used have been previously reported (4).

The authors wish to thank the National Research Council of Canada for generous financial support. We wish also to acknowledge the valuable discussions with Dr. E. B. Robertson.

1. T. S. SORENSEN. J. Amer. Chem. Soc. **89**, 3794 (1967).
2. T. S. SORENSEN. J. Amer. Chem. Soc. **89**, 3782 (1967).
3. N. C. DENO and R. R. LASTOMIRSKY. J. Amer. Chem. Soc. **90**, 4085 (1968).
4. P. H. CAMPBELL, N. W. K. CHIU, K. DEUGAU, I. J. MILLER, and T. S. SORENSEN. J. Amer. Chem. Soc. **91**, 6404 (1969).
5. N. C. DENO, J. BOLLINGER, N. FRIEDMAN, K. HAFER, J. D. HODGE, and J. J. HOUSER. J. Amer. Chem. Soc. **85**, 2998 (1963).
6. Unpublished work by N. W. K. Chiu in this laboratory.
7. M. J. JORGENSEN and D. R. HARTTER. J. Amer. Chem. Soc. **85**, 878 (1963).
8. E. B. ROBERTSON. Ph.D. Thesis. The University of Alberta, Edmonton, Alberta. 1964. pp. 23 and 98.
9. R. GILLESPIE. Acc. Chem. Res. **1**, 202 (1968).

Can. J. Chem. Downloaded from www.nrcresearchpress.com by 210.87.254.40 on 09/05/12
For personal use only.

Can. J. Chem. Downloaded from www.nrcresearchpress.com by 210.87.254.40 on 09/05/12
For personal use only.

Bicyclo[2,2,1]heptylphosphonates II.[1] Stéréochimie de l'addition de Diels–Alder du vinylphosphonate de diméthyle sur quelques cyclopentadiènes; étude par r.m.n.

HENRY J. CALLOT ET CLAUDE BENEZRA
Département de Chimie, Université d'Ottawa, Ottawa 2, Canada

Reçu le 30 avril 1970

La stéréochimie de l'addition de Diels–Alder du vinylphosphonate (**1**) sur le cyclopentadiène, l'hexachlorocyclopentadiène (**6**), le diméthoxytétrachlorocyclopentadiène (**8**) et le pentachlorocyclopentadiène (**10**) a été étudiée. La configuration des composés obtenus a été prouvée par corrélation chimique et surtout par r.m.n. L'étude des spectres de r.m.n. confirme la dépendance angulaire du couplage vicinal $^{31}P,^{1}H$ et donne une idée de l'électronégativité du groupe $(CH_3O)_2P(O)$—.

The stereochemistry of the Diels–Alder addition of the vinylphosphonate (**1**) to cyclopentadiene, hexachlorocyclopentadiene (**6**), dimethoxytetrachlorocyclopentadiene (**8**), and pentachlorocyclopentadiene (**10**) has been studied. The configuration of the compounds has been proved by chemical correlation and essentially by n.m.r. spectroscopy. The study of the n.m.r. spectra confirms the $^{31}P,^{1}H$ vicinal coupling dihedral angular dependence and suggests an electronegativity range for the $—P(O)(OCH_3)_2$ group.

Canadian Journal of Chemistry, **48**, 3382 (1970)

Bien que l'addition de Diels–Alder de phosphonates vinyliques sur des diènes conjugués soit connue depuis un certain nombre d'années (1–4), il ne semble pas que l'étude de la stéréochimie de cette réaction ait été entreprise. Cela vient sans doute de ce que la séparation des épimères *exo* et *endo* s'avère souvent difficile et n'a pu être réalisée dans plusieurs cas (3).

Nous avons entrepris l'étude de l'addition thermique du vinylphosphonate de diméthyle (**1**, $CH_2{=}CH—P(O)(OCH_3)_2$) sur différents cyclopentadiènes en pensant que, d'une part, les spectres de r.m.n. seraient plus simples, du fait de la présence des méthoxyles, que ceux des produits d'addition avec $CH_2{=}CHP(O)(OC_2H_5)_2$ (3), d'autre part, des résultats récents de ce laboratoire (5) nous permettant d'attribuer sans ambigüité la configuration *endo* ou *exo* au groupe diméthylphosphonique.

L'addition de **1** aux divers cyclopentadiènes est en général lente et ce fait semble montrer que l'effet électroattracteur du groupe $P(O)(OCH_3)_2$ est faible. Ce résultat, confirmé par l'étude des couplages en r.m.n. n'est pas surprenant et on sait, par exemple que bien que l'échange d'un hydrogène en α du groupe dimethylphosphonique soit réalisable, il ne l'est que dans des conditions énergiques, avec des bases fortes telles que les dérivés lithiés (6).

Ce travail décrit l'addition de $CH_2{=}CHP(O)(OCH_3)_2$ sur quatre cyclopentadiènes; tous les produits ont été séparés, caractérisés et leur structure démontrée essentiellement par r.m.n.

Addition de Diels–Alder du vinylphosphonate de diméthyle sur le cyclopentadiène

Les additions de Diels–Alder sur le cyclopentadiène conduisent généralement (**7**) à un mélange des deux isomères *endo* et *exo*. Avec comme diénophile le vinylphosphonate de diéthyle, Daniewski et Griffin (3) ont montré qu'un mélange 1:1 des deux isomères se forme. Ces deux auteurs n'ont pu séparer les deux épimères, ni leur attribuer de stéréochimie.

Dans le cas du vinylphosphonate de diméthyle, nous avons obtenu les isomères *exo* et *endo* dans un rapport 1.2:1 et les avons séparés par chromatographie sur colonne de silice (éq. 1).

L'attribution des configurations peut se déduire de l'examen en r.m.n. de l'hydrogène situé en tête de pont, H_4. Cet hydrogène est en effet couplé avec le phosphore lorsque le groupe diméthylphosphonique est *exo* ($^3J_{PH}$ = 7.5–8.5 Hz) alors qu'il n'y a pas de couplage décelable lorsqu'il est *endo* ($^3J_{PH} < 0.5$ Hz) (5). Le couplage vicinal *H*—C—C—*P* est en effet une fonction de l'angle dièdre φ (P, H) et suit une relation de type Karplus (8): il est maximum pour 0 et 180° et s'annule pour $\phi = 90°$, de la même facon que le couplage *H*—C—C—*H* (9). Nous attribuons la structure *exo* au composé **2** ($^3J_{PH_4}$ = 8.5 Hz) et *endo* au composé **3** ($^3J_{PH_4} \sim 0$).

La configuration *exo* du dérivé **2**, le moins polaire en chromatographie sur colonne est

[1]Bicyclo[2,2,1]heptylphosphonates I: voir réf. 5.

[1] 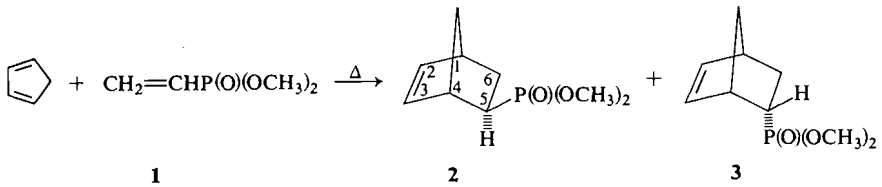

1 2 3

[2] 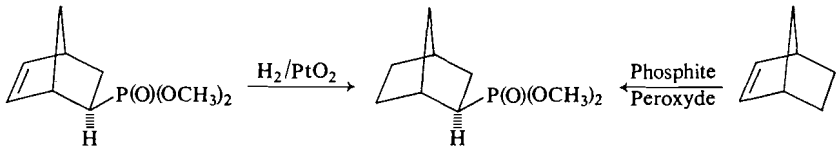

2 4 5

[3] 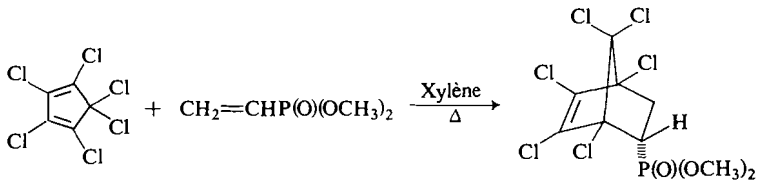

6 7

confirmée par son hydrogénation quantitative en dérivé saturé, **4**. La r.m.n. de **4** montre un couplage $^3J_{PH_4}$ = 8.5 Hz (l'irradiation du ^{31}P permet les attributions univoques des couplages P, H).

Nous avons pu obtenir ce même dérivé **4** en additionnant du phosphite de diméthyle sur le norbornène **5** en présence d'un générateur de radicaux, le peroxyde de benzoyle (éq. 2). Pratiquement toutes les additions radicalaires sur le norbornène **5** conduisent d'une façon prépondérante, sinon exclusive au dérivé *exo* (10). L'addition radicalaire de $HP(O)(OMe)_2$ ne semble pas faire exception à la règle.

Addition de 1 sur l'hexachlorocyclopentadiène et le diméthoxy-5,5 tétrachlorocyclopentadiène-1,3

Cette addition conduit dans les deux cas à un seul isomère, conformément à la "règle endo" d'Alder. L'hexachlorocyclopentadiène **6** donne le dérivé **7** auquel nous avons attribué la configuration *endo* (éq. 3). Outre les considérations d'ordre mécanistique qui, suivant la règle d'addition *endo* conduisent à considérer la formation d'un dérivé *exo* comme hautement improbable (cela tendrait en effet à rapprocher dans l'état de transition des groupes aussi volumineux que Cl et $(CH_3O)_2$-P(O)—), nous avons établi la structure du composé **7** en le transformant complètement en dérivé **3**. Cette dernière réaction a été effectuée en traitant le produit d'addition **7** par le sodium dans un mélange de THF et de méthanol, modification d'un procédé déjà décrit (11).

Il a d'ailleurs été établi que l'addition de diverses oléfines à l'hexachlorocyclopentadiène conduisait exclusivement à l'épimère *endo* (12). L'addition du vinylphosphonate de diéthyle à l'hexachlorocyclopentadiène ne conduit donc certainement pas, comme cela l'a été décrit (3) au mélange des isomères *endo* et *exo*. Les données de r.m.n. qui ont conduit les auteurs à cette conclusion erronée (aspect du signal du groupe éthyle) sont entièrement interprétables si l'on considère que le carbone porteur du groupe diéthylphosphonique est asymmétrique (13).

De même, nous attribuons la configuration *endo* au produit d'addition de **1** sur le diméthoxy-5,5 tétrachlorocyclopentadiène-1,3, **8** (éq. 4); d'une part, pour les mêmes raisons que nous avons invoquées plus haut (état de transition conduisant à l'*exo*, défavorable), d'autre part, la partie du spectre de r.m.n. attribuable aux pro-

Can. J. Chem. Downloaded from www.nrcresearchpress.com by 210.87.254.40 on 09/05/12
For personal use only.

[4] 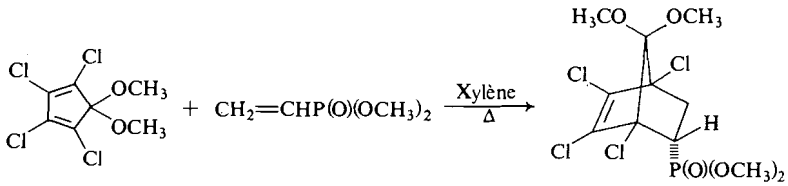

8 9

tons 5 et 6 est pratiquement superposable à la partie correspondante du spectre du composé **7**. Ces résultats sont en parfait accord avec les travaux de Williamson (12) sur l'addition de diverses oléfines au cyclopentadiène **6**.

Addition du vinylphosphonate de diméthyle 1 au pentachloro-1,2,3,4,5 cyclopentadiène 10

Cette addition pouvait conduire *a priori* aux quatre isomères, **11**–**14**. La formation du composé **14** est peu favorisée en raison de la forte interaction qui résulterait entre des groupes aussi volumineux que Cl ou $(CH_3O)_2P(O)$— dans l'état de transition. Nous n'en avons par trouvé trace.

Ce résultat semble général et Williamson *et al.* (14) ont récemment montré que l'addition du pentachlorocyclopentadiène **10** à diverses oléfines monosubstituées conduisait, dans des proportions égales, à trois isomères analogues des composés **11**, **12** et **13**.

Lorsque le pentachlorocyclopentadiène **10** est mis en réaction dans le xylène avec le vinylphosphonate de diméthyle pendant 3 h à 133°, après séparation d'une quantité importante de goudrons insolubles, on isole par chromatographie sur colonne de silice trois composés (dans le rapport 1:3 5:2.8) auxquels nous attribuons les structures **11**, **12**, et **13**.

La structure du composé **12**, le plus abondant, découle de l'examen de son spectre de r.m.n. L'hydrogène porté par le carbone C-7 apparaît à champ faible (δ = 4.05 p.p.m.) sous forme d'un doublet de doublet qui se réduit à un simple doublet par irradiation du ^{31}P à 40 MHz ($^4J_{PH}$ = 4.0 Hz) (5). Le H_7 est couplé au phosphore et à H_6 *endo* ($^4J_{H_{6n}H_7}$ = 1.5 Hz). Ces couplages en W sont caractéristiques des systèmes bicyclo[2,2,1]-heptaniques (15, 16).

La r.m.n. des composés **11** et **13** montrent que H_7 est *anti* par rapport à la double liaison; dans les deux composés, en effet, ils apparaissent sous forme d'un fin sigulet (pas de couplage longue-distance en W).

L'aspect, en r.m.n., des signaux des protons attachés aux carbones C-5 et C-6 est révélateur. Si l'on compare les absorptions attribuables à ces hydrogènes dans les spectres des composés **11** et **13** à celles correspondantes dans le composé **7** (où le groupe phosphoré est *endo*) on remarque une certaine similarité entre les composés **7** et **13** alors que le composé **11** semble nettement à part. Cette constatation nous avait conduits (17) à postuler une configuration *exo* pour le groupe $(CH_3O)_2P(O)$— dans le composé **11**.

Cette hypothèse a été confirmée par la réduction du composé d'addition **7** par le zinc dans l'acide acétique. Williamson *et al.* (18) ont montré qu'une telle réduction était stéréoselective et conduisait d'une façon prépondérante au dérivé *syn*-chloro. Dans notre cas, cette réduction conduit à 90% d'un composé identique à **13** et à 10% d'un composé identifié à **12** (éq. 5). Dans le composé **11**, H_7 apparaissant sous forme d'un fin singulet, est donc en position *anti* par rapport à la double liaison, comme dans le composé **13**. Dans ce dernier produit le groupe phosphoré étant *endo*, il s'ensuit que **11** a la structure *exo* indiquée plus haut.

Spectres de r.m.n. des composés 2, 3, 4, 7, 9, 11, 12, et 13

Les spectres de r.m.n. des composés décrits

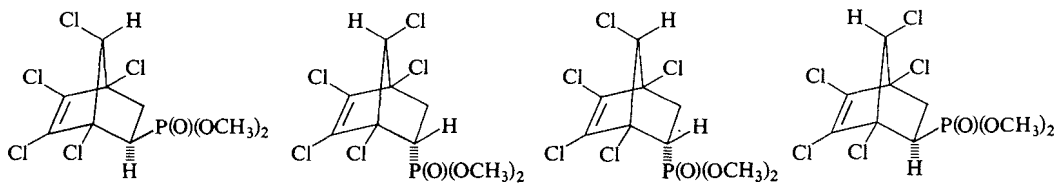

11 12 13 14

Can. J. Chem. Downloaded from www.nrcresearchpress.com by 210.87.254.40 on 09/05/12
For personal use only.

[5] 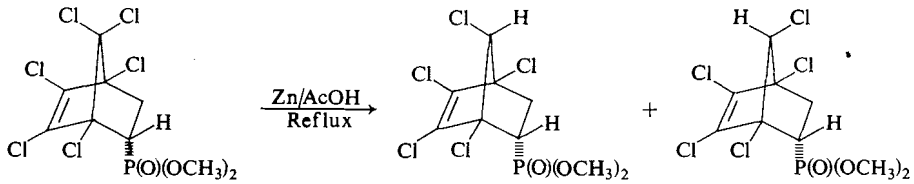

7 13(90%) 12(10%)

plus haut sont parfaitement en accord avec les structures proposées. En plus de ce qui a été dit précédemment, certains faits sont intéressants à noter. Si l'on compare le composé **9** avec les produits d'addition de l'hexachlorocyclopentadiène avec diverses oléfines étudiées par Williamson (12), on constate que les constantes de couplages $J_{5x,6x}$ = 9.5 Hz, $J_{5x,6n}$ = 5.0 Hz sont

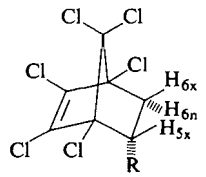

légèrement supérieures à celles trouvées pour R = CN (9.3 et 4.6 Hz respectivement); cela signifierait que le groupe $(CH_3O)P(O)$— est légèrement moins électronégatif que le groupe cyano. Ce résultat permet de comprendre la faible réactivité du vinylphosphonate diméthylique constatée dans notre étude. Il semble que l'effet inductif du groupe est ici le plus important.

Les couplages vicinaux $^{31}P,^{1}H$ sont en accord avec une dépendance angulaire de type Karplus. On trouve en effet $^{3}J_{PH}$ (ϕ = 0°) compris entre 16.9 et 17.6 Hz, $^{3}J_{H}$ (ϕ = 60°) compris entre 7.6 et 8.4 Hz et $^{3}J_{PH}$ (ϕ = 30°) entre 8 et 8.5 Hz. Ces valeurs sont légèrement supérieures à celles trouvées dans le cas d'hydroxyphosphonates (5).

Les couplages P—O—CH_3 sont tous compris entre 9.6 et 11.0 Hz, sauf dans le cas du dérivé **13** où il est anormalement bas: 5.2 Hz. Nous n'avons pas d'explication, pour l'instant, pour ce phénomène.

Partie expérimentale

Indications générales

L'hexachlorocyclopentadiène est un produit commercial (Hooker Chemical Corporation). Le cyclopentadiène utilisé a été préparé par distillation du bicyclopentadiène commercial. Le pentachlorocyclopentadiène a été préparé à partir d'hexachlorocyclopentadiène par la méthode décrite par Newcomer et McBee (19).

La préparation du vinylphosphonate diméthylique est décrite dans un brevet (20). Nous donnons ici le processus expérimental précis que nous avons suivi.

Les chromatographies sur colonne ont été effectuées sur du silica gel Mallinckrodt (cc-7 mesh: 100–200), les réactions ont été suivies par chromatographie en couche mince (c.c.m.).

Les spectres i.r. ont été mesurés sur l'IR 20 de Beckman. Nous ne donnons pas ici leur description détaillée; ils sont tous compatibles avec les structures proposées: les absorptions semblent caractéristiques du squelette bicyclo[2,2,1]heptane. Tous comportent des bandes très intenses: P=O (1210–1240 cm^{-1}) et P—O—C (~1050 cm^{-1}). Les doubles liaisons 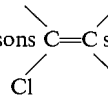 sont caractéristiques et apparaissent à 1600 cm^{-1}.

Les spectres de masse pris sur Hitachi–Perkin–Elmer RMU-6D seront décrits en détail dans une publication ultérieure.

Préparation du vinylphosphonate de diméthyle 1

On porte à reflux pendant 5 h un mélange de dibromoéthane (565 ml; 1240 g) et de triméthylphosphite (70 ml; 73 g) puis on distille sous vide. Après passage des produits de départ qui n'ont pas réagi, on recueille deux fractions distillant respectivement à 70–100 et à 100–130° sous 20 Torr.

La première fraction est redistillée (ébullition 179–183°/760 Torr) pour donner une huile incolore (15 g) identifiée par r.m.n. au méthylphosphonate de diméthyle (181°) 760 Torr *cf.* réf. 21.

Spectre de r.m.n. ($CDCl_3$, pris sur T-60 Varian): 1 d à 1.49 p.p.m. (3H, CH_3P, J_{PH} = 18.0 Hz); 1 d à 3.82 p.p.m. (6H, CH_3OP, J_{PH} = 11.6 Hz). Il est intéressant de noter que la réaction du dibromoéthane avec $P(OMe)_3$ donne des quantités à peu près équivalentes du produit attendu par réarrangement d'Arbuzov: $BrCH_2$-$CH_2P(O)(OCH_3)_2$ et d'un produit secondaire provenant de la réaction du bromure de méthyle sur le phosphite triméthylique.

$$BrCH_2CH_2Br + P(OCH_3)_3 \rightarrow BrCH_2CH_2P(O)(OCH_3)_2 + CH_3Br$$

$$CH_3Br + P(OCH_3)_3 \rightarrow CH_3P(O)(OCH_3)_2 + CH_3Br$$

Ceci n'a été, à notre connaissance, souligné nulle part.

La seconde fraction (25 ml) est traitée par la triéthylamine (15 ml) dans le benzène (40 ml) et le mélange laissé à température ordinaire pendant 24 h. Une fois filtrés les cristaux de bromhydrate de triéthylamine et le benzène évaporé, on recueille une fraction qui bout à 70–80°/10 Torr qui est composée de vinylphosphonate

Can. J. Chem. Downloaded from www.nrcresearchpress.com by 210.87.254.40 on 09/05/12
For personal use only.

Can. J. Chem. Downloaded from www.nrcresearchpress.com by 210.87.254.40 on 09/05/12
For personal use only.

diméthylique pur (13.5 g; litt. ébullition 72.5°/10 Torr réf. 22).

Spectre de r.m.n. ($CDCl_3$, pris sur T-60 Varian): 1 d à 3.81 p.p.m. (6H, CH_3OP, J_{PH} = 11.2 Hz); 1 m vers 6.5 p.p.m. (3H, système ABCX, CH_2=C*H*—P).

Réaction du cyclopentadiène avec le vinylphosphonate de diméthyle: composés 2 et 3

On chauffe pendant 18 h, à 160–170°, dans une bombe en acier, un mélange de cyclopentadiène (1.2 g), de vinylphosphonate diméthylique (2.0 g), et d'hydroquinone (50 mg). Après refroidissement, on ajoute de l'éther, filtre pour éliminer un résidu insoluble puis évapore le solvant. On obtient une huile (2.7 g) qui est chromatographiée sur silica gel (50 g.). On élue successivement le produit **2** (695 mg; éther/éther de pétrole, 3/7) puis le produit **3** (575 mg; éther/éther de pétrole 1/1). Les deux produits sont purifiés par microdistillation (70°/10 Torr).

Anal. Calc. pour composé **2**, $C_9H_{15}O_3P$: C, 53.47; H, 7.43; P, 15.35. Trouvé: C, 53.46; H, 7.75; P, 15.40.

Spectre de masse: pic moléculaire à *m/e* 202.

Anal. Calc. pour composé **3**, $C_9H_{15}O_3P$: C, 53.47; H, 7.43; P, 15.35. Trouvé: C, 53.36; H, 7.39; P, 15.33.

Spectre de masse: pic moléculaire à *m/e* 202.

Addition radicalaire du phosphite de diméthyle sur le norbornène: composé 4

On chauffe à reflux un mélange de norbornène (4.5 g) et de phosphite diméthylique (100 g) et on y ajoute du peroxyde de benzoyle (2 g) dans le tétrachlorure de carbone (20 ml). On chauffe à reflux 30 min supplémentaires puis distille sous vide (10 mm). On recueille successivement une fraction de tête contenant l'excès de phosphite puis le produit qui est redistillé à 127–132°/10 Torr. Huile incolore (84 g, soit 86% par rapport au norbornène de départ).

Anal. Calc. pour $C_9H_{17}O_3P$: C, 52.94; H, 8.33; P, 15.20. Trouvé: C, 52.76; H, 7.99; P, 14.95.

Spectre de masse: pic moléculaire à *m/e* 204.

Hydrogénation catalytique de 2: composé 4

Le composé **2** (100 mg) est dissous dans le méthanol et hydrogéné en présence de Pd/C à 2.7 atm pendant 22 h. On filtre, élimine le solvant sous vide. L'huile incolore (~100 mg) est identifiée à **4** (c.c.m , i.r., r.m.n.).

Addition de 1 sur l'hexachlorocyclopentadiène: composé 7

On chauffe pendant 46 h à 125–127° un mélange d'hexachlorocyclopentadiène (7 g), de vinylphosphonate diméthylique (4 g), d'hydroquinone (200 mg), et de xylène (30 ml). On refroidit, élimine le xylène sous vide et chromatographie l'huile sombre obtenue sur silica gel (100 g). Le mélange éther/éther de pétrole, 1/1, élue le composé **7** (4.1 g) qui cristallise lentement et est sublimé (130°/0.1 Torr) pour l'analyse; p.f. 44–46°.

Anal. Calc. pour $C_9H_9Cl_6O_3P$: C, 26.41; H, 2.20; P, 7.58; Cl, 52.08. Trouvé: C, 26.88; H, 2.19; P, 8.02; Cl, 51.81.

Addition de 1 sur le diméthoxy-5,5-tétrachlorocyclopentadiène: composé 9

On chauffe pendant 21 h à 122–123° un mélange de diméthoxytétrachlorocyclopentadiène (6 g), de vinylphosphonate diméthylique (4 g), d'hydroquinone (200 mg), et de xylène (20 ml). Après refroidissement, on élimine le xylène sous vide et chromatographie l'huile obtenue sur silica gel (100 g). Le produit **9** est élué par le mélange éther/éther de pétrole, 1/1, sous forme d'une huile (4.5 g) qui est microdistillée (130°; 0.1 Torr) pour l'analyse.

Anal. Calc. pour $C_{11}H_{15}Cl_4O_5P$: C, 33.00; H, 3.75; P, 7.75; Cl, 35.50. Trouvé: C, 33.47; H, 4.04; P, 8.03; Cl, 35.20.

Réaction de 1 avec le pentachloro-1,2,3,4,5 cyclopentadiène: composés 11, 12, et 13

On chauffe pendant 3 h à 133° un mélange de pentachlorocyclopentadiène (2.6 g; monomère, fraîchement distillé), de vinylphosphonate diméthylique (1.5 g), d'hydroquinone (200 mg) et de xylène (5 ml). La solution se colore fortement avec dépôt de polymères insolubles en cours de réaction. On refroidit, dilue à l'éther, filtre, élimine le solvant et chromatographie l'huile sur silica gel (35 g) en utilisant des mélanges chlorure de méthylène/chloroforme jusqu'au chloroforme pur. On élue successivement les composés **11** (70 mg), **12** (220 mg), et **13** (180 mg) qui tous trois cristallisent après évaporation du solvant et sont sublimés (125°/0.1 Torr) pour l'analyse.

Anal. Calc. pour composé **11** (p.f. 89–90°), $C_9H_{10}Cl_5O_3P$: C, 28.84; H, 2.67; P, 8.28; Cl, 47.13. Trouvé: C, 28.69; H, 2.86; P, 8.49; Cl, 47.18.

Anal. Calc. pour composé **12** (p.f. 62–64°), $C_9H_{10}Cl_5O_3P$: C, 28.84; H, 2.67; P, 8.28; Cl, 47.13. Trouvé: C, 28.96; H, 2.81; P, 8.48; Cl, 47.24.

Anal. Calc. pour composé **13** (p.f. 147–151°), $C_9H_{10}Cl_5O_3P$: C, 28.84; H, 2.67; P, 8.28; Cl, 47.13. Trouvé: C, 29.08; H, 2.66; P, 8.37; Cl, 47.10.

Traitement du produit d'addition 7 par Na/MeOH/THF: composé 2

On dissout le composé **7** (300 mg) dans un mélange de tétrahydrofurane (10 ml) et de méthanol (2 ml) et on refroidit à 0°. On ajoute du sodium (150 mg) par petites portions puis on dilue par du tétrahydrofurane (10 ml) et du methanol (3 ml) et rajoute du sodium (200 mg). Durant toute l'addition (2 h 15 min), on agite vigoureusement le mélange réactionnel. On isole le produit en ajoutant de l'eau (100 ml) et du benzène (50 ml), puis on lave la phase organique avec de l'eau et ensuite avec une solution saturée de chlorure de sodium. On sèche sur sulfate de sodium et élimine le solvant. On obtient une huile incolore (70 mg; 45%) identifiée à **2** (c.c.m., i.r., r.m.n.).

Réduction par le zinc dans l'acide acétique du composé 7: composés 12 et 13

On dissout **7** (210 mg) dans l'acide acétique glacial (8 ml) et y ajoute du zinc en poudre (500 mg). On porte à reflux pendant 20 h en agitant vivement puis, après refroidissement, on dilue par l'eau (50 ml), extrait trois fois au chloroforme, lave par une solution de carbonate de potassium à 10% puis à l'eau. Après évaporation du solvant, on obtient une huile (190 mg) qui cristallise. On identifie le produit à un mélange des composés **13** (90%) et **12** (10%) (c.c.m.; r.m.n.).

Spectres de r.m.n.

Les spectres de r.m.n. ont été mesurés sur le spectromètre Varian HA-100, les composés étant dissous dans

TABLEAU 1

Déplacements chimiques (δ p.p.m.)

H	2	3	4	7	9	11	12	13
1	2.97	2.94	2.32	—	—	—	—	—
2,3	6.20	6.12	—	—	—	—	—	—
4	3.09	3.16	2.53	—	—	—	—	—
5	1.2–2.10*	2.32	1.1–1.8*	3.16	3.00	2.69–2.91*	3.12	2.34–3.04*
6x	1.2–2.10*	2.00	1.1–1.8*	2.55	2.33	2.69–2.91*	2.49	2.34–3.04*
6n	1.2–2.10*	1.10–1.55*	1.1–1.8*	2.55	2.33	2.69–2.91*	2.49	2.34–3.04*
7	1.2–2.10*	1.10–1.55*	1.1–1.8*	—	—	4.96	4.05	4.30
CH_3	3.76	3.69	3.78	3.79	3.83	3.85	3.79	3.77
	3.735	3.66	3.75	3.76	3.86	3.77	3.76	3.79

*Non attribuable avec précision.

TABLEAU 2

Constantes de couplage (en Hz)

	2	3*	4	7	9	11	12	13
$J_{5,6x}$	n.m.†	10.0	n.m.	9.5	10.0	n.m.	10.2	n.m.
$J_{5,6n}$	n.m.	5.2	n.m.	5.0	5.0	n.m.	5.2	n.m.
$J_{6x,6n}$	n.m.	n.m.	n.m.	12.5	12.0	n.m.	12.2	n.m.
$J_{P,4}$	8.5	0	8.5	—	—	—	—	—
$J_{P,5}$	n.m.	15.0	n.m.	16.0	13.0	n.m.	15.2	n.m.
$J_{P,6x}$	n.m.	8.4	n.m.	8.0	7.6	n.m.	8.2	n.m.
$J_{P,6n}$	n.m.	n.m.	n.m.	17.6	17.4	n.m.	16.9	n.m.
J_{POCH_3}	10.6	10.5	9.6	11.0	10.0	5.2	11.0	10.6

*Pour le composé 3, on peut également mesurer: $J_{1,2} = J_{3,4} = 3.0$ Hz; $J_{2,3} = 5.6$ Hz; $J_{4,5} = 3.2$ Hz (alors que $J_{4,5} = 0$ pour 2) et enfin $J_{1,6x} = 10.0$ Hz.
†Non mesurable: n.m.

le deutériochloroforme. Les déplacements chimiques sont exprimés en p.p.m. et donnés en unités δ par rapport au TMS, référence interne. Les couplages sont exprimés en Hz (à 0.2 Hz près). Le découplage du ^{31}P a été réalisé à 40 MHz avec un découpleur de spin hétéronucléaire, n.m.r. Varian Specialties. Les résultats sont résumés dans tableaux 1 et 2.

Nous remercions le Conseil National de Recherche du Canada pour l'assistance financière (Octroi A-5496) accordée à ce travail.

1. E. C. LADD. U.S. Patent, 2 611 784. Sept. 23, 1952. Chem. Abstr. **47**, 9355 (1953).
2. E. C. LADD. U.S. Patent, 2 622 096. Dec. 16, 1952. Chem. Abstr. **47**, 9344 (1953).
3. W. M. DANIEWSKI et C. E. GRIFFIN. J. Org. Chem. **31**, 3236 (1966).
4. A. N. PUDOVIK, G. E. YASTREBOVA, V. I. NIKITINA, et YU-YU. SAMITOV. Zh. Obshch. Khim. **38**, 292 (1968); Chem. Abstr. **69**, 106815 j (1968).
5. C. BENEZRA. Tetrahedron Lett. 4471 (1969).
6. E. J. COREY et G. T. KWIATKOWSKI. J. Amer. Chem. Soc. **88**, 5654 (1966).
7. J. SAUER. Angew. Chem. Int. Edit. **6**, 16 (1967).
8. C. BENEZRA et G. OURISSON. Bull. Soc. Chim. Fr. 1825 (1966).
9. M. KARPLUS. J. Chem. Phys. **30**, 11 (1959).
10. H. STOCKMANN. J. Org. Chem. **29**, 245 (1964) et références citées.
11. P. G. GASSMAN et P. G. PAGE. J. Org. Chem. **29**, 160 (1964).
12. K. L. WILLIAMSON. J. Amer. Chem. Soc. **85**, 516 (1963).
13. C. BENEZRA et G. OURISSON. Bull. Soc. Chim. Fr. 2270 (1966).
14. K. L. WILLIAMSON, Y.-F. L. HSU, R. LACKO, et C. H. YOUN. J. Amer. Chem. Soc. **91**, 6129 (1969).
15. J. MEINWALD et Y. MEINWALD. J. Amer. Chem. Soc. **85**, 2514 (1963).
16. C. W. JEFFORD, B. WAEGELL et K. RAMEY. J. Amer. Chem. Soc. **87**, 2191 (1965).
17. H. J. CALLOT et C. BENEZRA. Chem. Commun. 485 (1970).
18. K. L. WILLIAMSON, Y.-F. L. HSU, et E. I. YOUNG. Tetrahedron, **24**, 6007 (1968).
19. J. S. NEWCOMER et E. T. MCBEE. J. Amer. Chem. Soc. **71**, 946 (1949).
20. H. ZENFTMAN et D. CALDER. Brit. Patent, 812 983. May 6, 1959. Chem. Abstr. **53**, 15647*f* (1959).
21. G. M. KOSOLAPOFF. Organophosphorus compounds. John Wiley and Sons, Inc., New York, N.Y. 1950.
22. M. I. KABACHNIK et T. YA MEDVED. Izv. Akad. Nauk. SSSR, Otdel. Khim. Nauk. 2142 (1959); Chem. Abstr. **54**, 10834*e* (1960).

Can. J. Chem. Downloaded from www.nrcresearchpress.com by 210.87.254.40 on 09/05/12
For personal use only.

Can. J. Chem. Downloaded from www.nrcresearchpress.com by 210.87.254.105 on 09/05/12
For personal use only.

Studies on pyrylium and thiopyrylium salts

D. M. McKINNON
Chemistry Department, University of Manitoba, Winnipeg, Manitoba

Received June 2, 1970

2*H*-Thiopyran-2-ones, 4*H*-thiopyran-4-ones, and 4*H*-pyran-4-ones may be reduced by lithium aluminum hydride to the corresponding thiopyranols or pyranols, which on treatment with perchloric acid are converted to pyrylium or thiopyrylium salts. The reaction fails with 2*H*-pyran-2-ones. Peracetate oxidation of 2*H*-thiopyran-2-thiones affords thiopyrylium salts, but with other pyran-2- and 4-thiones yields the corresponding ketones. The rearrangement of an acetylenic thiolester to thioflavone is described.

Canadian Journal of Chemistry, 48, 3388 (1970)

The treatment of various pseudo-bases with acid is a convenient method for the preparation of various heteroaromatic cations (1) Thus, the hydride reduction of pyranones or thiopyranones should provide a convenient route to 2- or 4-unsubstituted pyrylium, **1**, or thiopyrylium, **2**, salts via the pyranol or thiopyranol pseudo-bases. In fact, little is reported on this approach. 4*H*-Thiopyran-4-one (**3***a*) can be converted (2) to the thiopyrylium cation (**2***a*) by this method, and xanthydrol (**4***a*) and thioxanthydrol (**4***b*), which are available by reduction of the corresponding ketones, give the xanthylium (**5***a*) and thioxanthylium (**5***b*) cations respectively (3, 4) on treatment with acids. The reduction of 2*H*-pyran-2-ones **6**, Z = O, with lithium aluminum hydride gives acyclic products (5, 6) and no information appears to be available on the reduction of 2*H*-thiopyran-2-ones **7**, Z = O. Certain 2- or 4-unsubstituted pyrylium and thiopyrylium salts were needed for another investigation, and it seemed desirable to investigate this method to determine its scope and utility.

A representative variety of pyrones and thiopyrones was studied. Some of their benzo-derivatives were also included. In most cases, excepting the 2*H*-pyran-2-ones **6**, Z = O, these could be reduced successfully to the corresponding pseudo-bases, which were not isolated, but were converted directly to the pyrylium **1** or thiopyrylium **2** cations by treatment with perchloric acid. The structures of most of these products were confirmed by comparison with authentic specimens or by alternate syntheses, some of which are new.

When the 2*H*-thiopyran-2-one **7***a*, prepared by treatment of the corresponding thione **7***b*, with mercuric acetate, was reduced, using one quarter equivalent of lithium aluminum hydride, a crude

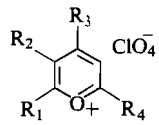

1

a $R_1 = R_2 = H$; $R_3 = R_4 = Ph$
b $R_1 = Ph$; $R_2 = R_3 = H$; $R_4 = Ph$
c $R_1, R_2 = (CH{=}CH)_2$; $R_3 = H$, $R_4 = Ph$

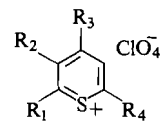

2

a $R_1 = R_2 = R_3 = R_4 = H$
b $R_1 = R_2 = H$; $R_3 = R_4 = Ph$
c $R_1 = H$; $R_2 = Ph$; $R_3 = H$; $R_4 = Ph$
d $R_1 = Ph$; $R_2 = R_3 = H$; $R_4 = Ph$
e $R_1, R_2 = (CH{=}CH)_2$; $R_3 = H$; $R_4 = Ph$

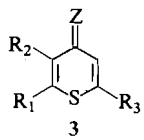

3

a $R_1 = R_2 = R_3 = H$; Z = O
b $R_1 = Ph$; $R_2 = H$; $R_3 = Ph$, Z = O
c $R_1, R_2 = (CH{=}CH)_2$; $R_3 = Ph$, Z = O
d $R_1 = Ph$; $R_2 = H$; $R_3 = Ph$; Z = S
e $R_1, R_2 = (CH{=}CH)_2$; $R_3 = Ph$, Z = S

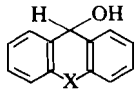

4

a X = O
b X = S

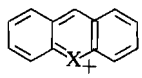

5

a X = O
b X = S

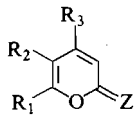

6

a R_1 = Ph; R_2 = H; R_3 = Ph, Z = O
b R_1, R_2 = (CH=CH)$_2$; R_3 = H, Z = O
c R_1 = Ph; R_2 = H; R_3 = Ph, Z = S
d R_1, R_2 = (CH=CH)$_2$; R_3 = H, Z = S

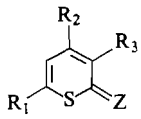

7

a R_1 = R_2 = Ph; R_3 = H, Z = O
b R_1 = R_2 = Ph; R_3 = H, Z = S
c R_1 = Ph; R_2 = H; R_3 = Ph, Z = O
d R_1 = Ph; R_2 = H; R_3 = Ph, Z = S

product was obtained which on treatment with acid afforded the thiopyrylium salt **2***b*. Similar treatment of the thiopyrone **7***c* afforded the thiopyrylium salt **2***c*. The structures of these were confirmed by alternate syntheses, employing the peracetate oxidation of the corresponding 2*H*-thiopyran-2-thiones, **7***b* and *d* respectively. These reactions are related to known reaction of 1,2-dithiole-3-thiones (7, 8) and 1,3-dithiole-2-thiones (9, 10), with which the thiopyranthiones are isoelectronic and have some similar structural features. The success of this reaction in the dithioles has been ascribed to the resistance of the dithiolium cation products to further oxidation (11), and similar considerations may hold here. However, similar oxidation of 4*H*-thiopyran-4-thiones **3**, Z = S, and pyranthiones **6** and **8**, Z = S, failed to give any salt-like product, and other factors appear also to be important. Only the corresponding pyranones or thiopyranones were isolated in these cases. Similar results have been reported for other oxidative studies (12).

This hydride reduction was unsuccessful when applied to two 2*H*-pyran-2-ones studied, 4,6-diphenyl-2*H*-pyran-2-one (**6***a*), and coumarin (**6***b*). The first of these gave a pale yellow oil, but treatment of this with perchloric acid gave only traces of salt-like material. In view of the low yield, the product may be a protonated form of some acyclic reduction product similar to those known (13, 14). The expected product, 2,4-diphenylpyrylium perchlorate (**1***a*) was prepared by the addition of phenyl magnesium bromide to 2-phenyl-4*H*-pyran-4-one (**8***a*), followed by treatment with acid, similar to known methods (15, 16). This product, m.p. 229°, did not correspond to that, m.p. 240°, reportedly prepared (17) from acetophenone and cinnamaldehyde using triphenylmethyl perchlorate. A repetition of this latter synthesis afforded in fact 2,6-diphenylpyrylium perchlorate (**1***b*), probably produced by cyclization of initially formed 1,5-diphenylpenta-2,4-dien-1-one. Indeed this diene has been shown (18) to form the salt (**1***b*) on oxidative cyclization.

The reduction of coumarin (**6***b*) gave a pale yellow oil. Treatment of this with perchloric acid gave apparently polymeric material. Tautomerism of the initially formed pseudo-base would give *o*-hydroxycinnamaldehyde, which might be expected to polymerize under the influence of acid. The success of this method when applied to the thio-2-pyrones **7**, Z = O, contrasted to the 2-pyrones **6**, Z = O, is probably a consequence of the greater electron-releasing ability of sulfur over oxygen affecting the ring-chain tautomeric equilibria of the pseudo-base.

Application of this reductive method to the 4*H*-pyran-4-ones **8**, Z = O, and the 4*H*-thiopyran-4-ones **3**, Z = O, gave unsatisfactory results when only the theoretical quantities (one quarter equivalent) of lithium aluminum hydride were used. In most cases starting materials were recovered, usually as the protonated forms (19) after the addition of perchloric acid. However, use of a ten-fold excess of reagent gave satisfactory results. Similar results are known in the reactions of certain ketones with Grignard reagents owing to complex formation (20). Indeed in the preparation of 2,4-diphenylpyrylium perchlorate (**1***a*) from the 4-pyrone **8***a* and phenyl

8

a R_1 = Ph; R_2 = R_3 = H; Z = O
b R_1 = Ph; R_2 = H; R_3 = Ph, Z = O
c R_1, R_2 = (CH=CH)$_2$; R_3 = Ph, Z = O
d R_1 = CH_3; R_2 = H; R_3 = CH_3, Z = O
e R_1 = Ph; R_2 = H; R_3 = Ph, Z = S
f R_1, R_2 = (CH=CH)$_2$; R_3 = Ph, Z = S
g R_1 = CH_3; R_2 = H; R_3 = CH_3, Z = S

PhC(SPh)=CHCOSPh

9

Can. J. Chem. Downloaded from www.nrcresearchpress.com by 210.87.254.105 on 09/05/12
For personal use only.

Can. J. Chem. Downloaded from www.nrcresearchpress.com by 210.87.254.105 on 09/05/12
For personal use only.

TABLE 1

Conversion of pyrones and thiopyrones to pyrylium and thiopyrylium salts

Starting pyrone	Source reference	Product	Yield (%)	Formula	Melting point (°C)	Analyses							
						Calculated (%)				Found (%)			
						C	H	Cl	S	C	H	Cl	S
3*b*	23	**2***d*	63	$C_{17}H_{13}ClO_4S$	186–187*								
3*c*	†	**2***e*	41	$C_{15}H_{11}ClO_4S$	163‡								
7*a*	†	**2***b*	39	$C_{17}H_{13}ClO_4S$	157	58.41	3.72	10.18	9.17	58.20	3.85	10.04	9.25
7*c*	26	**2***c*	47	$C_{17}H_{13}ClO_4S$	258–260	58.41	3.72	10.18	9.17	58.16	4.07	10.26	8.99
8*b*	27	**1***b*	41	$C_{17}H_{13}ClO_5$	230§								
8*c*	‖	**1***c*	51	$C_{15}H_{11}ClO_5$	178–179¶								

*Literature (24) 186–187°.
†This work.
‡Literature (25) 163°.
§Literature (28) 230°.
‖K. and K. Laboratories.
¶Literature (29) 178–179°.

Can. J. Chem. Downloaded from www.nrcresearchpress.com by 210.87.254.105 on 09/05/12
For personal use only.

magnesium bromide mentioned above, satisfactory results were only obtained when an excess of Grignard reagent was employed. Thus, 2,6-diphenyl-4*H*-pyran-4-one (**8***b*) and 2,6-diphenyl-4*H*-thiopyran-4-one (**3***b*) were converted to the salts **1***b* and **2***d* respectively. Similarly flavone (**8***c*) and thioflavone (**3***c*) were converted to flavylium perchlorate (**1***c*) and thioflavylium perchlorate (**2***e*) respectively. Thioflavone (**3***c*) was made by treatment of phenyl phenylthiolpropiolate with aluminum chloride. Presumably a Fries rearrangement of the thiophenolic ester first forms *o*-phenylpropiolylbenzenethiol, which cyclizes to the thioflavone. The product obtained was identical to that prepared by a known method, (21). In the presence of excess benzenethiol, phenyl 3-phenylthiothiolcinnamate (**9**) was obtained by further addition of mercaptan to the acetylenic ester.

This preparative method for pyrylium and thiopyrylium cations failed to give any salt-like product when applied to 2,6-dimethyl-4*H*-pyran-4-one (**8***d*) and 2-phenyl-4*H*-pyran-6-one (**8***a*). There is little apparent reason why these reactions failed to give the desired products, although possibly steric effects are significant, and in these cases hydride reduction gives alternate or further reduction products which cannot be converted to pyrylium salts. From the above results, it appears that this reductive method is satisfactory for the preparation of pyrylium and thiopyrylium salts from the corresponding pyrones or thiopyrones except in the case of the 2*H*-pyran-2-ones, **6**.

Experimental

Reductions were performed by lithium aluminum hydride supplied by Alfa Inorganics Ltd., in diethyl ether, previously dried over sodium. Ether or benzene extracts were dried over anhydrous sodium sulfate. Pyrones or thiopyrones were either available commercially or were synthesized according to the literature (See Table 1). New methods are described below. The i.r. spectra were obtained in liquid paraffin mulls on a Perkin–Elmer Model 337 spectrophotometer.

Preparation of 4,6-Diphenyl-2H-thiopyran-2-one (7a)

To 4,6-diphenyl-2*H*-thiopyran-2-thione (4 g) (22) in acetic acid (50 ml) at 60° was slowly added with shaking a saturated solution of mercuric acetate in acetic acid until the red color of the thione had disappeared. The mixture was thrown on ice and the yellow precipitate recrystallized from ethanol as yellow felted needles, m.p. 97–8°, lit. (22) 97–98° (92%).

Preparation of Phenyl 3-Phenylthiolpropiolate

To a solution of phenylpropiolyl chloride (30 g) in pyridine (100 ml) was slowly added phenylmercaptan (20 g). The mixture became warm and was shaken 1 h then poured into water. The ether extract was washed with dilute sodium hydroxide, dilute hydrochloric acid, and water, and dried. Evaporation gave a red oil which was used directly in the next reaction.

When phenylpropiolyl chloride (30 g) was treated with excess phenyl mercaptan under the same conditions, a red oil was obtained which partly crystallized on standing. The mixture was triturated with ethanol and the crude yellow solid recrystallized from ethanol as yellow plates, m.p. 138° (39%).

Anal. Calcd. for $C_{21}H_{16}OS_2$: C, 72.65; H, 4.60; S, 18.39. Found: C, 72.71; H, 4.29; S, 18.01.

Preparation of Thioflavone (3c)

The crude phenyl 3-phenylthiolpropiolate (10 g) prepared above was dissolved in dry benzene (50 ml) and treated with powdered anhydrous aluminum chloride (15 g). After 3 days the greenish solution was poured into water, and the dried benzene extract was evaporated to give a dark solid product. This was washed with cold ether and recrystallized from ethanol as colorless needles, m.p. 129–130° (68%). This was identical (mixed m.p. and i.r.) with an authentic specimen (21).

Reductions of 2H-Pyran-2-ones and 2H-Thiopyran-2-ones by Lithium Aluminum Hydride

To a stirred solution of the pyrone (2.00 mmoles) in anhydrous ether (200 ml) was added powdered lithium aluminum hydride (0.50 mmole). Usually a slight yellow coloration was evident. After ½ h ethyl acetate (10 ml) was added, and after a further 10 min, 10% dilute hydrochloric acid (10 ml) was added. The ether layer was separated, dried, and evaporated below 30° *in vacuo*. The crude pyranol products were used directly in the next stage.

Reductions of 4H-Pyran-4-ones and 4H-Thiopyran-4-ones by Lithium Aluminum Hydride

These were performed exactly as with the 2-pyrones, except that 5.00 mmoles of lithium aluminum hydride were used. Use of lesser amounts gave incomplete reaction. The crude pyranol products were used directly in the next stage.

Treatment of Pyranols and Thiopyranols with Perchloric Acid

The crude products obtained above by reduction of pyrones or thiopyrones were dissolved in cold acetic acid (5 ml) and 70% perchloric acid (0.5 ml) added. The salts either crystallized directly, or the mixtures were diluted with ether (50 ml) and scratched to induce crystallization. The crude products were recrystallized from acetic acid containing a trace of perchloric acid. The results are summarized in Table 1.

The reduction products of the pyrones **6***b* and **8***d* failed to give any salt-like material, and those of the pyrones **6***a* and **8***a* gave only traces (~5 mg).

Hydrogen Peroxide Oxidation of 4,6-Diphenyl-2H-thiopyran-2-thione (7b)

To the thione (0.5 g) (22), suspended in acetic acid (20 ml), was added 30% hydrogen peroxide solution (0.5 ml) and the mixture maintained at 30°. The mixture

Can. J. Chem. Downloaded from www.nrcresearchpress.com by 210.87.254.105 on 09/05/12
For personal use only.

became dark red in color, then slowly lightened to pale yellow. After 2 h 70% perchloric acid (0.6 ml) was added to the solution. Dilution with ether gave yellow needles which were recrystallized from acetic acid containing perchloric acid, m.p. 157° (66%). The compound **2***b* was identical (mixed m.p. and i.r.) to that prepared by the reductive method.

Hydrogen Peroxide Oxidation of 3,6-Diphenyl-2H-thiopyran-2-thione (7c)

Oxidation of this thione (26) was performed exactly as above. Yellow needles of **2***c* were obtained (99%), identical (mixed m.p. and i.r.), to that prepared by the reductive method.

Hydrogen Peroxide Oxidation of Thiones 3d, e; 6c, d; 8e, f, g

These reactions, performed under the same conditions as above, gave no salts on treatment with ether. The solutions were diluted with water, and the ether layers separated. Evaporation gave the corresponding carbonyl compounds in almost quantitative yields.

Reaction of 2-Phenyl-4H-pyran-4-one (8c) with Phenylmagnesium Bromide

To a solution of the pyrone (4.3 g) (30) in anhydrous ether (100 ml) was slowly added a solution of phenylmagnesium bromide prepared from bromobenzene (7.8 g) and magnesium (1.2 g) in anhydrous ether (100 ml). The solution initially became cloudy, but cleared towards the end of the addition. After 10 min the solution was poured into dilute hydrochloric acid (100 ml of 5% in water). The dried ether layer was concentrated to a red oil *in vacuo* at room temperature which on treatment with 70% perchloric acid (1 ml in acetic acid (10 ml)), and dilution with ether (20 ml) gave a yellow precipitate which was recrystallized from acetic acid containing perchloric acid, m.p. 227° (33%).

Anal. Calcd. for $C_{17}H_{13}ClO_5$: C, 61.35; H, 3.91; Cl, 10.67. Found: C, 61.17; H, 3.98; Cl, 10.83.

Reaction of Acetophenone and Cinnamaldehyde with Triphenylmethyl Perchlorate

This reaction was performed as described (17). The product, m.p. 230°, obtained was identical (mixed m.p. and i.r.) to that obtained from 2,6-diphenyl-4*H*-pyran-4-one by the reductive method outlined above, or by oxidative cyclization of 1,5-diphenylpentane-1,5-dione as described (28).

Financial support of this work by the National Research Council of Canada is gratefully acknowledged.

1. D. Beke. Advances in heterocyclic chemistry. Vol. 1. Academic Press, New York, 1963. p. 167.
2. I. Degani, R. Fochi, and C. Vincenzi. Tetrahedron Lett. 1167 (1963).
3. K. A. Hofmann, R. Roth, K. Hobold, and A. Metzler. Ber. **43**, 2624 (1910).
4. A. Werner. Ber. **34**, 3300 (1901).
5. L. R. Morgan. J. Org. Chem. **27**, 343 (1962).
6. K. Yamada. Bull. Chem. Soc. Jap. **35**, 1329 (1962).
7. E. Klingsberg. Chem. and Ind. 1568 (1960).
8. E. Klingsberg and A. Schreiber. J. Amer. Chem. Soc. **83**, 2934 (1961).
9. D. Leaver, W. A. H. Robertson, and D. M. McKinnon. J. Chem. Soc. 5104 (1962).
10. E. Klingsberg. J. Amer. Chem. Soc. **84**, 3410 (1962).
11. H. Prinzbach and E. Futterer. Advances in heterocyclic chemistry. Vol. 7. Academic Press, New York, 1966. p. 49.
12. M. El-Kaschef and M. H. Nosseir. J. Chem. Soc. 4643 (1963).
13. J. J. Basselier. Ann. Chim. (Paris), **6**, 1131 (1961).
14. C. Dufraisse, G. Rio, Y. Fellion, and J. J. Basselier. C.R. **252**, 32 (1961).
15. A. Baeyer and J. Piccard. Ann. **384**, 208 (1911).
16. W. Schneider. Ann. **432**, 297 (1923).
17. M. Simalty-Siemiatycki and R. Fugnitto. Bull. Soc. Chim. Fr. 1944 (1965).
18. W. Dilthey. Ber. **50**, 1008 (1917).
19. J. N. Collie and T. Tickle. J. Chem. Soc. **75**, 710 (1899).
20. C. G. Swain and H. B. Boyles. J. Amer. Chem. Soc. **73**, 870 (1951).
21. S. Ruhemann. Ber. **46**, 2197 (1913).
22. D. Leaver, D. M. McKinnon, and W. A. H. Robertson. J. Chem. Soc. 32 (1965).
23. F. Arndt, P. Nachwey, and J. Putch. Ber. **58**, 1633 (1925).
24. R. Wizinger and H. J. Angliker. Helv. Chim. Acta, **49**, 2046 (1966).
25. A. Luttringhaus, N. Engelhard, and A. Kolb. Ann. **654**, 189 (1962).
26. G. Laban and R. Mayer. Z. Chem. **7**, 227 (1967).
27. R. J. Light and C. R. Hauser. J. Org. Chem. **25**, 538 (1960).
28. M. Siemiatycki and R. Fugnitto. Bull. Soc. Chim. Fr. 538 (1961).
29. R. J. W. LeFevre. J. Chem. Soc. 2773 (1929).
30. W. Borsche and W. Peter. Ann. **453**, 158 (1927).

Can. J. Chem. Downloaded from www.nrcresearchpress.com by 210.87.254.40 on 09/05/12
For personal use only.

Detection of the intermediate in the aqueous acid catalyzed isomerization of *cis*-cinnamic acid[1]

M. B. HOCKING
Exploratory Research Laboratory, Dow Chemical of Canada, Limited, Sarnia, Ontario

Received June 4, 1970

The rates of isomerization of *cis*-cinnamic acid and of dehydration of β-hydroxy-β-phenylpropionic acid have been determined in strong HCl solutions. The ratio $k_{dehydration}/k_{isomerization}$ was found to be in the range 1.6 to 4 and has been used to account for the observed lengthy isomerization induction periods. Concentrations of a previously suggested intermediate, **5**, assuming its presence, have been calculated. Accounting for the concentration of intermediate present has enabled mathematical and experimental removal of the induction period from the kinetics. Attempted isolation of this intermediate resulted at least in positive detection of its presence.

Canadian Journal of Chemistry, 48, 3393 (1970)

Introduction

The isomerization of *cis*-cinnamic acid to the *trans* has been extensively studied in aqueous acid systems by Noyce and his co-workers (1), who have formulated the process as shown in Scheme 1, with $k_2 > k_1$. More recently, some attention has been given to the thermal isomerization of neat *cis*-cinnamic acid and the observed kinetics have been explained on the basis of a transitory carbonium ion intermediate (2), as shown in the sequence **1** → **2** → **3** in Scheme 2, without involvement of the hydrated intermediate **5**. The complete formulation of the aqueous acid isomerization process, outlined in Scheme 2, is based on Noyce (3–5), who reported the relative order of the rate constants as $k_3, k_4 \gg k_2 > k_1$. Since the rate constant for the neat isomerizations, when extrapolated to the same temperature and hydrogen ion concentration, was found to be of the same order of magnitude as that for an aqueous acid isomerization (2), it was suggested that the same mechanism was operating in the two systems.

While the latter fact, the extensive body of earlier data on the observed induction period for the isomerizations (1), and the faster alpha deuterium exchange concurrent with isomerization (1) all suggest involvement of an intermediate, they do not cast any light on the relative importance of **2** and **5**. Likewise, the faster rates of dehydration of **5** than isomerization of **1**, observed both by Noyce and ourselves, are only suggestive of the possibility of the intermediacy of **5**. This study endeavors to further substantiate the extent of involvement of **2** and **5** in the aqueous acid isomerization of *cis*-cinnamic acid by mathematical and chemical experiments.

Results and Discussion

As a measure of the importance of **5** as an intermediate an effort was made to find an aqueous acid solution in which the rate constant for the dehydration of **5** was likely to be smaller than, or more nearly the same as, the rate constant for the isomerization. Plots of log k *vs.* H_0 (6) for Noyce's dehydration and isomerization data at a number of different sulfuric acid strengths yielded a pair of smooth curves convergent at a point somewhere near a rate constant of 1×10^{-10} s^{-1} ($H_0 = +2.5$), conditions which were too remote from the practical, in time and acidity, for a kinetic study. However, it was considered that changing to an acid less favored for dehydrations than sulfuric might well not only change both the dehydration and isomerization rate constants for a particular hydrogen ion activity, but also affect

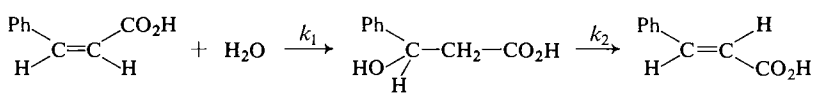

1 **5** **3**

SCHEME 1

[1]Contribution No. 184, Exploratory Research Laboratory, Dow Chemical of Canada, Limited, Sarnia, Ontario.

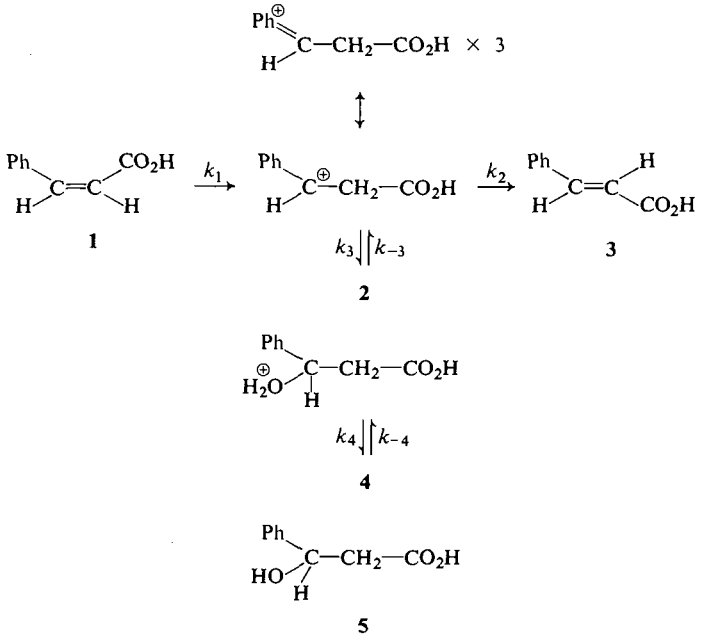

SCHEME 2

the slopes of the log k *vs.* H_0 plots such that convergence could be achieved at a higher acidity and rate constant. Both objectives were achieved in hydrochloric acid solutions, with significant reduction in the ratio $k_{\text{dehydration}}/k_{\text{isomerization}}$ (Table 1). However, it still appeared unlikely that it would be possible to arrange conditions such that the rate of dehydration would be slower than the rate of isomerization. Furthermore, the induction period in the isomerization experiments at lower acidity becomes so long (about 2 days, Tables 2 and 3) that kinetic data from further experimentation at lower acid values could be severely affected by unrelated errors. The increase in induction time and proportion reacted is a natural consequence of convergence of the rate constants for protonation of **1** and deprotonation of **2**. As these become more nearly equal a much larger proportion of **1** must have proceeded to **2** before steady state concentrations of **1** and **2** can be reached (7). The induction period is not, therefore, a consequence of a lag in the formation of **5** but only of the rate determining protonation of the alpha carbon of *cis*-cinnamic acid since the rate of hydration of **2** is relatively much faster (3). This conclusion, *i.e.* that alpha protonation to **2** is the rate determining step, was reached earlier on the basis of the large kinetic isotope effect (5) observed in sulfuric acid-d_2.

It was assumed, then, that the isomerization of *cis*-cinnamic acid to *trans* proceeds via two consecutive first order processes, $A \xrightarrow{k_1} B \xrightarrow{k_2} C$, where A = **1**, B = **2**, and C = **3**. Since upon completion the *cis* acid A is essentially completely converted to the *trans* C[2], equations which have been developed for this sequence (8) could be used to calculate a number of different variables from the data obtained. By the use of eq. 1, k_1 was calculated point-to-point by substitution of $[C]_t$, $[A]_0$, k_2, and t into an iterative

$$[1]\quad [C]_t = [A]_0\left[1 + \frac{1}{k_1 - k_2}(k_2 e^{-k_1 t} - k_1 e^{-k_2 t})\right]$$

computer program (Tables 3 and 4). Constant k_1 obtained in this way was the theoretical rate constant for the protonation of *cis*-cinnamic acid, and, as expected, was greater than $k_{\text{isomerization}}$, which was an experimentally determined resultant of k_1 and k_2. From the standpoint of showing

[2]Perhaps not completely true since 1.7% of the hydroxy acid **2** has been detected in the dehydration equilibrium in 52% H_2SO_4 (3).

Can. J. Chem. Downloaded from www.nrcresearchpress.com by 210.87.254.40 on 09/05/12
For personal use only.

TABLE 1

Comparison of rate of dehydration of β-phenyl-β-hydroxypropionic acid with the rate of isomerization of *cis*-cinnamic acid at 45.0 °C

Acid (weight %)	$-H_0$*	$k_{dehydration}$ ($s^{-1} \times 10^5$)	$k_{isomerization}$ ($s^{-1} \times 10^5$)	$\frac{k_{dehydration}}{k_{isomerization}}$	Isomerization induction period (%)
H_2SO_4 (34.8)	3.00	2.03†	0.109†	19	>15‡
HCl (25.9)	3.00	0.725	0.106§ 0.465	6.8 1.6	37
H_2SO_4 (41.8)	4.20	59.7†	1.49†	40	Slight
HCl (34.9)	4.20	34.8	1.06§ 9.30	33 3.7	5

*From data of ref. 6.
†Interpolated from data of ref. 1.
‡Induction period from ref. 1 is 15% at $H_0 = -3.6$.
§First order rate constant during induction period.

TABLE 2

Comparison of observed *vs.* calculated induction periods, and the calculated maximum concentration of the intermediate for the isomerization of *cis*-cinnamic acid*

Acid concentration (%)	Induction period		Hydroxy acid, **5**, concentration	
	Observed (s)	Calculated† (s)	Calculated maximum‡	Experimental
51.87 H_2SO_4	3.0×10^4	3.04×10^4	3.78%	—
58.05 H_2SO_4	Slight	5.37×10^3	2.0	—
25.9 HCl	1.6×10^5	1.71×10^5	36.1	5.3
34.9 HCl	5.0×10^3	5.17×10^3	16.5	—

*Sulfuric acid data derived from those of ref. 1.
†Calculated using eq. 3.
‡Calculated using eq. 4.

TABLE 3

Isomerization of *cis*-cinnamic acid to the *trans* in 25.9% HCl at 45.0°

Time ($s \times 10^{-4}$)	Optical density (o.d.)	(1-*trans*)* × 100	Experimental $k_{isomerization} \times 10^6$ s^{-1}	Calculated $k_1 \times 10^6$† s^{-1}
0	[0.549]	98.80		
2.28	0.553	98.29	0.76	3.01
10.00	0.610	90.81	0.95	3.17
10.92	0.617	89.90	0.98	3.04
16.62	0.662	83.99	1.05	2.53
17.32	0.665	83.60	1.03	2.42
43.86	0.923	62.86	1.06	1.03
62.22	1.102	26.25	2.15	2.94
68.70	1.142	21.00	2.27	3.02
77.34	1.186	15.22	2.44	3.15
77.91	1.192	14.44	2.49	3.21
196.6 (∞)	1.302			

*$(o.d._\infty - o.d._t / o.d._\infty - 0.540) \times 100$. 0.540 in this run corresponds to the calculated optical density expected for 100% *cis*-cinnamic acid initially. Reported as (1-*trans*) since this figure includes both β-hydroxy-β-phenylpropionic and *cis*-cinnamic acids.
†Calculated using eq. 1.

Can. J. Chem. Downloaded from www.nrcresearchpress.com by 210.87.254.40 on 09/05/12
For personal use only.

TABLE 4

Isomerization of *cis*-cinnamic acid to the *trans* in 34.9% HCl at 45.0°

Time ($s \times 10^{-3}$)	Optical density (o.d.)	(1-*trans*)* × 100	Experimental $k_{isomerization} \times 10^5$ s^{-1}	Calculated $k_1 \times 10^5$† s^{-1}	Calculated (%) hydroxy acid, 5‡
0	[0.709]	98.80			
0.54	0.710	98.68	2.48	2.56	4.35
1.62	0.715	98.17	1.16	0.59	10.53
2.16	0.726	97.06	1.39	2.14	12.50
2.70	0.734	96.24	14.19	2.80	13.98
3.66	0.803	89.23	3.11	6.64	15.56
5.16	0.895	79.89	4.35	8.06	16.32
6.66	0.982	71.06	5.13	8.51	15.82
8.22	1.073	61.82	5.85	8.94	14.68
9.06	1.112	57.86	6.04	8.89	13.97
10.20	1.171	51.87	6.44	9.10	12.89
11.76	1.248	44.06	6.97	9.51	11.46
14.10	1.334	35.32	7.38	9.50	9.45
16.26	1.399	28.73	7.67	9.54	7.74
18.72	1.460	22.53	7.96	9.61	6.26
22.68	1.524	16.04	8.07	9.40	4.35
86.40 (∞)	1.682	—	—	—	—

*(o.d.$_\infty$ − o.d.$_t$/o.d.$_\infty$ − 0.697) × 100. 0.697 in this run corresponds to the calculated optical density expected for 100% *cis*-cinnamic acid initially. Reported as (1-*trans*) since this figure includes β-hydroxy-β-phenylpropionic and *cis*-cinnamic acids.

†Calculated using eq. 1.

‡Calculated using experimental k_2 for dehydration of **2** in 34.9% HCl, and experimental $k_{isomerization}$ in eq. 2.

much less of a definite trend or induction period this calculated k_1 appears to be more reliable.

Other findings also lent support for the initial assumption. The concentration of the intermediate was calculated point for point using eq. 2 (Table 4). A plot of log [(1-*trans*)% − B%]

$$[2] \qquad [B]_t = \frac{[A]_0 k_1}{k_2 - k_1}(e^{-k_1 t} - e^{-k_2 t})$$

vs. t gave very nearly a straight line, without a sharp rate difference for the induction period (Fig. 1). Thus the isomerizations, if followed by loss of *cis*-cinnamic acid rather than the appearance of the *trans*, would be expected to give straight line first order plots. The maximum concentration of the intermediate and the time at which this occurred were calculated using eqs. 3 and 4 (8).

$$[3] \qquad \tau_{max} = 1/\kappa - 1 \cdot \ln \kappa$$

where $\tau = k_1 t$; $\kappa = k_2/k_1$

$$[4] \qquad \beta_{max} = \kappa^{\kappa/1-\kappa}$$

where $\beta = [B]_t/[A]_0 = [OH\ acid]/[cis]_0$

The calculated times agree quite closely with the observed induction periods (Table 2). A kinetic experiment conducted with the calculated proportions of β-hydroxy-β-phenylpropionic acid to *cis*-cinnamic acid present at the start also gave a first order kinetic plot with only a very slight slope change for the induction period (Fig. 1).

Further calculations showed that 36.1% of β-hydroxy-β-phenylpropionic acid (**5**) was evidently present at the end of the induction period in the lower dilution hydrochloric acid experiments, high enough to suggest the possibility of isolation. Preliminary blank experiments established that it was possible to quantitatively recover the hydroxy acid **5**, unchanged, from these aqueous acid solutions. Work-up of a number of isomerizations failed to yield this high percentage of the hydroxy acid **5**, but in all cases its presence was demonstrated. The most reliable experiment yielded 5.3% of **5**, and 21.5% (16.5% formed during the isomerization) of *trans*-cinnamic acid. Thus, the presence of **5** as an intermediate in the aqueous acid catalyzed isomerization of *cis*-cinnamic acid postulated by Noyce, has now been conclusively demonstrated. The amount detected was so much lower than that for which a blank work-up technique had been developed that isolation of the hydroxy acid was not attempted.

Conclusions

A previously derived set of equations has been used to calculate (*a*) k_1 independently of k_2 and thus to give a more reliable indication of the ratio k_2/k_1 when this is near to 1, (*b*) the maximum and the point-to-point concentration of the inter-

Can. J. Chem. Downloaded from www.nrcresearchpress.com by 210.87.254.40 on 09/05/12
For personal use only.

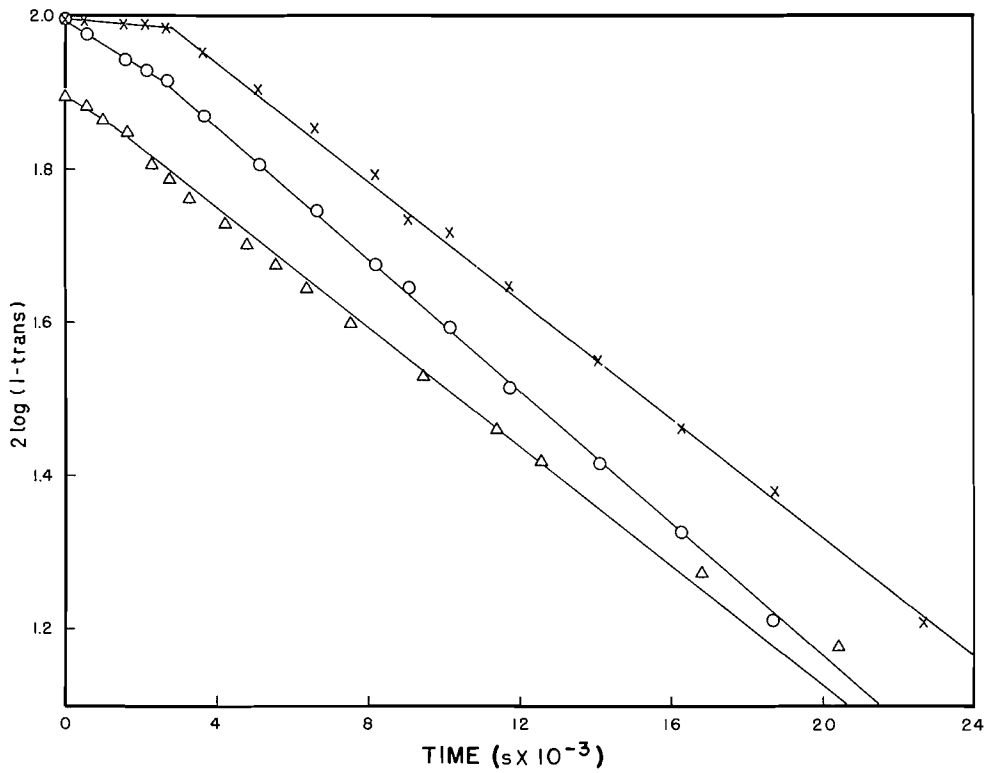

FIG. 1. First order plots of the isomerization of *cis*-cinnamic acid to the *trans* in 34.9% HCl at 45° = X; same data corrected for β-OH-β-phenylpropionic acid (**5**) present = 0; experiment with **5** present initially = △ (ordinate moved down 0.1 units).

mediate **5** and from this the actual concentration of *cis*-cinnamic acid present at any time, and (*c*) the theoretical induction period. It was possible to test the theoretical concentration of **5** by the first order plot, log [*cis*] *vs. t*, and to try an experiment starting with the calculated maximum concentration of **5**. Both treatments gave much improved linear plots. Finally, an attempt to isolate the intermediate **5**, was unsuccessful, although its presence was proved conclusively by n.m.r. spectroscopy.

Experimental

Materials

cis-Cinnamic acid was prepared by isomerization of the *trans*-acid under u.v. irradiation, as previously described (2). β-Hydroxy-β-phenylpropionic acid, purchased from K and K Laboratories, was recrystallized once from water (m.p. 92–94°, lit. 96°) before use. The HCl was Baker and Adamson reagent grade material.

General Kinetic Conditions

Progress of the reactions was followed by the increase in u.v. absorption of the reaction solution at 300 mμ using a Perkin–Elmer 350 spectrophotometer. The solution was held in a cell surrounded by a water-jacketed cell block held at 45.0 °C. The slower reactions were carried out on much larger solutions in an external thermostat from which aliquots were withdrawn and examined at intervals. For all the reactions a time-drive accessory was used to give a direct plot of absorbance *vs. t* at 300 mμ.

Kinetic Experiments

(a) Dehydration

At the higher acid concentration these runs were all complete in a relatively short time requiring only a reaction on the scale accommodated (3.1 ml) by the jacketed u.v. cell. An accurately weighed amount of about 10 mg of **5** was made up to a 25 ml solution in ethanol, while the acid-filled u.v. cell reached thermal equilibrium. Four drops of the solution of **5** were then added to the u.v. cell via a calibrated dropper (93 drops/ml) and the cell vigorously inverted several times to thoroughly mix the contents before returning it to the spectrophotometer. In these runs, the time elapsed from mixing to absorbance measurement was usually less than 3 min. The slower runs, scaled up about 15 times, were conducted in a tightly stoppered thermostatted flask. Aliquots (3.1 ml) were withdrawn as required, and absorbance changes followed for a period of 8–10 h before the aliquot was discarded. Runs at both hydrochloric acid concentrations proceeded smoothly to completion, and the first order rate constants obtained are recorded in Table 1.

Can. J. Chem. Downloaded from www.nrcresearchpress.com by 210.87.254.40 on 09/05/12
For personal use only.

(b) Isomerization

Solutions of *cis*-cinnamic acid in ethanol were used to initiate these experiments in a precisely analogous way to those with β-hydroxy-β-phenylpropionic acid. The chief anomaly consistently observed at both hydrochloric acid concentrations was a definite induction period (Tables 3 and 4).

(c) Combined Dehydration–Isomerization

The maximum concentration of β-hydroxy-β-phenylpropionic acid in the 34.9% HCl run was 16.5% (Table 2). The extent of formation of *trans*-cinnamic acid at the end of the calculated induction period should have been 20.1% and that found at the end of the observed induction period was 23%. The mole ratio of *cis*-cinnamic acid to β-hydroxy acid for these two situations was thus 3.83–1 and 3.66–1 respectively.

β-Hydroxy-β-phenylpropionic acid (3.2 mg; 13.4 mmoles) and *cis*-cinnamic acid (7.6 mg; 34.5 mmoles) were dissolved and made up to a volume of 10 ml in ethanol. With a calibrated dropper, 30 drops of this solution were added to 15 ml of 34.9% HCl at 45° and vigorously mixed. A u.v. cell was filled with an aliquot of this solution and the gradual rise in absorbance followed spectrophotometrically. The results are plotted in Fig. 1.

Attempted Isolation of Intermediate

(a) Blank Work-up

β-Hydroxy-β-phenylpropionic acid (30 mg) was dissolved in 25.9% HCl (100 ml) at 45° by stirring for 1 h. (This corresponds to the concentration of β-hydroxy acid expected from the large scale reaction following.) The HCl solution was cautiously neutralized with solid sodium bicarbonate (9) while being allowed to cool. After the solution was re-acidified to p*H* 2 with sodium bisulfate, and saturated with sodium chloride at 0° it was extracted with ether (5 × 20 ml). The combined extracts were dried ($MgSO_4$) and the ether removed at room temperature leaving 40 mg of pale brown crystalline solid. An n.m.r. spectrum of this material in deuteriochloroform showed that it consisted of β-hydroxy-β-phenylpropionic acid and traces of silicone grease.

(b) Attempted Isolation

cis-Cinnamic acid (0.9964 g of 95% *cis*, 5% *trans*) was dissolved, with 10 min stirring, in 25.9% HCl (500 ml) at 45 °C. This solution was tightly stoppered and thermostatted at 45° for 48 h, conditions calculated to yield the concentration of β-hydroxy acid present in the blank, and then allowed to cool as neutralization with solid sodium bicarbonate was begun. The remainder of the work-up was carried out in a precisely analogous way to the blank and yielded 1.22 g of colorless oil which slowly crystallized at room temperature. An n.m.r. spectrum of a portion of this oil in acetone-d_6 established that it consisted of 74.2% *cis*-cinnamic acid, 21.5% *trans*-cinnamic acid, and 5.3% β-hydroxy-β-phenylpropionic acid. The identity of the latter was confirmed by the superimposed peaks produced by addition to the n.m.r. solution of a small portion of the authentic material.

The 60 MHz n.m.r. spectrum of β-hydroxy-β-phenylpropionic acid in acetone-d_6 at room temperature consisted of what appeared to be a doublet[3] at 161.2 c.p.s., $J_{\alpha\beta} = 6.8$, $J_{\alpha\alpha} \simeq 0$ cycles; a triplet for the methine at 308.2 c.p.s., $J_{\beta,\alpha} = 6.8$ cycles: OH at 325 c.p.s.; and for the aromatics a complex multiplet from 430 to 450 c.p.s.

The author thanks H. D. Mak for obtaining all the n.m.r. spectra and E. C. Clarke for the use of his polynomial regression computer program and for writing a program for the solution of eq. 1 in the test for k_1.

1. D. S. NOYCE, P. A. KING, F. B. KIRBY, and W. L. REED. J. Amer. Chem. Soc. **84**, 1632 (1962).
2. M. B. HOCKING. Can. J. Chem. **47**, 4567 (1969).
3. D. S. NOYCE and C. A. LANE. J. Amer. Chem. Soc. **84**, 1635 (1962). J. Amer. Chem. Soc. **84**, 1641 (1962). D. S. NOYCE, P. A. KING, C. A. LANE, and W. L. REED. J. Amer. Chem. Soc. **84**, 1638 (1962).
4. D. S. NOYCE and H. S. AVARBOCK. J. Amer. Chem. Soc. **84**, 1644 (1962).
5. D. S. NOYCE, H. S. AVARBOCK and W. L. REED. J. Amer. Chem. Soc. **84**, 1647 (1962).
6. M. A. PAUL and F. A. LONG. Chem. Revs. **57**, 1 (1957).
7. E. S. GOULD. Mechanism and structure in organic chemistry. H. Holt and Co., New York, N.Y. 1959. p. 168.
8. A. A. FROST and R. G. PEARSON. Kinetics and mechanism. 2nd ed. John Wiley and Sons, Inc., New York, N.Y. 1961. pp. 166–171.
9. E. ERLENMEYER and G. HILGENDORFF. Biochem. Z. **35**, 134 (1911). Beil. **10**, 248.

[3]This could be a part of a more complex splitting pattern because of the adjacent optical center.

Can. J. Chem. Downloaded from www.nrcresearchpress.com by 210.87.254.40 on 09/05/12
For personal use only.

Can. J. Chem. Downloaded from www.nrcresearchpress.com by 210.87.254.40 on 09/05/12
For personal use only.

1,3-Dipolar cycloaddition reactions of 2-(2′-thienyl)aziridines

J. W. Lown and K. Matsumoto[1]
Department of Chemistry, University of Alberta, Edmonton, Alberta

Received June 3, 1970

The 1,3-dipolar cycloaddition of 2-(2′-thienyl)aziridines to a series of acetylenic and heteromultiple dipolarophiles leading to a series of new linked heterocycles is described. The versatility of these reactions suggests a general synthetic route to linked heterocycles.

Canadian Journal of Chemistry, **48**, 3399 (1970)

We have recently described the preparation of the hitherto unknown 2-(2′-thienyl)aziridines (1) and have shown that, despite the lower resonance energy of the thiophene ring (20 kcal mole^{-1} (2)) compared with benzene, 2-(2′-thienyl)-3-aroylaziridines undergo thermal cleavage of the 2–3 bond of the aziridine ring to azomethine ylides at moderate temperatures. The transient dipoles could be trapped with olefinic dipolarophiles affording 2-(2′-thienyl)pyrrolidines.

We report the examination of 1,3-dipolar cycloadditions of 2-(2′-thienyl)aziridines to acetylenic and heteromultiple bonds as a first approach to a general synthesis of linked heterocycles.

(a) Acetylenic Dipolarophiles

Both *cis*- and *trans*-3-benzoyl-1-cyclohexyl-2-(2′-thienyl)aziridine (**1**) reacted with dimethyl

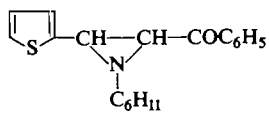

1

acetylenedicarboxylate to form a 1:1 adduct, the spectral data of which were consistent with the *cis*-2-pyrroline structure **2**, together with some of the pyrrole **3** (1). Heine *et al.* have shown that 3-pyrrolines are formed when 1,2,3-triphenylaziridine reacts with acetylenic esters (3) but Padwa and Hamilton isolated 2-pyrrolines like **2** when 3-aroylaziridines reacted with acetylenes (4). In the present work, addition of dimethyl acetylenedicarboxylate to 3-benzoyl-1-cyclohex-

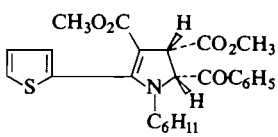

2

[1]NRCC Postdoctorate Fellow, 1969 to present.

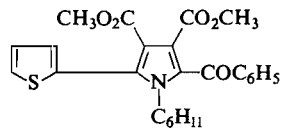

3

yl-3-deutero-2-(2′-thienyl)aziridine (91% deuterium incorporation) gave **5** in which both branches of the 12 Hz AB quartet due to the methine protons were diminished to an equal extent (20%). This discounts the *trans*-3-pyrroline structure **4** for the compound (which is in any case unlikely in view of the magnitude of the methine coupling) which would be expected to show one branch of the AB quartet diminished

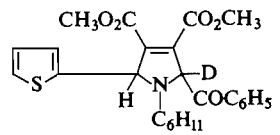

4

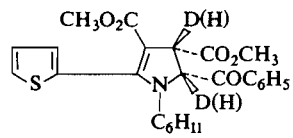

5

in intensity. The observed scrambling of the deuterium label in **5** suggests its formation by rapid prototropy of the 3-pyrroline **4** the intermediacy of which in this type of reaction was previously suggested by Padwa and Hamilton (4). The extent of deuterium incorporation in 1,3 dipolar addition products of 3-deuterated aziridines with reactive dipolarophiles is normally about 70–80% (27). The observed 20% incorporation with the powerful acetylenic dipolarophiles attests to the lability of the methine protons in the intermediate **4**.

Similar 2-(2′-thienyl)pyrroles prepared in this way are listed in Tables 1 and 2. Addition of

Can. J. Chem. Downloaded from www.nrcresearchpress.com by 210.87.254.40 on 09/05/12
For personal use only.

TABLE 1

5-Aroyl (or acyl) -2-(2′-thienyl)pyrroles*

No.	R_1	R_2	Melting point (°C)	Yield (%)†	Found C	Found H	Found N	Found S	Found Molecular ion (mass spectrum)	Calculated C	Calculated H	Calculated N	Calculated S	Calculated Molecular ion (mass spectrum)
a	CH_3CO_2	*m*-$NO_2C_6H_4$	161–162	32	60.58	4.88	5.47	6.16	496.1302	60.47	4.87	5.64	6.46	496.1304
b	CH_3CO_2	*p*-$CH_3C_6H_4$	194–195	53	66.65	5.75	2.90	6.92	465.1606	67.05	5.85	3.01	6.89	465.1610
c	CH_3CO_2	*p*-$CH_3OC_6H_4$	176–177	65	64.64	5.63	2.86	6.77	481.1557	64.85	5.65	2.91	6.66	481.1559
d	H	C_6H_5	179–180	32	70.08	5.89	3.63	8.14	393.1397	70.20	5.89	3.56	8.13	393.1398
e	H	*m*-$NO_2C_6H_4$	178–179	25	62.92	5.15	6.23	7.20	438.1807	62.70	5.49	6.36	7.28	438.1803
f	H	*p*-$CH_3C_6H_4$	177–179	26	70.97	6.19	3.71	7.95	407.1556	70.74	6.18	3.44	7.87	407.1555
g	H	*p*-$CH_3OC_6H_4$	157–158	39	68.55	6.46	3.24	7.68	423.1500	68.08	5.95	3.31	7.57	423.1505
h	H	2-Naphthyl	158–160	36	72.98	5.69	3.29	7.07	443.1540	73.10	5.68	3.16	7.23	443.1555

*Compounds of structure:

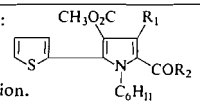

†Yield after recrystallization.

TABLE 2

Spectroscopic properties of 5-aroyl (or acyl) -2-(2′-thienyl)-pyrroles

No.	Infrared spectrum $CHCl_3$ (C=O)	Nuclear magnetic resonance spectrum ($CDCl_3$)δ: Aryl, thienyl, and (—CH=) protons	3-Carboxy methyl protons	4-Carboxy methyl protons	Aroyl substituent	*N*-Substituent	Absorption spectrum* ($CHCl_3$) λ_{max}	log ε
a	1677 1719	7.09–9.0(7H)m	3.65(3H)s	3.35(3H)s		3.7–4.2(1H)m 0.3–2.2(10H)m	314	3.52
b	1663 1720	7.0–8.0(7H)m	3.65(3H)S	3.33(3H)S	2.41(3H)s	0.3–2.2(10H)m 3.6–4.3(1H)m	264 310(sh)	4.34 3.38
c	1659 1721	6.7–8.1(7H)m	3.65(3H)s	3.38(3H)s	3.86(3H)s	0.5–2.3(10H)m 3.5–4.3(1H)m	293	4.32
d	1637 1705	7.0–8.0(9H)m	3.58(3H)s	—	—	0.5–2.6(10H)m 4.0–4.5(1H)m	303	4.21
e	1646 1715	7.0–8.7(8H)m	3.65(3H)s	—	—	0.6–2.8(10H)m 3.8–4.7(1H)m	308	4.19
f	1637 1707	7.0–8.1(8H)m	3.65(3H)s	—	2.46(3H)s	0.7–2.6(10H)m 3.9–4.6(1H)m	305	4.24
g	1637 1708	6.7–8.1(8H)m	3.64(3H)s	—	3.89(3H)s	0.6–2.8(10H)m 3.9–4.6(1H)m	308	4.35
h	1640 1711	7.0–8.5(10H)m	3.65(3H)s	—	—	0.6–2.8(10H)m 3.9–4.7(1H)m	311 293	4.29 4.22

*Absorption spectrum of compound $R_1 = CO_2CH_3$, $R_2 = C_6H_5$ previously reported (1) was λ_{max}: 250 (log ε 4.38), 300 mμ (sh) (log ε 3.80).

Can. J. Chem. Downloaded from www.nrcresearchpress.com by 210.87.254.40 on 09/05/12
For personal use only.

methyl propiolate to **1** gave only the 2-(2′-thienyl)-pyrrole **6**, evidently in this case the intermediate pyrroline was readily dehydrogenated by atmospheric oxygen. In contrast 1,2,3-triphenylaziridine afforded the 3-pyrroline **7** which showed a

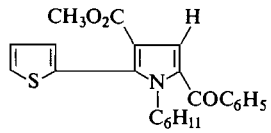

6

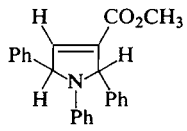

7

singlet for the methine protons, and no allylic coupling as was observed in the analogous compound prepared with ethyl propiolate by Heine *et al.* (3).

The orientation of addition in the case of **6** is based on the following evidence. The n.m.r. line positions of the carbomethoxy groups in the series of 2-(2′-thienyl)pyrroles **8** fall into two groups at 3.65 and 3.28–3.38 δ. By comparison

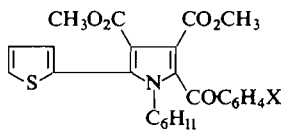

8

X	δ(CO$_2$CH$_3$)	
H	3.65	3.28
p-CH$_3$	3.65	3.33
p-CH$_3$O	3.65	3.38

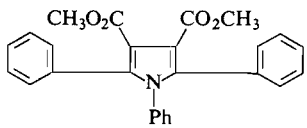

9

δ(CO$_2$CH$_3$) 3.69

in **9** in which the carbomethoxy groups are necessarily adjacent to an aromatic ring the line position was 3.69 δ, which allows the assignment of ester methyl groups in **8** as 3.65 (4-ester) and 3.28–3.38 δ (3-ester). It has been demonstrated that the ring current in thiophen does not differ significantly from that in benzene despite the observed differences in resonance energy (5).

Since the prepared series of adducts of 2-(2′-thienyl) aziridines with methyl propiolate all showed a carbomethoxy singlet at 3.65 δ they were accordingly assigned structure **6**. Careful examination of the i.r. spectrum of the acid **10** in carbon tetrachloride at different concentrations showed no evidence of *intra*-molecular hydrogen

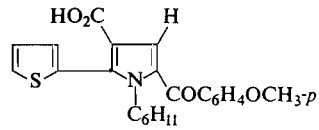

10

bonding such as might have been expected had the reverse mode of addition been adopted (6). The conclusions reached above with respect to the orientation of the addition of methyl propiolate in **6** are in agreement with studies of the addition of olefinic dipolarophiles to 2-(2′-thienyl)aziridines in which bulky addends were found to adopt positions remote from the 3-aroyl group which presumably exerts greater steric hindrance than does the 2-(2′-thienyl) group in this type of addition (1).

(b) Carbonyl Dipolarophiles

The 2-(2′-thienyl)aziridine **1** reacted readily with chloral in benzene to give the 2-(2′-thienyl)-oxazolidine **11**. The orientation of the 1,3-dipolar

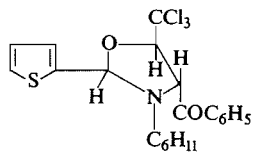

11

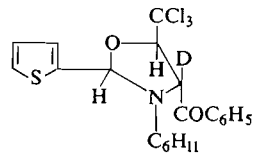

12

cycloaddition to the carbon bond was proven by a parallel reaction with 3-benzoyl-1-cyclohexyl-3-deutero-2-(2′-thienyl)aziridine (91% deuterium) to give **12**, the n.m.r. spectrum of which confirmed specific deuterium labelling (77%) at the 4-oxazolidine position by the modified AB quartet due to the *trans* 4,5-protons. This experiment disposes of the product of the alternative mode of addition, *i.e.* structure **13**. The method used to

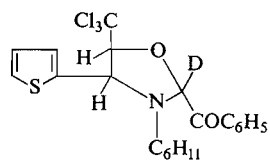

13

assign the full stereochemistry to oxazolidine structures obtained from analogous 2-aryl-3-aroylaziridines has been reported elsewhere (7).

Can. J. Chem. Downloaded from www.nrcresearchpress.com by 210.87.254.40 on 09/05/12
For personal use only.

The 2-(2′-thienyl)aziridine, **1**, reacted readily with diphenylcyclopropenone to give a 1:1 adduct assigned the 2-(2′-thienyl)-4-oxazoline structure **14** on the basis of its dipolarophilic activity (8, 9). For example, treatment of **14** with

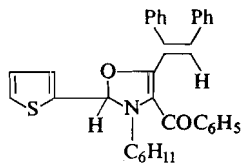

14

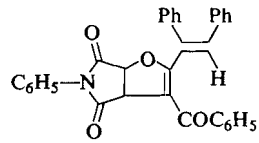

15

N-phenylmaleimide afforded the known dihydrofuran adduct **15** (9) in 82% yield with the expulsion of the 2-thiophen aldimine. The latter reaction shows that 4-oxazolines cleave thermally to 1,3-dipoles of the externally stabilized ketocarbene type even with a 2-substituent of substantially reduced resonance energy compared with an aryl group.

(c) Aryl Isothiocyanates as Dipolarophiles

We have reported that 3-aroyl-2-arylaziridines react with aryl isothiocyanates to form (*a*) 4-aroyl-5-arylamino-4-thiazolines, **16**, by 1,3-dipolar cycloaddition to the C=S bond followed by tautomerization and/or (*b*) 2-arylimino-4-aroyl-4-thiazolines **17** (10) (Scheme 1).

The novelty of this reaction and the observed marked dependence of the course of the reaction on the nature of the substituents both at the 1 and 2 positions of the aziridine ring demanded further investigation.

The 2-(2′-thienyl)aziridines bearing an *N*-cyclohexyl substituent reacted with a series of aryl isothiocyanates to give, after chromatography on alumina, 2-(2′-thienyl)-4-thiazolines and 2-arylimino-4-(2′-thienyl)-4-thiazolines ex-

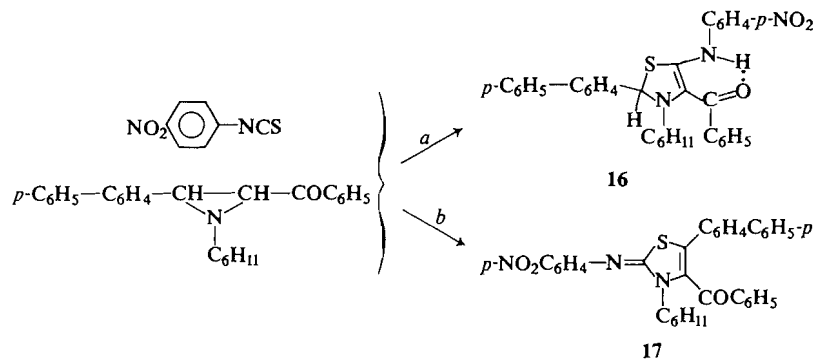

16

17

SCHEME 1

emplified by **18** and **19** respectively. In this set of reactions compounds of type *A* were by far the major products.

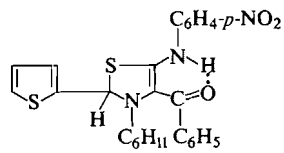

Type *A* **18**

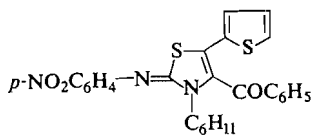

Type *B* **19**

The previously postulated initial product of 1,3-dipolar cycloaddition (10) was frequently detected in this series of reactions as an extremely labile species **20** before chromatographic separation of *A* and *B*. (Scheme 2). Compound **20** and similar structures tautomerized completely to the stable form **18** upon attempted chromatographic purification on neutral alumina or merely on standing in $CDCl_3$ solution so that the progress of this tautomerization could be followed by n.m.r. (see Fig. 1).

It was observed in this series that smaller *N*-substituents *e.g.* isopropyl instead of cyclohexyl lead to the exclusive formation of thiazolines of type *B*, regardless of solvent type. This result, which parallels that observed previously with 3-aroyl-2-arylaziridines, may now be given

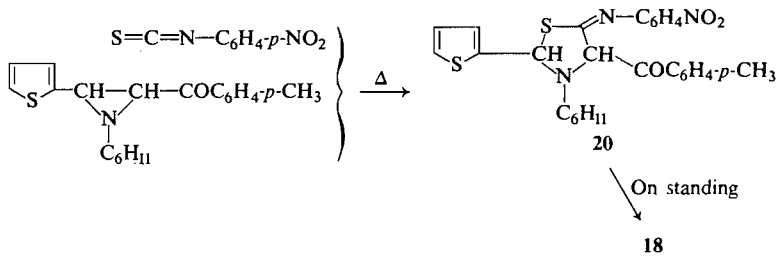

SCHEME 2

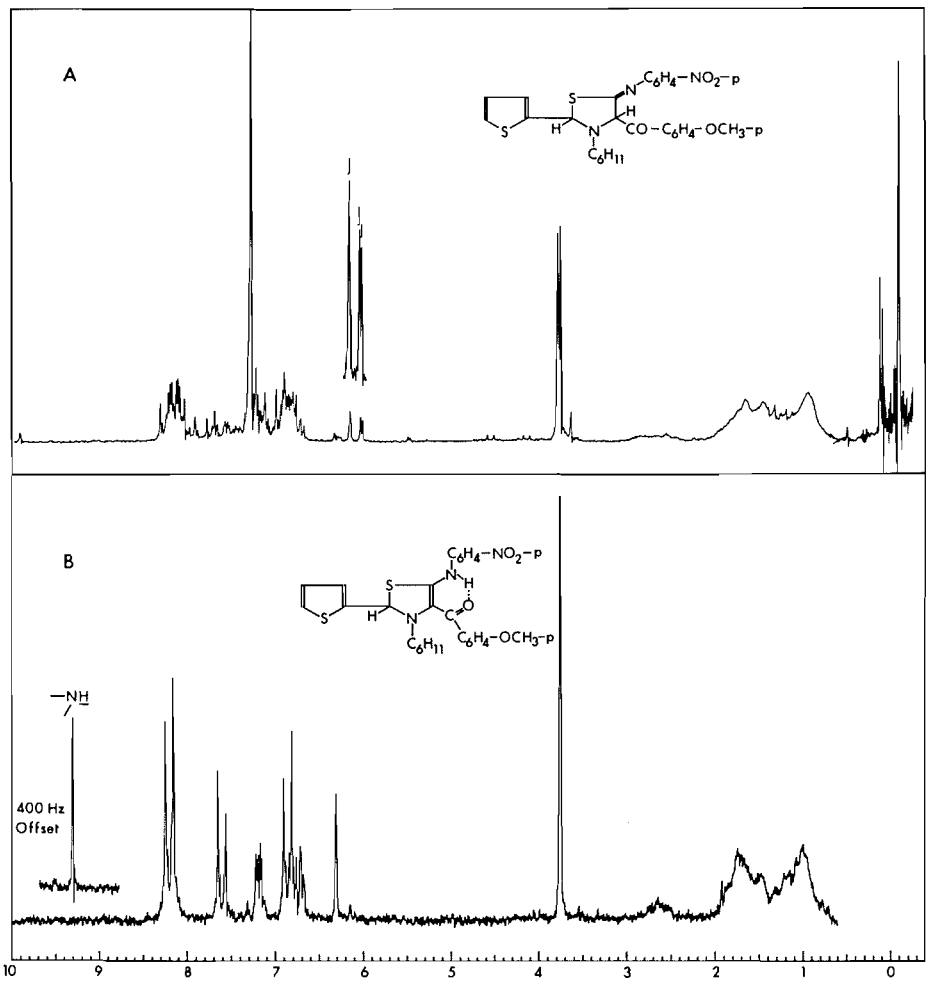

FIG. 1. The n.m.r. spectrum at 100 MHz of (A) labile intermediate in the reaction of 3-*p*-anisoyl-1-cyclohexyl-2-(2′-thienyl)aziridine with *p*-nitrophenyliso-thiocyanate. (B) 4-*p*-anisoyl-3-cyclohexyl-5-*p*-nitrophenyl-amino-2-(2′-thienyl)-4-thiazoline.

a plausible interpretation. Professor Stamm informed us that he has observed a similar tendency towards increased yield in the reaction of aziridines with carbon disulfide to form thiazolidin-2-thiones with smaller *N*-substituents (11) (Scheme 3). Steric hindrance to quaternization of the aziridine nitrogen when R is larger than CH_3 will tend to favor the competing 1,3-dipolar cycloaddition as observed when N is cyclohexyl for example.

Can. J. Chem. Downloaded from www.nrcresearchpress.com by 210.87.254.40 on 09/05/12
For personal use only.

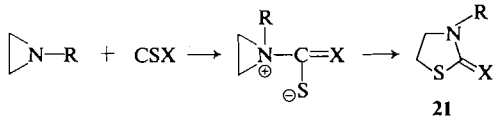

21

X = N—Ar (10)
X = S (11)

SCHEME 3

(d) Sulfonylimines as Dipolarophiles

The 2-(2′-thienyl)aziridine **1** reacted readily with *N*-(*m*-nitrobenzal)-*p*-nitrobenzene sulfonamide (12, 13) to give the thienyl imidazolidine **22** in 90% yield. A control reaction with the

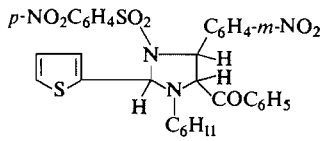

22

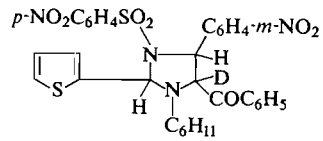

23

corresponding specifically 3-deuterated thienylaziridine afforded **23** in 94% yield, the n.m.r. spectrum of which confirmed the orientation of addition of the dipolarophile.

(e) Methyl Azodicarboxylate as Dipolarophile

The aziridine **1** added readily to methyl azodicarboxylate (3) in benzene to give the triazolidine **24** in 65% yield.

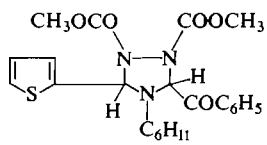

24

Inspection of the literature of heterocyclic chemistry reveals that many naturally occurring and synthetic compounds in which heterocycles are linked directly together often have valuable applications in agriculture and pharmacology. The representative examples shown in Chart 1 have been cast in a perhaps unfamiliar form to bring out this feature.

While specific syntheses have been developed for particular compounds and some of their analogues, no attempt at a general synthesis of linked heterocycles has been made hitherto. A general route to linked heterocycles would also be useful for studies of comparative reactivity in substitution reactions.

The demonstrated versatility and synthetic utility of 1,3-dipolar cycloadditions of substituted 3-aroylaziridines to heteromultiple bonds illustrated above suggests the general synthetic scheme (Scheme 4) for the formation of a wide variety of otherwise inaccessible linked heterocycles.

This approach has the advantages of (*i*) versatility, (*ii*) availability of starting materials, (*iii*) generally good yields, (*iv*) predictability of full stereochemistry of the new heterocyclic ring from considerations of the Woodward–Hoffmann rules to ring opening (in the case of aziridines (22) and oxiranes (23, 24)), and (*v*) a wide variety of substituents in the products.

In view of the recent demonstration of photolytic cleavage of epoxides to carbonyl ylides (23, 24), the application of epoxides in Scheme 4 is under examination.

Experimental

Melting points were determined on a Fisher–Johns apparatus and are uncorrected. The i.r. spectra were recorded on a Perkin–Elmer model 421 spectrophotometer, and only the principal, sharply defined peaks are reported. The n.m.r. spectra were recorded on Varian A-60 and A-100 analytical spectrometers. The spectra were measured on approximately 10–15% (w/v) solutions in $CDCl_3$, with tetramethylsilane as a standard. Line positions are reported in p.p.m. from the reference. Absorption spectra were recorded in 'spectro'-grade solvents on a Beckman DB recording spectrophotometer. Mass spectra were determined on an Associated Electrical Industries MS-9 double focusing high resolution mass spectrometer. The ionization energy, in general, was 70 eV. Peak measurements were made by comparison with perfluorotributylamine at a resolving power of 15 000. Kieselgel DF-5 (Camag, Switzerland) and Eastman Kodak precoated sheets were used for t.l.c. Microanalyses were carried out by Dr. C. Daesslé, Organic Microanalysis Ltd., Montreal, Quebec and by Mrs. D. Mahlow of this department.

General Preparation of 2-(2′-Thienyl)aziridines

The details of the method of preparation of most of the 2-(2′-thienyl)aziridines employed in this paper have been given elsewhere (1). One new aziridine was prepared, the physical and spectroscopic data of which follow.

Can. J. Chem. Downloaded from www.nrcresearchpress.com by 210.87.254.40 on 09/05/12
For personal use only.

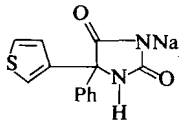

Sodium phethenylate
(anticonvulsant) (14)

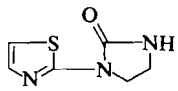

Niridazole
(schistomicidal amebicidal) (15)

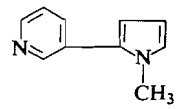

β-Nicotyrine
(insecticide) (16)

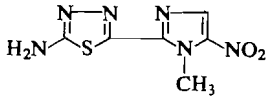

(Antimicrobial agent)
(17)

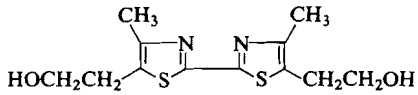

Vitachrome
(18)

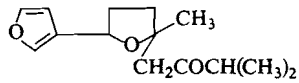

Furacin
(antibacterial) (19)

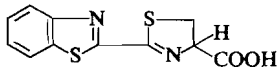

Luciferin
(20)

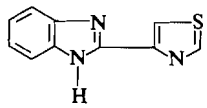

Thibendazole (21)
(Vermifuge)

CHART 1

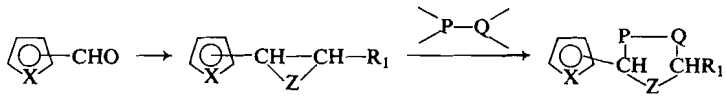

X = O; S; NR; —C=N—
Z = NR; NAr; O
P—Q = C=C; C≡C; O=C, S=C, N=C; N≡C; N=N
R_1 = COAr; COR; CO_2R; C≡N; Ar

SCHEME 4

1,2-Dibromo-1-(β-naphthoyl)-2-(2′-thienyl)ethylene

1,2-Dibromo-1-(β-naphthoyl)-2-(2′-thienyl)ethylene was prepared from 1-(β-naphthoyl)-2-(2′-thienyl)ethylene (25) by bromination in chloroform in 91% yield, m.p. 132–133°.

Anal. Calcd. for $C_{17}H_{12}BrOS$: C, 48.12; H, 2.85; Br, 37.68; S, 7.56. Found: C, 48.17; H, 2.87; Br, 37.39; S, 7.54.

The i.r. spectrum $\nu_{max}(CHCl_3)$: 1686 cm^{-1} (C=O). The n.m.r. spectrum δ TMS ($(CD_3)SO$): AB quartet centered at 6.28 and 6.81, J = 10.5 Hz (2H, 1, 2-protons); 7.5–8.5 (10H, multiplet, thienyl and naphthyl protons).

1-Cyclohexyl-3-(β-napthoyl)-2-(2′-thienyl)aziridine

This aziridine was prepared in the manner previously described (1) in 91% yield, m.p. 103–105° (*cis* and *trans* mixture).

Anal. Calcd. for $C_{23}H_{23}NSO$: C, 76.42, H, 6.41; N, 3.88; S, 8.87. Found: C, 76.65; H, 6.12; N, 3.72; S, 8.79.

The i.r. spectrum: $\nu_{max}(CHCl_3)$: 1663 cm^{-1} (C=O). The n.m.r. spectrum δ TMS ($CDCl_3$): 0.3–2.9 (11H, multiplet, cyclohexyl protons); 3.35 and 3.81 (2H, singlets, *cis* and *trans* 2,3-protons); 6.8–8.3 (10H, multiplet, thienyl and naphthyl protons).

Addition of 2-(2′-Thienyl)aziridines to Acetylenic Dipolarophiles

The additions of aziridines to dimethyl acetylenedicarboxylate and to methyl propiolate were carried out in the manner described in the following representative examples. Thereafter the analytical and spectral data on new thienyl pyrroles are summarized in Tables 1 and 2.

1-Cyclohexyl-3,4-dicarbomethoxy-5-(4-methoxybenzoyl)-2-(2′-thienyl)-2-pyrroline

A solution of 0.683 g (2 mmoles) of 1-cyclohexyl-3-(*p*-methoxybenzoyl-2-(2′-thienyl)aziridine and 0.286 g (2 mmoles) of dimethyl acetylenedicarboxylate in 30 ml dry benzene was refluxed for 5 h under nitrogen. The solution was concentrated to *ca.* 10 ml and subjected to chromatography on alumina (BDH). Elution with benzene

Can. J. Chem. Downloaded from www.nrcresearchpress.com by 210.87.254.40 on 09/05/12
For personal use only.

followed by benzene–ether (3:1) gave one main fraction. Evaporation of solvent gave a yellow oil, trituration of which with hexane gave a pale yellow crystalline solid which was recrystallized with ether–hexane (m.p. 160–162°) 0.543 g (56% yield).

Anal. Calcd. for $C_{26}H_{29}NSO_6$ (mol. wt. 483.1716): C, 64.59; H, 6.05; N, 2.90; S, 6.63. Found: ((mass spectrum) 483.1710) C, 64.57; H, 5.64; N, 2.95; S, 6.60.

The i.r. spectrum $\nu_{max}(CHCl_3)$: 1666 (aryl C=O), 1727 cm^{-1} (ester C=O). The n.m.r. spectrum δ TMS ($CDCl_3$): 0.6–2.2 (10H, multiplet, cyclohexyl protons); 2.6–3.2 (1H, multiplet, CH—N); 3.39 (3H, singlet, ester methyl protons); 3.45 (3H, singlet, ester methyl protons) 3.92 (3H, singlet, methoxyl protons); AB quartet centered at 4.34 and 5.56 (2H, J = 12 Hz, 4,5-protons); 6.8–8.5 (7H, multiplet, thienyl and aryl protons). Absorption spectrum λ_{max}(EtOH): 224 (log ε 4.26); 293 mμ (log ε 4.34).

1-Cyclohexyl-3,4-dicarbomethoxy-5-(4′-methylbenzoyl)-2-(2′-thienyl)-2-pyrroline

A solution of 0.650 g (2 mmoles) of 1-cyclohexyl-3-(*p*-methylbenzoyl)-2-(2′-thienyl)aziridine and 0.286 g (2 mmoles) of dimethyl acetylenedicarboxylate in 50 ml dry benzene was refluxed for 5 h under nitrogen and worked-up exactly as described above to give the 2-pyrroline, m.p. 143–146 °C, 0.478 g (51% yield).

Anal. Calcd. for $C_{26}H_{29}NSO_5$ (mol. wt. 467.1767): C, 66.82; H, 6.18; N, 2.91; S, 6.80. Found ((mass spectrum) 467.1762): C, 66.77; H, 6.25; N, 3.00; S, 6.80.

The i.r. spectrum $\nu_{max}(CHCl_3)$: 1675 (aryl C=O), 1732 cm^{-1} (ester C=O). The n.m.r. spectrum δ TMS ($CDCl_3$): 0.6–2.2 (10H, multiplet, cyclohexyl protons); 2.44 (3H, singlet, methylprotons); 3.39 (3H, singlet, ester methyl protons); 3.43 (3H, singlet, ester methyl protons); AB quartet centered at 4.39 and 5.56 (2H, J = 12.5 Hz, 4,5 protons); 6.8–8.4 (7H, multiplet, thienyl and aryl protons). Absorption spectrum λ_{max}(EtOH): 210 (log ε 4.13) 265 mμ (log ε 4.26).

Similar reaction of 1-cyclohexyl-3-(*p*-methoxybenzoyl)-2-(2′-thienyl)aziridine or 1-cyclohexyl-3-(*p*-methylbenzoyl)-2-(2′-thienyl)aziridine with 10 equiv. of dimethyl acetylenedicarboxylate afforded only the corresponding pyrroles and not the 2-pyrrolines. In the reaction of 1-cyclohexyl-3-(*m*-nitrobenzoyl)-2-(2′-thienyl)aziridine with only 1 equiv. of dimethyl acetylenedicarboxylate only the pyrrole was obtained directly.

Reaction of 3-Benzoyl-1-cyclohexyl-3-deutero-2-(2′-thienyl)aziridine with Dimethyl Acetylenedicarboxylate

The reaction between 0.933 g (3 mmoles) of 3-benzoyl-1-cyclohexyl-3-deutero-2-(2′-thienyl)aziridine (prepared according to a previously described procedure and containing *ca.* 91% deuterium incorporation by n.m.r. integration) and 0.426 g (3 mmoles) of dimethyl acetylenedicarboxylate was carried out in the manner described above, the product subjected to chromatography on alumina to yield (*a*) 5-benzoyl-3,4-dicarbomethoxy-1-cyclohexyl-2-(2′-thienyl)pyrrole, m.p. 158–160° (petroleum ether) 0.246 g (18% yield) and (*b*) 5-benzoyl-3,4-dicarbomethoxy-5-deutero-2-(2′-thienyl)-2-pyrroline, m.p. 140–141° (petroleum ether) 0.52 g (38% yield). The analytical and spectroscopic data on the labelled pyrroline were identical with that of the corresponding protium compound with the exception of the n.m.r. intensities of the methine protons which confirm equal labelling at the 4 and 5 positions. The n.m.r. spectrum δ TMS ($CDCl_3$): 0.5–2.0 (10H, multiplet, cyclohexyl protons); 2.5–3.3 (1H, multiplet CHN); 3.37 (3H, singlet, $COOCH_3$); 3.41 (3H, singlet $COOCH_3$); AB quartet centered at 4.34 and 5.52 (1.81H, J = 12 Hz, 4,5-protons); 6.8–8.4 (8H, multiplet aromatic protons).

Dehydrogenation of Pyrrolines to Pyrroles with Tetrachloro-1,4-benzoquinone

(a) 1-Cyclohexyl-3,4-dicarbomethoxy-5-(p-methoxybenzoyl)-2-(2′-thienyl)pyrrole

A mixture of 0.292 g (0.5 mmoles) of 1-cyclohexyl-3,4-dicarbomethoxy-5-(*p*-methoxybenzoyl)-2-(2′-thienyl)-2-pyrroline and 0.615 g (2.5 mmoles) of tetrachloro-1,4-benzoquinone in 20 ml dry chlorobenzene was heated under reflux with stirring for 4 days. The reaction mixture was cooled and 200 ml ether was added. The solution was washed with 4% aqueous sodium hydroxide solution containing 1% sodium bisulfite and then washed with water. The organic layer was dried ($MgSO_4$) and evaporation of the solvents gave a pale green solid which was recrystallized from ether–hexane, m.p. 176–177°, 0.103 g (43% yield). This compound was identical in all respects with the compound which was obtained by the reaction of 1-cyclohexyl-3-(*p*-methoxybenzoyl)-2-(2′-thienyl)aziridine with 10 equiv. of dimethyl acetylenedicarboxylate (Table 1).

(b) 1-Cyclohexyl-3,4-dicarbomethoxy-5-(p-methylbenzoyl)-2-(2′-thienyl)pyrrole

A mixture of 0.936 g (2 mmoles) of 1-cyclohexyl-3,4-dicarbomethoxy-5-(*p*-methylbenzoyl)-2-(2′-thienyl)-2-pyrroline and 2.460 g (0.01 mole) of tetrachloro-1,4-benzoquinone in 50 ml dry chlorobenzene was refluxed with stirring for 4 days. The mixture was worked-up exactly in the same manner as above, m.p. 194–195° (ethyl acetate – hexane), 0.288 g (31% yield). This compound was identical in all respects with the product which was obtained by reaction of the corresponding aziridine with 10 equiv. of dimethyl acetylenedicarboxylate (see Tables 1 and 2).

3,4-Dicarbomethoxy-1,2,5-triphenyl-3-pyrroline and 3,4-Dicarbomethoxy-1,2,5-triphenylpyrrole

These compounds had been prepared by Heine and Peavy (26) but the n.m.r. line positions required for the present studies had not been reported. Therefore the pyrrole was prepared by the procedures described above and then dehydrogenated with tetrachloro-1,4-benzoquinone.

(a) 3,4-Dicarbomethoxy-1,2,5-triphenyl-3-pyrroline

Melting point 158–159° (ethyl acetate – hexane), 93% yield.

Anal. Calcd. for $C_{26}H_{23}NO_4$ (mol. wt. 413.1627): C, 75.51; H, 5.61; N, 3.39. Found ((mass spectrum) 413.1623): C, 75.60; H, 5.75; N, 3.40.

The i.r. spectrum $\nu_{max}(CHCl_3)$: 1723 cm^{-1} (ester C=O). The n.m.r. spectrum δ TMS ($CDCl_3$): 3.60 (6H, singlet, ester methyl protons); 6.23 (2H, singlet, 2,5-protons); 6.1–7.5 (15H, multiplet, aryl protons).

(b) 3,4-Dicarbomethoxy-1,2,5-triphenylpyrrole

Melting point 196–197° (ethyl acetate – hexane).

Anal. Calcd. for $C_{26}H_{21}NO_4$ (mol. wt. 411.1471):

Can. J. Chem. Downloaded from www.nrcresearchpress.com by 210.87.254.40 on 09/05/12
For personal use only.

Can. J. Chem. Downloaded from www.nrcresearchpress.com by 210.87.254.40 on 09/05/12
For personal use only.

C, 75.92; H, 5.15; N, 3.41. Found ((mass spectrum) 411.1468); C, 75.68; H, 5.17; N, 3.69.

The i.r. spectrum $\nu_{max}(CHCl_3)$: 1717 cm^{-1} (ester C=O). The n.m.r. spectrum δ TMS ($CDCl_3$): 3.69, (6H, singlet, ester methyl protons); 6.7–7.4 (15H, multiplet, aryl protons). Absorption spectrum $\lambda_{max}(CHCl_3)$: 277 mμ (log ε 4.18).

Reaction of 1,2,3-Triphenylaziridine with Methyl Propiolate

A solution of 1.626 g (6 mmoles) of 1,2,3-triphenylaziridine and 0.504 g (6 mmoles) of methyl propiolate in 50 ml toluene was heated under reflux for 24 h. Evaporation of the solvent gave 3-carbomethoxy-1,2,5-triphenyl-3-pyrroline as a white solid, m.p. 195–196° (ethyl acetate – hexane), 1.391 g (65% yield).

Anal. Calcd. for $C_{24}H_{21}NO_2$ (mol. wt. 355.1573): C, 81.11; H, 5.96; N, 3.94. Found ((mass spectrum) 355.1573): C, 81.16; H, 5.92; N, 4.25.

The i.r. spectrum $\nu_{max}(CHCl_3)$: 1724 cm^{-1} (ester C=O). The n.m.r. spectrum δ TMS ($CDCl_3$): 3.63 (3H, singlet, ester methyl protons); 6.13 (2H, singlet, 2,5-protons); 6.3–7.7 (16H, multiplet, aromatic protons). Absorption spectrum $\lambda_{max}(CHCl_3)$: 298 mμ (log ε 3.34).

Dehydrogenation of 3-Carbomethoxy-1,2,5-triphenyl-3-pyrroline with Tetrachloro-1,4-benzoquinone

A solution of 0.710 g (2 mmoles) of 3-carbomethoxy-1,2,5-triphenyl-3-pyrroline and 0.984 g (4 mmoles) of tetrachloro-1,4-benzoquinone in 25 ml of *p*-xylene was heated under reflux for 8 h. The reaction mixture was worked-up as described above affording 3-carbomethoxy-1,2,5-triphenylpyrrole, m.p. 152–153° (ethyl acetate – hexane), 0.583 g (83% yield).

Anal. Calcd. for $C_{24}H_{19}NO_2$ (mol. wt. 353.1416): C, 81.56; H, 5.42; N, 3.96. Found ((mass spectrum) 353.1415): C, 82.06; H, 5.36; N, 3.88.

The i.r. spectrum $\nu_{max}(CHCl_3)$: 1702 cm^{-1} (ester C=O). The n.m.r. spectrum δ TMS ($CDCl_3$): 3.69 (3H, singlet, ester methyl protons); 6.8–7.4 (16H, multiplet aryl protons). Absorption spectrum $\lambda_{max}(CHCl_3)$: 279 mμ (log ε 4.26).

Hydrolysis of 3-Carbomethoxy-1-cyclohexyl-5-p-methoxybenzoyl-2-(2′-thienyl)pyrrole to 1-Cyclohexyl-3-carboxy-5-p-methoxybenzoyl-2-(2′-thienyl)pyrrole

A solution of 0.212 g (5 mmoles) of 3-carbomethoxy-1-cyclohexyl-5-*p*-methoxybenzoyl-2-(2′-thienyl)pyrrole and 155 mg (3.9 mmoles) of sodium hydroxide in 25 ml of 95% dimethylsulfoxide was heated to about 80° with stirring for 3 h. The solution was diluted with water and made slightly acidic with hydrochloric acid. A white crystalline solid precipitated and was collected and dried, m.p. 220–222°, 0.181 g (88% yield).

Anal. Calcd. for $C_{23}H_{23}NSO_4$ (mol. wt. 409.1348): C, 67.47; H, 5.66; N, 3.42; S, 7.83. Found ((mass spectrum) 409.1346): C, 67.26; H, 5.52; N, 3.59; S, 7.92.

The i.r. spectrum $\nu_{max}(CCl_3)$: 3000 (OH, *intermolecular hydrogen bonding, vide infra*), 1638 (aryl C=O), 1679 cm^{-1} (carboxyl C=O dimer). The n.m.r. spectrum δ TMS ($CDCl_3$): 0.5–2.7 (10H, multiplet, cyclohexyl protons); 3.88 (3H, singlet, methoxyl protons); 3.9–4.5 (1H, multiplet CHN): 6.8–8.0 (8H, multiplet, aromatic protons); 10.73 (1H, singlet, exchangeable with D_2O, carboxyl proton).

Examination of the i.r. spectrum at three different concentrations showed no evidence for the presence of *intra*-molecular hydrogen bonding but showed a free OH bond at 3428 cm^{-1} at high dilution which adopted a value of *ca.* 3000 cm^{-1} under conditions at which intermolecular hydrogen bonding was appreciable.

Reaction of 3-Benzoyl-1-cyclohexyl-2-(2′-thienyl)aziridine with Chloral

A solution of 0.933 g (3 mmoles) of 3-benzoyl-1-cyclohexyl-2-(2′-thienyl)aziridine and 0.442 g (3 mmoles) of chloral in 50 ml dry benzene was heated under reflux for 5 h. Evaporation of solvent gave a dark red oil which was subjected to chromatography on alumina (BDH). Elution with benzene gave one fraction. Evaporation of solvent and trituration of the residual oil with hexane gave 4-benzoyl-3-cyclohexyl-2-(2′-thienyl)-5-trichloromethyloxazolidine as a yellow solid, m.p. 88–90° (ether–hexane), 0.605 g (45% yield).

Anal. Calcd. for $C_{21}H_{22}NSCl_3O_2$: C, 54.96; H, 4.83; N, 3.05; S, 6.99; Cl, 23.18. Found: C, 54.84; H, 4.72; N, 2.89; S, 7.04; Cl, 23.46.

The i.r. spectrum $\nu_{max}(CHCl_3)$: 1677 cm^{-1} (aryl C=O). The n.m.r. spectrum δ TMS ($CDCl_3$): 0.3–3.0 (11H, multiplet, cyclohexyl and $\diagdown$CH—N$\diagup$ protons); 4.81 (1H, doublet, J = 4 Hz 5-proton); 5.31 (1H, doublet, J = 4 Hz, 4-proton); 6.61 (1H, singlet 2-proton); 6.8–8.4 (8H, multiplet, thienyl and aryl protons).

Reaction of 3-Benzoyl-1-cyclohexyl-3-deutero-2-(2′-thienyl)aziridine with Chloral

A mixture of 0.933 g (3 mmoles) of 3-benzoyl-1-cyclohexyl-3-deutero-2-(2′-thienyl)aziridine (91% D incorporation) and 0.442 g (3 mmoles) of chloral in 50 ml dry benzene was heated under reflux for 3 h. The reaction mixture worked-up exactly as described above affording 4-benzoyl-3-cyclohexyl-5-deutero-2-(2′-thienyl)-5-trichloromethyloxazolidine, m.p. 89–90°, 0.687 g (51% yield).

The n.mr. spectrum δ TMS ($CDCl_3$): 0.2–3.0 (11H, multiplet, cyclohexyl protons); 4.81 (1H, singlet, 5-proton); 5.31 (0.23H, doublet, 4-proton); 6.61 (1H, singlet, 2-proton); 6.8–8.4 (8H, multiplet, thienyl and phenyl protons).

By this experiment the orientation of the 1,3-dipolar addition of the chloral was confirmed.

Reaction of 3-Benzoyl-1-cyclohexyl-2-(2′-thienyl)-aziridine with Diphenylcyclopropenone

A solution of 0.933 g (3 mmoles) of 3-benzoyl-1-cyclohexyl-2-(2′-thienyl)aziridine and 0.620 g (3 mmoles) of diphenylcyclopropenone in 50 ml dry benzene was heated under reflux for 12 h. Evaporation of the solvent gave a yellow oil which was subjected to chromatography on alumina. Elution with benzene gave one fraction. Evaporation of solvent and trituration with hexane gave 4-benzoyl-3-cyclohexyl-5-(*cis*-1,2-diphenylvinyl)-2-(2′-thienyl)-4-oxazoline as a white solid, m.p. 108–110° (ether–hexane), 1.01 g (65% yield).

Anal. Calcd. for $C_{34}H_{31}NSO_2$ (mol. wt. 517): C, 78.87; H, 6.05; N, 2.71; S, 6.19. Found: ((mass spectrum) 517): C, 79.49; H, 6.47; N, 2.52; S, 6.15.

The i.r. spectrum $\nu_{max}(CHCl_3)$: 1715 cm^{-1} (aryl C=O). The n.m.r. spectrum δ TMS ($CDCl_3$): 0.3–2.2 (10H, multiplet, cyclohexyl protons); 2.5–3.2 (1H, multiplet,

Can. J. Chem. Downloaded from www.nrcresearchpress.com by 210.87.254.40 on 09/05/12
For personal use only.

TABLE 3

4-Aroyl-5-arylamino-2-(2′-thienyl)-4-thiazolines*

					Found					Calculated				
No.	R_4	R_5	Melting point (°C)	Yield† (%)	C	H	N	S	Molecular ion (mass spectrum)	C	H	N	S	Molecular ion (mass spectrum)
i	C_6H_5	*p*-$NO_2C_6H_4$	176–177	43	63.70	5.17	8.27	13.10	491.1338	63.52	5.13	8.55	13.05	491.1337
j	*p*-$CH_3C_6H_4$	*p*-$NO_2C_6H_4$	112	35	63.95	5.28	8.33	12.07	505.1496	64.13	5.38	8.31	12.68	505.1494
k	*p*-$CH_3OC_6H_4$	*p*-$NO_2C_6H_4$	193	61	62.55	5.25	7.92	12.45	521.1444	62.17	5.22	8.06	12.30	521.1443
l	2-Naphthyl	*p*-$NO_2C_6H_4$	125	64	66.54	5.14	7.88	11.51	541.1489	66.51	5.03	7.76	11.84	541.1494
m	*m*-$NO_2C_6H_4$	*p*-$NO_2C_6H_4$	184	42	58.16	4.60	10.19	11.62	536.1187	58.18	4.51	10.44	11.95	536.1189
n	C_6H_5	1-Naphthyl	163	12	—	—	5.84	13.29	496.1645	—	—	5.65	12.92	496.1643
o	*p*-$C_6H_5C_6H_4$	2-Naphthyl	174	15	—	—	5.01	11.19	572.1960	—	—	4.89	11.20	572.1956

*Compounds of structure:

†Yield after recrystallization.

TABLE 4

Spectroscopic properties of 4-aroyl-5-arylamino-2-(2′-thienyl)-4-thiazolines

	Infrared spectrum ($CHCl_3$)		Nuclear magnetic resonance spectrum ($CDCl_3$)δ					Absorption spectrum ($CHCl_3$)	
No.	N—H Bonded	C=O	Aryl protons	2-Proton	*N*-Alkyl groups	Aryl methyl	Chelated N—H	λ_{max} (mμ)	log ε
i	3050 br	1607 (s)	6.8–8.4 (12H) m	6.42 (1H) s	0.6–3.2 (11H) m C_6H_{11}		13.36 (1H) s	437 371 275	4.06 4.12 4.09
	3050 br	1599 (s)	6.7–8.4 (11H) m	6.43 (1H) s	0.5–2.2 (10H) m 2.3–3.0 (1H) m C_6H_{11}	2.40 (3H) s	13.38 (1H) s	440 370 281	4.12 4.03 4.15
k	3050 br	1607 (s)	6.6–8.4 (11H) m	6.40 (1H) s	0.5–2.3 (10H) m 2.3–3.0 (1H) m C_6H_{11}	3.86 (3H) s	13.43 (1H) s	450 371 292	4.19 4.09 4.11
	3050 br	1608 (s)	6.6–8.6 (14H) m	6.44 (1H) s	0.5–2.2 (10H) m 2.3–2.9 (1H) m	—	13.36 (1H) s	454 363 297	4.17 4.08 4.19
m	3050	1610 (sh)	6.8–8.6 (11H) m	6.30 (1H) s	0.5–2.9 (11H) m	—	13.66 (1H) s	462 320	4.23 4.05
n	3050	1610 (s)	6.6–8.5 (15H) m	6.42 (1H) s	0.5–3.0 (11H) m	—	13.35 (1H) s	428 280	3.80 4.16
o	3050 br	1606	6.6–8.5 (19H) m	6.44 (1H) s	0.5–2.3 (10 H) m 2.4–3.1 (1H) m	—	13.30 (1H) s	426 373 285	4.23 4.09 4.39

CH—N<): 5.15 (1H, singlet, 2-proton); 6.8–8.1 (15H, multiplet, aryl and vinyl protons).

Reaction of 4-Benzoyl-3-cyclohexyl-5-(cis-1,2-diphenylvinyl)-2-(2′-thienyl)-4-oxazoline with N-Phenylmaleimide

A solution of 0.259 g (5 mmoles) of 4-benzoyl-3-cyclohexyl-5-(*cis*-1,2-diphenylvinyl)-2-(2′-thienyl)-4-oxazoline and 0.10 g (5.8 mmoles) of *N*-phenylmaleimide in 25 ml of dry toluene was heated under reflux for 25 h. Evaporation of the solvent afforded an oil which was subjected to chromatography on alumina (BDH) with benzene as eluant affording one fraction. Evaporation of the solvent gave 3-benzoyl-2-(*cis*-1,2-diphenylvinyl)-6-phenyl-4,8-dihydrofurano-[4,5-*c*]-pyrrolin-2,5-dione, m.p. 220–224° (lit. m.p. 222–224° (9)), 0.24 g (82% yield). This compound was identical in all respects with that obtained by reaction of 4-benzoyl-3-cyclohexyl-5-(*cis*-1,2-diphenylvinyl)-2-phenyl-4-oxazoline with *N*-phenylmaleimide.

Reaction of 2-(2′-Thienyl)aziridines with Aryl Isothiocyanate.

General Method

The method is exemplified by two reactions in which the products were respectively a 5-arylamino-4-thiazoline and a 2-arylimino-4-thiazoline.

(a) Reaction of 3-Benzoyl-1-cyclohexyl-2-(2′-thienyl)-aziridine with p-Nitrophenyl Isothiocyanate

A solution of 0.933 g (3 mmoles) 3-benzoyl-1-cyclohexyl-2-(2′-thienyl)aziridine and 0.540 g (3 mmoles) of *p*-nitrophenylisothiocyanate in 50 ml of dry benzene was heated under reflux for 5 h under nitrogen. The solution was concentrated *in vacuo* to *ca.* 10 ml and chromatographed on grade 1 alumina (BDH). Elution with benzene afforded one main fraction which upon evaporation afforded 4-benzoyl-3-cyclohexyl-5-*p*-nitrophenylamino-2-(2′-thienyl)-4-thiazoline as orange crystals, m.p. 176–177° (ethyl acetate), 0.633 g (43% yield after recrystallization). Full details on this and other analogous 5-arylamino-2-(2′-thienyl)-4-thiazolines are summarized in Tables 3 and 4.

(b) Reaction of 1-Isopropyl-3-phenylbenzoyl-2-(2′-thienyl)aziridine with p-Nitrophenyl Isothiocyanate

A solution of 0.695 g (2 mmoles) of 1-isopropyl-3-*p*-phenylbenzoyl-2-(2′-thienyl)aziridine and 0.360 g (2 mmoles) of *p*-nitrophenyl isothiocyanate in 50 ml of dry benzene was heated under reflux for 5 h under nitrogen. The solvent was evaporated and the residual red oil was chromatographed on alumina with elution by benzene followed by chloroform, which gave one main fraction. Evaporation of solvent gave an orange oil, which by trituration with ethyl acetate gave 3-cyclohexyl-

Can. J. Chem. Downloaded from www.nrcresearchpress.com by 210.87.254.40 on 09/05/12
For personal use only.

Can. J. Chem. Downloaded from www.nrcresearchpress.com by 210.87.254.40 on 09/05/12
For personal use only.

TABLE 5

4-Aroyl-2-arylimino-5-(2′-thienyl)-4-thiazolines*

						Found					Calculated				
No.	R_2	R_3	R_4	Melting point (°C)	Yield (%)†	C	H	N	S	Molecular ion (mass spectrum)	C	H	N	S	Molecular ion (mass spectrum)
p	*p*-$NO_2C_6H_4$	C_6H_{11}	*p*-$CH_3C_6H_4$	107	33	63.74	5.05	8.50	12.87	503.1337	64.39	5.00	8.34	12.74	503.1336
q	*m*-$NO_2C_6H_4$	C_6H_{11}	*p*-$CH_3C_6H_4$	180	49	64.58	5.07	8.43	12.67	503.1338	64.39	5.00	8.34	12.74	503.1338
r	*p*-$NO_2C_6H_4$	$(CH_3)_2CH$	*p*-$C_6H_5C_6H_4$	254	32	66.37	4.28	7.84	11.90	525.1183	66.25	4.41	8.00	12.20	525.1181

*Compounds of structure:

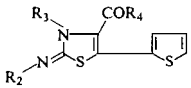

†Yield after recrystallization.

TABLE 6

Spectroscopic properties of 4-aroyl-2-arylimino-5-(2′-thienyl)-4-thiazolines

				Infrared spectrum ($CHCl_3$)		Nuclear magnetic resonance spectrum δ($CDCl_3$)			Absorption spectrum	
No.	R_2	R_3	R_4	C=O	C=N	Aryl protons	Aryl methyl	*N*-Alkyl groups	λ_{max} (mμ)	log ε
p	*p*-$NO_2C_6H_4$	C_6H_{11}	*p*-$CH_3C_6H_4$	1607	1597	6.8–8.3 (11H)m	2.38 (3H)s	0.5–2.5 (10H)m	425	3.73
									346	3.71
								3.8–4.5 (1H)m	264	4.49
q	*m*-$NO_2C_6H_4$	C_6H_{11}	*p*-$CH_3C_6H_4$	1608(s)	1598(s)	6.7–8.3 (11H)m	2.37 (3H)s	0.5–2.5 (10H)m	415	3.45
									345	3.55
								3.9–4.6 (1H)m	257	4.45
r	*p*-$NO_2C_6H_4$	$(CH_3)_2CH$	*p*-$C_6H_5C_6H_4$	1619(s)	1603(s)	6.9–8.4 (16H)m	—	1.62(6H)d	431	3.82
								4.4–5.1 (1H)m	339	3.81
									271	4.48

Can. J. Chem. Downloaded from www.nrcresearchpress.com by 210.87.254.40 on 09/05/12
For personal use only.

2-*p*-nitrophenylimino-4-*p*-phenylbenzoyl-5-(2′-thienyl)-4-thiazoline as a yellow solid, m.p. 254–255°, 0.334 g (32% yield).

Anal. Calcd. for $C_{29}H_{23}N_3S_2O_3$·(mol. wt. 525.1181); C, 66.25; H, 4.41; N, 8.00; S, 12.20. Found: ((mass spectrum) 525.1183): C, 66.37; H, 4.28; N, 7.84; S, 11.90.

The i.r. spectrum $\nu_{max}(CHCl_3)$: 1619 (C=O), 1603 (C=N). The n.m.r. spectrum δ TMS ($CDCl_3$): 1.62 (6H, doublet, isopropyl-methyl protons); 4.5–5.1 (1H, multiplet, isopropyl methine proton); 6.9–8.4 (16H, multiplet, thienyl and aryl protons). The analytical and spectral data on other 4-aroyl-2-arylimino-5-(2′-thienyl)-4-thiazolines are summarized in Tables 5 and 6.

Reaction of 2-(2′-thienyl)aziridine with N-(m-nitrobenzal)-p-nitrobenzenesulfonamide

A mixture of 0.933 g (3 mmoles) of 3-benzoyl-1-cyclohexyl-2-(2′-thienyl)aziridine and 1.005 g (3 mmoles) of *N*-(*m*-nitrobenzoyl)-*p*-nitrobenzenesulfonamide (27) in 50 ml of dry benzene was heated under reflux for 3 h. Evaporation of the solvent gave 5-benzoyl-1-cyclohexyl-3-(*N*-*p*-nitrobenzenesulfonyl)-4-*m*-nitrophenyl-2-(2-thienyl)imidazolidine as a pale yellow solid, m.p. 180–181° (ethyl acetate – hexane), 1.73 g (89% yield).

Anal. Calcd. for $C_{32}H_{30}N_4S_2O_7$: C, 59.43; H, 4.68; N, 8.66; S, 9.92. Found: C, 59.79; H, 4.67; N, 8.43; S, 9.79.

The i.r. spectrum $\nu_{max}(CHCl_3)$: 1690 (aryl C=O). The n.m.r. spectrum δ TMS ($(CD_3)_2SO$): 0.4–2.0 (10H, multiplet, cyclohexyl protons); 5.16 (1H, singlet, 4-proton, see below); 5.24 (1H, singlet, 5-proton); 6.48 (1H, singlet, 2-proton); 7.0–8.7 (16H, multiplet, thienyl and aryl protons).

Mass spectrum Calcd. for $C_{26}H_{23}N_3S$ (imidazole fragment ion): 457.1460. Found: 457.1464.

Reaction of 3-Benzoyl-1-cyclohexyl-3-deutero-2-(2′-thienyl)aziridine with N-(m-Nitrobenzal)-p-nitrobenzenesulfonamide

A mixture of 0.933 g (3 mmoles) of 3-benzoyl-1-cyclohexyl-3-deutero-2-(2′-thienyl)aziridine (91% deuterium incorporation) and 1.006 g (3 mmoles of *N*-(*m*-nitrobenzal)-*p*-nitrobenzenesulfonamide in 50 ml of dry benzene was refluxed for 3 h. Evaporation of the benzene gave the product as a pale yellow solid which was recrystallized from ethyl acetate – hexane, m.p. 180–181°, 1.833 g (94% yield).

The n.m.r. spectrum δ TMS ($(CD_3)_2SO$): 0.4–2.0 (10H, cyclohexyl protons); 5.16 (1H, singlet, 4-proton); 5.24 (0.3H, singlet, 5-proton); 6.48 (1H, singlet, 2-proton); 7.0–8.7 (16H, multiplet, thienyl and aryl protons).

Examination of the n.m.r. spectrum thus showed the position and extent of deuterium incorporation and confirmed the orientation of the 1,3-dipolar cycloaddition.

Reaction of 2-(2′-Thienyl)aziridines with Dimethyl Azodicarboxylate

(i) 5-Benzoyl-4-cyclohexyl-1,2-dicarbomethoxy-3-(2′-thienyl)-1,2,4-triazolidine

A solution of 0.933 g (3 mmoles) of 3-benzoyl-1-cyclohexyl-2-(2′-thienyl)aziridine and 0.438 g (3 mmoles) of dimethyl azodicarboxylate in 50 ml of dry benzene was heated under reflux for 5 h. The solution was concentrated to 10 ml and chromatographed on alumina (BDH) with elution by benzene, which gave one fraction. Evaporation of the solvent gave 5-benzoyl-4-cyclohexyl-1,2-dicarbomethoxy-3-(2′-thienyl)-1,2,4-triazolidine as a white solid, m.p. 141–142° (dec.) (ether–hexane), 0.887 g (65% yield).

Anal. Calcd. for $C_{23}H_{27}SN_3O_5$: C, 60.37; H, 5.95; N, 9.19; S, 7.01. Found: C, 60.33; H, 5.78; N, 8.82; S, 6.97.

The i.r. spectrum $\nu_{max}(CHCl_3)$: 1684 (aryl C=O), 1717 cm^{-1} (ester C=O). The n.m.r. spectrum δ TMS ($CDCl_3$): 0.5–2.0 (10H, cyclohexyl protons); 2.8–3.3 (1H, multiplet >N—CH—cyclohexyl proton); 3.66 and 3.71 (6H, singlets, ester methyl protons); 6.37 (1H, singlet, 5-proton); 6.58 (1H, singlet, 3 proton); 6.8–8.2 (8H, multiplet, thienyl and phenyl protons).

(ii) 4-Cyclohexyl-1,2-dicarbomethoxy-5-β-naphthoyl-3-(2′-thienyl)-1,2,4-triazoline

A solution of 1.807 g (5 mmoles) of 1-cyclohexyl-3-β-naphthoyl-2-(2′-thienyl)aziridine and 0.731 g (5 mmoles) of dimethyl azodicarboxylate in 50 ml of dry benzene was heated under reflux for 3 h. The reaction mixture was worked-up as described above affording the product as a white solid, m.p. 86° (dec.) (pentane), 2.08 g (82% yield).

Anal. Calcd. for $C_{27}H_{29}N_3SO_5$: C, 63.89; H, 5.76; N, 8.28; S, 6.32. Found: C, 63.91; H, 5.70; N, 8.20; S, 6.24.

The i.r. spectrum $\nu_{max}(CHCl_3)$: 1680 (aryl C=O), 1717 cm^{-1} (ester C=O). The n.m.r. spectrum δ TMS ($CDCl_3$): 0.5–2.2 (10H, multiplet, cyclohexyl protons); 2.8–3.3 (1H, cyclohexyl CH—N proton); 3.64 and 3.73 (6H, singlets, ester methyl protons); 6.43 (1H, singlet, 5-proton); 6.76 (1H, singlet, 3-proton); 6.8–8.3 (10H, multiplet, thienyl and aryl protons).

1. J. W. Lown and K. Matsumoto. Can. J. Chem. **48**, 2215 (1970).
2. S. Sunner. Acta Chem. Scand. **9**, 847 (1955).
3. H. W. Heine, R. E. Peavy, and A. J. Durbetaki. J. Org. Chem. **31**, 3924 (1966).
4. A. Padwa and L. Hamilton. J. Heterocycl. Chem. **4**, 118 (1967).
5. R. J. Abraham, R. C. Sheppard, W. A. Thomas, and S. Turner. Chem. Commun. 43 (1965).
6. L. J. Bellamy. The infra-red spectra of complex molecules. Second edition. Methuen, London, 1958. p. 96.
7. G. Dallas, J. W. Lown, and J. P. Moser. Chem. Commun. 278 (1970).
8. J. W. Lown, R. K. Smalley, G. Dallas, and T. W. Maloney. Can. J. Chem. **48**, 89 (1970).
9. J. W. Lown, R. K. Smalley, G. Dallas, and T. W. Maloney. Can. J. Chem. **48**, 103 (1970).
10. J. W. Lown, G. Dallas, and T. W. Maloney. Can. J. Chem. **47**, 3557 (1969).
11. H. Stamm. Pharm. Zent. **107**, 440 (1968), and personal communication.
12. G. Kresze and R. Albrecht. Chem. Ber. **97**, 490 (1964).
13. R. Albrecht, G. Kresze, and B. Mlakar. Chem. Ber. **97**, 483 (1964).
14. J. J. Spurlock. U.S. Pat. 2,366,221 (1945) through Chem. Abstr. **39**, 1736 (1945).
15. C. R. Lambert, M. Wilhelm, H. Striebel, F. Kradolfer, and R. Schmidt. Exper. **20**, (8) 452 (1964).

16. R. L. FRANK, R. W. HOLLEY, and D. M. WIKHOLM. J. Amer. Chem. Soc. **64**, 2835 (1942).
17. W. A. REMERS, G. J. GIBBS, and M. J. WEISS. J. Heterocycl. Chem. **6**, 835 (1969).
18. P. KARRER and M. C. SANZ. Helv. Chim. Acta, **27**, 619 (1944).
19. (*a*) R. M. ACHESON. An introduction to the chemistry of heterocyclic compounds. Second edition. Wiley, New York, 1967. p. 119. (*b*) A. J. BIRCH, R. A. MASSY-WESTRUP, S. E. WRIGHT, T. KUBOTA, T. MATSUURA, and M. D. SUTHERLAND. Chem. Ind., (London), 904 (1954). (*c*) T. KUBOTA and N. ICHIKAWA. Chem. Ind., (London), 902 (1954).
20. E. H. WHITE, F. MCCAPRA, and G. F. FIELD. J. Amer. Chem. Soc. **85**, 337 (1963).
21. H. D. BROWN, A. R. MATZUK, I. R. ILVES, L. H. PETERSON, S. A. HARRIS, L. H. SARETT, J. R. EGERTON J. J. YAKSTIS, W. C. CAMPBELL, and A. C. CUCKLER. J. Amer. Chem. Soc. **83**, 1764 (1961).
22. R. HUISGEN, W. SCHEER, and H. HUBER. J. Amer. Chem. Soc. **89**, 1753 (1967).
23. T. DO-MINH, A. M. TROZZOLO, and G. W. GRIFFIN. J. Amer. Chem. Soc. **92**, 1402 (1970).
24. D. R. ARNOLD and L. A. KARNISCHKY. J. Amer. Chem. Soc. **92** 1404 (1970).
25. R. PALLAUD and F. DELAVEAU. C. R. **237**, 1254 (1953).
26. H. W. HEINE and R. PEAVY. Tetrahedron Lett. 3123 (1965).
27. J. W. LOWN, J. P. MOSER, and R. WESTWOOD. Can. J. Chem. **47**, 4335 (1969).

Can. J. Chem. Downloaded from www.nrcresearchpress.com by 210.87.254.40 on 09/05/12
For personal use only.

Can. J. Chem. Downloaded from www.nrcresearchpress.com by 210.87.254.42 on 09/05/12
For personal use only.

The ^{19}F nuclear magnetic resonance spectra of antimony pentafluoride, *cis*-$Sb_3F_{16}^-$ and higher polyanions $Sb_nF_{5n+1}^-$

J. BACON, P. A. W. DEAN, AND R. J. GILLESPIE
Department of Chemistry, McMaster University, Hamilton, Ontario

Received March 26, 1970

The resonances in the ^{19}F nuclear magnetic resonance (n.m.r.), spectrum of antimony pentafluoride have been reassigned and it is shown that the fine structure observed in the spectrum of antimony pentafluoride in various inert solvents can only be explained by considering the effects of magnetic nonequivalence. Solutions of *t*-butyl fluoride and tetra-*n*-butylammonium hexafluoroantimonate in excess SbF_5/SO_2ClF are shown to contain the $Sb_3F_{16}^-$ and $Sb_4F_{21}^-$ anions which have *cis*-fluorine bridged structures. The coupling constants and chemical shifts in the n.m.r. spectra of $Sb_3F_{16}^-$, $Sb_4F_{21}^-$, $(SbF_5)_n$ and 1:1 and 2:1 complexes of SbF_5 are compared and discussed.

Canadian Journal of Chemistry, 48, 3413 (1970)

In a previous paper (1) it was shown that when *t*-butyl fluoride is allowed to react with SbF_5 and the product is dissolved in SO_2 the solution contains the trimethylcarbonium ion, the $Sb_2F_{11}^-$ anion, and the adduct $SbF_5.SO_2$. The $Sb_2F_{11}^-$ ion and $SbF_5.SO_2$ were unambiguously identified by means of their characteristic ^{19}F n.m.r. spectra (2, 3). In the absence of SO_2 the fluorine resonance of *t*-butyl fluoride/SbF_5 mixtures was a very broad line on which was superimposed the spectrum of SbF_5 which when present in sufficient excess remained as a finely dispersed insoluble phase. It was suggested that the main liquid phase consists of a fused salt $(CH_3)_3C^+Sb_nF_{5n+1}^-$ where the anion is a mixture of different polyanions $Sb_3F_{16}^-$, $Sb_4F_{21}^-$, etc., giving a complex but unresolved ^{19}F n.m.r. spectrum. However these polyanions, if formed, are decomposed in SO_2 solution to give $Sb_2F_{11}^-$ and $SbF_5.SO_2$ and no direct evidence for them was obtained. About this time Edwards *et al.* (4) reported the crystal structure of the compound $Br_2^+Sb_3F_{16}^-$ in which the anion was found to have the *trans*-fluorine bridged structure **1**.

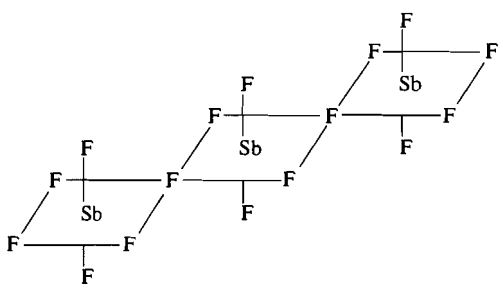

1

In another recent paper (5) it was shown that SO_2ClF is a much weaker base towards SbF_5 than SO_2 and hence it seemed possible that the higher polyanions such as $Sb_3F_{16}^-$ might be stable in this medium. This paper reports a study of the ^{19}F n.m.r. spectra of some *t*-BuF/SbF_5/SO_2ClF and $Bu_4NSbF_6/SbF_5/SO_2ClF$ solutions. The observed spectra are rather complicated and were only interpreted after a reinvestigation and reinterpretation of the closely related spectrum of liquid SbF_5. This is reported first in this paper.

^{19}F *Spectrum of Antimony Pentafluoride*

Hoffman, Holder, and Jolly (6) found the fluorine spectrum of liquid SbF_5 to consist of three peaks of relative areas 1/2/2, and therefore proposed the *cis*-fluorine bridged polymeric structure **2** for the liquid.

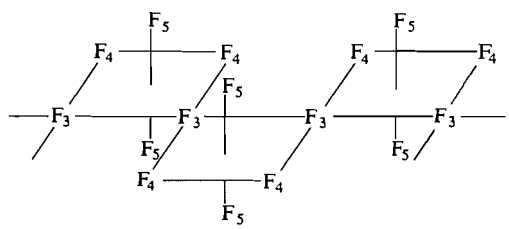

2

Here we have numbered structure **2** according to the uniform numbering scheme recently introduced (5) for the fluorines in both the $Sb_2F_{11}^-$ anion **3** and the 1:1 complexes **4** and 2:1 complexes **5** of SbF_5 with a base B.

This scheme in which numbering starts from the terminal fluorine opposite a fluorine bridge, or, if that is not present, opposite a donor molecule, and which gives the same number to chemically equivalent fluorines has the advantage that similar fluorines in different species are given the same number, simplifying the comparison of

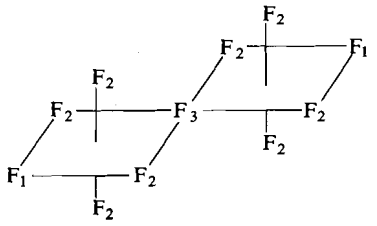

3

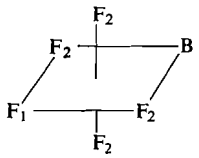

4

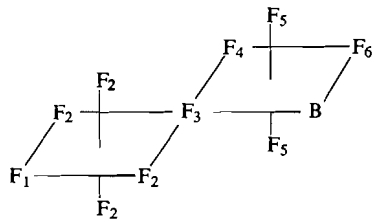

5

chemical shifts and coupling constants. Structure **2** should give rise to three chemically shifted resonances with the relative areas observed, and it is also in accord with the extremely high viscosity of SbF_5, which suggests a polymer of considerable length. The spectrum observed by Hoffman *et al.* (6) showed fine structure in two of the resonances, that at high field being split into a triplet ($J = 130 \pm 15$ Hz) and that in mid-spectrum appearing to be a septet ($J = 70 \pm 10$ Hz). The authors assigned the high-field resonance to the two fluorines (F_5) which are each *cis* to both of the bridging fluorines, split by coupling to the two fluorines (F_4) which are each *trans* to one bridging fluorine and *cis* to the other. In this interpretation, the resonance of the F_4 fluorines, split into a triplet by the coupling to the two F_5 fluorines, is further split by the smaller coupling to the bridging fluorines (F_3). Since $J_{45} \approx 2J_{34}$, the resulting triplet of triplets appears as a septet. The authors assumed $J_{35} < 30$ Hz.

We have found that the dilution of pure SbF_5 with Freon-114 ($CF_2Cl.CF_2Cl$), perfluorocyclobutane (C_4F_8), or arsenic pentafluoride increases the resolution in the fluorine spectrum markedly, presumably because a decrease in the polymer chain length and in the viscosity causes a narrowing of the natural width of the individual lines. The 56.4 MHz spectrum of a solution with the composition SbF_5/Freon-114 = 2.5, recorded at $-56°$, the temperature of best resolution, is shown in Fig. 1. The septet is quite well resolved, and two of the lines in the triplet at the high field end of the spectrum are split into doublets.

No simple explanation of the doublet splitting in the high-field resonance can be given on the basis of the interpretation of the spectrum proposed by Hoffman *et al.* (6). We now show that the spectrum of diluted SbF_5 can be satisfactorily interpreted by reassigning the chemical shifts and considering the effects of magnetic non-equivalence. The value of 130 Hz for J_{45} reported by Hoffman *et al.* (6) compares very favorably with literature values for J_{FF} in other *cis*-SbF_4X_2 species, *e.g.*, for the *cis*-polymer of SbF_4SO_3F, $J = 125$–128 Hz (7) and for the *cis*-$SbF_4(SO_3F)_2^-$ ion, $J = 122$–126 Hz (8). However, $J_{35} < 30$ Hz is somewhat surprising, since in $Sb_2F_{11}^-$ the coupling between the bridging fluorine and fluorines *cis* to it is 60 Hz (2). *Trans* couplings to the bridging fluorine in $Sb_2F_{11}^-$ are very small, perhaps <10 Hz, yet Hoffman *et al.* report $J_{34} = 70$ Hz for SbF_5. Clearly the earlier assignment is in error and the mid-field resonance should be assigned to F_5 and the high-field resonance to F_4, giving $J_{34} < 30$ Hz, $J_{35} = 70$ Hz, which is consistent with the $Sb_2F_{11}^-$ results.[1] Such a reassignment makes no difference to the first-order spectrum.

In the SbF_6 unit in the polymer all four of the coupling constants J_{35} are equal to each other, as are the four coupling constants J_{45}. The coupling between F_3 and F_4 cannot be described by a single value, however, since the *cis*-coupling, J_{34}, would be expected to be much larger than the *trans*-coupling, J_{34}', by comparison with the $Sb_2F_{11}^-$ ion. This situation is known as "magnetic non-equivalence" and generally results in spectra of greater complexity than expected from first-order considerations. We have, therefore, calculated theoretical six-spin spectra for the SbF_6 unit in the polymer, using

[1]Since the manuscript of this paper was submitted a paper has appeared (13) giving a better resolved ^{19}F n.m.r. spectrum of SbF_5 than that of Hoffman *et al.* (6). The authors attempt a first-order analysis of the spectrum but make the same incorrect chemical shift assignment as in the earlier work.

Can. J. Chem. Downloaded from www.nrcresearchpress.com by 210.87.254.42 on 09/05/12
For personal use only.

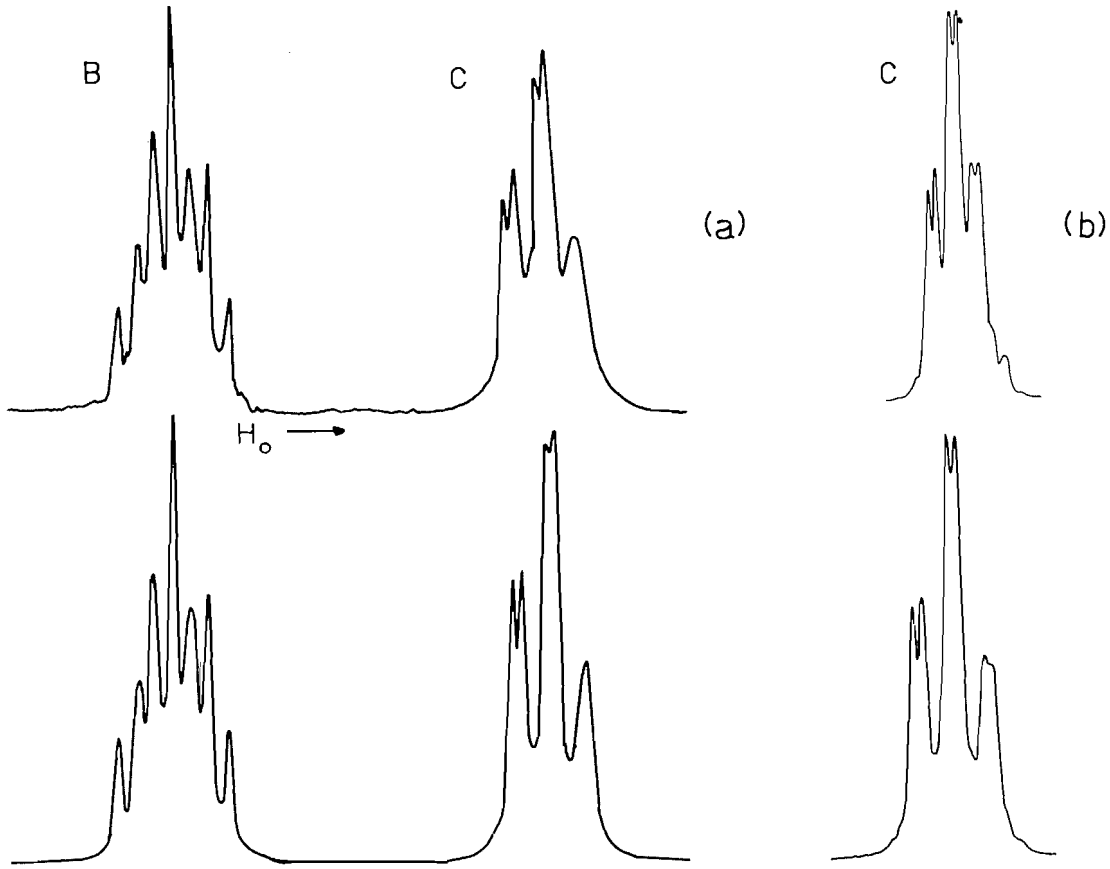

FIG. 1. (*a*) The 56.4 MHz ^{19}F spectrum of a solution of SbF_5 in Freon-114; mole ratio of SbF_5/Freon-114 = 2.5 (lowfield resonance A omitted). (*b*) The 94.1 MHz spectrum (highfield triplet only) of SbF_5 diluted with AsF_5. The calculated spectra are shown below; in (*b*) the horizontal scales are slightly different.

the general n.m.r. spectral program LAOCN3 of Bothner-By and Castellano (9). We find that the theoretical spectrum depends on six coupling constants, J_{35}, J_{45}, J_{34}, J_{34}', and the geminal coupling constants J_{33} and J_{44}. The one remaining coupling constant in the SbF_6 unit, J_{55}, has no effect on the spectrum. The theoretical spectrum consists of 128 lines, many of them quite closely spaced and overlapping. For this reason, a program NMRPLT was written which takes the line positions and intensities calculated by LAOCN3 and calculates the line shape as the sum of individual Lorentzian curves, given a value for the natural line width, and plots this summed line shape on an off-line plotting system. It is this plotted line shape which is compared with the experimental spectrum.

Trial six-spin spectra were calculated for SbF_5 using the initial values $J_{35} = 70$ Hz, $J_{45} = 130$ Hz, $J_{34} = 53$ Hz, $J_{34}' = 10$ Hz, $J_{33} = 25$ Hz, $J_{44} = 100$ Hz together with appropriate chemical shift values and an estimate of 30 Hz for the line width. J_{35} and J_{45} were varied until the splittings observed in the septet were reproduced. The other four coupling constants were then varied. When $J_{35} = 85.6$ Hz, $J_{45} = 144.3$ Hz, $J_{34} = 61.5$ Hz, $J_{34}' = -8.5$ Hz, $J_{33} = 25$ Hz, $J_{44} = 85$ Hz, and a 32 Hz line width is taken, the spectrum shown at the bottom of Fig. 1 is obtained. It is an excellent fit for the experimental spectrum. The same two lines of the triplet are split into doublets in both spectra, and the magnitude of these splittings and those in the septet are well reproduced (largest deviation 1.8 Hz, average deviation 1.4 Hz). The calculated line shape for the triplet resonance is shown in greater detail in Fig. 2, together with the individual lines making up the multiplet.

Can. J. Chem. Downloaded from www.nrcresearchpress.com by 210.87.254.42 on 09/05/12
For personal use only.

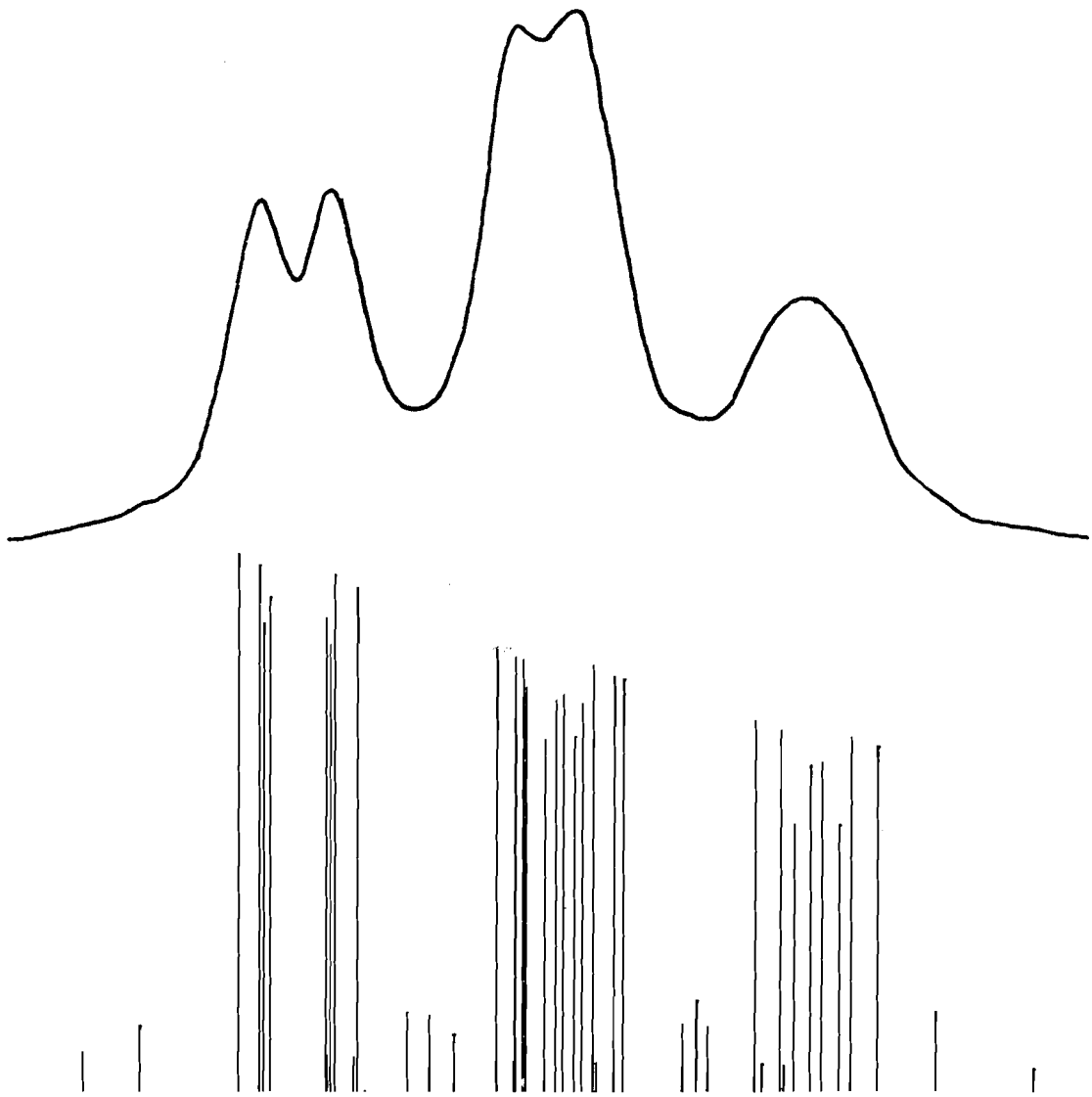

FIG. 2. Calculated line shape and individual lines for the highfield triplet in the 56.4 MHz ^{19}F spectrum of SbF_5/Freon-114 = 2.5.

Dilution of SbF_5 with Freon-114, C_4F_8, or AsF_5 has little effect on resonance A, that of the bridging fluorines, which remains a single broad peak. In our calculated spectrum, resonance A is a broad complex multiplet, showing less resolution than B and C, but still having some degree of structure. However, the theoretical spectrum was calculated for one SbF_6 unit only, *i.e.*, the coupling between a bridging fluorine and the fluorines of the neighboring SbF_6 unit was ignored. This coupling would result in a further splitting of the A resonance resulting, we may reasonably assume, in a broad line showing no structure as was experimentally observed.

The coupling constants for SbF_5 obtained above are all reasonable values. The only *trans*-coupling constant obtained, J_{34}', is less than 10 Hz as expected by analogy with the $Sb_2F_{11}^-$ ion. All the remaining coupling constants involve fluorines which are *cis* to one another, and are in the order $J_{45} > J_{35} > J_{44} > J_{34} > J_{33}$. The reason for this order is not clear, but it is interesting to note that the *cis* coupling between a given fluorine and the bridging fluorine is less

Can. J. Chem. Downloaded from www.nrcresearchpress.com by 210.87.254.42 on 09/05/12
For personal use only.

Can. J. Chem. Downloaded from www.nrcresearchpress.com by 210.87.254.42 on 09/05/12
For personal use only.

than that between the same fluorine and a non-bridging fluorine. The same relationship holds for the two *cis*-coupling constants in the $Sb_2F_{11}^-$ ion. The calculation of the theoretical spectrum is of interest chiefly because of the splitting of the F_c resonance due to magnetic non-equivalence. The effects of magnetic non-equivalence are quite striking. If J_{34} and J_{34}' are varied, the theoretical spectrum for resonance C shows splitting of the individual lines of the triplet into triplets, AB-like quartets, or doublets, depending on the relative values of J_{34} and J_{34}'. The successful calculation of the doublet splitting in the present case confirms the reassignment of chemical shifts proposed here and gives us a basis for understanding the fluorine spectra of species with two fluorine bridges *cis* to one another, as will be seen in the next section.

In principle, other combinations of the six coupling constants in the SbF_5 unit could give rise to essentially the same theoretical spectrum. This would seem to be unlikely, however, since the second order effects in the spectrum arise primarily from magnetic non-equivalence, suggesting that the only ambiguities in the coupling constants given lie in some of the relative signs and in a possible interchange of J_{34} with J_{34}' or J_{33} with J_{44}. Our assignment gives values consistent with those found for the analogous coupling constants in similar systems, as discussed above. Nonetheless, we have tested our assignment by calculating the theoretical spectrum at 94.1 MHz, using the same coupling constants. The calculated spectrum is very similar to the 56.4 MHz spectrum and shows all the same features except that all three lines of the high field triplet show a doublet splitting (Fig. 1). This splitting of all three lines of the triplet is observed in all the spectra we have recorded at 94.1 MHz, *e.g.*, SbF_5 diluted with AsF_5 (Fig. 1), and would appear to be an additional confirmation of the assignment.

t-Butyl Fluoride in SbF_5/SO_2ClF Solution

A sample having *t*-BuF/SbF_5/SO_2ClF = 1/2.5/2.2 was prepared, and its low temperature 56.4 and 94.1 MHz ^{19}F spectra and its proton spectrum were recorded. The proton spectrum showed the presence of the *t*-butyl ion $(CH_3)_3C^+$. The 94.1 MHz ^{19}F spectrum was more useful than the 56.4 MHz spectrum since not only is the spectrum more spread out, reducing the overlap of adjoining multiplets, but also the multiplets themselves are better resolved. The improved resolution occurs because the fluorine exchange can be effectively stopped at a slightly higher temperature at the 94.1 MHz operating frequency (−75° *vs.* −95° for 56.4 MHz) where the relaxation time is longer and the natural width less. The 94.1 MHz spectrum obtained at −75° is shown in Fig. 3. Given *t*-BuF/SbF_5 = 1/2.5, we might reasonably expect the solution to contain either equimolar amounts of the $Sb_2F_{11}^-$ and $Sb_3F_{16}^-$ ions or $Sb_2F_{11}^-$ and SbF_5 coordinated with the solvent, as is the case when SO_2 is the solvent. The spectrum of Fig. 3 shows seven main resonances. Resonance *a*, a broad signal 89.8 p.p.m. above $CFCl_3$, is in the bridging fluorine region. Resonance *c* at 112.4 p.p.m. is close to the resonance position found for the eight equivalent fluorines of $Sb_2F_{11}^-$ in SO_2 solution and appears to be a doublet of doublets. Resonances *f* and *g* are simple quintets (J = 100 ± 2 Hz) at 136.3 and 141.1 p.p.m. Resonances *b* and *e* are multiplets at 108.3 and 127.8 p.p.m., and the remaining resonance, *d*, is a broad peak at 117.9 p.p.m. We may first assign the quintet *f* and resonances *a* and *c* to the $Sb_2F_{11}^-$ ion. Peak *d* is due to SbF_6^-; for solutions of SbF_5 in HF (2) the resonance of SbF_6^- lies 5–6 p.p.m. above that of the eight equivalent fluorines in the $Sb_2F_{11}^-$ ion, in good agreement with the 5.6 p.p.m. shift between peaks *c* and *d*. The quintet *g* and multiplets *b* and *e* remain to be assigned.

Consider the structure **8** for *cis*-$Sb_3F_{16}^-$

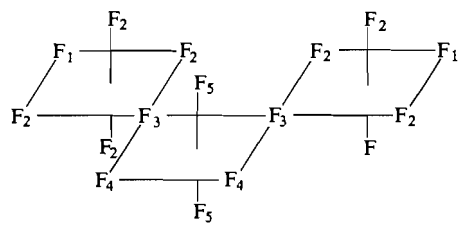

6

Assuming free rotation about the fluorine bridges there are five groups of chemically different fluorines in such an ion. If *trans* couplings are small, as is the case in the $Sb_2F_{11}^-$ ion and SbF_5, the resonance of the F_1 fluorines should be a quintet with $J \sim 100$ Hz. The quintet resonance *g* can therefore be assigned to these fluorines. $SbF_5.SO_2ClF$ would also give rise to a quintet with $J \sim 100$ Hz in the same region, but a strong doublet resonance of $SbF_5.SO_2ClF$ expected at

Can. J. Chem. Downloaded from www.nrcresearchpress.com by 210.87.254.42 on 09/05/12
For personal use only.

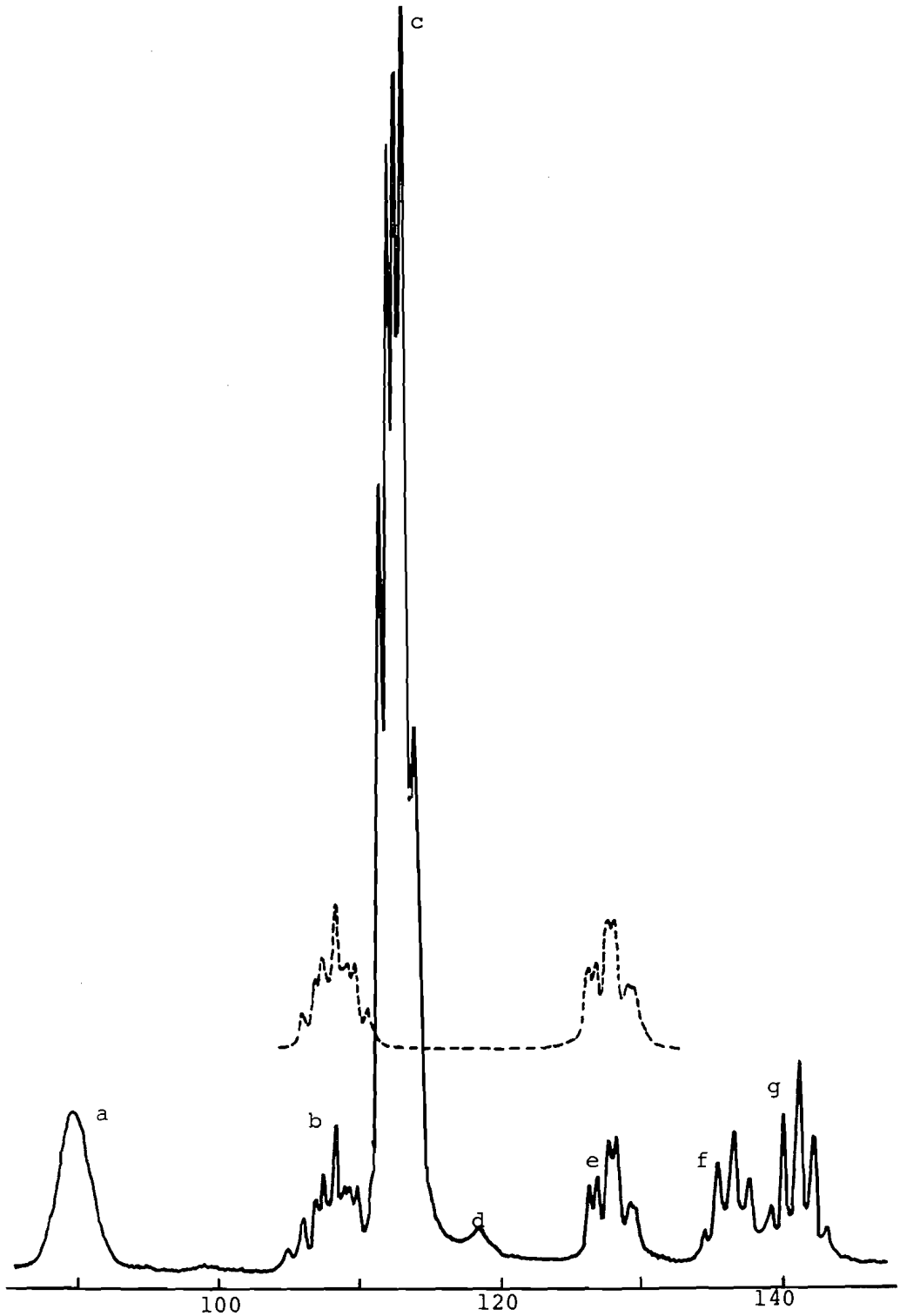

FIG. 3. The 94.1 MHz ^{19}F spectrum of *t*-butyl fluoride/2.5 SbF_5/2.2 SO_2ClF at $-75°$, F-on-Sb region only. The calculated spectrum for the multiplets *b* and *e* is shown by the dashed line.

Can. J. Chem. Downloaded from www.nrcresearchpress.com by 210.87.254.42 on 09/05/12
For personal use only.

105.1 p.p.m. (5) is not seen in the spectrum of Fig. 4, and therefore little or no $SbF_5.SO_2ClF$ is present. The resonance of the F_2 fluorines in *cis*-$Sb_3F_{16}^-$ should be a doublet of doublets, for the same reasons as in $Sb_2F_{11}^-$, and the bridging fluorines F_3 will give rise to a very complicated multiplet, since each F_3 will be coupled strongly (J = 50–80 Hz) to four F_2 fluorines, both F_5 fluorines, and one of the F_4 fluorines. If we assume that fluorines F_3 and F_2 of $Sb_3F_{16}^-$ make up part of resonances *a* and *c*, already assigned to the analogous fluorine atoms in the $Sb_2F_{11}^-$ ion present in this solution, then multiplets *b* and *e* can be assigned to fluorines F_5 and F_4 of the $Sb_3F_{16}^-$ ion. Resonance *c* shows an additional peak at high field, its position consistent with the presence of two overlapping doublets of doublets, at 112.4 and 113.2 p.p.m. We may note that resonance *e*, assigned to F_4, is a triplet showing the doublet splittings on all three lines in the 94.1 MHz spectrum, and on two lines only in the 56.4 MHz spectrum, the same as in the spectra of diluted SbF_5 discussed above. Multiplet *b* is a septet similar to that observed for the F_5 fluorines in SbF_5. The splittings in multiplets *b* and *e* are of the same order of magnitude as in SbF_5, but slightly different, as would be expected for a different species. We see therefore that the experimental spectrum can be interpreted on the basis of the spectrum of the $Sb_2F_{11}^-$ ion plus the spectrum of a new ion *cis*-$Sb_3F_{16}^-$, the spectrum of this ion having some of the features of the spectra of both the $Sb_2F_{11}^-$ ion and SbF_5. Since relative areas 2/8/1 are expected for the resonances from the $Sb_2F_{11}^-$ ion and relative areas $F_1/F_2/F_3/F_4/F_5$ = 2/8/2/2/2 for the *cis*-$Sb_3F_{16}^-$ ion equimolar amounts of the two ions should give relative areas $a/(b + c)/e/(f + g)$ = 3/18/2/4 in excellent agreement with the observed experimental areas 2.8/18.4/2/4.2. The spectral areas thus appear to confirm the proposed assignment.

Reference to the structural diagram for $Sb_3F_{16}^-$ (**8**) shows that the center SbF_6 unit of this ion should give rise to a spectrum similar to that of SbF_5, as is observed, and that the spectrum of the F_4 and F_5 fluorines should depend on the same six coupling constants. A trial LAOCN3 spectrum was calculated using values of J_{35} and J_{45} estimated from multiplet *b* and the final values obtained for the other four coupling constants in SbF_5, that is J_{35} = 91.5 Hz, J_{45} = 131.1 Hz, J_{34} = 61.5 Hz, J_{34}' = −8.5 Hz, J_{33} = 25 Hz, J_{44} = 85 Hz. The parameters were varied until the splittings in the spectra were well reproduced with the largest deviation 1.7 Hz and the average deviation 0.9 Hz. The final set of coupling constants is J_{35} = 85.6, J_{45} = 135.7, J_{34} = 79.3, J_{34}' = −11.1, J_{33} = 27.5, J_{44} = 112.5. The spectrum for multiplets *b* and *e* calculated with these parameters is shown in Fig. 3. The doublet splittings of the high field triplet *e* in the experimental spectrum (49.9, 45.0, 32.2 Hz, from low to high field) are particularly well reproduced in the calculated spectrum (50.1, 44.7, 31.9 Hz). The very small peak on the left hand side of the multiplet *b* is not reproduced in the calculated spectrum. It can probably be assigned to the low field half of the doublet of the AX_4 spectrum arising from a very small amount of $SbF_5.SO_2ClF$. The other half of this doublet presumably lies beneath the adjacent peak and indeed causes the intensity of this peak to be greater than is the calculated spectrum. The corresponding very weak quintet will lie under the quintet *g* and would be much too weak to be observed. The final set of coupling constants were also used to calculate a theoretical 56.4 MHz spectrum which compared very well with the experimental spectrum. In particular, only two of the lines in the high field triplet were split into doublets, as observed at 56.4 MHz. The difference in the spectra at 56.4 and 94.1 MHz is a second order effect, and in the limit of infinite chemical shift three equal doublet splittings would be observed. It may be noted that the fit between the experimental and calculated spectra is better than that obtained for the SbF_5 polymer. This is to be expected because in the latter the mixing of the F_3 spins with two additional F_3 spins is not allowed for in the simple six-spin approximation.

The n.m.r. spectra, area measurements, and calculated spectra given above clearly show the existence of the $Sb_3F_{16}^-$ ion in SO_2ClF. The observation of the effects of magnetic non-equivalence on the triplet resonance at 127.8 p.p.m. shows that the fluorine bridges in the $Sb_3F_{16}^-$ ion are *cis* to one another as is the case for SbF_5. If $Sb_3F_{16}^-$ were *trans*-bridged the four non-bridging fluorines in the center SbF_6 unit would be chemically equivalent, and give a single resonance split into a triplet by coupling to the two bridging fluorines, rather than the two multiplets observed experimentally. It is interesting to note that although the $Sb_3F_{16}^-$ ion in $Br_2^+Sb_3F_{16}^-$ has a *trans* structure no evidence for any appreciable concentration of such an ion

Can. J. Chem. Downloaded from www.nrcresearchpress.com by 210.87.254.42 on 09/05/12
For personal use only.

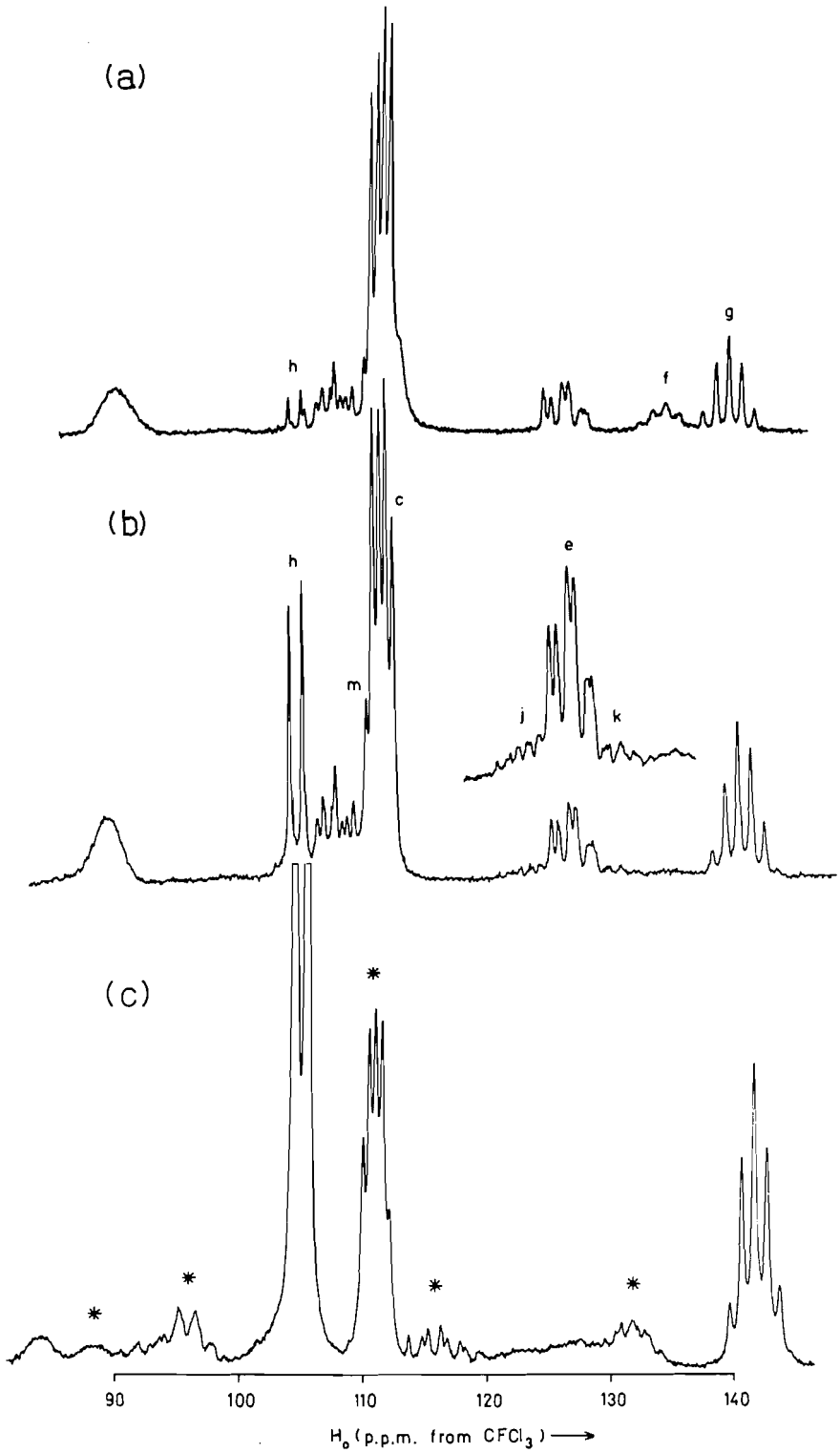

FIG. 4 (*a*). The 94.1 MHz ^{19}F n.m.r. spectrum (F-on-Sb region only) of a solution with $Bu_4NSbF_6/SbF_5/SO_2ClF$ = 1/1.97/12.4, at −90°. (*b*). The 94.1 MHz ^{19}F n.m.r. spectrum (F-on-Sb region only) of a solution with $Bu_4NSbF_6/SbF_5/SO_2ClF$ = 1/2.89/14.7, at −94°. (*c*). The 94.1 MHz ^{19}F n.m.r. spectrum (F-on-Sb region only) of a solution with SbF_5/SO_2ClF = 1/1.92, at −104°.

TABLE 1

Chemical shift data* for SbF_6^-, $Sb_2F_{11}^-$, and $Sb_3F_{16}^-$ in several solvents

Solvent	Ion	Chemical shifts				
		F_1	F_2	F_3	F_4	F_5
SO_2	$Sb_2F_{11}^-$	132.2	110.2	90.3		
SO_2ClF†	SbF_6^-		117.9			
	$Sb_2F_{11}^-$	136.4	113.2	89.7		
	$Sb_3F_{16}^-$	141.1	112.4	89.7	127.8	108.3
HF	SbF_6^-		125			
	$Sb_2F_{11}^-$	141.8	120.1	93.0		

*Chemical shifts in p.p.m. relative to $CFCl_3$. Fluorines are numbered as explained in the text. The data for SO_2 and HF as solvents is taken from refs. 1 and 10.
†The solution was about 1.9 molal in each of the $Sb_2F_{11}^-$ and $Sb_3F_{16}^-$ ions and the cation was $(CH_3)_3C^+$.

was found in the SO_2ClF solution that we studied. A few percent of the *trans* form should have been observable and we can only suppose that the lattice energy of Br_2^+ *trans*-$Sb_3F_{16}^-$ is sufficiently greater than that of Br_2^+ *cis*-$Sb_3F_{16}^-$ that the *trans* form is preferred in the solid state.

Table 1 summarizes the chemical shifts obtained for SbF_6^-, $Sb_2F_{11}^-$, and $Sb_3F_{16}^-$ in SO_2ClF and compares them with those previously found for SbF_6^- and $Sb_2F_{11}^-$ in SO_2 and HF (1, 10). It can be seen there is a considerable solvent effect on the chemical shift of $Sb_2F_{11}^-$ and SbF_6^- in the direction HF > SO_2ClF > SO_2. However, it would appear that the chemical shifts of the $Sb_2F_{11}^-$ ion in SO_2ClF is markedly dependent on both the nature of the cation and the concentration, unlike its behavior in the other solvents, while the chemical shifts of the $Sb_3F_{16}^-$ ion in SO_2ClF show little cation or concentration dependence (see below).

The 2:1 complexes of SbF_5 with the weak bases SO_2ClF, SO_2, and SOF_2 have the structure **5** (5). The half of this dimer containing the coordinated base presents a case which is, in principle, similar in many respects to that for the SbF_6 unit in liquid SbF_5 and the center SbF_6 unit in *cis*-$Sb_3F_{16}^-$. We might, therefore, expect similar values for certain fluorine–fluorine coupling constants in these cases; for example, J_{45} in $Sb_3F_{16}^-$ should be about the same as J_{45} and J_{56} in $Sb_2F_{10}B$. In a previous study (5), it was not possible to measure these coupling constants from the 56.4 MHz spectrum with any degree of accuracy, due mainly to second order effects and to line broadening at the low temperatures necessary to stop exchange. In the present work we have obtained the coupling constants of interest for the 2:1 complexes of SbF_5 with SO_2ClF, SO_2, and SOF_2, all in SO_2ClF solution, from low temperature 94.1 MHz spectra. These and the coupling constants previously measured (J_{12}, J_{13}) are shown in Table 2, together with the analogous coupling constants for $Sb_2F_{11}^-$ and $Sb_3F_{16}^-$. As expected, the corresponding coupling constants in the various species are similar in size.

Table 3 compares the chemical shifts for neat liquid SbF_5 and SO_2ClF solutions of *cis*-$Sb_3F_{16}^-$ and the 2:1 and 1:1 complexes of SbF_5 with SO_2ClF, SOF_2, and SO_2. It can readily be seen that fluorines given the same number in the system proposed have similar chemical shifts.

Evidence for Higher Polyanions in SO_2ClF Solutions

The ^{19}F n.m.r. spectra of the $RF/SbF_5/SO_2ClF$ mixtures discussed above can be duplicated using mixtures of Bu_4NSbF_6 and SbF_5 in SO_2ClF. As has been previously observed (1), decomposition of the *n*-Bu_4N^+ cation by SbF_5 occurs on standing; however, a negligible amount of reaction occurs if the solutions are made up rapidly and kept at liquid nitrogen temperature until used. Bu_4NSbF_6 itself is quite insoluble in SO_2ClF, but dissolves in the presence of SbF_5.

Figure 4*a* shows the −90° ^{19}F (94.1 MHz) n.m.r. spectrum of a solution having the composition $SbF_6^-/SbF_5/SO_2ClF$ = 1/1.97/12.4. The observation of two quintets *f* and *g* at 135.3 and 140.4 p.p.m. shows the solution to contain both $Sb_2F_{11}^-$ and *cis*-$Sb_3F_{16}^-$ (see above). A weak doublet *h* can be seen at 104.8 p.p.m., which by comparison with earlier work (5) can be assigned to $SbF_5 \cdot SO_2ClF$. Since the amount of the latter is clearly very small, this solution must also contain some $Sb_4F_{21}^-$; we suppose that in a solution having the stoichiometry SbF_6^-/SbF_5 = 1/2, an equilibrium distribution of at

Can. J. Chem. Downloaded from www.nrcresearchpress.com by 210.87.254.42 on 09/05/12
For personal use only.

TABLE 2

Coupling constants* for various species in SO_2ClF solution

Species	J_{12}	J_{23}	J_{34}	J_{35}	J_{36}†	J_{45}	J_{46}	J_{56}†
$Sb_2F_{11}^-$	101‡	60						
$Sb_3F_{16}^-$	99	54	79.3	85.6	−11.1	135.7	112.5	135.7
$(SbF_5)_2SO_2ClF$	93	44	100	100	~ 0	134	100	150
$(SbF_5)_2SOF_2$	95	49	97	102	~ 0	139	97	132
$(SbF_5)_2SO_2$	98	49	89	102	~ 0	132	101	132

*In Hz.
†J_{36} and J_{56} in the 2:1 complexes correspond to J_{34}' and J_{45} in $Sb_3F_{16}^-$.
‡For $Sb_2F_{11}^-$ in SO_2, $J_{12} = 102$, $J_{23} = 59$ Hz.

least three polyanions exists and that $Sb_4F_{21}^-$ is probably partly solvolyzed to $Sb_3F_{16}^-$ and $SbF_5.SO_2ClF$.

$$2Sb_3F_{16}^- \rightleftarrows Sb_4F_{21}^- + Sb_2F_{11}^-$$

At higher SbF_5/SbF_6^- ratios, further changes occur in the n.m.r. spectra of the solutions. When $SbF_6^-/SbF_5/SO_2ClF = 1/2.89/14.7$, the fluorine-on-antimony regions of the −94° spectrum is as shown in Fig. 4*b*. The quintet *f* is not seen, showing the absence of $Sb_2F_{11}^-$ in this solution and the doublet *h* is more intense. From the observation of three lines in the F-on-S region of the spectrum, it appears by comparison with a previous study (5) that both $SbF_5.SO_2ClF$ and $(SbF_5)_2SO_2ClF$ are present in solution, and comparison of the intensities of the F-on-S lines assignable to the monomer and dimer, shows that the mole ratio $SbF_5.SO_2ClF/(SbF_5)_2SO_2ClF = 30/1$. In fact, comparison with the F-on-Sb region of the −100° spectrum of a solution with $SbF_5/SO_2ClF = 1.00/1.92$ (Fig. 4*c*), where the starred resonances are attributable solely to $(SbF_5)_2$-SO_2ClF (5), shows that the F-on-Sb region of the present solution has no observable resonances attributable to $(SbF_5)_2SO_2ClF$. Furthermore, by calculation of the amounts of $SbF_5.SO_2ClF$ and $(SbF_5)_2SO_2ClF$ from the intensities of the three lines in the F-on-S region of the spectrum, we deduce that polyanions present have the average composition $(SbF_6^-)(SbF_5)_{2.43}$ and hence that the solution must contain larger polyanions than *cis*-$Sb_3F_{16}^-$. By comparison with the *cis*-bridged structure of $Sb_3F_{16}^-$ in these solutions, we expect that $Sb_4F_{21}^-$ will also be *cis*-bridged (7)

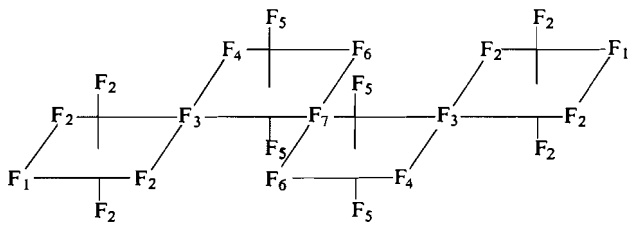

7

But for some intensity differences resulting from a change in the number of terminal and non-terminal SbF_6 units, such an anion would certainly have a ^{19}F n.m.r. spectrum similar to that of *cis*-$Sb_3F_{16}^-$, with the important difference that the fluorines F_4 and F_6, F_3 and F_7 are no longer chemically equivalent. The two apparently equally intense regions of resonance, *j* and *k*, on either side of the resonance *e* due to F_4 of *cis*-$Sb_3F_{16}^-$ (see Fig. 4*b*, inset) are in positions consistent with their being due to F_6 and F_4 of $Sb_4F_{21}^-$. Also, in the absence of either $Sb_2F_{11}^-$ or $(SbF_5)_2SO_2ClF$, the second double-doublet, *m* overlapping that due to F_2 of *cis*-$Sb_3F_{16}^-$, *c*, must be due to the fluorines F_2 in *cis*-$Sb_4F_{21}^-$ which will be coupled to both F_1 and F_3. No other separate resonances are observed, but it is likely that these overlap with their counterparts in the more intense $Sb_3F_{16}^-$ spectrum. The changes we observe on increasing the SbF_5/SbF_6^- ratio to 2.89 are thus consistent with production of *cis-cis*-$Sb_4F_{21}^-$ anion and not a *trans-trans* or *cis-trans* $Sb_4F_{21}^-$ anion; this anion also undergoes more solvolysis than $Sb_3F_{16}^-$.

At still higher SbF_5/SbF_6^- ratios, the spectra become increasingly complicated since the

Can. J. Chem. Downloaded from www.nrcresearchpress.com by 210.87.254.42 on 09/05/12
For personal use only.

TABLE 3

Chemical shift data* for SbF_5, and SbF_5 complexes in SO_2ClF solution

Species	Chemical shifts					
	F_1	F_2	F_3	F_4	F_5	F_6
SbF_5†			87.0	131.3	105.3	
$Sb_3F_{16}^-$	141.1	112.4	89.7	127.8	108.3	
$Sb_4F_{21}^-$		111.5‡		~131		~124
$(SbF_5)_2SO_2ClF$	141.6	110.9	85.2	130.3	95.9	113.4
$(SbF_5)_2SOF_2$	141.1	110.7	83.1	128.4	93.2	114.1
$(SbF_5)_2SO_2$	140.2	109.3	83.8	127.3	94.9	114.8
$SbF_5.SO_2ClF$	141.8	105.1				
$SbF_5.SOF_2$	138.6	102.6				
$SbF_5.SO_2$	136.6	102.0				

*Chemical shifts in p.p.m. relative to $CFCl_3$. The data for the 1:1 and 2:1 complexes of SbF_5 with SO_2ClF, SOF_2, and SO_2 is taken from ref. 5.
†Neat liquid SbF_5. Data taken from ref. 6 and converted to $CFCl_3$ scale.
‡Resonances found in the spectrum of the $Bu_4NSbF_6/SbF_5/SO_2ClF$ = 1/2.89/14.7 sample discussed in the text. The F_1, F_3, and F_5 resonances presumably lie under the corresponding resonances of the $Sb_3F_{16}^-$ ion.

TABLE 4

Cation and concentration dependence of chemical shifts for $Sb_2F_{11}^-$ in SO_2ClF and SO_2

Solvent	Cation	Temperature (°C)	Concentration (*m*)		Chemical shift		
			Cation	$Sb_2F_{11}^-$	F_1	F_2	F_3
SO_2ClF*	$(CH_3)_3C^+$	−95	3.84	1.92	136.4	113.2	89.7
SO_2ClF†	$(CH_3)_2C^+CH_2CH_3$	−85	0.72	0.44	134.2	107.3	84.4
SO_2ClF*	*n*-Bu_4N^+	−95	0.54	0.50	136.4	114.6	93.4
SO_2ClF*	*n*-Bu_4N^+	−94	0.68	0.23	135.3‡		
SO_2§	Cs^+	−60			131.2	109.1	89.4
SO_2§	$(CH_3)_3C^+$	−80	0.90	0.90	132.2	110.2	90.3
SO_2†	$(CH_3)_2C^+CH_2CH_3$	−85	0.09	0.09		111.5‖	91.0

*This work.
†Reference 11.
‡Only the resonance of F_1 was visible, those of F_2 and F_3 lying under the corresponding resonances of $Sb_3F_{16}^-$.
§Reference 1.
‖Only the resonances of F_2 and F_3 were visible, that of F_1 lying under the corresponding resonance of SbF_5SO_2.

amounts of $(SbF_5)_2SO_2ClF$ present become appreciable. However, using the intensities in the F-on-S region to estimate the amounts of the solvolysis products, as outlined for the previous solution, it is possible to show that still larger polyanions are being formed along with the solvolysis products. For instance, in the case of a solution where $SbF_6^-/SbF_5/SO_2ClF$ = 1/5.53/16.1, we deduce that the polyanions formed have the average formula $(SbF_6^-)(SbF_5)_{3.46}$. Hence, the existence of $Sb_5F_{26}^-$ is indicated; by analogy with $Sb_3F_{16}^-$ and $Sb_4F_{21}^-$ this presumably has the all *cis*-bridged structure. Presumably the higher polyanions also occur in solution when alkyl halides are ionized in SO_2ClF containing a sufficiently high concentration of SbF_5.

Cation and Concentration Dependence of Chemical Shifts

Table 4 shows various values obtained in this laboratory for the chemical shifts of $Sb_2F_{11}^-$ in SO_2ClF and SO_2 solution. Where the molality given for the cation differs from that given for $Sb_2F_{11}^-$, either SbF_6^- or $Sb_3F_{16}^-$ is also present in solution. We note that in SO_2ClF solution the resonances of $Sb_2F_{11}^-$ occur at higher field as the concentration of $Sb_2F_{11}^-$ is increased, but that there also appears to be a marked effect from the cation, solutions containing the tetrabutylammonium ion giving resonances at higher field than similar solutions having a carbonium ion as the cation. Table 5 shows the chemical shifts obtained for $Sb_3F_{16}^-$ in SO_2ClF when its concentration is varied or the cation changed. (The solutions of Table 5 also contain some $Sb_2F_{11}^-$ or $Sb_4F_{11}^-$ ion.) Here we note that all the chemical shifts are virtually constant, none changing by more than ~1 p.p.m. Clearly $Sb_3F_{16}^-$ is not very susceptible to cation and concentration effects.

Can. J. Chem. Downloaded from www.nrcresearchpress.com by 210.87.254.42 on 09/05/12
For personal use only.

TABLE 5

Cation and concentration dependence of chemical shifts for $Sb_3F_{16}^-$ in SO_2ClF

Cation	Temperature (°C)	Concentration (*m*)		Chemical shift				
		Cation	$Sb_3F_{16}^-$	F_1	F_2	F_3	F_4	F_5
$(CH_3)_3C^+$	−95	3.84	1.92	141.1	112.4	89.7	127.8	108.3
$(CH_3)_2C^+CH_2CH_3$	−85	0.72	0.28	140.7	111.9	89.0	128.2	107
n-Bu_4N^+	−94	0.68	0.45	140.4	111.9	90.2	127.1	108.0
n-Bu_4N^+	−94	0.58	0.40	140.9	112.0	89.6	127.3	108.0

Experimental

Fluorine n.m.r. spectra were obtained at 56.4 and 94.1 MHz using Varian DA-60 and HA-100 spectrometers, respectively. Both spectrometers were equipped with Varian variable temperature analytical probes and temperature controllers. Spectra were recorded in the HR centerband or sideband mode and calibrated by generating sidebands with an audio oscillator. Spectra were referenced relative to $CFCl_3$ by sample interchange. Fluorine chemical shifts and coupling constants were reproducible to better than 1 p.p.m. and about 1 Hz, respectively.

Antimony pentafluoride was obtained from Ozark Mahoning Company and distilled twice in glass apparatus in an atmosphere of dry air before use. *t*-Butyl fluoride and tetra-*n*-butylammonium hexafluoroantimonate were prepared and purified as previously described (1). The inert solvents AsF_5 (Ozark Mahoning Co.), Freon-114 (Matheson of Canada Ltd.), and perfluorocyclobutane (Matheson) were purified by vacuum fractionation. Sulfuryl chlorofluoride, SO_2ClF, was prepared from KSO_2F and chlorine by the method of Seel and Riehl (12). Sulfur dioxide present as an impurity in the product was removed by distilling the product onto about 5 g of SbF_5 on a vacuum line and distilling the SO_2ClF back out of the resulting solution, the SO_2 remaining behind as the adduct $SbF_5.SO_2$. The absence of SO_2 was confirmed by the absence of the characteristic ^{19}F n.m.r. spectrum of either $SbF_5.SO_2$ or $(SbF_5)_2SO_2$ (5) in the n.m.r. spectra of the SO_2ClF solutions.

Nuclear magnetic resonance samples of SbF_5 in the inert solvents were prepared by a method analogous to that used previously to prepare SbF_5/SO_2ClF samples (5). In a dry box an all-glass syringe was used to transfer SbF_5 into an n.m.r. tube fitted with a detachable tap, the tube was attached to a standard glass vacuum line and the required amount of solvent condensed in prior to sealing off. The n.m.r. sample of *t*-butyl fluoride in SbF_5/SO_2ClF was prepared on a vacuum line using a small flask with a detachable tap and n.m.r. tubes sealed to the flask. A small amount of SbF_5 (about 0.04 mole) and the appropriate amount of solvent were distilled into the flask in weighed amounts. A known volume of *t*-butyl fluoride was then allowed to evaporate into the reaction flask, giving a solution of known composition. The flask was then removed from the vacuum line and tilted so that a suitable volume of solution entered the n.m.r. tube, and the tube sealed off. To allow preparation of $SbF_5/Bu_4NSbF_6/SO_2ClF$ samples whilst keeping room temperature contact between Bu_4N^+ and SbF_5 minimal (the cation is decomposed by prolonged contact with the pentafluoride (1)), a glass apparatus was constructed as follows: two tubes of *ca.* 15 mm o.d., both closed at one end and open via 1/4 in. tubing at the other, were interconnected by 1/4 in. tubing; one of the large tubes had an n.m.r. tube attached at right angles to the interconnection. To prepare the samples, solids were put into the apparatus in the dry box; the salt was weighed into the tube with two sidearms and SbF_5 into the other. Both exits were closed with detachable tops; the whole apparatus was connected to a glass vacuum line via one of the detachable fittings and evacuated. SO_2ClF was condensed onto the SbF_5 and both exits sealed. On warming to room temperature the SbF_5 dissolved in the solvent and the solution was poured onto the Bu_4NSbF_6 via the interconnection. The salt dissolved on shaking. The resulting solution was quickly tipped into the n.m.r. sidearm and the n.m.r. tube sealed off. Samples were kept in liquid nitrogen until used. It was found that this method gave a negligible amount of the coloration due to decomposition of the Bu_4N^+ cation.

We thank the Directorate of Chemical Sciences of the United States Air Force Office of Scientific Research and the National Research Council of Canada for financial support of this work. We also thank Dr. R. A. Rothenbury who recorded the spectra of solutions of SbF_5 in Freon-114.

1. J. Bacon, P. A. W. Dean, and R. J. Gillespie. Can. J. Chem. **47**, 1655 (1969).
2. R. J. Gillespie and K. C. Moss. J. Chem. Soc. (A), 1170 (1966).
3. J. W. Moore, H. W. Baird, and H. B. Miller. J. Amer. Chem. Soc. **90**, 1358 (1968).
4. A. J. Edwards, G. R. Jones, and R. J. C. Sills. Chem. Commun. 1527 (1968).
5. P. A. W. Dean and R. J. Gillespie. J. Amer. Chem. Soc. **91**, 7260 (1969).
6. C. J. Hoffman, B. E. Holder, and W. L. Jolly. J. Phys. Chem **62**, 364 (1958).
7. R. J. Gillespie and R. A. Rothenbury. Can. J. Chem. **42**, 416 (1964).
8. R. C. Thompson, J. Barr, R. J. Gillespie, J. B. Milne, and R. A. Rothenbury. Inorg. Chem. **4**, 1641 (1965).
9. A. A. Bothner-By and S. M. Castellano. LAOCN3, The Mellon Institute, Pittsburgh.
10. M. Azeem, M. Brownstein, and R. J. Gillespie. Can. J. Chem. **47**, 4159 (1969).
11. J. Bacon and R. J. Gillespie. Unpublished results.
12. F. Seel and L. Riehl. Z. Anorg. Chem. **282**, 293 (1955).
13. T. K. Davies and K. C. Moss. J. Chem. Soc. (A), 1054 (1970).

Can. J. Chem. Downloaded from www.nrcresearchpress.com by 210.87.254.42 on 09/05/12
For personal use only.

Can. J. Chem. Downloaded from www.nrcresearchpress.com by 210.87.254.42 on 09/05/12
For personal use only.

Cyanoethylations and Michael additions. V.[1] The synthesis of allylic cyclohexenols by γ-cyanoethylation of α,β-unsaturated aldehydes and ketones. Part V[2, 3]

CH. R. ENGEL, V. S. SALVI, AND L. RUEST
Department of Chemistry, Laval University, Quebec, Quebec

Received May 19, 1970

It is shown that the cyanoethylation of 3β-acetoxy-21-methyl-5α-pregn-17-en-21-one results in part in the addition of acrylonitrile to the γ-position, with concomitant cyclization, and that therefore the cyclo-γ-cyanoethylations of α,β-unsaturated carbonyl compounds reported previously were not confined to aldehydes. However, the main reaction products of the conjugated ketone were α-cyanoethylated derivatives. A variation of the reaction time did not affect the proportion of α- and γ-cyanoethylated products; the implications of this finding on mechanistic considerations are discussed; in particular, an explanation based on the assumption of an equilibrium between reactants and α- and γ-cyanoethylated products is ruled out. It is shown that the γ-additions observed, particularly in the case of α,β-unsaturated aldehydes, are not due to steric hindrance, neither to an abnormal charge distribution in the anion. It is further shown that in the presence of base the propionitrile moiety of oxygen-cyanoethylated α,β-unsaturated aldehydes with a suitable geometry is transferred to the γ-position of the original aldehyde and that cyclization occurs so that the same products are obtained from such cyano-enol ethers as in the direct cyanoethylation of the free aldehydes. On the basis of this finding, a mechanism for the cyclo-γ-cyanoethylations of α,β-unsaturated carbonyl compounds, involving such a transfer reaction, can be tentatively proposed.

Canadian Journal of Chemistry, **48**, 3425 (1970)

In previous publications of this series (1, 3, 4, *cf.* also 2, 5, 6), we have shown that certain α,β-unsaturated aldehydes were cyanoethylated, in contradistinction to earlier findings reported in the literature, in the γ-position, with concomitant cyclization, and that these reactions thus led in high yield to allylic α′-cyano cyclohexenols. It was now of interest to investigate whether or not this reaction took a similar course in the case of α,β-unsaturated ketones. We decided to investigate the cyanoethylation of a ketone closely related to the aldehydes which had given rise to such cyclo-γ-cyanoethylations, 3β-acetoxy-21-methyl-5α-pregn-17-en-21-one (**5**), the methyl ketonic homolog of the first aldehyde investigated (3, 4).

A suitable synthetic precursor for the desired unsaturated methyl ketone **5** seemed the known (7, 8) 17-unsaturated pregnenoic acid **3**. Two classical methods are known for the preparation of such acids: the Favorsky rearrangement of 17,21-dihalogenated 20-ketones (*cf.* 7–12), and dehydration of the products obtained from Reformatzky reactions of 17-ketones (13–15).[4] According to the literature, none of the methods gives satisfactory yields but we considered the Reformatzky sequence promising since its shortcomings were not connected with the actual Reformatzky reaction but with the dehydration step (*cf.* 13, 15). One of us (C.R.E.) (17) has previously shown that such difficult dehydrations of β-hydroxy carboxylic esters could be circumvented by dehydroacetylation with base of the corresponding acetates, a finding independently confirmed by Linstead *et al.* (18). Therefore, 3β-acetoxy-5α-androstan-17-one (**1**) was transformed with ethyl bromoacetate and zinc to a mixture of the 3β,17β-dihydroxy 5α-pregnanoic ester **2** and the corresponding 3-monoacetate **2***a* in an overall yield of 80%; acetylation, under the conditions of Turner (19), gave the diacetoxy ester **2***b*. Treatment of this product with sodium ethylate in absolute ethanol gave in 77% yield the desired 3-hydroxy ethyl ester **3***b*. Analogous results were obtained when the Reformatzky reaction was carried out with methyl bromoacetate and the dehydroacetylation with sodium methylate (*cf.* **1** → **2***d*,*c* → **3***d*). According to Magrath *et al.* (15), the hydrolysis of such unsaturated esters with potassium hydroxide in methanol is unsatisfactory, but we obtained

[1]For paper IV of this series *cf.* ref. 1.

[2]This publication represents part XXXIV in the series on Steroids and Related Products. For paper XXXIII see ref. 1.

[3]Abbreviated in part from the doctoral thesis of L. Ruest, submitted to the School of Graduate Studies of Laval University, Quebec, Quebec, 1969; and from the "thèse de doctorat d'Etat ès-sciences", University of Paris, France, registered at the C.N.R.S. under the number A. O. 1987. For a preliminary report see ref. 2.

[4]The oxidation of 3β-acetoxy-5α-pregn-17-en-21-al (3, 4) with Jones' reagent (16) gave only an unsatisfactory yield (30%) of acid **3***a* (*cf.* Experimental).

Can. J. Chem. Downloaded from www.nrcresearchpress.com by 210.87.254.42 on 09/05/12
For personal use only.

excellent yields with potassium hydroxide in aqueous dioxane. The hydroxy acid **3** (7) was acetylated and the acetoxy acid **3***a* transformed with oxalyl chloride (*cf.* 20–22) into the acid chloride **6** which gave with dimethyl cadmium (*cf.* 23) the desired methyl ketone **5** in 80% yield, calculated from the hydroxy acid **3**.

The cyanoethylation of the unsaturated ketone **5**, under the conditions used in the case of analogous unsaturated aldehydes (1, 4), gave a product from which we isolated, after separation of 16% of the starting material (**5**), a mixture of α-cyanoethylated ketones (**4**A and B) (50% yield), a mixture of cyclized γ-cyanoethylation products (**7** and **8**) (23% yield), and very small quantities (2%) of a dehydration product of these cyclized derivatives, dienonitrile **9**.[5]

The elemental composition of the ketones **4**A and B indicates the addition of one acrylonitrile moiety. Their i.r. spectra show, apart from the usual acetate bands, the presence of a non-conjugated nitrile function, of a non-conjugated carbonyl function, and of a double bond. The trisubstituted nature of the double bond is confirmed by the n.m.r. spectra, which also show the 18- and 19-methyl groups and the methyl ketone moiety. Furthermore, there appears in each case a peak at 3.28 δ which we attribute to the allylic proton in position 20, α to the carbonyl function; the protons of the methylene group, α to the nitrile function, absorb at 2.25 δ. These data are compatible with structures **4**A and B, arising from a classical α-addition of acrylonitrile to the α,β-unsaturated ketone **5**, and cannot be reconciled with products arising from a γ-addition. The fact that only one acrylonitrile moiety was attached to ketone **5** seems plausible in view of the steric hindrance exerted by the 18-methyl group. The two α-cyanoethylated ketones **4**A and B must be epimeric in position 20.

The structure determination of the cyclized γ-cyanoethylation products, **7**, **8**, and **9**, followed that of the corresponding products of the previously described cyanoethylations of analogous aldehydes (1, 4). The elemental composition of the products corresponds again to the addition of one acrylonitrile moiety. The i.r. spectra of the cyclized hydroxy derivatives **7** and **8** reveal the presence of an acetoxy group, of an alcohol function, of a non-conjugated nitrile group, and of an isolated double bond; the position of the absorption band of the latter, at 1682 cm^{-1} (in $CHCl_3$) in the case of hydroxy nitrile **7**, and at 1675 cm^{-1} in the case of hydroxy nitrile **8**, corresponds well to that of a double bond endocyclic to a six-membered ring and exocyclic to a five-membered ring (*cf.* 4). The n.m.r. spectra confirm the presence of a trisubstituted double bond and reveal, apart from the 18- and 19-methyl groups, the methyl group attached in position 21. The proton of the alcohol function appears at 2.70 δ for alcohol **7** and at 2.52 δ for alcohol **8**. The 16^2-proton is seen as a triplet, centered at 3.08 δ in the case of alcohol **7**, and at 3.10 δ in the case of alcohol **8**. The 16-protons of these products are observed as multiplets, centered at 3.02 and 2.75 respectively. The olefinic proton of each alcohol is coupled allylically with the 16-proton. These data are compatible only with structures of cyclized γ-addition products of type **7** and **8** and cannot correspond to products arising from an addition in position α, followed by aldol cyclization (*cf.* 4).

The spectral characteristics of the dienonitrile **9** correspond entirely to the assigned structure. For details we refer to the Experimental and for their interpretation to the discussion (4) of the structures of analogous products formed by the γ-cyanoethylation of 3β-acetoxy-5α-pregn-17-en-21-al (**10**). Furthermore, both hydroxy nitriles **7** and **8** were transformed with *p*-toluenesulfonic acid in a mixture of acetic anhydride and acetic acid into dienonitrile **9**, in yields of 70 and 20%, respectively for alcohol **7** and alcohol **8**. If one extrapolates the findings on the parent aldehyde **10** (4), and assumes that during these dehydrations no epimerization in position 16 occurs, one has to assign to the γ-cyanoethylation products **7**, **8**, and **9** identical configurations in that position.

As mentioned above, the 16^2-proton of the hydroxy nitriles **7** and **8** appears as a triplet, produced by the coupling with the protons in position 16^1. Since the coupling constants are only of 3.2 Hz, they cannot arise from vicinal diaxial couplings and therefore the 16^2-proton of both isomers **7** and **8** must be equatorial, their nitrile function axial. If one now assumes that

[5]The α-cyanoethylated ketones **4**A and B form a eutectic adduct, in a ratio of 1:2, which is eluted from aluminum oxide after the pure ketone **4**A; the pure ketone **4**B could only be obtained by reducing the reaction time considerably (see below).

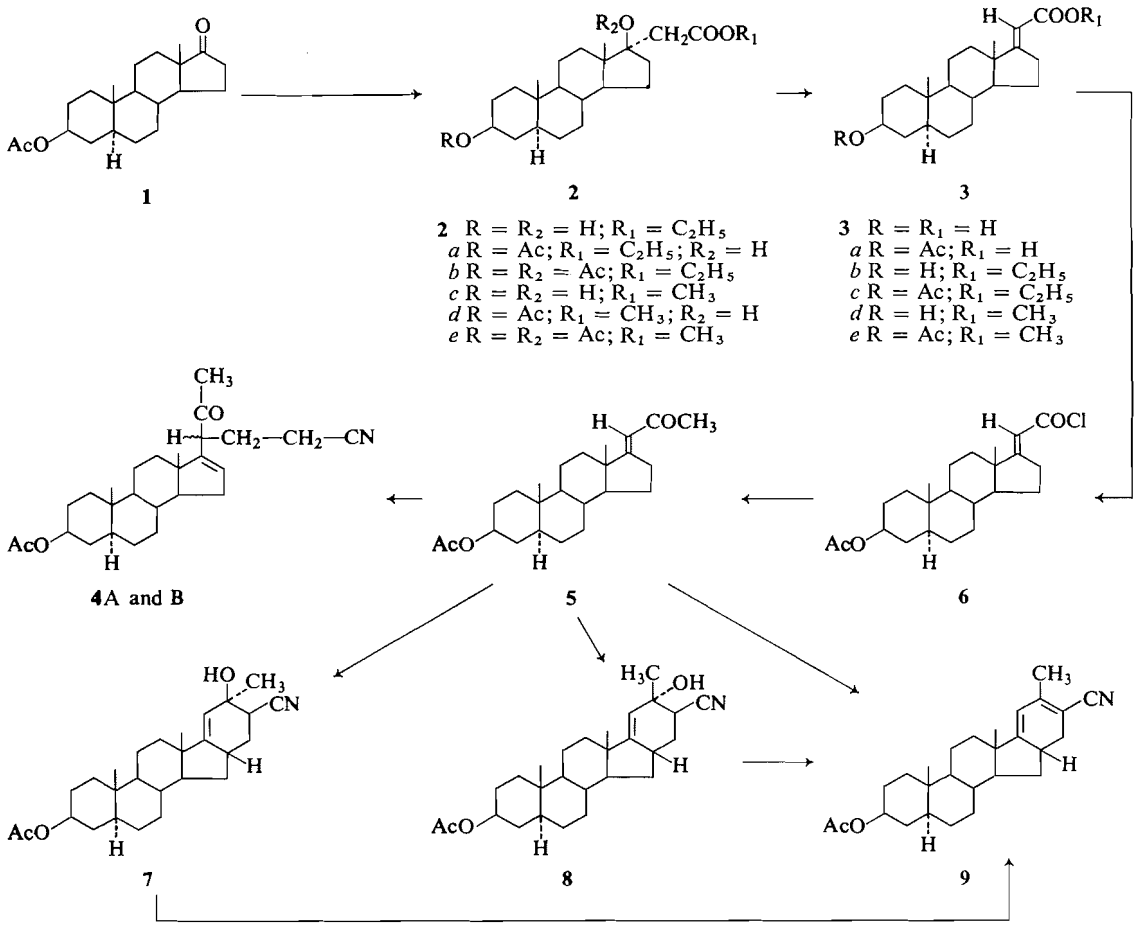

both hydroxy nitriles **7** and **8** have the same stereochemistry in position 16, one concludes that they must be 21-epimers. Therefore, the difference in chemical shifts of the 18-methyl group (seen at 0.83 δ in the case of alcohol **7** and at 0.76 δ in alcohol **8**), and of the 16-proton (which appears at 3.02 δ for alcohol **7** and at 2.75 δ for alcohol **8**) must be due to this difference in stereochemistry. We attribute the parallel deshielding of the 18-methyl group and the 16-proton of hydroxy nitrile **7** to the influence of a 21-substituent, the hydroxyl function, *cis* to both these groups. We thus conclude that the 16-hydrogen must be *cis* to the 18-methyl group and therefore β (compare also refs. 1 and 4). It follows that the configuration of the 16-nitrile function of alcohols **7** and **8** must be β. The assumption that the parallel deshielding effect of the 21-substituent of alcohol **7** on the 16-proton and the 18-methyl group is due to the hydroxyl function is confirmed by the facile dehydration of the product, which suggests a *trans* arrangement of the 21-hydroxyl group and the 16^2-hydrogen. Thus, we have to assign to the hydroxyl function of alcohol **7** a β-configuration, to that of alcohol **8** an α-configuration.

In previous publications of this series (4, 24) we have also given indirect evidence for a 16β-hydrogen configuration of the main cyclo-γ-cyanoethylation products of type **7** and **8**. If, as we have done, one extrapolates from the findings concerning aldehyde **10** that no significant epimerization in position 16 occurs during dehydration, (*cf.* 4), dienonitrile **9** must have a 16β-hydrogen configuration. However, this configuration is in opposition to Moscowitz' rule (25), relating the sign of the Cotton effect of a conjugated homodiene to its helicity, and we are thus in the same situation as in the case of the cyclo-γ-cyanoethylation of aldehyde **10** (4). We have amply discussed this discrepancy (1, 4) and

Can. J. Chem. Downloaded from www.nrcresearchpress.com by 210.87.254.42 on 09/05/12
For personal use only.

Can. J. Chem. Downloaded from www.nrcresearchpress.com by 210.87.254.42 on 09/05/12
For personal use only.

we have suggested that the exception to Moscowitz' rule may be due to the fact that one double bond of the diene system is exocyclic to a five-membered ring since in the D-homo series this discrepancy is not observed.

The experiments described show that the cyclo-γ-cyanoethylation observed in the case of an aldehyde of the steroid series (3, 4), an aldehyde of the D-homo steroid series (1), and an aldehyde of the decaline series (2, 6), applies also to an α,β-unsaturated ketone, with the important difference, however, that in that instance the cyclized γ-cyanoethylation products are not the sole addition products but rather that the main products arise from a "normal" α-addition.[6]

The Mechanism of the Cyclo-γ-cyanoethylation of α,β-Unsaturated Carbonyl Compounds

The reaction of ketone **5** with acrylonitrile allowed the experimental investigation of a hypothesis which seemed to explain the addition of acrylonitrile to the γ-position of α,β-unsaturated carbonyl compounds, in spite of the greater negativity, in the anion, of the α-carbon atom.[7] This hypothesis was based on the assumptions that the greater negativity of the α-carbon atom should not completely prevent addition to the γ-carbon atom, which represents also a negative center; and that there existed an equilibrium between reactants and α- and γ-addition products. While the γ-cyanoethylated products could now readily undergo aldol-cyclization to thermodynamically highly stable compounds, an analogous cyclization of α-addition products would lead to thermodynamically unfavored four-membered ring compounds. In the case of the products investigated by us, it could further be assumed that the free energy level of the cyclized γ-addition products should also be lower than that of the non-cyclized α-addition products; hence, the isolation, in high yield, of cyclized γ-addition products after reasonable reaction times would become plausible. Such a "thermodynamic" hypothesis had already been considered by Nielsen in order to rationalize the dimerization of 2-ethyl 2-hexenal (29) and would have explained the α-orientation of cyanoethylations of rigid *transoid* α,β-unsaturated carbonyl systems (30, 31), since in these instances the cage-like cyclized γ-addition products would not be thermodynamically favored. In a previous publication (24) we have shown that such a hypothesis could not be confirmed by the drastic reduction of the reaction time of acrylonitrile with 3β-acetoxy-5α-pregn-17-en-21-al (**10**), since even in that instance no α-addition products could be isolated. However, the cyanoethylation of ketone **5**, in which both α- and γ-addition products are formed, lent itself to a more convincing verification, since a variation of the reaction time should necessarily lead to a variation of the proportion of the addition products, if the "thermodynamic" hypothesis were accurate. We therefore subjected ketone **5** to cyanoethylations, under "standard" conditions, with the exception of the length of the reaction times. The results are summarized in Table 1. It can be seen that such a variation of the reaction time does not change the proportion of α- and γ-cyanoethylated products, and that the "thermodynamic" hypothesis has to be abandoned.[8]

Although the argument that the "atypical" γ-cyanoethylations were due to atypical charge distributions in certain anions derived from α,β-unsaturated carbonyl compounds (the γ-carbon atom being more negative than the α-carbon

TABLE 1

Proportion of α- and γ-cyanoethylation products of ketone **5** in relation to the reaction time

Reaction time	Proportion of α- and γ-cyanoethylated products
t*	2.08
$4t$	2.13
$12t$	2.10
$24t$	2.11

*t = 15 min at 24°, 25 min at 55°, and 60 min at 24°.

[6]After completion of our experiments, Wiemann *et al.* (26) published results confirmatory to ours. They report that addition of acrylonitrile to mesityl oxide does not only give, as previously observed by Bruson and Riener (27), an α,α-dicyanoethylated derivative, but also some cyclized γ-cyanoethylation product.

[7]For literature references see the discussion in Part II of this series (4) and in particular ref. 28 of the present paper.

[8]We also subjected one of the two isomeric α-addition products (**4A**) to the cyanoethylation conditions but were not able to observe the formation of any γ-cyanoethylated product; the main result was an epimerization in position 20, leading to isomer **4B**. In itself, this experiment is not conclusive because, in order to equilibrate a non-anionic α-addition product of type **4** to a cyclized addition product of type **7** or **8**, one would have to abstract a proton in position α to the nitrile function, whereas, evidently, the 20-proton should be abstracted far more readily.

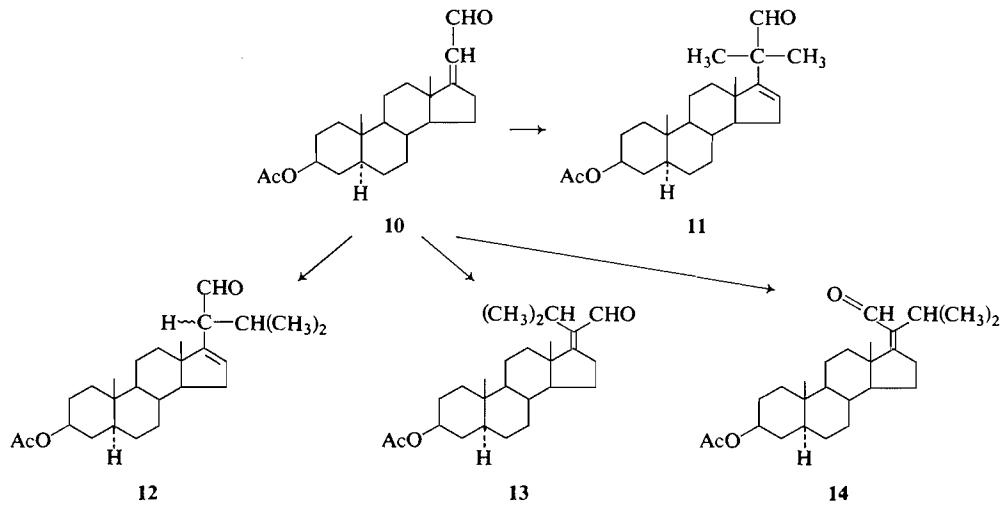

atom) was not attractive, we subjected, for experimental proof, aldehyde **10**, which had given in high yields cyclized γ-cyanoethylation products (3, 4), to the action of methyl iodide in the presence of *t*-butoxide in *t*-butanol, under the reaction conditions of Woodward *et al.* (32). After the recovery of 22% of starting material, we isolated in 98% the 20,20-dimethylated product **11** and did not detect a trace of a γ-addition product. The structure determination of the dimethylated aldehyde **11** was based on its elemental analysis and its spectral characteristics. The i.r. spectrum confirms the presence of the non-conjugated aldehyde function and of the isolated double bond of the five-membered ring, whose absorption band appears at 1605 cm^{-1}. The n.m.r. spectrum shows the four methyl groups (in positions 18, 19, and 20), the only olefinic proton (in position 16) and the proton of the aldehyde function. The experiment confirms that in the anion derived from aldehyde **10** the α-carbon atom is more negative than the γ-carbon atom.

We were also able to rule out the possibility that the γ-cyanoethylations observed were due to steric hindrance in the α-position, by subjecting aldehyde **10** to alkylation with a bulky reagent, isopropyl iodide. After recovery of 23% of starting material, three mono-α-alkylation products (**12**, **13**, and **14**) were isolated in 97% yield. Their mass (400) was indicative of the addition of one isopropyl moiety, which is plausible in view of the steric hindrance exerted by the 18-methyl group. Aldehyde **12** shows in the i.r. characteristic bands of a non-conjugated unsaturated aldehyde. In the n.m.r. one observes, among other signals, a not well defined triplet at 5.61 δ with a coupling constant of 2.5 Hz, which we assign to the olefinic proton in position 16, and a doublet at 11.04 δ (J = 4.5 Hz) which corresponds to the aldehydic proton coupled with the only proton in position 20. These spectral characteristics cannot satisfy a product arising from a γ-alkylation since such a derivative would possess either a conjugated carbonyl function or a tetra-substituted double bond in positions 16,17.

The aldehydes **13** and **14** absorb in the u.v. at 253 and 252 nm, respectively; these values correspond well to those calculated for such systems (33). In the i.r., aldehydes **13** and **14** show the typical absorptions of α,β-unsaturated aldehydes. In the n.m.r., no olefinic proton is visible and the aldehydic proton appears as a singlet. The 16-protons appear as multiplets, at 2.52 δ for aldehyde **13**, and at 2.40 δ for aldehyde **14**. The greater shielding of these protons in isomer **14** suggests the proximity of the isopropyl group. Again, these data exclude structures corresponding to an addition in position 16. Steric hindrance can therefore be eliminated as explanation for the observed γ-cyanoethylations.

In a previous publication (24), we have already excluded the possibility that the observed γ-cyanoethylations were not Michael-type reactions but that they represented Diels–Alder-like additions to an enolic form of the carbonyl derivatives.

Can. J. Chem. Downloaded from www.nrcresearchpress.com by 210.87.254.42 on 09/05/12
For personal use only.

Can. J. Chem. Downloaded from www.nrcresearchpress.com by 210.87.254.42 on 09/05/12
For personal use only.

The observation that no γ-cyanoethylation of α,β-unsaturated carbonyl compounds seems to occur in the case of a rigid *transoid* arrangement of the unsaturated system, for instance in the case of the cyanoethylation of isophorone (31) or of Woodward's tricyclic ketone (30), and the consideration of the particular stereochemistry of α,β-unsaturated carbonyl systems, such as aldehyde **10**, which lend themselves to cyclo-γ-cyanoethylations, made it conceivable that the occurrence of this reaction could be connected to the "geometric predisposition" of such molecules for a cyclo-addition (irrespective of the actual mechanism); indeed, in the cases in which the cyclo-γ-cyanoethylation occurs, the four carbon atoms of the anion tend to assume a *cisoid* arrangement.

Although one could now argue that the alternation of charges, both in the anion and in the electrophile, would favor a γ-addition (by placing the reactants through electrostatic forces in a favorable position), provided a suitable geometry of the anion exists,[9] such a hypothesis suffers from the consideration that the alternation of charges would also be quite favorable for an α-addition. However, the apparent importance of the geometric requirements suggested another hypothesis: that cyanoethylation occurred originally on the most negative center of the mesomeric anion, the oxygen, and that the intermediate anionic enol ether would be then transformed through a cyclic six-membered transition state (*cf.* representation **i**) to a γ-addition product; the driving force for the reaction would be the negative charge in the acrylonitrile moiety.

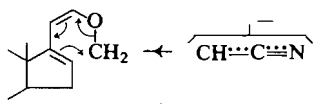

i

Alternatively, one could consider that the transfer would not be concerted but that the acrylonitrile would be released from the oxygen in the vicinity of the negative γ-carbon atom which would capture it immediately, before it could reach, after breaking through the solvent cage, the even more negative α-carbon atom, or before the anion could change its stereochemistry sufficiently for an α-addition[10] (*cf.* Scheme 1).

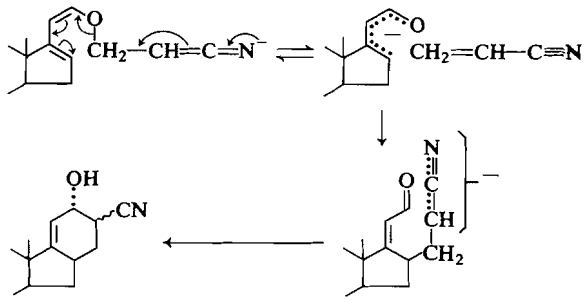

SCHEME 1

In order to investigate the validity of the hypothesis of such transfers, we synthesized from aldehyde **10** the isomeric oxygen-cyanoethylated enol ethers **16** and **17** by subjecting the aldehyde to the action of 3-hydroxypropionitrile and *p*-toluenesulfonic acid (for aldehyde acetylations with this catalyst, *cf.* ref. 34), and by treating the resulting acetal **15** with phosphorous oxychloride in pyridine (*cf.* 35). The enol ethers are unstable and are readily hydrolized to aldehyde **10**. Their mixture was separated by preparative t.l.c.

Treatment of the (analytically pure) mixture of the isomeric enol ethers **16** and **17** with *t*-sodium amylate in benzene at 55° gave a product containing small amounts of the unsaturated aldehyde **10** and which consisted primarily of the main cyanoethylation products of the free aldehyde **10**, the hydroxy nitriles **18** and **19**, and dienonitrile **20**. No reaction took place when the mixture of the enol ethers was heated in refluxing toluene; furthermore, it was necessary to employ for the transformation of the enol ether mixture to the cyclic products a higher concentration of base than in the direct cyanoethylation of aldehyde **10**.[11] Treatment with sodium amylate of the pure *cis* cyano enol ether **16**, also led to the cyclized products; however, these derivatives

[9]Such an assumption could explain, to some extent, that α,β-unsaturated ketones of type **5** are less prone to cyclo-γ-cyanoethylations than the corresponding aldehydes, since the "bulky" substituent of the carbonyl function would not favor a geometry suitable for a 1,4-addition.

[10]We are grateful to Professor Peter Yates, Toronto, Ontario, for his very helpful suggestions concerning a transfer mechanism, and to Professor G. Just, Montreal, Quebec, and Dr. J. Lessard, Sherbrooke, Quebec, for fruitful discussions.

[11]This is not surprising, since the proton α to the nitrile group is not abstracted as readily as the proton α to the conjugated carbonyl group of the aldehyde.

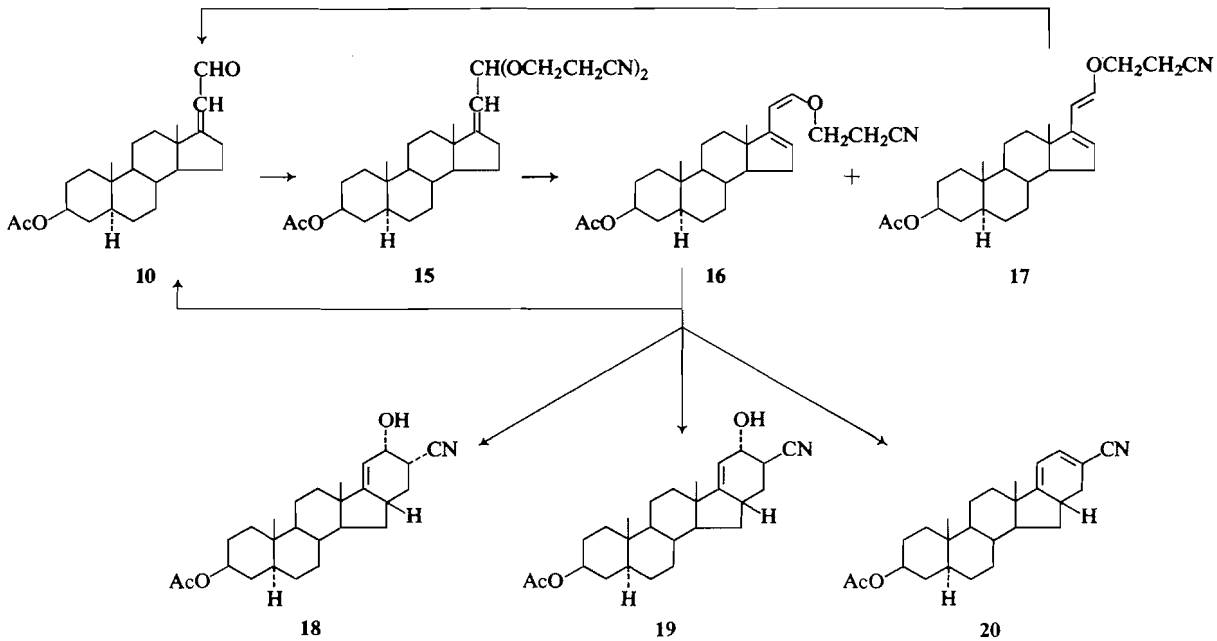

could not be obtained by treatment of the pure *trans* cyano enol ether **17**. In that case, the main products isolated were unchanged enol ether **17** and aldehyde **10**.

These experiments show that under basic conditions the transfer of acrylonitrile from the enolic oxygen of a suitably shaped enol ether of type **16** to the γ-position of the original carbonyl compound indeed takes place; they thus support the explanation of the γ-cyanoethylation based on a transfer reaction from oxygen to the γ-carbon atom. The fact that no transfer reaction occurs in the absence of base seems to indicate that either the negative charge in the propionitrile moiety of the enol ether represents a necessary driving force, or that the reaction is not concerted (*cf.* above). We intend to investigate this problem further. However, whatever the intimate mechanism of the transfer may be, such a reaction seems to represent, for the moment, the only explanation compatible with all experimental findings and accounts well for the importance of stereochemical factors in the orientation of cyanoethylations of α,β-unsaturated carbonyl compounds. We therefore suggest for the formation of cyclic γ-cyanoethylation products a pathway involving initial cyanoethylation on the oxygen, followed by a transfer reaction which, in turn, is followed by an aldol cyclization.

Experimental[12]

Ethyl 3β,17β-Dihydroxy-5α-pregnan-21-oate (2) and Ethyl 3β-Acetoxy-17β-hydroxy-5α-pregnan-21-oate (2a)

To a solution of 1.5 g of 3β-acetoxy-5α-androstan-17-one (1), m.p. 121–121.5°, in 25 ml of absolute benzene, 4.6 g of activated granular zinc and 25 ml of absolute ether were added; 10 ml of the solvents was removed by distillation; and 6.25 ml of ethyl bromoacetate was added. Another 20 ml of solvent was distilled off and after the strongly exothermic reaction had partly subsided, 8 ml of absolute dioxane was added and the mixture was refluxed for 2 h. After cooling, 40 ml of 2 *N* aqueous hydrochloric acid was added dropwise, with stirring, and the mixture was extracted with ether. The ethereal solution was washed with iced saturated sodium bicarbonate and with water and was dried over sodium sulfate. Removal

[12]The melting points were taken in evacuated capillaries and the temperatures were corrected. For column chromatography, neutral aluminum oxide Woelm, activity III, and Davison's silica gel 923 were employed. Thin-layer chromatography was performed with Merck-Darmstadt silica gel. The i.r. spectra were recorded on a Beckman IR-4 spectrophotometer and the u.v. spectra on a Beckman DK-1A instrument. The n.m.r. spectra were recorded on a Varian A-60 spectrometer, tetramethylsilane serving as internal standard and deuteriochloroform as solvent, if not otherwise stated. The rotatory dispersion curves were registered on a Jasco ORD/UV 5 spectropolarimeter, the mass spectra were taken on a Varian M-66 mass spectrometer. The microanalyses were performed by the late Mr. A. Bernhardt, Max Planck Institute for Coal Research, Mülheim, Germany, and by Dr. F. Pascher, Bonn, Germany, to whom we are much indebted.

Can. J. Chem. Downloaded from www.nrcresearchpress.com by 210.87.254.42 on 09/05/12
For personal use only.

Can. J. Chem. Downloaded from www.nrcresearchpress.com by 210.87.254.42 on 09/05/12
For personal use only.

of the solvent gave 3.22 g of a dark residue which was chromatographed on 100 g of aluminum oxide. Elutions with petroleum ether and petroleum ether – benzene mixtures (9:1, 4:1, and 1:1) gave 800 mg (42%) of *ethyl 3β-acetoxy-17β-hydroxy-5α-pregnan-21-oate (2a)*, m.p. 98–100°. A sample was recrystallized twice from hexane; m.p. 100–101°; $[\alpha]_D^{25}$ −30.1° (*c*, 1.00 in $CHCl_3$); ν_{max} (KBr) 3550 (hydroxyl), 1745 (acetate), 1735 (ethyl ester), 1290, 1270, 1245, 1188 (ester functions), 1080, 1035, and 1015 cm^{-1} (hydroxyl and acetate); n.m.r.: δ ($CDCl_3$) 0.85 (s) and 0.90 (s) (18- and 19-CH_3), 1.28 (t, J = 7.0 Hz) (O—CH_2—CH_3), 2.00 (s) (CH_3COO), 2.45 (d) and 2.58 (d) (AB system, J = 16.0 Hz) (20-CH_2), 4.15 (s) (exchanged with D_2O) (17β-OH), 4.19 (q, J = 7.0 Hz) (O—CH_2—CH_3), 4.68 (m) (3α-H); mass spectrum: *m/e* 420 (M^+), 402, 387, 360, 342, 333, 328, and 314.

Elutions with petroleum ether – benzene (1:4 and 1:9) and with pure benzene gave 667 mg (39%) of *ethyl 3β,17β-dihydroxy-5α-pregnan-21-oate, (2)*, m.p. 134–135°. A sample was recrystallized three times from ether – hexane for analysis; m.p. 139–140°; $[\alpha]_D^{25}$ −13.5° (*c*, 1.00 in $CHCl_3$); ν_{max} (KBr) 3490 and 3430 (hydroxyls), 1718, 1308, 1238, and 1204 (ester), 1080, 1044, and 1020 cm^{-1} (alcohols); n.m.r.: δ ($CDCl_3$) 0.82 (s) and 0.88 (s) (18- and 19-CH_3), 1.27 (t, J = 7.0 Hz) (O—CH_2—CH_3), 2.07 (s, large) (exchanged with D_2O) (3β-OH), 2.47 (d) and 2.55 (d) (AB system, J = 16.0 Hz) (20-CH_2), 3.55 (m) (3α-H), 4.17 (q, J = 7.0 Hz) (O—CH_2—CH_3), 4.22 (s) (exchanged with D_2O) (17β-OH).

Anal. Calcd. for $C_{23}H_{38}O_4$: C, 72.97; H, 10.12. Found: C, 73.01; H, 10.09.

Ethyl 3β,17β-Diacetoxy-5α-pregnan-21-oate (2b)

(a) From the Acetoxy Hydroxy Ethyl Ester 2a

A solution of 717 mg of ethyl 3β-acetoxy-17β-hydroxy-5α-pregnan-21-oate (**2a**), m.p. 100–101°, in 14 ml of acetic anhydride and 28 ml of acetic acid was treated at room temperature for 15 h with 680 mg of *p*-toluenesulfonic acid. To the cooled solution, 20 ml of methanol was added and the product was extracted with ether. The organic phase was washed with a cold saturated sodium bicarbonate solution and with water and was dried over sodium sulfate. Evaporation of the solvent gave 800 mg of crystalline ethyl 3β,17β-diacetoxy-5α-pregnan-21-oate (**2b**), m.p. 129–132°. A sample was recrystallized three times from ether–hexane for analysis; m.p. 141–141.5°; $[\alpha]_D^{25}$ +18.0° (*c*, 1.00 in $CHCl_3$); ν_{max} (KBr) 1750, 1740, 1735, 1250, and 1025 cm^{-1} (ester functions); n.m.r.: δ ($CDCl_3$) 0.84 (s) (18- and 19-CH_3), 1.22 (t, J = 7.0 Hz) (O—CH_2—CH_3), 2.00 (s) (3β- and 17β-CH_3COO), 2.62 (d) and 3.28 (d) (AB system, J = 14.0 Hz) (20-CH_2), 4.17 (q, J = 7.0 Hz) (O—CH_2—CH_3), 4.71 (m) (3α-H).

Anal. Calcd. for $C_{27}H_{42}O_6$: C, 70.10; H, 9.15. Found: C, 70.17; H, 8.98.

(b) From Ethyl 3β,17β-Dihydroxy-5α-pregnan-21-oate (2)

As described under (*a*), 649 mg of ethyl 3β,17β-dihydroxy-5α-pregnan-21-oate (**2**), m.p. 132–134°, was acetylated. There was obtained 780 mg of diacetate **2b**, m.p. 129–132°. Recrystallization raised the m.p. to 140–141°.

Methyl 3β,17β-Dihydroxy-5α-pregnan-21-oate (2c) and Methyl 3β-Acetoxy-17β-hydroxy-5α-pregnan-21-oate (2d)

A solution of 50 g of 3β-acetoxy-5α-androstan-17-one (**1**), m.p. 120–121°, was subjected, under the same reaction conditions as those described for the preparation of the ethyl esters **2** and **2a**, to the action of 140 g of zinc and 84 ml of methyl bromoacetate. The crude reaction product (87 g) was chromatographed on 2.6 kg of aluminum oxide. Petroleum ether – benzene (9:1 and 4:1) eluted 24.7 g (40.5%) of *methyl 3β-acetoxy-17β-hydroxy-5α-pregnan-21-oate (2d)*, m.p. 120–122°. A sample was recrystallized twice from ether – hexane for analysis; m.p. 123–124°; $[\alpha]_D^{23}$ −11.3° (*c*, 1.00 in $CHCl_3$); ν_{max} (KBr) 3540 (hydroxyl), 1735, 1282, 1245, and 1200 (esters), 1038 and 1002 cm^{-1} (hydroxyl and acetate); n.m.r.: δ ($CDCl_3$) 0.83 (s) and 0.88 (s) (18- and 19-CH_3), 1.99 (s) (CH_3COO), 2.46 (d) and 2.59 (d) (AB system, J = 16.0 Hz) (20-CH_2), 3.71 (s) (OCH_3), 4.11 (s) (exchanged with D_2O) (17β-OH), 4.70 (m) (3α-H); mass spectrum: *m/e* 406 (M^+), 388, 373, 346, 333, 328, and 314.

Anal. Calcd. for: $C_{24}H_{38}O_5$: C, 70.90; H, 9.42. Found: C, 71.13; H, 9.25.

Petroleum ether – benzene (1:1 and 1:4) and pure benzene eluted 21.3 g (39.3%) of *methyl 3β,17β-dihydroxy-5α-pregnan-21-oate (2c)*, m.p. 169–171°. Three recrystallizations from ether–hexane gave the analytical sample; m.p. 172–173°; [lit. (36): m.p. 179–181°]; $[\alpha]_D^{25}$ −12.7° (*c*, 1.05 in $CHCl_3$); ν_{max} (KBr) 3450 and 3370 (hydroxyls), 1710, 1300, 1205 (ester), 1078, 1042, 1030, and 1002 cm^{-1} (ester and hydroxyls); n.m.r.: δ ($CDCl_3$) 0.80 (s) and 0.86 (s) (18- and 19-CH_3), 1.87 (s) (exchanged with D_2O) (3β-OH), 2.46 (d) and 2.56 (d) (AB system, J = 16.0 Hz) (20-CH_2), 3.55 (m) (3α-H), 3.67 (s) (OCH_3), 4.11 (s) (exchanged with D_2O) (17β-OH).

Anal. Calcd. for: $C_{22}H_{36}O_4$: C, 72.49; H, 9.96. Found: C, 72.55; H, 9.87.

Methyl 3β,17β-Diacetoxy-5α-pregnan-21-oate (2e)

(a) From Methyl 3β-Acetoxy-17β-hydroxy-5α-pregnan-21-oate (2d)

A quantity of 22.7 g of hydroxy acetoxy methyl ester **2d**, m.p. 120–122°, was acetylated, as described for the corresponding ethyl ester **2a**, with acetic anhydride, acetic acid, and *p*-toluenesulfonic acid. There was obtained 23.5 g of methyl 3β,17β-diacetoxy-5α-pregnan-21-oate (**2e**), m.p. 99–101°. For analysis, a sample was recrystallized three times from hexane; m.p. 103–103.5°; $[\alpha]_D^{25}$ −16.0° (*c*, 1.00 in $CHCl_3$); ν_{max} (KBr) 1740 (large), 1240, 1198, and 1028 cm^{-1} (esters); n.m.r.: δ ($CDCl_3$) 0.84 (s) (18- and 19-CH_3), 1.99 (s) (3β- and 17β-acetates), 2.66 (d) and 3.28 (d) (AB system, J = 14.5 Hz) (20-CH_2), 3.65 (s) (OCH_3), 4.70 (m) (3α-H).

Anal. Calcd. for $C_{26}H_{40}O_6$: C, 69.61; H, 8.99. Found: C, 69.78; H, 8.81.

(b) From Methyl 3β,17β-Dihydroxy-5α-pregnan-21-oate (2c)

A quantity of 2.34 g of methyl 3β,17β-dihydroxy-5α-pregnan-21-oate (**2c**) was treated as described under (*a*) and gave 2.55 g of diacetate **2e**, m.p. 100–101°. The identity of the product with the above-described sample was

Can. J. Chem. Downloaded from www.nrcresearchpress.com by 210.87.254.42 on 09/05/12
For personal use only.

established by the determination of a mixture m.p. and by the comparison of the i.r. spectra.

Ethyl 3β-Hydroxy-5α-pregn-17-en-21-oate (3b)

To a refluxing solution of sodium ethylate in ethanol, prepared from 8.0 g of sodium and 370 ml of absolute ethanol, 9.5 g of ethyl 3β,17β-diacetoxy-5α-pregnan-21-oate (**2b**) in 170 ml of absolute ethanol was added. The mixture was refluxed for 10 min and then allowed to stand at room temperature for another 20 min. The product was poured into ice water and the mixture was extracted with ether. The ethereal layer was washed with water and dried over sodium sulfate. Evaporation of the solvent gave 7.1 g of a residue which, upon crystallization from ether–hexane, gave 4.66 g (63%) of *ethyl 3β-hydroxy-5α-pregn-17-en-21-oate (3b)*, m.p. 149–150.5°. A sample was recrystallized three times from ether–hexane for analysis; m.p. 152–152.5°; $[\alpha]_D^{24}$ + 14.0° (*c*, 1.00 in $CHCl_3$); λ_{max} (EtOH) 222 nm (ε 13 400); ν_{max} (KBr) 3480 (hydroxyl), 1695 (ester), 1650 (double bond), 1280, 1240, and 1180 (ester), 1075, 1050, and 1040 (ester and alcohol), 875 cm^{-1} (double bond); n.m.r.: δ ($CDCl_3$) 0.83 (s) (18- and 19-CH_3), 1.27 (t, J = 7.0 Hz) (O—CH_2—CH_3), 2.00 (s) (exchanged with D_2O) (3β-OH), 2.83 (m) (16-CH_2), 3.58 (m) (3α-H), 4.16 (q) (O—CH_2—CH_3), 5.54 (t, J = 2.5 Hz) (20-H).

Anal. Calcd. for $C_{23}H_{36}O_3$: C, 76.62; H, 10.07. Found: C, 76.84; H, 10.22.

The residue of the mother liquors of the crystallization of the crude product (2.45 g) was chromatographed on 82 g of aluminum oxide. Petroleum ether – benzene mixtures (4:1, 1:1, and 1:4) eluted 806 mg (11%) of the *unsaturated ester 3b*, m.p. 148–150°. Pure benzene eluted 320 mg (4%) of *ethyl 3β,17β-dihydroxy-5α-pregnan-21-oate (2)*, m.p. 139–140°, identified by a mixture m.p. and by the comparison of its i.r. spectrum with that of an authentic sample.

Taking into account the recovery of starting material, in the form of the dihydroxy adduct **2**, the yield of the unsaturated ester **3b**, amounted to 77%.

Acetate 3c

A quantity of 85 mg of the hydroxy ester **3b**, m.p. 149–150°, was treated for 15 h at room temperature with 1.5 ml of acetic anhydride in 3 ml of pyridine. The usual work-up gave 86 mg of ethyl 3β-acetoxy-5α-pregn-17-en-21-oate (**3c**), m.p. 74–76°. The product was recrystallized four times from hexane for analysis; m.p. 79–80°; $[\alpha]_D^{25}$ +14.0° (*c*, 1.00 in $CHCl_3$); λ_{max} (EtOH) 222 nm (ε 15 480); ν_{max} (KBr) 1745 (acetate), 1715 (ethyl ester), 1660 (double bond), 1280, 1250, and 1238 (esters), 1205, 1185, and 1170 (ethyl ester), 1042 and 1030 (esters), 862 cm^{-1} (double bond); n.m.r.: δ ($CDCl_3$) 0.80 (s) and 0.84 (s) (18- and 19-CH_3), 1.25 (t, J = 7.0 Hz) (O—CH_2—CH_3), 2.00 (s) (CH_3COO), 2.84 (m) (16-CH_2), 4.14 (q, J = 7.0 Hz) (O—CH_2—CH_3), 4.68 (m) (3α-H), 5.52 (t, J = 2.5 Hz) (20-H).

Anal. Calcd. for $C_{25}H_{38}O_4$: C, 74.59; H, 9.52. Found: C, 74.47; H, 9.50.

Methyl 3β-Hydroxy-5α-pregn-17-en-21-oate (3d)

To a refluxing solution of sodium methylate in methanol, prepared from 1.45 g of sodium and 70 ml of methanol, 1.74 g of methyl 3β,17β-diacetoxy-5α-pregnan-21-oate (**2e**), m.p. 99–101°, in 29 ml of absolute methanol was added. The mixture was refluxed for 10 min, was left for another 20 min at room temperature, and the product was extracted with ether. The ethereal solution was washed with water and dried over sodium sulfate. Evaporation of the solvent gave a residue (1.22 g) which, upon crystallization from ether–hexane, gave 753 mg (56%) of *methyl 3β-hydroxy-5α-pregn-17-en-21-oate (3d)*, m.p. 178–179°. A sample was recrystallized three times from ether-hexane for analysis; m.p. 180–181° [lit. (8): m.p. 174–176°]; $[\alpha]_D^{25}$ +32.7° (*c*, 1.00 in $CHCl_3$); λ_{max} (EtOH) 221 nm (ε 12 100); ν_{max} (KBr) 3480 (hydroxyl), 1700 (ester), 1652 (double bond), 1200 and 1180 (ester), 1049 and 1022 (ester and hydroxyl), 875 cm^{-1} (double bond); n.m.r.: δ ($CDCl_3$) 0.87 (s) (18- and 19- CH_3), 1.95 (s) (exchanged with D_2O) (3β-OH), 2.95 (m) (16-CH_2), 3.77 (m) (3α-H), 3.86 (s) (O—CH_3), 5.81 (t, J = 2.5 Hz) (20-H).

Anal. Calcd. for $C_{22}H_{34}O_3$: C, 76.26; H, 9.89. Found: C, 76.46; H, 9.78.

The residue of the mother liquors of the crystallization of the crude product (470 mg) was chromatographed on 12 g of aluminum oxide. Petroleum ether – benzene (1:1 and 1:4) eluted 310 mg (23%) of the *hydroxy ester 3d*, m.p. 177–179°. Pure benzene and benzene–ether (1:1) eluted 140 mg (4%) of *methyl 3β,17β-dihydroxy-5α-pregnan-21-oate (2c)*, m.p. 172–173°, identified by a mixture m.p. determination and by the comparison of its i.r. spectrum with that of an authentic sample.

Taking into account the recovery of starting material, in the form of the dihydroxy ester **2c**, the yield of the unsaturated ester **3d** amounted to 79%.

Acetate 3e

A quantity of 100 mg of the hydroxy ester **3d**, m.p. 179–180°, was acetylated with 1.5 ml of acetic anhydride in 3 ml of pyridine in the usual fashion. There was obtained 115 mg of the acetoxy ester **3e**, m.p. 193–194°. The product was recrystallized twice from ether–hexane for analysis; m.p. 194.5–195° [lit. (8): 193–194°]; $[\alpha]_D^{25}$ +15.0° (*c*, 1.00 in $CHCl_3$) [lit. (8): $[\alpha]_D^{17}$ +14.7° and +13.1°]; λ_{max} (EtOH) 221 nm (ε 15 500); ν_{max} (KBr) 1740 (acetate), 1725 (methyl ester), 1660 (double bond), 1245 (large) (esters), 1205, 1185, and 1170 (methyl ester), 1020 (acetate), 860 cm^{-1} (double bond); n.m.r.: δ ($CDCl_3$) 0.80 (s) and 0.84 (s) (18- and 19-CH_3), 2.00 (s) (CH_3COO), 2.82 (m) (16-CH_2), 3.67 (s) (O-CH_3), 4.70 (m) (3α-H), 5.53 (t, J = 2.5 Hz) (20-H).

Anal. Calcd. for $C_{24}H_{36}O_4$: C, 74.19; H, 9.34. Found: C, 74.09; H, 9.27.

3β-Hydroxy-5α-pregn-17-en-21-oic Acid (3)

(a) From Ethyl Ester 3b

A solution of 6.00 g of ethyl 3β-hydroxy-5α-pregn-17-en-21-oate (**3b**), m.p. 150–151°, in 300 ml of dioxane was refluxed with 50 ml of a 7 *N* aqueous potassium hydroxide solution, under nitrogen, for 5 h. The product was poured into ice water and the mixture was extracted with ether. The organic phase was washed with water and dried over sodium sulfate. Evaporation of the solvent gave 927 mg of *starting material, hydroxy ester 3b*, m.p. 149–150°. The aqueous phase of the ether extraction and the first water

Can. J. Chem. Downloaded from www.nrcresearchpress.com by 210.87.254.42 on 09/05/12
For personal use only.

washings were acidified with dilute sulfuric acid to the Congo-blue reaction and the precipitate was extracted with dichloromethane. The organic solution was washed with water and dried over sodium sulfate. Removal of the solvent gave 4.58 g of *3β-hydroxy-5α-pregn-17-en-21-oic acid (3)*, m.p. 242–244°. A sample was recrystallized twice from methanol for analysis; m.p. 245–246° [lit. (7): m.p. 249°, (8): m.p. 247–289°]; $[\alpha]_D^{25}$ +19.6° (*c*, 1.00 in C_2H_5OH) [lit. (8): $[\alpha]_D^{17}$ +25.8°]; λ_{max} (EtOH) 221 nm (ε 13 230); ν_{max} (KBr) 3400 (hydroxyl), 3220–2500 (associated hydroxyl of acid), 1685 (acid), 1650 (double bond), 1200–1188 (large band), 1040, and 1030 cm^{-1} (alcohol); n.m.r.: δ (C_5D_5N) 0.77 (s) and 0.85 (s) (18- and 19-CH_3), 1.98 (s) (exchanged with D_2O) (3β-OH), 3.06 (m) (16-CH_2), 3.76 (m) (3α-H), 5.82 (t, J = 2.5 Hz) (20-H), 9.35 (m) (exchanged with D_2O) (21-COOH).

Anal. Calcd. for $C_{21}H_{32}O_3$: C, 75.86; H, 9.70. Found: C, 75.89; H, 9.80.

Taking into account the recovery of starting material, the yield of acid **3** amounted to 98%.

(b) From Methyl Ester 3d

A solution of 250 mg of methyl 3β-hydroxy-5α-pregn-17-en-21-oate (*3d*), m.p. 179–180°, in 25 ml of dioxane was refluxed with 5 ml of an aqueous 7 *N* potassium hydroxide solution for 5 h, under nitrogen. After cooling, the mixture was poured into ice water and extracted with ether. The product was worked up as described under (*a*). There was obtained 40 mg of *starting material, hydroxy ester* **3***d*, m.p. 177–179°, and 200 mg of *hydroxy acid* **3**, m.p. 243–245°, identified by the determination of a mixture m.p. and the comparison of its i.r. spectrum with that of the sample described above, under (*a*). Taking into account the recovery of starting material, the acid was obtained in 98% yield.

Methylation

A solution of 68 mg of hydroxy acid **3**, m.p. 244–245°, in 5 ml of absolute methanol and 15 ml of absolute ether was treated at 0° with 5 ml of a 3.1% ethereal diazomethane solution. After 15 h, the excess diazomethane was destroyed with acetic acid and the solvents were removed *in vacuo*. Thus, 70 mg of *methyl 3β-hydroxy-5α-pregn-17-en-21-oate (3d)*, m.p. 175–177°, was obtained. The identity of the product was determined by a mixture m.p. and i.r. analysis.

3β-Acetoxy-5α-pregn-17-en-21-oic Acid (3a)

(a) By Acetylation of the Hydroxy Acid 3

A solution of 200 mg of hydroxy acid **3**, m.p. 243–245°, in 3 ml of pyridine was treated for 15 h with 1 ml of acetic anhydride. Subsequently, 3 ml of water was added and the mixture was refluxed for 45 min, cooled, and poured into ice water. The product was extracted with ether, the ethereal solution was washed with cold aqueous hydrochloric acid and with water. Removal of the solvent gave 224 mg of the acetoxy acid **3***a*, m.p. 229–232°. A sample was recrystallized twice from methanol for analysis; m.p. 235–236° [lit. (8): m.p. 234–236°]; $[\alpha]_D^{24}$ +16.2° (*c*, 1.25 in $CHCl_3$) [lit. (8): $[\alpha]_D^{17}$ +17.4°]; λ_{max} (EtOH) 221 nm (ε 14 500); ν_{max} (KBr) 2750–2500 (associated acid hydroxyl), 1735 (acetate), 1682 (acid), 1640 (double bond), 1260, 1240, and 1220 (acid and acetate), 1020 cm^{-1} (acetate); n.m.r.: δ (C_5D_5N) 0.78 (s) (18- and 19-CH_3), 1.99 (s) (CH_3COO), 3.04 (m) (16-CH_2), 4.77 (m) (3α-H), 5.80 (t, J = 2.5 Hz) (20-H), 12.4 (m) (exchanged with D_2O) (COOH).

Anal. Calcd. for $C_{23}H_{34}O_4$: C, 73.76; H, 9.15. Found: C, 73.63; H, 9.12.

(b) From Aldehyde 10

A solution of 1.00 g of 3β-acetoxy-5α-pregn-17-en-21-al (**10**) (3, 4) in 70 ml of absolute acetone was treated at 0° with 3 ml of Jones' reagent (16) and stirred for 20 min. The mixture was poured into ice water and extracted with dichloromethane. The organic phase was washed with water and dried over sodium sulfate. Evaporation of the solvent gave 1.025 g of a residue which, upon crystallization from methanol, gave 257 mg (25%) of acetoxy acid **3***a*, m.p. 229–231°. The mother liquors (750 mg) still contained some aldehyde **10** and were reoxidized under the same conditions. After the usual work-up and crystallization, another 50 mg (5%) of acetoxy acid **3***a*, m.p. 223–229°, was obtained. The mother liquors contained no more aldehyde **10**, or α,β-unsaturated acid **3***a*, and were not further investigated.

3β-Acetoxy-5α-pregn-17-en-21-oic Acid Chloride (6)

A solution of 1.5 g of acetoxy acid **3***a*, m.p. 235–236°, in 12 ml of absolute benzene was treated at 0° with a solution of 2 ml of oxalyl chloride in 10 ml of absolute benzene. The mixture was shaken periodically for 1 h at room temperature. Evaporation of the solvent and of the volatile substances under vacuum gave 1.56 g of acid chloride **6**, m.p. 162–164°; ν_{max} (KBr) 3080 (vinylic hydrogen), 1768 (acid chloride), 1740 (acetate), 1615 (double bond), 1240, 1062, 1035, and 1010 (acetate), 890 and 885, 860 and 850, 830 and 820 (doublets), 790 and 710 cm^{-1}.

Ethyl Ester 3c from Acid Chloride 6

Acid chloride **6**, prepared from 530 mg of acetoxy acid **3***a*, as described above, was dissolved in 6 ml of absolute benzene and treated with 3 ml of absolute ethanol. The mixture was refluxed for 10 min, the solvents were evaporated *in vacuo*, and 535 mg of *ethyl 3β-acetoxy-5α-pregn-17-en-21-oate (3c)*, m.p. 76–77°, was obtained. The identity of the product with an authentic sample (see above) was established by the determination of a mixture m.p. and by comparison of the i.r. spectra.

3β-Acetoxy-21-methyl-5α-pregn-17-en-21-one (5)

Methyl Grignard reagent was prepared from 800 mg of magnesium, 3.5 ml of methyl iodide and 40 ml of absolute ether. There were added 40 ml of absolute ether and, with stirring, 3.2 g of dry cadmium chloride. The mixture was refluxed for 1.5 h and rapidly filtered through sodium sulfate. To the filtrate there was added, within 5 min, with stirring, a solution of 1.56 g of acid chloride **6**, m.p. 165–166°, in 30 ml of absolute ether and 15 ml of absolute benzene. The mixture was refluxed for 1 h, cooled and treated portionwise with 20 ml of an aqueous 10% acetic acid solution. The product was extracted with ether, the organic solution was washed with iced sodium bicarbonate solution and with water, and was dried over sodium sulfate. Evaporation of the solvent gave 1.5 g of 3β-acetoxy-21-methyl-5α-pregn-17-en-21-one (**5**), m.p. 179–181°. A sample was recrystallized three times from ether–hexane for analysis; m.p. 183–184°; $[\alpha]_D^{25}$ −33.8° (*c*, 1.00 in $CHCl_3$); λ_{max} (EtOH) 241

Can. J. Chem. Downloaded from www.nrcresearchpress.com by 210.87.254.42 on 09/05/12
For personal use only.

nm (ε 12 650); ν_{max} (KBr) 1740 (acetate), 1688 and 1620 (Δ^{17}-21-keto doublet), 1255 (shoulder) and 1240 (acetate), 1202, 1185, 1030 (acetate), 860 cm^{-1} (double bond); ν_{max} ($CHCl_3$) 1730, 1685, 1615, 1255, 1230, 1028 cm^{-1}; n.m.r.: δ ($CDCl_3$) 0.78 (s) and 0.83 (s) (19- and 18-CH_3), 1.98 (s) (CH_3COO), 2.14 (s) (21-methyl-21-ketone), 2.82 (m) (16-CH_2), 4.70 (m) (3α-H), 5.92 (t, J = 2.0 Hz) (20-H).

Anal. Calcd. for $C_{24}H_{36}O_3$: C, 77.37; H, 9.74. Found: C, 77.31; H, 9.84.

Cyanoethylation of 3β-Acetoxy-21-methyl-5α-pregn-17-en-21-one (5)

(a) Under "Standard" Conditions (cf. 1, 4): Reaction Time: 3 h at 24°, 5 h at 55°, 12 h at 24°

To a solution of 9.00 g of 3β-acetoxy-21-methyl-5α-pregn-17-en-21-one (**5**), m.p. 183–184°, in 90 ml of absolute benzene was added, with stirring, under nitrogen, 1.5 ml of a 2 *N* solution of *t*-sodium amylate in benzene. To this mixture was added, dropwise and with stirring, in the course of 10 min, 31 ml of a 0.83 *M* acrylonitrile solution in benzene. The mixture was stirred at 24° for 3 h, at 55° for 5 h, and for 12 h at 24°. The product was poured into 800 ml of ice water containing 20 ml of an aqueous 0.1 *M* acetic acid solution and the precipitate was extracted with ether. The organic phase was washed with water and dried over sodium sulfate. Evaporation of the solvent gave 10.1 g of a product which was chromatographed on 300 g of aluminum oxide.

Pure petroleum ether and a mixture of petroleum ether and benzene (9:1) eluted 1.65 g of a mixture containing the starting material **5** and dienonitrile **9**. Fractional crystallization afforded 1.44 g of *starting material, 3β-acetoxy-21-methyl-5α-pregn-17-en-21-one (5)*, m.p. 181–183°, and 130 mg of *3β-acetoxy-16α-ethyl-16²-cyano-21-methyl-16²,21-cyclo-5α-pregna-17,21-diene (9)*, m.p. 186–189°. For analysis, a sample was recrystallized four times from ether–hexane; m.p. 194.5–195°; $[\alpha]_D^{25}$ −268.0° (*c*, 1.00 in $CHCl_3$); λ_{max} (EtOH) 295 nm (ε 9900); ν_{max} (KBr) 3020 (vinylic hydrogen), 2180 (conjugated nitrile), 1740 (acetate), 1660 and 1585 (conjugated double bonds), 1240 and 1028 cm^{-1} (acetate); ν_{max} ($CHCl_3$) 3005, 2245, 1725, 1710, 1609, 1255, 1028 cm^{-1}; n.m.r.: δ ($CDCl_3$) 0.84 (s) (18- and 19-CH_3), 2.00 (s) (CH_3COO), 2.03 (s) (21-CH_3), 2.32 (m) (16¹-CH_2), 2.67 (m) (16-H), 4.70 (m) (3α-H), 5.50 (d, J = 2.5 Hz) (20-H); optical rotatory dispersion (o.r.d.) (*c*, 0.00125 in CH_3OH): $[\alpha]_{500}$ −320, $[\alpha]_{400}$ −640, $[\alpha]_{350}$ −1920, $[\alpha]_{330}$ −4160, $[\alpha]_{314}$ −4800 (min), $[\alpha]_{294}$ −1600, $[\alpha]_{290}$ 0, $[\alpha]_{282}$ +3680, $[\alpha]_{270}$ +6560, $[\alpha]_{260}$ +8000, $[\alpha]_{246}$ +8400 (max), $[\alpha]_{236}$ +8150° (negative Cotton effect).

Anal. Calcd. for $C_{27}H_{37}O_2N$: C, 79.56; H, 9.15; N, 3.44. Found: C, 79.38; H, 9.13; N, 3.58.

In the above-described chromatogram, petroleum ether – benzene (4:1) eluted 1.15 g of *3β-acetoxy-21-oxo-21-methyl-5α,20ξ-chol-16-eno-24-nitrile (4A)*, m.p. 108–110°. Four recrystallizations from ether–hexane gave the analytical sample; m.p. 112.5–113°; $[\alpha]_D^{25}$ +118.5° (*c*, 1.00 in $CHCl_3$); ν_{max} (KBr) 3030 (vinylic hydrogen), 2230 (non-conjugated nitrile), 1735 (acetate), 1718 (ketone), 1620 (double bond), 1245 and 1028 cm^{-1} (acetate); n.m.r.: δ ($CDCl_3$) 0.87 (s) (18- and 19-CH_3), 1.99 (s) (CH_3COO), 2.13 (s) (methyl ketone), 2.25 (m) (CH_2—CN), 3.28 (m) (20-H), 4.70 (m) (3α-H), 5.42 (m) (16-H); o.r.d. (*c*, 0.02 in CH_3OH): $[\alpha]_{400}$ +270, $[\alpha]_{350}$ +480, $[\alpha]_{320}$ +1020, $[\alpha]_{300}$ +2010 (max), $[\alpha]_{290}$ +1320, $[\alpha]_{282}$ 0, $[\alpha]_{270}$ −1200, $[\alpha]_{258}$ −1590 (min), $[\alpha]_{240}$ −1170, $[\alpha]_{230}$ −900° (positive Cotton effect).

Anal. Calcd. for $C_{27}H_{39}O_3N$: C, 76.19; H, 9.24; N, 3.29. Found: C, 76.05; H, 9.33; N, 3.41.

Further elutions with petroleum ether – benzene (4:1) and with petroleum ether – benzene (1:1) afforded 3.30 g of a crystalline eutectic product formed of *keto nitriles 4A and B*; m.p. 95–98°. A sample was recrystallized ten times from ether–hexane for analysis; m.p. 102.5–103°; $[\alpha]_D^{25}$ −16.5° (*c*, 1.00 in $CHCl_3$); ν_{max} (KBr) 2240 (non-conjugated nitrile), 1745 (acetate), 1720 (ketone), 1620 (double bond), 1250, 1240, and 1035 cm^{-1} (acetate); n.m.r.: δ ($CDCl_3$) 0.78 (s), 0.82 (s) and 0.86 (s) (18- and 19-CH_3), 1.99 (s) (CH_3COO), 2.13 (s) (methyl ketone), 2.25 (m) (CH_2—CN), 3.28 (m) (20-H), 4.70 (m) (3α-H), 5.42 (m) and 5.56 (m) (olefinic 16-proton).

Anal. Calcd. for $C_{27}H_{39}O_3N$: C, 76.19; H, 9.24; N, 3.29. Found: C, 76.43; H, 9.49; H, 3.30.

According to the integration of the olefinic protons in the n.m.r. and to the rotation, the product is a eutectic compound formed in a proportion of 1:2 from keto nitriles **4A** and B.

Further elutions in the chromatogram with petroleum ether – benzene (1:4) and with pure benzene gave 1.50 g of *3β-acetoxy-21β-hydroxy-21α-methyl-16α-ethyl-16²β-cyano-16²,21-cyclo-5α-pregn-17-ene (7)*, m.p. 230–233°. A sample was recrystallized three times from ether for analysis; m.p. 240–240.5°; $[\alpha]_D^{25}$ −21.5° (*c*, 1.00 in $CHCl_3$); ν_{max} (KBr) 3460 (hydroxyl), 2225 (non-conjugated nitrile), 1730 (acetate), 1690 (double bond), 1248 (acetate), 1080, 1035, and 1025 cm^{-1} (acetate and alcohol); ν_{max} ($CHCl_3$) 3600, 3480, 3017, 2240, 1730, 1682, 1255, 1027 cm^{-1}; n.m.r.: δ ($CDCl_3$) 0.83 (s) (18-CH_3), 0.85 (s) (19-CH_3), 1.32 (s) (21α-CH_3), 1.99 (s) (CH_3COO), 2.70 (s) (exchanged with D_2O) (21β-OH), 3.02 (m) (16β-H), 3.08 (t, J = 3.2 Hz) (16²α-H), 4.68 (m) (3α-H), 5.05 (d, J = 2.5 Hz) (20-H).

Anal. Calcd. for $C_{27}H_{39}O_3N$: C, 76.19; H, 9.24; N, 3.29. Found: C, 75.99; H, 9.18; N, 3.32.

Benzene–ether (9:1) eluted 490 mg of *3β-acetoxy-21α-hydroxy-21β-methyl-16α-ethyl-16²β-cyano-16²,21-cyclo-5α-pregn-17-ene (8)*, m.p. 250–252°. A sample was recrystallized twice from ether for analysis; m.p. 254–254.5°; $[\alpha]_D^{25}$ +40.0° (*c*, 1.00 in $CHCl_3$); ν_{max} (KBr) 3400 (hydroxyl), 2220 (non-conjugated nitrile), 1725 (acetate), 1680 (double bond), 1270 and 1240 (shoulder) (acetate), 1080 and 1038 cm^{-1} (acetate and hydroxyl); n.m.r.: δ ($CDCl_3$) 0.76 (s) (18-CH_3), 0.87 (s) (19-CH_3), 1.34 (s) (21β-CH_3), 2.00 (s) (CH_3COO), 2.52 (s) (exchanged with D_2O) (21α-OH), 2.75 (m) (16β-H), 3.10 (t, J = 3.2 Hz) (16²α-H), 4.67 (m) (3α-H), 5.17 (d, J = 2.5 Hz) (20-H).

Anal. Calcd. for $C_{27}H_{39}O_3N$: C, 76.19; H, 9.24; N, 3.29. Found: C, 76.22; H, 9.11; H, 3.45.

The end fractions (1.6 g) of the chromatogram, eluted with pure ether and with ether–methanol mixtures, represented very complex mixtures of cyanoethylated products which could not be separated by chromatog-

Can. J. Chem. Downloaded from www.nrcresearchpress.com by 210.87.254.42 on 09/05/12
For personal use only.

raphy; they were not further examined; ν_{max} (KBr) 3450 and 3360 (large hydroxyl bands), 2230 (non-conjugated nitrile), 2170 (conjugated nitrile), 1735 (acetate), 1710 (shoulder) (carbonyl), 1640, 1620, and 1560 (large bands, unsaturations), 1250 and 1030 cm^{-1} (acetate).

In toto, considering the recovery of starting material (1.44 g, 16%), there were obtained 130 mg (1.6%) of dienonitrile **9**, 1.15 g (13.3%) of cyano ketone **4A**, 3.30 g (38%) of a eutectic mixture of cyano ketones **4A** and **B**, 1.50 g (17.3%) of hydroxy nitrile **7**, 490 mg (5.6%) of hydroxynitrile **8**, as well as 1.6 g of unidentified products; α-cyanoethylated products: 51.3%, γ-cyanoethylated products: 24.5%.

(b) Reaction Time: 15 min at 24°, 25 min at 55°, 60 min at 24°

A quantity of 2.15 g of the unsaturated ketone **5**, m.p. 183–184°, was subjected to the cyanoethylation reaction under identical conditions to those described under (*a*) but with the reaction times indicated in the title. The product (2.40 g) was chromatographed on 75 g of aluminum oxide. Petroleum ether – benzene (4:1) eluted 580 mg of a mixture of starting material and dienonitrile **9** from which, by crystallization, 28 mg of *dienonitrile* ***9***, m.p. 191–193°, and 535 mg of *starting material, ketone* ***5***, m.p. 181–183°, were isolated.

Elutions with petroleum ether – benzene (1:1) gave 405 mg of *cyano ketone* ***4A***, m.p. 107–109°, and 340 mg of *3β-acetoxy-21-oxo-21-methyl-5α,20ξ-chol-16-eno-24-nitrile (cyano ketone* ***4B****)*, m.p. 127–129°. A sample was recrystallized four times from ether–hexane for analysis; m.p. 133–133.5°; $[\alpha]_D^{25}$ −83.0° (*c*, 1.00 in $CHCl_3$); ν_{max} (KBr) 3030 (vinylic hydrogen), 2230 (non-conjugated nitrile), 1724 (acetate and ketone), 1615 (double bond), 1238 and 1022 cm^{-1} (acetate); ν_{max} ($CHCl_3$) 3018, 2242, 1723, 1712, 1610, 1255, 1226 cm^{-1}; n.m.r.: δ ($CDCl_3$) 0.78 (s) (18-CH_3), 0.85 (s) (19-CH_3), 1.98 (s) (CH_3COO), 2.12 (s) (methyl ketone), 2.25 (m) (CH_2CN), 3.28 (m) (20-H), 4.70 (m) (3α-H), 5.56 (m) (16-H); o.r.d. (*c*, 0.02 in $CHCl_3$): $[\alpha]_{400}$ −140, $[\alpha]_{350}$ −260, $[\alpha]_{310}$ −1280, $[\alpha]_{302}$ −1540 (min), $[\alpha]_{290}$ −800, $[\alpha]_{282}$ 0, $[\alpha]_{270}$ +1220, $[\alpha]_{257}$ +1470 (max), $[\alpha]_{245}$ +1280° (negative Cotton effect).

Anal. Calcd. for $C_{27}H_{39}O_3N$: C, 76.19; H, 9.24; N, 3.29. Found: C, 76.03; H, 9.19; N, 3.19.

Petroleum ether – benzene (1:4) eluted 188 mg of the *eutectic compound* of *ketones* ***4A*** *and* ***B***, m.p. 98–100°. Benzene and benzene–ether (9:1) eluted 310 mg of *cyano alcohol* ***7***, m.p. 233–235°, benzene–ether (4:1) 110 mg of *cyano alcohol* ***8***, m.p. 250–252°. Again, the last chromatogram fractions (310 mg) were complex mixtures.

In toto, there were obtained (yields calculated on the basis of the recovery of 435 mg of starting material): 28 mg (1.5%) of dienonitrile **9**, 405 mg (22.0%) of cyano ketone **4A**, 340 mg (18.5%) of cyano ketone **4B**, 188 mg of the eutectic mixture of cyano ketones **4A** and **B** (10.2%), 310 mg (16.8%) of cyano alcohol **7**, 110 mg (6%) of cyano alcohol **8**, and 310 mg of unidentified products; α-cyanoethylated products: 50.7%; γ-cyanoethylated products: 24.4%.

(c) Reaction Time: 1 h at 24°, 100 min at 55°, 4 h at 24°

A quantity of 2.00 g of the unsaturated ketone **5** was cyanoethylated under identical conditions as before but using the above-mentioned reaction times. There were obtained 400 mg of *starting material, ketone* ***5***, m.p. 179–181°; 30 mg (1.7%) of *dienonitrile* ***9***, m.p. 189–191°; 260 mg (14.8%) of *cyano ketone* ***4A***, m.p. 106–108°; 640 mg (35%) of the *eutectic mixture* of *ketones* ***4A*** *and* ***B***, m.p. 96–99°; 296 mg (16.2%) of *cyano alcohol* ***7***, m.p. 233–236°; 100 mg (5.5%) of *cyano alcohol* ***8***, m.p. 249–251°; and 340 mg of the above-mentioned complex and unidentified mixtures. The calculation of yields takes into account the recovery of starting material; α-cyanoethylated products: 49.8%; γ-cyanoethylated products: 23.4%.

(d) Reaction Time: 6 h at 24°, 10 h at 55°, 25 h at 24°

From the cyanoethylation of 2.00 g of ketone **5** with the above-mentioned reaction times, there were obtained 220 mg of *starting material, ketone* ***5***, m.p. 178–180°; 40 mg (2.1%) of *dienonitrile* ***9***, m.p. 190–192°; 201 mg (10.3%) of *cyano ketone* ***4A***, m.p. 107–109°; 785 mg (38.6%) of the *eutectic mixture* of *ketones* ***4A*** *and* ***B***, m.p. 98–100°; 322 mg (15.8%) of *cyano alcohol* ***7***, m.p. 230–233°; 108 mg (5.3%) of *cyano alcohol* ***8***, m.p. 250–252°; and 584 mg of the unidentified mixture; α-cyanoethylated products: 48.9%; γ-cyanoethylated products: 23.2%.

Treatment of Cyano Ketone ***4A*** *with t-Sodium Amylate and Acrylonitrile*

To a solution of 300 mg of 3β-acetoxy-21-oxo-21-methyl-5α,20ξ-chol-16-eno-24-nitrile ***4A***, m.p. 110–110.5°, in 8 ml of absolute benzene, 0.1 ml of a 1.3 *N* solution of *t*-sodium amylate in benzene and 1.0 ml of a 0.83 *M* acrylonitrile solution in benzene were added. The mixture was stirred for 3 h at 24°, for 5 h at 55°, and for 12 h at 24°. The usual work-up gave 310 mg of a crude product which was chromatographed on 15 g of aluminum oxide. Elutions with petroleum ether – benzene (1:1) gave 62 mg of *starting material, cyano ketone* ***4A***, m.p. 104–107°. Petroleum ether – benzene (1:4) and pure benzene eluted 236 mg of the *eutectic mixture* of the *ketones* ***4A*** *and* ***B***, m.p. 96–98°.

Dehydration of Cyano Alcohol ***7***

To a solution of 175 mg of 3β-acetoxy-21β-hydroxy-21α-methyl-16α-ethyl-16^2β-cyano-16^2,21-cyclo-5α-pregn-17-ene (**7**), m.p. 237–238°, in 8 ml of acetic acid and 4 ml of acetic anhydride, 170 mg of *p*-toluenesulfonic acid was added and the mixture was stirred at room temperature for 15 h. The product was treated with 5 ml of methanol and poured into ice water. The ether extract was washed with a cold saturated sodium bicarbonate solution and with water and was dried over sodium sulfate. Evaporation of the solvent gave 170 mg of a residue which gave upon crystallization from ether–hexane 91 mg of *dienonitrile* ***9***, m.p. 192–193.5°. The residue of the mother liquors (74 mg) was subjected to preparative t.l.c. (petroleum ether – ether 1:1) and thus gave another 28 mg (16%) of dienonitrile **9**, m.p. 190–192°. The identity of the product was established by the determination of a mixture m.p. and the comparison of the i.r. spectrum with that of an authentic sample. Total yield of *dienonitrile* ***9***: 70%.

Can. J. Chem. Downloaded from www.nrcresearchpress.com by 210.87.254.42 on 09/05/12
For personal use only.

Dehydration of Cyano Alcohol ***8***

Under the conditions described for alcohol **7**, 28 mg of 3β-acetoxy-21α-hydroxy-21β-methyl-16α-ethyl-16²β-cyano-16²,21-cyclo-5α-pregn-17-ene (**8**) was dehydrated with *p*-toluenesulfonic acid in acetic acid and acetic anhydride. The reaction product (26 mg) was subjected to preparative t.l.c., to give 6 mg of *dienonitrile* ***9***, m.p. 191–193° (20% yield).

*Methylation of 3β-Acetoxy-5α-pregn-17-en-21-al (**10**)*

To a solution of 600 mg of aldehyde **10** (3, 4), m.p. 159–160°, in 11 ml of absolute *t*-butanol there was added, under nitrogen and with stirring, a solution of potassium *t*-butoxide in *t*-butanol, prepared from 150 mg of potassium and 3.1 ml of *t*-butanol. Methyl iodide (0.36 ml) was added and the mixture was refluxed for 1 h. After cooling, the product was poured into ice water and extracted with ether. The organic phase was washed with cold 2 *N* hydrochloric acid, with iced sodium bicarbonate solution, and with water and was dried over sodium sulfate. Evaporation of the solvent gave 627 mg of a product which was acetylated with 1 ml of acetic anhydride in 3 ml of pyridine, for 15 h at room temperature. The usual work-up gave 640 mg of a product which was chromatographed on 80 g of silica gel. Benzene – ethyl acetate (97:3) eluted 470 mg of *3β-acetoxy-20,20-dimethyl-5α-pregn-16-en-21-al (**11**)*, m.p. 165–167°. A sample was recrystallized twice from ether–hexane for analysis; m.p. 168–169°; $[\alpha]_D^{25}$ +19.7° (*c*, 1.00 in $CHCl_3$); ν_{max} (KBr) 3050 (vinylic hydrogen), 2700 (aldehyde), 1740 (large acetate and aldehyde band), 1605 (double bond), 1250 and 1040 cm^{-1} (acetate); n.m.r.: δ ($CDCl_3$) 0.82 (s) and 0.85 (s) (18- and 19-CH_3), 1.18 (s) and 1.22 (s) (20,20-dimethyl), 1.99 (s) (CH_3COO), 4.68 (m) (3α-H), 5.65 (m) (16-H), 9.34 (s) (21-H).

Anal. Calcd. for $C_{25}H_{38}O_3$: C, 77.67; H, 9.91. Found: C, 77.62; H, 9.85.

Elutions with benzene – ethyl acetate (95:5 and 90:10) gave 135 mg of *starting material, aldehyde **10***, m.p. 155–157°. Considering this recovery, the total yield of methylation amounted to 98%.

Isopropylation of Aldehyde ***10***

To a solution of 2.00 g of aldehyde **10**, m.p. 159–160°, in 40 ml of *t*-butanol, a solution of potassium *t*-butoxide in *t*-butanol, prepared from 500 mg of potassium and 10 ml of *t*-butanol, was added. The solution was refluxed with 0.4 ml of isopropyl iodide for 2 h. The product was worked-up as described for the methylation experiment and yielded 2.20 g of a product which was acetylated with 7 ml of acetic anhydride in 18 ml of pyridine. The crude reaction product (2.23 g) was chromatographed on 300 g of silica gel. Elutions with benzene – ethyl acetate (97:3) gave 1.65 g of a mixture of three products which were separated by preparative t.l.c. (petroleum ether – ether 1:1). Thus there were isolated:

(*1*) 535 mg of *3β-acetoxy-20ξ-isopropyl-5α-pregn-16-en-21-al (**12**)*, m.p. 170–172°, ν_{max} (KBr) 3050 (vinylic hydrogen), 2700 (aldehyde), 1740 (acetate), 1730 (non-conjugated aldehyde), 1605 (double bond), 1250 and 1025 cm^{-1} (acetate); n.m.r.: δ ($CDCl_3$) 0.86 (s) (18- and 19-CH_3), 1.27 (ill-defined multiplet) [$(CH_3)_2CH$], 2.00 (s) (CH_3COO), 2.48 (m) (20-H), 4.71 (m) (3α-H), 5.61 (large triplet, J = 2.5 Hz) (16-H), 11.04 (d, J = 4.5 Hz) (21-H); mass spectrum: *m/e* 400 (M^+), 385, 371, 343.

(*2*) 530 mg of *3β-acetoxy-20-cis-isopropyl-5α-pregn-17-en-21-al (**13**)*,[13] λ_{max} (EtOH) 253 nm (ε 4000); ν_{max} (KBr) 2760 (aldehyde), 1740 (acetate), 1670 and 1610 (doublet of conjugated aldehyde), 1240 and 1025 cm^{-1} (acetate); n.m.r.: δ ($CDCl_3$) 0.85 (s) and 0.87 (s) (18- and 19-CH_3), 1.12 (d, J = 7.5 Hz) and 1.17 (d, J = 7.5 Hz) (isopropyl methyl groups), 2.02 (s) (CH_3COO), 2.52 (m) (16-CH_2), 4.70 (m) (3α-H), 9.43 (s) (21-H); mass spectrum: *m/e* 400 (M^+), 385, 371, 343.

(*3*) 545 mg of *3β-acetoxy-20-trans-isopropyl-5α-pregn-17-en-21-al (**14**)*,[14] λ_{max} (EtOH) 252 nm (ε 6400); ν_{max} (KBr) 2750 (aldehyde), 1745 (acetate), 1678 and 1615 (doublet of conjugated aldehyde), 1245 and 1025 cm^{-1} (acetate); n.m.r.: δ ($CDCl_3$) 0.85 (s) (18- and 19-CH_3), 1.00 (d, J = 7.0 Hz) and 1.17 (d, J = 7.0 Hz) (isopropyl methyl groups), 2.02 (s) (CH_3COO), 2.40 (m) (16-CH_2), 4.70 (m) (3α-H), 10.05 (s) (21-H); mass spectrum: *m/e* 400 (M^+), 385, 371, 343.

In the original column chromatogram, benzene – ethyl acetate (96:4 and 80:20) eluted 460 mg of *starting material, aldehyde **10***, m.p. 154–156°.

In summary, considering the recovery of starting material, there were obtained 32% (535 mg) of aldehyde **12**, 32% (530 mg) of aldehyde **13**, and 33% (545 mg) of aldehyde **14**.

It was not possible to prepare analytical samples of the isopropylated aldehydes since they decomposed upon recrystallization.

*3β-Acetoxy-21-bis(2′-cyanoethoxy)-5α-pregn-17-ene (**15**)*

From a solution of 10.0 g of 3α-acetoxy-5α-pregn-17-en-21-al (**10**), m.p. 160–161°, in 1 l of absolute benzene, 40 ml of solvent was removed. Freshly distilled hydracrylonitrile (2-hydroxypropionitrile) (110 ml) and 440 mg of *p*-toluenesulfonic acid were added and the mixture was refluxed for 15 h, moist benzene being removed periodically. After cooling, the mixture was poured into ice water containing sodium bicarbonate and the precipitate was extracted with ether. The organic solution was washed with a cold saturated sodium bicarbonate solution and with water and was dried over sodium sulfate. Removal of the solvent gave 13.4 g of a crude product which was chromatographed on 300 g of aluminum oxide, activity III. Petroleum ether – benzene (1:4) and pure benzene eluted 4.886 g of pure acetal **15**, m.p. 65–75°. Recrystallizations from acetone–hexane gave an analytical sample; m.p. 67–79°; $[\alpha]_D^{24}$ +34.1° (*c*, 0.945 in pyridine); ν_{max} (KBr) 2242 (nitrile), 1730 (acetate), 1675 (double bond), 1245 (acetate), 1040 cm^{-1} (acetal).

Anal. Calcd. for $C_{29}H_{42}O_4N_2$: C, 72.16; H, 8.77; N, 5.81. Found: C, 71.50; H, 8.72; N, 5.91.[15]

*3β-Acetoxy-21-(2′-cyanoethoxy)-5α-pregna-16,20-dienes (**16** and **17**)*

A solution of 1.2 g of acetal **15** in 5.0 ml of absolute toluene was added to a mixture of 0.24 ml of freshly

[13] *cis* With respect to the 13-position.

[14] *trans* Refers to the 13-position.

[15] No better values for carbon could be obtained.

Can. J. Chem. Downloaded from www.nrcresearchpress.com by 210.87.254.42 on 09/05/12
For personal use only.

distilled phosphorous oxychloride, 2.0 ml of pyridine, and 5 ml of absolute toluene. The mixture was stirred under nitrogen for 45 min at 95°, cooled and poured into 50 ml of cold saturated sodium bicarbonate solution. The product was extracted with benzene and was washed with saturated sodium bicarbonate and dried over sodium sulfate. Removal of the solvent gave 1.0 g of a crude product which crystallized from benzene – petroleum ether. Thin-layer chromatography indicated two components (**16** and **17**). They could not be separated by crystallization. A sample of the mixture was recrystallized twice for analysis; m.p. 172–173°; ν_{max} (KBr) 2250 (nitrile), 1715 (acetate), 1640 and 1575 (diene), 1260 (acetate), 1020 cm^{-1} (ether).

Anal. Calcd. for $C_{26}H_{37}N_3$: C, 75.87; H, 9.06; N, 3.40. Found: C, 75.62; H, 8.84; N, 3.15.

A sample of 110 mg of this product was subjected to preparative t.l.c. (petroleum ether – ether – ethyl acetate 6:4:1). Thus, 49 mg of homogenous *cis enol ether* ***16*** (R_F 0.57) was obtained; recrystallization from benzene – petroleum ether gave the analytical sample; m.p. 172–174°, $[\alpha]_D^{24}$ +36.4° (*c*, 0.985 in pyridine); λ_{max} (EtOH) 245 nm (ε 14 500); ν_{max} (KBr) 2250 (nitrile), 1720 (acetate), 1645 and 1635 (split band) (diene), 1575 (charact. band of the *cis* isomer), 1260 (acetate), 1025 cm^{-1} (ether); n.m.r.:[16] δ (C_5D_5N) 0.76 (s) and 0.82 (s) (18- and 19-CH_3), 1.96 (s) (CH_3COO), 2.88 (t, J = 6 Hz) (—CH_2—CN), 3.88 (t, J = 6 Hz) (—O—CH_2—), 4.7 (m) (ill def.) (3α-H), 5.56 (d, J = 13 Hz) (20-H), 6.78 (d, J = 13 Hz) (21-H); mass spectrum: *m/e* 411 (M^+), 396, 336, 265, 242, 228, 189.

Anal. Calcd. for $C_{26}H_{37}O_3N$: C, 75.87; H, 9.06; N, 3.40. Found: C, 75.67; H, 8.98; N, 3.32.

The *trans enol ether* ***17*** (38 mg, R_F 0.7) was recrystallized from benzene – petroleum ether; m.p. 154–158°; λ_{max} (EtOH) 254 nm (ε 12 800); ν_{max} (KBr) 2250 (nitrile), 1730 and 1720 (split band) (acetate), 1640 and 1635 (split band) (diene), 1250 (acetate), and 1025 cm^{-1} (ether); mass spectrum: *m/e* 411 (M^+), 396, 336, 265, 242, 228, 189.

Anal. Calcd. for $C_{26}H_{37}O_3N$: C, 75.87; H, 9.06; N, 3.40. Found: C, 76.07; H, 8.90; N, 3.65.

Reaction of the Mixture of Enol Ethers ***16*** *and* ***17*** *with t-Sodium Amylate*

A 1.85 *N* solution (0.18 ml) of *t*-sodium amylate in absolute benzene was added to a solution of 409 mg of the mixture of the enol ethers **16** and **17** in 5 ml of absolute benzene. The mixture was stirred under nitrogen at room temperature for 2 h. The product was poured into crushed ice (25 ml) and extracted with ether. The ethereal layer was washed with water and dried over sodium sulfate. Removal of the solvent gave 380 mg of a solid product which was separated by preparative t.l.c. (petroleum ether – ether – ethyl acetate 4:6:1). There was obtained 107 mg (25% yield) of *3β-acetoxy-16α-ethyl-16²α-cyano-16²,21-cyclo-5α-pregn-17-en-21α-ol* ***(18)***, m.p. 219–221°, not depressed upon admixture of an authentic sample (4). The identity of the product was further confirmed by the comparison of its i.r. spectrum with that of authentic material. There was further obtained 92 mg (20% yield) of *3β-acetoxy-16α-ethyl-16²β-cyano-16²,21-cyclo-5α-pregn-17-en-21α-ol* ***(19)***, m.p. 208–210°, not depressed upon admixture of an authentic sample. The i.r. analysis confirmed the structure. As a third component, 30 mg (7.3% yield) of *3β-acetoxy-16α-ethyl-16²-cyano-16²,21-cyclo-5α-pregna-17,21-diene* ***(20)***, m.p. 166–167°, λ_{max} (EtOH) 295 nm (ε 10 350), was obtained. The identity was confirmed by i.r. analysis and by the determination of a mixture m.p. Furthermore, 20 mg (5.6%) of *aldehyde* ***10*** was isolated.

When the same reaction was carried out on 510 mg of the mixture of enol ethers **16** and **17**, with a lower concentration of base (0.05 ml of a 1.85 *N t*-sodium amylate solution), no cyclization occurred.

Also, when 40 mg of this mixture of enol ethers **16** and **17** was heated for 25 h under reflux in toluene, no reaction took place.

Reaction of the Cis Enol Ether ***16*** *with t-Sodium Amylate*

A quantity of 0.03 ml of a 1.65 *N* sodium *t*-amylate solution in absolute benzene was added to 57 mg of enol ether **16**, in 1 ml of absolute benzene. The reaction was carried out as described above and there was obtained, by preparative t.l.c. of the product, 16 mg (28%) of hydroxy nitrile **18**, m.p. 219–221°, 9 mg (16%) of hydroxy nitrile **19**, m.p. 208–210°, and 2 mg (3%) of dienonitrile **20**, m.p. 166–167°.

Reaction of the Trans Enol Ether ***17*** *with t-Sodium Amylate*

A 1.65 *N t*-sodium amylate solution (0.015 ml) in absolute benzene was added to a solution of 29 mg of the *trans* enol ether **17**, in 1 ml of absolute benzene and the reaction mixture was stirred under nitrogen at room temperature for 2 h. The product was worked up as described above. The crude product (23 mg) was subjected to preparative t.l.c. There were obtained: 5 mg (17%) of the *starting material, trans enol ether* ***17***, and 3 mg (12%) of *aldehyde* ***10***. The products were identified in the usual fashion. No cyclized products of types **18**, **19**, and **20**, could be detected.

Sincere thanks are due to Mrs. J. Capitaine for expert assistance in some of the experiments and to Mr. D. Capitaine and Mrs. G. Pelletier for devoted technical assistance. One of us, (V.S.S.) gratefully acknowledges the award of a Laval University post-doctorate fellowship, another (L.R.) the award of NRCC scholarships. We express our appreciation to the National Research Council of Canada, to Ayerst Laboratories, Montreal, Quebec, and to the Schering Corporation, Bloomfield, New Jersey for financial support. We sincerely thank Ayerst Laboratories for providing us with starting material.

1. CH. R. ENGEL and L. RUEST. Can. J. Chem. **48**, 3136 (1970).
2. CH. R. ENGEL, J. LESSARD, L. RUEST, and S. BORY. Abstracts of communications. 5th International symposium on the chemistry of natural products. London, 1968, pp. 358–359.
3. CH. R. ENGEL and J. LESSARD. J. Amer. Chem. Soc. **85**, 638 (1963).

[16]Taken on a Varian HA 100 instrument. We are indebted to Prof. G. Just, Montreal, Quebec, for this spectrum.

4. CH. R. ENGEL and J. LESSARD. Can. J. Chem. **48**, 2819 (1970).
5. CH. R. ENGEL and J. LESSARD. Abstracts of communications. 2nd International symposium on the chemistry of natural products. Prague, 1962. p. 34.
6. (*a*) J. LESSARD and CH. R. ENGEL. Ann. ACFAS. **30**, 53 (1964). (*b*) J. LESSARD and CH. R. ENGEL. Ann. ACFAS. **34**, 42 (1967).
7. R. E. MARKER, H. M. CROOKS, JR., R. B. WAGNER, and E. L. WITTBECKER. J. Amer. Chem. Soc. **64**, 2089 (1942).
8. PL. A. PLATTNER, H. HEUSSER, and S. F. BOYCE. Helv. Chim. Acta, **31**, 603 (1948).
9. R. E. MARKER, H. M. CROOKS, JR., and R. B. WAGNER. J. Amer. Chem. Soc. **64**, 817 (1942).
10. P. L. JULIAN and W. J. KARPEL. J. Amer. Chem. Soc. **72**, 362 (1950).
11. F. SONDHEIMER, O. MANCERA, M. URQUIZA, and G. ROSENKRANZ. J. Amer. Chem. Soc. **77**, 4145 (1955).
12. J. ROMO and A. ROMO DE VIVAR. J. Amer. Chem. Soc. **79**, 1110 (1957).
13. T. REICHSTEIN, H. MÜLLER, C. MEYSTRE, and M. SUTTER. Helv. Chim. Acta, **22**, 741 (1939).
14. PL. A. PLATTNER and W. SCHRECK. Helv. Chim. Acta, **22**, 1178 (1939).
15. D. MAGRATH, D. S. MORRIS, V. PETROW, and R. ROYER. J. Chem. Soc. 2393 (1950).
16. (*a*) K. BOWDEN, I. M. HEILBRON, E. R. H. JONES, and B. C. L. WEEDON. J. Chem. Soc. **39** (1946). (*b*) A. BOWERS, T. G. HALSALL, E. R. H. JONES, and A. J. LEMIN. J. Chem. Soc. 2548 (1953).
17. CH. R. ENGEL. D. Sc. thesis. Swiss Fed. Inst. Techn. Zurich, Switzerland. 1951. pp. 35, 36, 62, 63, 65, 66.
18. R. P. LINSTEAD, L. N. OWEN, and R. F. WEBB. J. Chem. Soc. 1211, 1218, 1225 (1953).
19. R. B. TURNER. J. Amer. Chem. Soc. **75**, 3489 (1953).
20. R. ADAMS and L. H. ULICH. J. Amer. Chem. Soc. **42**, 599 (1920).
21. A. L. WILDS and C. H. SHUNK. J. Amer. Chem. Soc. **70**, 2427 (1948).
22. F. REBER, A. LARDON, and T. REICHSTEIN. Helv. Chim. Acta, **37**, 45 (1954).
23. H. HEUSSER, CH. R. ENGEL, P. T. HERZIG, and PL. A. PLATTNER. Helv. Chim. Acta, **33**, 2229 (1950).
24. S. BORY and CH. R. ENGEL. Bull. Soc. Chim. Fr. 3043 (1970).
25. A. MOSCOWITZ, E. CHARNEY, U. WEISS, and H. ZIFFER. J. Amer. Chem. Soc. **83**, 4661 (1961).
26. J. W. WIEMANN, J. CHABALIER, O. CONVERT, and M. L. BOUGUERRA. C. R. Acad. Sci. **264**, 1186 (1967).
27. H. A. BRUSON and T. W. RIENER. J. Amer. Chem. Soc. **65**, 18 (1943).
28. J. WARKENTIN and L. K. M. LAM. Can. J. Chem. **42**, 1676 (1964).
29. A. T. NIELSEN. J. Amer. Chem. Soc. **79**, 2524 (1957).
30. R. B. WOODWARD, F. SONDHEIMER, D. TAUB, K. HEUSLER, and W. M. MCLAMORE. J. Amer. Chem. Soc. **74**, 4223 (1954).
31. S. JULIA. C. R. Acad. Sci. **237**, 913 (1953). Bull. Soc. Chim. Fr. 780 (1954).
32. R. B. WOODWARD, A. A. PATCHETT, D. H. R. BARTON, D. A. J. IVES, and R. B. KELLY. J. Amer. Chem. Soc. **76**, 2852 (1954).
33. R. B. WOODWARD. J. Amer. Chem. Soc. **63**, 1123 (1941). J. Amer. Chem. Soc. **64**, 72, 76 (1942).
34. J. BÉDUWÉ. Bull. Soc. Chim. Belgique, **34**, 41 (1925).
35. O. ISLER, M. MONTAVON, R. RÜEGG, and P. ZELLER. Helv. Chim. Acta, **39**, 259 (1956).
36. K. GÄTZI. Helv. Chim. Acta, **22**, 753 (1939).

Can. J. Chem. Downloaded from www.nrcresearchpress.com by 210.87.254.42 on 09/05/12
For personal use only.

Can. J. Chem. Downloaded from www.nrcresearchpress.com by 210.87.254.105 on 09/05/12
For personal use only.

Electron spin resonance study of the 1,3,5-trinitrobenzene–NaOH system

A. R. NORRIS, A. BRECK, W. DEPEW, AND J. K. S. WAN
Department of Chemistry, Queen's University, Kingston, Ontario

Received July 14, 1969[1]

Electron spin resonance spectra were observed in an aqueous system containing 1,3,5-trinitrobenzene and concentrated sodium hydroxide at 0 to 40 °C. From the hyperfine structure of the spectra and temperature studies, it is concluded that the paramagnetic species is a radical generated by reduction of a 1,3,5-trinitrobenzene–OH^- σ-complex. The spectral assignments were supported by using deuterated 1,3,5-trinitrobenzene.

Canadian Journal of Chemistry, **48**, 3440 (1970)

Introduction

Nitroaromatic compounds can generally be converted into radical anions by accepting a charge transferred from a strong base (1). The rate and extent of radical anion formation and the stability of the anion depend on the nature of the solvent, the donor, and the acceptor. Few systematic studies have been made in this area particularly in systems involving 1,3,5-trinitrobenzene in which the predominant reaction with anions is the formation of σ-complexes.

Gold and Rochester (2) failed to observe radical anions from solutions of 1,3,5-trinitrobenzene in methanolic sodium methoxide or from solutions of 2,4,6-trinitroanisole in ethanolic sodium hydroxide. However, 1,3,5-trinitrobenzene and tert-butoxide give a very low concentration of radical anions in *t*-butanol and an appreciable concentration of radical anions in a *t*-butanol–dimethylsulfoxide mixture (3). Electron spin resonance spectra have been observed in basic solutions of 1,3,5-trinitrobenzene and ketones such as acetone, ethylmethyl ketone, diethyl ketone, and cyclohexanone (2), and during the course of a slow reaction between 1,3,5-trinitrobenzene and diethylamine both in the presence and absence of acetone (2, 4).

We wish to report here our observations on the paramagnetic species formed by 1,3,5-trinitrobenzene in concentrated aqueous NaOH solution.

Experimental

Eastman 1,3,5-trinitrobenzene was recrystallized several times from an ethanol–water mixture and dried *in vacuo* over silica gel, m.p. 122 °C. 1,3,5-Trinitrobenzene-d_3 was prepared as described by Buncel and Symons (5), recrystallized from ethanol–water, and dried *in vacuo* to constant weight, m.p. 120.5–121.5 °C. Analysis of the compound, using an i.r. technique described by Symons (6), indicated 91 ± 2% deuteration. "Spectrograde" solvents and reagent grade chemicals were used without further purification.

Samples were contained in a small, flat quartz cell placed in a variable temperature control insert. The e.s.r. spectra were recorded with a Varian 4500–10A X-band spectrometer equipped with a circulator microwave bridge and a Mark II field dial. The magnetic field was calibrated with a Varian F-8A flux meter by monitoring its transmitter frequency with a Hewlett-Packard frequency counter model 5245M. The microwave frequency was measured using the same electronic counter and a Hewlett-Packard frequency converter plug-in model 5256A.

Results and Discussion

The observations which follow arose from attempts to produce the 1,3,5-trinitrobenzene radical anion in the manner described by Kolker and Waters (7, 8). In those experiments the aromatic nitro compounds were dissolved in a 0.10 *M* solution of NaOH in 25% aqueous acetone to give solutions 10^{-2} *M* in the nitro compound. The solutions were then mixed with aqueous solutions 10^{-2} *M* in sodium dithionite and 0.10 *M* in NaOH and flowed through an e.s.r. cavity where e.s.r. spectra were recorded.

In our present experiments we have found that when an aqueous acetone solution (25 volume % water) is made 0.10 *M* in NaOH, two colorless liquid layers begin to form immediately with formation being complete within 30 min at 25 °C. At lower temperatures, *e.g.* at 0 °C, complete separation of the two layers may take several hours. The lower viscous layer which is approximately 3–5% of the total volume of the system, contains more than 50% of the base and little or no acetone. Thus, it is essentially a concentrated solution of sodium hydroxide in water. The lower layer is completely miscible with water but immiscible with acetone. Smaller amounts of total base added lead to smaller volumes of the lower

[1]Revision received June 5, 1970.

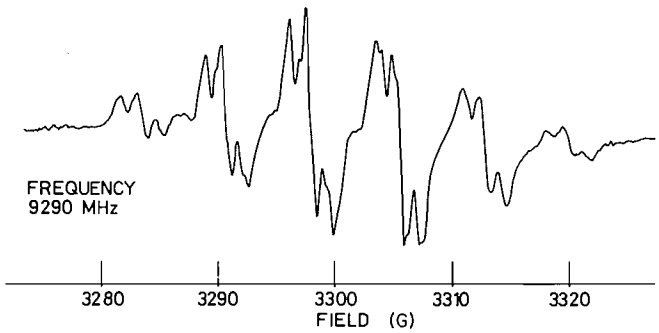

FIG. 1. The e.s.r. spectrum at 30 °C of the species resulting from the interaction of 1,3,5-trinitrobenzene and sodium hydroxide in aqueous solution.

layer. This suggests that the lower layer must contain a certain minimum concentration of NaOH in order for separation to occur.

On addition of 1,3,5-trinitrobenzene (TNB) to the two-layered solution at room temperature a deep wine-red color is formed immediately in the upper layer and a light red–brown color is formed more slowly in the lower layer. Upon standing, the lower layer becomes progressively darker in color (red) and the color of the upper layer fades to a light yellow or yellow–orange. Separation and titration of the two layers at this stage reveals that approximately 85% of the added base is in the lower layer. After 3 days at room temperature, the lower layer is deep brown in color and gives off a strong odor of ammonia. Repeated attempts to separate and characterize the nitroaromatics in this layer were not successful. Other workers have reported the production of 3,5,3′,5′-tetranitroazoxybenzene, 3,5-dinitrophenol and ammonia under similar reaction conditions (9–11).

A strongly basic deeply colored lower layer is also formed when an aqueous acetone solution (25 volume % water) which is 10^{-2} *M* in TNB is made 0.10 *M* in NaOH either at room temperature or at 0 °C. Similar results were obtained employing acetonitrile in place of acetone.

An e.s.r. study was undertaken to reveal the nature of the paramagnetic species formed in the above systems. In the aqueous acetone solutions no e.s.r. absorption was obtained from either the upper or the lower layer immediately after addition of TNB. After several hours at 0 °C, however, the lower layer, now a dark red in color, gave a poorly resolved multi-line e.s.r. spectrum. The resolution of the hyperfine structure of the spectrum increased with temperature up to 40 °C and the original spectrum was reproduced when the sample was returned to 0 °C. A typical spectrum taken at 30 °C is shown in Fig. 1. The spectrum diminished appreciably when the sample was warmed above 50 °C. No e.s.r. spectrum was obtained at any stage from the upper layer.

Although σ-complex **1** would be expected to be the predominant species present in the lower layer (10, 11) the observed e.s.r. spectrum cannot be satisfactorily explained either in terms of a species formed by electron transfer within an ion pair of **1** and Na^+ or on the basis of a radical such as **2** formed by the reduction of **1**. Alternative formulations based on species such as **3** and **4**, which are generated as a result of both substitution and electron transfer processes, seem unlikely in view of the coupling constants reported for these and analogous types of radicals (12, 13).

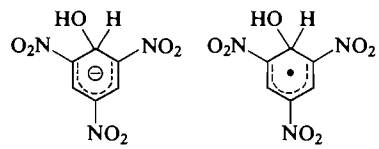

1 **2**

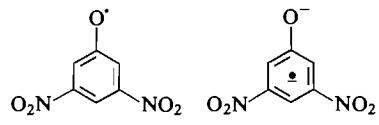

3 **4**

We suggest therefore that the spectrum is due to either **6** or **7**. Both could be generated via reduction of the σ-complex **5** by either Na^+ or uncomplexed TNB. Of the two, **7** might be expected to be the more stable.

Can. J. Chem. Downloaded from www.nrcresearchpress.com by 210.87.254.105 on 09/05/12
For personal use only.

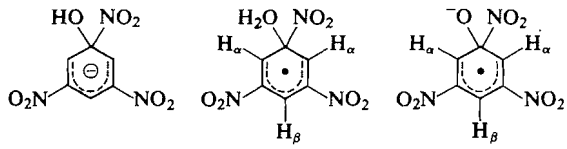

5 6 7

Though spectroscopic evidence for the existence of σ-complexes such as **6** is lacking these species must exist, probably as short-lived intermediates, since substitution of NO_2^- by OH^- is known to occur under the reaction conditions employed in these experiments (10, 11, 14).

An analysis of the spectrum in Fig. 1 in terms of the free radical **7** was made using the following spectral parameters: a_N (in the 3 and 5 positions) = 7.5 ± 0.2 G, $a_{H\alpha}$ = 7.0 ± 0.2 G, $a_{H\beta}$ = 1.4 ± 0.2 G, and maximum slope width 0.6 G. The value of a_H would be expected to be small (15); our e.s.r. studies consequently cannot distinguish between **6** and **7**.

Experiments using deuterated TNB support the above assignments. The spectrum observed at 30 °C (Fig. 2) consisted of five broad lines resulting from the interaction of the electron spin with the two equivalent nitrogen atoms.

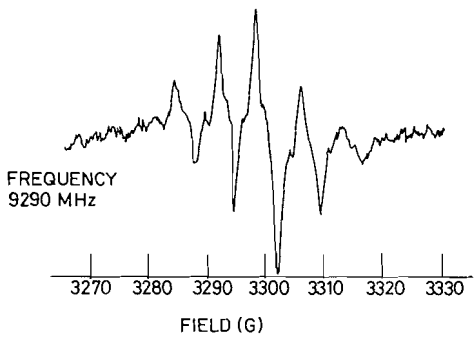

FIG. 2. The e.s.r. spectrum at 30 °C of the species resulting from the interaction of 1,3,5-trinitrobenzene-d_3 and sodium hydroxide in aqueous solution.

The requirements for a high ionic strength environment and a large concentration of σ-complex **5** probably account for the time lag between mixing of solutions and the appearance of an e.s.r. spectrum in the lower layer and for previous failures to observe free radical species in like systems.

Further experiments, designed to differentiate between **6** and **7** and to determine the nature of the reducing agent in this system, are anticipated.

Financial support by the National Research Council of Canada is gratefully acknowledged. One of us (W.D.) wishes to acknowledge support from the McLaughlin Research Fund of Queen's University, Kingston, Ontario. The authors also thank Professor M. C. R. Symons for several valuable suggestions.

1. E. BUNCEL, A. R. NORRIS, and K. E. RUSSELL. Quart. Rev. London, **22**, 127 (1968).
2. V. GOLD and C. H. ROCHESTER. J. Chem. Soc. 1692 (1964).
3. G. A. RUSSELL, E. G. JANZEN, and E. T. STROM. J. Amer. Chem. Soc. **86**, 1807 (1964).
4. R. E. MILLER and W. F. K. WYNNE-JONES. Nature, **186**, 149 (1960).
5. E. BUNCEL and E. A. SYMONS. Can. J. Chem. **44**, 771 (1966).
6. E. A. SYMONS. Ph.D. Thesis, Queen's University, Kingston, Ontario, 1969.
7. P. L. KOLKER and W. A. WATERS. Proc. Chem. Soc. 55 (1963).
8. P. L. KOLKER and W. A. WATERS. J. Chem. Soc. 1136 (1964).
9. A. CAHOURS. Ann. Chim. (3), **25**, 26 (1849).
10. V. GOLD and C. H. ROCHESTER. Proc. Chem. Soc. 403 (1960).
11. V. GOLD and C. H. ROCHESTER. J. Chem. Soc. 1710 (1964).
12. PETER B. AYSCOUGH. Electron spin resonance in chemistry, 1st Ed. Methuen and Co. Ltd., London, 1967. p. 287.
13. R. J. FABER and G. K. FRAENKEL. J. Chem. Phys. **47**, 2462 (1967).
14. J. SAUER and R. HUISGEN. Ang. Chem. **72**, 294 (1960).
15. PETER B. AYSCOUGH. Electron spin resonance in chemistry, 1st Ed. Methuen and Co. Ltd., London, 1967. p. 298.

Can. J. Chem. Downloaded from www.nrcresearchpress.com by 210.87.254.105 on 09/05/12
For personal use only.

Can. J. Chem. Downloaded from www.nrcresearchpress.com by 210.87.254.42 on 09/05/12
For personal use only.

NOTES

Stabilities of nickel–alkyl compounds

J. THOMSON AND M. C. BAIRD
Department of Chemistry, Queen's University, Kingston, Ontario

Received April 30, 1970

The compounds π-$C_5H_5Ni(PPh_3)R$ (R = Me, Et, *n*-Pr, *iso*-Pr, *n*-Bu, *sec*-Bu, *iso*-Bu) have been prepared and characterized. Thermal decomposition of these compounds in xylene solution yields, in all cases except the methyl, an olefin and an olefin isomerization catalyst.

Les composés π-$C_5H_5Ni(PPh_3)R$ (R = Me, Et, *n*-Pr, *iso*-Pr, *n*-Bu, *sec*-Bu, *iso*-Bu) ont étés préparés et caractérisés. La décomposition thermique de ces composés dans une solution de xylol produit, en touts cas sauf le méthyle, une oléfine et une catalyte d'isomérization d'oléfine.

Canadian Journal of Chemistry, **48**, 3443 (1970)

Transition metal alkyl compounds have been postulated as intermediates in a number of metal-catalyzed reactions of olefins, and several recent publications (1–5) have been concerned with reactions involving cleavage of metal–carbon σ-bonds. Thus Sneeden and Zeiss (1) have found that trialkyl chromium compounds decompose thermally to give mixtures of alkanes and olefins. Similar products have been reported from the thermal decomposition of *n*-butyl(tri-*n*-butylphosphine)copper(I) (2), diethyl (α,α'-dipyridal)-nickel(II) (3), and diethylbis(α,α'-dipyridal)-iron(II) (4), while reactions of Grignard reagents with transition metal halides have long been known (5) to yield olefins and alkanes, presumably from the decomposition of unstable alkyl–metal derivatives. Some compounds of platinum (6) and ruthenium (7), on the other hand, yield only an olefin, there apparently being no alkanes detected.

Although details of the mechanisms of the formation of the hydrocarbon products from the various systems studied may vary, it seems likely that the saturated hydrocarbons arise from homolytic fission of the metal–carbon bond to yield radicals. These can abstract a hydrogen atom from another alkyl group or the solvent, or can dimerize. Olefins are believed to arise from migration of a β-hydrogen atom to the metal to give an olefin–metal hydride complex (see eq. 1).

This reaction is often reversible, and is believed to be an important step in such reactions as the transition metal-catalyzed isomerization and hydrogenation of olefins (8).

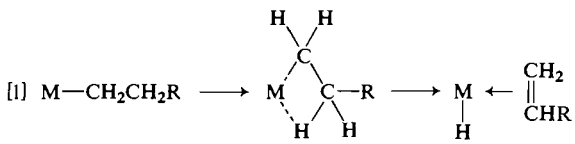

Prompted by some of the above-mentioned studies, we have investigated the properties of the homologous series π-$C_5H_5Ni(PPh_3)R$, where R = methyl, ethyl, *n*-propyl, *iso*-propyl, *n*-butyl, *sec*-butyl, *iso*-butyl and *tert*-butyl. This series is apparently unique, in that it appears to be the only one known in which the higher branched chain derivatives are stable enough to be isolated and characterized; even platinum *sec*- and *iso*-compounds are unknown, although the normal alkyl derivatives are extremely stable (9). Since the product distribution from the thermal decomposition of other metal alkyl compounds seems to depend greatly on both the metal and the nature of the ligands on it, it seemed of interest to investigate the influence of the nature of the alkyl groups.

We also wanted to test the assumption (1) that the stability sequence for metal–alkyl compounds is generally normal > secondary > tertiary. Much of the evidence in the literature pertaining to stabilities of organometallic compounds appears to be based not on direct observations of the compounds concerned, but solely on whether or not they could be prepared. It seemed important to clear up this point if possible because of its obvious bearing on the course of catalytic reactions involving metal–alkyl intermediates.

TABLE 1

Analytical figures for π-$C_5H_5Ni(PPh_3)R$, R = *iso*-Pr, *iso*-Bu

Compound	Found		Calculated	
	Carbon	Hydrogen	Carbon	Hydrogen
π-$C_5H_5Ni(PPh_3)$*iso*-Pr	73.84	6.08	72.75	6.35
π-$C_5H_5Ni(PPh_3)$*iso*-Bu	73.17	6.79	73.16	6.61

Experimental

The n.m.r. spectra were run on Bruker HX-60 and Varian T-60 spectrometers. Melting points were obtained on samples sealed in capillaries under nitrogen using a Gallenkamp melting point apparatus. Some of the operations described below were carried out in a Fisher "Isolator Lab" glovebox. A Beckman GC/2 chromatograph using a Sargent 1 MV full scale recorder and a thirty foot column of 20.8% propylene carbonate on activated alumina (10) was used for identification of hydrocarbons.

Preparation of the Compounds

The compounds π-$C_5H_5Ni(PPh_3)R$ (R = Me, Et, *n*-Pr, *n*-Bu, and *sec*-Bu) have been prepared previously by Yamazaki *et al.* (11) from the reaction of π-$C_5H_5NiPPh_3$-Cl(12) with the appropriate Grignard reagent. In our hands, the rather briefly described experimental procedure of these workers gave only poor yields of the desired products. The following procedure was found to give much better and more consistent results.

The appropriate Grignard reagent (0.02 mole) in 75 ml of a 2:1 benzene – ethyl ether solution was added slowly to a stirred, ice-cooled solution of π-$C_5H_5Ni(PPh_3)Cl$ (0.024 mole) in 100 ml benzene under nitrogen. During the reaction, the color changed from deep red to dark green. The reaction was stirred for 2 h, treated with 5 ml of ethanol to destroy any unreacted Grignard, and then the solvent was removed under reduced pressure.

The residue was redissolved in 50 ml of benzene and the resulting solution was passed through a column of activated alumina (Fisher, 80–200 mesh) which had been de-aerated by a stream of nitrogen. Using a 1:1 mixture of benzene-hexane, the dark green product was the first fraction to be eluted from the column; the volume of the solution was reduced to about 20 ml, 30 ml of hexane were added, and the solution was cooled overnight to give dark green crystals of the product.

The m.p. of the compounds reported previously (11) were in good agreement with the literature values (Table 2). The *iso*-propyl and *iso*-butyl derivatives are new compounds and were analyzed for carbon and hydrogen (Table 1). The former is very air-sensitive, even in the solid state, and a satisfactory analysis could not be obtained. However, its chemistry, n.m.r. spectrum and appearance showed that the material isolated was the desired *iso*-propyl compound.

All the compounds, with the exception of the *iso*-propyl derivative are reasonably stable in solution under nitrogen and even in air for short periods of time in the solid state. The *tert*-butyl derivative could not be prepared; attempts using *tert*-butyl Grignard led only to dark brown mixtures and evolution of isobutene.

The ^1H n.m.r. spectra of all compounds contained a multiplet at about τ 2.33 and a singlet at τ 4.78 $\pm$ 0.03 which may be assigned to the triphenylphosphine and cyclopentadienyl protons, respectively. The aliphatic regions of the spectra are characteristic for each compound, but the resonances overlap considerably and in most cases cannot be interpreted on a first order basis. However, the spectra all integrate satisfactorily for the expected numbers of protons.

TABLE 2

Melting points* of the compounds π-$C_5H_5Ni(PPh_3)R$

R	Melting point °C (lit.)	R	Melting point °C (lit.)
Me	125–126 (126–129)	*n*-Bu	88–89 (88–91)
Et	117–118 (118–120)	*iso*-Bu	91–93
n-Pr	70–71 (75–77)	*sec*-Bu	105–107 (111–112)
iso-Pr	97–99		

*All compounds melted with decomposition.

TABLE 3

Hydrocarbon products from the thermal decomposition of the compounds π-$C_5H_5Ni(PPh_3)R$

R	State	Composition of the gases evolved
Me	Solid	92% Methane, 8% ethane
	Solution	79% Methane, 21% ethane
Et	Solid	88% Ethylene, 12% ethane, trace of butane
	Solution	99% Ethylene, 1% ethane, trace of butane
n-Pr	Solid	99% Propylene, 1% propane
	Solution*	99% Propylene, 1% propane
iso-Pr	Solid	99% Propylene, 1% propane
	Solution	99% Propylene, 1% propane
n-Bu	Solid	87% But-1-ene, 7% *trans*-but-2-ene, 5% *cis*-but-2-ene, 1% butane
	Solution	81% But-1-ene, 11% *trans*-but-2-ene, 7% *cis*-but-2-ene, 1% butane
sec-Bu	Solid	60% But-1-ene, 23% *trans*-but-2-ene, 16% *cis*-but-2-ene, 1% butane
	Solution	63% But-1-ene, 21% *trans*-but-2-ene, 15% *cis*-but-2-ene, 1% butane
iso-Bu	Solid	98% *iso*-Butene, 2% isobutane
	Solution	99% *iso*-Butene, 1% isobutane

*The evolved gases in this case accounted for at least 85% of the nickel compound decomposed.

Thermal Decomposition

Solutions of each of the alkyl compounds in dry

Can. J. Chem. Downloaded from www.nrcresearchpress.com by 210.87.254.42 on 09/05/12
For personal use only.

TABLE 4
Results of the isomerization reactions

Initial gas	Gas composition after 24 h at 100 °C		
	But-1-ene	*trans*-But-2-ene	*cis*-But-2-ene
But-1-ene	75%	15%	10%
cis-But-2-ene	3%	7%	90%
trans-But-2-ene	2%	95%	3%

xylene (b.p. 139°) were refluxed for 1 h and the gases evolved were carried by a stream of nitrogen through a water-cooled condenser (to eliminate xylene) and trapped in a U tube immersed in liquid nitrogen. After decomposition was complete, as shown by a change in color of the solution from green to dark brown, the U tube was evacuated, closed off, and allowed to warm to room temperature. The gases in the U tube were sampled by syringe through a serum cap and identified by gas chromatography.

A different procedure was followed in the case of the methyl derivative because of the low m.p. of methane, one of the expected products. The decomposition was carried out on a solution in α-methylnaphthalene (b.p. 246°) at 140° in a closed, evacuated system and the evolved gases were identified by mass spectroscopy. Solid state decompositions were carried out similarly.

The results of the thermal decomposition of the alkyl–nickel compounds are shown in Table 3.

Isomerization of Butenes

The *n*-propylnickel compound (0.002 mole) in 8 ml dry toluene was placed in each of three Carius tubes and 0.02 mole of each of the linear butene isomers was frozen into each solution. The tubes were sealed, heated for 24 h at 100°, and the gases in the systems were sampled (Table 4).

Discussion

If decomposition temperatures can be taken as a rough guide to thermal stabilities, then the methyl compound is the most stable, followed by the ethyl. Although the *iso*-propyl derivative is relatively air-sensitive and is therefore the most difficult to isolate, it appears, surprisingly, to be more stable thermally than the *n*-propyl compound. Similarly the *sec*-butyl compound appears to be at least as stable as the *n*-butyl and *iso*-butyl compounds. Rausch *et al.* (13) have recently extended the series in the other direction and have shown that the phenyl (dec. 134–135°) and trifluoromethyl (m.p. 160–161° without dec.) compounds are even more stable.

In several cases, the ^{1}H n.m.r. spectra of the compounds in the aliphatic region are too complicated to make assignments without computer analyses. In the case of the methyl compound, the resonance of the methyl protons is centered at τ 10.42 and is a doublet because of coupling with the phosphorus (J = 6 Hz) of the triphenylphosphine. The spectrum of the *iso*-butyl compound contains a strong doublet at τ 9.10 which may be assigned to the six equivalent methyl protons coupled with the methine proton (J = 6 Hz) and a 1:1:1:1 quartet at τ 9.38 which may be assigned to the methylene protons coupled to the methine proton (J = 6 Hz) and the phosphorus atom (J = 9 Hz). The methine resonance would be a multiplet and probably lies under the other st ong lines. The spectrum of the *sec*-butyl compound contains a triplet (τ 9.30) and doublet (τ 8.87) which can be assigned to the two methyl groups. The spectra of the other compounds are too complicated to make assignments.

It has been shown (14) that there is a linear relation between the difference in chemical shifts of the methyl and methylene resonances of the ethyl groups of compounds CH_3CH_2X and the electronegativity of X. Normally the methyl triplet is at higher field than the methylene quartet, but there have been several reports (3, 15) of spectra of ethyl metal compounds in which the methylene resonance is at a similar or even higher field than the methyl resonance, presumably because of the low electronegativity of the metal. The spectrum of the ethyl compound, π-$C_5H_5Ni(PPh_3)Et$, is very similar to the spectra of several ethyl silicon and zinc compounds (15), and thus the π-$C_5H_5Ni(PPh_3)$ group appears to have a rather low electronegativity.

Decomposition of the methyl compound yielded products characteristic of homolysis, as expected. The ethyl compound also showed evidence of homolysis in the solid state, but in solution it and all the higher alkyl compounds yielded only olefins, presumably by β-elimination (eq. 1). In the case of the *n*-propyl compound, it was shown that the propylene produced accounted for at least 85% of the nickel–alkyl compound decomposed, and we assume that in all cases except the methyl, an olefin is the predominant product.

Can. J. Chem. Downloaded from www.nrcresearchpress.com by 210.87.254.42 on 09/05/12
For personal use only.

We have been unable to detect a nickel hydride by n.m.r., but the distribution of products from the *n*-butyl compound and the isomerization of but-1-ene in the presence of the decomposition products from the *n*-propyl compound suggest that such a compound does exist and that the β-elimination of an olefin is reversible. It should be possible to induce the *n*-butyl compound to isomerize to the *sec*-butyl isomer, a type of reaction which has been noted in cobalt (16) and platinum (6) systems.

Our results are very similar to those of Felkin and Swierczewski (17), who found that treatment of $NiCl_2(PPh_3)_2$ with *n*-BuMgBr yielded but-1-ene, presumably via an unstable butyl nickel compound. In contrast, Yamamoto *et al.* (3) found that the thermal decomposition of $Et_2(\alpha,\alpha'$-dipyridal)Ni yields predominantly ethane and butane, with relatively small amounts of ethylene. Clearly the nature of the ligands on the metal atom strongly influences not only the stability of a metal alkyl complex, but also the nature of the decomposition products.

Financial assistance by the National Research Council of Canada and the International Nickel Company of Canada is gratefully acknowledged.

1. R. P. A. Sneeden and H. H. Zeiss. J. Organometal. Chem. **16**, 449 (1969).
2. G. M. Whitesides, E. R. Stedronsky, C. P. Casey, and J. S. Filippo. J. Amer. Chem. Soc. **92**, 1426 (1970).
3. T. Saito, Y. Uchida, A. Misono, A. Yamamoto, K. Morifuji, and S. Ikeda. J. Amer. Chem. Soc. **88**, 5198 (1966).
4. *Idem.* J. Amer. Chem. Soc. **87**, 4652 (1965).
5. H. Gilman, R. G. Jones, and L. A. Wood. J. Amer. Chem. Soc. **76**, 3615 (1954).
6. J. Chatt, R. S. Coffey, A. Gough, and D. T. Thompson. J. Chem. Soc. (A), 190 (1968).
7. P. S. Hallman, B. R. McGarvey, and G. Wilkinson. J. Chem. Soc. (A), 3143 (1968).
8. C. W. Bird. Transition metal intermediates in organic synthesis. Academic Press, New York, N.Y. 1967.
9. E. Lodewijk and D. Wright. J. Chem. Soc. (A), 119 (1968).
10. T. McKenna. Anal. Chem. **32**, 1301 (1960).
11. H. Yamazaki, T. Nishido, Y. Matsumoto, S. Sumida, and N. Hagihara. J. Organometal. Chem. **6**, 86 (1966).
12. M. van den Akker and F. Jellinek. Rec. **86**, 897 (1967).
13. M. D. Rausch, Y. F. Chang, and H. B. Gordon. Inorg. Chem. **8**, 1355 (1969).
14. J. R. Cavanaugh and B. P. Dailey. J. Chem. Phys. **34**, 1099 (1961).
15. P. T. Narasimhan and M. T. Rogers. J. Amer. Chem. Soc. **82**, 5983 (1960).
16. Y. Takegami, C. Yokokawa, Y. Watanabe, and Y. Okuda. Bull. Chem. Soc. Jap. **37**, 181 (1964).
17. H. Felkin and G. Swierczewski. C.R. **266C**, 1611 (1968).

Radiolysis of gaseous isobutene by ^{60}Co γ-rays. III. Low boiling point condensation products

Jan A. Herman
Département de Chimie, Université Laval, Québec, Québec

Received May 4, 1970

During the γ-rays irradiation of gaseous isobutene the following low boiling point condensation products are formed: 2-methyl-1-butene, 2-methyl-2-butene, 1,1-dimethyl-cyclopropane, 3-methyl-1-butene, neopentane, isopentane, and *n*-pentane. All these products are formed in radical processes, as shown by the scavenging action of nitric oxide. The formation of the pentenes results from the reaction of the methylene radical with isobutene, whereas the reaction of the methyl radical with the monomer accounts for the production of pentanes.

Canadian Journal of Chemistry, **48**, 3446 (1970)

In recent papers (1, 2) we reported radiation chemical yields of decomposition products formed during radiolysis of gaseous isobutene. We noted (1) the presence of some condensation products, however their identification and quantitative analysis were poorly performed. Sparapany (3) studied the formation of the polymer in the irradiated monomer, and later Viswanathan and Kevan (4) reported the formation of C_8 and C_{12} products, but in both cases the irradiation was carried out on liquid isobutene and was specifically oriented toward ionic polymerization processes. Okamoto *et al.* (5) studied the gas-phase radiation induced polymerization of the isobutene and they established the ionic mechanism of this reaction. However,

Can. J. Chem. Downloaded from www.nrcresearchpress.com by 210.87.254.42 on 09/05/12
For personal use only.

We have been unable to detect a nickel hydride by n.m.r., but the distribution of products from the *n*-butyl compound and the isomerization of but-1-ene in the presence of the decomposition products from the *n*-propyl compound suggest that such a compound does exist and that the β-elimination of an olefin is reversible. It should be possible to induce the *n*-butyl compound to isomerize to the *sec*-butyl isomer, a type of reaction which has been noted in cobalt (16) and platinum (6) systems.

Our results are very similar to those of Felkin and Swierczewski (17), who found that treatment of $NiCl_2(PPh_3)_2$ with *n*-BuMgBr yielded but-1-ene, presumably via an unstable butyl nickel compound. In contrast, Yamamoto *et al.* (3) found that the thermal decomposition of $Et_2(\alpha,\alpha'$-dipyridal)Ni yields predominantly ethane and butane, with relatively small amounts of ethylene. Clearly the nature of the ligands on the metal atom strongly influences not only the stability of a metal alkyl complex, but also the nature of the decomposition products.

Financial assistance by the National Research Council of Canada and the International Nickel Company of Canada is gratefully acknowledged.

1. R. P. A. Sneeden and H. H. Zeiss. J. Organometal. Chem. **16**, 449 (1969).
2. G. M. Whitesides, E. R. Stedronsky, C. P. Casey, and J. S. Filippo. J. Amer. Chem. Soc. **92**, 1426 (1970).
3. T. Saito, Y. Uchida, A. Misono, A. Yamamoto, K. Morifuji, and S. Ikeda. J. Amer. Chem. Soc. **88**, 5198 (1966).
4. *Idem.* J. Amer. Chem. Soc. **87**, 4652 (1965).
5. H. Gilman, R. G. Jones, and L. A. Wood. J. Amer. Chem. Soc. **76**, 3615 (1954).
6. J. Chatt, R. S. Coffey, A. Gough, and D. T. Thompson. J. Chem. Soc. (A), 190 (1968).
7. P. S. Hallman, B. R. McGarvey, and G. Wilkinson. J. Chem. Soc. (A), 3143 (1968).
8. C. W. Bird. Transition metal intermediates in organic synthesis. Academic Press, New York, N.Y. 1967.
9. E. Lodewijk and D. Wright. J. Chem. Soc. (A), 119 (1968).
10. T. McKenna. Anal. Chem. **32**, 1301 (1960).
11. H. Yamazaki, T. Nishido, Y. Matsumoto, S. Sumida, and N. Hagihara. J. Organometal. Chem. **6**, 86 (1966).
12. M. van den Akker and F. Jellinek. Rec. **86**, 897 (1967).
13. M. D. Rausch, Y. F. Chang, and H. B. Gordon. Inorg. Chem. **8**, 1355 (1969).
14. J. R. Cavanaugh and B. P. Dailey. J. Chem. Phys. **34**, 1099 (1961).
15. P. T. Narasimhan and M. T. Rogers. J. Amer. Chem. Soc. **82**, 5983 (1960).
16. Y. Takegami, C. Yokokawa, Y. Watanabe, and Y. Okuda. Bull. Chem. Soc. Jap. **37**, 181 (1964).
17. H. Felkin and G. Swierczewski. C.R. **266C**, 1611 (1968).

Radiolysis of gaseous isobutene by ^{60}Co γ-rays. III. Low boiling point condensation products

Jan A. Herman
Département de Chimie, Université Laval, Québec, Québec

Received May 4, 1970

During the γ-rays irradiation of gaseous isobutene the following low boiling point condensation products are formed: 2-methyl-1-butene, 2-methyl-2-butene, 1,1-dimethyl-cyclopropane, 3-methyl-1-butene, neopentane, isopentane, and *n*-pentane. All these products are formed in radical processes, as shown by the scavenging action of nitric oxide. The formation of the pentenes results from the reaction of the methylene radical with isobutene, whereas the reaction of the methyl radical with the monomer accounts for the production of pentanes.

Canadian Journal of Chemistry, **48**, 3446 (1970)

In recent papers (1, 2) we reported radiation chemical yields of decomposition products formed during radiolysis of gaseous isobutene. We noted (1) the presence of some condensation products, however their identification and quantitative analysis were poorly performed. Sparapany (3) studied the formation of the polymer in the irradiated monomer, and later Viswanathan and Kevan (4) reported the formation of C_8 and C_{12} products, but in both cases the irradiation was carried out on liquid isobutene and was specifically oriented toward ionic polymerization processes. Okamoto *et al.* (5) studied the gas-phase radiation induced polymerization of the isobutene and they established the ionic mechanism of this reaction. However,

Can. J. Chem. Downloaded from www.nrcresearchpress.com by 210.87.254.40 on 09/05/12
For personal use only.

TABLE 1

G-Values of products as a function of the pressure

Products	Pressure (Torr)* 6	12	24	47	95
Allene	(100)	(100)	1.25 (100)	1.01 (100)	0.76 (100)
2-Methyl-1-butene	(64)	(70)	0.91 (73)	0.78 (77)	0.55 (72)
2-Methyl-2-butene	(23)	(30)	0.36 (29)	0.26 (26)	0.17 (23)
1,1-Dimethyl-cyclopropane	(1.2)	(5.2)	0.08 (6.1)	0.07 (7.3)	0.07 (8.7)
3-Methyl-1-butene	—	—	0.02 (1.3)	0.01 (1.2)	0.007 (0.9)
Neopentane	(53)	(46)	0.43 (34)	—	0.11 (15)
Isopentane	(14)	(23)	0.33 (26)	0.31 (31)	0.31 (41)
n-Pentane	—	(2.8)	0.04 (3.3)	0.04 (3.8)	0.02 (3.1)
1,4-Pentadiene (?)	—	—	—	0.02 (2.1)	0.02 (2.6)

*The relative yields are in parentheses.

about 70% of the stable decomposition products proceed via mechanisms involving excited neutral states of the monomer with elimination of radical fragments. A good example of the subsequent action of the radical fragment is the formation of about 60% of the total isobutane in radical reaction via disproportionation between tertiary butyl radicals (2, 6), the $t\text{-}C_4H_9^{\cdot}$ being formed efficiently by thermal hydrogen addition to the tertiary carbon in isobutene. Other radical fragments: ($:CH_2$, $CH_3^{\cdot}$, etc.) are present in the system and they react with the isobutene giving heavier products. In this work we account for some of these condensation products and propose mechanisms of their formation.

Experimental and Results

The experimental procedure was described previously (1, 2). Phillips research grade isobutene was purified by gas chromatography before use; it did not contain any compounds other than the monomer. Pure nitric oxide was obtained from Matheson and was used without any further purification. The irradiations were performed at a dose-rate around 2×10^{17} eV g^{-1} min^{-1} and the total doses did not exceed 2×10^{19} eV g^{-1}. The yields are calculated relative to the yields of allene in the unscavenged radiolysis experiments because the formation of this compound is dose and dose-rate independent at a given pressure, and it is also insensitive to radical scavengers (1). But the radiation yield of allene is pressure dependent (it decreases with increasing pressure), and its value at low pressure (< 20 Torr) is not well established. Therefore, we present the yields in two ways (Table1): *G*-values of the condensation products for pressures where dosimetry was well established, and relative yields (in brackets), taking as 100 the yield of allene at all pressures. Such a presentation has the advantage of illustrating the relation between some C_5 products and methylene or methyl radicals formed during the decomposition of the monomer into propene, allene, and propyne.

All products were completely scavenged by nitric oxide (~ 6%).

Discussion

The C_5 condensation products (with the exception of the minor 1,4 pentadiene) belong to two groups, each one resulting from processes involving either methylene radical or methyl radical. The pentenes can be derived from the reaction of methylene with isobutene in two distinct processes: insertion into a carbon—hydrogen bond or addition to a carbon—carbon double bond. The pentanes arise from the interaction of methyl radicals with isobutene or tertiary butyl radicals. The scavenging action of nitric oxide on all condensation products is an indication of radical mechanisms involved in the formation of these compounds. Indeed, one would not expect these products to be formed from butene ions based upon knowledge of the

Can. J. Chem. Downloaded from www.nrcresearchpress.com by 210.87.254.40 on 09/05/12
For personal use only.

Can. J. Chem. Downloaded from www.nrcresearchpress.com by 210.87.254.40 on 09/05/12
For personal use only.

ion–molecule chemistry of butenes (7). The charge transfer between iso-$C_4H_8^+$ (ionization potential (i.p.) = 9.23 eV) and NO (i.p. = 9.25 eV) must be excluded as an alternative scavenging

[1] $\text{iso-}C_4H_8^+ + NO \rightarrow \text{iso-}C_4H_8 + NO^+$

path of NO, because reaction 1 is slow (8), and therefore a much higher concentration of nitric oxide than that used in the present experiments would be required. This was corroborated in recent photolytical studies of isobutene by 10.0 and 11.6–11.8 eV radiation (9).

The 2-methyl-1-butene and the 2-methyl-2-butene are formed in an insertion reaction of $:CH_2$ into a carbon—hydrogen bond (10), eq. 2.

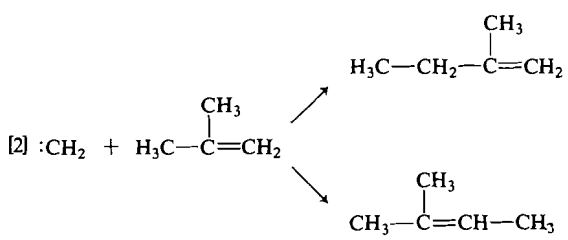

The distribution of these products relative to carbon—hydrogen bonds available in the isobutene is very close to statistical. This confirms the indiscriminate reaction of the $:CH_2$ radical with the C—H bond, as shown earlier by Doering (10*a*). The formation of these two branched pentenes is slightly pressure dependent, suggesting a small contribution of a collisional deactivation process. Apparently a stronger collisional deactivation process is needed for the formation of 1,1-dimethyl-cyclopropane, which results from the addition of $:CH_2$ across the carbon—carbon double bond, eq. 3. The addition

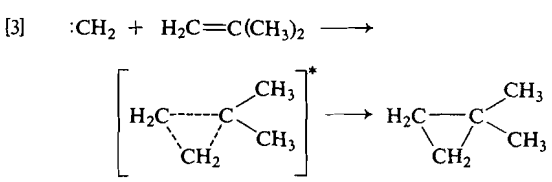

of methylene to a carbon—carbon double bond is known to produce a cyclopropane with more than enough excess energy to undergo further reaction, even to isomerize (11). It is possible that the minor product 3-methyl-1-butene results from an isomerization of the vibrationally excited 1,1-dimethyl-cyclopropane, eq. 4.

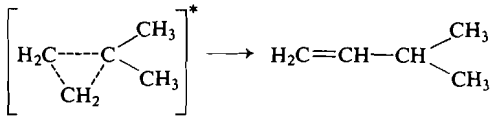

The total relative yields of pentenes formed in reactions 2, 3, and 4 is slightly higher than 100 for pressures above 12 Torr. We have shown that around 50% of propene is formed in unimolecular decomposition reaction, the remaining part being produced in ion–molecule reactions (2). It follows then, that at 47 Torr about half of the pentenes formed in reactions 2, 3, and 4 account for the methylene radicals produced simultaneously with propene. We have then to assume that other paths exist for $:CH_2$ formation. The decomposition of an excited isobutyl radical formed in a hot hydrogen addition is a possible path for the formation of methylene radicals.

[5] $(CH_3)_2C{=}CH_2 + H \rightarrow [(CH_3)_2CHCH_2]^* \rightarrow :CH_2 + C_3H_7^{\cdot}$

The energy required for reaction 5 is of an order which is easily accessible in radiation chemistry processes.

The constituents of the second group of C_5 products are isopentane, *n*-pentane, and neopentane. Isopentane is formed by $CH_3^{\cdot}$ addition to isobutene, eq. 6. Following Szwarc and co-workers (12) reaction 6 is about 20 times more

[6] $(CH_3)_2C{=}CH_2 + CH_3^{\cdot} \rightarrow (CH_3)_2CCH_2CH_3 \xrightarrow{+M} \text{isopentane}$

favorable than the hydrogen abstraction by $CH_3^{\cdot}$ from isobutene. In this case also there is a pressure dependence for process 6 as can be seen in Table 1. If the addition of a hot methyl radical is responsible in part for such behavior, it might also explain the formation of *n*-pentane. Indeed, the energy transmitted by a hot methyl may be sufficient to isomerize the transient complex to *n*-C_5H_{12}. The neopentane behaves quite differently compared to the other saturated pentanes. Its formation decreases strongly with increasing pressure recalling a similar trend of isobutane formation (1). The formation of neopentane is scavenged completely by nitric oxide, indicating that we deal with a radical process. A combination reaction between tertiary-butyl and methyl radicals might explain the formation of neopentane, eq. 7. Following Kutschke and co-workers

[7] $(CH_3)_3C^{\cdot} + CH_3^{\cdot} \rightarrow (CH_3)_4C$

(13) the combination reaction 7 is slightly more favorable than the disproportionation reaction involving the same radicals.

With increasing pressure the competition for methyl and tertiary-butyl radicals in other condensation reactions increases (including some polymerization processes), therefore the production of neopentane diminishes. Such behavior would not be expected for isopentane and *n*-pentane which are formed by hydrogen abstraction from isobutene by isopentyl or *n*-pentyl radicals.

The financial assistance of the National Research Council of Canada is gratefully acknowledged.

1. G. J. Collin and J. A. Herman. Can. J. Chem. **45**, 3097 (1967).
2. J. A. Herman and G. J. Collin. Can. J. Chem. **47**, 3837 (1969).
3. J. J. Sparapany. J. Amer. Chem. Soc. **88**, 1357 (1966).
4. N. S. Viswanathan and L. Kevan. J. Amer. Chem. Soc. **89**, 2482 (1967); Advan. Chem. Ser. **82**, 361 (1968).
5. K. Okamoto, K. Fueki, and Z. Kuri. J. Phys. Chem. **71**, 3222 (1967).
6. (*a*) H. M. Frey. Proc. Chem. Soc. 385 (1959); (*b*) R. Birrel and A. Trotman-Dickenson. J. Chem. Soc. 4218 (1960); (*c*) J. A. Garcia Dominguez, J. A. Kerr, and A. F. Trotman-Dickenson. J. Chem. Soc. 3357 (1962); (*d*) J. Terry and J. Futrell. Can. J. Chem. **46**, 664 (1968).
7. I. Koyano. J. Chem. Phys. **45**, 706 (1966). V. Aquilanti, A. Galli, A. Giardini-Guidoni, and G. G. Volpi. Trans. Faraday Soc. **63**, 926 (1967). F. Abramson and J. Futrell. J. Phys. Chem. **72**, 1994 (1968).
8. L. W. Sieck and J. H. Futrell. J. Chem. Phys. **48**, 1409 (1968).
9. J. Herman, K. Herman, and P. Ausloos. J. Chem. Phys. **52**, 28 (1970).
10. (*a*) W. v. Doering, R. G. Buttery, R. G. Laughlin, and N. Chandhuri. J. Amer. Chem. Soc. **78**, 3224 (1956); (*b*) W. v. Doering and H. Prinzbach. Tetrahedron, **6**, 24 (1959).
11. H. M. Frey. Progress in reaction kinetics. **2**, 151 (1964). Macmillan Co., New York.
12. R. P. Buckley, F. Leavitt, and M. Szwarc. J. Amer. Chem. Soc. **78**, 5557 (1956).
13. A. R. Blake, J. F. Henderson, and K. O. Kutschke. Can. J. Chem. **39**, 169 (1951).

Quaternization of quinazoline with methyl iodide

John W. Bunting and William G. Meathrel
Department of Chemistry, University of Toronto, Toronto 181, Ontario

Received June 9, 1970

Contrary to previous reports, the methylation of quinazoline with methyl iodide has been shown to produce both 1-methylquinazolinium iodide and 3-methylquinazolinium iodide. These quaternary salts are formed in the ratio of 5:1 in favor of the latter isomer.

Canadian Journal of Chemistry, **48**, 3449 (1970)

There are a number of reports in the literature (1–4) that suggest that the quaternization of quinazoline with methyl iodide gives exclusively the 3-methylquinazolinium ion **1**. Formation of the 1-methylquinazolinium ion **2** in this reaction

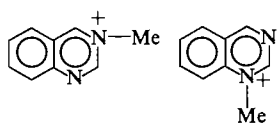

1 **2**

has never been observed. This conclusion is based upon the oxidation of the pseudo-base **3**, which **1** readily forms in aqueous solutions, to 3,4-dihydro-3-methyl-4-oxoquinazoline **4** by alkaline potassium ferricyanide.

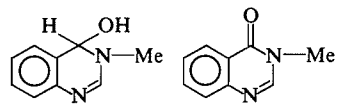

3 **4**

We have used n.m.r. spectroscopy to study the products of the methylation of quinazoline by methyl iodide, and wish to report that, contrary to previous reports in the literature, appreciable methylation of the N-1 atom does occur, although the main product is the 3-methylquinazolinium ion.

Results and Discussion

The n.m.r. spectrum (in trifluoroacetic acid) of the product from the methylation of quinazoline with methyl iodide is shown in Fig. 1. Two peaks

Can. J. Chem. Downloaded from www.nrcresearchpress.com by 210.87.254.40 on 09/05/12
For personal use only.

[7] $(CH_3)_3C^{\cdot} + CH_3^{\cdot} \rightarrow (CH_3)_4C$

(13) the combination reaction 7 is slightly more favorable than the disproportionation reaction involving the same radicals.

With increasing pressure the competition for methyl and tertiary-butyl radicals in other condensation reactions increases (including some polymerization processes), therefore the production of neopentane diminishes. Such behavior would not be expected for isopentane and *n*-pentane which are formed by hydrogen abstraction from isobutene by isopentyl or *n*-pentyl radicals.

The financial assistance of the National Research Council of Canada is gratefully acknowledged.

1. G. J. Collin and J. A. Herman. Can. J. Chem. **45**, 3097 (1967).
2. J. A. Herman and G. J. Collin. Can. J. Chem. **47**, 3837 (1969).
3. J. J. Sparapany. J. Amer. Chem. Soc. **88**, 1357 (1966).
4. N. S. Viswanathan and L. Kevan. J. Amer. Chem. Soc. **89**, 2482 (1967); Advan. Chem. Ser. **82**, 361 (1968).
5. K. Okamoto, K. Fueki, and Z. Kuri. J. Phys. Chem. **71**, 3222 (1967).
6. (*a*) H. M. Frey. Proc. Chem. Soc. 385 (1959); (*b*) R. Birrel and A. Trotman-Dickenson. J. Chem. Soc. 4218 (1960); (*c*) J. A. Garcia Dominguez, J. A. Kerr, and A. F. Trotman-Dickenson. J. Chem. Soc. 3357 (1962); (*d*) J. Terry and J. Futrell. Can. J. Chem. **46**, 664 (1968).
7. I. Koyano. J. Chem. Phys. **45**, 706 (1966). V. Aquilanti, A. Galli, A. Giardini-Guidoni, and G. G. Volpi. Trans. Faraday Soc. **63**, 926 (1967). F. Abramson and J. Futrell. J. Phys. Chem. **72**, 1994 (1968).
8. L. W. Sieck and J. H. Futrell. J. Chem. Phys. **48**, 1409 (1968).
9. J. Herman, K. Herman, and P. Ausloos. J. Chem. Phys. **52**, 28 (1970).
10. (*a*) W. v. Doering, R. G. Buttery, R. G. Laughlin, and N. Chandhuri. J. Amer. Chem. Soc. **78**, 3224 (1956); (*b*) W. v. Doering and H. Prinzbach. Tetrahedron, **6**, 24 (1959).
11. H. M. Frey. Progress in reaction kinetics. **2**, 151 (1964). Macmillan Co., New York.
12. R. P. Buckley, F. Leavitt, and M. Szwarc. J. Amer. Chem. Soc. **78**, 5557 (1956).
13. A. R. Blake, J. F. Henderson, and K. O. Kutschke. Can. J. Chem. **39**, 169 (1951).

Quaternization of quinazoline with methyl iodide

John W. Bunting and William G. Meathrel
Department of Chemistry, University of Toronto, Toronto 181, Ontario

Received June 9, 1970

Contrary to previous reports, the methylation of quinazoline with methyl iodide has been shown to produce both 1-methylquinazolinium iodide and 3-methylquinazolinium iodide. These quaternary salts are formed in the ratio of 5:1 in favor of the latter isomer.

Canadian Journal of Chemistry, **48**, 3449 (1970)

There are a number of reports in the literature (1–4) that suggest that the quaternization of quinazoline with methyl iodide gives exclusively the 3-methylquinazolinium ion **1**. Formation of the 1-methylquinazolinium ion **2** in this reaction

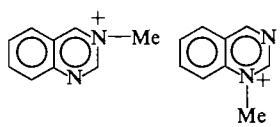

1 **2**

has never been observed. This conclusion is based upon the oxidation of the pseudo-base **3**, which **1** readily forms in aqueous solutions, to 3,4-dihydro-3-methyl-4-oxoquinazoline **4** by alkaline potassium ferricyanide.

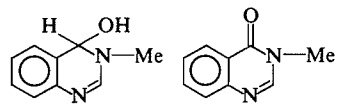

3 **4**

We have used n.m.r. spectroscopy to study the products of the methylation of quinazoline by methyl iodide, and wish to report that, contrary to previous reports in the literature, appreciable methylation of the N-1 atom does occur, although the main product is the 3-methylquinazolinium ion.

Results and Discussion

The n.m.r. spectrum (in trifluoroacetic acid) of the product from the methylation of quinazoline with methyl iodide is shown in Fig. 1. Two peaks

Can. J. Chem. Downloaded from www.nrcresearchpress.com by 210.87.254.105 on 09/05/12
For personal use only.

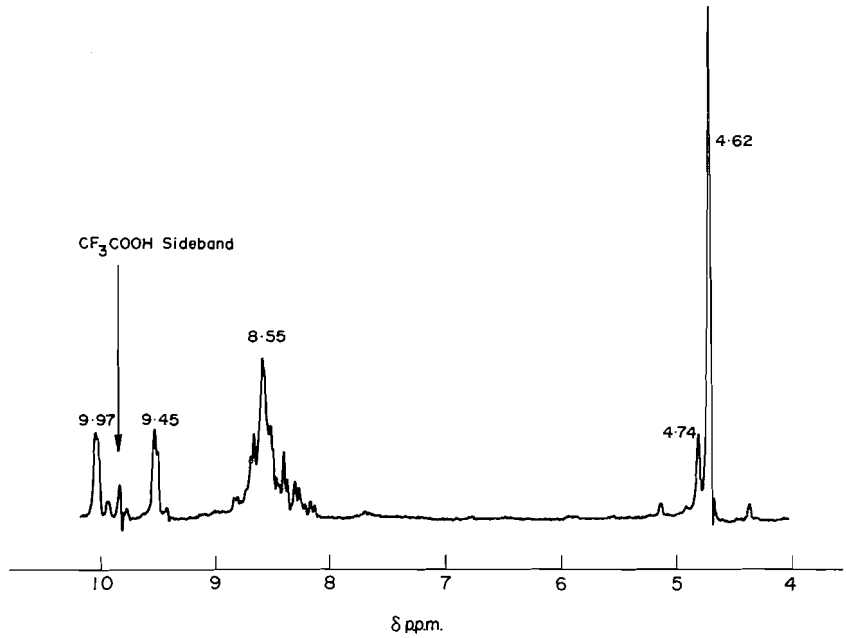

FIG. 1. The n.m.r. spectrum, in trifluoroacetic acid, of the product from the methylation of quinazoline with methyl iodide.

(δ 4.62, 4.74) which can be assigned to *N*-methyl groups are apparent, and have relative intensities of 5:1. The n.m.r. spectrum of the same reaction product in dilute aqueous acid solution (0.1 *N* HCl in D_2O) is shown in Fig. 2. Dual peaks, with relative intensities 5:1, appear at three places in this spectrum: δ 8.32, 8.45; 6.21, 6.34; and 3.53, 3.69. In aqueous acid solutions the 3-methylquinazolinium ion is known to exist as the cation **6** of the pseudo-base which is formed by hydroxide addition to C-4 (4). The dual peaks in

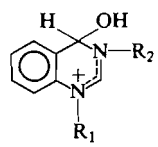

5

6 $R_1 = H; R_2 = Me$
7 $R_1 = R_2 = H$
8 $R_1 = Me; R_2 = H$
11 $R_1 = R_2 = Me$

the spectrum in Fig. 2 are readily assigned to protons in similar environments to those on C-2 and -4 and *N*-methyl protons respectively in a structure such as **5**. They compare well with the peaks at δ 8.42 (C(2)—H) and 6.38 (C(4)—H) in the n.m.r. spectrum of the covalently hydrated quinazoline cation **7** (5).

The similarities of the chemical shifts of these major and minor sets of peaks suggest that they arise from very similar chemical structures. We assign these structures as the covalent hydrates, **6** and **8**, of the 3-methylquinazolinium ion (major isomer) and 1-methylquinazolinium ion (minor isomer) respectively. Evidence in support of this structural assignment is presented in the following paragraphs.

When an aqueous solution of the mixture of *N*-methylquinazolinium ions was carefully titrated with aqueous potassium hydroxide, a white precipitate started to appear at p*H* 8.5. After the addition of one equivalent of alkali the precipitate was collected. The n.m.r. spectrum of this product in dilute aqueous acid indicated that only the major isomer was present, since the peaks for the minor isomer that were initially present (Fig. 2) were no longer observed. Oxidation of the original mixture of pseudo-bases with alkaline potassium ferricyanide gave a product that had an n.m.r. spectrum in which two peaks were assignable to *N*-methyl groups (δ 3.52 (major) and 3.80 (minor) in DMSO-d_6). Oxidation of **3** has previously been shown to give **4** (3).

Can. J. Chem. Downloaded from www.nrcresearchpress.com by 210.87.254.105 on 09/05/12
For personal use only.

Can. J. Chem. Downloaded from www.nrcresearchpress.com by 210.87.254.105 on 09/05/12
For personal use only.

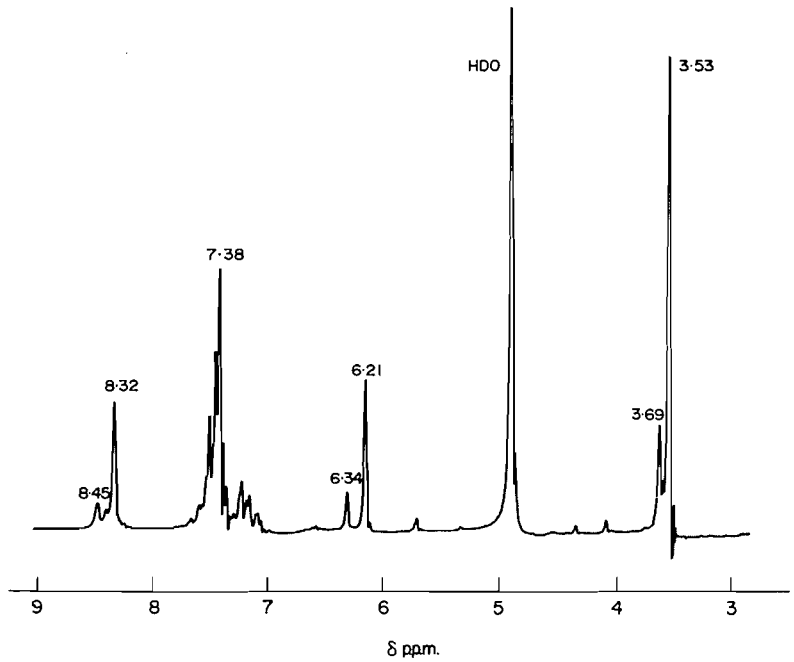

FIG. 2. The n.m.r. spectrum, in 0.1 *N* HCl in D_2O, of the product from the methylation of quinazoline with methyl iodide.

Thus this oxidized product should be a mixture of **4** and **9**. The methyl group in **9** has been

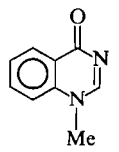

9

reported (6) to have a chemical shift of δ 3.8 in DMSO-d_6. On this basis, the minor oxidation product can be assigned to **9** and the major product must therefore be **4**. This was confirmed by oxidation of the precipitated pure pseudo-base to give a product which has only one peak (δ 3.52 in DMSO-d_6) in its n.m.r. spectrum that is assignable to an *N*-methyl group.

Since **4** is derived from the major product of the methylation of quinazoline, this indicates that this major product is **1** (previously reported to be the only product) and therefore **2** is the minor product. The presence of **9** in the oxidation products also eliminates the remote possibility that the two pseudo-bases contributing to the spectrum in Fig. 2 are stereoisomers of **6** arising from a slow inversion of N-3. Such stereoisomers would give rise to the same oxidation product, **4**.

The possibility that the dimethylated quinazoline dication **10** is the minor product of the reaction can be ruled out on the basis of the

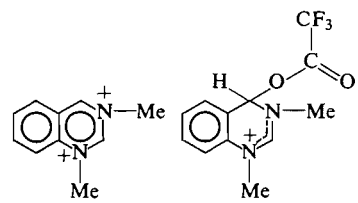

10 **12**

oxidation experiments discussed above and the following evidence. The pseudo-base **3** was treated with methyl iodide to give **11**. The n.m.r. spectrum of **11** in trifluoroacetic acid has peaks at δ 3.70 (singlet, 3H), 3.87 (singlet, 3H), 7.69 (center of multiplet, 5H) and 8.35 (singlet, 1H), while in D_2O the peaks are at δ 3.58 (singlet, 3H), 3.73 (singlet, 3H), 6.28 (singlet, 1H), 7.62 (center of multiplet, 4H), and 8.50 (singlet, 1H). There is a close correspondence between the spectra in these two solvents except for the peak at δ 6.28 in D_2O which seems to move downfield in trifluoroacetic acid and occurs along with the benzene ring protons in the multiplet centered at δ 7.69. This downfield shift can be explained by

Can. J. Chem. Downloaded from www.nrcresearchpress.com by 210.87.254.105 on 09/05/12
For personal use only.

a conversion of **11** into **12** in trifluoroacetic acid, with the downfield shift of C(4)—H resulting from the replacement of the hydroxyl group on C-4 by the more strongly electron-withdrawing trifluoroacetoxy group. The spectrum in trifluoroacetic acid is not consistent with what would be expected for the dication **10**. For **10**, the peaks for the protons on C-2 and -4 should be even further downfield than those for the protons on the same two carbon atoms in **1** (δ 9.45 and 9.97 in Fig. 1). Finally, oxidation of **11** did not give a product with an *N*-methyl peak at δ 3.80 as was observed for the minor oxidation product in the mixture of pseudo-bases.

It is interesting that the 1-methylquinazolinium ion forms the pseudo-base cation **8** rather than **13** which would result from nucleophilic addition at the more electron-deficient C-2. The formation of **8** can be explained by its enhanced stability due to amidinium-type resonance stabilization (7) which is not possible in **13**. This type of resonance stabilization has also been invoked to explain the stabilities of the cation of the pseudo-base of the 3-methylquinazolinium ion, **6**, and of the covalently hydrated quinazoline cation, **7**.

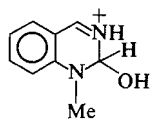

13

Methylation of a nitrogen heterocycle containing more than one azine nitrogen atom is expected to occur predominantly at the most basic nitrogen atom in the absence of opposing steric effects. Owing to the ready formation of a covalent hydrate by the quinazolinium ion (7), it is not possible to ascertain experimentally the site of protonation in quinazoline. Estimates have been made of the relative basicities of N-1 and -3 in quinazoline on the basis of an empirical equation that has been developed to generate estimates of pK_a values for substituted quinolines and isoquinolines (8). These considerations suggest that N-3 is probably only slightly more basic than N-1 and that the non-hydrated quinazolinium ion is probably a mixture of N(3)- and N(1)-protonated species in which the former predominates. Theoretical calculations of the electron density distribution in the quinazoline molecule also indicate that there is probably little difference in the basicities of the N-1 and -3 atoms in quinazoline (9–11). Thus, one would predict that N-3 should be only slightly favored over N-1 as the methylation site, and that methylation may possibly produce a mixture of the isomeric *N*-methylquinazolinium ions. Our experimental results are in accord with such a rationalization of this reaction.

It is noteworthy that the presence of substituents on C-4 can alter the preferred site of methylation from N-3 to -1 (3). This further confirms that there is little difference in the susceptibilities of N-1 and -3 to methylation, since the preferred site of attack may be readily influenced by the electronic and/or steric effects of substituents.

Experimental

The n.m.r. spectra were recorded on Varian T-60 or A-60 spectrometers using sodium 2,2-dimethyl-2-silapentane-5-sulfonate as internal reference.

Methylation of Quinazoline

(*A*) Quinazoline (1 g) was dissolved in ethanol (5 ml). Methyl iodide (1 ml) was added and the solution was refluxed for 4 h. The solvent was evaporated and the viscous residue dissolved in chloroform. The chloroform solution was extracted with dilute aqueous hydrochloric acid and the aqueous extracts were evaporated to yield a mixture of the hydroiodides of the pseudo-bases of the *N*-methylquinazolinium ions as a yellow viscous oil which solidified on standing; m.p. 89°.

Anal. Calcd for $C_9H_{11}N_2OI$: C, 37.4; H, 3.48; N, 9.69; I, 43.8. Found: C, 38.2;[1] H, 3.64; N, 9.64; I, 44.0.

(*B*) Quinazoline (1 g) and methyl iodide (1 ml) were allowed to stand at room temperature overnight. The excess methyl iodide was evaporated and the residue worked-up as described above.

The ratio of 1-methyl- to 3-methylquinazolinium ions in the trifluoroacetic acid solution was the same, within experimental error, for the products from quaternization in ethanol solution (method *A*) and the neat methyl iodide (method *B*).

3,4-Dihydro-4-hydroxy-3-methylquinazoline

Aqueous potassium hydroxide (1 *M*) was added dropwise to an aqueous solution (1 *M*) of the mixture of products from the quaternization reaction, until the p*H* reached 9.5. The white precipitate which had formed was filtered off and redissolved in water (2 ml) to which 1 drop of hydrochloric acid had been added. The pseudo-base was then reprecipitated by addition of potassium hydroxide solution; m.p. 161–162°, lit. m.p. 162–163° (1), 164–165° (2), 158° (3), 167–168° (4). Mass spectrum: molecular ion peak at 162; most intense peak at M-17 (loss of OH).

Anal. Calcd. for $C_9H_{10}N_2O$: C, 66.7; H, 6.21; N, 17.3. Found: C, 65.7;[1] H, 6.22; N, 17.2.

Methylation of 3,4-Dihydro-4-hydroxy-3-methylquinazoline

The pure pseudo-base (0.05 g) and methyl iodide (1 ml)

[1]Difficulty in obtaining satisfactory carbon analyses for this class of compound has been reported previously (12).

were refluxed in ethanol (3 ml) for 24 h. The reaction product was worked-up as described for the methylation of quinazoline.

Incubation of the pseudo-base cation with methyl iodide in ethanol, under the same conditions that were used for the methylation of quinazoline, did not result in the methylation of N-1.

Oxidation Experiments

The pseudo-base was treated with a solution of potassium ferricyanide (1 *M*) in aqueous potassium hydroxide (1 *M*) for 10–15 min. The oxidation products were extracted into chloroform; these extracts were dried over magnesium sulfate and the solvent removed on the rotary evaporator. Treatment of either the pseudo-bases or their oxidation products with strong alkali for excessive periods of time resulted in their decomposition products being present in the chloroform extracts.

This work was supported by a grant from the Ontario Department of University Affairs, and was carried out during the tenure (by W.G.M.) of an Ontario Graduate Fellowship.

1. S. Gabriel and J. Colman. Chem. Ber. **37**, 3643 (1904).
2. C. Schöpf and F. Oechler. Ann. Chem. **523**, 1 (1936).
3. D. J. Fry, J. D. Kendall, and A. J. Morgan. J. Chem. Soc. 5062 (1960).
4. A. Albert, W. L. F. Armarego, and E. Spinner. J. Chem. Soc. 5267 (1961).
5. J. W. Bunting and D. D. Perrin. J. Chem. Soc. (B) 433 (1966).
6. S. C. Pakrashi, J. Bhattacharyya, L. F. Johnson, and H. Budzikiewicz. Tetrahedron, **19**, 1011 (1963).
7. A. Albert and W. L. F. Armarego. Advan. Heterocycl. Chem. **4**, 1 (1965).
8. D. D. Perrin. J. Chem. Soc. 5590 (1965).
9. H. C. Longuet-Higgins and C. A. Coulson. J. Chem. Soc. 971 (1949).
10. A. H. Gawer and B. P. Dailey. J. Chem. Phys. **42**, 2658 (1965).
11. P. J. Black, R. D. Brown, and M. L. Heffernan. Aust. J. Chem. **20**, 1305 (1967).
12. C. J. Cooksey and M. D. Johnson. J. Chem. Soc. (B) 1191 (1968).

Electron spin resonance studies of radiation damage. Part IV.[1,2] The effect of photobleaching on the trapped radicals in gamma irradiated 2-methyltetrahydrofuran glasses at 77 °K

F. P. Sargent

Materials Science Branch, Atomic Energy of Canada Limited, Whiteshell Nuclear Research Establishment, Pinawa, Manitoba

Received June 16, 1970

The concentration of trapped radicals was found to decrease during the course of photobleaching trapped electrons in gamma irradiated 2-methyltetrahydrofuran glasses at 77 °K.

Canadian Journal of Chemistry, **48**, 3453 (1970)

The electron spin resonance (e.s.r.) spectra of gamma irradiated 2-methyltetrahydrofuran glasses at 77 °K consists of a narrow singlet 4 G wide due to a trapped electron and a broad septet of linewidth 10 G and hyperfine spacing of 20 G due to a trapped radical (1–3). The reported e.s.r. studies have been in agreement apart from one exception, namely, the effects of photobleaching. Smith and Pieroni (4) reported that photobleaching led to the complete removal of the singlet together with one third of the radical septet; however, Shirom and Willard (5) report no change in the intensity of radical spectrum within $\pm 2\%$ and Dainton and Salmon (2) report "no significant change took place in the background spectrum" (*i.e.* the radical) when the electron singlet was photobleached. We thought these differences were sufficiently important to re-investigate the photobleaching of these glasses.

Methyltetrahydrofuran, MTHF, was purified by the usual methods (2), but the final stages involved treatment with naphthalene and a sodium mirror on a vacuum line followed by distillation to a storage vessel containing a sodium mirror only. After several months there has been no deterioration of this mirror. Greaseless and O-ring free stopcocks were used throughout the vacuum system. Samples were prepared by distillation from the storage bulb to thin walled spectrosil e.s.r. tubes which had been flamed out at red heat. These were gamma

[1]For Part III, see ref. 8.
[2]AECL No. 3699.

Can. J. Chem. Downloaded from www.nrcresearchpress.com by 210.87.254.105 on 09/05/12
For personal use only.

were refluxed in ethanol (3 ml) for 24 h. The reaction product was worked-up as described for the methylation of quinazoline.

Incubation of the pseudo-base cation with methyl iodide in ethanol, under the same conditions that were used for the methylation of quinazoline, did not result in the methylation of N-1.

Oxidation Experiments

The pseudo-base was treated with a solution of potassium ferricyanide (1 *M*) in aqueous potassium hydroxide (1 *M*) for 10–15 min. The oxidation products were extracted into chloroform; these extracts were dried over magnesium sulfate and the solvent removed on the rotary evaporator. Treatment of either the pseudo-bases or their oxidation products with strong alkali for excessive periods of time resulted in their decomposition products being present in the chloroform extracts.

This work was supported by a grant from the Ontario Department of University Affairs, and was carried out during the tenure (by W.G.M.) of an Ontario Graduate Fellowship.

1. S. Gabriel and J. Colman. Chem. Ber. **37**, 3643 (1904).
2. C. Schöpf and F. Oechler. Ann. Chem. **523**, 1 (1936).
3. D. J. Fry, J. D. Kendall, and A. J. Morgan. J. Chem. Soc. 5062 (1960).
4. A. Albert, W. L. F. Armarego, and E. Spinner. J. Chem. Soc. 5267 (1961).
5. J. W. Bunting and D. D. Perrin. J. Chem. Soc. (B) 433 (1966).
6. S. C. Pakrashi, J. Bhattacharyya, L. F. Johnson, and H. Budzikiewicz. Tetrahedron, **19**, 1011 (1963).
7. A. Albert and W. L. F. Armarego. Advan. Heterocycl. Chem. **4**, 1 (1965).
8. D. D. Perrin. J. Chem. Soc. 5590 (1965).
9. H. C. Longuet-Higgins and C. A. Coulson. J. Chem. Soc. 971 (1949).
10. A. H. Gawer and B. P. Dailey. J. Chem. Phys. **42**, 2658 (1965).
11. P. J. Black, R. D. Brown, and M. L. Heffernan. Aust. J. Chem. **20**, 1305 (1967).
12. C. J. Cooksey and M. D. Johnson. J. Chem. Soc. (B) 1191 (1968).

Electron spin resonance studies of radiation damage. Part IV.[1,2] The effect of photobleaching on the trapped radicals in gamma irradiated 2-methyltetrahydrofuran glasses at 77 °K

F. P. Sargent

Materials Science Branch, Atomic Energy of Canada Limited, Whiteshell Nuclear Research Establishment, Pinawa, Manitoba

Received June 16, 1970

The concentration of trapped radicals was found to decrease during the course of photobleaching trapped electrons in gamma irradiated 2-methyltetrahydrofuran glasses at 77 °K.

Canadian Journal of Chemistry, **48**, 3453 (1970)

The electron spin resonance (e.s.r.) spectra of gamma irradiated 2-methyltetrahydrofuran glasses at 77 °K consists of a narrow singlet 4 G wide due to a trapped electron and a broad septet of linewidth 10 G and hyperfine spacing of 20 G due to a trapped radical (1–3). The reported e.s.r. studies have been in agreement apart from one exception, namely, the effects of photobleaching. Smith and Pieroni (4) reported that photobleaching led to the complete removal of the singlet together with one third of the radical septet; however, Shirom and Willard (5) report no change in the intensity of radical spectrum within $\pm 2\%$ and Dainton and Salmon (2) report "no significant change took place in the background spectrum" (*i.e.* the radical) when the electron singlet was photobleached. We thought these differences were sufficiently important to re-investigate the photobleaching of these glasses.

Methyltetrahydrofuran, MTHF, was purified by the usual methods (2), but the final stages involved treatment with naphthalene and a sodium mirror on a vacuum line followed by distillation to a storage vessel containing a sodium mirror only. After several months there has been no deterioration of this mirror. Greaseless and O-ring free stopcocks were used throughout the vacuum system. Samples were prepared by distillation from the storage bulb to thin walled spectrosil e.s.r. tubes which had been flamed out at red heat. These were gamma

[1]For Part III, see ref. 8.
[2]AECL No. 3699.

Can. J. Chem. Downloaded from www.nrcresearchpress.com by 210.87.254.40 on 09/05/12
For personal use only.

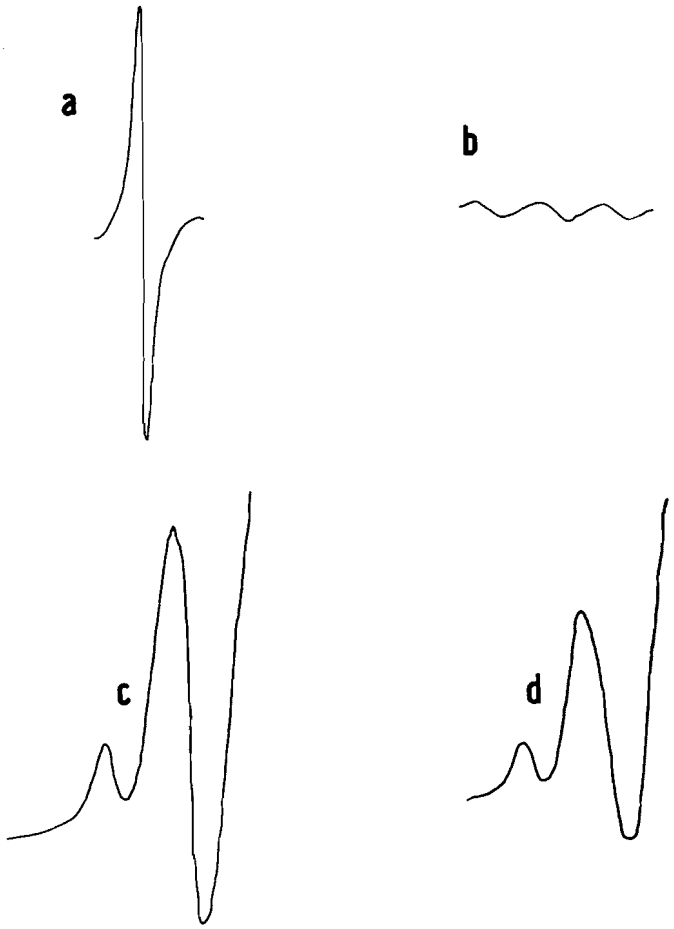

FIG. 1. Electron spin resonance spectra of gamma irradiated MTHF glasses. (*a*) and (*b*), center of spectrum at gain setting 25 before and after photobleaching. (*c*) and (*d*), high field lines of radical at gain setting 630 before and after photobleaching.

irradiated in liquid nitrogen in the dark to doses of the order of 10^{19} eV g^{-1}. The e.s.r. spectra were recorded at low microwave power levels of about 0.01 mW, using a Varian low power bridge together with a resistive termination to ensure no dispersive contribution to the signal. Photobleaching was performed with the unfiltered output of a tungsten projector lamp.

The e.s.r. spectra shown in Fig. 1 are only part spectra, *i.e.* only the central section before and after photobleaching is shown in (*a*) and (*b*) at gain setting 25 and only the high field lines of the septet are shown in (*c*) and (*d*) at gain setting 630. Clearly photobleaching leads to the complete removal of the singlet (see Fig. 1 (*a*) and (*b*)); in addition about 40% of the radicals are also removed (see Fig. 1 (*c*) and (*d*)). The decrease in the intensity of the radical septet was shown to be real because there was no change in the spectrometer sensitivity during photobleaching when a dual cavity was used with a reference sample of bleached MTHF glass, and the line shape of the singlet is Gaussian which contributes to a negligible extent to the outer radical lines. The effects of photobleaching were studied in detail, the sample being bleached *in situ* for a few seconds followed by taking spectra at gain settings of 25 and 630 to monitor the changes of the trapped electron singlet and the radical septet, respectively. The results are summarized in Table 1. These show that the loss of electrons and radicals *i.e.* E(NORM) and ΔR(NORM) are closely correlated, implying that the fraction of electrons lost which lead to radical removal

Can. J. Chem. Downloaded from www.nrcresearchpress.com by 210.87.254.40 on 09/05/12
For personal use only.

TABLE 1

Peak-to-peak first derivate electron spin resonance intensities as a function of photobleaching

Bleaching time	E*	E(NORM)	R†	$R - R_\infty$	ΔR(NORM)
0	16.4	1.0	11.2	4.6	1.0
6	13.4	0.82	10.4	3.8	0.83
13	11.0	0.67	9.8	3.2	0.70
23	8.0	0.49	9.0	2.4	0.52
33	6.2	0.38	8.4	1.8	0.39
43	5.0	0.30	8.0	1.4	0.30
53	4.2	0.26	7.8	1.4	0.26
73	3.0	0.18	7.4	0.8	0.17
93	2.2	0.13	7.0	0.4	0.1
∞(600)	0	0	6.6	0	0

*Intensity of electron signal at gain setting 25.
†Intensity of second high field septet line at gain setting 630.

remains constant throughout the course of photobleaching. We find that the presence of comparatively large amounts of water, *i.e.* sufficient to give a cloudy glass due to precipitation of ice, has little effect either on the yield of trapped electrons or on the fractional loss of radicals during photobleaching. The presence of air led to a decrease in the number of trapped electrons to about half the deaerated value; furthermore, the loss of radicals during photobleaching was completely inhibited.

To account for the removal of radicals during photobleaching it is necessary to invoke mechanisms similar to those of Smith and Pieroni (4). These all involve the neutralization of positive charge to form hydrogen atoms followed by addition to the radicals; however, we were unable to detect any hydrogen atoms during photobleaching. This could mean that the radical and the positive charge are trapped close together and might be trapped on the same molecule as suggested by Smith and Pieroni (4); however, this is only one of several possible explanations. The comparatively small amounts of electron scavenger *i.e.* 0.03 mole% biphenyl (4) or oxygen, necessary to inhibit radical loss suggest that the electrons are trapped in locations far removed from the positive charge and that photobleaching causes electrons to scan out large volumes of the matrix via successive detrapping and retrapping before encountering either the positive charge or an added solute. This model is essentially that of Dyne and Miller (6).

The substantial agreement between the results presented here and those of Smith and Pieroni (4) prompted us to closely examine the e.s.r. spectra of Dainton and Salmon (2). This revealed that their septet did in fact decrease in intensity by about one third when the electron was photobleached (7), although with respect to the singlet this decrease was only about two %.[3] Therefore, our results together with those of Smith and Pieroni (4) and those of Dainton and Salmon (2) are in substantial agreement. We are at a loss to explain the results of Shirom and Willard (5), but we wish to point out that their procedure for MTHF purification did not involve treatment with a sodium mirror. It is possible that sodium removes other impurities which, like oxygen and biphenyl (4), would inhibit the loss of radicals during photobleaching.

1. D. R. Smith and J. J. Pieroni. Can. J. Chem. **43**, 876 (1965).
2. F. S. Dainton and G. A. Salmon. Proc. Roy. Soc. London. Ser. A. **285**, 319 (1965).
3. J. Lin, K. Tsuji, and F. Williams. J. Amer. Chem. Soc. **90**, 2766 (1968).
4. D. R. Smith and J. J. Pieroni. Can. J. Chem. **43**, 2141 (1965).
5. M. Shirom and J. E. Willard. J. Phys. Chem. **72**, 1702 (1968).
6. P. J. Dyne and O. A. Miller. Can. J. Chem. **43**, 2696 (1965).
7. G. A. Salmon. Private communication.
8. F. P. Sargent. Can. J. Chem. **48**, 1780 (1970).

[3]The Dainton and Salmon spectra consist of a singlet of peak-to-peak intensity 2.66 in. and the penultimate high field radical peak is 0.20 in. After photobleaching the singlet, the radical intensity is 0.14 in. This decrease was measured more accurately on a photographically enlarged spectrum.

Can. J. Chem. Downloaded from www.nrcresearchpress.com by 210.87.254.40 on 09/05/12
For personal use only.

The vibrational spectra of ClF_2SbF_6, BrF_2SbF_6, and ClO_2SbF_6

H. A. CARTER AND F. AUBKE[1]

Department of Chemistry, The University of British Columbia, Vancouver 8, British Columbia

Received April 24, 1970

Infrared and Raman spectra of ClF_2SbF_6, BrF_2SbF_6, and ClO_2SbF_6 are reported. Vibrational frequencies for the BrF_2^+ cation are assigned. In all compounds various degrees of anion–cation interaction are found. The symmetry of the anion is reduced but no internal similarity between the three spectra is recognizable. In addition, strong coupling of vibrational modes for BrF_2SbF_6 is observed.

Canadian Journal of Chemistry, 48, 3456 (1970)

Can. J. Chem. Downloaded from www.nrcresearchpress.com by 210.87.254.5 on 09/05/12
For personal use only.

Over the last years the study of fluoro and oxy cations of the heavier halogens has received much attention (1). Hexafluoroarsenates and antimonates are found to be a good source of heterocations, because the interaction of halogen fluorides or oxyfluorides with the strong fluoride acceptors can proceed under F^- transfer. The four atom molecules ClF_3, BrF_3, and $FClO_2$ can serve well to illustrate this reaction type. The interaction results in the stable solid compounds ClF_2SbF_6 (2, 3), BrF_2SbF_6 (4, 5), and ClO_2SbF_6 (6, 7). Structural studies have been restricted to the Raman spectrum of ClF_2SbF_6 (8), an infrared spectrum of ClO_2SbF_6 (9), and an X-ray diffraction study of BrF_2SbF_6 (10). The structural interpretations of this class of compounds differ quite distinctively. The vibrational spectra of the related compounds ClO_2AsF_6 (11) and ClF_2AsF_6 (12, 13) have been interpreted using a strictly ionic model as evidenced by elaborate force constant calculations. A more cautious approach (8–10) has found some evidence for anion–cation interaction via fluorine bridge bonding in these compounds.

To clarify this point more fully for these related series of compounds, where a certain structural similarity would be expected, we have started a comparative study using infrared spectroscopy down to 250 cm^{-1} and Laser Raman spectroscopy.

A study of a number of related nitrogen oxy and fluoro hexafluoroarsenates and antimonates (14) had established a narrow range for the five i.r. and Raman active fundamentals, some minor discrepancies interpreted as site symmetry effects notwithstanding. In this study, the SbF_6^- group has been found to be slightly more sensitive towards distortion.

[1]To whom correspondence should be addressed.

Experimental

General

A monel metal vacuum line was employed for material transfer in all preparations. Two-part reaction vessels of monel equipped with Hoke valves were used. The solids were handled in a dry box containing a dry nitrogen atmosphere. All compounds studied were found to be highly reactive and very corrosive.

Materials

Antimony pentafluoride (Alpha Inorganic Chemical Corp.) was added to the reaction vessel in the dry box after purification. Chlorine and bromine trifluoride were obtained from Matheson Co. and purified by distillation. Chloryl fluoride was prepared by the reaction of $KClO_3$ with BrF_3 according to Woolf (7). Except for the use of monel metal vacuum line equipment and reactors, the reported preparative routes were employed (3, 4, 7). The reactions were followed by weight, with the most volatile component in an excess.

Instrumentation

The i.r. spectra were recorded on a Perkin–Elmer 457 grating spectrometer for the region of 400–250 cm^{-1}. Silver chloride and KSR-5 windows were used (Harshaw Chemicals) in all cases without any mulling agent. Raman spectra were obtained on a Cary 81 spectrophotometer equipped with a Spectra Physics Model 125 He–Ne Laser as a source of exciting light. The samples were contained in flat bottom Pyrex or silica tubes (5 mm o.d.). The tubes were flame sealed after charging in a dry box.

Results

The infrared and Raman frequencies with their intensities for the three hexafluoroantimonates together with the frequencies for $KSbF_6$ are listed in Table 1. The Raman spectra in the range of 900–300 cm^{-1} for all three heterocation compounds are reproduced in the figure.

Agreement with the previously published Raman spectrum of ClF_2SbF_6 (8) is good except for minor differences. We were not able to resolve a small splitting for $\nu_{1(ClF_2)}$ observed and interpreted by Gillespie and Morton as a factor group splitting. In addition we find a shoulder of weak

TABLE 1

The vibrational spectra of ClF_2SbF_6, BrF_2SbF_6, and ClO_2SbF_6 in cm^{-1}*

ClF_2SbF_6		ClO_2SbF_6		BrF_2SbF_6		$KSbF_6$	
Infrared	Raman	Infrared	Raman	Infrared	Raman	Infrared	Raman
1310 vw	1064 vw	1304 s	1314 w	715 ms	706 vs	655 s	661 s
					693 w	270 s	575 s
1295 vw	1040 vw	1290 s	1293 w	673 vs	679 s		294 m
1065 vw	833 m	1048 ms	1053 s	663 vs,br	641 s		278 m
830 s	810 vs	810 vw	706 m	638 s	552 vs		
803 s	662 vs	720 s,b	680 s	535 m,sh	523 m		
677 s	644 w	680 s,b	649 vs	523 ms	493 ms		
660 s	596 w	670 s	592 ms	495 ms	367 m		
				370 w,sh			
647 s	542 mw	640 s	588 ms	285 m,sh	284 m,sh		
604 s,sh	537 mw	586 m,s,b	518 m	270 m,sh	270 m		
582 mw	385 mw	515 s	308 s	265 m			
375 mw	292 w	305 m	288 m,sh				
290 w,sh	282 m	288 w	269 w				
283 w,sh	267 m	270 s,b					
265 s							

*v = very, w = weak, m = medium, s = strong, b = broad, sh = shoulder.

intensity at 644 cm^{-1}. We also agree with their reassignment of $\nu_{2(ClF_2^+)}$. Some very weak absorption peaks in our ClF_2SbF_6 spectrum are obviously due to ClO_2SbF_6 impurities, produced by hydrolysis or glass interactions. When Pyrex tubes are used as Raman cells, all SbF_6^- compounds showed very weak and diffuse background bands at $\sim$ 420 and $\sim$ 370^{-1}.

The infrared spectrum of ClO_2SbF_6 previously reported by us (9) is now extended down to 250 cm^{-1}. As discussed more fully in another paper (14), principal disagreement in the assignment of ν_4 for the undistorted SbF_6^- exists. A previously reported value of 350 cm^{-1} found for $LiSbF_6$ (15) is not confirmed even though the other assignments agree well. We find ν_4 at 270 cm^{-1} for $KSbF_6$ as well as for NO- and NO_2SbF_6 (14).

Discussion

Previously reported assignments for the cations ClO_2^+ (9, 11) and ClF_2^+ (8) are confirmed. As the only departure from previous reports, $\nu_{2(ClO_2^+)}$ appears to be split in the infrared.

Principal difficulties are encountered in the assignment of the vibrational frequencies ν_1 and ν_3 for BrF_2^+, because both are expected and found roughly in the same region as ν_1 and $\nu_{3(SbF_6^-)}$. This leads to poor resolution noticeable particularly in the i.r. spectrum. The bending $\nu_{2(BrF_2^+)}$ is found at 366 cm^{-1}. The intense vibration at 706 cm^{-1} in the Raman spectrum of BrF_2SbF_6 is best assigned as ν_1 and a strong shoulder in the infrared at 715 cm^{-1} is assigned as ν_3, which is not resolved in the Raman spectrum. This tentative assignment is in good agreement with the ClF_2^+ bands. The extremely high intensity of $\nu_{1(BrF_2^+)}$ which is found to be the strongest peak in the Raman spectrum is in contrast to the intensity of $\nu_1 ClF_2^+$. Assignment of the vibrational frequencies for the SbF_6^- group is more difficult. Instead of the three Raman active modes ν_1 [A_{1g}], ν_2 [E_g], and ν_5 [F_{2g}] expected for octahedral symmetry, all spectra show far more lines. This is reiterated by the i.r. spectra. In addition no similarity between the spectra for the three compounds is found.

Since no high resolution i.r. spectra for the compounds are available and the resolution of the low frequency bands in the Raman spectra is not too good, the discussion will be restricted to the higher frequency range shown in the figure. Involving the three fundamental frequencies ν_1, ν_2, and ν_3 of the SbF_6^- group, found at 661, 575, and 655 cm^{-1}, respectively, for $KSbF_6$.

The least difficulties are expected for BrF_2SbF_6, where the known crystal structure (10) should aid in interpreting the vibrational spectrum. As expected for a *cis*-fluorine bridged SbF_6 group, the symmetry is lowered from O_h to C_{2v}. In addition, arrangement of BrF_2SbF_6 in polymeric coiled chains with two molecules in the same chain per unit cell will lead to an overall symmetry D_2. The reported Br—$F_{bridging}$ distance of 2.29 Å is longer than the Br—F single bond distance of $\sim$1.70 Å

Can. J. Chem. Downloaded from www.nrcresearchpress.com by 210.87.254.5 on 09/05/12
For personal use only.

TABLE 2
Correlation diagram for the XF_6 species

Vibrational mode	Free molecule (O_h)	Distorted molecule (C_{2v})	Molecule in chain (D_2)
ν_1	A_{1g}	A_1	$A + B_2$
ν_2	E_g	A_1	$A + B_2$
		B_2	$B_3 + B_1$
ν_3 (or ν_4)	F_{1u}	A_1	$A + B_2$
		B_1	$B_3 + B_1$
		B_2	$B_3 + B_1$
ν_5	F_{2g}	A_1	$A + B_2$
		A_2	$A + B_2$
		B_1	$B_3 + B_1$

but shorter than the sum of the Van der Waals radii of about 3.30 Å. Therefore, the coupling of SbF_6 groups via BrF_2 units appears to be quite strong and has to be invoked to explain the multitude of bands found for the compound in the vibrational spectrum.

A brief correlation diagram illustrating the symmetry lowering and the coupling is found for the three fundamentals in Table 2. The absorption bands which are the components of ν_2 can be assigned. One finds in the infrared spectrum, bands at 535 (B_1), 523 (B_2), and 495 (B_3) cm^{-1} as expected. Only three of four expected modes appear in the Raman spectrum, 552 (A), 523 (B_2), and 493 (B_3) cm^{-1}, and it is assumed that the B_1 band in the Raman is obscured by the very intense band at 552 cm^{-1}.

It is also relatively easy to assign the two remaining A modes originating from ν_1 and ν_3 as the strong bands found at 678 and 641 cm^{-1}, respectively. Assignment of the weaker B modes in the Raman spectrum is very difficult due to the closely spaced A modes and $\nu_{1(BrF_2^+)}$ at 706 cm^{-1}. Only a weak shoulder is found at 690 cm^{-1} which is tentatively assigned as originating from ν_1. The above mentioned high intensity of the 706 cm^{-1} band suggests coupling between all the different A modes.

It should also be pointed out that coupling will likewise affect the BrF_2^+ vibrations, and for the chain modes, four components for ν_1 and ν_3 are expected of the type A, B_1, B_2, and B_3. The lack of resolution in the infrared region and the closely spaced bands in the Raman region do not allow a complete assignment beyond the point where the 706 cm^{-1} band is assigned as the A mode and the

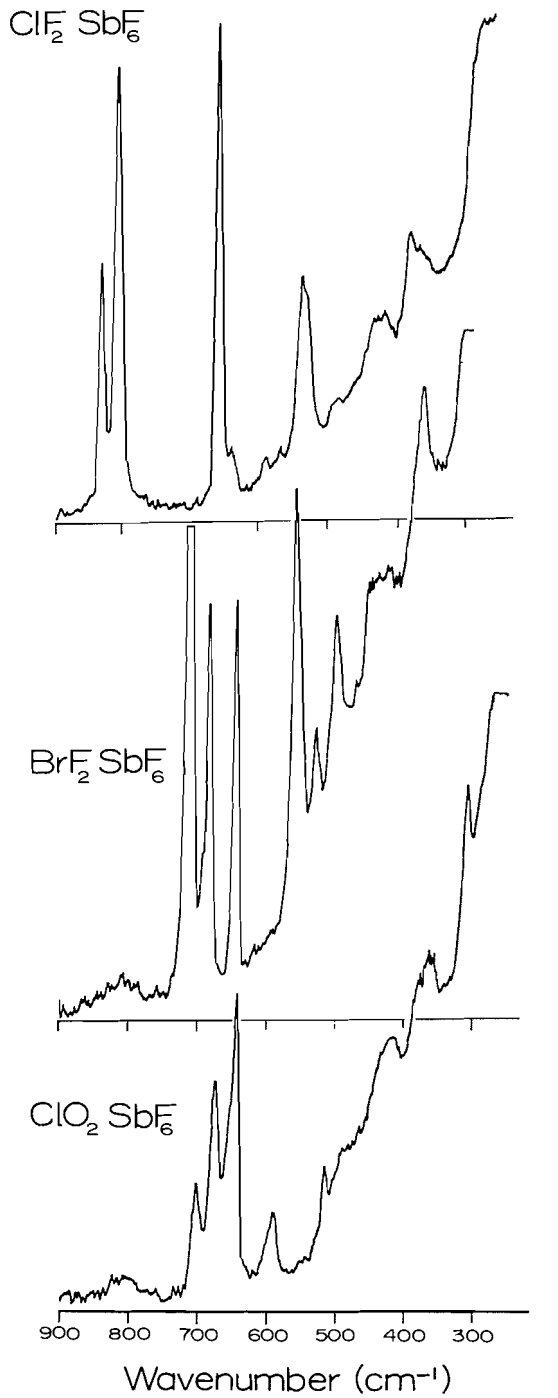

FIG. 1. The Raman spectra of ClF_2SbF_6, BrF_2SbF_6, and ClO_2SbF_6.

Can. J. Chem. Downloaded from www.nrcresearchpress.com by 210.87.254.5 on 09/05/12
For personal use only.

715 cm^{-1} shoulder as B_2 or B_3. It may also be possible that the shoulder at 690 cm^{-1} is better assigned as B_1 and belonging to BrF_2^+. Finally some of the B modes originating in ν_3 and ν_1 are found at 673, 663, and 638 cm^{-1} and again coupling and superposition may occur.

A similar approach cannot be used for the two remaining compounds ClO_2SbF_6 and ClF_2SbF_6 where the crystal structures are unknown.

The previous interpretation of the ClF_2SbF_6 spectrum (8) has invoked an identical molecular model as found for BrF_2SbF_6 (10). This is not confirmed by the vibrational spectra of both compounds. The apparent dissimilarity between the vibrational spectra for both compounds can have various reasons such as different crystal structures, a weaker ClF_2^+ linkage so that no coupling of vibrations can occur, or an entirely different molecular structure. The splittings found for ν_3 and ν_2 and the relaxation of the mutual exclusion rule for the 647 cm^{-1} band are in our opinion sufficient evidence for anion–cation interaction.

No certain assignment is possible for SbF_6^- in ClO_2SbF_6. Strong Raman active bands are found at 706, 680, and 649 cm^{-1} in the region of ν_1. Here, ν_2 appears not to be widely split; the small splitting of 4 cm^{-1} may possibly be caused by the crystalline field. These features are difficult to reconcile but again departure from an ionic model is apparent. Similar features as the shift of the anion frequencies to higher wavelengths are also found for $(ClO_2)_2SnF_6$ and are discussed there more fully (16).

We gratefully acknowledge the financial support received from the National Research Council of Canada. We are indebted to Dr. A. V. Bree for helpful discussion of the vibrational spectra and to Mr. E. Matter for his help in building the monel vacuum line and the metal reactors used in this study.

1. A. A. Woolf. Advan. Inorg. Chem. Radiochem. **9**, 217 (1966).
2. F. Seel and O. Dettmer. Angew. Chem. **70**, 163 (1958).
3. F. Seel and O. Dettmer. Z. Anorg. Allg. Chem. **301**, 113 (1959).
4. A. A. Banks, H. J. Emeleus, and A. A. Woolf. J. Chem. Soc. 2816 (1949).
5. J. Fischer, R. Liimatainen, and J. Bingle. J. Amer. Chem. Soc. **77**, 5848 (1955).
6. M. Schmeisser and W. Fink. Angew. Chem. **69**, 780 (1957).
7. A. A. Woolf. J. Chem. Soc. 4113 (1954).
8. R. J. Gillespie and M. J. Morton. Inorg. Chem. **9**, 616 (1970).
9. H. A. Carter, W. M. Johnson, and F. Aubke. Can. J. Chem. **47**, 4619 (1969).
10. A. J. Edwards and G. R. Jones. J. Chem. Soc. (A), 1467 (1969).
11. K. O. Christe, C. J. Schack, D. Pillipovich, and W. Sawodny. Inorg. Chem. **8**, 2489 (1969).
12. K. O. Christe and A. E. Pavlath. Z. Anorg. Allg. Chem. **335**, 210 (1965).
13. K. O. Christe and W. Sawodny. Inorg. Chem. **6**, 313 (1967).
14. A. M. Qureshi and F. Aubke. Can. J. Chem. In press.
15. G. M. Begun and A. C. Rutenberg. Inorg. Chem. **6**, 2212 (1967).
16. H. A. Carter, A. M. Qureshi, J. R. Sams, and F. Aubke. Can. J. Chem. In press.

The reaction of acetic acid and nitrogen dioxide

R. N. Pandey and Donald Barton
Department of Chemistry, Memorial University of Newfoundland, St. John's, Newfoundland

Received May 19, 1970

Nitric oxide was found to be an autocatalyst in the reaction of acetic acid and nitrogen dioxide at 470 and 527 °K in the vapor phase. The observed products, in addition to NO, were CO, CO_2, and CH_3NO_2.

Canadian Journal of Chemistry, **48**, 3459 (1970)

Autocatalysis by NO was observed in the reaction of NO_2 with formic acid (1) but not in the reactions of NO_2 with formaldehyde (2), acetaldehyde (3), glyoxal (4), and some other organic molecules. The peculiar hydrogen kinetic isotope effects which were found in the reaction of NO_2 with formaldehyde were interpreted in terms of a chain mechanism (5). However, the origin of the hydrogen isotope effects in the reaction of NO_2 with formic acid is still obscure (6) and the

Can. J. Chem. Downloaded from www.nrcresearchpress.com by 210.87.254.5 on 09/05/12
For personal use only.

715 cm^{-1} shoulder as B_2 or B_3. It may also be possible that the shoulder at 690 cm^{-1} is better assigned as B_1 and belonging to BrF_2^+. Finally some of the B modes originating in ν_3 and ν_1 are found at 673, 663, and 638 cm^{-1} and again coupling and superposition may occur.

A similar approach cannot be used for the two remaining compounds ClO_2SbF_6 and ClF_2SbF_6 where the crystal structures are unknown.

The previous interpretation of the ClF_2SbF_6 spectrum (8) has invoked an identical molecular model as found for BrF_2SbF_6 (10). This is not confirmed by the vibrational spectra of both compounds. The apparent dissimilarity between the vibrational spectra for both compounds can have various reasons such as different crystal structures, a weaker ClF_2^+ linkage so that no coupling of vibrations can occur, or an entirely different molecular structure. The splittings found for ν_3 and ν_2 and the relaxation of the mutual exclusion rule for the 647 cm^{-1} band are in our opinion sufficient evidence for anion–cation interaction.

No certain assignment is possible for SbF_6^- in ClO_2SbF_6. Strong Raman active bands are found at 706, 680, and 649 cm^{-1} in the region of ν_1. Here, ν_2 appears not to be widely split; the small splitting of 4 cm^{-1} may possibly be caused by the crystalline field. These features are difficult to reconcile but again departure from an ionic model is apparent. Similar features as the shift of the anion frequencies to higher wavelengths are also found for $(ClO_2)_2SnF_6$ and are discussed there more fully (16).

We gratefully acknowledge the financial support received from the National Research Council of Canada. We are indebted to Dr. A. V. Bree for helpful discussion of the vibrational spectra and to Mr. E. Matter for his help in building the monel vacuum line and the metal reactors used in this study.

1. A. A. Woolf. Advan. Inorg. Chem. Radiochem. **9**, 217 (1966).
2. F. Seel and O. Dettmer. Angew. Chem. **70**, 163 (1958).
3. F. Seel and O. Dettmer. Z. Anorg. Allg. Chem. **301**, 113 (1959).
4. A. A. Banks, H. J. Emeleus, and A. A. Woolf. J. Chem. Soc. 2816 (1949).
5. J. Fischer, R. Liimatainen, and J. Bingle. J. Amer. Chem. Soc. **77**, 5848 (1955).
6. M. Schmeisser and W. Fink. Angew. Chem. **69**, 780 (1957).
7. A. A. Woolf. J. Chem. Soc. 4113 (1954).
8. R. J. Gillespie and M. J. Morton. Inorg. Chem. **9**, 616 (1970).
9. H. A. Carter, W. M. Johnson, and F. Aubke. Can. J. Chem. **47**, 4619 (1969).
10. A. J. Edwards and G. R. Jones. J. Chem. Soc. (A), 1467 (1969).
11. K. O. Christe, C. J. Schack, D. Pillipovich, and W. Sawodny. Inorg. Chem. **8**, 2489 (1969).
12. K. O. Christe and A. E. Pavlath. Z. Anorg. Allg. Chem. **335**, 210 (1965).
13. K. O. Christe and W. Sawodny. Inorg. Chem. **6**, 313 (1967).
14. A. M. Qureshi and F. Aubke. Can. J. Chem. In press.
15. G. M. Begun and A. C. Rutenberg. Inorg. Chem. **6**, 2212 (1967).
16. H. A. Carter, A. M. Qureshi, J. R. Sams, and F. Aubke. Can. J. Chem. In press.

The reaction of acetic acid and nitrogen dioxide

R. N. Pandey and Donald Barton
Department of Chemistry, Memorial University of Newfoundland, St. John's, Newfoundland

Received May 19, 1970

Nitric oxide was found to be an autocatalyst in the reaction of acetic acid and nitrogen dioxide at 470 and 527 °K in the vapor phase. The observed products, in addition to NO, were CO, CO_2, and CH_3NO_2.

Canadian Journal of Chemistry, **48**, 3459 (1970)

Autocatalysis by NO was observed in the reaction of NO_2 with formic acid (1) but not in the reactions of NO_2 with formaldehyde (2), acetaldehyde (3), glyoxal (4), and some other organic molecules. The peculiar hydrogen kinetic isotope effects which were found in the reaction of NO_2 with formaldehyde were interpreted in terms of a chain mechanism (5). However, the origin of the hydrogen isotope effects in the reaction of NO_2 with formic acid is still obscure (6) and the

Can. J. Chem. Downloaded from www.nrcresearchpress.com by 210.87.254.105 on 09/05/12
For personal use only.

TABLE 1

Summary of the results of complete reactions at 526.5 °K*

Exp. No.	CH_3COOH		NO_2			Product, moles × 10^6				
	P_0	N_0	P_0	N_0	ΔP_f	CO	CO_2	CH_3NO_2	NO	$\Delta P_0/\Delta t$
1†	19.3	119	16.2	100	13.5	12	54	8	88	3.5
2†	19.6	121	27.9	173	23.0	24	85	13	164	5.3
3‡	19.6±0.1	121±1	60.7±0.5	376±5	46.8±0.6	62±1	152±1	30±1	§	10.7±1.2
4	19.6	121	86.9	537	47.7	61	159	§	§	20.0
5	10.2	63	59.8	369	24.3	29	82	22	§	7.0
6	10.8	67	59.9	372	§	§	§	§	§	6.2
7†	45.4	281	60.8	376	45.1	50	172	53	312	15.0
8†	45.5	281	60.0	371	45.4	58	168	§	307	12.0
9†	95.7	592	60.7	375	39.5	§	§	§	§	29.0
10†	95.7	592	60.4	374	35.5	§	§	§	§	23.5

*P_0, initial pressure in mm Hg; N_0 initial concentration in moles × 10^6; ΔP_f, final pressure change in mm Hg; $\Delta P_0/\Delta t$, initial rate of pressure rise in mm Hg s^{-1}.
†Excess acetic acid.
‡Results in this row are average of 5 to 8 runs.
§No analysis.

mechanism of the autocatalysis is unknown. The possibility was considered that autocatalysis is specifically related to the carboxyl group. In order to test this hypothesis information on the reactions of NO_2 with other carboxylic acids is required. In this note some results of an exploratory study of the reaction of NO_2 with acetic acid are reported. Further details may be found in ref. 7.

Experimental

The apparatus and procedure were similar to those previously described (6). Glacial acetic acid and acetic acid prepared from acetic anhydride were used. Acetic acid-*d* (CH_3COOD) was prepared from acetic anhydride and D_2O (7).

The products were divided into three fractions, the first collectable by toepler pump at −220 °C, the second at −120 °C, and finally the residue. The first fraction, mainly CO, was oxidized over hot CuO. The second fraction, mainly CO_2 and NO, was analyzed using a trap at −160 °C. The residue was analyzed for CH_3NO_2 in a gas infrared cell with CaF_2 windows. Attempts were made to detect N_2O in the CO_2 by means of gas chromatography using a silica gel column, and by using caroxite.

Results

Examples of pressure–time curves at 526.5 °K are illustrated in Fig. 1. Product yields, pressure changes, and initial rates of pressure change are listed in Table 1. Mole fractions of products assumed to arise from the methyl group are listed in Table 2. The cumulative analytical errors are such that about 5% of the nitrogen or of the carbon could be present as products other than CO, CO_2, CH_3NO_2, or NO. Small amounts of N_2 or of N_2O were suspected in the CO and CO_2 fractions, respectively, but were not identified and if present do not exceed 1% of the total nitrogen.

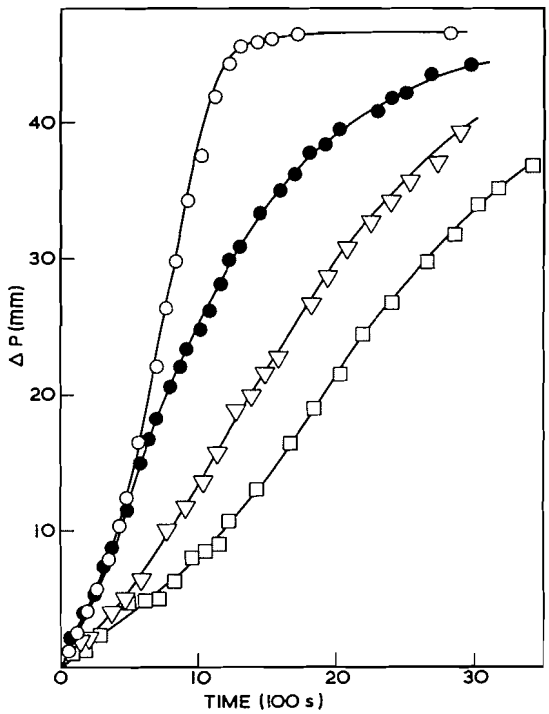

FIG. 1. Pressure–time curves at 526.5 °K. Reactant pressures are initial pressures. Experiment 29: ▽, CH_3COOH 19.6 mm, NO_2 60.4 mm; experiment 28*B*: □, CH_3COOD 19.6 mm, NO_2 60.4 mm; experiment 27: ●, CH_3COOH 19.6 mm, NO_2 60.4 mm, NO, 19.7 mm; experiment 50: ○, CH_3COOH 56.0 mm, NO_2 60.4 mm.

The rates of pressure rise are not particularly useful because of the complicated stoichiometry

Can. J. Chem. Downloaded from www.nrcresearchpress.com by 210.87.254.105 on 09/05/12
For personal use only.

TABLE 2
Fate of the methyl group*

P_0 CH_3COOH	P_0 NO_2	Mole fraction of methyl group products		
		CO	CH_3NO_2	CO
19.6	16.2	0.32	0.22	0.46
19.6	27.9	0.39	0.21	0.39
19.6	60.7	0.50	0.24	0.25
19.6	86.9	0.50	0.18	0.31
10.2	59.8	0.39	0.36	0.26
45.4	60.8	0.36	0.38	0.25

*P_0, initial reactant pressures in mm Hg.

and also because of the concurrent decomposition of NO_2. In any further study of the reaction the technique of Gagarina and Emanuel might be used, in which NO_2 is added first and the NO_2, O_2, and NO are allowed to approach equilibrium before the organic compound is added (8).

Experiments carried out at 470 °K, not reported here, gave results which were essentially the same as those at 527 °K.

Discussion

The shapes of the pressure–time curves are characteristic of autocatalytic reactions in which the rate expression contains a non-autocatalytic term, since the rate does not approach zero at zero time. In fact the curves resemble those observed for the reaction of NO_2 and formic acid (1, 6). The pressure–time curve of experiment 27, Fig. 1, with NO added initially, shows that NO is a catalyst. The results are consistent with the suggestion that the carboxyl group is related to catalysis by NO and indicate that further work should be profitable. However, since the oxidation of CH_4 by NO_2 is catalyzed by NO (at much higher temperatures) (8) the autocatalysis cannot be viewed as being due to some unique property of the carboxyl group.

The observation of a hydrogen isotope effect, as in experiment 28*B*, indicates the importance of carboxyl hydrogen abstraction.

Since the quantity of CO_2 which is produced in experiments with excess NO_2 (Table 1) exceeds that available from the carboxyl group, the methyl group is partially oxidized to CO_2. By assuming that the carboxyl group appears entirely as CO_2, the proportions of CO, CO_2, and CH_3NO_2 which are formed from the methyl group have been calculated and are listed in Table 2. Although reactions are known which are consistent in a qualitative way with the fate of the methyl group, the observed variation in the ratio $[CO_2]/[CO]$ as a function of pressure of NO_2 could not be accounted for. In columns 7–10 of Table 1 it can be seen that the final pressure change is smaller at a high pressure than at a low pressure of acetic acid, indicating that a high pressure of acetic acid favors formation of CH_3NO_2. This observation also could not be explained.

The results of this exploratory study indicate that a more detailed investigation should prove interesting in connection with reactions involving the methyl group as well as with the mechanism of autocatalysis.

Financial support from the National Research Council of Canada is gratefully acknowledged.

1. F. H. POLLARD and K. A. HOLBROOK. Trans. Faraday Soc. **53**, 468 (1957).
2. F. H. POLLARD and R. M. H. WYATT. Trans. Faraday Soc. **45**, 760 (1949).
3. A. E. PEDLER and F. H. POLLARD. Trans. Faraday Soc. **53**, 44 (1957). L. PHILLIPS and R. SHAW. Tenth Symposium on Combustion, 453 (1964).
4. J. H. THOMAS. Trans. Faraday Soc. **49**, 630 (1953)
5. D. BARTON. J. Phys. Chem. **65**, 1831 (1961).
6. D. BARTON and P. E. YANKWICH. J. Phys. Chem. **71**, 3455 (1967).
7. R. N. PANDEY. M.Sc. thesis. Memorial University of Newfoundland, St. John's, Newfoundland. 1967.
8. A. B. GAGARINA and N. M. EMANUEL. J. Phys. Chem. U.S.S.R., **33**, 90 (1959).

Can. J. Chem. Downloaded from www.nrcresearchpress.com by 210.87.254.105 on 09/05/12
For personal use only.

Can. J. Chem. Downloaded from www.nrcresearchpress.com by 210.87.254.105 on 09/05/12
For personal use only.

Canadian Journal of Chemistry

Published by THE NATIONAL RESEARCH COUNCIL OF CANADA

VOLUME 48 NOVEMBER 15, 1970 NUMBER 22

Ionic reactions occurring in the irradiation of carbon dioxide – oxygen mixtures at very high dose rates[1]

CLIVE WILLIS AND P. E. BINDNER

Physical Chemistry Branch, Chalk River Nuclear Laboratories, Atomic Energy of Canada Limited, Chalk River, Ontario

Received March 20, 1970

Ozone yields have been measured in CO_2–O_2 mixtures irradiated with single pulses from a Febetron 705 at a dose rate of 10^{26} eV g^{-1} s^{-1}. Low concentrations of carbon dioxide in oxygen rapidly reduce the yield from $G(O_3) = 12.8$ to $G(O_3) \approx 9$. At 300 Torr total pressure, as the oxygen concentration is reduced, the ozone yield decreases from this yield of $G(O_3) \approx 9$ to an extrapolated yield, at zero oxygen, of close to $G(O_3) = 7.8$. Changes of yields with composition are explained in terms of ionic reactions, the main neutralization process being

[14] $$O_2^+ + CO_4^- \rightarrow O + 2O_2 + CO$$

At 700–1500 Torr total pressure, the ozone yields are lower than that at 300 Torr. It is proposed that clustering of the ionic species affects the products of the neutralization reaction.

Sulfur hexafluoride suppresses the dissociative neutralization reaction and ozone yields from mixtures containing 1.5–2% SF_6 are those predicted from direct neutral dissociation processes in the pure gases.

Computer calculations are used to compare the experimental results to the proposed mechanism and, in general, a good fit is obtained.

Canadian Journal of Chemistry, **48**, 3463 (1970)

Introduction

Previous studies of the radiation chemistry of carbon dioxide – oxygen mixtures have been reported by Anderson and Best (1) and by Meaburn *et al.* (2).

Anderson and Best (1) carried out a very detailed study of the system at dose rates from 10^{19} to 10^{21} eV $g^{-1}s^{-1}$. In discussing the ionic mechanism they were unable to present precise conclusions. They did suggest, on kinetic grounds, that O_2^- and CO_4^- would be the predominant negative ions and that one or both of these was responsible for the rapid re-oxidation of carbon monoxide observed in the radiolysis of carbon dioxide at low dose rates (3).

Meaburn *et al.* (2) irradiated carbon dioxide – oxygen mixtures with single electron pulses at the much higher dose rate of about 2×10^{25} eV $g^{-1}s^{-1}$ as part of a survey of reactions of oxygen atoms. They studied the effect of sulfur hexafluoride on the yields but reported only isolated results which did not allow general conclusions to be made. They suggested that energy transfer from carbon dioxide to oxygen was important in the radiolysis so as to preclude any quantitative mechanistic speculations. However, they did speculate that either CO_3^- or CO_4^- was involved in the radiolysis mechanism.

We have previously studied the radiation chemistry of both pure oxygen (4) and pure carbon dioxide (5) with single electron pulses at high dose rates of 10^{26}–10^{27} eV $g^{-1}s^{-1}$, conditions similar to those of Meaburn *et al.* (2). As a result of these studies, we felt that the carbon dioxide – oxygen system warranted further study. We have measured ozone yields over the whole range of composition, with and without the addition of sulfur hexafluoride. A fairly complete ionic mechanism is proposed based on known reactions and, in particular, the ion neutralization steps are examined in detail.

Experimental

Irradiations

The source of electron pulses used in these experiments is a Febetron 705. This gives single, very intense pulses which were used to irradiate the gas mixture contained in

[1]AECL No. 3701.

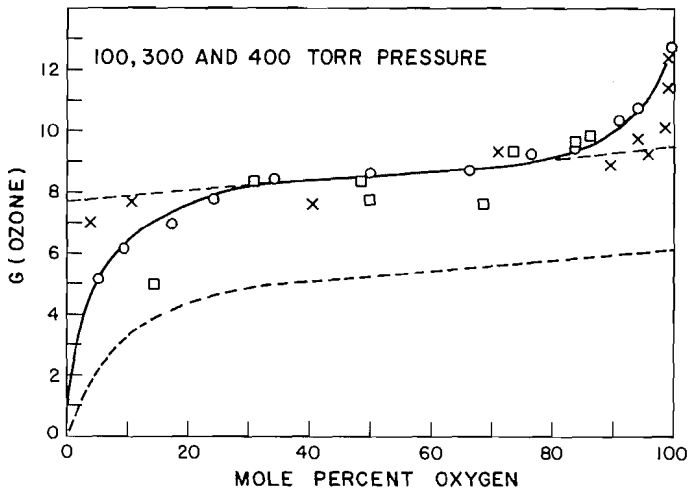

FIG. 1. Ozone yields from CO_2–O_2 mixture at 100, 300, and 400 Torr total pressure. □, 100 Torr dose rate 2×10^{26} eV $g^{-1}s^{-1}$; ○, 300 Torr dose rate 2×10^{26} eV $g^{-1}s^{-1}$; ×, 400 Torr dose rate $\sim 10^{25}$ eV $g^{-1}s^{-1}$; —, results taken from ref. 2; ----, yields in presence of SF_6 taken from Fig. 3.

a stainless steel cell fitted with a multiple reflection mirror system. More complete details are given elsewhere of the irradiation procedures and optical techniques (6–8).

Ozone Analysis

Ozone was determined by its optical absorption at 254 nm using the decadic extinction coefficient as (9, 10)

$$\varepsilon_{254\,nm} = 135\ cm^{-1}\ S.T.P.$$

The gas mixture in the cell was irradiated and the absorption at 254 nm measured about 200 ms after the irradiation pulse, when the ozone concentration had reached a limiting value. The ozone yield for a particular sample, then, was obtained by comparing the optical density at this wavelength to that obtained for pure oxygen. The usual corrections for pressure and relative stopping powers were made in calculating relative doses.

No carbon monoxide yields are presented as attempts to measure small concentrations of carbon monoxide in the presence of a large excess of oxygen have not given sufficient precision for the values to be meaningful.

Dosimetry

The mean dose absorbed in the cell over the volume illuminated by the analyzing light was determined by irradiating pure oxygen at various pressures. The yield of ozone from pure oxygen at pressures from 100–800 Torr at dose rates of 10^{25}–10^{27} eV $g^{-1}s^{-1}$ can be taken as $G(O_3) = 12.8 \pm 0.6$ (2, 4, 11, 12). For the conditions of the present experiments, the mean dose in the cell was about 0.1 Mrad per pulse delivered at a dose rate of approximately 10^{26} eV $g^{-1}s^{-1}$.

Materials

The oxygen, Matheson C.P. grade, was used directly from the cylinder. The carbon dioxide, Matheson "bone-dry", and sulfur hexafluoride, Matheson C.P. grade, were outgassed prior to use. All gas mixtures were thoroughly mixed by thermal cycling before irradiation.

Results

The ozone yields from single pulse irradiations of carbon dioxide – oxygen mixtures at a total pressure of 100 and 300 Torr are given in Fig. 1. Included on this figure are results taken from the paper of Meaburn *et al.* (2) for a total pressure of 400 Torr and a dose rate of 2×10^{25} eV $g^{-1}s^{-1}$. Actual values reported by Meaburn *et al.* (2) are based on nitrous oxide dosimetry taking $G(N_2) = 10$. As we have discussed elsewhere (5), the value at 2×10^{25} eV $g^{-1}s^{-1}$ should be close to $G(N_2) = 12.4$ and all values taken from this paper are corrected to this latter nitrogen yield.

The results show a rapid decrease in ozone yield from $G(O_3) = 12.8$ for pure oxygen to $G(O_3) \approx 9$ for 90% oxygen. As the amount of oxygen in the mixture is further decreased, the ozone yield decreases slowly until at $\sim 20\%$ oxygen the yield starts to decrease again more rapidly.

Ozone yields for carbon dioxide – oxygen mixtures at total pressures of 700 and 1500 Torr are given in Fig. 2. The values shown are qualitatively similar to those at the lower pressures given in Fig. 1 but are some 10–15% lower between 20 and 80% oxygen.

A limiting value for the ozone yield from pure carbon dioxide at 700 Torr for the present experimental conditions (stainless steel optical cell, etc.) at a dose rate of 10^{26} eV $g^{-1}s^{-1}$ has been measured to be $G(O_3) \leqslant 0.2$. This is comparable to

Can. J. Chem. Downloaded from www.nrcresearchpress.com by 210.87.254.105 on 09/05/12
For personal use only.

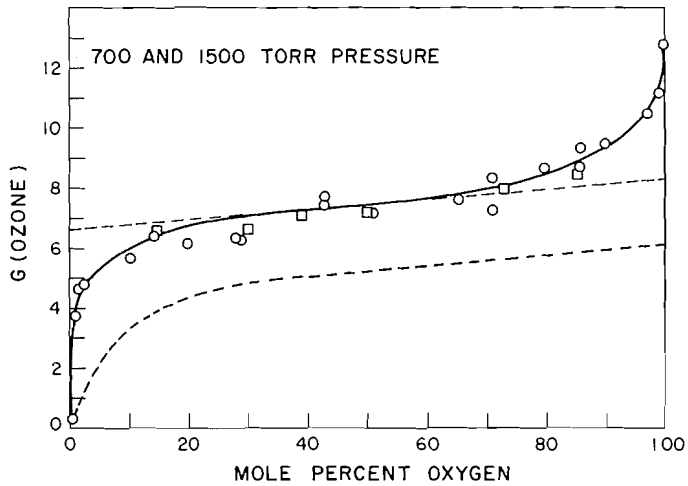

FIG. 2. Ozone yields from CO_2–O_2 mixtures at 700 and 1500 Torr total pressure. ○, 700 Torr dose rate 2×10^{26} eV $g^{-1}s^{-1}$; □, 1500 Torr dose rate 2×10^{26} eV $g^{-1}s^{-1}$; ---, yields in presence of SF_6 taken from Fig. 3.

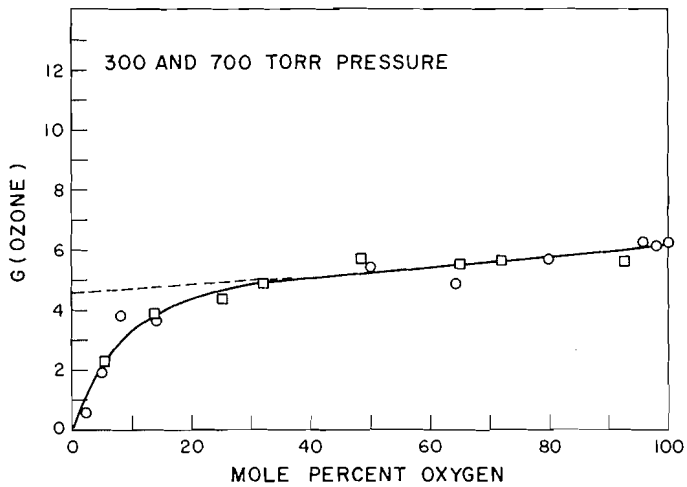

FIG. 3. Ozone yields from CO_2–O_2 mixtures at 300 and 700 Torr total pressure containing 1.5–2.0% SF_6. □, 300 Torr dose rate 2×10^{26} eV $g^{-1}s^{-1}$; ○, 700 Torr dose rate 2×10^{26} eV $g^{-1}s^{-1}$.

that previously reported (5) for the higher dose rate of 2×10^{27} eV $g^{-1}s^{-1}$ where $G(O_3) \leqslant 0.1$.

The effect of SF_6 on the product yields as a function of concentration has been previously reported for both pure oxygen (4) and pure carbon dioxide (5). In both cases, at a dose rate of 2×10^{27} eV $g^{-1}s^{-1}$, 0.1–0.2 mole% SF_6 was sufficient to produce a limiting effect. Ozone yields from carbon dioxide – oxygen mixtures at 300 and 700 Torr total pressure in the presence of 1.5–2.0 mole% added SF_6 are shown in Fig. 3. The results obtained at the two pressures are indistinguishable. Addition of SF_6 markedly reduces the observed yield of ozone throughout the range of compositions. Furthermore, the marked decrease in ozone yields on adding an amount of carbon dioxide to oxygen is not observed in the presence of SF_6.

Discussion

There is agreement between our ozone yields and those of Meaburn *et al.* (2) as shown in Fig. 1. It is the purpose of the following discussion to examine the underlying radiolytic mechanism which results in the yields observed.

The immediate precursor of all ozone formed

Can. J. Chem. Downloaded from www.nrcresearchpress.com by 210.87.254.105 on 09/05/12
For personal use only.

TABLE 1

Yields of primary processes in oxygen and carbon dioxide

Oxygen*		Carbon dioxide†	
Process	Yield (G units)	Process	Yield (G units)
$O_2 \rightsquigarrow O + O$	3.00	$CO_2 \rightsquigarrow CO + O$	4.05
$O_2 \rightsquigarrow O_2^+ + e$	3.17	$CO_2 \rightsquigarrow CO_2^+ + e$	2.30
$O_2 \rightsquigarrow O^+ + O + e$	0.10	$CO_2 \rightsquigarrow CO^+ + O + e$	0.46
		$CO_2 \rightsquigarrow O^+ + CO + e$	0.16
		$CO_2 \rightsquigarrow C^+ + 2O + e$	0.07
Yield of O atoms (excluding ion–molecule and ion–neutralization reactions)			
Oxygen		Carbon dioxide	
$G(O) = 2 \times 3.00 + 0.10 = 6.10$		$G(O) = 4.05 + 0.46 + 2 \times 0.07 = 4.65$	

*Yields taken from ref. 4.
†Yields taken from ref. 5.

in the radiolysis of carbon dioxide – oxygen mixtures is an oxygen atom. Meaburn *et al.* (2) have shown that "the pseudo-first order plots of ozone formation in carbon dioxide–oxygen mixtures are strictly linear and can be interpreted in terms of a single reaction,

[1] $$O(^3P) + O_2 + M \rightarrow O_3 + M$$

They could not exclude prior deactivation of $O(^1D)$ or the participation of the CO_3 molecule. However, their results show that ozone has no direct ionic mode of formation in the system.

The oxygen atoms produced in irradiated carbon dioxide – oxygen mixtures have two distinct origins: neutral, dissociative excitation processes, and ionic processes.

The primary processes and their yields for pure oxygen and pure carbon dioxide are summarized in Table 1. These values and their derivations are discussed fully in the two papers referred to. This table is presented here as the yields of the various primary processes will be used throughout the following discussion.

Yields in the Presence of SF_6

Sulfur hexafluoride reduces the yields of products of radiolysis of oxygen and of carbon dioxide by suppressing dissociative neutralization of ions (4, 5). The total yield of oxygen atoms from oxygen for processes other than dissociative neutralization will be that from direct dissociative excitation, shown in Table 1, plus that produced from the small amount of O^+ present via reaction 2.[2]

[2] $$O^+ + O_2 \rightarrow O_2^+ + O$$

The yield of oxygen atoms from pure oxygen in the presence of SF_6, then, is

$$G(O) = 6.10 + 0.10 = 6.2$$

The oxygen atom yield from carbon dioxide when dissociative neutralization is suppressed should be $G(O) = 4.65$. The O^+ ions in carbon dioxide do not directly yield oxygen atoms but react via reaction 3 to give O_2^+, yielding oxygen atoms only on dissociative neutralization.

[3] $$O^+ + CO_2 \rightarrow CO + O_2^+$$

Thus the yield of ozone formed in carbon dioxide – oxygen mixtures containing SF_6 is expected to give an extrapolated yield for 100% carbon dioxide of $G(O_3) = 4.65$ representing the yield of oxygen atoms. The yield of ozone should then vary with composition from $G(O_3) = 4.65$ to 6.2 from 0 to 100% oxygen.

The ozone yields in the presence of SF_6, shown in Fig. 3, are in very good agreement with the predictions made from the pure gases. The yield of ozone decreases steadily from $G(O_3) = 6.2 \pm 0.5$ for pure oxygen to an extrapolated yield of $G(O_3) = 4.5 \pm 0.5$ for

[2]All references to ionic reactions are given in Table 3 and will not be generally referred to throughout the text.

Can. J. Chem. Downloaded from www.nrcresearchpress.com by 210.87.254.105 on 09/05/12
For personal use only.

Can. J. Chem. Downloaded from www.nrcresearchpress.com by 210.87.254.105 on 09/05/12
For personal use only.

pure carbon dioxide. The fall-off in measured ozone yields below $\sim 25\%$ oxygen is presumably due to inefficient scavenging of oxygen atoms by the oxygen as discussed by Meaburn *et al.* (2).

The agreement between the predicted and experimental yields for these conditions excludes serious complications from energy transfer from carbon dioxide to oxygen as suggested by Meaburn *et al.* This suggestion was made as the value of the rate constant estimated for reaction 4 was an order of magnitude higher than that

[4] $$O(^3P) + O(^3P) + CO_2 \rightarrow O_2 + CO_2$$

generally accepted in the literature. They proposed that "energy transfer from carbon dioxide to oxygen leads to an instantaneous increase in oxygen atom concentration and a consequent over-estimate of the pseudo-bimolecular rate constant". We find no evidence for such energy-transfer processes.

Ionic Processes

Positive Ions

The predominant positive ions formed in oxygen and carbon dioxide will be O_2^+ and CO_2^+. However, for the sake of completeness, the fates of the other ions formed will be examined.

In pure oxygen, O^+ rapidly reacts to give O_2^+ via reaction 2. Addition of carbon dioxide should not affect the production of O_2^+ as O^+ can react with carbon dioxide to give O_2^+ via reaction 3.

[3] $$O^+ + CO_2 \rightarrow CO + O_2^+$$

The situation for the minor ions produced from carbon dioxide is more complex. Initially formed CO^+ and C^+, in pure carbon dioxide, will react as in [5] and [6]. Thus most positive ions

[5] $$CO^+ + CO_2 \rightarrow CO_2^+ + CO$$

[6] $$C^+ + CO_2 \rightarrow CO^+ + CO$$

will react to give CO_2^+ except for O_2^+ formed from O^+; and the CO_2^+ ion in carbon dioxide at the pressures of the present experiments will rapidly form $C_2O_4^+$ (16, 23) via reaction 7.

[7] $$CO_2^+ + 2CO_2 \rightarrow C_2O_4^+ + CO_2$$

Addition of oxygen to carbon dioxide will significantly change the reactions of the positive ions discussed above. As the concentration of oxygen is increased CO^+ will tend to react via [8] instead of [5]

[8] $$CO^+ + O_2 \rightarrow O_2^+ + CO$$

and C^+ via [9] instead of [6]. Moreover,

[9] $$C^+ + O_2 \rightarrow CO^+ + O$$

CO_2^+ and presumably $C_2O_4^+$, as will be discussed below, can also react with oxygen, yielding O_2^+.

[10] $$CO_2^+ + O_2 \rightarrow O_2^+ + CO_2$$

[11] $$C_2O_4^+ + O_2 \rightarrow O_2^+ + 2CO_2$$

When sufficient oxygen is added, then, all positive ions will end up as O_2^+ provided neutralization does not intercede.

Negative Ions

In both oxygen and carbon dioxide the predominant negative species formed initially will be the electron. Thermal electrons can attach to oxygen, via reaction 12, but apparently

[12] $$e + O_2 + M \rightarrow O_2^- + M$$

thermal electrons cannot attach directly to carbon dioxide. A very recent report (24) has shown CO_2^- to be stable but it is almost certainly a bent molecule and Franck Condon factors may exclude a rapid thermal attachment process (25). In pure oxygen, then, O_2^-, or a more complexed form ($O_{2_n}^-$) (4), will be the predominant negative species and in pure carbon dioxide the negative species will initially be the electron.[3]

In carbon dioxide – oxygen mixtures the O_2^- ion formed can react further to give CO_4^- (21).

[13] $$O_2^- + CO_2 + M \rightarrow CO_4^- + M$$

Whether CO_4^- or O_2^- is the predominant negative ion depends on concentrations, pressure, and dose rate.

Neutralization Reactions

We are now in a position to consider the product yield formed from the neutralization reactions. Which ions are involved in the neutralization step, for the dose rates of the present experiments, will be very dependent upon the

[3]Rigorously, this is only applicable for very low doses at very high dose rates. As oxygen is produced by the radiolysis it can compete for the electron with the neutralization step and at low dose rates (10^{16} eV g^{-1} s^{-1}), only very low doses will be required to produce sufficient oxygen for the O_2^- ion to be formed.

Can. J. Chem. Downloaded from www.nrcresearchpress.com by 210.87.254.105 on 09/05/12
For personal use only.

mixture considered. Below, by computer calculation, the contributions of each process will be given; however, the products of neutralization must first be considered.

In pure carbon dioxide the neutralization step will be

[18] $$C_2O_4^+ + e \rightarrow CO + O + CO_2$$

This reaction gives one oxygen atom as we have discussed elsewhere (5). In pure oxygen the neutralization step will be of the form

[15] $$O_2^+(O_2)_n + O_2^-(O_2)_m \rightarrow O + O + (n + m + 1)\,O_2$$

In reporting our results for pure oxygen (4) we discussed various neutralization processes involving the O_2^+ ion. Briefly, we concluded that if the electron, O_2^-, or O_4^- ions were involved, dissociative neutralization occurred yielding two oxygen atoms as shown in reaction 15. This reaction involving the electron or O_2^- has been treated theoretically by Chan (26, 27) who proposes an "electron-jump" tunnelling mechanism for the neutralization step. In ref. 4, we also considered neutralization by SF_6^-, c-$C_4F_8^-$, and O_3^- and concluded that two oxygen atoms were not formed (*i.e.* no dissociation of O_2^+ on neutralization). We were unable to determine if there was any dissociation of the negative species.

In carbon dioxide – oxygen mixtures the neutralization step, in addition to the reactions just given, will also include reactions of the form

[20] $$C_2O_4^+ + O_2^- \rightarrow CO + O + CO_2 + O_2$$

and

[14] $$O_2^+ + CO_4^- \rightarrow \text{Products}$$

Based on the "electron-jump" mechanism for neutralization by O_2^-, it is reasonable to suppose that the products of reaction 20 will be similar to those formed from neutralization of $C_2O_4^+$ by the bare electron, as in reaction 18. However, we cannot make any such predictions for the products of reaction 14.

There are three possibilities for this reaction:

(*i*) positive ion dissociation

[14*a*] $$O_2^+ + CO_4^- \rightarrow O + O + O_2 + CO_2$$

(*ii*) non-dissociative neutralization

[14*b*] $$O_2^+ + CO_4^- \rightarrow 2O_2 + CO_2$$

(*iii*) negative ion dissociation

[14*c*] $$O_2^+ + CO_4^- \rightarrow CO + O + 2O_2$$

The first of these, [14*a*], gives two oxygen atoms per neutralization; the second, [14*b*], none; and the third, [14*c*], one. As we shall see below, of these three possibilities only the process involving negative ion dissociation, [14*c*], giving one oxygen atom and one carbon monoxide molecule per neutralization, is consistent with the experimental results.

As is reported below in the section presenting computer calculated results, for carbon dioxide – oxygen mixtures between 30 and 70% oxygen, the predominant neutralization reaction is [14]. As carbon dioxide is added to oxygen, the measured ozone yields at all pressures shown in Figs. 1 and 2 decreases from the pure oxygen value of $G(O_3) = 12.8 \pm 0.6$ where two oxygen atoms are formed per neutralization. The ozone yields extrapolated from intermediate mixtures (30–70% oxygen) shown in Fig. 1 give $G(O_3) = 9.3 \pm 0.5$ for 100% oxygen and $G(O_3) = 7.7 \pm 0.5$ for 100% carbon dioxide. Subtracting from these values, the contributions from processes other than neutralization, the extrapolated yields from neutralization processes are, for 100% oxygen, $9.3 - 6.2 = 3.1$ and for 100% carbon dioxide $7.7 - 4.6 = 3.1$. Within experimental error these are equal to the ion pair yield for each of the gases, $W_{O_2} = 30.6$ eV per ion pair (28); $W_{CO_2} = 33.1$ eV per ion pair (29). One ozone (and hence one oxygen atom) then must be produced from each ion pair (*i.e.* per neutralization).

In this context it is important to note that Meaburn *et al.* (2) report that the yield of carbon monoxide from carbon dioxide is unaffected by up to at least 1% added oxygen. Since, at their dose rate, this is sufficient to significantly reduce the amount of $C_2O_4^+$ ions in the neutralization step and since, in pure carbon dioxide, one molecule of carbon monoxide is produced per neutralization, this observation strongly supports the above prediction that one carbon monoxide molecule is produced for each O_2^+ ion neutralized.

Computer Calculations

Computer calculations have been used to estimate the detailed contributions of all reactions to the final yields. The program used, originally written by Schmidt (30) as WR 16, calculates the concentrations of all species as a function of time during and following the irradiation pulse.

TABLE 2

Primary yields in carbon dioxide – oxygen mixtures

Percentage oxygen	Percentage of dose absorbed in oxygen	Initial yields (G units)							
		CO_2^+	CO^+	O^+	C^+	O_2^+	CO	O	e
100	100	—	—	0.10	—	3.17	—	6.10	3.27
90	86.7	0.31	0.06	0.11	0.01	2.75	0.56	5.91	3.24
80	74.4	0.59	0.12	0.11	0.02	2.36	1.08	5.73	3.20
70	62.9	0.85	0.17	0.12	0.03	1.99	1.56	5.57	3.16
60	52.2	1.10	0.22	0.13	0.03	1.65	2.01	5.40	3.13
50	42.1	1.33	0.27	0.13	0.04	1.33	2.44	5.26	3.10
40	32.7	1.55	0.31	0.14	0.04	1.04	3.10	5.12	3.08
30	23.8	1.76	0.35	0.15	0.05	0.75	3.21	4.99	3.06
20	15.4	1.95	0.39	0.16	0.05	0.49	3.56	4.87	3.04
10	7.5	2.13	0.43	0.16	0.06	0.24	3.89	4.76	3.02
0	0.0	2.30	0.46	0.16	0.07	—	4.21	4.65	2.99

TABLE 3

Ionic reactions in irradiated carbon dioxide – oxygen mixtures

	Reaction	Rate constant (cm^3 $molecule^{-1}$ s^{-1})	Reference No. or footnote
[2]	$O^+ + O_2 \rightarrow O_2^+ + O$	$2 \pm 1 \times 10^{-11}$	13
[3]	$O^+ + CO_2 \rightarrow O_2^+ + CO$	1.2×10^{-9}	13, 14
[5]	$CO^+ + CO_2 \rightarrow CO_2^+ + CO$	1.1×10^{-9}	15
[6]	$C^+ + CO_2 \rightarrow CO^+ + CO$	1.9×10^{-9}	15
[7]	$CO_2^+ + 2CO_2 \rightarrow C_2O_4^+ + CO_2$	3×10^{-28}	16*
[8]	$CO^+ + O_2 \rightarrow O_2^+ + CO$	2.0×10^{-10}	15
[9]	$C^+ + O_2 \rightarrow CO^+ + O$	$1.0 \pm 0.1 \times 10^{-10}$	15,17
[10]	$CO_2^+ + O_2 \rightarrow O_2^+ + CO_2$	1.0×10^{-10}	18
[11]	$C_2O_4^+ + O_2 \rightarrow O_2^+ + 2CO_2$	1.0×10^{-10}	†
[12]	$e + O_2 + M \rightarrow O_2^- + M$	2.0×10^{-30}	*‡
[13]	$O_2^- + CO_2 + M \rightarrow CO_4^- + M$	1.0×10^{-30}	*§
[14]	$O_2^+ + CO_4^- \rightarrow$ Products	2×10^{-6}	†
[15]	$O_2^+ + O_2^-.O_2 \rightarrow O + O + 2O_2$	2×10^{-6}	†
[16]	$O_2^+ + e \rightarrow O + O$	2×10^{-7}	22
[17]	$CO_2^+ + e \rightarrow CO + O$	2×10^{-7}	†
[18]	$C_2O_4^+ + e \rightarrow CO + O + CO_2$	2×10^{-7}	†
[19]	$CO_2^+ + O_2^- \rightarrow CO + O + O_2$	2×10^{-6}	†
[20]	$C_2O_4^+ + O_2^- \rightarrow CO + O + O_2 + CO_2$	2×10^{-6}	†

*This rate constant has units cm^6 $molecule^{-2}$ s^{-1}.
†This rate constant is assumed.
‡With O_2 as third body the rate constant is reported as $1.4 \pm 0.2 \times 10^{-29} (300/T)\, e^{-600/T}$ cm^6 $molecule^{-2}$ s^{-1} (19) and with CO_2 as the third body as $3.3 \pm 0.7 \times 10^{-30}$ cm^6 $molecule^{-2}$ s^{-1} between 300 and 525 °K (20).
§With O_2 as third body the rate constant is reported as 2×10^{-29} cm^6 $molecule^{-2}$ s^{-1} and with CO_2 as third body as 9×10^{-30} cm^6 $molecule^{-2}$ s^{-1} (21).

We have used this program before for extensive calculations of this type (4, 31). The primary yields of species, as a function of oxygen concentration in the mixture, are given in Table 2. These were interpolated from the yields in the pure gases assuming energy absorption proportional to electron density. The irradiation pulse was approximated by a step function with 2 ns steps. The ionic reactions of importance in carbon dioxide – oxygen mixtures and their rate constants used in the program are given in Table 3.

The calculated concentrations of ionic species as a function of time during and following the Febetron pulse are shown graphically in Figs. 4*a*, 4*b*, 4*c* for 10, 50, and 90% oxygen in carbon dioxide. The Febetron pulse shape is the same as that given elsewhere (4, 31) and is not repeated on the figures. Species given in Table 3 but not shown on the figures had maximum concentrations of less than 10^{-9} *M*.

It is clear from the figures that the predominant ionic species predicted are: O_2^+, CO_4^-, $C_2O_4^+$, O_2^-, and the electron. These species vary in importance with oxygen concentration very much as might be expected. Clearly none of the fragment ions from carbon dioxide (CO^+, O^+, C^+)

Can. J. Chem. Downloaded from www.nrcresearchpress.com by 210.87.254.105 on 09/05/12
For personal use only.

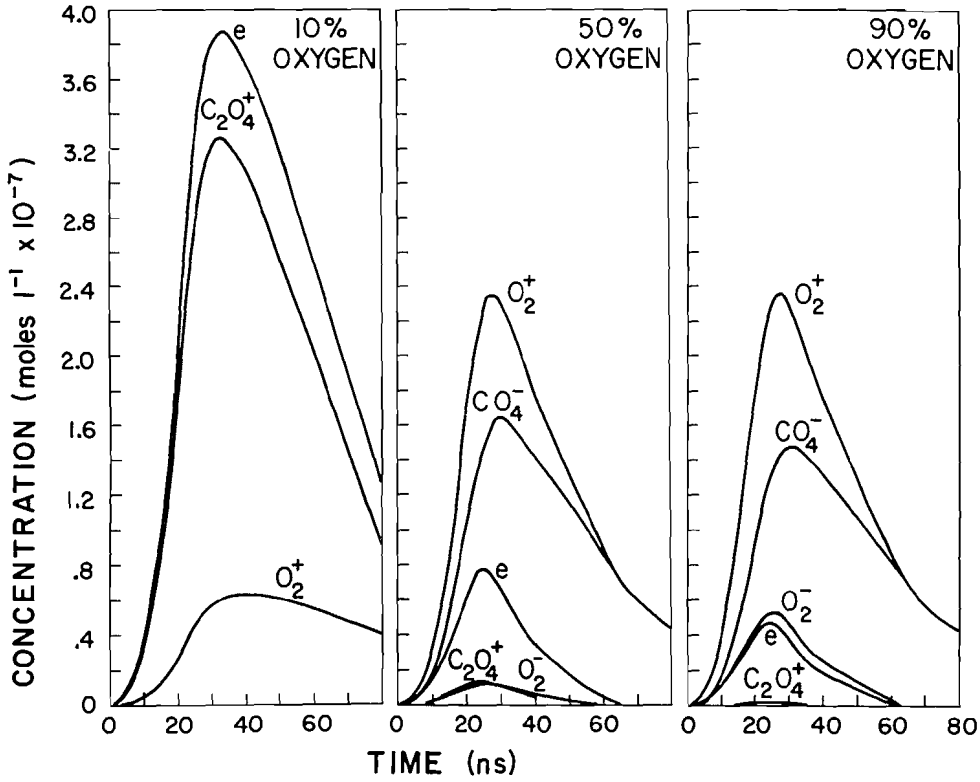

FIG. 4. Calculated concentration of ions in Febetron irradiated CO_2–O_2 mixtures: dose rate, 1.4×10^{26} eV $g^{-1}s^{-1}$; total dose, 1.515×10^{19} eV l^{-1}; pressure, 700 Torr; temperature, 25 °C. *A*, 10% O_2, 90% CO_2; *B*, 50% O_2, 50% CO_2; *C*, 90% O_2, 10% CO_2.

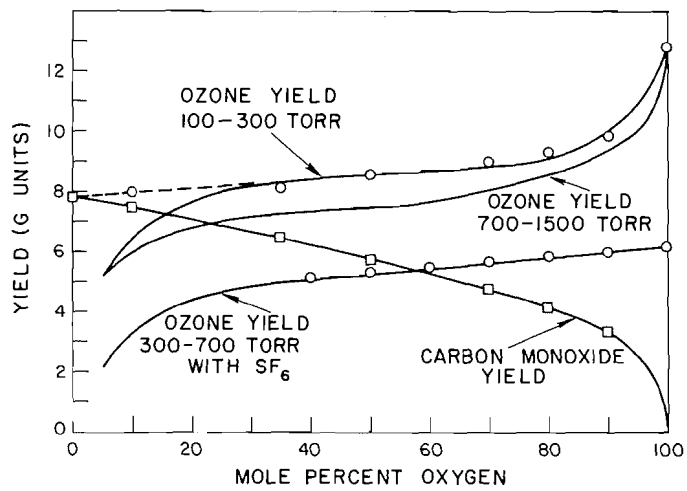

FIG. 5. Comparison of calculated and measured ozone yields from CO_2–O_2 mixtures at 700 Torr pressure. ○, calculated ozone yields with and without SF_6; □, calculated carbon monoxide yields. Curve marked ozone yield 100–300 Torr is taken from Fig. 1; curve marked ozone yield 700–1500 Torr is taken from Fig. 2; curve marked ozone yield 300–700 Torr with SF_6 is taken from Fig. 3 (carbon monoxide yields are all calculated).

Can. J. Chem. Downloaded from www.nrcresearchpress.com by 210.87.254.105 on 09/05/12
For personal use only.

Can. J. Chem. Downloaded from www.nrcresearchpress.com by 210.87.254.105 on 09/05/12
For personal use only.

will be directly neutralized: all will undergo ion–molecule reactions either with carbon dioxide or oxygen.

The yields of ozone and carbon monoxide calculated using the above program, and assuming each oxygen atom yields one molecule of ozone, are shown in Fig. 5. The calculated points shown are for a total pressure of 700 Torr and a dose rate of 1.4×10^{26} eV $g^{-1}s^{-1}$. Except at very high concentrations of oxygen, there is very little difference between the results calculated for 300 and 700 Torr and for this reason only those for 700 Torr are given.

The calculated yields of ozone are in very good agreement with the experimental curve for 100, 300, 400 Torr total pressure from Fig. 1. However, the experimental curve for 700–1500 Torr total pressure from Fig. 2 lies somewhat below this. Based on the reactions given in Table 3, there is no explanation for this. The difference cannot be accounted for by differences in reactions of neutral species since the yields with SF_6 are the same for 300 and 700 Torr and both agree well with the calculations.

At high oxygen concentrations different curves are expected for different pressures due to the pressure dependences of reactions 12 and 13

[12] $$e + O_2 + M \rightarrow O_2^- + M$$

[13] $$O_2^- + CO_2 + M \rightarrow CO_4^- + M$$

competing with the neutralization step. However, this should not give less than one oxygen molecule per neutralization.

It is possible that the lower yields observed at 700–1500 Torr represent inefficient production of ozone from oxygen atoms at these pressures. A more plausible explanation is the effect of clustering of ions leading to different neutralization products.

In the calculations, we have not considered clustering of the ions. In ref. 4 we discussed clustering of oxygen ions in pure oxygen and its effect on the neutralization reactions. It was postulated that neutralization occurred by the electron jump mechanism of Chan (26, 27) with the positive ion being neutralized while the negative species was still a considerable distance away.

The situation in carbon dioxide – oxygen mixtures, however, is different. The neutralization step envisaged for the present system,

[14c] $$O_2^+ + CO_4^- \rightarrow O + CO + 2O_2$$

is unlikely to occur by any tunnelling mechanism. Considerable energy must be realeased to the CO_4^- species to cause dissociation to CO, O, and O_2. Thus it is reasonable to suppose that neutralization occurs only after the positive and negative ions have coalesced. If this is the case, then, if there were any clustering of the ions, energy could be transferred to the clustered molecules suppressing dissociation.

On the basis of this explanation for the difference between the experimental curve for 300 Torr and that for 700 Torr, it would be expected that the results for the higher pressure of 1500 Torr would lie even lower. The results given in Fig. 2 for 1500 Torr do appear to be lower than those for 700 Torr but because of experimental errors, they are not conclusively so.

A recent paper has discussed clustering of ions in carbon dioxide – oxygen mixtures (32) and has given equilibrium constants for the constituents of the clusters. However, our present experiments are not sufficiently precise to apply this data in a quantitative manner.

All the above discussion assumes that $C_2O_4^+$ undergoes charge exchange with oxygen in a manner similar to CO_2^+. We have no evidence that this reaction does occur. Neutralization of $C_2O_4^+$ by an electron (and probably by O_2^-) very likely gives one oxygen atom and one molecule of carbon monoxide (5) which would agree with the observations. However, the rapid fall-off in ozone yield at fairly high oxygen concentrations requires less than two oxygen atoms to be produced per neutralization. For neutralization of $C_2O_4^+$ to be an explanation for this, it would require that O_2^+ could charge exchange to give $C_2O_4^+$, which is not probable.

Conclusions

We have presented an ionic mechanism for the radiolysis of carbon dioxide – oxygen mixtures at high dose rates using our results and drawing from previous observations of Meaburn *et al.* (2). In this mechanism, it has been necessary to propose a neutralization step involving dissociation of the originally negative fragment. It should, perhaps, be emphasized that the only proof we present for this neutralization reaction is its

[14c] $$O_2^+ + CO_4^- \rightarrow CO + O + 2O_2$$

agreement with the kinetic analysis presented. Possibly, some sort of geometrical restraint, such as that we have proposed for the case of neutralization of O_2^+ by O_3^- (4), leads to the break-up of the CO_4 fragment. However, further speculation must await a deeper understanding of gaseous ion-neutralization reactions, a very little understood region.

The present work has not been compared to the results obtained in the detailed study of Anderson and Best (1) because the conditions of their experiments are so widely different from ours. The major conclusions of these authors refer to the back reactions observed in the low dose rate radiolysis of carbon dioxide. It is hoped that a study of the radiation chemistry of carbon monoxide – oxygen mixtures at our high dose rates will enhance understanding of these back reactions. We are at present beginning work on this system.

At present we have no explanation for the difference in yields between 100–300 Torr and 700–1500 Torr other than clustering of ions, as has been discussed. Further work at different dose rates and pressures could give additional information on this effect. This work is now in progress and will be reported later.

We should like to thank Drs. A. W. Boyd and W. A. Seddon of CRNL for their careful reading of the manuscript.

1. A. R. ANDERSON and J. V. F. BEST. Advan. Chem. **82**, 231 (1968).
2. G. M. MEABURN, D. PERNER, J. LECLAVÉ, and M. BOURÈNE. J. Phys. Chem. **72**, 3920 (1968).
3. (*a*) A. R. ANDERSON and D. A. DOMINEY. Rad. Res. Rev. **1**, 269 (1968). (*b*) A. R. ANDERSON. Fundamental processes in radiation chemistry. *Edited by* P. Ausloos. John Wiley and Sons, Inc., New York. 1968. p. 281.
4. C. WILLIS, A. W. BOYD, M. J. YOUNG, and D. A. ARMSTRONG. Can. J. Chem. **48**, 1505 (1970).
5. C. WILLIS, A. W. BOYD, and P. E. BINDNER. Can. J. Chem. **48**, 1951 (1970).
6. C. WILLIS, A. W. BOYD, and O. A. MILLER. Can. J. Chem. **47**, 3007 (1969).
7. C. WILLIS, A. W. BOYD, and M. J. YOUNG. Can. J. Chem. **48**, 1515 (1970).
8. C. WILLIS, W. A. SEDDON, and M. J. YOUNG. AECL report. To be published.
9. W. B. DEMORE and O. RAPER. J. Phys. Chem. **68**, 412 (1964).
10. M. GRIGGS. J. Chem. Phys. **49**, 857 (1968).
11. J. A. GHORMLEY, C. J. HOCHANADEL, and J. W. BOYLE. J. Chem. Phys. **50**, 419 (1969).
12. A. W. BOYD, C. WILLIS, R. CYR, and D. A. ARMSTRONG. Can. J. Chem. **47**, 4715 (1969).
13. D. B. DUNKIN, F. C. FEHSENFELD, A. L. SCHMELTEKOPF, and E. E. FERGUSON. J. Chem. Phys. **49**, 1365 (1968).
14. F. C. FEHSENFELD, E. E. FERGUSON, and A. L. SCHMELTEKOPF. J. Chem. Phys. **44**, 3022 (1966).
15. F. C. FEHSENFELD, A. L. SCHMELTEKOPF, and E. E. FERGUSON. J. Chem. Phys. **45**, 23 (1966).
16. J. F. PAULSON, F. DALE, and R. L. MOSHER. Nature, **204**, 377 (1964).
17. J. L. FRANKLIN and M. S. B. MUNSON. 10th Combustion Symp. Comb. Inst., Pittsburgh. 1965. p. 561.
18. E. E. FERGUSON. Space research. Vol. VII. North Holland Publ. Co., Amsterdam. 1967. p. 135.
19. J. L. PACK and A. V. PHELPS. J. Chem. Phys. **44**, 1870 (1966).
20. J. L. PACK and A. V. PHELPS. J. Chem. Phys. **45**, 4316 (1966).
21. J. L. MORUZZI and A. V. PHELPS. J. Chem. Phys. **45**, 4617 (1966).
22. E. E. FERGUSON. Advan. in Electron. and Elec. Phys. **24**, 1 (1968).
23. S. M. SCHILDCROUT and J. L. FRANKLIN. J. Chem. Phys. **51**, 4055 (1969).
24. J. F. PAULSON. J. Chem. Phys. **52**, 963 (1970).
25. J. N. BARDSLEY. J. Chem. Phys. **51**, 3384 (1969).
26. F. T. CHAN. J. Chem. Phys. **49**, 2533 (1968).
27. F. T. CHAN. J. Chem. Phys. **49**, 2540 (1968).
28. G. G. MEISELS. J. Chem. Phys. **41**, 51 (1964).
29. W. P. JESSE and J. SADAUSKIS. Phys. Rev. **97**, 1668 (1965).
30. K. H. SCHMIDT. USAEC Research and Development Report, ANL-7199, 1966.
31. C. WILLIS, A. W. BOYD, and D. A. ARMSTRONG. Can. J. Chem. **47**, 3783 (1969).
32. N. G. ADAMS, D. K. BOHME, D. B. DUNKIN, F. C. FEHSENFELD, and E. E. FERGUSON. J. Chem. Phys. **52**, 3133 (1970).

Can. J. Chem. Downloaded from www.nrcresearchpress.com by 210.87.254.105 on 09/05/12
For personal use only.

Can. J. Chem. Downloaded from www.nrcresearchpress.com by 210.87.254.40 on 09/05/12
For personal use only.

Studies on hydrogen–oxygen systems in the electrical discharge. IV. Spectroscopic identification of the matrix-stabilized intermediates, H_2O_3 and H_2O_4

PAUL A. GIGUÈRE AND KAZIMIERA HERMAN
Centre de Recherches sur les Atomes et les Molécules, Université Laval, Québec, Québec

Received May 13, 1970

The infrared absorption of the products from electrically dissociated H_2O or D_2O vapor and other hydrogen–oxygen systems trapped at liquid nitrogen temperature was measured between 4000 and 300 cm^{-1}. Four new absorption bands were found in the deuterated systems at 857, 820, 760, and about 440 cm^{-1}. By isotopic substitution of ^{18}O the frequencies are shifted to 806, 775, 717, and ~420 cm^{-1} as expected for O—O vibrations. In the hydrogen systems this region is obscured by the strong libration bands of H_2O and H_2O_2 molecules. Temperature and composition effects show that more than one new species is involved. Accordingly the new spectra are assigned to the often postulated polyoxides, H_2O_3 and H_2O_4, stabilized in the water–peroxide matrix. The more abundant, and also more stable, H_2O_3 has a half-life of some 5 h at −65 °C.

The observed frequencies are consistent with zigzag chain structures linked by single covalent bonds as in hydrogen polysulfides. Relative concentrations of the polyoxides are estimated at 5 to 10 mole% depending on the composition of the starting material. Possible mechanisms of formation and decomposition are discussed.

On a étudié les spectres infrarouges entre 4000 et 300 cm^{-1} des produits piégés de la vapeur d'eau, H_2O ou D_2O, et autres systèmes oxhydriques dissociés dans une décharge électrique. Quatre nouvelles bandes apparaissent à 857, 820, 760 et environ 440 cm^{-1} dans les systèmes deutériés. Par substitution isotopique de ^{18}O les fréquences sont décalées à 806, 775, 717 et environ 420 cm^{-1} tel que prévu pour des vibrations O—O. Avec l'hydrogène ordinaire cette région est complètement obscurcie par les fortes bandes de libration des molécules H_2O et H_2O_2. Les effets de composition et de température confirment qu'il y a plus d'une nouvelle espèce moléculaire dans les produits piégés. Par analogie avec les polysulfures d'hydrogène il doit s'agir des polyoxydes H_2O_3 et H_2O_4. Le plus abondant et le plus stable des deux, H_2O_3 se décompose avec une demi-vie de l'ordre de cinq heures à −65 °C.

Les nouveaux spectres sont en accord avec des structures en chaînes reliées par des liaisons covalentes simples. La concentration molaire des polyoxydes varie entre 5 et 10% selon la composition des matériaux de départ. On discute brièvement les mécanismes possibles de formation et de décomposition.

Canadian Journal of Chemistry, **48**, 3473 (1970)

Introduction

The existence of higher oxides of hydrogen such as H_2O_3 and H_2O_4 has been postulated repeatedly since the original suggestion of Berthelot in 1880 (1). For a review of the question *cf.* the recent monograph by Venugopalan and Jones (2). In particular the trioxide[1] has been considered as a metastable intermediate in the reaction between ozone and hydrogen peroxide (4), and more recently in the radiation chemistry of aqueous systems, mainly from kinetics evidence (5–7). In the much studied material (2) condensed from electrically dissociated water vapor and other hydrogen–oxygen systems, H_2O_3 and H_2O_4 have been postulated on the basis of such experimental observations as oxygen evolution on warming (8), thermal analysis (9), or phase change (10). However, this interpretation has been questioned (11, 12). On the other hand, on kinetics grounds H_2O_3 is unlikely to be produced from known reactions although, thermodynamically speaking, it should be less unstable than H_2O_4 (13, 14). In the hope of settling the question this series of investigations was initiated a few years ago (15). Lately our effort was centered on infrared absorption of the frozen products, the technique considered most likely to provide definite evidence. Quite a few similar studies have been carried out in the past, both in this laboratory and elsewhere (16–23). Unfortunately, the many pitfalls and limitations of the method were not always fully appreciated.

[1]This is the logical name for H_2O_3 by analogy with hydrogen trisulfide, the accepted name of H_2S_3. The term sesquioxide has also been used in the past, specially by radiation chemists. However, according to the official nomenclature rules of the I.U.P.A.C. (3) there is no need to specify the combining ratio of the two elements in naming this kind of simple inorganic compound. As for the homologous series H_2O_2, H_2O_3, etc., it should be called the polyoxides, again by analogy with the hydrogen polysulfides. The often used superoxides is misleading since it is already reserved for combinations of the O_2^- ion with the more electropositive metals, like KO_2. Their oxidizing power is higher than the element in its standard state, contrary to the polyoxides.

Can. J. Chem. Downloaded from www.nrcresearchpress.com by 210.87.254.40 on 09/05/12
For personal use only.

Indeed, besides the many possible contaminants previously mentioned (24), the infrared absorption of these systems is a real chameleon. It changes considerably with the physical state (glassy *vs.* crystalline), composition (e.g. formation of a dihydrate $H_2O_2 \cdot 2H_2O$), mixed isotopic species (e.g. from traces of H_2O in D_2O), etc. Interpretation of the spectra is further complicated by the diffuse nature of the OH bands, and the overlapping of high frequency lattice modes in the region of the fundamentals. A large amount of experimental data (some 200 different spectra) was required to complete this investigation.

Experimental

The apparatus was essentially the same as used previously in this laboratory for studying the reactions of ozone with either atomic hydrogen (24) or ammonia (25). The combined plasma tube – low temperature infrared cell (Fig. 1) was constructed somewhat differently to make it more efficient and easier to handle. For instance, the large standard taper ground glass joint, which tended to freeze, was replaced by a flange joint (A) with 10 cm diameter O-ring. The injector tube (B) was positioned so as to provide the maximum trapping of the dissociated stream. This was found by trial to be quite critical, depending on the size of the injector orifice, its orientation towards, and distance from the cold plate. The injector entered the cell through a slanted 14/30 taper joint (C) lubricated with a little silicone grease. To minimize surface reactions the distance from the plasma (D) to the cold plate was kept as short as feasible (about 10 cm). The inlet vacuum stopcock (E) was of the greaseless type, with a Teflon plug and Viton O-ring to avoid contamination. At the same time it afforded better control of the gas stream than an ordinary glass stopcock. The inner coolant well, terminating in a Kovar seal and the copper plate holder (F), was insulated with Teflon tape. This was necessary to avoid sublimation of the sample, followed by condensation onto the colder metal parts during thermal treatments.

The outer windows, of cesium bromide, were sealed on with Cenco Vacuum Wax for easy removal and cleaning. To prevent attack due to evaporation of the sample the cell was opened to the air after each run. For the cold plate the most suitable material turned out to be Irtran-6 (Eastman Kodak's microcrystalline cadmium telluride). Besides its chemical inertness its transparency over the whole region covered here was satisfactory; about 50% as far as 350 cm^{-1} for a 3 mm thick plate. (Thinner plates had insufficient heat capacity.) One drawback was its dark color which prevented observation of the yellow tint usually associated with the glassy deposit. In contrast, rock-salt is clear, but it cuts off at 15 μ. Also, being hygroscopic, it was badly attacked by the sample on warming up. New silver chloride plates could be used for a few runs; thereafter, they tended to darken due to traces of ozone or under the electrical discharge (solarization). As for cesium bromide, it was found to react with

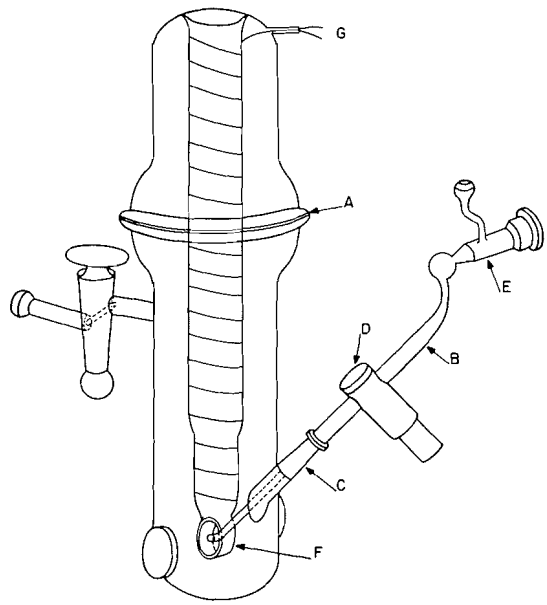

FIG. 1. Combined low temperature infrared absorption cell and microwave plasma tube.

hydrogen peroxide, even at −100 °C. The addition compound presumably thus formed showed some strong absorption bands, particularly one at 945 cm^{-1}.

The temperature of the sample was measured with an accuracy estimated at ± 1° C by means of a tiny copper–constantan thermocouple G inserted between the cold plate and the copper holder. An automatic digital potentiometer ("Megatronix", United Systems Corp.) gave direct readings of the temperature in °C. With liquid nitrogen the lowest temperature attainable was −189°. This rose by 4 or 5° when the microwave discharge was turned on due to surface recombination of the dissociated species. In the plasma itself, the temperature of the Pyrex tube was kept below 40° with an air blast through the microwave cavity. The power dissipated in the latter was somewhat below the maximum capacity of the generator ("Microtron" 200 W, Electro-Medical Supply).

Prior to a run the entire system was evacuated to 10^{-3} Torr by means of a large capacity oil diffusion pump, and then checked for leaks. A most sensitive test was the intense N_2O_3 band at 1305 cm^{-1} readily detected in the spectra of the trapped discharge products (17). Water vapor was admitted through a calibrated needle valve from a thoroughly deaerated liquid sample at room temperature. A suitable deposit, some 10 μ thick, was obtained after 2 h with an evaporation rate of some 0.15 g h^{-1} and a carrier gas to bring the pressure up to about 0.1 Torr. Faster rates (for instance 20 min without carrier gas) gave deposits of poor quality, partly crystalline, with a marked tendency to peel off the cold plate. The carrier gas was argon or krypton, either pure or mixed with hydrogen or oxygen as stated below. The heavy water was 99.7% pure D_2O. For the experiments

Can. J. Chem. Downloaded from www.nrcresearchpress.com by 210.87.254.40 on 09/05/12
For personal use only.

with isotopic oxygen the samples (Miles–Yeda Lab.) were 98.8% in deuterium and either 50 or 98% in ^{18}O. The $^{18}O_2$ gas had an isotopic purity of about 90%. In a few experiments hydrogen peroxide vapor, from a 99% solution (Buffalo Electro-Chemical Co.), was dissociated either in the microwave or a Tesla coil discharge. The spectra were recorded with a Perkin–Elmer double-beam spectrometer Model 621.

Results

The New Bands

As reported before (17–19), the spectra of the products from dissociated water vapor show no clear indication of new features arising possibly from some higher oxides of hydrogen (Fig. 2*A*). This is because of the very strong libration bands of H_2O and H_2O_2 molecules in the 700 to 900 cm^{-1} region where the O—O vibrations are expected.[2] Even in deposits containing as much as 50% hydrogen peroxide the O—O stretching band at 880 cm^{-1} is barely noticeable in the original glassy deposit. Only upon crystallization (Fig. 2*B*) does it emerge as a weak shoulder.[3] Fortunately, in fully deuterated systems that region is quite free, which enables observation of a new, fairly strong band at 760 cm^{-1} (Fig. 2*C* and *D*). Incidentally, the weak band reported previously at that frequency in the infrared spectra of crystalline D_2O_2 (27) must be ascribed to the hybrid molecules HDO, and HDO_2 from isotopic contamination of the samples. Recent measurements (28) have confirmed that relationship. The band at 760 cm^{-1} has been observed before in the reaction products of condensed ozone with atomic hydrogen or deuterium (21) or mixtures of the two isotopes (24). In addition a second, much weaker band at 820 cm^{-1} was found in the former system by Csejka *et al.* (21). These authors pointed out that the two new frequencies could fit the O—O stretching modes of hypothetical H_2O_4 molecules. However, the presence of organic contaminants in their samples, and the variation in relative intensity of the two bands, depending on the substrate, precluded any definite conclusion. In order to establish the identity of these new bands we have carried out the following sequence of tests. First, it was ascertained that they do not arise from some secondary reactions with the substrate. In fact, they could be reproduced on a variety of materials: Irtran-2 or -6, silver chloride, rock-salt, cesium bromide, etc. Contamination from the discharge tube itself, previously suspected (11, 15), is also ruled out as the bands were still present when the Pyrex tube was coated with phosphoric acid (to reduce hydrogen atoms recombination) or replaced by a fused quartz tube. With the latter the two bands at 820 and 760 cm^{-1}, as well as all the peroxide bands, were somewhat weaker, in agreement with recent observations made in this laboratory (29).

On the assumption that the two extra bands were due to some polyoxide species it was logical to search for other characteristic bands, particularly the chain bending, at lower frequencies. These should occur around 400 to 500 cm^{-1} by analogy, for instance, with the normal alkanes (30). Now that area is badly encumbered in both hydrogen and deuterium systems (Fig. 2). In the latter, however, some additional absorption was usually visible, specially in the crystallized samples, centered near 440 cm^{-1}. Exact location of the maximum is uncertain as it lies on the slope of the OD libration bands. In addition, a couple of sharp lattice bands of the dihydrate $D_2O_2 \cdot 2D_2O$ appear precisely at 430 and 395 cm^{-1} on crystallization (28). Nevertheless, the extra absorption is genuine as it is already detectable in the glassy deposit.

The Oxygen-rich Systems

In order to bring out more clearly the new absorption bands, specially the very weak ones at 820 and 440 cm^{-1}, it seemed logical to increase the concentration of oxygen in the starting material. This was achieved most simply by adding molecular oxygen to the carrier gas. Dissociating deuterium peroxide vapor should yield somewhat similar results, but at greater cost and complication. Addition of oxygen to the system increased markedly the intensity of the three new

[2]From a theoretical analysis of their spectra based on analogy with the vibrations of normal paraffin molecules the Russian authors (26) arrived at a group of calculated frequencies for the O_3 and O_4 skeleton of hydrogen polyoxides in the range from 1000 to 1100 cm^{-1}, in close agreement with some of their observed frequencies (20, 22, 23). However, the latter no doubt were due to some contamination as they have never been observed, either by us or by other workers (19, 21).

[3]This behavior was interpreted by some workers (19, 22, 23) as evidence against the formation of H_2O_2 in the trapped products. However, the present study of deuterated systems has confirmed that the peroxide bands show hardly any intensity increase on crystallization. Only their contour is altered appreciably. For instance, that at 880 cm^{-1} becomes slightly sharper, while the broad OD bending, centered around 1050 cm^{-1}, splits up into two components, ν_2 and ν_6, at 1090 and 1025 cm^{-1}.

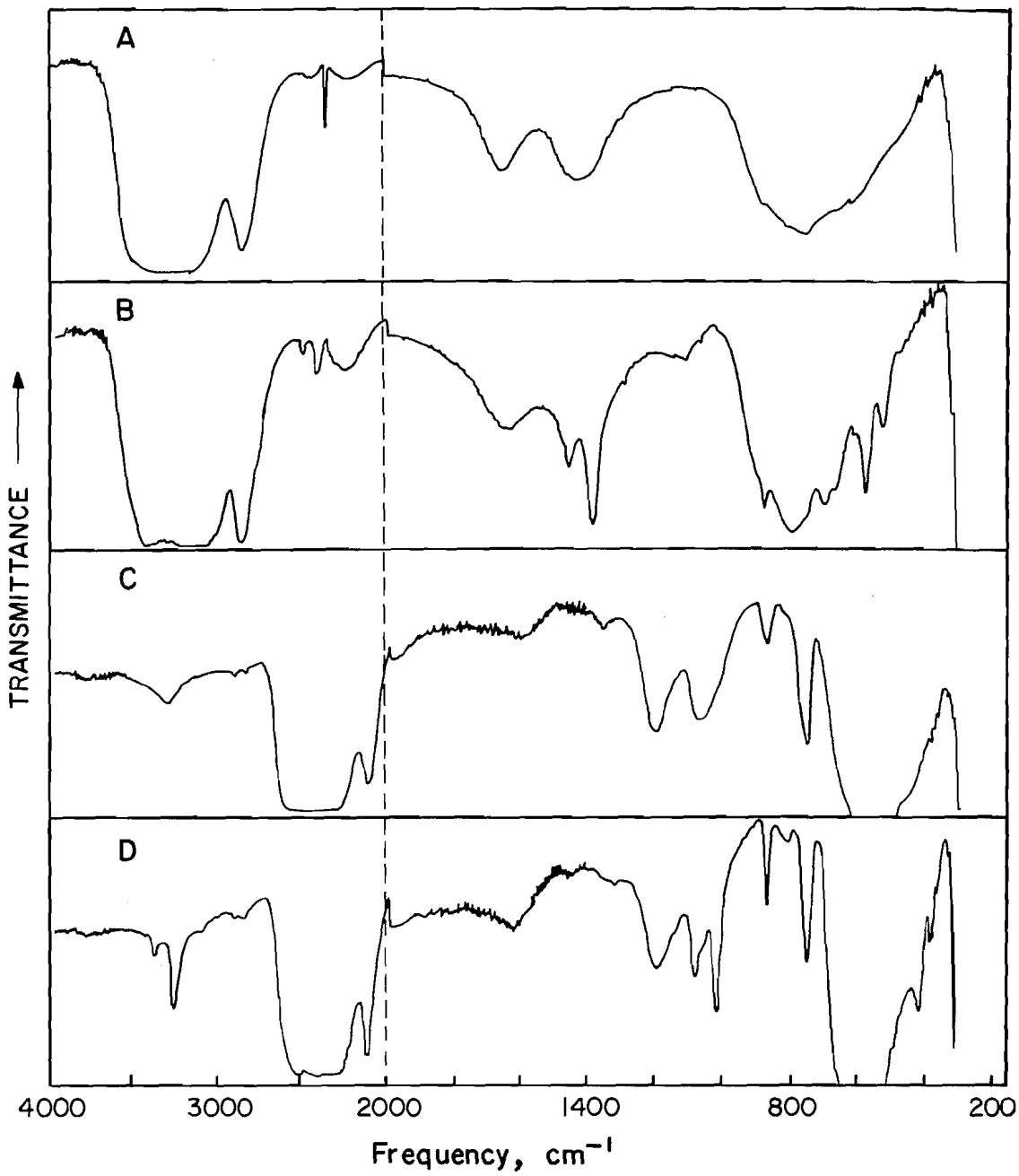

FIG. 2. Infrared spectra of the trapped products from dissociated H_2O vapor before crystallization (*A*), and after (*B*); D_2O before crystallization (*C*), and after (*D*).

bands, but not in the same ratio. For instance with a molar ratio O_2/D_2O of about 0.25 the absorption at 760 cm^{-1} was roughly doubled whereas it increased many fold for the other two bands. In contrast the peroxide bands were hardly affected, but those of water were somewhat reduced. This last remark also holds for the reaction products of liquid ozone with atomic hydrogen (21, 24). Even in dissociated $H_2O + O_2$ systems it was possible to detect extra absorption

Can. J. Chem. Downloaded from www.nrcresearchpress.com by 210.87.254.40 on 09/05/12
For personal use only.

Can. J. Chem. Downloaded from www.nrcresearchpress.com by 210.87.254.40 on 09/05/12
For personal use only.

at 760 and 450 cm^{-1} on top of the broad libration bands.

In an attempt to simulate the conditions of inert matrix isolation a few runs were made with krypton (m.p. -156.6 °C) as the carrier gas. At the same time the temperature of the sample holder was lowered to about $-196°$ by pumping over the liquid nitrogen, and the flow rate of dissociated gas was reduced to improve trapping. The concentration of O_2 was increased and that of D_2O vapor decreased making the ratio about 0.35. Still, their overall concentrations in krypton were much too high for true inert matrix isolation. This yielded somewhat clearer spectra, but more importantly, a fourth, very weak band at 875 cm^{-1} (Fig. 3*C*). Increasing the concentration of oxygen in the reagents also changed noticeably the physical properties of the sample. In general it was less transparent than in the case of dissociated water vapor alone. Then, on warming it began to devitrify at a slightly lower temperature ($-115°$). The crystallization could not be followed much above $-90°$ due to blistering of the thin film. This was due in part to evaporation of some trapped ozone since the spectra showed the sharp absorption peak at 1035 cm^{-1} on top of the OD bending bands,[4] and the weaker one at 702 cm^{-1}. On the other hand, adding deuterium gas to the heavy water vapor decreased the peroxide bands, and that at 760 cm^{-1} as well. However, very large concentrations (in excess of 5 to 1) of deuterium were required to suppress entirely the latter.

The ^{18}O Spectra

Definite identification of the new bands was achieved through an isotope effect. On substituting ^{18}O for ordinary oxygen the bands at 857, 820, and 760 cm^{-1} were shifted to 806, 775, and 717 cm^{-1}, respectively, as calculated for O—O vibrations. For N—O vibrations, for instance, the shifts would be only half as large. The bending band at about 450 cm^{-1} also seemed shifted to lower frequency, although it could not be ascertained exactly to what extent. The peroxide band at 880 cm^{-1} was shifted to lower frequency by the same ratio of 0.94. All the other bands moved very little, if at all, in accordance with OD vibrations (Table 1). Next an equimolar mixture of the two oxygen isotopes revealed clearly the triplet O—O band of the three isotopic species $D_2{}^{16}O_2$, $D_2{}^{16}O^{18}O$, and $D_2{}^{18}O_2$ and in the correct intensity ratios 1:2:1 (Fig. 3). As for the new bands, that at 760 cm^{-1} was transformed into a single broad peak with maximum near 740 cm^{-1}. This must be due to overlapping of a number of close components, a further indication that the species involved contains more than two oxygen atoms. Incidentally, this feature rules out assignment of that band to the hypothetical isomer of hydrogen peroxide, H_2O—O, suggested at one time (32).

The Thermal Decomposition

Since the new bands are not to be found in deuterium peroxide samples prepared in the electrical discharge (33) after melting, the implication is that they disappear on warming to room temperature. Furthermore, it is well known (2) that the oxygen evolution from the glassy deposit occurs mainly above $-100°$. Attempts to record the infrared spectrum as a function of temperature were inconclusive as the sample melted (around $-60°$) before showing appreciable decomposition. Luckily, a fairly constant temperature of about $-65°$ could be maintained by means of acetone – Dry Ice slush in the coolant well of the absorption cell. This made it possible to follow the evolution with time of the various bands by scanning periodically the most significant region (700 to 1300 cm^{-1}) under conditions as constant as feasible. From the relative intensities shown in Fig. 4 in arbitrary units it appears that over a period of 8 h the D_2O band at 1200 cm^{-1} decreased regularly by about one-third, and those of D_2O_2 (1090 + 1025 cm^{-1}) by somewhat less (about one-quarter). Evaporation of the sample into the evacuated cell was no doubt responsible for this, even if the infrared beam was on for brief periods only (4 or 5 min each hour). By contrast the 760 cm^{-1} band dropped by as much as four-fifths over the same time. Allowing for some slight evaporation the half-life of the species responsible is seen to be of the order of 5 h. Within the rather low accuracy of the intensity measurements, due to uncertain base line and alteration of band contour by continuing crystallization, the decay seemed to follow a zero-order law, as for diffusion controlled process. Unfortunately it was not possible to study likewise the other new bands for reasons already mentioned.

[4]This frequency, already reported before (24), is in agreement with recent measurements (31) on solid ozone in an oxygen matrix at 10 °K. In ^{18}O systems it was shifted to 976 cm^{-1}.

TABLE 1

Infrared absorption of the condensed products from various oxygen–deuterium systems

(Frequencies in cm^{-1})			
$D_2{}^{16}O$	$D_2{}^{18}O$	$D_2{}^{16/18}O$	Assignments
3390 m 3350 sh 3250 m 3120 sh	3390 m 3350 sh 3250 m 3120 sh	3390 m 3350 sh 3240 m 3120 sh	O—H stretch. (H_2O, H_2O_2)
2875 w	2860 w	2870 w	$\nu_2 + \nu_6$ (H_2O_2)
2530 s ~2420 sh 2290 vs	2530 s ~2400 sh ~2290 vs	2530 s ~2400 sh ~2280 vs	O—D stretch. (D_2O, D_2O_2)
2118 m	2103 m	2118 m	$\nu_2 + \nu_6$ (D_2O_2)
~1640 vw	~1650 vw	~1650 vw	ν_2 (H_2O)
1460 w	1460 w	1460 w	ν_2, ν_6 (H_2O_2)
1200 m	1200 m	1200 m	ν_2 (D_2O)
1090 m ~1070 sh 1025 s	1080 m ~1060 sh 1020 s	1085 m ~1065 sh 1020 s	ν_2, ν_6 (D_2O_2)
1035 w*	975 w*		$\nu_3(O_3)$
880 w	830 w	880 vw 855 w 830 vw	O—O stretch. (D_2O_2)
857 vw*	806 vw*		O—O stretch (D_2O_3, D_2O_4)
820 m*	775 m*		O—O stretch (D_2O_3, D_2O_4)
760 m	717 m	740 m	O—O stretch (D_2O_3, D_2O_4)
702 vw*	661 vw*		ν_2 (O_3)
585 s 530 m ~490 sh 430 w† 395 w	585 s 530 w ~490 sh 420 w 395 w	585 s 527 w ~490 sh 420 w 390 w	Lattice bands

*With added O_2 only.
†440 m with added O_2, due to O—O—O bend (D_2O_3, D_2O_4).

Discussion

The Hydrogen Polyoxides

The present results provide the first positive identification of stabilized polyoxides in the reactions of oxy-hydrogen systems. Previous evidence was either indirect or negative; for instance, the evolution of oxygen (8) or heat (9, 34) on warming the trapped products, or the presumed absence of hydrogen peroxide among the primary products of the reduction of liquid ozone by atomic hydrogen (19, 23). Such evidence is always liable to alternative explanation. The formation of traces of hydrogen trioxide in the pulse radiolysis of air-saturated water (5) and aqueous solutions of strong mineral acids (6) has been postulated mostly on kinetics grounds. In the latter case a fleeting ultraviolet absorption was ascribed to H_2O_3. However, this interpretation is somewhat hazardous because the u.v. absorption is only a continuum, and very similar to that of hydrogen peroxide. For obvious reasons there is no proof in our spectra that the new molecular species also contain hydrogen. This is a foregone conclusion in view of the chemical composition of the systems, and by analogy with the polysulfides, H_2S_3 and H_2S_4 (35). Other conceivable species, such as cyclic, single-bonded O_3 or O_4 molecules, seem highly improbable. In addition, their infrared spectra would be entirely different from the present ones.

The discovery of three new O—O stretching

FIG. 3. Infrared absorption spectra of the products from the electrically dissociated systems: $D_2{}^{18}O$ (*A*), $D_2{}^{16/18}O$ (*B*), and $D_2{}^{16}O + {}^{16}O_2$ (*C*), after crystallization at $-80°$ ($-90°$ for *C*).

Can. J. Chem. Downloaded from www.nrcresearchpress.com by 210.87.254.40 on 09/05/12
For personal use only.

Can. J. Chem. Downloaded from www.nrcresearchpress.com by 210.87.254.40 on 09/05/12
For personal use only.

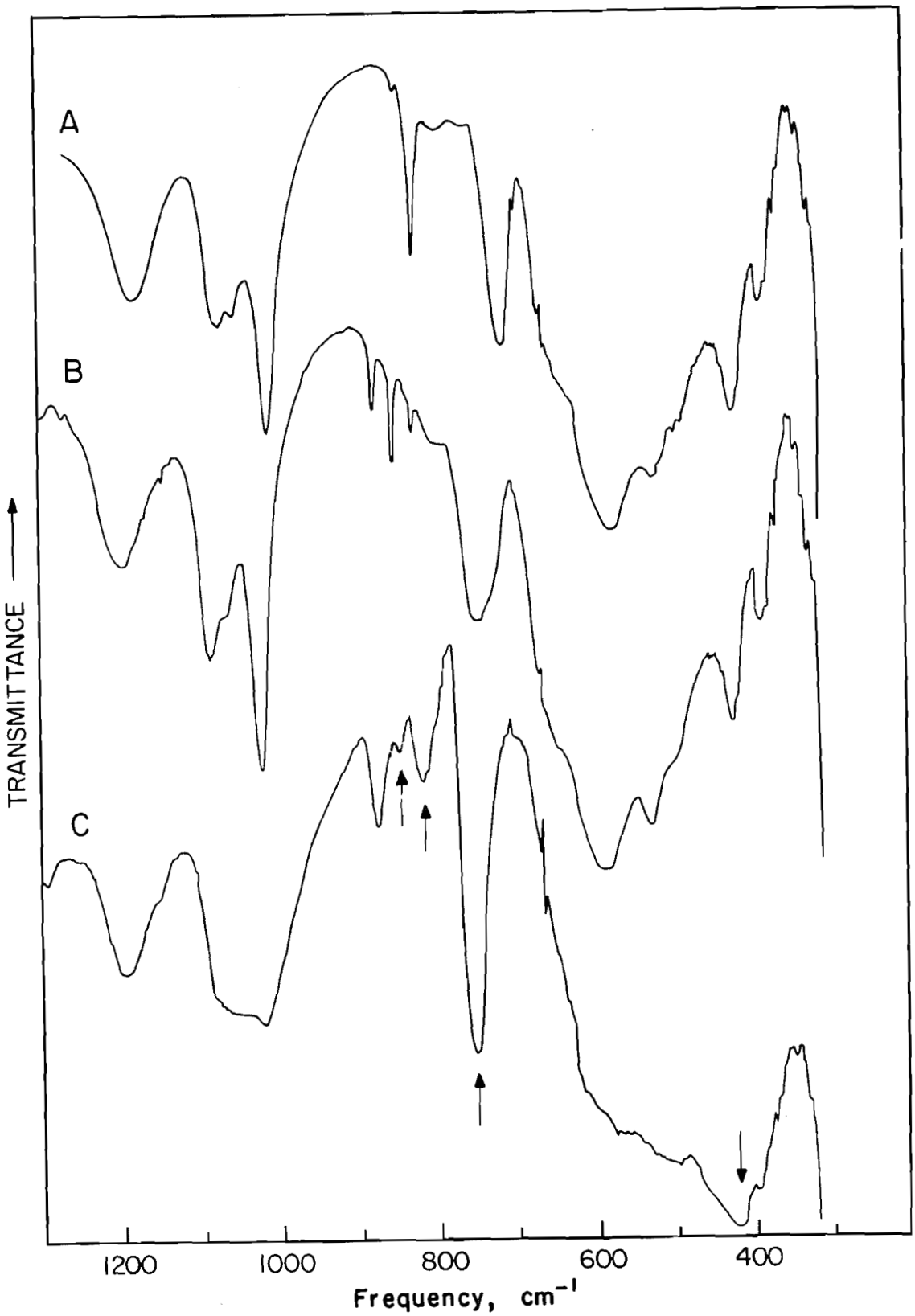

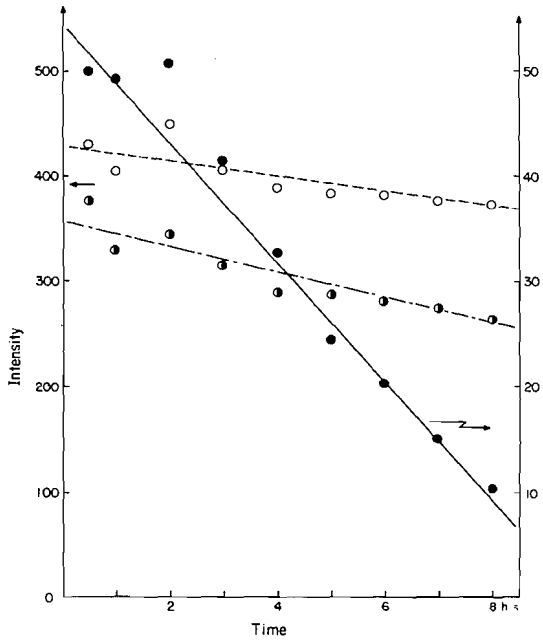

FIG. 4. Decrease in relative intensity at $-65°$ of the absorption bands of the trapped products from electrical dissociation of water vapor. ●, the polyoxide band at 760 cm^{-1}; ◑, the D_2O band at 1200 cm^{-1}; ○, the D_2O_2 bands at 1090/1025 cm^{-1}.

bands with slightly different temperature and composition patterns confirms the presence of more than one hydrogen polyoxide. This is in agreement with previous evidence such as the already noted variation in relative intensity of the two bands at 820 and 760 cm^{-1} (21), and the two distinct steps observed in calorimetric (34), manometric (15), and kinetics (36) studies of the warming process in the condensed products from dissociated water vapor. The present data are not sufficient to allow definite assignments to specific vibrations. A Raman investigation now underway should make this possible. Some of the vibrations of H_2O_3 and H_2O_4 must overlap as was observed in the analogous case of H_2S_3 and H_2S_4 (35). *A priori* one might conclude that the strong band at 760 cm^{-1} arises mainly from the antisymmetric O—O stretching of the most abundant species, namely H_2O_3. Indeed, thermodynamics indicate that it should be somewhat more stable than H_2O_4. As for the structure of these molecules, the present frequencies are consistent with zigzag chains held together by single bonds. The latter should have about the same lengths ($\sim$ 1.5 Å) as in hydrogen peroxide, and O—O—O angles of 100 to 120°. Internal rotation of the OH groups would be only weakly hindered in the free molecules; in the solid their orientation will be strongly dependent on hydrogen bonding, again as in hydrogen peroxide (37).

Other Polyoxides

Until a few years ago (38) there was no known example of molecules with more than two oxygen atoms joined by a single covalent bond. From thermochemical considerations (14) alkyl polyoxides should have about the same stability as the corresponding hydrogen compounds. On that basis the first claim (39) for the existence below $-30°$, of di-*ter*-butyl tetroxide was considered dubious (14). Subsequently the formation of di-*ter*-butyl- and *di*-cumyl trioxides was reported (40) and their decomposition process measured. The latter was found to be exothermic by about 23 kcal, with half-life of the order of $\frac{1}{2}$ h and 1 h, respectively at $-25°$. Much more stable are the perfluoroalkyl trioxides isolated and identified in recent years (41, 42). An infrared study of di-perfluoromethyl trioxide (43) has shown two strong bands in the O—O stretching region: the one at 773 cm^{-1} was assigned to the antisymmetric mode and the other, at 897 cm^{-1}, tentatively to the symmetric mode. By comparison with our data the latter seems of rather high frequency for such a vibration. A weak band at 810 cm^{-1}, assigned to a combination, might possibly belong to the symmetric mode. On the other hand, in the corresponding peroxide the O—O stretching frequency is 890 cm^{-1} (44). The situation in these molecules is quite different from that in hydrogen polyoxides; among other things there must be a strong coupling between the C—O and the O—O vibrations. As far as we know, no other spectroscopic study of alkyl trioxides has been published so far. The infrared, Raman, and n.m.r. spectra reported for di-*ter*-butyl trioxide (45) have been shown since to belong, in fact, to another compound (40). As for the tetroxides, there are indications from n.m.r. that traces may be formed in the preparation of di-perfluoromethyl trioxide (41).

It may be noted incidentally that the oxygen fluorides O_3F_2 and O_4F_2 synthesized in the electrical discharge (46) are not yet very well characterized from the structural viewpoint. Recently their reality has been questioned (47, 48). At any rate, if the case of O_2F_2 is any indication

Can. J. Chem. Downloaded from www.nrcresearchpress.com by 210.87.254.40 on 09/05/12
For personal use only.

Can. J. Chem. Downloaded from www.nrcresearchpress.com by 210.87.254.40 on 09/05/12
For personal use only.

(49), the O—O bonds in these compounds are certainly not of the single covalent type.

Thermodynamics and Kinetics

On thermodynamics grounds the very existence of hydrogen polyoxides seems rather marginal. Indeed, enthalpies of formation of the order of -13 kcal for H_2O_3 and $+5$ kcal for H_2O_4 have been estimated by Benson (14) from bond additivities and other group properties. The standard free energy of formation would be still less favorable because of the entropy term. From estimated thermodynamic functions (28) the latter would amount to some -4.5 kcal at 100 °K for H_2O_3. On the other hand these calculated quantities apply to the free molecules. In condensed phases hydrogen bonding and other intermolecular forces alter the picture considerably. The importance of that contribution to the stabilization of the intermediate species may be gauged from a rough estimate of the enthalpies of sublimation. From the experimental values of 12.2 kcal for ice and 15.6 kcal for H_2O_2, those for H_2O_3 and H_2O_4 must be of the order of 18 to 20 kcal. Therefore, the formation in the frozen matrix of both polyoxides from gaseous species is certainly an exothermic reaction.

The most likely process for the latter is via free radical recombination

$$[1] \qquad HO\cdot + HO_2\cdot = H_2O_3$$

and

$$[2] \qquad 2HO_2\cdot = H_2O_4$$

This must be so even in the reaction of atomic hydrogen with condensed ozone (13). Kinetically speaking formation of H_2O_3 is hampered by competition from the very fast disproportionation reactions. For H_2O_4 the situation is less unfavorable because the $HO_2\cdot$ radical is more inert than the hydroxyl, and higher steady state concentrations are possible. As for the decomposition of H_2O_3, it is not possible from the present data nor from previous calorimetric measurements to decide between the two possibilities

$$[3] \qquad H_2O_3 = H_2O + O_2$$

or

$$[4] \qquad H_2O_3 = H_2O_2 + \tfrac{1}{2}O_2$$

The alkyl trioxides studied so far (40, 41) decompose into the corresponding peroxide. If such were the case for hydrogen trioxide, then our estimates of its concentration in the samples would have to be doubled. These are based on the following reasoning.

The molar ratio of evolved oxygen to residual hydrogen peroxide in the case of dissociated water vapor has been found to vary between 0.15 and 0.2 (2). On the other hand the composition of the glassy deposit is usually close to that of the dihydrate $H_2O_2\cdot 2H_2O$. This leads to molar concentrations of polyoxides of 4 or 5% according to reaction 3 above. Obviously, somewhat higher concentrations are achieved in systems richer in oxygen.

Conclusions

The unique interest of the hydrogen polyoxides as higher members of the homologous series comprising H_2O and H_2O_2 stems from the great natural abundance of their constituent elements, and the wide diversity and importance of the chemical reactions between them. The long time and effort needed for their identification and characterization was due to the combined circumstances that they are quite labile, and require very special conditions for their formation, always as minor components, well camouflaged in water–hydrogen peroxide mixtures. It is likely that they were first obtained in the laboratory as long as 40 years ago (50), at the time when electrical dissociation of gases and vapors began to attract attention.

Quite apart from the considerable difficulty of concentrating and purifying them, the prospects for any practical use for of these polyoxides now appear rather slim. As pointed out before their oxidizing power is less than that of ozone, and even oxygen. On the other hand, their fundamental importance as intermediates, for instance, in the radiation chemistry of aqueous systems, or in the reactions (combustion, explosion, etc.) of hydrogen–oxygen mixtures hardly needs to be emphasized.

The authors are grateful to the National Research Council of Canada for continued financial assistance, and for other help in the form of samples of $D_2{}^{18}O$ (courtesy of Dr. L. Leitch) and analysis of band intensities by computerized methods (courtesy of Dr. R. N. Jones).

1. M. BERTHELOT. Compt. Rend. **90**, 656 (1880).
2. M. VENUGOPALAN and R. A. JONES. Chemistry of dissociated water vapor and related systems. Interscience Publishers, John Wiley and Sons, Inc., New York. 1968 Chap. 7.

3. I.U.P.A.C. J. Amer. Chem. Soc. **82**, 5529 (1960).
4. W. C. BRAY. J. Amer. Chem. Soc. **60**, 82 (1938).
5. G. CZAPSKI and B. J. J. BIELSKI. J. Phys. Chem. **67**, 2180 (1963).
6. B. H. J. BIELSKI and H. A. SCHWARZ. J. Phys. Chem. **72**, 3836 (1968).
7. K. SEHESTED, E. BJERGBOKKE, O. L. RASMUSSEN, and H. FRICKE. J. Chem. Phys. **51**, 3159 (1969).
8. E. OHARA. J. Chem. Soc. Jap. **61**, 569 (1940).
9. J. A. GHORMLEY. J. Amer. Chem. Soc. **79**, 1862 (1957).
10. J. A. GHORMLEY. J. Chem. Phys. **39**, 3539 (1963).
11. P. A. GIGUÈRE. ICSU Rev. **4**, 172 (1962).
12. P. A. GIGUÈRE. J. Chem. Phys. **42**, 2989 (1965).
13. S. W. BENSON. J. Chem. Phys. **33**, 306 (1960).
14. S. W. BENSON. J. Amer. Chem. Soc. **86**, 3922 (1964).
15. N. HATA and P. A. GIGUÈRE. Can. J. Chem. **44**, 869 (1966).
16. P. A. GIGUÈRE. J. Chem. Phys. **22**, 2085 (1954).
17. P. A. GIGUÈRE and K. B. HARVEY. J. Chem. Phys. **25**, 373 (1956).
18. P. A. GIGUÈRE and D. CHIN. J. Chem. Phys. **51**, 1685 (1959).
19. J. A. WOJTOWICZ, F. MARTINEZ, and J. A. ZASLOWSKY. J. Phys. Chem. **67**, 849 (1963).
20. T. V. YAGODOVSKAYA and L. I. NEKRASOV. Russ. J. Phys. Chem. **38**, 953 (1964).
21. D. A. CSEJKA *et al.* Study of Superoxidizers. Final Report, Air Force Office of Scientific Research, Washington 25, D.C. Document AD 617 964 (1965).
22. T. V. YAGODOVSKAYA and L. I. NEKRASOV. Russ. J. Phys. Chem. **40**, 698 (1966).
23. T. V. YAGODOVSKAYA and L. I. NEKRASOV. Russ. J. Phys. Chem. **41**, 108 (1967).
24. K. HERMAN and P. A. GIGUÈRE. Can. J. Chem. **46**, 2649 (1968).
25. K. HERMAN and P. A. GIGUÈRE. Can. J. Chem. **43**, 1746 (1965).
26. T. V. YAGODOVSKAYA, N. P. KLIMUSHINA, L. I. NEKRASOV, and YU. A. PENTIN. Russ. J. Phys. Chem. **41**, 369 (1967).
27. P. A. GIGUÈRE and C. CHAPADOS. Spectrochim. Acta, **22**, 1131 (1966).
28. J. L. ARNAU. Unpublished results.
29. P. BRUNET, X. DEGLISE, and P. A. GIGUÈRE. Can. J. Chem. **48**, 2041 (1970).
30. N. B. COLTHUP, L. H. DALY, and S. E. WIBERLEY. Introduction to infrared and Raman spectroscopy. Academic Press, Inc., New York. 1964.
31. L. LE BRUMANT, A. BARBE, and P. JOUVE. Compt. Rend. **268**, 549 (1969).
32. K. H. GEIB and P. HARTECK. Ber. **65**, 1551 (1932).
33. P. A. GIGUÈRE, E. A. SECCO, and R. S. EATON. Discuss. Faraday Soc. **14**, 104 (1953).
34. I. I. SKOROKHODOV, L. I. NEKRASOV, and N. I. KOBOZEV. RUSS. J. Phys. Chem. **35**, 994 (1961).
35. W. WIESER, P. J. KRUEGER, E. MULLER, and J. B. HYNE. Can. J. Chem. **47**, 1033 (1969).
36. R. A. JONES, W. CHAN, and M. VENUGOPALAN. J. Chem. Phys. **51**, 1273 (1969).
37. Y. AMAKO and P. A. GIGUÈRE. Can. J. Chem. **40**, 765 (1962).
38. W. E. DASENT. Nonexistent compounds. Marcel Dekker Inc., New York, 1965. p. 55.
39. N. A. MILAS and S. M. DJOKIC. Chem. Ind. London, 405 (1962).
40. P. D. BARTLETT and P. GÜNTHER. J. Amer. Chem. Soc. **88**, 3288 (1966).
41. P. G. THOMPSON. J. Amer. Chem. Soc. **89**, 4316 (1967).
42. L. R. ANDERSON and W. B. FOX. J. Amer. Chem. Soc. **89**, 4313 (1967).
43. R. P. HIRSCHMANN, W. B. FOX, and L. R. ANDERSON. Spectrochim. Acta, **25A**, 811 (1969).
44. J. R. DURIG and D. W. WERTZ. J. Mol. Spectry, **25**, 467 (1968).
45. N. A. MILAS and G. G. ARZOUMANIDIS. Chem. Ind. London, 66, (1966).
46. A. V. GROSSE, A. G. STRENG, and A. D. KIRSCHENBAUM. J. Amer. Chem. Soc. **83**, 1004 (1961).
47. R. D. SPRATLEY, J. J. TURNER, G. C. PIMENTEL. J. Chem. Phys. **44**, 2063 (1966).
48. I. J. SOLOMON, J. N. KEITH, A. J. KACMAREK, and J. K. RANEY. J. Amer. Chem. Soc. **90**, 5408 (1968).
49. R. H. JACKSON. J. Chem. Soc. 4585 (1960).
50. G. I. LAVIN and F. B. STEWART. Nature, **123**, 607 (1929).

Can. J. Chem. Downloaded from www.nrcresearchpress.com by 210.87.254.40 on 09/05/12
For personal use only.

The rubidium chloride – sodium chloride phase diagram

A. D. PELTON AND S. N. FLENGAS
Department of Metallurgy and Materials Science, University of Toronto, Toronto 181, Ontario

Received June 2, 1970

The phase diagram of the RbCl–NaCl system has been measured by the method of cooling curves. By combining these data with available thermochemical data for the system, the integral molar excess free energy of mixing at 800 °C has been calculated as $\Delta G^E = -632 X_{RbCl} X_{NaCl}$ cal/mole; and the integral molar excess entropy of mixing has been calculated as $\Delta S^E = -0.208 X_{RbCl} X_{NaCl}$ cal/°K mole. Estimated precisions are ±50 cal for ΔG^E and ±0.05 cal/°K mole for ΔS^E at $X_{RbCl} = X_{NaCl} = 0.5$.

Canadian Journal of Chemistry, 48, 3483 (1970)

Can. J. Chem. Downloaded from www.nrcresearchpress.com by 210.87.254.105 on 09/05/12
For personal use only.

Introduction

A knowledge of the thermodynamic properties of mixtures of alkali halides is important in the understanding of the fundamental properties of simple fused salt systems. Because of the solubility of the alkali metals in their molten halides, measurements of free energies using reversible electrochemical cells are not possible in these systems. In cases in which the system is a simple eutectic, and in which solid solubility is limited, however, an accurate knowledge of the phase diagram will permit thermodynamic properties to be calculated with quite a high precision. Such is the case in the RbCl–NaCl system.

Enthalpies of mixing in the molten RbCl–NaCl system have been measured calorimetrically at 810 °C by Hersh and Kleppa (1) who obtained the following equation for the integral molar enthalpy of mixing

$$[1] \quad \Delta H = X_{RbCl} X_{NaCl} (-770 - 80 X_{NaCl}) \text{ cal/mole}$$

where X_{NaCl} and X_{RbCl} are the mole fractions (1 cal = 4.1840 J).

Accurate heats of fusion and heat capacities are available (3, 4). Also, the limits of solid solubility have been measured (5). With the available data, then, as will be shown, quite precise thermodynamic calculations can be made.

Liquidi in the system were measured by Zhemchuzhnui and Rambach (2) in 1910, who reported that the system exhibited simple eutectic behavior. The accuracy of this work is questionable, however. The reported melting point of pure NaCl was 20 °K higher than the presently accepted (3) value, for instance. Murgulescu and Sternberg (6) also measured liquidi in this system. Their reported melting points for the pure salts and their eutectic temperature agree well with those measured in the present work. Their reported liquidi in the region of the eutectic point, however, are 10 to 20 °K lower than those determined in the present study. It is quite difficult to draw a phase diagram from their reported liquidus points so that the liquidi meet at the eutectic temperature. Thermodynamic calculations (7) based upon these results give positive excess entropies of liquid mixing. However, in all other binary alkali chloride systems for which data are available, negative excess entropies are found (7).

Experimental

Reagent grade NaCl was used. The RbCl (Matheson) was of 99+% purity. The salts were dried under vacuum and with dry HCl gas at 550 °C, and were stored in a vacuum desiccator.

Liquidus and eutectic points were found by the method of cooling curves. Measurements were carried out on samples of approximately 25 g in sealed, evacuated, quartz cells. A thermocouple was sheathed in close-fitting quartz tubes blown into the cells. The cells were placed in an Inconel metal sheath and lowered into a vertical tube furnace. By grounding the Inconel sheath, any spurious voltages induced in the thermocouple by the a.c. field of the furnace windings were entirely eliminated. The use of such a grounded sheath was found to be essential if accurate results are to be obtained. The melt filled the cells to a depth of about 3 cm, and the thermocouple sheath extended about 2 cm below the surface of the melt. Temperature differences over the depth of the melt were 0.25 °K or less.

The furnace was controlled by a variable auto-transformer. The furnace could be cooled at any desired rate by means of an electric motor which drove down the auto-transformer through a variable-ratio gear reductor. With cooling rates of less than 1 °K per min, supercooling could be kept to a tolerable level of 0.5 to 3 °K. A rate of 0.75 °K/min was adopted in all experiments. Supercooling was avoided as much as possible by vigorously rocking the entire furnace.

The output from the thermocouple was recorded on a 1 mV full-scale Sargent SRG recorder, with most of the

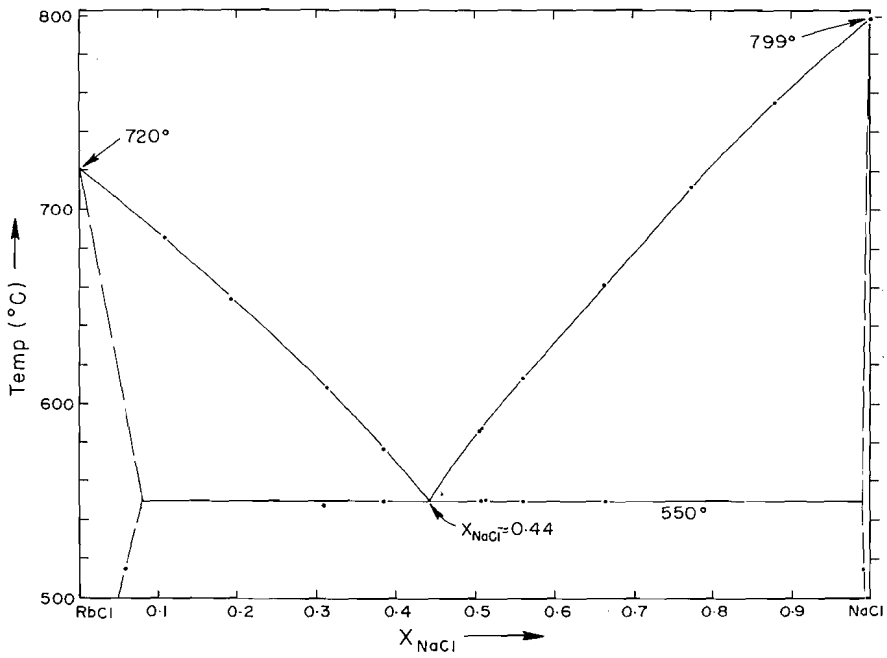

FIG. 1. The RbCl–NaCl phase diagram.

thermocouple output compensated by a Leeds and Northrup K3 potentiometer. A 24-gauge chromel–alumel thermocouple was used. The thermocouple was calibrated by the manufacturer, and the calibration was also checked against the melting points of pure tin, lead, and gold. The two calibrations were in agreement to better than 0.5 °K.

Results

Experimental liquidus and eutectic points are listed in Table 1. Except for one measurement, the various determinations of the eutectic temperature agree with a spread of 0.75 °K. The measured melting points of pure NaCl and RbCl (799.25 and 720 °C), compare well with the most recent literature values of 800 (3) and 722 °C (8). The phase diagram is shown in Fig. 1.

Short and Roy (5) used the method of interdiffusion to measure the solid solubility limits. These were found to be 6 mole% NaCl in RbCl and 0.8 mole% RbCl in NaCl at 515 °C. These two points are shown in Fig. 1. The solid solubility and solidus lines were then estimated as shown in Fig. 1 so as to give reasonable values for the slopes of these lines. The estimated solid solubilities at the eutectic temperature would seem to be accurate to ±50% or better. As will be shown later, these error limits will not give rise to appreciable errors in the thermodynamic calculations of the liquid state properties.

TABLE 1

Experimental liquidus and eutectic points in the RbCl–NaCl system

X_{NaCl}	T_L(°C)	T_E(°C)
0.0 (Pure RbCl)	720.0	
0.1088	685.5	—
0.1938	654.5	—
0.3118	608.25	548.25
0.3831	576.75	550.25
0.5056	585.75	550.5
0.5071	586.0	550.25
0.5602	613.0	550.25
0.6627	660.75	549.75
0.7744	711.5	—
0.8767	755.0	—
1.0 (Pure NaCl)	799.25	

The eutectic composition was found to be at $X_{NaCl} = 0.44$ at 550 °C.

Calculations

The van't Hoff relationship in the following form was used to calculate partial molar free energies of mixing of RbCl and NaCl along their respective liquidi.

$$[2] \quad \Delta\bar{G}_{ACl(T_L)} = (RT \ln a_{ACl(solidus)}) - T_L \int_{T_f}^{T_L} \Delta H_f \, d\left(\frac{1}{T}\right)$$

Can. J. Chem. Downloaded from www.nrcresearchpress.com by 210.87.254.105 on 09/05/12
For personal use only.

Can. J. Chem. Downloaded from www.nrcresearchpress.com by 210.87.254.105 on 09/05/12
For personal use only.

where $\Delta\bar{G}_{ACl(T_L)}$ is the partial molar free energy of mixing of ACl (RbCl or NaCl), with respect to the pure liquid standard state, at a point on its liquidus at T_L, T_L is the liquidus temperature, T_f is the fusion temperature of pure ACl, $a_{ACl\ (solidus)}$ is the activity of ACl on the solidus line at T_L with respect to the pure solid standard state, ΔH_f is the enthalpy of fusion of ACl.

For calculations along the NaCl liquidus, ΔH_f of NaCl is known with an accuracy of about $\pm 2\%$ (3) at T_f. Also, heat capacities of liquid and solid NaCl are known (4), and so ΔH_f may be written as a function of temperature. Solid solubility was taken to be 1 mole% at the eutectic temperature, and a linear solidus between the eutectic and the melting point of pure NaCl was assumed. The solid solution, being very dilute in RbCl, was assumed to be Raoultian with respect to the solvent, NaCl, so that $a_{NaCl\ (solidus)}$ could be calculated. Values of $(RT\ln a_{NaCl\ (solidus)})$ were never greater than about 15 cal, and so, errors introduced by uncertainties in the position of the solidus and by assuming Raoultian behavior are very small.

Values of the partial molar excess free energies of mixing, $\Delta\bar{G}^E_{NaCl}$, were calculated at each experimental point on the NaCl liquidus. Isothermal values of $\Delta\bar{G}^E_{NaCl}$ at 800 °C were then calculated using the Gibbs–Helmholtz equation and using the partial molar enthalpy of mixing calculated from eq. 1. Values of $\Delta\bar{G}^E_{NaCl}$ at 800 °C are shown in Fig. 2. (Enthalpies of mixing were assumed to be independent of temperature.) The six points were fitted by a least squares technique to an equation as follows

$$[3] \qquad \Delta\bar{G}^E_{NaCl} = -632X_{RbCl}^2 \quad \text{cal/mole}$$

The mean deviation was 12 cal. Error limits may be estimated by considering maximum probable errors in the heat of fusion, heat capacities, liquidus temperatures, and solid solubility calculations. The error in $\Delta\bar{G}^E_{NaCl}$ at $X_{NaCl} = X_{RbCl} = 0.5$ is probably about ± 50 cal.

Similar calculations were made for each experimental point along the RbCl liquidus. ΔH_f of RbCl is known with an accuracy of $\pm 2\%$ at T_f (3). The heat capacity, C_p, for solid RbCl is known (4), but C_p for liquid RbCl is not. In the calculations, a value of C_p for liquid RbCl of 16.0 cal/°K mole was chosen, as this is the value given in the literature (4) for both liquid NaCl and liquid KCl, and is close to the values (4) for various other molten halides. Probable errors

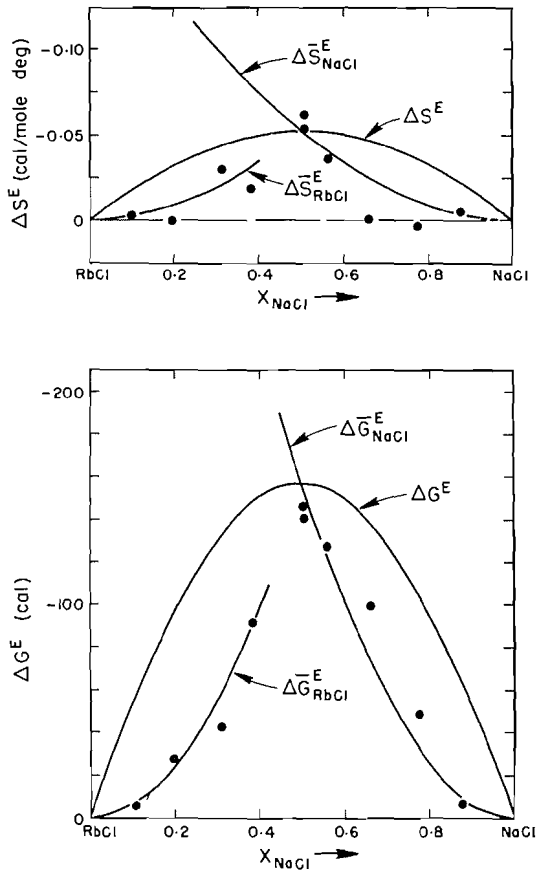

FIG. 2. Partial and integral molar excess free energies of mixing at 800 °C and partial and integral molar excess entropies of mixing in the RbCl–NaCl system from phase diagram calculations (lines are from least squares fits).

introduced by this assumption can be shown to be of the order of ± 25 cal. The calculation of $(RT\ln a_{RbCl\ (solidus)})$ was made assuming 8 mole% solid solubility at the eutectic temperature, assuming a linear solidus between the eutectic and the melting point of pure RbCl, and assuming that the solid solutions are Raoultian with respect to RbCl. Values of $(RT\ln a_{RbCl\ (solidus)})$ calculated in this manner were as large as 100 cal at temperatures near the eutectic. Probable errors introduced by the various assumptions are of the order of ± 100 cal.

Values of $\Delta\bar{G}^E_{RbCl}$ were calculated in this manner, and isothermal values at 800 °C were then calculated using the Gibbs–Helmholtz equation. Points are shown in Fig. 2. Also shown in Fig. 2 is the curve

$$[4] \qquad \Delta\bar{G}^E_{RbCl} = -632X_{NaCl}^2 \quad \text{cal/mole}$$

calculated from eq. 3 using the Gibbs–Duhem relation. Agreement with the calculated points is very good. This, then, shows that eq. 3, which was obtained by fitting only the points calculated from the NaCl liquidus, can probably be extrapolated with confidence to the "RbCl-side" of the system.

In view of the larger errors inherent in the calculations along the RbCl liquidus, the points calculated from this liquidus were not included in the least squares fit, and eqs. 3 and 4 were taken as the final "best" fits. A plot of the excess integral molar free energy of mixing

$$[5] \quad \Delta G^E = -632 X_{RbCl} X_{NaCl} \quad \text{cal/mole}$$

is also shown in Fig. 2. As has been shown, probable error limits in ΔG^E are ± 50 cal at $X_{RbCl} = X_{NaCl} = 0.5$.

Values of the partial molar excess entropy of mixing of NaCl, $\Delta \bar{S}^E_{NaCl}$, were calculated for each experimental point using the isothermal values of $\Delta \bar{G}^E_{NaCl}$ as in Fig. 2, and using values of $\Delta \bar{H}_{NaCl}$ calculated from eq. 1. Points are shown in Fig. 2. These six points were fitted to an equation as follows

$$[6] \quad \Delta \bar{S}^E_{NaCl} = -0.208 X_{RbCl}^2 \quad \text{cal/°K mole}$$

Values of $\Delta \bar{S}^E_{RbCl}$ were similarly calculated from the experimental points on the RbCl liquidus, and are also shown in Fig. 2. Agreement is very good with the curve

$$[7] \quad \Delta \bar{S}^E_{RbCl} = -0.208 X_{NaCl}^2 \quad \text{cal/°K mole}$$

A plot of the excess integral molar entropy of mixing is also shown in Fig. 2.

$$[8] \quad \Delta S^E = -0.208 X_{RbCl} X_{NaCl} \quad \text{cal/ °K mole}$$

Considering the errors in ΔG^E and ΔH, the error in ΔS^E at $X_{RbCl} = X_{NaCl} = 0.5$ is probably about ± 0.05 cal/°K mole.

Conclusions

The phase diagram of the RbCl–NaCl system has been measured. By combining the present results with other available thermochemical data for this system, excess free energies and excess entropies of mixing have been calculated with an estimated precision of ± 50 cal and ± 0.05 cal/°K mole, respectively, at $X_{RbCl} = X_{NaCl} = 0.5$. The precision was not great enough to permit the asymmetry terms in the concentration dependences of these properties to be determined, however.

The very small negative excess entropy of mixing observed in this system would indicate that ideal random mixing is closely approached. The small negative deviations from ideality could be due to a small degree of ordering on the cation sublattice as, for instance, is predicted by the quasichemical (9) theory.

A maintenance fellowship for one of us (A.D.P.) from Shell Canada Ltd., and financial assistance from the National Research Council of Canada are gratefully acknowledged.

1. L. S. HERSH and O. J. KLEPPA. J. Chem. Phys. **42**, 1309 (1965).
2. S. ZHEMCHUZHNUI and F. RAMBACH. Z. Anorg. Chem. **65**, 415 (1910).
3. A. S. DWORKIN and M. A. BREDIG. J. Phys. Chem. **64**, 269 (1960).
4. M. BLANDER. Molten salt chemistry. *Edited by* M. Blander. Interscience Publishers, New York. 1964. Chap. 2, p. 141.
5. J. M. SHORT and R. ROY. J. Amer. Ceram. Soc. New York. **47**, 149 (1964).
6. I. G. MURGULESCU and S. STERNBERG. Z. Phys. Chem. **219**, 114 (1962).
7. J. LUMSDEN. Thermodynamics of molten salt mixtures. Academic Press, New York. 1966. Chap. 4.
8. I. S. YAFFE and E. R. VAN ARTSDALEN. J. Phys. Chem. **60**, 1125 (1956).
9. T. FØRLAND. Fused salts. *Edited by* B. Sundheim. McGraw Hill, New York. 1964. Chap. 2, p. 87.

Can. J. Chem. Downloaded from www.nrcresearchpress.com by 210.87.254.105 on 09/05/12
For personal use only.

Can. J. Chem. Downloaded from www.nrcresearchpress.com by 210.87.254.6 on 09/05/12
For personal use only.

Decomposition of BrO studied by kinetic spectroscopy[1]

J. BROWN[2] AND GEORGE BURNS
Department of Chemistry, University of Toronto, Toronto 181, Ontario

Received April 13, 1970

Kinetics of BrO decomposition was studied between 293 and 673 °K using the technique of kinetic spectroscopy. At 293 °K the reaction rate is second order with respect to BrO and is independent of $[Br_2]$, $[O_2]$, and total pressure of diluent gas. The activation energy for decomposition obtained from rate measurements between 293 and 450 °K is 0.65 ± 0.05 kcal/mole. Above 450 °K this activation energy appears to increase to 4.5 kcal/mole. It is shown that, although kinetically the ClO and BrO decompositions are similar, the mechanism for BrO decomposition below 450 °K is much simpler than that of ClO. The reaction proceeds, most likely, via one step: $2\,BrO \rightarrow 2\,Br + O_2$, with Br_2O_2 being an activated complex, which has either linear or staggered configuration. ClO and BrO decomposition is compared with $H_2 + I_2 \rightleftharpoons 2\,HI$ reaction.

Canadian Journal of Chemistry, **48**, 3487 (1970)

Introduction

Although the kinetics of ClO decomposition have been investigated previously (1–7), a study of BrO decomposition using the flash photolysis technique has not been attempted. On the other hand, the kinetics of BrO formation in flash photolytic experiments has already been studied (8).

Experimental

The apparatus used in the present investigation has been described previously (9). British Drug Houses analytical reagent bromine (99.9%) was kept in contact with pure KBr for several days to remove other halogens; then it was distilled *in vacuo* over P_2O_5 the middle fraction was retained, following the procedure described elsewhere (10). Oxygen and argon were supplied by Matheson Co.; the minimum purity of these gases was reported by the manufacturers as 99.9%; they were used without further purification.

Results and Discussion

Bromine monoxide radical concentration was followed by measuring the peak areas of the microdensitometer trace at five wavelengths. Each peak is well separated from the other and the slope of the blank line, taken by flashing spectroscopic lamp alone, coincided, within the accuracy of the experiment, with the base line of the microdensitometer trace which shows BrO absorption (Fig. 1).

The mean peak area was calculated and this average taken as being proportional to [BrO]. A typical plot of the BrO peak area against time after flash is shown in Fig. 2. Figure 3 shows the plot of log [BrO] against time and $[BrO]^{-1}$ against time. It follows from Fig. 3 that at 293 °K, the reaction of BrO is second order with respect to BrO. In the present experiments, the bromine pressure was varied from 5 to 20 Torr, oxygen pressure from 150 to 750 Torr, while the total pressure was maintained constant by the addition of argon. In another series of experiments, the total pressure was varied from 169 to 785 Torr. Under all these variations, at room temperature, the rate of reaction was independent, within the accuracy of the experiment (±7%), of Br_2, O_2, and total gas concentrations. However, the absolute concentration of BrO produced depends upon $[Br_2]$ and $[O_2]$. In the present experiments, the maximum concentration of BrO was produced when the mixture containing 20 Torr of Br_2 and 1 atm of O_2 was flash photolyzed.

The decomposition of BrO was also studied over a temperature range between 293 and 673 °K (Fig. 4). However, the measurements became progressively more difficult with increase of temperature. This is most probably because the transparency of quartz to the radiation shorter than 2000 Å decreases with temperature, and it is this radiation that is responsible (8) for the production of BrO. In experiments at 673 °K, the accuracy of the measurement is not sufficient to differentiate between the first and second order for BrO decomposition. However, lower temperature results yield a relatively accurate value of the activation energy for second order decomposition of BrO (0.65 ± 0.05 kcal/mole). Although the accuracy of the activation energy above 450 °K is also satisfactory (4.5 ± 0.3 kcal/mole), this accuracy may very well be spurious.

[1]This work was supported in part by the Directorate of Chemical Sciences, Air Force Office of Scientific Research, Grant No. 506-66 and 1695-69.

[2]Present address: Ontario Hydro Research Division, 200 Kipling Avenue South, Toronto 18, Ontario.

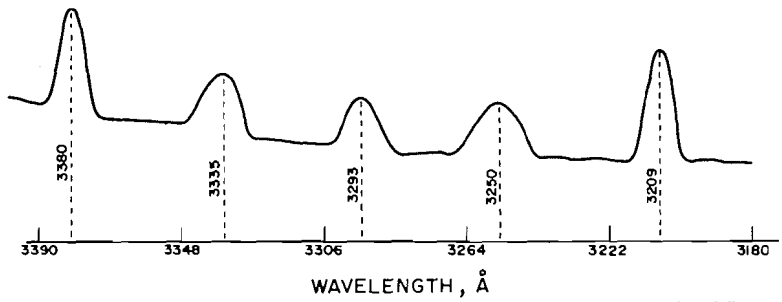

FIG. 1. Microdensitometer trace of BrO spectrum taken 100 μs after flash photolysis of Br_2 plus O_2 mixture at room temperature.

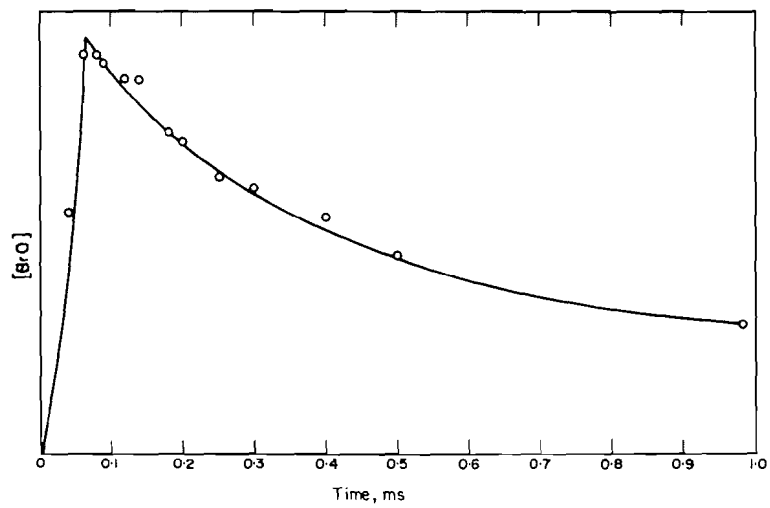

FIG. 2. Plot of [BrO] in relative units against time after flash initiation in a typical experiment.

Discussion

In order to explain the experimental results, it may be profitable to compare present data with the more thoroughly investigated ClO decomposition. The latter reaction was also found to be second order with respect to its halogen monoxide. The presently accepted scheme for the ClO decomposition was proposed by Benson and Buss (6)

[1] $$2\,ClO \rightleftharpoons ClOO + Cl$$

[2] $$Cl + ClOO \rightarrow Cl_2 + O_2$$

[3] $$ClOO\,(+M) \rightarrow Cl + O_2\,(+M)$$

Clyne and Coxon (3) provided evidence in support of the mechanism [1]–[3], as well as for the reaction

[4] $$2\,ClO + M \rightleftharpoons Cl_2O_2 + M$$

Johnston *et al.* (7) demonstrated unequivocally that the disappearance of the ClO radical depends upon the inert gas concentration (reaction 4).

It was generally suspected (3, 6) that BrO decomposition should be similar to ClO decomposition. However, it follows from the work of Burns and Norrish (8) that, unlike ClOO radical, BrOO is unstable. Thus, while the reaction

$$2\,Cl + O_2 \rightarrow 2\,ClO$$

which proceeds in two steps via ClOO, is very rapid, the reaction

$$2\,Br + O_2 \rightarrow 2\,BrO$$

does not occur (8). Clyne and Coxon (3) also reported that the reaction

$$Br + ClOO \rightarrow BrOO + Cl$$

seems not to occur. Further evidence for stability of ClOO can be deduced from the known efficiency of O_2 as a third body in Cl atom recombination re-

Can. J. Chem. Downloaded from www.nrcresearchpress.com by 210.87.254.6 on 09/05/12
For personal use only.

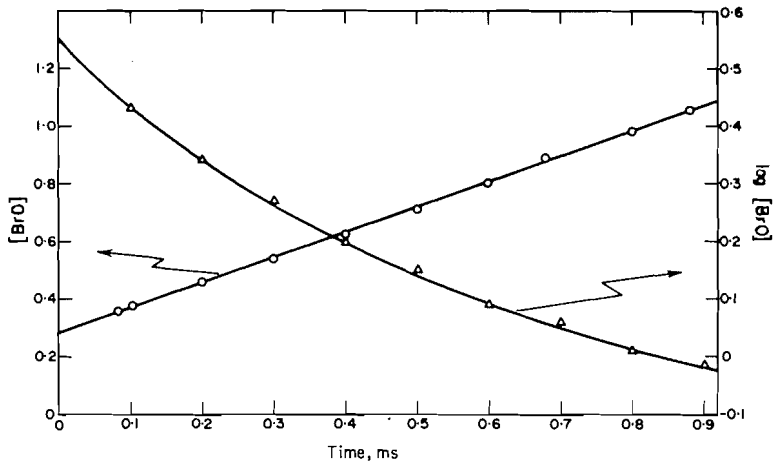

FIG. 3. log [BrO] and $[BrO]^{-1}$ (straight line) against time at 293 °K for a typical experiment. The ordinate is given in relative units.

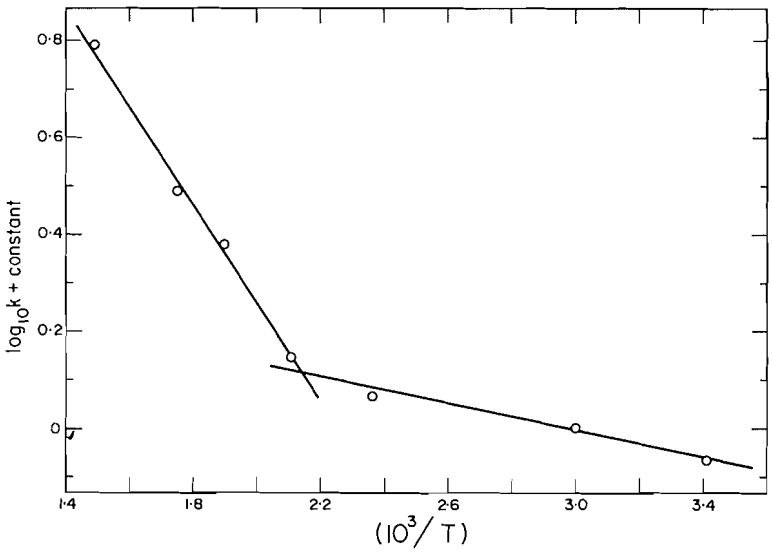

FIG. 4. Arrhenius plot for BrO decomposition reaction.

actions. Porter and Wright (1) reported that O_2 is 46 times more efficient than N_2 in Cl recombination. On the other hand, the efficiencies of O_2 and N_2 differ only by a factor of two (11) for the Br recombination. Blake, Browne, and Burns recently (12) calculated that the depth of the intermolecular potential between Br and O_2 is about 1 kcal/mole, while the intermolecular potentials for Br–N_2 and Br–Kr pairs are about 1.7 and 2.2 kcal/mole deep, respectively. On the other hand, the bond-dissociation energy for ClOO was estimated to be 7 kcal/mole (3) and 8 ± 2 kcal/mole (6). Furthermore, we were not able to find a third body dependence, and for this reason the reaction

[5] $$2\ BrO + M \rightarrow Br_2O_2 + M$$

is not substantiated in our experiments.

Therefore, present experimental data coupled with previous findings (8) yield the following scheme for BrO decomposition

[6] $$2\ BrO \rightleftharpoons Br_2O_2$$

[7] $$Br_2O_2 \rightarrow 2\ Br + O_2$$

Since the activation energy in [7] is, most probably, zero the activation energy for the

Can. J. Chem. Downloaded from www.nrcresearchpress.com by 210.87.254.6 on 09/05/12
For personal use only.

Can. J. Chem. Downloaded from www.nrcresearchpress.com by 210.87.254.6 on 09/05/12
For personal use only.

reaction 6, below 450 °K, is 0.65 kcal/mole. Therefore the Br_2O_2 is unstable and can be thought to be an "activated complex" which reacts either in one step, [7], or via

[8] $$Br_2O_2 \rightarrow BrOO + Br$$

[9] $$BrOO \rightarrow Br + O_2$$

The one step decomposition is preferred because the binding energy of BrOO is only 1 kcal/mole (12). Similar mechanism is not likely for ClO decomposition (3) on account of the endothermicity of the reaction

[10] $$2\ ClO \rightarrow 2\ Cl + O_2$$

of some 9.3 kcal/mole. Since reactions 7, 8, and 9 appear to be irreversible, one may expect that BrO decomposition should be faster than ClO decomposition. This conclusion is supported in the work of Clyne and Coxon (3, 13). Although we were unable to measure our rate constants, qualitatively, by examining our plates, we concur at this point with Clyne and Coxon (3, 13).

Thus we arrive at an interesting conclusion that, although the BrO decomposition is similar to the ClO decomposition, the mechanisms for the two reactions differ substantially.

We favor linear or staggered (14) configuration for the Br_2O_2 activated complex. This is because a trapezoidal (14) activated complex would provide a partial bond between two Br atoms, which would then rapidly recombine. Actually there seems to be no evidence that the presence of BrO accelerates Br_2 reappearance in flash photolysis experiments (11). The shape of the activated complex for some four center reactions is of considerable interest, both experimentally and theoretically (14–17).

Finally, it may be of interest to compare BrO and ClO recombination to the much studied $H_2 + I_2 \rightleftharpoons 2$ HI reaction. BrO decomposition appears to be very similar to HI decomposition. The mechanism of the latter reaction can be obtained from recent work of Sullivan (18). There, as in the present work, the linear or staggered activated complex leads to the formation of a new strong bond (either —O—O— or —H—H—). Thereafter, one halogen is lost, and then the other

[6a] $$2\ HI \rightleftharpoons H_2I_2$$

[8a] $$H_2I_2 \rightarrow H_2I + I$$

[9a] $$H_2I \rightarrow H_2 + I$$

As in the case of HI reaction, the BrO decomposition is relatively simple only at lower temperatures. Some complexities in the BrO decomposition seem to appear above 450 °K.

The BrO formation differs from the HI formation reaction. In the former case, rupture of Br—Br bond does not lead to the formation of BrO, because $2\ Br + O_2 \rightarrow BrO$ reaction is endothermic. Therefore, in order to produce BrO in flash photolysis experiments, it is necessary to break a strong O—O bond (8). On the other hand, the $H_2 + I_2$ reaction is initiated by rupture of the weak I—I bond (18).

There is an analogy between HI and ClO formation. In these cases, both reactions are initiated with rupture of the weak halogen–halogen bond. Although these mechanisms are similar, there is an appreciable difference in the absolute values of rate constants and activation energies in these two reactions.

This work was supported by the Defence Research Board, Grant No. 9530-54, the Directorate of Chemical Sciences, Air Force Office of Scientific Research, Grant No. 506-64 and Grant No. 506-66 and 1695-69, and the Petroleum Research Fund of the American Chemical Society.

We are grateful to Drs. M. A. A. Clyne and H. W. Cruse for the preprints of their papers on the formation, decay, and reactions of BrO radicals.

1. G. Porter and F. J. Wright. Discuss. Faraday Soc. **14**, 23 (1953).
2. M. A. A. Clyne and J. A. Coxon. Trans. Faraday Soc. **62**, 1175 (1966).
3. M. A. A. Clyne and J. A. Coxon. Proc. Roy. Soc. Ser. A, **303**, 207 (1968).
4. F. J. Lipscomb, R. G. W. Norrish, and B. A. Thrush. Proc. Roy. Soc. Ser. A, **233**, 445 (1956).
5. F. H. C. Edgecomb, R. G. W. Norrish, and B. A. Thrush. Proc. Roy. Soc. Ser. A, **243**, 24 (1957).
6. S. W. Benson and J. H. Buss. J. Chem. Phys. **27**, 1382 (1957).
7. H. S. Johnston, E. D. Morris, and J. Van den Bogaerde. J. Amer. Chem. Soc. **91**, 7712 (1969).
8. G. Burns and R. G. W. Norrish. Proc. Roy. Soc. Ser. A, **271**, 289 (1963).
9. J. Brown and G. Burns. Can. J. Chem. **47**, 4291 (1969).
10. G. B. Kistiakowsky and J. C. Sternberg. J. Chem. Phys. **21**, 2218 (1953).
11. J. K. K. Ip and George Burns. J. Chem. Phys. **51**, 3414 (1969).
12. J. A. Blake, R. J. Browne, and George Burns. J. Chem. Phys. In press.
13. M. A. A. Clyne and H. W. Cruse. Trans. Faraday Soc. In press.
14. R. M. Noyes. J. Chem. Phys. **48**, 323 (1968).
15. R. Hoffman. J. Chem. Phys. **49**, 3739 (1968).
16. L. C. Cusachs, M. Krieger, and C. W. McCurdy. J. Chem. Phys. **49**, 3740 (1968).
17. R. M. Noyes. J. Chem. Phys. **49**, 3741 (1968).
18. J. H. Sullivan. J. Chem. Phys. **46**, 73 (1967).

Can. J. Chem. Downloaded from www.nrcresearchpress.com by 210.87.254.40 on 09/05/12
For personal use only.

The complexing characteristics of insoluble selenides. 1. Silver selenide[1]

M. C. MEHRA[2] AND A. O. GUBELI
Department of Chemistry, Laval University, Quebec, Quebec

Received February 23, 1970

The aqueous solubility of the system silver selenide has been investigated in an inert atmosphere of nitrogen at a unit molar ionic strength and constant temperature of 25 °C. The experimental evidence indicates the formation of two aqueous species $[Ag_2(HSe)(OH)]$, and $[Ag(Se)_2(OH)]^{4-}$ in contact with the precipitated selenide in different regions of acidity. The former exists in acidic medium and has a pβ value of 48.49 ± 0.10 while the latter is stable only in alkaline conditions and has a pβ value of 24.07 ± 0.19. A mathematical treatment has been elaborated to identify and calculate the stability constants of such selenide complexes formed through a heterogeneous equilibrium.

Canadian Journal of Chemistry, **48**, 3491 (1970)

Introduction

In the course of systematic investigations on the solubility characteristics of metal chalcogenides, we have earlier reported on the formation of thiocomplexes of cadmium and zinc (1, 2). These complexes are not unique since other workers have also observed these characteristics in the solubility equilibria of the sulfides of antimony (3), mercury (4, 5), lead (6, 7), silver (8, 9), and cobalt (10). In some cases aqueous complexes of exceptionally high stabilities have been observed, *e.g.* the thiocomplexes of silver and mercury.

Surprisingly nothing is known on the similar interactions of insoluble selenides, though their precipitation characteristics are reported to be similar to their corresponding sulfides (11). This apparent lack of interest in the aqueous chemistry of metal selenides may in part be attributed to the low solubilities and also obnoxious character of the selenium compounds. Nevertheless, a knowledge of the comparative complexing properties of the analogous series of compounds derived from S, Se, and Te is desirable.

The solubility and complexing characteristics of silver selenide have been investigated in this study in order to compare its behavior with the corresponding sulfide. The natures of the aqueous species in contact with the precipitated selenide have been established under uniform experimental conditions.

Experimental

The aqueous solubility of this system has been determined over the entire pH range at a constant ionic strength of unity, controlled with pure sodium perchlorate at 25 °C. The precipitate at any desired pH was produced by mixing known volumes of standard radioactive silver perchlorate and an excess of sodium hydrogen selenide as precipitating ligand. The radiotracer ^{110}Ag employed in this study was obtained from A.E.C.L., Chalk River, Ontario, and all other reagents were of the analytical grade purity. The compound sodium hydrogen selenide was synthesized when necessary by a method similar to the synthesis of sodium hydrogen sulfide (12). The stock and all other solutions were prepared in deoxygenated and deionized double distilled water, and furthermore the aqueous medium was kept free of any other complexing ions. Only solutions of perchloric acid and sodium hydroxide were employed to control the pH of the medium. The system was equilibrated for a period of five days in a constant temperature water bath at 25 °C before making the final analytical determinations. In each case the equilibrated aqueous phase was analyzed for total silver (Ag_{tot}), ionic silver (Ag^+), total selenide (Se_{tot}), and the acidity (pH) of the system. A Polymetron type-42 pH meter with an expanded scale arrangement was employed with appropriate electrode assemblies, to measure the pH and Ag^+ concentrations of the medium, whereas a well type γ-ray scintillation spectrometer was utilized for the determination of Ag_{tot} radiometrically. The selenide total concentration was obtained iodimetrically by the method of Wood (13). The method was suitably modified and the end point in the titration was determined electrometrically on a Metrohm potentiograph E-336, using a platinum and a normal calomel cell assembly.

The precipitations and other experimental measurements were done in an inert atmosphere of nitrogen in specially constructed Pyrex glass vessels. The apparatus was so designed that air could be expelled by nitrogen before effecting selenide precipitations at any desired acidity. The aliquots from the reaction vessel were similarly carefully passed through a fritted glass filter by applying nitrogen pressure into an attached pipette from which a measured volume could be drawn for analytical determinations. It was established in preliminary experiments that this procedure gives reproducible results, moreover air oxidation of the selenium compound is thus minimized.

In a separate determination the physico chemical constants of this system, *i.e.*, solubility product of silver

[1]Presented in part at the 51st annual meeting of the C.I.C. Vancouver, British Columbia, June 1968.

[2]Present address: Department of Chemistry, University of Moncton, Moncton, New Brunswick, Canada.

Can. J. Chem. Downloaded from www.nrcresearchpress.com by 210.87.254.40 on 09/05/12
For personal use only.

selenide and the ionization constants of hydrogen selenide, were obtained under identical experimental conditions of ionic strength and temperature by the potentiometric technique. The details of the experimental procedures are cited elsewhere (12).

Theoretical

In the precipitation of silver selenide in an excess of sodium hydrogen selenide, any of the three species H_2Se, HSe^-, and Se^{2-} can give rise to aqueous complex formation. In some parallel determinations with sodium hydrogen sulfide it has, however, been established that either the aqueous complexing interactions of the molecular species H_2S are absent or they are too small to be of any special significance. Hence, it is assumed in this case as well that the species H_2Se does not function as a complexing ligand. In an aqueous medium, on the other hand, the species OH^- may be regarded as a complexing ligand particularly in alkaline conditions. The following equilibria then adequately represent the general complex formation conditions of the system.

$$[1]\quad Ag^+ + xH^+ + xSe^{2-} + yOH^- \rightleftharpoons [Ag(HSe)_x(OH)_y]^{1-(x+y)}$$

$$[2]\quad Ag^+ + xSe^{2-} + yOH^- \rightleftharpoons [Ag(Se)_x(OH)_y]^{1-(x+y)}$$

$$[3]\quad [H^+][OH^-] = K_w \quad (K_w = \text{ion product of water})$$

$$[4]\quad [Ag^+]^2[Se^{2-}] = K_{sp} \quad (K_{sp} = \text{solubility product})$$

$$[5]\quad [Se]_{tot} = [H_2Se] + [HSe^-] + [Se^{2-}] + [Se_{complex}]$$

In view of the low solubilities of the selenides (11), it is reasonable to assume that the term $[Se_{complex}]$ remains negligibly small and can even be neglected in reaction 5. Introduction of the two ionization constants, K_1K_2 of the diprotic acid H_2Se in reaction 5 and rearrangement lead to two more equations as follows

$$[6]\quad [Se]_{tot} = [HSe^-]\left[\frac{[H^+]}{K_1} + 1 + \frac{K_2}{[H^+]}\right]$$

$$[7]\quad [Se]_{tot} = [Se^{2-}]\left[\frac{[H^+]^2}{K_1K_2} + \frac{[H^+]}{K_2} + 1\right]$$

In eqs. 6 and 7 an approximation can be introduced such that concentration expressed by $[Se]_{tot}$ corresponds to concentration of HSe^- when $K_1 \gg [H^+] \gg K_2$ and likewise $[Se]_{tot}$ corresponds to concentration of species Se^{2-} when $K_2 \gg [H^+]$. These conditions may be expressed as

$$[8]\quad [Se]_{tot} = [HSe^-] \quad \text{when } K_1 \gg [H^+] \gg K_2$$

$$[9]\quad [Se]_{tot} = [Se^{2-}] \quad \text{when } K_2 \gg [H^+]$$

This implies that HSe^- and Ag^+ interactions will be apparent only when the p*H* of the medium is in between the values of the two ionization constants of the ligand acid, whereas the Se^{2-} reactions will show up only in the alkaline conditions when the p*H* is beyond the value of the second ionization constant of the H_2Se. It is further evident that at any other condition of acidity in the medium the concentrations of the species HSe^- and Se^{2-} shall be p*H* dependent, *i.e.* the solubility of the system will vary depending on the p*H* of the medium. It is interpreted to mean that if any complexing interactions do occur with either HSe^- or Se^{2-}, the system as a whole will exhibit certain characteristic solubility slopes, which will indicate the nature of interaction, hence the nature of the species formed.

A general mathematical treatment of the solubility data has already been elaborated for HS^-–metal interaction (2), which by suitable modifications can be adapted for HSe^-–silver complexing interactions as in this study. The characteristic solubility slopes for some postulated HSe^-–Ag^+ complexes are recorded in Table 1. The general complexing characteristics of the Se^{2-}–Ag^+ interactions can be similarly derived theoretically by taking into consideration the p*H* dependency of the ligand species as shown in reaction 7. We may divide the effect of p*H* on $[Se^{2-}]$ into three broad regions of acidity; before the first ionization constant of hydrogen selenide, in between the first and second ionization constants, and finally after the second ionization constant. These conditions can be mathematically expressed as shown in the following equations.

$$[10]\quad [Se]_{tot} = \frac{[Se^{2-}][H^+]^2}{K_1K_2} \quad \text{when } [H^+] \gg K_1 \gg K_2$$

$$[11]\quad [Se]_{tot} = \frac{[Se^{2-}][H^+]}{K_2} \quad \text{when } K_1 \gg [H^+] \gg K_2$$

$$[12]\quad [Se]_{tot} = [Se^{2-}] \quad \text{when } K_2 \gg K_1 \gg [H^+]$$

TABLE 1

Theoretical slopes of postulated selenide complex species of silver

Species	$\partial \log [Ag]_{tot}/\partial pH$			$\frac{\partial \log [Ag]_{tot}}{\partial p[Se]_{tot}}$
	$pH \ll pK_1$	$pK_1 \ll pH \ll pK_2$	$pK_2 \ll pH$	
Ag^+	−1	−0.5	0	+0.5
[Ag(HSe)]	0	−0.5	−1	−0.5
$[Ag(HSe)_2]^-$	+1	−0.5	−2	−1.5
$[Ag(HSe)_3]^{2-}$	+2	−0.5	−3	−2.5
$[Ag(HSe)_4]^{3-}$	+3	−0.5	−4	−3.5
$[Ag(HSe)(OH)_2]^{2-}$	+2	+1.5	+1	−0.5
$[Ag(HSe)_2(OH)]^{2-}$	+2	+0.5	−1	−1.5
$[Ag_2(HSe)(OH)]$	0	0	0	0
$[Ag(Se)]^-$	+1	+0.5	0	−0.5
$[Ag(Se)_2]^{3-}$	+3	+1.5	0	−1.5
$[Ag(Se)(OH)_2]^{3-}$	+3	+2.5	+2	−0.5
$[Ag(Se)_2(OH)]^{4-}$	+4	+2.5	+1	−1.5
$[Ag(Se)_2(OH)_2]^{5-}$	+5	+3.5	+2	−1.5
[Ag(OH)]	0	+0.5	+1	+0.5
$[Ag(OH)_2]^-$	+1	+1.5	+2	+0.5

The silver total concentration, $[Ag]_{tot}$, in an equilibrated system at any instant may be regarded as the sum of all the species formed in some significant concentrations. The equilibrium constant of general Se^{2-}–Ag^+ reaction expressed in reaction 2 can therefore be written as

$$[13] \quad \phi_{xy} = \frac{[Ag(Se)_x(OH)_y]^{1-(x+y)}}{[Ag^+][Se^{2-}]^x[OH^-]^y}$$

where the constant expressed by ϕ_{xy} is unique such that it always has a positive value even when there is no complex formation, *i.e.* the system consists only of simple free silver ions. In all other cases where seleno complexing does occur

$$[[Ag(Se)_x(OH)_y]^{1-(x+y)}] = [Ag]_{tot} = \text{sum of all the species in the solution}$$

We may therefore write eq. 13 as a function of $[Ag]_{tot}$ and the other experimental parameters, as

$$[14] \quad [Ag]_{tot} = \sum_{x=0}^{N-y} \sum_{y=0}^{N-x} \phi_{xy}[Ag^+][Se^{2-}]^x[OH^-]^y$$

where N in eq. 14 represents the coordination number of silver which is generally 4.

Equation 14 encompasses all the possible complex species. However, it is known that in such heterogeneous systems rarely more than two or three species are formed in appreciable concentrations. One can in fact say that for all practical purposes the total concentration of silver in solution represents the concentrations of these limited number of aqueous complexes. The experimental variations in the concentration of $[Ag]_{tot}$ as function of pH or $[Se]_{tot}$ can also be said to represent the variations in the concentration of a given complex, as a function of these variables.

In a given pH region and a certain concentration interval of the ligand, if the experimentally observed $[Ag]_{tot}$ corresponds to variations predicted for a given complex, one may conclude that $[Ag]_{tot}$ corresponds to the concentration of that particular complex. The complex is thus identified and its formation constant is calculated from known values of $[Ag]_{tot}$, pH, and $[Se]_{tot}$.

It is easy to visualize now that in the summation eq. 14 in a particular pH region and at a specific interval of $[Se]_{tot}$ only one dissolved species may be significant at a time, which may be represented by a general formula $[Ag(Se)_x(OH)_y]^{1-(x+y)}$. Assuming this to be true and introducing eqs. 10, 11, and 12 alternately into significant term, eq. 14 may be further divided into three equations for this significant species as

$$[15] \quad [Ag]_{tot} = \phi_{xy} \times \frac{[Ag^+][Se]_{tot}^x[K_1K_2]^x[OH^-]^y}{[H^+]^{2x}}$$

when $[H^+] \gg K_1 \gg K_2$

Can. J. Chem. Downloaded from www.nrcresearchpress.com by 210.87.254.40 on 09/05/12
For personal use only.

Can. J. Chem. Downloaded from www.nrcresearchpress.com by 210.87.254.40 on 09/05/12
For personal use only.

$$[16]\quad [Ag]_{tot} = \phi_{xy} \times \frac{[Ag^+][Se]_{tot}{}^x[K_2]^x[OH^-]^y}{[H^+]^x} \quad \text{when } K_1 \gg [H^+] \gg K_2$$

$$[17]\quad [Ag]_{tot} = \phi_{xy}[Ag^+][Se]_{tot}{}^x[OH^-]^y \quad \text{when } K_2 \gg [H^+]$$

Introducing eqs. 3 and 4 into eqs. 15, 16, and 17, the final expressions are

$$[18]\quad [Ag]_{tot} = \phi_{xy}K_{sp}{}^{\frac{1}{2}}[Se]_{tot}{}^{x-\frac{1}{2}}[K_1K_2]^{x-\frac{1}{2}} \times [K_w]^y[H^+]^{1-(2x+y)}$$

$$[19]\quad [Ag]_{tot} = \phi_{xy}K_{sp}{}^{\frac{1}{2}}[Se]_{tot}{}^{x-\frac{1}{2}}[K_2]^{x-\frac{1}{2}} \times [K_w]^y[H^+]^{\frac{1}{2}-(x+y)}$$

$$[20]\quad [Ag]_{tot} = \phi_{xy}K_{sp}{}^{\frac{1}{2}}[Se]_{tot}{}^{x-\frac{1}{2}} \times [H^+]^{-y}[K_w]^y$$

The theoretical solubility characteristics of the complex can be established as shown earlier in HS^-–metal complexing reactions (2) by differentiating eqs. 18, 19, and 20 with respect to the experimental variables, pH, and $[Se]_{tot}$ with one being constant at any particular instant. The final equations expressing the solubility slopes of the species at a constant $[Se]_{tot}$ are as given below in their logarithmic forms.

$$[21]\quad \frac{\partial \log [Ag]_{tot}}{\partial pH} = (2x + y - 1) \quad \text{when } [H^+] \gg K_1 \gg K_2$$

$$[22]\quad \frac{\partial \log [Ag]_{tot}}{\partial pH} = (x + y - \tfrac{1}{2}) \quad \text{when } K_1 \gg [H^+] \gg K_2$$

$$[23]\quad \frac{\partial \log [Ag]_{tot}}{\partial pH} = (y) \quad \text{when } K_2 \gg [H^+]$$

while at a specific pH the species will have a constant slope as a function of $[Se]_{tot}$ as given in eq. 24

$$[24]\quad \frac{\partial \log [Ag]_{tot}}{\partial p[Se]_{tot}} = (\tfrac{1}{2} - x)$$

Theoretically the knowledge of the numerical values of two of the four derivatives shown above is sufficient to establish the values of x and y in the general formula and hence the identity of the species in question. The exact nature of the species is, however, assured by comparing the experimentally observed solubility slopes with the theoretically derived characteristics for the same species (*cf.* Table 1).

In this manner careful investigations over the entire pH range, and at sufficiently well spaced $[Se]_{tot}$ intervals, lead to the identification of all the species formed in appreciable concentrations. In the case when more than one species may be formed in the same pH region as defined earlier, one can still establish their identities by observing the changes in the slopes of the solubility curves in the specific region of interest. Such interactions have been observed earlier for the Ag^+–$SeO_3{}^{2-}$ system (16).

An important point to be noted here is that validity of eqs. 21 through 24 depends on eqs. 18, 19, and 20, which shall be the case provided only one term with a nonzero value for the exponent of $[H^+]$ or $[Se]_{tot}$ is significant at a time in the summation. Fortunately this restriction holds true for polyprotic acids having a large difference in the values of their individual ionization constants. Furthermore, eqs. 21 through 24 show that one may expect pure seleno, pure hydroxy, or mixed seleno hydroxy species in the system depending on the values of x and y in the postulated complexes. The theoretical solubility slopes of a number of seleno silver complex species are recorded in Table 1.

In conclusion identification of a species formed becomes straightforward if only one complex is formed at a time. However, simultaneous formation of several species is also probable as discussed earlier. In the event when such species are formed in a systematic manner *i.e.* their characteristic slopes remain well defined in a specific region of acidity or $[Se]_{tot}$ interval, their identification can be successfully made by the method of comparison as shown in this study. On the other hand should the information from the solubility curves remain inconclusive, one can still identify the complex formed in the highest concentration from the experimental data. The natures and the stability constants of the underlying species, in such cases, are established by resorting to the system of simultaneous equations as has been shown in an earlier study (1). This treatment has the advantage that only species contributing significantly to $[Ag]_{tot}$ in solution are taken into account, thus eliminating the possibilities of negative values for their formation constants.

TABLE 2

Complex $[Ag(Se)_2(OH)]^{4-}$, $p\beta_{21}$*

p*H*	$p[Ag]_{tot}$	$p[Se]_{tot}$	$p[Ag^+]$	$p[OH^-]$	$p[Ag_c]$	$-p\beta_{21}$
12.50	7.25	1.87	25.97	1.50	7.44	23.77
12.75	6.80	1.83	25.98	1.25	6.86	24.03
13.00	6.78	1.89	25.95	1.00	6.83	23.90
13.00	6.00	1.59	26.10	1.00	6.01	24.27
13.05	5.90	1.61	26.09	0.95	5.90	24.36
13.07	5.85	1.58	26.10	0.93	5.85	24.34
13.10	5.80	1.58	26.10	0.90	5.80	24.42
13.12	5.74	1.58	26.10	0.88	5.74	24.40
12.70	5.87	1.18	26.30	1.30	5.88	24.08
12.80	5.72	1.20	26.29	1.20	5.72	24.17
12.90	5.79	1.18	26.30	1.10	5.79	23.97
13.05	5.62	1.20	26.29	0.95	5.62	24.02
13.17	5.47	1.23	26.28	0.83	5.47	24.10
13.20	5.40	1.19	26.30	0.80	5.40	24.08
13.30	5.34	1.14	26.32	0.70	5.34	23.96
13.45	5.17	1.20	26.29	0.55	5.17	24.07
13.60	5.07	1.20	26.29	0.40	5.07	24.02
13.70	5.02	1.11	26.34	0.30	5.02	23.84
13.75	4.95	1.10	26.34	0.25	4.95	23.84
13.82	4.87	1.14	26.32	0.18	4.87	23.91
13.85	4.72	1.10	26.34	0.15	4.72	23.97

*Experimental data from the solubility curves, Fig. 1.

The Formation Constant

The final expression for the over-all stability constant β, of a complex with HSe^- or Se^{2-} as ligand is given by eqs. 25 or 26, and depends on the nature of interaction, with Ag^+ ions.

$$[25]\quad \beta_{xy} = \frac{[Ag]_{tot}[K_2]^x[H^+]^{y-x}[Se^{2-}]^{\frac{1}{2}-x}}{K_{sp}{}^{\frac{1}{2}}K_w{}^y} = K_2{}^x\phi_{xy}$$

$$[26]\quad \beta_{xy} = \frac{[Ag]_{tot}[Se^{2-}]^{\frac{1}{2}-x}[H^+]^{+y}}{K_{sp}{}^{\frac{1}{2}}K_w{}^y} = \phi_{xy}$$

Results

The potentiometric determination with a silver and a standard Calomel electrode cell assembly gave the values of the two ionization constants of hydrogen selenide as $10^{-3.48}$ and $10^{-11.60}$, respectively, while the value of the solubility product of silver selenide from the same experimental data was $10^{-53.79}$, thereby showing the extreme insolubility of the compound. These data have been utilized in the present calculations wherever necessary.

The aqueous solubility data for silver selenide as a function of both the experimental variables, p*H* and $[Se]_{tot}$ are shown in Fig. 1, while the solubility variations (at a constant p*H*) as a function of $[Se]_{tot}$ are traced in Fig. 2. The salient features of these graphs are that in the former case two distinct solubility slopes are apparent; slope of zero in acidic regions and a positive slope of one in alkaline medium, while in the latter case a slope of 1.5 in alkaline medium is evident from the graphical data. Comparison of these characteristic slopes with the theoretical data in Table 1 readily confirms the possibility of two important species in the aqueous phase of silver selenide, which may be described by the formula $[Ag_2(HSe)(OH)]$ and $[Ag(Se)_2(OH)]^{4-}$.

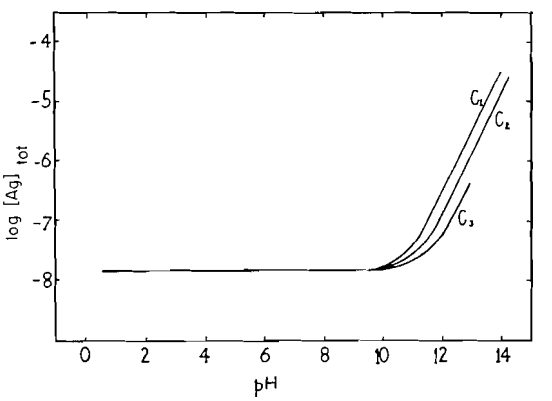

FIG. 1. Solubility curves of Ag_2Se as a function of p*H*. C_1, $[Se]_{tot} \simeq 0.0645\ M$; C_2, $[Se]_{tot} \simeq 0.0263\ M$; C_3, $[Se]_{tot} \simeq 0.0135\ M$: $[^{110}Ag]_{tot}$ (original) $= 4 \times 10^{-4}\ M$.

Formation Constant of $[Ag_2(HSe)(OH)]$

The average value of $[Ag]_{tot}$ in acidic medium was found to be $10^{-7.70}\ M$, this may be sub-

Can. J. Chem. Downloaded from www.nrcresearchpress.com by 210.87.254.40 on 09/05/12
For personal use only.

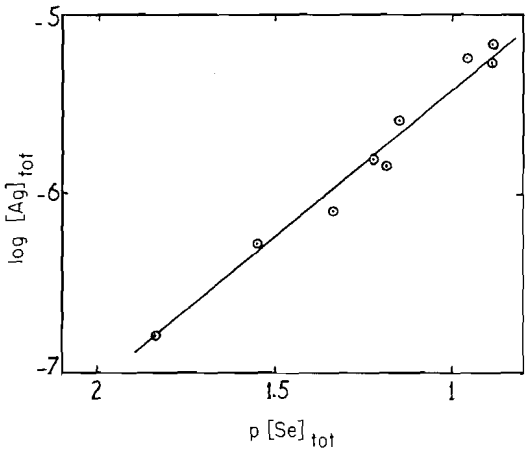

FIG. 2. Solubility curve of Ag_2Se as a function of $[Se]_{tot}$. $pH \simeq 12.5$; $[^{110}Ag]_{tot}$ (original) $= 4 \times 10^{-4}$ *M*.

stituted in eq. 25 to obtain the stability constant of this species.

$$\beta_{11} = \frac{[Ag_2(HSe)(OH)]}{[Ag^+]^2[HSe^-][OH^-]} = \frac{[Ag]_{tot}K_2}{K_{sp}K_w}$$

$$p\beta_{11} = p[Ag]_{tot} - pK_{sp} + pK_2 - pK_w$$
$$= 7.70 - 53.79 + 11.60 - 14.0$$
$$= -48.49 \pm 0.10$$

Formation Constant of Species $[Ag(Se)_2(OH)]^{4-}$

The experimental data from Fig. 1 in alkaline medium are recorded in Table 2. In this case $[Ag]_{tot}$ is regarded as the sum of two species, hence the concentration of the species $[Ag(Se)_2(OH)]^{4-}$ alone is obtained by subtracting the concentration of species described above.

$$[Ag]_{tot} = [Ag_2(HSe)(OH)] + [[Ag(Se)_2(OH)]^{4-}]$$

$$[[Ag(Se)_2(OH)]^{4-}] = [Ag]_{tot} - [Ag_2(HSe)(OH)] = [Ag]_c$$

The stability constant of the complex may be calculated from eq. 26 utilizing the data from Table 2, or from the following expression,

$$\beta_{21} = \frac{[[Ag(Se)_2(OH)]^{4-}]}{[Ag^+][Se^{2-}]^2[OH^-]}$$

$$= \frac{[Ag]_c}{[Ag^+][Se^{2-}]^2[OH^-]}$$

$$p\beta_{21} = pAg_c - pAg^+ - 2pSe^{2-} - pOH^-$$
$$= -24.07 \pm 0.19$$

In this case since solubility increases in the p*H* regions beyond pK_2 of hydrogen selenide, evidently Se^{2-} remains the principal complexing ligand in the medium.

Discussion

The data available on the physico chemical constants of metal selenides are very meagre; even the simple solubility product constants of metal selenides in an aqueous medium are not known with any certainty. In addition there is a considerable uncertainty on the reported values of the two ionization constants of hydrogen selenide (15). It therefore became essential to establish these constants under the same experimental conditions as utilized in the solubility studies, *i.e.* controlled ionic strength and temperature. We have already demonstrated the technique of obtaining these constants in a sulfide system by a potentiometric method (12, 14), which has been extended to the selenide system as well. The main advantage of this technique is that both the ionization constants of hydrogen selenide and the solubility product constant of silver selenide are obtained simultaneously from the same experimental data. Since reliable results have been obtained in sulfide systems, we presume the data obtained for H_2Se constants are also the best available so far. The solubility product of silver selenide has thus been experimentally established for the first time by this method.

The actual solubility of silver selenide is much higher than that calculated on the basis of simple solubility product alone, which certainly implies that some complex aqueous species are formed in the system. The analysis of the solubility data indicates the existence of at least two predominant species $[Ag_2(HSe)(OH)]$ and $[Ag(Se)_2(OH)]^{4-}$ in acidic and alkaline conditions, respectively. These unusual aqueous species appear to be exceptionally stable as shown by their formation constants. This is not surprising since in many sulfide systems such interactions have given rise to aqueous complexes of high stabilities (2, 4, 9). However, the surprising feature is that silver selenide solubility behavior is very different from that of its sulfide, where in the latter case only one species $[Ag(HS)_2]^-$ was noticed in neutral

Can. J. Chem. Downloaded from www.nrcresearchpress.com by 210.87.254.40 on 09/05/12
For personal use only.

Can. J. Chem. Downloaded from www.nrcresearchpress.com by 210.87.254.40 on 09/05/12
For personal use only.

medium besides the presence of a complex $[Ag_2(HS)(OH)]$, both in acidic and alkaline medium (12). Nevertheless in acidic conditions their behavior is parallel to the extent that both the selenide and the sulfide systems give a soluble species of the similar nature. However, the selenide complex (pβ, 48.49) is more stable than the sulfide species (pβ, 41.89) which may primarily be due to the greater insolubility of silver selenide. Comparatively speaking the absence of any HSe^- complexing in silver selenide equilibrium leaves the impression that this species acts as a poor complexing ligand, which appears justified too since in a parallel study on the complexing characteristics of H_2SeO_3 it has been shown that the species $HSeO_3^-$ has negligible complexing properties, while the species SeO_3^{2-} coordinates with silver with greater ease (16). The results of the present investigation supplement this view to a large extent since in alkaline conditions Se^{2-} complexing is well characterized (*cf.* Fig. 2). Hence, HSe^- is a weaker ligand than HS^-, while Se^{2-} is a stronger ligand than S^{2-} as shown in the respective determinations on silver systems. However, some more systems must be analyzed before any generalizations can be definitely ascribed to such interactions.

It is, nevertheless, clear that the increase in the solubility of the selenide precipitate is not due to any hydroxy complex formation as found in an independent investigation on the solubility characteristics of silver oxide (17). If it were so, the solubility in alkaline medium would have decreased as a function of increasing selenide concentration, even though a positive slope of unity as a function of p*H* might still remain the principal solubility feature. The actual results (*cf.* Figs. 1 and 2) show that the species formed incorporates one OH^- ion and two Se^{2-} ions, leading to the formation of an unusual species $[Ag(Se)_2(OH)]^{4-}$. We have also noticed similar solubility increases in the interactions of mercuric sulfide and selenide systems, which we think are due to the formation of mixed species as observed in this system (12). In this respect the solubility behavior of silver selenide in alkaline conditions is totally different from that of its sulfide, which hardly forms any mixed thio complexes in alkaline conditions. As far as known to the authors this is the first report on the aqueous species of insoluble selenides of metals.

The authors gratefully acknowledge the financial support provided by the National Research Council of Canada.

1. J. Ste-Marie, A. E. Torma, and A. O. Gubeli. Can. J. Chem. **42**, 662 (1964).
2. A. O. Gubeli and J. Ste-Marie. Can. J. Chem. **45**, 2101 (1967).
3. K. Dubey and S. Ghosh. Z. Anorg. U. Allgem. chem. **319**, 204 (1962).
4. G. Schwarzenbach and W. Widmer. Helv. Chem. Acta, **46**, 2613 (1963).
5. H. L. Barnes, S. B. Romberger, and M. Stemprok. Econ. Geol. **62**, 957 (1967).
6. J. J. Hemley. Econ. Geol. **48**, 113 (1953).
7. G. M. Anderson. Econ. Geol. **57**, 809 (1962).
8. W. D. Treadwell and H. Hepenstrick. Helv. Chem. Acta, **32**, 1872 (1949).
9. G. Schwarzenbach and W. Widmer. Helv. Chem. Acta, **49**, 111 (1966).
10. A. Mickwitz. Z. Anorg. Chem. **196**, 113 (1931).
11. J. W. Mellor. A comprehensive treatise on inorganic and theoretical chemistry. Longmans and Sons. 1930.
12. M. C. Mehra. Doctoral Dissertation, Laval University, Quebec, Quebec. 1968.
13. R. L. Wood. J. Amer. Chem. Soc. **80**, 1559 (1958).
14. J. Ste-Marie. Doctoral Dissertation, Laval University, Quebec, Quebec. 1966.
15. L. G. Sillen and A. E. Martell. Stability constants of metal ion complexes. Special publication no. 17. The Chemical Society, London. 1964.
16. M. C. Mehra and A. O. Gubeli. Radiochem. Radioanal. Lett. **2(2)**, 61 (1969).
17. A. O. Gubeli and J. Ste-Marie. Can. J. Chem. **45**, 827 (1967).

The chemical shift. I. Approximate theory and application to first row binary fluorides

F. G. HERRING

Department of Chemistry, University of British Columbia, Vancouver 8, British Columbia

Received February 5, 1970

Starting from the approximations of the i.n.d.o.-l.c.a.o.-s.c.f. method and using approximate Hartree–Fock perturbation theory, a method has been developed whereby the nuclear shielding of a nucleus for a first row element may be estimated. The method avoids the use of the average energy approximation. The method is demonstrated by calculating the ^{19}F chemical shifts in the first row binary fluorides relative to the fluorine molecule.

Canadian Journal of Chemistry, **48**, 3498 (1970)

Can. J. Chem. Downloaded from www.nrcresearchpress.com by 210.87.254.5 on 09/05/12
For personal use only.

The basic theory of nuclear magnetic shielding has been developed by Ramsey (1). This work indicates that the nuclear shielding of a nucleus is made up of two parts *i.e.* the Lamb term which may be evaluated from the ground state wavefunction and the paramagnetic term which is a second order contribution and requires a sum over excited states. It is the latter term which has proved to be the most difficult to evaluate as it requires a knowledge of excited state wavefunctions.

The work of Lipscomb and co-workers (2–4) has shown, within the framework of Hartree–Fock perturbation theory, that the nuclear magnetic shielding for a nucleus in a diatomic molecule may be calculated satisfactorily.

The treatment of larger molecular systems is, however, at a much more approximate level. Previous calculations of chemical shifts have all, with one exception (16), employed the average energy approximation to simplify the paramagnetic term (1, 5–13). This approximation results in an expression for the paramagnetic term as a function of bond order and charge density matrix elements for the ground state. The average energy approximation has the obvious defect that it fails to take into account the fact that there may be terms of opposite sign in the sum over excited states (14), although for some magnetic properties this approximation may be applicable (15). The inadequacy of this approximation has been demonstrated in the case of ClF (16). Thus in order to understand qualitatively the variations in chemical shift for a number of molecules it seems necessary that the average energy approximation be avoided.

Recently, in the light of extended basis set calculations, Hegstrom and Lipscomb (17) discussed the various approximations to the paramagnetic term and showed the relationship of these approximations to perturbed Hartree–Fock theory. This work indicated that certain "off-diagonal" self-consistency terms may be neglected, although there is no *a priori* reason for doing so, so that the calculation of the nuclear shielding may be simplified.

The purpose of the present work is to avoid the pitfalls of the average energy approximation by using approximate perturbed Hartree–Fock theory. In conjunction with this the necessary molecular wavefunctions will be obtained from the i.n.d.o.-l.c.a.o.-s.c.f. method, developed by Pople *et al.* (18). The calculations will be confined to those nuclei whose nuclear shielding is dominated by the paramagnetic term. It should be noted here that a similar theory, although different in detail, for the estimation of diamagnetic susceptibilities has been presented by Bley (19).

Theory

The approximate theory to be developed here follows the method known as Hartree–Fock perturbation theory (2, 17, 20). The one electron nature of the magnetic perturbations make this method particularly suitable for the estimation of the chemical shift. This has been amply demonstrated by the calculations of Lipscomb and co-workers (2–4). It is the aim of this work to estimate the chemical shift of a nucleus of a first row element in the framework of the i.n.d.o.-l.c.a.o.-s.c.f. method devised by Pople *et al.* (18) together with the necessary Hartree–Fock perturbation theory.

The requisite expressions for the chemical shift may be obtained from the following molecular Hamiltonian, in which all magnetic interactions, other than those contributing to the chemical shift directly, have been neglected (21, 22)

$$[1]\quad \mathscr{H} = \mathscr{H}_0 + \boldsymbol{H}\cdot\sum_{i=1}^{2N}\beta_e\boldsymbol{L}_{0i} + \sum_n \mu_n\cdot\sum_{i=1}^{2N} 2\beta_e\boldsymbol{L}_{ni}r_{ni}^{-3} + \tfrac{1}{2}r_e\sum_n\mu_n\cdot\sum_{i=1}^{2N}[(\boldsymbol{r}_{ni}\cdot\boldsymbol{r}_{ni})\mathbf{U} - \boldsymbol{r}_{0i}\boldsymbol{r}_{ni}]r_{ni}^{-3}\cdot\boldsymbol{H}$$

where $\mathscr{H}_0$ is the electronic Hamiltonian for the unperturbed $2N$-electron system, $\boldsymbol{L}_{0i}$ and $\boldsymbol{L}_{ni}$ are the dimensionless angular momentum operators for electron i about a common molecular origin and about the nucleus n, respectively (the electron position vectors $\boldsymbol{r}_{0i}$ and $\boldsymbol{r}_{ni}$ are similarly defined), $\boldsymbol{H}$ is the applied magnetic field, μ_n, the magnetic moment of the nucleus n, $\mathbf{U}$ is the unit dyadic, $\beta_e = e\hbar/2mc$ and $r_e = e^2/mc^2$.

The unperturbed electron Hamiltonian is approximated by a Hartree–Fock operator, which for a single electron is

$$[2]\quad h^0(1) = -\tfrac{1}{2}\Delta_1 - \sum_n z_n r_{n1}^{-1} + \sum_{j=1}^{2N}\langle\chi_j^0|\mathscr{O}_{12}|\chi_j^0\rangle$$

where $\mathscr{O}_{12} = r_{12}^{-1}(1 - P_{12})$ in which P_{12} permutes the electron coordinates (see ref. 20) and χ_j is a molecular spin orbital. The one electron nature of the magnetic perturbations in eq. 1 allows us to formalize the problem in the following way (assuming for simplicity a single nuclear spin $\mu \neq 0$)

$$[3]\quad [h^0(1) + \boldsymbol{H}\cdot\boldsymbol{h}^{100}(1) + \mu\cdot\boldsymbol{h}^{010}(1) + \mu\cdot\mathbf{h}^{001}(1)\cdot\boldsymbol{H} - \varepsilon_i]\chi_i(1) = 0$$

where $\boldsymbol{h}^{100}$, $\boldsymbol{h}^{010}$, and $\mathbf{h}^{001}$ correspond to the operators in eq. 1, whence, expanding ε_i and χ_i as double power series in μ and $\boldsymbol{H}$, we obtain the following expressions for those energy terms independent of μ and $\boldsymbol{H}$ and bilinear in them

$$[4]\quad E^0 = \sum_{i=1}^{2N}\left(\varepsilon_i^0 + \left\langle\chi_i^0\right|\left| -\tfrac{1}{2}\Delta_1 - \sum_n z_n r_{ni}^{-1}\right|\chi_i^0\right\rangle\right)$$

$$[5]\quad E^{011} = \mu\cdot\left\{\sum_{i=1}^{2N}\langle\chi_i^0|\mathbf{h}^{001}|\chi_i^0\rangle + \sum_{i=1}^{2N}(\langle\chi_i^{01}|\boldsymbol{h}^{100}|\chi_i^0\rangle + \langle\chi_i^{10}|\boldsymbol{h}^{010}|\chi_i^0\rangle)\right\}\cdot\boldsymbol{H}$$

There are no linear terms in μ and $\boldsymbol{H}$ since the perturbations $\boldsymbol{h}^{100}$ and $\boldsymbol{h}^{010}$ are imaginary. The first term in [5] corresponds to the Lamb term and the second term to the so-called paramagnetic term. This second term (in eq. 5) may be simplified using Dalgarno's Interchange Theorem (23) so that only one or other of the first order corrections need be calculated, *viz.*,

$$[6]\quad \begin{aligned} E^{011} &= \mu\cdot\left\{\sum_{i=1}^{2N}\langle\chi_i^0|\mathbf{h}^{001}|\chi_i^0\rangle + 2\sum_{i=1}^{2N}\langle\chi_i^{01}|\boldsymbol{h}^{100}|\chi_i^0\rangle\right\}\cdot\boldsymbol{H} \\ &= \mu\cdot\left\{\sum_{i=1}^{2N}\langle\chi_i^0|\mathbf{h}^{001}|\chi_i^0\rangle + 2\sum_{i=1}^{2N}\langle\chi_i^{10}|\boldsymbol{h}^{010}|\chi_i^0\rangle\right\}\cdot\boldsymbol{H}\end{aligned}$$

All that is required now is to write down the coupled equations necessary to obtain χ_i^{10} or χ_i^{01}. These have been given previously (2, 17, 20) and are

$$[7]\quad [h^0(1) - \varepsilon_i^0]\chi_i^{01}(1) + h^{01}\chi_i^0(1) + \sum_{j=1}^{2N}\{\langle\chi_j^{01}|\mathscr{O}_{12}|\chi_j^0\rangle + \langle\chi_j^0|\mathscr{O}_{12}|\chi_j^{01}\rangle\}\chi_j^0(1) = 0$$

The equations may be solved by expanding χ^{01} as a linear combination of zeroth order function, that is, we write

Can. J. Chem. Downloaded from www.nrcresearchpress.com by 210.87.254.5 on 09/05/12
For personal use only.

[8] $$\chi_i^{01}(1) = \sum_{p=2N+1}^{M} C'_{pi}\chi_p^0(1)$$

where the zeroth order functions are defined by

$$[h^0(1) - \varepsilon_i^0]\chi_i^0(1) = 0$$

and

$$\langle\chi_j^0|\chi_i^0\rangle = \delta_{ji}$$

i.e. solutions of the Hartree–Fock operator. It is only necessary for the sum in eq. 8 to be over unoccupied orbitals since mixing the occupied orbitals does not change the wavefunction. Substituting eq. 8 into eq. 7, premultiplying by χ_p^0 (1) and integrating, we have

[9] $$(\varepsilon_p^0 - \varepsilon_i^0)C'_{pi} + \langle\chi_p^0|\boldsymbol{h}^{010}|\chi_i^0\rangle + \sum_{j=1}^{2N}\sum_{q=2N+1}^{M}[\langle\chi_j^0\chi_p^0|r_{12}^{-1}|\chi_q^0\chi_i^0\rangle - \langle\chi_j^0\chi_p^0|r_{12}^{-1}|\chi_i^0\chi_q^0\rangle]C'_{qj}$$

$$+ \sum_{j=1}^{2N}\sum_{q=2N+1}^{M}[\langle\chi_q^0\chi_p^0|r_{12}^{-1}|\chi_j^0\chi_i^0\rangle - \langle\chi_q^0\chi_p^0|r_{12}^{-1}|\chi_i^0\chi_j^0\rangle]C'^*_{qj} = 0$$

We now change the basis set to the N doubly occupied orbitals

$$\phi_j^0(\chi_j^0(1) = \phi_j^0(1)\alpha,\ \chi_{j+1}^0(2) = \phi_j^0(1)\beta)$$

whence

[10] $$(\varepsilon_p^0 - \varepsilon_i^0)C'_{pi} + \langle\phi_p^0|h^{010}|\phi_i^0\rangle + \sum_{j=1}^{N}\sum_{q=N+1}^{M}[2\langle\phi_j^0\phi_q^0|r_{12}^{-1}|\phi_p^0\phi_i^0\rangle - \langle\phi_j^0\phi_i^0|r_{12}^{-1}|\phi_p^0\phi_q^0\rangle]C'_{qj}$$

$$+ \sum_{j=1}^{N}\sum_{q=N+1}^{M}[2\langle\phi_q^0\phi_j^0|r_{12}^{-1}|\phi_p^0\phi_i^0\rangle - \langle\phi_q^0\phi_i^0|r_{12}^{-1}|\phi_p^0\phi_j^0\rangle]C'^*_{qj} = 0$$

which is the equation derived by Lipscomb *et al.* (2–4). Now since both perturbations $\boldsymbol{h}^{010}(1)$ and $\boldsymbol{h}^{100}(1)$ are imaginary the C'_{pi} are imaginary thus $C'^*_{pi} = -C'_{pi}$ and keeping only those terms in eq. 10 for which $j = i$, we have

[11] $$(\varepsilon_p^0 - \varepsilon_i^0)C'_{pi} + \langle\phi_p^0|h^{010}|\phi_i^0\rangle + \sum_{q=N+1}^{M}[\langle\phi_q^0\phi_i^0|r_{12}^{-1}|\phi_p^0\phi_i^0\rangle - \langle\phi_i^0\phi_i^0|r_{12}^{-1}|\phi_p^0\phi_q^0\rangle] = 0$$

which corresponds to the method (*b*) of Langhoff, Karplus, and Hurst (21).

In addition to the neglect of the above off-diagonal self consistency terms one may also approximate eq. 11 by setting $q = p$, whence

[12] $$C'_{pi} = \frac{\langle\phi_p^0|h^{010}|\phi_i^0\rangle}{\varepsilon_p^0 - \varepsilon_i^0 + \langle\phi_p^0\phi_i^0|r_{12}^{-1}|\phi_i^0\phi_p^0\rangle - \langle\phi_i^0\phi_p^0|r_{12}^{-1}|\phi_i^0\phi_p^0\rangle}$$

which corresponds to the method suggested by Lipscomb and Hegstrom (17). These workers were careful to emphasize that the terms neglected above are not always small and that their magnitude can only be estimated by doing a fully coupled Hartree–Fock perturbation. However, within the framework of an approximate l.c.a.o.-s.c.f., it would seem reasonable to adopt eq. 12 and this is what has been done. The form of the energy denominator in eq. 12 arises as a consequence of the pure imaginary character of the perturbations involved (see, for example, ref. 2), therefore it differs from the usual singlet–singlet energy difference presumably used by Hendrickson and Kuznesof (13).

Substituting eq. 8 together with eq. 12 into eq. 6 we obtain

[13] $$E^{011} = \mu \cdot \left\{2\sum_{i=1}^{N}\langle\phi_i^0|\mathbf{h}^{001}|\phi_i^0\rangle + 4\sum_{i=1}^{N}\sum_{p=N+1}^{M}\langle\phi_i^0|\boldsymbol{h}^{010}|\phi_p^0\rangle\langle\phi_p^0|\boldsymbol{h}^{100}|\phi_i^0\rangle E_{pi}^{-1}\right\} \cdot \boldsymbol{H}$$

where $$E_{pi} = \varepsilon_p - \varepsilon_i + \langle\phi_p^0\phi_i^0|r_{12}^{-1}|\phi_i^0\phi_p^0\rangle - \langle\phi_i^0\phi_p^0|r_{12}^{-1}|\phi_i^0\phi_p^0\rangle$$

Can. J. Chem. Downloaded from www.nrcresearchpress.com by 210.87.254.5 on 09/05/12
For personal use only.

Comparing eq. 13, with the usual spin Hamiltonian for the nuclear shielding and dividing the chemical shift into a diamagnetic (σ^d) and a paramagnetic (σ^p) part, we can write for a diagonal component ($\alpha = x, y,$ or z) of the shielding tensor

$$[14a] \qquad \sigma^d_{\alpha\alpha} = r_e \sum_{i=1}^{N} 2\langle\phi_i^0|(r^2 - \alpha^2)r^{-3}|\phi_i^0\rangle$$

$$[14b] \qquad \sigma^p_{\alpha\alpha} = 8\beta_e^2 \sum_{i=1}^{N} \sum_{p=N+1}^{M} E_{pi}^{-1}\langle\phi_i^0|L_\alpha|\phi_p^0\rangle\langle\phi_p^0|L_\alpha r^{-3}|\phi_i^0\rangle$$

where the origin of L_α and r are taken to be the nucleus of interest (17).

The unperturbed l.c.a.o. molecular orbitals are to be evaluated using the i.n.d.o. (intermediate neglect of overlap) method devised by Pople *et al.* (18). Using the approximations of this theory the matrix elements of Hartree–Fock operator, expanded in an atomic orbital basis set ψ_μ, are given by

$$F_{\mu\mu} = U_{\mu\mu} + \sum_{\lambda} P^A_{\lambda\lambda}[(\mu\mu|\lambda\lambda) - \tfrac{1}{2}(\mu\lambda|\mu\lambda)] + \sum_{B \neq A} (P_{BB} - Z_B)\gamma_{AB} \quad (\mu \in A)$$

$$F_{\mu\nu} = \tfrac{1}{2}P_{\mu\nu}[3(\mu\nu|\mu\nu) - (\mu\mu|\nu\nu)] \quad (\mu \neq \nu, \mu \text{ and } \nu \in A)$$

$$F_{\mu\nu} = \tfrac{1}{2}(\beta_A^0 + \beta_B^0)S_{\mu\nu} - \tfrac{1}{2}P_{\mu\nu}\gamma_{AB} \quad (\mu \neq \nu)$$

where

$$P_{\mu\nu} = 2\sum_{i=1}^{N} C_{i\mu}C_{i\nu}$$

$$P_{AA} = \sum_{\mu}^{A} P_{\mu\mu}$$

and the remaining notation is that of Pople *et al.* The molecular coulomb and exchange integrals required in [14*b*] have the following form in the i.n.d.o. framework

$$\langle\phi_k\phi_l|r_{12}^{-1}|\phi_k\phi_l\rangle = \sum_{\mu\nu} \{C^2_{\mu k}C^2_{\nu l}[\gamma_{AB}(1 - \delta_{AB}) + \delta_{AB}(\mu\mu|\nu\nu)] + \delta_{AB}(1 - \delta_{\mu\nu})C_{\mu k}C_{\mu l}C_{\nu k}C_{\nu l}(\mu\nu|\mu\nu)\}$$

$$\langle\phi_k\phi_l|r_{12}^{-1}|\phi_l\phi_k\rangle = \sum_{\mu\nu} \{C_{\mu k}C_{\mu l}C_{\nu k}C_{\nu l}[\gamma_{AB}(1 - \delta_{AB}) + \delta_{AB}(\mu\mu|\nu\nu)] + \delta_{AB}(1 - \delta_{\mu\nu})C^2_{\mu k}C^2_{\nu l}(\mu\nu|\mu\nu)\}$$

It is now necessary to consider the evaluation of the magnetic integrals needed for eqs. 14*a* and 14*b*. We propose to consider, at the present, only those nuclei in which it is believed that changes in the nuclear shielding are manifested mainly in the paramagnetic term and that the Lamb term (dominated in the main by the 1s contribution for first row elements) remains essentially constant. Consequently for the present investigation we define the chemical shift (δ) as the difference between the paramagnetic nuclear shielding of the molecule in question (σ^p_x) and some arbitrarily chosen standard molecule (σ^p_s), *i.e.*

$$\delta = \sigma^p_x - \sigma^p_s$$

Cornwell (16, 20) has devised approximate expression for the angular momentum integrals in eq. 14*b*; these are

$$[15] \qquad \langle\phi_j|L_\alpha|\phi_p\rangle = i\sum_B (\boldsymbol{C}_p^B \times \boldsymbol{C}_j^B)_\alpha$$

$$\langle\phi_p|L_\alpha r^{-3}|\phi_j\rangle = i\langle r^{-3}\rangle_{Ap}(\boldsymbol{C}_p^A \times \boldsymbol{C}_j^A)_\alpha$$

where the summation runs over all atom B in the molecule, the components of the vectors $\boldsymbol{C}_p^B$ are the coefficients of the corresponding p_x, p_y, p_z orbitals and $\langle r^{-3}\rangle_{Ap}$ is the expectation value of r^{-3} for an electron in the valence p-orbitals on center A. The value of $\langle r^{-3}\rangle_{Ap}$ can be evaluated from $\xi^3/3$ where ξ

Can. J. Chem. Downloaded from www.nrcresearchpress.com by 210.87.254.5 on 09/05/12
For personal use only.

is the orbital exponent of a Slater 2p orbital. The approximate expressions in [15] are in the same spirit as the approximations inherent in the i.n.d.o. method in that overlap between different atoms is neglected and that only valence electrons are considered. Integrals of the form $\langle\phi_B|L_A r_A^{-3}|\phi_B\rangle$ although formally allowed in the z.d.o. approximation have been neglected due to their r^{-3} dependence.

In addition the rotational invariance of the i.n.d.o. method and the neglect of overlap terms in eq. 15 ensure that the present calculations are *gauge* invariant.

The approximate perturbed Hartree–Fock method employed here together with the appropriate approximation to the magnetic integrals (19) may be extended to spin–spin couplings, g-shifts etc.; such extensions are being considered.

Computational Details and Results

The i.n.d.o.-l.c.a.o.-s.c.f. program employed in this work was written in this laboratory for an IBM 360/67. The results of many s.c.f. calculations have been carefully checked against the previously published results of Pople *et al.* The estimation of the nuclear shielding is attached as an option to this program. All calculations are performed as indicated in the theoretical section. A computational point should be noted here, care must be taken in the use of eq. 12 when degeneracies are present and the nuclear shielding at a nucleus not at the origin of coordinates is being computed, *e.g.* the fluorine atom in CF_4. It is mandatory that the degenerate orbitals be symmetry adapted, otherwise the other arbitrary choices of orbitals can lead to different values of the nuclear shielding at different centers. In the present work the degenerate orbitals were symmetry adapted so that no problem arises.

In order to test the previously described theory it was decided to estimate the ^{19}F chemical shifts of the first row binary fluorides relative to the fluorine molecule. The results are given in Table 1. It will be seen that the results are in reasonable agreement with experimental values.

TABLE 1

^{19}F chemical shifts for the binary first row fluorides

Molecule*	Nuclear Shielding (p.p.m.)	δ_{F_2} (p.p.m.) Calcd.	Observed
F_2	−675	(0)	(0)†
OF_2	−366	+309	+149†
NF_3	−290	+385	+285†
NF_4^+	−452	+223	+213‡
CF_4	−202	+473	+491†
BF_3	−198	+477	+555†
BF_4^-	−150	+535	+575†
BeF_2	−18	+657	+599†
LiF	−84	+591	*ca.* +570§

*All molecular geometries are taken from ref. 27.
†Reference 28.
‡Reference 29.
§Reference 16.

Discussion

Chemical shifts for ^{19}F are usually interpreted in terms of changes in the high frequency (paramagnetic) contribution to the nuclear shielding. The present calculations have made the same assumption although variations in the Lamb (diamagnetic) term are not negligible (24), especially if we consider a series of molecules which have different geometries. The first conclusion that may be reached on the basis of the present calculations is that variations in the Lamb term are relatively small and that the avoidance of the average energy approximation has led to a reasonable description of the ^{19}F chemical shifts.

The ^{19}F chemical shifts have been computed with respect to the fluorine molecule. The calculations confirm that the principal contribution to the paramagnetic term in F_2 arises from a $\pi \rightarrow \sigma^*$ excitation. It may be noted that the value calculated here for the paramagnetic shielding for the ^{19}F nucleus in the F_2 molecule is in good agreement with the full calculation of Stevens and Lipscomb (4). This agreement, however, is no doubt somewhat fortuituous but does lead us to believe that the method outlined here may at least describe the major contributions to the nuclear shielding of a nucleus whose chemical shift depends mainly on the paramagnetic term.

It is noticeable from Table 1 that as the symmetry of the molecule in question increases there is an improvement between theory and experiment. Presumably this is due to the fact that as the molecule approaches T_d symmetry the paramagnetic term is dominated by excitations amongst the valence p orbitals and as a consequence, these terms neglected in the evaluation

Can. J. Chem. Downloaded from www.nrcresearchpress.com by 210.87.254.5 on 09/05/12
For personal use only.

of the molecular magnetic integrals (*i.e.* two-center 2s and 2p overlap integrals) are less important in determining the magnitude of the paramagnetic term.

Another manifestation of the approximations employed may be in the overestimation of the chemical shifts in OF_2 and NF_3. In OF_2, for example, the chemical shift is over-estimated (*i.e.* nuclear shielding underestimated) due to the neglect of 2s contribution in the $B_2 \rightarrow A_1$ excitations. Both of these orbitals are of σ-type and overlap effects are expected to be important. This is brought out by the fact that the computed paramagnetic term of OF_2 is only just over 50% of that measured by Flygare (26).

It is instructive to compare the relative chemical shifts of the three isoelectronic tetrahedral molecules BF_4^-, CF_4, and NF_4^+. Both calculation and experiment show that the ^{19}F chemical shift decreases, *i.e.* the ^{19}F resonance moves down field as the electronegativity of the central atom increases. As analysis of the calculation shows that on going from B, C, to N there is a marked decrease in the excitation energies (E_{pj}) which causes an increase in the absolute value of the ^{19}F nuclear shielding in NF_4^+ which in turn manifests itself as a lowering of the chemical shift (down field shift). This marked lowering of the excitation energies in NF_4^+ relative to CF_4 and BF_4^- is no doubt due to the fact that the energy difference between the valence orbitals on nitrogen and fluorine is much less than between carbon and fluorine and boron and fluorine; in other words the NF bond is more covalent.

In a subsequent paper it will be shown that the method described here adequately accounts for the ^{14}N chemical shifts in a number of nitrogen–oxygen–halogen compounds.

The communication of ref. 11 by C. D. Cornwell (16) is gratefully acknowledged. The author is grateful to K. A. R. Mitchell and D. P. Chong for many discussions. This work was supported by a grant from the National Research Council of Canada.

1. N. F. Ramsey. Phys. Rev. **77**, 567 (1950); **78**, 699 (1950); **83**, 540 (1951); **83**, 540 (1951); **86**, 243 (1952).
2. W. L. Lipscomb. Advan. Magnetic Resonance, **2**, 138 (1966).
3. R. M. Stevens, R. M. Pitzer, and W. N. Lipscomb. Chem. Phys. **38**, 550 (1963).
4. R. M. Stevens, and W. N. Lipscomb. J. Chem. Phys. **40**, 2238 (1964); **41**, 184 (1964); **41**, 3710 (1964); **42**, 3666 (1965).
5. M. Karplus and T. P. Das. J. Chem. Phys. **34**, 1683 (1961).
6. J. A. Pople. J. Chem. Phys. **37**, 53 (1962).
7. F. Prosser and L. Goodman. J. Chem. Phys. **38**, 374 (1963).
8. M. Karplus and J. A. Pople. J. Chem. Phys. **38**, 2803 (1963).
9. V. M. S. Gil and J. N. Murrell. Trans. Faraday Soc. **60**, 248 (1964).
10. J. A. Pople. Mol. Phys. **7**, 301 (1963).
11. J. E. Kent and E. L. Wagner. J. Chem. Phys. **44**, 3520 (1966).
12. D. W. Davies. Mol. Phys. **13**, 465 (1967).
13. D. N. Hendrikson and P. M. Kuznesof. Theoret. Chem. Acta, **15**, 57 (1969).
14. A. D. McLachlan. J. Chem. Phys. **32**, 1263 (1960).
15. M. Karplus. J. Chem. Phys. **33**, 941 (1960).
16. C. D. Cornwell. J. Chem. Phys. **44**, 874 (1966).
17. R. A. Hegstrom and W. N. Lipscomb. J. Chem. Phys. **46**, 1594 (1967).
18. J. A. Pople, D. L. Beveridge, and P. A. Dobosh. J. Chem. Phys. **47**, 2026 (1967).
19. W. R. Bley. Mol. Phys. **16**, 303 (1969).
20. C. D. Cornwell. Private communication.
21. P. W. Langhoff, M. Karplus, and R. P. Hurst. J. Chem. Phys. **44**, 505 (1966).
22. A. Abragam. Principles of nuclear magnetism. Oxford University Press, London. 1961. p. 170.
23. C. P. Slichter. Principles of magnetic resonance. Harper and Row, New York. 1963. Chap. 4.
24. J. O. Hirschfelder, W. Byers Brown, and S. T. Epstein. Advan. Quant. Chem. **1**, 256 (1964).
25. D. W. Davies. Nature, **207**, 75 (1965).
26. W. H. Flygare. J. Chem. Phys. **42**, 1157 (1965).
27. Sutton. Interatomic distances. Chem. Soc. Special Publications No. 11. 1958 and No. 18. 1965.
28. Emsley, Feeney, and Sutcliff. High resolution nuclear magnetic resonance spectroscopy. Vol. 2.
29. K. O. Christie, J. P. Guertin, A. E. Pavlath, and W. Sawodny. Inorg. Chem. **6**, 533 (1967).

Can. J. Chem. Downloaded from www.nrcresearchpress.com by 210.87.254.5 on 09/05/12
For personal use only.

Can. J. Chem. Downloaded from www.nrcresearchpress.com by 210.87.254.6 on 09/05/12
For personal use only.

The chemical shift. II. A study of ^{14}N chemical shifts in nitrogen–oxygen–halogen compounds

F. AUBKE, F. G. HERRING, AND A. M. QURESHI
Department of Chemistry, The University of British Columbia, Vancouver 8, British Columbia

Received March 2, 1970

The chemical shifts of the ^{14}N nucleus in a number of nitrogen–halogen–oxygen compounds have been estimated within the framework of the i.n.d.o.-l.c.a.o.-s.c.f. method using approximate perturbed Hartree–Fock theory. Generally good agreement with experiment is achieved. The calculations indicate that the variation in ^{14}N chemical shift is due to either changes in orbital angular momentum, or to the presence of low lying excited states, or to a combination of both effects.

Canadian Journal of Chemistry, 48, 3504 (1970)

Introduction

A fair number of ^{14}N nuclear magnetic resonance studies are reported over the last years and chemical shifts for many inorganic and organic molecules have been obtained. The variations observed in these chemical shifts are thought to be determined by changes in the paramagnetic (high frequency) term in Ramsey's expression, as is the case for a number of other nuclei, *e.g.*, ^{19}F. Estimation of these variations can be made using the theory developed by Pople (2), Karplus and Pople (3), and Prosser and Goodman (4). The expressions for the nuclear shielding developed by these workers entail a sum over charge densities and bond orders together with an average energy approximation.

The work of Kent and Wagner (5) on linear triatomic molecules and by Witanowski (6, 7) on a number of organic nitro compounds demonstrated that for a series of related compounds the variations in the ^{14}N chemical shifts are due mainly to changes in π-electron densities in the ground state of the molecules. The success of these calculations is no doubt due to the fact that the molecules considered were very similar and the variation in ΔE, treated as a constant parameter, is small. As indicated, it is the usual practice to treat ΔE as a parameter which may be varied from one series of closely related molecules to another. Hendrickson and Kuznesof (8) attempted to compute the ^{14}N chemical shifts for a number of structurally different nitrogen containing molecules by setting ΔE equal to the energy separating the first magnetically allowed excited state and the ground state, the results gave uniformly too high chemical shifts.

The validity of the application of the average energy approximation to the estimation of chemical shifts has been in some doubt since the work of Cornwell (9) on the CIF molecule, where a positive contribution to the paramagnetic term occurs in the sum over excited states leading to the apparently anomalous upfield ^{19}F chemical shift. In addition the recent work of Emsley (10–12) on fluorobenzene and other benzenoid molecules has indicated that the average energy approximation is not applicable in all cases. Consequently, it seems desirable that the average energy approximation be avoided.

The recent work of Herring (13) has shown that within the framework of the i.n.d.o.-l.c.a.o.-s.c.f. method (14) and approximate perturbed Hartree–Fock theory (15–17) the average energy approximation may be avoided. The calculation performed gave a reasonable description of the ^{19}F chemical shifts in the first row binary fluorides.

Qureshi, Ripmeester, and Aubke ((18) and references therein) carried out a study of ^{14}N nuclear magnetic resonance in some nitrogen–oxygen–halogen compounds. The results they obtained and those of other workers (19–22) provide an ideal test for the computational procedure given in ref. 13.

Theory and Results

The method used to estimate the ^{14}N chemical shifts revolves around approximate Hartree–Fock perturbation theory. The molecular Hamiltonian employed is

$$[1]\quad \mathcal{H} = \mathcal{H}_0 + \boldsymbol{H}\cdot\sum_{i=1}^{2N}\beta_e\boldsymbol{L}_{0i} + \sum_n \mu_n \cdot \sum_{i=1}^{2N} 2\beta_e \boldsymbol{L}_{ni} r_{ni}^{-3} + \frac{1}{2} r_c \sum_n \mu_n \cdot \sum_{i=1}^{2N} [(\boldsymbol{r}_{ni}\cdot\boldsymbol{r}_{0i})\mathbf{U} - \boldsymbol{r}_{0i}\boldsymbol{r}_{ni}] r_{ni}^{-3}\cdot\boldsymbol{H}$$

TABLE 1
Molecular geometries employed

Species	Symmetry	Bond distances (A°)	Angles (degree)	Reference
NO_3^-	D_{3h}	NO = 1.21	ONO = 120	26
NO_2^-	C_{2v}	NO = 1.236	ONO = 115.4	14
O''NNO'$_2$	C_s	NO' = 1.18		
		NO'' = 1.12	O'NO'' = 134	27
		NN = 2.08	O''NN = 110	
N_2O_4	D_{2h}	NN = 1.750	NNO = 133.7	26
		NO = 1.180	ONO = 108	
NOF	C_s	NF = 1.52	ONF = 110	26
		NO = 1.13		
NO_2F	C_{2v}	NO = 1.1798	ONO = 136	28
		NF = 1.467		
NF_3	C_{3v}	NF = 1.371	FNF = 102.9	29
ONF_3	C_{3v}	NO = 1.17	ONF = 116.45	30
		NF = 1.44	FNF = 101.33	
NF_4^+	T_d	NF = 1.48		31
N_2F_4	C_2	NF = 1.393	FNF = 103.7	31
		NN = 1.530		
trans-N_2F_2	C_{2h}	NF = 1.42	NNF = 103	23, This work
		NN = 1.25		
cis-N_2F_2	C_{2v}	NF = 1.42	NNF = 113	23, This work

where $\mathscr{H}_0$ is the electronic Hamiltonian for the unperturbed $2N$-electron system, $\boldsymbol{L}_{0i}$ and $\boldsymbol{L}_{ni}$ are the dimensionless angular momentum operators about a common molecular origin and about the nucleus n, respectively (the electron position vectors are similarly defined), $\boldsymbol{H}$ is the applied magnetic field, μ_n the magnetic moment of nucleus n, $\mathbf{U}$ is the unit dyadic, $\beta_e = e\hbar/2mc$ and $r_e = e^2/mc^2$. It can now be shown that, if a perturbation calculation is carried out with either the second or third terms in eq. 1 using the unperturbed molecular orbitals (ϕ_i^0) as zeroth order functions, the paramagnetic term $\sigma_{\alpha\alpha}^P$ ($\alpha = x, y,$ or z) is given by

$$[2] \qquad \sigma_{\alpha\alpha}^P = 8\beta_e^2 \sum_{i=1}^{N} \sum_{p=N+1}^{M} \langle \phi_i^0 | L_\alpha | \phi_p^0 \rangle C'_{pi}$$

where the first order coefficients are given by

$$[3] \qquad C'_{pi} = \frac{\langle \phi_p^0 | L_\alpha r^{-3} | \phi_i^0 \rangle}{\varepsilon_p^0 - \varepsilon_i^0 + K_{pi} - J_{pi}}$$

where ε_p^0 and ε_i^0 are the eigenvalues of the zeroth order problem and J_{pi} and K_{pi} are the molecular coulomb and exchange integrals, respectively. As noted in ref. 13, the energy denominator in eq. 2 does not correspond to the usual singlet–singlet transition energy which differs by $+K_{pi}$. This particular form arises from the preimaginary character of the perturbations in eq. 1. As a consequence the excitation energies quoted later cannot be related to the electronic spectra of the molecules concerned.

The zeroth order wave function is calculated using the i.n.d.o.-l.c.a.o.-s.c.f. method devised by Pople *et al.* (14). The expressions for the molecular electron repulsion integrals at this level of approximation have been given previously (13). The molecular magnetic integrals have been evaluated using the approximate formulas due to Cornwell (9).

The calculations have been performed on an IBM 360/67 computer using a program written in this laboratory (13). The estimation of the nuclear shielding is attached as an option to this program (13).

Table 1 shows the molecules studied in this work together with the geometries employed. For the *cis* and *trans* isomers of difluorodiazine additional calculations were performed to determine the N—N—F angle, using the bond distances N—F = 1.44 Å and N—N = 1.25 Å. The results obtained, 113° for *cis*-N_2F_2 and 103° for the *trans* isomer, are in good agreement with recent data reports by Bohn and Bauer (23) and in disagreement with previous reports (24).

Table 2 gives the results of our calculations of the nuclear shielding of the molecules studied here. The chemical shift is defined, in the present work, as the difference between the paramagnetic nuclear shielding of the molecule of interest and

Can. J. Chem. Downloaded from www.nrcresearchpress.com by 210.87.254.6 on 09/05/12
For personal use only.

TABLE 2

^{14}N nuclear shielding and chemical shifts

Species	Nuclear shielding (p.p.m.)	$\delta_{calcd.}$ (p.p.m.)	$\delta_{obs.}$* (p.p.m.)
NO_3^-	−286	(0)	(0)
NO_2^-	−621	−335	−250
$ONNO_2$	−348	−62	−67
$ONNO_2$	−605	−319	−302
N_2O_4	−277	+9	+11
NOF	−390	−104	−116
NO_2F	−246	+40	+65
ONF_3	−198	+88	+131
NF_3	−254	+32	+8
N_2F_4	−243	+43	+47
NF_4^+	−235	+51	—
trans-N_2F_2	−384	−98	−67
cis-N_2F_2	−347	−61	−5

*Experimental values taken from refs. 18, 19, 20, and 21.

some arbitrarily chosen standard (in this case NO_3^-). It can be seen that the results are in reasonable agreement with experiment.

Discussion

The ^{14}N chemical shifts may be qualitatively accounted for by a consideration of the variations of the orbital angular momentum with increasing or decreasing electronegativity of the attached atoms (25). The presence of a lone pair on the nitrogen atom leads to a large negative paramagnetic term and concomitant lowering of the chemical shift *i.e.* down field shift relative to a molecule in which the lone pair is absent. This behavior has been attributed (19, 22) to low lying excited states caused by the presence of the lone pair.

In order to investigate these ideas we have considered in some detail the terms that contribute to eq. 2. Since there are many terms contributing to this sum we have arbitrarily omitted any such that are less than ±10 p.p.m. Tables 3 and 4 give such an analysis for the isoelectronic molecules NO_2^- and NOF and it will be seen that the neglect of small terms leads only to slightly different values for the nuclear shielding.

A comparison of Tables 3 and 4 shows that the paramagnetic term in NO_2^- is dominated by a very large (−1100 p.p.m.) contribution from an $A_1 \rightarrow B_2$ ($\sigma \rightarrow \pi^*$) excitation in the x-direction (in the plane of the molecule perpendicular to the bisector, y-axis, of the ONO angle). In NOF this term is reduced nearly three-fold (−350 p.p.m.) due to (*i*) an increase in E_{pj} from 0.08 to 0.14 a.u. (a factor of 1.75) and (*ii*) a decrease in the molecular angular momentum integrals by a factor of approximately 1.5. The latter effect is caused by both a reduction of electron density at the nitrogen and that the $2_{p\pi}$ orbital on the fluorine atom in NOF contributes very little to the A'' orbital, whereas in NO_2^- both oxygen atoms contribute $2_{p\pi}$ orbitals to the B_2 orbital. The changes are reflected in reduction of orbital coefficients which in turn reduce the magnetic integrals.

A similar investigation of the terms contributing to the nuclear shielding in NO_3^- and

TABLE 3

Terms contributing to the principal components of the nuclear shielding tensor of the ^{14}N nucleus in NO_2^-*

Component	Excitation†	Contribution (p.p.m.)	E_{pi} (a.u.)	$\langle i\|L_\alpha\|p\rangle$ (a.u.)	$\langle p\|L_\alpha/r^3\|i\rangle$ (a.u.)
x	$A_1 \rightarrow B_2$	−46	0.44	+0.19	−1.01
	$A_1 \rightarrow B_2$	−1109	0.08	−0.91	+0.98
	$B_2 \rightarrow A_1$	−75	0.65	−0.52	+0.87
y	$B_1 \rightarrow B_2$	−40	1.09	+0.43	−0.95
	$B_1 \rightarrow B_2$	−129	0.40	−0.56	+0.85
	$B_1 \rightarrow B_2$	−145	0.18	+0.67	−0.37
	$B_2 \rightarrow B_1$	−134	0.75	+0.83	−1.14
z	$B_1 \rightarrow A_1$	−20	1.34	−0.37	+0.67
	$B_1 \rightarrow A_1$	−62	0.64	+0.61	−0.61
	$B_1 \rightarrow A_1$	+28	0.43	+0.43	+0.26
	$A_1 \rightarrow B_1$	−21	0.90	−0.33	+0.54
	$A_1 \rightarrow B_1$	−109	0.77	−0.83	+0.94

*Average nuclear shielding = −614 p.p.m.
†An $A_1 \rightarrow B_2$ excitation corresponds to a σ to π* excitation and an $A_1 \rightarrow B_1$ excitation corresponds roughly to a σ to σ* excitation.

Can. J. Chem. Downloaded from www.nrcresearchpress.com by 210.87.254.6 on 09/05/12
For personal use only.

TABLE 4

Terms contributing to the principal components of the nuclear shielding tensor of the ^{14}N nucleus in NOF*

Component	Excitation†	Contribution (p.p.m.)	E_p (a.u.)	$\langle i\|L_\alpha\|p\rangle$ (a.u.)	$\langle i\|L_\alpha r^{-3}\|p\rangle$ (a.u.)
x	$A'' \rightarrow A'$	−103	0.52	−0.44	+1.15
	$A'' \rightarrow A'$	+43	0.31	−0.47	−0.26
	$A' \rightarrow A''$	−354	0.14	−0.72	+0.63
y	$A' \rightarrow A''$	−15	1.25	−0.22	+0.45
	$A' \rightarrow A''$	−212	0.36	−0.73	+0.99
	$A' \rightarrow A''$	−56	0.37	+0.45	−0.43
	$A' \rightarrow A''$	−50	0.14	−0.19	+0.34
	$A'' \rightarrow A'$	−139	0.68	+0.83	−1.06
	$A'' \rightarrow A'$	−12	0.69	−0.31	+0.24
z	$A' \rightarrow A'$	−11	1.56	−0.30	+0.52
	$A' \rightarrow A'$	−170	0.48	+0.79	−0.96
	$A' \rightarrow A'$	+39	0.31	+0.26	+0.43
	$A' \rightarrow A'$	−26	0.30	+0.20	−0.38
	$A' \rightarrow A'$	−100	0.76	−0.80	+0.90
	$A' \rightarrow A'$	+13	0.44	−0.09	−0.60

*Average chemical shift = −384 p.p.m.
†An $A' \rightarrow A''$ excitation corresponds roughly to a σ to π^* excitation.

TABLE 5

Terms contributing to the principal components of the nuclear shielding tensor of the ^{14}N nucleus in NO_3^-*

Component	Excitation	Contribution (p.p.m.)	E_{pi} (a.u.)	$\langle i\|L_\alpha\|p\rangle$ (a.u.)	$\langle i\|L_\alpha r^{-3}\|p\rangle$ (a.u.)
x	$E' \rightarrow A_2''$	−35	1.20	−0.40	+0.99
	$E' \rightarrow A_2''$	−44	0.50	+0.30	−0.72
	$E' \rightarrow A_2''$	−181	0.23	−0.82	+0.47
	$A_2'' \rightarrow E'$	−97	0.91	−0.72	+1.16
y	This component identical to x-component				
z	$E' \rightarrow E'$	−34	1.55	−0.53	+0.93
	$E' \rightarrow E'$	−60	0.84	+0.70	−0.67
	$E' \rightarrow E'$	+22	0.55	−0.25	−0.44
	$E' \rightarrow E'$	−34	1.55	+0.53	−0.93
	$E' \rightarrow E'$	−60	0.84	−0.70	+0.67
	$E' \rightarrow E'$	+22	0.55	−0.25	−0.44

*Average chemical shift = −286 p.p.m.

NO_2F shows that the decrease in nuclear shielding on going from NO_3^- to NO_2F is due to a low lying $E' \rightarrow A_2''$ ($\sigma \rightarrow \pi^*$) excitation contributing to the y-component of the shielding tensor (see Table 5), but this contribution is absent in the y-component in NO_2F (see Table 6). This is brought about by the fact that the E' orbital is the highest occupied in NO_3^- whereas in NO_2F it is a symmetry determined B_1 orbital which does not contribute to any of the paramagnetic terms. The x- and z-components of the ^{14}N shielding tensors are essentially the same in both molecules.

The effect of the presence of a lone pair may now be investigated by considering the following pairs of molecules, NF_3 and ONF_3, NOF and FNO_2, and NO_2^- and NO_3^-. A break down of the terms contributing to the nuclear shielding of the ^{14}N nucleus in these molecules is given in Tables 3–8.

A consideration of Tables 7 and 8 shows that on going from NF_3 to ONF_3, the number of contributing excitations increases (because of the larger basis set); however, the nuclear shielding in ONF_3 is less than in NF_3. The reason for this appears to be the substantial reduction of the orbital angular momentum integrals in the ONF_3 molecule relative to NF_3. To illustrate this point consider the x-component of both ^{14}N nuclear shielding tensors. There are three contributions

Can. J. Chem. Downloaded from www.nrcresearchpress.com by 210.87.254.6 on 09/05/12
For personal use only.

TABLE 6

Terms contributing to the principal components of the nuclear shielding tensor of the ^{14}N nucleus in NO_2F*

Component	Excitation	Contribution (p.p.m.)	E_{pl} (a.u.)	$\langle i\|L_\alpha\|p\rangle$ (a.u.)	$\langle i\|L_\alpha r^{-3}\|p\rangle$ (a.u.)
x	$B_1 \rightarrow B_2$	−43	1.20	−0.49	+0.99
	$B_1 \rightarrow B_2$	−78	0.45	−0.50	+0.66
	$B_1 \rightarrow B_2$	−57	0.41	−0.51	+0.43
	$B_1 \rightarrow B_2$	−51	0.21	+0.49	−0.20
	$B_2 \rightarrow B_1$	−113	0.91	−0.83	+1.17
	$B_2 \rightarrow B_1$	−10	0.84	+0.31	−0.24
y	$A_1 \rightarrow B_2$	−12	1.30	+0.20	−0.67
	$A_1 \rightarrow B_2$	−16	0.51	−0.12	+0.61
	$A_1 \rightarrow B_2$	−90	0.22	+0.70	−0.27
	$B_2 \rightarrow A_1$	−30	0.61	−0.22	+0.80
	$B_2 \rightarrow A_1$	+30	0.33	−0.56	−0.16
	$B_2 \rightarrow A_1$	−64	0.77	−0.48	+0.96
z	$B_1 \rightarrow A_1$	−17	1.30	−0.33	+0.65
	$B_1 \rightarrow A_1$	−45	0.51	−0.49	+0.43
	$B_1 \rightarrow A_1$	+24	0.34	+0.27	+0.28
	$B_1 \rightarrow A_1$	−24	0.32	+0.55	−0.13
	$B_1 \rightarrow A_1$	−24	1.45	−0.42	+0.78
	$B_1 \rightarrow A_1$	−49	0.69	−0.60	+0.53
	$B_1 \rightarrow A_1$	+16	0.47	−0.45	−0.16
	$A_1 \rightarrow B_1$	−15	1.69	−0.38	+0.65
	$A_1 \rightarrow B_1$	−38	1.03	+0.52	−0.70
	$A_1 \rightarrow B_1$	−40	0.89	+0.56	−0.59
	$A_1 \rightarrow B_1$	+15	0.61	+0.31	+0.26

*Average chemical shift = −243 p.p.m.

TABLE 7

Terms contributing to the principal components of the nuclear shielding tensor of the ^{14}N nucleus in NF_3*

Component	Excitation	Contribution (p.p.m.)	E_{pl} (a.u.)	$\langle i\|L_\alpha\|p\rangle$ (a.u.)	$\langle i\|L_\alpha r^{-3}\|p\rangle$ (a.u.)
x	$E \rightarrow A_1$	−58	0.65	0.50	−0.71
	$A_1 \rightarrow E$	−101	0.67	−0.67	+0.96
	$A_1 \rightarrow E$	−103	0.35	+0.31	−1.11
y	$E \rightarrow A_1$	−58	0.65	0.50	−0.71
	$A_1 \rightarrow E$	−101	0.67	−0.67	+0.96
	$A_1 \rightarrow E$	−103	0.35	+0.31	−1.11
z	$E \rightarrow E$	−14	1.48	+0.31	−0.64
	$E \rightarrow E$	−97	0.70	−0.71	+0.90
	$E \rightarrow E$	−14	1.48	+0.31	−0.64
	$E \rightarrow E$	−97	0.70	−0.71	+0.90

*Average chemical shift = −249 p.p.m.

for NF_3, all of which have their energetic counterparts (*i.e.* excitation with similar energy) in ONF_3; comparing these we see the substantial reduction in angular momentum integrals. The presence of additional excitations in ONF_3 of somewhat higher energy does not compensate for the reduction of the three principal contributions. The presence of the additional oxygen reduces the p-orbital coefficients at the nitrogen *i.e.* the orbital angular momentum is reduced as the nitrogen atom approaches the spherically symmetric electron distribution of an inert gas (25).

Comparing Tables 4 and 6, which contain the results for FNO and FNO_2, again we see an increase in the number of excitations. In this case, however, it appears that the addition of an oxygen atom does affect at least one excitation substantially, *viz.* the $A' \rightarrow A''$ excitation of 0.14 a.u. in FNO is raised to 0.21 a.u. as a $B_1 \rightarrow B_2$ excitation in FNO_2. This can be at-

Can. J. Chem. Downloaded from www.nrcresearchpress.com by 210.87.254.6 on 09/05/12
For personal use only.

TABLE 8

Terms contributing to the principal components of the nuclear shielding tensor of the ^{14}N nucleus in ONF_3*

Component	Excitation	Contribution (p.p.m.)	E_{pi} (a.u.)	$\langle i\|L_\alpha\|p\rangle$ (a.u.)	$\langle p\|L_\alpha r^{-3}\|i\rangle$ (a.u.)
x	$A_1 \rightarrow E$	−31	1.35	+0.45	−0.88
	$A_1 \rightarrow E$	−17	0.81	+0.25	−0.51
	$A_1 \rightarrow E$	−53	0.60	−0.58	+0.52
	$A_1 \rightarrow E$	−35	0.46	+0.24	−0.63
	$E \rightarrow A_1$	−21	0.60	−0.27	+0.44
	$E \rightarrow A_1$	+17	0.37	+0.41	+0.15
	$E \rightarrow A_1$	−60	0.95	+0.64	−0.84
y	This component identical to x-component				
z	$E \rightarrow E$	−15	1.44	−0.25	+0.62
	$E \rightarrow E$	−74	0.71	+0.50	−1.00
	$E \rightarrow E$	+13	0.51	+0.18	+0.34
	$E \rightarrow E$	−15	1.44	−0.25	+0.34
	$E \rightarrow E$	−74	0.71	−0.50	+1.0
	$E \rightarrow E$	+13	0.51	+0.18	+0.34

*Average chemical shift = −191 p.p.m.

tributed to a lone pair effect of sorts. It should also be noted that, again, there is a substantial reduction in the orbital angular momentum. Therefore, in this pair of molecules we have a combination of both a lone pair effect and the reduction of orbital angular momentum.

At the other extreme it would appear that it is a lone pair effect that dominates the change in nuclear shielding on going from NO_2^- to NO_3^-, a comparison of Tables 3 and 5 shows this.

In conclusion then, it may be said that the variation of ^{14}N chemical shifts may be dominated by either changes in excitation energies or orbital angular momentum, or that there can be a combination of both effects, so it can be dangerous to ascribe changes in nuclear shielding to one or other of these effects exclusively.

Financial support from the National Research Council of Canada is gratefully acknowledged.

1. N. F. Ramsey. Phys. Rev. 77, 567 (1950); **78**, 699 (1950); **83**, 540 (1955); **86**, 243 (1952).
2. J. A. Pople. J. Chem. Phys. 37, 53 (1962).
3. M. Karplus and J. A. Pople. J. Chem. Phys. **38**, 2803 (1963).
4. F. Prosser and L. Goodman. J. Chem. Phys. **38**, 374 (1963).
5. J. E. Kent and E. L. Wagner. J. Chem. Phys. **44**, 3520 (1966).
6. M. Witanowski. J. Amer. Chem. Soc. **90**, 5683 (1968).
7. M. Witanowski and S. A. Shevelev. J. Mol. Spectrosc. **33**, 19 (1970).
8. D. N. Hendrikson and P. M. Kuznesof. Theoretica Chem. Acta, **15**, 57 (1969).
9. C. D. Cornwell. J. Chem. Phys. **44**, 874 (1966).
10. J. W. Emsley. J. Chem. Soc. A, 1387 (1968).
11. J. W. Emsley. J. Chem. Soc. A, 2018 (1968).
12. J. W. Emsley. J. Chem. Soc. A, 2735 (1968).
13. F. G. Herring. Can. J. Chem. This issue.
14. J. A. Pople, D. L. Beveridge, and P. A. Dobosh. J. Chem. Phys. **47**, 2026 (1967).
15. W. L. Lipscomb. Advan. Mag. Resonance, **2**, 138 (1966).
16. P. W. Langhoff, M. Karplus, and R. P. Hurst. J. Chem. Phys. **44**, 505 (1966).
17. R. A. Hegstrom and W. N. Lipscomb. J. Chem. Phys. **46**, 1594 (1967).
18. A. M. Qureshi, J. A. Ripmeester, and F. Aubke. Can. J. Chem. **47**, 4247 (1969).
19. J. Mason and W. van Bronswijk. Chem. Commun. 357 (1969).
20. J. H. Noggle, J. D. Baldeschwieler, and C. B. Colburn. J. Chem. Phys. 37, 182 (1962).
21. L. O. Anderson and J. Mason. Chem. Commun. 99 (1968).
22. L. O. Anderson, J. Mason, and W. van Bronswijk. J. Chem. Soc. A, 296 (1970).
23. R. K. Bohn and S. H. Bauer. Inorg. Chem. **6**, 309 (1967).
24. S. H. Bauer. J. Amer. Chem. Soc. **69**, 3104 (1947).
25. J. W. Emsley, J. Feeney, and L. H. Sutcliffe. High resolution magnetic resonance spectroscopy. Vol. 2. Pergamon Press, 1966. p. 1034.
26. L. E. Sutton. Interatomic distances. Chem. Soc. Spec. Publ. No. 11, 1958 and No. 18, 1965.
27. W. A. Yeranos and M. J. Joncich. Mol. Phys. **13**, 263 (1967).
28. A. C. Legon and D. J. Miller. J. Chem. Soc. 1736 (1968).
29. J. Sheridan and W. Gordy. Phys. Rev. **79**, 513 (1950).
30. K. Hedberg. Personal communication quoted by D. C. Frost, F. G. Herring, K. A. R. Mitchell, and I. A. Stenhouse. To be published.
31. R. K. Bohn and S. H. Bauer. Inorg. Chem. **6**, 304 (1967).

Can. J. Chem. Downloaded from www.nrcresearchpress.com by 210.87.254.6 on 09/05/12
For personal use only.

Can. J. Chem. Downloaded from www.nrcresearchpress.com by 210.87.254.6 on 09/05/12
For personal use only.

Studies on metal hydroxy compounds. XII. Thermal analyses, decomposition kinetics, and infrared spectra of copper basic oxysalts

P. RAMAMURTHY AND E. A. SECCO

Chemistry Department, St. Francis Xavier University, Antigonish, Nova Scotia

Received June 11, 1970

The thermal analyses of copper basic oxysalts of the type $Cu_2(OH)_2XO_y$, where X = S, C, Cl, Br, I, N, HC and y = 4, 3, or 2 reveal that decomposition occurs, in most cases, by dehydroxylation with concomitant disproportionation of the oxysalt. An outstanding exception to this pattern of decomposition is the basic sulfate. Calorimetric measurements along with related enthalpic values for the decomposition reaction are given.

The kinetics of thermal decomposition of the compounds are classified into three main categories: (*i*) three-dimensional contracting sphere model, (*ii*) first-order rate, and (*iii*) nucleation controlled rate processes.

The infrared spectral data of nine copper basic oxycompounds in the frequency region 4000–250 cm^{-1} are presented with their assignments. The fundamental infrared inactive modes of the anionic species SO_4^{2-}, NO_3^-, etc. become active by the presence of the copper hydroxide ligand indicating a lowering of symmetry in the anion.

Canadian Journal of Chemistry, **48**, 3510 (1970)

Introduction

This study extends our earlier studies on copper compounds (1) and deals with the copper basic oxysalts, *viz.* sulfate, nitrate, halates, etc. Tarte (2) reported on the infrared spectra of some of these copper derivatives, but his study was mainly concerned with the OH active region of the spectrum.

This report represents a more comprehensive physicochemical study of copper basic oxysalts which includes differential thermal analysis (DTA), thermogravimetry (TG), calorimetric measurements, decomposition kinetics, and infrared spectra. The discussion on the infrared spectra reported herein is intended to complement Tarte's work with attention focussed on the effect of the hydroxide on the prevailing symmetry of the XO_y group in the appropriate compound where X = S, C, Cl, Br, I, N, HC and y = 4, 3, or 2.

Experimental

All compounds used in this work, except the basic carbonate, were prepared in this laboratory by following known procedures; the basic carbonate was Fisher Scientific Purified grade. Brief descriptions of the methods of preparation are given below. All chemicals used were Reagent grade. In each preparation, unless otherwise specified, the precipitate was filtered and washed thoroughly with distilled water, which was followed by drying overnight at 110 °C.

$CuSO_4 \cdot 2Cu(OH)_2$ and $Cu(NO_3)_2 \cdot 3Cu(OH)_2$ were prepared by digesting CuO with medium concentrated aqueous solutions of copper sulfate and nitrate at 110 °C over a week respectively (3, 4).

Copper basic nitrite, formate, chlorate, bromate, and iodate were prepared by the action of the corresponding alkali salt on copper basic acetate (5). A two-fold excess of alkali salt with mechanical stirring at room temperature for 10 h was found most suitable for the preparations.

The identities of the compounds were confirmed by the available X-ray diffraction patterns (6, 7).

The heating curves, calorimetric measurements, and isothermal kinetic traces were recorded on a duPont Thermal Analyzer DTA-900 and TGA-950 with appropriate accessories and programming adjustments as previously described (1).

The heating rate used for most curves was 20 °C/min; however, in the case of overlapping steps, slower heating rates of 4 or 2 °C/min were used in an attempt to resolve the steps. An ambient atmosphere of dry N_2 (Matheson Prepurified Grade with a stated impurity of 0.003% O_2) was maintained during all the experiments unless otherwise specified.

The infrared spectra of the compounds were obtained by using the standard KBr disc technique in a Perkin–Elmer 521 spectrophotometer; KCl was used as the matrix material in a Beckmann IR-8 spectrophotometer to identify the intermediate products from $CuSO_4 \cdot 3Cu(OH)_2$ in differential thermal analysis.

Results and Discussion

Thermogravimetry

The results of thermogravimetry are presented in Table 1 and each compound is discussed in sequence. The proposed decomposition reactions for each compound, represented by the equation with its onset and terminal temperatures, are those which best fit the observed weight loss; the products of decomposition were confirmed by X-ray diffraction and correlated with DTA curves.

TABLE 1

Thermogravimetry results

Compound	Step number*	% of total weight lost: Observed	% of total weight lost: Calculated	Reaction
$Cu(NO_2)_2.3Cu(OH)_2$	1	27.72	27.75	[1]
$Cu(NO_3)_2.3Cu(OH)_2$	1	33.50	33.74	[2]
$CuCO_3.Cu(OH)_2$	1	28.01	28.05	[3]
$Cu(HCO_2)_2.3Cu(OH)_2$	1	33.01	32.29	[4*a*]
	1	28.50	28.70	[4*b*]
$CuSO_4.2Cu(OH)_2$	1	10.14	10.15	[5*a*]
	2	32.70	32.79	[5*b*]
$CuSO_4.3Cu(OH)_2.0.65H_2O$	1	14.08	14.13	[6]
	2	31.20	31.33	[5*b*]
$Cu(ClO_3)_2.3Cu(OH)_2$	1	28.60	28.67	[7*a*]
	2	59.73	53.69	[7*b*] and partial [7*c*]
$Cu(BrO_3)_2.3Cu(OH)_2$	1	42.53†	47.83	[8]
$Cu(IO_3)_2.3Cu(OH)_2{\cdot}2H_2O$	1	12.10	12.14	[9*a*]
	2	57.00	57.09	[9*b*]

*In all cases disproportionation of CuO was observed above 800 °C.
†Discrepancy between observed and calculated values for $Cu(BrO_3)_2.3Cu(OH)_2$ explained in text.

(1) $Cu(NO_2)_2.3Cu(OH)_2$

Decomposition occurs by dehydroxylation with simultaneous disproportionation of the nitrite to the oxide according to

$$[1]\quad Cu(NO_2)_2.3Cu(OH)_{2(s)} \xrightarrow{200\text{–}290\ ^\circ C} 4CuO_{(s)} + 3H_2O_{(g)} + 2NO_{(g)} + \tfrac{1}{2}O_{2(g)}$$

(2) $Cu(NO_3)_2.3Cu(OH)_2$

Dehydroxylation of the compound occurs with concomitant disproportionation of the nitrate to the oxide according to

$$[2]\quad Cu(NO_3)_2.3Cu(OH)_{2(s)} \xrightarrow{240\text{–}310\ ^\circ C} 4CuO_{(s)} + 3H_2O_{(g)} + 2NO_{2(g)} + \tfrac{1}{2}O_{2(g)}$$

Our observation that the weight loss occurs in a single step according to reaction 2 is at variance with the two-step thermogravimetry results of Bouillon and Wafelaer (7), who reported the loss of 3 moles of water at 120 °C with disproportionation occurring between 120–300 °C. Repeated attempts at slower heating rates in this laboratory have failed to resolve the two overlapping steps. There is a further inconsistency in their claim that the X-ray powder pattern of the product at 120 °C was identical to the pattern of the basic compound.

(3) $CuCO_3.Cu(OH)_2$

The compound breaks down via dehydroxylation accompanied by disproportionation of the carbonate as follows

$$[3]\quad CuCO_3.Cu(OH)_{2(s)} \xrightarrow{260\text{–}350\ ^\circ C} 2CuO_{(s)} + H_2O_{(g)} + CO_{2(g)}$$

(4) $Cu(HCO_2)_2.3Cu(OH)_2$

In nitrogen atmosphere the compound decomposes via dehydroxylation with simultaneous disproportionation of the formate to copper metal as follows

$$[4a]\quad Cu(HCO_2)_2.3Cu(OH)_{2(s)} \xrightarrow[N_2]{190\text{–}240\ ^\circ C} 3CuO_{(s)} + Cu_{(s)} + 4H_2O_{(g)} + CO_{(g)} + CO_{2(g)}$$

When the decomposition occurred in air the weight loss corresponds to CuO as the residue, that is

$$[4b]\quad Cu(HCO_2)_2.3Cu(OH)_{2(s)} \xrightarrow[air]{190\text{–}390\ ^\circ C} 4CuO_{(s)} + 4H_2O_{(g)} + 2CO_{2(g)}$$

(5) $CuSO_4.2Cu(OH)_2$

The first step is the dehydroxylation to the oxide and oxysulfate according to

$$[5a]\quad CuSO_4.2Cu(OH)_{2(s)} \xrightarrow{390\text{–}520\ ^\circ C} CuO_{(s)} + CuO.CuSO_{4(s)} + 2H_2O_{(g)}$$

which was followed by disproportionation of the oxysulfate

$$[5b]\quad CuO.CuSO_{4(s)} \xrightarrow{580\text{–}780\ ^\circ C} 2CuO_{(s)} + SO_{3(g)}$$

(6) $CuSO_4.3Cu(OH)_2.0.65\ H_2O$

The initial step corresponds to dehydration and dehydroxylation of the compound, *i.e.*

Can. J. Chem. Downloaded from www.nrcresearchpress.com by 210.87.254.6 on 09/05/12
For personal use only.

Can. J. Chem. Downloaded from www.nrcresearchpress.com by 210.87.254.6 on 09/05/12
For personal use only.

$$[6]\quad CuSO_4.3Cu(OH)_2.0.65H_2O_{(s)} \xrightarrow{150\text{–}400\ ^\circ C} 2CuO_{(s)} + CuO.CuSO_{4(s)} + 3.65H_2O_{(g)}$$

followed by disproportionation according to reaction 5*b*. These observations are concordant with those by Pannetier *et al.* (8)

(7) $Cu(ClO_3)_2.3Cu(OH)_2$

The first step involves dehydroxylation and decomposition of the chlorate according to

$$[7a]\quad Cu(ClO_3)_2.3Cu(OH)_{2(s)} \xrightarrow{210\text{–}350\ ^\circ C} 3CuO_{(s)} + CuCl_{2(s)} + 3H_2O_{(g)} + 3O_{2(g)}$$

which was followed by disproportionation of $CuCl_2$ and volatilization of CuCl, *i.e.*

$$[7b]\quad CuCl_{2(s)} \xrightarrow{400\text{–}680\ ^\circ C} CuCl_{(g)} + \tfrac{1}{2}Cl_{2(g)}$$

As in the thermogravimetry of the basic chlorides reported earlier (1), the observed weight loss for a CuO–$CuCl_2$ mixture is higher than the calculated value due to partial chlorination of the oxide as follows

$$[7c]\quad CuO_{(s)} + \tfrac{1}{2}Cl_{2(g)} \rightarrow CuCl_{(g)} + \tfrac{1}{2}O_{2(g)}$$

(8) $Cu(BrO_3)_2.3Cu(OH)_2$

Dehydroxylation occurs with concomitant disproportionation of the bromate to mainly the oxide as follows

$$[8]\quad Cu(BrO_3)_2.3Cu(OH)_{2(s)} \xrightarrow{200\text{–}250\ ^\circ C} 4CuO_{(s)} + Br_{2(g)} + \tfrac{5}{2}O_{2(g)} + 3H_2O_{(g)}$$

The observed weight loss value for reaction 8 is always lower than the calculated value. This discrepancy arises from the disproportionation of the bromate partially to bromide as well as the oxide shown by Dusek and Petru (9).

(9) $Cu(IO_3)_2.3Cu(OH)_2.2H_2O$

The first step corresponds to overlapping dehydration and dehydroxylation to form the oxide and the iodate according to

$$[9a]\quad Cu(IO_3)_2.3Cu(OH)_2.2H_2O \xrightarrow{120\text{–}360\ ^\circ C} 3CuO_{(s)} + Cu(IO_3)_{2(s)} + 5H_2O_{(g)}$$

the overlap of these processes is such that the anhydrous basic iodate can be prepared by heating isothermally at 200 °C. The final step is the disproportionation of the iodate to the oxide, *i.e.*

$$[9b]\quad Cu(IO_3)_{2(s)} \xrightarrow{370\text{–}600\ ^\circ C} CuO_{(s)} + I_{2(g)} + \tfrac{5}{2}O_{2(g)}$$

Lumme and Lumme (10) reported the preparation of basic chlorate, bromate, and iodate by incomplete precipitation of the copper mineral salt solution with NaOH. Their claim that two OH groups in the compound $Cu(XO_3)_2.3Cu(OH)_2$ on drying reacted with atmosphere CO_2 giving the product $Cu(XO_3)_2.CuCO_3.2Cu(OH)_2$ is in contrast to our observations. The dried basic halates, in this study, displayed no detectable sign of CO_2 uptake either by thermogravimetry or in their infrared spectra where the characteristic CO_3 bands are expected to be clearly evident even in very low concentration.

Differential Thermal Analysis

The results of DTA measurements are assembled in Table 2 and a discussion of the pertinent features of the compounds are given to accompany the TG results. Since all compounds displayed the endothermic peak at 1000 °C due to disproportionation of CuO to Cu_2O, this detail will not be included to avoid unnecessary repetition.

The basic nitrite, nitrate, and carbonate showed one main endotherm attributed to dehydroxylation and disproportionation of the mineral salt to the oxide.

The basic formate gave two characteristic thermal effects with the following peak temperatures: endotherm at 230 °C and sharp exotherm at 250 °C. The endotherm is assigned to dehydroxylation and concomitant disproportionation of the copper formate to CO, CO_2, H_2O, and Cu metal. The sharp exotherm is interpreted in terms of a secondary reaction between CO and CuO.

$CuSO_4.3Cu(OH)_2.0.65\ H_2O$ exhibited four endotherms plus an exotherm. These observations are in agreement with the results of Pannetier *et al.* (8) and Margulis (11). The initial endotherm at 110 °C due to dehydration is followed by a broad endotherm between 250–500 °C with centers at 300 and 420 °C. Margulis assigned the 300° peak to the loss of one molecule of water of zeolitic character according to

$$CuO.CuSO_4.2Cu(OH)_2.H_2O \rightarrow CuO.CuSO_4.2Cu(OH)_2 + H_2O$$

Pannetier *et al.* disputed the formula of the compound and its interpretation in terms of zeolitic water which appeared inconsistent with their infrared data.

TABLE 2
Differential thermal analysis

Compound	Peak number	Peak temperature (°C)	Reaction
$Cu(NO_2)_2.3Cu(OH)_2$	1	240	[1]
	2	1000	Disproportionation CuO†
$Cu(NO_3)_2.3Cu(OH)_2$	1	285	[2]
$CuCO_3.Cu(OH)_2$	1	300	[3]
$Cu(HCO_2)_2.3Cu(OH)_2$	1	230	[4*a*]
	2*	250	$CO_{(g)} + CuO_{(s)} \rightarrow Cu_{(s)} + CO_{2(g)}$
$CuSO_4.3Cu(OH)_2.0.65H_2O$	1	110	Dehydration
	2	300	[6*a*]
	3	420	[6*b*]
	4*	530	Crystallization of products
	5	810	[5*b*]
$CuSO_4.2Cu(OH)_2$	1	500	[5*a*]
	2*	530	Crystallization of products
	3	810	[5*b*]
$Cu(ClO_3)_2.3Cu(OH)_2$	1	295	[7*a*]
	2	500	Disproportionation $CuCl_2$
	3	880	[7*b*]
$Cu(BrO_3)_2.3Cu(OH)_2$	1	220	[8]
$Cu(IO_3)_2.3Cu(OH)_2.2H_2O$	1	200	Dehydration
	2	300	Dehydroxylation
	3*	380	Crystallization of products
	4	490	[9*b*]

*Indicate exotherms; all other numbers signify endotherms.
†Observed in all cases, but not cited to avoid unnecessary repetition.

In an attempt to clarify the dispute we have followed the progress of decomposition of $CuSO_4.3Cu(OH)_2$ between 110 and 530 °C by infrared spectroscopy and X-ray diffractometry. A solid bearing zeolitic water is expected to display the absorption band due to the bending mode of molecular water, δ_{OH}, in the infrared region of 1700–1600 cm^{-1} as observed by Bertsch and Habgood (12) and Carter *et al.* (13). Our infrared spectra of the compound heated up to 300 °C showed no absorption band characteristic of δ_{OH} which confirms the results of Pannetier and coworkers and prompts us to rule out the presence of zeolitic water in the basic sulfate.

The infrared spectra of the heat-treated basic sulfate at different temperatures are presented in Fig. 1. Spectrum *A* at 120 °C shows two strong bands at 1120 and 1080 cm^{-1} along with a medium intensity band at 980 cm^{-1}; these bands are usually identified with the SO_4 group of C_{3v} symmetry. The band at 940 cm^{-1} is due to OH bending which disappears by dehydroxylation at 375 °C, spectrum *C*. Heating the compound to 300 °C, spectrum *B*, reveals a new band at 1050 cm^{-1}; further heating, spectra *C*, *D*, *E*, and *F*, effects a merging of the band details attributed to the amorphous nature of the solid resulting in a broad band with shoulders barely in evidence. Finally, after heating for 30 min at 530 °C, the spectrum *G* regains its structural detail with four bands prominent: 1005, 1050, 1160, and 1235 cm^{-1}. These latter bands are identified with copper oxysulfate, $CuO.CuSO_4$ (14) and normally characteristic of SO_4 in C_{2v} symmetry.

The mode of decomposition at 300 °C can be expressed by

$$[6a]\quad CuSO_4.3Cu(OH)_{2(s)} \xrightarrow{300\ °C} CuO.CuSO_4.2Cu(OH)_{2(s)} + H_2O_{(g)}$$

with subsequent dehydroxylation of the basic oxysulfate according to

$$[6b]\quad CuO.CuSO_4.2Cu(OH)_2 \xrightarrow{420\ °C} CuO.CuSO_{4(s)} + 2CuO_{(s)} + 2H_2O_{(g)}$$

The exotherm at 530 °C is the effect of crystallization of the products which was confirmed by X-ray diffraction patterns; the 810 °C endotherm has its origin in decomposition of the oxysulfate to CuO according to [5*b*].

Can. J. Chem. Downloaded from www.nrcresearchpress.com by 210.87.254.6 on 09/05/12
For personal use only.

TABLE 3

Compound	Reaction	Temperature range (°C)	Heat of decomposition* ΔH/mole of H_2O formed (kcal)	Heat of decomposition* ΔH/mole of compound decomposed (kcal)	$-\Delta H_f^0$ (kcal/mole)† This work	$-\Delta H_f^0$ (kcal/mole)† Literature
$Cu(NO_2)_2.3Cu(OH)_2$	[1]	210–310		14.32±0.21	292.60	—
$Cu(NO_3)_2.3Cu(OH)_2$	[2]	250–340		66.94±0.11	372.56	415.70
	[2*a*]	250–340	4.80±0.02	14.46±0.06	372.56	415.70
$CuCO_3.Cu(OH)_2$	[3]	230–325		14.05±0.05	239.40	—
	[3*a*]	230–325	2.95±0.02	2.95±0.02	239.40	—
$CuSO_4.2Cu(OH)_2$	[5*a*]	430–510	7.00±0.12	14.00±0.25	385.32 (15)	—
$Cu(ClO_3)_2.3Cu(OH)_2$	[7*a*]	240–320	4.83±0.06	14.51±0.20	346.31	—
$Cu(IO_3)_2.3Cu(OH)_2$	[9*c*]	275–350	3.41±0.04	10.23±0.12	348.12	—
$Cu(IO_3)_2$	[9*b*]	410–520		31.13±0.26	53.35	—

*All determinations were done in duplicate; ΔH values are given with their average deviations.
†ΔH_f^0 values of compounds used in our calculations, unless stated otherwise, are from N.B.S. Circular No. 500 (1951). The above ΔH_f^0 values were calculated using Kopp's rule approximation (1).

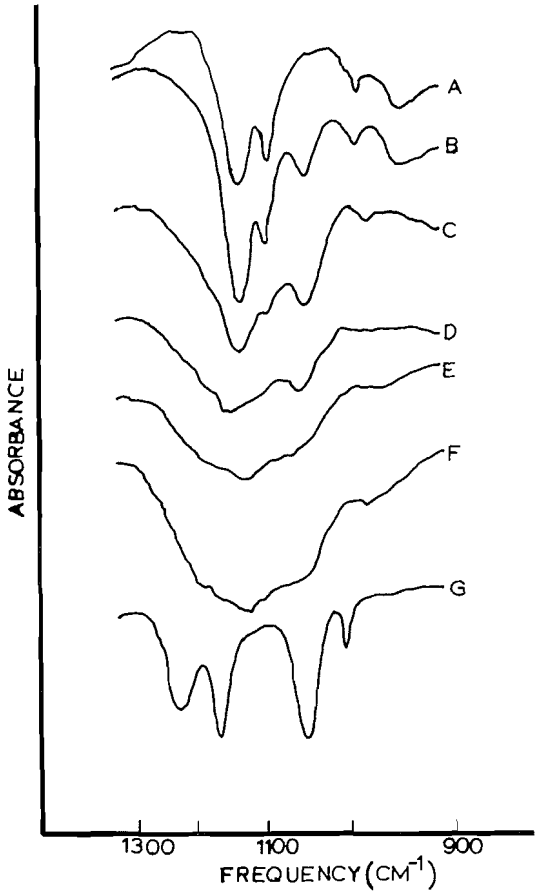

FIG. 1. Infrared spectra of $CuSO_4.3Cu(OH)_2$ annealed at different temperatures: *A*, 120 °C for 1 h; *B*, 300 °C for ½ h; *C*, 375 °C for ½ h; *D*, 400 °C for ½ h; *E*, 450 °C for ½ h; *F*, 475 °C for ½ h; *G*, 530 °C for ½ h.

$CuSO_4.2Cu(OH)_2$ undergoes dehydroxylation parallel to [6*b*] at 500 °C for the first endotherm. Crystallization of the products gives rise to an exothermic effect at 530 °C which is followed by the expected endotherm for oxysulfate decomposition [5*a*].

$Cu(ClO_3)_2.3Cu(OH)_2$ showed three endothermic effects: (*i*) dehydroxylation and disproportionation of the chlorate at 295 °C, (*ii*) disproportionation of $CuCl_2$ at 500 °C, and (*iii*) volatilization of CuCl at 880 °C.

$Cu(BrO_3)_2.3Cu(OH)_2$ gave a weak endotherm at 220 °C. The low intensity of this endotherm is the net result of an endotherm due to dehydroxylation and a concomitant exotherm due to disproportionation of the bromate.

$Cu(IO_3)_2.3Cu(OH)_2.2H_2O$ exhibited four thermal effects: (*i*) endotherm at 200 °C due to dehydration, (*ii*) dehydroxylation endotherm at 300 °C, (*iii*) exotherm at 380 °C due to crystallization of products, and (*iv*) iodate decomposition endotherm at 490 °C.

Calorimetric Measurements

The calorimetric results along with the related enthalpic values for the decomposition of the compounds are presented in Table 3 according to the equations given under thermogravimetry. The sole distinguishing feature between the thermogravimetric equation and the observed calorimetric reaction is the slightly different onset-terminal temperature limits which is included in Table 3.

The following reactions represent an alternate reaction path for the appropriate compound in

Can. J. Chem. Downloaded from www.nrcresearchpress.com by 210.87.254.6 on 09/05/12
For personal use only.

TABLE 4

Kinetic results for decomposition

Compound	Temperature range (°C)	Number of temperatures	Rate expression	Activation energy E_a (kcal)	log A
$Cu(NO_3)_2.3Cu(OH)_2$	230–260	4	$[1-(1-\alpha)^{1/3} = kt$	65.7±6.5	21.2
$CuSO_4.2Cu(OH)_2$	450–490	4	First order	45.5±3.1	12.7
$Cu(IO_3)_2.3Cu(OH)_2$	260–320	5	First order	29.7±2.6	11.2
$Cu(HCO_2)_2.3Cu(OH)_2$	190–220	4	$\alpha = kt^n$ $(\alpha < 0.4)$	18.9±1.0	6.0
			$-\ln(1-\alpha) = kt$ $(\alpha > 0.4)$	33.5±1.5	14.8
$Cu(NO_2)_2.3Cu(OH)_2$	200–250	5	$-\ln(1-\alpha) = (kt)^2$ $(\alpha < 0.7)$	17.6±1.0	7.0
			$-\ln(1-\alpha) = kt$ $(\alpha > 0.7)$	22.2±1.2	9.3
$Cu(BrO_3)_2.3Cu(OH)_2$	200–240	4	$-\ln(1-\alpha) = (kt)^2$	26.3±1.5	11.2
$Cu(ClO_3)_2.3Cu(OH)_2$	250–290	4	$-\ln(1-\alpha) = (kt)^3$	39.3±1.8	15.1
$CuCO_3.Cu(OH)_2$	290–340	5	$\ln \alpha/(1-\alpha) = kt + C$	42.4±3.5	15.5

addition to that described under thermogravimetry

[2*a*] $Cu(NO_3)_2.3Cu(OH)_{2(s)} \rightarrow 3CuO_{(s)} + Cu(NO_3)_{2(s)} + 3H_2O_{(g)}$

[3*a*] $Cu(CO_3)_2.Cu(OH)_{2(s)} \rightarrow CuO_{(s)} + CuCO_{3(s)} + H_2O_{(g)}$

[9*c*] $Cu(IO_3)_2.3Cu(OH)_{2(s)} \rightarrow 3CuO_{(s)} + Cu(IO_3)_{2(s)} + 3H_2O_{(g)}$

The ΔH_f^0 for the bromate, formate, and $CuSO_4.3Cu(OH)_2.0.65H_2O$ could not be evaluated because of overlapping processes; ΔH_f^0 for $Cu(IO_3)_2$ decomposition was determined since it was not available in the literature.

Our value of ΔH_f^0 for $Cu(NO_3)_2.3Cu(OH)_2$ differs from the literature value. $Cu(NO_3)_2$ disproportionates concomitantly with dehydroxylation in the decomposition reaction 2. If one assigns the experimentally observed ΔH of decomposition for the two combined processes to reaction 2*a*, a value of −425.04 kcal/mole is obtained which approaches the literature value.

The column of values for ΔH per mole of H_2O formed indicates lower values for the copper basic oxysalts relative to the copper basic halides and the parent $Cu(OH)_2$. This lower ΔH value is interpreted in terms of a weakening of the Cu—OH bond in the presence of the oxysalt anion species.

Reaction Kinetics Data

The experimental α, t data for the decomposition reactions were processed through a large number of kinetic rate expressions. The best linear relations between the experimental data and the known rate expressions over the maximum reaction fraction ($\alpha \sim 0.90$) for all compounds, excepting the nitrite and formate, and over the temperature range studied are given in Table 4.

The compounds studied can be classified on the basis of their reaction kinetics into three groups.

(*i*) Phase boundary control with the kinetic data fitting the three-dimensional contracting sphere model equation, *viz.*

$$1-(1-\alpha)^{1/3} = kt$$

where $k = (u/r)$; u, the velocity of movement of an interface and r, the distance or length of particle interface. The basic nitrate obeys this rate equation.

(*ii*) First-order rate kinetics with $CuSO_4.2Cu(OH)_2$ and $Cu(IO_3)_2.3Cu(OH)_2$ conforming to this rate equation throughout the reaction. The formate and nitrite follow a nucleation controlled relationship in the initial stage and then revert to the unimolecular decay law in the final stage.

(*iii*) Nucleation controlled rate processes.

The basic formate rate data fit a power law relationship in the initial accelerating stage up to $\alpha = 0.4$,

$$\alpha = kt^n$$

The basis of the power expression has been described by Jacobs and Tompkins (16) where the value of n is in the range 2–6; in this case n was found to be 2.1–2.7. The non-integral and temperature-dependent nature of n has been interpreted by Thomas and Tompkins (17) in

Can. J. Chem. Downloaded from www.nrcresearchpress.com by 210.87.254.6 on 09/05/12
For personal use only.

Can. J. Chem. Downloaded from www.nrcresearchpress.com by 210.87.254.6 on 09/05/12
For personal use only.

terms of nuclei growth rates dependent on nuclear size.

The basic nitrite, chlorate, and bromate kinetic data obey an Avrami–Erofeyeev (A–E) type equation,

$$-\ln (1 - \alpha) = (kt)^n$$

where n can have any integral value from 1 to 4.

For the nitrite and bromate $n = 2$ which implies either random nucleation followed by one-dimensional growth or extremely rapid nucleation followed by two-dimensional growth. One-dimensional growth is not a very efficient method of propagating a reaction in a three-dimensional particle although nuclei could grow linearly rapidly in one direction initially along a surface step and then proceed at a constant slower rate at right angles, resulting in a rectangular nucleus by one-dimensional growth. As the reaction accelerates the power exponent or n value should drop by one, since nucleation has become unimportant, leading to a first-order rate equation. The value of n can change from 2 to 1 when the interface between the product and reactant phases collapses before the reaction is complete leaving isolated blocks of material with no nuclei present. In isolated blocks each molecule possesses an equal probability for decomposition and the rate of reaction is proportional to the amount of undecomposed substance, *i.e.* first-order rate. This rate behavior is observed for the nitrite. However, no rate change-over was observed for the bromate which maintained a value of $n = 2$ up to $\alpha \sim 0.90$.

The A–E equation with $n = 3$ describes the decomposition rate for the chlorate which suggests either random nucleation followed by two-dimensional growth or extremely rapid nucleation with three-dimensional growth. However, the unsupported bare α, t data do not allow an interpretation of n, where $n = r + \lambda$; r is the number of molecular decompositions required to form a viable growth nucleus and λ represents the number of dimensions of active nucleus growth (18, 19).

The basic carbonate decomposition kinetics is described by the Prout–Tompkins (P–T) equation,

$$\ln [\alpha/(1 - \alpha)] = kt + c$$

which is based on a model involving linear and branching nuclei as proposed by Garner and Halles (20) and extended by Prout and Tompkins (21).

The pre-exponential A values of the Arrhenius equation for first-order rate kinetics in the solid state have been examined and interpreted by Shannon (22), Cordes (23), and the authors (1).

Infrared Spectral Data

The infrared spectral data of the compounds are presented in Tables 5 and 6. Since Tarte (2, 24) has already reported on the infrared spectra of basic sulfate, nitrate, formate, and carbonate in the OH active region we have restricted our spectral data in Table 5 to the anion band activity in these compounds. However, in the case of basic chlorate, bromate, iodate, and nitrite we have included in Table 6 the entire infrared region available to us.

The bands assigned to ν_{OH} and δ_{OH} are displaced to lower frequencies on deuteration with the ν_H/ν_D ratio falling in the range 1.33–1.35. The multiple bands assigned to OH can originate from a variety of Cu—O—H band distances incorporated in the lattice as suggested by Hartert and Glemser (25). The remaining bands unaffected by deuteration are assigned to anion or Cu—O modes. Each compound is discussed in tabular sequence.

The splitting of the degenerate ν_3 and ν_4 modes into two bands along with the appearance of ν_1 (infrared inactive in T_d symmetry) strongly suggests the SO_4 group in $CuSO_4 . 3Cu(OH)_2$ to possess C_{3v} symmetry. Two structural effects can account for this lowering of symmetry, (*i*) monodentate or tridentate SO_4 group and (*ii*) crystal field. Recognizing that it is virtually impossible to distinguish between these two effects in the absence of single crystal structural data, the formula–symmetry association as evident in this compound and $CuSO_4 . 2Cu(OH)_2$ tentatively suggests a tridentate SO_4.

The SO_4 group in $CuSO_4 . 2Cu(OH)_2$ exhibits C_{2v} symmetry on the basis that the degenerate ν_3 and ν_4 modes are split into three bands and ν_1 appears as a strong band. In conjunction with $CuSO_4 . 3Cu(OH)_2$ we speculate that $CuSO_4 . 2Cu(OH)_2$ incorporates a bidentate SO_4.

The NO_3 group in $Cu(NO_3)_2 . 3Cu(OH)_2$ shows a splitting of the degenerate ν_3 mode along with the appearance of the ν_1 mode (infrared inactive in D_{3h} symmetry) which is characteristic of C_{2v}

Can. J. Chem. Downloaded from www.nrcresearchpress.com by 210.87.254.6 on 09/05/12
For personal use only.

TABLE 5

Infrared absorption band frequencies*

Assignment	Frequency (cm^{-1})					
	$CuSO_4.3Cu(OH)_2$	$CuSO_4.2Cu(OH)_2$	$Cu(NO_3)_2.3Cu(OH)_2$	$CuCO_3.Cu(OH)_2$	$Cu(HCO_2)_2.3Cu(OH)_2$	
XO_4 or XO_3						
			1420 (s)	1520 (sh)	2800 (m)	ν_{CH}
		1155 (s)	1345 (s)	1500 (s)	2715 (m)	
ν_3	1120 (s)	1100 (s)		1425 (s)		
	1085 (s)	1080 (s)		1395 (s)	1535 (vs)	$\nu_{COO(asym)}$
					1370 (s)	π_{CH}
ν_1	980 (m)	990 (s)	1040 (m)	1095 (m)	1340 (s)	$\nu_{COO(sym)}$
		670 (m)	720 (m)	750 (m)	780 (s)	
ν_4	625 (m)	640 (s)		715 (m)	750 (m)	δ_{OCO}
	600 (s)	610 (s)			735 (m)	
ν_2	465 (m)	460 (m)	810 (s)	825 (s)		
	510 (m)	520 (m)	510 (s)	500 (s)	490 (s)	
	480 (m)	490 (s)	450 (m)	480 (s)	450 (s)	
ν_{Cu-O}	415 (m)	420 (s)	425 (m)	350 (s)	420 (m)	
	325 (s)	370 (m)	390 (w)	325 (s)	310 (s)	
		330 (s)	325 (m)			

*vs = very strong; s = strong; m = medium; w = weak; br = broad; sh = shoulder.

TABLE 6

Infrared absorption band frequencies*

Assignment	Frequency (cm^{-1})			
	$Cu(ClO_3)_2.3Cu(OH)_2$	$Cu(BrO_3)_2.3Cu(OH)_2$	$Cu(IO_3)_2.3Cu(OH)_2.2H_2O$	$Cu(NO_2)_2.3Cu(OH)_2$
ν_{OH}†	3550 (s)			
	3495 (s)	3500 (s)	3505 (s)	
	3440 (s)	3430 (s)		3455 (s)
	3345 (s)		3270 (s br)	3200 (br sh)
δ_{H_2O}†			1610 (m)	
δ_{OH}†	905 (s)	885 (m)		
	850 (sh)	840 (w)	965 (m)	1000 (m)
	825 (m)		895 (m)	910 (m)
	750 (m br)		845 (m br)	
	710 (m br)			770 (w)
	655 (s)			725 (s)
XO_3 or NO_2				
ν_3	990 (s)	790 (s)	775 (s)	1315 (m)
	955 (s)	750 (m)	735 (s)	
ν_1	930 (m)	700 (m)	700 (w)	1230 (s)
ν_2	590 (s)	520 (w)	365 (m)	810 (w)
ν_4	490 (s)	350 (s)	345 (w)	
	460 (m)	320 (w)	325 (m)	
ν_{Cu-O}	400 (s)	500 (s)	505 (s)	500 (s)
	325 (m)	420 (s)	430 (s)	420 (s)
	300 (w)			325 (m)

*s = strong; m = medium; w = weak; br = broad; sh = shoulder.
†Affected by deuterium substitution.

or C_s symmetry. The single crystal study of this compound shows the two oxygens of NO_3 to be attached to Cu along with four OH groups in a deformed octahedral arrangement (26). The symmetry of NO_3 remains C_{2v} or C_s in a monodentate or a bidentate configuration. The basic carbonate also displays C_{2v} or C_s symmetry for the CO_3 group (27).

The assignment of the formate frequencies is made according to Petrov *et al.* (28). The splitting of the formate bands could be due to (*i*) crystal field effects or (*ii*) interaction of two formate groups attached to the same Cu atom.

The NO_2 group in the basic nitrite possesses C_{2v} symmetry (29).

In the three basic halates, the XO_3 group experiences a removal of the degeneracies in the ν_3 and ν_4 modes indicating a lowering of the symmetry from C_{3v} to C_s (30, 31).

The Cu—O assignments were made in accordance with McDevitt and Baun (32).

The authors are indebted to the National Research Council of Canada for financial support of this research program and to Dr. Michael Falk, Atlantic Regional Laboratory, Halifax, for making the infrared facilities available to us.

1. P. Ramamurthy and E. A. Secco. Can. J. Chem. **47**, 2185, 2303, 3915 (1969).
2. P. Tarte. Spectrochim. Acta, **13**, 107 (1958).
3. E. Posnjak and G. Tunell. Amer. J. Science, **18**, 1 (1929).
4. J. Gauthier. Bull. Soc. Chim. France, 661 (1956).
5. J. Gauthier. Compt. Rend. **248**, 3170 (1959).
6. A.S.T.M. Index to powder diffraction file. 1963.
7. F. Bouillon and A. Wafelaer. Bull. Soc. Chem. Belg. **64**, 386 (1955).
8. G. Pannetier, J.-M. Bregeault, G. Djega-Mariadassou, and M. Grandon. Bull. Soc. Chim. France, 2616 (1963).
9. B. Dusek and F. Petru. Russ. J. Inorg. Chem. **13** (2), 307 (1968).
10. P. Lumme and H. Lumme. Suomen Kem. *B***35**, 120 (1962); *B***36**, 177 (1963); *B***36**, 192 (1963).
11. E. V. Margulis. Russ. J. Inorg. Chem. **7**, 935 (1962).
12. L. Bertsch and H. W. Habgood. J. Phys. Chem. **67**, 1621 (1963).
13. J. L. Carter, P. J. Lucchesi, and D. J. C. Yates. J. Phys. Chem. **68**, 1385 (1964).
14. V. V. Pechkovskii and M. S. Gaisinovich. Russ. J. Inorg. Chem. **9**, 1245 (1964).
15. T. R. Ingraham. Trans. Metall. Soc. AIME. **233**, 359 (1965).
16. P. W. M. Jacobs and F. C. Tompkins. Chemistry of the solid state. *Edited by* W. E. Garner. Butterworths Scientific Publications, London. 1955. Chap. 7.
17. J. G. N. Thomas and F. C. Tompkins. Proc. Roy. Soc. London. Ser. A. **209**, 550 (1951); **210**, 111 (1951).
18. P. W. M. Jacobs and A. R. Tariq Kureisky. Proceedings of Fourth International Symposium on

Can. J. Chem. Downloaded from www.nrcresearchpress.com by 210.87.254.6 on 09/05/12
For personal use only.

Reactivity of Solids. *Edited by* J. H. DeBoer. Elsevier Publications, Amsterdam. 1960. p. 352.
19. P. W. M. JACOBS. Kinetics of reactions in ionic systems. Vol. 4. Materials Science Research. *Edited by* T. J. Gray and V. D. Frechette. Plenum Press, New York. 1969. p. 44.
20. W. E. GARNER and H. R. HALLES. Proc. Roy. Soc. London. Ser. A. **139**, 576 (1933).
21. E. G. PROUT and F. C. TOMPKINS. Trans. Faraday Soc. **40**, 488 (1944).
22. R. D. SHANNON. Trans. Faraday Soc. **60**, 1902 (1964).
23. H. F. CORDES. J. Phys. Chem. **72**, 2185 (1968).
24. P. TARTE. Advan. Mol. Spectrosc. 1041 (1962).
25. E. HARTERT and O. GLEMSER. Z. Elektrochem. **60**, 1746 (1956).
26. W. NOWACKI and R. SCHEIDEGGER. Helv. Chim. Acta, **46**, 375 (1952).
27. K. NAKAMOTO, J. FUJITA, S. TANAKA, and M. KOBAYASKI. J. Amer. Chem. Soc. **79**, 4904 (1957).
28. K. J. PETROV, A. K. MOLODKUI, O. D. SARALIDZE, and O. M. IVANOVA. Russ. J. Inorg. Chem. **13**, 895 (1968).
29. K. NAKAMOTO. Infrared spectra of inorganic and coordination compounds. John Wiley & Sons, New York. 1962.
30. W. E. DASENT and T. C. WADDINGTON. J. Chem. Soc. 2429 (1966).
31. C. ROCCHICCIOLI. Compt. Rend. **242**, 2922 (1956); **249**, 236 (1959); **250**, 1232 (1960).
32. N. T. MCDEVITT and W. L. BAUN. Spectrochim. Acta, **20**, 799 (1964).

Can. J. Chem. Downloaded from www.nrcresearchpress.com by 210.87.254.6 on 09/05/12
For personal use only.

Can. J. Chem. Downloaded from www.nrcresearchpress.com by 210.87.254.5 on 09/05/12
For personal use only.

Studies on microcapsules. VII. Further characterization of sulfonated polyphthalamide microcapsules

KIKUKO TAKAHASHI, MASUMI KOISHI, AND TAMOTSU KONDO

Faculty of Pharmaceutical Sciences, Science University of Tokyo, Funagawara-machi, Shinjuku, Tokyo, Japan

Received April 6, 1970

Characterization was made on the sulfonated polyphthalamide microcapsules (SPPAM) prepared by making use of the interfacial polycondensation reaction of *p*-phthaloyl dichloride with mixtures of 4,4′-diaminostilbene-2,2′-disulfonic acid and diethylenediamine of varying mole ratios. The specific conductance of dialyzed dispersions of the H form of SPPAM in water was always higher than that of Na form microcapsule dispersions.

On the other hand, the former dispersions invariably gave a much lower p*H* in comparison with the latter. Cation binding experiments established increasing orders, $Ca^{2+} < Sr^{2+} < Ba^{2+}$ and $Li^+ < K^+$, NH_4^+, $Na^+ < Cs^+$, for the binding of di- and monovalent cations to SPPAM, respectively. The results were interpreted as showing that less hydrated ions are easier to adsorb on the negatively charged microcapsules. Finally, the feasibility of using SPPAM as ion-exchanger was indicated.

Canadian Journal of Chemistry, **48**, 3520 (1970)

Introduction

Recently, sulfonated polyphthalamide microcapsules (SPPAM) were prepared by making use of the interfacial polycondensation reaction between mixtures of a sulfonated and an unsulfonated diamines and a diacid chloride, and their electrophoretic behavior was studied in solutions of various inorganic salts (1). As a result, the cation binding was strongly suggested to sulfonic groups in the microcapsule membranes. This implies that SPPAM may serve as an ion-exchanger or, more specifically, a model for biological cells. Before applying SPPAM to practical uses, however, further information will be needed on their properties. Accordingly, this paper has aimed at characterizing SPPAM with particular emphasis on their cation binding ability.

Experimental

Preparation

SPPAM used in this work were prepared by the same method as in the previous work (1) except that polyethylene glycol was dropped from the solution to be encapsulated and a concentration of 5% was used for Span 85, as emulsifier. The diamines employed were 4,4′-diaminostilbene-2,2′-disulfonic acid diethylenediamine and they are abbreviated hereafter as DASSA and DEDA, respectively.

The microcapsules thus obtained were dispersed in deionized water with the aid of Tween 20 as dispersing agent after separating them from organic solvent by centrifugation.

Dialysis

In order to remove any remaining unreacted diamines, inorganic salts, and dispersing agent, the microcapsule dispersion was dialyzed in a cellophane tubing (Visking) against deionized water in a thermostat controlled at 40 °C with occasional shaking. The initial volume of dispersion to be dialyzed was about 200 ml. The dialysis was continued with changes of deionized water every 3 h until constant readings of p*H* and specific conductance were obtained.

Sulfur Content

The sulfur content of the microcapsule membranes was determined by usual elemental analysis with dried H form SPPAM. The H form SPPAM was obtained by treating the dialyzed Na form SPPAM with hydrochloric acid, followed by dialysis against deionized water.

Amount Bound of Cations

The determination of amount bound of various cations was carried out in the following manner. To a known volume of the dispersion of dialyzed SPPAM in a beaker was added an equal volume of salt solution, and the mixture was allowed to react for 1 h with continuous stirring. At the end of this period, the mixture was centrifuged at 12 000 r.p.m. for 5 min to remove the microcapsules. The supernatant liquid was filtered through a 0.45 μ millipore filter where necessary. An appropriate volume of the supernatant liquid was withdrawn by a pipette and analyzed.

In the binding experiments of monovalent cations, the H form SPPAM was used because the analysis of H^+ can be made more easily and accurately than the alkali metal ions. Therefore, the following ion-exchange reaction takes place between the microcapsules and monovalent cations in the solution

$$HS + M^+ \rightleftarrows MS + H^+$$

where S represents SPPAM and M^+ monovalent cations. The concentration of hydrogen ions thus liberated from the microcapsules was determined by means of conductometry or potentiometry, which gives directly the amount bound of the cations.

The binding of divalent cations was measured with the Na form SPPAM. Hence, the ion-exchange reaction is

$$2NaS + M^{2+} \rightleftarrows MS_2 + 2Na^+$$

where M^{2+} denotes divalent cations. The concentration

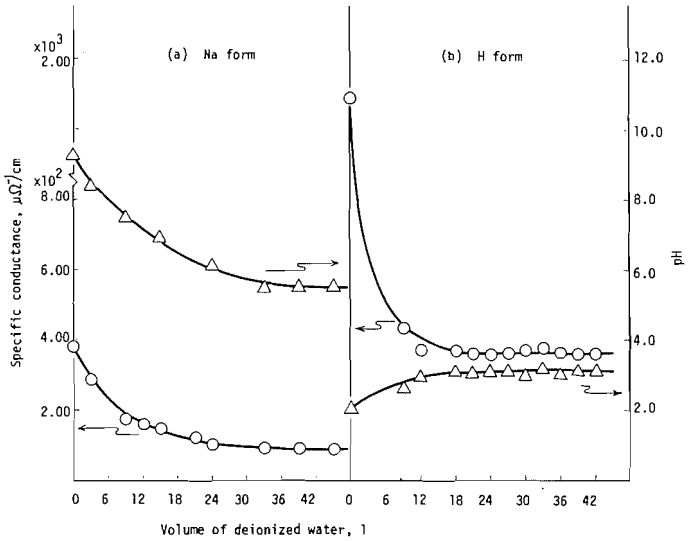

FIG. 1. Variations in specific conductance and p*H* during dialysis against water of dispersion of SPPAM prepared at 55.6 mole% of DASSA.

of divalent cations remaining in the supernatant was determined by chelatometric titration. The amount bound is given by the difference between the concentrations of divalent ions before and after mixing with the microcapsule dispersion.

Inorganic Salts

The inorganic salts used for binding experiments were chlorides of lithium, sodium, potassium, cesium, ammonium, calcium, barium, and strontium. All of these chlorides were of analytical reagent grade with a purity of more than 99.5%.

Results and Discussion

Dialysis and Elemental Analysis

In Fig. 1 are given the changes in specific conductance and p*H* during the dialysis of dispersions of Na form (Fig. 1(*a*)) and H form (Fig. 1(*b*)) SPPAM against the volume used of deionized water.

As the inorganic salts and unreacted diamines diffused out through their membranes and the cellophane tubing, both specific conductance and p*H* of the dispersion of Na form SPPAM decreased and then levelled off. The p*H* of the dialyzed dispersion was the same as that of deionized water, indicating the completion of dialysis. On the other hand, the specific conductance of the dispersion was higher than that of deionized water. This will be due to the sodium ions dissociated from the microcapsule membranes. Figure 2 seems to confirm this view, that

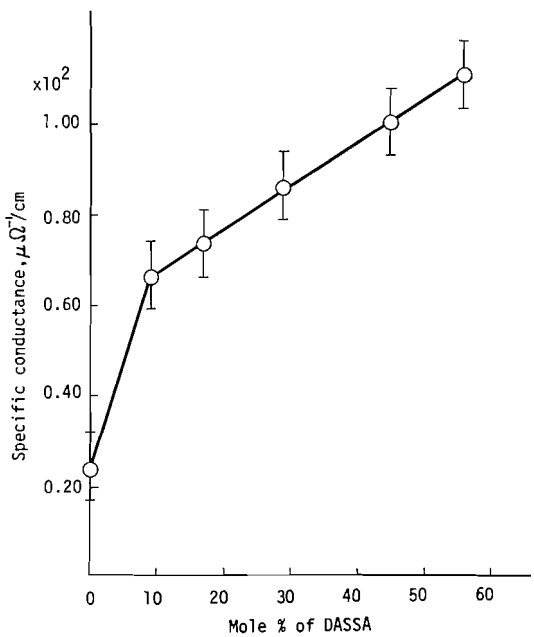

FIG. 2. Final specific conductances of dialyzed dispersions of Na form SPPAM as a function of mole% of DASSA in diamine mixtures.

there is an increase in specific conductance with increasing number of sodium sulfonate groups in the membranes.

The treatment of the dialyzed Na form SPPAM with excess hydrochloric acid gave the

Can. J. Chem. Downloaded from www.nrcresearchpress.com by 210.87.254.5 on 09/05/12
For personal use only.

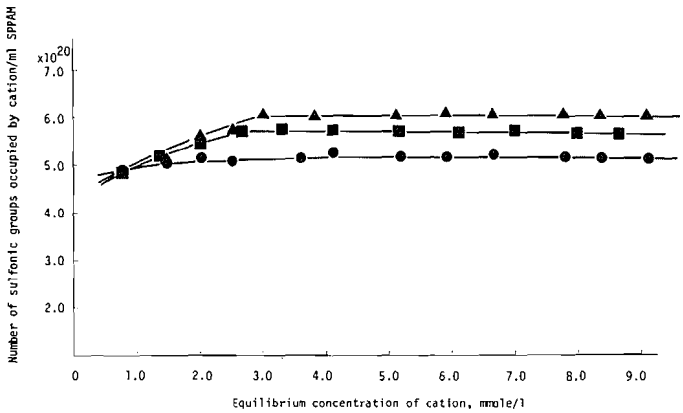

FIG. 3. Cation binding isotherms for Na form SPPAM at 20 °C (mole ratio of DASSA to DEDA in membranes is 0.173:1). Ba^{2+}, ▲; Sr^{2+}, ■; Ca^{2+}, ●.

dispersion a very high conductance and a low p*H* value. The excess hydrogen ions were removed very rapidly by redialysis against deionized water as shown in Fig. 1(*b*). The final high conductance and low p*H* values of the redialyzed dispersion will prove the conversion of the Na form to the H form.

The sulfur contents of microcapsule membranes increased with the increase in mole% of DASSA in the mixed diamines used for the preparation of SPPAM. Table 1 gives the molar ratios of DASSA to DEDA in the membranes. These values were calculated on the basis of the sulfur contents. An inspection of the table reveals that only a small portion of DASSA in the diamine mixtures can be chemically incorporated in the membranes. This should arise from the much lower reactivity of DASSA with the diacid chloride as compared with DEDA, since the interfacial polycondensation reaction occurs in the organic phase (2) and the partition coefficient is much smaller for DASSA than for DEDA (1).

Binding of Cations

The results of cation binding experiments are illustrated in Figs. 3 and 4. In these figures, the amounts bound of cations are expressed in terms of the number of sulfonic groups occupied by cations per ml of SPPAM. The volume of SPPAM was evaluated from the volume of aqueous phase encapsulated in the preparation and the dilution ratio of dispersion in later stages. This method of evaluation would be adequate for the purpose of the present work because the emulsification of aqueous phase in the first step of preparation of SPPAM was found to be complete, the microcapsule membrane thickness (less than 0.03 μ) was negligible compared with their mean diameter (about 3 μ), and the centrifugation was carried out in as low a field as possible to minimize the breakdown of the microcapsules.

From the binding isotherms shown in Fig. 3, it is evident that the divalent cation binding by SPPAM increases in the order $Ca^{2+} < Sr^{2+} < Ba^{2+}$, which is in accordance with the order of decreasing hydration for these three cations. As

TABLE 1

Mole ratios of DASSA to DEDA

In diamine mixtures	In microcapsule membranes
0.20:1	0.055:1
1.25:1	0.173:1
1.98:1	0.203:1
4.99:1	0.259:1

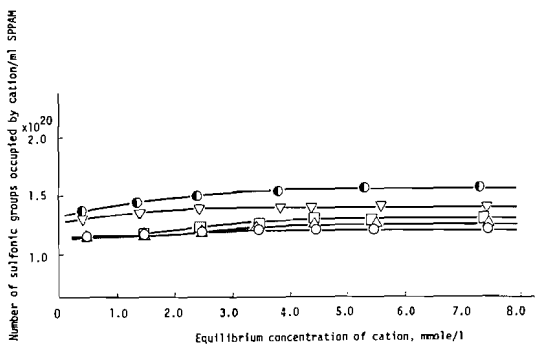

FIG. 4. Cation binding isotherms for H form SPPAM at 20 °C (mole ratio of DASSA to DEDA in membranes is 0.173:1). Cs^+, ◐; NH_4^+, □; K^+, △; Na^+, ▽; Li^+, ○.

Can. J. Chem. Downloaded from www.nrcresearchpress.com by 210.87.254.5 on 09/05/12
For personal use only.

the hydration of ions corresponds to the formation of ordered regions of water around the ions (3, 4), less hydrated ions would be easier to approach closely to and adsorb on the oppositely charged microcapsules. In view of this, the sequence of divalent cations in the present work seems to be a reflection of the above-mentioned tendency of ions. It is interesting to note here the cation order is the same as that already well established for the selective coefficient of ion-exchange resins (5). An increase in the molar ratio of DASSA to DEDA in the membranes brought about an increase in the binding ability of SPPAM to cations, owing to an increase in the number of sulfonic groups.

The amounts bound of monovalent cations were smaller than those of divalent cations by a factor of 3 or 4. As is seen from Fig. 4, an increasing order $Li^+ < K^+$, NH_4^+, $Na^+ < Cs^+$ is apparent for the binding of monovalent cations. The positions of Li^+ and Cs^+ in the sequence are likely to be correct, because the difference in their amount bound by SPPAM appears to be large enough to make this conclusion. Strongly structure-promoting lithium ions would be considerably harder to be captured by the microcapsules than are cesium ions. However, exact order of Na^+, K^+, and NH_4^+ is still uncertain because no significant difference was found in their binding.

The experimental findings reported so far would indicate the feasibility of using SPPAM as ion-exchanger since they were found to be a kind of ion-exchange membranes in nature; though there are no cross-linkings, contrary to ordinary ion-exchange membranes.

The authors are indebted to the Research Laboratory of Eisai Co., Ltd., Tokyo, for carrying out the elemental analysis in this work.

1. M. KOISHI, N. FUKUHARA, and T. KONDO. Can. J. Chem. **47**, 3447 (1969).
2. P. W. MORGAN and S. L. KWOKEK. J. Polymer Sci. **40**, 299 (1959).
3. H. S. FRANK and M. W. EVANS. J. Chem. Phys. **13**, 507 (1945).
4. H. S. FRANK and W. Y. WEN. Discuss. Faraday Soc. **24**, 133 (1957).
5. G. E. BOYD, J. SCHUBERT, and A. W. ADAMSON. J. Amer. Chem. Soc. **69**, 2818 (1947).

Can. J. Chem. Downloaded from www.nrcresearchpress.com by 210.87.254.5 on 09/05/12
For personal use only.

Can. J. Chem. Downloaded from www.nrcresearchpress.com by 210.87.254.42 on 09/05/12
For personal use only.

Coordination complexes of gallium(III) and indium(III) halides. VI. The structures of gallium(III) halide complexes with 1,10-phenanthroline

A. J. CARTY AND K. R. DYMOCK
Chemistry Department, University of Waterloo, Waterloo, Ontario

AND

P. M. BOORMAN
Chemistry Department, University of Calgary, Calgary, Alberta

Received June 29, 1970

Reaction of 1,10-phenanthroline (phen) with gallium trihalides yields the complexes $GaX_3(phen)$ (X = Cl, Br, I), $GaX_3(phen)_2$ (X = Cl, Br), and $GaX_3(phen)_3$ (X = Br, I). Raman and infrared measurements have established the structures of these compounds as $[GaX_2(phen)_2][GaX_4]$, $[GaX_2(phen)_2]X$, and $[Ga(phen)_3]X_3$. $GaI_3(bipy)$ (bipy = 2,2′-bipyridyl) has the structure $[GaI_2(bipy)_2][GaI_4]$. Raman and far-infrared measurements allow ready identification of GaX_4^- ions in these systems. The stereochemistry of the cation $[GaX_2(phen)_2]^+$ cannot be established from vibrational data alone.

Canadian Journal of Chemistry, **48**, 3524 (1970)

Introduction

2,2′-Bipyridyl reacts with gallium(III) halides to give the complexes $GaCl_3(bipy)$, $GaBr_3(bipy)_2$, and $GaI_3(bipy)$ (bipy = 2,2′-bipyridyl). The chloride and bromide complexes were shown by far-infrared spectroscopy to have the ionic structures $[GaCl_2(bipy)_2][GaCl_4]$ and $[GaBr_2(bipy)_2]Br$ (1). A single crystal X-ray study of $GaCl_3(bipy)$ confirmed this result and established a *cis* configuration for the cation $[GaCl_2(bipy)_2]^+$ (2). $GaI_3(bipy)$ was tentatively assigned the structure $[GaI_2(bipy)_2][GaI_4]$ on the basis of incomplete infrared measurements (1). We have now obtained additional evidence for the ionic dimer formulation of $GaI_3(bipy)$ from Raman measurements on the solid. In addition we now report a complete study of the corresponding reactions of GaX_3 (X = Cl, Br, I) with 1,10-phenanthroline. Infrared and Raman data have been used to suggest structures for all the complexes prepared. Preliminary X-ray data are reported for $GaBr_3(phen)$. Previous incomplete studies of the GaX_3/1,10-phenanthroline system established the existence of $GaCl_3(phen)_2$, $GaBr_3(phen)_3$, and $GaI_3(phen)_3$ (3) but no structural data were available for the solid compounds. $Ga(phen)_3(ClO_4)_3$ and $Ga(phen)_3(NO_3)_3$ are also known (4).

Experimental

Spectroscopic grade acetonitrile and acetone were dried over phosphorus pentoxide or Linde type 4A molecular sieves, then fractionated. Gallium trihalides (Fluka 99.99% purity) were handled on a conventional vacuum line.

Reaction of 1,10-Phenanthroline with Gallium Trichloride

Approximately 2 g of gallium trichloride was sublimed in vacuo from a weighed ampoule into a 3-necked flask containing acetone (50 ml) cooled to liquid nitrogen temperature. The flask was allowed to warm to room temperature to dissolve the halide. A quantity of 1,10-phenanthroline slightly less than that required for a 1:1 $GaCl_3$:ligand ratio in acetone (25 ml) was then added with stirring. Solvent (*ca.* 25 ml) was removed and the solution allowed to crystallize, yielding colorless prisms of $GaCl_3(phen)$. The crystals were filtered off, washed with acetone, and dried in vacuo. A slight excess of $GaCl_3$ is essential in this reaction to avoid contamination of the product by $GaCl_3(phen)_2$.

An analogous reaction using 2 moles of ligand per mole of $GaCl_3$ yielded the less soluble $GaCl_3(phen)_2$ as colorless crystals. The same product can be obtained from $GaCl_3(phen)$ in acetone by addition of one mole of 1,10-phenanthroline. The melting point, nitrogen and gallium analyses show that this complex is similar to that prepared by other workers (3).

Attempts to prepare $GaCl_3(phen)_3$ using either of the above complexes and excess 1,10-phenanthroline gave products which always contained a high percentage of bis product.

Reaction of 1,10-Phenanthroline with Gallium Tribromide

Colorless prisms of $GaBr_3(phen)$ and $GaBr_3(phen)_2$ were prepared as above using gallium tribromide in acetone. Reaction with an excess of 1,10-phenanthroline in boiling acetone gave the sparingly soluble tris adduct, $GaBr_3(phen)_3$, previously prepared (3) from diethyl ether. $GaBr_3(phen)$ can be converted to the bis or tris adducts using the stoichiometric amount of ligand in hot acetone.

Reaction of 1,10-Phenanthroline with Gallium Triiodide

The ligand (0.4 g) in acetone was carefully added dropwise to a stirred solution of gallium triiodide (1.0 g) in acetone (20 ml). The initial yellow precipitate dissolved on stirring to give a deep yellow solution. After filtration

TABLE 1
Microanalyses

Compound	Melting point (°C)	%C		%H		%N		%Ga	
		Calcd.	Found	Calcd.	Found	Calcd.	Found	Calcd.	Found
$GaCl_3(phen)$	362	40.45	40.36	2.30	2.30	7.86	7.46	19.57	19.09
$GaCl_3(phen)_2$	180–182					10.44	10.76	13.00	13.00
$[GaCl_2(phen)_2]PF_6$	350–355	44.60	44.02	2.50	2.35			14.97	14.48
$GaBr_3(phen)$	367–369	29.50	29.46	1.60	1.45	5.70	5.29	14.23	14.67
$GaBr_3(phen)_2$	297	42.10	42.09	2.40	2.66	8.40	7.86	10.40	10.20
$GaBr_3(phen)_3$*	210–211							8.20	8.08
$[GaBr_2(phen)_2]PF_6$	233–240	39.20	38.52	2.20	2.22			9.49	9.06
$GaI_3(phen)$	333–334	22.87	22.80	1.28	1.47	4.44	4.52	11.06	11.05
$GaI_3(phen)_3$*	366							7.03	7.08

*Compound similar to that reported previously (3), identified by m.p. and gallium analysis.

the solution was cooled overnight. The crystals of $GaI_3(phen)$ produced were recrystallized from acetonitrile as yellow needles.

Reaction of 1:1 or 1:2 molar quantities of $GaI_3(phen)$ and 1,10-phenanthroline in acetone or acetonitrile gave a brilliant yellow precipitate of the tris adduct $GaI_3(phen)_3$. Repeated attempts to prepare a bis adduct from acetone or acetonitrile failed.

Preparation of PF_6^- Salts

The complexes $GaCl_3(phen)$ and $GaCl_3(phen)_2$ were converted into the salt $[GaCl_2(phen)_2]PF_6$ by reaction with an excess of sodium hexafluorophosphate in boiling acetonitrile. Initial precipitates were discarded, pure products crystallizing as large prisms on standing. $[GaBr_2(phen)_2]PF_6$ was prepared in an analogous manner from $GaBr_3(phen)$ and $GaBr_3(phen)_2$. Infrared spectra of all these derivatives in the region 1650–700 cm^{-1} were run routinely to confirm the presence of uncoordinated PF_6^- ion (1).

Attempts to stabilize the ion $[GaI_2(phen)_2]^+$ with PF_6^- and BF_4^- were unsuccessful.

Microanalyses for all compounds prepared are shown in Table 1.

Physical Measurements

Microanalyses were performed by Chemalytics Inc., Tempe, Arizona and Alfred Bernhardt, 5251 Elbach über Engelskirchen Fritz Pregl Strasse, Germany.

Far-infrared measurements were made on Nujol mulls between caesium iodide plates using a Beckmann IR 12 spectrometer. All spectra were run on an expanded scale of 50 cm^{-1} per inch. Raman spectra were recorded on solids with a Cary 81 Helium–Neon laser equipped instrument using the 6328 Å exciting line. In both instances observed frequencies should be accurate to ± 2 cm^{-1}.

X-Ray measurements were made on Weissenberg Oscillation and Buerger precession cameras using a single crystal grown from acetone/benzene solution.

Results and Discussion

The reaction of gallium trihalides in acetone or acetonitrile solution with 1,10-phenanthroline yields the complexes $GaX_3(phen)$ (X = Cl, Br, I), $GaX_3(phen)_2$ (X = Cl, Br), $GaX_3(phen)_3$ (X = Br, I). The results contrast with similar reactions in diethyl ether (3) where only the complexes $GaCl_3(phen)_2$ and $GaX_3(phen)_3$ (X = Br, I) could be isolated. All the complexes prepared are stable and non-hygroscopic in air although the iodides are somewhat light sensitive. We find no evidence for complexes of stoichiometry $MX_3(phen)_{1.5}$ which are the main products from the reaction of 1,10-phenanthroline with indium trihalides in methyl cyanide or ethanol (5, 6).

Infrared and Raman Spectra

The structures of complexes of the types MX_3B_2, MX_3B (M = trivalent metal; B = 2,2′-bipyridyl, 1,10-phenanthroline) are of considerable current interest since many compounds with these stoichiometries are known for group III elements (7, 8). Moreover, recent work in the transition metal field (9, 10) has shown that structural assignments for several complex ions of the type *trans*-$[MX_2B_2]^+$ (M = Co, Cr, Rh, Ir) are in error. Indeed it now appears that *trans*-$[MX_2B_2]^+$ ions may not exist in the solid state (9). Utilizing the far-infrared (1), Raman (11), and X-ray data (2) for $GaCl_3(bipy)$ for comparison purposes we discuss possible stereochemical assignments for the complexes $GaX_3(phen)$, $GaX_3(phen)_2$, and $GaX_3(phen)_3$.

For $GaX_3(phen)$ (X = Cl, Br, I), several structural formulations are possible (1). By analogy with $GaCl_3(bipy)$ the most likely structure is ionic $[GaX_2(phen)_2][GaX_4]$. This deduction is confirmed for $GaCl_3(phen)$ by an analysis of the far-infrared (Table 2) and Raman (Table 3) spectra. In the far-infrared 1,10-phenanthroline absorbs weakly at 404, 257, and 240 cm^{-1} while Raman bands occur at 404 and 247 cm^{-1} (12, 13). In the complexes the 404 cm^{-1} band moves to higher frequency and increases in intensity in

Can. J. Chem. Downloaded from www.nrcresearchpress.com by 210.87.254.42 on 09/05/12
For personal use only.

TABLE 2

Far-infrared spectra (450–200 cm^{-1}) of gallium complexes*

Compound	Frequency (cm^{-1})					
$GaCl_3(phen)$	444(9)	427(16)	380(19)†	370(20)sh†	344(13)	
	318(19)	302(19)‡	235(17)	214(17)		
$GaCl_3(phen)_2$	440(7)	424(14)	312(20)	299(19)‡	267(3)	252(2)
	234(17)	214(17)				
$[GaCl_2(phen)_2]PF_6$	443(7)	425(12)	396(9)	379(6)sh	353(4)	
	315(20)	300sh(16)‡	294(18)‡	272(2)sh	248sh(7)	
	230(14)	218(14)	206(14)			
$GaBr_3(phen)$	441(5)	420(13)	310(14)	280(19)†	270(20)†	
	230sh(18)‡	221(19)‡				
$GaBr_3(phen)_2$	442(6)	424(12)	311(12)	223(20)‡		
$GaBr_3(phen)_3$	436(16)	426(17)	311(13)	275(9)	260(5)	215(17)
$[GaBr_2(phen)_2]PF_6$	442(6)	425(12)	311(11)	225(20)‡		
$GaI_3(phen)$	441(8)	423(13)	309(14)	221(19)sh†	210(20)†	
$GaI_3(phen)_3$	436(18)	425(20)	314(17)	273(11)	257(10)	
	212(19)					

*An arbitrary intensity of 20 is assigned to the strongest band in each spectrum for comparison purposes.
†Bands due to ν_3 of GaX_4^-.
‡Bands due to ν(Ga—X) of $GaX_2(phen)_2^+$ cation.

TABLE 3

Raman spectra (450–150 cm^{-1}) of gallium complexes

Compound	Frequency (cm^{-1})					
$GaCl_3(phen)$	432 vs	422 m	385 vw†	370 vs†	347 s‡	
	316 s	304 m§		239 vw	214 m	
$[GaCl_2(phen)_2]PF_6$	432 vs	423 w	316 s	302 m§	244 vw	
	220 m					
$GaCl_3(phen)_2$	431 vs	421 w	412 w	313 s	301 m§	
	239 m	212 s				
$GaBr_3(phen)$	429 vs	421 m	413 w	309 m	286 w†	
	278 w†	236 w	211vs‡	190 w	168 m	
$[GaBr_2(phen)_2]PF_6$	431 vs	315 m	309 m	228 m§	204 sh	170 sh
$GaBr_3(phen)_2$	433 vs	312 m	212 m§			
$GaBr_3(phen)_3$	428 s	310 m				
$GaI_3(phen)$	428 s	309 m	210 w†	144 vs*‡		
$GaI_3(bipy)$	358 w	219 m†	180 m	147 vs‡	131 m*	
$GaI_3(phen)_3$	430 m	312 w	247 w*			

*Spectra measured to 125 cm^{-1}.
†Bands due to ν_3 of GaX_4^-.
‡Bands due to ν_1 of GaX_4^-.
§Bands due to ν(Ga—X) of cation $[GaX_2(phen)_2]^+$.

both infrared and Raman spectra. The lower frequency bands cannot be traced with any degree of certainty in the complexes although several medium intensity features occur between 200 and 250 cm^{-1}. For $GaCl_3(phen)$, a broad intense absorption appears near 380 cm^{-1} which is absent from the spectra of $[GaCl_2(phen)_2]PF_6$, $GaBr_3(phen)$, and $GaI_3(phen)$. The corresponding Raman spectrum shows the presence of weak lines at 385 and 370 cm^{-1} with an intense band at 347 cm^{-1}. The Raman spectra of solutions containing the $GaCl_4^-$ ion show ν_3 at 381 cm^{-1} and ν_1 at 345 cm^{-1} (14). In the infrared of solid $Et_4N^+GaCl_4^-$ ν_3 occurs as a broad band at 373 cm^{-1} (15). These results together with the fact that simple tetrafluoroborate and hexafluorophosphate salts of the $[GaCl_2(phen)_2]^+$ cation can be prepared from $GaCl_3(phen)$ suggest that $GaCl_4^-$ ions are present in the $GaCl_3(phen)$. However, there still remains the question of the configuration of the cation and spectral assignments in the lower frequency region. The sharp intense absorption at 318 cm^{-1} in the infrared spectrum of $GaCl_3(phen)$ is present in all the complexes prepared and may be due to ν(Ga—N) and/or a ligand mode. For *cis*-$[GaCl_2(bipy)_2]^+X^-$ ν(Ga—Cl) is at 306 cm^{-1} (i.r.) and 307 cm^{-1} (R) (X = $GaCl_4^-$) and at 304 cm^{-1} (i.r.) and 307 cm^{-1} (R) (X = PF_6^-). We have concluded (11, 16) that the two ν(Ga—Cl) modes ($a + b$)

Can. J. Chem. Downloaded from www.nrcresearchpress.com by 210.87.254.42 on 09/05/12
For personal use only.

Can. J. Chem. Downloaded from www.nrcresearchpress.com by 210.87.254.42 on 09/05/12
For personal use only.

expected for a *cis* cation are almost degenerate in these systems, thus invalidating the possibility of assigning *cis* or *trans* stereochemistry from vibrational data alone. Similar conclusions apply to the phenanthroline complexes. Only one mode due to ν(Ga—Cl) of the $[GaCl_2(phen)_2]^+$ cation can be identified near 300 cm^{-1} in the infrared and Raman spectra (Tables 2 and 3). We should point out, however, that a wealth of X-ray powder and spectroscopic evidence for similar ions (9) indicates that the *trans* configuration is thermodynamically destabilized with respect to the *cis* isomer. Our single crystal X-ray data for $GaCl_3$(terpy) (terpy = 2,2′,2″-terpyridyl) also indicate that the *trans* isomer might be destabilized by a lengthening of *trans* Ga—Cl bonds (16). A *cis* configuration for the $GaCl_2(phen)_2^+$ cation therefore seems likely.

Infrared and Raman data for $GaCl_3(phen)_2$ indicate the absence of $GaCl_4^-$ ions. Comparison of the infrared (Fig. 1) and Raman (Fig. 2) spectra of $GaCl_3$(phen) and $GaCl_3(phen)_2$ as well as the synthesis of a PF_6^- derivative from $GaCl_3(phen)_2$ suggest a structure $[GaCl_2(phen)_2]Cl$ although the cation stereochemistry cannot be unequivocally established.

The structure $[GaBr_2(phen)_2]GaBr_4$ is also established for $GaBr_3$(phen). ν_3 of $GaBr_4^-$ appears as a doublet at 276 cm^{-1} in the infrared. In aqueous solutions of $GaBr_4^-$ ν_3 occurs at 278 cm^{-1} and ν_1 at 210 cm^{-1} (14, 17). The Raman spectrum of $GaBr_3$(phen) exhibits a weak doublet in the ν_3 region and a strong line at 211 cm^{-1} due to ν_s(Ga—Br) of $GaBr_4^-$. Comparison of the infrared (Fig. 3) and Raman (Fig. 4) spectra of $GaBr_3$(phen) and $[GaBr_2(phen)_2]PF_6$ confirms the above conclusions. Single crystal X-ray measurements for $GaBr_3$(phen) yield the following parameters: Ga_2Br_6, $(C_{12}H_8N_2)_2$, space group $P2_{1/c}$ (C_{2h}^5); a = 12.85 (9), b = 16.51 (8), c = 14.06 (4); β = 92° 15′; D_m = 2.20 g cm^{-3} (by flotation), D_c 2.17; Z = 4. There are no crys-

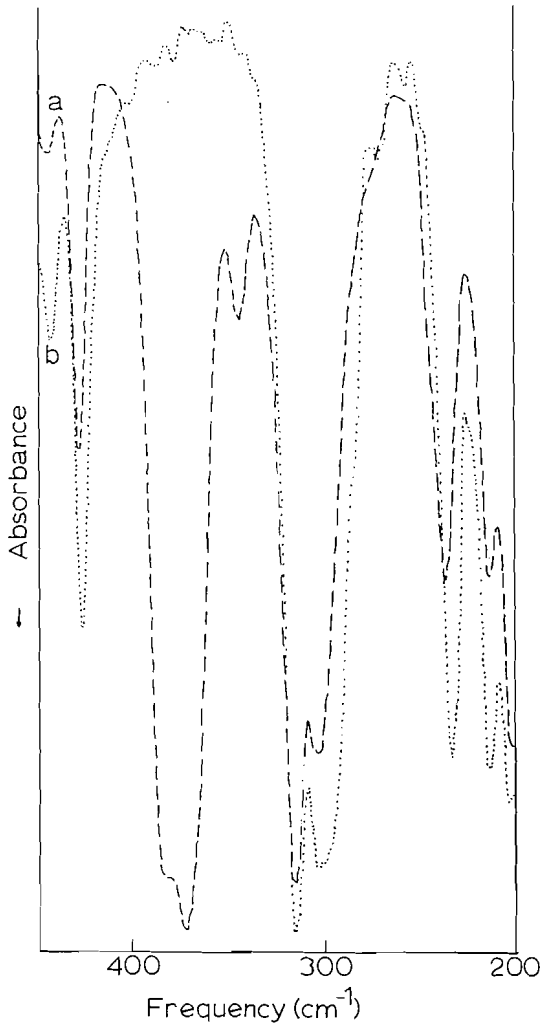

FIG. 1. Infrared spectra (450–200 cm^{-1}) of (*a*) $GaCl_3$(phen), (*b*) $GaCl_3(phen)_2$.

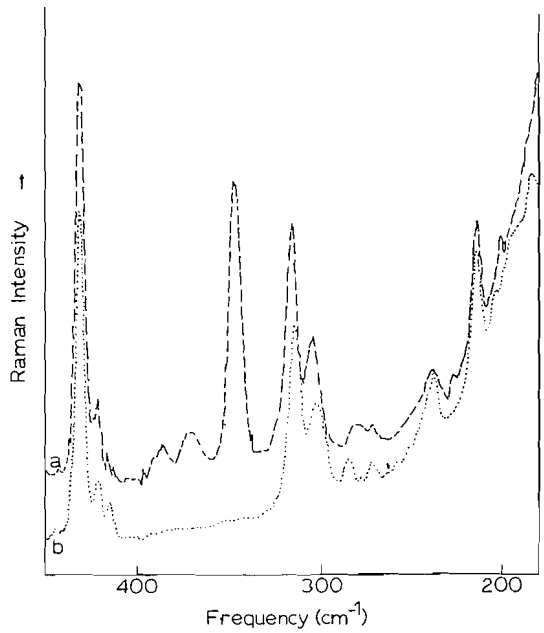

FIG. 2. Raman spectra (450–150 cm^{-1}) of (*a*) $GaCl_3$(phen), (*b*) $GaCl_3(phen)_2$.

Can. J. Chem. Downloaded from www.nrcresearchpress.com by 210.87.254.42 on 09/05/12
For personal use only.

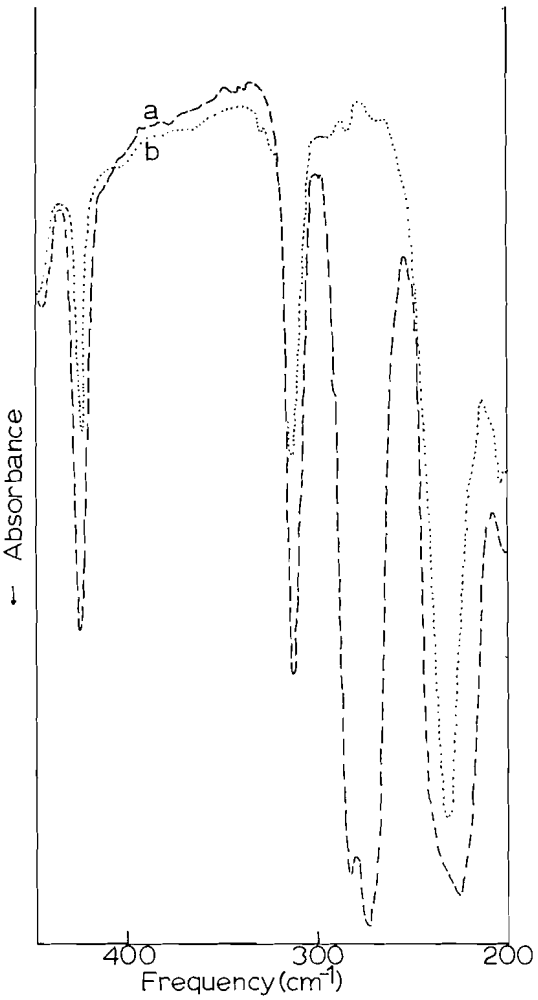

FIG. 3. Infrared spectra of (*a*) $GaBr_3(phen)$, (*b*) $[GaBr_2(phen)_2]PF_6$ in the region 450–200 cm^{-1}.

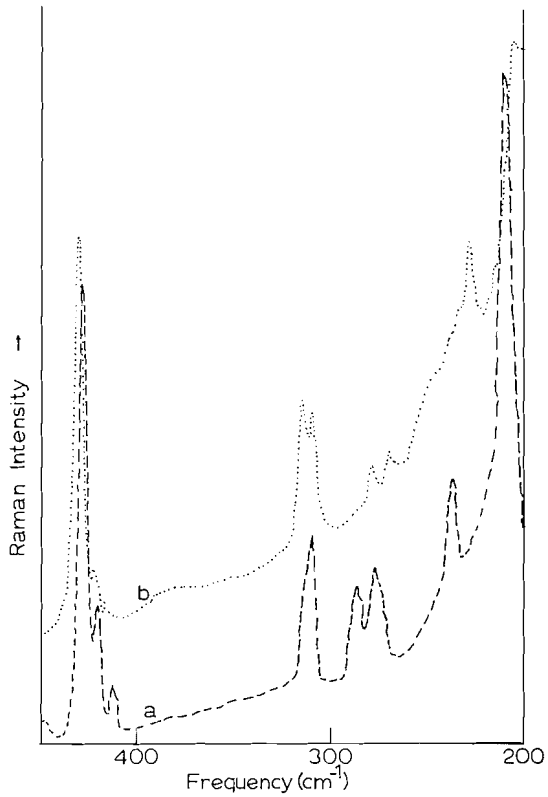

FIG. 4. Raman spectra of (*a*) $GaBr_3(phen)$, (*b*) $[GaBr_2(phen)_2]PF_6$ in the region 450–200 cm^{-1}.

tallographically imposed symmetry restrictions. Molecules of dimers occur on the general positions $x, y, z; \bar{x}, \bar{y}, \bar{z}$; $x, (\frac{1}{2}+y), (\frac{1}{2}-z)$; $x, (\frac{1}{2}-y), (\frac{1}{2}+z)$. On the basis of the above X-ray data a site symmetry analysis of the vibrational modes of $GaBr_4^-$ is trivial. However, for both $GaCl_3$-(phen) and $GaBr_3(phen)$ it is worth noting that $\nu_3(t_2)$ of GaX_4^- appears as a doublet in the infrared and Raman spectra. Comparison of the spectra of $GaBr_3(phen)$, $[GaBr_2(phen)_2]PF_6$, and $GaBr_3(phen)_2$ (Tables 2 and 3; Figs. 3 and 4) allows the following conclusions to be drawn: (*1*) the cation $[GaBr_2(phen)_2]^+$ is also present in $GaBr_3(phen)_2$; (*2*) ν(Ga—Br) for the cation appears at 221, 230 cm^{-1} ($GaBr_4^-$ salt), 228 cm^{-1} (PF_6^- salt), and 212 cm^{-1} (Br^- salt), (*3*) in no single case can both modes of a suspected *cis* cation be distinguished in *both* the infrared and Raman. Stereochemical assignments cannot be based on the number of ν(Ga—Br) bands.

Also of interest is the observation that ν(Ga—Br) of the cation $GaBr_2(phen)_2^+$ appears at higher frequency than ν_1 of $GaBr_4^-$ when for the analogous chloro complex ν_1 is higher by *ca.* 40 cm^{-1}. Intensity data are being collected for $GaBr_3(phen)$ in an attempt to find out whether these results are explicable in terms of Ga—Br bond lengthening in $GaBr_4^-$ or Ga—Br bond shortening in $GaBr_2(phen)_2^+$.

For $GaI_3(phen)$ the infrared spectrum is dominated by the appearance of a broad strong band at 210–221 cm^{-1}. In the Raman weak scattering occurs near 217 cm^{-1} with a very intense line at 144 cm^{-1}. Comparison with the Raman spectrum of aqueous GaI_4^- (18) shows ν_3 at 222 cm^{-1} and ν_1 at 145 cm^{-1}. The line positions in the infrared and Raman together

Can. J. Chem. Downloaded from www.nrcresearchpress.com by 210.87.254.42 on 09/05/12
For personal use only.

with the relative intensities leave little doubt that the ion GaI_4^- is present in the structure of GaI_3(phen). The analogous 2,2′-bipyridyl complex GaI_3(bipy) shows intense infrared absorption centered at 224 cm^{-1} with Raman lines at 219(m) and 147(vs). Again the spectra are consistent with the presence of GaI_4^-. These results suggest that both complexes be formulated $[GaI_2B_2][GaI_4]$ (B = 1,10-phenanthroline, 2,2′-bipyridyl). In view of the lack of infrared data below 200 cm^{-1} assignment of ν(Ga—I) modes for the cation cannot be attempted.

The tris complexes $GaX_3(phen)_3$ (X = I, Br) which were previously reported by Russian workers (3) have rather simple far-infrared and Raman spectra. Modes due to tetrahedral GaX_4^- and ν(Ga—Br) of $[GaBr_2(phen)_2]^+$ are clearly absent. Apart from the ligand bands near 430 cm^{-1} and the lines at *ca.* 310 cm^{-1}, no Raman scattering of significant intensity could be detected down to 125 cm^{-1}. The absence of halogen-sensitive bands in the spectra of $GaX_3(phen)_3$ (X = Br, I) implies structures of the type $[Ga(phen)_3]^{3+}3X^-$. Of the four infrared bands found in each spectrum above 200 cm^{-1}, those at 212 and 215 cm^{-1} are most likely ligand absorptions. We make no detailed attempt to assign the three bands between 260–315 cm^{-1} but note that for a D_3 cation two metal–nitrogen stretches ($a_2 + e$) are expected.

Conclusions

In addition to $GaCl_3(phen)_2$ and $GaX_3(phen)_3$ (X = Br, I) prepared by other workers (3) reaction of gallium trihalides with 1,10-phenanthroline gives GaX_3(phen) (X = Cl, Br, I) and $GaX_3(phen)_2$ (X = Br). The complexes GaX_3(phen) (X = Cl, Br, I), $GaX_3(phen)_2$ (X = Cl, Br), $GaX_3(phen)_3$ (X = Br, I) have structures $[GaX_2(phen)_2][GaX_4]$, $[GaX_2(phen)_2]X$, and $[Ga(phen)_3]X$, respectively. Identification of GaX_4^- ions in these complexes is simple when Raman and infrared data are utilized. Vibrational spectroscopy alone cannot distinguish *cis*-$GaX_2(phen)_2^+$ from *trans*-$GaX_2(phen)_2^+$. The structure of GaI_3(bipy) has now been shown to be $[GaI_2(phen)_2][GaI_4]$. As a final note it may be pointed out that cations of the type $[MX_2B_2]^+$ have now been firmly established for GaX_3(bipy) (X = Cl, I), $GaBr_3(bipy)_2$ (1), GaX_3(phen) (X = Cl, Br, I), $GaX_3(phen)_2$ (X = Cl, Br), InX_3-$(bipy)_{1.5}$ (X = Cl, Br, I) (5, 6, 13), $InX_3(phen)_{1.5}$ (X = Cl, Br, I) (19), Tl(bipy)X_3 (X = Br, I) (20), $TlX_3(bipy)_2$, $TlX_3(phen)_2$ (X = Cl, Br, I) (21) as well as for many derivatives prepared from the above by metathesis with MX (X = BF_4^-, PF_6^-, NO_3^- etc.).

This work was supported by the National Research Council of Canada. We thank Dr. A. Walker, Scarborough College, Scarborough, Ontario, for the use of infrared facilities.

1. A. J. Carty. Can. J. Chem. **46**, 3779 (1968).
2. R. Restivo and G. Palenik. Chem. Commun. 867 (1969).
3. B. N. Ivanov-Emin, L. A. Niselson, Y. A. I. Rabovik, and L. G. Larionova. Russ. J. Inorg. Chem. (Engl. Transl.) **5**, 583 (1961).
4. G. J. Sutton. Aust. J. Chem. **16**, 278 (1963).
5. A. J. Carty and D. G. Tuck. J. Chem. Soc. A, 1081 (1966).
6. R. A. Walton. J. Chem. Soc. A, 1485 (1967).
7. R. A. Walton. Coord. Chem. Rev. (1970). In press.
8. A. J. Carty. Coord. Chem. Rev. **4**, 29 (1969).
9. J. G. Gibson and E. D. McKenzie. J. Chem. Soc. A, 2637 (1969).
10. J. G. Gibson, R. Laird, and E. D. McKenzie. J. Chem. Soc. A, 2089 (1969).
11. A. J. Carty and P. M. Boorman. Unpublished results.
12. J. R. Ferraro, L. J. Basile, and D. L. Kovacic. Inorg. Chem. **5**, 391 (1966).
13. R. A. Walton. J. Chem. Soc. A, 61 (1969).
14. L. A. Woodward and A. A. Nord. J. Chem. Soc. 3721 (1956).
15. D. M. Adams, J. Chatt, J. M. Davidson, and J. Gerratt. J. Chem. Soc. 2189 (1963).
16. G. Beran, A. J. Carty, and G. Palenik. Chem. Commun. 222 (1970).
17. R. A. Plane and J. Nixon. J. Amer. Chem. Soc. **84**, 4445 (1962).
18. L. A. Woodward and G. H. Singer. J. Chem. Soc. 716 (1958).
19. A. J. Carty and D. G. Tuck. Unpublished results.
20. R. A. Walton. Inorg. Chem. **7**, 640 (1968).
21. (*a*) F. Ya Kulba, N. G. Yaroslavskii, L. V. Konovalov, A. V. Barsukov, and V. E. Mironov. Russ. J. Inorg. Chem. **13**, 79 (1968). (*b*) F. Ya Kulba, V. G. Mironov, Chin-Yang Ts'ung, and Z. G. Filippova. Russ. J. Inorg. Chem. **8**, 341 (1963).

Can. J. Chem. Downloaded from www.nrcresearchpress.com by 210.87.254.105 on 09/05/12
For personal use only.

Chemistry of 2-substituted adamantanes. I. Adamantanethione, its dimer and trimer[1]

J. W. GREIDANUS
Department of Chemistry, The University of Calgary, Calgary 44, Alberta

Received May 11 1970

The preparation of adamantanethione from adamantanone is reported, either via 2-ethoxy-2-adamantanethiol or directly with the aid of phosphorus pentasulfide. The conditions for the latter reaction were developed so as to give the highest yield (91%). Dimerization or trimerization of the thioketone under the influence of methanesulfonic acid leads to dispiro[1,3-dithietane-2.2′:4.2″-diadamantane], resp. trispiro[1,3,5-trithiane-2.2′:4.2″:6.2‴-triadamantane]. The spectral properties of the compounds are discussed, especially the n.m.r. spectrum of the thione in connection with the anisotropy of the thiocarbonyl group, and the aromatic solvent-induced shift.

Canadian Journal of Chemistry, 48, 3530 (1970)

The more successful synthetic methods for the preparation of aliphatic thioketones have only been developed in the last decade. Especially, Mayer *et al.* have contributed much to our present understanding and the topic has been reviewed (1).

Paquer and Vialle (2) very recently reported that use of the method of Bleisch and Mayer (1*b*) for the preparation of many thiones resulted in almost all cases where α-hydrogen was present in the formation of thione–enethiol mixtures, as was shown by v.p.c.

The use of sulfides of phosphorus for the conversion of simple aliphatic or alicyclic ketones has usually led to dimeric products (1*a*, 3) and it seems that among the aliphatic thiones, apart from perfluorothioketones (4), diphenyl cyclopropenethione (5), and some sulfur analogues of dimethylketene dimer (6), only thiofenchone (**1**) has been obtained in this manner as a pure compound (7).

Because pure simple aliphatic thioketones have been hard to obtain, and are often unstable, their chemistry as a whole has not been fully investigated. In particular the photochemistry, their potential in cyclo-addition reactions and spectral properties should be further investigated. Optical rotatory dispersion (o.r.d.) studies of aliphatic thioketones have been rare, this again as a result of the unavailability of stable pure thiones (8, 9).

After some initial work on the synthesis of the rather unstable cyclohexanethione by a variety of methods (mainly the reactions of ketone with hydrogen sulfide in the presence of acid or base catalyst (1*b*, 10)), it became clear to us that this compound would be unsatisfactory as a model compound for our study of the thiocarbonyl group in thioketones. Because of our research interest in the chemistry of adamantane compounds, we realized that adamantanethione (**2**) might be very suitable for our work with thioketones as its structure made enethiol formation

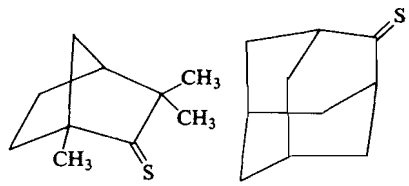

1 **2**

impossible. In addition, **2** would probably be a solid and as a result would be easier to purify than cyclohexanethione by means of crystallization or sublimation.

Compound **1** is one of the most stable aliphatic thiones known (1*a*) but if fairly stable pure **2** would become available it would have the advantage of a highly symmetrical environment of its thiocarbonyl group, when serving as a model compound.

In addition, adamantanethione would be an excellent starting material for the preparation of 2-adamantanethiol[2] and compounds derived from it.

If suitably substituted adamantanethiones could be secured by means of a generally applicable method for C=O to C=S conversion, a great number of thioketones would become accessible for study of the o.r.d. and circular dichroism (c.d.) of the thiocarbonyl chromo-

[1]Part of the results has appeared as a preliminary communication; see ref. 11.

[2]Details for the preparation of this thiol, which has been reported in our preliminary communication (11), will be published shortly.

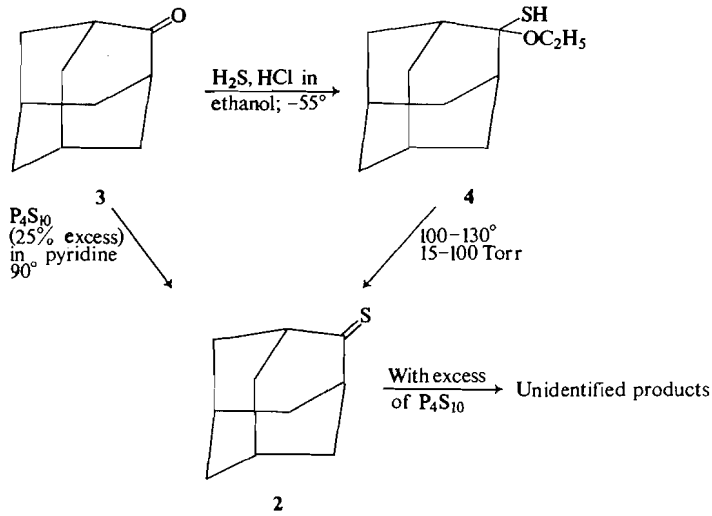

SCHEME 1

phore. Several optically active adamantanones have been reported and used for o.r.d.–c.d. studies (12). For the various reasons given it was decided to prepare adamantanethione and to explore some of its chemistry.

Results and Discussion

Adamantanethione

Adamantanethione could not be prepared satisfactorily by the method of Bleisch and Mayer (1*b*), *i.e.* by treatment of the ketone with H_2S at −70° in ethanol–ether, containing HCl. The major product of this reaction, an insoluble colorless powder, was identified as the trimer of the thione, to be referred to later.

When subsequently adamantanone (**3**) was heated with an excess of phosphorus pentasulfide in pyridine (20 h at 115°), a reaction took place, but no thioketone could be isolated. When the reaction was run at 25° for 90 h the thioketone was obtained in quantity for the first time. By adjusting the reaction times, the temperatures, and reagent ratios it was possible to raise the yield to 55% (this was the highest yield obtained at the time of our preliminary communication (11)), and eventually to more than 90% of crude thione, which contained only a trace of starting material as indicated by its i.r. spectrum.[3] A large excess of P_4S_{10} must be avoided as secondary reactions of the thione with P_4S_{10} will occur, especially at higher temperatures, with the formation of a yellow very viscous mass (Scheme 1).

The purity of the crude thione was determined by spectroscopic methods (n.m.r. and i.r.). Removal of ketone impurity by repeated recrystallization at low temperature (−50°) from petroleum ether or by repeated fractional sublimation *in vacuo* was a very tedious process and satisfactory results were only obtained if the quantity of impurity was low. The best purification method was chromatography on silica and elution with petroleum ether – benzene mixtures. If **2** is to be used for the preparation of 2-adamantanethiol it is not necessary to purify the crude thioketone as it is much easier to purify the thiol.

The thioketone **2** was also obtained when 2-ethoxy-2-adamantanethiol (**4**) was heated for 45 min at 100–130° under reduced pressure (15–100 Torr). The initially colorless, at that temperature, liquid geminal ethoxythiol (m.p. 30.5°) turned into an orange–red solid. This was found to be **2** of high purity. The not very stable geminal alkoxythiols are a little known class of compounds. Compound **4** was obtained when an attempt was made to prepare 2,2-adamantanedithiol using a procedure reported by Demuynck and Vialle (13). They reported that two representatives of this class of compounds easily lost a molecule of ethanol and formed enethiol. As

[3]A number of attempts to prepare the thioketone by reaction of adamantanone and phosphorus pentasulfide in toluene or carbon disulfide at 25°, or in heptane at 100° (this method has been reported (7) for the preparation of thiofenchone (**1**)) were not successful.

Can. J. Chem. Downloaded from www.nrcresearchpress.com by 210.87.254.105 on 09/05/12
For personal use only.

TABLE 1

Electronic absorption spectra of adamantanethione and some cyclic thioketones

Compound	Solvent	Main bands, mμ (log ε)	Minor bands and shoulders, mμ (log ε)	Reference
Adamantanethione	*n*-Hexane	240(4.10); 223 sh; 488(1.05)	450; 503; 514; 554(0.43)	
Thiofenchone	*n*-Hexane	240(4.00); 215(3.60); 488(1.04)	445; 501	1, 14
Thiocamphor	Cyclohexane	244(4.06); 214(3.62); 493(1.09)	450; 515; 551	1, 14
Androstane-17-thione	Dioxane	239(3.94); 492(1.11)		9

TABLE 2

The n.m.r. spectra (τ units) of **2** and **3** in CCl_4 and benzene

Compound	CCl_4		Benzene		
Adamantanone* (**3**)	7.58(2H)	7.98(12H)	7.52(2H)	8.32(8H)	8.45(4H)
Adamantanethione (**2**)	6.60(2H)	7.96(12H)	6.60(2H)	8.24(8H)	8.38(4H)

*The data for the spectrum in benzene correspond to those reported (15).

this is not possible in **2**, the formation of thione from **4** is not surprising.

Adamantanethione is a red–orange compound, with m.p. 173° and, like so many adamantane derivatives, it can be easily sublimed. Its i.r. spectrum shows a very strong absorption at 1150 cm^{-1}, in the general area (1025–1225 cm^{-1}) of the stretching frequencies for C=S (when bonded to elements other than nitrogen) according to Rao and Venkataraghavan (7) and close to the absorptions shown by some other homocyclic non-aromatic thiones: 1179 cm^{-1} in androstane-17-thione (9) and 1180 cm^{-1} thiofenchone (7).

The electronic absorption spectrum of adamantanethione in *n*-hexane shows two main bands at 488 (log ε 1.05) and 240 mμ (log ε 4.10) with several shoulders and minor bands. From the data in Table 1 it can be seen that the electronic absorption spectra of **2** and those of some other cyclic non-aromatic thioketones are very similar to each other, in the position as well as in the intensities of the bands.

The n.m.r. spectrum of **2** resembles that of adamantanone. For both compounds only two peaks are obtained in carbon tetrachloride, but in benzene three signals are observed (Table 2).

In our earlier communication (11) it was stated already that the n.m.r. results were yet another piece of evidence for the greater anisotropy of the C=S group as compared with the C=O group. The n.m.r. data obtained with thion esters (16, 17) and thiocamphor (17) have been explained on this basis. The n.m.r. data of Paquer and Vialle (2) for a great number of aliphatic thiones also show clearly the greater deshielding effect of the thiocarbonyl group (in general causing a downfield shift of 0.45–0.55 p.p.m. in the thiocarbonyl compound compared with the ketone). Very recently detailed information was published (18) on the geometry of positive and negative shielding regions surrounding the carbonyl group. As a result of a comparative study of camphor and thiocamphor at 220 MHz strong evidence has been presented that "the coordinate susceptibilities associated with the C=S function are quantitatively different from, but qualitatively similar to, those associated with the C=O function" (19). The evidence was in fact that the three coordinate susceptibilities for the thiocarbonyl group were stronger positive (shielding) or negative (deshielding) than those for the carbonyl group.

In our spectra the position of the signal for the tertiary protons adjacent to the thiocarbonyl function in **2** at τ 6.60 (in CCl_4) corresponds very well with that reported (2) at τ 6.64 for the methine protons in 2,4-dimethyl-3-pentanethione, and it shows that these bridgehead protons are more strongly deshielded than in the ketone. Compared with adamantane itself, all protons in these compounds are deshielded. This is to be expected as they would all be located in the ellipsoidal deshielding cone (18) of the C=O, and apparently of the C=S as well. When the same spectra are taken in benzene as solvent, it is found that the

Can. J. Chem. Downloaded from www.nrcresearchpress.com by 210.87.254.105 on 09/05/12
For personal use only.

Can. J. Chem. Downloaded from www.nrcresearchpress.com by 210.87.254.105 on 09/05/12
For personal use only.

aromatic solvent-induced shift of these same α-bridgehead protons is very small in the case of the ketone, and nil for the thioketone. The main peak, representing the other 12 protons on the adamantane skeleton has been shifted upfield (Table 2), and is now split into two peaks with integrated intensities corresponding to eight and four protons, of which the latter have the highest field position. If the geometry of polar solute – aromatic solvent collision "complexes" according to Ledaal (20) is accepted[4] the geometry in the case of adamantanone or adamantanethione in benzene would be:

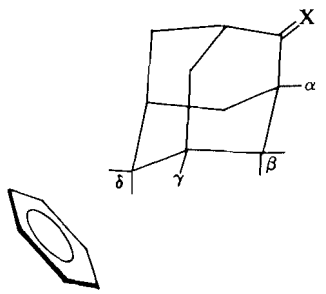

This would result in strongest shielding of the protons closest to the benzene ring, *i.e.* the four protons in the γ and δ position with respect to the C=X group. It is tempting to explain the signal in the highest field position on this basis. The eight β-protons are also moved to an upfield position in benzene, but the two α-bridgehead protons are virtually insensitive to the solvent change. The fact that the n.m.r. absorptions of equatorial protons α to the carbonyl function show very small aromatic solvent-induced shifts is well documented (21, 22). In adamantanone the α-protons are slightly deshielded (Table 2) and therefore appear to be on the same side of the reference plane (as first defined by Connolly and McCrindle (21)) as the carbonyl oxygen. It appears that for the thiocarbonyl group a similar reference plane can be drawn and this is not surprising.

Dimeric and Trimeric Adamantanethione

When pure, adamantanethione possesses considerable thermal stability, and it is recovered unchanged from its solution in toluene or *p*-xylene after 40–45 h of reflux (110, 138°, respectively).[5]

The formation of dimers, trimers, and polymers from aliphatic or alicyclic thioketones is a well-known reaction. When **2** was stirred in methanesulfonic acid at 22° the orange solid changed in about 5 min to a colorless product, which was shown to be the stable dimer of **2**, dispiro[1,3-dithietane-2.2′:4.2″-diadamantane] (**5**), m.p. 306–307° (see Scheme 2). Its n.m.r. spectrum (CCl_4) showed the bridgehead protons adjacent to the dithietane ring at τ 7.68 as a broad singlet (4H) and all other protons as a multiplet between τ 7.9 and 8.6 (24H). In the 100 MHz spectrum this multiplet is seen to consist of an AB quartet for the 16 methylene protons with a 1,3-relationship to the spiro carbon atoms with $J = 12$ Hz and a calculated τ 8.39 for H_A, 8.09 for H_B. The protons which have a 1,3-diaxial relationship to a C—S bond give probably the downfield signal at τ 8.09 (23). The other protons in the molecule cause a peak at τ 8.31. The trimer of **2**, trispiro[1,3,5-trithiane-2.2′:4.2″:6.2‴-triadamantane] (**6**), was obtained when a solution of the thioketone in ether was treated with some methanesulfonic acid (Scheme 2). It was insoluble in all solvents tried, but was purified by sublimation (250° at 0.05 Torr). The dimeric and trimeric nature of **5** and **6** was confirmed by their mass spectra, which showed M^+ at *m/e* 332 and 498.

Pyrolysis of the trimer **6** at 355° gave **2** in high yield (82%). Pyrolysis of trithianes has on occasion been used to prepare thioketones, especially alkyl aryl thioketones. In general pyrolytic methods can not be applied for the synthesis of aliphatic thiones (1*a*) because the 1,3,5-trithianes are frequently very stable and will only decompose under conditions which are destructive for the thioketones that are formed.

Reduction and Oxidation of Adamantanethione

Adamantanethione was found to be an excellent starting material for the preparation of 2-adamantanethiol (11), which in turn permits synthesis of a variety of 2-substituted sulfur containing adamantanes. With several other substituted adamantanones becoming more

[4]This model for benzene – polar solute association was successfully applied in the interpretation of aromatic solvent-induced shifts in camphor and thiocamphor (19).

[5]As a precaution against decomposition during storage **2** was usually stored at 0° in the dark, in a closed container.

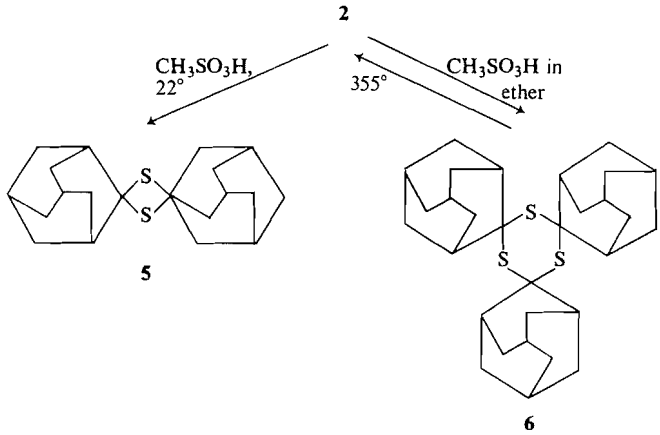

SCHEME 2

readily available, the corresponding thioketones, and thiols, will be accessible. Work in this direction, as well as on the oxidation of adamantanethione to its *S*-oxide, is in progress. Preliminary experiments indicate that unstable adamantanethione-*S*-oxide is formed upon oxidation with *m*-chloroperbenzoic acid; the product dissolved in CCl_4 shows in the n.m.r. spectrum two non-equivalent protons (the two bridgehead protons adjacent to the *S*-oxide group) at τ 5.98 and 7.11, as well as a main peak at τ 8.00, of the expected intensities. The *S*-oxide decomposes slowly into adamantanone on standing, even at $-10°$.

Experimental

The starting material adamantanone was initially prepared from adamantane,[6] later obtained commercially (Aldrich Chemical Company).

Melting points were determined on a Buchi melting point apparatus in sealed capillary tubes, and are uncorrected. The electronic absorption spectra were recorded on a Cary 15 instrument, the i.r. spectra on a Perkin-Elmer spectrophotometer, Model 337. The mass spectra were determined on a Varian-Mat CH-15 instrument at an ionization energy of 70 eV. The n.m.r. spectra were recorded at 60 or 100 MHz on Varian A-60 and HA-100 spectrometers, in the solvent indicated (concentrations 5–10% (w/w)). Tetramethylsilane (τ = 10) was used as internal standard. Microanalyses were carried out by Dr. C. Daesslé, Organic Microanalysis, Montreal, Quebec, and by Mrs. S. Swaddle of this department.

2-Ethoxy-2-adamantanethiol (4)

In a three-necked flask, equipped with gas-inlet tube and Dewar condenser, and cooled to $-75°$, 30 ml of liquid hydrogen sulfide was collected. A suspension of 15 g (0.10 mole) of adamantanone in a mixture of 110 ml of dry ethanol and 15 ml of dry ether, also cooled to $-75°$, was all at once added to the stirred liquid hydrogen sulfide; this gave a clear solution. The temperature was allowed to rise to $-55°$ and a stream of dry hydrogen chloride was introduced into the solution. After 30 min a colorless crystalline precipitate had been formed in the reaction mixture which turned gradually orange. After 1 h the flow of hydrogen chloride was stopped and the reaction mixture was kept at $-55°$ for 2 h. Then it was added to 500 ml of ice water and 500 ml of petroleum ether. (Caution! Great quantities of hydrogen sulfide gas escape.) The orange organic layer was washed four times with water, dried ($MgSO_4$) and evaporated *in vacuo* at room temperature till an orange oily residue was left. To this 150 ml of acetonitrile was added and the mixture was cooled to $-50°$ and filtered giving 12.1 g of almost colorless 2-ethoxy-2-adamantanethiol, m.p. 29.5–30.5° (yield 57%). After two crystallizations from acetonitrile the analytical sample was dried at 0.02 Torr; m.p. 30.5–31.5°. The product slowly decomposed, even at 0°, into an orange liquid.

Anal. Calcd. for $C_{12}H_{20}OS$: C, 67.87; H, 9.49. Found: C, 67.51; H, 9.79.

The i.r. spectrum ν_{max} (KBr): 2560 (weak, SH), 1103, 1087, 1070 (all very strong, C—O—C), 2975 cm^{-1} (CH_3); n.m.r. spectrum τ (CCl_4): 8.84 (triplet, 3H, J = 7Hz), 8.68 (singlet, 1H, SH), 6.41 (quartet, 2H, J = 7Hz), 7.5–8.6 (multiplet, 14H).

Adamantanethione (2)

(*a*) In a three-necked flask equipped with an efficient mechanical stirrer and a condenser with drying tube 48 g (0.32 mole) of adamantanone (**3**) was dissolved in 300

[6]Results using the photo-oximation of adamantane as reported by Müller *et al.* (24) were poor and similar to those described by Carpenter (25). Photo-oximation using nitrosylsulfuric acid (26) or oxidation of the hydrocarbon with chromyl chloride (27) did not afford the ketone in the desired quantity either. Oxidation of adamantane with sulfuric acid (28) proved to be the best method (unpublished results, J. W. Greidanus and W. J. Schwalm).

Can. J. Chem. Downloaded from www.nrcresearchpress.com by 210.87.254.105 on 09/05/12
For personal use only.

Can. J. Chem. Downloaded from www.nrcresearchpress.com by 210.87.254.105 on 09/05/12
For personal use only.

ml of dry pyridine (H_2O < 0.05%). The solution was heated in an oil bath to 90°, 17.8 g (0.04 mole) of phosphorus pentasulfide (P_4S_{10}) was added in portions in 10 min, and the reaction mixture was stirred vigorously for 11 h at 90°. The initially yellow solution turned red and a small quantity of an intensely colored violet–red glassy syrup was formed, covering the interior of the flask. After cooling the reaction mixture was added to 1.5 l of petroleum ether (boiling range 30–60°) and the mixture was four times extracted with water, twice with 2 *N* HCl, and again twice with water. After drying ($MgSO_4$) the solvent was removed *in vacuo*, leaving 48.0 g of orange adamantanethione (yield 90.5%). This product still contained a trace of starting material (C = O at 1725 cm^{-1} in the i.r. spectrum). Chromatography on a silica column (grade 950, Fisher, 60–200 mesh) with mixtures of petroleum ether and benzene in ratios 95:5 to 4:1, afforded the pure thioketone, m.p. 173–174°.

Anal. Calcd. for $C_{10}H_{14}S$: C, 72.23; H, 8.49; S, 19.28. Found: C, 71.97; H, 8.22; S, 19.14.

Mass spectrum: *m/e* 166 (M^+). The i.r. spectrum ν_{max} (CCl_4): 1150 cm^{-1} (very strong, C = S); n.m.r. spectrum in CCl_4 and benzene, see text and Table 2; electronic absorption spectra, see text and Table 1.

(*b*) In a small flask 1.45 g (6.8 mmole) of 2-ethoxy-2-adamantanethiol (**4**) was heated in an oil bath to 100–130° under a pressure of initially 100 Torr, later 15 Torr, for 45 min. The colorless liquid gradually turned orange and solidified. The product, 1.05 g, was virtually pure adamantanethione (**2**), yield 93%, identical to that prepared from adamantanone. After recrystallization from low boiling petroleum ether the m.p. was 173°.

The Dimer of Adamantanethione: Dispiro[1,3-dithietane-2.2′:4.2″-diadamantane] (5)

To 15 ml of reagent grade methanesulfonic acid, stirred at 22°, was added 3.32 g (0.02 mole) of adamantanethione. The orange color of the insoluble solid disappeared and a colorless powder was formed. After 1 h of stirring the reaction mixture was added to 200 ml of water. The crude product was recrystallized from hot 1,4-dioxane, giving 2.27 g (68%) of analytically pure dispiro[1,3-dithietane-2.2′:4.2″-diadamantane] (**5**), m.p. 306–307°.

Anal. Calcd. for $C_{20}H_{28}S_2$: C, 72.23; H, 8.49; S, 19.28. Found: C, 72.54; H, 8.62; S, 19.50.

Mass spectrum: *m/e* 332 (M^+). The i.r. spectrum ν_{max} (KBr): the seven strongest peaks in order of decreasing intensity between 800 and 1300 cm^{-1} are 964, 915, 1092, 1037, 1204, 1267, and 839 cm^{-1}; n.m.r. spectrum τ (CCl_4): 7.68 (broad singlet, 4H), between 7.95 and 8.54 (multiplet, 24H), see text.

The Trimer of Adamantanethione: Trispiro[1,3,5-trithiane-2.2′:4.2″:6.2‴-triadamantane] (6)

To a stirred solution of 4.98 g (0.03 mole) of adamantanethione in 50 ml of anhydrous ether was added dropwise 3 g of methanesulfonic acid. The addition of the first drop already caused formation of some colorless precipitate. When all the acid had been added, the reaction mixture was stirred for 90 min. After filtration and washing with 1,4-dioxane 4.01 g of colorless trispiro[1,3,5-trithiane-2.2′:4.2″:6.2‴-triadamantane] (**6**) was obtained (yield 80%), m.p. 354° (dec.). No solvent was found for recrystallization, but at 250–270° and 0.05 Torr the compound could be sublimed.

Anal. Calcd. for $C_{30}H_{42}S_3$: C, 72.23; H, 8.49. Found: C, 72.54; H, 8.45.

Mass spectrum: *m/e* 498 (M^+). The i.r. spectrum ν_{max} (KBr): the ten strongest peaks in order of decreasing intensity between 800 and 1300 cm^{-1} are 1092, 968, 1210, 1192, 843, 892, 1030, 1270, 1304, 797, and 821 cm^{-1}.

Thermal Decomposition of the Trimer of Adamantanethione (6)

In a test tube 0.50 g (1 mmole) of **6** was heated in a metal bath at 350–355° for 3 min. Decomposition started and a red liquid was formed. After cooling, the mixture was extracted with petroleum ether and 0.23 g of adamantanethione (**2**) was isolated. The insoluble material was found to be unchanged **6**, weighing 0.22 g. Taking the quantity of recovered trimer into account, the yield of thione was 82%.

We thank the National Research Council of Canada for financial support of this work.

1. (*a*) R. MAYER, J. MORGENSTERN, and J. FABIAN. Angew. Chem. Int. Ed. Engl. **3**, 277 (1964). (*b*) S. BLEISCH and R. MAYER. Chem. Ber. **100**, 92 (1967).
2. D. PAQUER and J. VIALLE. Bull. Soc. Chim. France, 3595 (1969).
3. E. CAMPAIGNE. Chem. Rev. **39**, 1 (1946). A. SCHÖNBERG. *In* Methoden der organischen chemie. Vol. IX, 4th ed. *Edited by* E. MÜLLER. G. Thieme Verlag, Stuttgart, 1955. p. 704.
4. E. G. HOWARD, JR. and W. J. MIDDLETON. U.S. Pat. 2970173 (1961); Chem. Abstr. **55**, 14311 (1961).
5. Y. KITIHARA and M. FINAMIZU. Bull. Chem. Soc. Japan, **37**, 1897 (1964). G. LABAN, J. FABIAN, and R. MAYER. Z. Chem. **8**, 414 (1968).
6. E. U. ELAM and H. E. DAVIS. J. Org. Chem. **32**, 1562 (1967).
7. C. N. R. RAO and R. VENKATARAGHAVAN. Spectrochim. Acta, **18**, 541 (1962).
8. E. CAMPAIGNE. *In* The chemistry of the carbonyl group. 1st ed. *Edited by* S. Patai. Interscience Publishers, New York, N.Y., 1966. p. 938.
9. C. DJERASSI and D. HERBST. J. Org. Chem. **26**, 4675 (1961).
10. R. MAYER, G. HILLER, M. NITZSCHKE, and J. JENTZSCH. Angew. Chem. Int. Ed. Engl. **2**, 370 (1963).
11. J. W. GREIDANUS and W. J. SCHWALM. Can. J. Chem. **47**, 3715 (1969).
12. G. SNATZKE and D. MARQUARDING. Chem. Ber. **100**, 1710 (1967). G. SNATZKE and G. ECKHARDT. Chem. Ber. **101**, 2010 (1968). W. S. BRIGGS, M. SUCHY, and C. DJERASSI. Tetrahedron Lett. 1097 (1968). G. SNATZKE and G. ECKHARDT. Tetrahedron, **24**, 4543 (1968).
13. M. DEMUYNCK and J. VIALLE. Bull. Soc. Chim. France, 1213 (1967).
14. J. FABIAN and R. MAYER. Spectrochim. Acta, **20**, 299 (1964).
15. H. W. GELUK and J. L. M. A. SCHLATMANN. Tetrahedron, **24**, 5361 (1968).
16. A. OHNO, T. KOIZUMI, and G. TSUCHIHASHI. Tetrahedron Lett. 2083 (1968).

17. S. SEARLES and D. L. SINCLAIR. 157th National Meeting of the American Chemical Society, Minneapolis, Minn., April 1969, Abstr. No. ORGN 128.
18. J. W. APSIMON, P. V. DEMARCO, D. W. MATHIESON, W. G. CRAIG, A. KARIM, L. SAUNDERS, and W. B. WHALLEY. Tetrahedron, **26**, 117 (1970).
19. P. V. DEMARCO, D. DODDRELL, and E. WENKERT. Chem. Commun. 1418 (1969).
20. T. LEDAAL. Tetrahedron Lett. 1683 (1968).
21. J. D. CONNOLLY and R. MCCRINDLE. Chem. Ind. (London), 379 (1965).
22. D. H. WILLIAMS and N. S. BHACCA. Tetrahedron, **21**, 1641 (1965); **21**, 2021 (1965). D. H. WILLIAMS and D. A. WILSON. J. Chem. Soc. (B), 144 (1966). M. FÉTIZON, J. GORÉ, P. LASZLO, and B. WAEGELL. J. Org. Chem. **31**, 4047 (1966).
23. F. W. VAN DEURSEN and P. K. KORVER. Tetrahedron Lett. 3923 (1967).
24. E. MÜLLER and G. FIEDLER. Chem. Ber. **98**, 3493 (1965). E. MÜLLER and H. G. PADEKEN. Chem. Ber. **99**, 2971 (1966).
25. C. R. CARPENTER. Ph.D. Thesis. The Pennsylvania State University, University Park, Pennsylvania, 1967.
26. H. WELZ. U.S. Pat. 2818380 (1957); Chem. Abstr. **52**, 9202*i* (1958).
27. C. C. HOBBS, JR. and B. HOUSTON. J. Amer. Chem. Soc. **76**, 1254 (1954); A. TILLOTSON and B. HOUSTON. J. Amer. Chem. Soc. **73**, 211 (1951).
28. H. W. GELUK and J. L. M. A. SCHLATMANN. Chem. Commun. 426 (1967). N. V. PHILIPS' GLOEILAMPENFABRIEKEN. Neth. Appl. 6509139 (1967); Chem. Abstr. **67**, 73246*c* (1967).

Can. J. Chem. Downloaded from www.nrcresearchpress.com by 210.87.254.105 on 09/05/12
For personal use only.

Can. J. Chem. Downloaded from www.nrcresearchpress.com by 210.87.254.6 on 09/05/12
For personal use only.

Multiple resonance n.m.r. study of 2α-fluoro-cholestan-3-one

C. W. M. GRANT[1] AND L. D. HALL
Department of Chemistry, The University of British Columbia, Vancouver 8, British Columbia

Received June 11, 1970

A detailed n.m.r. study has been made of 2α-fluoro-cholestan-3-one, with particular emphasis on the parameters of the nuclei attached to ring A. This study illustrates the potential of $^1H-\{^{19}F\}$ and $^{19}F-\{^1H\}$ heteronuclear decoupling experiments and of the $^1H-\{^1H\}$ INDOR technique as adjuncts to n.m.r. studies of fluorinated, and other, steroid derivatives.

Canadian Journal of Chemistry, 48, 3537 (1970)

Introduction

Although many studies of steroid derivatives by ^1H n.m.r. spectroscopy have amply demonstrated the power of this technique (1) for structural elucidation, it is obvious that the method also has many serious limitations. Of these, the most notable arises from the low sensitivity of proton chemical shifts with respect to changes in chemical and stereochemical environment. As part of a program to evaluate the potential of fluorine as a sensitive stereochemical probe for facilitating n.m.r. studies of steroids we have made a detailed study of 2α-fluoro-cholestan-3-one. In addition we have also investigated the potential of a variety of multiple resonance experiments, including the noise-modulated heteronuclear decoupling and $^1H-\{^1H\}$ INDOR[2] techniques. As will be seen, the latter technique enables one to probe successfully beneath the "methylene envelope" which, characteristically, complicates the ^1H n.m.r. spectra of steroids, and to determine the parameters of resonances which cannot be detected by direct measurement of the normal ^1H n.m.r. spectrum.

Experimental

All nuclear magnetic measurements were made with a modified Varian HA-100 spectrometer, operating in the frequency-swept mode.

The equipment required for the heteronuclear decoupling experiments has been described elsewhere (3). An account of the modifications necessary for the measurement of $^1H-\{^1H\}$ INDOR spectra has also been given previously (4).

The n.m.r. measurements were made with a *ca.* 25% (w/v) (0.63 *M*) solution of **1** in deuterochloroform containing sufficient trichlorofluoromethane, chloroform, or tetramethylsilane to establish a field-frequency lock. Since the tetramethylsilane interfered with the INDOR measurements, these were performed with the instrument locked onto the proton resonance of chloroform.

Analysis of the n.m.r. spectra were made with a modified version of the LAØCØØN III program, and an I.B.M. 360-67 computer in the U.B.C. Computer Centre.

2α-fluoro-cholestan-3-one (1) was prepared by the method described in the literature (5).

Results

The normal ^1H n.m.r. spectrum of **1** in a deuterochloroform–chloroform solution is given in Fig. 1*A*. The low field octet, assignable (*vide infra*) to the $H_{2\beta}$ proton exhibits a characteristically large (*ca.* 48 Hz) *geminal* coupling with the $F_{2\alpha}$ substituent. Irradiation at the resonance

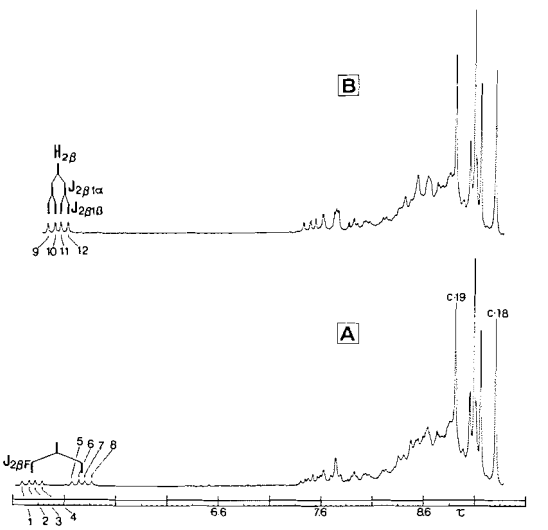

FIG. 1. The ^1H n.m.r. spectra (100 MHz) of 2α-fluoro-cholestan-3-one (**1**) in deuterochloroform–chloroform solution. A The normal proton spectrum. B The spectrum measured with simultaneous irradiation at the ^{19}F resonance frequency (94, 076, 140.0 Hz). The first-order assignment of the $H_{2\beta}$ resonance is indicated diagrammatically. The assignment of the *C*-methyl resonances follows previously established criteria (ref. 1).

[1]Recipient of an NRCC 1967 Science Scholarship, 1968–1970.

[2]An acronym coined by Baker (2) for InterNuclear DOuble Resonance.

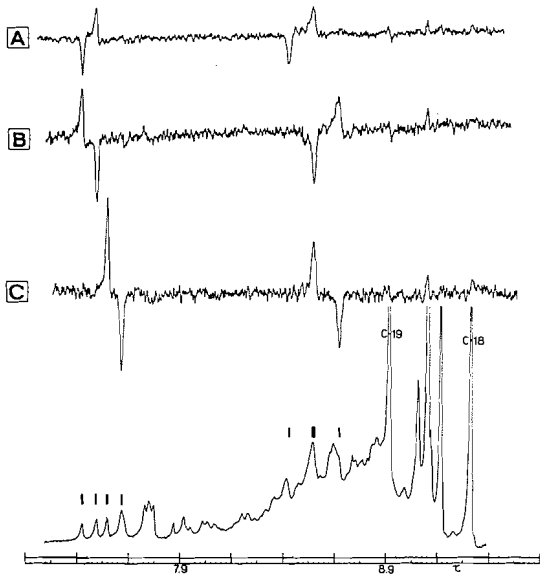

FIG. 2. The ^1H–{^1H} INDOR experiments performed on the ^{19}F decoupled spectrum of **1** in deuterochloroform–chloroform solution. Using the transition numbering system of Fig. 1, the spectrum in A corresponds to monitoring transition 12, B corresponds to monitoring transition 11, and C to transition 9. The composite assignment resulting from these spectra is shown diagrammatically above the normal proton spectrum. The chloroform resonance was used as the internal-reference signal for the field-frequency lock.

frequency of the fluorine substituent resulted (Fig. 1*B*) in the collapse of this octet to a quartet due to removal of the ^{19}F–$H_{2\beta}$ splitting. The changes which occur in the high-field region of Fig. 1*A* during fluorine decoupling are discussed later.

Two series of ^1H–{^1H} INDOR measurements were made. The first of these was performed[3] on the ^{19}F decoupled spectrum. The responses shown in Fig. 2*A* were obtained by monitoring transition 12 (using the numbering system of Fig. 1), while scanning a weak radio-frequency field through the methylene region. Sequential monitoring of transitions 11 and 9 gave the responses shown in Figs. 2*B* and *C*. The effective summation of these three sets of INDOR responses is shown diagrammatically above the normal spectrum in Fig. 2. It is important to note that for the purposes of this summation the frequency at which a particular transition gives an INDOR response is independent of whether the response is positive- or negative-going. The four, low-field INDOR responses confirm that the four, low field transitions of the normal spectrum belong to a single proton and indicate that it is one of the H_1 resonances. Perhaps more importantly the higher field set of INDOR responses now identify the transitions of the other H_1 resonance which are normally obscured by the resonances of the other methylene protons.

The second series of INDOR experiments, shown in Fig. 3, were obtained by monitoring in turn five of the transitions of the "normal" $H_{2\beta}$ resonance (no ^{19}F decoupling). Because of the decrease in the intensity of the transitions being monitored the effective signal-to-noise ratio for these responses is poorer than that of the responses shown in Fig. 2. Nevertheless, it is possible to make a summation of the individual

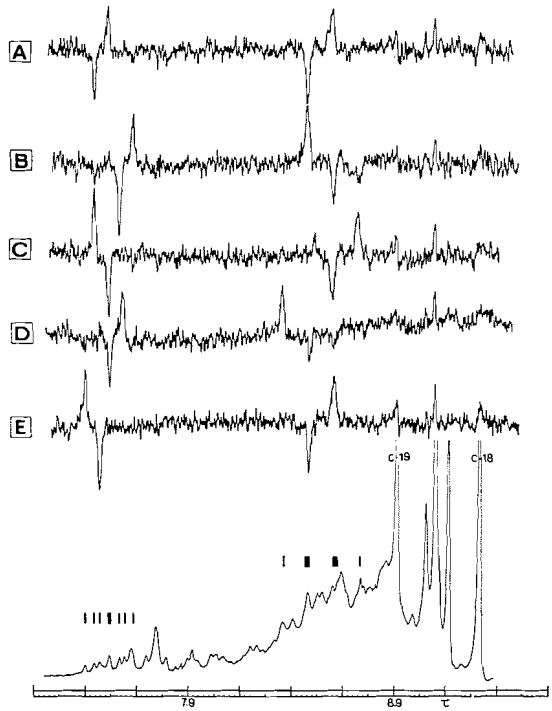

FIG. 3. The ^1H–^1H INDOR experiments performed on the normal spectrum of **1** in deuterochloroform–chloroform solution. The $H_{2\beta}$ transitions were monitored as follows: A transition 8; B transition 6; C transition 7; D transition 2; E transition 3. A diagrammatic summary of these responses is given above the normal spectrum. The chloroform resonance was used as the internal-reference signal for the field-frequency lock.

[3]All of the INDOR spectra shown in Figs. 2 and 3 were performed on a "first-run" basis and no special precautions were observed. To this extent, they may be regarded as "typical".

Can. J. Chem. Downloaded from www.nrcresearchpress.com by 210.87.254.6 on 09/05/12
For personal use only.

responses and obtain the complete set of transition frequencies for both of the H_1 resonances. Due to the fortuitous near equality of the spectral splittings, there is considerable degeneracy for the upfield C-1 proton.

In order to obtain a more complete set of n.m.r. parameters for ring A, it was necessary to identify the H_4 resonances. This was achieved as follows. Inspection of the lower field portion of the normal and ^{19}F decoupled methylene region (Fig. 4) indicated that in addition to the changes associated with the collapse of the known H_1 transitions, two further proton multiplets were subject to some decoupling; likely, these were from the H_4 protons.

Several of these transitions were clearly resolved and a series of INDOR experiments in which these transitions were monitored, made possible a reasonably accurate assignment, of the entire resonances of both the H_4 protons. Further responses were also observed around τ 8.4 and these were assigned to the H_5 resonance.

Close inspection of the INDOR spectra shown in Figs. 2 and 3 reveals that some responses occur at frequencies corresponding to the *C*-methyl resonances. Although it seems likely that these are instrumental artifacts arising from overloading of some amplifier stage in the spectrometer, further studies will be necessary before this rationale is proven.

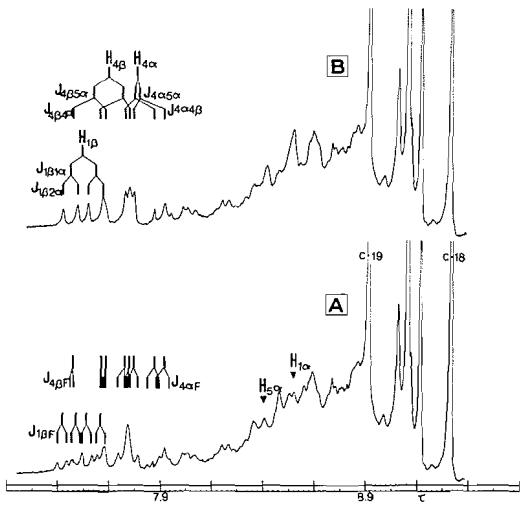

FIG. 4. Partial ^1H n.m.r. spectrum of the high field region of **1** in chloroform solution. The normal spectrum is shown in A, and the ^{19}F decoupled spectrum in B. The first-order assignments of these spectra were based on the data obtained from the INDOR experiments shown in Figs. 2 and 3 and from other INDOR measurements discussed in the text.

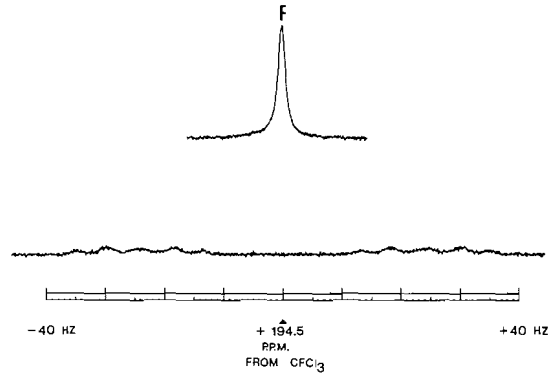

FIG. 5. ^{19}F n.m.r. spectra (94.07 MHz) of **1** in chloroform solution. The normal spectrum is shown in the lower trace. The inset was recorded at the same gain, but with simultaneous irradiation of the entire ^1H spectrum using a noise-modulated radio-frequency centered at 99,997,945.0 Hz.

The normal ^{19}F spectrum of **1** is shown in Fig. 5. The comparatively poor resolution of this spectrum is due to the fact that the ^{19}F substituent is part of a highly coupled proton spectrum and to the presence of a number of small, long-range couplings. In addition to the large *geminal* coupling with $H_{2\beta}$ (*ca.* 48 Hz) a number of smaller proton couplings are resolved.

Discussion

The experiments discussed in the previous section of this paper served to identify the resonances of all of the protons associated with ring A of derivative **1**. Comparison of the transitions assigned to the "normal" and ^{19}F decoupled resonances of $H_{1\alpha}$ and $H_{1\beta}$ provided an estimate of the magnitudes of the ^1H–^1H and ^{19}F–^1H couplings, which proved to be in reasonable accord with the estimates obtained by direct measurement of the ^{19}F spectrum (Fig. 5). These data are included in Table 1. Simulation of the spectra of the H_1 and $H_{2\beta}$ resonances using the parameters involving these three nuclei and the $F_{2\alpha}$ substituent, gave calculated transition energies which were in close accord with the experimental values; on this basis it was concluded that a full, iterative analysis was unnecessary. Interestingly, the ^1H–^1H couplings listed in Table 1 are identical, within experimental error, with those previously reported by Allinger *et al.* (6) for 2α-fluoro-5α-androstane-3,17-dione.

Can. J. Chem. Downloaded from www.nrcresearchpress.com by 210.87.254.6 on 09/05/12
For personal use only.

TABLE 1

Nuclear magnetic resonance parameters for the ring A resonances of 2α-fluoro-cholestan-3-one

Nucleus	Chemical shifts (τ-values, ϕ_c-value)*						
	$H_{1\alpha}$ 8.52	$H_{1\beta}$ 7.52	$H_{2\beta}$ 5.01	$H_{4\alpha}$ 7.79	$H_{4\beta}$ 7.65	H_5 8.47	$F_{2\alpha}$ ϕ_c + 194.5
	Coupling constants (Hz)						
$J_{1\alpha,1\beta}$ −12.2†	$J_{1\alpha,2\beta}$ 12.3†	$J_{1\beta,2\beta}$ 6.9†	$J_{F,2\beta}$ 48.0†	$J_{F,1\alpha}$ 11.5†	$J_{F,1\beta}$ 4.5†		
$J_{4\alpha,4\beta}$ −13.9‡	$J_{4\alpha,5\alpha}$ 2.06‡	$J_{4\beta,5\alpha}$ 14.43‡	$J_{F,4\alpha}$ 7.3‡	$J_{F,4\beta}$ −2.0§	$J_{F,5\alpha}$ ~0		

*Measured in deuterochloroform solution containing $CHCl_3$, $CFCl_3$ or TMS.
†The estimated error for these parameters is ±0.2 Hz.
‡The estimated error for these parameters is ±0.4 Hz.
§Estimated error ± 1.0 Hz.
NOTE: The error figures indicated by ‡ and § represent the limits between which the coupling constants were found to vary when the individual transitions were varied over the maximum possible limits.

Evaluation of the parameters of the H_4 and H_5 resonances proved to be more difficult. In spite of the small chemical shift separation of the two H_4 resonances a satisfactory estimate of the interproton couplings was readily made by examination of the ^{19}F decoupled spectra and by iterative, computer-based, analysis involving the $H_{4\alpha}$, $H_{4\beta}$, and H_5 resonances. However, because of several fortuitous degeneracies, many attempts were required before a full analysis which included the ^{19}F couplings could be made. It should be noted that the presence of a spin-1/2 heteronucleus was crucial for these assignments since in its absence it would have been impossible to assign the $H_{4\alpha}$ and $H_{4\beta}$ resonances. The ^{19}F–$H_{4\alpha}$ coupling was assigned an absolutely positive sign on the basis of previous studies (7).

We turn now to consider the conformational significance of the coupling constants determined for **1**. In a previous study, Abraham and Holker (8) had rationalized the *vicinal* H_1–H_2 couplings of the 2α-bromo analog (**2**) of the derivative we were studying, in terms of a slightly distorted chair conformation for ring A. Since the H_1–H_2 couplings of **1** are closely similar to those of **2** it seems probable that both systems have similar conformations. The remaining couplings determined for **1** appear to support this contention and hence, indirectly, the validity of the previous conclusions. Thus, the $H_{4\beta,5}$ coupling of 14.4 Hz clearly accords with a *trans-diaxial* relationship between these two protons. Furthermore, the magnitudes of the *vicinal* ^{19}F–^1H couplings are only consistent with a *gauche* relationship between the $F_{2\alpha}$ substituent and the two protons at C_1. Although there is a paucity of data concerning $^4J_{F,H}$ couplings the values listed in Table 1 for the couplings between $F_{2\alpha}$ and $H_{4\alpha}$ and $H_{4\beta}$ appear to be in reasonable accord with expectation (7).

One of the more interesting points which we wished to evaluate in the course of this study, was whether it might be possible to use a fluorine substituent to label a specific site of a steroid molecule for subsequent n.m.r. studies. It is obvious from the normal ^{19}F spectrum of **1**, shown in Fig. 5, that conventional ^{19}F measurements have little to recommend them. However, the detection of a ^{19}F resonance whilst simultaneously irradiating the proton spectrum appears to be a more attractive proposition. In the case of **1**, the ^1H resonances were spread over *ca.* 4.5 p.p.m. and continuous-wave ^{19}F–$\{^1H\}$ decoupling experiments only resulted in partial collapse of the proton couplings. However, noise-modulated ^{19}F–^1H decoupling effectively removed all of the proton couplings and, as is indicated in the insert of Fig. 5, the ^{19}F resonance was then detected as a reasonably sharp singlet.

In conclusion, it seems obvious that ^{19}F–$\{^1H\}$ and ^1H–$\{^{19}F\}$ heteronuclear decoupling experiments can considerably facilitate n.m.r. studies of fluorinated steroidal systems. In particular, the observation that noise-modulated irradiation of the entire ^1H spectrum can effectively reduce a ^{19}F resonance to a narrow singlet augurs well for the future of fluorine as a probe for evaluating the interaction of steroidal derivatives with other systems of biochemical significance, such as membranes. We also conclude that ^1H–$\{^1H\}$ INDOR measurements should find widespread application in a number of structural problems

Can. J. Chem. Downloaded from www.nrcresearchpress.com by 210.87.254.6 on 09/05/12
For personal use only.

commonly encountered in steroid chemistry. Clearly, the presence of a fluorine substituent is not a necessary prerequisite for such measurements.

This work was supported by the National Research Council of Canada. It is a pleasure to thank Paul Steiner of this laboratory for his advice concerning the INDOR measurements.

1. D. H. WILLIAMS and N. S. BHACCA. Applications of n.m.r. in organic chemistry. Holden-Day, 1964.
2. E. B. BAKER. J. Chem. Phys. **37**, 911 (1962).
3. R. ERNST. J. Chem. Phys. **45**, 3845 (1966); R. BURTON and L. D. HALL. Can. J. Chem. **48**, 59 (1970).
4. R. BURTON, L. D. HALL, and P. R. STEINER. Can. J. Chem. **48**, 2679 (1970).
5. S. NAKANISHI, K. MORITA, and E. JENSEN. J. Amer. Chem. Soc. **81**, 5259 (1959).
6. N. L. ALLINGER, M. A. DAROOGE, M. A. MILLER, and B. WAEGELL. J. Org. Chem. **28**, 780 (1963).
7. T. A. WITTSTRUCK, S. K. MALHOTRA, H. J. RINGOLD, and A. D. CROSS. J. Amer. Chem. Soc. **85**, 3038 (1963).
8. R. J. ABRAHAM and J. S. HOLKER. J. Chem. Soc. 806 (1963).

Can. J. Chem. Downloaded from www.nrcresearchpress.com by 210.87.254.6 on 09/05/12
For personal use only.

Can. J. Chem. Downloaded from www.nrcresearchpress.com by 210.87.254.105 on 09/05/12
For personal use only.

Studies in ferrocene derivatives. IX.[1] The dimerization of α-ferrocenyl carbonium ions[2]

W. M. HORSPOOL,[3] R. G. SUTHERLAND,[4] AND J. R. SUTTON
Department of Chemistry and Chemical Engineering, The University of Saskatchewan, Saskatoon, Saskatchewan
Received October 10, 1969[5]

Ferrocenylethylenes dissolve in 90% HCOOH to give solutions of the α-ferrocenyl carbonium ions in equilibrium with the unprotonated species. These subsequently react by an ionic-addition mechanism to give dimeric carbonium ions which can cyclize by both homo- and heteroannular pathways.

Canadian Journal of Chemistry, 48, 3542 (1970)

Both ferrocenylethylenes (1) and the corresponding carbinols (2) are protonated by strong acids to form α-ferrocenylcarbonium ions. These ions are stable, and give well resolved n.m.r. spectra. The stability of these carbonium ions, and the stereoselectivity of their reactions has given rise to speculation, and considerable controversy as to the electronic and structural factors responsible for this stability (3). In view of our work with ferrocenylethylenes, it was decided to investigate the acid strengths necessary for half-protonation of a series of these alkenes as a more direct probe of the stability of these carbonium ions rather than the kinetic approach previously adopted. During this work we observed that at acid strengths close to that required for half-protonation[6] an irreversible reaction of these carbonium ions took place and it was decided that this reaction required further investigation. At this time the possibilities of hydride transfer to α-ferrocenyl carbonium ions was also under study. Since the alkenes were readily protonated, and it was known that the formate ion was a good hydride donor (4), the protonation of ferrocenylethylenes by formic acid was investigated. It was found that these alkenes dissolved readily in 90% HCOOH to give a red solution which quickly becomes turbid, and an immiscible oil separated out in less than 2 min. A comparison of the reaction mixtures showed that the same product mixture was obtained in 40% H_2SO_4 and 90% HCOOH. This is not too surprising, since both acids have approximately the same strength, acidity function $Hr = -4.7$. Further experiments showed that the same reaction mixture was obtained no matter whether a ferrocenylethylene or the corresponding carbinol was used as substrate. It was also found that the reaction was a general one for all potential α-ferrocenyl carbonium ions, and that similar product mixtures could be obtained from potential 1-1[1]-ferrocenyl dications.

All of these reaction mixtures were extremely difficult to handle experimentally, and it was decided to concentrate our attention on the carbonium ion derived from 2-ferrocenylpropene **1**. Examination of the mass spectrum of the red oil derived from **1** after reaction in 90% HCOOH gave a molecular ion at *m/e* 452. The product is dimeric and it was first thought that it might have the structure **2**. This would be the expected product of an ionic addition mechanism, and would correspond to the product recently isolated by Goldberg *et al.* (5) from an alumina-catalyzed dehydration of 1-ferrocenylethanol. Although the analytical and mass spectra data fitted **2** the n.m.r. spectrum was significantly different. In particular, it lacked any proton resonance which could be confidently assigned to the olefinic proton, and additionally, the methyl region of the spectrum was exceedingly complex showing six non-equivalent methyl groups. The i.r. data was ambiguous with regard to the presence or absence of a double bond. Because of this several attempts were made to hydrogenate the product under increasingly severe conditions. No uptake of hydrogen was observed. This ruled out structure 2 since the hydrogenation of other ferrocenylbutenes, which had been synthesized unam-

[1]For part VIII see W. M. Horspool *et al.* (15).
[2]Reported in part at the 158th A.C.S. National Meeting, New York, N.Y., September 8–12, 1969. Abstract Orgn. 87.
[3]Department of Chemistry, The University, Dundee, Scotland.
[4]The author to whom correspondence may be addressed.
[5]Revision received June 16, 1970.
[6]2-Ferrocenylpropene is 1/2 protonated in 40% w/w H_2SO_4.

Can. J. Chem. Downloaded from www.nrcresearchpress.com by 210.87.254.105 on 09/05/12
For personal use only.

TABLE 1
Properties of dimers

Dimer	Molecular weight	C (%)	H (%)	Melting point (°C)
A	452	68.56	6.0	185–186
B	452	69.18	6.2	105–106
$C_{26}H_{28}Fe_2$	452	69.1	6.2	

biguously, could be accomplished under mild conditions.

At this stage the dimeric nature of the product had been established as had the lack of olefinic unsaturation which led to the conclusion that a ring was present in the product(s). Low temperature fractional crystallization showed that the oil was, in fact, a mixture. Crystallization from Skellysolve F at −70° gave dimer *A* as yellow crystals; the residue eventually crystallized when the solvent was changed to pentane to give dimer *B*. The properties of the dimers are given in Table 1. The resonance absorptions of both compounds account for all peaks observed in the crude dimeric mixture. The total yield of *A* and *B* was 85%, and the yields of *A* and *B*, based on integration of the n.m.r. spectrum, were 34 and 51% respectively.

Reaction Scheme I suggests that three saturated dimers may be formed. 2-Ferrocenylpropene (**1**) is protonated by the reaction medium to form the dimethyl-ferrocenyl carbonium ion which is attacked by a further molecule of **1** to give the dimeric carbonium ion **3**. Rather than deprotonate to form **2**, the carbonium ion **3** attacks the cyclopentadienyl rings to form either **4** or **5**, the former resulting from heteroannular cyclization, the latter from homoannular cyclization.

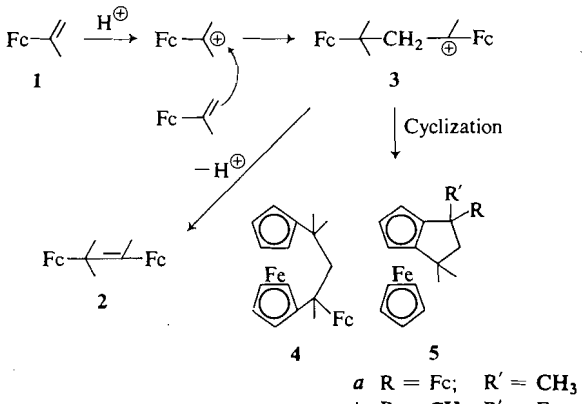

a R = Fc; R′ = CH_3
b R = CH_3; R′ = Fc

SCHEME 1

This scheme leads to three possible saturated structures, **4**, **5***a*, and **5***b* where the ferrocenyl substituent is *exo* (**5***a*) or *endo* (**5***b*) to the other iron atom. Two saturated dimers, *A* and *B*, were isolated from the reaction mixture and the n.m.r. spectra for *A* and *B* are recorded in Table 2.

The n.m.r. spectra of *A* and *B* are very similar, but quite distinct. They each have 17 ring protons, three methyl groups and one methylene group. Compelling evidence for a bridge in both *A* and *B* comes from the methylene resonance signal. In both cases this appears as an AB quartet at 60 MHz and can be assigned to a methylene group in a ring system with no protons on the adjacent carbon atoms; the *J* value of 12 Hz is also consistent with geminal coupling. More detailed analysis of the AB quartets by standard methods shows that the line separation in isomer *A* is 33 Hz which means that the true line positions are 7.45 and 7.95 τ respectively, while in isomer *B* the line separation is 45 Hz with the true line positions at 7.13 and 7.87 τ respectively. These spectra are compatible with both structures **4** and **5**.

The cyclization of suitable ferrocenealkanecarboxylic acids to give bridged ferrocenes has been investigated by many workers (8). All of these results show that three carbon units lead to [3] ferrocenophanes while four carbon units give homoannular cyclization exclusively. Very few exceptions are known; thus α,α-dimethyl-β-ferrocenyl propionic acid gave a 1:1 mixture of the homo- and heteroannularly cyclized products under forcing conditions (9). This information would lead us to expect that a carbonium ion such as **3** would cyclize heteroannularly to give **4** as the major product. However, the bulky ferrocenyl substituent could retard heteroannular cyclization leading to the formation of **5***a* or *b*. Unfortunately, it would be very difficult to distinguish between **5***a* and *b*, but it appears more likely that the bulky ferrocenyl group would be *exo* during the cyclization step and so **5***a* appears to be a more likely structure.

The problem then is to assign structures to dimers *A* and *B*. The latter compound was obtained in the greater yield and since heteroannular cyclization should be preferred we have given dimer *B* structure **4**. Additionally, the n.m.r. spectrum of dimer *A* is more compatible with **5** than **4**. Thus the methylene proton which is at highest field is that at 7.95 τ and it seems more likely that in the methylene group of the homo-

TABLE 2

The n.m.r. spectra for dimers *A* and *B**

Protons	Dimer *A*	Dimer *B*	Integral
Ring	6.6(b), 6.1(b), 5.95(b) 5.88(bs), 5.75(bs)	6.4(b), 6.2(b), 6.12(s) 5.83(s), 5.6(b)	17
Methyl	9.14(s), 8.64(s), 8.09(s)	8.75(s), 8.5(s), 8.4(s)	9
Methylene	7.7† (J = 12 Hz)	7.5‡ (J = 12 Hz)	2

*Spectra are reported in τ, solvent $CDCl_3$; s, singlet; b, broad; bs, broad singlet.
†Center of AB quartet.

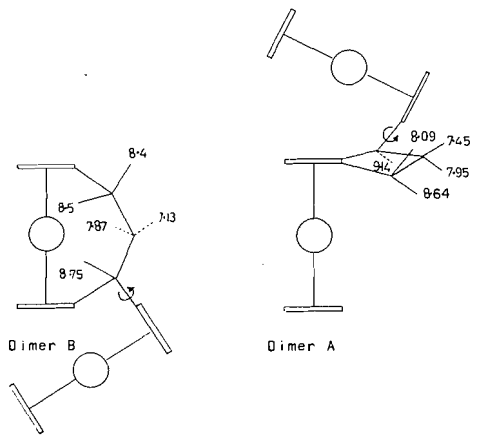

Fig. 1. Structure of dimers *A* and *B*.

annularly cyclized product **5***a*, one of the hydrogens will be in the field of the iron atom, *i.e.* effectively an "*endo*" situation whereas the other hydrogen will not be affected by such a shielding.[7] Our tentative assignments are shown in Fig. 1.

Experimental

Ferrocenylethylenes were prepared as previously described (6, 7). The n.m.r. spectra were recorded on a Varian A60 spectrometer in $CDCl_3$ solution. Mass spectra were recorded on an A.E.I., M.S. 12 instrument.

Reaction of 2-Ferrocenylpropene in 90% HCOOH

2-Ferrocenyl-2-propene (1.01 g, 0.04 mole) was added to rapidly stirred HCOOH (90%, 15 ml) over 8 min under a nitrogen atmosphere. The mixture was allowed to stand for 10 min while an oil separated out. The mixture was extracted with benzene (15 ml). The benzene layer was separated, washed free of acid (H_2O), dried (Na_2SO_4), and solvent removed. A viscous golden–yellow oil (0.84 g, 85%) remained. Crystallization was effected using Skellysolve F as solvent at −70 °C when a bright yellow solid was obtained. Repeated crystallization gave compound *A*, m.p. 185–186 °C. The solvent was changed to pentane when an isomer, compound *B*, was obtained, m.p. 105–106 °C. The yield of *A* and *B* as determined from n.m.r. spectra was 34 and 51% respectively.

The dimer can be separated from monomer by v.p.c. using 10% S.E. 30 on Chromosorb W (acid washed, D.M.C.S. treated) on a column 8′ × 1/8″. R_T of alkene is *ca.* 1 min and the dimeric mixture *ca.* 5 min at 225 °C.

We thank the University of Saskatchewan for the award of a research assistantship (J.R.S.) and the National Research Council of Canada for generous financial assistance.

[7]The assignment of the *endo* proton to the high field resonance is controversial. However, a considerable amount of support can be found for this assignment (10). The molecular anisotropy studies of Mulay *et al.* (11, 12) suggest that *endo* protons in ferrocenes should be deshielded. Unpublished results quoted in Abbate's thesis (13) show that the *endo* side of the ferrocene molecule is deshielding at one carbon distance from the ferrocene nucleus; however, the hydroxylic protons of ferrocenyl carbinols experience an upfield shift when in the vicinity of the metal (7, 14). Clearly more work is required in this area.

1. W. M. Horspool and R. G. Sutherland. Chem. Commun. 786 (1967).
2. M. Cais, J. J. Dannenberg, A. Eisenstadt, M. I. Levenberg, and J. H. Richards. Tetrahedron Lett. 1965 (1966).
3. (*a*) M. Cais. Organometal. Chem. Rev. 1, 435 (1966). (*b*) J. Feinberg and M. Rosenblum. J. Amer. Chem. Soc. **91**, 4324 (1969). (*c*) E. A. Hill and R. Wiesner. J. Amer. Chem. Soc. **91**, 509 (1969). (*d*) T. G. Traylor and J. C. Ware. J. Amer. Chem. Soc. **89**, 2304 (1967).
4. R. Grinter and S. F. Mason. Trans. Faraday Soc. 60, 889 (1964).
5. S. I. Goldberg, W. D. Loeble, and T. T. Tidwell. J. Org. Chem. **32**, 4070 (1967).
6. W. M. Horspool and R. G. Sutherland. Can. J. Chem. **46**, 3453 (1968).
7. W. M. Horspool, R. G. Sutherland, and J. R. Sutton. Can. J. Chem. **47**, 3085 (1969).
8. M. Rosenblum. Chemistry of the iron group metallocenes. Ferrocene, Ruthenocene, Osmocene. Pt. John Wiley and Sons, N.Y., 1965.
9. M. Rosenblum, A. K. Banerjee, N. Danieli, R. W. Fish, and V. Schlatter. J. Amer. Chem. Soc. **85**, 316 (1963).
10. M. L. Maddox, S. L. Stafford, H. D. Kaesz. Adv. Organometal. Chem. **3**, 1965.
11. L. N. Mulay and A. Attalla. J. Chem. Phys. **38**, 760 (1963).
12. L. N. Mulay and M. E. Fox. J. Chem. Phys. **38**, 760 (1963).
13. R. W. Fish and M. Rosenblum. Unpublished results, quoted by F. Abbate. Ph.D. Thesis. Brandeis University, Boston, Mass., 1966. p. 46.
14. E. A. Hill and J. H. Richards. J. Amer. Chem. Soc. **83**, 3840 (1961).
15. W. M. Horspool, R. G. Sutherland, and B. J. Thomson. Tetrahedron Lett. 2853 (1969).

Can. J. Chem. Downloaded from www.nrcresearchpress.com by 210.87.254.105 on 09/05/12
For personal use only.

Can. J. Chem. Downloaded from www.nrcresearchpress.com by 210.87.254.40 on 09/05/12
For personal use only.

Isobutane from acid-catalyzed dehydration of butanols

JOHN WARKENTIN AND KENNETH E. HINE[1]
Department of Chemistry, McMaster University, Hamilton, Ontario
Received January 5, 1970

Dehydration of the four isomeric butanols by strong acid at about 160° gives a C_4-fraction containing isobutane as well as the isomeric butenes. Isobutane probably arises by hydride transfer, from one or more donors including the substrate alcohol and hydrocarbons formed from it in the medium, to one or more carbonium ions including the *t*-butyl cation. Materials which react with 2,4-dinitrophenylhydrazine reagent to form 2,4-dinitrophenylhydrazones can be swept out of the hot acid solution with a stream of nitrogen.

Canadian Journal of Chemistry, 48, 3545 (1970)

Introduction

In the course of an experiment illustrating the utility of gas chromatography as an analytical tool (1) we found that acid catalyzed dehydration of 1- and 2-butanol yields an extra product which is eluted well before the isomeric butenes. Speculation that it might be methylcyclopropane (2) or an acyclic, saturated hydrocarbon (3) led us to treat the mixture with alkaline permanganate to destroy the alkenes. The remaining gas was shown, by comparison of the p.m.r. spectrum and of the g.l.p.c. retention time with those of authentic material, to be isobutane. It is formed also during dehydration of isobutyl alcohol and *t*-butyl alcohol.

Saturated hydrocarbons have been identified before among the products from treatment of alcohols with strong acid. Deno *et al.* (3) found that treatment of butanols, or of 2,2,4-trimethylpentenes, with 96% H_2SO_4 at 25° gave a hydrocarbon fraction the carbon content of which ranged principally from C_5–C_{18}. A small C_4-fraction was not identified further. Corresponding oxidized products include dienes and allylic cations with which they are in equilibrium (3). Although a direct comparison of our product mixture, from dehydration under preparative conditions at high temperature, with that of Deno *et al.* (3) is not warranted, it is likely that their C_4-fraction was also mostly isobutane and that the same mechanism operates under both sets of conditions. Presumably that mechanism is hydride transfer from a donor to a carbonium ion. Known donors of hydride ion to carbonium ions include alkenes (3), hydrocarbons (4), alcohols (5), and formic acid (6). Immediate cationic precursors of isobutane could be the *t*-butyl cation, the isobutyl cation or protonated methylcyclopropane (2).

The primary objective of this report is to communicate the identity of the saturated C_4-fragment and the dependence of the relative yield on alcohol structure. Some experiments aimed at identification of the sources of isobutane are also described.

Results and Discussion

Dehydration of alcohols by hot mineral acids is a complex process producing many products, the ratios of which are not highly reproducible. Part of the problem may stem from rearrangement of first-formed alkenes; a complication that can be overcome partly by sweeping the products out of the hot acid medium with an inert gas (Experimental section). In spite of this precaution the relative yields varied considerably, as did overall yields. The results are gathered in Table 1.

The striking features of the dehydrations are

TABLE 1

Dehydration of butanols at 164 ± 2° by H_2SO_4 in H_3PO_4*

C_4-Alcohol fed	Product distribution (relative percent)† Isobutane	1-Butene and isobutene‡	*trans*-2-Butene	*cis*-2-Butene
n-Butyl§	5–19	20–51	22–47	16–27
sec-Butyl§	2–6	31–46	29–36	23–27
iso-Butyl‖	25–43	42–66	7–11	2–5
t-Butyl‖	0.5–2.0	98–99	Trace	Trace

*Volume percent: H_2SO_4, 10; 85% H_3PO_4, 90.
†Overall yields of volatile C_4-products ranged from about 15% for *n*-butyl alcohol to 45% for *t*-butyl alcohol.
‡1-Butene and isobutene were not well separated in the column and are given together.
§Results represent the ranges from at least six runs. Two-fold decreases in the rate of sweeping with N_2 or in the rate of addition of alcohol did not cause the product distribution to leave the normal range.
‖Three runs.

[1]Much of this work was done by K.E.H. as part of a final-year, undergraduate laboratory course.

TABLE 2

Dehydration of mixtures of alcohols and of *n*-butyl-*t*-butyl ether

Reactants*	Acid†	Temperature (°C)	Product distribution (relative percent)			
			Isobutane	1-Butene and isobutene	*trans*-2-Butene	*cis*-2-Butene
Iso- and *t*-butyl alcohols (1:1)	1:9	170 ± 3	4.0	94.5	trace	trace
Iso- and *t*-butyl alcohols (3:1)	1:9	165 ± 2	6.3	89.5	2.0	1.4
n-Octyl and *t*-butyl alcohols (4:1)	1:9	165 ± 3	7.0	86.8	6.2	trace
n-Butyl-*t*-butyl ether	1:9	162–153	6.0	81.5	6.5	5.1
n-Butyl-*t*-butyl ether	1:9	97–95	4.3	87.2	3.8	3.0
n-Butyl-*t*-butyl ether	1:16	70–75	3.8	87.0	3.8	1.4

*The bracketed ratios refer to volumes and are in the order of listing of the components.
†H_2SO_4: 85% H_3PO_4, by volume.

the large fractions of isobutane that can be obtained and the fact that isobutyl alcohol gives the highest fraction of that product.

Several probes were made for likely sources of hydride ion. To detect transfer of the α-hydrogen from alcohols, eq. 1, or from their inorganic

[1] 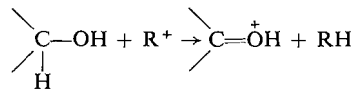

esters formed in the medium, the effect of feeding mixed alcohols (1° + 3°) was determined. A mixed ether, $(CH_3)_3COCH_2CH_2CH_2CH_3$, was also fed because it should provide the strongest test for the reaction of eq. 1. By leaving a molecule of *n*-butanol in the immediate proximity of a *t*-butyl cation, eq. 2, the system provides for a high local concentration of potential reducing agent. Table 2 gives the results of those experiments.

[2] 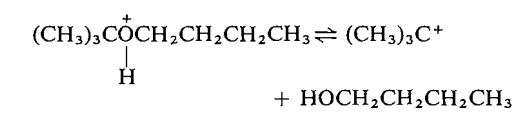

Although the relative yields of isobutane are increased (Table 2) by feeding an alcohol with alpha hydrogens along with *t*-butyl alcohol, or by feeding the ether, the increases over the yields from *t*-butyl alcohol alone (Table 1) are modest. This result, together with the fact that *t*-butyl alcohol alone gives isobutane, indicates that alpha hydrogens of alcohols are not the only available sources of hydride. In a highly-acidic medium, alcohols presumably are relatively poor reducing agents because protonation keeps the concentration of free alcohol low (eq. 1) or, in the case of eq. 2, because the lifetime of a newly-formed molecule of alcohol is short.

That alpha hydrogen transfer does occur was also indicated by the formation of carbonyl products, as required by eq. 1. Rapid bubbling of N_2 through the hot acid medium in a large-scale dehydration of isobutyl alcohol gave a liquid fraction which reacted with 2,3-dinitrophenylhydrazine. The purified product had λ_{max}(EtOH) 361 mμ in the u.v. spectrum, indicating the absence of α,β-unsaturation (7). There was no vinyl absorption in the ^1H spectrum and comparison with the n.m.r. spectrum of isobutyraldehyde-2,4-dinitrophenylhydrazone showed that the latter and other aldehyde derivatives were absent. In the mass spectrum the highest value of *m/e* was 308, which fits the formula ($C_{14}H_{20}N_4O_4$) for the dinitrophenylhydrazone of a saturated C_8-ketone. The complex n.m.r. spectrum (220 MHz) indicated a mixture, probably including geometric isomers. Separation and further identification was not attempted because the carbonyl components swept out may well represent only a small fraction of the total formed in the reactions. The presence of a C_8-ketone and the absence of isobutyraldehyde indicate clearly enough that the formation of carbonyl compounds is also complex, like the

Can. J. Chem. Downloaded from www.nrcresearchpress.com by 210.87.254.40 on 09/05/12
For personal use only.

Can. J. Chem. Downloaded from www.nrcresearchpress.com by 210.87.254.40 on 09/05/12
For personal use only.

hydrocarbon formation studied by Deno *et al.* (3).

Second and third increments of isobutyl alcohol were added to a dehydrating medium to probe for reduction of cations by the non-volatile organic residues that build up in the reaction vessel. The three batches of product showed no trend toward an increase in the relative yield of isobutane. This result suggests that the more effective hydride donors among the residues are relatively short-lived intermediates.

The identity of one important cationic precursor of isobutane can be inferred from some of the results. Low temperature hydrolysis of *n*-butyl-*t*-butyl ether (Table 2) left the *n*-butyl alcohol largely undehydrated, as indicated by the low yields of 2-butenes, but led to significant increases in the relative yields of isobutane, compared to those from *t*-butyl alcohol alone. Whatever the hydride donors are, it is very likely that the major acceptor under the mild conditions is the *t*-butyl cation. The same long-lived cation probably gives rise to most of the isobutane at the higher temperatures also, although some could come from the isobutyl cation or from protonated methylcyclopropane.[2]

It is not clear why isobutyl alcohol gives consistently higher relative yields of isobutane than the other butanols. Perhaps it surpasses 1-butanol and 2-butanol in this respect because it can form the *t*-butyl cation in fewer steps and because it has not only α-hydrogens but also a tertiary hydrogen to serve as hydride sources. Tertiary butyl alcohol, although it forms the most long-lived cation directly, has no good sources of hydride in the alcohol itself and presumably gives little isobutane because of the scarcity of suitable reducing agents.

Experimental

Alcohols and Acids

The butyl alcohols were commercial products free of dissolved hydrocarbons and other volatile impurities, as judged by g.l.p.c. analysis. Sulfuric acid, C.P. Reagent from C.I.L., 95.5% minimum H_2SO_4, and 85% phosphoric acid, Fisher Certified Reagent, were used directly as supplied.

n-Butyl-t-butyl Ether

To a mixture of *n*-butyl alcohol (200 ml) and 20% H_2SO_4 (200 ml) at 80°, in a 2 l, three-necked flask, was added, by drops during vigorous stirring, 100 ml of a solution of *t*-butyl alcohol (90%) in *n*-butyl alcohol (10%). When addition was complete the mixture was heated for 30 min more before it was cooled and the layers were separated. After the organic layer had been washed five times with 100 ml portions of saturated salt solution, g.l.p.c. analysis showed that it was composed of *n*-butyl alcohol (*ca.* 80%), *n*-butyl-*t*-butyl ether (*ca.* 20%) and an impurity (< 1%) believed to be *n*-butyl ether.

The mixed ether was purified by oxidation of the *n*-butyl alcohol in the mixture with alkaline $KMnO_4$ in water. Extraction with ether (5 × 100 ml), drying over K_2CO_3 and distillation of the ether left a residue (7.2 g) which was about 98% *n*-butyl-*t*-butyl ether (g.l.p.c.): n.m.r. (δ, CS_2): 3.20, t, OCH_2; 1.57–0.67, m, with 1.08, s, $(CH_3)_3C$, superimposed.

Identification of Isobutane

Into a 250 ml, three-necked flask fitted with paddle stirrer, gas inlet, dropping funnel, condenser, and drying tube was placed 150 ml of a solution of sulfuric acid (10% by volume) in 85% phosphoric acid (90% by volume). When a thermometer in the liquid registered 165°, *n*-butyl alcohol (20 ml) was added gradually (30–50 drops/min) while nitrogen was passed in above the liquid at 75 ml/min. The gas mixture was swept out through the water condenser and the drying tube into a trap cooled with liquid nitrogen. Gases were collected for 5 min after all the alcohol had been added. The products in the trap were then distilled in the vacuum line into an evacuated bulb charged with 250 ml of 1.0 *M* $KMnO_4$, 0.1 *N* in KOH. The oxidizing mixture was stirred for several hours at room temperature before the remaining gas above the solution was distilled, first into another trap and then into an n.m.r. tube containing CCl_4 and TMS. The tube was sealed and the spectrum was recorded at −20° with a Varian A-60 Spectrometer. It showed a doublet at δ 0.90, $J = 7$ Hz, and a multiplet centered at δ 1.67. Authentic isobutane gave the same spectrum except for small differences in the shapes of peaks in the multiplet. The retention volumes of the collected gas and of authentic isobutane on a 10′ SE 550 column were identical.

Composition of the Volatile Product

Dehydrations for determining product composition were analogous to the one described above but on a smaller scale. The quantity of acid was reduced to 50 ml and that of alcohol to 2 g. Instead of $KMnO_4$, the scrubbing bulb contained aqueous NaOH to remove SO_2 and other acidic components. The gas volume was read with the aid of a burette and levelling-bulb arrangement and the gas was introduced into the Aerograph A90-P3 gas chromatograph directly from the line by means of the Aerograph Gas Sampling Accessory. A 10′ × 1/4″ column packed with SE 550 (31%) on firebrick was used

[2]The presence of traces of 2-butenes among the products from dehydration of *t*-butyl alcohol at high temperatures must mean that cations other than *t*-butyl intervene. It has been argued, however, that $3° \rightarrow 1°$ rearrangements of cations are too endothermic to be important processes (8) and that bimolecular reactions can account for the rearrangements (9).

at room temperature with a helium flow rate of 20 ml/min. At 24° the relative retention times were: isobutane, 1.00; 1-butene plus isobutene, 1.39; *trans*-2-butene 1.80; *cis*-2 butene, 2.12. Ratios were determined by triangulation of peaks or by cutting and weighing the paper. They are not corrected for differences in thermal conductivity.

Hydrolysis of n-Butyl-t-butyl Ether

The ether (1.5 ml) was dropped into a stirring solution of H_2SO_4 (5 ml) in H_3PO_4 (45 ml) at 162°. The temperature of the mantel-heated flask dropped to 153° by the time addition was complete. Product gases were swept from the flask and analyzed as already described.

Carbonyl Compounds

Isobutyl alcohol (10 ml) was dropped into a paddle-stirred solution of sulfuric acid (75 ml) in pyrophosphoric acid (150 ml) at 165–170°. The flask was fitted with a fritted gas-delivery tube through which N_2 was blown below the acid surface. The effluent was passed through a downward-pointing, water-cooled condenser. About 5 ml of a two-phase mixture was collected. The upper, organic layer, on treatment with 2,4-dinitrophenylhydrazine reagent (10) deposited a red precipitate which was crystallized from ethanol and recrystallized from methanol to yield 0.0295 g, m.p., 98.5–100.5°; u.v. (EtOH): λ_{max} 361 mμ, ε_{max} 18 000 (based on $C_{14}H_{20}N_4O_4$, see text). The low field part of the n.m.r. spectrum was characteristic of the three aromatic protons of dinitrophenylhydrazones, with no absorption at δ 7.50, where

H—C=N

of isobutyraldehyde dinitrophenylhydrazone appears as a doublet. The high field portion of the spectrum totalled about 16H, taking the low-field integral as representing 3H, but was of such complexity as to suggest a mixture.

The isobutyl alcohol used in the experiment gave a negative test with the dinitrophenylhydrazine reagent.

This work was supported, in part, by the National Research Council of Canada. The Shell Oil Company of Canada, Oakville, Ontario, provided a sample of isobutane.

1. C. N. Reilly and D. T. Sawyer. Experiments for instrumental methods. McGraw-Hill Book Co., Inc., 1961. p. 256.
2. M. Saunders, E. L. Hagen, and J. Rosenfeld. J. Amer. Chem. Soc. **90**, 6882 (1968), and references therein.
3. N. C. Deno, D. B. Boyd, J. D. Hodge, C. U. Pittman, Jr., and J. O. Turner. J. Amer. Chem. Soc. **86**, 1745 (1964).
4. P. D. Bartlett, F. E. Condon, and A. Schneider. J. Amer. Chem. Soc. **66**, 1531 (1944).
5. P. D. Bartlett and J. D. McCollum. J. Amer. Chem. Soc. **78**, 1441 (1956).
6. R. Stewart. Can. J. Chem. **35**, 766 (1957).
7. J. R. Dyer. Applications of absorption spectroscopy of organic compounds. Prentice-Hall, Inc., 1965. p. 10.
8. G. J. Karabatsos and F. M. Vane. J. Amer. Chem. Soc. **85**, 729 (1963).
9. G. J. Karabatsos, F. M. Vane, and S. Meyerson. J. Amer. Chem. Soc. **83**, 4297 (1961); **85**, 733 (1963).
10. R. L. Shriner, R. C. Fuson, and D. Y. Curtin. The systematic identification of organic compounds. 4th Edition. John Wiley and Sons, Inc., New York' 1956. p. 111.

Can. J. Chem. Downloaded from www.nrcresearchpress.com by 210.87.254.40 on 09/05/12
For personal use only.

Can. J. Chem. Downloaded from www.nrcresearchpress.com by 210.87.254.40 on 09/05/12
For personal use only.

Termolecular ion–molecule reactions involving $C_3H_5^+$

A. G. HARRISON AND A. A. HEROD
Department of Chemistry, University of Toronto, Toronto 181, Ontario

Received May 13, 1970

The reaction of $C_3H_5^+$ with C_2D_4 to produce $C_5H_5D_4^+$ is shown to be second order in C_2D_4. The rate coefficients are in the range 10^{-24} to 10^{-25} cm^6 molecule^{-2} s^{-1} but decrease markedly with increasing ion kinetic energy. This decrease reflects the effect of the ion kinetic energy on the lifetime of the initial collision complex. Small differences in rate coefficients are observed depending on the source of the $C_3H_5^+$ ion but these are insufficient to distinguish between possibly different ionic structures. The reaction of $C_3H_5^+$ with C_2H_3F forms $C_5H_7^+$ in a reaction second order in C_2H_3F. The rate coefficients are also in the range 10^{-24} to 10^{-25} cm^6 molecule^{-1} s^{-1} and show a similar dependence on ion kinetic energy. These high third order rate constants are compared with data for other termolecular reactions and are shown to be consistent with the effect of molecular size on the third order rate constant.

Canadian Journal of Chemistry, 48, 3549 (1970)

Introduction

Recent work (1–3) has shown that the $C_5H_9^+$ ion observed in the high-pressure mass spectrum of ethylene originates predominantly by the reaction sequence shown in eqs. 1 and 2, where

[1] $$C_3H_5^+ + C_2H_4 \rightarrow C_5H_9^{+*}$$

[2] $$C_5H_9^{+*} + M \rightarrow C_5H_9^+ + M$$

the second step is the collisional stabilization of the complex formed in the initial ion–molecule collision. Experimental evidence (1) indicates that this overall termolecular reaction is quite rapid, presumably because the collision complex has a long lifetime. Recently Bowers *et al.* (3) have estimated an upper limit of $\sim 1.1 \times 10^{-4}$ s for the dissociative lifetime of the complex at thermal ion energies. No quantitative data on the overall rate of the reaction has been reported since in ethylene the $C_3H_5^+$ ion is produced by reaction 3[1] and, therefore, has an unknown and variable ion source residence time.

[3] $$C_2H_4^+ + C_2H_4 \rightarrow C_3H_5^+ + CH_3$$

A further termolecular reaction of the $C_3H_5^+$ ion has been observed in the vinyl fluoride system (4). The $C_3H_5^+$ produced by reaction of the molecular ion reacts further by reaction 4 to

[4] $$C_3H_5^+ + 2\,C_2H_3F \rightarrow C_5H_7^+ + (HF + C_2H_3F)$$

produce $C_5H_7^+$ in a reaction which has been shown (4) to be second order in C_2H_3F. Again no accurate value for the rate coefficient was obtained although it was estimated that it must be in the range 10^{-24} to 10^{-25} cm^6 molecule^{-2} s^{-1}.

The present work reports the results obtained in a quantitative study of these third-order reactions involving $C_3H_5^+$. The $C_3H_5^+$ reactant ions were produced directly by dissociative ionization of suitable derivatives and the formation of the appropriate product was followed as a function of the pressure of the added reactant gas. In the ethylene case C_2D_4 was used while C_2H_3F was used in the vinyl fluoride study. The use of C_2D_4 was necessary because in C_2H_4 the $C_3H_5^+$ ion is formed rapidly and in large yield by reaction 3. In contrast, in vinyl fluoride formation of $C_3H_5^+$ occurs predominantly by a third order reaction (4).

Experimental

The experiments were carried out using the medium pressure instrument described previously (5). The pertinent operating conditions were a source temperature of ~100 °C, a primary ion travel distance of 0.54 cm, and repeller voltages corresponding to 0.64, 0.96, and 1.60 eV ion exit energy. The electron beam was pulsed with the primary ion residence times being measured directly by the deflection technique described previously (5). Source pressures were measured directly using an MKS Baratron micromanometer.

The $C_3H_5^+$ reactant ions were produced by dissociative ionization of the various bromo derivatives, 1-bromopropene, 2-bromopropene, allyl bromide, and cyclopropyl bromide. Typical operating conditions were 1 to 3 μ of C_3H_5Br with the C_2D_4 pressure being varied from 0.5 to ~8 μ pressure and, for the vinyl fluoride studies, the C_2H_3F pressure being varied from 0.5 to ~18 μ. The electron energy was in the range 11 to 13eV nominal energy to avoid excessive fragment ion formation.

The C_3H_5Br compounds were obtained from Aldrich Chemical Co. and were purified by bulb-to-bulb distillation *in vacuo* with a middle fraction being retained

[1]The $C_3H_5^+$ has also been shown (2, 6) to be produced by the reaction sequence $C_2H_3^+ + C_2H_4 \rightarrow C_2H_5^+ + C_2H_2$, $C_2H_5^+ + C_2H_4 \rightarrow C_3H_5^+ + CH_4$.

Can. J. Chem. Downloaded from www.nrcresearchpress.com by 210.87.254.40 on 09/05/12
For personal use only.

for use. Ethylene-d_4 (98.2% isotopic purity) was obtained from Merck, Sharp and Dohme while the vinyl fluoride was obtained from Matheson and Co.

Results and Discussion

Reaction of $C_3H_5^+$ with C_3H_5Br

The mass spectra of the bromo compounds were studied as a function of pressure to determine the reactions occurring between the $C_3H_5^+$ fragment ion and the neutral molecule. In all cases the only products attributable to reaction of $C_3H_5^+$ were $C_4H_7^+$ (*m/e* 55) and $C_6H_9^+$ (*m/e* 81) formed by reactions 5 and 6. The total

[5] $C_3H_5^+ + C_3H_5Br \rightarrow C_4H_7^+ + C_2H_3Br$

[6] $C_3H_5^+ + C_3H_5Br \rightarrow C_6H_9^+ + HBr$

rate constant for disappearance of $C_3H_5^+$ varied between a low of 0.7×10^{-10} cm^3 molecule^{-1} s^{-1} for cyclopropyl bromide and a high of 7×10^{-10} cm^3 molecule^{-1} s^{-1} for allyl bromide, with the rate constants decreasing slightly with increasing ion exit energy. The ratio $C_4H_7^+/C_6H_9^+$ varied from a low of ~2.8 for 1-bromopropene (at 1.6 eV exit energy) to a high of ~18 for allyl bromide (at 0.64 eV exit energy) with the ratios in all cases decreasing slightly with increasing ion exit energy.

Reaction of $C_3H_5^+$ with C_2D_4

In addition to the ionic species characteristic of the C_3H_5Br system and those characteristics of the C_2D_4 system, in C_3H_5Br–C_2D_4 mixtures significant ion currents were observed at *m/e* 73 ($C_5H_5D_4^+$) and at *m/e* 42, 43, 44, and 45 corresponding to $C_3H_4D^+$, $C_3H_3D_2^+$, $C_3H_2D_3^+$, and $C_3HD_4^+$. The $C_5H_5D_4^+$ ion is the collisionally-stabilized product from condensation of $C_3H_5^+$ with C_2D_4, while the isotopically mixed ions from *m/e* 42 to 45 are those expected from decomposition of the $C_5H_5D_4^{+*}$ complex with isotopic mixing of the hydrogens and deuteriums. The same products were observed by Tiernan and Futrell (2) in tandem experiments where $C_3H_5^+$ was reacted with C_2D_4. The product distribution in the C_3 region could not be determined accurately in the present work because of overlap with products formed from reactions characteristic of the ethylene system. In the present study no products were detected analogous to the $C_5H_7^+$ ion observed (3, 6) at low pressures from reaction of $C_3H_5^+$ with C_2H_4.

The production of $C_5H_5D_4^+$ can be attributed to the third-order reactions 7 and 8, where either C_3H_5Br or C_2D_4 may act as the third body to stabilize the collision complex. For low extent of

[7] $C_3H_5^+ + C_2D_4 + C_3H_5Br \rightarrow C_5H_5D_4^+ + C_3H_5Br$

[8] $C_3H_5^+ + C_2D_4 + C_2D_4 \rightarrow C_5H_5D_4^+ + C_2D_4$

reaction of $C_3H_5^+$ eq. 9 may be derived where K is the conversion factor from source pressure in μ

$$[9] \quad \frac{I_{C_5H_5D_4^+}}{I_{C_3H_5^+} \cdot P_{C_2D_4}} = k_7 t K^2 P_{C_3H_5Br} + k_8 t K^2 P_{C_2D_4}$$

to concentration in molecule cm^{-3} units, t is the reaction time, and k_7 and k_8 are the relevant third order rate constants. At constant C_3H_5Br pressure a plot of the function on the left hand side of eq. 9 *vs.* $P_{C_2D_4}$ should yield a straight line, the third order rate constant being calculable from the slope.

Figure 1 shows typical results obtained for the cyclopropyl bromide – C_2D_4 system at the three different exit energies employed. From the slopes of such straight line plots we have evaluated the third-order rate constants summarized in Table 1. Each value is the average of two or more determinations which were found to be in agreement within 10%. No attempt has been made to evaluate k_7 from the intercepts of the plots since there is a distinct possibility that the intercept may contain a second-order contribution if the collision complex survives to reach the ion collector.

Several points should be noted concerning the results in Table 1. For all sources of $C_3H_5^+$ the third order rate constant decreases rapidly with increasing ion exit energy or, since for low conversion the average reactant ion kinetic energy $\bar{E} = Ee/3$ (7), with increasing reactant ion kinetic

TABLE 1

Rate coefficients for reaction
$C_3H_5^+ + 2\,C_2D_4 \rightarrow C_5H_5D_4^+ + C_2D_4$

	k(cm^6 molecule^{-2} s^{-1}) × 10^{25}		
Source of $C_3H_5^+$	0.64 eV*	0.96 eV*	1.6_0 eV*
Cyclopropyl bromide	8.4	4.6	2.3_5
Allyl bromide	14.1	7.1	3.4
2-Bromopropene	6.2	2.4_5	0.9_3
1-Bromopropene	3.6	2.1	0.1_0

*Ion exit energy.

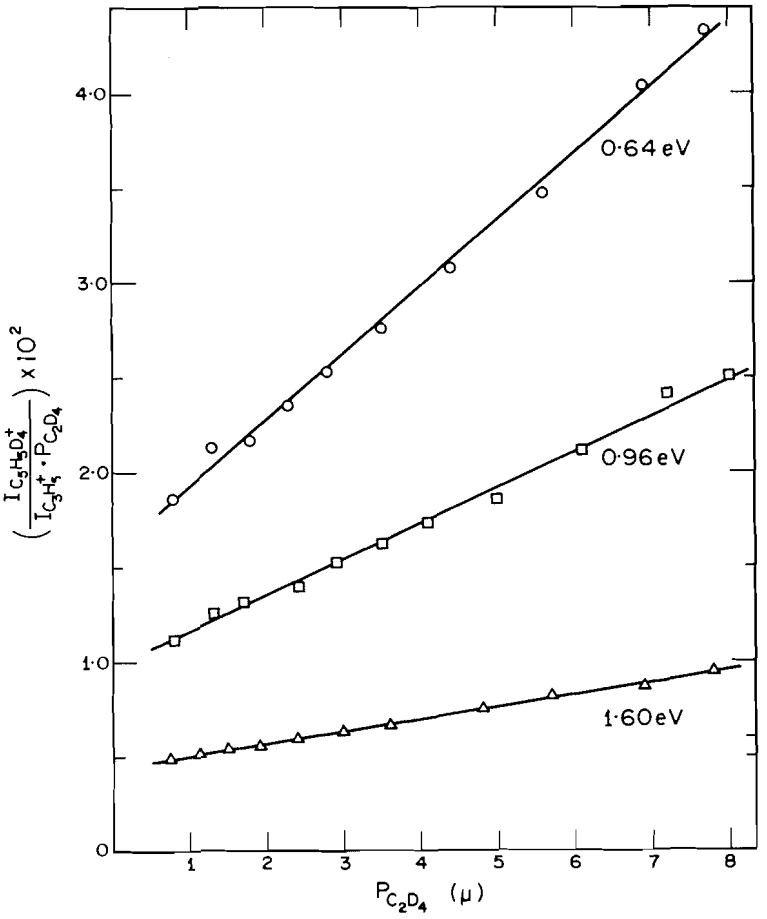

FIG. 1. Third order plot for cyclopropyl bromide – C_2D_4 system.

energy. This undoubtedly reflects the effect of the ion kinetic energy on the lifetime of the $C_5H_5D_4^{+*}$ collision complex. For a given ion kinetic energy the third order rate constant varies with the source of the $C_3H_5^+$ reactant ion, being lowest for 1-bromopropene and highest for allyl bromide (3-bromopropene). The various isomers were studied in the hope that the results might permit a distinction between the possible isomeric forms of the $C_3H_5^+$ ion, particularly the possibly cyclic ion from cyclopropyl bromide compared to the possibly acyclic ions from the other derivatives. The rate differences are not sufficiently large to permit such distinctions and it is probable that these differences arise from the effect of the differing internal energies of the reactant ions on the lifetime of the $C_5H_5D_4^+$ collision complex.

Reactions of $C_3H_5^+$ with C_2H_3F

Since the results in the above study indicated only minor effects attributable to the source of the $C_3H_5^+$ ion the reaction of $C_3H_5^+$ with C_2H_3F was studied only for the cyclopropyl bromide – C_2H_3F system. In such mixtures the reactions 10–12 lead to disappearance of $C_3H_5^+$.

[10] $C_3H_5^+ + C_3H_5Br \rightarrow$ products

[11] $C_3H_5^+ + C_2H_3F + C_3H_5Br \rightarrow C_5H_7^+ + (HF + C_3H_5Br)$

[12] $C_3H_5^+ + C_2H_3F + C_2H_3F \rightarrow C_5H_7^+ + (HF + C_2H_3F)$

Considering these three reactions, we may derive eq. 13 where $\sum I_{C_3H_5^+}$ represents the

Can. J. Chem. Downloaded from www.nrcresearchpress.com by 210.87.254.40 on 09/05/12
For personal use only.

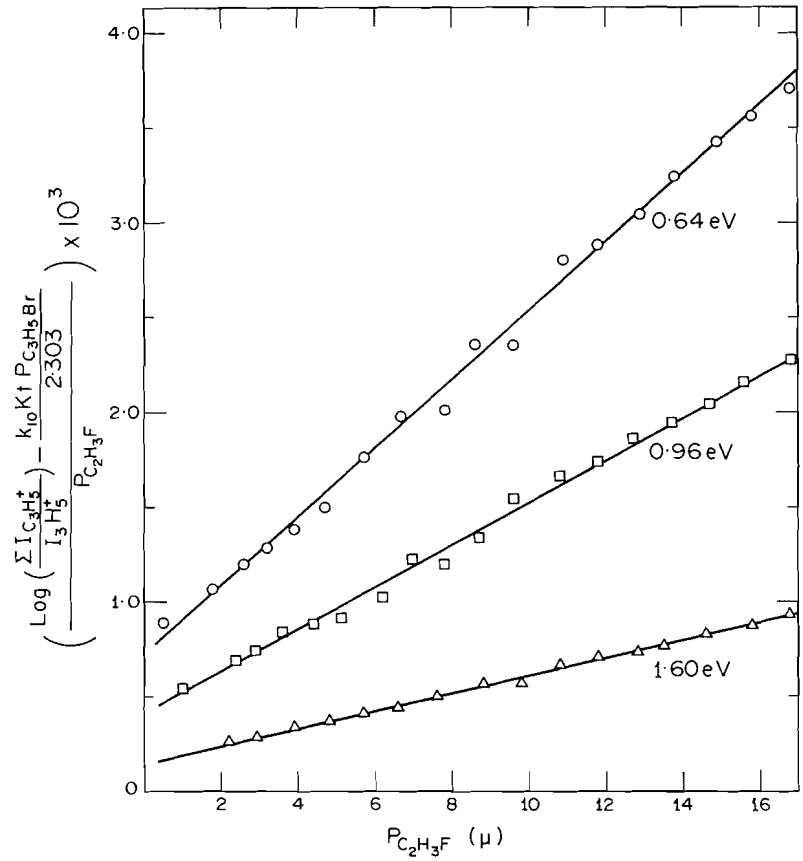

FIG. 2. Third order plot for cyclopropyl bromide – C_2H_3F system.

$$[13]\quad \frac{\log\left(\frac{\sum I_{C_3H_5^+}}{I_{C_3H_5^+}}\right) - \frac{k_{10}KtP_{C_3H_5Br}}{2.303}}{P_{C_2H_3F}} = \frac{k_{11}K^2tP_{C_3H_5Br}}{2.303} + \frac{k_{12}K^2tP_{C_2H_3F}}{2.303}$$

ion current for $C_3H_5^+$ and all products originating from reactions of $C_3H_5^+$ and K and t again represent, respectively, the conversion factor from pressure to source concentration and the reaction time. The second term in the numerator of the left hand side of the equation may be obtained from measurements in the absence of C_2H_3F.

Figure 2 shows typical results obtained at 0.64, 0.96 and 1.6_0 eV ion exit energy plotted in the form of eq. 13. As predicted, straight lines result. Repeat determinations (in agreement within 5%) yielded from the slopes the third order constants k_{13} (cm^6 molecule^{-2} s^{-1}), $8.8_4 \times 10^{-25}$ at 0.64 eV, $6.6_1 \times 10^{-25}$ at 0.96 eV and $3.5_3 \times 10^{-25}$ at 1.6_0 eV ion exit energy. As for the ethylene system the third order rate coefficients decrease rapidly with increasing average reactant ion kinetic energy. In this case the product ion observed is not the stabilized collision complex but the ion formed by elimination of HF from this complex. Why this reaction should require third-body intervention is not clear.

Conclusions

The present studies have shown that, in agreement with previous qualitative conclusions, the third order reaction of $C_3H_5^+$ with C_2D_4 is a rapid reaction leading to formation of the stabilized collision complex with a rate coefficient in the range 10^{-25} to 10^{-24} cm^6 molecule^{-2} s^{-1} for reactant ions with energies in the range 0.2 to 0.5 eV kinetic energy. Such a high rate coefficient is certainly adequate to explain the high yield of

Can. J. Chem. Downloaded from www.nrcresearchpress.com by 210.87.254.40 on 09/05/12
For personal use only.

$C_5H_9^+$ observed in the high pressure mass spectrum of ethylene. The third order reaction of $C_3H_5^+$ with vinyl fluoride also has a rate coefficient in the range 10^{-25} to 10^{-24} cm^6 molecule^{-2} s^{-1}, in agreement with the previous rough estimate, although the present work casts no further light on the question of why this reaction is third order since it does not involve simple stabilization of the ion-neutral collision complex.

Bohme (8) recently has reviewed the literature on ion-neutral termolecular association reactions and has found that an order-of-magnitude estimation of the rate coefficients may be obtained from the empirical relationship shown in eq. 14 where

$$k = 10^{-32.5\pm1} N^{6.24} \quad [14]$$

N is the number of atoms in the product ion cluster. For the reaction leading to $C_5H_5D_4^+$ formation this equation predicts a rate coefficient of $10^{-25.3\pm1}$ in reasonable agreement with the present experimental results.

The authors are indebted to the National Research Council of Canada for financial support.

1. J. J. MYHER and A. G. HARRISON. Can. J. Chem. **46**, 101 (1968).
2. T. O. TIERNAN and J. H. FUTRELL. J. Phys. Chem. **72**, 3080 (1968).
3. M. T. BOWERS, D. D. ELLEMAN, and J. L. BEAUCHAMP. J. Phys. Chem. **72**, 3599 (1968).
4. J. A. HERMAN and A. G. HARRISON. Can. J. Chem. **47**, 957 (1969).
5. S. K. GUPTA, E. G. JONES, A. G. HARRISON, and J. J. MYHER. Can. J. Chem. **45**, 3107 (1967).
6. A. A. HEROD and A. G. HARRISON. Int. J. Mass. Spect. Ion Phys. In press.
7. P. WARNECK. J. Chem. Phys. **46**, 513 (1967).
8. D. K. BOHME. Can. J. Chem. **47**, 1809 (1969).

Can. J. Chem. Downloaded from www.nrcresearchpress.com by 210.87.254.40 on 09/05/12
For personal use only.

Can. J. Chem. Downloaded from www.nrcresearchpress.com by 210.87.254.6 on 09/05/12
For personal use only.

Radicals derived from heteroaromatic systems. II. Thiazolyl radicals[1]

MRS. A. L. LEE, DONALD MACKAY, AND E. L. MANERY
Department of Chemistry, University of Waterloo, Waterloo, Ontario

Received May 29, 1970

2-Thiazolylhydrazine and all three thiazole carbonyl peroxides have been synthesized and examined as radical precursors in solution in benzene, bromobenzene, and cumene. Silver oxide oxidation of the hydrazine or thermal decomposition of the 2-peroxide gives good yields of 2-arylthiazoles but negligible amounts of esters; in cumene a trace of bicumyl is formed. The isomer ratios in bromobenzene and cumene fully support the involvement of 2-thiazolyl radicals (**1**).

The 4-carbonyl peroxide gives fair yields of 4-arylthiazoles but the phenyl ester is also a major product in benzene, indicative of reactions of both 4-thiazolyl radicals (**2**) and thiazole-4-carbonyloxy radicals. The 5-peroxide gives no products clearly diagnostic of 5-thiazolyl radicals (**3**) or thiazole-5-carbonyloxy radicals. Bicumyl is a major product of the reactions of the 4- and the 5-peroxides in cumene.

Canadian Journal of Chemistry, **48**, 3554 (1970)

In a continuing study of routes to, and reactions of, free radicals with the unpaired electron on a heteroaromatic ring an account has already been given of 3-pyridyl radicals (1), 2- and 3-thienyl radicals (2, 3) and 5-nitro-2-thienyl radicals (3). 2-Thiazolyl radicals (**1**) have been generated under Gomberg conditions in a variety of aromatic solvents (4), and thiazolyl and 4-methylthiazolyl radicals have been implicated in the reactions of benzoyl peroxide with thiazole (5, 6) and 4-methylthiazole (7). We now wish to describe the synthesis of 2-thiazolylhydrazine and of all three thiazole carbonyl peroxides and to examine all these as potential sources of the 2-, 4-, and 5-thiazolyl radicals (**1**, **2**, and **3**) in benzene, bromobenzene, and cumene as representative aromatic solvents. This permits a comparison of the three different sources of the 2-radical and of the decomposition pattern of the three isomeric peroxides in relation to one another.

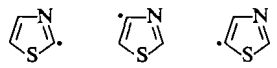

1 **2** **3**

No unsubstituted thiazolylhydrazines have been properly described, though Hantzsch-type syntheses have been applied to the preparation of the 2-isomer. Thus condensation of acetothiosemicarbazide and 1,2-dibromoethyl acetate followed by acid hydrolysis was claimed (8) to yield 2-thiazolylhydrazine hydrobromide, from which the base could be liberated as an unstable substance giving a hydrazone with acetophenone of m.p. 152–154°. Beyer *et al.* (9) reacted 1,2-dichloroethyl ether with acetophenone thiosemicarbazone and obtained a 65% yield of acetophenone 2-thiazolylhydrazone hydrochloride, m.p. 195°. With sodium acetate it gave the hydrazone, m.p. 155°, and with hot hydrochloric acid it gave 2-thiazolylhydrazine hydrochloride as an impure solid, m.p. 104°. The readily available 2-aminothiazole, however, has not been investigated as a starting point for the hydrazine.

Diazotization of 2-aminothiazole, followed by reduction with stannous chloride and treatment with ammonia, gave 2-thiazolylhydrazine (60%), m.p. 97–98°, stable indefinitely in the dark at room temperature. Its hydrochloride had m.p. 162–164°, unlike that reported by Beyer *et al.* (m.p. 104°), but the acetophenone hydrazone hydrochloride was identical (m.p. 195–198°) with an authentic sample (9).

The three isomeric thiazole carboxylic acids were prepared by published procedures (10–13). Attempts to make ethyl thiazole-2-carboxylate from ethyl thiooxamate and chloroacetaldehyde dimethyl acetal (*cf.* the free aldehyde (14)), and to directly deaminate the readily available ethyl 2-aminothiazole-4-carboxylate (12) to ethyl thiazole-4-carboxylate, failed.

Thiazole-2-carbonyl chloride, not hitherto described, was prepared from thionyl chloride and the sodium salt (1) as a low melting solid extremely sensitive to moisture. Treatment of the acid directly with thionyl chloride gave a different solid, perhaps the acid chloride hydrochloride; difficulties in the preparation of chlorides of thiazole-2-carboxylic acids have been attributed to the great ease with which the acids decarboxylate (15).

[1]For part I of this series see ref. 3.

Can. J. Chem. Downloaded from www.nrcresearchpress.com by 210.87.254.6 on 09/05/12
For personal use only.

The usual methods for diacyl peroxide production involving aqueous media (16) failed when applied to thiazole-2-carbonyl chloride. Under anhydrous conditions in pyridine containing ethereal hydrogen peroxide (1) a poor yield of the 2-carbonyl peroxide resulted. The method of Greene and Kazan (17) using the carboxylic acid, ethereal hydrogen peroxide and dicyclohexylcarbodiimide proved more effective (30–40% yields).

A variation of this method was applied to the 4- and 5-carbonyl peroxides, taking advantage of the solubility of the parent acids in aqueous media and the availability commercially of the water soluble 1-cyclohexyl-3-(2-morpholinoethyl)-carbodiimide metho-*p*-toluenesulfonate. Addition of 50% hydrogen peroxide to a solution in aqueous acetone of the acid and the diimide caused precipitation of the carbonyl peroxide (40–45% after crystallization). As well as being rapid and convenient this method avoids the rather hazardous ethereal hydrogen peroxide.

All three peroxides were crystalline solids, stable if kept in the cold and the dark. They melted sharply and detonated violently above their melting points.[2]

The 2-thiazolylhydrazine oxidations (18) were carried out with an excess of silver oxide in dilute (*ca.* 1%) solutions in benzene, bromobenzene, and cumene at room temperature; the three peroxides were decomposed by heating dilute solutions in the same solvents. All yields of thiazole and non-acidic products were determined by analytical g.l.c. against internal standards and are shown in Table 1 along with the yields of acid.[3]

The silver oxide oxidations gave, as well as considerable thiazole, moderate yields of 2-arylthiazoles, 12% from benzene, 11% from bromobenzene, and 10% from cumene. The isomers from bromobenzene were in the ratio *o*:*m*:*p* = 51:31:18; g.l.c. gave the ratio of *o*:*m* + *p* (unresolved), but isolation of the isomer mixture by preparative g.l.c. enabled the *m*:*p* ratio to be determined by quantitative i.r. analysis.

The yields of 2-cumylthiazoles may be somewhat in error since the reference isomers were not available for comparison. The peaks for the *m*- and *p*-isomers were only partially resolved and their ratio was determined by curve fitting. The areas were then compared with the bicumyl peak (a minor reaction product) on the basis of their carbon numbers.[4] Support for the identity of each component in the triple peak was obtained by preparative g.l.c. of the reaction products, with direct elution into a rapid scan gas-phase i.r. spectrophotometer. The expected (20) substitution pattern for *o*-, *m*-, and *p*-disubstituted benzene derivatives was observed in the region 750–850 cm^{-1}.

The *o*:*m*:*p* isomer ratios in bromobenzene and cumene are in agreement with those found in most arylation procedures (21) and point clearly to the involvement of 2-thiazolyl radicals (**1**). The affinity for the *o*-position is, however, remarkably lower than that observed in the reactions of 2-thiazolyl radicals, produced by the Gomberg method (4), in similar solvents, *e.g.* chlorobenzene and toluene.

Thiazole is a predictable (18) end product of the oxidation of the hydrazine with a metal oxide, though the yields are unusually high. Particularly noteworthy is the fact that the yield in cumene is comparable with that in benzene and not, as might have been supposed, much higher. Side chain hydrogen abstraction by 2-thiazolyl radicals is evidently not a favored process and the low yield of bicumyl (1%) is consistent with this. The possibility that the intermediate oxidation species, 2-thiazolylnitrene (Scheme 1, R = 2-thiazolyl), is capable of concerted decomposition to thiazole and nitrogen as well as of homolytic fragmentation might merit testing with deuterium labelling.

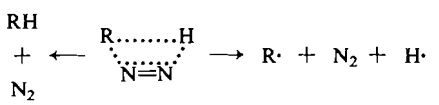

SCHEME 1

[2]On one occasion an unpurified specimen of the 2-peroxide spontaneously ignited.

[3]All yields are based on the simplified general eqs. 1 and 2.

[1] $RNHNH_2 + Ag_2O \rightarrow Ag + H_2O + RN{=}NH \rightarrow R\cdot + N_2 + H\cdot$

and

[2] $(RCO_2)_2 \rightarrow RCO_2\cdot + R\cdot + CO_2.$

[4]On the assumption that for equimolar amounts the signal area for cumylthiazole:bicumyl = 12:18 (the ratio of the numbers of carbon atoms in the molecules). The carbon number is claimed to be roughly proportional to signal area in flame ionization detection (19*a*).

Can. J. Chem. Downloaded from www.nrcresearchpress.com by 210.87.254.6 on 09/05/12
For personal use only.

TABLE 1

Products from 2-thiazolylhydrazine and thiazole carbonyl peroxides*

	Solvent ArH	Temperature (°C)	Acids RCO_2H	CO_2	Thiazole	Arylthiazole R—Ar	Ester RCO_2Ar	Other
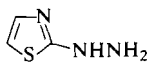	PhH				30.7	12.1		
	PhBr				18.7	10.9 (*o*:*m*:*p* = 51:31:18)		
	Cumene				23.4	9.8 (*o*:*m*:*p* = 40:35:25)		1.3 Bicumyl
$(RCO_2)_2$								
R =	PhH	80			18.2	36.9	1.5	4 RCO_2R (?)
	PhBr	100			21.1	54.5 (*o*:*m* + *p* = 49:51)		
	Cumene	100			72.1	23.1 (*o*:*m*:*p* = 43:32:25)		1.3 Bicumyl
R =	PhH	80	90		1.9	21.2	13.3	1 Ph_2
	PhBr	80	119.5	55	1.0	28.4 (*o*:*m* + *p* = 69:31)		
	Cumene	155	64					40.7 Bicumyl
R =	PhH	80	115		0.5		7.2	7.1 Ph_2
	PhBr	80	112.6	18.7	0.5			25 ?†
	Cumene	155	37					13.8 Bicumyl

*Yields are in moles percent moles of starting material.
†See footnote 5.

Can. J. Chem. Downloaded from www.nrcresearchpress.com by 210.87.254.6 on 09/05/12
For personal use only.

Thermal decomposition of thiazole-2-carbonyl peroxide in the same solvents gave good yields of 2-arylthiazoles, 37% from benzene, 54% from bromobenzene ($o:m + p = 49:51$) and 23% from cumene ($o:m:p = 43:32:25$), the isomer ratios being in excellent agreement with those obtained in the oxidation reactions. In cumene again there was only slight evidence (1% bicumyl) of side chain attack by 2-thiazolyl or other radicals. All three reaction mixtures showed small amounts of higher boiling components in their gas chromatograms. From benzene the ester phenyl thiazole-2-carboxylate was identified, but esters are clearly very minor products from this peroxide. In all its properties it resembles nicotinoyl peroxide (1) or a benzoyl peroxide and is quite unlike the dicarbonyl peroxides of thiophene.

The yields of thiazole-2-carboxylic acid and of carbon dioxide were not determined. Control experiments showed that the temperature and duration of the reactions caused extensive decarboxylation of the acid. This is reflected in the yields of thiazole, though the very high value in cumene points to an additional pathway, involving reactions of thiazolyl or thiazole carbonyloxy radicals with the substrate and not at the solvent side-chain.

Decomposition of thiazole-4-carbonyl peroxide in benzene and bromobenzene gave substantial amounts of acid (90 and 120%) and traces of thiazole (2 and 1%) which did not arise by decarboxylation of the carboxylic acid formed (control experiment). Carbon dioxide evolution (determined in bromobenzene only) was 55%. Strong evidence for the generation of 4-thiazolyl radicals (**2**) is provided by the yields of 4-arylthiazoles, 21% in benzene and 28% in bromobenzene, and in particular by the isomer ratio from the latter ($o:m + p = 69:31$). Thiazole-4-carbonyloxy radicals are also involved in nuclear attack, at least in benzene where a 13% yield of phenyl thiazole-4-carboxylate was observed; in bromobenzene the gas chromatogram showed minor peaks that might be attributable to esters. The percentage of ortho attack in bromobenzene by 4-thiazolyl radicals is noticeably higher than that by 2-thiazolyl radicals, suggesting that the former are more electrophilic.

The peroxide was rather insoluble in cumene at 80° and so the reaction was carried out under reflux. A control experiment showed that a 1% suspension of the acid in refluxing cumene suffered 60% decarboxylation. In line with this the amount of acid isolated from the decomposition reaction was low (64%). Bicumyl (41%) was the only simple non-acidic product formed in other than trace quantities. Whether the 4-thiazolyl or the thiazole-4-carbonyloxy radicals are responsible for the side-chain dehydrogenation leading to bicumyl is obscured by the decarboxylation of the acid. Both radical processes would lead to thiazole.

Thiazole-5-carbonyl peroxide also gave high yields of carboxylic acid and trace amounts of thiazole when decomposed in benzene and bromobenzene at 80° (again there was no decarboxylation of the carboxylic acid at this temperature, though there was a 19% yield of carbon dioxide from other sources measured in the bromobenzene reaction). There was no evidence whatsoever for the formation of 5-phenylthiazole or 5-bromophenylthiazoles. In the benzene reaction 7% of the phenyl ester was present, diagnostic of thiazole-5-carbonyloxy radicals. The only other simple product, in unexpectedly large amount (7%), was biphenyl (the 4-peroxide also produced a trace in benzene). The formation of biphenyl during peroxide decomposition in benzene is almost certainly a consequence of phenyl radical reactions. It has been noted in earlier work and an explanation has been suggested (3).

The bromobenzene decomposition gave one major and unidentified neutral product,[5] more volatile than a 5-bromophenylthiazole or a bromophenyl thiazole-4-carboxylate, neither of which was detected.

During the decomposition in cumene, in this case again carried out at reflux temperature, the production of thiazole-5-carboxylic acid must have been considerable, since 35% survived the reaction even though in a control experiment a 1% suspension of acid in refluxing cumene was 80% decarboxylated in the same time period. No products of nuclear attack on the solvent were detected, but there was substantial side chain attack leading to a 13% yield of bicumyl.

Though the mass balance of products derived from the three peroxides is far from complete,

[5]It had the same retention time as, but was not, *p*-dibromobenzene. On the basis of a comparable carbon number it was accorded a yield of 25%.

Can. J. Chem. Downloaded from www.nrcresearchpress.com by 210.87.254.6 on 09/05/12
For personal use only.

as Table 1 shows, it is clear that with respect to the formation of simple products at least, these peroxides show very different behavior. The decomposition pattern of the 2-peroxide is typical of that of an aroyl peroxide, reactive thiazolyl radicals being involved to the exclusion of thiazole carbonyloxy radicals. The 4-peroxide, like the thenoyl peroxides, gives thiazolyl and thiazole carbonyloxy radicals both of which are reactive towards the nucleus. By contrast the 5-peroxide gives radicals of low reactivity.

Experimental

General

Solvents were purified by conventional methods and fractionated. Petroleum ether refers to the fraction b.p. 35–60° unless otherwise stated. Anhydrous magnesium sulfate was used as drying agent for solutions in organic solvents.

The i.r. spectra were obtained on Beckman instruments: for routine work the IR5 or IR10; for quantitative analysis, the IR9; and for rapid scan analyses, the IR102. The n.m.r. analyses were done on a JEOL C60 spectrometer, absorptions being quoted in τ values against tetramethylsilane.

A Beckman GC-4 gas chromatograph with flame ionization was used for the analytical determinations. Preparative g.l.c. was performed on an Aerograph Autoprep Model 700 with a 10′ × 3/8″ column of 30% SE-30 silicone gum rubber on Chromosorb W. An F and M Model 810 was used in conjunction with the rapid scan Beckman IR102 spectrometer.

All the thiazole determinations were done at 100° on a 6′ × 1/4″ column of 25% Carbowax 20M on Chromosorb W pretreated with 3% potassium hydroxide; untreated columns caused tailing of the feebly basic thiazole. The internal standard was cyclopentanone for the benzene and bromobenzene reactions and bromobenzene for the cumene reactions, since the latter solvent had the same retention time as cyclopentanone.

Other columns, used as described later, for the GC-4 chromatograph are designated as follows: 6′ × 1/8″ 10% SE-30 on Chromosorb W, column A; 6′ × 1/8″ 3% SE-30 on Chromosorb W, column B; 6′ × 1/4″ 25% Apiezon L on Chromosorb W, column C; 6′ × 1/8″ 3% Apiezon L on Chromosorb W, 3% KOH, column D.

The following materials were available commercially. 1-Cyclohexyl-3-(2-morpholinoethyl)-carbodiimide metho-*p*-toluenesulfonate, all three bromobenzonitriles, and chloroacetaldehyde and its dimethyl and diethyl acetals from Aldrich; *m*- and *p*-bromophenacyl bromides from Eastman; *o*-bromoacetophenone from Sapon Laboratories. Thiazole, from K and K Laboratories, was of high purity (g.l.c.). 2-Aminothiazole, from Aldrich, was badly discolored and of poor m.p. 84–88°. It was purified by dissolving 10 g in the minimum hot ethanol and passing the hot solution through a 1″ layer of charcoal; the amine crystallized from the filtrate as colorless prisms, m.p. 88–89°.

Thioformamide was prepared just before use by gradually adding phosphorus pentasulfide to formamide in the cold, extracting the product with ether and evaporating.

2-Phenylthiazole

Reaction of thiobenzamide, m.p. 116.5–117.5° (lit. (22) m.p. 116°) and chloroacetaldehyde diethylacetal in ethanol containing a catalytic amount of piperidine gave 2-phenylthiazole (23). It had b.p. 96°/1 mm (lit. (23) b.p. 125°/18 mm), and was further purified by preparative g.l.c. Its picrate, m.p. 124–127°, was prepared in and crystallized from methanol.

Anal. Calcd. for $C_{15}H_{10}N_4O_7S$: N, 14.4. Found: N, 14.3.

2-Bromophenylthiazoles

A modification of Erlenmeyer's method (24) for the *p*-isomer was used. The bromothiobenzamides were made from the appropriate nitrile with hydrogen sulfide in pyridine–triethylamine solution (22). *o-Bromothiobenzamide* had m.p. 83–84°; ν(Nujol) 3335 cm^{-1} (NH). The *m-isomer* had m.p. 118–119°; ν(Nujol) 3330 cm^{-1} (NH). *p*-Bromothiobenzamide had m.p. 145–146° (lit. (25) m.p. 145°). The thioamide was refluxed with a three-fold excess of chloroacetaldehyde for 12 h. The solution was evaporated, ether and aqueous sodium carbonate were added, and the ether extract dried and worked-up to give crude product contaminated with the thioamide. *2-o-Bromophenylthiazole* was purified by steam distillation, isolated from the distillate with ether, and subjected to preparative g.l.c. at 250° to give an oil, n_D^{20} 1.6734.

Anal. Calcd. for C_9H_6BrNS: C, 45.0; H, 2.5; Br, 33.3; S, 13.35. Found: C, 45.0; H, 2.7; Br, 33.3; S, 13.2.

The *m-isomer*, also an oil, was similarly purified, n_D^{20} 1.6702.

Anal. Found: C, 44.8; H, 2.6; Br, 33.2; S, 13.3.

The *p*-isomer was purified by chromatography on alumina and crystallized from pentane as colorless needles, m.p. 50–51° (lit. (24) m.p. 52–53°).

4-Phenylthiazole

Phenacyl bromide (2.0 g, 0.01 mole) was added with stirring to a solution of thioformamide (1.0 g, 0.015 mole) in ether. After the spontaneous reaction had ceased the mixture was refluxed for 5 min and then washed with aqueous sodium carbonate. The residue from the ether was steam distilled and the distillate chilled to give crystalline product which was recrystallized from petroleum ether, m.p. 50–51° (lit. (23) m.p. 51–52°).

The *picrate* was prepared in methanol and crystallized from methanol–acetone as yellow prisms, m.p 164–166.5°.

Anal. Calcd. for $C_{15}H_{10}N_4O_7S$: N, 14.4. Found: N, 14.2.

4-Bromophenylthiazoles

The method just described was used for each, the *o*-bromophenacyl bromide being obtained by direct bromination of *o*-bromoacetophenone. *4-o-Bromophenylthiazole* was purified by distillation, b.p. 150–155°/10 mm.

Anal. Calcd. for C_9H_6BrNS: C, 45.0; H, 2.5; N, 5.8. Found: C, 45.6; H, 2.7; N, 5.0.

The *m-isomer* crystallized directly on work-up and was recrystallized from petroleum ether, as faintly pink crystals, m.p. 51–52°.

Anal. Found: N, 6.3.

Can. J. Chem. Downloaded from www.nrcresearchpress.com by 210.87.254.6 on 09/05/12
For personal use only.

The *p*-isomer was twice sublimed, m.p. 73.5–74° (lit. (24) m.p. 76–77°).

5-Phenylthiazole

Phenylacetaldehyde was brominated by treatment with 1 equiv. of pyridinium hydrobromide perbromide in methylene chloride, followed by immediate and thorough washing of the solution with aqueous sodium bicarbonate. The α-bromoaldehyde was purified by distillation and allowed to react with thioformamide as before. The 5-phenylthiazole was purified by steam distillation and crystallized directly pure, m.p. 43–43.5° (lit. (23) m.p. 40–41°).

2-Thiazolylhydrazine

2-Aminothiazole (10 g, 0.10 mole) was dissolved in 12 *N* hydrochloric acid (80 ml) and diazotized by the addition of concentrated aqueous sodium nitrite (7 g, 0.10 mole), which was slowly introduced under the surface with vigorous stirring. The internal temperature was maintained between -10 and $+5°$; remaining in this range was of critical importance. The diazonium solution was then reduced with a solution of stannous chloride (45 g $SnCl_2.2H_2O$, 0.20 mole) in 12 *N* hydrochloric acid (20 ml). During the reduction the temperature was kept below $-10°$. The heavy precipitate was filtered off, sucked dry, and washed thoroughly with ether; washing with methanol, or methanolic hydrochloric acid led to a substantial loss in yield.

The precipitate was covered with benzene (1 *l*), ammonia gas was passed through the solution to expel oxygen, water (10 ml) was added, and the benzene solution was saturated with ammonia gas. The solution was dried, filtered, and concentrated under reduced pressure until separation of solid began. Precipitation was completed by the addition of petroleum ether to give the hydrazine as a granular, almost colorless solid (7 g, 61%), m.p. 97–98°. Recrystallization from benzene – petroleum ether failed to improve the m.p. and resulted in some decomposition with the formation of a purple color.

It was found that larger scale preparations decomposed when the ammonia saturation of the benzene solution was attempted. It was also noted that the ammonia-saturated benzene solution decomposed if allowed to stand for several hours.

The hydrazine had $\nu(CCl_4)$ 3340 (NH), 1635 cm^{-1} (NH_2 deformation); λ_{max} (EtOH) 258 mμ (ε 5.96×10^4); $\tau(CDCl_3)$ 2.52 (4-H), 3.10 (5-H) as a quartet ($J_{4,5} = 4$ c.p.s.), 4.4 p.p.m., broad (three N—H's).

Anal. Calcd. for $C_3H_5N_3S$: C, 31.2; H, 4.4; N, 36.4: S, 28.0. Found: C, 31.2; H, 4.4; N, 36.6; S, 28.2.

The *hydrochloride* was formed as a colorless solid by passing dry hydrogen chloride into an ethereal solution of the hydrazine. Recrystallized from methanol–ether it gave almost colorless prisms, m.p. 162–164° (with decomposition).

Anal. Calcd. for $C_3H_6ClN_3S$: Cl, 23.4; N, 27.8. Found: Cl, 23.2; N, 27.6.

The *picrate*, m.p. 184–185°, was prepared in methanol and was recrystallized from aqueous methanol.

Anal. Calcd. for $C_9H_8N_6O_7S$: N, 24.4. Found: N, 24.4.

Acetone 2-Thiazolylhydrazone

The hydrazine (2.0 g, 0.017 mole) reacted exothermally in acetone (25 ml) when two drops of glacial acetic acid were added. The solution was further heated for a few minutes, cooled, and water (10 ml) was added. Recrystallization of the product from aqueous methanol (charcoal) gave the *hydrazone* (1.4 g, 53%) as large straw-colored prisms, m.p. 139–141°; $\nu(CCl_4)$ 3360 cm^{-1} (NH); $\tau(CDCl_3)$ −1.10 (NH), 2.50 (4-H), 3.15 (5-H) as a quartet ($J_{4,5} = 4$ c.p.s.), 7.90, 8.02 p.p.m. sharp singlets (two Me groups).

Anal. Calcd. for $C_6H_9N_3S$: N, 27.1; S, 20.6. Found: N, 27.1; S, 20.8.

Acetophenone 2-Thiazolylhydrazone

A solution of the hydrazine (170 mg, 1.5 mmoles) and acetophenone (180 mg, 1.5 mmoles) in methanol (20 ml) containing acetic acid (1 ml) was refluxed for 15 min. Addition of water (10 ml) with cooling gave the hydrazone which on recrystallization from aqueous methanol (charcoal) gave straw-colored prisms, m.p. 158–160°; $\nu(CCl_4)$ 3360 cm^{-1} (NH).

Anal. Calcd. for $C_{11}H_{11}N_3S$: N, 19.3; S, 14.7. Found: N, 19.3; S, 14.5.

The hydrazone hydrochloride precipitated when hydrogen chloride was passed into an ethereal solution of the hydrazone. It was recrystallized from methanol–ether as fine, almost colorless needles, m.p. 195–198°.

A *direct* synthesis of the hydrazone hydrochloride was achieved by a modification of Beyer's method (9). Acetophenone thiosemicarbazone, m.p. 118.5–119.5°, (0.03 mole) and chloroacetaldehyde diethyl acetal (0.04 mole) were refluxed ½ h in ethanol (10 ml) and 12 *N* hydrochloric acid (4 ml). The light red solution was pumped to dryness and triturated with ether–methanol to give a gummy solid, which was again similarly treated leaving the hydrochloride (60%) of high purity (i.r.). Recrystallization from methanol–ether gave material of m.p. 196–199°, undepressed in admixture with the above specimen.

Thiazolecarboxylic Acids

The 2-acid, m.p. 97–98° (lit. (10) m.p. 97–98°), was made by lithiation of 2-bromothiazole (26) followed by carbonation, and the 4-acid, m.p. 196–197° (lit. (12) m.p. 196–197°), by decarboxylation of the 4,5-di-acid at 180° (11, 12). The 5-acid, m.p. 222–223° (lit. (13) m.p. 218°), was obtained either by hydrolysis of its ethyl ester (11) or directly by lithiation and carbonation of 5-bromothiazole (10).

Thiazole-2-carbonyl Chloride

Moisture was rigidly excluded throughout. The dry sodium salt was refluxed with an excess of acid-free thionyl chloride for 1 h and the solution evaporated under reduced pressure. Slow distillation of the sticky residue at 2 mm gave the *acid chloride* as a yellow solid, m.p. 26–29°. It was used without further purification.

N-Phenyl Thiazole-2-carboxamide

Reaction of the acid chloride with 2 equiv of aniline in benzene and work-up of the benzene soluble fraction gave the *amide*; it was recrystallized from aqueous ethanol as colorless needles, m.p. 88–89°; $\nu(CCl_4)$ 3385 (NH), 1690, 1605 cm^{-1} (amide I and II bands).

Anal. Calcd. for $C_{10}H_8N_2OS$: N, 13.7; S, 15.7. Found: N 13.7; S, 15.8.

Can. J. Chem. Downloaded from www.nrcresearchpress.com by 210.87.254.6 on 09/05/12
For personal use only.

Phenyl Esters

Thiazole-2-carbonyl chloride was refluxed with a slight excess of phenol in pyridine for ½ h and the solution poured on ice. Recrystallization of the precipitate from aqueous ethanol gave *phenyl thiazole-2-carboxylate* as colorless prisms, m.p. 72–73°; ν(CCl_4) 1772, 1740 cm^{-1} (C=O doublet).

Anal. Calcd. for $C_{10}H_7NO_2S$: C, 58.5; H, 3.4; N, 6.8. Found: C, 58.6; H, 3.65; N, 6.9.

Thiazole-4-carboxylic acid was refluxed for 2 h with an excess of thionyl chloride. Evaporation gave the light yellow crystalline acid chloride which was treated as above. The *4-ester* formed colorless needles, m.p. 87–87.5°, from aqueous ethanol; ν(Nujol) 1750 cm^{-1} (C=O).

Found: C, 58.7; H, 3.6; N, 6.95.

The *5-isomer*, prepared similarly, was a colorless crystalline powder (aqueous ethanol), m.p. 57–58°; ν(CCl_4) 1742 cm^{-1} (C=O)

Found: C, 58.4; H, 3.4; N, 6.9.

Thiazole-2-carbonyl Peroxide

Powdered thiazole-2-carboxylic acid (2.58 g, 20 mmoles) was added to an ice-cold solution of *N,N'*-dicyclohexylcarbodiimide (4.12 g, 20 mmoles) in 1.5 *N* ethereal hydrogen peroxide (70 ml) and the whole stirred for 5 h at 0°. The mixture was then filtered and the precipitate washed with a small portion of ether. The ethereal solution was washed first with small portions of saturated aqueous ammonium sulfate, saturated aqueous potassium bicarbonate, and saturated aqueous ammonium sulfate again, and the solution was then dried. The original precipitate was stirred at 0° for 1 h with chloroform to extract further peroxide. The whole was filtered and the precipitate identified as *N,N'*-dicyclohexylurea by mixed m.p. with an authentic specimen. The yield of the urea at this point was 83%, but overall it was probably higher since it is somewhat soluble in chloroform.

The chloroform filtrate and the ether solution were combined and evaporated to dryness below room temperature to give crude peroxide, containing some dicyclohexylurea. At this point on one occasion the residue spontaneously and violently inflamed.

The residue was dissolved in a minimum amount of chloroform, and methanol was added with cooling to precipitate the colorless, crystalline peroxide which was filtered and air dried (30%), m.p. 98° (with brisk effervescence followed by detonation); ν(CCl_4) 1768, 1737 cm^{-1} (C=O doublet).

Anal. Calcd. for $C_8H_4N_2O_4S_2$: iodometric equiv. 128. Found: iodometric equiv. 125, 126.

Thiazole-4-carbonyl Peroxide

Thiazole-4-carboxylic acid (1.5 g, 12 mmoles) was dissolved in aqueous acetone (30 ml, 1:1) and the solution chilled in an ice-bath. A solution of 1-cyclohexyl-3-(2-morpholinoethyl)-carbodiimide metho-*p*-toluenesulfonate (7.0 g, 18 mmoles) in aqueous acetone (30 ml, 1:1) was added with stirring within 2 min, followed by 50% hydrogen peroxide (10 ml). Stirring was continued for 6 h at 0° and the *peroxide* was filtered off and washed thoroughly with aqueous sodium carbonate and water. Dried and recrystallized from petroleum ether – methylene chloride it formed colorless prisms (45%), m.p. 149° (followed by explosion); ν(Nujol) 1790, 1750 cm^{-1} (C=O doublet).

Anal. Found: iodometric equiv. 127.

Thiazole-5-carbonyl Peroxide

The method and scale for the 4-peroxide were used exactly. Recrystallization from petroleum ether – chloroform gave colorless prisms (40%), m.p. 129° (followed by explosion); ν(Nujol) 1805, 1770 cm^{-1} (C=O doublet).

Anal. Calcd. for $C_8H_4N_2O_4S_2$: N, 10.85; iodometric equiv. 128. Found: N, 10.7; iodometric equiv. 127.

Radical Reactions of the Hydrazine and Peroxides

General Work-up and Analytical Methods

Approximately 1% solutions of the hydrazine were stirred and treated portionwise with 2 mol equiv of freshly precipitated silver oxide at room temperature: nitrogen was evolved and the formation of water was evident. The mixtures were heated at 80° for 12 h and then distilled at atmospheric pressure through an efficient fractionating column. The distillate in each case was diluted with sufficient benzene to dissolve the water carried over; this solution was then brought to standard volume with the inclusion of an internal standard for the g.l.c. determination of thiazole. The residue was filtered from the silver and silver oxide which were thoroughly washed with benzene, the filtrate and washings being brought to a standard volume. Aliquots of this were taken for g.l.c. determination as required and brought to a known volume with inclusion of an appropriate internal standard.

One percent solutions of the peroxides were heated in the dark until decomposition was complete (12 to 24 h; followed iodometrically). The solutions were then filtered from any acidic or polymeric material and brought to a standard volume with benzene, aliquots being used for g.l.c. analysis as required. In the case of the 4- and 5-peroxides the carboxylic acid content (mainly the 4- and 5-carboxylic acids) was determined by taking aliquots of both the insoluble precipitate and of the standard solution and titrating them potentiometrically in aqueous methanol.

Gas chromatographic analyses were carried out essentially as described by Dal Nogare and Juvet (19*b*). The solutions from the reaction were analyzed against a calibration curve obtained with solutions of the authentic reference materials in varying concentrations, each containing a fixed concentration of internal standard. Peak areas were determined using either a planimeter or a disc integrator.

The reaction temperatures and the yields of all products are listed in Table 1. A brief account of each individual reaction follows, giving the reaction scale and the columns, temperature programs and internal standards used, and including, where necessary, a description of additional analytical determinations and isolation and characterization of products.

2-Thiazolylhydrazine

Benzene, 6.00 g (52.1 mmoles) in 600 ml; column A, 150 to 300°, bibenzyl. Thiazole was found in both the distillate and the residue. Evaporation of a portion of the reaction solution gave slightly impure 2-phenylthiazole which was steam distilled and identified as its picrate, mixed m.p. 124–127° with authentic picrate.

Can. J. Chem. Downloaded from www.nrcresearchpress.com by 210.87.254.6 on 09/05/12
For personal use only.

Bromobenzene, 5.90 g (51.3 mmoles) in 600 ml; column C, 250°, *o*, *o'*-dichlorobibenzyl. The *m*- and *p*-isomers could not be separated using a wide range of g.l.c. conditions, and to separate the *o*-isomer cleanly small sample injections (0.1 μl) were necessary.

The bulk of the solution was evaporated and the residue subjected to preparative g.l.c. to collect all three isomers together. The i.r. analysis of each of the three synthesized isomers showed the 683 cm^{-1} band in the meta- and the 830 cm^{-1} band in the para- to be uniquely characteristic and to be free of overlap from other bands in a mixture of *o*-, *m*- and *p*-somers. Using the absorbance–concentration curve obtained for the pure *m*- and pure *p*-isomers in carbon disulfide solutions, the concentrations of these in a carbon disulfide solution of the p.g.l.c. fraction were determined as being in the ratio of $m:p = 1.74:1$.

Cumene, 3.00 g (26.0 mmoles) in 100 ml, under purified nitrogen to avoid autoxidation of solvent; column A, 150 to 300°, 3-phenylthiophene (see footnote 4 for the basis of yield calculation). The meta and para peaks overlapped slightly and were resolved by curve analysis.

The p.g.l.c. was used to collect separately the 2-cumylthiazoles and the bicumyl using a temperature program from 200 to 250°. Only the tops of the three isomer peaks were collected. These were then re-chromatographed and directly eluted into the IR102 spectrometer. This confirmed the substitution pattern for each isomer, by the strong band at 750 cm^{-1} for the *o*-, 790 cm^{-1} for the *m*-, and 840 cm^{-1} for the *p*-cumylthiazole (16). The bicumyl fraction from the p.g.l.c. was crystallized from methanol giving material of m.p. and mixed m.p. 117–118°.

A control experiment using only silver oxide and cumene on the same scale as before and with the same work-up procedure showed the formation of a trace of bicumyl (0.0094 g). The corrected yield is shown in Table 1.

Thiazole-2-carbonyl Peroxide

The g.l.c. analyses were done exactly as for the hydrazine reactions.

Benzene, 0.510 g (1.99 mmoles) in 50 ml. A substance of retention time similar to that of the phenyl ester was observed in the chromatogram, possibly 2-thiazolyl thiazole-2-carboxylate.

In a control experiment in the same proportions thiazole-2-carboxylic acid was refluxed in benzene. The g.l.c. showed the formation of thiazole equivalent to 31% decarboxylation.

Bromobenzene, 0.427 g (1.67 mmoles) in 42.7 ml. The *m* to *p* ratio for the bromophenylthiazole isomers was not determined in this case.

Cumene, 0.300 g (1.17 mmoles) in 30 ml.

Thiazole-4-carbonyl Peroxide.

Benzene, 2.70 g (10.6 mmoles) in 270 ml; column B, 100 to 300°, 9,10-d chloroanthracene. Evaporation of most of the solution and alkaline hydrolysis of the residue gave impure 4-phenylthiazole which was isolated with ether and converted into its picrate, identical with synthetic picrate.

A small portion of the solution was washed with dilute acid and base. Evaporation of the benzene then left neutral high molecular weight material corresponding to an overall weight of 0.99 g.

Bromobenzene, 0.662 g (2.58 mmoles) in 60 ml; column D, 110 to 300°, biphenyl. The carbon dioxide evolved was trapped by passing a stream of purified nitrogen through the reaction solution and then into a solution of barium hydroxide (saturated, then diluted with an equal volume of water). The precipitate of barium carbonate was weighed. A blank was done using bromobenzene alone.

Cumene, 0.595 g (2.32 mmoles) in 60 ml; column B, 100 to 300°, biphenyl. A portion of the solution was evaporated. The crude residue was washed with dilute acid and base and chromatographed on alumina with petroleum ether – ether mixtures. Bicumyl of m.p. and mixed m.p. 117.5–119° was eluted.

Control Reactions. A 1% suspension of thiazole-4-carboxylic acid in benzene was refluxed for 24 h. The solvent was removed and the acid reweighed. There was no loss in weight. A similar control in refluxing cumene showed 60% decarboxylation.

Thiazole-5-carbonyl Peroxide

The g.l.c. analyses were done exactly as for the 4-peroxide.

Benzene, 0.995 g (3.89 mmoles) in 100 ml. A portion of the solution was evaporated and the residue extracted with ether. The ether solution was washed with dilute acid and base and the unextracted material was chromatographed on alumina. Petroleum ether eluted the biphenyl, which was twice crystallized from aqueous methanol, and had a mixed m.p. of 69–70°.

Bromobenzene, 0.533 g (2.08 mmoles) in 50 ml. An unidentified compound of shorter retention time than the bromophenylthiazoles was observed. On the basis of the molecule containing one benzene ring it could be assigned an approximate yield of 25%.

Cumene, 0.470 g (1.84 mmoles) in 50 ml. The bicumyl was again isolated and identified.

Control Reactions were carried out on the 5-acid, as described for the 4-acid, and showed that there was no decarboxylation in refluxing benzene, and 80% decarboxylation in refluxing cumene.

We wish to thank the National Research Council of Canada for support of this work.

1. M. C. Ford and D. Mackay. J. Chem. Soc. 1294 (1958).
2. M. C. Ford and D. Mackay. J. Chem. Soc. 4620 (1957).
3. D. Mackay. Can. J. Chem. **44**, 2881 (1966).
4. G. Vernin, B. Barré, H. J-M. Dou, and J. Metzger. C. R. 2025 (1969).
5. G. Vernin and J. Metzger. Bull. Soc. Chim. France, 2504 (1963).
6. H. J-M. Dou, G. Vernin, and J. Metzger. Tetrahedron Lett. 2223 (1967).
7. G. Vernin, H. J-M. Dou, and J. Metzger. Bull. Soc. Chim. France, 3280 (1968).
8. T. Matsukawa and S. Ban. Japan 8282 (1954). Chem. Abstr. **50**, 13999 (1956).
9. H. Beyer, H. Höhn, and W. Lässig. Chem. Ber. **85**, 1122 (1952).
10. H. C. Beyerman, P. H. Berben, and J. S. Bontekoe. Rec. Trav. Chim. **73**, 325 (1954).
11. H. Erlenmeyer and H. von Meyenburg. Helv. Chim. Acta, **20**, 204 (1937).

12. H. ERLENMEYER and CH. J. MOREL. Helv. Chim. Acta, **25**, 1073 (1942).
13. H. ERLENMEYER, E. SCHMID, and A. KLEIBER. Helv. Chim. Acta, **25**, 375 (1942).
14. H. ERLENMEYER, R. MARBET, and H. SCHENKEL. Helv. Chim. Acta, **28**, 924 (1945).
15. R. C. ELDERFIELD. Heterocyclic compounds. Vol. 5. John Wiley and Sons, Inc., New York, 1957. p. 630.
16. A. G. DAVIES. Organic peroxides. Butterworths. London, 1961. p. 63.
17. F. D. GREENE and J. KAZAN. J. Org. Chem. **28**, 2168 (1963).
18. R. L. HARDIE and R. H. THOMSON. J. Chem. Soc. 2512 (1957).
19. S. DAL NOGARE and R. S. JUVET, JR. Gas–liquid chromatography. Interscience Publishers, New York, 1962. (*a*) p. 220; (*b*) p. 256.
20. L. J. BELLAMY. The infrared spectra of complex molecules. 2nd Edition. Methuen and Co., London, 1958. p. 65.
21. G. H. WILLIAMS. Homolytic aromatic substitution. The Pergamon Press, Ltd., London, 1960. p. 46.
22. A. E. S. FAIRFULL, J. L. LOWE, and D. A. PEAK. J. Chem. Soc. 742 (1952).
23. H. ERLENMEYER, C. BECKER, E. SORKIN, H. BLOCH, and E. SUTER. Helv. Chim. Acta, **30**, 2059 (1947).
24. H. ERLENMEYER, J. ECKENSTEIN, E. SORKIN, and H. MEYER. Helv. Chim. Acta, **33**, 1271 (1950).
25. F. SAULMANN. Ber. **33**, 2636 (1900).
26. K. GANAPATHI and A. VENKATARAMAN. Proc. Indian Acad. Sci. **A22**, 362 (1945).

Can. J. Chem. Downloaded from www.nrcresearchpress.com by 210.87.254.6 on 09/05/12
For personal use only.

Can. J. Chem. Downloaded from www.nrcresearchpress.com by 210.87.254.5 on 09/05/12
For personal use only.

Synthesis of pyrazol-4-ols

M. J. NYE[1] AND W. P. TANG
Department of Chemistry, University of Guelph, Guelph, Ontario

Received July 6, 1970

3,5-Diphenylpyrazol-4-ol (**4**) has been prepared by four convenient routes starting with the following compounds: diphenylpropanetrione (**1**), 2-acetoxyl-1,3-diphenyl-1,3-propanedione (**5**), chalcone oxide (**7**), and 1,3-diphenyl-2-propanone (**10**).

Canadian Journal of Chemistry, **48**, 3563 (1970)

Pyrazoles bearing an oxygen atom in the 4-position have not been extensively studied, in contrast to the 3- and 5-oxygenated compounds. Two review articles have regarded such compounds as "relatively few" (1) and "relatively inaccessible" (2). We report here the experimental details of four synthetic routes to the previously unknown (3) 3,5-diphenylpyrazol-4-ol (**4**).

In route 1 treatment of diphenylpropanetrione (**1**) (4) (or its hydrate) with excess hydrazine (or its hydrate) gives an 88% yield of **4**. The mechanism involves the intermediacy of first **2***a* and then **3** (5), since either will produce **4** under the conditions of the reaction, and **2***a*[2] can be isolated as a by-product. Further support for the mechanism is given by the observation that if methylhydrazine is used instead of hydrazine, a good yield of **2***b* is produced and none of **12***a* (N-1 in formula **2** must bear a hydrogen for the reaction to proceed further). This route is based on the method for the preparation of **12***b* of Sachs and Röhmer (6).

Route 2 gives a 97% yield of **4** by treatment of 2-acetoxyl-1,3-diphenyl-1,3-propanedione (**5**) (7) with hydrazine hydrate. An intermediate (**6**)

[1]

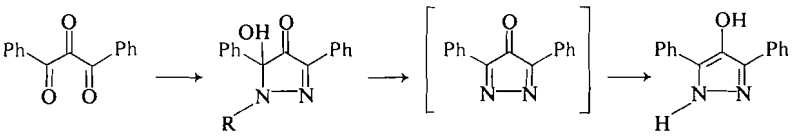

1 **2** **3** **4**

a R = H
b R = CH_3

[2]

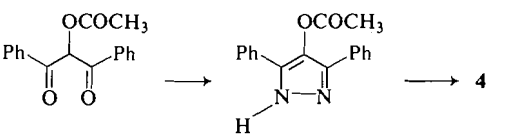

5 **6**

[3]

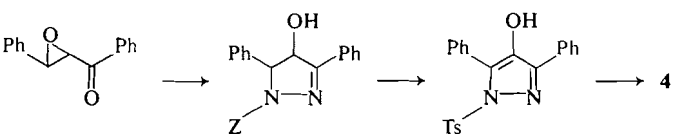

7 **8** **9**

a Z = *p*-Toluenesulfonyl (Ts)
b Z = H

[1]To whom correspondence should be addressed.
[2]Structural identification of this compound and other related hydrazones will be reported in a later paper.

Can. J. Chem. Downloaded from www.nrcresearchpress.com by 210.87.254.5 on 09/05/12
For personal use only.

is formed by a double condensation, and it can be isolated as a by-product if the temperature is kept low. This method has no close precedents in the literature.

Route 3 involves treatment of chalcone oxide (**7**) with *p*-toluenesulfonylhydrazide to give **8***a* which is oxidized by chromium trioxide to **9**, and then hydrolyzed by acid to **4** in a 20% overall yield. The first step of this synthesis is taken from the work of Padwa (8).

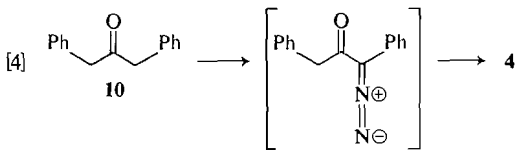

In route 4, 1,3-diphenyl-2-propanone is treated with *p*-toluenesulfonylazide and sodium ethoxide to give a 45% yield of **4**. This route is analogous to Regitz's preparation of **12***e* (9).

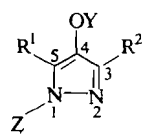

12

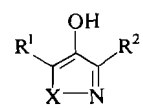

13

	R^1	R^2	Y	Z
a	phenyl	phenyl	H	CH_3
b	methyl	phenyl	H	H
c	phenyl	phenyl	$COCH_3$	H
d	phenyl	phenyl	$COCH_3$	CH_3
e	benzoyl	benzoyl	H	H

a X = O
b X = NH

Discussion

Probably the most versatile of the four routes is route 2, since on initial inspection it appears that by slightly modifying the reactants, compounds of general formula **12** can be prepared with different substituents at N-1, C-3, C-5, and O. In this laboratory we have only prepared compounds **4**, **12***a*, **12***c*, and **12***d* by this method, but in each case yields were excellent. Routes 1 and 4 on the other hand have variation of substituents limited to C-3 and C-5, and route 3 allows substituent variation at N-1, C-3, and C-5. However, on the last route, if N-1 carries a hydrogen atom, the chromium trioxide oxidation is not successful, probably because under the conditions used, which were similar to those used in the oxidation of **8***a*, **8***b* is more completely oxidized to **3** which would react further to give complex products (5).

From the point of view of yields and availability of starting materials, route 4 is probably the most attractive since 1,3-diphenyl-2-propanone is available from suppliers and is inexpensive, and the whole synthesis is carried out in one step. Routes 1 and 2 however are also attractive since the starting materials can be prepared from the available 1,3-diphenyl-1,3-propanedione in yields of 84 and 71% respectively.

In view of these four simple routes to pyrazol-4-ols, we point out that this area of chemistry need no longer be neglected. Indeed this group of compounds together with the isoxazoles (**13***a*) invites a much more thorough investigation since they are the main representatives of the heterocyclic system of general formula **13** (where X is a heteroatom) which has chemistry quite distinct from the isomeric 3- and 5-hydroxy analogues.

Experimental

Melting points were determined on a Meltemp apparatus and are uncorrected. Microanalyses were carried out by A. B. Gygli, Microanalysis Laboratories Limited, Toronto, Ontario. The reported i.r. spectra give only the principal sharply defined peaks. The n.m.r. spectra are reported in p.p.m. relative to internal tetramethylsilane.

Route 1

(*A*) A solution of 1.28 g (0.005 mole) of diphenylpropanetrione hydrate (4) in 15 ml 95% ethanol was treated with 0.51 g (0.01 mole) of 99–100% hydrazine hydrate in 1.5 ml ethanol. The reaction mixture became yellow and was refluxed on a water-bath for 30 min. On cooling, bright colorless prisms were formed, filtered, and washed with cold diluted ethanol. Yield: 1.033 g (87.5%), m.p. 231–233°. One recrystallization from ethanol gave 3,5-diphenylpyrazol-4-ol (**4**), m.p. 235–237°.

(*B*) A solution of 1.19 g (0.005 mole) of diphenylpropanetrione (4) in 25 ml absolute ethanol was treated with 0.51 g (0.01 mole) of 99–100% hydrazine hydrate in 1.5 ml ethanol. The color of triketone solution intensified on addition of hydrazine solution. The reaction mixture was worked-up as above, giving colorless prisms. Yield: 1.057 (89.6%), m.p. 231–233°. This substance was identical with the one prepared by method *A* by mixture m.p. and i.r. spectrum.

Anal. Calcd. for $C_{15}H_{12}N_2O$: C, 76.26; H, 5.12; N, 11.86. Found: C, 76.04; H, 5.28; N, 11.62.

The i.r. (KBr): 3222, 2520, 1591, 1263, 1150 cm^{-1}. The u.v. (95% EtOH, 25°): λ_{max} mμ (ε): 252 (22 700); 276 (shoulder, 17 100), 295 (shoulder, 10 040). The n.m.r.: (dimethyl sulfoxide-d_6): 7.45 (7H, multiplet: 6H aromatic, 1H hydroxyl exchangeable with D_2O); 8.02 (4H, multiplet, aromatic); 8.40 (1H, broad, NH).

(*C*) Into a stirred, cooled (ice-bath) solution of 1.025 g (0.004 mole) of diphenylpropanetrione (4) in 12 ml of methanol was dropped fairly rapidly a solution of 0.44 g (0.0088 mole) of 99–100% hydrazine hydrate in 2 ml of

Can. J. Chem. Downloaded from www.nrcresearchpress.com by 210.87.254.5 on 09/05/12
For personal use only.

methanol. During addition of hydrazine solution, some precipitates formed which soon dissolved to give a yellow solution. After stirring for 30 min, 70 ml of water was added resulting in heavy precipitation. The mixture was well chilled and the bright yellow prisms of 3,5-diphenyl-5-hydroxyl-4-pyrazolone were collected on a filter and washed with cold, diluted methanol, m.p. 120–122° (dec.). Further recrystallization from cold, diluted methanol gave the same m.p. (dec.). Yield: 89% (from 1,3-diphenylpropanetrione hydrate); 95.8% (from 1,3-diphenylpropanetrione). Recrystallization from hot solvents rendered a complete change of this substance (see below).

Anal. Calcd. for $C_{15}H_{12}N_2O_2$: C, 71.44; H, 4.80; N, 11.11. Found: C, 71.48; H, 5.08; N, 10.89.

The i.r. (KBr): 3368, 1747, 1714, 1306, 1197, 1018 cm^{-1}. The u.v. (95% EtOH, 25°): λ_{max} mμ (ε): 254 (19 100); 356 (3210). The n.m.r. (acetone-d_6): 6.32 (1H, broad, OH); 7.45 (8H, multiplet, aromatic), 8.08 (2H, multiplet, aromatic); 9.50 (1H, broad, NH).

Conversion of 3,5-diphenyl-5-hydroxyl-4-pyrazolone to the desired 3,5-diphenylpyrazol-4-ol (4) was effected by: (*a*) recrystallization in boiling ethanol, (*b*) heating at its melting temperature, or (*c*) treating with strong acids with dehydrating properties. Under conditions (*a*) and (*b*), orange-brown dirty substances were formed as side products. Under condition (*c*), a purple solution containing **3** formed initially and then gradually turned light brown. Crystallization from ethanol gave **4**. The yields ranged from 40–70%.

Route 2

A solution of 0.15 g of 99–100% hydrazine hydrate in 1 ml of 95% ethanol was added to a warm solution of 0.564 g 2-acetoxyl-1,3-diphenyl-1,3-propanedione (7) in 7 ml of 95% ethanol. The mixture was refluxed for 20 min and allowed to cool to room temperature. It was then poured into 20 ml of ice-water under slight agitation to give colorless prisms, m.p. 235–237°. The yield of **4** was 97%.

Route 3

Into a stirred, cooled (10–15°) solution of 0.784 g (0.002 mole) of 3,5-diphenyl-4-hydroxy-1-*p*-toluenesulfonyl pyrazoline (**8***a*) (8) in 100 ml acetone was added dropwise a standard chromic acid reagent[3] (*ca.* 1.5 ml) until a permanent brown color persisted. After 10 min, 500 ml of water were added and the mixture was stirred in an ice-bath for an additional hour. During this time, the initially waxy mass turned into yellow crystals which were filtered and washed with water; m.p. 150–155°. Recrystallization from ethanol afforded 3,5-diphenyl-1-*p*-toluenesulfonyl-pyrazol-4-ol (**9**) as slightly yellow plates, m.p. 161–163°, 0.465 g (59.6%). Another crystallization raised the m.p. to 165–167°.

[3]Prepared by dissolving 2.67 g chromium trioxide in 2.3 ml concentrated sulfuric acid diluted to a volume of 10 ml.

Anal. Calcd. for $C_{22}H_{18}N_2O_3S$: C, 67.66; H, 4.65; N, 7.18. Found: C, 67.74; H, 4.81; N, 7.13.

The i.r. (KBr): 3357, 3301, 1452, 1384, 1226, 1190, 1175 cm^{-1}. The u.v. (95% EtOH, 25°): λ_{max} mμ (ε): 224 (25 100), 275 (13 000), 289 (12 100), 370 (814). The n.m.r. (acetone-d_6): 2.38 (3H, singlet, CH_3); 7.48 (13H, multiplet, aromatic, including OH exchangeable with D_2O); 8.08 (2H, multiplet, aromatic).

Hydrolysis of this product to (**4**) was achieved by refluxing it in a mixture of concentrated HCl and acetic acid for 10 h. Recrystallization of the crude, colorless solids gave the desired product; colorless prisms, m.p. 233–235°; yield, *ca.* 70%.

Route 4

Into a well-stirred and well-cooled (ice-bath) solution of 1.05 g (0.005 mole) of 1,3-diphenyl-2-propanone in 15 ml of absolute ethanol was added a solution of 0.01 mole of sodium ethoxide in 10 ml absolute ethanol, followed immediately by rapid addition of a solution of 1 g of *p*-toluenesulfonyl azide (10) in 5 ml ethanol. The reaction mixture was then stirred for 1 h at ice-bath temperature. Dry ether (100 ml) was added to precipitate sodium salts of *p*-toluenesulfonamide which were filtered and well-washed with dry ether. The ethereal filtrate was extracted with 80 ml of water and the ethereal layer dried with sodium sulfate. Evaporation of ether at reduced pressure to a quarter of its initial volume afforded the almost colorless product as prisms, m.p. 232–236°. Further concentration of the filtrate gave two crops of the same material, m.p. 232–236°. The combined yield was 47%.

We thank the National Research Council of Canada for their financial support.

1. R. H. WILEY and P. WILEY. Pyrazolones, pyrazolidones and derivatives. John Wiley and Sons, New York, 1964. p. 111.
2. A. N. KOST and I. I. GRANDBERG. Advances in heterocyclic chemistry. Vol. 6. Academic Press, New York, 1966. p. 372.
3. M. J. NYE and W. P. TANG. 1st International Congress of Heterocyclic Chemistry, Albuquerque, New Mexico, June 1967, Abstracts No. 80; J. P. FREEMAN, J. J. GANNON, and D. L. SURBEY. J. Org. Chem. **34**, 187 (1969).
4. L. A. BIGELOW and R. S. HANSLICK. Org. Syn. Col. Vol. **2**, 244 (1943).
5. P. J. FAGAN, M. J. NYE, and W. P. TANG. 2nd International Congress of Heterocyclic Chemistry, Montpelier, France, July 1969, Abstracts No. A15.
6. F. SACHS and A. RÖHMER. Ber. **35**, 3307 (1902).
7. R. DE NEUFVILLE and H. v. PECHMANN. Ber. **23**, 3375 (1890).
8. A. PADWA. J. Org. Chem. **30**, 1274 (1965).
9. M. REGITZ and H. J. GEELHAAR. Ber. **101**, 1473 (1968).
10. W. v. E. DOERING and C. H. DEPUY. J. Amer. Chem. Soc. **75**, 5955 (1953). M. REGITZ, J. HOCKER, and A. LIEDHEGENER. Org. Syn. **48**, 36 (1968).

Can. J. Chem. Downloaded from www.nrcresearchpress.com by 210.87.254.6 on 09/05/12
For personal use only.

Structure of a diazecine derivative from the condensation of phthaloyl chloride with ethylenediamine

SAUL WOLFE AND S. K. HASAN
Department of Chemistry, Queen's University, Kingston, Ontario

Received May 8, 1970

The high dilution condensation of phthaloyl chloride with ethylenediamine has afforded not the benzodiazocine derivative **14**, as reported earlier, but a more complex compound (**17**) which has been found to be a bridged *di*benzodiazecine derivative. Treatment of **17** with ethanol causes alcoholysis of two of the four bridgehead lactam linkages. On heating, **17** isomerizes by a double ring → chain rearrangement to 1,2-diphthalimidoethane. The n.m.r. spectrum of **17** is discussed in terms of three possible conformations of the ten-membered ring.

Canadian Journal of Chemistry, **48**, 3566 (1970)

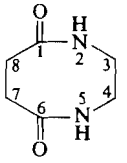

1

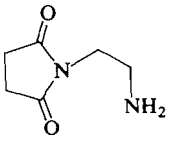

2

[1]

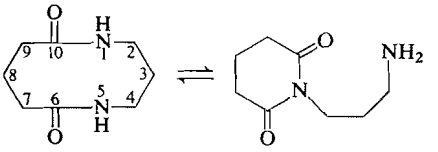

3 **4**

[2]

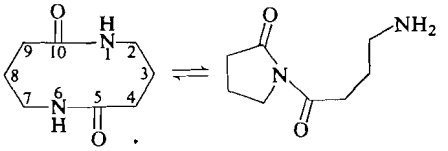

5 **6**

[3]

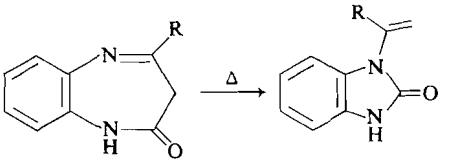

7 **8**

[4]

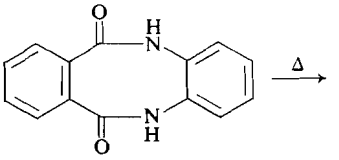

9

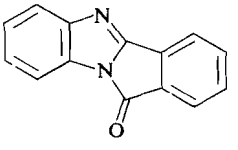

11

In the course of various studies in progress in this laboratory (1, 2) we became interested in certain properties of 1,6-dioxo-2,5-diazocines (**1**), in particular their behavior in dynamic n.m.r. experiments (3, 4) and the possibility of ring-chain tautomerism (**1** ⇄ **2**) (5). The latter behavior has been demonstrated for the 6,10-dioxo-1,5-diaza and 5,10-dioxo-1,6-diazacyclodecanes (**3** ⇄ **4** and **5** ⇄ **6**; eqs. 1 and 2) (6); and thermal rearrangement of the dihydrodiazepinone **7** to the imidazolidone **8**, eq. 3 (7) and of the dibenzodiazocines **9** and **10** to **11** and **12**, eqs. 4 and 5 respectively, has been achieved (8). In contrast, 2-aminoethylphthalimide (**13**) fails to cyclize to 1,6-dioxo-2,3,4,5-tetrahydro-2,5-benzodiazocine (**14**) (9), apparently because of the susceptibility of the phthalimido group to both the inter and intramolecular action of amines (10). A synthesis of the diazocine **14** has been reported by Stetter *et al.* (11), and the original intention of the present work was to repeat this synthesis and determine whether rearrangement of **14** to **13** could be demonstrated. Repetition of the work has afforded a compound having the reported (11) melting point, but the compound now obtained has been found not to be a simple diazocine.

In Stetter's synthesis (11), a 31.8% yield of **14**, m.p. 178°, was quoted. The spectral properties of the compound were not given, but the micro-

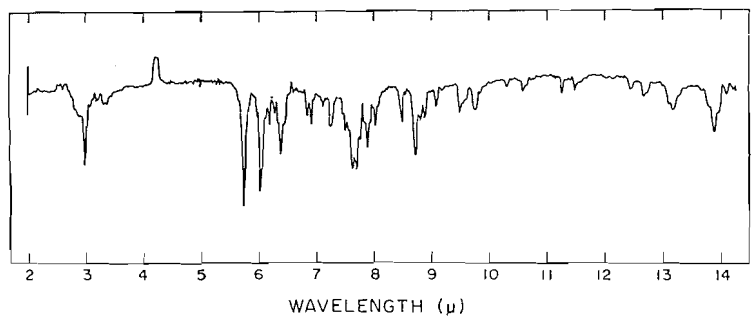

FIG. 1. The i.r. spectrum (in KBr) of **15**.

[5] 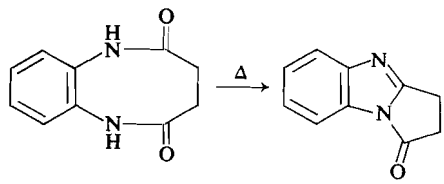

10 **12**

analysis and a molecular weight determination were presented which support the molecular formula $C_{10}H_{10}N_2O_2$. The preparation consisted of addition to benzene, through constant addition dropping funnels, of dilute benzene solutions

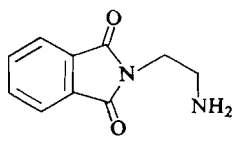

13

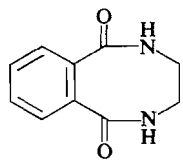

14

of phthaloyl chloride and ethylenediamine. Removal of polymer by filtration, followed by evaporation, trituration of the residue with hot ethanol, and concentration of the ethanol solution afforded the product. In the present work, this sequence of operations was followed as closely as possible (see Experimental), but in no case was the product of the ethanol treatment obtained in greater than 2.9% yield. Initial preparations of the material melted at 176–177°; later preparations yielded a substance having identical spectroscopic properties which melted at 192–194°.

The i.r. spectrum of the compound (Fig. 1) shows amide absorption at 3.05, 6.1, and 6.45 μ, and ester carbonyl absorption at 5.8 μ. The n.m.r. spectrum (Fig. 2) shows, among other peaks, a triplet at τ 8.77 and a quartet at τ 5.34, and indicates the presence of at least one ethyl group in the compound. The microanalysis indicates a formula $C_{20}H_{24}N_2O_6$, and this formula is confirmed by the high resolution mass spectrum (calcd. for $C_{20}H_{24}N_2O_6$, 412.1634; found, 412.1640). The mass spectrum also shows prominent peaks at 366 and 320 corresponding to loss of one and two molecules of ethanol from the molecular ion (calcd. for $M—C_2H_6O$, 366.1201; found, 366.1215). The spectroscopic data are consistent with structure **15**; in agreement with this formulation, **15** eliminates ethanol when heated above its melting point to give 1,2-diphthalimidoethane (**16**), m.p. 242–245°.

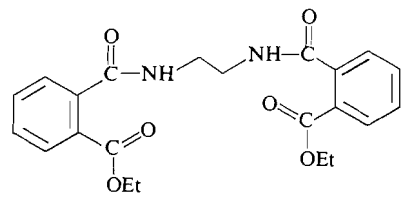

15

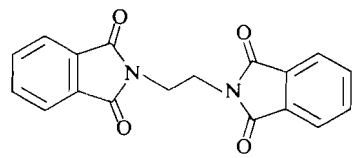

16

The diester **15** could only have been produced from a reaction of ethanol with a primary product of the initial condensation. Omission of the ethanol treatment or re-examination of the ethanol-insoluble material permitted the isolation of this primary product, m.p. 224–227° following crystallization from benzene. This compound has the molecular formula $C_{18}H_{12}N_2O_4$; although it is an isomer of **16**, the melting points,

Can. J. Chem. Downloaded from www.nrcresearchpress.com by 210.87.254.6 on 09/05/12
For personal use only.

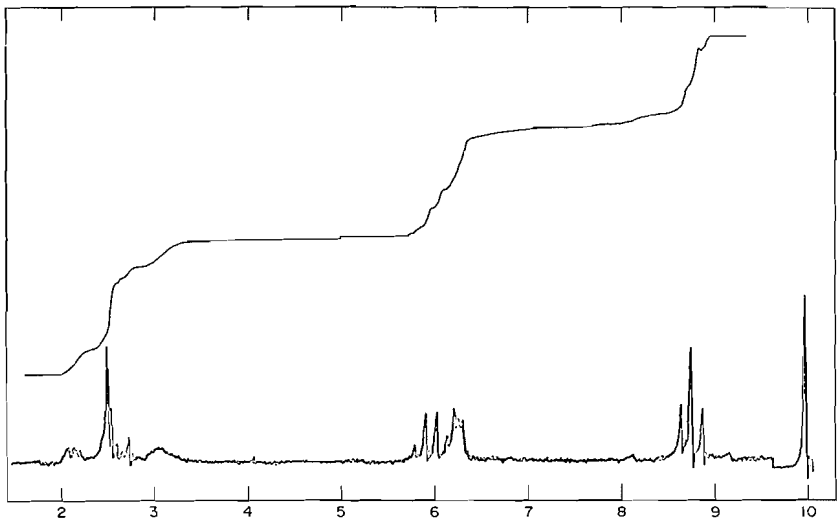

FIG. 2. The n.m.r. spectrum of **15**.

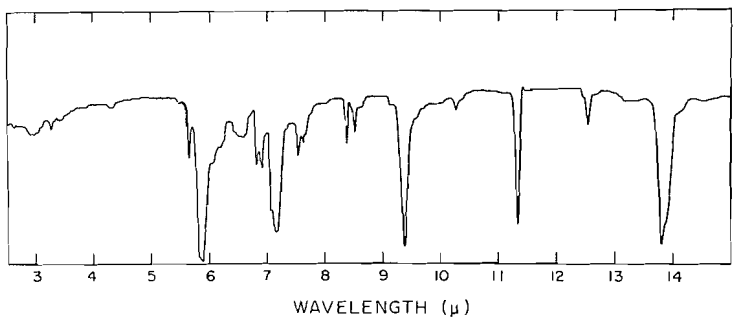

FIG. 3. The i.r. spectrum of 1,2-diphthalimidoethane.

solubility properties and spectroscopic behavior of the two compounds are different. The n.m.r. spectrum of **16** shows a doublet centered at τ 2.25 and a singlet at τ 5.98, in the ratio 2:1; the n.m.r. spectrum of the new compound shows a *multiplet* centered at τ 2.25 and a singlet at τ 5.90, also in the ratio 2:1. Consequently both compounds have eight aromatic protons and four equivalent methylene protons. The i.r. spectra of **16** and the new compound are displayed in Figs. 3 and 4; whereas **16** shows typical phthalimido bands at 5.62 (w) and 5.79 μ (s), the new compound has *strong* carbonyl absorption at 5.6 and 5.85 μ, indicative of a diacylimide structural unit (12). Structure **17**, 6,13-ethanodibenzo(*c*,*h*)(1,6)diazecine-5,7,12,14-tetraone is proposed for the condensation product. This structure is compatible with the spectroscopic data described above, and with the chemical properties of the compound.

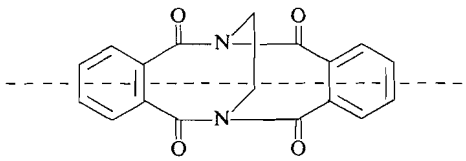

17

As a bridgehead lactam, **17** is expected to exhibit exceptional reactivity for its amide carbonyl groups (13); thus, brief refluxing with ethanol affords the diethyl ester **15**, as already anticipated by the isolation of **15** from the original work-up of the condensation reaction. Further, heating **17** above its melting point causes conversion to 1,2-diphthalimidoethane. This reaction is entirely analogous to the thermal rearrangement of 1,4,6,9-tetraketopyridazo[1,2-*a*]pyridazine (**18**) to N,N^1-bisuccinimide (**19**) eq. 6 (14).

We are unable to account for the difference

Can. J. Chem. Downloaded from www.nrcresearchpress.com by 210.87.254.6 on 09/05/12
For personal use only.

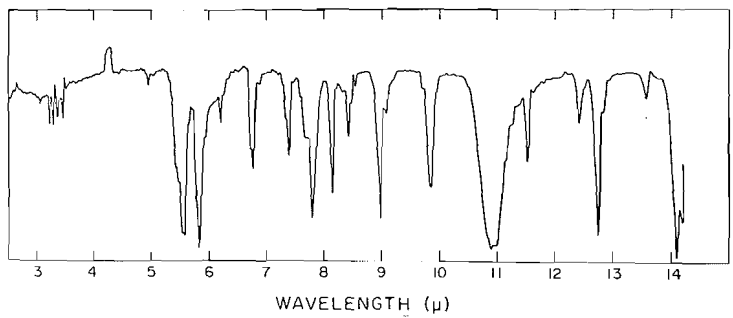

FIG. 4. The i.r. spectrum of **17**.

[6]

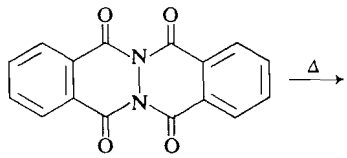

18

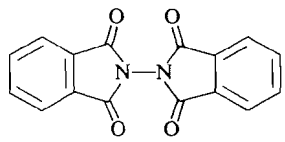

19

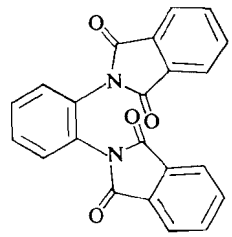

20

between the present results and those reported by Stetter. It is perhaps of interest to note that Paudler and Zeiler (8) have recently synthesized and characterized the dibenzodiazocine derivative **9**, m.p. 301–302.5°. The compound is not the same as that, m.p. 298°, claimed by Stetter *et al.* (11) from the high dilution condensation of *o*-phenylenediamine with phthaloyl chloride. The latter was shown (8) to be *o*-diphthalimidobenzene (**20**).

Compound **17** is a 2:1 adduct of phthaloyl chloride with ethylenediamine. Its mode of formation has not been examined, but it can be speculated that the benzodiazocine derivative **14**, formed initially, reacts with a second mole of phthaloyl chloride. The compound can be viewed either as a bridged dibenzodiazecine or as two connected benzodiazocines. In the latter case, the thermal rearrangement to diphthalimidoethane corresponds to ring → chain rearrangement of each diazocine ring, as originally envisaged for **14** → **13**. The rearrangement of **17** to **16** can then be described in terms of a sequence shown in eq. 7.

When **17** is viewed as a dibenzodiazecine derivative, three possibilities for stereoisomerism can be discerned, depending on the conformation of the ten-membered ring. These three conformations are most readily viewed in terms of their reflections across the mirror plane which bisects the molecule in all cases. Structure **22**, which has C_{2v} symmetry, is termed "mariner"; structure **23**, which has C_s symmetry, is termed "triclinium";[1] structure **24**, which has C_{2v} symmetry, is termed

[7]

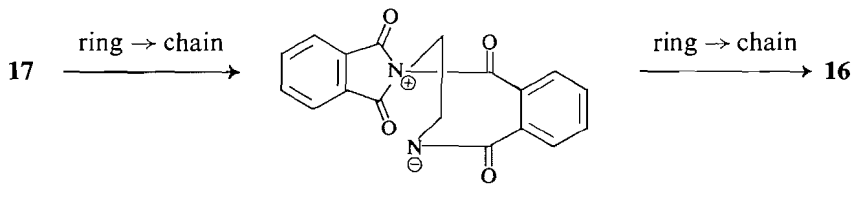

21

[1]Latin, *a couch* for reclining or eating

Can. J. Chem. Downloaded from www.nrcresearchpress.com by 210.87.254.6 on 09/05/12
For personal use only.

"saddle". On the basis of the aromatic chemical shifts, it appears possible to rule out conformation **24**. In the "saddle" the two benzene rings are face-to-face, and an upfield shift of about 1 p.p.m. could then be expected for the aromatic protons of **17** when compared to **16** (15). In fact, the two compounds have the same center of gravity of their aromatic protons.

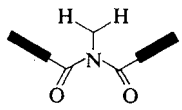

22
Mariner

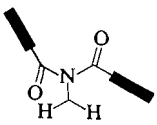

23
Triclinium

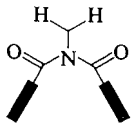

24
Saddle

Under conditions of slow ring inversion, the ethylene protons of **23** would be expected to give an AA'BB' pattern in the n.m.r. spectrum. At room temperature the spectrum shows a singlet for these protons. If **17** has the triclinium conformation, this result would imply rapid inversion of the ten-membered ring at room temperature on the n.m.r. time scale. Unfortunately, this point could not be checked because of the low solubility of **17** at lower temperatures. The evidence presented here does not, therefore, distinguish conformations **22** and **23**, and further work will be needed to resolve the conformational problem.

Experimental

Melting points were determined on a Fisher–Johns melting point apparatus, and are uncorrected. The i.r. spectra were recorded on a Beckman IR 5A instrument and were calibrated against the 6.238 μ peak of polystyrene. The n.m.r. spectra were obtained on Varian A60 or T60 spectrometers as 10% solutions in deuterochloroform, and were calibrated against tetramethylsilane as an internal standard. Mass spectra were recorded on a JEOL-JMS-O1SG double focussing mass spectrometer, at 75eV and 200 mμA. Microanalyses are by A. B. Gygli, Toronto, Ontario.

Absolute ethanol was prepared by distillation from magnesium ethoxide (16). Distilled benzene was dried over sodium wire and redistilled before use. Phosphorus pentachloride was purified by heating in a distillation apparatus on the steam bath to remove low boiling impurities such as phosphorus oxychloride (11). Phthalic anhydride was purified by sublimation (17). Ethylenediamine was dried over sodium metal (11). Small pieces of sodium were added in portions to ethylenediamine (40 ml) until the initial reaction was complete. Then additional sodium (total 2 g) was added and the mixture was refluxed for 1 h. The solvent was distilled, and the distillate redistilled, a fraction boiling at 115–116° being retained. This fraction shows singlets (ratio 1:1) at τ 7.13 and 8.17 in its n.m.r. spectrum. *The peak at τ 8.17 disappears* when the solution is shaken with D_2O.

Phthaloyl Chloride (17)

(*i*) Phthalic anhydride (14.8 g, 0.1 mole) and phosphorus pentachloride (22.0 g, 0.106 mole) were mixed and heated together for 12 h at 150–160°. A light brown liquid resulted, from which phosphorus oxychloride was removed by distillation at 40° under reduced pressure. The temperature of the bath was then raised to 240° and phthaloyl chloride was collected at 150–160°/40 mm. Redistillation gave a colorless liquid, b.p. 150–155°/20 mm; the yield was 11.1 g (54%). The i.r. spectrum shows peaks at 5.6 and 5.75 μ and the n.m.r. spectrum shows a multiplet at τ 2.2.

(*ii*) Phthaloyl chloride prepared by the procedure of Kyrides (18) gave identical results in the condensation reaction. Phthalic anhydride (74 g, 0.5 mole) and anhydrous zinc chloride (400 mg) were placed in a three-necked flask fitted with a dropping funnel, thermometer, and water cooled condenser. The mixture was heated to 200°, and thionyl chloride (59.5 g, 0.5 mole) was added dropwise during a 6 h period, the temperature being maintained at 200–230°. The mixture was then refluxed for an additional 5 h, and distilled at 115–120°/1 mm to give 20.5 g (20.5%) of phthaloyl chloride.

Reaction of Phthaloyl Chloride with Ethylenediamine (11)

Solutions of phthaloyl chloride (2.0 g, 0.01 mole) in dry benzene (200 ml) and dry ethylenediamine (1.2 g, 0.02 mole) in dry benzene (200 ml) were prepared. A four-necked flask was fitted with a magnetic stirrer, a nitrogen inlet, and a condenser with a drying tube attached. The flask was flame-dried, fitted with precision dropping funnels[2] and then charged, under nitrogen, with dry benzene (150 ml). The two reactants were added to the flask at room temperature at a rate of 5 drops every 4.2 s, the ethylenediamine being added through the center neck to minimize deposition of polymer on the walls of the flask. Addition was complete in 3 h, and the insoluble polymer was then removed by filtration. Evaporation of the filtrate gave a residue which was extracted with benzene (50 ml). Removal of the benzene afforded 0.5 g of a white solid. This was partially soluble in hot absolute ethanol (25 ml). The ethanol-insoluble part (319 mg) was recrystallized from benzene to give **17**, m.p. 224–227°.

Anal. Calcd. for $C_{18}H_{12}N_2O_4$ (mol. wt., 320.0797): C, 67.5; H, 3.75; N, 8.75. Found (320.0801): C, 67.4; H, 4.29; N, 8.59.

Concentration of the ethanol extract afforded 55 mg of **15** as colorless crystals, m.p. 192–194° or 176–177°.

Anal. Calcd. for $C_{22}H_{24}N_2O_6$ (mol. wt. 412.1634):

[2]Obtained as Catalog No. 7340 from Ace Glass Inc., Vineland, New Jersey.

Can. J. Chem. Downloaded from www.nrcresearchpress.com by 210.87.254.6 on 09/05/12
For personal use only.

C, 63.97; H, 5.87. Found (412.1614; 412.1640): C, 64.1; H, 5.82.

A mixture of **17** (48.5 mg) and absolute ethanol (15 ml) was refluxed for 0.5 h. Filtration and concentration of the filtrate yielded 10 mg (18.5%) of **15**, m.p. 190–193°, identified by its i.r. spectrum and by a mixture m.p. determination. Repetition of this experiment and extension of the reflux period to 20 h led to the formation of 1,2-diphthalimidoethane, m.p. 243–244° (lit. (19). 243–244°).

The ethyl ester **15** (9 mg) was heated to 200° and maintained at this temperature for 15 min. Cooling and crystallization of the material from absolute ethanol (1 ml) afforded 2 mg of 1,2-diphthalimidoethane, identified by its m.p., i.r. spectrum, and a mixture m.p. with an authentic specimen.

Compound **17** (26.9 mg) was heated for 15 min at 240–250°. The i.r. spectrum of the cooled residue was identical with that of 1,2-diphthalimidoethane. Recrystallization from ethanol yielded 1,2-diphthalimidoethane, m.p. 243–244°.

We thank the National Research Council of Canada for support of this work and for an equipment grant which made possible the purchase of the mass spectrometer. Helpful discussions with Professor James A. Moore are also gratefully acknowledged.

1. S. K. HASAN. Ph.D. Thesis. Queen's University, Kingston, Ontario. 1969.
2. J. R. CAMPBELL. Ph.D. Thesis. Queen's University, Kingston, Ontario. 1969.
3. G. BINSCH. *In* Topics in stereochemistry. Vol. 3. E. L. Eliel and N. L. Allinger, *Editors*. Wiley-Interscience, New York. 1968. p. 97.
4. S. WOLFE and J. R. CAMPBELL. Chem. Commun. 874 (1967).
5. P. R. JONES. Chem. Rev. **63**, 461 (1963).
6. G. I. GLOVER, R. B. SMITH, and H. RAPOPORT. J. Amer. Chem. Soc. **87**, 2003 (1965).
7. M. ISRAEL, L. C. JONES, and E. J. MODEST. Tetrahedron Lett. 4811 (1968).
8. W. W. PAUDLER and A. G. ZEILER. J. Org. Chem. **34**, 2138 (1969).
9. C. J. M. STIRLING. J. Chem. Soc. 4531 (1958).
10. S. WOLFE and S. K. HASAN. This issue.
11. H. STETTER, L. MARX-MOLL, and H. RUTZEN. Ber. **91**, 1775 (1958).
12. L. J. BELLAMY. The infra-red spectra of complex molecules. John Wiley and Sons, Inc., New York. 1962. p. 221; T. UNO and K. MACHIDA. Bull. Chem. Soc. Japan. **34**, 545 (1961); **35**, 1226 (1962).
13. M. DENZER and H. OTT. J. Org. Chem. **34**, 183 (1969).
14. E. HEDAYA, R. L. HINMAN, V. SCHOMAKER, S. THEODOROPULOS, and L. M. KYLE. J. Amer. Chem. Soc. **89**, 4875 (1967).
15. L. A. SINGER and D. J. CRAM. J. Amer. Chem. Soc. **85**, 1080 (1963).
16. A. I. VOGEL. A textbook of practical organic chemistry. Longmans, Green and Co., London. 1956. p. 169.
17. E. OTT. *In* Organic Syntheses. Coll. Vol. II. John Wiley and Sons, Inc., New York. 1943. p. 528.
18. L. R. KYRIDES. J. Amer. Chem. Soc. **59**, 206 (1937).
19. BEILSTEIN'S Handbuch der Organischen Chemie. Vol. XXI. Julius Springer Verlag, Berlin. 1935. p. 492.

Can. J. Chem. Downloaded from www.nrcresearchpress.com by 210.87.254.6 on 09/05/12
For personal use only.

Can. J. Chem. Downloaded from www.nrcresearchpress.com by 210.87.254.5 on 09/05/12
For personal use only.

Five-membered rings. II.[1] Inter and intramolecular reactions of simple amines with *N*-substituted phthalimides. Methylamine as a reagent for removal of a phthaloyl group from nitrogen

SAUL WOLFE AND S. K. HASAN
Department of Chemistry, Queen's University, Kingston, Ontario

Received May 8, 1970

A reexamination of the literature on inter and intramolecular reactions of amines with *N*-substituted phthalimides has led to the demonstration that methylamine is a convenient reagent for removal of a phthaloyl protecting group from nitrogen at room temperature. Application of this procedure (first described in 1896) to the Gabriel synthesis of primary amines and to peptide synthesis is recommended. The simplicity of the reaction is a consequence of the consecutive occurrence of two unexpectedly rapid processes: (*1*) methylaminolysis of one of the imide bonds; (*2*) intramolecular catalysis, by an *N*-methylamido group, of the hydrolysis or aminolysis of an adjacent phthalamido linkage.

Some unsuccessful attempts to prepare 2-aminoethylphthalimide are also described.

Canadian Journal of Chemistry, 48, 3572 (1970)

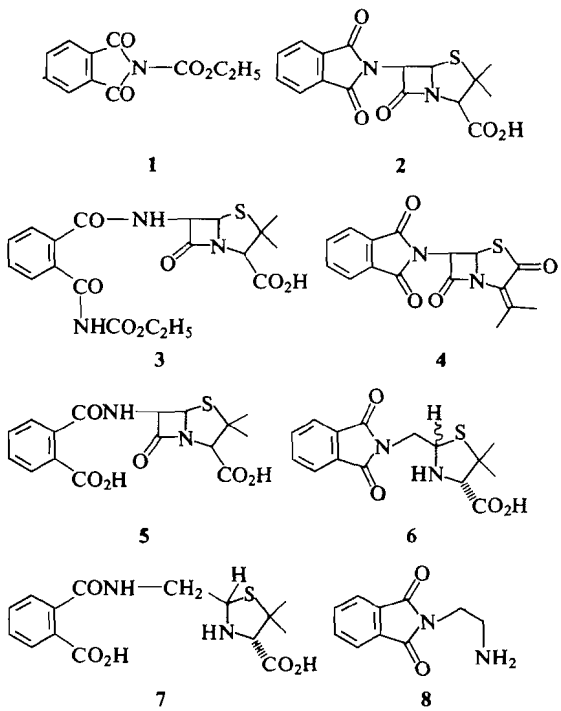

1 **2**

3 **4**

5 **6**

7 **8**

There is an extensive literature on the partial and total hydrolysis, aminolysis, and hydrazinolysis of *N*-substituted phthalimides (1, 2). The first stage of these reactions is of interest as a convenient synthetic route to phthalamic acid derivatives (3). The second has been the subject of numerous kinetic investigations (4) because of its relationship to mechanisms of intramolecular catalysis (5), and is also of synthetic importance as the final step in the Gabriel synthesis of primary amines (1). In the course of several synthetic investigations in progress in this laboratory, in which the phthalimido protecting group has been employed, a number of observations have been made recently which seem to indicate that this group is more sensitive to acyl cleavage than had been anticipated (6). Thus, (*A*): *N*-carbethoxyphthalimide (**1**) (Nefkens' reagent (7)) transfers its phthaloyl group at room temperature and p*H* 7.5 to 6-aminopenicillanic acid (6-APA) to form **2** (8). This reaction, devised by Nefkens (7), implies cleavage of one acyl linkage of **1** by the amino group of 6-APA, followed by ready ring closure of the phthalamate **3**; (*B*): the phthalimido group of the anhydropenicillin **4** undergoes hydrolysis to a phthalamic acid at p*H* 7.4 in DMSO–H_2O in the course of the reversal of the anhydropenicillin rearrangement (**4** → **5** (9)); (*C*): treatment of the epimeric 2-phthalimidomethylthiazolidinecarboxylic acids **6** with dilute potassium carbonate also effects conversion to a phthalamic acid (**7** (10)); (*D*): finally, 2-aminoethylphthalimide (**8**) cannot be isolated following neutralization of the hydrochloride (*cf.* 11), and the phthalimido group rapidly disappears from the solution. Although, as indicated by the references cited, none of these observations is without precedent, taken together they suggested that closer examination of some aspects of the cleavage of the acyl bonds of *N*-substituted phthalimides might be warranted.

von Braun and Pinkernelle noted in 1934 (12) that *N*-3-aminopropylphthalimide is not stable in

[1]Part I is S. K. Hasan *et al.* (41).

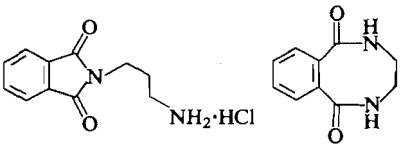

9 10

the form of the free base but can be characterized as the crystalline hydrochloride **9**. Later, after successful inter (13) and intramolecular (14) transfer of acyl groups from acyclic diacylimides had been achieved, Stirling (11) examined the possibility of ring-chain tautomerism of *N*-2-aminoethylphthalimide (**8** → **10**). The hydrobromide of **8** was prepared by treatment of the carbobenzoxy derivative with hydrogen bromide, but, as in von Braun's work, the free base could not be characterized. Neutralization of the hydrobromide produced only an unidentified acid, a small amount of ethylenediamine and none of the diazocine **10**. More recently, Peck has found that liberation of the *N*-methyl derivative of **8** from its hydrochloride proceeds with instantaneous hydrolysis to the phthalamic acid (15). All of these results indicated that a report by Spring and Woods (16) (in which no experimental details, yields or characterization of products were given) that **8** is obtained upon treatment of *N*-methylphthalimide with ethylenediamine required reexamination.

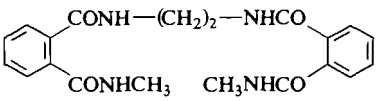

11

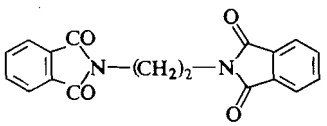

12

In 15 min at room temperature, the reaction in chloroform of equimolar quantities of ethylenediamine and *N*-methylphthalimide has now afforded a crystalline compound $C_{20}H_{22}N_4O_4$, m.p. 164–166°, which shows amide absorption in the i.r. spectrum at 3.1, 6.1–6.2, 6.4, and 6.6 μ. The compound is an adduct containing *two* units of *N*-methylphthalimide and one of ethylenediamine, and structure **11**, *N*,*N*′-(*N*,*N*′-dimethyl)-diphthalamidoethane is proposed. Refluxing of this compound in ethanol causes cyclization to 1,2-diphthalimidoethane (**12**). The same process can be observed in the mass spectrometer, which shows no molecular ion (17), but peaks at M-CH_3NH_2 (calcd. for $C_{19}H_{17}N_3O_4$: 351.1219; found: 351.1219) and M-$2CH_3NH_2$ (calcd. for $C_{18}H_{12}N_2O_4$: 320.0797; found: 320.0787). The compound can be considered to have formed by intermolecular reaction of ethylenediamine with two moles of *N*-methylphthalimide.

Extensive and unsuccessful efforts were also made in the present work to obtain **8** by neutralization of the hydrochloride and from the reaction of Nefkens' reagent with ethylenediamine. From the latter reactions only **12** and polymeric material were obtained. The hydrochloride of **8** was synthesized by the sequence shown in Chart 1; as in Stirling's work (11), neutralization of this compound under a variety of conditions afforded no recognizable monomeric product. From a reaction conducted under high dilution conditions with triethylamine in methylene chloride, a solution was obtained which displayed phthalimido absorption in the i.r. spectrum. However, removal of the solvent led to disappearance of these i.r. peaks, and heating of the residue afforded 1,2-diphthalimidoethane. It appears that **8** does not cyclize to a diazocine but, rather, undergoes polymerization with opening of the phthalimido ring. In this sense its behavior is quite different from that of the saturated analogs **13** and **14** (18), both of which undergo ready *intra*molecular cyclization to diazecine deriva-

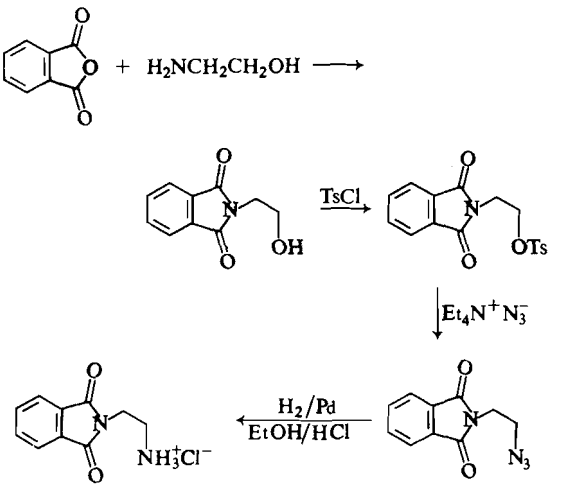

CHART 1. Synthesis of the hydrochloride of 2-aminoethylphthalimide

Can. J. Chem. Downloaded from www.nrcresearchpress.com by 210.87.254.5 on 09/05/12
For personal use only.

Can. J. Chem. Downloaded from www.nrcresearchpress.com by 210.87.254.5 on 09/05/12
For personal use only.

tives. All of these observations provide further evidence that *phthal*imides display exceptional reactivity towards an amino group.

One of Gabriel's synthetic routes to *N*-substituted diaminoalkanes (19) consisted of treatment of 2-bromoethylphthalimide with an aromatic amine, followed by removal of the phthaloyl group. An attempt by Ristenpart to extend this sequence to the synthesis of *alkyl*aminoethylamines met with mixed success (20). Diethylamine effected displacement of bromine from 2-bromoethylphthalimide, but ethylamine reacted at 0° in ethanol to form the *phthalamide* **15**, and methylamine reacted *at room temperature* in ethanol to give *N*-methylphthalimide. Similar behavior has occasionally been noted by other workers (1, 21–24), and it is not surprising, therefore, that a reported addition of amines to the *double bond* of *N*-vinylphthalimide (**16**) (25) could not be substantiated (26). We have found

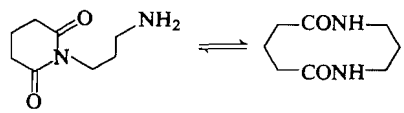

13

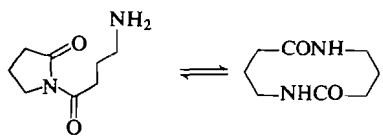

14

that ethylamine reacts with **16** to give a compound, m.p. 142–143° (lit. (26) 143.5–144.5°) whose spectral properties are consistent with the *phthalamide* structure **17**. The reaction of **16** with *methylamine* proceeded differently; shaking of a benzene solution of **16** at room temperature

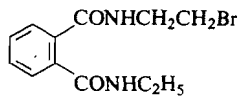

15

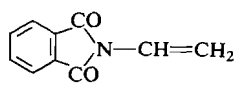

16

with excess 40% aqueous methylamine produced in 5 min, as in the case of ethylamine, a heavy precipitate. This was not the expected (26) *N*-methyl-*N'*-vinylphthalamide but, rather, *N,N'*-di*methyl*phthalamide **18**.

The possible existence of the series of reversible reactions shown in Scheme 1 has been discussed (21,27,28). Depending on the experimental conditions and on the nature of R_1 and R_2, one may expect selective formation of one of the imides (**19** or **21**), the unsymmetrical phthalamide **20** or the symmetrical phthalamides **22** and **23**. However, it does not appear to have been appreciated that forcing of the reaction of **19** to the imide **21** or the phthalamide **23** *corresponds to dephthaloylation* of **19**. All of the evidence cited above (1, 20, 21; and the formation of **18** from **16**) indicates that *aqueous methylamine* is a suitable reagent for this purpose. The generality of this statement can be demonstrated. In addition to **16**, phthalimide, 2-hydroxyethylphthalimide, *N*-methylphthalimide, phthaloylglycine and phthaloylalanine react with methylamine to give **18** at room temperature and with release of the original amino function. In the cases of the glycine and alanine derivatives (eq. 1), formation of the amino acids was quantitative.

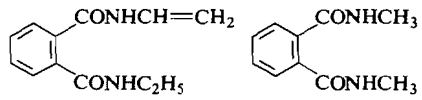

17 **18**

The initial stage in these reactions with methylamine presumably consists of the now well-documented aminolysis of one of the imide linkages. The second is considered to consist of intramolecular catalysis, by the new *N*-methylamido function, of the hydrolysis or aminolysis of the second phthalamido bond. Most studies of intramolecular catalysis of amide hydrolysis (4) have been performed under acidic conditions and are not directly applicable to the present system. However, mechanisms for intramolecular catalysis under neutral and alkaline conditions do exist (29, 30). At p*H* 7.8, methanol is eliminated from the methyl esters of phthalamic acid (k_2 = 3100 M^{-1} s^{-1}) and *N-methyl*phthalamic acid (k_2 = 12,400 M^{-1} s^{-1}) more rapidly (29) than from methyl *o*-formylbenzoate which had been described (31) as the most reactive known methyl ester. Imide formation from phthalamic acid derivatives is not confined to the esters; in neutral or basic aqueous solutions, the amide group is several orders of magnitude more effective as an intramolecular nucleophilic reagent towards ester *or amide* linkages than either the imidazolyl or carboxylate functions (30). For example, at 25.9° and p*H* 7.8, *N,N'*-dimethylphthalamide was converted to *N*-methylphthalimide with a rate constant of 7.6 M^{-1} s^{-1} (29).

The above kinetic studies refer to concentrations of the order of 1×10^{-4} *M* and, under

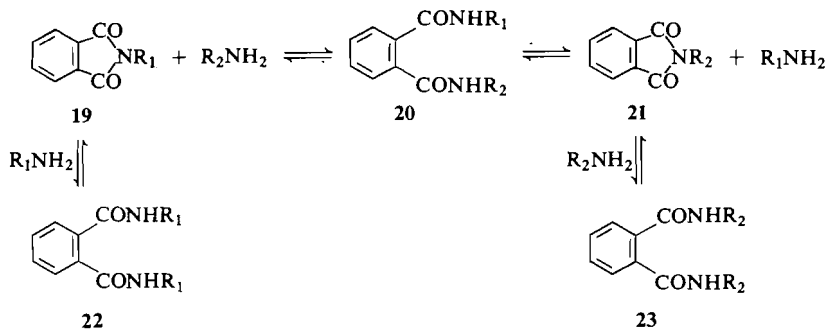

SCHEME 1

[1] 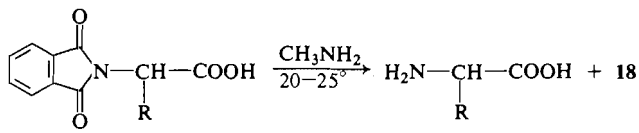

R = H, CH_3

[2] 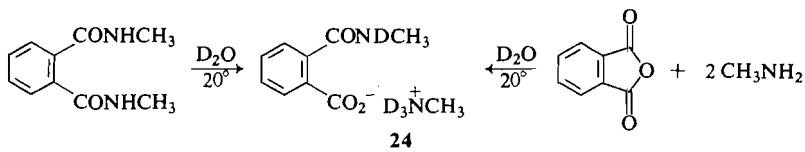

these conditions, the product is the imide. It seemed desirable to examine the hydrolytic behavior of *N,N'*-dimethylphthalamide, as a model substrate, at higher concentrations. This compound is surprisingly soluble in water; the n.m.r. spectrum of a 10% solution in deuterium oxide showed, initially, two singlets at τ 2.62 and 7.25 in the ratio 4:6. After 16 h at room temperature the spectrum consisted of a multiplet (4H) at τ 2.55–2.74 and two three-proton singlets at τ 7.19 and 7.5. The new spectrum was shown to be that of **24**, the methylammonium salt of *N*-methylphthalamic acid (eq. 2) in the following way. An exactly identical n.m.r. spectrum was obtained when a suspension of phthalic anhydride in deuterium oxide containing 2 mole equiv of methylamine was shaken for 12 h at room temperature. Acidification of each solution afforded *N*-methylphthalamic acid, which was converted to *N*-methylphthalimide upon treatment with diazomethane (29). The n.m.r. spectrum of a 10% solution of *N*-methylphthalamic acid (**25**) in deuterium oxide showed initially a multiplet (4H) at τ 2.07–2.77 and a singlet (3H) at τ7.17. After 16 h at room temperature the spectrum consisted of a multiplet (4H) centered at τ 2.4 and singlets at τ 7.17 (1.8 H) and 7.44 (1.2 H). This result indicates further hydrolysis of **25** to **26**, the methylammonium salt of phthalic acid. The relative intensities of the methyl singlets reflect the position of the equilibrium shown in eq. 3. These results demonstrate that, at the

[3] 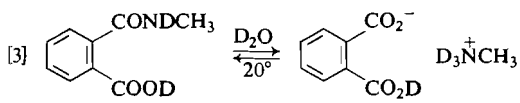

concentrations employed in preparative experiments, stepwise hydrolysis of an *N*-methylphthalamide proceeds readily in the absence of base. Rapid methylaminolysis of such a compound, as in the dephthaloylation described above, is therefore consistent with these properties.

Hydrazinolysis (32) is the generally accepted procedure for removal of the phthalimido group in the Gabriel synthesis (1) and in peptide synthesis (33), although base-catalyzed hydroxylaminolysis has been recommended recently as an alternative (34). The present methylamine procedure ought to provide a useful adjunct to these other methods because of its simplicity and the ease of removal of excess amine from reaction mixtures.

Can. J. Chem. Downloaded from www.nrcresearchpress.com by 210.87.254.5 on 09/05/12
For personal use only.

Can. J. Chem. Downloaded from www.nrcresearchpress.com by 210.87.254.5 on 09/05/12
For personal use only.

Experimental

Melting points were determined on a Fisher–Johns melting point apparatus, and are uncorrected. The i.r. spectra were recorded on a Beckman IR 5A instrument, and calibrated against the 6.238 μ peak of polystyrene. The n.m.r. spectra were obtained on Varian A60 or T60 spectrometers as 10% solutions in chloroform or deuterium oxide; tetramethylsilane (TMS) or trimethylsilyl-1-propanesulfonic acid (TSS) were employed as internal standards, as required. Mass spectra were recorded on a JEOL-JMS-01SG double focussing mass spectrometer, at 75 eV and 200 mμA. Microanalyses are by A. B. Gygli, Toronto, Ontario.

The t.l.c was performed on plates coated with silica gel or with alumina. Spots were developed in an iodine chamber and then observed, if necessary, under u.v. light. All solvents were distilled before use; ethanol, benzene, and ether were dried by standard procedures. Petroleum ether refers to a hydrocarbon fraction which boils at 30–60°. Magnesium sulfate was employed routinely as a drying agent.

N,N′-Dimethylphthalamide

Phthalimide (5.0 g, 0.034 mole) dissolved initially when added to 40% aqueous methylamine (7.5 ml), and after 1 min a heavy precipitation took place. This precipitate was collected and recrystallized from aqueous acetone to give 3.55 g (54.5%) of **18** as colorless needles, m.p. 206–207°. The i.r. spectrum shows peaks at 3.15, 6.15, and 6.45 μ.

N-Methylphthalimide

N,N′-Dimethylphthalamide (1.9 g, 0.01 mole) was heated for 15 min at 205–210°. Recrystallization from ethanol of the cooled residue afforded 1.4 g (87%) of *N*-methylphthalimide, m.p. 136–137° (lit. (21) 133°). The i.r. spectrum shows phthaloylamino absorption at 5.65 and 5.85 μ; the n.m.r. spectrum shows a multiplet at τ 2.07–2.4 (4H) and a singlet at τ 6.87 (3H).

Reaction of N-Methylphthalimide with Ethylenediamine

N-Methylphthalimide (483 mg, 0.003 mole) and anhydrous ethylenediamine (35) (180 mg, 0.003 mole) were stirred in chloroform (50 ml) for 15 min. Removal of the solvent afforded a viscous oil which crystallized upon treatment with ethanol–ether. Recrystallization from ethanol–ether gave 257 mg (56%) of **11**, m.p. 164–166°.

Anal. Calcd. for $C_{20}H_{22}N_4O_4 \cdot H_2O$: C, 60.00; H, 5.5; N, 14.00. Found: C, 59.66; H, 5.3; N, 13.89.

The mass spectrum shows peaks at *m/e* 351.1226, 351.1219 (calcd. for M-CH_3NH_2, *i.e.*, $C_{19}H_{17}N_3O_4$: 351.1219), and 320.0806, 320.0787 (calcd. for M-$2CH_3NH_2$, *i.e.*, $C_{18}H_{12}N_2O_4$: 320.0797); λ_{max}(KBr) 3.1, 6.1–6.2, 6.4–6.6 μ.

The compound (22 mg) was heated for 15 min at 160–170° and the cooled residue was then triturated with chloroform (2 ml). Recrystallization of the chloroform soluble material (16.55 mg) from ethanol afforded 1,2-diphthalimidoethane, m.p. 244°, identified by this m.p., a mixture m.p. and its i.r. and n.m.r. spectra (35).

Nefkens' Reagent (7)

Potassium phthalimide (55.5 g, 0.3 mole) was added to dimethylformamide (300 ml), and the suspension was cooled in an ice-salt bath. Ethyl chloroformate (30.8 g, 0.35 mole) was then added, with stirring, during a 15 min period. Stirring was continued for 1 h after the addition was complete and the reaction mixture was then poured into a mixture of ice and water (600 ml). The resulting precipitate was collected and dried. Recrystallization from ethanol afforded 31.8 g of *N*-carbethoxyphthalimide as colorless crystals, m.p. 78–80°.

Reaction of Nefkens' Reagent with Ethylenediamine

(*A*) Two methylene chloride solutions containing, respectively, *N*-carbethoxyphthalimide (4.4 g, 0.02 mole) and ethylenediamine (1.2 g, 0.02 mole) in 1000 ml of solvent were added, simultaneously and with stirring at room temperature, to methylene chloride (100 ml). Constant addition dropping funnels were employed for this addition (35) and a rate of 1 drop/s was maintained throughout. When the addition was complete, the solvent was removed under reduced pressure and the residue was triturated with chloroform (100 ml). The chloroform-soluble residue weighed only 195 mg. Two recrystallizations from methanol yielded 79 mg of 1,2-diphthalimidoethane, m.p. 243–244°.

(*B*) To a solution of *N*-carbethoxyphthalimide (2.2 g, 0.01 mole) in methylene chloride (200 ml) was added, at 0° and with stirring, a solution of ethylenediamine (600 mg, 0.01 mole) in methylene chloride (25 ml). The reaction mixture was stirred for 2 h after the addition was complete, and the solvent was then removed under reduced pressure. The residue was extracted with hot ethanol; cooling of this extract afforded 225 mg of material (in two crops) which showed both amide and phthaloylamino peaks in its i.r. spectrum (λ_{max}(KBr): 3.1, 5.65, 5.85, 6.1, 6.5 μ). The ethanol mother liquor was then evaporated and the residue dissolved in methylene chloride. Addition of ether to this solution precipitated 1.16 g of a white solid which, like the earlier material, showed both amide and phthaloylamino peaks in its i.r. spectrum. The constitutions of these materials were not investigated further.

2-Hydroxyethylphthalimide

(*A*) Following the procedure of Wenker (36), phthalic anhydride (74 g, 0.5 mole) and 2-aminoethanol (30.5 g, 0.5 mole) were heated together for 90 min at 175–190°. The resulting liquid solidified when cooled. Crystallization from chloroform – petroleum ether gave 90.5 g (95%) of material, m.p. 129–131° (lit. (36) 127–128°). The n.m.r. spectrum shows peaks at τ 2.24 (m, 4H), 6.14 (s, 4H) and 7.29 (s, 1H).

(*B*) A solution of *N*-carbethoxyphthalimide (1.1 g, 0.005 mole) in methylene chloride (20 ml) was added at room temperature to a solution of 2-aminoethanol (300 mg, 0.005 mole) in methylene chloride (20 ml). The mixture was stirred for 2 h and the solvent was then removed under reduced pressure. Crystallization of the residue from chloroform – petroleum ether afforded 481 mg (50.5%) of 2-hydroxyethylphthalimide, m.p. 129–130°, identical with the material prepared in *A*.

2-Phthalimidoethyl-p-toluenesulfonate

2-Hydroxyethylphthalimide (9.55 g, 0.05 mole) and *p*-toluenesulfonyl chloride (9.5 g, 0.05 mole) were melted together at 140°. The melt was maintained at this temperature for 5 min and then at 110–120° for an additional 14 h. This change of temperature was necessary because

Can. J. Chem. Downloaded from www.nrcresearchpress.com by 210.87.254.5 on 09/05/12
For personal use only.

N-vinylphthalimide was the major product which formed at the higher temperature (see below). Crystallization of the cooled reaction mixture from ethanol–acetone afforded 5.1 g of material. Recrystallization from the same solvent gave 4.6 g of 2-phthalimidoethyl-*p*-toluenesulfonate, m.p. 140–142° (lit. (37) m.p. 142°); λ_{max}(KBr) 5.65, 5.85 μ; n.m.r.: τ 2.25, 2.39, 2.77, 2.92 (9H), 5.77 (2H, t), 6.04 (2H, t, J = 5.0 Hz), 7.3 (3H, s).

When the above experiment was performed for 12 h in refluxing benzene or refluxing toluene, there was no reaction.

2-Azidoethylphthalimide

Tetraethylammonium chloride (8.25 g, 0.05 mole) was dissolved in methylene chloride (250 ml), and sodium azide (3.25 g, 0.05 mole) was added to this solution. The suspension was stirred for 3 h and then filtered. The insoluble material showed no absorption at 4.7 μ in the i.r. spectrum and the conversion of the chloride to tetraethylammonium azide was, therefore, judged to be complete. The solvent was removed from the filtrate, and the residue, suspended in dry acetone (100 ml), was employed directly in the next step.

2-Phthalimidoethyl-*p*-toluenesulfonate (5.2 g, 0.015 mole) was added to the above acetone suspension, the mixture refluxed for 18 h, and the solvent was then removed under reduced pressure. The residue was dissolved in chloroform (100 ml) and this solution was washed with four 25 ml portions of water, dried, and concentrated to a syrup which weighed 3.65 g. Trituration with ether and slow evaporation of the ether-soluble material afforded a crystalline compound. Two recrystallizations from ether – petroleum ether gave 2.2 g (68%) of 2-azidoethylphthalimide, m.p. 65–67°; λ_{max}(KBr) 4.7, 5.65, 5.85 μ; n.m.r.: τ 2.17 (4H, d), 5.94–6.55 (4H, m).

Anal. Calcd. for $C_{10}H_8N_4O_2 \cdot 0.5\ H_2O$: C, 53.4; H, 4.00. Found: C, 53.42; H, 3.73.

2-Aminoethylphthalimide Hydrochloride

2-Azidoethylphthalimide (2.0 g, 0.009 mole) was dissolved in ethanol (60 ml) containing *N* hydrochloric acid (36 ml, 0.036 mole) and 10% palladium-on-charcoal catalyst (400 mg). The mixture was hydrogenated at 45 p.s.i. for 4 h at room temperature. After removal of the catalyst and evaporation of the solvent, there was obtained 1.85 g of a white solid. Recrystallization from aqueous ethanol afforded 1.45 g (71%) of the desired compound, m.p. 270–272° (dec); λ_{max}(KBr) 3.5, 5.65, 5.85 μ; n.m.r. (D_2O): τ 2.17 (s, 4H), 5.95 (t, 2H, J = 5.5 Hz), 6.62 (t, 2H, J = 5.5 Hz).

Anal. Calcd. for $C_{10}H_{11}N_2O_2Cl$: C, 52.98; H, 4.85; N, 12.36. Found: C, 52.4; H, 4.84; N, 12.18.

Attempted Preparation of 2-Aminoethylphthalimide

(A) By Reduction of the Azide

(i) With Aluminum Amalgam (38)

Aluminum foil (100 mg) was cut into small strips (1 × 0.5 cm) and these were immersed for 15 s in 2% mercuric chloride solution and then, successively, into ethanol and ether. They were then added to a solution of 2-azidoethylphthalimide (512 mg, 0.0024 mole) in aqueous tetrahydrofuran (tetrahydrofuran, 27 ml; water, 3 ml). Evolution of hydrogen began after 1 min and the reaction soon became vigorous. The mixture was refluxed for 90 min and then cooled, filtered, and the filtrate concentrated to remove the tetrahydrofuran. The aqueous residue was extracted with five 10 ml portions of chloroform. Evaporation of the dried chloroform extract gave a greenish yellow liquid (333 mg), λ_{max}(KBr) 3.0, 4.7, 5.65, 5.85 μ. The peak at 4.7 μ indicated that the reduction was incomplete. The liquid crystallized from chloroform – petroleum ether to give 78 mg of material, λ_{max}(KBr) 3.0, 4.7, 5.9 μ. The n.m.r. spectrum showed singlets at τ 2.44 (4H), 4.1 (1H), 6.3, 6.45 (4H).

(ii) With Adams' Catalyst

2-Azidoethylphthalimide (253 mg) was dissolved in absolute ethanol (100 ml), platinum oxide (20 mg) was added, and the mixture was hydrogenated overnight at room temperature and atmospheric pressure. Removal of the catalyst and evaporation of the solvent gave 236 mg of a sticky solid. Treatment of an ethanol solution of this solid with petroleum ether afforded 35 mg of crystals, m.p. 138–140°, λ_{max}(KBr) 3.05, 5.95, 6.1, 6.5 μ. The t.l.c. examination (using chloroform) of the mother liquor showed it to consist of at least four compounds.

(iii) With Palladium-on-charcoal

2-Azidoethylphthalimide (135 mg) was dissolved in ethanol (50 ml) and 10% palladium–charcoal catalyst (50 mg) was added. The mixture was hydrogenated overnight at room temperature and 30 p.s.i. After removal of the catalyst and the solvent there was obtained a colorless syrup (137 mg), λ_{max}(KBr) 3.0, 5.65, 5.85, 6.1, 6.5 μ. The t.l.c. (chloroform:ethanol, 20:1) showed this syrup to be a mixture of at least four compounds. These appeared to be secondary products since the original hydrogenation mixture had shown only one spot upon examination by t.l.c.

(B) By Neutralization of the Amine Hydrochloride

(*i*) Triethylamine (100 mg, 0.001 mole) was dissolved in methylene chloride (200 ml), and 2-aminoethylphthalimide hydrochloride (226 mg, 0.001 mole) was added. The solution was stirred at room temperature for 30 min and then extracted with four 25 ml portions of water. After drying and evaporation of the organic layer there was obtained a light yellow solid (91 mg), λ_{max}(KBr) 3.0, 5.65, 5.85, 6.0, 6.2, 6.5 μ. This was triturated with chloroform. The chloroform soluble portion contained 18.3 mg of a light yellow solid, from which 2.6 mg of white crystals were obtained on recrystallization from chloroform – petroleum ether. The i.r. spectrum showed both amide absorption, at 3.0, 6.0, 6.5 μ, and phthaloylamino absorption at 5.65 and 5.85 μ, and suggested that the product was perhaps *N,N'*-diphthalimidoethylphthalamide. The chloroform insoluble residue was recrystallized from ethanol – petroleum ether to give 8.5 mg of material which was now insoluble in hot ethanol. This suggested that polymerization had occurred during the crystallization.

(*ii*) 2-Aminoethylphthalimide hydrochloride (113 mg, 0.005 mole) was dissolved in 0.5 ml of 1.04 *N* sodium deuteroxide – deuterium oxide and the n.m.r. spectrum of the resulting solution was run after various intervals. Broad multiplets were observed at τ 2.29–3.0 and 6.34–7.14. The multiplet at τ 6.34–7.14 appeared to split into two multiplets, at τ 6.27–6.67 and 6.67–7.14 after some time. No other information could be drawn from these spectra.

(*iii*) 2-Aminoethylphthalimide hydrochloride (22 mg) was suspended in methylene chloride (1 ml), and tri-

Can. J. Chem. Downloaded from www.nrcresearchpress.com by 210.87.254.5 on 09/05/12
For personal use only.

ethylamine was added dropwise until a clear solution was obtained. The i.r. spectrum of this solution was taken at various intervals. No change was detected during a 4 h period. At this point the spectrum showed no amide absorption but did have peaks at 3.3–3.55 μ, and 5.65 and 5.85 μ. The solution was then evaporated at room temperature and the residue triturated with chloroform. Evaporation of the chloroform extract afforded an oily solid, λ_{max}(KBr) 3.4, 4.1 (several peaks), 5.65, 5.85, 6.0, 6.5 μ (weak), which now appeared to be a polymer.

(*iv*) 2-Aminoethylphthalimide hydrochloride (113 mg, 0.5 mmole) was suspended in chloroform (200 ml), and a solution of triethylamine (100 mg, 0.001 mole) in chloroform (100 ml) was added dropwise at room temperature. The resulting clear solution was concentrated to a volume of 200 ml and then washed with four 25 ml portions of water, dried, and evaporated to give 51.7 mg of a syrup. The n.m.r. spectrum of this syrup showed peaks at τ 2.24 (d, 4H), 7.64–8.07 (m, 2H), 8.74 (m, 2H). No change was observed when the solution was shaken with deuterium oxide. The material was recovered from the n.m.r. tube and recrystallized from ethanol–ether to give a white solid (5.85 mg), λ_{max}(KBr) 3.1, 6.1, 6.5 μ. This solid melted partially near 240° and completely, with decomposition, at 254–260°. The compound (1.57 mg) was heated for 15 min at 160–165° and then cooled and extracted with chloroform (1 ml). The chloroform extract gave 0.91 mg of a light yellow solid identified as 1,2-diphthalimidoethane on the basis of its i.r. spectrum and thin layer chromatographic behavior.

N-Vinylphthalimide

2-Hydroxyethylphthalimide (19.1 g, 0.1 mole) and *p*-toluenesulfonyl chloride (19 g, 0.1 mole) were heated together at 130–160° for 8 h. The melt was then cooled. Two crystallizations from ethanol afforded 12.4 g of the product, λ_{max}(KBr) 5.65, 5.85 μ. The n.m.r. spectrum of this product showed it to be mostly *N*-vinylphthalimide with 2-phthalimidoethyl-*p*-toluenesulfonate as an impurity. Recrystallization from chloroform – petroleum ether and then again from ethanol gave *N*-vinylphthalimide (**16**), m.p. 78–80° (lit. (39) 83°), λ_{max}(KBr) 5.65, 5.85 μ. The n.m.r. spectrum shows two multiplets τ 1.97–2.35 and 5.8–6.35 in the ratio 4:3.

Reaction of Methylamine with N-Vinylphthalimide

A solution of *N*-vinylphthalimide (1.7 g, 0.01 mole) in benzene was added to 40% aqueous methylamine (5 ml, 0.065 mole) and the mixture was shaken. A white precipitate appeared in 5 min. It was collected and recrystallized from ethanol. The product (450 mg) melted at 206–208° and had λ_{max}(KBr) 3.1, 6.1, 6.25, 6.45 μ. The i.r. spectrum was the same as that of *N,N'*-dimethylphthalamide (**18**). It was found that the reaction was incomplete when equivalent amounts of the reactants were used and the precipitated product then appeared to be a mixture of *N*-vinylphthalimide and *N,N'*-dimethylphthalamide.

N-Ethyl-N'-vinylphthalamide (17) (25, 26)

N-Vinylphthalimide (500 mg, 0.0029 mole) was dissolved in benzene and a 33% aqueous solution of ethylamine (1 g, 0.0075 mole) was added. A white precipitate appeared after the mixture had been shaken for 5 min and this precipitate was collected after 30 min. It weighed 532 mg (84.5%). Recrystallization from benzene gave 340 mg, m.p. 142–143° (lit. (26) 143.5–144.5°), λ_{max}(KBr) 3.1, 6.15, 6.5 μ. The n.m.r. spectrum in deuterochloroform, after shaking with a drop of deuterium oxide, shows peaks at τ 2.39–2.75 (m, 4H), 6.24–6.75 (m, 5H), 8.82 (t, 3H, J = 7.0 Hz). The amide protons appeared as a broad peak at τ 2.9–3.29 because a decrease in the integral was noticed when the solution was shaken with deuterium oxide.

Reaction of Methylamine with 2-Hydroxyethylphthalimide

2-Hydroxyethylphthalimide (1.9 g, 0.01 mole) was dissolved in ethanol (50 ml) by warming on the steam bath. The solution was then cooled to room temperature and 40% aqueous methylamine (3 ml, 0.04 mole) was added. Stirring of the reaction mixture for 8 h followed by evaporation under reduced pressure afforded a crystalline solid. Recrystallization from ethanol yielded 994 mg (45%) of *N,N'*-dimethylphthalamide.

Reaction of α-Phthalimido Acids with Methylamine

(A) General Procedure for the Assay of Amino Acids (40)

The aqueous reaction mixture (10 μl) was chromatographed during 20 h on Whatman paper #3 with a 12:3:5 mixture of *n*-butanol:acetic acid:water as the developing solvent. Spots were detected under u.v. light and with the ninhydrin reagent. For quantitative determination, the spot corresponding to the amino acid was developed and then excised from the paper, extracted into acetone solution, and the intensity of the peak was measured at 570 nm against a known standard of the amino acid (25 μg).

(*B*) (*i*) Methylamine hydrochloride (135 mg, 0.002 mole) was dissolved in water (1 ml) and potassium carbonate (138 mg, 0.001 mole) was added followed by phthalimidoglycine (205 mg, 0.001 mole). The reaction mixture was left for 48 h and, after this time, the yield of glycine was 23%.

(*ii*) Phthaloylglycine (100 mg, 0.5 mmole) was dissolved in 1 ml of a 40% aqueous solution of methylamine. The yield of glycine after 48 h was 97%.

(*iii*) Phthaloylalanine (220 mg, 0.001 mole) was dissolved in a solution of methylamine hydrochloride (135 mg, 0.002 mole) in water (1 ml) containing potassium carbonate (138 mg, 0.001 mole). The yield of alanine after 48 h was 12%.

(*iv*) Phthaloylalanine (100 mg; 0.45 mole) was dissolved in 1 ml of a 40% aqueous methylamine solution. The yield of alanine after 48 h was quantitative.

Reaction of N,N'-Dimethylphthalamide with Water

N,N'-Dimethylphthalamide (200 mg, 0.001 mole) dissolved readily in deuterium oxide (2 ml). After 5 min, an n.m.r. spectrum of the solution showed peaks at τ 2.62 (s, 4H) and 7.25 (s, 3H). After standing overnight, the solution now showed peaks at τ 2.55–2.74 (m, 4H), 7.19 (s, 3H), and 7.5 (s, 3H). The i.r. spectrum of this latter deuterium oxide solution showed peaks at 6.18, 6.3, 6.4, 6.65 μ. The solution was acidified to p*H* 4 and extracted with three 25 ml portions of ethyl acetate. Evaporation of the dried ethyl acetate extract yielded 77 mg (46%) of

N-methylphthalamic acid (**25**); λ_{max}(KBr) 3.0, 5.8, 6.15, 6.45 μ. The n.m.r. spectrum of this acid in deuterium oxide showed peaks at τ 2.07–2.77 (m, 4H) and 7.17 (s, 3H). After this solution had stood overnight the n.m.r. spectrum showed peaks at τ 2.14–2.79 (m, 4H), 7.17 (s, 1.8H), 7.44 (s, 1.2H). Treatment of the *N*-methylphthalamic acid with diazomethane afforded *N*-methylphthalimide.

Reaction of Phthalic Anhydride with Methylamine

Methylamine hydrochloride (135 mg, 0.002 mole) was dissolved in deuterium oxide. Potassium carbonate (138 mg, 0.001 mole) was then added followed by phthalic anhydride (150 mg, 0.001 mole). The anhydride did not dissolve readily and, after 5 min, the n.m.r. spectrum of the supernatant liquid showed peaks at τ 2.6 (t), 7.17 (s) and 7.45 (s) in the ratio 35:25:58. The integral ratio indicates the presence of unreacted methylamine. When the mixture was stirred overnight the phthalic anhydride dissolved completely and the n.m.r. spectrum now showed peaks at τ 2.54–2.7 (m), 7.17 (s), and 7.45 (s) in the ratio 40:26:38. The ratio of the integrals of the multiplet to those of the two singlets is thus approximately 4:6. The n.m.r. spectrum is the same as that of an aqueous solution of *N,N'*-dimethylphthalamide at equilibrium. On standing for an additional 8 h, the solution deposited a crystalline material which was collected and dried to yield *N*-methylphthalimide (8 mg), m.p. 134–136°, identified by its i.r. spectrum and a mixture m.p. After removal of this material, the filtrate was acidified to p*H* 4 and extracted with three 15 ml portions of ethyl acetate. Evaporation of the dried ethyl acetate extract and trituration of the residue with ether yielded 85 mg of a foamy solid, λ_{max}(KBr) 3.0, 5.8, 6.15, 6.2, 6.45 μ, which appeared to be *N*-methylphthalamic acid. The n.m.r. spectrum in deuterium oxide showed, after 5 min, peaks at τ 2.14–2.79 (m, 4H) and 7.17 (s, 3H). Two days later the n.m.r. spectrum showed peaks at τ 2.27–2.69 (m, 4H), 7.17 (s, 1.8 H), 7.44 (s, 1.2 H). Treatment of the phthalamic acid with an excess of diazomethane afforded *N*-methylphthalimide.

We thank the National Research Council of Canada for support of this work.

1. M. S. Gibson and R. W. Bradshaw. Angew. Chem. Int. Ed. Eng., 7, 919 (1968).
2. E. Schröder and K. Lübke. The peptides. Vol. 1. Academic Press, New York, 1965. Chapt. I. J. F. S. McOmie. *In* Advances in organic chemistry. Vol. 3. R. A. Raphael, *editor*. Interscience, New York, 1963. p. 191.
3. R. A. Boissonas. *In* Advances in organic chemistry. Vol. 3. R. A. Raphael, *editor*. Interscience, New York, 1963. p. 159.
4. M. L. Bender, Y.-L. Chow, and F. Chloupek. J. Amer. Chem. Soc. **80**, 5380 (1958). G. Dahlgren and N. L. Simmerman. J. Phys. Chem. **69**, 3626 (1965). J. Brown, S. C. K. Su, and J. A. Shafer. J. Amer. Chem. Soc. **88**, 4468 (1966).
5. T. C. Bruice and S. J. Benkovic. Bioorganic mechanisms. Vol. 1. W. A. Benjamin, Inc., New York, 1966.
6. Y. Wolman. *In* The chemistry of the amino group. S. Patai, *editor*. Interscience Publishers, New York, 1968. p. 669.
7. G. H. L. Nefkens. Nature, **185**, 309 (1960). G. H. L. Nefkens, G. I. Tesser, and R. J. F. Nivard. Rec. Trav. Chim. **79**, 688 (1960).
8. S. Wolfe, J. C. Godfrey, C. T. Holdrege, and Y. G. Perron. Can. J. Chem. **46**, 2549 (1968).
9. S. Wolfe, R. N. Bassett, S. M. Caldwell, and F. I. Wasson. J. Amer. Chem. Soc. **91**, 7205 (1969).
10. S. Wolfe and S. K. Hasan. In preparation.
11. C. J. M. Stirling. J. Chem. Soc. 4531 (1958).
12. J. v. Braun and W. Pinkernelle. Ber. **67**, 1056 (1934).
13. E. Taschner, M. Kocór, and S. Meyer. Rocz. Chem. **26**, 692 (1952).
14. T. Wieland and H. Urbach. Ann. **613**, 84 (1958).
15. R. M. Peck. J. Org. Chem. **27**, 2677 (1962).
16. F. S. Spring and J. C. Woods. Nature, **158**, 754 (1946).
17. *cf.* K. Biemann. Mass spectrometry. Organic chemical applications. McGraw-Hill, Inc., New York, 1962. p. 46.
18. G. I. Glover, R. B. Smith, and H. Rapoport. J. Amer. Chem. Soc. **87**, 2003 (1965).
19. S. Gabriel. Ber. **22**, 2223 (1889).
20. E. Ristenpart. Ber. **29**, 2530 (1896).
21. F. S. Spring and J. C. Woods. J. Chem. Soc. 625 (1945).
22. K. Körmendy. Acta Chim. Acad. Sci. Hung. **17**, 255 (1958). K. Körmendy and J. Volford. Acta. Chim. Hung. **32**, 115 (1961).
23. J. Jenni, H. Kühne, and B. Prijs. Helv. Chim. Acta, **45**, 1163 (1962).
24. N. K. Datta and P. B. Talukdar. J. Ind. Chem. Soc. **43**, 461 (1966)
25. K. Yanagi. J. Org. Chem. **24**, 1121 (1959).
26. K. Kato. Nippon Kagaku Zasshi. **83**, 313 (1962).
27. H. S. Mosher. J. Amer. Chem. Soc. **68**, 1565 (1946).
28. H. J. Barber and W. R. Wragg. Nature, **158**, 514 (1946).
29. J. A. Shafer and H. Morawetz. J. Org. Chem. **28**, 1899 (1963).
30. M. T. Behme and E. H. Cordes. J. Org. Chem. **29**, 1255 (1964).
31. M. L. Bender and M. S. Silver. J. Amer. Chem. Soc. **84**, 4589 (1962).
32. H. R. Ing and R. H. F. Manske. J. Chem. Soc. 2348 (1926).
33. Reference 2, p. 12.
34. O. Neunhoeffer, G. Lehmann, D. Haberer, and G. Steinle. Ann. **712**, 208 (1968).
35. S. Wolfe and S. K. Hasan. Can. J. Chem. This issue.
36. H. Wenker. J. Amer. Chem. Soc. **59**, 422 (1937).
37. D. H. Peacock and U. C. Dutta. J. Chem. Soc. 1303 (1934).
38. E. J. Corey and M. Chaykovsky. J. Amer. Chem. Soc. **87**, 1345 (1965).
39. A. F. Nikolaev and S. N. Ushakov. Izv. Akad. Nauk. S.S.S.R. 1235 (1957); Chem. Abstr. **52**, 6283*b* (1958).
40. C. A. Atkins. Ph.D. Thesis. Queen's University, Kingston, Ontario, 1969.
41. S. K. Hasan, F. I. Wasson, and S. Wolfe. Can. J. Chem. **45**, 2000 (1967).

Can. J. Chem. Downloaded from www.nrcresearchpress.com by 210.87.254.5 on 09/05/12
For personal use only.

Can. J. Chem. Downloaded from www.nrcresearchpress.com by 210.87.254.42 on 09/05/12
For personal use only.

Hydrogen–deuterium exchange of medium ring cycloalkenes during deuterogenation with tris(triphenylphosphine)chlororhodium(I)[1]

J. G. Atkinson and M. O. Luke
Isotopic Laboratories, Merck Sharp & Dohme Canada Ltd., Pointe Claire/Dorval 700, Quebec

Received June 2, 1970

Cyclooctene, and, to a lesser extent, cycloheptene and cyclododecene undergo H–D scrambling during deuterogenation with tris(triphenylphosphine)chlororhodium(I), whereas this catalyst affords clean addition of two deuterium atoms to cyclohexene and 1-octene. Cyclooctene containing up to 0.4 deuterium atoms per molecule has been isolated after 50% reduction and the isotope shown to be randomly distributed about the ring. This unexpected exchange reaction has been accounted for in terms of the medium size ring effect (I-strain) and provides impressive further evidence for the reversible formation of a normally unobserved rhodium–alkyl species as an intermediate in the hydrogenation reaction.

Canadian Journal of Chemistry, **48**, 3580 (1970)

Introduction

The effective homogeneous hydrogenation catalyst tris(triphenylphosphine)chlororhodium(I) discovered by Wilkinson and co-workers (1) is known to be effective for the clean addition of deuterium to disubstituted olefins (2). Addition of the two hydrogen (or deuterium) atoms of the catalytically active species $RhCl(H_2)(PPh_3)_2$ to a monoolefin was originally thought to be synchronous (1), but now appears to proceed via a σ-bonded rhodium–alkyl intermediate. This type of intermediate was postulated first for the Wilkinson catalyst by Biellmann and Jung (2*c*) to explain the isomerization of an exocyclic double bond to an endocyclic position. Further evidence came from several reports of H–D scrambling during deuterogenation with $RhCl(PPh_3)_3$ (3, 4) including the recent work of Hussey and Takeuchi on deuterogenation of trisubstituted olefins (5).

The early promise of $RhCl(PPh_3)_3$ as a clean deuterogenation catalyst led us to investigate the possibility of its use to obtain 1,2-dideuterocyclooctane by the deuterogenation of cyclooctene. Our failure to obtain cleanly labelled material then prompted us to investigate the deuterogenation of this and other cycloalkenes in more detail.

Experimental

Material

Cyclohexene, cycloheptene, and cyclooctene were purified prior to use by passage through neutral alumina followed by distillation. Cyclododecene (Aldrich) and 1-octene (Chemical Samples Co., 99%) were used as received.

$RhCl(PPh_3)_3$ was prepared as described previously (1).

[1]Aspects of stable isotope chemistry, VIII. For part VII, see ref. 11.

Deuterogenation Procedure

The deuterogenations were carried out in 100 ml flasks fitted with a magnetic stirrer and attached to a graduated, deuterium reservoir. Catalyst, solvent, and substrate were added in the order indicated, the system evacuated and filled with deuterium gas 3 times, then stirring was started and continued until the desired amount of deuterium gas was absorbed.

Product Isolation

Reaction products and solvent were removed from the catalyst by evacuation of the reaction mixture and collection of volatiles in a liquid nitrogen cooled trap. Product cycloalkenes and/or cycloalkanes were freed of solvent by careful distillation. Cycloalkanes were shown to be free of olefin contamination by vapor phase chromatography (v.p.c.) ($AgNO_3$, 50 °C thermal conductivity detector), prior to mass and/or nuclear magnetic resonance (n.m.r.) analyses. Cyclohexene–cyclohexane mixtures were separated by preparative scale v.p.c. ($AgNO_3$). Cyclooctene–cyclooctane mixtures were separated with $AgClO_4$ (6). Cyclododecane was freed of residual unreduced cyclododecene by sacrificial recrystallization from pentane.

Analytical

Mass spectral analyses were done by the Morgan–Schaffer Corporation, Montreal.

Results and Discussion

Reduction of cyclooctene with deuterium gas in the presence of $RhCl(PPh_3)_3$ gave cyclooctane containing an average of two deuterium atoms per molecule but with isotopic species from d_0 to d_9 present. This unexpected result prompted us to examine the products of incomplete deuterogenation, during the course of which it was discovered that cyclooctene recovered after 50% reduction contains an average of 0.4 deuterium atoms per molecule with species from d_0 to d_4 present. This experiment was repeated several times and in each case similar results were obtained.

TABLE 1

Deuterium addition to cycloalkenes using tris(triphenylphosphine)chlororhodium(I)[a]

Product analyzed	[b,c]	[b,c]	[d,e]	[b,f]	[b,f]	[c,d]	[c,g]
Species and %							
d_0	67.13	11.81	13.20	99.79	0.88	3.80	10.38
d_1	26.06	28.81	29.37	0.21	2.03	5.42	13.26
d_2	5.74	50.23	30.70		97.09	87.83	65.14
d_3	0.89	7.79	14.48			2.85	8.13
d_4	0.18	1.07	6.95			0.10	2.16
d_5		0.09	3.13				0.56
d_6		0.02	1.38				0.28
d_7			0.53				0.09
d_8			0.21				
d_9			0.05				
d_{ave}	0.41	1.57	1.92	—	1.96	1.90	1.82
	1.98						

[a]All reductions were carried out at 25 °C and 1 atm D_2 pressure, with 0.08 moles cycloalkene and from 5.4×10^{-5} to 1.4×10^{-4} moles $RhCl(PPh_3)_3$ in 15 ml of solvent.
[b]After half reduction.
[c]In benzene.
[d]After complete reduction.
[e]In 1:1 benzene–ethanol.
[f]In 1:1 xylene–ethanol.
[g]Reduction was only 80% complete. The low d_{ave} value is probably due to deuterium in unreduced cyclododecene.

TABLE 2

Deuterium distribution in exchanged cyclooctene

By deuterium n.m.r.			By mass spectrometry		
	% of total D			%	
Position	Observed	Calculated*	Species	Observed	Calculated†
Vinyl	10	14	d_0	67.13	66.07
Allylic	38	29	d_1	26.06	27.82
Aliphatic	52	57	d_2	5.74	5.41
			d_3	0.89	0.65
			d_4	0.18	0.05

*Calculated assuming statistical distribution about the ring.
†Binomial distribution for C_8H_{14} containing an average of 0.41 deuterium atoms and 14 exchangeable hydrogen atoms.

Isotopic scrambling also accompanies deuterogenation of cycloheptene and cyclododecene although to a lesser extent than with cyclooctene, whereas 1-octene shows the expected clean addition of two deuterium atoms per molecule.

In sharp contrast to the behavior of medium ring cycloalkenes, cyclohexene gives 1,2-dideuterocyclohexane, and cyclohexene recovered after 50% of the theoretical deuterium gas uptake contains only traces of deuterium. The isotopic distribution patterns of the products of cycloalkene deuterogenation are shown in Table 1.

The results of mass spectral and deuterium n.m.r. (*cf.* ref. 7) analyses on the recovered cyclooctene are given in Table 2. The principal features of interest in this unexpected exchange are (*a*) that the deuterium n.m.r. shows the isotope to be nearly statistically distributed around the ring, and (*b*) that the mass distribution pattern is virtually identical to that calculated for a binomial distribution (8) of the isotopic species.

These results, the most striking illustration of H–D exchange yet reported for tris(triphenylphosphine)chlororhodium(I), have several important mechanistic implications.

Scheme 1, similar to that previously proposed (5), provides a route to all the observed isotopic species in partially deuterated cyclooctene. In the scheme, species such as **2**, **3**, and **4** must be in rapid equilibrium relative to steps -1, $-1'$, and *3* in order to account for the introduction of deuterium into all parts of the recovered olefin. The recent results of Gale (9) on the relative rates

Can. J. Chem. Downloaded from www.nrcresearchpress.com by 210.87.254.42 on 09/05/12
For personal use only.

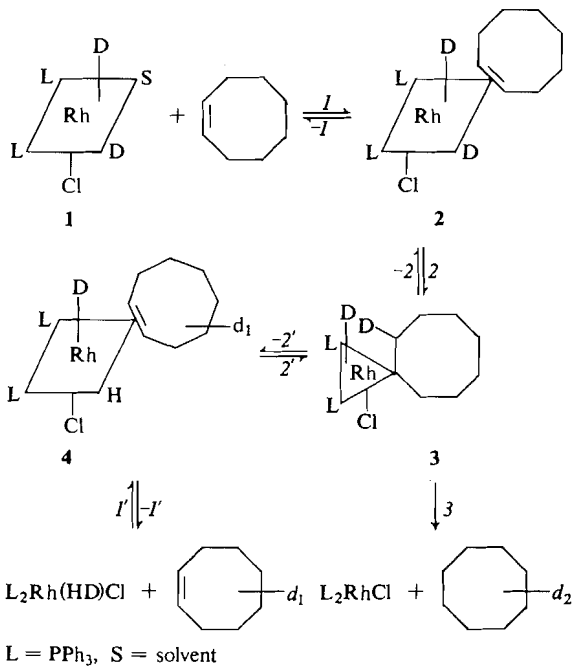

SCHEME 1

of reversible free-radical additions to cycloolefins seem to provide a reasonable explanation for our observations. In medium ring size compounds, there is an increase in non-bonded interactions (I-strain) in going from an sp^2- to an sp^3-hybridized carbon atom (10), which, in our case, would facilitate the reversion of **3** to **2** and/or **4**, and allow double bond migration to occur.[2,3]

The binomial distribution pattern observed (Table 2) means that only one hydrogen of the cyclooctene is exchanged per contact with the catalyst.[4] Since $Rh(D_2)Cl(PPh_3)_2$ (**1**) will always be the major hydride species in solution,[5] this result requires that the two deuterium atoms of **1** be non-equivalent and that only one of them is involved in equilibria such as that between **3** and **4**. However, we are unable to say at this point which of the deuterium atoms takes part in this previously unobserved selectivity.

The fact that in no case were products containing more than an average of two deuterium atoms per molecule obtained shows that exchange of RhHD, RhH_2, and $RhH(C_8H_{14}D)$ with D_2 is very slow under the conditions employed for reduction.

The unusual behavior of medium ring size compounds might also be explained in terms of transannular hydride (or hydrogen atom) shifts, but this possible route would not, in itself, give rise to the statistical deuterium distribution observed in this work.[6]

This work was supported by an Industrial Research Grant from the National Research Council of Canada. The deuterium n.m.r. was kindly supplied by Dr. L. F. Johnson of Varian Associates. The proton n.m.r. was provided by S. C. Ho and J. G. Lachambre of our Analytical Laboratory.

1. J. A. OSBORN, F. H. JARDINE, J. F. YOUNG, and G. WILKINSON. J. Chem. Soc. A, 1711 (1966).
2. (*a*) A. J. BIRCH and K. A. M. WALKER. J. Chem. Soc. C, 1894 (1966); (*b*) J. F. BIELLMANN and H. LIESENFELT. Bull. Soc. Chim. France, **12**, 4029 (1966); (*c*) J. F. BIELLMANN and M. J. JUNG. J. Amer. Chem. Soc. **90**, 1673 (1968).
3. W. VOELTER and C. DJERASSI. Chem. Ber. **101**, 58 (1968).
4. A. L. ODELL, J. B. RICHARDSON, and W. R. ROPER. J. Catal. **8**, 393 (1967).
5. A. S. HUSSEY and Y. TAKEUCHI. J. Amer. Chem. Soc. **91**, 672 (1969).
6. A. E. COMYNS and H. J. LUCAS. J. Amer. Chem. Soc. **79**, 4339 (1957).
7. L. K. MONTGOMERY, A. O. CLOUSE, A. M. CRELIER, L. E. APPLEGATE. J. Amer. Chem. Soc. **89**, 3453 (1967).
8. P. G. HOEL. Introduction to mathematical statistics. 3rd ed. John Wiley and Sons Inc., New York. 1962. p. 85.
9. L. H. GALE. J. Org. Chem. **34**, 81 (1969).
10. E. L. ELIEL. Stereochemistry of carbon compounds. McGraw-Hill Book Co., Inc., New York. 1962. p. 265.
11. P. BÉLANGER, J. G. ATKINSON, and R. S. STUART. Chem. Commun. 1067 (1969).
12. K. SCHRAGE and R. L. BURWELL, JR. J. Amer. Chem. Soc. **88**, 4555 (1966).

[2]It may be noted that no appreciable exchange with D_2 gas or solvent was observed in this work.

[3]The relative rates of deuterium absorption for cyclohexene and cyclooctene were 4:1. See ref. 5 for the possible significance of larger rate differences.

[4]For a similar example in heterogeneous catalysis see ref. 12.

[5]The formation of $Rh(H_2)Cl(PPh_3)_2$ and $Rh(HD)Cl(PPh_3)_2$ is also required to account for d_0 and d_1 cycloalkanes.

[6]A referee has suggested a viable modification of the proposed mechanism whereby a statistical deuterium distribution may result from a series of reversible coordination steps between $Rh(HD)Cl(PPh_3)_2$ and cyclooctene-d_1 generated in an initial *1* to $-1'$ process. This modification preserves the concept of the relative difficulty of step *3*, that is, facile reversion of **3** to **2** or **4**, with medium ring cycloalkenes as the driving force for isotopic scrambling. The probability of such a cage type phenomenon in these systems is unknown and it cannot be ruled out or confirmed on the basis of the present results.

An independent double bond isomerization reaction cannot be a major factor in achieving a statistical deuterium distribution in cyclooctene because in *n*-octane-d_2 the ratio of deuterium in methylene and methyl positions was shown by deuterium n.m.r. to be 1.13/1.

Can. J. Chem. Downloaded from www.nrcresearchpress.com by 210.87.254.42 on 09/05/12
For personal use only.

Can. J. Chem. Downloaded from www.nrcresearchpress.com by 210.87.254.40 on 09/05/12
For personal use only.

σ- and π-Bonding capabilities of $P\phi_3$, $As\phi_3$, and $Sb\phi_3$ in molybdenum hexacarbonyl derivatives

C. BARBEAU AND J. TURCOTTE
Department of Chemistry, Laval University, Quebec, Quebec

Received June 11, 1970

cis- and *trans*-$Mo(CO)_3(Sb\phi_3)_3$ and *cis*- and *trans*-$Mo(CO)_2(Sb\phi_3)_4$ have been prepared. The dipole moments of $Mo(CO)_5L$, *cis*-$Mo(CO)_4L_2$, and *cis*-$Mo(CO)_3L_3$ (L = $P\phi_3$, $As\phi_3$, and $Sb\phi_3$) as well as those of *cis*- and *trans*-$Mo(CO)_2(Sb\phi_3)_4$ have been measured.

As the infrared data for stretching as well as deformation vibrations do not clearly explain the differences in stability, ease of substitution, or dipole moments with the different ligands, we have used the model of variable donor–acceptor ability of ligands combined with the model of non-retention of charges on the metal to show the importance of steric hindrance in substituted metal carbonyls. It is also possible to differentiate the σ and π bonding capabilities of the ligands $P\phi_3$, $As\phi_3$, and $Sb\phi_3$. It is shown that $P\phi_3$ is a better donor or acceptor than $As\phi_3$ or $Sb\phi_3$.

Les dérivés *cis*- et *trans*-$Mo(CO)_3(Sb\phi_3)_3$, *cis*- et *trans*-$Mo(CO)_2(Sb\phi_3)_4$ ont été synthétisés. On a mesuré les moments dipolaires des dérivés $Mo(CO)_5L$, *cis*-$Mo(CO)_4L_2$, *cis*-$Mo(CO)_3L_3$ (L = $P\phi_3$, $As\phi_3$ et $Sb\phi_3$) ainsi que ceux des isomères *cis*- et *trans*-$Mo(CO)_2(Sb\phi_3)_4$.

Les données infrarouges des vibrations C—O, Mo—C, Mo—C—O et Mo—L ne permettent pas d'expliquer la facilité de substitution, la stabilité et les moments dipolaires des dérivés.

En utilisant le modèle du pouvoir donneur–accepteur variable des ligands et celui de la conductivité du métal central, nous avons pu montrer l'importance des effets stériques sur la stabilité des métaux carbonyle substitués et séparer les pouvoirs σ et π des donneurs $P\phi_3$, $As\phi_3$ et $Sb\phi_3$. On trouve que $P\phi_3$ est un meilleur donneur et un meilleur accepteur que $Sb\phi_3$ ou $As\phi_3$.

Canadian Journal of Chemistry, **48**, 3583 (1970)

Introduction

It is generally accepted that most ligands have a net charge-donating effect compared to carbon monoxide when substitution in metal carbonyls takes place. This effect is accompanied by a decrease in the C—O bond order, an increase in the M—C stretching frequency and in the M—C—O deformation frequency. The M—L bond and the partial dipole moments μL—M and μM—C should also reflect the changes occurring in the complex.

Study of the dipole moments in relation to the stability of the derivatives, to the ease and degree of substitution, and to the various bond strengths could provide a means to separate the σ- and π-bonding capabilities of the ligands.

Strohmeier and Hellmann (1) and Bigorgne and Messier (2) have developed equations which may be used to calculate partial moments in metal carbonyl derivatives. Strohmeier and coworkers (3) have deduced, from a number of measured dipole moments, a relation between partial moment, π-accepting ability of the ligand and stability of the compound.

In this work we wanted to compare compounds which are very similar. We have chosen derivatives of $Mo(CO)_6$ with triphenyl ligands, namely $P\phi_3$, $As\phi_3$, and $Sb\phi_3$. These three donors are known to replace up to three CO groups and they induce similar C—O stretching frequencies in carbonyls (4–7). The three group VA atoms show vacant d orbitals available for dπ–dπ back-bonding and the σ-donating ability of the ligand should be mainly controlled by the inductive effect of the phenyl groups.

Experimental

Molybdenum Hexacarbonyl Derivatives

$Mo(CO)_5L$

Using Strohmeier's technique (8), the monoderivatives with $P\phi_3$, $As\phi_3$, and $Sb\phi_3$ are prepared, in 50 to 80% yield, by refluxing for 24 h a solution of $Mo(CO)_6$ and excess donor (L) in petroleum ether (b.p. 65–110 °C). After cooling, the solution is filtered and the precipitate is freed from any remaining hexacarbonyl by sublimation at 60°C under vacuum. The purity of the white, soluble compounds is verified through their infrared spectra (6) and elemental analyses.

$Mo(CO)_4L_2$

The *cis* derivative with $P\phi_3$ is obtained through substitution of 1,5-cyclooctadiene molybdenum tetracarbonyl (9). On heating to 80 °C for 5 to 10 min, a solution of the diene and $P\phi_3$ in petroleum ether (b.p. 65–110 °C) yields a colorless solution which precipitates, on cooling, giving a 30% yield of *cis*-$Mo(CO_4)(P\phi_3)_2$.

The *trans* derivative is obtained when a solution of $Mo(CO)_6$ and $P\phi_3$ in benzene is heated or radiated with ultraviolet light.

The *cis* derivative $Mo(CO)_4(As\phi_3)_2$ precipitates from a solution of $Mo(CO)_6$ and $As\phi_3$ in petroleum ether which

Can. J. Chem. Downloaded from www.nrcresearchpress.com by 210.87.254.40 on 09/05/12
For personal use only.

has been radiated with a mercury vapor lamp for 9 to 12 h at room temperature, using the technique already described (10).

The *cis* derivatives $Mo(CO)_4(Sb\phi_3)_2$ and $Mo(CO)_4(As\phi_3)_2$ are obtained through thermal reaction in the same way as with the monoderivatives. Substitution occurs when a solution of the carbonyl and $Sb\phi_3$ or $As\phi_3$ is refluxed at 140 °C. The white compounds precipitate on cooling.

The infrared spectra in the C—O stretching region were used to differentiate *cis*- and *trans*-isomers.

$Mo(CO)_3L_3$

cis-$Mo(CO)_3(P\phi_3)_3$ and *cis*-$Mo(CO)_3(As\phi_3)_3$ are both precipitated when benzene solutions of cycloheptatriene molybdenum tricarbonyl and the donor are refluxed (11). $P\phi_3$ reacts within 10 min. whereas $As\phi_3$ reacts only after 10 h of treatment.

cis-$Mo(CO)_3(Sb\phi_3)_3$ is obtained, with a close to 100% yield, when a mixture of $Sb\phi_3$ and $Mo(CO)_6$ in petroleum ether is radiated with a high-pressure mercury vapor lamp (GE H100-A4/T) until no further precipitation occurs in solution.

trans-$Mo(CO)_3(Sb\phi_3)_3$ precipitates in very small quantities (15 to 25 mg) when a benzene solution of $Mo(CO)_6$ (1 g) containing excess donor (3 g), is radiated with mercury for at least 48 h. The compound is white, very sparingly soluble in benzene and chloroform, insoluble in ethanol, cyclohexane, and petroleum ether. In solution, it undergoes rapid isomerization at room temperature (total rearrangement inside 5 h in benzene).

Anal. Calcd: C, 55.25; H, 3.66. Found: C, 55.38; H, 3.99.

The number of bands in the infrared spectra (7), the dipole moment, and the solubility enable a differentiation between the *trans* isomer and the *cis* isomer.

$Mo(CO)_2L_4$

The yellow solution, obtained after 6 h of irradiating a benzene solution of 1 g $Mo(CO)_6$ and 3 g $Sb\phi_3$, contains the *cis* derivative, $Mo(CO)_2(Sb\phi_3)_4$, in small quantities. The solution is partially evaporated, then added to petroleum ether, and the cycle so repeated until *cis*-$Mo(CO)_2(Sb\phi_3)_4$ precipitates as a fine pale yellow substance. The yield varies between 5 and 10%. The compound is soluble in benzene and chloroform, partially soluble in cyclohexane, ethanol, tetrahydrofuran and acetone, and insoluble in petroleum ether. The solutions are not very sensitive to atmospheric oxygen. The solid compound is stable for months without a nitrogen atmosphere.

Anal. Calcd: C, 56.82; H, 3.86. Found: C, 56.76; H, 3.94.

Irradiating the above mixture for a period of 50 to 70 h produces much decomposition with a small amount of yellow precipitate. Its C and H contents are identical to the previous compound but its infrared spectrum is quite different. On the basis of infrared spectrum, dipole moment, and solubility, this compound is described as *trans*-$Mo(CO)_2(Sb\phi_3)_4$. The yield is very low (about 50 mg) and the solubility in benzene negligible (20 mg/100 ml) The yellow substance is very stable under atmospheric oxygen.

Anal. Calcd: C, 56.82; H, 3.86. Found: C, 56.71; H, 3.83.

A mixture of the *cis*- and *trans*-isomers is obtained whenever the irradiation time is less than 50 h and more than 8 h. Fractional precipitation from chloroform–ethanol (2:1) yields the same relative amounts of *cis*- and *trans*-$Mo(CO)_2(Sb\phi_3)_4$. No evidence for the formation of the *trans* isomer through irradiation of a solution containing only the *cis* isomer and $Sb\phi_3$ could be found.

Repeated experiments, involving irradiation of $Mo(CO)_6$ with $As\phi_3$ or $P\phi_3$ in benzene, were all unsuccessful in isolating a tetra derivative. The resulting solutions were, however, of the yellow color which would be expected if the tetra derivatives were present.

Infrared Spectra

Due to the very low solubility of a few compounds, all spectra were taken from Nujol mull with CsI windows.

For the region 3000–250 cm^{-1}, spectra were recorded on a Perkin–Elmer 621. A RIIC Fourier Spectrophotometer was used in collecting data between 300 and 80 cm^{-1}.

Dipole Moments

The dipole moments were measured in benzene with the apparatus and procedure as previously described (12). The calculations were based on Guggenheim's equation (13) when the refractive index was obtainable. In the case of very dilute solutions, an estimate of the slope of n_{12}^2 *vs.* molar fraction was made (12).

The dipole moment of *trans*-$Mo(CO)_2(Sb\phi_3)_4$ was measured by dissolving 8 mg of the isomer in 40 ml benzene.

Results and Discussion

Dipole Moments

The experimental dipole moments μ_G' are shown in Table 1. The values calculated according to Higasi's equation (14) are much higher in the poly-substituted carbonyl on account of the identical electronic polarization assigned to all compounds by the Higasi method. For comparative purposes, μ_G' has been reduced to a ligand – metal – carbon monoxide dipole moment μ_K. This is obtained by making use of the geometrical factor (Fig. 1) for the different derivatives and assuming no variation in the bond angles.

Dipole moments have been measured in benzene because of the low solubility of certain derivatives in cyclohexane. Measurements in cyclohexane of the mono and bis derivative with $Sb\phi_3$ show that no solvent effect occurs. Rapid *trans* → *cis* isomerization in solution prevented the measurement of the dipole moment of *trans*-$Mo(CO)_3(Sb\phi_3)_3$.

Substitution influences both the ligand–metal dipole moment μ_L and the metal – carbon monoxide moment μ_C. If these effects are interrelated, μ_K will show the total variation.

$$[1] \qquad \mu_K = \mu_L + \mu_C$$

It is seen from Table 1 and Fig. 2 that μ_K varies linearly only in the case of $Sb\phi_3$ and only up to

TABLE 1

Dipole moments (D) of molybdenum hexacarbonyl derivatives in benzene solution (25 °C)*

Compound	α	P_E (cm³)	γ′	μ_H ±0.05	μ_G' ±0.05	F	μ_K ±0.05	$\Delta\mu_K$
$Mo(CO)_5(Sb\phi_3)$	38.88	117	3.5	5.28	5.06	1	5.06	—
cis-$Mo(CO)_4(Sb\phi_3)_2$	63.57	200	6.8	6.75	6.41	$\sqrt{2}/2$	4.53	0.53
cis-$Mo(CO)_3(Sb\phi_3)_3$	76.54	284	10.2	7.40	6.93	$\sqrt{3}/3$	4.00	0.53
cis-$Mo(CO)_2(Sb\phi_3)_4$	39.99	367	13.6	5.35	4.37	$\sqrt{2}/2$	3.09	0.91
trans-$Mo(CO)_2(Sb\phi_3)_4$	13.74	367	13.6	3.14	0	—	0	—
$Mo(CO)_5(As\phi_3)$	43.37	114	3.4	5.57	5.38	1	5.38	—
cis-$Mo(CO)_4(As\phi_3)_2$	68.74	195	6.6	7.02	6.71	$\sqrt{2}/2$	4.74	0.64
cis-$Mo(CO)_3(As\phi_3)_3$	53.64	275	9.9	6.12	5.63	$\sqrt{3}/3$	3.25	1.49
$Mo(CO)_5(P\phi_3)$	43.59	112	3.3	5.59	5.40	1	5.40	—
cis-$Mo(CO)_4(P\phi_3)_2$	60.37	190	6.4	6.58	6.25	$\sqrt{2}/2$	4.42	0.98
cis-$Mo(CO)_3(P\phi_3)_3$	47.22	268	9.6	5.82	5.22	$\sqrt{3}/3$	3.01	1.41
$Mo(CO)_5(Sb\phi_3)$	28.52†	117	2.66	5.30	5.05†	1	5.05	—
cis-$Mo(CO)_4(Sb\phi_3)_2$	46.67†	200	5.27	6.79	6.39†	$\sqrt{2}/2$	4.52	0.53

*$\alpha = d\varepsilon_{12}/df_2$; P_E = molecular electronic polarization; $\gamma' = dn_{12}^2/df_2$; μ_H, μ_G = dipole moment calculated from Higasi and Guggenheim equations; F = geometrical factor.
†Dipole moments in cyclohexane.

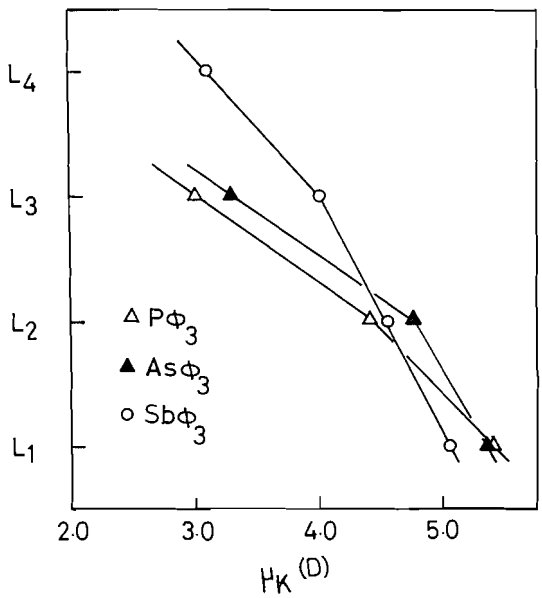

FIG. 1. Reduction of μ_G' to a linear dipole moment μ_K.

the tris derivative. μ_K^1 and μ_K^2 with $As\phi_3$ are similar to μ_K^1 and μ_K^2 with $Sb\phi_3$ whereas, with $P\phi_3$, only μ_K^1 is of the same magnitude as the other μ_K^1.

A sharp decrease in μ_K accompanies a fall in the stability of the compounds. Thus, solutions of *cis*-$Mo(CO)_3(P\phi_3)_3$ are more sensitive to oxygen than are solutions of *cis*-$Mo(CO)_3(As\phi_3)_3$ which, in turn, are more sensitive than solutions of *cis*-$Mo(CO)_3(Sb\phi_3)_3$. The fall of μ_K^4 with $Sb\phi_3$ seems to indicate that $Mo(CO)(Sb\phi_3)_5$, if it existed, would be very unstable. Repeated experiments to detect this compound have been unsuccessful. The sharp fall in μ_K^3 for $As\phi_3$ and $P\phi_3$ also tends to indicate that the tetra derivatives would hardly be stable. In fact, the only

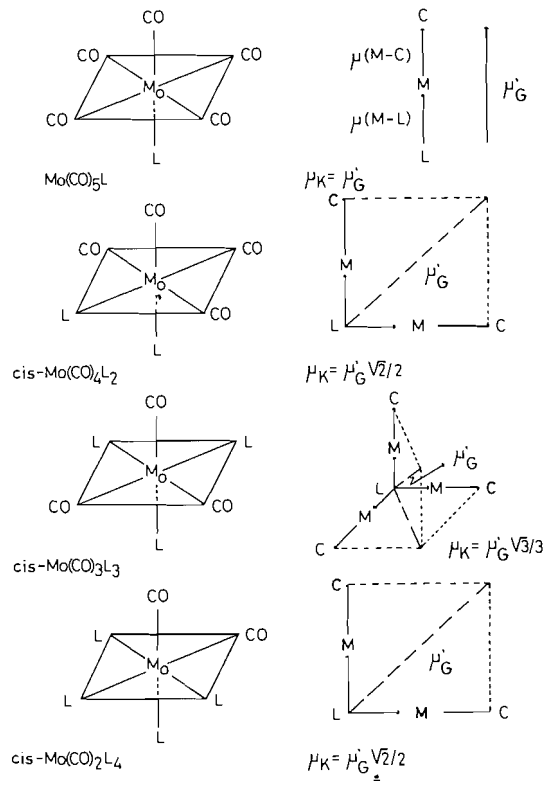

FIG. 2. Correlation between degree of substitution and μ_K.

Can. J. Chem. Downloaded from www.nrcresearchpress.com by 210.87.254.40 on 09/05/12
For personal use only.

Can. J. Chem. Downloaded from www.nrcresearchpress.com by 210.87.254.40 on 09/05/12
For personal use only.

TABLE 2

Infrared absorption bands of substituted metal carbonyls in the 2500–80 cm^{-1} region

Compound	Total bands possible (obsd)	ν(C—O) (±2 cm^{-1})	Total bands possible (obsd)	δ(M—C—O) (±2 cm^{-1})	Total bands possible (obsd)	ν(M—C) (±2 cm^{-1})	Total bands possible (obsd)	ν(M—L)† (±4 cm^{-1})
$Mo(CO)_6$	1(1)	2124*2027*1984	1(1)	590	1(1)	392*368 340*		
$Mo(CO)_5(Sb\phi_3)$	3(3)	2074 1988 1945	4(3)	608 579 525	3(3)	432 395 378	1(1)	154 190
cis-$Mo(CO)_4(Sb\phi_3)_2$	4(4)	2025 1894 1911 1927	6(4)	608 581 577 541	4(4)	472 432 402 387	2(2)	152 158 196 212
cis-$Mo(CO)_3(Sb\phi_3)_3$	2(2)	1933 1843	3(3)	622 591 514	2(2)	490 439	2(2)	146 162 192 214
cis-$Mo(CO)_2(Sb\phi_3)_4$	2(2)	1860 1806	3(3)	609 590 576	2(2)	513 492	4(2)	148 162 198 212
trans-$Mo(CO)_3(Sb\phi_3)_3$	3(3)	1961 1872 1842	5(3)	614 580 500	3(2)	460 448	3	
trans-$Mo(CO)_2(Sb\phi_3)_4$	1(1)	1816	2(1)	590	1(1)	436	1(1)	126 202
$Mo(CO)_5(As\phi_3)$	3(3)	2076 1991 1947	4(3)	608 582 528	3(3)	438 394 374	1(1)	156 212
cis-$Mo(CO)_4(As\phi_3)_2$	4(4)	2028 1868 1901 1915	6(3)	621 583 549	4(4)	475 447 401 379	2(2)	148 162 206 212
cis-$Mo(CO)_3(As\phi_3)_3$	2(2)	1941 1838	3(3)	630 596 505	2(2)	480 450	2(2)	140 156 208 218
$Mo(CO)_5(P\phi_3)$	3(3)	2075 1991 1946	4(2)	607 581	3(3)	446 401 374	1(1)	166 230
cis-$Mo(CO)_4(P\phi_3)_2$	4(4)	2016 1882 1898 1912	6(4)	614 588 581 550	4(4)	480 451 412 390	2(2)	156 170 222 236
cis-$Mo(CO)_3(P\phi_3)_3$	2(2)	1932 1833	3(3)	630 600 500	2(2)	480 443	2(2)	144 160 224 236
trans-$Mo(CO)_4(P\phi_3)_2$	1(1)	1887	2(2)	624 574	1(1)	400	1(1)	138 226

*Raman values (26).
†The two possible series are given.

Can. J. Chem. Downloaded from www.nrcresearchpress.com by 210.87.254.40 on 09/05/12
For personal use only.

evidence for the existence of these two compounds is the yellow color (initially colorless) of the irradiated solutions of the tris derivative in benzene in the presence of excess donor.

Infrared

The infrared spectra have been divided in four regions, corresponding to the different vibrational modes. The results are given in Table 2. Each region was studied for a relationship between changes observed in dipole moments and variations in the vibrational frequencies.

C—O

The assignments of the carbonyl stretching frequencies have already been made for most of these compounds (7) and the linear relationship between the degree of substitution and the mean value of the CO frequencies is well established (15). This linear relationship up to the tetra derivative, as shown in Fig. 3, could indicate a constant change in the electronic environment of the CO group. The slope is negative which corresponds to a lower π-acceptor capability of the ligands compared to CO. The mean values for $P\phi_3$, $As\phi_3$, and $Sb\phi_3$ are similar. The slightly lower values with $P\phi_3$ could indicate that $P\phi_3$ induces a higher negative charge on CO via π-bonding.

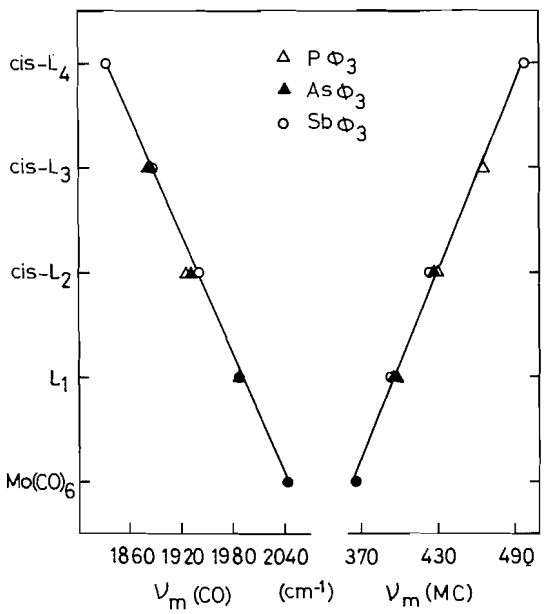

FIG. 3. Correlation between degree of substitution and mean stretching frequencies ν_m(C—O) and ν_m (Mo—C).

Mo—C

The region 350–700 cm^{-1} contains both the Mo—C stretching vibrations and the Mo—C—O deformation vibrations. According to Adams (16), the stretching vibrations occur at lower frequencies than the deformation vibrations which, for any derivative, vary very little from the deformation vibration in the unsubstituted carbonyl. As shown in Fig. 3, the linear relationship also holds. The slope is positive as expected if, through π-bonding, the Mo—C bond increases. Here again the mean values for $P\phi_3$, $As\phi_3$, and $Sb\phi_3$ are very close, with $P\phi_3$ inducing slightly higher values than $As\phi_3$ and $Sb\phi_3$.

This is in agreement with a stronger donating power for $P\phi_3$.

Mo—C—O

The mean values for this vibrational frequency, calculated from a smaller number of bands than the theoretically expected number, lie between 570 and 590 cm^{-1}. No important or consistent variation is therefore apparent.

Mo—L

The region 80–300 cm^{-1} shows many bands due to the donor molecule, C—Mo—C and C—Mo—L deformation vibrations (17). Two series of bands could be related to Mo—L stretching vibrations: one situated around 215 cm^{-1}, the other restricted to the 150 cm^{-1} region. Many authors (18–20) have assigned M—L stretching vibrations to bands in the neighborhood of 200 cm^{-1}. We tentatively consider the region around 150 cm^{-1} as the one containing the stretching vibrations of Mo—L because of the shift to lower frequencies of these bands with substitution. The bands in the 215 cm^{-1} region present a mean frequency which remains constant for all degrees of substitution. Comparison of this last behavior with that of Mo—C—O deformations leads us to consider the 215 cm^{-1} region as a possible one for deformation. However, the weak intensities and the width of the bands preclude us to discard the other assignment.

The infrared data do not show any major variations which could be linked to the differences in stability or dipole moments. $P\phi_3$ seems to be a stronger donating ligand than $As\phi_3$ or $Sb\phi_3$ and the Mo—P bond would appear to be stronger than Mo—As or Mo—Sb. The instability of the derivatives does not, however, reflect itself openly in the different vibrational modes.

TABLE 3

Net charges on ligands and COs with angular distortion in derivatives of $Mo(CO)_6$

Compound	δ_P Electron	δ_N Electron	μ_K (calcd) (D)	μ_K (Experimental) (D)	ϕ (deg)
$Mo(CO)_5(Sb\phi_3)$	0.35	0.07	5.10	5.06	—
cis-$Mo(CO)_4(Sb\phi_3)_2$	0.28	0.14	4.56	4.53	—
cis-$Mo(CO)_3(Sb\phi_3)_3$	0.21	0.21	4.03	4.00	—
cis-$Mo(CO)_2(Sb\phi_3)_4$	0.14	0.28	3.49	3.09	7
	$a = 2.8$ Å,			$b = 1.2$ Å,	$\delta_{Sb\phi_3} = 0.42$ electron*
$Mo(CO)_5(As\phi_3)$	0.40	0.08	5.36	5.38	—
cis-$Mo(CO)_4(As\phi_3)_2$	0.32	0.16	4.73	4.74	—
cis-$Mo(CO)_3(As\phi_3)_3$	0.24	0.24	4.09	3.25	10
	$a = 2.6$ Å,			$b = 0.95$ Å,	$\delta_{As\phi_3} = 0.48$ electron*
$Mo(CO)_5(P\phi_3)$	0.45	0.09	5.47	5.40	—
cis-$Mo(CO)_4(P\phi_3)_2$	0.36	0.18	4.48	4.42	—
cis-$Mo(CO)_3(P\phi_3)_3$	0.27	0.27	3.50	3.01	11
	$a = 2.5$ Å,			$b = 0.2$ Å,	$\delta_{P\phi_3} = 0.54$ electron*

*Net charges on ligands relative to an infinity of COs.

Charge Distribution

The derivatives of $Mo(CO)_6$ with $Sb\phi_3$ show a constant change in μ_K up to the tris derivative. They should constitute an excellent system on which Bigorgne's theory concerning the variation of donor–acceptor capability of ligands and the non-retention of negative charges by the metal (21) could be applied and verified.

Assuming that the total charge on the metal brought through σ-bonding remains constant and equal to the charge returned through π-bonding, the ratios $\mu_K^1/\mu_K^2/\mu_K^3$ should be a function of the distance separating the centers of gravity of positive and negative charges. The distance a, between the center of positive charges P and the metal M, and the distance b, separating the center of negative charges N and the metal, can be considered constant in all derivatives.

$$P \overset{a}{—} M \overset{b}{—} N$$

$Sb\phi_3$ has a stronger donating capability than CO. In a monoderivative, $Sb\phi_3$ will carry a positive charge equal to 5/6 of its net donating power relative to CO. Each CO will receive, through π-bonding, 1/6 of the negative charge. In a bis derivative the net donating capability of $Sb\phi_3$ has been reduced to 4/6 of its initial power while each CO carries 2/6 of the net negative charge. If δ represents the net donating power of a ligand, the dipole moments μ_K of the derivatives are as follows

$$[2] \qquad \mu_K^1 = \left(a + \frac{b}{5}\right)\frac{5}{6}\delta$$

$$[3] \qquad \mu_K^2 = \left(a + \frac{b}{2}\right)\frac{4}{6}\delta$$

$$[4] \qquad \mu_K^3 = \left(a + b\right)\frac{3}{6}\delta$$

$$[5] \qquad \mu_K^4 = \left(a + 2b\right)\frac{2}{6}\delta$$

In order that δ remains constant, b in the case of the three *cis* derivatives with $Sb\phi_3$ must be equal to $0.43a$. To determine b for the derivatives with $As\phi_3$ and $P\phi_3$ is difficult because μ_K^3 does not lie in line with μ_K^1 and μ_K^2. The ratio μ_K^1/μ_K^2 gives a value of b equal to $0.36a$ for $As\phi_3$ and $0.08a$ for $P\phi_3$. The center of gravity of the positive charges is taken on the donor atom mainly because the ligands show a stronger σ-donating power than π-accepting capability. Based on crystallographic data (22) and covalent radii, the distances a have been chosen as 2.5, 2.6, and 2.8 Å for $P\phi_3$, $As\phi_3$, and $Sb\phi_3$. In Table 3 are given the charges, in parts of electron, on the ligands and the resulting dipole moments μ_K.

As the infrared data are similar for derivatives with the same degree of substitution, it seems that the fall in μ_K and the decrease in stability cannot be explained on the basis of charges either on P or N.

Short a distances for $P\phi_3$ and $As\phi_3$ can bring about steric hindrance due to the phenyl groups, and this in turn induces instability. The longer Mo—Sb bond length would allow a tris derivative to exist without any distortion in the octahedron. The fall in μ_K^4 with $Sb\phi_3$ can be explained if steric

Can. J. Chem. Downloaded from www.nrcresearchpress.com by 210.87.254.40 on 09/05/12
For personal use only.

TABLE 4

σ- and π-capabilities of ligands and mean frequencies of Mo—L in derivatives of $Mo(CO)_6$

Compound	δ'_P (electron) σ	π	ν_m(Mo—L)*	
$Mo(CO)_5(Sb\phi_3)$	0.35	0.02_8	190	154
cis-$Mo(CO)_4(Sb\phi_3)_2$	0.28	0.04_7	204	155
cis-$Mo(CO)_3(Sb\phi_3)_3$	0.21	0.05_2	203	154
cis-$Mo(CO)_2(Sb\phi_3)_4$	0.14	0.04_7	205	155
	$\delta'_{Sb\phi_3} = 0.35\sigma, 0.02_8\pi$†			
$Mo(CO)_5(As\phi_3)$	0.40	0.04	212	156
cis-$Mo(CO)_4(As\phi_3)_2$	0.32	0.06_4	209	155
cis-$Mo(CO)_3(As\phi_3)_3$	0.24	0.07_3	213	148
	$\delta'_{As\phi_3} = 0.40\sigma, 0.04\pi$†			
$Mo(CO)_5(P\phi_3)$	0.45	0.07	230	166
cis-$Mo(CO)_4(P\phi_3)_2$	0.36	0.11	229	163
cis-$Mo(CO)_3(P\phi_3)_3$	0.27	0.12_4	230	152
	$\delta'_{P\phi_3} = 0.45\sigma, 0.07\pi$†			

*The two possible series are given.
†Capabilities of ligands relative to five COs.

hindrance opens the angle between adjacent $Sb\phi_3$ moieties by 7°. In $Mo(CO)_3(As\phi_3)_3$, repulsion of the phenyl groups would open the angle by 10°. With $b = 0.08a$ in the $P\phi_3$ series, the angle opening in $Mo(CO)_3(P\phi_3)_3$ is about the same as in $Mo(CO)_3(As\phi_3)_3$. The fact that neither tetra derivative with $As\phi_3$ or $P\phi_3$ could be isolated can also be explained by the steric hindrance. The yellow color of irradiated tris derivative solutions appearing only when excess donor is present shows the importance of the donor in enabling recombination with the metal before total dissociation occurs.

The presence of the center of gravity of negative charges so close to the metal leads us to conclude that *b* is determined by the total amount of negative charges returning via π-bonding, on the CO's and on the ligands. The *b* value obtained from dipole moments of molybdenum derivatives containing ligands with negligible π-accepting capability and offering no steric hindrance would represent the center of gravity of negative charges brought by the ligand's σ-bonding. From the values of μ_K with pyridine (23), which can be regarded as a very poor π-acceptor (24), N would be located at about mid-distance on the C—O axis. We have chosen 2.5 Å as the center of negative charges. However, this value deduced from only one type of derivatives could be in error up to 20%. This would put the center of negative charges either on the oxygen atom as suggested by Carroll (25) or on the carbon atom as proposed by Bigorgne (2). The δ values of Table 3 represent therefore the net donating power.

$$P \xleftarrow[\sigma]{\pi} M \xrightarrow{\pi} N$$

To obtain the σ-donating capacity, the δ values must be calculated for $b = 2.5$ Å. These corrected values δ′ are given in Table 4 together with the π-accepting capability. The values given for $P\phi_3$ are maximum values because *b* is taken as $0.08a$, which is very low considering the fact that the *trans* isomer is stable and that the fall in μ_K from $Mo(CO)_5P\phi_3$ to *cis*-$Mo(CO)_4(P\phi_3)_2$ is much greater than that to $Mo(CO)_4(As\phi_3)_2$. It seems therefore possible that the steric hindrance in $Mo(CO)_4(P\phi_3)_2$ would permit the existence of a *trans* isomer and would lower the dipole moment. Taking a *b* value close to that for $As\phi_3$ would give about the same departure from orthogonality in the tris derivative but it would imply an angle opening of about 6° in the bis derivative and a σ–π capacity of 0.42_6–0.04_4 electron for $P\phi_3$.

Studies on the kinetics of substitution of ligands by α,α′-bipyridyl in *cis*-disubstituted molybdenum hexacarbonyl derivatives have shown that the lability of the leaving groups follow the order $As\phi_3 \geqslant P\phi_3 > Sb\phi_3 \gg CO$ (9). It was hinted that the group lability reflects the Mo—L bond strength. On the other hand, Graham (24) has deduced from C—O force constants in mono-substituted molybdenum hexacarbonyl a relative σ-donor and π-acceptor scale for different

Can. J. Chem. Downloaded from www.nrcresearchpress.com by 210.87.254.40 on 09/05/12
For personal use only.

ligands. $Sb\phi_3$ was found to have an overall stronger σ–π bonding ability than $As\phi_3$ or $P\phi_3$, both of which were found similar. *En accord* with our results of dipole moments, the frequencies observed in the region 140–300 cm^{-1} are higher for $P\phi_3$ than for $As\phi_3$ or $Sb\phi_3$. It seems therefore that the metal–phosphorus bond is the strongest. Of the two series of frequencies which could be attributed to metal–ligand bond, one remains constant throughout substitution whereas the second series follows the same trend as that shown in the dipole moments. The mean frequencies of these two series are given in Table 4.

Conclusion

Stability in $Mo(CO)_6$ derivatives seems to be controlled by two factors. The first one is the *net* donating power of the ligand. If the ligand has a strong *net* donating power, the negative charges on the CO's will be large enough to induce instability. The second factor is the steric hindrance which becomes important whenever large groups are coordinated to the metal. This factor explains the anomalies in the stability and in the dipole moments of derivatives with $Sb\phi_3$, $As\phi_3$, and $P\phi_3$.

It appears that a *trans* isomer will be stable if the *cis* derivative undergoes internal steric repulsion. This is the case with $P\phi_3$ in the bis derivative and with $Sb\phi_3$ in the tetra derivative. In the tris derivative with $Sb\phi_3$, no steric hindrance has been found and consequently the *trans* isomer is very difficult to obtain and study because of a rapid *cis* isomerization. *trans*-$Mo(CO)_4(As\phi_3)_2$ or *trans*-$Mo(CO)_4(Sb\phi_3)_2$ should therefore be quite difficult to study in solution as predictably the isomerization to the *cis* isomer will be quite rapid.

By means of Bigorgne's model, it appears possible to separate σ- and π-bonding capabilities of ligands. This requires, however, precise measurements of the dipole moments of polysubstituted carbonyls. The ligands $Sb\phi_3$, $As\phi_3$, and $P\phi_3$ are mainly σ-donating ligands, with $P\phi_3$ being a better donor and acceptor than $As\phi_3$, which in turn is a better donor and acceptor than $Sb\phi_3$.

We thank the National Research Council of Canada for financial support.

1. W. Strohmeier and H. Hellmann. Ber. Bunsenges. Phys. Chem. **67**, 190 (1965).
2. M. Bigorgne and C. Messier. J. Organometal. Chem. **2**, 79 (1964).
3. W. Strohmeier, J. F. Guttenberger, and G. Popp. Chem. Ber. **98**, 2248 (1965).
4. G. Bouquet and M. Bigorgne. Bull. Soc. Chim. France, 433 (1962).
5. D. Benlian and M. Bigorgne. Bull. Soc. Chim. France, 1583 (1963).
6. Thomas A. Magee, Clifford N. Matthews, Tze Seng Wang, and John H. Wotiz. J. Amer. Chem. Soc. **83**, 3200 (1961).
7. R. Poilblanc and M. Bigorgne. Bull. Soc. Chim. France, 1301 (1962).
8. W. Strohmeier. Chem. Ber. **94**, 2490 (1961).
9. Mauro Graziani, Franco Zingales, and Umberto Belluco. Inorg. Chem. **6**, 1582 (1967).
10. C. Barbeau. Can. J. Chem. **45**, 161 (1967).
11. J. G. Verkade, R. E. McCarley, D. G. Hendricker, and Roy W. King. Inorg. Chem. **4**, 228 (1965).
12. C. Barbeau, L. Ricard, and J. Turcotte. Can. J. Chem. **48**, 1698 (1970).
13. J. W. Smith. Trans. Faraday Soc. **46**, 394 (1950).
14. K. Higasi. Bull. Inst. Phys. Chem. Res. Tokyo. 22805 (1963).
15. O. Kahn and M. Bigorgne. J. Organometal. Chem. **10**, 137 (1967).
16. D. M. Adams. J. Chem. Soc. 1771 (1964).
17. G. Bouquet, A. Loutellier, and M. Bigorgne. J. Mol. Struct. **1**, 211 (1967–1968).
18. C. G. Barlow and G. C. Holywell. J. Organometal. Chem. **16**, 439 (1969).
19. N. A. D. Carey and H. C. Clark. Inorg. Chem. **7**, 94 (1967).
20. A. C. Vandenbroucke, Jr., D. G. Hendricker, R. E. McCarley, and J. G. Verkade. Inorg. Chem. **7**, 1825 (1968).
21. M. Bigorgne. J. Organometal. Chem. Amsterdam, **2**, 68 (1964).
22. H. Luth, Mary R. Truter, and A. Robson. J. Chem. Soc. A, 28 (1969).
23. W. Strohmeier and W. Langhäuser. Z. Phys. Chem. **28**, 268 (1961).
24. W. A. G. Graham. Inorg. Chem. **7**, 315 (1968).
25. D. G. Carroll and S. P. Mc Glynn. Inorg. Chem. **7**, 1285 (1968).
26. L. H. Jones. J. Chem. Phys. **36**, 2375 (1962).

Can. J. Chem. Downloaded from www.nrcresearchpress.com by 210.87.254.40 on 09/05/12
For personal use only.

Can. J. Chem. Downloaded from www.nrcresearchpress.com by 210.87.254.40 on 09/05/12
For personal use only.

Cyclononatrienes *vs.* dihydroanthracenes

ROBERT R. FRASER AND ADEL JURAYDINI
Department of Chemistry, University of Ottawa, Ottawa, Canada

Received June 24, 1970

This paper provides evidence that three compounds previously assumed to be methoxyl derivatives of dihydroanthracenes (1) are actually cyclononatriene derivatives. The revised structural assignments, made on the basis of mass spectral and n.m.r. evidence, remove a previous inconsistency in their n.m.r. properties. The constancy of geminal coupling constants in all three cyclononatrienes is discussed.

Canadian Journal of Chemistry, 48, 3591 (1970)

A recent article in this journal reported an unusual feature in the n.m.r. spectra of three methoxylated dihydroanthracenes (1). In contrast to the appearance of a singlet for the methylene proton absorption in 9,10-dihydroanthracene (**1**) a nonequivalent AB quartet was observed for the methylene absorption in the 2,6-dimethoxy, 2,3,6,7-tetramethoxy, and 2,3,4,6,7,8-hexamethoxy derivatives, **2**, **3**, and **4** respectively. The authors interpreted this nonequivalence as being due to an increase in the barrier to interconversion between the two boat forms of the central dihydroanthracene ring. In view of the known flexibility of this ring system (2, 3, 4) and the lack of any obvious mechanism by which a non-adjacent methoxyl could influence this property, we undertook an investigation of the phenomenon.

A search of the literature revealed the fact that

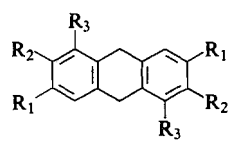

1 $R_1, R_2, R_3 = H$
2 $R_1 = OCH_3; R_2, R_3 = H$
3 $R_1, R_2 = OCH_3; R_3 = H$
4 $R_1, R_2, R_3 = OCH_3$

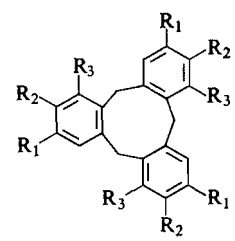

5 $R_1 = OCH_3; R_2, R_3 = H$
6 $R_1, R_2 = OCH_3; R_3 = H$
7 $R_1, R_2, R_3 = OCH_3$

the compound assumed to be **3** by Jimenez and co-workers (1) is actually the *cis,cis,cis*-cyclononatriene derivative, **6**, commonly referred to as cyclotriveratrylene.[1] Proof of structure was provided by two independent groups on the basis of chemical, n.m.r. and mass spectral evidence (5, 6). An alternate synthesis of this compound has also appeared (7). Recent additional evidence (8) shows that **6** exists in the symmetrical "crown" conformation shown in Fig. 1. This conformation is rigid and accounts for the observed n.m.r. nonequivalence of the methylene protons.

It remained then to prepare the compounds reported to have structures **2** and **4** and to deter-

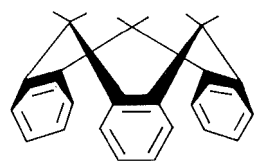

FIG. 1. Symmetrical "crown" conformation of **6**.

TABLE 1
Benzylic proton shifts* for the cyclononatrienes

Compound	δ_A	δ_B	J_{AB}(Hz)
5, m.p. 242–243° (lit. m.p. 245° (1))	4.749	3.619	−13.50
6, m.p. 227–228° (lit. m.p. 227° (1))	4.750	3.532	−13.65
7, m.p. 201–202° (lit. m.p. 202–203° (1))	4.418	4.033	−13.55

*In p.p.m. downfield from TMS.

[1]The trivial name, cyclotriveratrylene, stems from its synthesis in high yield by treatment of veratryl alcohol or veratrole and formaldehyde with acid. The correct name for **6**, 10,15-dihydro-2,3,7,8,12,13-hexamethoxy-5*H*-tribenzo[*a*,*d*,*g*]cyclononene is somewhat longer.

TABLE 2

Mass spectra of cyclononatrienes

5		6		6 (ref. 6)		7	
m/e	% Base	*m/e*	% Base	*m/e*	% Base	*m/e*	% Base
361	11	451	19	451	30	541	34
360	44	450	60	450	100	540	100
345	12	435	19	435	27	525	18
329	25	420	20	420	20	510	40
253	11	419	60	419	75	509	81
252	15	312	27	312	12	478	12
240	21	300	28	300	15	372	14
239	100	299	83	299	70	360	23
238	29	298	16	281	22	359	97
224	32	281	43	268	20	358	50
209	13	270	25	151	18	357	12
195	11	268	43			341	17
165	19	225	20			329	19
153	11	152	21			328	35
152	15	151	100			313	15
121	44					195	11
105	23					181	48

mine their mass spectra to establish whether or not they too were cyclononatriene derivatives. Samples of all three compounds in question were synthesized. They possessed physical constants and n.m.r. spectra (see Table 1) in agreement with those reported (1). The mass spectra of supposed **2** and **4** gave parent peaks and fragmentation patterns consistent only with structures **5** and **7**. The prominent peaks (>10% of base) for **5**, **6**, and **7** are recorded in Table 2. The presence of only one methylenic absorption in the n.m.r. of each requires that they all exist in the "crown" conformation, and the simplicity of the aromatic absorption (1) indicates identical substitution patterns for all three aromatic rings. The correct structures, therefore, are **5**, **6**, and **7**.

An additional aspect of the cyclononatrienes is of interest to us because of the unusual conformation of the methylene protons in **6** with respect to the benzene ring. It has been predicted on the basis of studies on a series of para-substituted benzyl tetrahydropyranyl ethers that protons in the conformation possessed by structure **6** would be insensitive to a para-substituent effect (9) since the angle ϕ, between the π orbitals of the benzene ring and the antisymmetric CH_2 group M.O. is ~80°. It can be seen that the effect of a methoxyl substituent on J_{gem} is negligible in contrast to the 0.5 Hz decrease noted in the tetrahydropyranyl ethers (9). Although the three geminal coupling constants for **5**, **6**, and **7** provide only mild corroboration of our proposal, the potential of this ring system for further testing substituent effects on geminal coupling constants is clear and work in this area has been initiated.

Experimental

The n.m.r. spectra were recorded on a Varian HA 100 n.m.r. spectrometer using 0.05 *M* solutions in deuterochloroform as solvent. The mass spectra were measured on a Hitachi Perkin–Elmer RMU-6D spectrometer using an ionization voltage of 70 eV. The compounds were readily prepared according to the procedures in (1). The only notable difference was that, in our hands, **5** was obtained in a yield of 1.5% after chromatography on silicic acid and elution with 10% ethyl acetate in hexane, followed by crystallization from ethyl acetate.

The authors thank the National Research Council of Canada for generous financial support.

1. F. G. JIMENEZ, M. C. PEREZAMADOR, and J. R. ALCAYDE. Can. J. Chem. **47**, 4489 (1969).
2. E. L. ELIEL, N. L. ALLINGER, S. J. ANGYAL, and G. A. MORRISON. Conformational analysis. Interscience Publishers, New York, N.Y. 1965. p. 242.
3. J. B. STOTHERS, private communication, reports that all attempts to observe individual conformations by low-temperature n.m.r. methods have been unsuccessful.
4. A. L. TERNAY, A. W. BRINKMAN, S. EVANS, and J. HERRMANN. Chem. Commun. 654 (1969).
5. A. S. LINDSEY. J. Chem. Soc. 1685 (1965); Chem. Ind. 823 (1963).
6. H. ERDTMAN, F. HAGLID, and R. RYHAGE. Acta Chem. Scand. **18**, 1249 (1964).
7. B. UMEZAWA, O. HOSHINO, H. HARA, K. OHYAMA, S. MITSUBAYASHI, and J. SAKAKIBARA. Chem. Pharm. Bull. Japan, **17**, 2240 (1969).
8. R. C. COOKSON, B. HALTON, and I. D. R. STEVENS. J. Chem. Soc. *B*, 767 (1968).
9. R. R. FRASER, P. HANBURY, and C. REYES-ZAMORA. Can. J. Chem. **45**, 2481 (1967).

Can. J. Chem. Downloaded from www.nrcresearchpress.com by 210.87.254.40 on 09/05/12
For personal use only.

Chemistry of 2-substituted adamantanes. II. Preparation of 2-adamantanethiol and some of its derivatives.[1] Aromatic solvent-induced shifts in their n.m.r. spectra

J. W. GREIDANUS

Department of Chemistry, The University of Calgary, Calgary 44, Alberta

Received May 11, 1970

Reduction ($NaBH_4$) of adamantanethione gives high yields of pure 2-adamantanethiol, from which several derivatives including the methyl sulfide, sulfoxide, and sulfone were prepared. The sulfenyl chloride was prepared and used *in situ*. From the n.m.r. spectra the aromatic solvent-induced shifts $\Delta = \tau(\text{benzene}) - \tau(CCl_4 \text{ or } CDCl_3)$ were determined, where possible.

Canadian Journal of Chemistry, 48, 3593 (1970)

Recently we reported the details for the preparation of adamantanethione (**2**), which can be obtained in a 90% yield from adamantanone (**1**) by treatment with phosphorus pentasulfide in pyridine (2) (Scheme 1). Reduction of **2** seemed an attractive method to prepare 2-adamantanethiol (**3**) which had not yet been reported. Its

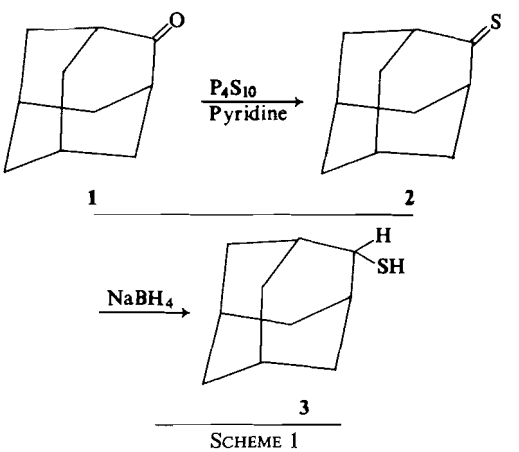

SCHEME 1

isomer, 1-adamantanethiol, has been prepared from the readily available 1-bromoadamantane via the isothiouronium salt (3). Ionic substitution reactions in adamantane derivatives occur much less readily at the secondary carbon than at the bridgehead positions (4). But even if it would be possible to prepare the 2-thiol from the 2-bromo compound in a good yield, then the starting material would still have to be prepared from the ketone: adamantanone → 2-adamantanol → 2-bromoadamantane.[2] For economic and practical reasons it seemed to us therefore unlikely that a more satisfactory method than the sequence **1** → **2** → **3** would become available for the preparation of 2-adamantanethiol, if a good reduction method could be found. As sodium borohydride reacts very readily with the thiocarbonyl group (7) and had been used successfully by others in a few cases (8), it was our first choice.

We now report the details for the preparation and purification of the thiol (**3**) and a number of derivatives (**4**–**10**).

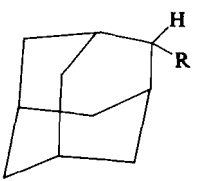

4 R = S—CH_3
5 R = SO—CH_3
6 R = SO_2—CH_3
7 R = 2-adamantyldithio
8 R = S-3,5-dinitrobenzoyl
9 R = S—Cl
10 R = S—phthalimido

Adamantanethione (**2**) was reduced with excess sodium borohydride in 1,2-dimethoxyethane at approximately 45°. We have used impure starting material (**2**) containing up to 30% of adamantanone (**1**) and found that the crude thiol, which on occasion contained large quantities of 2-adamantanol, can be easily and effectively purified via its yellow lead salt. In the experimental section the conversion of **2**, containing about 1% of ketone, into pure thiol is described (yield 85%). 2-Adamantanethiol sublimes readily (90°, 15 Torr), like so many adamantane derivatives.

The new thiol was converted into *S*-(2-adamantyl) 3,5-dinitrobenzoate (**8**), and by methylation (yield 83%) into 2-methylthioadamantane (**4**). The latter, a liquid, was oxidized with 1-chloro-

[1]Part of this work has been reported in a preliminary communication (1).

[2]Practical syntheses of 2-bromoadamantane from the secondary alcohol have been reported, using either phosphorus pentabromide (65% yield (5)) or thionylbromide (88% yield (6)).

Can. J. Chem. Downloaded from www.nrcresearchpress.com by 210.87.254.5 on 09/05/12
For personal use only.

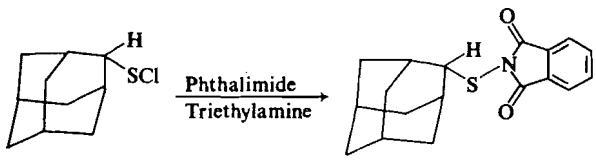

9 10

SCHEME 2

benzotriazole (9) to 2-methylsulfinyladamantane (**5**), or with hydrogen peroxide in acetic acid to the corresponding sulfone (**6**). Oxidation of **3** with iodine gave di-(2-adamantyl) disulfide (**7**).

As 2-adamantanesulfenyl chloride (**9**) seemed a compound of considerable potential in the synthesis of a variety of 2-adamantylthio-compounds, a reaction with the sulfenyl chloride, prepared by the general method of Emde (10), was carried out.

When *N*-chlorosuccinimide was added to 2-adamantanethiol (**3**) in benzene, a yellow–orange solution of **9** was obtained in less than 15 min. After filtration the solution was used for the reaction with phthalimide, giving *N*-(2-adamantylthio)-phthalimide (**10**) (Scheme 2), yield 72%.

The Nuclear Magnetic Resonance Spectra of Compounds 3–7

The n.m.r. spectra showed in general the typical pattern for a 2-monosubstituted adamantane (**11**), as reported by van Deursen and Korver (11). In Table 1 the observed chemical shifts (or calculated origin positions in the case of the AB systems) are presented for all protons where this was possible in compounds **3–7**, as well as for 2-adamantanol. Carbon tetrachloride or deuteriochloroform, and benzene were used as solvents.[3]

In most cases, a.s.i.s. values could be determined for the five protons H-2, H-4,9(*e*), and H-4,9(*a*) on the adamantane skeleton **11**, in addition to shift values for some other protons. Unfortunately it was impossible to get a.s.i.s. values

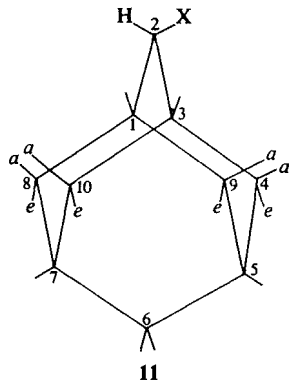

11

for the two other proton pairs H-8,10 (*a* and *e*) in any of the compounds, including 2-adamantanol.[4]

Our data show that the methyl protons in the sulfide **4**, sulfoxide **5** and sulfone **6** are becoming more deshielded in the order given in all solvents, but the aromatic solvent-induced shift $\Delta = \tau(\text{benzene}) - \tau(CCl_4 \text{ or } CDCl_3)$ increases from 0.21 p.p.m. for the sulfide to 0.69 p.p.m. for the sulfone, *i.e.* in the order of their expected dipole moments.[5]

In all cases where complete data could be collected, the a.s.i.s. values show that the equatorial (with respect to the substituent X) proton pair H-4,9(*e*), and H-2 (except in compound **7**) are shielded, while the axial pair H-4,9(*a*) is deshielded by the aromatic solvent.

The thiol proton in 2-adamantanethiol (**3**) shows virtually no solvent-induced shift in our experiments. It is interesting to note that in 1-adamantanethiol the thiol proton shows a downfield solvent shift of 0.13 p.p.m. for the same solvent pair (unpublished observations of the author). This fact shows clearly how much caution is required in the interpretation of aromatic solvent shift data.

The lack of data for the sulfoxide **5** in Table 1 is the result of the complexity of its n.m.r. spectrum, especially in the region where H-2, H-1,3, and H-4,9(*a*) were expected to have their

[3]As carbon tetrachloride and benzene are for various reasons an ideal pair (12) for the study of aromatic solvent-induced shifts (a.s.i.s.), deuteriochloroform was used only when solubility problems were met. Solvent shifts for the pair $CDCl_3$ and CCl_4 have been determined for a number of substituted cyclohexanones and in most cases were found to be small, although there were some striking exceptions (13). The shifts for the two solvent pairs as reported in this work are therefore not strictly comparable in all cases, but our mixed data fit well together and no trends, if noticeable, seem disturbed by the change of solvent.

[4]This compound was the only one for which the origin positions for the H-8,10 (*a* and *e*) protons could be determined by van Deursen and Korver (11) in $CDCl_3$ solution. In CCl_4 or benzene this was not possible, we found.

[5]The following dipole moments μ have been reported in benzene solution: dimethyl sulfide, 1.45 D (14); dimethyl sulfoxide, 3.9 D (15); dimethyl sulfone, 4.25 D (16).

Can. J. Chem. Downloaded from www.nrcresearchpress.com by 210.87.254.5 on 09/05/12
For personal use only.

Can. J. Chem. Downloaded from www.nrcresearchpress.com by 210.87.254.5 on 09/05/12
For personal use only.

TABLE 1

Chemical shift (τ units) of protons in compounds 3–7,* and in 2-adamantanol, and their aromatic solvent-induced shift Δ†

	3			4			5			6			7			2-adamantanol		
Protons‡	CCl_4	Benzene	Δ	CCl_4	Benzene	Δ	$CDCl_3$	Benzene	Δ	$CDCl_3$	Benzene	Δ	CCl_4	Benzene	Δ	CCl_4	Benzene	Δ
H-1,3					8.06					7.43	7.68	+0.25	7.90	7.79	−0.11			
H-2	6.68§	6.90§	+0.22	7.11	7.20	+0.09				6.88	7.31	+0.43	6.87	6.73	−0.14	6.23	6.40	+0.16
H-4,9(*e*)‖	8.49	8.62	+0.13	8.49	8.54	+0.05				8.38			8.47	8.54	+0.07	8.55	8.59	+0.04
H-4,9(*a*)‖	7.81	7.79	−0.02	7.82	7.68	−0.14				7.52	7.32¶	−0.20	7.86	7.72	−0.14	7.89	7.83	−0.06
H-8,10(*e*)‖					8.37					8.24								
H-8,10(*a*)‖					8.22					8.00								
—XH(X=O or S)	8.54§	8.53§	−0.01													8.60	8.96	+0.36
Methyl-H				7.96	8.17	+0.21	7.45	8.02	+0.57	7.13	7.82	+0.69						

*Solutions were 5–10% (w/w).
†Δ = τ(benzene) − τ(CCl_4 or $CDCl_3$). A positive value of the solvent shift indicates a shift to higher field, *i.e.* more shielding, in the aromatic solvent.
‡Designation as in text.
§Doublet, J = 7 Hz.
‖Representing one half of an AB quartet, J = 12 Hz.
¶Approximately; signal for H-4,9(*e*) could not be observed.

signals. We found it impossible to make the necessary assignments and seek the explanation for the far more complicated spectrum in the fact that the two bridgehead protons H-1,3 are not equivalent any more as a result of the adjacent sulfoxide group.

General conclusions regarding the shifts induced by aromatic solvents cannot be drawn from the data in Table 1. They are presented as a contribution to the gradually increasing body of information on these shifts which ultimately may make it possible to arrive at a more quantitative understanding of the phenomenon. At present the qualitative aspects are on many occasions not clear.

Experimental

Melting points were determined on a Büchi melting point apparatus in sealed capillary tubes, and are uncorrected. The i.r. spectra were recorded on a Perkin–Elmer spectrophotometer, Model 337. The mass spectra were determined on a Varian-Mat CH-15 instrument at an ionization energy of 70 eV. The n.m.r. spectra were recorded at 60 or 100 MHz on Varian A-60 and HA-100 spectrometers, in the solvent indicated, at concentrations 5–10% (w/w). Tetramethylsilane ($\tau = 10$) was used as internal standard. Microanalyses were carried out by Dr. C. Daesslé, Organic Microanalysis, Montreal, Quebec, and by Mrs. S. Swaddle of this Department.

2-Adamantanethiol (3)

To a stirred solution of 22.5 g (135 mmoles) of adamantanethione (**2**) (containing approximately 1% adamantanone) in 170 ml of 1,2-dimethoxyethane was added 3.0 g (80 mmoles) of sodium borohydride in small portions in 3 min. When the temperature of the reaction mixture had risen to about 45°, external cooling was started to keep the temperature from rising more. The orange color of the thione faded and after 10 min some colorless precipitate was present. To decompose excess borohydride, 10 ml of water was added dropwise, and then very slowly concentrated hydrochloric acid till p*H* 2 was reached. The reaction mixture was extracted four times with carbon tetrachloride. The extract was washed twice with water, dried ($MgSO_4$), and concentrated *in vacuo* giving 22.4 g of solid crude 2-adamantanethiol. It was dissolved in a mixture of 150 ml of 1,2-dimethoxyethane and 100 ml of ethanol. This solution was added to a stirred solution of 25.8 g (68 mmoles) of lead acetate in 250 ml of 70% ethanol. A bright yellow lead thiolate precipitated. After filtration, the lead salt was twice washed with water, then twice with acetone. After drying, 36.1 g of the fine yellow powder was obtained. This was suspended in 150 ml of water and 250 ml of petroleum ether (boiling range 30–60°) was added. Hydrogen sulfide was bubbled through the aqueous layer for 1 h and lead sulfide was removed by filtration. The aqueous and organic layers were separated, the petroleum ether was washed three times with water, dried ($MgSO_4$), and concentrated to dryness, giving 19.2 g of 2-adamantanethiol (**3**) (yield 85% from the thione), m.p. 153–155°.

An analytical sample of the thiol was obtained by sublimation at 90° and 15 Torr, m.p. 160–161°.

Anal. Calcd. for $C_{10}H_{16}S$: C, 71.37; H, 9.58; S, 19.05. Found: C, 71.42; H, 9.79; S, 18.81.

Mass spectrum: *m/e* 168 (M^+). The i.r. spectrum ν_{max}(KBr): 2560 cm^{-1} (weak, SH); for the n.m.r. spectrum, see Table 1 and text.

S-(2-Adamantyl) 3,5-Dinitrothiobenzoate (8)

Reaction of 2-adamantanethiol with 3,5-dinitrobenzoylchloride in the presence of pyridine afforded *S*-(2-adamantyl) 3,5-dinitrothiobenzoate (**8**), m.p. 171–172° after two recrystallizations from chloroform – petroleum ether.

Anal. Calcd. for $C_{17}H_{18}N_2O_5S$: C, 56.34; H, 5.01; N, 7.73. Found: C, 56.04; H, 4.95; N, 7.52.

The i.r. spectrum ν_{max}(KBr): 1660 (C=O), 1545 and 1350 cm^{-1} (C—NO_2), all very strong; n.m.r. spectrum $\tau(CDCl_3)$: between 0.75 and 1.00 (multiplet, 3H, aromatic protons), 5.71 (singlet, 1H, proton at C-2), between 7.67 and 8.50 (unresolved multiplet, 14H).

2-Methylthioadamantane (4)

To a solution of 8.40 g (50 mmoles) of **3** in 25 ml of methanol and 50 ml of 1,2-dimethoxyethane was added a solution of 2.6 g (65 mmoles) of sodium hydroxide in 20 ml of water. While this mixture was well stirred in a N_2-atmosphere, 7.56 g (60 mmoles) of dimethyl sulfate was added dropwise in 5 min and the reaction mixture was stirred for another 2 h. It contained a lower layer of the sulfide and after 200 ml of water had been added the reaction mixture was extracted three times with petroleum ether. After washing (H_2O), drying ($MgSO_4$), and concentration of the extract, 8.42 g of oil was obtained which was distilled at 95–97° and 4 Torr giving 7.50 g of 2-methylthioadamantane (yield 83%), n_D^{25} 1.5460.

Anal. Calcd. for $C_{11}H_{18}S$: C, 72.46; H, 9.95; S, 17.59. Found: C, 72.31; H, 9.94; S, 17.42.

Mass spectrum: *m/e* 182 (M^+). For the n.m.r. spectrum see Table 1 and text.

2-Methylsulfinyladamantane (5)

With 1-chlorobenzotriazole 1.46 g (8 mmoles) of **4** in methanol – methylene chloride (2:1) at −78° was converted into the corresponding sulfoxide using a recently reported method (9). 2-Methylsulfinyladamantane (**5**) was obtained in a 77% yield, m.p. 120°. After recrystallization from *n*-hexane (containing 5% benzene) shiny plates were obtained, m.p. 122–123°.

Anal. Calcd. for $C_{11}H_{18}OS$: C, 66.61; H, 9.15; S, 16.16. Found: C, 66.79; H, 8.99; S, 15.89.

Mass spectrum: *m/e* 198 (M^+). The i.r. spectrum ν_{max}(KBr): 1041 and 1030 cm^{-1} (very strong, SO stretching in sulfoxide); for the n.m.r. spectrum see Table 1 and text.

2-Methylsulfonyladamantane (6)

Oxidation of 0.88 g (4.8 mmoles) of **4** with hydrogen peroxide in glacial acetic acid gave a 60% yield of 2-methylsulfonyladamantane, m.p. 114.5–115.5°.

Anal. Calcd. for $C_{11}H_{18}O_2S$: C, 61.64; H, 8.47; S, 14.96. Found: C, 61.47; H, 8.41; S, 14.66.

Mass spectrum: *m/e* 214 (M^+). The i.r. spectrum ν_{max}(KBr): 1130 and 1275 cm^{-1} (very strong, SO_2); for the n.m.r. spectrum see Table 1 and text.

Can. J. Chem. Downloaded from www.nrcresearchpress.com by 210.87.254.5 on 09/05/12
For personal use only.

Di(2-adamantyl) Disulfide (7)

A solution of 1.27 g (5 mmoles) of iodine in 25 ml of ethanol was added dropwise to a stirred solution of 1.68 g (10 mmoles) of 2-adamantanethiol and 0.54 g (10 mmoles) of sodium methoxide in 50 ml of a 1:1 mixture of ethanol and 1,2-dimethoxyethane. The disulfide precipitated and was isolated by filtration (weight 1.61 g). It was very well soluble in carbon tetrachloride, benzene, ethylacetate, and petroleum ether, only slightly in hot acetonitrile or hot ethanol. It was twice recrystallized from benzene – acetonitrile (1:2) giving 1.32 g of di(2-adamantyl) disulfide (yield 79%), m.p. 275°.

Anal. Calcd. for $C_{20}H_{30}S_2$: C, 71.80; H, 9.04; S, 19.16. Found: C, 71.44; H, 8.95; S, 19.14.

Mass spectrum: *m/e* 334 (M^+). For the n.m.r. spectrum see Table 1 and text.

*N-(2-Adamantylthio)-phthalimide (**10**)*

A solution of 2-adamantanesulfenyl chloride (**9**) was prepared as follows (10): to a stirred suspension of 2.72 g (20.4 mmoles) of *N*-chlorosuccinimide in 30 ml of benzene was added a solution of 3.36 g (20 mmoles) of 2-adamantanethiol in 10 ml of benzene. The vigorously stirred reaction mixture turned yellow–orange and was filtered after 15 min.

The clear filtrate, containing the sulfenylchloride was added to 2.94 g (20 mmoles) of phthalimide in 20 ml of *N,N*-dimethylformamide containing 2.7 g (27 mmoles) of triethylamine. After 20 min of stirring at 25°, the reaction mixture was left standing for 40 h. After filtration to remove the formed triethylammonium chloride the filtrate was poured into 200 ml of water. After extraction with carbon tetrachloride (three times) the extract was washed with water, dried ($MgSO_4$), and concentrated till almost dry. Addition of 100 ml of petroleum ether, filtration, and drying of the product gave 4.5 g of almost colorless *N*-(2-adamantylthio)-phthalimide (72%), which could be recrystallized from ethanol; m.p. 166–167°.

Anal. Calcd. for $C_{18}H_{19}NO_2S$: C, 68.98; H, 6.11; N, 4.47; S, 10.23. Found: C, 69.20; H, 6.16; N, 4.28; S, 10.46.

Mass spectrum: *m/e* 313 (M^+). The i.r. spectrum ν_{max}(KBr): 1755 cm^{-1} (very strong, C=O); n.m.r. τ (CCl_4): 2.19 (multiplet, 4H, aromatic protons), 6.52 (singlet, 1H, proton at C-2), τ 6.4–8.7 (unresolved multiplet, 14H).

The author thanks The National Research Council of Canada for financial support of this work.

1. J. W. Greidanus and W. J. Schwalm. Can. J. Chem. **47**, 3715 (1969).
2. J. W. Greidanus. Can. J. Chem. This issue.
3. J. R. Geigy A.-G. Belg. Pat. 629 370 (1963); Chem. Abstr. **60**, 9167*c* (1964).
4. P. von R. Schleyer and R. D. Nicholas. J. Amer. Chem. Soc. **83**, 182 (1961). R. C. Fort, Jr. and P. von R. Schleyer. Chem. Rev. **64**, 277 (1964). C. R. Carpenter. Ph.D. Thesis. The Pennsylvania State University, University Park, Pennsylvania, 1967.
5. W. Hoek, J. Strating, and H. Wynberg. Rec. Trav. Chim. **85**, 1045 (1966).
6. S. Landa, J. Burkhard, and J. Vais. Z. Chem. **7**, 388 (1967).
7. J. C. Powers and F. H. Westheimer. J. Amer. Chem. Soc. **82**, 5431 (1960).
8. R. M. Dodson and P. B. Sollman. U.S. Pat. 2753361 (1956); Chem. Abstr. **51**, 2079 (1957). R. M. Dodson and P. B. Sollman. U.S. Pat. 2840577 (1958); Chem. Abstr. **53**, 453 (1959).
9. W. D. Kingsbury and C. R. Johnson. Chem. Commun. 365 (1969).
10. H. Emde. German Pat. 804572 (1951); Chem. Abstr. **46**, 529 (1952).
11. F. W. van Deursen and P. K. Korver. Tetrahedron Lett. 3923 (1967).
12. T. Ledaal. Tetrahedron Lett. 1683 (1968).
13. M. Fetizon, J. Goré, P. Laszlo, and B. Waegell. J. Org. Chem. **31**, 4047 (1966).
14. H. Lumbroso and G. Dumas. Bull. Soc. Chim. France, 651 (1955).
15. F. A. Cotton and R. Francis. J. Amer. Chem. Soc. **82**, 2986 (1960).
16. H. Lumbroso and R. Passerini. Bull. Soc. Chim. France, 1179 (1955).

Identification of 1-(4-methoxyphenyl)-1-methoxy-2-aminopropane diastereoisomers

K. Bailey

Research Laboratories, Food and Drug Directorate, Ottawa, Canada

Received April 29, 1970

A method for the assignment of *erythro* and *threo* configurations to the diastereoisomeric 1-(4-methoxyphenyl)-1-methoxy-2-aminopropanes and related compounds based on p.m.r. data is presented and discussed.

Canadian Journal of Chemistry, **48**, 3597 (1970)

The physiological activities of the (+) and (−) forms of the *erythro* and *threo* isomers of derivatives of phenylpropanolamine, $C_6H_5CH(OH)CH(CH_3)NH_2$ may be expected to differ, and a positive identification of the forms is essential in analysis and for investigations of structure–activity relationships (1). Synthetic compounds of the type $ArCH(OR^1)CHR^2NH_2$ (2, 3) are a case in point, and the difficulties in assigning configurations to the potentially hypo-

Can. J. Chem. Downloaded from www.nrcresearchpress.com by 210.87.254.5 on 09/05/12
For personal use only.

Di(2-adamantyl) Disulfide (7)

A solution of 1.27 g (5 mmoles) of iodine in 25 ml of ethanol was added dropwise to a stirred solution of 1.68 g (10 mmoles) of 2-adamantanethiol and 0.54 g (10 mmoles) of sodium methoxide in 50 ml of a 1:1 mixture of ethanol and 1,2-dimethoxyethane. The disulfide precipitated and was isolated by filtration (weight 1.61 g). It was very well soluble in carbon tetrachloride, benzene, ethylacetate, and petroleum ether, only slightly in hot acetonitrile or hot ethanol. It was twice recrystallized from benzene – acetonitrile (1:2) giving 1.32 g of di(2-adamantyl) disulfide (yield 79%), m.p. 275°.

Anal. Calcd. for $C_{20}H_{30}S_2$: C, 71.80; H, 9.04; S, 19.16. Found: C, 71.44; H, 8.95; S, 19.14.

Mass spectrum: *m/e* 334 (M^+). For the n.m.r. spectrum see Table 1 and text.

*N-(2-Adamantylthio)-phthalimide (**10**)*

A solution of 2-adamantanesulfenyl chloride (**9**) was prepared as follows (10): to a stirred suspension of 2.72 g (20.4 mmoles) of *N*-chlorosuccinimide in 30 ml of benzene was added a solution of 3.36 g (20 mmoles) of 2-adamantanethiol in 10 ml of benzene. The vigorously stirred reaction mixture turned yellow–orange and was filtered after 15 min.

The clear filtrate, containing the sulfenylchloride was added to 2.94 g (20 mmoles) of phthalimide in 20 ml of *N,N*-dimethylformamide containing 2.7 g (27 mmoles) of triethylamine. After 20 min of stirring at 25°, the reaction mixture was left standing for 40 h. After filtration to remove the formed triethylammonium chloride the filtrate was poured into 200 ml of water. After extraction with carbon tetrachloride (three times) the extract was washed with water, dried ($MgSO_4$), and concentrated till almost dry. Addition of 100 ml of petroleum ether, filtration, and drying of the product gave 4.5 g of almost colorless *N*-(2-adamantylthio)-phthalimide (72%), which could be recrystallized from ethanol; m.p. 166–167°.

Anal. Calcd. for $C_{18}H_{19}NO_2S$: C, 68.98; H, 6.11; N, 4.47; S, 10.23. Found: C, 69.20; H, 6.16; N, 4.28; S, 10.46.

Mass spectrum: *m/e* 313 (M^+). The i.r. spectrum ν_{max}(KBr): 1755 cm^{-1} (very strong, C=O); n.m.r. τ (CCl_4): 2.19 (multiplet, 4H, aromatic protons), 6.52 (singlet, 1H, proton at C-2), τ 6.4–8.7 (unresolved multiplet, 14H).

The author thanks The National Research Council of Canada for financial support of this work.

1. J. W. Greidanus and W. J. Schwalm. Can. J. Chem. **47**, 3715 (1969).
2. J. W. Greidanus. Can. J. Chem. This issue.
3. J. R. Geigy A.-G. Belg. Pat. 629 370 (1963); Chem. Abstr. **60**, 9167*c* (1964).
4. P. von R. Schleyer and R. D. Nicholas. J. Amer. Chem. Soc. **83**, 182 (1961). R. C. Fort, Jr. and P. von R. Schleyer. Chem. Rev. **64**, 277 (1964). C. R. Carpenter. Ph.D. Thesis. The Pennsylvania State University, University Park, Pennsylvania, 1967.
5. W. Hoek, J. Strating, and H. Wynberg. Rec. Trav. Chim. **85**, 1045 (1966).
6. S. Landa, J. Burkhard, and J. Vais. Z. Chem. **7**, 388 (1967).
7. J. C. Powers and F. H. Westheimer. J. Amer. Chem. Soc. **82**, 5431 (1960).
8. R. M. Dodson and P. B. Sollman. U.S. Pat. 2753361 (1956); Chem. Abstr. **51**, 2079 (1957). R. M. Dodson and P. B. Sollman. U.S. Pat. 2840577 (1958); Chem. Abstr. **53**, 453 (1959).
9. W. D. Kingsbury and C. R. Johnson. Chem. Commun. 365 (1969).
10. H. Emde. German Pat. 804572 (1951); Chem. Abstr. **46**, 529 (1952).
11. F. W. van Deursen and P. K. Korver. Tetrahedron Lett. 3923 (1967).
12. T. Ledaal. Tetrahedron Lett. 1683 (1968).
13. M. Fetizon, J. Goré, P. Laszlo, and B. Waegell. J. Org. Chem. **31**, 4047 (1966).
14. H. Lumbroso and G. Dumas. Bull. Soc. Chim. France, 651 (1955).
15. F. A. Cotton and R. Francis. J. Amer. Chem. Soc. **82**, 2986 (1960).
16. H. Lumbroso and R. Passerini. Bull. Soc. Chim. France, 1179 (1955).

Identification of 1-(4-methoxyphenyl)-1-methoxy-2-aminopropane diastereoisomers

K. Bailey

Research Laboratories, Food and Drug Directorate, Ottawa, Canada

Received April 29, 1970

A method for the assignment of *erythro* and *threo* configurations to the diastereoisomeric 1-(4-methoxyphenyl)-1-methoxy-2-aminopropanes and related compounds based on p.m.r. data is presented and discussed.

Canadian Journal of Chemistry, **48**, 3597 (1970)

The physiological activities of the (+) and (−) forms of the *erythro* and *threo* isomers of derivatives of phenylpropanolamine, $C_6H_5CH(OH)CH(CH_3)NH_2$ may be expected to differ, and a positive identification of the forms is essential in analysis and for investigations of structure–activity relationships (1). Synthetic compounds of the type $ArCH(OR^1)CHR^2NH_2$ (2, 3) are a case in point, and the difficulties in assigning configurations to the potentially hypo-

Can. J. Chem. Downloaded from www.nrcresearchpress.com by 210.87.254.6 on 09/05/12
For personal use only.

TABLE 1

The p.m.r. spectral data* from β-nitrostyrene derivatives

Compound	β-R	4-OCH_3	α-OCH_3	α-H	β-H	β-CH_3
5	NO_2	6.20	6.77	*ca.* 5.10 q (4, 8)	*ca.* 5.35 q (12, 8) and *ca.* 5.65 q (12, 4)	—
6*a*	NO_2	6.22	6.75	5.15	5.7 ⎫ α-H and β-H give	8.47 d (6.5)
6*b*	NO_2	6.20	6.85	5.15	5.7 ⎭ overlapping multiplet	8.76 d (6.5)
7	MH_2 7.77	6.21	6.77	5.90 t (6)	7.13 d (6)	—
8*a*	NH_2 8.30	6.20	6.78	~6.15 d?	6.85 m	8.93 d (6.5)
8*b*	NH_2 8.30	6.20	6.80	~6.28 d?	6.85 m	9.13 d (6.5)
9	N^+H_3 1.55	6.21	6.73	5.38 q (6.5, 7.5)	6.85 m	—
10*a*	N^+H_3 1.45	6.20	6.61	5.33 d (4.5)	6.50 m	8.72 d (6.5)
10*b*	N^+H_3 1.25	6.20	6.73	5.77 d (9)	6.55 m	8.72 d (6.5)
11	NH_2 8.22	6.25	—	*ca.* 7.60 q (13, 8) and *ca.* 7.32 q (13, 5.5)	*ca.* 6.88 m	8.92 d (6.5)

*τ-Values, measured with a Varian A-60A spectrometer using solutions *ca.* 15% in $CDCl_3$ containing TMS as internal standard, CH_3 signals were experimentally reproducible within ± 0.01 p.p.m. Chemical shift differences cited in the text were confirmed by measuring spectra of appropriate mixtures. Signals were singlets except when d = doublet, t = triplet, q = quartet, and m = multiplet, with first-order coupling constants (Hz) indicated. The α- and β-protons of **5**, **6** and **11** give complex signals and τ-values are approximate. The α-H of **8***a* and of **8***b* gives a doublet, one branch obscured by the 4-OCH_3. The spectrum of **8***b* was obtained only in the presence of **8***a*.

tensive derivatives **1** and **2** have been alluded to recently (3). In the present study the p.m.r. spectra of some derivatives of 4-methoxy-β-nitrostyrene (**3**) which exist as *erythro* and *threo* racemates, were examined in an attempt to assign their relative configurations by methods of conformational analysis.

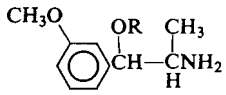

1 R = CH_3
2 R = C_2H_5

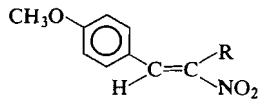

3 R = H
4 R = CH_3

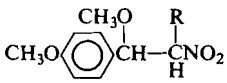

5 R = H
6 R = CH_3

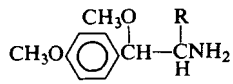

7 R = H
8 R = CH_3

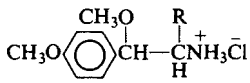

9 R = H
10 R = CH_3

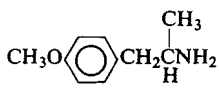

11

Nitrostyrenes react with methoxide ion in methanol to give methoxynitropropanes (2, 3), and the nitrostyrene **4** produces a mixture of the (±) *threo* and (±) *erythro* compounds **6** in the ratio major product *a*:minor *b* = 2:1 (by integrated p.m.r.). These isomers could not be separated by analytical t.l.c. using several systems. Reduction of the mixture **6** with lithium aluminum hydride afforded the amino compounds (±) **8** in the ratio major *a*:minor *b* = 3:2 (by p.m.r.). The high yield (90%) shows that the ratio change is not due to preferential reduction or recovery of one form, but that some racemization of the acidic β-carbon occurs under the influence of the reagent. A net inversion under these conditions is unreasonable and contraindicated by the observation that in both **6** and **8** the (generally similarly environed, see below) downfield β-CH_3 compound predominates. Compound (±) **7** was obtained similarly. The two diastereoisomers of **8** were separated in small amounts by column chromatography, and then converted into the (±) hydrochlorides **10**.

Salient features of the p.m.r. spectra of compounds **5**–**10** are presented in Table 1. Newman projections of the staggered-form rotamers corresponding with *erythro* and *threo* forms are depicted in Fig. 1. Assuming that steric interactions principally govern the relative conformational energies, rotamer **A** should dominate in every case. (In an investigation of ephedrine and ψ-ephedrine, Hyne (4) pointed out that such views must be held with caution). Hence, in compounds **6**, **8**, and **10**, effects on the α-OCH_3 and β-CH_3 due to electric fields and the magnetic anisotropies of the nitro and aryl groups respectively would be more marked in the *threo* form. Comparing **7** and **8** the (upfield) α-OCH_3 shifts on methylation of the β-carbon are very small in both series. However, when compounds **5** and **6** are compared there results an α-OCH_3 upfield shift of 0.08 p.p.m. for the minor product **6***b* and a downfield shift of only 0.02 p.p.m. for **6***a*.

Can. J. Chem. Downloaded from www.nrcresearchpress.com by 210.87.254.6 on 09/05/12
For personal use only.

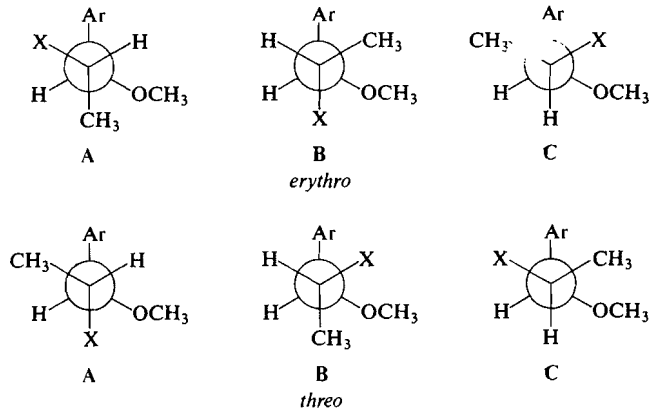

FIG. 1. *erythro* and *threo* **6**, **8**, and **10** where X = NO_2, NH_2, and N^+H_3 respectively.

Since the highly anisotropic NO_2 group would be expected to exert greater through-space effects than a CH_3 group, this indicates (assuming that rotamers about the C_α–C_β bond in **5** are roughly equally populated) that the upfield shift is due to resultant net shielding of the α-OCH_3 by the β-NO_2 group and therefore that the *threo* form is probably the minor product **6***b*. In compounds **8** the α-OCH_3 groups fall into similar electronic environments, but the β-CH_3 groups are seen to be disposed fairly similarly to their average in **6**.

The amino function of the ephedrines relatively deshields *gauche* protons (4). If the NO_2 shielded the *gauche* OCH_3 of *threo* **6**, on reduction the *threo* α-OCH_3 of **8** would be the more deshielded (0.05 p.p.m.) and changing inductive effects could account for the small upfield shift (0.03 p.p.m.) of the *erythro* α-OCH_3. However, if the NO_2 group deshielded the *gauche* α-OCH_3, the *threo* isomers would be the major components *a*, but it seems unlikely that the *erythro* α-OCH_3 would shift downfield by 0.05 p.p.m. (from 6.85 to 6.80τ) on reduction of the generally remote NO_2. These interpretations, favoring shielding of the α-OCH_3 by a *gauche* β-NO_2 require simultaneous relative shielding of the β-CH_3 by the *gauche* aromatic ring. A comparison of the β-CH_3 shifts in mixed and single samples of **8** and *p*-methoxyamphetamine (**11**) shows a large (0.21 p.p.m., **8***b*) and small (*ca.* 0.01 p.p.m., **8***a*) upfield shift results on α-methoxylation. Following the argument presented for **5** and **6** above the aryl group shields the *gauche* CH_3, and **8***b* is the *threo* isomer. The p.m.r. spectra (CS_2) (5) of *meso* and *dl*-2,3-diphenylbutane, in which the CH_3 and C_6H_5 groups are predominantly *gauche* and *trans* disposed respectively, demonstrated relative shielding of the CH_3 groups (at 9.04 and 8.78 respectively) by the *gauche* benzene ring, and a study of a 1,2-diphenyl-propyl series (6) showed a shielding of about 0.3 p.p.m. ($CDCl_3$) for a predominantly *gauche vs. trans* CH_3/C_6H_5 conformation.

The shielding effects of a NO_2 group qualitatively resemble those of a carbonyl function (7) and Barbieux and Martin (8) investigated *erythro* and *threo* ethyl α,β-dialkyl-*p*-methoxydihydrocinnamates. Coupling constants between the α and β protons were not reported, assignments were made on the basis that *gauche* aryl and carboethoxy groups in the *threo* isomers would result in a relatively upfield position of those ethyl protons (9). Their spectra show that an α-CH_3 is overall shielded (higher field) by anisotropic effects of a *gauche* compared with a *trans* carboxyl function.

Because the aryl and nitro groups of **6** and **8** rotate and different relative rotamer populations of **5**–**8** and **11** are expected, the criteria for comparative shielding effects are difficult to assess. However, these results leave little doubt that **6***b* and **8***b* are the *threo* isomers.

Conversion of isomers **8** into the amine salts **10** preserves the stereochemical integrity of each form. Table 1 shows that the more widely split α-H of **10** is from the minor component **10***b* and appears at higher field than in isomer **10***a*. Vicinal coupling constants of this magnitude (9 Hz) are generally associated with dihedral angles of about 180° (10), indicating that **10***b* exists largely in the **A** form (*erythro* or *threo*) and that the major product has relatively greater contributions from **B** and **C** type rotamers. Since

Can. J. Chem. Downloaded from www.nrcresearchpress.com by 210.87.254.6 on 09/05/12
For personal use only.

Can. J. Chem. Downloaded from www.nrcresearchpress.com by 210.87.254.6 on 09/05/12
For personal use only.

in **B** and **C** rotamers the α-protons are on average further away from the ammonium ion, overall relative shielding of the *gauche* protons by it (or its ion pair/ion complex moiety) is indicated. In **10***b* the α-H and α-OCH_3 are *both* upfield of their positions in diastereoisomer **10***a*. This simultaneous shielding seems reasonable for the **A** rotamer of the *threo* series where both the α-H and α-OCH_3 are *gauche* to the ionic moiety, and it follows that **10***b* and therefore **8***b* and **6***b* are the *threo* isomers, consistent with the evidence for **8** and **6** assignments presented above. The designation *threo* to the isomer **10***b* with larger coupling here is in line with results for ephedrines (4) and agrees with the magnitudes of the H_α–H_β coupling constants for the appropriate diastereoisomers of 1-substituted-1,2-diphenylpropanes (6).

In monosubstituted cyclohexanes, conformational (steric) preferences in aprotic solvents increase as $NO_2 < NH_2 < N^+H_3$ (12). The β-CH_3 groups of the salts **10** appear at the same chemical shift, again suggesting that *erythro* rotamers **B** and **C** (*gauche* aryl/CH_3) abnormally contribute. In these three forms the α-OCH_3 and β-N^+H_3 are *gauche*; possibly polar interactions have a stabilizing influence.

It is probable that for diastereomeric pairs similar to **6**, **8**, and **10** (*i.e.* with different aromatic substitutions), the (±) *threo* configuration may be assigned to the isomer with the relatively upfield α-H, β-CH_3, and/or α-OCH_3 signals, the latter two being easily visible and so diagnostically useful. The analysis may be extendable to the corresponding signals from compounds with other α-alkoxyl and β-alkyl groups, but this has not been investigated.

Experimental

Melting points are uncorrected. The known nitrostyrenes used here were prepared by the condensation of anisaldehyde with nitromethane or nitroethane using NH_4OAc/HOAc (11).

1-(4-Methoxyphenyl)-1-methoxy-2-nitroethane (5)

This was prepared by the general method of Howe *et al.* (3) from 4-methoxy-β-nitrostyrene (**3**). Crude yield (oil) 97%. Distillation (partial dec.) gave **5** (55%), b.p. 136°/2 mm, m.p. 50–51°; oil ν_{max} (film): 1555 and 1380 cm^{-1} (NO_2); (Nujol): 1550 and 1375 cm^{-1}; lit. m.p. 57–58° (2).

Anal. Calcd. for $C_{10}H_{13}NO_4$: C, 56.86; H, 6.20; N, 6.63. Found: C, 57.01; H, 6.29; N, 6.49.

1-(4-Methoxyphenyl)-1-methoxy-2-nitropropane (6)

This was obtained similarly from 4-methoxy-β-methyl-β-nitrostyrene, (**4**) in 95% yield as a pale yellow oil, examined and used without purification. The t.l.c. (silica gel and alumina, Et_2O, $CHCl_3$, C_6H_6, and C_6H_{14}: Me_2CO = 2:1) gave a single spot or streak, ν_{max} (film): 1555 and 1370 cm^{-1} (NO_2).

2-(4-Methoxyphenyl)-2-methoxyethylamine (7)

A crude sample of **5** (3.3 g) in dry ether (30 ml) was added dropwise to a stirred suspension of lithium aluminum hydride (2 g) in dry ether (50 ml). The mixture was kept at reflux for 5 h, cooled, and treated with ordinary ether (50 ml) followed by the cautious addition of water (6 ml). The ethereal suspension was filtered under weak vacuum and the ether solution dried ($MgSO_4$) and concentrated to give the amine **7** as a colorless oil, 1.9 g. This was quantitatively converted into the hydrochloride **9** using a saturated solution of hydrogen chloride in ether. Recrystallization from chloroform–hexane gave prisms, m.p. 162–163°, lit. 165–166.5°, dec. 186–187 (2) and 186–187° (13); ν_{max} (Nujol) 2800–2600 cm^{-1} (N^+H_3).

Anal. Calcd. for $C_{10}H_{16}ClNO_2$: C, 55.17; H, 7.41; N, 6.43. Found: C, 55.07; H, 7.50; N, 6.31.

The amine was regenerated from its hydrochloride by treatment with sodium carbonate solution and was extracted with chloroform.

1-(4-Methoxyphenyl)-1-methoxy-2-aminopropane (8)

The crude *erythro–threo* mixture **6** (4 g) was reduced in ether with lithium aluminum hydride (2 g), furnishing the amine **8** as a colorless oil (3.1 g, 90%). This was examined by p.m.r. and then adsorbed on to silica gel (50 g). Elution with chloroform (50 ml fractions, 350 ml) afforded the major component (0.23 g). Continued elution (700 ml) gave mixtures of **8***a* and **8***b* (1.39 g). Elution with 1% methanol (200 ml) and 2% methanol in chloroform (50 ml) gave **8***a* and **8***b* (0.51 g). Continued elution with 2% methanol in chloroform (500 ml) gave **8***b* containing traces of **8***a* (by t.l.c.) (0.22 g). Samples of **8***a*·HCl, m.p. 177–178 raised to 178–180° by recrystallization from $CHCl_3$ and **8***b*·HCl, m.p. 171–173 raised to 178–179° had mixed m.p. 160–162°. Their i.r. spectra (KBr) were similar, but the samples showed no detectable amounts of the other by i.r. and p.m.r.

Anal. Calcd. for $C_{11}H_{18}ClNO_2$: C, 57.00; H, 7.83; N, 6.05; Cl, 15.31. Found for **8***a*·HCl: C, 57.17; H, 7.61; N, 6.01; Cl, 15.25. Found for **8***b*·HCl: C, 56.87; H, 7.85; N, 5.97.

The author thanks Miss D. Verner for assistance with synthesis, and Mr. H. W. Avdovich for determining p.m.r. spectra.

1. G. A. Alles. J. Pharmacol. Exp. Ther. **47**, 339 (1933).
2. K. W. Rosenmund. Ber. Deut. Chem. Ges. **46**, 1034 (1913).
3. R. Howe, E. H. P. Young, and A. D. Ainley. J. Med. Chem. **12**, 998 (1969).
4. J. B. Hyne. Can. J. Chem. **39**, 2536 (1961).
5. A. A. Bothner-By and C. Naar-Colin. J. Amer. Chem. Soc. **84**, 743 (1962).
6. C. A. Kingsbury and D. C. Best. J. Org. Chem. **32**, 6 (1967).
7. K. Tori and K. Kuriyama. Tetrahedron Lett. 3939 (1964).

8. M. BARBIEUX and R. H. MARTIN. Tetrahedron Lett. 2919 (1965).
9. D. Y. CURTIN and S. DAYAGI. Can. J. Chem. **42**, 867 (1964).
10. M. KARPLUS. J. Chem. Phys. **30**, 11 (1959).
11. M. G. S. RAO, C. SRIKANTIA, and M. S. IYENGAR. Helv. Chim. Acta, **12**, 581 (1929); L. C. RAIFORD and D. E. FOX. J. Org. Chem. **9**, 170 (1944).
12. J. MCKENNA. Conformational analysis of organic compounds. Royal Institute of Chemistry Lecture Series No. 1 (1966).
13. B. REICHERT. Arch. Pharm. **274**, 369 (1936).

Reactions of trifluoromethyl and methyl radicals with ethylene oxide

S. H. JONES AND E. WHITTLE
Chemistry Department, University College, Cathays Park, Cardiff, Gt. Britain

Received June 15, 1970

The reaction between CF_3 radicals and ethylene oxide was studied in the range 60–228 °C using CF_3I as a radical source. For the reactions,

$$CF_3 + CH_2\text{—}CH_2O \xrightarrow{k_H} CF_3H + CH_2\text{—}CHO$$

$$CF_3 + CF_3 \xrightarrow{k_c} C_2F_6$$

we obtain

$$\log k_H/k_c^{1/2}(cm^{3/2}\ mole^{-1/2}\ s^{-1/2}) = (5.77 \pm 0.12) - (11.02 \pm 0.22)/\theta$$

where $\theta = 2.3RT$ kcal mole^{-1}.

Published data of Phibbs and Darwent on the reaction

[5] $$CH_3 + CH_2\text{—}CH_2O \rightarrow CH_4 + CH_2\text{—}CHO$$

have been re-calculated and it is suggested that both the original and re-calculated values of the activation energy E_5 are too low. The Arrhenius parameters for the reactions of CF_3 and CH_3 radicals with ethylene oxide are compared with those for related reactions.

Canadian Journal of Chemistry, **48**, 3601 (1970)

Can. J. Chem. Downloaded from www.nrcresearchpress.com by 210.87.254.6 on 09/05/12
For personal use only.

As part of a study of the vapor phase reactions of free radicals with cyclic compounds, we have determined Arrhenius parameters for the abstraction of hydrogen by CF_3 radicals from ethylene oxide. The radicals were generated by photolysis of CF_3I.

We have also re-calculated the data of Phibbs and Darwent (1) on the corresponding reaction involving CH_3 radicals with ethylene oxide. Their results on CH_3 + cyclopropane have also been re-interpreted. It is found that published data on the reaction between CH_3 radicals and ethylene oxide are anomalous and the system appears to require re-investigation.

Experimental

Ethylene oxide was purified by bulb-to-bulb distillation retaining a middle cut which was stored in liquid nitrogen. It was better than 99.9% pure as indicated by g.l.c. No impurities could be detected by i.r. spectroscopy.

Mixtures of CF_3I and ethylene oxide were photolyzed and the products analyzed using procedures described elsewhere (2).

Results

Blank experiments without photolysis showed that there is no dark reaction between CF_3I and ethylene oxide, EtO. When the mixture is photolyzed, important reactions are [1]–[3]. The

[1] $$CF_3I + h\nu \rightarrow CF_3 + I$$

[2] $$CF_3 + CH_2\text{—}CH_2O \rightarrow CF_3H + CH_2\text{—}CHO$$

[3] $$CF_3 + CF_3 \rightarrow C_2F_6$$

radical produced by reaction 2 is probably scavenged by various reactions producing iodides (2, 3). If CF_3H and C_2F_6 are formed only by reactions 2 and 3, the rate constants of which we donate by k_H and k_c respectively, then

[4] $$k_H/k_c^{1/2} = R_{CF_3H}/R_{C_2F_6}^{1/2}\ [EtO]$$

where R denotes rate of formation of product. The photolyses covered the range 60–228 °C and the results are given in Table 1. It is seen that at

8. M. BARBIEUX and R. H. MARTIN. Tetrahedron Lett. 2919 (1965).
9. D. Y. CURTIN and S. DAYAGI. Can. J. Chem. **42**, 867 (1964).
10. M. KARPLUS. J. Chem. Phys. **30**, 11 (1959).
11. M. G. S. RAO, C. SRIKANTIA, and M. S. IYENGAR. Helv. Chim. Acta, **12**, 581 (1929); L. C. RAIFORD and D. E. FOX. J. Org. Chem. **9**, 170 (1944).
12. J. MCKENNA. Conformational analysis of organic compounds. Royal Institute of Chemistry Lecture Series No. 1 (1966).
13. B. REICHERT. Arch. Pharm. **274**, 369 (1936).

Reactions of trifluoromethyl and methyl radicals with ethylene oxide

S. H. JONES AND E. WHITTLE
Chemistry Department, University College, Cathays Park, Cardiff, Gt. Britain

Received June 15, 1970

The reaction between CF_3 radicals and ethylene oxide was studied in the range 60–228 °C using CF_3I as a radical source. For the reactions,

$$CF_3 + CH_2\text{—}CH_2O \xrightarrow{k_H} CF_3H + CH_2\text{—}CHO$$

$$CF_3 + CF_3 \xrightarrow{k_c} C_2F_6$$

we obtain

$$\log k_H/k_c^{1/2}(cm^{3/2}\ mole^{-1/2}\ s^{-1/2}) = (5.77 \pm 0.12) - (11.02 \pm 0.22)/\theta$$

where $\theta = 2.3RT$ kcal mole^{-1}.

Published data of Phibbs and Darwent on the reaction

[5] $$CH_3 + CH_2\text{—}CH_2O \rightarrow CH_4 + CH_2\text{—}CHO$$

have been re-calculated and it is suggested that both the original and re-calculated values of the activation energy E_5 are too low. The Arrhenius parameters for the reactions of CF_3 and CH_3 radicals with ethylene oxide are compared with those for related reactions.

Canadian Journal of Chemistry, **48**, 3601 (1970)

Can. J. Chem. Downloaded from www.nrcresearchpress.com by 210.87.254.42 on 09/05/12
For personal use only.

As part of a study of the vapor phase reactions of free radicals with cyclic compounds, we have determined Arrhenius parameters for the abstraction of hydrogen by CF_3 radicals from ethylene oxide. The radicals were generated by photolysis of CF_3I.

We have also re-calculated the data of Phibbs and Darwent (1) on the corresponding reaction involving CH_3 radicals with ethylene oxide. Their results on CH_3 + cyclopropane have also been re-interpreted. It is found that published data on the reaction between CH_3 radicals and ethylene oxide are anomalous and the system appears to require re-investigation.

Experimental

Ethylene oxide was purified by bulb-to-bulb distillation retaining a middle cut which was stored in liquid nitrogen. It was better than 99.9% pure as indicated by g.l.c. No impurities could be detected by i.r. spectroscopy.

Mixtures of CF_3I and ethylene oxide were photolyzed and the products analyzed using procedures described elsewhere (2).

Results

Blank experiments without photolysis showed that there is no dark reaction between CF_3I and ethylene oxide, EtO. When the mixture is photolyzed, important reactions are [1]–[3]. The

[1] $$CF_3I + h\nu \rightarrow CF_3 + I$$

[2] $$CF_3 + CH_2\text{—}CH_2O \rightarrow CF_3H + CH_2\text{—}CHO$$

[3] $$CF_3 + CF_3 \rightarrow C_2F_6$$

radical produced by reaction 2 is probably scavenged by various reactions producing iodides (2, 3). If CF_3H and C_2F_6 are formed only by reactions 2 and 3, the rate constants of which we donate by k_H and k_c respectively, then

[4] $$k_H/k_c^{1/2} = R_{CF_3H}/R_{C_2F_6}^{1/2}\ [EtO]$$

where R denotes rate of formation of product. The photolyses covered the range 60–228 °C and the results are given in Table 1. It is seen that at

TABLE 1

Photolysis of CF_3I with ethylene oxide*

T (°C)	Photolysis time (s)	Reactant pressure (Torr) CF_3I	Reactant pressure (Torr) C_2H_4O	$R_{C_2F_6}$†	R_{CF_3H}†	$k_H/k_c^{1/2}$‡
60.6	3600	37.0	56.8	0.246	0.045	0.0332
60.8	3600	~100	116.4	0.224	0.112	0.0394
100.8	3600	~100	116.4	0.196	0.548	0.248
102.0	1800	40.7	57.3	0.395	0.330	0.214
142.4	1800	50.7	54.3	0.275	0.955	0.867
142.4	1800	60.0	27.5	0.238	0.460	0.891
187.6	1800	53.5	17.5	0.335	0.912	2.59
187.7	1800	45.5	31.4	0.308	1.63	2.69
227.9	1800	66.0	36.7	0.449	5.77	7.35
228.2	1800	68.6	21.9	0.413	3.21	7.15

*Reaction vessel volume 161.2 cm^3.
†Rates of formation of products in mole cm^{-3} s^{-1} × 10^{12}.
‡$k_H/k_c^{\frac{1}{2}}$ in $cm^{3/2}$ $mole^{-\frac{1}{2}}$ $s^{-\frac{1}{2}}$.

any given temperature the value of $k_H/k_c^{1/2}$ is independent of the pressure of EtO used. An Arrhenius plot was a good straight line from which

$$\log k_H/k_c^{1/2}\ (cm^{3/2}\ mole^{-1/2}\ s^{-1/2}) = (5.77 \pm 0.12) - (11.02 \pm 0.22)/\theta$$

where $\theta = 2.3RT$ (R in kcal deg^{-1} $mole^{-1}$).

Taking $A_c = 2.3 \times 10^{13}$ cm^3 $mole^{-1}$ s^{-1} and $E_c = 0$, (4, 5), we obtain the absolute Arrhenius parameters for reaction 2 given in Table 2. It is of interest to compare these results with data on the corresponding reaction 5. The only work on

[5] $CH_3 + CH_2{-}CH_2(O) \rightarrow CH_4 + CH_2{-}CH(O)$

this reaction is that of Phibbs and Darwent (1) who photolyzed mixtures of mercury dimethyl and EtO. Relevant reactions are [5] plus [6]

[6] $CH_3 + Hg(CH_3)_2 \rightarrow CH_4 + CH_2HgCH_3$

[7] $CH_3 + CH_3 \rightarrow C_2H_6$

and [7]. If CH_4 and C_2H_6 come only from these reactions then

$$[8] \quad \frac{R_{CH_4}}{R_{C_2H_6}^{1/2}} = \frac{k_6[Hg(CH_3)_2]}{k_7^{1/2}} + \frac{k_5[EtO]}{k_7^{1/2}}$$

Phibbs and Darwent obtained $E_5 - \frac{1}{2}E_7 = 9.6$ kcal $mole^{-1}$ but their work includes two sources of error. First they neglected the occurrence of reaction 6 by omitting the first term on the right-hand side of eq. 8. Secondly they obtained $E_5 - \frac{1}{2}E_7$ by plotting $R_{CH_4}/R_{C_2H_6}^{1/2}$ against $10^3/T$ instead of using the more usual $R_{CH_4}/R_{C_2H_6}^{1/2}$[EtO]. This introduces an error since they used a constant *pressure* of EtO so that the concentration of EtO varied with temperature. We have re-calculated the results correcting for this and also allowing for the occurrence of reaction 6 by using data of Rebbert and Steacie (6) who give

$$\log k_6/k_7^{1/2}\ (cm^{3/2}\ mole^{-1/2}\ s^{-1/2}) = 5.03 - 10.8/\theta$$

The re-calculated results show that about one third of the total methane is produced by reaction 6 which cannot therefore be neglected. Using

$$[9] \quad \log k_5/k_7^{1/2}\ (cm^{3/2}\ mole^{-1/2}\ s^{-1/2}) = (4.5 \pm 0.3) - (10.1 \pm 0.6)/\theta$$

eq. 8, we obtain eq. 9. The results show considerable scatter and the Arrhenius plot could well be curved.

Phibbs and Darwent also give data on

[10] $CH_3 + c\text{-}C_3H_6 \rightarrow CH_4 + c\text{-}C_3H_5$

from which they obtain $E_{10} - \frac{1}{2}E_7 = 10.2$ kcal $mole^{-1}$. Their data on reaction 10 was also re-calculated as described for EtO to give

$$\log k_{10}/k_7^{1/2}\ (cm^{3/2}\ mole^{-1/2}\ s^{-1/2}) = (4.7 \pm 0.7) - (11.7 \pm 1.3)/\theta$$

Discussion

It is known (7) that when CF_3 and CH_3 radicals abstract hydrogen from a given substrate RH, the activation energy difference $\Delta E = E(CH_3 + RH) - E(CF_3 + RH)$ is usually about

Can. J. Chem. Downloaded from www.nrcresearchpress.com by 210.87.254.42 on 09/05/12
For personal use only.

TABLE 2

Arrhenius parameters for reactions of CF_3 and CH_3 radicals with ethylene oxide and related molecules§

	E†	log A†	log k (400K)†	Reference‡
CF_3 + 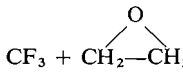	11.0	12.5	6.5	*a*
+ CH_3OCH_3	6.8	11.7	8.0	13
+ $CH_3C^*H_2OC^*H_2CH_3$	5.5	11.9	8.9	13
+	8.7	11.5	6.7	2
+ $CH_3C^*H_2CH_3$	6.4	11.7	8.2	14
CH_3 + 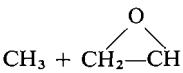	(9.6)	—	—	1
	(10.1)	(11.2)	(5.7)	*b*
+ CH_3OCH_3	10.0	11.6	6.1	13
+ $CH_3C^*H_2OC^*H_2CH_3$	9.7	12.0	6.7	15
+	13.3	11.8	4.5	9, 1
+ $CH_3C^*H_2CH_3$	10.3	11.9	6.3	16

*Hydrogen atom abstracted.
†E in kcal mole^{-1}, A and k in cm^3 mole^{-1} s^{-1}.
‡References: *a*, this work; *b*, re-calculated from data in ref. (1), see present text.
§Data in parentheses are suspect, see text.

2 to 3 kcal mole^{-1}. Exceptions to this rule are rare and usually involve a highly polar RH (8). We now find that $E(CF_3 + EtO) = 11.0$ kcal mole^{-1} (see Table 2), hence we expect $E(CH_3 + EtO)$ to be about 13 kcal mole^{-1} or possibly even higher since we have shown (2) that for RH = cyclopropane, $\Delta E = 4.6$ kcal mole^{-1}. Accordingly Phibbs and Darwent's result that $E(CH_3 + EtO) = 9.6$ kcal mole^{-1} seems anomalously low and our re-calculated value in eq. 9 seems little better. This suggestion is confirmed by our re-calculated value of $E_{10} - \frac{1}{2}E_7$ for cyclopropane which, although higher than Phibbs and Darwent's figure by 1.5 kcal mole^{-1}, is still low compared with the figure of 13.3 kcal mole^{-1} obtained by McNesby and Gordon (9, 2) using a more reliable competitive technique.

The above data is listed in Table 2 together with Arrhenius parameters for other related reactions. First we note that H abstraction by CF_3 from EtO is much more difficult than from $(CH_3)_2O$ or $(C_2H_5)_2O$ just as H abstraction by CF_3 from cyclopropane is more difficult than from the corresponding non-ring compound propane. In both cases, this is expected from Brown's I-strain theory (10). By analogy, we expect a similar drop in reactivity from $CH_3 + (CH_3)_2O$ or $(C_2H_5)_2O$ to CH_3 + EtO but this is not shown by the data in Table 2: hence we have a second reason for suggesting that the activation energy given there for CH_3 + EtO is too low. A more reasonable value would be about 14 kcal mole^{-1}.

We conclude that further experimental studies of the reaction between CH_3 radicals and EtO are desirable.

It might be expected that further conclusions could be drawn by comparing the data in Table 2 with that for CH_3 and CF_3 + ethyleneimine and dimethylamine. For CH_3 + ethyleneimine, separate Arrhenius parameters have been measured by Gray and Jones (11) for abstraction from N—H and C—H, using isotopic labelling. However for CF_3 + ethyleneimine, only overall Arrhenius parameters exist (12) so such discussion does not seem justified.

One of us (S.H.J.) wishes to thank the Science Research Council for a grant.

1. M. K. PHIBBS and B. DEB. DARWENT. Can. J. Res. **28B**, 395 (1950).
2. S. H. JONES and E. WHITTLE. Int. J. Chem. Kinetics, Nov. 1970.

Can. J. Chem. Downloaded from www.nrcresearchpress.com by 210.87.254.42 on 09/05/12
For personal use only.

3. E. R. MORRIS and J. C. J. THYNNE. Trans. Faraday Soc. **64**, 414 (1968).
4. P. B. AYSCOUGH. J. Chem. Phys. **24**, 944 (1956).
5. R. D. GILES and E. WHITTLE. Trans. Faraday Soc. **61**, 1425 (1965).
6. R. E REBBERT and E. W. R. STEACIE. J. Chem. Phys. **21**, 1723 (1953).
7. G. H. MILLER and G. O. PRITCHARD. J. Chem. Phys. **35**, 1135 (1961).
8. B. G. TUCKER and E. WHITTLE. Trans. Faraday Soc. **61**, 866 (1965).
9. J. R. MCNESBY and A. S. GORDON. J. Amer. Chem. Soc. **79**, 825 (1957).
10. H. C. BROWN and M. GERSTEIN. J. Amer. Chem. Soc. **72**, 2926 (1950).
11. P. GRAY and A. JONES. Trans. Faraday Soc. **61**, 2161 (1965).
12. E. R. MORRIS and J. C. J. THYNNE. Trans. Faraday Soc. **64**, 2124 (1968).
13. N. L. ARTHUR, P. GRAY, and A. A. HEROD. Can. J. Chem. **47**, 1347 (1969).
14. P. B. AYSCOUGH and E. W. R. STEACIE. Can. J. Chem. **34**, 103 (1956). G. O. PRITCHARD, H. O. PRITCHARD, H. I. SCHIFF, and A. F. TROTMAN-DICKENSON. Trans. Faraday Soc. **52**, 849 (1956).
15. J. LONG and G. SKIRROW. Trans. Faraday Soc. **58**, 1403 (1962).
16. W. M. JACKSON, J. R. MCNESBY, and B. DEB. DARWENT. J. Chem. Phys. **37**, 1610 (1962).

Chemical reactions in a Toepler pump

J. H. JOHNSON, R. H. KNIPE, AND A. S. GORDON
Chemistry Division, Research Department, Naval Weapons Center, China Lake, California 93555

Received April 21, 1970

Products have been generated in a Toepler pump from a variety of hydrocarbons and ketones. From the nature of the products, it is deduced that the mechanism must involve more processes than just mercury $^3P^0$ sensitization. These observations suggest that trace products from samples taken with a Toepler pump may be at least partly artifactual.

Canadian Journal of Chemistry, 48, 3604 (1970)

During the course of a photochemical investigation involving the production of trace amounts of carbon monoxide, we were plagued by extraneous production of carbon monoxide. Mechanical agitation of the mercury in a Toepler pump by gas bubbles was shown to be the source. Although it has been recognized that bubbling gases through mercury and other liquids gives rise to spectra of the gases (1), we have not found any report of the chemical reactions which occur during the process. This is a report on product formation by some classes of hydrocarbons and ketones.

An automatic Toepler pump with a 1 l expansion volume was used in these experiments. Some experiments were conducted by manually operating the pump to avoid electrical sparks between the contacts, and with the mercury grounded and foil wrapped around the outside of the pump to minimize electro-static discharges. No significant differences were observed between the results with the normal automatic operation and operation where extraneous electrical effects were minimized.

To gain a measure of the rate of formation of various products, the pressure of the reactant was held constant during the course of the experiments by setting the discharge valve to return the gases to the manifold rather than the collection system. The time for one complete cycle was about 1 min and the rates are reported in terms of total elapsed time for the experiments.

All the gas from the experiment was collected in a sample flask. CO and methane were analyzed on a sieve 5A column, temperature programmed from liquid N_2. While H_2 shows on a sieve column, its sensitivity is so low that H_2 values were obtained from duplicate runs into a mass spectrometer from the sample flask at liquid N_2 temperature. Calibration was via mixes of H_2 and CO_2 simulating the conditions of the experimental sample where H_2 was in the presence of a condensed phase at liquid N_2 temperature. Acetone, perfluoro acetone, diethylketone, and some saturated and unsaturated hydrocarbons were tested. The results are shown in Table 1.

It will be noted that acetone yields H_2 as well as CO and CH_4 as products. Since H_2 is produced, it indicates that dissociation is not exclusively via excited mercury $^3P^0$ sensitization. Similarly H_2 and CH_4 are found in the products from diethylketone in addition to the products expected from excited mercury sensitization.

Usually H_2 was the only product monitored

Can. J. Chem. Downloaded from www.nrcresearchpress.com by 210.87.254.42 on 09/05/12
For personal use only.

3. E. R. MORRIS and J. C. J. THYNNE. Trans. Faraday Soc. **64**, 414 (1968).
4. P. B. AYSCOUGH. J. Chem. Phys. **24**, 944 (1956).
5. R. D. GILES and E. WHITTLE. Trans. Faraday Soc. **61**, 1425 (1965).
6. R. E REBBERT and E. W. R. STEACIE. J. Chem. Phys. **21**, 1723 (1953).
7. G. H. MILLER and G. O. PRITCHARD. J. Chem. Phys. **35**, 1135 (1961).
8. B. G. TUCKER and E. WHITTLE. Trans. Faraday Soc. **61**, 866 (1965).
9. J. R. MCNESBY and A. S. GORDON. J. Amer. Chem. Soc. **79**, 825 (1957).
10. H. C. BROWN and M. GERSTEIN. J. Amer. Chem. Soc. **72**, 2926 (1950).
11. P. GRAY and A. JONES. Trans. Faraday Soc. **61**, 2161 (1965).
12. E. R. MORRIS and J. C. J. THYNNE. Trans. Faraday Soc. **64**, 2124 (1968).
13. N. L. ARTHUR, P. GRAY, and A. A. HEROD. Can. J. Chem. **47**, 1347 (1969).
14. P. B. AYSCOUGH and E. W. R. STEACIE. Can. J. Chem. **34**, 103 (1956). G. O. PRITCHARD, H. O. PRITCHARD, H. I. SCHIFF, and A. F. TROTMAN-DICKENSON. Trans. Faraday Soc. **52**, 849 (1956).
15. J. LONG and G. SKIRROW. Trans. Faraday Soc. **58**, 1403 (1962).
16. W. M. JACKSON, J. R. MCNESBY, and B. DEB. DARWENT. J. Chem. Phys. **37**, 1610 (1962).

Chemical reactions in a Toepler pump

J. H. JOHNSON, R. H. KNIPE, AND A. S. GORDON
Chemistry Division, Research Department, Naval Weapons Center, China Lake, California 93555

Received April 21, 1970

Products have been generated in a Toepler pump from a variety of hydrocarbons and ketones. From the nature of the products, it is deduced that the mechanism must involve more processes than just mercury $^3P^0$ sensitization. These observations suggest that trace products from samples taken with a Toepler pump may be at least partly artifactual.

Canadian Journal of Chemistry, 48, 3604 (1970)

During the course of a photochemical investigation involving the production of trace amounts of carbon monoxide, we were plagued by extraneous production of carbon monoxide. Mechanical agitation of the mercury in a Toepler pump by gas bubbles was shown to be the source. Although it has been recognized that bubbling gases through mercury and other liquids gives rise to spectra of the gases (1), we have not found any report of the chemical reactions which occur during the process. This is a report on product formation by some classes of hydrocarbons and ketones.

An automatic Toepler pump with a 1 l expansion volume was used in these experiments. Some experiments were conducted by manually operating the pump to avoid electrical sparks between the contacts, and with the mercury grounded and foil wrapped around the outside of the pump to minimize electro-static discharges. No significant differences were observed between the results with the normal automatic operation and operation where extraneous electrical effects were minimized.

To gain a measure of the rate of formation of various products, the pressure of the reactant was held constant during the course of the experiments by setting the discharge valve to return the gases to the manifold rather than the collection system. The time for one complete cycle was about 1 min and the rates are reported in terms of total elapsed time for the experiments.

All the gas from the experiment was collected in a sample flask. CO and methane were analyzed on a sieve 5A column, temperature programmed from liquid N_2. While H_2 shows on a sieve column, its sensitivity is so low that H_2 values were obtained from duplicate runs into a mass spectrometer from the sample flask at liquid N_2 temperature. Calibration was via mixes of H_2 and CO_2 simulating the conditions of the experimental sample where H_2 was in the presence of a condensed phase at liquid N_2 temperature. Acetone, perfluoro acetone, diethylketone, and some saturated and unsaturated hydrocarbons were tested. The results are shown in Table 1.

It will be noted that acetone yields H_2 as well as CO and CH_4 as products. Since H_2 is produced, it indicates that dissociation is not exclusively via excited mercury $^3P^0$ sensitization. Similarly H_2 and CH_4 are found in the products from diethylketone in addition to the products expected from excited mercury sensitization.

Usually H_2 was the only product monitored

Can. J. Chem. Downloaded from www.nrcresearchpress.com by 210.87.254.105 on 09/05/12
For personal use only.

TABLE 1

Products from Toeplering various compounds

Reactant	Pressure (cm)	Time (min)	Product	Amount produced (μmoles)
Acetone	20	60	CO	0.48
			CH_4	0.04
			H_2	0.17
1 Acetone to 1 Ethane	40	20	CO	0.07
			CH_4	0.05
Hexafluoroacetone	20	5	CO	0.07
1 Diethylketone to 4 Helium	20	60	CO	0.41
			CH_4	0.04
			H_2	0.35
Ethane	10	60	CO	0.01
			CH_4	0.05
			H_2	0.31
Butane	10	5	H_2	0.04
Ethene	10	60	H_2	0.27
Propene	10	60	H_2	0.21
Butene-1	10	60	H_2	0.12
trans-Butene-2	10	60	H_2	0.14
cis-Butene-2	10	10	H_2	0.09
cis-Butene-2	10	5	H_2	0.06

from hydrocarbons. A chromatographic analysis was made of the products from ethane and ethene. For ethane, the appearance of methane provided evidence of C—C bond breaking. Trace methane impurities in the ethene limited the detectability of products resulting from C—C bond breaking. Within the limits of detection, we could see no evidence of any product methane. The source of the small amount of CO from ethane is uncertain. It was observed that the amount of CO was dependent on the presence of O_2 and water in the reactant gas. The result for ethane quoted in Table 1 is for an experiment where care was taken to minimize O_2 and water, by pumping on the liquid ethane at liquid N_2 temperature and then distilling a small part of the pumped liquid ethane directly into the Toepler pump.

These observations show that taking samples via a Toepler pump may lead to artifactual compounds. Since these compounds can be confused with other reaction products from the sample, a Toepler pump technique is inappropriate when the samples are to be analyzed for trace products.

1. L. J. SCHOEN. Can. J. Phys. **38**, 967 (1960).

Can. J. Chem. Downloaded from www.nrcresearchpress.com by 210.87.254.105 on 09/05/12
For personal use only.

Can. J. Chem. Downloaded from www.nrcresearchpress.com by 210.87.254.42 on 09/05/12
For personal use only.

Pyrolysis of bicyclo[2.2.1]hepta-2,5-diene-2,3-dicarboxylic anhydride[1]

O. A. MAMER AND F. P. LOSSING
Division of Chemistry, National Research Council, Ottawa, Canada
AND
E. HEDAYA AND M. E. KENT
Union Carbide Research Institute, Tarrytown, New York 10591

Received July 20, 1970

The pyrolysis of the titled anhydride at low pressures and short contact times was found by both mass spectral and chemical experiments to involve an unusual decarboxylation to benzocyclobutenone. The latter subsequently decarbonylates to give a triad of C_7H_6 isomers: 5-vinylidenecyclopentadiene, ethynylcyclopentadiene, and benzocyclopropene. No evidence was found for dehydronorbornadiene, which would be expected on the basis of the pyrolysis of maleic anhydride or phthalic anhydride.

Canadian Journal of Chemistry, 48, 3606 (1970)

The pyrolysis of maleic anhydride (**1**) at 800–900° is known to give equimolar quantities of acetylene, carbon monoxide, and carbon dioxide (1). The utility of this type of fragmentation of a cyclic unsaturated anhydride is best exemplified by the pyrolysis of phthalic anhydride (**2**) where benzyne is obtained by consecutive (2) or concerted (1*b*) elimination of carbon monoxide and carbon dioxide. Recently, the preparation of bicyclo[2.2.1]hepta-2,5-diene-2,3-carboxylic anhydride (**3**) was described (3). This anhydride is a potential thermal source of the highly strained cyclic acetylene **4**, which itself may undergo novel thermal rearrangements, fragmentations, and cyclo-addition reactions. We have investigated the flash vacuum pyrolysis of **3** and have found instead that it undergoes an unusual sequential loss of carbon dioxide and carbon monoxide to ultimately give 5-vinylidenecyclopentadiene (fulvenallene, **5**) via benzocyclobutenone (**6**).

Compound **3** was first introduced into an oven coupled directly to the ionization source of a mass spectrometer at about 10^{-4} Torr and short contact times (10^{-3} s) (4). A low voltage scan revealed prominent thermal fragments at *m/e* 118 (C_8H_6O by isotopic distribution) and *m/e* 90 (Fig. 1): ionization potential (IP) (118, 700°) 8.99 eV; IP (90, 1000°) 8.88 eV. Co-pyrolysis of the anhydride with ethyl nitrite gave no evidence that methyl radicals were adding to a

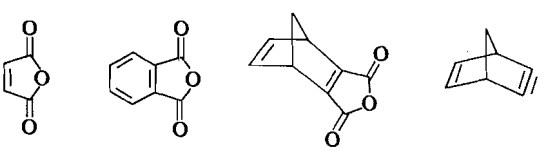

1 **2** **3** **4**

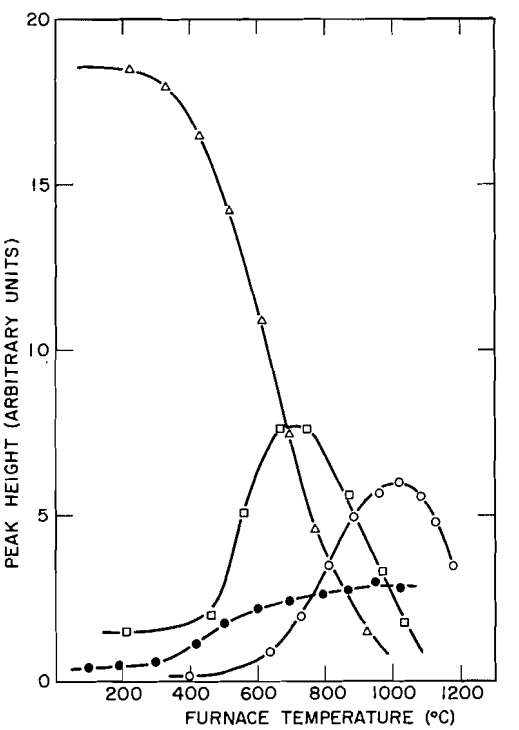

FIG. 1. Pyrolysis of bicyclo[2.2.1]hepta-2,5-diene-2,3-dicarboxylic anhydride (**3**): △, *m/e* 162; □, *m/e* 118; ○, *m/e* 90; ●, *m/e* 66.

[1]NRCC No. 11608.

Can. J. Chem. Downloaded from www.nrcresearchpress.com by 210.87.254.42 on 09/05/12
For personal use only.

thermal fragment. Finally, **3** was observed to be considerably less stable than either phthalic or *o*-methylphthalic anhydride. The latter did not fragment appreciably at temperatures $<800°$.

The identity of the *m/e* 118 and 90 products was determined by carrying out the above pyrolysis in an apparatus which closely duplicates the mass spectral pyrolysis conditions and where the pyrolysate is rapidly quenched on the surface of a dewar at liquid nitrogen temperatures (4*b*). Characterization of the pyrolysate obtained at 700° showed that the major product was benzocyclobutenone (**6**) while the pyrolysate at 900° consisted predominantly of fulvenallene (**5**) with minor amounts of benzocyclopropene (**7**) and ethynylcyclopentadiene (**8**). These were identical in all respects to authentic samples which had previously been obtained from the flash vacuum pyrolysis of 1,2-indanedione (5). This served to identify the *m/e* 118 (**6**) and *m/e* 90 products (**5**) detected in the mass spectral experiments.

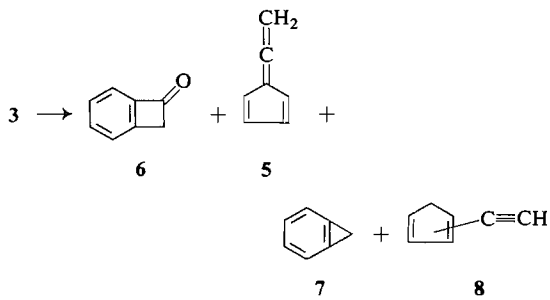

A plausible scheme accounting for facile formation of benzocyclobutenone (**6**) is shown in Scheme 1. Unusual features include a radical induced anhydride ring opening to give **10**.[2] Intermolecular radical addition–elimination reactions to carbonyl moieties have been previously proposed in the free radical initiated chlorocarbonylation of hydrocarbons with oxalyl chloride (6).

The final step for formation of **6** is depicted as involving a 1,3 or 1,5 hydrogen transfer of the biradical **9**. It is conceivable that the latter process

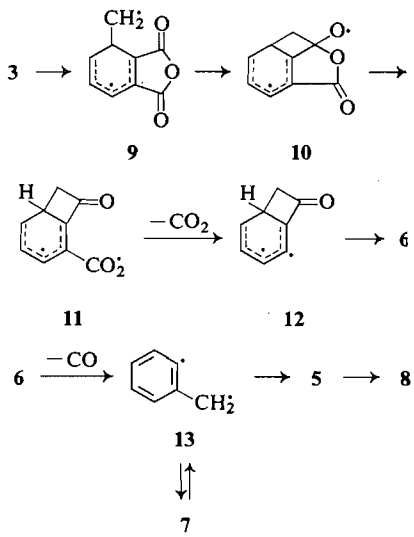

SCHEME 1

may go through intermediate carbene species stemming from 1,2 hydrogen shifts.

The formation of fulvenallene (**5**), benzocyclopropene (**7**), and ethynylcyclopentadiene (**8**) is best rationalized in terms of the 1,3-biradical **13** which undergoes ring-closure or ring contraction depending on the pyrolysis temperature. This process for authentic benzocyclobutenone was previously elucidated in an investigation of the flash vacuum pyrolysis of 1,2-indanedione (5).

It is interesting to compare the pyrolytic fragmentation observed for **3** with that induced by electron-impact. The 50 V mass spectrum for **3** has major peaks at *m/e* 162 (25.6%), 118 (10.6%), 90 (54.7%), and 66 (100%). A metastable was observed at *m/e* 68.8 which corresponds to $118^+ \rightarrow 90^+ + 28$. Thus, the electron impact induced fragmentation appears to parallel the pyrolytic fragmentation. However, the structure of the major intermediates may be very different. Scheme 2, for example, would be plausible based on the mass spectrum of phthalic anhydride which has major peaks at *m/e* 104 (C_6H_4CO) and 76 (C_6H_4) (2). It is noteworthy that attempts to detect, by mass spectroscopy, a pyrolytic fragment from phthalic anhydride corresponding to benzocyclopropenone (*m/e* 104) were unsuccessful (7). Similarly, in our chemical pyrolytic studies on **3**, no evidence was obtained for an intermediate corresponding to **14**.

In general, we believe that the practice of predicting pyrolytic fragmentations based on

[2]An alternative scheme involving initial anhydride ring cleavage was considered but discarded because of the observed low stability of **3** compared to *o*-methylphthalic anhydride. Also, subsequent intermediates did not have structural features consistent with the observed decarboxylation–decarbonylation sequence. Finally, Scheme 1 incorporates intermediates having greater bond strengths and radical stabilization of radical sites than those derived from initial anhydride ring cleavage.

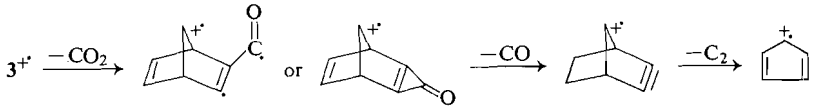

14

SCHEME 2

electron impact results or of inferring structures of prominent ions obtained by electron impact on the basis of pyrolytic studies should be exercised with caution (2, 8).

1. (*a*) F. O. RICE and M. T. MURPHY. J. Amer. Chem. Soc. **64**, 896 (1942); (*b*) A. L. Brown and P. D. Ritchie. J. Chem. Soc. C, 2007 (1968).
2. (*a*) S. MEYERSON. Rec. Chem. Progr. **26**, 257 (1965); (*b*) E. K. FIELDS and S. MEYERSON. Chem. Commun. 474 (1965); (*c*) E. K. FIELDS and S. MEYERSON. J. Org. Chem. **31**, 3307 (1966); (*d*) R. F. C. BROWN, D. V. GARDNER, J. F. W. MCOMIE, and R. K. SOLLY. Aust. J. Chem. **20**, 139 (1967).
3. J. R. EDMAN and H. E. SIMMONS. J. Org. Chem. **33**, 3808 (1968).
4. (*a*) F. P. LOSSING. *In* Mass Spectroscopy. *Edited by* C. A. McDowell. McGraw-Hill Book Co., Inc., New York. 1963. p. 442; (*b*) E. HEDAYA. Accts. Chem. Res. **2**, 367 (1969).
5. E. HEDAYA and M. E. KENT. J. Amer. Chem. Soc. **92**, 2149 (1970).
6. (*a*) M. S. KHARASCH, S. S. KANE, and H. C. BROWN. J. Amer. Chem. Soc. **64**, 1621 (1942); (*b*) E. HEDAYA and L. M. KYLE. J. Org. Chem. **32**, 197 (1967).
7. F. P. LOSSING and O. A. MAMER. Unpublished results.
8. (*a*) F. W. MCLAFFERTY. *In* Mass Spectrometry of Organic Ions. Academic Press, New York. 1963. p. 311; (*b*) O. A. MAMER, R. J. KOMINAR, and F. P. LOSSING. Org. Mass Spec. In press; (*c*) D. W. BRENT, J. D. HRIBAR, and D. C. DEJONGH. J. Org. Chem. **35**, 135 (1970).

Can. J. Chem. Downloaded from www.nrcresearchpress.com by 210.87.254.42 on 09/05/12
For personal use only.

Can. J. Chem. Downloaded from www.nrcresearchpress.com by 210.87.254.6 on 09/05/12
For personal use only.

Canadian Journal of Chemistry

Published by THE NATIONAL RESEARCH COUNCIL OF CANADA

VOLUME 48 DECEMBER 1, 1970 NUMBER 23

Recoil reactions in neutron-activated nickel carbonyl

O. H. WHEELER AND J. E. TRABAL
Puerto Rico Nuclear Center, Mayagüez, Puerto Rico

AND

D. R. WILES
Chemistry Department, Carleton University, Ottawa, Canada

Received February 20, 1970

Retention of ^{65}Ni in neutron-irradiated $Ni(CO)_4$ has been measured both in the pure form and in *n*-heptane and $Fe(CO)_5$ solutions, and mixed with triphenylphosphine ($P\phi_3$) in *n*-heptane solution. Retention was found to be nearly 100% in all cases except with high concentrations of $Fe(CO)_5$, where the retention dropped off strongly. It is concluded that the high retention is the result of rapid exchange of CO with inactive $Ni(CO)_4$. The effect of $Fe(CO)_5$ is considered to be a hot-zone reaction. The presence of triphenylphosphinenickel tricarbonyl was found not to affect the retention in $Ni(CO)_4$. This is taken to show that the ^{65}Ni atoms formed in crystalline $\phi_3PNi(CO)_3$ remain trapped in the lattice.

Canadian Journal of Chemistry, 48, 3609 (1970)

Neutron activation of metal carbonyls results in various fractions of the radioactive metal atoms remaining in, or reforming, the parent compound. Most thoroughly studied of the mononuclear carbonyls have been those of Group VI (1–3), which show retention of 40–70% of the radioactive atoms in their original form, the exact value being dependent to some extent on post-irradiation treatment. Heating the irradiated sample at a known temperature for various times usually results in an increase in retention. Zahn and Collins (3) have shown that with the Group VI carbonyls, heating the sample in carbon monoxide under pressure results in a very marked increase in retention, which increase is dependent on the pressure as well as on the time and temperature. Thus, availability of CO in the crystal seems to be a prime factor in the reaction.

This dependence on the presence of CO can be extrapolated to other cases where CO is not present in excess but which also show post-irradiation annealing effects. In such cases, the reaction may involve free carbon monoxide from radiolysis (3) or normal chemical dissociation (4). If the latter mechanism is valid, the process of recombination following nuclear reaction should be related to ligand exchange processes which often follow a similar dissociation pathway. This argument also applies, of course, to possible similar reactions which may occur at ambient temperature too quickly to allow chemical observation. In this context, one notes that $Fe(CO)_5$ and $Mn_2(CO)_{10}$, which are inert to exchange (and which thus do not make free CO available) have somewhat lower retention values (4, 5).

The present paper describes some studies made on nickel carbonyl. This compound, liquid at room temperature, is known (6) to exchange its carbonyls quite rapidly by a dissociation mechanism.

$$[1] \qquad Ni(CO)_4 \rightleftarrows Ni(CO)_3 + CO$$

$$[2] \qquad Ni(CO)_3 + {}^*CO \rightarrow ({}^*CO)Ni(CO)_3$$

Nickel carbonyl is also found (7) to be relatively insensitive to radiolysis. Direct evidence for the existence of $Ni(CO)_3$ has recently been given by Rest and Turner (8) who found that it is stable at 15 °K, although at 30 °K it recombines by the reverse of reaction 1. They were thus able to measure an infrared spectrum of what appeared to be a non-planar, C_{3v}, $Ni(CO)_3$ in the frozen matrix of $Ni(CO)_4$.

Can. J. Chem. Downloaded from www.nrcresearchpress.com by 210.87.254.6 on 09/05/12
For personal use only.

Experimental

All the operations with nickel carbonyl were carried out using a vacuum line mounted in a fume hood. Nickel carbonyl (K and K laboratories) was distilled into the vacuum line, and stored in a glass tube protected from light. The carbonyl was degassed and redistilled in vacuo before use. *n*-Heptane was fractionally distilled from sodium, and stored over sodium. All solutions were degassed in vacuo before irradiation.

Samples of nickel carbonyl ($\geqslant$ 800 mg) were sealed in evacuated tubes fitted with break seals. After neutron activation for 30 s in the PRNC swimming pool reactor to produce 2.56 h ^{65}Ni, the tubes were opened on the vacuum line, and the nickel carbonyl distilled at room temperature into a liquid nitrogen cooled trap. The activity of the distilled nickel carbonyl was determined by removing an aliquot with a hypodermic syringe through a silicone rubber septum. This aliquot was diluted with chloroform for counting. The empty activation tube was then opened to the air and washed with chloroform and with nitric acid. Aliquots of these extracts were also counted. Measurement of the activity was made with a well-type sodium iodide crystal and a single-channel pulse height analyzer.

$Ni(CO)_4$ could be distilled quantitatively in vacuum and since no decomposition was detected visually, the chemical recovery found by weighing was always $\sim$ 100%.

Neutron irradiation of samples containing iron carbonyl, *n*-heptane, or triphenylphosphine was done in the same way. The liquid present was totally transferred at room temperature *in vacuo* to remove it from the solid or adsorbed residues. No attempt was made to separate the volatile components, since ^{65}Ni was the only active species present and $Ni(CO)_4$ was the only nickel compound volatile at room temperature. Total recovery was confirmed in all cases by weighing the combined distillate. The activated $Ni(CO)_4$–$Fe(CO)_5$ solutions left a dark green solid, amounting to about 0.6–0.8%, by weight, of the total sample. This substance was most probably $Fe_3(CO)_{12}$, which is formed from $Fe(CO)_5$ by photolysis (9) and by radiolysis (4).

The triphenylphosphine was used as 5% solution, by weight, in *n*-heptane. Triphenylphosphinenickel tricarbonyl (m.p. 123 °C) was prepared by heating triphenylphosphine with nickel carbonyl in methanol, and recrystallizing from chloroform (11). Triphenylphosphine is reported (6) to react rapidly and quantitatively with nickel carbonyl at room temperature to give $\phi_3PNi(CO)_3$. In a tracer experiment using neutron-irradiated solid $\phi_3PNi(CO)_3$ suspended in *n*-heptane, distillation of the liquid in the usual manner gave no significant activity in the distillate. The same result was found when inactive $Ni(CO)_4$ was added to the solvent. This shows the absence of fast disproportionation reactions in the solid

$$[3] \qquad 2\phi_3PNi(CO)_3 \rightarrow (\phi_3P)_2Ni(CO)_2 + Ni(CO)_4$$

$$[4] \qquad \phi_3P^*Ni(CO)_3 + Ni(CO)_4 \rightleftharpoons \phi_3PNi(CO)_3 + {}^*Ni(CO)_4$$

The method of weighing the total distillate will give less reliable values where the amount of residual $Ni(CO)_4$ is small *i.e.* when the starting composition is ϕ_3P:Ni-$(CO)_4 \geqslant 1$. In such case the reported retention values will be proportionately too low. In all cases the retention values reported were determined by comparing the radioactivity of the vacuum distilled liquid with the total activity of all fractions.

Results and Discussion

The retention found in pure $Ni(CO)_4$ is 98.6 $\pm$ 1% as the average of 5 determinations using 30 s irradiations. Irradiation for 2 min gave a value of 97.1%, which is not a significantly different value.

Pure nickel carbonyl irradiated as a solid at −78 °C showed $R = 95 \pm 0.5\%$ independent of whether the separation was done by direct sublimation from the solid, or by vacuum distillation following melting or following dissolution of the solid in cold (−78 °C) *n*-heptane. By chloroform leaching of the residue following distillation less than 1% of the total activity was recovered in all cases.

Dilution of the samples to be irradiated with *n*-heptane did not cause significant change in the retention values, as is seen in Table 1. This behavior is to be contrasted with that of $Mn_2(CO)_{10}$ irradiated in benzene and other solvents (10), in which case the observed retention fell to an extremely low value. This was interpreted as representing the extent of failure of bond rupture, "primary retention". Rosenberg and Sugihara (11) found a retention of only 4.1% in nickel phthalocyanine, which shows that the nickel atom is given sufficient energy to break its bonds in the overwhelming majority of events. Thus we are dealing mainly with a reformation process in the present case. Hence we conclude that the radioactive nickel atom along with whatever of its ligands may remain attached diffuses unscavenged through the hydrocarbon solution, and collects further carbonyl groups

TABLE 1

Retention of Ni as $Ni(CO)_4$ for *n*-heptane solutions irradiated at room temperature. Values given are the average of 2 determinations

$Ni(CO)_4$ concentration (mole fraction)	Retention (%)
1.00	98.6
0.70	97.6
0.45	97.8
0.43	98.5
0.39	97.5
0.31	95.0
0.10	97.6

Can. J. Chem. Downloaded from www.nrcresearchpress.com by 210.87.254.6 on 09/05/12
For personal use only.

until the molecule is once more complete. That CO groups are in fact available through the dissociation shown in reaction 1 has already been demonstrated (6). We are at present unable to deduce anything further about the nature of the diffusing species, and shall call it $Ni(CO)_x$, where $0 \leqslant x \leqslant 3$. The detection of $C_6H_5Mn(CO)_5$ in neutron irradiated benzene solutions of $CpMn(CO)_3$ (5) shows that accretion of carbonyls does occur to some extent, although the very low yield may reflect the failure of Mn—CO dissociation to provide sufficient CO groups.

Results of experiments using $Fe(CO)_5$–$Ni(CO)_4$ solutions are given in Fig. 1. It is seen that the retention values remain only slightly affected by the presence of $Fe(CO)_5$ up to concentrations of nearly 50 mole %, and then decrease more strongly. Thus, the $Ni(CO)_4$ is destroyed by the recoil and, while the $Fe(CO)_5$ does hinder the reformation, it does so very inefficiently. The nature of the reaction involved is not known although according to Harris (12), such inefficient scavenging must occur within the hot zone itself rather than following diffusion.

To follow an earlier conclusion coming from the *n*-heptane experiments, the dilution will not of itself cause a decrease in retention. There remain two possibilities: (*1*) that the $Fe(CO)_5$ is somehow able to compete for the available CO molecules and leave too few for the nickel to recombine with. This would have to be a bulk effect resulting in overall decomposition of the $Ni(CO)_4$. Since this gross decomposition was not detected, this reaction can be eliminated; (*2*) that at high concentrations in the hot zone $Fe(CO)_5$ is able to prevent reaction of the nickel atoms beyond a certain very early unstable stage, either by scavenging the nickel compound at that stage to form a mixed iron–nickel carbonyl, or by blocking its access to nearby carbonyl groups. The effect of this scavenging, then, would be to prevent the formation of a critical intermediate which could react further with available carbonyl groups.

In other work (5) it was found that a very small quantity of $Fe(CO)_5$ greatly reduced the retention of ^{56}Mn in $CH_3CpMn(CO)_3$. The reaction is again unknown but from the present results one may conclude that it is not a reaction with CO but rather must be a scavenging of CH_3Cp, or of a manganese-containing species such as CH_3CpMn.

Some of the solutions irradiated had triphenylphosphine added to them before irradiation. The sample thus consisted of a slurry of $\phi_3PNi(CO)_3$ in heptane with some excess $Ni(CO)_4$. The results are shown in Fig. 2, which gives the retention in $Ni(CO)_4$ as a function of the mole fraction of total ϕ_3P in the mixture. The first part of the curve shows that the fraction of the ^{65}Ni found as $Ni(CO)_4$ is equal to the mole fraction of

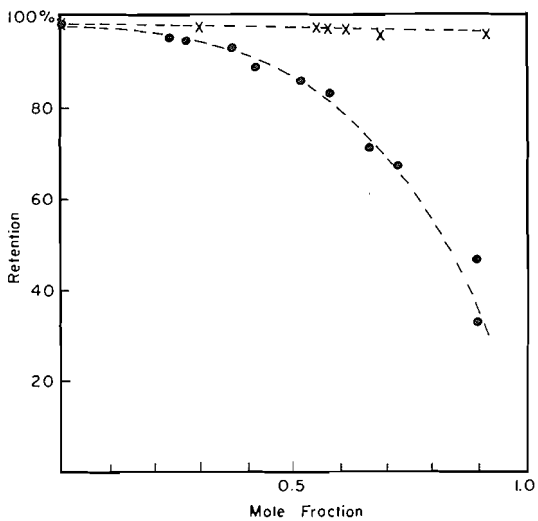

FIG. 1. Effect of dilution of the $Ni(CO)_4$ before irradiation: ×, *n*-heptane; ●, $Fe(CO)_5$. Mole fraction refers to the diluent.

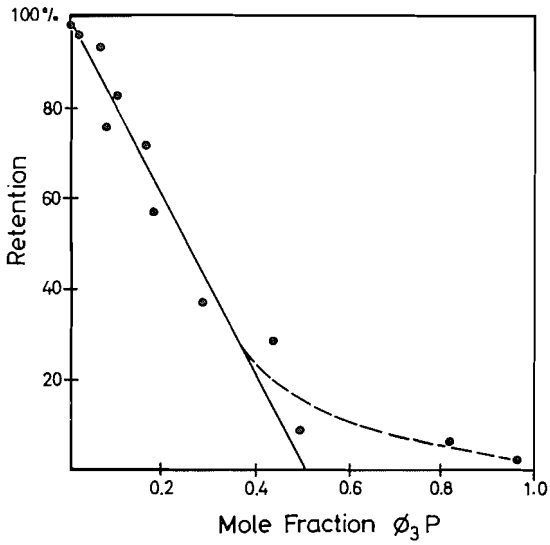

FIG. 2. Effect of adding ϕ_3P before irradiation. Mole fraction = $\phi_3P/(\phi_3P + Ni(CO)_4)$ disregarding chemical reaction. The solid line shows the effect expected for complete reaction to give $\phi_3PNi(CO)_3$, with no exchange.

unreacted $Ni(CO)_4$. This shows that either (*1*) there is no interaction whatsoever between the two components of the mixture or (*2*) the exchange between the components is rapid and complete. Since reactions 3 and 4 have been shown not to occur within the time of our experiment, one must conclude that the radioactive nickel atoms generated in the solid $\phi_3PNi(CO)_3$ remain in the solid during and after the nuclear reaction.

1. V. D. NEFEDOV and M. A. TOROPOVA. Zh. Neorg. Khim. **3**, 175 (1958).
2. P. REICHOLD and H. P. ANDERS. Radiochim. Acta, **5**, 44 (1966).
3. U. ZAHN, K. E. COLLINS, and C. H. COLLINS. Radiochim. Acta, **11**, 33 (1969).
4. S. R. NARAYAN and D. R. WILES. Can. J. Chem. **47**, 1019 (1969).
5. I. G. DEJONG, S. C. SRINIVASAN, and D. R. WILES. Can. J. Chem. **47**, 1327 (1969).
6. J. P. DAY, G. BASOLO, and R. G. PEARSON. J. Amer. Chem. Soc. **90**, 6927 (1968).
7. H. F. BARZYNSKI, R. R. HENTZ, and M. BURTON. J. Phys. Chem. **69**, 2034 (1965).
8. A. J. REST and J. J. TURNER. Chem. Commun. 1026 (1969).
9. H. BARZYNSKI and D. HUMMEL. Z. phys. Chem. **38**, 103 (1963).
10. U. ZAHN. Radiochim. Acta, **1**, 170 (1967).
11. H. E. ROSENBERG and T. T. SUGIHARA. *In* Chemical effects of nuclear transformations. Vol. 2. IAEA Vienna. 1965. p. 151.
12. W. E. HARRIS. Can. J. Chem. **39**, 121 (1961).

Can. J. Chem. Downloaded from www.nrcresearchpress.com by 210.87.254.6 on 09/05/12
For personal use only.

Can. J. Chem. Downloaded from www.nrcresearchpress.com by 210.87.254.6 on 09/05/12
For personal use only.

The kinetics and mechanism of the reactions between carbon monoxide and ruthenium(II) chlorides in solution

B. C. Hui and B. R. James
Department of Chemistry, University of British Columbia, Vancouver 8, British Columbia
Received July 9, 1970

The kinetics of formation of mono- and dicarbonyl complexes in two successive stages by direct carbonylation of ruthenium(II) chlorides in dimethylacetamide solution have been studied at 65–80° and up to 1 atm CO by gas uptake techniques. Both stages are first order in ruthenium. Formation of the monocarbonyl is independent of CO pressure; dicarbonyl formation is first order in CO at low pressures with the order decreasing towards zero with increasing pressure, and shows an inverse chloride dependence from 0.1–2.0 *M* added chloride. For both stages, the data are consistent with a mechanism involving predissociation. A similar mechanism is suggested for the corresponding reactions in 3 *M* HCl solution which had been studied earlier and which showed overall second-order kinetics.

Discussion on the related formation of molecular nitrogen complexes of ruthenium(II) is presented.

Canadian Journal of Chemistry, **48**, 3613 (1970)

Introduction

The growing interest in the uses of ruthenium complexes as homogeneous catalysts (1) prompts us to report new data on the mechanism of formation of ruthenium(II) chlorocarbonyls by direct carbonylation in a non-aqueous polar medium and consider in more detail some earlier data on a corresponding system in aqueous hydrochloric acid (2). Such reactions are of importance for more detailed understanding of catalytic reactions involving ruthenium carbonyls, and also for comparison with the mechanism of formation of transition metal dinitrogen (N_2) complexes formed from gaseous nitrogen.

Carbon monoxide had previously been found (2) to react with chlororuthenate(II) complexes in aqueous hydrochloric acid solutions at 80° and 1 atm pressure to form the carbonyl derivatives $[Ru(CO)(H_2O)Cl_4]^{2-}$ and $[Ru(CO)_2Cl_4]^{2-}$. The reactions involving ruthenium(II) chloro complexes in dimethylacetamide (DMA) were found to proceed quite differently kinetically and usually with faster rates than those in the aqueous medium, but we conclude that a common mechanism involving predissociation exists, which is consistent with the kinetic data for both solvent systems.

Experimental

Ruthenium(III) trichloride trihydrate was obtained as $RuCl_3.3H_2O$ (with 40.59% Ru) from Johnson Matthey Limited. Other materials used and the procedure used for following CO uptake at constant pressure have been described earlier (2–4). Ruthenium(II) chloride solutions in DMA were prepared by reaction of hydrogen with $RuCl_3.3H_2O$ solutions at room temperature as previously described (5).

Visible and ultraviolet spectra were recorded on a Perkin–Elmer 202 instrument, and infrared spectra were recorded on a Perkin–Elmer 137 as solutions taken directly from kinetic runs into 1 mm sodium chloride liquid cells.

The CO solubility in DMA has been measured previously (4) and is computed after allowance for the vapor pressure of solvent at various temperatures (6).

Results

The deep blue solutions of $Ru^{II}Cl_n$ in DMA (λ_{max} 650 nm, $\varepsilon = 1200$) absorbed CO very readily at pressures up to 1 atm in the temperature range 65–80°, the total uptake of CO corresponding closely to 2 moles of CO per mole of ruthenium as shown in Fig. 1. The absorption occurred in two distinct stages, the first mole of CO being taken up relatively rapidly (~1 h at 80°) and the second mole more slowly (~10 h). The absorption of the first mole of CO was accompanied by a color change from deep blue to green (λ_{max}

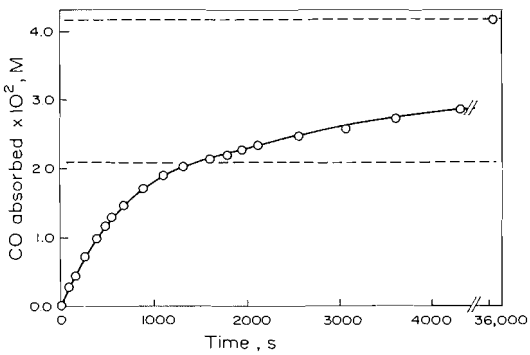

FIG. 1. Uptake of CO by a 0.021 *M* solution of Ru^{II} chloride in DMA (550 mm CO, 80°). The broken lines correspond to the uptake of 1 mole of CO and 2 moles of CO respectively, per mole of Ru^{II}.

Can. J. Chem. Downloaded from www.nrcresearchpress.com by 210.87.254.6 on 09/05/12
For personal use only.

385 nm, $\varepsilon = 1000$, λ_{max} 450 nm, $\varepsilon = 1000$), and of the second mole by a color change from green to yellow ($\lambda_{max} = 465$ nm, $\varepsilon = 430$). These observations suggest a two-step carbonylation reaction

$$[1] \qquad Ru^{II} + CO \rightarrow Ru^{II}(CO)$$

$$[2] \qquad Ru^{II}(CO) + CO \rightarrow Ru^{II}(CO)_2$$

Consistent with this, the infrared spectrum of a green $Ru^{II}(CO)$ solution showed a broad band at 1940 cm^{-1}, while the yellow $Ru^{II}(CO)_2$ solution showed two bands at 2040 and 1960 cm^{-1} indicative of *cis* carbonyls. The reaction is very similar to the one in aqueous HCl as regards the overall stoichiometry, the form of uptake curve, and color changes (2).

The formation of $Ru^{II}(CO)$ according to reaction 1 obeyed the first-order rate law

$$[3] \qquad -d[CO]/dt = d[Ru^{II}(CO)]/dt = k_1[Ru^{II}]$$

where k_1 is a true first-order rate constant being independent of CO concentration. Values of k_1 were determined using eq. 3 from the slopes of first-order log plots such as that depicted in Fig. 2; the stoichiometric relation

$$[4] \qquad [Ru^{II}] + [Ru^{II}(CO)] = [Ru^{II}]_{initial}$$

was used to estimate $[Ru^{II}]$ from the observed CO uptake. The values of k_1 thus obtained are summarized in Table 1. The rate was little affected on addition of LiCl up to 0.5 *M*; at higher chloride concentrations k_1 increased somewhat.

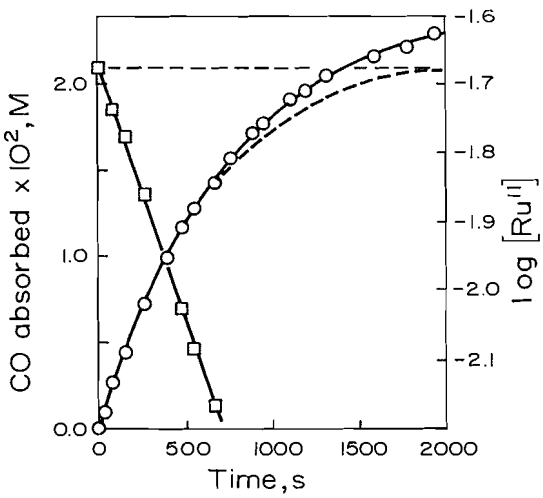

FIG. 2. Kinetic plot for the formation of Ru(CO) in DMA (0.021 *M* Ru^{II}, 550 mm CO, 80°). (○) CO absorbed; (□) log[Ru^{II}]. The broken line corresponds to the uptake of 1 mole of CO per mole of Ru^{II}.

TABLE 1

Summary of kinetic data for reaction 1

$[Ru^{II}]$ × 10^2 (*M*)	CO (mm)	[CO] × 10^3 (*M*)	k_1 × 10^3 (s^{-1})
2.10	725	4.70	1.49
2.10	550	3.56	1.57
2.10	408	2.65	1.45
2.10	267	1.73	1.45
2.10	149	0.97	1.26
1.58	550	3.56	1.45
1.05	550	3.56	1.46
0.53	550	3.56	1.28
2.10	725	4.70	1.93[a]
2.10	725	4.70	1.54[b]
2.10	725	4.70	1.32[c]
2.10	725	4.70	1.36[d]
2.10	725	4.70	2.03[e]
2.10	725	4.70	2.18[f]
2.10	730	4.71	1.05[g]
2.10	736	4.87	0.81[h]
2.10	741	4.95	0.52[i]

[a] 0.5 *M* H_2O.
[b] 0.1 *M* LiCl.
[c] 0.2 *M* LiCl.
[d] 0.5 *M* LiCl.
[e] 1.5 *M* LiCl.
[f] 2.0 *M* LiCl.
[g] 75°.
[h] 70°.
[i] 65°.

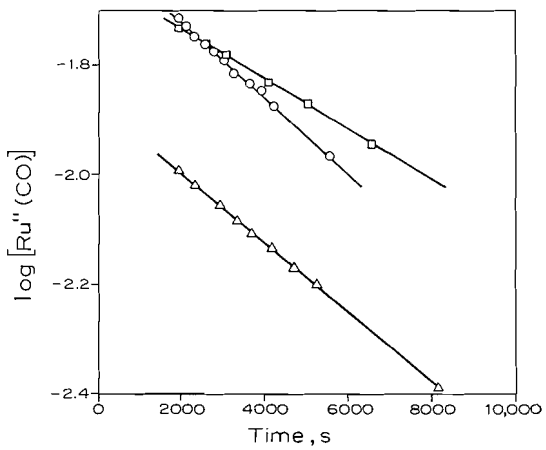

FIG. 3. First-order rate plots for the uptake of CO by $Ru^{II}(CO)$ solutions in DMA at 80°. (○) 0.021 *M* Ru^{II}, 550 mm CO; (□) 0.021 *M* Ru^{II}, 267 mm CO; (△) 0.011 *M* Ru^{II}, 550 mm CO.

Addition of 0.5 *M* H_2O also increased k_1 somewhat. The activation parameters were estimated from a good Arrhenius plot to be $\Delta H^{\ddagger} = 16.9 \pm 1$ kcal $mole^{-1}$, $\Delta S^{\ddagger} = -24 \pm 4$ e.u.

At constant [CO] and $[Cl^-]$, the formation of $Ru^{II}(CO)_2$ according to reaction 2 followed pseudo-first order kinetics, the rate being proportional to the residual concentration of $Ru^{II}(CO)$, *i.e.*

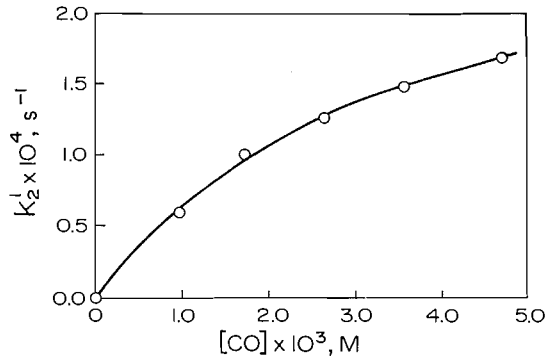

FIG. 4. Dependence of k_2' on [CO] in DMA at 80° (0.021 M Ru^{II}).

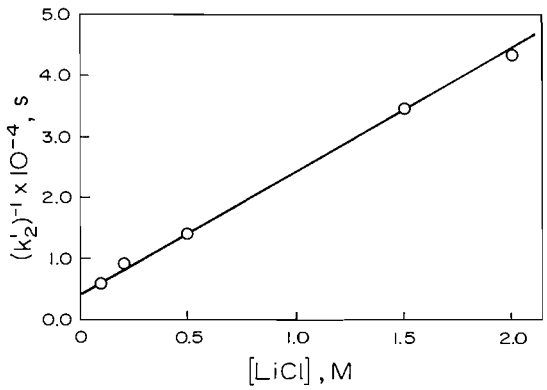

FIG. 5. Inverse dependence of k_2' on [LiCl] in DMA at 80° (0.021 M Ru^{II}, 725 mm CO).

$$[5] \quad -d[Ru^{II}(CO)]/dt = d[Ru^{II}(CO)_2]/dt = k_2'[Ru^{II}(CO)]$$

k_2' was evaluated from the slopes of first-order log plots such as shown in Fig. 3, and was independent of the initial $[Ru^{II}]$ from (0.53–2.10) × 10^{-2} M. Table 2 summarizes the kinetic data for k_2'. The kinetic dependence on CO is shown in Fig. 4 and indicates a first order at low concentrations but with decreasing order with increasing concentration, the rate approaching a limiting value (zero order). An inverse dependence on added chloride from 0.1–2.0 M is observed and a linear graph results from plotting $(k_2')^{-1}$ against $[Cl^-]$ (Fig. 5). The temperature dependence data for k_2' is summarized in Table 3.

Discussion

The kinetics for the first stage, showing a zero dependence on CO, indicate that formation of $Ru^{II}(CO)$ proceeds through a mechanism involving predissociation of the type

TABLE 2

Summary of kinetic data for reaction 2 at 80° unless otherwise noted

$[Ru^{II}(CO)]$ × 10^2 (M)	CO (mm)	[CO] × 10^3 (M)	k_2' × 10^4 (s^{-1})
2.10	725	4.70	1.68
2.10	550	3.56	1.48
2.10	408	2.65	1.26
2.10	267	1.73	1.00
2.10	149	0.97	0.59
1.58	550	3.56	1.23
1.05	550	3.56	1.43
0.53	550	3.56	1.38
2.10	725	4.70	1.34[a]
2.10	725	4.70	1.40[b]
2.10	725	4.70	1.09[c]
2.10	725	4.80	0.72[d]
2.10	725	4.70	0.29[e]
2.10	725	4.70	0.23[f]
2.10	732	4.71	1.07[g]
2.10	420	2.71	0.84[g]
2.10	737	4.87	0.71[h]
2.10	421	2.78	0.57[h]
2.10	742	4.95	0.38[i]
2.10	425	2.84	0.33[i]

[a] 0.5 M H_2O.
[b] 0.1 M LiCl.
[c] 0.2 M LiCl.
[d] 0.5 M LiCl.
[e] 1.5 M LiCl.
[f] 2.0 M LiCl.
[g] 75°.
[h] 70°.
[i] 65°.

TABLE 3

Formation of $Ru^{II}(CO)_2$ in DMA: effects of temperature on rate constants

Temperature (°C)	k_2 × 10^4 (s^{-1})	$k_{-2}[L]/k_4$ × 10^3 (M)
80	3.0	3.7
75	1.7	2.9
70	1.0	1.8
65	0.5	1.6

$$[6] \quad LRu^{II}Cl_n \underset{k_{-1}}{\overset{k_1}{\rightleftharpoons}} Ru^{II}Cl_n + L$$

$$[7] \quad Ru^{II}Cl_n + CO \xrightarrow{k_3} Ru^{II}(CO)Cl_n$$

(L may be Cl^-, DMA or, less likely, H_2O or OH^-). This mechanism yields the rate law,

$$[8] \quad -\frac{d[LRu^{II}Cl_n]}{dt} = -\frac{d[CO]}{dt} = \frac{k_1k_3[LRu^{II}Cl_n][CO]}{k_{-1}[L] + k_3[CO]}$$

When $k_3[CO] \gg k_{-1}[L]$, the rate law reduces to that observed (eq. 3). Since the rate is essen-

Can. J. Chem. Downloaded from www.nrcresearchpress.com by 210.87.254.6 on 09/05/12
For personal use only.

Can. J. Chem. Downloaded from www.nrcresearchpress.com by 210.87.254.6 on 09/05/12
For personal use only.

tially independent of CO even at the lowest pressure used it is impossible to test the system for an inverse dependence on L since the $k_3[CO]$ term in the denominator of eq. 8 always predominates. Consistent with this is the finding that the rate is independent of added chloride up to 0.5 *M*, although as noted before (7) no suitable inert anion could be found which could be substituted for chloride in order to maintain a constant ionic strength in these experiments. It is possible that L could be a Ru^{II} moiety, that is, the initial complex in solution is dimeric, but we have no evidence of this.[1]

The rate law for the reaction corresponding to reaction 1 in aqueous 3 *M* HCl, probably involving the $RuCl_4^{2-}$ species, was of the form $k[Ru^{II}][CO]$ and an inverse dependence on Cl^- was observed although the mechanism was not considered (2). The data could be consistent with reactions 6 and 7 with $L = Cl^-$; if $k_{-1}[Cl]$ is large compared with $k_3[CO]$, then the rate laws are equivalent with $k = k_1k_3/k_{-1}[Cl^-]$. The kinetic data for k (2) over the range 2.4–4.7 *M*, when the equilibrium distribution of chloro complexes present appears much the same (8), do show a reasonably direct inverse dependence on $[Cl^-]$ as required. The solubility of CO in water (9) is some ten times less than in DMA, and in the 3 *M* HCl the $k_{-1}[Cl^-]$ could predominate over the $k_3[CO]$ term and give rise to the observed different rate laws.

Thus we believe that the mechanism of carbonyl formation is the same in both solvent systems (both 3 *M* HCl and DMA have a dielectric constant in the range 30–40, and have similar coordinating ability (10 and references therein)) and involves predissociation. The expected dependence on CO is given by eq. 8. In 3 *M* HCl the system is in the first-order region and shows an inverse chloride dependence, and is in the zero-order region in DMA where no chloride (or L) dependence is expected. Further evidence for a predissociation step in the HCl system is provided by the activation parameters (2) $\Delta H^{\ddagger} = 19$ kcal mole^{-1}, $\Delta S^{\ddagger} = -5$ e.u., which are very similar to those reported for the reactions of chlororuthenate(II) with ethylene (7) ($\Delta H^{\ddagger} = 22.8$ kcal mole^{-1}, $\Delta S^{\ddagger} = -4$ e.u.) and formic acid (11) ($\Delta H^{\ddagger} = 23.5$ kcal mole^{-1}), $\Delta S^{\ddagger} = -5$ e.u.) in the same media, where the predissociation step

$$[9] \qquad RuCl_4^{2-} \rightleftharpoons RuCl_3^- + Cl^-$$

seems well substantiated.

In the DMA system, the maximum possible number of chlorides initially coordinated is 3 and a process such as

$$[10] \quad RuCl_3^- \rightleftharpoons RuCl_2 + Cl^- \text{ (solvent ligands omitted)}$$

seems more compatible with the $\Delta S^{\ddagger}$ value of -24 e.u. than equilibria involving lower chloro species since these would involve ionization to chloride and a cationic species and such a process for a corresponding $RhCl_3$ system has a much larger negative $\Delta S^{\ddagger}$ value (12). The somewhat lower $\Delta H^{\ddagger}$ value (16.9 kcal mole^{-1}) might be expected if these equilibria are solvent-assisted processes because of the somewhat greater donor power of DMA compared to H_2O (10).

The observed CO dependence of k_2' gives more definite evidence for a predissociation mechanism for the second stage of the reaction.

$$[11] \qquad Ru^{II}(CO)L \underset{k_{-2}}{\overset{k_2}{\rightleftharpoons}} Ru^{II}(CO) + L$$

$$[12] \quad Ru^{II}(CO) + CO \xrightarrow{k_4} Ru^{II}(CO)_2 \quad \text{(other ligands omitted)}$$

The rate law is of the form shown in eq. 8 and at constant [L] and [CO], the measured pseudo first-order constant k_2' is given by

$$k_2' = k_2k_4[CO]/(k_{-2}[L] + k_4[CO])$$

Hence,

$$[13] \qquad \frac{1}{k_2'} = \frac{1}{k_2} + \frac{k_{-2}[L]}{k_2k_4[CO]}$$

The plot of $(k_2')^{-1}$ *vs.* $[CO]^{-1}$ at 80°, shown in Fig. 6, is in accord with this relation and yields the values of k_2 and $k_{-2}[L]/k_4$ listed in Table 3. Results from more limited data at other tempera-

[1]NOTE ADDED IN PROOF:
Since this paper was submitted, Rose and Wilkinson (20) have reported that the blue Ru^{II} chloride solutions in water, 10 *M* HCl, methanol, and dimethylformamide are likely to contain the $Ru_5Cl_{12}^{2-}$ cluster, since the electron spin resonance spectrum of each solution was essentially identical to that of the anion isolated from methanol solutions. However, there is difficulty in interpreting the magnetic behavior of the systems which show about 1 unpaired electron per 5 Ru atoms for the Ru^{II} d^6 configuration. If $Ru_5Cl_{12}^{2-}$ exists in the DMA solution, our k_1 value (multiplied by 5) could refer to its slow dissociation by solvent to a monomeric, solvated $Ru^{II}Cl_n$ species. However, it is difficult to reconcile the kinetic data in the 3 *M* HCl media (2, 7, 11) with the existence of polymeric chlororuthenate(II) species, since a fractional dependence on Ru would be expected.

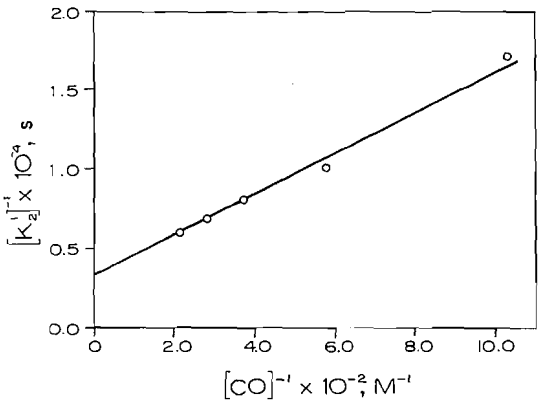

FIG. 6. Dependence of rate on the [CO] at 80° plotted in accord with eq. 8.

tures (Table 2) are also included. The observed linear plot of $(k_2')^{-1}$ against $[Cl^-]$ (Fig. 5) might suggest that L = Cl^-; the intercept from this plot according to (13) gives $k_2 \sim 2.5 \times 10^{-4}$ s^{-1}, in reasonable agreement with the value of 3.0×10^{-4} s^{-1} obtained from the CO data at 80° (Table 3). However, the slope of Fig. 5 gives $k_{-2}/k_4 \sim 3 \times 10^{-2}$ which is not consistent with $k_{-2}[Cl^-]/k_4 = 3.7 \times 10^{-3}$ M since this gives $[Cl^-] \sim 0.12$ M for the experiments with varying CO pressures with no added chloride. Further in these experiments, if L = Cl^- the $[Cl^-]$ would increase somewhat from the 0.021 M present at the conclusion of the first stage; some deviation in the first-order log plots of Fig. 3 would be expected although none was observed. The analysis thus suggests that L is more likely to be a solvent molecule. A good Arrhenius plot for k_2 gives $\Delta H_2^{\ddagger} = 28.1 \pm 1.5$ kcal mole^{-1} and $\Delta S_2^{\ddagger} = 5 \pm 2$ e.u., and the latter seems consistent with little charge separation in the transition state. The slowness of the second stage results then from the high activation energy required for the dissociation step.

The fact that the relative importance of the $k_{3(4)}[CO]$ and $k_{-1}[L]$ terms changes for the formation of $Ru^{II}(CO)$ and $Ru^{II}(CO)_2$ could result from L being chloride and solvent, respectively.

The linear plot of Fig. 5 is considered somewhat fortuitous since a constant ionic strength was not maintained for these experiments and the composition of the chloro complexes might vary; even the solubility of CO could be a function of added chloride. If the ionic strength and solubility effects are relatively small, Fig. 5 suggests that at 0.1–2.0 M added chloride a higher chloro complex exists, which reacts by dissociation of a chloride ligand at a rate similar to the dissociation rate of the complex present at no added chloride.

No detailed kinetics were reported for the formation of $Ru^{II}(CO)_2$ from $Ru^{II}(CO)$ in aqueous HCl solution, due to the slowness of the reaction.

The present results are relevant in view of the current interest in the mechanism of formation of molecular nitrogen complexes. Shilov and co-workers (13, 14) have concluded from kinetic studies that the formation of RuL_5N_2 complexes (L = Cl^-, H_2O, THF), and nitrogen exchange, in these complexes proceed via predissociations of the type

$$[14] \qquad RuL_6 \rightleftharpoons RuL_5 + L$$

$$[15] \qquad RuL_5 + N_2 \rightarrow RuL_5N_2$$

Borod'ko and Shilov state in a review (15) that this contrasts with the formation of carbonyl complexes which involve direct S_N2 reactions, although no references or details were given. The bonding properties of the isoelectronic CO and N_2 may be influenced by the presence of other coordinated ligands (16). Page and co-workers (17) have shown that the reaction of N_2 with $Ru(NH_3)_5H_2O^{2+}$ to form $Ru(NH_3)_5N_2^{2+}$ in aqueous solution is first order in both reactants. Similarly, Armor and Taube (18) have shown that $Ru(NH_3)_5H_2O^{2+}$ reacts with a number of other reagents including CO with overall second-order kinetics. The specific rate constants for these aquopentammineruthenium(II) reactions are all fairly similar but as pointed out by Page and co-workers (17) this does not distinguish between the two possible mechanisms: the ligands could have about the same nucleophilicity for ruthenium(II) be it in the direct S_N2 displacement (with loss of H_2O) or the step such as [15] in the S_N1 mechanism.

Our results stress the dangers of implying an S_N2 mechanism from overall second order kinetics for these carbonyl, and presumably nitrogen systems. It is necessary to extend the studies to higher CO and N_2 concentrations by using higher pressures, or in the present work, non-aqueous media, in attempts to detect a less than first-order dependence on the gas and inhibition by the leaving group.

We are pursuing studies on the kinetics of

Can. J. Chem. Downloaded from www.nrcresearchpress.com by 210.87.254.6 on 09/05/12
For personal use only.

formation of carbonyls by direct carbonylation of ruthenium complexes including those which are known to form molecular nitrogen complexes (19).

We thank the National Research Council of Canada for financial support and Johnson Matthey Limited for the loan of ruthenium. We would also like to thank one of the referees for helpful comments.

1. B. R. JAMES. Inorg. Chim. Acta Rev. In press.
2. J. HALPERN, B. R. JAMES, and A. L. W. KEMP. J. Amer. Chem. Soc. **88**, 5142 (1966).
3. B. R. JAMES and G. L. REMPEL. Can. J. Chem. **44**, 233 (1966).
4. B.R. JAMES, G. L. REMPEL, and F. T. T. NG. J. Chem. Soc. A, 2454 (1969).
5. B. C. HUI and B. R. JAMES. Chem. Commun. 198 (1969).
6. Dupont DMAC Product Information Bulletin, Wilmington, Delaware.
7. J. HALPERN and B. R. JAMES. Can. J. Chem. **44** 495 (1966).
8. A. L. W. KEMP. Ph.D. Dissertation, University of Chicago, Chicago, Illinois, 1964.
9. A. SEIDELL. Solubilities of inorganic and metal organic compounds. Vol. 1. Van Nostrand, New York. 4th ed. 1958.
10. B. R. JAMES and G. L. REMPEL, Discuss. Faraday Soc. **46**, 48 (1968).
11. J. HALPERN and A. L. W. KEMP. J. Amer. Chem. Soc. **88**, 5147 (1966).
12. B. R. JAMES and G. L. REMPEL. Can. J. Chem. **46**, 571 (1968).
13. A. K. SHILOVA and A. E. SHILOV. Kinetika i Kataliz, **10**, 267 (1969); Chem. Abstr. **71**, 25095 (1969).
14. A. K. SHILOVA, A. E. SHILOV, and Z. N. VOSTROKNUTOVA. Kinetika i Kataliz. In press.
15. Y. G. BOROD'KO and A. E. SHILOV. Russ. Chem. Rev. **38**, 355 (1969).
16. K. G. CAULTON, R. L. DEKOCK, and R. F. FENSKE. J. Amer. Chem. Soc. **92**, 515 (1970).
17. C. M. ELSON, I. J. ITZKOVITCH, and J. A. PAGE. Can. J. Chem. **48**, 1639 (1970).
18. J. N. ARMOR and H. TAUBE. J. Amer. Chem. Soc. **91**, 6874 (1969).
19. A. D. ALLEN, T. ELIADES, R. O. HARRIS, and P. REINSALU. Can. J. Chem. **47**, 1605 (1969).
20. D. ROSE and J. WILKINSON. J. Chem. Soc. A, 1791 (1970).

Can. J. Chem. Downloaded from www.nrcresearchpress.com by 210.87.254.6 on 09/05/12
For personal use only.

Can. J. Chem. Downloaded from www.nrcresearchpress.com by 210.87.254.42 on 09/05/12
For personal use only.

The reaction of atomic hydrogen with methyl cyanide

J. W. S. JAMIESON, G. R. BROWN,[1] AND J. S. TANNER
Department of Chemistry, Dalhousie University, Halifax, Nova Scotia

Received May 20, 1970

The reaction of hydrogen atoms, produced by electric discharge, with methyl cyanide vapor has been reinvestigated at seven different temperatures between 40 and 507 °C over a range of methyl cyanide flow rates from 2 to 25 μmoles/s. As in the previous limited investigation the products have been found to be hydrogen cyanide, methane, and ethane, but the present results indicate the presence of chain characteristics to a minor extent, propagated by CN. Kinetic parameters for formation of the products have been evaluated, as $k_{HCN} = 3.55 \times 10^{-12} e^{-5816/RT}$; $k_{CH_4} = 1.66 + 10^{-13} e^{-2990/RT}$; and $k_{C_2H_6} = 1.70 \times 10^{-12} e^{-7857/RT}$.

Canadian Journal of Chemistry, **48**, 3619 (1970)

Introduction

During a current investigation of the reaction of atomic hydrogen with ethyl cyanide it very soon became apparent that the results could only be explained by a chain mechanism. It therefore seemed desirable to study the reaction of atomic hydrogen with methyl cyanide, under the same conditions in the same reaction system, since it might also involve a chain mechanism to some extent, and the results of this study might clarify the mechanism of the ethyl cyanide reaction.

Experimental

Materials

Hydrogen was supplied by the Linde Gases Division, Union Carbide Canada Limited and acetonitrile (methyl cyanide) "Baker Analyzed" reagent, b.p. 81.6 °C, was purchased from the Fisher Scientific Company Limited.

Apparatus and Methods

The apparatus was a conventional fast flow system which has recently been described (1). In all experiments the flow rate of molecular hydrogen was 88.2 μmoles/s, which gave a pressure in the reaction system of 1.10 mm. The atomic hydrogen flow rates at the various temperatures were estimated from the maximum extent of the reactions of cyclic imines (2), which have been shown to give results in reasonable agreement with those based on the maximum extent of the reactions of ethyl chloride, formamide, or ethylenimine with hydrogen atoms.

Flow rates of methyl cyanide were estimated in experiments with the hydrogen discharge off. The methyl cyanide was trapped at liquid nitrogen temperature and then distilled into a known volume connected to a manometer which was used to measure the pressure of the vapor at ambient temperature.

The hydrogen cyanide produced was measured by titration with silver nitrate (3) and by gas chromatography, using a triacetin column (4). Ethane was separated from other products in a Le Roy still, after which it was measured in a gas burette and shown to be free of impurity by gas chromatography, using either a Beckmann No. 17329 di-*n*-butyl maleate column or a triacetin column. Methane was trapped quantitatively by the method of Demchuk and Gesser (5), measured in a gas burette and analyzed by gas chromatography, using a molecular sieve 5A column (1).

Results and Discussion

The results obtained at various temperatures are given[2] in Figs. 1, 2, and 3. Methane, ethane, and HCN were found to be the only products apart from a trace of unidentified solid. Figure 1 shows that the yield of methane decreased not only with increasing temperature but also with increasing flow rates of methyl cyanide at the higher temperatures. The maximum yields of the other products decreased, as shown in Figs. 2 and 3, at both 397 and 507 °C are due presumably to increased combination of hydrogen atoms on the wall of the reaction vessel at higher temperatures. At most temperatures the maximum amounts of both methyl radicals (measured as twice the ethane formed) and HCN produced were substantially higher than the flow rates of hydrogen atoms at these temperatures. Thus a chain mechanism is involved to a slight extent.

The results can be most simply interpreted in terms of the following mechanism

[1] $$H + CH_3CN \rightarrow CH_4 + CN$$

[2] $$H + CH_3CN \rightarrow CH_3 + HCN$$

[3] $$CN + H_2 \rightarrow HCN + H$$

[4] $$2CH_3 \rightarrow C_2H_6$$

[1] Present address: Department of Chemistry, McGill University, Montreal, P.Q.

[2] More complete data are available from the Depository of Unpublished Data, National Science Library, National Research Council of Canada, Ottawa, Canada.

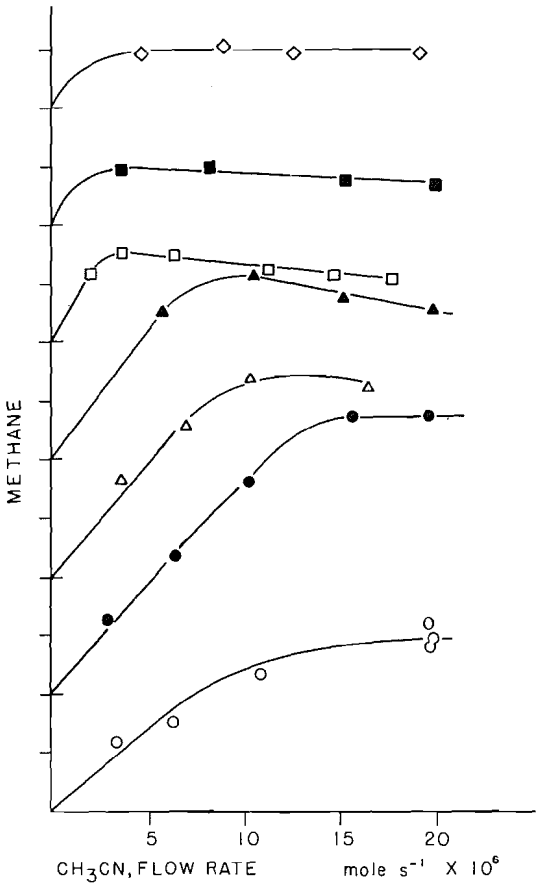

FIG. 1. Methane produced at 40° (○), 83° (●), 152° (△), 198° (▲), 306° (□), 397° (■), and 507 °C (◇). To avoid congestion of experimental points and curves, at each successively higher temperature the origin has been raised by two units along the ordinate axis which is divided into integral units of μmoles/s.

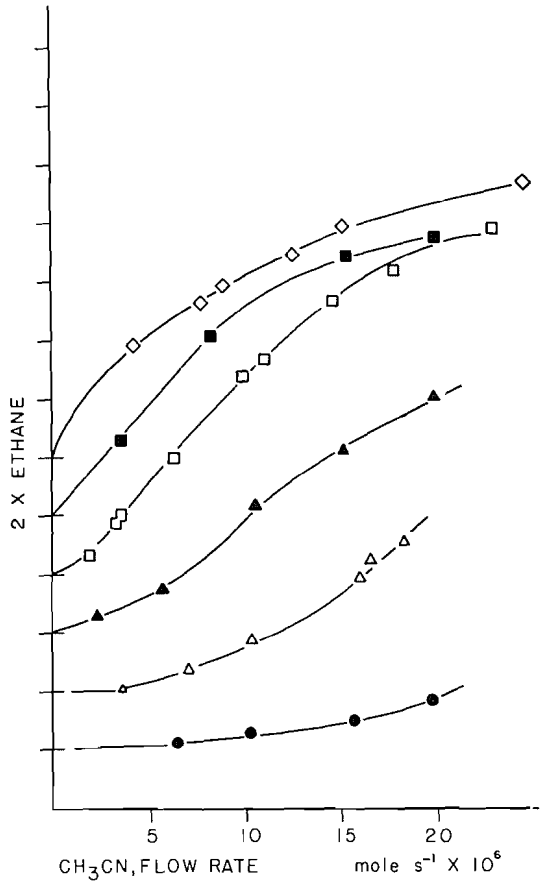

FIG. 2. Ethane produced × 2 at 83° (●), 152° (△), 198° (▲), 306° (□), 397° (■), and 507 °C (◇). As in Fig. 1, at each successively higher temperature the origin has been raised but only by one unit along the ordinate axis which is divided into integral units of μmoles/s.

It appears that reactions 1 and 2 are competitive primary steps. These reactions, together with the more typical hydrogen abstraction reaction

[5] $$H + CH_3CN \rightarrow H_2 + CH_2CN$$

have previously (6) been considered as possible primary steps. Although reaction 1 may seem to be somewhat unusual it appears to be inevitable since, as is shown below, cyanide radicals are the only feasible chain carriers apart from which the C—C bond is surely the weakest bond in methyl cyanide.

No evidence for the occurrence of reaction 5 has been observed in the present investigation although slight occurrence of this reaction followed by combination of CH_2CN radicals to succinonitrile (6) might account for the deposition of very small amounts of a solid product on the wall of the first cold trap.

It has been suggested (6) that reaction 2 followed by the reaction

[6] $$CH_3 + H_2 \rightarrow CH_4 + H$$

might propagate a chain, but recently it has been shown (1), in the present apparatus under similar conditions, that this reaction does not occur to an appreciable extent. Therefore, it is probable that the limited chain is carried by cyanide radicals, formed in reaction 1, which then react readily with molecular hydrogen to generate hydrogen atoms according to reaction 3.

Conclusive evidence that reaction 3 occurs

Can. J. Chem. Downloaded from www.nrcresearchpress.com by 210.87.254.42 on 09/05/12
For personal use only.

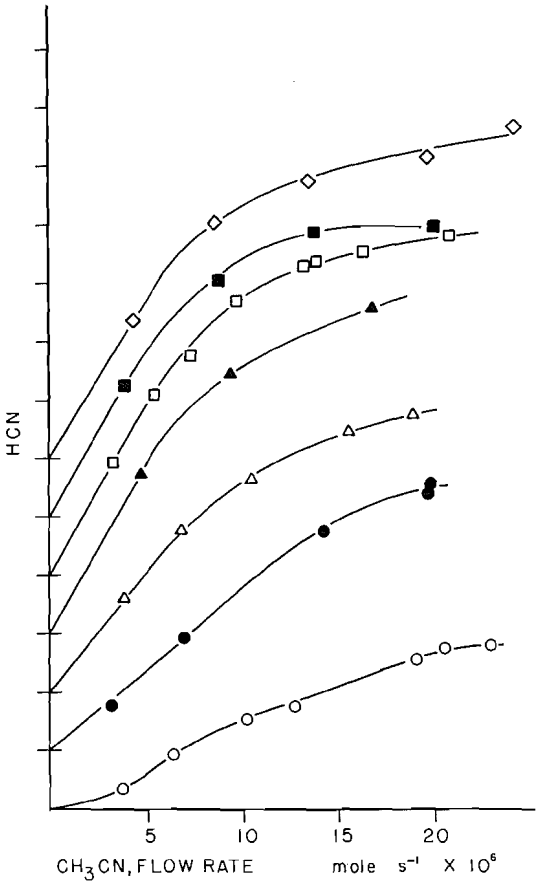

FIG. 3. HCN produced at 40° (○), 83° (●), 152° (△), 198° (▲), 306° (□), 97° (■), and 507 °C (◇). As in Fig. 1, at each successively higher temperature the origin has been raised but only by one unit along the ordinate axis which is divided into integral units of μmoles/s.

rapidly and quantitatively, when molecular hydrogen is present in high concentration, has been reported by Haggart and Winkler (7, 8) who have also shown that cyanide radicals react with methane to form both HCN and CH_3CN, presumably in the reactions

[7] $$CN + CH_4 \rightarrow HCN + CH_3$$

and

[8] $$CN + CH_4 \rightarrow CH_3CN + H$$

neither of which could compete favorably with reaction 3 in the present apparatus containing a large excess of molecular hydrogen. Reactions 7 and 8 might account for the decrease in methane production observed in the present study at high flow rates and higher temperatures but there appears to be no necessity to consider these reactions in the calculation of specific reaction rates from the results obtained at low reactant flow rates.

Chain termination seems to be largely due to the occurrence of reaction 2 as well as to the combination of hydrogen atoms at the reaction vessel wall. Another possible chain limiting reaction

[9] $$H + CH_3 \rightarrow CH_4$$

has been found not to occur appreciably in the present apparatus (1). It would, of course, also require a third body so that it would probably not compete favorably with bimolecular reactions such as reaction 4.

No evidence was found that cyanide radicals had combined to form cyanogen. Cyanogen was specifically sought but not found among the products in either the present study or related investigations (6, 9). It is, however, unlikely that cyanide radicals would interact appreciably with either hydrogen atoms or one another in the presence of a large excess of molecular hydrogen which would rapidly consume cyanide radicals according to reaction 3.

Under most conditions the amount of HCN produced was found to be approximately equal to the amount of methane plus twice the amount of ethane. Thus a reasonable material balance is implied.

As a result of kinetic calculations based on the mechanism of reactions 1 to 4 it appears that more quantitative statements can be made. If the rate of reaction 1 is calculated from the production of methane and the rate of reaction 2 is taken as the rate of production of methyl radicals (which is twice the rate of production of ethane, since reaction 4 probably occurs readily in the first cold trap), the sum of these two rates is virtually equal to the over-all rate of production of HCN. It can, of course, also be shown from the usual steady state treatment that

[10] $$A_1 e^{-E_1/RT} + A_2 e^{-E_2/RT} = A_{HCN} e^{-E_{HCN}/RT}$$

With the use of an IBM 360/50 computer the logarithms of the specific reaction rates have been calculated according to the usual second order expression for streamline flow, as has previously been reported (1), from the present data obtained at low methyl cyanide flow rates. Where possible the methane production was also estimated as [HCN − methyl] and the methyl radical produc-

Can. J. Chem. Downloaded from www.nrcresearchpress.com by 210.87.254.42 on 09/05/12
For personal use only.

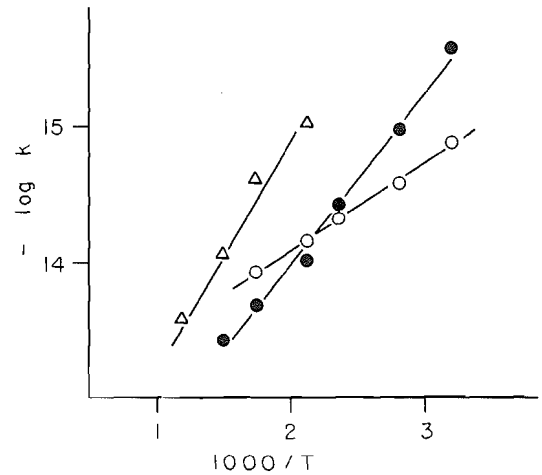

FIG. 4. Arrhenius plots for methane (○), methyl radical (△), and HCN (●).

tion was also estimated as [HCN − methane].

The Arrhenius plots are shown in Fig. 4, from which the specific reaction rates have been calculated as

$$k_1 = k_{\text{methane}} = 1.66 \times 10^{-13} e^{-2990/RT}$$

$$k_2 = k_{\text{methyl}} = 3.39 \times 10^{-12} e^{-7857/RT}$$

$$k_{\text{HCN}} = 3.55 \times 10^{-12} e^{-5816/RT}$$

At the mean temperature of 240 °C (513 °K), $k_1 + k_2 = 10^{-14}$ and $k_{\text{HCN}} = 1.2 \times 10^{-14}$, in satisfactory agreement with eq. 10, which implies that the present results are adequately accounted for by the mechanism of reactions 1 to 4.

One might wonder, however, why the reaction

[11] $$H + CH_4 \rightarrow H_2 + CH_3$$

is not involved since it has recently been shown (1) in the same reaction system that this reaction has an activation energy of 7.4 ± 1.1 kcal and a frequency factor of about 10^{-12} cm^3/molecule s. This difficulty might be avoided by adopting more recently suggested higher values (10–12) for the activation energy and frequency factor of reaction 11 but these values, albeit most interesting, were either measured indirectly or estimated from various data. Thus they could hardly be assumed to be as reliable as those cited above (1) which were obtained by direct measurement of both the activation energy and the frequency factor from an Arrhenius plot of data obtained at three widely different temperatures in experiments which at 500 °C showed that all the available hydrogen atoms were consumed in reaction 11 and all the methyl radicals thus formed appeared as ethane. Since there seems to be no justification for ruling out reaction 11 except that reaction 2 would be favored by higher concentrations of CH_3CN than CH_4, it might be necessary to include both reactions 2 and 11 in the mechanism, in which case it would not be possible to relate the rates of production of methane, methyl radical, and HCN so simply to the rates of individual reactions.

Financial assistance from the National Research Council of Canada is gratefully acknowledged. The authors are also grateful to Mr. D. W. Lemon for preparing and using some of the preliminary computer programs.

1. J. W. S. JAMIESON and G. R. BROWN. Can. J. Chem. **42**, 1638 (1964).
2. J. W. S. JAMIESON, G. R. BROWN, and W. K. HANCOCK. Can. J. Chem. **43**, 1973 (1965).
3. I. M. KOLTHOFF and E. B. SANDELL. Textbook of quantitative inorganic analysis. Macmillan, New York. 1948.
4. R. E. ISBELL. Anal. Chem. **35**, 255 (1963).
5. N. DEMCHUK and H. GESSER. Can. J. Chem. **41**, 1645 (1963).
6. W. FORST and C. A. WINKLER. Can. J. Chem. **33**, 1814 (1955).
7. C. HAGGART and C. A. WINKLER. Can. J. Chem. **37**, 1791 (1959).
8. C. HAGGART and C. A. WINKLER. Can. J. Chem. **38**, 329 (1960).
9. D. E. MCELCHERAN, M. H. J. WIJNEN, and E. W. R. STEACIE. Can. J. Chem. **36**, 321 (1958).
10. R. W. WALKER. J. Chem. Soc. A, 2391 (1968).
11. M. J. KURYLO and R. B. TIMMONS. J. Chem. Phys. **50**, 5076 (1969).
12. M. J. KURYLO, G. A. HOLLINDEN, and R. B. TIMMONS. J. Chem. Phys. **52**, 1773 (1970).

Can. J. Chem. Downloaded from www.nrcresearchpress.com by 210.87.254.42 on 09/05/12
For personal use only.

Mass spectrometric studies of chemical reactions in shock waves. Part II. The thermal decomposition of diazomethane

J. E. Dove and J. Riddick
Department of Chemistry, University of Toronto, Toronto 181, Ontario

Received[1] July 12, 1968

The thermal decomposition of CH_2N_2, highly diluted in Kr, has been studied in shock waves by using time-of-flight mass spectrometry to follow concentration changes in the reacting gas. Observations were made at pressures 45 to 95 Torr and temperatures 820 to 1200 °K. The principal products of reaction are C_2H_4, C_2H_2, and N_2. The primary step appears to be a second order unimolecular decomposition of CH_2N_2 into CH_2 and N_2; for this step, $\log k = (9.61 \pm 0.21) - (15\,800 \pm 1\,000)/2.303RT$ (cal mole^{-1} and cm^3 mole s units.) Some decomposition of CH_2N_2 into HCN and NH is also indicated.

The formation of C_2H_2 is believed to occur through vibrationally excited C_2H_4, formed by reaction between CH_2 and CH_2N_2. Calculations using the R.R.K.M. theory indicate that 50 ± 10% of the energy of this reaction appears as vibrational energy of the product C_2H_4.

Canadian Journal of Chemistry, **48**, 3623 (1970)

Introduction

Diazomethane is important as a source of methylene radicals (1), and the kinetics of thermal decomposition of gaseous diazomethane have been the subject of a number of investigations. Early experiments by Steacie (2) in a static system in the pressure range 40–200 Torr and at temperatures between 410 and 490 °K indicated that the decomposition was homogeneous and bimolecular, with an activation energy of approximately 36 kcal mole^{-1}. However, it has now been established (3–6) that at temperatures greater than 500 °K the initial step is the unimolecular reaction

[1] $$CH_2N_2 \rightarrow CH_2 + N_2$$

Shantarovich (4) studied the decomposition in a flow system using nitrogen carrier gas (total pressure about 20 Torr, temperature 600–700 °K) and obtained $k_1 = 0.8 \times 10^{11} \exp(-31\,750/RT)$ s^{-1}. Setser and Rabinovitch (5) have reported $k_1 = 1.2 \times 10^{12} \exp(-34\,000/RT)$ in 1:20 mixtures of diazomethane:*cis*-butene (total pressure 25 Torr, temperature range 505–530 °K), while Dunning and McCain (6) found $k_1 = 0.9 \times 10^{12} \exp(-32\,000/RT)$ in the presence of hydrogen (mixtures of 0.42 Torr diazomethane and 110 Torr hydrogen in the range 566–646 °K). Setser and Rabinovitch suggest that their measurements were made in the fall-off region and that their measured activation energy was about 1 kcal mole^{-1} lower than E_∞.

We have studied the kinetics and mechanism of thermal decomposition of gaseous diazomethane diluted with krypton, using shock wave techniques to obtain temperatures higher than those employed by previous investigators. It is to be expected on theoretical grounds that the pressure at which fall-off occurs will decrease with increasing temperature (7). The results of the present work show that the reaction is in the fall-off region under our experimental conditions (45–95 Torr, 820–1200 °K).

Experimental

A detailed description of the apparatus and its operation has been given previously (8). The equipment included a shock tube coupled to a Bendix Model 12 time-of-flight mass spectrometer. The gas mixture studied was compressed and heated extremely rapidly by means of a reflected shock wave. The chemically reacting gas was sampled continuously through an orifice of 0.1 mm diameter in the end plate of the shock tube, directly into the ion source of the mass spectrometer. The rapidly changing concentrations in the gas mixture were studied by recording about 20 mass spectra at known intervals of 10 to 100 μs. The temperature and pressure of the shock-heated gas were calculated from the measured value of the incident shock velocity.

Nitrogen was used as the driver gas in all of the experiments.

Materials

The krypton diluent was Matheson Research Grade and was used as supplied. (Stated minimum purity, 99.995%; O_2 less than 4 p.p.m.)

The nitrogen diluent was Union Carbide, Linde Gases Division, Certified Grade, of stated minimum purity, 99.995%. (O_2 content about 2 p.p.m.) It was passed slowly through a series of traps cooled in liquid nitrogen, to remove condensables.

Diazomethane was prepared by dropping a solution of N-methyl N-nitroso *p*-toluene sulfonamide in diethy-

[1]Revision received June 22, 1970.

Can. J. Chem. Downloaded from www.nrcresearchpress.com by 210.87.254.42 on 09/05/12
For personal use only.

Can. J. Chem. Downloaded from www.nrcresearchpress.com by 210.87.254.42 on 09/05/12
For personal use only.

lene glycol monobutyl ether into an evacuated flask containing a saturated solution of potassium hydroxide in ethylene glycol. The diazomethane vapor evolved was pumped through a trap cooled in solid carbon dioxide/acetone mixture and then condensed at −196 °C. Small quantities were prepared (not more than 0.2 g) and stored at −78 °C. No explosions occurred when using this method of preparation.

Deuterated diazomethane was prepared as follows. A sample of diazomethane was condensed into a trap containing anisole at −196 °C. The trap was allowed to warm up to room temperature, and the resultant solution of diazomethane in anisole was shaken for 5 min with three successive portions of a 50% solution of KOD in D_2O. The organic layer was then separated off and the diazomethane distilled under vacuum into a trap cooled in liquid nitrogen. The product was analyzed mass spectrometrically and found to be 88% deuterated (79% CD_2N_2, 19% $CHDN_2$, 2% CH_2N_2).

The experimental mixtures were prepared by manometric measurement in a conventional high vacuum apparatus and were mechanically stirred before use. Special precautions had to be taken because of the instability of gaseous diazomethane. The glass apparatus was preconditioned with diazomethane for extended periods in order to minimize the rate of heterogeneous decomposition. Decomposition in the metal shock tube was, however, relatively rapid, but was kept to a low level by ensuring that the shock wave was always initiated less than 20 s after admitting the gas to the shock tube. In order to observe the rate of depletion of diazomethane under room temperature conditions, separate experiments were made in which reaction mixtures in the storage vessel and in the shock tube were monitored mass spectrometrically. These experiments indicated that the extent of decomposition in the glass apparatus in 2 h, the maximum period for which mixtures were stored, was less than 20%, and in the shock tube was less than 6% in 20 s. The possibility of additional loss of diazomethane in the transfer lines, during the few seconds taken to fill the shock tube, cannot be excluded. The only gaseous products observed from the pre-shock decomposition were nitrogen and small amounts of ethylene. Since these are also found to be the principal products of the high temperature decomposition, it is unlikely that decomposition before shock heating had any major effects on the observed kinetics though it did have to be considered in the detailed interpretation of the results.

Calculation of Shock Wave Parameters

The temperature and pressure in the unreacted gas behind the reflected shock wave were calculated from the initial conditions and the incident shock wave velocity using the standard conservation relations (9) and published thermodynamic data (10, 11). Under our conditions the incident shock wave velocity was decreasing by about 5% per m, so that the velocity at the end plate of the shock tube was obtained by a short extrapolation. It was assumed that ideal shock reflection occurred and that rotational and vibrational equilibrium were established both in the incident and reflected shock waves.

Results and Discussion

Reaction Products and Mechanism

The results discussed in this section were obtained with a mixture of 2% diazomethane, 98% krypton. Mass spectra were recorded at 15 V electron energy in the mass range m/e = 12 to 50. The main peaks observed were at m/e = 14, 26, 27, 28, 42; because of the low ionizing voltage, it may safely be assumed that these ions were all singly charged.

Mass 42 is the diazomethane parent peak. It increased suddenly as the gas mixture was compressed by the shock wave, and then decayed exponentially with time. Herzberg and Shoosmith (12) have shown that the rate of the reaction between methylene and diazomethane is approximately equal to the collision rate. The main processes removing diazomethane are therefore considered to be reaction 1 and the secondary reaction

$$[2] \qquad CH_2 + CH_2N_2 \rightarrow C_2H_4^* + N_2$$

Mass 14 is almost certainly CH_2^+, and this identification was confirmed by labelling with deuterium. The CH_2^+ ion could arise by direct ionization of CH_2, but we believe that the major contribution is from fragmentation of $CH_2N_2^+$ in the mass spectrometer, as discussed later.

The peak at mass 28 increased progressively as the diazomethane disappeared, and it was invariably the largest product peak. It is believed to be the parent peak of ethylene formed in reaction 2. Under our experimental conditions the relative sensitivity of the mass spectrometer to C_2H_4 and N_2 is such that N_2 could account for less than 10% of peak 28.

Reaction 2 is highly exothermic and is likely to lead to the formation of ethylene in a highly excited vibrational state. Provided that the vibrational energy is high enough, the ethylene may then decompose by reaction 3.

$$[3] \qquad C_2H_4^* \rightarrow C_2H_2 + H_2$$

The excited ethylene may also be de-energized by collision

$$[4] \qquad C_2H_4^* + M \rightarrow C_2H_4 + M$$

The observation of a peak at mass 26 ($C_2H_2^+$) suggests that the products of reaction 3 were being detected.

There is also a major product peak at mass 27.

Can. J. Chem. Downloaded from www.nrcresearchpress.com by 210.87.254.42 on 09/05/12
For personal use only.

The three product peaks at $m/e = 26$, 27, and 28 increase simultaneously and, within experimental error, the ratios 26/28 and 27/28 are time-independent in a given experiment. The ratios are plotted as a function of temperature in Figs. 1 and 2. For comparison, the corresponding results for the mass spectrum of ethylene obtained under similar experimental conditions are included on the same diagram. The mass spectrum of ethylene has a slight temperature dependence, the extent of fragmentation increasing with increasing temperature. However, the dependence is small and there must be some other source of 26 and 27 in the diazomethane experiments. As we have seen, mass 26 can be accounted for as being due to acetylene formed in reaction 3. It might be suggested that vinyl radicals formed in the analogous reaction 5 are responsible for the peak at mass 27

[5] $$C_2H_4^* \rightarrow C_2H_3 + H$$

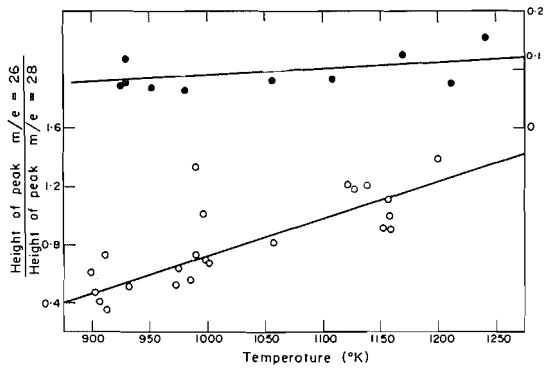

FIG. 1. Dependence of (height of peak $m/e = 26$)/(height of peak $m/e = 28$) on temperature. ○, diazomethane decomposition (left hand scale); ●, mass spectrum of ethylene (right hand scale).

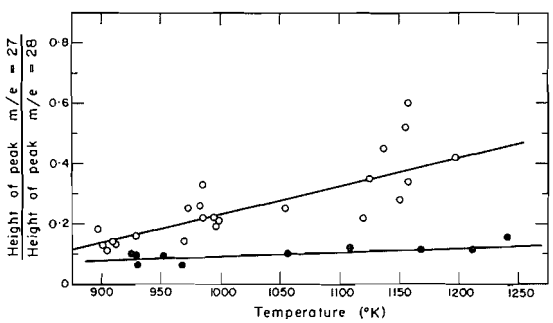

FIG. 2. Dependence of (height of peak $m/e = 27$)/(height of peak $m/e = 28$) on temperature. ○, diazomethane decomposition; ●, mass spectrum of ethylene.

However, we think this is not the source of mass 27, for the following reasons. Harrison and Lossing (13) have obtained a value of 65 ± 3 kcal mole^{-1} for $\Delta H_f(C_2H_3)$. Hence, the critical energy for the decomposition of ethylene to form a hydrogen atom and C_2H_3 is not less than 101 kcal mole^{-1}. As discussed later, the critical energy for reaction 3 is estimated to be about 77 kcal mole^{-1}, so that reaction 5 is expected to be very much slower than reaction 3. Furthermore, there is no evidence that mass peak 27 decreases once all the diazomethane has decomposed, so that the species involved is probably a stable molecule. This also eliminates the possibility that the peak at mass 27 might be due to enhanced fragmentation of the parent ion formed from $C_2H_4^*$.

A further possibility is that peak 27 is the result of ion–molecule reactions taking place in the ion source and involving the $C_2H_2^+$ or $C_2H_4^+$ ions. However, calculations indicated that the effect of ion–molecule reactions would probably be negligible (see also ref. 14). This was confirmed experimentally by obtaining the mass spectrum of a mixture of 1% ethylene + 1% acetylene in krypton at seven different temperatures in the range 1000–1026 °K. The average value of 27/28 was 0.1 (3), in good agreement with the results for ethylene in krypton (see Fig. 2), and it is concluded that ion–molecule reactions are not an important source of mass 27.

The above results lead to the conclusion that there must be a stable molecular product of mass 27. HCN fulfils this requirement and it could be formed in an alternative unimolecular decomposition

[6] $$CH_2N_2 \rightarrow HCN + NH$$

In order to substantiate the identification of mass 27 as HCN^+ rather than $C_2H_3^+$, isotope labelling experiments were carried out. The decomposition of 2% of deuterated diazomethane in krypton was studied at 780–1250 °K, and the results were analyzed to discover whether there was some unsuspected source of additional $C_2D_3^+$. The ratio (peak 30):(peak 32) is plotted as a function of temperature in Fig. 3. The "theoretical" lines in this figure and in Fig. 4 are calculated from the results for CH_2N_2 on the basis of the following assumptions: k_1 and k_6 are approximately the same for CH_2N_2, $CHDN_2$,

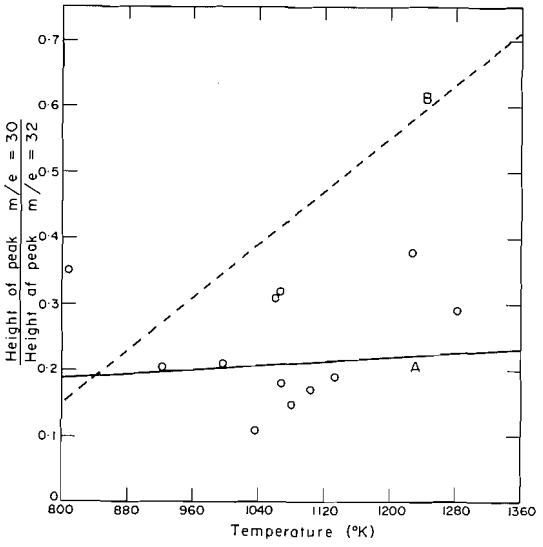

FIG. 3. Comparison of calculated and observed dependence of (height of peak $m/e = 30$)/(height of peak $m/e = 32$) on temperature, for deuterated diazomethane. Line *A*, calculated using results from experiments on CH_2N_2 and the mass spectrum of C_2H_4, assuming that the peak of $m/e = 27$ is not $C_2H_3^+$. Line *B*, calculated from the same results assuming that $m/e = 27$ is $C_2H_3^+$. ○, experimental results for CD_2N_2.

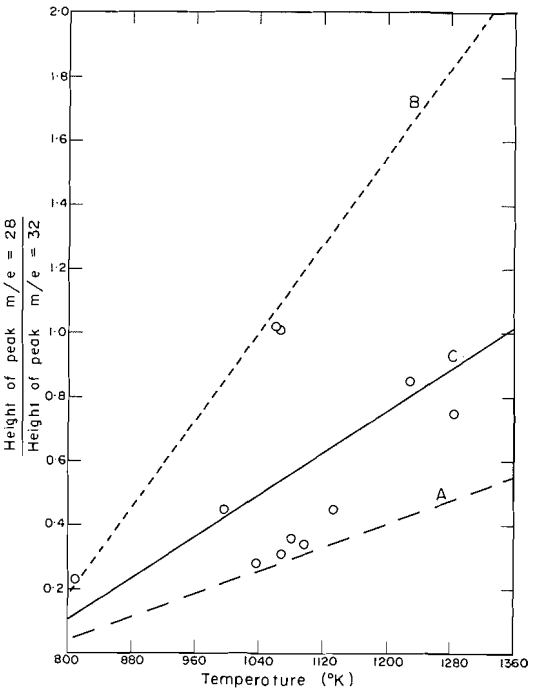

FIG. 4. Comparison of calculated and observed dependence of (height of peak $m/e = 28$)/(height of peak $m/e = 32$) on temperature, for deuterated diazomethane. Line *A*, calculated from the CH_2N_2 results and the mass spectrum of C_2H_4 allowing for the formation of DCN (but not C_2D_2). Line *B*, calculated from the CH_2N_2 results and the mass spectrum of C_2H_4 allowing for the formation of DCN and C_2D_2. ○, experimental results for CD_2N_2. Line *C*, experimental.

and CD_2N_2; CH_2, CHD, and CD_2 have approximately equal reactivity in reaction 2; the mass spectral sensitivities and fragmentation patterns for the deuterated compounds are the same as for their undeuterated analogues. It is apparent from Fig. 3 that peak 30 can be accounted for as the sum of the parent peak of $C_2H_2D_2$ and the $C_2D_3^+$ breakdown peak from C_2D_4, and we conclude that there is no additional source of $C_2D_3^+$; with reference to the CH_2N_2 experiments this suggests that the ion at $m/e = 27$ is not $C_2H_3^+$.

The isotope labelling experiments also give information about the formation of DCN. The 28/32 ratio is plotted against temperature in Fig. 4. The experimental values for this ratio are lower than expected if C_2D_2 and DCN are both formed at the same rate as C_2H_2 and HCN in the thermal decomposition of CH_2N_2, but those results can be explained if the rate of decomposition of C_2D_4* to form C_2D_2 and D_2 is about 0.3 times the rate of the corresponding decomposition of C_2H_4*. This is not an unreasonable postulate in view of the fact that Callear and Cvetanović (15) have obtained a value of 0.5 for the ratio of the rates of the mercury photosensitized decomposition of C_2D_4 and C_2H_4. The results of these isotope studies, therefore, appear to be consistent with our conclusion that some hydrogen cyanide is formed during the high temperature thermal decomposition of diazomethane.

Mass 42 never completely disappeared in our experiments, and in those cases where the decomposition of diazomethane was believed to be complete the residual peak at mass 42 was about 5% of the initial height. This is probably due to the formation of C_3H_6 by the reaction

[7] $$CH_2 + C_2H_4 \rightarrow C_3H_6$$

We also found small peaks at $m/e = 15$, 30, and 40. The peak at mass 40 is probably due to C_3H_4 from

[8] $$CH_2 + C_2H_2 \rightarrow C_3H_4$$

There is experimental evidence (1, 16) that CH_2 can abstract H atoms to form CH_3 and the peak

Can. J. Chem. Downloaded from www.nrcresearchpress.com by 210.87.254.42 on 09/05/12
For personal use only.

at $m/e = 15$ may be from methyl radicals formed in reaction 9.

[9] $$CH_2 + CH_2N_2 \rightarrow CH_3 + CHN_2$$

Herzberg and Travis (17) have detected both CH_3 and CHN_2 in the flash photolysis of diazomethane. The CH_3 radical could subsequently react to form ethylene and ethane (mass 30) *e.g.* by

[10] $$CH_3 + CH_2N_2 \rightarrow C_2H_5 + N_2$$

[11] $$C_2H_5 \rightarrow C_2H_4 + H$$

[12] $$2C_2H_5 \rightarrow C_2H_4 + C_2H_6$$

[13] $$2CH_3 \rightarrow C_2H_6$$

There was no evidence for the presence of CH_4. It is noted that methane is not a product of the photolysis of CH_2N_2, but small amounts of ethane are formed (18).

Kinetics of Unimolecular Decomposition of Diazomethane

The thermal decomposition of diazomethane was investigated over a temperature range of about 300° in each of three different mixtures: 2% CH_2N_2, 98% Kr (880–1160 °K); 1% CH_2N_2, 99% Kr (900–1200 °K); 1% CH_2N_2, 9% N_2, 90% Kr (820–1170 °K). In each individual experiment, semi-log plots of the height of mass peak 42 against time were linear to within experimental uncertainty (Fig. 5), suggesting that the rate has an approximately first order dependence on diazomethane concentration. However, as explained below, we believe that under our conditions the reaction was of second order overall, energizing collisions being rate determining. Accordingly, the first order slopes were divided by total gas concentrations to give second order rate constants for overall destruction of diazomethane; the results for the CH_2N_2 + Kr mixtures are plotted in Figs. 6 and 7.

We found that, at any given temperature, the rate constant so obtained was somewhat greater for the 2% mixture than for 1%. A detailed analysis of the results indicates that two effects are responsible for this difference: (*a*) diazomethane, and probably also reaction products, are more efficient than krypton in collisional energization; (*b*) even though the mixtures were relatively dilute, there is sufficient exothermicity to affect the observed rates appreciably. (Some curvature of the first order plots would then be expected, but previous experience (8) shows that

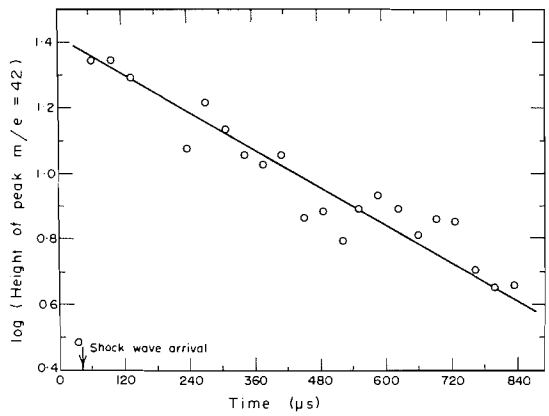

FIG. 5. First order plot of the disappearance of peak $m/e = 42$. 2% CH_2N_2 in krypton. Experimental conditions, 953 °K, 59.6 Torr.

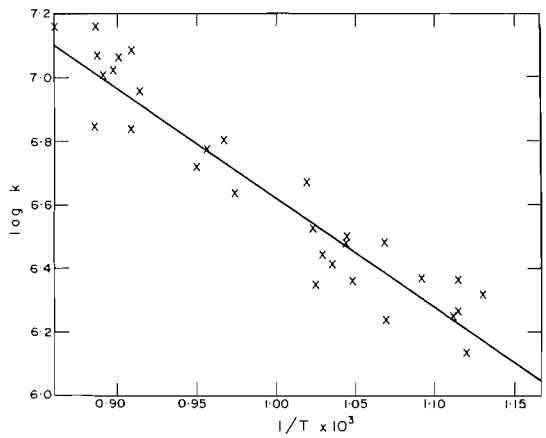

FIG. 6. Arrhenius plot of the overall rate constant (second order) for decomposition of diazomethane (2% CH_2N_2 in 98% Kr). k in l mole s units.

moderate curvature is very hard to detect in experiments of this type.) In principle, effects (*a*) and (*b*) can be separated from one another, to allow the calculation of the relative collision efficiency of diazomethane and krypton. However, in practice we found that this separation could not be achieved with satisfactory accuracy because pre-shock decomposition caused some uncertainty in the initial composition. We have, therefore, used our data to remove the two effects simultaneously. It may be shown that under the conditions of our experiments, $k = [k(1\%)]^2/k(2\%)$. $k(1\%)$ and $k(2\%)$ are second order rate constants for the 1 and 2% mixtures, measured over the same fractional extent of decomposition

Can. J. Chem. Downloaded from www.nrcresearchpress.com by 210.87.254.42 on 09/05/12
For personal use only.

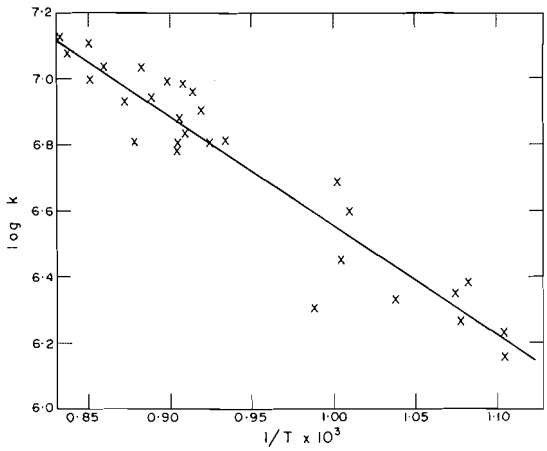

FIG. 7. Arrhenius plot of the overall rate constant (second order) for decomposition of diazomethane (1% CH_2N_2 in 99% Kr). k in l mole s units.

of diazomethane at the same initial temperature after shock reflection. k is then the overall rate constant for the decomposition of diazomethane in very dilute krypton. (The significance of k is further explained below.) The derivation of the expression for k assumes that the processes which remove diazomethane before arrival of the shock wave are approximately first order in diazomethane (this was checked experimentally), so that the pre-shock concentrations in the two mixtures remain in the ratio of about 1:2. Note, incidentally, that the extrapolation from the measured rates to k is in any case quite small. k usually differs from $k(1\%)$ by less than 30%.

In this way, we found $k = 10^{9.91} \exp(-15\,800/RT)$ cm^3 mole^{-1} s^{-1}. This can be interpreted as a rate constant for the decomposition of diazomethane which has been sufficiently diluted with krypton for the effects of exothermicity and of energizing collisions other than those between diazomethane and krypton to have been eliminated. However, the effects of secondary reactions, which also consume diazomethane, have not yet been removed. Since k_2 is approximately equal to the collision number (12), k_1' is very much smaller than k_2 in all of our experiments, and therefore the unimolecular rate is one half of the total rate of destruction of diazomethane. (Primed symbols refer to second order rate parameters of unimolecular reactions.) The effects of secondary reactions could, therefore, have been eliminated by multiplying $k(1\%)$ and $k(2\%)$ by $\frac{1}{2}$ before calculating k. However, the factor of $\frac{1}{2}$ can just as well be applied to k now, to give

$$k_1'_{,Kr} = 10^{9.61 \pm 0.21} \exp(-15\,800 \pm 1\,000/RT) \text{ cm}^3 \text{ mole}^{-1} \text{ s}^{-1}$$

as the second order rate constant for the unimolecular decomposition of diazomethane to CH_2 and N_2 with krypton as the only collision partner. The quoted uncertainties are derived from the standard deviations of the experimental data.

Addition of 9% N_2 did not change the observed rates significantly. We conclude that the collision efficiency of N_2 in the energization of diazomethane is most probably not more than 10 times that of Kr. Higher percentages of N_2 were not used, as otherwise seriously non-ideal behavior of the reflected shock waves might have occurred (19).

Our results can also yield information about the rates of reaction 6. Assuming that C_2H_4, C_2H_2, and HCN are formed entirely via reactions 1, 2, 3, 4, and 6, and provided that there is no major alternative path for the removal of CH_2 and C_2H_4, the quotient (HCN formed)/(C_2H_4 formed + C_2H_2 formed) = k_6'/k_1'. The results are represented as an Arrhenius plot in Fig. 8. From the graph, we find $E_6' - E_1' = 10.8$ kcal mole^{-1} and $A_6'/A_1' = 40$. These figures are tentative, because of the possibility that HCN is formed by another mechanism, as discussed later.

Our experimentally observed Arrhenius activation energy for the unimolecular decomposition to CH_2 and N_2 is much lower than that observed by other workers at lower temperatures. The lowness of this value confirms our supposition that the reaction was far into the second order

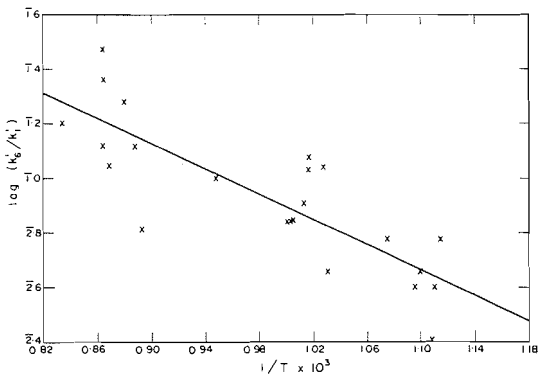

FIG. 8. Arrhenius plot of k_6'/k_1'.

Can. J. Chem. Downloaded from www.nrcresearchpress.com by 210.87.254.42 on 09/05/12
For personal use only.

Can. J. Chem. Downloaded from www.nrcresearchpress.com by 210.87.254.42 on 09/05/12
For personal use only.

region. Second order kinetics are in any case to be expected, since the reaction has been found (5) to be already in the fall-off region at comparable pressures and very much lower temperatures. (For technical reasons, the pressure could not be varied enough in our experiments to make a direct test of the second order dependence.) In considering such an activation energy, a standard procedure is to compare the results with the classical Kassel expression (20) for the low pressure second order rate constant of a unimolecular reaction

$$[14] \quad k = \lambda Z/(s-1)! \times (E^*/RT)^{s-1} \exp(-E^*/RT)$$

or when the inequality $E^* \gg (s-1)RT$ does not hold

$$[14a] \quad k = \lambda Z \sum_{r=0}^{s-1} (1/r!)(E^*/RT)^r \times \exp(-E^*/RT)$$

λ is a collision efficiency factor, Z is the collision number, and s is one half of the number of square terms contributing to the decomposition. E^* is the minimum energy required for dissociation, and is generally considered to be equal to the limiting high pressure Arrhenius activation energy, which is about 34 kcal mole^{-1} for diazomethane (4–6). To account for our experimental energy of activation of about 16 kcal mole^{-1}, we require $s \simeq 10$. This implies that at the temperature of our experiments, all of the internal degrees of freedom contribute to the dissociation.

The largeness of our value of s is surprising. Normally, s is closer to one half of the number of vibrational modes, and Johnson and Setser (21) have emphasized that there are good theoretical grounds to expect this, even at temperatures of 1000 °K or greater. Nevertheless, there are a number of cases in the literature where s has been found to be approximately equal to the total number of vibrational degrees of freedom (22–27). There is as yet no accepted explanation for these abnormally high values of s. Gutman *et al.* (27) have suggested that the behavior may be due to extensive departure from thermal equilibrium among molecules having less than the minimum critical energy and that this would lead to similar behavior for CO_2 at 5000 °K and for N_2O at 2500 °K, since their minimum critical energies for decomposition are respectively 125 and 60 kcal mole^{-1}. A simple extension of this argument to diazomethane would suggest that abnormally low values of s are to be expected at least as low as 1300 °K, since the minimum critical energy for decomposition is approximately 34 kcal mole^{-1}. However, because of the greater molecular complexity of CH_2N_2, it is not certain that this argument, even if valid for CO_2 and N_2O, can actually be extended in this manner.

It is of course possible that the assumed reaction mechanism is wrong and that under our conditions a chain mechanism is operative. However, we have been unable to propose a chain mechanism which satisfactorily accounts for both the reaction products and the observed kinetics. In particular, the complete absence of CH_4 is difficult to explain in this way. A further important point is that the measured rate constants are demonstrably lower than the values obtained by extrapolation of the low temperature results (see Fig. 9); an alternative mechanism would be kinetically preferred at higher tem-

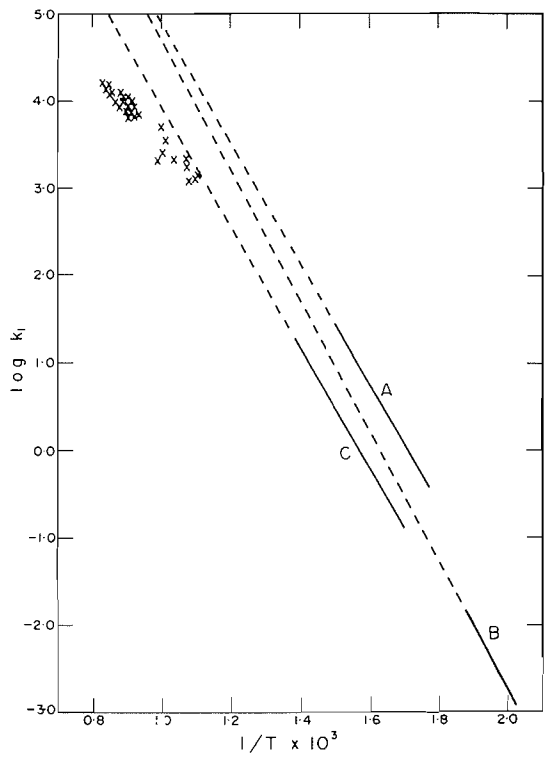

FIG. 9. Arrhenius plot of first order rate constant (k_1). ×, experimental results for 2% CH_2N_2; *A*, Dunning and McCain, ref. 6; *B*, Setser and Rabinovitch, ref. 5; *C*, Shantarovich, ref. 4. Dashed lines are extrapolations.

Can. J. Chem. Downloaded from www.nrcresearchpress.com by 210.87.254.42 on 09/05/12
For personal use only.

peratures only if it resulted in an increased rate of decomposition.

If, as we suggest, diazomethane can decompose by both reactions 1 and 6, we would expect the Arrhenius plots to be curved since $E_6' - E_1' = 10.8$ kcal mole^{-1}. Only in the case of the 2% mixture (Fig. 6) is there any evidence of curvature. However, the expected effects are small and within experimental error: correction of the results for reaction 6 leads to a decrease of 1 to 1.5 kcal mole^{-1} for E_1', and this change does not materially affect the above discussion.

Origin of the CH_2^+ Ion

The CH_2^+ ion which was observed in our mass spectra could arise by direct ionization of CH_2, or from fragmentation (28) of $CH_2N_2^+$. Considering these two alternatives, we note first that in our experiments peaks 14 and 42 disappeared simultaneously (Fig. 10). The results are rather scattered, but the trend is evident. (The intercept on the ordinate is probably due to some formation of C_3H_6 in the later stages, by reaction 7.) The average ratio of peak heights of 14 to 42 was about 0.25 at 850 °K and about 0.3 at 1100 °K. Since we found a corresponding ratio of only 0.05 in static measurements of the mass spectrum of diazomethane, this appears at first sight to show that substantial amounts of the methylene radical were being detected in our shock wave experiments. Nevertheless we believe that even at high temperatures the main contribution to mass 14 came in fact not from methylene but from fragmentation of the diazomethane parent ion. The difference between the static spectrum (where the diazomethane was taken from a room temperature source) and the shock wave spectra apparently arises from a temperature effect on the fragmentation pattern. Our reasons for this conclusion are as follows.

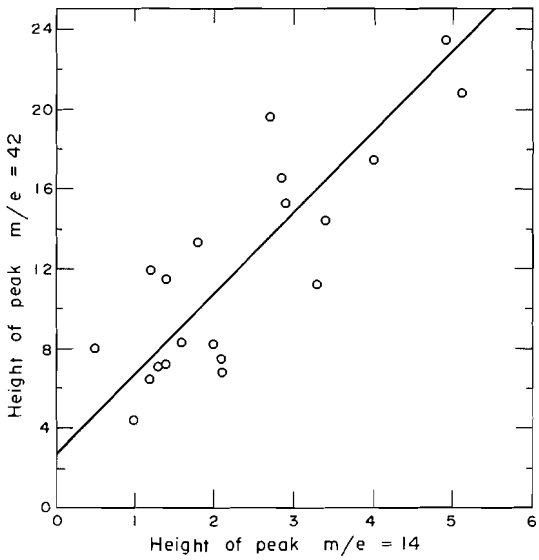

FIG. 10. Variation of peak $m/e = 14$ with peak $m/e = 42$ (peak heights in arbitrary units) during a single experiment.

Because reaction 2 is so fast (12), a stationary state in CH_2 radicals will be established very early in the reaction. Then $CH_2 = k_1/k_2$ and should thereafter remain constant throughout a given reaction; hence, the observed time dependence of the height of the 14 peak indicates that CH_2 is not the main source. Consideration of the temperature dependence of the relative heights of the 14 and 42 peaks leads to the same conclusion. Using our experimental activation energy for reaction 1 of 16 kcal mole^{-1}, we calculate that in our experiments the concentration of methylene radicals at the upper end of the temperature range should be about 10 times that at the lower end. As noted above, the ratio of 14 to 42 does increase slightly with temperature, but certainly not by a factor of 10. A possible complication is that the temperature dependence of the methylene concentration might, in principle, be reduced by the occurrence of the recombination reaction

$$[2a] \qquad 2CH_2 \rightarrow C_2H_4$$

However, calculations show that because reaction 2 is so fast, the effect of reaction 2*a* will be negligible in our experiments. The same calculations indicate that the methylene concentration probably never exceeds 1% of the initial concentration of diazomethane, giving further evidence that large peaks at mass 14 cannot be due primarily to methylene.

In this connection, we note that Berkowitz and Wexler (29) were unable to detect CH_2^+ from CH_2 formed in the pyrolysis of diazomethane, although they were able to identify CH_3 as a source of CH_3^+ when they pyrolyzed dimethyl mercury under the same conditions.

In our experiments, the sampled gas was expanded extremely rapidly from conditions of high temperature and high pressure into a vacuum. It is known that in such an expansion the number of collisions suffered by each molecule is quite small, and that the molecules tend to

Can. J. Chem. Downloaded from www.nrcresearchpress.com by 210.87.254.42 on 09/05/12
For personal use only.

retain most of their initial vibrational energy and even some of their rotational energy (30, 31). It appears that the diazomethane molecules were still sufficiently highly vibrationally excited when they reached the electron beam of the mass spectrometer for the fragmentation pattern of the resultant ions to be influenced. We have observed a similar effect in several other molecules, and this topic is currently under further investigation in our laboratory.

Kinetics of Formation of Acetylene

We now discuss the origin of the acetylene which we found in the reaction products. The heats of formation of methylene, diazomethane, and ethylene are taken to be 92 (32–35), 71 (5, 36, 37), and 9.2 kcal mole^{-1}, respectively, so that reaction 2 is approximately 154 kcal mole^{-1} exothermic. The heats of formation of diazomethane and methylene have been the subject of much discussion, but the values given are probably not in error by more than a few kcal. The large exothermicity of reaction 2 makes it likely that the ethylene will be formed in a highly excited vibrational state, since it is now established that in many cases a large fraction of the heat of reaction is retained as vibrational energy of the bond being formed. The vibrationally excited ethylene may decompose by reaction 3.

[3] $$C_2H_4^* \rightarrow C_2H_2 + H_2$$

Kistiakowsky and co-workers (38) have measured an activation energy of 50.5 kcal mole^{-1} for the thermal decomposition of ethylene, but the reaction mechanism was not definitely established; if the reaction is unimolecular, then the measurements were made in the fall-off region. Using literature values for the rate constant of reaction 3*a*,

[3*a*] $$C_2H_2 + H_2 \rightarrow C_2H_4$$

they estimated that the activation energy (minimum critical energy) for the unimolecular decomposition of ethylene into acetylene and hydrogen to be 77 kcal mole^{-1}. In agreement with this, a value of approximately 80 kcal mole^{-1} has recently been obtained by an analysis of data available in the literature on the nonequilibrium decomposition of ethylene (39). Thus, it seems likely the $C_2H_4^*$ formed in reaction 2 will have sufficient internal energy for reaction 3 to occur. This can account for the presence of a product peak at mass 26 ($C_2H_2^+$). The excited ethylene

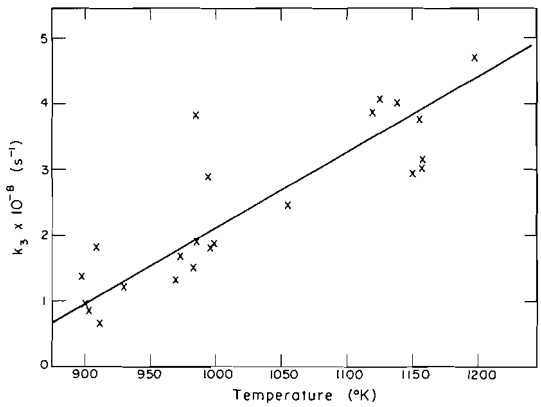

FIG. 11. Dependence of k_3 on temperature.

may also be de-energized by collision

[4] $$C_2H_4^* + M \rightarrow C_2H_4 + M$$

If all of the ethylene molecules formed in reaction 2 subsequently react by reactions 3 or 4, $k_3/k_4 =$ [M] × (acetylene produced)/(ethylene produced). The values of k_3 calculated from this equation on the assumption of unit collision efficiency in reaction 4 and using a mean collision diameter of 4.5 Å are plotted as a function of temperature in Fig. 11.

In order to investigate further the possibility that the acetylene in the reaction products was formed in reaction 3, we have made calculations of the rate of decomposition of vibrationally excited ethylene. According to the Rice–Ramsperger–Kassel–Marcus quantum-statistical theory of unimolecular reactions (40, 41), the specific rate of decomposition of critically energized molecules is given by

[15] $$k(E) = \frac{1}{h}\frac{Z^+}{Z}\frac{\sum P(E^+)}{N(E)}$$

If E_0 is the minimum energy required for decomposition, then $E^+ = E - E_0$. $N(E)$ is the density of energy states for the active degrees of freedom of the molecule at energy E, and $\sum P(E^+)$ is the sum of the degeneracies of all accessible energy states of the activated complex at energy E^+. Z^+ and Z are the products of the partition function for the adiabatic degrees of freedom of the activated complex and the molecule, respectively, and h is Planck's constant. Whitten and Rabinovitch (42) have shown that $N(E)$ and $P(E)$ may be closely approximated by the expressions

$$[16] \quad N(E) = (E + aE_Z)^{s-1}/\Gamma(s) \prod^{s} h\nu_i$$

$$[17] \quad \sum^{E} P(E) = (E + aE_Z)^{s}/\Gamma(s+1) \prod^{s} h\nu_i$$

where E_Z is the zero point energy, s the number of vibrational modes of frequency ν_i (where $i = 1$ to s) among which the vibrational energy is distributed, and a is an empirical correction factor given by

$$[18] \quad a = 1 - \frac{s-1}{s} \frac{\langle \nu^2 \rangle}{\langle \nu \rangle^2} \omega$$

Values of ω as a function of E/E_Z, obtained by matching the approximate summation with the computer-evaluated exact sums of harmonic vibrational-energy-level densities for 45 different molecules, are given in ref. 42 and are used in our calculation.

In evaluating $k(E)$ for the decomposition of ethylene to form acetylene and hydrogen we have assumed that the only adiabatic degrees of freedom are the overall rotations and that $Z^+/Z = 1$. We have used two different models: in model I the vibrational mode at 995 cm^{-1} has been equated to the reaction co-ordinate and the remaining frequencies assumed to be the same as for the ethylene molecule; in model II the C—H stretching frequencies ν_5, ν_9, and ν_{11} were lowered by 500 cm^{-1} and the C—C stretch and CH_2 deformation frequencies, ν_2 and ν_3, were increased by 200 cm^{-1}, the other properties of the model being the same as model I. The fundamental vibration frequencies for ethylene (43) are 3019, 1623, 1342, 825, 3272, 1050, 949, 943, 3106, 995, 2990, and 1444 cm^{-1}.

From Fig. 11, $k_3 = 2.6 \times 10^8$ s^{-1} at the middle of our temperature range (1020 °K). If we make the crude assumption that the C_2H_4* molecules formed in reaction 2 are monoenergetic we can estimate their vibrational energy, E, by matching the experimental value of k_3 with the value calculated from equation 15. Setting $E_0 =$ 77 kcal $mole^{-1}$, model I gives $E = 84$ kcal $mole^{-1}$, and model II gives $E = 86$ kcal $mole^{-1}$. Estimating the thermal vibrational energy of ethylene at 1020 °K to be 7.1 kcal $mole^{-1}$, and using 86 kcal $mole^{-1}$ for E (since model II is probably more realistic), it follows that 78.9 kcal $mole^{-1}$ or 51% of the exothermicity of reaction 2 is released as vibrational energy of the product ethylene.

Kirk and Tschuikow-Roux (39) have recently reexamined the available data for the relative rates of stabilization and decomposition of excited ethylene as a function of internal energy. From their graph we calculate that for $E = 86$ kcal $mole^{-1}$, and under our experimental conditions, the ratio (acetylene formed):(ethylene formed) is 0.10 in comparison with our experimental value of 0.60. However, the values of k_3 are based on the assumption of unit collision efficiency for krypton. Internal consistency of the calculated (model II) and experimental rate constant and the product ratio calculated from ref. 39 can be achieved by setting the collision efficiency of krypton equal to 0.1. The corresponding value of E is 80 kcal $mole^{-1}$. We do not consider those figures particularly significant in view of the arbitrary nature of the activated complex model and the inherent uncertainties in k_3 and in the graph by Kirk and Tschuikow-Roux. Furthermore, the ethylene molecules formed in reaction 2 are certainly not monoenergetic, but will have an (unknown) energy distribution arising from the energy distribution of the reactant molecules and the partitioning of the exothermicity among the products. However, using the value 154 kcal for the exothermicity of reaction 2, and noting that the calculated value of E is not very sensitive to the model used, we feel that we are justified in concluding that 50 ± 10% of this exothermicity goes into vibration. This value may be compared with recent results for the reaction $HI + CH_2N_2 \rightarrow CH_3I + N_2$. Hassler and Setser (37) find that the CH_3I contains 58 ± 2 kcal $mole^{-1}$ in the active degrees of freedom. This corresponds to approximately 70% of the heat of reaction if the value of 71 kcal $mole^{-1}$ is used for $\Delta H_f(CH_2N_2)$.

Acetylene has seldom been reported as a product of diazomethane decomposition at lower temperatures, but it has occasionally been detected in both thermal (4, 6) and photolytic (18) experiments. The absence or low incidence of acetylene under those conditions does not necessarily invalidate our proposed reaction mechanism, since k_3 is temperature dependent. Calculation of the temperature dependence of k_3 is complicated by the fact that there seems to be no way to determine *a priori* precisely how E, the vibrational energy of the C_2H_4* formed in reaction 2, will depend on temperature. By setting the temperature variation of E equal to

Can. J. Chem. Downloaded from www.nrcresearchpress.com by 210.87.254.42 on 09/05/12
For personal use only.

TABLE 1

Comparison of experimental and calculated rate constants for the reaction $C_2H_4^* \rightarrow C_2H_2 + H_2$

Temperature (°K)	k_3(experimental) $\times 10^{-8}$ (s^{-1})	k_3(calcd.) $\times 10^{-8}$ (s^{-1})	
		Model I	Model II
300	—	0.00	0.13
500	—	0.14	0.21
880	0.9	1.2	1.2
1020	2.6	2.6	2.6
1160	4.3	4.8	5.2

the temperature variation of the thermal equilibrium vibrational energy of ethylene and making use of the value of E deduced above for 1020 °K, the rate constants in Table 1 were calculated. In view of the gross assumptions involved, we regard the close agreement of the calculated and experimental dependences of k_3 on temperature as somewhat fortuitous. At lower temperatures, as E approaches the minimum critical energy, E_0, the calculated value of k_3 depends more strongly on the model used. On the basis of model II, the ratio (acetylene formed):(ethylene formed) at a total pressure of 50 Torr is 0.08 at 500 °K and 0.06 at 300 °K; model I predicts 0.05 at 500 °K and 0.00 at 300 °K. Earlier in this section we noted a possibility that the efficiency of krypton in collisional deactivation is as low as 0.1, in which case $E = 80$ kcal mole^{-1} at 1020 °K and it follows that $E \leqslant E_0$ for $T \leqslant 800$ °K and the ethylene would not have sufficient energy spontaneously to decompose into hydrogen and acetylene below this temperature. The calculations are inconclusive from a quantitative standpoint, but do demonstrate that the formation of acetylene at high temperatures and its absence at low temperatures can be reasonably explained.

Mechanism of Formation of Hydrogen Cyanide

The heats of formation of NH and HCN are taken to be 79 and 31 kcal mole^{-1}, respectively. Hence, reaction 6 is 38 kcal mole^{-1} endothermic, and our value of $E_6' \simeq 27$ kcal mole^{-1} is reasonable if the reaction is in fact in the second order region. NH radicals are much less reactive than CH_2 (44) and may eventually be removed via

[19] $$2NH \rightarrow N_2 + H_2$$

However, NH is isoelectronic with CH_2, so that reaction 20, the analogue of reaction 2, may occur, the methyleneimine formed then decomposes to form more HCN

[20] $$NH + CH_2N_2 \rightarrow CH_2NH + N_2$$

[21] $$CH_2NH \rightarrow HCN + H_2$$

Reaction 21 is in some ways comparable to the formation of CH_3CN, through ethyleneimine as intermediate, when NH reacts with C_2H_4 (44).

Hydrogen cyanide has been detected as a product when CH_2N_2 is decomposed in the presence of H_2 (6). Its formation was attributed to the reaction sequence

[22] $$CH_3 + CH_2N_2 \rightarrow CHN_2 + CH_4$$

[23] $$2CHN_2 \rightarrow 2HCN + N_2$$

As already noted, CH_4 was not detected in the present work, but CHN_2 could be formed by reaction 9. However, it is probable that CHN_2 would undergo rapid unimolecular decomposition, *viz.*

[24] $$CHN_2 \rightarrow CH + N_2$$

and reaction 23 is unlikely to be the main source of the quite large amounts of hydrogen cyanide produced.

Moore and Pimentel (45) have shown that photolysis of diazomethane in solid nitrogen produces CH_2NH and HCN. They suggest that the highly polar CH_2N_2 molecules have a head to tail orientation and that the CH_2 produced in the primary photolytic act attacks the N—N bond of an adjacent CH_2N_2 molecule

[25] $$CH_2 + CH_2N_2 \rightarrow \begin{matrix} H \\ \diagdown \\ C{=}\overset{+}{N}{-}\overset{-}{N} \\ \diagup \quad\quad \diagdown \\ H \quad\quad C \\ \quad\quad\quad H_2 \end{matrix} \rightarrow CH_2{=}NH + HCN$$

It is possible that the same reaction could be important in the gas phase.

Our results do not permit a definite choice between the several suggested mechanisms.

Can. J. Chem. Downloaded from www.nrcresearchpress.com by 210.87.254.42 on 09/05/12
For personal use only.

However, the production of HCN has an apparent activation energy of 27 kcal mole^{-1}. This would imply that reactions 9 and 25 together are < 0.01 times as fast as reaction 2 which has approximately unit collision efficiency. Hence, the observed proportion of HCN is an order of magnitude greater than can be explained by reactions 9 and 25, and to this extent our results support the hypothesis that diazomethane can decompose by reaction 6 as well as by reaction 1.

This work was supported by the National Research Council of Canada. We are grateful to Dr. L. C. Leitch for advice about the preparation of deuterated diazomethane.

1. W. B. DeMore and S. W. Benson. Advan. Photochem. **2**, 219 (1964).
2. E. W. R. Steacie. J. Phys. Chem. **35**, 1493 (1931).
3. F. O. Rice and A. Glasebrook. J. Amer. Chem. Soc. **56**, 2381 (1934).
4. P. S. Shantarovich. Dokl. Akad. Nauk. SSSR, **116**, 255 (1957).
5. D. W. Setser and B. S. Rabinovitch. Can. J. Chem. **40**, 1425 (1962).
6. W. J. Dunning and C. C. McCain. J. Chem. Soc. B, 119 (1966).
7. N. B. Slater. Theory of unimolecular reactions. Cornell University Press, Ithaca, New York. 1959. p. 162.
8. S. C. Barton and J. E. Dove. Can. J. Chem. **47**, 521 (1969).
9. C. D. Johnson and D. Britton. J. Chem. Phys. **38**, 1455 (1963).
10. C. B. Moore and G. C. Pimentel. J. Chem. Phys. **40**, 342 (1964).
11. B. J. McBride, S. Heimel, J. G. Ehlers, and S. Gordon. Thermodynamic properties to 6000 °K for 210 substances involving the first 18 elements. NASA SP-3001. National Aeronautics and Space Administration, Washington, D.C. 1963.
12. G. Herzberg and J. Shoosmith. Nature, **183**, 1801 (1959).
13. A. G. Harrison and F. P. Lossing. J. Amer. Chem. Soc. **82**, 519 (1960).
14. W. J. Felmlee, R. V. Petrella, and R. W. Diesen. Technical Report SL 175311a. The Dow Chemical Company, Midland, Michigan. 1966.
15. A. B. Callear and R. J. Cvetanović. J. Chem. Phys. **24**, 873 (1955).
16. M. L. Halberstadt and J. R. McNesby. J. Chem. Phys. **45**, 1666 (1966).
17. G. Herzberg and D. N. Travis. Can. J. Phys. **42**, 1658 (1964).
18. H. M. Frey. J. Amer. Chem. Soc. **82**, 5947 (1960).
19. H. Mark. NACA TM 1418. The National Advisory Committee for Aeronautics, Washington, D.C. 1958.
20. N. B. Slater. Theory of unimolecular reactions. Cornell University Press, Ithaca, New York. 1959. Chap. 2.
21. R. L. Johnson and D. W. Setser. J. Phys. Chem. **71**, 4366 (1967).
22. W. Tsang, S. H. Bauer, and M. Cowperthwaite. J. Chem. Phys. **36**, 1768 (1962).
23. R. W. Diesen. J. Chem. Phys. **39**, 2121 (1963).
24. W. O. Davies. J. Chem. Phys. **41**, 1846 (1964).
25. A. P. Modica and J. E. LaGraff. J. Chem. Phys. **43**, 3383 (1965).
26. A. P. Modica. J. Chem. Phys. **44**, 1585 (1966).
27. D. Gutman, R. L. Belford, A. J. Hay, and R. Pancirov. J. Phys. Chem. **70**, 1793 (1966).
28. G. S. Paulett and R. Ettinger. J. Chem. Phys. **39**, 825 (1963).
29. J. Berkowitz and S. Wexler. J. Chem. Phys. **37**, 1476 (1962).
30. J. B. Anderson, R. P. Andres, J. B. Fenn, and G. Maise. Proceedings of the 4th International Symposium on Rarefied Gas Dynamics, Toronto, July 1964. Vol. II. *Edited by* J. H. de Leeuw. Academic Press, Inc., New York. 1966. p, 106.
31. P. V. Marrone. Phys. Fluids, **10**, 521 (1967). (Earlier references there).
32. W. A. Chupka, J. Berkowitz, D. J. Meschi, and H. A. Tasman. Advan. Mass Spectrom. Proc. Conf. 2nd, Oxford, 1961. Macmillan Co., New York. 1963. p. 99.
33. H. Prophet. J. Chem. Phys. **38**, 2345 (1963).
34. V. H. Dibeler, M. Krauss, R. M. Reese, and F. N. Harllee. J. Chem. Phys. **42**, 3791 (1965).
35. W. A. Chupka and C. Lifshitz. J. Chem. Phys. **48**, 1109 (1968).
36. J. A. Bell. J. Chem. Phys. **41**, 2556 (1964).
37. J. C. Hassler and D. W. Setser. J. Amer. Chem. Soc. **87**, 3793 (1965).
38. I. D. Gay, R. D. Kern, G. B. Kistiakowsky, and H. Niki. J. Chem. Phys. **45**, 2371 (1966).
39. A. W. Kirk and E. Tschuikow-Roux. J. Chem. Phys. **51**, 2247 (1969).
40. R. A. Marcus and O. K. Rice. J. Phys. Colloid. Chem. **55**, 894 (1951).
41. R. A. Marcus. J. Chem. Phys. **20**, 359 (1952).
42. G. Z. Whitten and B. S. Rabinovitch. J. Chem. Phys. **38**, 2466 (1963).
43. G. Herzberg. Molecular spectra and molecular structure. II. Infrared and Raman spectra of polyatomic molecules. 2nd. ed. D. Van Nostrand Co. Inc., Princeton, New Jersey. 1950.
44. D. W. Cornell, R. S. Berry, and W. Lwowski. J. Amer. Chem. Soc. **88**, 544 (1966).
45. C. B. Moore and G. C. Pimentel. J. Chem. Phys. **43**, 63 (1965).

Can. J. Chem. Downloaded from www.nrcresearchpress.com by 210.87.254.42 on 09/05/12
For personal use only.

Can. J. Chem. Downloaded from www.nrcresearchpress.com by 210.87.254.6 on 09/05/12
For personal use only.

Spectra of cobalt(II) and nickel(II) in molten lead, stannous, and bismuth chlorides

K. W. FUNG AND K. E. JOHNSON
Department of Chemistry, University of Saskatchewan, Regina, Saskatchewan

Received March 12, 1970

From measurements of electronic spectra it is deduced that cobalt(II) is tetrahedrally coordinated in molten $PbCl_2$, $SnCl_2$, and $BiCl_3$, whereas nickel(II) adopts a coordination in $PbCl_2$ and $SnCl_2$ which is close to octahedral. $NiCl_2$ is insoluble in $BiCl_3$ and is formed by the reaction of NiS and $BiCl_3$ whereas CoS is soluble in $BiCl_3$. Solutions of Pd(II), Pt(II), Rh(III), and Ir(III) may be prepared in molten $PbCl_2$ but the spectra do not assist in assigning the coordination of the solute ions.

Canadian Journal of Chemistry, 48, 3635 (1970)

The spectra of cobalt(II) and nickel(II) have been studied in a wide variety of molten salts (1) ranging from alkali halides (2) through mixtures such as $CsCl–ZnCl_2$ (3) to oxyanion systems (4). Of the post-transition metal halides $PbCl_2$, $SnCl_2$, and $BiCl_3$ have received little attention as solvents for coordination studies although their structural properties have been examined. It so happens that all three solvents have considerable ionic character as demonstrated by the specific conductances but they are quite viscous (5) (*cf.* Table 1). Raman spectral data suggested that molten $PbCl_2$ (6) and $SnCl_2$ (7) did not contain simple units such as MCl_3^- or MCl_4^{2-} but rather were polymeric like the solids where the metal ions occupy apical positions in chains of trigonal pyramids (8, 9). These solvents were also of interest because of the possibility of forming heterometallic bonds as in $Pt(SnCl_3)_5^{3-}$ (10).

Experimental

Solvent Preparation

Lead Chloride

The Reagent grade salt was recrystallized from hot water, dried *in vacuo* at 120 °C for 2 days and further purified by HCl treatment (11).

TABLE 1

Conductance and viscosity of molten $PbCl_2$, $SnCl_2$, and $BiCl_3$ calculated from ref. 5

Salt	Temperature (°C)	Specific conductance (ohm^{-1} cm^{-1})	Viscosity (cP)
$PbCl_2$	532	6.001	3.87
$SnCl_2$	300	1.107	7.00 (7)
$BiCl_3$	270	0.446	29.41
KCl (Ionic)	787	2.203	1.15
$HgCl_2$ (Covalent)	289	3.534×10^{-5}	1.75

Stannous Chloride

The dihydrate was treated with acetic anhydride (12) and the crude anhydrous salt heated in an atmosphere of HCl to the melting point. HCl was passed through the melt for 3 h and then displaced by passing dry nitrogen for 4 h, after which the liquid was filtered through a glass frit, allowed to freeze and stored *in vacuo*.

Bismuth Chloride

The Reagent grade salt was dried in a current of HCl and distilled in first HCl and then dry nitrogen (13).

Preparation of Solutions

Concentrated solutions of *cobalt chloride* in $PbCl_2$, $SnCl_2$, and $BiCl_3$ and of *nickel chloride* in $PbCl_2$ and $SnCl_2$ were made by mixing known quantities of solvent and anhydrous solute (12), melting, and stirring by bubbling dry nitrogen. *Cobalt sulfide* prepared from cobalt chloride solution and H_2S and dried for two days at 200 °C, was added to molten $BiCl_3$ and the mixture filtered through a glass frit; the cobalt(II) concentration in the filtrate was determined colorimetrically (14). *Nickel sulfide* was prepared from nickel chloride solution and H_2S and also dried for two days at 200 °C.

Concentrated solutions of *platinum(II)*, *palladium(II)*, *iridium(III)*, and *rhodium(III)* in molten lead chloride were prepared by anodizing the given metal in a fritted compartment, a Sargent Model IV coulometric current source being employed.

Spectroscopic Measurements

Samples were prepared by mixing pure solvent and concentrated solution and were sealed under nitrogen in 1 cm^2 cross-section silica cells. The volumes of the solutions in the cells were obtained from their weights by assuming that the densities of the pure solvents and the solutions were identical (5).

Electronic spectra of melts were obtained with a Cary 14H spectrophotometer using a furnace described previously (15) and the absorption curves of the solutions and solvents were measured. The spectra were analyzed into Gaussian components by the method of Chatt *et al.* (16) using an IBM 360/50 computer.

Infrared spectra were recorded on a Beckman I.R. 12, the samples being prepared as KBr pellets which were dried *in vacuo* at 120° for two days.

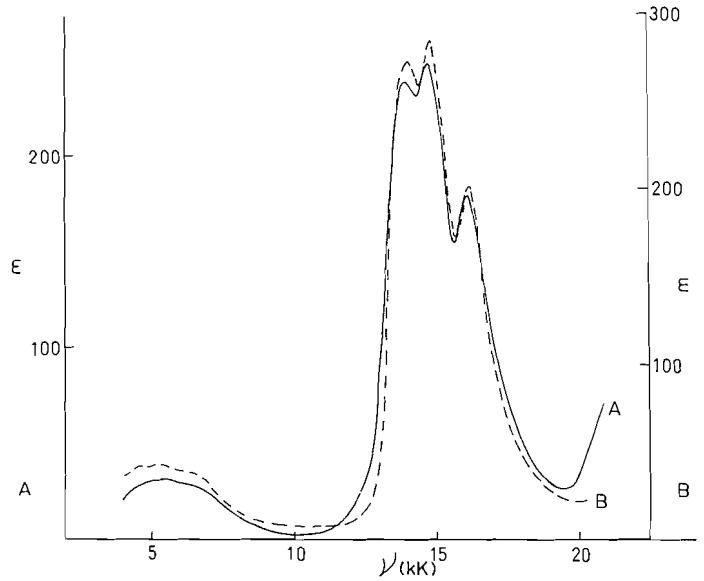

FIG. 1. Spectra of $CoCl_2$ in *A*, $PbCl_2$ at 532 °C and *B*, $SnCl_2$ at 300 °C.

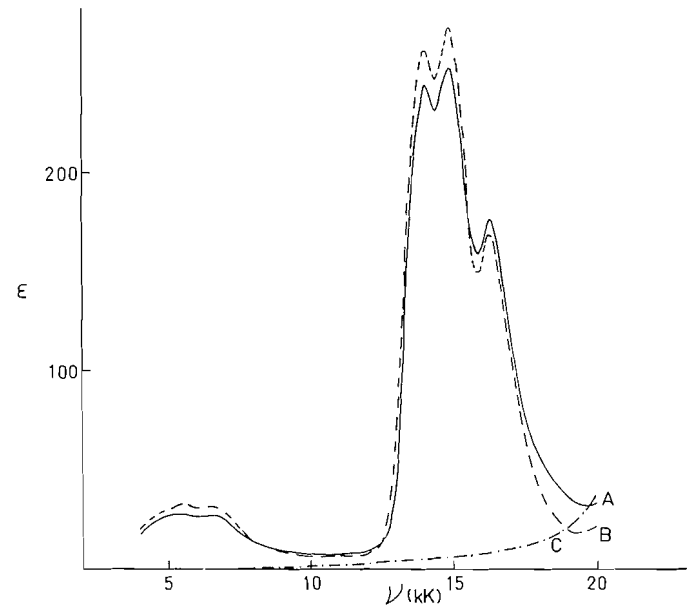

FIG. 2. Spectra of *A*, $CoCl_2$; *B*, CoS; and *C*, Bi_2S_3 in $BiCl_3$ at 270 °C.

Results

Figures 1 and 2 show the complete spectra of cobalt(II) in molten $PbCl_2$, $SnCl_2$, and $BiCl_3$ and Figs. 3, 4, and 5 show the visible spectrum of $CoCl_2$ in molten $SnCl_2$ and the spectra of $NiCl_2$ in molten $PbCl_2$ and $SnCl_2$. Gaussian components are included in the last three figures. Table 2 gives details of band positions (ν), molar absorptivities (ε), oscillator strengths (*f*), and the ligand field parameters (Δ, *B*, *C*, and β).

$NiCl_2$ was found to be insoluble in molten $BiCl_3$: even after filtering a molten mixture of the two, no nickel(II) was detectable in the filtrate. Whereas cobalt wire reacted with molten

Can. J. Chem. Downloaded from www.nrcresearchpress.com by 210.87.254.6 on 09/05/12
For personal use only.

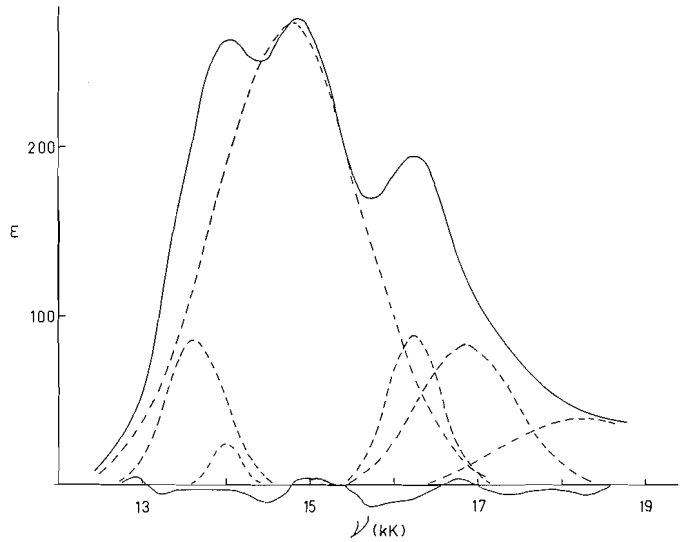

FIG. 3. Visible spectrum of $CoCl_2$ in $SnCl_2$ with Gaussian components (bottom solid line is the residual).

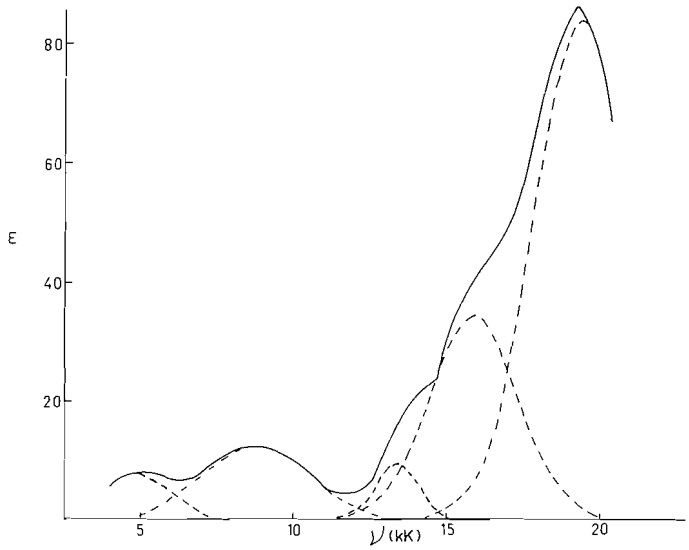

FIG. 4. Spectrum of $NiCl_2$ in $PbCl_2$ at 532 °C with Gaussian components.

$BiCl_3$ to form a violet solution of cobalt(II) and bismuth, nickel wire merely underwent a surface reaction, itself becoming darkened, while some bismuth was produced leading to a brown coloration of the melt; again no nickel(II) was found in the solution.

Since cobalt and nickel occur naturally as the sulfides, the solubility of CoS and NiS in molten $BiCl_3$ was investigated. CoS dissolved to give a green solution which froze to a green solid (*cf.* the blue solid from $CoCl_2$ and $BiCl_3$). NiS reacted with molten $BiCl_3$ to form insoluble $NiCl_2$ and a brown solution of Bi_2S_3 in $BiCl_3$; the filtrate from this mixture contained no Ni(II). The spectrum of CoS in $BiCl_3$ and 1/3 Bi_2S_3 in $BiCl_3$ are included in Fig. 2. The addition of $CoCl_2$ to the brown Bi_2S_3 solution turned it green and the addition of increasing amounts (up to 12 sulfide equivalents) of Bi_2S_3 to the CoS solution increased the intensity of the visible

Can. J. Chem. Downloaded from www.nrcresearchpress.com by 210.87.254.6 on 09/05/12
For personal use only.

Can. J. Chem. Downloaded from www.nrcresearchpress.com by 210.87.254.6 on 09/05/12
For personal use only.

TABLE 2

Spectral data for cobalt(II) and nickel(II)

System	Temperature (°C)	(kK) Found	(kK) Calcd.	ε	$f \times 10^4$	Assignment	Δ (cm^{-1})	B (cm^{-1})	C (cm^{-1})	β	Symmetry
$CoCl_2$ in $PbCl_2$	532	17.47	—	62.3	6.87	$^4A_1 \rightarrow {}^2H$	3300	695	2400	0.715	T_d
		16.54	—	71.0	3.39	$\rightarrow {}^2A_1(G)$					
		16.06	—	47.6	1.18	$\rightarrow {}^2T_2(G)$					
		14.62	Fitted	247	25.1	$\rightarrow {}^4T_1(P)$					
		13.92		20.5	0.36	${}^2E(G)$					
		13.51	Fitted	86.0	2.78	$\rightarrow {}^2T_1(G)$					
		12.90		24.4	0.77						
		5.76	Fitted	30.8	5.02	$\rightarrow {}^4T_1(F)$					
		3.46*	3.31	—	—	$\rightarrow {}^4T_2(F)$					
$CoCl_2$ in $SnCl_2$	300	18.13	—	42.2	3.66	$^4A_1 \rightarrow {}^2H$	3400	695	2500	0.715	T_d
		16.80	—	86.2	5.15	${}^2A_1(G)$					
		16.18		92.3	3.11	$\rightarrow {}^2T_2(G)$					
		14.72	Fitted	280	26.3	$\rightarrow {}^4T_1(P)$					
		13.94	Fitted	27.2	5.18	${}^2E(G)$					
		13.60	—	90.7	3.45	$\rightarrow {}^2T_1(G)$					
		5.90	Fitted	43.5	7.21	$\rightarrow {}^4T_1(F)$					
		3.55*	3.40	—	—	$\rightarrow {}^4T_2(F)$					
$CoCl_2$ in $BiCl_3$	270	17.51	—	71.8	7.50	$^4A_1 \rightarrow {}^2H$	3400	705	2400	0.725	T_d
		16.71	—	56.6	2.29	${}^2A_1(G)$					
		16.24	—	59.6	1.83	$\rightarrow {}^2T_2(G)$					
		14.84	Fitted	252	24.6	$\rightarrow {}^4T_1(P)$					
		13.80	Fitted	102	3.14	${}^2E(G)$					
		13.31		67.0	1.71	$\rightarrow {}^2T_1(G)$					
		5.90	Fitted	27.4	4.54	$\rightarrow {}^4T_1(F)$					
		3.55	3.39	—	—	$\rightarrow {}^4T_2(F)$					
CoS in $BiCl_3$	270	18.10	—	38.2	1.86	$^4A_1 \rightarrow {}^2H$	3400	695	2450	0.720	T_d
		16.81	—	128	5.57	${}^2A_1(G)$					
		16.25	—	82.7	2.47	$\rightarrow {}^2T_2(G)$					
		14.74	Fitted	270	25.4	$\rightarrow {}^4T_1(P)$					
		13.90	Fitted	83.1	1.79	${}^2E(G)$					
		13.42	—	75.1	1.84	$\rightarrow {}^2T_1(G)$					
		5.90	Fitted	32.0	5.01	$\rightarrow {}^4T_1(F)$					
		3.50*	3.40	—	—	$\rightarrow {}^4T_2(F)$					
$NiCl_2$ in $PbCl_2$	532	19.42	Fitted	86.3	14.0	$^3A_{2g} \rightarrow {}^3T_{1g}(P)$	5050	865	3650	0.830	Distorted O_h
		15.96	—	35.3	5.42	$\rightarrow {}^1T_{2g}(D)$					
		13.44	Fitted	9.4	0.66	$\rightarrow {}^1E_g(D)$					
		8.92	8.69	12.3	2.29	$\rightarrow {}^3T_{1g}(F)$					
		5.05	Fitted	6.9	0.77	$\rightarrow {}^3T_{2g}(F)$					
$NiCl_2$ in $SnCl_2$	300	20.70	Fitted	58.0	8.84	$^3A_{2g} \rightarrow {}^3T_{1g}(P)$	5500	910	4800	0.875	Distorted O_h
		18.54	—	13.8	2.06	$\rightarrow {}^1T_{2g}(D)$					
		16.11	Fitted	8.3	1.73	$\rightarrow {}^1E_g(D)$					
		10.14	9.46	7.0	1.06	$\rightarrow {}^3T_{1g}(F)$					
		5.51	Fitted	3.7	1.00	$\rightarrow {}^3T_{2g}(F)$					

*From infrared KBr pellet.

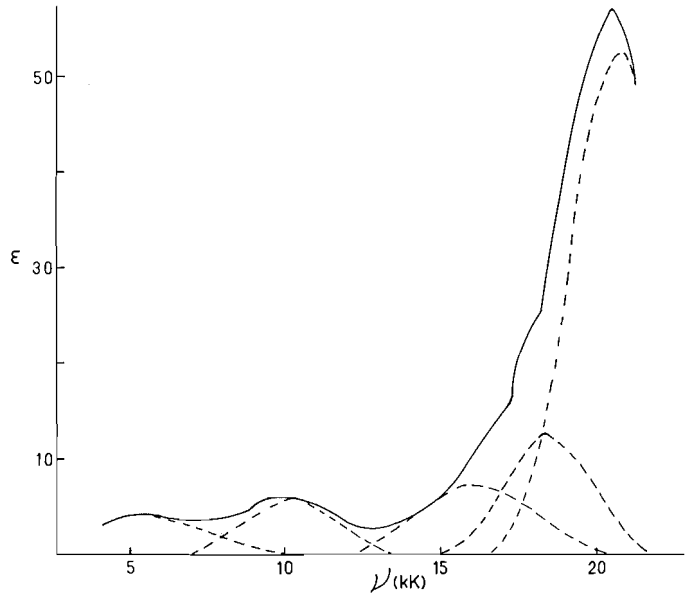

FIG. 5. Spectrum of $NiCl_2$ in $SnCl_2$ at 300 °C with Gaussian components.

band, particularly the high energy peak (unresolved).

The spectra of palladium(II), platinum(II), rhodium(III), and iridium(III) in molten $PbCl_2$ all consisted of a monotonous increase of absorption with increasing energy through the visible to the solvent cut-off at 21 kK (molar absorptivities in the red were: 22 for Pd(II) at 12.5 kK, 45 for Pt(II) at 13.3 kK, 28 for Rh(III) at 14.2 kK, and 26 for Ir(III) at 14.0 kK).

Discussion

Cobalt(II) Spectra

The cobalt(II) spectra in all three solvents are typical of tetrahedral coordination (1, 17) and have been assigned on this basis (Table 2). The splitting of the visible band is probably due to intermixing of quartet and doublet excited states or a slight distortion from a regular tetrahedron since it is somewhat large to be ascribed to spin–orbital coupling alone. From the energy of the strongest component of the visible band ($^4T_1 \leftarrow {}^4A_1(F)$) and the energy of the near infrared band ($^4T_1(F) \leftarrow {}^4A_1(F)$), a further weak transition (spin-allowed but electric dipole forbidden) is predicted at 3 kK. This band was located in a separate measurement on a KBr pellet containing frozen melt. The agreement between calculated and observed energies for this transition ($^4T_2(F) \leftarrow {}^4A_1(F)$) is satisfactory. The observed Δ values ($\sim$ 3.4 kK) are somewhat lower than those found for LiCl–KCl and this may result from the removal of negative charge from chloride to post-transition metal ion in the polymeric ligand.

CoS and $CoCl_2$ give almost identical spectra in $BiCl_3$ but the experiments with Bi_2S_3 and $BiCl_3$ mixtures indicate that the sulfide ion may complex with the cobalt ion even when added to CoS but complete transformation to CoS_4^{6-} was certainly not approached.

Nickel(II) Spectra

It is possible to assign *most* of the transitions of Ni(II) in both $PbCl_2$ and $SnCl_2$ as those of octahedral chromophores (18), in which case reasonable values of Δ, B, C, and β are obtained (Table 2). One can argue that the values are low for octahedral symmetry because of the polymeric nature of the ligands and can account for the high molar absorptivities if it is assumed that such ligands conveniently arrange to provide a distorted octahedral environment (*cf.* Fig. 6). However, the second most intense band in each case must be assigned as spin-forbidden. This situation has arisen in other investigations (1) and, in particular, the spectrum of Ni(II) in $PbCl_2$ closely resembles that of one of the species formed by Ni(II) in LiCl–KCl (19), and that of Ni(II) in $SnCl_2$ closely resembles that of

Can. J. Chem. Downloaded from www.nrcresearchpress.com by 210.87.254.6 on 09/05/12
For personal use only.

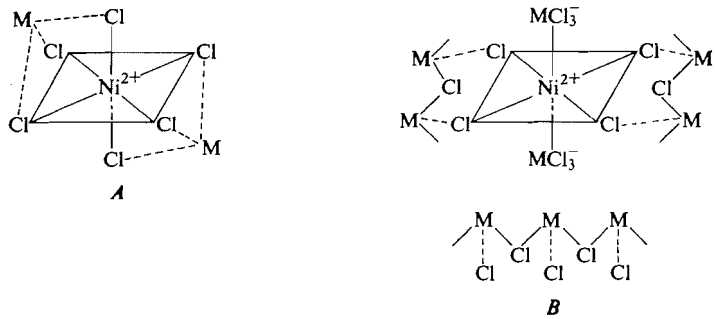

FIG. 6. Distortion of octahedral structure around Ni(II) caused by the polymeric nature of the ligand in post-transition metal halides: *A*, D_{3d} distortion (MCl_3^- as ligand); *B*, D_{4h} distortion and the polymeric chain structure of the melt.

one of the species formed by Ni(II) in $ZnCl_2$–CsCl (3). Smith and co-workers (19) label these species as types of **O** center to imply that their symmetry is approximately octahedral. Except for an overall intensity reduction, the spectrum of Ni(II) in Li_2SO_4–Na_2SO_4–K_2SO_4 eutectic melt looks very similar (1, 20). Whether we are dealing with pure **O** centers in $PbCl_2$ and $SnCl_2$ or with equilibrium mixtures of **O** and **T** (pseudo-tetrahedral) centers might become apparent from studies under way on Ni(II) in sundry mixtures of $PbCl_2$ and $SnCl_2$ with KCl.

The ability to separate cobalt and nickel by dissolution of the sulfides in molten $BiCl_3$ has, at least, some analytical significance.

The investigation of Pt(II), Pd(II), Rh(III), and Ir(III) in $PbCl_2$ was not very rewarding. For all four ions the absorption exceeded that obtained in molten LiCl–KCl (21) but, as no bands could be resolved, it is not possible to say whether the coordination differed in the two solvents.

This work was supported by the National Research Council of Canada, including a grant for the purchase of the Cary 14H spectrophotometer. We are grateful to L. G. Boxall for help in computer programming and G. P. Smith for providing details of some spectra prior to publication.

1. K. E. JOHNSON and J. R. DICKINSON. *In* Advances in molten salt chemistry. Vol. II. *Edited by* G. P. Smith, J. Braunstein, and G. Mamantov. Plenum Press, New York. To be published.
2. H. A. OYE and D. M. GRUEN. Inorg. Chem. **4,** 1173 (1965).
3. W. E. SMITH, J. BRYNESTAD, and G. P. SMITH. J. Chem. Phys. In press.
4. R. A. BAILEY, M. EL GUINDY, and J. A. WALDEN. Inorg. Chem. **8,** 2526 (1969).
5. G. J. JANZ (*Editor*). Molten salts handbook. Academic Press, Inc., New York. 1967.
6. K. BALASUBRAHMANYAM and L. NANIS. J. Chem. Phys. **40,** 2657 (1964).
7. J. H. R. CLARKE and C. SOLOMONS. J. Chem. Phys. **47,** 1823 (1967).
8. K. SAHL and J. ZEMANN. Naturwiss. **48,** 651 (1961).
9. R. E. RUNDLE and D. E. OLSON. Inorg. Chem. **3,** 596 (1964).
10. R. D. CRAMER, R. V. LINDSAY, JR., C. T. PREWITT, and U. G. STOLBERG. J. Amer. Chem. Soc. **87,** 658 (1965).
11. J. D. VAN NORMAN, J. S. BOOKLESS, and J. J. EGAN. J. Phys. Chem. **70,** 1276 (1966).
12. G. BRAUER (*Editor*). Handbook of preparative inorganic chemistry. Vols. 1 and 2. Academic Press, Inc., New York. 2nd ed. 1965.
13. S. J. YOSIM, A. J. DARNELL, W. G. GEHMAN, and S. W. MAYER. J. Phys. Chem. **63,** 231 (1959).
14. R. E. KITSON. Anal. Chem. **22,** 664 (1950).
15. K. E. JOHNSON, J. R. MACKENZIE, and J. N. SANDOE. J. Chem. Soc. A, 2644 (1968).
16. J. CHATT, L. E. ORGEL, and G. A. GAMLEN. J. Chem. Soc. 486 (1958).
17. R. L. CARLIN. *In* Transition metal chemistry. Vol. 1. *Edited by* R. L. Carlin, Marcel Dekker, New York. 1965. p. 1.
18. L. SACCONI. *In* Transition metal chemistry. Vol. 4. *Edited by* R. L. Carlin. Marcel Dekker, New York. 1968. p. 199.
19. J. BRYNESTAD, C. R. BOSTON, and G. P. SMITH. J. Chem. Phys. **47,** 3179 (1967).
20. J. R. DICKINSON and K. E. JOHNSON. To be published.
21. J. R. DICKINSON and K. E. JOHNSON. Can. J. Chem. **45,** 1631 (1967); **45,** 2457 (1967).

Can. J. Chem. Downloaded from www.nrcresearchpress.com by 210.87.254.6 on 09/05/12
For personal use only.

Nuclear magnetic resonance studies of multi-site chemical exchange. I. Matrix formulation of the Bloch equations[1]

L. W. Reeves and K. N. Shaw
Department of Chemistry, University of Waterloo, Waterloo, Ontario

Received May 20, 1970

A concise matrix formulation of chemical exchange effects on a nuclear magnetic resonance (n.m.r.) spectrum using the Bloch equations is described. The method accommodates many-site exchange processes, site-dependent relaxation times, differing site populations, and saturation effects in a steady-state first-order spectrum. The simple two-site exchange system is analyzed in detail and saturation effects in this system are studied numerically. Alternative forms of the basic lineshape equation are derived, all of which are readily adapted to efficient computer calculations for complete lineshape fitting to obtain kinetic data for complicated chemical exchange processes.

Canadian Journal of Chemistry, 48, 3641 (1970)

Can. J. Chem. Downloaded from www.nrcresearchpress.com by 210.87.254.40 on 09/05/12
For personal use only.

Introduction

The Bloch equations (1) have served as an excellent basis for the phenomenological description of the lineshape characteristics of n.m.r. spectra for liquids. These equations are readily modified to take into account chemical exchange effects (2, 3), thus allowing a simple physical interpretation of such effects in n.m.r. Of course, it is assumed that use of the modified Bloch equations is restricted to first-order spectra (4) so that the nuclear spin isochromats (1) associated with distinct sites of differing Larmor frequency may be considered to be independent except for chemical exchange effects. It is known at this point that complete steady-state lineshape fitting, throughout the temperature region in which the n.m.r. spectra are modified by chemical exchange, is the most satisfactory method of determining rate constants and activation parameters for exchange processes (5, 6). The study of multi-site exchange processes requires the numerical computation of lineshape functions and hence a matrix formulation of such processes in n.m.r. allows the most general, convenient, and lucid method of analysis. Although matrix formulations of exchange processes have been described (7–10, 26), inconsistent analyses are still apparent in the literature and little thought has been given to efficient numerical methods for routine studies. Thus the aim of this paper is to present a simple concise matrix formulation of the modified Bloch equations describing multi-site exchange processes, as a basis for a series of experimental studies of a wide range of chemical exchange systems. All Cartesian components of the nuclear magnetization are included and the separability of the longitudinal and transverse relaxation equations in the presence of chemical exchange is considered. This allows an analysis of saturation effects, as normally encountered in exchange lineshape studies which leads to a set of conditions for maximum signal-to-noise ratio and minimal lineshape distortion. This feature is important when the study of exchange processes in dilute solutions leads the experimentalist to compromise with larger than normal H_1 fields to achieve the signal-to-noise ratio in a recorded spectrum necessary for a reliable complete lineshape fit. Using a method similar to that suggested by Gordon and McGinnis (11),[2] an efficient numerical analysis has been developed and programmed. The computation of a given lineshape function is based upon a single diagonalization of a complex matrix, and an inversion of the resultant transformation matrix, for an arbitrary number of spectral data points. Previous applications (12–15) of a matrix formulation for exchange processes are unnecessarily clumsy and uneconomic of computer time, in that a direct and uncritical application requires a complex matrix inversion (7) for each spectral data point. The efficient computation of lineshape functions becomes very important in the iterative fitting of these functions to digitized experimental data (20). Apart from the much smaller computing costs (more than two orders of magnitude reduction in computation time using the present scheme) the matrix formulation described here

[1]This work was supported by the National Research Council of Canada in grants to L.W.R.

[2]We are grateful to a referee for pointing out this earlier independent suggestion.

Can. J. Chem. Downloaded from www.nrcresearchpress.com by 210.87.254.40 on 09/05/12
For personal use only.

enables yet more complicated multi-site chemical exchange processes to be tackled. Succeeding papers will include experimental applications to chemical systems which are both complicated and time-consuming to analyze when viewed in terms of the techniques being used at present.

Modified Bloch Equations

Suppose that we consider n distinct sites of differing Larmor frequency, ω_i, and that exchange effects in general modulate all frequency differences, $|\omega_i - \omega_j|$. Following McConnell (3), a transfer of nuclear magnetization may be described for the ξ-mode in the form

$$[1] \qquad d\xi_i/dt = \sum_{\substack{j=1 \\ j\neq i}}^{n} [k_{ji}\xi_j - k_{ij}\xi_i]$$

The indices refer to site and the double indices refer to first order transfer rate constants between sites such that $k_{ij}\xi_i$ represents the rate of transfer of ξ-mode magnetization *from site i to site j*. This form of notation is important in defining matrix elements for a multi-site exchange process. The time-dependence of the u-mode magnetization associated with site-i may now be expressed in the Bloch form

$$[2] \quad \frac{du_i}{dt} = -\left[\frac{1}{T_{2i}} + \sum_{j\neq i}^{n} k_{ij}\right]u_i + \sum_{j\neq i}^{n} k_{ji}u_j + w_i v_i$$

with $w_i = (\omega - \omega_i)$; where ω is the angular frequency of the oscillatory radio frequency field defining the normal rotating frame of reference, ω_i is defined as the site-i resonance frequency, and T_{2i} is the corresponding spin–spin relaxation time including a contribution from magnetic field inhomogeneity. The total u-mode magnetization for the system is then given by

$$u = \sum_{i=1}^{n} u_i$$

the site magnetization isochromats being independent except for transfer effects. Considering this magnetization as a column vector, $\boldsymbol{u}$, we may write [2] in matrix form to include all sites

$$[3] \qquad d\boldsymbol{u}/dt + \mathbf{R}_2 \cdot \boldsymbol{u} - \mathbf{w} \cdot \boldsymbol{v} = 0$$

with

$$\mathbf{R}_2 = \mathbf{T}_2 + \mathbf{K}$$

$\mathbf{T}_2$ is a diagonal $n \times n$ matrix with general element ${T_{2i}}^{-1}$, $\mathbf{K}$ is the transfer rate matrix, $n \times n$, with elements

$$[3a] \quad K_{ii} = \sum_{\substack{j=1 \\ j\neq i}}^{n} k_{ij} \text{ and } K_{ij} = -k_{ji}, j \neq i$$

where $\mathbf{w}$ is a diagonal frequency deviation matrix, $n \times n$ with element w_i, and $\boldsymbol{v}$ is the v-mode magnetization vector, with element v_i.

The off-diagonal elements of the rate matrix $\mathbf{K}$ are individual first-order rate constants for each pair of sites, and the diagonal elements are the sums of rate constants *from each* site-i. Thus the diagonal elements represent the overall rate processes for n sites. Also any column has a zero sum, consistent with detailed balance of rate processes

$$K_{ii} + \sum_{j\neq i}^{n} K_{ji} = 0$$

Similar matrix equations can be written for the v- and z-mode magnetization transfers involved in a chemical exchange process

$$[4] \qquad d\boldsymbol{v}/dt + \mathbf{R}_2 \cdot \boldsymbol{v} + \mathbf{w} \cdot \boldsymbol{u} = -\omega_1 \boldsymbol{M}_z$$

$$[5] \quad d\boldsymbol{M}_z/dt + \mathbf{R}_1 \cdot \boldsymbol{M}_z - \omega_1 \boldsymbol{v} = M_0 \mathbf{T}_1 \cdot \boldsymbol{P}$$

where

$$\omega_1 = \gamma H_1 \qquad \mathbf{R}_1 = \mathbf{T}_1 + \mathbf{K}$$

$\mathbf{T}_1$ is a diagonal spin–lattice relaxation matrix, $n \times n$ with element ${T_{1i}}^{-1}$, T_{1i} being the spin–lattice relaxation time for site-i. $\boldsymbol{P}$ is a column vector of the fractional populations for each site. We note that

$$\sum_{i=1}^{n} P_i = 1$$

and

$$[6] \qquad M_{0i} = M_0 P_i$$

where M_{0i} is the thermal equilibrium value for the z-mode magnetization in site-i, and M_0 is the corresponding total magnetization.

Solving the coupled matrix eqs. 3–5, the steady-state v-mode magnetization is given explicitly by

$$[7] \qquad \boldsymbol{v} = -\omega_1 M_0 \mathbf{C}^{-1} \cdot \boldsymbol{\varepsilon}_2 \cdot \boldsymbol{\varepsilon}_1 \cdot \mathbf{T}_1 \cdot \boldsymbol{P}$$

Can. J. Chem. Downloaded from www.nrcresearchpress.com by 210.87.254.40 on 09/05/12
For personal use only.

with

$$\mathbf{C} = \mathbf{I} + \omega_1^2 \boldsymbol{\varepsilon}_2 \cdot \boldsymbol{\varepsilon}_1 + \boldsymbol{\varepsilon}_2 \cdot \mathbf{w} \cdot \boldsymbol{\varepsilon}_2 \cdot \mathbf{w}$$

$\mathbf{I}$ is the unit $n \times n$ matrix, and $\boldsymbol{\varepsilon}_1$ and $\boldsymbol{\varepsilon}_2$ are the inverse matrices corresponding to $\mathbf{R}_1$ and $\mathbf{R}_2$, respectively.

For an arbitrary reference frequency ω_0, an independent frequency variable x may be defined as

$$x = \omega - \omega_0$$

such that for site-i

$$[8] \qquad w_i = x - \Omega_i$$

$$\Omega_i = \omega_i - \omega_0$$

where Ω_i is the chemical shift with respect to ω_0. The vector $\boldsymbol{v}$ now defines the steady-state n.m.r. absorption mode spectrum as a function of x

$$[9] \qquad V(x) = \sum_{i=1}^{n} v_i(x) = \boldsymbol{I} \cdot \boldsymbol{v}$$

The elements of the matrix $\mathbf{w}$ in [7] are defined by [8] and $\boldsymbol{I}$ is the row vector with each of the n elements equal to unity.

The corresponding matrix equations for the steady-state u- and z-mode magnetizations are now given in accordance with [3]–[5] and in terms of $\boldsymbol{v}$ as

$$[10] \qquad \boldsymbol{u} = \boldsymbol{\varepsilon}_2 \cdot \mathbf{w} \cdot \boldsymbol{v}$$

$$[11] \qquad \boldsymbol{M}_z = M_0 \boldsymbol{\varepsilon}_1 \cdot \mathbf{T}_1 \cdot \boldsymbol{P} + \omega_1 \boldsymbol{\varepsilon}_1 \cdot \boldsymbol{v}$$

This formulation allows a compact and versatile description of general nuclear magnetization transfer effects in a first-order n.m.r. spectrum, including those associated with spin–lattice relaxation (16, 17) and nuclear spin transition saturation.

Saturation Effects

Under normal steady-state conditions, a saturation factor S' may be defined in the form

$$S' = \frac{1}{1 + \omega_1^2 T_1 T_2} \qquad 0 < S' \leqslant 1$$

Now, since in the presence of chemical exchange saturation effects are described through the matrix $\mathbf{C}$ in [7] and, in particular, are contained in that part defined as

$$[12] \qquad \mathbf{S}' = \mathbf{I} + \omega_1^2 \boldsymbol{\varepsilon}_2 \cdot \boldsymbol{\varepsilon}_1$$

it is convenient to replace ω_1^2 by an equivalent parameter β defined in terms of an average saturation factor S' as

$$\beta = \frac{(1 - S')}{S'} \left\langle \frac{1}{T_1 T_2} \right\rangle \qquad 0 \leqslant \beta < \infty$$

where the relaxation part is also an average value for all sites. In this way [12] is written in the form

$$[13] \qquad \mathbf{S}' = \mathbf{I} + \beta \boldsymbol{\varepsilon}_2 \cdot \boldsymbol{\varepsilon}_1$$

A complete analysis of saturation effects would include the interrelationship with the deviation from steady-state conditions (18). Under normal experimental conditions, however, locked-field spectrometers allow a very good approximation to the required slow passage conditions and the above formulation is adequate.

The effects of saturation on the n.m.r. absorption mode lineshape have been studied for a particular two-site (A- and B-sites) chemical exchange system described by the spectral parameters: $P_A = 0.5$, $2\Omega = |\Omega_A - \Omega_B| = 10.0$ Hz and $T_{2A} = T_{2B} = 0.64$ s. Also, as is usual for liquid systems, it is assumed that $T_{1A} = T_{2A}$. The spin–spin relaxation time, T_{2A}, chosen corresponds to a Lorentzian full-width at half-maximum of 0.5 Hz and 2Ω is the chemical shift between sites in the absence of exchange, *cf.* [8]. By means of an iterative numerical analysis, using [7] and [9], values of the saturation parameters β and S' were determined corresponding to a prescribed mean deviation of the lineshape function, $V(x)$, from that for the reference limit of zero saturation ($\beta = 0$). A mean percentage deviation, ΔV, was defined for N data points as

$$\Delta V = (1/N) \sum_{i=1}^{N} [(V_i'(x) - V_i(x))/V_i'(x)] \cdot 100$$

in which $V_i'(x)$ and $V_i(x)$ are the reference and saturated lineshape function values, respectively, corresponding to the frequency value x_i. The results of such an analysis are shown in Fig. 1 for $\Delta V = 5\%$ by plots of β and S' as a function of $\log_{10}(k/2\Omega)$. It is seen that saturation effects for a fixed magnitude of the irradiation radio frequency (r.f.) magnetic field, $2H_1$, are most severe in the limits of very slow ($k \ll \Omega$) and very fast ($k \gg \Omega$) exchange corresponding to spectral lines of minimal width (0.5 Hz). For a mean

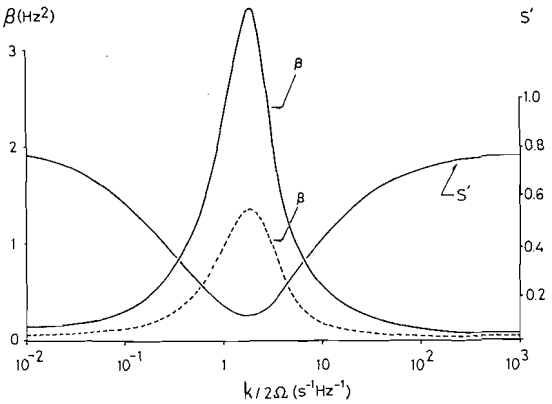

FIG. 1. Computed saturation parameters, β and S', for equal population two-site exchange system corresponding to 5% (—) and 2% (---) mean deviation from zero saturation reference absorption mode lineshape, for $T_1 = T_2 = 0.64$ s.

deviation $\Delta V = 5\%$ the values of H_1 for $k/2\Omega = 0.01$ and 1.0 are computed for ^{1}H n.m.r. ($\gamma_H = 2.7 \times 10^4$ rad s^{-1} G^{-1}) to be 0.56×10^{-2} and 9.4×10^{-2} mG, respectively. It is of interest to note that these fields correspond to a spectral frequency distribution of only 0.002 and 0.04 Hz.[3] As H_1 is increased, saturation gives rise to a general broadening of spectral lines and leads to an increased apparent first-order rate constant, k. A 5% deviation as considered above may lead to an error in a fitted k value of 5–10%. However, an irradiation field for an exchange system satisfying $k \sim \Omega$ of a magnitude approximately 20 times greater than that for $k \ll \Omega$ has been shown above to be acceptable. In the region for which $k \sim \Omega$, the spectral lines are of maximal width ($\sim \Omega$ rad s^{-1}) and hence minimum intensity. Spectral line intensity is linearly proportional to H_1 only in the absence of saturation effects. Nevertheless, it is seen that the intensity and hence signal-to-noise ratio of a recorded lineshape may be increased to levels acceptable for the measurement of reliable data for complete lineshape fitting without adverse distortion due to saturation, by increasing H_1 following an experimental linearity check for negligible saturation in the slow exchange limit. Relative H_1 field strengths corresponding to negligible saturation distortion may be estimated over a complete range of the parameter $k/2\Omega$ from Fig. 1, and hence reliable spectra for complete lineshape fitting may be obtained, in effect, in the limit of zero saturation.

[3]Grunwald *et al.* (28) have shown experimentally that H_1 fields an order of magnitude greater than those calculated above give negligible distortion due to saturation for chemical exchange systems. This implies that in actual fact a complicated combination of steady-state passage conditions and r.f. power levels (H_1) determine the observed saturation effects.

Zero Saturation Limit

For a general n-site exchange system, this limit may be defined by $\omega_1 \to 0$ ($\omega_1 = \gamma H_1$) and thus the modified Bloch equation describing the steady-state z-mode magnetization is given in accordance with [5] as

$$\boldsymbol{M}_z = M_0 \boldsymbol{\varepsilon}_1 \cdot \mathbf{T}_1 \cdot \boldsymbol{P}$$

with $\boldsymbol{\varepsilon}_1$ the inverse of the matrix $\mathbf{R}_1$.

In the absence of chemical exchange

$$\mathbf{R}_1 \equiv \mathbf{T}_1$$

and

$$[14] \qquad \boldsymbol{M}_z = M_0 \boldsymbol{P}$$

That is, the z-mode magnetization in each site is directly proportional to the site fractional populations, P_j, and is independent of spin–lattice relaxation effects. This condition is shown to be valid also in the presence of chemical exchange for all exchange rates and is considered in detail for a general two-site system in the following section.

The modified Bloch equations describing chemical exchange in the limit of zero saturation reduce to two coupled equations given in accordance with [3], [4], and [14] as

$$[15] \qquad \begin{aligned} \mathrm{d}\boldsymbol{u}/\mathrm{d}t + \mathbf{R}_2 \cdot \boldsymbol{u} - \mathbf{w} \cdot \boldsymbol{V} &= 0 \\ \mathrm{d}\boldsymbol{V}/\mathrm{d}t + \mathbf{R}_2 \cdot \boldsymbol{V} + \mathbf{w} \cdot \boldsymbol{u} &= -\omega_1 M_0 \boldsymbol{P} \end{aligned}$$

from which the steady-state v-mode magnetization is given explicitly by

$$[16] \qquad \boldsymbol{V} = -\omega_1 M_0 \mathbf{C}^{-1} \cdot \boldsymbol{P}$$

with

$$\mathbf{C} = \mathbf{R}_2 + \mathbf{w} \cdot \boldsymbol{\varepsilon}_2 \cdot \mathbf{w}$$

Again the steady-state n.m.r. absorption mode spectrum is determined as a function of the independent frequency variable, x, by $V(x)$ as defined in [9]. Equation 16 is to be compared with the more generally formulated [7]. In the limit of zero saturation, [16] shows that the n.m.r. absorption intensity is linearly related to the effective magnitude of the irradiating r.f. mag-

Can. J. Chem. Downloaded from www.nrcresearchpress.com by 210.87.254.40 on 09/05/12
For personal use only.

Can. J. Chem. Downloaded from www.nrcresearchpress.com by 210.87.254.40 on 09/05/12
For personal use only.

netic field, H_1, and is independent of spin–lattice relaxation effects for all chemical exchange rates. Within the limits discussed in the preceding section, [16] is the expression defining the lineshape function $V(x)$ normally used in the analysis of steady-state n.m.r. data.

Although the absorption mode lineshape function, $V(x)$, is given explicitly by [16] in terms of the *real* matrix **C**, the independent variable x is contained in the frequency deviation matrix **w** and hence an evaluation of $V(x)$ over a specified frequency range requires an inversion of the matrix **C** for each value of x.

An alternative formulation in the limit of zero saturation based upon the coupled Bloch equations [15] allows a much simplified calculation of $V(x)$. Following Pople *et al.* (19), a transverse magnetization, $\boldsymbol{G}$, may be defined for an n-site exchange system in vector form as

$$[17] \qquad \boldsymbol{G} = \boldsymbol{u} + \mathrm{i}\boldsymbol{V}$$

where the vector component V_j describes the v-mode magnetization associated with the j-site.

In accordance with [15], the steady-state transverse magnetization is now given by

$$\boldsymbol{G} = -\mathrm{i}\omega_1 M_0 [\mathbf{R}_2 + \mathrm{i}\mathbf{w}]^{-1} \cdot \boldsymbol{P}$$

and the corresponding *complex* lineshape function $G(x)$ follows as

$$[18] \quad G(x) = -\mathrm{i}\omega_1 M_0 \boldsymbol{I} \cdot [\mathbf{R}_2 + \mathrm{i}\mathbf{w}]^{-1} \cdot \boldsymbol{P}$$

where $\boldsymbol{I}$ is the vector with each of n elements equal to unity, *cf.* [9]. The absorption mode lineshape function, $V(x)$, is simply the imaginary part of $G(x)$, *cf.* [17]. The independent variable x appears only in the diagonal matrix **w**, *cf.* [8], and thus it is possible to transform the matrix $[\mathbf{R}_2 + \mathrm{i}\mathbf{w}]$ into a completely diagonal form, hence allowing a ready evaluation of $G(x)$ following a single matrix diagonalization. Now consider the matrix **R**

$$[19] \qquad \mathbf{R} = [\mathbf{T}_2 + \mathbf{K} - \mathrm{i}\boldsymbol{\Omega}]$$

such that

$$[\mathbf{R}_2 + \mathrm{i}\mathbf{w}] = \mathbf{R} + \mathrm{i}x\mathbf{I}$$

In these equations $\boldsymbol{\Omega}$ is an $n \times n$ diagonal matrix with element Ω_j, the chemical shift for the j-site, *cf.* [8], and **I** is the unit $n \times n$ matrix. In terms of the diagonalized matrix $\boldsymbol{\Lambda}$ corresponding to **R**, [18] may be expressed in the form

$$[20] \quad G(x) = -\mathrm{i}\omega_1 M_0 \boldsymbol{I} \cdot \mathbf{S} \cdot [\boldsymbol{\Lambda} + \mathrm{i}\,x\mathbf{I}]^{-1} \cdot \mathbf{S}^{-1} \cdot \boldsymbol{P}$$

where **S** is the matrix which diagonalizes **R**, *viz.*

$$[21] \qquad \boldsymbol{\Lambda} = \mathbf{S}^{-1} \cdot \mathbf{R} \cdot \mathbf{S}$$

Following this transformation, the evaluation of inverse matrix elements is reduced to the determination of reciprocal diagonal elements of the matrix $[\boldsymbol{\Lambda} + \mathrm{i}x\mathbf{I}]$, and the complex function $G(x)$ is defined in component form by

$$[22] \quad G(x) = -\mathrm{i}\omega_1 M_0 \times \sum_{j=1}^{n} I_j \sum_{k=1}^{n} \sum_{l=1}^{n} S_{jl}(S^{-1})_{lk} P_k / [\lambda_l + \mathrm{i}x]$$

where λ_l is the lth diagonal element of the matrix $\boldsymbol{\Lambda}$. S_{jl} and $(S^{-1})_{jl}$ are the jlth elements of the transformation matrices **S** and $\mathbf{S}^{-1}$, respectively. As the matrix elements involved are all complex, the computation of each spectral data point defined by $G(x)$ requires a number of operations in complex arithmetic on a digital computer. These operations are relatively slow and hence the absorption mode lineshape function, $V(x)$, is finally given in terms of operations in real arithmetic only by defining a matrix **B** as the real part of the matrix $\mathbf{S} \cdot [\boldsymbol{\Lambda} + \mathrm{i}x\mathbf{I}]^{-1} \cdot \mathbf{S}^{-1}$. That is, in accordance with [20]

$$V(x) = A\boldsymbol{I} \cdot \mathbf{B} \cdot \boldsymbol{P}$$

in which A is a normalization constant, and the matrix elements $\boldsymbol{B}_{jk}$ are given by

$$B_{jk} = \sum_l \{a_{jkl}\lambda_l^{\mathrm{R}} + b_{jkl}[\lambda_l^{\mathrm{I}} + x]\}/d_l$$

where a_{jkl} and b_{jkl} (and λ_l^{R} and λ_l^{I}) are the real and imaginary parts of $S_{jl}(S^{-1})_{lk}$ (and λ_l), respectively. d_l is defined in terms of the independent variable x as

$$d_l = [\lambda_l^{\mathrm{R}}]^2 + [\lambda_l^{\mathrm{I}} + x]^2$$

Analogous to [22], $V(x)$ is now given as

$$[22a] \qquad V(x) = A \sum_{j=1}^{n} I_j \sum_{k=1}^{n} B_{jk} P_k$$

A computer program (available from the authors) based upon [21], [22*a*] has been developed and has been shown to give reliable and efficient iterative total lineshape analyses for multi-site exchange systems.

Although specific details will be discussed in

Can. J. Chem. Downloaded from www.nrcresearchpress.com by 210.87.254.40 on 09/05/12
For personal use only.

following papers dealing with experimental applications (20), one aspect of the general iterative fitting procedure should be outlined at this point. In the $(m + 1)$th iteration, the refined rate constant for any two-sites i and j is determined as

$$k_{ij}^{m+1} = k_{ij}^{m} + \Delta k_{ij}$$

and thus in accordance with [3*a*], [19]

$$\mathbf{R}^{m+1} = \mathbf{T}_2 + (\mathbf{K}^m + \Delta\mathbf{K}) - i\boldsymbol{\Omega}$$

$$= \mathbf{T}_2 + \mathbf{K}^{m+1} - i\boldsymbol{\Omega}$$

the elements of the matrix $\Delta\mathbf{K}$ being simply the incremental rate constants Δk_{ij}. Now, in the mth iteration, transformation matrices have been determined in accordance with [21] such that

$$\boldsymbol{\Lambda}^m = (\mathbf{S}^{-1})^m \cdot \mathbf{R}^m \cdot \mathbf{S}^m$$

$\boldsymbol{\Lambda}^m$ being the diagonal matrix corresponding to the rate matrix $\mathbf{R}^m$. Thus in the $(m + 1)$th iteration, it follows that a matrix $\boldsymbol{\Lambda}'$ determined by

$$\boldsymbol{\Lambda}' = (\mathbf{S}^{-1})^m \cdot \mathbf{R}^{m+1} \cdot \mathbf{S}^m$$

is approximately diagonal. The matrix $\boldsymbol{\Lambda}'$ may now be diagonalized exactly with considerable reduction in computation time. The $(m + 1)$th iteration transformation matrices, $\mathbf{S}^{m+1}$ and $(\mathbf{S}^{-1})^{m+1}$ are readily obtained as follows

$$\boldsymbol{\Lambda}^{m+1} = \mathbf{T}^{-1} \cdot \boldsymbol{\Lambda}' \cdot \mathbf{T}$$

$$= (\mathbf{S}^{-1})^{m+1} \cdot \mathbf{R}^{m+1} \cdot \mathbf{S}^{m+1}$$

with $\mathbf{S}^{m+1} = \mathbf{S}^m \cdot \mathbf{T}$ and $(\mathbf{S}^{-1})^{m+1} = \mathbf{T}^{-1} \cdot (\mathbf{S}^{-1})^m$. Having defined the complex matrices $\boldsymbol{\Lambda}^{m+1}$, $\mathbf{S}^{m+1}$, and $(\mathbf{S}^{-1})^{m+1}$ in this manner, the computation of the lineshape for the rate constants k_{ij}^{m+1} reduces to an application of [22*a*].

Two-Site Exchange System

The complex matrix formulation of chemical exchange processes developed in the preceding section is most readily illustrated through an analysis of the simple two-site system in the limit of zero saturation.

Consider the system with exchange sites A and B defined by relative chemical shifts (rad s^{-1}) $\Omega_A = -\Omega$ and $\Omega_B = \Omega$ in terms of the independent frequency variable x (rad s^{-1}) with $\omega_0 = \frac{1}{2}(\omega_A + \omega_B)$[4] *cf.* [8], and fractional site populations P_A and P_B. The relaxation, rate, and chemical shift matrices are then determined in accordance with [3]–[5] and [18] as

$$\mathbf{T}_1 = \begin{pmatrix} \frac{1}{T_{1A}} & 0 \\ 0 & \frac{1}{T_{1B}} \end{pmatrix}$$

$$\mathbf{T}_2 = \begin{pmatrix} \frac{1}{T_{2A}} & 0 \\ 0 & \frac{1}{T_{2B}} \end{pmatrix}$$

$$\mathbf{K} = \begin{pmatrix} k_A & -k_B \\ -k_A & k_B \end{pmatrix}$$

$$\boldsymbol{\Omega} = \begin{pmatrix} -\Omega & 0 \\ 0 & \Omega \end{pmatrix}$$

in which T_{1A} and T_{2A} (s) are the spin–lattice and spin–spin relaxation times, respectively, for the A-site and k_A (s^{-1}) is the first-order rate constant for transfer *from* the A-site. It should be noted that the rate constants and site populations are related, in terms of detailed balance for rate processes, by

[23] $$P_A k_A = P_B k_B$$

In the limit of zero saturation, the z-mode magnetization is given by [5] as

$$M_z = M_0 \boldsymbol{\varepsilon}_1 \cdot \mathbf{T}_1 \cdot \boldsymbol{P}$$

with

$$\boldsymbol{\varepsilon}_1 = (\mathbf{R}_1)^{-1} = \frac{1}{D}\begin{pmatrix} \frac{1}{T_{1B}} + k_B & k_B \\ k_A & \frac{1}{T_{1A}} + k_A \end{pmatrix}$$

and

$$D = \frac{1}{T_{1A}T_{1B}} + \frac{k_A}{T_{1B}} + \frac{k_B}{T_{1A}}$$

Using [23], it is readily shown that the matrix product $\boldsymbol{\varepsilon}_1 \cdot \mathbf{T}_1 \cdot \boldsymbol{P}$ reduces to $\boldsymbol{P}$ in this limit, thus showing the validity of the modified Bloch equations as expressed in [15]. For analytic simplicity it will now be assumed that the spin–spin relaxation times for the two sites are the

[4] ω_A is the resonance frequency for the A-site in terms of the independent frequency variable ω, and is given as $\omega_A = \omega_0 - \Omega$.

Can. J. Chem. Downloaded from www.nrcresearchpress.com by 210.87.254.40 on 09/05/12
For personal use only.

same so that the matrix $\mathbf{T}_2$ becomes a scalar matrix, *viz.* $(1/T_2)\mathbf{I}\cdot\mathbf{I}$ is the 2×2 unit matrix. The exchange matrix $\mathbf{R}$, defined by [19], may now be expressed in the form

$$[24] \qquad \mathbf{R} = \frac{1}{T_2}\mathbf{I} + [\mathbf{K} - i\boldsymbol{\Omega}]$$

The diagonal matrix $\boldsymbol{\Lambda}$ corresponding to $[\mathbf{K} - i\boldsymbol{\Omega}]$ is now defined by

$$\boldsymbol{\Lambda} = \mathbf{S}^{-1} \cdot [\mathbf{K} - i\boldsymbol{\Omega}] \cdot \mathbf{S}$$

cf. [21].

If, initially, an equal population system is considered, the diagonal elements of the matrix $\boldsymbol{\Lambda}$ above are given by

$$[25] \qquad \lambda = k \pm \alpha \qquad \alpha = (k^2 - \Omega^2)^{1/2}$$

with $k = k_A = k_B$. The associated transformation matrices, $\mathbf{S}$ and $\mathbf{S}^{-1}$, are

$$[26] \qquad \mathbf{S} = \begin{pmatrix} 1 & 1 \\ -\beta_- & \beta_+ \end{pmatrix} \qquad \mathbf{S}^{-1} = \frac{k}{2\alpha}\begin{pmatrix} \beta_+ & -1 \\ \beta_- & 1 \end{pmatrix}$$

where $\beta_\pm = (\alpha \pm i\Omega)/k$. As the matrix $[\mathbf{K} - i\boldsymbol{\Omega}]$, or $\mathbf{R}$, is non-Hermitian, the matrix elements λ are in general complex and the row vectors defining the transformation matrix, $\mathbf{S}$, are complex and non-orthogonal. These vectors are normalized in accordance with the condition

$$S_{jj}^* S_{jj} + S_{lj}^* S_{lj} = 1$$

for $j,l = 1,2$ and S_{jj}^* the complex conjugate of S_{jj}. It should also be noted that all normalization constants have been combined in the factor $k/2\alpha$ in [26].

The complex lineshape function, $G(x)$, in accordance with [20] and [24]–[26] takes on the form

$$[27] \qquad G(x) = -i\omega_1 M_0 \boldsymbol{I} \cdot \mathbf{S} \cdot [\boldsymbol{\Lambda} + (1/T_2 + ix)\mathbf{I}] \cdot \mathbf{S}^{-1} \cdot \mathbf{P}$$

The parameter α, as defined in [25], may be real or pure imaginary for $k > \Omega$ and $k < \Omega$, respectively. Thus, from [27], the complex lineshape function for rate constants in the range $0 \leqslant k \leqslant \Omega$ is expressed in terms of a real parameter ε as

$$[28] \qquad G(x) = iA\left\{\frac{(1 + ik/\varepsilon)}{r + i(x + \varepsilon)} + \frac{(1 - ik/\varepsilon)}{r + i(x - \varepsilon)}\right\}$$

with

$$A = -\tfrac{1}{2}\omega_1 M_0$$

$$r = 1/T_2 + k$$

and

$$\varepsilon = (\Omega^2 - k^2)^{1/2}$$

The constant A is merely an overall intensity normalization factor. The associated lineshape function for rate constants in the range $\Omega \leqslant k < \infty$ is

$$[29] \qquad G(x) = iA\left\{\frac{(1 - k/\alpha)}{(r + \alpha) + ix} + \frac{(1 + k/\alpha)}{(r - \alpha) + ix}\right\}$$

Equations 28 and 29 allow a lucid and concise description of the n.m.r. absorption lineshape function, $V(x)$, for the equal population two-site chemical exchange system. In general, the diagonal matrix elements λ, as defined in [25], determine the positions and linewidths of the component spectral lines and the matrix $\mathbf{S}$, as defined in [26], determines the intensities of these lines.

Thus for $0 \leqslant k \leqslant \Omega$, [28] defines absorption mode components corresponding to modified Lorentzian lines described by the lineshape function

$$[30] \qquad V(x) = A\left\{\frac{(r + k) + (k/\varepsilon)x}{r^2 + (x + \varepsilon)^2} + \frac{(r + k) - (k/\varepsilon)x}{r^2 + (x - \varepsilon)^2}\right\}$$

In the absence of exchange, $k = 0$ ($r = 1/T_2$, $\varepsilon = \Omega$) and [30] shows that the spectrum consists of pure Lorentzian lines centered at $X = \pm\Omega$ (rad s^{-1}) with full-widths at half-maximum of $2/T_2$ (rad s^{-1}). This is consistent with the normal definitions of 2Ω as the chemical shift between sites and T_2 as the parameter describing spectral linewidth in the absence of exchange effects (21). In the presence of exchange, the spectral components may be considered in terms of a superposition of pure Lorentzian and associated dispersion functions, the degree of mixing being determined by the factor k/ε in [30]. For example, for the component centered at $x = \varepsilon$, $V_+(x)$ is given by

$$[31] \qquad V_+(x) = A\left\{\frac{r}{r^2 + (x - \varepsilon)^2} - \frac{k}{\varepsilon}\left[\frac{(x - \varepsilon)}{r^2 + (x - \varepsilon)^2}\right]\right\}$$

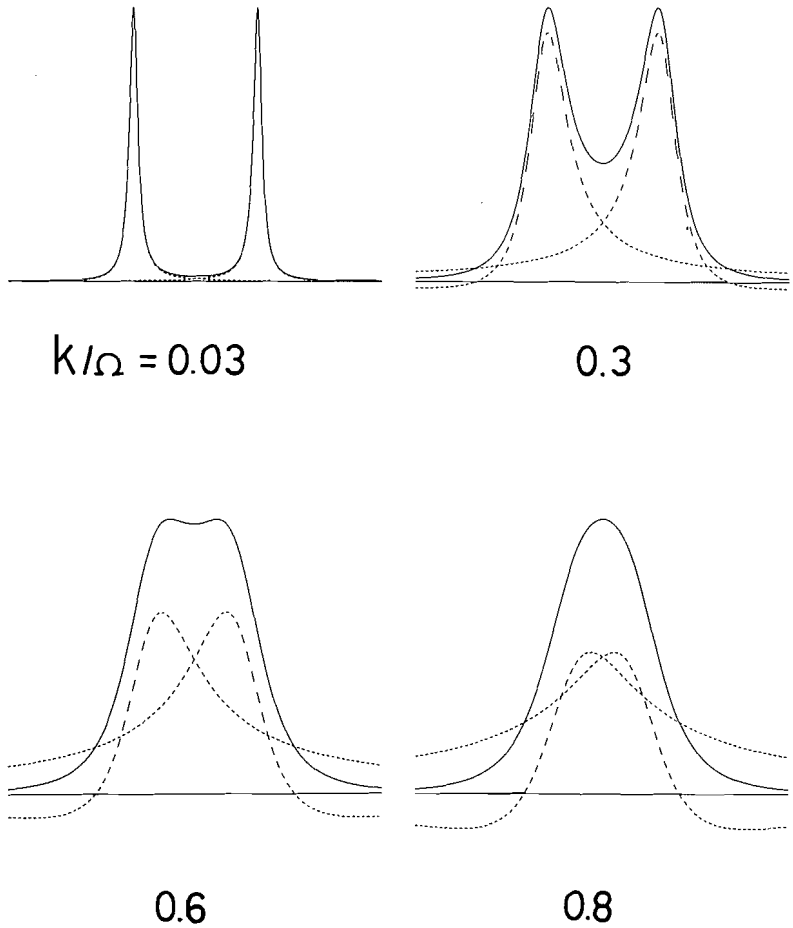

FIG. 2. Modified Lorentzian component spectral lines (---) and resultant absorption mode lineshape function (—), $V(x)$, for equal population two-site exchange system and slow exchange ($k < \Omega$).

Thus it is shown that the Lorentzian type component has a full-width at half-maximum of $2(1/T_2 + k)$, linearly increasing with k, and a position $\varepsilon < \Omega$ such that the component separation, 2ε, decreases with increasing k. These basic lineshape characteristics for the exchange system under consideration are shown in Figs. 2 and 3 for varying values of k/Ω.

For clarity, the computed lineshapes shown have been normalized, through the factor A, to an arbitrary maximum independent of k. Figure 2 shows the form of the modified Lorentzian component lines for $k/\Omega < 1$ as described by [30]; whereas Fig. 3 shows the total Lorentzian and associated dispersion functions, as defined for $k/\Omega < 1$ by $V_+(x)$ in [31] and a corresponding function $V_-(x)$ for the component centered at $x = -\Omega$, determining the overall lineshape function $V(x)$.

Experimentally, use of an r.f. phase-sensitive detector allows the observation of an n.m.r. signal proportional to a specific component of the transverse nuclear magnetization $\boldsymbol{G}(x)$, *cf.* [17], as an oscillatory linearly polarized component at the irradiation frequency, ω, in the fixed laboratory frame of reference. The direction of a specific component of transverse magnetization is defined by the relative phase difference, ϕ, between the detector reference r.f. field vector and the r.f. irradiation field vector, $\boldsymbol{H}_1(\omega)$, defining the u-axis of the normal rotating frame of reference as used in the preceding theoretical derivations. Thus in the absence of exchange effects, by setting $\phi = 90°$, the specific compon-

Can. J. Chem. Downloaded from www.nrcresearchpress.com by 210.87.254.40 on 09/05/12
For personal use only.

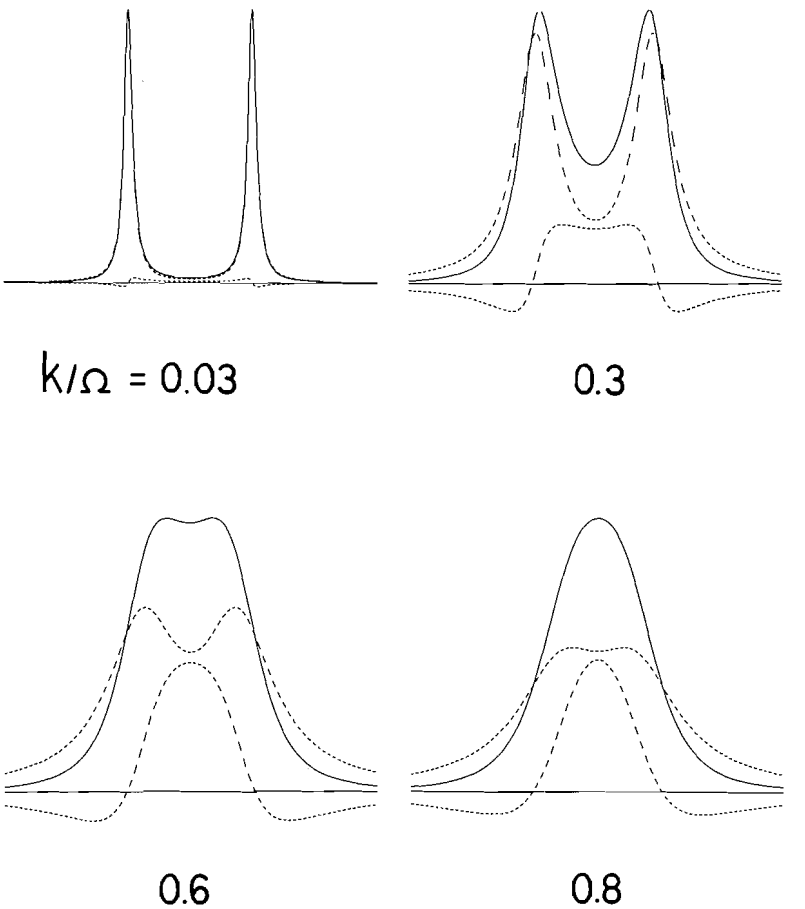

FIG. 3. Total Lorentzian $[V_+(x) + V_-(x)]$ (---) and associated dispersion $[U_+(x) + U_-(x)]$ (---) functions, and resultant absorption mode lineshape function (—), $V(x)$, for equal population two-site exchange system and slow exchange ($k < \Omega$).

ent corresponding to the v-mode magnetization vector V, *cf.* [17], is observed giving rise to an absorption mode spectrum as described by the lineshape function $V(x)$. This spectrum consists of pure Lorentzian lines (assuming a simple $1/T_2$-type spin–spin relaxation mechanism) centered at $x = \pm\Omega$; or $\omega = \omega_0 \pm \Omega$ with $\omega_0 = \frac{1}{2}(\omega_A + \omega_B)$, ω_A being the resonance frequency for the A-site in the laboratory reference frame. The associated dispersion mode spectrum is described by a lineshape function $u(x)$ given in accordance with [28] as

$$[32] \quad u(x) = -A\left\{\frac{(x+\varepsilon) - kr/\varepsilon}{r^2 + (x+\varepsilon)^2} + \frac{(x-\varepsilon) + kr/\varepsilon}{r^2 + (x-\varepsilon)^2}\right\}$$

with

$$[33] \quad u_+(x) = -A\left\{\frac{(x-\varepsilon)}{r^2 + (x-\varepsilon)^2} + \frac{k}{\varepsilon}\left[\frac{r}{r^2 + (x-\varepsilon)^2}\right]\right\}$$

This form of spectrum is observed by setting $\phi = 0$. The first term in [33] describes the dispersion mode line centered at $x = +\Omega$ in the absence of exchange effects.

In the presence of chemical exchange for $k < \Omega$, the mixing of normal absorption and dispersion mode n.m.r. signals associated with the v- and u-mode components, respectively, of the transverse magnetization in the rotating frame of reference may now be considered

Can. J. Chem. Downloaded from www.nrcresearchpress.com by 210.87.254.40 on 09/05/12
For personal use only.

Can. J. Chem. Downloaded from www.nrcresearchpress.com by 210.87.254.40 on 09/05/12
For personal use only.

qualitatively in terms of the behavior of the transverse components of the individual nuclear spin isochromats. A spin isochromat, $\boldsymbol{M}(x,\phi)$, is defined to be the resultant vector magnetization due to all spins having a particular Larmor frequency and relative phase (with respect to the u-axis of the rotating frame of reference) in a macroscopic sample (1). In the absence of chemical exchange, T_2 is the relaxation time describing the isochromat dephasing and consequential spectral linewidth due to local magnetic field inhomogeneity, giving rise to distributions of Larmor frequencies centered at the A- and B-site resonance frequencies, $x = \pm\Omega$, respectively. This type of isochromat dephasing is a coherent effect. It should be noted that there is also a small contribution to such a relaxation time due to natural lifetime limiting of any nuclear spin state. In the presence of chemical exchange, however, the individual spin isochromats are involved in a transfer between sites corresponding to distinct local magnetic fields (chemical shifts) at completely random times. Conversely, it may be considered that each spin isochromat experiences a randomly fluctuating local magnetic field with a fundamental frequency component in the associated frequency distribution of krad s^{-1}. This random process alters the form of isochromat dephasing, which may be described in terms of a probability function (22, 23) for the isochromat relative phase distribution, the time average effect for all isochromats being observed as an effective mixing of the normal u- and v-mode transverse magnetizations, as described by [30] and [32] and for a particular component spectral line by [31] and [33]. It should be emphasized that the function $V(x)$, *cf.* [30], by definition describes the signal as observed in the presence of exchange processes for the phase sensitive detector relative phase $\phi = 90°$, and this will always be referred to as the absorption mode signal. Now, if the fundamental frequency associated with the fluctuating local magnetic field due to a chemical exchange process becomes comparable to the frequency difference between exchange sites, 2Ω, the modification of the basic T_2 isochromat dephasing is expected to be most significant. This is actually observed in the form of maximal broadening and coalescence of the component spectral lines for rate constants $k \simeq \Omega$. For rate constants $k \simeq \Omega$, in accordance with [30], the component line Lorentzian and associated dispersion functions may be combined as

$$[34]\quad V(x) = V_+(x) + V_-(x) = A\left\{r\left[\frac{1}{r^2 + (x+\varepsilon)^2} + \frac{1}{r^2 + (x-\varepsilon)^2}\right] + \frac{k}{\varepsilon}\left[\frac{(x+\varepsilon)}{r^2 + (x+\varepsilon)^2} - \frac{(x-\varepsilon)}{r^2 + (x-\varepsilon)^2}\right]\right\}$$

Thus it is seen that the lineshape characteristics are strongly dependent upon the second term, in addition to the broadening described by the parameter r, due to the factor $k/\varepsilon \to \infty$. It is this factor that describes the well known (24) sensitivity of the observed absorption mode lineshape to rate constant for a particular chemical shift difference between exchange sites in the region about component line coalescence. In accordance with [34], for $k = \Omega$ ($\varepsilon = 0$) the second term now makes no effective contribution to the lineshape function $V(x)$ and thus the spectrum consists of a single Lorentzian line centered at $x = 0$ with full-width at half-maximum of $2r = 2[1/T_2 + \Omega]$ and intensity factor $2r$. Qualitatively, this is consistent with the simple isochromat model for exchange effects previously discussed. As the rate of isochromat transfer between exchange sites increases, or conversely as the fundamental frequency associated with the fluctuating local magnetic field for an isochromat increases, the time average contribution from the normal dispersive u-mode magnetization is maximized and then effectively cancelled out for the particular condition $k = \Omega$. This cancellation coincides with an exact averaging of the component line separation, 2ε, to zero. Also, for all rate constants $k > \Omega$ there is no effective contribution to the lineshape from a dispersive type function.

For rate constants $k > \Omega$, the absorption mode lineshape function, $V(x)$, is given in accordance with [29] as

$$[35]\quad V(x) = A\left\{(1 + k/\alpha)\left[\frac{r-\alpha}{(r-\alpha)^2 + x^2}\right] + (1 - k/\alpha)\left[\frac{r+\alpha}{(r+\alpha)^2 + x^2}\right]\right\}$$

Can. J. Chem. Downloaded from www.nrcresearchpress.com by 210.87.254.40 on 09/05/12
For personal use only.

with

$$r = \frac{1}{T_2} + k$$

$$\alpha = (k^2 - \Omega^2)^{1/2}$$

That is, the spectrum consists of a modified Lorentzian line centered at $x = 0$ which may be described as the superposition of two Lorentzian components, that giving a positive contribution to $V(x)$ being defined as

$$V_+(x) = A(1 + k/\alpha)\left[\frac{r - \alpha}{(r - \alpha) + x^2}\right]$$

This component has a full-width at half-maximum of $2(r - \alpha)$ (rad s^{-1}) and an intensity factor $(1 + k/\alpha)$. The parameters r and α determine a linewidth which decreases with increasing k and a maximum value for the intensity factor of 2. The other component defined in [35] gives a negative contribution and is a Lorentzian function with linewidth $2(r + \alpha)$, increasing linearly with k, and intensity factor $(1 - k/\alpha)$.[5] Again, for $k \sim \Omega$ the lineshape is strongly dependent upon the factor k/α (as $\alpha \to 0$) and the observed lineshape is particularly sensitive to the rate constant k in this region.

In the limit of very fast exchange ($k \gg \Omega$) the component $V_+(x)$ becomes dominant and the absorption mode spectrum consists of a single Lorentzian line

$$V(x) = 2A\left\{\frac{1/T_2}{(1/T_2)^2 + x^2}\right\}$$

centered at $x = 0$ with linewidth $2/T_2$ (rad s^{-1}). The intensity factor 2 is consistent with the fact that the intensities associated with the component lines at $x = \pm\Omega$ in the limit of slow exchange ($k \ll \Omega$), *cf.* [30], are now combined for the single line centered at the mean Larmor frequency, $x = \frac{1}{2}(\omega_A + \omega_B) = 0$. These lineshape characteristics are shown in Fig. 4 for two values of k/Ω, where again the computed lineshapes have been normalized to an arbitrary maximum independent of k.

A similar matrix treatment for the more general unequal population, $P_A \neq P_B$, two-site exchange system using the fundamental eqs. [23], [24], and [27] leads to complex lineshape functions, $G(x)$, for $0 \leqslant k \leqslant \Omega$

$$[36] \quad G(x) = iA\left\{\frac{(1 + ik/\varepsilon) - (1 - 2P_A)\Omega/\varepsilon}{r + i(x + \varepsilon)} + \frac{(1 - ik/\varepsilon) + (1 - 2P_A)\Omega/\varepsilon}{r + i(x - \varepsilon)}\right\}$$

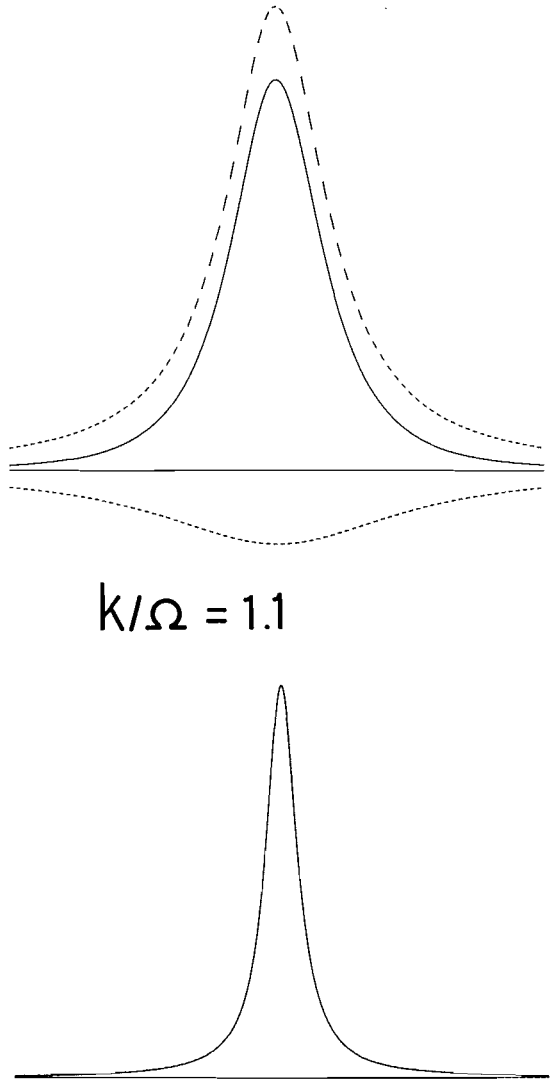

FIG. 4. Lorentzian components (---) and resultant absorption mode lineshape (—), $V(x)$, for equal population two-site exchange system and fast exchange ($k > \Omega$).

[5]Gutowsky *et al.* (29) have also noted similar distinct contributions to the lineshape function, $V(x)$, for an uncoupled two-site exchange system in the fast exchange limit.

Can. J. Chem. Downloaded from www.nrcresearchpress.com by 210.87.254.40 on 09/05/12
For personal use only.

and for $\Omega \leqslant k < \infty$

$$[37] \quad G(x) = iA\left\{\frac{(1 - k/\alpha) - i(1 - 2P_A)\Omega/\alpha}{(r + \alpha) + ix} + \frac{(1 + k/\alpha) + i(1 - 2P_A)\Omega/\alpha}{(r - \alpha) + ix}\right\}$$

where the characteristic parameters are defined by

$$\varepsilon = [\Omega^2 - k^2 - 2i(1 - 2P_A)k\Omega]^{1/2}$$

$$\alpha = [k^2 - \Omega^2 + 2i(1 - 2P_A)k\Omega]^{1/2}$$

$$r = 1/T_2 + k$$

with

$$k = \tfrac{1}{2}(k_A + k_B)$$

$$2\Omega = \omega_B - \omega_A = \Omega_B - \Omega_A$$

and

$$\omega_0 = \tfrac{1}{2}(\omega_A + \omega_B)$$

A is the normalization factor defined previously, *cf.* [28]. In this case the parameters ε and α remain complex, but they may be compared directly with the analogous parameters used in the analysis of the equal population system. It is readily seen that [36] and [37] reduce to [28] and [29] for the particular system in which $P_A = P_B = 1/2$. An analysis of the absorption mode lineshape function in terms of [36] and [37] is complicated by the complex parameters ε and α. However, it is interesting to note that these parameters now determine both component line position (imaginary part) and linewidth (real part) for all rate constants k, whereas in the equal population case the real parameters ε and α determined only line position or linewidth, respectively.

Now consider a general population two-site exchange system analogous to that already discussed with site chemical shifts (rad s^{-1}) $\Omega_A = -\Omega$ and $\Omega_B = \Omega$. In the limit of slow exchange ($k \ll \Omega$), in accordance with [36] it is shown that the absorption mode lineshape function, $V(x)$, simplifies to the form

$$[38] \quad V(x) = A\left\{P_A\left[\frac{r}{r^2 + (x + \Omega)^2}\right] + (1 - P_A)\left[\frac{r}{r^2 + (x - \Omega)^2}\right]\right\}$$

Thus in the absence of exchange ($k = 0$), the spectrum consists of pure Lorentzian lines centered at $x = -\Omega$ and $x = +\Omega$ with intensity factors P_A and $(1 - P_A) = P_B$, respectively, and full-width at half-maximum of $2/T_2$ (rad s^{-1}). In the limit of very fast exchange ($k \gg \Omega$), the second term in [37] becomes dominant and the absorption mode spectrum consists of a single Lorentzian line

$$[40] \quad V(x) = 2A\left\{\frac{1/T_2}{(1/T_2)^2 + (x - (1 - 2P_A)\Omega)^2}\right\}$$

centered at $x = (1 - 2P_A)\Omega$ with a linewidth $2/T_2$. That is, for the unequal population system, the spectral line in this limit is positioned away from the mean frequency $x = \frac{1}{2}(\Omega_A + \Omega_B) = 0$ towards the resonance frequency corresponding to the larger population exchange site, consistent with a previous derivation (19).

Finally, for the general population exchange system under consideration, [36] and [37] may be reformulated (25) to give a simple analytical expression for the absorption mode lineshape function, $V(x)$, valid for all rate constants $0 \leqslant k < \infty$

$$[41] \quad V(x) = A\left\{\frac{(r + k)B + (x + (1 - 2P_A)\Omega)C}{B^2 + C^2}\right\}$$

where

$$B = (1/T_2)(r + k) + \Omega^2 - x^2$$

$$C = 2[rx - (1 - 2P_A)k\Omega]$$

All other parameters are those as previously defined. This lineshape equation is, of course, equivalent to the familiar Gutowsky–Holm expression (21) for a two-site exchange system.

Summary

A variety of n.m.r. methods for studying chemical exchange processes in liquids has developed over the past decade (5, 6). The application of these methods, both theoretically and experimentally, is not straightforward and only comparatively recently has there developed a growing awareness of the systematic errors involved and the experimental care required in the determination of reliable kinetic data. Although many approximate methods have been introduced to allow a simplified estimation of the first-order rate constant for a specific exchange process, at a given temperature, from steady-state

Can. J. Chem. Downloaded from www.nrcresearchpress.com by 210.87.254.40 on 09/05/12
For personal use only.

n.m.r. spectral characteristics; at this time, it is known that the general method of complete fitting of a theoretical lineshape function to experimental data is apparently the only method yielding reliable kinetic data. However, the lineshape equation describing the simplest exchange process, between two uncoupled nuclear spin sites, is sufficiently complicated to require computer calculations. Thus as studies are extended to more complicated chemical systems of systematic interest, it is necessary to have available an efficient lineshape fitting procedure for a general *n*-site exchange system. This paper outlines a matrix formulation of the modified Bloch equations describing exchange effects, applicable only to first-order n.m.r. spectra, which allows a concise and relatively simple analysis of *n*-site exchange systems and which is also very readily adapted to computer programming. Of course, the description of second-order (tightly coupled) nuclear spin systems undergoing exchange requires a full spin density matrix treatment and matrix methods similar to those applied in the first-order case have been used to develop programs for the analysis of these even more complicated systems (25), independently of Binsch (27). The general two-site exchange system, being the best known example, has been analyzed in detail and it is shown that the matrix formulation leads to a lucid description of the lineshape characteristics consistent with previous treatments (19, 21). Alternative forms of the basic absorption mode lineshape equation have been derived corresponding to specific assumptions for the nuclear spin relaxation processes involved. The application of these equations in a completely automatic iterative lineshape fitting of digitized steady-state n.m.r. data, and details of the computer programs required, will be described in future publications.

The authors are indebted to Dr. C. H. Holm of the Shell Development Company, Emeryville, California for providing a computer program which leads to the work described here.

1. F. BLOCH. Phys. Rev. **70**, 460 (1946).
2. H. S. GUTOWSKY, D. W. MCCALL, and C. P. SLICHTER. J. Chem. Phys. **21**, 279 (1953).
3. H. M. MCCONNELL. J. Chem. Phys. **28**, 430 (1958).
4. R. K. WANGSNESS and F. BLOCH. Phys. Rev. **89**, 728 (1953).
5. L. W. REEVES. *In* Advan. Phys. Org. Chem. Vol. III. *Edited by* V. Gold. Academic Press, London. 1965. p. 187.
6. C. S. JOHNSON. Advan. Mag. Res., Vol. 1. *Edited by* J. S. Waugh. Academic Press, New York. 1965. p. 33.
7. A. ABRAGAM. Principles of Nuclear Magnetism. Oxford Univ. Press, London. 1961. pp. 447, 504.
8. R. A. SACK. Mol. Phys. **1**, 163 (1958).
9. P. W. ANDERSON and P. R. WEISS. Rev. Mod. Phys. **25**, 269 (1953).
10. P. W. ANDERSON. J. Phys. Soc. Jap. **9**, 316 (1954).
11. R. G. GORDON and R. P. MCGINNIS. J. Chem. Phys. **49**, 2455 (1968).
12. E. J. WELLS, R. C. FERGUSON, J. G. HALLETT, and L. K. PETERSON. Can. J. Chem. **46**, 2733 (1968).
13. J. BACON, R. J. GILLESPIE, J. S. HARTMAN, and U. R. K. RAO. Mol. Phys. **18**, 561 (1970).
14. J. R. YANDLE and J. P. MAHER. J. Chem. Soc. A, 1549 (1969).
15. G. M. WHITESIDES and J. S. FLEMING. J. Amer. Chem. Soc. **89**, 2855 (1967).
16. H. M. MCCONNELL and D. D. THOMPSON. J. Chem. Phys. **26**, 958 (1957).
17. S. FORSEN and R. A. HOFFMAN. J. Chem. Phys. **39**, 2892 (1963).
18. R. R. ERNST and W. ANDERSON. Rev. Sci. Instr. **36**, 1969 (1965).
19. J. A. POPLE, W. G. SCHNEIDER, and H. J. BERNSTEIN. High Resolution NMR. McGraw-Hill, Inc., New York. 1959. p. 219.
20. K. N. SHAW and L. W. REEVES. To be published.
21. H. S. GUTOWSKY and C. H. HOLM. J. Chem. Phys. **25**, 1228 (1956).
22. B. MULLER and M. BLOOM. Can. J. Phys. **38**, 1318 (1960).
23. M. BLOOM, L. W. REEVES, and E. J. WELLS. J. Chem. Phys. **42**, 1615 (1964).
24. A. ALLERHAND, H. S. GUTOWSKY, J. JONAS, and R. A. MEINZER. J. Amer. Chem. Soc. **88**, 3185 (1966).
25. K. N. SHAW. Ph.D. Thesis, University of British Columbia, Vancouver, British Columbia. 1970.
26. H. S. GUTOWSKY, R. L. VOLD, and E. J. WELLS. J. Chem. Phys. **43**, 4107 (1965).
27. G. BINSCH. J. Amer. Chem. Soc. **91**, 1304 (1969).
28. E. GRUNWALD, A. LOEWENSTEIN, and S. MEIBOOM. J. Chem. Phys. **27**, 630 (1957).

Can. J. Chem. Downloaded from www.nrcresearchpress.com by 210.87.254.6 on 09/05/12
For personal use only.

Isolation and structure of monochaetin, a metabolite of the fungus *Monochaetia compta*[1,2]

H. SPENCER[3] AND Y. K. MO

Department of Chemistry and Chemical Engineering, University of Saskatchewan, Saskatoon, Saskatchewan

AND

G. TERTZAKIAN,[4] G. P. SLATER, R. H. HASKINS, AND L. R. NESBITT

Prairie Regional Laboratory, National Research Council of Canada, Saskatoon, Saskatchewan

Received April 10, 1970

A new metabolite has been isolated from the fungus *Monochaetia compta*. The properties and reactions of the metabolite suggest that it is 6,8*a*-dihydro-4-acetyl-8-methyl-6-oxo-7(3-methyl-2-oxo)-pentyl-1*H*-2-benzopyran-1-one (**2***a*).

Canadian Journal of Chemistry, 48, 3654 (1970)

A fungus (PRL 1754) was isolated from wild rose hips (*Rosa acicularis* Lindl.) and identified as *Monochaetia compta* (or possibly *Cryptostictis cynosbati* (Fckl) Sacc. (Melanconiales) (1)). The only member of the Melanconiales for which a metabolite has been reported (2) is *Gloeosporum musarum* (Cke et Mass.) which produced the carotenoid canthaxanthin (4,4′-diketo-β-carotene) (3). The present fungus deposited white crystals m.p. 202.5–203.5° in potato dextrose agar cultures. Constancy of m.p., t.l.c. and p.m.r. spectroscopy, and mass spectral analysis attested to the homogeneity of the new metabolite, which analyzed for $C_{18}H_{20}O_5$. We propose the name monochaetin for this compound and describe work which suggests that its structure is represented by **2***a*.

The p.m.r. spectrum of monochaetin in deuterochloroform solution (Fig. 1) was interpreted as follows: τ 9.03 (3H), a triplet (J = 7 Hz), CH_3CH_2—; 8.3 (2H), a multiplet CH_3CH_2-CH—; 6.81 (1H), a sextet $CH_3CH_2CHCH_3$; 8.87 (3H), a doublet (J = 6 Hz) CH_3CH_2-$CHCH_3$. Double irradiation experiments confirmed the appropriate mutual couplings of this group. Since the methine sextet occurred at a low field position it follows that the next carbon atom was not substituted by hydrogen but by an electronegative atom or group. In view of the i.r. spectrum (see below) a carbonyl group seemed the most probable. A singlet τ 8.67 (3H) was assigned as

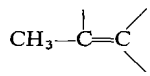

and a singlet at τ 7.87 (3H) was interpreted as being due either to a methyl ketone or to an *O*-acetyl group. Chemical tests confirmed that this was a methyl ketone; no acetic acid could be detected after monochaetin was hydrolyzed with sulfuric acid but iodoform was generated by an alkaline solution of iodine and potassium iodide. The remaining peaks were at τ 6.25 (1H), double-doublet (J's = 2 and 13 Hz); 5.90 (1H), a doublet (J = 13 Hz); 4.72 (1H), doublet (J = 0.5 Hz); 4.00 (1H), singlet —CH=C<, a very small coupling to the methyl group at τ 7.87 was revealed by a sharpening of this peak on double irradiation at the frequency of the methyl group, so that the substitution of this double bond could be written

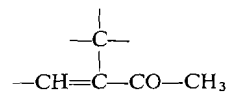

τ 3.20 (1H), double doublet (J's = 0.5 and 2 Hz).

The i.r. spectrum of monochaetin (chloroform) had two sharp bands at 1788 and 1718 cm^{-1} (Fig. 2), which could be assigned to an enol-lactone (or vinyl ester) and a saturated ketone, respectively. A third broad band at 1650–1640 cm^{-1}, together with the bands at 1605 and 1532 cm^{-1} were interpreted as an α,β-α′,β′-dienone and an α,β-unsaturated ketone. The broad

---

[1]Issued as NRCC No. 11515.

[2]Taken in part from the M.Sc. Thesis of Y. K. Mo, University of Saskatchewan, Saskatoon, Saskatchewan, 1969.

[3]NRCC Postdoctorate Fellow, 1965–1966. Present address: Imperial Chemical Industries Ltd., Pharmaceuticals Division, Alderley Park, Macclesfield, Cheshire SK10 4TG, England.

[4]NRCC Postdoctorate Fellow, 1962–1964. Present address: Raylo Chemicals Ltd., Edmonton, Alberta.

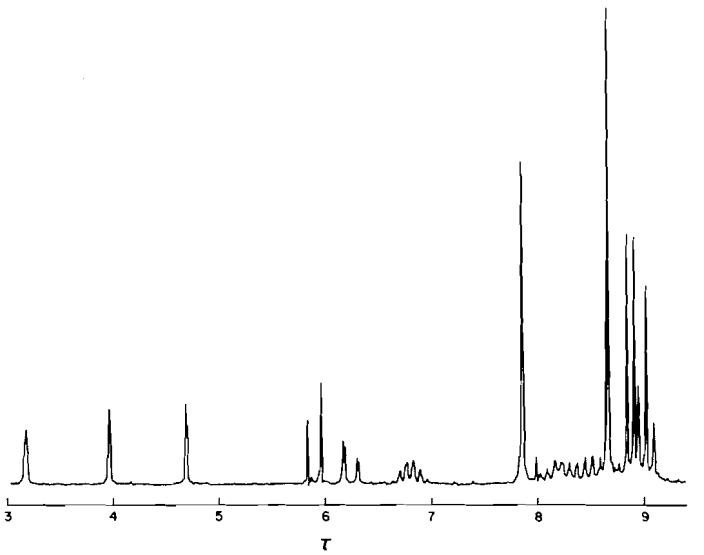

FIG. 1. The p.m.r. spectrum of monochaetin in deuterochloroform solution.

carbonyl band was at lower frequency than is usually suggested for these groups (4), however, this is probably due to the extended conjugation in monochaetin. Additional support for these assignments was provided by the u.v. spectrum (ethanol–water) which had two maxima at 248 (ε 5.83 × 10^3) and 343 nm (ε 2.53 × 10^4). The high extinction coefficients of these absorptions suggested that they were associated with a conjugated unsaturated ketone rather than with an aromatic chromophore. Since an α,β-α′,β′-dienone absorbs close to 244 nm (5) at least one more double bond and several substituents are needed to extend the absorption to the observed maximum at 343 nm.

Treatment of monochaetin with sodium borohydride gave a product, $C_{18}H_{22}O_5$ (**10**), whose i.r. spectrum (KBr) had bands at 3555 and 3380 cm^{-1} (OH) and 1760 cm^{-1} (enol lactone). The band at 1718 cm^{-1} was missing, showing that only the saturated carbonyl group was reduced. The u.v. absorption spectrum was identical to that of monochaetin, confirming that the dienone and α,β-unsaturated ketone functions were not affected. The p.m.r. spectrum of the acetylated reduction product (**11**, $C_{20}H_{24}O_6$) in deuterochloroform, was similar to that of monochaetin but with the following differences. The three protons of the acetate group gave rise to a singlet at τ 7.98. The proton attached to the same carbon atom as the *O*-acetyl appeared as a quartet at τ 4.79. There was a single two proton doublet at τ 6.68 in place of the two separate one proton signals which in monochaetin were at τ 6.25 and 5.9. The signal due to the methine proton in the *sec*-butyl chain had moved upfield. Double irradiation experiments showed that it was located at τ 8.1 and was coupled to the quartet at τ 4.79 as also was the doublet at τ 6.68. Irradiation at the frequency of the quartet caused the doublet to collapse to a singlet at τ 6.68. This spectrum was consistent only with the presence of the group $—CH_2CH(OAc)CH(CH_3)CH_2CH_3$ in this derivative which would have been formed from the $—CH_2COCH(CH_3)CH_2CH_3$ side chain in monochaetin.

Hydrogenation of monochaetin over Adam's catalyst at atmospheric pressure resulted in the rapid uptake of 3 moles of hydrogen with the formation of a crystalline hexahydro derivative **12**. Yields of this crystalline derivative were low but the mother liquors, from which the crystalline hexahydro compound had been isolated, could be further hydrogenated with a slow absorption of hydrogen to give a crystalline octahydromonochaetin **13** in good yield. Neither of the hydrogenated derivatives showed any absorption in the u.v. region. In its i.r. spectrum hexahydromonochaetin did not show any hydroxyl peaks so that it was formed from monochaetin by reduction of three carbon–carbon double bonds. The i.r. spectrum of octahydromonochaetin did have an O—H stretching band at 3390 cm^{-1} and differs from the hexahydro derivative in that a

Can. J. Chem. Downloaded from www.nrcresearchpress.com by 210.87.254.6 on 09/05/12
For personal use only.

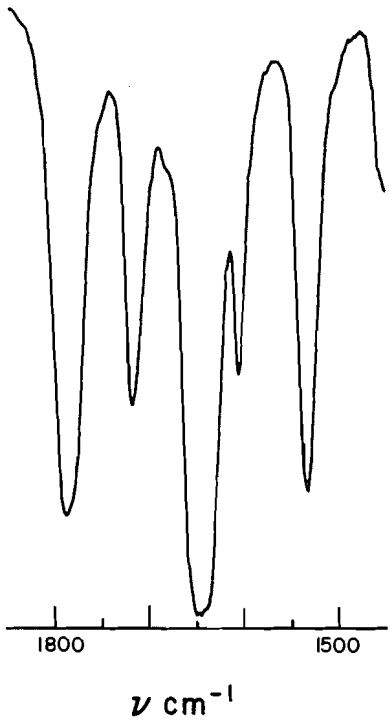

FIG. 2. Part of the i.r. spectrum of monochaetin (chloroform solution).

carbonyl group had been reduced. The p.m.r. spectra of both hydrogenated derivatives, in pyridine-d_5, were too complicated to permit a full analysis but one point is significant. Both spectra contained two high field, three proton, doublets. In octahydromonochaetin these were at τ 8.75 (J = 7 Hz) and 8.9 (J = 6 Hz). Double irradiation experiments showed that the lower field one was coupling to a sextet at τ 7.10 and hence was due to the methyl group in the *sec*-butyl chain. The upper field one was coupling to a multiplet at τ 6.82. Neither of the hydrogenated products had a three proton singlet near τ 8.67 which there had been in the spectrum of monochaetin. This was interpreted as indicating that there was in monochaetin the group

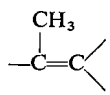

which gave the singlet at τ 8.67 and which had been transformed by hydrogenation into

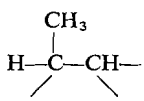

which gave rise to the doublet at τ 8.91.

Monochaetin was insoluble in water and in sodium carbonate solution but dissolved readily in dilute aqueous sodium hydroxide, from which it was recovered unchanged by the addition of acid. The amount of monochaetin recovered depended upon the temperature and the time that elapsed before acidification. After only a few minutes in alkali at room temperature the recovery was quantitative but prolonged heating caused a degradation of the molecule which is discussed in detail at a later point. Such behavior is characteristic of α- or γ-pyrones and lactones. The presence of a γ-pyrone system in monochaetin was discounted because of the complete failure of attempts to form pyrylium salts by treating ethereal solutions of monochaetin with dry hydrogen chloride gas. Confirmatory evidence for the presence of a lactone ring was obtained by allowing monochaetin to react with concentrated ammonia. This resulted in the formation of a new derivative, $C_{18}H_{23}O_5N$ (**14**), formed by the addition of the elements of ammonia. The new compound was insoluble in aqueous acids but had bands in the i.r. at 3400, 3260, and 3150 and 1672 cm^{-1}, and its p.m.r. spectrum had two broad peaks, each one proton, at τ 2.48 and 2.86, compatible with a primary amide. Only a lactone could have been converted into a primary amide with the addition of the elements of ammonia. Further evidence for the enolic nature of this lactone came from the reaction of monochaetin with Tollen's reagent. Although the p.m.r. spectrum of monochaetin had not shown any aldehydic protons a silver mirror was formed in the reaction with Tollen's reagent, implying that an aldehyde group was generated in the alkaline solution, as would be the case with an enol lactone.

The reaction between monochaetin and *N*-bromosuccinimide (1.1 mole) in carbon tetrachloride resulted in the formation of a crystalline monobromo derivative **4**. The p.m.r. spectrum of monobromomonochaetin (in deuterochloroform) was identical to that of monochaetin except for the one proton singlet at τ 4.70 which had been eliminated by bromination. Since this proton was readily replaced by bromine it must have been allylic, but in order to account for its unusually low field position in the p.m.r. spectrum, we suggest that it is allylic to two double bonds and α to a carbonyl group. With two moles of *N*-bromosuccinimide two hydrogen atoms were replaced. This dibromo derivative **5** reacted with

Can. J. Chem. Downloaded from www.nrcresearchpress.com by 210.87.254.6 on 09/05/12
For personal use only.

Can. J. Chem. Downloaded from www.nrcresearchpress.com by 210.87.254.6 on 09/05/12
For personal use only.

potassium carbonate with the elimination of HBr to give a crystalline product, $C_{18}H_{17}O_5Br$ (**6**), which showed in its p.m.r. spectrum (in $CDCl_3$) the peaks of the *sec*-butyl group at τ 9.03 (3H, triplet); 9.00 (3H, doublet); 8.40 (2H, multiplet); 6.50 (1H, sextet); the methyl ketone at 8.30 (3H, singlet), and the vinylic methyl group at 7.75 (3H, singlet). Two other protons gave rise to singlets at τ 3.32 and 1.23. The u.v. spectrum of this compound (in 50% aqueous ethanol) was different from that of monochaetin and its other derivatives, having maxima at 270 (ε 1.35×10^4), 360 (ε 1.0×10^4), and 555 nm (ε 3.03×10^3).

As mentioned earlier, heating monochaetin with aqueous sodium hydroxide caused a degradation and two smaller fragments were isolated. The first of these was acetic acid, characterized as its *p*-bromophenacyl ester, and isolated in 15% yield. Since it has already been demonstrated that there was no *O*-acetyl in monochaetin the acetic acid must have been formed from the methyl ketone via a retro-Aldol or retro-Claisen reaction. The other product was a non-volatile gum **1** (44% yield) which formed a crystalline 2,4-dinitrophenylhydrazone (**1***a*) having the formula $C_{22}H_{26}O_6N_4$. After allowance for the 2,4-dinitrophenylhydrazine residue this led to $C_{16}H_{22}O_3$ as the formula of the ketonic gum **1**. The u.v. spectrum (in 50% aqueous ethanol) of the ketone showed a single maximum at 282 nm (ε 2720) which moved to 300 nm (ε 3490) on adding 0.5 *N* potassium hydroxide, indicative of a phenolic compound. The formation of a red precipitate with diazotized aniline confirmed the phenolic nature of this product. The formation of a phenolic degradation product, under the conditions of this reaction, from a non-aromatic starting material was further strong evidence that there was in monochaetin a dienone function in a six-membered ring. The i.r. spectrum (liquid film) of the gum **1**, showed hydrogen bonded OH at 3342 cm^{-1} and a ketonic carbonyl at 1705 cm^{-1}. In its p.m.r. spectrum ($CDCl_3$) a two proton signal (broad singlet) at τ 3.5 was assigned to aromatic protons. Two singlets, each (τ 6.27 and 6.47) were assigned as benzylic protons α to the carbonyl groups, and two other singlets (τ 7.87 and 7.95, three protons each) as CH_3CO— and CH_3-aryl respectively. The protons of a *sec*-butyl group were still present as in monochaetin itself. In deuteroacetone as solvent the two aromatic protons had different chemical shifts, occurring at τ 3.4 and 3.5. The signals were broad but became clearly resolved as mutually coupled doublets (J = 1.6 Hz) upon

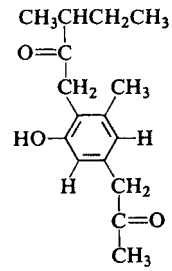

1

double irradiation at τ 6.47 indicating that the protons were *meta* to each other and confirming that the methylene group at τ 6.47 was α to the ring. The structure of this compound must be **1** or an isomer of this in which the positions of the nuclear substituents are interchanged.

We propose the structure **2***a* for monochaetin as the only one which incorporates all of the structural elements which have been identified and which satisfactorily explains the observed chemistry. For example, in dilute alkali the

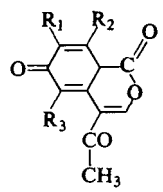

2

	R_1	R_2	R_3
a	$CH_2COCH(CH_3)CH_2CH_3$	CH_3	H
b	CH_3	$CH_2COCH(CH_3)CH_2CH_3$	H
c	H	$CH_2COCH(CH_3)CH_2CH_3$	CH_3
d	$CH_2COCH(CH_3)CH_2CH_3$	H	CH_3
e	CH_3	H	$CH_2COCH(CH_3)CH_2CH_3$
f	H	CH_3	$CH_2COCH(CH_3)CH_2CH_3$

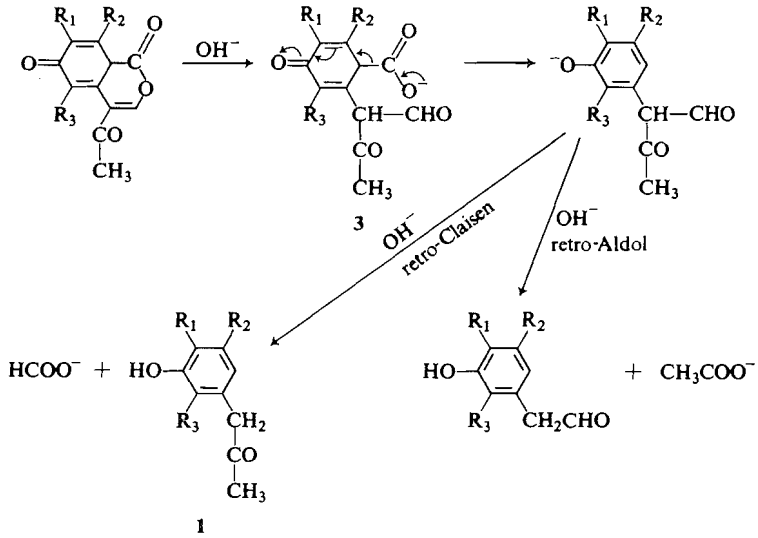

SCHEME 1

lactone ring would open as shown in Scheme 1 to give the anion **3** which is an aldehyde and would react with Tollen's reagent to give a silver mirror. Prolonged heating with alkali could cause further reaction as shown, accounting for the formation of the isolated products. The proposed structure also incorporates a chromophoric group which could reasonably be expected to give the observed u.v. spectrum *viz.*

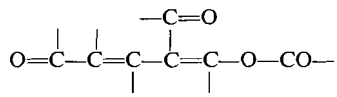

The structure also contains a proton which is allylic to two double bonds and α to a carbonyl group, which according to Shoolery's rules (6) would resonate close to the observed value at τ 4.70 in the p.m.r. spectrum. One would expect this proton to be the one most easily replaced by reaction with *N*-bromosuccinimide leading to the monobromo derivative **4**. The next most easily replaceable hydrogen would be the one allylic to one double bond and α to a carbonyl group so that the dibromo derivative would be **5** for which the spectra are consistent. Elimination of HBr could occur to give **6** which being a quinone methide ought to be colored, as observed.

The low resolution mass spectrum of monochaetin (Table 1) also lends support to the proposed structure, **2***a*, as indicated by the following

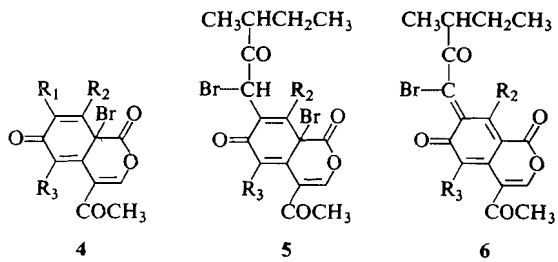

4 **5** **6**

brief description of the fragmentation. One mode of α-cleavage of the methyl ketone would account for the abundant ion at *m/e* 43 (CH_3CO^+). The alternative mode of cleavage would result in the loss of CH_3 to give ion *m/e* 301 and subsequent loss of CO to give ion *m/e* 273. The latter could then lose CO_2 (from the lactone ring) to produce ion *m/e* 229.

The ions *m/e* 259 (loss of C_4H_9) and 85 ($C_5H_9O^+$) are indicative of the two possible modes of α-cleavage of the *sec*-butyl ketone. Each of these ions could then lose CO, accounting for the ions *m/e* 231 and 57, respectively. A metastable peak at 38.3 confirmed the fragmentation of ion *m/e* 85 to 57. Loss of CO from ion *m/e* 231 would account for ion *m/e* 203 (this is supported by the occurrence of a metastable ion at *m/e* 178), and subsequent loss of ketone would lead to the base peak *m/e* 161.

Alternative structural proposals such as **2***b* and **2***c* were discounted because they could not

Can. J. Chem. Downloaded from www.nrcresearchpress.com by 210.87.254.6 on 09/05/12
For personal use only.

TABLE 1
The mass spectrum of monochaetin

m/e	Relative abundance	m/e	Relative abundance
29	20.0	145	2.6
29.5m	0.06	146	2.5
32	2.0	148	5.3
38.3m	0.06	159	22.7
39	6.0	160	5.3
41	12.0	161	100.0
43	26.6	162	14.0
44	2.0	163	1.3
51	3.3	169m	0.2
53	2.0	175	5.3
55	2.6	178m	0.06
57	50.0	182	1.0
58	2.3	187	6.0
63	3.3	188	3.0
65	2.3	189	4.0
77	8.0	190	6.0
78	4.0	203	21.3
79	2.0	204	6.0
85	5.3	214	3.3
89	1.3	216	6.0
91	4.0	218	1.3
102	1.3	229	1.3
103	6.0	231	44.7
105	2.6	232	16.7
106	1.7	233	2.3
115	4.7	243	4.7
116	1.7	244	1.0
119	2.0	259	1.0
131	3.3	273	0.8
132	9.3	301	1.2
133	2.7	316	20.0
137	2.3	317	4.0
		318	0.5

account for the elimination of HBr. Structures such as **2***d* and **2***e* would have degraded with alkali to give a phenol having protons on adjacent nuclear positions for which the coupling constant would have been about 6 Hz and hence these two structures are untenable. The structure **2***f* was considered less likely than **2***a* because it contains the unit

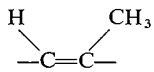

in which detectable coupling between the methyl group and the vinylic proton would be expected.

Other locations of the lactone ring were also considered but deemed unsatisfactory. No structures based upon the system **7** could account for the p.m.r. spectrum of monochaetin, while the systems **8** and **9** could not provide a satisfactory explanation for either the u.v. spectrum or for the loss of the lactone carbonyl group upon treatment with sodium hydroxide.

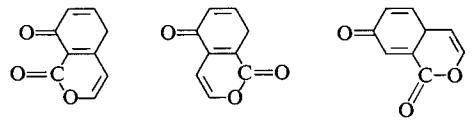

7 **8** **9**

Experimental

General Directions

The p.m.r. spectra were determined using either a Varian HA-100 or a Varian T-60 spectrometer with TMS as an internal standard. The i.r. spectra were recorded on a Perkin-Elmer 21 spectrometer and u.v. spectra were determined using a Cary 14. Mass spectra were determined on an A.E.I. MS 12 spectrometer. A Fisher hot stage m.p. apparatus was used for all m.p.'s, which are uncorrected.

Growth

A medium consisting of 1% dextrose and 1% Difco Yeast extract (50 ml) was inoculated with the organism *Monochaetia compta* (PRL 1754) and incubated at 24°, on a rotary shaker, for 4 days. The cells were collected and dispersed in water (100 ml) and the suspension spread with a small paint brush upon the growth medium, which consisted of Difco Potato Dextrose agar enriched with 20 g/l of dextrose and contained in pyrex dishes (31 cm × 46 cm, 500 ml of agar per dish) covered with aluminum lids. The cultures were incubated at 24 to 26° for 30 days.

Extraction

The whole agar culture was freeze-dried and the residue extracted exhaustively with chloroform. The white solid resulting from evaporation of the extract was washed with light petroleum (30–60°) to remove oils. The yield of monochaetin determined at this point was 1.85 g/l of agar. Treatment with charcoal and several crystallizations from ethanol gave pure monochaetin, m.p. 202.5–203.5°, $[\alpha]_D^{25} = 1040 \pm 10°$ (*c*, 0.3 $CHCl_3$), λ_{max} (50% aqueous ethanol) 248 (ε 5.83 × 10^3) and 343 nm (ε 2.53 × 10^4).

Anal. Calcd. for $C_{18}H_{20}O_5$: C, 68.34; H, 6.37. Found: C, 68.26; H, 6.45.

Test for O-Acetyl

Sulfuric acid (2 *N*, 50 ml) was steam distilled until 100 ml of distillate had been collected. This was discarded and a fresh quantity of distillate (50 ml) was obtained to serve as a blank. Monochaetin (95.7 mg) was added to the sulfuric acid and the mixture heated under reflux for 1.5 h. The residual solution was again steam distilled to obtain 50 ml of distillate. Both the blank and the distillate after reaction had the same p*H* (4.8) and each required the same quantity of standard sodium hydroxide solution (0.2 ml, 0.036 *N*) to take the p*H* to 8.

Sodium Borohydride Reduction

Monochaetin (316 mg, 1.0 m*M*) and sodium borohydride (28 mg, 0.75 m*M*) were dissolved in dry methanol (15 ml) and stirred at room temperature for 2 h. The resulting solution was acidified with dilute sulfuric acid (15 ml) and extracted with chloroform. The chloroform was evaporated and the residue separated by preparative layer chromatography. The major product, **10**, crystallized from ethanol (96 mg, 30% yield), m.p. 105–107°. In

Can. J. Chem. Downloaded from www.nrcresearchpress.com by 210.87.254.6 on 09/05/12
For personal use only.

Can. J. Chem. Downloaded from www.nrcresearchpress.com by 210.87.254.6 on 09/05/12
For personal use only.

the u.v. it had λ_{max} (ethanol) 247 (ε 6.07 × 10^3) and 352 nm (ε 2.32 × 10^4).

Anal. Calcd. for $C_{18}H_{22}O_5$: C, 67.91; H, 6.97. Found (mol. wt. (mass spectroscopy) 318): C, 67.69; H, 7.05.

Acetylation of the Sodium Borohydride Reduction Product

The above reduction product **10** (31 mg) was dissolved in pyridine (0.5 ml) and acetic anhydride (0.5 ml) and allowed to stand at room temperature overnight. Water (1 ml) was added to the reaction mixture and the acetyl derivative **11** collected (24 mg, 69% yield) and crystallized from aqueous ethanol, m.p. 216–217°.

Anal. Calcd. for $C_{20}H_{24}O_6$: C, 66.65; H, 6.71. Found (mol. wt. (mass spectroscopy) 360): C, 66.83; H, 6.66.

Catalytic Hydrogenation

Monochaetin (459 mg) was dissolved in ethanol (100 ml) that had been distilled from magnesium ethoxide and the solution was shaken with hydrogen in the presence of Adams' platinum oxide (197.9 mg). Rate of uptake changed abruptly after 1.66 h when 120 ml of hydrogen had been absorbed (theoretical uptake for the catalyst and three double bonds, 122.4 ml). After filtering the catalyst, the solution was concentrated and a white precipitate (78 mg) formed. This was purified by chromatography on a silicic acid column. *Hexahydromonochaetin* (**12**) crystallized from methanol, m.p. 247–248°. No absorption in the u.v. region.

Anal. Calcd. for $C_{18}H_{26}O_5$: C, 67.06; H, 7.89. Found (mol. wt. (mass spectroscopy) 322): C, 67.05; H, 7.89.

The mother liquors were returned to hydrogenate until the uptake of hydrogen ceased. The filtrate was concentrated and *octahydromonochaetin* (**13**), m.p. 220–221°, precipitated upon standing. No absorption in the u.v. region.

Anal. Calcd. for $C_{18}H_{28}O_5$: C, 66.64; H, 8.70; Found (mol. wt. (mass spectroscopy) 324): C, 66.65; H, 8.90.

Effect of Alkali on Monochaetin

Monochaetin (24.4 mg) was dissolved in 0.02 *N* sodium hydroxide (6 ml) with a little gentle warming and immediately acidified with *N* sulfuric acid. The precipitate was collected and dried (16.8 mg) and crystallized from aqueous ethanol. The recovered material had m.p. 202.5–203.5°, and was identical with monochaetin (mixed m.p., i.r.) (starting material, m.p. 202.5–203.5°).

Hydrolysis of Monochaetin

Monochaetin (328 mg) was heated with 5% sodium hydroxide (23 ml) at reflux, in a nitrogen atmosphere, for 1.5 h. The cooled solution was acidified with dilute sulfuric acid and steam distilled until 100 ml of distillate had been collected. The residual liquor was extracted thoroughly with ether–chloroform (4:1) and the dried extract evaporated and fractionated by silicic acid column chromatography. Elution with chloroform–benzene (85:15) yielded a gum, **1**, which appeared to be homogenous (t.l.c.). In the u.v. (1:1 aqueous ethanol) it had λ_{max} 282 nm (ε 2720) which shifted in alkali to 300 nm (ε 3490).

The 2,4-dinitrophenylhydrazone derivative, **1***a*, had m.p. 180°.

Anal. Calcd. for $C_{22}H_{26}O_6N_4$: C, 59.72; H, 5.92; N, 12.66. Found: C, 59.97; H, 5.89; N, 12.55.

Mass of parent ion calcd. for $C_{22}H_{26}O_6N_4$: 442.1852. Found: 442.1847. (High resolution measurements by Dr. A. M. Hogg, University of Alberta, Edmonton, Alberta.)

The acids in the steam distillate were neutralized with 0.02 *N* sodium hydroxide and the solution evaporated to dryness. To the salts, dissolved in water (2 drops) was added *p*-bromophenacyl bromide (1.1 mole) in ethanol (100 ml) and the solution was boiled for 30 min. The solvent was evaporated and the residue chromatographed on silicic acid. Elution with $CHCl_3$–C_6H_6 (85:15 v/v) gave *p*-bromophenacyl acetate, m.p. 84° (lit. (7) m.p. 86°). The i.r. spectrum was identical with that of a standard sample.

Reaction with Ammonia

Monochaetin (200 mg) was dissolved in concentrated ammonia (8 ml) and warmed for 20 min. The solution was diluted with water and the precipitate (150 mg) collected and crystallized from aqueous ethanol to give needle-like crystals, m.p. 238–239°. In the u.v., the product **14** had λ_{max} 247 (ε 5.38 × 10^3) and 356 nm (ε 1.96 × 10^4).

Anal. Calcd. for $C_{18}H_{23}O_5N$: C, 64.85; H, 6.71; N, 4.20. Found (mol. wt. (mass spectroscopy) 333): C, 65.11; H, 6.80; N, 4.32.

Monobromomonochaetin (4)

Monochaetin (316 mg, 1 m*M*) was heated with *N*-bromosuccinimide (178 mg 1 m*M*) and a trace of benzoyl peroxide in carbon tetrachloride (30 ml). After 2 h the reaction mixture was washed with water (30 ml), dried, and evaporated to give a yellow solid (390 mg) which crystallized from ethanol as colorless needle-like crystals, m.p. 224–225°. The parent ion in the mass spectrum (mass 394) showed the appropriate isotope distribution for a compound containing one bromine atom.

Anal. Calcd. for $C_{18}H_{19}O_5Br$: C, 54.68; H, 4.81. Found: C, 54.67; H, 4.83.

Dibromomonochaetin (5)

Monochaetin (121 mg, 0.38 m*M*) was heated with *N*-bromosuccinimide (157 mg, 0.88 m*M*) and a trace of benzoyl peroxide in carbon tetrachloride (35 ml) overnight. The reaction mixture was washed with water, dried, and evaporated to give a gum (120 mg) which was separated by preparative t.l.c. on silica gel using chloroform–ether–benzene (7:2:1). The major product was a gum which decomposed to a considerable extent in 2–3 days at room temperature but was stable indefinitely at liquid nitrogen temperature. The parent ion in the mass spectrum (*m/e* 472) showed the appropriate isotope distribution for a compound containing two bromine atoms. In the u.v. it had λ_{max}(EtOH) 225 (ε 9 × 10^3), 267 (ε 1.4 × 10^4), and 357 nm (ε 1.45 × 10^4).

Anal. Calcd. for $C_{18}H_{18}O_5Br_2$: C, 45.58; H, 3.83. Found: C, 45.33, H, 3.70.

Dehydrobromination of Dibromomonochaetin

Dibromomonochaetin (80 mg) and potassium carbonate were heated together in ethanol (30 ml) for 2 h. The reaction mixture was filtered and acidified with dilute sulfuric acid, then water (15 ml), benzene (15 ml), and chloroform (15 ml) were added. The aqueous phase was separated and the non-polar layer was dried and evaporated. The residue was fractionated by preparative t.l.c.

and a crystalline product (**6**) (18 mg) m.p. 109–110° was obtained from the yellow band on the t.l.c. plates. The u.v. had λ_{max}(EtOH) 270 (ε 1.35 × 10^4), 360 (ε 1.0 × 10^4), and 555 nm (ε 3.03 × 10^3).

Anal. Calcd. for $C_{18}H_{17}O_5Br$: C, 54.98; H, 4.35. Found (mol. wt. (mass spectroscopy) 392): C, 55.22; H, 4.46.

We wish to thank Mr. M. Mazurek for measuring the 100 MHz p.m.r. spectra and Mr. J. Fisher for recording the mass spectra. Two of us (H.S. and Y.K.M.) wish to acknowledge the generous financial support of the National Research Council of Canada and one of us (Y.K.M.) thanks the University of Saskatchewan for the award of a teaching assistantship.

1. E. F. GUBA. *In* Monochaetia and Pestalotia. Harvard University Press, Cambridge, Mass., 1961. p. 263.
2. S. SHIBATA, S. NATORI, and S. U. UDAGAWA. *In* List of fungal products. University of Tokyo Press, Tokyo, 1964. p. 24.
3. F. J. PETRACEK and L. Z. ZECHMEISTER. Arch. Biochem. Biophys. **61**, 137 (1956).
4. L. J. BELLAMY. *In* The infra-red spectra of complex molecules. Methuen, London, 1958. p. 132.
5. A. I. SCOTT. *In* Interpretation of the ultraviolet spectra of natural products. Pergamon Press, Oxford, 1964. p. 255.
6. R. M. SILVERSTEIN and G. C. BASSLER. *In* Spectrometric identification of organic compounds. John Wiley and Sons, New York, N.Y., 1967. p. 141.
7. A. I. VOGEL. *In* Elementary practical organic chemistry. Part 2. Longmans, London, 1966.

Can. J. Chem. Downloaded from www.nrcresearchpress.com by 210.87.254.6 on 09/05/12
For personal use only.

Can. J. Chem. Downloaded from www.nrcresearchpress.com by 210.87.254.5 on 09/05/12
For personal use only.

Preparation and characterization of some α,α-disubstituted-α-hydroxythiolesters

WILMA E. ELIAS
Department of Chemistry, University of Victoria, Victoria, British Columbia

Received December 9, 1969[1]

A series of α,α-disubstituted-α-hydroxythiolesters has been prepared from ketone cyanohydrins by the Pinner reaction. The esters have been characterized both by classical methods and by analysis of their i.r. n.m.r., and u.v. spectra.

Canadian Journal of Chemistry, **48**, 3662 (1970)

Introduction

In view of the widely-known hydrogenolytic and reductive desulfurization reactions which organic thio compounds undergo in the presence of Raney nickel (1, 2) and other reducing agents (3, 4 and, for instance, refs. given in 5*a*), and of the hydrogenolysis reactions of carbonyl compounds with vicinyl oxygen-containing groups (*e.g.* refs. given in 5*b* and 6, but compare with 7), it was considered that an examination of the reactions of α-hydroxythiolesters with a number of reducing agents would be of interest. Since α-hydroxythiolesters are not reported in the literature it was necessary to develop a method for the preparation of these compounds. This paper reports the synthesis and characterization of a number of compounds of structure $RR'C(OH)COSC_2H_5$.

Several methods for the preparation of thiolesters have been developed,[2] among them reaction of an acyl halide or acid anhydride with the appropriate thiol, transesterification, reaction of an acyl halide with the appropriate lead mercaptide, and the Pinner reaction. In view of the presence of the tertiary alcohol hydroxyl in the compounds desired, the latter method suggested itself as the most likely to be of general use. The acid-catalyzed addition of an alcohol across the triple bond of a nitrile, followed by hydrolysis of the imidate salt[3] (eq. 1)

[1] $RCN + R'OH + \text{anhydrous } HX \rightarrow$

$$RC(=NH\cdot HX)OR' \xrightarrow{\text{hydrolysis}} RCO_2R' + NH_4^+ + X^-$$

was first reported by Pinner and Klein (9) and has since been used quite extensively but, although some cyanohydrins have been treated with alcohols and some nitriles with thiols, no report of the reaction of cyanohydrins with thiols has been found.[4]

Results and Discussion

The thioimidate hydrochlorides were prepared according to the 'standard' procedure for bringing about the Pinner acid-catalyzed reaction. The necessity for maintaining the reaction temperature close to 0 °C was manifested during one preparation which was allowed, inadvertently, to warm under its own heat of reaction; there was generated an odor far more powerful and obnoxious than that associated with the normal process. The resultant mixture was not analyzed, but it was assumed that this indicated the formation of at least some thionamide (10 and refs. therein, 14). Only a slight excess of thiol was used, since reaction of imidate salts with excess alcohol is a synthetic route to ortho esters (10 and refs. therein).

Crystalline thioimidate hydrochlorides were obtained from only a few of the cyanohydrins (marked with an asterisk in Table 1); large masses of granular, white crystals were obtained in each case. Reaction mixtures which did not deposit crystals became very viscous, frequently set to a glass, and often developed colors ranging from yellow to deep orange.

No attempt was made to isolate the thioimidate hydrochlorides, which were converted directly to the corresponding α-hydroxythiolesters as described in the experimental section, *i.e.*, the thiolesters were purified only by distillation through a short Vigreux column, during which a fore-run and two or three fractions were collected.

[1]Revision received July 27, 1970.

[2]A brief review is given in ref. 8.

[3]The nomenclature of compounds RC(=NH)OR′ is confused; they have been called iminoethers, iminoesters, imidic esters, imidoates, imidates, imidoethers, and imidoesters. The convention adopted by Roger and Neilson (10) in naming them imidates, will be followed in this series of papers. Chemical Abstracts lists these compounds as esters of imidic acids.

[4]No recent, comprehensive review of the Pinner reaction is known to the author, but several partial reviews are available (10–13).

Can. J. Chem. Downloaded from www.nrcresearchpress.com by 210.87.254.5 on 09/05/12
For personal use only.

TABLE 1

Preparation, physical properties, and analysis of $RR'C(OH)COSC_2H_5$

Compound No.	Substituents R	Substituents R′	Reaction time (days)	Yield† thiolester (%)	Boiling points (°C)‡ Reduced pressure	Boiling points (°C)‡ Atmospheric pressure	η_D§	d_4‖	Molar refractivities Calculated¶	Molar refractivities Found	Saponification equivalent Calculated	Saponification equivalent Found	Sulfur content (%) Calculated	Sulfur content (%) Found
1	CH_3	CH_3	7*	59.2	90–95/19–20	200–203	1.4155 (28)	1.051 (29)	39.258	39.26	148.2	143.5, 145.0	21.60	20.31, 20.91 **††
2	CH_3	C_2H_5	20*	53.3	89–92/20–21	211–214d./710	1.4773 (28)	1.053 (27)	43.905	43.55	162.2	155.0, 157.0	19.73	19.42, 19.22, 19.22**‡‡
3	C_2H_5	C_2H_5	14	25.6	101–103/20	219–223					176.3	166.0, 167.5	18.19	15.31, 15.75**§§
4	CH_3	n-C_3H_7	13	73.2	68–76/1	223–224.5	1.4752 (25)				176.3	167.4, 166.1, 163.3		
5	CH_3	i-C_3H_7	14	59.4	60–63/1	221–224.5	1.4689 (25)	0.9978 (25)	48.552	49.19	176.3	170.9, 174.9, 177.5	18.19	18.08, 18.04
6	CH_3	n-C_6H_{13}	15	79.4	150–158/8	267.5–270	1.4733 (24.5)				218.4	211.3, 211.7, 215.9		
7	C_2H_5	n-C_4H_9	13	64.8	113–116/2.5	250.5–252	1.4732 (24.5)	0.9764 (25)	57.846	58.73	204.3	202.7, 200.7	15.69	15.58, 15.63
8	CH_3	C_6H_5—CH_2	15	80.2	176–185/11–20	281.5–288.5	1.5424 (26)	1.0968 (26)	63.693	64.55	224.3	217.7, 218.2, 224.3		
9	Cyclohexyl		3*	65.7	122–125/7	261.5–262.5	1.5092 (26.5)	1.096 (26)	51.143	51.57	188.3	185.9, 182.5	17.03	16.71, 16.65
10	2-Methylcyclohexyl		16	31	110–125/5									
11	3-Methylcyclohexyl		11*	62.8	106–110/3	184.5–185.5	1.5030 (27.5)	1.0608 (27.5)	56.818	56.38	202.3	199.0, 196.5, 202.6	15.85	15.74, 15.75‖‖
12	4-Methylcyclohexyl		11	79.5	107–109/3	267.5–268	1.5030 (27)	1.0627 (27)	56.818	56.28	202.3	198.1, 200.0, 205.1	15.85	15.67, 15.64
13	Cyclopentyl		2*	74.9	103–107/7	240.5–242	1.4984 (27)	1.1025 (26)	46.496	46.36	174.3	176.1, 175.7, 181.1	18.39	18.18

*Crystalline thioimidate hydrochlorides were obtained.
†The sum of the weights of all fractions with reasonably small b.p. ranges was used to calculate the percentage of the theoretical yield. All yields are for the conversion of cyanohydrin to the ester.
‡Boiling points are given for the fractions used to determine the physical constants, including spectra and upon which the quantitative analyses are based. The figures to the right of the oblique indicate the pressure (mm of Hg) at which the distillation was conducted.
§Temperatures at which the determinations were made are given in parentheses.
‖The determinations were made in semimicro pycnometers such as described by Schneider (25). Temperatures at which determinations were made are given in parentheses.
¶Calculated, using the atomic parameters reported by Vogel, as summarized by D. J. Pastro and C. R. Johnson (28).
**Analyses denoted by ** were carried out by the author, using the Parr-bomb combustion method, followed by gravimetric determination of the sulfate. Other analyses were carried out by the Alfred Bernhardt Laboratory, Mulheim, Germany.
††Spectroscopic measurements were carried out on a preparation which analyzed for 21.79% S.
‡‡Spectroscopic measurements were carried out on a preparation which analyzed for 19.72 and 19.84% S.
§§Spectroscopic measurements were carried out on a preparation which analyzed for 15.26 and 15.41% S.
‖‖Anal. Calcd.: C, 59.37; H, 8.97. Found: C, 59.59; H, 8.86 (on a sample which had been stored for some months).

Can. J. Chem. Downloaded from www.nrcresearchpress.com by 210.87.254.5 on 09/05/12
For personal use only.

Examination of the data presented in Table 1 shows that, although the yields of thiolesters were variable, the synthesis is practicable. (The esters derived from diethyl ketone and 2-methylcyclohexanone were formed in lower yield, and were obtained in a much less pure state, than the other compounds.)

The α-hydroxythiolesters were characterized by classical methods and by their spectroscopic properties.[5] The results of the classical analyses are summarized in Table 1; in addition, three of the esters have been hydrolyzed to the corresponding α-hydroxyacids, as described in the experimental section.

In analyzing the spectra, cognizance of the impurities in **3** and **10** has been made, and information concerning these compounds has been included only where it is non-equivocal and completely in accord with that obtained for the other compounds. This is emphasized by enclosing compound numbers (**3**) and (**10**) in parentheses wherever used.

Nuclear Magnetic Resonance Spectra

Quartets at 2.82–2.92 p.p.m. and triplets at 1.16–1.26 p.p.m. confirmed the presence of the $S—CH_2—CH_3$ group (15*a*, *b*, 16); in some instances, further splitting indicated the magnetic non-equivalence of the methylene protons. The presence of the OH group was confirmed by deuterium oxide exchange.

Ultraviolet Spectra

All solutions were scanned over the region 200–670 mμ. For all compounds there was a single, reasonably sharp peak the base of which tailed off more gradually on the short wavelength side than on the long. As seen from Table 2*a*, absorption was not intense, but occurred at almost identical wavelengths for all but **1** and was in the region expected. The ultraviolet spectra of thiolesters are not widely reported in the literature, but data for three aliphatic esters have been included in Table 2*b*.

Infrared Spectra

The i.r. spectra were examined for bands for OH, C=O, C—S, and C=C groups. No evidence of carbon–carbon unsaturation was detected, indicating the stability of the tertiary hydroxyl group to the experimental conditions employed in the preparation of these compounds. On the other hand, characteristic absorptions for C=O in the range 5.89–5.99 μ (20–22), C—S in the range 7.00–7.05 μ (22) and, except for (**10**) one to three bands not present in the precursors in the range 9.92–10.75 μ (22), were found. Except for **8**, the OH group gave a band or shoulder at 2.73–2.78 μ and a band at 2.80–2.86 μ; **8** showed only a band at 2.8 μ.

TABLE 2
Ultraviolet spectra of thiolesters

Compound	λ_{max} (mμ)	ε_{max} ($\times 10^{-3}$)	Reference
(a) α-Hydroxythiolesters			
1	259	16.6	
4	243	3.16	
5	242.7	2.65	
6	243	3.30	
7	240.5	3.06	
8	243	3.80	
9	242.7	1.74	
11	243	3.37	
12	241.3	5.0	
13	243	3.31	
(b) Thiolesters reported in the literature			
n-Butyl thiolacetate	≃230	4.0	17
2-Methylcyclohexyl thiolacetate	231.5	4.5	18
2-hydroxy-3-chloropropyl thiolacetate	≃230	4.0	19

Thus, both the classical and spectroscopic analyses provide evidence that compounds of the desired structures were obtained, and were obtained in a sufficient state of purity to serve all practical purposes, by the simple purification method described. Furthermore, it can be concluded that the reaction of ethane thiol with ketone cyanohydrins is a reaction of at least reasonable generality, and hence that the work reported here extends the scope of the Pinner reaction. However, it cannot be claimed that the method is general for the production of α,α-disubstituted-α-hydroxythiolesters, since it rests upon the availability of the requisite cyanohydrins and thus will be mainly confined to esters derived from methyl and some ethyl open-chain, and alicyclic ketones.

Experimental

Preparation of the Cyanohydrins

The cyanohydrins were prepared either by the method of Cox and Stormont (23) or of Bucherer and Grolee (24). In instances where the cyanohydrin was not isolated in a

[5]Details of the mass spectra of these compounds will be presented in a subsequent paper.

TABLE 3
Ketone cyanohydrins

Ketone	Boiling point of cyanohydrin (°C/mm of Hg)
Ethyl *n*-butyl	82–84/4
Methyl benzyl	141–144/8
2-Methylcyclohexanone	103–104/5
3-Methylcyclohexanone	106–110/4.5
4-Methylcyclohexanone	118–121/7
Cyclopentanone	81–83/3

pure state, a mixture of the washed extracts and benzene was rendered anhydrous by removal of the benzene–water azeotrope under the vacuum created by a water aspirator. Boiling points not given in Beilstein are listed in Table 3.

Preparation of the α-Hydroxythioimidate Hydrochlorides

Either a mixture of cyanohydrin (1 *M* quantity) and ethyl mercaptan (1.1 *M* quantity) in anhydrous ether or benzene was prepared, or the mercaptan was added to the anhydrous benzene solution of cyanohydrin prepared from 1 *M* quantity of ketone. This mixture was then cooled in an ice bath and hydrogen chloride was passed in to saturation; the weight of hydrogen chloride taken up by the solution was not measured. The anhydrous mixture was then allowed to stand in the refrigerator either until a good crop of glistening white crystals was obtained, or for some days or weeks; typical reaction times are given in Table 1.

Preparation of the α-Hydroxythiolesters

Water was added to the crystalline thioimidate hydrochlorides after removal of the supernatant liquid by decantation; water was added directly to the whole syrup or glass. In either case, steam was passed through the aqueous mixture until the distillate was free from water-insoluble material. The thiolesters, which separated from the cooled distillates as colorless oils, were extracted into ether or benzene and these extracts were worked-up in the usual manner. Final purification consisted of distillation at reduced pressure through a small Vigreux column; boiling points and other physical properties are shown in Table 1.

All esters prepared were clear, colorless liquids of unpleasant odor, an odor which lingered on the skin for several hours after contact. During storage in the refrigerator, the esters from 2- and 3-methylcyclohexanone formed some crystals, which disappeared as soon as the flasks were removed from the refrigerator. All esters were insoluble in water but soluble in methanol, ethanol, ether, benzene, carbon tetrachloride, and chloroform.

Hydrolysis of α-Hydroxythiolesters

Three of the esters were converted to the corresponding α-hydroxyacids (I, $RR'C(OH)CO_2H$). The melting points are uncorrected. Required for I, $R = R' = CH_3$, m.p. 79°; found, m.p. 78.5–79°. Required for $R = CH_3$, $R' = C_2H_5$, m.p. 68–73° (lit. 27*a*); found, m.p. 67.5–68°. Required for I, $R = R' = C_2H_5$, m.p. 79–80° (lit. 27*b*); found, m.p. 78–79°.

Nuclear Magnetic Resonance Spectra

The n.m.r. spectra were determined at 60 MHz on a Varian HA60 spectrometer at room temperature. Deuterochloroform was used as solvent, the solutions being approximately 10% (v/v) in concentration. All chemical shifts are reported as δ values with respect to tetramethylsilane used as an internal standard.

Ultraviolet Spectra

The u.v. spectra were recorded on a Unicam SP700 spectrophotometer. Chloroform was used as solvent, and solutions were approximately 10^{-4} *M*.

Infrared Spectra

The i.r. spectra were recorded either on a Perkin–Elmer 337 or Beckmann IR-4 spectrophotometer, using chloroform as solvent.

ADDENDUM: Since the original writing of this manuscript the synthesis of *S*-methyl thiomandelate ($C_6H_5CH(OH)COSCH_3$) from tri(methylmercapto)acetophenone has been reported (26).

The author gratefully acknowledges the aid of Dr. R. U. Lemieux, University of Alberta, Edmonton, Alberta, with whom the problem was discussed during the early stages of work, and of Miss P. A. Cockrill, Miss H. L. Dougan, and Mrs. P. J. Hoibak, who rendered invaluable assistance in the laboratory.

Gratitude is also expressed to the University of Victoria and to the National Research Council of Canada for financial assistance.

1. E. MOSSETIG. Org. React. **8**, 218 (1954).
2. H. HAUPTMANN and W. F. WALTER. Chem. Rev. **62**, 348 (1962).
3. J. D. DUTCHER, J. R. JOHNSON, and W. F. BRUCE. J. Amer. Chem. Soc. **67**, 1736 (1945).
4. J. R. JOHNSON and J. B. BUCHANAN. J. Amer. Chem. Soc. **75**, 2103 (1953).
5. J. MARCH. Advanced organic chemistry. McGraw-Hill Book Co., New York, 1968. (*a*) p. 556; (*b*) p. 893.
6. H. O. HOUSE. Modern synthetic reactions. W. A. Benjamin, Inc., New York, 1965. pp. 56, 57.
7. H. ADKINS. Org. React. **8**, 1 (1954).
8. E. M. REID. Organic chemistry of bivalent sulfur. Vol. IV. Chemical Publishing Co. Inc., New York, 1962. pages 24 ff and 63 ff.
9. A. PINNER and F. KLEIN. Ber. **10**, 1889 (1877).
10. R. ROGER and D. G. NEILSON. Chem. Rev. **61**, 179 (1961).
11. R. H. SHRINER and F. W. NEUMANN. Chem. Rev. **35**, 351 (1944).
12. E. N. ZIL'BERMAN and A. E. KULIKOVA. Zh. Obshch. Khim. **30**, 3999 (1960); Chem. Abstr. **55**, 22126 (1961).
13. E. N. ZIL'BERMAN. Russ. Chem. Rev. (English translation), **31**, 620 (1962).
14. R. H. HARTIGAN and J. B. CLOKE. J. Amer. Chem. Soc. **67**, 709 (1945).
15. A. SCHONBERG and K. PRAEFCKE. (*a*) Chem. Ber., **99**, 237 (1966); (*b*) Chem. Ber. **99**, 2433 (1966).
16. A. SCHONBERG and K. PRAEFCKE. Chem. Ber. **100**, 778 (1967).
17. L. H. NODA, S. A. KUBY, and H. A. LARDY. J. Amer. Chem. Soc. **75**, 913 (1953).
18. J. I. CUNNEEN. J. Chem. Soc. 134 (1947).
19. B. SJOBERG. Z. Phys. Chem. **52B**, 209 (1942).

Can. J. Chem. Downloaded from www.nrcresearchpress.com by 210.87.254.5 on 09/05/12
For personal use only.

20. K. IGARASHI and T. HONMA. J. Org. Chem. **32**, 2521 (1967).
21. A. W. BAKER and G. H. HARRIS. J. Amer. Chem. Soc. **82**, 1923 (1960).
22. R. A. NYQUIST and W. J. POTTS. Spectrochim. Acta, **7**, 514 (1959).
23. R. F. B. COX and R. T. STORMONT. Org. Syn. **15**, 1 (1935).
24. H. BUCHERER and A. GROLEE. Ber. **39**, 1224 (1906).
25. F. SCHNEIDER. Qualitative organic microanalysis. John Wiley and Sons, Inc., New York, 1946. p. 98.
26. G. A. RUSSELL and L. A. OCHRYMOWYCZ. J. Org. Chem. **34**, 3618 (1969).
27. BEILSTEIN. III, (*a*) 324, (*b*) 338.
28. D. J. PASTRO and C. R. JOHNSON. Organic structure determination. Prentice-Hall, Inc., Englewood Cliffs, N.J., 1969. p. 71.

Can. J. Chem. Downloaded from www.nrcresearchpress.com by 210.87.254.5 on 09/05/12
For personal use only.

Can. J. Chem. Downloaded from www.nrcresearchpress.com by 210.87.254.105 on 09/05/12
For personal use only.

Complexes of Group III trimethyls with diamines

A. STORR AND B. S. THOMAS
Chemistry Department, University of British Columbia, Vancouver 8, British Columbia

Received June 30, 1970

Direct combination of the Lewis acids, Me_3M (where M = B, Al, Ga, or In), and the diamines, $Me_2N(CH_2)_nNMe_2$ (where n = 1, 2, or 3) has given two series of complexes. A range of 1:1 complexes can be isolated with $Me_2NCH_2NMe_2$ as ligand. With the other diamines, use of a 1:1 molar ratio of reactants yields crystalline 2:1 complexes with two moles of Me_3M per mole of ligand. Excluding the reaction between Me_3B and $Me_2NCH_2NMe_2$, 2:1 complexes can be isolated by reacting the various Lewis acids with the appropriate molar quantity of the diamines. The complexes have been characterized by i.r. and proton n.m.r. spectroscopy and molecular weight measurements.

A number of complexes of Me_3Ga with methyl substituted ethylenediamines have been prepared and the effects of substitution on the nitrogen ligand atoms studied. Pyrolysis of these complexes has demonstrated the ready elimination of methane and has resulted in the formation of condensed Ga—N species.

Canadian Journal of Chemistry, 48, 3667 (1970)

Introduction

The formation of molecular addition complexes between aluminum alkyls and difunctional bases has received much attention. Brüser *et al.* (1) and Thiele *et al.* (2) have shown that Me_3Al forms 2:1 complexes with $MeO(CH_2)_2OMe$, $MeO(CH_2)_2NMe_2$, $Me_2N(CH_2)_2NMe_2$, and $Et_2N(CH_2)_2NEt_2$ and 1:1 complexes with $MeO(CH_2)_2NMe_2$, 2,2′-bipyridyl and 1,10-phenanthroline. Thiele and Brüser (3) have reported that both 1:1 and 2:1 complexes may be formed between Me_3Al and 1,4-dioxane, *N*-methylmorpholine and *N,N′*-dimethylpiperazine. Fetter *et al.* (4, 5) have investigated the formation of complexes between Me_3Al and the compounds $Me_2N(CH_2)_nNMe_2$ (where n = 0, 1, 2, or 3). They proposed that 1:1 complexes are formed when the nitrogen atoms of the ditertiary base are separated by one or no intervening methylene groups, while 2:1 complexes are formed when the separation is by two or more methylene groups.

Fetter and Bartocha (6) have investigated the reactions of Me_3Al with various methyl hydrazines. They have demonstrated that 1:1 complexes are formed initially but that, in the cases of the partially substituted hydrazines, methane is evolved and a condensed Al—N framework produced. Clemens *et al.* (7) and Nielsen and Sisler (8), in a similar study using Et_3Al as Lewis acid, again demonstrated the formation of 1:1 complexes with hydrazine ligands and the ready elimination of ethane from a number of the complexes.

In sharp contrast little has been written concerning the formation of complexes between Me_3B and difunctional bases. Brüser and Thiele (9) have reported that 2:1 complexes of Me_3B are formed with $R_2N(CH_2)_2NR_2$ (where R = Me or Et) and that no reaction was observed between Me_3B and 2,2′-bipyridyl.

In the present investigation we have extended the information already available on difunctional base – Group III Lewis acid interactions by making a systematic study of the tertiary diamines, $Me_2N(CH_2)_nNMe_2$ (where n = 1, 2, or 3), as ligands towards the trimethyl derivatives, Me_3M (where M = B, Al, Ga, and In), as Lewis acids. As an extension of this study we have investigated the formation of complexes between Me_3Ga and the partially substituted ethylenediamines, $Me_{2-x}H_xN(CH_2)_2NMe_{2-y}H_y$ (where x = 0, 1, or 2 and y = 1 or 2), and the subsequent elimination of methane from these complexes.

Experimental

Materials were handled in a conventional high vacuum line or in a glove box under an atmosphere of oxygen-free dry nitrogen. Benzene was dried by refluxing over potassium for several days and then distilled.

Starting Materials

The diamines were dried over calcium hydride and then distilled under reduced pressure. Trimethyl boron (K and K Laboratories, Inc.) and trimethyl aluminum (Alfa Inorganics, Inc.) were vacuum distilled before use. Trimethyl gallium and trimethyl indium were prepared by reaction of dimethyl mecury with a slight excess of the appropriate metal at approximately 120° for several days in a sealed, thick-walled glass tube. Trimethyl gallium was purified by vacuum distillation and trimethyl indium by vacuum sublimation.

Spectra

Definitive i.r. spectra were recorded on a Perkin-Elmer Model 457 spectrometer (4000–250 cm^{-1}). The samples were run as benzene or cyclohexane solutions, the cells being loaded in the glove box.

TABLE 1

Physical properties of some complexes of Group III Lewis acids with tertiary diamines

Compound	Melting point (°C)	Molecular weight data		^{1}H n.m.r. data			
		Found	Calculated	τ_{CH_2}	τ_{NMe_2}	$\Delta(\tau_{NMe_2} - \tau_{CH_2})$	τ_{MMe_3}
$Me_2NCH_2NMe_2$	Liquid	—	—	7.50	7.92	0.42	—
$Me_3B \cdot Me_2NCH_2NMe_2$	32–35	152	158	6.81	8.02	1.21	9.84
$Me_3Al \cdot Me_2NCH_2NMe_2$	33–35	179	174	6.87	8.10	1.23	10.51
$Me_3Ga \cdot Me_2NCH_2NMe_2$	Liquid	216	217	6.87	7.99	1.12	10.34
$Me_3In \cdot Me_2NCH_2NMe_2$	Liquid	264	262	7.07	8.06	0.99	10.24
$Me_3Al \cdot Me_2NCH_2NMe_2 \cdot AlMe_3$	103–106	254	246	6.24	8.01	1.77	10.61
$Me_3Ga \cdot Me_2NCH_2NMe_2 \cdot GaMe_3$	82	226	332	6.74	8.04	1.30	10.17
$Me_3In \cdot Me_2NCH_2NMe_2 \cdot InMe_3$	53–56	282	422	6.97	8.04	1.07	10.14
$Me_2N(CH_2)_2NMe_2$	Liquid	—	—	7.74	7.96	0.22	—
$Me_3B \cdot Me_2N(CH_2)_2NMe_2 \cdot BMe_3$	98–105	174	228	7.61	8.17	0.66	9.81
$Me_3Al \cdot Me_2N(CH_2)_2NMe_2 \cdot AlMe_3$	136–139	270	260	7.54	8.31	0.77	10.61
$Me_3Ga \cdot Me_2N(CH_2)_2NMe_2 \cdot GaMe_3$	102–103	350	346	7.65	8.22	0.51	10.34
$Me_3In \cdot Me_2N(CH_2)_2NMe_2 \cdot InMe_3$	90–93	440	436	7.74	8.24	0.50	10.24
$Me_2N(CH_2)_3NMe_2$	Liquid	—	—	7.84 and 8.47	7.96	—	—
$Me_3B \cdot Me_2N(CH_2)_3NMe_2 \cdot BMe_3$	114–122	244	242	8.12	8.12	—	9.91
$Me_3Al \cdot Me_2N(CH_2)_3NMe_2 \cdot AlMe_3$	166–169	276	274	8.21	8.21	—	10.54
$Me_3Ga \cdot Me_2N(CH_2)_3NMe_2 \cdot GaMe_3$	140	362	359	8.24	8.24	—	10.24
$Me_3In \cdot Me_2N(CH_2)_3NMe_2 \cdot InMe_3$	81–83	456	450	8.24	8.24	—	10.21

Proton n.m.r. spectra were obtained on Varian HA-100 and T-60 instruments. The benzene solutions were prepared in the glove box and the sample tubes sealed off to prevent oxidation and hydrolysis. All τ values are referred to benzene as $\tau_{C_6H_6} = 2.84$ p.p.m. Concentrations of all the solutions were kept roughly the same (~ 0.3 *M*) in an attempt to minimize any concentration dependence of the signals.

Molecular Weights

Molecular weight determinations were conducted cryoscopically using benzene as solvent. The apparatus was designed to provide a nitrogen blanket over the solution to prevent atmospheric interference.

Preparative Details

The complexes were all prepared by the same general method which can be illustrated by the preparation of $Me_3Al \cdot Me_2NCH_2NMe_2 \cdot AlMe_3$.

Trimethyl aluminum (0.4630 g, 6.42 mmoles) was condensed into an evacuated flask and *N,N,N′,N′*-tetramethylmethylenediamine (0.3280 g, 3.21 mmoles) was added by vacuum transfer. The mixture was allowed to warm slowly to room temperature to yield the white crystalline complex, $Me_3Al \cdot Me_2NCH_2NMe_2 \cdot AlMe_3$ (m.p. 103–106°; mol. wt. 254, calcd. 246).

The complexes can be purified by vacuum sublimation at temperatures ranging from 25–100°, without loss of free Lewis acid or amine. Selected properties are listed in Table 1. Melting points are uncorrected.

Analysis

The compounds described were not subjected to chemical analysis since they were all prepared on a high-vacuum line from purified starting materials and as nothing is lost by this technique the method of preparation itself constitutes an analysis (10). In all cases proton n.m.r. confirmed the various stoichiometries upon integration of the signals and further confirmation of compound formation is reflected in the sharp melting points and molecular weight data of most of the compounds. In the experiments where 2:1 complexes are formed using a 1:1 molar ratio of reactants a stoichiometric amount of free ligand was always recovered, and the complexes formed exhibited identical proton n.m.r., melting points, molecular weights etc. to the authentic 2:1 complexes. In decompositions involving the formation of methane the latter was always measured using a Toepler pump.

Pyrolysis Studies

The 1:1 complexes of trimethyl gallium and the *N*-methyl-, *N,N*-dimethyl-, *N,N′*-dimethyl-, and *N,N,N′*-trimethylethylenediamines and the 2:1 complex with *N,N′*-dimethylethylenediamine were pyrolyzed. As an example of the procedure used the details for the pyrolysis of $Me_3Ga \cdot MeNH(CH_2)_2NMeH \cdot GaMe_3$ are given below.

The bis(trimethyl gallium)-*N,N′*-dimethylethylenediamine complex (0.395 g, 1.24 mmoles) was weighed into a 100 ml round-bottomed flask fitted with a break-seal side-arm and a tap adaptor. The flask was cooled to −196°, evacuated, sealed off, and then warmed to 120° for several days. It was then attached to the vacuum line via the break-seal arm, cooled to −196°, and the break-seal ruptured. The volume of methane evolved was measured by means of a Toepler pump. (Found 55.2 ml, 2.46 mmoles).

The pyrolysis products were purified by vacuum sublimation at temperatures ranging from 40–110°. A summary of the data obtained is presented in Table 2.

Results and Discussion

The reactions of $Me_2NCH_2NMe_2$ with the trimethyl derivatives Me_3M, (where M = B, Al,

Can. J. Chem. Downloaded from www.nrcresearchpress.com by 210.87.254.105 on 09/05/12
For personal use only.

TABLE 2

Experimental data for pyrolysis studies

Complex	Pyrolysis data CH_4 evolved/ mole complex	Product	Molecular weight data Found	Calculated*
$Me_3Ga \cdot H_2N(CH_2)_2NMeH$	1.58	Yellow oil	390	345
$Me_3Ga \cdot H_2N(CH_2)_2NMe_2$	0.95	Yellow oil	396	373
$Me_3Ga \cdot MeNH(CH_2)_2NMeH$	1.20	White solid m.p. 217–220°	410	373
$Me_3Ga \cdot MeNH(CH_2)_2NMe_2$	0.75	Yellow oil	374	401
$Me_3Ga \cdot MeNH(CH_2)_2NMeH \cdot GaMe_3$	1.99	White solid m.p. > 250° dec.	—	—

*Calculated for dimeric pyrolysis product.

Ga, or In), in equimolar ratios yield the 1:1 complexes, $Me_3M \cdot Me_2NCH_2NMe_2$. Cryoscopic molecular weight determinations show that the complexes are monomeric in benzene solution (see Table 1). Fetter *et al.* (4) have prepared the aluminum compound $Me_3Al \cdot Me_2NCH_2NMe_2$ and report that it is associated in benzene solution (degree of association 1.38). On the basis of their n.m.r. data, which shows only one N—Me proton signal, Fetter *et al.* suggested a chelate structure for the complex with both nitrogen atoms coordinating to the aluminum which becomes five-coordinate. Several other workers have proposed chelate structures for complexes of this type (3, 6, 7, 11). However, in the present systems, it is felt that either an intramolecular rearrangement could alternate the coordinated nitrogen atom via a transition state involving the five-coordinate arrangement proposed by Fetter *et al.* (4), or, more likely, intermolecular exchange via a rapid dissociative mechanism could take place, which would better explain the observed n.m.r. spectra especially for those complexes involving acceptor atoms which show little tendency for five-coordination in this type of compound.

In general the reactions of the Lewis acids Me_3M (where M = B, Al, Ga, or In) with the diamines $Me_2N(CH_2)_nNMe_2$ (where n = 1, 2, or 3) in the correct stoichiometric ratios have yielded the 2:1 complexes $Me_3M \cdot Me_2N(CH_2)_n$-$NMe_2 \cdot MMe_3$. The one exception was the reaction of Me_3B with $Me_2NCH_2NMe_2$ which produces the 1:1 complex and free Me_3B. Selected properties of the complexes are summarized in Table 1. The majority of the complexes are monomeric in benzene solution. This is in contrast with the results of Fetter *et al.* (4) and Fetter and Moore (5) who report a slight association for some of their aluminum complexes. Trimethyl boron exhibits a marked tendency to form only 1:1 complexes with the diamines under study. Thus, $Me_3B \cdot Me_2NCH_2NMe_2 \cdot BMe_3$ could not be isolated and $Me_3B \cdot Me_2N(CH_2)_2$-$NMe_2 \cdot BMe_3$ is ~ 30% dissociated in benzene solution. The latter compound has been reported previously by Thiele and Brüser (3) to have a similar melting point range (93–103° with evolution of Me_3B) and molecular weight (167) to those found in this investigation. It appears that with increasing carbon chain length in the diamine ligands the stability of the 2:1 complexes with Me_3B (and also with Me_3Ga and Me_3In) increases. The propanediamine complex with trimethyl boron, $Me_3B \cdot Me_2N(CH_2)_3NMe \cdot$-$BMe_3$, is a well-defined stable crystalline solid which is monomeric in benzene solution. Presumably the reduced basicity of the second nitrogen atom in a diamine after complexing the first nitrogen atom is more pronounced the shorter the connecting carbon chain, as might be expected, leading to the observed trend in stabilities for the 2:1 complexes. However, the nature of the acceptor moiety must play a critical role since the reverse situation is presented by diamine complexes of the stronger boron Lewis acids BF_3 and 'BH_3'. Brown *et al.* (12) have reported that $F_3B \cdot H_2N(CH_2)_2NH_2$ is unstable while the 2:1 complex, with 2 moles of BF_3 per mole of diamine, may be crystallized from water. Similarly Gatti and Wartik (13) have shown that $H_3B \cdot Me_2N(CH_2)_2NMe_2$ may be prepared by dissolving the 2:1 complex in $Me_2N(CH_2)_2NMe_2$ at 60° but the product when isolated from solution soon reverts to the 2:1 complex $H_3B \cdot Me_2N$-$(CH_2)_2NMe_2 \cdot BH_3$ at room temperature. The latter authors attribute this rather unexpected preference for the bis-adduct to lattice stabiliza-

Can. J. Chem. Downloaded from www.nrcresearchpress.com by 210.87.254.105 on 09/05/12
For personal use only.

TABLE 3

Infrared spectroscopic data for some complexes of Group III Lewis acids with tertiary diamines in benzene solution

Complex	ν_{asym}M—C*	ν_{sym}M—C*	ν M—N*
$Me_3B \cdot Me_2NCH_2NMe_2$	1080 s	974 s	678 s†
$Me_3B \cdot Me_2N(CH_2)_2NMe_2 \cdot BMe_3$	1070 s	975 s	676 s†
$Me_3B \cdot Me_2N(CH_2)_3NMe_2 \cdot BMe_3$	1071 m	979 m	673 s†
$Me_3Al \cdot Me_2NCH_2NMe_2$	616 vs	572 m	520 s
$Me_3Al \cdot Me_2NCH_2NMe_2 \cdot AlMe_3$	616 vs	562 m	522 vs
$Me_3Al \cdot Me_2N(CH_2)_2NMe_2 \cdot AlMe_3$	620 vs	588 s	525 s
$Me_3Al \cdot Me_2N(CH_2)_3NMe_2 \cdot AlMe_3$	622 vs	570 m	525 s
$Me_3Ga \cdot Me_2NCH_2NMe_2$	600 s	540 vs	510 s
$MeGa \cdot Me_2NCH_2NMe_2 \cdot GaMe_3$	570 s	540 vs	509 s
$Me_3Ga \cdot Me_2N(CH_2)_2NMe_2 \cdot GaMe_3$	570 s	542 vs	511 m
$Me_3Ga \cdot Me_2N(CH_2)_3NMe_2 \cdot GaMe_3$	586 s	542 vs	511 m
$Me_3In \cdot Me_2NCH_2NMe_2$	520 m	480 vs	466 sh
$Me_3In \cdot Me_2NCH_2NMe_2 \cdot InMe_3$	515 m	480 vs	463 s
$Me_3In \cdot Me_2N(CH_2)_2NMe_2 \cdot InMe_3$	522 s	480 vs	465 sh
$Me_3In \cdot Me_2N(CH_2)_3NMe_2 \cdot InMe_3$	520 w?	478 vs	465 sh

*vs = very strong, s = strong, m = medium, w = weak, sh = shoulder.
†Recorded in cyclohexane solution.

tion effects resulting from considerations of symmetry.

The proposal of Fetter *et al.* (4) that the reaction of Me_3Al with tertiary diamines yields 1:1 complexes when the nitrogen atoms of the base are separated by one or no intervening methylene groups, while 2:1 complexes are formed when the separation is by two or more methylene groups is viewed by the present authors to be only partially correct. Thus, $Me_3Al \cdot Me_2NCH_2NMe_2 \cdot AlMe_3$ as prepared by us is a well-defined crystalline solid which is monomeric in benzene solution. Indeed it appears that $Me_2NCH_2NMe_2$ provides the intermediate case where both 1:1 and 2:1 complexes may be formed. Similar 2:1 complexes with $Me_2NCH_2NMe_2$ and Me_3Ga and Me_3In can be prepared and sublimed unchanged but these are dissociated in benzene solution. Presumably, on dissociation, the 1:1 complexes and free Lewis acids are in rapid equilibrium with the 2:1 complexes in solution since the proton n.m.r. spectra show only single peaks for the methylene, N—Me and M—Me protons. The molecular weight data indicate that both complexes (Ga and In) are ~ 50% dissociacted in benzene solution.

The relative acceptor strengths of the Lewis acids studied towards the diamine ligands may be tentatively inferred from the dissociation data calculated from the molecular weights of the various complexes. The three Lewis acids, Me_3Al, Me_3Ga, and Me_3In all form complexes in each series reported in Table 1. However, in the $Me_3M \cdot Me_2NCH_2NMe_2 \cdot MMe_3$ compounds, the gallium and indium derivatives are ~ 50% dissociated in benzene solution suggesting that these complexes are weaker than the corresponding aluminum complex. The trimethyl boron moiety does not form a 2:1 complex in this series indicating that it is perhaps the weakest of the Lewis acids studied. Hence the following tentative order of Lewis acidity, which has already been proposed by Stone (14) for the complexes with trimethylamine, $Me_3N \cdot MMe_3$, is suggested: $Me_3Al > Me_3Ga \sim Me_3In > Me_3B$.

Infrared Spectra

Selected vibrational frequencies from the i.r. spectra of the complexes in benzene solution are listed in Table 3. The tentative assignments of the asymmetric and symmetric M—C stretching vibrations and of the M—N stretching vibrations are made on the basis of previous assignments for similar donor–acceptor compounds, proposed by other workers. The assignments of the B—C and B—N stretching frequencies follows from those of Sawodny and Goubeau (15) for the compound $Me_3N \cdot BMe_3$. The assignment of the aluminum, gallium, and indium frequencies follows from the compilation of spectral data of Coates *et al.* (16–18) and Wade *et al.* (19–21). With increasing atomic number of the acceptor atom the various frequencies are observed to decrease indicating the operation of the expected mass effect.

Substituted Ethylenediamine Complexes

The reaction of Me_3Ga with a series of ethylenediamines of general formula $Me_{2-x}H_xN$-

Can. J. Chem. Downloaded from www.nrcresearchpress.com by 210.87.254.105 on 09/05/12
For personal use only.

TABLE 4

Physical properties of complexes of Me_3Ga with some partially methylated ethylenediamines

Complex	Melting point (°C)	Molecular weight data	
		Found	Calculated
$Me_3Ga \cdot H_2N(CH_2)_2NH_2$	118–125	226	175
$Me_3Ga \cdot H_2N(CH_2)_2NH_2 \cdot GaMe_3$	143–146	296	289
$Me_3Ga \cdot MeNH(CH_2)_2NH_2$	Liquid	184	189
$Me_3Ga \cdot MeNH(CH_2)_2NH_2 \cdot GaMe_3$	55–58	307	303
$Me_3Ga \cdot Me_2N(CH_2)_2NH_2$	Liquid	201	203
$Me_3Ga \cdot Me_2N(CH_2)_2NH_2 \cdot GaMe_3$	59–62	314	317
$Me_3Ga \cdot MeNH(CH_2)_2NMeH$	Liquid	197	203
$Me_3Ga \cdot MeNH(CH_2)_2NMeH \cdot GaMe_3$	60–62	334	317
$Me_3Ga \cdot Me_2N(CH_2)_2NMeH$	Liquid	220	217
$Me_3Ga \cdot Me_2N(CH_2)_2NMeH \cdot GaMe_3$	68–70	340	331

$(CH_2)_2NMe_{2-y}H_y$ (where $x = 0$, 1, or 2 and $y = 1$ or 2) in the correct stoichiometric ratio yields the 2:1 complexes with 2 moles of Me_3Ga per mole of diamine. Selected properties of the complexes are tabulated in Table 4. The compounds are, in general, sharp melting crystalline solids, which are monomeric in benzene solution. With one mole of Me_3Ga per mole of diamine, 1:1 complexes were obtained as colorless oils. These appear to be stable with respect to disproportionation to the 2:1 complexes and ligands since they have negligible vapor pressures and free ligands cannot be recovered from the reaction sphere. This is in sharp contrast to the behavior observed using $Me_2N(CH_2)_2NMe_2$ as the ligand. The 1:1 complex of ethylenediamine itself, however, is an unstable solid which decomposes slowly at room temperature to the 2:1 complex and free amine. It will be noted (Table 4), that the 2:1 complexes of Me_3Ga with the partially methylated ethylenediamines have considerably lower melting points (ranging between 55–70°) than either $Me_3Ga \cdot Me_2N(CH_2)_2NMe_2 \cdot GaMe_3$ (143–146°) or $Me_3Ga \cdot H_2N(CH_2)_2NH_2 \cdot GaMe_3$ (102–103°), suggesting that they have correspondingly lower lattice energies. If this is true, then perhaps the lattice stabilization effects proposed by Gatti and Wartik (13) to account for the preferred stability of $H_3B \cdot Me_2N(CH_2)_2NMe_2 \cdot BH_3$ over the corresponding monoadduct are insufficient in the present Me_3Ga complexes to stabilize the 2:1 complexes and thus cause disproportionations as illustrated in eq. 1. No

[1] $$2Me_3Ga \cdot HNMe(CH_2)_2NMe_2 \rightarrow Me_3Ga \cdot HNMe(CH_2)_2NMe_2 \cdot GaMe_3 + HNMe(CH_2)_2NMe_2$$

doubt steric factors, and possibly hydrogen-bonding, also play important roles in the formation and stability of the 1:1 complexes.

The i.r. spectra of the 1:1 and 2:1 complexes of Me_3Ga and the partially substituted ethylenediamines again displayed characteristic Ga—C asymmetric and symmetric stretching vibrations in the 570–580 cm^{-1} and 540–550 cm^{-1} regions of the spectra respectively. Absorptions attributable to ν_{Ga-N} modes occurred in the range 500–515 cm^{-1}, although no clear cut trend was observed in these frequencies with changing extent of methylation of the amine ligand. This contrasts with the behavior of 'BH_3' (22) and 'GaH_3' (23) as Lewis acids to monofunctional methylamines where substitution of dimethylamine for trimethylamine as donor increases the position of the M—N stretching modes by some 25–30 cm^{-1} in each case.

Pyrolysis Studies

Although the data are in some instances non-stoichiometric, pyrolysis of the 1:1 complexes of Me_3Ga with the partially methylated diamines appears to yield methane and isolable dimeric Ga—N systems. In a previous pyrolysis study (24) it was demonstrated that $Me_2NHGaMe_3$ and $MeNH_2GaMe_3$, under suitable conditions eliminate methane to yield the dimer $(Me_2NGaMe_2)_2$ and the trimer $(MeNHGaMe_2)_3$ respectively. It was concluded that steric requirements are critical for alkyl substituents on nitrogen in these cyclic compounds. In the present examples it appears that the preference for dimeric products is a dominant feature in the pyrolyses. It is expected that in the original

Can. J. Chem. Downloaded from www.nrcresearchpress.com by 210.87.254.105 on 09/05/12
For personal use only.

complexes the Me_3Ga moiety is bonded to the nitrogen atom with the greatest number of hydrogen atoms attached, and it is assumed that molecule elimination occurs intramolecularly from adjacent gallium and nitrogen atoms, followed by coordinative saturation via cyclization or polymerization. Fetter and Bartocha (6) have reached similar conclusions regarding complexes of Me_3Al with methylhydrazines and attribute the effect to steric hindrance of the methyl groups attached to nitrogen.

Thus it appears that four membered, $(Ga—N)_2$, rings are formed on pyrolysis of the 1:1 complexes *e.g.* eq. 2.

[2] $2Me_3Ga \cdot HMeN(CH_2)_2NMeH \rightarrow$

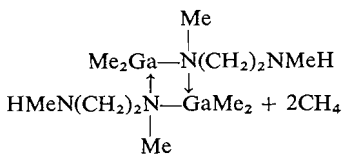

Pyrolysis of the 2:1 complex $Me_3Ga \cdot MeNH(CH_2)_2NMeH \cdot GaMe_3$ gave 2 moles of methane and a white solid, insoluble in common organic solvents, and presumably polymeric. The results suggest the formulation,

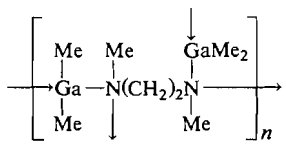

as a possible arrangement for the product.

We thank the National Research Council of Canada for financial support.

1. W. Brüser, K.-H. Thiele, and H. K. Muller. Z. Chem. **2**, 342 (1962).
2. K.-H. Thiele, H. K. Muller, and W. Brüser. Z. Anorg. Chem. **345**, 194 (1966).
3. K.-H. Thiele and W. Brüser. Z. Anorg. Chem. **348**, 179 (1966).
4. N. R. Fetter, B. Bartocha, F. E. Brinckman, and D. W. Moore. Can. J. Chem. **41**, 1359 (1963).
5. N. R. Fetter and D. W. Moore. Can. J. Chem. **42**, 885 (1964).
6. N. R. Fetter and B. Bartocha. Can. J. Chem. **39**, 2001 (1961).
7. D. F. Clemens, W. S. Brey, and H. H. Sisler. Inorg. Chem. **2**, 1251 (1963).
8. R. P. Nielsen and H. H. Sisler. J. Chem. Soc. 3818 (1962).
9. W. Brüser and K.-H. Thiele. Z. Anorg. Chem. **349**, 310 (1967).
10. G. E. Coates. J. Chem. Soc. 2003 (1951).
11. M. S. Bains and D. C. Bradley. Can. J. Chem. **40**, 1350 (1962).
12. C. A. Brown, E. L. Muetterties, and E. G. Rochow. J. Amer. Chem. Soc. **76**, 2537 (1954).
13. A. R. Gatti and T. Wartik. Inorg. Chem. **5**, 329 (1966).
14. F. G. A. Stone. Chem. Rev. **58**, 101 (1958).
15. W. Sawodny and J. Goubeau. Z. Phys. Chem. **44**, 227 (1965).
16. G. E. Coates and R. N. Mukherjee. J. Chem. Soc. 1295 (1964).
17. O. T. Beachley and G. E. Coates. J. Chem. Soc. 3241 (1965).
18. O. T. Beachley, G. E. Coates, and G. Kohnstam. J. Chem. Soc. 3248 (1965).
19. J. E. Lloyd and K. Wade. J. Chem. Soc. 2662 (1965).
20. J. R. Jennings and K. Wade. J. Chem. Soc. A, 1333 (1967).
21. J. R. Jennings, I. Pattison, K. Wade, and B. K. Wyatt. J. Chem. Soc. A, 6108 (1967).
22. R. C. Taylor. Nature, **182**, 390 (1958).
23. N. N. Greenwood, E. J. F. Ross, and A. Storr. J. Chem. Soc. A, 706 (1966).
24. A. Storr. J. Chem. Soc. A, 2605 (1968).

Can. J. Chem. Downloaded from www.nrcresearchpress.com by 210.87.254.105 on 09/05/12
For personal use only.

Can. J. Chem. Downloaded from www.nrcresearchpress.com by 210.87.254.42 on 09/05/12
For personal use only.

Structural and conformational studies on tetrahydroprotoberberine alkaloids

C. K. Yu and D. B. MacLean
Department of Chemistry, McMaster University, Hamilton, Ontario

AND

R. G. A. Rodrigo and R. H. F. Manske
Department of Chemistry, University of Waterloo, Waterloo, Ontario

Received June 29, 1970

Two new tetrahydroprotoberberine alkaloids are reported, one from *Corydalis thalictrifolia* and the other from *Corydalis tuberosa*. The former is apparently identical with a previously described synthetic compound. The latter is a des-methyl derivative of the first. Both compounds are 13-methyltetrahydroprotoberberines in which the hydrogens at C-13 and -14 are *cis* to one another. An examination has been made of the p.m.r. spectra of the two new bases and of several 13-methyltetrahydroprotoberberines of established structure and stereochemistry. The spectra can be used to assign the relative stereochemistry of these 13-methyl compounds.

Canadian Journal of Chemistry, **48**, 3673 (1970)

From *Corydalis thalictrifolia* Franch. (1) and from *Corydalis tuberosa* DC (*C. Cava* (L.) Schweigg. et. Körte) (2) a number of tetrahydroprotoberberines and several 13-methyltetrahydroprotoberberines have been isolated along with alkaloids of other isoquinoline systems. We report here the isolation and structure of two new alkaloids, one from each of these species, which are tetrahydroprotoberberines with 13-methyl groups. In the course of this investigation we examined the p.m.r. spectra of many of the known 13-methyltetrahydroprotoberberines. From this work it is evident that p.m.r. can be used to assign the relative configuration at C-13 and -14 in this series of alkaloids.

The first of the two new alkaloids, $C_{21}H_{23}NO_4$, from *C. thalictrifolia*, was assigned the trivial name, cavidine, **1**. The base was optically inactive, melted at 192° and had λ_{max}(MeOH) 285 mμ in its u.v. spectrum. The i.r. spectrum showed the absence of carbonyl or hydroxyl absorption but had absorption in the 2700–2800 cm^{-1} region. The mass spectrum of cavidine has a molecular ion at *m/e* 353 (35) and fragment ions at *m/e* 338 (7.5), 192 (5.5), 190 (4.5), and 162 (100).[1] This fragmentation pattern can be rationalized, Scheme 1, on the basis of structure **1** for cavidine (3) but the mass spectrum does not define the substitution pattern. The p.m.r. spectrum confirmed the nature of the substituent groups and enabled them to be assigned to the positions shown in structure **1**.

The 100 MHz p.m.r. spectrum of **1** in $CDCl_3$ is shown in Fig. 1. The presence of a $\rangle CH—CH_3$ group is apparent from the signal centered at 0.98 δ, $J = 7$ Hz, and the presence of two methoxyl groups and of one methylenedioxy group by the signals at 3.88 (area 6) and 5.93 (area 2), respectively. The presence of four protons in the aromatic region is established by integration but the spectrum in the aromatic

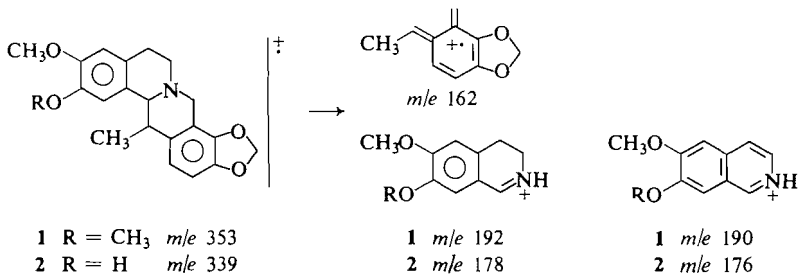

1 R = CH_3 *m/e* 353
2 R = H *m/e* 339

1 *m/e* 192
2 *m/e* 178

1 *m/e* 190
2 *m/e* 176

SCHEME 1

[1]Intensities are given in parentheses.

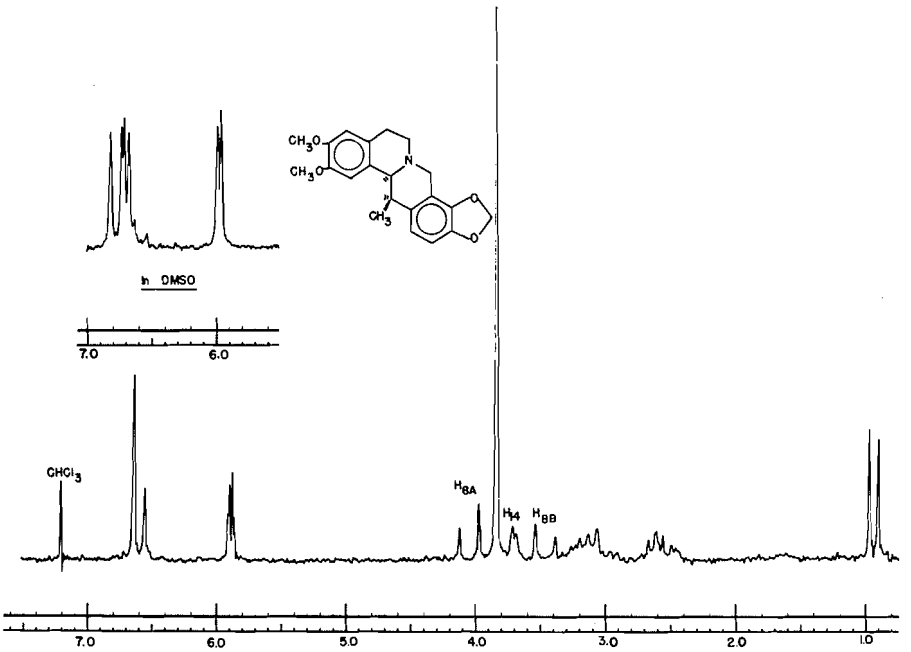

FIG. 1. The 100 MHz p.m.r. spectrum of cavidine.

region in $CDCl_3$ is disappointing in that it is impossible to draw any conclusions about the substitution pattern. In DMSO, however, two singlets and an AB quartet were clearly discernible (see inset Fig. 1). The presence of an AB quartet centered at 4.07 and 3.52 δ, $J_{H_AH_B}$ = 15 Hz, ascribed to the protons at C-8, indicates that there is an oxygen substituent at C-9 (3). The signal centered at 3.74 δ is attributed to the proton at H-14 which is coupled (J = 3 Hz) to the adjacent *cis* proton at C-13 (*vide infra*). The remaining unassigned signals in the aliphatic region arise from protons at C-13, -5, and -6.

The spectroscopic examination indicated that cavidine is a 13-methyltetrahydroprotoberberine with a methylenedioxy group at C-9 and C-10 in ring D and with two methoxyl groups in ring A. This substitution pattern is similar to that in thalictrifoline (1) and in an alkaloid described by Taguchi and Imaseki (4) which they designated "Base II". They showed that Base II was a stereoisomer of thalictrifoline by converting both alkaloids to a common dehydro base. Upon reduction the dehydro base gave a mixture of ±-thalictrifoline and ±-Base II (m.p. 191–192). Jeffs (5, 6) has inferred that the C-13 and -14 hydrogens in Base II are *cis* while in thalictrifoline they are *trans* to one another. ±-Base II has a m.p. close to that of cavidine. Moreover, the i.r. and p.m.r. spectra of cavidine are similar to those published by Taguchi and Imaseki (4) for ±-Base II. It seems likely that cavidine and ±-Base II are identical but we were unable to obtain a sample of the latter for a direct comparison. Nevertheless, the evidence above along with that presented below for apocavidine defines the structure of cavidine.

The second base, also optically inactive, $C_{20}H_{21}NO_4$, now named apocavidine, **2** is a demethylated derivative of **1**. This was apparent from an examination of its mass spectrum and its p.m.r. spectrum. The mass spectrum showed a molecular ion at *m/e* 339 and fragment ions at *m/e* 178 (6), 176 (4), and 162 (100) which are accounted for in Scheme 1. The p.m.r. spectrum (Fig. 2) in $CDCl_3$ shows signals corresponding to a single CH—CH_3 (0.98 δ, J = 7 Hz), a single methoxyl at 3.87 δ, and a methylenedioxy group centered at 5.93 δ. The aromatic region integrates for four aromatic protons and there is present an AB quartet corresponding to the protons at C-8 and a doublet corresponding to the proton at C-14. The phenolic hydroxyl shows up as a broad signal centered near 5.68 δ. The relationship of

Can. J. Chem. Downloaded from www.nrcresearchpress.com by 210.87.254.42 on 09/05/12
For personal use only.

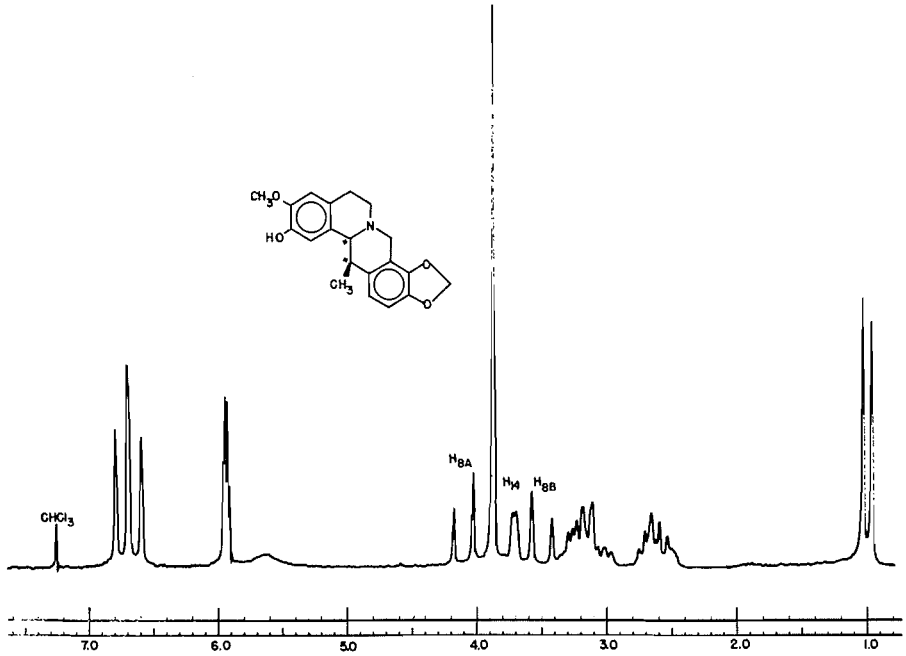

FIG. 2. The 100 MHz p.m.r. spectrum of apocavidine.

1 and **2** was confirmed by conversion of **2** to **1** by treatment with diazomethane.

From double irradiation experiments and through nuclear Overhauser effect (n.O.e) studies (7, 8) it was possible to assign the position of the OH group in apocavidine. First, we were able to establish that the proton to which the *C*-methyl group is coupled is also coupled to the signal centered at 3.71 δ which must therefore be attributed to C-14. Irradiation at 3.71 δ causes the low field aromatic proton at 6.78 δ to sharpen relative to the aromatic proton at 6.58 δ. Thus we can assign the signal at 6.78 δ to H-1. Irradiation at 2.6 δ sharpens the signal at 6.58 δ relative to that at 6.78 δ. Thus the signal at 6.58 δ can be assigned to C-4. The irradiated proton must be one of those at C-5. We were then able to show that upon irradiation of the methoxyl signal the area of the signal at 6.58 δ increased by 23% but that the area of the signal at 6.78 δ was unaffected. Thus we can assign the methoxyl group to C-3 and the hydroxyl group to C-2.

The conformation of the 13-methyltetrahydroprotoberberines has been discussed by Jeffs (5, 6). He has concluded that, in those compounds in which the C-13 and -14 hydrogens are *cis* to one another, the quinolizidine system assumes a *trans* conformation. The C-13 methyl will adopt an axial conformation and all compounds of this stereochemistry exhibit Bohlmann bands in their i.r. spectra. The two new bases described above fall into this category since both have Bohlmann bands in their i.r. spectra. The diastereomeric compounds in which the hydrogens at C-13 and -14 are *trans* to one another are considered by Jeffs to adopt a *cis*-quinolizidine conformation for, to do otherwise, would result in strong non-bonded interactions between the C—CH_3 and the hydrogens at C-1 and -12. As expected, compounds of this configuration, *e.g.*, meso-corydaline and thalictrifoline, do not exhibit Bohlmann bands.

It seemed to us that the p.m.r. spectra of these compounds should also be diagnostic of their configuration. Accordingly we examined the spectra of a number of these compounds as shown in Table 1. Only two alkaloids with the hydrogens at C-13 and -14 *trans* to one another were available, namely, thalictrifoline and meso-corydaline. The spectrum of thalictrifoline is shown in Fig. 3. It is obvious that there are three noticeable differences between the two groups of diastereomers. The first is the chemical shift of the C—Me group, the second is the coupling

Can. J. Chem. Downloaded from www.nrcresearchpress.com by 210.87.254.42 on 09/05/12
For personal use only.

TABLE 1

Signals of ring C protons in the p.m.r. spectra of some 13-methyltetrahydroprotoberberines*

		Chemical shift in p.p.m. (δ)				Coupling constant Hz
		H-8A	H-8B	13-CH_3	H-14	$J_{H_{13}-H_{14}}$
(+)-Corydaline	$R_1 = R_2 = R_3 = R_4 = R_5 = CH_3$; $R_6 = H$	4.19	3.49	0.97	3.68	3.0
Meso-corydaline	$R_1 = R_2 = R_3 = R_4 = R_6 = CH_3$; $R_5 = H$	4.13	3.97	1.48	3.62	7.5
(+)-Corybulbine	$R_1 = R_3 = R_4 = R_5 = CH_3$; $R_2 = R_6 = H$	4.20	3.55	0.99	3.70	3.0
(+)-Thalictricavine	$R_1 + R_2 = CH_2$; $R_6 = H$; $R_3 = R_4 = R_5 = CH_3$	4.21	3.52	0.99	3.69	3.0
(+)-Thalictrifoline	$R_1 = R_2 = R_6 = CH_3$; $R_3 + R_4 = CH_2$; $R_5 = H$	4.02	3.89	1.48	3.68	7.5
(±)-Cavidine	$R_1 = R_2 = R_5 = CH_3$; $R_3 + R_4 = CH_2$; $R_6 = H$	4.07	3.52	0.98	3.74	3.0
(±)-Apocavidine	$R_2 = R_5 = CH_3$; $R_3 + R_4 = CH_2$; $R_1 = R_6 = H$	4.08	3.50	0.98	3.71	3.0

*The compounds have the following general structure:

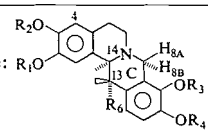

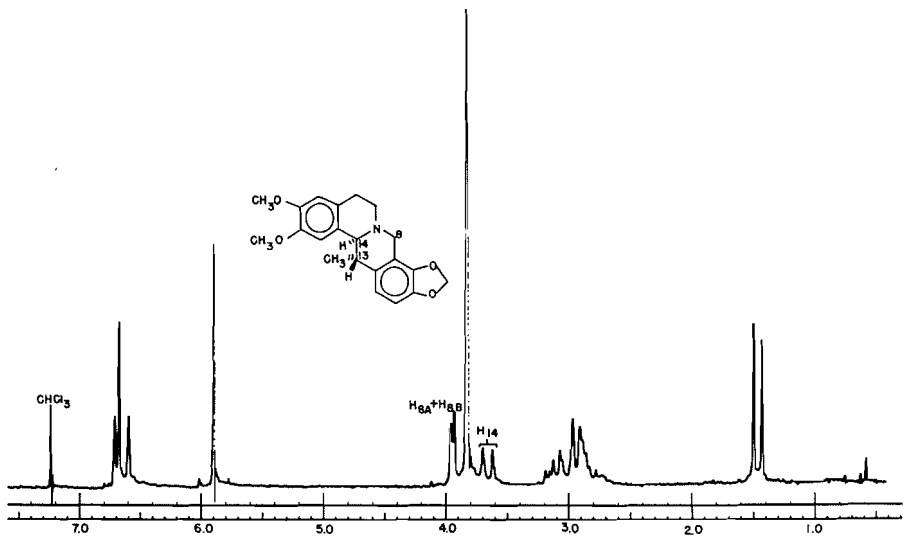

FIG. 3. The 100 MHz p.m.r. spectrum of thalictrifoline.

constant between the protons at C-13 and -14, and the third is the chemical shift of the two protons at C-8. The chemical shift of the C—Me in those compounds with *cis* hydrogens is near 1.0 δ while it is near 1.5 δ in the systems with *trans* hydrogens at these centers, an observation also made by Shamma *et al.* (9) for two synthetic 13-methyltetrahydroprotoberberines. In the systems in which the hydrogens are *trans* the *C*-methyl group lies nearly in the plane of ring D and is, therefore, deshielded. The coupling constants between H-13 and -14 are *ca.* 3.0 Hz

Can. J. Chem. Downloaded from www.nrcresearchpress.com by 210.87.254.42 on 09/05/12
For personal use only.

Can. J. Chem. Downloaded from www.nrcresearchpress.com by 210.87.254.42 on 09/05/12
For personal use only.

in the systems with *cis* hydrogens and *ca.* 7.5 Hz in the systems with *trans* hydrogens. These coupling constants are expected for the systems in which the dihedral angle approaches 90° in one case and 180° in the other. The H-14 signal is clearly visible in all spectra.

In all the spectra of the *cis* compounds the protons at C-8 appear as an AB quartet ($J \approx 16$ Hz) with a large chemical shift (0.6–0.7 p.p.m.) between them. The lower field proton is probably equatorial and deshielded by the aromatic ring D, the lone pair on the adjacent nitrogen, and the oxygen at C-9. In the two compounds with *trans* hydrogens at C-13 and -14 the difference in chemical shift of the two protons at C-8 is very much smaller (0.1–0.2 p.p.m.) with the high field proton moving downfield. Thus the p.m.r. spectra are diagnostic of the configuration of these systems. The results of the p.m.r. study are in complete accord with and lend support to the stereochemical assignment made on the basis of i.r. and conformational arguments. Diagrams A and B are typical representations of *cis*- and *trans*-fused tetrahydroprotoberberines.

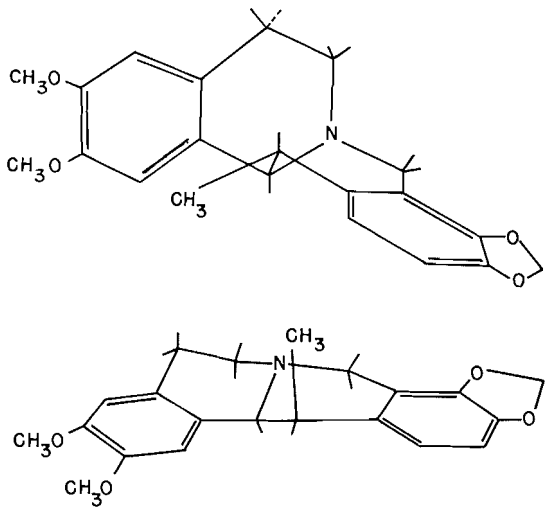

The p.m.r. spectroscopy has been used previously to assign conformation in saturated cyclic systems in which nitrogen occupies a bridgehead position (10, and refs. cited therein). It has been shown that in *trans*-fused systems the two protons on the methylene adjacent to nitrogen have a much larger difference in chemical shift than the analogous protons in a *cis*-fused system and that the proton at lower field in the *trans*-fused system is the equatorial proton. The difference in chemical shift has been attributed to the deshielding effect of the lone pair on the nitrogen. In the *trans*-fused system only one proton, the equatorial one, is deshielded by the lone pair. In the *cis*-fused system both protons are equally affected since the lone pair bisects the angle between the geminal protons.

Experimental

Methods

Mass spectra were recorded on a CEC 21-110B double-focusing mass spectrometer. For high resolution work spectra were recorded on plates and accurate mass measurements were made using perfluorokerosene as a marker (11).

The p.m.r. spectra were recorded using the frequency sweep mode of a Varian HA-100 spectrometer. Samples were dissolved in $CDCl_3$ using added TMS as the internal locking signal. Chemical shifts were measured relative to TMS using a V4315 frequency counter incorporated in the instrument. Double irradiation was achieved by employing a Hewlett-Packard 201C audiogenerator at the desired frequency. A Beckmann IR 10 spectrometer was used to record i.r. spectra and a Cary 14 spectrometer was used for the u.v. spectra.

Isolation of Apocavidine

The mixture of bases derived from *C. tuberosa* (2) from which tetrahydropalmatine, corydaline, thalictricavine etc. had been separated either as free bases or as salts was redissolved in ether and the solution shaken in a separatory funnel with 40% potassium hydroxide solution. There was formed a sparingly soluble potassium salt which remained suspended in the lower aqueous layer. The addition of a little fresh water facilitated the removal of the lower layer along with the suspended potassium salt. This procedure was repeated with fresh potassium hydroxide solution until no further solid separated. The combined aqueous extract was washed once with a generous volume of ether, partly neutralized with hydrochloric acid, and treated with an excess of ammonium chloride. The separated phenolic base was removed by filtration, washed with water, and suspended in dilute hydrochloric acid. A very sparingly soluble hydrochloride then formed. The latter was converted to the free base which, when crystallized from methanol, melted at 175°. The substance retained solvent of crystallization very tenaciously and consequently gave unsatisfactory elemental analyses.

Anal. Calcd. for $C_{20}H_{21}O_4N \cdot \frac{1}{2}CH_3OH$ (before drying): C, 69.3; H, 6.5; N, 3.9. Found: C, 69.0; H, 6.7; N, 4.0.

The u.v. spectrum: λ_{max}(MeOH) 288 mμ, log ε_{max} 3.85; ν_{OH} ($CHCl_3$) 3550 cm^{-1}. The molecular formula was confirmed by high resolution mass spectrometry.

Mol. Wt. Calcd. for $C_{20}H_{21}NO_4$: 339.147. Found: 339.147.

Methylation of Apocavidine

Apocavidine (50 mg) was dissolved in methanol (50 ml) and excess diazomethane in ether added to the solution

which was then allowed to stand for 36 h in a refrigerator. The solvent was allowed to evaporate and the residue recrystallized from methanol when it deposited colorless rectangular plates melting sharply at 192° (42 mg).

Anal. Calcd. for $C_{21}H_{23}O_4N$: C, 71.4; H, 6.6, 2 × OMe 17.6. Found: C, 71.6; H, 6.9; OMe, 17.6.

The i.r. spectrum of the compound in $CHCl_3$ was identical with that of cavidine (Base II). The molecular formula was confirmed by high resolution mass spectrometry.

Mol. Wt. Calcd. for $C_{21}H_{23}NO_4$: 353.163. Found: 353.161.

Isolation of Cavidine (Base II) from C. thalictrifolia

The mother liquor derived from *C. thalictrifolia* (1) from which no further thalictrifoline could be separated slowly deposited a sparingly soluble base which was recrystallized twice from $CHCl_3$–MeOH. It consisted of colorless to pale pink deep rectangular plates which melted at 176°. Upon chromatography on silica gel in benzene–acetone (4:1) it could be separated into two fractions the faster moving upon removal of the solvent and recrystallization from MeOH yielded cavidine, m.p. 192°. The slower fraction was shown to be protopine, m.p. 209°, by comparison of its i.r. and p.m.r. spectra with an authentic sample.

We thank the National Research Council of Canada for financial support of this work.

1. R. H. F. MANSKE. Can. J. Res. B**21**, 111 (1943).
2. R. H. F. MANSKE. J. Amer. Chem. Soc. **75**, 4928 (1953).
3. C.-Y. CHEN and D. B. MACLEAN. Can. J. Chem. **46**, 2501 (1968).
4. H. TAGUCHI and I. IMASEKI. J. Pharm. Soc. Japan, **84**, 955 (1964).
5. P. W. JEFFS. Exper. **21**, 690 (1965).
6. P. W. JEFFS. Alkaloids, **9**, 41 (1967).
7. F. A. L. ANET and A. J. R. BOURN. J. Amer. Chem. Soc. **87**, 5250 (1965).
8. J. K. SAUNDERS, R. A. BELL, C.-Y. CHEN, D. B. MACLEAN, and R. H. F. MANSKE. Can. J. Chem. **46**, 2876 (1968).
9. M. SHAMMA, C. D. JONES, and J. A. WEISS. Tetrahedron, **25**, 4347 (1969).
10. T. A. CRABB and E. R. JONES. Tetrahedron, **26**, 1217 (1970).
11. K. BIEMANN. Pure Appl. Chem. **9**, 95 (1964).

Can. J. Chem. Downloaded from www.nrcresearchpress.com by 210.87.254.42 on 09/05/12
For personal use only.

Can. J. Chem. Downloaded from www.nrcresearchpress.com by 210.87.254.105 on 09/05/12
For personal use only.

Silylcarbonium ions from the reaction of silylcarbinols with boron trifluoride

A. G. Brook and K. H. Pannell[1]
Department of Chemistry, University of Toronto, Toronto 181, Ontario

Received April 29, 1970

The behavior of silylcarbonium ions, Si—C$^+$, generated from various types of α-silylcarbinol with boron trifluoride under a variety of conditions of temperature and solvent has been examined. Four distinct types of reaction have been observed, depending on the conditions and the structure of the carbinol. These are: 1,2-migration of aryl groups from silicon to carbon, yielding a fluorosilane; Friedel–Crafts substitution of the carbonium ion on an aromatic substrate; elimination of the elements of water to give a vinylsilane; and isomerization to the β-silylcarbonium ion by hydrogen migration, followed by elimination of the silyl group to give a simple fluorosilane and an alkene (*i.e.* a β-elimination). Factors affecting the partitioning between these pathways are discussed.

Canadian Journal of Chemistry, **48**, 3679 (1970)

The classic work of Sommer *et al.* (1) on the reaction of chloroalkylsilanes with Lewis acids clearly established that silylcarbonium ions $\equiv$Si—$\overset{+}{\underset{|}{C}}$— could be readily generated and that these tended to exhibit two types of behavior, (*a*) migration of an alkyl group from silicon and/or (*b*) migration of hydrogen from the adjacent carbon to give a β-silylcarbonium ion (eq. 1).

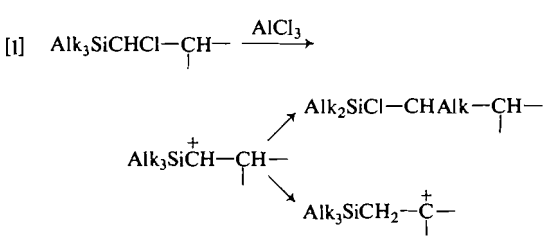

The behavior of these species has been recently reviewed (2). Studies by Kumada *et al.* (3) indicated that silyl groups also migrated readily from silicon to carbon, and studies by Eaborn and Jeffrey (4) showed small amounts of aryl migration from silicon to carbon took place when compounds such as dimethylarylsilylmethyl ethyl ether were treated with aqueous alcoholic hydrogen fluoride. All of these reactions have been described in the literature as analogs of a Wagner–Meerwein rearrangement (eq. 2) although no unambiguous evidence for the formation of a free siliconium ion has been found.

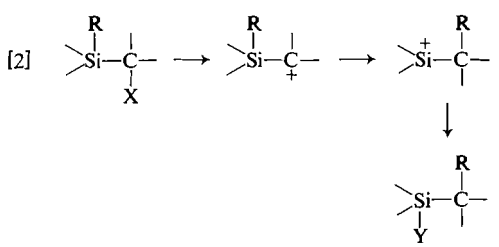

The existence in this laboratory of a wide variety of α-silylcarbinols (α-hydroxysilanes) (5) offered the possibility of providing a wide variety of silylcarbonium ions which could serve for the further study of these reactions, in particular the migration of aryl groups from silicon to carbon, which at the time our work was initiated was relatively unknown. A preliminary account of part of this work has already appeared (6) and this paper will present and discuss the data obtained in greater detail.

As isomerizing agent for the silylcarbinols, gaseous boron trifluoride was employed, this having proven to be much more effective than boron fluoride etherate (since reactions could be completed in minutes, rather than hours or days) and much milder than aluminum chloride, which is known to lead to cleavage of aromatic groups from silicon (7).

In the course of the study on the various silylphenyl carbinols two reactions were observed, 1,2-migrations from silicon, and Friedel–Crafts substitution reactions. It is convenient to present the results in sections related to the general structure of the carbinols studied.

In virtually all of the reactions of silylcarbinols with boron trifluoride, it appears quite clear, as will be subsequently established, that relatively free silylcarbonium ions, Si—$\overset{+}{C}$, are generated, and the discussion of data to follow will pre-

[1]From the Ph.D. thesis of K. H. Pannell, University of Toronto, Toronto, Ontario, 1966.

[3] 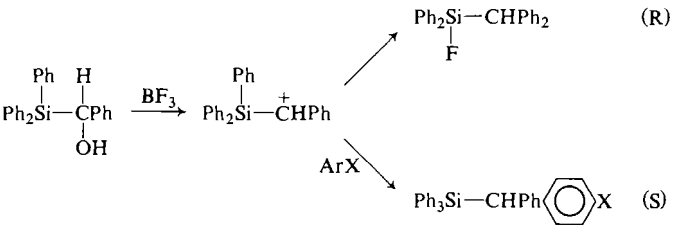

suppose the formation and existence of these species. However, no direct evidence in support of the isomeric siliconium ions was found during the course of this work.

Silylmonophenylcarbinols: $R_3SiCHOHAr$

When silylmonophenylcarbinols were treated in various solvents with gaseous BF_3, two distinct kinds of reaction were observed; rearrangement (R), involving migration of an aryl group from silicon to the carbon originally bearing the hydroxyl group (during which process an Si—F bond is formed) and, Friedel–Crafts substitution (S), in which the intermediate silylcarbonium ion reacts with an aromatic solvent, *e.g.* eq. 3.

In all cases where substituted aromatics were used as solvents, only para-substituted derivatives were isolated, and no evidence for other positions of substitution was noted.

Table 1 summarizes the data obtained with silylmonophenylcarbinols. Several trends are evident which appear to have straightforward explanations.

(*a*) For a given silylcarbinol at a given temperature, the greater the electron-donating ability of the substituent on the aromatic ring of the solvent, the greater is the proportion (given as a percent here and elsewhere) of substitution product obtained: *e.g.* as solvents at 23°; toluene ≈ *tert*-butylbenzene ≈ anisole, 100 S; benzene, 50 S; fluorobenzene, 0 S. Obviously the more reactive the solvent is toward electrophilic substitution, the more favored the intermolecular Friedel–Crafts reaction would be.

(*b*) For a given silylcarbinol in a given solvent, the higher the temperature, the greater the proportion of rearrangement; *e.g.* for triphenylsilylphenylcarbinol in benzene; 5°, 10 R; 23°, 50 R; 80°, 100 R. Since the two competing reactions will have different activation energies the reaction with the higher activation energy will experience the greater acceleration in rate with increasing temperature (8). It follows that the activation energy for rearrangement is greater than that for substitution.

(*c*) The more electron-donating the para-substituent on the phenyl group attached to the carbinol carbon, the greater is the amount of rearrangement product formed: *e.g.* in benzene at 23°, OMe, 100 R; CMe_3, 78 R; H, 50 R; Cl, 44 R. This infers that stabilization of the proposed benzyl type silylcarbonium ion intermediate ($Ph_3SiCH^+—C_6H_4X$-*p*) facilitates rearrangement relative to substitution. It has been demonstrated by Nenitzescu (9) that electron-donating substituents on the aromatic ring in benzyl carbonium ions increase the rate of the Friedel–Crafts reactions of the ions by stabilization of the transition state; hence it is clear from our results that such substituents stabilize the transition state of the 1,2-migrations from silicon to an even greater extent.

(*d*) The more electron-donating the para-substituents on the aromatic rings attached to silicon, the greater is the proportion of rearrangement: *e.g.* in benzene at 23°, CMe_3, 100 R; H, 50 R; Cl, 0 R. Since the rearrangement process can be conceived as an intramolecular electrophilic attack by the carbonium ion on the aromatic groups attached to silicon, it follows that the more susceptible these are to electrophilic attack the more readily the rearrangement should take place.

(*e*) Trimethylsilylphenylcarbinols fail to rearrange, and either undergo Friedel–Crafts substitution with an aromatic solvent exclusively, or, in a non-aromatic solvent, yield polymer. The failure to observe the migration of alkyl groups infers that much greater energy is required for alkyl migration from silicon to carbon than for aryl migration, as would have been expected, and the formation of substitution products indicates that the activation energy for this process is lower than for alkyl migration. The polymer formation observed in the absence of an

Can. J. Chem. Downloaded from www.nrcresearchpress.com by 210.87.254.105 on 09/05/12
For personal use only.

TABLE 1

Proportion (%) of rearrangement (R) and Friedel–Crafts substitution (S) for silylmonophenylcarbinols with various solvents and temperatures*†

Compound	Solvent	Temperature (°C) 5	23	80	Other
$Ph_3SiCHOHPh$	C_6H_6	10 R 90 S	50 R 50 S	100 R	
	C_6H_5Me		100 S		30 R 70 S‡
	C_6H_5F		100 R		85 R 15 S§
	C_6H_5OMe		100 S		
	$C_6H_5CMe_3$		100 S		
	C_6H_{14}‖		100 R		
$Ph_3SiCHOHC_6H_4OMe$-*p*	C_6H_6	100 R	100 R	100 R	
	$C_6H_5CMe_3$		100 S		
	C_6H_{14}		100 R		
$Ph_3SiCHOHC_6H_4CMe_3$-*p*	C_6H_6	64 R 36 S	78 R 22 S	100 R	
	C_6H_5Me		100 S		
	C_6H_{14}		100 R		
$Ph_3SiCHOHC_6H_4Cl$-*p*	C_6H_6	33 R 66 S	44 R 56 S	80 R 20 S	
	C_6H_5Me		100 S		
	C_6H_{14}		100 R		
(p-$Me_3CC_6H_4)_3SiCHOHPh$	C_6H_6		100 R		
	C_6H_5Me		100 S		
(p-$ClC_6H_4)_3SiCHOHPh$	C_6H_6		100 S		
	C_6H_{14}		100 R		
$Me_3SiCHOHPh$	C_6H_5X¶		100 S		
	C_6H_{14}		Polymer		

*Reaction being studied is:

$$R_3SiCHOHR' \xrightarrow[BF_3]{ArX} R_2FSiCHRR'(R) + R_3SiCHR'C_6H_4X\text{-}p(S).$$

†Proportions of products, accurate to about 5%, were estimated by n.m.r. techniques and are given as percentages. Isolated yields generally confirmed the proportions given. For details of the reactions see the Experimental section.
‡Temperature of run was 110°.
§Temperature of run was −40°.
‖C_6H_{14} is *n*-hexane.
¶X = H, OMe, CMe_3, or F.

TABLE 2

Products from silyldiphenylcarbinols with BF_3 at 23°

Compound	Solvent	Product	%
Ph_3SiCPh_2OH	C_6H_5Me	$Ph_2FSiCPh_3$	100 R
$Ph_2MeSiCPh_2OH$	C_6H_5Me	$PhMeFSiCPh_3$	100 R
$PhMe_2SiCPh_2OH$	C_6H_5Me	$Me_2FSiCPh_3$	100 R
Me_3SiCPh_2OH	C_6H_{14}	$Me_2FSiCMePh_2$	100 R
1-NpPhMeSiCPh$_2$OH	C_6H_6	1-NpMeFSiCPh$_3$	90 R
		PhMeFSiCPh$_2$-1-Np	10 R*

*Product detected by n.m.r. but not isolated.

aromatic solvent probably arose from attack of the carbonium ion on the aromatic ring of a second molecule.

Silyldiphenylcarbinols

In contrast to the competing reactions observed with silylmonophenylcarbinols, silyldiphenylcarbinols were observed to undergo rearrangement only, as indicated in Table 2. In view of the sterically hindered nature of the intermediate carbonium ion, it perhaps is not surprising that Friedel–Crafts substitution with an aromatic solvent did not occur. As was inferred earlier, and is now evident, in any competition between alkyl and aryl migration from silicon to carbon, only the latter occurs, since only aryl migration was observed in diphenylmethyl- or phenyldimethylsilyldiphenyl-

Can. J. Chem. Downloaded from www.nrcresearchpress.com by 210.87.254.105 on 09/05/12
For personal use only.

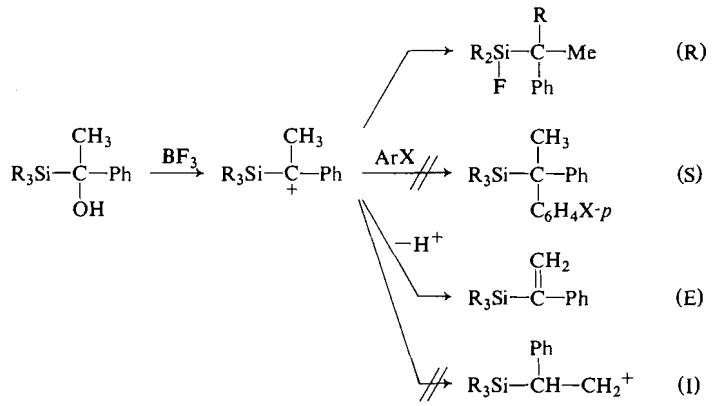

SCHEME 1

TABLE 3

Results of the reaction of silylmethylphenylcarbinols with BF_3*

Compound	Solvent	Temperature (°C)			
		−40	23	32	110
$Ph_3SiCOHMeC_6H_4OMe$	C_6H_5Me	100 E	100 E		100 E
	C_5H_{12}	100 R		10 R 90 E	
$Ph_3SiCOHMeC_6H_5$	C_6H_5Me	70 R 30 E	100 E		100 E
	C_5H_{12}	100 R		100 R	
$Ph_3SiCOHMeC_6H_4Cl$	C_6H_5Me	80 R 20 E	66 R 33 E		100 E
	C_5H_{12}	100 R		100 R	

*R ≡ $Ph_2FSiCMePh(C_6H_4X\text{-}p)$; E ≡ $Ph_3SiC(C_6H_4X\text{-}p)=CH_2$.

carbinols. However, in contrast to the situation with silylmonophenylcarbinols, trimethylsilyldiphenylcarbinol was observed to undergo alkyl rearrangement rather than polymer formation. When either a phenyl or an α-naphthyl group was capable of undergoing migration, as with 1 - naphthylphenylmethylsilyldiphenylcarbinol, phenyl migration occurred about nine times more frequently than naphthyl migration, the latter possibly being inhibited by the steric requirements of the transition state.

Silylmethylarylcarbinols: $R_3SiCOHMeC_6H_4X\text{-}p$

When an alkyl group is attached to the carbonium ion generated from a silylcarbinol with boron trifluoride, additional types of reaction other than rearrangement (R) or Friedel–Crafts substitution (S) may occur. Elimination of a proton (E) would constitute an overall dehydration of the parent carbinol. In addition the possibility exists, previously observed in other cases (10), of isomerization (I) caused by hydrogen migration, converting the original silylcarbonium ion to its β-isomer, which could then react in a variety of ways. Of the four possible reactions outlined in Scheme 1, only rearrangement and proton elimination were observed with the silylmethylarylcarbinols. The results obtained are presented in Table 3. Friedel–Crafts substitution may not occur because of steric considerations, as was proposed to explain the behavior of the silyldiphenylcarbinols. The failure of the tertiary ion to isomerize to the primary (β) carbonium ion (I) is understandable because of unfavorable differences in stability.

Of the two processes elimination and rearrangement, it is evident from Table 3 that the former is favored by higher temperature. The nature of the solvent also plays an important role in determining the relative importance of the two reactions, pentane (non-solvating) favoring rearrangement but toluene (ion-solvating) favoring elimination. It is also evident that para-sub-

Can. J. Chem. Downloaded from www.nrcresearchpress.com by 210.87.254.105 on 09/05/12
For personal use only.

TABLE 4

Products from triphenylsilylphenyl-*p*-substituted benzylcarbinols treated with BF_3 in toluene at various temperatures*

Carbinol	Products, %Yields R†	E‡	Stilbene (*cis–trans*)§	Ph_3SiF	Ph_3SiOH
−40°					
$Ph_3SiCOHPhCH_2C_6H_4CMe_3$-*p*	17	0	67(50–50)	36	19
$Ph_3SiCOHPhCH_2C_6H_5$	27	0	38(90–10)	20	17
$Ph_3SiCOHPhCH_2C_6H_4Cl$-*p*	51	0	38(100–0)	13	25
110°					
$Ph_3SiCOHPhCH_2C_6H_4CMe_3$-*p*	0	37	53(28–72)	12	19
$Ph_3SiCOHPhCH_2C_6H_5$	0	33	26(90–10)	6	18
$Ph_3SiCOHPhCH_2C_6H_4Cl$-*p*	0	28	43(90–10)	5	29

*Yields reported are of isolated material. The *cis–trans* proportions are based on spectroscopic data.
†R ≡ $Ph_2FSiCPh_2CH_2C_6H_4X$-*p*.
‡E ≡ 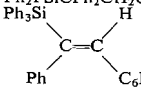
§Stilbene ≡ $PhCH{=}CHC_6H_4X$-*p*(*cis–trans* proportions) ≡ IE′.

stituents on the aryl groups attached to carbon play an important role in determining whether rearrangement or elimination is the major reaction occurring, electron-donating substituents (*e.g.* OMe) favoring elimination, presumably because charge delocalization by the aromatic ring attached to carbon in the transition state is of paramount importance.

Silyl-p-substituted Benzylphenylcarbinols: $Ph_3SiCOHPhCH_2C_6H_4X$-p

The *p*-substituted-benzylphenylcarbinols were formed by treatment of benzoyltriphenylsilane with the appropriate Grignard reagent (eq. 4).

[4] $Ph_3SiCOPh + X{-}C_6H_4{-}CH_2MgX \longrightarrow$ 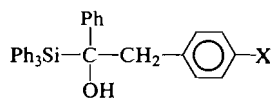

Treatment of these carbinols with BF_3 could be expected to yield silylcarbonium ions which could attack the toluene used as solvent (S), rearrange (R), or directly lose a proton to form a silyl-substituted stilbene (E). Additionally, hydrogen migration could occur (I) to give the isomeric β-silylcarbonium ion, a reasonable reaction here since the β-ion would also be benzylic in character and thus of comparable stability. This β-ion could lose a proton to give, by this alternative route, the same silylstilbene, but loss of a proton from a β-silylcarbonium ion is not commonly observed (11). The alternative process available to the β-silylcarbonium ion, elimination of the silyl group as triphenylfluorosilane, IE′, with the formation of an alkene, in this case a stilbene, is well-documented behavior commonly observed in β-elimination reactions (11). These possibilities are outlined in Scheme 2.

The reaction products from the carbinols examined gave evidence that each of the possible reaction pathways except Friedel–Crafts substitution had occurred: again, as in previous situations involving tertiary carbonium ions, steric effects presumably preclude substitution taking place. The reaction mixtures were sufficiently complex that estimation of the proportions of various products could not be carried out from n.m.r. spectral data alone, and the data reported in Table 4 are isolated yields, and thus not very precise in some cases. In the separation of the products by column chromatography some triphenylfluorosilane was hydrolyzed to triphenylsilanol, so that the sum of the yields of these two products constitutes some measure of the overall amount of elimination of silicon (IE′) occurring from the β-silylcarbonium ions.

As is evident from the data in Table 4, the reactions are highly temperature sensitive. At −40°, rearrangement of an aryl group from silicon to carbon (R) or isomerization of the α-silylcarbonium ion to the β-ion, followed by loss of silicon (IE′), were the only processes observed, no silylstilbene, the product of simple

Can. J. Chem. Downloaded from www.nrcresearchpress.com by 210.87.254.105 on 09/05/12
For personal use only.

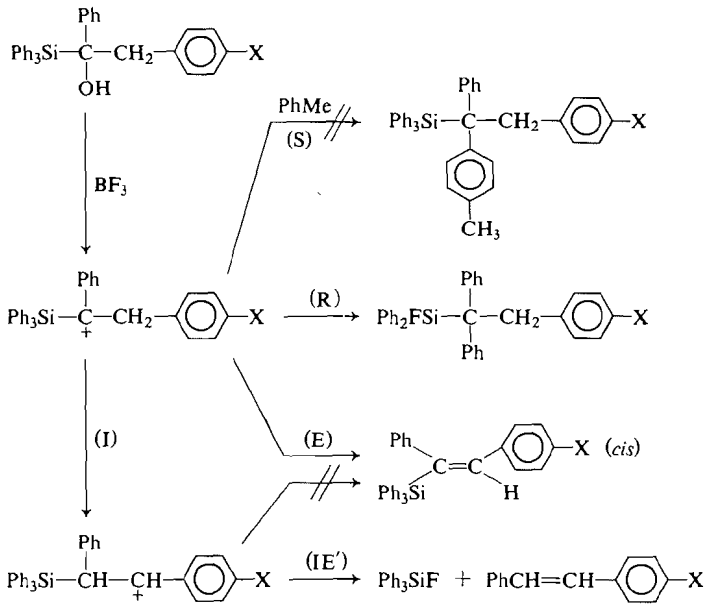

SCHEME 2

elimination (E), being detected. Less rearrangement and more isomerization occurred when the benzyl group had an electron-donating substituent attached, presumably because isomerization would be more favorable when the new β-ion could be stabilized whereas the α-ion would be relatively unaffected by substituents on the benzyl group. A surprising amount of the stilbene resulting from the IE′ process was the *cis*-isomer.

At the elevated temperature (110°), no rearrangement product was detected. Elimination of a proton from the α-silylcarbonium ion (E) yielding silylstilbene was a major reaction and the silylstilbenes isolated were shown by comparison with authentic samples to be exclusively the isomers where both aryl groups were *cis* to one another, suggesting that less steric interaction occurs between *cis*-aryl groups than when an aryl group and a triphenylsilyl group are *cis* to one another. The other process occurring at 110° was again isomerization–elimination (IE′) since significant amounts of fluorosilane and silanol and *cis*- and *trans*-stilbenes were isolated.

It seems probable that the silylstilbenes observed arise solely by loss of a proton from the α-silylcarbonium ion. Loss of a proton from β-silylcarbonium ions is not normally observed, loss of silicon being the usual process (11). In the present work, and as a test of the source of the silylstilbenes, the β-silylcarbinol 1-phenyl-2-triphenylsilylethanol was treated with BF_3 in toluene (eq. 5); triphenylfluorosilane was isolated in high yield. No silylalkene, the product of proton elimination, could be detected. Hence, we believe the silylstilbene arises solely by loss of a proton from the α-silylcarbonium ion, whereas fluorosilane and *cis*- and *trans*-stilbenes are the only products produced by any β-silylcarbonium ion formed.

Since treatment of either the *cis*- or *trans*-stilbene with BF_3 under the reaction conditions caused no isomerization, it appears that the proportions of *cis*- and *trans*-stilbenes obtained from the reaction of the silylcarbinols with BF_3 are somehow specifically related to their silylcarbonium ion precursors. While it would be possible to speculate as to a possible explanation for the proportions in which they are formed it seems more prudent to await further information.

Aliphatic Silylcarbinols

Three triphenylsilylcarbinols having only hydrogen or aliphatic groups attached to the carbinol carbon were subjected to treatment with BF_3 in hexane and in toluene.

Triphenylsilylcarbinol was found to resist reaction and was recovered unchanged after

Can. J. Chem. Downloaded from www.nrcresearchpress.com by 210.87.254.105 on 09/05/12
For personal use only.

TABLE 5
Products from germylcarbinols with BF_3

Compound	Solvent	Temperature (°C)	Products	Results with Si analog
$Ph_3GeCHOHPh$	C_6H_6	23	100 S	50 R 50 S
	C_6H_6	80	5 R 95 S	100 R
	C_6H_5F	−20	100 S	—
	C_6H_{14}	23	100 R	100 R
$Ph_3GeCOHPh_2$	ArX or C_6H_{14}	23	100 R	100 R

[5] $Ph_3SiCH_2CHOHPh \xrightarrow[C_6H_5Me]{BF_3} Ph_3SiCH_2\overset{+}{C}HPh \nearrow Ph_3SiF + CH_2{=}CHPh$; $\overset{+}{C}HPh \not\rightarrow Ph_3SiCH{=}CHPh$

treatment with BF_3 in hexane at 23°, or in toluene at either 40 or 110°. Similarly 1-triphenylsilylethanol failed to react in hexane or toluene at 23°. This inertness may be due to the instability of the anticipated carbonium ions, since it is known that under the reaction conditions employed neither methanol nor ethanol undergoes Friedel–Crafts reactions (12).

2-Triphenylsilyl-2-propanol reacted with BF_3 to give only isopropenyltriphenylsilane, the dehydration product, under a variety of reaction conditions including hexane at 23°, or toluene at −40 or +110 °C.

Germylcarbinols and Carbinols:
$Ph_3GeCPhOHR(R = H, Ph)$,
$Ph_3CCHOHPh$

The reactions of boron trifluoride with a few germylcarbinols were investigated to compare with the behavior of the analogous silicon compounds. The data are summarized in Table 5.

Both the germylmono- and diphenylcarbinols behaved rather like their silicon analogs, although the germylmonophenyl carbinols showed a greater tendency to undergo substitution rather than rearrangement under similar conditions, compared with their silicon analogs.

When 1,2,2,2-tetraphenylethanol was treated with boron fluoride for comparison purposes in a variety of solvents at various temperatures, under all conditions the only product formed was tetraphenylethylene (eq. 6).

[6] $Ph_3C{-}CHOHPh \xrightarrow{BF_3} Ph_3C{-}\overset{+}{C}HPh \rightarrow Ph_2\overset{+}{C}{-}CHPh_2 \rightarrow Ph_2C{=}CPh_2$

Thus the reactions of the carbinols $Ph_3MCHPhOH$ (M = C, Si, Ge) with boron fluoride depend noticeably on the nature of the atom M. Each carbinol can be presumed to have formed the carbonium ion $Ph_3M\overset{+}{C}HPh$.

In non-aromatic solvents, each underwent rearrangement involving migration of phenyl from M to the adjacent electron-deficient carbon atom. In aromatic solvents, as the atom M changes from Ge to Si to C, it is observed that the amount of Friedel–Crafts substitution of the original carbonium ion diminishes relative to the amount of 1,2-phenyl migration. One of the reasons for this may be the decreasing size of M, resulting in differing steric effects. In particular, with the smaller size of carbon, there will be an increase in the steric repulsions between the three phenyl groups attached to M, increasing the driving force for migration. Additionally, the smaller the atom M is, the more sterically shielded the carbonium ion is likely to be, making approach of the aromatic solvent necessary for Friedel–Crafts substitution more difficult. Both these effects will tend to increase the amount of 1,2-migration and reduce the amount of substitution on changing M from Ge to Si to C.

Carbonium Ions

In the discussion so far it has been assumed that carbonium ion intermediates were created by reaction of the silylcarbinols with BF_3. Some fairly compelling evidence for these assumptions exists as will be described below.

Attempts to trap silylcarbonium ions as methyl ethers by adding the deep red solution, formed

Can. J. Chem. Downloaded from www.nrcresearchpress.com by 210.87.254.105 on 09/05/12
For personal use only.

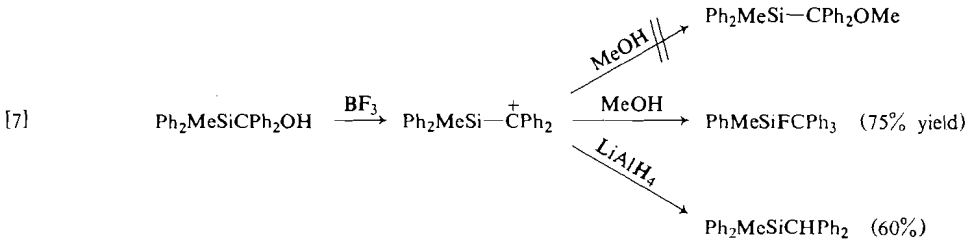

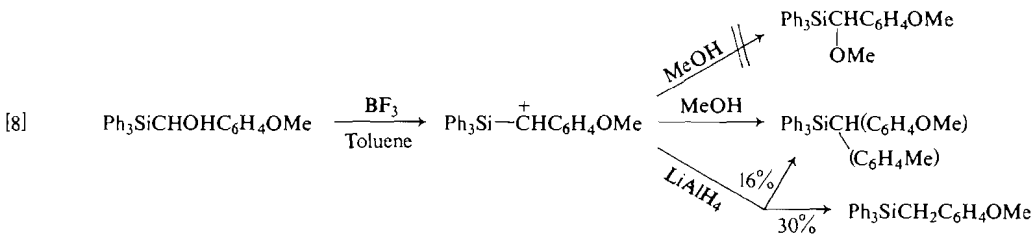

by addition of BF_3 to a solution of diphenylmethylsilyldiphenylcarbinol in toluene at $-40°$, to methanol at $-60°$ failed, since only the normal rearrangement product phenylmethyltritylfluorosilane was obtained (eq. 7). However, when the deep red solution was treated with ethereal lithium aluminum hydride, following the procedure of Brown for trapping carbonium ions as the hydride derivative (13) a 60% yield of diphenylmethylsilylphenylmethane was isolated, strongly suggestive of an intermediate carbonium ion.

Similarly, the deep red solution formed at $-40°$ from triphenylsilyl-*p*-methoxyphenylcarbinol with BF_3 in toluene when treated with methanol failed to yield the methyl ether, the Friedel–Crafts substitution product with toluene being obtained in greater than 80% yield. However, when treated with ethereal lithium aluminum hydride, a mixture of the hydride and the Friedel–Crafts product was obtained (eq. 8). These results indicate that under conditions where either rearrangement or substitution was normally found to occur exclusively, low temperature quenching led to the formation of compounds logically explicable in terms of an intermediate carbonium ion.

We have sought further evidence for the existence of the carbonium ions by obtaining n.m.r. spectra of various species following the general procedures developed by Olah *et al.* (14). Thus dissolving the silylcarbinols in a mixture of antimony pentachloride – sulfur dioxide at -60 °C gave rise to deeply colored solutions whose n.m.r. spectra were readily interpretable as due to silylcarbonium ions being present in high yield.

Table 6 presents the data for the various silylcarbonium ions observed, together with the data of Olah *et al.* (14, 15) for related carbonium ions. In general the spectra were not clean and integration always indicated too many aromatic protons. This, coupled to the inability to recover recognizable products after quenching with methanol, suggests that extensive cleavage of the aromatic groups on silicon took place. Aryl–silicon bonds are well known to be susceptible to cleavage under these conditions (16). In view of these observations it is apparent that the n.m.r. spectra obtained for the silylalkylcarbonium ions are the more useful in illustrating the existence of the silylcarbonium ions because the alkyl resonances may be compared to those of the related carbonium ions. The phenyl resonances although in general appearing to be in the expected region may contain significant amounts of $C_6H_5^+$ ion or related species thus confusing the spectra in this region.

The preceding data make it possible to explain the reactions of boron trifluoride with the silylcarbinols as involving silylcarbonium ion intermediates which rearrange, or which undergo elimination reactions. Certain details of the over-

Can. J. Chem. Downloaded from www.nrcresearchpress.com by 210.87.254.105 on 09/05/12
For personal use only.

TABLE 6

The n.m.r. spectra of silylcarbonium ions in $SbCl_5$:SO_2 at $-60°$

Ions	Resonance position δ
$Ph_3SiCPhMe^+$	3.61 (s) ($SiCMe^+$), 7.3–8.4 (Aryl)
$Ph_3SiCMeC_6H_4F^+$	3.58 (s) ($SiCMe^+$), 7.3–8.4 (Aryl)
$Ph_3SiCPh_2^+$	7.5–8.3 (Aryl)
$PhMe_2SiCPh_2^+$	0.75 (s, Me), 7.7–8.3 (Aryl)
$Ph_3SiC(C_6H_4OMe)CH_2Ph^+$	4.4 (OMe), 4.6 (s) ($C—CH_2Ph^+$), 7.0–8.0 (Aryl)
$Ph_3SiCPhCH_2Ph^+$	5.2 (s) (CH_2Ph), 7.0–8.5 (Aryl)
$PhEtCMe^+$	3.5 (s) (CMe^+)
Me_3C^+	3.83 (s)
$Ph_3CCPh_2^+$	7.4–8.3 (Aryl)
$Ph_2CCH_2Ph^+$	5.1 (s) (CH_2Ph), 7.1 (m) (CH_2Ph), 7.5–8.3 (Aryl)

all mechanism have not been clearly resolved however. There is no evidence that siliconium ions are intermediate species in the rearrangement reactions. No products were isolated from any reaction whose formation would have involved reaction of a siliconium ion with an aromatic substrate. Further, when triphenylsilanol in toluene was treated with BF_3 in the hope of forming triphenylsiliconium ion, which could then react with the aromatic substrate, only tris(triphenylsiloxy)boron was formed. If siliconium ions are not involved, as seems probable, then the degree to which fluoride ion or some other anion is involved in the migration process, and the timing of the silicon–fluorine bond formation relative to aryl migration from silicon to carbon is not yet clearly established. Recent studies in these laboratories (17) have shown that silyldiazoalkanes, on treatment with acid, a process presumed to give silylcarbonium ions (or ion pairs), give the simpler addition product $R_3SiCHXR$, with no rearrangement product being formed (eq. 9). However, if the diazo

$$[9]\quad R_3SiCN_2R' + HX \rightarrow R_3Si—\overset{+}{C}HR' \rightarrow R_3SiCHXR \qquad (X^-)$$

compound is treated with $BF_3 \cdot Et_2O$ (under conditions where some water may be present) or if the addition product $R_3SiCHXR$ is treated with $BF_3 \cdot Et_2O$, then the expected rearrangement and Friedel–Crafts substitution products are obtained (18) (eq. 10).

$$[10]\quad \begin{matrix} R_3SiCN_2R \\ \text{or} \\ R_3SiCHXR \end{matrix} \xrightarrow[\text{toluene}]{BF_3 \cdot Et_2O \text{ in}} R_2SiCHR_2 + \underset{F}{R_3SiCHPhC_6H_4Me\text{-}p}$$

It is therefore evident that more than the mere formation of a simple silylcarbonium ion is required for rearrangement to occur, and it is obvious that BF_3 is a particularly good reagent for effecting rearrangements of aryl groups from silicon to carbon. However, a clearer understanding of the processes involved and their timing must await further studies.

Experimental

The silylcarbinols employed in this study were known compounds prepared according to published routes as noted below for each family: silylphenylcarbinols (5), silyldiphenylcarbinols (19, 20), silylphenylbenzylcarbinols (5), silylphenylmethylcarbinols (5), and silylalkylcarbinols (21).

The solvents employed were reagent grade and the boron trifluoride (Matheson) was used direct from the cylinder without purification.

Most reactions were carried out following a standard procedure. The silylcarbinol was dissolved in the desired solvent in a 100 ml round-bottomed flask under nitrogen, and the solution was stirred magnetically. Cooling when desired was effected by Dry Ice – acetone or ice-baths, and reactions at elevated temperatures were usually carried out at reflux.

Boron trifluoride was rapidly bubbled directly into the solution until the effluent gases fumed, which was taken as an indication that excess boron fluoride had been added. This usually required only a few seconds. In many

Can. J. Chem. Downloaded from www.nrcresearchpress.com by 210.87.254.105 on 09/05/12
For personal use only.

Can. J. Chem. Downloaded from www.nrcresearchpress.com by 210.87.254.105 on 09/05/12
For personal use only.

TABLE 7

Products from the reactions of silylcarbinols with BF_3

Reagent or solvent	Product	Yield* (%)	Melting point (°C)	Analysis† C	Analysis† H
(a) Products from $Ph_3SiCHOHPh$					
C_6H_5OMe	$Ph_3SiCHPhC_6H_4OMe$-*p*	87‡	172–174	84.15	6.17
				84.46	6.27
C_6H_5Me	$Ph_3SiCHPhC_6H_4Me$-*p*	79‡	185–186		§
C_6H_{14}	$Ph_2FSiCHPh_2$	94‖	154–155	81.53	5.71
				81.61	5.82
(b) Products from $Ph_3SiCHOH(C_6H_4Cl$-p)					
C_6H_5Me	$Ph_3SiCH(C_6H_4Cl$-*p*$)(C_6H_4Me$-*p*$)$	66¶	160–161	80.88	5.73
				80.85	5.74
C_6H_{14}	$Ph_2FSiCHPh(C_6H_4Cl$-*p*$)$	75	102–104	74.49	5.00
				74.47	4.92
(c) Products from $Ph_3SiCHOH(C_6H_4CMe_3$-p)					
C_6H_5Me	$Ph_3SiCH(C_6H_4CMe_3$-*p*$)(C_6H_4Me$-*p*$)$	65	144–145	87.04	7.30
				87.01	7.32
C_6H_{14}	$Ph_2FSiCHPh(C_6H_4CMe_3$-*p*$)$	86	147–149	82.01	6.88
				81.42	6.97
(d) Products from $(p$-$XC_6H_4)_3SiCHOHPh$					
C_6H_6	$(p$-$ClC_6H_4)_3SiCHPh_2$	68	194–196	70.23	4.37
				69.97	4.42
C_6H_6	$(p$-$Me_3CC_6H_4)_2FSiCHPh(C_6H_4CMe_3$-*p*$)$	70	154–156	82.70	8.40
				82.50	8.32
C_6H_5Me	$(p$-$Me_3CC_6H_4)_3SiCHPh(C_6H_4Me$-*p*$)$	59	206–207	86.76	8.61
				86.03	8.30
(e) Products from $Ph_nMe_{3-n}SiCOHPh_2$					
C_6H_5Me	$Ph_2FSiCPh_3$	85‡**	186–187	83.82	5.67
				83.50	5.69
C_6H_5Me	$PhMeFSiCPh_3$	83‡	150–151	81.61	6.06
				82.12	6.03
C_6H_5Me	$Me_2FSiCPh_3$	70	134–135	78.68	6.60
				78.50	6.62
C_6H_5Me	$Me_2FSiCMePh_2$	56	††	74.34	7.41
				74.65	7.24
(f) Products from $Me_3SiCHOHPh$					
C_6H_5OMe	$Me_3SiCHPh(C_6H_4OMe$-*p*$)$	64	57–58‡‡	75.49	8.19
				75.15	7.75
$C_6H_5CMe_3$	$Me_3SiCHPh(C_6H_4CMe_3$-*p*$)$	53	§§	81.02	9.38
				81.00	9.15
C_6H_5Me	$Me_3SiCHPh(C_6H_4Me$-*p*$)$	78	35–36‡	79.92	8.72
				79.77	8.53
C_6H_6	$Me_3SiCHPh_2$	70	74–75‖‖		§
C_6H_5F	$Me_3SiCHPh(C_6H_4F$-*p*$)$	52	49–50‡	74.36	7.14
				74.23	7.21

*Yields are based on material isolated from 0.5 g runs in 50 ml of solvent at a temperature of either 23° or as otherwise noted.
†Top line, calculated values; second line, found values.
‡Recrystallized from methanol.
§Identified by mixed m.p. with authentic sample.
‖In C_6H_5F, yield was 85%; in C_6H_6 at 80°, yield was 77% after recrystallization from petroleum ether (b.p. 90–100°). Reduction of product with $LiAlH_4$ gave $Ph_2HSiCHPh_2$ m.p. 130–132°.
Anal. Calcd. for $C_{25}H_{22}Si$: C, 85.64; H, 6.33. Found: C, 85.58; H, 6.18.
¶Recrystallized from petroleum ether (b.p. 90–100°).
**On reduction with $LiAlH_4$, $Ph_2HSiCPh_3$ was obtained ,m.p. 152–154°, from petroleum ether.
Anal. Calcd. for $C_{31}H_{26}Si$: C, 87.27; H, 6.14. Found: C, 87.35; H, 6.01.
††Liquid: b.p. 55°/0.02 mm.
‡‡Recrystallized from pentane at −70°.
§§High boiling liquid purified by chromatography on alumina.
‖‖Recrystallized from ethanol.

TABLE 8

Data from reactions of silylcarbinols $Ph_3SiCOHMe(C_6H_4X\text{-}p)$ in various solvents

X of reagent	Solvent	Product	Temperature (°C)	Yield (%)	Melting point (°C)	Analysis C	Analysis H
H	C_6H_5Me	$Ph_3SiCPh{=}CH_2$*	23	82	133–135†	‡	
H	C_5H_{12}	$Ph_2FSiCMePh_2$	32	58	88–90§	81.61	6.06
						81.35	6.05
Cl	C_6H_5Me	$Ph_3SiC(C_6H_4Cl\text{-}p){=}CH_2$	110‖	81	123–124†	78.64	5.33
						78.14	5.18
Cl	C_5H_{12}	$Ph_2FSiCMePh(C_6H_4Cl\text{-}p)$	32	60	106–108§	74.87	5.32
						74.69	5.32
OMe	C_6H_5Me	$Ph_3SiC(C_6H_4OMe\text{-}p){=}CH_2$	−40¶	90	100–101†	82.59	6.16
						82.61	6.08
OMe	C_5H_{12}	$Ph_2FSiCMePh(C_6H_4OMe\text{-}p)$	−40	64	112–113§	78.54	6.07
						78.31	6.01

*The u.v. spectrum, λ_{max} (EtOH) 249 mμ (8800).
†Recrystallized from ethanol.
‡Identified by mixed m.p. with authentic sample.
§Recrystallized from methanol.
‖The u.v. spectrum, λ_{max} (EtOH) 255 mμ (10 800).
¶The u.v. spectrum, λ_{max} (EtOH) 264 (10 000), 268 (10 300), 272 mμ (s) (9600).

of the reactions highly colored (red–yellow) intermediate solutions were observed. Reactions were worked-up by quenching in water followed by ether extraction. Where mixtures of products were obtained they were identified by comparison with the spectra of authentic samples, and the ratio of the products was determined by n.m.r. integration. Several typical examples are given below, and the results of all reactions will be found in Tables 7–10.

Nuclear Magnetic Resonance

Nuclear magnetic resonance was extensively employed in this work to establish the ratio of mixtures of products. While the positions of absorptions associated with particular groups varied very little between the members of a family of compounds (*e.g.* *p*-CMe_3, δ 1.20–1.32; *p*-OMe, δ 3.64–3.73; *p*-Me, δ 2.25–2.29; Si—C*H*— δ 4.08–4.3 p.p.m., etc.) absorptions associated with many frequently encountered combinations of compounds were readily identified. Thus, for example, from the reaction of triphenylsilylphenylcarbinol with BF_3 in toluene (eq. 11), the products formed, benzhydryldiphenylfluorosilane and *p*-methylbenzhydryltriphenylsilane were easily distinguished, and the proportions readily established by integration. In the fluorosilane, the benzylic

[11] $Ph_3SiCHOHPh \rightarrow Ph_2FSiCHPh_2 + Ph_3SiCHPhC_6H_4Me\text{-}p$

proton occurred as a doublet, at δ 4.1 p.p.m., $J = 7$ Hz, being split by the adjacent fluorine whereas the *p*-tolyl compound could be estimated quantitatively both by the benzylic proton which occurred as a singlet at δ 4.36 p.p.m., and by the intensity of the methyl signal at 2.25 p.p.m.

In the compounds containing methoxyphenyl groups the four aromatic protons usually were observed as an AB quartet at about 6.7–6.9 p.p.m., separate from the other aromatic proton signals, indicating unambiguously that substitution had occurred in the para position, but *p*-tolyl- or *p*-*t*-butylphenyl- signals usually overlapped other aromatic protons.

The ^{19}F spectra of a variety of compounds, *e.g.* $Ph_2FSiCHPh_2$, $Ph_2FSiCPh_3$, etc. were consistent with the structures assigned. Details of some typical spectra are given in Table 11.

Reaction of Triphenylsilylphenylcarbinol in Hexane at 23 °C

Boron trifluoride was bubbled into a solution of 0.5 g (1.37 mmole) of triphenylsilylphenylcarbinol in 50 ml of hexane for a few seconds until the effluent gases fumed. The reaction mixture was quenched in water, and the ether extracts, after drying with magnesium sulfate, were evaporated to dryness to give a colorless oil which was crystallized from petroleum ether (b.p. 90–100°) to give 0.47 g (94%) of benzhydryldiphenylfluorosilane, $Ph_2FSiCHPh_2$, m.p. 154–155°; n.m.r. (CCl_4); δ 4.1 (1H, d, $J = 7$, SiC*H*), 7.1–7.2 p.p.m. (20H, m, Ar).

Reaction of Triphenyl-p-chlorophenylcarbinol in Toluene at 23°

Boron trifluoride was bubbled into a solution of 0.5 g (1.25 mmole) of triphenylsilyl-*p*-chlorophenylcarbinol in 50 ml of toluene at 23°. After quenching with water and extraction with ether, the dried ether layer was evaporated under reduced pressure to give a colorless oil which was crystallized from petroleum ether (b.p. 90–100°) to give 0.35 g (66%) of triphenyl-*p*-chloro-*p'*-methylbenzhydrylsilane, $Ph_3SiCH(C_6H_4Cl\text{-}p)$ ($C_6H_4Me\text{-}p$), m.p. 160–161°; n.m.r. (CCl_4); δ 2.26 (3H, s, Me), 4.36 (1H, s, SiC*H*), 6.85–7.3 p.p.m. (23H, m, Ar).

Reaction of Phenyldimethylsilyldiphenylcarbinol in Toluene at −40°

Boron trifluoride was bubbled into a solution of 2.0 g (6.4 mmole) of the above carbinol in 50 ml of toluene at −40 °C for 30 s. An immediate red coloration appeared and persisted over 30 min, at which time the mixture was removed from the cold bath and allowed to warm to

Can. J. Chem. Downloaded from www.nrcresearchpress.com by 210.87.254.105 on 09/05/12
For personal use only.

TABLE 9

Products from reactions of $Ph_3SiCOHPh(CH_2C_6H_4X\text{-}p)$ in toluene at various temperatures

X of reagent	Temperature of reaction (°C)	Product	Yield (%)	Melting point (°C)	Analysis C	Analysis H
Cl	−40	$Ph_2FSiCPh_2(CH_2C_6H_4Cl\text{-}p)$	51	134–135.5	77.93 78.18	5.31 5.23
		cis-$PhCH{=}CHC_6H_4Cl\text{-}p$*	38			
		Ph_3SiF	13	62–64	†	
		Ph_3SiOH	25	153–154	†	
Cl	110	$Ph_3SiCPh{=}CHC_6H_4Cl\text{-}p$‡	28	151–152.5	81.23 81.30	5.32 5.33
		trans-$PhCH{=}CHC_6H_4Cl\text{-}p$*	4	131–132.5	†	
		cis-$PhCH{=}CHC_6H_4Cl\text{-}p$*	40			
		Ph_3SiF	5	62–64	†	
		Ph_3SiOH	29	153–154	†	
CMe_3	−40	$Ph_2FSiCPh_2(CH_2C_6H_4CMe_3\text{-}p)$	17	167	83.98 84.12	6.85 6.82
		trans-$PhCH{=}CHC_6H_4CMe_3\text{-}p$§	35	95–97	†	
		cis-$PhCH{=}CHC_6H_4CMe_3\text{-}p$‖	32			
		Ph_3SiF	36	63–64	†	
		Ph_3SiOH	19	153–154	†	
CMe_3	110	$Ph_3SiCPh{=}CHC_6H_4CMe_3\text{-}p$¶	37	209–211	87.75 87.82	6.93 6.82
		trans-$PhCH{=}CHC_6H_4CMe_3\text{-}p$§	37	96–97	91.49 91.06	8.57 8.63
		cis-$PhCH{=}CHC_6H_4CMe_3\text{-}p$‖	15			
		Ph_3SiF	12	63–64	†	
		Ph_3SiOH	17	152–154	†	
H	−40	$Ph_2FSiCPh_2(CH_2Ph)$	27	135–136	83.78 83.70	5.93 6.18
		trans-$PhCH{=}CHPh$*	3	124–125	†	
		cis-$PhCH{=}CHPh$*	38			
		Ph_3SiF	20	63–64	†	
		Ph_3SiOH	16	153–154	†	
H	110	$Ph_3SiCPh{=}CHPh$**	35	110–112	87.61 87.30	5.97 5.88
		trans-$PhCH{=}CHPh$*	3	124–125	†	
		cis-$PhCH{=}CHPh$*	26			
		Ph_3SiF	4	63–64	†	
		Ph_3SiOH	14	153–154	†	

*The u.v. spectrum was in accord with data of ref. 24.
†Identified by mixed melting point with an authentic sample.
‡λ_{max} (EtOH) 298 mμ (18 800).
§λ_{max} (EtOH) 298 (27 600), 311 mμ (27 600).
‖λ_{max} (EtOH) 263 mμ (14 000).
¶λ_{max} (EtOH) 269 mμ (19 400).
**λ_{max} (EtOH) 265 mμ (20 800).

room temperature. As warming occurred, the red color began to fade, and when gone, the mixture was quenched in water and extracted with ether. After drying the extracts over magnesium sulfate, the ether was removed yielding a white solid, which after recrystallization from cyclohexane gave 1.42 g (70%) of triphenylmethyldimethylfluorosilane, $Me_2FSiCPh_3$, m.p. 134–135°; n.m.r. (CCl_4); δ 0.23 (6H, d, $J = 7.5$, Me_2SiF), 7.25 p.p.m. (15H, s, Ar).

Generation and Trapping of Diphenylmethylsilyldiphenylcarbonium Ion

A solution of 0.3 g (0.79 mmole) of diphenylmethylsilyldiphenylcarbinol in 50 ml of toluene at −40° was treated with BF_3 for a few seconds. A deep red suspension was formed and persisted as long as the temperature was kept cold. Addition of the suspension with vigorous stirring to an ether solution of excess lithium aluminum hydride at −40° led to immediate loss of the red color. After warming to room temperature and aqueous acid work-up, the dried ether extracts gave an oil which on recrystallization from methanol gave 0.17 g (59%) of diphenylmethylbenzhydrylsilane, m.p. 104–105°, identified by mixed m.p. with an authentic sample.

Trapping of Triphenylsilyl-p-methoxyphenylcarbonium Ion

Boron fluoride was bubbled into a solution of 1.6 g (4.0 mmole) of triphenylsilyl-*p*-methoxyphenylcarbinol in 50 ml of toluene at −40 °C. A pale red solution was formed which was slowly added to a solution of excess

Can. J. Chem. Downloaded from www.nrcresearchpress.com by 210.87.254.105 on 09/05/12
For personal use only.

TABLE 10

Data for products of reactions of triphenylgermylcarbinols with BF_3 in various solvents at 23°

Solvent	Reagent	Product	Yield (%)	Melting point (°C)	Analysis C	Analysis H
C_6H_6	$Ph_3GeCHOHPh$	$Ph_3GeCHPh_2$	81	158–160*	†	
C_6H_5Me	$Ph_3GeCHOHPh$	$Ph_3GeCHPhC_6H_4Me$-*p*	84	176–178	79.20 79.84	5.82 6.06
C_6H_5F	$Ph_3GeCHOHPh$	$Ph_3GeCHPh(C_6H_4F$-*p*$)$	74	156–157*	76.10 75.58	5.15 5.25
C_6H_{14}	$Ph_3GeCHOHPh$	$Ph_2FGeCHPh_2$	77	147–148‡	72.69 72.67	5.13 5.27
C_6H_{14}	$Ph_3GeCOHPh_2$	$Ph_2FGeCPh_3$§	78	202–204	76.14 76.35	5.12 5.18

*Recrystallized from methanol.
†Identified by mixed m.p. with an authentic sample.
‡Recrystallized from petroleum ether (b.p. 90–100°).
§When solvent was toluene, yield of $Ph_2FGeCPh_3$ was 70%. On reduction with $LiAlH_4$, $Ph_2HGeCPh_3$ was obtained, m.p. 164–166° from ethanol.
Anal. Calcd. for $C_{31}H_{26}Ge$: C, 79.03; H, 5.56. Found: C, 79.37; H, 5.54.

TABLE 11

The n.m.r. data of typical reaction products

Compound	$\delta(CCl_4)$ p.p.m.
$Ph_2FSiCHPh_2$	7.1–7.2 (m, Ar); 4.1 (d, J = 7 Hz, CH)
$Ph_2FSiCHPhC_6H_4CMe_3$-*p*	7.1–7.3 (m, Ar); 4.08 (d, J = 7 Hz, CH); 1.28 (s, CMe_3)
$Me_2FSiCHPh_2Me$	7.2 (s, Ph); 1.73 (s, broad, C—Me); 0.14 (d, J = 7.5 Hz, Me_2Si)
$Ph_3SiCHPhC_6H_4OMe$-*p*	7.0–7.2 (m, Ph); 6.71 (AB q, J = 8 Hz, $\nu_0\delta_2$ = 15.5 Hz, C_6H_4OMe); 3.68 (s, OMe); 4.3 (s, CH)
(*p*-$Me_3CC_6H_4)_3SiCHPhC_6H_4Me$-*p*	6.9–7.3 (m, Ar); 4.31 (s, CH); 2.28 (s, ArMe); 1.30 (s, CMe_3)
$Ph_2FGeCHPh_2$	7.2 (m, Ph); 4.45 (d, J = 4 Hz, CH)
$Me_3SiCHPhC_6H_4F$-*p*	7.0–7.5 (m, Ar); 3.42 (s, CH); 0.02 (s, Me_3Si)

lithium aluminum hydride in ether at −40°. The red color disappeared. After warming to room temperature, and aqueous work-up, the dried ether extracts gave an oil on removal of the solvent. Recrystallization from 1:1 ethanol–hexane gave 0.03 g (16%) of *p*-methoxy-*p'*-methylbenzhydryltriphenylsilane, m.p. 164°, identified by mixture m.p. Concentration of the mother liquors gave 0.48 g (30%) of *p*-methoxybenzyltriphenylsilane, m.p. 103–105°, identified by spectra and mixed m.p.

Reaction of Triphenylsilylphenylbenzylcarbinol with BF_3 in Toluene at −40°

Boron trifluoride was bubbled through a solution of 1.0 g (2.20 mmole) of the carbinol in 50 ml of toluene. A red color was formed immediately which soon faded. When colorless, water was added and the mixture was extracted with ether, the extracts being dried over anhydrous magnesium sulfate. Removal of the ether gave a viscous oil whose i.r. spectrum showed no absorption in the 2.7–2.8 μ (SiO—H) region. The oil was chromatographed on a 1 × 5″ silica gel column. Elution with hexane (250 ml) gave 0.15 g (38%) of an oil shown to be *cis*-stilbene by comparison of its spectral properties with published data (10–12). Further elution with 250 ml hexane gave an oil containing both *trans*-stilbene and triphenylfluorosilane, from which was isolated 0.007 g (3%) of *trans*-stilbene, m.p. 123–124°, identified by mixed m.p. On further elution with 400 ml of hexane, an oil was isolated which crystallized from methanol to yield 0.12 g (20%) of triphenylfluorosilane, m.p. 62–64°, identified by mixed m.p. Elution with 500 ml of carbon tetrachloride yielded a white solid which was recrystallized from methanol to yield 0.27 g (27%) of 1,1,2-triphenylethyldiphenylfluorosilane, m.p. 135–136°. Finally, elution with 125 ml of benzene gave material which, after crystallization from carbon tetrachloride, afforded 0.10 g (16%) of triphenylsilanol, m.p. 153–154°. Chromatography of authentic triphenylfluorosilane on a similar

Can. J. Chem. Downloaded from www.nrcresearchpress.com by 210.87.254.105 on 09/05/12
For personal use only.

Can. J. Chem. Downloaded from www.nrcresearchpress.com by 210.87.254.105 on 09/05/12
For personal use only.

column under similar conditions led to conversion of part of the fluorosilane to silanol.

Reaction of Triphenylsilylphenylbenzylcarbinol with BF_3 in Toluene at 110°

Boron trifluoride was bubbled into a solution of 0.9 g (1.98 mmole) of carbinol in 50 ml of refluxing toluene for a few seconds. No colored species were formed. Work-up in the usual manner gave an oil which was crystallized from boiling methanol to give 0.30 g (35%) of α-triphenylsilyl-*cis*-stilbene, m.p. 110–112°, shown to be identical to a material produced by an alternate route (22).

Solvent was removed from the mother liquors under reduced pressure and the oil was chromatographed on a 1 × 3″ silica gel column. Elution with 500 ml of hexane gave 0.095 g (26%) of *cis*-stilbene, identified by its spectral properties. From the next 150 ml of hexane was isolated 0.005 g (3%) of *trans*-stilbene, m.p. 122–124°, identified by mixed m.p. From the next 300 ml of hexane was isolated 0.023 g (4%) of triphenylfluorosilane, m.p. 62–64°, identified by mixed m.p. Elution with 150 ml of carbon tetrachloride yielded an additional 0.05 g (total 0.30 g, 34%) of triphenylsilyl-*cis*-stilbene. Finally, elution with 150 ml of benzene yielded, after recrystallization from carbon tetrachloride, 0.077 g (14%) of triphenylsilanol, m.p. 152–154°, identified by mixed m.p.

Reaction of Triphenylsilylmethylphenylcarbinol with BF_3 in Toluene at −40 °C

Boron trifluoride was bubbled into a solution of 0.5 g (1.32 mmole) of the carbinol in 50 ml of toluene at −40° for a few seconds. Aqueous work-up as usual gave a solid, shown by n.m.r. spectrum to consist of α-triphenylsilylstyrene and 1,1-diphenylethyldiphenylfluorosilane in the ratio of 3:2. The solid was dissolved in hexane and chromatographed on a 1 × 3″ column of neutral Woelm alumina. Elution with 150 ml of hexane gave 0.11 g (23%) of α-triphenylsilylstyrene, which after recrystallization from petroleum ether (b.p. 60–70°) had m.p. 132–134°. A mixed m.p. with an authentic sample was not depressed. Further elution with 200 ml of hexane gave 0.21 g (41%) of the fluorosilane, m.p. 88–90° after recrystallization from methanol.

Treatment of Triphenylsilylpropanol in Toluene at 23 °C

Boron fluoride was bubbled into a solution of 0.5 g (1.53 mmole) of 2-triphenylsilyl-2-propanol in 50 ml of toluene. No coloration was observed and the reaction was worked-up in the normal manner. Removal of the solvents left a white solid that was recrystallized from ethanol to yield 0.42 g (89%) of isopropenyltriphenylsilane, m.p. 94–95 °C. A mixed m.p. with an authentic sample was not depressed. When the reaction was repeated in pentane 0.35 g (72%) of isopropenyltriphenylsilane was obtained.

Treatment of 2-Triphenylsilyl-1-phenylethanol in Toluene at 23 °C

Boron fluoride was bubbled into a solution of 0.5 g (1.35 mmole) of 2-triphenylsilyl-1-phenylethanol in 50 ml toluene. The reaction mixture was worked-up in the normal manner to leave a solid that was recrystallized from methanol to yield 0.21 g (56%) of triphenylfluorosilane, m.p. 62–63 °C, identified by mixed m.p. with an authentic sample.

Synthesis of cis- and trans-p-t-Butylstilbene

A mixture of 5.0 g (0.0276 mole) of *p-t*-butylbenzyl chloride and 7.24 g (0.0276 mole) of triphenylphosphine was heated for 13 h in 5 ml of benzene. Filtration gave 5.2 g (46%) of *p-t*-butylbenzyltriphenylphosphonium chloride, m.p. 206–209° with decomposition.

To 5.2 g (0.013 mole) of the phosphonium salt in ether was added slowly 2.0 ml (0.013 mole) of phenyllithium in ether. After stirring for 3 h, a solution of 1.35 g (0.012 mole) of benzaldehyde in 10 ml of ether was added slowly. After stirring for 16 h, the reaction was worked-up with aqueous acid, and the dried ether extracts afforded a sticky solid, which was crystallized from methanol. This yielded 0.53 g of *trans-p-t*-butylstilbene, m.p. 96–97° which on recrystallization had m.p. 99–100°.

Anal. Calcd. for $C_{18}H_{20}$: C, 91.53; H, 8.47. Found: C, 91.10; H, 8.65.

The n.m.r.: (CCl_4), δ 7.2–7.5 (complex, aryl), 7.0 (s, vinyl), 1.32 p.p.m. (s, CMe_3); u.v.: λ_{max} (MeOH), 298 (ε, 27 600), 311 mμ (ε, 27 600).

Solvent from the mother liquor from the above was removed under reduced pressure and the residual material was treated with 1–2 ml of carbon tetrachloride, some insoluble material being filtered off. The solution was transferred to a 1/2 × 10″ alumina column, and was eluted with hexane. Virtually no material was eluted in the first 350 ml of solvent, but the next 200 ml yielded 0.40 g (14%) of *cis-p-t*-butylstilbene as a viscous oil, characterized by its spectra. The n.m.r.: (CCl_4), δ 7.2 (s, Ar) 7.1 (s, Ar), 6.5 (s, =C*H*), 1.28 p.p.m. (s, CMe_3); u.v.: λ_{max} (MeOH), 263 mμ (ε, 14 000).

Further elution of the column with 100 ml of carbon tetrachloride yielded 0.22 g of the *trans*-isomer (total 0.75 g, 27%).

Treatment of Triphenylgermylphenylcarbinol in Benzene at 23 °C

Boron fluoride was bubbled into a solution of 0.3 g (7.3 mmole) of triphenylgermylphenylcarbinol in 50 ml of benzene. No coloration was observed and the reaction mixture was quenched in water, extracted with ether, and dried with magnesium sulfate. Removal of the solvents under reduced pressure left a white solid. The solid was recrystallized from methanol to yield 0.28 g (81%) of benzhydryltriphenylgermane, m.p. 158–160 °C. A mixed m.p. with an authentic sample was not depressed.

Treatment of 1,2,2,2-Tetraphenylethanol in Anisole at −40 °C

Boron fluoride was bubbled into a solution of 0.35 g (1.0 mmole) of 1,2,2,2-tetraphenylethanol in 50 ml of anisole. A red coloration was observed but this faded very quickly and the reaction was quenched in water and extracted with ether. After drying with magnesium sulfate the solvents were removed under reduced pressure to leave a white solid that was recrystallized from benzene to yield 0.21 g (63%) of tetraphenylethylene, m.p. 227 °C. A mixed m.p. with an authentic sample was not depressed. A repeat of the reaction with 0.2 g (5.7 mmole) of the carbinol in 50 ml of hexane at 23° produced 0.11 g (58%) of tetraphenylethylene as the only product detected.

Treatment of Triphenylsilanol with BF_3 in Toluene

Boron fluoride was bubbled into a solution of 0.5 g

(1.83 mmole) of triphenylsilanol in 50 ml of toluene at 23 °C. No coloration was observed and the reaction was quenched in water after about 30 s. The reaction mixture was extracted with ether and dried with magnesium sulfate. The solvents were removed under reduced pressure leaving a white solid that was recrystallized from methanol yielding 0.37 g (83%) of tris(triphenylsiloxy)-boron, $(Ph_3SiO)_3B$, (23) m.p. 153–154 °C.

Anal. Calcd. for $C_{54}H_{45}O_3Si_3B$: C, 77.58; H, 5.56. Found: C, 77.41; H, 5.42.

This research was supported by the National Research Council of Canada. The authors are indebted to the Dow Corning Corporation and the National Research Council of Canada for Scholarships to K.H.P. in 1964–1965, and 1965–1966, respectively.

1. L. H. Sommer, D. Bailey, J. Gould, and F. C. Whitmore. J. Amer. Chem. Soc. **76**, 801 (1954) and references therein.
2. C. Eaborn and R. W. Bott. Organometallic compounds of group IV elements. Vol. 1. Part 1. Marcel Decker Inc., New York. 1968. p. 443.
3. M. Kumada, J. Nakajima, M. Ishikawa, and Y. Yamomoto. J. Org. Chem. **23**, 292 (1958).
4. C. Eaborn and J. C. Jeffrey. J. Chem. Soc. 137 (1957).
5. A. G. Brook, G. E. LeGrow, and D. M. MacRae. Can. J. Chem. **45**, 239 (1967).
6. A. G. Brook, K. H. Pannell, G. E. LeGrow, and J. J. Sheeto. J. Organometal. Chem. **2**, 491 (1964).
7. C. Eaborn. Organosilicon compounds. Butterworths, London. 1960. p. 155.
8. E. S. Gould. Mechanism and structure in organic chemistry. Holt Dylan. 1959. p. 489.
9. C. D. Nenitzescu, S. Titeica, and V. Ioan. Acta Chim. (Acad. Sci. Hung.) **12**, 195 (1957).
10. C. Eaborn and R. W. Bott. Organometallic compounds of group IV elements. Vol. 1. Part 1. Marcel Decker Inc., New York. 1968. p. 445.
11. C. Eaborn and R. W. Bott. Organometallic compounds of group IV elements. Vol. 1. Part 1. Marcel Decker Inc., New York. 1968. p. 382.
12. A. Schriesheim. *In* G. Olah, Friedel-Crafts and related reactions. Vol. 2. Interscience Publishers, New York. 1964. Chapt. 18.
13. H. C. Brown and H. M. Bell. J. Org. Chem. **27**, 1928 (1962).
14. G. Olah, M. B. Comisarow, C. A. Cupas, and C. U. Pitman, Jr. J. Amer. Chem. Soc. **87**, 2997 (1965).
15. G. Olah and C. U. Pitman, Jr. J. Amer. Chem. Soc. **87**, 3507 (1965).
16. C. Eaborn and R. W. Bott. Organometallic compounds of group IV elements. Vol. 1. Part 1. Marcel Decker Inc., New York. 1968. p. 428.
17. A. G. Brook and P. F. Jones. Chem. Commun. 1324 (1969).
18. A. G. Brook and P. F. Jones. Unpublished work.
19. A. G. Brook. J. Amer. Chem. Soc. **80**, 1886 (1956).
20. A. G. Brook, C. M. Warner, and M. McGrisken. J. Amer. Chem. Soc. **81**, 981 (1958).
21. H. Gilman and G. C. Lichtenwalter. J. Amer. Chem. Soc. **80**, 2680 (1958).
22. A. G. Brook, K. H. Pannell, and D. G. Anderson. J. Amer. Chem. Soc. **90**, 4374 (1968).
23. N. F. Orlov, B. N. Dolgov, and M. G. Vorenkov. Khim i Prakt, Primenie Kremneorg. Soedinenii, Trudy Konf., Leningrad. 1958. No. 1. pp. 161–169 (C.A. **54**, 4360A (1960)).
24. P. Schmid. U.S. Atomic Energy Commission, UCRL-8883, 1959. p. 114.

Can. J. Chem. Downloaded from www.nrcresearchpress.com by 210.87.254.105 on 09/05/12
For personal use only.

Can. J. Chem. Downloaded from www.nrcresearchpress.com by 210.87.254.42 on 09/05/12
For personal use only.

The near-infrared spectra of some simple aldehydes[1]

G. LUCAZEAU[2] AND C. SANDORFY
Département de Chimie, Université de Montréal, Montréal, Québec

Received July 13, 1970

The near-infrared spectra of CH_3CHO, CD_3CHO, CH_3CDO, CF_3CHO, $CHCl_2CHO$, and CCl_3CHO were measured from 4000 to 9000 cm^{-1} in solution at room and liquid nitrogen temperatures. Assignments are made and cases of Fermi resonance are examined. A few potential and anharmonicity constants are obtained. Solvent effects affecting fundamentals and overtones are discussed.

Canadian Journal of Chemistry, **48**, 3694 (1970)

Introduction

The infrared spectrum of acetaldehyde was thoroughly studied by Pitzer and Weltner (1) and by Evans and Bernstein (2) and some of its deuterated homologues were examined by Cossee and Schachtschneider (3) and by Capwell (4). The spectra of CCl_3CHO and $CHCl_2CHO$ were studied by Lucazeau and Novak (5, 6) and that of CF_3CHO by Berney (7). Some interesting cases of Fermi resonance were observed (2–8) and some parts of the near-infrared spectra were measured (9, 10). This and the increasing attention given to anharmonicity in the analysis of vibrations of polyatomic molecules induced us to measure the spectra of acetaldehyde and some of its derivatives in the overtone-region, that is, in the near infrared from 4000 to 9000 cm^{-1}.

The following molecules were examined: CH_3CHO, CH_3CDO, CD_3CHO, CF_3CHO, CCl_3CHO, and $CHCl_2CHO$. Most of the spectra were measured in solution, in a 1:1 mixture of CCl_3F (freon-11) and $CF_2Br—CF_2Br$ (freon 114-B-2) which gives a good glass at liquid nitrogen temperature.

This solvent, first used by Durocher and Sandorfy (11, 12), is highly translucent in the near infrared and makes it possible to work at low temperatures and thereby to obtain better resolved solution spectra than has been hitherto possible. We measured our spectra at 298 and at 83 °K. In certain cases vapor and crystal phase spectra were also taken. Our aim was to assign as many bands as possible in the near-infrared part of the spectra, to study cases of anharmonic resonances which are found, determine the values of anharmonicity and potential constants whenever possible, to make observations on intensity ratios of fundamentals and overtones, and on solvent effects affecting these.

Experimental

All the spectra were determined on a Cary-14 spectrometer.

The purification of the compounds has been described in a recent publication on their far-ultraviolet spectra (14). The solvent and low temperature techniques used were described in earlier publications from this laboratory (11–13).

The great vapor pressure of CF_3CHO, CH_3CHO, CD_3CHO, and CH_3CDO allowed us to examine them as gaseous samples at pressures near 600 mm Hg. For the last three compounds, the spectra are not well resolved and we present only the spectrum of CH_3CHO (Fig. 1). The resolution is progressively improved in the spectra in solution at 295 °K, at 85 °K, and in the solid state (Figs. 1–9). All solutions were prepared under vacuum by condensing the compounds into a graduated cylinder containing the solvent cooled by liquid nitrogen. The concentrations were 0.1 ± 0.05 *M*.

Solid samples were obtained by condensation of the vapor on a quartz window cooled by liquid nitrogen. The extinction coefficients in the near-infrared region were so low that we were obliged to prepare thick solid samples (a hundred times thicker than in the fundamental region).

To circumvent the problem of scattered light, we projected gaseous helium onto the condensed sample. Thus we could observe bands with ε values less than 0.05. For CF_3CHO we observed a phase change, as shown by the 3000 cm^{-1} region: the ν_{CH} band which was split into three components becomes unique after this treatment (Fig. 8) while $\nu_{02,CO}$ keeps the same intensity. (The indices 0 and 2 stand for the vibrational quantum numbers. So ν_{02} is a first overtone.)

Generally this treatment favors the formation of a vitreous phase (this was the case for CF_3CHO and CCl_3CHO) and it lowers the amount of scattering. No changes due to polymer formation were observed in the spectra.

---

[1]Photocopies of a more detailed version of this paper including Tables I to VII may be obtained free of charge, upon request, from the Depository of Unpublished Data, National Science Library, National Research Council of Canada, Ottawa, Canada.

[2]Permanent address: Laboratoire de Chimie-Physique du C.N.R.S., 2 rue Henri Dunant, Thiais 94, France.

Can. J. Chem. Downloaded from www.nrcresearchpress.com by 210.87.254.42 on 09/05/12
For personal use only.

Assignments

Assignments of overtones and combination tones are usually more uncertain than those of the fundamentals. This is because of the great number of possible combinations, and the difficulty of predicting the values of anharmonicity constants. We found the following criteria useful in making assignments.

(*a*) For methyl or aldehydic CH vibrations, deuteration of the respective group was used.

(*b*) CO vibrations shift to lower frequencies in the order gas → solution (295 °K) → pure liquid (295 °K) → glassy solution (85 °K) → vitreous solid (85 °K) → crystal (85 °K). (The shift amounts to about 20 cm^{-1} from the gas to the solid for the fundamental and about 40 cm^{-1} for the first overtone.)

The vibrations due to the aldehydic CH bond show the opposite trend. This has been established for the fundamentals by Evans and Bernstein (2) and by Lucazeau and Novak (5). This trend is maintained in the overtones (about 40 and 80 cm^{-1}, respectively).

Methyl CH_3 vibrations are much less sensitive to changes in physical state.

We made the assumption that bands of a mixed type have an intermediate type of behavior concerning this characteristic shifting.

All this is confirmed by the coherent picture which is obtained by the application of the above rules.

(*c*) Characteristic changes in the relative intensities of close lying bands with the change in physical state often reveal the presence of a Fermi resonance and this can be helpful in the identification of certain bands (15).

(*d*) In may cases anharmonicities are approximately preserved in going from one molecule to another and this can also be used in making assignments.

(*e*) Intensities can be helpful in certain cases.

(*f*) In cases of Fermi resonance certain assignments can be eliminated by looking at the terms of the perturbing Hamiltonian (see below).

The following symbols are used throughout this paper: ν_{01}, ν_{02}, ν_{03}, ... fundamental and overtones of stretching vibrations; δ_{01}, δ_{02}, δ_{03}, ... the same for bending vibrations.

The indices of the anharmonicity constants (X_{111}, X_{121}, ...) stand for the normal coordinates where 1 represents the (mainly) aldehydic CH stretching motion, 2 the in-plane bending of the aldehydic CH bond (δ), 3 the C=O stretching frequency, and 4 the CH_3 stretching frequencies. The potential constant X_{122} couples ν_{CH} and $2\delta_{CH}$.

Anharmonic Resonances

The energy levels of anharmonic vibrations are usually computed from perturbation formulas. In polyatomic molecules it often happens that a combination or overtone has nearly the same energy and the same symmetry as a fundamental and that, at the same time, there is a large anharmonic term in the potential which "couples" them. In this case the usual formulas which give the energies to the second order cannot be used and the related part of the perturbational secular determinant must be solved separately.

Supposing that the intensity of the combination band can always be taken for zero compared to the fundamental we obtain (17) for ΔE^0, the separation of the unperturbed states

$$[1] \qquad \Delta E^0 = \Delta E(\rho - 1)/(\rho + 1)$$

where ΔE is the observed separation of the interacting vibrational states and ρ is their observed (integrated) intensity ratio.

The interaction W_{nm} has the form

$$[2] \qquad W_{nm} = \int \Psi_n^* H' \Psi_m \, d\tau$$

where Ψ_n is usually a fundamental and Ψ_m a combination band and $d\tau$ represents integration for all normal coordinates.

Although the best known cases of Fermi resonance are those between the fundamental of one vibration and the first overtone of another, this is by no means the only possibility. In fact Fermi resonance is possible between two overtones or combination tones and more than two vibrations can participate in Fermi resonance. Since, in the case of aldehydes we observed several cases of Fermi resonance where none of the partners are fundamentals we computed the value of W_{nm} for the cases which are of importance for the interpretation of their near-infrared spectra. (Details are given in a more complete manuscript deposited at the National Science Library along with the tables. See also refs. 18 and 19.)

The cases of such superior Fermi resonances which we observed were produced by the three vibrations which can be approximately localized

Can. J. Chem. Downloaded from www.nrcresearchpress.com by 210.87.254.42 on 09/05/12
For personal use only.

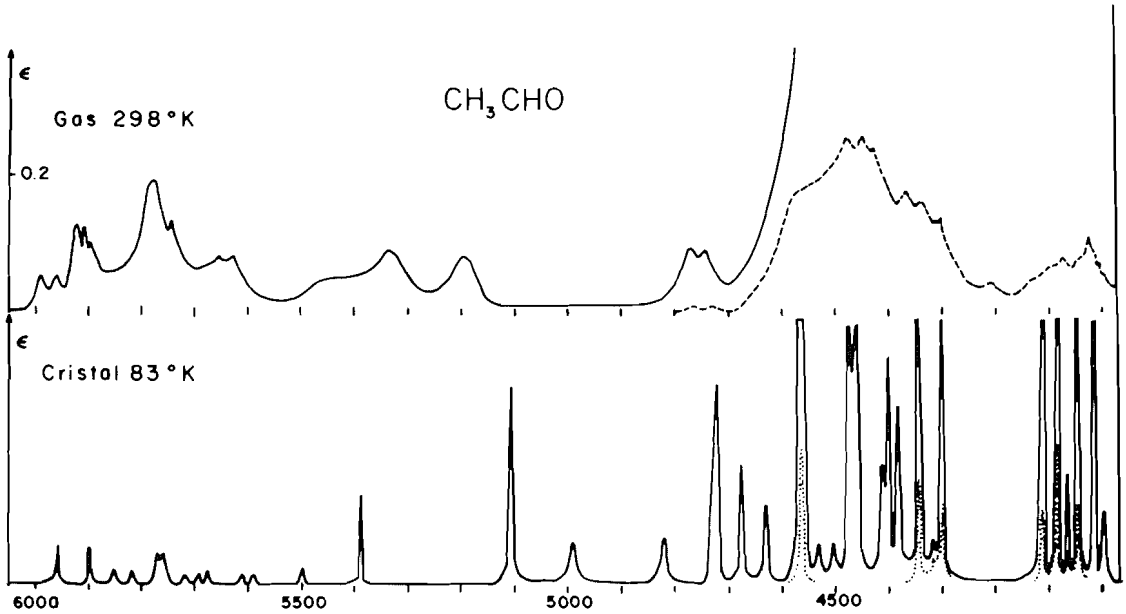

FIG. 1. The near-infrared spectrum of acetaldehyde from 4000 to 6000 cm^{-1}. Dashed curves: the ordinate is to be multiplied by four. Wave numbers against molecular extinction coefficients.

in the aldehyde group ($-\overset{H}{\overset{/}{C}}{=}O$): q_1 the (mainly) C—H stretching mode, q_2 the (mainly) C—H (in-plane) deformation mode, and q_3 the (mainly) C=O stretching mode.

All cases involve the same potential constant k_{122}. (Index 1 stands for the aldehydic CH stretching vibration and 2 for the bending of the CHO group.) However, because of the approximations which are implied in (1) we do not expect to obtain the same numerical values in all cases. Outside of the approximations proper to the perturbational treatment we had to suppose that one of the partners in all the resonances has zero intensity. This is partly justified by the fact that one of the partners is always a combination of a higher order than the other (binary against ternary etc.). We could not take into account electric anharmonicity. This could affect appreciably the measured intensities and, through eq. 1, it could influence the unperturbed frequencies computed from Fermi doublets.

The measured intensities which enter in the calculation of ρ are, of course, approximate. The band areas were measured with a planimeter assuming an approximate Cauchy (Lorentz) shape, and intensity ratios are believed to be accurate to ±10 p.c. only.

For these reasons we shall not attempt to interpret variations in the values of the constants which can be obtained from different bands in the spectra.

Anharmonic resonances of higher order are also possible. The one of the next higher order is due to the off-diagonal terms of the quartic part of the potential and is sometimes called Darling–Dennison resonance (20).

None of the anharmonic resonances we observed required the inclusion of such higher terms for its interpretation, however.

Results

(1) Methyl CH Vibrations

Between 6000 and 5600 cm^{-1} we find a number of peaks and shoulders which are due to CH_3 vibrations as shown by their complete disappearance in the spectra (Figs. 1 to 4) of CD_3CHO, CF_3CHO, and CCl_3CHO. Supposing the degeneracy due to the C_{3v} symmetry of the methyl group lifted, there are three CH stretching fundamentals which could give three overtones and three other binary combinations between them. Furthermore, the three CH_3 bending modes near 1460 and 1380 cm^{-1} could give 18 combinations of the $\nu + 2\delta$ type. This means 24 bands in this area and there are, of course, other

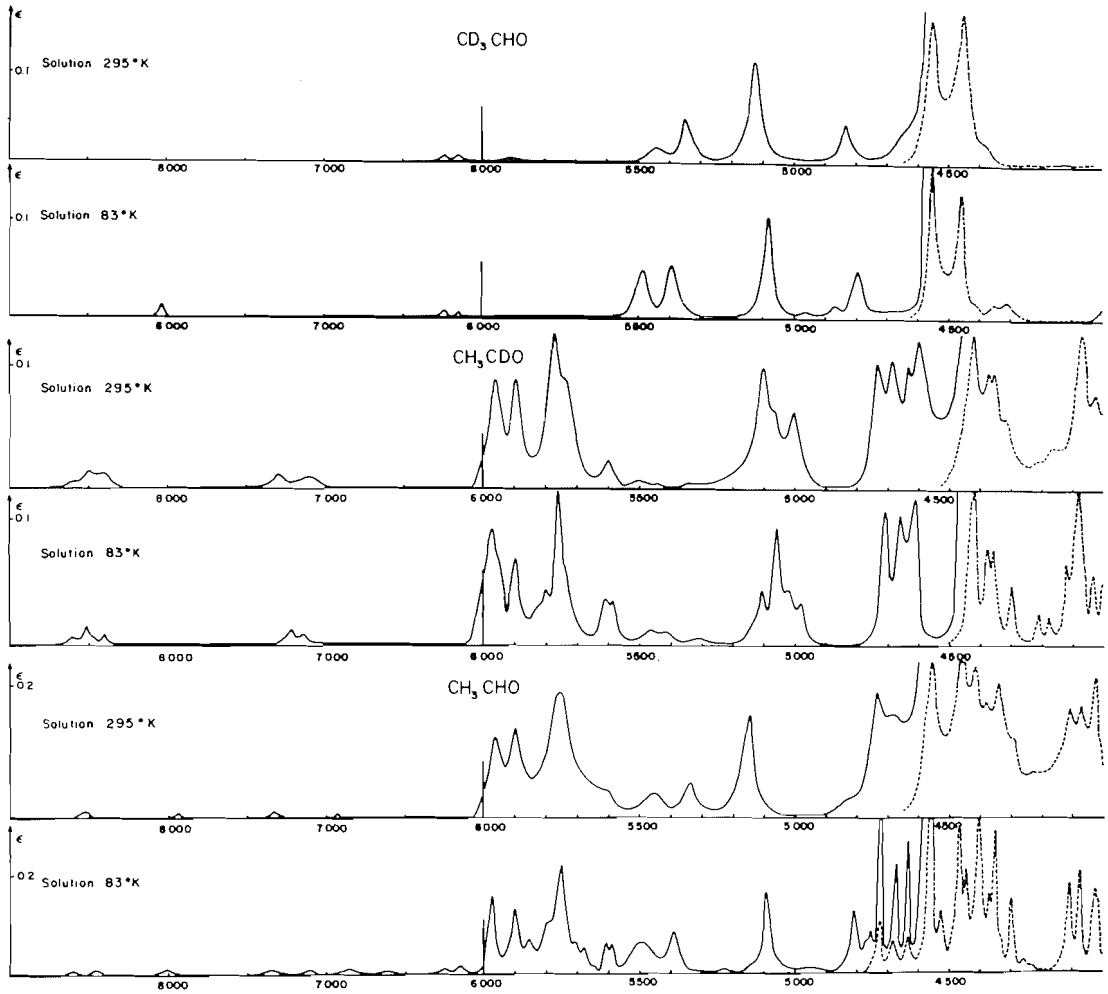

FIG. 2. The near-infrared spectra of acetaldehyde and its deuterated homologues in 0.1 *M* solution at 295 and 85 °K.

possible combinations. Thus we renounce assigning these bands individually. A relatively clear picture is obtained for the crystalline film spectrum of acetaldehyde (Fig. 1). We have made tentative assignments for this particular case. They are given in Table 1.[1] The anharmonicity constants which can be obtained from them were computed from simple second order perturbation formulas. For overtones

$$X_{ii} = \nu_{i,01} - (\nu_{i,02}/2)$$

and for combination tones

$$X_{ij} = \nu_{\text{comb.}} - (\nu_{i,01} + \nu_{j,01})$$

In making the assignment we supposed that the order of frequencies of the bands at the fundamental level is preserved at the level of the overtones so that if, for example $\nu_{a,01} > \nu_{s,01}$, also $\nu_{a,02} > \nu_{s,02}$, etc. (a and s stand for antisymmetric and symmetric, respectively). This is tantamount to supposing that the anharmonicities do not change the order of the frequencies of overtones (and combinations) with respect to the fundamentals. We obtained values for the anharmonicity constants ranging from 15 to 30 cm^{-1}. The molecular extinction coefficients of the CH_3 fundamentals are weak, of the order of $\varepsilon = 10$. The respective overtones have about $\varepsilon = 0.2$, a factor of about 50.

In $CHCl_2CHO$, the remaining methyl hydro-

Can. J. Chem. Downloaded from www.nrcresearchpress.com by 210.87.254.42 on 09/05/12
For personal use only.

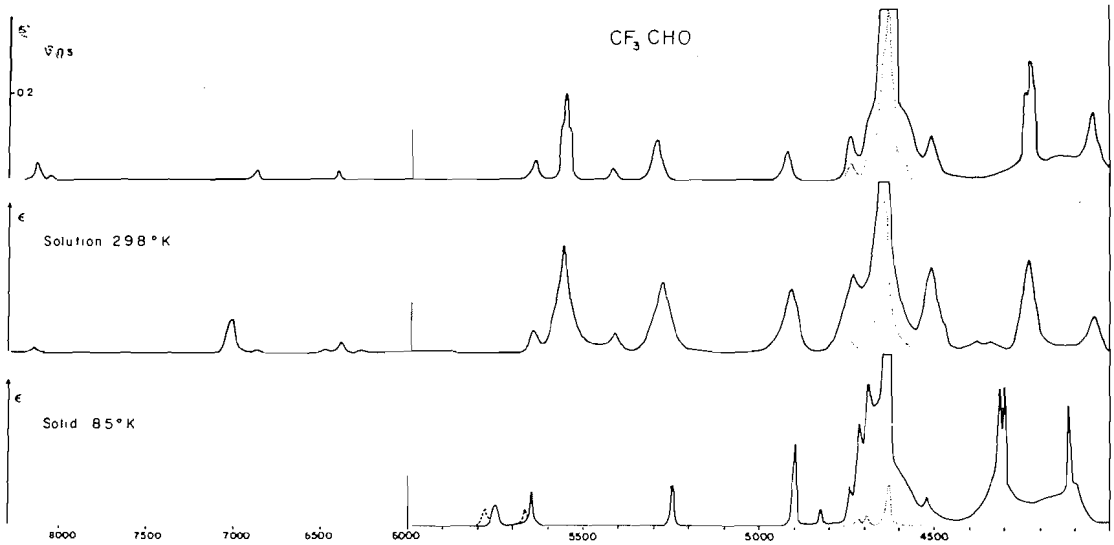

FIG. 3. The near-infrared spectrum of CF_3CHO. Dotted curves: the ordinate is to be multiplied by four. Dashed curves: crystal.

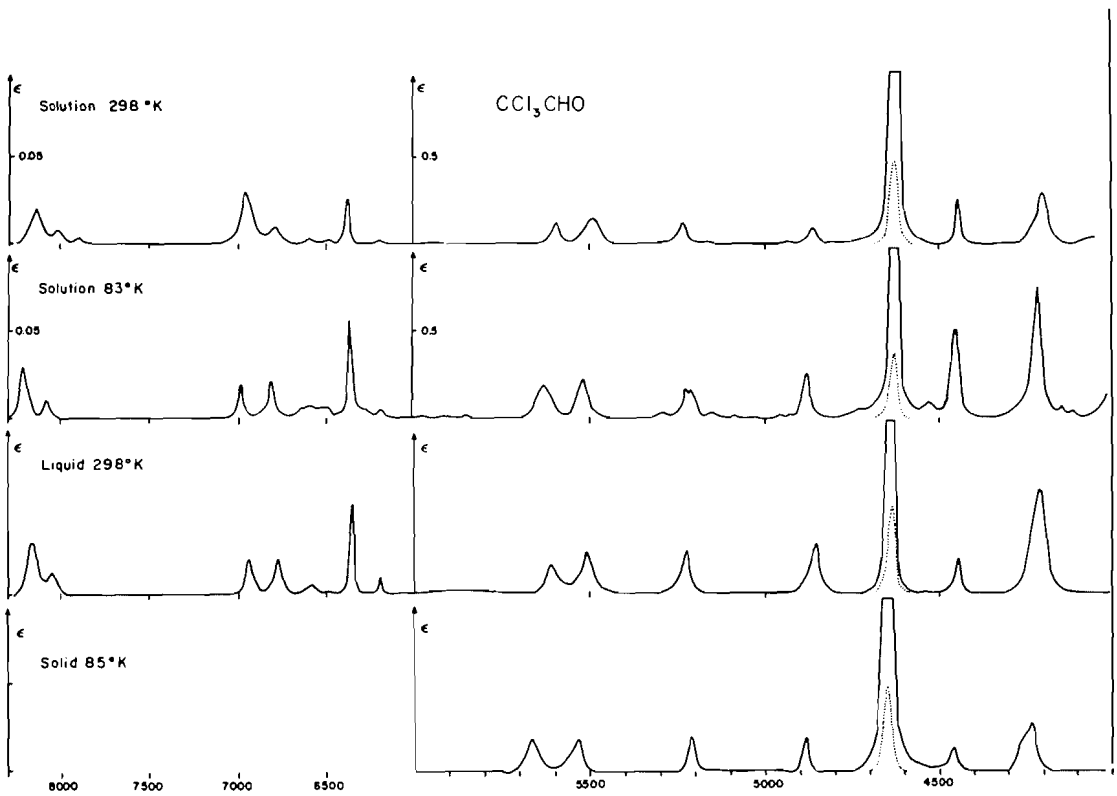

FIG. 4. The near-infrared spectrum of CCl_3CHO. Dotted curves: the ordinate is to be multiplied by four.

Can. J. Chem. Downloaded from www.nrcresearchpress.com by 210.87.254.42 on 09/05/12
For personal use only.

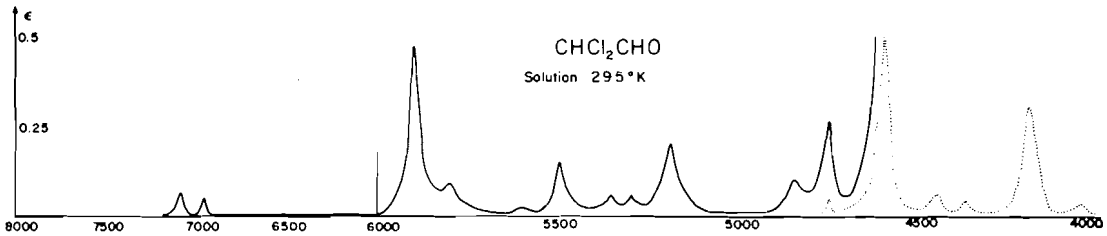

FIG. 5. The near-infrared spectrum of $CHCl_2CHO$ in solution. Dotted curve: the ordinate is to be multiplied by three.

gen gives a well defined overtone at 5894 cm^{-1} ($\varepsilon = 0.4$). The fundamental (6) is at 3011 ($\varepsilon = 6$) so that $X_{11} = 64\ cm^{-1}$. At both levels there is a weaker band due to the *gauche* isomer (5789 and 2963 cm^{-1}, respectively) giving $X_{11} = 69\ cm^{-1}$. The relative values of X_{11} for the case of $CHCl_2CHO$ (one hydrogen) and CH_3CHO (three hydrogens) (15 to 30 cm^{-1}) are in line with considerations of Siebrand and Williams (21) concerning the division of the anharmonic contribution to the energy between bonds ending at a common atom.

The second overtones of the CH_3 stretching vibrations and the combinations among them yield weak bands in the 8600–8400 cm^{-1} region. Most of them are likely to be complex. Their molecular extinction coefficients are about 0.01 or less, about a thousand times weaker than their fundamentals.

Between 4300 and 4850 cm^{-1} we find a number of strong combination bands (ε between 1 and 2 for the strongest). By comparing the spectra of CH_3CHO with those of CD_3CHO, CH_3CDO, and the halogenated aldehydes we can identify three groups of bands. Starting at the low frequency end of this range there are about five CH_3 stretching + CH_3 bending combination bands (Table II), followed at higher frequencies by aldehydic CH stretching + CO stretching and by CH_3 stretching + CO stretching combinations (see below).

The coupling constants for the $\nu + \delta$ type CH_3 bands are of the order of $X_{ij} = 15$–$30\ cm^{-1}$ if our assignments made according to the above hypothesis are correct.

(2) Aldehydic CH Vibrations

The C—H stretching fundamental is affected by a pronounced Fermi resonance which was reported by previous authors (1–8). We remeasured these bands in our solvent at a concentration of 0.1 *M* (Figs. 6–9, Table II).

As is seen, the conditions are not simple. For CH_3CHO there is a large splitting yielding bands at 2852 and 2761 cm^{-1} at 83 °K. Both bands are at least doublets, however. The advantage of measuring the spectra at low temperature appears clearly on Fig. 6. There is a changeover in the intensities of the overlapping bands at 2761 and 2739 (low temperature values) in going from room to liquid nitrogen temperature, which may be due partly to the solvent affecting the two bands differently and partly to the sharpening of the bands leading to changed overlap conditions. In CD_3CHO only the two main bands at 2843 and 2746 cm^{-1} are observed. The other two bands which intervene in the CH_3 containing molecules are likely to be the first overtone of the 1425 deformation mode (2850 cm^{-1}) and the combination of 1425 and 1342 cm^{-1} (2728 cm^{-1}). So this is a complicated case of multiple resonance. We computed the unperturbed frequencies form [1] by taking mean values for the small splittings.

The unperturbed frequencies, the W_{12} and k_{122} values are given in Table III. The average value of W_{12} is 50 cm^{-1} for the acetaldehydes in solution at 83 °K and that of k_{122} is 100 cm^{-1} under the same conditions.

CCl_3CHO has only one strong band which is probably slightly affected by resonance with its two weak neighbors. The ε values are diminished by a factor of about three with respect to acetaldehyde.

In the gas phase spectrum of CF_3CHO the CH band shows some rotational contour with an apparent *Q* branch. It is probably in weak resonance with its neighbor at 2734 cm^{-1} which has a similar shape (Fig. 8). This spectrum was first published by Berney (7). We also measured

Can. J. Chem. Downloaded from www.nrcresearchpress.com by 210.87.254.42 on 09/05/12
For personal use only.

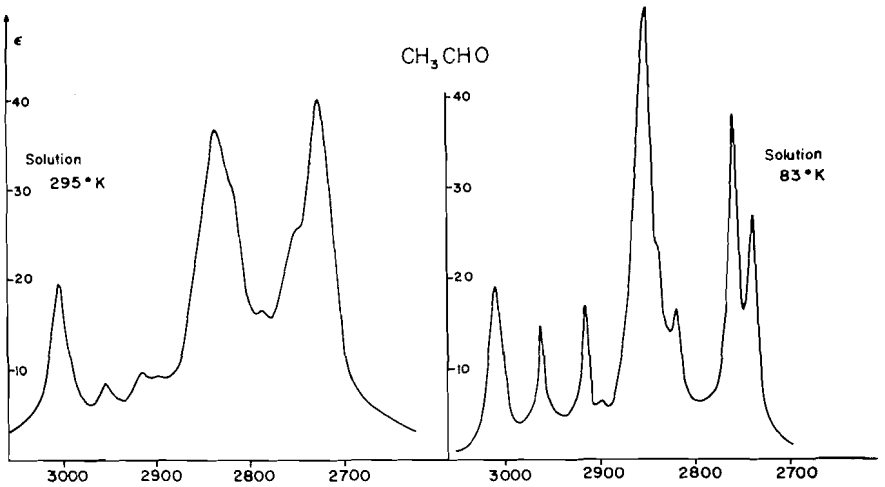

FIG. 6. The region of the ν_{CH_3} and ν_{CH} fundamentals of CH_3CHO in solution.

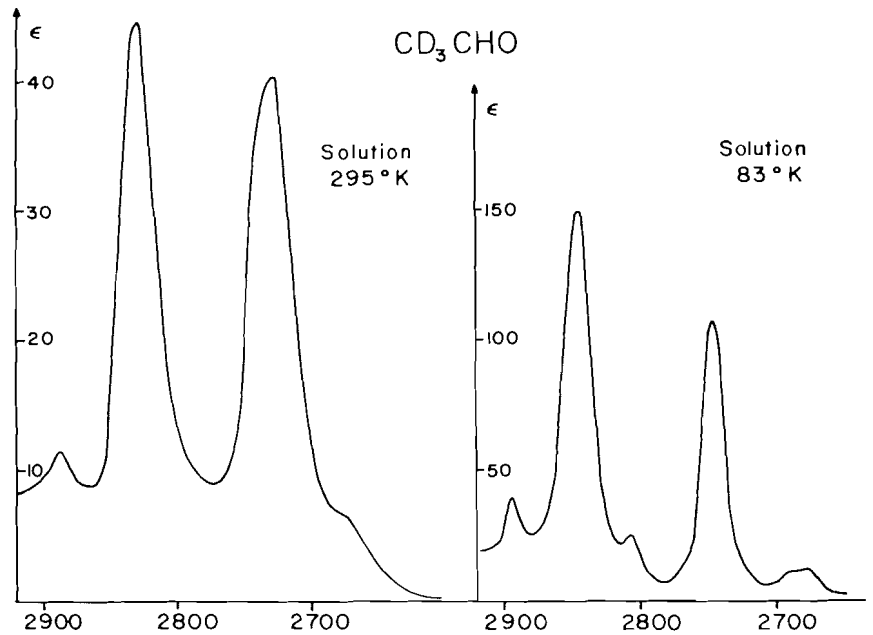

FIG. 7. The region of the ν_{CH} fundamental of CD_3CHO in solution.

the spectrum of the solid at 77 °K. There is a spectacular difference between the spectrum of the glass[3] (solid curve on Fig. 8) and that of the crystalline solid. The relative intensities of two weak bands at 2765 and 2724 cm^{-1} probably in weak resonance with the fundamental, are also affected. A similar observation can be made in the corresponding overtone region. In spite of the weakness of $\delta_{02,CH}$ (2685 cm^{-1}) and the presence of a third combination band in the fundamental region for halogenated aldehydes, k_{122} was computed and found equal to 72 and 105 cm^{-1}, respectively, for CCl_3CHO and $CHCl_2CHO$ in solution at 295 °K. These values are very similar to those obtained in the same

[3]We found the same frequency, 2918 cm^{-1}, as Berney for this molecule in a CO_2 matrix.

Can. J. Chem. Downloaded from www.nrcresearchpress.com by 210.87.254.42 on 09/05/12
For personal use only.

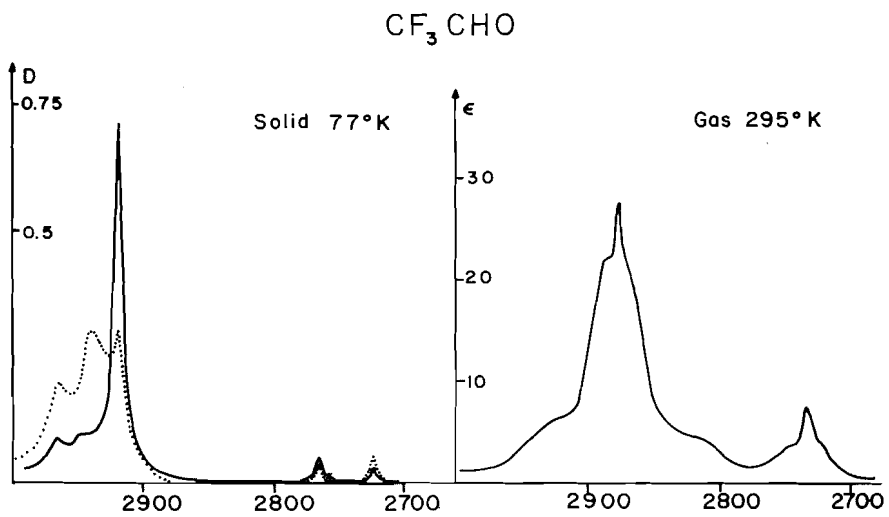

FIG. 8. The region of the ν_{CH} fundamental of CF_3CHO. Dotted curve: crystal; solid curve: glass.

physical state at the first overtone level. The agreement is less good for CF_3CHO (105 cm^{-1} at the fundamental level).

The first overtone region of the CH vibration, seems to "inherit" the Fermi resonance found at the fundamental level.

We find two bands in the spectra of CH_3CHO and CD_3CHO separated by about 100 cm^{-1}, respectively, at 5385, 5502 cm^{-1} ($\varepsilon = 0.11$) and 5386, 5487 cm^{-1} in solution at 85 °K ($\varepsilon = 0.08$). For CH_3CHO the band at 5502 seems to be broadened by the neighboring CH_3 absorptions[4] while this is not the case for CD_3CHO. This, with the effect of temperature on the intensity of this band (see below) can be closely related to the observations made at the fundamental level. We computed $W_{12} = 53$, $k_{122} = 75$ cm^{-1} for both compounds at 85 °K, that is 25% less than the value computed at the fundamental level and this may be due to the approximations already mentioned. Other data are compiled in Tables III and V.

When the bands do not have an equal intensity (CF_3CHO, CD_3CHO in solution at 295 °K, CH_3CHO in the gaseous and crystalline phases), the stronger one is always at the lower frequency and therefore must have strong CH stretching character. This implies that the ternary $\nu + 2\delta$ combination is the one borrowing intensity from the binary $2\nu_{CH}$ and not the opposite.

The contrary was true at the fundamental level, ν_{CH} having a higher frequency than $2\delta_{CH}$. To explain this reversal, we computed the anharmonic coupling constant from the unperturbed frequency $\nu + 2\delta$ for CD_3CHO in solution at 295 °K and obtained

$$X_{12} = \tfrac{1}{2}[(\nu_{01} + \delta_{02}) - \nu_{01} - \delta_{02}] = -77 \text{ cm}^{-1}$$

At the same time, the unperturbed frequencies of ν_{02} and δ_{02} yield

$$X_{11} = \nu_{01} - (\nu_{02}/2) = -95 \text{ cm}^{-1}$$

and

$$X_{22} = \delta_{02} - (\delta_{02}/2) = -1 \text{ cm}^{-1}$$

The larger value of X_{11} compared to X_{12} explains the observed reversal of frequencies in going from the fundamental level to the first overtone level. (For related formulas see ref. 16, p. 206.)

A similar situation is encountered with fluoral (gas) (Fig. 3). From $\nu + \delta$ we obtain $X_{12} = (\nu_{01} + \delta_{01}) - \nu_{01} - \delta_{01} = 6$ cm^{-1} and from $\nu + 2\delta$, $X_{11} = -66$ and $X_{22} = -6$ cm^{-1}. The large value of X_{11} suffices to reverse the order of the bands.

For $CHCl_2CHO$ $X_{12} = +20$ or 19 cm^{-1}, $X_{11} = -68$ cm^{-1}, and $X_{22} = +3$ cm^{-1}.

It is seen that the X_{12} coupling constant has widely different values for the different molecules.

[4]In fact, smaller bands ($\varepsilon \simeq 0.01$) at this frequency can be observed in the spectrum of CH_3CDO and can be attributed to combinations of δ_{CH_3} modes.

Can. J. Chem. Downloaded from www.nrcresearchpress.com by 210.87.254.42 on 09/05/12
For personal use only.

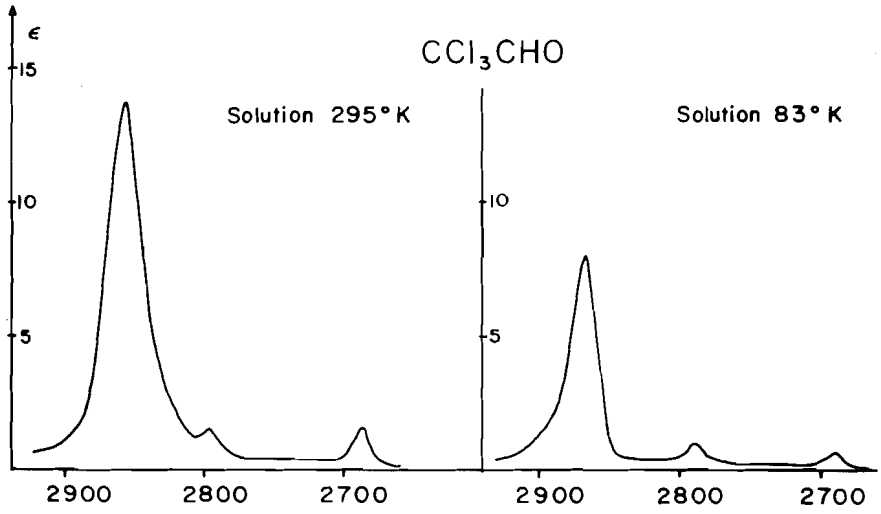

FIG. 9. The region of the ν_{CH} fundamental of CCl_3CHO in solution.

In the cases where the coincidence of 2ν and ν + 2δ is quasi-perfect we must have the same mixture of ν and δ, in the two bands resulting from Fermi resonance. The respective anharmonicity constants are given in Table VI. $X_{12} = -71$ cm^{-1} for CH_3CHO in solution at 85 °K, $X_{11} = -92$, $X_{22} = +6$ very close to those for CD_3CHO where the two bands were of unequal intensity. This confirms our interpretation of the reversal of the order of the two bands in the latter case. For CCl_3CHO $X_{12} = +4$ or $+10$, $X_{11} = -72$, $X_{22} = -4$ cm^{-1} in solution at 85 °K.

At the level of the second overtone of CH_3CHO and CD_3CHO we find a weak band. There is a possibility of a Fermi resonance between ν_{03} and $\nu_{02} + \delta_{02}$ so that there should be two bands in this area. Actually we find two bands for CCl_3-CHO and CF_3CHO with the one at higher frequency stronger. This was so at the level of ν_{01} but not at the level of ν_{02}. Whether there is a switch back in the order of the frequencies, or only the relative intensities change we cannot tell.

(3) The C=O Stretching Bands

The fundamentals were measured by previous authors (1–7). We measured the first, second, and third overtones.

A typical case is that of chloral. The respective molecular extinction coefficients are ε = 550, 10, 0.1, and 0.03. The anharmonicity constants computed from $\nu_{01} - (\nu_{02}/2)$, $(\nu_{02}/2) - (\nu_{03}/3)$, and $(\nu_{03}/3) - (\nu_{04}/4)$ are, $X_{33} = -8$, -14, and -11, respectively, showing the validity of the second order perturbation approach. Only the intensity of the third overtone seems to be relatively high.

For gaseous CF_3CHO we obtain the anharmonicity constants -11, -10, and -10 in the same order.

For acetaldehyde in solution at 295 °K we obtain -4 and -10 for the first two levels.

This is a case of low anharmonicity with no apparent complications.

(4) Combination between CH_3, CH, and CO Vibrations

These combinations are the most intense in the spectra. There is Fermi resonance between $\nu_{01,CO} + \nu_{01,CH}$ and $\nu_{01,CO} + \delta_{02,CH}$ as well as between $\nu_{02,CO} + \nu_{02,CH}$ and $\nu_{02,CO} + \delta_{02,CH}$. These bands are in the 4500 and 6200 cm^{-1} areas (Table 1).

We obtain again k_{122} (about 90 cm^{-1} for acetaldehyde, Table III). For X_{13} the unperturbed frequencies give -32 in the case of acetaldehyde at 295 °K. It is $+4$ for chloral and -1 for fluoral.

Combination between CO and CH_3 stretching bands are numerous because of the degenerate CH_3 bands. The average value of X_{34} is about 6 cm^{-1}.

Other data are given in Table VI.

(5) Environmental Effects

In Buckingham's theory (18) (23, 24) it is predicted that the gas to solution shifts of the

Can. J. Chem. Downloaded from www.nrcresearchpress.com by 210.87.254.42 on 09/05/12
For personal use only.

Can. J. Chem. Downloaded from www.nrcresearchpress.com by 210.87.254.42 on 09/05/12
For personal use only.

fundamental, first, and second overtones ··· of a diatomic vibrator are in a proportion 1:2:3: ··· This relation does not depend on the actual potential between solute and solvent molecules but only on the validity of the second order perturbation calculation. Since some of the vibrations we encounter in the aldehydes can be considered as localized in a CH or CO bond we thought it interesting to check upon the validity of Buckingham's relation. We have gas to solution (or glass) values in two cases only but we measured the shift from room to liquid nitrogen temperature in all possible cases, in the same solvent. Since a change in temperature may be supposed to have a similar effect on the solute as going from one solvent to the other it is reasonable to study Buckingham's relation in this case too.

Table VII contains a few typical results. It is seen that the 1:2:3 relation is fairly well kept for both the gas to solution and 295, 85 °K shifts for the CO and CH stretching vibrations but less well for the CH than for the CO. This is in keeping with the larger anharmonicity of the CH stretching motion. It seems that we are at the limit of the second order approach in the latter case. As mentioned above ν_{CO} undergoes a red shift whereas ν_{CH} undergoes a blue shift. This is not due to the anharmonicities which have the same sign and comparable magnitudes. The δ_{CH} bands show much smaller shifts. Also their anharmonicities are small. The combinations $\nu_{CO} + \nu_{CH}$, $\nu_{CO} + \delta_{CH}$ and $\nu_{CH} + \delta_{CH}$ exhibit a somewhat irregular behavior. However, with a few exceptions, the shifts of the combinations are fairly close to the sum of the shifts of the respective fundamentals. This is closer to being true for CH + CH than for CH + CO combinations. In view of the errors inherent in the method of computing the unperturbed frequencies we cannot hope to draw more precise information from our data.

Anharmonicity constants should be environment-independent to the second order (24, 25). This is approximately verified in the cases we have studied (Table VI).

Conclusions

The near-infrared spectra of aldehydes are dominated by the overtones of CH_3, aldehydic CH and CO stretching vibrations, and combinations between these and with δ_{CH_3} and δ_{CH} deformation vibrations. Several cases of Fermi resonance are found. The most pronounced are of the type ν–2δ, 2ν–$(\nu + 2\delta)$, 3ν–$(2\nu + 2\delta)$. In all these cases first order anharmonic resonance seems to suffice to interpret the phenomenon. We found no cases of higher order anharmonic resonances although these might make slight contributions to the observed ones.

The value of the potential constant k_{122} was computed from observed Fermi doublets. Six anharmonicity constants were also computed.

Buckingham's 1:2:3 relation concerning solvent shifts is approximately valid and the shifting of combination bands is seen to have a connection with that of the corresponding fundamentals.

We are indebted to the National Research Council of Canada for financial help.

1. K. S. Pitzer and W. Weltner. J. Amer. Chem. Soc. **71**, 2842 (1949).
2. J. C. Evans and H. J. Bernstein. Can. J. Chem. **34**, 1083 (1956).
3. P. Cossee and J. H. Schachtschneider. J. Chem. Phys. **44**, 97 (1966).
4. R. J. Capwell, Jr. J. Chem. Phys. **49**, 1436 (1968).
5. G. Lucazeau and A. Novak. Spectrochim. Acta, **25A**, 1615 (1969).
6. G. Lucazeau and A. Novak. J. Mol. Struct. **5**, 85 (1970).
7. C. V. Berney. Spectrochim. Acta, **25A**, 793 (1969).
8. E. L. Saier, L. R. Cousins, and M. R. Basila. J. Phys. Chem. **66**, 232 (1962).
9. E. Taillandier et M. Taillandier. C. R. Acad. Sci. Paris, **257**, 1522 (1963).
10. M. P. Groenewege and H. A. Van Vucht. Mikrochim. Acta, **2**, 471 (1955).
11. G. Durocher and C. Sandorfy. J. Mol. Spectry. **20**, 410 (1966).
12. C. Sandorfy. Can. Spectry. **10** (4), 85 (1965).
13. M. Asselin, G. Bélanger, and C. Sandorfy. J. Mol. Spectry. **30**, 96 (1969).
14. G. Lucazeau and C. Sandorfy. J. Mol. Spectry. **35**, 214 (1970).
15. J. Fernandez Bertran, L. Ballester, L. Dobrihalova, N. Sanchez, and R. Arrieta. Spectrochim. Acta, **25A**, 1765 (1968).
16. G. Herzberg. Infrared and Raman spectra. Vol. II. Van Nostrand, Princeton, New Jersey. 1950.
17. J. Overend. Infrared spectroscopy and molecular structure. *Edited by* Mansel Davis. Elsevier-London. 1963. p. 352.
18. A. D. Buckingham. Proc. Roy. Soc. **A248**, 169 (1958).
19. P. Barchewitz. Spectroscopie infrarouge. I. Gauthier-Villars, Paris. 1961. p. 189.
20. B. T. Darling and D. M. Dennison. Phys. Rev. **57**, 128 (1940).
21. W. Siebrand and D. F. Williams. J. Chem. Phys. **49**, 1860 (1968).
22. A. D. Buckingham. Proc. Roy. Soc. **A255**, 32 (1960).
23. A. D. Buckingham. Trans. Faraday Soc. **56**, 753 (1960).
24. G. Durocher and C. Sandorfy. J. Mol. Spectry. **22**, 347 (1967).

Can. J. Chem. Downloaded from www.nrcresearchpress.com by 210.87.254.40 on 09/05/12
For personal use only.

Thermolysis of thiete 1,1-dioxide and related species[1]

J. F. KING, P. DE MAYO, C. L. MCINTOSH, K. PIERS, AND DAVID J. H. SMITH
Department of Chemistry, University of Western Ontario, London 72, Ontario

Received June 18, 1970

Thiete 1,1-dioxide (**1**) rearranges to 5*H*-1,2-oxathiole-2-oxide (**3**) on heating in solution or in the vapor phase. The presence of phenol in the solution leads to formation of phenyl 2-propene-1-sulfonate (CH_2=$CHCH_2SO_2OPh$) in 15% yield. The results are rationalized in terms of a mechanism involving vinylsulfene (**2**). Flash thermolysis of some thietane 1,1-dioxides (**16**) and 3-thietanone 1,1-dioxides (**15**) gave products derived from extrusion processes, but 3-thietanol 1,1-dioxide (**17**) yielded, among other products, acetaldehyde and formaldehyde. The latter is believed to arise by "desulfinylation" of sulfene (CH_2=SO_2) formed along with the enol form of acetaldehyde by cycloreversion from **17**.

Canadian Journal of Chemistry, 48, 3704 (1970)

The present paper represents the results of the researches of two groups working in the same area, but, initially at least, with somewhat different aims and approaches. One group was primarily interested in finding new reactions involving the intermediacy of sulfenes (RR'C=SO_2) as part of a systematic investigation[2] of the chemistry of these species. The objectives of the second group were simply the generation of a sulfene and its possible isolation and trapping at low temperature, by a high temperature–short contact time technique (flash thermolysis[3]) in the context of a general study of reactions under such conditions. For reasons detailed in the discussion of the individual experiments, thiete 1,1-dioxide (**1**) and certain other four-membered ring sulfones appeared to be promising substrates for the formation of sulfenes by thermolysis, and from the evidence presented herein it would appear that this expectation has, in some measure, been fulfilled. Part of this work has been summarized in two preliminary communications (3, 4).

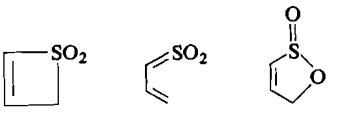

1 **2** **3**

[1]Organic sulfur mechanisms Part 7 and Flash thermolysis Part 3; for the previous part in each series see ref. 1.

[2]See refs. 1 and 2 and earlier papers cited.

[3]The term "thermolysis" (Shorter Oxford Dictionary (S.O.D.) "decomposition or dissociation by heat") was selected rather than the demotic "pyrolysis". The latter, unrecognized by the S.O.D., presumably derives its signification from pyro- "done with, caused or produced by fire" and therefore appeared inappropriate.

Results and Discussion

Liquid and Low Temperature Vapor Phase Thermolyses

At the time this work was begun it seemed to us that thiete 1,1-dioxide (**1**) might undergo either (or both) of the following thermally-induced reactions: (*i*) rearrangement to vinylsulfene (**2**) analogous to the formation of butadiene from cyclobutene, (*ii*) fragmentation (not necessarily concerted) with formation of acetylene and sulfene (CH_2=SO_2) itself. Either of these processes would be a new way of forming sulfenes which might well have advantages for looking at some of the properties of sulfenes not readily investigated by previously known routes to these species. We accordingly set out to obtain a sufficient quantity of **1** to investigate its thermolysis.

The synthesis of thiete 1,1-dioxide (**1**) was first reported by Dittmer and Christy (5), but we found it convenient to prepare **1** from 3-thietanol 1,1-dioxide (**4***a*) which was readily available via the sulfene–ketene acetal cycloaddition described by Truce and Norell (6). Dehydration of **4***a* to **1** was effected in 80–90% overall yield by converting **4***a* to the phenylmethanesulfonate ester (**4***b*) (via the sulfene (7)), and treating the latter with triethylamine.

Thermal rearrangement of **1** was carried out successfully in the vapor phase and in solution, both procedures giving a good yield of a material shown below to be the cyclic sulfinic ester **3**.[4] For the gas phase reactions we used a simple quartz

[4]By analogy with the designation "sultone" for a cyclic sulfonic ester, the name "sultine" has been suggested (8–10) for a cyclic sulfinic ester. Brevity commends its use.

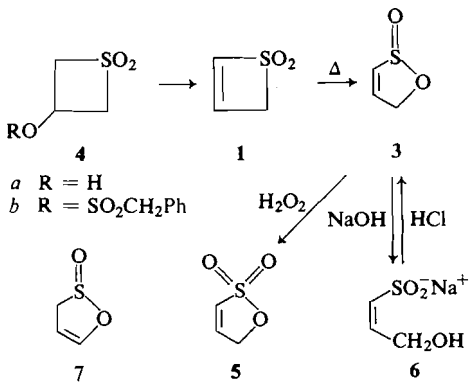

tube heated by an oven and leading into a U-tube cooled in a Dry Ice – acetone trap and connected to a vacuum pump. The pressure was measured between the trap and the pump; this is not regarded as indicating the pressure in the tube, but merely as a way of comparing one run with another. With an oven temperature above 390° and a pressure reading of 0.005 mm, thiete dioxide (**1**) was completely converted to the sultine (**3**). At 350° and 0.05 mm both **1** and **3** were present in the product; in another run at 350° but with a pressure of 0.3 mm, the product was estimated to contain more than 70% of **3** and less than 30% of **1**. In runs at 390 and 450° we obtained 80–90% yields of product estimated to be >90% sultine (**3**).

Liquid phase thermolysis of degassed benzene solutions at 220° for 20 min was also found to give the sultine (**3**) in good yield. In cyclohexane solution at 220° the result was much the same as in benzene, but in xylene the product was a dark brown material containing a small amount of **3**; under the same conditions **3** was also found to be similarly decomposed.

Rigorous proof of the cyclic sulfinate structure (**3**) was obtained as follows. Elemental analysis and mass spectrometric determination of the molecular weight showed the molecular formula to be $C_3H_4O_2S$. The i.r. spectrum showed only weak absorption between 1300 and 1400 cm^{-1}, clearly indicating the absence of a sulfonyl group whereas a very strong band at 1135 cm^{-1} (together with a slightly weaker band at 985 cm^{-1}) strongly suggested a sulfinic ester (11); confirmation of this was obtained by peroxide oxidation of **3** to **5**. Sultone **5** has been described somewhat sketchily (12, 13); these sources report melting points of 78 and 83–84°, respectively, in acceptable agreement with our value, 83–84°. The i.r. spectrum of **5** shows very strong bands at 1360 and 1190 cm^{-1}, characteristic of a sulfonic ester (11), while the n.m.r., spectrum showed a multiplet around 7.0 p.p.m. and an apparent triplet of the same integrated intensity at 5.1 p.p.m. Though the formation of **5** makes the possibility that the thermolysis product might have the isomeric enol sulfinate structure (**7**) distinctly remote, the question was settled by treating it with one equivalent of dilute sodium hydroxide. The i.r. spectrum of the product (**6**) showed absorption due to sulfinate anion and hydroxyl functions but nothing ascribable to a carbonyl group, as would have been expected from **7**. Acidification with hydrochloric acid converted the sulfinate salt back to **3**, showing that the alkaline treatment had not led to any deep-seated changes in the material.

The n.m.r. spectrum is in full agreement with structure **3** and possesses features of interest. The spectrum shows an ABXY pattern in which $\delta_A = 5.06$, $\delta_B = 5.41$, $\delta_X = 6.70$, $\delta_Y = 6.90$ p.p.m, J_{AB} −15.9, J_{AX} 2.55, J_{AY} −1.84, J_{BX} 2.70, J_{BY} −1.57, and J_{XY} 6.43 Hz. Protons A and B are obviously those of the methylene group, the pronounced difference in chemical shift between them being in excellent agreement both with recent observations on the anisotropy of the sulfinyl group (succinctly summarized in ref. 14) and with the spectra of the following closely related compounds: (*a*) **8**, $\delta_A = 5.42$, $\delta_B = 5.78$ p.p.m., J_{AB} 13.5 Hz (15), (*b*) **9**, $\delta_A = 5.31$, $\delta_B = 5.98$ p.p.m., J_{AB} 14 Hz (8), and (*c*) **10** (obtained by flash thermolysis as described in the next section), $\delta_A = 5.32$, $\delta_B = 5.72$, $\delta_X = 6.81$ p.p.m., J_{AB} −16.0, J_{AX} 2.21, J_{BX} 1.95 Hz. The previous work on the anisotropy of the sulfinyl group (*cf.* ref. 14) clearly indicates proton A in each of the above cases is the one *cis* to the sulfinyl oxygen.

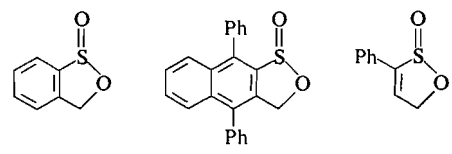

8 **9** **10**

Not long after we had encountered the formation of **3** from **1**, Dittmer *et al.* made a preliminary announcement (16) of a similar rearrangement of a substituted naphthothiete

Can. J. Chem. Downloaded from www.nrcresearchpress.com by 210.87.254.40 on 09/05/12
For personal use only.

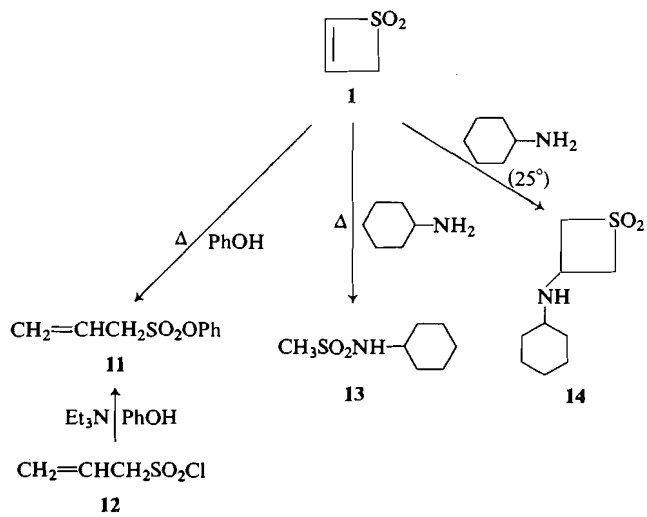

sulfone when heated in the presence of 9,10-dihydroanthracene. There was no indication in their abstract (16) that these authors were particularly concerned about the possible intermediacy of a sulfene and we therefore carried on with our study. Much more recently these authors have published a full account of their work (8) in which they refer to "an intermediate (dipolar or diradical in character)" which is represented by a sulfene structure and two other canonical forms. As we had surmised, the study of sulfenes was clearly not the primary purpose of their investigation and there is in fact relatively little overlap between their work and ours.

Having firmly established structure **3** for the thermolysis product, we turned our attention to the problem of gaining information about its mechanism of formation. Since it seemed likely to us that vinylsulfene (**2**) was a precursor of the sultine (**3**), and since trapping of an alleged intermediate is traditionally a good piece of circumstantial evidence for a mechanism, we tried a number of experiments with potential sulfene traps. Aniline, *o*-chloroaniline, or cyclohexanol led to only small amounts of brown intractable material, but phenol gave the hoped for ester **11** in roughly 15% yield. The ester (**11**) was identified by its spectra and an orthodox preparation from 2-propene-1-sulfonyl chloride (**12**), presumably via 1,2-addition to vinylsulfene (**2**) (17). When the sultine (**3**) was similarly heated with phenol only a brown tar was obtained, showing that the ester (**11**) did not arise from **3**.

In the hope of finding a more efficient trapping agent than phenol, we tried heating **1** with cyclohexylamine. The product, obtained in good yield, was, unexpectedly, *N*-cyclohexyl*methane*sulfonamide (**13**). The origin of **13** is not established but a plausible mechanism is suggested by the observation that cyclohexylamine and **1** react at room temperature to give the simple addition product **14**. Thermal decomposition of **14** could lead to sulfene and *N*-vinyl-*N*-cyclohexylamine, followed by reaction of sulfene with cyclohexylamine to give **13**. Such a fragmentation of **14** finds close parallel in the fission of 3-thietanol 1,1-dioxide to acetaldehyde and formaldehyde on flash thermolysis (see below).

Trapping experiments in the vapor phase gave only negative results. Neither 1–2 mm of ammonia (to trap sulfenes) nor 30 mm of oxygen (to trap possible free radical intermediates) gave any sign of products derived from reaction with the would-be trapping reagents.

As mentioned above, vinylsulfene (**2**) has been implicated (17) in the reaction of 2-propene-1-sulfonyl chloride (**12**) with triethylamine and methanol-*d*. It therefore seemed conceivable that vinylsulfene so generated might yield the sultine **3** provided sulfene traps were absent, but experiments at 0 and −40° gave no sign of **3**. This result was disappointing but not really surprising in view of the difference in reaction conditions, the requirement of a *cisoid* conformation of **2** to form **3**, and the speed and variety of other reaction paths available to **2**.

Another experiment was attempted which also gave negative results, though in this instance it is

Can. J. Chem. Downloaded from www.nrcresearchpress.com by 210.87.254.40 on 09/05/12
For personal use only.

Can. J. Chem. Downloaded from www.nrcresearchpress.com by 210.87.254.40 on 09/05/12
For personal use only.

the result that would be expected from the vinylsulfene mechanism. It was argued that if the reaction were not an electrocyclic ring opening but merely a homolytic cleavage to the diradical (in which each of the odd electrons is orthogonal to the π-bond) which then closed to the sultine **3**, a similar (though presumably slower) reaction might be observed on thermolysis of trimethylene sulfone, the saturated analogue of **1**. Trimethylene sulfone was found to be stable to conditions which completely converted **1** to **4**, but at 580° in the quartz tube it decomposed to give no recognizable products other than starting material nor any indication of a sultine. On flash thermolysis trimethylene sulfone also behaved differently from thiete 1,1-dioxide (**1**), as is described below.

Flash Thermolytic Experiments

The original object of these experiments was the generation of sulfene. It was hoped that this could be achieved by inducing what would now be termed the reversal of a 2s + 2a addition in a cyclic sulfone. This assumed, probably unjustifiably, an analogy of sulfene with ketene. Generated in this way the sulfene might possibly be trapped at liquid nitrogen temperature where it would be available for reaction with subsequently added reagents and, eventually, for spectroscopic examination. The first of these objects has been achieved since the completion of the presently described experiments, and has been described elsewhere (1).

The apparatus used for the thermolytic experiments is described in the Experimental section. It consists of a flow system[5] wherein the heated products are quenched rapidly by impinging on a liquid nitrogen-cooled cold-finger. The contact times were of the order of 1–5 ms. A similar apparatus has been described by Hedaya (19).

The first substances examined were the ketosulfones **15***a*, *b*, and *c* because of their ready availability and because, in principle, ketene could be one of the products. However, the not surprising observation was made that all three substances lost sulfur dioxide and carbon monoxide virtually quantitatively to give ethylene, isobutylene, or styrene respectively. This presumably entails the extrusion of one of the small fragments followed by coupling to give the three-membered ring. A second extrusion then follows. There is analogy for all the separate steps of the sequence.

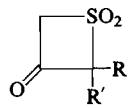

15

a R = R′ = H
b R = R′ = Me
c R = H, R′ = Ph

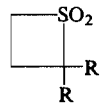

16

a R = H
b R = Me

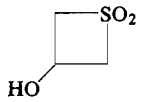

17

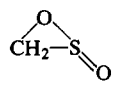

18

The thermolysis of thiete 1,1-dioxides was then investigated. The parent substance (**1**) itself gave, at 615°, the sultine **3** already obtained and characterized as described in the preceding section. Similarly 2-phenyl 1,1-thiete dioxide at 455° gave the sultine **10**. Under these conditions fragmentation did not occur, and at higher temperature, as was later found, loss of the elements of sulfur monoxide[6] took place (4). No sultine could be obtained from the thermolysis of 2,2-dimethyl thiete 1,1-dioxide.

The thermolysis of thietane 1,1-dioxide (**16***a*) itself gave cyclopropane, propylene, and sulfur dioxide (Table 1). Similarly 2,2-dimethylthietane 1,1-dioxide (**16***b*) gave 3-methyl-1-butene, 2-methyl-2-butene, 2-methyl-1-butene, and sulfur dioxide. The initial process would appear to be homolysis of the carbon–sulfur bond followed normally by formation of the 1,3-diradical and closure (or hydrogen migration). The formation of cyclopropane and propene from such a 1,3-radical has been proposed by Flowers and Frey from a study of the photolysis of cyclobutanone (23). The ratio of methylbutene formed in the thermolysis of 2,2-dimethylthietane 1,1-dioxide is close to that found by Flowers and Frey (24) in the

[5]The system derives from that of F. P. Lossing who over the years has pioneered this technique (see for instance ref. 18 and many subsequent papers from Dr. Lossing's laboratories). More recently, and roughly contemporarily with our own work E. Hedaya and his collaborators (19) have made several important and elegant contributions to the area.

[6]By analogy with the term "desulfonylation" (20) which refers to loss of sulfur dioxide, we designate the loss of sulfur monoxide as "desulfinylation". The process has been observed with episulfoxides (21) and sulfones at high temperature (22).

TABLE 1

Thermolysis of thietane and thietanone 1,1-dioxides

Compound	Temperature (°C)	Pressure (μ) Pump	Pressure (μ) Furnace	Time (min)	Products (%) SO_2	Hydrocarbons		
						Ethylene		
15*a*	930	1	200	30	98.5	96.1		
	940	5	100	30	96.0	99.7		
						Isobutylene		
15*b*	940	1	100	30	97.3	96.5		
	945	1	100	30	95.3	93.5		
						Styrene		
15*c*	930	1	100	30	97.2	97.6		
	950	1	50	15	92.5	91.5		
						Ethylene	Propylene	Cyclopropane
16*a**	960	7	90	15	69.1	Trace	43.5	51.2
	950	5	110	15	50.6		46.2	52.5
						1-Methyl-2-butene	3-Methyl-1-butene plus 2-Methyl-1-butene	
16*b*	950	5	150	15	79.5	21.2	15.6	
	950	4	100	15	50.2	20.8	15.9	

*At 800° and 10–20 μ **16***a* gave in addition to the hydrocarbons a small amount of starting material (< 15%) and ~ 10% of the saturated sultine analogous to 3.

TABLE 2

Products of thermolysis of 3-thietanol 1,1-dioxide (**17**) at 935°

Product		MeCHO	$MeCH(OMe)_2$	$CH_2(OMe)_2$	EtCHO	MeCOMe	CH_2=CHCHO	C_2H_6	C_2H_4	SO_2
Yield	Run 1	2.8	24.0	6.4	23.1	26.8	2.3	1.4	10.0	42
	Run 2	4.5	23.3	6.9	21.1	23.2	4.5	1.4	6.9	—*

*Not determined.

pyrolysis of dimethylcyclopropane. 3-Methyl-1-butene and 2-methyl-2-butene plus 2-methyl-1-butene were formed in the ratio of 1.0:0.96 as against 1.0:0.77 from the thietane 1,1-dioxide. At 800° and 10–20 μ, conditions sufficiently mild to give back a little unreacted starting material, **16***a* also gave a small amount (~ 10%) of the saturated sultine, 1,2-oxathiolane 2-oxide (25), presumably from the initially formed diradical.

Concurrent with the thermolysis of the thiete dioxides the flash thermolysis of 3-thietanol 1,1-dioxide (**17**) was also investigated. Here it was hoped that occurrence of the desired fission could be detected by the observation of the formation of acetaldehyde. This (in its enolic form) would be, together with sulfene, the product of a reversed 2a + 2s addition. The product mixture obtained was complex (see Table 2). When thermolyzed with no trapping agent on the cold-finger, only a small percentage of chloroform-soluble material was obtained and a large amount of polymer was formed. When methanol (intended as a trap for any sulfene formed) was deposited on the cold-finger the products listed were obtained in the indicated yields.

The formation of some of the products could be readily explained. Extrusion of sulfur dioxide could give acetone and propionaldehyde by hydrogen migration or by closure to cyclopropanol and rearrangement. Some dehydration to thiete 1,1-dioxide could occur, and the high temperature rearrangement of this was known (4) to give acrolein.

The formation of acetaldehyde and its dimethyl acetal indicated that a third mechanism of decomposition was operative which could have been that originally desired. At the same time the formation of formaldehyde required explanation. Both observations can be rationalized if it be assumed that the initially formed sulfene rearranges to the cyclic isomer **18** which then undergoes desulfinylation (4). It would appear that the desulfinylation of sulfenes is a general process at temperatures above 700–800°. For instance, it has

Can. J. Chem. Downloaded from www.nrcresearchpress.com by 210.87.254.40 on 09/05/12
For personal use only.

Can. J. Chem. Downloaded from www.nrcresearchpress.com by 210.87.254.40 on 09/05/12
For personal use only.

been further observed that methanesulfonyl chloride at 940° also gives formaldehyde, ethenesulfonyl chloride above 800° gives chloroacetaldehyde (presumably from chloromethyl sulfene), and 1,3-dithietane 1,1,3,3-tetroxide ("sulfene dimer") (26) at 900° yields formaldehyde as well as sulfur dioxide and ethylene.[7] These results are readily and consistently accounted for by assuming thermal fragmentation or rearrangement to form a sulfene, followed by desulfinylation. It should be further pointed out that with those systems for which there is evidence for sulfene formation at the lower temperatures, *only* the desulfinylation product is found at the higher temperatures.

In the 3-thietanol 1,1-dioxide experiment, if the foregoing be true, the yield of sulfur dioxide should equal that of the acetone and propionaldehyde combined; this is indeed approximately so. The remaining sulfur is extruded as SO and was observed as a red material on the Dewar surface which was transformed into a yellow insoluble polymer on being warmed to room temperature. This behavior is compatible with the disproportionation of sulfur monoxide to disulfur monoxide and conversion of the latter to poly(sulfur oxide) (27).

Discussion of the Mechanism of the Rearrangement of 1 → 3

The evidence given above describing experiments on thiete 1,1-dioxide (**1**) and related compounds is not sufficient to prove the intermediacy of vinylsulfene (**2**) in the rearrangement of **1** to **3**, but taken with other data does contribute to a persuasive circumstantial case for the sulfene mechanism. The argument may be summarized by the following points. (*a*) Thermal opening of four-membered rings containing an endocyclic double bond has in other instances been shown to be a cyclic, concerted process. (*b*) The product expected from trapping of a sulfene has been obtained in one case; the low yield in this reaction and the failure of other trapping experiments can be reasonably attributed to one or more of the following: (*i*) instability of the trapped product, (*ii*) fast unimolecular reaction of vinylsulfene (**2**), (*iii*) diversion of the course of the reaction by preliminary interception of the starting material by the would-be trapping reagent. (*c*) The thermolysis of trimethylene sulfone (**16***a*), which cannot undergo analogous ring opening, gives different products, probably by a completely different route, from **1**.[8] (*d*) High temperature flash thermolysis of **1** gives the desulfinylation product, acrolein, and derivatives of **1** which have been similarly treated react analogously (3, 4). (*e*) Considerable evidence is now available concerning the "abnormal" route to and from sulfenes, and, in particular, there is independent evidence of formation of a substituted cyclic sulfinic ester from a vinylsulfene. Points (*a*)–(*d*) have already been discussed in recounting the experiments, but the final aspect of the argument, (*e*), requires amplification.

Point (*e*) concerns "abnormal" addition to sulfenes, which has been defined (3), as one leading to a sulfinyl derivative; this contrasts with "normal" addition which gives a sulfonyl derivative. By this definition formation of the sultine **3** from vinylsulfene (**2**) (and also of **18** from sulfene) would be an "abnormal" addition and a mention of the present status of such addition would seem relevant.

To complement our earlier approach to this question (28), we have recently obtained strong evidence (29) for the formation of methylsulfene from the α-chlorosulfinate anion. This reaction is the reverse of "abnormal" addition and shows that the free energy of the transition state for the "abnormal" route is not impossibly high. As the terminology implies, the "normal" addition ordinarily has the lower activation energy, but for reactions such as those discussed in this paper and earlier (28), in which the "normal" process merely gives back starting material, product formation via the "abnormal" route would seem eminently reasonable.

In addition to our general observations on the "abnormal" reaction, we have recently en-

[7]D. L. Verdun and D. R. K. Harding, unpublished observations in these laboratories.

[8]The formation of a small amount of saturated sultine from **16***a* could be taken as indicating that **1** and **16***a* react by similar mechanisms, the cyclopropane and propylene merely arising from further reaction of the saturated sultine. Control experiments by D. R. K. Harding in these laboratories, however, show that the saturated sultine is *less* susceptible to thermal decomposition than **16***a* and only 25%, at the most, of the products from **16***a* could arise via the sultine. At the same time the complete absence of desulfonylation products for **1** over a temperature range from 615–950° (4, 10) strongly suggests that the homolysis mechanism which easily accounts for the products from **16***a* cannot be important in the thermolysis of **1**.

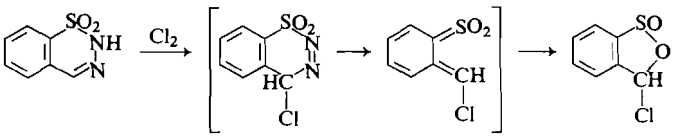

19 20 21 22

countered another reaction for which our preferred mechanism is a cyclization of a vinylsulfene to a sultine. The benzothiadiazine **19** on reaction with chlorine in an anhydrous medium gives **22** (30, and B. L. Huston and L. J. Danks, unpublished observations). An attractive rationalization of this observation is that **20**, the primary product of chlorination, undergoes a reverse Diels–Alder reaction with loss of nitrogen to give **21**, which then cyclizes in the same way as **2** to give **22**.

Experimental

Melting points were determined on a Kofler hot stage and are uncorrected. The i.r. spectra were obtained with a Beckman IR-10 spectrophotometer using sodium chloride cells. The n.m.r. spectra were determined either on a Varian A-60 or a Varian HA-100 instrument. The t.l.c. was carried out using Camag Kieselgel DF 5. Degassing of sealed tubes prior to thermolysis was carried out by freezing the mixture in liquid N_2, pumping with a vacuum pump for a few minutes, thawing, and then repeating the procedure twice more.

1,1-Dioxy-3-thietanyl Phenylmethanesulfonate (4b)

3-Thietanol 1,1-dioxide (**17**) (1 g, 8.2 mmoles), prepared by the method of Truce and Norell (6), and phenylmethanesulfonyl chloride (1.71 g, 9.0 mmoles) were dissolved in dry tetrahydrofuran (40 ml). Triethylamine (1.01 g, 10 mmoles) was added dropwise and with stirring to this solution and the mixture stirred for 1 h further. The solvent was then evaporated under reduced pressure; the residue was taken up in methylene chloride and this solution washed with water, dried, and the solvent evaporated leaving a colorless residue (2.2 g). Recrystallization from methylene chloride gave a product (2.01 g, 89%) melting at 189–190°.

Anal. Calcd. for $C_{10}H_{12}O_5S$: C, 43.49; H, 4.38; S, 23.20. Found: C, 43.62; H, 4.34; S, 23.01.

Thiete 1,1-Dioxide (1)

1,1-Dioxy-3-thietanyl phenylmethanesulfonate (1.0 g, prepared as above) was suspended in benzene (50 ml) at 50°. A solution of triethylamine (3.6 ml) in benzene (10 ml) was added and the mixture stirred for 1 h further. The solvent was evaporated and the residue extracted with ether (three portions of 60 ml). The solvent of the combined extracts was evaporated and the residue recrystallized from benzene – petroleum ether giving a product (360 mg, 96%) melting at 47–49° and showing i.r. and n.m.r. spectra agreeing well with those already reported (5, 31).

Low Temperature Thermolysis of Thiete 1,1-Dioxide (1)

(a) In the Gas Phase

The gas phase thermolyses were carried out in a quartz test tube (30 cm long and 1 cm outside diameter) fitted with a B10 male ground glass joint. The latter was connected to a Pyrex U-tube which could be cooled by immersing the lower part in a Dewar flask containing a Dry Ice – acetone mixture. Thiete 1,1-dioxide (100 mg; 0.96 mmole) was placed at the closed end of the quartz tube, which was then fitted with the U-tube and evacuated to 0.02 mm Hg (measured between the cold trap and the pump). In the meantime the quartz tube was heated to 450° by means of a furnace so arranged that the closed end containing the organic material protruded about 3 cm out of the furnace. After about 45 min all of the thiete 1,1-dioxide had passed through the tube and a yellow liquid with a sharp irritating odor had collected in the U-tube (88 mg, 85%). This liquid was distilled twice in a small cold-finger distillation apparatus; b.p. 90°/15 mm. The i.r. spectrum (CCl_4) showed absorption at 3090(w), 2920(w), 2860(w), 1600(w), 1445(w), 1335(w), 1280(m), 1195(w), 1135(s), 1085(m), 1005(m), 985(s), 920(m), 705(s), 645(m), 615(m). The n.m.r. values given in the Results and Discussion were obtained from a spectrum determined on the HA-100 instrument using the LAOCOON III computer program. The signs of the coupling constants could not be rigorously assigned; those giving best agreement between observed and computed spectra are given.

Anal. Calcd. for $C_3H_4O_2S$: C, 34.60; H, 3.87; S, 30.79. Found: C, 34.45; H, 3.85; S, 30.68.

Thermolyses carried out at 450° and 0.005 mm and at 390° and 0.005 mm in the same apparatus gave similar results.

The above quartz thermolysis tube was fitted with a tubulation at the closed end to allow gases to be added during the reaction. In one experiment ammonia was passed through the tube during the thermolysis of a sample of thiete 1,1-dioxide (60 mg). A second trap cooled in liquid nitrogen was added to retain the ammonia. The pressure measured between the liquid nitrogen trap and the pump varied between 1 and 2 mm. The product contained in the front trap (50 mg) was shown by i.r. and t.l.c. to be an approximately 1:1 mixture of thiete 1,1-dioxide (**1**) and the cyclic sulfinic ester (**3**); there was no indication of any product derived from reaction with ammonia. When a sample of thiete 1,1-dioxide was passed through the tube at 450° in the presence of a rapid stream of oxygen (pressure between the traps and pump > 30 mm), the product (43 mg) was also found by i.r. and t.l.c. to be 1:1 mixture of thiete 1,1-dioxide and the sultine (**3**) with no sign of material derived from any reaction with oxygen.

(b) In Solution

Thiete 1,1-dioxide (**1**) (15 mg) was dissolved in benzene

Can. J. Chem. Downloaded from www.nrcresearchpress.com by 210.87.254.40 on 09/05/12
For personal use only.

Can. J. Chem. Downloaded from www.nrcresearchpress.com by 210.87.254.40 on 09/05/12
For personal use only.

(1 ml) contained in a thick-walled Pyrex tube (outer diameter 1 cm). The sample was degassed and sealed under reduced pressure and the tube heated in a Carius oven at 280° for 10 min. The tube was cooled and the benzene evaporated leaving an oil (11 mg) identical in i.r. spectrum and t.l.c. behavior with the sultine (**3**) obtained from the gas phase thermolyses.

Similar thermolyses at 220° for 30 min and 230° for 10 min gave products containing both unreacted thiete 1,1-dioxide and the sultine (**3**). Use of xylene as the solvent in an experiment carried out at 270° for 45 min led to a dark brown product which was shown by t.l.c. to have, amongst others, one component with the same R_f value as the sultine (**3**). Similar treatment of sultine **3** also gave an extensively decomposed material.

Reaction of Sultine 3 with Sodium Hydroxide

The sultine (**3**) (45 mg, 0.43 mmole) was dissolved in 0.1 *N* sodium hydroxide (4.3 ml) and the solution stirred at room temperature for 2 h. The water was evaporated under reduced pressure leaving a gummy residue, insoluble in ether, methylene chloride, or chloroform, which was taken up in methanol (2 ml). A small portion of this was deposited on a sodium chloride plate and the solvent evaporated leaving a film; the i.r. spectrum of this film showed bands at 1020 and 960 characteristic of sulfinate anions (11), a very strong hydroxyl band at 3300, absorption presumably due to water around 1650 and no sign of any peaks between 1700 and 200 cm^{-1}.

The methanol was evaporated from the major portion remaining above and the residue dissolved in 5 *N* HCl (3 ml). The solution was saturated with sodium chloride and continuously extracted with methylene chloride for 26 h. The organic extract was dried with magnesium sulfate and the solvent evaporated leaving an oil (28 mg) which was identified as sultine **3** by i.r., t.l.c., and v.p.c.

Oxidation of Sultine 3 with Hydrogen Peroxide

The sultine (**3**) (49 mg) was dissolved in a solution (1 ml) obtained by mixing glacial acetic acid (3 ml) with 30% hydrogen peroxide solution (0.8 ml), and the resulting solution refluxed for 2 h. The reaction mixture was cooled, poured into water, and extracted with methylene chloride. The methylene chloride extracts were washed with saturated sodium carbonate solution, dried over magnesium sulfate, and the solvent evaporated, leaving a nearly colorless solid (40 mg) which on recrystallization from ether melted at 83–84°. Preparation of the unsaturated sultone (**5**) has been reported (without experimental details) previously; reported m.p. 78° (12) and 83–84° (13). The i.r. spectrum displayed strong bands at 1360 and 1190 cm^{-1}, the n.m.r. spectrum showed only a complex multiplet around 7.0 and an apparent triplet at 5.1 p.p.m. with the same integrated intensity as the other band.

Thermolysis of Thiete 1,1-Dioxide in Benzene–Phenol

Thiete 1,1-dioxide (90 mg) was dissolved in benzene (1 ml) contained in a thick-walled Pyrex tube as described above and phenol (0.3 g) added. The tube was degassed and sealed under vacuum and heated in a Carius oven at 220° for 30 min. The dark brown reaction mixture was taken up in ether and washed with portions of 10% aqueous sodium hydroxide and water. The ether solution was dried over magnesium sulfate and the solvent evaporated leaving a dark brown oil (25 mg) which showed bands at 1370 and 1140 cm^{-1} characteristic of a sulfonic ester. A number of similarly executed runs gave the following results: (*i*) 15 mg heated at 270–280° for 10 min gave 7 mg of crude product, (*ii*) 12 mg heated at 270–280° for 15 min gave 8 mg of crude product, (*iii*) 40 mg heated at 185° for 2 h gave 4 mg of crude product, (*iv*) 400 mg heated at 250° for 15 min gave 80 mg of crude product.

The crude product (~ 150 mg) from a number of such runs was subjected to preparative t.l.c. using benzene as the developing solvent. The purified sulfonate (~ 70 mg) obtained from the chromatography was distilled in a glass tube (b.p. 85°/0.005 mm) and the distillate subjected to preparative v.p.c., (GE-SE 30 on Chrom W at 140°). The sample of phenyl 2-propene-1-sulfonate so obtained had $n_D^{25} = 1.5216$, strong i.r. bands at 1390, 1370, 1170, 1150, and 870 cm^{-1}, and the following n.m.r. signals: 7.5 (5H, s), a multiplet between 5.4 and 6.4 (3H), and a doublet at 4.1 p.p.m. (2H).

*Preparation of Phenyl 2-Propene-1-sulfonate (**11**) from 2-Propene-1-sulfonyl Chloride (**12**)*

Triethylamine (2 ml) in methylene chloride (5 ml) was added dropwise to a stirred solution of 2-propene-1-sulfonyl chloride (**12**) (500 mg) and phenol (1 g) in methylene chloride (50 ml) at room temperature. The stirring was continued for 1 h after the addition. The reaction mixture was then washed with 2 *N* HCl, 10% aqueous NaOH, and water, respectively. The methylene chloride extract was dried and the solvent evaporated yielding a colorless oil (500 mg). A specimen for analysis, determination of physical properties, and comparison with the material from the thermolytic experiments was obtained by v.p.c. as described above; the i.r. and n.m.r. spectra were identical to those of the specimen of (**11**) obtained from thiete 1,1-dioxide (**1**); $n_D^{25} = 1.5211$.

Anal. Calcd. for $C_9H_{10}O_3S$: C, 54.53; H, 5.08; S, 16.18. Found: C, 54.59; H, 4.85; S, 16.28.

Reaction of Sultine 3 with Phenol

The sultine (**3**) (80 mg) was dissolved in benzene (1 ml) in a thick-walled Pyrex tube and phenol (0.5 g) added. The tube was degassed, sealed under vacuum, and heated at 245° for 15 min. The dark brown reaction mixture was taken up in ether (10 ml) and washed with dilute NaOH and water. The organic phase was dried and the solvent evaporated leaving a brown tar (5 mg) which showed no distinctive features either on t.l.c. or in its i.r. spectrum.

Attempted Trapping of the Sulfene with Amines and Cyclohexanol

These experiments were carried out in degassed solutions in dry benzene in sealed tubes as described above.

Aniline (0.5 ml) was added to a solution of thiete 1,1-dioxide (**1**) (45 mg) in benzene (0.5 ml) and the mixture heated at 240° for 30 min to give an almost black product which was diluted with methylene chloride and washed with 2 *N* HCl and water. Evaporation of the solvent gave a small amount (5 mg) of a dark brown residue showing no distinct features on t.l.c. *o*-Chloroaniline (0.5 ml) in benzene (0.5 ml) containing the thiete dioxide (30 mg) was heated for 20 min at 220°. Similar work-up gave only a few milligrams of brown product showing only a brown streak on t.l.c. Cyclohexanol (0.5

Can. J. Chem. Downloaded from www.nrcresearchpress.com by 210.87.254.40 on 09/05/12
For personal use only.

ml) was added to a solution of the thiete dioxide (30 mg) in benzene (0.5 ml) which was then heated at 230° for 15 min. The residue (3 mg) obtained after work-up was a dark brown tar showing no distinct spots on t.l.c.

Cyclohexylamine (0.6 ml) was added to a solution of thiete 1,1-dioxide (40 mg) in benzene (0.3 ml) and the mixture heated at 220° for 30 min. The reaction product was poured into methylene chloride (15 ml) and washed with dilute HCl. Evaporation of the solvent gave a residue (45 mg), which after sublimation melted at 102–104°; this was identified as *N*-cyclohexyl methanesulfonamide (**13**) by comparison of m.p., mixed m.p., i.r., and n.m.r. spectra with an authentic specimen (m.p. 104–105°, after recrystallization from methanol) prepared from methanesulfonyl chloride; reported melting points are 105–106.5 (32) and 106° (33).

Reaction of Thiete 1,1-Dioxide with Cyclohexylamine at Room Temperature

Cyclohexylamine (38 mg) was added to thiete 1,1-dioxide (40 mg) and the mixture shaken at room temperature for 1 to 2 min, after which time the mixture had crystallized. Recrystallization from ether gave crystals 3-(*N*-cyclohexylamino)-thietane 1,1-dioxide (**14**), melting at 93–94°.

Anal. Calcd. for $C_9H_{17}NO_2S$: C, 53.19; H, 8.43; N, 6.89. Found: C, 53.37; H, 8.53; N, 6.79.

Reaction of 2-Propene-1-sulfonyl Chloride with Triethylamine

A solution of the propenesulfonyl chloride (15 mg) in dry ether was slowly treated at 0° with a solution (1 ml) prepared by mixing triethylamine (0.2 ml) with ether (10 ml). A precipitate formed; the solution was stirred at 0° for 30 min. It was then washed with diluted HCl. The t.l.c. showed no sign of the cyclic sulfinate ester. Similar experiments carried out at room temperature and −40° showed no significant indication of the presence of the cyclic sulfinic ester.

Hydrogenation of Thiete 1,1-Dioxide

Thiete 1,1-dioxide (120 mg) was added to a suspension of prehydrogenated 5% Pd on barium carbonate catalyst (200 mg) in ethyl acetate (10 ml), and the mixture shaken with hydrogen. Hydrogen uptake was complete in 20 min. Filtration and evaporation of the solvent gave the product (118 mg) which on crystallization from ethyl acetate – pentane gave trimethylene sulfone **16***a* (112 mg) m.p. 73–75°; reported m.p. 74–75° (*cf.* ref. 5). Use of 5% Pd on charcoal catalyst also gave trimethylene sulfone but only in about 30% yield.

2-Phenyl-3-thietanone 1,1-Dioxide

3,3-Diethoxy-2-phenylthietane 1,1-dioxide (6) (10 g) was dissolved in concentrated hydrochloric acid (100 ml) and stirred for 18 h. The crystalline precipitate (8.2 g) was triturated with chloroform and the residue crystallized from benzene–dioxane to give 5.6 g (71%) of the thietanone (evidently the enol form), m.p. 172–174°; ν_{max}(Nujol), 3100 (broad), 1680, 1265, 1105 cm^{-1}; $\delta(CD_3COCD_3)$: 7.92 (5H, m) 4.55 (2H, s); λ_{max}(EtOH), 265 nm (ε 13 200).

Anal. Calcd. for $C_9H_8O_3S$: C, 55.10; H, 4.11; S, 16.31. Found: C, 55.11; H, 4.13; S, 16.23.

The chloroform soluble portion gave, after chromatography, 3-ethoxy-2-phenyl 2-thiete 1,1-dioxide, m.p. 132–132.5° [lit. (6) 132–134°]; $\delta(CDCl_3)$: 1.4 (3H, t, J = 7 Hz), 4.15 (4H, q, J = 7 Hz), 4.57 (2H, s), 7.40 (5H, m). The thietanone gave with diazomethane 3-methoxy-2-phenyl 2-thiete 1,1-dioxide, m.p. 132–132.5; $\nu_{max}(CHCl_3)$ 1662, 1307, 117 cm^{-1}; $\delta(CDCl_3)$: 3.90 (3H, s), 4.59 (2H, s), 7.39 (5H, m); λ_{max}(EtOH) 264 nm (ε 14 500).

2-Phenyl-2-thiete 1,1-Dioxide

3-*N*,*N*-dimethylamino-2-phenylthietane 1,1-dioxide (34) (1 g) was dissolved in 50 ml of a methanol–chloroform mixture and 0.85 ml methyl iodide added. After 24 h the crystals (1.05 g) of quaternary salt were isolated by filtration, m.p. 212°. The salt (3 g) was dissolved in water (120 ml) and 3 g silver oxide added. The triethylamine was removed, with warming under reduced pressure, and the product isolated with methylene chloride to give, after crystallization from methylene chloride – light petroleum (60–80°), the thiete 1,1-dioxide (1.1 g; 74%), m.p. 94.5–95°, identical in all respects with the material prepared by Wells and Abbott (34) by a different route.

*2,2-Dimethyl-thietane 1,1-Dioxide (**16***b*)

2,2-Dimethylthiete 1,1-dioxide (640 mg) (35) in ethanol was hydrogenated over palladized charcoal (100 mg, 5%) until one molecular equivalent of hydrogen was absorbed. The crude product, m.p. 61–62° was sublimed to give 580 mg of the thietane 1,1-dioxide, m.p. 70–71°; $\nu_{max}(CCl_4)$ 1323, 1128 cm^{-1}; $\delta(CCl_4)$ 1.57 (6H, s), A_2X_2 at δ_A = 4.14, δ_X = 6.57 $J_{AA'}$ 18.59 Hz, $J_{XX'}$ 17.70 Hz, J_{AX} 6.48 Hz, $J_{AX'}$ 10.43, $J_{A'X}$ 10.43 and $J_{A'X'}$ 6.48 Hz.[9]

Anal. Calcd. for $C_5H_{10}O_2S$: C, 44.77; H, 7.52; S, 23.85. Found: C, 44 81; H, 7.36; S, 23.76.

High Temperature Reactions

The apparatus used for most of these experiments is shown schematically in Fig. 1*a*. In a later modification, the Dewar system has been greatly enlarged and is followed by a second Dewar as shown in Fig. 1*b*. A description of the oven of the first type follows.

The furnace unit was a brass cylinder 11 × 2.5 (diam.) × $\frac{1}{8}$ in. and was wrapped with 9 coils of $\frac{1}{4}$ in. copper tubing (water cooling). The ends of the cylinder were two $\frac{3}{8}$ in. brass flanges 5 in. in diameter. An end plate, with a $\frac{1}{2}$ in. O-ring connector, a Hastings gauge, and two pairs of metal-to-porcelain through connectors, was bolted to one end of the cylinder. A second plate with a 1 in. O-ring butt connector was bolted to the other end. Vacuum seal was maintained with $\frac{1}{8}$ in. Viton O-rings. The reactor tube was inserted through the $\frac{1}{2}$ in. O-ring connector into the cylinder. This tube consisted of an inner $\frac{1}{8}$ in. i.d. ceramic thermocouple well and an outer $\frac{1}{2}$ in. o.d. ceramic tube. The two tubes were fused to Pyrex glass of the same diameter and were joined together at the inlet end outside the end plate. A $\frac{1}{8}$ in. stainless steel shielded MgO insulated chromel–alumel thermocouple was used and was attached to a Barber–Coleman Model 471 temperature controller. The first 4 in. of the outer tube were wound with 6 ft of 22 gauge Nichrome spaced between turns of $\frac{1}{8}$ in. asbestos rope, and covered

[9]Calculated spectrum using a LAOCOON III computer program with iteration.

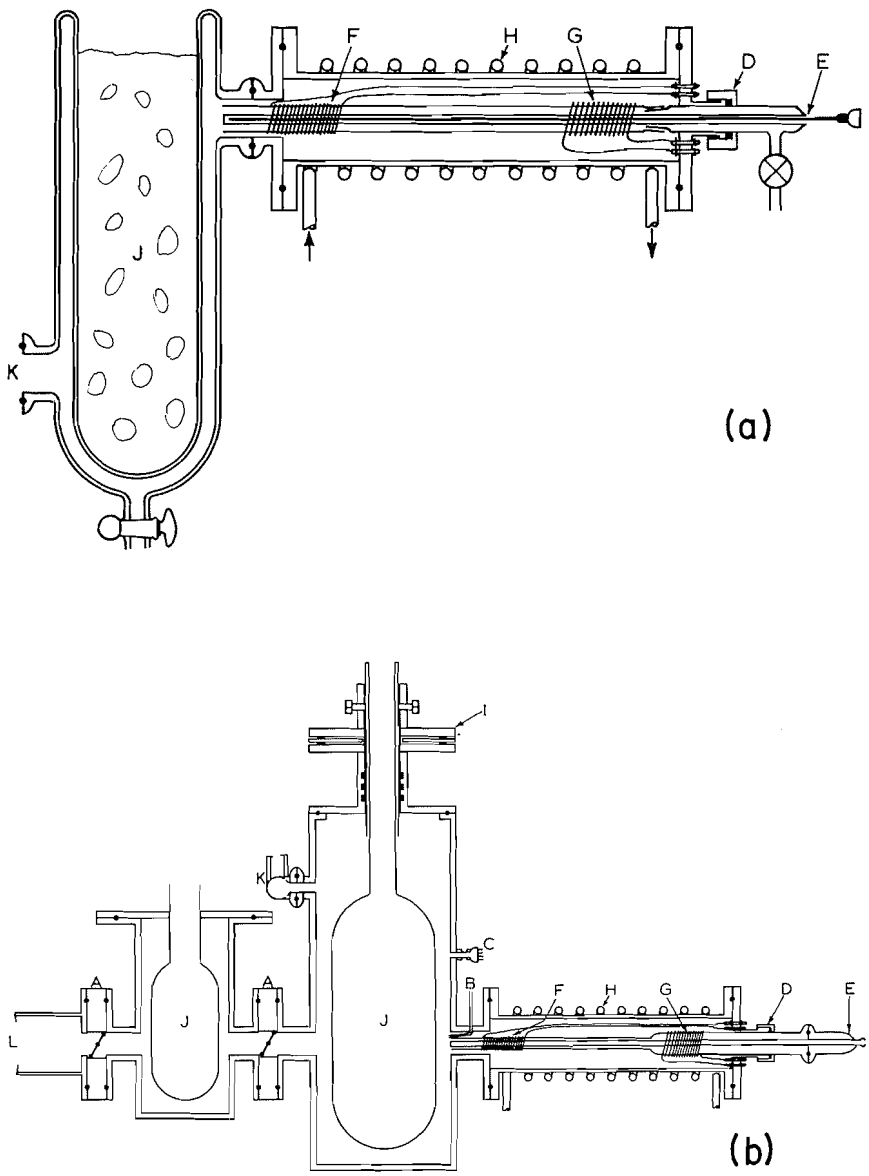

FIG. 1. (*a*, *b*) A, quarter-swing butterfly valves; B, trapping agent inlet; C, vacuum gauge*; D, vacuum seal coupling; E, thermocouple well; F, main oven; G, sublimation oven; H, water-cooling coil; I, ball bearing race; J, liquid nitrogen cold-finger; K, connection leading to the sample-handling manifold; L, connection to main pump.
*The apparatus in Fig. 1*a* also has a Hastings gauge located adjacent to the vacuum seal coupling D and is not shown on the drawing.

with a layer of asbestos paper. The last 4 in. were loosely bound with an additional 4 ft of the same wire. The ends of both wirings were attached to the through-connectors.[10] Liquids after distillation from the Dewars or U-tube collectors were transferred in the usual way through a vacuum line. Gases were collected in a 75 ml stainless steel bomb filled with $\frac{3}{16}$ stainless steel balls, the whole being cooled in liquid nitrogen. The apparatus was evacuated using a Welch Model 1403 pump and a Consolidated Vacuum Corporation VMF-20 oil diffusion pump. The pressure was monitored at several stations using Hastings gauges. In more recent modifications we have used a Speedivac ED-500 pump. In the presently

[10]More recently platinum–iridium wire has been used to permit the attainment of temperatures up to 1300°.

Can. J. Chem. Downloaded from www.nrcresearchpress.com by 210.87.254.40 on 09/05/12
For personal use only.

Can. J. Chem. Downloaded from www.nrcresearchpress.com by 210.87.254.40 on 09/05/12
For personal use only.

described experiments pressures of the order of 100 μ were used. More recently pressures between 1–40 μ have been routine.

For analytical purposes, calibrating compounds in known amounts were added to the products. These are specified in the text. Sulfur dioxide was also estimated iodometrically.

Contact times were calculated from the formula

$$T = 0.16 \frac{V_r \cdot p \cdot t}{T_r \cdot m}$$

where P is the pressure, V_r the volume of the hot zone of reactor, T_r the reaction temperature (°K), t the time of reaction (s), m the moles of material passed. The contact times used were of the order of ms, but in view of the dubious significance of the term so derived the values should only be given a relative sense.

The thermolyses for these relatively non-volatile substances were carried out by placing a known weight of material in the first section of the furnace. The material was slowly sublimed through the hot zone with a small stream of nitrogen to minimize back sublimation. Any starting material which did sublime backwards was washed out and weighed. Traps were cooled in liquid nitrogen. All materials were shown to be sublimed unchanged.

Thermolyses

*(a) Thietane 1,1-Dioxide (**16a**)*

(*i*) Approximately 80 mg of the substance was thermolyzed at 465, 595, and 765° (100 μ). The only non-gaseous material observed was starting material in 92.5, 78.6, and 36.5% yield, respectively.

(*ii*) Approximately 90 mg of the substance was thermolyzed at 950° at 100 μ. After completion of the reaction and cooling, 5.0 ml of propane gas was added. The mixture was analyzed on a 5 ft × $\frac{3}{16}$ in. 10% Ethofat on chromosorb P column at 100°. The products were identified by i.r. and retention time as ethylene, propylene, and SO_2 (see Table 1).

*(b) 2,2-Dimethyl-thietane 1,1-Dioxide (**16b**)*

(*i*) At 465 and 610° (180 μ) 71 and 40% recoveries were obtained.

(*ii*) Thermolysis at 950° (120 μ) using methyl formate as calibrating compound gave, using a 5 ft × $\frac{3}{16}$ in. Porapak S at 150° column, the results in Table 1. The products were identified by i.r. spectra and v.p.c. retention time, and the hydrocarbons also by n.m.r.

*(c) 3-Thietanone, 2,2-Dimethyl- and 2-Phenyl-3-thietanone 1,1-Dioxides (**15a**, b, and c, respectively)*

About 200 mg of the ketone was thermolyzed at near 930° (~ 200 μ). Propane, *n*-pentanol, and *n*-propanol were used as the calibrating compounds, respectively. The columns used were 5 ft × $\frac{3}{16}$ in. Porapak S at 80° for the first analysis, 20 × $\frac{1}{4}$ in. 10% FFAP on chromosorb P at 110° for the second and third. In the first and third cases the SO_2 analysis was confirmed iodometrically. The results are contained in Table 1.

*(d) 3-Thietanol 1,1-Dioxide (**17**)*

(*i*) Methanol (0.5 ml) was placed in the trap (a U-tube) and 200 mg of the alcohol thermolyzed at 935° (110 μ). Methyl formate (calibrating compound) was added, the products washed with 0.5 ml methanol, and the mixture analyzed (20 × $\frac{1}{4}$ in. 10% FFAP on chromosorb P at 50°). The following substances were isolated and the means of identification are indicated parenthetically: acetaldehyde (n.m.r., v.p.c.), dimethoxymethane (i.r., n.m.r., v.p.c.), propionaldehyde (v.p.c., 2,4-dinitrophenylhydrazone), acetone (i.r., n.m.r., v.p.c., 2,4-dinitrophenylhydrazone), acetaldehyde dimethyl acetal (i.r. n.m.r., v.p.c.), acrolein (v.p.c., 2,4-dinitrophenylhydrazone).

(*ii*) A cold-finger trap was used omitting methanol. A thermolysis at 940° (100 μ) with propane as calibrating compound gave ethane, ethylene, and sulfur dioxide identified by v.p.c. retention time and i.r. spectrum. The results are given in Table 2.

*(e) Thiete 1,1-Dioxide (**1**)*

146 mg of the dioxide were thermolyzed at 615° (10 μ). Undecomposed material (55 mg) was recovered and 64 mg (70%, based on unrecovered starting material) of the sultine (**3**) was obtained.

(f) 2-Phenylthiete 1,1-Dioxide

200 mg of the dioxide were thermolyzed at 455° (50 μ). A mixture of phenyl vinyl ketone (10) and the sultine (**10**) was obtained. This was separated by thin-layer chromatography (eluent: $CHCl_3$) to give the pure sultine (55 mg, 27%), m.p. 74.5–75.5°, $\nu_{max}(CCl_4)$ 1135, 1028 cm^{-1}, and an *ABX* pattern at $\delta_A = 5.32$, $\delta_B = 5.72$, $\delta_X = 6.81$, $J_{AB} = 15$, $J_{AX} = 2.21$, and $J_{BX} = 1.95$ Hz, and a five proton singlet at 7.47.

Anal. Calcd. for $C_9H_8O_2S$: C, 60.00; H, 4.48; S, 17.77. Found: C, 60.18; H, 4.57; S, 17.87.

We are grateful to Professor J. B. Stothers for his aid in obtaining and interpreting the calculated n.m.r. spectra, Dr. D. N. Harpp (McGill University) for kindly supplying us with the experimental details for preparing the saturated sultine, and Mr. D. R. K. Harding for completing certain of the experiments. This work was supported by the Petroleum Research Fund, administered by the American Chemical Society, and by the National Research Council of Canada.

1. J. F. KING, P. DE MAYO, and D. L. VERDUN. Can. J. Chem. **47**, 4509 (1969).
2. J. F. KING and T. W. S. LEE. J. Amer. Chem. Soc. **91**, 6524 (1969).
3. J. F. KING, K. PIERS, D. J. H. SMITH, C. L. MCINTOSH, and P. DE MAYO. Chem. Commun. 31 (1969).
4. C. L. MCINTOSH and P. DE MAYO. Chem. Commun. 32 (1969).
5. D. C. DITTMER and M. E. CHRISTY. J. Org. Chem. **26**, 1324 (1961).
6. W. E. TRUCE and J. R. NORELL. J. Amer. Chem. Soc. **85**, 3231, 3236 (1963).
7. J. F. KING and T. DURST. J. Amer. Chem. Soc. **87**, 5684 (1963).
8. D. C. DITTMER, R. S. HENION, and N. TAKASHINA. J. Org. Chem. **34**, 1310 (1969).
9. R. S. HENION. Ph.D. thesis. Syracuse University, Syracuse, New York. 1967. *Cited by* R. S. Henion, Eastman Organic Chemical Bulletin, **41**, No. 3 (1969).
10. C. L. MCINTOSH. Ph.D. thesis. University of Western Ontario, London, Ontario. 1968.
11. L. J. BELLAMY. *In* Organic sulfur compounds. Vol. 1. *Edited by* N. Kharasch. Pergamon Press, Oxford. 1961. p. 47.

12. G. MANECKE, J. DANHÄUSER, and C. REICH. Angew Chem. **70**, 503 (1958).
13. J. H. HELBERGER and G. MUELLER. Ger. Pat. 1,146,870; Chem. Abs. **59**, 11259 (1963).
14. C. R. JOHNSON and W. O. SIEGL. J. Amer. Chem. Soc. **91**, 2796 (1969).
15. J. KOMERY. M.Sc. thesis. University of Western Ontario, London, Ontario. 1969.
16. D. C. DITTMER, R. S. HENION, and N. TAKASHINA. 153rd National Meeting of the American Chemical Society, Miami, Florida. April 1967. Abstract 101.
17. W. E. TRUCE and R. W. CAMPBELL. J. Amer. Chem. Soc. **88**, 3599 (1966).
18. R. F. POTTIE, A. G. HARRISON, and F. P. LOSSING. J. Amer. Chem. Soc. **83**, 3204 (1961).
19. E. HEDAYA. Accounts of chemical research. **2**, 367 (1969).
20. J. L. KICE. *In* Organic sulfur compounds. Vol. 2. *Edited by* N. Kharasch and C. Y. Meyers. Pergamon Press, Oxford. 1966. p. 115.
21. G. E. HARTZELL and J. N. PAIGE. J. Amer. Chem. Soc. **88**, 2616 (1966).
22. E. K. FIELDS and S. MEYERSON. J. Amer. Chem. Soc. **88**, 2836 (1966).
23. M. C. FLOWERS and H. M. FREY. J. Chem. Soc. 2758 (1960).
24. M. C. FLOWERS and H. M. FREY. J. Chem. Soc. 3953 (1959).
25. D. N. HARPP and J. G. GLEASON. Tetrahedron Lett. 1447 (1969).
26. G. OPITZ and H. R. MOHL. Angew Chem. Intern. Ed. **8**, 73 (1969).
27. P. W. SCHENK and R. STEUDEL. Angew Chem. Intern. Ed. **4**, 402 (1965).
28. T. DURST and J. F. KING. Can. J. Chem. **44**, 1859 (1966).
29. J. F. KING and R. P. BEATSON. Chem. Commun. 663 (1970).
30. J. F. KING, A. HAWSON, D. M. DEAKEN, and J. KOMERY. Chem. Commun. 33 (1969).
31. N. S. BHACCA, L. F. JOHNSON, and J. N. SHOOLERY. N.m.r. Spectra Catalog, Varian Associates. 1962. Spectrum no. 22.
32. S. I. BURMISTROV and V. I. MARKOV. Z. Obsch. Khim. **31**, 1665 (1961). (Consultants Bureau Translation p. 1552).
33. Y. UEDA, H. YANO, and T. MOMOSE. Chem. Pharm. Bull. Japan. **12**, 5 (1964).
34. J. N. WELLS and F. S. ABBOTT. J. Med. Chem. **9**, 489 (1966).
35. W. E. TRUCE, J. R. NORELL, J. E. RICHMAN, and J. P. WALSH. Tetrahedron Lett. 1677 (1963).

Can. J. Chem. Downloaded from www.nrcresearchpress.com by 210.87.254.40 on 09/05/12
For personal use only.

Can. J. Chem. Downloaded from www.nrcresearchpress.com by 210.87.254.5 on 09/05/12
For personal use only.

Simple and quick method for the dielectric study of solid powders

K. K. SRIVASTAVA, G. F WRIGHT, S. L. KHANNA,[1] IQBAL KRISHAN, AND R. K. NAYAR
Department of Chemistry, University of Toronto, Toronto 181, Ontario

Received June 8, 1970

The dielectric constant values for many substances have been determined at a frequency of 1 MHz by the method discussed in the paper. In some cases, these values have also been determined by other commonly used methods and show a good agreement.

Canadian Journal of Chemistry, **48**, 3716 (1970)

Introduction

The method was essentially suggested by Knoke (1) who carried out the moisture-content measurements of some solid powders. It is based on the principle of immersion, *i.e.* the dielectric constant of liquid mixture is varied until the introduction of powder does not cause any more change. Incidentally no data seem to be available on dielectric measurements based on this method. The authors have found that the method is not only extremely quick but also provides reliable results. The limitations of this method have also been discussed here which were omitted by Knoke probably because he was only interested in the measurement of moisture-content.

Apparatus Used

(A) Dielectrometer

The dielectric constant values have been determined with the help of a Dielectrometer (2), designed and fabricated by one of us (K.K.S.).

(B) Dielectric Cell [2] *(Type PD-797)*

The cell was supplied by Haardt and Co., G.M.B.H., West Germany. It contains two measuring systems, both being concentric cylindrical plates of nearly equal dimensions (capacities: 5.33 pF and 5.4 pF) located one above the other in a glass tube. The two systems can be separately connected to the Dielectrometer by the help of a switch. Figure 1 gives the sketch of the cell.

Chemicals

The following liquids were chosen for the calibration of the dielectric cell.

Cyclohexane (L.R., B.D.H.) was fractionally distilled and the middle cut was dried over sodium which was subsequently distilled (b.p. 80 °C).

Carbon tetrachloride (A.R., B.D.H.) was distilled over sodium and the middle cut (b.p. 76.5 °C) was collected for use.

Benzene (E. Merck) was distilled once and the middle fraction (b.p. 80 °C) was further crystallized before use.

Decalin (Reidel, Pure Grade) was used as such.

Their accepted values for dielectric constant at 20 °C are 2.023, 2.238, 2.284, and 2.160 respectively.

Experimental

The cell is first calibrated with substances of known dielectric constant values. This is done by filling the cell consecutively with liquids of known values and noting the dielectrometer readings for the upper measuring system. A plot of these readings against the dielectric constant values gives the calibration curve, shown in Fig. 2. Next, the cell is filled up to well above the upper measuring system with decalin (or any other non-polar substance of low dielectric constant) and the dielectrometer settings are noted for the upper as well as the lower measuring systems. A few drops of nitrobenzene (or any other polar substance of high dielectric constant) are then added into the cell which is shaken thoroughly. Again the dielectrometer settings for the upper and the lower systems are noted. This procedure is repeated several times by adding more and more nitrobenzene. A graph is then plotted with the dielectrometer readings for the upper system as abscissa and the differences of readings between the upper and lower settings as ordinate. This graph, called the compensation curve, should be a straight line, shown in Fig. 1.

Lastly, the cell is filled with decalin and enough of powdered sample is added into the cell so as to cover the lower measuring system. After the solid particles of the sample settle down and the liquid in the upper measuring system becomes clear, the dielectrometer readings for both the measuring systems are taken. Thereafter, a small amount of nitrobenzene is added into the cell which is shaken thoroughly. After the powder settles down, the dielectrometer readings for both the systems are again noted. This procedure is repeated a few more times by adding further quantities of nitrobenzene into the cell. The plot of dielectrometer readings for the upper system against the differences in readings between the two sys-

---

[1]Present address: Physics Department, York College, York, Pennsylvania.

[2]The authors are grateful to Dr. Bal Krishna of Allahabad University, Allahabad, India, for lending the cell.

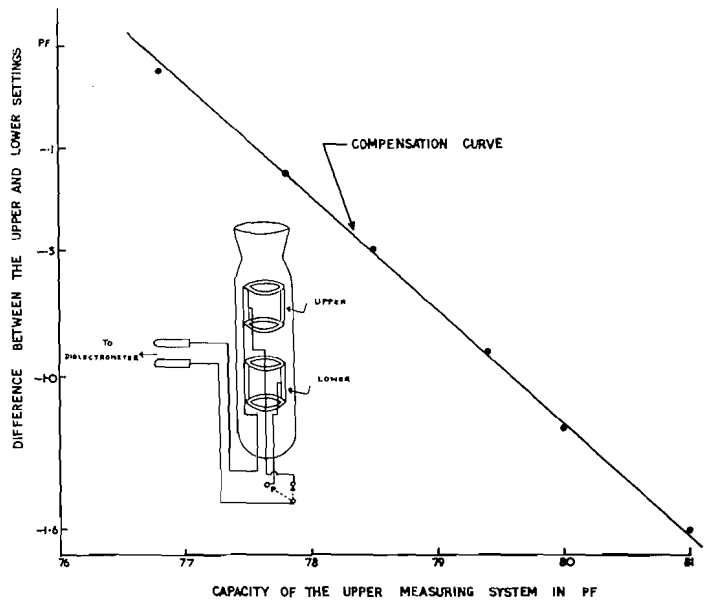

FIG. 1. Variation of the difference between the upper and lower systems with the dielectric constant of the immersion mixture.

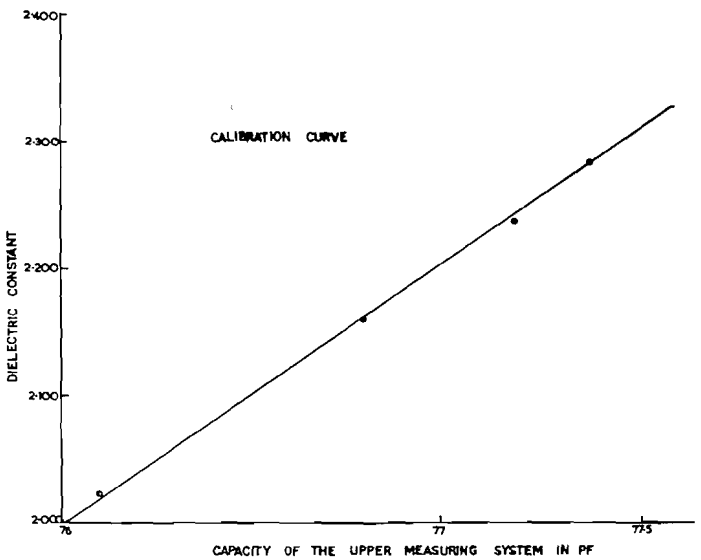

FIG. 2. Variation of the capacitance of the upper measuring system with the known dielectric constants.

tems should also be a straight line and is called the analysis curve, shown in Fig. 3. The scale used for this curve should be the same as that for the compensation curve. It may be mentioned that the analysis curves for all the substances are found to be straight lines.

The point of intersection of the analysis curve with the compensation curve indicates graphically when the capacity of the measuring cell, filled with the immersion liquid, is equal to the capacity of the measuring cell with the powder sample immersed in the immersion mixture. The abscissa value for the point of intersection of these two curves is noted and corresponding value of dielectric constant is obtained from the calibration curve.

All the observations[3] were made at 20 °C. Table 1 lists the experimental substances, their manufacturers, melting points whenever it could be determined, and the measured values of dielectric constant.

[3]These measurements were made in the Department of Physics of Panjab University, Chandigarh, India.

Can. J. Chem. Downloaded from www.nrcresearchpress.com by 210.87.254.5 on 09/05/12
For personal use only.

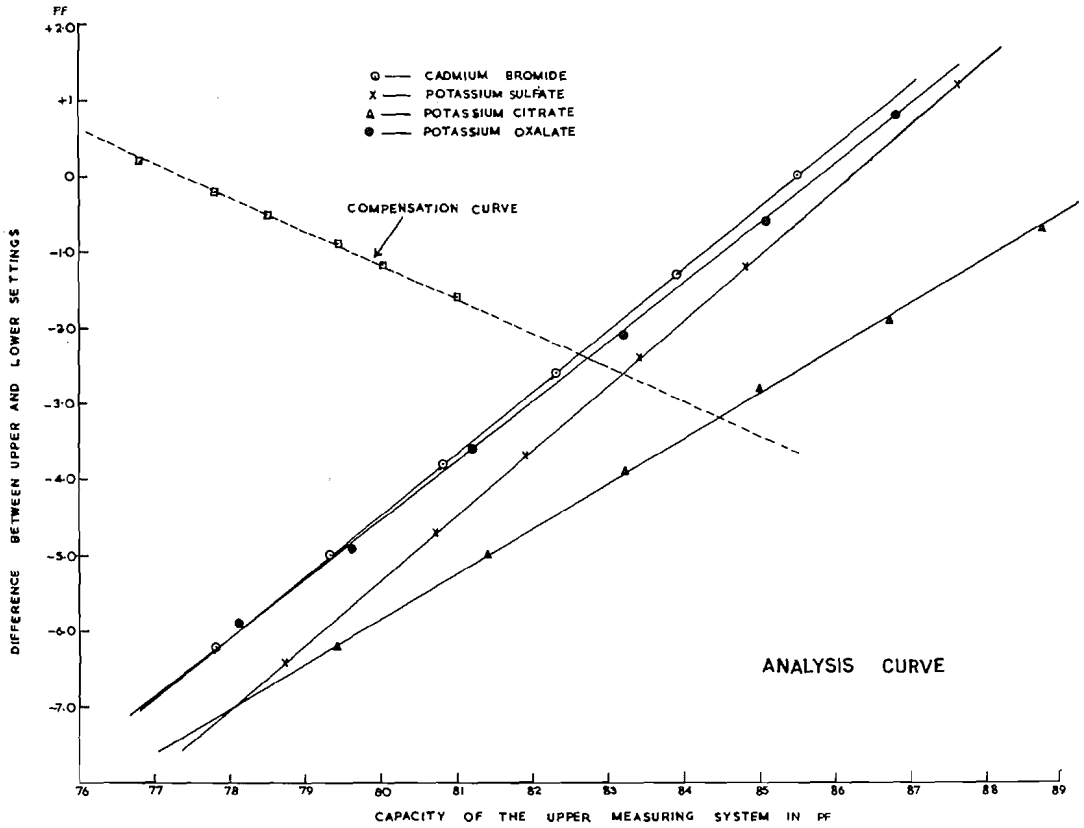

FIG. 3. Variation of the difference between the upper and lower systems with the dielectric constant of the immersion mixture containing powder.

TABLE 1

Dielectric constants of substances under study

Substance	Source	Melting point (°C)		Dielectric constant
		Observed	Literature	
Potassium nitrate	Merck			2.78
Boric acid	A.R., B.D.H.			2.34
Urea	May & Baker	132.5	132.7	2.73
Diaminoethanetetraacetic acid	L.R., B.D.H.			2.76
Triphenylamine	Dr. Theodor Schuchardt (West Germany)	127.0	126.5	2.46
Tribenzylamine	Fluka (Switzerland)	92.0	92.0	2.56
Tetrabutylammonium iodide	Dr. Theodor Schuchardt	144.0	—	2.41
Tetraethylammonium iodide	Dr. Theodor Schuchardt			2.51
Aluminum potassium sulfate	L.R., B.D.H.			3.36
N,N,N′,N′-Tetramethyl-*p*-phenylenediamine dihydrochloride	Dr. Theodor Schuchardt			4.18
Cadmium bromide	L.R., B.D.H.			3.34
Potassium sulfate	Merck			3.46
Potassium citrate	L.R., B.D.H.			3.72
Potassium oxalate	L.R., B.D.H.			3.36
p-Chloroaniline	Dr. Theodor Schuchardt	70	70–72	3.12
p-Toluidine	German (repacked)			2.65
Lithium carbonate	L.R., B.D.H.			2.73
Benzophenone	Dr. Theodor Schuchardt	48.5	—	2.95

Can. J. Chem. Downloaded from www.nrcresearchpress.com by 210.87.254.5 on 09/05/12
For personal use only.

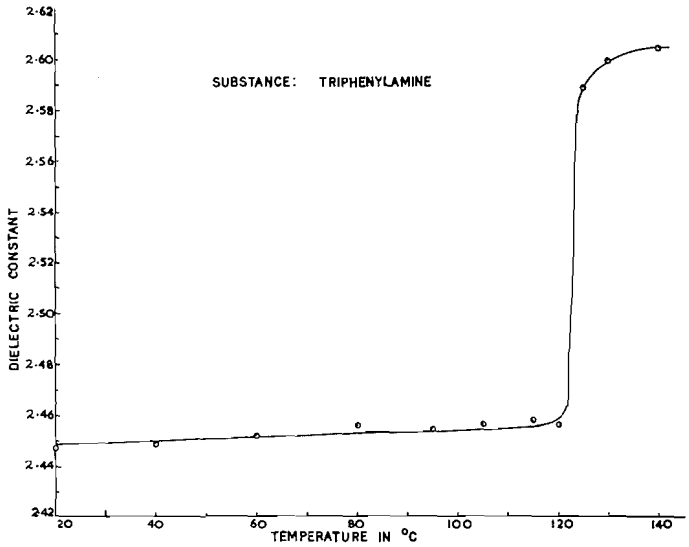

FIG. 4. Variation of dielectric constant with temperature for triphenylamine.

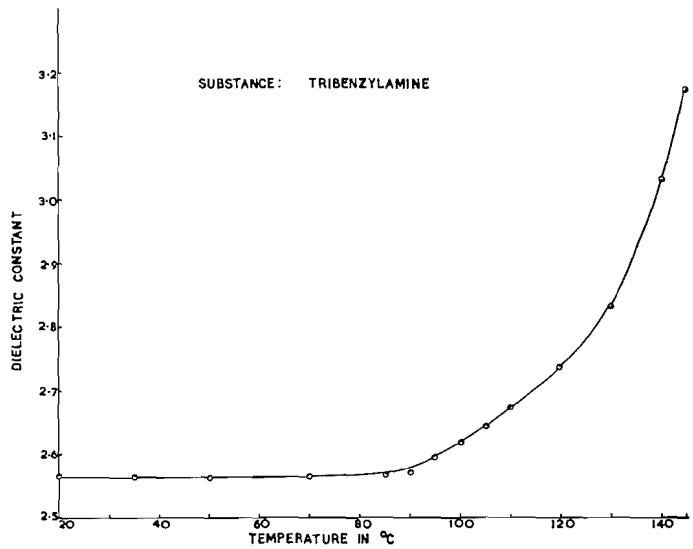

FIG. 5. Variation of dielectric constant with temperature for tribenzylamine.

Discussion

The air-capacity of the lower cell is slightly greater than that of the upper cell. For liquids, having lower values of dielectric constant, the lead-capacitances are not negligible in comparison to the air-capacitances of the cells. The measured capacitance of the upper system, therefore, shows a greater value than the lower system which makes the difference a positive number. As we increase the dielectric constant of the liquid-mixture, the lead-capacity starts getting less and less significant which makes the difference a negative quantity. Obviously, therefore, this method would give slightly higher values for powders having large values of dielectric constant, because the effective lead-capacity of the lower system, having the dielectric material, will not be negligible. Another limiting factor is the solubility of the experimental substance in the immersion mixture. The sample must exist in the solid state

Can. J. Chem. Downloaded from www.nrcresearchpress.com by 210.87.254.5 on 09/05/12
For personal use only.

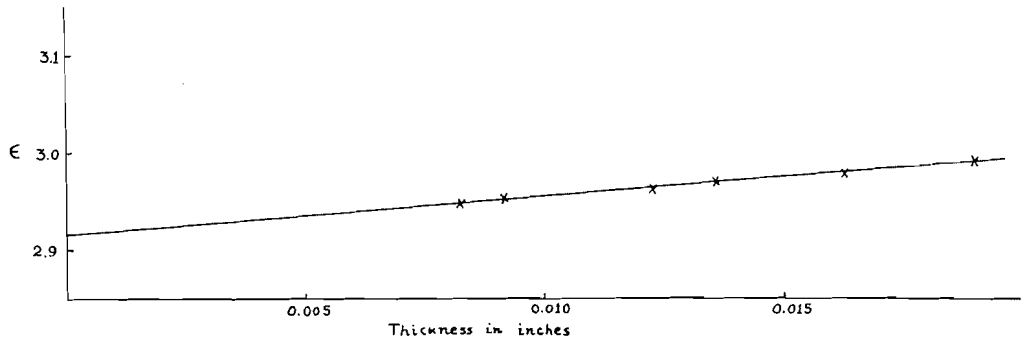

FIG. 6. Dielectric constant of benzophenone.

(covering the lower system) while the measurements are being made. Its slight solubilization during shaking of the cell would not affect the results as the dielectric constant of the immersion mixture is varied uniformly through the entire region of the cell. If the substance has a tendency to dissolve during the time of measurements, then the analysis curve would not be a straight line.

The dielectric constants of triphenylamine and tribenzylamine, which could easily be melted in the laboratory, were also determined at different temperatures by using a simple cylindrical cell (3). At freezing points, these substances show values of 2.45 and 2.56 (see Figs. 4 and 5) which agree with those obtained by the immersion method, *i.e.* 2.46 and 2.56. Bedard *et al.* in this laboratory, made a series of benzophenone wafers of varying thicknesses and measured their dielectric constants by another method (4). His observations are shown in Fig. 6. His extrapolated value of dielectric constant is 2.916 as against 2.95 obtained by the immersion method. In consideration of the fact that benzophenone is the substance among those examined which has an appreciable, though slight, solubility in decalin it appears that there is much to recommend the immersion method for determination of the dielectric constant of solids to high precision.

Conclusions

The immersion method gives reasonably good values of dielectric constant of solids. It should be considered as alternative, if not preferable to other methods now in use. The limitation of the immersion method is undue solubility of the candidate substance in the immersion medium.

1. VON S. KNOKE. Z. Elektrochem. **43**, 749 (1937).
2. J. K. VIJ and K. K. SRIVASTAVA. Indian J. Pure Appl. Phys. 7, 394 (1969).
3. P. K. SHARMA and K. K. SRIVASTAVA. Oyo Denki Kenkyusho Iho, Japan, **16**, 53 (1964).
4. M. BEDARD, H. HUBER, J. L. MYERS, and G. F WRIGHT. Can. J. Chem. **40**, 2278 (1962).

Can. J. Chem. Downloaded from www.nrcresearchpress.com by 210.87.254.5 on 09/05/12
For personal use only.

Nuclear magnetic resonance study of anions derived from some carbon acids

C. A. FYFE
Chemistry Department, University of Guelph, Guelph, Ontario

AND

A. ALBAGLI AND ROSS STEWART
Chemistry Department, University of British Columbia, Vancouver 8, British Columbia

Received June 22, 1970

High resolution n.m.r. spectroscopy has been used to investigate the interaction of several nitrophenylmethanes with base and to characterize the species thus produced. In hexamethylphosphoramide (HMP) containing sodium methoxide, the n.m.r. spectra reveal that the anions present are formed by simple proton loss and this enables the u.v. spectra of these carbanions to be assigned. In less basic systems u.v. absorption occurs at lower wavelengths and n.m.r. spectroscopy reveals the presence of radical-anions.

Previously observed spectral shifts brought about by solvent changes are thought to be due in whole or in part to the formation of radical anions and/or radicals. These are formed by electron transfer from carbanion to a neutral molecule of the nitro compound; this process is particularly important under less basic conditions, which cause the nitro compound to be only partly dissociated.

Canadian Journal of Chemistry, **48**, 3721 (1970)

Can. J. Chem. Downloaded from www.nrcresearchpress.com by 210.87.254.42 on 09/05/12
For personal use only.

Introduction

Carbon acids, such as those based on the fluorene, 4,4′-dinitrodiphenylmethane, and 4,4′-4″-trinitrotriphenylmethane moieties, have been widely used as indicators and as the basis of acidity scales (1–7).

However, different pK_a values and different u.v. spectral characteristics have been reported by different groups of workers; λ_{max}, in particular, is found to be markedly solvent dependent (Table 1). The purpose of the present study was to use high resolution n.m.r. to characterize the ionic species formed by the interaction of these acids with base, and to thus determine their u.v. spectral parameters. Hexamethylphosphoramide (HMP), which provides with hydroxide ion extremely basic systems, was used as solvent in most cases. It was found that side reactions became more important in less basic systems, such as those obtained with dimethyl sulfoxide. The results for the different carbon acids are quite diagnostic and will be discussed individually.

Experimental

The n.m.r. spectra were recorded at 60 MHz on a JEOL C-60H spectrometer and at 100 MHz on a Varian H.A.-100 spectrometer. Chemical shifts are reported in p.p.m. from an internal tetramethylsilane reference. Calculated spectra were obtained using a copy of the program LAOCOON III suitably modified for use on an I.B.M. 360/70 computer. The e.s.r. spectra were recorded on a Varian E3 spectrometer. The u.v. spectra were measured using matched cells on a Cary 16 spectrometer. The compounds used have been previously described and had melting points in agreement with published values (1).

Results

Section A. 4,4′-Dinitrodiphenylmethane (1) and Derivatives

The n.m.r. spectrum of a 0.8 *M* solution of **1** in HMP consists of a sharp resonance at $\delta = -4.45$ (relative intensity 1) due to the two methylene hydrogens, and an AA′XX′ multiplet (relative intensity 4) centered at $\delta = -8.0_4$ due to the aromatic ring hydrogens (Fig. 1A). The addition of less than one equivalent of anhydrous sodium methoxide to this solution gives an intense green coloration and causes a decrease in the intensity of the spectrum of the acid substrate and the appearance of a new spectrum at higher fields (Fig. 1B). Both spectra appear simultaneously and are quite sharp, indicating a relatively slow rate of exchange between the two species, and also the absence of any radicals which could exchange with either. As judged by the intensity of the aromatic resonances, the conversion is, within experimental error, quantitative. When slightly more than one equivalent of base is added, there is complete conversion into the second species (Fig. 1C). The new spectrum, consisting of a sharp resonance at $\delta = -5.4_4$ (relative intensity 1) and an AA′XX′ multiplet centered at $\delta = -7.2_7$ (relative intensity 8), $J_{AA'} = J_{XX'} = 2.1$, $J_{AX} = J_{A'X'} = 8.0$, $\nu_0\delta = 81$ Hz, is in agreement

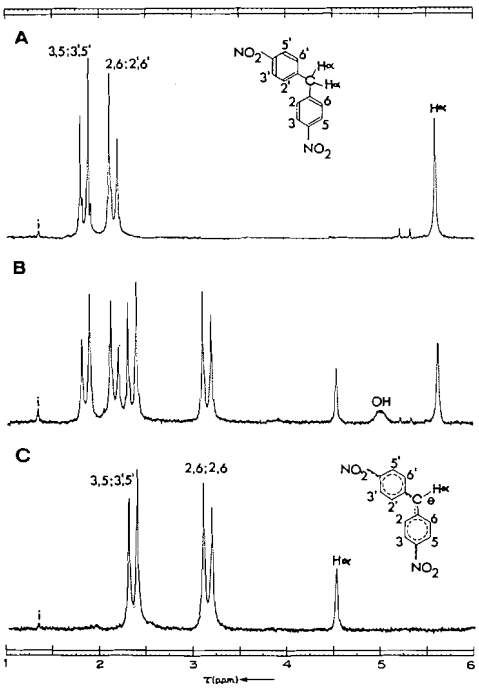

FIG. 1. The 100 MHz n.m.r. spectra of: (A) A 0.8 *M* solution of **1** in HMP. (B) This solution after the addition of one-half an equivalent of anhydrous sodium methoxide. (C) This solution after the addition of one equivalent of anhydrous sodium methoxide.

with the formation of an anion by proton removal from the α-carbon atom as indicated in Fig. 1C.

The electronic structure of the ion can be represented by the principal resonance forms **2**, **3**, and **4** or by the single formulation **5** where both of the phenyl—C_α bonds have some double bond character, and the negative charge is delocalized

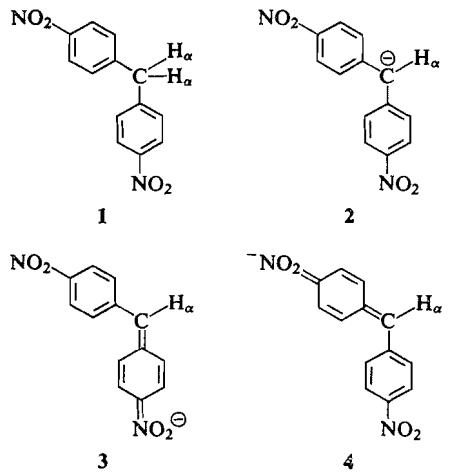

1 **2**

3 **4**

over the whole system. The upfield shift in the aromatic resonances observed in going from the substrate to the ion is in accord with the distribution of the negative charge into the rings.

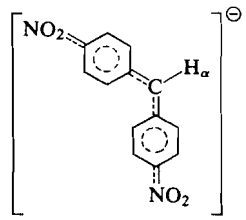

5

If the partial double bond character of the C_α—phenyl bonds indicated in **5** were large enough to restrict the rotation of the phenyl groups on an n.m.r. time scale, the aromatic resonances would appear as any ABXY spectrum. That such a spectrum is not observed (Fig. 1C), indicates that the barrier to rotation effected by the charge delocalization is not large enough at room temperature to be detectable by n.m.r., but not necessarily that there has been no effect. Restriction of rotation of this type, caused by delocalization into an aromatic ring system of a charge formally localized on a substituent has been observed previously in the anions of picramides (8, 9), *p*-nitrophenylacetonitrile (10, 11) and other compounds (11). That it does not occur in the present case may be due to the much larger extent to which the charge is delocalized. Hückel molecular orbital (H.m.o.) calculations employing the heteroatom parameters used by Caveng and Zollinger (12) show a decrease in the bond order of the C_α—phenyl bond from 0.641 in the carbanion of *p*-nitrophenylacetonitrile to 0.558 in the carbanion of **1**, in agreement with the trend indicated by the n.m.r. data. Identical n.m.r. results are obtained when a 0.05 *M* solution is used. On the basis of this evidence for the absence of side reactions and the quantitative conversion, the u.v. spectral parameters were determined directly from these solutions using short path-length cells (0.1 and 0.01 mm). Because of the large extinction coefficient, dilution by a factor of about ten was necessary for accurate measurements. After recording the spectrum, a check was made to ensure that additional base did not increase the absorption. Since the profile of the spectrum was unchanged it was assumed that a quantitative conversion to the anion had occurred, as indicated by the n.m.r. study of the

Can. J. Chem. Downloaded from www.nrcresearchpress.com by 210.87.254.42 on 09/05/12
For personal use only.

Can. J. Chem. Downloaded from www.nrcresearchpress.com by 210.87.254.42 on 09/05/12
For personal use only.

more concentrated solution. The spectral parameters found were: $\lambda_{max} = 787$ nm, $\varepsilon_{max} = 58\,300$ l mole^{-1} cm^{-1}.

Somewhat different results are obtained when the solvent system is altered. Thus, the addition of 10–20% methanol to a solution containing a mixture of ion and substrate in HMP (which already contains a small amount of methanol liberated in the formation of the ion) causes substantial broadening of the spectrum of the substrate but does not affect the spectrum of the ion. This is possibly a consequence of exchange between the substrate and radical-anions produced in the system. At higher methanol concentrations there is severe broadening and eventual disappearance of both spectra.

The addition of anhydrous sodium methoxide to a 0.6 *M* solution of **1** in DMSO causes slight broadening of the resonances of the neutral substrate and gives rise to a new spectrum which can be assigned to the ion; H_α at $\delta = -5.61$ and the aromatic protons as an AA′XX′ spectrum centered at $\delta = -7.25$ and with $J = 8.5$, $\nu_0\delta = 68$ Hz. Further addition of base increases the concentration of the ionic species to about 30–40%. Beyond this point, further addition of base causes extreme broadening and eventual disappearance of both spectra, possibly again the consequence of exchange reactions with paramagnetic species.

Identical results were obtained from analogs of **1** which are substituted on C_α with a methyl or phenyl group. Neither of these compounds shows any evidence for restricted rotation, which makes less likely the possibility that the symmetrical spectra observed for the parent compound are due to fortuitously identical chemical shifts within the 2,6- and 3,5-ring hydrogen pairs. There is a general similarity in the n.m.r. and u.v. spectral parameters for all the ions, consistent with their having a common electronic basis.

Section B. 3,4′-Dinitrodiphenylmethane (6)

The n.m.r. spectrum of a 0.7 *M* solution of **6** in HMP shows a sharp resonance at $\delta = -4.43$ (relative intensity 1) due to the two methylene protons, and a series of lines at low field (relative intensity 4) due to the two aromatic rings (Fig. 2A). Of these, the resonances due to the 4′-ring can be picked out owing to their symmetry. They consist of an AA′XX′ multiplet centered at $\delta = -8.05$ with $J_{AA'} = 2.2$, $J_{XX'} = 2.2$, $J_{AX'} = J_{A'X} = 0.5$, $J_{AX} = J_{A'X'} = 8.2$ and $\nu_0\delta_{AX} = 46.1$ Hz. The addition of an equimolar quantity of anhydrous sodium methoxide to this solution causes the appearance of a new spectrum at higher fields, and a broadening and decrease in intensity of the substrate peaks until eventually they become one broad absorption superimposed on which is the spectrum of the second species (Fig. 2B). Addition of more base causes the complete disappearance of the substrate spectrum without the second spectrum attaining the full intensity expected. In some experiments there was also broadening of the spectrum of the second species. These effects could be reversed by the passage of oxygen through the system, and are again thought to be due to the presence of paramagnetic species.

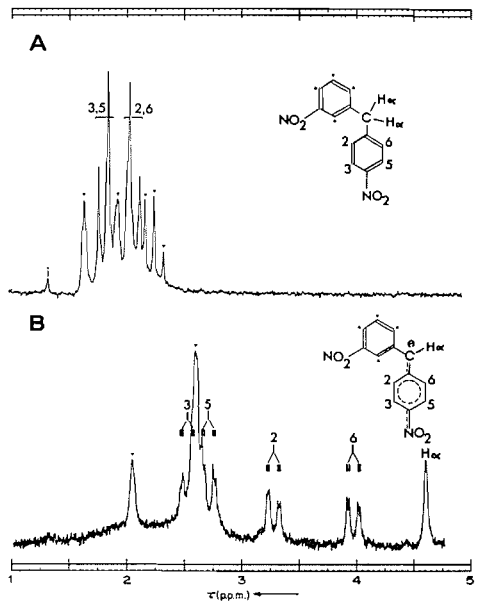

FIG. 2. The 100 MHz n.m.r. spectra of: (A) A 0.7 *M* solution of **6** in HMP. (B) This solution after the addition of one equivalent of anhydrous sodium methoxide.

The second spectrum can be rationalized in terms of the ion **7** as shown in Fig. 2B, where the resonances at $\delta = -7.95$ and $\delta = -7.38$ are assigned to the 2 and 4, 5, 6 hydrogens of the asymmetrical ring respectively, and the hydrogens of the symmetrical ring are thought to give rise to four "doublets" of major splittings ~9 Hz, and smaller splittings ~2 Hz centered at $\delta = -6.02$, -6.70, -7.26, and -7.44 p.p.m. However, if this is the case, then part of the "doublet" at $\delta = -7.44$ must be considered hidden by the resonances of the second ring. Some evidence in favor of this assignment is that it is possible to produce

almost complete decoupling of the doublet at $\delta = -6.02$ by irradiation of the one centered at $\delta = -7.26$ and vice versa, and it is also possible to achieve partial decoupling of the multiplet at $\delta = -6.7$, by irradiation at $\delta = -7.44$.

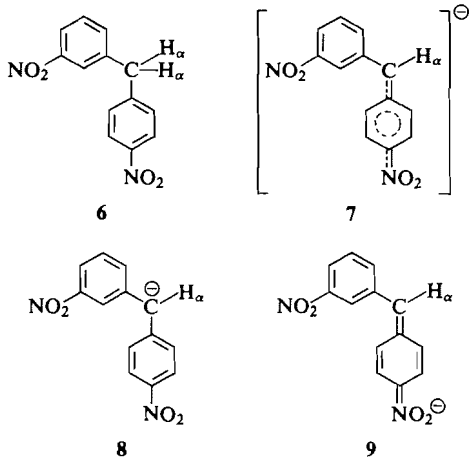

6 **7**

8 **9**

Implicit in the assignment discussed above and indicated in Fig. 2B, is the postulate that, in this case, there is no longer free rotation on the n.m.r. time scale about the C_α—phenyl bond in the symmetrically substituted ring. This can be rationalized in terms of the electronic structure expected for the ion. The resonance forms which will contribute in the case will be **8** and only a singlet structure **9** where the charge is delocalized into an aromatic ring, due to the inability of the nitro group in the 3 position to delocalize the charge by a mesomeric effect. The subsequent restriction of the negative charge to a single ring system might well give rise to a higher rotational barrier as indicated by the spectrum.

Although, as discussed above, side reactions occur in this system, they seem to be less important in the more dilute solutions. Thus complete conversion to the ion can be effected by the careful stepwise addition of an equivalent of base to a 0.05 *M* solution of the compound in HMP. From this solution, the u.v. spectral parameters can be evaluated and are $\lambda_{max} = 593$ nm, $\varepsilon_{max} = 28\,000$ l mole^{-1} cm^{-1}.

Section C. 4,4′4″-Trinitrotriphenylmethane (9)

The n.m.r. spectrum of a 0.8 *M* solution of **9** in HMP consists of a single resonance at $\delta = -6.60$ due to the methine hydrogen, and an AA′XX′ multiplet centered at $\delta = -8.02$; $J_{AA'} = J_{XX'} = 2.0$, $J_{AX'} = J_{A'X} = 0.5$, $J_{AX} = J_{A'X'} = 8.2$, and $\nu_0\delta_{AX} = 54$ Hz, due to the hydrogens on the three equivalent rings (Fig. 3A). Addition of anhydrous base to this solution causes the appearance of a second spectrum and a decrease in the intensity of the original one (Fig. 3B). The second spectrum consists of a second AA′XX′ multiplet centered at $\delta = 7.56$, with $J_{AA'} = J_{XX'} = 2.0$, $J_{AX'} = J_{A'X} = 0.5$, $J_{AX} = J_{A'X'} = 8.7$ and $\nu_0\delta_{AX} = 50.8$ Hz, and is in agreement with the formation of the ion **10** as indicated in Fig. 3. There is no broadening of either spectrum, and complete conversion to the ion is possible with the addition of further base (Fig. 3B). Similar results are obtained with a 0.05 *M* solution, and on the basis of the complete ionization and absence of side reactions indicated by the n.m.r. spectra, the u.v. spectral parameters of the ion can be determined directly: $\lambda_{max} = 775$ nm, $\varepsilon_{max} = 43\,000$ l mole^{-1} cm^{-1}. In DMSO solution, very similar changes in the n.m.r. spectra are observed, but broadening of the

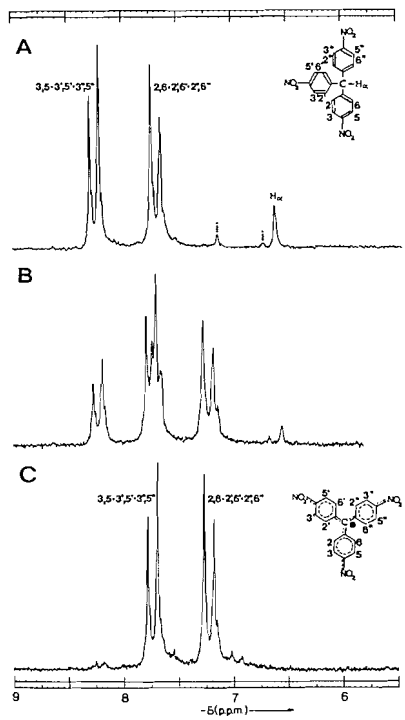

FIG. 3. The 100 MHz n.m.r. spectra of: (A) A 0.8 *M* solution of **9** in HMP. (B) This solution after the addition of 0.6 equivalent of anhydrous sodium methoxide. (C) This solution after the addition of slightly more than one equivalent of sodium methoxide.

Can. J. Chem. Downloaded from www.nrcresearchpress.com by 210.87.254.42 on 09/05/12
For personal use only.

TABLE 1.

The u.v. spectral data of nitrophenylmethanes in strongly basic solutions

	HMP/NaOMe		DMSO/EtOH/NaOEt		MeOH/NaOMe	
Compound	λ_{max}(nm)	ε(l mole^{-1} cm^{-1})	λ_{max}(nm)	ε(l mole^{-1} cm^{-1})	λ_{max}(nm)	ε(l mole^{-1} cm^{-1})
1	787	58 300*	704 707	40 600† 41 900**	534	28 000‡
6	593	28 000*	550 570	31 700† 28 800**	430¶	
9	775	43 400*	707 809 810	19 300† 30 300§ 63 000‖	530	25 600‡

*Values determined in this work in HMP containing sodium methoxide.
†Values determined by Bowden and Stewart (1) in ethanolic DMSO containing 0.01 *M* sodium ethoxide.
‡Values determined by Kroeger and Stewart (2) in methanolic DMSO containing 0.01 *M* sodium methoxide.
§Value determined in this work in DMSO containing sodium methoxide $\varepsilon_{DMSO} \sim 70\%$ of the ε_{HMP}.
‖Value determined by Ritchie and Uschold (3) in DMSO.
¶Value determined in this work in methanolic sodium methoxide; the molar absorptivities are not reported since the compound was ionized to only a small extent.
**Value redetermined in this work in 90% DMSO – ethanol – 0.01 *M* sodium ethoxide.

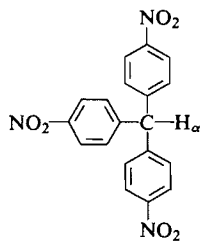

9

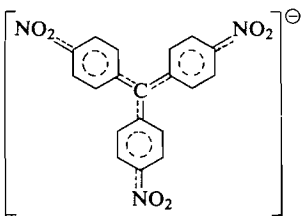

10

spectrum of both the molecule and the ion occurs after the substrate is about 80% ionized. It is difficult to infer from the n.m.r. spectrum of the ion anything about possible barriers to rotation in this case, as the ion is symmetrical about each C_α—phenyl bond.

Discussion

As noted in the introduction, discrepancies exist in values of the spectroscopic parameters of the anions, and the acid dissociation constants of the parent carbon acids as determined by different workers. The λ_{max} and ε_{max} values obtained in the present work by direct measurement are compared with existing literature values from equilibrium measurements in different solvents in Table 1.

The very large changes in λ_{max} in changing from basic methanol to basic DMSO solution recorded in Table 1 for **1** and **9** have also been found in the present work for **6**, and by Ritchie and Uschold for **9** in going from basic ethanol to basic DMSO. The differences shown in Table 1 are too large to be accounted for in terms of solvent effects on the spectral parameters, and an explanation is sought in terms of chemical effects.

In each of the solvent systems quoted in Table 1, it had been assumed that the action of the base on the substrate was that of proton abstraction. In fact, a variety of reactions between aromatic nitro compounds are possible (13), and all give rise to intensely colored solutions.

We find that in systems less basic than HMP–alkoxide, severe line-broadening occurs in the n.m.r. spectra of both ion and substrate, indicative of the formation of radicals.

Russell and Janzen (14) have shown that *o*- and *p*-nitrotoluenes produce radicals and radical-anions in DMSO-*t*-butyl alcohol solutions containing a deficient amount of base.

[1*a*] $O_2NC_6H_4CH_3 + B^- \rightleftarrows O_2NC_6H_4CH_2^- + BH$

[1*b*] $O_2NC_6H_4CH_2^- + O_2NC_6H_4CH_3 \rightleftarrows O_2NC_6H_4CH_2\cdot + O_2NC_6H_4CH_3^{\cdot-}$

The mechanism shown in eqs. 1*a* and *b* is thought to be quite general, the main limiting feature being the availability of unreacted substrate for the second step. The formation of radicals will then be favored for weaker acids and for less basic solvent systems.

In the present work, n.m.r. spectroscopy of solutions of **1**, **6**, and **9** has indicated the presence of radicals in systems that are less basic than HMP–methoxide. The e.s.r. studies of such systems indicate at least a 10^{-4} *M* concentration of radical-anions in solutions containing 10^{-2} *M* substrate. It is thought that the presence of radical-anions (and/or radicals) is a reason for the

Can. J. Chem. Downloaded from www.nrcresearchpress.com by 210.87.254.42 on 09/05/12
For personal use only.

discrepancies noted in Table 1, to the extent that, for the less basic systems, the measurements may in fact be based to a considerable extent on the visible spectra of radical-anions or radicals rather than on carbanions formed by simple proton loss from the carbon acids.

It is obvious from these results that only carbon acids which ionize by simple proton abstraction should be used to determine acidity functions. Information regarding the ionization should be obtained using more than one analytical technique since the traditional method, u.v. spectrophotometry, is inadequate for the identification of the ionization process.

1. K. BOWDEN and R. STEWART. Tetrahedron **21**, 261 (1965).
2. D. J. KROEGER and R. STEWART. Can. J. Chem. **45**, 2163 (1967).
3. C. D. RITCHIE and R. E. USCHOLD. J. Amer. Chem. Soc. **87**, 1721, 2752 (1967); **90**, 2821 (1968).
4. E. C. STEINER and J. M. GILBERT. J. Amer. Chem. Soc. **87**, 382 (1965); **89**, 2751 (1967).
5. (*a*) A. STREITWEISER, JR., E. CIUFFARIN, J. H. HAMMONS, and J. I. BRAUMAN. J. Amer. Chem. Soc. **89**, 59 (1967). (*b*) A. STREITWEISER, JR., E. CUIFFARIN, and J. H. HAMMONS. J. Amer. Chem. Soc. **89**, 63 (1967).
6. R. KUHN and D. REWICKI. Tetrahedron Lett. 3513 (1965), 383 (1964); Liebigs Ann. **706**, 250 (1967).
7. H. RAPOPORT and G. SMOLINSKY. J. Amer. Chem. Soc. **80**, 2910 (1968).
8. K. L. SERVIS. J. Amer. Chem. Soc. **87**, 5495 (1965).
9. M. R. CRAMPTON and V. GOLD. J. Chem. Soc. B, 893 (1966).
10. M. R. CRAMPTON. J. Chem. Soc. B, 85 (1967).
11. C. A. FYFE. Can. J. Chem. **47**, 2331 (1969).
12. P. CAVENG and H. ZOLLINGER. Helv. Chim. Acta, **50**, 866 (1967).
13. E. BUNCEL, A. R. NORRIS, and K. E. RUSSELL. Quart. Rev. London, **22**, 123 (1968).
14. G. A. RUSSELL and E. G. JANZEN. J. Amer. Chem. Soc. **84**, 4153 (1962); **89**, 300 (1967).

Can. J. Chem. Downloaded from www.nrcresearchpress.com by 210.87.254.42 on 09/05/12
For personal use only.

Can. J. Chem. Downloaded from www.nrcresearchpress.com by 210.87.254.42 on 09/05/12
For personal use only.

Organic sulfur compounds. VII.[1] Some reactions of benzothiazine hydroxamic acids

R. T. COUTTS, SHARON J. MATTHIAS, AND (in part) E. MAH and N. J. POUND
Faculty of Pharmacy and Pharmaceutical Sciences, University of Alberta, Edmonton

Received June 15, 1970

Treatment of (3,4-dihydro-4-hydroxy-3-oxo-2*H*-1,4-benzothiazin-2-yl)acetic acid (**1***a*) with sodium hydroxide yields the corresponding lactam, *i.e.* (3,4-dihydro-3-oxo-2*H*-1,4-benzothiazin-2-yl)acetic acid, together with the α,β-unsaturated acid, 3,4-dihydro-3-oxo-2*H*-1,4-benzothiazine-$\Delta^{2,\alpha}$-acetic acid. The 6-methyl- and 6-bromo-derivatives of **1***a* behaved similarly when reacted with sodium hydroxide but when 3,4-dihydro-4-hydroxy-3-oxo-2*H*-1,4-benzothiazine was so treated a more complex reaction occurred.

Methyl (6-bromo-3,4-dihydro-4-hydroxy-3-oxo-2*H*-1,4-benzothiazin-2-yl)acetate was also treated with hydrochloric acid. The two products isolated were (6-bromo-3,4-dihydro-3-oxo-2*H*-1,4-benzothiazin-2-yl)acetic acid and (6-bromo-7-chloro-3,4-dihydro-3-oxo-2*H*-1,4-benzothiazin-2-yl)acetic acid.

The action of hydrochloric acid on 3,4-dihydro-4-hydroxy-7-methyl-3-oxo-2*H*-1,4-benzothiazine also gave two products. One was the corresponding lactam; the other was unexpected and has been tentatively identified as bis[2-(3,4-dihydro-7-methyl-3-oxo-2*H*-1,4-benzothiazine].

Canadian Journal of Chemistry, **48**, 3727 (1970)

Some reference compounds were required to help identify metabolic degradation products of benzothiazine hydroxamic acids. For this reason, derivatives of (3,4-dihydro-4-hydroxy-3-oxo-2*H*-1,4-benzothiazin-2-yl)acetic acid (**1***a*) were reacted with aqueous sodium hydroxide and with dilute hydrochloric acid, and the major products were identified.

When a solution of the acid **1***a* in aqueous sodium hydroxide was heated under reflux, then acidified, three products were isolated, none of which retained the hydroxamic acid group. One product was the lactam, (3,4-dihydro-3-oxo-2*H*-1,4-benzothiazin-2-yl)acetic acid (**2***a*), which was

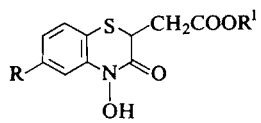

1

	R	R^1
a	H	H
b	Me	H
c	Br	Me
d	Br	H
e	H	Me

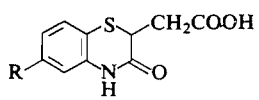

2

	R
a	H
b	Me
c	Br

characterized by means of elemental analysis, m.p., and i.r. data. The mechanism of its formation from **1***a*, which involves a reduction, is not immediately apparent[2] but presumably the hydroxylamine **3** is an intermediate product of the reaction and would be capable of oxidation–reduction. Heller *et al.* (1) explained the reported (2) formation of small quantities of aniline and azoxybenzene by the action of acid on phenylhydroxylamine as due to irrelevant oxidation–reduction of the latter.

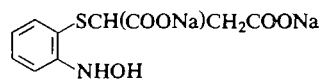

3

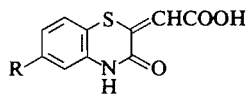

4

R

a H
b Me
c Br

Another product of the action of sodium hydroxide on **1***a* was a yellow solid which analyzed satisfactorily for $C_{10}H_7NO_3S$. Its mass spectrum showed a molecular ion at *m/e* 221 and fragment ions at *m/e* 204, 203, 177, 176, and 175 which are identified as $(M\text{-}OH)^+$, $(M\text{-}H_2O)^+$, $(M\text{-}CO_2)^+$, $(M\text{-}CO_2H)^+$, and $(M\text{-}CO_2H_2)^+$ respectively. The presence of a carbonyl absorption band at 1670 cm^{-1} in the i.r. spectrum of this product was consistent with an α,β-unsaturated carbonyl function. For these reasons, the product was deduced to be 3,4-dihydro-3-oxo-2*H*-1,4-benzothiazine-$\Delta^{2,\alpha}$-acetic acid (**4***a*) and this deduction was confirmed when the same

[1]Part VI see R. T. Coutts *et al.* (12).

[2]A referee suggested that a possible source of reducing power was the formation to some extent of —SH bonds which could form disulfide and, in so doing, would reduce some of the NHOH groups. The referee also suggested that the isolation of the disulfide, **7**, might lend some support to this theory.

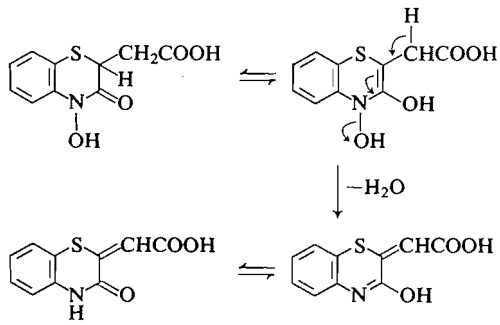

SCHEME 1

compound was obtained by the interaction of *o*-aminothiophenol and acetylene dicarboxylic acid (3). A possible mechanism for the formation of **4***a* from **2***a* can be envisaged (Scheme 1).

The third product of the action of sodium hydroxide on **1***a* was isolated in very low yield and not identified.

In the same manner, the action of sodium hydroxide on (6-methyl-3,4-dihydro-4-hydroxy-3-oxo-2*H*-1,4-benzothiazin-2-yl)acetic acid (**1***b*) yielded (6-methyl-3,4-dihydro-3-oxo-2*H*-1,4-benzothiazin-2-yl)acetic acid (**2***b*) and 6-methyl-3,4-dihydro-3-oxo-2*H*-1,4-benzothiazine-$\Delta^{2,\alpha}$-acetic acid (**4***b*).

When methyl (6-bromo-3,4-dihydro-4-hydroxy-3-oxo-2*H*-1,4-benzothiazin-2-yl)acetate (**1***c*) was dissolved in aqueous sodium hydroxide and the solution was allowed to stand at 20° for 2 days, the only product isolated on acidification of the solution was the corresponding acid **1***d*. When, however, the ester **1***c* was treated with boiling aqueous sodium hydroxide, the two major products were the lactam-acids, (6-bromo-3,4-dihydro-3-oxo-2*H*-1,4-benzothiazin-2-yl)acetic acid (**2***c*) and 6-bromo-3,4-dihydro-3-oxo-2*H*-1,4-benzothiazine-$\Delta^{2,\alpha}$-acetic acid (**4***c*). A third minor product was not identified.

The simpler hydroxamic acid, 3,4-dihydro-4-hydroxy-3-oxo-2*H*-1,4-benzothiazine (**5***a*) was also treated with boiling aqueous sodium hydroxide. A high melting solid precipitated from the basic solution. Its i.r. spectrum showed absorption bands attributable to the CO_2^- anion and to N—H stretching which suggested that reduction had occurred and sodium (*o*-aminophenylthio)acetate (**6**) had been formed. This was confirmed when acidification of a solution of the salt gave 3,4-dihydro-3-oxo-2*H*-1,4-benzothiazine (**5***b*).

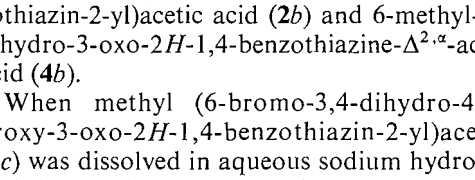

5

	R	R^1
a	OH	H
b	H	H
c	OH	Me
d	H	Me

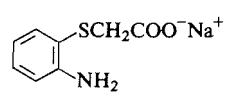

6

The filtrate remaining after the removal of **6** was acidified and yielded two products. One was the lactam (**5***b*) and the other was shown to be 2,2′-diaminodiphenyldisulfide (**7**) by means of its mass spectrum and by comparison with an authentic sample of the diamine.

The bromo-ester **1***c* was also treated with aqueous hydrochloric acid and this yielded two products. Once again, reduction by an unknown mechanism gave the previously described lactam **2***c*. The second product contained chlorine. Previous observations (4) on the action of hydrochloric acid on related compounds permitted the identification of this product as (6-bromo-7-chloro-3,4-dihydro-3-oxo-2*H*-1,4-benzothiazin-2-yl)acetic acid (**8**). The compound analyzed

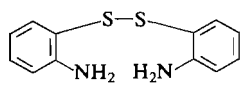

7

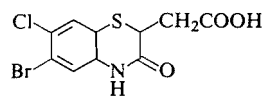

8

satisfactorily for $C_{10}H_7BrClNO_3S$ and i.r. data supported this structure. The mass spectrum of **8** showed groups of ions of *m/e* 339, 337, and 335 $[M]^+$; 321, 319, and 317 $[M\text{-}18]^+$; and 293, 291, and 289 $[M\text{-}46]^+$ which can be explained as illustrated in Scheme 2. Two 1-proton singlets, located at τ 2.35 and 2.67 in the n.m.r. spectrum of the chlorinated product, indicated that the two hydrogen atoms in the aromatic ring were in positions para to one another, and in agreement with the postulated structure (**8**).

It was also of interest to investigate the action of hydrochloric acid on 3,4-dihydro-4-hydroxy-7-methyl-3-oxo-2*H*-1,4-benzothiazine (**5***c*) since nucleophilic attack by chloride ion, which occurs at carbon-7 in other benzothiazine hydroxamic acids (4), would not be possible in this instance. Two solid products were isolated from this reaction. The major one was the lactam, (**5***d*), the structure of which was confirmed by elemental analysis, n.m.r. spectroscopy, and mass spectral evidence. The mass spectrum displayed abundant

Can. J. Chem. Downloaded from www.nrcresearchpress.com by 210.87.254.42 on 09/05/12
For personal use only.

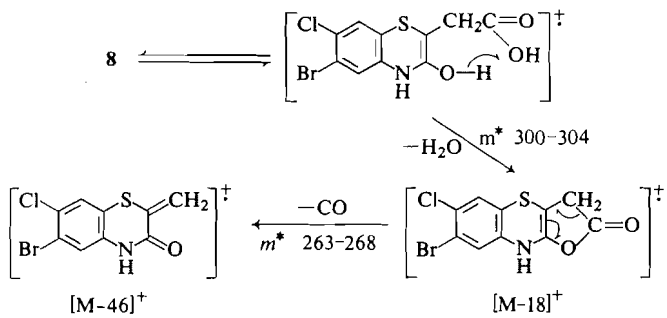

SCHEME 2

ions of *m/e* 179, 150, and 134 which correspond to M^+, $[M\text{-}HCO]^+$, and $[M\text{-}HCS]^+$ fragments. Similar ions are observed (5) in the spectrum of **5***b*. The minor product analyzed satisfactorily for $C_{18}H_{16}N_2O_2S_2$. Its n.m.r. spectrum showed peaks which corresponded to three methyl group protons, three aromatic protons, an NH proton, and a CH proton. Its mass

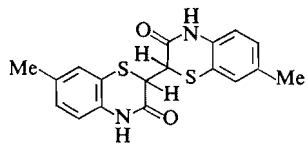

9

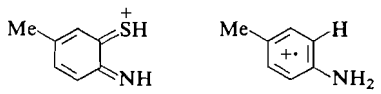

10 **11**

spectrum showed only four ions of relative abundance greater than 10%, *i.e. m/e* 356, 138, 107, and 18, and accurate mass measurements confirmed that the first three of these were $[C_{18}H_{16}N_2O_2S_2]^+$, $[C_7H_8NS]^+$, and $[C_7H_9N]^+$. From this evidence, it is concluded that the minor product is probably bis[2-(3,4-dihydro-7-methyl-3-oxo-2*H*-1,4-benzothiazine] (**9**). The two fragment ions $[C_7H_8NS]^+$ and $[C_7H_9N]^+$ are the results of complex rearrangements and presumably possess structures **10** and **11**.

Experimental

Melting points are uncorrected. The i.r. spectra were measured on KBr discs except where indicated with a Beckman IR-10 spectrophotometer. Mass spectra were measured with an A.E.I. MS-9 or MS-12 spectrometer at an ionization potential of 70 eV using the direct insertion technique, and n.m.r. spectra were recorded on a Varian A-60 spectrometer using DMSO-d_6 as solvent and TMS as standard.

The α-(*o*-nitrophenylthio)-esters (**12***a*, *b*, and *c*), used in the syntheses of the hydroxamic acids described below, were prepared by the literature (6) method.

Preparation of Hydroxamic Acids (1)

General Method

A solution of sodium borohydride (1.0 g) in water (5 ml) was added to a suspension of palladium(10%)-on-charcoal (0.1 g) in water (5 ml). Dioxane (5 ml) was added to the mixture and nitrogen gas bubbled through it (1–2 min). The substituted α-(*o*-nitrophenylthio)-ester (1.0 g), dissolved in a minimum of dioxane, was added to the reduction mixture dropwise over a period of 15–30 min. Nitrogen gas was bubbled through the reaction mixture during the addition of ester and for an additional 15 min.

The reaction mixture was filtered and the charcoal washed with portions of water and dioxane. The washings were added to the filtrate and the filtrate acidified with concentrated hydrochloric acid, keeping the temperature below 30°. The solid hydroxamic acid which precipitated was removed by filtration. Additional product was obtained by extraction of the filtrate with ether, re-extracting the ether layer with 10% sodium hydroxide solution, and acidifying the basic layer with concentrated hydrochloric acid, keeping the temperature below 30°. If no precipitate formed, the acidic solution was extracted with ether, the ether layer was dried (Na_2SO_4) and evaporated to yield the hydroxamic acid.

If no precipitate formed when the original filtrate was acidified, the acidified filtrate was subjected to the same extraction procedure as that described immediately above.

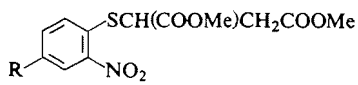

12

R

a H

b Me

c Br

(3,4-Dihydro-4-hydroxy-3-oxo-2H-1,4-benzothiazin-2-yl)acetic Acid (1a)

When dimethyl α-(4-methyl-2-nitrophenylthio)succinate (**12***a*) (3 g) was reduced using the general method, the pale yellow product (1.51 g), m.p. 190–192° (aqueous MeOH) was not the methyl ester **1***e*. Hydrolysis had

Can. J. Chem. Downloaded from www.nrcresearchpress.com by 210.87.254.42 on 09/05/12
For personal use only.

Can. J. Chem. Downloaded from www.nrcresearchpress.com by 210.87.254.42 on 09/05/12
For personal use only.

occurred during the reduction and the title compound, lit. (7) m.p. 186–188°, was formed. The i.r. spectrum: 1640 (hydroxamate C=O), 1690 (acid C=O), 3300 cm^{-1} (broad), (hydrogen bonded OH).

*(6-Methyl-3,4-dihydro-4-hydroxy-3-oxo-2H-1,4-benzothiazin-2-yl)acetic Acid (**1b**)*

This compound was obtained similarly as a pale yellow solid (0.71 g), m.p. 187–188° when dimethyl α-(4-methyl-2-nitrophenylthio)succinate (**12***b*) (2 g) was reduced using the general method. The i.r. spectrum: 1650 (hydroxamate C=O), 1685 (acid C=O), 3000 cm^{-1} (broad) (hydrogen bonded OH).

Anal. Calcd. for $C_{11}H_{11}NO_4S$: C, 52.16; H, 4.38. Found: C, 52.44; H, 4.44.

*Methyl (6-Bromo-3,4-dihydro-4-hydroxy-3-oxo-2H-1,4-benzothiazin-2-yl)acetate (**1c**)*

This compound was obtained as a white solid (1.38 g), m.p. 159–161° when dimethyl α-(4-bromo-2-nitrophenylthio)succinate (**12***c*) (2 g) was reduced by the general method. Literature (6) m.p. 165–167°. The i.r. spectrum: 1740 (ester C=O), 1665 (hydroxamate C=O), 3450 cm^{-1} (broad) (hydrogen bonded OH).

Action of Alkali on Benzothiazine Hydroxamic Acids

*(a) 3,4-Dihydro-4-hydroxy-3-oxo-2H-1,4-benzothiazin-2-yl)acetic Acid (**1a**)*

This hydroxamic acid (1.6 g) was dissolved in 10% sodium hydroxide (50 ml) and heated under reflux for 1 h. The dark red reaction mixture was cooled and acidified carefully with concentrated hydrochloric acid and product A (0.927 g) precipitated. The filtrate was allowed to stand and product B (0.08 g) precipitated. The filtrate from product B was then extracted with ether, the ether layer dried (Na_2SO_4) and evaporated to yield product C (0.25 g).

None of these products gave a violet color with ethanolic ferric chloride solution.

Product A was repeatedly recrystallized from methanol to give 3,4-dihydro-3-oxo-2*H*-1,4-benzothiazine-$\Delta^{2,\alpha}$-acetic acid (**4***a*) as a yellow–green powder, m.p. 280–282°, lit. (3) m.p. 278° (d). The i.r. spectrum was identical to that of an authentic sample of **4***a*, prepared by the lit. (3) method.

Anal. Calcd. for $C_{10}H_7NO_3S$ (mol. wt. 221): C, 54.29; H, 3.19; N, 6.33. Found ((mass spectrum) 221): C, 54.49; H, 3.49; N, 6.52.

Product C was recrystallized from aqueous methanol to give (3,4-dihydro-3-oxo-2*H*-1,4-benzothiazin-2-yl)-acetic acid (**2***a*) as a white powder, m.p. 189–191°, lit. (8) m.p. 195–196°.

The i.r. spectrum: 1665 (amide C=O), 1695 (acid C=O), 3200 cm^{-1} (NH).

Anal. Calcd. for $C_{10}H_9NO_3S$: C, 53.79; H, 4.06; N, 6.27; S, 14.36. Found: C, 53.60; H, 4.07; N, 6.42; S, 13.88.

Minor product B was not investigated further.

*(b) (6-Methyl-3,4-dihydro-4-hydroxy-3-oxo-2H-1,4-benzothiazin-2-yl)acetic Acid (**1b**)*

A solution of this hydroxamic acid (1 g) in 10% sodium hydroxide (50 ml) was heated under reflux for 1 h, cooled, and acidified with concentrated hydrochloric acid. Product A (0.29 g) precipitated. The filtrate was allowed to stand and product B (0.333 g) formed and was removed. Extraction of the resulting filtrate with ether yielded only a negligible amount of product, which was discarded.

Neither of the products A or B gave a violet color with ethanolic ferric chloride solution.

Product A was recrystallized from methanol to yield (6-methyl-3,4-dihydro-3-oxo-2*H*-1,4-benzothiazine-$\Delta^{2,\alpha}$-acetic acid (**4***b*) as a yellow powder, m.p. 307–309° (dec.).

The i.r. spectrum: 1659 (α,β-unsaturated C=O), 3300–2700 cm^{-1} (OH, NH).

Anal. Calcd. for $C_{11}H_9NO_3S$ (mol. wt. 235): C, 56.16; H, 3.86; N, 5.95. Found ((mass spectrum) 235): C, 55.66; H, 3.90; N, 5.57.

Product B was repeatedly crystallized from methanol to give (6-methyl-3,4-dihydro-3-oxo-2*H*-1,4-benzothiazin-2-yl)acetic acid (**2***b*) as a cream colored powder, m.p. 237–239°. The i.r. spectrum: 1670 (amide C=O), 1700 (acid C=O), broad absorption 2800–3300 cm^{-1} (OH) with peak at 3280 cm^{-1} (NH).

Anal. Calcd. for $C_{11}H_{11}NO_3S$: C, 55.68; H, 4.67; N, 5.90. Found: C, 56.24; H, 4.57; N, 6.24.

*(c) Methyl (6-Bromo-3,4-dihydro-4-hydroxy-3-oxo-2H-1,4-benzothiazin-2-yl)acetate (**1c**)*

(*i*) The title hydroxamic acid (0.55 g) was dissolved in 10% sodium hydroxide (30 ml) and the solution allowed to stand at room temperature for 43 h. The solution was clarified by filtration and the filtrate acidified carefully with concentrated hydrochloric acid to precipitate (6-bromo-3,4-dihydro-4-hydroxy-3-oxo-2*H*-1,4-benzothiazin-2-yl)acetic acid (**1***d*) as a cream colored solid (0.31 g) m.p. 215–217° (MeOH). This product gave a violet color with ethanolic ferric chloride solution. The i.r spectrum: 1643 (hydroxamate C=O), 1700 (acid C=O), 3200 cm^{-1} (broad, OH).

Anal. Calcd. for $C_{10}H_8BrNO_4S$: C, 37.75; H, 2.52; N, 4.40; S, 10.07. Found: C, 37.91; H, 2.63; N, 4.41; S, 9.66.

(*ii*) The hydroxamic acid (2.3 g) was dissolved in 10% sodium hydroxide solution (100 ml) and heated under reflux for 45 min. The reaction mixture was cooled and acidified carefully with concentrated hydrochloric acid and product A (1.5 g) precipitated. The filtrate was allowed to stand and product B (0.479 g) separated as a pale yellow solid. The filtrate from product B was then extracted with ether, the ether layer dried (Na_2SO_4) and evaporated to yield product C (0.169 g) as a brown solid.

None of these products gave a violet color with ethanolic ferric chloride solution.

Product A was repeatedly crystallized from aqueous methanol to give 6-bromo-3,4-dihydro-3-oxo-2*H*-1,4-benzothiazine-$\Delta^{2,\alpha}$-acetic acid as an orange powder (**4***c*), m.p. 244–246°. The i.r. spectrum: 1665 (α,β-unsaturated C=O), 3400–2800 cm^{-1} (OH, NH).

Anal. Calcd. for $C_{10}H_6BrNO_3S$: C, 40.02; H, 2.02; N, 4.67. Found: C, 40.11; H, 2.28; N, 5.09.

Product B was recrystallized from methanol to give (6-bromo-3,4-dihydro-3-oxo-2*H*-1,4-benzothiazin-2-yl)-acetic acid (**2***c*) as a white powder, m.p. 251–253°. The i.r. spectrum: 1663 (amide C=O), 1707 (acid C=O), 3178 cm^{-1} (NH).

Anal. Calcd. for $C_{10}H_8BrNO_3S$: C, 39.75; H, 2.67; N, 4.64; S, 10.61. Found: C, 39.49; H, 2.68; N, 4.72; S, 10.52.

Product C was a brown solid, m.p. 269–272° which was not investigated further.

Can. J. Chem. Downloaded from www.nrcresearchpress.com by 210.87.254.42 on 09/05/12
For personal use only.

(d) 3,4-Dihydro-4-hydroxy-3-oxo-2H-1,4-benzothiazine (5a)

The title hydroxamic acid (1.87 g) was dissolved in 10% sodium hydroxide solution (20 ml) and heated under reflux for 1 h. The reaction mixture was cooled and product A (0.29 g) precipitated. The filtrate was acidified with concentrated hydrochloric acid and product B (0.95 g) was deposited. The filtrate from product B was allowed to stand and product C (0.32 g) precipitated. None of these products gave a violet color with ethanolic ferric chloride solution.

Product A was dissolved in ethanol, filtered, and reprecipitated with ether to give the sodium salt of α-(*o*-aminophenylthio)acetic acid (**6**) as white crystals, m.p. > 340°. The i.r. spectrum: 1635, 1363 (CO_2^-), 3410 cm^{-1} (NH).

Anal. Calcd. for $C_8H_8NO_2SNa$: N, 6.83. Found: N, 6.65.

The sodium salt was dissolved in a minimum of water, filtered, and acidified with 10% hydrochloric acid to yield 3,4-dihydro-3-oxo-2*H*-1,4-benzothiazine (**5***b*) as a white powder, m.p. 171–173°, lit. (9) m.p. 179°. It had an i.r. spectrum identical with that of an authentic sample: 1661 (C=O), 3208 cm^{-1} (NH).

Product B (m.p. > 340°) was treated with 10% sodium hydroxide solution. The insoluble fraction (0.50 g) was recrystallized from aqueous ethanol to give 2,2′-diaminodiphenyldisulfide (7) as yellow plates, m.p. 90–91°, lit. (10) m.p. 93–94°. The i.r. spectrum: 3480, 3300, 1610 cm^{-1} (NH). Mass spectrum: 248 (47) $[C_{12}H_{12}N_2S_2]^+$, 125 (38) $[C_6H_7NS]^+$, 124 (100) $[C_6H_6NS]^+$ *m/e* (relative abundance).

Product C was recrystallized from aqueous ethanol to give 3,4-dihydro-3-oxo-2*H*-1,4-benzothiazine (**5***b*) as a white powder, m.p. 170–173°, lit. (9) m.p. 179°. The i.r. spectrum was identical with that of an authentic sample.

Action of Hydrochloric Acid on Methyl (6-Bromo-3,4-dihydro-4-hydroxy-3-oxo-2H-1,4-benzothiazin-2-yl)-acetate (1c)

The title hydroxamic acid (1.0 g) was suspended in 10% hydrochloric acid (30 ml) and heated under reflux for 30 min. The hydroxamic acid failed to dissolve but the solution turned a yellow color and the crystalline structure of the suspended material altered in appearance. The hot reaction mixture was filtered to give product A (0.41 g). The filtrate was then cooled and product B (0.33 g) precipitated. The filtrate from product B was then extracted with ether, the ether solution dried (Na_2SO_4) and evaporated to yield product C (0.07 g). None of these products gave a violet color with ethanolic ferric chloride solution.

Products A and B had similar i.r. spectra. These two products were combined and crystallized from ethanol to give (6-bromo-7-chloro-3,4-dihydro-3-oxo-2*H*-1,4-benzothiazin-2-yl)acetic acid (**8**) as a white solid, m.p. 269–271°. The i.r. spectrum: 1643, 1700 (C=O), 3181 cm^{-1} (NH). Mass spectrum: 339 (7), 337 (25), 335 (19); 321 (1.5), 319 (5), 317 (3.5); 293 (25), 291 (100), 289 (68) *m/e* (% relative abundance). The n.m.r. spectrum: 2.35, 2.67 τ (1-proton singlets) (aromatic protons).

Anal. Calcd. for $C_{10}H_7BrClNO_3S$: C, 35.67; H, 2.09; N, 4.16; S, 9.52. Found: C, 35.69; H, 2.17; N, 4.01; S, 9.77.

The filtrate remaining from the recrystallization of **8** was flooded with water to give a white solid which had an i.r. spectrum identical with that of product C. These two products were combined and recrystallized from aqueous ethanol to give (6-bromo-3,4-dihydro-3-oxo-2*H*-1,4-benzothiazin-2-yl)acetic acid (**2***c*) as a white solid, m.p. 251–253°. The i.r. spectrum was superimposable on that of the sample of **2***c* formed, as described above, by the action of sodium hydroxide on **1***c*.

(5-Methyl-2-nitrophenylthio)acetic Acid and its Methyl Ester

3-Chloro-4-nitrotoluene (17.2 g) and thioglycolic acid (9.2 g) were added to a solution of sodium bicarbonate (24 g) in 50% ethanol (200 ml) and the mixture was heated under reflux for 15 h. The solution was concentrated and extracted with ether. The ether extract was discarded. The aqueous layer was acidified with hydrochloric acid and the solid which separated was crystallized from aqueous ethanol to give *(5-methyl-2-nitrophenylthio)acetic acid* as a yellow solid (12.5 g), m.p. 148–150°. The i.r. spectrum (Nujol mull): 3400 to 2400 (acid OH); 1720 (C=O); 1500, 1328 cm^{-1} (NO_2).

Anal. Calcd. for $C_9H_9NO_4S$: C, 47.57; H, 3.99; N, 6.16. Found: C, 48.01; H, 4.12; N, 6.58.

A portion (10.4 g) of the above acid was heated under reflux for 22 h in methanol (150 ml) containing concentrated sulfuric acid (10 ml). The solution was cooled and reduced in volume. *Methyl (5-methyl-2-nitrophenylthio)-acetate* separated as a yellow solid (10.62 g), m.p. 73–74° (from ethanol). The i.r. spectrum (Nujol mull): 1730 (C=O); 1495, 1328 cm^{-1} (NO_2).

Anal. Calcd. for $C_{10}H_{11}NO_4S$: C, 49.78; H, 4.60; N, 5.81. Found: C, 49.61; H, 4.74; N, 5.95.

3,4-Dihydro-4-hydroxy-7-methyl-2H-1,4-benzothiazine (5c)

Methyl (5-methyl-2-nitrophenylthio)acetate (3 g) was reduced using the general method for the preparation of hydroxamic acids. The *hydroxamic acid* (**5***c*) was obtained as a colorless solid (1.58 g), m.p. 148–150° (from aqueous ethanol). It gave a purple color with ferric chloride solution. The i.r. spectrum (Nujol mull): 3080 (OH); 1668, 1630 cm^{-1} (hydroxamate C=O) (11). The n.m.r. spectrum: 7.75 (s, 3, CH_3), 6.37 (s, 2, CH_2), 2.58 to 3.08 (m, 3, aromatic protons), −0.52 τ (s, 1, OH; exchanged in D_2O).

Anal. Calcd. for $C_9H_9NO_2S$: C, 55.37; H, 4.65; N, 7.17. Found: C, 55.77; H, 4.88; N, 7.05.

Action of Hydrochloric Acid on 3,4-Dihydro-4-hydroxy-7-methyl-2H-1,4-benzothiazine (5c)

The title compound (0.36 g) was heated under reflux for 2.5 h in dioxane (10 ml) and dilute hydrochloric acid (10 ml). The filtered solution was cooled and diluted with water and a product (0.23 g), m.p. 180–185°, separated. When treated with chloroform, a portion (27 mg), m.p. 293–297° remained insoluble. Treatment of this solid with boiling benzene gave *bis[2-(3,4-dihydro-7-methyl-3-oxo-2H-1,4-benzothiazine)]* (**9**) as a colorless solid, m.p. 305–308°. The i.r. spectrum (Nujol mull): 3300 or 3240 (NH); 1682, 1662 cm^{-1} (C=O). The n.m.r. spectrum

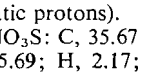

7.87 (s, 3, CH_3), 4.75 (s, 1, CH—C=O), 2.70–3.25 (m, 3, aromatic protons), −0.8 τ (NH). Mass spectrum: 356 (59) [Accurate mass Calcd. for $C_{18}H_{16}N_2O_2S_2$:

356.0654. Measured: 356.0651], 138 (100) [Accurate mass Calcd. for C_7H_8NS: 138.0378. Measured: 138.0378], 107 (95) [Accurate mass Calcd. for C_7H_9N: 107.0735. Measured: 107.0735] *m/e* (% relative abundance).

Anal. Calcd. for $C_{18}H_{16}N_2O_2S_2$: C, 60.67; H, 4.49. Found: C, 60.48; H, 4.70.

The chloroform-soluble portion of the crude reaction product was recrystallized from benzene and yielded *3,4-dihydro-7-methyl-3-oxo-2H-1,4-benzothiazine* (**5***d*, 76 mg) as a colorless solid, m.p. 201–203°. The i.r. spectrum (Nujol mull): 3195 or 3095 (NH); 1675 cm^{-1} (C=O). The n.m.r. spectrum: 7.77 (s, 3, CH_3), 6.57 (s, 2, CH_2CO), 2.55 to 3.07 (m, 3, aromatic protons), −0.45 τ (broad s, 1, NH; exchanged in D_2O). Mass spectrum: 179 (75) $[M]^+$, 150 (100) $[M\text{-}HCO]^+$ *m/e* (% relative abundance).

Anal. Calcd. for C_9H_9NOS: C, 60.31; H, 5.06; N, 7.81. Found: C, 60.13; H, 5.03; N, 8.01.

1. H. E. Heller, E. D. Hughes, and C. K. Ingold. Nature, **166**, 909 (1951).
2. E. Bamberger. Ann. **424**, 297 (1921).
3. L. K. Mushkalo and V. A. Brezemskaya. Ukr. Khim. Zh. **18**, 163 (1952); Chem. Abstr. **48**, 13692 (1954).
4. R. T. Coutts and N. J. Pound. Can. J. Chem. **48**, 1859 (1970).
5. R. T. Coutts and K. W. Hindmarsh. Org. Mass Spectrom. **3**, 105 (1970).
6. R. T. Coutts, H. W. Peel, and E. M. Smith. Can. J. Chem. **43**, 3221 (1965).
7. R. T. Coutts, D. L. Barton, and E. M. Smith. Can. J. Chem. **44**, 1733 (1966).
8. W. H. Mills and J. B. Whitworth. J. Chem. Soc. 2738 (1927).
9. M. A. T. Rogers and W. A. Sexton. J. Chem. Soc. 1619 (1947).
10. G. M. Badger and N. Kowanko. J. Chem. Soc. 1652 (1957).
11. R. T. Coutts, K. W. Hindmarsh, S. J. Powell, J. L. Pound, and E. M. Smith. Can. J. Pharm. Sci. **3**, 49 (1968).
12. R. T. Coutts, S. J. Matthias, and H. W. Peel. Can. J. Chem. **48**, 2448 (1970).

Can. J. Chem. Downloaded from www.nrcresearchpress.com by 210.87.254.42 on 09/05/12
For personal use only.

Can. J. Chem. Downloaded from www.nrcresearchpress.com by 210.87.254.40 on 09/05/12
For personal use only.

Gypsum, disodium pentacalcium sulfate, and anhydrite solubilities in concentrated sodium chloride solutions[1]

D. N. GLEW AND D. A. HAMES
Exploratory Research Laboratory, Dow Chemical of Canada Limited, Sarnia, Ontario

Received June 11, 1970

The solubility of gypsum and anhydrite have been determined at 65 °C in aqueous 3.0 to 6.1 *m* NaCl solutions. Gypsum solubility at 30 °C has been determined in 5.9 *m* NaCl and in saturated sodium chloride. At 65 °C gypsum reacts with sodium chloride solutions more concentrated than 3.7 *m* NaCl to form disodium pentacalcium sulfate, $Na_2Ca_5(SO_4)_6.3H_2O$, which is isomorphous with calcium sulfate hemihydrate. The solubility of this double salt has been determined at 65 °C in aqueous 4.0 to 6.3 *m* NaCl solutions.

Canadian Journal of Chemistry, 48, 3733 (1970)

Introduction

Although many phase equilibrium studies have been made of the geologically important $CaSO_4$–$NaCl$–H_2O system, the relative solubilities of gypsum, hemihydrate, and anhydrite in concentrated sodium chloride brines are uncertain at 65 °C. All recent solubility measurements in concentrated sodium chloride solutions have been made (1–5) by determining the saturation calcium ion concentration and assuming an equal concentration for the dissolved sulfate ion. Arguments for this equality have been given by Zen (2). While this assumption may be true for gypsum solubility in concentrated brines at ambient temperatures, the equivalence of calcium and sulfate is contrary to observation above 65 °C, where the sulfate ion levels are shown to be significantly lower than those for calcium (6); this early work provides the first evidence for the reaction of gypsum with concentrated sodium chloride brines to form a double salt.

Eipeltauer (7) and Powell (8) described the reaction of gypsum with concentrated brine at 80 °C to form a double salt, described as a sodium-containing calcium sulfate hemihydrate. In solubility experiments starting with gypsum in concentrated brines at 70 °C, Zen (2) identified the final solid phase as bassanite, calcium sulfate hemihydrate, but did not recognize that sodium ions replaced calcium isomorphously within the hemihydrate lattice. In similar gypsum solubility measurements with concentrated sodium chloride brines between 70 and 95 °C, Marshall and Slusher (1) reported the formation of stoichiometric disodium pentacalcium sulfate, Na_2SO_4.$5CaSO_4.3H_2O$, which was shown to be petrographically identical with that found by Hill and Wills (9) in the $CaSO_4$–Na_2SO_4–H_2O system. Without X-ray analysis Marshall and Slusher (1) were unaware that the solid disodium pentacalcium sulfate was isomorphous with the sodium-containing calcium sulfate hemihydrate reported to be non-stoichiometric by Powell (8).

To better define the $CaSO_4$–$NaCl$–H_2O system at 65 °C, we have determined the solubilities of gypsum and anhydrite and for the first time have measured the solubility of the double salt prepared in situ with a range of concentrated sodium chloride solutions at 65 °C. The uncertainty of the formula and structure of the double salt formed from the reaction of gypsum with concentrated sodium chloride brines at higher temperatures has been unequivocally resolved by our identification of disodium pentacalcium sulfate by chemical, X-ray, and differential thermal analyses.

Experimental

Materials

Water was laboratory-distilled. Sodium chloride was Fisher certified, reagent grade and was dried before use. Gypsum and anhydrous calcium sulfate (orthorhombic β-anhydrite, which we refer to as anhydrite) were both Baker analyzed reagents. This anhydrite contained some gypsum impurity, detected by X-ray analysis, which was removed by heating at 400 °C for 24 h immediately prior to solubility determination. Anhydrite was also prepared from the gypsum by heating at 400 °C for 24 h.

Calcium sulfate hemihydrate was prepared by refluxing a 5 wt % gypsum suspension in a continuously stirred aqueous 18 wt % $CaCl_2$ solution for 4.5 h. Within this time the gypsum was completely transformed into calcium sulfate hemihydrate without formation of anhydrite.

Glauberite was prepared by the stirred reaction at 75 °C of gypsum with aqueous 24 wt % Na_2SO_4 for 2 days (9).

[1]Contribution No. 177.

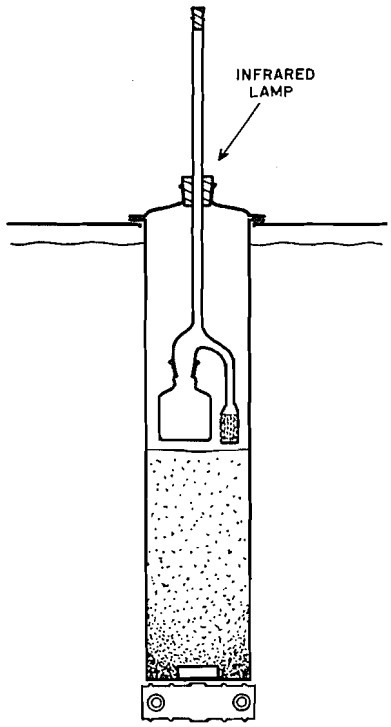

FIG. 1. Solubility apparatus.

Disodium pentacalcium sulfate was formed with continuous stirring (*i*) at 65 °C by heating gypsum for less than one day with 6.4 *m* NaCl solutions and for increasing periods of up to 11 days for 5.5 *m* NaCl, (*ii*) at 75 °C by reaction of gypsum with glauberite in the presence of aqueous 12 wt % Na_2SO_4 (9). Freshly prepared samples contained excess adsorbed water which was removed by evacuation at 2 Torr for 24 h. No further water was removed by evacuation for 63 h.

Apparatus

All solubilities were determined in the apparatus, shown in Fig. 1, which consisted of a cylindrical vessel, 7.5 cm diameter, 40 cm deep, with a 9.5 cm ground-glass flange at its upper end. The vessel was immersed to a depth of 35 cm in a covered liquid thermostat which controlled the temperature of the vessel contents to better than ±0.05 °C. Super- and subsaturated solutions, initially half-filling the vessel, were brought into equilibrium with excess solid by continuous vigorous agitation and grinding of a magnetic stirring bar. We particularly stress the importance of both the vigorous stirring and grinding of the solid between the stirring bar and the flat bottom of the vessel because these lead to rapid equilibration. The flanged lid of the vessel contains a rubber stopper supporting the solution sampling device, which consists of 7 mm diameter, 40 cm long tube carrying at its lower end a coarse fritted-glass filter and a 50 cm^3 sample bottle attached via 19/22 joint. The upper end of the 7 mm tube was stoppered to prevent escape of water vapor and both the tube and flanged lid were heated by an infrared lamp to slightly above thermostat temperature to prevent water condensation. Using this solubility apparatus no water losses were detected for numerous experiments over 30-day periods at 65 °C.

Method

Gypsum and anhydrite solubilities at 65 °C were determined from subsaturation by adding 0.07 g-mole of the solids to 500 g H_2O containing sodium chloride. Frequent sampling showed that equilibrium with gypsum was established in less than 2 days with 3 to 5 *m* NaCl solutions, but determinations were made between 4 and 16 h near to sodium chloride saturation due to the more rapid formation of disodium pentacalcium sulfate. Equilibrium with anhydrite was attained within 4 days as shown by regular sampling for up to 6 weeks. Disodium pentacalcium sulfate was formed in situ from gypsum with aqueous sodium chloride at 65 °C as described earlier, after which 5 days were required for equilibrium with 6.4 *m* NaCl, increasing to 11 days for equilibrium with 4.0 *m* NaCl.

Stirrers were stopped 30 min before sampling to permit settling of the solid which eliminated possible entrance of solids into the sample bottles via the fritted-glass filters. Sample bottles, previously placed above the solution and in thermal equilibrium with it, were lowered and a 15–20 g sample was withdrawn via the glass frits. The sample bottles were removed, stoppered, weighed, diluted to 50 g with water, and reweighed. Weighed aliquots of the diluted solution were analyzed invariably for chloride by potentiometric titration, calcium by EDTA titration, and sulfate by gravimetric barium sulfate determination. The accuracy of determination for chloride was ±0.2%, for calcium less than ±0.5%, and for sulfate ±2.8%. Sodium ion concentration was calculated from the electroneutrality relationship for the solution $(Na^+) = (Cl^-) + 2(SO_4^{2-}) - 2(Ca^{2+})$. All concentrations are expressed as molality, mole/kg H_2O.

The solids, after attainment of equilibrium, were filtered from solution on a fritted-glass funnel and washed with benzene and then acetone. The solid was immediately identified by its X-ray diffraction powder pattern using Cu K_α radiation on a Phillips recording X-ray diffractometer. The dehydration temperature of the solid was determined by differential thermal analysis using a Dupont thermograph. The chemical composition was determined by dissolving the solid in water and analyzing for calcium and sulfate. The solid water content was determined by weight loss on heating at 400 °C for 16 h.

To establish the stability of disodium pentacalcium sulfate with concentrated sodium chloride solutions at 30 °C, the solid was prepared in situ at 65 °C, as described above, and the whole system was cooled at 30 °C.

Results and Discussion

(*a*) *Characterization of Disodium Pentacalcium Sulfate*

The reaction at 65 °C of gypsum with solutions more concentrated than 3.7 *m* NaCl yields a double-salt solid phase and a supernatant liquid

Can. J. Chem. Downloaded from www.nrcresearchpress.com by 210.87.254.40 on 09/05/12
For personal use only.

Can. J. Chem. Downloaded from www.nrcresearchpress.com by 210.87.254.40 on 09/05/12
For personal use only.

containing more calcium than sulfate and less sodium than chloride ions: this indicates removal of sodium and sulfate ions in the formation of the double salt and enrichment of the solution in calcium ion.

The X-ray diffraction pattern for the double-salt, determined on the final solid phase for each of the eight solubility experiments reported in Table 3, was identical with our calcium sulfate hemihydrate pattern and with that for disodium pentacalcium sulfate prepared by the reaction of gypsum with glauberite in 12 wt % Na_2SO_4 at 75 °C (9). We agree with ASTM card 2-0675 and with Powell's (8) patterns for calcium sulfate hemihydrate.

Our chemical analyses of double-salt samples, which were in equilibrium with eight different solutions between 4.0 and 6.4 *m* NaCl, gave an experimental SO_4^{2-}/Ca^{2+} mole ratio of 1.201 ± 0.002. Six evacuated samples of three separate preparations were dehydrated a 420 °C and lost 6.22 ± 0.02 wt % H_2O. These results correspond to the ratios by weight of 16.25:77.53:6.22 for Na_2SO_4:$CaSO_4$:H_2O, compared with the theoretical ratios 16.20:77.63:6.17 for the double-salt $Na_2SO_4.5CaSO_4.3H_2O$. This is the same salt that Hill and Wills (9) prepared from the reaction of gypsum with aqueous sodium sulfate. Our chemical analyses show that the non-stoichiometric formu a of Powell (8) is wrong.

Differentia! thermal analysis of the solids at a heating rate of 20 °C/min gave onset temperatures for dehydration endotherms at 235 ± 2 °C for the double salt compared with 200 ± 2 °C for calcium sulfate hemihydrate. No difference in onset temperature or in endotherm curve shape was observed for eight samples of the double salt prepared under the widely different conditions. In contrast to the double-salt curve which showed only an endotherm up to 450 °C, our samples of calcium sulfate hemihydrate showed both an endotherm and exotherm (8).

The invariant X-ray diffraction pattern, chemical composition, and differential thermal analysis (DTA) endotherm temperature for double-salt samples prepared in different ways support the formula $Na_2Ca_5(SO_4)_6.3H_2O$, disodium pentacalcium sulfate, which we denote by PS, in which two sodium ions isomorphously replace calcium in a hemihydrate-like lattice, the replacement being stoichiometric over two hemihydrate unit cells (10).

TABLE 1

Gypsum solubility in aqueous sodium chloride at 65.15 °C

Sodium chloride m_{NaCl} (mole NaCl/kg H_2O)	Gypsum solubility S_G (mole $CaSO_4$/kg H_2O)
3.00	0.0583
3.01	0.0583
3.50	0.0585
3.50	0.0585
3.96	0.0580
3.98	0.0582
4.49	0.0569
4.51	0.0568
5.06	0.0558
5.09	0.0556
5.10	0.0557
5.16	0.0555
5.22	0.0551
5.50	0.0545
5.54	0.0546
6.16	0.0522

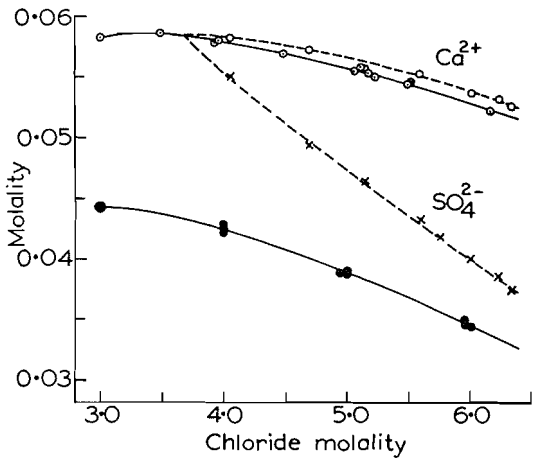

FIG. 2. Solution concentration in the $CaSO_4$–NaCl–H_2O system as a function of chloride molality at 65 °C. ⊙, gypsum solubility; ○, calcium ion, and ×, sulfate ion in equilibrium with PS; ●, β-anhydrite solubility.

(b) Gypsum Solubility

Gypsum solubilities at 65.15 °C in sodium chloride solutions between 3 *m* NaCl and saturation are given in Table 1 and shown in Fig. 2. Our solubilities are in agreement with earlier measurements (1, 2) but have considerably less scatter, with an experimental error, assessed from replicate determinations, of 0.00011 *m* on calcium concentration. In these experiments where the calcium and sulfate molalities are equal, the change of the gypsum solubility S_G, in mole $CaSO_4$/kg H_2O, with the aqueous sodium chlo-

TABLE 2

Gypsum solubility in concentrated aqueous sodium chloride

Temperature (°C)	Sodium chloride m_{NaCl} (mole NaCl/kg H_2O)	Gypsum solubility S_G (mole $CaSO_4$/kg H_2O)		Reference
29.80	5.90	0.0471		This work
25	5.82	0.0465	(0.0466)	4
30	5.55	0.0453	(0.0492)	3
35	5.94	0.0483	(0.0479)	2
29.80	6.15 s*	0.0463		This work
25	6.11	0.0453	(0.0452)	4
25	6.13	0.0489	(0.0450)	1
35	6.17	0.0463	(0.0468)	2

*s = saturated with halite.

ride molality m_{NaCl} is expressed by the equation

$$[1] \quad S_G = 0.05243 + 0.00396\, m_{NaCl} - 0.000652\, m_{NaCl}^2$$

with a standard error on a single determination of 0.00019 *m* which is of the same magnitude but slightly larger than the error assessed from replicate determinations.

Gypsum solubilities at 29.80 °C with 5.90 and 6.15 *m* NaCl, obtained following the decomposition of solid PS as described in section (*c*), are compared with literature values in Table 2. The values in parentheses are calculated from our solubilities for the other authors' conditions of temperature and composition. Our measurements are in good agreement with that of Madgin and Swales (4) and Zen (2), but are in poor agreement with the low value of Bock (3) and the high value of Marshall and Slusher (1).

(c) Solubility of PS

Calcium and sulfate molalities in equilibrium at 65.15 °C with PS, formed in situ by reaction of gypsum with aqueous sodium chloride, are given in Table 3 and shown in Fig. 2. The calcium molalities are slightly larger and the sulfate molalities are considerably smaller than for gypsum: the chloride molalities m_{Cl^-} are correspondingly larger than those for sodium.

In the formation of PS the amount of sodium and sulfate removed from solution depends on the initial excess of undissolved gypsum: with larger excesses of gypsum more PS is formed so that the solution becomes correspondingly more depleted in sodium and sulfate and enriched in calcium. Thus earlier measurements (1, 2) in the region for PS formation are incomplete and misleading since the non-stoichiometric sulfate concentration was neither measured nor taken into consideration.

TABLE 3

Solubility of PS in aqueous sodium chloride at 65.15 °C

Chloride ion m_{Cl^-} (mole Cl^-/kg H_2O)	PS solubility (Ca^{2+}) (mole Ca^{2+}/kg H_2O)	(SO_4^{2-}) (mole SO_4^{2-}/kg H_2O)
4.05	0.0582	0.0550
4.70	0.0573	0.0492
5.15	0.0556	0.0465
5.60	0.0554	0.0432
5.75	—	0.0417
6.02	0.0537	0.0400
6.24	0.0532	0.0384
6.34	0.0524	0.0373

The solubility and stability of solid PS with concentrated aqueous sodium chloride at 30 °C was assessed by preparing PS at 65 °C in the normal manner then cooling to 30 °C and following the composition of the stirred solution phase. Results presented in Fig. 3 (*a*) for 5.90 m_{Cl^-} and (*b*) for 6.15 m_{Cl^-}, saturated with sodium chloride, show the initial equal decreases of calcium and sulfate concentrations caused by the precipitation of gypsum from the solutions. After 10 days the calcium concentrations dropped only slowly whereas the sulfate concentrations increased rapidly up to the calcium levels, showing the back-reaction at 30 °C of the solid PS with the solution to form gypsum. The solution compositions after 30 and 36 days gave the gypsum solubilities at 29.80 °C reported in Table 2. X-Ray analysis of the solid phases after 40 days in (*a*) confirmed gypsum only and in (*b*), gypsum and halite.

Can. J. Chem. Downloaded from www.nrcresearchpress.com by 210.87.254.40 on 09/05/12
For personal use only.

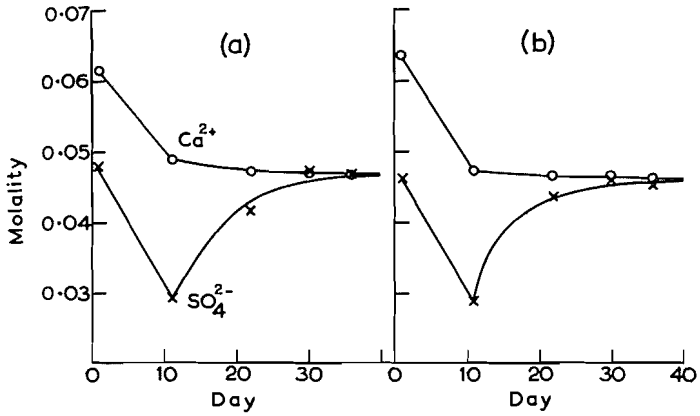

FIG. 3. Solution concentration for PS transformation to gypsum at 30 °C (*a*) in 5.90 *m* NaCl and (*b*) in 6.15 *m* NaCl. ○, calcium ion and ×, sulfate ion.

(d) Anhydrite Solubility

Anhydrite solubilities S_A, in mole $CaSO_4$/kg H_2O, at 65.15 °C in aqueous sodium chloride with between 3 and 6 *m* NaCl are presented in Table 4 and shown in Fig. 2. Solubilities are for our anhydrite prepared from gypsum, while those in parentheses refer to the commercial sample of anhydrous calcium sulfate. With equal calcium and sulfate concentrations, the solubility variation with sodium chloride molality is given by

$$[2] \quad S_A = 0.04217 + 0.00269\, m_{NaCl} - 0.000664\, m_{NaCl}^2$$

with a standard error of 0.00034 *m*.

Contrary to Zen's work at 70 °C (2) over a period of 6 weeks we find no evidence for the transformation of anhydrite to gypsum at 65 °C. The solid phase at the termination of all experiments invariably was shown by X-ray analysis to be β-anhydrite.

TABLE 4

Anhydrite solubility in aqueous sodium chloride at 65.15 °C

Sodium chloride m_{NaCl} (mole NaCl/kg H_2O)	Anhydrite solubility S_A (mole $CaSO_4$/kg H_2O)
3.01	0.0442
3.01	0.0442
4.01	0.0420
4.01	(0.0428)
4.02	0.0426
4.94	0.0387
5.01	(0.0389)
5.01	(0.0391)
5.95	0.0350
5.98	0.0346
6.00	(0.0343)

(e) Gypsum, PS, and Anhydrite Stability

The calcium times sulfate molality product S_G^2 for gypsum, $MP_{PS} = Ca^{2+}.SO_4^{2-}$ for PS, and S_A^2 for anhydrite at 65.15 °C are plotted against chloride ion molality in Fig. 4. The molality products are represented by the least squares regressions

$$[3] \quad S_G^2 = 0.002806 + 0.000413\, m_{NaCl} - 0.0000696\, m_{NaCl}^2$$

$$[4] \quad MP_{PS} = 0.005334 - 0.000530\, m_{Cl^-}$$

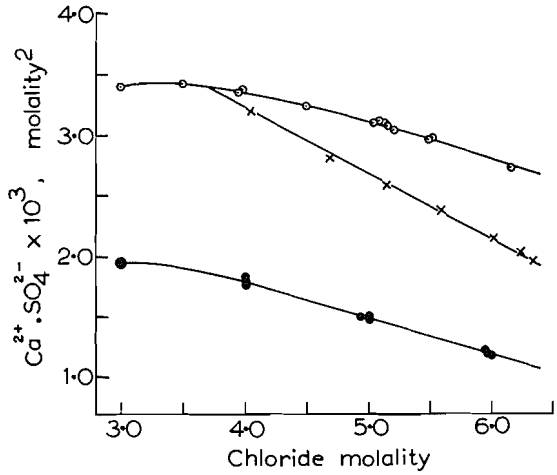

FIG. 4. Dependence of molal product $Ca^{2+}.SO_4^{2-}$ on chloride molality. ⊙, gypsum; ×, PS; ●, anhydrite.

Can. J. Chem. Downloaded from www.nrcresearchpress.com by 210.87.254.40 on 09/05/12
For personal use only.

$$[5] \qquad S_A^2 = 0.001967 + 0.000127\, m_{NaCl} - 0.0000429\, m_{NaCl}^2$$

giving a standard error on single determination of 0.000023, 0.000022, and 0.000029, respectively. The error for PS is unrealistic and is too small compared with the known error on sulfate determination.

The intersection of the S_G^2 and MP_{PS} curves in Fig. 4, where the right-hand side of eqs. 3 and 4 are equal, shows that gypsum is unstable with respect to PS in solutions more concentrated than 3.68 *m* NaCl. At higher molalities the sodium ion from solution competes with calcium and stabilizes the lattice of PS. In all of our experiments at 65 °C anhydrite is the most stable phase of calcium sulfate, into which both gypsum and PS will transform on attainment of equilibrium with the solutions more concentrated than 3 *m* NaCl.

Ostroff (11) observed the dehydration of gypsum to β-anhydrite via a hemihydrate intermediate after 10 days with aqueous 2.8 *m* NaCl at 90.5 °C. Since the hemihydrate which was reported would actually be PS, we expected the similar transformation of PS to anhydrite. Trace quantities of anhydrite do form from PS vigorously stirred with saturated sodium chloride solutions at 65 °C after 6 days, whereas PS equilibrated with 4.7 *m* NaCl at 65 °C show only a trace of anhydrite after 30 days. In contrast we find that gypsum is completely converted via the PS intermediate to anhydrite in the presence of 12 wt % Na_2SO_4 within 40 days at 75 °C. Since anhydrite is the thermodynamically most stable phase under these conditions, the transformation of PS into anhydrite is limited kinetically.

1. W. L. Marshall and R. Slusher. J. Phys. Chem. **70**, 4015 (1966).
2. E-An Zen. J. Petrology, **6**, 124 (1965).
3. E. Bock. Can. J. Chem. **39**, 1746 (1961).
4. W. M. Madgin and D. A. Swales. J. Appl. Chem. **6**, 482 (1956).
5. J. D'Ans, D. Bredtschneider, H. Eick, and H. E. Freund. Kali und Steinsalz (Ser. 1), Heft **9**, 17 (1955).
6. G. Arth and Crétien. Bull. Soc. Chim. [3], **35**, 778 (1906).
7. E. Eipeltauer. Zement-Kalk-Gips. **9**, 501 (1956).
8. D. A. Powell. Aust. J. Chem. **15**, 868 (1962).
9. A. E. Hill and J. H. Wills. J. Amer. Chem. Soc. **60**, 1647 (1938).
10. O. W. Flörke. Neues Jb. Miner. Abh. **84**, 189 (1952).
11. A. G. Ostroff. Geochim. Cosmochim. Acta, **28**, 1363 (1964).

Can. J. Chem. Downloaded from www.nrcresearchpress.com by 210.87.254.40 on 09/05/12
For personal use only.

Can. J. Chem. Downloaded from www.nrcresearchpress.com by 210.87.254.42 on 09/05/12
For personal use only.

Solvolytic reactivity of bridgehead substituted tricyclo[4.4.0.0^{3,8}]decanes (twistanes)[1]

R. C. BINGHAM[2] AND P. VON R. SCHLEYER
Department of Chemistry, Princeton University, Princeton, New Jersey 08540

AND

Y. LAMBERT AND P. DESLONGCHAMPS
Département de Chimie, Université de Sherbrooke, Sherbrooke, Québec

Received June 18, 1970

Several bridgehead substituted twistanes (tricyclo[4.4.0.0^{3,8}]decanes) have been prepared and their solvolysis rates determined. 1-Twistyl derivatives react only slightly faster than the corresponding bicyclo-[2.2.2]octyl derivatives and about 10^3 more slowly than 1-adamantyl derivatives. Although the ground states of all three of these molecules are essentially free from angle strain, they differ in the degree of nonbonded interactions, which is the main reason for the decrease in 1-twistyl and 1-bicyclo[2.2.2]octyl reactivity.

Canadian Journal of Chemistry, **48**, 3739 (1970)

Bridged polycyclic hydrocarbon derivatives with their rigid, fixed conformations are ideal substrates for the study of the effect of changes of geometry on reactivity (1). For carbonium ion processes, the bridgehead positions are best in this regard for reactions there tend to be uncomplicated mechanistically (1, 2). Furthermore, the rates of bridgehead solvolyses are very sensitive to structural effects and large reactivity differences are observed (1, 3, 4).

A comparison of the behavior of 1-adamantyl bromide (**1**) and 1-bicyclo[2.2.2]octyl bromide (**2**) is particularly apt (1, 4*a*). Both substrates have very nearly the same ground state geometry around the reaction site and yet their solvolysis rates differ by more than three powers of ten! Qualitatively, we have ascribed this difference to the increase in $C_1 \ldots C_4$ nonbonded repulsive interactions during the solvolysis of **2** which has no counterpart in the reaction of **1** (1). This argument has been supported by quantitative conformational analysis (4).

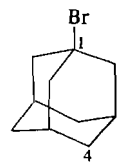

1
(1)*

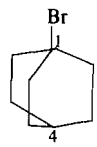

2
(7×10^{-4})*

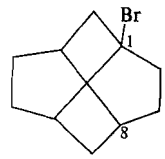

3
(2×10^{-3})*

*(k_{rel}, 100°, 80% ethanol)

As a further check of this hypothesis, we have investigated the solvolysis or 1-twistyl bromide (**3**), 1-twistyl chloride (**4**) (5*a*), and 1-twistyl tosylate (**5**). These compounds have become readily available through the realization of a one-step synthesis of 8-acetoxy-4-tricyclo-[4.4.0.0^{3,8}]decanone (8-acetoxy-4-twistanone (5*b*). 1-Twistanol (5*a*) was converted by standard procedures to its tosylate (**5**) and bromide (**3**) derivatives. The solvolysis rates of **3**–**5** are sum-

[1]This work was supported at Princeton by grants from the National Science Foundation, the National Institutes of Health (AI-07766), and the Petroleum Research Fund, administered by the American Chemical Society and at Sherbrooke by the National Research Council of Canada, Ottawa and Ayerst Laboratories, Montreal.

[2]National Institutes of Health Predoctoral Fellow, 1967–1970.

TABLE 1
Solvolysis Data

Compound	Solvent	Temperature (°C)	k (s^{-1})	$\Delta H^{\ddagger}$ (kcal/mole)	$\Delta S^{\ddagger}$ (e.u.)
1-Adamantyl bromide (**1**)[a]	80% EtOH	100.0	1.26×10^{-3}	22.4	−12.3
1-Bicyclo[2.2.2]octyl bromide (**2**)[b]	80% EtOH	100.0	9.05×10^{-7}[c]	26.0	−16.9
1-Twistyl bromide (**3**)	80% EtOH	124.8	$2.36 \pm .04 \times 10^{-5}$	24.6	−18.4
		150.1	$1.62 \pm .02 \times 10^{-4}$		
		100.0	2.79×10^{-6}[c]		
		25.0	5.25×10^{-10}[c]		
1-Twistyl chloride (**4**)	50% EtOH	124.4	$3.24 \pm .06 \times 10^{-5}$	26.6	−12.8
		150.1	$2.66 \pm .04 \times 10^{-4}$		
		100.0	3.37×10^{-6}[c]		
		25.0	3.27×10^{-10}[c]		
1-Twistyl tosylate (**5**)	CH_3COOH	75.2	$1.73 \pm .05 \times 10^{-4}$	23.6	−8.3
		100.0	$1.78 \pm .11 \times 10^{-3}$		
		25.0	4.74×10^{-7}[c]		

[a]Reference 2*b* and references cited therein.
[b]P. Brennersen *et al.* (9).
[c]Calculated.

marized in Table 1 along with the relevant data for model compounds **1** and **2**.

The twistyl derivatives, like most bridgehead substrates (1), solvolyze without rearrangement. In 80% aqueous ethanol, **3** gives 60% 1-twistanol and 40% of the corresponding ethyl ether. Similarly, acetolysis of **5** gives only unrearranged 1-acetoxytwistane.

The twistyl (**3**) and bicyclo[2.2.2]octyl (**2**) systems are closely related geometrically. In both the angles are not expected to deviate significantly from tetrahedral. The bridgehead. . .bridgehead distances in **2** ($C_1 \ldots C_4$) and in **3** ($C_1 \ldots C_8$) are probably quite similar and are quite different from the chair-type 1,4-C,C distances in adamantane (**1**). Therefore, it is not surprising to find that the solvolysis rates of **2** and **3** are quite similar, both compounds being appreciably slower than **1** (Table 1). This finding supports the qualitative explanation for the reactivity difference between **1** and **2** mentioned above (1).

The slightly enhanced reactivity of **3** relative to **2** is probably due to a torsional effect (4*a*, 6). The addition of the ethylene bridge to **2** to give **3** enhances the "twisting" in the bicyclo[2.2.2]-octyl portion of the molecule (7). In **2** the dihedral angles between the C—Br bond and the adjacent methylene C—H's should be significantly larger than the similar dihedral angles involving the C—Br bond in **3**. This interaction is relieved upon ionization enhancing the rate of **3** relative to **2** (6).

The magnitude of the effect appears smaller than expected on the basis of a first order conformational analysis (6). Possibly this is due to the average D_3 conformation of bicyclo[2.2.2]-octane itself (7) and to a compensating bond angle deformation in **3** introduced by the greater "twisting" in this system.

Torsional effects in carbonium ions will be discussed in greater detail and the results of a full computer conformational analysis (4) of the reactivity of **3** will be presented in forthcoming publications.

Experimental

1-Twistyl Bromide (3)

To freshly distilled thionyl bromide (2.5 ml, 32.2 mmoles) dissolved in dichloromethane (15 ml) and cooled in an ice-bath was added a solution of 1-twistanol (1.53 g, 10.1 mmoles) in dichloromethane (12 ml). The reaction mixture was left for 1 h at room temperature and refluxed for 1.5 h. Pentane was added and the organic phase was washed with saturated sodium carbonate solution, water, and dried over magnesium sulfate. Evaporation of the solvent gave crude crystalline **3** (2.75 g) which was obtained pure by column chromatography over alumina (Wöelm, neutral, grade 1) with pentane (1.82 g, 85% yield). The analytical sample was obtained by sublimation; m.p. 125–127 °C.

Anal. Calcd. for $C_{10}H_{15}Br$: C, 55.81; H, 6.98. Found: C, 55.82; H, 7.03.

1-Twistyl Tosylate (5)

In a 50 ml three-neck round-bottom flask fitted with a magnetic stirrer, condenser, nitrogen inlet, dropping funnel, and a rubber stopper for syringe inlet was placed

Can. J. Chem. Downloaded from www.nrcresearchpress.com by 210.87.254.42 on 09/05/12
For personal use only.

Can. J. Chem. Downloaded from www.nrcresearchpress.com by 210.87.254.42 on 09/05/12
For personal use only.

200 mg (1.32 mmoles) of 1-twistanol in 20 ml anhydrous ether. A 1.67 *M* solution of methyl lithium (1.2 ml, 1.95 mmoles) was added with a syringe, taking care that the tip of the syringe remained in the solution throughout the addition. The solution was then gently refluxed for 15 min. After cooling, 500 mg (2.65 mmoles) of freshly recrystallized *p*-toluenesulfonyl chloride in 10 ml anhydrous ether was added rapidly. The solution was then gently refluxed for 30 min. After cooling the solution was filtered, and the solvent was removed *in vacuo*. The remaining oil was mixed with 3 ml pyridine and after 5 min was poured into about 50 ml ice water. The solid ester precipitated from the ice water, was filtered, and dried *in vacuo* to give 235 mg (58% yield). The product was dissolved in about 30 ml of 30–60° petroleum ether, treated with charcoal, and crystallized by cooling the solution to −78° to give an analytically pure sample; m.p. 87–88°.

Anal. Calcd. for $C_{17}H_{22}SO_3$: C, 66.67; H, 7.19. Found: C, 66.75; H, 7.32.

1-Ethoxytwistane

A mixture containing triethyloxonium fluoroborate (2.3 g), dry dichloromethane, and anhydrous sodium carbonate (600 mg) was prepared and vigorously stirred for 15 min. 1-Twistanol (200 mg, 1.31 mmoles) in dichloromethane (5 ml) was added and the mixture left at room temperature for 4 h. Ether was added, the organic layer was washed with water, dried over magnesium sulfate, and evaporated to dryness. Pure 1-ethoxytwistane (150 mg, 66% yield) was obtained by chromatography on alumina (Woelm, neutral, grade 1) with petroleum ether (b.p. 30–60 °C). The analytical sample was obtained by distillation.

The n.m.r.: τ(CCl_4, TMS) 6.68 (—OCH_2; quadruplet, J = 7 c.p.s.) and 8.93 (CH_3, triplet, J = 7 c.p.s.).

Anal. Calcd. for $C_{12}H_{20}O$: C, 80.00; H, 11.11. Found: C, 80.30; H, 11.38.

Kinetic Methods

The kinetics of the aqueous ethanol solvolyses were measured in the usual manner (8). Solvolysis rates in anhydrous acetic acid were determined conductimetrically with a Wayne-Kerr Model B331 Impedance Bridge, capable of 0.1% accuracy. The conductivity cell used had bright platinum electrodes, a cell constant of 0.3, and a volume of approximately 25 ml. Typically, 10^{-3} *M* solutions were used. At least twelve conductance measurements were taken during the first three half-lives of the reaction. The raw conductance data were then fitted to the first order rate equation by means of a least squares computer program. This conductance method accurately produces literature data.

Product Analyses

Compound **3** (96.5 mg, 0.45 mmole) was dissolved in 80% aqueous ethanol (3 ml) containing sodium carbonate (78.5 mg, 0.74 mmole). This mixture (in a sealed tube) was heated with an oil bath (temperature 130 °C) during 21 h. Water was added (30 ml) and the mixture was extracted with ether. The ethereal extract was dried over magnesium sulfate, filtered, and evaporated to dryness yielding a solid residue (63.7 mg).

Thin-layer chromatography showed the presence of three compounds identified as 1-ethoxytwistane, 1-twistanol, and unreacted starting material. This result was confirmed by v.p.c. analyses which showed only three peaks: 1-twistanol (38%), 1-ethoxytwistane (25%), and 1-twistyl bromide (38%). Identification was made by comparison of their respective retention times with those of authentic samples. The individual products could also be isolated by column chromatography (Fisher Florisil (100–200 mesh)). Elution of a 60 mg sample with petroleum ether (b.p. 30–60 °C) gave **3** (18 mg), elution with benzene – petroleum ether (1:1) gave 1-ethoxytwistane (15 mg), and elution with benzene–ether (5 and 10%) gave 1-twistanol (26 mg). The i.r. spectra of these three compounds were identical with those of authentic samples.

A similar result was obtained for the acetolysis of **5**. The unrearranged acetate product was identified by conversion to 1-twistanol via lithium aluminum hydride and comparison of v.p.c. retention time and i.r. spectra with those of authentic alcohol.

1. R. C. Fort, Jr., and P. v. R. Schleyer. Adv. Alicyclic Chem. **1**, 283 (1966).
2. (*a*) J. L. Fry, C. J. Lancelot, L. K. M. Lam, J. M. Harris, R. C. Bingham, D. J. Raber, R. E. Hall, and P. v. R. Schleyer. J. Amer. Chem. Soc. **92**, 2538 (1970). (*b*) D. J. Raber, R. C. Bingham, J. M. Harris, J. L. Fry, and P. v. R. Schleyer. J. Amer. Chem. Soc. **92**, 5977 (1970). (*c*) D. N. Kevill, K. C. Kolwyck and F. L. Weitl. J. Amer. Chem. Soc. In press. (*d*) J. M. Harris, D. J. Raber, R. E. Hall, and P. v. R. Schleyer. J. Amer. Chem. Soc. In press.
3. P. v. R. Schleyer and R. D. Nicholas. J. Amer. Chem. Soc. **83**, 2700 (1961).
4. (*a*) G. J. Gleicher and P. v. R. Schleyer. J. Amer. Chem. Soc. **89**, 582 (1967). (*b*) P. v. R. Schleyer, P. R. Isele, and R. C. Bingham. J. Org. Chem. **33**, 1239 (1968); W. G. Dauben and C. D. Poulter. J. Org. Chem. **33**, 1237 (1968). (*c*) R. C. Bingham, W. F. Sliwinski, and P. v. R. Schleyer. J. Amer. Chem. Soc. **92**, 3471 (1970); S. A. Sherood, R. G. Bergman, G. J. Gleicher, and D. Morris. J. Amer. Chem. Soc. **92**, 3469 (1970).
5. (*a*) A. Belanger, Y. Lambert, and P. Deslong champs. Can. J. Chem. **47**, 795 (1969). (*b*) A. Belanger, J. Poupart, and P. Deslongchamps. Tetrahedron Lett. 2127 (1968).
6. P. von R. Schleyer. J. Amer. Chem. Soc. **86**, 1854, 1856 (1964); **89**, 701 (1967).
7. O. Ermer and J. D. Dunitz. Helv. Chim. Acta, **52**, 1861 (1969). Also see A. F. Cameron, G. Ferguson, and D. G. Morris. J. Chem. Soc. (**B**), 1249 (1968).
8. H. C. Brown and Y. Okamoto. J. Amer. Chem. Soc. **77**, 3619 (1955).
9. P. Brennersen, C. A. Grob, R. A. Jackson, and M. Ohta. Helv. Chim. Acta, **48**, 146 (1965).

Can. J. Chem. Downloaded from www.nrcresearchpress.com by 210.87.254.105 on 09/05/12
For personal use only.

Structural preferences for the double bond position in some unsaturated 3,3-diphenylpyrrolidines

M. M. A. HASSAN AND A. F. CASY
Faculty of Pharmacy and Pharmaceutical Sciences, University of Alberta, Edmonton, Alberta

Received April 24, 1970

The reaction between 3,3-diphenyl-3-cyano-1-methylpropyl isocyanate and ethyl magnesium bromide leads to 2-ethyl-5-methyl-3,3-diphenyl-1-pyrroline rather than the isomeric 2-ethylidenepyrrolidine. The protonated *N*-methyl analogue (identical with a major metabolite of methadone) retains the 1-pyrroline structure, but the free base is a *cis–trans* mixture of the corresponding 2-ethylidenepyrrolidines; the *cis* Me/Ph isomer preponderates and is the sole product (obtained as a quaternary salt) when the mixture is treated with methyl iodide. 5-Methyl-2-methylene-3,3-diphenylpyrrolidine, a lower homologue of the methadone metabolite, isomerizes to a 1-pyrroline derivative when protonated or methylated. All structural conclusions are based on i.r. and p.m.r. spectroscopic evidence.

Canadian Journal of Chemistry, **48**, 3742 (1970)

The base derived from the product of reaction between 3,3-diphenyl-3-cyano-1-methylpropyl isocyanate (**1**) and ethyl magnesium bromide

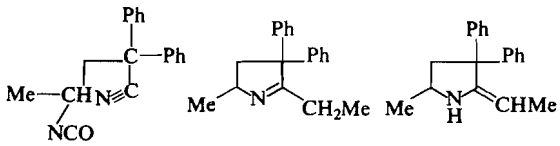

1 **2*a*** **2*b***

may be formulated either as a 1-pyrroline **2*a*** or a pyrrolidine **2*b*** since it gives reactions typical of both forms (1). We prepared this base in connection with work upon the metabolism of methadone (2), and report here its structural preference together with that of its derivatives on the basis of spectroscopic evidence.

The p.m.r. spectrum of the base **2** in $CDCl_3$ displays signals characteristic solely of the endocyclic alkene **2*a***, in particular a quartet and a triplet typical of an ethyl group (details in Experimental).[1] The i.r. spectrum of the base (film) shows bands at 1700 and 1630 cm^{-1} of medium intensity as seen in acyclic ketimines and attributed to C=N stretching (3), and spectroscopic features of the base hydrochloride establish that the *endo* structure is retained in the protonated form. Treatment of the pyrroline **2** with dimethylsulfate gives a tertiary base which may be isolated as a hydriodide. Evidence for the pyrroline structure **3** of this salt and its identity with a major

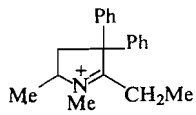

3

metabolite of methadone has been given elsewhere (2). The *N*-methyl base corresponding to **3** may also be obtained from 1,5-dimethyl-3,3-diphenylpyrrolid-2-one (2). A freshly distilled sample derived from this source had spectroscopic properties which showed it to be a *cis–trans* mixture of the exocyclic alkenes **4** and **5**. Thus its

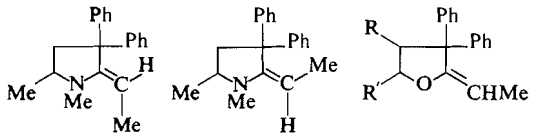

4 *trans* Me/Ph

5 *cis* Me/Ph

6 *a* R = H; R′ = Me; *b* R = Me; R′ = H

p.m.r. spectrum displayed duplicate vinylic (quartets), vinylic methyl (doublets), 5-methyl (doublets) and *N*-methyl signals of similar, but not equal, intensities, while its i.r. spectrum showed an intense band at 1650 cm^{-1}. This i.r. band is assigned to $\nu_{C=C}$ and its high intensity is attributed to the polarizing influence of the adjacent nitrogen atom; the $\nu_{C=C}$ bands of the related tetrahydrofurans **6*a*** and **6*b***, are similarly of high intensity (4). One of the four methyl doublets of the p.m.r. spectrum of the *t*-base mixture in various solvents appeared much lower field (δ 1.72) than the other three which formed an overlapping multiplet near δ 1.0, best resolved in benzene. Signal assignments were aided by the

[1]The p.m.r. evidence upon **2** and its analogues does not preclude the existence of minor components, but if other structural isomers are present in the various samples they must represent less than 10% of the total.

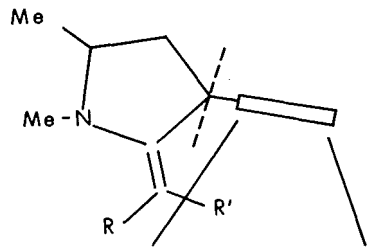

FIG. 1. Diagram of Dreiding model of *cis* and *trans* 2-ethylidene-1,5-dimethyl-3,3-diphenylpyrrolidine (**4** and **5**) viewed from above. The rectangle and dotted line represent the end on views of the two phenyl substituents at C-3.

fact that the vinylic methine protons exchanged for deuterium when the base in $CDCl_3$ was shaken with D_2O, with the result that their signals disappeared. The methyl doublets which simultaneously collapsed to singlets (δ 1.72 and 0.95) were thus identified as the vinylic methyl resonances.

A favored conformation for the exocyclic alkenes **4** and **5** is probably one in which the two 3-phenyl groups are orientated as in Fig. 1, the plane of one of the rings being almost at right angles to the mean plane of the pyrrolidine ring; in this arrangement non-bonded interactions are at a minimum (4, 5). This conformation removes the R vinylic substituent from the aromatic influence and its chemical shift should be in the normal range of a group attached to a carbon–carbon double bond; the R′ substituent, however, falls within the diamagnetic screening zone of the aromatic group and its p.m.r. signal should occur at an unusually high field position. On these grounds the vinylic methine signal at δ 4.33 (within normal range) (6) and the methyl signal at δ 0.95 (upfield of normal range) are assigned to the *cis* Me/Ph isomer **5**, and the signals at δ 3.72 (HC=, high field) and δ 1.72 (MeC=, normal) to the *trans* isomer **4**. The lower field vinylic signal was clearly the more intense, hence the *cis* form preponderates, and the more intense of the two *N*-methyl signals is therefore assigned to the same isomer. This assignment was corroborated by data upon the 2-methylene analogue **7**; the chemical shift of the *N*-methyl group of this derivative (δ 2.68) was closer to that of the major ethylidene isomer (δ 2.63) than that of the minor (δ 2.78). It is concluded that the vinylic methyl group in *trans* **4** has a small deshielding influence on the *N*-methyl protons.

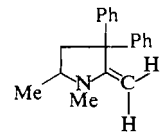

7

In **7**, the higher field vinylic signal is assigned to the methine proton *cis* to the 3-phenyl substituent, and the lower field signal to the *trans* proton from arguments already discussed. Vinylic chemical shifts calculated using these values and the geminal shielding parameter of methyl attached to a C=C double bond (σ_{gem} Me −0.44 p.p.m.) (7) agree closely with the observed shifts of vinylic protons in the ethylidene derivatives **4** and **5** (see Scheme 1); this result shows that vinylic protons suffer similar degrees of aromatic shielding in **7** and the isomers **4** and **5**.

The p.m.r. spectrum of the total product of reaction between the mixture of bases **4** and **5** and methyl iodide displayed a *single* 5-methyl and vinylic methyl doublet. This establishes that the *exo*-cyclic alkene salt, **8**, consists of only *one* of

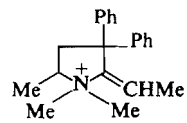

8

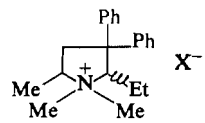

9

the two possible geometrical isomers. The lower field doublet (δ 1.67) in the spectrum of **8** is assigned to 5-methyl because of its broad nature (attributed to ^{14}NCCH coupling, known to amount to about 2 Hz in quaternary salts) (8) and by comparison of its chemical shift with that of 5-methyl in the saturated analogue **9** (δ 1.58). The upfield doublet (δ 1.21) is therefore due to the vinylic methyl group, and its high field position shows that the quaternary salt **8** has a *cis* Me/Ph configuration. The *trans* isomer is probably unfavored on steric grounds since models show that this structure entails interactions between vinylic methyl and *both* of the *N*-methyl groups. The $\nu_{C=C}$ band of the quaternary salt **8** was much weaker than that of the corresponding free base mixture **4** and **5**, and this results supports the argument of the intense absorption seen in the latter being due to the polarizing influence of the ring nitrogen atom; in the quaternary salt **8** the absence of a nitrogen

Can. J. Chem. Downloaded from www.nrcresearchpress.com by 210.87.254.105 on 09/05/12
For personal use only.

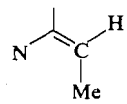

$\nu_{cis\text{-}H} = -3.25 - 0.44 = -3.69$; observed, 3.73 p.p.m. (δ)

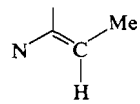

$\nu_{trans\text{-}H} = -3.81 - 0.44 = -4.35$; observed, 4.35 p.p.m. (δ)

SCHEME 1

lone-pair of electrons precludes the resonance interaction $\ddot{N}\!\!\curvearrowright\!\!-C{=}C \leftrightarrow \overset{+}{N}{=}C{-}\overset{-}{C}$.

The 2-methylene analogue of the bases **4** and **5** also had a preferred exocyclic alkene structure **7** since its p.m.r. spectrum showed two broad vinylic methine signals and its i.r. spectrum, an intense $\nu_{C=C}$ band at 1650 cm^{-1}. In the spectrum of a purified sample in $CDCl_3$, the vinylic resonances were considerably broadened (w_H 13 Hz), indicating their exchangeable nature. This conclusion was confirmed by the diminution of the signal intensities when D_2O was added. Pronounced broadening of these signals was not seen in the spectrum of the base **7** in DMSO-d_6, a solvent which presumably reduces the proton exchange rate by its hydrogen bonding properties. Protonation of **7** occurs at the exocyclic carbon atom of the methylene group rather than at nitrogen (giving **10**), as is clear from the

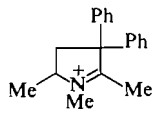

10

appearance of a broad 3-proton signal at δ 2.48 and the disappearance of the vinylic methine signals when trifluoroacetic acid is added to the base in $CDCl_3$. The signal at δ 2.48, assigned to vinylic methyl in **10**, was of greatly reduced intensity in the spectrum of the acidified base in $CDCl_3$—D_2O. Methylation of **7** also occurred at the same exocyclic carbon atom to yield the hydriodide of the methadone metabolite **3**.

This study shows that 1-pyrrolines of type **2** are more stable than corresponding pyrrolidines with an exocyclic alkene substituent at C-2; the latter structures are only favored in cases where pyrroline formation entails the cleavage of an N—C bond (**4**, **5**, and **7**) or the generation of severe non-bonded interactions (**8**). The governing influence of steric factors in determining preference for *cis–trans* Me/Ph geometry in the five-membered ethylidene derivatives **5** and **8** is also apparent in the tetrahydrofuran analogues **6***a*, **6***b*, and **11**.

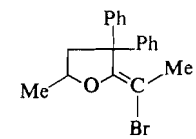

11

In the first two the *trans* isomers are preferred as is evident by the normal resonance positions of their vinylic methyl [δ 1.66 (**6***a*), 1.63 (**6***b*)] and high field vinylic methine signals [δ 3.95 (**6***a*), 4.03 (**6***b*)] (4). In the bromo derivative **11** (9), however, the vinylic methyl chemical shift is very close to that of *cis* **5** (δ 0.95) after allowance is made for the deshielding influence of a geminal bromine atom ($\nu_{Me,\ corrected} = 1.53 - 0.56$[2] = δ 0.97); hence **11** has a *cis* configuration as anticipated from the relative bulk of the bromo and methyl substituents.

Experimental

The p.m.r. spectra were recorded on a Varian A-60 spectrometer using $CDCl_3$ as solvent unless otherwise stated. Chemical shifts are expressed in δ units with TMS as internal standard; in most cases only signals diagnostic of endocyclic or exocyclic alkene structures are reported. The i.r. spectra of salts were recorded as Nujol mulls and bases as liquid films.

The p.m.r. spectrum of base **2**, b.p. 135–140°/0.3 mm (1, 2) showed a quartet at 2.13, *J* 6.5 Hz (2-CH_2Me) and a triplet at 1.08, *J* 6.5 Hz (2-CH_2*Me*). The spectrum of **2** hydrochloride, m.p. 160–162° (2) showed the same signals at 2.78 and 1.27 (*J* 7.5 Hz).

The mixture of bases **4** and **5** derived from the reaction of 1,5-dimethyl-3,3-diphenylpyrrolid-2-one with ethyl lithium (2) distilled at 131–133°/0.1 mm.

Anal. Calcd. for $C_{20}H_{23}N$: C, 86.6; H, 8.4. Found: C, 86.5; H, 8.4.

The mixture had the following p.m.r. characteristics:

[2]Calculated from ν_{Me} in propene (δ 1.72) and 2-bromopropene (δ 2.28) (10).

Can. J. Chem. Downloaded from www.nrcresearchpress.com by 210.87.254.105 on 09/05/12
For personal use only.

quartets at 4.33 (major) and 3.72, *J* 7 Hz (vinylic methine); singlets at 2.78 and 2.63 (major) (N—*Me*); doublets at 1.72 and 0.95, *J* 7 Hz (vinylic methyl), and at 1.12 and 1.07, *J* 5.6 Hz (5-*Me*). In benzene these signals had the chemical shifts: 4.38, 3.92, *J* 7 Hz (vinylic methine); 2.68, 2.50 (N—*Me*); 1.72, 1.17, *J* 7 Hz (vinylic methyl); 1.17, 1.02 *J* 6 Hz (5-*Me*).

1,5-Dimethyl-3,3-diphenyl-2-methylene Pyrrolidine (7)

Compound **7** (5 g) b.p. 120°/0.1 mm, was prepared by treating 1,5-dimethyl-3,3-diphenylpyrrolid-2-one (8.5 g) with methyl lithium obtained from lithium (0.9 g) and methyl iodide (6 g) in ether at −40 °C.

Anal. Calcd. for $C_{19}H_{21}N$: C, 86.6; H, 8.05. Found: C, 86.9; H, 8.4.

The undistilled base had the following p.m.r. characteristics: broad singlets at 3.8 and 3.25, width at half height (w_H) ~ 3 Hz (vinylic methines); singlet at 2.68 (N—Me); doublet at 1.1, *J* 6.5 Hz (5-*Me*). The vinylic methine singlets were at 3.73 and 3.13 ($w_H \sim 3$) in DMSO-d_6, and were replaced by a broad singlet at 148, $w_H \sim 4$ Hz of relative intensity 3 (vinylic methyl) in $CDCl_3$–TFA. The p.m.r. spectrum of the product of reaction between **7** and methyl iodide showed signals characteristic of **3** (2) namely; a multiplet at 5.15 (5-methine); a singlet at 4.03 (N—Me); a quartet near 3.0 (2-CH_2Me); and a triplet at 0.7, *J* 7 Hz (2-CH_2Me).

A mixture of **4** and **5** (4.2 g), dimethyl sulfate (1.4 ml), and benzene (25 ml) was heated under reflux for 1 h and cooled. The solid which separated was recrystallized from ethanol–ether to give **8** (X = $MeSO_4^-$) (3.5 g), m.p. 235–237°, lit. (1) 227–230°.

Anal. Calcd. for $C_{22}H_{29}NO_4S$: C, 65.5; H, 7.2; N, 3.5. Found: C, 65.6; H, 7.2; N, 3.3.

The methiodide **8** (X = I^-) m.p. 185–187°, was prepared similarly and crystallized as a hemihydrate, ν_{max} 3420 cm^{-1} (H_2O).

Anal. Calcd. for $C_{21}H_{26}IN$, 0.5 H_2O: C, 58.9; H, 6.35; N, 3.3. Found: C, 59.3; H, 6.1; N, 2.95.

Its p.m.r. spectrum showed singlets at 3.68 and 3.63 (N—*Me*); doublets at 1.27, *J* 6.5, (w_H of each doublet line ~ 3 Hz) (5-*Me*) and 1.21, *J* 7.5 (vinylic methyl). The quaternary salt **9** (X = $MeSO_4^-$), m.p. 68–70°, prepared from 1,5-dimethyl-3,3-diphenyl-2-ethylpyrrolidine (11) and dimethyl sulfate, also crystallized as a hemihydrate, ν_{max} 3500 cm^{-1} (H_2O).

Anal. Calcd. for $C_{22}H_{31}NO_4S$, 0.5 H_2O: C, 63.7; H, 7.8. Found: C, 63.9; H, 7.8.

Its p.m.r. spectrum showed a multiplet, centered at 4.6 (5-methine), singlets at 3.67 ($MeSO_4^-$), 3.42 and 2.98 (N—*Me*), a doublet at 1.58, *J* 6.5 Hz with broadened lines ($w_H \sim 2$ Hz) (5-Me), plus a deformed triplet with separations ~ 7 Hz at 1.0 (2-CH_2Me).

The authors thank Dr. A. B. Simmonds, Chelsea College of Science and Technology, London, for a sample of the bromo derivative **11**, and the Medical Research Council of Canada for financial support.

1. H. Bretschneider, W. Klotzer, W. Sachsenmaier, and M. Sander. Monatsh. Chem. **90**, 688 (1959).
2. A. H. Beckett, J. F. Taylor, A. F. Casy, and M. M. A. Hassan. J. Pharm. Pharmacol. **20**, 754 (1968).
3. A. F. Casy and M. M. A. Hassan. J. Chem. Soc. (B), 631 (1969).
4. A. F. Casy and M. M. A. Hassan. Tetrahedron, **23**, 4075 (1967).
5. P. S. Portoghese and D. A. Williams. J. Heterocycl. Chem. **6**, 307 (1969).
6. D. Chapman and P. D. Magnus. Introduction to practical high resolution nuclear magnetic resonance spectroscopy. Academic Press, London, 1966.
7. S. W. Tobey. J. Org. Chem. **34**, 1281 (1969).
8. Y. Kawazoe, M. Tsuda, and M. Ohnishi. Chem. Pharm. Bull. (Tokyo), **15**, 214 (1967).
9. N. R. Easton, S. J. Nelson, V. B. Fish, and P. N. Craig. J. Amer. Chem. Soc. **75**, 3751 (1953).
10. F. A. Bovey. NMR data tables for organic compounds. Vol. 1. Interscience, New York, 1967.
11. A. F. Casy and M. M. A. Hassan. J. Med. Chem. **12**, 337 (1969).

Hydrophobic folding of maltose in aqueous solution

J. L. Neal and D. A. I. Goring

Pulp and Paper Research Institute of Canada and Department of Chemistry, McGill University, Montreal, Quebec

Received April 10, 1970

The apparent specific thermal expansibilities of glucose, cellobiose, and maltose were compared to show that the maltose molecule folds in solution and undergoes intramolecular hydrophobic bonding.

Canadian Journal of Chemistry, **48**, **3745** (1970)

An examination of a molecular model of glucose reveals that certain surfaces are hydrophobic in character. Presumably, the net effect of glucose on the structure of liquid water is a sum of the effects of the hydrophilic —OH groups and the hydrophobic surfaces (1). If a dimer of glucose were able to rotate about its glycosidic linkage such that the hydrophobic surfaces were juxtaposed, these surfaces would bond intramolecularly (2) and thus increase the net hydrophilic character of the molecule. On the other hand, if such a conformational arrange-

Can. J. Chem. Downloaded from www.nrcresearchpress.com by 210.87.254.105 on 09/05/12
For personal use only.

quartets at 4.33 (major) and 3.72, *J* 7 Hz (vinylic methine); singlets at 2.78 and 2.63 (major) (N—*Me*); doublets at 1.72 and 0.95, *J* 7 Hz (vinylic methyl), and at 1.12 and 1.07, *J* 5.6 Hz (5-*Me*). In benzene these signals had the chemical shifts: 4.38, 3.92, *J* 7 Hz (vinylic methine); 2.68, 2.50 (N—*Me*); 1.72, 1.17, *J* 7 Hz (vinylic methyl); 1.17, 1.02 *J* 6 Hz (5-*Me*).

1,5-Dimethyl-3,3-diphenyl-2-methylene Pyrrolidine (7)

Compound **7** (5 g) b.p. 120°/0.1 mm, was prepared by treating 1,5-dimethyl-3,3-diphenylpyrrolid-2-one (8.5 g) with methyl lithium obtained from lithium (0.9 g) and methyl iodide (6 g) in ether at −40 °C.

Anal. Calcd. for $C_{19}H_{21}N$: C, 86.6; H, 8.05. Found: C, 86.9; H, 8.4.

The undistilled base had the following p.m.r. characteristics: broad singlets at 3.8 and 3.25, width at half height (w_H) ~ 3 Hz (vinylic methines); singlet at 2.68 (N—Me); doublet at 1.1, *J* 6.5 Hz (5-*Me*). The vinylic methine singlets were at 3.73 and 3.13 ($w_H \sim 3$) in DMSO-d_6, and were replaced by a broad singlet at 148, $w_H \sim 4$ Hz of relative intensity 3 (vinylic methyl) in $CDCl_3$–TFA. The p.m.r. spectrum of the product of reaction between **7** and methyl iodide showed signals characteristic of **3** (2) namely; a multiplet at 5.15 (5-methine); a singlet at 4.03 (N—Me); a quartet near 3.0 (2-CH_2Me); and a triplet at 0.7, *J* 7 Hz (2-CH_2Me).

A mixture of **4** and **5** (4.2 g), dimethyl sulfate (1.4 ml), and benzene (25 ml) was heated under reflux for 1 h and cooled. The solid which separated was recrystallized from ethanol–ether to give **8** (X = $MeSO_4^-$) (3.5 g), m.p. 235–237°, lit. (1) 227–230°.

Anal. Calcd. for $C_{22}H_{29}NO_4S$: C, 65.5; H, 7.2; N, 3.5. Found: C, 65.6; H, 7.2; N, 3.3.

The methiodide **8** (X = I^-) m.p. 185–187°, was prepared similarly and crystallized as a hemihydrate, ν_{max} 3420 cm^{-1} (H_2O).

Anal. Calcd. for $C_{21}H_{26}IN$, 0.5 H_2O: C, 58.9; H, 6.35; N, 3.3. Found: C, 59.3; H, 6.1; N, 2.95.

Its p.m.r. spectrum showed singlets at 3.68 and 3.63 (N—*Me*); doublets at 1.27, *J* 6.5, (w_H of each doublet line ~ 3 Hz) (5-*Me*) and 1.21, *J* 7.5 (vinylic methyl). The quaternary salt **9** (X = $MeSO_4^-$), m.p. 68–70°, prepared from 1,5-dimethyl-3,3-diphenyl-2-ethylpyrrolidine (11) and dimethyl sulfate, also crystallized as a hemihydrate, ν_{max} 3500 cm^{-1} (H_2O).

Anal. Calcd. for $C_{22}H_{31}NO_4S$, 0.5 H_2O: C, 63.7; H, 7.8. Found: C, 63.9; H, 7.8.

Its p.m.r. spectrum showed a multiplet, centered at 4.6 (5-methine), singlets at 3.67 ($MeSO_4^-$), 3.42 and 2.98 (N—*Me*), a doublet at 1.58, *J* 6.5 Hz with broadened lines ($w_H \sim 2$ Hz) (5-Me), plus a deformed triplet with separations ~ 7 Hz at 1.0 (2-CH_2Me).

The authors thank Dr. A. B. Simmonds, Chelsea College of Science and Technology, London, for a sample of the bromo derivative **11**, and the Medical Research Council of Canada for financial support.

1. H. Bretschneider, W. Klotzer, W. Sachsenmaier, and M. Sander. Monatsh. Chem. **90**, 688 (1959).
2. A. H. Beckett, J. F. Taylor, A. F. Casy, and M. M. A. Hassan. J. Pharm. Pharmacol. **20**, 754 (1968).
3. A. F. Casy and M. M. A. Hassan. J. Chem. Soc. (B), 631 (1969).
4. A. F. Casy and M. M. A. Hassan. Tetrahedron, **23**, 4075 (1967).
5. P. S. Portoghese and D. A. Williams. J. Heterocycl. Chem. **6**, 307 (1969).
6. D. Chapman and P. D. Magnus. Introduction to practical high resolution nuclear magnetic resonance spectroscopy. Academic Press, London, 1966.
7. S. W. Tobey. J. Org. Chem. **34**, 1281 (1969).
8. Y. Kawazoe, M. Tsuda, and M. Ohnishi. Chem. Pharm. Bull. (Tokyo), **15**, 214 (1967).
9. N. R. Easton, S. J. Nelson, V. B. Fish, and P. N. Craig. J. Amer. Chem. Soc. **75**, 3751 (1953).
10. F. A. Bovey. NMR data tables for organic compounds. Vol. 1. Interscience, New York, 1967.
11. A. F. Casy and M. M. A. Hassan. J. Med. Chem. **12**, 337 (1969).

Hydrophobic folding of maltose in aqueous solution

J. L. Neal and D. A. I. Goring

Pulp and Paper Research Institute of Canada and Department of Chemistry, McGill University, Montreal, Quebec

Received April 10, 1970

The apparent specific thermal expansibilities of glucose, cellobiose, and maltose were compared to show that the maltose molecule folds in solution and undergoes intramolecular hydrophobic bonding.

Canadian Journal of Chemistry, **48**, **3745** (1970)

An examination of a molecular model of glucose reveals that certain surfaces are hydrophobic in character. Presumably, the net effect of glucose on the structure of liquid water is a sum of the effects of the hydrophilic —OH groups and the hydrophobic surfaces (1). If a dimer of glucose were able to rotate about its glycosidic linkage such that the hydrophobic surfaces were juxtaposed, these surfaces would bond intramolecularly (2) and thus increase the net hydrophilic character of the molecule. On the other hand, if such a conformational arrange-

Can. J. Chem. Downloaded from www.nrcresearchpress.com by 210.87.254.6 on 09/05/12
For personal use only.

TABLE 1

Coefficients of $\phi_2 = A_0 + A_1T + A_2T^2 + A_3T^3$ and derived data

Sugar	Concentration (weight fraction)	A_0 (ml g^{-1})	$A_1 \times 10^3$ (ml $g^{-1}°C^{-1}$)	$A_2 \times 10^4$ (ml $g^{-1}°C^{-2}$)	$A_3 \times 10^6$ (ml $g^{-1}°C^{-3}$)	$(d\phi_2/dT)4°C \times 10^3$ (ml $g^{-1}°C^{-1}$)	$\frac{d\phi_2/dT}{N/M}$
Glucose	0.021	0.604	0.98	− 0.12	0.08	0.89	0.0321
Cellobiose	0.027	0.599	0.80	− 0.06	0	0.75	0.0321
Maltose	0.023	0.598	0.96	− 0.15	0.17	0.85	0.0363

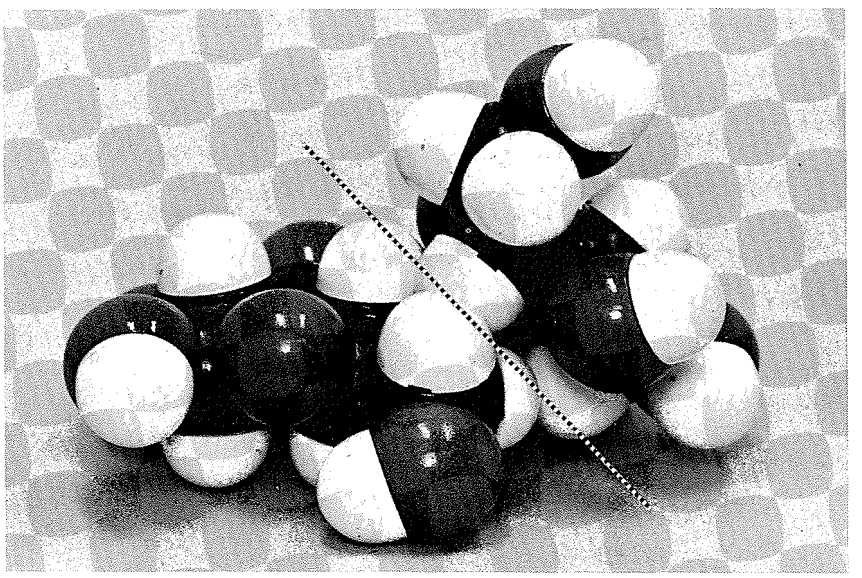

FIG. 1. A Stuart-Brieleb model of maltose in the "folded" conformation. Hydrogen atoms H4 and 2H6 on the reducing sugar are in contact with H3 and H5 on the non-reducing end (see dotted line). It was not possible to arrange a model of the cellobiose molecule into a similar conformation.

ment is restricted, the hydrophobic surfaces would be exposed to the water as in glucose. It is likely that the β 1–4 glycosidic linkage is less flexible than the α 1–4 glycosidic linkage (3). Thus the disaccharide, cellobiose should be less capable of such intramolecular hydrophobic folding than maltose.

A useful diagnostic tool for the above effect would be the change of the apparent specific volume, ϕ_2 of the solute with change in temperature, T. In a previous report (1) it was shown for a variety of non-electrolytes dissolved in water, that $d\phi_2/dT$ is high for hydrophilic solutes and low for hydrophobic solutes. Non-electrolytes rich in —OH groups, such as carbohydrates, were found to show rather high values of $d\phi_2/dT$ (1, 4, 5).

Accordingly, the thermal expansion of dilute solutions of glucose, cellobiose and maltose were determined by the methods described previously (1, 6). The results are expressed in terms of the coefficients of the best-fit polynomials shown in Table 1. Values of $d\phi_2/dT$ at 4 °C are also given in Table 1.

The results show clearly that $d\phi_2/dT$ for maltose is greater than the value for cellobiose and the difference is well above the reproducibility of $\pm$ 0.02 $\times$ 10^{-3} ml $g^{-1}°C^{-1}$ in $d\phi_2/dT$. In order to compare the behavior of the disaccharides with that of glucose, it is necessary to make allowance for the difference of hydroxyl content by dividing $d\phi_2/dT$ by N/M when N is the number of —OH groups per sugar residue and M is the molecular weight of a sugar residue. As shown in Table 1, the value of $d\phi_2/dT/N/M$ for glucose is equal to that of cellobiose while both are less than the figure for maltose.

Examination of the molecular models of the

Can. J. Chem. Downloaded from www.nrcresearchpress.com by 210.87.254.6 on 09/05/12
For personal use only.

two disaccharides reveals that maltose can fold together readily to screen hydrophobic surfaces while the cellobiose molecule cannot (Fig. 1). Thus the results in Table 1 are in keeping with the expected behavior of the two disaccharides and indicate the presence of intramolecular hydrophobic bonding in maltose in aqueous solution. Similar effects have recently been proposed for the oligomers of polypropylene glycol in aqueous solution (7). It is interesting to note that the conformation shown in Fig. 1 corresponds roughly with the conformation (X) which was invoked by Rees (8) to interpret the optical rotations of α–1,4 oligomers in dimethyl sulfoxide and aqueous solutions. However, Rees's arguments were based on hydrogen bonding rather than the hydrophobic bonding proposed in the present work.

Finally it should be mentioned that the insolubility of cellulose in water or aqueous alkali has been attributed by Rees and Skerrett (9) to hydrophobic bonding between the ribbon-like cellulose chains arranged in stacks (10). Also, Goring (11) has suggested that the flocculation of cellulose fibers in aqueous suspension may be associated with hydrophobic bonding between nonpolar cellulose surfaces on the fibers.

1. J. L. Neal and D. A. I. Goring. J. Phys. Chem. **74**, 658 (1970).
2. W. Kauzman. Adv. Protein Chem. **14**, 1 (1959).
3. M. Ihnat and D. A. I. Goring. Can. J. Chem. **45**, 2353 (1967).
4. M. Wahba and K. Aziz. J. Text. Inst. **53**, T291 (1962).
5. M. V. Ramiah and D. A. I. Goring. J. Polym. Sci. C**11**, 27 (1965).
6. J. L. Neal. Ph.D. Thesis. McGill University, Montreal, Quebec, 1969.
7. L. S. Sandell and D. A. I. Goring. Macromol. **3**, 50 (1970).
8. D. A. Rees. J. Chem. Soc. (B) 877 (1970).
9. D. A. Rees and R. J. Skerrett. Carbohyd. Res. **7**, 334 (1968).
10. J. O. Warwicker and A. Wright. J. Appl. Polym. Sci. **11**, 659 (1967).
11. D. A. I. Goring. Pulp Pap. Mag. Can. **67**, T519 (1966).

Preparation and properties of 5-nitro-, 7-nitro-, and 5,7-dinitrooxindole

R. T. Coutts, K. W. Hindmarsh, and E. Mah

Faculty of Pharmacy and Pharmaceutical Sciences, University of Alberta, Edmonton, Alberta

Received June 17, 1970

The preparation and the mass spectra of the title compounds are discussed.

Canadian Journal of Chemistry, **48**, 3747 (1970)

An attempt to prepare 8-nitroquinoline *N*-oxide by oxidizing 8-nitroquinoline with hydrogen peroxide was unsuccessful. Mainly starting material was recovered from this attempt but in addition a small amount of a red compound, m.p. 256–257°, was isolated which analyzed satisfactorily for $C_8H_6N_2O_3$. An examination of the i.r. spectrum of this solid showed bands ascribable to the presence of an NH, carbonyl, and nitro group. The compound was subjected to mass spectrometry. The M^+ peak was located at *m/e* 178 and an accurate mass determination indicated a molecular formula of $C_8H_6N_2O_3$. This evidence suggested that the red compound was the hitherto unknown 7-nitrooxindole (**1***a*).

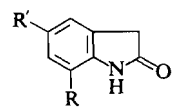

1

	R	R′
a	NO_2	H
b	H	H
c	H	NO_2
d	NO_2	NO_2

An abundant ion in the mass spectrum of this product appeared at *m/e* 160 and the presence of a strong metastable ion at *m/e* 143.8 indicated that the fragment ion was due to the direct loss of 18 mass units (*i.e.* water) from the molecular ion. A mass spectrum of oxindole (**1***b*) was

Can. J. Chem. Downloaded from www.nrcresearchpress.com by 210.87.254.6 on 09/05/12
For personal use only.

two disaccharides reveals that maltose can fold together readily to screen hydrophobic surfaces while the cellobiose molecule cannot (Fig. 1). Thus the results in Table 1 are in keeping with the expected behavior of the two disaccharides and indicate the presence of intramolecular hydrophobic bonding in maltose in aqueous solution. Similar effects have recently been proposed for the oligomers of polypropylene glycol in aqueous solution (7). It is interesting to note that the conformation shown in Fig. 1 corresponds roughly with the conformation (X) which was invoked by Rees (8) to interpret the optical rotations of α–1,4 oligomers in dimethyl sulfoxide and aqueous solutions. However, Rees's arguments were based on hydrogen bonding rather than the hydrophobic bonding proposed in the present work.

Finally it should be mentioned that the insolubility of cellulose in water or aqueous alkali has been attributed by Rees and Skerrett (9) to hydrophobic bonding between the ribbon-like cellulose chains arranged in stacks (10). Also, Goring (11) has suggested that the flocculation of cellulose fibers in aqueous suspension may be associated with hydrophobic bonding between nonpolar cellulose surfaces on the fibers.

1. J. L. Neal and D. A. I. Goring. J. Phys. Chem. **74**, 658 (1970).
2. W. Kauzman. Adv. Protein Chem. **14**, 1 (1959).
3. M. Ihnat and D. A. I. Goring. Can. J. Chem. **45**, 2353 (1967).
4. M. Wahba and K. Aziz. J. Text. Inst. **53**, T291 (1962).
5. M. V. Ramiah and D. A. I. Goring. J. Polym. Sci. C**11**, 27 (1965).
6. J. L. Neal. Ph.D. Thesis. McGill University, Montreal, Quebec, 1969.
7. L. S. Sandell and D. A. I. Goring. Macromol. **3**, 50 (1970).
8. D. A. Rees. J. Chem. Soc. (B) 877 (1970).
9. D. A. Rees and R. J. Skerrett. Carbohyd. Res. **7**, 334 (1968).
10. J. O. Warwicker and A. Wright. J. Appl. Polym. Sci. **11**, 659 (1967).
11. D. A. I. Goring. Pulp Pap. Mag. Can. **67**, T519 (1966).

Preparation and properties of 5-nitro-, 7-nitro-, and 5,7-dinitrooxindole

R. T. Coutts, K. W. Hindmarsh, and E. Mah

Faculty of Pharmacy and Pharmaceutical Sciences, University of Alberta, Edmonton, Alberta

Received June 17, 1970

The preparation and the mass spectra of the title compounds are discussed.

Canadian Journal of Chemistry, **48**, 3747 (1970)

An attempt to prepare 8-nitroquinoline *N*-oxide by oxidizing 8-nitroquinoline with hydrogen peroxide was unsuccessful. Mainly starting material was recovered from this attempt but in addition a small amount of a red compound, m.p. 256–257°, was isolated which analyzed satisfactorily for $C_8H_6N_2O_3$. An examination of the i.r. spectrum of this solid showed bands ascribable to the presence of an NH, carbonyl, and nitro group. The compound was subjected to mass spectrometry. The M^+ peak was located at *m/e* 178 and an accurate mass determination indicated a molecular formula of $C_8H_6N_2O_3$. This evidence suggested that the red compound was the hitherto unknown 7-nitrooxindole (**1***a*).

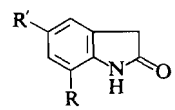

1

	R	R′
a	NO_2	H
b	H	H
c	H	NO_2
d	NO_2	NO_2

An abundant ion in the mass spectrum of this product appeared at *m/e* 160 and the presence of a strong metastable ion at *m/e* 143.8 indicated that the fragment ion was due to the direct loss of 18 mass units (*i.e.* water) from the molecular ion. A mass spectrum of oxindole (**1***b*) was

Can. J. Chem. Downloaded from www.nrcresearchpress.com by 210.87.254.40 on 09/05/12
For personal use only.

Can. J. Chem. Downloaded from www.nrcresearchpress.com by 210.87.254.40 on 09/05/12
For personal use only.

recorded for comparison purposes. Neither $OH^{\bullet}$ nor H_2O was expelled from the molecular ion; the initial fragmentations in oxindole were the expulsion of a CO molecule followed by a hydrogen radical. It is conceivable, therefore, that the nitro group in the 7-position participates in the loss of H_2O from the molecular ion of **1***a* (Scheme 1). A similar involvement of a nitro-group has been suggested (1) to explain the loss of an OH radical from *o*-nitroaniline on electron bombardment.

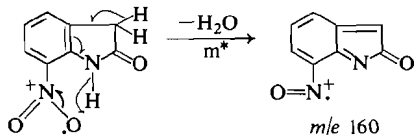

m/e 178 (**1***a*) *m/e* 160

SCHEME 1

Other abundant ions in the mass spectrum of **1***a* were found at *m/e* 178, 161, 131, 103, and 76 and may be accounted for as shown in Scheme 2.

To substantiate these conclusions, the mass spectra of two other nitrooxindoles (**1***c* and *d*) were required. A literature search revealed that only one nitrooxindole, *i.e.* 5-nitrooxindole (**1***c*), is known (2). An earlier claim (3) that 6-nitrooxindole had been prepared has been refuted (2). This derivative (**1***c*) was obtained by nitrating oxindole using the literature method; however, by raising the reaction temperature slightly, some of the dinitro-derivative (**1***d*) was also formed.

The mass spectrum of 5-nitrooxindole (**1***c*) was comparable to that of oxindole (**1***b*). No [M—OH] or [M—H_2O] fragments were observed in **1***c*. The initial fragment ions were of mass 150, 149, and 148, *i.e.* [M—CO], [M—HCO], and [M—NO] respectively. In contrast, the mass spectrum of 5,7-dinitrooxindole (**1***d*) fragmented in a manner similar to that of **1***a*. The molecular ion and [M—OH], [M—H_2O], and [M—OH—NO] fragment ions were observed at *m/e* 223, 206, 205, and 176 respectively.

The mechanism by which 5-nitrooxindole is formed from 8-nitroquinoline is not known. It may involve the initial formation of 3-hydroxy-8-nitroquinoline, in view of the fact that a similar oxidation of quinoline-8-carboxylic acid is known (4) to give 3-hydroxyquinoline-8-carboxylic acid.

Experimental

Melting points are uncorrected. The i.r. spectra were recorded as Nujol mulls. Mass spectra were measured by Dr. A. M. Hogg and his associates with an A.E.I. MS-9 or MS-12 spectrometer at an ionization potential of 70 eV, and n.m.r. spectra were recorded by Mrs. S. Li on a Varian A-60 spectrometer using TMS as standard and DMSO-d_6 as solvent. Mr. W. F. Dylke performed the microanalyses.

*7-Nitrooxindole (**1a**)*

Hydrogen peroxide (30%, 4 ml) was added to a solution of 8-nitroquinoline (1.74 g) in glacial acetic acid (20 ml) and the solution was warmed to 65–70° for 3 h. The mixture was then concentrated, basified with sodium carbonate solution and extracted with chloroform. Removal of the chloroform gave a solid (1.15 g) which was recrystallized from acetone. A red product (90 mg), m.p. 256–257°, was obtained. The i.r. spectrum: 3200 (NH); 1730 (C=O); 1515, 1350, 845 cm^{-1} (NO_2). The mass spectrum: 178 (M^+, 100); 161 (19); 160 (20); 131 (27); 104 (27); 103 (32); 77 (28); 76 (19); 51 (24); 50 (12); 18 (14) *m/e* (% relative abundance).

Anal. Calcd. for $C_8H_6N_2O_3$: C, 53.94; H, 3.39; N, 15.73. Found: C, 53.95; H, 3.16; N, 15.46.

Evaporation of the acetone filtrate from **1***a* gave 8-nitroquinoline.

*5-Nitrooxindole (**1c**)*

A solution of oxindole (6.65 g) in concentrated sul-

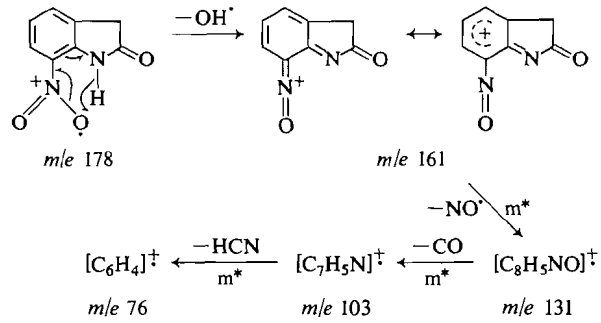

m/e 178 *m/e* 161 *m/e* 76 *m/e* 103 *m/e* 131

SCHEME 2

furic acid (25 ml) was cooled to $-5°$ and maintained at this temperature throughout the reaction. Fuming nitric acid (2.1 ml) was added dropwise and after the addition was complete the solution was allowed to stand at $-5°$ for 30 min then poured into ice. The product (6.21 g) had m.p. 200–210°. Only after four recrystallizations from 50% acetic acid and then five recrystallizations from aqueous ethanol was the title compound obtained as a yellow solid, m.p. 241–243° [lit. (2) m.p. 240–241°]. The i.r. spectrum: 3180 (NH); 1716 (C=O); 1508, 1332 cm^{-1} (NO_2). The mass spectrum: 178 (M^+, 100); 150 (6); 149 (10); 148 (8) *m/e* (% relative abundance).

Anal. Calcd. for $C_8H_6N_2O_3$: C, 53.94; H, 3.39; N, 15.73. Found: C, 53.72; H, 3.21; N, 15.51.

5,7-Dinitrooxindole (1d)

The reaction immediately above was repeated on a twofold scale except that the reaction temperature was maintained at $+5°$. The crude product (9.40 g) had m.p. 150–172°. Repeated recrystallizations from acetone/ethanol gave the title compound as a pale brown solid, m.p. 248–250°. The i.r. spectrum (Nujol mull): 3200 (NH); 1751 (C=O); 1534, 1340, 842 cm^{-1} (NO_2). The mass spectrum: 223 (M^+, 100); 206 (11); 205 (17); 176 (20) *m/e* (% relative abundance). The n.m.r. spectrum: 6.18 (S, 2, CH_2); 1.28 and 1.58 (two 1-proton collapsed doublets, $J = 1.9$, aromatic protons); -1.7 τ (broad S, 1, NH, exchanged in D_2O).

Anal. Calcd. for $C_9H_5N_3O_5$: C, 43.06; H, 2.26; N, 18.83. Found: C, 43.04; H, 2.35; N, 18.54.

1. H. BUDZIKIEWICZ, C. DJERASSI, and D. H. WILLIAMS. Mass spectrometry of organic compounds. Holden-Day, San Francisco, 1967. p. 516.
2. W. C. SUMPTER, M. MILLER, and M. E. MAGAN. J. Amer. Chem. Soc. **67**, 499 (1945).
3. W. BORSCHE, H. WEUSSMANN, and A. FRITZSCHE. Chem. Ber. **57**, 149 (1924).
4. E. OCHIAI, C. KANEKO, I. SHIMADA, Y. MURATA, T. KOSUGE, S. MIYASHITA, and C. KAWASAKI. Chem. Pharm. Bull. (Tokyo), **8**, 126 (1960).

Can. J. Chem. Downloaded from www.nrcresearchpress.com by 210.87.254.40 on 09/05/12
For personal use only.

Acylation of 2-methyl-2-thiazoline

T. DURST AND J. DU MANOIR
Department of Chemistry, University of Ottawa, Ottawa 2, Canada

Received June 10, 1970

The acylation of 2-methyl-2-thiazoline initially reported by Sheehan *et al.* (1) has been reinvestigated and reinterpreted. The initially formed 2-chloro-*N*-acylthiazolidine (*e.g.* **8**) can be dehydrohalogenated to a 2-methylene-*N*-acylthiazolidine by reaction with triethylamine or converted to a 2-hydroxy-*N*-acylthiazolidine on addition of water. Contrary to the earlier report no 2-methyl-*N*-acyl-4-thiazolines are produced when the reaction is carried out in benzene at 60° and in the presence of excess triethylamine.

Canadian Journal of Chemistry, **48**, 3749 (1970)

In 1956 Sheehan *et al.* (1) reported in connection with the synthesis of penicillins a study of the reaction of 2-methyl-2-thiazoline (**1**) with phthaloylglycyl chloride (**2***a*). Two acylated products were described. A "low temperature adduct" assigned the 2-methylene-3-phthaloylglycine structure (**3***a*) was obtained when the reaction was carried out in benzene at room temperature in the presence of one equivalent of triethylamine. This material reportedly crystallized with one mole of water. In benzene at 60°, and in the presence of excess triethylamine, acylation led to a so-called "high temperature adduct" formulated as 2-methyl-3-phthaloylglycyl-4-thiazolidine (**4***a*). The structure proof of **3***a* and **4***a* and their relationship to each other was based mainly on hydrogenation of **4***a* and "crude **3***a* containing triethylammonium chloride" to the saturated thiazolidine **6**. The mechanism of the formation of **4***a* was suggested to involve the tautomerism **1** → **5**.

In connection with another problem in which we required some simple *N*-acyl-4-thiazolines we attempted to prepare such compounds according to the conditions outlined for the formation of the "high temperature adduct". Reaction of *p*-nitrobenzoyl chloride (**2***b*) with 2-methyl-2-thiazoline in benzene at 60° (excess triethylamine) gave a yellow crystalline product in 96% yield. The structural assignment of this material as 2-methylene-3-*p*-nitrobenzoylthiazolidine (**3***b*) was made on the basis of its elemental analysis

furic acid (25 ml) was cooled to $-5°$ and maintained at this temperature throughout the reaction. Fuming nitric acid (2.1 ml) was added dropwise and after the addition was complete the solution was allowed to stand at $-5°$ for 30 min then poured into ice. The product (6.21 g) had m.p. 200–210°. Only after four recrystallizations from 50% acetic acid and then five recrystallizations from aqueous ethanol was the title compound obtained as a yellow solid, m.p. 241–243° [lit. (2) m.p. 240–241°]. The i.r. spectrum: 3180 (NH); 1716 (C=O); 1508, 1332 cm^{-1} (NO_2). The mass spectrum: 178 (M^+, 100); 150 (6); 149 (10); 148 (8) *m/e* (% relative abundance).

Anal. Calcd. for $C_8H_6N_2O_3$: C, 53.94; H, 3.39; N, 15.73. Found: C, 53.72; H, 3.21; N, 15.51.

5,7-Dinitrooxindole (1d)

The reaction immediately above was repeated on a twofold scale except that the reaction temperature was maintained at $+5°$. The crude product (9.40 g) had m.p. 150–172°. Repeated recrystallizations from acetone/ethanol gave the title compound as a pale brown solid, m.p. 248–250°. The i.r. spectrum (Nujol mull): 3200 (NH); 1751 (C=O); 1534, 1340, 842 cm^{-1} (NO_2). The mass spectrum: 223 (M^+, 100); 206 (11); 205 (17); 176 (20) *m/e* (% relative abundance). The n.m.r. spectrum: 6.18 (S, 2, CH_2); 1.28 and 1.58 (two 1-proton collapsed doublets, $J = 1.9$, aromatic protons); -1.7 τ (broad S, 1, NH, exchanged in D_2O).

Anal. Calcd. for $C_9H_5N_3O_5$: C, 43.06; H, 2.26; N, 18.83. Found: C, 43.04; H, 2.35; N, 18.54.

1. H. BUDZIKIEWICZ, C. DJERASSI, and D. H. WILLIAMS. Mass spectrometry of organic compounds. Holden-Day, San Francisco, 1967. p. 516.
2. W. C. SUMPTER, M. MILLER, and M. E. MAGAN. J. Amer. Chem. Soc. **67**, 499 (1945).
3. W. BORSCHE, H. WEUSSMANN, and A. FRITZSCHE. Chem. Ber. **57**, 149 (1924).
4. E. OCHIAI, C. KANEKO, I. SHIMADA, Y. MURATA, T. KOSUGE, S. MIYASHITA, and C. KAWASAKI. Chem. Pharm. Bull. (Tokyo), **8**, 126 (1960).

Acylation of 2-methyl-2-thiazoline

T. DURST AND J. DU MANOIR
Department of Chemistry, University of Ottawa, Ottawa 2, Canada

Received June 10, 1970

The acylation of 2-methyl-2-thiazoline initially reported by Sheehan *et al.* (1) has been reinvestigated and reinterpreted. The initially formed 2-chloro-*N*-acylthiazolidine (*e.g.* **8**) can be dehydrohalogenated to a 2-methylene-*N*-acylthiazolidine by reaction with triethylamine or converted to a 2-hydroxy-*N*-acylthiazolidine on addition of water. Contrary to the earlier report no 2-methyl-*N*-acyl-4-thiazolines are produced when the reaction is carried out in benzene at 60° and in the presence of excess triethylamine.

Canadian Journal of Chemistry, **48**, 3749 (1970)

In 1956 Sheehan *et al.* (1) reported in connection with the synthesis of penicillins a study of the reaction of 2-methyl-2-thiazoline (**1**) with phthaloylglycyl chloride (**2***a*). Two acylated products were described. A "low temperature adduct" assigned the 2-methylene-3-phthaloylglycine structure (**3***a*) was obtained when the reaction was carried out in benzene at room temperature in the presence of one equivalent of triethylamine. This material reportedly crystallized with one mole of water. In benzene at 60°, and in the presence of excess triethylamine, acylation led to a so-called "high temperature adduct" formulated as 2-methyl-3-phthaloylglycyl-4-thiazolidine (**4***a*). The structure proof of **3***a* and **4***a* and their relationship to each other was based mainly on hydrogenation of **4***a* and "crude **3***a* containing triethylammonium chloride" to the saturated thiazolidine **6**. The mechanism of the formation of **4***a* was suggested to involve the tautomerism **1** → **5**.

In connection with another problem in which we required some simple *N*-acyl-4-thiazolines we attempted to prepare such compounds according to the conditions outlined for the formation of the "high temperature adduct". Reaction of *p*-nitrobenzoyl chloride (**2***b*) with 2-methyl-2-thiazoline in benzene at 60° (excess triethylamine) gave a yellow crystalline product in 96% yield. The structural assignment of this material as 2-methylene-3-*p*-nitrobenzoylthiazolidine (**3***b*) was made on the basis of its elemental analysis

Can. J. Chem. Downloaded from www.nrcresearchpress.com by 210.87.254.105 on 09/05/12
For personal use only.

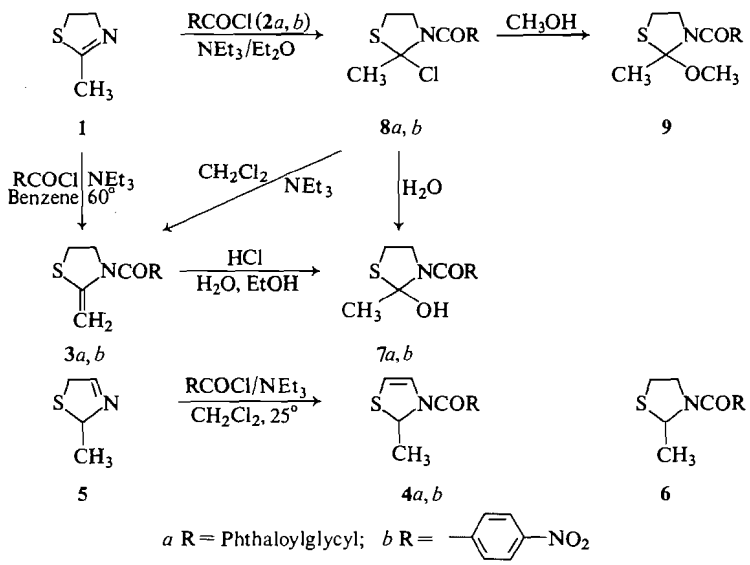

SCHEME 1

and spectroscopic properties. In particular, the n.m.r. spectrum showed absorption at δ 3.17 (t, J = 6.5 c.p.s., 2H), 4.13 (t, J = 6.5 c.p.s., 2H), 4.70 (d, J = 2.5 c.p.s., 1H), and 5.01 (d, J = 2.5 c.p.s., 1H). When the reaction was carried out in benzene or methylene chloride at room temperature (one equivalent of triethylamine) **3***b* was again the only acylation product. In contrast, 2-methyl-3-*p*-nitrobenzoyl-4-thiazoline (**4***b*), the product analogous to Sheehan's high temperature adduct which was prepared by acylation of 2-methyl-3-thiazoline (**5**) (2), showed n.m.r. peaks at δ 1.66 (d, J = 6.0 c.p.s., 3H) and 5.6–6.5 (m, 3H) consisting of two vinyl and the methine hydrogen.

In view of the results described above and the unusually facile isomerization required to explain the formation of **4***a* (1) it was decided to re-investigate the reactions described by Sheehan and co-workers. In our hands, phthaloylglycylation of **1** in benzene at 60° led to 2-methylene-3-phthaloylglycylthiazolidine (**3***a*) in 57% yield. The n.m.r. spectrum of **3***a* showed the expected similarities with **3***b*; peaks were observed at δ 3.13 (t, J = 6.5 c.p.s., 2H), 4.17 (t, J = 6.5 c.p.s., 2H), 4.63 (s, 2H), 4.88 (d, J = 2.0 c.p.s., 1H), 5.60 (d, J = 2.0 c.p.s., 1H), and 7.7–8.1 (m, 4H). The *N*-acyl-4-thiazoline isomer **4***a*, claimed by Sheehan's group to be formed under the above conditions was again obtainable only by reaction of phthaloylglycyl chloride with 2-methyl-3-thiazoline. The spectroscopic properties of **4***a* also parallelled those of **4***b* and are recorded in the Experimental section.

The i.r. spectrum of either **3***a* or **4***a* showed no evidence of the presence of water of crystallization, an observation which was corroborated by the elemental analyses. We have found however that a "hydrated" adduct, actually the tertiary alcohol **7***a*, can be produced if the acylation is carried out in benzene at room temperature followed by trituration of the initial precipitate with water (Sheehan's condition for formation of his low temperature adduct), or if the reaction is carried out in dry ether in the absence of triethylamine and the precipitate is again reacted with water. For example, addition of **2***a* to a solution of **1** in dry ether gave an immediate precipitate which became pink on exposure to air. Treatment of this material, formulated as **8***a* with water led to **7***a* m.p. 156–158° (overall yield from **1**, 75%), while addition to a solution of triethylamine in methylene chloride afforded the 2-methylene thiazolidine **3***a* (60%). When dissolved in methanol, **8***a* was converted to the methyl ether **9**.

The i.r. spectrum of **7***a* ($CHCl_3$) showed intramolecular hydrogen bonding in the 3400 cm^{-1}

Can. J. Chem. Downloaded from www.nrcresearchpress.com by 210.87.254.105 on 09/05/12
For personal use only.

region, while n.m.r. peaks were at δ 1.60 (s, 3H), 2.8–3.2 (m, 2H), 3.3–3.6 (m, 2H), 4.30 (s, 2H), 6.5 (broad s, 1H, exchanged on D_2O treatment), and 7.5–8.1 (m, 4H). The analytical and spectroscopic properties of the methyl ether **9** were also consistent with its formulation.

Comparison of our results for the reaction of phthaloylglycyl chloride with 2-methyl-2-thiazoline with those reported earlier is rather difficult in view of the discrepancies in physical properties between our compounds and those reported earlier. The reported m.p. of Sheehan's "high temperature adduct" to which was assigned the structure **3***a* is 197–199°, while we find for **3***a* a m.p. of 180–181°. The tertiary alcohol **7***a* melts at 157–159°, while the m.p. of the "hydrated low temperature adduct" is given as 186–188°. Furthermore the m.p. of the 4-thiazoline **4***a* is 175–177°.

The formation of **3** or **7** in the acylation of 2-methyl-2-thiazoline depends on the solubility properties of the intermediate **8**. If **8** is insoluble, the addition of water to the reaction mixture produces **7**. On the other hand, if **8** is soluble it is readily converted to **3** on reaction with triethylamine.

In summary, the acylation of 2-methyl-2-thiazoline yields an intermediate 2-chloro-*N*-acylthiazolidine which is converted to a variety of products depending on reaction conditions (see Scheme 1). The hydrogenation reactions referred to earlier which were key reactions in Sheehan's structure assignment included hydrogenation of "crude low temperature adduct containing triethylammonium chloride" in dry dioxane as solvent. It is suggested that the saturated thiazolidine **6** obtained in this way was probably formed either from hydrogenolysis of the chloride **8***a* (3) still present in the crude precipitate, or that of the alcohol **7***a* itself (4, 5). Under the conditions described for the formation of the "high temperature adduct", *i.e.* benzene and triethylamine at 60°, 2-methyl-2-thiazoline (**1**) does not rearrange to 2-methyl-3-thiazoline (**5**) and *N*-acylated 4-thiazolines are not formed from **1** when the acylation reactions are carried out under these conditions (1, 6).

The tertiary alcohols **7***a* and *b* represent unusually stable alcohols in which the carbon bearing the hydroxyl group is attached to two other heteroatoms (*e.g.* N, O, or S). Other derivatives of this type having moderate stability, *e.g.* **10** have recently been reported by Rothe and co-workers (4, 5, 7). Unlike the compounds described by these workers **7***a* and *b* are stable in aqueous acid and are in fact produced in over 80% yield on exposure of **3***a* and *b* to hot aqueous ethanolic HCl.

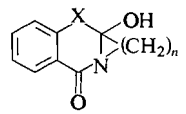

10

X = O, S, NR
n = 2–7, 11

Considerable efforts have been made to establish the tetrahedral nature of the intermediate in the transfer of acyl groups (8) from nitrogen to nitrogen, oxygen to nitrogen, sulfur to nitrogen and vice versa. The alcohols **7***a* and *b* are thus of some additional interest since they represent readily isolable examples of such species.

Experimental

Unless otherwise specified i.r. spectra were obtained as chloroform solutions on a Beckman IR-20 and n.m.r. spectra as $CDCl_3$ solutions on a Varian Associates T-60 spectrophotometer. Usual work-up refers to washing of the reaction mixture with water, drying the organic extracts over anhydrous $MgSO_4$, and evaporating the solvent at reduced pressure.

*p-Nitrobenzoylation of 2-Methyl-2-thiazoline (**1**)*

To 20 ml of benzene at 60° containing 5 ml of triethylamine and 1.01 g (10 mmole) of **1** was added dropwise 2.0 g (11 mmole) of *p*-nitrobenzoyl chloride in 20 ml of benzene. The solution became intensely yellow and was kept at 60° for an additional 15 min then worked-up to yield, after recrystallization from methylene chloride – pentane, 2.41 g (96%) of **3***b*, m.p. 108–110°; i.r. 1645, 1520, and 1360 cm^{-1}.

Anal. Calcd. for $C_{11}H_{10}N_2O_3S$: C, 52.80; H, 4.03; N, 11.20. Found: C, 52.53; H, 4.01; N, 10.78.

When the reaction was carried out in methylene chloride at room temperature for 1 h a 79% yield of **3***b* was obtained.

*p-Nitrobenzoylation of 2-Methyl-3-thiazoline (**5**)*

2-Methyl-3-thiazoline (1.01 g, 10 mmole) and 1.8 ml of triethylamine were dissolved in 15 ml of methylene chloride at 0°. To this solution was added dropwise 2.0 g (11 mmole) of *p*-nitrobenzoyl chloride in 5 ml of methylene chloride. The reaction mixture became initially yellow then gradually red as it warmed to room temperature.

Can. J. Chem. Downloaded from www.nrcresearchpress.com by 210.87.254.105 on 09/05/12
For personal use only.

Can. J. Chem. Downloaded from www.nrcresearchpress.com by 210.87.254.105 on 09/05/12
For personal use only.

The reaction mixture was worked-up after 2.5 h to yield 1.56 g (63%) of **4***b* as yellow crystals m.p. 90–92° (ether–pentane); i.r. peaks at 1640, 1522, and 1350 cm^{-1}.

Anal. Calcd. for $C_{11}H_{10}N_2O_3S$: C, 52.80; H, 4.03; N, 11.20. Found: C, 52.38; H, 4.06; N, 10.83.

Hydration of 2-Methylene-3-p-nitrobenzoylthiazolidine (3b)

Thiazolidine **3***b* (1.60 g) was dissolved in 16 ml of ethanol and added to 4 ml of 10% HCl solution. The reaction was warmed on a steam bath for 10 min then diluted with 40 ml of water. Filtration yielded 1.37 g (80%) of solid which on recrystallization from methylene chloride – pentane gave **7***b* as slightly yellowish prisms, m.p. 111–112°. The i.r. peaks, 3420, 3340, 1650, 1510, and 1337 cm^{-1}; n.m.r. absorption at δ 2.40 (s, 3H), 3.1–3.4 (m, 2H), 3.6–4.0 (m, 2H), 6.9–7.3 (broad s, 1H, exchanged on D_2O treatment), and 7.9–8.5 (m, 4H).

Anal. Calcd. for $C_{11}H_{12}N_2O_4S$: C, 49.25; H, 4.51; N, 10.45. Found: C, 49.45; H, 4.87; N, 10.60.

Phthaloylglycylation of 2-Methyl-2-thiazoline (1)

(a) In Methylene Chloride at 25°

To a solution of 1.01 g (10 mmole) of **1** and 5 ml of triethylamine in 10 ml of methylene chloride was added over a period of 5 min 2.3 g (10 mmole) of **2***a* in 10 ml of methylene chloride. The reaction was worked-up after 10 min to yield 2.15 g (74%) of slightly yellow solid which was recrystallized several times from methylene chloride – pentane to give **3***a*, m.p. 180–181°; i.r. 1775(m), 1715(vs), 1682(s), 1382(m), 1108(m), 953(m), and 870(w).

Anal. Calcd. for $C_{14}H_{12}N_2O_3S$: C, 58.33; H, 4.20; N, 9.72. Found: C, 57.74; H, 4.33; N, 9.45.

(b) In Benzene at 25°

To a solution of 1.01 g (10 mmole) of **1** and 1.1 g (10 mmole) of triethylamine in benzene was added over a period of 30 min 2.0 g (11 mmole) of acid chloride **2***a*. The reaction mixture was stirred for an additional 30 min, filtered (2.4 g), and the filtrate triturated with 75 ml of water. The yield of water insoluble material was 1.1 g (40%) identified by comparison of n.m.r. and i.r. spectra as **7***a* (see below).

(c) In Benzene at 60°

The reaction was carried out as described (1) using 10 mmole of thiazoline **1**, 11 mmole of acid chloride **2***a*, and excess triethylamine. The reaction mixture was worked-up by washing with water, drying, and evaporating the benzene layer. The yield of **3***a* was 1.65 g (57%).

(d) In Ether in the Absence of Triethylamine

To a solution of 1.25 g of thiazoline **1** in 20 ml of dry ether was added slowly 3.0 g of acid chloride **2***a* in 10 ml of dry ether. An immediate colorless precipitate formed which rapidly became pink. This material to which structure **8***a* was assigned was quickly filtered and then treated as described below.

Reaction of 8a with H_2O

The precipitate obtained from 1.25 g thiazoline **1** and 3.0 g of **2***a* was stirred with 10 ml of H_2O. The colorless solid so obtained was filtered and dried, yield 2.85 g (75%) of **7***a*, m.p. 156–158°. The i.r. peaks were at 3420(w), 3360(w), 1770(m), 1710(vs), 1670(s), 1515(m), 1380(s), 1125(m), 1105(s), and 943(m) cm^{-1}.

Anal. Calcd. for $C_{14}H_{14}N_2O_4S$: C, 54.90; H, 4.61; N, 9.15. Found: C, 55.09; H, 4.44; N, 8.84.

Reaction of 8a with CH_3OH

The pink precipitate (1.65 g, 51%), obtained by adding 2.5 g acid chloride **2***a* to 1.01 g of thiazoline **1**, was stirred with 10 ml of methanol for 15 min. The colorless material so obtained had m.p. 151–153°; yield 73% from **8***a*, 35% from **1**. The i.r. peaks were at 1770(s), 1715(vs), 1650(s), 1380(s), 1300(s), 1105(s), and 948(s) while n.m.r. absorption occurred at δ 2.15 (s, 3H), 3.52 (s, 3H), 2.7–4.0 (m, 4H), and 7.6–8.0 (m, 4H).

Anal. Calcd. for $C_{15}H_{16}N_2O_4S$: C, 56.25; H, 5.04. Found: C, 56.27; H, 5.03.

Phthaloylglycylation of 2-Methyl-3-thiazoline (5)

To a solution of 3.03 g of **5** and 15 g of triethylamine in 50 ml of methylene chloride was added 7.5 g of freshly recrystallized **2***a*. After 1 h the reaction mixture was worked-up to yield 2.2 g (25%) of **4***a* as a slightly yellow solid m.p. 173–176°. Recrystallization from $CHCl_3$–ether gave product m.p. 175–177°. The n.m.r. spectrum of **4***a* showed peaks at δ 1.83 (d, J = 6.0 c.p.s., 3H), 4.64 (s, 2H), 6.0–6.4 (m, 2H, due to overlap of the methine with an olefinic hydrogen), 6.72 (d, J = 4.5 c.p.s., 1H), and 7.9–8.3 (m, 4H). The i.r. frequencies were 1775(m), 1715(vs), 1682(s), 1382(s), 1308(m), 1108(m), and 953(m) cm^{-1}.

Anal. Calcd. for $C_{14}H_{12}N_2O_3S$: C, 58.33; H, 4.20; N, 9.72. Found: C, 58.57; H, 4.20; N, 9.32.

Hydration of 3a to 7a

Thiazolidine **3***a* (105 mg) was heated on a steambath with 2 ml of ethanol and 5 ml of 10% HCl until the solution was homogeneous (approximately 5 min). The solution was allowed to cool and the colorless precipitate filtered. Yield, 87 mg (80%), identified as **7***a* by comparison of n.m.r. spectra and by mixed m.p.

The financial assistance of Bristol Laboratories (Syracuse, New York) and the National Research Council of Canada is acknowledged.

1. J. C. Sheehan, C. W. Beck, K. R. Henery-Logan, and J. J. Ryan. J. Amer. Chem. Soc. **78**, 4478 (1956).
2. M. Thiel, F. Asinger, and K. Schmiedel. Ann. **611**, 121 (1958).
3. P. N. Rylander. Catalytic hydrogenation of platinum metals. Academic Press, New York and London, 1967. pp. 405–432.
4. M. Rothe and R. Steinberger. Tetrahedron Lett. 2467 (1970).
5. M. Rothe, W. Schindler, R. Pudill, T. Tòth, and D. Jacob. Tetrahedron Lett. 5127 (1969).
6. L. A. Cohen and B. Witkop. *In* Molecular rearrangements. *Edited by* P. de Mayo. Interscience Publishers Inc., New York, 1964. pp. 974–975.
7. M. Rothe and R. Steinberger. Tetrahedron Lett. 649 (1969).
8. D. R. Robinson. J. Amer. Chem. Soc. **92**, 3138 (1970), and references therein.

Studies in isoxazole chemistry. IV. Isoxazoles via isoxazolines

R. G. MICETICH[1]
R & L Molecular Research Ltd., 8045 Argyll Road, Edmonton 82, Alberta

Received April 8, 1970

4- or 5-Chloro- or cyanoisoxazoles, 5-chloromethylisoxazoles, and 5-methylisoxazoles were made by the 1,3-dipolar cycloaddition of nitrile oxides to α-halogeno- or α-alkoxyolefins. In the case of *cis*- and *trans*-1,2-dichloroethylene, (**5***a* and *b*) the intermediate *cis*- and *trans*-4,5-dichloroisoxalines (**6***a* and *b*) were isolated. Both **6***a* and *b* were dehydrochlorinated with base to give the 4-chloroisoxazole (**7***a*) exclusively. The *cis*-isomer **6***a* reacted faster than the *trans*-isomer **6***b*. The reactions were found to be specific in every reaction since only one isomer was isolated. The structures of the products were established from n.m.r. spectral analysis.

Canadian Journal of Chemistry, **48**, 3753 (1970)

Can. J. Chem. Downloaded from www.nrcresearchpress.com by 210.87.254.105 on 09/05/12
For personal use only.

In continuation of our work on the preparation of isoxazoles via isoxazolines (1, 2) we decided to study the 1,3-dipolar cycloaddition of nitrile oxides to α-halogeno- and α-alkoxyolefins. Cycloadditions involving bromoethylenes have been reported to produce isoxazoles via unstable isoxazolines (3–7), and Bianchi and Grünanger have recently described a convenient route to isoxazoles by converting 2-isoxazolines to their bromo derivatives followed by dehydrobromination (8). 1,3-Dipolar cycloadditions are stereoselective (9) and the synthesis of isoxazolines by this method usually produces the thermodynamically more stable isomer (10). The reaction of a nitrile oxide with an olefin substituted in the α-position with a suitable leaving group such as halogen, alkoxy, amino, or nitro, is hence a potentially useful method of preparing a variety of specifically substituted isoxazoles (see Scheme 1). By using other dipoles such as nitrile imines, diazoalkanes, and azides, this same approach could lead to similarly substituted pyrazoles (11) and triazoles.

By using appropriately substituted ethylenes it should be possible to obtain either the 3,4-disubstituted isoxazoles **7** or the 3,5-disubstituted compounds **4** from these reactions, as illustrated in Scheme 1.

The n.m.r. spectroscopy is a convenient method of establishing the substitution pattern of these isoxazoles, since the C_4-proton signals in compounds of type **4** are usually found at *ca.* τ 3.2 (see ref. 12), while the C_5-proton signals of compounds **7** are found further downfield at *ca.* τ 1.0. This method is especially useful when both isomers, for example **4***a* and **7***a*, or **4***b* and **7***c* are available.

2,5-Dichlorobenzonitrile oxide (**1**) was chosen as the dipole for this study because it is fairly stable at room temperature (13), can be isolated, and gave high yields of cycloaddition products (1, 2). All the α-halogeno- and α-alkoxyolefins used in this study are commercially available. These reactions were found to be selective (9, 10), and the n.m.r. spectrum of the product from every reaction showed the presence of only one isomer (either **4** or **7**). In most cases the intermediate isoxazoline (**3** or **6**) was not detected, since it was transformed spontaneously into the isoxazole (**4** or **7**). It was only with *cis*- (**5***a*) and *trans*-1,2-dichloroethylene (**5***b*), that the *cis*- (**6***a*) and *trans*-4,5-dichloroisoxazoline (**6***b*) were isolated. In agreement with the findings of Huisgen (9) on similar systems, the *trans*-isomer **5***b* was found to react at least five times as fast as the *cis*-isomer **5***a*.

The 4,5-dichloroisoxazolines **6***a* and *b* could be expected to undergo dehydrochlorination to give either **4***a* or **7***a*. Both **6***a* and *b* reacted readily with sodium hydroxide in methanol to form the 4-chloroisoxazole (**7***a*). No trace of the 5-isomer **4***a* was found in the n.m.r. spectrum of the crude product. A preliminary study showed that although both isomers **6***a* and *b* underwent rapid dehydrochlorination with base, the *cis*-isomer **6***a* reacted faster than the *trans*-isomer **6***b*. Thus an n.m.r. analysis of the reaction product after 10 s at room temperature (25 °C) showed complete dehydrochlorination in the case of the *cis*-isomer **6***a*, but only *ca.* 66% reaction with the *trans*-isomer **6***b*. Triethylamine in ether reacted very slowly with **6***a* and *b*.

[1]Present address: Raylo Chemicals Ltd., 8045 Argyll Road, Edmonton 82, Alberta.

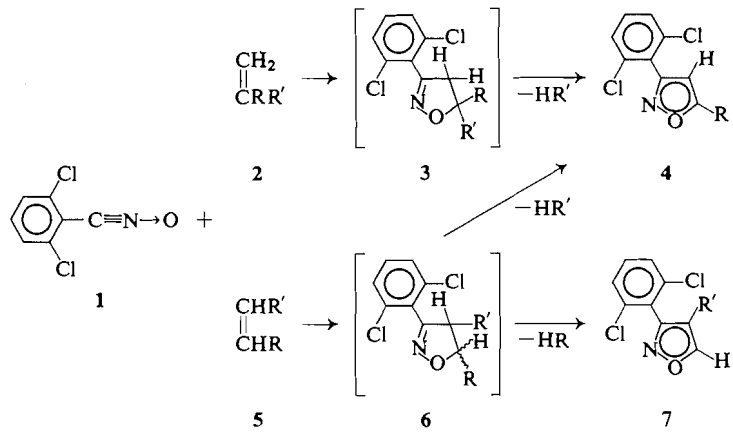

2 and **3**
a R = R′ = Cl
b R = CN, R′ = Cl
c R = CH_3, R′ = Br
d R = CH_2Cl, R′ = Cl

4
a R = Cl
b R = CN
c R = CH_3
d R = CH_2Cl

5 and **6**
a R = R′ = Cl (*cis*)
b R = R′ = Cl (*trans*)
c R = OEt, R′ = CN
d R = CH_3, R′ = Br

7
a R′ = Cl
c R′ = CN

SCHEME 1

In the case of the bromoolefins **2***c* and **5***d*, there was i.r. spectroscopic evidence for the concurrent formation of oximes similar to those recently reported in reactions with acetylenes (14, 15). We have not yet investigated this aspect in detail.

Experimental

The instruments used were those described previously (1). 2,5-Dichlorobenzonitrile oxide **1** was made as described by Grundmann and Dean (13). A sample of 3-ethoxyacrylonitrile **5***c* was obtained from Kay-Fries Chemicals Inc., New York 10017; all other olefins were purchased from commercial sources.

General Procedure

(*a*) 2,6-Dichlorobenzonitrile oxide (5.6 g, 0.03 mole) was added to a stirred solution of the olefin (0.036 mole) in dry THF (10 ml) cooled in an ice-bath. In some cases an exothermic reaction took place. After 1/2 h the solution was left at room temperature until the reaction was complete. The course of the reaction was followed by the disappearance of the nitrile oxide band in the i.r. spectrum of the reaction mixture. When the reaction was complete the mixture was concentrated under reduced pressure and triturated with a small volume of cold dry ether. The solid furoxan was removed by filtration and the ether solution concentrated. The residue, if solid, was crystallized, and if liquid, was distilled under reduced pressure.

(*b*) The reaction was done as described above except that the solvent used was ether (50 ml). Triethylamine (10 ml) was added after 24 h at room temperature. After a further 2 days at ambient temperature the mixture was washed with water, dried ($MgSO_4$), and concentrated under reduced pressure.

3-(2,6-Dichlorophenyl)-5-chloroisoxazole (4a)

1,1-Dichloroethylene (**2***a*) by method *a* gave a 72% yield of **4***a*, b.p. 119°/0.8 mm, m.p. 34–37°; see ref. 2.

3-(2,6-Dichlorophenyl)-trans-4,5-dichloroisoxazoline (6b)

Trans-1,2-dichloroethylene (**5***b*) after 3 days (method *a*) gave a 76% yield of **6***b*, m.p. 109–112° (hexane). The n.m.r. ($CDCl_3$) τ 2.59 (s, 3H), 3.40 (s, 1H), 4.34 (s, 1H). The C-4 and -5 protons in this case gave sharp singlets, which is surprising in view of the fact that other similar *trans*-isoxazolines show $J_{4,5}$ of *ca.* 6 Hz (16). This effect is probably due to hydrogen bonding and steric interactions which compress the dihedral angle of the vicinal hydrogen atoms to about 90° resulting in singlets for these protons (17).

Anal. Calcd. for $C_9H_5Cl_4NO$: C, 37.90; H, 1.76; N, 4.91. Found: C, 38.20; H, 1.81; N, 4.68.

3-(2,6-Dichlorophenyl)-cis-4,5-dichloroisoxazoline (6a)

Cis-1,2-dichloroethylene (**5***a*), required 2 weeks (method *a*) for the reaction to be complete. The product was purified by elution from a silica column using ether:hexane (1:19). Fractions (400 ml) were collected and monitored by the i.r. spectrum and weight of the residue after evaporation. Fractions 4 to 8 were collected and recrystallized from carbon tetrachloride when 1.7 g (20%) of **6***a*, m.p. 98–100° was obtained. The n.m.r. ($CDCl_3$) τ 2.57 (s, 3H), 3.22 (d, 1H), 4.05 (d, 1H), $J_{4,5}$

Can. J. Chem. Downloaded from www.nrcresearchpress.com by 210.87.254.105 on 09/05/12
For personal use only.

Can. J. Chem. Downloaded from www.nrcresearchpress.com by 210.87.254.105 on 09/05/12
For personal use only.

6.5 Hz. The reported $J_{4,5}$ for similar *cis*-isoxazolines is *ca.* 11 Hz (16).

Anal. Calcd. for $C_9H_5Cl_4NO$: C, 37.90; H, 1.76; N, 4.91. Found: C, 38.20; H, 1.68; N, 5.11.

3-(2,6-Dichlorophenyl)-5-cyanoisoxazole (4b)

2-Chloroacrylonitrile (**2***b*) (method *a*) gave 93% of **4***b*, m.p. 115–117° (CCl_4). The n.m.r. ($CDCl_3$) τ 2.59 (s, 3H), 2.94 (s, 1H).

Anal. Calcd. for $C_{10}H_4Cl_2N_2O$: C, 50.21; H, 1.67; N, 11.72; Cl, 29.71. Found: C, 50.26; H, 1.45; N, 11.76; Cl, 29.41.

3-(2,6-Dichlorophenyl)-4-cyanoisoxazole (7c)

3-Ethoxyacrylonitrile (**5***c*) (method *a*) gave 60% of 7*c*, m.p. 97–98° (hexane). The n.m.r. ($CDCl_3$) τ 0.95 (s, 1H), 2.57 (s, 3H).

Anal. Calcd. for $C_{10}H_4Cl_2N_2O$: C, 50.21; H, 1.67; N, 11.72; Cl, 29.71. Found: C, 50.21; H, 1.90; N, 11.73; Cl, 29.10.

3-(2,6-Dichlorophenyl)-5-methylisoxazole (4c)

Both 1-bromopropene (**5***d*) and 2-bromopropene (**2***c*) by method *b*, gave the same product **4***c* (b.p., i.r., and n.m.r. spectra identical) in yields of 73 and 95% respectively. The compound was a faint yellow oil, b.p. 110°/0.1 mm. The n.m.r. ($CDCl_3$) τ 2.60 (s, 3H), 3.89 (s, 1H), 7.51 (s, 3H). The signals at τ 3.89 and 7.51 although apparent singlets showed considerable broadening due to coupling between the C_4-proton and the C_5-methyl protons.

Anal. Calcd. for $C_{10}H_7Cl_2NO$: C, 52.68; H, 3.07; N, 6.14; Cl, 31.14. Found: C, 52.36; H, 2.97; N, 5.91; Cl, 30.80.

Method *a* in both cases gave a crude product which showed a strong broad i.r. absorption band at *ca.* 3200 cm^{-1}, and no band at 2300 cm^{-1}. Treatment of this reaction product in ether with triethylamine immediately gave a strong sharp band at 2300 cm^{-1}.

3-(2,6-Dichlorophenyl)-5-chloromethylisoxazole (4d)

2,3-Dichloropropene (**2***d*) (method *a*) gave 65% of **4***d*, b.p. 144–146°/0.3 mm. The n.m.r. (CCl_4) τ 2.69 (s, 3H), 3.63 (s, 1H), 5.33 (s, 2H).

Anal. Calcd. for $C_{10}H_6Cl_3NO$: C, 45.72; H, 2.29; N, 5.33. Found: C, 45.78; H, 2.36; N, 5.50.

3-(2,6-Dichlorophenyl)-4-chloroisoxazole (7a)

A 3 *M* solution of sodium hydroxide in methanol (2.7 ml, 0.008 mole) was added slowly to a stirred mixture of **6***a* or *b* (2.28 g, 0.008 mole) in methanol (35 ml). After 15 min the mixture was concentrated, the residue shaken with water (50 ml), and extracted with ethyl acetate (3 × 50 ml). The combined organic layers were dried ($MgSO_4$), filtered, and solvent removed when 1.9 g (100 %) of the 4-chloroisoxazole 7*a* was obtained. Recrystallization from hexane gave 1.6 g (86 %) of crystals m.p. 84–85°. The n.m.r. ($CDCl_3$) τ 1.37 (s, 1H), 2.58 (s, 3H).

Anal. Calcd. for $C_9H_4Cl_3NO$: C, 43.45; H, 1.61; N, 5.63; Cl, 42.86. Found: C, 43.71; H, 1.80; N, 5.38; Cl, 42.39.

Comparison of Rates of Dehydrochlorination of 6a and b

A solution of sodium hydroxide in methanol (1 ml of a 1 *M* solution, 0.001 mole) was added in one lot with shaking to a solution of **6***a* or *b* (280 mg, *ca.* 0.001 mole) in methanol (30 ml) at room temperature. After 10 s the equilibrium was frozen by adding hydrochloric acid (1 ml of a 3 *M* solution, 0.003 mole). The solutions were taken to dryness and an n.m.r. spectrum ($CDCl_3$) run on each residue.

The residue from **6***a* showed two sharp signals at τ 1.40 and 2.56 which is characteristic of 7*a* above.

The residue from **6***b* showed sharp signals at τ 1.40 and 2.56 characteristic of 7*a* and at τ 3.40 and 4.33 characteristic of **6***b*. The integration ratio of the signals at τ 1.40, 3.40, and 4.33 was 2:1:1 showing that there was *ca.* 66% conversion of **6***b* to 7*a*.

The author wishes to thank Dr. R. U. Lemieux, director of research, for his guidance and encouragement and Messrs. R. A. Fortier and R. R. Thomas for their capable technical assistance. We also wish to thank Kay-Fries Chemicals Inc., New York 10017, for the sample of 3-ethoxyacrylonitrile.

1. R. G. MICETICH. Can. J. Chem. **48**, 467 (1970).
2. R. G. MICETICH. Org. Prep. Proced. In press.
3. G. S. D'ALCONTRES and G. LO VECCHIO. Gazz. Chim. Ital. **90**, 1239 (1960).
4. P. GRÜNANGER. Gazz. Chim. Ital. **84**, 359 (1958).
5. G. S. D'ALCONTRES and P. GRÜNANGER. Gazz. Chim. Ital. **80**, 831 (1950).
6. M. CHRISTL. Ph.D. Thesis, University of Munich, Munich, West Germany, 1969.
7. A. QUILICO. *In* The chemistry of heterocyclic compounds. Interscience Publishers, New York, 1962. p. 32.
8. G. BIANCHI and P. GRÜNANGER. Tetrahedron, **21**, 817 (1965).
9. R. HUISGEN. Angew. Chem. Int. Ed. **2**, 565, 633 (1963).
10. N. K. KOCHETKOV and S. D. SOKOLOV. *In* Advances in heterocyclic chemistry. Vol. 2. Academic Press, New York, 1963. p. 377.
11. A. N. KOST and I. J. GRANDBERG. *In* Advances in heterocyclic chemistry. Vol. 6. Academic Press, New York, 1966. p. 381.
12. A. BATTAGLIA, A. DONDONI, and F. TADDEI. J. Heterocycl. Chem. 7, 721 (1970).
13. C. GRUNDMANN and J. M. DEAN. J. Org. Chem. **30**, 2809 (1965).
14. S. MORROCCHI, A. RICCA, A. ZANOROTTI, G. BIANCHI, R. GANDOLFI, and P. GRÜNANGER. Tetrahedron Lett. 3329 (1969).
15. A. BATTAGLIA and A. DONDONI. Tetrahedron Lett. 1221 (1970).
16. M. C. AVERSA, G. CUMM, and M. CRISAFULLI. Gazz. Chim. Ital. **98** 42 (1968).
17. M. KARPLUS. J. Chem. Phys. **30**, 11 (1959). M. KARPLUS and D. H. ANDERSON. J. Chem. Phys. **30**, 6 (1959).

Gaseous reactions and luminescence initiated by triboelectricity

S. DE PAOLI AND O. P. STRAUSZ
Department of Chemistry, University of Alberta, Edmonton, Alberta

Received August 10, 1970

Mercury shaken at room temperature in the presence of reduced pressure of a hydrocarbon, CO_2, acetone, N_2–H_2 mixture, etc., induces visible fluorescence and chemical transformations in the gaseous material.

Canadian Journal of Chemistry, 48, 3756 (1970)

Can. J. Chem. Downloaded from www.nrcresearchpress.com by 210.87.254.42 on 09/05/12
For personal use only.

The appearance of electrification upon rubbing together dissimilar substances is a familiar phenomenon, which is commonly referred to as frictional electrification or triboelectrification.[1] The source of this electrification is the separation of electrical charges caused by contact potential differences. The friction serves merely to bring about intimate surface contact; polished disks of steel and glass when pressed firmly together and then separated show charge separation. This type of charging between metal and glass also occurs when the metal is liquid such as mercury. In this case rubbing is not necessary, mere contact is capable of generating static charges (1).

Triboelectrification is frequently accompanied by optical phenomena, called triboluminescence. Triboelectrification and triboluminescence of solids, in particular, have been widely investigated. The companion triboluminescence of the triboelectrification of liquid mercury – glass system, however, has received attention only in the past decade (2 – 6) in spite of its discovery centuries ago (7, 8), and apparently no previous study has been reported on the chemistry of gaseous triboelectrical discharges. We have recently initiated a study of these phenomena, in which two particular aspects were explored: visual observation of optical phenomena and a survey of chemical reactions.

The luminescences were produced in a similar fashion as described by earlier workers (6, 7). Evacuated glass ampules were filled with a few Torr of gas material and sealed. The ampules were shaken manually or in a small laboratory vibrator. Luminescence occurs on relative motion of the mercury to the glass as the electrons trapped on unfilled surface sites of the glass jump back to the positively charged mercury pool (6). The effect on the visible emission of the nature of the filling gas, its pressure, temperature, the nature of the wall material and its surface conditions modified by subjecting it to various treatments prior to use were investigated.

Four tube materials, Pyrex glass, Vycor #7910, fused quartz, and plexiglass were examined. They all proved to be effective to produce light. The following gases were investigated: Ne (intense orange-red); He, Ar, Kr, Xe, H_2, CH_4, biacetyl, C_2H_4, air, Hg (no gas added) (light blue); CO (greenish-blue); N_2 (violet blue).

The use of sodium amalgam instead of pure mercury had the effect of changing the color and suppressing the intensity of emission. A Wood's alloy (Bi, Pb, Sn, and Cd, 50; 26.7; 13.3; 10.0) melting at 70 °C with neon gave the same characteristic orange-red color as with mercury.

The intensity of emission could be increased by increasing the area of contact surface through the use of glass spirals in the tube. The lamp constructed in this manner was suitable for the slow photolysis of acetone vapor.

Earlier spectroscopic studies (2, 5) have shown the presence of He and Ar lines in the luminescence spectra of He and Ar filled luminescence tubes. In order to produce emission from He an excitation energy in excess of 20 eV is required. This suggests that in reactive systems chemical reactions should occur. To investigate the chemistry of these systems, procedures were followed that were similar to those in the luminescence studies. Pyrex vessels (50–100 cc) containing a few grams of mercury were filled with methane (10–50 Torr) and sealed under vacuum. Shaking of the tube in a small laboratory shaker (1–10 h) led to extensive decompositions. The products are listed in Table 1 with yields expressed in relative gas chromatogram peak areas. The most interesting product is $(CH_3)_2Hg$, formed in moderately high yields. Some other examples of gaseous reactions are also listed in

[1]From the Greek word tribos, which means rubbing.

TABLE 1

Product yields from the triboelectrical discharge decomposition of hydrocarbons and acetone*

Substrate	Pressure (Torr)	Relative gas chromatogram peak areas of products										
		Me_2Hg	C_2H_2	C_2H_4	C_2H_6	H_2	C_3H_8	C_3H_6	CH_4	C_4†	MeHgEt	CO
CH_4	10	128	60	52	45	29	17	2	—	—	—	—
C_3H_8	10	55	60	32	112	12	—	50	145	35	11	—
CH_3COCH_3	12	621	—	—	137	—	23	27	107	45	—	814
C_2H_4	11	171	2014	—	208	62	72	147	333	—	191	—
H_2	8.3	40	396	—	130	—	42	21	—	17	—	—
C_2H_4	6.6											

*Conversions ranged from 5 to 30%.
†C_4-hydrocarbons.

the table, of which the synthesis of ammonia and hydrazine from a 3:1 mixture of N_2 and H_2 is noteworthy.

Similar reactions could be brought about by bubbling the appropriate gases through a pool of mercury.

The mechanisms of these reactions are obviously complex. The processes include electrical breakdown and direct and sensitized photolysis.

These phenomena have implications for gas phase kinetic studies. It is possible to produce spurious reactions in the Toepler pump and in other equipment where moving mercury surfaces are in contact with glass or gas materials. This possibility was checked and from hydrocarbons and acetone, we would indeed produce non-condensable gases on extensive pumping.

The authors wish to thank the National Research Council of Canada for financial support.

1. J. A. MEDLEY. Brit. J. Appl. Phys. Supp. 2, **28** (1953). W. R. HARPER. Advan. Phys. **6**, 365 (1957).
2. L. J. SCHOEN. Can. J. Phys. **38**, 967 (1960).
3. K. IKENOUE and Y. SASADA. Mem. Defense Acad. Jap. II, 49 (1962); II, 57 (1962).
4. J. L. SHERMAN, C. E. CARDWELL, D. Q. LAMB, Jr., and C. E. MANDEVILLE. Bull. Amer. Phys. Soc. **11**, 77 (1966).
5. G. L. DYBWAD and C. E. MANDEVILLE. Phys. Rev. **161**, 527 (1967).
6. G. L. DYBWAD. J. Appl. Phys. **40**, 4977 (1969).
7. A. WOLF. A History of Science, Technology and Philosophy in the 16th and 17th centuries. MacMillan, New York. 1935. p. 303.
8. FRA. HAUKSBEE. Phil. Trans. Roy. Soc. London, **24**, 2130 (1705). I. Newton Optics, or A treatise of the reflections, refractions, inflection and colours of light. 2nd ed. (1718) Qu. 8.

Kinetics of the exchange reaction of dimethylarsenic deuteride with diethylarsine

W. R. CULLEN AND W. R. LEEDER
Chemistry Department, University of British Columbia, Vancouver 8, British Columbia

Received May 8, 1970

The exchange reaction $(CH_3)_2AsD + (C_2H_5)_2AsH \rightleftharpoons (CH_3)_2AsH + (C_2H_5)_2AsD$ can be monitored by conventional nuclear magnetic resonance spectroscopy. The equilibrium constant in diethyl ether-d_{10} solution is 1.2 ± 0.1 and the rate constant for the forward reaction is $4.95 \pm 0.25 \times 10^{-5}$ l mole^{-1} s^{-1} at 35°. Dimethylarsine exchanges rapidly with methanol-d_4 and bis(trifluoromethyl)arsinic deuteride.

Canadian Journal of Chemistry, **48**, 3757 (1970)

Knowledge of the rate of exchange of secondary arsine protons, as in reaction 1, was important in determining the mechanism of the addition of secondary arsines to hexafluorobutyne-2,

$$[1]\quad (CH_3)_2AsD + (C_2H_5)_2AsH \underset{k_{-1}}{\overset{k_1}{\rightleftharpoons}} (CH_3)_2AsH + (C_2H_5)_2AsD$$

because the distribution of the deuterium label in the products of the competitive reaction described by reaction 2, would give mechanistic information

$$[2]\quad \left.\begin{matrix}(CH_3)_2AsD\\(C_2H_5)_2AsH\end{matrix}\right\} + CF_3C{\equiv}CCF_3 \rightarrow \begin{matrix}(CH_3)_2AsC(CF_3){=}C(CF_3)\binom{D}{H}\\(C_2H_5)_2AsC(CF_3){=}C(CF_3)\binom{H}{D}\end{matrix}$$

Can. J. Chem. Downloaded from www.nrcresearchpress.com by 210.87.254.42 on 09/05/12
For personal use only.

TABLE 1

Product yields from the triboelectrical discharge decomposition of hydrocarbons and acetone*

Substrate	Pressure (Torr)	Relative gas chromatogram peak areas of products										
		Me_2Hg	C_2H_2	C_2H_4	C_2H_6	H_2	C_3H_8	C_3H_6	CH_4	C_4†	MeHgEt	CO
CH_4	10	128	60	52	45	29	17	2	—	—	—	—
C_3H_8	10	55	60	32	112	12	—	50	145	35	11	—
CH_3COCH_3	12	621	—	—	137	—	23	27	107	45	—	814
C_2H_4	11	171	2014	—	208	62	72	147	333	—	191	—
H_2	8.3	40	396	—	130	—	42	21	—	17	—	—
C_2H_4	6.6											

*Conversions ranged from 5 to 30%.
†C_4-hydrocarbons.

the table, of which the synthesis of ammonia and hydrazine from a 3:1 mixture of N_2 and H_2 is noteworthy.

Similar reactions could be brought about by bubbling the appropriate gases through a pool of mercury.

The mechanisms of these reactions are obviously complex. The processes include electrical breakdown and direct and sensitized photolysis.

These phenomena have implications for gas phase kinetic studies. It is possible to produce spurious reactions in the Toepler pump and in other equipment where moving mercury surfaces are in contact with glass or gas materials. This possibility was checked and from hydrocarbons and acetone, we would indeed produce non-condensable gases on extensive pumping.

The authors wish to thank the National Research Council of Canada for financial support.

1. J. A. MEDLEY. Brit. J. Appl. Phys. Supp. 2, **28** (1953). W. R. HARPER. Advan. Phys. **6**, 365 (1957).
2. L. J. SCHOEN. Can. J. Phys. **38**, 967 (1960).
3. K. IKENOUE and Y. SASADA. Mem. Defense Acad. Jap. II, 49 (1962); II, 57 (1962).
4. J. L. SHERMAN, C. E. CARDWELL, D. Q. LAMB, Jr., and C. E. MANDEVILLE. Bull. Amer. Phys. Soc. **11**, 77 (1966).
5. G. L. DYBWAD and C. E. MANDEVILLE. Phys. Rev. **161**, 527 (1967).
6. G. L. DYBWAD. J. Appl. Phys. **40**, 4977 (1969).
7. A. WOLF. A History of Science, Technology and Philosophy in the 16th and 17th centuries. MacMillan, New York. 1935. p. 303.
8. FRA. HAUKSBEE. Phil. Trans. Roy. Soc. London, **24**, 2130 (1705). I. Newton Optics, or A treatise of the reflections, refractions, inflection and colours of light. 2nd ed. (1718) Qu. 8.

Kinetics of the exchange reaction of dimethylarsenic deuteride with diethylarsine

W. R. CULLEN AND W. R. LEEDER
Chemistry Department, University of British Columbia, Vancouver 8, British Columbia

Received May 8, 1970

The exchange reaction $(CH_3)_2AsD + (C_2H_5)_2AsH \rightleftharpoons (CH_3)_2AsH + (C_2H_5)_2AsD$ can be monitored by conventional nuclear magnetic resonance spectroscopy. The equilibrium constant in diethyl ether-d_{10} solution is 1.2 ± 0.1 and the rate constant for the forward reaction is $4.95 \pm 0.25 \times 10^{-5}$ l mole^{-1} s^{-1} at 35°. Dimethylarsine exchanges rapidly with methanol-d_4 and bis(trifluoromethyl)arsinic deuteride.

Canadian Journal of Chemistry, **48**, 3757 (1970)

Knowledge of the rate of exchange of secondary arsine protons, as in reaction 1, was important in determining the mechanism of the addition of secondary arsines to hexafluorobutyne-2,

$$[1]\quad (CH_3)_2AsD + (C_2H_5)_2AsH \underset{k_{-1}}{\overset{k_1}{\rightleftharpoons}} (CH_3)_2AsH + (C_2H_5)_2AsD$$

because the distribution of the deuterium label in the products of the competitive reaction described by reaction 2, would give mechanistic information

$$[2]\quad \left.\begin{matrix}(CH_3)_2AsD\\(C_2H_5)_2AsH\end{matrix}\right\} + CF_3C{\equiv}CCF_3 \rightarrow \begin{matrix}(CH_3)_2AsC(CF_3){=}C(CF_3)\binom{D}{H}\\(C_2H_5)_2AsC(CF_3){=}C(CF_3)\binom{H}{D}\end{matrix}$$

Can. J. Chem. Downloaded from www.nrcresearchpress.com by 210.87.254.105 on 09/05/12
For personal use only.

Can. J. Chem. Downloaded from www.nrcresearchpress.com by 210.87.254.105 on 09/05/12
For personal use only.

only if no significant exchange occurred between the reactants and/or products (1).

Proton transfer reactions have been studied using a wide variety of methods (2), including specialized fast reaction techniques (3). However, reaction 1 was slow enough to be followed by simple integration of the nuclear magnetic resonance (n.m.r.) spectrum of the reaction mixture.

Experimental and Results

Starting Materials and Techniques

A vacuum system was used for the manipulation of volatile substances. Nuclear magnetic resonance spectra were run on Varian A 60 (^{1}H spectra in p.p.m. downfield from external TMS), and HA 100 (^{19}F spectra in p.p.m. upfield from internal $CFCl_3$) spectrometers. Methanol-d_4 (99.9%), diethyl ether-d_{10}, deuterium chloride, and D_2O were purchased from Merck, Sharp and Dohme of Canada Ltd. Bis(trifluoromethyl)-arsine was prepared from tetrakis(trifluoromethyl)diarsine by reacting this with hydrogen chloride in the presence of mercury (4). The ^{1}H n.m.r. spectrum showed a septet centered at 5.08 p.p.m. (J_{CF_3-H} = 9.2 Hz) and the ^{19}F n.m.r. spectrum a doublet centered at 42.3 p.p.m. Bis(trifluoromethyl)arsenic deuteride was similarly prepared using deuterium chloride. The ^{1}H n.m.r. spectrum of the product indicated that some hydride was present. The material was shaken with D_2O for two weeks to yield pure bis(trifluoromethyl)arsenic deuteride. The gas phase infrared spectrum of the deuteride run on a Perkin–Elmer 457 instrument showed main bands at 1548 m, 1190 s, 1168 s, 1120 s, 734 cm^{-1}. Dimethylarsenic deuteride and diethylarsine were prepared as previously described (1).

Proton Exchange Reactions and Kinetics

Weighed portions of materials whose exchange was to be followed, plus a measured amount of solvent when used, were sealed in n.m.r. tubes and kept frozen until they were to be studied. The tubes were quickly warmed to room temperature and placed immediately in the n.m.r. spectrometer. Care was taken to isolate the starting materials with a layer of solvent, to try to prevent any unnecessary exchange before the mixing was complete.

In a typical experiment, 0.118 g of diethylarsine, then diethyl ether-d_{10}, and finally 0.036 g of dimethylarsenic deuteride were sealed in an n.m.r. tube. Upon quickly warming the tube to 35°, the exchange was followed by integrating over the methyl peaks of dimethylarsine and dimethylarsenic deuteride. Figure 1 shows typical spectra in this region run at a sweep width of 50 c.p.s. The following results were found.

t(s)*	Concentration of $(CH_3)_2AsD$ (moles/l)
3 600†	0.458
3 765	0.459
3 870	0.452
7 935	0.337
8 100	0.341
8 220	0.331
10 080	0.303
10 260	0.301
10 425	0.306
11 940	0.271
12 030	0.280
12 120	0.278

*t = 0 is arbitrary.
†Previous to this time the methyl peaks of the hydride and deuteride were not separated well enough for reliable integration.

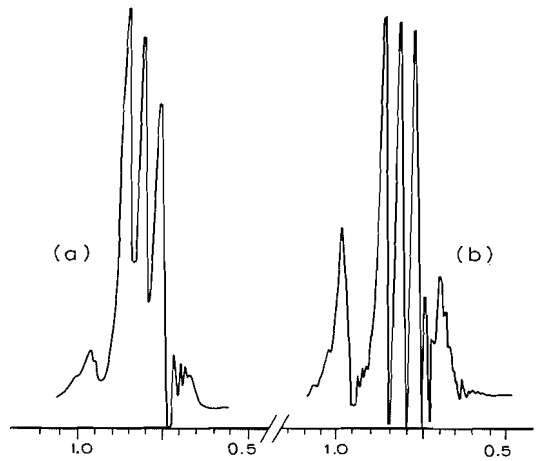

FIG. 1. ^{1}H n.m.r. spectra of the CH_3 region in mixtures of $(CH_3)_2AsH$ and $(CH_3)_2AsD$. (*a*) Mainly $(CH_3)_2AsD$, (*b*) a higher proportion of $(CH_3)_2AsH$.

The following reaction scheme yields a kinetic rate law which corresponds with the experimental results

$$[3] \qquad AD + BH \xrightarrow{k_1} AH + BD$$

$$[4] \qquad AH + BD \xrightarrow{k_{-1}} AD + BH$$

If the following abbreviations for concentrations are made: at $t = 0$, [AD] = a and [BH] = b; at $t = t$, [AH] = x = [BD] and [AD] = $a - x$; the rate law from reactions 3 and 4 is

$$[5] \qquad dx/dt = k_1(a - x)(b - x) - k_{-1}x^2$$

TABLE 1

The rate and equilibrium constants for the proton exchange reactions*

Reactant A	Concentration of A (mole/l)	Reactant B	Concentration of B (mole/l)	Solvent	K	k_1
$(CH_3)_2AsD$	4.32	$(C_2H_5)_2AsH$	5.95	Neat	1.315	—
$(CH_3)_2AsD$	3.74	$(C_2H_5)_2AsH$	6.24	Neat	1.335	5.9×10^{-5}
$(CH_3)_2AsD$	1.12	$(C_2H_5)_2AsH$	2.43	$(C_2D_5)_2O$	1.1	4.7×10^{-5}
$(CH_3)_2AsD$	0.852	$(C_2H_5)_2AsH$	2.19	$(C_2D_5)_2O$	1.365	5.2×10^{-5}
$(CH_3)_2AsD$	0.275	$(C_2H_5)_2AsH$	2.71	$(C_2D_5)_2O$	†	†
$(CH_3)_2AsH$	2.46	$(CF_3)_2AsD$	1.76	$(C_2D_5)_2O$	0.28	‡
$(CH_3)_2AsH$	0.187	$(CF_3)_2AsD$	0.450	$(C_2D_5)_2O$	0.36	‡

*The reaction temperature is ~ 35°.
†Due to the small amount of dimethylarsenic deuteride used, the diethylarsine peaks overlapped seriously in the n.m.r. spectrum.
‡Too fast to measure.

Solving eq. 5 and using the equilibrium constant, $K = k_1/k_{-1}$, gives the result

$$[6] \quad k_{-1}t = \frac{1}{\sqrt{-q}} \ln \left(\frac{2cx + d - \sqrt{-q}}{2cx + d + \sqrt{-q}} \right)$$

where $q = 4Kab(K - 1) - K^2(a + b)^2$, $c = (K - 1)$, and $d = -K(a + b)$. Plotting t against $\ln (2cx + d - \sqrt{-q})/(2cx + d + \sqrt{-q})$ gives a straight line as seen in Fig. 2. From the slope, k_{-1}, and thus k_1, can be determined from a knowledge of the value of K.

A number of exchange reactions of dimethylarsine or dimethylarsenic deuteride were monitored by n.m.r., as described above, and the results are summarized in Table 1.

Discussion

Of the different proton exchanges of hydrides with dimethylarsine investigated (Table 1), only the reaction described by eq. 1 could be studied kinetically. The proton exchange of the arsines corresponds with a rate law [5] based on the mechanism outlined in reactions 3 and 4 whose solution is eq. 6. The rate constants (k_1) for the exchanges done neat and in diethyl ether-d_{10} solvent, are 5.9×10^{-5} and $4.95 \pm 0.25 \times 10^{-5}$ l mole^{-1} s^{-1} at 35°. The equilibrium constants are 1.335 ± 0.020 and 1.2 ± 0.1, respectively.

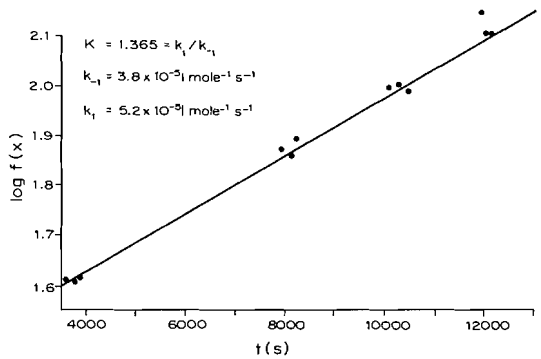

FIG. 2. Plot of $\log f(x)$ against time (eq. 6) for the reaction of $(CH_3)_2AsD$ with $(C_2H_5)_2AsH$ in $(C_2D_5)_2O$ solution.

The range of concentrations that could be satisfactorily used for these rate studies was very small, as will now be explained. Since the equilibrium in reaction 1 was to the right, it was desirable to study the exchange from the left side to increase the relative difference in concentrations between the dimethylarsenic deuteride and hydride monitored during the reaction. At high dimethylarsenic deuteride concentrations, relative to diethylarsine, there were too few protons exchanged at equilibrium to make integration practical. Consequently, the diethylarsine concentration had to be the greater of the two to give satisfactory results. Due to the overlap of small diethylarsine peaks in the n.m.r. spectra, with the methyl peaks for dimethylarsine, dimethylarsenic deuteride could not be less than 1/3 of the concentration of diethylarsine. If it were less than this, analysis was impossible as is seen in the last diethylarsine example in Table 1. The optimal relative concentrations were used for the rate studies in the three successfully analyzed experiments. It was found when the concentrations were changed absolutely and not relatively, these exchanges obeyed the same rate law and had similar rate constants. The exchange of these hydrides was slightly faster when done neat than when done in diethyl ether-d_{10}.

The exchange rate of bis(trifluoromethyl)-arsenic deuteride with dimethylarsine was studied in the hope of finding another slow exchange system that could be used in the competitive addition to hexafluorobutyne-2. (*c.f.* reaction 2) The rate of exchange in reaction 7 was found to be

Can. J. Chem. Downloaded from www.nrcresearchpress.com by 210.87.254.105 on 09/05/12
For personal use only.

too fast to measure by n.m.r. integration techniques. Calculation of the equilibrium constant, 0.32 ± 0.06 in diethyl ether-d_{10} at 35° was possible, however. Consequently these hydrides are

[7] $(CF_3)_2AsD + Me_2AsH \rightleftharpoons (CF_3)_2AsH + Me_2AsD$

unsuitable for a competitive addition reaction, as they would exchange protons to a significant extent before addition to the acetylene occurred.

Dimethylarsine adds to hexafluorobutyne-2 in methanol solvent much faster than in ether and the product is 100% *trans* isomer (1), when the reaction is carried out in methanol-d_4 the 1:1 adduct is 85% deuterated (5). However, we have now found a fast exchange takes place between dimethylarsine and methanol-d_4 so that an interpretation of the deuterium content of the adduct in terms of the mechanism of the addition reaction is not possible.

The mechanism involved in these exchanges is open to speculation. An ionic or four-centered mechanism can meet the kinetic requirements. Meiboom and co-workers (6, 7) have indicated that the water–methanol proton transfer is non-ionic in a neutral solution, but ionic when traces of bases or acids are present. At 25° the rate of the non-ionic process ($k_1 \sim 10^0$ l mole^{-1} s^{-1}) is much slower than the trace acid or base induced ionic process ($k_1 \sim 10^6$ l mole^{-1} s^{-1}). It is possible that the arsines are strong enough bases to promote an ionic exchange between themselves and methanol. However, the slow rate for the dimethylarsenic deuteride – diethylarsine exchange ($\sim 10^{-3}$ l mole^{-1} s^{-1}) seems to be against an ionic mechanism. Thus a four-centered mechanism could very well be the main path for the arsine exchange mechanism as depicted in reaction 8. This 4-center mechanism is favored by

[8] $$(CH_3)_2AsD + (C_2H_5)_2AsH \rightleftharpoons \begin{bmatrix} (C_2H_5)_2As & \cdots & H \\ \vdots & & \vdots \\ D & \cdots & As(CH_3)_2 \end{bmatrix} \rightleftharpoons (C_2H_5)_2AsD + (CH_3)_2AsH$$

Gold and Satchell (2) for amine proton transfers, as well as by other authors for various related proton exchanges such as the tin hydride – tin deuteride exchange (8).

The authors wish to thank the National Research Council of Canada for financial support.

1. W. R. Cullen and W. R. Leeder. Can. J. Chem. **47**, 2137 (1969).
2. V. Gold and D. P. N. Satchell. Quart. Rev. **9**, 51 (1955).
3. E. F. Caldin. Fast reactions in solution. Blackwell Scientific Publications, Oxford. 1964.
4. W. R. Cullen. Can. J. Chem. **39**, 1855 (1961).
5. W. R. Leeder. Ph.D. thesis. University of British Columbia, Vancouver 8, B.C. 1970.
6. Z. Luz, D. Gill, and S. Meiboom. J. Chem. Phys. **30**, 1540 (1959).
7. E. Grunwald, C. F. Jumper, and S. Meiboom. J. Amer. Chem. Soc. **81**, 4664 (1962).
8. W. P. Neumann and R. Sommer. Angew. Chem. Internat. Ed. **2**, 517 (1963).

Concerning rhenium nitrogen fluoride and technetium nitrogen fluoride

M. Cowie, C. J. L. Lock,[1] and J. Ozog
Institute for Materials Research, McMaster University, Hamilton, Ontario

Received July 31, 1970

We have shown that the reported (1) X-ray powder pattern of "ReNF" is that of NH_4ReO_4 and we suggest that the X-ray powder pattern of "TcNF" is that of $(NH_4)_2TcF_6$. In light of these results we suggest that the existence of the discrete phases ReNF and TcNF has not been proven.

Canadian Journal of Chemistry, 48, 3760 (1970)

Introduction

La Valle *et al.* (1) have reported the existence of the compounds ReNF and TcNF which might be expected to have similarities to ZrNF, and ThNF (2). Apart from analytical data and X-ray powder results, no physical properties were reported. It became apparent as a result of our experiments that some of the data reported by La Valle *et al.* have been misinterpreted. We were able to prepare a black solid by the method

[1]To whom correspondence should be addressed.

Can. J. Chem. Downloaded from www.nrcresearchpress.com by 210.87.254.105 on 09/05/12
For personal use only.

too fast to measure by n.m.r. integration techniques. Calculation of the equilibrium constant, 0.32 ± 0.06 in diethyl ether-d_{10} at 35° was possible, however. Consequently these hydrides are

[7] $(CF_3)_2AsD + Me_2AsH \rightleftharpoons (CF_3)_2AsH + Me_2AsD$

unsuitable for a competitive addition reaction, as they would exchange protons to a significant extent before addition to the acetylene occurred.

Dimethylarsine adds to hexafluorobutyne-2 in methanol solvent much faster than in ether and the product is 100% *trans* isomer (1), when the reaction is carried out in methanol-d_4 the 1:1 adduct is 85% deuterated (5). However, we have now found a fast exchange takes place between dimethylarsine and methanol-d_4 so that an interpretation of the deuterium content of the adduct in terms of the mechanism of the addition reaction is not possible.

The mechanism involved in these exchanges is open to speculation. An ionic or four-centered mechanism can meet the kinetic requirements. Meiboom and co-workers (6, 7) have indicated that the water–methanol proton transfer is non-ionic in a neutral solution, but ionic when traces of bases or acids are present. At 25° the rate of the non-ionic process ($k_1 \sim 10^0$ l mole^{-1} s^{-1}) is much slower than the trace acid or base induced ionic process ($k_1 \sim 10^6$ l mole^{-1} s^{-1}). It is possible that the arsines are strong enough bases to promote an ionic exchange between themselves and methanol. However, the slow rate for the dimethylarsenic deuteride – diethylarsine exchange ($\sim 10^{-3}$ l mole^{-1} s^{-1}) seems to be against an ionic mechanism. Thus a four-centered mechanism could very well be the main path for the arsine exchange mechanism as depicted in reaction 8. This 4-center mechanism is favored by

[8] $$(CH_3)_2AsD + (C_2H_5)_2AsH \rightleftharpoons \begin{bmatrix} (C_2H_5)_2As & \cdots & H \\ \vdots & & \vdots \\ D & \cdots & As(CH_3)_2 \end{bmatrix} \rightleftharpoons (C_2H_5)_2AsD + (CH_3)_2AsH$$

Gold and Satchell (2) for amine proton transfers, as well as by other authors for various related proton exchanges such as the tin hydride – tin deuteride exchange (8).

The authors wish to thank the National Research Council of Canada for financial support.

1. W. R. Cullen and W. R. Leeder. Can. J. Chem. **47**, 2137 (1969).
2. V. Gold and D. P. N. Satchell. Quart. Rev. **9**, 51 (1955).
3. E. F. Caldin. Fast reactions in solution. Blackwell Scientific Publications, Oxford. 1964.
4. W. R. Cullen. Can. J. Chem. **39**, 1855 (1961).
5. W. R. Leeder. Ph.D. thesis. University of British Columbia, Vancouver 8, B.C. 1970.
6. Z. Luz, D. Gill, and S. Meiboom. J. Chem. Phys. **30**, 1540 (1959).
7. E. Grunwald, C. F. Jumper, and S. Meiboom. J. Amer. Chem. Soc. **81**, 4664 (1962).
8. W. P. Neumann and R. Sommer. Angew. Chem. Internat. Ed. **2**, 517 (1963).

Concerning rhenium nitrogen fluoride and technetium nitrogen fluoride

M. Cowie, C. J. L. Lock,[1] and J. Ozog
Institute for Materials Research, McMaster University, Hamilton, Ontario

Received July 31, 1970

We have shown that the reported (1) X-ray powder pattern of "ReNF" is that of NH_4ReO_4 and we suggest that the X-ray powder pattern of "TcNF" is that of $(NH_4)_2TcF_6$. In light of these results we suggest that the existence of the discrete phases ReNF and TcNF has not been proven.

Canadian Journal of Chemistry, 48, 3760 (1970)

Introduction

La Valle *et al.* (1) have reported the existence of the compounds ReNF and TcNF which might be expected to have similarities to ZrNF, and ThNF (2). Apart from analytical data and X-ray powder results, no physical properties were reported. It became apparent as a result of our experiments that some of the data reported by La Valle *et al.* have been misinterpreted. We were able to prepare a black solid by the method

[1]To whom correspondence should be addressed.

Can. J. Chem. Downloaded from www.nrcresearchpress.com by 210.87.254.105 on 09/05/12
For personal use only.

described for ReNF with an X-ray powder pattern identical to that described for ReNF, but the white crystalline starting material which we assumed was $(NH_4)_2ReF_6$, and which we had heated to give "ReNF" had an identical X-ray powder pattern. As a result we have investigated this system in greater detail.

We found that the two methods of making K_2ReF_6 (1, 2) used by La Valle *et al.* gave mixtures whose composition varied considerably with the reaction conditions. All mixtures contained considerable amounts of $KReO_4$ which was difficult to separate from K_2ReF_6 except by hand picking the single crystals. Unless this separation was carried out very carefully the perrhenate ion carried through the procedure used to give $(NH_4)_2ReF_6$ and yielded NH_4ReO_4. Both gave black products on heating at 300°, but unless heating was continued for some time, the products contain the starting ammonium salts as shown by X-ray powder diffraction patterns. The ammonium salts were extracted with water when both black residues were found to be amorphous. A comparison of the X-ray powder data for "ReNF" (1) and ammonium perrhenate (3) given in Table 1 shows clearly that the two are the same. It is clear that the sample of "ReNF" used by La Valle *et al.* for X-ray studies must have contained considerable amounts of NH_4ReO_4, and it is possible to see, in light of our experiments, how this could have occurred.

TABLE 1

Comparison of the X-ray diffraction patterns of NH_4ReO_4 and "ReNF"

NH_4ReO_4 (3)		"ReNF" (1)	
d	*I*	*d*	*I*
5.361	70	5.334	s
3.504	100	3.492	s+
3.245	13	3.240	m+
2.942	17	2.938	s−
2.680	3	—	—
2.581	20	2.576	m
2.3749	9	—	—
2.2477	13	2.240	m+
2.1791	20	2.174	s−
2.0800	9	2.073	m
1.9803	1	—	—
1.9391	5	1.932	w+
1.9193	11	1.914	m+
1.8479	11	1.842	m+
1.7885	20	1.782	s−
1.7685	5	1.764	w
1.7511	9	1.748	m+
1.6189	7	1.614	m
1.5647	3	1.561	m−
1.5267	7	1.524	m
1.5156	5	1.513	m
1.4706	3	1.470	w+
1.4182	7	1.419	m+
1.4108	9	1.409	s−
1.4009	3	—	—
1.3817	3	1.381	m−
1.3558	5	1.354	m+
1.3472	3	1.347	w
1.3397	3	1.339	w+
1.3155	5	1.315	w+
1.2793	1	1.280	m−
1.2647	1	1.265	m−
1.2504	1	—	
1.2390	3	—	
1.2251	1	—	
1.2192	3	1.219	m
Others			
a = 5.883 Å		a = 5.88 Å	
c = 12.979 Å		c = 13.00 Å	

*d = interplanar spacing; I = intensity; s = strong; m = medium; w = weak.

We have shown, however, that the reaction described by La Valle *et al.* does take place. $(NH_4)_2ReF_6$, on heating at 300° in nitrogen, did give a black product, and we assume that NH_3 and HF were emitted from the sample since $(NH_4)_2SiF_6$ (identified by an X-ray powder pattern) collected in the cooler part of the tube. The black residue was not crystalline, however, as shown by its X-ray powder pattern, and the decomposition residues obtained by us varied in weight more than those of La Valle *et al.* Despite the excellent thermogravimetric and analytical results of La Valle *et al.*, we feel that further evidence is needed to prove the existence of ReNF as a discrete phase.

We have not attempted to prepare TcNF, but by comparison with the rhenium system one can argue that the X-ray data given for "TcNF" (1) are really those of ammonium hexafluorotechnate. The X-ray data presented by La Valle *et al.* can be indexed using hexagonal unit cell parameters of a = 5.98 Å and c = 4.79 Å. The parameters are very close to those reported for $(NH_4)_2TcF_6$ (4) but are not in themselves significant since the unit cell parameters of monoclinic TcO_2, with which TcNF might be isostructural, are a = 5.53 Å, b = 4.79 Å, c = 5.53 Å, and β = 120° (5) and it would be very difficult to distinguish between the $(NH_4)_2TcF_6$ cell and a TcO_2 (or MoO_2 or ReO_2) type cell. It should be possible, however, to differentiate between the two types of cell on the basis of the intensities of the lines.

It is not necessary to consider previous transition metal nitride fluoride structure types in the comparison since thorium and zirconium nitride fluorides (6) have the LaOF structure which in

Can. J. Chem. Downloaded from www.nrcresearchpress.com by 210.87.254.105 on 09/05/12
For personal use only.

TABLE 2

Comparison of X-ray powder data for "TcNF" with $(NH_4)_2ReF_6$, ReO_2, and MoO_2

"TcNF" (1)		$(NH_4)_2ReF_6$*		ReO_2 (3)		MoO_2 (3)	
d	*I*	*d*	*I*	*d*	*I*	*d*	*I*
5.200	s	5.209	88				
4.791	s	4.785	39			4.78	20
3.502	s	3.511	100	3.40	100	3.41	100
2.985	m+	3.006	51	2.79	20	2.80	30
2.533	m+	2.544	40	2.40	100	2.433	50 }
						2.420	85 } 225
						2.405	40 }
						2.397	50 }
2.279	s−	2.286	59				
2.173	m+	2.172	10	2.17	20	2.176	30 }
						2.171	10 } 40
1.959	m−	1.970	20				
1.871	m	1.869	30	1.85	20	1.833	35
1.815	m	1.822	37				
1.760	m+	1.761	29				
1.738	w−	1.736	12	1.69	10	1.713	55
						1.704	80
						1.692	50
1.519	m	1.523	30	1.52	40	1.597	10
						1.540	25
						1.530	40
						1.522	35
1.497	m	1.497	5				
1.435	m−	1.438	12	1.44	20	1.463	25
1.407	m	1.407	7	—		1.402	10
						1.397	50
1.377	m−	1.383	14	1.385	30	1.379	30
1.361	w+	1.357	8			1.351	10
		1.237	3	Others		1.340	10
		1.194	11			Others	
		1.162	12				
		1.109	9				
		1.071	18				

*This work.

turn is derived from CaF_2 (7). Most LaOF structures are cubic or tetragonal. The only known hexagonal structures have a rhombohedral cell with a about 7 Å and α about 33°, which do not correspond to the parameters for TcNF. A comparison of the data for TcNF with those for $(NH_4)_2ReF_6$, ReO_2 (3), and MoO_2 (3) is made in Table 2. It can be seen that the TcNF data correspond to those for $(NH_4)_2ReF_6$ but not to those for ReO_2 and MoO_2. It appears, therefore, that the X-ray powder data reported for "TcNF" are those of $(NH_4)_2TcF_6$, and we suggest that the existence of the phase TcNF has not been proved.

Experiments

Analyses were performed by conventional methods. Ammonia was determined by titration after being distilled from a 3 *M* sodium hydroxide solution of the salt. Rhenium fluoride compounds were decomposed with molten potassium in a vacuum. The residue was first attacked with a few ml of methanol to destroy any residual potassium. The mixture was extracted with water to remove fluoride ion. The residual rhenium metal was dissolved in hydrogen peroxide and determined as tetraphenylarsonium perrhenate (8). X-Ray photographs were recorded for powdered samples mounted in quartz tubes by the Debye–Scherrer technique using nickel-filtered copper Kα radiation.

Anal. Found for $KReO_4$: K, 13.2; Re, 64.1; K_2ReF_6: K, 20.0; Re, 50.7; NH_4ReO_4: NH_3, 6.0; Re, 68.7; $(NH_4)_2ReF_6$: NH_3, 10.0; Re, 56.1.

Weight loss of $(NH_4)_2ReF_6$ on heating at 300 °C: 29.9% and 33.8%. X-Ray powder patterns of $KReO_4$, NH_4ReO_4, and $(NH_4)_2SiF_6$ samples obtained by us were essentially identical with those reported in the Powder Index (3). Data for K_2ReF_6 and $(NH_4)_2ReF_6$ could be indexed in terms of the published parameters (4).

We thank the National Research Council of Canada for financial support.

1. D. E. LaValle, R. M. Steele, and W. T. Smith, Jr. J. Inorg. Nucl. Chem. **28**, 260 (1966).
2. E. Weise. Z. anorg. Chem. **283**, 377 (1956).

Can. J. Chem. Downloaded from www.nrcresearchpress.com by 210.87.254.105 on 09/05/12
For personal use only.

3. Powder diffraction File, Amer. Soc. Testing and Materials, Pa., U.S.A. Cards 7–13, $(NH_4)_2SiF_6$; 10–252, NH_4ReO_4; 8–14, $KReO_4$; 5–0452, MoO_2; 17–600, ReO_2.
4. R. D. PEACOCK. J. Chem. Soc. 1291 (1956).
5. W. H. ZACHARIASEN. Acta Chem. Scand. **9**, 1378 (1955).
6. R. JUZA, R. SIEVERS, and W. JUNG. Naturwiss. **53**, 551 (1966).
7. A. F. WELLS. Structural inorganic chemistry. 3rd ed. Oxford University Press, Oxford. 1962. p. 388.
8. H. H. WILLARD and C. C. SMITH. Ind. Eng. Chem. Anal. Ed. **11**, 305 (1939).

An external heavy atom effect on biacetyl in the gas phase?

A. W. JACKSON AND A. J. YARWOOD
Department of Chemistry, McMaster University, Hamilton, Ontario

Received June 5, 1970

The luminescence intensity of biacetyl in the gaseous phase at 303 °K was studied, and the external heavy atom effect of xenon on the luminescence excited at 405 nm was re-examined. The effect on the phosphorescence lifetime was also investigated. In contrast to an earlier report, the external heavy atom effect of xenon on the triplet state of biacetyl is very small and probably negligible.

Canadian Journal of Chemistry **48**, 3763 (1970)

Can. J. Chem. Downloaded from www.nrcresearchpress.com by 210.87.254.105 on 09/05/12
For personal use only.

The dissipation of electronic energy in molecules is affected by the environment, and the rate constants governing the radiative and radiationless processes are modified. Apart from changes due to phase and temperature the major effects (1) are those associated with perturbations (*a*) by oxygen, nitric oxide or paramagnetic ions or molecules, (*b*) in systems with charge-transfer complexes, and (*c*) by atoms of high atomic number (heavy atom effect).

External heavy atoms can affect the absorption from the ground electronic state to the first excited triplet state, the rate constants of the radiationless processes to and from the triplet state, and the rate constant of the radiative transition from the triplet to the singlet state (phosphorescence).

The increase in $T_1 \leftarrow S_0$ absorptions by heavy atoms was first shown by Kasha (2) for the chloronaphthalene – ethyl iodide system. Later, many other examples (*e.g.* refs. 3–6) were discovered and the enhancement of $T_1 \leftarrow S_0$ absorptions by an external heavy atom effect is well documented. However, there are conflicting reports in the literature concerning the relative importance of the external heavy atom effect on the radiationless process to and the radiative and radiationless processes from the triplet state (7, 8).

The early research used ethyl iodide as the perturbing species but more recently xenon has been used as an external heavy atom. (The advantage is that xenon does not absorb in the ultraviolet region.) Robinson (9) suggested that xenon enhanced the intersystem crossing from the singlet to the triplet in solid benzene at 4.2 °K since the fluorescence was quenched. Wilkinson and co-workers (10) demonstrated convincingly this effect in liquids, by showing that the quantum yield of triplets was increased by xenon quenching of the singlet states of polynuclear aromatic compounds. Cundall and Voss (11) showed that xenon dissolved in xylene also increased the triplet state yield. Studies of gaseous systems have also shown the effect of external heavy atoms, thus the fluorescence of toluene is quenched by xenon (12).

It has been suggested recently (13) that xenon can interact with π^*-n triplet states since the intensity of phosphorescence of biacetyl in the gas phase decreased in the presence of xenon. However, xenon has only a very small effect on the lifetime of the triplet state of hexafluoroacetone (14) so we have re-examined the biacetyl–xenon system and investigated the external heavy atom effect on the lifetime of triplet biacetyl in the gas phase.

Experimental

The biacetyl (MCB Chromatoquality) was distilled at −78 °C and stored in the dark at −196 °C. The xenon was Airco research grade.

The total luminescence studies used a 50 W medium pressure Hg lamp (Gates Omnirange) as the light source and the 405 nm line was isolated using a narrow band filter (maximum transmission at 403 nm, transmits 1% at 386 and 430 nm). A portion of the incident light reflected from a quartz plate and was monitored by a photocell (935). The 10 cm long quartz cell was T shaped and the emitted light was observed through a Suprasil

3. Powder diffraction File, Amer. Soc. Testing and Materials, Pa., U.S.A. Cards 7–13, $(NH_4)_2SiF_6$; 10–252, NH_4ReO_4; 8–14, $KReO_4$; 5–0452, MoO_2; 17–600, ReO_2.
4. R. D. PEACOCK. J. Chem. Soc. 1291 (1956).
5. W. H. ZACHARIASEN. Acta Chem. Scand. **9**, 1378 (1955).
6. R. JUZA, R. SIEVERS, and W. JUNG. Naturwiss. **53**, 551 (1966).
7. A. F. WELLS. Structural inorganic chemistry. 3rd ed. Oxford University Press, Oxford. 1962. p. 388.
8. H. H. WILLARD and C. C. SMITH. Ind. Eng. Chem. Anal. Ed. **11**, 305 (1939).

An external heavy atom effect on biacetyl in the gas phase?

A. W. JACKSON AND A. J. YARWOOD
Department of Chemistry, McMaster University, Hamilton, Ontario

Received June 5, 1970

The luminescence intensity of biacetyl in the gaseous phase at 303 °K was studied, and the external heavy atom effect of xenon on the luminescence excited at 405 nm was re-examined. The effect on the phosphorescence lifetime was also investigated. In contrast to an earlier report, the external heavy atom effect of xenon on the triplet state of biacetyl is very small and probably negligible.

Canadian Journal of Chemistry **48**, 3763 (1970)

Can. J. Chem. Downloaded from www.nrcresearchpress.com by 210.87.254.42 on 09/05/12
For personal use only.

The dissipation of electronic energy in molecules is affected by the environment, and the rate constants governing the radiative and radiationless processes are modified. Apart from changes due to phase and temperature the major effects (1) are those associated with perturbations (*a*) by oxygen, nitric oxide or paramagnetic ions or molecules, (*b*) in systems with charge-transfer complexes, and (*c*) by atoms of high atomic number (heavy atom effect).

External heavy atoms can affect the absorption from the ground electronic state to the first excited triplet state, the rate constants of the radiationless processes to and from the triplet state, and the rate constant of the radiative transition from the triplet to the singlet state (phosphorescence).

The increase in $T_1 \leftarrow S_0$ absorptions by heavy atoms was first shown by Kasha (2) for the chloronaphthalene – ethyl iodide system. Later, many other examples (*e.g.* refs. 3–6) were discovered and the enhancement of $T_1 \leftarrow S_0$ absorptions by an external heavy atom effect is well documented. However, there are conflicting reports in the literature concerning the relative importance of the external heavy atom effect on the radiationless process to and the radiative and radiationless processes from the triplet state (7, 8).

The early research used ethyl iodide as the perturbing species but more recently xenon has been used as an external heavy atom. (The advantage is that xenon does not absorb in the ultraviolet region.) Robinson (9) suggested that xenon enhanced the intersystem crossing from the singlet to the triplet in solid benzene at 4.2 °K since the fluorescence was quenched. Wilkinson and co-workers (10) demonstrated convincingly this effect in liquids, by showing that the quantum yield of triplets was increased by xenon quenching of the singlet states of polynuclear aromatic compounds. Cundall and Voss (11) showed that xenon dissolved in xylene also increased the triplet state yield. Studies of gaseous systems have also shown the effect of external heavy atoms, thus the fluorescence of toluene is quenched by xenon (12).

It has been suggested recently (13) that xenon can interact with π^*-n triplet states since the intensity of phosphorescence of biacetyl in the gas phase decreased in the presence of xenon. However, xenon has only a very small effect on the lifetime of the triplet state of hexafluoroacetone (14) so we have re-examined the biacetyl–xenon system and investigated the external heavy atom effect on the lifetime of triplet biacetyl in the gas phase.

Experimental

The biacetyl (MCB Chromatoquality) was distilled at −78 °C and stored in the dark at −196 °C. The xenon was Airco research grade.

The total luminescence studies used a 50 W medium pressure Hg lamp (Gates Omnirange) as the light source and the 405 nm line was isolated using a narrow band filter (maximum transmission at 403 nm, transmits 1% at 386 and 430 nm). A portion of the incident light reflected from a quartz plate and was monitored by a photocell (935). The 10 cm long quartz cell was T shaped and the emitted light was observed through a Suprasil

side window. The transmitted light was detected by a photocell (935). The luminescence passed through a glass filter (Corning CS 3-71) and was measured by a photomultiplier (1P28)–electrometer combination. The relative luminescence intensity, Q_{p+f}, is defined as $(I_e - I_e^\circ)/(I_t^\circ - I_t)g$ where I_e and I_t are the emitted and transmitted intensities in the presence (e) and the absence (0) of biacetyl. g is the factor that takes into account that the emitted light from the center section of the cell is observed.

In the study of the triplet lifetime a xenon discharge lamp with a decay time of 3.8×10^{-6} s was used, and the incident light passed through a broad band glass filter (CS 5-60). The emitted light was detected as in the continuous intensity study, except that the response time of the photomultiplier was reduced to less than 2×10^{-6} s and its output displayed on an oscilloscope and photographed. The total energy dissipated in the xenon lamp to obtain one lifetime measurement was about 1.8 J.

The experiments were carried out at 30 °C in a mercury-, grease-, and metal-free system. For a single measurement the cell was filled with biacetyl to the required pressure and the appropriate amount of xenon added. The attainment of equilibrium was checked using the photocell that measured the transmitted light intensity. Condensation of biacetyl on the walls of the cell was not detected. Studies at higher temperatures did not show the significant increase in the light absorbed that would be expected if liquid biacetyl were present at the lower temperatures. The lifetime was measured, then the continuous luminescence intensity and the lifetime remeasured. In all cases the lifetimes measured at the beginning and the end agreed to within 2%. The xenon was then recovered but the biacetyl was discarded. For a further measurement of the biacetyl lifetime the cell was filled with a new sample of biacetyl and a different pressure of xenon added. This technique was used since the biacetyl lifetime depended on the length of time the sample remained in the cell. The decrease in the lifetime was not due to oxygen quenching but may be caused by condensation products formed in the system.

Results and Discussion

At high light intensities the lifetime of the triplet biacetyl varies with the incident light intensity (16). The flash intensity used in this study is quite low and no dependence of the triplet lifetime on intensity is expected. Accordingly, the triplet lifetime of 1.76×10^{-3} s reported in Table 1 for biacetyl at 30 °C may be compared with the 1.8×10^{-3} s reported by Kaskan and Duncan (15) for biacetyl at 25 °C at moderate light intensity.

The mechanism that describes the luminescence behavior of biacetyl at low pressures excited at 405 or 436 nm is (16)

[1] $$B + h\nu \rightarrow {}^1B$$

[2] $$^1B \rightarrow {}^3B$$

TABLE 1

Effect of xenon on the luminescence and lifetime of biacetyl at 30 °C

Xe pressure (Torr)	Q_{p+f}	τ_p (10^{-3} s)	1/100 τ_p (s^{-1})
0	60.6	1.76	5.68
191	59.9	1.75	5.71
369	58.5	1.68	5.95
520	58.3	1.74	5.75
644	57.2	1.64	6.10
848	60.8	1.66	6.02

[3] $$^1B \rightarrow B + h\nu_f$$

[4] $$^3B \rightarrow B + h\nu_p$$

[5] $$^3B \rightarrow B$$

and the following process was added when xenon was present (13).

[6] $$^3B + Xe \rightarrow B + Xe$$

Thus at a fixed temperature and pressure of biacetyl the reciprocal of the lifetime of the triplet state of biacetyl would be expected to vary linearly with the xenon pressure ($1/\tau_p = k_4 + k_5 + k_6[Xe]$ from a steady state treatment). The lifetime data of Table 1 were assumed to be precise to 2% and the slope was calculated for the least squares line; $k_6 = (7 \pm 3) \times 10^2\ M^{-1}\ s^{-1}$ at 30 °C.

There is a discrepancy between these results and those reported earlier (13), where a larger quenching rate constant was found. In their study of the triplet state of hexafluoroacetone, Kutschke and co-workers observed a small decrease in the lifetime when a high pressure of xenon was added (14). However, they suggested that an oxygen impurity in the xenon was sufficient to explain the data. Triplet biacetyl at 25 °C is quenched by oxygen with a rate constant of 8.55×10^{-13} cc molecule^{-1} s^{-1} (15), so the xenon need only contain about 1 p.p.m. of oxygen to explain the data of Table 1. The studies on Q_{p+f} confirm the very small (probably negligible) effect of xenon on the phosphorescence of biacetyl at 25 °C. The earlier data (13) can also be explained by oxygen being present in the xenon (17).

In conclusion, the effect of xenon on the triplet lifetime of biacetyl in the gaseous phase at 30 °C is very small, so the external heavy atom effect on this π^*-n triplet state is very small and probably negligible. This supports the proposal of Vanquickenborne and McGlynn (18), that the external heavy atom effect on any triplet carbonyl

Can. J. Chem. Downloaded from www.nrcresearchpress.com by 210.87.254.42 on 09/05/12
For personal use only.

compound is not very large and that the effect on π^*-n triplet states is less than that on π^*-π triplet states.

We thank the National Research Council of Canada for financial support.

1. S. P. McGlynn, T. Azumi, and M. Kinoshita. Molecular spectroscopy of the triplet state. Prentice-Hall, New Jersey. 1969.
2. M. Kasha. J. Chem. Phys. **20**, 71 (1952).
3. L. S. Forster. J. Chem. Phys. **26**, 1761 (1957).
4. S. P. McGlynn, R. Sunseri, and N. Christodouleas. J. Chem. Phys. **37**, 1818 (1962).
5. A. Grabowska. Spectrochim. Acta, **19**, 307 (1963).
6. D. R. Kearns and W. A. Case. J. Amer. Chem. Soc. **88**, 5087 (1966).
7. S. P. McGlynn, G. W. Daigre, and F. J. Smith. J. Chem. Phys. **39**, 675 (1963).
8. S. Siegel and H. S. Judeikis. J. Chem. Phys. **42**, 3060 (1965).
9. G. W. Robinson. J. Mol. Spectrosc. **6**, 58 (1961).
10. A. R. Horrocks, A. Kearvell, K. Tickle, and F. Wilkinson. Trans. Faraday Soc. **62**, 3393 (1966).
11. R. B. Cundall and A. J. R. Voss. Chem. Commun. 902 (1968).
12. C. S. Burton and W. A. Noyes, Jr. J. Chem. Phys. **49**, 1705 (1968).
13. A. Cook, G. P. Semeluk, and I. Unger. Can. J. Chem. **47**, 4527 (1969).
14. A. Gandini, D. A. Whytock, and K. O. Kutschke. Ber. Bunsenges. Phys. Chem. **72**, 296 (1968).
15. W. E. Kaskan and A. B. F. Duncan. J. Chem. Phys. **18**, 427 (1950).
16. W. A. Noyes, Jr., G. B. Porter, and J. E. Jolley. Chem. Rev. **56**, 49 (1956).
17. G. P. Semeluk. Private communication.
18. L. Vanquickenborne and S. P. McGlynn. J. Chem. Phys. **45**, 4755 (1966).

Can. J. Chem. Downloaded from www.nrcresearchpress.com by 210.87.254.42 on 09/05/12
For personal use only.

Pulse radiolysis of liquid ethanol: reaction kinetics of the radicals[1]

J. W. Fletcher, P. J. Richards, and W. A. Seddon
Physical Chemistry Branch, Atomic Energy of Canada Limited, Chalk River Nuclear Laboratories, Chalk River, Ontario

Received April 1, 1970

In the pulse radiolysis of alkaline ethanol solutions the conjugate base CH_3CHO^- is not formed from the α-ethanol radical CH_3CHOH, *i.e.*

$$CH_3CHOH + CH_3CH_2O^- \not\rightarrow CH_3CHO^- + CH_3CH_2OH$$

This is contrary to the observation in aqueous alkaline solutions of ethanol of a rapid equilibrium between CH_3CHOH and CH_3CHO^-.

The small quantity of CH_3CHO^- which is produced in the present system is consistent with the formation of the ethoxy radical CH_3CH_2O and its subsequent reaction with the ethoxide ion $CH_3CH_2O^-$.

Canadian Journal of Chemistry, **48**, 3765 (1970)

Introduction

The radical ion $RCHO^-$ has been assumed (1, 2) to be formed by reaction *1f* in basic alcohol solutions

$$[1]\quad RCHOH + RCH_2O^- \underset{1r}{\overset{1f}{\rightleftharpoons}} RCHO^- + RCH_2OH$$

This assumption is based on the previous observation (3, 4) of the rapid dissociation of RCHOH in aqueous solutions of alcohol at high p*H* to form $RCHO^-$ via the equilibrium

$$[2]\quad RCHOH + OH^- \rightleftharpoons RCHO^- + H_2O$$

The corresponding equilibrium in aqueous solution is observed (5–10) for the hydroxyl radical

$$[3]\quad OH + OH^- \rightleftharpoons O^- + H_2O$$

This note reports evidence that reaction *1f* is not rapid enough to be an important process in alkaline ethanol. However, a small yield of

[1]AECL No. 3717.

compound is not very large and that the effect on π^*-n triplet states is less than that on π^*-π triplet states.

We thank the National Research Council of Canada for financial support.

1. S. P. McGlynn, T. Azumi, and M. Kinoshita. Molecular spectroscopy of the triplet state. Prentice-Hall, New Jersey. 1969.
2. M. Kasha. J. Chem. Phys. **20**, 71 (1952).
3. L. S. Forster. J. Chem. Phys. **26**, 1761 (1957).
4. S. P. McGlynn, R. Sunseri, and N. Christodouleas. J. Chem. Phys. **37**, 1818 (1962).
5. A. Grabowska. Spectrochim. Acta, **19**, 307 (1963).
6. D. R. Kearns and W. A. Case. J. Amer. Chem. Soc. **88**, 5087 (1966).
7. S. P. McGlynn, G. W. Daigre, and F. J. Smith. J. Chem. Phys. **39**, 675 (1963).
8. S. Siegel and H. S. Judeikis. J. Chem. Phys. **42**, 3060 (1965).
9. G. W. Robinson. J. Mol. Spectrosc. **6**, 58 (1961).
10. A. R. Horrocks, A. Kearvell, K. Tickle, and F. Wilkinson. Trans. Faraday Soc. **62**, 3393 (1966).
11. R. B. Cundall and A. J. R. Voss. Chem. Commun. 902 (1968).
12. C. S. Burton and W. A. Noyes, Jr. J. Chem. Phys. **49**, 1705 (1968).
13. A. Cook, G. P. Semeluk, and I. Unger. Can. J. Chem. **47**, 4527 (1969).
14. A. Gandini, D. A. Whytock, and K. O. Kutschke. Ber. Bunsenges. Phys. Chem. **72**, 296 (1968).
15. W. E. Kaskan and A. B. F. Duncan. J. Chem. Phys. **18**, 427 (1950).
16. W. A. Noyes, Jr., G. B. Porter, and J. E. Jolley. Chem. Rev. **56**, 49 (1956).
17. G. P. Semeluk. Private communication.
18. L. Vanquickenborne and S. P. McGlynn. J. Chem. Phys. **45**, 4755 (1966).

Can. J. Chem. Downloaded from www.nrcresearchpress.com by 210.87.254.5 on 09/05/12
For personal use only.

Pulse radiolysis of liquid ethanol: reaction kinetics of the radicals[1]

J. W. Fletcher, P. J. Richards, and W. A. Seddon
Physical Chemistry Branch, Atomic Energy of Canada Limited, Chalk River Nuclear Laboratories, Chalk River, Ontario

Received April 1, 1970

In the pulse radiolysis of alkaline ethanol solutions the conjugate base CH_3CHO^- is not formed from the α-ethanol radical CH_3CHOH, *i.e.*

$$CH_3CHOH + CH_3CH_2O^- \not\rightarrow CH_3CHO^- + CH_3CH_2OH$$

This is contrary to the observation in aqueous alkaline solutions of ethanol of a rapid equilibrium between CH_3CHOH and CH_3CHO^-.

The small quantity of CH_3CHO^- which is produced in the present system is consistent with the formation of the ethoxy radical CH_3CH_2O and its subsequent reaction with the ethoxide ion $CH_3CH_2O^-$.

Canadian Journal of Chemistry, **48**, 3765 (1970)

Introduction

The radical ion $RCHO^-$ has been assumed (1, 2) to be formed by reaction *1f* in basic alcohol solutions

$$[1]\quad RCHOH + RCH_2O^- \underset{1r}{\overset{1f}{\rightleftharpoons}} RCHO^- + RCH_2OH$$

This assumption is based on the previous observation (3, 4) of the rapid dissociation of RCHOH in aqueous solutions of alcohol at high p*H* to form $RCHO^-$ via the equilibrium

$$[2]\quad RCHOH + OH^- \rightleftharpoons RCHO^- + H_2O$$

The corresponding equilibrium in aqueous solution is observed (5–10) for the hydroxyl radical

$$[3]\quad OH + OH^- \rightleftharpoons O^- + H_2O$$

This note reports evidence that reaction *1f* is not rapid enough to be an important process in alkaline ethanol. However, a small yield of

[1]AECL No. 3717.

CH_3CHO^- is formed by an independent process. Estimates of the rate constants involved are made. Consequences of this on the mechanism proposed for the chain reaction in alkaline alcohol solutions of N_2O are discussed.

Experimental

The experimental procedures were the same as previously described (11). Solutions were irradiated with 0.5 μs electron pulses from a 2 MeV Van de Graaff accelerator with doses ranging from 1 to 10 krad/pulse. The initial yields and mode of decay were calculated by computer analysis of the decay curves.

Results and Discussion

We observe that the pulse radiolysis of pure neutral ethanol gives an optical absorption in the ultraviolet (u.v.) (Fig. 1) due to a single species which decays by second order kinetics. Its spectrum and decay are like those observed previously in both pure and aqueous ethanol solutions and ascribed to the CH_3CHOH radical (3, 4, 12).

An absorption at 350 mμ attributed to CH_3CHO^- the basic form of CH_3CHOH has been observed (3, 4) to be formed from CH_3CHOH in alkaline aqueous ethanol. However, we observed that in alkaline ethanol this absorption at 350 mμ[2] has an optical density (o.d.) about 25% of the intensity relative to the o.d. of CH_3CHOH at 250 mμ. That this absorption at 350 mμ was due to CH_3CHO^- was confirmed by pulsing solutions of ethanol containing acetaldehyde. This produces CH_3CHO^- via reaction 4 (11).

[4] $\quad e^- + CH_3CHO \rightarrow CH_3CHO^-$

For kinetic studies spectral overlap was minimized by monitoring CH_3CHOH at 255 mμ and CH_3CHO^- at 350 mμ. When necessary in alkaline solutions a small correction due to the absorption of CH_3CHO^- at 255 mμ was applied assuming the absorption spectrum of CH_3CHO^- was the same in aqueous and nonaqueous ethanol.

Our results show that equilibrium 1 between CH_3CHOH and CH_3CHO^- is not rapidly attained. It is possible to estimate an upper limit

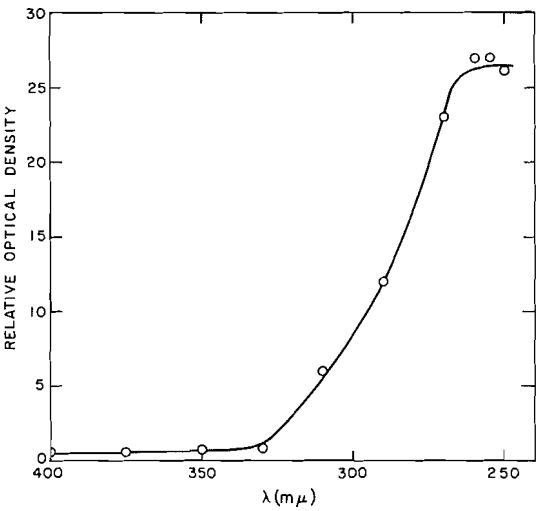

FIG. 1. Absorption spectrum of the CH_3CHOH radical in pure ethanol. No absorption due to CH_3CHO^- is present in pure ethanol. Relative optical density extrapolated to zero time using second order kinetics.

for k_{1f} by assuming that there is a pseudo first order decay of CH_3CHOH from reaction *1f* underlying our observed second order decay of this species. On this basis the first halflife of CH_3CHOH is 0.4 ms in 1.5 *M* ethoxide solution and would correspond to $k_{1f} \leqslant 1 \times 10^3\ M^{-1}\ s^{-1}$ ($k_{1f} \leqslant 0.693\ [CH_3CH_2O^-]/t_{\frac{1}{2}}$). As the CH_3CHO^- we observe in alkaline solutions is formed immediately ($t_{\frac{1}{2}} \leqslant 1$ μs) it is evidently not formed via reaction *1f*. Furthermore since CH_3CHOH decays by a second order process and CH_3CHO^- decays by a much slower essentially first order process, equilibrium 1 is not rapidly attained.

As the CH_3CHO^- we observe in alkaline solutions is formed immediately, its precursor must be very short lived. A logical precursor of CH_3CHO^- is the ethoxy radical CH_3CH_2O. The formation of the alkoxy radical (RCH_2O) in alcoholic solutions has been indicated previously by steady state radiolysis (from product analysis and use of a deuterium tracer) (1, 13) and pulse radiolysis competition studies (14). They estimated the yields of $G(RCH_2O) \lesssim 2$ with a halflife $t_{\frac{1}{2}}(RCH_2O) \lesssim$ microseconds. Assuming that the ethoxy radical normally decays by reaction 5, then, in alkaline solutions reaction 6 can compete with reaction 5 thus producing CH_3CHO^-.

[2]This absorption has also been reported by Arai *et al.* J. Phys. Chem. **74**, 2102 (1970) since submission of this note.

Can. J. Chem. Downloaded from www.nrcresearchpress.com by 210.87.254.5 on 09/05/12
For personal use only.

TABLE 1
Relevant rate constants

Reaction number	Rate constants (M^{-1} s^{-1}) k_f	k_r	pK§ (radical)	Reference number
1	$< 10^3$	$\leqslant 20 \pm 10$		This work
	$\sim 10^3$			*
2	$\sim 10^9$	$\sim 10^5$	11.6	3
3	4×10^9			†
	3×10^9			10
		$> 7.2 \times 10^5$		6
		3.6×10^5	11.8 ± 2	5
			11.8	7
			11.9	8
5	4×10^4 M^{-1} s^{-1} $< k_5 <$ 10^7 M^{-1} s^{-1}			This work
6	$k_6 > 8 \times 10^7$ M^{-1} s^{-1}			This work
7	$2k_7 = (1.4 \pm 0.5) \times 10^9$ M^{-1} s^{-1} (ethanol)			This work
	$2k_7 = (1.0 \pm 0.1) \times 10^9$ M^{-1} s^{-1} (ethanol)			‡
	$2k_7 = (1.4 \pm 0.4) \times 10^9$ M^{-1} s^{-1} (aq. ethanol)			12, 16
	$2k_7 = (2.0 \pm 0.6) \times 10^9$ M^{-1} s^{-1} (aq. ethanol)			17

*Calculated in this paper from data on methanol in refs. 2 and 15.
†Calculated in ref. 9 from data in ref. 5.
‡Calculated in this paper from data in ref. 12.
§Where K = [radical ion][H$^+$]/[radical].

[5] $CH_3CH_2O + CH_3CH_2OH \rightarrow CH_3CH_2OH + CH_3CHOH$

[6] $CH_3CH_2O + CH_3CH_2O^- \rightarrow CH_3CH_2OH + CH_3CHO^-$

In support of eq. 6 we observe that the initial concentration of CH_3CHO^- increases with increasing ethoxide concentration to a maximum value at about 0.1 M ethoxide. In solutions containing 8 mM ethoxide ion the initial concentration of CH_3CHO^- is about one half the maximum value (observed above 0.1 M ethoxide solution). Under this condition reaction 5 will be as fast as reaction 6. Hence $k_6/k_5 \sim [CH_3CH_2OH]/[CH_3CH_2O^-] \sim 2 \times 10^3$. We observe no building up of CH_3CHOH on a time scale $\geqslant 1$ μs so $k_5 > 4 \times 10^4$ M^{-1} s^{-1}. This leads to a value of $k_6 > 8 \times 10^7$ M^{-1} s^{-1}. Similar estimates for k_5 and k_6 can be calculated from the observation that the formation of CH_3CHO^- is complete in < 1 μs in 8 mM ethoxide ion solution. In the limit, k_5 should be less than 10^7 M^{-1} s^{-1} since it is very unlikely that k_6 will be greater than 10^{10} M^{-1} s^{-1}.

We observe the decay of CH_3CHO^- to be pseudo first order and independent of ethoxide concentration with $t_{\frac{1}{2}} = 2$ ms, corresponding to a second order rate constant 20 M^{-1} s^{-1}. Reaction *1r* is the only mode of decay of CH_3CHO^- consistent with the observations.

Since we observe that CH_3CHOH decays by second order kinetics and since the decay is independent of ethoxide concentration, CH_3CHOH presumably is disappearing by the occurrence of reaction 7 (1).

[7] $2CH_3CHOH \rightarrow CH_3CHO + CH_3CH_2OH \rightarrow (CH_3CHOH)_2$

Our measured decay constant is $2k_7 = (1.6 \pm 0.4) \times 10^6 \times \varepsilon_{255\ m\mu}$. Assuming $G(CH_3CHOH) = 6.5$ molecules/100 eV from product analysis data (1), it is possible to calculate the extinction coefficient for CH_3CHOH $\varepsilon_{255\ m\mu} = 870 \pm 70$ M^{-1} cm^{-1} which gives $2k_7 = (1.4 \pm 0.5) \times 10^9$ M^{-1} s^{-1}. This rate constant is in agreement with the value $2k_7 = (1.0 \pm 0.1) \times 10^9$ M^{-1} s^{-1} calculated from the data of Taub and Dorfman (12) using the ratio of extinction coefficients $(\varepsilon_{255}/\varepsilon_{297}) = 3$ (Fig. 1).

Table 1 summarizes the various measured and estimated rate constants. For comparison it includes previously determined constants in aqueous solutions.

It is interesting to note the marked difference in rates for the ionic reactions between the aqueous (reactions 2, 3) and nonaqueous

Can. J. Chem. Downloaded from www.nrcresearchpress.com by 210.87.254.5 on 09/05/12
For personal use only.

(reaction 1) systems. This difference cannot easily be explained but appears to be due to a medium effect rather than a property of the radical or radical ion.

The observed slowness of reaction *1f* in our pulse radiolysis data for ethanol (which by analogy can be generalized to other alcohols) has consequences for the interpretation of the steady state radiolysis results (1, 2, 15) in alkaline solutions of N_2O in alcohols. Since reaction *1f* is slow, the observed limiting yield of N_2 and acetaldehyde at high N_2O concentrations (15) will be governed by the termination step [7′] of the chain mechanism, rather than the previously suggested reaction 8.

[7′] $2\ RCHOH \rightarrow$ termination

[8] $2\ RCHO^- \rightarrow$ termination

In fact, in ethanol we find no evidence for reaction 8 but rather that CH_3CHO^- decays slowly presumably via [*1r*].

Our general mechanism is summarized below:

Initiation

$$RCH_2OH \text{—}\sim\!\!\rightarrow e^- + RCHOH + \text{products}$$

$$e^- + N_2O \rightarrow N_2 + O^-$$

Propagation

[*1f*] $RCHOH + RCH_2O^- \rightarrow RCHO^- + RCH_2OH$

$$RCHO^- + N_2O \rightarrow RCHO + N_2 + O^-$$

$$O^- + RCH_2OH \rightarrow RCHOH + OH^-$$

Termination

[7′] $2\ RCHOH \rightarrow$ termination

This mechanism indicates that the limiting observed rate of formation of N_2 and RCHO would be given by

$$[9]\quad G(N_2 \text{ or } RCHO) = k_{1f}[RCH_2O^-] \times \left(\frac{100N(G(e^-) + G(RCHOH))}{2k_7 I}\right)^{\frac{1}{2}}$$

where I is the dose rate (eV l^{-1} s^{-1}) and N is Avogadro's number.

Since this system has not been studied in ethanol solution, we will test our conclusions in the methanol system since it would be expected to be very similar. Methanol solutions saturated with N_2O and containing 0.1 M methoxide irradiated at a dose rate $I = 5.6 \times 10^{18}$ eV $l^{-1}s^{-1}$ gives values[3] of $G(N_2) \approx 100$ (15) and $G(HCHO) \approx 80$ (2). Assuming that the radical recombination rate constant $2k_7 \approx 10^9\ M^{-1}\ s^{-1}$ for methanol (similar to ethanol) and $G(CH_2OH) + G(e) \approx 8$, then from eq. 9 the rate constant for radical reaction with methoxide is k_{1f} (methanol) $\sim 10^3\ M^{-1}\ s^{-1}$. This is consistent with our pulse radiolysis data for ethanol. It should also be noted that our eq. 9 fits more closely the observed (15) methoxide concentration dependence than that predicted by the previous mechanisms (2).

We wish to thank Drs. A. W. Boyd and P. R. West for their helpful suggestions and Mr. M. J. Young for aid in the experimental work.

1. G. R. Freeman. Actions Chimiques et Biologiques des Radiations **14**, 73 (1970).
2. G. K. Sibirskaya and A. K. Pikaev. Bull. Acad. Sci. USSR Div. Chem. Sci. 2248 (1968).
3. K. D. Asmus, A. Henglein, A. Wigger, and G. Beck. Ber. Bunsenges Phys. Chem. **70**, 756 (1966).
4. M. Simic, P. Neta, and E. Hayon. J. Phys. Chem. **73**, 3794 (1969).
5. B. L. Gall and L. M. Dorfman. J. Amer. Chem. Soc. **91**, 2199 (1969).
6. G. V. Buxton. Trans. Faraday Soc. **65**, 2150 (1969).
7. J. L. Weeks and J. Rabani. J. Phys. Chem. **70**, 2100 (1966).
8. J. Rabani and M. S. Matheson. J. Phys. Chem. **70**, 761 (1966).
9. F. S. Dainton and S. A. Sills. Proc. Chem. Soc. 223 (1962).
10. G. E. Adams, J. W. Boag, and B. D. Michael. Trans. Faraday Soc. **61**, 492 (1965).
11. J. W. Fletcher, P. J. Richards, and W. A. Seddon. Can. J. Chem. **48**, 1645 (1970).
12. I. A. Taub and L. M. Dorfman. J. Amer. Chem. Soc. **84**, 4053 (1962).
13. J. J. J. Myron and G. R. Freeman. Can. J. Chem. **43**, 1483 (1965).
14. F. S. Dainton, I. V. Janovsky, and G. A. Salmon. Chem. Commun. 335 (1969).
15. W. V. Sherman. J. Phys. Chem. **71**, 4245 (1967).
16. L. M. Dorfman and I. A. Taub. J. Amer. Chem. Soc. **85**, 2370 (1963).
17. W. A. Seddon and A. O. Allen. J. Phys. Chem. **71**, 1914 (1967).

[3]We estimate these G values from graphs given in the references.

Can. J. Chem. Downloaded from www.nrcresearchpress.com by 210.87.254.5 on 09/05/12
For personal use only.

Basicities of organometallic and other bases using the visible absorption maximum of the reference acid and its conjugate base

R. A. N. McLean and J. D. Umpleby[1]
Department of Chemistry, University of British Columbia, Vancouver 8, British Columbia
and
Department of Inorganic Chemistry, University of Bristol, Woodland Road, Bristol 8, England

Received June 19, 1970

The shift in the visible absorption maximum of hexanitrodiphenylamine has been used as a measure of the base strengths of some organometallic and organic bases. It is not possible to obtain a quantitative measure for stronger bases as the hexanitrodiphenylamine anion is produced. The order of base strengths for the organometallic bases studied is found to be $Me_3SiSMe < Me_3CSMe < Me_3SnSMe \approx Me_3SiNMe_2$.

Canadian Journal of Chemistry, **48**, 3769 (1970)

Following studies (1–3) on the relative base strengths of organometallic bases, using the shift in the C—D stretching frequency in $CDCl_3$ and in the proton resonance in $CHCl_3$, we have attempted to devise a method of measuring relative base strengths using the shift in the ultraviolet or visible absorption maximum of a suitable reference acid. Very little work has been done on the effect of hydrogen bonding on the electronic spectra of aromatic primary and secondary amines and alcohols, but it has been observed that bases shift the absorption maxima to lower energy (4 and references therein).

As those silicon containing organometallic bases which we wished to study undergo reaction with phenols, we examined some amines as reference acids. Diphenylamine showed only a small shift in its absorption maximum even with the strongest of the bases under investigation. However, upon substitution of electron-withdrawing groups on the phenyl rings, larger shifts were observed with stronger bases, and it was found that 2,2′-4,4′-6,6′-hexanitrodiphenylamine (HNDA), despite its insolubility in all non-polar solvents except benzene, is most suitable. In acidic, or weakly basic solutions the yellow form of the amine (λ_{max} 370–383 nm) is present; whilst in strongly basic solutions the red anion (λ_{max} 415–418 nm) is formed.

We attempted to measure the interaction between the bases and HNDA in dilute solutions of a non-interacting solvent. However, it was not possible to do this, as solvents in which HNDA is soluble (*e.g.* ether, dioxane, and benzene), cause greater shifts in the absorption maximum than some of the bases under investigation. Therefore, the spectra of HNDA were run as approximately 5×10^{-5} *M* solutions in the base with the pure base reference. The position of the absorption maximum in some representative bases is given in Table 1.

The extinction coefficients of the bands around 370–380 nm are $\approx$ 15 000 and of the bands at 418 nm $\approx$ 25 000. None of the bases studied produced two maxima, *i.e.* only partially deprotonated HNDA, so that it appears that the energy barrier to deprotonation is small and narrow. It is obvious that the method is not specific for stronger bases. In fact all amines studied, except pyridine, produced an absorption maximum at 418 nm. Thus only a small amount of activation energy is required to completely remove the proton from HNDA to produce the red anion. Therefore, only differences in the basicity of very weak bases can be measured using the technique.

Even with weak bases there is only just a

TABLE 1
Absorption maximum of HNDA in bases

Base	λ_{max}(nm)
Ether	375.5
Dioxane	376.5
Benzene	382
Pyridine	383.5
Piperidine	418
Butylamine	418
Me_3SiNMe_2	418
Me_3CSMe	371
Me_2HCSMe	371.5
Me_3SiSMe	370
Me_3SnSMe	415.5

[1]Present address: KDStV Burgundia-Leipzig zu Dusseldorf, Chlodwigstrasse 88, 4 Dusseldorf, West Germany.

Can. J. Chem. Downloaded from www.nrcresearchpress.com by 210.87.254.105 on 09/05/12
For personal use only.

significant but reproducible shift in the band for the compounds, in which we are particularly interested, Me_3CSMe and Me_3SiSMe. Despite this, the order of base strength $Me_3SiSMe < Me_3CSMe < Me_3SnSMe$ is the same as that found in the two previous studies of these compounds (2, 3), although in these studies the carbon sulfide was significantly more basic than the silicon analogue. The most significant result here is that Me_3SnSMe is a considerably stronger base than the other two. The previous explanation that the inductive donation of charge from the less electronegative tin atom increases the basicity of the sulfur atom seems reasonable. As expected, Me_3SiNMe_2 is a considerably stronger base than its sulfur analogue, and the oxygen bases are somewhat stronger than the sulfur bases.

It is interesting to note that non-polar benzene significantly shifts the absorption maximum to lower energy compared to the weakest of the bases examined here. It seems likely that a charge transfer interaction between the aromatic rings produces this effect. This type of interaction probably also accounts for the anomalous position of pyridine, which is not a very weak base, and, in general, it is unlikely that this technique can be used to compare the base strengths of any species with aromatic rings.

In conclusion it can be pointed out that none of the results obtained from this method are capable of direct quantitative comparison, but the order of the base strengths of weak organometallic bases can be estimated.

One of us (R.A.N.M.) thanks the Salters' Company and the Killam Fellowship Committee of the University of British Columbia for financial support, and we are grateful to Dr. E. W. Abel for his interest in this work.

1. E. W. ABEL, D. A. ARMITAGE, and G. R. WILLEY. Trans. Faraday Soc. **60**, 1257 (1964).
2. E. W. ABEL, D. A. ARMITAGE, and D. B. BRADY. Trans. Faraday Soc. **62**, 3459 (1966).
3. E. W. ABEL, D. A. ARMITAGE, and S. P. TYFIELD. J. Chem. Soc. A, 554 (1967).
4. A. B. SANNIGRAHI and A. K. CHANDRA. J. Phys. Chem. **67**, 1106 (1963).

Can. J. Chem. Downloaded from www.nrcresearchpress.com by 210.87.254.105 on 09/05/12
For personal use only.

Can. J. Chem. Downloaded from www.nrcresearchpress.com by 210.87.254.5 on 09/05/12
For personal use only.

Spin–orbit relaxation of $Hg(6^3P_1)$ by various gases

A. C. VIKIS, G. TORRIE, AND D. J. LE ROY
Lash Miller Chemical Laboratories, University of Toronto, Toronto 181, Ontario

Received September 1, 1970

The enhanced rate of the mercury photosensitized decomposition of C_2H_4 under incomplete quenching conditions caused by various added gases (1) has been used to obtain quantum yields, ϕ^{*0}, for the spin–orbit relaxation process $Hg(6^3P_1) \xrightarrow{Q} Hg(6^3P_0)$. Values of ϕ^{*0} for $C(CH_3)_4$, c-C_3H_6, NH_3, ND_3, H_2O, and D_2O were all > 0.5 while CO_2 quenches predominately to the ground state.

Canadian Journal of Chemistry, **48**, 3771 (1970)

In a recent investigation (1) of the enhancement by CO of the mercury photosensitized decomposition of C_2H_4 under incomplete quenching conditions, we concluded that the effect was due to $Hg(6^3P_0)$ rather than Hg*CO eximer formation. It was deduced that the quantum yield,[1] ϕ^{*0}, for the spin–orbit relaxation process $Hg(6^3P_1) \xrightarrow{Q} Hg(6^3P_0)$ was not much less than unity in the case of CO. This conclusion is in disagreement with the recent results of Callear and Hedges (2) who determined ϕ^{*0} for CO and a number of other gases; in line with earlier results, summarized in refs. 3, 4, 5, they found low values of ϕ^{*0} for all gases (except N_2).

However, more recently Callear and McGurk (6) have shown that their earlier results (2) were in error; using a new technique they obtained results in line with ours (1), *i.e.* $\phi^{*0} \approx 0.85$ for CO. They have also found relatively large values of ϕ^{*0} for other gases.

In the present communication we present the results of ϕ^{*0} measurements on a number of gases. A summary of our results to date is given in Table 1. A more detailed report, together with results on other gases will be published in this Journal in the near future. Values of ϕ^{*0} determined by the method of London *et al.* (1) or Callear and McGurk (6) should prove useful in clarifying the theoretical interpretation (7, 8) of the spin–orbit relaxation process.

The present results were obtained using the method described previously (1, type D) and based on the following mechanism

[1] $\quad Hg + h\nu^* \longrightarrow Hg^*$

[2] $\quad Hg^* \xrightarrow{1/\tau^*} Hg + h\nu^*$

[3] $\quad Hg^* + Q \xrightarrow{k_Q^{*g}} Hg + Q'$

[4] $\quad Hg^* + Q \xrightarrow{k_Q^{*0}} Hg^0 + Q''$

[5] $\quad Hg^* + C_2H_4 \xrightarrow{k_E^{*g}} Hg + C_2H_2 + H_2$

[6] $\quad Hg^0 + C_2H_4 \xrightarrow{k_E^{0g}} Hg + C_2H_2 + H_2$

[7] $\quad Hg^0 + Q \xrightarrow{k_Q^{0g}} Hg + Q'''$

[8] $\quad Hg^0 \xrightarrow{1/\tau^0} Hg$

in which Hg*, Hg^0, and Hg represent $Hg(6^3P_1)$, $Hg(6^3P_0)$, and $Hg(6^1S_0)$, respectively. Reaction 8 includes all processes, including radiative decay, which are first order or pseudo-first order under our experimental conditions. Results obtained in our laboratory indicate that k_E^{*0} for the process $Hg^* + C_2H_4 \xrightarrow{k_E^{*0}} Hg^0 + C_2H_4'$ is negligible and this reaction is omitted from the mechanism.

If I/I_0 is the ratio of the fluorescence from Hg* in the presence of Q to that in its absence and if S/S_0 is the ratio of the rate of formation of H_2 in the presence of Q to that in its absence, then

[9] $\quad I_0/I = 1 + (k_Q^{*g} + k_Q^{*0})[Q]/\{1/\tau^*) + k_E^{*g}[C_2H_4]\}$

[1]Defined as $\phi^{*0} = k^{*0}/(k^{*0} + k^{*g})$; see below.

TABLE 1

Rate constants and quantum yields for spin–orbit relaxation[a]

Q	k_Q^{*0} ($M^{-1}\,s^{-1} \times 10^{-9}$)	$k_Q^{*g} + k_Q^{*0}$ ($M^{-1}\,s^{-1} \times 10^{-9}$)		ϕ^{*0}
$C(CH_3)_4$	8.0 ± 0.4	—	(14)[b]	0.5_7
c–C_3H_6	8.2 ± 2.0	12.4 ± 0.6	(13)	0.6_6
NH_3	45 ± 6	54 ± 6	(50.4)	0.8
ND_3	67 ± 6	62 ± 5	(17.4)	~1
H_2O	10 ± 2	*ca.* 9	(16.7)	~1
D_2O	6 ± 0.5	*ca.* 6.3	(8.1)	~1
CO_2	<0.2	29	(28.0)	<0.01
CO	63 ± 19[c]	58.6 ± 0.9[c]	(55.9)	~1[c]

[a]Plus and minus values are average deviations obtained from determinations at three or more C_2H_4 pressures.
[b]Values in parentheses are taken from ref. 4, physical determinations, process II.
[c]Reference 1.

and

$$[10]\quad [(S/S_0)(I_0/I) - 1]^{-1} = \frac{\phi_E^{*g} k_E^{*g} k_Q^{0g}}{\phi_E^{0g} k_E^{0g} k_Q^{*0}} + \{(1/\tau^0) + k_E^{0g}[C_2H_4]\} \frac{\phi_E^{*g} k_E^{*g}}{\phi_E^{0g} k_E^{0g} k_Q^{*0}} \frac{1}{[Q]}$$

where ϕ_E^{*g} and ϕ_E^{0g} are the efficiencies of H_2 formation resulting from reactions 5 and 6, respectively. The values of $[C_2H_4]$ were in the range 5×10^{-3} to 25×10^{-3} Torr and those of [Q] were in the range 10^{-2} to 2 Torr. The total pressure was kept constant at 20 Torr using argon; it can therefore be assumed that ϕ_E^{*g} and ϕ_E^{0g} were constant in all experiments.

For each of the gases, Q, a number of values of S/S_0 and I_0/I at various values of [Q] were determined for each of a series of values of $[C_2H_4]$. For a given value of $[C_2H_4]$, the left hand side of eq. 10 was plotted against $1/[Q]$. The slopes of these curves were then plotted against $[C_2H_4]$ to obtain values of $\phi_E^{*g} k_E^{*g}/\phi_E^{0g} k_Q^{*0}$. The values of k_Q^{*0} given in Table 1 were obtained by assuming $\phi_E^{*g} \approx \phi_E^{0g}$ and using the published value of k_E^{*g} (4).

Values of $k_Q^{t} = k_Q^{*g} + k_Q^{*0}$ were obtained from Stern–Volmer plots; the required values of $1/\tau^*$ were obtained as described previously (1).

The method (1) does not, of course, distinguish between H_2 formed in reactions 5 and 6 and that formed as the result of reactions 3 or 7. For this reason the compounds listed in Table 1 were limited to those for which the rate of formation of H_2 in the absence of C_2H_4 was less than 10% of the rate in the presence of C_2H_4 for the range of [Q] used in the measurements.

The present results constitute the first quantitative evidence that spin–orbit relaxation is predominant in $Hg(6^3P_1)$ atom photosensitization. Thus, caution should be exercised in ascertaining whether $Hg(6^3P_1)$ or $Hg(6^3P_0)$ reactions are being studied, especially in systems where more than one quencher is present and/or incomplete quenching conditions with respect to $Hg(6^3P_1)$ emission prevail. The previous qualitative evidence of Penzes *et al.* (9, 10) of relatively high $Hg(6^3P_0)$ concentrations in the presence of $C(CH_3)_4$, NH_3, and H_2O is in line with this work.

The authors gratefully acknowledge the financial support received from the National Research Council of Canada.

1. G. London, A. C. Vikis, and D. J. Le Roy. Can. J. Chem. **48**, 1420 (1970).
2. A. B. Callear and R. E. M. Hedges. Trans. Faraday Soc. **66**, 605 (1970).
3. H. E. Gunning and O. P. Strausz. Advan. Photochem. **1**, 209 (1963).
4. R. J. Cvetanović. Progr. Reaction Kinet. **2**, 41 (1964).
5. J. G. Calvert and J. N. Pitts. Photochemistry. John Wiley and Sons, Inc., New York, 1966.
6. A. B. Callear and J. McGurk. To be published.
7. P. G. Dickens, J. W. Linnett, and O. Sovers. Discuss. Faraday Soc. **33**, 52 (1962).
8. V. K. Bykhovskii and E. E. Nikitin. Opt. Spectry. **16**, 111 (1964).
9. S. Penzes, A. J. Yarwood, O. P. Strausz, and H. E. Gunning. J. Chem. Phys. **43**, 4524 (1965).
10. S. Penzes, O. P. Strausz, and H. E. Gunning. J. Chem. Phys. **45**, 2322 (1966).

Can. J. Chem. Downloaded from www.nrcresearchpress.com by 210.87.254.5 on 09/05/12
For personal use only.

Can. J. Chem. Downloaded from www.nrcresearchpress.com by 210.87.254.42 on 09/05/12
For personal use only.

Canadian Journal of Chemistry

Published by The National Research Council of Canada

VOLUME 48 DECEMBER 15, 1970 NUMBER 24

Surface tensions of binary liquid systems. I. Mixtures of nonelectrolytes[1]

V. T. Lam[2] and G. C. Benson

Division of Chemistry, National Research Council of Canada, Ottawa, Canada

Received July 9, 1970

Surface tensions were measured for the ten binary liquid systems: cyclopentane + carbon tetrachloride, cyclopentane + tetrachloroethylene, cyclopentane + benzene, cyclopentane + toluene, cyclohexane + tetrachloroethylene, cyclohexane + benzene, cyclohexane + toluene, cyclohexane + *cis*-decalin, cyclohexane + *trans*-decalin, and benzene + *o*-xylene. The system cyclohexane + benzene was studied at 20 and 30 °C. Measurements for the other nine systems were carried out at 25 °C. The principle of corresponding states was used to correlate the surface tension results with other properties of the pure component liquids and of their binary mixtures.

Canadian Journal of Chemistry, **48**, 3773 (1970)

Introduction

There are very few binary liquid systems in the literature for which surface tensions as well as the excess properties of the bulk phase have been investigated. Such systems are needed for examining theories of the surface tension of mixtures.

Previous publications from our laboratory have reported values of the excess thermodynamic functions for a number of binary nonelectrolyte systems (1–5). The purpose of the present paper is to describe surface tension measurements for ten of these systems over the whole concentration range, and to consider some theoretical analyses of the results. The ten binary liquid systems studied were formed by mixing cyclopentane with carbon tetrachloride, tetrachloroethylene, benzene, and toluene; cyclohexane with tetrachloroethylene, benzene, toluene, *cis*-decalin, and *trans*-decalin; and benzene with *o*-xylene.

Experimental

Materials

Research grade (Phillips Petroleum Co.) benzene, toluene, and cyclohexane were used without further purification. The other primary component liquids were obtained from several different commercial sources and were further purified in an F. & M. preparative gas chromatograph (Model 775). Reference should be made to previous publications for details of the chromatographic purification of cyclopentane (3), carbon tetrachloride (6), tetrachloroethylene (5), *o*-xylene (2), and *cis*- and *trans*-decalin (4).

Table 1 lists the values of the density (d^{25} g cm^{-3}), refractive index (n_D^{20}) and surface tension (γ dyn cm^{-1}) characterizing the component liquids used in the surface tension studies. The densities and surface tensions were measured at 25 °C, the refractive indices at 20 °C. In the case of cyclohexane and of benzene, surface tensions were also determined at 20 and 30 °C. Included in Table 1 for comparison are values of the densities, refractive indices, and surface tensions taken from the literature (7–10).

Mixtures with known compositions were prepared by weight from the pure components. Precautions were taken to minimize evaporation losses during the preparation and subsequent determination of the surface tension.

Apparatus and Operational Procedure

Surface tensions of the pure liquids and of their binary mixtures were measured by the maximum bubble pressure technique originally developed by Sugden (11). Our apparatus, which is similar to that described by Quayle (12), consists of a double tube bubbler, a manometer filled with *p*-xylene, and a mercury aspirator. Bubbles of dry air, presaturated with vapor of the pure liquid or mixture under investigation, are slowly drawn alternately through the small and larger tips of the bubbler. The pressure differential P developed by the mercury aspirator is measured on the xylene-filled manometer using a precision cathetometer reading to 0.001 cm.

---

[1]NRCC No. 11 570.

[2]NRCC Postdoctorate Fellow 1967–1969. Present address: Département de Chimie, Faculté des Sciences, Université de Sherbrooke, Sherbrooke, Québec.

TABLE 1

Densities, refractive indices, and surface tensions for component liquids

Component	d^{25} (g cm^{-3})			n_D^{20}			γ^a (dyn cm^{-1})	
	Observed	Literature	Reference	Observed	Literature	Reference	Observed	Literature[b]
Cyclopentane	0.74034	0.74045	7	1.40638	1.40645	7	21.85	21.87
Cyclohexane	0.77389	0.77389	7	1.42625	1.42623	7	24.38	24.40
							24.81[c]	
							23.78[d]	
Benzene	0.87362	0.87370	7	1.50115	1.50112	7		28.20[e]
							28.86[c]	
							27.60[d]	
Toluene	0.86242	0.86230	7	1.49693	1.49693	7	27.94	27.92
o-Xylene	0.87590	0.87596	7				29.44	29.48
Carbon tetrachloride	1.58436	1.58433	8	1.46018	1.46005	8	26.13	26.14
Tetrachloroethylene	1.61432	1.61446	9	1.50576	1.50534	9	31.30	31.80
cis-Decalin	0.89288	0.89291	10	1.48090	1.48098	10	32.24	31.60
trans-Decalin	0.86596	0.86592	10	1.46949	1.46932	10	29.97	29.38

[a]At 25 °C unless otherwise indicated.
[b]Interpolated from values in (8).
[c]At 20 °C.
[d]At 30 °C.
[e]Value adopted for calibration of bubbler.

[1] $$P = Hgd'$$

where H is the difference in levels of the manometer fluid of density d', and g is the constant of gravitational acceleration. The value of the surface tension, γ, is given by Sugden's formula

[2] $$\gamma = A[P + 0.69\, rgd]$$

where A is a function of the radii of cross-section of the two bubbler orifices, r is the radius of the larger orifice (0.0631 cm in our apparatus), and d is the density of the liquid under investigation. The small orifice of our bubbler has a radius of approximately 0.01 cm and it is unnecessary to know this value accurately since A is treated as a constant of the apparatus.

The bubbler was calibrated frequently with research grade benzene; assuming a surface tension of 28.20 dyn cm^{-1} for this material at 25 °C (8), the apparatus constant A was found to have a value of 2.750×10^{-3} cm, reproducible within $\pm 0.2\%$. With the temperature of the bubbler controlled at 25.00 ± 0.01 °C, values of the surface tension were normally reproducible within ± 0.03 dyn cm^{-1}. Surface tensions for all of the systems were measured at 25 °C, with the exception of cyclohexane + benzene which was studied at 20 and 30 °C. Equilibrium was established quite rapidly in all cases and there was no evidence of time effects at rates of bubble formation slower than one bubble per second.

Values of d for binary mixtures, containing mole fraction x_i of component i with molecular weight M_i and molar volume V_i, were obtained from the relation

[3] $$d = (x_1M_1 + x_2M_2)(x_1V_1 + x_2V_2 + V^E)^{-1}$$

using values of V^E, the molar excess volume, calculated from smoothed representations of experimental volumes of mixing. Suitable Redlich–Kister forms for V^E at 25 °C are available for all of the systems studied (1–5).[3] The overall error of the value of d determined in this way is estimated to be less than ± 0.0002 g cm^{-3}.

Results

The surface tensions measured for the pure components have already been reported in Table 1. The experimental results (x_1, γ) for the ten binary systems are summarized in Table 2 which also contains values of the excess surface tension γ^E. The latter quantity is defined by the relation[4]

[4] $$\gamma^E = \gamma - x_1\gamma_1 - x_2\gamma_2$$

[3]In the case of the system cyclohexane(*1*) + benzene(*2*) densities of the pure components at 20 and 30 °C were estimated from their values at 25 °C using the coefficients of expansion given in Table 4. The variation of V^E with temperature was neglected and values of V^E at 25 °C were used in calculating densities of mixtures at 20 and 30 °C.

The excess volumes of the system cyclohexane(*1*) + tetrachloroethylene(*2*) were determined recently in our laboratory by the dilatometric method described in ref. 13. The unpublished results are represented by the equation

$$V^E(\text{cm}^3\ \text{mole}^{-1}) = x_1(1 - x_1)[2.0644 - 0.4648(1 - 2x_1)]$$

with a standard error of estimate $\sigma_v = 0.008$ cm^3 mole^{-1}.

[4]This terminology follows the usage of most authors (14). However, recently the designation of γ^E as an "excess function" has been criticized on the grounds that it does not have the usual connotation of a deviation from ideal solution behavior (15).

Can. J. Chem. Downloaded from www.nrcresearchpress.com by 210.87.254.42 on 09/05/12
For personal use only.

Can. J. Chem. Downloaded from www.nrcresearchpress.com by 210.87.254.42 on 09/05/12
For personal use only.

where γ_1 and γ_2 are the surface tensions of the pure components.

For each system, the subscripts *1* and *2* are assigned to the two components in the order used in the name of the system.

The method of least squares was used to fit each set of results for γ^E with a Redlich–Kister form of equation

$$[5] \quad \gamma^E = x_1(1 - x_1) \sum_{j=1}^{n} c_j(1 - 2x_1)^{j-1}$$

containing n adjustable coefficients, c_j. In each case, n was varied and the minimum number of coefficients needed to represent the results (consisting of n_{obs} values) adequately, was found by examining the standard error of estimate.

$$[6] \quad \sigma_\gamma = [\sum(\gamma_{obs}{}^E - \gamma^E)^2/(n_{obs} - n)]^{\frac{1}{2}}$$

Values of the coefficients obtained in this way are given in Table 3 along with the corresponding values of σ_γ. Plots of the experimental results for γ^E and of their least squares representations by eq. 5 are shown in Figs. 1–3.

There have been very few other determinations of the surface tensions of the present systems. It appears that only cyclohexane + benzene has been investigated previously (16, 17). Values of γ^E for this system obtained from the surface tensions at 20 and 30 °C reported recently by Suri and Ramakrishna (17) are included in Fig. 1 for comparison with our results. At 20 °C there is reasonable agreement between the two investigations but Suri and Ramakrishna's values at 30 °C are appreciably smaller in magnitude than our results. The two investigations therefore indicate quite different excess surface entropies.

The relative behavior of the excess surface tensions of the present systems parallel, fairly closely, the behavior of the excess enthalpies studied previously. Thus, the excess surface tensions of cyclopentane + tetrachloroethylene mixtures are larger in magnitude than those of cyclopentane + carbon tetrachloride (at corresponding concentrations of cyclopentane), and our previous calorimetric studies indicated that the excess enthalpies of cyclopentane + tetrachloroethylene (5) are greater than those of cyclopentane + carbon tetrachloride (3). Again, in the alicyclic–aromatic systems formed by mixing cyclopentane or cyclohexane with benzene

TABLE 2

Experimental values of the surface tension of binary mixtures[a]

Cyclopentane + carbon tetrachloride at 25 °C			Cyclopentane + tetrachloroethylene at 25 °C			Cyclopentane + benzene at 25 °C		
x_1	γ	γ^E	x_1	γ	γ^E	x_1	γ	γ^E
0.2176	25.17	−0.03	0.1115	29.86	−0.39	0.1095	27.00	−0.51
0.3003	24.77	−0.07	0.1993	28.81	−0.61	0.2078	26.00	−0.88
0.3922	24.38	−0.07	0.2966	27.77	−0.72	0.3168	25.18	−1.01
0.4976	23.92	−0.08	0.4117	26.66	−0.75	0.4055	24.60	−1.03
0.6037	23.44	−0.11	0.4901	25.96	−0.70	0.5042	24.02	−0.98
0.6920	23.04	−0.13	0.6081	24.92	−0.63	0.5949	23.50	−0.92
0.7987	22.63	−0.08	0.7031	24.16	−0.50	0.6959	22.99	−0.79
0.8981	22.19	−0.09	0.8107	23.31	−0.33	0.7993	22.51	−0.62
			0.9127	22.55	−0.13	0.8972	22.13	−0.37

Cyclopentane + toluene at 25 °C			Cyclohexane + tetrachloroethylene at 25 °C			Cyclohexane + benzene at 20 °C		
x_1	γ	γ^E	x_1	γ	γ^E	x_1	γ	γ^E
0.1072	27.09	−0.20	0.0918	30.19	−0.48	0.1056	27.86	−0.57
0.2012	26.34	−0.37	0.2112	29.13	−0.71	0.2041	27.14	−0.90
0.3268	25.49	−0.46	0.3090	28.18	−0.98	0.3033	26.54	−1.09
0.3920	25.08	−0.47	0.4141	27.45	−0.98	0.3962	26.15	−1.11
0.4959	24.46	−0.46	0.5139	26.81	−0.93	0.5063	25.73	−1.08
0.5081	24.39	−0.46	0.6081	26.23	−0.86	0.6077	25.42	−0.98
0.5973	23.87	−0.43	0.7065	25.71	−0.70	0.6922	25.26	−0.80
0.6961	23.33	−0.37	0.8128	25.15	−0.52	0.7957	25.03	−0.60
0.8093	22.78	−0.23	0.8920	24.81	−0.32	0.8949	24.96	−0.28
0.8980	22.30	−0.17						

TABLE 2 (*Concluded*)

Cyclohexane + benzene at 30 °C			Cyclohexane + *cis*-decalin at 25 °C			Cyclohexane + *trans*-decalin at 25 °C		
x_1	γ	γ^E	x_1	γ	γ^E	x_1	γ	γ^E
0.1004	26.79	−0.43	0.1152	31.46	0.12	0.1031	29.45	0.05
0.1056	26.64	−0.56	0.2121	30.62	0.05	0.2031	28.97	0.13
0.2004	26.08	−0.75	0.3001	29.90	0.02	0.3067	28.36	0.10
0.2041	25.99	−0.83	0.4105	29.07	0.06	0.3982	27.84	0.09
0.2041	26.08	−0.74	0.5105	28.33	0.10	0.4709	27.43	0.10
0.2916	25.58	−0.90	0.6052	27.56	0.08	0.5935	26.75	0.10
0.3033	25.44	−1.00	0.6969	26.86	0.10	0.6906	26.19	0.08
0.3925	25.09	−1.01	0.7988	26.03	0.07	0.8042	25.61	0.13
0.3962	25.06	−1.03	0.8963	25.30	0.10	0.9013	24.99	0.06
0.4914	24.75	−0.97						
0.5063	24.67	−0.99						
0.5958	24.49	−0.84						
0.6077	24.37	−0.91						
0.6922	24.22	−0.74						
0.6970	24.25	−0.69						
0.7957	24.01	−0.55						
0.7959	24.06	−0.50						
0.8940	23.91	−0.27						
0.8949	23.89	−0.29						

Cyclohexane + toluene at 25 °C			Benzene + *o*-xylene at 25 °C		
x_1	γ	γ^E	x_1	γ	γ^E
0.1048	27.22	−0.35	0.0955	29.32	−0.01
0.2148	26.66	−0.52	0.1973	29.11	−0.09
0.3135	26.09	−0.73	0.3038	28.94	−0.12
0.3674	25.82	−0.81	0.4053	28.84	−0.10
0.3982	25.81	−0.72	0.4975	28.72	−0.10
0.5050	25.37	−0.77	0.6121	28.58	−0.10
0.5918	25.13	−0.70	0.6847	28.53	−0.06
0.7455	24.72	−0.57	0.7905	28.35	−0.11
0.8268	24.55	−0.44			
0.8833	24.51	−0.29			
0.8924	24.49	−0.28			

[a]Units: γ and γ^E, dyn cm^{-1}.

TABLE 3

Values of coefficients for eq. 5 determined by method of least squares[a]

System	Temperature (°C)	c_1	c_2	c_3	σ_γ
Cyclopentane + carbon tetrachloride	25	−0.400	0.384		0.019
Cyclopentane + tetrachloroethylene	25	−2.895	−1.333		0.017
Cyclopentane + benzene	25	−3.997	−1.154	−1.369	0.029
Cyclopentane + toluene	25	−1.890	−0.486		0.018
Cyclohexane + tetrachloroethylene	25	−3.911	−1.140		0.046
Cyclohexane + benzene	20	−4.429	−1.680		0.028
	30	−3.965	−1.420		0.037
Cyclohexane + toluene	25	−3.116	−0.366		0.038
Cyclohexane + *cis*-decalin	25	0.363			0.047
Cyclohexane + *trans*-decalin	25	0.485			0.032
Benzene + *o*-xylene	25	−0.440			0.026

[a]Units: c_j and σ_γ, dyn cm^{-1}.

Can. J. Chem. Downloaded from www.nrcresearchpress.com by 210.87.254.42 on 09/05/12
For personal use only.

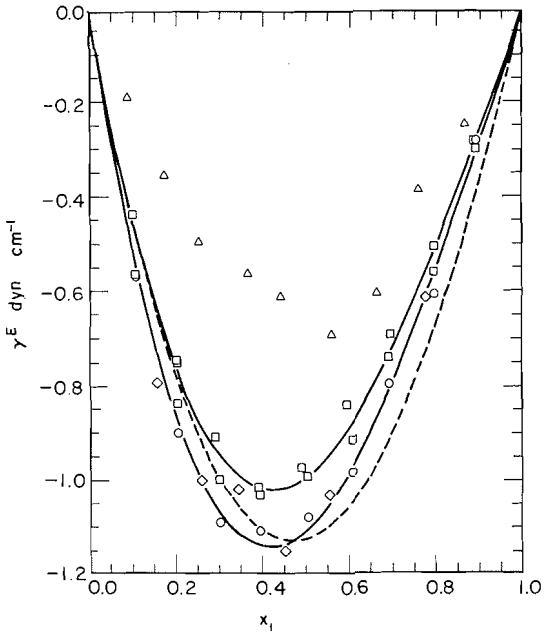

FIG. 1. Excess surface tension of cyclohexane + benzene mixtures. Our results: 20 °C, ○; 30 °C, □. Solid curves are least squares representations by eq. 5. Broken curve was calculated from theory of corresponding states at 25 °C. Results of Suri and Ramakrishna (17): 20 °C, ◇; 30 °C, △.

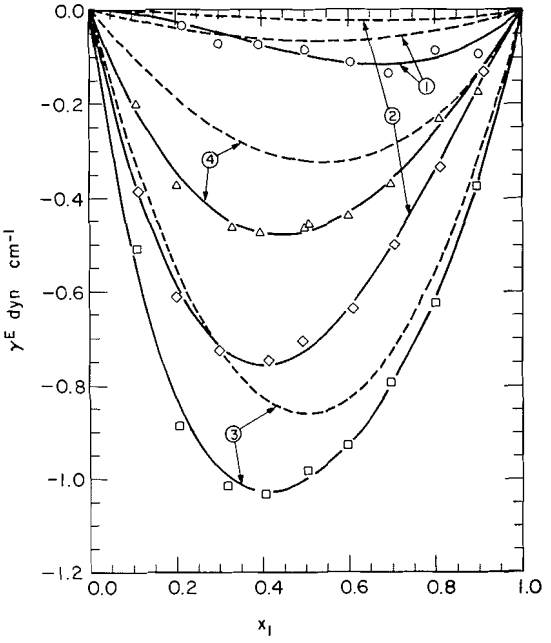

FIG. 2. Excess surface tension of mixtures at 25 °C. Systems: **1**, cyclopentane + carbon tetrachloride, ○; **2**, cyclopentane + tetrachloroethylene, ◇; **3**, cyclopentane + benzene, □; **4**, cyclopentane + toluene, △. Solid curves are least squares representations by eq. 5. Broken curves were calculated from theory of corresponding states.

and with toluene, the magnitudes of both the excess surface tension and the excess enthalpy (1) decrease from benzene to toluene. The excess enthalpies of cyclohexane + decalin mixtures (4) are fairly small at 25 °C and the curves are sigmoid in shape; the excess surface tensions of these systems are also small and appear to be positive, but the precision of the measurements is too low to allow a meaningful comparison of their relative behavior.

Analyses of Results

A number of theoretical treatments have been developed to express the surface tension of a binary mixture in terms of properties of the pure components and of the bulk mixture (14, 18–21). In general, some model of the surface region is also required.

Analyses of our excess surface tensions according to the theories of Guggenheim (19), Hoar and Melford (20), and Shereshefsky (21) were investigated. In most cases, excess surface tensions calculated from regular solution theories (19, 20) using molecular areas obtained from molar volumes on the basis of close-packed spherical molecules, and interaction energy parameters derived from excess enthalpy data, differed considerably (by a factor of 2 or more) from the experimental results. However, good representations of the experimental γ^E values could be achieved with these theories and with the treatment of Shereshefsky (21) provided one or two of the parameters occurring in the formulas were adjusted empirically to give a least squares fit. Unfortunately the values obtained for these parameters were generally of questionable physical significance when interpreted as molecular areas, numbers of surface layers, etc.

A more interesting correlation of our results was obtained by using the Flory theory of mixtures (22) in combination with the reduced surface tension equation formulated recently by Patterson and Rastogi (23). The remainder of this section summarizes the formulas used in this treatment, and describes the numerical results of its application to our systems.

Can. J. Chem. Downloaded from www.nrcresearchpress.com by 210.87.254.42 on 09/05/12
For personal use only.

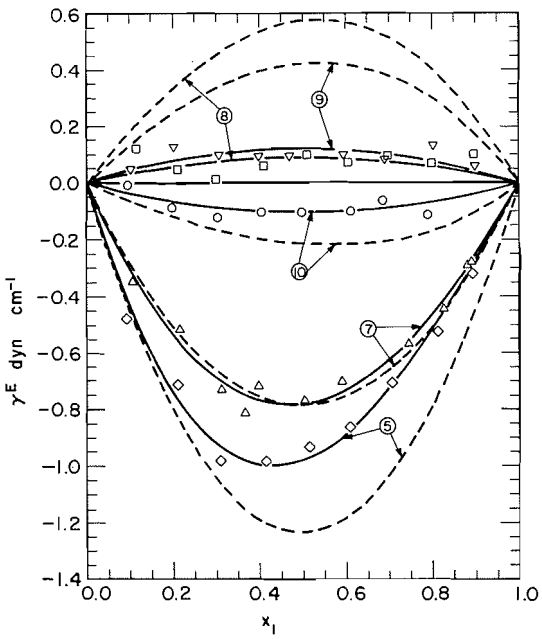

FIG. 3. Excess surface tension of mixtures at 25 °C. Systems: **5**, cyclohexane + tetrachloroethylene, ◇; **7**, cyclohexane + toluene, △; **8**, cyclohexane + *cis*-decalin, □; **9**, cyclohexane + *trans*-decalin, ▽; **10**, benzene + *o*-xylene, ○. Solid curves are least squares representations by eq. 5. Broken curves were calculated from theory of corresponding states.

Corresponding States Theory and Surface Tension

Patterson *et al.* (24, 25) have drawn attention to the close connection between the theory of mixtures developed by Flory (22) and the Prigogine corresponding states theory (26) employing a simple cell model of the liquid state in which the configurational energy is inversely proportional to the volume (*i.e.* a van der Waals liquid). The equation of state for materials conforming to the principle of corresponding states can be expressed in a "universal" form through the use of suitable characteristic values (*i.e.* reduction parameters) p^*, V^*, and T^* for the pressure, volume, and temperature, respectively. In Flory's treatment the reduced equation of state takes the form

$$[7] \qquad \tilde{T} = (\tilde{V}^{-\frac{1}{3}} - 1)/\tilde{V}^{\frac{4}{3}}$$

in the limit of zero pressure. The tilde is used in eq. 7 to indicate the reduced values of the temperature and volume defined by

$$[8] \qquad \tilde{T} = T/T^*$$

and

$$[9] \qquad \tilde{V} = V/V^*$$

Values of p^*, V^*, and T^* for pure materials can be obtained from a knowledge of the coefficient of expansion α and of the isothermal compressibility β, using the relations

$$[10] \qquad \tilde{V} = [(1 + (4\alpha T/3)/(1 + \alpha T)]^3$$

and

$$[11] \qquad p^* = (\alpha/\beta)T\tilde{V}^2$$

in combination with eqs. 7 to 9.

Patterson and Rastogi (23), in their extension of the corresponding states theory to deal with surface tension, used as the reduction parameter, the quantity

$$[12] \qquad \gamma^* = k^{\frac{1}{3}}p^{*\frac{2}{3}}T^{*\frac{1}{3}}$$

where k is the Boltzmann constant. Starting from the work of Prigogine and Saraga (27), they derived a reduced surface tension equation which in the case of a van der Waals liquid can be written in the form

$$[13] \quad \tilde{\gamma}(\tilde{V}) = M\tilde{V}^{-5/3} - \left(\frac{\tilde{V}^{1/3} - 1}{\tilde{V}^2}\right) \ln\left(\frac{\tilde{V}^{1/3} - 0.5}{\tilde{V}^{1/3} - 1}\right)$$

In this equation, M represents the fractional reduction in nearest neighbors for a cell at the surface compared with one in the bulk of the liquid. On the basis of a close-packed lattice, M should have a value of 0.25. However, Patterson and Rastogi found that a least squares treatment of surface tension results for a variety of polyatomic liquids led to a best value of 0.29 for M and we have adopted this in our own use of eq. 13.

Theoretical estimates of the surface tensions of the present component liquids at 25 °C were obtained from the relation

$$[14] \qquad \gamma = \gamma^*\tilde{\gamma}(\tilde{V})$$

using the formulas outlined above for the characteristic and reduced surface tensions. The values of V, α, and β employed in these calculations are listed in Table 4, along with the results

Can. J. Chem. Downloaded from www.nrcresearchpress.com by 210.87.254.42 on 09/05/12
For personal use only.

TABLE 4

Corresponding states calculation of surface tension of component liquids at 25 °C

Component	V (cm^3 mole^{-1})	$10^3\alpha^a$ (deg^{-1})	$10^6\beta^a$ (atm^{-1})	p^* (J cm^{-3})	V^* (cm^3 mole^{-1})	T^* (°K)	γ_{Theory} (dyn cm^{-1})	$\Delta\gamma$ (theory − expt.) (dyn cm^{-1})
Cyclopentane	94.73	1.325	135.1	509.0	72.27	4531	21.16	−0.69
Cyclohexane	108.76	1.217	115.5	530.2	84.27	4720	23.39	−0.99
Benzene	89.43	1.217	98.12	624.1	69.30	4720	26.08	−2.12
Toluene	106.84	1.071	95.0	542.5	84.65	5040	26.48	−1.46
o-Xylene	121.21	0.963	83.1	538.4	97.75	5342	28.79	−0.65
Carbon tetrachloride	97.09	1.212	109.1	558.2	75.28	4730	24.29	−1.84
Tetrachloroethylene	102.73	1.020	76.5	630.4	82.08	5177	30.52	−0.78
cis-Decalin	154.84	0.851	70.1	542.6	127.30	5739	32.04	−0.20
trans-Decalin	159.66	0.865	77.0	504.6	130.93	5683	30.12	0.15

[a]Sources for the values of α and β are given in refs. 2–5, 28.

computed for p^*, V^*, and T^*.[5] The theoretical values of the surface tension and deviations between these and the experimental results are given in the last two columns of the table.

We have also applied eq. 13 (with $M = 0.29$) to mixtures, on the assumption that they are equivalent to single component liquids with the characteristic values

$$[15]\quad \langle V^* \rangle = x_1 V_1^* + x_2 V_2^*$$

$$[16]\quad \langle p^* \rangle = \phi_1 p_1^* + \phi_2 p_2^* - \phi_1\phi_2 X_{12}/(\phi_2 + s_{12}\phi_1)$$

and

$$[17]\quad \langle T^* \rangle = \langle p^* \rangle \Big/ \left(\frac{\phi_1^* p_1^*}{T_1^*} + \frac{\phi_2^* p_2^*}{T_2^*}\right)$$

which are implicit in Flory's theory. The excess surface tension can then be expressed as

$$[18]\quad \gamma^E = \langle \gamma^* \rangle \tilde{\gamma}(\tilde{V}) - x_1\gamma_1^*\tilde{\gamma}(\tilde{V}_1) - x_2\gamma_2^*\tilde{\gamma}(\tilde{V}_2)$$

where $\langle \gamma^* \rangle$ is obtained from eqs. 12, 16, and 17 and $\tilde{V}$ is the reduced volume satisfying eq. 7 at a reduced temperature of $T/\langle T^* \rangle$. In eq. 16 ϕ_1 and ϕ_2 are segment fractions defined by

$$[19]\quad \phi_i = x_i V_i^*/\langle V^* \rangle$$

and s_{12} is the ratio of molecular surface areas of contact (per segment) for each species. If the molecules are approximately spherical, the relation

$$[20]\quad s_{12} = (V_2^*/V_1^*)^{\frac{1}{3}}$$

is generally assumed (30). The quantity X_{12} is a constant characterizing the difference in the energy of interaction between segments of unlike molecules, from the average of the interactions in the pure component liquids. X_{12} is usually treated as an adjustable parameter (29, 30) and its value is selected to obtain a fit between the calculated and experimental values of some property of the mixture (such as the excess enthalpy or excess volume).

Compatible values of s_{12} and X_{12} for the present systems at 25 °C are given in Table 5. In all cases, the value of s_{12} has been obtained from eq. 20. With one exception, the values of X_{12} are based on experimental excess enthalpies (2–5, 28); however, in the case of cyclohexane + tetrachloroethylene, X_{12} was selected to give a least squares fit of the excess molar volumes (as represented by the equation in footnote 3), since excess enthalpies were not available.

Excess surface tensions were calculated for all of the systems at 25 °C. The results are shown as broken curves in Figs. 1–3. The standard deviation, σ, between the theoretical and smoothed experimental curves is also given in Table 5, along with a comparison of theoretical and experimental values of γ^E for equimolar mixtures.

Discussion

The principle of corresponding states provides estimates of the surface tension of the component

[5]The values of α and β are the same as employed in previous calculations from our laboratory (2–5, 28), and in most cases the values of p^*, V^*, and T^* are identical with those used in our earlier applications of the Flory theory (2–4, 28, 29). A few minor differences arise from the adoption of slightly different molar volumes.

Can. J. Chem. Downloaded from www.nrcresearchpress.com by 210.87.254.42 on 09/05/12
For personal use only.

TABLE 5

Corresponding states calculation of surface tension of binary mixtures at 25 °C

No.	System	s_{12}	X_{12} (J cm^{-3})	γ^E (0.5)(dyn cm^{-1}) Theory	γ^E (0.5)(dyn cm^{-1}) Expt.	σ (dyn cm^{-1})
1	Cyclopentane + carbon tetrachloride	1.014	4.07	−0.07	−0.10	0.04
2	Cyclopentane + tetrachloroethylene	1.043	12.73	−0.02	−0.72	0.52
3	Cyclopentane + benzene	0.986	33.37	−0.86	−1.00	0.16
4	Cyclopentane + toluene	1.054	18.65	−0.33	−0.47	0.12
5	Cyclohexane + tetrachloroethylene	0.991	45.18	−1.23	−0.98	0.20
6	Cyclohexane + benzene	0.937	38.44	−1.13	−1.05[a]	0.09[a]
7	Cyclohexane + toluene	1.002	28.30	−0.78	−0.78	0.02
8	Cyclohexane + *cis*-decalin	1.147	2.365	0.58	0.09	0.36
9	Cyclohexane + *trans*-decalin	1.158	1.791	0.43	0.12	0.23
10	Benzene + *o*-xylene	1.122	11.38	−0.21	−0.11	0.08

[a]Refers to average of experimental results at 20 and 30 °C.

liquids which are of the right order of magnitude and which exhibit very nearly the same relative order as the experimental results. In most cases, however, there is a tendency for the theoretical values to be lower than the experimental. Auxiliary calculations indicate that the theoretical values are quite sensitive to the value of M, and that the overall agreement is improved for our set of pure liquids by using a value of about 0.295 (instead of 0.29) for this parameter.

Estimates of γ^E for mixtures involve essentially a difference of γ values and are not changed significantly by minor changes in M. In most respects, the calculated γ^E curves show the same pattern of relative behavior as observed experimentally. Agreement between theory and experiment is quite good (*i.e.* within 2 to 3 times the standard error) for the systems cyclopentane + carbon tetrachloride, cyclohexane + benzene, cyclohexane + toluene, and benzene + *o*-xylene. Although the sign of γ^E is predicted correctly, calculations for the two decalin systems and for cyclopentane + tetrachloroethylene show large discrepancies. This is not unexpected since difficulties arise in applying the Flory theory to these three systems. The excess enthalpy curves for the decalin systems are unusual in shape, and some difficulty was experienced previously in fitting and correlating the excess enthalpies and excess volumes according to the Flory treatment (4). Use of the other values of s_{12} and X_{12} given in ref. 4, which were determined by treating both s_{12} and X_{12} as adjustable parameters, does not improve the estimates of γ^E for these systems. In the case of cyclopentane + tetrachloroethylene, excess volumes, calculated with the parameters given in Tables 4 and 5, show large deviations from experiment; thus, in an equimolar mixture, the theoretical and experimental (5) values of the excess volume are −0.154 and −0.007 cm^3 mole^{-1}, respectively.

Finally, it should be noted that in most theories of the surface tension of mixtures, negative values of γ^E result from surface adsorption of the component of lower surface tension. The corresponding states treatment of mixtures, described above, is somewhat unorthodox, since the application of eq. 13 to an equivalent single component liquid effectively ignores differences in concentration occurring at the surface of the mixture. Our calculations indicate that the principle of corresponding states can produce useful estimates of the excess surface tension without considering such concentration effects and without adjusting any parameters to fit the surface properties of the mixtures.

The authors wish to thank Mr. P. J. D'Arcy and Mr. C. J. Halpin for valuable technical assistance in the experimental work.

1. A. E. P. Watson, I. A. McLure, J. E. Bennett, and G. C. Benson. J. Phys. Chem. **69**, 2753 (1965).
2. J. Singh, H. D. Pflug, and G. C. Benson. J. Phys. Chem. **72**, 1939 (1968).
3. T. Boublík, V. T. Lam, S. Murakami, and G. C. Benson. J. Phys. Chem. **73**, 2356 (1969).
4. G. C. Benson, S. Murakami, V. T. Lam, and J. Singh. Can. J. Chem. **48**, 211 (1970).
5. J. Polák, S. Murakami, V. T. Lam, and G. C. Benson. J. Chem. Eng. Data, **15**, 323 (1970).
6. S. Murakami and G. C. Benson. J. Chem. Thermodyn. **1**, 559 (1969).
7. American Petroleum Institute. Research Project 44. Selected values of properties of hydrocarbons and related compounds. Chemical Thermodynamic Properties Center, A. and M. College of Texas, College Station, Texas.

Can. J. Chem. Downloaded from www.nrcresearchpress.com by 210.87.254.42 on 09/05/12
For personal use only.

8. J. TIMMERMANS. Physico-chemical constants of pure organic compounds. Vol. I and II. Elsevier Press, Inc., New York. 1950 and 1965.
9. R. R. DREISBACH. Advan. Chem. Ser. No. 22, 411 (1959).
10. D. L. CAMIN and F. D. ROSSINI. J. Phys. Chem. **59**, 1173 (1955).
11. S. SUGDEN. J. Chem. Soc. **121**, 858 (1922); J. Chem. Soc. **125**, 27 (1924).
12. O. R. QUAYLE. Chem. Rev. **53**, 439 (1953).
13. H. D. PFLUG and G. C. BENSON. Can. J. Chem. **46**, 287 (1968).
14. R. DEFAY, I. PRIGOGINE, A. BELLEMANS, and D. H. EVERETT. Surface tension and adsorption. John Wiley and Sons, New York. 1966.
15. R. W. MISSEN. Ind. Eng. Chem. Fundam. **8**, 81 (1969).
16. J. TIMMERMANS. The physico-chemical constants of binary systems in concentrated solutions. Vol. 1. Interscience Publishers, New York. 1959.
17. S. K. SURI and V. RAMAKRISHNA. J. Phys. Chem. **72**, 3073 (1968).
18. J. C. ERIKSSON. Advan. Chem. Phys. **6**, 145 (1964).
19. E. A. GUGGENHEIM. Trans. Faraday Soc. **41**, 150 (1945).
20. T. P. HOAR and D. A. MELFORD. Trans. Faraday Soc. **53**, 315 (1957).
21. J. L. SHERESHEFSKY. J. Colloid Interfac. Sci. **24**, 317 (1967).
22. P. J. FLORY. J. Amer. Chem. Soc. **87**, 1833 (1965).
23. D. PATTERSON and A. K. RASTOGI. J. Phys. Chem. **74**, 1067 (1970).
24. D. PATTERSON, S. N. BHATTACHARYYA, and P. PICKER. Trans. Faraday Soc. **64**, 648 (1968).
25. D. PATTERSON and G. DELMAS. Trans. Faraday Soc. **65**, 708 (1969).
26. I. PRIGOGINE (with the collaboration of A. Bellemans and V. Mathot). The molecular theory of solutions. North-Holland Publ. Co., Amsterdam. 1957. Chaps. 16 and 17.
27. I. PRIGOGINE and L. SARAGA. J. Chim. Phys. **49**, 399 (1952).
28. G. C. BENSON and J. SINGH. J. Phys. Chem. **72**, 1345 (1968).
29. S. MURAKAMI, V. T. LAM, and G. C. BENSON. J. Chem. Thermodyn. **1**, 397 (1969).
30. A. ABE and P. J. FLORY. J. Amer. Chem. Soc. **87**, 1838 (1965).

Can. J. Chem. Downloaded from www.nrcresearchpress.com by 210.87.254.42 on 09/05/12
For personal use only.

Can. J. Chem. Downloaded from www.nrcresearchpress.com by 210.87.254.40 on 09/05/12
For personal use only.

Excess enthalpy, volume, and Gibbs free energy of *n*-propanol – isopropanol mixtures at 25 °C[1]

JIŘÍ POLÁK,[2] SACHIO MURAKAMI,[3] G. C. BENSON, AND H. D. PFLUG[4]
Division of Chemistry, National Research Council of Canada, Ottawa, Canada

Received July 31, 1970

The results of calorimetric, dilatometric, and circulation still studies of the system *n*-propanol – isopropanol at 25 °C are reported. Examination of the behavior of the excess properties indicates that deviations from ideality can be attributed mainly to the formation of mixed association complexes.

Canadian Journal of Chemistry, **48**, 3782 (1970)

Introduction

Previous publications (1–7) from our laboratory have described the measurement of various thermodynamic properties for a number of binary alcohol systems. The present paper reports the results of similar studies of the system *n*-propanol – isopropanol at 25 °C. Values of the molar excess enthalpy and molar excess volume were obtained from direct calorimetric and dilatometric measurements. Excess Gibbs free energies were derived from determinations of vapor–liquid equilibria.

Experimental

(i) Materials

The component liquids used in the course of this investigation were commercial reagents which were purified in an F & M preparative gas chromatograph (Model 775). *n*-Propanol (from Eastman Organic Chemicals), and isopropanol (Spectroquality from Matheson, Coleman and Bell) were passed through a column (6 ft long and 3/4 in. diameter) packed with Poropak Q, held at an oven temperature of 152 °C. The products were checked with a Model 154 Perkin–Elmer analytical chromatograph, using a column containing 10% PEG 1000 on Chromosorb G (NAW) at 100 °C, and no impurities were detected (*i.e.* level less than 0.01%). The refractive index, n_D, and vapor pressure, p^0, the latter measured ebulliometrically, were determined for each material at 25 °C; these results are listed in Table 1, along with values from standard data compilations (8, 9) and other sources (4, 5, 10). It should be noted that the refractive indices measured in the present investigation are both lower than the values given in the MCA Tables (9) and are closer to the results published by Brown and Smith (10). Also, the present vapor pressures differ from the API values (8) and are in better agreement with results obtained previously by the static method in our laboratory for different preparations of the alcohols (4, 5).

(ii) Apparatus and Techniques

Successive dilution techniques were used in determining the excess enthalpies and the excess volumes. The calorimeter and dilatometer have been described previously (2, 11). All of the measurements were made at 25.00 ± 0.01 °C. The uncertainties in the results for an equimolar mixture are estimated to be approximately ±0.3 J mole^{-1} for the excess enthalpy and ±0.0005 cm^3 mole^{-1} for the excess volume.

Vapor–liquid equilibria were studied in a circulation still. Details of the design and of the operating technique are given in ref. 12. The pressure in the still was measured with a quartz spiral gage (Texas Instruments) which was calibrated by comparison with a mercury manometer. For each point, the pressure was adjusted until a temperature of 25.000 ± 0.005 °C was obtained in the still head. The vapor pressures listed in Table 1 were determined with the still filled with the pure components. In the case of mixtures, equilibrium conditions were maintained for several hours before removing samples of the liquid and condensed vapor phases. These were analyzed chromatographically in the Perkin–Elmer 154, using a column filled with Poropak Q and an oven temperature of 156 °C. Tests of the method of analysis, employing samples of known composition, indicated an accuracy of ±0.08 mole%.

Results

The results of the calorimetric and dilatometric measurements on the system *n*-propanol (**1**) – isopropanol (**2**) at 25.00 °C are listed in Table 2. There, values of the molar excess enthalpy, H^E, and values of the molar excess volume, V^E, are listed for various mole fractions, x_1, of *n*-propanol.

The first three columns of Table 3 summarize the results of the vapor–liquid studies (also at 25.00 °C); x_1 and y_1 are the mole fractions of *n*-propanol in the equilibrium liquid and vapor phases at pressure p. The last column of the table contains the corresponding values of the molar

---

[1]NRCC No. 11 593.

[2]NRCC Postdoctorate Fellow 1968–1970. Present address: Department of Chemical Engineering, University of Ottawa, Ottawa, Canada.

[3]NRCC Postdoctorate Fellow 1967–1969. Present address: Department of Chemistry, Faculty of Science, Osaka City University, Sumiyoshi-ku, Osaka, Japan.

[4]NRCC Postdoctorate Fellow 1965–1967. Present address: Metallgesellschaft-AG, Frankfurt/M, Germany.

TABLE 1

Properties of component liquids at 25 °C

Component	Refractive index n_D		Vapor pressure p^0 (mm Hg)	
	Measured	Literature	Measured	Literature
n-Propanol	1.38304	1.38355 (9) 1.38314 (10)	21.24	20.48 (8) 21.06 (4)
Isopropanol	1.37487	1.37527 (9) 1.37497 (10)	43.56	44.49 (8) 43.35 (5)

TABLE 2

Experimental values of the molar excess enthalpy and molar excess volume of *n*-propanol (**1**) – isopropanol (**2**) mixtures at 25 °C

x_1	H^E (J mole^{-1})	x_1	H^E (J mole^{-1})	x_1	V^E (cm^3 mole^{-1})
0.0304	− 6.1	0.5351	−48.6	0.0180	−0.0016
0.0324	− 6.4	0.5635	−47.9	0.0456	−0.0042
0.0685	−13.2	0.5668	−47.5	0.0851	−0.0076
0.0749	−14.2	0.5722	−47.0	0.1346	−0.0115
0.1133	−20.6	0.5868	−47.1	0.1966	−0.0157
0.1418	−24.6	0.6050	−46.4	0.2577	−0.0193
0.1618	−27.7	0.6216	−45.1	0.3155	−0.0217
0.2135	−34.1	0.6284	−44.5	0.3695	−0.0234
0.2170	−34.0	0.6768	−41.6	0.4194	−0.0246
0.2644	−39.3	0.6865	−40.7	0.4640	−0.0251
0.3181	−43.4	0.7269	−37.5	0.4822	−0.0249
0.3187	−43.0	0.7390	−36.1	0.5210	−0.0247
0.3746	−46.7	0.7759	−32.6	0.5664	−0.0240
0.4155	−47.9	0.7905	−30.7	0.6168	−0.0228
0.4186	−48.1	0.8265	−26.7	0.6700	−0.0210
0.4317	−48.5	0.8405	−24.9	0.7200	−0.0189
0.4549	−48.7	0.8749	−20.2	0.7713	−0.0165
0.4650	−48.9	0.8887	−18.3	0.8217	−0.0136
0.4680	−48.7	0.9253	−12.6	0.8696	−0.0104
0.4854	−49.2	0.9320	−11.6	0.9151	−0.0070
0.5139	−48.9	0.9668	− 5.8	0.9519	−0.0039
0.5141	−48.7	0.9699	− 5.3	0.9811	−0.0014
0.5180	−48.4				

excess Gibbs free energy defined by

$$[1] \qquad G^E = RT(x_1 \ln \gamma_1 + x_2 \ln \gamma_2)$$

where R is the gas constant, T is the absolute temperature, and γ_1 and γ_2 are the activity coefficients of the two components in the liquid phase. Values of the activity coefficients were obtained from the results for the vapor–liquid equilibria by means of the equations

$$[2] \qquad \ln \gamma_i = \ln (y_i p/x_i p_i^0) + (B_{ii} - V_i^0)(p - p_i^0)/RT + (1 - y_i)^2 p\delta/RT$$

and

$$[3] \qquad \delta = 2B_{12} - B_{11} - B_{22}$$

The calculation employed our results for the vapor pressures of the pure components, p_i^0, molar volumes V_i^0 from ref. 9, and virial coefficients B_{11}, B_{22}, and B_{12} equal to -1959, -1777, and -1866 cm^3 mole^{-1}, respectively. The latter values were estimated from critical point data (13) according to the empirical correlation developed by O'Connell and Prausnitz (14).

The area test (15) was used to examine the consistency of the (x_1, y_1, p) values. A plot of $\ln (\gamma_1/\gamma_2)$ against x_1 showed a relatively large scatter but, after smoothing the values with a polynomial form, the difference of the positive and negative areas under the smoothed $\ln (\gamma_1/\gamma_2)$ curve was less than 5%. This discrepancy is reasonable in view of the fairly large errors in-

Can. J. Chem. Downloaded from www.nrcresearchpress.com by 210.87.254.40 on 09/05/12
For personal use only.

TABLE 3

Vapor–liquid equilibria of
n-propanol (1) – isopropanol (2) mixtures at 25 °C

x_1	y_1	p (mm Hg)	G^E (J mole^{-1})
0.0677	0.0306	42.01	−12
0.1302	0.0641	40.39	−26
0.1895	0.0994	38.92	−33
0.2601	0.1473	37.16	−37
0.3314	0.1969	35.66	−30
0.3996	0.2429	34.19	−37
0.4542	0.2874	33.02	−33
0.5889	0.4146	29.98	−30
0.6406	0.4715	28.75	−33
0.6901	0.5309	27.65	−28
0.7288	0.5757	26.78	−33
0.7656	0.6208	26.07	−28
0.7938	0.6626	25.39	−28
0.8356	0.7225	24.52	−25
0.8725	0.7776	23.80	−18
0.9058	0.8285	23.10	−20

herent in the determination of the vapor–liquid equilibria.

The results for H^E, V^E, and G^E are presented graphically in Figs. 1 and 2. The scatter of the points for G^E again reflects the uncertainties in the results for the vapor–liquid equilibria. The overall error in the value of G^E for an equimolar mixture is estimated to be about ± 7 J mole^{-1}. The continuous curves in Figs. 1 and 2 are smoothed representations of the experimental results by the Redlich–Kister form

$$[4] \quad X^E = x_1x_2[c_1 + c_2(x_2 - x_1) + c_3(x_2 - x_1)^2 + \cdots]$$

where X^E is H^E, V^E, or G^E. Appropriate values of the coefficients for each function, determined by least squares analyses, are given in Table 4 along with σ, the standard error of estimate associated with the use of the representation.

The equation

$$[5] \quad TS^E = H^E - G^E$$

relates the molar excess entropy, S^E, to the molar excess enthalpy and the molar excess Gibbs free energy. This was used to construct the curve for TS^E (shown in Fig. 1) from the smoothed values of H^E and G^E.

Discussion

The results in Fig. 1 show that the entropy term, $-TS^E$, makes a relatively small contribution to the excess Gibbs free energy and that deviations of the system *n*-propanol – isopropanol

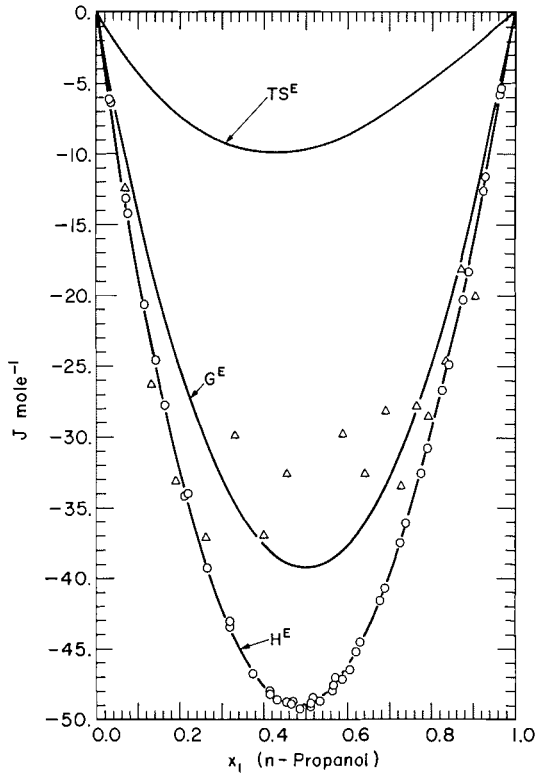

FIG. 1. Molar excess enthalpies, Gibbs free energies, and entropies of *n*-propanol (1) + isopropanol (2) mixtures at 25 °C. Experimental results H^E ○; G^E △. — H^E and G^E least squares representations by eq. 4; TS^E obtained from eq. 5.

from ideality are primarily energetic in origin (at 25 °C). Dispersive interactions between pairs of like and unlike molecules must be nearly equal in this system and it is reasonable to attribute the deviations from ideal behavior mainly to changes in hydrogen bonding. On this basis, the excess enthalpy of a binary alcohol mixture is the net result of positive and negative terms arising respectively from the breaking of hydrogen bonds between like alcohol molecules and from the formation of bonds between unlike molecules. Evidently the tendency to form mixed association complexes predominates in *n*-propanol – isopropanol mixtures at 25 °C.

It is interesting to compare the thermodynamic behavior of the present system with that of systems formed by mixing methanol with the various isomeric butanols (7). The behavior of the present system parallels most closely that of the system methanol – *sec*-butanol although

Can. J. Chem. Downloaded from www.nrcresearchpress.com by 210.87.254.40 on 09/05/12
For personal use only.

TABLE 4

Values of coefficients for least squares fit of results by eq. 4

Function X^E	c_1	c_2	c_3	σ
H^E (J mole^{-1})	−195.44	−13.41	2.81	0.19
V^E (cm^3 mole^{-1})	− 0.09932	− 0.00650	0.00872	0.00016
G^E (J mole^{-1})	−156.7			5.5

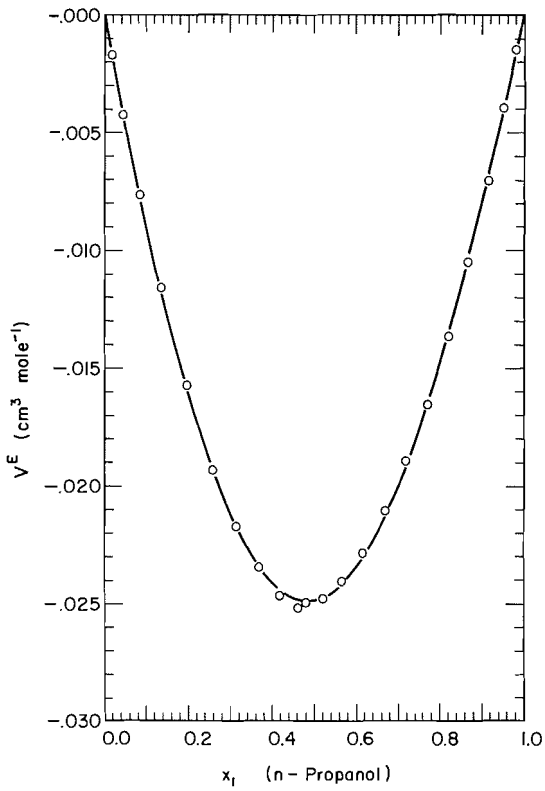

FIG. 2. Molar excess volumes of *n*-propanol (**1**) + isopropanol (**2**) mixtures at 25 °C. Experimental, ○; solid line is the least squares representation by eq. 4.

there is no variation in the sign of TS^E as observed for the latter. Both systems comprise a normal and a secondary alcohol and it appears that the formation of hydrogen bonds between unlike molecules plays an important role in determining their excess properties. However, the bonding of unlike molecules in the present system is accompanied by a decrease in volume, in contrast to the anomalous positive excess volumes observed for methanol – *sec*-butanol (7).

The authors thank Mr. P. J. D'Arcy and Mr. C. J. Halpin for technical assistance in all phases of the experimental work.

1. A. E. POPE, H. D. PFLUG, B. DACRE, and G. C. BENSON. Can. J. Chem. **45**, 2665 (1967).
2. H. D. PFLUG and G. C. BENSON. Can. J. Chem. **46**, 287 (1968).
3. H. D. PFLUG, A. E. POPE, and G. C. BENSON. J. Chem. Eng. Data, **13**, 408 (1968).
4. J. SINGH and G. C. BENSON. Can. J. Chem. **46**, 2065 (1968).
5. J. SINGH, H. D. PFLUG, and G. C. BENSON. Can. J. Chem. **47**, 543 (1969).
6. G. C. BENSON and H. D. PFLUG. J. Chem. Eng. Data. **15**, 382 (1970).
7. J. POLÁK, S. MURAKAMI, V. T. LAM, H. D. PFLUG, and G. C. BENSON. Can. J. Chem. **48**, 2457 (1970).
8. American Petroleum Institute. Research Project 44 Selected values of properties of hydrocarbons and related compounds. Texas A & M University, College Station Texas. Loose-leaf sheets dated April 30, 1956.
9. Manufacturing Chemists Association Research Project. Selected values of properties of chemical compounds. Carnegie Institute of Technology, Pittsburgh, Pa. Loose-leaf sheets dated Dec. 31, 1960 and June 31, 1961.
10. I. BROWN and F. SMITH. Aust. J. Chem. **15**, 1 (1962).
11. S. MURAKAMI and G. C. BENSON. J. Chem. Thermodyn. **1**, 559 (1969).
12. J. POLÁK, S. MURAKAMI, V. T. LAM, and G. C. BENSON. J. Chem. Eng. Data, **15**, 323 (1970).
13. A. P. KUDCHADKER, G. H. ALANI, and B. J. ZWOLINSKI. Chem. Rev. **68**, 659 (1968).
14. J. P. O'CONNELL and J. M. PRAUSNITZ. Ind. Eng. Chem. Process Design Develop. **6**, 245 (1967).
15. O. REDLICH and A. T. KISTER. Ind. Eng. Chem. **40**, 345 (1948).

Can. J. Chem. Downloaded from www.nrcresearchpress.com by 210.87.254.40 on 09/05/12
For personal use only.

The nature of the coordination bond in metal complexes of substituted pyridine derivatives. V. 4-Methylpyridine complexes of Zn(II), Cd(II), and Hg(II)

M. C. SEARS, W. V. F. BROOKS, AND D. G. BREWER
Department of Chemistry, University of New Brunswick, Fredericton, New Brunswick
Received[1] September 2, 1969

In this paper, an attempt is made to interpret the π-bonding between a 4-methylpyridine ligand and the divalent ions of zinc, cadmium, and mercury, using the previously introduced R_π parameter. To do this, the ν_{12} mode in the complexes is assigned and confirmed by a normal coordinate analysis based on a valence force field model.

Canadian Journal of Chemistry, **48**, 3786 (1970)

Can. J. Chem. Downloaded from www.nrcresearchpress.com by 210.87.254.105 on 09/05/12
For personal use only.

Introduction

The variation in the pure ring deformation mode in some substituted pyridine ligands has previously been interpreted (1, 3, 4) as reflecting the amount of π-bonding between the pyridine nitrogen and some first row transition metals. The π-bonding in these complexes ranged from large (Cu, Ni, etc.) to small (Zn) and the question arises as to whether the R_π parameter calculated is sensitive enough in complexes containing only small amounts of π-bonding. The Zn–Cd–Hg series was felt to be appropriate to answer this question.

Experimental

The reagents and the preparation of the 4-methylpyridine complex of Zn(II) have been described in a previous paper of this series (1).

The complex of Cd(II) was prepared by adding the ligand (2 moles) into the metal chloride solution (1 mole) in absolute alcohol with constant stirring. The resulting precipitate was filtered, washed several times with absolute alcohol and anhydrous ether, and dried in a vacuum desiccator over sulfuric acid.

The Hg(II) complex was prepared according to procedures described in the literature (2).

Microanalysis results for the complexes are found in Table 1.

The infrared spectra of the complexes in the region between 4000–200 cm^{-1} were recorded on a Beckman IR-12 filter/grating spectrometer. In the region 4000–400 cm^{-1}, the potassium bromide disk method was used. The infrared spectra of the solid compounds in the region 400–200 cm^{-1} were recorded as Nujol mulls with polyethylene windows. The spectrometer was constantly purged with dry air and wavelength calibration of the spectrometer was checked against the rotational spectra of water vapor. The spectra were obtained using standard settings as outlined in the Beckman IR-12 instruction manual. The reproducibility of the spectra was found to be ± 0.20 cm^{-1}. The infrared spectra in the region below 200 cm^{-1} were measured by means of a Perkin–Elmer model 301 spectrometer, which has been described elsewhere (3).

The calculations of the metal–ligand stretching force constants were carried out by means of an IBM 360 computer.

Results and Discussion

(I) Infrared Spectra and the Metal–Nitrogen (Ligand) Stretching Force Constants

The observed metal–nitrogen stretching frequencies of 4-methylpyridine complexes of some metal chlorides are found in Table 2. The assignment of the metal–nitrogen stretching frequency for the 4-methylpyridine complex of Zn(II) is the same as that of a previous paper in this series (4). The assignment of the metal–nitrogen stretching frequency for the 4-methylpyridine complexes of Cd(II) and Hg(II) is based on a comparison of their spectra with those of similar metal complexes with bromide instead of chloride.

The data in Table 2 indicate that coordination between 4-methylpyridine and different metal ions gives different metal–nitrogen stretching frequencies which decrease in the following order

$$Zn(II) > Hg(II) > Cd(II)$$

The above order for Zn(II) and Hg(II) is in agreement with the results of a study (5) of the magnetic susceptibilities of 4-methylpyridine complexes of Zn(II), Hg(II), and Cd(II) chlorides. The authors state that the metal–nitrogen bond is stronger for the 2:1 complex of Zn(II) than for the 1:1 complex of Hg(II). However, the Cd(II) complex used in that study was a 2:1 complex and the order for Cd(II), therefore, does not agree with our 1:1 complex of Cd(II).

In the previous papers of this series, not all of the force constants were adjusted nor were all of the observed frequencies fitted by calculated ones. With the availability of a larger, faster computer and appropriate programs it became possible to do a more complete vibrational analysis. We still considered only a simplified model, the in-plane

[1]Revision received July 27, 1970.

TABLE 1

Preparation of metal complexes with 4-methylpyridine

Metal	Ratio (ligand/metal)	Calculated (%)					Found (%)				
		C	H	N	Metal	Cl	C	H	N	Metal	Cl
Zn(II)	2:1	44.68	4.38	8.69	20.27	21.98	44.50	4.29	8.49	19.55	22.32
Cd(II)	1:1	26.07	2.55	5.07	40.66	25.65	25.95	2.54	5.16	40.04	26.27
Hg(II)	1:1	19.77	1.94	3.84	55.01	19.45	19.81	1.94	3.82	52.67	19.95

TABLE 2

Summary of relevant data for complexes studied

Complex	Stereochemistry	Absorption band (cm^{-1}) (M–N)	Metal–nitrogen force constants (mdyn/Å)	ν_{12} mode (cm^{-1})	R_π values	First ionization potentials of metals (eV)
$Zn(CH_3C_5H_4N)_2Cl_2$	Tetrahedral	238	2.26	1034	−4.5	9.39
$Hg(CH_3C_5H_4N)Cl_2$	Dimeric (1 bridged Cl)	121	0.87	1037	−1.5	10.43
$Cd(CH_3C_5H_4N)Cl_2$	Dimeric (2 bridged Cl)	104	0.81	1036	−2.5	8.99

TABLE 3

Molecular parameters used in the calculation (3, 11–13)

$\alpha_1 = \alpha_1' = 118° 32'$	$r_1 = r_1' = 1.3944$ Å
$\alpha_2 = \alpha_2' = 121° 18'$	$r_2 = r_2' = 1.3945$ Å
$\alpha_3 = \alpha_3' = 120° 10'$	$r_3 = r_3' = 1.3402$ Å
$\beta_1 = \beta_1' = 123° 53'$	$r_4 = r_4' = 1.0805$ Å
$\beta_2 = \beta_2' = 120° 14'$	$r_5 = r_5' = 1.0803$ Å
$\beta_3 = \beta_3' = 115° 53'$	$r_6(CH_3) = 1.53$ Å
$\nu_1 = 118° 20'$	$r_7(Zn) = 2.06$ Å
$\nu_2 = \nu_3 = 120° 50'$	$r_7(Hg) = 2.60$ Å
$\delta_1 = 116° 50'$	$r_7(Cd) = 2.46$ Å
$\delta_2 = 3 = 121° 35'$	

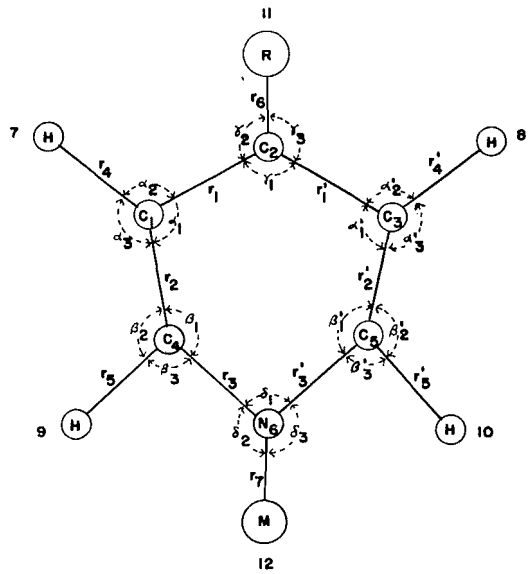

FIG. 1. The 1:1 complex model of 4-substituted pyridine–Zn(II), Cd(II), Hg(II) complexes.

vibrations of a metal atom plus a single ligand (Fig. 1, Table 3, refs. 11–13). This approximation should be adequate since the coupling of the groups through the metal atom is probably small (6). The methyl group of the ligand was treated as a single particle having the mass of the group. We used a set of 42 independent force constants which were adjusted to give a least squares fit to 49 observed frequencies of three complexes. The programs used were based on those of Schachtschneider (7). The observed and calculated frequencies are given in Table 4 and the final diagonal force constants are in Table 5. The final off-diagonal force constants are in the Depository of Unpublished Data.[2] The final force constants do not, of course, represent a unique set (14); but the diagonal stretching constants do, we feel, give a reliable measure for comparing bond strengths.

Comparison of the metal–nitrogen stretching force constants gives the same order as that obtained for the metal–nitrogen stretching frequencies, *i.e.*, Zn(II) > Hg(II) > Cd(III).

As in previous studies (3, 4) the metal–nitrogen stretching frequency is apparently directly related

[2]Photocopies may be obtained free of charge, upon request, from the Depository of Unpublished Data, National Science Library, National Research Council of Canada, Ottawa, Canada.

Can. J. Chem. Downloaded from www.nrcresearchpress.com by 210.87.254.105 on 09/05/12
For personal use only.

TABLE 4

Fundamental vibrational frequencies of metal complexes of 4-methylpyridine

Description	Vibrational frequency (cm^{-1})					
	Zn(II)		Hg(II)		Cd(II)	
	Obsd.	Calcd.	Obsd.	Calcd.	Obsd.	Calcd.
A_1 species						
ν(M—N)	238	241	121	123	104	106
ν_{6a}, ring, R-sensitive	550	545	532	523	538	529
ν_1, ring, β(C—M)	1032	960	1012	948	1020	956
ν_{12}, ring	1034	1022	1037	1026	1036	1023
ν_{18}, ν(C—R), β(C—H)	1218	1162	1215	1158	1217	1161
ν_{9a}, β(C—H)	1230	1244	1225	1237	1230	1235
R-sensitive	1432	1419	1428	1417	1433	1417
ν_{19a}, ν(C—C, C—N)	1505	1509	1501	1505	1506	1512
ν_{8a}, ν(C—C)	1617	1643	1614	1637	1620	1649
B_2 species						
ν(M—N)	207	196		92		92
ν_{15}, R-sensitive	421	423	420	412	420	412
ν_{6b}, ring	669	685	668	679	667	666
ν_{18b}, β(C—H)	1103	1114	1098	1112	1101	1107
ν_3, β(C—H)	1120	1159	1117	1157	1120	1159
ν_{14}, ν(C—C, C—N)	1332	1348	1332	1340	1337	1348
ν_{19b}, ν(C—C, C—N)						
β(C—R, C—H)	1458	1468	1457	1463	1458	1458
ν_{8b}, ν(C—C)	1561	1581	1558	1567	1560	1566

TABLE 5

Valence force constants (diagonal)

Force constant number	Force constant (mdyn/Å)			Description of force constant
	Zn(II)	Hg(II)	Cd(II)	
1	7.21	7.12	7.25	C—C stretch (top)
2	7.42	7.65	7.53	C—C stretch (bottom)
3	8.59	8.66	8.62	C—N stretch
4	5.00	5.00	5.00	C—H stretch
5	5.85	5.90	5.99	C—CH_3 stretch
6	2.26	0.87	0.81	M—N stretch
7	0.68	0.62	0.65	C—C—C angle (H)
8	0.16	0.20	0.20	C—C—C angle (CH_3)
9	2.01	2.06	2.21	C—N—C angle
10	0.74	0.78	0.67	C—C—N angle
11	0.91	0.88	0.90	Wag on C—C—C angle (H)
12	0.88	0.91	0.90	Wag on C—C—C angle (CH_3)
13	0.33	0.06	0.06	Wag on C—N—C angle (M)
14	0.76	0.76	0.76	Wag on C—C—N angle

to the metal–nitrogen stretching force constant. Also, the magnitude of the metal–nitrogen stretching frequency may be employed as a measure of the coordination bond strength for complexes of pyridine derivatives.

The stereoconfigurations of the 4-methylpyridine complexes of the divalent metal ions are listed in Table 2.

There are two halogen-sensitive bands in the spectra of the Zn(II) complex (tetrahedral configuration, ML_2X_2) which correspond to the A_1 and B_1 species of the C_{2v} point group.

In the Hg(II) complex one ν(Hg—Cl) vibration occurs at 321 cm^{-1} in agreement with the work of Clark and Williams (8). The complex is therefore deduced to be dimeric (9) with the terminal halogen vibration at 321 cm^{-1} and the bridged halogen vibration below 200 cm^{-1}.

The Cd(II) complex shows only badly resolved bands above 200 cm^{-1}. This suggests that all the

Can. J. Chem. Downloaded from www.nrcresearchpress.com by 210.87.254.105 on 09/05/12
For personal use only.

metal chlorine vibrations are below 200 cm^{-1} and are bridged halogens. Apparently, the Cd(II) complex is also dimeric (9).

(II) The Relative Strength of the π-Coordination Bond in the Complexes

The vibrational frequencies of the ν_{12} mode (pure ring deformation (1, 10)), together with the corresponding R_π values, of the divalent metal complexes of 4-methylpyridine are listed in Table 2. The R_π values were calculated according to the equation (given in ref. 1)

$$R_\pi = \nu_{ML} - (1.002\nu_L - 3.60)$$

where ν_{ML} and ν_L are the ν_{12} frequencies of the complex and free ligand, respectively. As in the previous study (4) the R_π values are quite small, and therefore the π-bond in these complexes is very weak. The coordination bond is then primarily σ in character.

The relative magnitude of the ν_{12} frequency, as well as the R_π values of these complexes are in the following order

$$Hg(II) > Cd(II) > Zn(II)$$

The π-bonding tendency of chlorine should proceed in the order Zn, Cd, Hg; hence that of 4-methylpyridine should follow the reverse order.

The R_π values calculated using the previously published formula (1) are small. It appears that the R_π parameter remains essentially constant for systems with very weak π-bonds.

We wish to thank Dr. P. Wong, National Research Council of Canada, Ottawa for obtaining the infrared spectra below 200 cm^{-1} as well as the National Research Council of Canada and the University of New Brunswick who provided the necessary funds for this investigation.

1. P. T. T. Wong and D. G. Brewer. Can. J. Chem. **46**, 131 (1968).
2. D. Cook. Can. J. Chem. **42**, 2523 (1964).
3. P. T. T. Wong and D. G. Brewer. Can. J. Chem. **46**, 139 (1968).
4. D. G. Brewer, P. T. T. Wong, and M. C. Sears. Can. J. Chem. **46**, 3137 (1968).
5. S. A. Zaveri and M. G. Datar. J. Indian Chem. Soc. **12**, 830 (1964).
6. K. Nakamoto, P. J. McCarthy, R. Ruby, and A. E. Martell. J. Amer. Chem. Soc. **83**, 1066 (1961).
7. J. H. Schachtschneider. Technical Report No. 263–62 of Shell Development Company.
8. R. J. H. Clark and C. S. Williams. Inorg. Chem. **4**, 350 (1965).
9. G. E. Coates and D. Ridley. J. Chem. Soc. **166** (1964).
10. E. Spinner. J. Chem. Soc. 3860 (1963).
11. M. A. Porai-Koshits, L. O. Atovmyan, and G. N. Tishchenko. Zh. Struckt. Khim. **1**, 337 (1960).
12. R. Zanetti. Gazz. chim. ital. **90**, 1428 (1960).
13. D. Grdenić and I. Krslanović. Arhiv. Kem. **27**, 143 (1955).
14. S. Toman and J. Pliva. J. Mol. Spectry, **21**, 362 (1966).

Can. J. Chem. Downloaded from www.nrcresearchpress.com by 210.87.254.105 on 09/05/12
For personal use only.

Can. J. Chem. Downloaded from www.nrcresearchpress.com by 210.87.254.5 on 09/05/12
For personal use only.

Temperature dependence of the 1555 cm^{-1} infrared absorption band in liquid D_2O: inflection points

R. Oder and D. A. I. Goring
Physical Chemistry Section, Pulp and Paper Research Institute of Canada
and
Department of Chemistry, McGill University, Montreal 110, Quebec

Received[1] October 27, 1969

The temperature dependence curves of the peak height, frequency, and half-width of the infrared intermolecular combination band absorbing at 1555 cm^{-1} in liquid D_2O has been observed to behave sigmoidally between 5 and 70 °C. No evidence of sharp discontinuities has been obtained but inflection points in the rather broad temperature interval of about 25 to 40 °C have been observed. Results are discussed in terms of structural changes occurring in the liquid.

Canadian Journal of Chemistry, 48, 3790 (1970)

Introduction

In an earlier infrared study of the intermolecular 2125 cm^{-1} absorption band in liquid water (1), a well defined inflection point at 32 °C was obtained on plotting the peak height *vs.* temperature. There was no clear evidence for a similar effect in the temperature dependence of the frequency, but the data indicated the possibility of an inflection between 30 and 40 °C.

Whether there is acceptable evidence for the existence of higher order transitions in liquid water has been a subject of controversy for some time. Numerous authors have reported the presence of anomalies in the temperature dependence of certain properties of water (1–8). Others have claimed all such effects are artefacts and no discontinuities beyond experimental error are evident (9–12). Luck and Ditter have concluded that discontinuities may be detected experimentally, but that their occurrence is an artefact and not a direct indication of transitions in water structure (13, 14). Nevertheless, the persistence of reports of anomalous behavior especially between 30 and 40 °C from spectral, volume, viscosity, and other types of studies lends some validity to the concept of a transition in liquid water.

The purpose of the present work was to investigate the effects of temperature on the peak height and the frequency of the 1555 cm^{-1} infrared absorption band of liquid D_2O, and to obtain the thermal dependences of its intensity and half-width. Spectra were recorded between 5 and 70 °C and at least one deformation band contour was included at each temperature.

[1]Revision received May 26, 1970.

Experimental

Infrared Measurements

Infrared spectra were recorded linearly in % transmission and wavenumber with a Unicam SP-100G double beam vacuum grating spectrophotometer. During runs, the sample and reference cell wells were purged with dry nitrogen. All spectra were recorded with an empty reference cell well, and a sample cell with CaF_2 windows. Lead shims used as spacers were amalgamated with mercury to make tightly sealed liquid cells. Path lengths, chosen to give combination band peaks of about 50 to 60% transmission, were measured by the interference pattern method (15) and checked frequently but found to remain unchanged for the duration of the experimental work. One cell was used throughout the study and its path length was 16.0 ($\pm$0.2) μ.

For temperature control, the CaF_2 cell was placed in a tightly fitting water jacket through which circulated a dilute water–glycol solution from a control bath. The sample temperature was measured with a copper–constantan thermocouple and could be determined to $\pm$0.3 °C.

The heavy water used was 99.7% D_2O from Merck, Sharp and Dohme. Samples were checked for HDO content by measuring the HDO absorption at 3400 cm^{-1}. The HDO content was never greater than 1.0%. The airtightness of the cells was verified by observing only a 1% decrease in transmission in the 3400 cm^{-1} absorption band in a D_2O sample over a period of 26 h (16). This corresponded to a change in concentration of less than 0.1% HDO.

An average of four spectra were taken of the combination band region at each temperature. For the deformation region one or two spectra only were recorded. Scan times used were from 50 to 80 cm^{-1} per min. Spectra of CaF_2 windows were recorded at varying temperatures but no trends with temperature were noted: thus the effects due to window materials were assumed to remain constant. Losses due to scattering and reflection amounted to about 10% T (T = transmission).

The infrared spectrophotometer was calibrated with water vapor absorption lines and liquid indene. Frequency calibrations are accurate to $\pm$1.0 cm^{-1}. Reproducibility was checked by taking standard spectra of a polystyrene film.

Can. J. Chem. Downloaded from www.nrcresearchpress.com by 210.87.254.5 on 09/05/12
For personal use only.

The instrument was operated with automatic slit programming resulting in spectral slit widths of 2.0 to 5.0 cm^{-1}. The effect of finite slit widths on recorded absorption spectra was investigated but was found to be negligible (16–18).

Analytical Methods

The major features of liquid D_2O transmittance curves in the frequency range investigated (900–2000 cm^{-1}) are shown in Fig. 1. The sharp intense band ν_2, centered at 1215 cm^{-1} arises from the fundamental intramolecular deformation mode (19). The less intense broad band overlapping the high frequency wing of the deformation band and with maximum absorption at 1555 cm^{-1} is due to intermolecular restricted rotation. It is most generally assigned to a combination of the deformation mode with a lower frequency librational mode (19, 20), and is designated ν_{2+L}. Also shown is the background curve arising from CaF_2 cell windows. The liquid D_2O spectrum after correction for window effects is shown by the solid lines. In all measurements, window effects have been taken into account.

The frequency of maximum absorption of the broad combination band was determined by the method illustrated in Fig. 2. A tracing of the recorded band contour was inverted and superimposed on the original spectrum with maximum overlap of the two curves. A base-line PQ was drawn between the two minima and a perpendicular drawn from its midpoint R to intersect the original spectrum at S. The frequency at S was then measured in wavenumbers and called ν_0. For the much sharper deformation mode, ν_0 was read directly from the recorded spectrum.

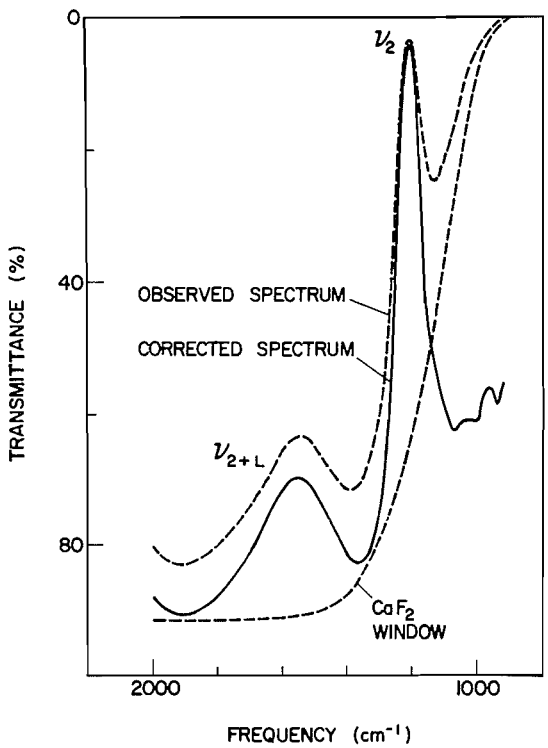

FIG. 1. Infrared absorption curves of liquid D_2O showing effect of correction for CaF_2 windows.

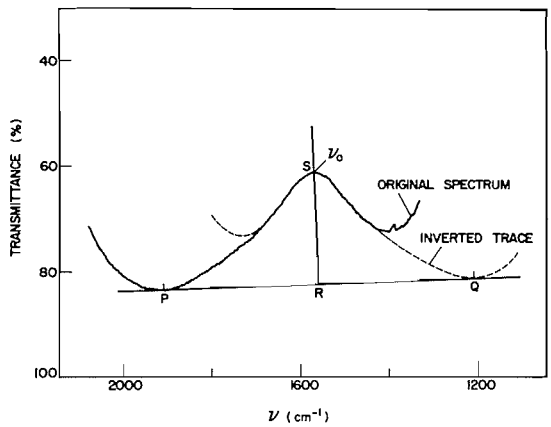

FIG. 2. Schematics of ν_0 determination for the combination band.

In determining both the extinction coefficient and the half-width of the bands, the minimum on the high frequency side of the combination band was taken as base-line transmittance, T_0. The molecular extinction coefficient at maximum absorption, ε_{max}, was derived from (21)

$$[1] \qquad \varepsilon_{max} = \frac{1}{ct} \log_{10} \left[\frac{T_0}{T}\right]_{\nu_0}$$

where T is the transmittance at frequency $\nu = \nu_0$, t is the thickness of the absorbing layer, and c is the concentration of the absorbing species; c has a value of 55.14 moles/l for D_2O (19). The half-width was determined from the two points at which the horizontal line at half maximum absorption cut the corrected infrared curve. At higher temperatures, an extrapolation (Fig. 1) on the low frequency side was necessary.

The peak height, ΔT_m, of the combination band of liquid H_2O was determined previously (1) from the interval between the minimum and the maximum transmittance of the band on its low frequency side, without compensation for window effects. This measurement is affected by the increasing degree of overlap of the combination and deformation bands on increasing temperature, and in D_2O by the curved base-line resulting from significant CaF_2 absorption in the vicinity of its combination band. In the present work, the difference in transmittance between the minimum and the maximum on the high frequency side of the combination band, after correction for window effects, was measured and was designated $\Delta T_m'$.

The experimental standard deviations of the infrared parameters determined for the combination band are given in Table 1. The experimental standard deviation of ν_0 for the deformation band was ± 1.0 cm^{-1}.

Results

Detailed numerical results for the combination band are given in Table 1 and the data are displayed graphically in Figs. 3 and 4.

TABLE 1

Temperature dependence of infrared parameters for the 1555 cm^{-1} band in liquid D_2O

Temperature (°C)	$\Delta T_m'$* (%)	ν_0† (cm^{-1})	$\Delta\nu_{1/2}$‡ (cm^{-1})	ε_{max}§
4.2	23.9	1570	230	1.50
6.8	23.9	1567	235	1.50
10.0	23.6	1565	235	1.48
13.6	23.1	1560	240	1.44
17.0‖	—	1560	—	—
19.7	22.3	1557	250	1.39
27.2	21.4	1555	255	1.34
30.6	21.2	1553	255	1.31
34.0	21.0	1550	260	1.30
38.0	20.9	1550	260	1.29
39.6‖	—	1552	—	—
46.2	20.4	1545	262	1.26
48.4	20.2	1542	270	1.24
52.6	19.8	1539	270	1.22
62.3	18.6	1529	275	1.13
66.0	18.4	1520	280	1.12

*Standard deviation = 0.2. T_l = 38 °C.
†Standard deviation = 1.5. T_l = 26 °C.
‡Standard deviation = 2.5. T_l = 31 °C.
§Standard deviation = 0.01; T_l = 38 °C.
‖Frequency range recorded was not sufficient to give $\Delta T_m'$, $\Delta\nu_{1/2}$, or ε_{max}

The temperature dependence of $\Delta T_m'$ obtained for liquid D_2O is shown in Fig. 3. The similarity in the peak height behavior to that observed earlier by Salama and Goring (1) is evident; both show a marked decrease with increase of temperature and a variation of slope near the middle of the temperature range investigated.

The temperature dependence found for the extinction coefficients of the combination band is also shown in Fig. 3. As expected, the behavior of ε_{max} is similar to that of peak height.

Observed frequencies of maximum absorption in heavy water are plotted in Fig. 4 together with values reported by Bayly, Kartha, and Stevens (19). An overall frequency shift of about $-0.8\ cm^{-1}/°C$ was obtained for liquid D_2O.

In contrast to the other infrared parameters measured, the half-width of the combination band increased on temperature elevation as shown by Fig. 4. Since the half-width is increasing with temperature, the decrease in ε_{max} shown in Fig. 3 does not necessarily mean a decrease in absorption intensity. An approximate evaluation of the intensity of the absorption was obtained by calculating the band area from

$$[2] \qquad \text{Area} = K \cdot \varepsilon_{max} \cdot \Delta\nu_{1/2}$$

in which the proportionality factor K has a value of 1.57 for a pure Cauchy (Lorentz) absorption profile and 1.06 for a pure Gaussian profile (22).

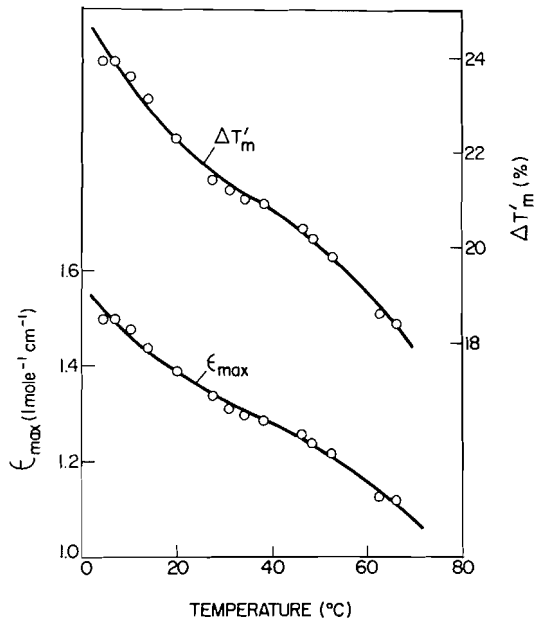

FIG. 3. Peak heights and ε_{max} *vs.* temperature for the combination band of heavy water. The curves are the least square 3rd degree polynomials.

For the intermolecular combination band, the actual shape of the band contour was found to be temperature dependent (23). However, it was possible to characterize the extent to which each absorption band profile was Cauchy or Gaussian in character and thus to determine at each temperature a K value (16) from which the band area could be calculated by eq. 2. In this manner, it was found that the combination band intensity decreased non-linearly with rising temperature by about 30% in liquid D_2O between 5 and 70 °C.

The infrared parameters of the deformation band absorbing at 1215 cm^{-1} in D_2O were found to be but slightly affected by temperature. Observed frequency trends are shown in Fig. 5 together with values taken from the literature. The magnitude of the shift was about $-0.1\ cm^{-1}/°C$ in good agreement with the results of Draegert *et al.* (20). With increasing temperature the maximum extinction coefficient was observed to increase slightly.

Discussion

Inflection Behavior

The first question to be discussed is whether or not the data collected indicate the presence of inflections in the temperature dependence of

Can. J. Chem. Downloaded from www.nrcresearchpress.com by 210.87.254.5 on 09/05/12
For personal use only.

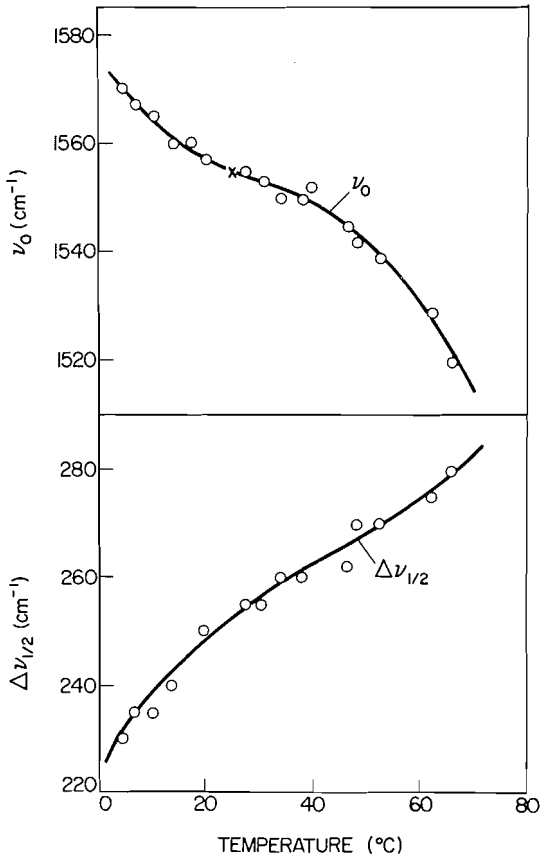

FIG. 4. Frequency and half-width *vs.* temperature for combination band of heavy water. The curves are the least square 3rd degree polynomials.

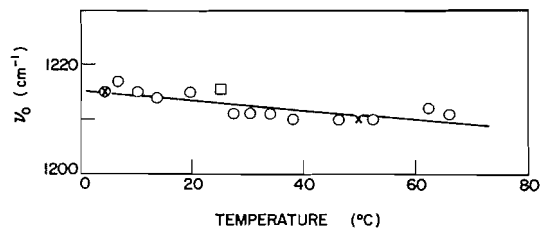

FIG. 5. Frequency *vs.* temperature for the deformation band of liquid D_2O. The crosses are data from Ford and Falk (24) and the square is from Bayly *et al.* (19).

the combination band parameters of liquid heavy water. Inspection of the results suggests that there is sigmoidal behavior in all trends shown in Figs. 3 and 4. Sigmoidal behavior was not apparent in the frequency *vs.* temperature plots shown in Fig. 5 for the deformation band. Here the total shift in frequency between 5 and 70 °C is an order of magnitude less than that of the combination band and thus any similar effect, were it present, would be too minute for detection.

A quantitative characterization of the temperature-dependence curves of the combination band was obtained by computer-fitting of polynomials of the form

$$[3] \qquad P = A_0 + A_1T + A_2T^2 + \ldots + A_nT^n$$

to the experimental data points by the method of least squares. In eq. 3, P represents the infrared parameter under investigation, A_0, A_1, A_2, A_n are coefficients, T is temperature in °C, and n is degree of the polynomial. Improvement of fit with increasing n was tested for by comparing the variance V about a polynomial of degree n with that of the $n + 1$ degree polynomial: whichever n gave the smallest V was taken as the degree of the polynomial giving the best approximation of the experimental data. The variance was given by

$$[4] \qquad V = \sum_m \delta_m^2/(m - n - 1)$$

where δ_m is the deviation of an experimental point from the least square polynomial and m is the number of points (25).

The polynomial curves thus obtained are drawn in Figs. 3 and 4. For all parameters of the combination bands the analysis showed that "best fit" was achieved with a third degree polynomial. On going to a fourth degree polynomial the value of V increased. The temperatures (T_i) calculated from the coefficients of the third degree polynomial curves for their points of inflection fell between 26 and 38 °C (Table 1).

It must be admitted that the validity of the inflection in any individual temperature-dependence trend shown in Figs. 3 and 4 is somewhat open to question. However, the combined observations of sigmoidal behavior for all of the infrared parameters studied suggest that the inflections observed are genuine effects and not experimental artefacts. This mutual reinforcement may be illustrated further by combining, for all the parameters, normalized deviations of the derivative dP/dT from the least square straight line through dP/dT *vs.* T. The procedure was as follows. For each series of experimental points, values of $dP/dT_{\text{experimental}}$ at various T were generated by a least square, seven point, moving quadratic analysis (1). The least-square straight line through $dP/dT_{\text{experimental}}$ *vs.* T was then computed and deviations from this were

Can. J. Chem. Downloaded from www.nrcresearchpress.com by 210.87.254.5 on 09/05/12
For personal use only.

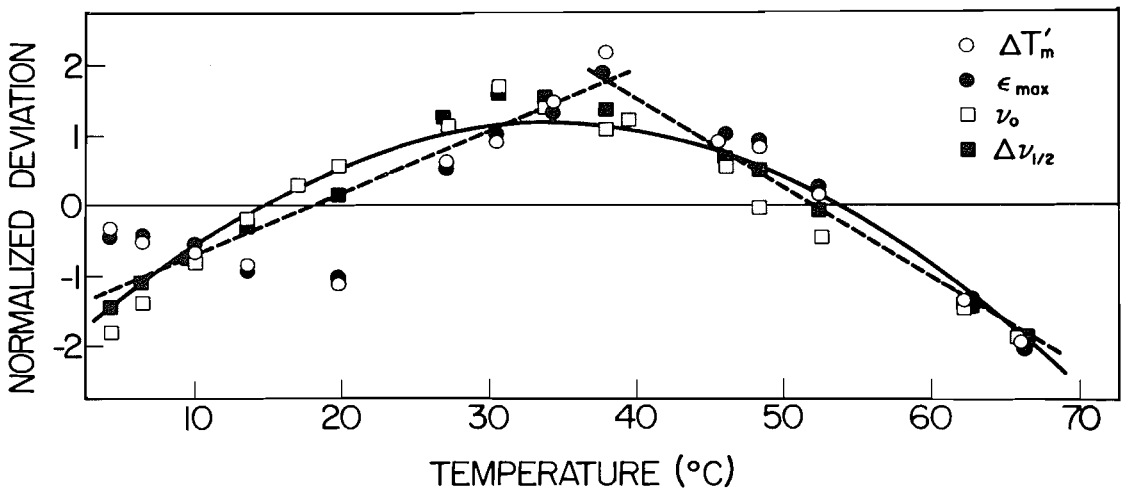

FIG. 6. Normalized deviation *vs.* temperature for the infrared absorption parameters of liquid heavy water. The abscissa coincides with the least square straight line through the points. The curve is the least square quadratic and the two sloping lines are the least square straight lines through points above and below 35 °C.

normalized such that the mean deviation of $dP/dT_{experimental}$ from the straight line was unity. The normalized deviation $(dP/dT_{experimental} - dP/dT_{least\ square})_N$ was then plotted against T. Points so derived, covering all the data for the combination band, are shown in Fig. 6. The normalized deviations derived from the half-width data were reversed in sign to accommodate the reverse inflection shown by $\Delta\nu_{1/2}$ *vs.* T (Fig. 4).

Although the points in Fig. 6 show considerable scatter, it is quite apparent that they are not randomly distributed about the abscissa. The standard deviations for the least-square straight line and quadratic through the points are given in Table 2. The high F-ratio (26) shows that a quadratic is a much better fit than a straight line through dP/dT *vs.* T. This means that P *vs.* T is better approximated by a 3rd degree than a 2nd degree polynomial. Interestingly, significant improvement over the quadratic can be obtained by plotting two least-square straight lines, one each for the points above and below 35 °C. This suggests that two intersecting quadratics are a better approximation to the trends shown in Figs. 3 and 4 than a single cubic.

TABLE 2

Standard deviations (s.d.) and F-ratios for curves fitted to data shown in Fig. 6

Single straight line	Quadratic		Two straight lines	
s.d.	s.d.	F-ratio	s.d.	F-ratio
1.16	0.52	230	0.42*	30

*Mean for two lines.

Interpretation of Trends

At this stage it is possible to attempt a qualitative explanation of the trends observed in terms of the "mixture" concept of liquid water. Walrafen (27–30) has given a good description of the two major species in a mixture model. The structured component consists of an assembly of water molecules of C_{2v} symmetry held in regular array by tetrahedral hydrogen bonding and resembling ice on a local scale. This is in equilibrium with an unstructured component in which molecules are not bound by the directional covalent interactions usually associated with hydrogen bonding but by other forces.

In Walrafen's model, increase of temperature causes "melting" of the structured component which is initially the more rapid but slows down somewhat at higher temperatures (28–30). This type of behavior would be expected to give a monotonic decrease in the numerical value of the first derivative of a species-dependent parameter with increase of temperature. In the present work, the temperature-dependence curves of the infrared parameters of the combination band show that up to about 25 °C the slopes are indeed

Can. J. Chem. Downloaded from www.nrcresearchpress.com by 210.87.254.5 on 09/05/12
For personal use only.

Can. J. Chem. Downloaded from www.nrcresearchpress.com by 210.87.254.5 on 09/05/12
For personal use only.

gradually decreasing. However, above 40 °C the slope starts to increase again. Something new must be taking place in the liquid water system to account for this resurgence of slope change. A possibility is that, as the structured component melts to give more and more unstructured water on temperature increase, the nature of the unstructured component changes from that of a pure librator to a mixture of librating and rotating molecules. The postulate implies that at lower temperature complete rotation of water molecules is inhibited in both structured and unstructured regions but that between 25 and 40 °C rotation of unstructured molecules begins to occur. Magat (2) first suggested the onset of rotation as an explanation for observed anomalous behavior of liquid water in this temperature range. Attempts to find direct evidence for rotational motion in liquid water from its spectra have proved unsuccessful. However, as pointed out by Luck and Ditter (14), water spectra in CCl_4 solutions do show evidence of rotation, and the inability to observe a corresponding motion in the pure liquid indicates that the proportion of truly free molecules is small, not that it is negligible.

It is important to note that the observed sigmoidal effect in the temperature-dependence curves is slight. This indicates that the equilibrium between librators and rotators in the unstructured species represents a minor perturbation only, the main trends being governed by equilibrium between structured and unstructured components in liquid water. The optimum bands to investigate for such effects are thus intermolecular bands originating from librational motion. Some authors studying the temperature dependence of fundamental intramolecular band parameters have found no inflections (29–31). Luck and Ditter have published several examples of discontinuities in the temperature dependence of the frequency of infrared bands of liquid water (13, 32). However, these authors conclude that the effects are due not to sharp transitions in the structure of the liquid but rather to particular combinations of the parameters of the overlapping bands corresponding to the individual species present in water (13, 14).

In conclusion, it should be emphasized that despite the better fit to the straight lines in Fig. 6, the data show that the inflection taking place is a gradual one. As Falk and Kell (10) noted, there is no convincing evidence for sharp kinks or sudden discontinuities over a narrow temperature range in the pure liquid. It is possible that, in systems which have a large interface with water, the inflection is sharpened considerably to give fairly sudden changes over a much narrower temperature range. The prevalence of such transitional behavior in interface water has been proposed recently by Drost-Hansen (33), and may account for the transitions observed in carbohydrate–water systems (34, 35), and in dilute solutions (36). Drost-Hansen has also made the interesting suggestion that the high window–surface to liquid–volume ratio in the short path length cells used could be responsible for the previously noted anomaly in ΔT_m *vs.* T (33). However, with a path length of 10 μ, the surface-to-liquid ratio is only 0.1 $m^2\ g^{-1}$, several orders of magnitude lower than the internal surface of a structure such as that of a water-swollen cellulose fiber (37). With such a small surface-to-liquid ratio it seems unlikely that surface effects are playing an important role in the behavior observed in the present work.

The authors wish to thank Dr. H. I. Bolker for his guidance in the early stages of the investigation and Mr. N. Ness for assistance in running the spectrophotometer. We are indebted also to Mr. P. Lamb of the McGill Computing Centre for his generous help in developing the computer procedure used.

1. C. Salama and D. A. I. Goring. J. Phys. Chem. **70**, 3838 (1966).
2. M. Magat. J. Phys. Radium, Paris, **6**, 179 (1935).
3. F. Feates and D. J. G. Ives. J. Chem. Soc. 2798 (1956).
4. F. Franks and D. J. G. Ives. J. Chem. Soc. 741 (1960).
5. R. Goldstein and S. S. Penner. J. Quant. Spectrosc. Radiat. Transfer **4**, 441 (1964).
6. W. Drost-Hansen. Ind. Eng. Chem. **57**, No. 4, 18 (1965).
7. M. J. Blandamer, M. F. Fox, and M. C. R. Symons. Nature, **214**, Pt. 1, 163 (1967).
8. Y. Chen and W. H. Orttung. J. Phys. Chem. **72**, 3069 (1968).
9. E. W. Rusche and W. B. Good. J. Chem. Phys. **45**, 4667 (1966).
10. M. Falk and G. S. Kell. Sci. **154**, 1013 (1966).
11. S. D. Hamann and N. K. King. Nature, **215**, 1963 (1967).
12. R. Cini and M. Torrini. J. Chem. Phys. **49**, 2826 (1968).
13. W. A. P. Luck. Ber. Bunsenges. Phys. Chem. **69**, 626 (1965).
14. W. A. P. Luck and W. Ditter. Z. Naturforschg. **24b**, 482 (1969).
15. W. J. Potts, Jr. Chemical infrared spectroscopy. Vol. I. Techniques. J. Wiley and Sons, New York. 1963. p. 114.

16. R. ODER. M.Sc. thesis. McGill University, Montreal, Quebec. 1969.
17. R. N. JONES and R. VENKATARAGHAVAN. Spectrochim. Acta, **23A**, 925 (1967).
18. A. ROESLER. Infrared Phys. **5**, 51 (1965).
19. J. G. BAYLY, V. B. KARTHA, and W. H. STEVENS. Infrared Phys. **3**, 211 (1963).
20. D. A. DRAEGERT, N. W. B. STONE, B. CURNETTE, and D. WILLIAMS. J. Opt. Soc. **56**, 64 (1966).
21. R. N. JONES and C. SANDORFY. Techniques of organic chemistry. Vol. 9. Weissberger, Interscience, New York. 1956. Chap. 4. p. 271.
22. C. LALAU. Spectrochim. Acta, **14**, 181 (1959).
23. R. ODER and D. A. I. GORING. To be published.
24. T. A. FORD and M. FALK. Can. J. Chem. **46**, 3579 (1968).
25. O. L. DAVIES. Statistical methods in research and production. Hafner, New York. 1957. p. 32.
26. O. L. DAVIES. Statistical methods in research and production. Hafner, New York. 1957. p. 66.
27. G. E. WALRAFEN. J. Chem. Phys. **40**, 3249 (1964).
28. G. E. WALRAFEN. J. Chem. Phys. **44**, 1546 (1966).
29. G. E. WALRAFEN. J. Chem. Phys. **47**, 114 (1967).
30. G. E. WALRAFEN. Hydrogen-bonded solvent systems. Taylor and Francis, London. 1968. pp. 9–29.
31. M. FALK and T. A. FORD. Can. J. Chem. **44**, 1699 (1966).
32. W. A. P. LUCK and W. DITTER. Ber. Bunsenges. Phys. Chem. **72**, 365 (1968).
33. W. DROST-HANSEN. Ind. Eng. Chem. **61**, No. 11, 10 (1969).
34. M. V. RAMIAH and D. A. I. GORING. J. Polymer Sci. C**11**, 27 (1965).
35. M. WAHBA and K. AZIZ. J. Text. Inst. **53**, T291 (1962).
36. V. V. MORARIU and R. V. BUCUR. J. Mol. Struct. **2**, 349 (1968).
37. J. E. STONE and A. M. SCALLAN. Pulp Paper Mag. Can. **66**, T407 (1965).

Can. J. Chem. Downloaded from www.nrcresearchpress.com by 210.87.254.5 on 09/05/12
For personal use only.

The thermal decomposition of benzoic acid

KEITH WINTER AND DONALD BARTON
Department of Chemistry, Memorial University of Newfoundland, St. John's, Newfoundland
Received[1] September 29, 1969

The thermal decomposition of benzoic acid has been studied in a Pyrex reaction vessel at 475, 486, and 499 °C over the pressure range 5 to 40 Torr. The main products, CO_2 and C_6H_6, were accompanied by smaller quantities of CO, H_2, and biphenyl. The percentage of conversion varied from less than 1% for initial rate experiments to over 90% in attempts to obtain a material balance. Moderately reproducible initial rates of formation of CO_2 were obtained after the vessel had been conditioned by pyrolysis of benzoic acid. The order for the initial rate of formation of CO_2, 1.20 ± 0.03 at 475 °C and 1.28 ± 0.04 at 499 °C, is discussed in terms of a combination of first and three-halves order reactions. Formation of both C_6H_5D and C_6H_6 in the presence of $C_6D_5CD_3$ is accepted tentatively as evidence of formation of benzene by both molecular and radical processes.

Canadian Journal of Chemistry, **48**, 3797 (1970)

Can. J. Chem. Downloaded from www.nrcresearchpress.com by 210.87.254.42 on 09/05/12
For personal use only.

Although the kinetics of the thermal decomposition of a number of monocarboxylic acids have been studied, no general relationship between structure and mechanism has appeared. In fact, the mechanisms of decomposition of the simple acids have not been firmly established.

For example, Blake and Hinshelwood (1) found that formic acid reacts at the surface of glass reaction vessels, but in carbon coated vessels they proposed homogeneous molecular dehydration and decarboxylation reactions. On the other hand Sims and Watson (2) obtained evidence of radical reactions. Puzzling observations in the work of Blake and Hinshelwood were the second order kinetics and low Arrhenius parameters for dehydration.

Blake and Jackson (3) found that the dehydration of acetic acid also followed second order kinetics below 600 °C in a silica reaction vessel but above 700 °C the order was found to be one. The order for decarboxylation was one over the entire temperature range of 530 to 762 °C. Although it was proposed that all reactions were homogeneous and molecular, reproducible rates were obtained only after the vessel had been conditioned by repeated pyrolysis of acetic acid, causing the rates to fall to minimum and reproducible values. The question arises whether or not the reactions are entirely homogeneous if conditioning of the vessel is required.

In the presence of toluene Back and Sehon (4) found that the rate of decarboxylation of phenylacetic acid was almost independent of the surface-to-volume ratio of the reaction vessel and proposed that the main reaction was carbon–carbon bond breakage. However, the results of a similar study (5) of the pyrolysis of diphenylacetic acid showed that reactions occurred at the surface.

Smith and Blau (6) found only the products propene and carbon dioxide in a study of the thermal decomposition of 3-butenoic acid, and that the rate was only slightly dependent upon the surface-to-volume ratio of the vessel. Homogeneous decarboxylation by transfer of the carboxyl hydrogen atom to the terminal carbon atom was proposed.

In view of the primitive state of the study of the carboxylic acids, and their diverse behavior, studies of various types of acids seemed appropriate. We report here the results of an exploratory study of benzoic acid, in which a number of reaction mechanisms suggested for other acids appeared to be impossible or unlikely.

Experimental

Benzoic acid (Fisher primary standard for Calorimetry) was melted, cooled, ground, degassed at 0 °C, melted and again degassed. Toluene-d_8 (Stohler Isotope Chemicals) was used without treatment other than degassing. Benzene (Fisher spectro-grade), CO_2, CO, and H_2 (Matheson) were used without treatment.

The vacuum system was of conventional design, using stopcocks and high vacuum silicone grease. The 1 l spherical Pyrex reaction vessel was located in a furnace controlled by a platinum probe and relay. The temperature was measured with chromel–alumel thermocouples. Pressure was determined using a Pyrex spoon gauge located in an air furnace along with various stopcocks and a 5 l flask used sometimes for introducing reactants. The null position of the spoon gauge was detected by focussing the image of the filament of a tungsten lamp on two phototransistors, using a glass bead at the tip of the spoon gauge arm and a lens. For a series of pressure measure-

[1]Revision received July 20, 1970.

TABLE 1

Products of the decomposition of benzoic acid in a 1.162 l reaction vessel at 498.5 °C*

Time (s)	Moles of acid × 10^6		Product, moles × 10^6			
	Initial	Unreacted	CO_2	C_6H_6	CO	H_2
2 000	768	676	27.3	—	6.7	0.27
2 600	769	—	28.6	—	10.3	0.58
9 000	792	566	139	121	27.9	1.65
10 500	717	488	143	137	40.3	0.72
12 000	756	—	513	—	28.0	6.0
16 000	783	415	249	210	74.6	2.7
62 200	808	34	649	510	95.1	8.6
16 000	229	123	76.6	66	9.9	0.46

*Spaces indicate no analysis performed.

ments with a fixed pressure of air in the reaction vessel the average deviation was 0.13 Torr. The pressure was measured by means of a large bore mercury manometer and a cathetometer.

The products could be separated by means of traps and a Toepler pump into four fractions; those volatile at −196; −116; −45 °C; and the remainder. The first fraction was analyzed for H_2 and CO by means of a CEC 21-614 mass spectrometer. The second and third fractions were also examined by means of the mass spectrometer. Only CO_2 was detectable in the second fraction and only C_6H_6 in the third. A few analyses for C_6H_6 were performed using an infrared gas cell. The final fraction could be titrated with NaOH in neutralized ethanol. The final (solid) fraction was also examined by means of a Perkin–Elmer RMU-6 mass spectrometer.

Results

Successive experiments exhibited a decreasing initial rate of formation of CO_2 until the rate became moderately reproducible. For example, consider three experiments performed in sequence. The reaction vessel had been evacuated continuously overnight with the diffusion pump in operation, and an experiment at 17.7 Torr of benzoic acid was the first experiment of the day. The reaction produced 2.39×10^{-6} mole of CO_2 in 600 s. The second experiment of the day, using the same starting pressure, was carried out $1\frac{1}{2}$ h later with no treatment of the vessel except for the few minutes of pumping required to reduce the pressure to 10^{-6} Torr. The reaction produced 1.58×10^{-6} mole of CO_2 in 600 s. In the third experiment, which was carried out $1\frac{1}{2}$ h after the second, 1.65×10^{-6} mole of CO_2 was produced. The latter two experiments are typical of those designated as experiments carried out in a conditioned reaction vessel. Pumping overnight with the fore pump or with the diffusion pump, or isolating the reaction vessel overnight, destroyed the conditioning and it was particularly difficult to condition the vessel after venting. For example, a series of experiments carried out after venting followed by 5 days of continuous pumping yielded 10.35, 7.76, and 7.26×10^{-6} mole of CO_2. A series carried out on the following day yielded 6.53, 5.32, 5.26, and 5.23×10^{-6} mole of CO_2. The final three were designated as carried out in a conditioned vessel. At one time during the study the normal leakage of air into the vessel during a run was considered as a possible source of erratic results and high reaction rates. The deliberate addition of air into the reaction vessel during a run, at pressures several times that normally present, caused only a small increase in rate. Exposure to air before a run, even at 10^{-6} Torr for a long period, results in an absence of conditioning as defined above, while a much higher pressure during a run does not seriously affect the conditioning. On completion of the study no surface deposit of carbon was visible. This contrasts with the condition for reproducible rates found by Blake and Hinshelwood, who deposited a visible film of carbon on the surface by pyrolyzing a hydrocarbon (1).

Products from experiments in a conditioned vessel are listed in Table 1. Some biphenyl and smaller amounts of other aromatic compounds were found in the solid fraction. It was found that $\sim 10^{-3}$ mole of benzoic acid could be manipulated through the air furnace and recovered with less than 2% loss, or $\sim 0.02 \times 10^{-3}$ mole. The difference between the number of moles of acid introduced and that recovered plus the number of moles of CO and CO_2 produced varies from 0.02×10^{-3} to 0.06×10^{-3} mole. These results suggest that some products other than CO and CO_2 may arise from the carboxyl group. If the

Can. J. Chem. Downloaded from www.nrcresearchpress.com by 210.87.254.42 on 09/05/12
For personal use only.

TABLE 2

Order, Arrhenius parameters, and rate constants of the formation of carbon dioxide

Temperature (°C)	Rate constant* × 10^5	Order
475.1	$1.040 \pm 0.002\, l^{0.20}\, m^{-0.20}\, s^{-1}$	1.20 ± 0.03
498.5	$7.07 \pm 0.02\, l^{0.28}\, m^{-0.28}\, s^{-1}$	1.28 ± 0.04

*Rate constant from middle of concentration range using the mean order: $k = 10^{13.4} \exp(-62\,200/RT)\, l^{0.24}\, s^{-1}$.

difference between the initial and recovered quantities of benzoic acid is compared with the quantity of CO plus CO_2, the percentage of missing carboxyl group is apparently rather large for experiments carried to a low percentage of reaction. Such a conclusion is not justified because of the difficulty experienced in manipulating benzoic acid.

A very small amount of methane was found occasionally, presumably from pyrolysis of the stopcock lubricant.

The initial rates of formation of carbon dioxide in a conditioned vessel are shown in Fig. 1 and the orders and Arrhenius parameters in Table 2. The Arrhenius parameters are obtained from the middle of the concentration range using the mean order, *i.e.* by supposing that the order is not temperature dependent. Comments on this procedure are to be found below. A few data on the initial rate of formation of CO and of H_2 are given in Table 3.

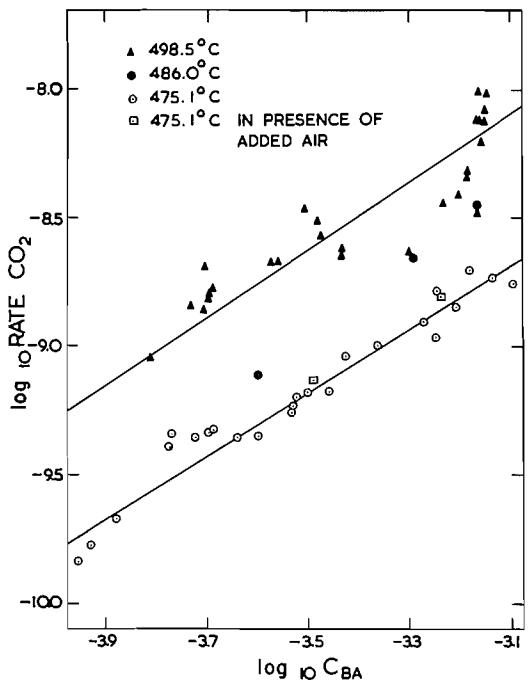

FIG. 1. Initial rate of formation of CO_2. Dimensions are moles l^{-1} s^{-1} and moles l^{-1}.

The occurrence of biphenyl is consistent with the presence of phenyl radicals. Confirmation of this was sought by adding toluene-d_8 to the reacting system and measuring the C_6H_5D content of the benzene. The results are summarized in Table 4.

Discussion

The results are discussed in terms of the elementary reactions 1–12.

[1] $C_6H_5COOH \rightarrow C_6H_5 + COOH$

[2] $COOH + M \rightarrow CO_2 + H + M$

[3] $COOH + M \rightarrow CO + OH + M$

[4] $C_6H_5COOH + H \rightarrow C_6H_5CO_2 + H_2$

[5] $C_6H_5COOH + OH \rightarrow C_6H_5CO_2 + H_2O$

[6] $C_6H_5COOH + C_6H_5 \rightarrow C_6H_6 + C_6H_5CO_2$

[7] $C_6H_5CO_2 \rightarrow C_6H_5 + CO_2$

[8] $2C_6H_5 \rightarrow (C_6H_5)_2$

[9] $C_6H_5 + H \rightarrow C_6H_6$

[10] $C_6H_5 + OH \rightarrow C_6H_5OH$

[11] $C_6H_5COOH \rightarrow C_6H_6 + CO_2$

[12] $C_6H_5 + C_6D_5CD_3 \rightarrow C_6H_5D + C_6D_5CD_2$

The rate expression for CO_2 formation is treated as a combination of a first order term with one of the next higher common order, three-halves.

$$d[CO_2]/dt = [C_6H_5COOH]A_1 \exp(E_1/RT) + [C_6H_5COOH]^{3/2} A_{3/2} \exp(E_{3/2}/RT)$$

While more complex mechanisms and other combinations of order are conceivable, we have chosen a simple mechanism which can serve as a basis for discussion. A mechanism for the first order part is composed of reactions 1, 2, and 9 in

Can. J. Chem. Downloaded from www.nrcresearchpress.com by 210.87.254.42 on 09/05/12
For personal use only.

TABLE 3

Initial rate of formation of CO and of H_2

Temperature (°C)	Acid concentration ($ml^{-1} \times 10^3$)	Rate of formation of CO ($ml^{-1}\ s^{-1} \times 10^{12}$)	Rate of formation of H_2 ($ml^{-1}\ s^{-1} \times 10^{12}$)
498.5	0.333	615	19
498.5	0.339	476	10
498.5	0.661	2880	132
498.5	0.655	1550	78
498.5	0.662	3390	190
498.5	0.705	2670	120
486.0	0.253	590	3.7
486.0	0.516	575	13
486.0	0.682	1160	23
475.1	0.251	51	1.8
475.1	0.377	204	3.7
475.1	0.658	400	8.3

TABLE 4

Formation of C_6H_5D in the presence of $C_6D_5CD_3$ at 498.5 °C

Initial pressure of acid (Torr)	Initial ratio $[C_6D_5CD_3]/[C_6H_5COOH]$	Ratio in products $[C_6H_5D]/[C_6H_6]$	Percentage reaction
33.0	1.74	0.058	39
33.1	2.97	0.074	29
9.5	32.4	0.138	49
32.9*	3.27	0.081	63

*Reaction vessel not conditioned.

which reaction 1 is rate-controlling, or of reaction 11. The homogeneous reaction 1 cannot make a major contribution because $D(C_6H_5—COOH)$ is approximately 97 kcal $mole^{-1}$, calculated from the ΔH_f^0 values of C_6H_5COOH, COOH, and C_6H_5 which are reported to be respectively -69.9 (7), -53 (8), and 80 (9) kcal $mole^{-1}$. By using the average order, *i.e.* by neglecting any temperature dependence of order and supposing the activation energy to be the same for both mechanisms, the experimentally found order is obtained if $A_1 \approx 1.7 \times 10^{12}\ s^{-1}$ and $A_{3/2} \approx 1.0 \times 10^{14}\ l^{0.5}\ mole^{-0.5}\ s^{-1}$. The values of A_1 and of E_1 are normal and favor the homogeneous reaction 11 rather than the heterogeneous reactions 1 or 11. The complete rate expression is obtained by combining with reaction 11 the long chain reaction sequence 1, 2, 4, 6, 7, and 8. The resulting rate expression is

$$d[CO_2]/dt = k_{11}[C_6H_5COOH] + k_6(k_1/k_8)^{1/2}[C_6H_5COOH]^{3/2}$$

For $E_1 \approx 97$ and $E_8 \approx 0$, an acceptable value of E_6 will yield an activation energy of 65 kcal $mole^{-1}$ as observed. The ratios $[CO_2]/[H_2]$ give the chain lengths according to this mechanism. The limited exploratory data on the rate of formation of hydrogen do not, however, correspond to reaction 4, as the major reaction of atomic hydrogen. The chain mechanism gives for hydrogen formation

$$d[H_2]/dt = (k_1k_2)/(k_2 + k_3)[C_6H_5COOH]$$

while the data show that the order is much greater than one. The origin of the bulk of the hydrogen is not apparent; a bimolecular reaction of benzoic acid, producing H_2 might occur but the nature of such a reaction is not obvious.

The scatter in the values for the initial rate of formation of CO_2 is presumably due to surface reaction(s) even in the conditioned vessel. Surface reactions are therefore favored although the Arrhenius parameters appear to be normal for homogeneous reactions. Confirmation of this is found if the temperature dependence of the order is considered. The orders were obtained from 27 measurements at 498.5 °C and from 25 at 475.1 °C by treating the data by the least-squares method. The attached errors suggest that there is justification in considering the order to be

Can. J. Chem. Downloaded from www.nrcresearchpress.com by 210.87.254.42 on 09/05/12
For personal use only.

Can. J. Chem. Downloaded from www.nrcresearchpress.com by 210.87.254.42 on 09/05/12
For personal use only.

temperature dependent. The rate constants for the two terms so obtained are

$$k_1 = 10^{7.2} \exp(-45\,000/RT)\,s^{-1}$$

and

$$k_{3/2} = 10^{17} \exp(-72\,500/RT)\,l^{1/2}\,m^{-1/2}\,s^{-1}$$

The pre-exponential factor in k_1 is outside the normal range for homogeneous unimolecular reactions and the activation energy is low, indicating a major contribution by a heterogeneous reaction.

If D(CO—OH) $\approx$ 45 kcal mole^{-1} and D(COO—H) $\approx$ 20 kcal mole^{-1} (4), the homogeneous reaction 3 does not contribute to CO formation but a heterogeneous reaction 3 is possible. The rate of formation of CO would be

$$d[CO]/dt = (k_1k_3)/(k_2 + k_3)[C_6H_5COOH]$$

Although the experiments on CO formation were of the exploratory type, and the data are scattered, the results suggest that the order is much greater than one and that reaction 3 is not the main source of CO. When the results of studies of CO formation from other acids are considered it becomes apparent that the results of a detailed study of CO formation from benzoic acid would be of considerable interest. Blake and Hinshelwood (1), observing that the reaction forming CO from HCOOH in carbon coated reactors was second order, suggested that CO is formed by a unimolecular reaction of $(HCOOH)_2$. The pre-exponential factor in that case is very small and of the correct order of magnitude for a combination of the monomer–dimer equilibrium constant with a unimolecular rate constant. Also (below 600 °C) the dehydration reaction of acetic acid is second order (3). The molecular dehydration reaction of acetic acid which produces water and ketene is not analogous to the molecular dehydration reaction of formic acid which produces water and hydrogen. The reaction forming carbon monoxide and phenol from benzoic acid would be more nearly analogous to the dehydration reaction of formic acid than to that of acetic acid. It is of interest to note that while the three molecular reactions described above are not analogous reactions, second order reactions may occur in all cases. The origin of such a common behavior is not clear.

Phenyl radicals are present, as shown by the detection of C_6H_5D in four experiments, the results of which are summarized in Table 4. Although a detailed study of the effect of toluene on the rate and stoichiometry is desirable, a provisional interpretation of the results may be made. If it is assumed that benzene is produced only according to reactions 6 and 12, the ratio of the rates of formation of C_6H_6 and C_6H_5D is

$$d[C_6H_5D]/d[C_6H_6] = (k_6/k_{12})[C_6D_5CD_3]/[C_6H_5COOH]$$

In the first experiment the ratio $[C_6D_5CD_3]/[C_6H_5COOH]$ is $\sim$1.7 initially and $\sim$2.8 finally while in the second experiment the ratio is $\sim$3.0 initially and $\sim$4.7 finally, *i.e.*, the ratio is greater by a factor of $\sim$1.7 throughout. The ratio $[C_6H_5D]/[C_6H_6]$ increases by a factor of 1.3. Arguing similarly for the second and third experiments, the ratio $[C_6D_5CD_3]/[C_6H_5COOH]$ is increased by a factor of $\sim$20 initially and $\sim$60 finally while the ratio $[C_6H_5D]/[C_6H_6]$ is increased by only 2.4. Although complete scavenging of phenyl radicals has not been obtained, the results suggest that a substantial quantity of benzene is formed via reactions other than 6 and 12, such as the molecular elimination reaction 11.

The authors are grateful to Dr. Leslie B. Sims of the University of Arkansas for helpful comments on this work and to the National Research Council of Canada for financial assistance.

1. P. G. Blake and Sir Cyril Hinshelwood. Proc. Roy. Soc. A**255**, 444 (1960).
2. (*a*) S. W. Watson. M.Sc. Thesis. Michigan State University, East Lansing, Michigan. 1967. (*b*) Leslie B. Sims. Private communication.
3. P. G. Blake and G. E. Jackson. J. Chem. Soc. B, 94 (1969).
4. M. H. Back and A. H. Sehon. Can. J. Chem. **38**, 1261 (1960).
5. M. H. Back and A. H. Sehon. Can. J. Chem. **38**, 1271 (1960).
6. G. G. Smith and S. E. Blau. J. Phys. Chem. **68**, 1231 (1964).
7. J. D. Cox. Tetrahedron, **18**, 1337 (1962).
8. S. W. Benson. J. Chem. Educ. **42**, 502 (1965).
9. A. S. Rodgers, D. M. Golden, and S. W. Benson. Ber. Bunsenges. Phys. Chem. **72**, 253 (1968).

Can. J. Chem. Downloaded from www.nrcresearchpress.com by 210.87.254.42 on 09/05/12
For personal use only.

Ethylene exchange in $PtCl(C_5H_7O_2)(\pi\text{-}C_2H_4)$

C. E. HOLLOWAY AND J. FOGELMAN
Department of Chemistry, York University, Downsview, Ontario

Received July 7, 1970

The kinetics of exchange of free with complexed ethylene in the system $PtCl(acac)(\pi\text{-}C_2H_4)$ have been investigated over a temperature and concentration range by proton magnetic resonance. First order kinetics are observed with respect to each component with no solvent dependence of rate. The activation energy and entropy are 2.7 kcal $mole^{-1}$ and -36 cal deg^{-1} $mole^{-1}$, respectively. A five coordinate intermediate is suggested, with complete retention of configuration at the platinum.

Canadian Journal of Chemistry, **48**, 3802 (1970)

Introduction

Previous studies on ethylene exchange in Pt(II) and Rh(1) complexes have been carried out using nuclear magnetic resonance (n.m.r.) and isotopic labelling techniques (1–4). In many cases rapid exchange is reported, such that the proton resonance spectrum is effectively averaged and only lower limits to the exchange rate can be determined. Differences in the estimated order of magnitude of the exchange between free and coordinated ethylene have been attributed to the operation of the E.A.N. rule in the case of Rh(1) complexes (5). The nature of the groups attached to the olefinic carbon atoms have also been observed to affect the exchange rate for complexes of substituted olefins (6). However, little quantitative work has been carried out, partly because of the intramolecular reorientation of the coordinated olefin (4, 5, 7). Thus at temperatures where line shape analysis of the ethylene exchange might be attempted, it is usually found that the rotation of the coordinated ethylene is also affecting the spectrum and considerably complicating the analysis. The present study has avoided this problem since the complex studied has only a small separation (at 60 MHz) between non-equivalent ethylenic protons, and also has an intermediate rate of free-complexed ethylene exchange. Thus it has been possible to choose concentrations and temperatures which are in the slow region of intermolecular exchange while in the fast limit of intramolecular reorientation. The solubilities of the two components curtail investigations to polar organic solvents, in which solvent participation in the exchange mechanism would not be expected to be very important. The results show that such participation is, within experimental error, negligible.

With platinum there arises the problem of two isotopic species, ^{195}Pt and ^{196}Pt, the former having a spin ($I = 1/2$) and a natural abundance of 33.7%. The proton spectra therefore contain peaks for the derivatives of both isotopes, again complicating line shape analysis. At the slow limit of exchange, allowance for the relative abundance of the species present can be made in calculations of the lifetimes of the coordinated ethylene. Coalescence of the proton spectra of the two isotopic derivatives does not occur, even above room temperature, in the absence of free ethylene (7). Thus any collapse observed in the present system must be occurring by an indirect exchange process via the free ethylene. Statistically, therefore, the rate governing such collapse will be several times slower than the rate of free-complexed ethylene exchange. In the slow region studied here, the effect of ^{195}Pt–^{196}Pt exchange has therefore been neglected. This does lead to introduction of errors when using the complexed ethylene line shape, at the faster rates, but the overall results suggest that the free ethylene line shapes are not seriously affected.

Experimental

The complex $PtCl(acac)(\pi\text{-}C_2H_4)$, where *acac* is the oxygen bonded chelated acetylacetonato group, was prepared and purified by literature methods (8, 9). Solutions were prepared in deuterochloroform or in benzene. Those containing excess ethylene were prepared by weighing the complex into a 5 mm o.d. n.m.r. tube and adding a known volume of a concentrated stock solution of ethylene. The tube was then sealed with a cap and a sealing cement. The concentration of ethylene in the stock solution was calculated by adding small known volumes of acetone or cyclohexane and integrating the n.m.r. peak areas. Variations in ethylene concentration were made by dilution of the stock solution.

Most of the kinetic data was obtained at room temperature in the limit of slow exchange. By lowering the temperature, the rate dependence and activation parameters were obtained. Some variation in ethylene

TABLE 1

$PtCl(acac)(\pi\text{-}C_2H_4)$ exchange with C_2H_4

No.	Solvent	[Pt complex] $\times 10^3 M$	(C_2H_4) $\times 10^4 M$	$1/\tau_{Pt}$	$1/\tau_{C_2H_4}$	k l mole^{-1} s^{-1} $\times 10^{-3}$
1	$CDCl_3$	0.809	In excess		2.01	2.48
		0.943			2.58	2.74
		1.13			3.39	3.00
		7.30			17.43	2.39
		9.13			22.61	2.47
		12.20			34.18	2.80
2	$CDCl_3$	In excess	10.8	2.38		2.21
			16.2	3.85		2.38
			27.9	8.50		2.79
			32.4	10.92		3.37
3	C_6H_6	3.31	In excess		8.33	2.52
		7.66			16.46	2.15
		15.9			36.44	2.29

concentration was detected on varying the temperature. However, by observing only the line shape of the free ethylene such variations could be ignored provided that the kinetics with respect to free ethylene were first order.

A Varian A-60 spectrometer was used, TMS being added to samples where appropriate as an internal reference. The spectra were obtained under conditions of low radio frequency power to avoid saturation, and the slowest sweep available (0.1 c.p.s.).

Results and Discussion

In general, Pt(II) complexes undergo ligand exchange according to the rate equation 1 (10).

$$[1] \qquad \text{Rate} = k_1[\text{Pt}] + k_2[\text{Pt}][\text{L}]$$

where k_1 is the rate constant for a solvent induced step and k_2 is a second order rate constant. Usually a strongly solvated species, for example in aqueous solution, is being dealt with in which the pseudo first order solvent induced step plays a significant role. Since the solvents used in this work, chloroform and benzene, are relatively weak donors, it is expected that the value of k_1 will be negligible. The rate process can thus be simplified to a second order process with a single rate constant, eq. 2.

$$[2] \qquad \text{Rate} = k[\text{Pt}][\text{L}]$$

The parameter obtainable from n.m.r. studies is the mean lifetime (τ) of a particular site, which is inversely proportional to the rate of site exchange. This can be expressed for the general case of exchange between two sites;

$$[3] \qquad \tau_A^{-1} = \text{Rate}/[\text{A}] = k[\text{A}]^a[\text{B}]^b/[\text{A}]$$

Thus the orders of reaction (a and b) with respect to each component are obtainable from log plots of τ values *vs.* concentration. The actual measurement of the τ values has been extensively discussed (11), and approximate methods are available for extracting them from particular features of the n.m.r. line shapes. In the present case concentrations were selected to keep the rate slow, hence the equation for large τ values [4] is applicable;

$$[4] \qquad 1/T_2' = 1/T_2 + 1/\tau$$

where $1/T_2'$ and $1/T_2$ are the linewidths in radians per second of a particular resonance with and without exchange, respectively. The derivation of eq. 4 implies that the separation of the resonances for the exchanging sites is large compared to the inverse of the half-height linewidths, and the τ values large enough to prevent appreciable overlap of the peaks. This is adequately satisfied in the present case (7).

The results in Table 1 show the room temperature rate dependence of the exchange process on concentration. The kinetics were determined from the linewidth of the species in excess, hence for first order kinetics with respect to that species the actual concentration of the excess component is not required (eq. 3). The order of reaction was determined from plots of eq. 1 and log plots of eq. 3. The graphical results of eq. 1 are shown in Fig. 1 and confirm that the solvent assisted step k_1 has no importance. The plots indicate two other features of interest, the first being the similarity between the rates in deuterochloroform and benzene. The second is the departure from linearity of the plot taken from the lifetimes of the coordinated ethylene. The deviation is such as to make the apparent rate of exchange increase

Can. J. Chem. Downloaded from www.nrcresearchpress.com by 210.87.254.42 on 09/05/12
For personal use only.

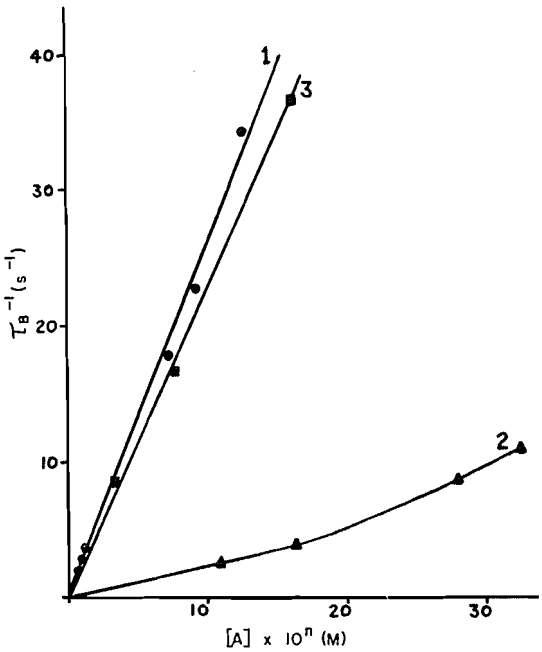

FIG. 1. Concentration dependence of rate. (*1*) A = C_2H_4; B = complex in $CDCl_3$; $n = 3$. (*2*) A = complex; B = C_2H_4 in $CDCl_3$; $n = 4$. (*3*) A = C_2H_4; B = complex in C_6H_6; $n = 3$.

faster than it should with increasing concentration. At these higher concentrations the induced ethylene exchange between platinum isotopes begins to become important. The linewidth of the ^{196}Pt derivative thus has an additional broadening effect which causes underestimation of the complexed ethylene τ value. Log plots of eq. 3 indicate a 1.0 order of reaction with respect to free ethylene and a 1.25 order with respect to complex, the latter reflecting the systematic error due to the additional contribution to linewidth. The rate process for ethylene exchange can thus be described in terms of eq. 2, the platinum complex undergoing attack by the free ethylene. The rate constant for the exchange in deuterochloroform is $2.65 \pm 0.2 \times 10^3$, and in benzene is $2.32 \pm 0.2 \times 10^3$ with units of l $mole^{-1}$ s^{-1}.

Activation parameters for the system can be obtained in the usual manner from the temperature dependence of the rate constant. Because of the errors introduced into the linewidth of the complexed ethylene, and the possible variation in free ethylene concentration with temperature, the kinetics were measured in the presence of excess ethylene only. Thus the linewidth of free

TABLE 2

Temperature dependence of exchange rate*

Number	Temperature (°C)	ln τ^{-1}	(T, °A) $\times 10^3$	Activation energy (kcal $mole^{-1}$)
1	−54.5	1.028	4.57	2.90
	−46.0	1.376	4.40	
	−40.0	1.537	4.29	
	−32.0	1.652	4.15	
	−20.0	1.919	3.95	
2	−40.0	1.924	4.29	2.44
	−36.0	1.933	4.22	
	−31.5	2.156	4.14	
	−26.0	2.223	4.05	
	−20.0	2.308	3.95	
	−15.0	2.403	3.87	
	− 6.0	2.523	3.74	

*Activation energy $E_a = 2.65 \pm 0.2$ kcal $mole^{-1}$; activation entropy $\Delta S = -36 \pm 5$ cal deg^{-1} $mole^{-1}$.

ethylene is used to obtain τ values, which are consequently independent of the actual free ethylene concentration. The results for the temperature dependent study are given in Table 2. A plot of the Arrhenius equation, log τ^{-1} *vs.* the inverse of the absolute temperature, gives a reasonable straight line the slope of which is a measure of the activation energy. The activation entropy is calculated from the thermodynamical formulation of rate constants, using the appropriate relationship for reactions in solution (12).

The activation parameters support the idea of a facile attack of free ethylene on the complex to give a five coordinate intermediate which then loses a molecule of ethylene. The n.m.r. spectrum of a concentrated solution of the platinum complex and ethylene, in which rapid exchange occurs, shows the individual methyl sites of the acetylacetonato group (7). Thus the configuration of the ligand about the platinum is retained during the exchange process. This is certainly in agreement with the expected behavior of a square planar platinum(II) species, in which the incoming ligand attacks essentially via the metal p_z valence orbital. However, in this case the group to be displaced is the one with the largest *trans* effect. Displacement of the ligand *trans* to the ethylene would involve partial dissociation of the acetylacetonato group and formation of a *trans* bis-ethylene complex. A derivative of Zeise's salt, *trans*-$PtCl_2(\pi\text{-}C_2H_4)_2$, is known to exist at −80 °C and has been suggested as a model of the intermediate to be expected in reactions of this type (13). Thus the systems studied by Cramer (3) have been discussed in terms of such

Can. J. Chem. Downloaded from www.nrcresearchpress.com by 210.87.254.42 on 09/05/12
For personal use only.

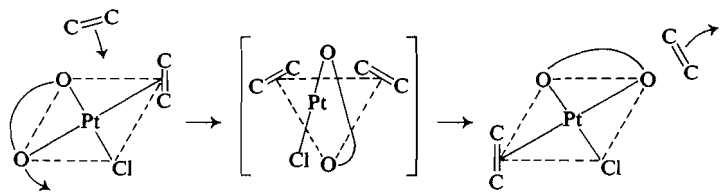

FIG. 2. Associative mechanism for exchange.

an intermediate. It has also been used to provide an explanation of the catalytic effects of allyltriethylarsonium cation and trichlorostannate(II) anion (13, 14) in the formation of platinum–olefin complexes. In the present case the entropy of activation suggests a highly ordered activated complex, which is not consistent with dissociation of a platinum–oxygen bond. The disruption in the delocalized acetylacetonato π-bond would also contribute unfavorably to the energy of activation. The scheme shown in Fig. 2 represents a possible pathway for the exchange process in which initial attack *trans* to the platinum–ethylene bond is followed by an intramolecular rearrangement of the ligands. Thus the oxygen atom *trans* to the ethylene is labilized, and on attack by free ethylene swings into the fifth coordination position along the p_z direction. A bis-ethylene intermediate is thus formed which can then lose one of the ethylenes, allowing the acetylacetonato group to swing back into the *xy* plane. Because of the initial *trans* attack the configuration of the ligands is unchanged, as is required by the n.m.r. spectrum under conditions of rapid exchange. Using the notation of Langford and Gray (16), the mechanism is essentially of the A type, the intermediate having the two high *trans* effect ligands sharing π-orbital interactions in the trigonal plane. The values of the activation parameters show that the exchange rate is governed to a considerable degree by the entropy of activation. The enthalpy of activation is much smaller than for most substitution reactions of platinum(II) complexes, although the general tendency for good entering ligands (also good *trans* labilizers) is being followed. In fact the enthalpy term is approaching the activation energy usually associated with diffusion controlled reactions in organic solvents (typically 2–3 kcal). It is interesting to note that the enthalpy is also much smaller than the activation enthalpy for intramolecular reorientation of the complexed olefin (7). The reaction might be considered to follow the interchange I pathway, there being no metastable intermediate formed. Here the kinetics are envisioned as being controlled by the rate at which the two components come into contact in the correct orientation.

The question as to the nature of the ethylene attack has been briefly investigated using an approach similar to that of Cramer (6). Displacement of the ethylene by substituted olefins is well known (9), and it should be possible to form the complex of *trans*-1,2 dichloroethylene by a simple exchange reaction

$$PtCl(acac)(\pi\text{-}C_2H_4) + C_2H_2Cl_2 \rightarrow PtCl(acac)(\pi\text{-}C_2H_2Cl)_2 + C_2H_4$$

Free ethylene formed in solution will undergo exchange with the initial complex as determined above, enabling its concentration to be calculated and hence the rate of displacement to be estimated. However, when excess of the dichloroethylene is added to a chloroform solution of the platinum ethylene complex and sealed into an n.m.r. tube, no change in the spectrum is observed over a period of several hours at room temperature. The rate of the displacement is thus quite a different order of magnitude to that for the ethylene case. Olefins bearing electronegative substituents should be poorer σ-donors and better π-acceptors than ethylene. Thus a process involving nucleophilic attack of the olefin on the platinum should be less favored for the dichloroethylene than for ethylene itself. The resultant complex, by analogy with the olefin complexes of Rh(I), should be more stable for the dichloroethylene case. Thus the observations support the contention (6, 15) that, in substitution reactions of this type, the initial formation of a σ-bond is the important step in the formation of the activated complex.

The financial support of the National Research Council of Canada for this work is gratefully acknowledged.

1. A. PANUNZI, R. PALUMBO, C. PEDONE, and G. PAIARO. J. Organomet. Chem. 5, 586 (1966).

Can. J. Chem. Downloaded from www.nrcresearchpress.com by 210.87.254.42 on 09/05/12
For personal use only.

2. J. A. KIEFT and K. NAKAMOTO. J. Inorg. Nucl. Chem. **30**, 3103 (1968).
3. R. CRAMER. Inorg. Chem. **4**, 445 (1965).
4. R. CRAMER. J. Amer. Chem. Soc. **86**, 217 (1964).
5. R. CRAMER. J. Amer. Chem. Soc. **89**, 5377 (1967).
6. R. CRAMER. J. Amer. Chem. Soc. **89**, 4621 (1967).
7. C. E. HOLLOWAY, G. HULLEY, B. F. G. JOHNSON, and J. LEWIS. J. Chem. Soc. A, 53 (1969).
8. A. WERNER. Chem. Rev. 2584 (1901).
9. D. GIBSON, J. LEWIS, and C. OLDHAM. J. Chem. Soc. A, 72 (1967).
10. F. BASOLO and R. G. PEARSON. Mechanism of inorganic reactions. John Wiley and Sons, New York. (1967).
11. J. A. POPLE, W. G. SCHNEIDER, and H. J. BERNSTEIN. High resolution nuclear magnetic resonance. McGraw-Hill, New York. 1959.
12. K. J. LAIDLER. Theories of chemical reaction rates. McGraw-Hill, New York. 1969. Chap. 3.
13. G. DOLCETTI, R. PIETROPAOLO, and U. BELLUCO. Inorg. Chem. **9**, 553 (1970).
14. R. PIETROPAOLO, G. DOLCETTI, M. GIUSTINIANI, and U. BELLUCO. Inorg. Chem. 549 (1970).
15. H. G. SCHUSTER-WOLDAN and F. BASOLO. J. Amer. Chem. Soc. **88**, 1657 (1966).
16. C. H. LANGFORD and H. B. GRAY. Ligand substitution processes. W. A. Benjamin Inc., New York. 1965.

Can. J. Chem. Downloaded from www.nrcresearchpress.com by 210.87.254.42 on 09/05/12
For personal use only.

Can. J. Chem. Downloaded from www.nrcresearchpress.com by 210.87.254.5 on 09/05/12
For personal use only.

Studies in solvolysis. Part II.[1] Some comments on the ion-pair mechanism for displacements at a primary carbon atom

JOHN M. W. SCOTT[2]
Chemistry Department, University of Calgary, Calgary, Alberta

Received May 11, 1970

The implication of Sneen and co-workers (2–5) that all S_N2 substitutions at a primary carbon atom probably proceed via the intermediate production of an intimate ion-pair is examined with respect to the reactions of the methyl halides (MeX; X = F, Cl, Br, I) with various nucleophiles (H_2O, OH^-, F^-, Cl^-, Br^-, I^-, CN^-, CSN^-, $S_2O_3^{2-}$) in water. By establishing certain rules concerning the behavior of derived reactivity scales (essentially ρ values) as contrasted with absolute reactivity scales (observed rate constants), it is concluded that Sneen and Larsen's mechanistic description is consistent with the experimental facts, and that in such cases the substitution process involves a pre-equilibrium constant, K_e, which is independent of the attacking nucleophile. This is followed by a rate determining bimolecular rate constant, k_n, which depends on the ion pair and the nature of the nucleophile. The observed rate (k^0) is given by $k^0 = K_e k_n$. A method of calculating K_e is described and values of k_n for nine nucleophiles attacking the four methyl halide ion-pairs are reported along with a number of confirmatory calculations. It is concluded that the classical Hughes–Ingold S_N2 Heitler–London description of these reactions is inadequate. Some further suggestions to place the new mechanistic description on a firmer experimental basis are made.

Canadian Journal of Chemistry, **48**, 3807 (1970)

Introduction

Recently Sneen and co-workers (2–5) have postulated that solvolytic displacements in highly nucleophilic (aqueous) media take place entirely by nucleophilic attack on an intimate ion-pair intermediate, to the exclusion of any reaction with the initial state of the reactant. This particular mechanism for aliphatic substitution is a part of the more generalized mechanism developed by Winstein (6–8) and numerous colleagues (see also ref. 9–11).

$$[1]\qquad \begin{array}{ccccccc} & & \overset{k_1}{\rightleftharpoons} & & \overset{k_3}{\rightleftharpoons} & & \overset{k_5}{\rightleftharpoons} \\ RX & & R^+X^- & & R^+||X^- & & R^+ + X^- \\ & \overset{k_2}{\downarrow} & & \overset{k_4}{\downarrow} & & \overset{k_6}{\downarrow} & \\ & P & & P & & P & \end{array} \qquad \begin{array}{c} \\ \\ \overset{k_{4n}}{\downarrow} \\ P \end{array}$$

where various species along the reaction coordinate derived from the substrate (RX) are the intimate- or tight-ion-pair (R^+X^-), the solvent-separated-ion-pair ($R^+||X^-$), and finally the kinetically free ions (R^+, X^-). This mechanism (reaction 1) specifically assumes that the substrate and each of the ionic modifications of that species are capable of reacting with a nucleophile to give the product (P). The rate constants $k_1 \rightarrow k_6$ form the ionic components of the mechanism and the rate constants $k_{1n} \rightarrow k_{4n}$ constitute the nucleophilic parts of the overall substitution process. In any particular situation of solvent, substrate, temperature, and pressure, the relative kinetic significance of the ten rate constants is the proper mechanistic question. The relative importance of each of the ten rate constants is a matter of energetics.

One of the distinctive features of the Winstein scheme is the de-emphasis of concerted processes. Indeed, if we accept Sneen's hypothesis (4) that the k_{1n} step is kinetically insignificant then truly concerted processes are absent in the overall sequence, *i.e.*, at every stage the nucleophilic and ionizing components of the reaction are kinetically separate. This proposal is consistent with and reminiscent of an earlier observation of Moelwyn-Hughes (12) who suggested that unitary processes in solution are exceptional.[3] The push–pull (13) description is likewise abandoned; "pushing" and "pulling" being distinct kinetic processes.

For secondary centers attached to good leaving groups, *e.g.* sec-octyl *p*-bromobenzene sulfonate, and activated primary centers (*p*-methoxybenzyl chloride) reacting in nucleophilic media, Sneen and co-worker (4) consider that a truncated

[1]For Part I, see ref. 1.

[2]Honorary Visiting Professor on leave from the Chemistry Department, Memorial University of Newfoundland, St. Johns, Newfoundland. This is the address to which all correspondence regarding this paper should be sent.

[3]Moelwyn-Hughes writes "Nature, it would seem, prefers to bring about material changes through a concerted set of reactions rather than through one elementary reaction." A unitary process is "one elementary reaction" with no intermediates and one transition state.

Can. J. Chem. Downloaded from www.nrcresearchpress.com by 210.87.254.5 on 09/05/12
For personal use only.

version of reaction 1 will suffice to cope with the experimental facts

$$[2] \qquad RX \underset{k_2}{\overset{k_1}{\rightleftharpoons}} R^+X^- \overset{k_{2n}}{\rightarrow} P$$

The absence of k_{1n} in reaction 2 is notable, for this means that the classical S_N2 reaction previously considered to take place by the Heitler–London mechanism (14, 15) is kinetically unimportant. Indeed, Sneen and Larsen (4) specifically state that "attack on covalent carbon seldom, if ever, occurs" and they challenge others to produce evidence to the contrary, *i.e.* evidence which will sustain the reality of the k_{1n} process. The validity of this challenge is recognized: the purpose of the present paper is to further vindicate the ion-pair mechanism for primary centers since these are the most likely alkyl halides to react by the k_{1n} route.

Certain further features of the Sneen mechanism are worthy of mention. The application of the steady-state theorem to reaction 2 gives, for the observed rate constant k^0,

$$[3] \qquad k^0 = k_1k_{2n}/(k_2 + k_{2n}) = k_1/(1 + \alpha)$$

where α is given by the expression

$$[4] \qquad \alpha = k_2/k_{2n}$$

The quantity α is important since the magnitude of this parameter defines three relatively distinct kinetic (not mechanistic) regions. In region I, α is small (<0.01) and hence k_1 becomes the rate determining step. This region might be identified with the traditional S_N1 mechanism in solvents of high nucleophilicity, *i.e.* an ion-pair intermediate is formed which reacts by paths which have no further kinetic significance, since the rate constants associated with these processes are all faster than k_1.

In region II, which might arbitrarily be defined by[4] $0.01 < \alpha < 100$, the rates of removal of the intimate ion-pair by k_2 (internal return) or k_{2n} (nucleophilic attack) are comparable and the steady-state expression given in eq. 3 is appropriate to this region. In region III, α becomes large ($\alpha > 100$) and eq. 3 assumes an alternative limiting form

$$[5] \qquad k^0 = k_1k_{2n}/k_2 = K_ek_{2n}$$

Whereas the kinetic behavior of RX in region I fits nicely into the traditional S_N1 classification, regions II and III represent mechanisms of a kind not accommodated by the S_N1–S_N2 scheme of Hughes–Ingold (15). Certainly reactions in these regions have S_N2 characteristics since the nucleophilic components of the observed rate are partly or wholly rate determining. However, the original formulation of the S_N2 reaction was conceived in terms of a rate determining bimolecular nucleophilic attack on the *initial state* of RX, not an ion-pair.

The quantity "α" discussed above is best considered as a selectivity parameter. In region I, the ion-pair is highly selective in that it largely proceeds to product without internal return. In region II, internal return becomes appreciable and in the middle of region II, when $\alpha = 1$, the selectivity of the ion-pair falls to zero, *i.e.*, the rates of internal return and product formation are equal. In region III, internal return is the dominant process and the ion-pair again becomes highly selective, but in an opposite sense to that displayed in region I.

A careful distinction must be drawn between the stability of the intermediate (thermodynamic) and its selectivity (kinetic). The former depends on the difference in free energy between RX and the ion-pair. The latter depends solely on the difference in free energy of the transition states which define the paths of its destruction. That selectivity and stability may be related is not denied since as substances become more reactive, the implied contraction of the free energy ordinates will bring reactants, intermediates, and transition states closer together in free energy and paralleled alterations in selectivity and stability are possible. Nevertheless, the stability of the intermediate does not formally[5] influence the kinetics since it may be shown that the free energy of activation in all kinetic regions does not depend on the free energy of the intermediate.

For most solvolytic substrates, k_2 appears to be the fastest step of all the processes in reaction 1. The reasons why this is so have been elaborated by Ritchie (16) in a useful summary of the broad features of the Winstein mechanism. If k_2 is indeed the fastest step then displacements taking place by the Sneen mechanism do so in kinetic region III as defined above. Ritchie's proposals concerning k_2 and hence α are to some extent

[4]Sneen and Larsen (4) operationally define this region by the expression $0.1 < \alpha < 10$.

[5]The "paralleled alterations" mentioned above represent the "informal" influence of stability on reactivity. This would be an extra-thermodynamic relationship between rates and equilibria.

Can. J. Chem. Downloaded from www.nrcresearchpress.com by 210.87.254.5 on 09/05/12
For personal use only.

contradicted by two studies reported by Sneen and Larsen, both of which lead to empirical values of α in the vicinity of unity. However, the interpretations given by the latter authors are not unique, since they assume the k_{2n} step to be simple, whereas in reality it may involve a "mixed kinetics" situation, *i.e.*, be a combination of k_{2n} and k_3 (see reaction 1). The empirical value of α would then be given by

$$[6] \qquad \alpha = k_2/(k_{2n} + k_3)$$

whereas the true value of α is as defined by eq. 4. As far as we can ascertain, the empirical data do not distinguish between a single rate constant or two rate constants for the destruction of the ion-pair aside from the k_2 process. In cases where solvent separated ion-pairs become important, the inclusion of a further rate constant (k_3) in the denominator of eq. 4 (to give eq. 6) will obviously reduce α, *i.e.*, the empirical value will be lower without contradicting Ritchie's considerations with respect to the k_2 step. Internal return is clearly an elusive phenomenon (16). As we pointed out earlier, an accurate assessment of the kinetic significance of the rate constants in reaction 1 constitutes the primary mechanistic question. Sneen and co-workers may not have accomplished such an assessment for the systems they investigated but this does not detract from the importance of their work.

The ion-pair mechanism represents a major departure from current thinking with respect to the definite bimolecular displacement, and because this is so, further numerical justification is mandatory.

In the remainder of this paper we present quantitative evidence which supports the ion-pair mechanism for primary centers reacting in water. The evidence derives from an evaluation of the kinetic behavior of methyl halides with a range of nucleophiles in this solvent. We believe that most primary compounds react in water in kinetic region III (see above) and hence the mechanism is defined by the parameters K_e and k_{2n}. A device for calculating K_e and k_{2n} for the primary systems constitutes the major contribution of this paper.

Linear Free Energy Relationships

Linear free energy relationships (l.f.e.r.) will play a central role in establishing the ion pair mechanism for primary centers reacting in water. The necessary l.f.e.r. will be developed in a formal way. This will not represent a proliferation of reactivity scales (17) but rather will emphasize the importance of derived reactivity scales which have, under certain well defined conditions, considerable mechanistic significance. In essence we are concerned here with an interpretation of ρ values but under conditions which are relatively restricted, compared to the general use of the l.f.e.r. of Hammett (18), Taft (19), etc. The treatment offered leads naturally to the Swain–Scott equation (20) and a version of the Hammett equation.

For the reaction

$$[7] \qquad R + N \xrightarrow{k_n}{}^{6} (R\text{---}N) \rightarrow \text{Product}$$

we define two sets of reactivity numbers, $\theta_1, \theta_2, \theta_3, \cdots, \theta_r$ associated with substrates $R_1, R_2, R_3, \cdots, R_r$ and $\phi_1, \phi_2, \phi_3, \cdots, \phi_n$ associated with nucleophiles $N_1, N_2, N_3, \cdots, N_n$ such that the rate constants k_n (*cf.* reaction 2) are given by

$$[8] \qquad \log k_n = \rho_n\theta + C_r^n$$

where N is fixed and R is variable, *e.g.* (the OH^- ion reacting with ion-pairs derived from MeX (X = F, Cl, Br, I) and

$$[9] \qquad \log k_n = \rho_r\phi + C_n^r$$

where R is fixed and N is variable (*e.g.* the methyl bromide ion-pair reacting with a series of nucleophiles, H_2O, OH^-, CN^- etc.). The quantities C_r^n and C_n^r are constants.

In general, the species R may be the initial state of RX or any of the subsequent modifications of this species in reaction 1, each of which will be associated with a distinct characteristic reactivity number. The quantities ρ_r and ρ_n are selectivity numbers which give a *derived* measure of the reactivity of the R and N species, respectively. The log k_n, ρ, θ, and ϕ numbers provide a formal framework to establish a derived reactivity scale for the process represented by eq. 7. The log k_n numbers are empirical and in principle can be absolutely characterized for any R–N pair. The derived ρ numbers can be established relative to a standard arbitrarily chosen R–N pair. The θ and ϕ numbers may be usefully considered as "intrinsic" reactivity numbers; their most important property is their uniqueness, *i.e.* whether or not a single number will suffice to characterize the reactivity of any particular R or N species.

[6] To avoid the proliferation of subscripts "n" here refers to "$2n$" in eq. 2.

Can. J. Chem. Downloaded from www.nrcresearchpress.com by 210.87.254.5 on 09/05/12
For personal use only.

Any departure from uniqueness will manifest itself by a breakdown of the linear free energy relationship derived from eqs. 8 and 9. Operationally we may insist that the original θ and ϕ scales remain valid and that departures from the scales arise from interactions which were not included in the original scale.[7]

We believe that the ρ scale, under certain circumstances, may be of greater mechanistic significance than the log k scale with the proviso that changes in ρ derive only from structural alterations for a fixed process. In most cases ρ values derive from a diversity of changes, *e.g.* alterations in the reaction type, the solvent, and the temperature.

The form of eqs. 8 and 9 is similar to expressions derived by Dewar and co-workers (23, 24) from the perturbed molecular orbital method (25), otherwise these equations constitute a working hypothesis to be verified *a posteriori*.

The derived reactivity scale (ρ) has been implied in some recent writings of Dewar (25). This scale, represented by the ρ numbers, is established empirically from the $\log k_n$ numbers in the following way. Consider an arbitrarily chosen standard nucleophile characterized by a selectivity number ρ_{ns}. From eq. 8

$$[10] \qquad \log k_n^s = \rho_{ns}\theta + C_r^{ns}$$

and for any other nucleophile (ρ_n)

$$[11] \qquad \log k_n = \rho_n\theta + C_r^n$$

Eliminating θ between eqs. 10 and 11 gives

$$[12] \quad \log k_n = (\rho_n/\rho_{ns}) \log k_n^s - (\rho_n/\rho_{ns})C_r^{ns} + C_r^n = (\rho_n/\rho_{ns}) \log k_n^s + C_1$$

where C_1 is a constant related to the constants in eqs. 11 and 12. Equation 12 is a version of the familiar Hammett equation (18) and has been used in the way envisaged here[8] by Hammond and Kochi (26) and particularly by Streitwieser (27) in a discussion of the reactivity of a series of arylmethyl chlorides and tosylates reacting in a variety of solvolytic media. In both of the above mentioned studies (26, 27) the solvolytic reaction was considered to be a unitary process, *i.e.* the equation was applied to the overall rate (k^0).

We must now examine the important question of the uniqueness of the θ scale which underpins eq. 12, *i.e.* consider the factors which might lead to a breakdown of the l.f.e.r.'s derived from this equation. Equation 12 is most likely to accommodate a wide range of R structures when the steric requirements of the standard and other nucleophiles are identical. Thus for small nucleophiles, *e.g.* H_2O, OH^-, F^-, CN^- etc., eq. 12 might be expected to accommodate primary, secondary, and tertiary centers. However, bulky nucleophiles such as $(CH_3)_3N$ when paired with water or lyate ion are likely to give a less satisfactory correlation. This will lead to an ill-defined derived reactivity scale, *i.e.* the ρ_n/ρ_{ns} value may not be constant over a wide range of R structures. In addition to the more obvious limitations mentioned above, eq. 12 is likely to show limitations of a more subtle kind.

If it is assumed explicitly that the displacement reaction proceeds via the ion-pair mechanism then the observed rate constant for the displacement k^0 cannot be substituted directly into eq. 12, since k^0 (eq. [5]) includes a K_e term whereas eq. 12 refers only to the k_n quantity. Since

$$[13] \qquad \log k_n = \log k^0 - \log K_e$$

combining eq. 12 with eq. 13 gives

$$[14] \quad \log k^0 - \log K_e = (\rho_n/\rho_{ns}) \times [\log k_s^0 - \log K_e] + C_1$$

If $\log K_e$ changes randomly with R then no correlation between $\log k_s^0$ and $\log k^0$ is to be anticipated. If, on the other hand, linear relationships exist between $\log K_e$ and the quantities $\log k^0$ and $\log k_s^0$ of the form

$$[15] \qquad \log K_e = \gamma \log k^0 + \beta$$

and

$$[16] \qquad \log K_e = \gamma_s \log k_s^0 + \beta_s$$

where γ, γ_s, β, and β_s are constants. A linear correlation between $\log k^0$ and $\log k_s^0$ will result, but the slope of the correlation will differ from ρ_n/ρ_{ns} by a factor $(1 - \gamma_s)/(1 - \gamma)$, *i.e.*

$$[17] \quad \log k^0 = (\rho_n/\rho_{ns})[(1 - \gamma_s)/(1 - \gamma)] \times \log k_s^0 + C_2$$

where the constant C_2 is related to the constant terms in eqs. 14, 15, and 16. The above considerations show that in general, ρ_n/ρ_{ns} cannot be

[7]For a more detailed discussion of such problems, see refs. 21 and 22.

[8]Not using the benzoic acids to define the σ scale.

Can. J. Chem. Downloaded from www.nrcresearchpress.com by 210.87.254.5 on 09/05/12
For personal use only.

established from the rate constants characteristic of an *indirect* displacement; the only processes which appear to meet the required conditions for establishing the constants in eq. 12 are the reactions of triaryl carbonium ions with nucleophiles

[18] $$Ar_3C^+ + N \rightarrow Ar_3CN$$

recently studied by Ritchie *et al.* (28), Taft *et al.* (29), and Hill and Meuller (30). Sufficient data are available from these studies to establish the constants in eq. 12 for the lyate ion and water and when these quantities are known, log K_e may be established for the methyl halides via eq. 14 using observed rates (k^0) of displacement of these substances with the same reagents (H_2O and OH^-).

Two rather drastic assumptions are inherent in these calculations. The first is concerned with the accommodation of all reacting centers by a single line (eq. 12 or eq. 14). This has been carefully discussed above. Since the steric requirements of water and lyate ion are virtually identical, these reagents are particularly favorable in this respect. Secondly, it is assumed that the reactions of the triaryl carbonium ions with nucleophiles constitutes a unitary process. As yet, there is no direct evidence to contradict this assumption. However, the principle of microscopic reversibility demands that the reaction of carbonium ions with nucleophiles follows the reverse path given in reaction 1. Hence the reaction of the trityl ions is not of necessity a unitary process, but might take place via

[19] $$Ar_3C^+ + N^- \rightleftharpoons Ar_3C^+||N^- \rightarrow \text{Product}$$

which is a truncated version of the reverse of reaction 1. As with reaction 2, eq. 12 may give rise to kinetic regions depending on the variation of relative values of rate constants in reaction 19, as R^+ and N^- vary. Here we assume explicitly that the attack of nucleophiles on the trityl carbonium ions is a unitary process.

The validity of the two assumptions discussed above appears to be vindicated by the order which they bring to the reactions of the methyl halides with nucleophiles. No better justification can be envisaged.

We continue our discussion by returning to eq. 9 and examine the evaluation of the ρ_r/ρ_{rs} as opposed to the ρ_n/ρ_{ns} parameters. For a standard substrate R_s and any other substrate R, eq. 9 gives

[20] $$\log k_n^s = \rho_{rs}\phi + C_{ns}^r$$

and

[21] $$\log k_n = \rho_r\phi + C_n^r$$

Eliminating ϕ between eqs. 20 and 21 gives

[22] $$\log k_n = (\rho_r/\rho_{rs}) \log k_n^s - (\rho_r/\rho_{rs})C_{ns}^r + C_n^r$$
$$= (\rho_r/\rho_{rs}) \log k_n^s + C_3$$

where C_3 is a constant related to the constant terms in eqs. 20 and 21. From eq. 13

[23] $$\log k_n = \log k^0 - \log K_e$$

and

[24] $$\log k_n^s = \log k_s^0 - \log K_{es}$$

combining eqs. 22, 23, and 24 gives

$$\log k^0 - \log K_e = (\rho_r/\rho_{rs})[\log k_s^0 - \log K_{es}] + C_3$$

Therefore

$$\log k^0 = (\rho_r/\rho_{rs}) \log k_s^0 - (\rho_r/\rho_{rs}) \log K_{es} + \log K_e + C_3$$

For any R/R_s pair, log K_e and log K_{es} are constants and do not vary as the structure of the nucleophile is altered. Hence the term $(\rho_r/\rho_{rs}) \log K_{es} + \log K_e + C_3$ can be represented by a single constant C_4, giving

[25] $$\log k^0 = (\rho_r/\rho_{rs}) \log k_s^0 + C_4$$

It follows from these considerations that the ion pair mechanism does not influence the ρ_r/ρ_{rs} parameter in the same manner as in the variable R fixed N/N_s case and in the instance of eq. 25, ρ_r/ρ_{rs} can be established using the *observed* rate constants (k^0) from an *indirect* displacement. Equation 25 is a slightly modified form of the Swain–Scott equation (20) and requires no further comment.

The application of eqs. 12, 14, and 25 to the relevant data will be considered in the following sections.

Results and Discussion

The Calculation of ρ_r/ρ_{rs} Values for the Methyl Halides

In Table 1 all the available bimolecular rate constants for the attack of nucleophiles on the methyl halides (MeX, X = F, Cl, Br, and I) in water are recorded for $T = 25$ °C. The solvolysis rates in water have been corrected for the molar concentration of the solvent (55.5 mole l^{-1}). Of the 36 rate constants recorded in Table 1, 24 are empirical and the remainder have been calculated

TABLE 1

Observed and calculated bimolecular rate constants for the attack of various nucleophiles in water on MeX (X = F, Cl, Br, I), T = 25 °C

Reference	Reagent		$-\text{Log } k^0$ (mole^{-1} l s^{-1}) MeF	MeCl	MeBr	MeI
31	H_2O		10.84	9.36	8.13	8.87
32	OH^-		7.92*‡	5.22	3.86	4.18
33	$S_2O_3^{2-}$		6.37*	3.01	1.49	1.43
32	I^-		7.67	4.75	3.21	3.46
32	F^-		9.61*	7.81	6.46	7.16
32	Br^-		7.80*	6.27	3.68*	4.39
32	Cl^-		8.56	6.67*	5.30	5.51
34	CN^-		7.15*	4.16*	2.68*	3.22
35	SCN^-		7.52*	4.71*	3.26*	3.45
		ρ_r/ρ_{rs}†	0.65±0.07	0.95±0.01	1	1.12±0.03
		C_4†	−5.40±0.42	−1.60±0.05	0	0.21±0.09

*Calculated via the modified Swain–Scott equation (20) (eq. 26).
†Least squares values of the constants appropriate to eq. 25. The rates in water have been corrected for the molar concentration of the solvent.
‡Experimental value −6.22 considered to be in error, see text.

via eq. 25 (see below) and are marked with an asterisk. Of the 24 empirical rate constants, one, that appropriate to the attack of lyate ion on MeF, deviates considerably from the line defined by MeBr = R_s (Fig. 1). Since the other correlations are excellent (MeCl *vs.* MeBr, MeI *vs.* MeBr, see Fig. 2) and the H_2O, Cl^- and I^- points for MeF are both well separated and adequately correlated, it is reasonable to conclude that the rate constant for the attack of OH^- on MeF is in error. In subsequent calculations the interpolated rate constant for this particular process will be used. The slopes and intercepts of the MeF, MeCl, and MeI lines (R_s = MeBr) have been calculated by the method of least squares and these are recorded in Table 1. The slopes (ρ_r/ρ_{rs}) give a derived reactivity scale for the methyl halides relative to ρ_{rs} = 1 for MeBr, which is in the order MeF > MeCl > MeBr > MeI assuming low selectivity to be associated with high reactivity and *vice versa*. The basis of the latter assumption merits further discussion.

The relationship between selectivity and reactivity, *i.e.* between the derived (ρ) and absolute (k^0) reactivity scales, does not appear to have attracted much theoretical attention (but see ref. 25) and we are unaware of any use of the derived scales as tools for mechanistic diagnosis. Brown and co-worker (36) have used the selectivity concept extensively in their quantitative treatment of aromatic substitution. However, the emphasis in their studies differs from that presented here.

The only theoretical tools for discussing selectivity and reactivity sequences appears to be the Bell–Evans–Polanyi (B.E.P.) (see ref. 25) free energy (G) reaction coordinate diagram. The B.E.P. diagram usually contains a series of substrate–reagent curves which remain parallel up to the various points of intersection. The points of intersection define the transition states for the various substrate–reagent species. Under the parallel constraint no variations in selectivity are possible since all the reagent–substrate curves intersect at the same angle.[9] Alterations in selectivity require the parallel constraint to be relaxed for either the substrate or the reagent curves separately or for both. Whereas the subsequent algebraical manipulations are straightforward when the parallel constraint is imposed

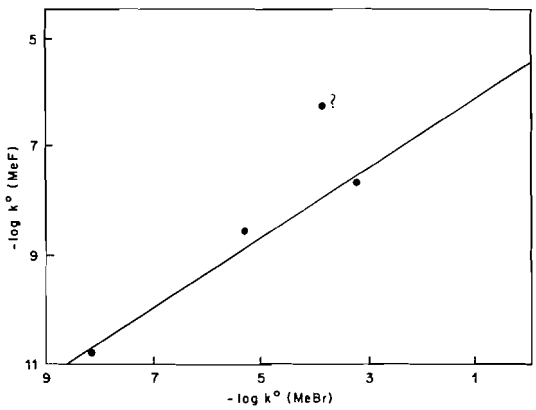

FIG. 1. Swain–Scott correlation for MeF *vs.* MeBr.

[9]Brönsted exponents are usually interpreted this way (37).

Can. J. Chem. Downloaded from www.nrcresearchpress.com by 210.87.254.5 on 09/05/12
For personal use only.

Can. J. Chem. Downloaded from www.nrcresearchpress.com by 210.87.254.5 on 09/05/12
For personal use only.

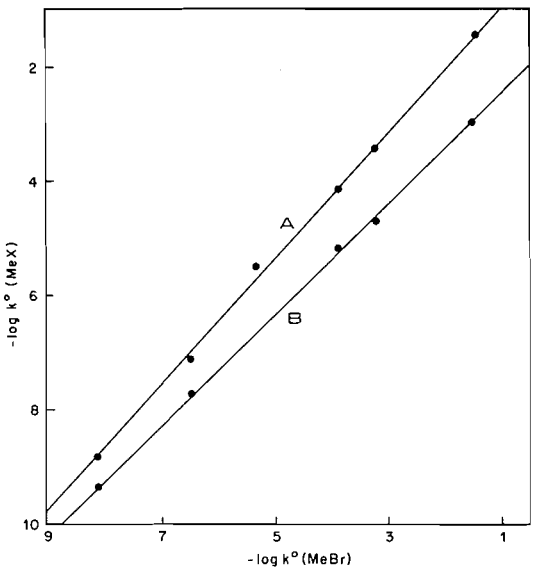

FIG. 2. Swain–Scott correlation for MeX (ordinate A = MeI, B = MeCl) and MeBr (abscissa).

on the B.E.P. diagram, no formal treatment appears possible when this parallel constraint is relaxed. However, a visual inspection of a B.E.P diagram when the parallel constraint is relaxed seems to suggest that high selectivity will be invariably associated with low reactivity and *vice versa.*

The hypothesis linking selectivity to reactivity in a definite way is limited to a unitary process, hence any departure from the anticipated correlation between selectivity sequences (ρ) and reactivity sequences (k^0) would imply that the process (k^0) under consideration is not unitary. The latter assumption is an important working hypothesis in this paper and its adequacy cannot be judged in isolation but must be considered against the overall background of the ideas presented.

It is important to note that the derived reactivity scale (ρ_r/ρ_{rs}) for the methyl halides does *not* correlate with the log k^0 scale which is typically MeF < MeCl < MeI < MeBr for most of the nucleophiles listed in Table 1. In light of the considerations discussed above, the lack of correlation between the log k^0 and ρ_r/ρ_{rs} scales provides an important mechanistic clue. It follows that if the ρ_r/ρ_{rs} scale is postulated to measure the reactivity of the ion-pair (the ρ_r/ρ_{rs} values obtained from eq. 25 are independent of K_e), then the log K_e term, which is included in the log k^0 scale, must show an opposite sequence to the log k_n values and, for the methyl halides, the trend in log K_e with structure must dominate the observed (log k^0) scale. This partly accounts for the odd sequence of reactivity displayed by the methyl halides on the log k^0 scale, the bromide invariably being the most reactive. This has been noted frequently (38, 39) although no satisfactory hypothesis has yet emerged.

The ρ_r/ρ_{rs} quantities for the methyl halides give excellent correlations with the gas phase enthalpies of ionization for these molecules and for the force constants of the C—X bonds (Figs. 3 and 4). These correlations are particularly significant since no such correlation exists on the log k^0 scale, which is not in a well-behaved halogen sequence (see above), in spite of the fact that the halogens form one of the most regular series in the periodic table. This regularity is manifested by all the thermodynamic quantities likely to influence the displacement. *i.e.* the C—X bond dissociation

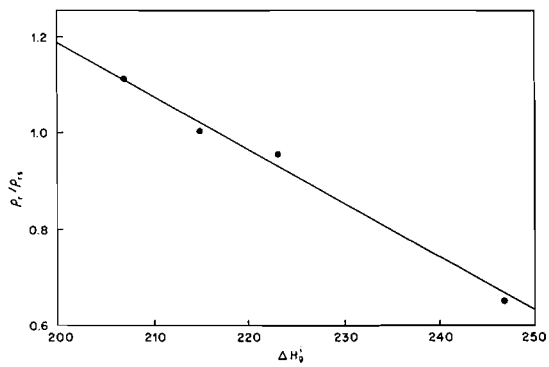

FIG. 3. Correlation between selectivity parameter ρ_r/ρ_{rs} and the gas phase heat of ionization of MeX (ΔH_g^i, X = F, Cl, Br, I).

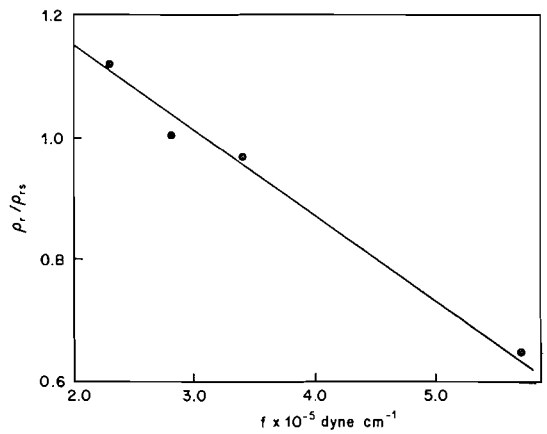

FIG. 4. Correlation between selectivity parameter ρ_r/ρ_{rs} and the force constant (f) of the C—X bond.

Can. J. Chem. Downloaded from www.nrcresearchpress.com by 210.87.254.5 on 09/05/12
For personal use only.

energies and force constants, the electron affinities of the halogen atoms, and the solvation energies of the halogen anions.

Since the ρ_r/ρ_{rs} scale derives ultimately from the log k_n scale, definite restrictions are now placed on the trends to be anticipated for log K_e and log k_n. Firstly, the log k_n values for any particular nucleophile must follow the sequence MeF > MeCl > MeBr > MeI. If the log K_e values derived from eq. 14 fail to produce this sequence for log k_n, the technique for calculating log K_e (eq. 14) must be considered suspect. Secondly, the log k_n values should show a quantitative relationship with ρ_r/ρ_{rs} and likewise correlate with various internal parameters of the MeX molecules, *e.g.*, the gas phase heats of ionization (ΔH_g^i) and the C—X force constants (f). All of these conditions are met with considerable precision as will be shown in the following section.

The Calculation of ρ_n/ρ_{ns} for H_2O/OH^- from the Trityl Carbonium Ion Reactions

The Evaluation of K_e and k_n for the Methyl Halides

In Table 2 we have collected the bimolecular rate constants for four carbonium ions reacting with water (w) and lyate ion (l) in water at 25 °C. The plot of log k_{nw} (ordinate) *vs.* log k_{nl} (abscissa) is shown in Fig. 5 and covers a sufficient range of reactivity on either axis to establish the constants in eq. 12 with reasonable precision although the data are meagre. A least squares treatment of the correlation gives

$$[26] \quad \log k_{nw} = (1.51 \pm 0.13) \log k_{nl} - (5.97 \pm 0.22)$$

Substituting the constants from eq. 26 into eq. 14 allows log K_e to be evaluated for each of the

TABLE 2

Bimolecular rate constants for the reaction of trityl cations with water (w) and lyate ion (l), T = 25 °C

Trityl cation	log k_{nw}*	log k_{nl}	Reference
Crystal violet	−6.62	−0.69	28
Malachite green	−5.42	0.34	28
p-Nitro malachite green	−5.50	0.75	28
Tris-*p*-MeO	−0.67‡	3.37†	29, 30

*Pseudo first order rates have been divided by 55.5 mole l^{-1}. The rates in ref. 28 were reported with this correction.

†Calculated on the basis that k_{nl}/k_{nw} at 25 °C is the same as at 30 °C. These processes have low activation energies and the error introduced by this assumption is at most 0.1 log k unit. This is not serious.

‡The values in refs. 29 and 30 are in excellent agreement; log k_{nw} without the solvent concentration correction is 1.11 in both references.

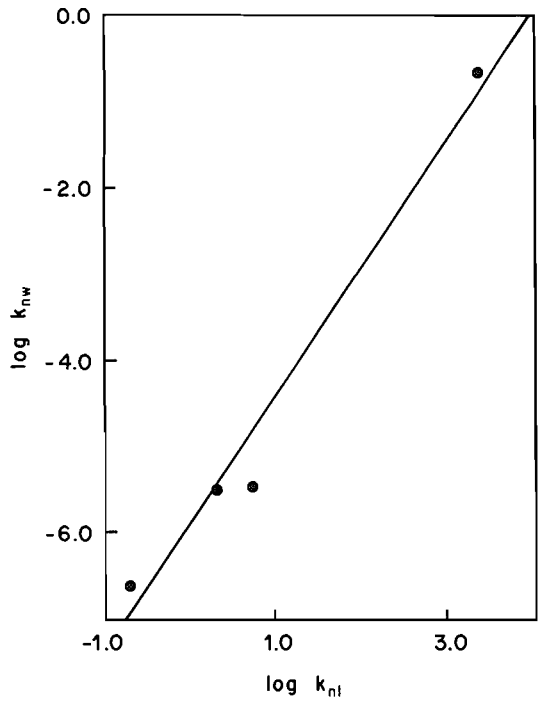

FIG. 5. Correlation between bimolecular rate constants for the attack of water (w, ordinate) and hydroxide ion (l, abscissa) for various trityl cations.

methyl halides using the water and lyate ion bimolecular rate constants recorded in Table 1. Since log K_e is now known, log k_n can be evaluated from each of the rate constants in Table 1 using eq. 13. Sample plots of log k_n *vs.* (*a*) the heat of ionization of MeX in the gas phase, (*b*) the C—X bond valence stretch force constant, and (*c*) the ρ_r/ρ_{rs} derived reactivity parameters are given in Figs. 6, 7, and 8.

The correlations are all satisfactory and demonstrate forcefully, particularly (*c*), that the model is internally consistent. In Fig. 9 sample plots of log k_n vs. log k_{nl} are presented using the lyate ion as the standard nucleophile. The slopes of these plots measure ρ_n/ρ_{ns} (relative to $OH^- = 1$) for all the nucleophiles listed in Table 1. Graphical values of these parameters are recorded in Table 3 along with the other parameters mentioned in the present section. In Fig. 10 a correlation between ρ_n/ρ_{ns} and log k_n for MeI is presented. The correlation is inferior to that of ρ_r/ρ_{rs} *vs.* log k_n and appears to be curved, possibly as a consequence of the greater range in the log k_n values as ρ_n/ρ_{ns} is varied. We do not, however, propose to discuss this correlation further at the present time.

Can. J. Chem. Downloaded from www.nrcresearchpress.com by 210.87.254.5 on 09/05/12
For personal use only.

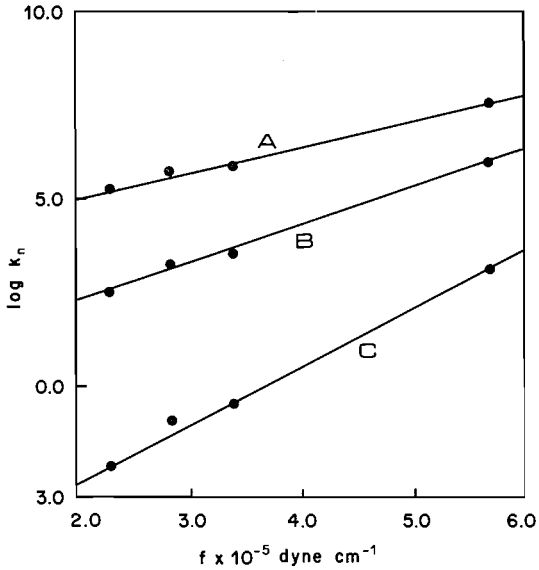

FIG. 6. Correlation between bimolecular rate of attack of various nucleophiles (A = $S_2O_3^{2-}$, B = OH^-, and C = H_2O) on the methyl halide ion pairs *vs.* the heat of ionization of MeX in the gas phase (ΔH_g^i, X = F, Cl, Br, I).

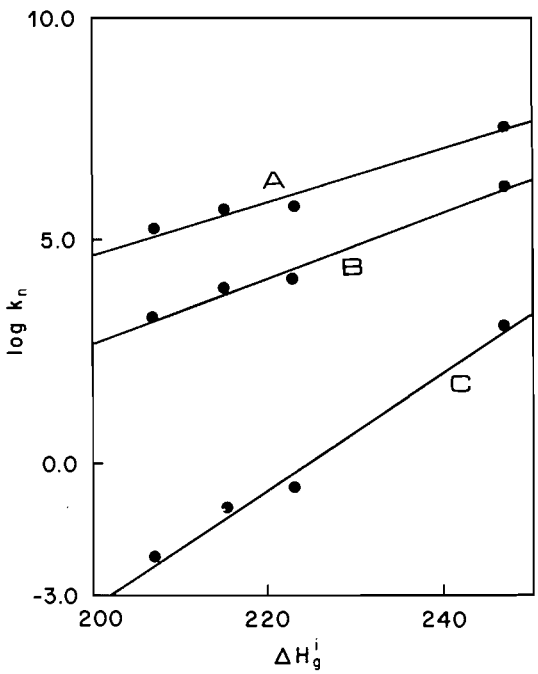

FIG. 7. Correlation between bimolecular rate of attack of various nucleophiles (A = $S_2O_3^{2-}$, B = OH^-, C = H_2O) on the methyl halide ion pairs *vs.* the force constant (f) of the C—X bond (X = F, Cl, Br, I).

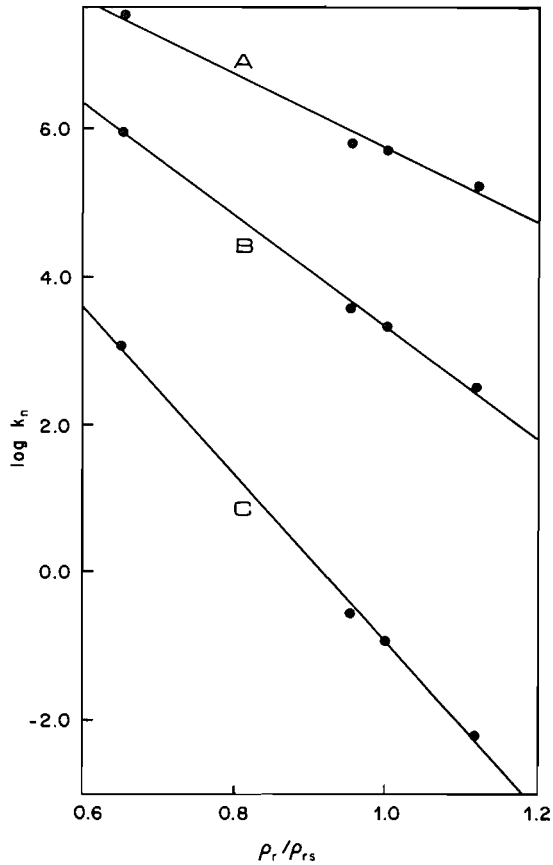

FIG. 8. Correlation between bimolecular rates of attack of various nucleophiles (A = $S_2O_3^{2-}$, B = OH^-, C = H_2O) *vs.* the selectivity parameter ρ_r/ρ_{rs} obtained from the Swain–Scott correlation (Figs. 1 and 2).

Some Further Confirmatory Evidence

The free energy changes for the overall process

[27] $MeX(g) \rightleftharpoons MeX(aq) \rightleftharpoons Me^+X^-(aq)$ X = F, Cl, Br, I

might be expected to show a correlation with the free energy changes for the process

[28] $HX(g) \rightleftharpoons H^+(aq) + X^-(aq)$ X = F, Cl, Br, I

since changes in ΔG for the reactions symbolized by reaction 28 depend solely on the solvation properties of X^-, the solvation of the proton being a constant factor in the reaction series. Essentially the model assumes that the role of the methyl cation in the ion-pair (reaction 27) is to replace one or possibly two water molecules in the primary solvation sheath of the halogen anion. The enthalpy changes for the process (reaction 28) are known (41) and the related entropy changes can be readily computed from the gas phase

TABLE 3

Rate constants and other parameters characterizing the ion-pair mechanism for the methyl halides, $T = 25$ °C

Parameter	Anion	MeF	MeCl	MeBr	MeI	ρ_n/ρ_{ns}	Reference
$\log K_e$		−13.90	−8.81	−7.19	−6.68	—	This work
ΔH_g^{i*}		247	223	215	207	—	40
f(C—X)†		5.70	3.40	2.84	2.29	—	41
$\log k_n$	H_2O	3.06	−0.55	−0.94	−2.19	1.51	This work
	OH^-	5.98	3.59	3.33	2.50	1.00	"
	$S_2O_3^{2-}$	7.53	5.80	5.70	5.25	0.64	"
	I^-	6.23	4.06	3.98	3.22	0.86	"
	F^-	4.29	1.00	0.73	−0.48	1.37	"
	Br^-	6.10	2.54	3.51	2.29	1.09	"
	Cl^-	5.34	2.14	1.89	1.17	1.22	"
	CN^-	6.75	4.65	4.51	3.46	0.97	"
	SCN^-	6.38	4.10	3.93	3.23	0.91	"

*In kcal/mole.
†In dyn $cm^{-1} \times 10^{-5}$.

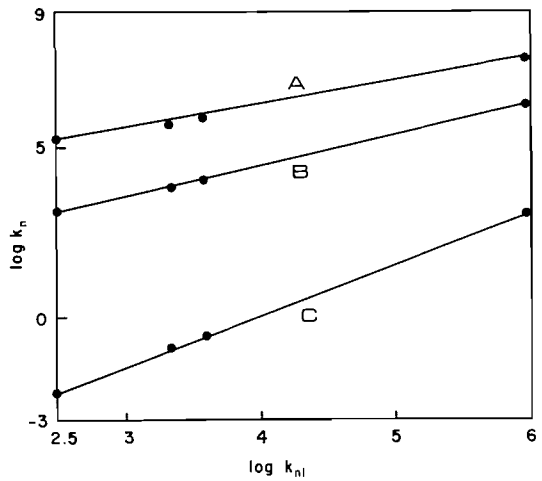

FIG. 9. Correlation between bimolecular rates of attack of various nucleophiles (ordinate) (A = $S_2O_3^{2-}$, B = I^-, C = H_2O) on the methyl halide ion pairs *vs.* the bimolecular rates of attack of lyate ion on these species.

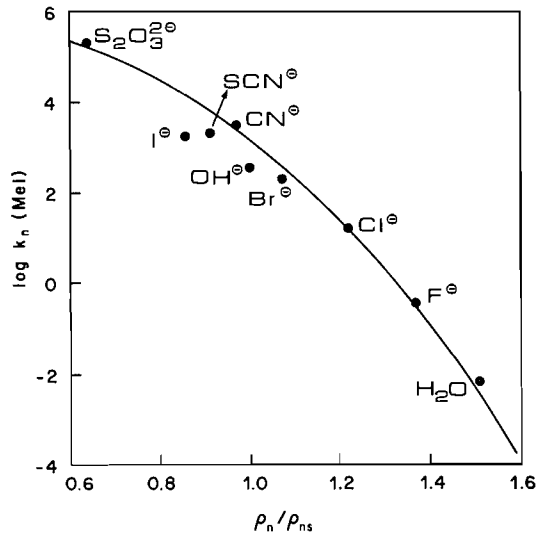

FIG. 10. Correlation of bimolecular rate constants of various nucleophiles on the methyl iodide ion pair *vs.* the selectivity of the nucleophiles ρ_n/ρ_{ns}. The OH^- ion used as a standard, *i.e.* $\rho_n = 1$, $N_s = OH^-$.

entropies of HX and the related ions in solution. Since two ions are produced in the transfer of the HX molecules from gas to solution, the problem of single ion entropies does not arise. The enthalpy and entropy terms can be combined in the usual way to give the values ΔG for the four processes summarized by reaction 28.

The overall free energy changes accompanying the two processes in reaction 27 can be computed from the log K_e values reported in this paper and the initial state data measured by Glew and Moelwyn-Hughes (42).

The correlation (Fig. 11) between the partly kinetic and purely thermodynamic quantities is excellent and provides further confirmation that the log K_e quantities in Table 3 are meaningful. The data for this calculation are recorded in Table 4.

The slope of the correlation (Fig. 11) might be considered as giving a rough measure of charge on the ion pair. Depending on how ΔG varies with charge (40) we estimate "*e*" to be between 0.76–0.87, which is reasonable.

Summary and Final Comments

The final order of reactivity on the log k^0 scale for the methyl halides in both the solvolysis reaction and the definite bimolecular displace-

Can. J. Chem. Downloaded from www.nrcresearchpress.com by 210.87.254.5 on 09/05/12
For personal use only.

TABLE 4

Thermodynamic data relevent to eqs. 27 and 28, T = 25 °C

HX/MeX	ΔH(g → s)†	S_g‡	S_{ion}§	ΔS‖	ΔG	log K_e*	ΔG_e*	$\Delta G_{g\to s}$*¶	ΔG**
HF	−11.6	41.9	−2.30	−37.85	0.3	−13.90	18.97	−0.2	18.77
HCl	−17.4	44.5	13.20	−24.28	−10.17	−8.81	12.02	−0.6	11.42
HBr	−19.95	47.6	19.29	−21.96	−13.4	−7.19	9.81	−0.85	8.96
HI	−19.2	49.7	26.14	−17.21	−14.10	−6.68	9.11	−0.95	8.16

*MeX data; the data without asterisks are for the HX compounds.
†Reference 41, chap. 18, p. 846.
‡Reference 41.
§Reference 43.
‖Corrected to a standard state of 1 mole/l in both phases by subtracting 6.35 e.u. from the gas phase entropies reported for p = 1 atm.
¶Calculated from data in ref. 40.
**Calculated from $\Delta G = \Delta G_e + \Delta G_{g\to s}$.

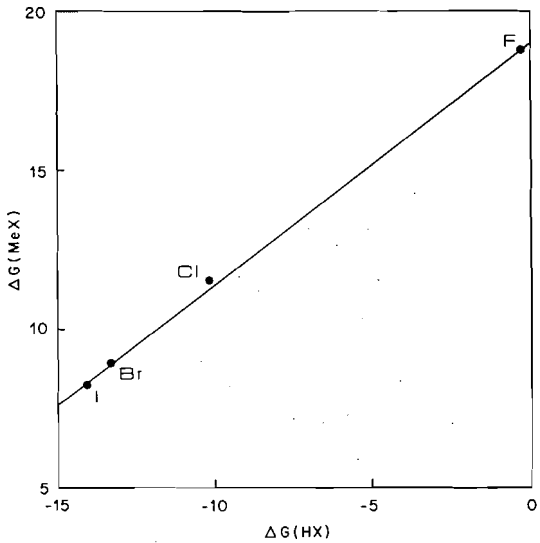

FIG. 11. Correlation between free energies of dissolution of the hydrohalic acids (HX, X = F, Cl, Br, I) and the free energies of dissolution of the methyl halide ion pairs (MeX, X = F, Cl, Br, I).

ments is now seen to be the result of two opposing sequences, the heterolytic ion-pair formation sequence (K_e) MeI > MeBr > MeCl > MeF combined with a bond forming sequence MeF > MeCl > MeBr > MeI, the former being dominant in the overall process. However, it is important to note that the bond forming process is not concerted in the sense that the incoming group provides the main driving force for the expulsion of the leaving group usually represented by

$$[29]\quad \overset{\frown}{N^-}\cdots CH_3\overset{\frown}{-}X \rightarrow [N\cdots \overset{\delta+}{C}H_3\cdots \overset{\delta-}{X}] \rightarrow N{-}CH_3 + X^-$$

Rather, the MeX molecule must become activated before the displacement process can occur. The high charge on the ion pair (see above) suggests that this species is held together primarily by electrostatic rather than covalent forces and the role of the incoming nucleophile is to reduce the electrostatic interaction to a level where the anion can escape. In this sense, bond making and bond breaking processes are not truly concerted in the manner represented in reaction 29. The formation of a new bond is a distinct kinetic process. The rapidity of these processes (see Table 3) and the small kinetic solvent isotope effect ($k(H_2O)/k(D_2O)$, see ref. 44)[10] suggests that the interaction between the ion pair and the nucleophile is relatively weak.

The extension of the ideas presented here to a wider series of RX structures is obviously desirable. The study of an extended range of nucleophiles attacking the triaryl carbonium ions is also required, including a thorough study with hydroxide ion to complement Taft's study of the water reactions (24). This would establish the constants in eq. 26 with greater certainty. A direct determination of the selectivities of the various ions in Table 1 would also result from such studies and establish whether these are independent of the nature of the reacting carbon center. At the present time we predict that this will be so, since the consistency of the two approaches offered by eqs. 12, 14, and 25 would seem to preclude any alternative. As long as the nucleophiles are of a similar size, the ρ_n/ρ_{ns} scale is likely to be unique and well defined, *i.e.* an appropriate linear free energy relationship exists.

One possible source of error in the calculations is the constant term (−5.97) in eq. 26 which may

[10]A more detailed account of the significance of the kinetic solvent isotope effect with respect to the mechanism of the displacement will appear elsewhere.

Can. J. Chem. Downloaded from www.nrcresearchpress.com by 210.87.254.5 on 09/05/12
For personal use only.

be inappropriate for primary centers. If this is so, the reported values of log K_e and log k_n will be relatively correct, but their absolute magnitudes will remain uncertain. We see no obvious way of overcoming this difficulty at the present time.

Finally, we believe that the evidence presented here provides substantial support for Sneen and Larsen's contention (4) that the mechanism of the displacement process at a primary carbon atom does not take place via the classical S_N2 Heitler–London mechanism. We fully concur with their viewpoint stated earlier; "direct attack on covalent carbon seldom if ever occurs" and by inference many of the conceptual difficulties associated with the S_N1–S_N2 mechanistic dichotomy (45) recede.

The patience, stimulation, encouragement, and criticisms of Dr. R. E. Robertson and his research team are gratefully acknowledged. Thanks are also due to the National Research Council of Canada for continued financial support and to Memorial University of Newfoundland for the granting of a year's leave of absence. Finally, the author wishes to thank the University of Calgary for its hospitality during his year of stay from September 1969 to August 1970.

1. J. M. W. Scott and J. G. Winter. Can. J. Chem. **46**, 2887 (1968).
2. H. Weiner and R. A. Sneen. J. Amer. Chem. Soc. **87**, 287 (1965).
3. H. Weiner and R. A. Sneen. J. Amer. Chem. Soc. **87**, 292 (1965).
4. J. W. Larsen and R. A. Sneen. J. Amer. Chem. Soc. **91**, 6021 (1969).
5. J. W. Larsen and R. A. Sneen. J. Amer. Chem. Soc. **91**, 362 (1969).
6. S. Winstein, P. E. Klinedist, Jr., and G. C. Robinson. J. Amer. Chem. Soc. **83**, 885 (1961) and references therein.
7. S. Winstein, P. E. Klinedist, Jr., and E. Clippinger. J. Amer. Chem. Soc. **83**, 4986 (1961).
8. S. Winstein, R. Baker, and S. G. Smith. J. Amer. Chem. Soc. **86**, 2072 (1964).
9. H. L. Goering and J. F. Levy. J. Amer. Chem. Soc. **84**, 3853 (1962).
10. H. L. Goering and R. W. Thies. J. Amer. Chem. Soc. **90**, 2967 (1962).
11. H. L. Goering, J. T. Doi, and K. D. McMichael. J. Amer. Chem. Soc. **86**, 1951 (1964).
12. E. A. Moelwyn-Hughes. The kinetics of reactions in solution. Clarendon Press, Oxford, England. 1947. Chap. I. p. 16.
13. C. G. Swain. J. Amer. Chem. Soc. **70**, 1119 (1948).
14. A. Streitwieser, Jr. Chem. Rev. **56**, 571 (1956).
15. C. K. Ingold. Structure and mechanism in organic chemistry. Cornell University Press, Ithaca, N.Y. 1953. Chap. 7.
16. C. D. Ritchie. Solute-solvent interactions. *Edited by* C. D. Ritchie and J. F. Coetzee. Marcel Dekker, New York and London. 1969. Section 4, p. 272.
17. C. D. Ritchie and W. F. Sager. Progress in physical organic chemistry. Vol. 2 *Edited by* A. J. Streitwieser, R. W. Taft, and S. Cohen. Interscience, John Wiley, London and New York. 1965.
18. L. P. Hammett. Physical organic chemistry. McGraw-Hill Book Co., Inc., New York. 1940. Chap. 7.
19. R. W. Taft, Jr. Steric effects in organic chemistry. *Edited by* M. S. Newman. John Wiley and Sons, Inc., New York. 1956. Chap. 13.
20. C. G. Swain and C. B. Scott. J. Amer. Chem. Soc., **71**, 141 (1953).
21. E. Grunwald and J. Leffler. Rates and equilibria of organic reactions. John Wiley and Sons, Inc., New York. 1963.
22. H. Benson and J. M. W. Scott. Can. J. Chem. **46**, 2896 (1968).
23. M. J. S. Dewar and R. J. Sampson. J. Chem. Soc. 2924 (1956).
24. M. J. S. Dewar and R. J. Sampson. J. Chem. Soc. 2789 (1957).
25. M. J. S. Dewar. Molecular orbital theory of organic chemistry. McGraw-Hill Book Co., Inc., New York. 1969.
26. G. Hammond and J. Kochi. J. Amer. Chem. Soc. **75**, 3445 (1953).
27. A. Streitwieser, Jr. Molecular orbital theory for organic chemists. John Wiley and Sons Inc., New York. 1961. Chap. 12.
28. C. D. Ritchie, G. A. Skinner, and V. G. Badding. J. Amer. Chem. Soc. **89**, 2063 (1967).
29. R. W. Taft, R. A. Diffenbach, and K. Sano. J. Amer. Chem. Soc. **88**, 4747 (1966).
30. E. A. Hill and W. J. Meuller. Tetrahedron Lett. **21**, 2565 (1968).
31. R. E. Robertson. Advances in physical organic chemistry. Vol. 4. *Edited by* A. J. Streitweiser, Jr. and R. W. Taft. Interscience, John Wiley, London and New York. 1967. p. 213 and references therein.
32. R. H. Bathgate and E. A. Moelwyn-Hughes. J. Chem. Soc. 2642 (1959).
33. E. A. Moelwyn-Hughes. The kinetics of reactions in solution. Clarendon Press, Oxford, England. Chap. 5, p. 127.
34. A. V. Willi and C. M. Wong. J. Amer. Chem. Soc. **90**, 5999 (1968).
35. G. C. Lalor and E. A. Moelwyn-Hughes. J. Chem. Soc. 2201 (1965).
36. H. C. Brown and L. M. Stock. Advances in physical organic chemistry. *Edited by* V. Gold. Academic Press, Inc., London and New York. 1963. p. 35 and references therein.
37. R. P. Bell. Acid–base catalysis. Oxford Univ. Press, Oxford, England. 1949. Chap. 7.
38. R. E. Robertson and R. L. Heppolette. Proc. Roy. Soc. London, **A252**, 273 (1959).
39. R. E. Robertson and J. M. W. Scott. J. Chem. Soc. 1596 (1961).
40. R. E. Robertson, J. M. W. Scott, and R. L. Heppolette. Can. J. Chem. **37**, 803 (1959).
41. E. A. Moelwyn-Hughes. Physical chemistry. Pergamon Press, London and New York. 1957. Chap. 12. p. 509.
42. D. N. Glew and E. A. Moelwyn-Hughes. Discuss. Faraday Soc. 15 (1953).
43. V. P. Vasil'ev, E. K. Zolotarev, A. F. Kapustinskii, K. P. Mishchenko, E. A. Podgornaya, and K. B. Yatsimirski. Russian J. Phys. Chem. **34**, 840 (1960).
44. R. E. Robertson and P. M. Laughton. Solute–solvent interactions. *Edited by* C. D. Ritchie and J. Coetzee. Marcel Dekker, New York and London. 1969. Section 7. p. 424.
45. V. Gold. J. Chem. Soc. 4632 (1956).

Can. J. Chem. Downloaded from www.nrcresearchpress.com by 210.87.254.5 on 09/05/12
For personal use only.

Can. J. Chem. Downloaded from www.nrcresearchpress.com by 210.87.254.6 on 09/05/12
For personal use only.

Studies related to the mechanism of action of cardiac glycosides. On the reactions of thiols with unsaturated lactones and on the structure of the compound previously reported as ouabagenin. The preparation and properties of authentic ouabagenin[1]

J. Bryan Jones and Hugh W. Middleton
Department of Chemistry, University of Toronto, Toronto 181, Ontario

Received June 12, 1970

In connection with mechanism of action studies on cardiac glycosides, the reactions of α-pyrone, γ-crotonolactone, digitoxigenin, and ouabagenin have been studied. No Michael addition reactions were observed with the cardenolide aglycones. The compound previously reported in the literature as ouabagenin has been shown to be 1β,3β,5β,11α,14β,19,21-heptahydroxycard-20,22-enoic acid and the preparation and properties of authentic ouabagenin are described.

Canadian Journal of Chemistry, **48**, 3819 (1970)

During investigations designed to evaluate which, if any, chemical reactions might be involved in the physiological activity of cardiac glycosides it was noted that thiols protect against the cardiotoxic activity of cardiac glycosides (1). Furthermore, sulfhydryl groups are known to be involved in the mechanism of action of the sodium–potassium ion active transport ATP[2]-ase enzymes of nerve cells (2); the enzyme is strongly inhibited by cardiac glycosides (2) and the data available are consistent with the cardiotoxic action of cardiac glycosides being due to their inhibition of such enzymes.

In this regard it was noted that the normal substrate ATP, of the active transport enzymes, and cardenolides could adopt conformations of similar steric dimensions in which the lactone ring of the cardenolide occupied the same position in space as the ATP phosphate grouping displaced *in vivo* by the enzymic nucleophile (3).[3]

These data, coupled with the observations that cardiac glycosides lose all or part of their cardiotonic and cardiotoxic activity upon saturation or epimerization of the C-17 lactone ring (1, 5–7) and that such a chemical transformation results in a significant lowering of their ATP-ase inhibitory action (7, 8), led us to investigate the possibility that the active cardenolides and bufadienolides might be bound to their receptor site via a Michael addition reaction with a receptor nucleophile, such as a cysteine thiol residue, as illustrated in Scheme 1 for the cardenolide lactone ring system. The Michael addition reaction **1** → **2** → **3** could not occur for the saturated, and largely inactive, lactone ring analogues of the cardenolides **1**.

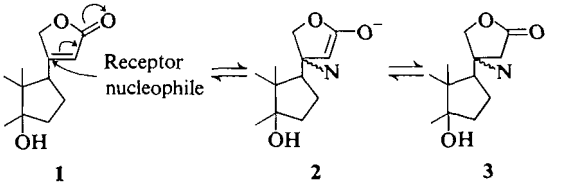

Scheme 1

Initially model studies with simple thiols were carried out using the readily available compounds α-pyrone (**4**) and γ-crotonolactone (**5**) as being structurally representative of the lactones occurring in bufadienolides and cardenolides respectively.[4]

The first experiments were carried out on α-pyrone (**4**) using α-toluene thiol as a simple and convenient model for *in vivo* cysteine thiol groups (12). At room temperature in aqueous methanolic solution α-pyrone was found to react completely

[1]Abstracted from the Ph.D. Thesis of H. W. Middleton (26).

[2]Adenosinetriphosphate.

[3]Unfortunately, the recently determined (4) three dimensional structure of hydrated disodium ATP does not enable any conclusions to be drawn regarding the conformation of ATP when it is at the active site of the active transport enzyme.

[4]It was realized that the use of β-substituted lactones would have provided more suitable models of the cardiac glycosides, especially in view of the known reluctance of thiols to undergo Michael addition when β-substituents are present in the conjugated system (9–11). However, owing to the difficulties involved in carrying out such reactions on cardenolides and in interpreting their p.m.r. spectra, it was decided to delineate the reaction conditions, and to obtain reference p.m.r. spectra of the products, on the simplest model compounds available.

4

5

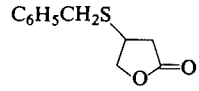

6

with one equivalent of benzyl thiol anion, as evidenced by the disappearance of vinylic proton peaks from the p.m.r. spectrum. However, the overall spectrum was unassignable to any one compound and t.l.c. analysis showed the reaction mixture to be a very complex one. The i.r. spectrum of the mixture showed a sharp absorption band at 1740 cm^{-1} indicating a saturated lactone or ester to be present but all attempts to resolve the mixture, including distillation and a variety of chromatographic methods, were unsuccessful. Upon lowering the temperature to $-35°$, a slower reaction occurred to give (by t.l.c.) a mixture of four unstable compounds each of which rapidly decomposed on keeping at 0° and in the hope of inducing greater product stability attention was turned to the reactions of cysteine and its derivatives. Cysteine, its methyl ester, and *N*-acetylcysteine methyl ester were found to react rapidly with α-pyrone but again the numbers of products obtained and the difficulties encountered of product decomposition during attempted purification precluded any conclusions being drawn. At this stage further work on α-pyrone was postponed since although the problem was chemically challenging, the complexity of the reactions encountered would have rendered any conclusions drawn to be of little *in vivo* relevance.

The reactions of the cardenolide lactone analogue, γ-crotonolactone (4-hydroxybut-2-enoic acid lactone, **5**) were studied next. Again the reactions with α-toluene thiol anion were considered first and, as expected, an extremely facile Michael reaction to give 3-benzylthio-4-hydroxybutyric acid lactone (**6**, quantitative yield by p.m.r.) was observed in both aqueous and methanolic solutions. Although the Michael addition product **6** underwent reverse Michael cleavage very readily, a 46% yield of the pure compound could be isolated. The addition reaction was found to be extremely fast in the p*H* range 8–11, and was still very rapid at physiological p*H* (7.4). As expected from related work (3), the thio-lactone **6** did not react further when excess α-toluene thiol was used.

From the point of view of providing a reference spectrum to assist in analyzing those of the corresponding glycoside compounds, the p.m.r. pattern of **6** was particularly encouraging since all but a few of the peaks occurred at chemical shifts (δ 1.97–4.38 and aromatic protons at δ 7.22 p.p.m.) which were outside the cardiac aglycone envelope of ~ δ 0.8–2.2 p.p.m.

Attention was then turned towards the reaction of γ-crotonolactone with cysteine and its derivatives since the properties of the thiol group of the latter compounds should be much closer to that of the *in vivo* thiol nucleophile than for α-toluene thiol. Disappointingly, our studies in both aqueous and methanolic solutions, on the reactions of **5** with the anions of cysteine, *N*-acetylcysteine, and *N*-acetylcysteine methyl ester did not prove to be definitive since it was not possible to purify the reaction mixtures sufficiently to enable the products to be fully characterized. However, spectral and other evidence did indicate that the expected thiol Michael additions were occurring.

Although the principal interest of this investigation was a study of the reaction of cardenolide-like unsaturated lactones with potentially important *in vivo* nucleophiles, the fact that saturated lactone cardenolides retained some cardiac activity (5, 6) prompted us to consider whether or not any significant interaction of such saturated γ-lactones with the active transport ATP-ase cysteine thiol group(s) could be expected. Reppe and his co-workers (13) had reported that γ-butyrolactone (7) interacted with thiols to give initially the product of carbonyl addition in a reversible reaction, and that under more vigorous conditions γ-thiolbutyric acids were formed. The generality of this reaction was confirmed by the formation of 4-benzylthiolbutyric acid (**8**, R = H) in 50% yield following extended refluxing of α-toluene thiol anion and γ-butyrolactone in aqueous solution (Scheme 2). The acid **8** (R = H) was further characterized as its methyl ester **8** (R = Me). The initial formation of the carbonyl addition product **9** was also confirmed by its isolation from anhydrous benzene solution. The i.r. spectrum of **9** showed no lactone carbonyl absorption but contained a band at 1570 cm^{-1} attributable to the C—O^- stretching vibration. (Sodium methoxide shows a

Can. J. Chem. Downloaded from www.nrcresearchpress.com by 210.87.254.6 on 09/05/12
For personal use only.

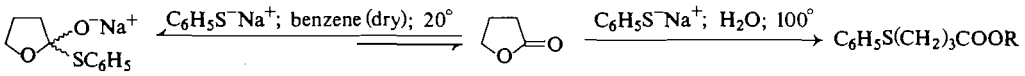

9 7 8

SCHEME 2

similar i.r. absorption band.) Due to solubility and stability problems, a satisfactory p.m.r. spectrum of **9** could not be obtained. On the basis of these results it was concluded that under aqueous *in vivo* conditions such interactions of thiol nucleophiles with the saturated lactone cardenolides were unlikely to be of much significance.

With the Michael addition conditions for the formation of compounds such as **6** delineated, and with the p.m.r. spectra available as reference standards, the reactions of α-toluene thiol with cardenolide aglycones themselves were examined.

Digitoxigenin (**10**) was selected as being a typical cardenolide aglycone and attempts were made to effect the addition of α-toluene thiol under a variety of conditions. These ranged from refluxing the reactants in benzene in the presence of potassium carbonate, in tetrahydrofuran containing methylamine, and using sodium α-toluene thiolate in tetrahydrofuran, methanol and aqueous methanol solutions. Only in the methanolic solutions at pH > 8, was any reaction observed

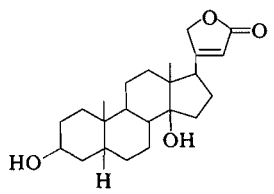

10

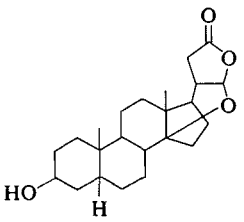

11

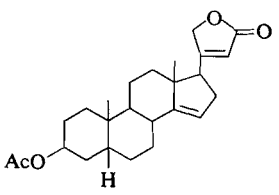

12

and the only detectable product proved to be isodigitoxigenin (**11**). The formation of **11** from digitoxigenin is known to be facile in basic media (14) and the α-toluene thiol anion present in these reactions thus functions only as the base needed to effect isomerization.

In order to eliminate the problem caused by the formation of the iso-derivative under the basic reaction conditions necessary to effect any Michael reaction digitoxigenin was converted to 3β-acetyl-$\Delta^{14,15}$-anhydrodigitoxigenin (**12**). However, yet again no Michael reaction with α-toluene thiol could be effected.

Owing to the insolubility of digitoxigenin in solutions containing relatively large proportions of water, attention was turned towards ouabagenin (**15**) in the hope that the additional hydroxyl groups would enable reactions to be carried out under conditions approximating more closely those obtaining *in vivo*. However, as described below, these proposed investigations were somewhat delayed by the discovery that the compound reported in the literature (15, 16) as ouabagenin did not in fact have the assigned structure **15**.

A satisfactory procedure for the hydrolysis of ouabain (**13**) to its aglycone was first reported by Mannich and Siewert (15). The method involved conversion of ouabain to ouabagenin-1,19-acetonide (**14**) followed by hydrolysis of the acetonide with hot aqueous ethanolic hydrochloric acid to give a compound m.p. 235–238° which was not unreasonably considered to be ouabagenin. Subsequently Djerassi and Ehrlich (16) had cause to reinvestigate the hydrolysis reactions and obtained the same material with a slightly higher m.p. of 242–243°.

The compound we obtained from the hydrolysis of ouabain had m.p. 247–248° and possessed other physical properties virtually identical with those reported (15, 16). However, it was noticed that the i.r. carbonyl stretching frequencies at 1717(sh), 1729, and 1826 cm^{-1} were outside the ranges of 1790–1778 and 1758–1736 cm^{-1} normally associated (17) with the cardenolide carbonyl groups (see Table 1).

The possibility that this difference was due in some way to hydrogen bonding in the solid state[5]

[5]For crystalline digitoxigenin, X-ray studies have shown the lactone carbonyl to be hydrogen-bonded to the C-3β hydroxyl group (19).

Can. J. Chem. Downloaded from www.nrcresearchpress.com by 210.87.254.6 on 09/05/12
For personal use only.

TABLE 1

Cardiac aglycone carbonyl stretching frequencies

	Infrared carbonyl frequencies (cm^{-1})						
	1825	1800	1775	1750	1725		
		Band I		Band II			
Normal cardenolide range (17)		1790–1778		1758–1736			
Ouabain (**13**)*		1785		1735			
Ouabagenin acetonide (**14**)*		1785, 1775		1735			
True ouabagenin (**15**)*		1782		1736			
Compound m.p. 247–248 (**16**)*	1826				1729	1719	
Abnormal cardenolides							
Calotropagenin (18)	1831		1779				1719†
Gitoxigenin*		1821	1788		1760		1718

*In both Nujol and KBr.
†Also contains the C-19 aldehyde peak.

was eliminated since the deuterated derivative obtained on replacement of all exchangeable protons by deuterium (with D_2O) exhibited an identical i.r. spectrum in the carbonyl region. The broad i.r. bands in the 3700–2400 cm^{-1} region were indicative of a carboxylic acid and since the hydrolysis of the acetonide **14** was performed under somewhat vigorous conditions (15, 16), the possibility was considered that hydrolysis of the cardenolide lactone ring might have occurred and that the m.p. 247–248° material was not ouabagenin but was in fact the corresponding acid, 1β,3β,5β,11α,14β-19,21-heptahydroxycard-20:22-enoic acid (**16**). This view was substantiated by the successful hydrolysis of **14** to true ouabagenin (**15**) under much milder conditions *viz.* with refluxing 0.004 *N* 50% aqueous ethanolic hydrochloric acid for 90 s. The ouabagenin (**15**) obtained (33% of pure material) showed a normal i.r. pattern in the carbonyl region (Table 1) and its i.r. spectrum was distinctly different from that of **16** in the hydroxyl, carbonyl, and fingerprint regions. It was best purified by dissolving in absolute ethanol or dioxane followed by slow precipitation with diethyl ether or benzene respectively. The samples obtained in this way contained one molecule of ethanol or dioxane respectively of crystallization.

A comparison of other physical properties confirmed that the two compounds were different and were not merely dimorphs. For example, **15** (with one dioxane of crystallization) has m.p. 265–266°, an R_f of 1.0 on t.l.c. analysis on DEAE cellulose with *n*-butanol development, and is very soluble in water. In contrast, the corresponding data for **16** are, respectively, 247–248°, $R_f = 0$, and slightly soluble. Owing to solubility difficulties, and to the ease with which **15** and **16** equilibrate, the u.v. and p.m.r. spectra of the two compounds in a variety of solvents were not very helpful in distinguishing the structural differences. The differences observed in the chemical properties of the two compounds (summarized in Chart 1) were also consistent with the assignment of their structures as the lactone and hydroxy acid respectively.

A further difference in properties of **15** and **16** was manifested by their reaction with methanol. With methanol containing a trace of triethylamine both compounds yielded the methyl ester **17**; however, in the absence of base ouabagenin itself was unreactive and only the acid **16** was converted to **17** on treatment with pure methanol.

The isolation of the acid **16** instead of the expected ouabagenin **15** from the original hydrolyses (15, 16) can be ascribed to the fact that **15** and **16** equilibrate in solution and as the hydrolysis proceeds the extremely insoluble acid **16** crystallizes out thereby displacing the equilibrium progressively until no ouabagenin remains in solution.

Another factor which may contribute to the preferential isolation of the hydroxyacid **16** is the possibility of hydrogen bonding between the C-11α hydroxyl and C-21 hydroxyl groups. Such hydrogen bonding would require ring C to have a very deformed chair, or possibly twist boat, conformation and octant rule analyses[6] of literature (20) optical rotatory dispersion data on

[6]A detailed account of the analyses is given in the Ph.D. thesis of H. W. Middleton (26).

Can. J. Chem. Downloaded from www.nrcresearchpress.com by 210.87.254.6 on 09/05/12
For personal use only.

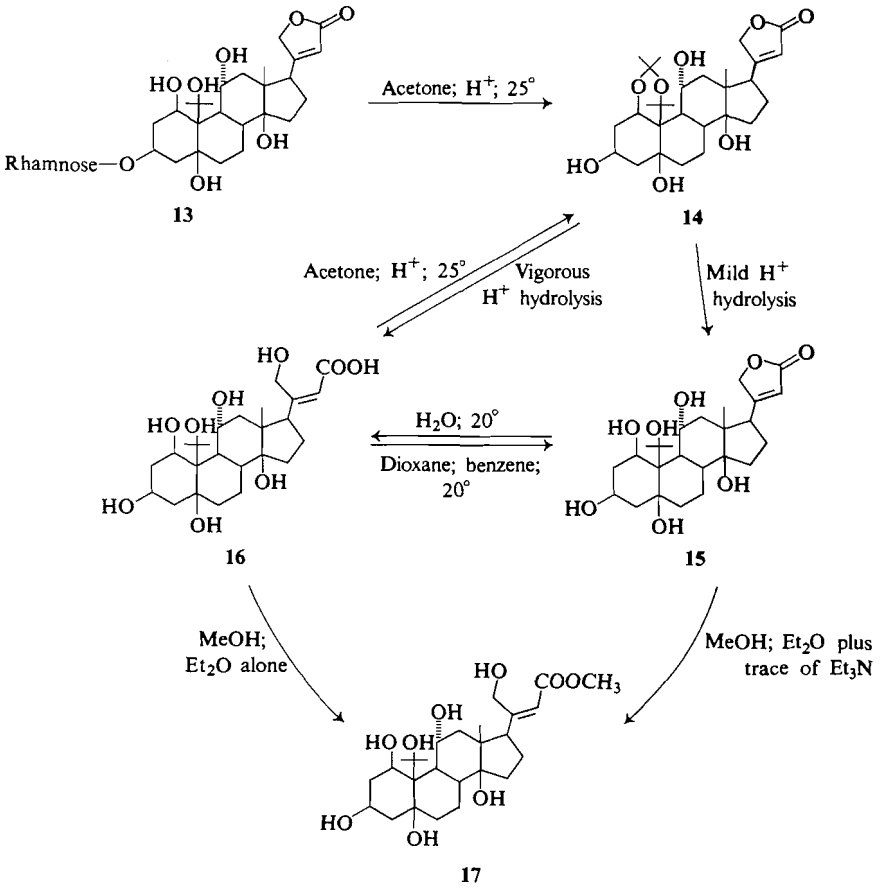

CHART 1

cardenolide 11-ketones are in accord with this suggestion.[7] Such hydrogen bond stabilization of the acid form may well be of general importance in cardiac glycoside or aglycone chemistry since where similar possibilities exist, for example for calotropagenin and gitoxigenin, the i.r. spectra are also anomalous in the carbonyl region (Table 1) suggesting that these two also are not the aglycones but are in fact interconvertible mixtures of the lactones and the corresponding acids. Obviously, however, much further work is needed before the above suggestion can be corroborated.

In view of the effort which had been expended to prepare an authentic sample of ouabagenin it was discouraging to find that, as for digitoxigenin, it did not react with α-toluene thiol under a broad range of conditions. The remote possibility existed that Michael addition was being prevented by the steric bulk of the benzyl group of the α-toluene thiol nucleophile. However, ouabagenin and digitoxigenin failed to react even with the least hindered of all thiol nucleophiles, hydrogen sulfide. As expected the model lactone γ-crotonolactone reacted smoothly (80% yield) with hydrogen sulfide to give the product of bis-Michael addition **18**.

Our inability to demonstrate the hoped for

[7]The deformation, towards a boat-like conformation, required of ring C is much greater than that apparent from the X-ray structure determination of digitoxigenin (19). However, the structural differences between digitoxigenin (**10**) and the acid **16** are sufficiently great to preclude direct extrapolation of the digitoxigenin X-ray conclusions to **16**. Futhermore the presence in **16** of a hydroxy acid function at C-17 in place of the lactone moiety, and of a C-11 hydroxyl group, would destroy the contribution made by the C-3 hydroxyl-lactone carbonyl hydrogen bond towards stabilizing the digitoxigenin ring conformations observed in the crystalline state.

Can. J. Chem. Downloaded from www.nrcresearchpress.com by 210.87.254.6 on 09/05/12
For personal use only.

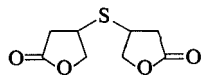

18

Michael additions with the aglycones **10** and **15** was disappointing but not altogether unexpected since, as noted previously, the presence of the substituent on the β-carbon of the conjugated system was known to be undesirable (9–11). Thus from the above data it can only be concluded that *in vivo* Michael addition of a thiol group to the lactone rings of cardenolides can not be of much importance with respect to either the cardiotonic or cardiotoxic properties. However, the reactivity of the C-23 carbonyl of cardenolides and bufadienolides (21) towards methoxide ion indicates that a similar interaction of the cardiac glycosides with a nucleophile of the active transport ATP-ase or a related intermediate may well be important and further studies which may clarify this question are in progress.

Experimental

Melting points were determined on a Fisher–Johns block and are uncorrected. The i.r. spectra were obtained on Beckman I.R. 8, and Perkin–Elmer 237-B and 521 spectrophotometers and p.m.r. spectra on a Varian A-60 or HA-100 instrument. The u.v. spectra were measured on a Perkin–Elmer 350 spectrophotometer and optical rotations on a Bendix–Ericsson ETL-NPL Automatic Polarimeter Type 143 A.

Merck silica gel G or Macherey, Nagal and Co. MN-cellulose 300 DEAE powder were used as the t.l.c. adsorbents. The spots were visualized by spraying with 50% aqueous *p*-toluenesulfonic acid followed by heating to 100° in the case of silica plates, or in the case of the cellulose plates by spraying with hot methanolic sodium hydroxide solution containing *m*-dinitrobenzoic acid. All compounds characterized were purified until analysis by t.l.c., and where appropriate, g.l.c. (3.8% SE-30 on Chromosorb G column) showed no impurities.

Compounds

α-Pyrone (**4**) b.p. 89° (6 Torr) was obtained in 41% yield by pyrolysis of coumalic acid (Aldrich) (22).

4-Hydroxybut-2-enoic acid lactone (γ-crotonolactone, **5**) b.p. 83–87° (9 Torr) was prepared from 2-acetoxyfuran in 60% yield (23).

Ouabain and digitoxigenin were obtained from Sigma and Mann respectively.

Reaction of 4-Hydroxybut-2-enoic Acid Lactone (4) with α-Toluenethiol

α-Toluenethiol (2.95 g, 24 mmoles) was dissolved in 2.6 *N* sodium methoxide (9.16 ml, 24 mmoles) and the mixture added at 20° to a stirred solution of 4-hydroxybut-2-enoic acid lactone (2.1 g, 24 mmoles) in methanol (10 ml). After the addition was complete the reaction solution was brought to p*H* 4 almost immediately (10 s) with 7.27 *N* methanolic hydrogen chloride (3.3 ml, 24 mmoles). The solution was concentrated by rotary evaporation at 20° and the crude product was fractionated to give 1.5 g of *3-benzylthio-4-hydroxybutyric acid* (**6**) b.p. 132–133° (0.35 Torr), i.r. (CCl_4) 1794 and 690 cm^{-1} (C—S); p.m.r. (CCl_4) δ 1.97–2.86 (m, 2, C-2 CH_2), 3.22–3.52 (m, 1, C-3 CH), 3.68 (s, 2, $C_6H_5CH_2$), 3.72–4.38 (m, 2, C-4 CH_2) and 7.22 (s, 5, C_6H_5) p.p.m.

Anal. Calcd. for $C_{11}H_{12}O_2S$: C, 63.13; H, 5.78; S, 15.32. Found: C, 63.14; H, 5.79; S, 15.29.

Similar yields of **6** were obtained in aqueous methanol in the p*H* range 7.4–11.

The Reaction of α-Toluenethiol with γ-Butyrolactone

(a) Sodium α-toluenethiolate (1.46 g, 11.6 mmoles, obtained by evaporating to dryness a methanol solution containing equimolar amounts of α-toluenethiol and sodium methoxide) was added at 20° to a vigorously stirred solution of γ-butyrolactone (0.94 g, 11.6 mmoles) in anhydrous benzene (20 ml). After 2 h the undissolved thiolate was filtered off under dry nitrogen and the filtrate diluted with anhydrous diethyl ether. The precipitate formed was collected under dry nitrogen, washed with anhydrous diethyl ether and dried *in vacuo* to give the sodium salt of *2-benzyl-2-hydroxytetrahydrofuran* (**9**) (0.5 g), i.r. (Nujol) 1550 cm^{-1} (C—O^-).

(b) A mixture of α-toluenethiol (14.6 g, 0.116 mole) in 11.6 *N* aqueous sodium hydroxide (10 ml, 0.116 mole) and γ-butyrolactone (9.3 g, 0.116 mole) was refluxed under nitrogen for 5 days. The cooled reaction mixture was then neutralized with 1 *N* hydrochloric acid (116 ml, 0.116 mole) and the solution extracted with diethyl ether (3 × 40 ml). The combined ether extracts were dried ($MgSO_4$), evaporated, and the crude product obtained was fractionally distilled twice to give 11.5 g of *4-benzylthiobutyric acid* (**8**, R = H) b.p. 148–150° (0.09 Torr), n_D^{20} 1.5531; i.r. (CCl_4) 3550–2400, 1718, and 690 cm^{-1} (C—S); p.m.r. (CCl_4) δ 1.7–2.05 (m, 2, CH_2CH_2COOH), 2.2–2.6 (m, 4, CH_2COOH and SCH_2CH_2); 3.59 (s, 2, $C_6H_5CH_2$), 7.18 (s, 5, C_6H_5), and 8.2 (s, 1, $COOH$) p.p.m.

Anal. Calcd. for $C_{11}H_{14}O_2S$: C, 62.83; H, 6.71; S, 15.25. Found: C, 63.01; H, 6.82; S, 15.08.

Treatment of the thioacid **8** (R = H) with ethereal diazomethane gave the *methyl ester* **8** (R = Me) in quantitative yield, b.p. 112° (0.07 Torr), i.r. (CCl_4) 1748 cm^{-1}.

Anal. Calcd. for $C_{12}H_{16}O_2S$: C, 64.25; H, 7.19; S, 14.29. Found: C, 64.40; H, 7.15; S, 14.18.

The Reaction of Digitoxigenin with α-Toluenethiol under Basic Conditions

Digitoxigenin (25 mg, 0.66 mmole) was added with stirring under nitrogen at 20° to a solution of α-toluenethiol (0.8 g, 6.6 mmoles) in methanol (10 ml) containing 1 *N* aqueous sodium hydroxide (0.66 ml, 6.6 mmoles). After stirring for a further 6 h the reaction mixture was neutralized with 1 *N* aqueous hydrochloric acid (0.66 ml, 6.6 mmoles), filtered, and the filtrate evaporated at room temperature. The residual solid was recrystallized from

Can. J. Chem. Downloaded from www.nrcresearchpress.com by 210.87.254.6 on 09/05/12
For personal use only.

Can. J. Chem. Downloaded from www.nrcresearchpress.com by 210.87.254.6 on 09/05/12
For personal use only.

methanol – diethyl ether to give 16 mg of isodigitoxigenin[8] (**11**) m.p. 270–271°, identical in all respects with an authentic sample prepared in 66% yield as described by Jacobs and Gustus (14).

*The Preparation of 3β-Acetyldigitoxigenin and 3β-Acetyl-$\Delta^{14(15)}$-digitoxigenin (**12**)*

3β-Acetyldigitoxigenin, m.p. 226–227° (lit. (24) m.p. 227°), was obtained in 69% yield by acetylation of digitoxigenin with acetic anhydride in pyridine (24). Its subsequent dehydration with phosphorous oxychloride (24) gave 3β-acetyl-$\Delta^{14(15)}$-digitoxigenin (**12**, 46% yield), m.p. 183–184°, $[\alpha]_D^{22}$ $-11.4 \pm 0.2°$ (*c* 6 in $CHCl_3$) (lit. (24) m.p. 182–184°, $[\alpha]_D^{15}$ $-11.6 \pm 2°$ (*c* 0.95 in $CHCl_3$)). The anhydro compound **12** did not react with α-toluenethiol in basic methanol solution.

*The Preparation of Ouabagenin Acetonide (**14**)*

(a) From Ouabain

Ouabagenin acetonide (**14**) m.p. 304–305° (lit. (16) m.p. 302–304°) was prepared in 81% yield by hydrolysis of ouabain octahydrate following the procedure reported by Djerassi and Ehrlich (16).

*(b) From Authentic Ouabagenin **15**, the Cardenoic Acid **16**, and the Methyl Ester **17***

Any one of compounds **15**, **16**, or **17** (100 mg) was dissolved in acetone containing a trace of hydrogen chloride and the solution seeded with a crystal of ouabagenin acetonide. Crystals began to separate after a short time and after keeping for several hours at 20°, the product was collected, washed with acetone (40 ml), then with anhydrous diethyl ether (60 ml) and dried *in vacuo*. The ouabagenin acetonide (80% yield) obtained from each reaction was identical in all respects with authentic material.

*The Preparation of 1β,3β,5β,11α,14β,19,21-Heptahydroxycard-20,22-enoic Acid (**16**)*

(a) From Ouabagenin Acetonide

A solution of the acetonide (2.4 g, 5.1 mmoles) in 50% aqueous ethanol (30 ml) containing 2 *M* aqueous acetic acid (0.5 ml) was heated under reflux for 30 min. The cooled (20°) reaction mixture was then concentrated by rotary evaporation and the solid which separated was filtered off, triturated with hot *n*-butanol, and recrystallized from a large volume of cold ethanol (14). The acid **16** obtained (1.1 g) had m.p. 247–248°, $[\alpha]_D^{22}$ 11.3 ± 0.8 (*c* 1.5 in H_2O) (lit. (16, 25) m.p. 242–244°, $[\alpha]_D^{17}$ 11.3 (*c* 1.3 in H_2O)), i.r. (Nujol) 1729 and 1717 cm^{-1}, u.v. (CH_3OH) 220.5 nm (ε 9150).

*(b) From Authentic Ouabagenin (**15**)*

Authentic ouabagenin (containing one dioxane of crystallization, 0.5 g, 9.8 mmoles) was dissolved in water (2 ml). After 2 min crystals began to separate and after keeping at 0° for a further 1 h the mixture was filtered. The crystalline solid obtained was washed with first hot *n*-butanol (10 ml) and then with anhydrous diethyl ether (60 ml) and dried *in vacuo* at 20° to give 0.44 g of the acid **16** identical in all respects to the sample obtained above.

*The Preparation of Authentic Ouabagenin (**15**)*

(a) From Ouabagenin Acetonide

The acetonide (0.58 g, 1.1 mmoles) was added all at once to refluxing 50% aqueous ethanol (50 ml) containing 2 *N* aqueous hydrochloric acid (0.1 ml). Heating under reflux was continued for a further 90 s after which time the solution was cooled rapidly to 20°, filtered, and the filtrate rotary evaporated to dryness at 30°. The residue was dissolved in warm ethanol (40 ml), the solution filtered, and anhydrous diethyl ether (160 ml) added. The precipitate formed was collected, and after being recycled through the latter ethanol – diethyl ether procedure, was dried, *in vacuo* at 20° to give 0.18 g of *authentic ouabagenin* (containing ethanol of crystallization[9]), i.r. (Nujol) 1782 and 1736 cm^{-1}, u.v. (H_2O) 218.5 nm (ε 14800).

Anal. Calcd. for $C_{23}H_{34}O_8$.1 EtOH: C, 62.0; H, 8.27. Found: C, 61.79; H, 8.09.

*(b) From the Acid **16***

The cardenoic acid **16** (100 mg, 0.22 mmole) was dissolved in warm dioxane (20 ml) and anhydrous benzene (50 ml) was then added to the filtered solution. After keeping for 5 h at 10°, the precipitated solid was filtered, washed with anhydrous diethyl ether and dried *in vacuo* at 20° to give 84 mg of authentic ouabagenin (15, containing one dioxane of crystallization[9]) m.p. 265–266°, i.r. and u.v. absorptions were identical with those of the sample obtained above except for differences due to solvent of crystallization.

Anal. Calcd. for $C_{23}H_{34}O_8$.1 dioxane: C, 61.6; H, 7.98. Found: C, 61.66; H, 8.12.

*The Preparation of Methyl 1β,3β,5β,11α,14β,19,21-Heptahydroxycard-20,22-enoate (**17**)*

*(a) From the Parent Acid **16***

The acid **16** (100 mg, 0.22 mmole) was dissolved in methanol (25 ml) and after keeping for 20 min at 20°, anhydrous diethyl ether (75 ml) was added. After 12 h the crystals which separated from the solution were filtered off, washed with diethyl ether, and dried to give 85 mg of the *methyl ester* **17** m.p. 264–265°, i.r. (Nujol) 1706 cm^{-1}, u.v. (MeOH) 221.5 nm (ε 9090).

Anal. Calcd. for $C_{24}H_{38}O_9$: C, 61.29; H, 8.06. Found: C, 61.46; H, 8.04.

(b) From Authentic Ouabagenin

Ouabagenin (containing one dioxane of crystallization, 100 mg, 1.21 mmoles) was dissolved in methanol (25 ml) containing one drop of triethylamine. After keeping for

[8]Although p.m.r. spectra were recorded for each of the cardenolide compounds discussed in this paper, no data have been included in the experimental section since the complexity of the spectra obtained makes a mere listing of chemical shifts, peak multiplicities, etc. rather pointless. The p.m.r. data were in accord with each structure assignment made and copies of all spectra are available from the authors on request.

[9]Due to the presence of solvent of crystallization, anomalously low m.p. values were often observed for ouabagenin samples. The value quoted for ouabagenin·1 dioxane is considered the most reliable.

20 min at 20° diethyl ether (75 ml) was added and the methyl ester **17** (70 mg) isolated as described above.

No reaction was observed in the absence of triethylamine.

*The Preparation of 3,3'-Di-(4-Hydroxybutyric Acid Lactone) Sulfide (**18**)*

Hydrogen sulfide was bubbled through a solution of 4-hydroxybut-2-enoic acid lactone (4.4 g, 53 mmoles) in methanol (40 ml) containing triethylamine (0.54 g, 53 mmoles). After passing the gas for 20 min the solution was neutralized with 2 *M* methanolic hydrogen chloride and the solution concentrated by 80%. The precipitated triethylamine hydrochloride was filtered off and washed with diethyl ether (20 ml) and the combined filtrates evaporated to dryness at 20°. The residue was recrystallized, with charcoal treatment, firstly from methanol – diethyl ether and finally from chloroform – diethyl ether to give 3.5 g of the *thio-ether* **18** m.p. 107–108°, i.r. ($CHCl_3$) 1782 cm^{-1}; p.m.r. ($CDCl_3$) δ 2.53–2.9 (m, 4, C-2 CH_2), 3.48–4.25 (m, 6, C-2 CH_2 and C-3 CH) and 4.5–4.78 (m, 4, C-4 CH_2) p.p.m.

Anal. Calcd. for $C_8H_{10}O_4S$: C, 47.10; H, 4.90; S, 15.68. Found: C, 47.36; H, 5.11; S, 15.78.

This work was generously supported by the Ontario Heart Foundation. We are also grateful to Dr. C. Djerassi for providing seed crystals of ouabagenin acetonide.

1. E. Pieragnole, E. Pretolani, and S. Tura. Minerva Cardioangiol. **5**, 592 (1957).
2. J. C. Skou. Progr. Biophys. Mol. Biol. **14**, 131 (1964) and references therein.
3. H. W. Middleton and J. B. Jones. Proc. Can. Fed. Biol. Soc. **12**, 210 (1969); H. W. Middleton. Arch. Biochim. Biophys. **136**, 280 (1970).
4. O. Kennard, N. W. Isaacs, J. C. Coppola, A. J. Kirby, S. Warren, W. D. S. Motherwell, D. G. Watson, D. L. Wampler, D. H. Chenery, A. C. Larson, K. A. Kerr, and L. R. Di Sanseverino. Nature, **225**, 333 (1970).
5. K. K. Chen and F. G. Henderson. J. Pharmacol. Exp. Ther. **111**, 365 (1964).
6. J. B. Kahn and S. B. Cohen. J. Pharmacol. Exp. Ther. **121**, 234 (1967).
7. K. Repke. Proc. 2nd Int. Pharmacol. Meeting, (Prague), **4**, 65 (1965).
8. H. Matsui and A. Schwartz. Biochim. Biophys. Acta, **151**, 655 (1968).
9. D. E. Duggan and R. M. Noll. Arch. Biochim. Biophys. **109**, 388 (1965).
10. E. Boyland and L. F. Chasseaud. Biochem. J. **99**, 138 (1966).
11. C. J. Cavallito and T. H. Haskell. J. Amer. Chem. Soc. **67**, 1991 (1945).
12. *cf.* J. B. Jones and J. N. Barker. Can. J. Chem. **48**, 1574 (1970) and previous papers.
13. W. Reppe *et al.* Ann. **596**, 170 (1955).
14. W. A. Jacobs and E. L. Gustus. J. Biol. Chem. **78**, 573 (1928).
15. C. Mannich and G. Siewert. Ber. **75**, 737 (1942).
16. C. Djerassi and R. Ehrlich. J. Org. Chem. **19** 1351 (1954).
17. R. N. Jones and B. S. Gallagher. J. Amer. Chem. Soc. **81**, 5242 (1959).
18. O. P. Mittal, C. H. Tamm, and T. Reichstein. Helv. Chim. Acta, **45**, 907 (1962).
19. I. L. Karle and J. Karle. Acta Cryst. (B), **25**, 434 (1969).
20. C. Djerassi, O. Halpern, V. Halpern, O. Schindler, and C. H. Tamm. Helv. Chim. Acta, **41**, 250 (1958).
21. A. Stoll, A. Hoffmann, and W. Kreis. Helv. Chim. Acta, **17**, 1334 (1934).
22. H. E. Zimmermann and R. M. Pauffler. J. Amer. Chem. Soc. **82**, 1514 (1960).
23. F. D'Alelio, C. J. Williams, and C. L. Wilson. J. Org. Chem. **25**, 1025 (1960).
24. F. Hunzicker and T. Reichstein. Helv. Chim. Acta, **28**, 1472 (1945).
25. J. P. Mathieu and A. Petit. Constantes selectionnees pouvoir rotatoir naturel. Masson et Cie, Paris, 1956.
26. H. W. Middleton. Ph.D. Thesis. University of Toronto, Toronto, Ontario, 1968.

Can. J. Chem. Downloaded from www.nrcresearchpress.com by 210.87.254.6 on 09/05/12
For personal use only.

Reactions of sodium *N,N*-diethyldithiocarbamate with some organic solvents

P. R. Heckley, D. G. Holah, A. N. Hughes, and F. Leh
Department of Chemistry, Lakehead University, Thunder Bay, Ontario

Received July 7, 1970

Sodium *N,N*-diethyldithiocarbamate reacts smoothly with methylene chloride (even in the presence of various transition metal ions) to give the dithiocarbamate ester $Et_2NC(S)SCH_2S(S)CNEt_2$ in very high yield. With chloroform and acetonitrile, proton abstraction occurs followed by partial decomposition of the *N,N*-diethyldithiocarbamic acid so formed to give diethylammonium *N,N*-diethyldithiocarbamate.

Canadian Journal of Chemistry, **48**, 3827 (1970)

Can. J. Chem. Downloaded from www.nrcresearchpress.com by 210.87.254.105 on 09/05/12
For personal use only.

Although there is a very considerable literature on the synthesis of metal *N,N*-dialkyldithiocarbamate complexes in aqueous solutions (1), it is only recently that reactions between metal halides and sodium *N,N*-diethyldithiocarbamate (Nadtc) have been examined under anhydrous conditions (2). In almost all cases, the metal–dtc complex is the major product although in certain reactions aimed at the synthesis of pentakis-(*N,N*-dimethyldithiocarbamato)Nb(V), an organic product, tetramethylthiuram disulfide [$(Me_2NCS_2)_2$] has been isolated (3). It appears that the metal is reduced to Nb(IV) and the tetramethylthiuram disulfide is produced via the radical $Me_2NCS_2^{\cdot}$. In no case, however, has there been mention of the possibility of a reaction between Nadtc and the anhydrous organic solvent.

As a continuation of our work on anhydrous metal halide – dtc systems (4), we have carried out reactions between sodium *N,N*-diethyldithiocarbamate and halides of Nb(V), Ta(V), Pa(V), and Mo and W (in various oxidation states) in several organic solvents under anhydrous and inert atmosphere conditions. These reactions produce not only the expected metal halide – dtc complexes (to be reported in separate papers) but also totally unexpected organic products formed by reactions of the Nadtc with the solvents. Indeed, in some reactions, the organic products are formed in very high yield to the almost complete exclusion of the metal halide – dtc complex. We therefore now report our findings concerning the reactions of sodium *N,N*-diethyldithiocarbamate with methylene chloride, chloroform, and acetonitrile under strictly anhydrous, oxygen-free conditions.

The Nb(V) and Ta(V) chlorides and bromides react vigorously and exothermically with Nadtc in methylene chloride to form the appropriate metal–dtc complexes together with varying amounts of an organic product analyzing for $C_{11}H_{22}N_2S_4$. Formation of the organic product is suppressed if the reaction mixture is cooled below reflux temperatures and the Nadtc added slowly. With the corresponding metal iodides, the complex formation is very slow but the reaction mixture, on vigorous agitation at room temperature for long periods, gives the expected complex and moderate yields of the organic product. If the reaction mixture is heated under reflux, the organic product is formed in almost quantitative yield to the virtual exclusion of the metal–dtc complex. That the complex is not an intermediate in the formation of the organic product is shown by the fact that mixtures of Nadtc and methylene chloride give excellent yields (>90%) of the organic material on heating under reflux briefly.

Mass spectrometric studies confirm the molecular weight of 310 and show that the dtc grouping is still present (peak at *m/e* 148). Further evidence for the presence of the dtc grouping comes from the i.r. spectrum which is very similar to that of Nadtc. The n.m.r. studies show a ratio of 12 methyl protons as a triplet at τ 8.71 ($J = 7$ Hz) to eight methylene protons as a poorly defined quartet at τ 6.2 to two other methylene protons as a sharp singlet at τ 4.63. Thus, the molecule is symmetrical and has the structure $Et_2NC(S)SCH_2S(S)CNEt_2$. The mass spectrometric fragmentation pattern is also in excellent agreement with this structure with very strong peaks at *m/e* 194 and 116 corresponding to the fragmentation $[Et_2NC(S)SCH_2S(S)CNEt_2]^{\cdot+} \rightarrow [Et_2NC(S)SCH_2S]^+$ (*m/e* 194) + $[Et_2NC{\equiv}S]^+$ (*m/e* 116). Other peaks in the spectrum are considerably weaker and appear to correspond with further fragmentation of these ions.

Can. J. Chem. Downloaded from www.nrcresearchpress.com by 210.87.254.105 on 09/05/12
For personal use only.

There has been one very brief report (5) that the analogous compound $Me_2NC(S)SCH_2S(S)CNMe_2$ can be prepared by the action of sodium *N,N*-dimethyldithiocarbamate on methylene chloride in ethanol under reflux for 2 h. No further details were given except that the reaction is said to occur with other dihalides.

The mechanism of formation of the organic product is of some interest. Clearly, nucleophilic displacement of chloride by dtc groups occurs but, even when a very large excess of methylene chloride is present, $Et_2NC(S)SCH_2S(S)CNEt_2$ is the only organic product formed. This suggests that the mono-displacement intermediate $Et_2NC(S)SCH_2Cl$ is very short lived and that the second chlorine atom is displaced by intramolecular attack of the nitrogen atom or the sulfur atom of the thiocarbonyl group to give a cyclic intermediate **1** or **2**. Both of these intermediates would be very susceptible to nucleophilic attack by dtc to give the observed product, *i.e.* the reaction could be an example of neighboring group participation. The reaction does not occur if Nadtc·$3H_2O$ is used.

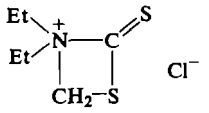

1

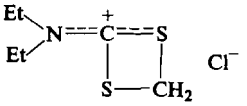

2

The reaction of Nadtc with chloroform (free from ethanol) is completely different. The dithiocarbamate dissolves readily in boiling chloroform and evaporation of the reaction mixture after several hours gives a little sodium chloride and a good yield of a colorless solid (m.p. 82°) analyzing for $C_9H_{22}N_2S_2$ or $C_9H_{20}N_2S_2$. The i.r. spectrum is very similar to that of Nadtc and the mass spectrum at 70° (direct inlet) shows the highest mass at *m/e* 149 (*i.e.* dtcH). Mass spectra taken at higher temperatures show peaks above *m/e* 149 but these spectra are not reproducible and it is clear that thermal decomposition occurs.

The n.m.r. spectrum shows (taking into account the elemental analyses) four methyl groups as two partially superimposed triplets at τ 8.5–9.0, two identical methylene groups as a quartet at τ 6.88 (J = 7 Hz), two other methylene groups as a quartet at τ 5.94 (J = 7 Hz), and two acidic protons as a singlet at τ 0.83. The product is not stable in chloroform solution for long periods and the n.m.r. spectrum becomes considerably modified during several days. The n.m.r. spectrum confirms that the molecular formula is $C_9H_{22}N_2S_2$.

The chloroform–dtc reaction product reacts with boiling methylene chloride to give the compound $Et_2NC(S)SCH_2S(S)CNEt_2$ which strongly suggests that the *N,N*-diethyldithiocarbamate ion is present. This is confirmed by treating the chloroform–dtc reaction product with a Ni(II) salt in ethanol solution which gives an immediate precipitate of $Ni(dtc)_2$ identical (X-ray powder pattern) with an authentic sample.

This evidence strongly suggests that the compound is diethylammonium *N,N*-diethyldithiocarbamate ($Et_2NCS_2^- \; Et_2\overset{+}{N}H_2$) and this was confirmed by synthesis of an authentic sample by treatment of Nadtc with diethylammonium chloride in benzene.[1] The i.r. and n.m.r. spectra and the X-ray powder pattern of the authentic sample are identical in all respects with those of the chloroform–dtc reaction product.

The diethylammonium salt is almost certainly derived from partial decomposition of *N,N*-diethyldithiocarbamic acid formed by abstraction of a proton from chloroform by dtc. Confirmation of this proton abstraction is given by the reaction of Nadtc with deuteriochloroform in which the diethylammonium salt heavily deuterated in the diethylammonium group is formed. The n.m.r. spectrum of the deuterated salt is almost identical to that of the material produced from chloroform except that the two acidic protons at τ 0.83 have vanished and the quartet due to the methylene groups in the diethylammonium ion (τ 6.88) is somewhat less intense than the quartet due to the methylene groups in the dtc grouping. Presumably, some deuterium exchange has occurred. The mass spectrum at 70° shows the highest significant peak at *m/e* 150 (dtcD). Moreover, the deuterated product is isostructural (X-ray powder pattern) with the undeuterated product. The most likely reaction path is outlined in Scheme 1. The later stages of this scheme are effectively the decomposition of *N,N*-dialkyldithiocarbamic acids as established by Zahradník and Zuman (6) although recent work (7) suggests that the intermediate **3** plays

[1]This compound is commercially available from Eastman Organic Chemicals, Rochester, New York.

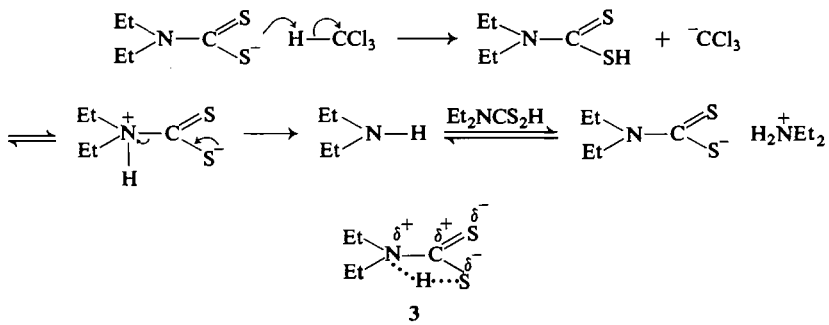

3

SCHEME 1

an important part in the decomposition and shows that steric inhibition of solvation markedly affects the rate of decomposition.

The initial step is very similar to proton abstraction from chloroform by strong base as used in the generation of dichlorocarbene (8). In this case, however, the fate of the probable intermediate $^{-}CCl_3$ is uncertain although the production of sodium chloride indicates that dichlorocarbene is formed. All attempts to trap the dichlorocarbene with cyclohexene according to the published method (8) were unsuccessful. This, however, is not unexpected in view of the number of highly reactive species already present in the reaction mixture.

It is also interesting to note that other sulfur-containing nucleophiles such as the thiophenolate ion (PhS^{-}) react only very slowly with chloroform (9).

A similar reaction occurs between Nadtc and the slightly acidic protons of acetonitrile and again, the product is diethylammonium *N,N*-diethyldithiocarbamate.

Thus, when the common non-aqueous solvents, methylene chloride, chloroform, and acetonitrile are used as solvents for reactions between metal halides and dithiocarbamates, the resulting metal complexes may be contaminated with organic products. This is particularly true in the case of methylene chloride although with chloroform and acetonitrile, the organic product still contains the dithiocarbamate ion which is able to react with metal ions in the normal manner.

It should also be mentioned that methylene chloride, chloroform, and acetonitrile appear to be inert towards the common sulfur-containing ligands, potassium ethylxanthate and toluene-3,4-dithiol.

Experimental

The i.r. spectra were recorded in Nujol mulls using a Beckman IR12 spectrophotometer while n.m.r. measurements were made with a Varian Associates model A60-A spectrometer in chloroform or deuteriochloroform solution with chloroform or tetramethylsilane as internal reference. Mass spectra were obtained using an Hitachi–Perkin–Elmer model RMU-7 double focussing mass spectrometer fitted with a direct inlet system. X-Ray powder diffraction studies were carried out in Lindemann X-ray capillaries and powder diffraction photographs were recorded using a Debye–Scherrer type powder camera (114.6 mm diameter) with nickel filtered copper-K_α radiation produced by a Phillips PW1130 3KW X-Ray Generator.

All reactions were carried out in dry, nitrogen-filled glove boxes in which samples were also prepared for physical measurements. Commercial Nadtc·$3H_2O$ was dehydrated under high vacuum (10^{-6} Torr) at 100°. Solvents were dried and stored over molecular sieves in the glove box.

Reaction of Nadtc with Methylene Chloride

Sodium *N,N*-diethyldithiocarbamate (1.29 g) was heated under reflux (2.5 h) with methylene chloride (20 ml) to give a pale greenish solution and a small amount of colorless residue (NaCl). The solid was removed by centrifugation, the solution was reduced to low bulk (5 ml), and ether was added dropwise until precipitation of a colorless solid was complete. The solid was removed by filtration and vacuum dried to give pure methylene bis(*N,N*-diethyldithiocarbamate) (1.01 g, 86.4%), m.p. 70–71°.

Anal. Calcd. for $C_{11}H_{22}N_2S_4$: C, 42.6; H, 7.1; N, 9.0; S, 41.3. Found: C, 42.8; H, 7.1; N, 8.8; S, 40.8.

Reaction of Nadtc with Chloroform

The sodium *N,N*-diethyldithiocarbamate (1.87 g) was mixed with dry, ethanol-free chloroform (30 ml) and the mixture was heated under reflux for 17 h. The mixture was then cooled to room temperature and was chromatographed twice on silica gel using chloroform as the eluting solvent. The eluate was evaporated to give a viscous mass which, on treatment with petroleum ether (30–40°), crystallized to give colorless needles of the crude product. Pure diethylammonium *N,N*-diethyldithiocarbamate

Can. J. Chem. Downloaded from www.nrcresearchpress.com by 210.87.254.105 on 09/05/12
For personal use only.

(m.p. 82–82.5°) was obtained as colorless needles (0.49 g, 40%) from the crude product by recrystallization from a chloroform – petroleum ether mixture.

Anal. Calcd. for $C_9H_{22}N_2S_2$: C, 48.6; H, 9.9; N, 12.6; S, 28.8. Found: C, 48.0; H, 8.9; N, 11.7; S, 28.2.

The product was identical in all respects with an authentic sample of diethylammonium *N,N*-diethyldithiocarbamate.

Synthesis of Authentic Diethylammonium N,N-Diethyldithiocarbamate

To sodium *N,N*-diethyldithiocarbamate (1.28 g) in dry benzene (75 ml) was added diethylamine hydrochloride (0.81 g). The mixture was heated under reflux for 18 h, cooled to room temperature, and the residue was extracted with benzene until no further material dissolved. The sodium chloride residue was discarded and the various benzene extracts were combined and chromatographed on silica gel. The eluate was evaporated to dryness to give pale yellow needles of the product which was recrystallized from carbon tetrachloride and petroleum ether (30–40°) to give colorless needles (1.16 g, 70%) of diethylammonium *N,N*-diethyldithiocarbamate (m.p. 82–83°).

Reaction of Nadtc with Acetonitrile

Sodium *N,N*-diethyldithiocarbamate (3.07 g) was mixed with dry acetonitrile (30 ml) and the mixture was heated under reflux for 19 h. During this time, a very small amount of a colorless solid which was not Nadtc or NaCN (X-ray powder patterns) was precipitated. On cooling to room temperature, the mixture was filtered to remove the precipitate and the solution was evaporated under reduced pressure. The resulting oily material was extracted with cold methylene chloride and the extracts were immediately chromatographed on silica gel. The eluate was evaporated and the pale yellow oil obtained was crystallized from a mixture of carbon tetrachloride and petroleum ether (30–40°) to give colorless crystals (0.93 g, 46.5%) of diethylammonium *N,N*-diethyldithiocarbamate identical in all respects with an authentic sample.

We thank the Senate Research Committee of Lakehead University, Thunder Bay, Ontario, the National Research Council of Canada, and the Ontario Department of University Affairs for generous financial support of this work.

1. See, for example, the review by D. COUCOUVANIS. Progr. Inorg. Chem. **11**, 233 (1970).
2. K. W. BAGNALL, D. BROWN, and D. G. HOLAH. J. Chem. Soc. A, 1149 (1968).
3. D. C. BRADLEY and M. H. GITLITZ. J. Chem. Soc. A, 1152 (1969).
4. D. BROWN, D. G. HOLAH, and C. E. F. RICKARD. J. Chem. Soc. A, 786 (1970).
5. J. C. THOMAS. U.S. Pat. 2 384 577 (1945). Chem. Abstr. **40**, 177 (6), (1946).
6. R. ZAHRADNÍK and P. ZUMAN. Chem. Listy, **52**, 231 (1958).
7. S. J. JORIS, K. I. ASPILA, and C. L. CHAKRABARTI. J. Phys. Chem. **74**, 860 (1970); R. R. VANDEBEEK, S. J. JORIS, K. I. ASPILA, and C. L. CHAKRABARTI. Can. J. Chem. 2205 (1970); K. I. ASPILA, V. S. SASTRI, and C. L. CHAKRABARTI. Talanta, **16**, 1099 (1969).
8. W. VON E. DOERING and A. K. HOFFMAN. J. Amer. Chem. Soc. **76**, 6162 (1954).
9. J. HINE. J. Amer. Chem. Soc. **72**, 2438 (1950).

Can. J. Chem. Downloaded from www.nrcresearchpress.com by 210.87.254.105 on 09/05/12
For personal use only.

Can. J. Chem. Downloaded from www.nrcresearchpress.com by 210.87.254.105 on 09/05/12
For personal use only.

Some observations on isotopic scramblings accompanying acetolysis in the 2-norbornyl system

C. C. Lee, Bo-Sup Hahn, L. K. M. Lam,[1] and D. J. Woodcock
Department of Chemistry and Chemical Engineering, University of Saskatchewan, Saskatoon, Saskatchewan

Received June 18, 1970

Evidence is presented to show that in the acetolysis of isotopically labeled *exo*- or *endo*-2-norbornyl brosylate (*exo*- or *endo*-**1**-OBs) in NaOAc buffered HOAc, the initially formed product, *exo*-**1**-OAc, could undergo further isotopic scrambling during its subsequent contact with the reaction medium. These scramblings in the acetate apparently involved relatively large amounts of rearrangement of the label from C-2 to -3. After partial acetolysis of *exo*- or *endo*-**1**-OBs-2-*d*, n.m.r. analysis showed that the recovered *endo*-brosylate was unchanged, while the D-label in the recovered *exo*-brosylate has definitely rearranged from C-2 to -1 and probably also to C-6. Thus, in the acetolysis of labeled *exo*-**1**-OBs as commonly carried out in HOAc–NaOAc, isotopic scramblings could occur not only in the solvolysis reaction itself, but also prior to the reaction due to internal return giving rise to scrambled brosylate and subsequent to the reaction due to further scrambling in the initial product. Other mechanistic implications of the results are also discussed.

Canadian Journal of Chemistry, **48**, 3831 (1970)

In the original work on the acetolysis of *exo*-2-norbornyl-2,3-$^{14}C_2$brosylate (*exo*-**1**-OBs-2,3-^{14}C) (1, 2), because the label was present at both C-2 and -3, it was not possible to observe directly any 3,2-hydride shifts. In our earlier work on the acetolysis of *exo*- and *endo*-**1**-OBs-2-*t* (3), small amounts (about 1–2%) of the *t*-label were found at the C-3 position of the resulting product, *exo*-**1**-OAc-*x*-*t*. Since treatment of *exo*-**1**-OAc-2-*t* in HOAc–NaOAc at 25° also gave rise to some isotopic scrambling with about 1% of the label rearranged to C-3 (3), it was concluded that most, if not all, of the overall 3,2-hydride shifts observed in the acetolysis of the brosylate could have resulted from the subsequent ionization, in the reaction mixture, of the initially formed acetolysis product. The present paper deals with further studies confirming this conclusion, some of the data from these studies having been reported previously in preliminary form (4). It is well known that the acetolysis of *exo*-**1**-OBs is accompanied by internal returns (5, 6). The present paper also describes our attempts in evaluating the nature and extents of the isotopic scrambling arising from internal returns in the recovered brosylate after partial acetolysis.

Results and Discussion

Given in Table 1 are the *t*-distributions in the 2-norbornyl skeleton of the *exo*-**1**-OAc-*x*-*t* samples obtained from the various experiments using *t*-labeled materials. The methods of degradation from which these distributions were obtained have already been described (3). For comparison, some of the results (experiments I, II, and III) reported by Lee and Lam (3) are also included in Table 1. The data in Table 1 indicate that there was extensive isotopic scrambling not only in the acetolysis of *exo*- or *endo*-**1**-OBs-2-*t*, but also when the acetolysis product was allowed to be in contact with the reaction mixture. This was demonstrated by experiments III and IV when *exo*-**1**-OAc-2-*t* was stirred at 25° or heated under reflux in NaOAc buffered HOAc. More rearrangement was observed at the higher temperature; but interestingly, the relative increase in rearrangement is much greater to C-3 than to the other positions. In experiment V, the acetolysis of *endo*-**1**-OBs-2-*t* at 30° for 64 days was found to give 6.3 and 4.7% overall rearrangement of the *t*-label to C-3 in duplicate runs. The precision of these values was not as good as those obtained in experiments I–IV, possibly because of lesser reproducible control of the experimental conditions during the prolonged reaction time. However, the extent of rearrangement to C-3 in experiment V was greater than those observed in experiments I–III. When the reaction time in the acetolysis of *endo*-**1**-OBs-2-*t* was reduced from 64 to 2 days (experiment VI), the amount of net rearrangement to C-3 was greatly decreased, again suggesting that the acetolysis product, *exo*-**1**-OAc-*x*-*t*, could undergo subsequent ioniza-

[1]Present address: Department of Chemistry, University of Windsor, Windsor, Ontario.

Can. J. Chem. Downloaded from www.nrcresearchpress.com by 210.87.254.105 on 09/05/12
For personal use only.

TABLE 1

Tritium distributions in the *exo*-2-norbornyl-*x*-*t* acetate (*exo*-1-OAc-*x*-*t*) from various experiments

Experiment	Reaction	Specific activity of *exo*-1-OH-*x*-*t* (c.p.m./mmole)*		Tritium content (%)							
				C-2		C-3		C-1,4,7		C-5,6	
		Run 1	Run 2	Run 1	Run 2	Run 1	Run 2	Run 1	Run 2	Run 1	Run 2
I†	*exo*-1-OBs-2-*t* in HOAc–NaOAc, 25°, 24 h	339 300	300 100	34.3	35.6	1.8	2.1	37.3	35.7	26.6	26.6
II†	*exo*-1-OBs-2-*t* in HOAc–NaOAc, 45°, 24 h	121 300	117 600	38.3	38.0	1.3	1.3	40.1	40.0	20.2	20.7
III†	*exo*-1-OAc-2-*t* in HOAc–NaOAc, 25°, 24 h	157 600	150 400	96.0	96.5	1.0	1.1	2.2	1.7	0.8	0.7
IV	*exo*-1-OAc-2-*t* in HOAc–NaOAc, reflux, 20 h	116 600	109 100	90.7	90.5	4.8	4.1	3.2	3.9	1.3	1.4
V	*endo*-1-OBs-2-*t* in HOAc–NaOAc, 30°, 64 days	141 300	135 800	41.4	42.5	6.3	4.7	32.8	32.8	19.5	20.0
VI	*endo*-1-OBs-2-*t* in HOAc–NaOAc 30°, 2 days	214 100	198 500	54.0	54.0	1.0	0.2	25.0	26.0	20.0	19.8
VII	Norbornene in HOAc-*O*-*t* – NaOAc reflux, 20 h	7 710	7 740	5.6	2.2	51.8	56.3	27.8	23.8	14.8	17.7

*The *exo*-1-OH-*x*-*t* was derived from the corresponding *exo*-1-OAc-*x*-*t* and was assayed as the α-naphthylurethan; it contained 100% of the *t*-activity.
†Data from ref. 3.

TABLE 2

Data from the treatment of norbornene with excess HOAc-*O-t* in the presence of NaOAc

Reactants used				*exo*-2-Norbornyl acetate					
HOAc-*O-t*				Carrier added (mmole)		Specific activity (c.p.m./mmole)		Yield (%)†	
Volume (ml)*	Specific activity (c.p.m./mmole)	Norbornene (mmole)	NaOAc (mmole)	Run 1	Run 2	Run 1	Run 2	Run 1	Run 2
25	525 300	20	22	19.5	22.0	9 120	13 600	1.7	2.9
30	923 400	20	100	17.5	19.5	23 300‡	33 100‡	2.3	3.6
50	774 400	7.5	270	18.9	24.3	4 070	2 130	1.3	0.9
100	774 400	7.5	1125	18.4	20.0	3 570	3 100	1.1	1.1

*Larger volumes were necessary to bring all reactants into solution in the experiments involving large amounts of NaOAc.
†Calculated from isotopic dilution, an illustration is given in the Experimental.
‡These samples were further diluted and degraded to give the isotopic distributions listed under experiment VII, Table 1.

tion in the reaction mixture to give isotopic scramblings which led to relatively larger amounts of overall rearrangement to C-3.

A possible route for locating the *t*-label at C-3 of the *exo*-**1**-OAc-*x-t* product would be via an elimination–addition process involving the addition of HOAc to the norbornene formed during the acetolysis of the 2-labeled brosylates. This possibility was investigated by a study on the addition of *O*-tritiated HOAc (HOAc-*O-t* from $Ac_2O + H_2O$-*t*) to norbornene in the presence of NaOAc. The results are given in Table 2. It can be seen that using NaOAc:norbornene molar ratios ranging from 1.1 to 150, refluxing in excess HOAc-*O-t* for 20 h resulted in the formation of only about 1–4% *exo*-**1**-OAc-*x-t* based on the norbornene. Since the acetolysis of *exo*-**1**-OBs gave rise to only 4% elimination products consisting of 98% nortricyclene and 2% norbornene (7), and since only 1–4% of the norbornene could be converted to *exo*-**1**-OAc under the acetolysis conditions, addition of HOAc to norbornene likely is not a major pathway responsible for the rearrangement of the label from C-2 to -3 in the acetolysis of *exo*- or *endo*-**1**-OBs-2-*t*.

If no rearrangement occurs in the addition of HOAc-*O-t* to norbornene, the resulting tritiated *exo*-**1**-OAc should have all the *t*-label located at the C-3 position. The two samples of *exo*-**1**-OAc-*x-t* obtained from the treatment of norbornene with the HOAc-*O-t* of highest specific activity (Table 2) were degraded and the isotopic distributions are given in Table 1 as experiment VII. The extensive isotopic scramblings observed in these samples further indicate the great propensity of the 2-norbornyl system to undergo cationic rearrangements, even when the cationoid species were generated from the reaction of norbornene with NaOAc buffered HOAc.

In a study on the π-route to the norbornyl cation from the solvolysis in HOAc–urea of 2-(Δ^3-cyclopentenyl)-2-^{14}C-ethyl *p*-nitrobenzenesulfonate (**2**-ONs-2-^{14}C), the resulting *exo*-**1**-OAc-*x*-^{14}C product was found to have the ^{14}C-label located essentially only at the C-3, -5, and -7 positions (*exo*-**1**-OAc-3,5,7-^{14}C) (8). This observation indicated that in this reaction, the amount of 3,2-hydride shift that took place in the resulting 2-norbornyl cation was negligible (the maximum extent of such 3,2-shifts could be no more than about 0.5%). If the *exo*-**1**-OAc-3,5,7-^{14}C obtained from such a reaction were treated with HOAc–NaOAc and the isotopic distribution in the recovered *exo*-**1**-OAc-*x*-^{14}C was ascertained, the data could provide an unequivocal demonstration that 3,2-shifts have occurred in the recovered acetate. The results from such an experiment, together with the earlier data of Lee and Hahn (8), are given in Table 3. These results clearly confirmed the conclusion that further isotopic scramblings in the initially formed acetolysis product could take place during its subsequent contact with the reaction medium. They also indicated that these further scramblings definitely gave rise to some overall 3,2-shifts, resulting, in the case with *exo*-**1**-OAc-3,5,7-^{14}C, in the rearrangement of some ^{14}C-label from C-3 to -2.

In the studies on internal returns, initially, it was intended to subject *exo*- and *endo*-**1**-OBs-2-*t* to partial acetolysis and then degrade the recovered brosylate to ascertain the nature and extent of the isotopic scrambling that might have resulted from the return processes. This was

Can. J. Chem. Downloaded from www.nrcresearchpress.com by 210.87.254.105 on 09/05/12
For personal use only.

Can. J. Chem. Downloaded from www.nrcresearchpress.com by 210.87.254.105 on 09/05/12
For personal use only.

TABLE 3

^{14}C-Distributions in the *exo*-2-norbornyl-*x*-^{14}C acetate (*exo*-**1**-OAc-*x*-^{14}C) from various experiments

Experiment	Reaction	Specific activity for 100% ^{14}C (c.p.m./mmole)*		^{14}C-Content (%)									
				C-2		C-3		C-1,4		C-7		C-5,6	
		Run 1	Run 2	Run 1	Run 2	Run 1	Run 2	Run 1	Run 2	Run 1	Run 2	Run 1	Run 2
VIII†	**2**-ONs-2-^{14}C in HOAc–urea 60°, 30 h	87 800	98 400	0.0	0.0	27.8	27.9	0.0	0.0	24.1	22.8	48.1	49.3
IX‡	As in VIII	92 800		0.0		27.3		0.0		23.7		49.0	
X	*exo*-**1**-OAc-3,5,7-^{14}C from IX in HOAc–NaOAc 25°, 24 h	153 400	153 800	2.8	1.7	21.5	21.7	1.4	0.9	27.4	28.2	46.9	47.5

*Corresponding to the specific activity of the *cis*-cyclopentane-1,3-dicarboxylic acid derived from the degradation of the *exo*-**1**-OAc-*x*-^{14}C.
†Data from ref. 8.
‡Part of the *exo*-**1**-OAc-3,5,7-^{14}C product was diluted with inactive carrier and then degraded; the remainder was utilized for the two runs in experiment X.

Can. J. Chem. Downloaded from www.nrcresearchpress.com by 210.87.254.105 on 09/05/12
For personal use only.

accomplished with the *endo*-epimer. After acetolysis at 75° for approximately one half-life, the recovered *endo*-brosylate was treated with anhydrous tetramethylammonium acetate in dry acetone to give *exo*-**1**-OAc-2-*t* (3) which on subsequent conversion to norcamphor (3) results in the loss of more than 99% of the *t*-activity. This finding indicated that the recovered brosylate was essentially unrearranged *endo*-**1**-OBs-2-*t*, confirming the conclusion of no rearrangement or racemization due to return to *endo*-brosylate, which was arrived at from the equality of the titrimetric and polarimetric rates for the acetolysis of *endo*-**1**-OBs (9).

Incidentally, in the direct displacement reaction of *endo*-**1**-OBs-2-*t* with $(CH_3)_4NOAc$ in acetone, under strictly anhydrous conditions, it was possible to obtain *exo*-**1**-OAc-2-*t* with about 99.5% of the *t*-label accounted for at C-2 (3). Such samples of *exo*-**1**-OAc-2-*t* were used in experiments III and IV (Table 1), and it could also be converted to *exo*-**1**-OBs-2-*t* and utilized in experiments I and II (Table 1) (3). However, this reaction of *endo*-**1**-OBs-2-*t* with $(CH_3)_4NOAc$ could give rise to samples of *exo*-**1**-OAc-*x*-*t* with varying amounts up to about 10% of the *t*-label rearranged from C-2 to the rest of the norbornyl skeleton. Possibly, failure of maintaining absolutely anhydrous conditions during the reaction could have contributed to the formation of cationic pathways which led to isotopic scrambling (the $(CH_3)_4NOAc$ is extremely hygroscopic and its exposure to the atmosphere such as in weighing may require further drying for several days under vacuum over P_2O_5 before its use). B. L. Murr (private communications) has also noted such scramblings in the reaction between *endo*-**1**-OBs-2-*d* and $(CH_3)_4NOAc$, and he has found that the use of tetrabutylammonium acetate in benzene, instead of $(CH_3)_4NOAc$ in acetone, would eliminate this difficulty.

When *exo*-**1**-OBs-2-*t* was treated with anhydrous $(CH_3)_4NOAc$ in dry acetone, instead of obtaining only the product of direct displacement, *endo*-**1**-OAc-2-*t*, both *exo*- and *endo*-**1**-OAc were produced (about 70% *exo*- and 30% *endo*-), and the *t*-label in this mixed product was found to be extensively scrambled upon degradation. These behaviors are analogous to the observations of Schaefer and Weinberg (10, 11), who noted that the reaction of optically active *endo*-**1**-OH with triphenylphosphine and bromine gave optically active *exo*-**1**-Br via a bimolecular displacement, while the same reaction utilizing optically active *exo*-**1**-OH resulted in the formation of only some optically active *endo*-**1**-Br, the major product being racemic *exo*-**1**-Br (some nortricyclene was also formed). Obviously, any degradation of *exo*-**1**-OBs-*x*-*t* involving treatment with $(CH_3)_4NOAc$ could not give meaningful results.

Closson and coworkers (12) have reported that *exo*-**1**-OTs may be cleaved without rearrangement to give *exo*-**1**-OH by treatment with sodium naphthalene anion radical in tetrahydrofuran solution. When *exo*-**1**-OBs-2-*t* was treated by this method, the resulting *exo*-**1**-OH-*x*-*t* was also found to show extensive isotopic scrambling. Presumably, H–T exchange under these highly basic conditions could have contributed to the apparent lability of the *t*-label. The use of *exo*-**1**-OBs-2-*t* as a substrate thus is unlikely to lead to a successful study on the problem of internal returns. An alternative is to employ ^{14}C-labeled *exo*-**1**-OBs and cleave the recovered brosylate after partial acetolysis by sodium naphthalene. H. L. Goering (private communication) has indicated to us that he is planning to study internal returns in the 2-norbornyl system utilizing ^{14}C as label.

In order to avoid the necessity of degrading the recovered brosylate in the internal return studies, D-labeling and n.m.r. analysis could be employed, although such a method would be of less accuracy than analogous studies utilizing radioactive tracers. Experiments were carried out using *endo*- or *exo*-**1**-OBs-2-*d*, prepared as previously reported (13). After the substrate was acetolyzed in the presence of NaOAc for approximately one half-life, the recovered brosylate was examined by n.m.r. The spectra obtained are shown in Fig. 1. With *endo*-**1**-OBs-2-*d*, the spectra before and after partial acetolysis were essentially identical (Fig. 1*A*). There was no detectable H-absorption for the C-2 proton (4.7 p.p.m. region), indicating no rearrangement due to returns to *endo*-brosylate, in complete accord with the results obtained from studies with *endo*-**1**-OBs-2-*t*.

The *exo*-**1**-OBs-2-*d* employed in the partial acetolysis (Fig. 1*B*) appeared to contain traces of H-absorption at C-2 (4.4 p.p.m. region). After acetolysis at 25° for 100 min, the recovered *exo*-**1**-OBs-*x*-*d* (Fig. 1*C*) definitely showed a

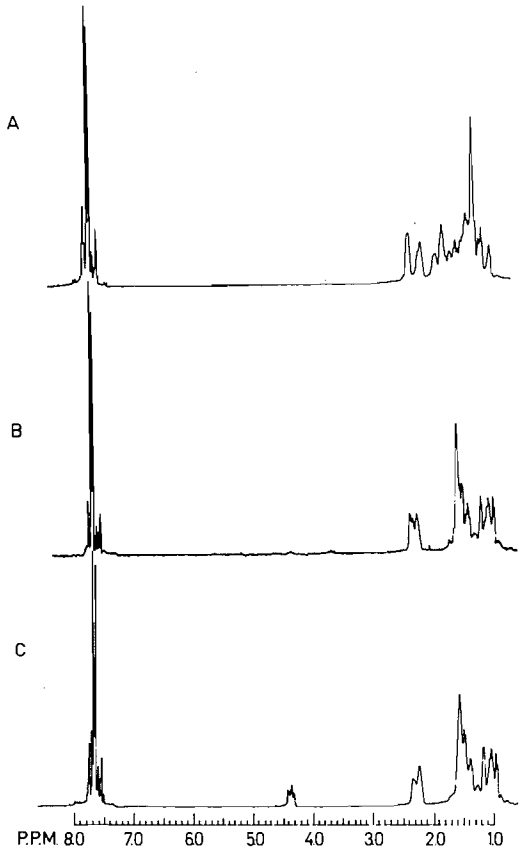

FIG. 1. The n.m.r. spectra. *A*, *endo*-2-Norbornyl-2-*d* brosylate (*endo*-**1**-OBs-2-*d*) before acetolysis and the same compound recovered after partial acetolysis; *B*, *exo*-**1**-OBs-2-*d* before acetolysis; *C*, *exo*-**1**-OBs-*x*-*d* recovered after partial acetolysis of *exo*-**1**-OBs-2-*d*.

significant increase in H-absorption at C-2. This was accompanied by a decrease in absorption for one of the bridge-head protons, the peak at 2.35 p.p.m. has decreased while the one at 2.25 p.p.m. remained essentially unchanged. These findings definitely indicated the scrambling of the D-label from C-2 to -1 in the recovered brosylate. Integration of Fig. 1*C*, using the absorption of the aromatic protons as an internal standard of 4.0 H, gave an estimated D-distribution of 0.4 ± 0.1 D at C-2, 0.4 ± 0.1 D at C-1,4 and 0.3 ± 0.1 D for the rest of the norbornyl skeleton (the integrated H-absorptions in the 0.8–1.8 p.p.m. region having changed from about 8.0 H in Fig. 1*B* to about 7.7 H in Fig. 1*C*). Although the small changes in integrated areas in the 0.8–1.8 p.p.m. region of Fig. 1*B* and *C* do not constitute a conclusive proof of 6,2-shifts, the probable presence of some D-label at C-3,5–7 does tend to suggest that scrambling of the D-label from C-2 to -6, as well as to C-1, has occurred as a result of internal returns during the acetolysis of *exo*-**1**-OBs-2-*d*.

From the above results, it is apparent that in the acetolysis of *exo*-**1**-OBs as commonly carried out in HOAc–NaOAc, isotopic scramblings could occur not only in the solvolysis reaction itself, but also prior to the reaction due to internal returns that gave rise to scrambled *exo*-**1**-OBs, and subsequent to the reaction due to ionization in the reaction medium of the initially formed product. Detailed quantitative analysis of the overall isotopic distributions obtained from labeled substrates would thus be fairly complicated. In interpreting such results, Roberts and coworkers (1, 2), and Lee and Lam (3) have used a qualitative approach. In treating the results such as those from experiments I and II (Table 1), Lee and Lam (3) have partitioned the overall *t*-distribution into contributions from processes in which C-1 and -2 are equivalent (Wagner–Meerwein shift), C-1, -2, and -6 are equivalent (Wagner–Meerwein and 6,2-shifts), and all carbon positions are equivalent (Wagner–Meerwein, 6,2- and 3,2-shifts). From more quantitative analyses of the data, such as by the elegant method of Collins and Lietzke (14), rate ratios for cation–anion collapse to 6,2- or 3,2-shifts (k_s/k_6 or k_s/k_3) could be evaluated. In this treatment, however, no provision was made for the possibility of further scrambling of the initial product in the solvolysis medium. When the reaction conditions are more likely to lead to kinetic control, such as in the π-route formation of the norbornyl cation from solvolysis of **2**-ONs-2-^{14}C in HOAc–urea or H_2O–acetone–$NaHCO_3$ (8), essentially no 3,2-shift was detected, and treatment of the scrambling data using the method of Collins and Lietzke (14) has led to the conclusion that both the norbornonium ion (corner-protonated nortricyclene) (**3**) and edge-protonated nortricyclene (**4**) are involved in product formation, and that ion **3** is the more stable of the two species.

Goering and Schewene (15) have studied the energy difference between the classical and non-classical norbornyl cations by investigating the $HClO_4$-catalyzed ionization of *exo*-**1**-OAc in HOAc. In the present work, isotopic scramblings have been found in the labeled *exo*-**1**-OAc even in NaOAc buffered HOAc (experiments III and

Can. J. Chem. Downloaded from www.nrcresearchpress.com by 210.87.254.105 on 09/05/12
For personal use only.

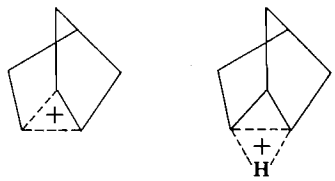

3 4

IV, Table 1). Data from such studies indicated that proportionally an extraordinarily large amount of net rearrangement from C-2 to -3 has occurred. In interpreting these results, even a qualitative partitioning into different contributing processes is not possible because all the apparent 3,2-shifts did not lead to all carbon positions becoming equivalent. In these cases, it appears that the process responsible for the rearrangement of the label from C-2 to -3 may be faster than other scrambling processes such as Wagner–Meerwein and 6,2-shifts. On the other hand, the formolysis of *exo*-**1**-OBs-2-*t* at 25° has been found to give a net rearrangement of about 6% of the label from C-2 to -3 (16). The overall *t*-distribution in the product from this formolysis reaction, however, could be rationalized qualitatively by the different contributing processes, with the assumption that 3,2-shifts together with Wagner–Meerwein and 6,2-shifts would result in the complete equivalence of all carbon positions. This apparent difference in the interpretation of the effects of 3,2-shifts in the formolysis of *exo*-**1**-OBs-2-*t* and in the reaction of *exo*-**1**-OAc-2-*t* in HOAc–NaOAc would appear to require some explanation. In this regard, it is pertinent to consider some spectroscopic data from the literature.

From the examination of the n.m.r. spectra of *exo*-**1**-OH in F_3CCOOH–H_2SO_4 under various conditions, with the amount of H_2SO_4 ranging from 5–60% and the temperature ranging from 0–40°, Fraenkel and coworkers (17) have concluded that under these conditions, 3,2- and 6,2-hydride shifts take place faster than Wagner–Meerwein rearrangements. Thus it appears that there could be some similarities in the processes of scrambling in the reaction of *exo*-**1**-OAc in HOAc–NaOAc and in the treatment of *exo*-**1**-OH in F_3CCOOH–H_2SO_4. In sharp contrast to the findings of Fraenkel and coworkers (17), the norbornyl cation generated in "super acid" by Schleyer and coworkers (18, 19) behaved quite differently. At temperatures between −5 and +37°, a one-peak n.m.r. spectrum was observed, indicating the equivalence of all protons on the n.m.r. time scale. When the temperature was lowered to −60°, the 3,2-hydride shift could be "frozen out", and it was estimated that at −120°, the 3,2-shift was slower than the 6,2-shift and the Wagner–Meerwein rearrangement by a minimum factor of $10^{8.8}$ (however, *cf.* ref. 20).

From considerations of data from Raman spectroscopy, ^{13}C n.m.r. and ^{1}H n.m.r. at very low temperatures down to −156°, Olah and coworkers (21–23) have recently concluded that the stable norbornyl cation is the nonclassical norbornonium ion or corner-protonated nortricyclene **3**, with its geometry corresponding to that of nortricyclene rather than that of norbornane. The 6,2,1-hydrogen migrations about the cyclopropane ring would, therefore, involve little if any change in the carbon skeleton of **3**. On the other hand, the 3,2-shift would require a lengthening of the 6,2 C—C bond distance in the transition state, resulting in a higher activation energy and a loss of σ-delocalization energy. It was further suggested that in the limiting case, when all the delocalization energy is lost prior to the transition state for the 3,2-shift, the classical ion could be considered an intermediate. In the formolysis of *exo*-**1**-OBs-2-*t* at 25° (16), subsequent ionization of the formate product probably contributed to some extent to the observed 6% overall 3,2-shifts. However, formolysis is likely to follow a **Lim** solvolysis mechanism (24, 25), involving relatively extensive dissociation and a long lifetime for the carbonium ion. Analogous to the behavior in super acid at room temperature, any 3,2-shift together with the 6,2,1-shifts would render all carbon positions equivalent. In the reaction of *exo*-**1**-OAc in HOAc–NaOAc, which involves a poor leaving group in a buffered medium, the degree of dissociation is likely not very extensive. Tight ion-pairs may be produced with the cationoid species retaining the norbornane geometry. 3,2-Shifts may occur at the ion-pair stage. Since *endo–endo* 3,2-hydride shifts are very unlikely (26–28), the process would involve *exo–exo* 3,2-shifts with the hydrogen migration occurring on the same side as the acetate group. Professor P. v. R. Schleyer has suggested to us that by hydrogen bonding-type of solvation, *exo–exo* 3,2-hydride shifts at the ion-pair stage may be facilitated. The mechanism of such a *cis*-shift would be analogous to that

Can. J. Chem. Downloaded from www.nrcresearchpress.com by 210.87.254.105 on 09/05/12
For personal use only.

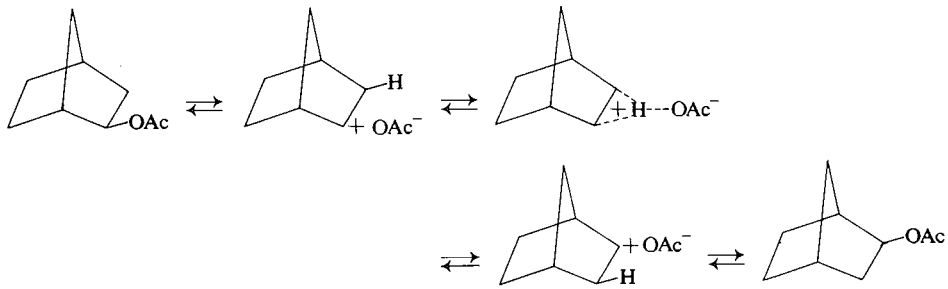

SCHEME 1

proposed by Cram and Tadanier (29) in their interpretation of the stereochemistry of hydrogen participation in the solvolysis of the tosylates of the diastereomeric 3-cyclohexyl-2-butanols. The processes involved may be depicted by Scheme 1.

Finally, with regard to isotopic scramblings accompanying internal returns, the present studies indicated the probable rearrangement of the label from C-2 to both C-1 and -6. This finding could be explained by a mechanism involving 6,2,1-hydrogen shifts in the nonclassical ion **3** before return to covalent brosylate. An alternative or concurrent mechanism could involve returns to brosylate from both **3** and **4**, and such a mechanism would also suggest the competitive formation of **3** and **4** from *exo*-**1**-OBs. The possibility of competitive formations of two ions in the acetolysis of *exo*-**1**-OBs may be of some mechanistic significance. Recently, Lee and Hahn (30) have shown that in the acetolysis of 2-labeled *exo*-dehydro-2-norbornyl brosylate, the different results on the extent of isotopic scrambling previously reported by two groups of workers (31, 32) are both correct, the difference being attributable to a temperature effect due to the competitive formation of two intermediate ions. It is of interest to note that in experiments I and II (Table 1), significant differences in the *t*-distributions in the products were found for the acetolysis of *exo*-**1**-OBs-2-*t* carried out at 25 and 45°. Comparing the data from the two temperatures, it appears that the acetolysis at 25° resulted in more rearrangement of the label to C-5,6 and less to C-1,4,7, while at 45°, there was more rearrangement to C-1,4,7 and less to C-5,6. When these data were first reported (3), no explanation for these differences was offered. With the precedent established on the effects of temperature in the *exo*-dehydro-2-norbornyl system (30), and in view of the possibility of competitive formations of **3** and **4**, there is the possibility that in the acetolysis of *exo*-**1**-OBs, at lower temperatures, more product is formed from edge-protonated nortricyclene **4**, while at higher temperatures, more product is produced from the more stable ion **3**. Further studies to clarify or confirm these suggestions regarding competitive reactions and temperature effects in the 2-norbornyl system would appear to be worthwhile.

Experimental

*Acetolysis of endo-**1**-OBs-2-t and Treatment of Labeled exo-**1**-OAc in HOAc–NaOAc*

The methods for the preparation of *endo*-**1**-OBs-2-*t* and *exo*-**1**-OAc-2-*t* and for the degradation of the *exo*-**1**-OAc-*x*-*t* product from the various experiments are the same as those previously described by Lee and Lam (3). The treatment of *exo*-**1**-OAc-2-*t* in HOAc–NaOAc and the acetolysis of *endo*-**1**-OBs-2-*t* (experiments IV–VI, Table 1) also followed the procedures of Lee and Lam (3) except for the changes in reaction temperature and reaction time as given in Table 1.

The acetolysis of **2**-ONs-2-^{14}C in HOAc–urea (experiment IX, Table 3) and the degradation of the acetate product to establish the ^{14}C-distribution followed the same procedures described by Lee and Hahn (8). The treatment of *exo*-**1**-OAc-3,5,7-^{14}C in HOAc–NaOAc (experiment X, Table 3) was carried out under the same conditions used by Lee and Lam for experiment III (3).

Addition of HOAc-O-t to Norbornene

HOAc-*O*-*t* was prepared by the dropwise addition of a slight excess of Ac_2O to H_2O-*t* followed by refluxing the resulting material for 2 h. The HOAc-*O*-*t*, b.p. 118–119°, was recovered by fractional distillation in the presence of about 1% $KMnO_4$.

In a typical experiment, 1.88 g (20 mmole) of norbornene and 1.80 g (22 mmole) of NaOAc were dissolved in 25 ml of HOAc-*O*-*t* and the resulting material was refluxed for 20 h. Periodically during the refluxing, the small amount of norbornene that had collected on the condenser was rinsed down with some of the reaction mixture. At the end of the 20 h, cracked ice was introduced and a known weight of inactive *exo*-**1**-OAc was added as carrier. Most of the HOAc-*O*-*t* was then removed by fractionation and the residue was extracted several times

Can. J. Chem. Downloaded from www.nrcresearchpress.com by 210.87.254.105 on 09/05/12
For personal use only.

Can. J. Chem. Downloaded from www.nrcresearchpress.com by 210.87.254.105 on 09/05/12
For personal use only.

with 25-ml portions of petroleum ether. The combined extract was washed successively with water, 10% K_2CO_3 solution, and again water. After drying over $MgSO_4$, the solution was concentrated using a rotatory evaporator. From the residue, pure *exo*-**1**-OAc-*x*-*t* was recovered by preparative v.p.c. (3/8 in. copper column packed with 25% Carbowax 20M on Chromosorb P, operating at 150°).

As an illustration of the isotope dilution calculations, for the experiment described above, the specific activity of the HOAc-*O*-*t* was 525,300 c.p.m./mmole; the amount of *exo*-**1**-OAc carrier added was 19.5 mmole; and the specific activity of the recovered *exo*-**1**-OAc-*x*-*t* was 9120 c.p.m./mmole. If *x* mmole of active *exo*-**1**-OAc was formed before its dilution by the inactive carrier, then

$$525\,300\,x = (x + 19.5)9120$$

$$x = 0.34 \text{ mmole}$$

The yield was $(0.34/20) \times 100 = 1.7\%$.

Internal Return Studies

The *endo*- and *exo*-**1**-OBs-2-*d* were prepared as described by Lee and Wong (13).

The *endo*-**1**-OBs-2-*d* (3.0 g, 9 mmole), in 30 ml of HOAc containing NaOAc (0.82 g, 10 mmole), was heated at 75° for 60 min (approximately one half-life estimated from the rate of solvolysis (9) of *endo*-**1**-OBs in HOAc–KOAc). The resulting material was poured into ice–water and extracted with ether. The extract was washed with water and $NaHCO_3$ solution, dried over $MgSO_4$ and concentrated by the removal of practically all of the ether. From the residue, about 1.0 g of brosylate was recovered upon crystallization from ether – petroleum ether.

The *exo*-**1**-OBs-2-*d* (3.0 g) was also subjected to partial acetolysis and about 1.0 g of brosylate was recovered as described above for the *endo*-epimer except that the temperature used was 25° and the reaction time was 100 min (approximately one half-life estimated from the rate of solvolysis (5) of *exo*-**1**-OBs in HOAc–KOAc).

The n.m.r. spectra of the various samples of deuterated *endo*- and *exo*-**1**-OBs were determined in CCl_4 solution using an HA100 spectrometer.

The financial support given by the National Research Council of Canada is gratefully acknowledged.

1. J. D. Roberts and C. C. Lee. J. Amer. Chem. Soc. **73**, 5009 (1951).
2. J. D. Roberts, C. C. Lee, and W. H. Saunders, Jr. J. Amer. Chem. Soc. **76**, 4501 (1954).
3. C. C. Lee and L. K. M. Lam. J. Amer. Chem. Soc. **88**, 2831 (1966).
4. C. C. Lee, B.-S. Hahn, and L. K. M. Lam. Tetrahedron Lett. 3049 (1969).
5. S. Winstein and D. Trifan. J. Amer. Chem. Soc. **74**, 1154 (1952).
6. S. Winstein and K. C. Schreiber. J. Amer. Chem. Soc. **74**, 2165 (1952).
7. S. Winstein, E. Clippinger, R. Howe, and E. Vogelfanger. J. Amer. Chem. Soc. **87**, 376 (1965).
8. C. C. Lee and B.-S. Hahn. J. Amer. Chem. Soc. **91**, 6420 (1969).
9. S. Winstein and D. Trifan. J. Amer. Chem. Soc. **74**, 1147 (1952).
10. J. P. Schaefer and D. S. Weinberg. J. Org. Chem. **30**, 2635 (1965).
11. J. P. Schaefer and D. S. Weinberg. J. Org. Chem. **30**, 2639 (1965).
12. W. D. Closson, P. Wriede, and S. Bank. J. Amer. Chem. Soc. **88**, 1581 (1966).
13. C. C. Lee and E. W. C. Wong. J. Amer. Chem. Soc. **86**, 2752 (1964).
14. C. J. Collins and M. H. Lietzke. J. Amer. Chem. Soc. **89**, 6565 (1967).
15. H. L. Goering and C. B. Schewene. J. Amer. Chem. Soc. **87**, 3516 (1965).
16. C. C. Lee and L. K. M. Lam. J. Amer. Chem. Soc. **88**, 5355 (1966).
17. G. Fraenkel, P. D. Ralph, and J. P. Kim. Can. J. Chem. **43**, 674 (1965).
18. P. v. R. Schleyer, W. E. Watts, R. C. Fort, Jr., M. B. Comisarow, and G. A. Olah. J. Amer. Chem. Soc. **86**, 5679 (1964).
19. M. Saunders, P. v. R. Schleyer, and G. A. Olah. J. Amer. Chem. Soc. **86**, 5680 (1964).
20. C. J. Collins and C. E. Harding. J. Amer. Chem. Soc. **91**, 7194 (1969).
21. G. A. Olah, A. Commeyras, and C. Y. Lui. J. Amer. Chem. Soc. **90**, 3882 (1968).
22. G. A. Olah and A. M. White. J. Amer. Chem. Soc. **91**, 3954 (1969).
23. G. A. Olah and A. M. White. J. Amer. Chem. Soc. **91**, 3956 (1969).
24. S. Winstein, E. Grunwald, and H. W. Jones. J. Amer. Chem. Soc. **73**, 2700 (1951).
25. S. Winstein and H. Marshall. J. Amer. Chem. Soc. **74**, 1120 (1952).
26. P. v. R. Schleyer. J. Amer. Chem. Soc. **89**, 699 (1967).
27. G. E. Gream. Rev. Pure Appl. Chem. **16**, 25 (1966).
28. J. L. Fry and G. J. Karabatsos. *In* Carbonium ions. Vol. II. G. A. Olah and P. v. R. Schleyer, *editors*. Interscience Publishers, New York, 1970. Pp. 521–571.
29. D. J. Cram and J. Tadanier. J. Amer. Chem. Soc. **81**, 2737 (1959).
30. C. C. Lee and B.-S. Hahn. J. Amer. Chem. Soc. **92**, 2583 (1970).
31. J. D. Roberts, C. C. Lee, and W. H. Saunders, Jr. J. Amer. Chem. Soc. **77**, 3034 (1955).
32. S. J. Cristol, T. C. Morrill, and R. A. Sanchez. J. Amer. Chem. Soc. **88**, 3087 (1966).

Can. J. Chem. Downloaded from www.nrcresearchpress.com by 210.87.254.6 on 09/05/12
For personal use only.

Mesquite gum. I. The 4-*O*-methylglucuronogalactan core

G. O. ASPINALL AND C. C. WHITEHEAD
Department of Chemistry, Trent University, Peterborough, Ontario, Canada
AND
Department of Chemistry, University of Edinburgh, Edinburgh, Scotland

Received July 6, 1970

A re-examination of mesquite gum has shown that partial hydrolysis of the gum furnishes a mixture of acidic oligosaccharides including 6-*O*-(4-*O*-methyl-β-D-glucopyranosyluronic acid)-D-galactose (**1**), 4-*O*-(4-*O*-methyl-α-D-glucopyranosyluronic acid)-D-galactose (**2**), 6-*O*-(β-D-glucopyranosyluronic acid)-D-galactose (**3**), *O*-(4-*O*-methyl-β-D-glucopyranosyluronic acid)-(1→6)-*O*-β-D-galactopyranosyl-(1→6)-D-galactose (**4**), and *O*-(4-*O*-methyl-α-D-glucopyranosyluronic acid)-(1→4)-*O*-β-D-galactopyranosyl-(1→3)-D-galactose (**5**). A series of degradations of the gum affords successively, arabinose-free degraded gum A, carboxy-reduced degraded gum A, and degraded gums B and C. Degraded gum C contains a high proportion of 1→3′ linked β-D-galactopyranose residues. The structure of the 4-*O*-methylglucuronogalactan core of the gum is re-assessed in the light of these and other results.

Canadian Journal of Chemistry, **48**, 3840 (1970)

Earlier investigations by White (1–4) and by Smith and his collaborators (5–7) showed that mesquite gum, the exudate from *Prosopsis juliflora*, is a highly branched polysaccharide with residues of L-arabinose, D-galactose, and 4-*O*-methyl-D-glucuronic acid. Some of the main structural features of the gum were established by both workers but differences in the modes of linkage of D-glucuronic acid (or its 4-methyl ether) to D-galactose residues were reported. Cuneen and Smith (5) isolated on partial acid hydrolysis of the gum a mixture of monomethyl derivatives of the aldobiouronic acids, 4-*O*- and 6-*O*-(D-glucopyranosyluronic acid)-D-galactoses. The second aldobiouronic acid was later shown to be 6-*O*-(4-*O*-methyl-β-D-glucopyranosyluronic acid)-D-galactose (7). In contrast, White (3) isolated from the methylated gum a partially methylated aldobiouronic acid for which the structure, 3-*O*-(2,3,4-tri-*O*-methyl-D-glucopyranosyluronic acid)-2,4-di-*O*-methyl-D-galactose, was assigned. The present investigation was undertaken to re-examine the linkages in these oligosaccharides and to ascertain the distribution of the 1→3′ and 1→6′ linkages between D-galactopyranose residues in the interior chains of the gum. The degradations performed on mesquite gum are summarized in the flow sheet labelled Scheme 1.

The purified gum acid, which was obtained by precipitation from an acidified solution of the gum, was shown to be chemically homogeneous within acceptable limits by chromatography on diethylaminoethylcellulose (8). Partial acid

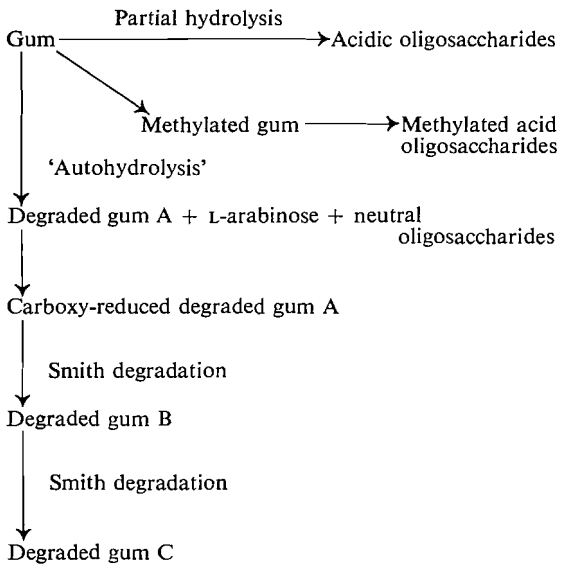

SCHEME 1

hydrolysis of the gum gave a series of acidic oligosaccharides which were separated by chromatography on diethylaminoethyl–Sephadex, followed by filter sheet chromatography, to give five acidic oligosaccharides (**1–5**) and three fractions containing mixtures of higher oligosaccharides. Oligosaccharide **1** was identified as the previously characterized 6-*O*-(4-*O*-methyl-β-D-glucopyranosyluronic acid)-D-galactose. The structure of oligosaccharide **2** was established as 4-*O*-(4-*O*-methyl-α-D-glucopyranosyluronic acid)-D-galactose by methylation analysis, and the configuration of the glycosidic linkage was

Can. J. Chem. Downloaded from www.nrcresearchpress.com by 210.87.254.6 on 09/05/12
For personal use only.

assigned on the basis of the observed specific rotation ($[\alpha]_D$ +94°) and by the presence of a doublet (τ 4.84; J = 3 Hz) in the n.m.r. spectrum of the disaccharide glycitol which was characteristic of an α-D-glycoside (9). Oligosaccharide **3**, which was isolated only in small amounts, was characterized as 6-*O*-(β-D-glucopyranosyluronic acid)-D-galactose by methylation analysis and by conversion into a crystalline derivative.

Oligosaccharides **4** and **5** were not isolated in sufficient quantity to permit the formation of crystalline derivatives. Their structures were established on the basis of their specific rotations, by paper chromatography of various transformation products, and by gas chromatography of fragments formed from the methylated trisaccharides and methylated modified derivatives. The structure, *O*-(4-*O*-methyl-β-D-glucopyranosyluronic acid)-(1→6)-*O*-β-D-galactopyranosyl-(1→6)-D-galactose, was assigned to oligosaccharide **4** on the basis of the following observations: (*i*) partial hydrolysis gave oligosaccharide **1**; (*ii*) partial hydrolysis of the carboxy-reduced trisaccharide glycoside afforded a disaccharide which was indistinguishable from 6-*O*-β-D-galactopyranosyl-D-galactose and whose structure was confirmed by methylation analysis; (*iii*) g.l.c. showed that methanolysis of the methylated trisaccharide furnished methyl glycosides of 2,3,4-tri-*O*-methylglucuronic acid, and 2,3,4- and 2,3,5-tri-*O*-methylgalactose,[1] whilst methanolysis of the methylated trisaccharide glycitol gave methyl glycosides of 2,3,4-tri-*O*-methylglucuronic acid and 2,3,4-tri-*O*-methylgalactose, together with 1,2,3,4,5-penta-*O*-methylgalactitol. The following observations permitted the assignment of the structure, *O*-(4-*O*-methyl-α-D-glucopyranosyluronic acid)-(1→4)-*O*-β-D-galactopyranosyl-(1→3)-D-galactose, for oligosaccharide **5**: (*i*) partial hydrolysis gave oligosaccharide **2**; (*ii*) methanolysis of the methylated trisaccharide gave methyl glycosides of 2,3,4-tri-*O*-methylglucuronic acid, and 2,3,6- and 2,4,6-tri-*O*-methylgalactose; (*iii*) the presence of a 3-*O*-substituted reducing galactose residue was established by conversion of the trisaccharide into methyl furanosides which were selectively oxidized with sodium periodate and reduced with sodium borohydride to give 3-*O*-substituted arabinofuranose units whose presence was detected by methylation analysis; (*iv*) the presence of the 3-*O*-substituted reducing galactose residue was further indicated by controlled oxidation of the trisaccharide with lead tetraacetate to give an alkali-stable 2-*O*-substituted lyxose residue.

4-Me-β-D-G*p*A-(1→6)-D-Gal (**1**)
4-Me-α-D-G*p*A-(1→4)-D-Gal (**2**)
β-D-G*p*A-(1→6)-D-Gal (**3**)
4-Me-β-D-G*p*A-(1→6)-β-D-Gal*p*-(1→6)-D-Gal (**4**)
4-Me-α-D-G*p*A-(1→4)-β-D-Gal*p*-(1→3)-D-Gal (**5**)

The three higher acidic oligosaccharide fractions were chromatographically homogeneous, but further examination of the fractions indicated that each contained a mixture of components. Although the separation of individual oligosaccharides was not feasible, some structural information was obtained by methylation analysis of the oligosaccharides, the oligosaccharide glycitols, and the products of alkaline degradation. For example, extended treatment of oligosaccharide fraction 7 with oxygen-free lime-water resulted in the disappearance of galactopyranose end groups, branch points, and 3-*O*-substituted galactose residues. This observation is consistent with the transformation of oligosaccharides (such as **6**), which contain 1→3′ linked galactose residues in chains interior to units of aldobiouronic acids (**1** or **3**), to *O*-glycosyl metasaccharinic acids (**7**) (see Scheme 2).

Since these experimental results failed to provide evidence for the formation of an oligosaccharide containing a 3-*O*-(D-glycopyranosyluronic acid)-D-galactose linkage, a sample of methylated mesquite gum was prepared for depolymerization under the conditions used earlier by White (3). An exhaustive series of fractionations was carried out on the products of methanolysis (see Experimental section), but no indication was obtained for the formation of the partially methylated aldobiouronic acid, 3-*O*-(2,3,4-tri-*O*-methyl-D-glucopyranosyluronic acid)-2,4-di-*O*-methyl-D-galactose, nor could a crystalline derivative of the type reported by White (3) be isolated. The presence of fully or partially etherified derivatives (**8**–**11**) of aldobiouronic acids **1** and **2** was clearly indicated. In so far as residues of 3-*O*-substituted 2,4-di-*O*-methyl-D-galactose were present in oligosaccharides formed on methanolysis of methylated mesquite gum they were constituents either of

[1]Where sites of substitution permit, methylation of reducing galactose and arabinose residues in *N*,*N*-dimethylformamide (10) gives rise to both pyranose and furanose derivatives.

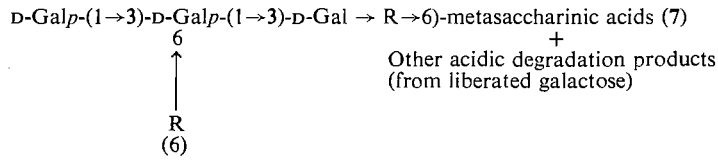

R = 4-Me-β-D-GpA-(1→6)-D-Galp-(1- or β-D-GpA)-(1→6)-D-Galp-(1-

SCHEME 2

partially etherified neutral oligosaccharides, *e.g.* derivatives of 3-*O*-D-galactopyranosyl-D-galactose, or of higher acidic oligosaccharides such as oligosaccharide **5**. We conclude therefore that the linkages of D-glucuronic acid (or the 4-methyl ether) to D-galactose residues are of two types only, namely β-D-(1→6′) and α-D-(1→4′), and that those of the 1→3′ type reported by White (3) were based on valid conclusions from the incomplete data obtained by the techniques then available.

2,3,4-Me_3-α-D-GpA-(1→4)-2,3,6-Me_3-D-Gal (**8**)
2,3,4-Me_3-β-D-GpA-(1→6)-2,3,4-Me_3-D-Gal (**9**)
2,3,4-Me_3-β-D-GpA-(1→6)-2,4-Me_2-D-Gal (**10**)
2,3,4-Me_3-β-D-GpA-(1→6)-2-Me-D-Gal (**11**)

The mixtures of methyl glycosides of methylated sugars formed on methanolysis of methylated mesquite gum and of the reduced methylated gum were examined by gas chromatography (Table 1). The identities of the more fully substituted derivatives of arabinose and galactose were confirmed by g.l.c. of the corresponding methylated aldonolactones. The results confirm and extend earlier observations by White (1) and Cuneen and Smith (6) who identified 2,3,5-tri- and 3,5-di-*O*-methyl-L-arabinose, 2,4-di-*O*-methyl-D-galactose, and 2,3,4-tri-*O*-methyl-D-glucuronic acid as cleavage products from the methylated gum. In addition, 2,5-di-*O*-methylarabinose together with smaller amounts of 2,3,4-tri-*O*-methylrhamnose, 2,3-di-*O*-methylarabinose, 2,3,4,6-tetra-, 2,3,4-tri-, and 2,3,6-tri-*O*-methylgalactose, and 2,3-di-*O*-methylglucuronic acid have now been shown to be present. 2-*O*-Methyl-D-galactose was recognized as a further constituent of the gum by examination of hydrolysis products, but the structural significance of this sugar must be regarded as unproven since the axial 4-hydroxyl group of 3-*O*-substituted D-galactose residues is known to be difficult to methylate. No monomethyl ethers of arabinose could be detected amongst the cleavage products from the methylated gum and no evidence for branching through residues of this sugar has been obtained. The recognition of variously substituted arabinose residues in the gum prompted an examination of oligosaccharides formed on controlled hydrolysis of the gum and these experiments are reported in the following paper (11). The formation of acidic oligosaccharide **3** on partial hydrolysis of the gum, taken together with the detection of 2,3-di-*O*-methylglucuronic acid and 2,3,4-tri-*O*-methylrhamnose as minor products from the methylated gum indicates the presence of a small proportion of unmethylated D-glucuronic acid residues and suggests that these units may be 4-*O*-substituted by (presumably L-) rhamnose residues as in gum arabic (12) and *Araucaria bidwillii* gum (13).

Mesquite gum, like many other exudate gums (14, 15), may be degraded by controlled acid hydrolysis to give a degraded polysaccharide essentially devoid of arabinose residues. Autohydrolysis of gum acid afforded degraded gum A. A sample of degraded gum A was methylated and the cleavage products from the methylated degraded gum (Table 1) were examined by gas chromatography of the methyl glycosides formed on methanolysis. The highly branched nature of the interior portion of the gum was clearly shown

TABLE 1

Methanolysis products from methylated gum and methylated degraded gum A

Methyl glycosides	Methylated gum*	Methylated degraded gum A*
2,3,4-Me_3 Rhamnose	+	tr
2,3,5-Me_3 Arabinose	+ + +	tr
2,3-Me_2 Arabinose	+	n.d.
2,5-Me_2 Arabinose	+ +	tr
3,5-Me_2 Arabinose	+ + + +	tr
2,3,4-Me_3 Glucuronic acid	+ + +	+ + +
2,3-Me_2 Glucuronic acid	+	n.d.
2,3,4,6-Me_4 Galactose	+	+ +
2,3,4-Me_3 Galactose	+	+ + +
2,3,6-Me_3 Galactose	+	+
2,4,6-Me_3 Galactose	n.d.	+
2,4-Me_2 Galactose	+ + + +	+ + +

*tr = trace; n.d. = not detected.

Can. J. Chem. Downloaded from www.nrcresearchpress.com by 210.87.254.6 on 09/05/12
For personal use only.

Can. J. Chem. Downloaded from www.nrcresearchpress.com by 210.87.254.6 on 09/05/12
For personal use only.

with residues of glucuronic acid (or the 4-methyl ether) as end groups. Galactose residues, with the exception of those which were 4-*O*-substituted by 4-*O*-methylglucuronic acid residues as in the aldobiouronic acid (**2**), were mutually joined by 1→3′ and/or 1→6′ linkages. Comparison of the cleavage products from methylated mesquite and from the methylated degraded gum indicated that the dominant site of attachment of arabinose-containing side-chains was by 1→3′ linkages to 6-*O*-substituted galactose residues as in the partial structure (**12**).

. . .6)-β-D-Gal*p*-(1. . . **12**, where R = [L-Ara*f*]$_n$. . .)
3
↑
R

In order to obtain information on the distribution of 1→6′ and 1→3′ linkages between galactose residues in the interior chains of the gum, degraded gum A was converted into the carboxy-reduced derivative (16), which was degraded by Smith's procedure (17) of sequential periodate oxidation, borohydride reduction, and mild acid hydrolysis, to give degraded gum B. Degraded gum B similarly afforded degraded gum C. Degraded gums B and C were examined by (*a*) paper chromatography of oligosaccharides formed on partial acid hydrolysis, (*b*) analysis of reagent consumed during periodate oxidation, and (*c*) gas chromatography of the methyl glycosides of methylated sugars formed on methanolysis of the methylated derivatives (Table 2). The results clearly indicated that the sequence of reactions had resulted in removal of most of the outer chains and that degraded gum C approximated to a linear 1→3′ linked β-D-galactan. Degraded gum C, however, still contains one branch point per 10–12 residues. It is probable, therefore, that the interior chains of the galactan framework of mesquite gum which still remain in degraded gum C, like those in the interior chains of gum arabic (18) and other *Acacia* gums (19, 20), are of the ramified type (as in **13**) rather than consisting of a single 1→3′ linked chain with comb-like branches (as in **14**). Evidence from the specific rotations of the degraded polysaccharides and of oligosaccharides formed in small amount on autohydrolysis of the gum (11) suggests that all the galactose residues, whether in 1→3′ or 1→6′ linkages, have the β-D-configuration.

TABLE 2

Relative proportions of methanolysis products from methylated degraded gums B and C

Methyl glycosides	Gum B	Gum C
2,3,4,6-Me_4 Galactose	1.5	1.5
2,3,4-Me_3 Galactose	1	0.5
2,4,6-Me_3 Galactose	4	15
2,4-Me_2 Galactose	1	1.8

Residues of 4-*O*-methyl-D-glucuronic acid (and presumably also of the small proportion of D-glucuronic acid) terminate outer chains in degraded gum A. Acidic oligosaccharides **1**, **4**, and probably **3**, presumably arise from the extremities of chains of 1→6′ linked β-D-galactopyranose residues. This type of linkage has been recognized in a number of other polysaccharides of the same general type (15). On the other hand, although some of these polysac-

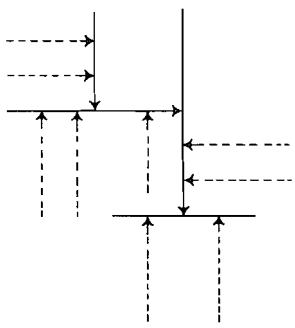

(13)

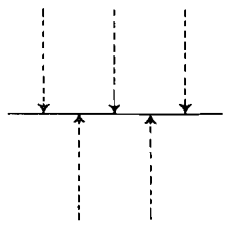

(14)

——— chains of 1→3′ linked β-D-galactopyranose units
- - - - - - - - - chains of 1→6′ linked β-D-galactopyranose units
→ 1→6′ linkages at branch points

Can. J. Chem. Downloaded from www.nrcresearchpress.com by 210.87.254.6 on 09/05/12
For personal use only.

charides also give rise on partial hydrolysis to the aldobiouronic acid (**2**), such units have not been placed within the overall molecular architecture. In mesquite gum, two observations, (*i*) the characterization of the trisaccharide (**5**) and (*ii*) the isolation of the fully etherified aldobiouronic acid (**8**) from the methylated gum, indicate that units of the aldobiouronic acid themselves carry no side-chains and that they are joined to the next D-galactose residues by 1→3′ linkages. Since virtually all the 3-*O*-substituted galactose residues in the gum are also 6-*O*-substituted, it is probable that units of the aldobiouronic acid (**2**) are attached as side-chains to the exterior chains of 1→6′ linked galactose residues as in the partial structure (**15**).

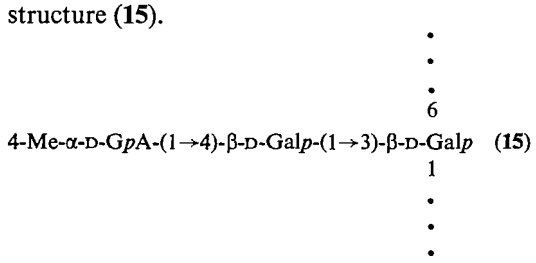

(**15**)

The present results permit the formulation of the following partial structure (**16**) for the 4-*O*-methylglucuronogalactan framework of mesquite gum in which the known structural features are accommodated. The following paper provides evidence for the sequences and types of linkage between L-arabinofuranose and other sugar residues in the acid-labile outer chains of the gum.

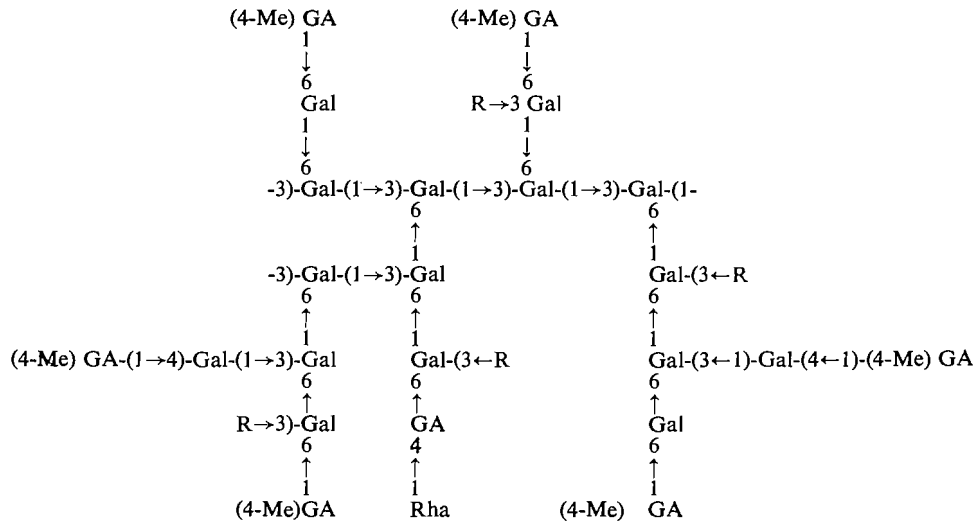

(**16**)

Experimental

General Methods

Paper chromatography was carried out in the following solvent systems (v/v): (*A*) ethyl acetate – pyridine – water (10:4:3); (*B*) ethyl acetate – acetic acid – formic acid – water (18:3:1:4); (*C*) ethyl acetate – acetic acid – formic acid – water (18:8:3:9); (*D*) ethyl acetate – pyridine – acetic acid – water (5:5:1:3); (*E*) 1-butanol – ethanol – water (4:1:5, upper layer).

Gas-liquid partition chromatography was carried out on columns of acid-washed Celite coated with: (*a*) 3% (w/w) of neopentylglycol adipate polyester at 150°; (*b*) 5% (w/w) of polyethyleneglycol adipate polyester at 175°; (*c*) 3% (w/w) of silicone gum XE-60 at 125°; and (*d*) 10% (w/w) of polyphenyl ether [*m*-bis-(*m*-phenoxyphenoxy)benzene] at 200°. Retention times (*T*) are quoted relative to methyl 2,3,4,6-tetra-*O*-methyl-β-D-glucopyranoside. Paper ionophoresis was performed in borate buffer at p*H* 10. Evaporations were carried out under reduced pressure at bath temperatures not exceeding 40°. Unless otherwise stated, optical rotations were observed for aqueous solutions at *ca.* 18°.

Small-scale methylations of oligosaccharides were performed by the method of Kuhn *et al.* (10). Uronic acid was determined by the carbazole method (21). Degrees of polymerization of oligosaccharides were determined by measurement of carbohydrate content by the phenol – sulfuric acid reagent (22) before and after reduction with sodium borohydride.

Isolation of Gum Acid

Mesquite gum was obtained as hard vitreous amber-yellow nodules, embedded with bark, twigs, and other foreign material. The nodules (50 g) were dispersed in water (150 ml), insoluble material was removed by filtration through muslin, the solution was acidified with dilute hydrochloric acid, and polysaccharide was precipitated by pouring the solution into ethanol (6 volumes). The polysaccharide was twice reprecipitated and redissolved in water to give a solution which was freeze-dried to afford gum acid (28 g), $[\alpha]_D$ +60° (*c*, 2.0), [Found:

Can. J. Chem. Downloaded from www.nrcresearchpress.com by 210.87.254.6 on 09/05/12
For personal use only.

uronic acid, 17%]. Hydrolysis of the gum gave galactose and arabinose as the main neutral sugar components together with a trace of rhamnose.

A portion of the gum acid (470 mg) was chromatographed on diethylaminoethylcellulose (phosphate form) (8) and the column was eluted with sodium dihydrogen phosphate buffer (p*H* 6) of increasing concentrations and finally with 0.5 *M* potassium chloride. The major peak eluted with 0.25 *M* buffer contained *ca.* 75% of the polysaccharide. The uronic acid content of the minor peaks was estimated by the carbazole method (21), and the results showed that all peaks, with the single exception of a neutral peak eluted with 0.005 *M* buffer and amounting to less than 5% of the whole, contained similar proportions of acid. The polysaccharide preparation was used without further purification in later experiments.

Partial Hydrolysis of Mesquite Gum

Mesquite gum (20 g) in 0.5 *N* sulfuric acid (2000 ml) was heated under reflux for 1.5 h. The cooled solution was neutralized with barium carbonate and filtered, and the filtrate was concentrated (to 200 ml). After treatment with Amberlite resin IR-120(H), the solution was further concentrated and adsorbed on a column (20 × 3 cm) of diethylaminoethyl–Sephadex A-25 (formate form). The column was eluted with water (1500 ml) to remove neutral sugars, and then 0.05 *M* formic acid to give fractions (total weight 3.1 g) containing acidic sugars. Acidic sugars were separated in sufficient quantity by filter-sheet chromatography in solvents *B* and *C* to give oligosaccharide fractions **1** (480 mg), **2** (205 mg), **3** (150 mg), **4** (210 mg), **5** (87 mg), **6** (150 mg), **7** (140 mg), and **8** (22 mg).

Examination of Oligosaccharide Fractions 1–8

Oligosaccharide **1**, $R_{galactose}$ 0.65 in solvent *B*, M_G 1.06, had $[\alpha]_D$ +20° (*c*, 1.0), and gave 4-*O*-methylglucuronic acid and galactose on hydrolysis. Methanolysis of the methylated derivative gave products which were shown by g.l.c. on column *a* to have the retention times of methyl glycosides of 2,3,4-tri-*O*-methylglucuronic acid, and 2,3,4- and 2,3,5-tri-*O*-methylgalactose. Methanolysis of the methylated glycitol similarly afforded 1,2,3,4,5-penta-*O*-methylgalactitol and methyl glycosides of 2,3,4-tri-*O*-methylglucuronic acid. Methylation of the disaccharide with methyl sulfate and sodium hydroxide, and methyl iodide and silver oxide furnished the methyl ester methyl glycoside hexamethyl ether of 6-*O*-(β-D-glucopyranosyluronic acid)-D-galactose, m.p. 89–90° and mixed m.p. (with sample of m.p. 90–91°) 90°.

Oligosaccharide **2**, $R_{galactose}$ 0.75 in solvent *B*, M_G 0.69, had $[\alpha]_D$ + 94° (*c*, 0.5), gave 4-*O*-methylglucuronic acid and galactose on hydrolysis, and contained 48% of uronic acid. The g.l.c. on column *a* of the methanolysis products from the methylated derivative showed the presence of methyl glycosides of 2,3,4-tri-*O*-methyl glucuronic acid and 2,3,6-tri-*O*-methylgalactose. Methanolysis of the methylated glycitol similarly afforded 1,2,3,5,6-penta-*O*-methylgalactitol and methyl glycosides of 2,3,4-tri-*O*-methylglucuronic acid. The p.m.r. spectrum of the disaccharide glycitol in deuterium oxide showed a doublet (τ 4.84, *J* 3 Hz) attributable (9) to the anomeric proton of an α-D-glycoside. The disaccharide (150 mg) was converted into the methyl ester methyl glycosides by standing overnight in methanolic 1% hydrogen chloride (10 ml), and then heating under reflux for 0.75 h. The cooled solution was neutralized with silver carbonate, filtered, and concentrated to a syrup which was treated with sodium borohydride (200 mg) in water (10 ml) for 18 h. Excess of borohydride was destroyed with Amberlite resin IR-120(H), the reduced disaccharide was methylated with methyl sulfate and sodium hydroxide, and the methylated disaccharide (105 mg) was isolated by extraction with chloroform. The methylated disaccharide was hydrolyzed with *N* hydrochloric acid at 100° for 6 h, and the neutralized hydrolysate was concentrated to a syrup. The syrup was fractionated on a cellulose column (35 × 2 cm) with light petroleum (b.p. 100–120°) – 1-butanol (7:3), saturated with water as eluant, to give (*i*) 2,3,4,6-tetra-*O*-methyl-D-glucose (45 mg), m.p. 79–80° and mixed m.p. (with sample of m.p. 81–82°) 79–80°, and (*ii*) 2,3,6-tri-*O*-methyl-D-galactose (32 mg), which was characterized by conversion into 2,3,6-tri-*O*-methyl-D-galactonolactone, m.p. 98–99° and mixed m.p. (with sample of m.p. 97–98°) 97–98°.

Oligosaccharide **3**, $R_{galactose}$ 0.26 in solvent *B*, M_G 1.14, gave glucuronic acid and galactose on hydrolysis, contained 46% of uronic acid, and was chromatographically indistinguishable from 6-*O*-(β-D-glucopyranosyluronic acid)-D-galactose. The g.l.c. on columns *a* and *b* of the methanolysis products from the methylated derivative showed the presence of methyl glycosides of 2,3,4-tri-*O*-methylglucuronic acid, and 2,3,4- and 2,3,5-tri-*O*-methylgalactose. Methanolysis of the methylated glycitol likewise furnished 1,2,3,4,5-penta-*O*-methylgalactitol and methyl glycosides of 2,3,4-tri-*O*-methylglucuronic acid. The disaccharide was characterized by conversion into the methyl ester methyl glycoside hexamethyl ether, m.p. 86–87° and mixed m.p. (with sample of 90–91°) 86–88°.

Oligosaccharide **4**, $R_{galactose}$ 0.15 in solvent *B*, M_G 0.92, $[\alpha]_D$ +2° (*c*, 1.0), contained 29% of uronic acid and was shown to be a trisaccharide. Partial hydrolysis gave 4-*O*-methylglucuronic acid, galactose, and oligosaccharide **1**. Methanolysis of the methylated trisaccharide and of the methylated trisaccharide glycitol gave methyl glycosides of 2,3,4-tri-*O*-methylglucuronic acid and 2,3,4-tri-*O*-methylgalactose from both, methyl glycosides of 2,3,5-tri-*O*-methylgalactose from the former, and 1,2,3,4,5-penta-*O*-methylgalactitol from the latter [g.l.c. on columns *a* and *b* respectively]. The trisaccharide (50 mg) was converted into the methyl glycoside of the carboxy-reduced derivative as described for oligosaccharide **2**. The reduction product was heated in 0.5 *N* sulfuric acid at 100° for 0.5 h. The neutralized hydrolysate was separated by filter sheet chromatography in solvent *B* to give a disaccharide (6 mg), $[\alpha]_D$ +25° (*c*, 0.5), $R_{galactose}$ 0.31, which gave galactose only on hydrolysis and was chromatographically indistinguishable from 6-*O*-β-D-galactopyranosyl-D-galactose. Methanolysis of the methylated disaccharide afforded methyl glycosides of 2,3,4,6-tetra-, and 2,3,4- and 2,3,5-tri-*O*-methylgalactose [g.l.c. on column *b*].

Oligosaccharide **5**, $R_{galactose}$ 0.24 in solvent *B*, M_G 0.72, $[\alpha]_D$ +56° (*c*, 1.0), contained 31% of uronic acid and was shown to be a trisaccharide. Partial hydrolysis gave 4-*O*-methylglucuronic acid, galactose, and oligosaccharide **2**. Methanolysis of the methylated trisaccharide and of the reduced [$LiAlH_4$] methylated trisaccharide

TABLE 3

Methylation of oligosaccharide fractions 6–8 and derivatives

Cleavage products from methylated derivatives	Oligosaccharide fractions*§							
	6			7			8	
	a	*b*	*c*	*a*	*b*	*c*	*a*	*b*
2,3,4-Me_3 Glucuronic acid†	+	+	+	+	+	+	+	+
2,3,4,6-Me_4 Galactose†	+	+		+	+	tr	+	+
2,3,4-Me_3 Galactose†	+	+	+	+	+	+	+	+
2,3,5-Me_3 Galactose†‡	+		tr	+		tr	+	
2,4,6-Me_3 Galactose†	tr			+	+		+	+
2,5,6-Me_3 Galactose†‡				+		tr	+	
2,4-Me_2 Galactose†	n.d.						n.d.	+
1,2,3,4,5-Me_5 Galactitol		+			+			+
1,2,3,5,6-Me_5 Galactitol		+			+			+

*a, Methylation of oligosaccharide fraction; *b*, methylation of oligosaccharide glycitol; *c*, methylation of oligosaccharide fraction after treatment with lime-water.
†As methyl glycosides.
‡From methylation of reducing sugar unit.
§tr = trace; n.d. = not detected.

gave methyl glycosides of 2,3,6- and 2,4,6-tri-*O*-methylgalactose from both, 2,3,4-tri-*O*-methylglucuronic acid from the former, and 2,3,4-tri-*O*-methylglucose from the latter [g.l.c. on columns *a* and *b*, and *b* respectively].

Oligosaccharide **5** (20 mg) was kept in methanolic 4% hydrogen chloride (2 ml) at room temperature for 165 min [$[\alpha]_D$ $+56° \rightarrow +42°$ (constant)]. The solution was neutralized with silver carbonate, filtered, and concentrated to a syrup which consisted of one major product, $R_{galactose}$ 0.46 in solvent *B*, and a trace of starting material. A portion (5 mg) of the syrup was oxidized with periodic acid (3 mg) in water (2 ml) at 5° for 1 h. Periodic and iodic acids were precipitated by neutralization with barium hydroxide, the solution was centrifuged, and barium ions were removed from the supernatant liquid by treatment with Amberlite resin IR-120(H). The solution containing the oxidation product was reduced with potassium borohydride (15 mg) for 18 h. Excess of borohydride was destroyed with Amberlite resin IR-120(H), the solution was concentrated, and boric acid was removed by repeated distillations with methanol. Partial hydrolysis of the degraded trisaccharide gave 4-*O*-methylglucuronic acid, galactose, arabinose, and oligosaccharide **2**. Methanolysis of the methylated degraded trisaccharide gave methyl glycosides of 2,3,4-tri-*O*-methylglucuronic acid, 2,3,6-tri-*O*-methylgalactose, and 2,5-di-*O*-methylarabinose [g.l.c. on columns *a* and *b*].

Lead tetraacetate (10 mg) in acetic acid (1 ml) was added to oligosaccharide **5** (12 mg) in water (0.5 ml) and acetic acid (1 ml), and the solution was kept for 15 min. Hydrogen sulfide was passed through the solution to precipitate lead salts, and the filtered solution was concentrated to a syrup which contained one major component, $R_{galactose}$ 1.13 in solvent *B*, which gave a characteristic pink stain with aniline oxalate, and a trace of starting material. Hydrolysis of a portion of the syrup gave lyxose, galactose, and oligosaccharide **2**. The remainder of the oxidized syrup was kept in oxygen-free saturated lime-water (15 ml) for 10 days. The solution was neutralized with Amberlite resin IR-120(H), filtered, and concentrated to a syrup, which contained a single reducing sugar, $R_{galactose}$ 0.59 in solvent *B*, gave no stain with triphenyltetrazolium hydroxide thus indicating the presence of a 2-*O*-substituted reducing unit (23), and yielded lyxose, galactose, and oligosaccharide **2** on partial hydrolysis.

Oligosaccharide fractions 6, 7, and 8 were homogeneous by paper chromatography and had $R_{galactose}$ 0.06 and 0.30 in solvents *B* and *C*, 0.02 and 0.20, and 0.01 and 0.13 respectively. Ionophoresis later showed that fraction 6 was heterogeneous, M_G 0.7 and 0.9, but only one component was detected in fraction 8. Partial hydrolysis of fractions 6, 7, and 8 gave galactose and oligosaccharides **1**, **3**, and **4**. Samples of each oligosaccharide fraction, the corresponding glycitols, and the products from treatment of fractions 6 and 7 with oxygen-free saturated lime-water for 7 days, were methylated and the methanolysis products from the various methylated derivatives were examined by g.l.c. [see Table 3].

Methylated Mesquite Gum

Gum nodules (30 g) were dissolved in water (100 ml) by stirring overnight, insoluble material was removed by filtration, and methylation was carried out by the addition of methyl sulfate (200 ml) and aqueous 30% sodium hydroxide (400 ml) during 4 h. After six further treatments the partially methylated gum was isolated by extraction with chloroform, converted into the silver salt (19.7 g), and methylated further with methyl iodide and silver oxide to give methylated mesquite gum (15 g), $[\alpha]_D$ $+59°$ (*c*, 0.8 $CHCl_3$),[Found: OMe, 43.1%], whose i.r. spectrum showed negligible hydroxyl absorption. A sample of the methylated gum was heated in methanolic 4% hydrogen chloride at 100° for 18 h, and after neutralization with silver carbonate the methanolysate was examined by g.l.c. on columns *a*, *b*, and *d* [see Table 4]. A portion of the methanolysate was hydrolyzed in *N* sulfuric acid at 100° for 12 h, and the hydrolysate was oxidized with bromine water for 3 days. Examination of the resulting mixture of aldonolactones by g.l.c. on column *b* showed the presence of components with the retention times of 2,3,5-tri- (*T*, 1.74), 2,3- (*T*, 8.1), 2,5-

Can. J. Chem. Downloaded from www.nrcresearchpress.com by 210.87.254.6 on 09/05/12
For personal use only.

TABLE 4

Gas-liquid chromatography of methanolysate from methylated mesquite gum

Methyl glycosides of	Relative retention times (T) on*								
	Column *a*			Column *b*			Column *d*		
2,3,4-Me_3 Rhamnose					0.46			0.43	
2,3,5-Me_3 Arabinose	0.49		0.63	0.54		0.72	0.49		(0.63)
2,3-Me_2 Arabinose		1.19			1.49				
2,5-Me_2 Arabinose		1.49			1.79		0.71		1.08
3,5-Me_2 Arabinose	0.83		1.98	1.05		2.40	(0.63)		0.84
2,3,4,6-Me_4 Galactose		1.77						1.59	
2,3,4-Me_3 Galactose		6.54			7.02		2.55		2.82
2,3,6-Me_3 Galactose	2.74	3.54	4.07	(3.13)	3.95	4.52			
2,4-Me_2 Galactose	13.5		15.5				3.66		4.21
2,3,4-Me_3 Glucuronic acid	2.28		2.99	2.40		3.13	1.75		2.18
2,3-Me_2 Glucuronic acid				7.7	8.45	10.3			

*Figures in parentheses represent T values for methyl glycosides whose anomers were detected in separate non-overlapping peaks; no figures are quoted for T values where no individual glycoside of an individual sugar was detected with certainty on a particular column.

(T, 14.8), and 3,5-di-*O*-methylarabinonolactone (T, 5.41), and 2,3,4,6-tetra- (T, 6.80) and 2,3,6-tri-*O*-methylgalactonolactone (T, 13.6).

Lithium aluminum hydride (200 mg) in tetrahydrofuran (8 ml) was added slowly to methylated mesquite gum (150 mg) in tetrahydrofuran (8 ml). The mixture was stirred for 30 min, and then heated under reflux for 3 h. Excess of hydride was destroyed by the addition of ethyl acetate, water was added, and the mixture was acidified to pH 4 by the addition of dilute sulfuric acid. The mixture was extracted with chloroform, and the extract was concentrated and poured into light petroleum to give reduced methylated gum (50 mg), $[\alpha]_D$ +61° (*c*, 1.0 $CHCl_3$), [Found: OMe, 39.4%]. A sample of the reduced methylated gum was methanolyzed and the resulting methyl glycosides were examined by g.l.c. on columns *a* and *b*. Similar products to those formed from methylated mesquite gum were detected except that methyl glycosides of 2,3,4-tri-*O*-methylglucose replaced those of 2,3,4-tri-*O*-methylglucuronic acid [T, 2.29 and 3.36, and 2.39 and 3.58 on columns *a* and *b* respectively]. No glycosides of 2,3-di-*O*-methylglucuronic acid or its reduction product, 2,3-di-*O*-methylglucose, could be detected.

Partial Methanolysis of Methylated Mesquite Gum

In order to simulate the conditions used by White in the examination of cleavage products from methylated mesquite gum (3), methylated gum (13 g) in methanolic 4% hydrogen chloride (110 ml) was heated under reflux for 5 h. The cooled solution was neutralized with silver carbonate, filtered, and concentrated to a syrup. The syrup was extracted five times with light petroleum at 100°, and the petrol-insoluble residue was dissolved in chloroform and concentrated to a syrup (3.0 g).

A portion of the petrol-insoluble residue was treated with dilute sodium hydroxide at pH 12 for 2 h. Sodium ions were removed with Amberlite resin IR-120(H), and the resulting solution was adsorbed on diethylaminoethyl–Sephadex A-25 (formate form) and separated into an acidic fraction (340 mg) and a neutral fraction (460 mg). The neutral fraction was hydrolyzed with N hydrochloric acid (25 ml) at 100° for 15 h, and the solution was neutralized and concentrated to a syrup. A portion (65 mg) of the syrup was separated by filter sheet chromatography in solvent E to give two major components, 2-*O*-methyl-D-galactose (21 mg), m.p. 148–150° and mixed m.p. (with sample of m.p. 149–151°) 148–151°, and 2,4-di-*O*-methyl-D-galactose, m.p. 101–103°, together with small amounts of 2,3,4-tri-*O*-methylgalactose, and 2,5- and 3,5-di-*O*-methylarabinose, which were identified by g.l.c. of their methyl glycosides, and traces of arabinose and an unidentified sugar (possibly a mono-*O*-methylarabinose).

A further quantity (1.8 g) of the petrol-insoluble residue was fractionally distilled under reduced pressure (0.005 mm) to give fractions 1 (34 mg, b.p. 88–160°), 2 (393 mg, b.p. 160–180°), and 3 (300 mg, b.p. 180–210°). The g.l.c. of fraction 1 showed the presence of methyl glycosides of 2,5- and 3,5-di-*O*-methylarabinose. Treatment of the fraction with methanolic hydrogen chloride caused no further depolymerization. The g.l.c. of fraction 2 showed the presence of methyl glycosides of the sugars in fraction 1 together with 2,4-di-*O*-methylgalactose. Further treatment of fraction 2 with methanolic hydrogen chloride gave in addition small amounts of methyl glycosides of 2,3,4-tri-*O*-methylglucuronic acid and 2,3,4-tri-*O*-methylgalactose. The g.l.c. of fraction 3 showed the presence of methyl glycosides of 2,4-di-*O*-methylgalactose, and, after methanolysis, of 2,3,4-tri-*O*-methylglucuronic acid, and 2,3,4- and 2,3,6-tri-*O*-methylgalactose. A sample of fraction 3 was remethylated, and the product was methanolyzed and acetylated. The g.l.c. indicated the formation of derivatives of 2,3,4-tri-*O*-methylglucuronic acid, 2,3,4,6-tetra-, and 2,3,4-, 2,3,6-, and 2,4,6-tri-*O*-methylgalactose. Treatment of a portion of fraction 3 with methanolic ammonia afforded a syrup from which no crystalline derivative could be obtained.

Separation of Acidic Oligosaccharide Fractions

The remainder of fraction 3 was saponified with dilute sodium hydroxide at pH 12.5 and fractionated by chromatography on diethylaminoethyl-Sephadex A-25 (formate form) as described previously to give neutral fraction 3A (160 mg) and acidic fraction 3B (90 mg). The g.l.c. of fraction 3A showed the presence of methyl glycosides of 2,4-di-*O*-methylgalactose, and, after treat-

Can. J. Chem. Downloaded from www.nrcresearchpress.com by 210.87.254.6 on 09/05/12
For personal use only.

TABLE 5

Cleavage products from partially methylated acidic oligosaccharide fractions 3B(*i*)–3B(*iii*)

Fraction	Cleavage products*	Cleavage products after remethylation
3B(*i*)	2,3,4-Me_3 Glucuronic acid 2,3,4-Me_3 Galactose 2,3,6-Me_3 Galactose 2,4-Me_2 Galactose (tr)	2,3,4-Me_3 Glucuronic acid 2,3,4-Me_3 Galactose 2,3,6-Me_3 Galactose
3B(*ii*)	2,3,4-Me_3 Glucuronic acid 2,3,4-Me_3 Galactose (tr) 2,4-Me_2 Galactose	2,3,4-Me_3 Glucuronic acid 2,3,4-Me_3 Galactose
3B(*iii*)	2,3,4-Me_3 Glucuronic acid 2,4-Me_2 Galactose 2-Me Galactose†	2,3,4-Me_3 Glucuronic acid 2,3,4-Me_3 Galactose

*tr = trace.
†Detected by paper chromatography of hydrolysate.

ment with methanolic hydrogen chloride, of a small amount of 2,3,4-tri-*O*-methylgalactose. Methylation of fraction 3A, followed by methanolysis and acetylation of the methyl glycosides, afforded derivatives of 2,3,4,6-tetra-, and 2,3,4-, 2,3,6- (trace), and 2,4,6-tri-*O*-methylgalactose (g.l.c.), indicating the presence in fraction 3A of partially methylated neutral oligosaccharides containing galactose residues mutually joined by 1→3′ and 1→6′ linkages.

Methanolysis of fraction 3B afforded methyl glycosides of 2,3,4-tri-*O*-methylglucuronic acid, 2,3,6- and 2,3,4-tri-, and 2,4-di-*O*-methylgalactose [g.l.c. of methyl glycosides on column *a* and of acetylated methyl glycosides on column *c*]. A portion of fraction 3B was remethylated, and the product was methanolyzed and acetylated. The g.l.c. indicated the formation of derivatives of 2,3,4-tri-*O*-methylglucuronic acid and 2,3,4-tri-*O*-methylgalactose as major products, and in smaller amounts of 2,3,6- and 2,4,6-tri-*O*-methylgalactose.

In an attempt to separate partially methylated acidic oligosaccharides containing galactose residues unsubstituted at C-6, fraction 3B (75 mg) in pyridine (2 ml) was heated with triphenylmethyl chloride (80 mg) at 100° for 1 h. The t.l.c. indicated no formation of products of increased chromatographic mobility due to tritylation, but the unchanged components were separated by preparative t.l.c. to give fractions 3B(*i*), 3B(*ii*), and 3B(*iii*). Samples of these fractions were methanolyzed and the resulting methyl glycosides (column *b*) and/or the derived acetates (column *c*) were examined by g.l.c. Further samples of the fractions were remethylated and the methanolysis products were similarly examined. The results are summarized in Table 5.

Degraded Gum A

Gum acid (25.5 g) in water (1275 ml) was boiled under reflux for 24 h, and the cooled solution was poured into ethanol (6 l) containing 1% of hydrochloric acid. The precipitated degraded polysaccharide was twice reprecipitated, redissolved in water, and the solution was freeze-dried to give degraded gum A (7.0 g), $[\alpha]_D$ −8° (*c*, 1) [Found: uronic acid (carbazole method), 40%]. Hydrolysis of the degraded polysaccharide gave acidic sugars, galactose, and only a trace of arabinose.

Degraded gum A (5 g) was methylated, as described for mesquite gum, with methyl sulfate and 30% sodium hydroxide. The partially methylated polysaccharide was isolated as the silver salt (2.5 g) which was further methylated with methyl iodide and silver oxide to give methylated degraded gum A (1.2 g), $[\alpha]_D$ −5° (*c*, 1.0 $CHCl_3$), [Found: OMe, 43.6%]. A sample of the methylated polysaccharide was heated in methanolic 4% hydrogen chloride at 100° for 18 h, and after neutralization with silver carbonate the methanolysate was examined by g.l.c. on columns *a* and *b* [for retention times of methyl glycosides see Table 4]. The results are quoted in Table 1.

Carboxy-reduced Degraded Gum A

Degraded gum A (9 g) was kept in water (600 ml) containing ethylene oxide (100 ml) at room temperature for 3 days during which time the p*H* rose from 2 to 7.1. Excess of ethylene oxide was removed by evaporation, and the glycol ester (9.5 g) was removed by precipitation with ethanol, dissolved in water, and the solution was freeze-dried. The glycol ester (9.4 g) was treated with acetic anhydride and pyridine in formamide (24) to give glycol ester acetate (15.7 g). Lithium borohydride (16 g) in tetrahydrofuran (250 ml) was added to glycol ester acetate (15.5 g) in tetrahydrofuran (250 ml) with immediate formation of a precipitate. The reaction mixture was stirred at room temperature for 2 h, and then heated under reflux for 18 h with stirring. Excess of hydride was destroyed by the careful addition of water. The mixture was then acidified to p*H* 3 by the addition of dilute sulfuric acid, dialyzed, concentrated (to 200 ml), and freeze-dried to give carboxy-reduced degraded gum A (6.8 g), $[\alpha]_D$ +50° (*c*, 1.0). Hydrolysis of the polysaccharide gave galactose and 4-*O*-methylglucose, and small amounts of arabinose and glucose but no acidic sugars.

Degraded Gum B

Carboxy-reduced degraded gum A (6.8 g) was oxidized by sodium metaperiodate (17.12 g) in water (1000 ml) for 7 h [consumption of oxidant, measured spectrophoto-

Can. J. Chem. Downloaded from www.nrcresearchpress.com by 210.87.254.6 on 09/05/12
For personal use only.

Can. J. Chem. Downloaded from www.nrcresearchpress.com by 210.87.254.6 on 09/05/12
For personal use only.

metrically (25), was constant and corresponded to 0.87 mole of reagent per sugar residue]. The excess of periodate was destroyed by the addition of ethylene glycol, the solution was dialyzed to remove sodium iodate and concentrated, and potassium borohydride (5 g) was added in two portions during 3 days. The excess of borohydride was destroyed and sodium ions were removed by treatment of the solution with Amberlite resin IR-120(H), and the solution was concentrated several times with methanol to remove boric acid as methyl borate, and furnished polyalcohol as a syrup (3.6 g). The polyalcohol was hydrolyzed with *N* sulfuric acid at room temperature for 3 h, and the solution was neutralized with barium hydroxide and barium carbonate, filtered, and treated with Amberlite resin IR-120(H). The solution was then concentrated and poured into ethanol (6 volumes). The precipitated polysaccharide was washed with ethanol and dissolved in water, and the solution was freeze-dried to give degraded gum B (1.2 g), $[\alpha]_D$ +18° (*c*, 1.0). The supernatant solution from the above precipitation was concentrated to a syrup (2.0 g). Paper chromatography showed glycerol to be the main component and that no reducing sugars were present. Hydrolysis of the syrup gave small amounts of galactose and arabinose.

Hydrolysis of degraded gum B gave galactose and a trace of arabinose. Partial hydrolysis of the degraded gum in 0.5 *N* sulfuric acid at 100° for 1 h gave as major components oligosaccharides with the mobilities of 3-*O*-β-D-galactopyranosyl-D-galactose and the polymer-homologous trisaccharide, and as a minor component 6-*O*-D-galactopyranosyl-D-galactose. Degraded gum B (200 mg) was methylated with methyl iodide and sodium hydride in dimethylsulfoxide as described by Sandford and Conrad (26), and furnished methylated degraded gum B (83 mg), $[\alpha]_D$ −24° (*c*, 1.0 $CHCl_3$) [Found: OMe, 43.8%]. A sample of the methylated polysaccharide was methanolyzed and g.l.c. of the resulting methyl glycosides on columns *a* and *b* showed the presence of components listed in Table 2, the relative proportions being determined by measurement of peak areas on the chromatograms.

Degraded Gum C

Degraded gum B (800 mg) was oxidized with sodium metaperiodate [consumption of reagent, 0.78 mole per sugar residue], reduced with sodium borohydride, and hydrolyzed with *N* sulfuric acid at room temperature as described previously, to give degraded gum C (360 mg), $[\alpha]_D$ +19° (*c*, 1.0). Partial hydrolysis of the polysaccharide gave galactose as the sole monosaccharide, 3-*O*-galactopyranosylgalactose, and in small amount 6-*O*-galactopyranosylgalactose. Oxidation of the polysaccharide with sodium metaperiodate resulted in the consumption of 0.25 mole of reagent per sugar residue. Degraded gum C (80 mg) was methylated with methyl iodide and sodium hydride in dimethylsulfoxide to give methylated degraded gum C (30 mg), $[\alpha]_D$ −16° (*c*, 1.0 $CHCl_3$). A sample of the methylated polysaccharide was methanolyzed to give methyl glycosides of the sugars listed in Table 2 [g.l.c. on columns *a* and *b*].

The authors wish to acknowledge financial support from the National Research Council of Canada, and, during the early stages of the investigation, the award of a scholarship (to C.C.W.) by the Brewing Industry Research Foundation, Nutfield, Surrey, England. Grateful thanks are expressed to Dr. D. A. Rees for helpful advice and to Dr. H. S. Isbell for a generous supply of mesquite gum.

1. E. V. WHITE. J. Amer. Chem. Soc. **68**, 272 (1946).
2. E. V. WHITE. J. Amer. Chem. Soc. **69**, 622 (1947).
3. E. V. WHITE. J. Amer. Chem. Soc. **69**, 2264 (1947).
4. E. V. WHITE. J. Amer. Chem. Soc. **70**, 367 (1948).
5. J. I. CUNEEN and F. SMITH. J. Chem. Soc. 1141 (1948).
6. J. I. CUNEEN and F. SMITH. J. Chem. Soc. 1146 (1948).
7. M. ABDEL AKHER, F. SMITH, and D. SPRIESTERSBACH. J. Chem. Soc. 3637 (1952).
8. H. NEUKOM, H. DEUEL, W. J. HERI, and W. KUNDIG. Helv. Chim. Acta, **43**, 64 (1960).
9. J. M. VAN DER VEEN. J. Org. Chem. **28**, 564 (1963).
10. R. KUHN, H. TRISCHMANN, and I. LÖW. Angew. Chem. **67**, 52 (1955).
11. G. O. ASPINALL and C. C. WHITEHEAD. Can. J. Chem. Following paper, this issue.
12. G. O. ASPINALL, A. J. CHARLSON, E. L. HIRST, and R. YOUNG. J. Chem. Soc. 1696 (1963).
13. G. O. ASPINALL and J. P. MCKENNA. Carbohyd. Res. **7**, 244 (1968).
14. F. SMITH and R. MONTGOMERY. Chemistry of plant gums and mucilages. Reinhold Publ. Corp., New York, 1959.
15. G. O. ASPINALL. Advan. Carbohyd. Chem. Biochem. **24**, 333 (1969).
16. D. A. REES and J. W. B. SAMUEL. Chem. Ind. London, 2008 (1965).
17. I. J. GOLDSTEIN, G. W. HAY, B. A. LEWIS, and F. SMITH. Methods Carbohyd. Chem. **5**, 361 (1965).
18. D. M. W. ANDERSON, SIR EDMUND HIRST, and J. F. STODDART. J. Chem. Soc. C, 1959 (1966).
19. D. M. W. ANDERSON, SIR EDMUND HIRST, and J. F. STODDART. J. Chem. Soc. C, 1476 (1967).
20. D. M. W. ANDERSON and A. C. MUNRO. Carbohyd. Res. **12**, 9 (1970) and references there cited.
21. E. A. MCCOMB and R. M. MCCREADY. Anal. Chem. **24**, 1630 (1952).
22. T. E. TIMELL. Sv. Papperstidn. **63**, 668 (1960).
23. D. S. FEINGOLD, G. AVIGAD, and S. HESTRIN. Biochem. J. **64**, 351 (1956).
24. J. F. CARSON and W. D. MACLAY. J. Amer. Chem. Soc. **68**, 1015 (1946).
25. G. O. ASPINALL and R. J. FERRIER. Chem. Ind. London, 1216 (1957).
26. P. A. SANDFORD and H. E. CONRAD. Biochem. **5**, 1508 (1966).

Can. J. Chem. Downloaded from www.nrcresearchpress.com by 210.87.254.105 on 09/05/12
For personal use only.

Mesquite gum. II. The arabinan peripheral chains

G. O. ASPINALL AND C. C. WHITEHEAD
Department of Chemistry, Trent University, Peterborough, Ontario, Canada
and
Department of Chemistry, University of Edinburgh, Edinburgh, Scotland

Received July 6, 1970

Autohydrolysis of mesquite gum affords a series of arabinose-containing oligosaccharides [*A*–*Q*] whose structures have been established. It is concluded that the majority of these oligosaccharides originate from peripheral chains in the gum containing the following sugar sequences:

(**1**) α-L-Ara*f*-(1 → 6)-α-D-Gal*p*-(1 → 3)-α-L-Ara*f*-(1 → 3)-L-Ara*f*-(1- and

(**2**) β-L-Ara*f*-(1 → 2)-β-L-Ara*f*-(1 → 2)-β-L-Ara*f*-(1 → 2)-β-L-Ara*f*-(1 → 2)-α-L-Ara*f*-(1 → 4)-β-L-Ara*p*-(1 → 3)-L-Ara*f*-(1- .

Canadian Journal of Chemistry, **48**, 3850 (1970)

During a re-examination of the 4-*O*-methylglucuronogalactan core of mesquite gum (1) the detection of 2,3- and 2,5-di-*O*-methylarabinose as cleavage products of the methylated gum, in addition to the 2,3,5-tri- and 3,5-di-*O*-methyl-L-arabinose previously detected by Cuneen and Smith (2) and White (3), indicated that the acid-labile peripheral chains of the gum are more complex than was formerly supposed. In order to obtain more detailed information on the structure of these peripheral chains, the sugars liberated during the preparation of degraded gum A (1) have been separated chromatographically to give a series of arabinose-containing oligosaccharide fractions A–Q. With the exception of fraction G these oligosaccharides were sufficiently homogeneous for complete structure determination. In most cases insufficient quantities of individual oligosaccharides were available for characterization by the formation of crystalline derivatives. Structure determination involved (*a*) determination of degree of polymerization (4), (*b*) gas chromatographic examination of cleavage products from the methylated derivatives of the oligosaccharides themselves, the oligosaccharide glycitols, and, in some cases, the aldobionic acids formed on bromine oxidation, (*c*) periodate oxidation of the derived phenylosazones (5), (*d*) examination of the products of degradation with cold dilute alkali, and (*e*) examination of products of partial acid hydrolysis. Since L-arabinose and D-galactose are well established as the main neutral constituents of the gum, assignments of configuration of glycosidic linkages have been made, where possible, on the basis of molecular rotations.

Methylation analyses of oligosaccharides A and B were identical and similar linkages were also shown by periodate oxidation of the non-identical phenylosazones. Molecular rotational data indicated that the disaccharides were respectively 3-*O*-α- and 3-*O*-β-L-arabinofuranosyl-L-arabinose. Oligosaccharides C–F were a series of related compounds and the results of experiments from which structures have been assigned are summarized in Table 1. Oligosaccharide fraction G was probably a mixture of higher homologues resulting from the addition of two or more arabinofuranose residues to the trisaccharide D since the fraction contained both arabinofuranose and galactopyranose non-reducing end groups.

Chains of sugar residues as shown in structure **1** may be proposed to account for the formation of oligosaccharides C–F and the probable components of oligosaccharide fraction G. Since the galactopyranosyl linkage in the sequence **1** is probably the most resistant to acid hydrolysis, oligosaccharide A is likely to arise from arabinofuranose units which are two or more residues interior to the galactopyranose residue. The present evidence does not exclude the possibility that units of the disaccharide could also originate

α-D-Gal*p*-(1 → 3)-α-L-Ara*f*-(1 → 3)-L-Ara (D)
α-D-Gal*p*-(1 → 3)-L-Ara (C)
-α-L-Ara*f*-(1 → 6)-α-D-Gal*p*-(1 → 3)-α-L-Ara*f*-(1 → 3)-α-L-Ara*f*-(1 → 3)-L-Ara*f*-(1- **(1)**
α-L-Ara*f*-(1 → 6)-α-D-Gal*p*-(1 → 3)-L-Ara (E) α-L-Ara*f*-(1 → 3)-L-Ara (A)
α-L-Ara*f*-(1 → 6)-α-D-Gal*p*-(1 → 3)-α-L-Ara*f*-(1 → 3)-L-Ara (F)

TABLE 1

Characterization of oligosaccharide fractions C–F

Oligosaccharide	C		D	E		F		G
Degree of polymerization				3		4		5
$[M]_D°$	+480			+284		+172		
Oligosaccharides formed on								
(*i*) Partial hydrolysis of oligosaccharide			C	C		C		C
(*ii*) Partial hydrolysis of oligosaccharide glycitol			C			C		C
Degradation by alkali	+ve		+ve			+ve		
Cleavage products from methylated derivatives*	*a*	*b*	*a*	*a*	*b*	*a*	*b*	*a*
2,3,4,6-Me_4 Galactose†	+	+	+					+
2,3,4-Me_3 Galactose†				+	+	+	+	+
2,3,5-Me_3 Arabinose†				+	+	+	+	+
2,5-Me_2 Arabinose†	+		+	+		+	+	+
1,2,4,5-/1,3,4,5-Me_4 Arabinitol		+			+		+	

*a From methylated oligosaccharide. *b* From methylated oligosaccharide glycitol.
†As methyl glycosides.

TABLE 2

Characterization of oligosaccharide fractions H–K

Oligosaccharide	H		I		J		K	
Degree of polymerization	2		3		4		5	
$[M]_D°$	+285		+414				+820	
Oligosaccharides formed on partial hydrolysis			H		H, I		H, I, J	
Cleavage products from methylated derivatives*	*a*	*b*	*a*	*b*	*a*	*b*	*a*	*b*
2,3,5-Me_3 Arabinose†	+	+	+	+	+	+	+	+
3,5-Me_2 Arabinose†	+		+	+	+	+	+	+
3,4-Me_2 Arabinose†‡	+		n.d.§		+		+	
1,2,4,5-/1,3,4,5-Me_4 Arabinitol		+		+		+		+

*a From methylated oligosaccharide. *b* From methylated oligosaccharide glycitol.
†As methyl glycosides.
‡Where sites of substitution permit, methylation of reducing arabinose residues in *N*,*N*-dimethylformamide (6) gives mainly furanose derivatives and pyranose derivatives were not always detected.
§n.d., not detected.

from arabinofuranose residues exterior to the galactopyranose residue.

Oligosaccharides H–K were shown by methylation and other experiments (see Table 2) to be members of a polymer-homologous series. The first member of the series was additionally characterized by the formation of crystalline derivatives from the hydrolysis of the methylated disaccharide. The liberation of these oligosaccharides on autohydrolysis of the gum was implied by the earlier methylation results of Cuneen and Smith (2) and White (3) which indicated the presence of chains of $1 \rightarrow 2'$ linked L-arabinofuranose residues.

Oligosaccharide L was chromatographically indistinguishable from 3-*O*-β-L-arabinopyranosyl-L-arabinose. Although the observed specific rotation ($[\alpha]_D$ +156°) was lower than those previously reported, *e.g.* $[\alpha]_D$ +220° (7), all other assigned structural features were confirmed by methylation analysis (see Table 3), by the formation of a phenylosazone of the correct melting point, and by the analysis of the products of periodate oxidation of the phenylosazone (5). Methylation analyses of oligosaccharides M and N and of the derived aldobionic acids were identical, and in the former case the assigned linkage was confirmed by the absence of mesoxaldehyde 1,2-bisphenylhydrazone and formaldehyde as products of periodate oxidation of the derived phenylosazone. Molecular rotational data indicated that the disaccharides were respectively 4-*O*-α- and 4-*O*-β-L-arabinofuranosyl-L-arabinose. Oligosaccharides O, P, and Q were

Can. J. Chem. Downloaded from www.nrcresearchpress.com by 210.87.254.105 on 09/05/12
For personal use only.

TABLE 3

Characterization of oligosaccharide fractions L–Q

Oligosaccharide	L		M		N		O		P		Q	
Degree of polymerization	2		2		2		3		4		5	
$[M]_D°$	+443		+17		+242		+165				+206	
Oligosaccharides formed on												
(*i*) Treatment with alkali									H		I	
(*ii*) Partial hydrolysis of oligosaccharide							L				L, O, P	
(*iii*) Partial hydrolysis of oligosaccharide glycitol							L not detected				L not detected	
Cleavage products from methylated derivatives*	*a*	*b*	*a*	*b*	*a*	*b*	*a*	*b*	*a*	*b*	*a*	*b*
2,3,5-Me_3 Arabinose†			+	+	+	+	+	+	+	+	+	+
2,3,4-Me_3 Arabinose†	+	+										
2,3-Me_2 Arabinose†			+		+		+	+	+	+	+	+
2,5-Me_2 Arabinose†	+						+		+			
3,5-Me_2 Arabinose†									+	+	+	+
1,2,4,5-/1,3,4,5-Me_4 Arabinitol		+						+		+		+
1,2,3,5-Me_4 Arabinitol			+		+							

*a From methylated oligosaccharide. *b* From methylated oligosaccharide glycitol.
†As methyl glycosides.

shown by methylation and partial fragmentation studies (see Table 3) to be a series of higher saccharides resulting from the successive addition of arabinofuranose residues to the non-reducing unit of disaccharide L. Comparison of the molecular rotations of oligosaccharides L ($[M]_D$ +443°) and O ($[M]_D$ +165°) suggests that the additional arabinofuranose residue in O has the α-L-configuration. In contrast, comparison of the molecular rotations of oligosaccharides O and Q ($[M]_D$ +206°) implies that the two outermost arabinofuranose residues have the β-L-configuration. This conclusion is consistent with the detection of oligosaccharides H and I as alkali-stable degradation products from oligosaccharides P and Q. Chains of sugar residues as shown in structure **2** may therefore be proposed to account for the formation of oligosaccharides H–K, L, M, and O–Q.

Although controlled acid hydrolysis of mesquite gum results in preferential cleavage of the acid-labile arabinofuranosyl bonds, some hydrolysis of the more resistant galactopyranosyl linkages occurs and small quantities of neutral galactose-containing oligosaccharides and acidic oligosaccharides were isolated. The neutral oligosaccharides were shown to be 3-*O*-β-D-galactopyranosyl-D-galactose (R), 6-*O*-β-D-galactopyranosyl-D-galactose (S), and the polymer-homologous trisaccharide (T). The acidic sugars were shown to include oligosaccharides **1**–**4**, which had been characterized previously (1), together with higher oligosaccharides to which arabinofuranose residues were still attached. The liberation of these oligosaccharides requires the hydrolysis of only one galactopyranosyl bond in the outer chains, whereas the release of the trisaccharide **5** (1), which was not detected in the autohydrolysate of the gum, and would have required the cleavage of contiguous galactopyranosyl bonds, would be improbable under conditions of limited hydrolysis of the more stable bonds.

A considerable number of oligosaccharides, containing a variety of different linkages, have been characterized as partial hydrolysis products from mesquite gum, but all the linkages recog-

β-L-Ara*f*-(1 → 2)-β-L-Ara*f*-(1 → 2)-β-L-Ara*f*-(1 → 2)-β-L-Ara*f*-(1 → 2)-L-Ara (K)
β-L-Ara*f*-(1 → 2)-β-L-Ara*f*-(1 → 2)-β-L-Ara*f*-(1 → 2)-L-Ara (J)
β-L-Ara*f*-(1 → 2)-β-L-Ara*f*-(1 → 2)-L-Ara (I)
β-L-Ara*f*-(1 → 2)-L-Ara (H) α-L-Ara*f*-(1 → 4)-L-Ara*p* (M)
-β-L-Ara*f*-(1 → 2)-β-L-Ara*f*-(1 → 2)-β-L-Ara*f*-(1 → 2)-β-L-Ara*f*-(1 → 2)-α-L-Ara*f*-(1 → 4)-β-L-Ara*p*-(1 → 3)-L-Ara*f*- (**2**)

β-L-Ara*p*-(1 → 3)-L-Ara (L)
α-L-Ara*f*-(1 → 4)-β-L-Ara*p*-(1 → 3)-L-Ara (O)
β-L-Ara*f*-(1 → 2)-α-L-Ara*f*-(1 → 4)-β-L-Ara*p*-(1 → 3)-L-Ara (P)
β-L-Ara*f*-(1 → 2)-β-L-Ara*f*-(1 → 2)-α-L-Ara*f*-(1 → 4)-β-L-Ara*p*-(1 → 3)-L-Ara (Q)

Can. J. Chem. Downloaded from www.nrcresearchpress.com by 210.87.254.105 on 09/05/12
For personal use only.

Can. J. Chem. Downloaded from www.nrcresearchpress.com by 210.87.254.105 on 09/05/12
For personal use only.

nized are of types inferred from the identification of cleavage products from the methylated polysaccharide (1). Nevertheless, the possibility of some of the six arabinobioses arising from artifact formation must be considered. 3-*O*-β-L-Arabinopyranosyl-L-arabinose (L) is known to be a major product from the acid-catalyzed reversion of L-arabinose (8), but, in the absence of other equilibrium-controlled reversion products such as 4-*O*-β-L-arabinopyranosyl-L-arabinose, it may be regarded as a genuine degradation product of mesquite since it is readily formed from the higher oligosaccharides O and Q. Artifact formation by kinetically controlled transglycosylation is also considered unlikely in view of the correspondence between the linkages in the isolated oligosaccharides and those indicated by the methylation analysis of the parent polysaccharide. However, in view of the isolation of two pairs of disaccharides, each pair differing only in the configurations of the glycosidic linkages, the further possibility of acid-catalyzed anomerization cannot yet be discounted. 4-*O*-α-L- (M) and 4-*O*-β-L-Arabinopyranosyl-L-arabinose (N) were isolated in the approximate proportions of 2:1. Whereas molecular rotational considerations indicated that units of the former disaccharide (M) provided the two non-reducing residues in the trisaccharide (O), no evidence was obtained that units of the latter disaccharide (N) formed part of other oligosaccharide sequences. Likewise, of the disaccharides, 3-*O*-α-L- (A) and 3-*O*-β-L-arabinofuranosyl-L-arabinose (B), which were isolated in similar amounts, units of the former (A) only have been recognized as constituents of more extended sequences (F and, possibly, components of fraction G). The structural significance, therefore, of disaccharides B and N remains unproven on present evidence.

The results presented in this and the previous paper (1) show clearly the highly complex structure of mesquite gum. In the absence of evidence for branching in the peripheral chains, all the arabinose-containing oligosaccharides formed on autohydrolysis of the gum, with the exception of the disaccharides B and N, appear to be derived from the basic structural sequences **1** and **2**. These chains are indicated as R in structure **16** in the previous paper (1). The implication that the pentasaccharides K and Q represent overlapping regions from type **2** chains suggests that these chains have a minimum size of seven L-arabinose residues. In an earlier study, Dutton and Unrau (9) obtained evidence for the presence of chains containing at least six arabinose residues. Although the disaccharides, 3-*O*-α-D-galactopyranosyl-L-arabinose (C) and 3-*O*-β-L-arabinopyranosyl-L-arabinose (L), have been isolated as partial hydrolysis products from peripheral chains of a number of exudate gums (10, 11), the presence of isolated D-galactopyranose and L-arabinopyranose residues within chains of L-arabinofuranose residues has not been previously observed.

Experimental

The general experimental procedures were as described in Part I (1).

Autohydrolysis of Gum and Fractionation of Liberated Oligosaccharides

Gum acid (30 g) in water (1500 ml) was boiled under reflux for 24 h, and the cooled solution was concentrated and poured into ethanol (6 volumes). A sample of the precipitated polysaccharide was hydrolyzed giving *inter alia* a substantial proportion of arabinose. The partially degraded gum in water (500 ml) was boiled under reflux for a further 12 h and the degraded polysaccharide (7.1 g), $[\alpha]_D$ −1° (*c*, 1.0), was precipitated with ethanol, and shown to give only traces of arabinose on hydrolysis. The combined supernatant liquids from the autohydrolyses were concentrated to a syrup which was adsorbed on a column (30 g) of diethylaminoethyl-Sephadex A-25 (formate form). Neutral sugars were eluted with water (2 l), and the eluate was concentrated to a syrup (15 g). The column was then eluted with 0.5 *M* formic acid to give acidic sugars (3.5 g).

Chromatographic examination of the mixture of neutral sugars showed the presence of arabinose, galactose, rhamnose, and a series of oligosaccharides. The sugars were adsorbed on a column of charcoal–Celite (1:1, 300 g) and monosaccharides (9 g) were eluted with water. The column was then eluted with water containing increasing proportions of ethanol. Appropriate fractions were combined and mixtures of oligosaccharides were further separated by filter sheet chromatography in solvents *A* or *B* to give oligosaccharides A to T (Table 4).

Chromatographic examination of the mixture of acidic sugars showed the presence of components similar to those previously isolated on partial hydrolysis of the gum (1). Filter sheet chromatography of a portion (0.6 g) of the syrup in solvent *C* gave fractions 1 (55 mg), 2 (104 mg), 3 (83 mg), 4 (42 mg), and 5 (29 mg). Further separation of fraction 3 by filter sheet chromatography in solvent *B* gave fractions 3*a* (22 mg) and 3*b* (37 mg). Fractions 4 and 5 were further separated by filter sheet ionophoresis to give fractions 4*a* (12 mg), 4*b* (17 mg), 5*a* (8 mg), 5*b* (6 mg), and 5*c* (4 mg).

Characterization of Arabinose-containing Oligosaccharides A–Q

Hydrolysis of oligosaccharides A, B, and H–Q gave arabinose only, and of oligosaccharides C–G galactose and arabinose. Degrees of polymerization were deter-

TABLE 4

Separation of oligosaccharide fractions A–T

Fraction	Weight (mg)	% EtOH in eluant	$[\alpha]_D°$	$R_{galactose}$ in solvents			M_G
				A	*B*	*E*	
A	23	0–5	0	1.48	1.26	1.23	0.39
B	25	5–10	+125	1.40	1.35		0.4
C	150	0–5	+154	0.73	0.52		0.62
D	12	5–10		0.53	0.30		
E	32	10	+64	0.72	0.24		
F	5	15	+30	0.69	0.20		
G	3	15			0.09		
H	137	5–10	+101	1.44	1.36	1.23	0.29
I	48	15	+98	1.29	0.81		
J	6	15		1.20	0.55		
K	30	15	+121	1.14	0.32		
L	94	0–5	+156	0.86	0.73		0.61
M	27	0–5	+6	1.28	1.07		0.12
N	12	5	+86	1.28	1.19		0.12
O	13	10	+40	1.32	0.78		
P	5	5–10		1.12	0.56		
Q	13	15	+30	1.02	0.37		
R	6	5		0.43	0.30		
S	32	0–5	+23	0.38	0.31		
T	10	5–10	+17	0.11	0.10		

TABLE 5

The g.l.c. of methylated sugar derivatives*

Sugar	Relative retention times (*T*) on columns *a* and *b* of					
	Methyl glycosides		Sugars		Aldonolactones	
	a	*b*	*a*	*b*	*a*	*b*
2,3,4-Me_3 Arabinose	0.89	1.03	2.49	3.14		
2,3,5-Me_3 Arabinose	0.49 0.64	0.55 0.72	1.78	2.21	1.45	1.75
2,3-Me_2 Arabinose	1.19 1.49	1.49 1.82			6.37	7.93
2,4-Me_2 Arabinose	1.86	2.18				
2,5-Me_2 Arabinose	1.50 2.71	1.78 3.17			14.2	14.2
3,4-Me_2 Arabinose	1.56 3.30	1.99 4.13				10.7
3,5-Me_2 Arabinose	0.85 1.97	1.03 2.35			4.48	5.42
2,3,4,6-Me_4 Galactose	1.76	1.80				

Alditol	Alditols	
	a	*b*
1,2,4,5-/1,3,4,5-Me_4 Arabinitol	0.89	0.99
1,2,3,5-/1,2,3,4-Me_4 Arabinitol		1.12

*Compounds whose retention times differed by more than ≃5% were sufficiently resolved to detect both components,

mined and small-scale methylations of oligosaccharides and derivatives were performed as described previously (1). The methylated oligosaccharides were characterized by g.l.c. of the methanolysis products, and also in the case of oligosaccharides B, H, N, O, and Q, of the aldonolactones formed on hydrolysis followed by bromine oxidation. The relative retention times (*T*) of various methylated derivatives of arabinose and of 2,3,4,6-tetra-*O*-methylgalactose on columns *a* and *b* are listed in Table 5. Partial hydrolyses of arabinose-containing oligosaccharides and oligosaccharide glycitols were carried out at 100° for 1 h in 0.02 *N* sulfuric acid. Alkaline degradations were performed in oxygen-free saturated lime-water at room temperature. Phenylosazones were prepared and their products from periodate oxidation were analyzed as described by Hough *et al.* (5). The results of these experiments have been summarized in Tables 1–3 or are quoted below.

Further Examination of Oligosaccharides A–Q

Oligosaccharide A afforded a phenylosazone, m.p. 212–213° [λ_{max} 255 (ε, 18 000), 310 (ε, 9800), 394 nm

Can. J. Chem. Downloaded from www.nrcresearchpress.com by 210.87.254.105 on 09/05/12
For personal use only.

Can. J. Chem. Downloaded from www.nrcresearchpress.com by 210.87.254.105 on 09/05/12
For personal use only.

(ε, 18 300) (ethanol)]. Periodate oxidation of the phenylosazone gave formaldehyde (1.1 mole) but no mesoxaldehyde 1,2-bisphenylhydrazone.

Oligosaccharide B afforded a phenylosazone, m.p. 215–217° and mixed m.p. (with sample of phenylosazone of oligosaccharide A) 205° [λ_{max} 255 (ε, 20 100), 309 (ε, 12 100), 390 nm (ε, 22 200) (ethanol)]. Periodate oxidation of the phenylosazone gave formaldehyde (0.85 mole) but no mesoxaldehyde 1,2-bisphenylhydrazone.

Oligosaccharide C furnished a phenylosazone, m.p. 232–233° and mixed m.p. (with sample, m.p. 235°) 233° [λ_{max} 257 (ε, 18 000), 310 (ε, 10 800), 394 nm (ε, 20 500) (ethanol)]. Periodate oxidation of the phenylosazone gave formaldehyde (1.0 mole) but no mesoxaldehyde 1,2-bisphenylhydrazone.

Oligosaccharide H (40 mg) was methylated with methyl sulfate and 30% aqueous sodium hydroxide, and then with methyl iodide and silver oxide. The methylated disaccharide was hydrolyzed to give (*i*) 2,3,5-tri-*O*-methyl-L-arabinose (12 mg), which was characterized by conversion into 2,3,5-tri-*O*-methyl-L-arabinonamide, m.p. 135–136° and mixed m.p. (with sample, m.p. 137–138°) 135–136°, and (*ii*) 3,4-di-*O*-methyl-L-arabinose (14 mg), which was characterized by conversion into 3,4-di-*O*-methyl-L-arabinonamide, m.p. 123–125° and mixed m.p. (with sample, m.p. 127–128°) 124–125°.

Oligosaccharide L furnished a phenylosazone, m.p. 233–234° (lit. (7) m.p. 234°) [λ_{max} 256 (ε, 23 100), 309 (ε, 12 400), 395 nm (ε, 22 500) (ethanol)]. Periodate oxidation of the phenylosazone gave formaldehyde (1.1 mole) but no mesoxaldehyde 1,2-bisphenylhydrazone.

Oligosaccharide M was oxidized with bromine water, the resulting aldobionic acid was methylated, and g.l.c. of the hydrolysis products from the methylated derivative showed the presence of 2,3,5-tri-*O*-methylarabinose and 2,3,5-tri-*O*-arabinonolactone. The disaccharide furnished a non-crystalline phenylosazone which was purified by t.l.c. [λ_{max} 256 (ε, 18 900), 307 (ε, 11 700), 390 nm (ε, 20 000, assumed)]. Periodate oxidation resulted in the consumption of 1.8 mole of reagent, traces (0.046 mole) of formaldehyde were liberated, and no mesoxaldehyde 1,2-bisphenylhydrazone was formed.

Oligosaccharide N was oxidized with bromine water, the resulting aldobionic acid was methylated, and g.l.c. of the hydrolysis products from the methylated derivative showed the presence of 2,3,5-tri-*O*-methylarabinose and 2,3,5-tri-*O*-methylarabinonolactone.

Characterization of Oligosaccharides R–T

Oligosaccharide R gave galactose only on hydrolysis and was chromatographically indistinguishable from 3-*O*-β-D-galactopyranosyl-D-galactose. Methanolysis of the methylated disaccharide gave methyl glycosides of 2,3,4,6-tetra-, and 2,4,6- and 2,5,6-tri-*O*-methylgalactose [g.l.c. on columns *a* and *b*].

Oligosaccharide S gave galactose only on hydrolysis and was chromatographically indistinguishable from 6-*O*-β-D-galactopyranosyl-D-galactose. Methanolysis of the methylated disaccharide gave methyl glycosides of 2,3,4,6-tetra- and 2,3,4-tri-*O*-methylgalactose [g.l.c. on column *a*]. Similar methanolysis of the methylated disaccharide glycitol gave methyl glycosides of 2,3,4,6-tetra-*O*-methylgalactose, and 1,2,3,4,5-penta-*O*-methylgalactitol [g.l.c. on column *b*].

Oligosaccharide T was a trisaccharide which gave galactose only on hydrolysis and was chromatographically indistinguishable from *O*-β-D-galactopyranosyl-(1 → 6)-*O*-β-D-galactopyranosyl-(1 → 6)-D-galactose. Partial hydrolysis gave oligosaccharide S. Methanolysis of the methylated trisaccharide and of the methylated trisaccharide glycitol gave methyl glycosides of 2,3,4,6-tetra- and 2,3,4-tri-*O*-methylgalactose from both, together with methyl glycosides of 2,3,5-tri-*O*-methylgalactose from the former and 1,2,3,4,5-penta-*O*-methylgalactitol from the latter [g.l.c. on columns *a* and *b*].

Examination of Acidic Oligosaccharide Fractions

Chromatographic examination of oligosaccharide fractions 1, 2, 3*a*, and 3*b* and of the products of partial hydrolysis, reduction and hydrolysis, and/or methanolysis of the methylated derivatives established their identity with the previously characterized oligosaccharides **2**, **1**, **3**, and **4** (1).

Oligosaccharide fractions 4*a*–5*c* were chromatographically similar to the previously examined fractions 6 and 7 (1). Hydrolysis of fractions 4*b*, 5*b* and 5*c* gave arabinose in addition to galactose and acidic oligosaccharides. Hydrolysis of the glycitols from fractions 4*b* and 5*b* gave *inter alia* arabinose and galactitol. Methanolysis of methylated fraction 5*b* gave methyl glycosides of 2,3,5-tri-*O*-methylarabinose, 2,3,4,6-tetra- and 2,3,4-, 2,4,6- and 2,5,6-tri-*O*-methylgalactose, and 2,3,4-tri-*O*-methylglucuronic acid.

The authors wish to acknowledge financial support from the National Research Council of Canada, and, during the early stages of the investigation, the award of a scholarship (to C.C.W.) by the Brewing Industry Research Foundation, Nutfield, Surrey, England. Thanks are also expressed to Dr. D. A. Rees for helpful advice.

1. G. O. ASPINALL and C. C. WHITEHEAD. Can. J. Chem. Preceding paper, this issue.
2. J. I. CUNEEN and F. SMITH. J. Chem. Soc. 1146 (1948).
3. E. V. WHITE. J. Amer. Chem. Soc. **68**, 272 (1946).
4. T. E. TIMELL. Sv. Papperstidn. **63**, 668 (1960).
5. L. HOUGH, D. B. POWELL, and B. M. WOODS. J. Chem. Soc. 4799 (1956).
6. R. KUHN, H. TRISCHMANN, and I. LÖW. Angew. Chem. **67**, 32 (1955).
7. J. K. N. JONES. J. Chem. Soc. 1672 (1953).
8. J. K. N. JONES and W. H. NICHOLSON. J. Chem. Soc. 27 (1958).
9. G. G. S. DUTTON and A. M. UNRAU. Can. J. Chem. **41**, 1417 (1963).
10. F. SMITH and R. MONTGOMERY. Chemistry of plant gums and mucilages. Reinhold Publ. Corp., New York, 1959.
11. G. O. ASPINALL. Advan. Carbohyd. Chem. Biochem. **24**, 333 (1969).

Can. J. Chem. Downloaded from www.nrcresearchpress.com by 210.87.254.40 on 09/05/12
For personal use only.

Halogen exchange in reactions of boron halides with *o*-(trifluoromethyl)-phenyltrimethyl derivatives of silicon and tin

T. CHIVERS
Department of Chemistry, The University of Calgary, Calgary 44, Alberta

Received July 20, 1970

The reaction of boron trifluoride with *o*-$CF_3C_6H_4SnMe_3$ in carbon tetrachloride gives *o*-$CF_3C_6H_4BF_2$, which with aqueous potassium fluoride is converted to K[*o*-$CF_3C_6H_4BF_3$]. Boron trichloride and *o*-$CF_3C_6H_4SnMe_3$ undergo halogen exchange to give, after hydrolysis, *o*-$CCl_3C_6H_4B(OH)_2$. Halogen exchange also occurs between boron trichloride and *o*-$CF_3C_6H_4Y$ (Y = H, $SiMe_3$) to give boron trifluoride and *o*-$CCl_3C_6H_4Y$. The long range HF and FF nuclear magnetic resonance (n.m.r.) coupling constants observed for *o*-$CF_3C_6H_4$-derivatives are briefly discussed.

Canadian Journal of Chemistry, **48**, 3856 (1970)

Introduction

Perfluoroalkyl derivatives of boron are unstable with respect to fluorine migration from the organic group to boron unless a group which may π-bond strongly with boron is linked to it (1, 2). Perfluorovinyl-(3) and perfluorophenyl-boron (4–6) compounds show greater stability with respect to fluorine migration from the side chain to boron. In connection with our interest in the structure-stability relationships of fluorocarbon–boron compounds we have investigated the reaction of *o*-$CF_3C_6H_4SnMe_3$ with boron trifluoride and with boron trichloride as a possible route to the hitherto unknown *o*-$CF_3C_6H_4BX_2$(X = F, Cl) derivatives.

Experimental

General

Manipulations which involved air sensitive materials were carried out in a dry nitrogen atmosphere or with the aid of a vacuum system. Infrared spectra were recorded on a Perkin–Elmer model 337 instrument using sodium chloride or potassium bromide optics, and were calibrated with a polystyrene film. A Varian HA 100 spectrometer was used for the ^{19}F n.m.r. spectra with CCl_3F as internal reference. The ^1H n.m.r. spectra were obtained for 20% solutions in carbon tetrachloride with a Varian A60 instrument. Boron trihalides, benzotrifluoride, and *o*-bromobenzotrifluoride were purchased commercially and used without further purification. *o*-(Trifluoromethyl)phenyltrimethyltin (7) and *o*-(trifluoromethyl)phenyltrimethylsilane (8) were prepared according to the literature.

Analyses were performed by Dr. A. Bernhardt, Mulheim, Germany, and by Dr. A. Daesslé, Montreal, Quebec.

Preparation of o-(Trifluoromethyl)phenylboron Difluoride

Boron trifluoride (1.40 g, 20.6 mmole) was condensed into a Carius tube containing *o*-(trifluoromethyl)phenyltrimethyltin (2.27 g, 7.6 mmole) in carbon tetrachloride (10 ml, freshly distilled from P_2O_5). The tube was sealed off and allowed to come to room temperature. A white precipitate was slowly deposited and after 2 days volatile products were transferred to the vacuum line and fractionated through traps at 0, −30, −78, and −182° to give *o*-(trifluoromethyl)phenylboron difluoride (−30°) (1.18 g, 6.1 mmole), carbon tetrachloride (−78°), and boron trifluoride (−182°) (0.40 g, 5.9 mmole). A white, air-sensitive solid residue in the tube was identified by its infrared spectrum (9) as trimethyltin tetrafluoroborate (1.88 g, 7.55 mmole).

o-(Trifluoromethyl)phenylboron difluoride was characterized by its fluorine analysis, and by conversion to K[*o*-$CF_3C_6H_4BF_3$] (see below).

Anal. Calcd. for $C_7H_4BF_5$: F, 49.0. Found: F, 48.5.

Preparation of Potassium o-(Trifluoromethyl)phenyltrifluoroborate

o-(Trifluoromethyl)phenylboron difluoride (2.17 g, 11.2 mmole) was condensed onto a solution of potassium fluoride (0.65 g, 11.2 mmole) in water (20 ml). A white precipitate (2.21 g) was obtained, which was recrystallized twice from water to give potassium *o*-(trifluoromethyl)-phenyltrifluoroborate (1.24 g, 4.9 mmole) which effervesced at 179–181° to give a white solid m.p. 255°.

Anal. Calcd. for $C_7H_4BF_6K$: C, 33.4; H, 1.6; F, 45.2. Found: C, 33.0; H, 1.8; F, 44.9.

The infrared spectrum (Nujol) showed bands at 1631m, 1571w, 1311s, 1260s, 1190s, 1172s, 1160s, 1118s, 1102s, 1066s, 1030s, 1005m, 960s, 910w, 776s, 748s, 697w, 647w cm^{-1}.

Reaction of o-(Trifluoromethyl)phenyltrimethyltin with Boron Trichloride

Excess of boron trichloride and *o*-(trifluoromethyl)-phenyltrimethyltin (4.18 g, 13.9 mmole) were allowed to react at 25° in a sealed, evacuated Carius tube. The reaction mixture was a colorless liquid after 2 h. After 18 h, some white crystals had formed and the supernatant solution was deep blue. After 2 days, volatile products were transferred to the vacuum line to give boron trifluoride (0.85 g, 12.5 mmole) identified by comparison of its infrared spectrum with that of an authentic sample. The blue liquid residue in the tube was treated with petrol (40–60°; 100 ml) and insoluble white crystals were filtered off and identified by their infrared spectrum and m.p. as dimethyltin dichloride (1.95 g, 8.8 mmole).

Can. J. Chem. Downloaded from www.nrcresearchpress.com by 210.87.254.40 on 09/05/12
For personal use only.

Solvent was removed from the filtrate (which was subjected to atmospheric hydrolysis at this stage) under vacuum to give a yellow solid residue, which was recrystallized from cyclohexane to give white crystals of *o*-(tri*chloro*methyl)phenylboronic acid (1.56 g, 6.5 mmole) m.p. 111–113° with effervescence.

Anal. Calcd. for $C_7H_6BCl_3O_2$: C, 35.1; H, 2.5. Found: C, 35.8; H, 2.6.

The ^1H n.m.r. spectrum ($CDCl_3$) showed a broad singlet at τ5.7 [$I = 45$; $B(OH)_2$] and multiplets at τ2.0 ($I = 23$), and at τ2.5 ($I = 68$) (aromatic protons). I = Integrated area. The infrared spectrum (Nujol) showed a broad band at 3340 cm^{-1} (O—H stretch) and strong bands at 790, 740, and 713 cm^{-1} (C—Cl stretch).

Preparation of o-(Trichloromethyl)phenyltrimethylsilane

o-(Trifluoromethyl)phenyltrimethylsilane (3.07 g, 14.1 mmole) and an excess of boron trichloride were kept in a sealed, evacuated tube at 25° for 24 h. The liquid reaction mixture, which was colorless, was cooled and volatile products were transferred to the vacuum line and shown to contain boron trifluoride (infrared spectrum). The involatile liquid residue (3.73 g) was distilled to give *o*-(trichloromethyl)phenyltrimethylsilane b.p. 82–83°/0.04 mm (3.22 g, 12.1 mmole).

Anal. Calcd. for $C_{10}H_{13}SiCl_3$: C, 44.9; H, 4.9; Cl, 39.75. Found: C, 45.05; H, 5.1; Cl, 39.5.

The ^1H n.m.r. spectrum (20% in CCl_4) showed a singlet at τ9.60 (Me_3Si) and multiplets at τ1.90, τ2.25, and τ2.73 (1:1:2, aromatic protons) in the ratio 100:44. The infrared spectrum (liquid film) showed bands at 3058w, 2953m, 2895w, 1458m, 1410m, 1265s, 1181m, 1170m, 1123s, 1073m, 1051m, 911w, 866vs, 842vs, 790vs, 770sh, 730vs, 705s, 698sh, 683sh, 630m, 620m, 451w cm^{-1}.

Reactions of Benzotrifluoride with Boron Trichloride

(a) 1:1 Molar Ratio

Benzotrifluoride (12.6 g, 86.4 mmole) and a slight excess of boron trichloride (10.4 g, 88.6 mmole) were left in a sealed, evacuated tube at 25° for 2 days. Volatile products were transferred to the vacuum line and shown to contain boron trifluoride (infrared spectrum). The involatile liquid residue was shown to be benzotrichloride (16.4 g, 84.0 mmole) by comparison of its infrared spectrum with that of an authentic sample.

(b) 3:1 Molar Ratio

Benzotrifluoride (20.9 g, 143 mmole) and boron trichloride (5.6 g, 48 mmole) were left in a sealed, evacuated tube at 25° for 1 day. Boron halides were separated from other products by vacuum transfer at −78°. Distillation of the liquid residue gave benzotrifluoride b.p. 102° (12.9 g, 88 mmole) and a liquid residue which was shown by its infrared spectrum to be benzotrichloride (9.8 g, 50 mmole).

Results and Discussion

In the reaction of *o*-$CF_3C_6H_4SnMe_3$ with boron trifluoride in dry carbon tetrachloride the expected Sn—C_{aryl} cleavage occurs to give *o*-$CF_3C_6H_4BF_2$ and a white precipitate of trimethyltin tetrafluoroborate.

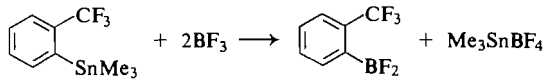

On exposure to air *o*-$CF_3C_6H_4BF_2$ fumes strongly, and the salt $K[o\text{-}CF_3C_6H_4BF_3]$ is formed when *o*-$CF_3C_6H_4BF_2$ is condensed onto an aqueous solution of potassium fluoride (*cf.* $K(C_6F_5BF_3)$) (10).

When *o*-$CF_3C_6H_4SnMe_3$ and an excess of boron trichloride were allowed to react in a sealed tube at ambient temperature, white crystals of dimethyltin dichloride slowly formed and the supernatant liquid was blue.[1] Volatile products were shown to contain boron trifluoride, and the involatile liquid product, after hydrolysis, was identified as *o*-$CCl_3C_6H_4B(OH)_2$. Apparently, halogen exchange between boron trichloride and the trifluoromethyl group occurred either prior to or concomitant with Sn—C_{aryl} cleavage to give *o*-$CCl_3C_6H_4BCl_2$ which, on hydrolysis, would give *o*-$CCl_3C_6H_4B(OH)_2$.

In support of this suggestion we have observed that halogen exchange occurs at ambient temperatures between boron trichloride and either $C_6H_5CF_3$ or *o*-$CF_3C_6H_4SiMe_3$ to give the corresponding *o*-$CCl_3C_6H_4$-derivative in good yield.

Halogen exchange also takes place between boron tribromide and *o*-$CF_3C_6H_4SiMe_3$ and this reaction can be conveniently monitored by recording the ^1H n.m.r. spectrum of the reaction

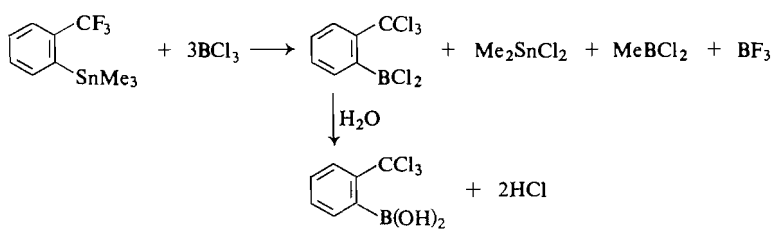

[1]A red color was observed in the reaction between $(C_6F_5)_2Sn(n\text{-}Bu)_2$ and boron tribromide (15). In the example above, it appears that the coloration is sensitive to the presence of trace impurities, since in one experiment the supernatant liquid was red.

Can. J. Chem. Downloaded from www.nrcresearchpress.com by 210.87.254.40 on 09/05/12
For personal use only.

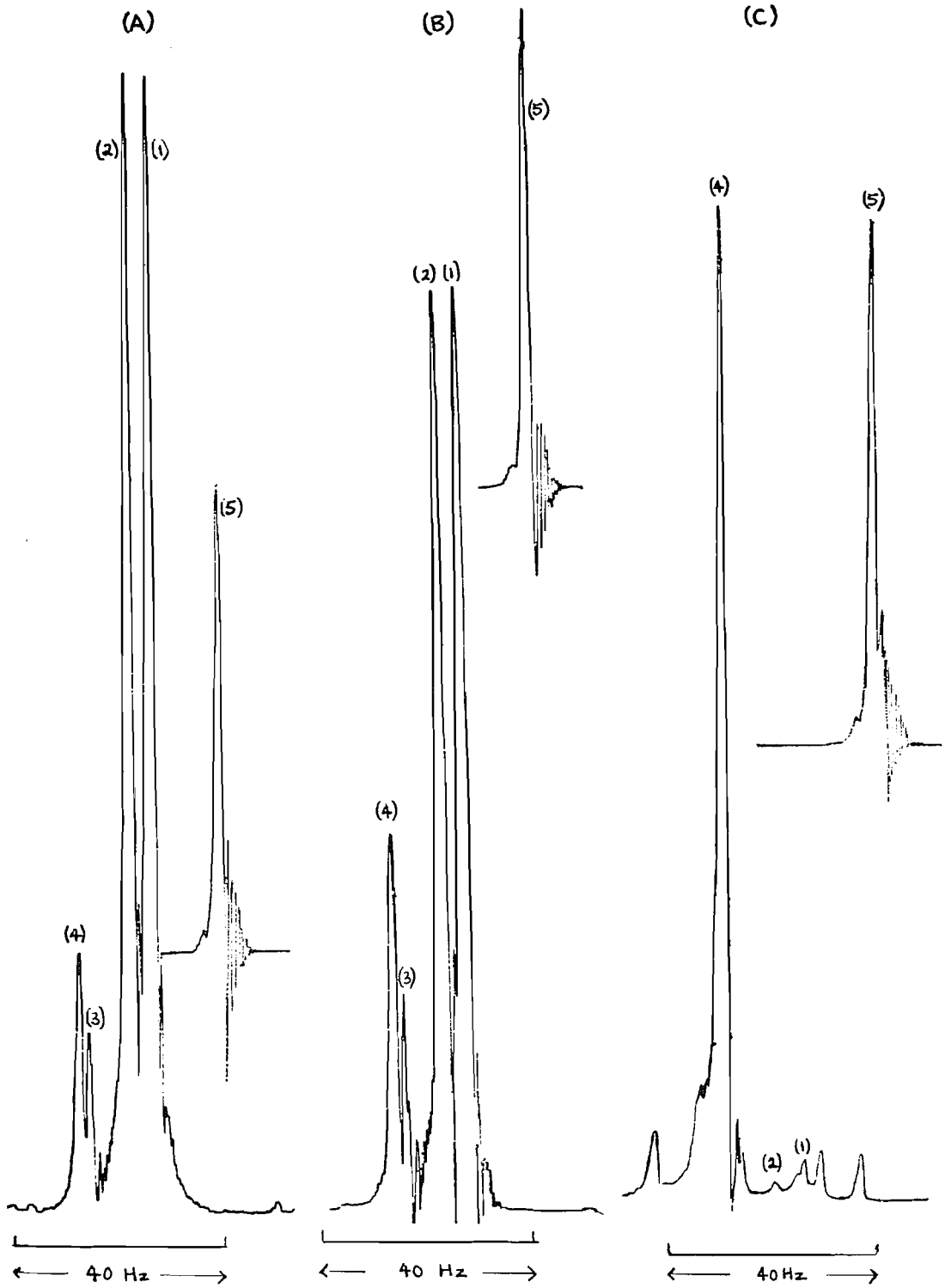

FIG. 1. 60 MHz ^{1}H n.m.r. spectra of BBr_3 and *o*-$CF_3C_6H_4SiMe_3$ after (*A*) 8 h; (*B*) 13 h; (*C*) 12 days. Peaks are due to (*1*) *o*-$CF_3C_6H_4SiMe_3$; (*2*) *o*-$CF_2BrC_6H_4SiMe_3$; (*3*) *o*-$CFBr_2C_6H_4SiMe_3$; (*4*) *o*-$CBr_3C_6H_4SiMe_3$; (*5*) external Me_4Si.

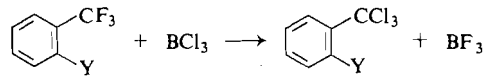

(Y = H, $SiMe_3$)

mixture at various time intervals (Fig. 1). A slight excess of boron tribromide was condensed into an n.m.r. tube containing *o*-$CF_3C_6H_4SiMe_3$ and the tube was sealed off under vacuum. After 8 h, the ^1H n.m.r. spectrum of the reaction mixture showed, in addition to a complex multiplet assigned to aromatic protons, a single peak due to *o*-$CF_3C_6H_4Si\mathit{Me}_3$ (*1*) and three other peaks at lower frequency presumably due to *o*-$CF_2BrC_6H_4Si\mathit{Me}_3$ (*2*), *o*-$CFBr_2C_6H_4Si\mathit{Me}_3$ (*3*), and *o*-$CBr_3C_6H_4Si\mathit{Me}_3$ (*4*). The relative intensity of peak *4* increases with time at the expense of peaks *1* and *2*, until after 12 days the predominance of peak *4* indicates that the reaction has gone to completion. Halogen exchange for the BCl_3/*o*-$CF_3C_6H_4SiMe_3$ system can also be followed by recording the ^1H n.m.r. spectrum of the reaction mixture, but overlapping of the peaks due to mixed halogen species is observed in this case.

However, attempts to use the halogen exchange reaction between boron trihalides and *o*-$CF_3C_6H_4$- derivatives selectively to displace either one or two fluorines of the CF_3 group by another halogen on a preparative scale have been unsuccessful, possibly due to disproportionation during the work-up procedure. For example, benzotrifluoride and boron trichloride in a 3:1 molar ratio gave benzotrichloride (35%) and unreacted benzotrifluoride (62%) as the major products.

Displacement of fluorine by chlorine in organic systems has been achieved using aluminum trichloride, but heating is normally required (11). The mild conditions used in the above examples are noteworthy, although fluorine–chlorine exchange between fluorohaloalkanes and boron trichloride has previously been observed in a study of the boron halide catalyzed haloalkylation of benzene (12).

$$3F(CH_2)_nCl + BCl_3 \rightarrow 3Cl(CH_2)_nCl + BF_3$$

Although we have not made a detailed study of the mechanism of halogen exchange, it seems likely that abstraction of fluoride ion by the boron trihalide to give a tetrahaloborate intermediate is involved, as has been demonstrated for exchange reactions between boron tribromide and some metal and non-metal chlorides (13).

The ^1H n.m.r. spectra of *o*-$CF_3C_6H_4SiMe_3$ and *o*-$CF_3C_6H_4SnMe_3$ both show 1:3:3:1 quartets at τ9.80 and τ9.66, respectively, due to coupling between the methyl protons and the 3 equivalent fluorines of the trifluoromethyl group, J_{HF} = 1.0 and 0.8 Hz, respectively. The coupling is formally through 6 bonds (5σ and 1 aromatic) and is significantly greater than that observed for the corresponding *o*-fluorophenyl derivatives where coupling through 5 bonds occurs, $J_{HF} \sim 0.5$ Hz (14).

The ^{19}F n.m.r. spectrum of K[*o*-$CF_3C_6H_4BF_3$] in 50% acetone solution shows a 1:3:3:1 quartet for —CF_3 fluorines at 58.9 p.p.m. due to coupling with $(—BF_3)^-$ fluorines, J_{FF} = 10.0 Hz. The ^{19}F n.m.r. spectrum of *o*-$CF_3C_6H_4BF_2$ as a neat liquid shows a broad singlet (—CF_3) at 61.2 p.p.m. (peak width at half height = 17.0 Hz). Broad, unresolved absorptions are observed for B—F fluorines in these two compounds at 79.6 p.p.m. (—BF_2) and 138.8 p.p.m. $(—BF_3)^-$, respectively. The latter value is close to that observed for B—F fluorines in K[$C_6F_5BF_3$] (134.25 p.p.m.) (10).

The early part of this work was carried out during the tenure of a Tutorial Fellowship at the University of Sussex. The author thanks Dr. D. R. M. Walton for a gift of *o*-(trifluoromethyl)phenyltrimethyltin. Financial support from the National Research Council of Canada is gratefully acknowledged.

1. T. Chivers. Chem. Commun. 157 (1967).
2. T. D. Parsons, J. M. Self, and L. H. Schaad. J. Amer. Chem. Soc. **89**, 3446 (1967).
3. S. L. Stafford and F. G. A. Stone. J. Amer. Chem. Soc. **82**, 6238 (1960).
4. R. D. Chambers and T. Chivers. J. Chem. Soc. 3933 (1965).
5. A. G. Massey and A. J. Park. J. Organometal. Chem. Amsterdam, **2**, 245 (1964); **5**, 218 (1965).
6. J. L. W. Pohlmann and F. E. Brinckman. Z. Naturforsch. **20**b, 5 (1965).
7. C. Eaborn, H. L. Hornfeld, and D. R. M. Walton. J. Organometal. Chem. Amsterdam, **10**, 529 (1967).
8. L. W. Frost. J. Amer. Chem. Soc. **78**, 3855 (1956).
9. H. C. Clark and R. J. O'Brien. Inorg. Chem. **2**, 1020 (1963).
10. R. D. Chambers, T. Chivers, and D. A. Pyke. J. Chem. Soc. 5144 (1965).
11. M. Hudlicky. Chemistry of organic fluorine compounds. Pergamon Press, London. 1961. p. 190.
12. G. A. Olah and S. J. Kuhn. J. Org. Chem. **29**, 2317 (1964).
13. P. M. Druce, M. F. Lappert, and P. N. K. Riley. Chem. Commun. 486 (1967).
14. T. Chivers. Unpublished data.
15. J. L. W. Pohlmann, F. E. Brinckman, G. Tesi, and R. E. Donadio. Z. Naturforsch. **20**b, 1 (1965).

Can. J. Chem. Downloaded from www.nrcresearchpress.com by 210.87.254.40 on 09/05/12
For personal use only.

Can. J. Chem. Downloaded from www.nrcresearchpress.com by 210.87.254.105 on 09/05/12
For personal use only.

Donor–acceptor interactions in Friedel–Crafts systems. The $CH_3COCl.AlCl_3$ addition compound

D. CASSIMATIS AND J. P. BONNIN
Ecole Polytechnique, Département de Génie Chimique, Montréal, Québec

AND

T. THEOPHANIDES
Université de Montréal, Département de Chimie, Montréal, Québec

Received June 30, 1970

The infrared spectra of CH_3COCl and $CH_3COCl.AlCl_3$ have been studied from 4000 to 300 cm^{-1} with a Perkin–Elmer 621 grating spectrophotometer. The results indicate that the addition compound $CH_3COCl.AlCl_3$ exists under three structures, two ionic and one dative structure. The distinct ionic structures are the carbonium type structure $[H_3C—C\dddot{=}O]^+[AlCl_4]^-$ with a carbonyl band at 2200 cm^{-1} (type 1) and a structure visualized as a hybrid between resonating structures

$$[CH_3—C{\equiv}O^+ \leftrightarrow CH_3—\overset{+}{C}{=}O \leftrightarrow \overset{+}{C}H_3{=}C{=}O][AlCl_4]^-$$

where the mesomeric limit form corresponding to the hyperconjugation is preponderant, with a carbonyl band at 2300 cm^{-1} (type 2). Vibrational assignments have been made for the two ions and supported by normal coordinate analysis. Two sets of force constants have been derived on the basis of the generalized force field for the two ionic structures to provide a correspondence between observed and calculated frequencies. Evidence would seem to show that the active species in the Friedel–Crafts ketone synthesis is the oxocarbonium type 1 acetylium ion.

Canadian Journal of Chemistry, **48**, 3860 (1970)

Introduction

Extensive work has been carried out to elucidate the structure of donor–acceptor addition compounds presumed to initiate Friedel–Crafts reactions (1). The conclusions reached on the structure of these compounds are based on the investigation of thermal properties, such as heats of formation and of electrical properties, such as conductivity and dipole moments. The most important contributions, however, arise from spectrochemical investigations, namely, the interpretation of the infrared spectra of the addition compounds of organic molecules containing the carbonyl group with the metal halide Lewis acid catalysts of the Friedel–Crafts reactions. These catalysts have an electron deficient central metal atom capable of accepting electrons from the carbonyl group of the organic compound.

The formation of the addition compound induces intramolecular displacement of negative charges from the donor to the acceptor molecule which results principally in a bathochromic or hypsochromic shift of the carbonyl stretching frequency ν(C=O).

From infrared evidence combined with X-ray analysis Susz and co-workers (2) came to the conclusion that these donor–acceptor addition compounds are of two distinct, well-defined structures:

(*1*) A structure corresponding to the hypsochromic shift with strong bands in the 2200 cm^{-1} region indicating the existence of the triple bond of the oxocarbonium ion $[R—C\dddot{=}O]^+$ isoelectronic with the R—C≡N molecule which also absorbs in the 2200 cm^{-1} region. This suggests the ionic structure

$$[R—C\dddot{=}O]^+[MX_{n+1}]^-$$

(*2*) A structure with a dative bond. In this structure the carbonyl group shares a pair of electrons with the electron deficient metal of the Lewis acid catalyst, thus forming a new covalent bond between the oxygen and the metal atoms.

The corresponding strong bathochromic shift of the order of 150–200 cm^{-1} of the carbonyl stretching frequency indicates the presence of a perturbed carbonyl bond which has lost some of its double bond character because of an electron displacement towards the oxygen atom.

All the investigated ketone – Lewis acid halide addition compounds and some of the acyl halide – Lewis acid halide addition compounds are of this dative bond structure

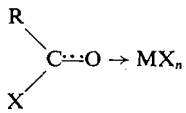

Susz and Wuhrmann (3) prepared the equimolar compound of CH_3COCl and $AlCl_3$ in the form of a white powder, which when heated decomposes at about 65 °C. During this preparation of the 1:1 addition compound $CH_3COCl.AlCl_3$ the possibility of the formation of a small fraction of the Illari compound $CH_2{=}CClO\text{-}AlCl_2$ was not, however, excluded. From the presence of the unique strong infrared absorption at 2300 cm^{-1} Susz and Wuhrmann suggested the resonance formula

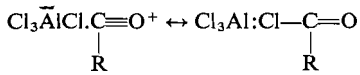

with a greater contribution of the limiting ionic structure over the non ionized form.

Cook (4) prepared the 1:1 addition compound $CH_3COCl.AlCl_3$ by direct mixture of the reactants in the absence of any solvent which resulted in a viscous liquid as opposed to the white powder obtained by Susz and Wuhrmann. This viscous liquid showed two strong infrared absorptions, at 2300 and 2203 cm^{-1}, the latter being absent from the Susz and Wuhrmann spectra.

In a first attempt to explain the two infrared absorptions, Cook assigned the 2300 cm^{-1} band to the $\nu(C{\equiv}O)$ stretching vibration of the free acetylium ion $[CH_3C{\equiv}O]^+$ and the 2200 cm^{-1} band to the complexed acetylium ion $[CH_3CO...AlCl_3]^+$ based on the possible analogy to the bathochromic shift of the dative structure, *i.e.* the lowering of carbonyl frequencies when complexed with Lewis acids.

In a later paper Cook (5) reversed the above assignments, *i.e.* the 2200 cm^{-1} band is now assigned to the free acetylium ion $[CH_3C{\equiv}O]^+$ and the 2300 cm^{-1} assigned to the complexed ion $[CH_3CO...AlCl_3]^+$ based on the possible analogy to the hypsochromic shift observed in nitrile addition compounds of the type $CH_3CN.AlCl_3$, where the complex has a higher CN stretching frequency than the free nitrile.

The discrepancies between the conclusions reached by Susz and Wuhrmann (3) and Cook (4) concerning the physical state of the addition compound $CH_3COCl.AlCl_3$, the additional 2200 cm^{-1} absorption band observed by Cook and the results obtained by Susz and Cassimatis (6) in investigations of the corresponding addition compounds of the aromatic molecules, where only the 2200 cm^{-1} infrared absorption band was observed, have led the authors of this paper to re-examine the infrared spectra of the $CH_3COCl.AlCl_3$ addition compound, to establish the structure of the active species in the ketone synthesis and subsequently determine the nature of the acetylating agent in the Friedel–Crafts reactions.

Independent of the assignment of the infrared absorptions in the 2200–2300 cm^{-1} region, the hypothesis of the complexed ion seemed to us to be contrary to the general idea of electron displacements in the donor–acceptor bond. It is difficult to conceive the possibility that the already electron deficient ion $[CH_3CO]^+$ shares a pair of its electrons with the electron deficient metal of the Lewis acid catalyst in a system of the type $[CH_3{-}C{\equiv}O...AlCl_3]^+\ Cl^-$. The recent X-ray (8) and infrared (10) studies also rule out the possibility of a complex of the above-mentioned type.

Experimental

Preparation

A solution of 0.05 mole of CH_3COCl in 50 ml of CCl_4 was introduced slowly into a suspension of 0.05 moles of powdered $AlCl_3$ in CCl_4. All the manipulations of the reactants, solvents, and solutions have been carried out in a dry box under strictly anhydrous conditions.

The mixture was agitated and heated slowly until nearly all the $AlCl_3$ passed into solution. Then the solution was decanted. The undissolved solid portion of $AlCl_3$ was negligible. By slowly cooling the solution, a colorless viscous liquid mass was deposited on the inner walls of the reaction flask which corresponds to the description of the complex made by Boeseken (7) and Cook (4).

The viscous compound was dried under vacuum to remove any CCl_4 or CH_3COCl which might have been retained in the product. Spectrographic analysis of the decanted liquor showed it to be a trace solution of CH_3COCl in CCl_4. This and chemical analysis were sufficient to lead the authors to conclude that this viscous, colorless mass was the 1:1 addition compound. This very simple but careful method of preparation was adopted by the authors as it seemed more likely to avoid experimental difficulties and thus diminish the possibility of undesirable side reactions or contamination of the product, which may occur with methods entailing the more lengthy manipulations found in previously described preparations.

Materials

Acetyl chloride was reagent grade, Baker and Adamson quality. Anhydrous aluminum chloride was certified

Can. J. Chem. Downloaded from www.nrcresearchpress.com by 210.87.254.105 on 09/05/12
For personal use only.

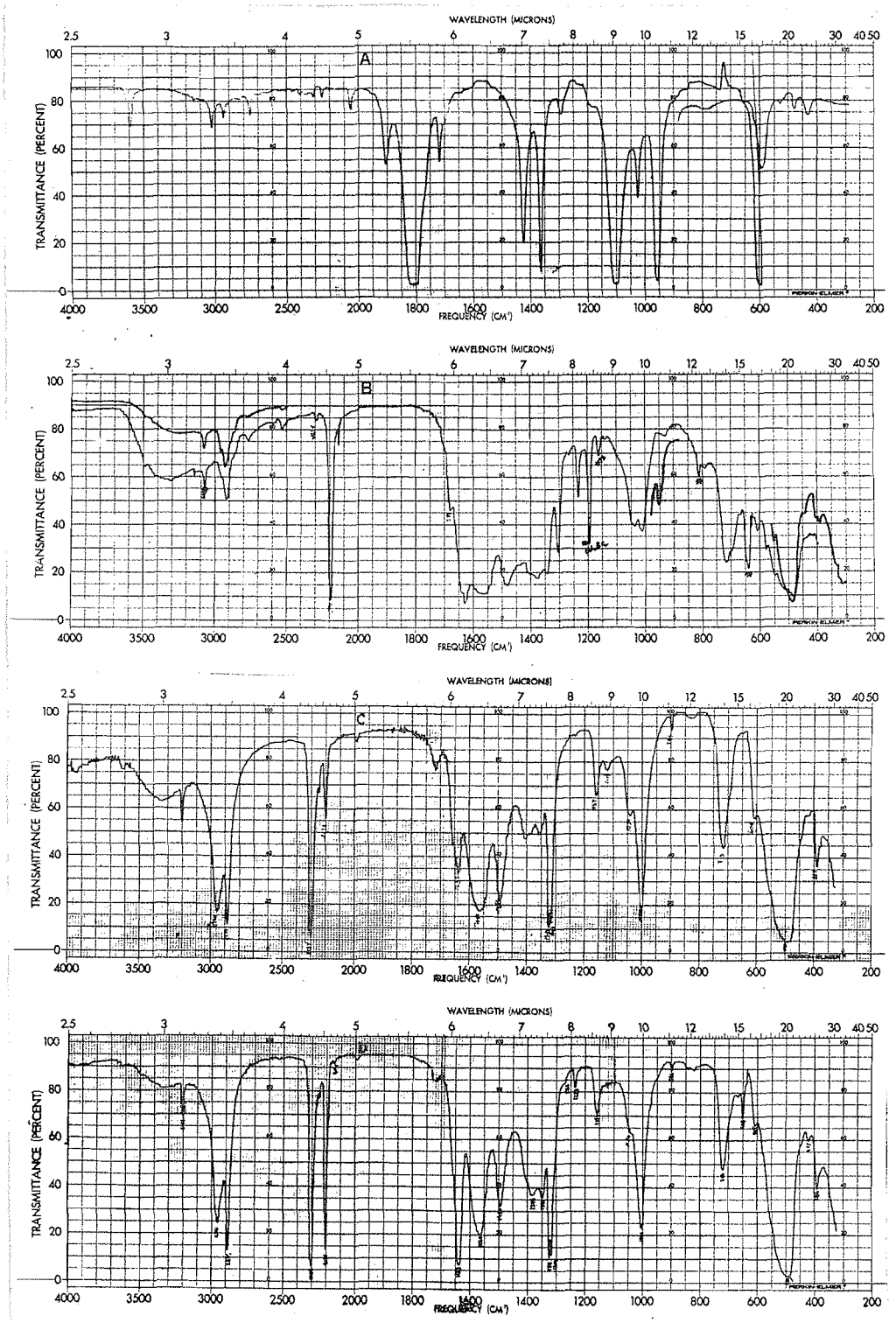

FIG. 1. Infrared spectra of (*A*) CH_3COCl (liquid); (*B*) $CH_3COCl.AlCl_3$ (type 1) suspension in CH_2Br_2; (*C*) $CH_3COCl.AlCl_3$ (type 2); and (*D*) mixture of type 1 and type 2.

Can. J. Chem. Downloaded from www.nrcresearchpress.com by 210.87.254.105 on 09/05/12
For personal use only.

TABLE 1

Observed vibrational frequencies and assignments

CH_3COCl (Liquid)	Assignment CH_3COCl	$CH_3COCl.AlCl_3$ Type 1	Type 2	Mixture	Assignment
3600	$2\nu_{CO}$				
			3200 m	3200 m	$2\nu(C—O\rightarrow)$
3025 m	$\nu_a(CH)$, $\nu_a(CH)$	2950 m	2950 s	2950 s	$\nu_a(CH)$
2940 w	$\nu_s(CH)$	2925 m	2878 s	2878 s	$\nu_s(CH)$
2760 w					
			2300 vs	2300 vs	$\nu(—C{=}O^+)$ stret. (2)
		2200 vs		2200 s	$\nu(—C{=}O^+)$ stret. (1)
2060 w	$2\rho_{CH_3}$				
1905 m	$2\nu_{CC}$				
1805 vs	ν_{CO}				
1717 w					
		1630 vs	1635 ms	1633 vs	
		1560 s	1560 s	1560 s	$\nu(—C{:}{:}O\rightarrow)$ stret.
1425 s	δ_{CH_3}, δ_{CH_3}	1478 s	1495 s	1490 s	
1368 s	δ_{CH_3}	1380 sb	1380 sb	1378 ms	$\delta_a(CH_3)$ (1, 2)
		1345 ms	1350 m	1346	
		1306 m	1322	1322	$\delta_s(CH_3)$ (1, 2)
			1315	1315	
1100 vs	$\rho_{CH_3}(+\nu_{CC})$				
1028 m	ρ_{CH_3}	1010 ms	1000 s	1000 s	$\rho_{CH_3}(1, 2)$, $\nu(C—C)$ (2)
955 s	$\nu_{CC}(+\rho_{CH_3})$	945			$\nu(C—C)$ (1)
		716 m	716 m	716 m	$\nu(O\rightarrow Al)$
				648	
595 s	$\nu_{(C-Cl)}$		604 w	605 w	$\nu(C—Cl)$
		495 sb	495 sb	495 sb	$\nu(Al—Cl)$
475 m	γ_{CO}				
430	ρ_{OCCl}	400			
		382 m	390 m	390 m	$\gamma(CCO)$ (1, 2)
(347) m*	δ_{CCCl}				
(238)*	τ_{CH_3}				

*Overend *et al.* (9).

Fisher reagent. Carbon tetrachloride was distilled, b.p. 63 °C and kept over molecular sieves. The solvents were of spectroscopic grade. The solutions were obtained by decanting the liquid from saturated solutions of the addition compound, always under strictly anhydrous conditions.

Analysis

The analysis for carbon and hydrogen was made by Schwarzkopf Microanalytical Laboratories 56-19, 37th avenue Woodside, N.Y. 11377, and by Dr. C. Daesslé, Organic Microanalyses, 5757 Decelles Ave., Montreal, Quebec. The analyses for chloride and aluminum were made in our laboratory.

Anal. Calcd. for $CH_3COCl.AlCl_3$: C, 11.33; H, 1.43; Cl, 66.95; Al, 12.73%. Found: C, 12.23; H, 1.29; Cl, 65.90; Al, 12.50%.

Spectra

A Perkin–Elmer 621 grating spectrophotometer was used to record the spectra. Suspensions of the compounds in Nujol, hexachlorobutadiene or in different solvents were prepared under strictly anhydrous conditions for the determination of the infrared spectra. The infrared spectra of liquid CH_3COCl and $CH_3COCl.AlCl_3$ recorded between NaCl or KBr plates are shown in Fig. 1. Suspensions of the $CH_3COCl.AlCl_3$ in CH_2Br_2 were deposited on the NaCl or KBr windows and the solvent allowed to evaporate before recording the spectra. The observed vibrational frequencies of CH_3COCl and $CH_3COCl.AlCl_3$ are listed in Tables 1 and 2. The vibrational assignment of CH_3COCl is similar to that reported by Overend *et al.* (9).

Results and Discussion

The infrared spectrum of the freshly prepared $CH_3COCl.AlCl_3$ presented the 2200 cm^{-1} infrared absorption, similar to that found with aromatic molecules containing the carbonyl group complexed with the Friedel–Crafts catalysts (6). The infrared absorption at 2300 cm^{-1} previously found in Susz and Wuhrmann (3) and Cook's (4) spectra was absent. Together with the 2200 cm^{-1} band, we observed a medium intensity band at 1010 cm^{-1} assigned to the methyl rocking shifted from 1100 cm^{-1} for the free CH_3COCl molecule to 1010 cm^{-1} for the complex $CH_3COCl.AlCl_3$ and a band at 945 cm^{-1} which is assigned to the C—C stretching vibration (see structure **1**). From the presence of the 2200 cm^{-1} absorption band only, we could

Can. J. Chem. Downloaded from www.nrcresearchpress.com by 210.87.254.105 on 09/05/12
For personal use only.

Can. J. Chem. Downloaded from www.nrcresearchpress.com by 210.87.254.105 on 09/05/12
For personal use only.

TABLE 2

Fundamental frequencies of the acetylium ions

		Type 1		Type 2					
Species	Mode	This work $CH_3COCl.AlCl_3$	Calculated	Susz and Wuhrmann (3) $CH_3COCl.AlCl_3$	Cook (5) $CH_3COCl.GaCl_3$	Gates and Steele (10) $CH_3COCl.SbCl_5$	This work $CH_3COCl.AlCl_3$	Calculated	Assignments
A_1	ν_1	2925	2924	2950	2870	2870	2878	2878	CH_3 sym. stret.
	ν_2	2200	2200	2305	2300	2295	2300	2300	CO stretching
	ν_3	1306	1306	1312	1310	1319	1322	1328	CH_3 sym. def.
	ν_4	945	945	1000		1001 950	1000	1001	CC stretching
E	ν_5	2950	2949	2950	2944	2940	2950	2955	CH_3 asym. stret.
	ν_6	1380	1380	1380		1360	1380	1373	CH_3 asym. def.
	ν_7	1010	1010	1000	1000	1001	1000	1009	CH_3 rocking
	ν_8	382	384	—	—	390	390	392	CCO deformation

Can. J. Chem. Downloaded from www.nrcresearchpress.com by 210.87.254.105 on 09/05/12
For personal use only.

suggest that the structure of the addition compound is of the ionic type $[CH_3C{\equiv}O]^+[AlCl_4]^-$. However, it will be shown below that this is not the case and that some further distinction between two ionic structures must be made, because of the appearance of the 2300 cm^{-1} band.

Taking the viscous colorless mass of $CH_3COCl.AlCl_3$ as a super-cooled liquid, we tried to crystallize the compound by redissolving it in such solvents as CCl_4, CS_2, C_6H_6, $CHCl_3$, CH_3CN, etc., but met with no success; on the contrary, the colorless mass took on a greyish tint and became more and more viscous. Further attempts to crystallize this mass resulted in the formation of grey-white spots agglomerated in the product. It is at this point that the infrared spectra presented both the 2200 and the 2300 cm^{-1} absorption bands with variable relative intensities, the intensity of the 2200 cm^{-1} band diminishing as that of the 2300 cm^{-1} band increased (see Fig. 2). Finally, the viscous liquid mass which was deposited on the inner walls of the reaction flask was treated following Susz and Wuhrmann's procedure of eliminating the last traces of solvent and acetyl chloride. This resulted in a grey-white powder which when heated decomposes at 75 °C. The infrared spectra of this grey-white powder showed the 2300 cm^{-1} band similar to that reported by Susz and Wuhrmann.

Together with the 2300 cm^{-1} absorption band we observed a strong band at 1000 cm^{-1}, which is described for reasons explained later as a mixture of the methyl-rocking and the symmetrical C—C stretching vibration shifted from 1100 and 955 cm^{-1} for the free CH_3COCl molecule to 1000 cm^{-1} for the complex $CH_3COCl.AlCl_3$ (see structure **2**).

For comparison of the infrared spectra of the free CH_3COCl and the complex $CH_3COCl.AlCl_3$ molecules, it should be mentioned here that Overend *et al.* (9) assigned two strong bands at 1109 and 958 cm^{-1} of the free CH_3COCl molecule to the mixture of the methyl rocking and carbon–carbon stretching vibrations.

It is clear from these spectra that the freshly prepared addition compound $CH_3COCl.AlCl_3$ characterized by the 2200 cm^{-1} band is partially transformed into a compound which shows the 2300 cm^{-1} absorption band. Here we must exclude any suggestion of a decomposition since

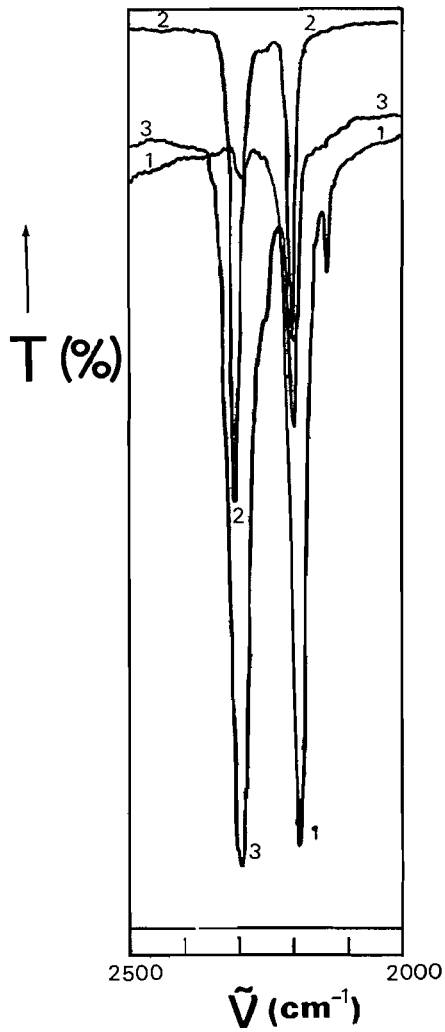

FIG. 2. Intensity variations of the infrared absorption bands in the region 2300–2200 cm^{-1} of the addition compound $CH_3COCl.AlCl_3$.

the chemical analysis was always in conformity with the 1:1 addition compound.

The variable relative intensities of the two carbonyl absorptions at 2200 and 2300 cm^{-1}, the shifted C—C stretching band at 945 and 1000 cm^{-1}, and the two strong bands at 1630 and 1560 cm^{-1}, led us to conclude that the addition compound $CH_3COCl.AlCl_3$ exists under two distinct ionic structures (*1*, *2*) and the dative structure (*3*):

(*1*) The oxocarbonium type structure

$$[H_3C{-}C{\equiv}O^+][AlCl_4]$$

with the carbonyl vibration at 2200 cm^{-1}, the methyl rocking at 1010 cm^{-1} and the C—C symmetrical stretching vibration at 945 cm^{-1} results from conjugative mesomeric displacements which occur within the C—O group. The displacement of negative charges of the oxygen atom in the same atomic octet towards the carbonyl bond increases the covalency, that is, the multiplicity of the double bond, until the internal energy of the system is minimized and a stable molecular condition is reached.

(*2*) The "ketene-like" structure which could be described as a hybrid between the resonating structures

$$[CH_3—C\equiv O^+ \leftrightarrow CH_3—\overset{+}{C}=O \leftrightarrow \overset{+}{C}H_3=C=O][AlCl_4]^-$$

where the mesomeric limit form corresponding to the hyperconjugation is preponderant, with a carbonyl group vibration at 2300 cm^{-1}, the methyl rocking and carbon–carbon stretching C—C vibration at 1000 cm^{-1}. It is well-known that in compounds containing the structure C=C=O such as ketenes, for example, the two double bonds have the single (1130 cm^{-1}) and triple bond (2160 cm^{-1}) infrared frequencies because of strong interaction. The "ketene-like" structure of the acetylium ion containing the structure C=C=O has bands at 1000 cm^{-1} corresponding to the C—C stretching vibration and at 2300 cm^{-1} corresponding to the carbonyl group vibration.

To explain the structure of this cation, let us consider the system $H_3C—\overset{+}{C}=O$ in the transition state. Due to the electrical demand of the unsaturated center from the surrounding structure, the methyl group exerts an inductive effect towards the central carbon. The unequal sharing of the electrons between the hydrogen atoms and the carbon atom, due to the inductive mechanism of electron displacements, induces a dipole on the carbon–carbon bond with the effect of decreasing the C—C distance

$$\begin{matrix} & H & \\ & \searrow & \\ [H \rightarrow & C\cdots C=O:]^+ & [AlCl_4]^- \\ & \nearrow & \\ & H & \end{matrix}$$

The above conclusions are in agreement with X-ray experimental results obtained by Boer (8) for the $CH_3COF.SbF_5$ addition compound, where the C—C distance of 1.378 Å is considerably shorter than the corresponding bond distances of 1.458 and 1.460 Å in the iso-electronic species $CH_3C\equiv N$ and $CH_3C\equiv CH$, respectively. The C—O distance of 1.15 Å in the addition compound is shorter than the C—O distance of 1.22 Å in the acetyl chloride.

(*3*) In addition to the bands in the 2200–2300 cm^{-1} region, we observe in the infrared spectra of the addition compound $CH_3COCl.AlCl_3$ the two strong bands at 1630 and 1560 cm^{-1}. These bands are assigned to the perturbed carbonyl frequency (C—O→) of the dative structure

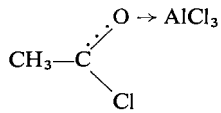

Detailed studies of the dative structure of these addition compounds have been made by Susz and Cassimatis (6) using $TiCl_4$ in place of $AlCl_3$. It should be mentioned here that $CH_3COCl.TiCl_4$ presents only the dative structure.

The fact that the C—O absorption band at 2300 cm^{-1} has been found in the infrared spectra of $CH_3COCl.AlCl_3$ only when in the solid state, is in general agreement with the findings of Susz and Wuhrmann (3) and Gates and Steele for $CH_3COCl.SbCl_5$ (10). The rise of the C—O stretching frequency from 2200 cm^{-1} in the viscous state to 2300 cm^{-1} in the solid state of the $CH_3COCl.AlCl_3$ cannot be explained as being due to the difference in the physical state of the addition compound. The observed shift of 100 cm^{-1} is too large to be attributed to the interaction of the lattice vibrations with the molecular C—O vibration.

To assess the vibrational spectra of the type 1 and 2 ions presents a somewhat difficult problem because they have always been obtained together with the infrared spectrum of the dative structure addition compound. However, having in mind the assignment made by Susz and Cassimatis (6) and Cassimatis *et al.* (11) for the addition compound $CH_3COCl.TiCl_4$, characterized by the frequencies 1630, 1560, 1155, and 1030 cm^{-1}, it is possible to proceed with the assignment of the four fundamental bands of the A_1 species and the four degenerate of the E species of the acetylium ion.

The bands of 2925, 2950 cm^{-1} and 2878, 2950 cm^{-1} for the infrared spectra of the type 1 and 2 ions, respectively, are assigned without

Can. J. Chem. Downloaded from www.nrcresearchpress.com by 210.87.254.105 on 09/05/12
For personal use only.

Can. J. Chem. Downloaded from www.nrcresearchpress.com by 210.87.254.105 on 09/05/12
For personal use only.

ambiguity to the symmetric and asymmetric C—H stretching vibrations.

The bands 1010, 1306, 1380 cm^{-1} of the infrared spectra of the type 1 ion and the bands 1000, 1322, and 1375 cm^{-1} of that of the type 2 ion are close to those of the rocking, symmetric, and asymmetric deformations normally found for the methyl group and can be immediately assigned to this group.

The assignment of the C—C stretching vibrations presents a certain difficulty. Gates and Steele (10) have assigned the C—C stretching vibration to the shoulder of the strong band at 1000 cm^{-1}. However, the 1000 cm^{-1} band in our spectra of the type 2 ion (2300 cm^{-1}) shows no shoulder. As the C—C absorption should be found in the region of 850 to 1000 cm^{-1}, we are obliged to make a double assignment for the 1000 cm^{-1} which is described as a mixture of the methyl rocking and carbon–carbon stretching vibrations. This is in good agreement with the Teller–Redlich product rule. The use of the C—C frequencies found for CH_3CN and CD_3CN and the corresponding value of 1000 cm^{-1} for the type 2 ion yields 920 cm^{-1} for the C—C stretching frequency of the CD_3CO^+ ion. This band exists in the infrared spectra of Gates and Steele (10) but it was not given any assignation.

The existence of a weak band at 950 cm^{-1} in the infrared spectra of the type 1 ion (2200 cm^{-1}) allows us to assign this frequency to the C—C vibration of this ion.

We are now left with one fundamental, the C—C—O bending. By analogy with the C—C—N bending vibration at 370 cm^{-1} for the CH_3CN molecule and the C—C—C bending at 336 cm^{-1} for the CH_3—C≡C—H molecule, we assign the medium intensity band at 390 cm^{-1} to the C—C—O bending vibration.

The Al—Cl infrared absorption of the $AlCl_4^-$ or of the dative complex is visible at 495 cm^{-1} in the form of a strong and broad band.

Finally, the medium band at 716 cm^{-1} may be attributed to the O → Al vibration and would correspond to the 540 cm^{-1} absorption band observed but not assigned by Gates and Steele (10) for the O → Sb vibration. However, these two frequencies seem to be higher than expected and would imply a bond order nearing one.

Once the double ionic structure of the addition compound $CH_3COCl.AlCl_3$ had been established, the problem was to determine which of the two ionic structures may be considered the active species in the mechanism of the Friedel–Crafts ketone synthesis. To this end, we examined and compared the infrared spectra of solutions of $CH_3COCl.AlCl_3$ in various solvents. The addition compound was found to be scarcely soluble in solvents such as CCl_4, CS_2, $CHCl_3$, CH_3CN, C_6H_6, etc. The infrared spectra of these solutions, apart from minor variations, were composed of the absorption bands of the free CH_3COCl and of the corresponding solvent. This led us to conclude that the addition compound does not exist in solution in the above-mentioned solvents, it dissociates to give the free acetyl chloride. However, solutions of $CH_3COCl.AlCl_3$ in nitrobenzene showed only the 2200 cm^{-1} absorption band. The band at 2300 cm^{-1} was never observed in spectra of solutions of these addition compounds. Even the type 2 addition compound characterized by the 2300 cm^{-1} band in the condensed phase, presented in solution in nitrobenzene only the 2200 cm^{-1} band. This is in accordance with previous results of Cassimatis *et al.* (11) and the findings of Cook (5) for solutions of $CH_3COCl.AlCl_3$ and $CH_3COCl.GaCl_3$ in nitrobenzene, who indicated that the 2300 cm^{-1} band was greatly reduced or disappeared and that a new band was observed at 2195 cm^{-1}. It seems therefore from this spectrographic evidence that, if a kinetic step of acetylium ion exists in Friedel–Crafts reactions, the active ion must be of the oxocarbonium type 1 structure, since it is the only one found in solution. It may also be of significance to mention that the Friedel–Crafts acetophenone synthesis was carried out using the addition compound $CH_3COCl.AlCl_3$ and benzene. The yield of acetophenone obtained from the oxocarbonium type 1 structure was of the order of 75% and was always superior by about 20–25% to that obtained from the type 2 structure. Further work, particularly an investigation of the rates of Friedel–Crafts reactions, where no infrared spectrographic evidence exists for the kinetic step of ion formation, would be desirable to determine unambiguously the structure of the acetylium ion active in Friedel–Crafts reactions.

Normal Coordinate Analysis

A normal coordinate analysis was carried out primarily for the purpose of deriving a set of

Can. J. Chem. Downloaded from www.nrcresearchpress.com by 210.87.254.105 on 09/05/12
For personal use only.

TABLE 3
Elements of the F-matrix

A_1 species		E species	
Element	Assignment	Element	Assignment
$F_{11} = f_r + 2f_{rr}$	CH sym. stretching	$F_{55} = f_r - f_{rr}$	CH asym. stretching
$F_{12} = \sqrt{3}f_{rt}$	CH sym. stret.—CO stret.	$F_{56} = [f_{r\alpha}' - f_{r\alpha}]d$	CH as. stret.—CH_3 as. def.
$F_{13} = \frac{\sqrt{2}}{2}[2f_{r\alpha} + f_{r\alpha}' - 2f_{r\beta} - f_{r\beta}']d$	CH sym. stret.—CH_3 sym. deform.	$F_{57} = [f_{r\beta}' - f_{r\beta}]d$	CH as. stret.—CH_3 rocking
$F_{14} = \sqrt{3}f_{rs}$	CH sym. stret.—CC stret.	$F_{58} = \frac{\sqrt{6}}{2}f_{\theta r_1}{}^x$	CH as. stret.—CCO bending
$F_{22} = f_t$	CO stretching	$F_{66} = [f_\alpha - f_{\alpha\alpha}]d^2$	CH_3 asym. deform.
$F_{23} = \frac{\sqrt{6}}{2}[f_{t\alpha} - f_{t\beta}]d$	CO stret.—CH_3 sym. deform.	$F_{67} = [f_{\alpha\beta}' - f_{\alpha\beta}]d^2$	CH_3 as. deform.—CH_3 rock.
$F_{24} = f_{rt}$	CO stret.—CC stret.	$F_{68} = \frac{\sqrt{6}}{2}f_{\theta\alpha_{23}}{}^x d^2$	CH_3 as. deform.—CCO bend.
$F_{33} = \left[\frac{1}{2}(f_\alpha + f_\beta) + f_{\alpha\alpha} + f_{\beta\beta} - 2f_{\alpha\beta} - f_{\alpha\beta}'\right]d^2$	CH_3 sym. deform.	$F_{77} = [f_\beta - f_{\beta\beta}]d^2$	CH_3 rocking
$F_{34} = \frac{\sqrt{6}}{2}[f_{\alpha s} - f_{s\beta}]d$	CH_3 sym. deform.—CC stret.	$F_{78} = \frac{\sqrt{6}}{2}f_{\theta\beta_1}{}^x d^2$	CH_3 rock.—CCO bending
$F_{44} = f_s$	CC stretching	$F_{88} = f_\theta d^2$	CCO bending

*The force constant units are: f, mdyn/Å; F stret., mdyn/Å; F bend., mdyn Å; F stret.-bend., mdyn. In evaluating the 25 bond force constants which are not all independent, the following relations must be considered:

$$2f_{r\alpha} + f_{r\alpha}' + 2f_{r\beta} + f_{r\beta}' = 0$$
$$f_{s\alpha} + f_{\beta\beta} = f_{t\alpha} + f_{t\beta} = 0$$
$$f_\alpha + 2f_{\alpha\alpha} + 2f_{\alpha\beta} + f_{\alpha\beta}' = 0$$
$$f_\beta + 2f_{\beta\beta} + 2f_{\alpha\beta} + f_{\alpha\beta}' = 0$$

Can. J. Chem. Downloaded from www.nrcresearchpress.com by 210.87.254.105 on 09/05/12
For personal use only.

force constants for each of the two ions and thereby to check and support our proposed vibrational assignment anticipating that the derived sets of force constants would give more insight into the difference in the bonding of the two ionic structures.

A vibrational assignment was made and thereafter a set of symmetry force constants, for each ion, was derived by a process of successive approximations, in such a way that when these force constants were introduced into the secular equations resulting from the **FG**-matrix method (12), these equations reproduced frequencies in best agreement with the observed frequencies.

A normal coordinate treatment was made by Gates and Steele (10) for the type 2 acetylium ion with a slightly different vibrational assignment. The derived force constants by Gates and Steele were quite different from those derived in this work. For the carbonium ion (2200 cm^{-1}) no X-ray analysis has been made since it is found only in the viscous state. Consequently its symmetry is unknown. However, for the sake of comparison, a similar coordinate analysis was made as for the type 2 acetylium ion (2300 cm^{-1}) assuming C_{3v} symmetry with tetrahedral angles for the methyl group and CH, CC, and CO bond lengths of 1.09, 1.46, and 1.13 Å, respectively.

The geometry and the parameters of the C_{3v} model of the acetylium ion are shown in Fig. 3. The potential function used is the general quadratic valence force field. The symmetry of the $[CH_3CO]^+$ ion requires only twenty independent F force constants. They are ten A_1 and ten E symmetry force constants. The elements of the **G** and **F** matrices have been calculated and found in agreement with those given before for the C_{3v} model of the BH_3CO and CH_3CN molecules (13, 15). However, we repeat the **F** matrix in Table 3 for the convenience of the reader.

Using the assignment given in Table 2 we derived for each of the two symmetry species a set of force constants. The procedure followed was the usual one found in the literature for the calculation of force constants by the **FG**-matrix method. A starting set of force constants available from similar molecules is introduced in each one of the two secular equations for the symmetric species A_1 and E. In our case these sets were taken from Duncan's (14) statistical data on

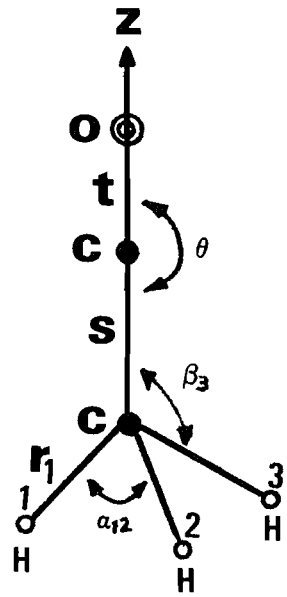

FIG. 3. Structural parameters of the C_{3v} acetylium ion; r = CH bond length, s = CC bond length, t = CO bond length. α(HCH) = β(CCH) = 109° 28′; for type 1, r = 1.09 Å, s = 1.46 Å, t = 1.13 Å; for type 2, r = 1.06 Å; s = 1.38 Å, t = 1.15 Å.

the CH_3—C group. The search type problem was to vary these constants judiciously so as to obtain the best fit to all observed frequencies.

During the course of these calculations we found that the A_1 frequencies were rather insensitive to five of the six off-diagonal force constants and it was reasonable to constrain them to zero. This was not the case for the F_{34} (CH_3 sym. deform—CC stretching) and it was possible to converge on a solution when F_{34} was allowed negative values in the range of -0.45 ± 0.05 for the type 1 ion and -0.69 ± 0.05 for the type 2 ion. Only F_{56}, F_{57}, and F_{68} of the E species needed to be constrained to zero.

The values of force constants for the two types of acetylium ion which reproduced the best agreement between the calculated and observed frequencies are shown in Tables 4 and 5. Alongside these force constants are given their uncertainty intervals within which the convergence is still possible. Small variations in some of the force constants within the given limits lead to changes in the calculated frequencies of less than 1%. However, it must be noticed that these limits simply determine the domain of uncertainty within which the set of force constants may be

TABLE 4

Symmetry force constants of C_{3v} acetylium ions*

Force constants A_1 species	Value			Force constant, E species	Value		
	Type 1	Type 2	Reference 14		Type 1	Type 2	Reference 14
F_{11}	4.92±0.05	4.73±0.05	4.95±0.08	F_{55}	4.63±0.05	4.62±0.05	4.82±0.12
F_{12}	0.00±0.01	0.00±0.01		F_{56}	0.00±0.03	0.00±0.03	−0.10±0.03
F_{13}	0.00±0.05	0.00±0.05	0.07±0.02	F_{57}	0.00±0.03	0.00±0.03	0.10±0.03
F_{14}	0.00±0.05	0.00±0.05	0.0	F_{58}	−0.07±0.03	−0.07±0.03	
F_{22}	17.73±0.06	18.58±0.06	18.96†	F_{66}	0.453±0.004	0.452±0.004	0.55±0.02
F_{23}	0.00±0.04	0.00±0.04		F_{67}	0.03±0.02	0.03±0.02	0.01±0.02
F_{24}	0.00±0.01	0.00±0.01		F_{68}	0.00±0.02	0.00±0.02	
F_{33}	0.590±0.004	0.58±0.004	0.59±0.02	F_{77}	0.690±0.004	0.663±0.004	0.66±0.02
F_{34}	−0.45±0.05	−0.69±0.05	−0.37±0.02	F_{78}	−0.03±0.02	−0.03±0.02	
F_{44}	5.70±0.10	6.72±0.10	5.26±0.08	F_{88}	0.349±0.006	0.352±0.006	

*The force constant units are: stretching, mdyn/Å; bending, mdyn Å; stret.-bend., mdyn.
†BH_3CO (15).

TABLE 5

Bond force constants of the C_{3v} acetylium ion*

Type 1†	Type 2‡
$f_r = 4.73$	$f_r = 4.66$
$f_s = 5.70$	$f_s = 6.73$
$f_t = 17.73$	$f_t = 18.58$
$f_{rr} = 0.096$	$f_{rr} = 0.037$
$f_{rs} = f_{rt} = 0.00$	$f_{rs} = f_{rt} = 0.00$
$f_{st} = 0.35$	$f_{st} = 0.00$
$f_{s\alpha} = -f_{s\beta} = -0.168$	$f_{s\alpha} = -f_{s\beta} = 0.268$
$f_{t\alpha} = -f_{t\beta} = 0.00$	$f_{t\alpha} = -f_{t\beta} = 0.00$
$f_{r\alpha}' = f_{r\alpha} = f_{r\beta} = f_{r\beta}' = 0.00$	$f_{r\alpha}' = f_{r\alpha} = f_{r\beta} = f_{r\beta}' = 0.00$
$f_\beta = 0.325$	$f_\beta = 0.368$
$f_\alpha = 0.359$	$f_\alpha = 0.354$
$f_{\alpha\beta} = -0.098$	$f_{\alpha\beta} = -0.094$
$f_{\alpha\beta}' = -0.074$	$f_{\alpha\beta}' = -0.069$
$f_{\beta\beta} = -0.111$	$f_{\beta\beta} = -0.086$
$f_{\alpha\alpha} = -0.022$	$f_{\alpha\alpha} = -0.048$
$f_\theta = 0.212$	$f_\theta = 0.222$
$f_{\theta r_1}{}^x = -0.039$	$f_{\theta r_1}{}^x = -0.041$
$f_{\theta\alpha_{23}}{}^x = 0.00$	$f_{\theta\alpha_{23}}{}^x = 0.00$
$f_{\theta\beta_1}{}^x = -0.012$	$f_{\theta\beta_1}{}^x = -0.013$

*Units of force constant: mdyn/Å.
†$r = 1.09$ Å; $s = 1.46$ Å; $t = 1.13$ Å.
‡$r = 1.06$ Å; $s = 1.38$ Å; $t = 1.15$ Å.

found. They are relative to the imposed constraints and can give the same false picture of the accuracy of force constants as the standard errors calculated by Duncan (14). These limits give a more realistic response to the multimodel search problem of force constants calculations than the standard errors often found in the literature on the subject.

As expected, the derived set of force constants for the type 2 ion reproduces the frequencies of the $[CD_3CO]^+$ ion listed by Gates and Steele (10). Because of that, a more satisfactory assignment of the $[CD_3CO]^+$ frequencies was possible. It has the advantage of avoiding the double assignment of the 834 cm^{-1} band to the A_1 and E species made by Gates and Steele. In addition, the then unassigned 920 cm^{-1} band is now assigned to C—C stretching (see Table 6).

The force constant of $F_{44} = 5.70$ mdyn/Å found for the C—C bond of the type 1 ion is somewhat greater than that found by Duncan for the $CH_3—C\equiv X$ molecules of 5.26 ± 0.08 mdyn/Å. However, this difference is slight enough to allow us to conclude that the type 1 ion is of the carbonium type structure $[CH_3—C\equiv O]^+$ similar to that of the molecules studied by Duncan. On the contrary the force constant of $F_{44} = 6.72$ mdyn/Å for the C—C bond of the

Can. J. Chem. Downloaded from www.nrcresearchpress.com by 210.87.254.105 on 09/05/12
For personal use only.

TABLE 6
Fundamental frequencies of $[CH_3CO]^+$ and $[CD_3CO]^+$ ions

		$[CH_3CO]^+$		$[CD_3CO]^+$		
Species	Mode	Observed	Calculated	Observed (10)	Calculated	Assignments
A_1	ν_1	2878	2872	2049	2056	CH_3 sym. stret.
	ν_2	2300	2300	2297	2302	CO stretching
	ν_3	1322	1328	1056	1050	CH_3 sym. def.
	ν_4	1000	1001	920	916	CC stretching
E	ν_5	2950	2955	2209	2204	CH_3 asym. stret.
	ν_6	1380	1373	980	982	CH_3 asym. def.
	ν_7	1000	1009	834	809	CH_3 rocking
	ν_8	390	392	370	367	CCO deformation

type 2 ion is appreciably higher than that of 5.26 ± 0.08 mdyn/Å found by Duncan. Nevertheless, this result is compatible with Boer's X-ray analysis (8) of the CH_3COF, SbF_5 which has shown a particularly short C—C bond length of 1.378 Å in comparison with the value of 1.46 Å in the isoelectronic molecules CH_3CN and CH_3CCH. Furthermore, the force constants $F_{11} = 4.73 \pm 0.06$ mdyn/Å (C—H stretching symmetric) and $F_{55} = 4.63 \pm 0.06$ mdyn/Å (C—H stretching asymmetric) are somewhat lower for the type 2 acetylium ion than those usually found for similar molecules of 4.95 ± 0.08 and 4.82 ± 0.12 mdyn/Å, respectively.

The increase of the C—C and the lowering of the C—H stretching constants led us to support the conclusion that a "ketene-like" structure exists for the type 2 ion which could be described as a hybrid between the resonating structures,

$$CH_3—C\equiv O^+ \leftrightarrow CH_3—\overset{+}{C}=O \leftrightarrow \overset{+}{C}H_3=C=O$$

where the mesomeric limit form corresponding to the hyperconjugation carries a heavy weight. The rather large increase of the force constant $f_{C=O}$ from 17.7 (type 1) to 18.6 mdyn/Å (type 2) is not unexpected because of resonance structure alterations of the C—C and C—O distances. The structure of the type 2 ion, the force constants of which are different from those of the type 1 acetylium ion, would imply an interaction effect between the C—C and C—O bond due to hyperconjugation, or delocalization of electrons spread over the entire unsaturated system which stabilizes it by lowering its energy.

The infrared evidence of the two distinct ionic structures of the addition compound $CH_3COCl.AlCl_3$ may be explained by the localization of the electrons in the less stable type 1 acetylium ion and delocalization of electrons in the "resonance stabilized" type 2 ion.

This viewpoint is in opposition to the hypothesis expressed in the literature (4) of complexed ions, but is compatible with the fact that the addition compounds of substituted benzoyl halides (6, 11, 16) present only one C—O infrared band in the region of 2200 cm^{-1} which corresponds to the C—O infrared absorption of the type 1 ion. If the hypothesis of the complexed ion were compatible with the real structure, there is no reason why the addition compounds of the aroyl halides should not show the 2300 cm^{-1} absorption band corresponding to the complexed ions.

D.C. gratefully acknowledges a grant from the National Research Council of Canada.

1. G. OLAH. Friedel-Crafts and related reactions. Interscience Publisher, Inc., New York. 1963.
2. B. P. SUSZ. Compt. Rend. **248**, 2569 (1959).
3. B. P. SUSZ and J.-J. WUHRMANN. Helv. Chim. Acta, **40**, 971 (1957).
4. D. COOK. Can. J. Chem. **37**, 48 (1959).
5. D. COOK. Can. J. Chem. **40**, 480 (1962).
6. B. P. SUSZ and D. CASSIMATIS. Helv. Chim. Acta, **44**, 395 (1961).
7. J. BOESEKEN. Rec. Trav. Chim. Pays-Bas, **19**, 19 (1900).
8. F. P. BOER. J. Amer. Chem. Soc. **88**, 1572 (1966).
9. J. OVEREND, R. A. NYQUIST, J. C. EVANS, and W. J. POTTS. Spectrochim. Acta, **17**, 1205 (1961).
10. P. N. GATES and D. STEELE. J. Mol. Struct. **1**, 349, (1967).
11. D. CASSIMATIS, P. GAGNAUX, et B. P. SUSZ. Helv. Chim. Acta, **43**, 425 (1960).
12. E. B. WILSON, J. C. DECIUS, and P. C. CROSS. Molecular vibrations. McGraw-Hill. 1955.
13. A. G. MEISTER. J. Chem. Phys. **16**, 951 (1948).
14. J. L. DUNCAN. Spectrosc. Acta, **20**, 1197 (1964).
15. G. W. BETHKE and M. K. WILSON. J. Chem. Phys. **26**, 1118 (1957).
16. D. CASSIMATIS and B. P. SUSZ. Helv. Chim. Acta, **44**, 943 (1961).

Can. J. Chem. Downloaded from www.nrcresearchpress.com by 210.87.254.105 on 09/05/12
For personal use only.

Can. J. Chem. Downloaded from www.nrcresearchpress.com by 210.87.254.6 on 09/05/12
For personal use only.

Electron paramagnetic resonance spectra of some sulfur-containing radicals

P. S. H. BOLMAN, I. SAFARIK, D. A. STILES, W. J. R. TYERMAN, AND O. P. STRAUSZ
Department of Chemistry, University of Alberta, Edmonton, Alberta

Received June 8, 1970

The e.p.r. spectra from the low temperature matrix photolysis of several mercaptans, disulfides, and cyclic sulfides have been recorded and compared to those obtained in the photolysis of these materials adsorbed on a porous Vycor glass. The spectra of the adsorbed radicals are characterized by an enhanced thermal stability and a shift of the highest sulfur *g*-value to higher fields. The only free radical product in the photolysis of mercaptans and disulfides is the thiyl radical. The cyclic sulfides $CH_2—(CH_2)_n—S$ appear to yield $\cdot CH_2—(CH_2)_n—S\cdot$ type diradicals, while the cyclic disulfide $CH_2—CH_2—CH—(CH_2)_4$-COOH gives the $\cdot S—(CH_2)_2—CH—(CH_2)_4COOH$ diradical.

Canadian Journal of Chemistry, 48, 3872 (1970)

Introduction

Cleavage of the S—H bond is the only significant primary step in photolysis of alkane thiols (1, 2). The photolytic and radiolytic behavior of disulfides, a system of biological significance, has been characterized in terms of a number of different overall processes. Rosengren measured the u.v. absorption spectra of photolyzed thiols (2) and disulfides (3) in matrices, and proposed that "hot" thiyl radicals formed which rapidly underwent further reaction. In contrast, long lived paramagnetic species are present in disulfides, γ-irradiated (4) or photolyzed (5) at 77 °K, and on the basis of similarities with e.p.r. spectra from thiols, these are identified as thiyl radicals. In long-chain disulfides C—H cleavage also seems to occur (5).

The primary aim of the present study was to shed further light on the free radical products of the condensed phase photolysis of simple alkyl thiols, disulfides, and cyclic sulfides through e.p.r. spectroscopy. Turkevich and Fujita (6) have shown that methyl radicals from the photolysis of methyl iodide can be stabilized by adsorption on porous Vycor glass, and we have also used this technique in the hope of obtaining more structural features in the e.p.r. spectra.

Experimental

The experimental arrangements and techniques used for recording the electron paramagnetic spectra have been described (7). The magnetic field was calibrated with Fremy's salt or a Harvey–Wells n.m.r. precision Gaussmeter. The microwave frequency was measured with a Hewlett Packard Model X5328 frequency meter.

Treatment of the porous Vycor glass (Corning No. 7930; 96% SiO_2 and 3% B_2O_3) used as the adsorbent and preparation of samples was performed according to the method of Turkevich and Fujita (6).

Vapor phase chromatography was employed to isolate the desired component of mixtures. Samples were transferred to quartz irradiation tubes and degassed, using conventional high vacuum techniques. The tubes were sealed off under vacuum and samples were irradiated at 77 °K, generally with the output of a Hanovia medium pressure mercury lamp. Some samples were photolyzed in the spectrometer cavity with a high pressure mercury arc as a light source. Each source produces light of wavelength $\lambda > 2200$ Å.

Materials

Methane thiol, ethane thiol, diethyl disulfide, and *n*-propyl disulfide were American Petroleum Institute standard samples and were used without further purification. *n*-Propane thiol (B.D.H.) and all other materials (Aldrich) were purified whenever necessary by g.l.c.

Trifluoromethane thiol was obtained by hydrolysis of the mercurial, $(CF_3S)_2Hg$, prepared by heating HgF_2 and CS_2 together at 250 °C (8). The $CF_3S_2CF_3$ (Peninsular Chemicals) was degassed and roughly fractionated on the vacuum line before use; the mass spectrum showed no impurities.

Results

Monoradicals

The e.p.r. spectra taken at 77 °K of u.v. irradiated solid mercaptans (methyl, ethyl, *n*-propyl, *n*-pentyl, *n*-hexyl, *t*-butyl) and disulfides (dimethyl, diethyl, and di-*n*-propyl) are quite similar and they all show the familiar sulfur pattern with *g*-values about 2.058, 2.025, and 2.001, indicating the formation of R—S · radicals by cleavage of the S—H or S—S bonds. After 5 min irradiation, e.p.r. spectra were detected in the thiols; the signal intensity increased to a

Can. J. Chem. Downloaded from www.nrcresearchpress.com by 210.87.254.6 on 09/05/12
For personal use only.

steady value in a few hours. In comparison, the signals from the disulfides were weak even after several hours of photolysis. In the photolysis of the mercaptans a search was made for the spectrum of hydrogen atoms, but without success. Thus it appears that removal of atoms either by recombination or abstraction is fast.

The spectrum of *t*-butyl mercaptan is simpler than that of the other alkyl mercaptans because of the absence of any α-hydrogens in the radical. This is evident from the two spectra given for comparison in Fig. 1*a* for the *t*-butyl and *b* for the *n*-propyl thiyl radical. The e.p.r. spectrum obtained from the irradiation of *n*-propyl mercaptan adsorbed on the Vycor glass is shown in Fig. 1*c*. From comparison of spectra *b* and *c*, a considerable upfield shift of the highest *g*-value (from 2.058 to 2.042) and a narrowing of the lines is apparent when the radicals are adsorbed on Vycor. This is a general distinction and is further illustrated by the spectra of neat and adsorbed di-*n*-propyl disulfide in Fig. 1*d* and *e*. It should also be noted that there is a closer resemblance between the disulfide and mercaptan spectra in the adsorbed state than there is in the solid phase.

On warming the samples above 77 °K, the spectra obtained from methane and ethane thiols showed little change in line shape below the melting points. The spectrum from *n*-propyl mercaptan became more asymmetric at 103 °K, the original spectrum returning on cooling to 77 °K.

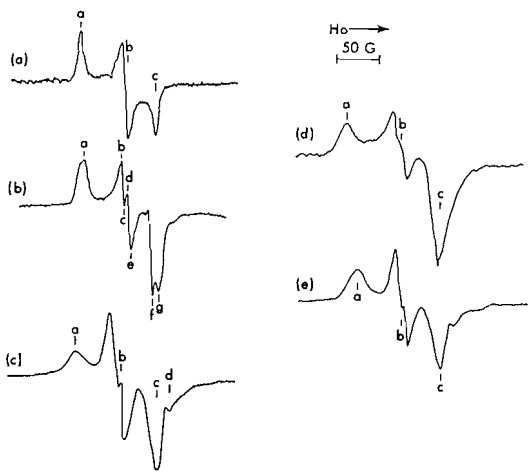

FIG. 1. The e.p.r. spectra of photolyzed thiols and disulfides: (*a*) *t*-butyl mercaptan, (*b*) *n*-propyl mercaptan, (*c*) *n*-propyl mercaptan (on Vycor), (*d*) di-*n*-propyl disulfide, (*e*) di-*n*-propyl disulfide (on Vycor), (for a list of *g*-values see Table 1).

On warming however, an ill-resolved multiplet formed (~140 °K) which persisted on re-cooling the sample to 77 °K. Rather similar changes were observed in the spectra from the other *n*-alkane thiols, although the initial broadening occurred at slightly higher temperatures. For *t*-butyl mercaptan, the spectrum collapsed into a single line at ~130 °K. On re-cooling to 77 °K, the original spectrum reappeared. The spectra decayed rapidly when the matrices were heated to temperatures greater than 150 °K.

Radicals adsorbed on Vycor glass showed higher thermal stability with rapid decay commencing only above 200 °K.

Three trifluoromethyl compounds, CF_3SH, CF_3SSCF_3, and $(CF_3S)_2Hg$, expected to give $CF_3S\cdot$ radicals, were also irradiated under similar conditions to those above. They yielded similar spectra which are therefore assigned to the $CF_3S\cdot$ radical. These spectra, in contrast to the alkyl thiyl radical spectra, contain only two principal lines.

The *g*-values of all thiyl radicals investigated here are summarized in Table 1.

Diradicals

Four cyclic sulfides, thiacyclopropane, -butane, -pentane, -hexane, and one cyclic disulfide, 6,8-thioctic acid have been investigated.

Thiacyclopropane photolyzed in its own matrix at 77 °K did not yield any e.p.r. signal but photolysis of adsorbed thiacyclopropane afforded a signal, consisting of a broad singlet with a line width of about 90 G centered at a *g*-value of 2.005.

Thiacyclobutane photolyzed in its own matrix at 77 °K yielded a spectrum, Fig. 2*a*, similar to the "sulfur pattern" with *g*-values 2.058, 2.026, and 1.997. There was no sign of a proton hyperfine structure due to the terminal methylene group at the carbon end of the $\cdot S—CH_2—CH_2—CH_2\cdot$ radical which is thought to be the initial product of the photolysis. Photolysis of the adsorbed material yielded a somewhat different spectrum, Fig. 2*b*, which apart from the "sulfur pattern" shows extra lines.

In the photolysis of both thiacyclopropane and thiacyclobutane adsorbed on Vycor, a line at half field (~1550 G) is also apparent. It is, however, weak and very difficult to distinguish from signals derived from the Vycor itself.

The spectra obtained in the photolysis of thiacyclopentane in its own matrix and in the

TABLE 1

Line positions of e.p.r. spectra from photolyzed thiols and disulfides (77 °K)

Substrate	Assigned g-values of line positions		
Methane thiol	a. 2.058 b. 2.034 c. 2.030	d. 2.025 e. 2.018 f. 2.005	
Ethane thiol	a. 2.064 b. 2.058 c. 2.032 d. 2.029	e. 2.025 f. 2.022 g. 2.018 h. 2.011	i. 2.008 j. 2.003 k. 1.993
n-Propane thiol	a. 2.059 b. 2.028 c. 2.024	d. 2.023 e. 2.020 f. 1.999	g. 1.997
n-Pentane thiol	a. 2.061 b. 2.029 c. 2.025	d. 2.019 e. 2.001 f. 1.982	
n-Hexane thiol	a. 2.062 b. 2.043 c. 2.030 d. 2.026	e. 2.020 f. 2.000 g. 1.980 h. 1.965	
t-Butyl thiol	a. 2.057	b. 2.024	c. 2.001
Dimethyl disulfide	a. 2.058 b. 2.033	c. 2.021 d. 2.010	e. 1.998 f. 1.984
Diethyl disulfide	a. 2.073 b. 2.036 c. 2.030	d. 2.022 e. 2.018 f. 2.009	g. 2.003 h. 1.996 i. 1.989
Di-*n*-propyl disulfide	a. 2.059 b. 2.025 c. 2.001		
Trifluoromethane thiol	a. 2.029	b. 2.005	
Perfluorodimethyl disulfide	a. 2.034	b. 2.004	
$(CF_3S)_2Hg$		b. 2.004	
n-Propyl thiol	a. 2.054 b. 2.026	c. 2.000 d. 1.992	On Vycor
Di-*n*-propyl disulfide	a. 2.043 b. 2.025	c. 2.001	On Vycor

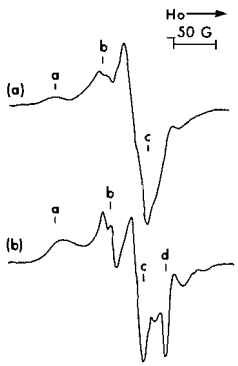

FIG. 2. The e.p.r. spectra of photolyzed thiacyclobutane: (*a*) in its own matrix (g-values: a. 2.058, b. 2.026, c. 1.997), (*b*) adsorbed on Vycor (g-values: a. 2.058, b. 2.024, c. 2.003, d. 1.993).

adsorbed state are shown in Fig. 3. The former spectrum features a composite pattern and has an overall line width of about 150 G. The line shape of the latter spectrum is similar to the former but some of the lines have been shifted to considerably higher fields. Both spectra quickly lose structure on warming and collapse into a broad line at 120 °K which gradually diminishes with further warming and completely disappears around 200 °K. The g-values of the two spectra are listed in Table 2.

The spectrum of thiacyclohexane was quite similar to that of thiacyclopentane, except that some of the lines were shifted slightly.

6,8-Thioctic acid in acetonitrile gave a spectrum very similar to that of the *t*-butyl thiyl

Can. J. Chem. Downloaded from www.nrcresearchpress.com by 210.87.254.6 on 09/05/12
For personal use only.

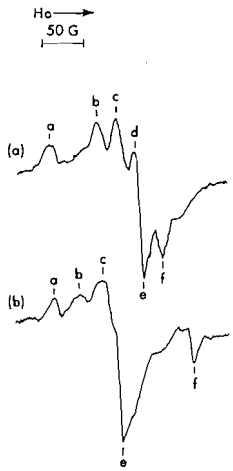

FIG. 3. The e.p.r. spectra of photolyzed thiacyclopentane (*a*) in its own matrix, (*b*) adsorbed on Vycor, (for a list of *g*-values see Table 2).

TABLE 2

Line positions of e.p.r. spectra from photolyzed thiacyclopentane (77 °K) in its own matrix (*1*) and on Vycor (*2*)

	Assigned *g*-values of line positions	
(*1*)	a. 2.055	d. 2.007
	b. 2.028	e. 2.001
	c. 2.017	f. 1.991
(*2*)	a. 2.039	d. —
	b. 2.026	e. 2.001
	c. 2.015	f. 1.963

radical. The *g*-values of the lines are 2.056, 2.027, and 2.002.

Discussion

Axially asymmetric radicals locked in random orientations exhibit basically three line e.p.r. spectra (9). The anisotropy is particularly large when the unpaired electron is localized on an atom with large spin-orbit coupling as is the case with sulfur. Thus, organo-sulfur radicals yield characteristic spectra with a considerable *g*-value anisotropy referred to as the "sulfur pattern".

Kurita and Gordy (10) from their study on irradiated single crystals of L-cystine·HCl, derived a model for organo-sulfur radicals with coplanar sp^2 hybrid structures.

Their results indicate that the three principal *g*-values for L-cystine·HCl are $g_{xx} = 2.003$, $g_{yy} = 2.025$, and $g_{zz} = 2.053$, the last axis lying along the C—S· bond which in the radical has rotated thermally from its position in the undamaged original molecule.

In agreement with this, the prominent feature of the spectra from all the non-fluorinated molecules listed in Table 1, is their basic three line structure with lines close to $g = 2.002$, 2.023, and 2.060, indicating that the major free radical modes of decomposition are

$$RSH + h\nu \rightarrow RS\cdot + H$$

$$RSSR + h\nu \rightarrow 2RS\cdot$$

The spectra from thiols and the corresponding disulfides are very similar, but not identical. This difference may be explained as being largely due to matrix interactions with the radicals, as no difference is discernible when the spectra of different adsorbed mercaptans or adsorbed disulfides are compared (*cf.* Fig. 1).

The spectrum obtained from *t*-butyl mercaptan attributed to the *t*-butyl thiyl radical is different from those of the *n*-alkyl thiyl radicals in that it shows no hyperfine structure. This is expected since α-protons causing the splittings are absent in this radical. On warming this sample the spectrum collapsed into a single line near the position of the central line ($g = 2.024$), indicating that the radical was able to rotate. However, near $g = 2.0$ there were also some very weak lines, which may be due to an alkyl radical. In the gas phase, it is believed (1) that *t*-butyl mercaptan can lose either H or SH on photolysis yielding a thiyl or an alkyl radical. In the condensed phase SH loss appears to be a minor process.

The spectrum in photolyzed *n*-hexyl mercaptan shows intense lines extending to lower *g*-values in addition to three lines in the positions of the thiyl spectra. A similar spectrum was detected in γ-irradiated dioctyl disulfide (4) and is attributed to radicals formed by C—H cleavage. Evidently both thiyl and alkyl radicals are present in photolyzed *n*-hexyl mercaptan. The weak high-field lines in *n*-pentyl mercaptan are explained in an analogous manner.

The behavior of the spectra on warming the matrix suggests that methane and ethane thiyl radicals decay at temperatures where rotation in the lattice is still restricted. Apparently the heavier thiyl radicals are able to rotate to some extent before decaying.

As mentioned above the C—S bond in the radical appears to be rotated from its position in the undamaged molecule. It seems reasonable

Can. J. Chem. Downloaded from www.nrcresearchpress.com by 210.87.254.6 on 09/05/12
For personal use only.

Can. J. Chem. Downloaded from www.nrcresearchpress.com by 210.87.254.6 on 09/05/12
For personal use only.

to assume that such a rotation of the bond might be hindered when the molecule is adsorbed on the Vycor glass and partially "locked in" through interaction with the surface. Interaction of the unpaired electron with the surface could affect the energy of the sp^2 hybrid and p-orbitals on the sulfur to a different extent. This would then explain the high-field shift of g_{zz}.

The observed increased thermal stability of the adsorbed radicals is expected since adsorption decreases the mobility of radicals. It is the consequence of this enhanced stability of adsorbed radicals which accounts for the characteristic rate differences of decay between matrix and Vycor glass photolyses. Adsorption seems to prevent cage recombination of the geminate thiyl radical pairs in disulfide photolyses and thus increases the apparent rate of photolysis. In the photolysis of mercaptans, cage recombination is unimportant because of the ease by which H atoms escape the cage.

The spectra of the $CF_3S\cdot$ radical are unusual in that they exhibit only two principal g-values suggesting that the radical has axial symmetry. In the photolysis of CF_3SH two additional lines (not recorded in Table 1) were also present, separated by 504 ± 5 G and centered at a g-value of 2.01. They are almost certainly due to H atoms.

The spectra obtained from the photolysis of cyclic sulfides are consistent with a $\cdot CH_2(CH_2)_n—S\cdot$ type diradical carrier, the intermediacy of which has been invoked in the gas phase photolysis of these molecules (11).

The photolysis of thiacyclobutane in a matrix yields a spectrum which can be identified with the sulfur pattern. Since there are no additional lines that could be assigned to the terminal CH_2 group of the diradical, it seems probable that recombination has taken place at the aliphatic part and the spectrum in fact is due to a diradical with unpaired electrons located on the two end sulfur atoms with no spin exchange taking place.

When thiacyclobutane is photolyzed on the Vycor glass the spectrum contains extra lines apart from the sulfur pattern. Although the intensity distribution of these lines cannot be derived and no definite assignment can be made, one explanation is that they may be due to the $—CH_2\cdot$ moiety of the primary diradical. In this case adsorption prevents recombination and stabilizes the primary radicals.

In contrast to thiacyclobutane the e.p.r. spectra of thiacyclopentane and thiacyclohexane photolyzed either in their own matrices or on Vycor glass, do not show any distinguishing feature. In both cases, hyperfine lines in addition to the sulfur pattern appear, indicating the presence of a $\cdot CH_2(CH_2)_n—S\cdot$ type diradical. Trapping on the Vycor glass again results in a shift of the low-field g-value.

The spectrum of photolyzed 6,8-thioctic acid (12, 13) features a clean sulfur pattern and it is likely due to the diradical

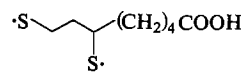

The close similarity with the spectrum of the t-butyl thiyl radical seems to suggest there is little interaction between the free spins in the diradical.

We thank the National Research Council of Canada for financial support and Mr. G. Bigam for helpful assistance.

1. J. G. Calvert and J. N. Pitts. *In* Photochemistry. John Wiley & Sons, Inc., London, 1966.
2. K. J. Rosengren. Acta Chem. Scand. **16**, 1461 (1962).
3. K. J. Rosengren. Acta Chem. Scand. **16**, 1418 (1962).
4. F. W. Truby. J. Chem. Phys. **36**, 2227 (1962); **37**, 2777 (1962).
5. J. J. Windle, A. K. Wiersema, and A. L. Tappel. J. Chem. Phys. **41**, 1996 (1964).
6. J. Turkevich and Y. Fujita. Sci. **152**, 1619 (1966).
7. D. A. Stiles, W. J. R. Tyerman, O. P. Strausz, and H. E. Gunning. Can. J. Chem. **44**, 2149 (1966).
8. R. L. Dannley and R. G. Taborsky. J. Org. Chem. **22**, 1275 (1957).
9. F. K. Kneubuhl. J. Chem. Phys. **33**, 1074 (1960).
10. Y. Kurita and W. Gordy. J. Chem. Phys. **34**, 282 (1961).
11. P. Fowles, M. de Sorgo, A. J. Yarwood, O. P. Strausz, and H. E. Gunning. J. Amer. Chem. Soc. **89**, 1352 (1967); and unpublished results from this laboratory.
12. R. B. Whitney and M. Calvin. J. Chem. Phys. **23**, 1750 (1955).
13. E. E. Smissman and J. R. J. Sorenson. J. Org. Chem. **30**, 4008 (1965).

Applications of proton magnetic resonance to rotational isomerism in halotoluene derivatives. IV. α,α,2,4,6-Pentachlorotoluene in carbon disulfide, an exchanging ABC system

HELEN G. GYULAI, B. J. FUHR,[1] H. M. HUTTON,[2] AND T. SCHAEFER
Chemistry Department, University of Manitoba, Winnipeg, Manitoba

Received July 15, 1970

The p.m.r. of α,α,2,4,6-pentachlorotoluene in carbon disulfide solution displays hindered rotation about the sp^2–sp^3 carbon–carbon bond, causing broadening and collapse of the proton resonance spectrum. A full line-shape analysis using the computer program DNMR gives an activation energy of 14.2 ± 0.3 kcal/mole, a frequency factor of 11.9 ± 0.2, an enthalpy of activation of 13.7 ± 0.3 kcal/mole, and an entropy of activation of −4.4 ± 1 e.u. These data are compared with the activation parameters obtained in methylcyclohexane and toluene-d_8 solutions from different line shapes.

Canadian Journal of Chemistry, 48, 3877 (1970)

Can. J. Chem. Downloaded from www.nrcresearchpress.com by 210.87.254.6 on 09/05/12
For personal use only.

Introduction

The barrier to rotation about the sp^2–sp^3 carbon–carbon bond in α,α,2,4,6-pentachlorotoluene (PCT), dissolved in methylcyclohexane ($C_6H_{11}CH_3$) and in toluene-d_8 (C_7D_8), was previously (1) determined by fitting the temperature dependent ring proton spectra, AB parts of ABX spectra, to theoretical line-shapes. In polar solvents the solubility of PCT is too low at low temperatures to allow of a reliable barrier determination.

In view of the many possible systematic errors which bedevil rate studies by n.m.r. (2, 3), it was deemed desirable to determine the barrier in PCT by another method. It was decided to use an n.m.r. line-shape technique but to alter the solvent, the spectral type, and the line-shape fitting technique as much as possible from the conditions of the previous study (1). Now, in carbon disulfide (CS_2), the proton resonance spectrum corresponds to a tightly coupled ABC spectrum, in contrast to the ABX spectra obtained in $C_6H_{11}CH_3$ and C_7D_8. Solubility changes at low temperatures present no problem and the dielectric constants of all three solvents are uniformly low (2.0–2.6). Furthermore, the program DNMR (4) devised by Binsch (5) is designed to cope with an ABC spectrum which reduces to an A_2B spectrum at higher temperatures. The only parameter, therefore, which is the same as in the previous work is the spectrometer operating at 60 MHz. At the time of the experiments no other frequency was available to us.

This paper briefly describes the results obtained for PCT in CS_2 solution and compares them to the previous data (1).

[1]Holder of an NRCC bursary, 1968–1969.
[2]University of Winnipeg, Winnipeg, Manitoba.

Experimental

The PCT was prepared as before (1) and was dissolved as 15 mole % solution in CS_2 containing tetramethylsilane (TMS) as an internal reference and locking signal. After degassing by the freeze–pump–thaw technique, p.m.r. spectra were obtained at 60 MHz at various temperatures in the manner described previously (1).

Results and Discussion

(1) Spectral Analysis at Low Temperatures

In Fig. 1 the p.m.r. spectrum at −34 °C is assigned to the protons as designated in the structural formula **1**. At 73 °C the average coupling $({}^5J^{BC} + {}^5J^{AC})/2 = 0.31 \pm 0.02$ Hz. At −34 °C the coupling ${}^5J^{BC} \approx 0.1$ Hz is not resolved but causes a broadening of the peaks arising from H_B and H_C, the latter proton lying in the plane of the ring and coupling predominantly to H_A.

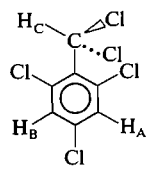

1

In order to find the intrinsic temperature dependence of the chemical shifts and coupling constants, several low temperature spectra were analyzed using the computer program LAOCN3 (6). The parameters are given in Table 1 where it is seen that the variation of these parameters with temperature is small. The internal shift of

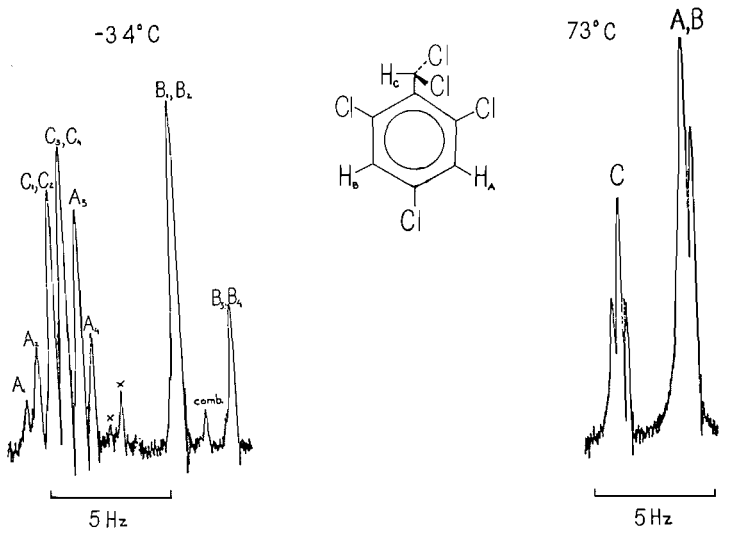

FIG. 1. The p.m.r. spectrum at 60 MHz of a 15 mole % solution of α,α,2,4,6-pentachlorotoluene in carbon disulfide at −34 and 73 °C. The two impurity peaks are marked with an X at −34 °C. The larger impurity peak is due to α,α,α,2,4,6-hexachlorotoluene. The peak marked comb. can be considered a combination line. As is obvious from the spectrum, the magnetic field is swept from left to right.

TABLE 1

Chemical shifts* and coupling constants† of some low temperature spectra of α,α,2,4,6-pentachlorotoluene in carbon disulfide as analyzed by LAOCN3

Temperature (°C)	ν_A	ν_B	ν_C	J_{AB}	J_{AC}	J_{BC}
−65	440.10	434.58	440.75	2.12	0.52	0.13
−61	440.14	434.54	440.71	2.15	0.49	0.10
−58	439.90	434.51	440.58	2.16	0.53	0.11
−50	440.44	434.81	440.71	2.15	0.51	0.10
−40	440.52	434.95	440.71	2.18	0.44	0.07
−34	440.68	435.11	440.82	2.14	0.50	0.10

*In Hz, at 60 MHz, to low field of tetramethylsilane; probable errors do not exceed 0.02 Hz.
†In Hz; probable errors do not exceed 0.03 Hz.

the ring protons, ν_{AB}, is constant to within 0.2 Hz in the range −65 to −34 °C. This parameter will have the largest effect on the line-shape because it is this shift which is averaged by the 180° flips of the dichloromethyl group. The shift of the methine proton apparently does not change with temperature in this range.

In the initial calculation of the theoretical spectra, the shift and coupling parameters used were those found at −34 °C. To obtain the best fits it was found necessary to alter some of the absolute shift parameters by as much as 0.5 Hz, but the coupling constants and the internal shift ν_{AB} were held constant in all line-shape calculations. The effective transverse relaxation times, T_2^{eff}, were calculated at each temperature from the width at half-height of the impurity peak due to the hexachlorotoluene. The input parameters used in the final line-shape calculations are summarized in Table 2.

(2) Line-shape Analysis and Rate Constants

Line-shape calculations were done using the line-shape theory (5) and computer program DNMR (4) adapted to an IBM 360/65 computer. A large number of calculated spectra with various rate constants[3] were plotted on a Calcomp plotter and were compared visually with the experimental spectra. Each spectrum spanned 25 Hz and consisted of approximately 1000 points. The experimental and the calculated spectra at five representative temperatures are shown in Fig. 2.

[3]In ref. 5 the formulation of the exchange operator was not obvious to us. One of us (H. G. G.) has given a heuristic derivation of this operator (7) and the interested reader may write for a copy.

Can. J. Chem. Downloaded from www.nrcresearchpress.com by 210.87.254.6 on 09/05/12
For personal use only.

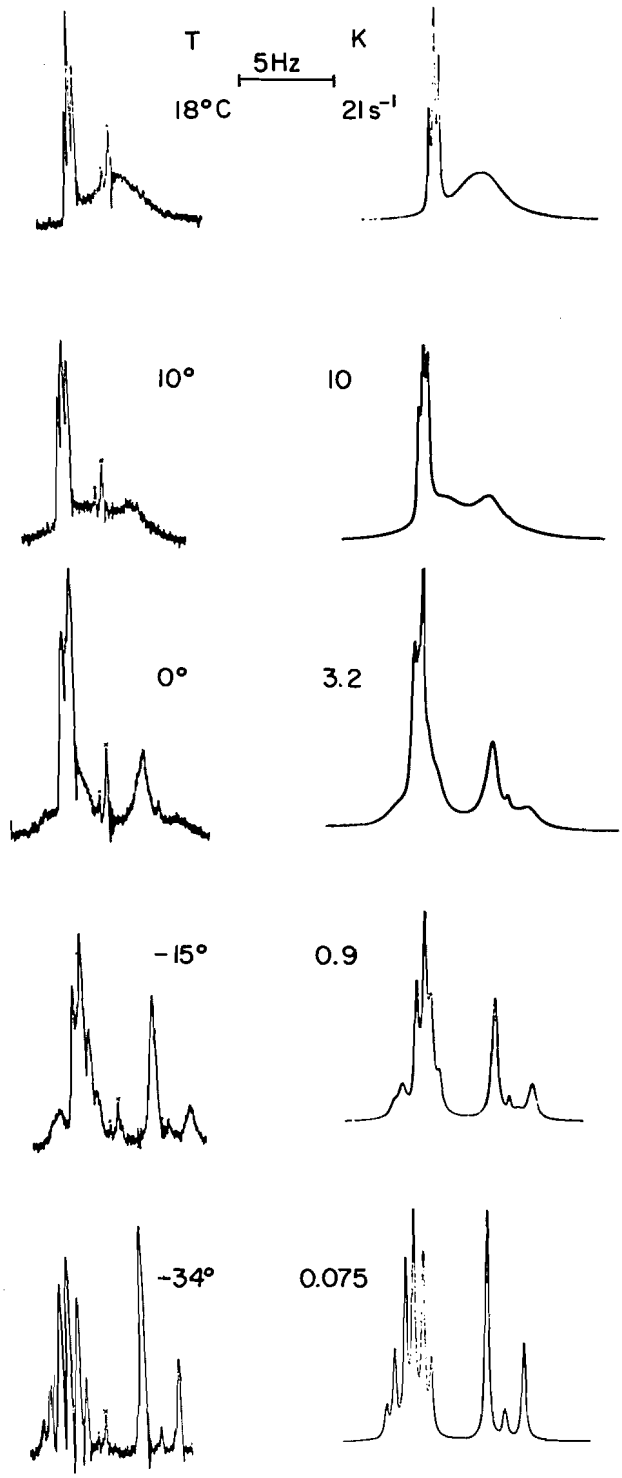

FIG. 2. Observed and calculated spectra at five representative temperatures, and rate constants, K, for α,α,2,4,6-pentachlorotoluene in carbon disulfide. Note that on sharp peaks the recorder pen comes down sharply on the right hand side in a "ring" and this effect is naturally absent in the computed spectrum.

Can. J. Chem. Downloaded from www.nrcresearchpress.com by 210.87.254.6 on 09/05/12
For personal use only.

TABLE 2

The parameters used in calculating the line-shapes for α,α,2,4,6-pentachlorotoluene in carbon disulfide

Temperature (°C)	ν_A (Hz)	ν_B (Hz)	ν_C (Hz)	J_{AB} (Hz)	$J_{\bar{A}C}$ (Hz)	J_{BC} (Hz)	T_2^{eff} (s)	K (s^{-1})
−34	440.69	435.11	440.82	2.15	0.51	0.12	1.38	0.075
−15	440.95	435.37	440.85	2.15	0.51	0.12	1.38	0.90
0	441.26	435.65	441.22	2.15	0.51	0.12	1.52	3.2
10	441.39	435.81	441.20	2.15	0.51	0.12	1.87	10.0
18	441.08	435.11	440.82	2.15	0.51	0.12	2.80	21.0
30	441.28	435.70	441.20	2.15	0.51	0.12	1.90	38.0
47	441.14	435.56	441.15	2.15	0.51	0.12	1.90	160
62	441.11	435.53	441.09	2.15	0.51	0.12	1.5	400
73	441.16	435.58	441.13	2.15	0.51	0.12	1.5	1000

TABLE 3

Activation parameters* for the hindered rotation in α,α,2,4,6-pentachlorotoluene in three solutions

Parameter	Methylcyclohexane solution	Toluene-d_8 solution	CS_2 solution	Three solutions combined
E_a (kcal/mole)	14.3±0.6	15.2±0.2	14.22±0.27	14.24±0.27 kcal/mole
log A	12.0±0.5	12.7±0.2	11.93±0.20	11.95±0.21
$\Delta H^{\neq}$ (kcal/mole)	13.7±0.6	14.6±0.2	13.69±0.27	13.68±0.27 kcal/mole
$\Delta S^{\neq}$ (e.u.)	−4.4±2.2	−1.1±0.7	−4.38±1.0	−4.37±1.0 e.u.
$\Delta G^{\neq}$ (kcal/mole)	15.0±0.2 (at 303.9 °K)	14.9±0.1 (at 303.5 °K)	14.86±0.10 (at 291 °K)	— kcal/mole

*The quoted errors are standard deviations.

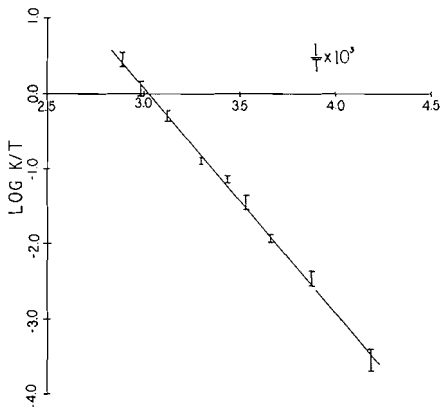

FIG. 3. A plot of log K/T *vs.* reciprocal temperature for the hindered rotation of α,α,2,4,6-pentachlorotoluene as a 15 mole % solution in carbon disulfide. The error bars come from the estimated error in the rate constant, K. The least squares straight line is drawn in and the correlation coefficient is 0.9987.

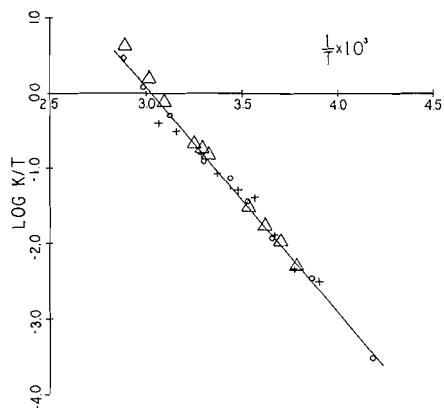

FIG. 4. As in Fig. 3 but for three solutions: (○) carbon disulfide, (△) toluene-d_8, + methylcyclohexane, all 15 mole % in the pentachlorotoluene. Data for the latter two solvents were taken from ref. 1. The least square line is given, correlation coefficient being 0.9948.

It should be stressed that in the experimental spectra the sharp peaks, whose linewidths were less than 0.2 Hz, are always apparently better resolved than in the calculated spectra. This arises primarily from the fact that the recorder pen comes down sharply after passing through the peak, a "ringing effect". Because the chemical environment of the methine proton does not change when the dichloromethyl group rotates through π radians, its resonance peaks remain sharp throughout the temperature range but change from a doublet at low rates of exchange to a triplet at high rates of exchange (virtual coupling). Equal T_2's were employed for all three protons although, in principle, the methine proton

Can. J. Chem. Downloaded from www.nrcresearchpress.com by 210.87.254.6 on 09/05/12
For personal use only.

may have had a larger T_2, leading to the sharper recorded peaks. We did not make provision for more than one T_2 in the computer program and, in any case, the linewidths of the peaks are very likely controlled by the magnetic field inhomogeneity and/or instability of the internal lock over the recording period.

The estimated errors in the rate constants lie near 10% in the intermediate rate region and are somewhat higher at either extreme. In Table 2 the rate constants are given as obtained by best visual fits at the various temperatures.

(3) Derivation of Activation Parameters

Plots of log K ($r = 0.9989$) and log K/T *vs.* $1/T$ were prepared in the usual way. Figure 3 shows a plot of log K/T *vs.* $1/T$, correlation coefficient $r = 0.9987$, and the error bars in log K/T are also given. In Fig. 4 a composite plot of our rate data in $C_6H_{11}CH_3$ (1), C_7D_8 (1), and in CS_2 is displayed, $r = 0.9948$. In Table 3 the activation parameters are compared for all three solutions and the composite parameters are given as well. Apparently the systematic errors in the different analyses are small.

We are grateful to the National Research Council of Canada for financial assistance, to B. W. Goodwin for help with the computer program, and to Dr. G. Binsch for helpful comments.

1. B. J. Fuhr, B. W. Goodwin, H. M. Hutton, and T. Schaefer. Can. J. Chem. **48**, 1558 (1970).
2. G. Binsch. *In* Topics in stereochemistry. Volume 3. *Edited by* E. L. Eliel and N. L. Allinger. Interscience Publishers, New York. 1968.
3. A. Allerhand, H. S. Gutowsky, J. Jonas, and R. A. Meinzer. J. Amer. Chem. Soc. **88**, 3185 (1966).
4. G. Binsch and D. A. Kleier. Computer program DNMR.QCPE. Chemistry Department, Indiana University, Bloomington, Indiana. No. 140.
5. G. Binsch. J. Amer. Chem. Soc. **91**, 1304 (1969).
6. S. Castellano and A. A. Bothner-By. J. Chem. Phys. **41**, 3863 (1964).
7. Helen G. Gyulai. M.Sc. thesis. University of Manitoba, Winnipeg, Manitoba, 1970.

Can. J. Chem. Downloaded from www.nrcresearchpress.com by 210.87.254.6 on 09/05/12
For personal use only.

Stereospecific synthesis of *cis*- and *trans*-2-(3,4,5-trimethoxyphenyl)-cyclopropylamines[1]

PAUL D. COOPER[2]
Department of Pharmacology, University of Toronto, Toronto, Ontario
Received July 6, 1970

The title compounds were synthesized as models for examining stereochemical requirements of the mescaline receptor. By analogy with indolic psychotomimetic drugs, the pseudo-indolic structure of the *cis* compound should endow it with greater psychotomimetic activity than the *trans* isomer might possess. A special synthetic sequence was obligatory for the preparation of the *cis* isomer because the usual intermediates were either unreactive or were epimerized during subsequent transformations. Observed differences in the i.r. and n.m.r. spectra of the key intermediates, *cis*- and *trans*-2-(3,4,5-trimethoxyphenyl)-cyclopropanecarboxylic acids, are due to electronic factors introduced secondary to the stereochemical fixation of the functional groups. It is suggested that this unavoidable electronic perturbation must be taken into account in future considerations of drug-receptor interaction.

Canadian Journal of Chemistry, **48**, 3882 (1970)

Can. J. Chem. Downloaded from www.nrcresearchpress.com by 210.87.254.40 on 09/05/12
For personal use only.

Introduction

Most structure-activity work concerning mescaline (**1**) has involved modification of nuclear substituents in number, position, and type (1) and it has been shown that more than one nuclear substitution pattern produces effective hallucinogens (2).

This present work was undertaken to provide mescaline analogs with fixed conformations in the side-chain. Alterations in the side-chain of mescaline have received relatively little attention (3), with the notable exception of α-methylmescaline (**2**) which is several times more potent than mescaline (4).

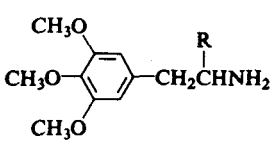

1 R = H
2 R = CH_3

We propose that the potentiating effect of the α-methyl group in compound **2** is due to the preferential stabilization of one of the two staggered conformations of **2**. Newman rotamer representations I and II (equivalent to compound **1**) show that conformation II would likely be favored energetically relative to I: if the NH_2 group is unionized, there are both steric and electrostatic repulsions between it and the aromatic ring, while if it is ionized (NH_3^+) the resultant electrostatic attraction toward the aromatic ring would likely be offset by a larger steric repulsion term due to the hydration of NH_3^+. Examining the rotamers III and IV (equivalent to compound **2**) it would appear that the situation is different: any tendency for the NH_2 or the NH_3^+ group to remain distant from the aromatic ring, as in IV, would be offset by steric repulsion of the methyl group by the aromatic ring. Conformations such as III would therefore be favored over those such as IV to a greater extent than I would be favored relative to II.

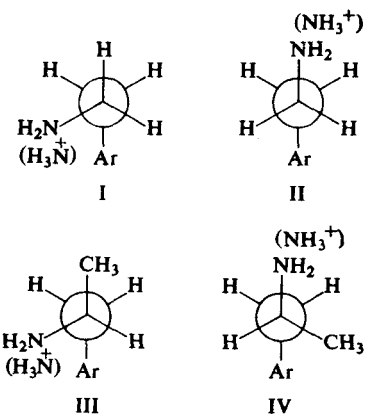

A pseudo-indolic conformation such as III more closely resembles potent indolic hallucinogens like LSD or psilocybin than does IV. While mescaline might be induced, at the expense of some bioreceptive energy, to assume a pseudo-

[1]This work was supported by a grant from the Government of Ontario, Department of University Affairs.
[2]Present address: Faculty of Pharmacy, University of Montreal, Montreal, Quebec.

indolic conformation, I, at the receptor or enzyme site where it may act, an initial preference for such a conformation, as induced by the α-methyl group in III, might reduce to a critical degree the entropic demands placed on the bioreceptive system whose partial requirements are for an indole-like structure.

The pharmacological study of conformationally rigid analogs of mescaline should offer a means of challenging such a hypothesis. We have reported (5) some pharmacological properties of one such analog, *trans*-2-(3,4,5-trimethoxyphenyl)-cyclopropylamine (**3**), a structural hybrid of mescaline and of the antidepressant, *trans*-2-phenylcyclopropylamine (**4**).

Details of the synthesis of **3** were not given. We now wish to describe two different syntheses of **3** as well as the stereospecific synthesis of its *cis* isomer, **5** (see Scheme 1).

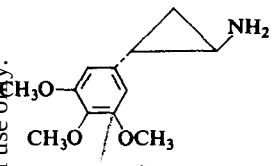

3

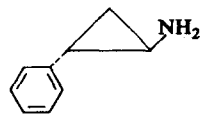

4

For the synthesis of **3**, 3,4,5-trimethoxybenzaldehyde was condensed with an excess of malonic acid in the presence of pyridine and piperidine to give *trans*-3,4,5-trimethoxycinnamic acid (**6**) in near quantitative yield. This was converted into the methyl ester, **7**, which was in turn converted into the tert-butyl ester, **8**, by ester interchange. The ester **8** reacted with dimethylsulfoxonium methylid in DMSO to give *trans*-2-(3,4,5-trimethoxyphenyl)-cyclopropanecarboxylic acid (**9**) which was transformed by a modified Curtius sequence into the desired amine, **3**.

Entry into the *cis* series was provided by the preparation of *cis*-3,4,5-trimethoxycinnamic acid (**10**) produced by u.v. irradiation of **6**. The isomeric acids were readily separated by fractional precipitation from their alkaline solution, using t.l.c. to monitor the separation. Structural assignment of *cis*-3,4,5-trimethoxycinnamic acid to the major photochemical product was based on formation of the identical hydrogenation product from the respective *cis* and *trans* methyl esters, **7** and **11**, which would each be expected to give methyl 3,4,5-trimethoxydihydrocinnamate (**12**).

As it was found that **10** was transformed, by treatment with thionyl chloride and tert-butanol, into the *trans* tert-butyl ester, **8**, instead of into the desired *cis* tert-butyl ester, the *cis* ethyl ester, **13**, was prepared by conventional treatment with ethanol and sulfuric acid. Reaction of **13** with dimethylsulfoxonium methylid in DMSO produced, instead of the expected *cis* cyclopropane acid, **14**, the *trans* isomer, **9**. Since it was later found that neither **14** nor **13** are epimerized by solutions of potassium tert-butoxide in DMSO, the transformation of **13** into **9** likely implicates carbanion intermediate formation by attack of the ylid reagent on the olefinic bond in **13**, rather than an epimerization of starting material or product.

Further attempts to methylenate the double bond of **13** using various modifications of the Simmons–Smith reaction gave only the starting ester or complex mixtures.

Controlled lithium aluminum hydride reduction of the carboxylate function in the *cis*, **13**, and *trans*, **15**, ethyl esters gave the corresponding *cis* and *trans* 3,4,5-trimethoxycinnamyl alcohols, **16** and **17** respectively, in good yields and stereochemically pure. Each of the alcohols, **16** and **17**, reacted with diethyl zinc and methylene iodide to give the corresponding *cis* and *trans* isomers of 2-(3,4,5-trimethoxyphenyl)-cyclopropylcarbinol, **18** and **19** respectively. The carbinol **19** was also obtained by lithium aluminum hydride reduction of ethyl *trans*-2-(3,4,5-trimethoxyphenyl)-cyclopropanecarboxylate (**20**) confirming the structure assigned to **19**.

Oxidation of the *cis* and *trans* carbinols with nickel peroxide gave the corresponding *cis* and *trans* cyclopropane acids, **14** and **9** respectively. The acid **14** was then converted into *cis*-2-(3,4,5-trimethoxyphenyl)-cyclopropylamine (**5**) by the modified Curtius reaction.

Results and Discussion

A comparison of the n.m.r. spectra of the cyclopropane acids, **9** and **14**, shows that the hydrogen, H_X is at lower field in the *cis* isomer **14** than it is in the *trans* isomer, **9**. This could result from a combination of factors, including inductive effects as well as magnetic and electric field effects due to the anisotropy of the aryl group (6).

The i.r. spectra of the *trans* isomers, **9** and **25**, of the carboxylic acid and the acyl azide respectively, show small but discernible shifts of the

Can. J. Chem. Downloaded from www.nrcresearchpress.com by 210.87.254.40 on 09/05/12
For personal use only.

Can. J. Chem. Downloaded from www.nrcresearchpress.com by 210.87.254.40 on 09/05/12
For personal use only.

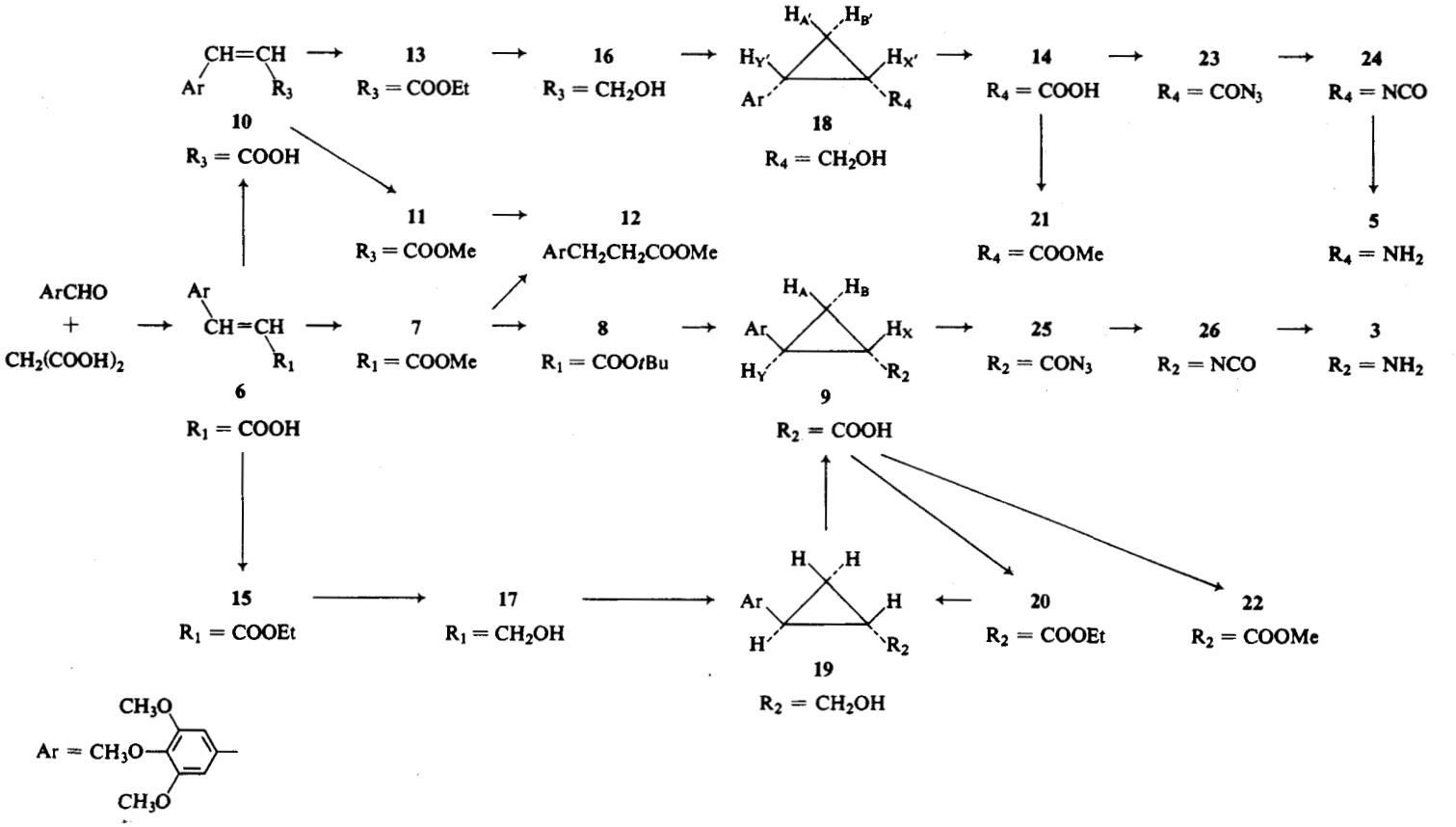

SCHEME 1. Reaction sequence for the synthesis of *cis* (**5**) and *trans* (**3**) 2-(3,4,5-trimethoxyphenyl)-cyclopropylamines

carbonyls to lower frequencies relative to their *cis* isomers **14** and **23**.

These differences should be manifested in some chemical properties of the target amines, **3** and **5**, such as their pK_b's, their nucleophilicity and other parameters which might play an important role at the level of drug-receptor interaction. Similar forces could equally well be in effect in open-chain analogs of phenethylamines when once their conformations are "frozen" by combination with receptors. Such factors should be considered in addition to direct steric aspects of the interaction of these amines with bioreceptive systems.

Experimental

Corrected capillary melting points are reported. The n.m.r. spectra ($CDCl_3$) were recorded on a Varian A-100 Spectrometer, u.v. spectra (water containing one equivalent of sodium bicarbonate) on a Bausch and Lomb Spectronic 505, and i.r. spectra on a Beckman IR-5 Spectrophotometer using $CHCl_3$ unless otherwise stated. Although only principal absorption bands are given, differences in the spectra of *cis* and *trans* isomers in the region 1420–1290 cm^{-1} (C—H deformations) allowed them to be distinguished, one from the other, in each case. Reaction mixtures and products were routinely examined by t.l.c. (Silica Gel H) using petroleum ether – acetone to separate *cis–trans* pairs and benzene – ethyl acetate to separate cyclopropanes from cinnamates. Elemental analyses were performed by Micro-Tech Laboratories, Skokie, Ill.

trans-3,4,5-Trimethoxycinnamic Acid (6)

To 150 ml pyridine and 3 ml piperidine was added gradually with stirring and occasional cooling, 100 g of (0.96 mole) malonic acid. After the malonic acid had dissolved, 84 g (0.43 mole) of 3,4,5-trimethoxybenzaldehyde was added. The mixture was stirred at 25° for 12 h,[3] and then at 80–100° until carbon dioxide evolution ceased. The solution was cooled and gradually poured into a vigorously stirred mixture of 2 l of ice and water containing 250 ml concentrated hydrochloric acid. The precipitate was collected and washed with water until the filtrates gave a negative test for Cl^-. The filter cake was dried at 50° *in vacuo* to give 98 g (96%) of **6**, m.p. 126–127° (lit. (7) m.p. 124–125°). The u.v. spectrum: λ_{max} 294 mμ (ε 7500) and 228 mμ (ε 9500). The i.r. spectrum: ν_{max} 3300–2500 (COO—H), 1675 (C=O), 1625 cm^{-1} (C=C).

trans-Methyl 3,4,5-Trimethoxycinnamate (7)

A solution of 13.4 g (0.056 mole) of **6** in 250 ml methanol and 5 ml concentrated sulfuric acid was refluxed for 4 h and then allowed to cool slightly. An excess of anhydrous sodium carbonate was then added in small portions with agitation. The mixture was filtered hot and the filter cake rinsed with hot methanol. The combined filtrates were concentrated *in vacuo* to 75 ml and poured into 500 ml of rapidly stirred cold water. The precipitate was collected, rinsed with water until the filtrates were neutral, and dried *in vacuo* to give 13.0 g (92%) of **7**, m.p. 98–99° (lit. (8) m.p. 96.5–97°).

trans-Ethyl 3,4,5-Trimethoxycinnamate (15)

Using 10.0 g of **6**, 100 ml of anhydrous ethanol, and 5 ml concentrated sulfuric acid and following the procedure of **7**, there was obtained 10.4 g (94%) of **15**, m.p. 68.5–70° (lit. (9) m.p. 68°); the i.r. spectrum: ν_{max} 1700 (C=C), 1630 cm^{-1} (C=C).

trans-t-Butyl 3,4,5-Trimethoxycinnamate (8)

Method A

A solution of 72 g (0.285 mole) **7** and 1.5 g (0.065 mole) sodium metal in 800 ml anhydrous tert-butanol was refluxed for 16 h and then evaporated to dryness *in vacuo*. The residue was partitioned between 1700 ml boiling 30–60° petroleum ether and 300 ml water. The organic phase gave, upon evaporation, 35 g (42%) of almost pure **8**. A sample recrystallized from 30–60° petroleum ether and sublimed at 140° (0.1 mm) had m.p. 78.5–79.5°.

Anal. Calcd. for $C_{16}H_{22}O_5$: C, 65.28; H, 7.53. Found: C, 65.75; H, 7.52.

The solids suspended in the aqueous phase were collected, rinsed neutral with water, and dried to give 30.5 (42% recovery) of **7**. The aqueous filtrates were acidified to recover 10.8 g of **6**.

Method B

A solution of 1.5 g of **6** in 5 ml thionyl chloride was allowed to stand at 25° for 2 h over a porcelain chip. Excess of thionyl chloride was removed *in vacuo* and the residue was treated with a solution of 0.9 ml pyridine in 4 ml tert-butanol. The suspension was shaken for 30 min and then evaporated to dryness *in vacuo*. The residue was partitioned between hot 30–60° petroleum ether and dilute hydrochloric acid. The organic phase gave, upon evaporation, 0.46 g (25%) of **8**, m.p. 73–74.5°, undepressed on admixture with product from method A. The solid remaining in the aqueous phase (1.06 g, m.p. 174–182°) gave the acid **6** on alkaline hydrolysis and is probably the acid anhydride.

trans-2-(3,4,5-Trimethoxyphenyl)-cyclopropanecarboxylic Acid (9)

Method A

This was prepared from the ester **8** and dimethylsulfoxonium methylid by following a procedure described for the synthesis of *trans*-2-phenylcyclopropanecarboxylic acid (10). From 44 g (0.15 mole) of **8** was obtained 20 g (52%) of **9**, m.p. 138–139°, homogeneous on t.l.c. as the methyl ester **22**. The i.r. spectrum: ν_{max} 3300–2500 (COO—H), 1695 (C=O), 1003, 990 cm^{-1} (C—O—C or cyclopropane). The n.m.r. spectrum: τ 3.65 (s, 2, Ar), 6.17 (d, 9, CH_3), 7.44 (octet, 1, H_Y), 8.13 (octet, 1, H_X), 8.39 (octet, 1, H_B), and 8.65 (octet, 1, H_A) p.p.m., J_{AB} 4.7, J_{AX} 8.4, J_{AY} 6.7, J_{BX} 4.9, J_{XY} 4.2 Hz.

Anal. Calcd. for $C_{13}H_{16}O_5$: C, 61.89; H, 6.39. Found: C, 61.78; H, 6.28.

trans-Ethyl 2-(3,4,5-Trimethoxyphenyl)-cyclopropanecarboxylate (20)

This was prepared in quantitative yield by reaction of the acid **9** with diazoethane, m.p. 47–49°.

[3]Although solution was complete in a few hours, CO_2 evolution depended on continued agitation.

Can. J. Chem. Downloaded from www.nrcresearchpress.com by 210.87.254.40 on 09/05/12
For personal use only.

Can. J. Chem. Downloaded from www.nrcresearchpress.com by 210.87.254.40 on 09/05/12
For personal use only.

trans-2-(3,4,5-Trimethoxyphenyl)-cyclopropylcarbinol (19)

Method A

To a solution of 0.6 g (0.0021 mole) of **20** in 10 ml anhydrous ether at 0° was added with stirring, under N_2, a suspension of 0.052 g (0.0013 mole) of lithium aluminum hydride in 10 ml ether over 40 min. The mixture was stirred a further 2 h at 0° and 2 h at 25°. Most of the ether was then removed by filter stick, the residue resuspended in 15 ml fresh ether, and decomposed with 3 ml of saturated aqueous sodium bisulfate. The aqueous phase was extracted with ether, the combined ether phases dried over Na_2SO_4 and freed of ether *in vacuo*. The residual oil was dried by repeated flash evaporation of its benzene solution at 40° (10 mm) to give 0.50 g (88%) of **19** as a pale yellow oil, homogeneous on t.l.c.; ν_{max} 3575, 3450 (OH), 1025, 1005 cm^{-1} (C—O—C or cyclopropane).

The alcohol, **19**, was characterized as its 3,5-dinitrobenzoate ester, m.p. 133–135°.

Anal. Calcd. for $C_{20}H_{20}N_2O_9$: C, 55.54; H, 4.66. Found: C, 55.77, H, 4.67.

trans-3,4,5-Trimethoxycinnamyl Alcohol (17)

This was prepared by a method analogous to method A used for preparing the alcohol **19**, except that the final ether solution was washed with aqueous sodium bicarbonate after the sodium bisulfate treatment to avoid acid-catalyzed decomposition of the product. The alcohol **17** was obtained in 81% yield as a yellow oil, and was homogeneous on t.l.c. A sample was further purified by distillation, b.p. 145–147° (0.15 mm). The i.r.: ν_{max} 3575, 3450 (OH), 1580 cm^{-1} (C=C and Ar).

Anal. Calcd. for $C_{12}H_{16}O_4$: C, 64.28; H, 7.19. Found: C, 63.88; H, 7.14.

A sample of the undistilled alcohol took up 90% of H_2 equivalent to one C=C when hydrogenated over 10% Pd–C/HOAc at 760 mm.

trans-2-(3,4,5-Trimethoxyphenyl)-cyclopropylcarbinol (19)

Method B

To a stirred solution of 0.46 ml (0.56 g, 0.0046 mole) of diethyl zinc in 2 ml dry benzene at 0° under nitrogen was added 0.22 g (0.001 mole) of **17** dissolved in 2 ml of dry benzene. After the initial frothing had subsided, the solution was maintained at 15° while a solution of 0.52 ml (1.7 g, 0.0064 mole) of methylene iodide in 1.5 ml dry benzene was added gradually, with stirring, from a micrometer burette over 1 h.[4]

The clear yellow solution became cloudy after the first 24 min of addition time, and a caramel-colored oil began to separate after 42 min. At the end of 1 h, 5 ml of ether was added and the mixture was then decomposed by gradual addition of 2 ml saturated ammonium chloride with stirring at 0° for 10 min. The organic phase was washed with 2 ml saturated ammonium chloride, then with 2 ml saturated aqueous sodium bicarbonate, and finally freed of solvents *in vacuo*. The residual oil was partitioned between warm water and 30–60° petroleum ether. The aqueous phase from this partition was saturated with sodium sulfate and the resultant emulsion was extracted with ether. The ether extract, on evaporation *in vacuo*, gave 0.155 g (66%) of **18**, relatively pure by t.l.c. and having the same i.r. spectrum as material prepared by method A.

trans-2-(3,4,5-Trimethoxyphenyl)-cyclopropanecarboxylic Acid (9)

Method B

A mixture of 0.20 g of **19**, 0.10 g of sodium bicarbonate and 1.1 g of nickel peroxide[5] in 5 ml water was shaken for 26 h at 25°. The suspension was filtered through Celite and the solids washed with water. The combined filtrates were extracted with ether and the aqueous phase freed of ether *in vacuo*. The aqueous phase was then acidified with dilute hydrochloric acid, the precipitate collected, washed with water, and dried to give 0.092 g (43%) of pale yellow solid, m.p. 131.5–134°. An admixture with **9** prepared by method A had m.p. 135–137°.

trans-2-(3,4,5-Trimethoxyphenyl)-cyclopropylamine (3)

This was prepared by a method analogous to that used for the preparation of *trans*-2-phenylcyclopropylamine (12). From 15.7 g (0.062 mole) of **9** was obtained first the acyl azide **25**, 14.7 g (85%), m.p. 84–87°. The i.r. ν_{max} 2145 (N_3), 1690 cm^{-1} (C=O). This gave, on heating, the isocyanate 30, ν_{max} 2270 cm^{-1} (NCO). The isocyanate was decomposed by 50% NaOH at 0° to give the amine **3**, ν_{max} (CCl_4) 3370, 3300 cm^{-1} (NH_2). The hydrochloride was prepared with dry hydrogen chloride gas in ether, 9.2 g (71%), m.p. 203–204° dec.

Anal. Calcd. for $C_{12}H_{18}NO_3Cl$: C, 55.55; H, 6.99; N, 5.41. Found: C, 55.44; H, 6.92; N, 5.27.

cis-3,4,5-Trimethoxycinnamic Acid (10)

A solution of 70 g (0.294 mole) of **6** in 400 ml water containing 25 g (0.298 mole) of sodium bicarbonate was irradiated with stirring in a Pyrex vessel[6] by an air-cooled AH-4 Hg lamp for 6 days at 56°. Water was added each day to replace evaporative losses. The progress of the isomerization was followed by isolating the mixed acids from small aliquots of the solution, converting them into mixed methyl esters, **7** and **11**, and examining the mixture by t.l.c., which showed one new major component. At the end of 6 days, the product ratio was constant, with the new component in excess. Irradiation was stopped, the solution cooled to 25° and partially neutralized with 18% hydrochloric acid to obtain 19.5 g (28%) of the starting *trans* acid, **6**. Successive additions of dilute hydrochloric acid caused the precipitation of the photoproduct **10** as fractions of 80–100% purity, depending on the cut. Reprecipitation of these fractions from aqueous

[4]Longer addition times resulted in the formation of degradation products while shorter times left considerable starting material behind, which was difficult to separate from the product. The addition of 1 equiv of glyme to complexate any zinc iodide formed, completely inhibited the methylenation reaction.

[5]Prepared by a reported method (11) except that 12% sodium hypochlorite solution was used; the nickel peroxide obtained had an activity of 0.46×10^{-2} g-atom of available O_2 per g.

[6]The use of a quartz vessel gave lower *cis*/*trans* ratios presumably because it transmits 270 mμ, one of the absorption maxima of the *cis* acid, **10**.

Chem. Brewed from www.nrcresearchpress.com by 210.87.254.40 on 09/05/12
For personal use only.

sodium bicarbonate solution gave 20 g (28.6%) of almost pure **10**. A sample recrystallized from boiling carbon tetrachloride had m.p. 114–116° and was homogeneous on t.l.c. The u.v. spectrum λ_{max} 270 (ε 4200) and 221 mμ (ε 7700). The i.r. spectrum: ν_{max} 3300–2500 (COO—H), 1680 (C=O), 1620 cm^{-1} (C=C).

Anal. Calcd. for $C_{12}H_{14}O_5$: C, 60.49; H, 5.93. Found: C, 60.72; H, 5.93.

A sample treated with diazomethane and then hydrogenated at 760 mm over 10% Pd–C in glacial acetic acid gave a product **12** having an i.r. spectrum the same as that of a sample of **6** treated likewise, ν_{max} 1720 cm^{-1}, no C=C.

Attempted Preparation of cis-t-Butyl-3,4,5-trimethoxycinnamate

Following method B for preparation of **8**, the acid **10** gave, with thionyl chloride, mostly black, water-soluble products along with small amounts of the *trans* ester, **8**, and the *trans* acid, **6**.

cis-Ethyl 3,4,5-Trimethoxycinnamate (13)

Using 21.5 g of **10** and following the procedure for synthesis of **15**, there was obtained 21.8 g (90.5%) of **13**, m.p. 43–47°. A sample recrystallized from 30–60° petroleum ether[7] had m.p. 50.5–52.5°, ν_{max} 1710 (C=O), 1620 cm^{-1} (C=C). A sample hydrolyzed by aqueous ethanolic sodium hydroxide gave the *cis* acid, m.p. 114–116°, undepressed on admixture with **10**.

Attempted Preparation of cis-2-(3,4,5-Trimethoxyphenyl)-cyclopropanecarboxylic Acid (14) from 13

Method A

A sample of **13** was treated in a manner analogous to that applied to **8** (dimethylsulfoxonium methylid in DMSO). There was obtained only the *trans* cyclopropane acid, **9**, m.p. 135.5–138°, undepressed on admixture with authentic **9**.

Method B

The *cis* ester **13** was treated with zinc-copper and methylene iodide according to the standard Simmons–Smith procedure (13). Only the starting ester was recovered.

Method C

The *cis* ester **13** was treated with diazomethane and copper sulfate according to a reported method (14) of cyclopropane ring formation. Only starting material was isolated.

Method D

The *cis* ester **13** was treated with diethyl zinc and methylene iodide according to method B for the synthesis of **19**. The product contained about 30% of the starting ester plus 10% each of seven other components.

cis-3,4,5-Trimethoxycinnamyl Alcohol (16)

Using the method described for synthesis of the *trans* alcohol **17**, but starting from 10.2 g (0.038 mole) of **13**, and distilling the product *in vacuo*, there was obtained 6.7 g (77%) of **16** as a pale yellow oil, b.p. 138–140° (0.25 mm), homogeneous on t.l.c., ν_{max} 3575, 3450 (OH) 1580 cm^{-1} (C=C and Ar).

Anal. Calcd. for $C_{12}H_{16}O_4$: C, 64.28; H, 7.19. Found: C, 63.95; H, 7.19.

cis-2-(3,4,5-Trimethoxyphenyl)-cyclopropylcarbinol (18)

Using method B for the synthesis of the *trans* carbinol **19** but starting with 6.0 g (0.027 mole) of **16**, 14.8 g (0.12 mole) of diethyl zinc, and 13.6 ml (45 g, 0.17 mole) of methylene iodide and adding the latter over 45 min, there was obtained 3.5 g (64%) of **18** as a viscous liquid, homogeneous on t.l.c., ν_{max} 3575, 3450 (OH), 1022, 1005 cm^{-1} (C—O—C or cyclopropane). The 3,5-dinitrobenzoate ester had m.p. 125–127°.

Anal. Calcd. for $C_{20}H_{20}N_2O_9$: C, 55.54; H, 4.66. Found: C, 55.75; H, 4.65.

cis-2-(3,4,5-Trimethoxyphenyl)-cyclopropanecarboxylic Acid (14)

This was prepared by the same procedure as method B for the *trans* acid **9**. From 3.5 g of **18** was obtained 2.35 g (64%) of **14**, m.p. 65–66.5°. On sublimation at 120° (0.1 mm), an allotroph, m.p. 114–115° was formed. A mixture of the two forms had m.p. 114–115°. Both forms gave the same i.r., ν_{max} 3300–2500 (COO—H), 1700 (C=O), 1005 cm^{-1} (C—O—C or cyclopropane) and were indistinguishable and homogeneous on t.l.c., as methyl esters, **21**. The n.m.r. ($CDCl_3$): τ 3.54 (s, 2, Ar), 6.24 (s, 9, CH_3), 7.46 (octet, 1, $H_{Y'}$), 7.99 (octet, 1, $H_{X'}$), 8.42 (octet, 1, $H_{B'}$), and 8.68 p.p.m. (octet, 1, $H_{A'}$), $J_{A'B'}$ 5.0, $J_{A'X'}$ 8.4, $J_{A'Y'}$ 8.2, $J_{B'X'}$ 5.5, $J_{X'Y'}$ 9.0 Hz.

Anal. Calcd. for $C_{13}H_{16}O_5$: C, 61.89; H, 6.39. Found: C, 61.76; H, 6.38.

Attempted Epimerization of 14

A solution of 0.035 g of **14** in 0.6 ml of DMSO containing 0.06 g potassium tert-butoxide was allowed to stand at 25° for 20 h. The solvent was removed *in vacuo* and the residue was dissolved in 1 ml water. The solution was acidified with dilute hydrochloric acid and the precipitate collected, washed and dried to obtain a solid, m.p. 64–66°, undepressed on admixture with the lower melting allotroph of **14**.

Attempted Epimerization of cis-Ethyl 3,4,5-Trimethoxycinnamate (13) and of trans-2-(3,4,5-Trimethoxyphenyl)-cyclopropanecarboxylic Acid 9

When samples of these compounds were separately treated with potassium *t*-butoxide in DMSO, each sample was recovered unchanged.

cis-2-(3,4,5-Trimethoxyphenyl)-cyclopropylamine (5)

When 1.0 g of the *cis* cyclopropane acid **14** was treated according to the sequence for synthesis of the *trans* amine, **3**, there was obtained 0.96 g (90%) of the acyl azide **23**, ν_{max} 2145 (N_3), 1700 cm^{-1} (C=O), m.p. 61–65°, followed by the isocyanate **24**, ν_{max} 2270 cm^{-1} (NCO) and the amine **5**, 0.35 g (54%), m.p. 62–63°. ν_{max} (CCl_4) 3370 3300 (NH_2), 1015 cm^{-1} (C—O—C or cyclopropane), and its hydrochloride, m.p. 208–209° dec. An admixture of the salt and that of the *trans* amine **3**, had m.p. 188–197° dec.

Anal. Calcd. for $C_{12}H_{18}NO_3Cl$: C, 55.55; H, 6.99; N, 5.41. Found: C, 55.80; H, 7.04; N, 5.38.

[7]The ester decomposed extensively if left in petroleum ether solution at 25° for 10 days but was stable as a dry solid.

The author wishes to thank Dr. G. Duncan, Faculty of Pharmacy, University of Toronto, Toronto, Ontario, for running the n.m.r. spectra.

1. F. BENNINGTON, R. D. MORIN, L. C. CLARK, and R. P. FOX. J. Org. Chem. **23**, 1979 (1958).
2. A. T. SHULGIN, T. SARGENT, and C. NARANJO. Nature, **221**, 537 (1969).
3. (*a*) F. BENNINGTON, R. D. MORIN, and L. C. CLARK. J. Org. Chem. **21**, 1545 (1956). (*b*) A. T. SHULGIN. Exper. **19**, 127 (1963).
4. (*a*) P. HEY. Quart. J. Pharm. Pharmacol. **20**, 129 (1947). (*b*) D. I. PERETZ, J. R. SMYTHIES, and W. C. GIBSON. J. Ment. Sci. **101**, 317 (1955). (*c*) A. T. SHULGIN, S. BUNNELL, and T. SARGENT. Nature, **189**, 1011 (1961).
5. G. C. WALTERS and P. D. COOPER. Nature, **218**, 298 (1968).
6. T. A. WITTSTRUCK and E. N. TRACHTENBERG. J. Amer. Chem. Soc. **89**, 3810 (1967).
7. F. BENNINGTON, R. D. MORIN, and L. C. CLARK. J. Org. Chem. **21**, 1545 (1956).
8. M. W. KLOHS, M. D. DRAPER, and F. KELLER. J. Amer. Chem. Soc. **76**, 2843 (1954).
9. K. FREUDENBERG and H. SCHRAUBE. Chem. Ber. **88**, *16* (1955).
10. C. KAISER, B. M. TROST, J. BEESON, and J. WEINSTOCK. J. Org. Chem. **30**, 3972 (1965).
11. K. NAGAKAWA, R. KONAKA, and T. NAKATA. J. Org. Chem. **27**, 1597 (1962).
12. J. WEINSTOCK. J. Org. Chem. **26**, 3511 (1961).
13. H. E. SIMMONS and R. D. SMITH. J. Amer. Chem. Soc. **81**, 4256 (1957).
14. D. L. MUCK and E. R. WILSON. J. Org. Chem. **33**, 419 (1968).

Can. J. Chem. Downloaded from www.nrcresearchpress.com by 210.87.254.40 on 09/05/12
For personal use only.

Infrared and Raman spectra and vibrational assignment of methylene cyclopropane-h_6 and -d_6

J. E. BERTIE AND M. G. NORTON
Department of Chemistry, University of Alberta, Edmonton, Alberta

Received June 30, 1970

Infrared spectra have been recorded in the range 4000 to 20 cm^{-1} for methylene cyclopropane-h_6 and -d_6 in the gas phase, and from 4000 to 200 cm^{-1} for methylene cyclopropane-h_6 in the liquid phase. Raman spectra have been recorded for the liquid phases of both species. The fundamental modes of vibration have been assigned using i.r. band contours and Raman depolarization ratios, with the exception of the i.r. inactive A_2 modes which were not observed. An interesting feature is the occurrence of remarkably small isotope shifts for certain modes.

Canadian Journal of Chemistry, 48, 3889 (1970)

Can. J. Chem. Downloaded from www.nrcresearchpress.com by 210.87.254.5 on 09/05/12
For personal use only.

Introduction

Vibrational assignments have been made for only a relatively small number of molecules containing the cyclopropane ring (1–10). Apart from cyclopropane, complete assignments have been published for cyanocyclopropane (7), methyl cyclopropane (8), and bromocyclopropane (9). The remainder of the work on cyclopropane derivatives has been directed mainly toward determining characteristic frequencies for the cyclopropane ring (10). The symmetry of the three molecules studied (7–9) in detail is low, hindering the definitive assignment of the spectra from purely spectroscopic evidence. The relatively high symmetry, C_{2v}, of methylene cyclopropane makes this molecule a desirable one to study in order to support the assignments with purely spectroscopic evidence, and hence to obtain definitive information to further our knowledge of the vibrations of the cyclopropane ring. It is of particular interest to observe the changes in the ring vibrations and force constants caused by the presence of the very distorted sp^2 hybridization on the ring C-1. The detailed assignment of methylene cyclopropane is, further, of interest in connection with the deuterium isotope effects in the formation of methylene cyclopropane-d_2 and -d_4 from methylene pyrazoline-d_2 and -d_4 (11).

Since the initial preparation of methylene cyclopropane by Gragson *et al.* (12) in 1951, its vibrational spectrum has been investigated in the i.r. and Raman by Blau (13) who attempted the assignment of the 24 normal modes. Blau used an approximate normal coordinate calculation to help in making assignments and, later, Loewenstein (14) used a more general force-field and made some reassignment of the spectra. Nevertheless it was not possible for these authors to make a complete assignment of the spectrum. There is no published information on the vibrational spectrum of methylene cyclopropane-d_6.

In this paper the assignment of the i.r. and Raman spectra of methylene cyclopropane-h_6 and -d_6 are discussed. The results of normal-coordinate calculations upon these molecules will be submitted to this journal shortly.

Experimental

Methylene cyclopropane and methylene cyclopropane-d_6 were prepared by the pyrolysis of 1-methylene pyrazoline, h_6 and d_6 respectively, at 200 °C (11). Gas liquid chromatography using a β,β-oxydipropionitrile column at 20 °C revealed no impurities for the hydrogen isotope. The n.m.r. spectra gave no indication of impurity for the h_6 isotope, but indicated 0 to 3% of H in the d_6 isotope, distributed randomly between the ethylenic and methylenic positions. This undoubtedly indicates between 0 and 18% of C_4D_5H impurity in the C_4D_6. No other impurity could be detected, except for a trace of water.

The i.r. spectra between 200 and 4000 cm^{-1} were taken with a Beckman I.R. 12 spectrophotometer. The instrument was calibrated using standard gases (15) and the Beckman fiducial marker accessory. The frequencies quoted are accurate to ± 0.5 cm^{-1} up to 2000 cm^{-1} and ±1 cm^{-1} above 2000 cm^{-1}. The resolution was generally better than 1 cm^{-1} between 4000 and 650 cm^{-1} and better than 2.5 cm^{-1} between 650 and 200 cm^{-1}. The i.r. spectra between 30 and 200 cm^{-1} were obtained using a Beckman-R.I.I.C. FS 720 interferometer, and using a sine plus cosine Fourier transform. The gas cells had a 10 cm path length and were fitted with either cesium iodide or polyethylene windows. The gas pressures were between 2 and 60 cm of mercury for C_4H_6 and between 2 and 20 cm of mercury for C_4D_6. The gas temperature was usually + 37 °C, but was about −40 °C for a few spectra recorded to check for hot bands and difference bands. Liquid spectra of C_4H_6 were taken from 200 to 4000 cm^{-1} in a low temperature cell with CsI windows, using a .005 in. spacer.

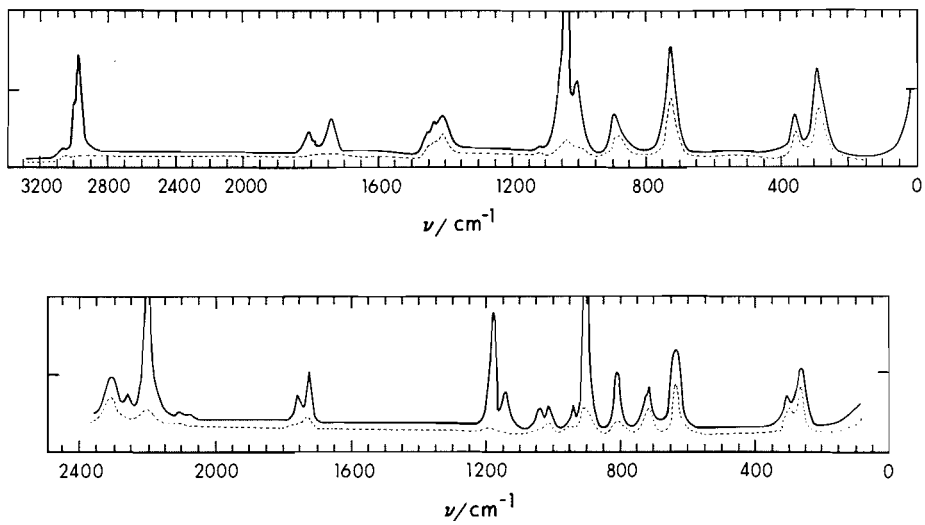

FIG. 1. Raman spectrum of C_4H_6 (upper), and C_4D_6 (lower), liquids at about 22 °C.

Raman spectra were recorded on a Perkin-Elmer L.R.-1 spectrophotometer using a 7 mW He–Ne laser and 90° excitation. The instrument was calibrated using carbon tetrachloride and benzene Raman lines, and the frequencies quoted are accurate to ± 5 cm^{-1}. The resolution was better than 10 cm^{-1}. The Raman samples were liquid and were contained in thick-walled glass tubing, about 1 mm i.d., flattened and polished at the ends, and sealed by a stopcock capable of sealing a few atmospheres internal pressure. The sample temperature was about 22 °C. Late in the course of this work a Raman spectrophotometer became available consisting of a Carson's Laboratories model 10SP Ar^+/Kr^+ laser, a Spex model 1401 monochromator, a cooled FW130 photomultiplier, and photon counting electronics. The Raman spectrum of C_4H_6 was obtained with this instrument and, using the 4880 Å Ar^+ line at about 140 mW power output, spectra with a resolution of about 1 cm^{-1} and a frequency accuracy of ± 1 cm^{-1} were obtained. The sample was the liquid at about 22 °C, sealed into a m.p. capillary tube. The Raman spectrum for C_4H_6 reported in this paper is that obtained from this instrument, while the spectrum for C_4D_6 is that obtained from the Perkin-Elmer L.R. 1. The spectrum of C_4D_6 could not be re-run on the new instrument because no sample was available at that time.

Results

The Raman spectra are shown in Fig. 1, and the frequencies are listed in Table 1. The i.r. spectrum of the gas is shown in Fig. 2 for C_4H_6 between 200 and 4000 cm^{-1}, and in Fig. 3 for C_4D_6 between 200 and 3200 cm^{-1}. No features, apart from the broad, unresolved, pure-rotational absorption, were found for either isotope below 200 cm^{-1}. The spectrum of liquid C_4H_6 is shown in Fig. 4. Table 2 presents the frequencies of the i.r. absorption features for gaseous and liquid C_4H_6, along with a description of the gas phase band contour, and the proposed assignment. For C_4D_6, too little material was available to permit spectra of the liquid to be recorded. Table 3 presents the frequencies of the i.r. absorption features for gaseous C_4D_6, along with a description of the band contours, and the proposed assignment. In Tables 2 and 3 weak combination or overtone bands have been included only if an identifiable band contour was observed. Figs. 5–10 show the i.r. spectra of gaseous C_4H_6 or C_4D_6 in specific regions, and show the proposed resolution of multiple bands into A-, B-, or C-type band contours. For convenience, Table 4 presents a brief symmetry coordinate description of each mode next to the mode number. This description does not, in most cases, accurately describe the normal coordinate. The numbering of the modes follows Herzberg (16).

Our i.r. spectra of C_4H_6 gas are more extensive and were run at higher resolution than those of Blau, but show essentially the same features, subject to resolution differences, except that we do not observe the band at 695 cm^{-1} reported by him. Blau's Raman spectrum of C_4H_6 contains a number of features, at 596, 663, 922, 969, and 1476 cm^{-1} that we have not observed. We believe that we would have observed them had they been present in our sample. The i.r. spectra reported

Can. J. Chem. Downloaded from www.nrcresearchpress.com by 210.87.254.5 on 09/05/12
For personal use only.

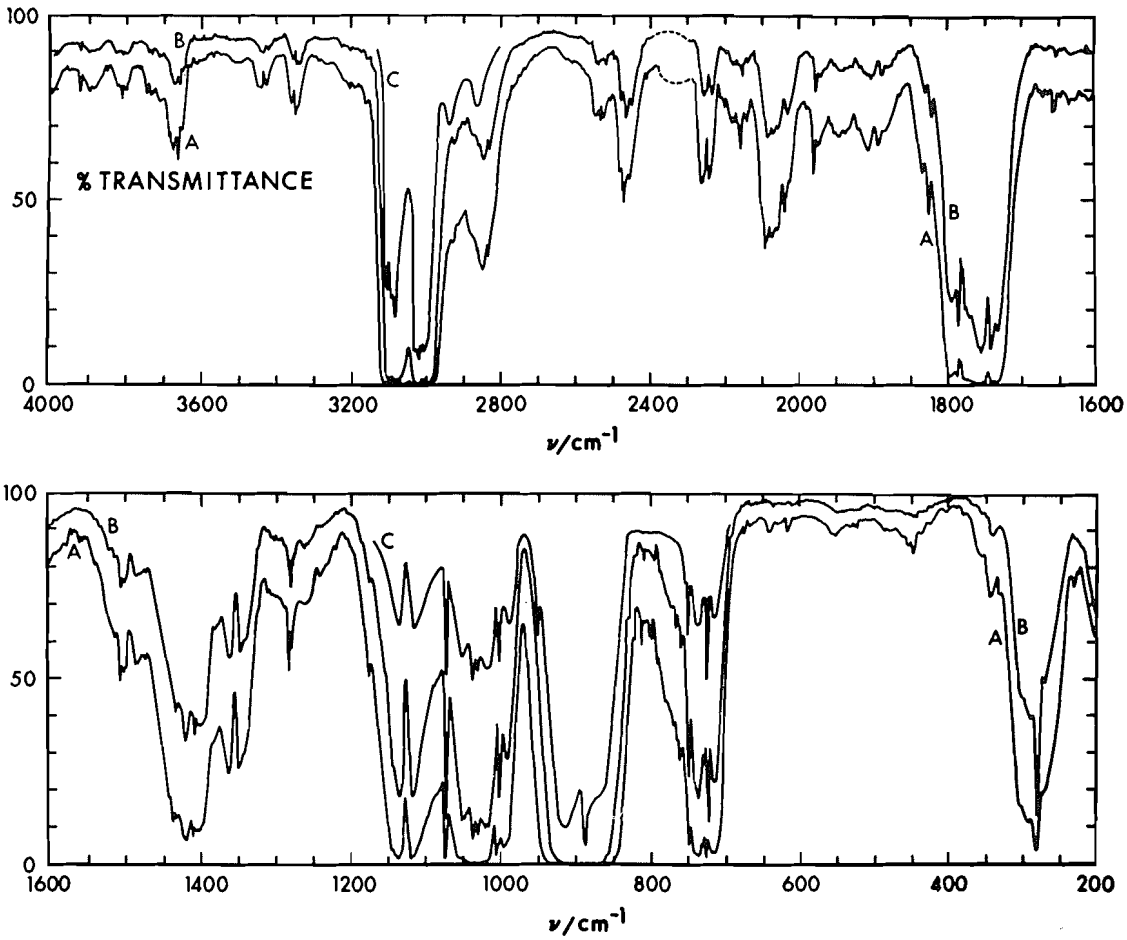

FIG. 2. The i.r. spectrum of C_4H_6 gas at about 34 °C. The gas pressures are: curve *A*, 580 mm of Hg; curve *B*, 250 mm of Hg; curve *C*, 60 mm of Hg. The path length is 10 cm.

here for liquid C_4H_6, and for gaseous C_4D_6, and the Raman spectrum of C_4D_6 reported here, are, to our knowledge, the first to be published.

Discussion

(a) Molecular Structure and Infrared Band Contours

The structure of methylene cyclopropane has been determined by Laurie and Stigliani (17) by microwave spectroscopy; the only assumption required was that the ethylenic carbon–hydrogen bond length is 1.088 Å (17). The molecule belongs to the C_{2v} point group (16). Taking the ring plane to be the *xz* plane, the 24 normal modes form the following representation of the group:

$$8A_1 + 4A_2 + 7B_1 + 5B_2$$

The Raman depolarization ratios help to identify the A_1 modes, the bands unique to the Raman spectrum arise from the A_2 modes, and the band contours in the i.r. spectrum of the gas characterize the absorption by the A_1, B_1, and B_2 modes.

The i.r. band contours may be calculated (18) from a knowledge of the moments of inertia. Using Laurie and Stigliani's (17) data we calculate the moments of inertia of C_4D_6 to be 37.6, 92.5, and 116.8, a.m.u. Å^2, and the band contours to be of Ueda and Shimanouchi's (18) type 17 for both C_4H_6 and C_4D_6.

The A_1, B_1, and B_2 modes may thus be

Can. J. Chem. Downloaded from www.nrcresearchpress.com by 210.87.254.5 on 09/05/12
For personal use only.

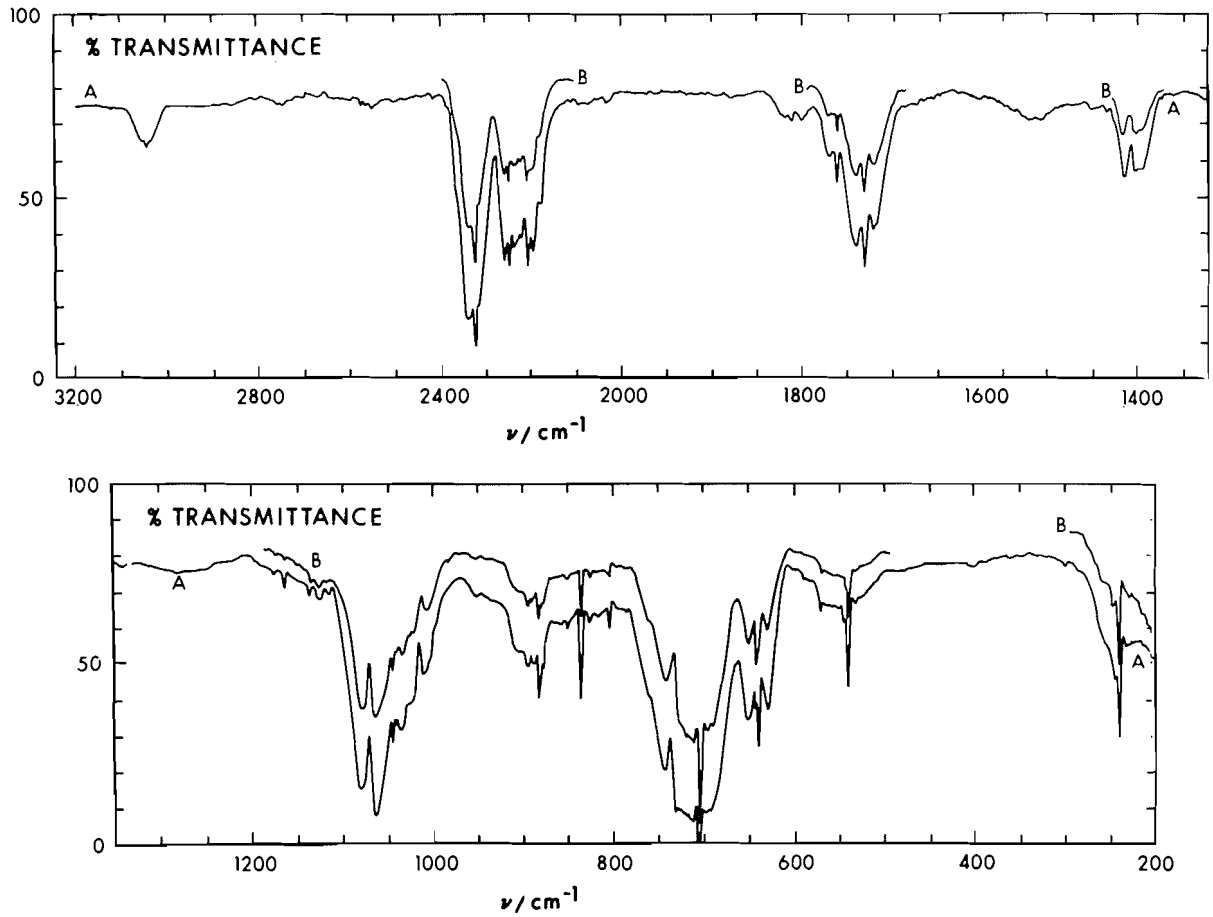

FIG. 3. The i.r. spectrum of C_4D_6 gas at about 34 °C. The gas pressures are: curve *A*, 200 mm of Hg; curve *B*, 100 mm of Hg. The path length is 10 cm.

identified by their A, B, C band contours respectively.

(b) Assignment for C_4H_6

(i) C—H Stretching Vibrations

The i.r. active fundamentals to be assigned are an A_1 and a B_1 ethylenic mode and A_1, B_1, and B_2 methylenic modes. The ethylenic B_1 and the methylenic B_2 modes are expected at a higher frequency than the other three modes, as they arise from the asymmetric stretch of the CH_2 group. The spectrum from 2900 to 3150 cm^{-1} is shown in Fig. 5.

Two regions of absorption are noted: the higher frequency band consisting of a B- and a C-type contour, while the one at lower frequency contains one B and two A bands. The assignment of the C-type band at 3069.5 cm^{-1} to the B_2 methylenic stretch, ν_{20}, and the B feature at 3086.2 cm^{-1} to the B_1 ethylenic stretch, ν_{13}, follows immediately. The other B_1 mode (B_1 methylenic stretch, ν_{14}) is found at 2996.0 cm^{-1}. The A_1 feature at 3008.3 cm^{-1} is assigned to the A_1 ethylenic stretch, ν_1, and the A_1 band at 2999.3 cm^{-1} to the A_1 methylenic stretch, ν_2, for the following reasons: (*a*) The Raman line at 2988 cm^{-1} is considerably more intense than that at 2997 cm^{-1}. Both lines are strongly polarized and therefore arise from A_1 modes. Somewhat intuitively, one expects the methylenic stretch to cause a greater polarizability change than the ethylenic stretch, and therefore to yield a more intense Raman line. Thus we assign the methylenic stretch to low frequency of the ethylenic stretch.

Can. J. Chem. Downloaded from www.nrcresearchpress.com by 210.87.254.5 on 09/05/12
For personal use only.

TABLE 1

Raman spectrum of C_4H_6 and C_4D_6 liquid

C_4H_6*			C_4D_6†		
Frequency‡	Intensity	Depolarization ratio	Frequency†	Intensity	Depolarization ratio
288	2	0.75	253	3	0.75
356	1	0.75	304	1	0.75
724	3	0.7	642	4	0.65
890	1	0.75	708	1.5	0.75
1000	1.5	0.1	804	3	0.35
1034	10	0.1	900	10	0.1
1125	0.1	0.75	946	1.5	0.1
1411	1	0.75	1019	0.6	0.75
1435	1	0.4	1048	1	~0.3
1453	0.1	?	1144	1	0.1
1736	0.5	0.1	1172	5	0.1
1784	0.05	?	1725	1	0.3
1805	0.4	0.1	1753	0.5	0.2
2988	2.5	0.1	2202	9	0.03
2997	1.2	0.1	2258	0.3	0.1
3060	0.3	0.75	2310	1.5	0.75

*Frequencies accurate to ± 1 cm^{-1}.
†Frequencies accurate to ± 5 cm^{-1}.
‡Frequency units are cm^{-1}.

(*b*) The higher frequency A_1 band is the more intense in the i.r., and, from the assumed geometry of the molecule, the bond moment approximation, assuming equal bond moments for all C—H bonds, predicts that the ethylenic stretch has a greater dipole moment change along the *z* axis than the methylenic stretching mode, and therefore has a greater absorption intensity.

The i.r. inactive A_2 vibration expected near ν_{20} or ν_{13} may contribute to the broad depolarized Raman feature at 3050 to 3080 cm^{-1}, but, because this is not resolved, we cannot make a reliable assignment of this mode.

(ii) The C=C Stretching Vibration

In the range 1600 to 2000 cm^{-1}, only two strong A-type features are found in the i.r. spectrum, at 1786.0 and 1742.2 cm^{-1} (Fig. 6). One of these features must be due to the C=C stretch, ν_3. The lower frequency feature, at 1742.2 cm^{-1}, corresponds to a medium intensity Raman peak (polarized), while the 1786.0 cm^{-1} feature gives rise to only a very weak band in the Raman. On this basis, we prefer the assignment of ν_3 to 1742.2 cm^{-1}, and assign the 1786.0 band to $2\nu_{22}$, enhanced by Fermi resonance with ν_3. The high frequency for a C=C stretching mode, 1742.2 cm^{-1}, undoubtedly arises primarily from the large kinetic coupling with the symmetric ring stretching mode which, itself, arises from the large angle (~150°) between the C=C bond and the ring C—C bonds. A similar effect is known to exist for C=O stretching modes (19).

(iii) The Ring Vibrations

Three ring vibrations are expected: the A_1 symmetric stretching mode (the ring breathing mode), the B_1 asymmetric stretching mode, and the A_1 deformation mode. The ring breathing mode (ν_6) is readily identified at 1034 cm^{-1} by its very strong Raman intensity, and by the A-type band at 1037.4 cm^{-1} in the i.r. (Fig. 7). The second Q branch at 1030.3 cm^{-1} decreases in intensity relative to that at 1037.4 cm^{-1} when the gas is cooled and is believed to be a hot band, probably originating from the 279.6 cm^{-1} energy level. The remaining A_1 and B_1 modes must be at considerably lower frequencies than 1037.4 cm^{-1}. The only A-type band meeting this requirement is at 723.8 cm^{-1} and we assign this to the A_1 ring deformation mode (ν_8). The B_1 asymmetric ring stretching mode should be between the two A_1 modes, and is assigned at 895 cm^{-1} (Fig. 8), to the only B-type band in this region.

(iv) The CH_2 Deformation Vibrations

The ethylenic CH_2 group gives rise to an A_1 deformation, an A_2 torsion, a B_1 rocking, and a B_2 wagging mode. The A_1 and B_2 modes are well characterized in substituted ethylenes (20, 21) at 1410 to 1420 cm^{-1}, and near to 890 cm^{-1} respectively. We therefore assign the A-type feature at 1411.0 cm^{-1} (Fig. 6) to the A_1 ethylenic

Can. J. Chem. Downloaded from www.nrcresearchpress.com by 210.87.254.5 on 09/05/12
For personal use only.

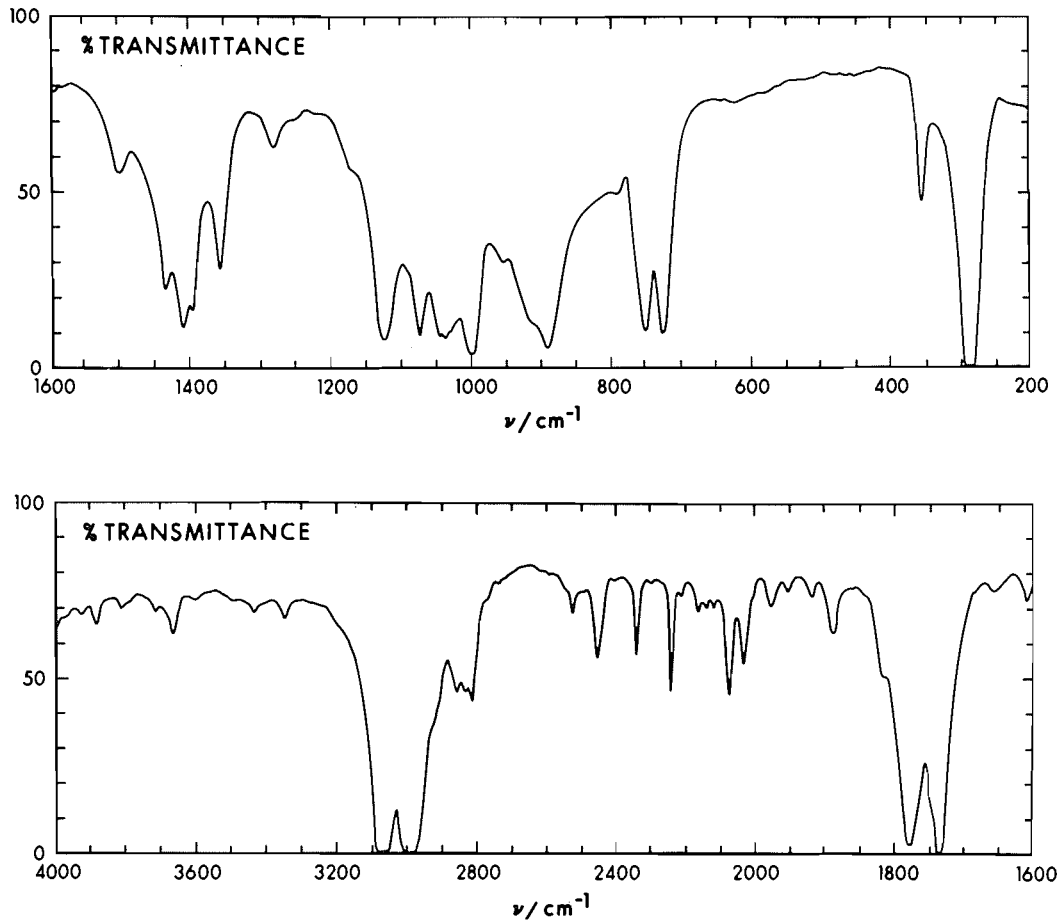

FIG. 4. The i.r. spectrum of C_4H_6 liquid at about -45 °C. The exact path length is unknown but is less than or equal to 0.005 in.

deformation (ν_5), and the intense C-type band at 890.5 cm^{-1} to the B_2 ethylenic wag (ν_{22}) (Fig. 8).

The A_2 torsion is not observed in the Raman spectrum. The B_1 rocking motion of the ethylenic group is not so uniquely determined. Early work, summarized by Sheppard and Simpson (20), placed this mode at around 1280 cm^{-1} in di-substituted ethylenes of the type $RR'C{=}CH_2$. Torkington (22) preferred the assignment of the ethylenic rock to 1062 cm^{-1} in isobutene and 1040 cm^{-1} in propene. Meyer and Gunthard, in a study of 2-bromo-propene (23), assign this mode to a band at 925 cm^{-1}. A recent study of isobutene (21) in the gas, liquid, and solid states assigns the A_1 ethylenic deformation to 1416 cm^{-1} and the B_1 ethylenic rock to 975 cm^{-1}. In view of this uncertainty we discuss this assignment with the other B_1 modes later.

The methylenic CH_2 groups give rise to an A_1 and a B_1 deformation, an A_1 and a B_1 wag, an A_2 and a B_2 twist, and an A_2 and a B_2 rock. The A_1 deformation is found near 1475 cm^{-1} (1, 5) in cyclopropane, and at 1490 cm^{-1} in ethylene oxide (24). The i.r. spectrum of methylene cyclopropane shows a weak A-type band at 1436.5 cm^{-1} (Fig. 6) coincident with a polarized Raman line, and a very weak Q branch (A or C band contour) at $\sim$ 1500 cm^{-1}, where no Raman band was detected. The Raman activity of the 1436.5 cm^{-1} feature suggests it arises from a fundamental transition and we assign it to the A_1 methylenic deformation (ν_4). The band at 1508 cm^{-1} may be due to $2\nu_{23}$. The only remaining A_1

Can. J. Chem. Downloaded from www.nrcresearchpress.com by 210.87.254.5 on 09/05/12
For personal use only.

Can. J. Chem. Downloaded from www.nrcresearchpress.com by 210.87.254.5 on 09/05/12
For personal use only.

TABLE 2

Infrared absorption frequencies* of methylene cyclopropane-h_6

Gas† frequency		Band contour	Liquid‡ frequency	Assignment
279.6	mw	C	290	ν_{24}
355	w	B	355	ν_{19}
723.8	m	A	725	ν_8
728	vw	A	—	hot band?
748.6	mw	C	748	ν_{23}
888.0	vw	C	—	hot band
890.5	vs	C	889	ν_{22}
895		B	~900	ν_{18}
951	vw	C	950	$\nu_8 + \nu_{24}$
1000.0	vw	A	—	hot band
1002.6	m	A	999	ν_7
1030.3	mw	C	—	hot band
1037.4	ms	A	1036	ν_6
—	ms	—	—	ν_{10}
1073.0	ms	C	1072	ν_{21}
1125.3	ms	B	1122	ν_{17}
1244	vvw	B	—	?
1280.5	vw	C	1279	$\nu_{24} + \nu_7$
1354.4	mw	B	1357	ν_{16}
1410	m	B	1397	ν_{15}
1411.0	wm	A	1409	ν_5
1436.5	wm	A	1434	ν_4
~1500	w	A?	1497	$2\nu_{23}$?
1742.2	s	A	1737	ν_3
1786.0	s	A	1777	$2\nu_{22}$
1822	w	A	1814	$\nu_{23} + \nu_{21}$
1896	vw	B	1888	$\nu_7 + \nu_{18}$
1948	vw	A		$\nu_{22} + \nu_{21}$
~1980	vw	A	1984	$2\nu_7$
2138	vvw	A	2142	$2\nu_{21}$
2160	vw	A	2169	$\nu_{23} + \nu_5$
2248	w	B	2241	$2\nu_{17}$
2350	vw	A?	2340	$\nu_6 + \nu_{16}$
2467	w	A	2452	$\nu_{16} + \nu_{17}$
2996.0	s	B	§	ν_{14}
2999.3	m	A	§	ν_2
3008.3	vs	A	§	ν_1
3069.5	s	C	§	ν_{20}
3086.2	s	B	§	ν_{13}
3348	vw	A	3350	$\nu_{20} + \nu_{24}$
3435	vw	B	3436	?
3665	w	A	3660	?
3820	vw	A	3810	$\nu_{20} + \nu_{23}$
3928	vvw	C	3921	$\nu_{18} + \nu_9(A_2)$

*Frequency units are cm^{-1}.
†At about 30 °C.
‡At −40 °C.
§The bands were too intense to measure.

mode, the A_1 wag, is found at 1002.6 cm^{-1} characterized by a polarized Raman band and an A-type i.r. absorption (Fig. 7).

We now consider the three B_1 modes: methylenic deformation, methylenic wag, and ethylenic rock. The spectrum shows two undisputable B contours at 1125.3 cm^{-1} (Figs. 2 and 7) and 1354.4 cm^{-1} (Figs. 2 and 6). In addition to these there is a very weak B contour at 1244 cm^{-1} (Fig. 2). The presence of a further B-type band at ~ 1410 cm^{-1} is suggested by the i.r. bandshape in the region

TABLE 3

Infrared absorption frequencies* of methylene cyclopropane-d_6 vapor

Gas frequency		Band contour	Assignment
240	mw	C	ν_{24}
304	vw	B	ν_{19}
537.5	mw	C	ν_{23}
541.5	vw	C	hot band?
637.0	m	A	ν_8
639.5	vw	A	hot band
650.5	vvw	C	$\nu_6 - \nu_{24}$
705.0	vs	C	ν_{22}
735	m	B	ν_{18}
804.2	vw	A	ν_7
835.5	w	C	ν_{21}
882	vw	C	$\nu_{24} + \nu_8$
895	mw	A	ν_6
1017	m	B	ν_{17}
1043	mw	A?	$\nu_{19} + \nu_{18}$?
1047	mw	C	$\nu_{24} + \nu_7$
1073	s	B	ν_{16}
1122	w	B	ν_{15}
1139	w	A	ν_5
1168	w	A	ν_4
1410	mw	B?	impurity
1727.7	ms	A	ν_3
1758.0	m	A	$\nu_{17} + \nu_{18}$
1805	vw	B	$\nu_{16} + \nu_8$
2179.0	m	B	ν_{14}
2202.3	ms	A	ν_2
2239.5	w	A	hot band
2241.7	s	A	ν_1
2315.2	s	C	ν_{20}
2321.1	s	B	ν_{13}
3038	mw	A	impurity

*Frequency units are cm^{-1}.

TABLE 4

Symmetry co-ordinate description of the normal modes

ν_1	A_1 Symmetric ethylenic stretch
ν_2	A_1 Symmetric methylenic stretch
ν_3	C=C Stretch
ν_4	A_1 Methylenic deformation
ν_5	A_1 Ethylenic deformation
ν_6	A_1 Ring stretch
ν_7	A_1 Methylenic wag
ν_8	A_1 Ring deformation
ν_9	A_2 Methylenic stretch
ν_{10}	A_2 Methylenic twist
ν_{11}	A_2 Methylenic rock
ν_{12}	A_2 Ethylenic torsion
ν_{13}	B_1 Asymmetric ethylenic stretch
ν_{14}	B_1 Symmetric methylenic stretch
ν_{15}	B_1 Methylenic deformation
ν_{16}	B_1 Ethylenic rock
ν_{17}	B_1 Methylenic wag
ν_{18}	B_1 Ring deformation
ν_{19}	In-plane C=C—C deformation
ν_{20}	B_2 Asymmetric methylenic stretch
ν_{21}	B_2 Methylenic twist
ν_{22}	Ethylenic wag
ν_{23}	B_2 Methylenic rock
ν_{24}	Out-of-plane C=C—C deformation

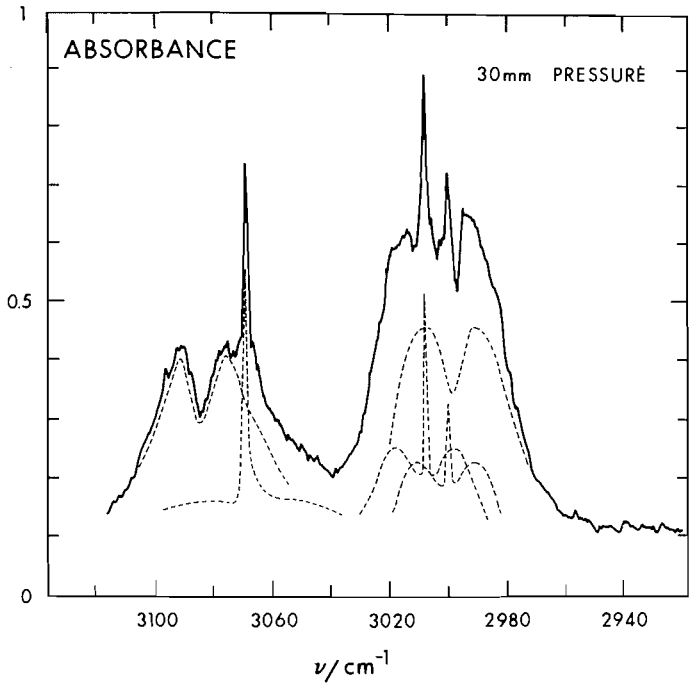

FIG. 5. The i.r. spectrum (solid line) of C_4H_6 gas, between 2920 and 3140 cm^{-1}, at about 34 °C, 10 cm path length. The dashed lines represent our proposed separation of the bands into A-, B-, and C-type contours.

1390 to 1450 cm^{-1} (Fig. 6), which is not consistent with there being just two A_1 fundamentals plus two A_1 hot bands in this region. Further, the Raman line at 1411.0 cm^{-1} (Fig. 1) is depolarized, suggesting the presence of a non-A_1 vibration at this frequency, in addition to the A_1 vibration observed in the i.r. Further, in the spectrum of the liquid (Fig. 4), there is a clearly separated band at 1397 cm^{-1}, in addition to bands corresponding to the A_1 features. We therefore assign the 1410 cm^{-1} B-type i.r. band to the B_1 methylenic deformation. The in-phase and out-of-phase methylenic deformations are therefore separated by 27 cm^{-1}, which is similar to the separation in ethylene oxide (24) and cyclopropane (1, 5) (20 and 41 cm^{-1} respectively).

In cyclopropane, the a_2' and e′ methylenic wags are assigned at 1070 cm^{-1} and 868 cm^{-1} respectively (5). The A_1 wag in C_4H_6 corresponds more clearly to the e′ mode in C_3H_6 and the B_1 wag to the a_2' mode. Therefore we expect the B_1 methylenic wag to occur at a higher frequency than the A_1 wag (1002.6 cm^{-1}). The B-type band at 1125.3 cm^{-1} is therefore assigned to the B_1 methylenic wagging vibration, ν_{17}, and the B_1 ethylenic rocking vibration, ν_{16}, can only be assigned to the band at 1354.4 cm^{-1}. This is a high frequency for such a vibration, but this assignment appears to be forced on us. There is a weak B-type band at $\sim$ 1244 cm^{-1} that was considered to possibly arise from the ethylenic rock, but it is absent in the spectrum of the liquid, and seems unlikely to arise from a fundamental transition.

The B_2 methylenic twisting and rocking vibrations give rise to two C-type features at 1073 cm^{-1} (Figs. 2 and 7) and 748.6 cm^{-1} (Fig. 2). The relative positions of these motions have been established unambiguously in cyclobutane (25) and in studies on solid cyclopropane (4), and we therefore assign the twist (ν_{21}) to 1073.0 cm^{-1} and the rock (ν_{23}) to 748.6 cm^{-1}.

The two remaining i.r. active fundamentals, a B_1 in-plane, and a B_2 out-of-plane, $=CH_2$ wagging vibration, have yet to be assigned. A C-type contour is observed at 279.6 cm^{-1} with a weak B-type contour at 355 cm^{-1} (Fig. 2). These modes are better resolved in the liquid spectrum

Can. J. Chem. Downloaded from www.nrcresearchpress.com by 210.87.254.5 on 09/05/12
For personal use only.

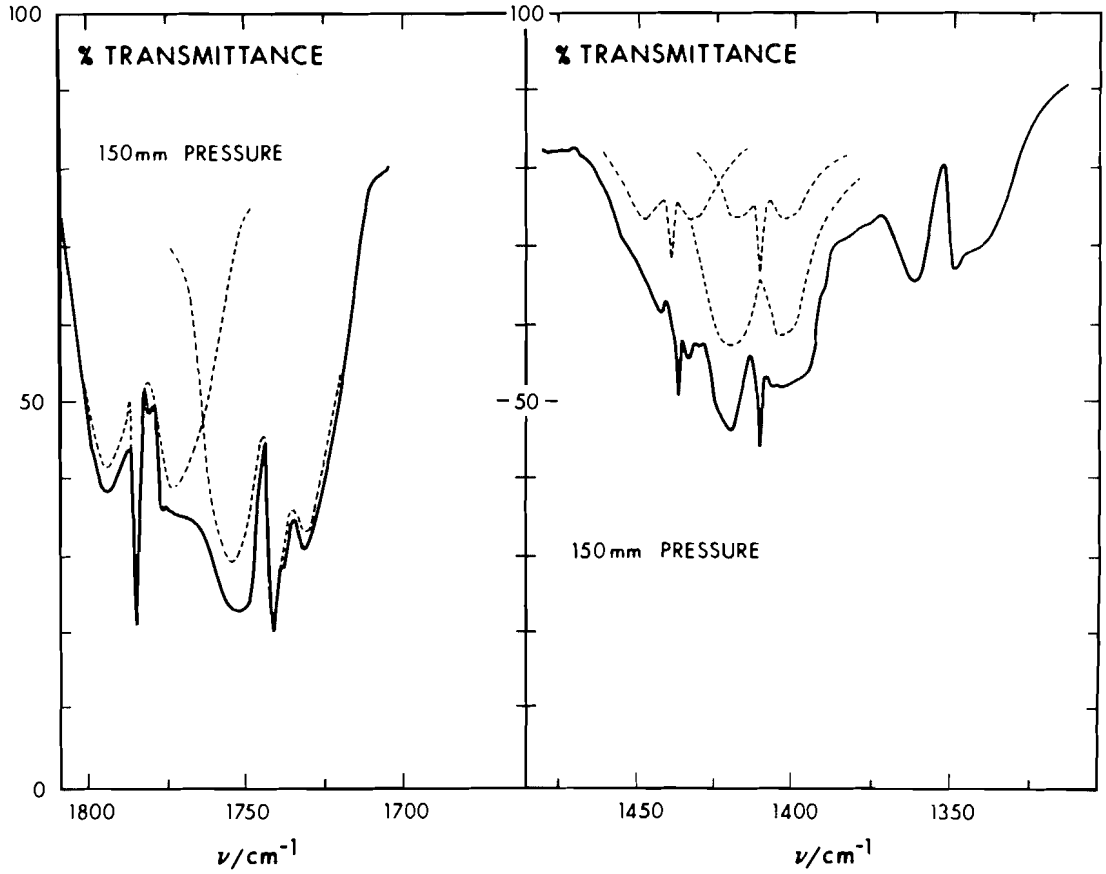

FIG. 6. The i.r. spectrum (solid line) of C_4H_6 gas, between 1700 and 1810 cm^{-1} and between 1300 and 1475 cm^{-1}, at about 34 °C, 10 cm path length. The dashed lines represent our proposed separation of the band into A- and B-type contours. The B-type band at 1354 cm^{-1} is self-evident.

(Fig. 4) and confirm the presence of a band centered at 355 cm^{-1} in the gas spectrum. Both modes are observed in the Raman spectrum and are depolarized (Fig. 1). The in-plane wag (ν_{19}) is thus assigned to the band at 355 cm^{-1} and the out-of-plane motion (ν_{24}) to that at 279.6 cm^{-1}.

The A_2 modes were not observed in this work.

(c) Assignment of C_4D_6

(i) C—D Stretching Vibrations

These occur between 2340 and 2160 cm^{-1} (Fig. 9) and can be assigned by direct comparison with the assignment of the light compound as: B_1 ethylenic stretch, ν_{13}, 2321.1 cm^{-1}; B_2 methylenic stretch, ν_{20}, 2315.2 cm^{-1}; A_1 ethylenic stretch, ν_1, 2241.7 cm^{-1}; A_1 methylenic stretch, ν_2, 2202.3 cm^{-1}; B_1 methylenic stretch, ν_{14}, 2179.0 cm^{-1}. The A_2 methylenic stretch was not observed.

(ii) C=C Stretching Vibration

As in the spectra of C_4H_6, two A_1 features are found in the i.r. at 1758.0 and 1727.7 cm^{-1} (Fig. 3) and in the Raman (Fig. 1). The higher frequency band is weaker in both the i.r. and Raman and may be due to a combination of two intense B-type modes at 1017 and 735 cm^{-1}, enhanced by Fermi resonance. We thus assign ν_3, C=C stretch, to 1727.7 cm^{-1}. The shift of this mode on deuteration (1742.2 to 1727.7 cm^{-1}) is remarkably small, but these assignments appear to be the most reasonable for each compound. If 1742.2 cm^{-1} is accepted for C_4H_6, the C_4D_6 frequency may be expected at about 1660 cm^{-1}, and there is clearly no band of significant

Can. J. Chem. Downloaded from www.nrcresearchpress.com by 210.87.254.5 on 09/05/12
For personal use only.

Can. J. Chem. Downloaded from www.nrcresearchpress.com by 210.87.254.5 on 09/05/12
For personal use only.

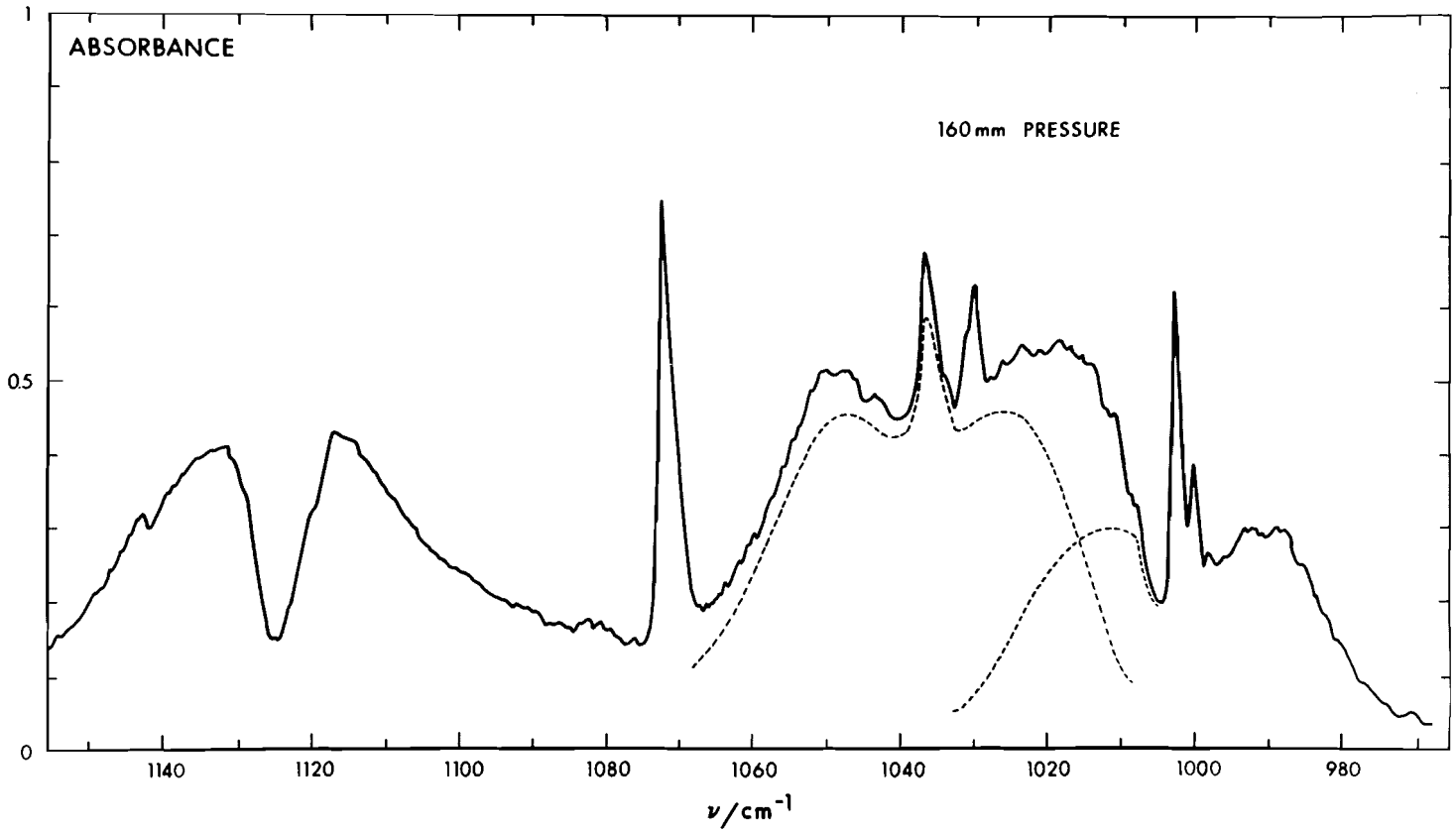

FIG. 7. The i.r. spectrum (solid line) of C_4H_6 gas, between 970 and 1150 cm^{-1}, at 34 °C, 10 cm path length. The dashed lines represent our proposed separation of the two A-type contours between 970 and 1060 cm^{-1}. The C-type band at 1073 cm^{-1} and the B-type band at 1125 cm^{-1} are self-evident.

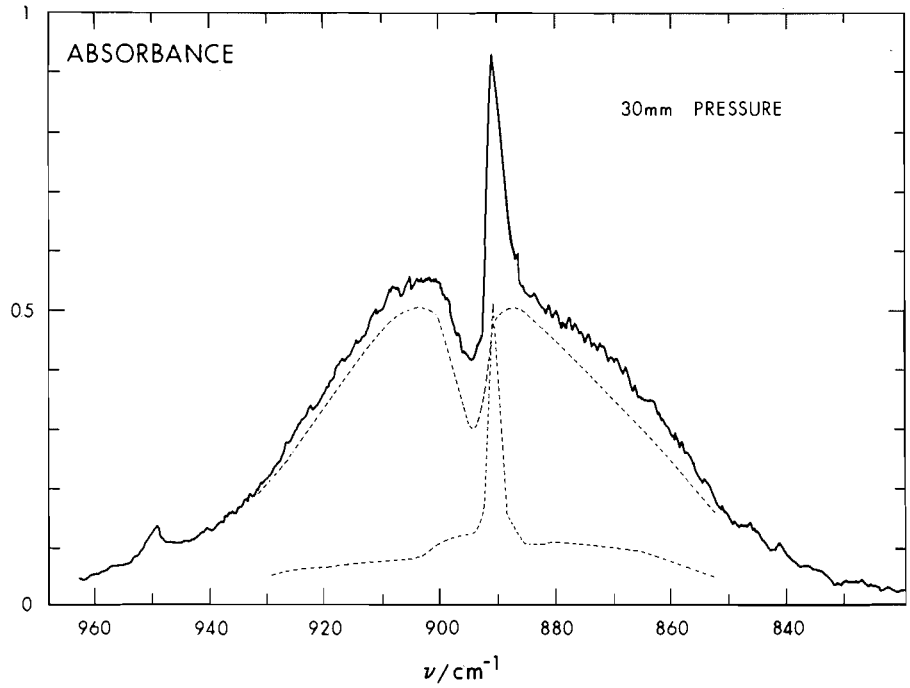

FIG. 8. The i.r. spectrum (solid line) of C_4H_6 gas, between 820 and 960 cm^{-1}, at 34 °C, 10 cm path length. The dashed lines represent our proposed resolution of the band into a B- and a C-type contour.

intensity in that region. Conversely, if 1727.7 cm^{-1} is accepted for C_4D_6, the C_4H_6 frequency would be expected near to 1810 cm^{-1}. While weak bands do occur in this region it does not seem reasonable to prefer them to the strong 1742.2 cm^{-1} band for this assignment.

(iii) The Ring Vibrations

By analogy with C_4H_6 we assign the feature at 900 cm^{-1} (Fig. 1), the most intense Raman band, to the ring breathing mode, ν_6. There is a somewhat imperfect A-type band in the i.r. at 895 cm^{-1} (Fig. 3), consistent with this assignment. The A_1 ring deformation (ν_8) is assigned to the well-defined A-type i.r. band at 637.0 cm^{-1}, which is nearly coincident with a partly polarized Raman band. The B_1 ring deformation (ν_{18}), is assigned to the only B-type i.r. band between the two A_1 frequencies, at 735 cm^{-1}.

(iv) The CD_2 Deformation Vibrations

We must assign an A_1 deformation, an A_2 torsion, a B_1 rock, and a B_2 wag for the ethylenic group, and an A_1 and a B_1 deformation, an A_1 and a B_1 wag, an A_2 and a B_2 twist, and an A_2 and a B_2 rock for the methylenic groups.

There are clearly C-type bands (Fig. 3) at 537.5 cm^{-1}, 705.0 cm^{-1}, 835.5 cm^{-1}, and 882 cm^{-1}. The strongest of these bands, at 705.0 cm^{-1} is assigned to the ethylenic wagging mode (ν_{22}), which usually yields strong i.r. absorption, at any rate in non-deuterated ethylenes (20, 21), and does so in C_4H_6 (see Discussion, section *b*, *iv*). For the same reasons as in C_4H_6 (Discussion, section *b*, *iv*) we assign the lower frequency band, 537.5 cm^{-1} to the methylenic rock (ν_{23}) and we assign the B_2 methylenic twist (ν_{21}) to the more intense of the remaining C-type bands, at 835.5 cm^{-1}.

The three B_1 modes must be assigned to the three B-type bands, at 1122, 1073, and 1017 cm^{-1} (Figs. 3 and 10). The 1122 and 1073 cm^{-1} bands are assigned to the B_1 methylenic deformation (ν_{15}) and the ethylenic rock (ν_{16}) respectively. This assignment yields a 20.5 and 20.7% respectively isotope shift on deuteration. The 1017 cm^{-1} feature must then be assigned to the B_1 methylenic wagging mode (ν_{17}). This assignment implies a surprisingly small isotope shift of 9.6% for this mode, compared with 19.8% for the A_1 methylenic wag. However, the product rule is

Can. J. Chem. Downloaded from www.nrcresearchpress.com by 210.87.254.5 on 09/05/12
For personal use only.

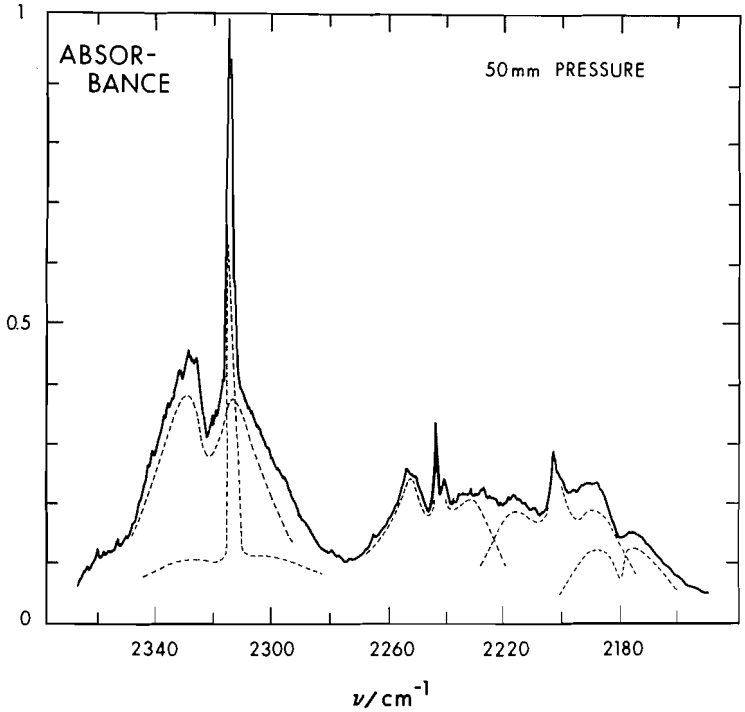

FIG. 9. The i.r. spectrum of C_4D_6 gas, between 2140 and 2380 cm^{-1}, at about 34 °C, 10 cm path length. The dashed lines represent our proposed separation of the bands into A-, B-, and C-type contours.

well satisfied by this assignment, and there is no viable alternative.

The three A_1 modes are less easy to assign confidently. The remaining A-type bands in the i.r. spectrum are all very weak (Figs. 3 and 10), and we must use the Raman polarization data as an aid to assignment. There are weak A-type infrared bands at 1168 (Fig. 10), 1139 (Fig. 10), and 804.2 cm^{-1} (Fig. 3), all of which correspond to polarized Raman lines. There are also two Q branch lines at 1043 and 1047 cm^{-1} which can best be separated into a C-type band at 1047 cm^{-1} and an A-type band at 1043 cm^{-1} (Fig. 10). There is a partly polarized Raman band at 1048 cm^{-1} which could arise from overlapping A- and C-type bands, or could arise from a single A-type band. The i.r. Q branches at 1047 and 1043 cm^{-1} could be assigned as an A-type band plus a hot band. At any rate there is clearly an A-type band at 1043 or 1047 cm^{-1}, or both.

The 804.2 cm^{-1} band is assigned to the A_1 methylenic wag (ν_7) and the A_1 methylenic deformation (ν_4) is assigned to the 1168 cm^{-1} band. In cyclopropane (5) and ethylene oxide (24) the symmetric methylenic deformation is strong in the Raman of the deuterated derivative, in contrast with its Raman intensity for the light species, perhaps because of coupling with the symmetric ring stretching mode. The occurrence of the same Raman intensity change supports the assignment of the symmetric CH_2 deformation at 1436.5 cm^{-1} in C_4H_6 and 1168 cm^{-1} in C_4D_6.

The A_1 ethylenic deformation can be assigned to the A_1 bands at 1139 cm^{-1} or at 1043 cm^{-1}. We prefer to assign it to the 1139 cm^{-1} band because of (*a*) the large isotopic shift (26%) if we assign it at 1043 cm^{-1} (compared to 21% in propylene (26)), and (*b*) there being no clear explanation of the 1139 cm^{-1} feature in terms of combinations, while the 1043 cm^{-1} band can be assigned as $\nu_{19} + \nu_{18}$, which is expected at 1039 cm^{-1}. However, as will be seen in section 4*d* this assignment does not fit the product rule well, while assigning the A_1 ethylenic deformation to 1043 or 1047 cm^{-1} does fit the product rule well.

No evidence as to the frequencies of the A_2 modes was obtained.

The two remaining modes, the in-plane (B_1)

Can. J. Chem. Downloaded from www.nrcresearchpress.com by 210.87.254.5 on 09/05/12
For personal use only.

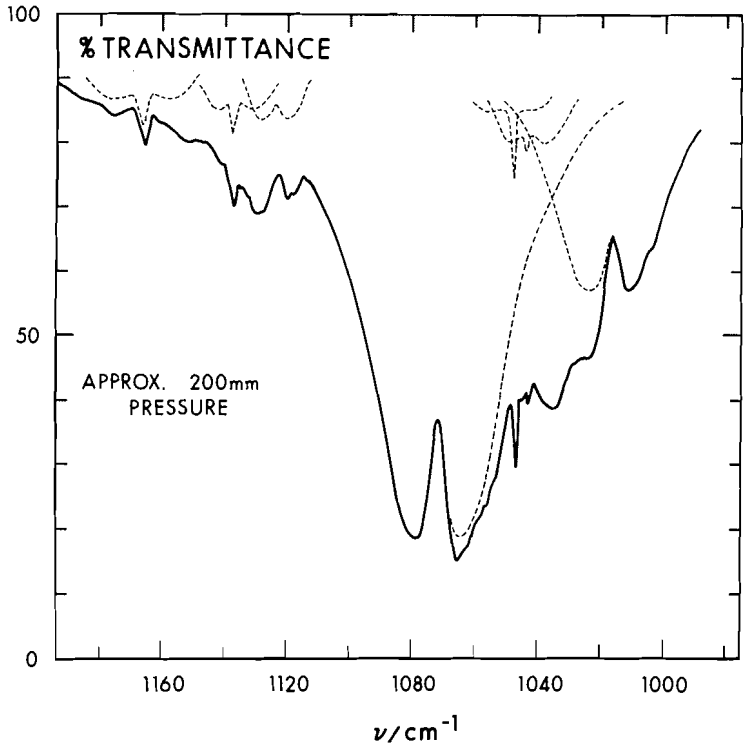

FIG. 10. The i.r. spectrum of C_4D_6 gas, between 980 and 1180 cm^{-1} at about 34 °C, 10 cm path length. The dashed lines represent our proposed separation of the band into A-, B-, and C-type contours.

(ν_{19}), and out-of-plane (B_2) (ν_{24}), wagging of the $=CD_2$ group are observed as the weak B-type band at 304 cm^{-1}, and the medium C-type band at 240 cm^{-1} respectively.

(v) Impurity Bands

The i.r. bands at 3030 and 1410 cm^{-1} and the Raman band at 946 cm^{-1} can not be readily assigned to C_4D_6 and are believed to arise from impurities. Because of these bands, and because of some very small isotopic shifts implied by the above assignments, we examined our C_4D_6 carefully for impurities (see Experimental), and have found no evidence for any impurity other than 18% or less of C_4D_5H. Further study of C_4D_6 was prevented by the very limited supply of sample, and the considerable difficulty of making more.

(d) Product Rule

The "product rule" for the A_1 modes, using the above assignment is 4.71 (5.33 theoretical). This implies either (*1*) large anharmonic effects influence the frequencies of the A_1 modes or (*2*) a wrong assignment. The latter may be the more likely, because the product rule factor becomes 5.2 if ν_5 is assigned at 1047 cm^{-1} in C_4D_6 instead of at 1139 cm^{-1}. However this assignment leaves the more intense 1139 cm^{-1} band unassigned and creates anomalies in the relative frequencies of the different CD_2 deformation modes in C_4D_6. We regard the assignment of ν_5 in C_4D_6 as uncertain between these two options.

The agreement between the observed and calculated values in the B_1 block is satisfactory, 4.55 and 4.76 respectively. This is within the usual range of anharmonic effects, and supports the assignment above.

In the B_2 block the observed "product rule" is 3.46 *vs.* 3.39 calculated. This implies an overall small negative anharmonicity. The ethylenic wagging mode has been shown to have a negative anharmonicity in asymmetrically disubstituted ethylenes (20) and it is reasonable to suppose that the other out of plane motion (ν_{24}) will behave similarly to give the small net negative anharmonicity required to fit the product rule exactly.

Can. J. Chem. Downloaded from www.nrcresearchpress.com by 210.87.254.5 on 09/05/12
For personal use only.

We thank Dr. R. J. Crawford for the C_4D_6 and for some of the C_4H_6 used in this study. Mr. R. S. Swindlehurst recorded the n.m.r. spectra. The work was supported by the National Research Council of Canada.

1. A. W. Baker and R. C. Lord. J. Chem. Phys. **23**, 1636 (1955).
2. P. M. Mathai, G. G. Shepherd, and H. L. Welsh. Can. J. Phys. **34**, 1448 (1956).
3. Hs. H. Gunthard, R. C. Lord, and T. K. McCubbin, Jr. J. Chem. Phys. **25**, 768 (1956).
4. C. Brecher, E. Krikorian, J. Blanc, and R. S. Halford. J. Chem. Phys. **35**, 1097 (1961).
5. J. L. Duncan and D. C. McKean. J. Mol. Spectrosc. **27**, 117 (1968).
6. J. B. Bates, D. E. Sands, and W. H. Smith. J. Chem. Phys. **51**, 105 (1969).
7. L. H. Daly and S. E. Wiberley. J. Mol. Spectrosc. **2**, 177 (1958).
8. L. M. Sverdlov, N. P. Krainov, and N. I. Prokofeva. Fiz. Probl. Spektrosk. Akad. Nauk. S.S.S.R, Mater. Soveshch., Leningrad, **1**, 363 (1960); Chem. Abstr. **59**, 12303*a*.
9. W. G. Rothschild. J. Chem. Phys. **44**, 3875 (1966).
10. H. E. Simmons, E. P. Blanchard, and H. D. Hartzler. J. Org. Chem. **31**, 295 (1966), and references quoted therein. Also W. G. Rothschild. J. Chem. Phys. **44**, 1712 (1966).
11. R. J. Crawford and D. M. Cameron. J. Amer. Chem. Soc. **88**, 2589 (1966).
12. J. T. Gragson, K. W. Greenlee, J. M. Derfer, and C. E. Boord. J. Amer. Chem. Soc. **75**, 3344 (1953).
13. E. J. Blau. University Microfilms. Mic. 58–730: 1953. Ph.D. Thesis, Ohio State University, Columbus, Ohio, 1953.
14. W. B. Loewenstein. University Microfilms. Mic. 60–82. Ph.D. Thesis, Ohio State University, Columbus, Ohio, 1954.
15. I.U.P.A.C. Tables of wavenumbers for the calibration of infrared spectrometers. Butterworths Scientific Publications, Ltd., London, 1961.
16. G. Herzberg. Infrared and Raman spectra. D. Van Nostrand Company, Inc., New York, 1945.
17. V. W. Laurie and W. M. Stigliani. J. Amer. Chem. Soc. **92**, 1485 (1970).
18. T. Ueda and T. Shimanouchi. J. Mol. Spectrosc. **28**, 350 (1968).
19. J. O. Halford. J. Chem. Phys. **24**, 830 (1956); P. von R. Schleyer and R. D. Nicholas. J. Amer. Chem. Soc. **83**, 182 (1961).
20. N. Sheppard and D. M. Simpson. Quart. Rev. **6**, 1 (1952).
21. W. Luttke and S. Braun. Ber. Bunsenges. **71**, 34 (1967).
22. P. Torkington. J. Chem. Phys. **17**, 1279 (1949).
23. R. Meyer and Hs. H. Gunthard. Spectrochim. Acta, **23** (A), 2341 (1967).
24. R. C. Lord and B. Nolin. J. Chem. Phys. **24**, 656 (1956).
25. R. C. Lord and D. G. Rea. Unpublished; cited by R. C. Lord and I. Nakagawa. J. Chem. Phys. **39**, 2951 (1963), and in ref. 1.
26. R. C. Lord and P. Venkateswarlu. J. Opt. Soc. Amer. **43**, 1079–1085 (1953).

Can. J. Chem. Downloaded from www.nrcresearchpress.com by 210.87.254.5 on 09/05/12
For personal use only.

Can. J. Chem. Downloaded from www.nrcresearchpress.com by 210.87.254.42 on 09/05/12
For personal use only.

Etude spectroscopique des dérivés du peroxyde d'hydrogène. IV. L'acide de Caro, H_2SO_5

JOSÉ L. ARNAU ET PAUL A. GIGUÈRE
Centre de Recherches sur les Atomes et les Molécules, Université Laval, Québec 10, Québec

Reçu le 3 juillet 1970

On a mesuré pour la première fois les spectres i.r. et Raman de H_2SO_5 pur à l'état cristallin entre 4000 et 30 cm^{-1}. La plupart des vibrations fondamentales de la molécule ont été identifiées par analogie avec celles des molécules de H_2SO_4 et H_2O_2, ainsi que l'ion HSO_5^-. On a également repéré une douzaine de vibrations de réseau. Contrairement à l'expectative la vibration de valence O—O se trouve à une fréquence légèrement supérieure (886 cm^{-1}) à celle de H_2O_2 cristallin. Les deux groupes hydroxyles sont nettement différents, tant du point de vue spectroscopique que chimique. Le groupe OH ionisable forme des liaisons hydrogène intermoléculaires assez fortes comme dans H_2SO_4. Par contre le groupe O_2H, peu ionisable, participe à une liaison hydrogène intramoléculaire. La maille élémentaire du cristal doit contenir plus de deux molécules.

The i.r. and laser Raman spectra of pure, crystalline Caro's acid, H_2SO_5, were measured for the first time between 4000 and 30 cm^{-1}. Most of the fundamental vibrations of the molecule could be identified by comparison with those of the H_2SO_4, H_2O_2 and HSO_5^- species. In addition, a dozen or so of lattice modes were recorded. The O—O stretching frequency is slightly higher (886 cm^{-1}) than in solid H_2O_2, contrary to expectation. The two hydroxyl groups are quite different, both chemically (Caro's acid is essentially monobasic) and spectroscopically. The ionizable OH group forms strong intermolecular hydrogen bonds, as in H_2SO_4. However, the non-ionizable O_2H group is engaged mainly in intramolecular hydrogen bonding. The unit cell of the crystalline acid must contain more than two molecules.

Canadian Journal of Chemistry, 48, 3903 (1970)

Introduction

L'acide monopersulfurique découvert par Caro en 1898 (1) a été très peu étudié jusqu'ici du point de vue structural. La raison en est que l'acide pur est difficile à préparer vu son caractère instable (*danger d'explosion*!), fortement réactif et hygroscopique. Sa composition et sa structure HO—SO_2—O—OH ont été établies par d'Ans et Friederich (2–4). Aucune étude par les méthodes de diffraction n'a encore été rapportée à notre connaissance. La seule étude spectroscopique connue est celle de Simon (5) qui a mesuré le spectre Raman sans toutefois attribuer les fréquences observées. Son but était surtout de confirmer l'absence de liaison S—H, laquelle aurait pu expliquer le caractère monobasique de l'acide. En i.r. seul le sel $KHSO_5$, son monohydrate, et leurs équivalents deutériés ont été étudiés (6). Intuitivement on peut imaginer la configuration de la molécule H_2SO_5 en remplaçant un atome d'hydrogène par un groupe OH dans la molécule bien connue H_2SO_4. Il nous a semblé qu'une étude spectroscopique utilisant les techniques modernes pourrait fournir des précisions utiles à savoir, par exemple, comment la liaison O—O se compare à celle des autres dérivés du peroxyde d'hydrogène (7), ou encore l'influence du pont peroxyde sur les fréquences fondamentales du groupe SO_2, et enfin le type de liaisons hydrogène dans le cristal.

Partie expérimentale

L'acide pur a été préparé par la méthode classique (2) suivant la réaction

[1] $$H_2O_2 + HSO_3Cl \rightarrow H_2SO_5 + HCl$$

et isolé par centrifugation, tel que décrit récemment par Kyrki (8). Le peroxyde d'hydrogène, titrant 99% en poids, avait été obtenu par distillation fractionnée sous vide du produit commercial à 80% (BECCO). Quant à l'acide chlorosulfurique, le produit "Reagent Grade" de Eastman Organic Chemicals a été employé. Le produit original frais peut servir tel quel, mais après un certain temps au contact de l'air il s'altère. Il faut alors le redistiller, sinon il devient impossible de cristalliser l'acide de Caro. Une autre précaution à observer concerne l'agitation de la solution tout au long de la réaction. Il faut, en effet, éliminer le gaz chlorhydrique au fur et à mesure de sa formation; autrement il finit par s'oxyder. Le chlore ainsi produit colore la solution en jaune, et il est presque impossible de l'éliminer par succion. De plus, il empêche le produit final de cristalliser.

Après quelques essais infructueux nous avons mis au point le dispositif illustré sur la fig. 1. L'acide chlorosulfurique dans un petit ballon était refroidi à environ −45° dans un bain de chlorobenzène maintenu à son point de congélation par addition périodique d'azote liquide. Un courant d'azote gazeux sec introduit par le tube latéral assurait l'agitation ainsi que l'atmosphère inerte. Le peroxyde d'hydrogène dans un petit entonnoir relié au ballon par un rodage, était ajouté goutte à goutte au moyen d'un robinet à clef de Teflon. Une fois tout le peroxyde ajouté, en quantité stoechiométrique, le mélange liquide était ramené à température ordinaire tout en maintenant le courant d'azote. Il se formait alors une sorte de mousse qui disparaissait après un certain

Can. J. Chem. Downloaded from www.nrcresearchpress.com by 210.87.254.42 on 09/05/12
For personal use only.

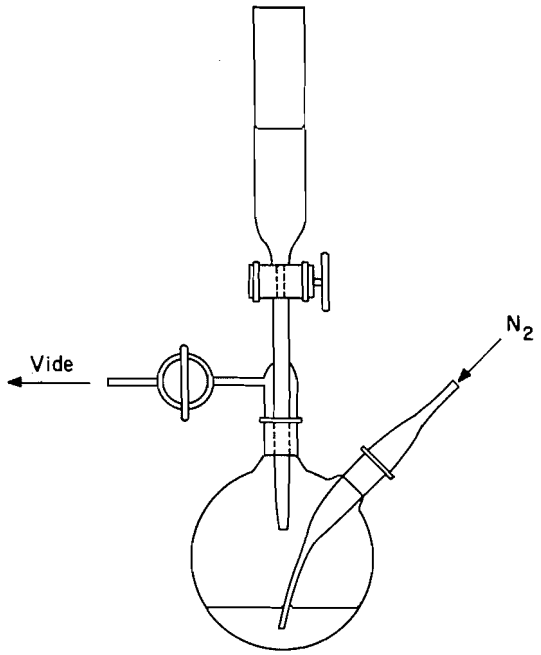

FIG. 1. Appareil utilisé pour préparer l'acide de Caro en atmosphère inerte.

temps laissant la solution claire et visqueuse. On arrêtait alors le courant gazeux, on fermait le robinet d'évacuation et on refroidissait de nouveau la solution qui se séparait en deux couches; le peracide liquide et un peu de solution-mère surnageant. Peu après, la cristallisation se produisait brusquement.

Par centrifugation dans un tube à essai muni d'un diaphragme de verre fritté les cristaux étaient débarrassés de la solution-mère. Le volume de celle-ci était toujours faible vu le rendement assez élevé de la réaction. Le peracide était alors fondu (vers 45 °C) puis recristallisé sous forme d'aiguilles transparentes: point de fusion d'environ 47° tel que rapporté par Kyrki. Il se conservait sans décomposition appréciable pendant plusieurs semaines dans un récipient hermétique et au réfrigérateur. On n'en préparait jamais plus de 5 g. à la fois à cause du danger d'explosion mentionné par divers auteurs (4, 5, 9) lequel, heureusement, ne s'est jamais matérialisé dans notre cas.

Les échantillons pour les spectres Raman étaient relativement faciles à préparer; soit en versant directement le produit liquide de la réaction dans un tube conique et en le cristallisant, soit, pour le spectrographe à laser, en scellant dans un mince capillaire de Pyrex un peu du solide fondu puis recristallisé. Les deux types d'échantillons ne montraient pas de différences notables dans leurs spectres, ce qui confirme bien la faible proportion de solution-mère dans le premier cas. Pour l'i.r., cependant, la préparation des échantillons fut extrêmement délicate vu le caractère à la fois corrosif, hygroscopique et instable du peracide. Aussi fallait-il travailler en atmosphère inerte, et protéger toutes les parties métalliques de la cellule d'absorption en les recouvrant de ruban de Teflon. Quant aux fenêtres portant l'échantillon, la plupart des matériaux courants se sont avérés inutilisables. Par exemple, NaCl, CaF_2 et AgCl catalysent la décomposition de l'acide de Caro; par ailleurs KBr, CsBr et Irtran-2 (Eastman Kodak) sont sensibles aux oxydants énergiques. Seules de minces (2mm) fenêtres de silicium élémentaire poli ont permis d'obtenir des échantillons convenables.

Pour préparer les échantillons toutes les méthodes courantes ont été essayées sans succès; soit par dispersion dans le nujol, le fluorolube ou la graisse Kel-F, soit en faisant réagir sur la fenêtre refroidie des couches minces superposées des deux réactifs de départ. Eventuellement on a eu recours à la technique qui avait été mise au point dans ce laboratoire pour les spectres de l'ion H_3O^+ en solution dans SO_2 liquide (10). Une goutte de peracide liquide (soit le produit original de la réaction, soit le solide fondu) était introduite, rapidement, et sous un fort courant d'azote sec, entre les deux fenêtres de silicium dans le porte-échantillon. Après refroidissement jusqu'à environ $-100°$ on évacuait la cellule et on laissait réchauffer l'échantillon pour le cristalliser. On a réussi par la même technique à obtenir quelques bons spectres avec des fenêtres neuves de AgCl en procédant très vite pour devancer la décomposition du peracide. Dans ce cas l'échantillon cristallisait pendant le refroidissement. Des tentatives pour obtenir le spectre infrarouge en solution très diluée dans un solvant inerte n'ont pas donné de résultats. Ainsi le peracide semblait complètement insoluble dans le tétrachlorure de carbone; ce dernier, même après purification prolongée, devenait trouble et coloré au contact de l'acide. Les spectres ont été enregistrés avec les mêmes instruments que précédemment (7), sauf pour le Raman à excitation laser qui a été décrit ailleurs (11).

Interprétation des spectres

Les figs. 2, 3 et 4 sont une reconstitution des spectres i.r. et Raman de l'acide de Caro pur. Les fréquences au maximum des principales bandes sont données au tableau 1 avec les attributions proposées. Ces dernières, en l'absence de toute donnée expérimentale sur la structure, ont été faites en prenant comme modèle la molécule H_2SO_4 et en y remplaçant un atome d'hydrogène par un groupe OH. Dans ce modèle l'indétermination principale vient de l'orientation des groupes OH et OOH. Dans l'hypothèse, *a priori* assez peu probable, où ces deux groupes seraient situés dans un même plan perpendiculaire à celui du groupe SO_2 on aurait une configuration de symétrie C_s. Autrement, il n'y aurait aucun élément de symétrie. Dans le premier cas la représentation réductible serait $12\,A' + 6\,A''$; mais dans ce cas comme dans l'autre les dix-huit modes doivent être actifs aussi bien en i.r. qu'en Raman. Le nombre de bandes observées ne peut donc servir de critère ici. Simon (5) avait conclu

Can. J. Chem. Downloaded from www.nrcresearchpress.com by 210.87.254.42 on 09/05/12
For personal use only.

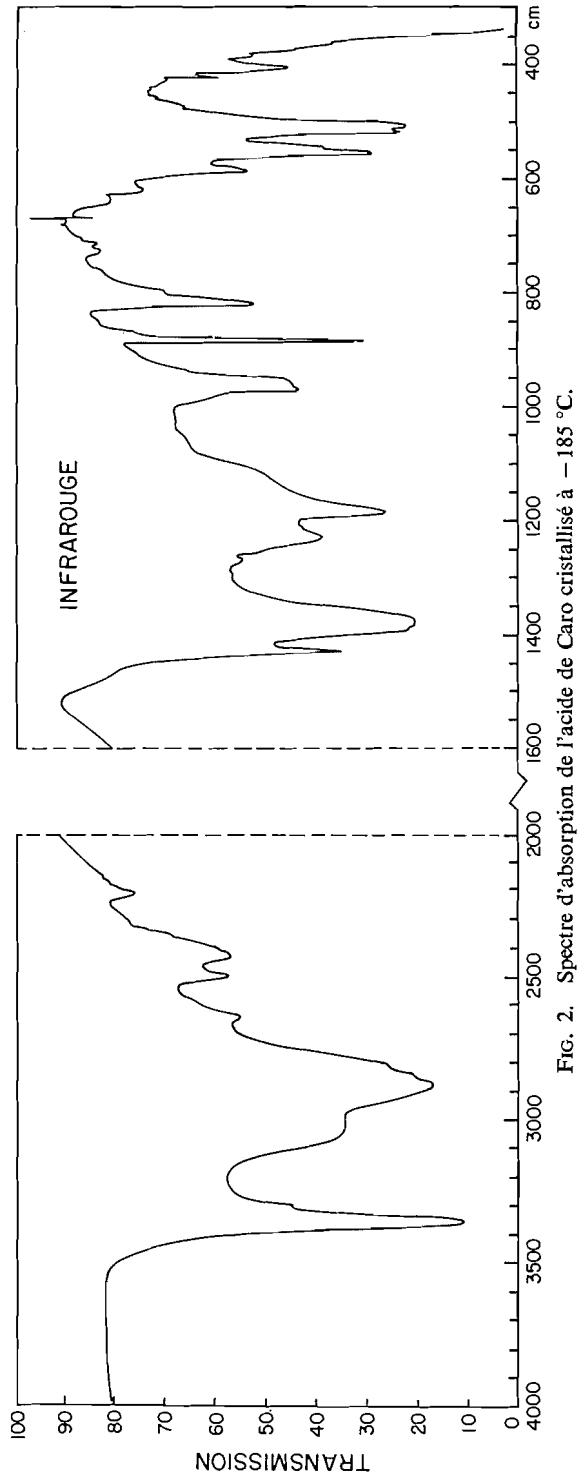

FIG. 2. Spectre d'absorption de l'acide de Caro cristallisé à −185 °C.

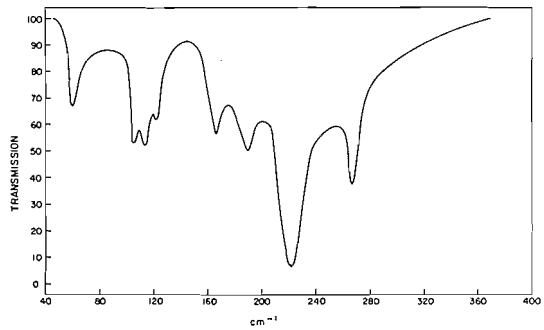

FIG. 3. Bandes d'absorption de H_2SO_5 cristallin dans l'infrarouge lointain.

que la molécule H_2SO_5 n'avait aucune symétrie vu le grand nombre de bandes, quinze ou seize, dans ses spectres Raman. Il faut noter toutefois que plusieurs de ces bandes sont en fait des composantes différentes d'une même vibration (tableau 1).

Les vibrations OH

On sait déjà que les deux groupes OH sont loin d'être équivalents dans H_2SO_5. En effet l'acide de Caro est essentiellement monobasique, le pK de seconde ionisation étant de l'ordre de 10 (6). On peut expliquer cette caractéristique à l'aide des structures de résonance suivantes:

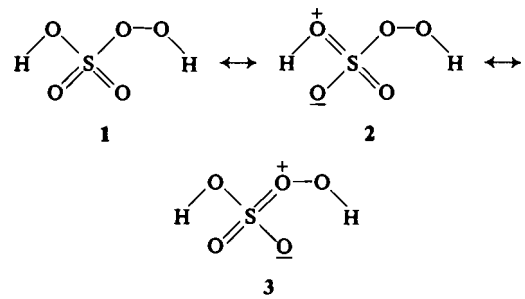

1 **2**

3

Ainsi la structure électronique **2** fait apparaître une charge positive sur l'oxygène du groupe hydroxyle, rendant ainsi le proton très ionisable. Rien de tel ne se produit dans la structure **3**, le groupe perhydroxyle s'opposant à la transmission des effets d'induction.

La non-équivalence des deux groupes OH est confirmée dans les spectres infrarouges par la présence de deux bandes de valence nettement différentes d'aspect: la première à 3350 cm^{-1}, assez fine (moins de 100 cm^{-1} à mi-hauteur), et la seconde beaucoup plus large, avec maximum vers 2890 cm^{-1}. Par analogie avec H_2SO_4 (12) cette dernière doit appartenir au groupe OH ionisable. L'autre, par ailleurs, se trouve à peu près à la même fréquence que la vibration de valence (à 3340 cm^{-1}) dans la molécule H_2O_2, (13). Quant à sa faible largeur, elle est due, d'après nous, à la formation d'une liaison hydrogène intramoléculaire. En effet, la géométrie de la molécule semble particulièrement favorable à une telle chélation puisqu'il existe deux degrés de liberté de rotation autour des liaisons S—O et O—O, (toutes deux essentiellement simples) dans ce cycle à cinq atomes. La distance O ··· H minimale (fig. 5) devient alors passablement inférieure à la somme des rayons de van der Waals, 2.6 Å (14). Comme cette liaison intramoléculaire est fortement angulaire, l'amortissement de la vibration de valence O—H est beaucoup moindre que pour une liaison linéaire de même longueur totale. Il n'existe pas de critère pour évaluer les paramètres de ces liaisons coudées à partir des données spectrales. Par contre, les liaisons intermoléculaires réalisées par le groupe OH ionisable doivent avoir à peu près les mêmes caractéristiques que dans H_2SO_4; soit une énergie de quelque 6 kcal $mole^{-1}$ et une distance O .... O de 2.67 Å (12).

Récemment on a publié des spectres i.r. (15) qui présentent dans la région de 3μ le même aspect que les nôtres: soit un massif très large aux environs de 3000 cm^{-1} et un pic assez aigu situé entre 3500 et 3600 cm^{-1}. Il s'agit d'acides α-hydroxycarboxyliques dans lesquels une liaison hydrogène intramoléculaire serait très improbable, semble-t-il. On a interprété ces spectres dans l'hypothèse de groupes OH libres. Une telle explication ne nous paraît pas applicable ici car les conditions sont beaucoup plus favorables à des liaisons hydrogène, tant inter- que intramoléculaires. Vu les nombreux sites accepteurs de proton dans ce cristal l'existence de groupes OH libres serait vraiment extraordinaire. En outre, une fréquence de 3350 cm^{-1} est sûrement trop basse pour une vibration O—H "libre". Par ailleurs les divers épaulements qu'on observe (fig. 2) sur les deux principales bandes de valence O—H résultent probablement des mouvements en phase et hors de phase dans différentes molécules de H_2SO_5 (tout probablement plus de deux) dans la maille primitive. La présence de dimères cycliques, comme dans les acides fluo- et chlorosulfuriques (16), est également une possibilité.

Can. J. Chem. Downloaded from www.nrcresearchpress.com by 210.87.254.42 on 09/05/12
For personal use only.

Can. J. Chem. Downloaded from www.nrcresearchpress.com by 210.87.254.42 on 09/05/12
For personal use only.

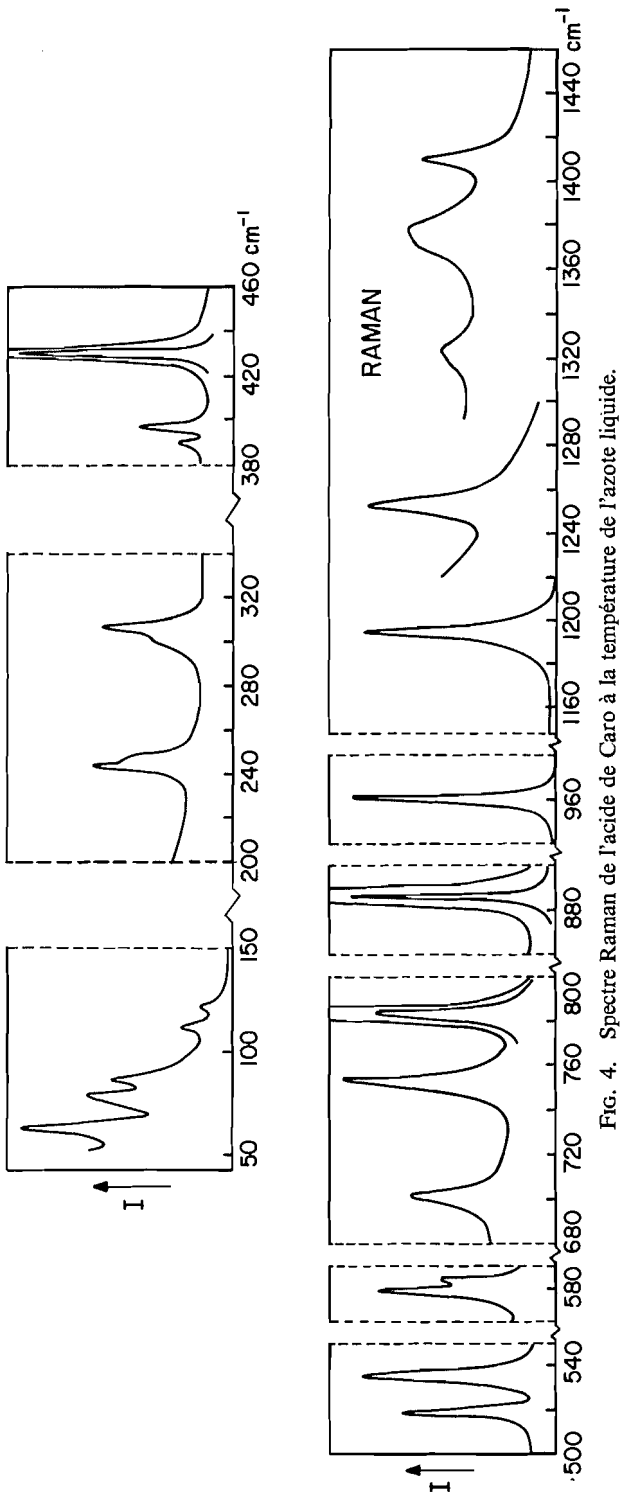

FIG. 4. Spectre Raman de l'acide de Caro à la température de l'azote liquide.

TABLEAU 1

Fréquences (en cm^{-1}) et attribution des principales bandes de vibration de H_2SO_5

Raman				
*	†	‡	Infrarouge§	Modes
			3365 FF	valence O—H (intra.)
			3352 FF	
			3302 ép.	
			~3030 m.l.	valence O—H (inter.)
			2890 FF	
			2802 ép.	
			2643 f	
			2501 f	
			2425 f	(2 × 1227)?
			2297 ff	
			2213 ff	
1414	1412	1420	1426 m.	valence S=O asym.
	1380	1382	1380 FF	déformation OOH
	~1325			
	1254		1250 ép.	déformation SOH
1211			1227 m.	
	1197	1195	1181 F	valence S=O sym.
1108			1130 ép. l.	
988	963	~960	965 m.	valence S—OH
923		956	955 ép.	
872	886	886	885 F	valence O—O
831			816 m.	valence S—O_2H
	788	774	~795 ép.	
	754			torsion OH?
	702			torsion OH?
580	585	580		
	580	~575	580 m.	torsion OH?
			551 F	
541	538	536	~540 ép.	rotation dans le plan SO_2
	521	517	513 FF	
(493)		514	505 FF	cisaillement SO_2
498		~435		
(425)	432	428	417 ff	rotation dans le plan (HO—S—O_2H)
	398	395	401 f	torsion du squelette
(358)	391	~390		
	307	293		déformation SOO
	300	~285		
			265	réseau
	249	~245		cisaillement OSOO
(225)	245	236		
			222	torsion (S—OO)
			190	réseau
			166	”
	121	~115	122	”
	113	108	114	”
			106	”
	92	87		”
	81	77		”
	65	59	63	”

*D'après Simon (5).
†A — 185 °C.
‡A température ambiante.
§ff = très faible; f = faible; m = médium; F = forte; FF = très forte; ép. = épaule; l = large.

Tout comme les vibrations de valence, les vibrations de déformation OH sont facilement identifiables par comparaison avec les modes antisymétriques correspondants dans H_2SO_4 (1240 cm^{-1}), et H_2O_2 (1375 cm^{-1}). Notons que dans le spectre i.r. de l'ion HSO_5^- Kyrki (6) a trouvé une fréquence plus basse (3270 cm^{-1}) pour la vibration O—H, et une plus élevée (1421 cm^{-1}) pour la déformation de l'angle OOH que dans l'acide pur. Ces différences appréciables dénotent un renforcement de la liaison hydrogène dans l'ion. Il se peut que celle-ci soit effectivement bifurquée, la composante intermoléculaire se trouvant renforcée, soit à cause d'un empilement

Can. J. Chem. Downloaded from www.nrcresearchpress.com by 210.87.254.42 on 09/05/12
For personal use only.

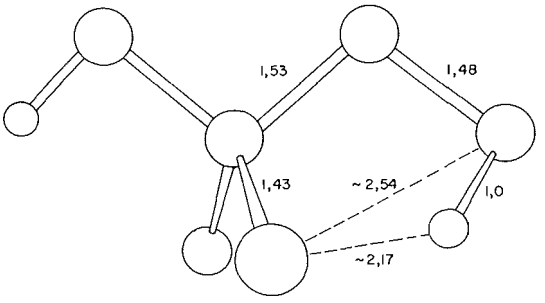

FIG. 5. Modèle représentant la configuration approximative de la molécule de H_2SO_5. (Distances en Å).

plus favorable dans le réseau cristallin, soit à cause des charges ioniques. Quant aux modes de torsion OH, leur identification dans nos spectres est assez ambigüe. Toujours par analogie avec les molécules H_2SO_4 et H_2O_2 à l'état solide on peut prévoir pour ces modes des fréquences comprises entre 600 et 800 cm^{-1}. En i.r. cette région ne montre aucune absorption notable, alors qu'en Raman deux bandes, à peine visibles à température ambiante, apparaissent très nettement à 702 et 754 cm^{-1} à la température de l'azote liquide. Vu leur comportement identique quant à la température elle doivent appartenir à des vibrations du même type. Par ailleurs elles semblent un peu fortes pour des torsions OH, surtout étant donné l'absence d'équivalents en i.r. De toute façon leur séparation est trop grande pour des composantes du même mode. Remarquons que la deutériation, difficilement réalisable en pratique, serait de peu d'utilité ici puisque les bandes décalées devraient tomber dans la région de 500 à 550 cm^{-1} déjà encombrée par les modes de déformation de SO_2.

Les vibrations du squelette

La fréquence relativement élevée de la vibration O—O dans H_2SO_5 (comp. 881 cm^{-1} dans H_2O_2 cristallin) est un peu inattendue vu la forte augmentation de masse du groupe substituant. L'effet de masse se fait évidemment beaucoup plus sentir dans les dérivés bi-substitués comme $S_2O_8^{2-}$ où la fréquence O—O est abaissée jusqu'à 830 cm^{-1} (17). On ne possède pas encore assez de données sur les hydroperoxydes pour discerner l'influence sur cette fréquence de divers facteurs possibles. Parmi ceux-ci il y a d'abord les effets de couplage qui doivent être importants dans ce cas-ci étant donné le voisinage des vibrations de valence O—O et S—O. Un calcul de constantes de force, une fois connus les paramètres de structure, pourrait nous renseigner là-dessus. Viennent ensuite les effets électroniques qui peuvent affecter le caractère des liaisons. Par exemple la vibration de valence S—O_2H montre ici un abaissement d'environ 160 cm^{-1} par rapport à la vibration S—OH. Il semble donc, d'après ce critère, que le caractère double de cette liaison soit diminué par la présence du groupe peroxyde. Cette conclusion est en accord avec les prévisions de la théorie des liaisons de valence étant donné que la structure canonique **3** donnée plus haut doit contribuer moins que la structure **2** à la résonance de la molécule. Il serait intéressant de vérifier cette conclusion par une étude aux rayons-X de la structure cristalline de H_2SO_5.

Quant aux vibrations S—O, leur attribution ne pose pas de problème. Ces vibrations ont déjà été étudiées en détail dans de nombreuses molécules, ce qui a conduit à des corrélations empiriques. Ainsi d'après les relations de Daasch (18) la somme des électronégativités des groupes OH et OOH dans l'acide de Caro serait d'environ 6.0. Quant au rapport des vibrations de valence S=O symétrique et antisymétrique, il suit d'assez près la corrélation établie par Robinson (19). De plus, les constantes de force de rappel des liaisons S=O et S—OH évaluées à environ 10.7 et 5.7 respectivement selon l'équation semi-empirique de Gillespie et Robinson (20), sont légèrement plus élevée que dans H_2SO_4. Elles correspondent à des ordres de liaison de 1.87 et 1.36 respectivement. Notons enfin que la présence de trois et même quatre composantes (*e.g.* deux en i.r. et deux en Raman) des vibrations du groupe SO_4 est une indication assez sûre que la maille élémentaire du cristal contient plus de deux molécules.

Ce travail a pu être exécuté grâce à une subvention du Conseil National de Recherches du Canada.

1. H. CARO. Z. Angew. Chem. **11**, 845 (1898).
2. J. D'ANS et W. FRIEDERICH. Ber. **43**, 1880 (1910).
3. J. D'ANS et W. FRIEDERICH. Z. Elektrochem. **17**, 849 (1911).
4. J. D'ANS et W. FRIEDERICH. Z. Anorg. Chem. **73**, 325 (1912).
5. A. SIMON. Z. Anorg. Chem. **242**, 369 (1939).
6. J. R. KYRKI. Suom. Kem. **B38**, 199 (1965).
7. J. L. ARNAU et P. A. GIGUÈRE. J. Mol. Struct. **3**, 483 (1969).
8. J. KYRKI. Ann. Univ. Turku. Ser. A, I, N° 61 (1963).
9. J. O. EDWARDS. Chem. Eng. News, **33**, 3336 (1955).
10. M. SCHNEIDER et P. A. GIGUÈRE. C. R. **267B**, 551 (1968).

Can. J. Chem. Downloaded from www.nrcresearchpress.com by 210.87.254.42 on 09/05/12
For personal use only.

11. R. E. MILLER, D. L. ROUSSEAU, and G. E. LEROI. Tech. Rept. No. 22, ONR Contract 1858 (27), May 1967, DDC Accession No. AD651646.
12. P. A. GIGUÈRE et R. SAVOIE. Can. J. Chem. **38**, 2467 (1960).
13. W. C. SCHUMB, C. N. SATTERFIELD, et R. I. WENTWORTH. Hydrogen peroxide. Reinhold Publ. Corp., New York, 1955.
14. L. PAULING. The nature of the chemical bond. 3rd Ed. Cornell University Press, Ithaca, N.Y., 1960.
15. J. A. KANTERS, J. KROON, A. F. PEERDEMAN, et J. A. VLIEGENTHART. Nature, **222**, 370 (1969).
16. R. SAVOIE et P. A. GIGUÈRE. Can. J. Chem. **42**, 277 (1964).
17. A. SIMON et H. RICHTER. Z. Anorg. Chem. **315**, 196 (1959).
18. L. W. DAASCH. Spectrochim. Acta, **12**, 257 (1959).
19. E. A. ROBINSON. Can. J. Chem. **39**, 247 (1961).
20. R. J. GILLESPIE et E. A. ROBINSON. Can. J. Chem. **41**, 2074 (1963).

Can. J. Chem. Downloaded from www.nrcresearchpress.com by 210.87.254.42 on 09/05/12
For personal use only.

Can. J. Chem. Downloaded from www.nrcresearchpress.com by 210.87.254.42 on 09/05/12
For personal use only.

Molar excess volumes in binary systems of *n*-hexadecane and 1-*n*-chloroalkanes at 25 °C

E. L. Heric and B. M. Coursey
Department of Chemistry, University of Georgia, Athens, Georgia

Received June 5, 1970

The molar excess volumes at 25 °C in nine binary systems of *n*-hexadecane with 1-*n*-chloroalkanes from 4 through 18 carbons have been calculated from density measurements. The applicability of Brønsted and Koefoed's congruence principle to the excess volumes was investigated.

Canadian Journal of Chemistry, **48**, 3911 (1970)

Introduction

Brønsted and Koefoed's congruence principle (1) has been used to correlate both excess thermodynamic equilibrium (2–8) and activation (9–11) properties of *n*-alkane mixtures. The principle states that at constant temperature and pressure the properties may be related to the average chain length

$$[1] \qquad n = x_1 n_1 + x_2 n_2$$

In eq. 1 subscripted x and n refer to the mole fraction and chain length of the indicated component.

The congruence principle has also been applied to systems of *n*-alkane derivatives (12–14). Again the basis for the approach is the carbon chain length.

By combining the congruence principle with the variation of the concentration of the substituent group, Brown *et al.* (15) were able to correlate heats of mixing in *n*-alkane – *n*-alcohol systems. Heric and Coursey (16) modified the latter approach, and have applied it to viscosity in the systems reported here. They compared viscosity in the present systems with that in systems where the halide was replaced by its *n*-alkane homomorph. A well-defined, systematic dependence of behavior on the halide chain length was shown.

The viscosity was treated through the excess molar Gibbs free energy of activation for flow, Δ^*G^E. For a binary mixture

$$[2] \quad \Delta^*G^E = RT[\ln \nu M - x_1 \ln \nu_1 M_1 - x_2 \ln \nu_2 M_2]$$

where ν is the kinematic viscosity and M is molecular weight. Equation 2 is obtained by combining the Eyring viscosity equation (17)

$$[3] \qquad \nu = (hN/V) \exp(\Delta^*G/RT)$$

with the definition of ideal mixture viscosity as mole fraction additivity of Δ^*G of the pure components. In eq. 3 h and N are the Planck and Avogadro constants, and V is the molar volume.

Viscosity, in terms of Δ^*G^E, was described by

$$[4] \quad \Delta^*G_{h_i,j}{}^E - \Delta^*G_{i,j}{}^E = x_{h_i}(1 - x_{h_i}) \times [a_0 + a_1(2x_{h_i} - 1)]$$

In eq. 4 i and j are *n*-alkanes, h_i is the halide homomorph of i, and a_0 and a_1 are empirical constants. a_0 values for the systems were related to halide chain length by

$$[5] \qquad a_0 = \alpha \exp(-\beta n_{h_i}),$$

where α and β are also empirical constants. a_1 values were not related to the halide chain length other than to show that they decreased with increasing chain length and became negligibly small above 1-chlorooctane.

The applicability of eqs. 4 and 5 was taken to show that the interaction in these systems could be resolved into two factors. One arises through mixing of the CH_2 and CH_3 groups, as found in *n*-alkane mixtures. This was called a "homogeneous" factor, to distinguish it from the "heterogeneous" factor arising when a group not present in one component is present in the other mixture component. Mixing of *n*-alkanes with 1-chloroalkanes, by this terminology, thus involves both homogeneous and heterogeneous factors.

The purpose of this work is to show that the molar excess volumes in the present systems may also be treated in the mathematical form expressed in eqs. 4 and 5. Densities, refractive indices, and refractivity intercepts in these systems have been reported (18). The densities lead to the excess molar volumes reported here, by the assumption that ideal volume is equal to the

TABLE 1

Excess volumes at 25.00 °C: binary systems containing *n*-hexadecane – 1-chloroalkanes (h_i,j), *n*-hexadecane – *n*-alkanes (i,j) or differences between them (h_i,j − i,j) (x = mole fraction of *n*-hexadecane; V^E in ml mole^{-1})

x	$V_{h_i,j}^E$	$V_{i,j}^E$	$(V_{h_i,j}^E - V_{i,j}^E)$
	n-Hexadecane – 1-chlorobutane		
0.1495	0.25		
0.2967	0.40		
0.4418	0.44	(−1.57±0.1)*	(2.01±0.1)*
0.5454	0.41		
0.6777	0.37		
0.8309	0.22		
	n-Hexadecane – 1-chloropentane		
0.1532	0.26		
0.2897	0.36		
0.4420	0.39	(−0.92±0.05)*	(1.34±0.05)*
0.5367	0.41		
0.6903	0.36		
0.8323	0.19		
	n-Hexadecane – 1-chlorohexane		
0.1413	0.21	−0.36	0.56
0.1478	0.23	−0.38	0.58
0.1944	0.25	−0.46	0.70
0.2058	0.26	−0.47	0.73
0.3072	0.35	−0.57	0.90
0.4454	0.35	−0.60	0.98
0.5320	0.39	−0.56	0.95
0.5438	0.39	−0.55	0.94
0.6893	0.34	−0.42	0.76
0.8311	0.24	−0.23	0.47
	n-Hexadecane – 1-chlorooctane		
0.1502	0.14	−0.18	0.34
0.2936	0.25	−0.28	0.52
0.3835	0.28	−0.29	0.57
0.4348	0.29	−0.28	0.58
0.5265	0.29	−0.26	0.56
0.6890	0.26	−0.19	0.44
0.8454	0.17	−0.07	0.23
	n-Hexadecane – 1-chlorodecane		
0.1457	0.14	−0.07	0.19
0.2910	0.19	−0.10	0.30
0.4463	0.23	−0.10	0.34
0.4487	0.25	−0.10	0.34
0.5414	0.21	−0.10	0.34
0.5466	0.25	−0.10	0.34
0.5758	0.24	−0.09	0.33
0.6979	0.22	−0.06	0.28
0.8427	0.18	−0.04	0.16
0.8464	0.16	−0.04	0.16
	n-Hexadecane – 1-chlorododecane		
0.1515	0.04	−0.02	0.08
0.1862	0.06	−0.02	0.10
0.2216	0.07	−0.02	0.11
0.3003	0.11	−0.02	0.13
0.4564	0.13	−0.02	0.15
0.4930	0.13	−0.02	0.15
0.4970	0.13	−0.02	0.15
0.5030	0.13	−0.02	0.15
0.5038	0.14	−0.02	0.15
0.5553	0.11	−0.02	0.14
0.6988	0.10	−0.02	0.12
0.8222	0.09	−0.01	0.09
0.8423	0.12	−0.01	0.08
0.8458	0.09	−0.01	0.08
0.8918	0.05	−0.01	0.06

TABLE 1 (*Concluded*)

x	$V_{h_i,j}^E$	$V_{i,j}^E$	$(V_{h_i,j}^E - V_{i,j}^E)$
	n-Hexadecane – 1-chlorotetradecane		
0.1514	0.05	0.00	0.05
0.3014	0.08	0.00	0.07
0.4365	0.09	0.00	0.09
0.4391	0.09	0.00	0.09
0.5484	0.07	0.00	0.09
0.6928	0.07	0.00	0.08
0.8300	0.05	0.00	0.05
0.8527	0.05	0.00	0.04
0.8764	0.02	0.00	0.04
	n-Hexadecane – 1-chlorohexadecane		
0.1550	0.02	0.00	0.03
0.2969	0.03	0.00	0.04
0.4487	0.06	0.00	0.05
0.5536	0.05	0.00	0.05
0.7085	0.05	0.00	0.04
0.8447	0.01	0.00	0.03
0.8532	0.03	0.00	0.02
	n-Hexadecane – 1-chlorooctadecane		
0.1535	0.00		
0.2941	0.02		
0.4551	0.04	(0.00±0.01)*	(0.02±0.01)*
0.5450	−0.01		
0.6982	0.01		
0.8554	0.02		

*Values at equimolarity; obtained by interpolation or extrapolation.

mole fraction additivity of the molar volumes of the pure components.

The method of density determination has been described (18). It followed commonly accepted procedures and precautions.

Results

Experimental molar excess volumes for the systems of *n*-hexadecane with the 1-chloroalkanes are given in column 2 of Table 1. The data were adequately fitted by the method of least squares by the equation

$$[6] \quad V_{h_i,j}^E = x_{h_i}(1 - x_{h_i})[B_0 + B_1(2x_{h_i} - 1)]$$

with weighting factors that have been described (19). The coefficients in eq. 6 for the various systems are listed in columns 2 and 3 of Table 2, together with the errors of the fit in columns 4 and 5.

For the difference in the molar excess volumes, we let

$$[7] \quad V_{h_i,j}^E - V_{i,j}^E = x_{h_i}(1 - x_{h_i}) \times [b_0 + b_1(2x_{h_i} - 1)]$$

where

$$[8] \quad b_0 = \lambda \exp(-\omega n_{h_i}).$$

In eqs. 7 and 8, constants b, λ, and ω correspond

Can. J. Chem. Downloaded from www.nrcresearchpress.com by 210.87.254.42 on 09/05/12
For personal use only.

TABLE 2

Coefficients for least squares fit of eqs. 6 and 7; component j is *n*-hexadecane

Components i and h_i	B_0	B_1	Error (ml mole^{-1}) Standard*	Maximum	b_0	b_1	Error (ml mole^{-1}) Standard*	Maximum
1-Chlorobutane *n*-Butane, 1-Chlorobutane	1.75	0.31	0.01	0.02				
1-Chloropentane *n*-Pentane, 1-Chloropentane	1.66	0.21	0.02	0.03				
1-Chlorohexane *n*-Hexane, 1-Chlorohexane	1.56	0.04	0.02	0.04	3.88	0.98	0.00	0.01
1-Chlorooctane *n*-Octane, 1-Chlorooctane	1.19		0.01	0.01	2.27	0.61	0.01	0.01
1-Chlorodecane *n*-Decane, 1-Chlorodecane	0.98		0.02	0.05	1.38	0.19	0.00	0.00
1-Chlorododecane *n*-Dodecane, 1-Chlorododecane	0.51		0.02	0.05	0.61	0.03	0.00	0.01
1-Chlorotetradecane *n*-Tetradecane, 1-Chlorotetradecane	0.35		0.01	0.02	0.36		0.00	0.01
1-Chlorohexadecane *n*-Hexadecane, 1-Chlorohexadecane	0.19		0.01	0.02	0.19		0.00	0.01
1-Chlorooctadecane *n*-Octadecane, 1-Chlorooctadecane	0.06		0.02	0.03				

*$[\sum_{\text{system mixtures}}$ (error of ordinate of ith mixture datum)^2/number of mixtures in system$]^{1/2}$

TABLE 3

Error in $V_{h_i,j}^E - V_{i,j}^E$ in ml mole^{-1} at equimolarity calculated with λ and ω values obtained through eq. 9; component j is *n*-hexadecane

Component h_i	$V_{h_i,j}^E - V_{i,j}^E$ From coefficients b_0, b_1 in Table 2	From λ and ω of eq. 8	Error, as column 2 minus column 3
1-Chlorobutane	(2.01±0.1)*	(1.73±0.1)*	(0.28)*
1-Chloropentane	(1.34±0.05)*	(1.30±0.1)*	(0.04)*
1-Chlorohexane	0.97	0.98	−0.01
1-Chlorooctane	0.57	0.56	0.01
1-Chlorodecane	0.34	0.32	0.02
1-Chlorododecane	0.15	0.18	−0.03
1-Chlorotetradecane	0.09	0.10	−0.01
1-Chlorohexadecane	0.05	0.06	−0.01
1-Chlorooctadecane	(0.02)*	(0.03)*	(−0.01)*

*Values based upon interpolation or extrapolation.

to *a*, α, and β in eqs. 4 and 5, except that each group of constants is concerned with a different property. Each group is unrelated to the other.

The consideration of eq. 7 requires $V_{i,j}^E$ for the *n*-alkane mixtures at mole fractions that correspond to those listed in Table 1. Molar excess volumes of the binary systems of *n*-hexadecane with the *n*-alkane homomorphs of 1-chlorobutane, 1-chloropentane, and 1-chlorooctadecane are poorly defined at 25 °C, so only the remaining six systems can be used to establish b_0, b_1, λ, and ω.

Of these six systems, only in *n*-hexadecane – *n*-hexane have measured values of $V_{i,j}^E$ been utilized. Our procedure for the other systems was to obtain $V_{i,j}^E$ through the congruence principle (20). Column 3 of Table 1 shows the results of these calculations. They are based upon smoothed $V_{i,j}^E$ for *n*-hexadecane – *n*-hexane mixtures that have been reported by one of us (11, 21). Also included in column 4, as well as in column 5 and in Tables 2 and 3, are quantities for systems containing 1-chlorobutane, 1-chloropentane, and 1-chlorooctadecane which will be commented upon below.

The values of $V_{i,j}^E$ in column 3 of Table 1 were combined with those of $V_{h_i,j}^E$ from B_0 and B_1 of Table 2 to give the $V_{h_i,j}^E - V_{i,j}^E$ listed in column 4 of Table 1. The last were fitted to eq. 7 and the constants are given in columns 6 and 7 of

Can. J. Chem. Downloaded from www.nrcresearchpress.com by 210.87.254.42 on 09/05/12
For personal use only.

Can. J. Chem. Downloaded from www.nrcresearchpress.com by 210.87.254.42 on 09/05/12
For personal use only.

Table 2, together with the errors of the fit in columns 8 and 9.

Combination of eqs. 7 and 8 gives at equimolarity

$$[9] \quad \ln (V_{h_i,j}^E - V_{i,j}^E) = \ln (\lambda/4) - \omega n_{h_i}$$

The data are plotted in Fig. 1, together with the line obtained by the method of least squares with $\lambda = 21.006$ and $\omega = 0.27869$. The data were weighted according to the uncertainty of the l.h.s. of eq. 9 (22). That uncertainty was obtained as $(e_{h_i,j}^2 + e_{i,j}^2)^{1/2}$, where e is the standard error in the indicated systems. $e_{h_i,j}$ is given in column 4 of Table 2. $e_{i,j}$ has been assumed to be the same, ± 0.03 ml mole^{-1}, as that in the system *n*-hexadecane – *n*-hexane, to which the congruence principle is applied in obtaining the other $V_{i,j}$ values. In Table 3 the values of $V_{h_i,j}^E - V_{i,j}^E$ at equimolarity calculated with b_0 are compared with values calculated with λ and ω.

Extrapolation of eq. 8 to the first, second, and last systems in the tables, those systems not used in evaluating λ and ω, has been performed. The $V_{h_i,j}^E - V_{i,j}^E$ calculated with λ and ω are listed in column 3 of Table 3. In column 2 of Table 3 values of $V_{h_i,j}^E - V_{i,j}^E$ obtained through the method stated for that column are given. This requires values from columns 2 and 3 of Table 1, just as in the other systems of this type. For the mixtures containing the alkanes, measurements of $V_{i,j}^E$ are not available. Instead, an indirect method has been used. Desmyter and van der

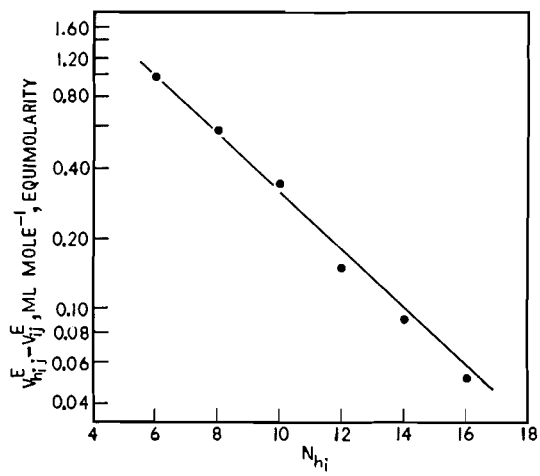

FIG. 1. Plot of eq. 9 for systems of *n*-hexadecane – 1-chloroalkanes and *n*-hexadecane – *n*-alkanes at 25.00 °C. h_i and i are homomorphs and j is *n*-hexadecane.

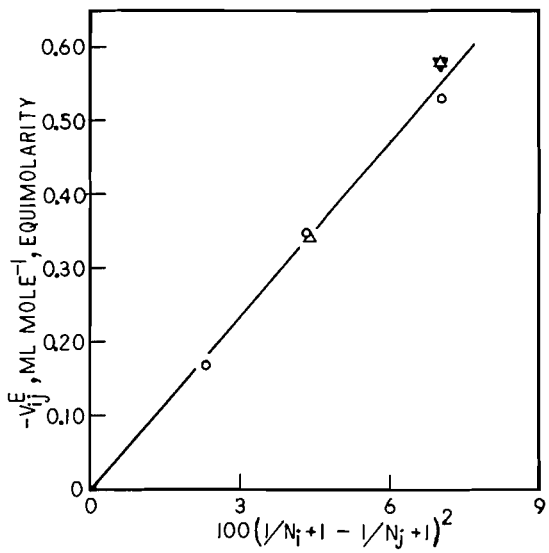

FIG. 2. Plot of eq. 10 for *n*-alkane – *n*-alkane systems. (△) Desmyter and van der Waals (5); (○) Gómez-Ibáñez and Liu (23); (▼) Heric and Brewer (11).

Waals (5) showed that their results at 20 °C for equimolar *n*-alkane mixtures between component limits of 5 and 16 carbons could be represented by

$$[10] \quad V_{i,j}^E = \left(\frac{1}{n_i + 1} - \frac{1}{n_j + 1}\right)^2$$

A similar plot for equimolar *n*-alkane mixtures at 25 °C is given in Fig. 2. Extrapolation and interpolation of that plot for the *n*-alkane components of present interest yields the corresponding values of $V_{i,j}^E$ given in column 3 of Table 1.

Discussion

$V_{h_i,j}^E$ are positive for all of the *n*-hexadecane – 1-chloroalkane systems. As the coefficients B_0 of eq. 6 show in Table 2, the trend is one of increasing values with the decrease in halide chain length. The fit of eq. 6 to these systems is in agreement with the uncertainty of the measured $V_{h_i,j}^E$, with the greatest standard error ± 0.02 ml mole^{-1}. The sign of $V_{h_i,j}^E$ is the opposite of that of $V_{i,j}^E$ in the systems involving the *n*-alkane homomorphs of the halides. For $V_{i,j}^E$, larger negative values are found as the chain length of the halide homomorph decreases. A comparison of the two types of systems is given in Fig. 3, for a chain length of six carbons. The asymmetry in both is similar in that the maximum deviation from ideality occurs on the *n*-hexadecane-poor side. The asymmetry is

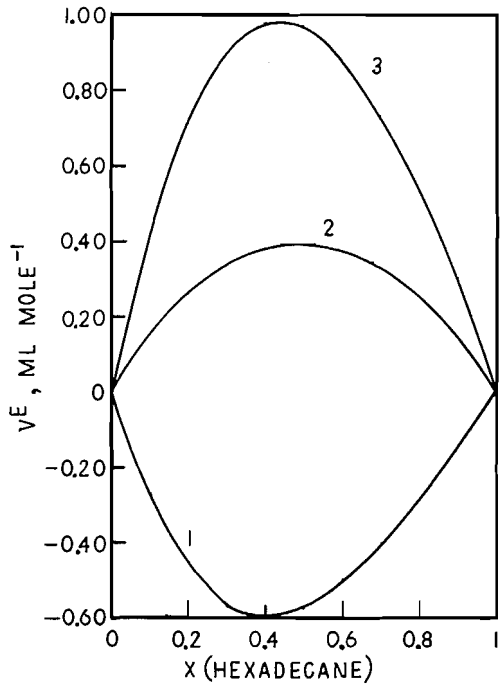

FIG. 3. V^E at 25.00 °C for *n*-hexadecane with *n*-hexane and with 1-chlorohexane. Curve *1* is for *n*-hexadecane – *n*-hexane (homogeneous factor). Curve *2* is for *n*-hexadecane – 1-chlorohexane (homogeneous and heterogeneous factors). Curve *3* is for the difference between the two systems (heterogeneous factor).

considerably less in the system containing the halide, however. This qualitative comparison of relative asymmetry in the two types of systems at given chain length is also found for the other chain lengths for which asymmetry occurs.

The conclusions from this work are dependent upon both $V_{h_i,j}{}^E$ and $V_{i,j}{}^E$. Both the accuracy and precision of the latter require comment. The accuracy of applying the congruence principle as used here has been illustrated by Hijmans (20). His results show that the agreement between calculated and experimental values is variable, but generally within 0.02 ml mole^{-1}. The agreement varies for different systems. Figure 1 shows that this small error in a system would not significantly affect the relationship established here.

Another question of accuracy arises through a comparison of the data used here for the *n*-hexadecane – *n*-hexane system which we have reported (11), with those from Desmyter and van der Waals (5) and Gómez-Ibáñez and Liu (23). All three sources agree on the asymmetry of $V_{i,j}{}^E$ in the system, but the $V_{i,j}{}^E$ and x_j coordinates of the maxima are different in each source. They are: −0.62, 0.35 (5); −0.59, 0.35 (23); and −0.60 ml mole^{-1}, 0.40 (11). All three sources agree for $x_j \geqslant 0.6$, while different source pairs agree over different composition ranges for $x_j < 0.6$. The disagreement between different sources is such that the error which might arise by the use of data from any of the sources again would not significantly affect the relationship established in Fig. 1. We have used our data from among the three sources, even though our precision is the poorest, because the present work thereby involves a consistent data source.

A third matter bearing on accuracy arises in the system *n*-hexadecane – *n*-tetradecane. V^E in that system has been determined experimentally (11). V^E is not zero there, as predicted with the congruence principle. Rather the small V^E values pass from positive to negative as the concentration of *n*-hexadecane is decreased. The sign transition is near equimolarity, however, and the average V^E is near zero. Again the effect of this small error on present conclusions is not significant.

The precision of $V_{i,j}{}^E$ for the various chain lengths has been assumed to be the same as that in the system *n*-hexadecane – *n*-hexane, because obtaining the former from the latter involves no additional experimental uncertainty. The application of the congruence principle is purely a geometrical operation.

For the coefficients of eq. 7, based upon the systems of 6 through 16 carbons, Table 2 shows that there is a systematic behavior. Both b_0 and b_1 increase with decreasing chain length. The fit of eq. 7 is uniformly excellent, reflecting the fact that values of $V_{h_i,j}{}^E$ and $V_{i,j}{}^E$ have been smoothed prior to their use in that equation.

The use of $V_{h_i,j}{}^E - V_{i,j}{}^E$ at equimolarity to obtain the coefficients λ and ω of eq. 8 is actually a test of the coefficient b_0 because the difference in V^E reduces to $b_0/4$ at that composition. Figure 1 and Table 3 show the fit of eq. 8 is good, with no disagreement in the systems of 6 through 16 carbons greater than 0.03 ml mole^{-1}. A clear correlation of the behavior with the carbon chain length exists in these systems.

The extension of eq. 8 to the other systems in Table 3 yields results of differing quality. For the system with 18 carbons the agreement is quite good, to 0.01 ml mole^{-1}. Here the $V_{i,j}{}^E$ obtained from Fig. 2 by interpolation is at a very low

Can. J. Chem. Downloaded from www.nrcresearchpress.com by 210.87.254.42 on 09/05/12
For personal use only.

Can. J. Chem. Downloaded from www.nrcresearchpress.com by 210.87.254.42 on 09/05/12
For personal use only.

abscissa value. Thus, even though a chain length of 18 carbons is outside the component range used in establishing the linearity, this has little effect. Moreover, the b_0 value for that system obtained from λ and ω of eq. 8 is quite small. For these reasons the significance of the agreement in this system is difficult to assess unambiguously. While both *n*-octadecane and 1-chlorooctadecane must be treated as supercooled liquids at 25 °C, that fact is of no consequence to the results.

For the systems of four and five carbons, there is yet greater uncertainty over the error shown in Table 3. Nevertheless, consideration of the possibility of such extrapolation to these systems seems to be warranted during this work. For the system with five carbons, $V_{i,j}{}^E$ must be obtained by extrapolation in Fig. 2 to an abscissa value approximately double that of the range over which linearity has been established. The disagreement in Fig. 2 between the different literature values for a given abscissa indicate an uncertainty in the extrapolated ordinate of about 0.05 ml mole^{-1} in $V_{i,j}{}^E$. The standard error in $V_{h_i,j}{}^E$ for that chain length, ± 0.02 ml mole^{-1} is negligible by comparison. A reasonable estimate of the uncertainty in extrapolating eq. 8 to that chain length is also 0.1 ml mole^{-1}. The agreement in Table 3 for this chain length, 0.04 ml mole^{-1}, is, therefore, within the estimated uncertainty.

For the system with four carbons the disagreement in Table 3 is considerably greater, 0.28 ml mole^{-1}. However, the uncertainties in the values compared may be quite great here. $V_{i,j}{}^E$ must be obtained by extrapolation in Fig. 2 to an abscissa value almost triple that of the range of established linearity. An uncertainty of about 0.1 ml mole^{-1} in $V_{i,j}{}^E$ may arise from this, assuming the extrapolation is valid. Such validity is questionable, however. Holleman and Hijmans (24) have shown experimentally that heats of mixing in *n*-alkane systems show considerable deviation from the congruence principle when the difference in component chain lengths becomes excessive. This may be a consequence of departure from the implied assumption in the congruence principle that the strengths of the van der Waals forces of the components are suitably similar. The change in the strength of these forces with chain length is greater at the lower end. Thus, extending eq. 10 to a chain length of four carbons for one of the components may be outside the validity of that equation. The extrapolation must treat *n*-butane as a superheated liquid at that temperature, which well illustrates the significantly smaller van der Waals forces of that component. It follows that the disagreement in Table 3 for this system may not be due to the failure of eq. 8 at that chain length. The assignment of an uncertainty of 0.1 ml mole^{-1} for the extrapolation of eq. 8 to a chain length of four is an arbitrary estimate, as it was for a chain length of five.

In terms of the foregoing, while the results must be qualified at four and five carbons, the agreement shown in column 4 of Table 3 for the other systems is good. While it may be that the coefficients b_1 of eq. 7 are also systematically related to chain length, present data are insufficient to establish this.

Equation 8 predicts that b_0 is sufficiently small at a chain length of 20 carbons that it is indistinguishable from zero within an experimental error of ± 0.02 ml mole^{-1}. That is, beyond this chain length the effect of the halide group is so small that $V_{h_i,j}{}^E$ and $V_{i,j}{}^E$ are the same whether h_i or i is mixed with *n*-hexadecane. Thus, the mixing effect in either case is essentially due to the hydrocarbon chains.

It is striking that both Δ^*G^E and V^E in these systems can be treated by the same approach. It must be emphasized, however, that the gross similarity in behavior of these two properties does not extend beyond that point. This is evident from a comparison of Figs. 3 and 4. Thus both properties show positive deviation from ideality for *n*-hexadecane – 1-chlorohexane, where both homogeneous and heterogeneous factors are involved. The homogeneous factor, in the system *n*-hexadecane – *n*-hexane, is positive for Δ^*G^E and larger than when both homogeneous and heterogeneous factors are present. The heterogeneous factor here is negative. That is, viscous flow is relatively enhanced in the system containing the halide, probably due to the decrease in dipole–dipole interaction in the halide when mixed with the *n*-alkane.

The homogeneous factor is negative for V^E. Thus the heterogeneous factor must be positive here, and larger than V^E when both homogeneous and heterogeneous factors are present; that is, larger than in the system containing the halide. The volumetric behavior may be explained by assuming an expansion when there is a decrease in dipole–dipole interactions. The latter is the heterogeneous factor.

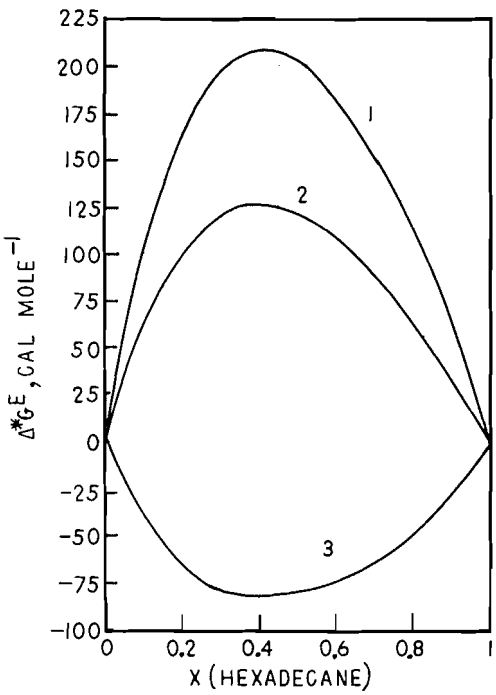

FIG. 4. Δ^*G^E at 25.00 °C for *n*-hexadecane with *n*-hexane and with 1-chlorohexane. Curve *1* is for *n*-hexadecane – *n*-hexane (homogeneous factor). Curve *2* is for *n*-hexadecane – 1-chlorohexane (homogeneous and heterogeneous factors). Curve *3* is for the difference between the two systems (heterogeneous factor).

It follows from Figs. 3 and 4 that there is no consistent correlation in these systems between free volume behavior and viscous flow. While the heterogeneous effects show the commonly assumed enhancement of flow accompanying volume increase, the overall relationship between V^E and Δ^*G^E is that the former may reflect either expansion or contraction in a system exhibiting positive deviation from ideal viscous flow.

Extension of the study of the systematic behavior of each of Δ^*G^E and V^E in the present systems to a common *n*-alkane other than *n*-hexadecane will reveal more on the generality of the approach. It may be limited to series of related systems in which the *n*-alkane chain length is relatively long. In our laboratory we are now studying mixtures of the same halides included here with *n*-hexane as the second component.

Acknowledgment is made to the donors of the Petroleum Research Fund, administered by the American Chemical Society, for support of this research.

1. J. N. BRØNSTED and J. KOEFOED. Kgl. Danske Videnskab Selskab. Mat. fys. Medd. **22**, 1 (1946).
2. J. H. VAN DER WAALS and J. J. HERMANS. Rec. Trav. Chem. Pays-Bas. **69**, 971 (1950).
3. TH. HOLLEMAN. Physica, **29**, 274 (1963).
4. J. A. FRIEND, J. A. LARKIN, A. MAROUDAS, and M. L. MCGLASHAN. Nature, **198**, 683 (1963).
5. A. DESMYTER and J. H. VAN DER WAALS. Rec. Trav. Chem. Pays-Bas. **77**, 53 (1958).
6. TH. HOLLEMAN. Physica, **29**, 585 (1963).
7. J. A. BARKER and M. LINTON. J. Chem. Phys. **38**, 1853 (1963).
8. G. W. NEDERBRAGT and J. J. DE JONG. Appl. Sci. Res. A. **3**, 125 (1953).
9. B. M. COURSEY and E. L. HERIC. Mol. Phys. **13**, 287 (1967).
10. B. M. COURSEY and E. L. HERIC. Can. J. Chem. Eng. **47**, 410 (1969).
11. E. L. HERIC and J. G. BREWER. J. Chem. Eng. Data, **14**, 55 (1969).
12. M. DIAZ PEÑA and F. F. MARTIN. Annales Real. Soc. Espan. Fis. Quim. (Madrid), **59**, 323, 331 (1963).
13. A. E. POPE, H. D. PFLUG, B. DACRE, and G. C. BENSON. Can. J. Chem. **45**, 2665 (1967).
14. R. S. RAMALHO and M. RUEL. Can. J. Chem. Eng. **46**, 167, 456 (1968).
15. I. BROWN, W. FOCK, and F. SMITH. Aust. J. Chem. **17**, 1106 (1964).
16. E. L. HERIC and B. M. COURSEY. Can. J. Chem. Eng. In press.
17. S. GLASSTONE, K. J. LAIDLER, and H. EYRING. The theory of rate processes. McGraw-Hill, New York. 1941. p. 484.
18. E. L. HERIC and B. M. COURSEY. J. Chem. Eng. Data. In press.
19. E. L. HERIC. J. Chem. Eng. Data, **11**, 66 (1966).
20. J. HIJMANS. Mol. Phys. **1**, 307 (1958).
21. E. L. HERIC and J. G. BREWER. J. Chem. Eng. Data, **12**, 574 (1967).
22. J. TOPPING. Errors of observation and their treatment. Reinhold Publ. Corp., New York. 1957. Chap. 3, p. 88.
23. J. D. GÓMEZ-IBÁÑEZ and C.-T. LIU. J. Phys. Chem. **67**, 1388 (1963).
24. TH. HOLLEMAN, J. HIJMANS. Physica, **31**, 64 (1965).

Can. J. Chem. Downloaded from www.nrcresearchpress.com by 210.87.254.42 on 09/05/12
For personal use only.

Can. J. Chem. Downloaded from www.nrcresearchpress.com by 210.87.254.6 on 09/05/12
For personal use only.

Etude des mouvements de molécules linéaires en phase liquide par analyse du profil des bandes d'absorption infrarouge. I. Oxyde nitreux

J. VINCENT-GEISSE, J. SOUSSEN-JACOB, NGUYEN-TAN TAI, ET D. DESCOUT

Groupe de Recherches n° 3 du C.N.R.S., Département de Recherches Physiques, Faculté des Sciences, 9, quai Saint Bernard, Paris (5°), France

Reçu le 13 juillet 1970

On a effectué la mesure de la largeur et du profil des 3 bandes de vibration fondamentales et de quelques harmoniques de la molécule N_2O en solution dans un grand nombre de solvants. Dans le cas de quelques solvants non polaires les largeurs des bandes observées semblent déterminées par des mouvements de rotation de la molécule dissoute; dans les autres cas on ne peut négliger les variations du potentiel intermoléculaire. On a d'autre part calculé les fonctions de corrélation et les moments correspondants; les chiffres obtenus sont interprétés dans l'hypothèse où la largeur est due aux mouvements de rotation et de diffusion rotationnelle de la molécule; ils se montrent sensiblement en accord avec la théorie dans le cas des solvants non polaires. Nous donnons de plus une valeur approchée du couple de rappel agissant sur la molécule N_2O en milieu liquide.

Measurements have been made of the width and profile of the three fundamental vibration bands and of some harmonics of the N_2O molecule in solution in a large number of solvents. In the case of some non polar solvents the widths of the bands observed appear to be determined by rotational motions of the solute molecules; in other cases variations in the intermolecular potential cannot be neglected. The correlation functions and corresponding moments were then calculated; the values obtained are interpreted using the hypothesis that the width arises as a result of rotation and rotational diffusion movements of the molecule; they appear approximately in agreement with theory in the case of non polar solvents. In addition, we give an approximate value of the torque acting on the N_2O molecule in liquid medium.

Canadian Journal of Chemistry, 48, 3918 (1970)

Introduction

L'étude en phase liquide du profil des bandes d'absorption dans l'i.r. et de la transformée de Fourier correspondante, est susceptible de nous fournir des renseignements sur le mouvement des molécules au sein du liquide. Le profil des bandes est déterminé par les fluctuations de fréquence dues aux variations aléatoires du potentiel intermoléculaire et par les mouvements de rotation des molécules (1, 2). Dans le cas général, le problème est très complexe; nous en avons examiné quelques exemples dans des articles précédents (3, 4). Si l'on veut comparer les résultats expérimentaux à ceux indiqués par la théorie, il est nécessaire de choisir une molécule pour laquelle on prévoit que des simplifications sensibles seront apportées au schéma général; ceci nous a amenés à étudier des molécules linéaires. Dans ce dernier cas, en effet, il n'existe que deux degrés de liberté de rotation équivalents autour d'axes perpendiculaires à l'axe nucléaire et un seul moment d'inertie; si ces molécules sont de plus assez légères et peu polaires, on peut penser que, au moins dans certains solvants, l'effet dû à la rotation des molécules l'emportera sur les fluctuations du potentiel et pourra donner lieu à une interprétation théorique satisfaisante. Nous avons choisi ici la molécule N_2O qui remplit les conditions précédentes.

Nous avons observé tout d'abord avec le plus de précision possible le profil des trois bandes fondamentales d'absorption de N_2O dans un grand nombre de solvants, ainsi que celui de quelques harmoniques et mesuré leur largeur. Nous avons calculé ensuite les fonctions de corrélation correspondantes et les moments d'ordre 2 et 4. Nous examinerons successivement les différents résultats obtenus et nous tenterons de les interpréter à la lumière de la théorie (2, 5, 6).

Molécule N_2O

Les trois modes fondamentaux se montrent actifs en i.r.; les vibrations de valence ν_1 et ν_3 sont parallèles à l'axe de la molécule et la vibration de déformation ν_2 doublement dégénérée, perpendiculaire à l'axe, ainsi que l'indique la fig. 1. Les harmoniques $2\nu_1$ et $2\nu_3$ sont des bandes parallèles; des deux sous-niveaux 020, seul celui de type Σ^+ donne lieu à une transition $2\nu_2$ active en i.r., parallèle à l'axe et en résonance de Fermi avec ν_1.

Le spectre de N_2O à l'état gazeux a été observé par de nombreux auteurs (en particulier 7–12)

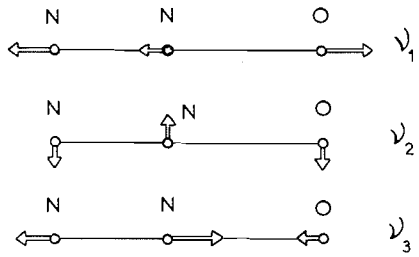

FIG. 1. Vibrations de la molécule N_2O.

et la littérature nous fournit, outre les fréquences des fondamentales, celles d'une quantité considérable d'harmoniques et de combinaisons, accompagnées le cas échéant des fréquences des bandes chaudes correspondantes. En effet, le niveau ν_2 se situe à une fréquence assez basse, de sorte que sa population n'est pas négligeable à la température de nos expériences (environ 13%) et les transitions à partir de ce niveau apparaissent dans le spectre. Ayant étudié dans ce travail les trois modes fondamentaux et le premier harmonique de chacun d'eux, nous présentons dans le tableau 1 les nombres d'ondes indiqués le plus récemment dans la littérature pour ces bandes et les bandes chaudes correspondantes.

En ce qui concerne la rotation, notons que le moment d'inertie de la molécule N_2O est 67.10^{-40} g cm^2.

Etude expérimentale

(a) Largeurs

Les largeurs des différentes bandes ont été déterminées en examinant dans chaque cas deux à trois spectres. On a construit les courbes en densité optique en rapportant le spectre de la solution à celui du solvant. On a opéré ainsi pour 18 substances, mais il n'a évidemment pas été possible d'obtenir dans tous les cas à la fois les largeurs des trois bandes fondamentales et de leurs harmoniques. La bande $2\nu_2$ en particulier n'apparaît que dans très peu de solvants, ceux-ci absorbant en général dans cette région sous l'épaisseur nécessitée par la faible solubilité de N_2O.

La concentration des solutions étudiées, mesurée approximativement en se référant à l'intensité donnée par la littérature pour les bandes à l'état gazeux, était en général très faible et ne dépassait pas 0.1 à 0.2 mole/l, sauf pour la bande $2\nu_1$, dont l'étude n'a été possible dans certains cas qu'au moyen d'une cuve à pression (p = 5 kg/cm^2 environ).

L'oxyde nitreux utilisé provenait de l'Air Liquide et titrait 99.99%. Les solvants étaient des produits très purs de différentes firmes, autant que possible pour spectrophotométrie.

Dans la majorité des cas, les spectres et plus particulièrement ceux ayant servi au calcul des fonctions de corrélation, ont été enregistrés sur un spectromètre Perkin–Elmer modèle 225. Quelques spectres cependant ont été obtenus avec d'autres appareils (Perkin–Elmer 112 à simple faisceau avec prisme de LiF, 521, Beckman IR 12 pour $2\nu_1$ sous pression, Cary 14 pour $2\nu_3$). Les conditions étaient toujours telles que la largeur spectrale de fente s se trouvait inférieure à 1/5 de la largeur $\Delta\nu_{1/2}$ de la bande. Dans le cas des spectres utilisés pour le calcul des fonctions de corrélation, les rapports $\Delta\nu_{1/2}/s$ étaient de 35 à 20 pour ν_1, 6 à 5 pour ν_2 et 18 à 8 pour ν_3.

(b) Fonctions de corrélation et moments

La fonction de corrélation, partie réelle de la transformée de Fourier de la courbe représentant le coefficient d'absorption k en fonction de la pulsation ω s'écrit

$$[1] \qquad \Phi(t) = \int_{\text{bande}} k(\omega) \cos(\omega - \omega_0)t \, d\omega$$

à un facteur de normalisation près. (La partie imaginaire est nulle dans le cas de bandes symétriques.) On a calculé les fonctions de corrélation à partir de cette formule de la manière suivante

$$[2] \qquad \Phi(t) = \frac{\int_{\text{bande}} \log \frac{I_0}{I} \, d\,[\sin(\omega - \omega_0)t]}{\int_{\text{bande}} \log \frac{I_0}{I} \, d\omega}$$

Les deuxième et quatrième moments sont donnés par l'expression

$$[3] \qquad M(n) = \int k(\omega)(\omega - \omega_0)^n d\omega / \int k(\omega) d\omega$$

avec $n = 2$ ou 4

Ces calculs ont été programmés en langage Fortran IV pour l'ordinateur CDC 6600. Nous avons déterminé de plus le logarithme népérien de $\Phi(t)$ et les points correspondants sont localisés sur un graphe donné par la machine en même temps que les valeurs de t, $\Phi(t)$, $\ln \Phi(t)$, $M(2)$ et $M(4)$; t est compris entre 0.05 et 5 ps.

Des difficultés de différents ordres se sont révélées dans l'évaluation de $\Phi(t)$ et des moments; nous allons les passer en revue. De toutes manières, comme nous l'avons vu, tous les spectres utilisés pour ce calcul ont été enregistrés sur le spectromètre 225 et l'on a bien entendu choisi dans chaque cas celui ou ceux des spectres qui nous semblaient les meilleurs, avec en particulier les ailes les plus précises. Lorsque les solvants présentaient une bande d'absorption relativement intense à l'emplacement des ailes de la bande étudiée, l'erreur en découlant nous a paru justifier l'abandon des courbes $\ln \Phi(t)$ correspondantes.

En ce qui concerne le domaine d'intégration, il s'étendait sur un intervalle de nombres d'ondes de 10 à 15 fois la largeur de la bande ν_1, de 15 à 20 fois celle de la bande ν_2 plus étroite que la précédente et de 15 à 25 fois celle de la bande ν_3 qui, plus intense que les autres, se situe en outre dans une région spectrale plus favorable.

L'un des plus gros problèmes que nous ayons rencontré dans cette étude est celui des bandes chaudes impossibles à séparer des fondamentales dans l'ignorance où nous nous trouvons de leur forme et de leur largeur. Dans le cas de la vibration ν_3 cependant, l'éloignement de la

Can. J. Chem. Downloaded from www.nrcresearchpress.com by 210.87.254.6 on 09/05/12
For personal use only.

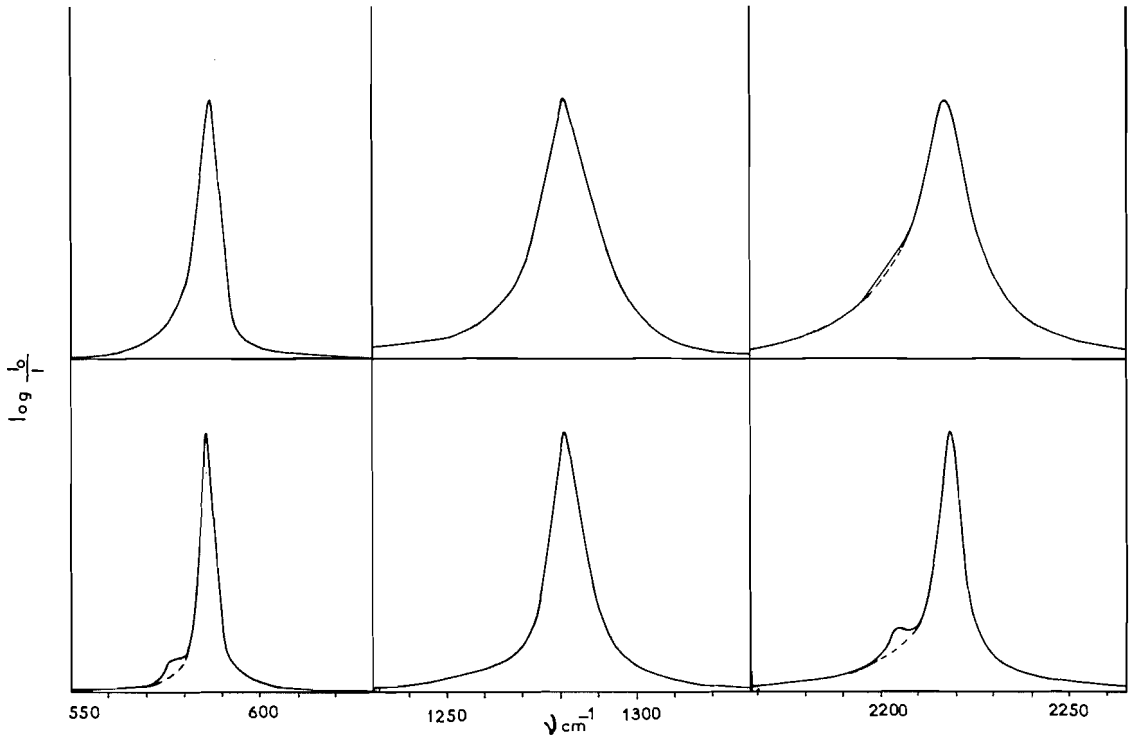

FIG. 2. Spectres de N_2O: en haut dans l'hexane, en bas dans le tétrachlorure de carbone: ν_2, 586 cm^{-1}; ν_1, 1281 cm^{-1}; ν_3, 2216 cm^{-1}.

bande chaude (-14.2 cm^{-1}) permet de considérer comme non perturbé le côté de la bande principale qui lui est opposé. Aussi a-t-on calculé pour cette vibration les $\Phi(t)$ en symétrisant la demi-courbe située du côté des hautes fréquences. De toutes manières, la bande parasite apparaissant toujours sous forme d'épaulement (plus ou moins accentué selon la largeur de la fondamentale, comme le montre la fig. 2), nous avions primitivement opéré en supprimant cet épaulement de la façon indiquée sur la figure. Un exemple de calcul à partir de la courbe entière et de la demi-courbe est donné sur la fig. 3: nous constatons que les points expérimentaux se placent beaucoup mieux au voisinage d'une droite, conformément à ce que prévoit la théorie, dans le cas de la symétrisation des demi-courbes. C'est au contraire toute la courbe en densité optique que nous avons utilisée pour la vibration ν_1, où la bande chaude est trop proche de la bande principale pour ne pas l'influencer des deux côtés, sans même qu'on puisse observer un épaulement (fig. 2). Dans le cas de ν_2 enfin, accompagnée de part et d'autre par deux bandes chaudes dont on ne connaît pas la répartition, il est seulement possible d'éliminer l'épaulement situé à 9.4 cm^{-1} de la fondamentale, du côté des basses fréquences (fig. 2).

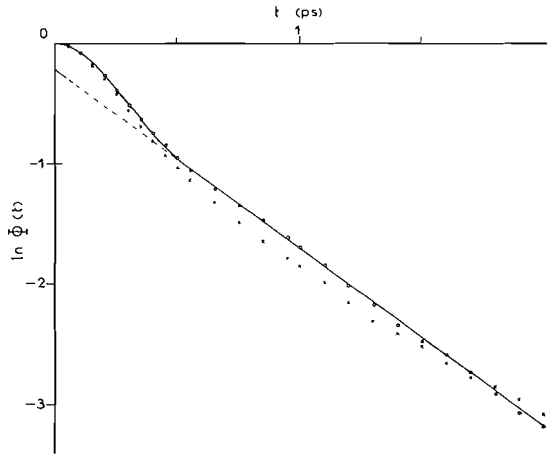

FIG. 3. ln $\Phi(t)$ de ν_3 dans l'hexane: ×, à partir de la courbe d'absorption entière; ○, à partir du double de la demi-courbe hautes fréquences.

Largeur des bandes. Résultats et discussion

Nous avons rassemblé dans le tableau 2 l'ensemble des largeurs des bandes fondamentales et des premiers harmoniques. Pour chaque vibration, la première colonne donne le nombre d'ondes du maximum d'absorption, la seconde la largeur à mi-hauteur et la troisième le double de la demi-largeur correspondant soit aux basses fréquences ($2\Delta_1$), soit aux hautes fréquences ($2\Delta_2$), à cause de l'existence de bandes chaudes

Can. J. Chem. Downloaded from www.nrcresearchpress.com by 210.87.254.6 on 09/05/12
For personal use only.

Can. J. Chem. Downloaded from www.nrcresearchpress.com by 210.87.254.6 on 09/05/12
For personal use only.

TABLEAU 1

Nombres d'ondes à l'état gazeux

Fondamentales	$\nu(cm^{-1})$	Référence	Bandes chaudes	$\nu(cm^{-1})$	Référence	Harmoniques	$\nu(cm^{-1})$	Référence	Bandes chaudes	$\nu(cm^{-1})$	Référence
ν_1	1284.9	(9)	$\nu_1 + \nu_2 - \nu_2$	1291.5	(10)	$2\nu_1$	2563.3	(9)	$2\nu_1 + \nu_2 - \nu_2$	2577.1	(8)
ν_2	588.8	(9)	$(2\nu_2)^0 - \nu_2$ $(2\nu_2)^2 - \nu_2$	579.3 590.4	(11) (11)	$2\nu_2$	1168.1	(10)	$3\nu_2 - \nu_2$	1160.3	(10)
ν_3	2223.7	(9)	$\nu_3 + \nu_2 - \nu_2$	2209.5	(12)	$2\nu_3$	4417.4	(9)	$2\nu_3 + \nu_2 - \nu_2$	4388.9	(8)

TABLEAU 2

Largeurs en cm^{-1}

	ν_1			ν_2			ν_3			$2\nu_1$			$2\nu_2$		$2\nu_3$	
Solvant*	ν	$\Delta\nu_{1/2}$	$2\Delta_1$	ν	$\Delta\nu_{1/2}$	$2\Delta_1$	ν	$\Delta\nu_{1/2}$	$2\Delta_2$	ν	$\Delta\nu_{1/2}$	$2\Delta_1$	ν	$\Delta\nu_{1/2}$	ν	$\Delta\nu_{1/2}$
n-C_5H_{12}							2217	18.0	17.4	2558	23.3	20.0				
n-C_6H_{14}	1280.7	17.0	14.5	586.6	7.3	7.0	2216.5	17.4	16.6	2557	22.0	18.8				
C_6H_{12}	1281.5	16.2	14.8				2218	14.0	13.6							
c-C_5H_{10}	1281.5	16.5	15.9				2217	14.9	14.6	2557	21.4	17.2				
c-C_6H_{12}	1281	14.5	12.4	586	6.0	5.7	2216	11.5	11.5	2556	17.4	16.0				
$C_2Cl_3F_3$	1282.5	12.5	11.8	587.5	5.3	5.0	2219.5	9.7	9.3	2558	20.6	18.5			4409.6	12.3
CCl_4	1281.3	11.2	10.2	586	4.3	4.0	2216	8.1	7.7	2556.2	18.5	17.2	1161	8.5	4406.5	11.8
C_2Cl_4	1281.2	10.2	9.5	585.6	4.5	4.1	2217	8.8	8.6	2555.5	15.4	15.0			4405	11.9
CS_2	1279.3	12.5	11.2	583.5	6.0	5.8	2214.5	10.5	10.4	2551.5	18.0	17.5	1156	13.1	4400	13.7
C_6H_6	1281	14.3	12.9	583.5	6.5	6.1	2219.4	9.6	8.9	2557	25.8	23.6				
$CHCl_3$	1282	17.3	16.1	584	7.6	7.3	2220.5	9.8	9.6	2557.5	32.5	31.2			4410	14.0
$CHBr_3$	1281	14.2	13.8				2218.4	8.3	8.3	2555	31.0	31.0			4407	14.3
CH_2Cl_2				584.8	5.6	5.2	2222.4	9.4	9.1							
CH_2I_2	1280	11.9	11.9				2217.8	8.0	8.0							
CH_3CN	1285	12.9	12.5	585.5	6.6	6.2	2228	12.5	11.7	2563	26.5	25.0				
CH_3NO_2	1284.5	12.8	11.9				2228.3	10.5	10.1							
$(CH_3)_2CO$	1283	14.2					2226.5	14.0	12.7	2563	31.3	26.4				
p-$C_4H_8O_2$							2225.5	12.0	11.7	2562	31.5	25.6				

*C_6H_{12} = 1-hexène; *c*-C_5H_{10} = cyclopentane; $C_2Cl_3F_3$ = 1,1 2-trichlorotrifluoroéthane; *p*-$C_4H_8O_2$ = paradioxanne.

Can. J. Chem. Downloaded from www.nrcresearchpress.com by 210.87.254.6 on 09/05/12
For personal use only.

qui perturbent, comme nous l'avons indiqué plus haut, l'une ou l'autre moitié de la bande principale.

L'interprétation des résultats est très simple dans le cas des bandes parallèles. Si l'élargissement par rotation est le seul qui intervienne, il doit être le même pour toutes les bandes parallèles, fondamentales ou harmoniques qui doivent donc présenter la même largeur. En ce qui concerne les bandes perpendiculaires, nous montrerons un peu plus loin que, toujours dans l'hypothèse d'un effet rotationnel prépondérant et, moyennant quelques conditions supplémentaires que nous mettrons en évidence, leur largeur doit être la moitié de celle des bandes parallèles. Ce rapport entre les largeurs ressort également des calculs de Favro (13) qui traite le cas où la diffusion rotationnelle est le seul effet existant; de l'expression qu'il donne du coefficient d'absorption d'une bande parallèle à un axe principal d'inertie numéroté 1, il vient: $\Delta\nu_{1/2} = (D_2 + D_3)/\pi c$, D_2 et D_3 étant les constantes de diffusion rotationnelle relatives aux rotations autour des deux autres axes.

Dans le cas qui nous intéresse, si l'axe 1 est l'axe nucléaire, $D_1 = 0$ et $D_2 = D_3 = D$, d'où

$$[4] \qquad (\Delta\nu_{1/2})_{\parallel} = 2D/\pi c \text{ et } (\Delta\nu_{1/2})_{\perp} = D/\pi c$$

Nous nous attendons donc à trouver des largeurs égales pour les bandes ν_1, ν_3, $2\nu_1$, $2\nu_2$, $2\nu_3$ et deux fois plus petites pour ν_2.

Si nous examinons le tableau 2, nous voyons que ces prévisions théoriques ne sont jamais exactement satisfaites, mais qu'elles le sont sensiblement, pour les bandes mesurées, dans le cas d'un certain nombre de solvants non polaires. Ailleurs on observe des déviations plus ou moins importantes, soit que les largeurs de ν_1 et ν_3 ne soient pas les mêmes, soit que celles des harmoniques diffèrent, soit que le rapport 2 ne soit pas respecté entre les largeurs de ν_1 et ν_3 et celle de ν_2. Finalement le pentane et l'hexane se présentent comme les solvants dans lesquels les actions intermoléculaires sont les plus faibles et l'effet rotationnel nettement prépondérant. Dans l'acétone, au contraire, les largeurs égales de ν_1 et ν_3 laisseraient penser que l'effet de rotation est dominant, mais la grande largeur de $2\nu_1$ montre que cette conclusion serait erronée. Assez souvent les largeurs de ν_1 et ν_3 sont différentes; le tableau 2 montre que la plus large des deux est alors ν_1, qui serait donc davantage sensible aux effets intermoléculaires; comme de plus, cette dernière présente, à cause de la résonance de Fermi, une certaine proportion de transition $2\nu_2$, les anomalies observées peuvent s'expliquer par cet effet et il est plus sûr de prendre en considération la largeur de ν_3 (ou $2\Delta_2$). Nous avons réuni dans le tableau 3 les constantes de diffusion rotationnelle calculées pour ν_3 (à partir de $2\Delta_2$) au moyen de la relation [4], lorsque cette diffusion semble le processus prépondérant dans l'élargissement. Sur ce tableau, le pentane et l'hexane viennent en tête pour la valeur de D; c'est dans ces solvants que la diffusion rotationnelle apparaît la plus rapide; le sulfure de carbone et le tétrachlorure de carbone, quoique réputés inertes, se situent loin derrière et montrent d'ailleurs de nombreuses anomalies.

TABLEAU 3

Constantes de diffusion rotationnelle

Solvant*	D (10^{12} s^{-1})
n-C_5H_{12}	0.82
n-C_6H_{14}	0.78
c-C_5H_{10}	0.69
c-C_6H_{12}	0.54
C_6H_{12}	0.64
$C_2Cl_3F_3$	0.44
CS_2	0.49
CCl_4	0.36
C_2Cl_4	0.40

*Pour les solvants, voir légende du tableau 2.

Nous voyons donc l'intérêt que présente l'étude de plusieurs bandes dans l'interprétation des chiffres obtenus. Un très petit nombre de solvants seulement donne des résultats en accord avec l'hypothèse de l'existence du seul effet de diffusion rotationnelle. Dans la plupart des cas on ne peut pas négliger l'effet de la fluctuation du potentiel intermoléculaire.

Fonctions de corrélation

Les figs. 4 et 5 donnent quelques-unes des courbes obtenues pour ln $\Phi(t)$ en fonction de t. Nous voyons qu'elles comprennent, comme prévu (5) et comme on l'observe généralement (14), une partie parabolique à l'origine et une partie linéaire qui commence au voisinage de $t_d = 0.35$ ps. Avant de procéder à l'examen détaillé de ces courbes et à leur interprétation, nous allons tout d'abord rappeler quelques résultats théoriques et en tirer des conclusions qui nous seront utiles par la suite.

La fonction de corrélation nous fournit des

Can. J. Chem. Downloaded from www.nrcresearchpress.com by 210.87.254.6 on 09/05/12
For personal use only.

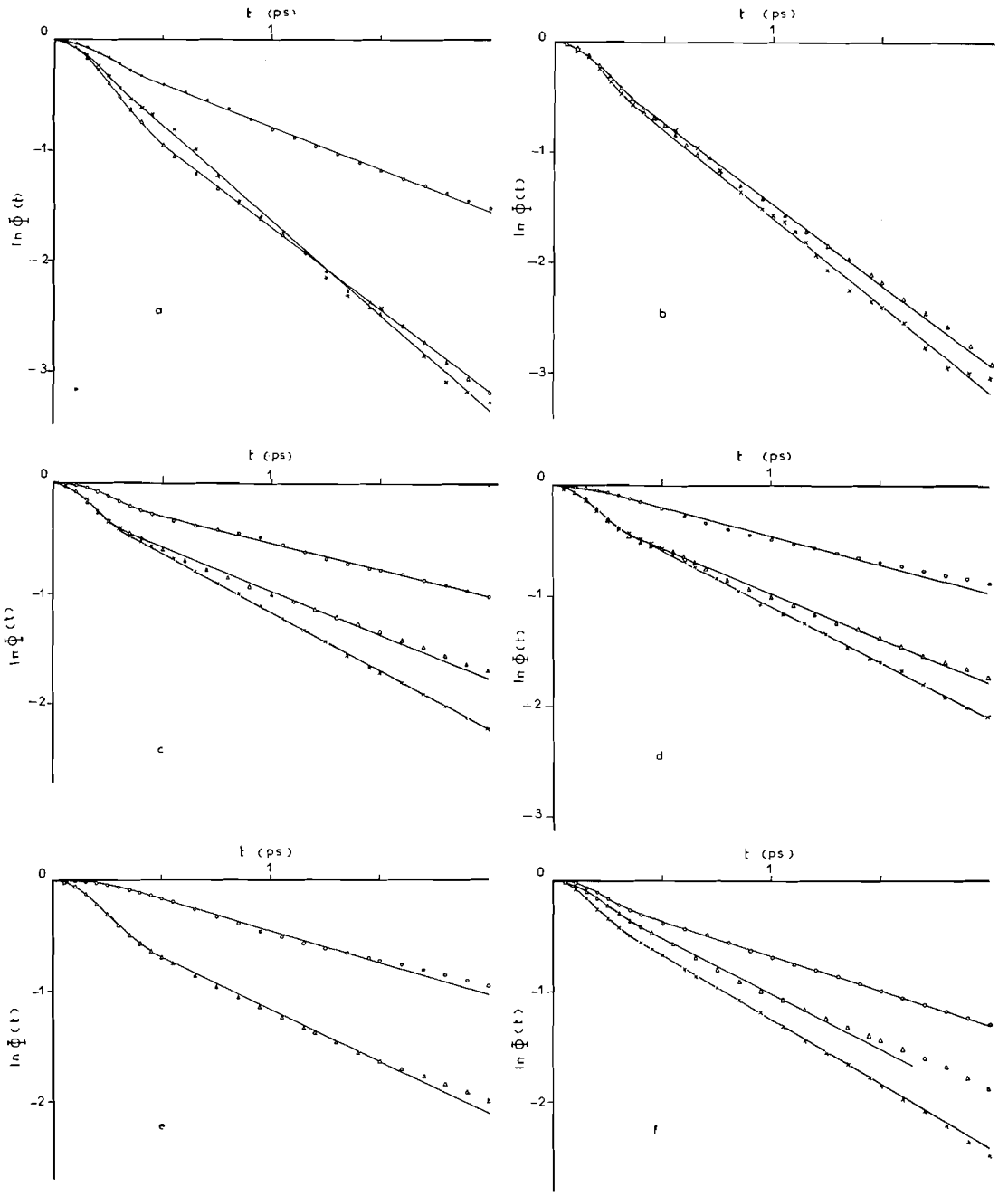

FIG. 4. ln $\Phi(t)$ de ν_1, ν_2 et ν_3 dans différents solvants ×, ν_1; ○, ν_2; △, ν_3. Solvants: *a*, hexane; *b*, cyclopentane; *c*, tétrachlorure de carbone; *d*, tétrachloroéthylène; *e*, 1,1,2-trichlorotrifluoroéthane; *f*, sulfure de carbone.

renseignements sur le comportement moyen d'une molécule en fonction du temps (5). Si l'on admet que la rotation et la diffusion rotationnelle sont les processus les plus importants dans l'élargissement des bandes, $\Phi(t)$ correspond à la valeur moyenne à l'instant t de l'expression $\vec{u}(0).\vec{u}(t)$ dans laquelle $\vec{u}$ représente le vecteur unitaire de l'axe parallèle à la direction de la vibration envisagée: $\Phi(t) = \langle \vec{u}(0).\vec{u}(t) \rangle$. Dans le cas d'une vibration parallèle à l'axe, $\Phi(t) = \cos \varphi$,

Can. J. Chem. Downloaded from www.nrcresearchpress.com by 210.87.254.6 on 09/05/12
For personal use only.

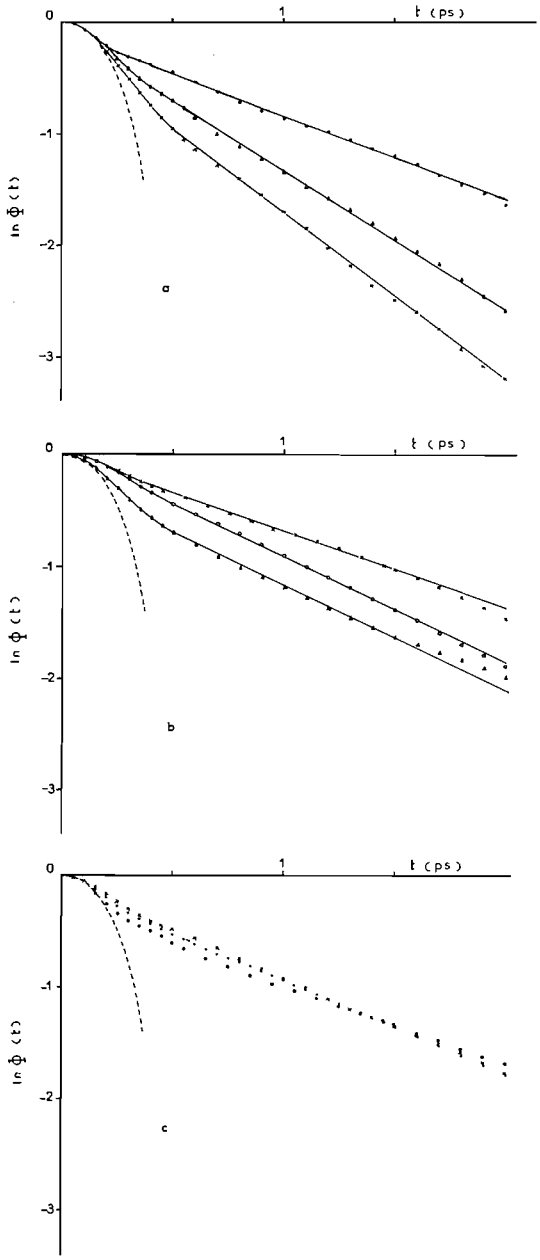

FIG. 5. ln $\Phi(t)$ de ν_3 dans différents solvants: ---, rotateur libre. Solvants: *a*, ×, hexane; △, hexène; ○, bromoforme; *b*, △, 1,1,2-trichlorotrifluoroéthane; ○, nitrométhane; ×, diiodométhane; *c*, ○, tétrachlorure de carbone; ●, chloroforme; ×, dichlorométhane.

φ étant l'angle dont a tourné, en moyenne, la molécule entre les instants 0 et t. L'interprétation est moins immédiate dans le cas d'une vibration perpendiculaire. Si nous attachons à la molécule en rotation un système d'axes cartésiens, une composante donnée d'une vibration perpendiculaire dégénérée tourne d'un angle que l'on peut calculer facilement et qui dépend de sa position par rapport aux axes; faisant ensuite la moyenne sur toutes les orientations possibles, on trouve qu'une composante perpendiculaire a tourné en moyenne, pendant le même temps t, d'un angle ψ tel que

$$[5] \qquad \cos^2\psi = \cos\varphi$$

Ce calcul ne s'applique qu'à des angles inférieurs à $\pi/2$. Nous avions présenté, dans une publication antérieure (15) une formule légèrement différente de [5] en considérant un temps suffisamment court pour que l'axe de rotation n'ait pas changé, mais les deux formules donnent le même résultat

$$[6] \qquad \psi^2 = \varphi^2/2$$

pour des petits angles c'est à dire pratiquement pour des angles φ inférieurs à 60°. De l'égalité [5] découle une relation intéressante entre les fonctions de corrélation relatives à une bande parallèle et à une bande perpendiculaire.

Considérons d'abord les parties exponentielles des fonctions de corrélation, c'est-à-dire les droites des graphiques ln $\Phi(t)$. En supposant, en première approximation, que ces droites passent par l'origine, nous pouvons écrire $\Phi(t) = e^{-t/\tau}$ pour les bandes parallèles et $\Phi(t) = e^{-t/\tau'}$ pour les bandes perpendiculaires. L'égalité [5] nous donne

$$[7] \qquad \tau' = 2\tau$$

Les bandes correspondantes présenteraient un profil de Lorentz et des largeurs respectives

$$[8] \qquad (\Delta\nu_{1/2})_{\parallel} = 1/\pi c\tau$$

et

$$[9] \qquad (\Delta\nu_{1/2})_{\perp} = 1/\pi c\tau' = \tfrac{1}{2}(\Delta\nu_{1/2})_{\parallel}$$

Nous retrouvons ainsi très simplement la relation déjà signalée plus haut. En réalité les droites ne passent pas par l'origine et les conclusions développées ci-dessus ne sont qu'approchées. Toutefois en considérant le cas où l'écart est le plus grand, celui de la bande ν_3 dans l'hexane, pour laquelle nous avons une ordonnée à l'origine voisine de -0.20, et en traçant une droite moyenne passant cette fois par l'origine nous obtenons $\tau = 0.61$ ps au lieu de la valeur 0.64 initialement trouvée. Cette approximation est donc acceptable dans la totalité des cas pour

Can. J. Chem. Downloaded from www.nrcresearchpress.com by 210.87.254.6 on 09/05/12
For personal use only.

$t > 0.35$ ps et le profil se rapproche de celui de Lorentz dans la partie centrale de la bande. La partie linéaire des courbes ln $\Phi(t)$ commence pour des valeurs de l'angle φ ou ψ qui ne dépassent généralement pas 60°. Il est donc légitime de développer cos φ et $e^{-t/\tau}$ en se limitant aux premiers termes. On obtient ainsi

$$1 - \frac{\varphi^2}{2} = 1 - \frac{t}{\tau}$$

ou

$$\varphi^2 = 2\frac{t}{\tau}$$

et

$$\psi^2 = \frac{t}{\tau}$$

Ces relations expriment que nous sommes dans la région de diffusion rotationnelle où, par définition, nous avons

$$\varphi^2 = 4Dt$$

et

$$\psi^2 = 2Dt$$

D étant la constante de diffusion correspondante. Nous avons donc

$$[10] \qquad D = \frac{1}{2\tau} = \frac{1}{\tau'}$$

Voyons maintenant ce qui se passe aux temps très courts, dans la partie non linéaire des courbes. On peut écrire

$$\Phi(t) = 1 - \frac{\varphi^2}{2} = 1 - \frac{\dot{\varphi}^2}{2}t^2$$

$\dot{\varphi}$ représentant la vitesse angulaire quadratique moyenne. Appliquant le théorème de l'équipartition de l'énergie cinétique et tenant compte du fait qu'une moléculaire linéaire possède deux degrés de liberté de rotation, on obtient

$$[11] \qquad \dot{\varphi}^2 = 2kT/I$$

La fig. 4 représente les fonctions de corrélation liées à plusieurs vibrations fondamentales, dans des solvants variés; celles de ν_1 et ν_3 devraient être confondues et celles de ν_2 se déduire des précédentes par une affinité de rapport 1/2. Nous voyons que ceci n'est jamais exactement vérifié, mais s'en rapproche le plus dans le cas de l'hexane. Nous avons porté dans le tableau 4 les constantes τ, τ' et D calculées d'après la pente des droites et les relations [10]. Les chiffres indiqués pour D, dans le cas de ν_3, coïncident sensiblement avec ceux du tableau 3, comme on pouvait s'y attendre.

TABLEAU 4
Constantes tirées de ln $\Phi(t)$

Solvant*		τ ou τ'(ps)	$D(10^{12}\,s^{-1})$	t_d(ps)
n-C_6H_{14}	ν_1	0.60	0.83	0.30
	ν_2	1.23	0.81	0.35
	ν_3	0.64	0.78	0.45
c-C_5H_{10}	ν_1	0.63	0.79	0.35
	ν_3	0.68	0.74	0.35
CS_2	ν_1	0.86	0.58	0.35
	ν_2	1.61	0.62	0.35
	ν_3	1.00	0.50	0.35
CCl_4	ν_1	0.94	0.53	0.35
	ν_2	2.08	0.48	0.40
	ν_3	1.27	0.39	0.35
C_2Cl_4	ν_1	1.00	0.50	0.30
	ν_2	1.90	0.53	0.30
	ν_3	1.24	0.40	0.35
C_6H_6	ν_1	0.73	0.68	0.35
	ν_2	1.48	0.67	0.45
	ν_3	0.96	0.50	0.35
$C_2Cl_3F_3$	ν_2	1.75	0.57	0.35
	ν_3	1.07	0.47	0.40
C_6H_{12}	ν_3	0.79	0.63	0.35
CH_3CN	ν_1	0.80	0.62	0.15
	ν_2	1.60	0.62	0.50
$(CH_3)_2CO$	ν_1	0.84	0.59	0.40
	ν_3	0.69	0.72	0.40
$C_4H_8O_2$	ν_3	1.06	0.47	0.35
CH_3NO_2	ν_3	1.03	0.48	0.15
$CHCl_3$	ν_1	non linéaire		
	ν_3	1.16	0.43	0.30
$CHBr_3$	ν_3	1.31	0.38	0.25
CH_2Cl_2	ν_3	1.13	0.44	0.30
CH_2I_2	ν_1	non linéaire		
	ν_3	1.50	0.33	0.35

*Pour les solvants, voir légende du tableau 2.

Sur la fig. 5 sont tracées les fonctions de corrélation se rapportant à la même vibration ν_3 dans plusieurs solvants; nous y avons ajouté la courbe correspondant à la rotation libre, tirée de la relation [11]. Nous voyons que la courbe expérimentale reste au départ assez proche de celle du rotateur libre, pour un certain nombre de solvants non polaires et en particulier l'hexane et qu'au contraire, elle se situe toujours au dessus pour les solvants polaires. Sur la fig. 5c où sont portées les fonctions relatives à CCl_4, CH_2Cl_2, $CHCl_3$, nous constatons que le comportement aux temps longs est sensiblement le même, mais qu'il diffère aux temps courts, le temps de rotation libre se montrant plus grand pour CCl_4. D'après toutes ces courbes le temps t_d, à partir duquel commence la diffusion rotationnelle, est voisin de 0.35 ps et de l'ordre de grandeur du temps de libre parcours moyen d'une molécule. Le temps de rotation libre, maximal et voisin de 0.15 ps dans les substances non polaires, est inférieur à 0.05 ps, et donc non lisible sur les courbes, dans la plupart des solvants polaires. L'angle de rota-

Can. J. Chem. Downloaded from www.nrcresearchpress.com by 210.87.254.6 on 09/05/12
For personal use only.

tion correspondant à t_d varie avec le solvant; il est compris entre 60° pour l'hexane et 38° pour l'iodure de méthylène. L'angle de rotation libre se montre bien inférieur à cette valeur, contrairement à ce qui avait été dit dans un article précédent (15).

En résumé, l'examen des fonctions de corrélation nous apporte de nombreux renseignements, complémentaires de ceux fournis par les largeurs de bandes et en accord avec les conclusions tirées de celles-ci. Notons toutefois qu'ici nous n'avons plus aucun critère qui nous permette d'apprécier l'importance relative des différents effets, car presque toutes les courbes ln $\Phi(t)$ présentent une partie rectiligne, même dans les cas où, d'après les largeurs de bandes, nous avions jugé que les fluctuations de fréquence dues aux variations du potentiel intermoléculaires se montraient assez grandes.

Deuxième et quatrième moments

Aux temps courts, cos $(\omega - \omega_0)t$, dans la relation [1], peut se développer en fonction de t. Compte tenu de la définition des moments, [3], il vient

$$[12] \qquad \Phi(t) = 1 - M(2)\frac{t^2}{2!} + M(4)\frac{t^4}{4!}$$

D'autre part les moments $M(2)$ et $M(4)$ se calculent à partir des équations classiques du mouvement de rotation et des valeurs moyennes des dérivées successives, par rapport au temps, de l'angle de rotation. Dans le cas des vibrations parallèles des molécules linéaires on a (5)

$$[13] \qquad M(2) = \langle \dot{\varphi}^2 \rangle = \frac{2kT}{I}$$

et

$$[14] \qquad M(4) = 8\left(\frac{kT}{I}\right)^2 + \frac{\langle C^2 \rangle}{I^2}$$

où C représente le moment des forces de rappel agissant sur la molécule, par unité d'angle d'écart.

Le développement [12] n'est autre que celui de cos φ.

$$\cos\varphi = 1 - M(2)\frac{t^2}{2!} + M(4)\frac{t^4}{4!}$$

Nous avons de même

$$\cos\psi = 1 - M'(2)\frac{t^2}{2!} + M'(4)\frac{t^4}{4!}$$

et l'application de la relation [5] nous fournit l'égalité [15] $M'(2) = M(2)/2$, et une autre, que nous n'expliciterons pas ici, pour $M(4)$.

TABLEAU 5
Moments

Solvant*		$M(2)$ (10^{24} s^{-2})	$M(4)$ (10^{50} s^{-4})	$\langle C^2 \rangle^{1/2}$ (kT/rad)
n-C_6H_{14}	ν_1	13.1	9.6	3.8
	ν_2	6.1	3.1	
	ν_3	15.0	13.3	4.8
c-C_5H_{10}	ν_1	14.0	10.6	4.1
	ν_3	12.2	8.7	3.5
CS_2	ν_1	15.6	18.1	5.9
	ν_2	6.1	3.1	
	ν_3	9.0	6.2	
CCl_4	ν_1	14.7	15.4	5.3
	ν_2	4.2		
	ν_3	16.9	22.7	6.8
C_2Cl_4	ν_1	14.4	15.6	5.4
	ν_2	2.0		
	ν_3	12.2	9.9	3.8
$C_2Cl_3F_3$	ν_3	12.0	8.7	3.6
C_6H_{12}	ν_3	13.3	11.4	4.4
CH_3CN	ν_1	6.5		
CH_3NO_2	ν_3	6.0		
$CHCl_3$	ν_3	12.0	12.3	4.6
$CHBr_3$	ν_3	15.3	24.6	7.1
CH_2Cl_2	ν_2	2.7		
	ν_3	9.4		
CH_2I_2	ν_3	5.6		

*Pour les solvants, voir légende du tableau 2.

Dans le cas de N_2O et à la température, $T = 313$ °K, de nos expériences $M(2) = 12.9$ 10^{24} c.g.s. (ν_1 et ν_3).

Nous avons porté dans le tableau 5 les valeurs des moments dans tous les cas où l'absorption dans les ailes est connue avec précision. Dans la colonne donnant $M(2)$ nous voyons que l'accord entre valeur théorique et valeur expérimentale est généralement satisfaisant pour les solvants non polaires pour ν_1 et ν_3. Par contre le moment mesuré est très inférieur au moment théorique dans l'acétonitrile, le nitrométhane, le dichloro- et le diiodométhane; dans ces solvants la vitesse angulaire est donc inférieure à celle qui résulterait de la relation [13]; la cause en est probablement l'existence d'une interaction relativement forte entre molécules de solvant et de soluté.

Nous n'avons calculé le quatrième moment que dans les cas où le deuxième moment est voisin de sa valeur théorique et nous en avons alors déduit le couple quadratique moyen en prenant kT (216 cm^{-1}) comme unité. Ces valeurs peuvent être comparées à celles données par Gordon (6) pour CO liquide ($4kT$) et par Cabana *et al.* (16) pour CH_4 (280 cm^{-1}); les chiffres obtenus semblent donc raisonnables.

La détermination des fonctions de corrélation et surtout celle des moments présente généralement de grandes difficultés. Dans le cas d'une molécule simple comme N_2O, elle se montre toutefois suffisamment précise pour nous permettre de comparer la théorie et l'expérience et de calculer un certain nombre de grandeurs relatives à la dynamique moléculaire en phase liquide.

1. S. BRATOS et J. RIOS. C. R. Acad. Sci. **269**, 90 (1969).
2. S. BRATOS, J. RIOS, et Y. GUISSANI. J. Chem. Phys. **52**, 439 (1970).
3. J. JACOB, J. LECLERC, et J. VINCENT-GEISSE. J. Chim. Phys. **66**, 970 (1969).
4. J. SOUSSEN-JACOB, J. VINCENT-GEISSE, D. BEAULIEU, et J. TSAKIRIS. J. Chim. Phys. **67**, 1118 (1970).
5. R. G. GORDON. Advances in magnetic resonance. *Edited by* J. S. Waugh. Academic Press, Inc., New York. Vol. 3. 1968. p. 1.
6. R. G. GORDON. J. Chem. Phys. **41**, 1819 (1964).
7. M. L. GRENIER-BESSON. Cah. Phys. **68**, 5 (1956); **69**, 8 (1956).
8. J. PLIVA. J. Mol. Spectrosc. **12**, 360 (1964).
9. J. PLIVA. J. Mol. Spectrosc. **27**, 461 (1968).
10. R. P. GROSSO et T. K. MC CUBBIN. J. Mol. Spectrosc. **13**, 240 (1964).
11. K. LAKSHMI, K. N. RAO, et H. H. NIELSEN. J. Chem. Phys. **24**, 811 (1956).
12. E. K. PLYLER, E. D. TIDWELL, et A. G. MAKI. J. Res. Nat. Bur. Stand. **68A**, 79 (1964).
13. L. D. FAVRO. Phys. Rev. **119**, 53 (1960).
14. C. E. FAVELUKES, A. A. CLIFFORD, et B. CRAWFORD. J. Phys. Chem. **72**, 962 (1968).
15. J. VINCENT-GEISSE, J. SOUSSEN-JACOB, et NGUYEN TAN TAI. C. R. Acad. Sci. **268**, 1020 (1969).
16. A. CABANA, R. BARDOUX, et A. CHAMBERLAND. Can. J. Chem. **47**, 2915 (1969).

Can. J. Chem. Downloaded from www.nrcresearchpress.com by 210.87.254.6 on 09/05/12
For personal use only.

Can. J. Chem. Downloaded from www.nrcresearchpress.com by 210.87.254.5 on 09/05/12
For personal use only.

Spectroscopic studies on some chromones

JAMES B. GALLIVAN
American Cyanamid Company, Central Research Division, Stamford, Connecticut

Received June 22, 1970

Absorption and luminescence spectra were measured for chromone, 4-chromanone, and four photoproducts formed by the addition of extramolecular multiple bonds to photo-excited chromone. Absorption spectra in polar and non-polar solvents at room temperature revealed a low lying $n \rightarrow \pi^*$ singlet transition in all of these systems. The cycloaddition products and 4-chromanone showed a weak fluorescence in polar solvents which was not observed in non-polar solvents, suggesting a solvent reordering, or at least increased mixing of low lying n,π^* and π,π^* singlet states. No fluorescence could be detected from chromone in either type of solvent. At 77 °K in polar solvents, all of these systems displayed a concentration independent, intense phosphorescence of intermediate lifetime (25 to 200 ms). The lifetime data, combined with the vibrational analyses of the phosphorescence spectra, phosphorescence polarization results, and oxygen induced singlet–triplet absorption spectra support the concept of a lowest energy triplet state of mixed orbital character. More detailed studies on chromone demonstrated a concentration dependent phosphorescence in non-polar solvents, with the "normal" chromone phosphorescence dominant below 10^{-4} *M*. At higher concentrations a lower energy, broad band phosphorescence was observed, which in spite of physical aggregation in the ground state, can be ascribed to a chromone exciplex.

Canadian Journal of Chemistry, **48**, 3928 (1970)

Introduction

The para oxo-benzopyran, chromone, has received far less spectroscopic attention than its ortho isomer, coumarin. Much of the interest in coumarin results from its widespread occurrence in plant life and its physiological effects on plants and animals (1). In certain respects, a spectroscopic study of chromone is more intriguing, and potentially of more value to photochemists because of the possibility of low lying n,π^* excited states, which are not expected in the lactone, coumarin. Differences in the photochemical reactivity of these two systems have been reported and the role of lowest triplet states of different orbital character has been suggested (2).

To provide some of the essential spectroscopic data on chromone, absorption and luminescence measurements were carried out at various concentrations in several solvents at room temperature and at 77 °K. Because of some interesting observations made on chromone itself, the study was extended to include 4-chromanone and a number of cyclo-addition products resulting from photochemical reactions of chromone with extramolecular multiple bonds. The gross absorption and luminescence features are similar for the systems studied, with patterns of excited state energies, spectral profiles, and phosphorescence lifetimes providing additional insight into the electronic distribution and structural properties of each system.

Various experimental techniques including polarized phosphorescence, singlet–triplet absorption by oxygen perturbation, and electron spin resonance (e.s.r.) spectra were used to examine the nature of the phosphorescent state. The results of these experiments together with criteria available for designating excited state orbital character were used to assess the nature of the lowest triplet state of the chromones. Certain of the results led to contradictory conclusions, while others were ambiguous and could be rationalized in favor of either an n,π^* or π,π^* assignment. These results demonstrate the dangers of making orbital assignments based on a single criterion, and suggest that designations of mixed orbital character may be more appropriate for complex, particularly non-planar, carbonyl compounds.

Experimental

Details concerning the syntheses and purifications of the compounds used in this study have been reported elsewhere (2). All the essential information on solvents and instrumentation can be found in an earlier paper on coumarin (3). The high pressure cell used for oxygen induced singlet–triplet absorption spectra was modeled after the cell used by Evans (4).

Results and Discussion

Chromone

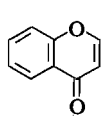

The ultra violet (u.v.) absorption spectrum of

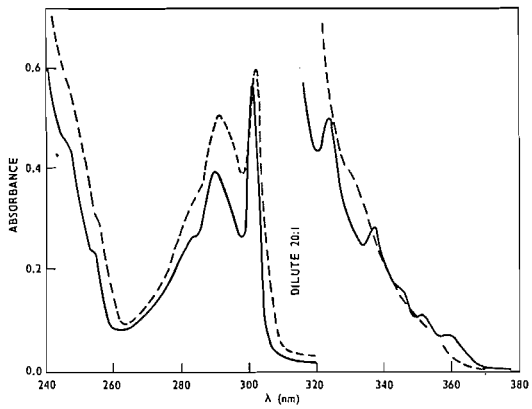

FIG. 1. Ultraviolet absorption spectra of chromone in 3 methylpentane (—) and 2-methyl-tetrahydrofuran (---) at room temperature. The long wavelength portion was run at 10^{-2} M in a 1 cm cell, the shorter wavelength portion at 5×10^{-4} M in a 1 mm cell.

chromone (Fig. 1) shows several strong bands in the 300 to 200 nm region, as well as a much weaker transition to longer wavelengths. Band maxima and extinction coefficients for the near u.v. absorption bands of chromone in 3-methylpentane (3MP) are given in Table 1. In 2-methyltetrahydrofuran (MTHF), the bands in the long wavelength, weak transition are broadened and blue shifted, so that band maxima are not clearly indicated. The magnitude of the extinction coefficients, and the direction of the solvent effect are both consistent with an $n \rightarrow \pi^*$ assignment to this transition (5). The strong transitions are broadened and slightly (1–2 nm) red shifted in MTHF. When coupled with the intensity of these bands, these features clearly indicate the $\pi \rightarrow \pi^*$ nature of these transitions.

In polar solvents (ethanol or MTHF) at 77 °K, chromone exhibits an intense, deep blue phosphorescence of short lifetime. At 10^{-3} M in MTHF, an apparent mean lifetime of 38 ($\pm$5) ms was obtained from the initial slope of the decay curves. Beyond ~1.5 lifetimes a longer lived component of 65 $\pm$ 15 ms was also observed. These lifetimes showed a strong solvent dependence and varied significantly as a function of concentration in a given solvent. These features did not change as the chromone was passed through successively more rigorous purification procedures, indicating that these are inherent properties of the molecule. Because of these complexities, a more thorough analysis of the phosphorescence lifetime of chromone, both from the experimental and theoretical points of view, is probably warranted. Within the broader context of this study it suffices to say that such factors as strong solvent interactions, which may influence the orbital composition of the lowest triplet state, and the prospects of emission from several different conformations of the triplet state, must be considered.

TABLE 1

Band maxima and approximate extinction coefficients for the near ultra violet transitions of chromone in 3-methylpentane at 25 °C

Band system	λ_{max} (nm)	$\log \varepsilon$ (M^{-1} cm^{-1})
A	360, 352, 345 337, 324	0.70, 0.78, 0.90* 1.18, 1.30
B	301, 290, 283	4.04, 3.90, 3.72
C	255, 246, 239 227, 223, 216 202	3.68, 3.93, 4.09 4.17, 4.20, 4.21 4.50

*Because of the underlying absorption from the tail of the strong band at 301 nm, there is an uncertainty of $\pm$25% in these values of ε.

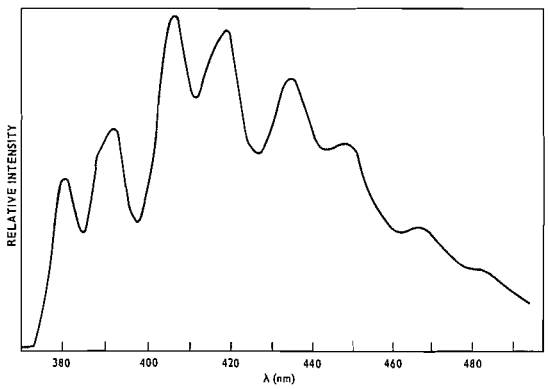

FIG. 2. Phosphorescence spectrum of 10^{-3} M chromone in 2-methyltetrahydrofuran at 77 °K.

The phosphorescence spectrum (Fig. 2) shows a complex vibrational profile, consisting of what appears to be two separate ~1650 cm^{-1} progressions built on the 0–0 band at 380 nm and another on the 0 + ~700 cm^{-1} band at ~391 nm. The spacing probably corresponds to the dominant ~1650 cm^{-1} progression observed in the phosphorescence spectra of n,π^* carbonyl triplets such as benzophenone and acetophenone, and attributed to the symmetric carbonyl stretching vibration (6). The 0–1 band and the other bands spaced at ~n × 1650 cm^{-1} from it, are somewhat distorted suggesting contributions from the ~700 cm^{-1} and other ring vibrations.

Can. J. Chem. Downloaded from www.nrcresearchpress.com by 210.87.254.5 on 09/05/12
For personal use only.

Can. J. Chem. Downloaded from www.nrcresearchpress.com by 210.87.254.5 on 09/05/12
For personal use only.

Contributions from these lower energy vibrations are clearly indicated in the phosphorescence of acetophenone (6), but they do not display the intensity of the 0–1 band of chromone. The presence of the carbonyl within the ring system might be expected to result in a more prominent contribution from a simultaneously excited ring vibration.

All attempts to observe an e.s.r. triplet signal from chromone were unsuccessful. This fact, coupled with the relatively short lifetime (38 ms) and the small energy gap ($\sim$1500 cm^{-1}) between the lowest singlet and triplet states, is at least suggestive of a lowest triplet state of n,π^* character. In addition, the phosphorescence (0–0 band) was found to be positively (+6, +10, and +5%) polarized with respect to excitation into the π,π^* transitions at 323, 300, and 255 nm, respectively. These results indicate significant in-plane polarization and based on first order spin–orbit coupling considerations could be used as a criterion for n,π^* classification of the lowest triplet state (7). Any such conclusion would have to be qualified, however, since clear-cut distinctions between $n \rightarrow \pi^*$ and $\pi \rightarrow \pi^*$ transitions become obscured as a molecule deviates from planarity. In addition, contributions from other than the 0–0 band at the emission wavelength monitored (380 nm) could yield parallel results through vibronic spin–orbit interactions (8). In fact, it would seem that in systems of low symmetry and uncertain geometry, polarization results of the magnitude noted here are of questionable value in making orbital assignments.

Attempts to measure the singlet–triplet absorption spectrum by phosphorescence excitation and by direct absorption proved to be unsuccessful. The main difficulties in measuring the $S_0 \rightarrow T_1$ transition are associated with the small energy gap between S_1 and T_1, and consequently the necessary overlap of the spin-allowed and spin-forbidden absorption bands at high chromone concentrations. Whereas the heavy atom perturbations failed to clearly resolve the $S_0 \rightarrow T_1$ contribution in the tail of the $S_0 \rightarrow S_1$ band, the O_2 perturbation technique (4) did so quite clearly (Fig. 3). The spectrum and single maximum are features which resemble the $S_0 \rightarrow T_1$ absorption spectra of 4-hydroxy and 4-methoxy acetophenone under similar conditions (9). Comparison with Fig. 2 demonstrates the good overlap between this absorption and the 0–0 band of the phosphorescence.

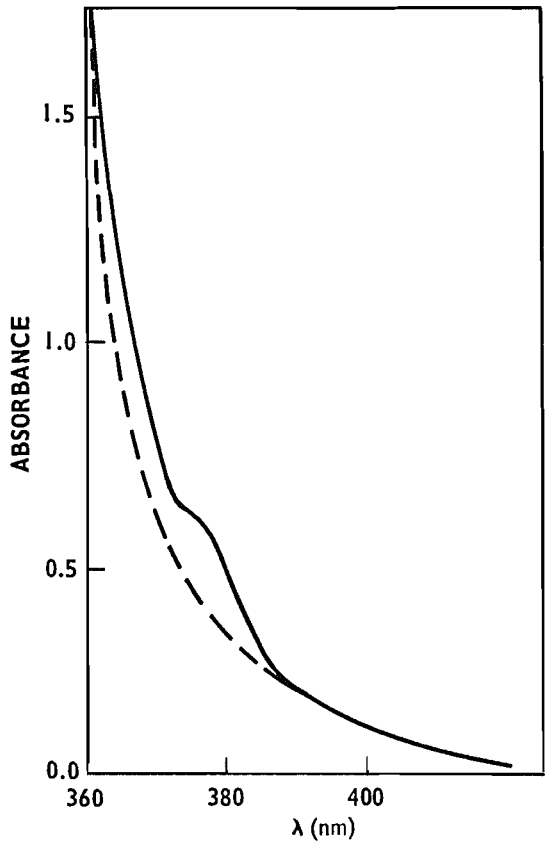

FIG. 3. Long wavelength tail of 0.1 *M* chromone in chloroform at atmospheric pressure (---) and under 1600 p.s.i. of O_2 (—).

The enhancement of $S_0 \rightarrow T_1$ absorption in aromatic carbonyls under O_2 pressure has been used (9) as a criterion for designating the lowest triplet state as π,π^*, and parallels a similar criterion used for heavy atom enhancement (10). The basis for these criteria is that n,π^* triplets undergo inherently strong spin–orbit coupling with the singlet manifold, whereas this coupling is inherently weak for π,π^* lowest triplets. As a consequence the magnitude of the spin–orbit coupling induced by the external perturbation due to oxygen or heavy atoms, is inconsequential in the case of n,π^* systems already exhibiting relatively strong $S_0 \rightarrow T_1$ absorption. In the case of π,π^* systems with vanishingly weak $S_0 \rightarrow T_1$ absorption, the same external perturbation increases spin–orbit coupling to an extent that makes the transition observable. The extinction coefficient of the induced absorption at 380 nm for chromone in chloroform under 1800 p.s.i.

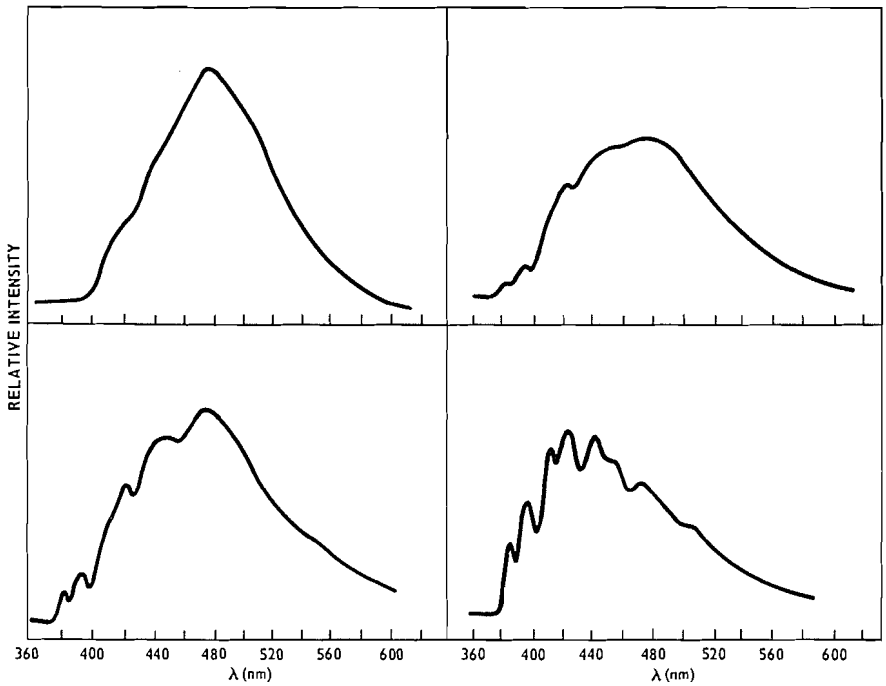

FIG. 4. Phosphorescence spectra of chromone in 3 MP at 77 °K as a function of concentration. Top L, 5×10^{-3} M; top R, 5×10^{-4} M; bottom L, 10^{-4} M; bottom R, 10^{-5} M.

of O_2 is ~ 0.1 M cm^{-1} from which a radiative lifetime for the triplet state of ~ 40 ms. can be estimated (11). By comparison, ε(380 nm) at atmospheric pressure is at least a factor of 20 smaller, so that τ_0 is certainly approaching 1 s. These results and calculations underscore π,π^* character in the lowest triplet state, but is such a designation of this state really warranted?

Dym and Hochstrasser (12) have pointed out that aromatic ketones having molecular symmetry lower than the C_{2v} symmetry of the C—C(O)—C group, likely have configurationally mixed states and no longer have strictly n and π type orbitals. Such designations may also be inappropriate for a non-symmetrical, non-planar system such as chromone. Recently Hirota (13) reported that the lowest triplet state of 3,4-dimethylacetophenone in a durene host crystal is of n,π^* character, based on the exceptionally large zero field splitting parameters ($D \sim 0.25$ cm^{-1}) observed. In durene he reported a mean phosphorescence lifetime of 30 ± 10 ms, but we have found that this lifetime increased to ~ 70 ms in 3MP and ~ 200 ms in ethanol. In the latter solvent, a D of ~ 0.11 cm^{-1} was found, precisely the magnitude expected for a π,π^* triplet state. These observations demonstrating the solvent reorientation of essentially isoenergetic triplet levels and/or the phenomenon of configurational mixing of n and π type orbitals, suggest that it may be more appropriate to deemphasize simple orbital designations. Based on the accumulated experimental observations for chromone, where different criteria suggest different orbital character, it may be most appropriate to stress the mixed orbital character of the lowest triplet state.

In 3MP at 77 °K, chromone phosphorescence shows a striking concentration dependence. At $\sim 10^{-5}$ M, the spectrum is essentially identical to that observed in MTHF, while a broad structureless component of significantly longer lifetime appears at lower energies at higher concentrations. At 5×10^{-3} M, the broad band emission completely dominates the spectrum (Fig. 4), and τ_m measured at 470 nm is ~ 0.4 s, an order of magnitude longer than that measured in MTHF.

The concentration dependence of chromone phosphorescence in 3MP at 77 °K, parallels the observations associated with excimer fluorescence (14). Although excimer phosphorescence has been reported for several systems (15), some of the

Can. J. Chem. Downloaded from www.nrcresearchpress.com by 210.87.254.5 on 09/05/12
For personal use only.

Can. J. Chem. Downloaded from www.nrcresearchpress.com by 210.87.254.5 on 09/05/12
For personal use only.

reports have been disputed and the phenomenon has not been demonstrated to be a significant radiative process. Because excimer phosphorescence is at least suggested by the spectra, this concentration dependent emission was studied in greater detail. At 5×10^{-3} *M* in 3MP at room temperature, the u.v. absorption spectrum showed no indication of any ground state interaction that could be construed as dimer or charge-transfer complex formation. However, on cooling to 77 °K, the chromone tended to aggregate and much of the solid material came out of solution. Because of the aggregation and scatter due to the solid material, the glass was not transparent and no meaningful absorption spectra were obtained. The same complications, to a slightly lesser degree, were encountered with 5×10^{-4} *M* solutions. Because of this ground state association (aggregation) which occurred on cooling, one must be careful about terming the emitting species an excimer or an exciplex (16). The visible cloudiness and long wavelength scattering noted in the absorption spectra indicate that the ground state aggregation involves large numbers of physically associated molecules. On excitation, the energy is delocalized over an unknown number of molecules and this microcrystalline unit phosphorescence as a separate entity. Since there is no evidence that a chemically stable ground state complex is formed, the radiative unit in this case could be termed an exciplex. At 10^{-3} *M* in 3MP at 77 °K, the phosphorescence is depolarized for all excitation wavelengths, a result consistent with emission from a conglomerate of solute molecules. No e.s.r. signal could be detected from such a sample, in spite of the relatively long lived (0.4 s) phosphorescence.

At room temperature in degassed solutions, and at 77 °K in both polar and non-polar glasses, no fluorescence could be detected from chromone. Thus, the luminescence features of chromone are essentially those of an aromatic ketone such as acetophenone, with the total luminescence being phosphorescence. The appearance of at least several components in the phosphorescence decay curves is a puzzling, yet intriguing, feature. The possibility of emission from several different lowest triplet state conformations seems feasible, since molecular models (Dreiding) indicate that the γ-pyrone ring is not strictly planar in the ground state. A number of different geometrical configurations would appear possible in the relatively high energy (~76 kcal) triplet state. The energy differences between different conformations may be unresolved by low resolution spectroscopy, yet may influence spin–orbit coupling factors sufficiently to yield different lifetimes.

Chromone Photoadducts

Chromone undergoes photoaddition reactions to olefins and acetylenes, with the 1:1 adducts being primary photoproducts (2). The adducts formed on reaction with tetramethylethylene (**1**), 1,1 dimethoxyethylene (**2**), cyclopentene (**3**), and butyne-2 (**4**) are represented by the following structures, and the spectroscopic features of each were examined.

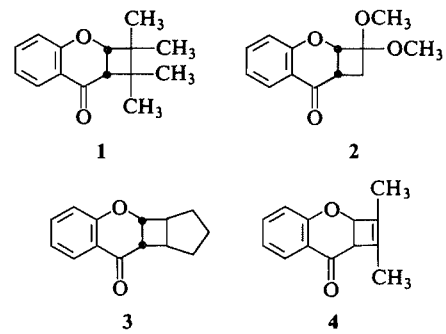

The near u.v. absorption spectra of the above compounds in 3MP are summarized in Table 2.

TABLE 2

Band maxima and approximate extinction coefficients for the near ultra violet transitions of some chromone photoadducts at 25 °C in 3-methylpentane

Compound	λ_{max}(nm)	log ε (M^{-1} cm^{-1})
1	375, 358	1.15, 1.47*
	323	3.52
	258, 250	3.90, 3.92
	217	4.37
2	368	0.92*
	322	3.52
	257, 251	3.82, 3.89
	217	4.36
3	375, 357	1.18, 1.40*
	321	3.66
	258, 250	3.71, 3.82
	216	4.27
4	364, 350	1.48, 1.60*
	317	3.37
	257, 250	3.65, 3.78
	216	4.26

*Because of the underlying absorption from the tail of the strong band at ~ 320 nm, there is an uncertainty of ±25% in these values of ε.

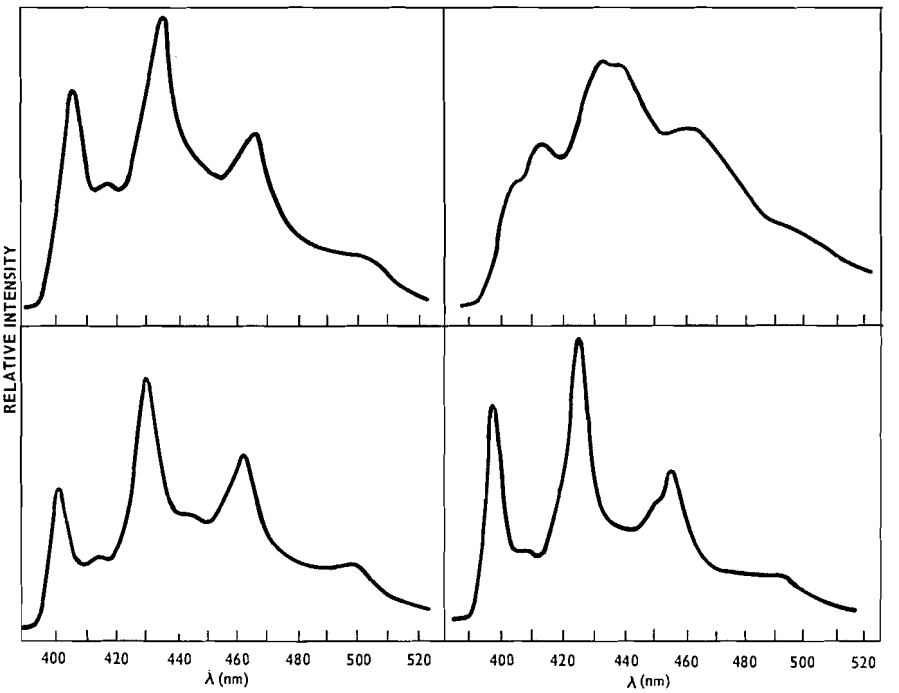

FIG. 5. Phosphorescence spectra of chromone-cyclo-adducts formed on reaction with top L, tetramethylethylene; top R, dimethoxyethylene; bottom L, cyclopentene; bottom R, butyne-2.

Comparison with Table 1 shows strong parallels between these systems and chromone. In MTHF and ETOH the weak transition is lost in the tail of the stronger transition to shorter wavelengths, while the intense bands display solvent broadening and red shifts. These features, as were noted for chromone, are consistent with n,π^* and π,π^* bands, respectively.

In MTHF at 77 °K an intense blue phosphorescence was observed from all four samples. The phosphorescence spectra are shown in Fig. 5 with significant differences in vibrational detail apparent. All spectra are red shifted with respect to chromone phosphorescence, with the triplet state energies increasing from 24 600 to 25 150 cm^{-1} across the series.

Whereas **1**, **3**, and **4** show well resolved vibrational bands, the spectrum of **2** is quite diffuse, with the 0–0 band considerably less intense than in chromone itself. The $\sim$1650 cm^{-1} carbonyl frequency dominates the spectra of the former three, so that the gross features resemble the n,π^* phosphorescence spectra of various aromatic carbonyls (6). It would appear that the more rigid four membered ring systems subject the pyrone ring to more strain and the only prominent vibration excited corresponds to the carbonyl stretching frequency. Restriction of the excitation energy to the benzo ring and the adjacent carbonyl results in the obvious parallel to acetophenone. The diffuseness of the phosphorescence of **2** must result from the strong mesomeric effect of the methoxy groups, which usually results in significant changes in the electronic spectra of simpler systems (17).

The mean phosphorescence lifetimes of **1** through **4** at 10^{-3} *M* in MTHF at 77 °K are $\sim$100, 230, 48, and 25 ms, respectively. As was the case with chromone, a longer lived component was resolved beyond a single lifetime in each case. These longer lived tails in the decay curves exceeded the indicated lifetimes by as little as 15% (**2**) and as much as 50% (**3**). The lifetime of **4** is $\sim$3 times that of acetophenone, while the 230 ms lifetime of **2** puts it in a region usually associated with lowest π,π^* triplets (7). However, polarization measurements on the 0–0 band of the phosphorescence of all four compounds show positive polarizations of comparable magnitudes ($\sim +10\%$) with respect to excitation into both

Can. J. Chem. Downloaded from www.nrcresearchpress.com by 210.87.254.5 on 09/05/12
For personal use only.

Can. J. Chem. Downloaded from www.nrcresearchpress.com by 210.87.254.5 on 09/05/12
For personal use only.

of the lower energy π,π^* transitions. This invariance of the phosphorescence polarization for these systems suggests that a common mechanism accounts for the polarization, and common orbital character may prevail throughout the series.

At room temperature in degassed ethanol solvents, all of these adducts exhibit very weak ($\phi_F \sim 10^{-4}$) broad band fluorescence with onsets at ~340 nm, and poorly resolved maxima near 377, 408, and 430 nm. The fluorescence of **2** was somewhat more intense (× 3) than the others, but even for that adduct, fluorescence was still very weak relative to the phosphorescence. At 77 °K in ethanol the intense phosphorescence is the only detectable luminescence so that the ϕ_P/ϕ_F ratio of **2** must be $\gg$100. The absence of fluorescence in 3MP solvent may be indicative of a solvent reversal of low lying singlet states of comparable energies, or at least may reflect increased mixing of these states due to a narrowing of the energy gap between states. The absorption spectra reveal that the $n \rightarrow \pi^*$ and $\pi \rightarrow \pi^*$ transitions are more strongly overlapped than is the case with chromone, so either of the two alternatives is plausible. Another possible interpretation of the weak fluorescence in the alcohol solvent is that the emitting species is protonated, a consideration which will be discussed in more detail when the results for 4-chromanone are examined (vide infra).

The phosphorescence lifetime data reflect the same complexities noted for chromone and at this stage can only be rationalized along parallel lines (vide supra). An obvious alternative explanation is to associate the multi-component decay curves with phosphorescent impurities. However, the internal consistencies within the series, the good agreement between the phosphorescence excitation spectra and absorption spectra, and the obvious parallels to chromone all suggest that the spectra observed are due to the indicated species.

4-Chromanone

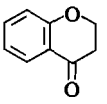

In contrast to chromone, the pyrone ring of 4-chromanone contains no double bond. Its ultraviolet absorption spectrum in 3MP is summarized in Table 3. In both MTHF and ETOH the weak bands at longer wavelengths disappear, while the stronger bands are red shifted. In these solvents a moderately intense phosphorescence (0–0 band at 393 nm) was observed. The spectrum (Fig. 6), shows the dominant ~1650 cm^{-1} vibrational progression, with the lower energy (~700 cm^{-1}) vibrations evident but weak.

TABLE 3

Band maxima and approximate extinction coefficients for the near ultra violet transitions of 4-chromanone in 3-methylpentane at 25 °C

λ_{max}(nm)	log $\varepsilon(M^{-1}\ cm^{-1})$
363, 347	1.00, 1.08*
322(sh), 312	3.51, 3.58
252, 246	3.92, 4.00
219(sh), 213	4.27, 4.43

*Because of the underlying absorption from the tail of the strong band at 312 nm, there is an uncertainty of ± 25% in these values of ε.

The phosphorescence lifetime of 4-chromanone in MTHF is 90 ms, as calculated from the initial slope of the decay curve. As with all the other chromones examined, a longer lived component (~120 ms) was evident beyond one lifetime. The 0–0 band of the phosphorescence shows positive (~ +8%) polarization with respect to 325 and 265 nm excitation. No e.s.r. triplet signal could be detected from either MTHF or ethanol solutions at 77 °K. The singlet–triplet absorption spectrum measured under 1600 p.s.i. of O_2 paralleled that observed for chromone with λ_{max} of the enhanced band at ~392 nm. All of these features match

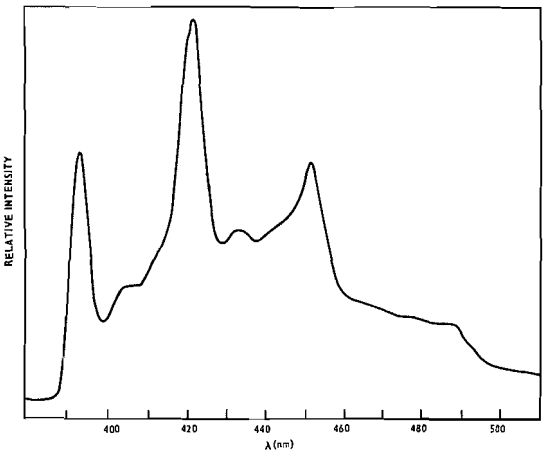

FIG. 6. Phosphorescence spectrum of 4-chromanone in 2-methyltetrahydrofuran at 77 °K.

Can. J. Chem. Downloaded from www.nrcresearchpress.com by 210.87.254.5 on 09/05/12
For personal use only.

those of chromone and the chromone–olefin cycloadducts, so the triplet warrants comparable classification.

The results reported here for 4-chromanone are at variance with those reported recently by Graber *et al.* (18). It is clear from these and other results that the excited state properties of 4-chromanone should be linked with chromone and its derivatives, rather than with the lactone coumarin and its derivatives. The basic differences in these two distinct types of compounds seem to be consistent with expected differences between lactones and simple aromatic ketones. Using acetophenone as a model compound, and considering the accumulated results on the chromones, it seems quite realistic to consider the excited state properties of the latter as essentially those of an aromatic ketone. The relatively long lifetimes, the multi-component character of the phosphorescence decay curves, and the greater complexity of the phosphorescence spectra, indicate that such a simplification is valid only as a first approximation. Whereas the simple aromatic ketones, such as acetophenone, have low lying triplet states that can be orbitally defined in a given environment (19), chromone and the related compounds studied here possess phosphorescent states that aren't as easily classified. The luminescence from all of these chromones consists almost entirely of a short lived phosphorescence in approximately the same spectral region, all showing the prominent $\sim 1650\ cm^{-1}$ vibrational progression associated with the symmetrical carbonyl stretching frequency. All of these features differ very strikingly from the luminescence features which characterize the coumarins (3).

In degassed ethanol solution at room temperature, 4-chromanone showed a very weak ($\phi_F \sim 10^{-4}$) broad band fluorescence, with λ_{max} at ~ 410 nm. Both the spectrum and intensity of the emission are comparable to the chromone photoadducts under similar conditions. As was the case with the chromone photoadducts, no fluorescence was observed in 3MP, so the rationale used to explain these observations for the latter compounds is invoked here. Other possible alternatives which could account for the weak fluorescence include fluorescence from impurities or from a protonated species. To test the latter possibility, a 5×10^{-3} *M* solution of 4-chromanone in 3MP was slowly acidified, but this did not result in the appearance of any fluorescence. A similar concentration of chromone in deuterated methanol (Merck-Uvasol®, >99% CD_3OD for Spectroscopy) was examined, and the weak broad band fluorescence noted was spectrally similar, but several times stronger than the corresponding ethanol sample. A weaker, but somewhat similar fluorescence was observed from the CD_3OD blank, so that quantitative comparisons as to relative yields were difficult. These results do not provide any evidence for a protonated fluorescence species, and while fluorescent impurities cannot be ruled out entirely, the solvent dependencies and internal consistencies argue against such a possibility.

Summary

Various spectroscopic methods, including such absorption and luminescence techniques as oxygen induced singlet–triplet absorption and polarized phosphorescence spectra, as well as e.s.r. spectroscopy of the triplet state, were used to investigate the excited state properties of some chromones. Chromone, 4-chromanone, and photoadducts of chromone with tetramethylethylene, dimethoxyethylene, cyclopentene, and butyne-2 were found to have weak low lying singlet states consistent with an n,π^* orbital designation. All of these compounds, except chromone, exhibited very weak ($\phi_F \sim 10^{-4}$) fluorescence in polar solvents, which was not observed in non-polar solvents. These observations were attributed either to solvent inversion of the lowest singlet state from n,π^* to π,π^* character, or simply increased configurational mixing of these states due to the decreased energy separation in polar solvents. All systems were strongly phosphorescent, with mixed orbital character indicated for the lowest triplet states. Although π,π^* contributions to the lowest triplet state of 4-chromanone were indicated, the distinctly π,π^* features reported for this compound in the recent literature (18) were not confirmed.

In non-polar solvents, the luminescence features noted for chromone at higher concentrations were associated with chromone aggregates. Since the aggregation in the ground state did not result in the formation of a new chemically stable species, the phosphorescent species was termed an exciplex. The return to optically clear glasses and monomer luminescence properties at $\sim 10^{-5}$ *M* attested to the poor solubility of chromone in

such solvents at reduced temperatures. The photochemical reactivity of chromone can be interpreted consistently on the basis of the spectroscopic results reported here.

The author would like to thank J. W. Hanifin of Lederle Labs. for providing the compounds reported in this study. He is also grateful to J. Koren for running the absorption spectra under oxygen pressure, and to J. S. Brinen for the e.s.r. measurements. He is especially indebted to J. S. Brinen and M. K. Orloff for helpful discussions and some valuable suggestions.

1. S. UNDENFRIEND. Fluorescence assay in biology and medicine. Academic Press, New York. 1962. p. 432.
2. J. W. HANIFIN and E. COHEN. J. Amer. Chem. **91**, 4494 (1969).
3. J. B. GALLIVAN. Mol. Photochem. **2**, 191 (1970).
4. D. F. EVANS. J. Chem. Soc. 1351 (1957).
5. H. H. JAFFE and M. ORCHIN. Theory and applications of ultraviolet spectroscopy. John Wiley and Sons, New York, 1965. p. 186.
6. M. KASHA. Radiat. Res. Suppl. **2**, 243 (1960).
7. S. P. MCGLYNN, T. AZUMI, and M. KINOSHITA. Molecular spectroscopy of the triplet state. Prentice-Hall, Inc., Englewood Cliffs, New Jersey. 1969. p. 246.
8. S. K. CHAKRABARTI. Mol. Phys. **16**, 467 (1969) and references therein.
9. D. A. WARWICK and C. H. J. WELLS. Spectrochim. Acta, **24A**, 589 (1968).
10. D. R. KEARNS and W. A. CASE. J. Amer. Chem. Soc. **88**, 5087 (1968).
11. N. J. TURRO. Molecular photochemistry. W. A. Benjamin, Inc., New York. 1965. p. 48.
12. S. DYM and R. M. HOCHSTRASSER. J. Chem. Phys. **51**, 2458 (1969).
13. N. HIROTA. Chem. Phys. Lett. **4**, 305 (1969).
14. C. A. PARKER. Photoluminescence of solutions. Elsevier Publ. Co., Amsterdam. 1969 p. 355.
15. (*a*) G. CASTRO and R. M. HOCHSTRASSER. J. Chem. Phys. **45**, 4352 (1966). (*b*) E. C. LIM and S. K. CHAKRABARTI. Mol. Phys. **13**, 293 (1967). (*c*) G. J. HOIJTINK *et al.* Chem. Phys. Lett. **1**, 609 (1968). (*d*) E. A. CHANDROSS and C. J. DEMPSTER. J. Amer. Chem. Soc. **92**, 704 (1970).
16. J. B. BIRKS. Molecular luminescence. *Edited by* E. C. Lim. W. A. Benjamin, Inc., New York. 1969. p. 907.
17. P. E. STEVENSON. J. Mol. Spectry. **15**, 220 (1965).
18. D. R. GRABER, M. W. GRIMES, and A. HAUG. J. Chem. Phys. **50**, 1623 (1969).
19. A. A. LAMOLA. J. Chem. Phys. **47**, 4810 (1967).

Can. J. Chem. Downloaded from www.nrcresearchpress.com by 210.87.254.5 on 09/05/12
For personal use only.

Can. J. Chem. Downloaded from www.nrcresearchpress.com by 210.87.254.5 on 09/05/12
For personal use only.

Fluorinated carbohydrates. Part V.[1] Nuclear magnetic resonance data on pyranose and furanose derivatives of 3-deoxy-3-fluoro-D-glucose[2]

A. B. FOSTER AND R. HEMS

Chester Beatty Research Institute, Institute for Cancer Research, Royal Cancer Hospital, London, S.W.3, Great Britain

AND

L. D. HALL

Department of Chemistry, The University of British Columbia, Vancouver 8, British Columbia

Received June 15, 1970

The n.m.r. spectra of a series of 3-fluorinated glucose derivatives have been measured; spectral assignments were confirmed by $^1H-\{^{19}F\}$ heteronuclear decoupling experiments. The ^{19}F spectral parameters illustrate a variety of stereospecific dependencies, the most noteworthy being that of $^4J_{F,H}$ couplings, for which $^4J_{e,e}$ = *ca.* + 4.0 Hz while $^4J_{e,a}$ = *ca.* − 1.5 Hz.

Canadian Journal of Chemistry, 48, 3937 (1970)

Introduction

The wide and increasing range of specifically fluorinated pyranose and furanose sugar derivatives (2, 3) and glycosyl fluorides (4, 5) now available, makes possible a meaningful study of n.m.r. data with regard to the angular and configurational dependencies of *vicinal*, *geminal*, and *long-range* (^4J and ^5J), $^{19}F-^1H$ couplings. The particular advantage of fluorinated carbohydrates in this respect is that, in many cases, definition of conformation on the basis of $^1H-^1H$ couplings establishes with reasonable precision the geometrical relationship of the fluorine atoms with respect to all, or most, of the protons in the same molecule.

We now report n.m.r. data and first order analyses for derivatives of 3-deoxy-3-fluoro-D-glucose and related derivatives. This study establishes[3] the generality of several conclusions based on previous (6) studies of glycopyranosyl fluoride derivatives.

Results and Spectral Assignments

Several of the derivatives of 3-deoxy-3-fluoro-D-glucose studied herein have been described previously (2), but some additional compounds have been synthesized. Treatment of 3-deoxy-3-fluoro-D-glucose (which has now been obtained crystalline) with boiling 2% methanolic hydrogen chloride gave a syrupy mixture of glycosides. After zinc chloride-catalyzed benzylidenation of this mixture, crystalline methyl 4,6-*O*-benzylidene-3-deoxy-3-fluoro-β-D-glucopyranoside was isolated and further characterized as the 2-*O*-acetyl derivative (**3**). The anomeric configuration assigned on the basis of $[\alpha]_D$ values (−48 and −57° respectively) was confirmed by the n.m.r. data discussed below. Treatment of 1,2,4,6-tetra-*O*-acetyl-3-deoxy-3-fluoro-β-D-glucopyranose (**1**) (2) with zinc chloride – acetic anhydride gave the α-anomer (**2**).

It it most convenient to discuss separately the furanose and pyranose derivatives.

Pyranose Derivatives, 1–6

The derivatives available for this study are listed with structures. Since assignments of the spectra of fluorinated sugar derivatives are reasonably complex a typical example will be discussed in some detail. Although assignments can be made directly, access to a $^1H-^{19}F$ heteronuclear decoupler greatly simplifies the problem; this point will also be illustrated. The chemical shifts and coupling constants found for derivatives **1–6** are listed in Tables 1 and 2 respectively.

The p.m.r. spectrum of a solution of 1,2,4,6-tetra-*O*-acetyl-3-deoxy-3-fluoro-β-D-glucopyranose (**1**) (deuterochloroform) is shown in Fig. 1. The doublet to lowest field (τ 4.35) can be assigned intuitively to the anomeric proton and

---

[1]The paper also constitutes Part VIII of a series from University of British Columbia entitled "Studies of Specifically Fluorinated Carbohydrates".

[2]A preliminary report of some of these results has been published: see ref. (1).

[3]The results obtained during a simultaneous study of derivatives of 2-deoxy-2-fluoro-D-altrose and of 2-deoxy-2-fluoro-D-allose will be reported elsewhere by L. D. Hall, Ingvar Johansson, and Bengt Lindberg.

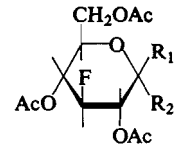

1 $R_1 = OAc$; $R_2 = H$
2 $R_1 = H$; $R_2 = OAc$

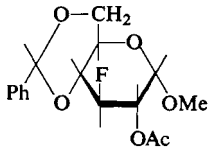

3

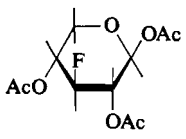

4

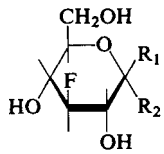

5 $R_1 = OH$; $R_2 = H$
6 $R_1 = H$; $R_2 = OH$

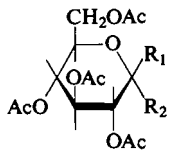

7 $R_1 = OAc$; $R_2 = H$
8 $R_1 = H$; $R_2 = OAc$

the magnitude of the splitting (8.3 Hz) immediately indicates that H-1 and -2 are *trans*-diaxially disposed. The complex pattern of 16 lines centered at highest field (τ 6.25) can be assigned to H-5; and for the present it will be assumed that the largest splitting (10.0 Hz) corresponds to $J_{4,5}$. To low field of this resonance is a series of transitions of total integrated intensity 2.5 protons. The initial intensity build-up and the separations shown by some of the transitions are characteristic of the AB part of an ABX-system (7) in which the A resonance is further coupled to another nucleus of spin 1/2, and are assigned on this basis to the C-6 protons: the splittings corresponding to $J_{5,6_1}$ and $J_{5,6_2}$ can be identified. The remaining three transitions of intensity 0.5 protons, have two couplings of *ca.* 9.0 Hz, and correspond with the triplet centered at τ 5.3 which also integrates for 0.5 protons. The separation between these two triplets corresponds to a coupling of 51.2 Hz which is known to be characteristic of a *geminal* ^{19}F–^{1}H coupling and this implies that these six transitions constitute the H-3 resonance. If this is correct, then $J_{2,3}$ and $J_{3,4}$ are both large (*ca.* 9 Hz) which implies that H-2, -3, and -4 are all axially oriented and hence that the fluorine substituent at C-3 is equatorially

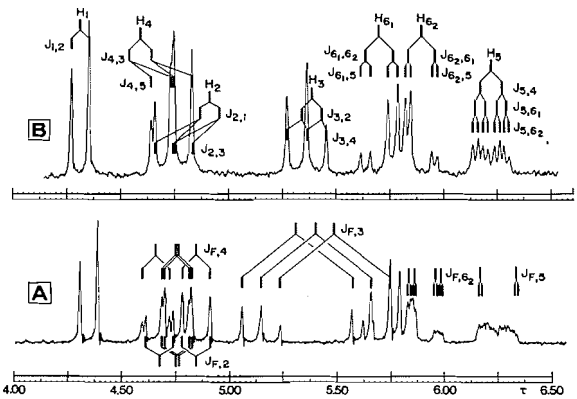

FIG. 1. Partial 100 MHz p.m.r. spectra of 3-deoxy-3-fluoro-β-D-glucopyranose tetraacetate (**1**) in $CDCl_3$ solution. A, Normal spectrum; B, ^{19}F decoupled spectrum obtained by applying a strong radiofrequency field at 94 075 740 Hz. The first-order assignments are as indicated. The two spectra were recorded with different gains.

oriented. The analysis thus far indicates that the derivative **1** has the β-D-*gluco* configuration.

It now remains to complete the assignment of the complex pattern centered at τ 4.8 which consists of the overlapping transitions of the H-2 and -4 resonances. Although this can be done by direct inspection of the ^{1}H spectrum it is easier to make use of the data from the ^{19}F spectrum, shown in Fig. 2. The magnitude of the largest splitting corresponds to the previously assigned *geminal* F–H_3 coupling, whereas the triplet structure implies that $J_{F,2} \simeq J_{F,4} \simeq 12.8$ Hz. Using these values, together with the various proton couplings previously obtained from the H-1, -3, and -5 resonances, enables a complete assignment to be made for the H-2 and -4 resonances. Again, this assignment is consistent with the β-D-*gluco* configuration. This conclusion is further supported by comparison of the chemical shift data of this compound with that of the α- and β-anomers of D-glucose pentaacetate **7**

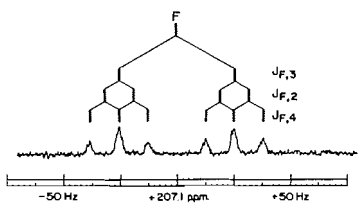

FIG. 2. The ^{19}F magnetic resonance spectrum (94.07 MHz) of 3-deoxy-3-fluoro-β-D-glucopyranose tetraacetate (**1**) in $CDCl_3$ solution containing *ca.* 20% CCl_3F (Freon-11).

Can. J. Chem. Downloaded from www.nrcresearchpress.com by 210.87.254.5 on 09/05/12
For personal use only.

Can. J. Chem. Downloaded from www.nrcresearchpress.com by 210.87.254.5 on 09/05/12
For personal use only.

TABLE 1

Chemical shifts (τ-values, ϕ-values) for pyranose derivatives (measured from normal spectra)

Derivative	H-1	H-2	H-3	H-4	H-5_a	H-6_1	H-6_2	OAc	^{19}F	Others
1*	4.35	4.77	5.40	4.75	6.25	5.71	5.91	7.92 (2), 7.93, 7.95	+196.2	
2*	3.69	‡	5.25	‡	5.7	———	6.1	7.90, 7.93, 7.97 (2)	+200.4	
3†	5.98	4.61	5.47	6.58	7.01	5.92	6.59	8.29	+198.6*	OMe 6.82; Ph. *ca.* 2.7 PhCH 4.83
4*	4.29	4.86	5.43	4.93	6.52	—	—	7.93 (3)	+195.3	H-5_e 5.82
7*	4.26	4.7	———	5.0	6.13	5.68	5.91	7.93, 7.96, 8.00 (2), 8.02	—	
8*	3.69	4.92	4.52	4.87	5.6	———	6.0	7.82, 7.92, 7.96, 7.98, 7.99	—	

*In $CDCl_3$ solution.
†In C_6D_6 solution.
‡Broad multiplet, τ 4.6–5.0.

TABLE 2

Coupling constants (Hz) for pyranose derivatives

Derivative	$J_{1,2}$	$J_{2,3}$	$J_{3,4}$	$J_{4,5a}$	$J_{5,6_1}$	$J_{5,6_2}$	$J_{6_1,6_2}$	$J_{F,2}$	$J_{F,3}$	$J_{F,4}$	Others
1*	8.3	8.9	9.2	10.0	4.3	2.5	12.5	12.8	51.2	12.8	$J_{F,5}$ 1.1; $J_{F,6_2}$ 1.5
2*	3.2	*ca.* 9.4	*ca.* 9.4	←	§		→	12.5	52.0	12.5	$J_{F,1}$ 4.0
3†	7.5	9.3	9.0	10.0	4.7	9.4	10.6	14.1	53.0	15.1	$J_{F,6_1}$ 2.0; $J_{F,5}$ 1.5
4*	6.5	*ca.* 7.9	*ca.* 7.9	8.0	—	—	—	12.4	49.4	12.4	$J_{4,5e}$ 5.0; $J_{5a,5e}$ 12.2 $J_{F,5e}$ 4.2
7*	8.0‡	*ca.* 9.0	*ca.* 9.0	*ca.* 9.0	4.5	2.4	12.5	—	—	—	
8*	3.5	10.2	*ca.* 9.0	*ca.* 9.5	§	§	§	—	—	—	

*In $CDCl_3$ solution.
†In C_6D_6 solution.
‡In $(CD_3)_2CO$ solution.
§Unresolved multiplets.

(8) and **8** (8) respectively, which are also listed in Table 1.

Conclusive confirmation of the above assignment follows comparison of the "normal" spectrum (Fig. 1A) with the "fluorine-decoupled" spectrum shown in Fig. 1B.

The p.m.r. spectrum of the α-anomer (**2**) also clearly supports the assigned structures. Thus, the spectrum showed four acetyl resonances together with the requisite ring proton resonances. The anomeric proton resonance showed as a triplet due to the additional coupling with the fluorine atom. This point will be discussed later.

The D-xylopyranose derivative (**4**) (1) was of considerable interest because its p.m.r. spectrum (deuterochloroform) (Fig. 3) demonstrated very clearly the stereospecific requirements for $^4J_{F,H}$ coupling. The observation of large *vicinal* ^1H–^1H couplings in the resonances of the anomeric (6.5 Hz) and one of the C_5-protons (8.0 Hz) indicates that this derivative has the β-configuration and exists preferentially at room temperature in the $^4C_1$-D conformation. The remainder of the assignment then follows; it is interesting to note the close similarity between this spectrum and that of the corresponding β-D-*gluco* derivative (**1**) shown in Fig. 1. Neither the H-1 nor the H-5$_a$ resonances show detectable coupling with the fluorine substituent; thus for this derivative, $^4J_{F,a} < 0.5$ Hz. In marked contrast, the H-5*e* resonance is clearly coupled with the fluorine, giving $^4J_{F,e} = 4.2$ Hz.

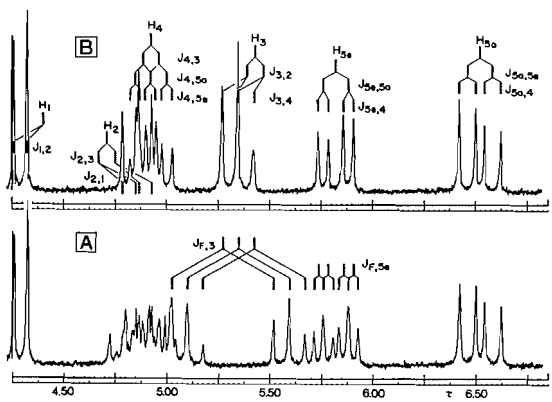

FIG. 3. Partial 100 MHz p.m.r. spectra of 3-deoxy-3-fluoro-β-D-xylopyranose triacetate (**4**) in $CDCl_3$ solution. A, Normal spectrum; B, ^{19}F decoupled spectrum obtained by irradiation at 94 075 899.0 Hz. The two spectra were recorded with the same spectrometer gain. Although no assignment is indicated for the H-2 and -4 resonance of A, every transition can in fact be allocated.

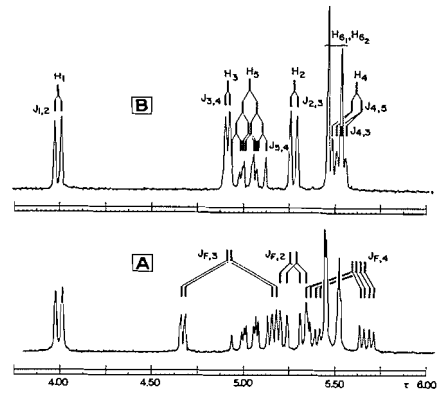

FIG. 4. Partial 100 MHz p.m.r. spectra of 3-deoxy-3-fluoro-1,2-*O*-isopropylidene-α-D-glucofuranose 5,6-carbonate (**9**) in $CDCl_3$ solution. A, Normal spectrum; B, ^{19}F decoupled spectrum obtained by strong irradiation at 94 074 700 Hz. The two spectra were recorded at different gains. The first-order assignments are indicated. It is not possible to assign unequivocally the couplings between H_5–H_{6_1} and H_5–H_{6_2}.

*Furanose Derivatives, **9–16***

The spectra of 3-deoxy-3-fluoro-1,2-*O*-isopropylidene-α-D-glucofuranose 5,6-carbonate (**9**) (2), shown in Fig. 4 are typical of those obtained from the furanose derivatives we have studied. The doublet to lowest field (τ 4.00) is assigned to H-1, which gives $J_{1,2} = 3.9$ Hz. The tripleted doublet at τ 4.67 integrates for 0.5 proton and the other transitions of the resonance of this proton are recognized at τ 5.17. Since the separation between the two halves of this resonance is *ca.* 50 Hz which is characteristic of a *geminal* ^{19}F–^1H coupling, this resonance is assigned to H-3. Irradiation of the H-1 resonance, under frequency-sweep conditions, with a decoupling field of *ca.* 10 Hz resulted in the removal of one of the smaller splittings ($J_{1,3}$ *ca.* 0.7 Hz), leaving $J_{3,4}$ as either 0.7 or 2.5 Hz. The same decoupling experiment removed the 3.6 splitting from the two doublets at τ 5.22 and 5.33 which were thus identified as the H-2 transitions. The larger splitting of this particular resonance was assigned to $J_{F,2}$ (10.8 Hz) and the small, incompletely resolved, splitting (*ca.* 0.7 Hz) to $J_{2,3}$. This enabled the completion of the H-3 assignment giving $J_{3,4} = 2.5$ Hz. A splitting of this same magnitude was observed in the quartet (integral, 0.5 proton) as τ 5.67 and in the partially obscured transitions at *ca.* τ 5.4. The separation between these two quartets (29.2 Hz) was assumed to be $J_{F,4}$ and the remaining splitting (5.1 Hz) was taken as $J_{4,5}$. A splitting of this same magnitude

Can. J. Chem. Downloaded from www.nrcresearchpress.com by 210.87.254.5 on 09/05/12
For personal use only.

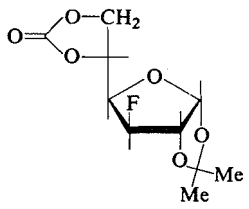

9

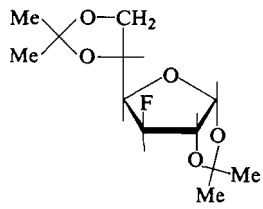

10

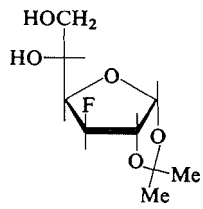

11

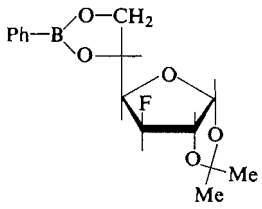

12

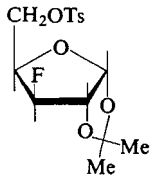

13

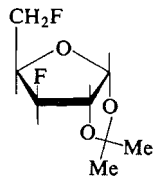

14

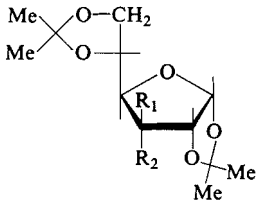

15 R_1 = OAc; R_2 = H
16 R_1 = H; R_2 = OAc

was observed in the octet at τ 5.04, identifying that as the H-5 resonance and giving the H_5–H_6 couplings (6.6, 7.5 Hz). The H-6 resonances were incompletely resolved at *ca.* τ 5.5. This analysis was supported by the couplings obtained from the ^{19}F spectrum (10.5, 30 and 50 Hz), and provides conclusive proof that the compound has the D-*gluco* (or L-*ido*) configuration and excludes the possibility that it has the D-*allo* configuration. The chemical shifts and coupling constants for 3-*O*-acetyl-1,2;5,6-di-*O*-isopropylidene-α-D-glucofuranose (**15**) (9) and the corresponding allofuranose derivative (**16**) (10), together with those of the other furanose derivatives are listed in Tables 3 and 4.

Discussion

The first-order parameters obtained by direct measurement of the various spectra are summarized in Tables 1–4; it is indeed fortunate that in most cases the chemical shift separations between the individual resonances are sufficient for these analyses to be entirely adequate. The coupling constants are considered to have a maximum error of ±0.5 Hz. The chemical shifts are taken from the "normal" spectra; the power dissipated by the decoupler is sufficient to warm the sample which causes significant changes in some of the proton shifts.

Since the 4,6-*O*-benzylidene derivative **3** has two, *trans*-fused six-membered rings it is not possible for this derivative to undergo any gross conformational-inversion processes. It is appropriate, therefore, to take this system as the model for all of the pyranose derivatives. The close similarity between the *vicinal* ring proton couplings of **3** and those of the other D-*gluco* derivatives (**1**, **2**, **7**, **8**) suggests that they all favor the $^4C_1$-D conformation **A**. However, the somewhat smaller values observed for the *vicinal* ^{19}F–^1H couplings of **1** and **2** compared with those

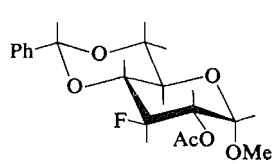

(A)

Can. J. Chem. Downloaded from www.nrcresearchpress.com by 210.87.254.5 on 09/05/12
For personal use only.

Can. J. Chem. Downloaded from www.nrcresearchpress.com by 210.87.254.5 on 09/05/12
For personal use only.

TABLE 3

Chemical shifts (τ-values ϕ-values) for furanose derivatives (measured from normal spectra)

Derivative	H-1	H-2	H-3	H-4	H-5	$H\text{-}6_1$	$H\text{-}6_2$	$C(Me)_2$	^{19}F	Others
9*	4.00	5.28	4.92	5.53	5.04	*ca.* 5.5		8.51, 8.68	+207.1	
10*	4.08	5.33	5.02	←	5.65	6.15	→	8.52, 8.58 8.66, 8.70	+208.0	
11*	4.08	5.34	4.92	5.83	←	6.0—6.4	→	8.53, 8.70	+209.4	
12*	4.16	5.33	4.93	5.79	←	*ca.* 5.6	→	8.55, 8.71	+207.8	
13*	4.14	5.36	5.10	5.3—5.9		—	—	8.59, 8.73	+210.6	$PhCH_3$, 7.61 Ph, 2.24, 2.71
14*§	4.04	‡	*ca.* 5.0	‡	‡	—	—	8.51, 8.68	+209.5 +231.2	
15*	4.14	5.51	4.75	←	5.75	6.0	→	8.51, 8.62 8.70 (2)	—	OAc, 7.94
16†	4.46	5.40	5.08	5.73	5.89	6.1—6.2		8.56, 8.66 8.76, 8.88	—	OAc, 8.28

*In $CDCl_3$ solution.
†In C_6D_6 solution.
‡Broad multiplet, τ 5.1–5.8.
§See ref. 20 for details of synthesis.

TABLE 4

Coupling constants (Hz) for furanose derivatives

Derivative	$J_{1,2}$	$J_{2,3}$	$J_{3,4}$	$J_{4,5}$	$J_{5,6_1}$	$J_{5,6_2}$	$J_{6_1,6_2}$	$J_{F,2}$	$J_{F,3}$	$J_{F,4}$	Others
9*	3.9	0.7	2.5	5.1	6.6	7.5	‡	10.8	49.9	29.2	$J_{1,3}$ 0.7
10*	3.7	0.8	<1.5	←		‡	→	10.5	*ca.* 49	*ca.* 28	
11*	3.3	*ca.* 0.5	2.0	8.0	←	‡	→	10.5	50.0	28.8	
12*	3.6	*ca.* 0.5	2.0	7.2	←	‡	→	10.5	50.0	28.9	
13*	3.8	*ca.* 0.5	*ca.* 2	*ca.* 7	—	—	—	10.5	50.5	*ca.* 25	J_{Ts} 8.1
14*	3.1	←	‡	→	—	—	—	←	‡	→	
15*	3.6	*ca.* 0.5	*ca.* 2	←		‡	→	—	—	—	
16†	3.7	4.7	8.0	4.9	←	‡	→	—	—	—	

*In $CDCl_3$ solution.
†In C_6D_6 solution.
‡Unresolved.

Can. J. Chem. Downloaded from www.nrcresearchpress.com by 210.87.254.5 on 09/05/12
For personal use only.

of **3** suggest either that the former both have a somewhat flatter pyranose ring than that of **3**, or, that they are undergoing some rapid, chair–chair conformational inversion process. A similar comment can be made concerning the D-xylopyranose derivative **4** which also has smaller *vicinal* ^1H–^1H and ^{19}F–^1H couplings than **3**. Nevertheless, these derivatives **1–4** demonstrate that the *vicinal* ^{19}F–^1H coupling of a moiety such as that shown in **B** should fall in the range 12.4–15 Hz.

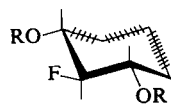

(B)

The D-xylopyranose derivative **4** demonstrates very clearly the stereospecific requirements of ^4J, ^{19}F–^1H couplings, which is the same as that found (11) for glycopyranosyl fluorides. The equatorially oriented fluorine substituent couples preferentially with the equatorially oriented C-5 proton. Although **4** shows no detectable coupling between the C-3 fluorine atom and either H-5_a or -1_a, the observation of a fluorine coupling in the H-5_a resonance of **1** shows that $^4J_{F_e,H_a}$ couplings can have detectable magnitude. As reported previously (12) it is a simple matter to determine the absolute signs of ^{19}F–^1H couplings by double-resonance experiments. In this way we have established that $^4J_{F_e,H_e}$ couplings are absolutely positive in sign and vary between +4 and +5.2 Hz, while $^4J_{F_e,H_a}$ couplings are absolutely negative in sign and vary between −1.1 and 0 Hz. Thus, the stereospecificity and signs of $^4J_{F,H}$ couplings parallel those of $^4J_{H,H}$ couplings (13), although the former are of larger magnitude.

A detailed discussion of these ^4J, ^{19}F–^1H couplings and also the ^5J, ^{19}F–^1H couplings is reserved for a future publication.

The close similarity between the couplings of the 3-fluoro-furanose derivatives **9–16** listed in Table 4, and the couplings previously reported (14) for derivatives of 1,2-*O*-isopropylidene-α-D-glucofuranose, including **15**, suggests that both sets of derivatives have the same conformational symmetry. The previous workers had concluded that these derivatives favor the $^3T_2$ conformation **C**. There is no particular justification for changing this assignment at this time although, as Steiner and Hall *et al.* have discussed in detail elsewhere

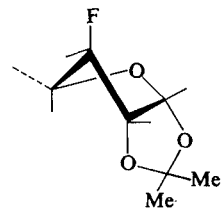

(C)

(15), the evidence in favor of this conformation over other conformations which are either immediately adjacent, or close, in the pseudorotational cycle, is rather slender.

If the previous conformational assignment is retained, the F_3–H_2 coupling (*ca.* 10.5 Hz) corresponds to a dihedral separation of *ca.* 30°, whereas the F_3–H_4 coupling (*ca.* 20 Hz) corresponds to a dihedral angle of *ca.* 150°. These values may be compared with the *vicinal* ^{19}F–^1H couplings (*ca.* 12.5 Hz) of the pyranose derivatives (**1–4**), which corresponds, nominally, to a dihedral separation of *ca.* 60°. If these *vicinal* couplings were in strict accord with a "$\cos^2 \phi$" relationship, $J_{30°}$ should be greater than $J_{60°}$, whereas the reverse situation is true. It is not yet known whether this disagreement reflects a configurational dependence (16) which is known (6) to be important for *vicinal* ^{19}F–^1H couplings, or whether it indicates that such couplings are intrinsically dependent upon ring size. Unfortunately, a value for $J_{180°}$ is not available at this time; the values obtained for glycopyranosyl fluorides are not admissible because of the additional electronegativity effect (6) of the lactol oxygen.

If ^{19}F n.m.r. is to be used as a sensitive steric probe, it will be necessary to know the conformational properties of a C—F group of a fluorinated carbohydrate derivative. The close similarity between the various ^1H–^1H couplings of the fluoro derivatives outlined in this paper and those of the corresponding oxygen containing derivatives, suggests that the C—F group is conformationally equivalent to a C—OR group. More incisive evidence supporting this contention follows a comparison of the composition of an equilibrated solution of 3-deoxy-3-fluoro-D-glucose (**5**, **6**) with the composition of comparable solutions of D-glucose and of 3-deoxy-D-*ribo*-hexose (17). Whereas the solutions of D-glucose and 3-fluoro-3-deoxy-D-glucose contain no detectable quantities of the furanose forms, a solu-

Can. J. Chem. Downloaded from www.nrcresearchpress.com by 210.87.254.5 on 09/05/12
For personal use only.

tion of 3-deoxy-D-*ribo*-hexose does (17). This point will be discussed in greater detail elsewhere. Assignment of the ^{19}F resonances of **5** and **6** followed from the known stereospecific dependencies of ^{3}J and ^{4}J, ^{19}F–^{1}H couplings.

It is of importance to note that the ^{19}F chemical shifts of these derivatives (+193 to +208 p.p.m.) are very significantly higher than those of the glycopyranosyl fluorides we have previously (5, 6) studied (+116.9 to 151.9 p.p.m.). Insofar as the chemical shifts of "primary" fluoro-carbohydrates come in the range +213 to +235 p.p.m. (18) it is evident that a ^{19}F chemical shift measurement gives a rapid, positive identification of the position of a fluorine substituent attached to a carbohydrate ring system.

Experimental

Melting points are uncorrected. Thin-layer chromatography was performed on microscope slides or glass plates (3.25 in. sq.) with Kieselgel G (Merck, 7731) and detection with iodine vapor or concentrated sulfuric acid.

The n.m.r. spectra were measured, as described elsewhere (6), with a modified Varian HA-100 spectrometer operating in the "frequency-swept" mode for ^{1}H resonances and (at 94 MHz) in the "locked, field-swept" mode for ^{19}F resonances. The ^{1}H–$\{^{19}F\}$ heteronuclear decoupling experiments utilized instrumentation described elsewhere (19).

*3-Deoxy-3-fluoro-*D*-glucose (5, 6)*

On storage over phosphorus pentaoxide for 2 months a sample of the syrupy, chromatographically homogeneous sugar (2) crystallized. Recrystallization from ethanol gave material having m.p. 114–115°, $[\alpha]_D^{25}$ + 66° (*c* 0.7, water). No mutarotation was observed and the n.m.r. spectrum (methyl sulfoxide, internal tetramethylsilane) contained, *inter alia*, doublets of comparable integrated area at τ 3.14 (*J* 6.5 Hz) and τ 3.50 (*J* 4.5 Hz) attributable to the equatorial and axial anomeric hydroxyl groups in the β- and α-pyranose forms respectively.

Anal. Calcd. for $C_6H_{11}FO_5$: C, 39.6; H, 6.05; F, 10.4. Found: C, 39.3; H, 5.9; F, 10.4.

*1,2,4,6-Tetra-O-acetyl-3-deoxy-3-fluoro-*α*-*D*-glucose (2)*

A solution of the β-tetraacetate (2) (0.75 g) and zinc chloride (0.2 g) in acetic anhydride (5 ml) was heated (8) at *ca.* 100° for 10 min and then poured into ice-water (150 ml). The mixture was extracted with chloroform in the usual manner and the product was eluted from Kieselgel (Merck, 7734) with benzene–ether (9:1). The major, chromatographically homogeneous fraction was recrystallized from benzene – light petroleum (b.p. 60–80°) to give the title compound (0.6 g, 80%), m.p. 109–111°, $[\alpha]_D^{25}$ + 88° (*c* 1, chloroform).

Anal. Calcd. for $C_{14}H_{19}FO_9$: C, 48.0; H, 5.4; F, 5.4. Found: C, 47.7; H, 5.5; F, 5.9.

*Methyl 4,6-O-Benzylidene-3-deoxy-3-fluoro-*β*-*D*-glucopyranoside*

A solution of 3-deoxy-3-fluoro-D-glucose (1 g) in 2% methanolic hydrogen chloride was boiled under reflux and monitored by t.l.c. (ethyl acetate – ethanol, 9:1). After 5 h only traces of starting material (R_F 0.40) remained and the major product had R_F 0.5. The cooled solution was neutralized ($PbCO_3$), filtered, and concentrated. The syrupy residue (1.1 g) was treated with benzaldehyde (10 ml) and zinc chloride (1 g) at room temperature. Reaction was complete (t.l.c.) after 2 h. The solution was poured into a vigorously stirred mixture of ice-water (40 ml) and light petroleum (40 ml, b.p. 60–80°). The product (1.67 g) was collected, washed with light petroleum, and recrystallized from ethanol – light petroleum to give the title compound (0.66 g, 42%), m.p. 176–177°, $[\alpha]_D^{25}$ − 48° (*c* 1, chloroform).

Anal. Calcd. for $C_{14}H_{17}FO_5$: C, 59.3; H, 6.0; F, 6.7. Found: C, 59.3; H, 5.9; F, 6.7.

With acetic anhydride and pyridine in the usual manner, the title compound gave the acetate (3) (68%), m.p. 137–138°, $[\alpha]_D^{25}$ − 57° (*c* 1, chloroform).

Anal. Calcd. for $C_{16}H_{19}FO_6$: C, 58.9; H, 5.8; F, 5.8. Found: C, 58.7; H, 5.8; F, 5.8.

This work was supported variously by grants (to L.D.H.), from the National Research Council of Canada and the National Cancer Institute of Canada, from N.A.T.O. (to A.B.F. and L.D.H.) [grant number 352(1968–69)], and to the Chester Beatty Research Institute (Institute of Cancer Research; Royal Cancer Hospital) from the Medical Research Council and the British Empire Cancer Campaign for Research. The equipment used for the heteronuclear decoupling experiments was purchased with a major equipment grant (to L.D.H.; No. E 1338) from the National Research Council of Canada.

1. A. B. FOSTER, R. HEMS, L. D. HALL, and J. F. MANVILLE. Chem. Commun. 158 (1968).
2. A. B. FOSTER, R. HEMS, and J. M. WEBBER. Carbohyd. Res. **5**, 292 (1967). G. ADAMSON, A. B. FOSTER, L. D. HALL, and R. H. HESSE. Chem. Commun. 309 (1969). A. D. BARFORD, A. B. FOSTER, J. H. WESTWOOD, and L. D. HALL. Carbohyd. Res. **11**, 287 (1969).
3. J. E. G. BARNETT. Advan. Carbohyd. Chem. **22**, 177 (1967).
4. F. MICHEEL and A. KLEMER. Advan. Carbohyd. Chem. **16**, 85 (1961).
5. L. D. HALL and J. F. MANVILLE. Can. J. Chem. **47**, 361, 379 (1969).
6. L. D. HALL, J. F. MANVILLE, and N. BHACCA. Can. J. Chem. **47**, 1 (1969); L. D. HALL and J. F. MANVILLE. Can. J. Chem. **47**, 19 (1969); Chem. Commun. 37 (1968).
7. J. A. POPLE, W. G. SCHNEIDER, and H. J. BERNSTEIN. High resolution nuclear magnetic resonance. McGraw-Hill, 1959.
8. M. L. WOLFROM and A. THOMPSON. Methods Carbohyd. Chem. **2**, 211 (1963) and references therein.
9. H. OHLE and L. V. VARGHA. Ber. **62**, 2425 (1929).
10. W. SOWA and G. H. S. THOMAS. Can. J. Chem. **44**, 836 (1963).
11. A. B. FOSTER, R. HEMS, L. D. HALL, and J. F. MANVILLE. Chem. Commun. 158 (1968).
12. L. D. HALL and J. F. MANVILLE. Carbohyd. Res. **9**, 11 (1969).

13. L. D. HALL and J. F. MANVILLE. Advances in chemistry series. No. 74. S. Hanessian, *editor*. *In* Deoxy sugars; Carbohyd. Res. **8**, 295 (1968).
14. R. J. ABRAHAM, L. D. HALL, L. HOUGH, and K. A. MCLAUCHLAN. J. Chem. Soc. 3699 (1962).
15. P. R. STEINER. M.Sc. Thesis, University of British Columbia, Vancouver, B.C., 1969. L. D. HALL, P. R. STEINER, and C. PEDERSEN. Can. J. Chem. **48**, 1155 (1970).
16. H. BOOTH. Tetrahedron Lett. 411 (1965).
17. S. J. ANGYAL. Private communication.
18. L. EVELYN and L. D. HALL. Chem. Ind. (London), 183 (1968).
19. R. BURTON and L. D. HALL. Can. J. Chem. **48**, 59 (1970).
20. A. B. FOSTER and R. HEMS. Carbohyd. Res. **10**, 168 (1969).

Can. J. Chem. Downloaded from www.nrcresearchpress.com by 210.87.254.5 on 09/05/12
For personal use only.

Can. J. Chem. Downloaded from www.nrcresearchpress.com by 210.87.254.105 on 09/05/12
For personal use only.

Fluorinated carbohydrates. Part VI.[1] Studies of derivatives of 3-deoxy-3-fluoro-D-galactose[2]

J. S. BRIMACOMBE[3]
Chemistry Department, The University, P.O. Box 363, Birmingham 15, Great Britain

AND

A. B. FOSTER, R. HEMS, AND J. H. WESTWOOD
Chester Beatty Research Institute, Institute of Cancer Research, Royal Cancer Hospital, London, S.W.3, Great Britain

AND

L. D. HALL
Department of Chemistry, The University of British Columbia, Vancouver 8, British Columbia

Received June 17, 1970

A synthesis of 3-deoxy-3-fluoro-D-galactose from 1,2:5,6-di-*O*-isopropylidene-α-D-gulofuranose is described. The ^{1}H and ^{19}F n.m.r. spectra of several derivatives of D-galactose and of its 3-deoxy-3-fluoro derivative have been assigned in accord with previously established stereospecific dependencies.

Canadian Journal of Chemistry, 48, 3946 (1970)

Introduction

Secondary sulfonate groups attached to five and six membered carbocycles can be displaced by fluoride ion using the combination tetra-alkylammonium fluoride-dipolar aprotic solvent (2). In the carbohydrate field, 1,2:5,6-di-*O*-isopropylidene-3-*O*-toluene-*p*-sulfonyl-α-D-allofuranose (**5**) was converted (3) (~ 75%) into 3-deoxy-3-fluoro-1,2:5,6-di-*O*-isopropylidene-α-D-glucofuranose using tetrabutylammonium fluoride in methyl cyanide. We now report a further application of this reagent in the synthesis of 3-deoxy-3-fluoro-D-galactose. Fluorinated hexoses are of interest as potential antitumor agents in connection with the inhibition of glycolysis (4).

Results and Discussion

1,2:5,6-Di-*O*-isopropylidene-α-D-gulofuranose is now readily available (5) and the 3-toluene-*p*-sulfonate (6) (**1**) reacted completely during 48 h with tetrabutylammonium fluoride in methyl cyanide at 60° to give a mixture of 3-deoxy-1,2:5,6-di-*O*-isopropylidene-α-D-*erythro*-hex-3-enofuranose (7) (**2**) and 3-deoxy-3-fluoro-1,2:5,6-di-*O*-isopropylidene-α-D-galactofuranose (**3**) in the ratio *ca.* 1:1.3. The chromatographic properties of compounds **2** and **3** were too similar to permit a convenient large-scale separation but, after platinum-catalyzed hydrogenation of the mixture at room temperature the crystalline fluoro derivative **3** and 3-deoxy-1,2:5,6-di-*O*-isopropylidene-α-D-*xylo*-hexofuranose (**4**) were readily separable by chromatography on Kieselgel.

It is interesting to note the difference in response of tosylates **1** and **5** to tetrabutylammonium fluoride – methyl cyanide. The latter compound reacts much more slowly (3) but apparently gives only fluoride.

Although H-2 is *trans* to the toxyloxy group in compound **5**, presumably elimination does not occur because a bridgehead double bond would result.

Treatment of the fluoro diketal **3** with an aqueous ethanolic suspension of Amberlite IR-120 (H^+) resin gave crystalline 3-deoxy-3-fluoro-D-galactose (**6**). With acetic anhydride – sodium acetate, the fluoro sugar **6** gave 1,2,4,6-tetra-*O*-acetyl-3-deoxy-3-fluoro-β-D-galactose (**7**) which could be isomerized (8) with zinc chloride – acetic anhydride into the α-anomer **8**.

Treatment of 3-deoxy-3-fluoro-D-galactose (**6**) with boiling 1% methanolic hydrogen chloride for 13 h gave a mixture of products. Chromatog-

---

[1]This paper also constitutes Part IX of a series from University of British Columbia entitled "Studies of specifically fluorinated carbohydrates".

[2]A preliminary report of some of these results has been published; see ref. 1.

[3]Present address: Department of Chemistry, The University, Dundee, Scotland.

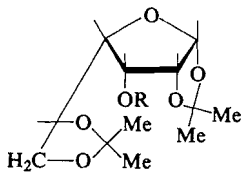

1 R = Ts
13 R = Bz

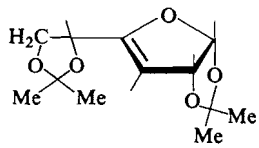

2

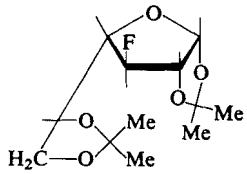

3

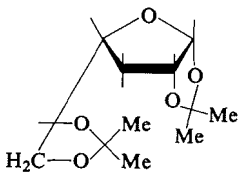

4

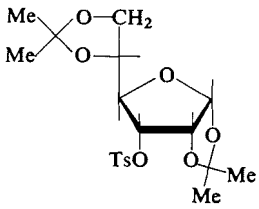

5

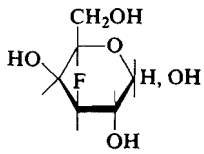

6

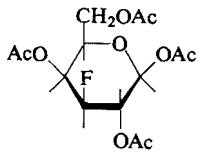

7

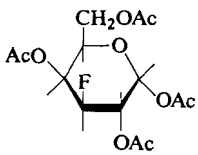

8

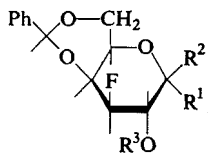

9 R^1 = OMe; R^2 = R^3 = H
10 R^1 = OMe; R^2 = H; R^3 = Ac
11 R^1 = R^3 = H; R^2 = OMe
12 R^1 = H; R^2 = OMe; R^3 = Ac

raphy on silica gel gave a small amount of material which was not further investigated but was tentatively identified as methyl 3-deoxy-3-fluoro-β-D-galactofuranoside. The major product was a mixture, *viz.*, methyl 3-deoxy-3-fluoro-α,β-D-galactopyranoside, in which the α-anomer preponderated. Zinc chloride-catalyzed benzylidenation of the mixture, followed by chromatography on silica gel gave methyl 4,6-*O*-benzylidene-3-deoxy-3-fluoro-α-D-galactopyranoside (**9**, 56%) and the β-anomer (**11**, 31%). The anomers **9** and **11** gave crystalline acetates, **10** and **12** respectively.

The proof of the structure of the derivatives in this study rests heavily on their ^1H and ^{19}F n.m.r. data. Hence particular care was taken to obtain detailed analyses of the spectra of certain key compounds, together with several related model compounds. The n.m.r. data obtained by first-order analysis of the spectra of derivatives **3**, **7**, **8** and the model systems **13–16** are given in Tables 1–4; for convenience the pyranose and furanose systems are listed separately.

To the best of our knowledge no detailed

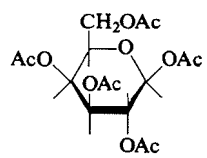

13

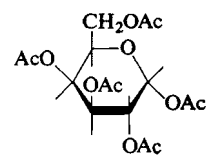

14

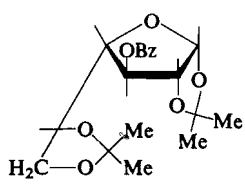

15

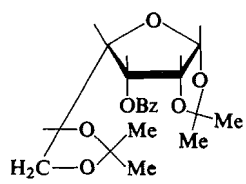

16

Can. J. Chem. Downloaded from www.nrcresearchpress.com by 210.87.254.105 on 09/05/12
For personal use only.

TABLE 1

Chemical shifts (τ-values, ϕ_c-values) of galactopyranose derivatives

Derivative	H_1	H_2	H_3	H_4	H_5	H_{6_1}	H_{6_2}	OAc	^{19}F
7*	4.36	4.62	5.30	4.41	←	5.76–6.08	→	7.88; 7.94 7.96; 8.00	+200.7
8*	3.59	4.60	5.14	4.31	←	5.60–6.05	→	7.89; 7.92 8.00; 8.02	+204.3
13*	4.25	4.67	4.87	4.56	←	5.68	→	7.84; 7.89 7.97 (2); 8.02	—
14†	3.68	4.80	4.63	5.50	←	5.77–6.01	→	7.85 (2); 7.97 7.99; 8.01	—

*In $CDCl_3$ solution.
†In $(CD_3)_2CO$ solution.

TABLE 2

Coupling constants (Hz) for galactopyranose derivatives

Derivative	$J_{1,2}$	$J_{2,3}$	$J_{3,4}$	$J_{4,5}$	$J_{5,6_1}$	$J_{5,6_2}$	$J_{6_16_2}$	$J_{F,2}$	$J_{F,3}$	$J_{F,4}$	Others
7*	8.1	9.5	3.8	~0.5	‡			11.5	47.4	5.6	
8*	3.6	10.0	3.6	1.0	‡			11.4	47.5	~6.4	$J_{F,1}$ ~ 4.8
13*	7.6	10.2	3.3	~0.5	‡			—	—	—	
14†	3.3	10.0	2.9	1.4	‡			—	—	—	

*In $CDCl_3$ solution.
†In $(CD_3)_2CO$ solution.
‡Indeterminate.

analysis has previously been given for the ring-proton resonances of the pentaacetates of α- and β-D-galactopyranose.[4] The coupling constants are much as would be anticipated with perhaps, the exception of the rather small value of $J_{4,5}$. It seems highly probable that this reflects the configurational dependence of *vicinal* ^1H–^1H coupling constants (9–11). Thus, the C_4—O_4 bond is antiparallel (see **A**) to the C_5—H_5 bond as also is the C_5—O_5 bond with respect to the C_4—H_4 bond.

The close similarity between the ^1H–^1H couplings of compounds **13** and **14** and their counterparts in the 3-deoxy-3-fluoro-D-galactose

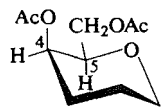

A

systems, **7** and **8** respectively, is self evident. Insofar as the coupling constants listed in Table 2 are probably only accurate to ±0.5 Hz, most of the pairs of couplings are identical within experimental error. This provides extremely strong evidence for the structures of **7** and **8**.

The ^{19}F–^1H couplings of compounds **7** and **8** provide further supporting evidence. Thus, we had previously established (12) that in the 3-deoxy-3-fluoro-D-glucose system, $J_{F,2} \simeq 13$ Hz, which is reasonably close to the values observed for $J_{F,2}$ in compounds **7** and **8**. That $J_{F,4}$ of compounds **7** and **8** is of smaller magnitude than $J_{F,4}$ of the D-*gluco* compounds (~ 13 Hz) was not anticipated; this may be another example

[4]A referee noted that Lemieux and Stevens (21) had previously reported $J_{1,2}$ 8.4 Hz for the β-anomer (13). He also commented that the small size of $J_{4,5}$ of galactopyranose derivatives had been noted before by Coxon and Fletcher (22) and by Cone and Hough (23). Neither of these papers proffered any rationale for their observation.

Can. J. Chem. Downloaded from www.nrcresearchpress.com by 210.87.254.105 on 09/05/12
For personal use only.

TABLE 3

Chemical shifts (τ-values; ϕ_c-values) of *galacto*- and *gulo*-furanose derivatives

Derivative	H_1	H_2	H_3	H_4	H_5	H_{6_1}	H_{6_2}	Me	^{19}F	Others
3*	4.10	5.28	5.18	5.92	5.66	5.94	6.20	8.48; 8.57 8.65; 8.67	+187.9	
15*	3.98	5.27	4.83	5.83	5.52	5.86	6.06	8.42; 8.59 8.64; 8.67	—	Ph† 2.0, 2.5
16*	4.13	5.06	4.66	5.83	5.13	5.84	6.36	8.50; 8.58 8.62; 8.70	—	Ph† 2.0, 2.5

*In $CDCl_3$ solution.
†Complex multiplet.

TABLE 4

Coupling constants (Hz) for *galacto*- and *gulo*-furanose derivatives

Derivative	$J_{1,2}$	$J_{2,3}$	$J_{3,4}$	$J_{4,5}$	$J_{5,6_1}$	$J_{5,6_2}$	$J_{6_1 6_2}$	$J_{F,2}$	$J_{F,3}$	$J_{F,4}$
3*	3.9	0.5	3.3	6.9	~6.2	6.4	8.0	15	51.6	23.7
15*	3.9	0.5	2.5	8.1	6.5	6.8	8.5	—	—	—
16*	4.0	5.6	6.4	9.0	6.5	7.1	8.4	—	—	—

*In $CDCl_3$ solution.

of the configurational dependence of *vicinal* ^{19}F–^1H couplings (13, 14).

It is interesting to note that the geminal F_3—H_3 couplings of compounds **7** and **8** are smaller than their counterparts in the D-*gluco* series (*ca.* 51 Hz). This relationship is formally analogous to that shown by glycopyranosyl fluorides (13) where compounds in the D-*manno* series (**B**) give smaller couplings than do their D-*gluco* counterparts (**C**).

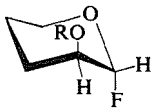

B

J_{gem} *ca.* 49 Hz

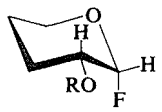

C

J_{gem} *ca.* 53.5 Hz

The ^4J coupling of *ca.* 4.8 Hz between the F-3 and H-1 substituents of the α-tetraacetate **8** is again in accord with the known stereospecificity of such couplings (15).

Analysis of the ^1H n.m.r. spectra of the 3-*O*-benzoyl-1,2:5,6-di-*O*-isopropylidene derivatives of D-galactose (**15**) and D-gulose (**16**) was straightforward and unambiguous. Comparison of the data obtained for these derivatives, listed in Tables 3 and 4, with that obtained for the 3-fluoro derivative (**3**) indicates quite unequivocally that the latter has the D-galacto configuration.

There is also a close similarity between the ring-proton couplings of compounds **3** and **15** and those previously published (16) for 3-*O*-acetyl-1,2:5,6-di-*O*-isopropylidene-α-D-glucofuranose {$J_{1,2}$ 3.6, $J_{2,3}$ < 0.5 Hz} and for (12) 3-deoxy-3-fluoro-1,2:5,6-di-*O*-isopropylidene-α-D-glucofuranose (**17**) {$J_{1,2}$ 3.7, $J_{2,3}$ *ca.* 0.8 Hz}. On this basis alone it might be concluded that both **3** and **17** favor the same $^3T_2$ conformation, **D**. However, this is an over-simplified and inaccurate description; the apparent similarity between the values of $J_{3,4}$ and of $J_{F,4}$ for **3** and **17** do not allow for the difference of configuration at C-4. The coupling constants for compound **3** appear to be best rationalized on the basis of a *preference* for a conformation approximating to either the V_2 or ^1V conformation (**E**, **F** respectively). Either of these conformations would have the merit of positioning the *cis* oriented C_3—F and C_4—H_4 bonds in an eclipsed, or nearly so, orientation. Furthermore, either of these conformations would allow the C_2—H_2 and C_3—H_3 bonds to have the near-90° dihedral separation which is unequivocally dictated by their near-zero coupling constant.

Although it is not possible to distinguish unequivocally between **E** or **F**, it has often been assumed in the past[5] that the ring oxygen of a furanose sugar is one of the "in-plane" atoms:

[5]See refs. 17–19 and references cited therein.

Can. J. Chem. Downloaded from www.nrcresearchpress.com by 210.87.254.105 on 09/05/12
For personal use only.

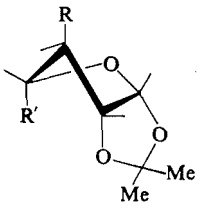

D

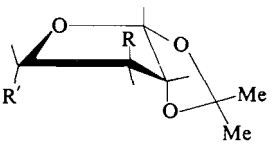

E

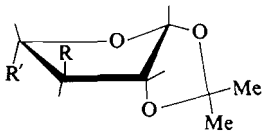

F

continuation of that assumption into the present discussion would clearly require the conclusion that **3** favors the V_2 conformation, **E**. In any event, a chemically significant fact emerges from the inter-comparison between derivatives **3** and **17**. Namely, that the inversion of configuration at C-4 causes the furanose ring to change its conformation. Inspection of molecular models indicates that either the V_2 or ^1V conformations would reduce the non-bonded interaction which would otherwise exist if **3** favored the $^3T_2$ conformation.

As has been discussed in detail elsewhere (17, 18) it is questionable whether it is realistic to couch any conformational discussion of a furanose system in terms of a single, exclusively populated conformation. The present discussion reinforces a previous suggestion (17, 18) that even *approximate* conformational evaluations of furanose systems can yield *chemically* significant conclusions. In the present situation, it could well be that the derivative has both the ^1V and the V_2 conformers significantly populated, and that the observed coupling constants represent a time-average of the couplings of these two forms. There is no way of distinguishing between these two models.

In summary, the n.m.r. parameters of the derivatives discussed above are in close accord with previously established stereospecific dependencies.

Experimental

Melting points are uncorrected. Thin-layer chromatography was performed using Kieselgel (Merck, 7731) and detection with iodine vapor or concentrated sulfuric acid. Unless otherwise stated, column chromatography was performed on Kieselgel (Merck, 7734). Gas–liquid chromatography was performed on a Pye 104 instrument with flame ionization detection using a column of poly(ethylene glycol adipate) at 165°. Light petroleum refers to the fraction b.p. 60–80°.

The n.m.r. spectra were measured with a modified (20) Varian HA-100 spectrometer operating in the "frequency sweep" mode for ^1H resonances and (at 94 MHz) in the "locked, field-sweep" mode for ^{19}F resonances.

3-Deoxy-3-fluoro-1,2:5,6-di-O-isopropylidene-α-D-galactofuranose

A mixture of 1,2:5,6-di-*O*-isopropylidene-3-*O*-toluene-*p*-sulfonyl-α-D-gulofuranose (6) (2.5 g), tetrabutylammonium fluoride (8.8 g, 5.5 mole), and acetonitrile (25 ml, distilled from phosphorus pentaoxide) was stirred at 60–65° and monitored by t.l.c. (benzene–ether, 9:1). After 48 h, no starting material ($R_F \sim 0.2$) survived and the product had $R_F \sim 0.5$. The reaction mixture was concentrated under diminished pressure and the syrupy residue was eluted from silica gel (Hopkin & Williams) with ether – light petroleum (1:1) to yield a syrupy major product (1.3 g), b.p. 90–100° (bath)/0.1 mm, which was homogeneous in t.l.c., but which, on examination by g.l.c., ν_{max}(liquid) 1660 cm^{-1} (C=C) showed two components in approximately equal proportions, with retention times of *ca.* 20 (identical with that of 1,2:5,6-di-*O*-isopropylidene-D-*erythro*-hex-3-enofuranose (7)) and 28 min.

A solution of the product mixture in ethanol (80 ml) was hydrogenated at atmospheric pressure over 5% palladized charcoal (600 mg). After 4 h, uptake of hydrogen was complete and the product showed two components in g.l.c. (retention times 28 and 41 min) and t.l.c. (benzene–ether, 9:1; $R_F \sim 0.5$ and ~ 0.2). Filtration of the mixture and concentration under diminished pressure yielded a syrup which showed no i.r. absorption at *ca.* 1660 cm^{-1}.

Column chromatography (benzene–ether, 9:1) of the mixture yielded, as the faster moving component, 3-deoxy-3-fluoro-1,2:5,6-di-*O*-isopropylidene-α-D-galactofuranose (0.65 g, 41%), m.p. 48–49° [from ether – light petroleum (b.p. 80–100°)], $[\alpha]_D^{25}$ −30° (*c* 1, chloroform).

Anal. Calcd. for $C_{12}H_{19}FO_5$: C, 55.0; H, 7.3; F, 7.3. Found: C, 55.4; H, 7.35; F, 7.3.

Further elution with benzene–ether (6:1) gave a product (0.58 g, 34%), m.p. 78.5–80° (from light petroleum), $[\alpha]_D^{25}$ −32° (*c* 4.0, ethanol) which was identical with 3-deoxy-1,2:5,6-di-*O*-isopropylidene-α-D-*xylo*-hexose (m.p. 81°, $[\alpha]_D^{20}$ −31.8° (ethanol)).

3-Deoxy-3-fluoro-D-galactose

A solution of 3-deoxy-3-fluoro-1,2:5,6-di-*O*-isopropylidene-α-D-galactofuranose (0.23 g) in ethanol (10 ml) and water (20 ml) was stirred at 60–65° with Amberlite IR-120 (H^+) resin (*ca.* 2 ml). The hydrolysis was monitored by t.l.c. (ethyl acetate) and was shown to be complete in 6 h. Concentration of the filtered solution gave a chromatographically homogeneous crystalline product which, on recrystallization from ethyl acetate – ethanol, yielded 3-deoxy-3-fluoro-D-galactose (0.147 g, 91%), m.p. 114–116°, $[\alpha]_D^{25}$ +87° → +76° (24 h, equil., *c* 0.5, water), $R_F \sim 0.3$ (t.l.c., ethyl acetate – ethanol, 9:1), and R_G 2.04 (chromatography on Whatman No. 1 paper,

Can. J. Chem. Downloaded from www.nrcresearchpress.com by 210.87.254.105 on 09/05/12
For personal use only.

Can. J. Chem. Downloaded from www.nrcresearchpress.com by 210.87.254.105 on 09/05/12
For personal use only.

butanol – acetic acid – water, 5:2:3, brown spot with aniline hydrogen phthalate).

Anal. Calcd. for $C_6H_{11}FO_5$: C, 39.6; H, 6.05; F, 10.5. Found: C, 39.5; H, 5.9; F, 10.9.

1,2,4,6-Tetra-O-acetyl-3-deoxy-3-fluoro-α- and -β-D-galactopyranose

When 3-deoxy-3-fluoro-D-galactose (180 mg) was treated with a boiling solution of sodium acetate (100 mg) in acetic anhydride (5 ml) for 10 min and the β-tetraacetate was isolated in the usual manner, the title compound (120 mg, 35%) was obtained m.p. 126–127° (from ethanol – light petroleum), $[\alpha]_D^{25}$ +35° (*c* 0.8, chloroform).

Anal. Calcd. for $C_{14}H_{19}FO_9$: C, 48.0; H. 5.4. Found: C, 48.15; H, 5.25.

A solution of the foregoing β-anomer (130 mg) and zinc chloride (100 mg) in acetic anhydride (4 ml) was heated at *ca.* 100° for 10 min (8), then poured into ice-water (40 ml) and extracted with chloroform (4 × 25 ml) in the usual way. Column chromatography (light petroleum – ether, 1:2) then yielded a homogeneous fraction (110 mg) which, after two recrystallizations from ethanol – light petroleum, afforded the α-tetraacetate (40 mg, 32%), m.p. 97–99°, $[\alpha]_D^{25}$ +126° (*c* 1.1, chloroform). (Found: C, 48.3; H, 5.3.)

Methyl Glycosidation of 3-Deoxy-3-fluoro-D-galactose

A solution of 3-deoxy-3-fluoro-D-galactose (200 mg) in 1% methanolic hydrogen chloride (2 ml) was heated under reflux, and the reaction was followed by t.l.c. (ethyl acetate – ethanol, 95:5). After 13 h, only traces of starting material ($R_F \sim 0.2$) remained and there were two major products ($R_F \sim 0.4$, ~ 0.6). The cooled reaction mixture was neutralized ($PbCO_3$), filtered, and concentrated under diminished pressure. Column chromatography (ethyl acetate – ethanol, 95:5) of the residue gave first a product (46 mg, $R_F \sim 0.6$) which was apparently homogeneous since the n.m.r. spectrum, (D_2O, Perkin–Elmer R-10) showed, *inter alia*, singlets at τ 6.62 and 5.02 attributable, respectively, to OMe and H-1. After recrystallization from ethyl acetate, the compound had m.p. 101–102°, $[\alpha]_D^{25}$ −13° (*c* 0.6, ethanol).

Anal. Calcd. for $C_7H_{13}FO_5$: C, 42.9; H, 6.6. Found: C, 43.1; H, 6.5.

This minor product, which was not further investigated, is possibly methyl 3-deoxy-3-fluoro-β-D-galactofuranoside.

The n.m.r. spectrum (pyridine, Perkin–Elmer R-10) of the second product (152 mg, $R_F \sim 0.4$) eluted from the column contained two signals (ratio *ca.* 3:2) attributable to OMe groups. Crystallization of the mixture from ethyl acetate gave methyl 3-deoxy-3-fluoro-α-D-galactopyranoside, m.p. 160–170°, $[\alpha]_D^{25}$ +150° (*c* 1, methanol) containing (n.m.r.) a small amount of the β-anomer.

Anal. Calcd. for $C_7H_{13}FO_5$: C, 42.9; H, 6.6; F, 9.7. Found: C, 42.9; H, 6.6; F, 9.9.

After treatment of the pyranoside mixture (200 mg) with zinc chloride (200 mg) and benzaldehyde (3 ml) at room temperature in the usual manner for 16 h, only traces of starting material survived (t.l.c., chloroform) and two major products at ($R_F \sim 0.2$, $\sim$ 0.3) were present. Column chromatography (chloroform) of the mixture afforded, first, a product (162 mg, 56%) which was recrystallized from ethanol – light petroleum to give methyl 4,6-*O*-benzylidene-3-deoxy-3-fluoro-α-D-galactopyranoside, m.p. 160–161°, $[\alpha]_D^{25}$ +144° (*c* 0.5 chloroform).

Anal. Calcd. for $C_{14}H_{17}FO_5$: C, 59.2; H, 6.0. Found: C, 58.8; H, 5.9.

The acetate had m.p. 158–159°, $[\alpha]_D^{25}$ +152° (*c* 0.5, chloroform).

Anal. Calcd. for $C_{16}H_{19}FO_6$: C, 58.9; H, 5.8. Found: C, 58.45; H, 5.6.

Eluted second was material (90 mg, 31%) which, on recrystallization from ethanol – light petroleum, gave methyl 4,6-*O*-benzylidene-3-deoxy-3-fluoro-β-D-galactopyranoside, m.p. 197–199° $[\alpha]_D^{25}$ −36° (*c* 0.55, chloroform). (Found: C, 59.3; H, 5.7). The acetate had m.p. 168–169°, $[\alpha]_D^{25}$ +8° (*c* 0.5, chloroform). (Found: C, 59.35; H, 6.0).

3-O-Benzoyl-1,2:5,6-di-O-isopropylidene-α-D-gulofuranose

Treatment of 1,2:5,6-di-*O*-isopropylidene-α-D-gulofuranose (5) (1 g) with dry pyridine (20 ml) and benzoyl chloride (1.66 g) in the usual way gave the title benzoate (1.1 g), m.p. 153.5–154.5°, $[\alpha]_D^{25}$ +55° (*c* 0.5, chloroform).

Anal. Calcd. for $C_{19}H_{24}O_7$: C, 62.6; H, 6.6. Found: C, 62.9; H, 6.9.

Spectral Assignments

The overall assignments of the ^1H n.m.r. spectra of derivatives **3**, **7**, **8**, **13**, **14**, **15**, and **16** were generally straightforward, with the sole exception of the C-5, -6 proton resonances of the pyranose derivatives **7**, **8**, **13**, **14**. These resonances were so closely coupled that an analysis was not accessible without recourse to computer techniques; it was not deemed worthwhile to attempt this. Fortunately the other ring-proton resonances were sufficiently chemically shifted to enable a first order analysis to be applied.

The spectrum of the α-tetraacetate (**8**), which is typical of those obtained from the pyranose derivatives, is shown in Fig. 1. The anomeric proton at low field showed as a triplet in this instance because of approximately equal couplings with both H-2 and F-3. The β-anomer **7** showed no such coupling with F-3. Clearly resolved in Fig. 1 is the rather small coupling between H-4 and -5. It is interesting to note the increased intensity build up in the H-3 quartet at τ 4.7 of the transitions associated with $J_{2,3}$; the intensity slant of the corresponding $J_{2,3}$ transitions is less marked. This reflects the difference in second order perturbations of the two halves of the H-3 resonance, the higher-field being the more weakly coupled to H-2.

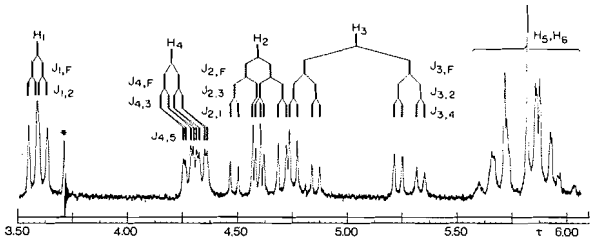

FIG. 1. Partial 100 MHz p.m.r. spectrum of 3-deoxy-3-fluoro-α-D-galactopyranose tetraacetate (**8**) in $CHCl_3$ solution. The first-order assignments are as indicated. The peak at τ *ca.* 3.7 is the high-field ^{13}C satellite of the chloroform solvent.

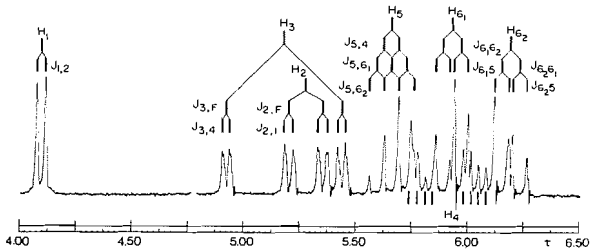

FIG. 2. Partial 100 MHz p.m.r. spectrum of 3-deoxy-3-fluoro-1,2:5,6-di-*O*-isopropylidene-α-D-galactofuranose (**3**) in $CDCl_3$ solution. The first-order assignments are as indicated.

The ^1H n.m.r. spectrum of 3-deoxy-3-fluoro-1,2:5,6-di-*O*-isopropylidene-α-D-galactofuranose (**3**), shown in Fig. 2, is a nice illustration as to the complexity of a spectrum which can be assigned intuitively, without recourse to either decoupling or computer facilities. Straightforward matching of the spectral splittings suffices to identify all of the transitions. It is important to note that several of the resonances, particularly those of H-2 and -3, evidence a number of long-range couplings which are not detailed in this paper; they will be discussed in another context elsewhere.

It is a pleasure for one of us (L.D.H.) to thank the National Research Council of Canada for their generous financial support and, in particular, for the provision of an equipment grant (E 1338) to cover the cost of the heteronuclear decoupler. Two of us (A.B.F. and L.D.H.) thank N.A.T.O. for a research grant (No. 352) and the work was also supported in part by grants to the Chester Beatty Research Institute from the Medical Research Council and the British Empire Cancer Campaign for Research.

1. J. S. BRIMACOMBE, A. B. FOSTER, R. HEMS, and L. D. HALL. Carbohyd. Res. **8**, 249 (1968).
2. H. B. HENBEST and W. R. JACKSON. J. Chem. Soc. 954 (1962).
3. A. B. FOSTER, R. HEMS, and J. M. WEBBER. Carbohyd. Res. **5**, 292 (1967).
4. J. ADAMSON and A. B. FOSTER. Carbohyd. Res. **10**, 517 (1969).
5. W. M. ZU RECKENDORF. Angew. Chem. **79**, 151 (1967).
6. J. S. BRIMACOMBE, P. A. GENT, and M. STACEY. J. Chem. Soc. (C) 567 (1968).
7. F. WEYGAND and H. WOLZ. Ber. **85**, 256 (1952).
8. M. L. WOLFROM and A. THOMPSON. Methods Carbohyd. Chem. **2**, 213 (1963).
9. H. BOOTH. Tetrahedron Lett. 411 (1965).
10. B. COXON. Tetrahedron, **21**, 3481 (1965).
11. L. D. HALL and J. F. MANVILLE. Can. J. Chem. **47**, 19 (1969).
12. A. B. FOSTER, R. HEMS, and L. D. HALL. Can. J. Chem. This issue.
13. L. D. HALL, J. F. MANVILLE, and N. BHACCA. Can. J. Chem. **47**, 1 (1969).
14. L. D. HALL and J. F. MANVILLE. Chem. Commun. **37**, (1968).
15. A. B. FOSTER, R. HEMS, L. D. HALL, and J. F. MANVILLE. Chem. Commun. 158 (1968).
16. R. J. ABRAHAM, L. D. HALL, L. HOUGH, and K. A. MCLAUCHLAN. J. Chem. Soc. 3699 (1962).
17. P. R. STEINER. M.Sc. Thesis, University of British Columbia, Vancouver, British Columbia, 1969.
18. L. D. HALL, P. R. STEINER, and C. PEDERSEN. Can. J. Chem, **48**, 1155 (1970).
19. J. D. STEVENS and H. G. FLETCHER. J. Org. Chem. **33**, 1799 (1968).
20. R. BURTON and L. D. HALL. Can. J. Chem. **48**, 59 (1970).
21. R. U. LEMIEUX and J. D. STEVENS. Can. J. Chem. **43**, 2059 (1965).
22. B. COXON and H. G. FLETCHER. Chem. Ind. (London), 662 (1964).
23. C. CONE and L. HOUGH. Carbohyd. Res. **1**, 1 (1965).

Can. J. Chem. Downloaded from www.nrcresearchpress.com by 210.87.254.105 on 09/05/12
For personal use only.

Can. J. Chem. Downloaded from www.nrcresearchpress.com by 210.87.254.42 on 09/05/12
For personal use only.

Deoxidation studies with cyclopropylcarbinol

A. J. CESSNA[1] AND C. C. LEE

Department of Chemistry and Chemical Engineering, University of Saskatchewan, Saskatoon, Saskatchewan

Received May 11, 1970

The liquid products from the deoxidation with cyclopropylcarbinol in KOH–$CHBr_3$ were identified as cyclopropylcarbinyl, cyclobutyl, and allylcarbinyl alcohols, bromides, and the various ethers, with dicyclopropylcarbinyl ether as the most abundant product. In addition, small amounts of methylene bromide, cyclopropanecarboxaldehyde, and cyclobutanone were also found. The deoxidation with cyclopropylcarbinol-α-^{14}C gave rise to isotopically scrambled cyclopropylcarbinol-x-^{14}C, with about 22% of the ^{14}C-label rearranged from C-α to the cyclopropyl group.

Canadian Journal of Chemistry, 48, 3953 (1970)

In a 1964 review on carbonium ions, Deno (1) briefly stated that deoxidation with cyclopropylcarbinol-α,α-d_2 (**1**-OH-α-d_2) gave principally 1,3-butadiene-1,1-d_2, indicating that no isotopic scrambling has occurred in the cyclopropylcarbinyl cation produced under the conditions of very short life expected for deoxidation. A more detailed analysis of the hydrocarbon products from the alkaline deoxidation of **1**-OK with bromoform was reported by Bayless *et al.* (2). Among the 11% yield of hydrocarbon products, 1,3-butadiene, bicyclobutane, cyclobutene, methylenecyclopropane, ethylene, and acetylene were found and their formation was attributed to processes involving highly energetic intramolecular cationic paths, such as carbon–hydrogen insertion, carbon-skeleton rearrangement, and fragmentation. In these earlier studies, the nature of the liquid products apparently has not been investigated. In the present work, the liquid products from deoxidation studies with **1**-OH were examined. The reaction was carried out in concentrated KOH (3, 4), since in this medium the presence of excess hydroxide ions may allow for the formation of rearranged alcohols such as cyclobutanol (**2**-OH) and allylcarbinol (**3**-OH). Moreover, Lee and Hahn (5) have found that the deoxidation with 2-phenyl-1-^{14}C-ethanol in KOH–$CHBr_3$ gave rise to some isotope position rearranged 2-phenyl-2-^{14}C-ethanol. Analogously, deoxidation studies with **1**-OH-α-^{14}C in KOH-$CHBr_3$ should be capable of yielding data on the extents of isotopic scrambling, if any, in the recovered **1**-OH-x-^{14}C.

The liquid products from the deoxidation with **1**-OH using a **1**-OH:$CHBr_3$ molar ratio of 1.0:0.5 or 1.0:1.0 are given in Table 1. The identifications of the various products were based on peak enhancement in the vapor phase chromatogram utilizing authentic samples and by examination of their n.m.r. spectra (the spectra of some of the authentic compounds, namely, the isomeric bromides, **1**-Br, **2**-Br, and **3**-Br, and the isometric ethers, **1**-O1, **1**-O2, and **1**-O3 are shown in Fig. 1). The **1**-OH-α-^{14}C (6) was subjected to a similar deoxidation using an equimolar amount of $CHBr_3$ and the recovered **1**-OH-x-^{14}C was degraded by oxidation to cyclopropanecarboxylic acid, followed by conversion to cyclopropylamine (6). The resulting activity data, showing the extents of isotopic scrambling from C-α to the cyclopropyl group, are summarized in Table 2.

The results in Tables 1 and 2 demonstrate that cationic processes do play important roles in deoxidation reactions. As originally suggested by Skell and Starer (7, 8), highly energetic carbonium ions may be formed via intermediate carbenes, eq. 1. In the cyclopropylcarbinyl

$$[1]\quad RO^- + CBr_2 \xrightarrow{-Br^-} ROCBr \rightarrow R^+ + CO + Br^-$$

system, interconversions between cyclopropylcarbinyl, cyclobutyl, and allylcarbinyl cations are well known (6, 9), and reactions between these ions and the available nucleophiles (OH^-, Br^-, and the various RO^-) would account for

[1]Holder of an NRCC Studentship, 1966–1969.

TABLE 1

Liquid products from deoxidation with cyclopropylcarbinol (1-OH)

Products*	Composition (%)† Experiment 1‡	Experiment 2‡
Two unidentified peaks	1.1	2.0
Allylcarbinyl bromide§	0.5	0.9
Cyclobutyl bromide§	1.5	5.2
Cyclopropylcarbinyl bromide§	0.1	0.2
Diallylcarbinyl ether‖	0.2	0.4
Allylcarbinyl cyclobutyl ether‖	0.2	0.2
Methylene bromide	0.4	0.9
Allylcarbinyl cyclopropylcarbinyl ether	1.6	2.5
Dicyclobutyl ether‖	0.1	0.3
Cyclobutyl cyclopropylcarbinyl ether¶	7.1	10.8
Allylcarbinol	0.3	0.8
Dicyclopropylcarbinyl ether	34.7	34.2
Cyclobutanol	0.6	4.3
Cyclopropylcarbinol	51.4	37.4

*Listed in the order of increasing retention times which ranged from 16 to 172 min under the conditions used for the v.p.c. analyses by the analytical column.

†Based on the relative areas of the various peaks in the v.p.c.

‡Experiments 1 and 2 were carried out using 1-OH:$CHBr_3$ molar ratios of 1.0:0.5 and 1.0:1.0, respectively.

§The actual amounts of these isomeric bromides formed in the deoxidation reaction may be different from the composition shown because 1-Br was found to undergo some rearrangement to 2-Br and 3-Br in the v.p.c. column under the conditions employed (see preparation for 1-Br in the Experimental section).

‖Authentic samples of these ethers were not synthesized and their tentative identifications were based on their n.m.r. spectra.

¶Containing small quantities of cyclobutanone and cyclopropanecarboxaldehyde, which amounted to about 0.1 and 0.2% respectively, in experiment 2.

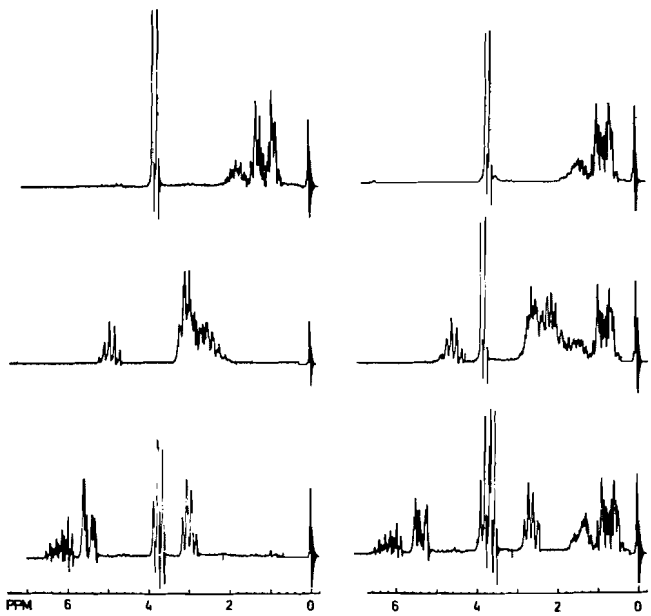

FIG. 1. The n.m.r. spectra. Left column, top to bottom, respectively, are the spectra of cyclopropylcarbinyl, cyclobutyl, and allylcarbinyl bromides; right column, top to bottom, respectively, are the spectra of dicyclopropylcarbinyl, cyclobutyl cyclopropylcarbinyl, and allylcarbinyl cyclopropylcarbinyl ethers.

Can. J. Chem. Downloaded from www.nrcresearchpress.com by 210.87.254.42 on 09/05/12
For personal use only.

TABLE 2

Activity data and isotopic scrambling in the recovered cyclopropylcarbinol-x-^{14}C from deoxidation with cyclopropylcarbinol-α-^{14}C

Compound assayed	Specific activity* (c.p.min/mmole)		Rearrangement (%)	
	Run 1	Run 2	Run 1	Run 2
c-C_3H_5COOH†	120 500	102 300		
c-$C_3H_5NH_2$‡	25 900	23 300	21.5	22.8

*Determined by a liquid scintillation counter, with appropriate corrections for quenching.
†Assayed as *N*-phenylcyclopropanecarboxamide.
‡Assayed as *N*-cyclopropylbenzamide.

most of the products given in Table 1. However, the possibility that some of these products might also have been derived from concerted displacements involving the nucleophiles and the alkoxybromocarbene, ROCBr, could not be excluded. Moreover, as the **1**-OH was converted to **2**-OH and **3**-OH, these rearranged alcohols likely could themselves undergo deoxidation reactions and contribute to the overall product distribution. Since *c*-$C_3H_5CH_2O^-$ would be the most abundant nucleophile present in the reaction mixture, it is not surprising that, aside from the recovered **1**-OH, the product obtained in the highest yield was dicyclopropylcarbinyl ether (**1**-O**1**) (Table 1).

It is of interest to note that CH_2Br_2 was found among the reaction products (Table 1). The formation of this compound could be attributed to hydride abstraction by dibromocarbene; for example, a process involving *c*-$C_3H_5CH_2O^-$ would give rise to cyclopropanecarboxaldehyde, eqs. 2*a* and *b*. Similarly, if cyclobutoxide were

[2*a*] $$c\text{-}C_3H_5CH_2O^- + CBr_2 \rightarrow c\text{-}C_3H_5CHO + CHBr_2^-$$

[2*b*] $$CHBr_2^- + H_2O \text{ or } ROH \rightarrow CH_2Br_2 + HO^- \text{ or } RO^-$$

involved, cyclobutanone would be produced. Actually, both cyclopropanecarboxaldehyde and cyclobutanone were detected among the products in the present study. Starer (10) has also noted the formation of CH_2Br_2 and CH_3CH_2CHO in the deoxidation of 1-propoxide and has suggested the possibility of hydride abstraction.

From Table 2, it is seen that, unlike the reported absence of isotopic scrambling in the gaseous 1,3-butadiene product (1), the **1**-OH-x-^{14}C recovered from the deoxidation with **1**-OH-α-^{14}C under the present conditions showed about 22% rearrangement of the ^{14}C-label from C-α to the cyclopropyl group, presumably to the C-2 and -3 methylene carbons of the ring. A thorough study of the stereochemistry of such cyclopropylcarbinyl to cyclopropylcarbinyl rearrangements has recently been reported by Wiberg and Szeimies (11). From the present work it is seen that as in the deamination of **1**-NH_2-α-^{14}C (6), the three methylene carbons in the recovered **1**-OH-x-^{14}C have not attained complete equivalence. Some of the excess ^{14}C at C-α undoubtedly was due to unreacted **1**-OH-α-^{14}C. Another possibility that might have contributed to more ^{14}C at C-α would be a concerted displacement by OH^- on *c*-C_3H_5-$^{14}CH_2OCBr$ to produce unrearranged **1**-OH-α-^{14}C. Thus the present ^{14}C-scrambling results once again suggest that both deoxidation and deamination reactions may involve similar, though not necessarily identical, rearrangement processes; such a conclusion was also arrived at in a comparison of the deoxidation and deamination reactions with the 1-^{14}C-1-propyl system (12).[2]

Experimental

*Preparation of Cyclopropylcarbinyl, Cyclobutyl, and Allylcarbinyl Bromides (**1**-Br, **2**-Br, and **3**-Br)*

Compounds **1**-Br and **2**-Br were prepared by the reaction of triphenylphosphine with the corresponding alcohol and carbon tetrabromide in anhydrous ether (13–15). The yields obtained for **1**-Br and **2**-Br, both boiling within the range of 109–113° (lit. (9) b.p. of a 2:1 mixture of **1**-Br and **2**-Br, 110.5–112.0°), were 90 and 50%, respectively. Initially v.p.c. analysis of the **1**-Br

[2]For a recent review on "free carbonium ions" generated from the decomposition of diazonium ions, deoxidation and anodic oxidation of carboxylic acids, see Keating and Skell (17).

Can. J. Chem. Downloaded from www.nrcresearchpress.com by 210.87.254.42 on 09/05/12
For personal use only.

Can. J. Chem. Downloaded from www.nrcresearchpress.com by 210.87.254.42 on 09/05/12
For personal use only.

using an Aerograph 200 chromatograph with flame ionization detector with a 25 ft 1/8 in. copper column packed with 25% β,β′-oxidipropionitrile on 60/80 mesh Chromatosorb P, AW, operating at a column temperature of 85° and N_2 carrier gas flow rate of 35 ml/min, showed the appearance of varying amounts of **2**-Br and **3**-Br. (The above v.p.c. column operated under the conditions described will be referred to as the analytical column.) However, it was later found that the use of a 10 ft 1/8 in. stainless steel column packed with 25% FFAP indicated that both the **1**-Br and **2**-Br obtained in these preparations were essentially pure (less than 2% impurities), suggesting that the **1**-Br could undergo some rearrangement, presumably on the copper walls of the column, during v.p.c. analysis with the analytical column.

Compound **3**-Br was prepared by the reaction of **3**-OH with PBr_3 in CH_2Cl_2 as described by Roberts and Mazur (9) for the reaction of **1**-OH with PBr_3. Fractionation gave a 60% yield of crude product, b.p. 102–110°, the v.p.c. analysis of which (FFAP stainless steel column) showed the presence of about 10% impurities. The final purification was effected by preparative v.p.c. using a Model 15 Pye chromatograph with a 15 ft 3/8 in. copper column packed with 25% β,β′-oxidipropionitrile on 60/80 mesh Chromosorb P, AW, operating at a column temperature of 90° and N_2 carrier gas flow rate of 75 ml/min. (This column operated under the conditions described will be referred to as the preparative column.) The b.p. of the purified **3**-Br was 97° at 717 mm (literature (9), b.p. 99–100°). The n.m.r. spectra of **1**-Br, **2**-Br, and **3**-Br are shown in Fig. 1.

Preparation of Dicyclopropylcarbinyl, Cyclobutyl Cyclopropylcarbinyl, and Allylcarbinyl Cyclopropylcarbinyl Ethers (1-O1, 1-O2 and 1-O3)

These ethers were prepared by the reaction of **1**-Br with the corresponding sodium alkoxide, **1**-ONa, **2**-ONa, or **3**-ONa. In the preparation of **1-O1**, 5.0 g (0.07 mole) of **1**-OH in 100 ml of anhydrous ether was stirred with an equivalent amount of Na to give the alkoxide and then 9.4 g (0.07 mole) of **1**-Br was added. After the mixture was refluxed for 5 h, apparently a fair amount of unreacted material was still present. In an attempt to raise the reaction temperature, 40 ml of acetone was introduced and the reaction mixture was refluxed for a further 5 h. More ether was then added and the resulting material was washed with water and dried over $MgSO_4$. Fractional distillation gave 4.1 g of crude product, b.p. 140–150°, the v.p.c. analysis of which showed the presence of about 20% impurities. Pure **1-O1**, b.p. 148–149°, was obtained after separation by v.p.c. using the preparative column.

Both preparations of **1-O2** and **1-O3** were then carried out simultaneously and in these cases the acetone was introduced at the beginning of the reaction. The use of acetone as a means of raising the reaction temperature turned out to be an error, and the major product obtained in these reactions was mesityl oxide from the condensation of acetone. However, in each preparation, a small fraction, b.p. 138–148°, (1–2 g) was obtained and it contained the desired ether. Pure **1-O2** or **1-O3** was separated from these crude fractions by v.p.c. using the preparative column. The n.m.r. spectra of **1-O1**, **1-O2** and **1-O3** are shown in Fig. 1.

Deoxidation with 1-OH

The reaction was carried out under conditions similar to those used by Lee and Hahn (5). Compound **1**-OH (2.0 g, 0.028 mole) was refluxed for 1 h on an oil bath with a concentrated KOH solution (15 g KOH in 6.0 ml H_2O). This mixture was cooled to about 100° and 3.53 or 7.06 g (0.014 or 0.028 mole) of $CHBr_3$ was added in one batch. After the initial vigorous reaction had subsided, the mixture was refluxed for 1 h. Water (60 ml) was then added and the resulting material was continuously extracted with ether for 24 h. The extract was dried over $MgSO_4$, concentrated, and subjected to v.p.c. analysis using the analytical column.

In order to identify the minor components, the products from six runs as described above were combined and then separated by v.p.c., using the preparative column, into various fractions, each containing one or more components. The n.m.r. spectra of each of these fractions were examined and each fraction was also analyzed by the analytical column, with identifications made by peak enhancement using known compounds. As it turned out with the analytical column, cyclobutanone (Aldrich) and cyclopropanecarboxaldehyde (prepared by reaction of *c*-C_3H_5CN with $LiAlH_4$ (16)) have the same retention time as cyclobutyl cyclopropylcarbinyl ether (**1-O2**). However, with a 25 ft 1/8 in. column packed with 20% bis-2-(2-methoxyethoxy)ethyl ether on 60/80 mesh firebrick, these three products were resolved into their individual components.

Deoxidation with 1-OH-α-^{14}C

Compound **1**-OH-α-^{14}C was prepared as described by Mazur *et al.* (6) and it was subjected to deoxidation using an equivalent amount of $CHBr_3$ as in the deoxidation with **1**-OH. The resulting **1**-OH-x-^{14}C was recovered from the reaction mixture with the aid of inactive **1**-OH as carrier. After purification by preparative v.p.c. it was degraded by oxidation to cyclopropanecarboxylic acid, followed by conversion to cyclopropylamine via the Schmidt reaction as previously described (6).

The financial support given by the National Research Council of Canada is gratefully acknowledged.

1. N. C. Deno. Progr. Phys. Org. Chem. **2**, 129 (1964).
2. J. Bayless, L. Friedman, J. A. Smith, F. B. Cook, and H. Shechter. J. Amer. Chem. Soc. **87**, 661 (1965).
3. P. S. Skell and I. Starer. J. Amer. Chem. Soc. **84**, 3962 (1962).
4. P. S. Skell and R. J. Maxwell. J. Amer. Chem. Soc. **84**, 3963 (1962).
5. C. C. Lee and B.-S. Hahn. Can. J. Chem. **45**, 2129 (1967).
6. R. H. Mazur, W. N. White, D. A. Semenow, C. C. Lee, M. S. Silver, and J. D. Roberts. J. Amer. Chem. Soc. **81**, 4390 (1959).
7. P. S. Skell and I. Starer. J. Amer. Chem. Soc. **81**, 4117 (1959).

8. P. S. SKELL and I. STARER. J. Amer. Chem. Soc. **82**, 2971 (1960).
9. J. D. ROBERTS and R. H. MAZUR. J. Amer. Chem. Soc. **73**, 2509 (1951).
10. I. H. STARER. Ph.D. Thesis. Pennsylvania State University, 1960.
11. K. B. WIBERG and G. SZEIMIES. J. Amer. Chem. Soc. **92**, 571 (1970).
12. C. C. LEE and K.-M. WAN. J. Amer. Chem. Soc. **91**, 6416 (1969).
13. I. M. DOWNIE, J. B. HOLMES, and J. B. LEE. Chem. Ind. London, 900 (1966).
14. J. B. LEE and I. M. DOWNIE. Tetrahedron, **23**, 359 (1967).
15. J. HOOZ and S. S. H. GILANI. Can. J. Chem. **46**, 86 (1968).
16. L. I. SMITH and E. R. ROGIER. J. Amer. Chem. Soc. **73**, 4047 (1951).
17. J. T. KEATING and P. S. SKELL. *In* Carbonium ions. Vol. 2. G. A. Olah and P. v. R. Schleyer, *editors*. Interscience Publishers, New York, 1970. pp. 573–653.

Can. J. Chem. Downloaded from www.nrcresearchpress.com by 210.87.254.42 on 09/05/12
For personal use only.

Synthesis of vitamin K_1 analogs. A new class of vitamin K_1 antagonists

J. LOWENTHAL AND M. N. ROY CHOWDHURY[1,2]
Department of Pharmacology and Therapeutics, McIntyre Medical Sciences Building, McGill University, Montreal 109, Quebec

Received July 8, 1970

The synthesis of two analogs of vitamin K_1, namely, 2-chloro (**2**) and 2-bromo (**3**) analogs, is described. The separation of *cis* and *trans* isomers of both these compounds on preparative t.l.c. is reported along with the spectral data.

Canadian Journal of Chemistry, **48**, 3957 (1970)

With the object of synthesizing vitamin K_1, **1**, analogs of potential biological interest, and of investigating the influence of substituents in position 2 of the naphthoquinone nucleus on biological activity, the synthesis of 2-chloro and 2-bromo analogs of vitamin K_1 was undertaken. These two analogs of vitamin K_1 were found to constitute a new class of vitamin K_1 antagonists, the chloro analog having been shown to be the most active one (1–3). In this communication, we now report the synthesis and characterization of these two analogs of vitamin K_1, namely, 2-chloro-3-phytyl-1,4-naphthoquinone (**2**) and 2-bromo-3-phytyl-1,4-naphthoquinone (**3**).

The synthesis was carried out essentially according to the published procedures (4–8) with some modifications. We have used activated manganese dioxide as the oxidizing agent in the final oxidation step, *i.e.*, in the oxidation of 2-halo-3-phytyl-1,4-naphthohydroquinone to 2-halo-3-phytyl-1,4-naphthoquinone (*vide* Experimental). We were also able to separate the *cis* and *trans* isomers (9, 10) of both the synthetic chloro and bromo analogs by means of t.l.c. on silica gel. Both the isomers of the chloro and bromo analogs were further characterized by n.m.r. spectroscopy (11).

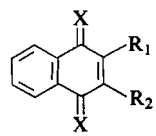

1 X = O; R_1 = CH_3; R_2 = $C_{20}H_{39}$
2 X = O; R_1 = Cl; R_2 = $C_{20}H_{39}$
3 X = O; R_1 = Br; R_2 = $C_{20}H_{39}$

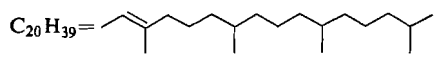

Experimental

Experiments were carried out in the dark and under nitrogen. The i.r. spectra were recorded on a Perkin–Elmer model 257 spectrophotometer. The u.v. spectra were taken in ethanol on a Beckman DB-G recording spectrophotometer. The n.m.r. spectra were recorded on Varian A-60 spectrometer with tetramethylsilane as an

[1]To whom enquiries concerning this paper should be addressed.
[2]Present address: Ontario Cancer Institute, Department of Medicine, 500 Sherbourne Street, Toronto 5, Ontario.

8. P. S. SKELL and I. STARER. J. Amer. Chem. Soc. **82**, 2971 (1960).
9. J. D. ROBERTS and R. H. MAZUR. J. Amer. Chem. Soc. **73**, 2509 (1951).
10. I. H. STARER. Ph.D. Thesis. Pennsylvania State University, 1960.
11. K. B. WIBERG and G. SZEIMIES. J. Amer. Chem. Soc. **92**, 571 (1970).
12. C. C. LEE and K.-M. WAN. J. Amer. Chem. Soc. **91**, 6416 (1969).
13. I. M. DOWNIE, J. B. HOLMES, and J. B. LEE. Chem. Ind. London, 900 (1966).
14. J. B. LEE and I. M. DOWNIE. Tetrahedron, **23**, 359 (1967).
15. J. HOOZ and S. S. H. GILANI. Can. J. Chem. **46**, 86 (1968).
16. L. I. SMITH and E. R. ROGIER. J. Amer. Chem. Soc. **73**, 4047 (1951).
17. J. T. KEATING and P. S. SKELL. *In* Carbonium ions. Vol. 2. G. A. Olah and P. v. R. Schleyer, *editors*. Interscience Publishers, New York, 1970. pp. 573–653.

Synthesis of vitamin K_1 analogs. A new class of vitamin K_1 antagonists

J. LOWENTHAL AND M. N. ROY CHOWDHURY[1,2]
Department of Pharmacology and Therapeutics, McIntyre Medical Sciences Building, McGill University, Montreal 109, Quebec

Received July 8, 1970

The synthesis of two analogs of vitamin K_1, namely, 2-chloro (**2**) and 2-bromo (**3**) analogs, is described. The separation of *cis* and *trans* isomers of both these compounds on preparative t.l.c. is reported along with the spectral data.

Canadian Journal of Chemistry, **48**, 3957 (1970)

With the object of synthesizing vitamin K_1, **1**, analogs of potential biological interest, and of investigating the influence of substituents in position 2 of the naphthoquinone nucleus on biological activity, the synthesis of 2-chloro and 2-bromo analogs of vitamin K_1 was undertaken. These two analogs of vitamin K_1 were found to constitute a new class of vitamin K_1 antagonists, the chloro analog having been shown to be the most active one (1–3). In this communication, we now report the synthesis and characterization of these two analogs of vitamin K_1, namely, 2-chloro-3-phytyl-1,4-naphthoquinone (**2**) and 2-bromo-3-phytyl-1,4-naphthoquinone (**3**).

The synthesis was carried out essentially according to the published procedures (4–8) with some modifications. We have used activated manganese dioxide as the oxidizing agent in the final oxidation step, *i.e.*, in the oxidation of 2-halo-3-phytyl-1,4-naphthohydroquinone to 2-halo-3-phytyl-1,4-naphthoquinone (*vide* Experimental). We were also able to separate the *cis* and *trans* isomers (9, 10) of both the synthetic chloro and bromo analogs by means of t.l.c. on silica gel. Both the isomers of the chloro and bromo analogs were further characterized by n.m.r. spectroscopy (11).

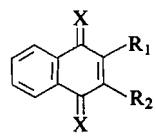

1 X = O; $R_1 = CH_3$; $R_2 = C_{20}H_{39}$
2 X = O; R_1 = Cl; $R_2 = C_{20}H_{39}$
3 X = O; R_1 = Br; $R_2 = C_{20}H_{39}$

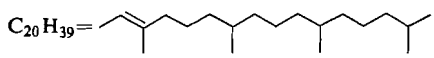

Experimental

Experiments were carried out in the dark and under nitrogen. The i.r. spectra were recorded on a Perkin–Elmer model 257 spectrophotometer. The u.v. spectra were taken in ethanol on a Beckman DB-G recording spectrophotometer. The n.m.r. spectra were recorded on Varian A-60 spectrometer with tetramethylsilane as an

[1]To whom enquiries concerning this paper should be addressed.
[2]Present address: Ontario Cancer Institute, Department of Medicine, 500 Sherbourne Street, Toronto 5, Ontario.

Can. J. Chem. Downloaded from www.nrcresearchpress.com by 210.87.254.40 on 09/05/12
For personal use only.

Can. J. Chem. Downloaded from www.nrcresearchpress.com by 210.87.254.40 on 09/05/12
For personal use only.

internal standard. Mass spectra were determined on an AEI MS-902 spectrometer. Microanalyses were carried out by Dr. F. Pascher, Bonn, and Dr. C. Daesslé, Montreal, Quebec.

2-Chloro-3-phytyl-1,4-naphthoquinone (2)

A solution of 2.11 g (11 mmoles) of 2-chloro-1,4-naphthoquinone (**2***a*, X = O, R_1 = Cl, R_2 = H) in 60 ml of ether was shaken repeatedly with 3 to 4 g portions of sodium hydrosulfite until the color of the solution became pale yellow. The ethereal solution was finally washed with saturated sodium chloride solution containing little sodium hydrosulfite, filtered, and dried over anhydrous sodium sulfate and evaporated to dryness to give 1.9 g of dry, cream-colored 2-chloro-1,4-naphthohydroquinone (**2***b*, X = OH, R_1 = Cl, R_2 = H). To a solution of this naphthohydroquinone in 40 ml of freshly distilled (over Na) dioxane, were added 2.96 g of phytol and 1 ml of boron trifluoride etherate; the mixture was kept in the dark for 6 h and then heated to 65° for ½ h. Ether was then added, and the organic layer was washed with H_2O, then with 2.5% sodium hydroxide solution containing sodium hydrosulfite, and finally with saturated sodium chloride solution containing sodium hydrosulfite. The resulting ethereal solution of 2-chloro-3-phytyl-1,4-naphthohydroquinone (**2***c*, X = OH, R_1 = Cl, R_2 = $C_{20}H_{39}$) was dried over anhydrous sodium sulfate and to this solution (60 ml) 1.5 g of activated manganese dioxide[3] was added. The mixture was stirred for 10 min, filtered over sodium sulfate and Celite, and evaporated to dryness to give 2.9 g of a brownish oil. The oil was chromatographed twice over Florisil; elution with petroleum ether (b.p. 30–60°) gave 1.82 g (39% yield, based on phytol) of *2-chloro-3-phytyl-1,4-naphthoquinone (2)*. λ_{max}(EtOH) 241 mμ (log ε 3.91), 245(4.20), 251(4.22), 267(4.11), and 275(4.16);[4] ν_{max} 1665 cm^{-1} (C=O), 1605 (C=C), 1595 (aromatic), 1296 (aromatic); δ 8.22–7.82 (m, 4H, aromatic protons), 5.26 (t, 1H, C—CH=C), 3.65 (d, 2H, Ar—CH_2—C), 1.93 and 1.8 (s, 3H each, —$C(CH_3)$=C, *cis* and *trans* methyls), 1.33 (chain CH_2's), and 1.02, 0.97, 0.90 (chain CH_3's); M^+ 472 (minor), 470 (major) (corresponding respectively, to Cl^{37} and Cl^{35}), M-225 247 (minor), 245 (major) (12).

Anal. Calcd. for $C_{30}H_{43}ClO_2$: C, 76.60; H, 9.15; Cl, 7.55. Found: C, 76.69; H, 9.35; Cl, 7.67.

The *cis* and *trans* isomers of 2-chloro analog were separated by preparative t.l.c. on silica gel using (9:1) hexane – *n*-butylether as the eluting solvent; R_f *cis* 0.49, R_f *trans* 0.45; ratio of *cis*:*trans* = 1:4. Both the *cis* and *trans* isomers of the chloro analog **2** gave identical n.m.r. spectra, except for the difference in chemical shifts of the peak corresponding to the olefinic methyl group in the region of 1.94 to 1.80 p.p.m.; in the n.m.r. spectrum of the *trans* isomer, the olefinic methyl protons appeared as a singlet only at 1.93 p.p.m., while the olefinic methyl protons of the *cis* isomer appeared only at 1.80 p.p.m.

2-Bromo-3-phytyl-1,4-naphthoquinone (3)

The 2-bromo analog **3** was synthesized in 40% yield (based on phytol), starting with 2-bromo-1,4-naphthoquinone (**3***a*, X=O, R_1=Br, R_2=H) and following the procedure as described above for the 2-chloro analog, **2**. The brown oil obtained after manganese dioxide oxidation of 2-bromo-3-phytyl-1,4-naphthohydroquinone (**3***c*, X=OH, R_1=Br, R_2=$C_{20}H_{39}$), was chromatographed twice on Florisil; elution with 2% ether in petroleum ether (b.p. 30–60°) gave *2-bromo-3-phytyl-1,4-naphthoquinone (3)*: λ_{max}(EtOH) 242 mμ (log ε 3.92), 246(4.22), 252(4.25), 270(4.17), 278(4.20);[4] ν_{max} 1675 cm^{-1} (C=O), 1600 (C=C), 1580 (aromatic), 1280 (aromatic); δ 8.2–7.8 (m, 4H, aromatic protons), 5.3 (t, 1H, C—CH=C), 3.7 (d, 2H, Ar—CH_2—C=) 1.87 and 1.70 (s, 3H each, —$C(CH_3)$=C, *cis* and *trans* methyls), 1.23 (chain CH_2's), and 0.91, 0.89, 0.81 (chain CH_3's); M^+ 516 and 514 (corresponding, respectively, to Br^{81} and Br^{79}), M-225 291, 289 (12). Mass spectrometric determination of the exact mass confirmed the molecular formula as $C_{30}H_{43}BrO_2$.[5]

The *cis* and *trans* isomers of the 2-bromo analog **3** were separated by t.l.c. in the same way as described above for the chloro-compound **2**; R_f *cis* 0.40, R_f *trans* 0.35; ratio of *cis*:*trans* 1:6. As already described for the 2-chloro analog **2**, n.m.r. spectra of the *cis* and *trans* isomers of the bromo derivative **3** differ only in the chemical shifts of their olefinic methyl protons, the *trans* methyl signal appeared at 1.87 p.p.m. while the methyl protons of the *cis* isomer appeared at 1.70 p.p.m.

1. J. Lowenthal, J. A. MacFarlane, and K. M. McDonald. Exper. **16**, 428 (1960).
2. J. Lowenthal and J. A. MacFarlane. Proceedings of the first international pharmacological meeting, 1963, Stockholm. Vol. VII. *Edited by* K. J. Brunings. Pergamon Press, New York. p. 333.
3. J. Lowenthal and J. A. MacFarlane. J. Pharmacol. Exp. Ther. **147**, 130 (1965).
4. O. Isler and K. Doebel. Helv. Chim. Acta, **37**, 225 (1954).
5. L. F. Fieser, M. Tishler, and N. L. Wendler. J. Amer. Chem. Soc. **62**, 2861 (1940).
6. R. Hirschmann, R. Miller, and N. L. Wendler. J. Amer. Chem. Soc. **76**, 4592 (1954).
7. R. J. Woods and J. D. Taylor. Can. J. Chem. **35**, 941 (1957).
8. O. Isler, H. Mayer, R. Rüegg, and J. Würsch. Vitamins and hormones, **24**, 331–347 (1966).
9. H. Mayer, U. Gloor, O. Isler, R. Rüegg, and O. Wiss. Helv. Chim. Acta, **47**, 221 (1964).
10. O. Isler and M. Montavon. Bull. Soc. Chim. France, **1965**, 2403 (1965).
11. L. M. Jackman, R. Rüegg, G. Ryser, C. von Planta, U. Gloor, H. Mayer, P. Schudel, M. Kofler, and O. Isler. Helv. Chim. Acta, **48**, 1332 (1965).
12. S. J. Di Mari, J. H. Supple, and H. Rapoport. J. Amer. Chem. Soc. **88**, 1226 (1966).

[3]Obtained from Winthrop Laboratories, New York, N.Y.

[4]Absence of an absorption maximum in 310–330 mμ region of the u.v. spectrum may be of interest, because, as was pointed out by one of the referees, phylloquinones exhibit a weak, broad maximum in this region (most often at 325–327 mμ).

[5]Satisfactory elemental analysis could not be obtained for the bromo analog presumably due to the light-sensitive and unstable nature of the compound.

An electron spin resonance study of the mechanism of intermolecular cation exchange reactions

T. E. GOUGH[1] AND P. R. HINDLE
Department of Chemistry, University of Waterloo, Waterloo, Ontario

Received July 22, 1970

A survey of the effects, as detected by electron spin resonance spectroscopy, of adding NaX (X^- = Ph_4B^-, ClO_4^-, I^-) to sodium-semiquinone ion pairs is given. When X^- = Ph_4B^- triple ion formation was observed, but when X^- = ClO_4^- or I^- intermolecular cation scrambling occurred. It is postulated that such scrambling reactions proceed via the triple ion.

Canadian Journal of Chemistry, **48**, 3959 (1970)

Can. J. Chem. Downloaded from www.nrcresearchpress.com by 210.87.254.5 on 09/05/12
For personal use only.

Recent papers (1–5) have reported the electron spin resonance spectra of systems in which a diamagnetic electrolyte was added to an ion-pair of a radical anion. These systems share two common features: the radical anion has two equivalent sites at which ionic association can occur, and the ion-pair has the same cation as the added electrolyte. Such a situation has lead to two results, expressed by the equilibria 1 and 2.

$$[1] \qquad MA + M^+ \underset{k_{-1}}{\overset{k_1}{\rightleftharpoons}} M^+ + AM$$

$$[2] \qquad MA + M^+ \underset{k_{-2}}{\overset{k_2}{\rightleftharpoons}} M_2A^+$$

In [1] intermolecular scrambling of M^+ proceeds via a mechanism in which the incoming cation associates with the uncomplexed site of the anion while the outgoing cation simultaneously leaves the complexed site; the rate constants k_1 and k_{-1} were found to be rapid within the time scale of the electron spin resonance experiment (1, 2). In [2], k_2 and k_{-2} were found to be slow so that well resolved spectra of the ion-pair, MA, and the triple ion, M_2A^+, were simultaneously observable (3, 5). Here we report the influence of the anion of the added electrolyte upon such systems when A^- is a semiquinone.

The results for the addition of sodium tetraphenylboride to solutions of sodium-semiquinone ion-pairs in tetrahydrofuran have already been published (3) and are described by [2]. Well resolved sodium hyperfine structure was observed for both MA and M_2A^+, showing k_2 and k_{-2} to be slow. When small amounts of sodium perchlorate were added to sodium-semiquinone ion-pairs in tetrahydrofuran, the sodium hyperfine structure became somewhat broadened while, in general, the triple ion spectrum was broad and showed no sodium hyperfine structure. However, for the triple ion [2,3-dimethyl-*p*-benzosemiquinone-Na_2]$^+$ over the temperature range -80 to -60 °C sodium septets, identical to those observed in the presence of sodium tetraphenylboride, were resolvable. This triple ion is the most favorable of the series for which to observe sodium splittings in the presence of exchange, having the largest value of a_{Na} at low temperatures. Larger additions of sodium perchlorate produced spectra with broad lines and hyperfine splitting constants typical of the corresponding unassociated semiquinone anion: raising the temperature, or adding more salt, caused these lines to sharpen. Were it not for the fact that the smaller additions show equilibrium 2 to be present, the effect of the larger additions might be interpreted in terms of equilibrium 1. Addition of very small amounts of sodium iodide destroyed the sodium hyperfine structure of the ion-pairs; further additions reproduced the effects of adding sodium perchlorate, generating a "time-averaged" spectrum. Sodium iodide was much more effective in inducing exchange than was an equal amount of sodium perchlorate. In summary, our results show that the rate of cation scrambling generated by the addition of a second electrolyte to a semiquinone ion-pair depends upon the anion of the added electrolyte, and furthermore, that this rate increases with decreasing dissociation constant of the added electrolyte.

It is difficult to incorporate these observations into [1] as a mechanism for the cation exchange reaction. However, they can be readily incorporated into [2] as shown in [3], where X^- is the added anion.

[1]To whom all correspondence should be addressed.

[3] $$MA + MX \underset{k_{-3}}{\overset{k_3}{\rightleftharpoons}} MAM^+ + X^-$$

Consider the reaction whereby the triple ion dissociates forming the ion-pair. When X^- has little affinity for M^+ (*e.g.* $X^- = Ph_4B^-$) this dissociation proceeds as in [2] and is slow since it involves cleavage of the A–M interaction. However, should X^- have a strong affinity for M^+ then it will attack the triple ion, forming the M–X interaction as the A–M interaction is weakened. Thus the rate of dissociation of the triple ion should increase as the strength of the MX interaction increases, *i.e.* as the dissociation constant of MX decreases. The situation for the formation of triple ion is somewhat more complicated; however, a possible disposition of the energies of reactants, activated complexes, and products is given in Fig. 1. We are at present attempting a more quantitative analysis of these systems to investigate these proposed mechanisms for cation scrambling reactions.

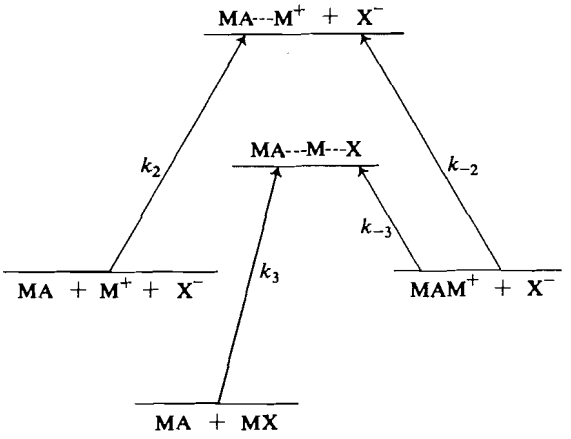

FIG. 1. Possible relative energies of reactants, activated complexes, and products involved in intramolecular cation exchange reactions. The subscripts 2 and 3 refer to the mechanisms 2 and 3 of the text.

This work received financial support from the National Research Council of Canada.

1. R. F. ADAMS and N. M. ATHERTON. Trans. Faraday Soc. **64**, 7 (1968).
2. A. W. RUTTER and E. WARHURST. Trans. Fraday Soc. **64**, 2338 (1968).
3. T. E. GOUGH and P. R. HINDLE. Can. J. Chem. **47**, 3393 (1969).
4. T. E. GOUGH and P. R. HINDLE. Trans. Faraday Soc. **66**, 2420 (1970).
5. S. A. AL-BALDAWI and T. E. GOUGH. Can. J. Chem. **48**, 2798 (1970).

Can. J. Chem. Downloaded from www.nrcresearchpress.com by 210.87.254.5 on 09/05/12
For personal use only.

Can. J. Chem. Downloaded from www.nrcresearchpress.com by 210.87.254.40 on 09/05/12
For personal use only.

An hydration scale for ketones in polar aprotic solvents[1]

ROSS STEWART AND JOHN D. VAN DYKE[2]
Department of Chemistry, University of British Columbia, Vancouver, British Columbia

Received July 16, 1970

An hydration scale (W_0) for aqueous sulfolane and dimethyl sulfoxide (DMSO) has been developed that represents the effect of the solvent on the equilibrium hydration of a series of trifluoroacetophenones; $ZH_2O \overset{K_d}{\rightleftharpoons} Z + H_2O$. The equilibrium constants are correlated with the substituent parameter σ^+; $\rho^+ = -1.62$ for dehydration. The function W_0, defined as $W_0 = pK_d + \log [Z]/[ZH_2O] = -\log (f_Z/f_{ZH_2O} \cdot a_{H_2O})$ is zero for pure water and rises to a value of 2.72 in 99 mole% sulfolane. W_0 in aqueous DMSO is negative from 0 to 85 mole% DMSO, meaning that these systems hydrate the ketones to a greater extent than does pure water.

Canadian Journal of Chemistry, 48, 3961 (1970)

Carbonyl compounds undergo hydration reactions to give *gem* diols provided that the attached groups are small or contain strongly electronegative atoms (1). We have used the general Hammett overlap method (2) to determine (*a*) the thermodynamic equilibrium constants for the hydration of a series of ring-substituted trifluoroacetophenones (standard state, water) and (*b*) the hydrating ability of solvent mixtures that range from pure water to 99 mole% tetramethylene sulfone (sulfolane) or dimethyl sulfoxide (DMSO). To preserve the analogy with Hammett-type acidity functions the equilibrium equation is written so that the hydrate is on the left and the ketone on the right.

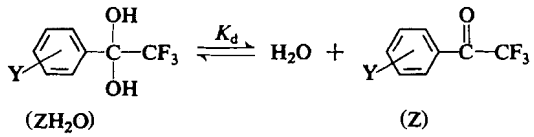

(ZH$_2$O) (Z)

The dehydration constant, K_d, takes the form

$$[1] \qquad K_d = \frac{[Z]}{[ZH_2O]} \cdot \frac{f_Z}{f_{ZH_2O}} \cdot a_{H_2O}$$

Therefore

$$[2] \quad pK_d = -\log\left(\frac{[Z]}{[ZH_2O]}\right) - \log\left(\frac{f_Z a_{H_2O}}{f_{ZH_2O}}\right)$$

We define W_0 as

$$[3] \qquad W_0 = -\log\left(\frac{f_Z a_{H_2O}}{f_{ZH_2O}}\right)$$

Combining [2] and [3] gives

$$[4] \qquad W_0 = pK_d + \log\frac{[Z]}{[ZH_2O]}$$

The symbol W_0 seems appropriate for this function since water is a component of the equilibrium. The subscript indicates the substrate's charge.

Values of log $[Z]/[ZH_2O]$ were obtained at 31.4° using both ^{19}F n.m.r. and ultraviolet (u.v.) spectroscopy, the latter being used at high water concentrations where solubility problems made n.m.r. measurements difficult or impossible. Excellent agreement between the two techniques was achieved.

The only ketone not previously prepared (3), 3-methoxy-α,α,α-trifluoroacetophenone, was obtained by the action of 3-methoxyphenylmagnesium bromide on trifluoroacetic acid; b.p. 60° at 2 Torr.

Anal. Calcd. for $C_9H_7OF_3$: C, 52.95; H, 3.45; F, 27.92. Found: C, 52.74; H, 3.49; F, 28.1.

The anchor compound is 4-methoxy-α,α,α-trifluoroacetophenone whose pK_d in water was found to be 0.84. (This value was obtained by adding a solution of this ketone in aqueous sulfolane to water so that the concentration of water was actually 99.90 mole%.) Methanesulfonic acid was added as catalyst to most of the solutions, because equilibrium was reached

[1]Taken from the Ph.D. thesis of J. D. Van Dyke, 1970.
[2]Present address: Polymer Corporation, Sarnia, Ontario.

Can. J. Chem. Downloaded from www.nrcresearchpress.com by 210.87.254.40 on 09/05/12
For personal use only.

extremely slowly in solutions whose water content was low. Experiments at higher water content showed the position of the hydration equilibrium to be unaffected by acid, except for the dimethylamino compound. Table 1 lists the pK_d values (in water) determined by the overlapping technique and Fig. 1 shows the effect of substituents on pK_d (4). It is interesting to note that the substituent parameter that governs the hydration equilibrium is σ^+ rather than σ (5), and this presumably reflects the importance of resonance interaction between para substituents and the carbonyl group (5).

Figure 2 shows the variation of W_0 with solvent composition for aqueous sulfolane and aqueous DMSO. It is clear that sulfolane has a greater dehydrating action in these systems than does DMSO, in sharp contrast to their effect on hydroxide ion basicity (6). Figure 2 reveals that aqueous systems containing up to 85 mole% DMSO are *more hydrating* with respect to trifluoroacetophenones than is pure water.

The activity of water in aqueous DMSO decreases faster than does the water concentration and in aqueous sulfolane it decreases more slowly than does the water concentration (7). The W_0 values are in the reverse order and this must result from the f_Z/f_{ZH_2O} term in eq. 3 being strongly solvent dependent. We believe that the ketone hydrate, because of its *gem* diol character, fits into the water structure without greatly perturbing it whereas the presence of sulfolane tends to exclude the ketone hydrate from the association pattern, causing f_{ZH_2O} to rise. DMSO, on the other hand, appears to form stronger associations with the hydrate than does water, causing f_{ZH_2O} in these solutions to fall (8).

Acidity scales have been found to be more substrate dependent than was originally thought (9) and we have little hope that hydration scales will be better behaved. Nonetheless, the concept should be of considerable value for determining hydration equilibrium constants in water (or any other standard state) of compounds whose degree of hydration is too high or too low for direct measurement.

TABLE 1

pK_d values of ketones
Y-$C_6H_4COCF_3$ in water at 31.4°

Y	pK_d
4-$(CH_3)_2N$	−0.86
4-CH_3O	0.84
4-CH_3	1.46
3-CH_3	1.77
H	1.89
4-F	1.91
3-CH_3O	1.99
3-F	2.50
3-NO_2	3.15

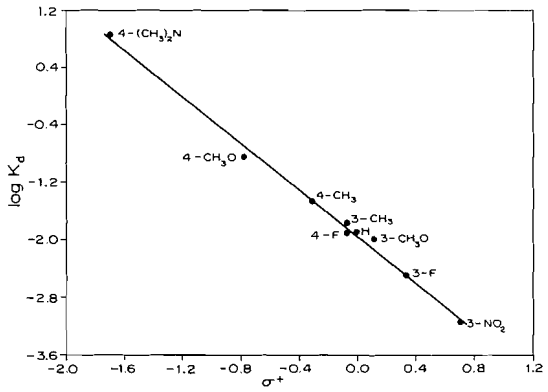

FIG. 1. Effect of substituents on equilibrium constants for the dehydration of trifluoroacetophenone hydrates; $\rho^+ = -1.62$, correlation coefficient, 0.997.

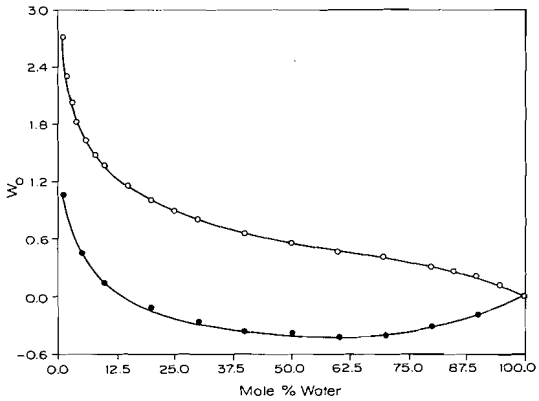

FIG. 2. Plots of W_0 determined with trifluoroacetophenone indicators against solvent composition for sulfolane–water mixtures (○) and DMSO–water mixtures (●) containing 0.1 *M* methanesulfonic acid.

The support of the National Research Council of Canada and the H. R. MacMillan Foundation is gratefully acknowledged.

1. R. P. BELL. Advan. Phys. Org. Chem. **4**, 1 (1966). P. LE HENAFF. Bull. Soc. Chim. France, **11**, 4687 (1968).
2. M. A. PAUL and F. A. LONG. Chem. Rev. **57**, 1 (1957).
3. R. STEWART and R. VAN DER LINDEN. Can. J. Chem. **38**, 399 (1960); A. MENDEL. J. Organometal. Chem. **6**, 97 (1966). E. T. MCBREE, S. RESCONICH, L. R. BEHOLAV, and H. P. BRAENDLIN. J. Org. Chem. **28**, 3579 (1963).

4. See also P. GREENZAID, Z. LUZ, and D. SAMUEL. J. Amer. Chem. Soc. **89**, 749 (1967).
5. J. HINE. Physical Organic Chemistry. McGraw-Hill Book, Co., Inc. New York, N.Y. 1962.
6. R. STEWART and J. P. O'DONNELL. Can. J. Chem. **42**, 1681 (1964).
7. J. KENTTAMAA and J. J. LINDBERG. Suomen. Kemistilehti, **B33**, 98 (1960). R. L. BENOIT and G. CHOUX. Can. J. Chem. **46**, 3215 (1968). R. L. BENOIT. Private communication.
8. V. S. GRIFFITHS and G. SOCRATES. Trans. Farday Soc. **63**, 673 (1967). Y. POCKER, J. E. MEANY, B. J. NIST, and C. ZADOROJNY. J. Phys. Chem.**73**, 2879 (1969). Y. POCKER and D. G. DICKERSON. J. Phys. Chem. **73**, 4005 (1969). B. G. COX and P. T. MCTIGUE. Aust. J. Chem. **22**, 1637 (1969).
9. R. H. BOYD. *In* Solute–Solvent Interactions. *Edited by* J. F. COETZEE and C. D. RITCHIE. Marcel Dekker Inc., New York, 1969.

Bromination and chlorination of *exo,exo*-5,6- and *endo,endo*-5,6-dideuterionorbornene; on the mechanism of nortricyclyl bromide and chloride formation[1]

NICK H. WERSTIUK AND IVAN VANCAS
Department of Chemistry, McMaster University, Hamilton, Ontario

Received May 21, 1970

Proton (deuteron) loss from C-6 to form tricyclic product occurs with *exo* and *endo* stereoselectivity when bromine and chlorine, respectively, are added to *exo,exo*-5,6- and *endo,endo*-5,6-dideuterionorbornene. These data strongly suggest that elimination occurs predominately from **6** in bromination and from **4** in chlorination or alternatively from the unsymmetrically bridged ions **2** and **3**, respectively.

Canadian Journal of Chemistry, **48**, 3963 (1970)

Typically, the addition of a polar reagent E^+Y^- electrophilically to norbornene yields 3-E-nortricyclene as one of the major products (1*a–j*).[2] Although bridged ions of the type **1***a* and **1***b* have been considered as possible intermediates in the additions, no information about the mechanism of tricyclic product formation has been available. To gain information on this problem, a study of the complete set of additions has been undertaken. This communication reports new and interesting mechanistic information obtained from a preliminary study with the electrophilic reagents Br_2 and Cl_2 and the substrates *exo,exo*-5,6- and *endo,endo*-5,6-dideuterionorbornene (2). The results are listed in Tables 1 and 2.

To interpret the observed *exo* and *endo* stereoslectivities in bromination and chlorination, respectively, the data already accumulated on 1,3 elimination in norbornyl systems are used. That is, *endo* stereoselectivity at least should be observed if proton loss occurs prior to a 1,2 Wagner–Meerwein shift or complete participation of the C_1—C_6 bond (1, 3–5). Importantly also, Berson and Grubb (6) have shown that the 6,2 hydrogen shift occurs *endo* → *endo* in the 2-carboxy-3-methyl-5-norbornyl cation.

That a radical process does not contribute to tricyclic product formation in this study is seen from (*a*) the data accumulated on the reaction of radicals with norbornene (7–11), (*b*) Poutsma's study (1*h*) on the chlorination of norbornene, and (*c*) the data in entries 6 and 7, Table 1. That scrambling of deuterium via hydrogen shifts is not important is indicated by the following facts. The products of the reactions are 70% *syn*-2,7-dibromide, 10% 2,3-*trans*-dibromide, 10% nortricyclyl bromide, and 10% other dibromides in CCl_4–Br_2; 40% *syn*-2,7-dichloride, 55% nortricyclyl chloride, and 5% other dichlorides in CCl_4–Cl_2. Furthermore, n.m.r. integration data from *endo,endo*-5,6-dideuterio-*syn*-7-norbornenyl bromide, (C-1 and -2 protons) prepared *via* the bromination of *exo,exo*-5,6-dideuterionorbornene (2) has shown that extensive deuterium scrambling does not occur within the limits of detection (5–10%).

Therefore, if *exo,exo*-5,6-di-deuterionorborn-

[1]Presented in part at the 52nd Annual Meeting of the Chemical Institute of Canada, Montreal, Quebec, May, 1969.

[2]In ref. 1: (*c*) bromine and *N*-bromosuccinimide; (*d*) *N,N*-dibromosulfonamide; (*e*) *N*-bromosuccinimide in wet DMSO; (*f*) *N*-bromosuccinimide in H_2SO_4, *t*-BuOH; (*g*) 2,4-dinitrobenzenesulfonylbromide and chloride; (*h*) chlorine and hypochlorous acid; (*i*) iodobenzenedichloride; (*j*) lead tetraacetate.

Can. J. Chem. Downloaded from www.nrcresearchpress.com by 210.87.254.40 on 09/05/12
For personal use only.

4. See also P. GREENZAID, Z. LUZ, and D. SAMUEL. J. Amer. Chem. Soc. **89**, 749 (1967).
5. J. HINE. Physical Organic Chemistry. McGraw-Hill Book, Co., Inc. New York, N.Y. 1962.
6. R. STEWART and J. P. O'DONNELL. Can. J. Chem. **42**, 1681 (1964).
7. J. KENTTAMAA and J. J. LINDBERG. Suomen. Kemistilehti, **B33**, 98 (1960). R. L. BENOIT and G. CHOUX. Can. J. Chem. **46**, 3215 (1968). R. L. BENOIT. Private communication.
8. V. S. GRIFFITHS and G. SOCRATES. Trans. Farday Soc. **63**, 673 (1967). Y. POCKER, J. E. MEANY, B. J. NIST, and C. ZADOROJNY. J. Phys. Chem.**73**, 2879 (1969). Y. POCKER and D. G. DICKERSON. J. Phys. Chem. **73**, 4005 (1969). B. G. COX and P. T. MCTIGUE. Aust. J. Chem. **22**, 1637 (1969).
9. R. H. BOYD. *In* Solute–Solvent Interactions. *Edited by* J. F. COETZEE and C. D. RITCHIE. Marcel Dekker Inc., New York, 1969.

Bromination and chlorination of *exo,exo*-5,6- and *endo,endo*-5,6-dideuterionorbornene; on the mechanism of nortricyclyl bromide and chloride formation[1]

NICK H. WERSTIUK AND IVAN VANCAS
Department of Chemistry, McMaster University, Hamilton, Ontario

Received May 21, 1970

Proton (deuteron) loss from C-6 to form tricyclic product occurs with *exo* and *endo* stereoselectivity when bromine and chlorine, respectively, are added to *exo,exo*-5,6- and *endo,endo*-5,6-dideuterionorbornene. These data strongly suggest that elimination occurs predominately from **6** in bromination and from **4** in chlorination or alternatively from the unsymmetrically bridged ions **2** and **3**, respectively.

Canadian Journal of Chemistry, **48**, 3963 (1970)

Typically, the addition of a polar reagent E^+Y^- electrophilically to norbornene yields 3-E-nortricyclene as one of the major products (1*a–j*).[2] Although bridged ions of the type **1***a* and **1***b* have been considered as possible intermediates in the additions, no information about the mechanism of tricyclic product formation has been available. To gain information on this problem, a study of the complete set of additions has been undertaken. This communication reports new and interesting mechanistic information obtained from a preliminary study with the electrophilic reagents Br_2 and Cl_2 and the substrates *exo,exo*-5,6- and *endo,endo*-5,6-dideuterionorbornene (2). The results are listed in Tables 1 and 2.

To interpret the observed *exo* and *endo* stereoslectivities in bromination and chlorination, respectively, the data already accumulated on 1,3 elimination in norbornyl systems are used. That is, *endo* stereoselectivity at least should be observed if proton loss occurs prior to a 1,2 Wagner–Meerwein shift or complete participation of the C_1—C_6 bond (1, 3–5). Importantly also, Berson and Grubb (6) have shown that the 6,2 hydrogen shift occurs *endo* → *endo* in the 2-carboxy-3-methyl-5-norbornyl cation.

That a radical process does not contribute to tricyclic product formation in this study is seen from (*a*) the data accumulated on the reaction of radicals with norbornene (7–11), (*b*) Poutsma's study (1*h*) on the chlorination of norbornene, and (*c*) the data in entries 6 and 7, Table 1. That scrambling of deuterium via hydrogen shifts is not important is indicated by the following facts. The products of the reactions are 70% *syn*-2,7-dibromide, 10% 2,3-*trans*-dibromide, 10% nortricyclyl bromide, and 10% other dibromides in CCl_4–Br_2; 40% *syn*-2,7-dichloride, 55% nortricyclyl chloride, and 5% other dichlorides in CCl_4–Cl_2. Furthermore, n.m.r. integration data from *endo,endo*-5,6-dideuterio-*syn*-7-norbornenyl bromide, (C-1 and -2 protons) prepared *via* the bromination of *exo,exo*-5,6-dideuterionorbornene (2) has shown that extensive deuterium scrambling does not occur within the limits of detection (5–10%).

Therefore, if *exo,exo*-5,6-di-deuterionorborn-

[1]Presented in part at the 52nd Annual Meeting of the Chemical Institute of Canada, Montreal, Quebec, May, 1969.

[2]In ref. 1: (*c*) bromine and *N*-bromosuccinimide; (*d*) *N,N*-dibromosulfonamide; (*e*) *N*-bromosuccinimide in wet DMSO; (*f*) *N*-bromosuccinimide in H_2SO_4, *t*-BuOH; (*g*) 2,4-dinitrobenzenesulfonylbromide and chloride; (*h*) chlorine and hypochlorous acid; (*i*) iodobenzenedichloride; (*j*) lead tetraacetate.

Can. J. Chem. Downloaded from www.nrcresearchpress.com by 210.87.254.5 on 09/05/12
For personal use only.

TABLE 1

Data for bromination of deuterionorbornenes

Substrate*	Entry	Initial M concentration norborenene	Conditions†	Fractional % loss of 1 D
exo,exo-di-d-	1	0.10	25°; CCl_4	41.
	2	0.55	0°; CCl_4	44‡
	3	0.06	0°; CH_2Cl_2	46
endo,endo-di-d-	4	0.07	0°; CCl_4	26
	5	0.16	0°; CCl_4	25
	6§	0.06	0°; CH_2Cl_2	14
	7§	0.13	0°; CH_2Cl_2; degassed, hydroquinone	17
	8§	0.0022	0°; CH_2Cl_2	13
	9	0.0022	0°; CH_2Cl_2	24
	10	0.0022	0°; CH_2Cl_2	28
	11‖	0.0089	0°; CH_2Cl_2	18
	12‖	0.0090	0°; CH_2Cl_2	17

*The dideuterionorbornenes composed of 80.8% d_2, 17.4% d_1, and 1.8% d_0 species (1.79 D/molecule) were 85–90% stereochemically pure at C_5—C_6.
†A solution of Br_2, of equivalent molarity to the norbornene, in the appropriate solvent was added to the norbornene and an equimolar amount of pyridine unless stated otherwise.
‡The n.m.r. integral data showed a loss of *ca.* 44% of 1-D.
§The dideuterionorbornene in CH_2Cl_2 was added to a solution of Br_2–pyridine in CH_2Cl_2.
‖2,6-Lutidine was used.

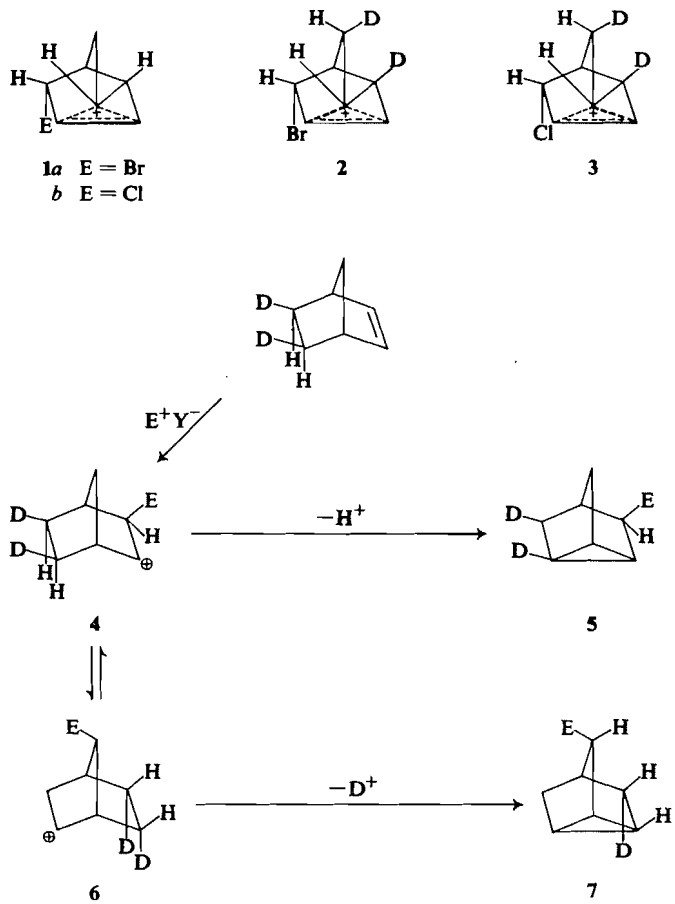

SCHEME 1

Can. J. Chem. Downloaded from www.nrcresearchpress.com by 210.87.254.5 on 09/05/12
For personal use only.

TABLE 2

Data for chlorination of deuterionorbornenes

Substrate	Entry	Initial M concentration norbornene	Conditions*	Fractional % loss of 1-D
exo,exo-di-d-	1†	0.084	0°; CCl_4	28
	2†	0.084	0°; CCl_4	29
endo,endo-di-d-	3†	0.13	0°; CCl_4	48
	4‡	0.04	0°; CH_2Cl_2; O_2 added	59
	5‡	0.04	0°; CH_2Cl_2	59

*As in Table 1.
†Cl_2 was swept into the solution with dry N_2.
‡Cl_2 in CH_2Cl_2 was added to the norbornene–pyridine–CH_2Cl_2 solution.

ene is considered, for example, and cationic species[3] are involved (Scheme 1), the *exo* and *endo* stereoselectivities observed in the bromination and chlorination, respectively, indicate that proton (deuteron) loss occurs in bromination (E = Br) predominately, if not completely, from **6** and in chlorination (E = Cl) from **4**. An attractive alternative, worthy of consideration is that proton (deuteron) loss occurs from the unsymmetrical norboronium ions **2** and **3**,[4] respectively. That **6** or **2** is preferred when E = Br may be a consequence of (*a*) the strain introduced into the system by 2,3 bromonium ion formation and (*b*) bromine-4 participation.

Finally the data listed in Tables 1 and 2 show that (*a*) a change in solvent from CCl_4 to CH_2Cl_2, (*b*) dilution, and (*c*) a change in the base from pyridine to 2,6-lutidine each has little or no effect on the stereochemistry of the 1,3 elimination. The order of addition (see entries 8, 9, 10, Table 1) does however have some effect on the stereoselectivity.

Financial assistance from the National Research Council of Canada and the Department of University Affairs (Ontario) is gratefully acknowledged. The author is indebted to Professor D. B. MacLean who provided for unlimited use of mass spectrometry facilities.

[3]A carbene could be formed by loss of a proton from the cations **4** or **6**. However, no deuterium would be lost unless a complicated mechanism operates that requires protonation at the δ^- center as insertion into the *endo*-C—D bond and loss of D^+ occur more or less consecutively. The bromination and chlorination of 2,3-dideuterionorbornene are planned to check this possibility.

[4]The heavier dotted line is intended to designate the "stronger" of the bridging bonds. In **2** more charge is concentrated on C-1 and in **3** more charge is concentrated on C-2.

1. (*a*) P. B. D. DE LA MARE and R. BOLTON. Electrophilic additions to unsaturated systems. Elsevier, New York, 1966. Chapts. 6 and 7. (*b*) T. G. TRAYLOR. Electrophilic additions to strain olefins. Account. Chem. Res. **2**, 152 (1969). (*c*) J. D. ROBERTS, E. K. TURNBULL, W. BENNETT, and R. ARMSTRONG. J. Amer. Chem. Soc. **72**, 3116 (1950); H. KWART and L. KAPLAN. J. Amer. Chem. Soc. **76**, 4072 (1959). (*d*) A. C. OEHLSCHLAGER, C. D. KENNEDY, and L. H. ZALKOW. J. Org. Chem. **31**, 1682 (1966). (*e*) D. R. DALTON, V. P. DUTTA, and D. C. JONES. J. Amer. Chem. Soc. **90**, 5498 (1968). (*f*) L. H. ZALKOW and A. C. OEHLSCHLAGER. J. Org. Chem. **29**, 1625 (1964). (*g*) H. KWART and K. K. MILLER. J. Amer. Chem. Soc. **78**, 5678 (1954). (*h*) J. D. ROBERTS, F. O. JOHNSON, and R. A. CARBONI. J. Amer. Chem. Soc. **76**, 5692 (1954); M. POUTSMA. J. Amer. Chem. Soc. **87**, 4293 (1965). (*i*) D. D. TANNER and G. C. GRADLEY. J. Org. Chem. **33**, 38 (1968). (*j*) K. ALDER, H. F. FLODE, and H. WURTZ. Ber. **91**, 609 (1958).
2. N. H. WERSTIUK. Can. J. Chem. **48**, 2310 (1970).
3. A. NICKON and N. H. WERSTIUK. J. Amer. Chem. Soc. **89**, 3914 3915 (1967).
4. C. J. COLLINS and BEN M. BENJAMIN. J. Amer. Chem. Soc. **89**, 1632 (1967).
5. N. H. WERSTIUK. Unpublished results.
6. J. A. BERSON and P. W. GRUBB. J. Amer. Chem. Soc. **87**, 4016 (1965).
7. D. I. DAVIES and S. J. CRISTOL. Advances in free radical chemistry. Vol. 1. G. H. Williams, *editor*. Academic Press London, 1965. pp. 159–169.
8. F. W. STACEY and J. F. HARRIS, JR. Organic reactions. Vol. 13. J. Wiley and Sons, Inc., 1969. pp. 150–376.
9. H. KWART and J. L. NYCE. J. Amer. Chem. Soc. **86**, 2601 (1964).
10. N. A. LEBEL. J. Amer. Chem. Soc. **82**, 623 (1960).
11. N. A. LEBEL, P. D. BEIRNE, E. R. KARGER, J. C. POWERS, and P. M. SUBRAMANIAN. J. Amer. Chem. Soc. **85**, 3199 (1963).

Can. J. Chem. Downloaded from www.nrcresearchpress.com by 210.87.254.5 on 09/05/12
For personal use only.

Base-catalyzed protium–deuterium exchange in bicyclo[2.2.1]heptanones

NICK H. WERSTIUK AND ROLAND TAILLEFER
Department of Chemistry, McMaster University, Hamilton, Ontario

Received September 28, 1970

The rates of NaOD-catalyzed protium–deuterium *exo* exchange in fenchan-2,5-dione (**2**) and 1-methyl-5-oxo-camphene (**3**) are 200 and 7, respectively, relative to epiisofenchone (**1**). The *endo* exchange rates in **2** and **3** are 1840 and 4, respectively, relative to **1**. These data give information about the relative importances of conjugative, conformational, inductive, strain, and steric effects which may arise when a carbonyl group or a double bond is situated 1,3 to an enolizable center in the 2.2.1 system.

Canadian Journal of Chemitsry, **48**, 3966 (1970)

Can. J. Chem. Downloaded from www.nrcresearchpress.com by 210.87.254.42 on 09/05/12
For personal use only.

Recently, interest in studies of the rates and stereochemistry of base-catalyzed protium–deuterium exchange in bicyclo[2.2.1]heptanones (1–5) has been high.

Our interest in the chemistry of bicyclo[2.2.1]-heptan-2,5-diones has led us to a study of base-catalyzed protium–deuterium exchange in the 2,5-dione system. This communication (Table 1) reports the *exo* and *endo* exchange rates in epi-isofenchone (**1**), fenchan-2,5-dione (**2**), and the 1-methyl-5-oxo-camphene (**3**). Compound **3** was included in the study as a standard for strain (4), conformational (10), and steric effects which could arise by the introduction of an sp^2 center in the system. To calibrate our data with those of Tidwell, norcamphor (**4**) was also run (entry 4). Our experimental value of 3.9×10^{-2} l mole^{-1} s^{-1} for the *exo* exchange rate compares well with Tidwell's (5.5×10^{-2}) (4) considering that slightly different dioxane–D_2O ratios were used in the two studies.[1]

TABLE 1

Second order rate constants of NaOD-catalyzed deuterium exchange in ketones at 25.0° in 60% dioxane–D_2O

Substrate	Entry	k_2 (l mole^{-1} s^{-1})*†	Relative rates *exo*	Relative rates *endo*
1 *exo*	1	9.9×10^{-3}	1	
endo		2.5×10^{-5}		1
2 *exo*	2	2.0‡	200	
endo		4.6×10^{-2}		1840
3 *exo*	3	6.8×10^{-2}	7	
endo		7.3×10^{-5}		3
4 *exo*	4	3.9×10^{-2}	4	

*Second order rate constants (an average of 3–4 runs) were obtained by dividing the measured pseudo-first order rate constant by the base concentration which was in the range of 0.008–0.16 *M*. Rates were reproducible with a maximum deviation of $< \pm 5\%$, except *endo*-**1** and *exo*-**2**, where the deviations were ± 14 and $\pm 10\%$, respectively.

†That the *exo* exchange was the faster was established by n.m.r. studies on (*a*) the diacetates of the di-*endo*-diols obtained from the deuteriodiones and (*b*) deuteriocamphenilan-2,5-diones.

‡Since *exo* exchange is very fast ($t_{1/2} \simeq 16$ s; [OD$^-$] 0.02 *M*.) k_2 *exo* was obtained by considering the extent of reaction $d_0 \rightarrow d_1$ after 1–4 min (for 3 runs), obtaining $t_{1/2}$, using the expression $t_{1/2} = \ln 2/k$ and dividing the pseudo-first order rate constant k by the base concentration.

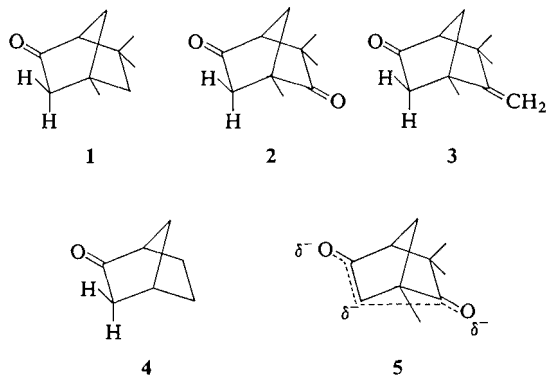

The results show that in the exchange process, (*a*) considerable rate enhancement, 200 for *exo* and 1840 *endo*, occurs when a carbonyl group is arranged 1,3 from the enolizable center (entries 1 and 2), (*b*) homoallylic stabilization[2] is certainly much less important than homoenolic stabilization and is probably small (entries 1 and 3), (*c*) the conformational and steric effects of an sp^2 center are small, and (*d*) the torsional effect (6) of a bridgehead methyl group is not much larger than that of hydrogen (entries 1 and 4).

[1]The kinetic procedure, similar to that described by Tidwell (4), was developed independently. Typically, an aliquot was quenched in acetate–phosphate buffer and the ketone (**1**, **3**, and **4**) was isolated by preparative gas chromatography. Deuterio-**2** was reduced to the diol and converted to the diacetate before the deuterium content was determined. Control experiments with deuteriated buffer and $LiAlD_4$ showed that exchange did not occur in the quenching and reduction stages. Deuterium analyses were done mass spectrometrically.

[2]Since the carbonyl group is much more effective than a double bond conjugatively and inductively in carbanion chemistry, a maximum enhancement of *ca.* 10 might be expected for *exo* exchange in **3**. Since the observed enhancement is 7, the results establish definitely that homoallylic stabilization and strain effects are small.

Recently, there has been some discussion as to whether enol or enolate intermediates and/or transition states are involved in NaOD–D_2O and MeONa–MeOD catalyzed enolizations (4, 7, 8). Although the magnitude of the inductive effect alone of the carbonyl group is not known exactly, the magnitudes and the difference in the degrees of enhancement for the *exo* and *endo* exchange suggest that some conjugation does occur to the 1,3 carbonyl group to yield a delocalized species of the type **5**. Our data, therefore, give some support for an enolate-like transition state for enolization, at least in the dione system.

That *endo* exchange is enhanced more than *exo* may be a consequence of several factors. Since the degree of charge development should be less in the more reactant-like transition state for *exo* exchange, the demand for stabilization via delocalization and therefore sensitivity to the 1,3 carbonyl group would be less in the *exo* case. A possibility worthy of consideration is that the *exo* and *endo*-hydrogens in dione **2** are different conformationally[3] from those in **1**, so that homoenolic stabilization (13) is more facile for *endo* cleavage. Further studies on this and other 2,5-dione systems are presently underway.

[3]That the 2,5-dione may exist in a twist conformation (cyclohexa-1,4-dione exists in a twist-boat conformation (9–12)) has been indicated by theoretical calculations and n.m.r. studies. An X-ray structure determination of the 2,5-dione is planned.

We wish to thank the National Research Council of Canada and the Department of University Affairs (Ontario) for financial support.

1. A. F. THOMAS and B. WILLHALM. Tetrahedron Lett. 1309 (1965).
2. J. M. JERKUNICA, S. BORČIĆ, and D. E. SUNKO. Tetrahedron Lett. 4465 (1965).
3. A. F. THOMAS, R. A. SCHNEIDER, and J. MEINWALD. J. Amer. Chem. Soc. **89**, 68 (1967).
4. T. T. TIDWELL. J. Amer. Chem. Soc. **92**, 1448 (1970).
5. P. BARRACLOUGH and D. W. YOUNG. Tetrahedron Lett. 2293 (1970).
6. P. VON R. SCHLEYER. J. Amer. Chem. Soc. **89**, 701 (1967).
7. J. WARKENTIN and C. BARNETT. J. Amer. Chem. Soc. **90**, 4629 (1968).
8. J. F. BUNNETT and L. A. RETALLICK. J. Amer. Chem. Soc. **89**, 423 (1967).
9. N. L. ALLINGER and C. B. BOYCE. J. Amer. Chem. Soc. **83**, 5028 (1961).
10. G. F. WRIGHT and F. LANTENSCHLAEGER. Can. J. Chem. **41**, 1972 (1963).
11. A. MOSSEL, C. ROMMERS, and E. HARRINGO. Tetrahedron Lett. 1247 (1963).
12. M. V. BHATT, G. SRINIVASAN, and P. NEELAKANTAN. Tetrahedron Lett. 21 and 291 (1965).
13. A. NICKON and J. L. LAMBERT. J. Amer. Chem. Soc. **88**, 1905 (1966).

Interaction of *s*-butyl peroxy and alkoxy radicals

R. HIATT AND LUDEK ZIGMUND
Department of Chemistry, Brock University, St. Catharines, Ontario

Received September 8, 1970

Contrary to previous suggestions, the interactions of 2 *s*-butyl peroxy radicals yields no di-*s*-butyl peroxide. Di-*s*-butyl peroxide has been shown to result from mixing *s*-butyl hydroperoxide with oxalyl chloride, presumably via 2 *s*-butyoxy radicals produced in a solvent cage from homolysis of di-*s*-butyl peroxyoxalate formed *in situ*.

Canadian Journal of Chemistry, **48**, 3967 (1970)

The interaction of non-tertiary peroxy radicals has been suggested (1) to proceed via a rapid hydrogen transfer via a cyclic transition state available to tetroxides formed by these species, though not open to di-tertiary tetroxides, which yield alkoxy radicals and oxygen in a solvent cage (2). The extreme rapidity of, and kinetic isotope effects on *sec*-peroxy – *sec*-peroxy radical interaction tend to corroborate this supposition (3); however, the fact that Co^{II}-catalyzed decomposition of *s*-BuO_2H yielded some 3% of *s*-Bu_2O_2 (4) has remained an obstacle, since for *t*-BuO_2H + Co^{II}, the yield of *t*-Bu_2O_2 was en-

[1] 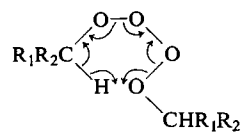

$$R_1R_2CO + O_2 + R_1R_2CHOH$$

Can. J. Chem. Downloaded from www.nrcresearchpress.com by 210.87.254.42 on 09/05/12
For personal use only.

Recently, there has been some discussion as to whether enol or enolate intermediates and/or transition states are involved in NaOD–D_2O and MeONa–MeOD catalyzed enolizations (4, 7, 8). Although the magnitude of the inductive effect alone of the carbonyl group is not known exactly, the magnitudes and the difference in the degrees of enhancement for the *exo* and *endo* exchange suggest that some conjugation does occur to the 1,3 carbonyl group to yield a delocalized species of the type **5**. Our data, therefore, give some support for an enolate-like transition state for enolization, at least in the dione system.

That *endo* exchange is enhanced more than *exo* may be a consequence of several factors. Since the degree of charge development should be less in the more reactant-like transition state for *exo* exchange, the demand for stabilization via delocalization and therefore sensitivity to the 1,3 carbonyl group would be less in the *exo* case. A possibility worthy of consideration is that the *exo* and *endo*-hydrogens in dione **2** are different conformationally[3] from those in **1**, so that homoenolic stabilization (13) is more facile for *endo* cleavage. Further studies on this and other 2,5-dione systems are presently underway.

[3]That the 2,5-dione may exist in a twist conformation (cyclohexa-1,4-dione exists in a twist-boat conformation (9–12)) has been indicated by theoretical calculations and n.m.r. studies. An X-ray structure determination of the 2,5-dione is planned.

We wish to thank the National Research Council of Canada and the Department of University Affairs (Ontario) for financial support.

1. A. F. THOMAS and B. WILLHALM. Tetrahedron Lett. 1309 (1965).
2. J. M. JERKUNICA, S. BORČIĆ, and D. E. SUNKO. Tetrahedron Lett. 4465 (1965).
3. A. F. THOMAS, R. A. SCHNEIDER, and J. MEINWALD. J. Amer. Chem. Soc. **89**, 68 (1967).
4. T. T. TIDWELL. J. Amer. Chem. Soc. **92**, 1448 (1970).
5. P. BARRACLOUGH and D. W. YOUNG. Tetrahedron Lett. 2293 (1970).
6. P. VON R. SCHLEYER. J. Amer. Chem. Soc. **89**, 701 (1967).
7. J. WARKENTIN and C. BARNETT. J. Amer. Chem. Soc. **90**, 4629 (1968).
8. J. F. BUNNETT and L. A. RETALLICK. J. Amer. Chem. Soc. **89**, 423 (1967).
9. N. L. ALLINGER and C. B. BOYCE. J. Amer. Chem. Soc. **83**, 5028 (1961).
10. G. F. WRIGHT and F. LANTENSCHLAEGER. Can. J. Chem. **41**, 1972 (1963).
11. A. MOSSEL, C. ROMMERS, and E. HARRINGO. Tetrahedron Lett. 1247 (1963).
12. M. V. BHATT, G. SRINIVASAN, and P. NEELAKANTAN. Tetrahedron Lett. 21 and 291 (1965).
13. A. NICKON and J. L. LAMBERT. J. Amer. Chem. Soc. **88**, 1905 (1966).

Interaction of *s*-butyl peroxy and alkoxy radicals

R. HIATT AND LUDEK ZIGMUND
Department of Chemistry, Brock University, St. Catharines, Ontario

Received September 8, 1970

Contrary to previous suggestions, the interactions of 2 *s*-butyl peroxy radicals yields no di-*s*-butyl peroxide. Di-*s*-butyl peroxide has been shown to result from mixing *s*-butyl hydroperoxide with oxalyl chloride, presumably via 2 *s*-butyoxy radicals produced in a solvent cage from homolysis of di-*s*-butyl peroxyoxalate formed *in situ*.

Canadian Journal of Chemistry, **48**, 3967 (1970)

The interaction of non-tertiary peroxy radicals has been suggested (1) to proceed via a rapid hydrogen transfer via a cyclic transition state available to tetroxides formed by these species, though not open to di-tertiary tetroxides, which yield alkoxy radicals and oxygen in a solvent cage (2). The extreme rapidity of, and kinetic isotope effects on *sec*-peroxy – *sec*-peroxy radical interaction tend to corroborate this supposition (3); however, the fact that Co^{II}-catalyzed decomposition of *s*-BuO_2H yielded some 3% of *s*-Bu_2O_2 (4) has remained an obstacle, since for *t*-BuO_2H + Co^{II}, the yield of *t*-Bu_2O_2 was en-

[1] 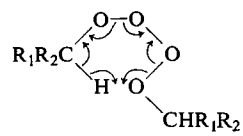

$$R_1R_2CO + O_2 + R_1R_2CHOH$$

Can. J. Chem. Downloaded from www.nrcresearchpress.com by 210.87.254.42 on 09/05/12
For personal use only.

Can. J. Chem. Downloaded from www.nrcresearchpress.com by 210.87.254.42 on 09/05/12
For personal use only.

tirely consistent with its being formed by interaction of 2 t-$BuO_2\cdot$'s, uninfluenced by the presence of metal ions (2, 4).

At the time that this was reported, we explained our inability to observe any s-Bu_2O_2 resulting from the solely free-radical-induced decomposition of s-BuO_2H as an experimental difficulty in detecting small amounts of this substance (2). Now, having considerably more experience in analyzing for s-Bu_2O_2 by g.l.c. (5), we have repeated the decomposition of s-BuO_2H by radicals produced from thermal decomposition of di-t-butyl peroxyoxalate (DBPO). Typically, 0.665 mmol of DBPO plus 1.22 mmol of s-BuO_2H in 10 ml of benzene heated at 45 °C for 5 h gave 1.19 mmol of t-BuOH, 0.458 mmol of s-BuOH, and 0.549 mmol of butanone, as well as CO_2 and O_2. No s-Bu_2O_2 was found though as little as 0.002 mmol could have been readily detected by the g.l.c. analysis (5). It thus appears that free s-butyl peroxy radicals *do not* yield s-Bu_2O_2 on interaction.

The production of s-Bu_2O_2 when s-BuO_2H is decomposed by Co^{II} must therefore be influenced by the metal ion, possibly via an ion–radical complex having some oxonium-like character.

$$[2]\quad [s\text{-}BuO\cdot Co^{II}] \leftrightarrow [s\text{-}BuO^{+}Co^{II}] \xrightarrow{s\text{-}BuO_2H} s\text{-}Bu_2O_2 + [Co^{III}OH^{-}]$$

So far, of course, no one has demonstrated that two s-butoxy radicals if produced together in a solvent cage (*e.g.*, $2\ s\text{-}BuO_2\cdot \xrightarrow{?} [2\ s\text{-}BuO\cdot + O_2]$) would in fact combine to give s-Bu_2O_2, as well as diffusing apart or disproportionating the other choices open. While combination *vs.* diffusion has been examined for 2 t-$BuO\cdot$'s under various circumstances (6), for s-$BuO\cdot$'s, the difficulty has been to establish experimental conditions where the radicals are both generated pairwise, and recombination is observable (5).

We believe this has now been accomplished through attempts to synthesize di-s-butyl peroxyoxalate. Though s-butyl peroxyesters are known to be particularly labile (7), we had hoped that at very low temperatures the conditions used to prepare DBPO (8) (*i.e.*, hydroperoxide, oxalyl chloride, and pyridine) would work. However, as low as −50°, the major products using s-BuO_2H were CO, CO_2, and butanone, with no evidence of free-radical-type products from the reactants or the solvent.

TABLE 1

Products from reacting 13.75 mmol of s-BuO_2H with 7.0 mmol of oxalyl chloride in 20 ml of toluene at 0 °C

Product	Amount, mmol	mol/mol of s-BuO_2H
Acetaldehyde	0.561	0.0408
Butanone	6.88	0.500
s-BuOH	3.67	0.267
s-Bu_2O_2	0.018	0.0013
Bibenzyl	0.044	0.0032
CO	0.63	0.046
CO_2	0.65	0.047
O_2	0.038	0.0028
$C_2H_4 + C_2H_6$	0.036	0.0026

Utilizing the method developed by Milas *et al.* (9) of using no pyridine, but removing evolved HCl by aspiration during the course of reaction, while not yielding any isolatable peroxalate, did result in products strongly suggestive of its formation (in low yield) and followed by homolysis. Table 1 shows those products identified by g.l.c. analysis from a typical run. The yield of conspicuously radical-type products is small, and it is not yet clear why the yield of acetaldehyde is not more nearly matched by that of bibenzyl (though, in the absence of contrary evidence, we are free to suggest that at this temperature, most ethyl radicals prefer to disproportionate, or to dimerize, rather than to abstract from toluene).

The obviously alternate route to s-Bu_2O_2, unreacted s-BuO_2H + s-BuOH (or s-BuCl from s-BuOH + HCl) can be rejected on two grounds; (*1*), reactions of H_2O_2 or hydroperoxides with alcohols or alkyl chlorides is a classically bad way to prepare *sec*-alkyl peroxides; (*2*) in our experiments the presence of s-Bu_2O_2 was always

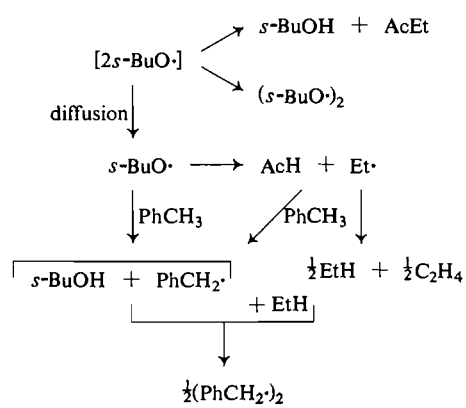

linked with the presence of bibenzyl, AcH, and O_2. Moreover, taking the yield of AcH as a fair approximation to the amount of *s*-butyl peroxyoxalate produced and decomposing homolytically, the yield of *s*-Bu_2O_2, $\sim 6\%$ of the initially produced caged radicals, is eminently reasonable in view of results with *t*-BuO· (2, 6).

Finally, the instability of *sec*-alkyl peroxyesters has been ascribed to concerted decomposition through a cyclic transition state, leading to ketone plus carboxylic acid (7). If this had been the case with di-*s*-butyl peroxyoxalate, a good yield of oxalic acid would be expected. In no case was oxalic acid found among the products, though it was shown to be stable under the conditions of reaction. While we yet have hopes of isolating di-*s*-butyl peroxyoxalate, we are, at the same time, exploring the reasons for our present failure; results to be published in due course.

The authors gratefully acknowledge financial support received from the National Research Council of Canada.

1 G. A. RUSSELL. J. Amer. Chem. Soc. **79**, 3871 (1957).
2 R. HIATT, T. MILL, and F. R. MAYO. J. Org. Chem. **33**, 1416 (1968) and references therein.
3. J. A. HOWARD and K. U. INGOLD. J. Amer. Chem. Soc. **90**, 1056 (1968); **90**, 1058 (1968).
4. R. HIATT, K. C. IRWIN, and C. W. GOULD. J. Org. Chem. **33**, 1430 (1968).
5. R. HIATT and S. SZILAGYI. Can. J. Chem. **48**, 615 (1970).
6. H. KIEFFER and T. G. TRAYLOR. J. Amer. Chem. Soc. **89**, 6667 (1967).
7. L. J. DURHAM, L. GLOVER, and H. S. MOSHER. J. Amer. Chem. Soc. **82**, 1508 (1960).
8. P. D. BARTLETT, E. P. BENZING, and R. E. PINCOCK. J. Amer. Chem. Soc. **82**, 1762 (1960).
9. N. A. MILAS, D. G. ORPHANOS, and R. J. KLEIN. J. Org. Chem. **29**, 3099 (1964).

Can. J. Chem. Downloaded from www.nrcresearchpress.com by 210.87.254.42 on 09/05/12
For personal use only.